ANGEWANDTE CHEMIE
International Edition in English
Volume 29 Number 1
January 1990
Pages 1–112

NMR Microscopy— Fundamentals, Limits and Possible Applications

New Analytical Methods (39)

By Winfried Kuhn

Dedicated to Professor Karl Hermann Hausser on the occasion of his 70th birthday

Alongside the numerous applications of NMR spectroscopy to structural elucidation in analytical chemistry, and to biochemical and morphological studies by NMR tomography, NMR microscopy makes possible a whole new range of applications. These include imaging, the investigation of biological objects such as plants and small animals, and also the observation of microscopic structures and structural changes in polymers and ceramics. NMR spectroscopy can also be conducted combinationally as volume-selective spectroscopy, whereby it is possible to spatially resolve the NMR-specific parameters: spin density ϱ, chemical shifts δ, and the relaxation times T_1 and T_2. The numerous well developed methods available make it possible to study dynamic processes by fast imaging with a temporal resolution in milliseconds. This not only allows the imaging of moving objects without incurring movement artefacts but also the measurement of diffusion constants in isotropic and anisotropic diffusion—in the latter case allowing, in principle, the determination of the complete diffusion tensor. The spatially resolved measurement of the relaxation times yields information on molecular mobility and bonding, e.g. the bonding of water, or other solvents, to polymers, the mobility of fluids in polymers or ceramics, or the three-dimensional evaluation of pore size in porous materials. In biomedicine, NMR microscopy allows the observation of growth on the cellular level, the study of embryos, and the development of therapeutic methods in animal experiments. It can lead to a drastic reduction in the number of animal experiments, and in combination with volume-selective spectroscopy gives valuable information on in-vivo metabolism.

1. Introduction

The physical phenomenon of NMR was discovered in 1946 by *Felix Bloch* and *Eduard Purcell*.[1, 2] Since then it has developed into one of the most fascinating methods available to physicists, chemists, biologists and medical practitioners.

Up to the 1970s NMR was used almost exclusively for structural analysis in chemistry, and for the measurement of such parameters as magnetic shielding tensors, electrical field gradient tensors and coupling tensors in molecular physics. Since the end of the 1970s, however, NMR has become important in the investigation of biochemical processes in vivo and in vitro, as an imaging method (NMR tomography), in the observation of morphological changes in tissues, and as a diagnostic aid in clinical practice. The combination of imaging and spectroscopic techniques allows volume-selective spectroscopy.

[*] Dr. W. Kuhn
Fraunhofer-Institut für zerstörungsfreie Prüfverfahren
Hauptabteilung Medizintechnik
Ensheimer Strasse 48, D-6670 St. Ingbert (FRG)

 © VCH Verlagsgesellschaft mbH, D-6940 Weinheim, 1990 0570-0833/90/0101-0001 $ 02.50/0

In clinical diagnosis either resistive or superconducting magnets with horizontal bores of between 60 and 100 cm are used, whereby the magnetic field strengths lie between 0.23 T and 2.4 T. These strengths correspond to proton resonance frequencies of 9.6 to 100 MHz. Magnetic field gradients with a strength of about 10 $mT m^{-1}$ (1 $G cm^{-1}$) allow a maximum spatial resolution of 5 mm^3 for whole-body systems.

As an example of the clinical application of NMR tomography, Figure 1 shows a sagittal section through the human head. The magnetic field strength was 0.28 T, corresponding

Fig. 1. Sagittal section through a human head. Slice thickness 5 mm, pixel resolution 1 mm^2, field strength 0.28 T, spin-echo image as sum of eight echoes of a multiecho recording.

to a proton resonance frequency of 11.6 MHz. The in-plane spatial resolution, termed pixel resolution (as the smallest element of an image is called a 'pixel'), is about 1 mm^2.

When discussing spatial resolution it is important to differentiate between the in-plane resolution and the resolution perpendicular to the slice thickness. The pixel resolution is normally far higher than that through the slice. Only occasionally in NMR tomography is an isotropic resolution obtained. The reasons for this difference in resolution lie firstly in the nature of the experiment, and secondly in the attainable signal-to-noise ratio (SNR). In a two-dimensional NMR imaging experiment a slice is normally selected by applying a selective RF pulse in the presence of a constant magnetic field gradient. The RF pulse has a bandwidth dependent upon its shape and duration .The slice thickness is then determined by the bandwidth of the pulse and the strength of the gradient. Hence an isotropic spatial resolution requires a pulse with a very narrow bandwidth, or extremely strong field gradients. Both of these are difficult to realize (see Section 3.2).

In three-dimensional experiments these restrictions do not exist, as no selective pulse is required for slice selection, instead spatial information in two directions is obtained by orthogonal field gradients of varying strength that act to phase-encode the signal. An isotropic resolution is thus more easily attainable in a three-dimensional experiment. The SNR achievable for the smallest detectable volume element (the *voxel*), and the size of the object under investigation, determine the maximum attainable resolution.

In biomedical research, in which the range of applications of NMR spectroscopy embraces the in-vivo observation of metabolic processes and morphological changes in tissues in animal experiments, magnets with horizontal bore sizes between 15 and 40 cm, and magnetic field strengths between 7.05 (^1H: 300 MHz) and 4.7 T (200 MHz) are used. The best spatial resolution obtainable with these instruments, using field gradients up to 100 $mT m^{-1}$, is about 1 mm^3.

A completely new dimension is opened up by the most recent NMR application, NMR microscopy, both in the spatial resolution attainable and the access to information at a molecular level. The first example of the realization of an NMR microscope was published in *Nature* in 1986.[3] The authors studied ova from *Xenopus laevis* (African clawed toad), and obtained for the first time images with a truly microscopic resolution of $13 \times 13 \times 250$ μm^3. NMR microscopy was made possible by magnets of high field strength, and strong magnetic field gradients. The highest magnetic field strength available for NMR is currently 14.1 T (600 MHz proton resonance frequency). Typically, the magnetic field strengths used for NMR microscopy lie between 7.05 (300 MHz) and 14.1 T. Table 1 shows a comparison of typical parameters and fields of application of currently available systems.

Commercial NMR microscopes are offered as supplementary add-ons to high-resolution and solid-state NMR spectrometers. They consist of a probe head with an integrated gradient system, a control unit for the gradient system for producing gradient pulses, and a modulation unit for RF

Winfried Kuhn, born February 5, 1949, studied engineering physics at the Technical College in Aachen (1971–1976) and subsequently physics (1976–1980) at the Institute of Technology in Aachen and at the University of Heidelberg. Following his Diplomarbeit at the Max Planck Institute for Medical Research in Heidelberg under Prof. Dr. K. H. Hausser, he completed his doctorate (1980–1983) at the same institute under Prof. U. Haeberlen. From 1982 until 1986 he was scientific co-worker and leader of the Instrumental Analytical Section (Chemistry/Biology) at the University of Bremen. 1986–1989 he worked for Fa. Bruker in Rheinstetten developing the NMR microscope. Since April 1, 1989 he has been in charge of the Magnetic Resonance Research Group at the Fraunhofer Institute for Nondestructable Analytical Methods in St. Ingbert.

Table 1. Comparison of NMR imaging systems.

	^{1}H-resonance frequency [MHz]	Magnetic field strength [T]	Object size [cm]	Spatial resolution [mm^3]	Application: Imaging on
NMR tomography (clinical diagnostics)	9.6–100	0.23–2.4	< 100	ca. 5	head and extremities
Tomography and in vivo spectroscopy (biomedical research)	41–200	1.00–4.7	< 30	ca. 2	animals such as rabbits, rats or mice
Mini-imaging	300–400	7.05–9.4	< 12	ca. 5×10^{-3}	rats, mice
NMR-microscopy	200–600	4.70–14.1	< 2.5	ca. 10^{-5}	mice, insects, polymers

pulses allowing modulation of both the amplitude and the phase of the pulse. With these gradient systems gradient strengths of about 1 Tm^{-1} are achievable. The highest resolution reached so far in the author's laboratory, and probably also worldwide, is $10 \times 10 \times 100$ μm^3.[4] This corresponds to a voxel volume of 10^{-5} mm^3 (Fig. 2).

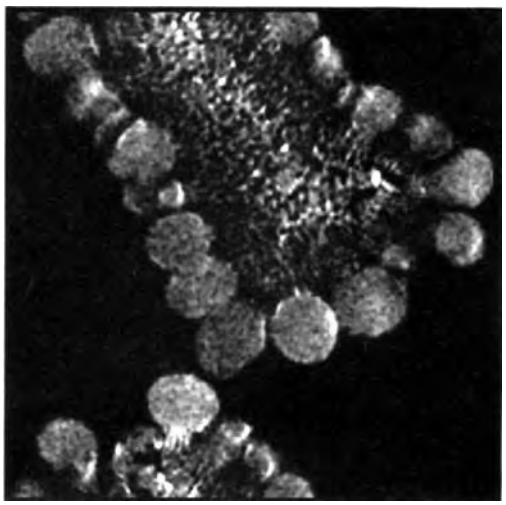

Fig. 2. Section through a leaf of the plant *Mesembryanthemum cristallinum*. The leaf of this plant is covered with oxalate crystals. Within the section the veins and some plant cells are visible. A spin-echo image is shown, recorded at a field strength of 7.05 T with a slice-thickness of 100 μm and a pixel resolution of 10^2 μm^2.

Various synonyms are used for NMR imaging. In medicine the term normally employed is "magnetic resonance imaging" (MRI), but "NMR imaging" and "spatially resolved nuclear magnetic resonance" are also used. For resolutions up to $100 \times 100 \times 1000$ μm^3 the term "mini-imaging" is common, and for superior resolutions the terms "micro-imaging" or "NMR-microscopy" are used.

2. Basic Principles of NMR Imaging

In a conventional NMR experiment, the object is placed in a static homogeneous magnetic field $\boldsymbol{B}$, which is related to the field strength $\boldsymbol{H}$ by the permeability constant μ_0 and the relative permeability μ_r [Equation (1)].

$$\boldsymbol{B} = \mu_0 \mu_r \boldsymbol{H} \tag{1}$$

In a sample with identical nuclei in an identical environment, e.g. the protons in water, all the spins experience the same magnetic field $\boldsymbol{B}$, and thus, from the resonance condition (2), have the same resonance frequency ω.

$$\omega = \gamma \boldsymbol{B} \tag{2}$$

The constant of proportionality γ is the nuclear gyromagnetic ratio, and has a value dependent upon the type of nuclei.

Nuclei in differing magnetic environments experience different magnetic fields, this being generally true of nuclei experiencing different chemical bonds. In NMR this manifests itself as discrete signals corresponding to the various chemical shifts.

This means that the resultant signal may be assigned to a given nucleus within the molecule, i.e. is localized within the molecule, but no spatial localization of the spins/molecules is possible as each nuclear species experiences a field independent of its position $\boldsymbol{r} = (x, y, z)$.

No possibility exists in such a homogeneous static magnetic field $\boldsymbol{B}_0$ of obtaining a spatial localization of the nuclei by means of their resonance frequency. The way to achieve spatially resolved NMR spectroscopy was discovered independently by *Damadian*[5] and *Lauterbur*[6] at the beginning of the 1970s. Spatially resolved magnetic resonance is made possible by superimposing a time dependent linear gradient field $\boldsymbol{G}(\boldsymbol{r}, t)$ onto the static magnetic field $\boldsymbol{B}_0$ [Eq. (3)].

$$\boldsymbol{B}(\boldsymbol{r}, t) = \boldsymbol{B}_0 + \boldsymbol{G}(\boldsymbol{r}, t) \tag{3}$$

The gradient field $\boldsymbol{G}(\boldsymbol{r}, t)$ has a linear dependence on the position, and as the nuclear resonance frequency is proportional to the magnetic field, there is then a linear relationship between the resonance frequency ω and the spatial position $\boldsymbol{r}$ [Eq. (4)].

$$\omega(\boldsymbol{r}, t) = \gamma \boldsymbol{B}(\boldsymbol{r}, t) \tag{4}$$

It should be emphasized that the gradient field has a *linear* dependence upon position, this means that the magnetic field gradients are *constant*.

The contribution made by each component of the gradient field to $\boldsymbol{B}_0 + \boldsymbol{G}(\boldsymbol{r}, t)$ is determined by the spatial derivative of the gradient field. The field gradient may be represented by a tensor having nine components [Eq. (5)].

$$\operatorname{grad} \boldsymbol{G}(\boldsymbol{r}, t) = \begin{pmatrix} \frac{\partial B_x}{\partial x} & \frac{\partial B_x}{\partial y} & \frac{\partial B_x}{\partial z} \\ \frac{\partial B_y}{\partial x} & \frac{\partial B_y}{\partial y} & \frac{\partial B_y}{\partial z} \\ \frac{\partial B_z}{\partial x} & \frac{\partial B_z}{\partial y} & \frac{\partial B_z}{\partial z} \end{pmatrix} \tag{5}$$

Usually $\boldsymbol{B}_0$ is of the order of 8 T, while the gradients are about 0.001 T. Hence the components perpendicular to the static magnetic field may be neglected, and only the components parallel to $\boldsymbol{B}_0$ lead to a spatial dependence of the resonance frequency (Fig. 3).

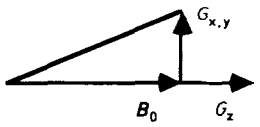

Fig. 3. Contribution of the gradient fields G_z and $G_{x,y}$ to $\boldsymbol{B}_0$. Only the components parallel to $\boldsymbol{B}_0$ make a contribution to the effective magnetic field $\boldsymbol{B}(r,t)$.

In practice the only tensor components having any influence on the resonance frequency in the sample are g_x, g_y and g_z [Eq. (6)–(8)].

$$g_x = \left(\frac{\partial B_z}{\partial x}\right) \tag{6}$$

$$g_y = \left(\frac{\partial B_z}{\partial y}\right) \tag{7}$$

$$g_z = \left(\frac{\partial B_z}{\partial z}\right) \tag{8}$$

These components may be represented as the components of a field gradient vector $\boldsymbol{g}$.

The superposition of the magnetic fields, and their effect on the nuclear resonance is shown in Figure 4. For $-x_0$,

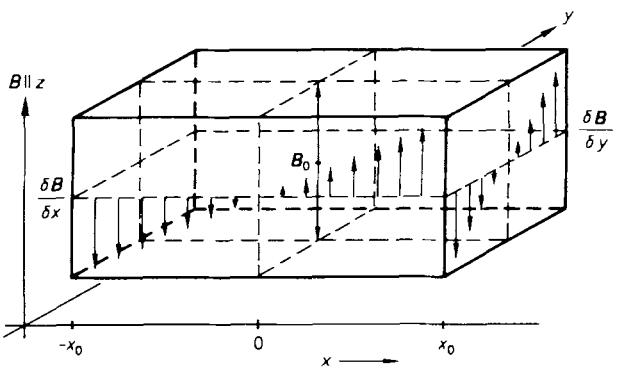

Fig. 4. Representation of the three-dimensional distribution of the gradient field $\boldsymbol{G}(\boldsymbol{r})$. The gradient fields change linearly over the sample volume. For $-x_0, -y_0, -z_0 < x,y,z < 0$, $\boldsymbol{B}(\boldsymbol{r}) < \boldsymbol{B}_0$, for $0 < x,y,z < x_0, y_0, z_0$, $\boldsymbol{B}(\boldsymbol{r}) > \boldsymbol{B}_0$ where $\boldsymbol{B}(\boldsymbol{r})$ is the resultant magnetic field.

$-y_0, -z_0 < x,y,z < 0$ the static magnetic field $\boldsymbol{B}_0$ is weakened by the influence of the gradient field $\boldsymbol{G}(x, y, z)$, and for $0 < x,y,z < x_0, y_0, z_0$ it is strengthened [Eqs. (9) and (10)].

$$\boldsymbol{B}(x,y,z) = \boldsymbol{B}_0 + \boldsymbol{G}(x,y,z) \tag{9}$$

$$\boldsymbol{B}(x,y,z) = \boldsymbol{B}_0 + \boldsymbol{gr} \tag{10}$$

From the resonance condition, the resonance frequency in the left half of the cubic volume is lower, in the right half higher, than ω_0 [Eq. (11)]. The spread of frequencies and

$$\omega(\boldsymbol{r}) = \omega_0 + \gamma \boldsymbol{gr} \tag{11}$$

hence the attainable spatial resolution is then directly proportional to the gradient strength $|\boldsymbol{g}|$ and the dimensions of the object $\Delta\boldsymbol{r} = (\Delta x, \Delta y, \Delta z)$ [Eq. (12)]. The gradient strengths

$$\Delta\omega = \gamma \boldsymbol{g} \Delta\boldsymbol{r} \tag{12}$$

determine the maximum spatial resolution attainable in an NMR imaging experiment.

3. Experimental Methods of NMR Microscopy

The excitation of nuclei within a sample is a result of irradiation with coherent electromagnetic waves. In general the RF pulse has an inexactly defined frequency spectrum from a few to several hundred kHz about the resonance frequency ω_0 of the nuclei in the static magnetic field $\boldsymbol{B}_0 = (0, 0, B_0)$, this being dependent upon the duration of the pulse. In the following discussion the simplification will be made that the static magnetic field lies parallel to the z axis of the coordinate system, and that only the z component B_0 of the field must be taken into consideration. Since nuclei subjected to a coherent irradiating RF field emit coherent RF waves, which may be detected by means of an appropriate coil, it is possible to apply a large number of different pulse experiments to the object, each yielding different characteristic information.

In the NMR spectroscopy of fluids such pulse experiments are used for the separation of coupling constants and chemical shifts, and in solid state NMR for line narrowing or for the decoupling/elimination of physical interactions, e.g. the dipolar coupling of protons or of protons and ^{13}C nuclei.

In NMR imaging a large number of different pulse sequences exist that, for example, allow very rapid imaging or images with a contrast weighted by the spin-spin or spin-lattice relaxation times. Of the numerous methods of NMR imaging available only three have proven to be of significant value.

3.1. Projection Reconstruction Techniques

These methods were used by *Lauterbur* in the early days of NMR imaging, and are now only used in special situations such as polymer imaging, or the spatially resolved measurement of spin-lattice and spin-spin relaxation times (relaxometry).[7] The reasons for this are the long measuring times and the relatively complicated data handling. These methods do however have the advantage of a very short time delay between the excitation of the nuclei and signal detection, thus allowing imaging of samples having very short spin-spin relaxation times. This also permits the detection of a large number of spin echoes in the case of relatively long spin-spin relaxation times. This is useful in relaxometry as it makes a multi-exponential fit to the relaxation curve possible, and thus enables tissue characterization.

3.2. Spin Echo Methods Based on a *Hahn*'s Spin Echo Pulse CP Sequence

The production of spin echoes by the method of *E. Hahn*,[8] uses a 90-τ-180-τ-echo sequence (Fig. 5). During the first period τ, the transverse component M_{xy} of the magnetization to a coherent state, and thus to a detectable echo. The path of the magnetization during such an experiment is shown in Figure 6.

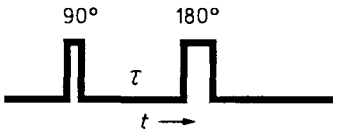

Fig. 5. Hahn spin-echo pulse-sequence. The excitation of the spin-system is achieved by a broad-band 90° pulse. The magnetization is refocussed by a 180° RF pulse. In this figure non-selective pulses are shown. This means that the pulses have a large (approx. 100 kHz) bandwidth, but this is not sharply-defined.

netization $\boldsymbol{M}$ loses phase coherence, i.e. is dephased under the influence of local inhomogeneities in the static magnetic field, and of the physical interactions with the nuclei. The 180° high-frequency pulse leads to a refocussing of the mag-

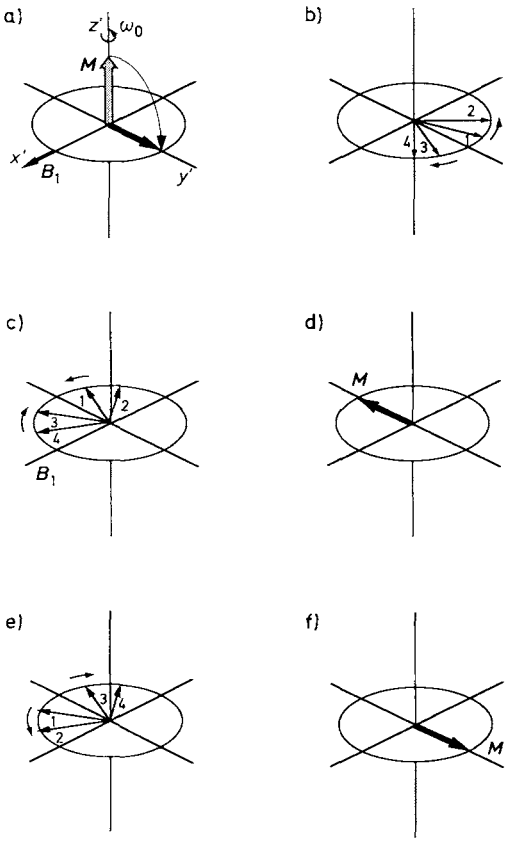

Fig. 6. Path of the magnetization during a spin-echo experiment. a) In the coordinate system rotating at the resonance frequency ω_0, the magnetization $\boldsymbol{M}$ lies parallel to the static magnetic field $\boldsymbol{B}(r) = (0,0,\boldsymbol{B}_0)$, i.e. along z'. The 90° pulse rotates the magnetization at resonance along the y'-axis, by means of an RF field $\boldsymbol{B}_1$ parallel to the x'-axis. b) The magnetization begins to dephase under the influence of local field inhomogeneities and gradients. c) The 180° pulse rotates the components of magnetization about the x'-axis, but the individual components continue to rotate in the same sense as previously. d) This leads to a coherent state after a time 2τ. This is known as a spin-echo, and is detectable. e) The magnetization starts once more to dephase, the steps (b)–(f) may be multiply repeated until the transverse magnetization M_{xy} disappears due to spin-lattice relaxation.

Spatial resolution of the nuclei is only possible by the combination of a spin-echo sequence with the appropriate magnetic field gradients. All of the following discussion of spin-echo sequences is based on the sequence shown in Figure 7.

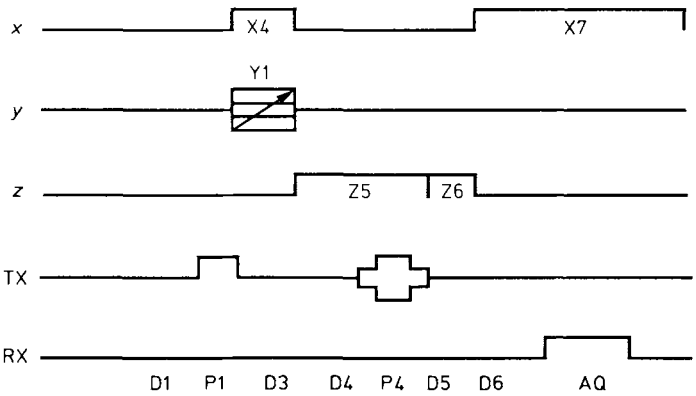

Fig. 7. The spin-echo sequence with x, y and z-gradients is shown; this is based upon the Hahn pulse sequence shown in Figure 5. Following a broad-band 90° pulse the magnetization dephases under the influence of local field inhomogeneities and the magnetic field gradients X4 and Y1 that have an exactly defined amplitude and duration. The amplitude of Y1 changes in the course of a two-dimensional imaging experiment by the increment IY1 [Eq. (13)]. X4 dephases the magnetization in the x'-y' plane of the rotating coordinate system. After the slice-selective 180° pulse P4 in the presence of gradient Z5, the magnetization is refocussed to a spin-echo by the read-gradient X7. The amplitude of the gradient Z5 and the bandwidth of the selective RF pulse determine the thickness of the selected slice. The amplitude of gradient X7 determines the in-plane resolution. TX = transmitter channel; RX = receiver channel.

In order to facilitate the description of the pulse sequence we shall consider a coordinate system rotating at the resonance frequency ω_0. After the 90° excitation pulse P1, the magnetization $\boldsymbol{M}$ at resonance is parallel to the y' axis of the rotating coordinate system, and hence only the component M_y exists. This pulse has a sufficiently large bandwidth to excite all nuclei of one species, and one isotope thereof. Under the influence of the dephasing gradient X4, and of local field inhomogeneities the transverse component of the magnetization dephases in the x'-y' plane. The incrementable phase-encoding gradient Y1 occurs simultaneously with the gradient X4. This gradient imposes on the NMR signal a phase φ characteristic of its strength I. This phase is stepped in increments $\Delta\varphi$ during the course of the experiment, as the strength I of Y1 increases or decreases by a definite increment IY1. The strength I of a gradient $g_\alpha(\alpha = x, y, z)$ is given by the time integral of the gradient [Eq. (12′)].

$$I = \int_0^{t'} g_\alpha \, dt \qquad (12')$$

For a two-dimensional image consisting, for example, of a 256 × 256 element matrix, one requires for the second image dimension 256 single experiments where the phase φ of the NMR signal at position y changes between each experiment in accord with Equation (13).

$$\Delta\varphi = \gamma \int IY1\, y\, dt \qquad (13)$$

Figure 8a shows phase-encoded spin-echoes, where the phase encoding is accomplished by gradients of varying strengths. The phase-corrected Fourier transformation of

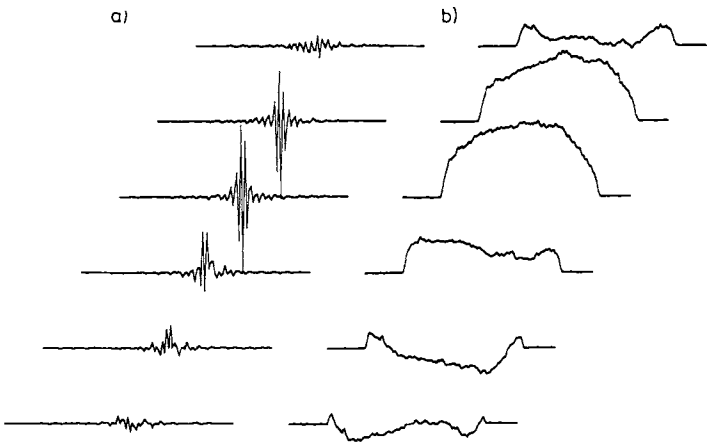

Fig. 8. a) Phase-encoded spin echoes from a two-dimensional spin echo experiment. b) Fourier transform of the spin echoes. One-dimensional phase-encoded profiles of the object in the direction of the read-gradient X7 are shown. The width of the profile is defined by the amplitude of the gradient X7.

these spin echoes is shown in Figure 8b. The spatial information in the first dimension is encoded by the application of the read-gradient X7 in the x direction. This gradient rephases the magnetization dephased by X4, and thus leads to a spin echo. The condition for complete rephasing of the signal is that the equality (14) be fulfilled, where the trans-

$$\int_0^{D3} X4\, dt = \int_0^{D6+AQ/2} X7\, dt \qquad (14)$$

verse magnetization dephased during the period D3 by the gradient X4 (see Fig. 7) is then rephased by the read gradient X7 during the period D6, which is required to stabilize the read gradient, and the acquisition time AQ. If the condition (14) is fulfilled, then a spin echo occurs with a maximum at the time AQ/2. As the echo maximum appears at the midpoint of the acquisition time, a symmetrical echo is detected, which is a condition for the ensuing Fourier transformation of the data.

In a two-dimensional imaging experiment, slice selection is achieved by a high-frequency (RF) pulse (P4) (Fig. 7) having an excitation angle of 180° and a defined bandwidth $\Delta\omega$ in the presence of a gradient Z5 perpendicular to the selected slice. RF pulses with a defined bandwidth are obtained by appropriate amplitude and phase modulation of electromagnetic waves having the carrier frequency ν_0. The Fourier theorem indicates that the duration of the pulse determines the excitation bandwidth space in the frequency range, and the carrier frequency of the pulse determines the position of the selected slice. In our example the gradient is parallel to the z axis of the coordinate system and the selected slice is perpendicular to this.

For slice selection, RF pulses with a $\sin(x)/x$ modulation or a Hermite modulation[9] are commonly used, whereby a $\sin(x)/x$ pulse of 4 ms duration gives, after Fourier transformation, an approximately square pulse with a bandwidth of 1170 Hz. For a z gradient of strength 100 $mT\,m^{-1}$ this corresponds according to Equation (15) to a slice thickness of 270 μm (Δz = slice thickness, $\Delta\omega$ = RF pulse bandwidth,

$$\Delta z = \frac{\Delta\omega}{(\gamma g)} \qquad (15)$$

γ = gyromagnetic ratio of nucleus ($\gamma_{^1H} = 42.58\ MHz\,T^{-1}$), g = strength of slice-selection gradient).

Figure 9 shows two examples of slice-selective RF pulses used in practice. These pulses are characterized by their favorable geometry for slice selection: The $\sin(x)/x$ pulse (Fig. 9a) has very steep sides and a flat plateau, corresponding to a sharply defined rectangular profile resulting from homogeneous excitation of all spins within the slice. However, at the pulse powers as are required for a 180° pulse there exists sideband modulation, which results in a partial excitation of nuclei in the vicinity of the slice. The Hermite pulse (Fig. 9c) has somewhat shallower sides, but better sideband characteristics. Figures 9b and 9d show the Fourier transformations of the RF pulses shown in Figures 9a and 9c, respectively.

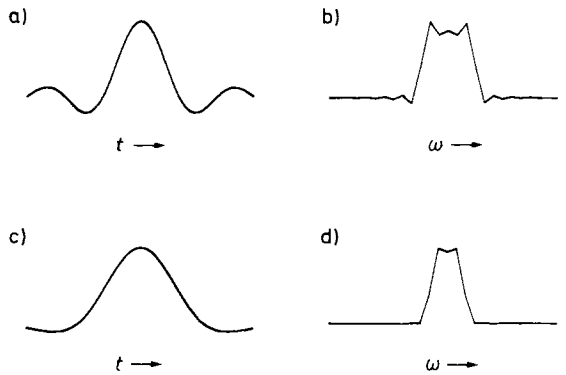

Fig. 9. RF modulation functions for slice-selective pulses. a) $\sin(x)/x$ modulation. b) Fourier transformed and phase-encoded spectrum of (a). c) Hermite function. d) Fourier transformed and phase-encoded spectrum of (b).

In principle it is possible to choose any desired slice within the object by an appropriate combination of gradients and of the carrier frequency of the slice-selective RF pulse; a mechanical alteration of the position of the object within the magnet is in general not necessary. Figure 10 illustrates effective slice selection by changing the resonance frequency in the presence of a slice-selective gradient.

The spin-echo methods include all pulse sequences having 180° refocussing pulses, and are very insensitive to inhomogeneities in the static magnetic field, thus giving images with a good signal-to-noise ratio and excellently reproducing the object profile. As a 90°–180° pulse sequence is used, the magnetization must be almost completely relaxed prior to each fresh repetition. In practice this implies a delay of at least T_1 between concluding data acquisition and the next excitation, and preferably of 3–5 T_1. These delays are in many cases of the order of seconds and lead to relatively long imaging times.

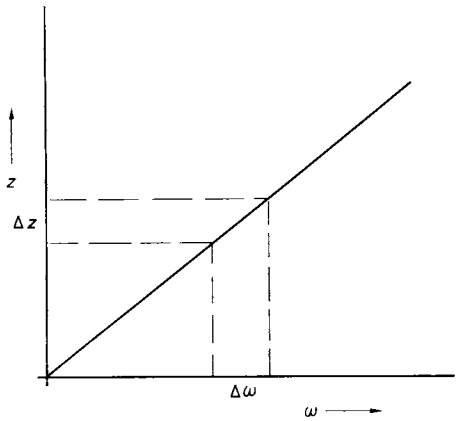

Fig. 10. Relationship of the bandwidth $\Delta\omega$ and the slice-thickness Δz in the presence of a gradient in the z-direction. The sharpness of the profile is given by the amplitude of the slice-gradient. For a given gradient strength the slice-thickness is proportional to the bandwidth of the pulse.

3.2.1. *Multi-slice Imaging*

Multi-slice imaging makes possible the imaging of a number of slices (e.g. 4, 8, 16, 32) in the same time as is necessary in a single-slice spin-echo experiment for one slice. The excitation of the spins within the sample is achieved by slice-selective 90° and 180° RF pulses. As the excitation bandwidth and profile should be the same for both pulses (both pulses affect the magnetization of the same slice), the pulses must be of differing power. As the pulses have differing profiles or even different sidebands, depending upon the pulse form, it is almost impossible to avoid some degree of overlap between neighboring slices. Effects due to overlapping may be minimized by means of a well planned excitation sequence, e.g. in an eight-slice experiment by exciting the slices in the order 1-3-5-7-2-4-6-8. The magnetization from previously excited slices relaxes following detection while the other slices are excited and detected. Thus, the relaxation delay necessary in a single slice experiment can be utilized to acquire the signals from several slices, without increasing the time required for the total experiment. Figure 11 shows the basic pulse sequence for multi-slice imaging, with two selective excitation pulses, and the corresponding gradient sequence for spatially encoding the magnetization.

The negative gradient Z3 refocusses the magnetization that is dephased by the gradient Z5 applied during the selective RF pulse P3. The duration of the latter is normally of the order of milliseconds, and for optimal rephasing the parameters are related by Equation (16).

$$Z3 = \frac{-Z5 \times P3}{(2 \times D3)} \tag{16}$$

Figure 12 shows the slice selection for a multi-slice experiment corresponding to the sequence shown in Figure 11.

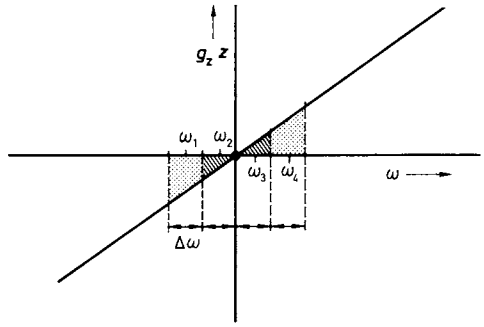

Fig. 12. A multi-slice selection is shown. The resonance frequency ω varies in the field gradient g_z, having a linear dependence with the spatial coordinate in the z-direction. The resonance frequency of the nuclei in the respective slices is ω_1 to ω_4. The bandwidth for a slice is $\Delta\omega$, determined by the duration of the selective RF pulse. The excitation of the individual slices occurs in the order slice 2 with frequency ω_2, slice 4 with frequency ω_4, slice 1 with frequency ω_1 and finally slice 3 with ω_3. This excitation sequence minimizes the effects of overlap between neighboring slices, and allows the relaxation of the spins in the slices already excited during the excitation and detection of the subsequent slices. In this experiment the repetition time is only 1/4 that of a single-slice experiment.

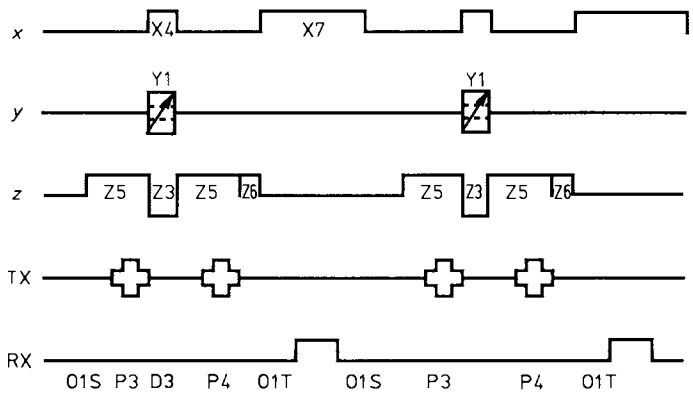

Fig. 11. Multi-slice pulse sequence with slice-selective 90° and 180° pulses. In contrast to the sequence shown in Figure 7, the spin system is excited with a defined bandwidth by the selective RF pulse P3. During this pulse the slice gradient Z5 is applied. During P3, which normally lasts several milliseconds, the magnetization is dephased by Z5. This dephasing is corrected by the negative gradient Z3, which is applied in the same direction as Z5 for a time D3. The gradient strength Z3 and Z5 are related by Equation (16). The frequency O1S defines the position of the selected slice, the frequency O1T is the receiver frequency.

3.2.2. *Multi-echo Imaging*

Multi-echo imaging is based on a Hahn echo sequence, in which, instead of a single echo, a series of echoes are generated by a sequence of slice-selective 180° RF pulses, and are detected and stored as separate data sets. Each of these echoes has the same phase encoding, and hence a complete image can be reconstructed from each echo. Figure 13 shows the multi-echo pulse sequence employed by the author, in which the phase-refocussing gradient Y2 refocusses the magnetization dephased by the phase-encoding gradient Y1.

Since the intensity of the spin echoes falls off exponentially at a rate determined by the spin-spin relaxation time T_2 [Eq. (17)], then T_2 weighted images are obtained following reconstruction.

$$M_{x,y}(t) = M_0 e^{-\frac{t}{T_2}} \tag{17}$$

According to *H. W. Spiess*[17] the spin-spin relaxation time T_2 of the nuclear spins is correlated with the mobility of the molecule via the rotation-correlation time τ_c [Eq. (18)].

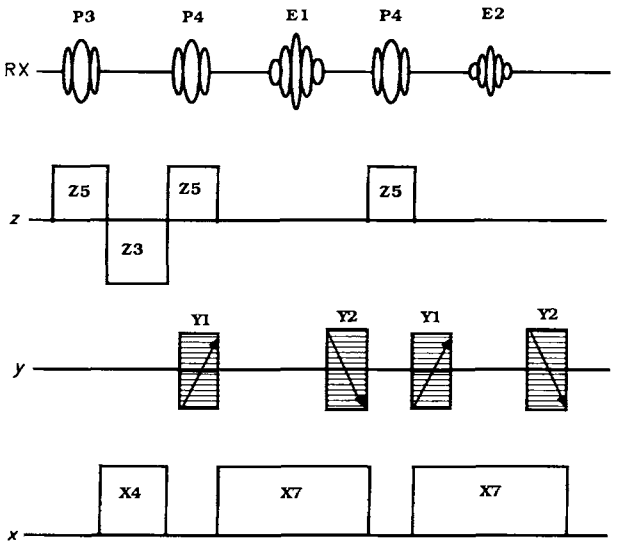

Fig. 13. Multi-echo single-slice pulse sequence. The nuclei here are excited, as in a multi-slice experiment, slice-selectively by narrow band RF pulses (P3, P4) in the presence of magnetic field gradients (Z5). Other than in the previously described methods (Fig. 7 and 12), in a multi-echo experiment a series of echoes (E1, E2, ...) are detected, not just as single echo, and the echoes are generated by repeated application of selective 180° pulses (P4) following the excitation of the system with a 90° pulse (P3). Unlike in the single-echo methods, after the detection of an echo the dephasing of the magnetization by the phase gradients Y1 is cancelled again by the gradients Y2; the strengths of the two gradients change inversely proportionally to each other from phase increment to phase increment. The advantage of this method is a prolonging of the time up to the total decay of the transversal magnetization. The amplitudes of the echoes in this experiment decrease with the relaxation time T_2. Since up to 128 echoes can be detected in the experiment, spatially resolved determination of T_2 is possible, thus enabling a parameter-selective image analysis [7].

$$\frac{1}{T_2} = \frac{1}{5}\gamma^4\left(\frac{h}{2\pi}\right)^2 I(I+1)\, r^{-6} \times \left(3\tau_c + \frac{5\tau_c}{1+\omega^2\tau_c^2} + \frac{2\tau_c}{1+4\omega^2\tau_c^2}\right) \qquad (18)$$

I is the nuclear quantum number and $r = |\boldsymbol{r}|$ the separation of the interacting nuclei, ω the resonance frequency and h the Planck constant.

Multi-echo imaging now offers the possibility of spatially resolved T_2 measurements. Hence this method gives unique access to the molecular dynamics in given regions of the sample. From the images of a multi-echo sequence it is possible to construct a "T_2-image". In a "T_2-image" the image intensity is proportional to the spin-spin relaxation time, and with this one obtains an insight into the homogeneity of the T_2 relaxation. Intensity profiles then allow the spatially resolved measurement of T_2 gradients. The summation of all the T_2 weighted images gives an image of extraordinarily rich contrast, which frequently allows the recognition of fine structures otherwise not normally seen. Possible uses of this method in polymer-research are, for example, the quantitative evaluation of the bonding of water or solvent-protons to polymer chains, and the spatial distribution of these over the complete polymer volume. Furthermore, this method offers the possibility of characterizing malignant and healthy tissue with a high spatial resolution, both in biomedical applications on humans, and in animal experiments. Multi-echo imaging is certainly one of the most valuable NMR imaging methods, both with respect to the image contrast obtained, and to the investigation of molecular dynamics.

3.2.3. *Chemical Shift Selective Imaging*

Chemical shift selective imaging is really the typical NMR imaging method. By this method images are produced only from nuclei having a given chemical shift. Hence it is possible in biomedical applications to obtain images showing the spatial distribution of water or fat in a tissue sample, an organ in vivo, or a plant. It also appears to be possible to image other metabolites, such as inorganic phosphate or phosphocreatine using ^{31}P-NMR imaging, or the metabolization of ^{13}C-labeled substances using ^{13}C-NMR imaging. The application of this method is relatively easy at high magnetic field strengths, and the spectral lines in question are well separated.

The chemical species to be detected is selectively excited by an RF pulse with a narrow bandwidth, such as a Gaussian pulse with a bandwidth of a few hundred hertz, and only this species is then detected (cf. Fig. 14). The subsequent course

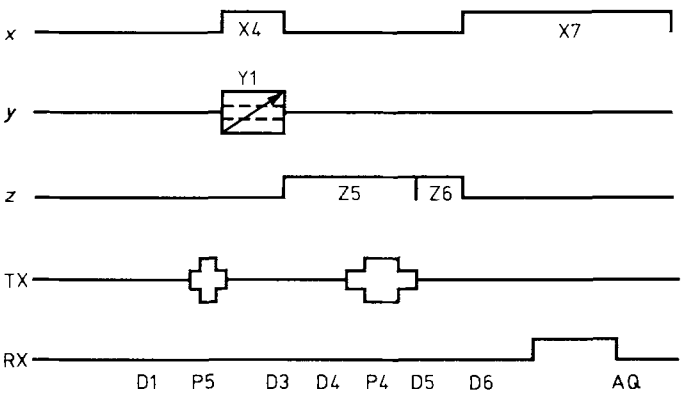

Fig. 14. Pulse sequence for the acquisition of a chemical shift selective image. The selection according to the chemical shift of a nuclear species is achieved by a gaussian 90° pulse having a narrow bandwidth. The pulse's carrier frequency corresponds to the resonance frequency of the species to be imaged. The further course of the experiment is identical to that shown in Figure 7.

of the experiment is that of a normal spin-echo experiment as described in Section 3.2, with the difference that during the experiment only magnetization excited on the basis of the chemical shift is further manipulated by the RF pulses, and then detected.

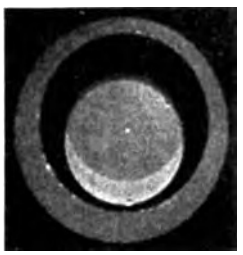

Fig. 15. Proton image of a phantom consisting of a 10-mm NMR tube filled with water, and containing a 5-mm tube filled with oil. The proton resonance frequency is 500 MHz. The chemical shift of the lipid with respect to the water protons is clearly visible.

Figures 15 and 16 demonstrate the excellent selection of chemically different species, in this case fat and water. The object consisted of a 10-mm NMR tube filled with water and containing a 5-mm tube filled with oil. This experiment was conducted at 11.74 T, corresponding to a proton resonance frequency of 500 MHz.

Fig. 16. Left: Chemical shift selective water image of the same sample as in Figure 15. Right: Chemical shift selective image of the sample's lipid protons. In both cases excitation is achieved with a gaussian pulse of approximately 600-Hz bandwidth.

3.2.4. T_1 Imaging

The return of the magnetization of thermal equilibrium following excitation by a 90° RF pulse, is described by the relaxation times T_1 and T_2. T_2 describes the loss of phase-coherence of the spin system, T_1 the relaxation of the magnetization parallel to the static magnetic field. The T_1 relaxation is given by

$$M_z(t) = \boldsymbol{M}_0(1 - e^{-\frac{t}{T_1}}) \tag{19}$$

The measurement of the spin-lattice time T_1 in NMR spectroscopy is performed using inversion-recovery[11] and saturation-recovery[12] pulse sequences. The combination of these pulse sequences with imaging methods (Fig. 17) allows the acquisition of T_1-weighted images from which spatially resolved spin-lattice relaxation times may be determined. This allows, on the one hand, inferences to be made about the molecular mobility at various positions of the sample, and, on the other, the possibility of a stronger contrast between regions with differing T_1 times.

Figure 17a shows an inversion-recovery imaging sequence. In this sequence the z-component M_z of the magnetization is inverted by the 180° pulse. After the delay VD, during which the longitudinal component of the magnetization relaxes due to spin-lattice interactions, this part of the total magnetization is detected using a spin-echo sequence. The echo amplitude is hence determined by both relaxation times [Eq. (20)].

$$M_y(t) = \boldsymbol{M}_0(1 - \beta e^{-\frac{VD}{T_1}})\,(1 - 2e^{-\frac{TR}{T_2}} e^{-\frac{TE}{2T_1}} + e^{-\frac{TE}{T_2}}) \tag{20}$$

TR is the repetition time of the experiment, TE the echo delay, β is 2 for inversion recovery, and 1 for saturation recovery experiments.

Figure 17b shows a saturation-recovery pulse-sequence. In this the magnetization is saturated by a rapid sequence of 90° pulses. The further course of the experiment is as given above.

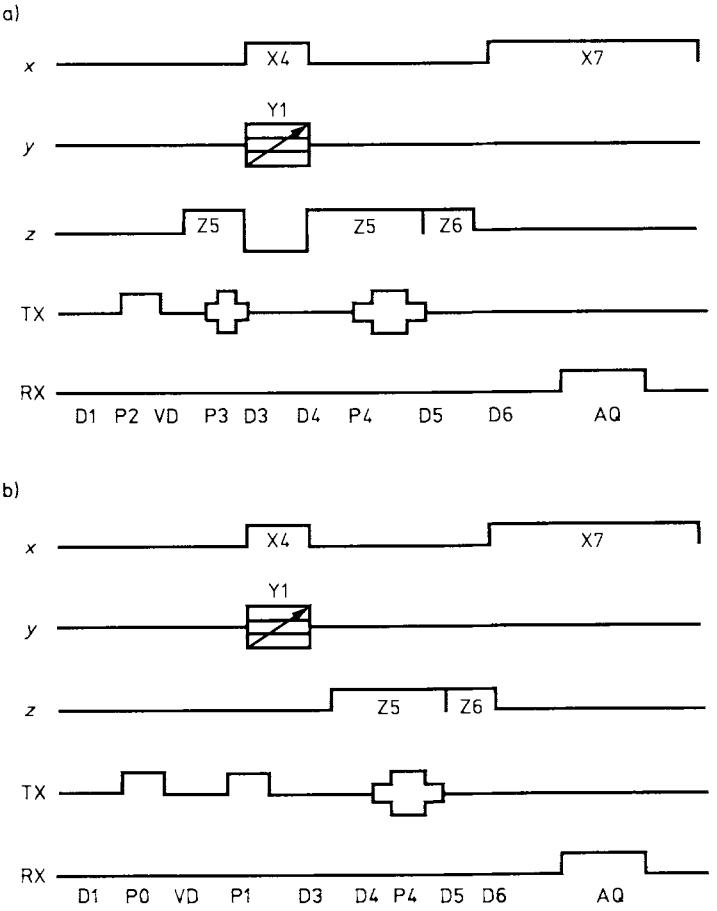

Fig. 17. a) Inversion-recovery imaging sequence. The inversion of the magnetization is achieved by a broad-band 180° pulse at the start of the pulse sequence. After a delay VD, during which the magnetization can relax along the z'-axis parallel to $\boldsymbol{B}_0$, a conventional spin-echo experiment (Fig. 7) is conducted. Depending upon the length of the delay VD, the images have a strong weighting according to the spin-lattice relaxation time. A series of inversion-recovery images with varying delays VD allows the spatially resolved measurement of T_1. b) Saturation-recovery sequence. The saturation of the magnetization is achieved by an aperiodic saturation sequence, in which the separation between consecutive pulses is reduced in geometric succession. The further course of the experiment is analogous to that of Figure 17a. The saturation-recovery sequence has the advantage over the inversion-recovery sequence that it is not necessary to wait between successive applications of the sequence, as the magnetization is saturated, and must not return to thermal equilibrium. This makes possible rapid T_1 weighted imaging.

As T_1 is correlated to molecular mobility, and also shows a clear dependence upon $1/(1 + \omega^2\tau_c^2)$, T_1 weighted images are an excellent means of visualizing molecular dynamic properties. Owing to the dependence of T_1 on the field strength, these methods are well suited to spatially resolved, field strength dependent, T_1 measurements. These measurements yield information about the physical interactions contributing to the relaxation.

3.3. Gradient Reversal Methods

Measurements with the spin-echo methods described in Sections 3.2 to 3.2.4 generally require a considerable delay between the individual experiments of at least T_1, and preferably 3–5 T_1, to allow for the relaxation of the longitudinal magnetization. In recent years, a large number of different pulse sequences have been developed in order to make rapid

imaging possible. The most popular, and for NMR microscopy the most important methods are the FLASH (*F*ast *L*ow *A*ngle *Sh*ot) methods,[13] which refocus the magnetization by gradient reversal instead of by a 180° refocussing pulse (Fig. 18).

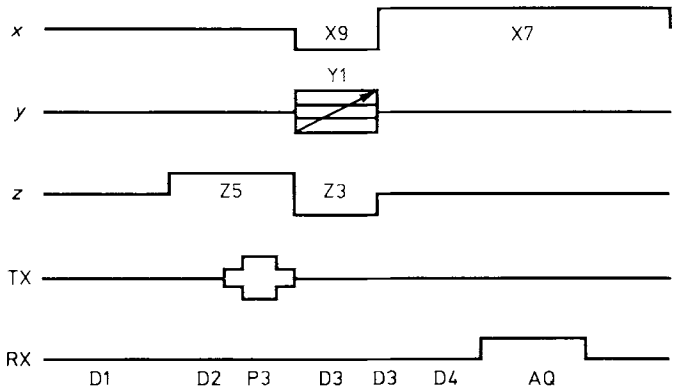

Fig. 18. Pulse sequence for rapid imaging with the FLASH sequence [13]. The magnetization is excited through a small angle from the z-axis by the RF pulse P3 in the presence of the slice-gradient Z5. The transverse components of the magnetization are then dephased by the gradients X9 and Y1 during the time D3. The Y1 gradient is turned off, and the gradient X9 reversed to give the read gradient X7. This leads to a rephasing of the transverse magnetization known as a gradient-echo.

The excitation of the spin system is accomplished in this pulse sequence by means of a slice-selective RF pulse with a small excitation angle. Under the influence of the gradient X9 the magnetization in the x'-y'-plane is dephased. The gradient Y1 simultaneously phase-encodes the second dimension of the slice. After a delay D3 the gradient X9 is reversed, this leads to a rephasing of magnetization of the observed slice, and finally once more to a coherent state that is detected as a "gradient echo". The FLASH sequence has the advantage that the short repetition time allows the acquisition of images within very short times of between 100 ms and a few seconds.

The disadvantage of this method is its sensitivity to inhomogeneities in the static magnetic field. As there is no 180° RF pulse in the FLASH sequence, only the magnetization that is dephased by the gradient X9 is refocussed. Magnetization that is dephased by main field inhomogeneities or susceptibility gradients at boundaries will not be refocussed by the gradient reversal. This magnetization makes only a small contribution to the signal, and leads to a poorer signal-to-noise ratio than in a spin-echo experiment, but may give an enhanced image contrast.

Since gradient reversal methods do not necessarily require that the magnetization is in thermal equilibrium prior to the pulse sequence, these methods are currently the only practical methods for rapid imaging. In combination with short acquisition times and very short gradient stabilization times of less than 100 μs (as are possible in a microscopy system), it is possible to acquire gradient reversed images with a matrix size of 128 × 64 in about 100 ms.

These very short imaging times allow the examination of relatively fast kinetics by NMR imaging. Figure 19 shows a glass-tube which is filled with water and contains a rectangular piece of plastic and is rotating at about 2 Hz. Despite the rotation of the sample the images are remarkably sharp.

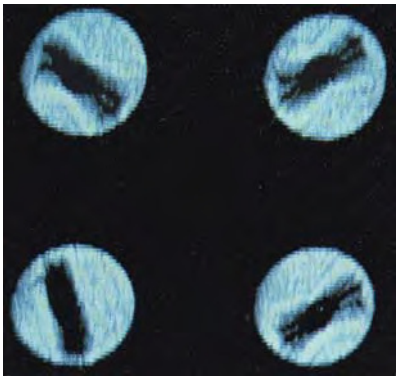

Fig. 19. Images of an NMR tube rotating at 2 Hz. The tube was filled with water and contained a submerged piece of plastic. These images were obtained with a snapshot-FLASH sequence [14] during the rotation of the tube. The imaging time was 90 ms per image for a matrix of 64 × 128 points. The gradient strengths used were 300 mTm^{-1} for the read and phase-encoding gradients and 200 mTm^{-1} for the slice gradient. The measurements were made at a field strength of 7.05 T.

4. Contrast Determining Parameters

Other than in the case of X-ray tomography, in which the contrast is determined only by the absorption of the X-rays, image contrast in NMR imaging is determined by the spin density and by the relaxation times T_1 and T_2 within the sample. By the appropriate choice of acquisition parameters it is possible to obtain an image contrast with a well defined relationship to certain physical properties of the object under investigation.

On using a spin-echo sequence for the acquisition of an image, the image contrast for a pixel is determined by the signal strength $S(\mathrm{TE,TR})$ [Eq. (21)][15] from the corresponding voxel.

$$S(\mathrm{TE,TR}) = \varrho\left(1-2e^{-\frac{TR}{T_1}}e^{-\frac{TE}{2T_1}}+e^{-\frac{TR}{T_2}}\right)e^{-\frac{TE}{T_2}} \qquad (21)$$

By appropriate choice of the parameters spin-echo time TE and repetition time TR, it is possible to weight the image contrast according to the spin density ϱ, or the relaxation times T_1 and T_2 [Eq. (21)].

For the gradient reversal method the signal strength is given by Equation (22).[16] By varying the excitation angle

$$S = \varrho\frac{\left(1-e^{-\frac{TR}{T_1}}\right)e^{-\frac{TE}{T_2}}\sin\theta}{1-e^{-\frac{TR}{T_1}}e^{-\frac{TR}{T_2}}-\left(e^{-\frac{TR}{T_1}}-e^{-\frac{TR}{T_2}}\right)\cos\theta} \qquad (22)$$

θ, spin-echo time TE and the repetition time TR it is also possible by this method to produce different image contrasts.

4.1. Spin Density

The spin density ϱ is determined by the number of nuclei of a certain species, e.g. water protons, lipid protons, in a

defined volume element. From the intensity of the signals in the spectrum, or from the integral of the image profile, it is possible to obtain the relative, or by calibration, the absolute metabolic concentration. Pure spin density images can be obtained with a spin-echo pulse sequence by choosing the parameters $TR \gg T_1$ and $TE \ll T_2$. For these parameters the signal strength $S(TE,TR)$ is only a function of the spin density ϱ, i.e. the image contrast is determined by the spin density within each voxel. In this situation the profile gives a quantitative determination of the metabolites imaged. In order to reduce the imaging time it is common to choose a shorter repetition time TR, generally $TR = T_1$. When this is the case, and when $TE \ll T_1$ and $TE \ll T_2$ are still valid, the signal intensity S of the NMR signal is, according to Equation (21), $0.63\,\varrho$, and is independent of other parameters.

4.2. Spin-Lattice Relaxation Time T_1

The spin-lattice relaxation time T_1 describes the return of the z component of the magnetization to thermal equilibrium, following the excitation of the spin system by an RF pulse.

In the case of proton imaging, the spin-lattice relaxation time is almost completely determined by the proton-proton dipolar coupling. In the case of other nuclei, such as ^{31}P in adenosine triphosphate, the contribution of the magnetic anisotropy of the phosphorus nuclei must also be considered. For the relaxation rate $1/T_1$, in the case of homonuclear dipolar coupling of nuclei I having isotropic motion one obtains Equation (23),[17] from which it can be seen that the

$$\frac{1}{T_1} = \frac{2}{5}\gamma^4\left(\frac{h}{2\pi}\right)^2 I(I+1)\,r^{-6}\left(\frac{\tau_c}{1+\omega^2\tau_c^2} + \frac{4\tau_c}{1+4\omega^2\tau_c^2}\right) \quad (23)$$

spin-lattice relaxation rate $1/T_1$ is dependent upon the correlation time τ_c of the molecule concerned. When the mobility of the molecule is restricted, as is generally the case in biological and polymeric samples, the relaxation rate $1/T_1$ is a function of the resonance frequency ω of the nuclei, and is hence dependent upon the magnetic field strength. From T_1-weighted images, or spatially resolved T_1 measurements (see Section 3.2.4), it is possible to estimate the mean intermolecular separation r if the correlation time τ_c is known, or, conversely, to determine the correlation time if r is known.

From Equation (21) one can derive the experimental conditions for T_1-weighted spin-echo images: For $TE \ll T_1 T_2$ one obtains Equation (24). An analogous condition for the

$$S(TR, T_1) = \varrho\,(1 - e^{-\frac{TR}{T_1}}) \quad (24)$$

gradient reversal method [Eq. (25)] is obtained from Equation (22) by choosing $TE \ll T_2$ and $TR \gg T_2$.

$$S(\theta) = \varrho \sin\theta \quad (25)$$

4.3. Spin-Spin Relaxation Time T_2

The spin-spin relaxation time T_2 exhibits a dependence upon the molecular correlation time of the molecule[17] in much the same way as the spin-lattice relaxation time T_1 does. Although the constant term $3\,\tau_c$ in Equation (26) [= Eq. (18)] shows that the dependence upon the magnetic field strength is significantly less. This makes the T_2 value an

$$\frac{1}{T_2} = \frac{1}{5}\gamma^4\left(\frac{h}{2\pi}\right)^2 I(I+1)\,r^{-6} \times \left(3\tau_c + \frac{5\tau_c}{1+\omega^2\tau_c^2} + \frac{2\tau_c}{1+4\omega^2\tau_c^2}\right) \quad (26)$$

ideal parameter for the characterization of molecular dynamic properties, as T_2 values measured at differing frequencies may still be compared with each other.

Pure T_2-weighted images are obtained by choosing $TR \gg T_1$. The signal intensity is hereby a function of the spin-echo time TE and the spin-spin relaxation time T_2 [Eq. (27)]. The image contrast in this case is determined only

$$S(TE, T_2) = \varrho\, e^{-\frac{TE}{T_2}} \quad (27)$$

by the spin-density ϱ and the ratio TE/T_2.

5. Limits to the Spatial Resolution of the NMR Microscope

The attainable resolution of the NMR microscope is limited by physical and technical factors.[18] Physical factors are: the line width and the chemical shift of the NMR signal, diffusion processes, and susceptibility gradients, both within the object and at its boundaries. Technical factors may be magnetic field inhomogeneity or instability, non-linearity of the magnetic field gradients, and the achievable signal-to-noise ratio.

5.1. Physical Limitations

5.1.1. Signal Line Width

The line width of the NMR signal $\Delta\nu$ is defined as the width of a Lorentzian line at half the maximum height where

$$\Delta\nu = \frac{1}{\pi T_2} \quad (28)$$

T_2 is the spin-spin relaxation time of the nuclei.

Equations (12) and (28) give the maximum obtainable spatial resolution Δx for a given spin-spin relaxation time T_2 as:

$$\Delta x = \frac{2}{\gamma g_x T_2} \quad (29)$$

In the following discussion three commonly encountered cases will be considered: NMR microscopy of a) samples similar to water, b) biological material, c) solids.

In water-like samples the T_2 times are between several hundred milliseconds and seconds. With regard to Equations (23) and (26) the situation of extreme narrowing pertains, i.e. the terms $\omega^2\tau_c^2$ are much smaller than unity, and

hence may be neglected. The relaxation rates then show no further dependence upon the field strength. For example Equation (29) shows that to obtain a pixel resolution of 10 μm for a sample having a T_2 of 1 s, a gradient strength of 0.7 mTm^{-1} (=0.07 G/cm) is necessary. In biological samples the signal line width may reach 100 Hz, depending upon the environment of the nuclei. This corresponds to a T_2 of about 3 ms. To obtain a spatial resolution of 10 μm in this situation requires a gradient strength of at least 235 mTm^{-1}.

In solids the line width may reach 50 kHz due to the dipolar coupling of protons to each other. For a resolution of only 1 mm a gradient strength of 1100 mTm^{-1} is required. For the realization of such an experiment these very strong gradients must be switched within 20 μs. This would induce enormous eddy currents in the electrically conducting parts of the magnet, which would have a strong effect on the magnetization. The experiment is also unrealizable in practice owing to the level of self-induction present.

From these considerations it is apparent that it should be possible to achieve resolution in the μm range for water-like samples and biological samples, but that, with the spin-echo and gradient-reversed methods described above, resolution of this order is impossible for solids. Possible techniques for achieving this are the combination of rotating gradients with the magic-angle spinning (MAS) frequency of the sample,[19] or of multipulse sequences with imaging methods[20–22] or RF pulse field gradients.[23] Fortunately the spin-spin relaxation times of many polymers lie in the millisecond range, and hence allow high resolution imaging by conventional methods.

5.1.2. *Chemical Shift*

The magnetic environment of a particular nuclear species can vary greatly within a sample. It is characterized by the chemical shift δ of the resonance signal in the spectrum, which is defined according to Equation (30).

$$\delta = (\omega_{signal} - \omega_{reference})/\omega_{reference} \tag{30}$$

The chemical shift δ is dependent upon the pH value, upon paramagnetic ions that may concentrate in particular regions of the sample, and upon temperature effects. This leads to a spread $\Delta\nu$ of the resonance frequencies of a molecular species over a definite range. The frequency range of the chemical shift of a nuclear species within a sample is proportional to the magnetic field strength B_0 [Eq. (31)], where the range of the chemical shift $\Delta\delta$ depends upon the magnetic environment of the nuclei

$$\Delta\nu = \gamma\,\Delta\delta\,B_0\,10^{-6} \tag{31}$$

The attainable resolution Δx for a given range of chemical shifts $\Delta\delta$ of a nuclear species, and for a given magnetic field strength B_0 is given by Equation (32). For example, to obtain

$$\Delta x = \frac{1}{g}\gamma\,\Delta\delta\,B_0\,10^{-6} \tag{32}$$

a resolution of 10 μm at a field strength of 9.4 T (400 MHz proton resonance frequency), and for a chemical shift range $\Delta\delta \approx 0.05$ for water in biological material, a gradient strength of 50 mTm^{-1} is necessary.

5.1.3. *Molecular Diffusion*

The influence of molecular diffusion on the attainable spatial resolution in NMR microscopy will be discussed under the following two aspects:

a) Molecular diffusion is certainly a resolution limiting factor if between excitation and detection the nuclei diffuse into a neighboring voxel. The maximum time allowed in a spin-echo experiment for a well defined resolution may be estimated with the help of classical thermodynamics.[24] Consider a group of particles at the center of the voxel ($x = 0$) at time $t = 0$. Under the influence of Brownian molecular motion the particles diffuse according to Fick's first law, so that at time t the expectation value of their distance from the origin is given by Equation (33). In a spin-

$$\Delta x = \sqrt{\overline{x^2}} = \sqrt{2Dt} \tag{33}$$

echo experiment the spatial resolution is only defined if, during the echo time TE, the spins do not leave the voxel in which they were excited, i.e. when the relationship (34) holds.

$$TE \leq \frac{(\Delta x)^2}{2D} \tag{34}$$

For a 10-μm voxel, and a sample consisting of pure water ($D = 2 \times 10^{-9}$ m^2/s) this implies that TE < 25 ms. In biological material and in polymers, the diffusion constant generally has a considerably lower value than that of free water. Further, in microscopy experiments TE normally lies between 1 and 20 ms, and hence, by the arguments given above, diffusion presents no limitation to the attainable resolution.

b) According to *Carr* and *Purcell*,[25] the relaxation of the transverse magnetization under the influence of T_2 in the presence of a magnetic field gradient $|\boldsymbol{G}|$ and diffusion is given by Equation (35).

$$M_{xy}(t) = \boldsymbol{M}_0\, e^{-\frac{t}{T_2}}\, e^{-\frac{1}{12}\gamma^2 G^2 D t^3} \tag{35}$$

This clearly leads to line broadening if the diffusion term M_D [Eq. (36)] reaches a similar order of magnitude to the

$$M_D = e^{-\frac{1}{12}\gamma^2 G^2 D t^3} \tag{36}$$

$$M_{T_2} = e^{-\frac{t}{T_2}} \tag{37}$$

T_2 term M_{T_2} [Eq. (37)]. For water (diffusion constant $D = 2 \times 10^{-9}$ m^2/s) it may be calculated that the gradient strength required for, e.g., a spatial resolution of 10 μm is 4 mTm^{-1}. Since the maximum gradients in an NMR microscope are always stronger than this, molecular diffusion at room temperature presents no limitation to the attainable spatial resolution.

5.2. Technical Limitations

Alongside physical considerations, technical factors must also be bourne in mind when considering the limits of spatial

resolution. Under consideration are imperfections in the apparatus, and the signal-to-noise ratio. The former may be due to magnetic field inhomogeneity, temporal instability or to nonlinearities in the gradient field.

5.2.1. Homogeneity and Stability of the Static Magnetic Field

The homogeneity of superconducting high field magnets currently in use for high resolution NMR spectroscopy, is characterized by the inhomogeneity factor f [Eq. (38)],

$$f = \frac{\Delta B}{B_0} \tag{38}$$

where f is appropriately $3 \times 10^{-8}\ h^{-1}$. In order to maintain a given resolution the inhomogeneity or instability ΔB of the static magnetic field $\boldsymbol{B}_0$ must be smaller than, or equal to, the inhomogeneity induced by the gradients during the entire experiment, i.e.

$$\Delta B = g\Delta x \tag{39}$$

By considering the inhomogeneity factor f one obtains a pixel size

$$\Delta x = f\frac{B_0}{g} \tag{40}$$

For a gradient strength of 100 $mT\,m^{-1}$ using a 10 T magnet, Equation (40) indicates that a maximum resolution of 3 μm is obtainable. If the gradient strength is 750 $mT\,m^{-1}$, then the resolution is 0.4 μm. In both instances an experimental duration not exceeding 1 h is assumed. For an "overnight" experiment having a duration of 15 h, one obtains resolutions of only 45 μm and 6 μm respectively for the two situations given above.

Hence magnetic field inhomogeneities and instabilities can have an effect on the attainable spatial resolution in NMR microscopy.

5.2.2. Magnetic Field Gradient Linearity

Unfortunately, magnetic field gradients are in general only constant in theory. In practice a coil is of finite length, and because of the limited space available, the length to diameter ratio is fixed. Hence a constant field gradient over the total length and diameter of the coil is unrealizable. Further distortion of the gradient field linearity is to be expected due to the coil construction, and to the distribution of the coil windings, which are normally multilayered.

This means that the magnetic field gradients within a gradient coil are spatially dependent, and may only be approximately described by a series expansion [Eq. 41)].

$$\boldsymbol{g} = \boldsymbol{g}(x) = a_1\boldsymbol{g}_1 x + a_2\boldsymbol{g}_2 x + a_3\boldsymbol{g}_3 x + \ldots \tag{41}$$

A consequence of gradient field nonlinearity is image distortion, and associated with this a degradation of the spatial resolution in the nonlinear regions of the field. Commercially available gradient systems give gradients that at the gradient center are linear to within 1% over a diameter of about 10 mm and 3% over 20 mm. These errors have no perceptible effect on image quality.

5.2.3. Signal-to-Noise Ratio

As in every NMR experiment, the signal-to-noise ratio determines the measuring time and attainable resolution in NMR microscopy. An improvement in the signal-to-noise ratio of the FID by a factor of 2 gives the same improvement in the image, or about a quarter of the measuring time for the same signal-to-noise ratio with the same resolution. Unfortunately however, the SNR for the acquisition of a high-resolution NMR spectrum from a sample is not identical with the SNR in an image, since in imaging the signal from a defined slice is divided between all the pixels of the image. Hence, the SNR per pixel is significantly worse than in a one-dimensional spectrum.

An improvement of the in-plane resolution by a factor of 2 in both dimensions reduces the voxel volume by a factor of 4, and necessitates about a factor of 16 more data accumulations to maintain the same SNR. Similarly, halving the slice-thickness while maintaining constant in-plane resolution requires 4 times the number of data accumulations. The volume dependence of the SNR as given by *Hoult* and *Richards*[26] [Eq. (42)] is the most significant limiting factor

$$\mathrm{S/N} \sim V \tag{42}$$

for the attainable SNR in NMR microscopy. Equation (42) implies that for an improvement in the spatial resolution of, for example, 10^3 μm^3 from 100^3 μm^3, the SNR deteriorates by a factor of 1000, and thereby the number of accumulations required for the same SNR increases by a factor of 10^6. This argument assumes that the sample volume and the diameters of the transmission and reception coils remain constant. From Equation (42) it is also possible to derive the dependence of the SNR upon the resonance frequency [Eq. (43)]. This relation is shown in Figure 20, and indicates

$$\frac{\mathrm{S}}{\mathrm{N}} \sim \sqrt[4]{\omega_0^7} \tag{43}$$

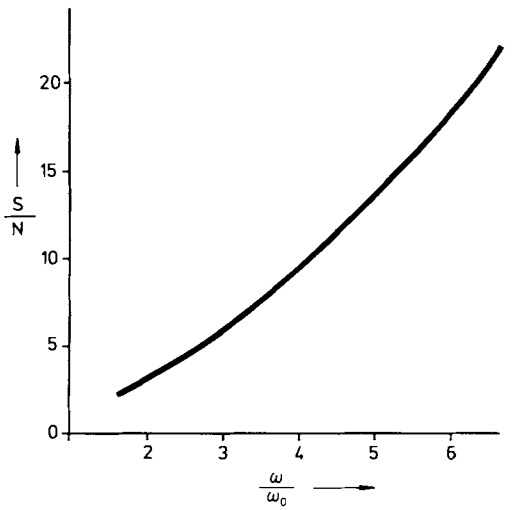

Fig. 20. Signal-to-noise ratio as a function of the resonance frequency ω and thus of the field strength of the static magnetic field [Eq. (43)] referred to $\omega_0 = 100$ MHz (S/N ≡ 1).

that on the basis of the SNR, NMR microscopy can only be usefully conducted at the highest possible field strengths.

A further interesting aspect is the dependence of the SNR upon the bandwidth $\Delta\omega$ of the receiver, or equivalently the spectral width of the image.

$$\frac{S}{N} \sim \frac{1}{\sqrt{\Delta\omega}} \tag{44}$$

Equation (44) shows that reducing the bandwidth diminishes the noise, but, however, this increases the time required for data acquisition. In spin-echo imaging the data must be symmetrically acquired, i.e. the echo maximum occurs midway through the detection period, because of data processing

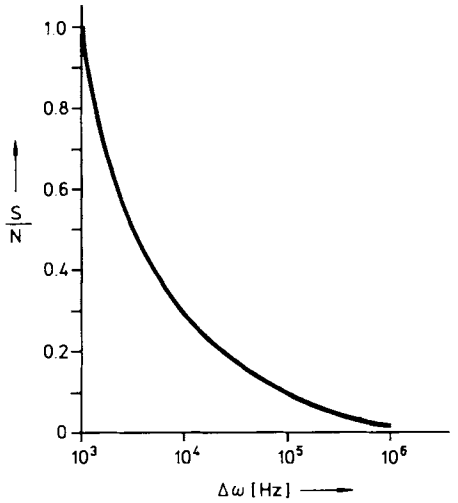

Fig. 21. Signal-to-noise ratio as a function of the detector bandwidth $\Delta\omega$ [Eq. (44)].

requirements (the FT). If the number of data points is kept constant then reducing the bandwidth leads to an increase in the spin-echo time TE. This in turn leads to losses due to T_2 in the echo intensity and so to a worsening in the SNR. Both circumstances are illustrated in Figures 21 and 22.

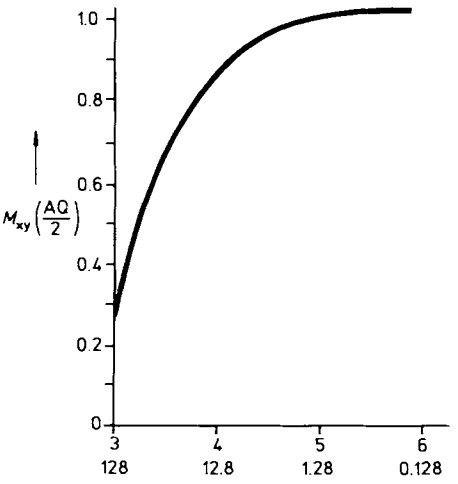

Fig. 22. Signal amplitudes $M_{xy}(t)$ after half acquisition time $T_2 = 100$ ms and data acquisition times between 128 μs and 128 ms (lower values of the abscissa: t[ms]) for 512 data points and bandwidths $\Delta\omega$ of 1–100 kHz (upper values of abscissa: $\lg(\Delta\omega)$).

Cooling of the receiver system is a further, but not very practicable, way of reducing the noise. This is because the sample, especially a biological sample, must generally be maintained at a given temperature, and thermally isolating the receiver coil from the sample would lead to the coil having a more unfavorable filling factor, and thus once more to a poorer signal-to-noise ratio.

The preceeding discussion indicates that, at least for samples such as biological samples that have relatively long spin-spin relaxation times and consequently narrow line widths, the SNR is the limiting factor for the attainable spatial resolution in NMR microscopy.

6. Applications of NMR Microscopy

As is clear from Section 5 the low sensitivity of NMR microscopy means that it will not in the forseeable future achieve resolutions comparable with those of optical microscopy (approx. 0.5 μm). So when judged by this criterion the NMR microscope presents no competition to the optical microscope, and its price is also uncompetitive. Useful applications of NMR microscopy lie only in the areas where it has special properties, such as:

a) The non-destructive investigation of samples, especially over longer time scales. These include observing the course of a disease in animal models and the slow diffusion of fluids in polymers;
b) the imaging of spin density leading to a quantitative assessment of concentrations;
c) chemical shift selective imaging for determining the spatial distribution of substances in a sample;
d) the investigation of dynamic processes by means of relaxation-time weighted images (see Sections 3.2.2 and 3.2.4);
e) the evaluation of dynamic properties by measuring the diffusion constants[27–29] of differing chemical species, or by evaluating the diagonal elements of the diffusion tensor (it may even be possible to completely determine the diffusion tensor);
f) the spectroscopy of defined partial volumes of the whole sample[30–36] or multidimensional spectroscopic imaging;[37–38]
g) the determination of flow velocities and profiles of fluids or viscous materials in capillaries or tubes.[39,40]

The above shows the incomparably broad range of applications of NMR microscopy which is not restricted by pure considerations of spatial resolution. In the following sections a few of the numerous possible applications will be discussed.

6.1. Biomedical Applications

The range of biomedical applications includes pharmaceutical research, pharmaceutical kinetics, therapeutic monitoring, and basic biomedical and biophysical research. These may be conducted on animal models for animals up to the size of a mouse or rat, on cell cultures and tissue samples in vivo and in vitro. The attainable spatial resolution with mice lies in the range from 50–130 μm, and rats at about 150 μm.

For cell cultures and tissue samples it may be better than 10 μm.

Figures 23 and 24 illustrate the use of NMR spectroscopy in arteriosclerosis research and show proton images from part of an artery. Figure 23a shows a longitudinal section;

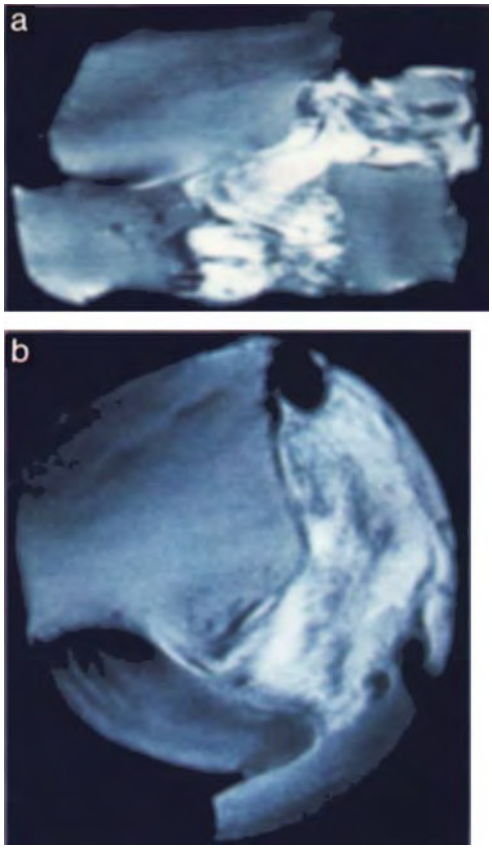

Fig. 23. Tissue sample from an artery, $B_0 = 7.05$ T. a) x-z-section, proton image. No chemical shift selection was applied. Two regions of differing intensity may be discerned. On the basis of the measuring parameters, TR = 500 ms, TE = 6.56 ms, it is to be expected that the lighter part of the image shows the lipid protons, as the spin-lattice relaxation time of these protons is several hundred milliseconds, while the T_1 of water lies in the range 1–3 s. The resolution in the x-direction is 36 μm, in the z-direction 92 μm, with a slice-thickness of 900 μm. $g_x = 100$, $g_z = 50\ \mathrm{mT\,m^{-1}}$. b) x-y-section, proton image. The in-plane resolution is now 36 μm isotropically, the slice-thickness 900 μm. Here also, the lighter part of the image shows the distribution of the lipid. $g = 100\ \mathrm{mT\,m^{-1}}$.

the region of low signal intensity represents a separation of the signals from water and lipids, that of high intensity a superposition. The high intensity of the lipid protons is a consequence of their relatively short (in comparison to water) spin-lattice (T_1) relaxation times, of several hundred milliseconds. This leads to almost complete relaxation and a strong lipid signal, whereas under the prevalent measuring conditions, water with its relatively long T_1 of about 1 s, is partially saturated. Figure 23b shows a section perpendicular to that of Figure 23a, and in this the two regions of differing intensity are clearly shown.

Figure 24 shows a chemical shift selective image (c.f. Section 3.2.3) of the lipid signal.[10] The excitation of the lipid signal is achieved with a Gaussian 90° pulse having a narrow bandwidth of about 600 Hz. The suppression of the water

Fig. 24. Chemical shift selective lipid proton image. The lipid protons were selectively excited by a narrow bandwidth 90° gaussian pulse. The short T_1 of the lipid protons allows the repetition time to be reduced to 200 ms. The other parameters are as for Figure 23b.

signal illuminates the contrast-rich structure in this part of the artery. In further studies[41] it was possible with chemical shift selective saturation-recovery imaging experiments (c.f. Section 3.2.4) to obtain spatially resolved measurements of the spin-lattice relaxation times for the water and lipid protons.

Figure 25 shows a section through the abdominal region of a healthy mouse anaesthetized with pentabarbital. In Figure 25a, the spine, spinal chord, back muscles, kidneys, stomach, spleen and liver are all clearly recognizable. Figure 25b is a zoom image of the kidney region with a pixel resolution of 60 μm × 60 μm and a slice thickness of 800 μm. For comparison Figure 25c shows an ex-vivo mouse kidney with a resolution of $36 \times 36 \times 320\ \mu m^3$.

With a mouse animal model it has been possible to follow the time course of a ceruletide-induced pancreatitis over a time period of 8 h,[42] (see Fig. 25d).

The influence of the spin-echo time is shown in Figure 26. Here, two sections through the abdominal region of a mouse are shown, obtained with TR = 3 s and a TE value of 32 ms (Fig. 26a, b) and of 12 ms, respectively (Fig. 26c, d). The regions of tissue having relatively short T_2 times make very little contribution to the signal when TE = 32 ms, but are first visible when TE = 12 ms.

Alongside the biomedical applications of NMR microscopy in animal experiments, this technique also finds numerous applications in plant research. Figures 27a and 27b each show the same sectional plane through a leaf from the plant *Bryophyllum tubiflore*. In the NMR microscopic image the vascular bundles and the cells, which have a size of ca. 40 μm in this plant, are easily recognizable. The changes in contrast in the regions of the cells are a result of the changes in the susceptibility of the cell membranes. In the light-microscopic image shown for comparison, the cells are clearly recognizable, but the dimensions of the vascular bundle are not determinable.

Figure 28 shows a spin-echo time study of a leaf from the plant *Mesembryanthemum cristallinum*.[4] The low intensity areas of the epidermis are a consequence of the very short spin-spin relaxation times of the water-protons in these areas. With decreasing TE these areas become lighter, and with a very short TE (TE = 4 ms) the intensity becomes almost uniform. This leads one to conclude that at the leaf's

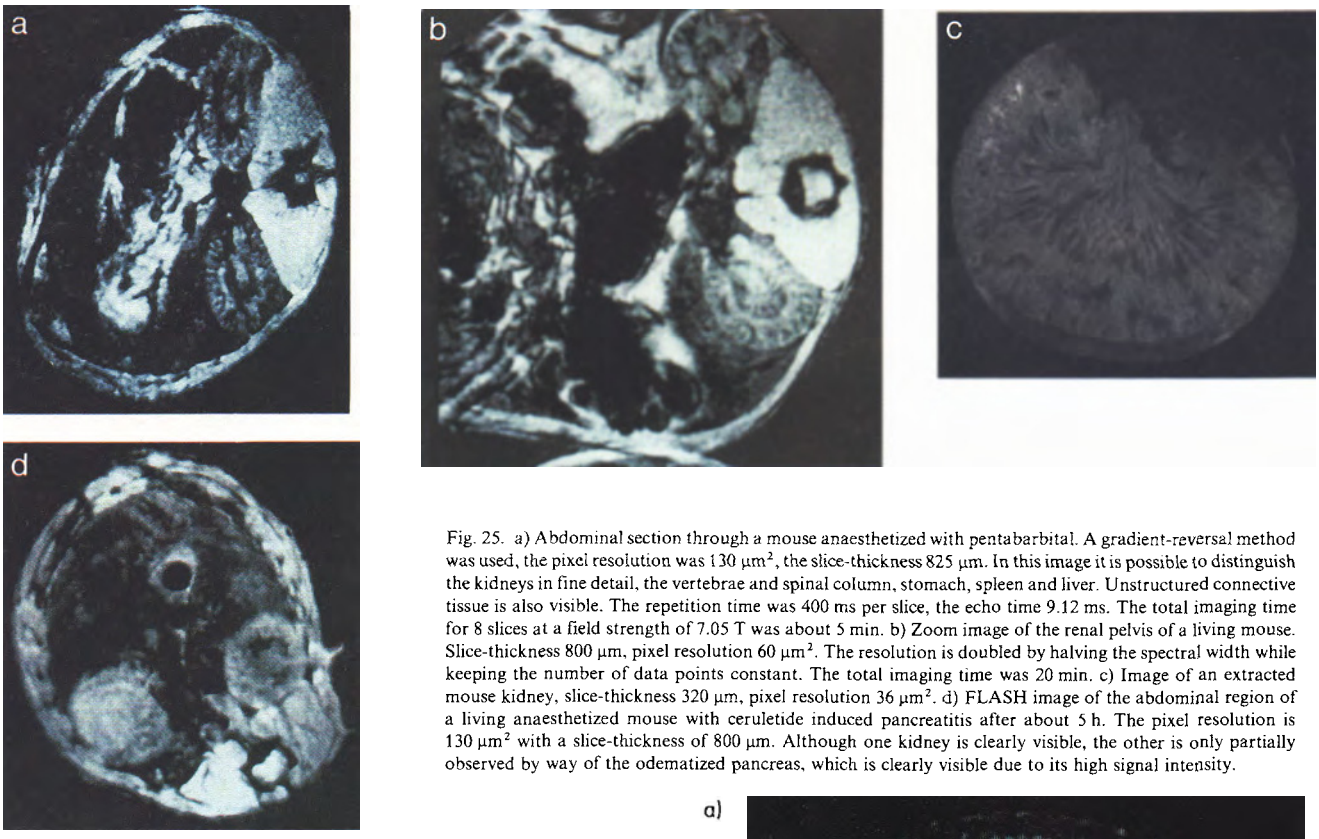

Fig. 25. a) Abdominal section through a mouse anaesthetized with pentabarbital. A gradient-reversal method was used, the pixel resolution was 130 μm^2, the slice-thickness 825 μm. In this image it is possible to distinguish the kidneys in fine detail, the vertebrae and spinal column, stomach, spleen and liver. Unstructured connective tissue is also visible. The repetition time was 400 ms per slice, the echo time 9.12 ms. The total imaging time for 8 slices at a field strength of 7.05 T was about 5 min. b) Zoom image of the renal pelvis of a living mouse. Slice-thickness 800 μm, pixel resolution 60 μm^2. The resolution is doubled by halving the spectral width while keeping the number of data points constant. The total imaging time was 20 min. c) Image of an extracted mouse kidney, slice-thickness 320 μm, pixel resolution 36 μm^2. d) FLASH image of the abdominal region of a living anaesthetized mouse with ceruletide induced pancreatitis after about 5 h. The pixel resolution is 130 μm^2 with a slice-thickness of 800 μm. Although one kidney is clearly visible, the other is only partially observed by way of the odematized pancreas, which is clearly visible due to its high signal intensity.

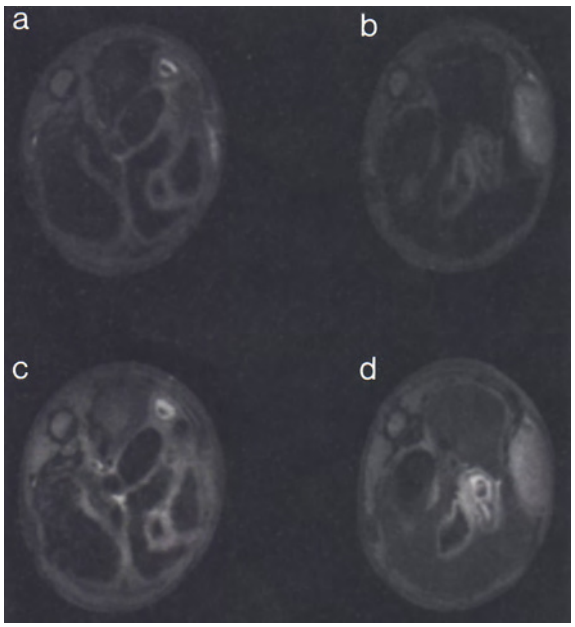

Fig. 26. Spin-echo images of the abdominal region of an anaesthetized mouse with an implanted tumour, the pixel resolution was 100^2 μm^2, the slice-thickness 500 μm. TR = 3 s, a) Slice 1, TE = 32 ms. b) Slice 2, TE = 32 ms. c) Slice 1, TE = 12 ms. d) Slice 2, TE = 12 ms. Field strength 9.4 T (by kind permission of Dr. M. Mattingly).

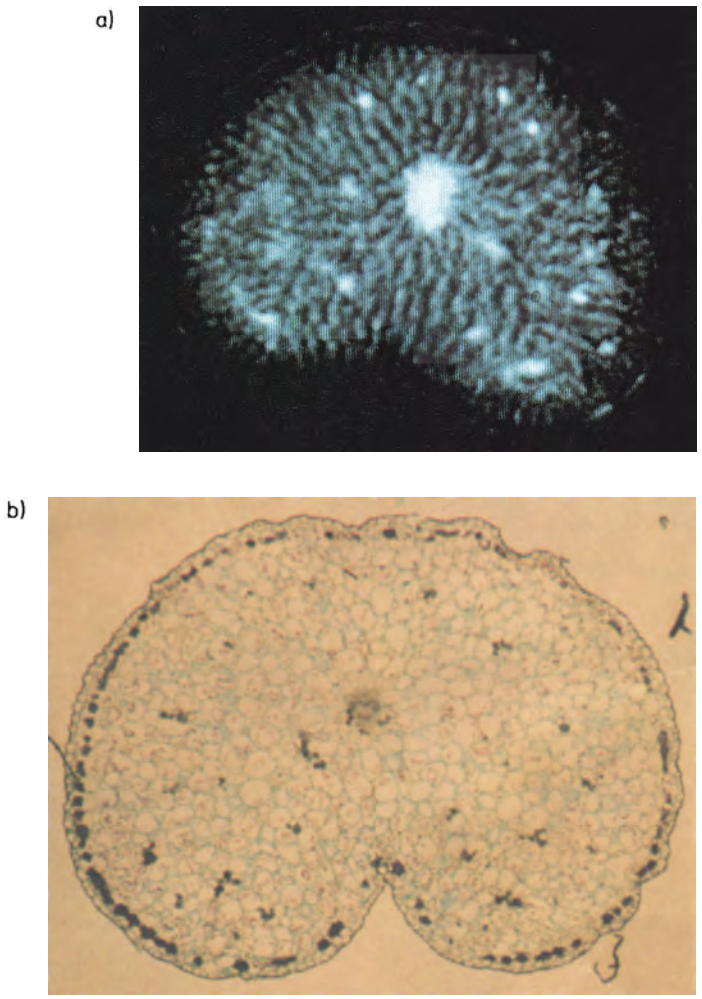

Fig. 27. Cross-section through a leaf of the plant *Bryophyllum tubiflore*. a) NMR microscopic image (7.05 T) with a resolution of $15 \times 15 \times 250$ μm^3. The vascular bundle, the individual plant cells, and the epidermis are clearly recognizable. b) Light-microscopic image. The cells have a diameter of ca. 40 μm (by kind permission of Dr. *W. Hartung*, Universität Würzburg).

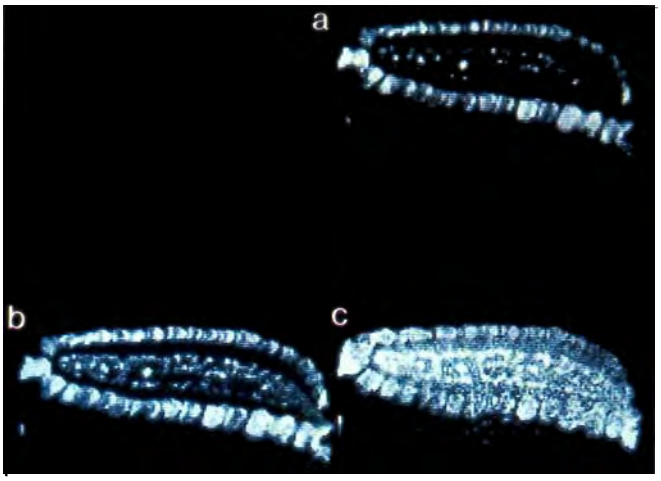

Fig. 28. Spin-echo image of *Mesambryanthenum cristallinum*. Influence of TE on the image contrast. a) TE = 18.24 ms. b) TE = 11.00 ms. c) TE = 4.40 ms.

edges the protons are relatively immobile, possibly due to the water being bound to the cellular compartments, but that the proton density throughout the leaf (except within the vein is almost constant). Further applications of NMR microscopy are the determination of the self-diffusion coefficient of water in plants,[43] changes in the water content of plant stems,[44] staging the growth of algae,[45] or, for example, studying morphology with relaxation agents.[46] The first measurements of water transport in plants by ^{17}O imaging using ^{17}O-labeled water have already been reported.[47] This, and other work[48] show that ^{17}O-labeled water is an excellent relaxation agent for biomedical applications, since its protons have a smaller T_1 than the protons of "normal water", and it is completely non-toxic. NMR microscopic investigations of intact multicellular tumor spheroids have been published in the course of the last two years.[49]

6.2. Uses of NMR Microscopy in Materials Science

NMR microscopy can be of great help in investigating the structure and dynamics of polymers, ceramics and building materials.[50, 51] Applications in the field of materials research may be classified as static or as time-dependent, depending on the nature of the experiment. *Blümich* and *Spiess*[52] give an exemplary description of the following investigations:

- The pore-distribution in unsintered ceramic.[53] The radial pore distribution was measured by proton-density images of absorbed fluids.
- The distribution of binding agent in unsintered ceramics.[54] Low molecular weight polymers and waxes are used as binding agents. With the predicted line width it should be possible to obtain images of still higher resolution.
- The distribution of pollutants in wood.[55] Pollutants in wood can change the relaxation times of the water protons. The distribution of pollutants as well as that of vaccines such as fungicides or bactericides appears to be possible.
- Fluid distributions within polymers.[56] The distribution of fluids such as water or solvents in polymers, and their diffusion in polymers or other materials is detectable.[57–60]
- Expansion-induced crystallization.[61] The proton relaxation times of the polymer protons is modified by this.
- Inhomogeneous temperature distributions,[62] e.g. in melts.
- Cross-linking of polymers as a function of various spatial, and relaxation-time-dependent values.[63]
- Diffusion processes from fluids into solids, and interfluid diffusion.

Figure 29 shows the interdiffusion of a water layer under a layer of isopropanol. The boundary between the liquids is clearly seen, owing to the difference in their susceptibilities.

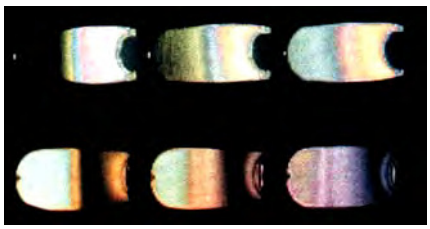

Fig. 29. Chemical shift selective spin-echo images of the interdiffusion of ethanol in water over a period of 18 h. The upper part shows the diffusion of the ethanol in water based on the protons of the methyl group; below: image of the corresponding water distribution. A gaussian RF pulse with an excitation bandwidth of ca. 700 Hz was used for the chemical shift selective excitation. The spatial resolution of the in-plane image is about 30 μm.

The difference in the susceptibilities leads to a strong local magnetic field gradient at the boundary, and hence to a dephasing of the spins. By using chemical-shift selective imaging it is possible to observe the time course of the diffusion for both fluids. The spatially resolved concentration ratio at any time may be obtained from the image profiles.

Figure 30 shows a spin-echo image with an echo-time TE = 4.5 ms of a plastic sample reinforced with fiber glass having varying water contents of between 1% and 20%. The

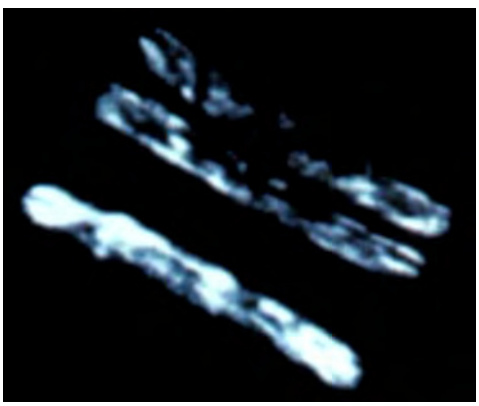

Fig. 30. Spin-echo image (20 recordings) of fiber-glass reinforced epoxy rods with water content between 1% and 20%. Pixel resolution 138 μm², slice thickness approx. 1 mm, TE = 4.5 ms, TR = 1 s.

fiber glass structures may be seen clearly. The resolution is 138 μm in the plane, with a slice thickness of about 1 mm. The images show projections of the sample in the z-direction, i.e. no slice selection was applied.

6.3. Dynamic NMR Microscopy

An interesting, novel application of NMR microscopy developed by *Callaghan* et al.[64] concerns the measurement of molecular translation. The phase shift of the NMR signal which arises when the echo being detected is preceded by a pair of intense gradient pulses separated by the phase-inverting 180° rf-pulse is used as probe. The *P*ulsed *G*radient *S*pin *E*cho[65] (PGSE) pulse sequence can be used to measure the probability $P(\boldsymbol{r}' - \boldsymbol{r}, \Delta)$, that nuclei initially at $\boldsymbol{r}$ at the first gradient pulse will move to $\boldsymbol{r}'$ at the second gradient pulse at a time Δ later. By combining PGSE and imaging methods it is possible to map $P(\boldsymbol{r}' - \boldsymbol{r}, \Delta)$ in a heterogeneous sample[64] (Fig. 31).

In the case of superposed self-diffusion and flow $P(\boldsymbol{r}' - \boldsymbol{r}, \Delta)$ is a gaussian function whose width is determined by the local molecular self-diffusion coefficient and whose center is determined by the local velocity of the particles. In the method described by *Callaghan* et al. this width and offset are computed for each pixel in the image space and thus separate maps are obtained for the molecular diffusion and the flow velocity. This dynamic imaging method has potential applications in both biological and materials science. A recent in vivo study of water transport in wheat grains has furnished valuable information about transport mechanisms and circulation pathways.[43] The diffusion constant of water was determined in vivo for various regions of the wheat grain: thus a diffusion constant D of $10^{-9}\,m^2\,s^{-1}$ was obtained for the vascular bundle and of $5 \times 10^{-10}\,m^2\,s^{-1}$ for the endosperm.

The method has also been applied to the rheological study of polymer solutions.[66] Figure 31 shows the basic Pulsed Gradient Spin Echo pulse sequence combined with an imaging sequence to obtain spatially resolved maps of diffusion processes. After slice selection the magnetization in the selected slice dephases under the influence of a very intense magnetic field gradient of a strength of several hundred Gauss/cm. Only the magnetization which is not influenced by diffusion will be completely rephased after the 180°-rf-pulse through the second intense field gradient of the same strength and duration. Spatial resolution occurs through both gradients G_x and G_y during the acquisition period. Figure 32 shows stacked profile plots for the velocity and diffusion maps of viscous polyethylene oxide solutions (PEO) flowing through a 700 μm capillary.[66] Figure 32a reproduces the behavior of a solution with low polyethylene oxide concentration (0.5%). The solution behaves as a Newtonian fluid, exhibiting the usual Poiseuille velocity profile. Figure 32b reveals that the higher concentrated polymer solution (4.5%) is non-Newtonian and behaves as a shear-thinning fluid. In the lower section of the figure there is evidence of enhanced longitudinal self diffusion in the region of higher shear rate, illustrating the ability of NMR microscopy to provide additional information at the molecular level.

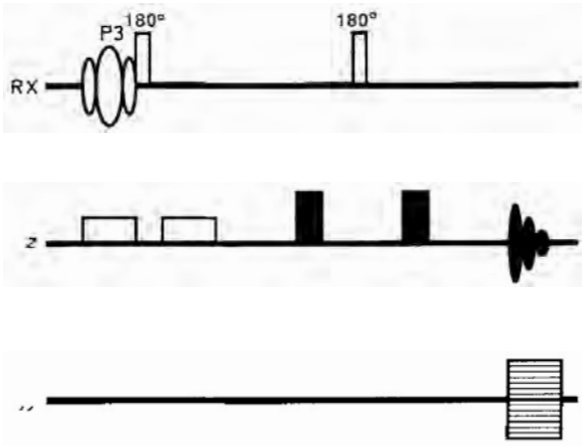

Fig. 31. Basic pulsed gradient spin-echo pulse sequence combined with an imaging sequence developed by *Callaghan* et al. [64]. After slice selection the magnetization in the selected slice dephases under the influence of a very intense magnetic field gradient (several 1000 $mT\,m^{-1}$). Only the magnetization which is not influenced by diffusion will be completely rephased after the 180° RF pulse through the second intense field gradient of the same strength and duration. Spatial resolution effected by the two orthogonal gradients G_x and G_y during the acquisition period.

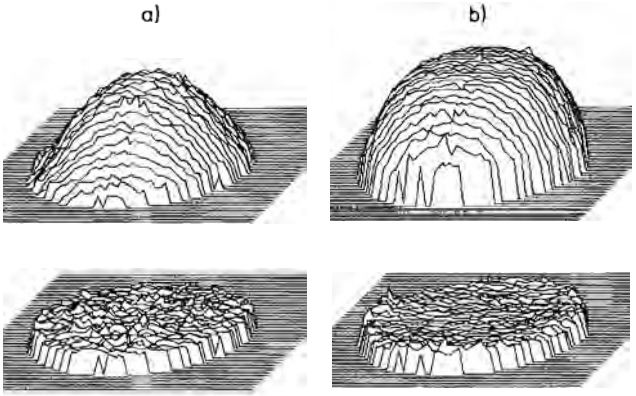

Fig. 32. Velocity map (above) and profile of the longitudinal diffusion (below) for aqueous solution of polyethylene oxide (PEO) flowing through a 700 μm I.D. teflon capillary (with kind permission of Prof. *Callaghan*). a) PEO concentration 0.5% w/v. Maximum velocity is 6.0 $mm\,s^{-1}$. The velocity profile corresponds to a power-law fluid behavior with exponent n = 1 (Newtonian fluid). b) PEO concentration 4.5%. The maximum velocity is likewise 6.0 $mm\,s^{-1}$. However, in this case, the liquid exhibits non-Newtonian behavior due to the increased shear forces at the capillary edge. The profile of the longitudinal diffusion is enlarged compared to that in Figure 32a.

7. Future Prospects

NMR microscopy is still in its early stages of development both as regards methods and apparatus. Therefore, it is not yet possible to ascertain the scope of potential applications. The use of microresonators could make possible the investigation of single cells, or of small groups of cells, enabling metabolic studies to be carried out. Resolutions of about 1 μm/pixel are conceivable. Using miniresonators it could be possible to study biopsy samples morphologically as well as biochemically, with a high spatial and spectroscopic resolution. Hence it is advantageous to work at very high field strengths: for example, 11.7 T (500 MHz)-widebore, and 14.1 T (600 MHz) magnets currently exist. In the future even stronger magnets should be available.

The use of special pulse sequences for the sensitive detection of low-concentration nuclei, such as ^{13}C in labeled substances by using polarization transfer,[67] allows the monitoring of metabolic pathways and of the distribution of metabolites by volume-selective spectroscopy. Similar information may be expected from volume-selective spectral editing as proposed by *Kimmich* et al.[68, 69]

The observation of rapid dynamic processes by application of the appropriate method (Ref. [70] and Section 3), now lies within the realm of the possible, and also allows the observation of motion without artifacts. The combination of gradients with sample rotation, as well as zero and multiquantum imaging, will make high-resolution solid-state imaging routine within the near future, allowing a new route to spatially resolved dynamic studies in solids.

For making possible the development of NMR microscopy I would like to thank Prof. G. Laukien and T. Keller (Bruker, Rheinstetten). Dr. D. Müller, Dr. Mark Mattingly and many colleagues at Bruker (Karlsruhe), Spectrospin (Zürich), and Bruker (Billerica, MA, USA) provided indispensible and encouraging assistance. I would especially like to thank Prof. Dr. K. H. Hausser and Prof. Dr. U. Haeberlen for numerous very helpful discussions and suggestions, and the following for collaborative experiments: Priv.-Doz. Dr. Dr. G. Rohr, Klinikum Mannheim der Universität Heidelberg, Dr. W. E. Hull, Deutsches Krebsforschungszentrum Heidelberg, and Prof. Dr. A. Haase, Universität Würzburg. For permission to publish the images obtained in collaborative experiments I am grateful to Prof. M. Asdente, University of Milan, Prof. U. Zimmermann, Universität Würzburg, Dr. M. Mattingly, Bruker (Billerica) and Dr. Dr. G. Rohr, Klinikum Mannheim der Universität Heidelberg.

Received: March 21, 1989 [A 744 IE]
German version: *Angew. Chem. 102* (1990) 1

[1] F. Bloch, W. W. Hansen, M. Packard, *Phys. Rev. 69* (1946) 127.
[2] E. M. Purcell, H. C. Torrey, R. V. Pound, *Phys. Rev. 69* (1946) 37.
[3] J. B. Aguayo, S. J. Blackband, J. Schoeniger, M. A. Mattingly, M. Hintermann, *Nature (London) 322* (1986) 190.
[4] L. Walter, A. Balling, U. Zimmermann, A. Haase, W. Kuhn, *Planta (1990)*, in press.
[5] R. Damadian, *Science (Washington) 171* (1971) 1151.
[6] P. C. Lauterbur, *Nature (London) 242* (1973) 190.
[7] K. Gersonde, T. Tolxdorff, L. Fesberg, *Magn. Reson. Med. 2* (1985) 390.
[8] E. L. Hahn, *Phys. Rev. 80* (1950) 580.
[9] W. S. Warren, *J. Chem. Phys. 81* (1984) 5437.
[10] L. Pavesi, P. L. Oreste, A. Colombo, W. Kuhn, E. Tremoli, M. Asdente, *8th Int. Symp. Atheroscler.* (Siena, Italy 1988).
[11] R. L. Vold, J. S. Waugh, M. P. Klein, D. E. Phelps, *J. Chem. Phys. 48* (1968) 383.
[12] R. Freeman, H. Hill, *J. Chem. Phys. 54* (1971) 3367.
[13] A. Haase, J. Frahm, D. Matthaei, W. Hänicke, K. D. Merboldt, *J. Magn. Reson. 67* (1986) 217.
[14] A. Haase, *Magn. Reson. Med.*, in press.
[15] R. Graumann, A. Oppelt, E. Stetter, *Magn. Reson. Med. 3* (1986) 707.
[16] D. D. Stark, W. G. Bradley: *Magnetic Resonance Imaging*, The C. V. Mosby, St. Louis, MO, USA 1988.
[17] H. W. Spiess, *NMR Basic Princ. Prog. 15* (1978).
[18] F. Laukien: *Feasibility Study of an NMR Microscope*, Massachusetts Institute of Technology, Boston, MA, USA 1984.
[19] D. G. Cory, J. W. M van Os, W. S. Veeman, *J. Magn. Reson. 76* (1988) 543.
[20] S. Emid, J. H. N. Creyghton, *Physica B128* (1985) 81.
[21] P. J. McDonald, J. J. Attard, D. G. Taylor, *J. Magn. Reson. 72* (1987) 224.
[22] G. C. Chingas, J. B. Miller, A. N. Garroway, *J. Magn. Reson. 66* (1986) 530.
[23] H. M. Cho, C. J. Lee, D. N. Shykind, D. P. Weitekamp, *Phys. Rev. Lett. 55* (1985) 1923.
[24] R. Becker, *Theorie der Wärme*, Springer, Berlin 1975.
[25] H. Y. Carr, E. M. Purcell, *Phys. Rev. 94* (1954) 630.
[26] D. I. Hoult, R. E. Richards, *J. Magn. Reson. 24* (1976) 71.
[27] R. A. Meyer, T. R. Brown, *J. Magn. Reson. 76* (1988) 393.
[28] J. Stepisnik, *Prog. Nucl. Magn. Reson. Spectrosc. 17* (1985) 187.
[29] P. Stilbs, *Prog. Nucl. Magn. Reson. Spectrosc. 19* (1987) 1.
[30] D. I. Hoult, *J. Magn. Reson. 33* (1979) 183.
[31] M. Garwood, T. Schleich, B. D. Ross, G. B. Matson, W. D. Winters, *J. Magn. Reson. 65* (1985) 239.
[32] M. R. Bendall, R. E. Gordon, *J. Magn. Reson. 53* (1983) 365.
[33] R. J. Ordidge, A. Connelly, J. A. B. Lohman, *J. Magn. Reson. 66* (1986) 283.
[34] W. P. Aue, S. Müller, T. A. Cross, J. Seelig, *J. Magn. Reson. 56* (1984) 350.
[35] P. R. Luyten, A. J. H. Marien, B. Sijtsma, J. A. den Hollander, *J. Magn. Reson. 67* (1986) 148.
[36] A. Haase, *Magn. Reson. Med. 3* (1986) 963.
[37] A. A. Maudsley, S. K. Hilal, W. H. Perman, H. E. Simon, *J. Magn. Reson. 51* (1983) 147.
[38] A. Haase, D. Matthaei, *J. Magn. Reson.*, in press.
[39] P. C. Lauterbur, *Nature (London) 336* (1988) 310.
[40] C. F. Jenner, Y. Xia, C. D. Eccles, P. T. Callaghan, *Nature (London) 336* (1988) 399.
[41] M. Asdente, L. Pavesi, P. L. Oreste, A. Colombo, W. Kuhn, E. Tremoli: *Evaluation of atherosclerotic lesions using NMR microimaging, Atherosclerosis*, in press.
[42] W. Kuhn, G. Rohr: *Imaging of Ceruletide-Induced Pancreatitis in the Mouse by NMR Microscopy (Magn. Reson. Biol. Syst. Proc. Intern. Conf. 13th* (ICMRBS) (Madison, WI, USA 1988)).
[43] C. D. Eccles, P. T. Callaghan, C. F. Jenner, *Biophys. J. 53* (1988) 77.
[44] G. A. Johnson, J. Brown, P. J. Kramer, *Proc. Natl. Acad. Sci. USA 84* (1987) 2752.
[45] L. G. Harrison, S. D. Luck, B. Munasinghe, L. D. Hall, *J. Cell Sci. 91* (1988) 79.
[46] A. Connelly, J. A. B. Lohman, B. C. Loughman, H. Quiquampoix, R. G. Ratcliff, *J. Exp. Bot. 38* (1987) 1713.
[47] G. D. Mateescu, G. M. Yvars, D. I. Pazara, N. A. Alldridge, J. C. LaManna, W. D. Lust, M. Mattingly, W. Kuhn: *Combined $^{17}O/^{1}H$ Magnetic Resonance Microscopy in Plants, Animals and Materials: Present Status and Potential* (Proc. 3rd Conf. Int. Isot. Soc. (Innsbruck 1988)).
[48] G. D. Mateescu, G. M. Yvars, D. I. Pazara, N. A. Alldridge, J. C. LaManna, W. D. Lust, M. Mattingly, W. Kuhn: *Oxygen-17: A Physiological, Biochemical and Anatomical MRI Contrast Agent (Proc. Annu. Meet. Soc. Magn. Reson. Med. 7th* (San Francisco 1988)).
[49] L. O. Sillerud, J. P. Freyer, M. Mattingly: *Proton NMR Microscopy of Intact Multicellular Tumor Spheroids, (Proc. Annu. Meet. Soc. Magn. Reson. Med. 6th* (New York 1987)).
[50] J. L. Koenig, *Eur. Spectrosc. News 80* (1988) 36.
[51] B. Blümich, *Angew. Chem. 100* (1988) 1460; *Angew. Chem. Int. Ed. Engl. 27* (1988) 1406.
[52] B. Blümich, H. W. Spiess, *Proc. BMFT Symp. Materialforschung* (Hamm 1988).
[53] W. A. Ellingson, J. L. Ackerman, L. Garride, J. D. Weynand, R. A. diMilia, *Ceram. Eng. Sci. Proc. 8* (1987) 503.
[54] L. Garrido, J. L. Ackerman, W. A. Ellingson, J. D. Weyand, *Proc. Conf. Compos. Adv. Ceram.* (Cocoa Beach, FL, USA 1988).
[55] L. D. Hall, V. Vasanthan, *Wood Sci. Technol. 20* (1986) 329.
[56] W. P. Rothwell, D. R. Holecek, J. A. Kershaw, *J. Polymer Sci., Polym. Lett. Ed. 22* (1984) 241.
[57] S. Blackband, P. Mansfield, J. R. Barnes, A. Clague, S. A. Rice, *SPE Form Eval. 1* (1986) 31.
[58] L. D. Hall, V. Rajanayagam, C. Hall, *J. Magn. Reson. 68* (1986) 185.
[59] G. C. Chingas, J. Miliken, H. A. Resing, T. Tsang, *Synth. Met. 12* (1985) 131.
[60] S. Blackband, P. Mansfield, *J. Phys. C19* (1986) L49.
[61] J. L. Ackerman, *Application Note*, Doty Scientific Instruments, USA 1988.
[62] B. H. Suits, D. White, *J. Appl. Phys. 60* (1986) 3772.
[63] P. O. Frickland, *Int. SAMPE Tech. Conf. 18* (1986) 876.
[64] P. T. Callaghan, C. D. Eccles, Y. Xia, *J. Phys. E21* (1988) 820.
[65] E. O. Stejskal, J. E. Tanner, *J. Chem. Phys. 42* (1965) 288.
[66] Y. Xia, P. T. Callaghan, *Makromolekulare Chemie, Symposia Series* (1988), in press.
[67] L. O. Sillerud, D. B. van Hulsteyn, R. H. Griffey, *J. Magn. Reson. 76* (1988) 380.
[68] A. Knüttel, R. Kimmich, K.-H. Spohn, *J. Magn. Reson. 81* (1989) 570.
[69] A. Knüttel, R. Kimmich, *J. Magn. Reson. 78* (1988) 205.
[70] R. J. Ordidge, R. Coxon, A. Howseman, B. Chapman, R. Turner, M. Stehling, P. Mansfield, *Magn. Reson. Med. 8* (1988) 110.

Biologically Active Analogues of the Extracellular Matrix: Artificial Skin and Nerves

By Ioannis V. Yannas*

In memoriam Professor Piero Pino

Animal development starts as a single cell which proliferates into several new cells; these differentiate into highly specialized tissues, organs, and limbs; and the small but functioning organism eventually grows into its full scale. Throughout development the extracellular matrices, which are complex macromolecular networks, also undergo dramatic changes. Matrix transformations occasionally control the much more well-studied changes in number and type of differentiating cells. Extracellular matrix (ECM) networks are typically broken down enzymatically to oligopeptides and are then resynthesized (remodeled) to form insoluble and nondiffusible macromolecular structures which confer stability of shape to multicellular systems. Mature ECM, such as skin, tendon, cartilage, and blood vessels, provides stiffness and strength to tissues and organs. Remodeling of ECM also occurs in adult organisms, during wound healing. An understanding of the role that ECM plays during development or wound healing can be obtained by use of synthetic ECM analogues. Several simple chemical ECM analogues have been synthesized and a few have been found to possess remarkable biological activity. One of these analogues has induced the partial regeneration of skin in an adult guinea pig wound model as well as in man. Peripheral nerve has been regenerated in another animal model by use of a similar ECM analogue. In all these mammalian lesions it is well-known that regeneration does not occur spontaneously. These analogues are graft copolymers of collagen and chondroitin 6-sulfate (a glycosaminoglycan) in the state of highly hydrated and covalently cross-linked gels. Procedures are summarized for synthesis of copolymers with adjusted physicochemical properties, such as the rate at which they degrade enzymatically when implanted, the elements of their pore structure, and the degree of collagen crystallinity. ECM analogues have provided a novel window into the complexities of morphogenesis and regeneration and they have pointed towards entirely new directions in the medical treatment of serious organ dysfunction and organ loss. An ECM analogue has already become the basis of a new clinical treatment for massively burned patients. An interpretation of the results leads to a hypothesis about the nature of ECM during development. Since biological activity appears only when the physicochemical parameters fall within very narrow limits, it is intriguing to speculate that these experiments describe a single insoluble growth factor which is specific for skin synthesis. Such an insoluble growth factor appears to be just as essential to skin development as are the much more well-known soluble growth factors. A different ECM analogue appears to induce nerve regeneration, possibly because each tissue requires its own developmentally active ECM.

1. Introduction

Most tissues consist of cells and a largely insoluble, nondiffusible extracellular matrix (ECM). In multicellular systems the ECM confers stiffness, strength, and, therefore, stability of shape. Although the composition and structure of ECM varies from one tissue to the next, these matrices are typically highly hydrated macromolecular networks composed of various amounts of glycoproteins such as collagen, elastin, fibronectin, laminin, and chondronectin, as well as of glycosaminoglycans (GAG), including hyaluronic acid, chondroitin 6-sulfate, dermatan sulfate, and heparan sulfate. Glycosaminoglycans usually occur as polysaccharide chains covalently attached to a protein core (proteoglycan). Macromolecular components of the ECM are synthesized in cells and are secreted in the extracellular space where further physicochemical modification, for example, crystallization and covalent cross-linking of macromolecular chains, takes place.[1, 2]

The ECM between two cell layers of different origins is frequently referred to as a basal lamina or basement membrane, illustrated in Figure 1.[2–5] The basal lamina must play a profound role during organization of cells into functional units (morphogenesis) since its removal by selective enzymatic treatment in well-defined developmental models suppresses morphogenesis completely.[3] Throughout life, but with special urgency during development, the basal lamina is degraded, resynthesized, and degraded further as tissue remodeling occurs. Remodeling of the basal lamina is also a very active process during healing of wounds.[4] During each of these processes cells and matrix interact closely and probably iteratively. These specific interactions are being studied intensively and important advances in understanding are rapidly being made.[1, 2, 5] Nevertheless, the precise molecular mechanisms underlying critical cell–matrix or cell–cell interactions during development are not well under-

[*] Prof. I. V. Yannas
Fibers and Polymers Laboratory,
Massachusetts Institute of Technology
Cambridge, MA 02139 (USA)

 © VCH Verlagsgesellschaft mbH, D-6940 Weinheim, 1990 0570-0833/90/0101-0020 $ 02.50/0

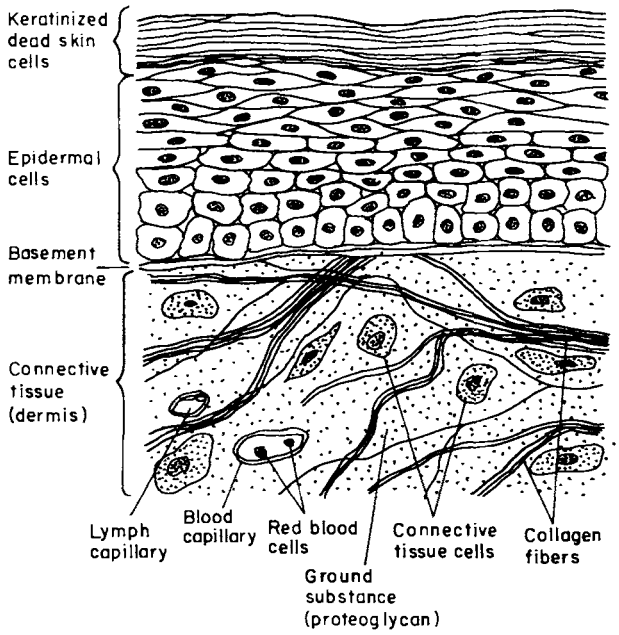

Fig. 1. A highly schematic view of skin which highlights the position of the basement membrane between the cellular epidermis and the largely noncellular dermis. The basement membrane is an extracellular matrix which typically occupies the interface between different tissues. The term basement membrane is often used interchangeably with basal lamina; however, some authors distinguish between the two terms, using each to describe a larger or smaller number of layers of interfacial matrix. (Redrawn from [97] with permission.)

stood,[3, 6] partly due to unavailability of well-defined and biologically active matrices for such investigations.[6]

Chemical analogues of the ECM provide a new probe into the complex processes of development. The analogues synthesized so far are graft copolymers of collagen and one each of several glycosaminoglycans and are, admittedly, very simple models of the chemically complex ECMs. Nevertheless, careful control of the cross-link density has yielded macromolecular networks which degrade under the action of tissue enzymes over a period that ranges from days to weeks. The essential transience of the ECM during development and wound healing can thereby be deliberately adjusted and its effect on cell–matrix and cell–cell interactions can be studied. Furthermore, control of the volume fraction of pores and of the average pore diameter has yielded gels with levels of hydration and specific surface area which extend over wide ranges. Since certain cell types interact very intimately with the surface of these ECM analogues, the opportunity presents itself to study systems in which the density of cells interacting with the matrix is varied widely.

The major constituent of these chemical ECM analogues is collagen, the fibrous protein which accounts for about one-third of the total protein in vertebrates. An unusual amino-acid composition and a characteristic wide-angle X-ray diffraction pattern distinguish collagen clearly from other tissue components.[1, 7] Various levels of structural order in collagen are illustrated in Figure 2. Collagen can be extracted from connective tissues such as cattle skin (hide) and tendon in relatively pure form and can be dispersed in aqueous acetic acid or other solvents in the form of either a solution of individual triple-helical macromolecules or a suspension of particles comprising naturally cross-linked aggregates of such macromolecules. The solid state can be recovered by either evaporation of the solvent or precipitation of the protein by use of a nonsolvent. The reconstituted collagen thereby prepared can be fashioned into membranes (films), tubes, fibers, or tape. Although collagen in the form of reconstituted membranes or sutures has been implanted surgically by several investigators since at least 1943,[8–12] the interaction between a casually reconstituted collagen and host tissue is passive and largely amounts to degradation of the triple-helical collagen molecules by collagenases secreted by cells adjacent to the implant.

By contrast with casually reconstituted collagens, the collagen analogues of the ECM described in this review interact in an active and highly specific manner with cells which migrate from adjacent tissues into the implanted analogues. The term regeneration template, or simply template, has been used to distinguish these biologically active forms of collagen.[13] Templates are recognized by their ability to induce tissue regeneration in a well-defined animal lesion (wound) for which it has been previously demonstrated that regeneration does not occur spontaneously. At least five physicochemical features distinguish templates from biologically inactive collagens, namely, the chemical composition of the macromolecular network (collagen/GAG ratio), the density of cross-links between the macromolecules, the average diameter of pores in the range 1–1000 μm, the fraction of collagen which is present in a highly crystalline (banded) form, and the volume fraction of water. The first three of these parameters have been studied rather assiduously. In addition, templates may be seeded with cells prior to implantation, a procedure which has been found to affect their

Ioannis V. Yannas studied chemistry at Harvard College, Cambridge, MA (BA, 1957). He then studied chemical engineering at the Massachusetts Institute of Technology (MIT), Cambridge (MS, 1959) and physical chemistry at Princeton University, Princeton, NJ (MS, 1965; PhD, 1966). Since 1966, he has been on the faculty of MIT and currently teaches graduate courses on deformation of polymers and on physical properties of biological polymers. His primary research activities have focused on the design of medical devices based on natural polymers, such as the design of an artificial skin for the treatment of burn patients and the design of a nerve prosthesis. Currently, he is focusing on the synthesis of physicochemical analogues of the extracellular matrix for the study of tissue regeneration in mammals. Prof. Yannas has authored or co-authored over 130 publications and has been granted 10 patents. He was elected member of the Institute of Medicine of the National Academy of Sciences (USA). He has received awards for his synthesis of an artificial skin from the American Chemical Society, Society for Biomaterials, and the Society of Plastics Engineers.

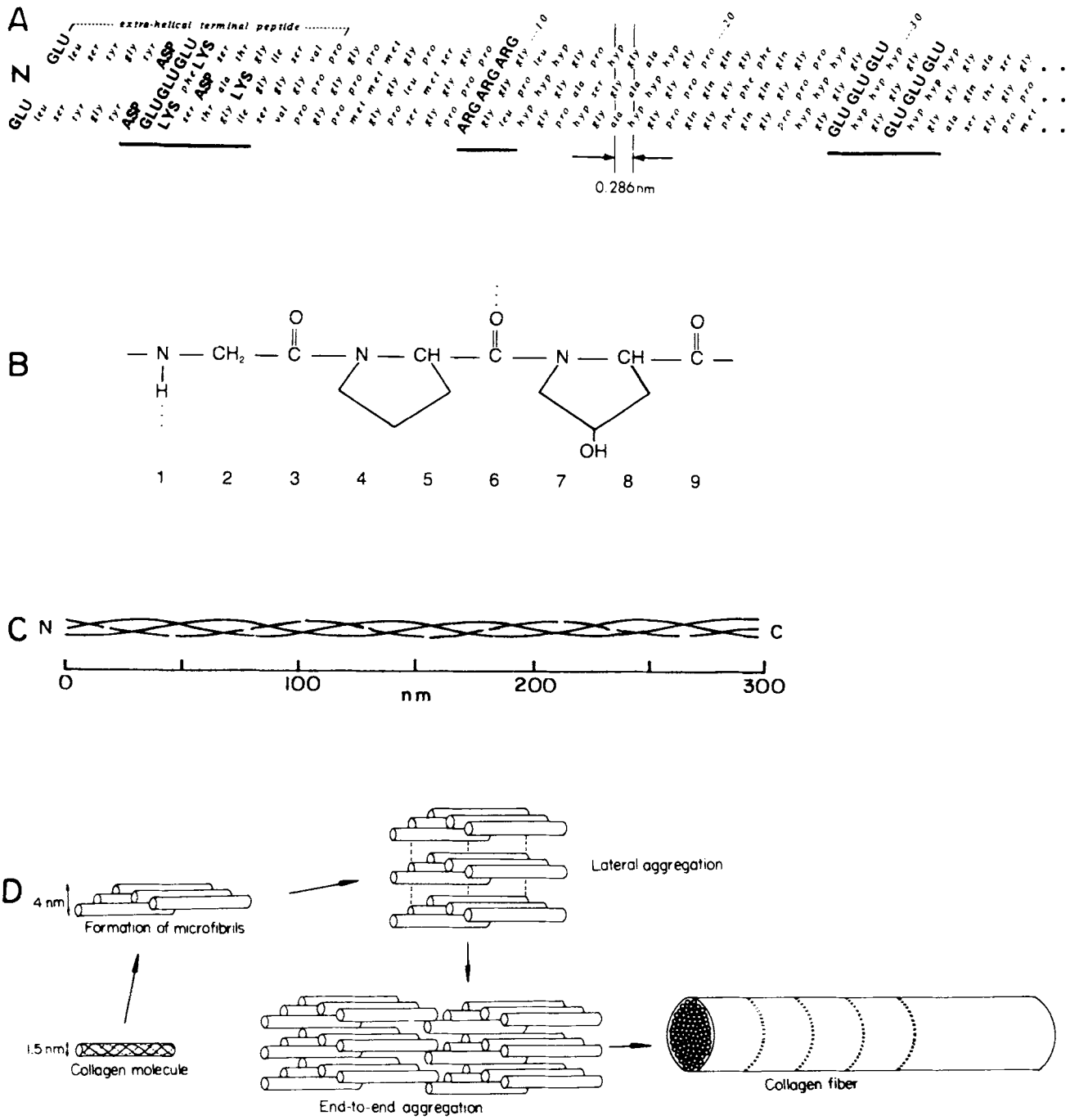

Fig. 2. Collagen, like other proteins, is distinguished by several levels of structural order. A: Primary structure—the complete sequence of amino acids along each polypeptide chain. An example is the triple chain sequence of type-I calf-skin collagen at the *N*-terminus of the molecule. Roughly 5% of a complete molecule is shown. No attempt has been made to indicate the coiling of the chains. Amino-acid residues participating in the triple helix are numbered, and the residue-to-residue spacing (0.286 nm) is shown as a constant within the triple-helical domain, but not outside it. Bold capitals indicate charged residues which occur in groups (underlined). (Reprinted from [98] with permission.) B: Secondary structure—the local configuration of a polypeptide chain. The triplet sequence Gly-Pro-Hyp illustrates elements of collagen triple-helix stabilization. The numbers identify peptide backbone atoms. The conformation is determined by *trans* peptide bonds (3 ---4, 6---7, and 9---1), fixed rotation angle of bond in proline ring (4---5), limited rotation of proline past the C=O group (bond 5---6), interchain hydrogen bonds (dots) involving the NH hydrogen at position 1 and the C=O at position 6 in adjacent chains, and the hydroxyl group of hydroxyproline, possibly through water-bridged hydrogen bonds. (Reprinted from [99] with permission.) C: Tertiary structure—the global configuration of polypeptide chains, representing the pattern according to which the secondary structures are packed together within the unit substructure. A schematic view of the type-I collagen molecule, a triple helix 300 nm long. (Reprinted from [100] with permission.) D: Quaternary structure—the unit supramolecular structure. The most widely accepted unit is one involving five collagen molecules (microfibril). Several microfibrils aggregate end to end and also laterally to form a collagen fiber, which exhibits a regular banding pattern under the electron microscope with a period of 65 nm. (Reprinted from [101] with permission.)

biological activity equally as strongly as do physicochemical manipulations.

Tissue, organ, and limb regeneration occur quite differently in various species. In amphibians, such as the salamander and the immature frog (tadpole), an entire amputated limb can be regenerated.[14] At the other extreme, spontaneous regeneration of most tissues in adult mammals is not observed.[15, 16] For example, the epidermis (the outer tissue layer of skin; cf. Fig. 1) is regenerated in adult mammals provided there is an underlying bed of dermis (the inner

layer). On the other hand, spontaneous regeneration of the dermis does not occur;[17, 18] instead, synthesis of nonphysiological connective tissue (scar) takes place. Likewise, peripheral nerves of mammals, such as the sciatic nerve in the rat, do not regenerate sufficiently well to bridge 15-mm-long gaps between the two cut stumps; a nonphysiological tissue (neuroma) is instead synthesized at the end of each stump.[19, 20]

The macromolecular matrices discussed below modify strongly the kinetics and mechanism of the wound healing process in certain adult mammalian species, including man. One of these has suppressed scar synthesis and has induced almost total synthesis of dermis in the guinea pig and in man. A similar matrix has induced synthesis of sciatic nerve in the rat over a 15-mm-long gap. Both are copolymers formed by chemically grafting chains of chondroitin 6-sulfate onto collagen fibers. Following nomenclature recommended by IUPAC,[21] these polymers have been referred to as collagen-*graft*-chondroitin 6-sulfate copolymers, or generically, as collagen-*graft*-glycosaminoglycan copolymers, or briefly, as CG copolymers. Since the biological activity is dependent on their ultrastructure, we will use the term copolymer matrix to denote the porous, hydrated, insoluble gel which results following physical processing of the copolymer. Implant refers to the sterile surgical device which is grafted at the site of the lesion.

This review surveys the coupling between the physicochemical features of CG copolymer matrices and the results of biological assays which are related, directly or indirectly, to regeneration. These connections show that very few copolymer matrices with narrowly defined structure act as if they are developmentally active ECM analogues. Several implications of such analogy in the study of development and in the experimental treatment of tissue loss are briefly discussed.

2. Synthesis of Collagen–GAG Graft Copolymers

Regeneration templates have so far been based on the family of collagen–GAG copolymers. Glycosaminoglycans that have been grafted onto collagen include chondroitin 6-sulfate, chondroitin 4-sulfate, heparan sulfate, heparin, dermatan sulfate, and keratan sulfate.[21, 22] Of these, chondroitin 6-sulfate is the member that has been studied most assiduously and the data presented in this review are based on collagen-*graft*-chondroitin 6-sulfate copolymers. There is currently no evidence in the literature which suggests that this composition is uniquely suited for biological activity; the original choice of this GAG, as well as of the predominantly type-I collagen extracted from bovine hide, was largely dictated by their availability in large enough quantity from suppliers in the early 1970s, when these copolymers were first synthesized.[22]

In fact, basal lamina, the particular ECM whose biological activity appears to be mimicked by collagen–GAG templates, has a chemically distinct composition,[23–27] consisting primarily of the following macromolecular species: collagen type IV, with a unique amino-acid composition, a highly flexible macromolecular configuration which is a collagen triple helix only in relatively small part, and an ultrastructure which does not consist of collagen-type fibrils but which rather strongly resembles a threadlike, open network or a scaffold;[24, 25, 27] three glycoproteins, namely, laminin, entactin, and fibronectin; and heparan sulfate, a GAG which is part of a proteoglycan.[24, 26] Future studies of developmental events could be profitably based on synthesis of a chemical analogue of the basement membrane which closely simulates the currently recognized composition of this specialized tissue.

The evidence obtained so far has shown clearly that significant, and apparently unprecedented, regeneration of dermis and peripheral nerve has been induced by the chemically far simpler, well-defined collagen–GAG copolymers described below. The choice of a rudimentary chemistry, although providing only a very rough model of the naturally occurring extracellular matrix, has made it possible to focus attention on the physical aspects of matrix structure. Specifically, the pore structure, the macromolecular network structure, and the fractional crystallinity have been deliberately varied and have been recognized as essential components of the observed biological activity of these templates.

Grafting of GAG chains onto collagen is conveniently carried out by first forming a coprecipitate of collagen and GAG and then treating this condensed state under conditions which favor formation of covalent bonds between the two macromolecules. Coprecipitation requires the presence of sulfate groups on the GAG and an acidic pH.[28] Hyaluronic acid, the only GAG which is nonsulfated, does not precipitate collagen out of solution.[28] Every one of the other members of this family of polysaccharides does cause precipitation; however, the precipitates formed in aqueous acetic acid readily dissolve when the pH is adjusted to neutrality.[28] The precipitate is an ionic complex probably formed by interaction between the anionic sulfate groups of the GAG and the amino groups in collagen, which are positively charged at acidic pH.[28–30]

Collagen–GAG coprecipitates can be made insoluble without use of a chemical cross-linking agent simply by drastic dehydration. This procedure is based on the discovery that removal of water below ca. 1 wt.% insolubilizes collagen; gelatin, the totally amorphous state of collagen, also requires drastic dehydration in order to become insoluble.[31, 32] The nature of cross-links formed can be inferred from results of earlier, independent studies using chemically modified gelatins. Gelatin that had been modified either by esterification of the carboxylic groups of aspartyl/glutamyl residues or by acetylation of the ε-amino groups of lysyl residues remained soluble in aqueous solvents after exposure of the solid protein to high temperature, whereas unmodified gelatins lost their solubility.[33] Insolubilization of collagen and gelatin following severe dehydration has been, accordingly, interpreted as the result of drastic removal of the aqueous product of a condensation reaction which led to formation of interchain amide links.[31] The proposed mechanism was consistent with results, obtained by titration, showing that the number of free carboxylic groups and free amino groups in collagen were both significantly decreased following high-temperature treatment.[34, 35]

Removal of water to the extent necessary to achieve a density of cross-links in excess of 10^{-5} moles of cross-links per gram of dry gelatin, corresponding to an average molec-

ular weight between cross-links, M_c, of about 70 kDa, was achieved within hours by exposure to temperatures in excess of 105 °C under atmospheric pressure.[36] The possibility that the cross-linking achieved under these conditions was caused by a pyrolytic reaction was ruled out on the basis of calorimetric data.[37] Furthermore, chromatographic data showed that the amino-acid composition of collagen remained intact after exposure to 105 °C for several days.[38,39] In fact, it was observed that the gelatin can be cross-linked by exposure to temperatures as low as 25 °C provided that a sufficiently high vacuum was present to achieve the drastic moisture removal which drives the reaction.[31]

Exposure of highly hydrated collagen to temperatures in excess of ca. 37 °C is known to cause reversible melting of the triple-helical structure.[40] The melting point increases with the collagen–diluent ratio from 37 °C, the helix–coil transition of the infinitely dilute solution, to ca. 120 °C for collagen swollen with as little as 20 wt% diluent[40] and up to ca. 210 °C, the melting point of anhydrous collagen.[32] Accordingly, it is possible to cross-link collagen using the drastic dehydration procedure described above without loss of the triple-helical structure. It is simply necessary to adjust the moisture content of collagen to a level sufficiently low to prevent melting prior to exposure to the high temperatures required for rapid dehydration. Conservation of the triple helix following prolonged exposure of solid, anhydrous collagen to 105 °C has been confirmed by wide-angle X-ray diffraction and IR spectroscopy as well as by measurement of the components of the optical activity tensor.[32,38]

The simple self-cross-linking treatment also cross-links GAG chains to collagen.[41] The reaction kinetics are outlined in Figure 3. The mechanism probably involves condensation of amino groups of collagen with carboxylic groups of glucuronic acid residues on the repeat unit of chondroitin 6-sulfate (Scheme 1), an alternating copolymer of D-glucuronic acid and an *O*-sulfate derivative of *N*-acetyl-D-galactosamine.[28]

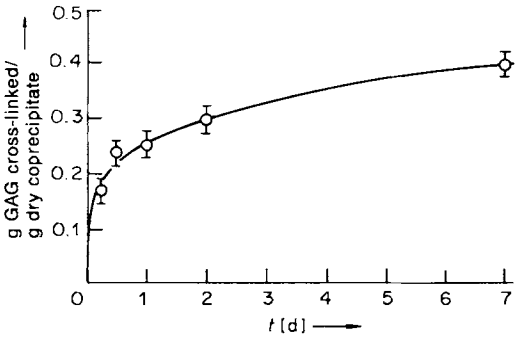

Fig. 3. Kinetics of cross-linking of chondroitin 6-sulfate, a glycosaminoglycan, to collagen following heating at 105 °C under 6.7 Pa (0.050 Torr). The mechanism of cross-linking is most probably interchain amide condensation involving ε-amino groups of lysyl residues on collagen chains with carboxylic groups on glucuronic acid residues in neighboring GAG chains. (Reprinted from [41] with permission.)

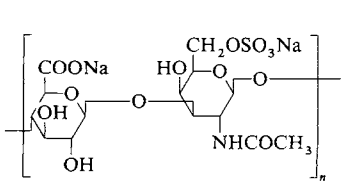

Scheme 1. Sodium chondroitin 6-sulfate.

Dehydration treatment cross-links as much as 40% of the GAG originally coprecipitated with collagen. Relative amounts of at least 10 wt% GAG (total dry copolymer basis) can be covalently bound to collagen and M_c can be varied in the range 2.5–25 kDa.[41] Proof of formation of a macroscopic network is based on inability to extract GAG from collagen under conditions of temperature and ionic strength where GAG separates readily and quantitatively from the coprecipitate.[41] Independent evidence of covalent cross-linking derives from the ability of the network to support an equilibrium tensile force under conditions where the network behaves as an ideal rubber and from the equilibrium swelling behavior (see below).[41]

Dialdehydes have been long known in the leather industry as effective tanning agents[42,43] and in histological laboratories as useful fixatives.[44] Both of these applications are based on the reaction between the dialdehyde and the ε-amino group of lysyl residues in the protein, which induces formation of interchain cross-links.[45–47] The nature of the cross-link formed has been the subject of controversy, primarily due to the complex, apparently polymeric, character of the glutaraldehyde reagent. Considerable evidence supports the proposed anabilysine structure, derived from two lysine side chains and two molecules of glutaraldehyde (Scheme 2).[47]

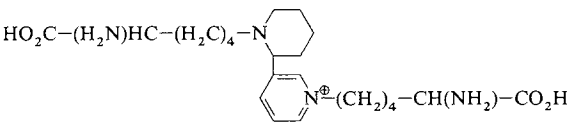

Scheme 2.

Evidence for other mechanisms has been presented.[48] By comparison with other aldehydes, glutaraldehyde has shown itself to be a particularly effective cross-linking agent,[42,43] as judged, for example, by its ability to decrease the average molecular weight between cross-links, M_c.[49] A wide range of M_c values provides the experimenter with a series of collagens in which the enzymatic degradation rate can be studied over a wide range, thereby affording implants which effectively disappear from the tissue between a few days and several weeks following implantation. Such experimental flexibility is indispensable in efforts to establish, by scanning over the experimental range, whether a threshold degradation rate exists below which the implant exhibits biological activity. Scanning is particularly useful in studies which involve an "unknown" animal lesion, that is, one which involves a different animal species or a wound on a different tissue site of a given species. Exposure of the collagen–GAG coprecipitate to aqueous glutaraldehyde in a neutral medium destabilizes the ionic macromolecular complex and the yield of graft copolymer is accordingly very low.[41] Destabilization of the complex and correspondingly low yields of graft copolymer also occur when the ionic strength of the aqueous medium exceeds about 0.25.[41] Up to about 3 wt% GAG (dry copolymer basis) can be incorporated at pH 3 and physiological ionic strength (0.15).[41] By controlling the source of collagen, glutaraldehyde concentration, and time of expo-

sure, networks with M_c in the range 5–40 kDa can be prepared.[41]

Although the mechanism of the reaction between glutaraldehyde and collagen at neutral pH is understood in part, the reaction in acidic media has not been studied extensively. There is little doubt that covalent cross-linking is involved, since gelatin films prepared from collagen that has been previously exposed to glutaraldehyde support an equilibrium force almost indefinitely when stretched in 1 M NaCl at 70 °C to various levels of extension;[41, 49] by contrast, gelatin prepared from untreated collagen dissolves readily in the hot medium. Likewise, little is known about the mechanism by which GAG chains attach themselves tenaciously to collagen following treatment of the coprecipitate in glutaraldehyde. What is clear is that a gelatin–GAG complex prepared from a collagen–GAG coprecipitate that was treated in aqueous acidic glutaraldehyde successfully resists elution of the attached GAG under conditions (3-h immersion in 1 M NaCl at 70 °C) where the untreated gelatin separates from the attached GAG in just seconds.[41] Additional evidence that glutaraldehyde-treated collagen–GAG coprecipitates have been converted into covalently cross-linked networks is based on the ability of their gelatinized states to support equilibrium tensile forces.[41]

Current preparation procedures for collagen–GAG copolymers make use both of drastic dehydration and glutaraldehyde treatments for reasons that are related to the requirements for a biologically active implant. Dehydration of the highly porous solid produced by freeze-drying (see below) stiffens the coprecipitate by introducing cross-links, thereby preventing pore collapse following prolonged exposure of the foam to ambient humidity. Pore collapse leads to irreversible loss of the high specific surface of the implant and results in complete loss of biological activity. In addition, both drastic dehydration and exposure to glutaraldehyde are, each in its own right and for reasons related to the protein cross-linking reaction which is promoted, efficient procedures for sterilization of the copolymer prior to implantation.[41] Both of these treatments have been used to prepare a medical device, occasionally referred to as artificial skin or artificial dermis, which has been used to treat successfully over 100 massively burned patients without clinical evidence of toxicity.[50, 51] Dehydration cross-linking, which amounts to self-cross-linking as described above, obviously does not lend toxicity to these implants. Glutaraldehyde, on the other hand, is a toxic substance and devices treated with it require thorough rinsing before use. Additional steps are occasionally followed, such as storage of the implant in media that react with residual reagent.[49]

3. Physicochemical Processing and Characterization of Copolymer Matrices

Although the chemical identity of collagen–GAG copolymers is a necessary element of their biological activity, it is not a sufficient one. In addition to chemical composition and cross-link density, biological activity also depends strongly on the degree of copolymer crystallinity and on the porous structure of these matrices. It is interesting to consider physicochemical methods for preparing and characterizing solids which are (1) primarily noncrystalline and cannot, therefore, be analyzed adequately using X-ray crystallography, (2) totally insoluble in all solvents and cannot be characterized by measurement of colligative or transport properties in states of infinite dilution, and (3) physically heterogeneous (porous) states, which are not completely defined unless detailed reference is made to the scale of heterogeneity and to the specific surface involved.

Network properties of cross-linked collagen–GAG copolymers can be analyzed structurally by methods based on the theory of rubber elasticity. If it can be demonstrated that the equilibrium force supported by a rubber is almost entirely entropic in origin and that, consequently, energetic interactions can be neglected by comparison, it is possible to compute directly the cross-link density of the network from measurements of the equilibrium modulus.[52] Collagen specimens with a high fraction of crystallinity, such as films cast at room temperature from a neutral buffer or naturally occurring tendon fibers, must be converted into gelatin before they show rubberlike elastic behavior.[53] Insoluble collagen that has been converted into gelatin by immersion in physiological saline between 65 and 80 °C for 1 h displays a resistance to uniaxial stretching (tensile modulus) which is directly proportional to the density of cross-links c (moles of cross-links per gram of dry polymer) and inversely proportional to M_c.[41, 49, 53] Collagen–GAG copolymers show similar behavior provided that the collagen is maintained in a gelatinized condition during measurement.[41, 49] These relationships demonstrate that, unlike collagen, cross-linked and swollen gelatin is a network in which the chains are random coils.[54] Below about 65 °C recrystallization of gelatin occurs, leading to development of significant energetic interactions and these relationships fail.[49] In the range of applicability of the ideal rubberlike model, the constitutive relation (1)[52, 55] describes the tensile behavior of appropriately gelatinized collagen[53] and collagen–GAG copolymers.[41, 49]

$$\sigma = (\varrho R T/M_c) V_2^{1/3} (\alpha - 1/\alpha^2) \quad (1)$$

In Equation (1), σ is the equilibrium stress (Nm^{-2}) supported by the swollen specimen; α is the stretched specimen length divided by the unstretched length (extension ratio); V_2 is the volume fraction of dry protein; and ϱ is the density of dry protein. The hypothesis that a specimen behaves as if it were an ideal rubber can be confirmed by observing a linear relation with zero intercept between σ and the strain function $(\alpha - 1/\alpha^2)$ and by establishing a direct proportionality between σ and the absolute temperature at constant value of the extension ratio, as stipulated by Equation (1).

When a sample is smaller than about 1 cm it becomes impractical to use tensile measurements to study network structure. The swelling behavior of small specimens can be used in such cases to calculate M_c. The method is based on the theory of *Flory* and *Rehner*,[55, 56] who showed that the volume fraction of a swollen polymer, V_2, depends on M_c through Equation (2).

$$\ln(1 - V_2) + V_2 + \chi V_2 - (\varrho V_{mol\,1}/M_c)(V_2^{1/3} - V_2/2) = 0 \quad (2)$$

In Equation (2) $V_{mol\,1}$ is the molar volume of the solvent, ϱ is the density of the polymer, and χ is a constant character-

istic of a specific polymer–solvent pair at a particular temperature. Although independent methods for estimating χ have been described,[55] it is possible to obtain M_c from tensile measurements for a given polymer–solvent system and use it to compute a single value of χ for a large number of network variants that can be prepared from the same polymer or copolymer. Equation (2) holds under conditions where the network behaves as an ideal rubber. The use of Equation (2) is illustrated in Figure 4. Values of M_c comput-

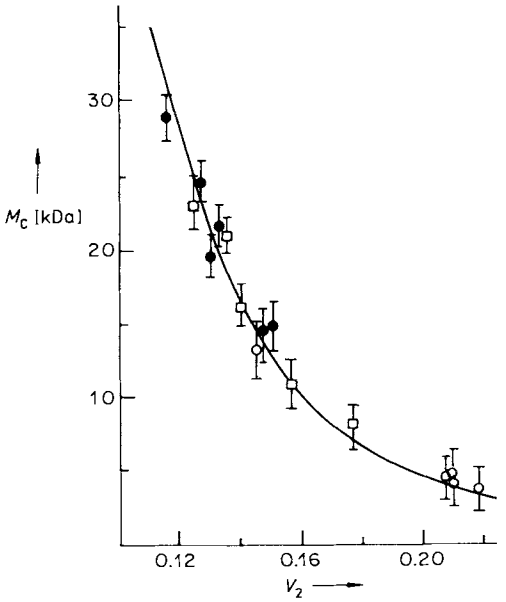

Fig. 4. Relation between the average molecular weight between cross-links, M_c, and the volume fraction of gelatinized collagen (gelatin), V_2. The swelling agent is 0.19 M citric acid/phosphate buffer solution, pH 7.4 at 80 °C. Experimental data obtained after cross-linking with various aldehydes: ●, formaldehyde; ○, glutaraldehyde; □, glyoxal. The curve is predicted by Equation (2) with $\chi = 0.52 \pm 0.04$. (Redrawn from [49] with permission.)

ed by use of Equation (1) or (2) provide insight into the structure of the network. For example, since the average molecular weight of an amino-acid residue in collagen is about 93,[57] an M_c value of 14 kDa corresponds to a not very tightly cross-linked network with an average network chain of approximately 151 amino acids. Amino-acid analysis of naturally occurring collagen from tendon yields about 27 mol% lysyl residues;[57] on the average, therefore, a lysyl residue occurs once every 37 residues. If we make the assumption, justified above, that glutaraldehyde attacks only lysyl residues, we conclude that an M_c value of 14 kDa implies that very roughly only 25% of the available ε-amino groups have reacted.

Structural order in collagen, as in other proteins, occurs at several discrete levels of the structural hierarchy. We follow below the nomenclature proposed by *Linderstrøm-Lang*[58] and *Kauzmann*[59] to describe generally structural order in proteins and we apply it to the structure of collagen[32] (Fig. 2). The *primary structure* of collagen is the complete sequence of amino acids along each of three polypeptide chains as well as the location of interchain cross-links in relation to this sequence. The *secondary structure* is the local configuration of a polypeptide chain that results from satisfaction of stereochemical angles and hydrogen-bonding potential of peptide residues. The *tertiary structure* refers to the global configuration of polypeptide chains; it represents the pattern according to which the secondary structures are packed together within the collagen molecule and it constitutes the unit substructure that can exist as a stable entity in solution (the triple-helical molecule). The fourth order or *quaternary structure* denotes the unit supermolecular structure, comprising several molecules packed in a specific lattice, which constitutes the basic element of the solid state. Higher levels of order, eventually leading to gross anatomical features which can be readily seen with the naked eye, have been proposed.[60, 61]

Crystallinity in collagen can be detected at two discrete levels of structural order: the tertiary (triple helix) (cf. Fig. 2C) and the quaternary (lattice of triple helices) (cf. Fig. 2D). Biochemists have used optical rotation, circular dichroism and viscometry as reliable methods of detecting in solution the conversion of triple-helical collagen to randomly coiled gelatin;[54] however, the use of optical methods to analyze the gelatin content of solid specimens, such as films cast from solution, has been complicated partly because of the optically anisotropic character of the solid state of this protein. Procedures for the quantitative analysis of collagen and gelatin in solid specimens that are imperfectly crystalline have been developed in order to study the substantial increase in enzymatic degradation rate which is observed when collagen is converted into gelatin.[62, 63] The presence of an intact tertiary structure (triple helix) can be detected in the

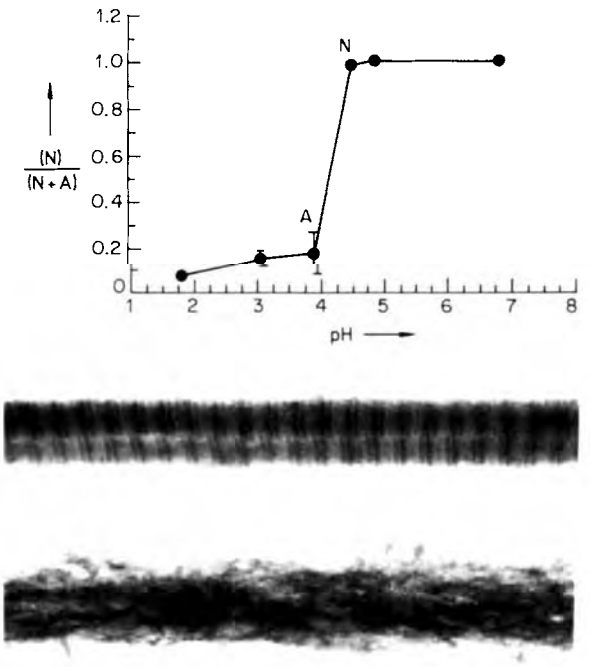

Fig. 5. The banding pattern of collagen fibers from bovine hide persists down to pH 4.25 ± 0.30 in 0.05 M acetic acid (N). The period is 65 nm. The fraction of banded fibrils $\frac{(N)}{(N+A)}$ was determined by transmission electron microscopy. Below pH 4.25 ± 0.30 the banding disappears from almost all fibers while the fiber diameter increases, indicative of swelling in the aqueous acetic acid diluent. Electron microscopy shows that a small fraction of banded fibrils, about 10% or less, persist below the transition even after long exposure to the swelling medium. The transformation abolishes the quaternary structure (packing order of helices, Fig. 2D) but leaves the tertiary structure (triple helix, Fig. 2C) intact. While banded collagen aggregates blood platelets, nonbanded collagen does not. Collagen periodicity, 65 nm. (Reprinted from [70] and [71] with permission.)

solid state by mid- and far-IR spectroscopy using "helical marker" bands which provide a quantitative measure of the extent to which a given collagen preparation has been converted into gelatin.[32, 64] Measurements of optical rotation with solid specimens also yield a quantitative analysis of gelatin in solid specimens, provided that the tensorial character of optical activity is taken into consideration and corrections are also made to account for the frequent presence of birefringence in collagen specimens.[65]

Electron microscopy has yielded the periodic banding pattern of collagen fibrils[66 - 69] and can also be used to provide a quantitative estimate of the length-average fraction of fibrils which possess discernible banding in a preparation of collagen fibrils.[70, 71] This morphological procedure can be supplemented with measurements of small-angle X-ray scattering.[72] Use of these procedures has led to the finding that the well-known loss of banding pattern that collagen fibrils undergo in aqueous acetic acid occurs relatively sharply at pH 4.25 ± 0.30 (Fig. 5).[71] Combined use of electron microscopy and IR spectroscopy showed that this transition amounts to disordering of the lattice but not to loss of the triple-helical structure.[71] Changes in pH can therefore be used to abolish selectively the quaternary structure while maintaining the tertiary structure intact. This experimental strategy has made it possible to show that the well-known phenomenon of blood platelet aggregation by collagen fibers is a specific property of the quaternary, rather than tertiary, structure.[71] Collagen has been prepared in a "thrombore-sistant" form, therefore, by selectively "melting out" the packing order of helices while preserving the helices intact.[71] Figure 6 illustrates the banding pattern observed with collagen–GAG copolymer matrices. Notice that short segments of banded collagen fibrils occasionally interrupt long segments of nonbanded fibrils (Fig. 6, inset).

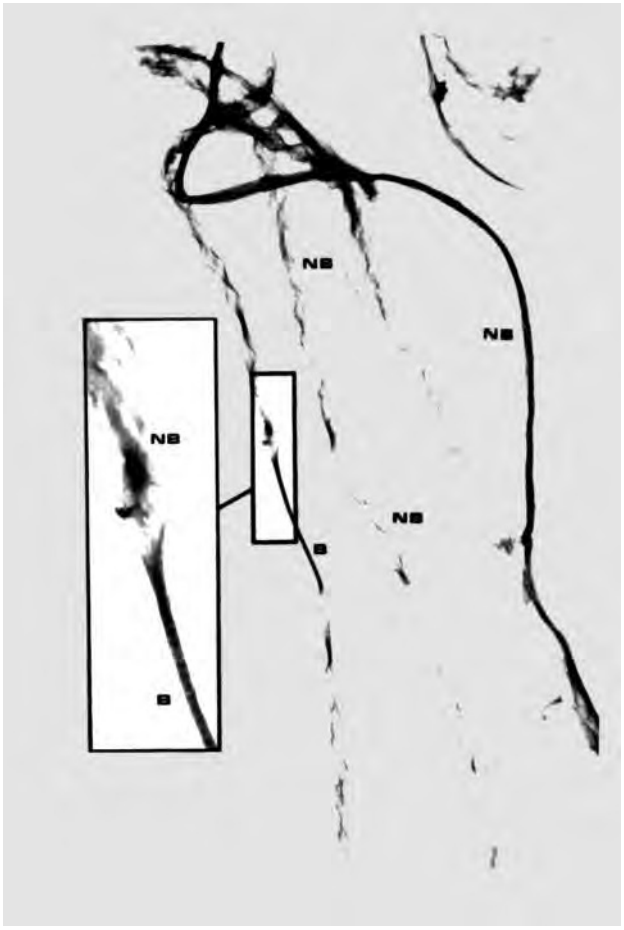

Fig. 6. Following exposure to pH below 4.25 ± 0.30, the banding pattern of type-I bovine-hide collagen practically disappears. Short lengths of banded collagen (B) do, however, persist next to very long lengths of nonbanded collagen (NB), which has tertiary but not quaternary structure. This preparation does not induce platelet aggregation provided that the fibers are prevented from recrystallizing to form banded structures when the pH is adjusted to neutral in order to perform the platelet assay. Stained with 0.5 wt% phosphotungstic acid. Banded collagen period, about 65 nm. (Reprinted from [70] with permission.)

The porosity of a collagen–GAG copolymer is an indispensable component of its biological activity.[73] Pores are incorporated by first freezing a very dilute suspension of the collagen–GAG coprecipitate and then inducing sublimation of the ice crystals by exposing the frozen suspension to vacuum at low temperatures.[74] The resulting pore structure is, therefore, a negative replica of the network of ice crystals (dendrites). It follows that control of the conditions of ice-crystal nucleation and growth can lead to a large variety of pore structures. In practice, the average pore diameter decreases with decreasing temperature of freezing, while the orientation of pore-channel axes also depends on the magnitude of the heat-flux vector during freezing. In experimental implants the mean pore diameter has ranged between about 1 and 800 μm, volume fractions have ranged up to about 0.995, the specific surface has been varied between about 10^4 and 10^8 mm^2 per gram of matrix, and the orientation of pore-channel axes in cylindrical implants has ranged from strongly uniaxial to random to highly radial. Figure 7 illustrates the range of porous structures that can be made accessible by control of the kinetics of ice nucleation and crystal growth as well as control of the heat-flux vector.

The biological activity of collagen–GAG copolymers depends generally on the structure of the porous matrix, that is, on the volume fraction, specific surface, mean pore size, and orientation of pores in the matrix. Determination of these properties is based on principles of stereology,[75, 76] the discipline which relates the quantitative statistical properties of three-dimensional structures to those of their two-dimensional sections or projections. In reverse, stereological procedures allow reconstruction of certain aspects of three-dimensional objects from a quantitative analysis of planar images.[76] Semi-automated or fully automated apparatus for quantitative image analysis has greatly facilitated stereological measurements. A plane that goes through the two-phase structure may be sampled by random points (Fig. 8A), by a regular pattern of points (Fig. 8B), by a near-total sampling using a very dense array of points (Fig. 8C), or by arranging the sampling points to form a continuous line (Fig. 8D). It can be shown[75, 76] that the volume fraction of pores, V_V, is equal to the fraction of total test points which fall inside pore regions, P_P, also equal to the total area fraction of pores, A_A (Fig. 8C), or, finally, the line fraction of pores, L_L, for a linear point array in the limit of infinitely close point spacing (Fig. 8D) [Eq. (3)].

$$V_V = P_P = A_A = L_L \tag{3}$$

The sampling methods illustrated in Figure 8 are the basis of all operations in stereology and are referred to as point counting (Fig. 8A, B), areal analysis (Fig. 8C), and lineal

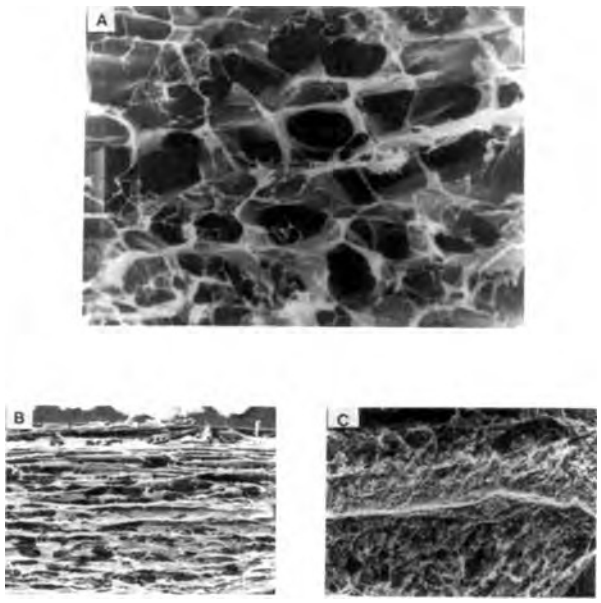

Fig. 7. Porous structures which can be obtained with collagen–GAG copolymers by adjusting the kinetics of crystallization of ice to the appropriate magnitude and direction (scanning electron microscopy). Pores form when the ice dendrites are eventually sublimed. The porous structure of collagen–GAG matrices is the negative replica of the ice-crystal structure which is formed when the dilute suspension of collagen–GAG coprecipitate particles is quenched below 0 °C. A: The orientation of pore-channel axes shown in this view is random and characterizes matrices which have induced skin regeneration. Average pore diameter, about 100 μm; pore volume fraction, about 0.99. B: Strong uniaxial orientation of pore-channel axes is shown in this cross-section of a 1.5-mm diameter cylindrical matrix which was used to induce regeneration of rat sciatic nerve across a gap. Average pore diameter, about 100 μm. C: Radial orientation of pore-channel axes yields an implant which induced synthesis of a sciatic nerve regenerate that was much less functional than when the orientation was uniaxial. Cylinder diameter: 1.5 mm. Average pore diameter, about 50 μm. (Courtesy of Massachusetts Institute of Technology.)

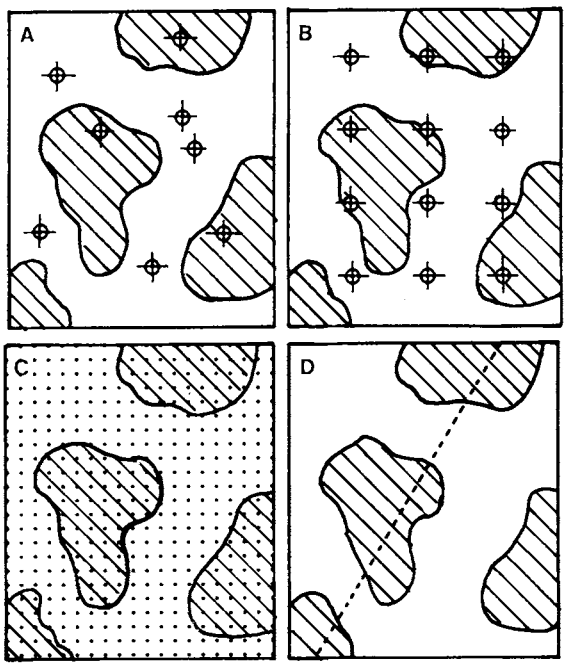

Fig. 8. Schematic representation of four procedures commonly used to sample a field in stereological analysis. These procedures have been used to study the porous structure of collagen–GAG matrices [74] and yield values for average pore diameter, pore volume fraction, and other features. In this illustration, a phase A (cross-hatched) is embedded in a continuous phase B (white background). A: Random point count. B: Systematic point count. C: Areal analysis. D: Lineal analysis. (Reprinted from [76] with permission.)

analysis (Fig. 8D). Clearly, randomness in the selection of a sampling procedure is of critical importance. Nearly complete characterization of the details of pore structure in collagen–GAG matrices has been obtained by systematic use of these procedures.[74]

4. Biological Activity and Matrix Structure

"Biological activity" is defined in a highly operational manner. Definitions are necessarily couched in terms of a highly specific assay, itself defined strictly in operational terms. Studies with collagen–GAG matrices have focused on regeneration of specific tissues which are well-known not to regenerate spontaneously. The problem, therefore, is one of constructing assays to study the effect of certain structural features of collagen–GAG matrices on the de novo synthesis of a given tissue. This problem appears on the surface to be somewhat analogous to the search for experimental strategies to study the effect of a family of heterogeneous catalysts on the yield of a macromolecular product in a well-defined reactor.

The activity of regeneration matrices has been studied in two relatively well established environments: the full-thickness, excised skin wound in the guinea pig and in man;[17, 18] and the 10-mm, as well as the 15-mm, transected gap in the sciatic nerve of the rat.[19, 20] Both of these "reactors" are wounds produced by a routine surgical procedure and in both cases the "kinetics" and the "mechanism" of the normal wound healing "reaction" have been studied rather extensively. Normal healing of a full-thickness skin wound is characterized by contraction of the wound perimeter toward the wound interior, which begins within several hours after the skin has been excised. It is considered to be over when contraction has ceased, roughly after 2 weeks, and scar tissue has been synthesized (Fig. 9A).[17, 18] Scar is distinctly different from normal skin in several ultrastructural features as well as in its optical and mechanical properties. Healing of transected sciatic nerve occurs by formation of a neuroma at each of the two cut ends (Fig. 10).[19, 20] This haphazardly growing tissue fails to reconnect with the opposite side and the result is paralysis.

The most obvious difference between a regeneration matrix and a catalyst is that the former is consumed during the course of the reaction. Implanted collagen–GAG matrices are degraded by collagenases,[77, 78] specific enzymes which attack the triple-helical molecule at one specific locus. Two characteristic products result: the *N*-terminal three-quarter fragment and the *C*-terminal one-quarter fragment, both of which are spontaneously denatured to gelatin at physiological temperatures.[77] The gelatinized fragments are then cleaved by several nonspecific proteases. Collagenases are naturally present in healing wounds and are credited with the degradation of collagen fibers at the site of trauma. At about the same time that degradation of collagen and of other ECM components proceeds in the "woundbed" these components are being synthesized by cells in the woundbed. The combined process is referred to as remodeling.[2–4] The balance between the rates of the two processes has been frequently considered to be an important feature of wound healing.[79–81]

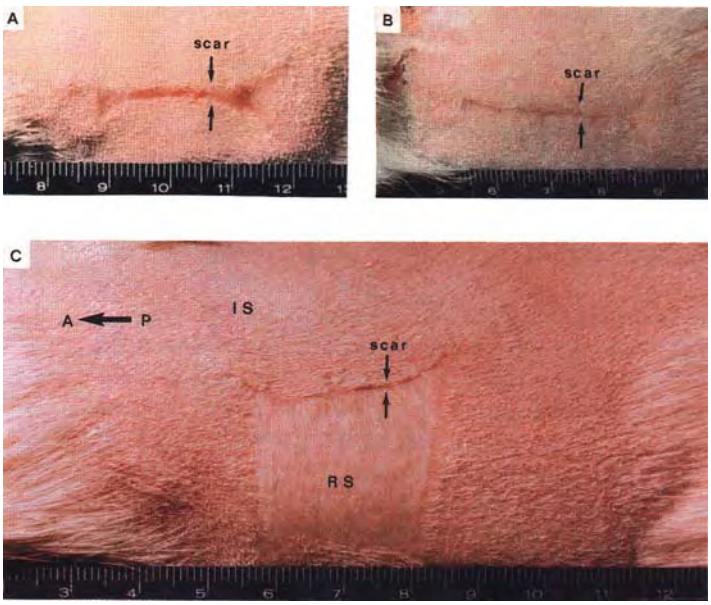

Fig. 9. The end result from healing of a full-thickness guinea pig skin wound which was treated in various ways. A: Untreated skin wound closes by contraction in about 20 days, forming a "linear scar" (arrow). Fifty percent of wound area is lost by contraction by day 8 ± 1. B: Skin wound treated with active collagen–GAG matrix, not seeded with cells, closes by strongly delayed contraction in about 40 days (arrow). Fifty percent of wound area is lost by contraction by day 27 ± 2. C: Skin wound treated with active collagen–GAG matrix seeded with skin cells does not close by contraction. Although some contraction of wound perimeter does occur, the wound closes essentially by synthesis of new skin, complete with dermis and epidermis but hairless, which forms within the wound perimeter. RS, regenerated skin. IS, intact guinea pig skin; AP, anterior-posterior axis of animal. The original wound perimeter is eventually transformed into a line of scar (arrows) which separates regenerated skin from intact skin. The scale is marked in cm. (Courtesy of Massachusetts Institute of Technology.)

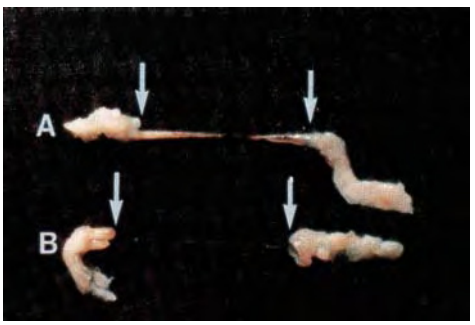

Fig. 10. Explants of rat sciatic nerve obtained six weeks after two treatments of a 15-mm gap. Silicone tubing was removed from the explants prior to photography. A: Regenerated sciatic nerve of rat spanned the entire 15-mm gap (arrows) which had been bridged with a collagen–GAG cylindrical implant; pore structure similar to the one shown in Figure 7B. The matrix was formed within a silicone rubber tube and the cut ends of the nerve were ensheathed within the ends of the tube. The new nerve totally replaced the enzymatically degradable CG matrix which occupied a 15-mm length within the silicone tube. B: A thin strand of connective tissue, but no nerve, grew across the 15-mm gap when the latter was bridged with an empty silicone tube. (Reprinted from [88] with permission.)

The availability of chemical ECM analogues that are degraded by collagenase over a relatively wide time scale makes it possible to study quantitatively the effects of ECM transience on a model wound healing process. After the ECM analogue has been brought in close physicochemical contact with the woundbed and after establishing that cells from the woundbed are migrating freely inside the pore structure of the analogue one can ask: How does a deliberate variation in the degradation rate of the ECM affect the mechanism of wound healing? Although the system of interest is a model wound, it is vitally important to establish a carefully designed in vitro experiment which can provide definitive tests of hypotheses about interactions between the matrix and specific components of the woundbed. Conclusive test results on isolated mechanistic steps frequently cannot be obtained in the complex in vivo model.

The degradation rate of collagen–GAG matrices in collagenase can be conveniently measured in vitro by at least two methods, which yield comparable results. In the first, a suspension of the finely comminuted implant is incubated in a stirred, standardized bath of collagenase. Degradation produces oligopeptides which are determined by a photometric procedure.[82, 83] The second assay is a mechanochemical method in which small strips of matrix are stretched in a standardized bath of collagenase and the kinetics of degradation are monitored by measuring the force necessary to maintain the specimen at fixed extension.[22, 49, 62] Whereas the first method measures the amount of solubilized protein, the second monitors the amount of undigested protein which persists in the form of a stress-bearing network. Additional study is necessary to correlate the information obtained by each of these two, apparently complementary, procedures. Certain interesting strategies for control of implant resistance to collagenolytic action have emerged from the use of in vitro assays. A systematic study of degradation rates of collagen specimens cross-linked with formaldehyde, glyoxal, and glutaraldehyde in the M_c range ca. 5 to 25 kDa showed an approximately 15-fold monotonous increase in the rate constant with increase in the molecular weight between cross-links.[49, 62] An approximately 10-fold increase in degradation rate with conversion to gelatin was also observed.[62] A particularly novel finding was a fivefold increase in resistance to collagenolysis as the relative amount of chondroitin 6-sulfate grafted onto collagen was increased to about 8 wt%; no further increase in resistance was observed beyond that level.[49, 81]

In vivo studies have confirmed the validity of these in vitro effects during the first 7–10 days following implantation; however, during the second week, important and revealing deviations from in vitro predictions have become evident. For example, increase in M_c led to acceleration of the rate at which subcutaneously implanted matrices were degraded[73] during the 10 days following implantation, while grafting of collagen with chondroitin 6-sulfate decreased the rate of implant degradation during that period.[22, 81] Both of these early results were expected from the in vitro studies. However, during the second week it was observed that implants in which the amount of grafted GAG exceeded about 2 wt% showed a net increase both in total dry weight and in relative collagen content; by contrast, implants in which the GAG content was lower or was zero continued to lose weight monotonously and maintained a constant relative collagen content during this period.[22, 73, 81] Histological studies showed that net increases in total dry weight followed by increases in relative collagen content were associated with synthesis of new connective tissue in very close proximity to the degrading matrix.[73, 81] These findings showed that the simple in vitro assays for degradation rate of matrices had

important predictive power which, however, was apparently limited to events occurring during the early phases of wound healing.

The effect of physicochemical manipulations of the matrix on the kinetics and mechanism of wound healing has turned out to be remarkable. One of the most obvious events that follows a total surgical removal (excision) of skin in rodents and in man is contraction of the wound perimeter. In the rodent model, where the contraction is especially vigorous, this process stops when two apposed wound edges have come in approximate contact and scar tissue has been synthesized in the narrow space separating the two edges (cf. Fig. 9A). In the human, contraction stops at an earlier stage with a greater amount of scar tissue separating the wound edges. It is now clear that skin wound contraction can be delayed so that it starts about 10 days after the wound is generated, rather than within 1–2 days after trauma, provided that the collagen–GAG matrices possess a narrowly defined constellation of properties: the resistance to degradation is higher than a critical level (Fig. 11), corresponding to

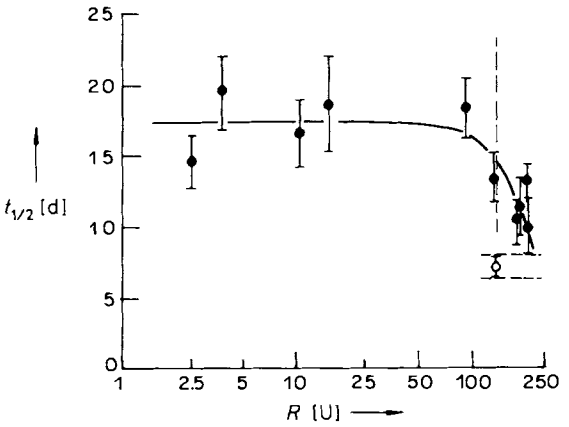

Fig. 11. Variation of the skin wound half-life with degradation rate R (in collagenase) of collagen–GAG matrix. The half-life $t_{1/2}$ is the time required for a wound to contract to 50% of the original area. The degradation is in empirical units, which are defined in terms of an in vitro assay. A somewhat arbitrary broken vertical line is drawn near $R = 140$ enzyme units. This line shows the level of degradation rate above which the half-life of matrices rapidly drops to the level of the ungrafted wound (○). The horizontal scale is logarithmic. (Reprinted from [84] with permission.)

loss of about 50% of dry implant weight within 10 days; and the average pore diameter is between 20 and 120 μm (Fig. 12), corresponding to a specific surface in the approximate range 10^6–10^7 mm^2 per gram of dry matrix.[84] Furthermore, preliminary studies have shown that collagen banding in implants must be maintained at near-zero levels (Fig. 6) while the triple-helical structure remains intact[71, 84] and that the pore volume fraction must be higher than about 0.95.[84]

When collagen–GAG matrices, which can significantly delay the onset of wound contraction, are seeded with a minimum density of easily separable skin cells (basal cells) from the same animal and the cell-seeded matrices are then grafted, wound healing is affected in an even more profound way. In this case, not only is the onset of wound contraction delayed by approximately 10 days but, a few days after it starts, contraction is arrested midway before complete clo-

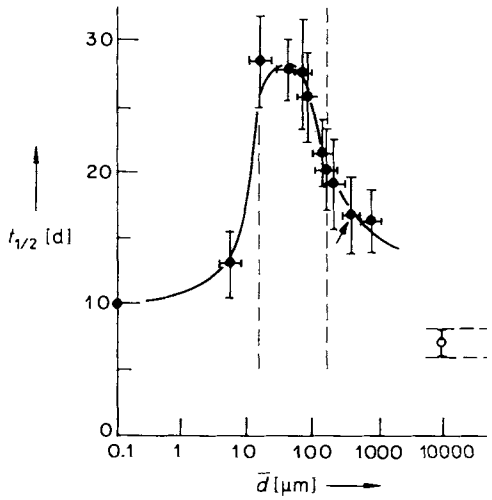

Fig. 12. Variation of half-life of skin wound with the average pore diameter of collagen–GAG matrices used as grafts for full-thickness skin wounds in the guinea pig. The vertical broken lines at about 20 and 120 μm mark the limits of matrix activity. Outside these approximate limits the wound half-life rapidly drops to the level of the ungrafted wound (○). The horizontal scale is logarithmic. (Reprinted from [84] with permission.)

sure; its direction is then reversed and the wound perimeter expands over several days until it slows down and finally stops expanding (Fig. 13). Several weeks after grafting, the area enclosed by the wound perimeter is about 65% of the original wound area and new skin, complete with a dermis and an epidermis, fills this area (cf. Fig. 9C).[85] If the matrix has not been previously seeded with skin cells, contraction is still delayed significantly, but the wound perimeter eventually closes with formation of scar (cf. Fig. 9B). The new skin synthesized with the help of cell-seeded matrices is hairless, but there is strong evidence from light scattering studies[86] as well as histological studies[84, 85, 87] that it is distinct from scar and is similar, though not identical, to normal skin. Morphological and physical (light scattering) evidence that distinguishes new skin from scar is illustrated in Figures 14

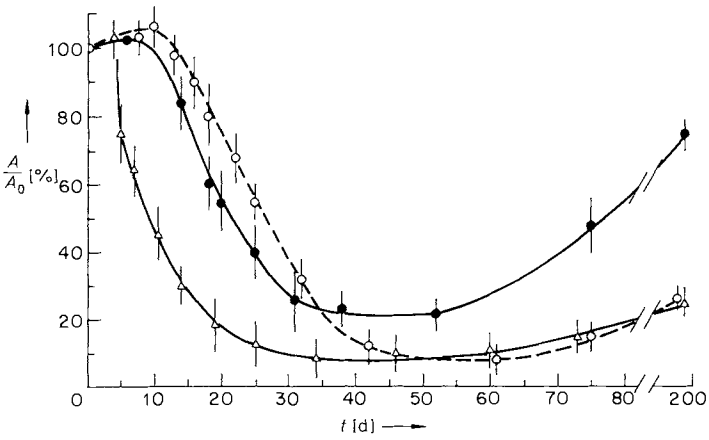

Fig. 13. Change in the original wound area, A_0, with time observed when full-thickness guinea pig skin wounds were grafted with active collagen–GAG matrices (△), active cell-free collagen–GAG matrices (○), and active cell-seeded collagen–GAG matrices (●). Active cell-free matrices delayed significantly the onset of wound contraction but did not eventually lead to arrest of contraction and skin regeneration. Active cell-seeded matrices delayed the onset of contraction, eventually arrested it, and induced skin regeneration within a woundbed which was expanding in area. (Reprinted from [84] with permission.)

and 15. The skin wound contraction kinetics are summarized in Figure 16. The kinetic data separate collagen–GAG matrices into three classes, namely, inactive matrices, active matrices which are not seeded with cells, and active matrices which are seeded with an adequate number of cells. Other collagen–GAG matrices have induced regeneration of almost intact rat sciatic nerve across a gap of 15 mm without the need for cell seeding (Fig. 10).[88]

Although the epidermis regenerates readily over an intact or partly intact dermal bed, it is well-known that de novo synthesis of the dermis does not occur spontaneously.[17, 18] Likewise, even though the rat sciatic nerve is regenerated spontaneously across a 5-mm gap or occasionally across a 10-mm gap (provided that the cut ends of the nerve are inserted in a saline-filled rubber tube), no such spontaneous regeneration is observed across a 15-mm gap.[19, 20] The appropriate use of collagen–GAG matrices leads to synthesis both of skin, complete with dermis and epidermis (cf. Fig. 15), and of new sciatic nerve (cf. Fig. 10A). It is this ability to induce de novo synthesis of nearly physiological

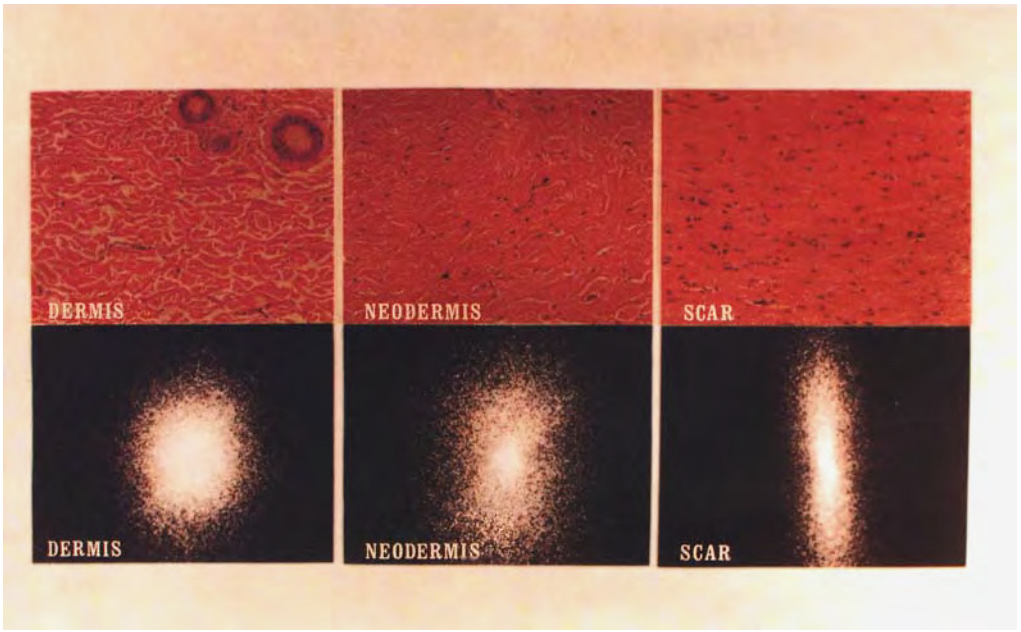

Fig. 14. Comparison of histological data obtained by light microscopy of tissue sections (top row) with small-angle patterns obtained by scattering a visible laser beam from the same tissue sections (bottom row). Tissue sections were stained with hematoxylin and eosin, but the nature of the histological stain does not appear to affect the light-scattering patterns. Left: View of normal guinea pig dermis shows a relatively random arrangement of collagen fibers and an elliptical scattering pattern. Middle: Regenerated dermis shows a less random orientation of collagen fibers and a scattering pattern which is clearly more anisometric than is true for intact dermis. Right: Dermal scar shows a highly oriented array of collagen fibers and a scattering pattern which is very highly anisometric. (Reprinted from [13] with permission.)

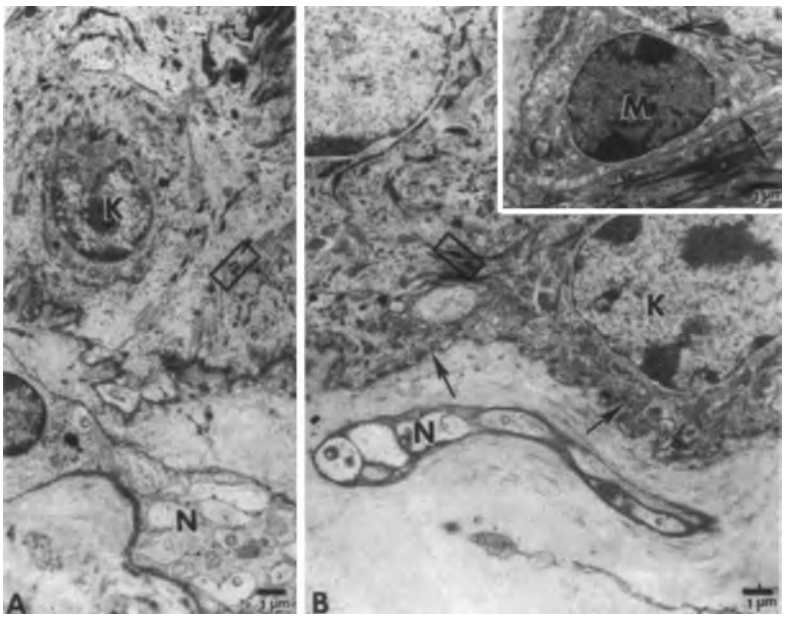

Fig. 15. A: Normal guinea pig skin viewed in the electron microscope. The epidermis is formed by keratinocytes (K) joined by junctional complexes (desmosomes enclosed). Note characteristic unmyelinated nerve fiber (N) within dermis. Bar: 1 μm. B: Regenerated skin 14 months after grafting wound with an active collagen–GAG matrix which had been seeded with skin cells. The neoepidermis is formed by keratinocytes (K) that are identical to intact skin. Desmosomes (enclosed) and basal lamina (arrows) are well-formed and normal in appearance. Melanocytes (M, inset) containing characteristic melanosomes (arrows, inset) also repopulate the neoepidermis, where they function normally in pigment production and donation. A dermal nerve fiber (N), similar to those of normal skin, is also observed. Bars in photo and in inset: 1 μm. (Reprinted from [81] with permission.)

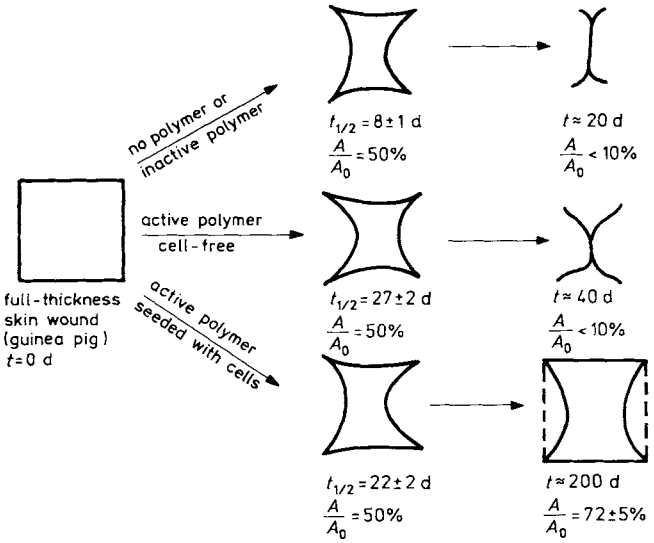

Fig. 16. The kinetics of contraction of full-thickness guinea pig skin wounds separate collagen–GAG matrices into three classes. An inactive matrix does not delay wound contraction significantly relative to the ungrafted control and eventually allows formation of "linear scar". An active, cell-free matrix delays wound contraction by about 20 days but eventually allows full contraction to occur. An active matrix, which has been seeded with a minimal number of skin cells, delays contraction significantly, later arrests it, and eventually induces synthesis of a new dermis and epidermis within an expanding wound perimeter (cf. Fig. 9). (Reprinted from [90] with permission.)

Fig. 17. A massively burned patient has been treated with autograft (left) and with a collagen–GAG matrix (right). The original clinical study of 10 patients by Dr. John F. Burke and his co-workers at Massachusetts General Hospital [50] has been expanded by a randomized clinical trial involving 106 patients [51]. Both studies concluded that a bilayer wound cover, made from a top layer of silicone rubber and a bottom layer of an active collagen–GAG matrix ("artificial dermis", "artificial skin"), performs as well as the autograft. The surgical procedure makes use of a collagen–GAG matrix which is not seeded with cells. About 15 days following grafting, the silicone layer is removed exposing a new dermal bed which is then grafted with a thin, autoepidermal graft. The conventional autograft requires removal not only of the epidermis but also of a layer of dermis, about one-half the thickness of the patient's dermis. The autografting procedure leaves a slowly healing, scarred donor site; the artificial skin procedure leaves a rapidly healing, almost unscarred donor site. (Photo of Dr. *J. F. Burke*.)

tissue under conditions where such synthesis does not occur spontaneously that characterizes regeneration matrices from the very large array of collagen or collagen–GAG matrices which are biologically inactive in this respect.

The clinical applications of ECM analogues appear to be unprecedented. Patients who have suffered massive burns and have lost a large fraction of their skin require immediate replacement of the lost skin area in order to gain back control of their dehydration rate as well as to stem large-scale infection. The best treatment currently is the skin autograft, that is, the patient's own skin, which can be obtained only after subjecting the patient to a serious operation. Clinical studies have shown that an ECM analogue virtually identical to the one which delays contraction in the guinea pig, induces synthesis of new dermis within about 15 days in patients with massive burns.[50] The new dermis forms a suitable bed on which to graft a thin layer of the patient's epidermis, which can be obtained without a serious operation, and the open wound is thereby closed permanently (Fig. 17). A recent randomized clinical trial involved 106 patients, all massively burned. This 11-hospital trial has confirmed the early finding[50] and has shown that treatment with the ECM analogue gives results which are clinically equivalent to treatment with the autograft.[51] The inability of patients to synthesize dermis spontaneously makes this clinical finding especially interesting. It is very likely that other tissues that do not regenerate spontaneously during wound healing can be induced to do so if appropriately synthesized ECM analogues are used to treat them.

It is fairly obvious that the unusual biological activity of certain collagen–GAG matrices is due to specific cell–matrix interactions which take place when these matrices are in contact with the skin woundbed or with the cut end of the nerve. What are these interactions? Electron-microscopic studies of skin wounds have shown that cells (monocytes) attach themselves particularly intimately to the collagen–GAG surface, which is itself coated with a thin layer of a fibrinlike network (Fig. 18A, B).[89] The attached cells are in close proximity on the matrix surface and most probably interact with each other. No such cell–matrix interaction is observed in a normally healing skin wound (Fig. 18C)[89] even though there are locally present, by all accounts, substantial amounts of various collagens, various GAGs, and other ECM components, all of which are undergoing remodeling, that is, degradation and synthesis. Why is contraction delayed or even arrested in the presence of active matrices? It has been hypothesized[90] that cell–matrix interactions of the type illustrated in Figures 18A and 18B may prevent differentiation of cells in the woundbed to myofibroblasts, the cells which have been credited with the contraction of wounds during normal healing.[91] This hypothesis is based on the observation that there is depletion of myofibroblasts on about day 10 following injury in woundbeds which have been treated with active matrices relative to untreated woundbeds on the same day.[89, 90]

The necessary attributes of a regeneration matrix can be most simply understood in terms of a highly specific cell–matrix interaction which diverts decisively the mechanism of wound healing away from contraction and scar synthesis to arrest of contraction and tissue regeneration in the woundbed.[84] The quantitative relations between matrix structure and wound contraction kinetics (cf. Figs. 11–13) can be used to deduce the physicochemical requirements: What seems to be necessary is the presence of a collagen–GAG surface which is (1) sufficiently extensive (upper limit of pore diameter; cf. Fig. 12), (2) sufficiently nondiffusible over a period of about 10 days (upper limit of degradation rate; cf. Fig. 11), and (3) endowed with pores which are sufficiently large to

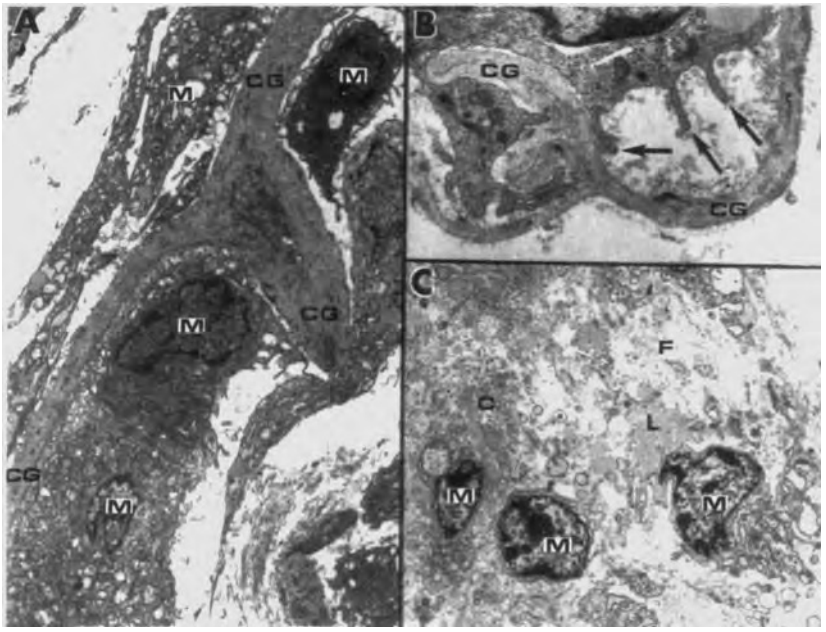

Fig. 18. Characteristic cell–matrix interactions observed when an active collagen–GAG matrix is in contact with the woundbed. The model wound is the full-thickness skin wound in the guinea pig. A, B: Seven days after grafting with a collagen–GAG matrix, mononuclear cells (M) formed an apparently continuous monolayer along the surfaces of pores in the matrix. Arrows in B indicate pseudopods extending from cells to the matrix surface. C: The ungrafted wound shows a random admixture of mononuclear cells, lipid (L), fibrin (F), and host collagen (C). Magnification: A, 3000X; B, 9500X; C, 2000X. CG = collagen-*graft*-glycosamino glycan copolymer. (Photo of Dr. *G. F. Murphy*.)

allow ready access to cells migrating into the woundbed (lower limit of pore diameter; cf. Fig. 12).[84] Additional criteria currently being studied include an apparent requirement for nearly zero crystallinity (banding) (cf. Fig. 6) and a pore volume fraction in excess of 0.95. Although skin regeneration requires that the matrix be seeded with a critical density of cells, the physicochemical structure suffices, by itself, to delay wound contraction (cf. Figs. 13 and 16) and probably sets the biological stage for regeneration to occur. In studies of nerve regeneration it has also been observed that a matrix that has not been seeded with cells can, in fact, induce synthesis of new, functional tissue over large gaps.[88, 92]

5. Conclusion

We conclude that a set of well-defined physicochemical manipulations suffices to yield insoluble but degradable, porous, cell-free macromolecular matrices which possess remarkable biological activity. Even when these matrices have not been previously seeded with cells, they modify profoundly the mechanism of healing in skin and nerve wounds. These matrices are very simple chemical analogues of the ECM. Nevertheless, deliberate changes in macromolecular network structure and in pore structure can be made and confirmed readily. These well-defined matrices can then be used to answer important questions about aspects of the mechanism of tissue remodeling which distinguish conventional wound healing from normal development or from regeneration. Such questions are currently intractable due principally to the lack of appropriately standardized preparations of biologically active ECMs.[6]

The physicochemical characteristics of collagen–GAG matrices that define the boundaries of biological activity in the skin wound model are quite narrow (cf. Figs. 11 and 12). So narrow is this description of active matrices in this animal model that the evidence probably defines a single substance. Unlike the vast majority of biologically active substances, the matrix defined in this context is insoluble and cannot be characterized by a molecular weight, as soluble macromolecules usually are; it lacks a precise three-dimensional configuration and, therefore, cannot be described by X-ray crystallography; and it is highly porous rather than forming a homogeneous phase. Nevertheless, the data define a network which maintains its nondiffusible character in the presence of collagenolytic activity and is sufficiently well endowed with surface area to enable high densities of cells to interact with it, and possibly with each other, in its presence. Accordingly, we have hypothesized that the data define a unique substance which acts as an insoluble growth factor[84] during skin development. Rather than allow the woundbed to contract and synthesize scar this matrix induces synthesis of partly physiological tissue. If it does that much the substance most probably possesses mitogenic activity and should, therefore, be considered a growth factor.

There is agreement that some kind of ECM, probably a variant or precursor of the mature basal lamina, mediates the critical interaction between epithelial and mesenchymal cells which leads to morphogenesis of several tissues during development.[4, 93] The specific matrix described by the data in Figures 11–13 must be present in order for the epithelial cells seeded into it, together with the mesenchymal cells which migrate into it from the underlying woundbed, to yield new skin. It is reasonable to hypothesize quite simply that the collagen–GAG matrix is responsible for that critical cell–cell interaction. In fact, it has been observed that if only epithelial and mesenchymal cells, but no matrix, are present in the woundbed, healing proceeds without any evidence of regeneration.[94] This line of reasoning supports the hypothesis that the regeneration matrix described here is a functional analogue of the basal lamina. This analogue mediates a critical epithelial–mesenchymal cell interaction during morphogenesis of skin and nerve before it becomes totally degraded and diffuses away from the woundbed. The final outcome of skin morphogenesis is not only a new dermis and

epidermis but also a new basal lamina (cf. Figs. 1, 15A, and 15B). In the process, the collagen–GAG matrix became completely degraded and is not visible in electron-microscopic views of newly synthesized skin (Fig. 15B). Similarly, residual fragments of collagen–GAG matrix are eventually not visible any more in sciatic nerve regenerates.

Another possibility emerges form the finding that the swollen, nonbanded type-I collagen present in the regeneration matrix (Fig. 6) does not aggregate platelets, whereas type-I banded collagen is very active.[71] It is well-known that one of the first events following tissue injury is platelet aggregation and degranulation with release of platelet-derived growth factor (PDGF), a powerful mitogen of cells of mesenchymal origin that participate in normal wound healing processes.[95, 96] Although PDGF is known to be secreted by platelets during the early phase of wound healing, other cells, principally macrophages, are also known to synthesize this growth factor in later stages of wound healing.[95, 96] Since the regeneration matrix does not aggregate platelets, PDGF is probably not secreted in woundbeds which have been treated with the matrix, and the strongly proliferative effect of this mitogen is , therefore, absent in such woundbeds, at least in the early stages of response to injury. I hypothesize that the absence of PDGF during the early phase of healing is the critical factor which diverts the kinetics and mechanism of the wound healing process away from contraction and relatively random cell proliferation towards the suspension, or even arrest, of contraction (Fig. 13) and the organization of cells into orderly arrays (Fig. 18) which synthesize new skin rather than scar (Figs. 14 and 15).

It is interesting to speculate on the structural, rather than functional, similarity between the basal lamina and the regeneration matrix. Inspection of Figure 6 opens up the intriguing possibility that type-I collagen, which is almost entirely nonbanded due to the swelling action of the diluent possesses an ultrastructure (quaternary structure) that simulates the threadlike, open network or scaffold ultrastructure[24, 25, 27] of type-IV collagen in the basal lamina. Like collagen IV in the basal lamina, but unlike collagen types I, II, and III, swollen type-I collagen (Fig. 6) does not form fibrils, except in very few locations. On the other hand, whereas the polypeptide chains in swollen, nonbanded collagen possess the triple-helical structure (tertiary structure) characteristic of type-I collagen along their entire length, the polypeptide chains of the basal lamina are partly nonhelical.[24, 25, 27] Other differences obviously extend to the amino-acid composition of the collagens, which is characteristic of collagen type IV in the basal lamina. Nevertheless, it would be extremely interesting to attempt the synthesis of collagen–GAG matrices which are based on collagen IV and which incorporate macromolecules known to be present in the basal lamina, such as heparan sulfate and laminin. There is no question that synthetic chemistry can make enormous contributions to the understanding of the role of the ECM during development.

Regeneration of rat sciatic nerve is induced by a similar, though distinct, collagen–GAG matrix. Evidence obtained so far indicates that the ECM analogue that induces sciatic nerve regeneration to occur most rapidly and completely is degraded more rapidly and has a smaller average pore diameter than does the analogue which induces skin synthesis.[81, 88, 92] It is intriguing to contemplate the possibility that morphogenesis of each type of tissue or organ requires a distinct ECM, with chemical composition and physicochemical structure that are specialized for the particular developmental task. Such hypotheses can be tested with the help of new ECM analogues.

Shape and form, the two indispensable attributes of developing systems, require not only an actively differentiating and proliferating cell population but also transient extracellular matrices which order the cells in space and probably induce transcription of genetic information. In the future I anticipate the synthesis of increasingly sophisticated but still well-defined macromolecular analogues of various ECMs which can be used to answer critical questions of development and of healing.

Received: June 28, 1989 [A 745 IE]
German version: *Angew. Chem. 102* (1990) 21

[1] K. A. Piez, A. H. Reddi (Eds.): *Extracellular Matrix Biochemistry*, Elsevier, New York 1984.
[2] E. D. Hay (Ed.): *Cell Biology of Extracellular Matrix*, Plenum Press, New York 1981.
[3] J. Darnell, H. Lodish, D. Baltimore: *Molecular Cell Biology*, Scientific American Books, New York 1986.
[4] W. F. Loomis: *Developmental Biology*, Macmillan, New York 1986.
[5] R. L. Trestad (Ed.): *The Role of Extracellular Matrix in Development*, Alan R. Liss, New York 1984.
[6] A. H. Reddi in [1], Chapter 10.
[7] a) M. E. Nimni (Ed.): *Collagen*, CRC Press, Boca Raton 1988; b) [7a], *Vol. I, Biochemistry*.
[8] F. O. Schmitt, *Ann. Rev. Biophys. Chem. 14* (1985) 1.
[9] H. C. Grillo, J. Gross, *J. Surg. Res. 2* (1962) 69.
[10] J. I. Abbenhaus, R. A. MacMahon, J. G. Rosenbrantz, B. C. Paton, *Surg. Forum 16* (1965) 477.
[11] M. Chvapil, R. Holusa, *J. Biomed. Mater. Res. 2* (1968) 245.
[12] A. L. Rubin, K. H. Stenzel in L. Stark, G. Agarwal (Eds.): *Biomaterials*, Plenum Press, New York 1969, pp. 157–184.
[13] I. V. Yannas, *Encycl. Polym. Sci. Eng. 13* (1988) 317.
[14] H. Wallace: *Vertebrate Limb Regeneration*, Wiley, New York 1981.
[15] H. Roels in L. E. Glynn (Ed.): *Tissue Repair and Regeneration*, Elsevier/North Holland Biomedical Press, Amsterdam 1981, pp. 265–270.
[16] E. E. Peacock, Jr., in S. I. Schwartz, G. T. Shires, F. C. Spencer, E. H. Storer (Eds.): *Principles of Surgery*, McGraw-Hill, New York 1984, p. 289.
[17] R. E. Billingham, P. B. Medawar, *J. Anat. 89* (1955) 114.
[18] R. E. Billingham, P. B. Medawar, *J. Exp. Biol. 28* (1951) 385.
[19] G. Lundborg, *Acta Orthop. Scand. 58* (1987) 145.
[20] G. Lundborg, L. B. Dahlin, N. Danielsen, R. H. Gelberman, F. M. Longo, H. L. Powell, S. Varon, *Exp. Neurol. 76* (1982) 361.
[21] W. Ring, I. Mita, A. D. Jenkins, N. M. Bikales, *Pure Appl. Chem. 57* (1985) 1427.
[22] I. V. Yannas, J. F. Burke, C. Huang, P. L. Gordon, *Polym. Prepr. Am. Chem. Soc. Div. Polym. Chem. 16* (1975) 209.
[23] N. A. Kefalides, *Int. Rev. Connect. Tissue Res. 6* (1973) 63.
[24] J. H. Fessler, G. Lunstrum, K. G. Duncan, A. G. Campbell, R. Sterne, H. P. Bachinger, L. J. Fessler in [5], pp. 207–219.
[25] E. J. Miller in [5], pp. 139–156.
[26] H. K. Kleinman, M. L. McGarvey, J. R. Hassell, G. R. Martin, A. B. von Evercooren, M. Dubois-Dalcq in [5], pp. 123–143.
[27] T. F. Linsenmayer, J. M. Fitch, R. Mayne in [5], pp. 145–172.
[28] M. B. Mathews: *Connective Tissue*, Springer, New York 1975.
[29] B. P. Toole, D. A. Lowther, *Biochem. J. 109*, (1968) 857.
[30] V. Podrazky, F. S. Steven, D. S. Jackson, J. B. Weiss, S. J. Leibovich, *Biochim. Biophys. Acta 229* (1971) 690.
[31] I. V. Yannas, A. V. Tobolsky, *Nature (London) 215*, (1967) 509.
[32] I. V. Yannas, *Rev. Macromol. Chem. C 7* (1972) 49.
[33] J. Bello, H. Riese-Bello, *Sci. Ind. Photogr. 29* (1958) 361.
[34] F. H. Silver, *Ph.D. Dissertation*, Massachusetts Institute of Technology 1977.
[35] F. H. Silver, I. V. Yannas, E. W. Salzman, *J. Biomed. Mater. Res. 13* (1979) 701.
[36] I. V. Yannas, A. V. Tobolsky, *J. Macromol. Chem. 1* (1966) 723.
[37] I. V. Yannas, A. V. Tobolsky, *Eur. Polym. J. 4* (1968) 257.

[38] N.-H. Sung, *Ph.D. Dissertation*, Massachusetts Institute of Technology 1972.
[39] J. H. Bowes, J. E. Taylor, *J. Am. Leather Chem. Assoc. 66* (1971) 96.
[40] P. J. Flory, R. R. Garrett, *J. Am. Chem. Soc. 80* (1958) 4836.
[41] I. V. Yannas, J. F. Burke, P. L. Gordon, C. Huang, R. H. Rubenstein, *J. Biomed. Mater. Res. 14* (1980) 107.
[42] C. W. Cater, *J. Soc. Leather Trades Chem. 47* (1963) 259.
[43] J. H. Bowes, C. W. Cater, *J. Appl. Chem. 14* (1964) 296.
[44] D. Hopwood in J. D. Bancroft, A. Stevens (Eds.): *Theory and Practice of Histological Techniques*, Churchill Livingstone, Edinburgh 1977, Chapter 2.
[45] F. M. Richards, J. R. Knowles, *J. Mol. Biol. 37* (1968) 231.
[46] P. M. Hardy, A. C. Nicholls, H. N. Rydon, *J. Chem. Soc. Perkin Trans. 1, 1976, 958.*
[47] P. M. Hardy, G. J. Hughes, H. N. Rydon, *J. Chem. Soc. Perkin Trans. 1, 1976, 2282.*
[48] M. E. Nimni, D. T. Cheung, B. Strates, M. Kodama, K. Sheikh in [7a], *Vol. III, Biotechnology*, Chapter 1.
[49] C. Huang, *Sc.D. Dissertation*, Massachusetts Institute of Technology 1974.
[50] J. F. Burke, I. V. Yannas, W. C. Quinby, Jr., C. C. Bondoc, W. K. Jung, *Ann. Surg. 194* (1981) 413.
[51] D. Heimbach, A. Luterman, J. Burke, A. Cram, D. Herndon, J. Hunt, M. Jordan, W. McManus, L. Solem, G. Warden, B. Zawacki, *Ann. Surg. 208* (1988) 313.
[52] L. R. G. Treloar: *The Physics of Rubber Elasticity*, 4th ed. Clarendon Press, Oxford 1975.
[53] N. M. Wiederhorn, G. V. Reardon, *J. Polym. Sci. 9* (1952) 4, 314.
[54] A. Veis: *The Macromolecular Chemistry of Gelatin*, Academic Press, New York 1964.
[55] P. J. Flory: *Principles of Polymer Chemistry*, Cornell University Press, Ithaca 1953.
[56] P. J. Flory, J. Rehner, *J. Chem. Phys. 11* (1943) 512.
[57] J. E. Eastoe in G. N. Ramachandran (Ed.): *Treatise on Collagen, Vol. 1, Chemistry of Collagen*, Academic Press, London 1967, Chapter 1.
[58] K. Linderstrøm-Lang; *Lane Medical Lectures, Proteins and Enzymes*, Stanford University Press, Stanford, CA, 1952, p. 58.
[59] W. Kauzmann, *Adv. Protein Chem. 14* (1959) 1.
[60] E. Baer, J. J. Cassidy, A. Hiltner in [7a], *Vol. II, Biochemistry and Biomechanics*, Chapter 9.
[61] I. V. Yannas, C. Huang, *J. Polym. Sci. Polym. Phys. Ed. 10* (1972) 577.
[62] C. Huang, I. V. Yannas, *J. Biomed. Mater. Res. Symp. 8* (1977) 137.
[63] P. H. von Hippel, W. F. Harrington, *Biochim. Biophys. Acta 36* (1959) 427.
[64] P. L. Gordon, C. Huang, R. C. Lord, I. V. Yannas, *Macromolecules 7* (1974) 954.
[65] I. V. Yannas, N.-H. Sung, C. Huang, *J. Phys. Chem. 72* (1976) 2935.
[66] C. E. Hall, M. A. Jakus, F. O. Schmitt, *J. Am. Chem. Soc. 64* (1942) 1234.
[67] C. Wolpers, *Klin. Wochenschr. 22* (1943) 624.
[68] J. H. Highberger, J. Gross, F. O. Schmitt, *J. Am. Chem. Soc. 72* (1950) 3321.
[69] J. H. Highberger, J. Gross, F. O. Schmitt, *Proc. Natl. Acad. Sci. USA 37* (1951) 286.
[70] M. J. Forbes, *M. S. Dissertation*, Massachusetts Institute of Technology 1980.
[71] M. Sylvester, I. V. Yannas, E. W. Salzman, *Thromb. Res., 55* (1989) 135.
[72] R. S. Bear, *J. Am. Chem. Soc. 64* (1942) 727.
[73] I. V. Yannas in P. Dineen (Ed.): *The Surgical Wound*, Lea & Febiger, Philadelphia 1981, Chapter 15.
[74] N. Dagalakis, J. Flink, P. Stasikelis, J. F. Burke, I. V. Yannas, *J. Biomed. Mater. Res. 14* (1980) 511.
[75] E. E. Underwood: *Quantitative Stereology*, Addison-Wesley, Reading 1969.
[76] H. F. Fischmeister in *Proc. Int. Symp. RILEM/IUPAC*, Prague 1973, Final Report Part II, p. C-439.
[77] D. E. Woolley in [1], Chapter 4.
[78] J. Gross, C. M. Lapiere, *Proc. Natl. Acad. Sci. USA 48* (1962) 1014.
[79] C. L. Mainardi in J. Uitto, A. J. Perejda (Eds.): *Connective Tissue Disease*, Marcel Dekker, New York 1987.
[80] I. V. Yannas, J. F. Burke, *J. Biomed. Mater. Res. 14* (1980) 65.
[81] I. V. Yannas in [7a], *Vol. III, Biotechnology*, Chapter 4.
[82] I. Mandl, J. D. Maclennan, E. L. Howes, *J. Clin. Invest 32* (1953) 1323.
[83] I. V. Yannas, E. Lee, M. D. Bentz in C. G. Gebelein (Ed.): *Applied Bioactive Polymeric Materials*, Plenum, New York 1988, pp. 313–318.
[84] I. V. Yannas, E. Lee, D. P. Orgill, E. M. Skrabut, G. F. Murphy, *Proc. Natl. Acad. Sci. USA 86* (1989) 933.
[85] I. V. Yannas, J. F. Burke, D. P. Orgill, E. M. Skrabut, *Science Washington DC 215* (1982) 174.
[86] A. Ferdman, I. V. Yannas, *Trans. Soc. Biomater. 10* (1987) 207.
[87] I. V. Yannas, D. P. Orgill, E. M. Skrabut, J. F. Burke in C. G. Gebelein (Ed.): *Polymeric Materials and Artificial Organs, ACS Symp. Ser. 256*, Am. Chem. Soc., Washington 1984, Chapter 13.
[88] I. V. Yannas, D. P. Orgill, J. Silver, T. V. Norregaard, N. T. Zervas, W. C. Schoene in C. G. Gebelein (Ed.): *Advances in Biomedical Polymers*, Plenum, New York 1987, pp. 1–9.
[89] G. F. Murphy, D. P. Orgill, I. V. Yannas, *Lab. Invest.*, in press.
[90] I. V. Yannas in G. Abatangelo, J. M. Davidson (Eds.): *Cutaneous Development, Aging and Repair, Fidia Research Series, Vol. 18*, Liviana Press, Padova 1989, p. 131.
[91] G. Gabbiani, G. B. Ryan, G. Majno, *Experientia 27* (1971) 549.
[92] I. V. Yannas, C. Krarup, A. Chang, T. V. Norregaard, N. T. Zervas, R. Sethi, *Soc. Neurosci. Abstr. 13* (1987) 1043.
[93] E. D. Hay in [2], Chapter 12.
[94] K. Troxel, I. V. Yannas, unpublished data.
[95] R. Ross, *Cell 46* (1986) 155.
[96] S. E. Lynch, J. C. Nixon, R. B. Colvin, H. N. Antoniades, *Proc. Natl. Acad. Sci. USA 84* (1987) 7696.
[97] cf. [3], Chapter 5, Fig. 552.
[98] J. A. Chapman, D. J. S. Hulmes in A. Ruggeri, P. M. Motta (Eds.): *Ultrastructure of the Connective Tissue Matrix*, Martinus Nijhoff, Boston 1984, Chapter 1, Fig. 1.
[99] K. A. Piez in [1], Chapter 1, Fig. 1.6.
[100] K. A. Piez in [1], Chapter 1, Fig. 1.22.
[101] M. E. Nimni, R. D. Harkness in [7], Chapter 1, Fig. 10.

Replication Experiments with Nucleotide Base Analogues

By Peter Strazewski and Christoph Tamm*

The principles governing the replication fidelity of genomes are not fully understood yet. *Watson* and *Crick*'s base-pairing principle for matched deoxyribonucleotide (DNA) bases can explain why the guanine–cytosine and adenine–thymine base pairs are approximately one hundred times more stable thermodynamically than mismatched combinations. In vitro, DNA polymerases reduce the number of mismatched base pairs to about 10^{-6} per Watson-Crick base pair. Replication fidelity can further be enhanced to a mutation probability of 10^{-10} or less in vivo if optimal conditions for DNA synthesis are provided by polymerase-assisting proteins and DNA-repairing enzymes. The precise reasons for the formation of mismatched base pairs (mispairs), which are responsible for a substantial part of DNA mutations, are still in debate. Although it is agreed that a template-directed "reading" of the hydrogen-substitution pattern in the heterocyclic bases is crucial for proper base pairing during DNA synthesis, it is not clear which type of "misreading" leads to mispairs. Misreading may be due to a non-Watson–Crick base pairing as well as to a change in the hydrogen-substitution pattern, leading to Watson–Crick-like mispairs. The surprising discovery of the selective and quantitative DNA-polymerase-catalyzed formation of a pyridine–pyrimidine base pair (involving a nucleotide base analogue) indicated that rare tautomeric forms in template DNA strands can lead to Watson–Crick-like mispairings that are hardly recognized by the polymerase's proofreading activity. This reveals new pathways for substitution mutations (replication-dependent DNA point mutations) and suggests a new type of mutagen in vivo.

1. Introduction

1.1. Essential Contacts

To evolve on earth, the structures of living matter had to satisfy four basic requirements. (1) They had to be sufficiently complex and stable to store imprinted genetic (i.e., inheritable) information. (2) Their surface had to be accessible to a template-directed reading so that the information could be accurately passed on to offspring (replication). (3) They had to be able to influence their "dead" environment in such a way that it would serve their own reproduction. In other words, they must have had a biological activity which would turn their immediate surroundings into a phenotype. Such a controlled environment would have helped them to compete against a great variety of replicating structures carrying other genetic information (selection). (4) They must have consisted of metastable information units to allow their carrier to evolve under the influence of natural selection (mutability allowing adaptation).

This information carrier is deoxyribonucleic acid (DNA). It can be divided into two classes of DNA regions: DNA stretches that encode amino acid sequences in proteins (exons) and noncoding stretches. Coding DNA sequences, which probably are a minor part of most DNA, can pass on their message to the phenotype through *DNA–ribo(mono)nucleotide* contacts assisted by transcription proteins. After being transcribed into an "active form" carried by ribonucleic acid (RNA), the translation of this type of information into proteins relies on *RNA–RNA* contacts (codon–anticodon binding between the DNA transcript, messenger RNA, and the amino-acid carrier, transfer RNA) and *RNA–protein* contacts (selective, enzymatic aminoacylation of the appropriate transfer RNAs). The RNA–RNA contacts are assisted by proteins and ribosomal RNA and are governed by the universal genetic code using triplet codons. The nature of the RNA–protein contacts, recently referred to as the second genetic code,[1] is not well understood yet. Both coding and noncoding DNA sequences can influence the phenotype through direct *DNA–protein* contacts as well. These provide possibilities to regulate the expression of coding sequences, are responsible for changes in the topology of DNA (e.g., unwinding), and allow a tight packing of DNA in chromosomes. *DNA–DNA* contacts are necessary for the chemical stabilization of DNA itself through the formation of a DNA double helix. They also dominate the exchange of DNA fragments during genetic recombination, which is the basis for sexual reproduction. Finally, *DNA–deoxyribo(mono)nucleotide* contacts—with the help of replication proteins—allow all genetic information to be copied and thus serve in DNA replication.

1.2. Various Forms of Base–Base Interactions

Of all these vital contacts (Section 1.1), those between nucleotide residues are the best known, because they involve only four different information units. The information is coded by the sequence of four heterocyclic nucleotide bases; adenine, guanine, cytosine, and uracil/thymine. In spite of the relatively simple structure of these bases (compared to the 20 structures of amino-acid side chains), a variety of contacts between them are known (Fig. 1). The most common contacts are hydrogen bonds that result in base pairing.

[*] Prof. Dr. C. Tamm
Institut für Organische Chemie der Universität
St. Johanns-Ring 19, CH-4056 Basel (Switzerland)
Dr. P. Strazewski
University Chemical Laboratory
Lensfield Road, GB-Cambridge CB2 1EW (UK)

 © VCH Verlagsgesellschaft mbH, D-6940 Weinheim, 1990 0570-0833/90/0101-0036 $ 02.50/0

Base pairings following the Watson–Crick rules[2] (Fig. 1a) take part in the formation of matched antiparallel double strands from DNA and/or RNA single strands. *Watson–Crick base pairs* always contain one purine base (guanine, adenine) and one pyrimidine base (cytosine, uracil/thymine); guanine pairs with cytosine and adenine with uracil (in RNA) or thymine (in DNA). Their structures, as well as the structures of *Hoogsteen pairs*, where a purine base adopts the unusual *syn* conformation around the glycosidic bond (Fig. 1b), and *wobble pairs*, where the C_2 pseudosymmetry of Watson–Crick pairs is broken (Fig. 1c), are well established thanks to X-ray crystallographic evidence. Hoogsteen and wobble pairs play an important role in alternative base-pairing modes in RNA and in DNA mutagenesis. Other types of base–base contacts are *reversed base pairs*, where two strands are assumed to be oriented parallel (Fig. 1d), and *base triplets* in DNA triple strands (Fig. 1e). These structures are constructed following the patterns of hydrogen donors and acceptors in the bases and have not yet been proven. Parallel strands are thought to exist in unusual DNA or RNA secondary structures.[3] Triple-stranded DNA sequences stabilize an unusual secondary structure that induces sharp bends in DNA double strands (H-DNA).[4] Triple-stranded DNA might also play a role in the initiation of recombination events.

All these base pairings can be formed under the instruction of the genetic information carried by DNA, either correctly or incorrectly. The "incorrect" pairs, which can lead to mutated forms of DNA, RNA, or proteins, are presently of great interest, because their formation is not as well understood as the formation of Watson–Crick pairs. Mutations are the consequence of unusual contacts, not only between nucleotide bases, but also between proteins and DNA or RNA. Yet, the most hazardous or meaningful ones (to the cell) are mutations which arise in DNA, because only they are inheritable and only they can give rise to a large amount of mutated products. Therefore, we shall focus on base pairings and mispairings formed during DNA replication.

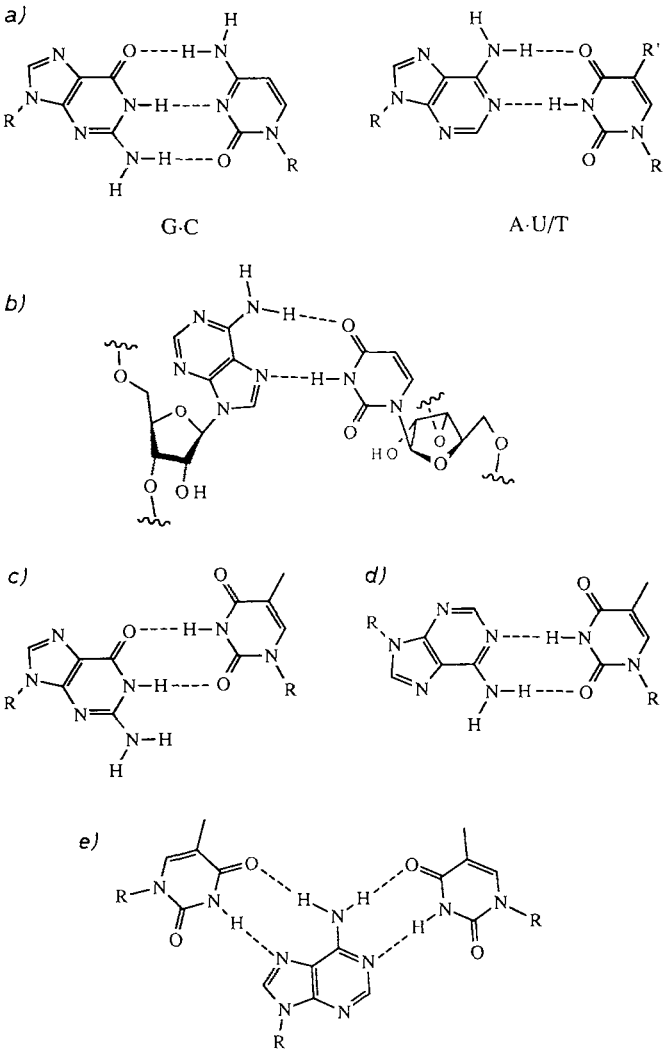

Fig. 1. Base–base interactions between nucleotides. R = β-D-ribofuranosyl or 2'-deoxy-β-D-ribofuranosyl, R' = H or CH_3. a) Watson–Crick base pairs G · C and A · U (R = ribosyl, R' = H) or A · T (R = deoxyribosyl, R' = CH_3). b) Hoogsteen pairs, e.g., A(*syn*) · U. c) Wobble pairs, e.g., G · T (wobble). d) Reversed base pairs, e.g., A · ⊥ (or ∀ · T). e) Base triplets, e.g., T · A · T.

1.3. Hydrogen-Substitution Patterns of Nucleotide Bases

Nucleotides (deoxyribonucleotides are simply referred to as nucleotides in this article) are chemically quite stable, because they are covalently bound in DNA as phosphoric acid diesters. Additionally, a quite strong secondary structure efficiently protects the bases from chemical modification and hydrolysis, because they are buried in the central core of the double helix. Nevertheless, nucleotides in DNA appear to be metastable with respect to replication (muta-

Christoph Tamm was born in 1923 in Basel. He studied at the University of Geneva and the University of Basel, where he received his Ph.D. in 1948 under Tadeus Reichstein. From 1949 to 1952, he worked as a postdoc with Oskar P. Wintersteiner, Squibb Institute for Medical Research, New Brunswick, NJ, and with Erwin Chargaff, Columbia University, New York. After his habilitation in 1953 in Basel, he worked in the Pharmaceutical Research Department at Sandoz AG, Basel (1957–1961). In 1961, he was appointed associate professor and in 1966 professor at the University of Basel. Tamm is a member of numerous research and government committees for science. His interests include the structure, synthesis, and biosynthesis of bioactive microbial metabolites, the use of enzymes in synthesis, and the synthesis of nucleosides and polynucleotides.

Peter Strazewski was born in 1958 in London. He studied at the University of Basel and received his Ph.D. in 1986 under Christoph Tamm. Since 1988, he has worked as a postdoc with Olga Kennard, University Chemical Laboratory, Cambridge (UK). His interests include the synthesis of natural products and the synthesis and X-ray analysis of oligonucleotides.

ble). The reason is the possible formation of mismatched base pairs that do not follow the Watson–Crick rules. Therefore, the base-paired nucleotides should be treated as the information-carrying units, rather than the single-stranded nucleotides.

In a strict sense, only one particular feature of the nucleotide base is crucial in governing the storage and transfer of genetic information, namely, the hydrogen-substitution pattern of the heterocycle, that is, the pattern of hydrogen acceptors and donors on the exposed side of the base. Hence, if the pattern changes before replication in such a way that the base can form normal hydrogen bonds to a different nucleotide base, the information content would be changed after replication.

How can a hydrogen-substitution pattern change in such a way? Figure 2 shows four alternative ways of changing a pattern of three donors/acceptors aligned in an anchored plane (the "information plane"), like the arrangement of H atoms and nonbonding electron pairs in a heterocyclic nucleotide base. The most trivial change is addition or removal of a proton, leaving a charged plane (Fig. 2a). This change can be neutralized by the reverse reaction or by removal or addition, respectively, of a different proton, thereby leading to a tautomer of the initial pattern (Fig. 2b). Base pairs that use these types of altered H-substitution patterns can have a Watson–Crick-like geometry but a different information content and they can therefore cause mutations. Another way of changing the pattern is to shift the reading frame out of the information plane (following the principle "no information is also information") (Fig. 2c). In nature, this is possible because the missing part of the information will be replaced by the solvent, which provides a huge reservoir of easily adjustable H donors and acceptors. Wobble pairs (cf. Fig. 1c) are base pairs with a shifted reading frame. They, too, have an altered information content and can cause mutations. Finally, we know that some natural information planes, the purine bases, carry heterocyclic H atoms and nonbonding electron pairs all around the plane. Changing the reading frame from one side of the information plane to the other can provide a different pattern. This can be achieved by simply rotating the anchored information plane by 180° (Fig. 2d). Hoogsteen pairs (cf. Fig. 1b) are arranged in such a way that another part of the purine base contains the reading frame. Some Hoogsteen pairs cause mutations as well. These basic possibilities can also be combined and offer still more ways of changing a hydrogen-substitution pattern. Examples are protonated Hoogsteen pairs and tautomeric wobble pairs.

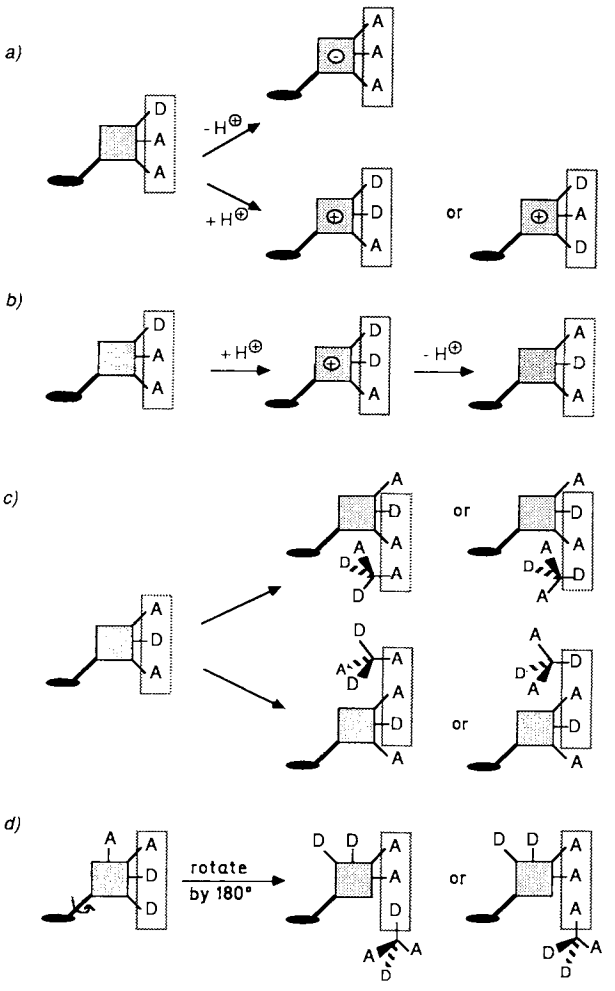

Fig. 2. Ways of changing the H-donor/acceptor substitution pattern of a nucleotide base. Shaded boxes: anchored information planes (schematic nucleotides), D = H donor, A = H acceptor, $D_2A_2 = H_2O$. Dotted lines: reading frame. a) Deprotonation or protonation. b) Tautomerization. c) Shift of the reading frame. d) Presentation of an alternative substitution pattern.

1.4. Nucleotide Base Analogues

A good way to find out which type of erroneous reading can occur in a DNA polymerase is to investigate modified nucleotide bases (analogues) with a reduced or altered capability of forming hydrogen bonds with the natural nucleotides. The behavior of such nucleoside triphosphate analogues during DNA synthesis might give an insight into what kinds of H-substitution patterns of an incoming nucleotide base are allowed by a polymerase. The use of these analogues as template nucleotides would clarify which H bonds are necessary for accurate DNA synthesis.

The modified nucleosides chosen for this purpose can all be considered to be structural analogues of deoxycytidine (Fig. 3). 1-(2′-Deoxy-β-D-ribofuranosyl)-2(1*H*)-pyridone (**1**)

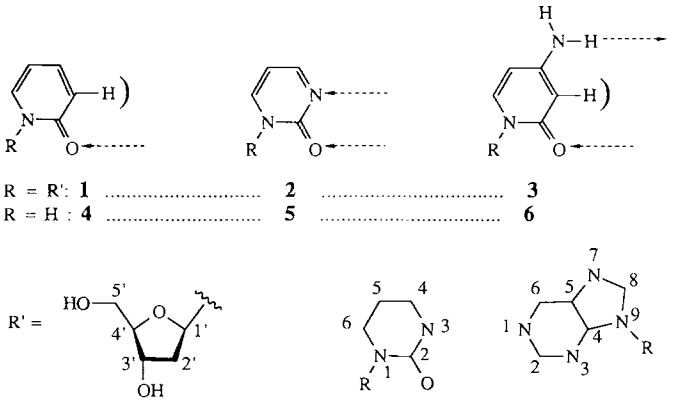

Fig. 3. Nucleoside analogues 1-(2′-deoxy-β-D-ribofuranosyl)-2(1*H*)-pyridone (**1**) and -pyrimidone (**2**) and 4-amino-1-(2′-deoxy-β-D-ribofuranosyl)-2(1*H*)-pyridone (**3**). Arrows indicate H-acceptor or -donor sites. Parentheses around H-3 in **4** and **6** mark repulsive interactions with the imino proton on N-3 of thymidine or on N-1 of deoxyguanosine upon Watson–Crick base pairing. Below: Conventional numbering of 2′-deoxy-β-D-ribofuranosyl and of pyrimidine and purine nucleoside bases.

is a nucleoside analogue that can form only one hydrogen bond (with the carbonyl oxygen of C-2). Additionally, the nucleosides deoxyguanosine (dG) and thymidine (dT), which bear an imino H atom, are prevented from base pairing with **1** because of the interactions between the protruding H-3 of the analogue and the imino protons on N-1 and N-3 of dG and dT, respectively (cf. Fig. 3 for the conventional numbering of purine and pyrimidine nucleosides). Attractive interactions between H-3 and an H acceptor like N-3 of deoxycytidine (dC) or N-1 of deoxyadenosine (dA) are expected to be present in the corresponding base pairs, but are much weaker than a normal H bond between two nitrogen atoms.

1-(2′-Deoxy-β-D-ribofuranosyl)-2(1*H*)-pyrimidone (**2**, "4-deamino-2′-deoxycytidine"; Fig. 3) is a dC base analogue lacking the 4-amino group, which is the only H donor of dC. In contrast to **1**, compound **2** could in principle form base pairs with dG (two H bonds) and dT (one H bond). Compound **2** also lacks a proton that would allow base pairing with dC or dA, but there are no constraints preventing dC or dA from base pairing with an N-3-protonated form of **2** in the polymerase.

As in **1**, H-3 in 4-amino-1-(2′-deoxy-β-D-ribofuranosyl)-2(1*H*)-pyridone (**3**, "3-deaza-2′-deoxycytidine"; Fig. 3) will prevent the analogue from base pairing with dG or dT. Pairings with dC or dA also seem rather unfavorable, because all bases have an H donor on N-4 (the rotation of aromatic amino groups out of the π conjugation is hindered) and the interactions between H-3 of **3** and N-3 of dC or N-1 of dA are expected to be very weak (as in **1**).

The expected or presumed base pairings between analogues **1**–**3** and the natural nucleosides only make sense if, during the polymerization reaction in the enzyme, both bases are uncharged and lie wholly in their predominant tautomeric form and if the positioning of both bases is Watson–Crick-like. If, nonetheless, an unexpected base pairing occurs in enzymatic in vitro experiments that allow the formation of base pairs with the analogues, one would have to consider either the formation of a protonated or rare tautomeric form in one of the bases (changes of the pattern depicted in Fig. 2a or 2b) or the dislocation of one of the bases with respect to the reading frame (Fig. 2c and 2d).

The enzymatic test reactions require synthesis of the modified bases, their stereochemically defined glycosylation, and an efficient 5′-triphosphorylation reaction. The use of the nucleoside analogues as template nucleotides in a DNA oligomer requires, besides their monophosphorylation, that the reaction conditions of a chemical DNA synthesis and of an enzymatic DNA chain elongation are compatible with these substrates, which are more sensitive than the natural compounds.

2. Synthesis of Nucleoside and Nucleotide Base Analogues

2.1. Modified Mononucleotides

2.1.1. Synthesis of Nucleoside Analogues

2-Pyridone (**4**) and 2-pyrimidone (**5**) are commercially available, but 4-amino-2-pyridone (**6**) had to be synthesized from other compounds and suitably derivatized. Our first approach (Scheme 1a) was based on published syntheses from the early 1960s and started from 2-chloropyridine (**7**), which was first oxidized to the *N*-oxide **8**, then nitrated to give the 4-nitro compound **9**. Hydrogenation of **9** gave **10**, which underwent methanolysis to yield 4-amino-2-methoxypyridine (**11**). The amino group was protected by acetylation to give **12**. Compound **12** could be used instead of **6** in the glycosylation reaction leading to **3**. Later, *Currie* et al.[5] synthesized **6** via a more straightforward route (Scheme 1b). 1-Methoxy-1-buten-3-yne (**13**) was homologized to ester **14**, which, upon aminolysis, provided compound **6**.

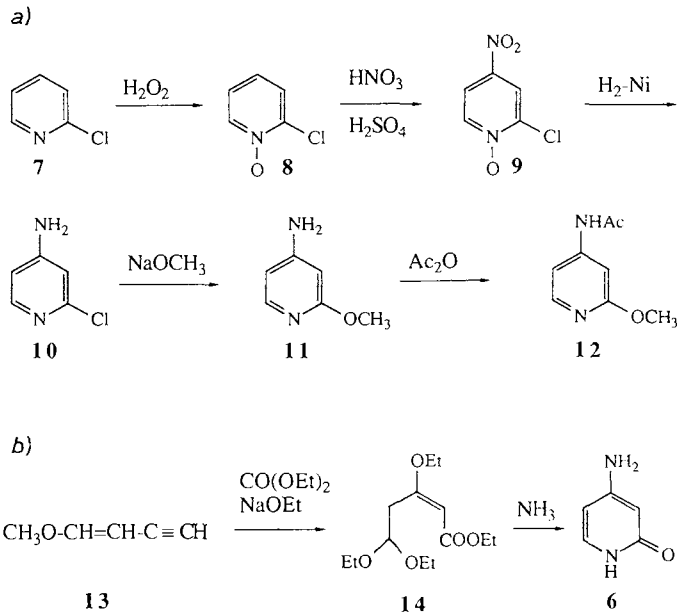

7 **8** **9** **10** **11** **12** **13** **14** **6**

Scheme 1. Syntheses of base analogues: a) **12**; b) **6**.

In all nucleoside analogues **1**–**3** the glycosylation was achieved through the well-known reaction of the 1-chloro-2-deoxyribofuranose derivative **15** with an activated form of the base heterocycle (Scheme 2a). The bases **4** and **5** were activated as mercury(II) salts **16** and **17**, respectively, whereas base **12** already represented an activated form of **6**. Condensation of **16**, **17**, and **12** with compound **15** in an inert solvent yielded **18**, **19** and **20**, respectively, as a mixture of α and β anomers in at the time satisfactory amounts.[6–10] The anomeric mixtures were separated by chromatography on silica or alumina to obtain the desired pure β anomers.

One well-known drawback of the above glycosylation procedure was the low thermal stability of **15**; under the reaction conditions, large amounts of its elimination product, **21**, are formed. This could be avoided by using the more stable methyl glycoside **22** and a more convenient base activation method (Scheme 2b). Base **5** was trimethylsilylated to give **23**, which, in the presence of trimethylsilyl trifluoromethanesulfonate (**24**) as demethoxylation agent, was glycosylated with **22** to give **19**.[11]

The yield of the desired β anomer, however, was relatively low. This problem could be solved by an alternative approach which profits from the procedure for deoxygenation of alcohols developed by *Barton* et al.[12] 2-Deoxyribofura-

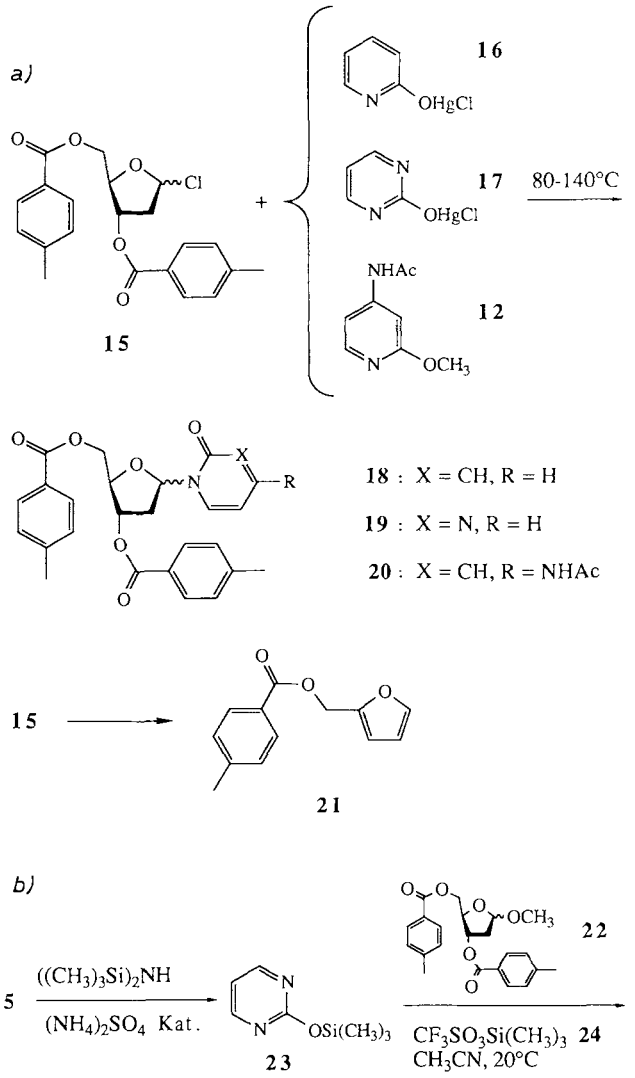

Scheme 2. Glycosylation using a) **15** and b) **22**.

nose derivatives usually react unspecifically on C-1 unless special care has been taken both in the synthesis of anomerically pure 1α-chloro-2-deoxyribose derivative α-**15** and in the choice of glycosylation conditions to suppress its anomerization (cf. Refs. [13–14]). Suitably derivatized ribofuranose will yield only β anomers on glycosylation, owing to the neighboring group participation of a 2α-tosyl[15] or a 2α-benzoyl group.[5,16] Glycosylation is best performed at room temperature with commercially available and stable 1-*O*-acetyl-2,3,5-*O*-tribenzoyl-β-D-ribofuranose (**25**)[5] or 1,2,3,5-tetra-*O*-acetyl-β-D-ribofuranose,[17a] pertrimethylsilylated bases, and a Lewis acid like trimethylsilyl trifluoromethanesulfonate (**24**) or tin tetrachloride to cleave the 1-acetoxy group. An example of our presently preferred synthesis of the 2'-deoxy-β-D-ribofuranoside **34** is depicted in Scheme 3. Aminopyridone (**6**) was bis-silylated to give the activated base **26**, which was glycosylated in situ with **25** in the presence of tin tetrachloride to yield the nucleoside analogue **27**.[5] The anomerically pure product was *N*-acetylated to give **28**, which was then selectively debenzoylated to yield **29**. Bis-silylation of **29** at the 3' and 5' positions with 1,3-dichloro-1,1,3,3-tetraisopropylsiloxane (**30**) afforded the ribose derivative **31**. These usually high-yield reactions must be followed by a two-step deoxygenation procedure.[18] First, a radicophilic functional group (thiocarbonate or xanthogenate) is attached to the 2'-oxygen atom. We use as a routine reagent *p*-tolyl chlorothioformate (**32**). The thiocarbonate **33** is chromatographically stable and can either be isolated in good yields or transformed in situ with tributyltin hydride to give the 2'-deoxy compound **34**.[17b]

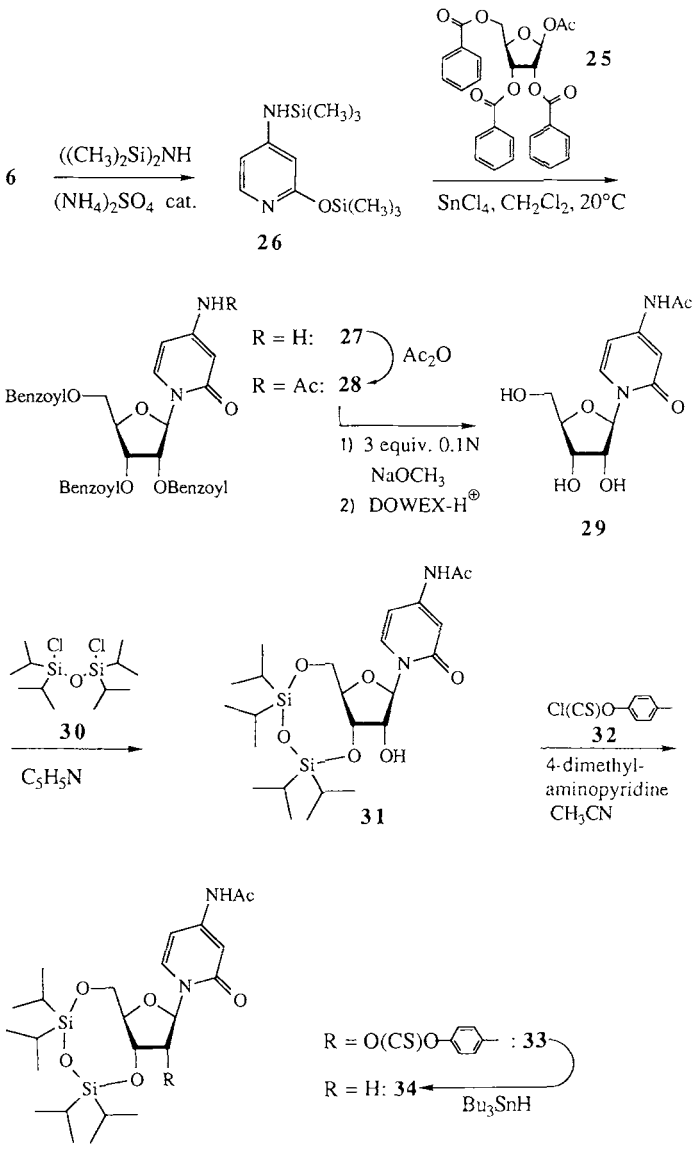

Scheme 3. Glycosylation using **25**.

2.1.2. *Phosphorylations*

Depending on the purpose of the phosphorylated products, different phosphorylation procedures were investigated. The first phosphorylation was performed on pyridone nucleoside **1**. The use of bis(2,2,2-trichloroethyl) phosphorochloridate, an attractive phosphorylating agent owing to its 5'-selectivity,[19] early revealed that **1** is more labile than the natural pyrimidone nucleosides dT and dC.[6] Pyridinium mono-2-cyanoethyl phosphate,[20] together with a

condensing agent like dicyclohexylcarbodiimide (DCC) or mesitylenesulfonyl chloride, was found to be the reagent of choice for 3'- and 5'-phosphorylations.[21-23] The 2-cyanoethyl group was removed with ammonia (via β-elimination) to give the ammonium salts of the phosphoric acid monoesters.

In order to obtain the nucleoside 5'-monophosphates directly, an alternative route has been developed (Scheme 4a).[24] Treatment of the nucleoside analogues **1**–**3** with a

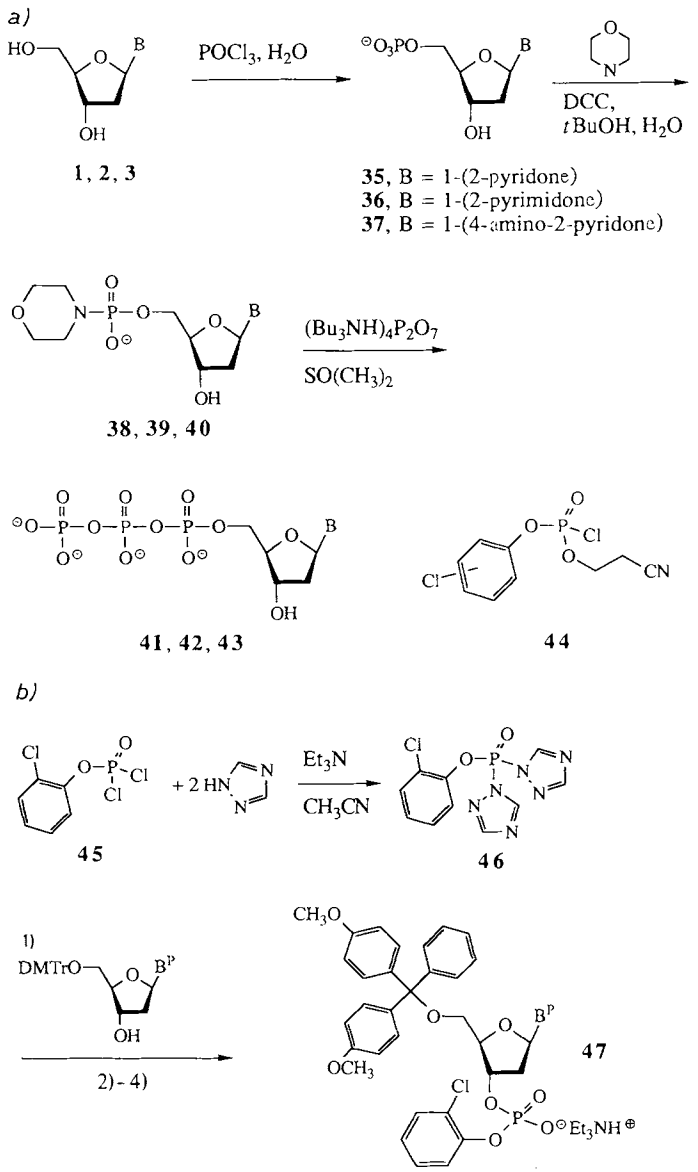

Scheme 4. a) 5'-Phosphorylations. b) 3'-Phosphorylations. B^P (protected bases): 9-(N^2-isobuturylguanine), 1-(N^4-anisoylcytosine), or 1-{N^4-(1-methylpyrrolidine-2-ylidene)cytosine} [39] and 9-{N^6-(1-methylpyrrolidine-2-ylidene)adenine} [40]. No protecting group on 1-(thymine). 1) Partially protected nucleoside; 2) Et_3N/pyridine/H_2O; 3) aq. Et_3NH HCO_3, extraction into $CHCl_3$; 4) chromatography on SiO_2, precipitation.

mixture of phosphorus oxychloride and a small amount of water afforded the 5'-phosphorylated compounds **35**–**37** in high yields.[25-27] No 3'-phosphorylation and no cleavage of the bases could be detected. Of the three analogues, pyrimidone nucleoside **2** contains the most acid- and base-labile glycosidic linkage.[25] Therefore, this direct phosphorylation procedure was ideal for its 5'-phosphorylation. Compounds **35**–**37** were chemically transformed into the corresponding triphosphates **41**–**43** according to the procedure of *Moffat* and *Khorana*[28-29] through the formation of the reactive phosphoramidates **38**–**40** (Scheme 4a).[27]

Another type of phosphate of the nucleoside analogues is required in the synthesis of DNA oligomers. The building blocks needed for the phosphotriester methodology are standard fully protected nucleoside 3'-monophosphate triesters. Acid-labile di- or monomethoxytrityl groups were used as temporary 5'-protecting groups and N^6-benzoyl, N^4-anisoyl, and N^2-isobuturyl amides were chosen for permanent protecting groups for the adenylate, cytidylate, and guanylate derivatives.[30-32] The *p*-chlorophenyl (later *o*-chlorophenyl) group was used as a permanent phosphate protecting group; these groups could be selectively cleaved by the 1,1,3,3-tetramethylguanidinium salt of (*E*)-4-nitrobenzaldehyde (later (*E*)-2-nitrobenzaldehyde) oxime in the final deprotection step after the last condensation reaction.[33-34] Suitable phosphorylating agents were *p*- and *o*-chlorophenyl 2-cyanoethyl phosphorochloridate (**44**). The 2-cyanoethyl group was used as a transient phosphate protecting group in order to render the building block lipophilic and purifiable on silica gel. Before each condensation step, this group had to be removed in situ with a base like triethylamine or *tert*-butylamine.[31,32,35-37]

Recently, we found that an eluent system for the chromatography of highly polar substrates, such as amino acids (ethyl acetate/methanol/water 4:1:0.1–0.7), was ideal for the purification of the anionic, fully protected building blocks **47** as their triethylammonium salts on fine silica (40–63 μm) by "flash chromatography", without cleavage of the very acid-labile 5'-dimethoxytrityl function. This procedure not only allowed us to omit the 2-cyanoethyl phosphate protecting group (which proved thermally slightly unstable on longer storage) and its in situ deprotection, but also enabled us to use a simpler phosphorylating agent, *o*-chlorophenyl phosphorodichloridate (**45**). Scheme 4b summarizes our presently favored phosphorylation procedure adopted from *Chattopadhyaya* and *Reese*[38a]; this procedure uses in situ phosphorodiimidazolidate derivative **46** as the reactive phosphorylation species for the synthesis of triester building blocks **47**.[38b]

2.2. Condensations of Nucleotides

2.2.1. *Syntheses in Solution*

At the beginning of our studies in the early 1970s, research into oligodeoxynucleotide synthesis had not yet established a preferred approach. The mild condensation reagents needed for the couplings according to *Gilham* and *Khorana*'s phosphodiester approach,[41] in particular DCC as a coupling reagent, seemed to be appropriate for our needs, since, during the studies with nucleoside analogue **1**, it became clear that we were dealing with unstable substrates.[6-7] Nevertheless, *Falk* et al.,[21] following *Letsinger* and *Ogilvie*,[20] used the initial version of the phosphotriester approach. A comparison of these phosphotriester-coupling yields for various polythymidine nucleotides with those derived from

Khorana and *Vizsolyi*'s[42] diester synthesis misleadingly indicated the superiority of the latter method.

Indeed, promising results were obtained in investigations on the synthesis of di- and trinucleotides containing pyridone (**4**) and pyrimidone (**5**) with this 5′ → 3′ diester method using the easily accessible nucleoside 5′-phosphates as building blocks, where the nucleophilic attack in the condensation reaction is carried out by a secondary alcohol function.[22, 23, 25, 26, 43, 44] In contrast, *Weimann* and *Khorana*'s[45] 3′ → 5′ diester method using nucleoside 3′-phosphates as building blocks resulted interestingly in the formation of dimeric pyrophosphates (self-condensation products).[23] These results enabled us to plan a synthetic strategy for the stepwise construction of longer oligonucleotides containing modified bases.

The plan for an enzymatic chain elongation involving the analogues is essentially divided into two parts, the synthesis of a wholly natural primer strand and that of three template strands bearing **1**, **2**, and **3** in defined positions.[46] The enzyme chosen for the replication experiments was the DNA-dependent *Escherichia coli* DNA polymerase I (pol I, E.C. 2.7.7.7.), which requires a DNA template and a DNA (or, in vivo, RNA) primer strand, with a minimal length of seven to nine nucleotides for both strands. The DNA should be double-stranded and for this experiment the template strand should be somewhat longer than the primer strand. The following sequences were elucidated (Scheme 8 summarizes the experimental setup and results): a tridecameric template strand, 5′-d(TpTpNpCpGpTpCpApApApApTpC)-3′, where N stands for **1**–**3** (in the following, template **I**, **II**, and **III**, respectively), and an octameric primer strand, 5′-d(GpApTpTpTpTpGpA)-3′. Note that the primer strand is complementary to the 3′ end of the template strand, leaving five nucleotides to act as the effective template with N in its center.

The primer strand was prepared by dinucleotide block synthesis (Scheme 5).[47] Since the diester method works with secondary alcohols, which, as nucleophiles, are relatively unreactive owing to steric hindrance, the formation of pyrophosphates was a common side reaction (nonactivated phosphate groups compete with 3′-OH functions). This led to low yields of the desired products (Scheme 5). The second problem was the anionic nature of reactants and products (phosphoric acid diesters), which needed to be separated on ion-exchange resins. The purification was quite tedious and the resolution of products of similar length rather difficult. Clearly, the phosphodiester method met its limits with the synthesis of an octamer.

Therefore, we reconsidered the phosphotriester approach,[35, 48] undertook two block syntheses of template **I**, and compared the diester with the triester method.[31] Although it was possible to carry out a substantial part of the synthesis, we had to abandon diester chemistry. The triester synthesis (Scheme 6) was based on standard fully protected nucleoside 3′-phosphotriesters (Section 2.1.2). The deprotected tridecamer was purified by preparative layer and ion-exchange chromatography and reversed-phase HPLC. A part of it was digested with phosphodiesterase I, and HPLC analysis of the mixture of monomers gave the expected base ratios. The preparation of template **II** was carried out essentially in the same way.[32] In addition to the HPLC analysis

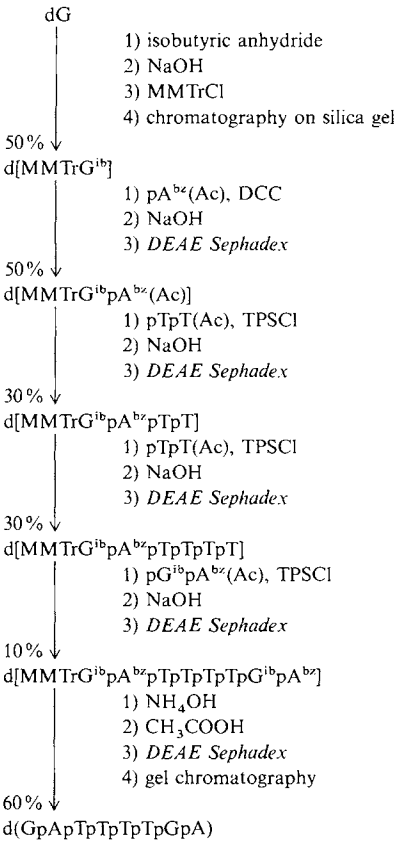

Scheme 5. Total synthesis of octadeoxynucleoside heptaphosphate GATTTTGA in solution using 5′ → 3′-phosphodiester methodology. Abbreviations: ^{ib} = N^2-isobuturyl; ^{bz} = N^6-benzoyl; (Ac) = 3′-*O*-acetyl; MMTr = 5′-*O*-[diphenyl(4-methoxyphenyl)]methyl (monomethoxytrityl ether); p = phosphoric acid diester; DCC = dicyclohexylcarbodiimide; TPSCl = 2,4,6-triisopropylbenzenesulfonyl chloride; DEAE-Sephadex = strong anion-exchange resin.

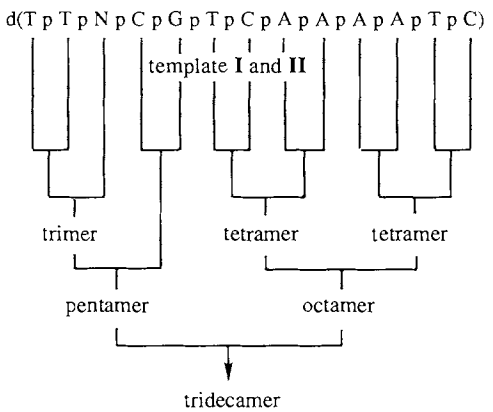

Scheme 6. Block synthesis of tridecadeoxynucleoside dodecaphosphate TTNCGTCAAAATC (N = **1**, template **I**; N = **2**: template **II**) in solution using phosphotriester methodology.

of the phosphodiesterase-I-digested oligomer, a sequence analysis according to the Maxam–Gilbert procedure[49a] showed the correct nucleotide sequence.

The results obtained from the incorporation and replication experiments (see Section 3.2) encouraged us to continue our synthetic work. The need for rather large amounts (50–100 mg per oligomer) of very pure oligomers that can be

analyzed by ^1H NMR, ^{15}N NMR, and CD spectroscopy and, if crystallizable, by X-ray diffraction again suggested the use of the block-synthesis strategy and the by now well-known triester approach in solution. We are now synthesizing as efficiently as possible five self-complementary oligomers: two hexamers (called TZ and CZ), two heptamers (called TT and CC), and one octamer (called TC). The reason for the choice of these sequences will be discussed in Section 3.3.

TZ 5′-d(CpGpTpNpCpG)-3′, dN = **3**
CZ 5′-d(CpGpCpNpCpG)-3′, dN = **3**
TT 5′-d(CpGpCpTpGpCpG)-3′
CC 5′-d(CpGpCpCpGpCpG)-3′
TC 5′-d(CpGpCpTpCpGpCpG)-3′

The trinucleotide sequences NCG, GCG, and CGC occur in several oligomers and therefore serve as blocks A, B, and C, respectively (Scheme 7). The central bases (outlined in Scheme 7) are labeled with highly enriched ^{15}N isotopes. They were synthesized from labeled urea (for labeled dT), uracil and ammonia (for labeled dC), and ammonia (for labeled **3**) according to the procedure depicted in Scheme 1b.[49b] The synthetic strategy is partly based on a modern solution procedure, the "filtration method" developed by *Chaudhuri* et al.[50] It is a triester method (5′ → 3′ chain elongation) that works with monomeric building blocks; we chose the ones already discussed in Section 2.1.2 (**47**, Scheme 4b). According to the authors, the use of a highly efficient coupling mixture results in coupling yields that are good enough to allow as many as five coupling cycles to be carried out without chromatographic purification of the intermediates (in our synthesis, three coupling cycles).

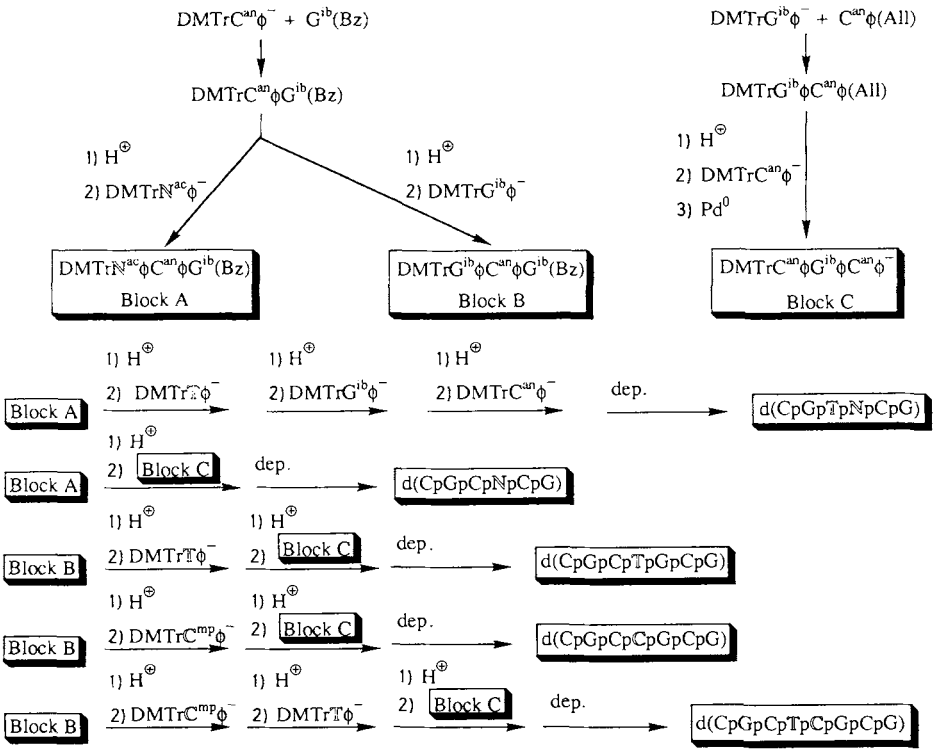

Scheme 7. Triester block synthesis of two hexamers, two heptamers, and one octamer in solution. ^{an} = N^4-anisoyl; ^{ib} = N^2-isobutyryl(Bz) = 3′-benzoyl; ϕ = 2-chlorophenyl phosphate; ϕ(All) = allyl 2-chlorophenyl phosphate; ϕ⁻ = triethylammonium 2-chlorophenyl phosphate; dN^{ac} = 4-[^{15}N]-acetamido-1-(2′-deoxy-β-D-ribofuranosyl)-[1,3-$^{15}N_2$]2(1*H*)-pyridone; T = [1,3-$^{15}N_2$]-thymidine; dC^{mp} = N^4-(1-methylpyrrolidine-2-ylidene)-[1,3-N^4-$^{15}N_3$]-2′-deoxycytidine.

2.2.2. *Syntheses on Solid Supports*

The chemical lability of **1** and **2** prevented the use of a solid-support synthesis, because the risk of obtaining a mixture of tridecamers with partly depyridinated or depyrimidinated residues after the final purification was too high. The additional 4-amino group in **3** rendered the nucleoside much more stable, presumably owing to the strong + M effect of this function in *para* position to the glycosidic linkage. Cleavage of the base was no longer a major problem, so a solid-support synthesis of template **III** was envisaged. At the time, one could choose between the rapid phosphite[51,52] and the phosphotriester methodology. The phosphoramidite method[53a] mostly used nowadays had not been established for routine work yet. Preliminary studies showed that, in the phosphite methodology, the drastic coupling conditions resulted in symmetrically coupled byproducts and lower yields than achieved with triester chemistry.[53b] Moreover, the latter and slower method had the advantage of being more flexible; for example, it allowed the use of di- or trimeric building blocks. Since our experience with the nucleotide analogues and triester chemistry in solution was good, we decided to continue with that approach.

The whole synthesis was run in a manually controlled closed system where the solutions could be added to the column containing the solid support through an eight-way valve by a slight over-pressure of dry nitrogen gas. Since the now widely used controlled-pore glass (CPG) was unknown at the beginning of this synthesis, the best solid support was found to be styrene cross-linked with 1% divinylbenzene. During the synthesis of template **III**, the reaction conditions

were optimized and tested in the synthesis of the octameric primer strand GATTTTGA.[10, 37] The building blocks for template **III** were monomers, dimers, and trimers with the same structures as used in the syntheses of templates **I** and **II** (cf. Section 2.1.2). However, GATTTTGA was synthesized using entirely monomeric building blocks.

Different coupling reagents were tested; mesitylenesulfonyl-3-nitro-1,2,4-triazol-1-ide/1-butylimidazole (minimum condensation time on solid support: 10 min) reacted fastest and afforded the best yields. The superiority of 1-butylimidazole as catalyst over the commonly used 1-methylimidazole has already been observed in phosphorylation reactions using reagent **44**.[31] It can be explained by the enhanced nucleophilicity of the butyl derivative, which is a major determinant in a rate-determining step of the coupling reaction.[10] Still more nucleophilic catalysts like 4-(dimethylamino)pyridine 1-oxide, introduced by *Efimov* et al.,[54] even enabled the triester method to compete with the coupling times of the rapid phosphoramidite method (condensation time: ca. 1 min). In consequence the average coupling yield in the optimized synthesis of the octamer was 98% and no capping of unreacted residues was necessary.

The final deprotection procedure had to be modified for template **III**, because the standard treatment with concentrated ammonia at 55 °C failed to hydrolyze the N^4-acetyl group of the base analogue. The base protection in N^4-acetyl-3-deaza-2'-deoxycytidylate, an amide derived from an enamine, proved to be more stable towards hydrolysis than an amide derived from an amidine, as in N^4-anisoyldeoxycytidylate. After cleavage of the permanent phosphate protecting groups and partial release of the product from the solid support with benzaldehyde oximate, and after total release from the solid support and cleavage of the benzoyl, anisoyl, and isobuturyl protecting groups with ammonia, a subsequent hydrolysis with 1 M NaOH for 30 min successfully deacetylated the base analogue in the tridecamer. Interestingly, the generation of a polyanion with benzaldehyde oximate afforded good enough protection for the other phosphoric acid diester bonds, which were not cleaved during final treatment with strong base.

HPLC analysis of the purified products showed apparent homogeneity; in the case of template **III**, this was confirmed by the appearance of a single band after polyacrylamide gel electrophoresis of the 5'-^{32}P-phosphorylated product. The phosphodiesterase I digestion of both the tridecamer and octamer resulted in the expected composition of mononucleotides upon HPLC analysis.[10, 37]

3. Base Pairing with Modified Nucleotides

3.1. Prokaryotic DNA Polymerases as a Model System

Escherichia coli DNA polymerase I (pol I) is the best characterized prokaryotic DNA-synthesizing enzyme.[55, 56] It has a molecular weight of 103 000 Da and consists of three domains (Fig. 4). The polymerase domain contains a template-DNA binding site, a DNA 3'-terminus binding site for the primer strand, and a nucleoside triphosphate (dNTP) binding site. The 3'-5'-exonuclease domain contains another 3'-terminus binding site, which can also bind a nucleoside

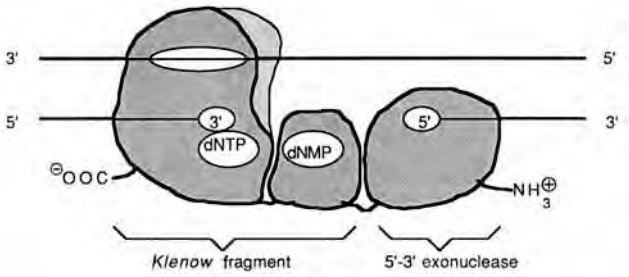

Fig. 4. Schematic drawing of DNA-bound *E. coli* DNA polymerase I (after *Joyce* and *Steitz* [57]).

monophosphate (dNMP). This domain excizes freshly polymerized 3'-terminal nucleoside 5'-monophosphates from the growing strand and therefore functions as a proofreading activity. These domains are together called the Klenow fragment or large (proteolytic) fragment having a molecular weight of 68 000 Da. Both domains require magnesium ions for proper functioning. The small fragment with a molecular weight of 35 000 Da, the 5'-3'-exonuclease domain, removes DNA ahead of the growing point of a DNA chain.[57, 58]

This enzymatic system served as a model enzyme for DNA synthesis. The aim was to determine whether our analogues would be accepted in the dNTP binding site or in the template DNA binding site of the polymerase and how they would behave in comparison to the natural substrates. Since preparations of *E. coli* DNA polymerase I were known to contain some concomitant DNA nuclease activity (possibly causing DNA digestion), an alternative, related enzyme, *Micrococcus luteus* DNA polymerase, having a much lower DNA nuclease activity, was also tested.

3.2. Enzymatic Reactions

3.2.1. In Vitro DNA Polymerase-Catalyzed Incorporations Using Modified Nucleoside Triphosphates[59]

All three triphosphate analogues, **41**, **42**, and **43** (Scheme 4a), can be considered to be dCTP structure analogues. Therefore, they were used in place of dCTP to measure the rate of incorporation into DNA. Polymerase was added to a mixture of activated calf thymus DNA ("random" sequences which act as template and primer), dATP, dGTP, TTP, [α-^{32}P]TTP, and increasing amounts of one of the analogues **41**–**43** (1 to 50 equivalents relative to natural triphosphates). After 30 min the reaction was quenched and the resulting DNA precipitated and washed. The rate of nucleotide incorporation was measured by scintillation counting of the radioactivity in the product.

The results were identical for both enzymes, pol I and *M. luteus* DNA polymerase, and did not depend on the addition of the analogues. This indicated that the polymerization continued until the first dCMP was to be incorporated and no incorporation of compounds **41**–**43** occurred. Alternatively, the analogues could have been incorporated, but the further synthesis inhibited. To test this, dCTP was added after the first incubation period and the reaction was quenched after another 30 min. The rate of incorporation increased and was practically identical to the rate measured

after an incubation with all four natural nucleoside triphosphates. This means that the polymerases cannot incorporate compounds **41**–**43** into DNA. When thymus DNA was replaced by synthetic poly-d(GC) and [α-^{32}P]dGTP was used at a constant concentration with increasing amounts of **41**, **42**, and **43**, essentially the same result was obtained.

Possible inhibition of the polymerase by **41**–**43** could not be ruled out. In order to measure an inhibition, a mixture of *M. luteus* DNA polymerase, thymus DNA or poly-d(GC), [α-^{32}P]TTP or [α-^{32}P]dGTP, respectively, and all the natural nucleoside triphosphates (only dGTP and dCTP for poly-d(GC)) was incubated with increasing amounts of **41**, **42**, and **43** under the same conditions as above. A very weak inhibition was observed with both templates and all three analogues. The DNA synthesis on the natural template was inhibited to 50% and on poly-d(GC) to 70% by a 50-fold excess of **41**, **42**, or **43**.

With an additional series of experiments, we intended to elucidate the type of inhibition by **41**–**43**. To a mixture of *M. luteus* DNA polymerase and thymus DNA, three natural nucleoside triphosphates were added in constant amounts and one—dATP or dCTP—in increasing amounts followed by incubation for 15 min. The dependence of DNA synthesis (i.e., reaction velocity v) on substrate concentration ([S], where S is dATP or dCTP) could be studied in this way. The dependence was measured once without and once with a 50-fold excess of one of the inhibitors **41**–**43**. In the experiments without inhibitor the rate of DNA synthesis, v, increased rapidly with increasing amounts of S to reach v_{max}. The same happened in the presence of each of the three inhibitors, but there v_{max} reached only 50% of the value without inhibitor. A Lineweaver–Burke plot[60] ($1/v$ versus $1/[S]$) for the experiments with and without inhibitor revealed that analogues **41**–**43** are uncompetitive inhibitors.

3.2.2. *In Vitro DNA Polymerase-Catalyzed Incorporations Using Modified Nucleotides in the DNA Template Strand*

As described in Section 2.2, three template strands have been constructed containing one analogue each. The primer GATTTTGA was to be elongated enzymatically (Scheme 8). First, the functioning of the primer and the templates **I**, **II**, and **III** as a DNA matrix for the Klenow fragment (pol I*) had to be tested. Only the large fragment of *E. coli* DNA polymerase I was used for all further studies, because the results derived from replication experiments with the whole enzyme would have seriously complicated the interpretations owing to the presence of the extra 5′-3′-exonuclease activity (cf. Section 3.1) and its capability of excizing mono- to decameric nucleotide fragments out of a DNA double strand after replication.[55]

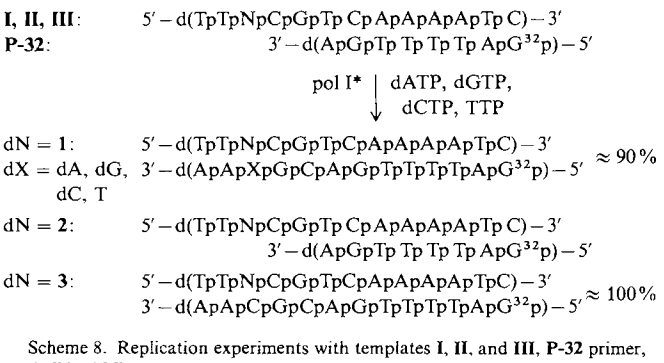

Scheme 8. Replication experiments with templates **I**, **II**, and **III**, **P-32** primer, dATP, dGTP, dCTP, and TTP using the Klenow fragment of *E. coli* DNA polymerase I (pol I*).

Pol I* was added to a mixture containing the necessary coagents (buffer, $Mg^{2\oplus}$ salt, etc.), [α-^{32}P]dCTP, the first nucleotide to be incorporated, and equimolar amounts of template **I**, **II**, or **III** and primer. The solutions were incubated for 90 min. After quenching the polymerization reactions, the products were separated by HPLC and the amount of incorporated radioactivity was determined by scintillation counting. In comparison to runs without enzyme, in all experiments most of the radioactive labeling was found in a peak ascribed to the prolonged primer d(GpApTpTpTpTpGpA[^{32}p]C). Hence, the functioning of the replication system was confirmed. The primer strand was then labeled on its 5′ end with [γ-^{32}P]dATP by polynucleotide kinase and purified by HPLC to give d([^{32}p]GpApTpTpTpTpGpA) (**P-32** primer).[10]

For the replication experiments,[61] equimolar amounts of template **I**, **II**, or **III** and **P-32** primer, together with dATP, dGTP, dCTP, and TTP were dissolved in a solution of buffer salts and additives and the mixture was heated to 60 °C for 5–10 min (standard procedure for the destruction of possible undesired secondary structures). Then, it was slowly cooled to allow the formation of the primer–template double helix. Pol I* was added and the mixture was incubated for 30 min. After quenching the reaction, the replication products were, on one hand, directly analyzed by gel electrophoresis and radiography and, on the other hand, sequenced and radiographed according to the Maxam–Gilbert procedure.[49]

Our interpretations of the results from the radiograms of the sequenced (Fig. 5) and unsequenced products (not shown) are depicted in Scheme 8.[61] With template **I** the elongation of the **P-32** primer proceeded to about 90%. The nucleotides were incorporated correctly when directed by a

Fig. 5. Radiogram of sequenced **P-32** primer after elongation by pol I* (according to *Maxam* and *Gilbert* [49a]). Lanes 1–4: Replication of template **III**. Lanes 5–8: Replication of template **I**. Lanes 9–12: Replication of template **II**, here the bands beyond 3′-terminal A are inconclusive. G, R, Y, C: G-, purine-, pyrimidine-, and C-specific strand-cleaving conditions, respectively.

natural template base, but the synthetic analogue led to non-specific incorporation. The replication of template **II** did not lead to any significant primer elongation. The most surprising result was obtained with template **III**. **P-32** primer was elongated to 100%. The incorporations opposite the natural bases were correct and base analogue **3** directed a specific incorporation of deoxycytidylate.

3.2.3. Mutagenicity Tests in Vivo

Bloch et al.[62] performed growth inhibition experiments and activity tests in vivo with 3-deazapyrimidine ribonucleoside analogues (e.g., 3-deazauridine and 3-deazacytidine) and found that the analogues were converted into the 5′-triphosphates but were not incorporated into either RNA or DNA. (Nucleoside 5′-triphosphates cannot be used in vivo, because ionic substrates will not penetrate cell membranes.) These results were confirmed by our own in vitro incorporation experiment using 3-deaza-2′-deoxycytidine 5′-triphosphate (**43**; cf. Section 3.2.1).

Nevertheless, *Bickle*[63] carried out in vivo mutagenicity tests with compound **3**, since the results with template **III** (Scheme 8) suggested that if deoxynucleoside analogue **3** were 5′-triphosphorylated and incorporated into DNA opposite deoxycytidylate in vivo, C → G transversions would result after a further round of replication. Specific transversion mutagens are very rare, so it would be of great help to have such a compound at hand. Unfortunately, both the standard Ames test[64] and the more sensitive "lambda-mutatest" developed by *Devoret*[65] revealed that, within a wide concentration range of compound **3**, no mutagenicity was detectable. We concluded that no incorporation into DNA occurred, although, presumably, the nucleoside analogue was 5′-triphosphorylated in the cells.

3.3. Interpretation of the Experimental Results

3.3.1. Structural Features Required for Nucleotide Incorporation

None of the experiments with the analogue triphosphates **41**–**43** led to an incorporation through a DNA polymerase. According to the information gained from successful incorporations of a variety of nucleotide analogues,[55] as well as from polymerase complexation stabilities of the natural compounds,[66] the primary binding of a nucleoside triphosphate in pol I is highly reversible, quite weak, and only moderately selective with respect to the base structure.

Therefore, it is reasonable to assume that all three compounds, being structurally closely related to the native dCTP, are able to form a complex in the triphosphate binding site of the polymerase. Yet, the reduced capability of **41**–**43** to form hydrogen bonds with any template base (Fig. 3) makes them rather weak competitors to the natural nucleoside triphosphates also present. As discussed in Section 1.4, alternative binding modes involving rare tautomers, protonated base pairs, or reading frame shifts must be ruled out for these analogue triphosphates, since no incorporation occurred at all.

3.3.2. Replication of Templates I and II

The structure of a nucleotide analogue bearing a 2-pyridone (e.g., **1**) is such that no base pairing with an imino proton of a nucleotide base (deoxyguanylate and thymidylate) can occur (cf. Section 1.4). The unspecific incorporations opposite **1** directed by template **I** included dGMP and TMP (Fig. 5). This suggests that, before polymerization, the base must have been cleaved from **1**, leaving an "abasic" site. Pol I ist capable of replicating abasic sites at a slower rate.[67]

The experiment with template **II** most probably failed owing to the exceptional instability of analogue **2** (cf. Section 2.1.2). The order of chemical stabilities of the base analogues is **3** > **1** > **2**. Yet, even the most stable template **III** showed a certain proneness towards strand cleavage, particularly between the nucleotide analogue **3** and its 5′-neighbor, thymidylate, if incubated in a buffer solution with polynucleotide kinase at room temperature for 6 h.[10] Although a reversed-phase HPLC purification of all three templates was carried out shortly before use,[10] the strands were not tested for their content of **1**–**3**. We assume that, even if template **II** was correct shortly before use, it must have been destroyed on heating to 60 °C immediately before the addition of pol I* (cf. Section 3.2.2), since the same treatment of template **I** most probably caused the even more stable analogue **1** to depyridinate.

The replication experiments with templates **I** and **II** demonstrate that the nucleotide base analogues must be sufficiently stable, not only during their chemical synthesis, but, equally important, under replication reaction conditions. Thus, the design of further analogues has to be planned very carefully.

3.3.3. Replication of Template III: The Structure of a Pyridine–Pyrimidine Pair in Polymerase-Bound DNA

To understand the specific incorporation of deoxycytidylate opposite analogue **3** in template **III**, we need to list all the theoretically possible arrangements of nucleotide base pairings in a polymerase containing the analogue in the template strand (Fig. 6). Analogue **3** in the amino-keto form cannot form a base pair with any nucleotide in the Watson–Crick arrangement, because there are always interactions between protruding hydrogen atoms that prevent the bases from coming close enough to form hydrogen bonds (Fig. 6a, first column). Theoretically, there are two alternative arrangements, the wobble position where one of the bases is shifted towards the major groove of the DNA double helix (Fig. 6a, second column) and that where the same base is shifted towards the minor groove (Fig. 6a, third column). In these positions, pairings with some purine and pyrimidine nucleotides would be sterically feasible; the most favorable pairing should be the one with deoxyguanylate. Since no deoxyguanylate was found opposite analogue **3** within the limits of accuracy of the Maxam–Gilbert procedure, we conclude that no formation of such a base pair in the wobble position is possible in the polymerase.

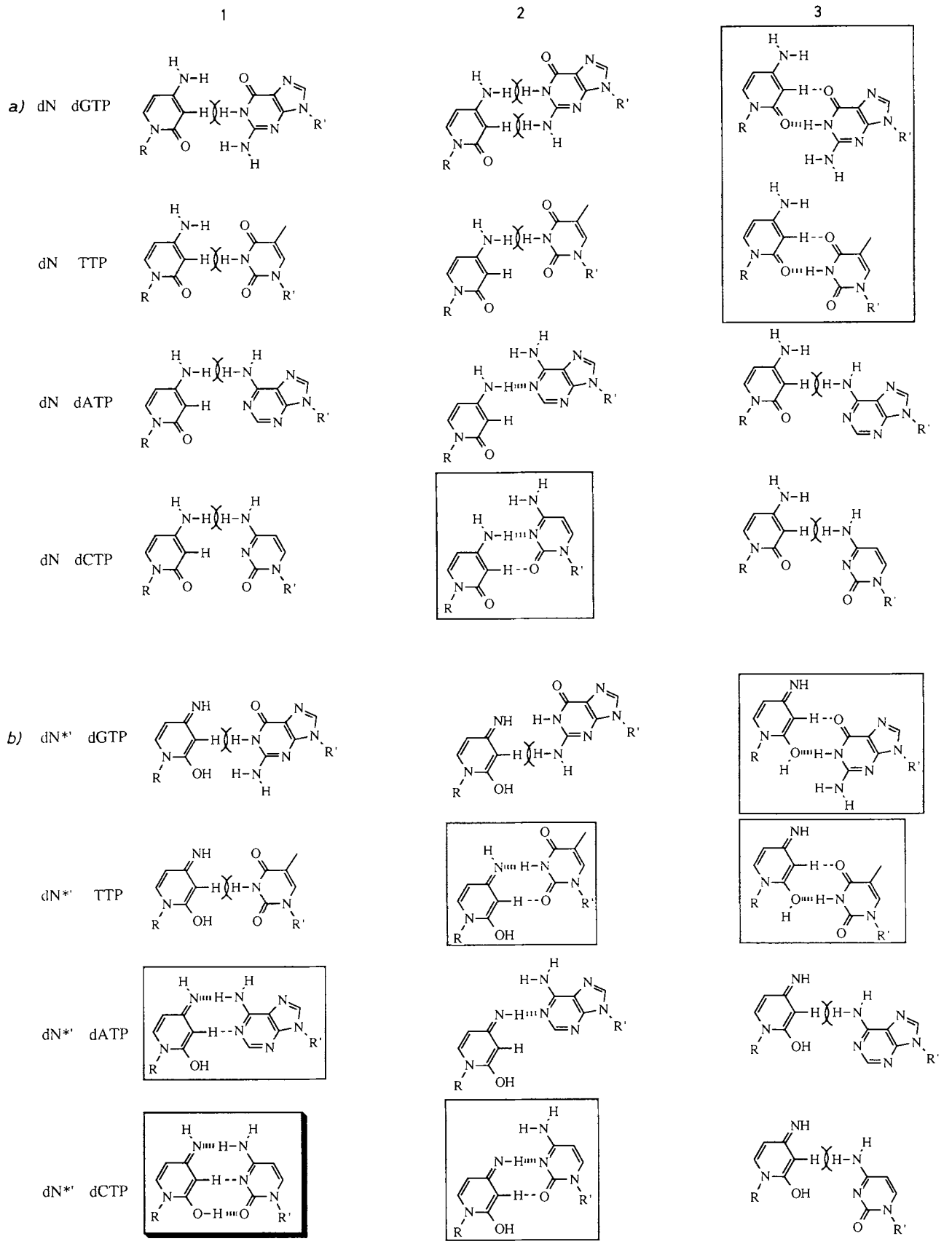

Fig. 6. Theoretically possible arrangements of nucleotide bases in a DNA polymerase between a) base analogue **3** (dN), b) tautomeric form of **3** (dN*'), and four natural deoxynucleotides in their normal tautomeric forms. First column, Watson–Crick-like arrangement; second column, wobble arrangement with incoming nucleotide shifted into major groove of DNA double helix; third column, as second, but with incoming nucleotide shifted into minor groove. R = DNA backbone; R' = 2'-deoxy-β-D-ribofuranosyl 5'-triphosphate. (III): hydrogen bonds between heteroatoms, (- - -): weak attractive interactions. Crossed bows symbolize steric hindrance (repulsion). Simple frames: more than one, but less than two H bonds per base pair. Shaded frame: two H bonds. In dN*' the position of H-N^4 (*syn* or *anti*) was chosen deliberately to provide optimal base pairing.

The tautomeric imino-enol form[*] of analogue **3** (dN*', Fig. 6b), in contrast, can form two hydrogen bonds with deoxycytidylate and less than two with deoxyadenylate in the Watson–Crick arrangement. In principal, base pairings with deoxyguanylate and thymidylate in a wobble position are also imaginable, but the sole incorporation of deoxycytidylate proves that, at high misincorporation frequencies, the Watson–Crick arrangement is the only accepted one in the polymerase.

Another form of base-pair arrangement should be considered. The incoming nucleoside triphosphates could be in their alternative tautomeric forms, presenting another hydrogen-substitution pattern. In particular, the lactim form of deoxyguanylate (dG*TP) and one imino form of deoxyadenylate (3*H*-dA*TP) would match the amino-keto form of analogue **3** in the Watson–Crick arrangement (Fig. 7). Both

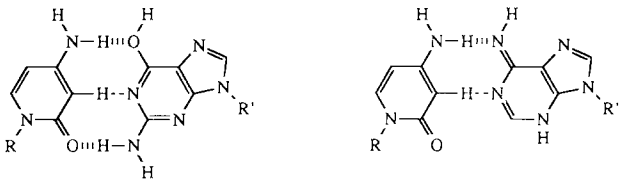

3 · dG*TP **3** · 3*H*-dA*TP

Fig. 7. Theoretically possible base-pair arrangements in a DNA polymerase between **3** (in the template) and rare tautomeric forms of nucleoside triphosphates dG*TP and 3*H*-dA*TP. R = DNA backbone; R' = 2'-deoxy-β-D-ribofuranosyl 5'-triphosphate.

tautomeric forms are known to be rare in the sense that their occurrence is 10^{-3} to 10^{-5} per monomeric molecule of the normal form in solution.[68] Again, since we did not observe such an incorporation, we argue that in the polymerase's binding site for nucleoside triphosphates the rare tautomeric forms are excluded. This is consistent with our finding that the tautomeric form of the triphosphate analogue **43**, dN*'TP, which was shown to be rare (see below), was not incorporated into DNA (Sections 3.2.1 and 3.3.1), as well as with other mutagenesis experiments (discussed in Ref. [69]).

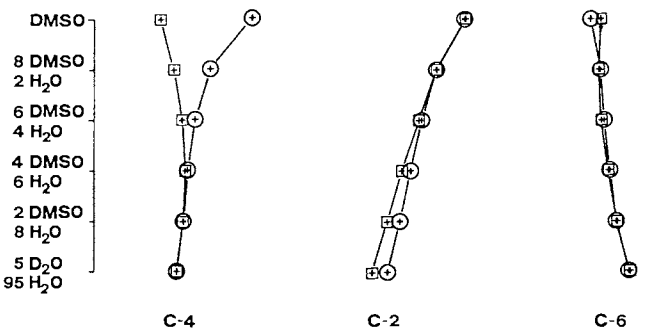

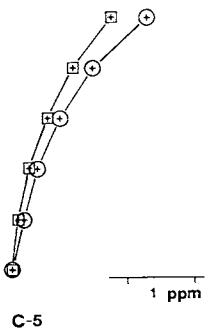

Fig. 8. Superimposition of δ(C) curves derived from the dependence of ^{13}C NMR spectra of base carbon atoms of 2'-deoxycytidine (squares) and 3-deaza-2'-deoxycytidine (circles) on solvent composition (from *Strazewski* [70]). DMSO = [D_6]dimethyl sulfoxide.

The question of the amount of the tautomeric imino-enol form of the nucleoside analogue **3** in water was answered by a comparative ^{13}C NMR study on the nucleosides **3** and deoxycytidine.[70] The tautomeric forms of deoxycytidine (dC* and dC*') are too rare in both water and dimethyl sulfoxide (DMSO) to be observable by ^{13}C NMR spectroscopy. Therefore, the differences in the chemical shifts of the carbon atoms in the sugar moiety of dC on gradually changing from DMSO to water are thought to be derived mainly from conformational changes, and the differences in the chemical shifts of the carbon atoms in the base of dC are ascribed mainly to the differences in solvation or hydration. The same holds true for the analogue. The δ(C) curves of both compounds are quite similar and differ largely in the range of $\Delta\delta_3^{dC} = 0.1-0.3$ when the "relative" δ(C) values of the corresponding carbon atoms are compared independently of the "absolute" chemical shift values (Fig. 8). The largest differences were $\Delta\delta = 0.5$ for C-5 and 1.4 for C-4 in pure DMSO, but with higher water contents the δ(C) curves become practically superimposable. This is plausible because, especially when none or only very little water is around, we expect another hydration mode in the proximity of the 4-amino group, dependent on whether an additional proton acceptor (N-3) is present or not.

A substantial, that is, spectroscopically observable shift of the tautomeric equilibrium of analogue **3**, on gradually changing from DMSO to water, should be observable as a difference in the δ(C) values for the C-4 atoms as well, but only concomitant with a difference in the δ(C) values for the C-2 atoms (dN → dN*'). In **3** the differences Δδ(C) for C-4 and C-2 between the pure DMSO and the pure water value are $\Delta\delta_{H_2O}^{DMSO} = 1.17$ and 1.16, respectively, and in dC 0.25 and 1.44, respectively. The difference derived from a change in the tautomeric form is expected to be at least $\Delta\delta_{H_2O}^{DMSO} = 2$ (when an external standard is used).[71] Since the shapes of the δ(C) curves for the C-2 atoms in the two compounds are very similar (Fig. 8), we conclude that no shift of the tautomeric equilibrium of the analogue could be observed. The ^1H NMR spectrum of compound **3** in DMSO shows two amino protons; therefore, the main tautomeric form of the analogue in aqueous solution must be the amino-keto form.

In spite of its rarity, only the imino-enol form of analogue **3** can apparently form a strong enough base pair with a nucleoside triphosphate to launch a polymerization reaction by the enzyme; the hydrogen-substitution pattern of this form is the same as in deoxyguanylate (Fig. 6b). This provides a sufficient explanation of the selective incorporation of deoxycytidylate directed by analogue **3** in template **III**.

[*] In the following, an asterisk represents the unusual tautomeric form at C-4 substituents of pyri(mi)dine and at C-6 substituents of purine nucleotides and a prime sign the unusual tautomeric form at C-2 substituents of pyri(mi)dine and purine nucleotides.

3.3.4. *A Model Mechanism of Nucleotide Base Pairing and Polymerization*

How do these interpretations compare to the so far known mechanism of nucleotide polymerization and replication fidelity? Since the present model of polymerization is mostly based on experiments with pol I*, some recent results and views shall be briefly presented.

Benkovic et al.[72–74] investigated the kinetics of DNA synthesis by pol I*. Their conclusions are summarized in Scheme 9 (taken from Ref. [74]). First, the enzyme is loaded

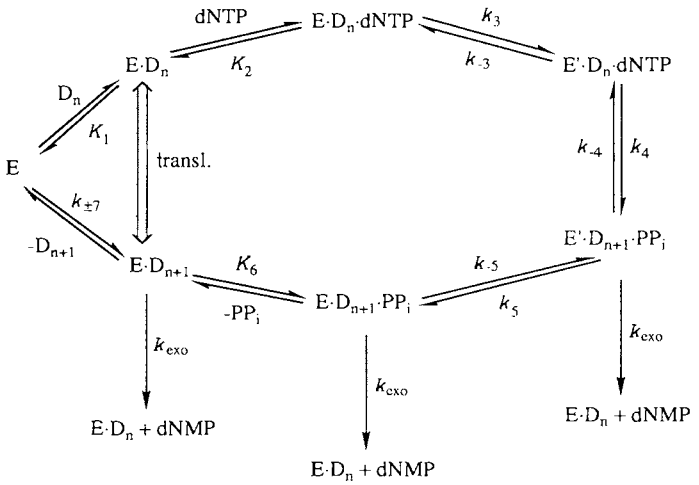

Scheme 9. Kinetic model for DNA synthesis and proofreading by *E. coli* DNA polymerase I (from *Kuchta* et al. [74]). E, enzyme; D_n, primer/template; PP_i, pyrophosphate; D_{n+1}, elongated primer/template.

with DNA template and primer strands (K_1). A primary complexation of a nucleoside triphosphate follows (K_2). The first rate-limiting step consists of a conformational change (E → E') of the whole complex ($k_{\pm 3}$). Then, in a quite rapid (i.e., at most only partly rate-limiting) polymerization step, the covalent bond between primer and complexed mononucleotide is formed ($k_{\pm 4}$), producing a prolonged primer and a bound pyrophosphate molecule. After these steps, the highest discrimination between correct and incorrect nucleotide is achieved (approximately $1:10^4$ to $1:10^6$). At this stage, the proofreading activity of pol I* (Fig. 4) can cleave the freshly made linkage to release a nucleoside 5'-monophosphate (k_{exo}). Another conformational change ($k_{\pm 5}$) has been proposed in order to allow a second (observed) discrimination between matched and mismatched primer termini. Owing to a decreased dissociation rate of mismatch-containing DNA, the proofreading activity is given an opportunity to remove most of the remaining mismatches (k_{exo}). Diffusion of pyrophosphate away from the complex (K_6) generates an intermediate complex that can follow three pathways: decomplexation of the template–primer ($k_{\pm 7}$), leading to an interruption of continuous (processive) DNA synthesis, cleavage of the last primer residue (k_{exo}), or a rate-limiting translocation, regenerating a free nucleoside triphosphate binding site (processive DNA synthesis).

During the first discrimination ($k_{\pm 3}$), the correct nucleoside triphosphate is thought to allow a rapid enough change from E to E', while the enzyme that binds an incorrect nucleoside triphosphate will stay long enough in its primary form E for the diffusion of dNTP away from the complex. The polymerization rate constant $k_{\pm 4}$ also varies, depending on whether a correct or an incorrect nucleotide is bound covalently. Interestingly, the proofreading activity (k_{exo}) is not only relatively inefficient in comparison to the polymerase activity, but also unselective towards the excision of nucleoside monophosphates. Correct and incorrect nucleotides can both be excized if the conditions are favorable. This particularly happens when the polymerization or its following steps slow down (i.e., become rate-limiting) owing to either the formation of a badly matched base pair or to the presence of a formerly unrecognized mispair in the position directly behind the last pair. At present, the precise (steric) reasons why mispairings cause the replication process to slow down are unclear.

Steitz et al. performed X-ray analyses on pol I* with bound TMP,[75] 5'-d(AGACCGCCCGG)-3'·5'-d(CCGGGCGG)-3', and $p(T)_4$.[76] These studies and additional structural investigations by protein engineering[57] surprisingly suggest a quite remote position of the proofreading site—about eight base pairs away from the active site of polymerization. The structure of a primer strand about to be proofread is proposed to be partly melted out, leaving the last four primer bases unpaired (Fig. 9).[76] The slowing of polymerization

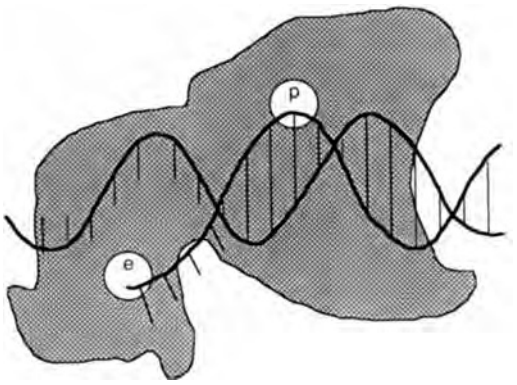

Fig. 9. Schematic drawing of pol I*/DNA with polymerase active site p. The DNA 3'-terminus is bound to exonuclease active site e (after *Freemont* et al. [76]).

by mismatched pairs, allowing the primer strand to move to the proofreading site, was proposed to be due to a recognizing element ("reading head") located in the polymerase active site.[58] At present, this model has no experimental support, since no X-ray data showing the polymerase active site in interaction with a template strand and a nucleoside triphosphate are available yet.

Ferrin et al.[66, 77, 78] studied pol I* interactions with nucleoside triphosphates and oligoribonucleotides as templates (oligoribonucleotides were used to prevent enzymatic degradation) by NMR spectroscopy (nuclear magnetic relaxation of enzyme-bound manganese ions and nuclear Overhauser effect studies). One important conclusion of these studies was a tentative interpretation of the structural conditions involved in primary dNTP binding and the first discrimination step, corresponding to K_2 and $k_{\pm 3}$, respectively, in Scheme 9. *Ferrin* et al. proposed[66] that, in a first step, the

nucleoside triphosphate binds to the enzyme and interacts with the enzyme-bound magnesium ion only via its terminal γ-phosphoryl group (Scheme 10). Although the triphosphate

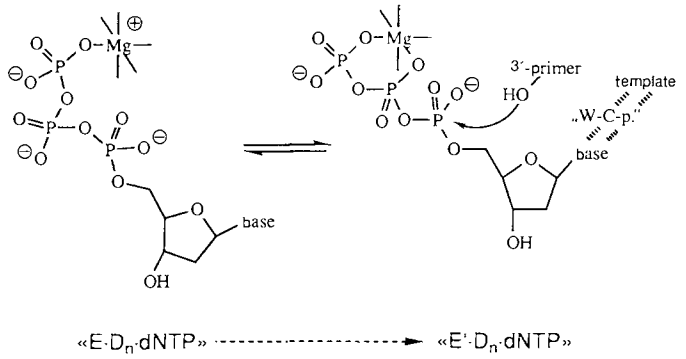

Scheme 10. Proposed interactions between $Mg^{2\oplus}$ (bound to the primer–template–pol I' complex) and dNTP prior to the actual polymerization step (after *Ferrin* et al. [77] and *Ferrin* and *Mildvan* [66]). "W-C-p." represents the formation of a Watson–Crick pair.

bases adopt, together with primer and template, a B-DNA conformation, this primary binding is not very selective with respect to the four bases of the nucleoside triphosphates and is highly reversible (K_2 in Scheme 9). In the rate-limiting step, the so-called verification step, in which a conformational change was assumed before,[72] *only if a Watson–Crick base pair, but not a wobble base pair,* can form between the substrate and the template bases does the β-phosphoryl group of the substrate also coordinate to the enzyme-bound magnesium ion ($k_{\pm 3}$). The formation of a six-membered chelate ring ($-Mg^{2\oplus}$–O–γP–O–βP–O–) decreases the distance between the α-phosphoryl group and the entering 3′-OH group of the primer strand and additionally accelerates the cleavage of the pyrophosphate leaving group. The substitution reaction $k_{\pm 4}$ follows.

This model mechanism, although speculation, rationalizes our replication experiments with analogues **41**–**43** and template **III** quite well and proves to be a useful working hypothesis. The triphosphates **41**–**43** were not incorporated, because $k_{\pm 3}$ was much too slow compared to the backward reaction of E · D_n · dNTP, owing to both the lack of H bonds and the interactions of the protruding hydrogen atoms in the pyridone analogues (Fig. 3), which prevented the formation of E′ · D_n · dNTP. More favorable protonated or tautomeric forms could not be used, because they were too rare to compete significantly with the binding of natural substrates.

However, this rarity could be used as a bottleneck passage in the case of replication of template **III**. The only way of bypassing analogue **3** in the template would be to use its rare tautomeric form as the nucleoside triphosphate base-binding (templating) residue. In our replication experiments we did not measure the polymerization velocities or turnovers from nucleoside tri- to monophosphates, so we cannot give any precise information about the kinetics of, say, the incorporation and proofreading of deoxycytidylate opposite analogue **3** in template **III**. Yet, since this reaction was complete in a time used for the replication of natural strands (cf. Section 3.2.2), it is reasonable to assume that the arrangement of the pyridine–pyrimidine pair during polymerization was Watson–Crick-like.

3.3.5. The Computed Structure of a Pyridine–Pyrimidine Pair in Enzyme-Free DNA

Basic considerations[79] and the latest crystallographic results[80] suggest that an unusual tautomeric form, although rare in the free nucleoside, can be stabilized by base pairing and base stacking.

Therefore, we carried out a preliminary computer modeling study (in collaboration with *K. Müller*, Hoffmann–La Roche, Basel, using the proprietary united-atom force field MOLOC) on a pyridine–pyrimidine pair containing the rare tautomeric form of analogue **3** and deoxycytidylate. The mispair was placed in the middle of a double-stranded B-DNA pentamer. The relaxation process of this DNA fragment, which was similar in sequence to the analogue-containing part of template **III**, resulted in an extended form of the base-pair arrangement depicted in Fig. 6b (bottom left) with an inserted, tightly hydrogen-bonded water molecule in the minor groove between the two base oxygen atoms.[69] Although this analysis did not represent a systematic comparative study of different conformational minima and therefore only showed one of perhaps several local minima, the base pair of interest resembled a normal Watson–Crick base pair astonishingly well (Fig. 10). The relaxed fragment

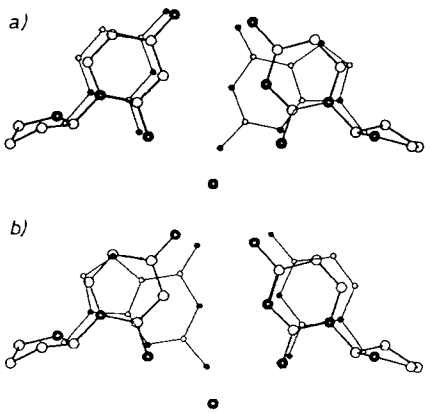

Fig. 10. Structural comparison between a modeled base pair and a standard Watson–Crick base pairs. Larger circles: 3-Deaza-2′-deoxycytidylate/2′-deoxycytidylate pair (dN*′ · dC) after relaxation of a modeled B-DNA pentamer [5′-d(pTpTpINpGpC)-3′] · [5′-pGpCpCpApA)-3′] (pdIN = 3-deaza-2′-deoxycytidylate) with an inserted water molecule in the minor groove (single circle stands for O atom of H_2O). Smaller circles: a) dC · dG base pair; b) dG · dC base pair (superimposition) from a canonical B-DNA [69].

still resembled qualitatively a normal B-DNA, indicating that pyri(mi)dine–pyrimidine, pairs can be present in DNA without greatly disrupting its overall secondary structure (Fig. 11).

There are several possibilities for the structure of our mispair. It may prefer to stay in a rare tautomeric state in solution, it could rearrange into a wobble pair with normal tautomeric forms, or it could be present in an equilibrium with both alternatives. A combined spectroscopic and crystallographic investigation of DNA double strands containing pyri(mi)dine–pyrimidine pairs is being undertaken (cf. Section 2.2.1 and Scheme 7).

In conclusion, the replication experiment with template **III** and the modeling study suggest that in the polymerase, the

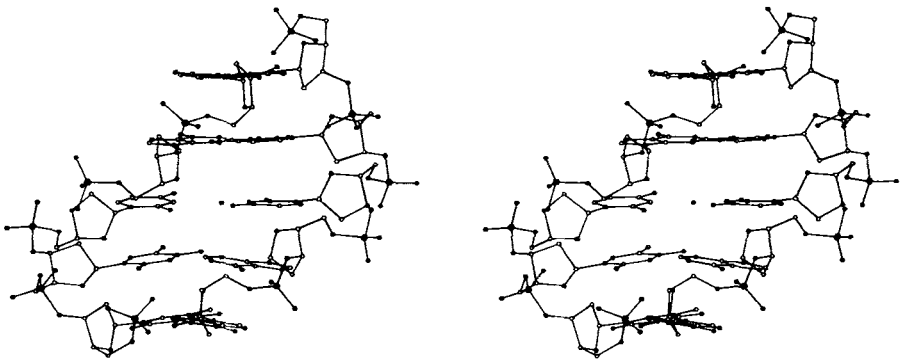

Fig. 11. Stereoview into the minor groove of the relaxed pentamer (cf. Fig. 10) including a water molecule (dot).

base-pair separation (C-1′–C-1′ distance) in the active site is not necessarily a determinant for nucleotide incorporation, whereas in a free double-helical DNA, constraints derived from the sugar–phosphate backbone and the hydration layer are likely to force the mispair to a close to normal separation. The dominant parameter for selectivity of incorporation and thus replication fidelity appears to be the hydrogen-substitution pattern of the template nucleotide base, which is read by the incoming nucleoside triphosphate base in a defined way. The position of the reading frame is strictly confined to a Watson–Crick-like arrangement of the bases (Fig. 2a, b, and d). A shifting of this position into a wobble arrangement (Fig. 2c) must be hindered by the surrounding enzyme.

3.3.6. Potential Medical Applications

What can be said about the practical applicability of nucleoside or nucleotide base analogues? One valuable use takes advantage of the potential mutagenicity of nucleoside analogues making them powerful synthetic antiviral agents.[81] Nowadays, the most prominent compound is the antiretroviral agent 3′-azido-3′-deoxythymidine (AZT, active against the AIDS virus HIV), which is a nucleoside sugar analogue. A variety of similar analogues have been prepared, among which the most interesting were shown to be the 2′,3′-dideoxy, 3′-azido-3′-deoxy, and 3′-deoxy-3′-fluoro derivatives.[82, 83] When applied in vivo, these compounds are thought to be stepwise triphosphorylated and incorporated into DNA by the retroviral RNA-dependent DNA polymerase called reverse transcriptase. This and other viral polymerases are known to replicate with a much lower fidelity[84] than, for example, bacterial polymerases such as pol I and, in fact, are therefore used by biochemists as agents for producing DNA mutations.

This larger tolerance of accepting modified nucleotides might allow the enzyme to incorporate nucleotide base analogues as well, although this has been shown not to be the case with 3-deazapyrimidine ribo- and deoxyribonucleosides (cf. Section 3.2.3) and nonviral polymerases. We think that there is a hope of finding an antiretroviral activity in combining base with sugar modifications. The first should lead to mispairings and, hence, to substitution mutations; the latter terminates the polymerization reaction due to the lack of a nucleophilic group in the 3′-position. At the very least, one could imagine a potential synergistic effect of such an analogue, when used together with AZT, which would allow a lower dosage of the still problematic anti-AIDS drug. Therefore, it will be interesting to test the dC and T analogues **48**–**53** for their toxicity and antiviral activity (Fig. 12).

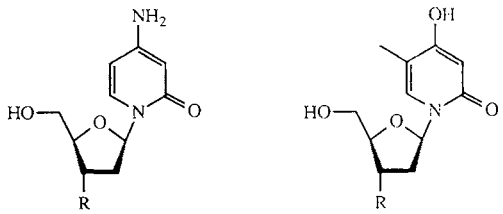

R = H: **48**, N_3: **49**, F: **50**

51, **52**, **53**

Fig. 12. 3-Deaza analogues of 2′,3′-dideoxycytidine (**48**), 3′-azido-2′,3′-dideoxycytidine (**49**), 3′-fluoro-2′,3′-dideoxycytidine (**50**), 3′-deoxythymidine (**51**), 3′-azido′-3′-deoxythymidine (**52**), and 3′-fluoro-3′-deoxythymidine (**53**).

3.3.7. Nucleotide Analogues Mimicking Ionized and Rare Tautomeric Forms of Natural Nucleotide Bases

The other, more indirect use for nucleotide base analogues is based on their ability to provide an unusual hydrogen-substitution pattern if used as modified template nucleotides in replication experiments. Examples for natural and synthetic variants of nucleoside bases are shown in Figure 13.

Only a few of these analogues were used to study misincorporations by polymerases. These led to various mispairings. N^4-Hydroxydeoxycytidylate is a (C · G → T · A and A · T → G · C) transition mutagen. It has a stabilized imino form, compared to deoxycytidylate and possesses an enhanced preference for the formation of base pairs with deoxyadenylate. The hydrogen-substitution pattern is the same as that in one rare tautomeric form of dC, dC*, and therefore should mimic its binding preferences (discussed in Ref. [69]) (Fig. 14a). 5-Bromo- and 5-fluorouridylate are also transition mutagens. The occasional mispairings with deoxyguanylate are due to their enhanced acidity, which allows the formation of Watson–Crick-like $^{Br}U^{\ominus}$ · G and $^{F}U^{\ominus}$ · G pairs at physiological pH.[85] Therefore, these compounds mimic the binding preferences of deprotonated thymidylate (Fig. 14b).

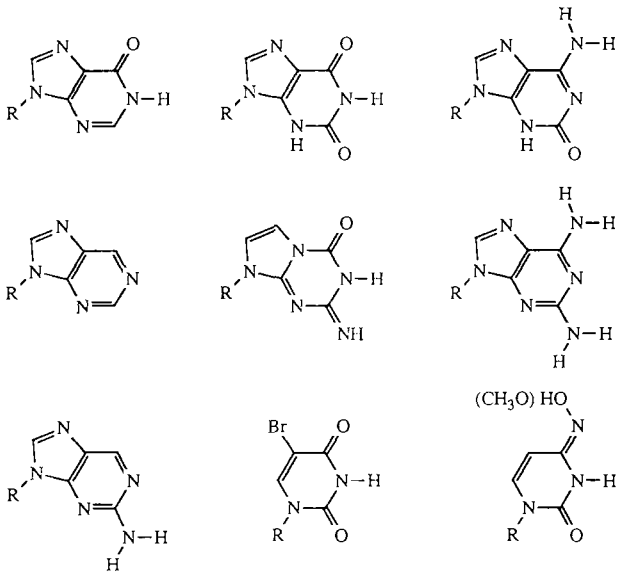

Fig. 13. Some natural and synthetic nucleoside base analogues. From left to right: 2′-deoxyinosine, -xanthosine, -isoguanosine, -nebularine, -5-aza-7-deazaguanosine, -ribosyl-2,6-diaminopurine, -ribosyl-2-aminopurine, -5-bromouridine, -N^4-methoxy-, and -N^4-hydroxycytidine. R = 1′-(2′-deoxy-β-D-ribofuranosyl).

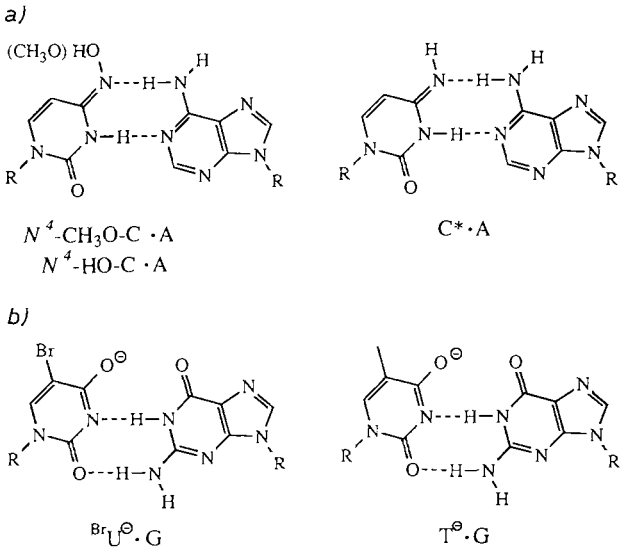

Fig. 14. Mimicry a) of a rare tautomeric form of deoxycytidine, dC*, by N^4-methoxy- or -hydroxycytidine and b) of a deprotonated form of thymidine by 5-bromodeoxyuridine in Watson–Crick-like base pairs.

2-Aminopurine (AP) as a template adenine analogue usually directs the incorporation of thymidylate, but quite often forms a base pair with deoxycytidylate, leading to A · T → G · C transitions.[86] The favored formation of a Watson–Crick-like [AP · C]$^{\oplus}$ mispair in a polymerase is responsible for the mutagenicity of AP (Fig. 15a).[87] The frequency of A · T → T · A transversions that could be derived from the formation of AP · A pairs (a wobble pair, Fig. 15b) was found to be at least an order of magnitude smaller.[88] Yet, the thermodynamic stability of a DNA duplex containing an [AP · C]$^{\oplus}$ pair was shown by *Eritja* et al.[89] to be lower than that containing an AP · A wobble pair. This led for the first time to the proposition that wobble pairs might be disfavored in polymerases, because of steric restrictions, so that a

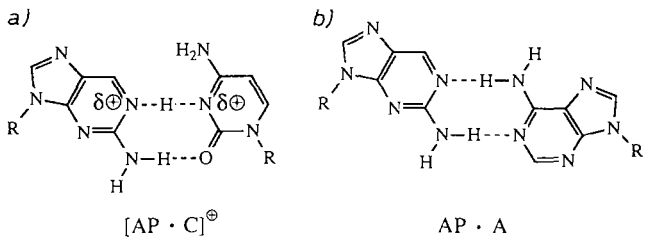

Fig. 15. a) Protonated Watson–Crick-like base pair between deoxyribosyl-2-aminopurine and deoxycytidine; b) neutral wobble base pair between deoxyribosyl-2-aminopurine and deoxyadenosine.

less stable base pair would be incorporated instead. Similar replication experiments with deoxyxanthosine (Fig. 13) as a template base revealed a still larger discrepancy between the favored incorporations by the eukaryotic DNA polymerase α and the measured thermodynamic stabilities of DNA duplexes that contain the analogue.[90] The incorporation preferences directed by deoxyxanthosine (X) were T > C ≫ A ≈ G, as opposed to the stabilities X · T > X · G > X · A ≈ X · C. This result was a first clear indication that the polymerase imposes constraints on substrate–template interactions, which can result in the more rapid formation of base mispairs having a lower stability in the final product DNA.

Naturally occurring O^6-methyldeoxyguanylate (d(O^6-meG)) and O^4-methylthymidylate (O^4-meT), derived from selective *O*-methylation by a methylating mutagen, are highly mutagenic DNA residues. Upon replication, they have a strong preference to direct the misincorporation of thymidylate and deoxyguanylate, respectively, because they bear an altered H-substitution pattern. ^{1}H NMR studies of DNA-duplex fragments bearing O^6-meG · C, O^6-meG · T, O^4-meT · A, and O^4-meT · G pairs show that the nonmutagenic O^6-meG · C and O^4-meT · A pairs form relatively stable wobble pairs (O^4-meT · A is likely to be protonated) and the mutagenic O^6-meG · T and O^4-meT · G pairs are Watson–Crick-like mispairs, apparently of relatively low thermodynamic stability in the duplex (Fig. 16).[91] Additionally,

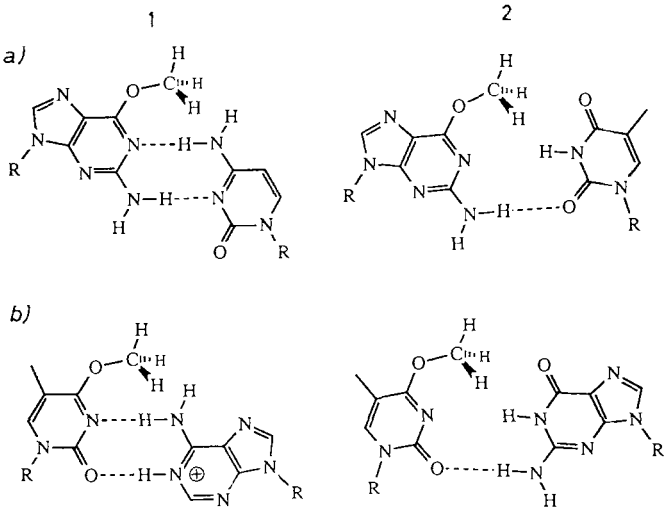

Fig. 16. Structures derived from ^{1}H NMR studies of base pairs between a) O^6-methyldeoxyguanosine and deoxycytidine (left) or thymidine (right), b) O^4-methylthymidine and deoxyadenosine (left) or deoxyguanosine (right) in B-DNA (after *Li* et al. [91]). Base pairs in left column, nonmutagenic wobble pairs; right column, mutagenic Watson–Crick-like pairs.

^{31}P NMR spectra of the d(O^6-meG)-containing compounds showed that the O^6-meG · C pair caused a much greater distortion of the sugar–phosphate backbone than did the O^6-meG · T pair, particularly in the strand opposing the alkylated base.[92] Once more, it was concluded that in a polymerase the wobble arrangement is unsuitable for polymerization.

This view is strongly supported by our experiments with template **III** that led to the formation of a pyridine–pyrimidine base pair which is presumed to be rather unstable.[93] Additionally, in this experiment the formation of a pyridine–pyrimidine base pair (and not a pyridine–purine base pair, e.g., pyridine–adenine, cf. Fig. 6b) occurred with a selectivity of 100%. This shows that the formation of a short base pair, although assumed to be unlikely because such a base pair is too unstable, can be very much favored and underlines that the stability of base pairs in a polymerase must be different from that in the free DNA.

Also, this result suggests that **3** has similar base-pairing preferences to dC*, another rare tautomer of deoxycytidylate, by mimicking its hydrogen-substitution pattern. A restriction regarding the quality of the analogy of the hydrogen-substitution pattern in compound **3** has to be noted. The real tautomer dC* does not have a hydrogen atom in the 3-position allowing, in principle, base pairing with an imino-proton-bearing nucleotide in a Watson–Crick-like arrangement. Besides the nonmutagenic binding of deoxyguanylate, there is still a chance that dC* might also direct the incorporation of thymidylate, a possible reason why C · T pairs do form in vitro.

4. Formation and Structure of Mispairs in DNA

4.1. Predicted and Evidenced Structures of Mispairs

4.1.1. Tautomeric Mispairs

Among various suggestions for the structures of mispairs responsible for the formation of substitution mutations, the first and most popular were the tautomeric transition mispairs A* = C, A = C*, G* = T, and G = T* proposed by *Watson* and *Crick*;[94] these mispairs were perfectly complementary with respect to the Watson–Crick rules. Owing to the presumed short lifetime of the rare tautomers in such mispairs in DNA, their existence could only be verified indirectly.

In 1976, 23 years later, *Topal* and *Fresco*[95] were able to lend support to the proposed structures through comparison of in vivo transition frequencies with the tautomeric equilibria of free nucleosides. Additionally, they suggested that transversions (purine–pyrimidine substitutions) could sufficiently be explained through the formation of tautomeric purine–purine pairs. These mispairs were assumed to be arranged as Hoogsteen pairs. Since two anomalies in the same base were thought to be improbable, one purine base would be a rare tautomer and the other a *syn* conformer. In the mixed G · A pair, either G*(*anti*) would form a base pair with A(*syn*) or A*(*anti*) would form a base pair with G(*syn*). The authors did not propose the straightforward and also "complementary" G(*anti*) · A(*anti*) or G(*anti*) · A(*syn*) pair without rare tautomeric forms, perhaps because tautomerization was regarded as an important reason for the formation of mispairs.

According to the authors,[95] rare tautomers could occur in the template nucleotide bases as well as in the nucleoside triphosphates and the *syn* conformers would, for steric reasons, only be allowed in the triphosphate binding site. The comparison of in vivo transversion frequencies with the tautomeric equilibria and the *syn–anti* equilibria of the purine nucleosides showed the consistency of this approach. Pyrimidine–pyrimidine pairs were thought to be unable to form base pairs within the duplex geometry. This led to the first and famous model, called "pathways for substitution mutations".[95]

This very influential paper explained for the first time, *average* mutation frequencies with simple thermodynamic parameters (equilibrium constants of *spontaneous* tautomerizations and *syn–anti* rotations) without the need of tautomerization-inducing forces. Unfortunately, from that time on, the pyrimidine–pyrimidine pairs seemed to be banned or at least denigrated by some researchers working on mismatches, polymerase mechanisms, and the like in vitro (discussed in Ref. [69]).

Later, exact measurements of the tautomerization equilibria of the free bases and the nucleosides revealed that, in fact, the mutation frequencies hardly ever correspond to these thermodynamic parameters (cf., e.g., Refs. [68, 79]). Moreover, it became clear that average mutation frequencies were by no means representative for the behavior of replicating DNA. Results accumulated showing that the probabilities of a specific substitution mutation depended strongly on the relative concentrations of the nucleoside triphosphates,[96] on the template sequence,[97–100] and on the polymerase.[101–103] The reasons for these differences, like the factors responsible for the error discrimination in polymerases (cf. Section 3.3.4), are still in dispute, though rare tautomeric forms are seldom invoked (for latest discussions see Refs. [74, 104, 105]). Thus, some researchers increasingly doubted whether rare tautomeric forms, particularly believed to occur in nucleoside triphosphates, would play a major role in mutagenesis.

On the other hand, the occurrence of pyrimidine–pyrimidine pairs could no longer be denied, since, recently, the in vitro replication of a natural template by polymerase α holoenzyme demonstrated clearly the existence of C · T and T · T pairs.[105, 106] In fact, biologists who have been performing in vivo mutagenesis experiments have never seemed to worry about the proposed inability of the polymerase to synthesize pyrimidine–pyrimidine pairs.

Therefore, the "pathways for substitution mutations" must be modernized. Obviously, all possible mispairs are involved in mutagenesis. To explain the reasons for their formation, in particular when occurring at a high frequency, we suggest that one should reconsider the formation of rare tautomeric forms not in the nucleoside triphosphate, but in the template bases. Yet, the greatest hindrance to the establishment of an important role for rare tautomeric forms in mutagenesis has still to be mentioned.

4.1.2. *Wobble Pairs*

The rapid development of useful synthetic and analytical procedures in chemistry, in particular the automated synthesis of oligodeoxynucleotides on a 10-micromolar scale, modern reversed-phase HPLC, and 2D ^{1}H NMR techniques, stimulated intensive investigations into the structure of short DNA oligomers of defined length and sequence. The combined analysis of a DNA duplex by circular dichroism and ^{1}H NMR in solution, and by X-ray crystallography in a single crystal provide the best means to ascertain the structure of a particular sequence. Of special interest are sequences bearing one or two mismatched base pairs.

As in the field of in vitro mutagenesis, the best analyzed structures are the purine–pyrimidine and the purine–purine mispairs. Oligomers containing the G · T pair were crystallized in A-, B-, and Z-DNA, the "dehydrated" right-handed, the normal right-handed, and the left-handed form, respectively. Irrespective of the overall conformation of the double helix, the bases form a wobble pair (Fig. 17a).[107–109] The A · C pair could also be crystallized in a B-DNA oligomer and proved to be very similar to the G · T pair in geometry, although it is probably protonated on N-1 of adenylate (Fig. 17b).[110–113] Both mispairs caused little disruption of

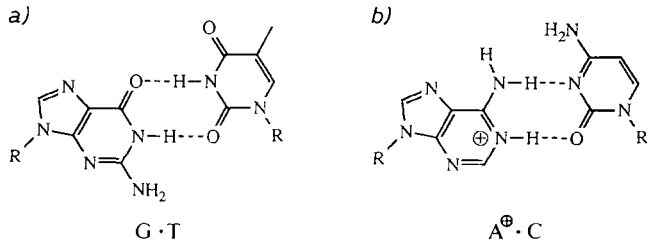

Fig. 17. a) G · T wobble pair, b) A$^{\oplus}$ · C wobble pair, schematized from X-ray data.

the DNA backbone in comparison with the native oligomer (without a mispair).

In the case of purine–purine pairs, only the G · A pair has been characterized crystallographically. It exists in several isomeric forms, dependent on the neighboring sequence. The first found was a Hoogsteen pair that induced a very slight disturbance in the DNA backbone (Fig. 18a);[114] another is

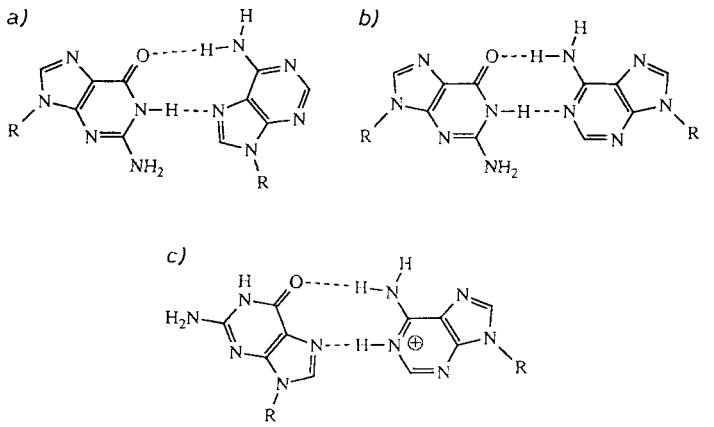

Fig. 18. a) G · A(*syn*), b) G · A, c) G(*syn*) · A$^{\oplus}$, schematized from X-ray data.

a Watson–Crick-like *anti–anti* pair, which is a little bit wider (Fig. 18b).[115] The structures of these mispairs are consistent with the ^{1}H NMR spectral data available.[116–122] *Gao* and *Patel*[123] suggested in a recent NMR study that, depending on the pH, the G · A pair could also exist in a third, protonated form, a Hoogsteen pair where G is the *syn* conformer (Fig. 18c). Very recently, this was confirmed by the crystal structure of G(*syn*) · A$^{\oplus}$.[124]

Gao and *Patel*'s work and a (mismatch repair) protein binding study on transition mispairs,[125] which showed a high sequence and pH dependence of G · T and, especially, A · C pairs, indicates that the structures of mispairs can be quite flexible and are very sensitive to their immediate surroundings.

Unfortunately, there is no crystallographic data of DNA available yet that contains a pyrimidine–pyrimidine mismatch in a duplex. Based on the ^{1}H NMR spectrum of a C · T-containing oligomer, it was proposed that this pair is an extended Watson–Crick-like type of base pair having a water molecule inserted in the gap in the minor groove, roughly similar to our computed mispair (cf. Fig. 10).[121] ^{1}H NMR spectra of oligomers containing T · T and C · C pairs suggest the wobble arrangement for the T · T pair and, although less certain, the strong pH dependence on the structure of the C · C pair is indicative for a protonated wobble pair or a variant of it.[126] Again, a high flexibility (nonrigidity) of those structures is expected, as their low thermodynamical stability suggests. In any case, it seems that none of the mismatches contain rare tautomeric forms.

4.2. Conclusions

4.2.1. *The Wobble Pair/Tautomeric Pair Conflict*

The crystallographic evidence led a substantial body of researchers to abandon the idea of rare tautomeric forms being involved in mutagenesis. The formation of wobble pairs was thought to be responsible for at least the transition mutations. The formation of purine–purine Hoogsteen pairs seems to explain adequately transversion mutations, again without the need of rare tautomeric forms.

However, various results involving experiments with a DNA polymerase contradict this point of view; some are mentioned in Sections 3.3.4 and 3.3.7, some are discussed in Ref. [69]. Therefore, we feel that the formation of Hoogsteen and wobble pairs without rare tautomeric forms cannot be responsible for all the substitution mutations found in vivo. In particular, the strong differences in substitution frequencies that usually occur at different sites (hot spots) are very badly explained by such a seemingly uninfluenced, random mode of misincorporation. Some influences that could have an effect on the sequence dependence of the probability of formation of, for instance, wobble pairs in polymerases are thought to be derived from differently stabilizing base-stacking interactions.[127a] But, considering there is a choice between only four different nearest neighbors that can stack more or less well with a wrong base at the primer end, the variability of the so stabilized mispairs is much too small to explain the enormous differences in substitution frequencies often found. Moreover, although it is known that in vivo

replication is assisted by DNA single-strand binding proteins, which are thought to destack the bases in the template strand prior to polymerization, thus enhancing the replication fidelity substantially,[127b] hot spots still occur in vivo.

Another more fundamental argument against wobble pair formation in polymerases is the function of the enzyme itself. In discussions about error discrimination mechanisms, it should always be taken into account that polymerases, prokaryotic and eukaryotic, are highly evolved proteins which presumably developed under the main constraint of not being selected unless the replication fidelity was high enough. The first restriction one can think of in order to enhance the replication fidelity, is to ensure a fixed reading frame (cf. Section 1.3, Figs. 2c and 2d), that is, to suppress or prevent the formation of wobble and Hoogsteen pairs (Fig. 1c and 1b, respectively). This can be achieved through a "clinch pocket" (or "binding cleft snugly fitting correct base pairs"[105]) provided by the protein. A much more difficult problem is to ensure a particular hydrogen-substitution pattern, that is, to prevent the bases from being (de)protonated and tautomerized (Fig. 2a and 2b), since these rapid and sterically nondemanding protolytic reactions presumably cannot be suppressed so well. It seems that the normal hydrogen-substitution patterns of the nucleotide triphosphate bases are relatively stable, whereas the template bases are more accessible to Brønsted acids and bases.

This evolutionary principle of replication fidelity strongly contrasts with the principle of another template-directed process, translation, where the proven formation of wobble pairs in the third codon position between mRNA and tRNA is not restricted, but selected by nature. There the purpose is a deliberate "infidelity of reading", in order to develop a degenerate universal code.

Hence one can assume that the formation of wobble pairs in polymerases is rather rare and will be responsible for some mutational background which can always be measured after replication and is not very site-specific. There must be some other mechanism that can lead to quite high substitution frequencies despite the replication fidelity of polymerases. The so formed mispairs should be inconspicuous; that is, they must be poorly recognized as mispairs in the polymerase.

After they have passed the crucial period in the enzyme, they will be released into solution and governed by forces inherent to hydrated, double-helical DNA. These were shown to be such that usually a most stable, normal tautomeric form is formed at the cost of a Watson–Crick-like geometry, resulting in the crystallographically observed normally tautomeric wobble and Hoogsteen pairs. At this stage, the role of wobble and Hoogsteen pairs becomes dominant in mutagenesis, because these structures can further be recognized and excized by post-replicative repairing exonucleases.

4.2.2. Rare Tautomeric Forms in the Template Strand In Vitro

It is at present difficult to prove directly the involvement of rare tautomeric forms in vitro, because of their transient appearence. Apart from our indirect evidence for a possible mutagenesis due to rare tautomeric forms in DNA template strands, there are other results which point in the same direction,[69, 128, 129] including results from X-ray crystallography. *Lippert* et al. showed that N^4-imino-1-methylcytosine (which corresponds to C^*) could be stabilized by coordination of N^4 to a platinum(IV) ion.[130] *Chattopadhyaya* et al. found a T^* residue in a Watson–Crick-like $T \cdot T^*$ pair between two non-double-helical DNA strands.[80]

Although no base pair involving a rare tautomer has been observed in an actual DNA double helix, the above results prove that forces derived from interactions present in all biological systems, such as metal coordination, base stacking, and base pairing, are able to overcome that apparent instability of rare tautomers. This means that the measured tautomeric equilibria of the free bases or even of the nucleosides represent the physico-chemical state of rare tautomeric forms neither in a protein-free DNA duplex nor in polymerase-bound DNA. The replication system seems not to be proof against kinetically labile forms in the template strand which can cause replication errors if the mispair escapes the proofreading. Such a form is a protonated or deprotonated template base or a rare tautomeric form of a template base. These forms differ from normal forms only very slightly when stacked into a DNA helix and might therefore be a "problematic" source of substitution mutations for the polymerase.

It would be very helpful, if the stability of Watson–Crick-like tautomeric or ionized mispairs within the active site of a polymerase could somehow be determined experimentally in vitro. The use of nucleotide base analogues with an altered H-substitution pattern proved to be a useful tool for the elucidation of a pathway for substitution mutations. Further investigations will be undertaken, in particular to study pol I's proofreading activity towards pyrimidine–pyrimidine base pairs.

Perhaps it would be of use to find mutagens which cause substitution mutations upon replication of their "victim" DNA, but do not cause any physical damage to it. The mode of action of such a *mild mutagen* should be a reversible reaction with DNA which is hazardous (mutagenic) when the reactant, a template nucleotide base, is replicated, but otherwise harmless owing to its kinetic lability. We suspect that there are means of tautomerizing DNA bases, particularly when they are in the easily accessible, single-stranded form. Yet, finding external mild mutagens that would produce substitution mutations in DNA upon replication in vitro (we like to call them "tauterogens") seems to be quite difficult, because it is not obvious what sort of molecules might possess the needed selectivity enabling them just to protonate or deprotonate and, hence, subsequently tautomerize DNA bases without reacting otherwise (e.g., with the polymerase).

4.2.3. Tautomerizing Mutagens in Vivo?

The most interesting possibility is the existence of tauterogens in vivo, since they would account for various kinds of mutation pressures inherent to all living cells. At present, there is no answer to the question of how an increased production of substitution mutations within a few cell genera-

tions might be achieved in vivo. The sudden production of secondary mutations in the initial stage of cancer growth and the sudden switching from an unactivated immune cell to a cell rapidly producing somatic substitution mutations in the genes that encode the antibody proteins are two examples. There must be a way of activating mutagens within a cell. These mutagens should not be dangerous in the sense that they damage the genome irreversibly (because the cell would die); they should merely cause substitution mutations in the offspring of the cell. Proteins with their immense variety of acidic and basic functional groups have deprotonating or protonating facilities. DNA-binding proteins might be candidates for this type of mild mutagen. They would act very discretely—just binding to DNA, tautomerizing a nucleotide base during replication, and diffusing off again—and therefore their biological activity could be difficult to detect.

The idea of the existence of "tauterogenic" DNA-binding proteins being responsible for a considerable amount of substitution mutations in vivo is exciting for several reasons. First, of all, if such proteins and their corresponding genes were found and identified, they might be very effective when used as, say, a cytostatic or other pharmaceutical. Moreover, a substantial part of the observed DNA sequence dependence of substitution mutations could be attributed to them, since they are expected to act very selectively. This property is known from other DNA-binding proteins, such as transcription factors and restriction enzymes. Last but not least, these mutagenic DNA-binding proteins, like all proteins, would be the almost direct products (via RNA) of DNA itself. This would enable the genome to have direct control over its own mutability; and this would answer some questions about how a given genome maintains a directional mutation pressure (e.g., a biased G + C content or a codon pressure, that is, the nonrandom use of synonymous codons) throughout many generations, in spite of the selection pressures possibly counteracting this tendency. Clearly, this is beyond the scope of this article (cf. Ref. [131]). The last part of our conclusions is at present devoid of any experimental evidence and therefore quite speculative. Still, it should encourage discussions and experimental investigations.

We should like to thank all collaborators who have significantly contributed to the project during the past years (alphabetical order): R. Altermatt, P. Bühlmayer, N. Cerletti, R. Charczuk, S. De Bernardini, W. Falk, R. Glaser, G. Graf, I. Gregor, P. Kohler, C. A. Leach, Ch. Papageorgiou, H. D. Schneider, U. Séquin, E. Volz, M. Wachtl, and F. Waldmeier. We also thank Prof. Thomas Bickle (Biocenter of the University of Basel, Department of Microbiology) and Priv.-Doz. Dr. K. Müller, F. Hoffmann–La Roche AG, Basel, for their engaged collaboration, as well as to Dr. Bill Hunter and Dr. Madeleine Moore (Chemical Laboratory, University of Cambridge, UK) for their corrections of the manuscript. The financial support from the Swiss National Science Foundation is gratefully acknowledged.

Received: December 16, 1988 [A 742 IE]
German version: *Angew. Chem. 102* (1990) 37

[1] C. de Duve, *Nature (London) 333* (1988) 117.
[2] J. D. Watson, F. H. C. Crick, *Nature (London) 171* (1953) 737.
[3] a) N. B. Ramsing, T. M. Jovin, *Nucleic Acid Res. 16* (1988) 6659; b) J. H. van de Sande, N. B. Ramsing, M. W. Germann, W. Elhorst, B. W. Kalisch, E. von Kitzing, R. T. Pon, R. C. Clegg, T. M. Jovin, *Science (Washington, D.C.) 241* (1988) 551.
[4] a) S. M. Mirkin, V. I. Lyamichev, K. N. Drushlyak, V. N. Dolorynin, S. A. Filippov, M. D. Frank-Kamenetskii, *Nature (London) 330* (1987) 495; b) Y. Kohwi, T. Kohwi-Shigematsu, *Proc. Natl. Acad. Sci. USA 85* (1988) 3781; c) J. C. Harvey, M. Shimizu, R. D. Wells, *ibid. 85* (1988) 6292.
[5] B. L. Currie, R. K. Robins, M. J. Robins, *J. Heterocycl. Chem. 14* (1977) 475.
[6] U. Séquin, C. Tamm, *Helv. Chim. Acta 52* (1969) 1219.
[7] U. Séquin, C. Tamm, *Helv. Chim. Acta 55* (1972) 1196.
[8] P. Kohler, E. Volz, U. Séquin, C. Tamm in L. B. Townsend, R. S. Tipson (Eds.): *Nucleic Acid Chemistry, Part 1*, Wiley-Interscience, New York 1978, p. 283.
[9] M. Wachtl, *Dissertation*, Universität Basel 1980.
[10] R. Charczuk, *Dissertation*, Universität Basel 1986.
[11] R. Altermatt, C. Tamm, *Helv. Chim. Acta 68* (1985) 475.
[12] D. H. R. Barton, W. B. Motherwell, *Pure Appl. Chem. 53* (1981) 15.
[13] J. R. Williamson, S. G. Boxer, *Nucleic Acids Res. 16* (1988) 1529, and references therein.
[14] H. Rosenmeyer, F. Seela, *Helv. Chim. Acta 71* (1988) 1573, and references therein.
[15] C. Papageorgiou, C. Tamm, *Tetrahedron Lett. 27* (1986) 555.
[16] C. Papageorgiou, C. Tamm, *Helv. Chim. Acta 70* (1987) 138.
[17] a) R. Zou, M. J. Robins, *Can. J. Chem. 65* (1987) 1436; b) C. Tamm, P. Strazewski, G. Hong, unpublished.
[18] M. J. Robins, J. S. Wilson, F. Hansske, *J. Am. Chem. Soc. 105* (1983) 4059.
[19] F. Eckstein, K. H. Scheit, *Angew. Chem. 79* (1967) 317; *Angew. Chem. Int. Ed. Engl. 6* (1967) 362.
[20] R. L. Letsinger, K. K. Ogilvie, J. Am. Chem. Soc. 91 (1969) 3350.
[21] W. Falk, C. Tamm, *Helv. Chim. Acta 55* (1972) 1928.
[22] I. Gregor, U. Séquin, C. Tamm, *Helv. Chim. Acta 58* (1975) 712.
[23] N. Cerletti, C. Tamm, *Helv. Chim. Acta 60* (1977) 1182.
[24] M. Yoshikawa, T. Kato, T. Takenishi, *Bull. Chem. Soc. Jpn. 42* (1969) 3505.
[25] E. Volz, C. Tamm, *Helv. Chim. Acta 61* (1978) 2579.
[26] F. Waldmeier, C. Tamm, *Helv. Chim. Acta 61* (1978) 1648.
[27] P. Kohler, M. Wachtl, C. Tamm, *Helv. Chim. Acta 63* (1980) 2488.
[28] J. G. Moffat, H. G. Khorana, *J. Am. Chem. Soc. 83* (1961) 649.
[29] J. G. Moffat, *Can. J. Chem. 42* (1964) 599.
[30] S. De Bernardini, F. Waldmeier, C. Tamm, *Helv. Chim. Acta 64* (1981) 2142.
[31] S. De Bernardini, G. Graf, C. A. Leach, P. Bühlmayer, F. Waldmeier, C. Tamm, *Helv. Chim. Acta 66* (1983) 639.
[32] R. Altermatt, C. Tamm, *Helv. Chim. Acta 68* (1985) 475.
[33] C. B. Reese, R. C. Titmas, L. Yau, *Tetrahedron Lett. 1978*, 2727.
[34] C. B. Reese, L. Yau, *Tetrahedron Lett. 1978*, 4443.
[35] C. A. Leach, F. Waldmeier, C. Tamm, *Helv. Chim. Acta 64* (1981) 2515.
[36] H.-D. Schneider, C. Tamm, *Helv. Chim. Acta 66* (1983) 350.
[37] R. Charczuk, C. Tamm, *Helv. Chim. Acta 70* (1987) 717.
[38] a) J. B. Chattopadhyaya, C. B. Reese, *Tetrahedron Lett. 1979*, 5059; b) C. Tamm, P. Strazewski, G. Hong, M. Walser, H. Eschenhof, unpublished.
[39] L. J. McBride, R. Kierzek, S. L. Beaucage, M. H. Caruthers, *J. Am. Chem. Soc. 108* (1986) 2040.
[40] L. J. McBride, M. H. Caruthers, *Tetrahedron Lett. 24* (1983) 2953.
[41] P. T. Gilham, H. G. Khorana, *J. Am. Chem. Soc. 80* (1958) 6212.
[42] H. G. Khorana, J. P. Vizsolyi, *J. Am. Chem. Soc. 83* (1961) 675.
[43] N. Cerletti, C. Tamm, *Heterocycles 5* (1976) 245.
[44] N. Cerletti, U. Séquin, C. Tamm, W. Zürcher, *Helv. Chim. Acta 61* (1978) 2589.
[45] G. Weimann, H. G. Khorana, *J. Am. Chem. Soc. 84* (1962) 419.
[46] N. Cerletti, *Dissertation*, Universität Basel 1976.
[47] P. Bühlmayer, G. Graf, F. Waldmeier, C. Tamm, *Helv. Chim. Acta 63* (1980) 2469.
[48] F. Waldmeier, S. De Bernardini, C. A. Leach, C. Tamm, *Helv. Chim. Acta 65* (1982) 2472.
[49] a) A. Maxam, W. Gilbert, *Proc. Natl. Acad. Sci. USA 74* (1977) 560; b) C. Tamm, P. Strazewski, M. Walser, unpublished.
[50] a) B. Chaudhuri, C. B. Reese, K. Weclawek, *Tetrahedron Lett. 25* (1984) 4037; b) M. V. Rao, C. B. Reese, *Nucleic Acids Res. 20* (1989) 8221.
[51] R. L. Letsinger, W. B. Lursford, *J. Am. Chem. Soc. 98* (1976) 3655.
[52] M. D. Matteucci, M. H. Caruthers, *J. Am. Chem. Soc. 103* (1981) 3185.
[53] a) S. L. Beaucage, M. H. Caruthers, *Tetrahedron Lett. 22* (1981) 1859; b) C. Tamm, R. Charczuk, unpublished.
[54] V. A. Efimov, O. G. Chakhmakheva, V. S. A. Ovchinnikov, *Nucleic Acids Res. 13* (1985) 3651.
[55] A. Kornberg: *DNA Replication*, Freeman, San Francisco 1980.
[56] A. Kornberg: *1982 Supplement to DNA Replication*, Freeman, San Francisco 1982.

[57] C. M. Joyce, T. A. Steitz, *Trends Biochem. Sci. 12* (1987) 288.
[58] T. A. Steitz in R. M. Burnett, H. J. Vogel (Eds.): *Biological Organization: Macromolecular Interactions at High Resolution*, Academic Press, Orlando 1987, p. 45.
[59] M. Wachtl, P. Kohler, C. Tamm, *Helv. Chim. Acta 63* (1980) 2495.
[60] H. Lineweaver, D. Burke, *J. Am. Chem. Soc. 56* (1934) 658.
[61] R. Charczuk, C. Tamm, B. Suri, T. Bickle, *Nucleic Acids Res. 14* (1986) 9530.
[62] a) A. Bloch, G. Dutschman, *J. Med. Chem. 16* (1973) 294; b) A. Bloch, M. C. Wang, *Biochem. Pharmacol. 21* (1972) 1063.
[63] T. Bickle, Biozentrum, Universität Basel, personal communication.
[64] B. N. Ames, *Science (Washington, D.C.) 204* (1979) 587.
[65] R. Devoret, *Sci. Am. 241* (1979) no. 2, p. 40.
[66] L. J. Ferrin, A. S. Mildvan, *Biochemistry 25* (1986) 5131.
[67] T. A. Kunkel, R. M. Schaaper, L. A. Loeb, *Biochemistry 22* (1983) 2378.
[68] R. Rein, M. Shibata, R. Garduno-Juarez, T. Kieber-Emmons in E. Clementi, R. H. Sarma (Eds.): *Structure and Dynamics: Nucleic Acids and Proteins*, Adenine press, New York 1983, p. 269.
[69] P. Strazewski, *Nucleic Acids Res. 16* (1988) 9733.
[70] P. Strazewski, *Nucleic Acids Res. 16* (1988) 5191.
[71] H. Rosemeyer, F. Seela, *J. Org. Chem. 52* (1987) 5136.
[72] V. Mizrahi, R. N. Henrie, J. F. Marlier, K. A. Johnson, S. J. Benkovic, *Biochemistry 24* (1985) 4010.
[73] R. D. Kuchta, V. Mizrahi, P. Benkovic, K. A. Johnson, S. J. Benkovic, *Biochemistry 26* (1987) 8410.
[74] R. D. Kuchta, P. Benkovic, S. J. Benkovic, *Biochemistry 27* (1988) 6716.
[75] D. L. Ollis, P. Brick, R. Hamlin, N. G. Xuong, T. A. Steitz, *Nature (London) 313* (1985) 762.
[76] P. S. Freemont, J. M. Friedman, L. S. Beese, M. R. Sanderson, T. A. Steitz, *Proc. Natl. Acad. Sci. USA 85* (1988) 8924.
[77] L. J. Ferrin, R. A. Beckman, L. A. Loeb, A. S. Mildvan in V. L. Schramm, F. C. Wedler (Eds.): *Manganese in Metabolism and Enzyme Function*, Academic Press, New York 1986, p. 259.
[78] L. J. Ferrin, A. S. Mildvan, *Biochemistry 24* (1985) 6904.
[79] M. J. Scanlan, I. H. Hillier, *J. Am. Chem. Soc. 106* (1984) 3737.
[80] R. Chattopadhyaya, S. Ikuta, K. Grzeskowiak, R. E. Dickerson, *Nature (London) 334* (1988) 175.
[81] R. K. Robins, *Chem. Eng. News 64* (1986) no. 1, p. 28.
[82] H. Mitsuya, S. Broder, *Nature (London) 325* (1987) 773.
[83] P. Herdewijn, J. Balzarini, E. De Clercq, R. Pauwels, M. Baba, S. Broder, H. Vanderhaeghe, *J. Med. Chem. 30* (1987) 1270.
[84] J. Weber, F. Grosse, *Nucleic Acids Res. 17* (1989) 1379.
[85] a) P. H. Driggers, K. L. Beattie, *Biochemistry 27* (1988) 1729; b) L. C. Sowers, R. Eritja, B. Kaplan, M. F. Goodman, G. V. Fazakerley, *J. Biol. Chem. 263* (1988) 14, 794.
[86] M. F. Goodman, E. W. Branscomb in T. B. L. Kirkwood, R. F. Rosenberger, D. J. Galas (Eds.): *Accuracy in Molecular Processes*, Chapman & Hall, London 1986, p. 191.
[87] L. A. Sowers, G. V. Fazakerley, R. Eritja, B. E. Kaplan, M. F. Goodman, *Proc. Natl. Acad. Sci. USA 83* (1986) 5434.
[88] D. Mhaskar, M. F. Goodman, *J. Biol. Chem. 259* (1984) 11, 713.
[89] R. Eritja, B. E. Kaplan, D. Mhaskar, L. A. Sowers, J. Petruska, M. F. Goodman, *Nucleic Acids Res. 14* (1986) 5869.
[90] R. Eritja, D. M. Horowitz, P. A. Walker, J. P. Ziehler-Martin, M. S. Boosalis, M. F. Goodman, K. Itakura, B. E. Kaplan, *Nucleic Acids Res. 14* (1986) 8135.
[91] B. F. L. Li, P. F. Swann, M. W. Kalnik, M. Kouchakdijan, D. J. Patel in J. W. Jaroszewski, K. Schaumberg, H. Kofod (Eds.): *NMR Spectroscopy in Drug Research, Alfred Benzon Symposium 26*, Munksgaard, Kopenhagen 1988, p. 309.
[92] P. Swann, University College London, personal communication.
[93] a) F. Aboul-ela, D. Koh, I. Tinoco, Jr., *Nucleic Acids Res. 13* (1985) 4811; b) H. Werntges, G. Steger, D. Riesner, H.-J. Fritz, *ibid. 14* (1986) 3773.
[94] J. D. Watson, F. H. C. Crick, *Nature (London) 171* (1953) 964.
[95] M. D. Topal, J. R. Fresco, *Nature (London) 263* (1976) 285.
[96] A. R. Fersht, J. W. Knill-Jones, W.-C. Tsui, *J. Mol. Biol. 156* (1982) 37.
[97] J. E. Patten, A. G. So, K. M. Downey, *Biochemistry 23* (1984) 1613.
[98] G. G. Hillebrand, A. H. McCluskey, K. A. Abbott, G. G. Revich, K. L. Beattie, *Nucleic Acids Res. 12* (1984) 3155.
[99] G. G. Hillebrand, K. L. Beattie, *J. Biol. Chem. 260* (1985) 3116.
[100] M.-D. Lai, K. L. Beattie, *Biochemistry 27* (1988) 1722.
[101] T. A. Kunkel, *J. Biol. Chem. 260* (1985) 5787.
[102] T. A. Kunkel, *J. Biol. Chem. 260* (1985) 12, 866.
[103] T. A. Kunkel, P. S. Alexander, *J. Biol. Chem. 261* (1986) 160.
[104] M. E. Reyland, I. R. Lehman, L. A. Loeb, *J. Biol. Chem. 263* (1988) 6518.
[105] J. Petruska, M. F. Goodman, M. S. Boosalis, L. A. Sowers, C. Cheong, I. Tinoco, Jr., *Proc. Natl. Acad. Sci. USA 85* (1988) 6252.
[106] M. S. Boosalis, J. Petruska, M. F. Goodman, *J. Biol. Chem. 262* (1987) 14, 689.
[107] T. Brown, O. Kennard, G. Kneale, D. Rabinovich, *Nature (London) 315* (1985) 604.
[108] G. Kneale, T. Brown, O. Kennard, D. Rabinovich, *J. Mol. Biol. 186* (1985) 805.
[109] P. S. Ho, C. A. Frederick, G. J. Quigley, G. A. van der Marel, J. H. van Boom, A. H. Wang, A. Rich, *EMBO J. 4* (1985) 3617.
[110] W. N. Hunter, T. Brown, N. N. Anand, O. Kennard, *Nature (London) 320* (1986) 552.
[111] W. N. Hunter, T. Brown, O. Kennard, *Nucleic Acids Res. 15* (1987) 6589.
[112] L. C. Sowers, G. V. Fazakerley, H. Kim, L. Dalton, M. F. Goodman, *Biochemistry 25* (1986) 3983.
[113] M. W. Kalnik, M. Kouchakdijan, B. F. L. Li, P. F. Swann, D. J. Patel, *Biochemistry 27* (1988) 100.
[114] O. Kennard, *J. Biomol. Struct. Dyn. 3* (1985) 205.
[115] G. G. Prive, U. Heinemann, S. Chandrasegaran, L.-S. Kan, M. L. Kopka, R. E. Dickerson, *Science (Washington, D.C.) 238* (1987) 498.
[116] T. A. Early, J. Olmsted, D. R. Kearns, A. G. Lezius, *Nucleic Acids Res. 5* (1978) 1955.
[117] D. J. Patel, S. A. Kozlowski, L. A. Marky, J. A. Rice, C. Broka, J. Dallas, K. Itakura, K. J. Breslauer, *Biochemistry 21* (1982) 437.
[118] L. S. Kan, S. Chandrasegaran, S. M. Pulford, P. S. Miller, *Proc. Natl. Acad. Sci. USA 80* (1983) 4263.
[119] D. J. Patel, S. A. Kozlowski, S. Ikuta, K. Itakura, *Biochemistry 23* (1984) 3207.
[120] D. J. Patel, S. A. Kozlowski, S. Ikuta, K. Itakura, *Biochemistry 23* (1984) 3218.
[121] D. J. Patel, S. A. Kozlowski, S. Ikuta, K. Itakura, *Fed. Proc. Fed. Am. Soc. Exp. Biol. 43* (1984) 2663.
[122] D. Hare, L. Shapiro, D. J. Patel, *Biochemistry 25* (1986) 7445.
[123] X. Gao, D. J. Patel, *J. Am. Chem. Soc. 110* (1988) 5178.
[124] T. Brown, A. Leonard, E. D. Booth, J. Chambers, *J. Mol. Biol. 207* (1989) 455.
[125] J. Jiricny, S.-S. Su, S. G. Wood, P. Modrich, *Nucleic Acids Res. 16* (1988) 7843.
[126] M. Kouchakdijan, B. F. L. Li, P. F. Swann, D. J. Patel, *J. Mol. Biol. 202* (1988) 139.
[127] a) L. N. Mendelman, M. S. Boosalic, J. Petrusca, M. F. Goodman, *J. Biol. Chem. 264* (1989) 14415; b) M. D. Topal, N. K. Sinha, *ibid. 258* (1983) 12274.
[128] Y. Kuchino, F. Mori, H. Kasai, H. Inoue, S. Iwai, K. Miura, E. Ohtsuka, S. Nishimura, *Nature (London) 327* (1987) 77.
[129] J. Fresco, S. Broitman, A. E. Lane in B. Alberts, C. F. Fox (Eds.): *Mechanistic Studies of DNA Replication and Genetic Recombination*, Academic Press, New York 1980, p. 753.
[130] B. Lippert, H. Schöllhorn, U. Thewaldt, *J. Am. Chem. Soc. 108* (1986) 6616.
[131] P. Strazewski, *J. Molec. Evol.* (1990), in press.

Communications may be submitted in English *or* in German. Further details regarding the submission of communications can be found in the "Notice to Authors" reproduced in the January issue of the journal. Copies thereof may be obtained from the editorial office upon request.

NMR Study of Nuclear Spin Polarization during Chemical Reactions with Ortho Hydrogen**

By *Joachim Bargon,** *Jörg Kandels,* and *Klaus Woelk*

Since the discovery of the CIDNP phenomenon,[1, 2] nuclear spin polarization effects in NMR spectra of chemical reactions have traditionally been ascribed to radical intermediates.[3] *Bowers* and *Weitekamp*[4, 5] showed, however, that very similar phenomena can also be observed in chemical reactions involving spin-polarized hydrogen. Thus, the cause of a nuclear spin polarization found by NMR spectroscopy is not unambiguous. Indeed, NMR polarization signals have been observed in the past during hydrogenation in the presence of organometallic catalysts[6] and often wrongly interpreted as CIDNP effects.[7] Here we describe the experimental elucidation of the cause of nuclear spin polarization by a method involving the two isomers of molecular hydrogen (i.e., ortho and para hydrogen).

So far, nuclear spin polarizations during hydrogenations have been investigated exclusively by using para hydrogen, as reflected in the acronyms PASADENA (*P*arahydrogen *A*nd *S*ynthesis *A*llows *D*ynamically *E*nhanced *N*uclear *A*lignment)[5] or PHIP (*P*ara *H*ydrogen *I*nduced *P*olarization).[8, 9] We have now studied these effects with both ortho and para hydrogen.[10]

Molecular hydrogen contains two protons having nuclear spin $I = 1/2$. These spins couple to give a total spin 1 (triplet-state nuclear spin in ortho hydrogen) or 0 (singlet-state nuclear spin in para hydrogen). At room temperature, the small energy difference between the two spin isomers can be neglected. Owing to the threefold degeneracy of the triplet state, the ratio of the two isomers at room temperature is 75% ortho to 25% para. Hydrogenation with H_2 in this ratio leads to intermediates and final products whose NMR signals are characterized by the slight difference in thermal occupation ($\Delta N/N \approx 10^{-5}$) of the nuclear spin states in the magnetic field.

If, on the other hand, only one of the two spin isomers—for example, para hydrogen—is used in the hydrogenation, then, in the intermediates and final products, the only nuclear spin states occupied are those exhibiting singlet character with respect to the protons undergoing transfer. All other states remain unoccupied. This enormous difference in occupation leads to strong emission and absorption signals in the NMR spectrum.

The mixture can be enriched in ortho hydrogen by exploiting the fact that, at low temperatures, the two spin isomers are not equally adsorbed on surfaces (theory of the hindered rotator[11]). Gas chromatography on alumina as a diamagnetic adsorber at 77 K thus affords a mixture enriched in ortho hydrogen.[12] This method yields a mixture containing about 80% ortho and 20% para hydrogen.

A mixture enriched in para hydrogen can be obtained by making use of the fact that, in the presence of a paramagnetic adsorber (active charcoal), a thermal equilibrium is established between ortho and para hydrogen. At low temperatures, therefore, para hydrogen is favored energetically.[13] In this way, we obtained a mixture of approximately 46% ortho and 54% para hydrogen at 77 K.

The isomer ratio in the mixture was determined by difference measurement with two thermal conductivity cells that exploit the differing specific heats of the two spin isomers at low temperatures (77 K).[14]

The enriched hydrogen obtained in this way was directly bubbled via a capillary into the sample tube of a ^1H NMR FT spectrometer (80 MHz) and used to hydrogenate acrylonitrile in the presence of Wilkinson catalyst, tris(triphenylphosphane)chlororhodium(I), in [D_6]benzene [Eq. (a)].

$$CH_2=CH-CN + H_2 \xrightarrow[C_6D_6]{(Ph_3P)_3RhCl} CH_3-CH_2-CN \qquad (a)$$

For kinetic reasons, the polarization signal of the reaction product propionitrile is maximal only after bubbling hydrogen into the reaction mixture at a constant rate for 30 s. Successive NMR pulses must therefore be separated by a corresponding period of time. The result of the NMR study is summarized in Figure 1.

Figure 1a shows the polarization signal of propionitrile during the hydrogenation with enriched ortho hydrogen, Figure 1b the complementary signal observed with enriched para hydrogen. Comparison of these two spectra reveals that the sequence of emission and absorption is reversed. The intensity ratio of the two spectra varies between 1:4 and 1:5.

This finding is explained as follows: During the hydrogenation, ortho and para hydrogen participate independently in the reaction. In principle, therefore, the total intensity I of the NMR signal of the reaction product should be obtainable by adding the intensities of ortho and para hydrogen weighted according to their relative amounts in the mixture. For hydrogenation with hydrogen in thermal equilibrium at room temperature (75% ortho and 25% para hydrogen), Equation (b) holds.

$$I_{thermal} = 1/4\ I_{para} + 3/4\ I_{ortho} \qquad (b)$$

The difference in occupation of the nuclear spin levels, which determines the signal intensity $I_{thermal}$, obeys the Boltzmann distribution and thus is several orders of magnitude smaller (ca. 10^{-5}) than the difference in occupation determining the signal intensities I_{para} and I_{ortho}. Therefore, it can be neglected (see Fig. 1c). Equation (c) is thereby obtained.

$$I_{ortho} = -\ 1/3\ I_{para} \qquad (c)$$

[*] Prof. Dr. J. Bargon, Dipl.-Phys. J. Kandels, Dipl.-Chem. K. Woelk
Institut für Physikalische Chemie der Universität
Wegelerstrasse 12, D-5300 Bonn 1 (FRG)

[**] This work was supported by the Fonds der Chemischen Industrie. We thank Prof. Dr. *W. Keim*, Technische Hochschule Aachen, Prof. Dr. *U. Nagel*, Universität Tübingen, Prof. Dr. *H. Hoberg*, Max-Planck-Institut, Mülheim a. d. Ruhr, and Prof. Dr. *M. Dosière*, Université Mons, Belgium, for valuable discussions.

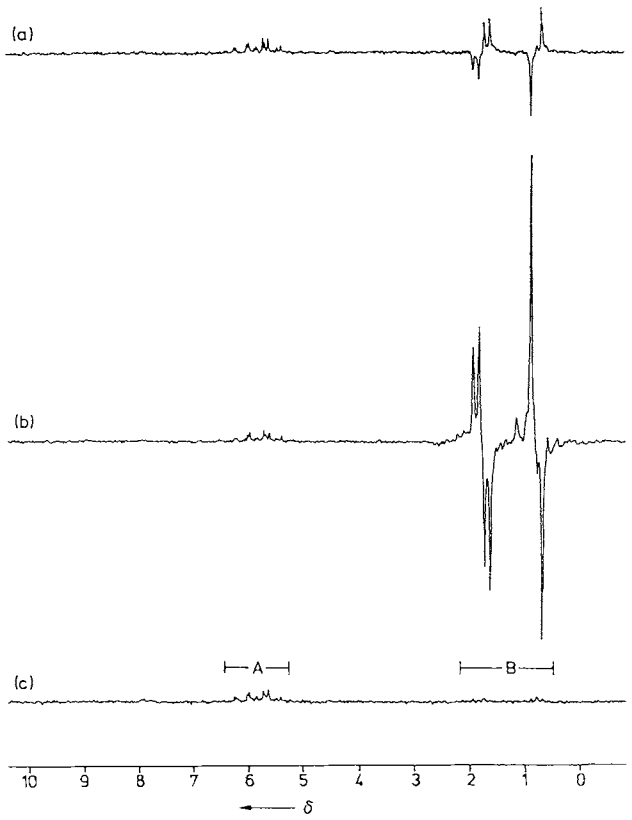

Fig. 1. Wilkinson catalyst (20 mg) and acrylonitrile (200 μL) dissolved in 1 mL of C_6D_6: NMR spectra at 80 MHz with a 45° pulse; A = acrylonitrile; B = propionitrile; NMR pulse after hydrogenation for 30 s with (a) enriched ortho hydrogen (I_{ortho}) and (b) enriched para hydrogen (I_{para}). c) NMR pulse several minutes after termination of the hydrogenation. The propionitrile nuclear spin system is relaxed; the weak thermal signal $I_{thermal}$ remains.

This equation holds only for pure ortho or pure para hydrogen. Adjustment for the experimentally accessible isomer ratios (thermal conductivity measurement) gives an intensity ratio between 1:5 and 1:6. This result agrees, within the limits of error, with the intensity ratio obtained from the experimental spectra.

According to the considerations above, the complementary behavior of the two spin isomers in hydrogenations is independent of the strength of the applied magnetic field and thus applicable to hydrogenations performed outside the NMR spectrometer, though these reactions display different polarization patterns.[15]

Received: June 20, 1989 [Z 3403 IE]
German version: *Angew. Chem. 102* (1990) 70

CAS Registry numbers:
$CH_2=CHCN$, 107-13-1; H_2, 1333-74-0.

[1] J. Bargon, H. Fischer, *Z. Naturforsch. A 22* (1967) 1551.
[2] H. R. Ward, R. G. Lawler, *J. Am. Chem. Soc. 89* (1967) 5518.
[3] A. R. Lepley, G. L. Closs: *Chemically Induced Magnetic Polarization*, Wiley, New York 1973.
[4] C. R. Bowers, D. P. Weitekamp, *Phys. Rev. Lett. 57* (1986) 2645.
[5] C. R. Bowers, D. P. Weitekamp, *J. Am. Chem. Soc. 109* (1987) 5541.
[6] R. L. Sweany, J. Halpern, *J. Am. Chem. Soc. 99* (1977) 8335.
[7] The interpretation of the data of P. F. Seidler, H. E. Bryndza, J. E. Frommer, L. S. Stuhl, R. G. Bergman, *Organometallics 2* (1983) 1701, must be corrected accordingly.
[8] T. C. Eisenschmid, R. U. Kirss, P. P. Deutsch, S. I. Hommeltoft, R. Eisenberg, J. Bargon, R. G. Lawler, A. L. Balch, *J. Am. Chem. Soc. 109* (1987) 8089.
[9] R. U. Kirss, T. C. Eisenschmid, R. Eisenberg, *J. Am. Chem. Soc. 110* (1988) 8564.
[10] We therefore propose that the acronym PHIP, introduced by *Eisenberg*, be reinterpreted as "Polarized Hydrogen Induced Polarization".
[11] Y. L. Sandler, *J. Phys. Chem. 58* (1945) 58.
[12] M. Dosière, *J. Chem. Educ. 62* (1985) 891.
[13] P. J. Durrant, B. Durrant: *Introduction in Advanced Inorganic Chemistry*, Longmans, Green, London 1962, pp. 368–371.
[14] T. W. Bradshaw, J. O. W. Norris, *Rev. Sci. Instrum. 58* (1987) 83.
[15] M. G. Pravica, D. P. Weitekamp, *Chem. Phys. Lett. 145* (1988) 255.

A New Route to Highly Enantiomerically Enriched (*Z*)-(1-Methyl-2-butenyl)boronic Esters**

By *Rainer Stürmer**

The (*Z*)-(1-methyl-2-butenyl)boronic ester **1** is a reliable reagent for chain lengthening of aldehydes to homoallyl alcohols **2** with full reagent control of the diastereoselectivity.[1,2]

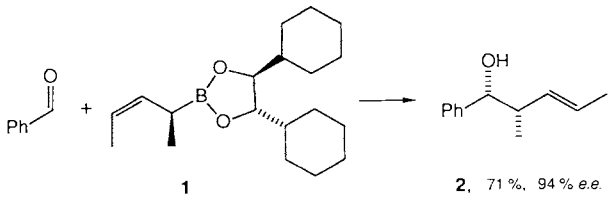

1 **2**, 71%, 94% *e.e.*

Here we describe a new, simple route to the boronic esters **1** from the Grignard reagent **3** and the borate **4**; this approach combines, for the first time, a racemization due to 1,3-metallotropic shift[3] with a kinetic resolution of a race-

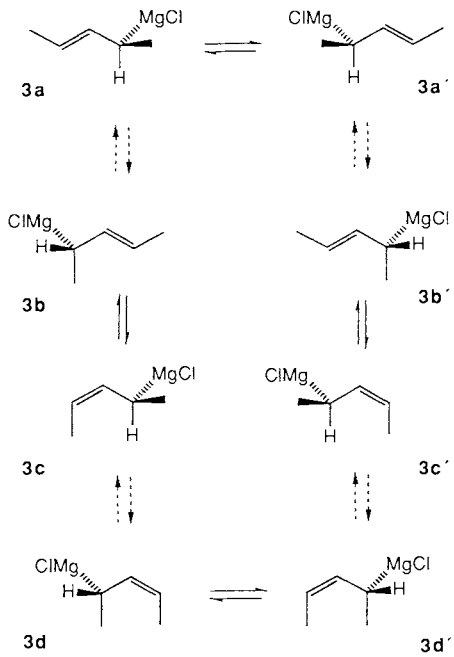

[*] Dipl.-Chem. R. Stürmer
Fachbereich Chemie der Universität
Hans-Meerwein-Strasse, D-3550 Marburg (FRG)

[**] This work was supported by the Deutsche Forschungsgemeinschaft (SFB 260, partial project with Prof. Dr. *R. W. Hoffmann*) and by the "Graduiertes Kolleg Metallorganische Chemie", Universität Marburg. I thank Prof. Dr. *R. W. Hoffmann* for his friendly support of this work.

mate.[4] The Grignard reagent **3** consists of an equilibrium mixture of enantiomers, diastereomers, and conformational isomers owing to rotation around formal single bonds[5] and 1,3-metallotropic shift.[6] Borate **4** reacts preferentially with **3b, b'**[7] to afford an 89% yield of the pentenylboronic esters **1** and **5**, which have (*Z*) configurations (cf. Ref. [8]).

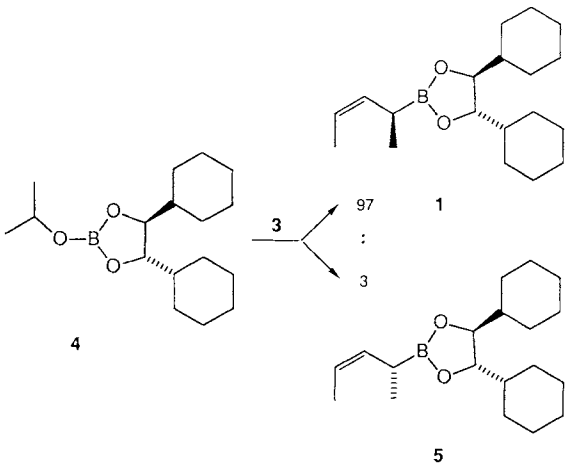

Furthermore, the chiral borate **4** differentiates between the enantiomers **3b, b'**, so that **1** can be obtained with a diastereomeric excess of 94% by kinetic resolution of a racemate. This was established by reaction of **1** with benzaldehyde and determination of the enantiomeric purity of alcohol **2**. The glycol from which **4** is derived and thus the reagent **1** are readily accessible in either enantiomeric form.[2, 9]

Experimental Procedure

A 0.85 M solution (6.0 mL, 5.1 mmol) of (1-methyl-2-butenyl)magnesium chloride (**3**) in THF was added dropwise over 15 min to a solution of (4*S*,5*S*)-2-isopropyloxy-4,5-dicyclohexyl-1,3,2-dioxaborolane (**4**; prepared from 1,2-dicyclohexylethane-1,2-diol and triisopropyl borate by distillative removal of the isopropanol) in 20 mL of THF at −78 °C. The solution was allowed to warm overnight to room temperature and the products were hydrolyzed by addition of a saturated solution (15 mL) of NH_4Cl. The aqueous phase was extracted with 3 × 20 mL of ether and the organic phase was dried over $MgSO_4$ and concentrated. The colorless oily residue was chromatographed with CH_2Cl_2 (column 30 × 2 cm, silica gel 60), affording 1.38 g (89%) of boronic ester **1**. For spectroscopic data and determination of the enantiomeric purity by addition to benzaldehyde, see [2].

Received: September 8, 1989 [Z 3544 IE]
German version: *Angew. Chem. 102* (1990) 62

CAS Registry numbers:
1, 105065-55-2; **3a**, 124316-45-6; **3c**, 79719-32-7; **4**, 124316-46-7; **5**, 124377-56-6; 1,2-dicyclohexylethan-1,2-diol, 120850-91-1; triisopropyl borate, 5419-55-6.

[1] K. Ditrich, T. Bube, R. Stürmer, R. W. Hoffmann, *Angew. Chem. 98* (1986) 1016; *Angew. Chem. Int. Ed. Engl. 25* (1986) 1028.
[2] R. W. Hoffmann, K. Ditrich, G. Köster, R. Stürmer, *Chem. Ber. 122* (1989) 1783.
[3] J. D. Morrison in J. D. Morrison (Ed.): *Asymmetric Synthesis, Bd. 1*, Academic Press, New York 1983, Chapter 1, p. 3.
[4] H. B. Kagan, J. C. Fiaud, *Top. Stereochem. 18* (1988) 249.
[5] H. Marsch, K. Harms, W. Massa, G. Boche, *Angew. Chem. 99* (1987) 706; *Angew. Chem. Int. Ed. Engl. 26* (1987) 696.
[6] D. A. Hutchison, K. R. Beck, R. A. Benkeser, J. B. Grutzner, *J. Am. Chem. Soc. 95* (1973) 7075.
[7] The borylation presumably proceeds with allylic inversion. The isomers **3d, d'** should be disfavored energetically owing to 1,3-allylic strain and therefore contribute little to the formation of **1**.
[8] M. Andersen, B. Hildebrandt, G. Köster, R. W. Hoffmann, *Chem. Ber. 122* (1989) 1777.
[9] E. N. Jacobsen, I. Markò, W. S. Mungall, G. Schröder, K. B. Sharpless, *J. Am. Chem. Soc. 110* (1988) 1968.

Inverse Amine-Stabilized Sulfenes $F_2C{=}SO_2$ and $FHC{=}SO_2$ **

By *Hans Pritzkow, Klaus Rall, Stefan Reimann-Andersen,* and *Wolfgang Sundermeyer**

Dedicatd to Professor Gerhard Fritz on the occasion of his 70th birthday

Over the past couple of decades several research groups have attempted the isolation of a sulfene $R_2C{=}SO_2$ (thione *S,S*-dioxide) in free form as a species analogous to SO_3,[1] but, owing to the exceptional reactivity of the C=S double bond, success has thus far only been achieved in demonstrating indirectly the existence of such a species in situ by (cyclo)additions. Double bonds between carbon and elements of the second or higher periods could, however, not only be stabilized by sterically demanding substituents but also by addition of Lewis bases to the element with the larger atomic radius. An earlier indication of the stabilization of sulfenes by tertiary amines[2] finally led to a better insight into the bonding in such adducts, in that we were able to isolate amine-stabilized sulfonylsulfenes **A** with quinuclidine as base.[3, 4]

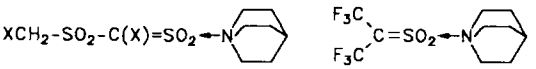

A, X = H, Cl, Br, CF_3, CH_3 **B**

X-ray structure analyses showed that quinuclidine normally coordinates to the sulfur atom with an S–N distance which is greater than that of an S–N single bond, irrespective of the type of substituents X on the sulfene carbon atom, and that the C–S distance (1.66 Å) almost equals that of an isolated C–S double bond. This is even more evident in the case of the first symmetrically substituted sulfene **B**, which was obtained, not under the usual "sulfene forming conditions (α-H-sulfonyl halide + amine) but by aminolysis of 1,3-dithietane *S*-oxides.[5] This implies that the resonance structure $R_2\overset{\ominus}{C}-\overset{\oplus}{S}O_2$ with the sulfur atom as electrophilic center[6, 7] is essential for a description of the electron distribution in sulfenes.

We have now succeeded, however, in obtaining definite proof that sulfenes can also be stabilized via the C atom (resonance structure $R_2\overset{\oplus}{C}-\overset{\ominus}{S}O_2$; inverse amine-stabilization). A first indication of the C atom having electrophilic character was obtained on attempting to synthesize dichlorosulfene, when trichloromethane sulfinate was formed by nucleophilic addition of chloride[8] (cf. also later works[9, 10]). According to all spectroscopic data, we had already obtained an inverse amine-stabilized sulfene $Me_3\overset{\oplus}{N}-CHF-SO_2^{\ominus}$ upon reaction of fluoromethanesulfonyl chloride **1** with trimethylamine; however, we were unable to isolate any crystals suitable enough for an X-ray structure analysis.[9] Whereas quinuclidine likewise adds inversely, but the product readily decomposes,[3] in the reaction of **1** with triethylamine the isolation and crystallization of the fluorosulfene adduct **2** (m.p. 159 °C (decomp.) is possible.

[*] Prof. Dr. W. Sundermeyer, Dr. H. Pritzkow, Dipl.-Chem. K. Rall, Dipl.-Chem. S. Reimann-Andersen
Anorganisch-chemisches Institut der Universität
Im Neuenheimer Feld 270, D-6900 Heidelberg 1 (FRG)

[**] This work was supported by the Deutsche Forschungsgemeinschaft (Priority program) and the Fonds der Chemischen Industrie.

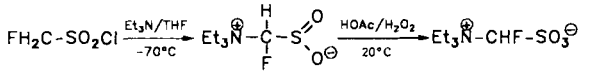

1 2 3

In the 84.7-MHz ^{19}F-NMR spectrum of **2** a doublet appears at $\delta = -164.8$ ($^2J_{HF} = 46.6$ Hz), and the 200-MHz ^{1}H-NMR spectrum[11] shows the expected diastereotropism of the methylene protons of the base as evidence of the addition to the sulfene C atom. The X-ray diffraction analysis of **2**[11] finally confirms the molecular structure (Fig. 1). Both

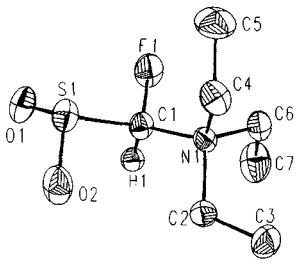

Fig. 1. Crystal structure of **2**. Important distances [Å] and angles [°]: S1–O 1.479(1), 1.485(1), S1–C1 1.904(1), C1–N1 1.515(2), C1–F1 1.370(2): O1–S1–O2 111.3(1), O1–S1–C1 96.7(1), O2–S1–C1 100.3(1), S1–C1–N1 117.9(1), S1–C1–F1 107.2(1), N1–C1–F1 107.1(1).

the C–N bond (1.515 Å) as well as the C–S bond (1.904 Å) are longer than the values quoted in the literature for C–N and C–S single bonds. By oxidation with peracetic acid, **2** can be converted into the corresponding sulfonate **3**,[12] which, like **2**, was characterized by its elemental analysis and mass spectrum.

The inverse amine-stabilized difluorosulfene **5** was obtained via a completely different route: by symmetrical ring cleavage of tetrafluoro-1,3-dithietane 1,1,3,3-tetroxide **4** with triethylamine.[13]

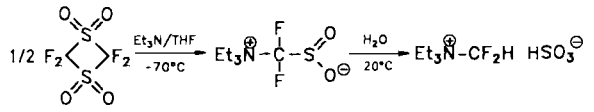

4 5 6

The 84.7-MHz ^{19}F-NMR spectrum of **5** shows a singlet at $\delta = -99.6$ ($(CD_3)_2SO$). The X-ray structure analysis reveals bond lengths comparable with those in **2** and confirms the inverse stabilization and the zwitterionic structure of the

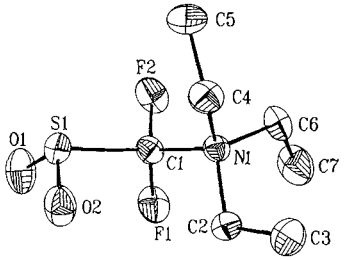

Fig. 2. Crystal structure of **5**. Important distances [Å] and angles [°]: S1–O 1.471(1), 1.470(2), S1–C1 1.949(2), C1–N1 1.521(2), C1–F 1.349(2), 1.346(2); O1–S1–O2 112.4(1), O1–S1–C1 96.7(1), O2–S1–C1 102.9(1), S1–C1–N1 120.3(1), S1–C1–F1 109.5(1), S1–C1–F2 106.5(1), N1–C1–F, 107.0(1), F1–C1–F2 105.7(1).

sulfene (Fig. 2). In contrast to **2**, **5** rapidly hydrolyzes to the (difluoromethyl)triethylammonium hydrogensulfite **6**.[14]

Thus, it could be demonstrated that sulfenes are usually coordinated by amines at the S atom, that they contain a C=S double bond in the adducts, and that they can be recovered again from the adducts. The two sulfenes $FHC{=}SO_2$ and $F_2C{=}SO_2$—the same may be expected of $H_2C{=}SO_2$, for which a structure analysis of the adduct has still to be carried out[15]—are, on the other hand, inversely amine-stabilized at the C atom. They are then present as zwitterions, have thereby lost all relation to the original sulfene, and react with cleavage of the C–S bond on attempted renewed recovery of the sulfene.

Received: August 17, 1989 [Z 3509 IE]
German version: *Angew. Chem. 102* (1990) 80

CAS Registry numbers:
1, 42497-69-8; **2**, 124462-75-5; **3**, 124481-52-3; **4**, 73090-23-0; **5**, 124462-76-6; **6**, 124462-78-8.

[1] B. G. Lenz, B. Zwanenburg, in *Houben-Weyl-Müller: Methoden der Organischen Chemie, Band E 11*, Thieme, Stuttgart 1985, p. 1326.
[2] G. Opitz, D. Bücher, *Tetrahedron Lett. 1966*, 5263.
[3] U. Hartwig, H. Pritzkow, W. Sundermeyer, *Chem. Ber. 121* (1988) 1435.
[4] J. Waldi, *Dissertation*, Universität Heidelberg 1989.
[5] U. Hartwig, H. Pritzkow, K. Rall, W. Sundermeyer, *Angew. Chem. 101* (1989) 224; *Angew. Chem. Int. Ed. Engl. 28* (1989) 221.
[6] G. Opitz, *Angew. Chem. 79* (1967) 161; *Angew. Chem. Int. Ed. Engl. 6* (1967) 107.
[7] L. A. Paquette, J. P. Freeman, R. W. Houser, *J. Org. Chem. 34* (1969) 2901.
[8] T. Kempe, T. Norin, *Acta. Chem. Scand. Ser. B 28* (1974) 609.
[9] U. Rheude, W. Sundermeyer, *Chem. Ber. 118* (1985) 2208.
[10] R. Allmann, W. Hanefeld, M. Krestel, B. Spangenberg, *Angew. Chem. 99* (1987) 1175; *Angew. Chem. Int. Ed. Engl. 26* (1987) 1133.
[11] **2**: space group *Pcab*; $a = 11.981(2)$, $b = 12.260(2)$, $c = 13.544(3)$ Å, $V = 1989$ Å^3, $Z = 8$. 2349 observed reflections ($I \geq \sigma_I$, two-circle diffractometer, $Mo_{K\alpha}$ radiation, ω scan). The refinement (S, F, O, N, C anisotropic, H isotropic) gave $R = 0.058$, $R_w = 0.059$ [16].—200-MHz ^{1}H NMR ($CDCl_3$): four signals in the ratio 9:3:3:1 at $\delta = 1.25$(t), 3.40(q), 3.75(q), 4.30(d, $^2J_{HF} = 46.6$ Hz).
[12] **3**: yield 81%: m.p. 193–194 °C.—90-MHz ^{1}H NMR ($(CD_3)_2SO$): three signals in the ratio 9:6:1 at $\delta = 1.36$(t), 3.75(m), 6.06 (d, $^2J_{HF} = 43.1$ Hz).—84.7-MHz ^{19}F NMR ($(CD_3)_2SO$): $\delta = -161.8$ (d, $^2J_{HF} = 43.1$ Hz).
[13] **5**: space group $P2_12_12_1$; $a = 8.460(5)$, $b = 9.161(5)$, $c = 12.989(7)$ Å, $V = 1007$ Å^3, $Z = 4$. 1807 observed reflections ($I \geq 2\sigma_I$, four-circle diffractometer, $Mo_{K\alpha}$ radiation, ω scan). The refinement (S, F, O, N, C anisotropic, H isotropic) yielded $R = 0.044$, $R_w = 0.044$ [16]; 90-MHz ^{1}H NMR ($(CD_3)_2SO$): two signals in the ratio 9:6 at $\delta = 1.36$(t), 3.78(q).
[14] **6**: 90-MHz ^{1}H NMR ($(CD_3)_2SO$): three signals in the ratio 9:6:1 at $\delta = 1.38$(t), 3.72(q), 7.47 (t, $^2J_{HF} = 57.1$ Hz).—84.7-MHz ^{19}F NMR ($(CD_3)_2SO$): $\delta = -111.2$ (d, $^2J_{HF} = 57.1$ Hz).
[15] J. F. King, S. Skonieczny, *Phosphorus Sulfur 1985*, 11.
[16] Further details of the crystal structure investigations are available on request from the Fachinformationszentrum Karlsruhe, Gesellschaft für wissenschaftlich-technische Information mbH, D-7514 Eggenstein-Leopoldshafen 2 (FRG), on quoting the depository number CSD-54097, the names of the authors, and the journal citation.

Synthesis and Structure of the Stable Tellurium Nitride $(ClTeNSN)_3N$ **

By *Herbert W. Roesky,* Jörg Münzenberg,* and *Mathias Noltemeyer*

All that is known about the tellurium nitrides that have been reported so far is that they are highly explosive.[1] Nothing

[*] Prof. Dr. H. W. Roesky, Dipl-Chem. J. Münzenberg, Dr. M. Noltemeyer
Insitut für Anorganische Chemie der Universität
Tammannstrasse 4, D-3400 Göttingen (FRG)

[**] This work was supported by the Deutsche Forschungsgemeinschaft, the Volkswagen Foundation, and the Fonds der Chemischen Industrie.

is known about their structure or their bonding, and even their stoichiometry is still a matter of debate. In connection with our studies on metal- and nonmetal-nitrogen compounds we recently reported the synthesis of a titanium imide nitride in which the imide and nitride functions are bridged by titanium atoms. We were surprised to find that this compound first decomposes above 200 °C.[2] This prompted us to try to stabilize tellurium-nitrogen bonds in the same way by bridge functions.[3] We now report on a tellurium nitride that is stable and non-explosive at room temperature.

For the synthesis of $(ClTeNSN)_3N$ **3**, tellurium(IV) chloride **1** was allowed to react with *N,N'*-bis(trimethylsilyl)sulfur diimide **2** in the molar ratio 1:1 (with slight excess of **2**) at 0 °C in toluene. Cleavage of chlorotrimethylsilane (other byproducts could not be unequivocally characterized) resulted in formation of **3** as a yellow solid, which decomposed violently above 207 °C. An elemental analysis[4] confirmed the composition of **3** and gave no indication of a compound of the initially expected composition Cl_2TeN_2S.[5] In the FD-mass spectrum, only Te_2Cl_2NSN is observed as heaviest fragment (*m/z* 388, ^{128}Te, ^{130}Te).

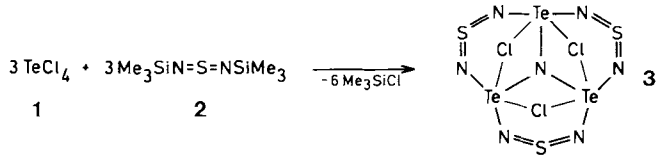

Final proof of the structure of **3** followed from the X-ray structure analysis of crystals which were obtained from dimethylformamide (DMF). Three molecules of DMF are coordinated via the oxygen atoms to the tellurium atoms of **3** (Fig. 1).

The three tellurium atoms form a puckered twelve-membered ring with the three bridging NSN ligands and a six-membered ring with the three bridging chlorine atoms. In the plan view (Fig. 1, top) it is clear that the three tellurium atoms are bridged by a further nitrogen atom, N(1).[6] The side view (Fig. 1, bottom) shows the trigonal-pyramidal arrangement of the $Te_3N(1)$ unit. The Te^{IV} atoms in **3**·3 DMF have a distored octahedral environment, as has already been described for $(TeCl_4)_4$.[7] The DMF molecules bound to the free coordination sites of the Te atoms are, according to the large Te–O distance (250.5 pm), only weakly coordinatively bound. The Te–N(1) bond lengths (mean value 206.1 pm) lie in the same range as those of known compounds with covalent Te–N bonding ($PhC(NSiMe_3)_2TeCl_3$ 209.6 pm;[8] $(Ph_3PNTeCl_3)_2$ 199.6 pm[3]). Also the remaining six Te–N bonds are of comparable length (mean value 203.3 pm). The S–N (mean 152.4 pm) and Te–Cl distances (mean 284.5 pm) are consistant with those in $Me_4Si_2N_4S_2$[9] (mean value 150.7 pm) and $[Te_3Cl_{13}]^{\ominus}$[10] (mean value 284.1 pm),[11] respectively. In the titanium compound[2] mentioned at the beginning the nitridic nitrogen deviates 104 pm from the plane of the metal atoms, whereas in the case of the tellurium compound **3** the deviation is only 40 pm.

The incorporation of the nitridic nitrogen atom could proceed via an $NS^{\oplus}$ ion, in analogy to the observation made by *Martinengo* et al.,[12] that $[Co_6N(CO)_{15}]^{\ominus}$ is formed from the nitrogen-free complex dianion and nitrosyl tetrafluoroborate. Summarizing, it can be established that: compound **3** is the first structurally confirmed tellurium nitride and at the same time the first compound in which three atoms are bound via NSN ligands to give a twelve-membered ring and the first compound that contains several TeN_3 units as structural groups.

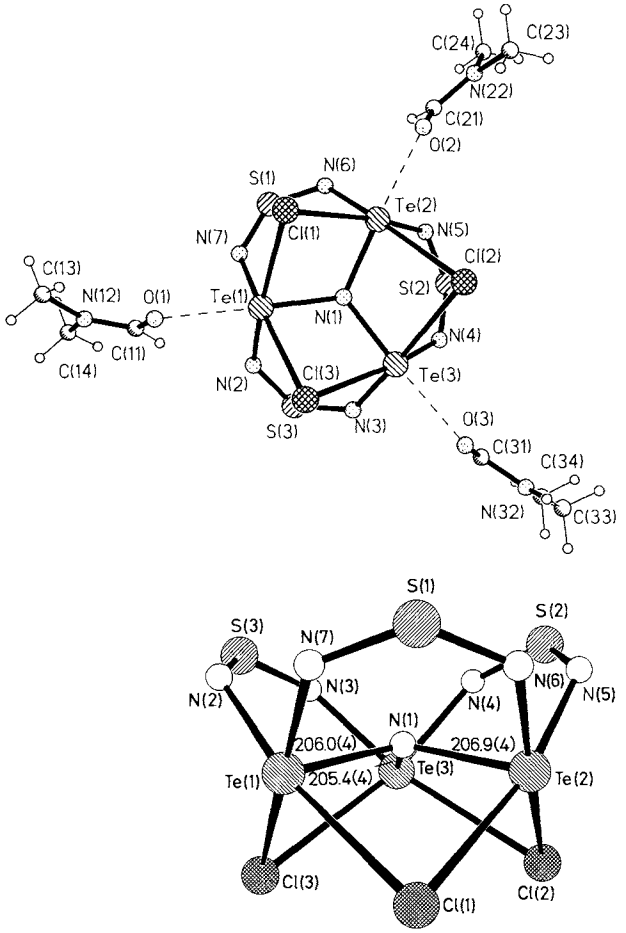

Fig. 1. Crystal structure of **3**·3 DMF. Above: top view. Below side view of the molecule without DMF molecules. Selected bond lenghts [pm] and angles [°]: Te(1)-Cl(1) 285.9(2), Te(1)-N(1) 206.0(4), Te(1)-N(7) 201.6(4), Te(1)-Cl(3) 282.6(2), Te(1)-N(2) 203.0(4), Te(2)-Cl(1) 283.7(2); Cl(1)-Te(1)-Cl(3) 99.6(1), Cl(1)-Te(1)-N(1) 80.9(1), Cl(3)-Te(1)-N(1) 82.0(1), Cl(1)-Te(1)-N(2) 169.8(1), Cl(3)-Te(1)-N(2) 85.3(1), N(1)-Te(1)-N(2) 91.0(2), Cl(1)-TeC1)-N(7) 87.3(1), N(1)-Te(1)-N(7) 91.3(2), N(2)-Te(1)-N(7) 86.7(2).

Experimental

A solution of **1** (3.50 g, 13 mmol) in toluene (120 mL) was treated dropwise at 0 °C with a solution of **2** (3.10 g, 15 mmol) in toluene (40 mL). The solution turned orange and a yellow solid precipitated. This was filtered off and washed with chloroform. 2.2 g (74%) of **3** was obtained. Recrystallization from dimethylformamide afforded, after several days storage at room temperature, yellow crystals of the composition $(ClTeNSN)_3N$·3 DMF. We cannot say with certainty whether a rearrangement takes place during the recrystallization. The solvate-free compound melts with decomposition at 207 °C.—IR: $\tilde{\nu}$[cm^{-1}] = 1120 vs sh, 1090 s, 1060 s, 1060 vs sh, 680 s, 570 s, 520 s. A ^{125}Te-NMR spectrum could not be obtained because of the sparing solubility of **3** in DMF. Nor could a suitable nitrogen-free solvent be found for ^{15}N-NMR investigations.

Received: August 16, 1989 [Z 3505 IE]
German version: *Angew. Chem. 102* (1990) 73

[1] H. Garcia-Fernandez, *Bull. Soc. Chim. Fr. 1973*, 1210; *C. R. Hebd. Seance Acad. Sci. 258* (1964) 2579; O. Schmitz-DuMont, B. Ross, *Angew. Chem. 79* (1967) 1061; *Angew. Chem. Int. Ed. Engl. 6* (1967) 1071.
[2] H. W. Roesky, Y. Bai, M. Noltemeyer, *Angew. Chem. 101* (1989) 788; *Angew. Chem. Int. Ed. Engl. 28* (1989) 754.
[3] J. Münzenberg, H. W. Roesky, M. Noltemeyer, *Chem. Ber. 122* (1989) 1915.
[4] Analysis of **3** (M_r = 683.39): found (calcd.): N 14.2% (14.35), Cl 16.4 (15.57).
[5] According to A. V. Zibarev, G. G. Furin, G. G. Yakobson, Izv. *Akad. Nauk SSR Ser. Khim. 12* (1985) 2775, $Te_3N_2SCl_2$ should be formed from **1** and **2**. This compound, however, has not been unequivocally characterized.

[6] Compare: C. Spang, F. T. Edelmann, M. Noltemeyer, H. W. Roesky, *Chem. Ber. 122* (1989) 1247.
[7] B. Buss, B. Krebs, *Angew. Chem. 82* (1970) 446; *Angew. Chem. Int. Ed. Engl. 9* (1970) 463; *Inorg. Chem. 10* (1971) 2795.
[8] E. Hey, C. Ergezinger, K. Dehnicke, *Z. Naturforsch. B44* (1989) 205.
[9] H. W. Roesky, *Angew. Chem. 91* (1979) 112; *Angew. Chem. Int. Ed. Engl. 18* (1979) 91.
[10] B. Krebs, V. Paulat, *Angew. Chem. 85* (1973) 662; *Angew. Chem. Int. Ed. Engl. 12* (1973) 666.
[11] **3**·3 DMF (M_r = 902.7): space group $P2_1/c$, a = 1205.3(6), b = 1104.3(6), c = 2040.8(10) pm, β = 100.92(3)°, V = 2.6672 nm^3, Z = 4, δ_{calcd} = 2.25 × 10^6 gm^{-3}, $\mu(Mo_{K\alpha})$ = 3.83 mm^{-1}, crystal dimensions 0.4 × 0.4 × 0.4 mm^3, STOE four-circle diffractometer, 4657 reflections up to 2θ = 45°, 3463 symmetry independent and 3156 with $F_0 > 3\sigma(F_0)$ used in the refinement (SHELX 76): R = 0.025 R_w = 0.027, $w^{-1} = \sigma^2(F_0) + 0.0001\,F_0^2$.—Further details of the crystal structure investigation are available on request from the Fachinformationszentrum Karlsruhe, Gesellschaft für wissenschaftlich-technische Information mbH, D-7514 Eggenstein-Leopoldshafen 2 (FRG), on quoting the depository number CSD-54036, the names of the authors, and the journal citation.
[12] S. Martinengo, G. Ciani, A. Sironi, B. T. Heaton, J. Mason, *J. Am. Chem. Soc. 101* (1979) 7095.

The Ultimate Carcinogen, *O*-Acetyl-*N*-(2-fluorenyl)hydroxylamine ("*N*-Acetoxy-2-aminofluorene"), and Its Reaction in vitro to Form 2-[*N*-(Deoxyguanosin-8-yl)amino]fluorene **

By *Ferdinand Bosold* and *Gernot Boche* *

After 2-acetylaminofluorene (**1a**) had been patented in 1940 as an insecticide (although it was never used), it became the most widely studied model carcinogen for aromatic amines owing to its high toxicity.[1]

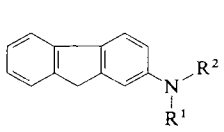

1a, $R^1 = COCH_3$, $R^2 = H$
1b, $R^1 = H$, $R^2 = OCOCH_3$
1c, $R^1 = COCF_3$, $R^2 = OCOCH_3$
1d, $R^1 = H$, $R^2 = OH$

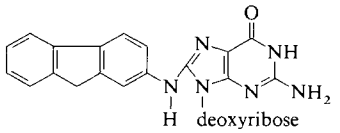

2

Not **1a** but rather the metabolite *O*-acetyl-*N*-(2-fluorenyl)hydroxylamine ("*N*-acetoxy-2-aminofluorene", **1b**) was thereby strongly implicated as an important ultimate carcinogen.[2, 3] Thus, primarily (80%) 2-[*N*-(deoxyguanosin-8-yl)amino]fluorene (**2**), that is, a DNA adduct, was isolated from rat liver (after DNA cleavage). Compound **2**, which bears no acetyl group on the fluorenylamine N atom,[4] has also been isolated from rat kidney and liver[5a] as well as from the bladder and liver of dogs.[5b] Also noteworthy is the high persistence in vivo of the DNA adduct containing **2** as a structural element.[6] Isomeric adducts in which the deoxyguanosine (dG) moiety is bonded, for example, to one of the ring C atoms of the aminofluorene moiety, have not been found. Reaction of an oligonucleotide with *O*-acetyl-*N*-(2-fluorenyl)-*N*-(trifluoroacetyl)hydroxylamine (**1c**) also afforded **2** (after DNA cleavage) as the sole adduct, thus indicating that **1b** is the active species.[7] All attempts to isolate the putative species **1b**, either formed in vivo or in vitro, or to synthesize it and study its reactivity with (bio)nucleophiles, have failed so far.[8] Here we describe the preparation of the title compound **1b** and its reaction in vitro with dG, which affords **2** as the sole adduct.[9]

1d $\xrightarrow[\text{THF, } \leq -40\,^\circ C]{CH_3CO-CN,\ Et_3N}$ **1b** $\xrightarrow[-40 \text{ to } 20\,^\circ C]{dG,\ H_2O/THF}$ **2** (14%)

Compound **1b** was prepared, in analogy to the procedure of *Prabhakar, Lobo,* and *Marques*,[10] from *N*-(2-fluorenyl)-hydroxylamine (**1d**) and acetyl cyanide in tetrahydrofuran (THF) at ≤ −40 °C. The crystalline product rapidly decomposes above −40 °C,[11] so that elemental analysis and mass-spectrometric analysis were not possible and the characterization had to be based on the ^{1}H NMR spectrum (see *Experimental Procedures*). Reaction of **1b** with dG was accomplished by adding an aqueous solution of dG to **1b** in THF at −40 °C. Noteworthy is the 14% yield of the dG adduct **2**, since the yields of the corresponding dG adducts of the *N*-acetoxyarylamines studied in Ref. [11] are at least a factor of two smaller.

In conclusion, since, in vivo and in the reaction of **1c** with an oligonucleotide, as described above, only the one non-*N*-acetylated dG adduct **2** is formed, the sole formation of **2** in the reaction of the title compound **1b** with dG is strong evidence that **1b** is indeed the ultimate carcinogen, which also leads in this case (if not generally[3]) to **2**.

Experimental Procedures

1b: A solution of acetyl cyanide (690 mg, 10.0 mmol) in 25 mL of THF was added dropwise to a vigorously stirred solution of **1d** (1.97 g, 10.0 mmol) and Et_3N (1.11 g, 11.0 mmol) in 50 mL of THF cooled to −40 to −50 °C. The temperature should not be allowed to rise above −40 °C! After 2 h, approximately 50 mL of THF was removed under vacuum and 30 mL of petroleum ether (b.p. 40–60 °C) cooled to −40 °C was added. After immediate filtration (frit at −78 °C), the filtrate was diluted with 180 mL of petroleum ether (b.p. 40–60 °C; −40 °C) and kept at −78 °C for about 1 h. The resulting colorless crystals were collected by filtration at −78 °C, washed with petroleum ether (−78 °C), dried under vacuum at −40 °C, and stored at −78 °C. Yield: 1.43 g (60%). Rapid decomposition occurs above −40 °C, the material turning black. ^{1}H NMR (400 MHz, [D$_8$]THF, 233 K): δ = 2.18 (s, 3H, CH_3), 3.84 (s, 2H, CH_2), 6.99 (d, 1H, aryl-H), 7.20 (s, 1H, aryl-H), 7.21 (d, 1H, aryl-H), 7.30 (t, 1H, aryl-H), 7.49 (d, 1H, aryl-H), 7.70 (d, 1H, aryl-H), 7.71 (t, 1H, aryl-H), 9.77 (s, broad, 1H, N-H).

2: dG (800 mg, 3.00 mmol) in 30 mL of H_2O was added to **1b** (0.72 g, 3.00 mmol) in 80 mL of THF at −40 °C. After the reaction mixture had warmed to room temperature, 100 mL of H_2O was added, the mixture was extracted with ether, and the ether phase was discarded. After addition of a further 200 mL of H_2O, the mixture was extracted eight times with ether. Compound **2** crystallized from the ether phase. The purification of **2** (and the search for other possible adducts) was carried out by chromatography with a special GC instrument (Chromatotron) ($CHCl_3$:CH_3OH = 7:3 on silica gel 60PF). Yield: 190 mg (14%). Compound **2** was characterized by comparison of its ^{1}H NMR spectrum with that of an authentic sample [4d].

Received: August 14, 1989 [Z 3496 IE]
German version: *Angew. Chem. 102* (1990) 99

CAS Registry numbers:
1b, 64253-17-4; **1d**, 53-94-1; **2**, 73051-69-1; dG, 961-07-9; acetyl cyanide, 631-57-2.

[*] Prof. Dr. G. Boche, F. Bosold
Fachbereich Chemie der Universität
Hans-Meerwein-Strasse, D-3550 Marburg (FRG)

[**] This work was supported by the Deutsche Forschungsgemeinschaft, the Fonds der Chemischen Industrie, and BASF AG.

[1] T. S. Scott: *Carcinogenic and Chronic Toxic Hazards of Aromatic Amines*, Elsevier, Amsterdam 1962.
[2] a) C. M. King, I. B. Glowinski, *EHP Environ. Health Perspect. 43* (1983) 42; b) C. M. King, *Cancer Res. 34* (1974) 1403; c) W. T. Allaben, C. M. King, *J. Biol. Chem. 259* (1984) 12128; d) T. J. Flammang, F. F. Kadlubar in A. R. Boobies, J. Caldwell, F. DeMatteis, C. R. Elcombe (Eds.): *Microsomes and Drug Oxidations*, Taylor and Francis, London 1985, p. 190; e) S. S. Thorgeirsson in H. Greim, R. Jung, M. Kramer, H. Marquardt, F. Oesch (Eds.): *Biochemical Basis of Chemical Carcinogenesis*, Raven Press, New York 1984, p. 47; f) C.-C. Lai, E. C. Miller, J. A. Miller, A. Liem, *Carcinogenesis 9* (1988) 1295.
[3] *N*-Sulfoxy-2-aminofluorene is presumably the ultimate carcinogen in the livers of young male C57B1/6JxC3H/HeJF$_1$ (B6C3F$_1$) mice: C.-C. Lai, J. A. Miller, E. C. Miller, A. Liem, *Carcinogenesis 6* (1985) 1037; see also [2f].
[4] a) C. C. Irving, R. A. Veazey, *Cancer Res. 29* (1969) 1799; b) E. Kriek, *Chem. Biol. Interact. 1* (1969) 3; c) E. Kriek, *Cancer Res. 32* (1972) 2042;

d) E. Kriek, J. G. Westra, *Carcinogenesis 1* (1980) 459; e) Review: F. A. Beland, F. F. Kadlubar, *EHP Environ. Health Perspect. 62* (1985) 19; f) Review: H.-G. Neumann, *J. Cancer Res. Clin. Oncol. 112* (1986) 100.
[5] a) W. T. Allaben, C. C. Weis, N. F. Fullerton, F. A. Beland, *Carcinogenesis 4* (1983) 1067; b) H. P. Morris, W. H. Eyestone, *J. Natl. Cancer Inst. (US) 13* (1953) 1139.
[6] F. A. Beland, K. L. Dooley, C. D. Jackson, *Cancer Res. 42* (1982) 1348.
[7] D. L. Johnson, T. M. Reid, M.-S. Lee, C. M. King, L. J. Romano, *Biochemistry 25* (1986) 449.
[8] A. C. Huggett, J. L. Cone, S. S. Thorgeirsson, P. P. Roller, *J. Org. Chem. 52* (1987) 4933, and references therein; see also [11] and references therein.
[9] Conformation of **2** and reaction of **1b** with the model nucleophile *N*-methylaniline: M. Famulok, F. Bosold, H. George, A. Heimbel, C. Meier, S. Schröder, G. Boche, *Chem Ber.*, in press.
[10] S. Prabhakar, A. M. Lobo, M. M. Marques, *Tetrahedron Lett. 23* (1982) 1391.
[11] The recently reported *N*-acetoxy compounds of β-naphthylamine (M. Famulok, F. Bosold, G. Boche, *Tetrahedron Lett. 30* (1989) 321), 4-aminobiphenyl (M. Famulok, F. Bosold, G. Boche, *Angew. Chem. 101* (1989) 349; *Angew. Chem. Int. Ed. Engl. 28* (1989) 337), and aniline (M. Famulok, G. Boche, *ibid. 101* (1989) 470 and *28* (1989) 468) are much more stable than **1b**.

Elucidation of the Structure of Hormaomycin **

By *Ellen Rössner, Axel Zeeck,** and *Wilfried A. König*

Dedicated to Professor Hans Zähner on the occasion of his 60th birthday

The novel peptide lactone hormaomycin produced by *Streptomyces griseoflavus* is selectively active against some gram-positive bacteria, and, in addition, influences both aerial mycelium formation as well as the production of secondary metabolites.[1] It thus belongs to the intercellular signal substances, of which the A factor (Khokhlov factor) is thus far the best known.[2] Hormaomycin differs fundamentally in its structure, however, from this comparably simple γ-lactone. Such signal substances are attracting increasing interest for the exploration of microbial secondary metabolism.[3] We report here on the elucidation of the structure of hormaomycin.

Hormaomycin, $C_{55}H_{69}ClN_{10}O_{14}$, contains the known amino acids *allo*-threonine (a-Thr), isoleucine (Ile) and (3-methyl)phenylalanine (Phe(3-Me)) as well as the new amino acids 4-[(*Z*)-propenyl]proline (Pro(4-Pe)) and 3-(2-nitrocyclopropyl)alanine (Ala(3-Ncp)). Phe(3-Me) and Ala(3-Ncp) each occur twice in the molecule. NMR and mass spectra point to an acylation of the N-terminal of the peptide chain by chlorine-containing *N*-hydroxypyrrole-2-carboxylic acid (Chpca).[1]

To determine the stereochemistry of the known amino acids (a-Thr, Ile, Phe(3-Me)) the acidic total hydrolyzate of hormaomycin (6N HCl/glacial acetic acid 1/1, 110 °C, 48 h), after esterification with methanol/HCl and acetylation with trifluoroacetic anhydride $(Tfa)_2O$, was analyzed chromatographically on Chirasil-Val[4] or XE-60-α-pea.[5] The amino acids known to be contained in hormaomycin could be identified as D-*allo*-threonine, L-isoleucine, and L-*threo*-(3-methyl)phenylalanine (two molecules).[1b] The stereochemistry of the new amino acids (2 × Ala(3-Ncp), Pro(4-Pe)) could not be determined by this method without the synthesis of suitable reference compounds.

The OH group of D-*allo*-threonine is esterified, as is recognizable by the downfield position of the β-CH signal of the a-Thr building block ($\delta = 5.35$) in the ^{1}H-NMR spectrum (200 MHz, $CDCl_3$) of hormaomycin. The amino acid participating with the C-terminal in the lactone bonding was determined by reduction of the ester group with $LiAlH_4$ (four mol equivalents $LiAlH_4$, THF, 0 °C, 3 h). After derivatization *N,O*-bis(trifluoroacetyl)-4-[(*Z*)-propenyl]prolinol ($m/z = 333$ ($[M]^{\oplus}$), 206 ($[M-CH_2OCOCF_3]^{\oplus}$)) could be detected in the GC/MS analysis of the hydrolyzed reaction product. The results of the structure elucidation so far indicate the partial formula **1** in which Ⓧ and Ⓨ are peptide chains of five amino acids (L-Ile, 2 × L-*threo*-Phe(3-Me), 2 × Ala(3-Ncp)).

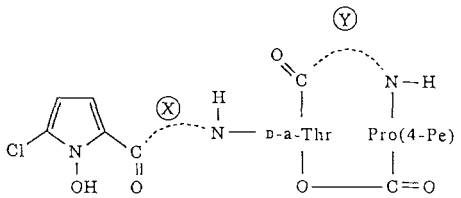

1

The sequences in the peptide lactone ring and in the side chain could be clarified by combining the results of several mass spectrometric and NMR spectroscopic investigations. Partial hydrolyzates of hormaomycin (e.g. 12 N HCl/glacial acetic acid 1/1, room temperature, 48 h) contained two tripeptides, which were identified as the trifluoroacetylated methyl esters by GC/MS coupling (Table 1).

Table 1. Peptides contained in the partial hydrolyzates of hormaomycin (derivatized to trifluoroacetylated methyl esters).

Peptide	Characteristic ions in the EI-mass spectrum (*m/z*)
N-Tfa-Phe(3-Me) · Ile-OCH_3	402 $[M]^{\oplus}$, 230 $[M-(OC\text{-}Ile\text{-}OCH_3)]^{\oplus}$
N,O-Bis(Tfa)-a-Thr · Phe(3-Me)-OCH_3	427 $[M-COOCH_3]^{\oplus}$, 266 $[M-OC\text{-}Phe(3\text{-}Me)\text{-}OCH_3)]^{\oplus}$, 192 $[Phe(3\text{-}Me)\text{-}OCH_3]^{\oplus}$
N-Tfa-Phe(3-Me) · Ile · Pro(4-Pe)-OCH_3	539 $[M]^{\oplus}$, 371 $[M-(Pro(4\text{-}Pe)\text{-}OCH_3)]^{\oplus}$, 230 $[M-(OC\text{-}Ile\cdot Pro(4\text{-}Pe)\text{-}OCH_3)]^{\oplus}$, 168 $[Pro(4\text{-}Pe)\text{-}OCH_3]^{\oplus}$

The open-chain hormaomycin methyl ester **2** (see Scheme 1), which no longer exhibits a biological activity comparable with hormaomycin,[1c] proved to be an important derivative for the mass spectrometric investigation. **2** is readily accessible from hormaomycin (methanol, catalytic amounts of K_2CO_3, room temperature, 12 h).[1a] Its FAB mass spectrum shows a sequence of ions, all of which can be characterized (Scheme 1). The successive cleavage of Pro(4-Pe)-OCH_3, Ile, and Phe(3-Me) starting from the esterified C-terminal of the peptide chain confirms the sequence of the tripeptide Phe(3-Me) · Ile · Pro(4-Pe) detected in the partial hydrolyzate. All the quoted fragment ions excluding the fragment *m/z* 418 show the typical isotopic

[*] Prof. Dr. A. Zeeck, Dr. E. Rössner
Institut für Organische Chemie der Universität
Tammannstrasse 2, D-3400 Göttingen (FRG)
Prof. Dr. W. A. König
Institut für Organische Chemie der Universität
Martin-Luther-King-Platz 6, D-2000 Hamburg 13 (FRG)

[**] This work was supported by the Deutsche Forschungsgemeinschaft (Ze 120/14-1). We thank Priv.-Doz. Dr. *H. Wolf*, Stuttgart, and Dr. *N. Andres*, Tübingen, for supplying the crude hormaomycin and Herrn Dipl.-Chem. *R. Machinek* for recording the ROESY spectra.

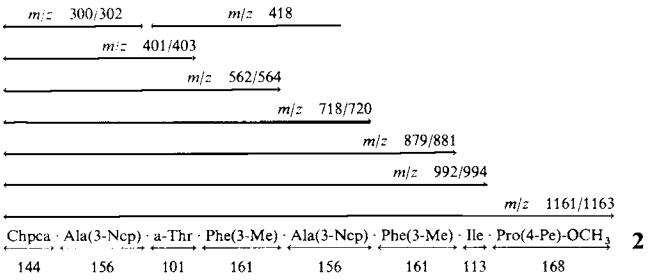

Scheme 1. Sequence ions of hormaomycin methyl ester **2** in the FAB-mass spectrum (*m*-nitrobenzyl alcohol as matrix, positive ions). Ion pairs with $\Delta(m/z) = 2$ confirm the presence of a Cl atom (m/z 1161, $[M + H]^{\oplus}$ for ^{35}Cl). The molecular weights of the individual building blocks are given below.

distribution for a Cl atom. As can be deduced from Scheme 1, the fragment m/z 418 is formed by cleavage of the amide bonds at the two Ala(3-Ncp) building blocks. The FAB-mass spectrum also shows a fragment ion of high intensity at m/z 144/146. It arises from the Cl-containing Chpca building block, which hitherto could not be detected in the total and partial hydrolyzates of hormaomycin. The sequence thus derived for the open-chain methyl ester **2** can be assumed for the natural product. The partial formula **1** can thus be extended as follows: Ⓧ = Ala(3-Ncp), Ⓨ = Phe(3-Me) · Ala(3-Ncp) · Phe(3-Me) · Ile.

ROESY(rotating-frame Overhauser enhancement spectroscopy)-NMR experiments[6] on the intact natural product could independently confirm parts of the sequence. Most of the numerous NOE effects[1b] are of no significance for the sequence analysis, but can be helpful for the (still outstanding) conformational analysis of the lactone ring. The NOE effects from the ROESY spectrum of hormaomycin that are of significance for a sequence analysis are collected in Table 2; however, the complete sequence could not be derived in this way.

Table 2. NOE effects between neighboring amino acids in the ^{1}H-ROESY-NMR spectrum (200 MHz, $CDCl_3$) of hormaomycin.

Amino acid	δ_H	Amino acid	δ_H
Ala(3-Ncp) I	3.49 (H_α)	Phe(3-Me) I	6.80 NH)
Phe(3-Me) II	4.37 (H_α)	Ala(3-Ncp) I	6.58 (NH)
Ala(3-Ncp) II	5.15 (H_α)	a-Thr	9.08 (NH)
Ile	4.62 (H_α)	Pro(4-Pe)	3.98 (5-H_b)

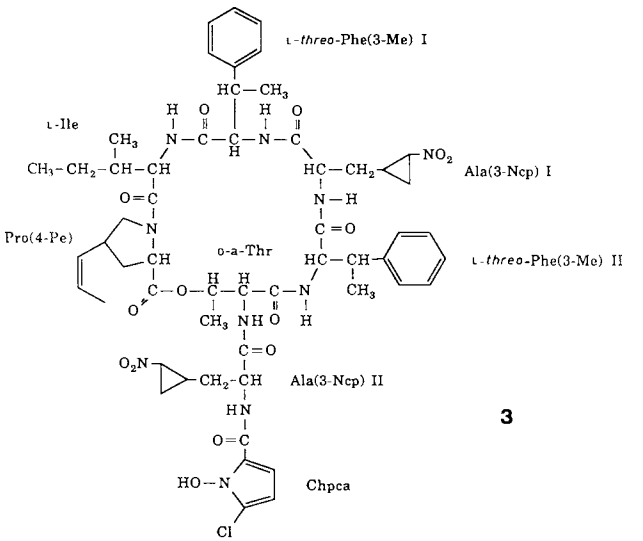

3

The combined data quoted here yielded the constitution **3** for hormaomycin. Peptide lactones of this structural type have hitherto not been described as microbial secondary metabolites.

Received: August 18, 1989 [Z 3512 IE]
German version: *Angew. Chem. 102* (1990) 84

CAS Registry numbers:
2, 124177-47-5; *N*-Tfa-Phe(3-Me)-Ile-OCH_3, 124177-48-6; *N,O*-Bis(Tfa)-a-Thr-Phe(3-Me)-OCH_3, 124177-49-7; *N*-Tfa-Phe(3-Me)-Ile-Pro(4-Pe)-OCH_3, 124177-50-0; hormaomycin, 121548-21-8.

[1] a) N. Andres, H. Wolf, H. Zähner, E. Rössner, A. Zeeck, W. A. König, V. Sinnwell, *Helv. Chim. Acta 72* (1989) 426; b) E. Rössner, *Dissertation*, Universität Göttingen 1989; c) N. Andres, *Dissertation*, Universität Tübingen 1989.

[2] a) A. S. Khokhlov, L. N. Anisova, I. I. Tovarova, E. M. Kleiner, I. V. Kovalenko, O. I. Krasilnikova, E. Y. Kornitskaya, S. A. Pliner, *Z. Allg. Mikrobiol. 13* (1973) 647; b) E. M. Kleiner, S. A. Pliner, V. S. Soifer, V. V. Onoprienko, T. A. Balashova, B. V. Rosynov, A. S. Khokhlov, *Bioorg. Khim. 2* (1976) 1142; c) K. Mori, *Tetrahedron Lett. 22* (1981) 3431; d) *Tetrahedron 39* (1983) 3107.

[3] a) U. Gräfe, I. Eritt, F. Hänel, W. Friedrich, M. Roth, B. Röder, E. J. Bormann in H. Kleinkauf, H. von Döhren, H. Dornauer, G. Nesemann (Eds.): *Regulation of Secondary Metabolite Formation*, VCH Verlagsgesellschaft, Weinheim 1986, p. 225; b) H. Ohashi, Y. Zheng, T. Nihira, Y. Yamada, *J. Antibiot. 42* (1989) 1191.

[4] H. Frank, G. J. Nicholson, E. Bayer, *J. Chromatogr. Sci. 15* (1977) 174.

[5] I. Benecke, W. A. König, *Angew. Chem. 94* (1982) 709; *Angew. Chem. Int. Ed. Engl. 21* (1982) 709; *Angew. Chem. Suppl. 1982*, 1605.

[6] a) H. Kessler, C. Griesinger, R. Kerssebaum, K. Wagner, R. R. Ernst, *J. Am. Chem. Soc. 109* (1987) 607; b) H. Kessler, M. Gehrke, C. Griesinger, *Angew. Chem. 100* (1988) 507; *Angew. Chem. Int. Ed. Engl. 27* (1988) 490.

$[BP_2]^{3\ominus}$ and $[BAs_2]^{3\ominus}$, Zintl Anions with Propadiene Structure

By *Hans-Georg von Schnering,* Mehmet Somer, Martin Hartweg,* and *Karl Peters*

Dedicated to Professor Christoph Rüchardt on the occasion of his 60th birthday

Depending on the elements involved and on the state of aggregation, triatomic 16-electron systems display all conceivable forms of coupling and bond orders, be it in monomers such as $BeCl_2(g)$, CO_2, ClCN and N_2O, in oligomers such as $(BOCl_3)_3$, or in the various polymers with different coordination, e.g. compounds of the structure type SiO_2, SiS_2, AlOCl, SnO_2, CaF_2 etc. Such variations can also be realized as partial structures in salt-like compounds, if a formal transfer of electrons from electropositive cations to an anion $[MX_2]^{n\ominus}$ is assumed as described by *Zintl*[1]. The expression $(e_M + 2e_X + ne) = 16$ holds true for the electron balance, and interatomic linkages as are found in the above mentioned compounds are expected for the partial structure of $[MX_2]^{n\ominus}$. In the case of heteroaromatic polyanions this treatment naturally contains a certain arbitrariness, which becomes apparent with big differences between M and X (M also "cation", formation of isolated $X^{m\ominus}$ anions); nevertheless, it is extremely valuable for systematic considerations and for the planning of syntheses. *Juza* et al.[2] have already detected polymeric partial structures $^3_\infty[MX_{4/2}]^{3\ominus}$ with tetra-

[*] Prof. Dr. H. G. von Schnering, Dr. M. Somer, Dr. M. Hartweg, Dr. K. Peters
Max-Planck-Institut für Festkörperforschung
Heisenbergstr. 1, D-7000 Stuttgart 80 (FRG)

hedral coordination of M for Li_3AlN_2 and Li_3GaN_2 as well as for Li_3AlP_2 and Li_3AlAs_2. Topological variants of these three-dimensional network structures are known with $^3_\infty[MX_{4/2}]^{2\ominus}$ (M = Si, Ge, Sn; X = P, As)[3] and with $^3_\infty[MX_{4/2}]^{1\ominus}$ ($M^{\oplus}$, $X^{2\ominus}$).[4] Tetrahedral chains of the SiS_2-type structure characterize the partial structures $^1_\infty[MX_{4/2}]^{n\ominus}$ of K_2SiP_2,[5] Rb_2SiAs_2,[6] and Na_3AlAs_2.[7] Especially interesting, however, are the isolated linear propadienes such as $[CN_2]^{2\ominus}$ and $[BN_2]^{3\ominus}$, because of their properties as synthetic building blocks (synthons), even though units like $[NiO_2]^{2\ominus}$[8] and $[ZnP_2]^{4\ominus}$[9] differ only slightly from them.

Ternary boron phosphides and arenides were hitherto unknown. They are formed from the elements or even from BP and/or BAs respectively at 1000–1100 K.[10] We obtained K_3BP_2 **1** and K_3BAs_2 **2** as bright yellow crystals and yellow-red crystals, respectively. X-ray structure analyses [11] and vibrational spectra confirm the presence of propadiene systems. The bond lengths $d_{B-P} = 176.7$ and $d_{B-As} = 186.8$ pm, have a Pauling bond order PBO = 1.9, and compare very well with those expected for double bonds, based on the bond distances in BP and BAs taken as single bonds ($d_1 = 196.5$ and 206.9 pm). As expected, the bonds are somewhat weaker than in $[BN_2]^{3\ominus}$[12] ($d_{B-N} = 133.6$ pm; $d_1 = 156.5$ pm; PBO = 2.1), whose propadiene structure was already established spectroscopically by *Goubeau* and *Anselment*[13] in 1961. The bond length and bond order in the anion $[BP_2]^{3\ominus}$ complement the corresponding values in the phosphorus analogues of borazine $R_3R'_3(BP)_3$[14] ($d_{B-P} = 184$ pm, PBO = 1.5) quite well.

The crystal structure (Fig. 1) of the isotypic compounds **1** and **2** is a model example for illustrating Nature's economy in matching widely different local building blocks to simple, optimum ensembles. A molecular 1,2,3-tripotassium diphosphaboracyclopropane could, e.g., satisfy the classical valences of all atoms in **1**, but not the striving for a higher coordination of the peripheral K atoms. For stoichiometric reasons this can only be achieved when the P atoms as minority component show an even higher coordination. Should potassium be on average fourfold or sixfold coordinated then phosphorus must have the coordination numbers (CN) 8 and 12, respectively, because K_3BP_2 ($\triangleq M_3M'X_2 \triangleq M''_2X$) is, in principle, a 2:1 compound. Accordingly, the structure of **1** in fact is a variant of the AlB_2 type, whereby the P atoms form the corners of trigonal prisms whose centers are 3/4 occupied by K atoms. $P_2(K_3\square)$. The B atom could occupy the hole $\square$ (CN 6), the center of the P_3-triangle adjacent thereto (CN 3), or one of the prism edges (CN 2). The latter is the case, and the formation of the propadiene structure $[P=B=P]^{3\ominus}$ apparently is not enforced by the composition of **1** and **2**, respectively. The defect 6^3 networks of K atoms are reorganized to pentagon ribbons (Fig. 1), whereby short K–K distances are avoided ($d_{K-K} \geq 331.5$ pm instead of 269 pm in AlB_2). Five K atoms surround each $[BP_2]^{3\ominus}$ unit (pentagonal bipyramids K_5P_2 surround the B atom with $d_{B-K} = 307.2-331.5$ pm). The six d_{K-P} distances in each case are for K1 330.2–399.3 pm ($\bar{d} = 355.2$ pm) and for K2 338.0–378.9 pm ($\bar{d} = 354.0$ pm). The P atoms are bound to one B atom and are coordinated by nine K atoms (instead of twelve).

Three internal vibrations can be expected for the anion $[BX_2]^{3\ominus}$ with $D_{\infty h}$ symmetry: $\Gamma_{vib} = \Sigma_g^+(RE, \nu_1) + \Sigma_u^+(IR, \nu_2) + \Pi_u(IR, \nu_3)$, with an isotope splitting (^{11}B, ^{10}B) in the IR active modes ν_2 and ν_3. In each case, a doublet of very high frequency (ν_2) and a low-lying triplet (site-symmetry-splitting; ν_3)—besides the lattice modes with $\tilde{\nu} < 200\ cm^{-1}$ are also observed in the IR spectra (Fig. 2). As expected $\tilde{\nu}(^{11}B)/\tilde{\nu}(^{10}B)$ is in each case 0.95/1,[14] and the force constants f, f', d [$N \cdot cm^{-1}$] determined according to *Siebert*[15] are 3.78, 0.60, 0.20 for **1** and 3.00, 0.30, 0.18 for **2**. These values give bond orders of 1.8 and 1.9, respectively,

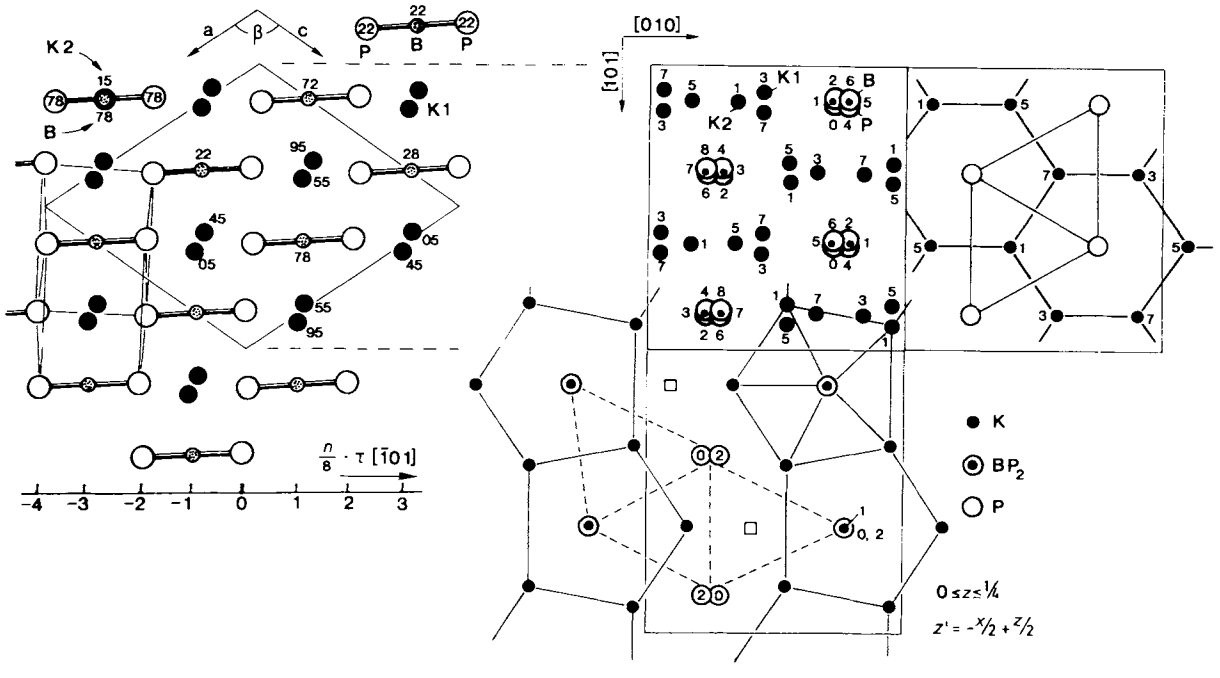

Fig. 1. Left: Projection of the structure of **1** along [010] with y in $n/100$; [101] corresponds to the hexagonal a-axis of an AlB_2 structure, [$\bar{1}$01] its fourfold c-axis (direction of the axes of the trigonal prisms). Right: Projection along [$\bar{1}$01] $\triangleq c'$ with the real atom positions (z' approximation in $n/8$). The idealized AlB_2-type structure is also shown. The connecting lines merely delineate the AlB_2 unit cells and the 6^3 network, the heights z' only the position of the defects $\square$. Along c' there are sequences of four P atoms with two alternatingly inserted B atoms (··· P–B–P ··· P–B–P), whereas only 3/4 of the M positions are occupied (MMM $\square$). Below: Section of the real structure parallel to [$\bar{1}$01]. The defects $\square$ break the 6^3 graphite network into bent chains, and the M partial structure becomes reformed to chains of condensed five-membered rings (increase in $d_{M\ M}$). One of the pentagonal bipyramids made up of 5 K + 2 P around the B atoms is indicated.

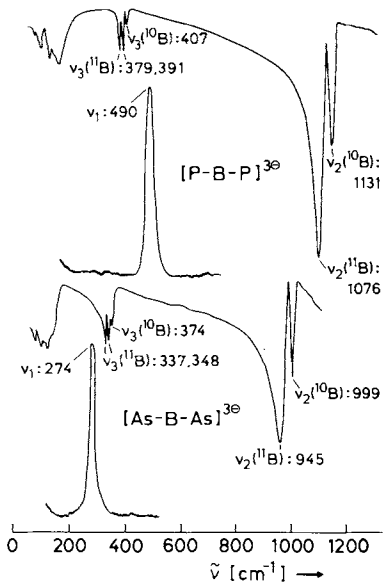

Fig. 2. IR and Raman spectra of **1** and **2**.

which are in excellent agreement with the above PBO's derived from the bond lengths.

K_3BP_2 reacts vigorously with water, alkalis and acids. It also reacts with NH_3 and chloroalkanes in THF, but in each case to give heterogeneous products which have not as yet been identified.

According to the most recent theoretical studies by *Pyykkö* and *Zhao*[16] a bond length of 183 pm is expected in the anion of **1**. The respective calculated vibrational wave numbers are 451 (ν_1) 1003 (ν_2) and 389 cm^{-1} (ν_3). On average, the calculated wave numbers are 5% smaller than the observed wave numbers, while the calculated bond length (6 pm) is 3% greater than the observed bond length. This discrepancy could be associated with shortcomings in the calculations; on the other hand, the deviations fit quite well to *Badger*'s rule, according to which $\tilde{\nu} \sim f^{1/2} \sim d^{-3/2}$.[17] In the K_3BP_2 crystal the effective charges in the $[BP_2]^{3\ominus}$ anion are certainly smaller, through interactions with the cations, than in the gaseous group. The shortening of d_{B-P} compared to that calculated is thus understandable. This effect, however, is possibly also an indication of considerable asymmetry in the electron density of the strongly polarized P atoms. Therefore we are planning to determine the nuclear distances by neutron diffraction.

Received: August 15, 1989 [Z 3502 IE]
German version: *Angew. Chem. 102* (1990) 63

[1] E. Zintl, *Angew. Chem. 52* (1939) 1.
[2] R. Juza, F. Hund, *Naturwissenschaften 4* (1946) 121; R. Juza, W. Schulz, *Z. Anorg. Allg. Chem. 269* (1952) 1.
[3] H. Pfister, *Acta Crystallogr. 11* (1958) 221.
[4] H. Hahn, G. Frank, W. Klinger, A. Meyer, G. Störger, *Z. Anorg. Allg. Chem. 271* (1953) 153.
[5] B. Eisenmann, M. Somer, *Z. Naturforsch. 396* (1984) 736.
[6] J. Wolf, D. Weber, H. G. von Schnering, *Z. Naturforsch. B41* (1986) 731.
[7] G. Cordier, H. Ochmann, *Z. Naturforsch. B43* (1988) 1538.
[8] H. Riek, R. Hoppe, *Z. Anorg. Allg. Chem. 400* (1973) 311; B. Nowitzki, R. Hoppe, *Croat. Chim. Acta 57* (1984) 537.
[9] B. Eisenmann, M. Somer, *Z. Naturforsch. B*, in press.
[10] The compounds were synthesized from the pure elements or from K, pnicogen and BP or BAs, respectively. The starting components (molar ratio: K:B:pnicogen = 3:1:2) were heated in sealed Nb crucibles (protective tube: quartz) for 4 h at 1000 (K_3BAs_2) and 1100 K (K_3BP_2), respectively, and cooled within 40 h to room temperature.
[11] Crystallographic data: **1**: $C2/c$ (No. 15), $a = 936.2(2)$, $b = 889.4(2)$, $c = 901.3(2)$ pm, $\beta = 110.99(2)^\circ$, $\varrho_{calcd} = 1.802$ g cm^{-3}; $N(hkl)[N'(hkl)] = 702[523]$ with $I > 3\,\sigma(I)$; $R_{aniso} = 0.034$. **2**: $C2/c$ (No. 15), $a = 960.8$, $b = 910.8(7)$, $c = 919.4(6)$ pm, $\beta = 111.68(3)^\circ$, $\varrho_{calcd} = 2.468$ g cm^{-3}, $N(hkl)[N'(hkl)] = 739[608]$ with $I > 3\,\sigma(I)$, $R_{aniso} = 0.067$. —For details of the crystal structure determinations, cf. M. Somer, M. Hartweg, K. Peters, H. G. v. Schnering, *Z. Kristallogr.*, in press.
[12] H. Yamane, S. Kikkawa, M. Koizumi, *J. Solid State Chem. 71* (1987) 1.
[13] V. J. Goubeau, W. Anselment, *Z. Anorg. Allg. Chem. 310* (1961) 248.
[14] H. V. R. Dias, P. P. Power, *Angew. Chem. 99* (1987) 1320; *Angew. Chem. Int. Ed. Engl. 26* (1987) 1270.
[15] H. Siebert, *Z. Anorg. Allg. Chem. 273* (1953) 170.
[16] P. Pyykkö, Y.-F. Zhao, private communication, 1989.
[17] R. M. Badger, *J. Chem. Phys. 2* (1934) 128; *ibid. 3* (1935) 710.

Synthesis of (+)-Terrein from L-Tartaric Acid

By *Hans-Josef Altenbach** and *Winfried Holzapfel*

(+)-Terrein is a metabolic product of several types of fungi.[1] It was first isolated as long ago as 1935, but it was not until 1955 before its correct structure could be elucidated.[1b,2] Compound **1**, which is readily obtainable fermentatively but does not exhibit any noticeable biologically activity, has found interest as an enantiomerically pure, highly functionalized cyclopentanoid building block, for example, for prostaglandin precursors.[3] The synthesis of terrein proved to be problematical because of its high sensitivity towards acids and bases, but in the meantime three routes to *rac*-**1** have been reported.[4]

We planned to synthesize optically active terrein **1** from the suitably protected L-tartaric acid derivative **2**, for the absolute configuration of **1** had been derived by *Barton* et al. by degradation down to the natural tartaric acid.[2] This idea was all the more attractive, as a simple retrosynthetic strategy to form both double bonds in **1** by Wittig-Horner olefinations leads to a C_2 symmetrical bisketophosphonate **3** as key compound, which appeared to be easily accessible from the tartrate **2**[5] (Scheme 1).

As protection for the alcohol functions of the tartaric acid, we chose the *tert*-butyldimethylsilyl group since it can be cleaved under such mild conditions that an isomerization (and racemization) to the isoterrein with *cis* arrangement of the hydroxy groups is avoided.

Compound **2** was obtained in 95% yield under standard conditions[6] by reaction of L-diethyl tartrate with *tert*-butyl(dimethyl)silyl chloride and imidazole in dimethylformamide. Surprisingly, upon reaction of **2** with four equivalents of diethyl lithiomethylphosphonate analogously to a synthetic method described by *Corey* et al.[7] for β-ketophosphonates (two equivalents are needed for the deprotonation of the bisketophosphonate **3** that is formed), mainly the Knoevenagel product **5** derived from **3** was isolated; in addition, small amounts of **4**, the desired product of an intramolecular Wittig-Horner reaction of **3**, was formed. Apparently, a cyclic intermediate is immediately formed, since the open-chain diadduct **3** could not be trapped, not even by quenching with acetic acid at −78 °C. The highest yields of the olefination product **4** required for the further step of the synthesis were obtained when two equivalents of acetic acid were first added after addition of the lithiomethylphospho-

[*] Prof. Dr. H.-J. Altenbach, Dr. W. Holzapfel
Fachbereich Chemie und Chemietechnik, Organische Chemie,
Universität-Gesamthochschule-Paderborn
Warburger Strasse 100, D-4790 Paderborn (FRG)

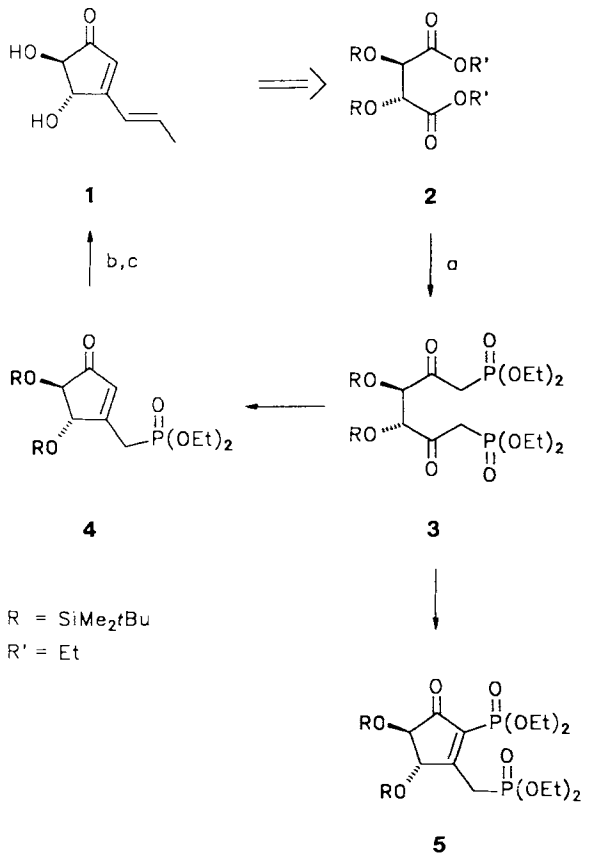

Scheme 1. a) 4 equiv. $LiCH_2PO(OEt)_2$, THF, $-78\,^{\circ}C \rightarrow -20\,^{\circ}C$, 1 h; 2 equiv. HOAc, 20 h, room temperature (RT); flash chromatography. b) NaH, THF, CH_3CHO (monomeric), 18 h, RT; medium-pressure liquid chromatography (MPLC): silica gel, CH_2Cl_2. c) 6.5 equiv. Et_4NCl, 6 equiv. $KF \cdot 2\,H_2O$, CH_3CN, 30 h, RT, MPLC: silica gel, CH_2Cl_2.

nate and warming of the reaction solution to $-20\,^{\circ}C$, and then stirring continued for 20 h at room temperature before the reaction was worked-up in aqueous solution. Under these conditions the product ratio **4**:**5** is 4:1. Owing to the large difference in their polarity **4** and **5** can be readily separated chromatographically and **4** [m.p. 54 °C (ether); $[\alpha]_D^{20} = +42.1^{\circ}$ ($c = 1.07$ in $CHCl_3$)] is obtained in 61% yield based on **2**. Introduction of the side chain in the required *E*-configuration was achieved smoothly via Wittig-Horner olefination of **4** with acetaldehyde. The product, which was obtained as a colorless oil, and whose spectral properties were consistent with those of the compound obtained by silylation of (+)-terrein,[8] is very labile and was allowed to react directly with Et_4NF—generated in situ from Et_4NCl and $KF \cdot H_2O$[9]—for cleavage of the alcohol protecting group. **1** was obtained in 42% yield based on **4**; its melting point, ^1H- and ^{13}C-NMR spectroscopic data, and rotation [m.p. 122 °C (CH_2Cl_2); $[\alpha]_D^{20} = 164^{\circ}$ ($c = 0.37$ in H_2O)] were identical with those of natural terrein.[1]

Remarkably, with this simple reaction sequence it appears that not only the synthesis of the optically active terrein is shorter and more effective than all the previously described routes to the racemate, but also that, with the intermediates, readily accessible enantiomerically pure five-membered ring building blocks are available which should be useful for the synthesis of other target materials, for example carbocyclic nucleoside analogues.

Received: September 6, 1989 [Z 3539 IE]
German version: *Angew. Chem. 102* (1990) 64

[1] a) H. Raistrick, G. Smith, *Biochem. J. 29* (1935) 606; *ibid. 31* (1937) 987; b) J. G. Grove, *J. Chem. Soc. 1954*, 4693; c) A. W. Dunn, I. D. Entwistle, R. A. W. Johnstone, *Phytochemistry 14* (1975) 2081; d) S. Kamata, H. Sakai, A. Hirota, *Agric. Biol. Chem. 47* (1983) 2637, and references cited therein.
[2] D. H. R. Barton, E. Miller, *J. Chem. Soc. 1955*, 1028.
[3] G. W. Clark, P. D. Hammesfahr, P. B. Hudson, L. A. Mitscher, K. Shirahata, J. Sulko, T. Veysoglu, *Heterocycles 13* (1979) 163, and references cited therein.
[4] J. Auerbach, S. M. Weinreb, *J. Chem. Soc. Chem. Commun. 1974*, 298; D. H. R. Barton, L. A. Hulshof, *ibid. 1977*, 1103; A. J. H. Klunder, W. Bos, B. Zwanenburg, *Tetrahedron Lett. 22* (1981) 4557.
[5] For further syntheses of five-membered ring systems from tartaric acid see: K. Ogura, M. Yamashita, G. Tsuchihachi, *Tetrahedron Lett. 1976*, 759; F. Barrière, D. H. R. Barton, J. Cleophax, A. Gateau-Olesker, S. Gero, F. Tadj, *ibid. 26* (1985) 3121; E. J. Corey, K. Niimura, Y. Konishi, S. Hashimoto, Y. Hamada, *ibid. 27* (1986) 2199; H. J. Bestmann, T. Moenius, *Angew. Chem. 98* (1986) 1007; *Angew. Chem. Int. Ed. Engl. 25* (1986) 994. Review on tartaric acid as chiral building block: D. Seebach, E. Hungerbühler, *Mod. Synth. Methods 1980*, 1.
[6] E. J. Corey, A. Venkateswarlu, *J. Am. Chem. Soc. 94* (1972) 6190.
[7] E. J. Corey, G. T. Kwiatkowski, *J. Am. Chem. Soc. 88* (1966) 5652, *ibid. 90* (1968) 6816.
[8] T. Veysoglu, L. A. Mitscher, *Tetrahedron Lett. 22* (1981) 1299.
[9] B. L. Carpino, A. J. Sau, *J. Chem. Soc. Chem. Commun. 1979*, 514.

Structure–Magnetism Relationship in $[Ti^{III}\text{-}O\text{-}Ti^{III}]^{4\oplus}$ Complexes**

By *Axel Bodner, Stefan Drueke, Karl Wieghardt,* Bernhard Nuber,* and *Johannes Weiss*

Structure-magnetism relationships in homobinuclear transition metal complexes containing two paramagnetic metal ions joined by an oxo bridge with octahedrally arranged ligands are currently the subject of intensive study.[1] Depending upon a) the electronic configuration of the two metal ions and b) the geometry of the $[M\text{–}O\text{–}M]^{n\oplus}$ moiety, which is puckered or linear, the intramolecular interaction of the spins can be antiferromagnetically or ferromagnetically coupled or even uncoupled. In complexes of type **A** containing a di-μ-carboxylato-μ-oxodimetal(III) structural unit, a strong antiferromagnetic behavior was observed for the iron(III) complex [d^5, high spin(hs)],[2] a strong ferromagnetic behavior for the analogous vanadium(III) complex (d^2),[3] and, finally, a weak ferromagnetic or weak antiferromagnetic, or even a decoupled behavior for the manganese(III) complex (d^4, hs). Compounds with a linear $[M\text{–}O\text{–}M]^{n+}$ unit (type **B**) show, e.g., strong antiferromagnetic coupling for Fe^{III} (d^5, hs),[5] ferromagnetic coupling for V^{III},[3] and antiferromagnetic coupling for Cr^{III}.[6]

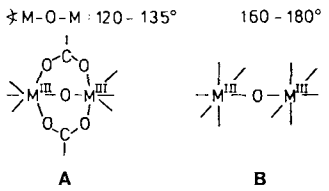

[*] Prof. Dr. Karl Wieghardt, Dipl-Chem. A. Bodner, Dr. S. Drüeke
Lehrstuhl für Anorganische Chemie I der Universität
Postfach 10 21 48, D-4630 Bochum (FRG)
Dr. B. Nuber, Prof. Dr. J. Weiss
Anorganisch-chemisches Institut der Universität
Im Neuenheimer Feld 270, D-6900 Heidelberg (FRG)

[**] This work was supported by the Fonds der Chemischen Industrie.

Surprisingly, nothing has thus far been reported in the literature about the magnetic properties of the electronically simplest complexes **A** and **B** containing two titanium(III) ions (d^1). We have therefore synthesized the complexes **1** and **2** and studied their magnetic properties.

$[L_2Ti_2(\mu\text{-}O)(\mu\text{-benzoato})_2](PF_6)_2$ **1**
$[L_2Ti_2Cl_4(\mu\text{-}O)]$ **2**
(L = *N*,*N*′,*N*″-trimethyl-1,4,7-triazacyclononane)

Figure 1 shows the structure of the cation **1**.[7] Two distorted octahedrally coordinated Ti^{III} ions are coupled with each other via a μ-oxo group as well as two symmetrical benzoato-

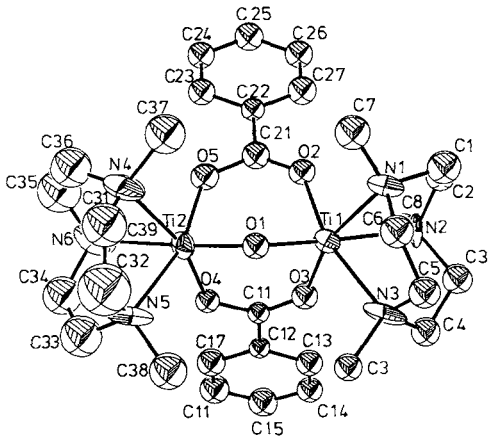

Fig. 1. Structure of the binuclear dication in crystals of **1**. Important bond lengths [Å] and angles [°] in **1**: Ti1-O1 1.81(2), Ti1-O2 2.03(2), Ti1-O3 2.06(2), Ti1-N1 2.24(2), Ti1-N2 2.34(2), Ti1-N3 2.20(2), Ti2-O1 1.84(2), Ti2-O4 2.05(2), Ti1-O5 2.04(2), Ti2-N4 2.23(2), Ti2-N5 2.21(2), Ti2-N6 2.30(2), Ti1···Ti2 3.198(4); Ti1-O1-Ti2 122.7(8), N-Ti-N 77.4(8) (average), O4-Ti2-O5 91.9(6), O2-Ti1-O3 92.7(6).

groups. The $[Ti\text{–}O\text{–}Ti]^{4\oplus}$ unit is bent [122.7(8)°]; the mean $Ti\text{–}O_\mu$ distance (1.82(2) Å) is very short. The $Ti\text{–}O_\mu$ bonds have a strong *trans* influence on the *trans* Ti–N bonds, which are about 0.10 Å longer than the corresponding *cis* Ti–N bonds. The Ti···Ti distance is 3.198(4) Å; it rules out a direct Ti–Ti bonding.[8] As follows from a comparison of the dimensions in analogous complexes of type **A**,[2–4] the distances and angles within the μ-oxo-bis-di-μ-carboxylato-μ-oxo-dimetal(III) unit are very similar.

The structure of **2** has not been determined, but it is highly probable that it contains a linear $[Ti^{III}\text{–}O\text{–}Ti^{III}]^{4\oplus}$ unit.

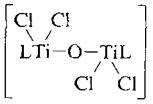

2

The magnetic properties of **1** and **2** differ drastically: crystals of **1** are *diamagnetic* at 298 K,[9] whereas **2** shows a temperature independent magnetic moment (90–298 K) of 1.72 μ_B per Ti^{III} center, which corresponds exactly to the spin-only value of one unpaired electron per Ti atom.

Thus, in **1** a very strong intramolecular spin-spin coupling of the two d^1 electrons is observed ($\boldsymbol{H} = -2JS_1 \cdot S_2$; $S_1 = S_2 = 1/2$; $-J > 400\ cm^{-1}$), whereas in **2** these electrons are uncoupled.

Figure 2 shows the X-band ESR spectrum of a powdered sample of **1** at 20 °C.[10] ESR spectroscopy is substantially more sensitive for the detection of unpaired electrons than measurements of the susceptibility on solid samples by the Faraday method. Three signals are observed. The two outer signals are strongly temperature dependent, and below 130 K they are no longer detectable. The signal at $g \approx 2.0$ is temperature independent; it can be ascribed to a paramagnetic impurity with $S = 1/2$ ground state ($LTiCl_3$ or $L_2Ti_2(\mu\text{-}O)(\mu\text{-benzato})_2]^{3\oplus}$).[11] The two temperature dependent signals are ascribed to an excited state of **1** with $S = 1$ which is no longer populated at low temperatures ($S = 0$ ground state).[12]

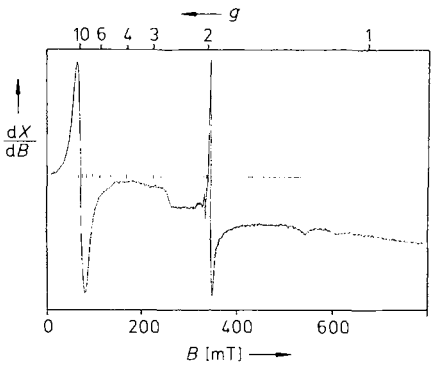

Fig. 2. ESR spectrum (X-band) of a solid sample of **1** at 246 K (20.0 mW/10 dB; 9.4232 GHz).

The bonds between the Ti atoms and the bridging O-atoms are the shortest bonds in **1** and **2**. It is therefore practicable for the following discussion to choose coordinates in which this bonding vector coincides with the *z*-axis; the d_{z^2} orbital in both complexes is then the energetically highest lying d-orbital and the d_{xy} orbital the energetically lowest lying (occupied) d-orbital. Since the d_{z^2} orbitals in **1** and **2** are unoccupied, a classical magnetic superexchange via the oxo bridges in **2** *cannot* explain the strong coupling. As shown in Figure 3 (left), however, it can be due to a

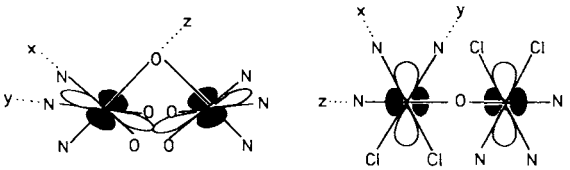

Fig. 3. Schematic representation of the overlap of the $d^1_{x^2-y^2}$ orbitals in **1** (left) and of the parallel $d^1_{x^2-y^2}$ orbitals in **2** (right).

symmetry allowed through-space overlapping of the two d_{xy} orbitals. In **1**, such an interaction leads to an $S = 0$ ground state (diamagnetism).[13] In the case of a linear $Ti^{III}\text{–}O\text{–}Ti^{III}$ group with longer Ti···Ti distance the d_{xy}-d_{xy} overlap would have δ symmetry and would be very weak (Fig. 3, right). The assumption of such a bridging geometry is consistent with the observed paramagnetism of **2**.

1 and **2** are good examples for demonstrating that the analysis of the possible magnetic orbitals in a given structure type of a binuclear complex can qualitatively correctly describe the observed coupling.[1b]

Experimental

1: A suspension of 1 g of $TiCl_3$ in 15 mL of dry CH_3CN was heated under reflux in an inert atmosphere (Ar) until a deep-blue solution was obtained. This was then treated dropwise with a solution of 1.2 g of *N,N',N''*-trimethyl-1,4,7-triazacyclononane (L) in 10 mL of CH_3CN. After 30 minutes' stirring at 20 °C a turquoise colored precipitate of $LTiCl_3$ was recovered by filtration (yield: 92%). UV/VIS (CH_3CN): $\lambda_{max} = 690$ nm ($\varepsilon = 30$); μ_{eff} (293 K) = 1.7 μ_B. 20 mL of a methanolic solution of 0.5 g of $LTiCl_3$ and 1 g of sodium benzoate was heated under reflux in an inert atmosphere (Ar) for 30 min. The resulting black-violet solution was treated with 1 g of $NaPF_6$. After 12 h at 5 °C, black-violet crystals of **1** were formed in 80% yield. IR (KBr): $\tilde{\nu} = 1541$ [$\tilde{\nu}_{as}$(C–O)], 1397 [ν_s(C–O)], 685 cm^{-1} [ν_{as}(Ti–O–Ti)]; UV/VIS (CH_3CN): $\lambda_{max} = 450$ ($\varepsilon = 2100$), 595 (sh) nm.—**2**: a solution of 0.8 g of L in 20 mL of dimethylformamide which contained about 1% H_2O was purged with argon and treated with 0.5 g of $TiCl_3$. The resulting suspension was heated under reflux for 30 min. After cooling to 5 °C a bright blue, microcrystalline precipitate of **2** was recovered by filtration (yield 45%). IR(KBr): $\tilde{\nu} = 745$ cm^{-1} [ν_a (Ti–O–Ti)]; UV/VIS (CH_3CN): $\lambda_{max} = 570$ nm ($\varepsilon = 520$ mol^{-1} cm^{-1}), 750 nm (sh). Magnetic moment: $\mu = 1.7$ μ_B per Ti atom (90–298 K). All the complexes gave correct elemental analyses (C,H,N,Cl).

Received: August 22, 1989 [Z 3517 IE]
German version: *Angew. Chem. 102* (1990) 60

[1] a) R. D. Willett, D. Gatteschi, O. Kahn Hrsg.: *Magneto-Structural Correlation in Exchange Coupled Systems, NATO ASI Ser. Ser. 140*, D. Reidel, Dordrecht, Holland 1985; b) O. Kahn, *Angew. Chem. 97* (1985) 837; *Angew. Chem. Int. Ed. Engl. 24* (1985) 834.

[2] a) J. R. Hartman, R. L. Rardin, P. Chaudhuri, K. Pohl, K. Wieghardt, B. Nuber, J. Weiss, G. C. Papaefthymiou, R. B. Frankel, S. J. Lippard, *J. Am. Chem. Soc. 109* (1987) 7387; b) S. J. Lippard, *Angew. Chem. 100* (1988) 353; *Angew. Chem. Int. Ed. Engl. 27* (1988) 344.

[3] M. Köppen, G. Fresen, K. Wieghardt, R. M. Llusar, B. Nuber, J. Weiss, *Inorg. Chem. 27* (1988) 721. The *J* value reported here for $[L_2V_2(O)(ac)_2]I_2 \cdot 2H_2O$ is incorrect. The correct value is $J > +200$ cm^{-1}: P. Knopp, K. Wieghardt, B. Nuber, J. Weiss, W. S. Sheldrick, *Inorg. Chem.*, in press.

[4] a) K. Wieghardt, U. Bossek, B. Nuber, J. Weiss, J. Bonvoisin, M. Corbella, S. E. Vitols, J. J. Girerd, *J. Am. Chem. Soc. 110* (1988) 7398; b) S. Ménage, J. J. Girerd, A. Gleizes, *J. Chem. Soc. Chem. Commun. 1988*, 431; c) J. E. Sheats, R. S. Czernuszewicz, G. C. Dismukes, A. L. Rheingold, V. Petrouleas, J. Stubbe, W. H. Armstrong, R. H. Beer, S. J. Lippard, *J. Am. Chem. Soc. 109* (1987) 1435.

[5] K. S. Murray, *Coord. Chem. Rev. 12* (1974) 1.

[6] a) J. Ferguson, H. U. Güdel, *Austr. J. Chem. 26* (1973) 505; b) J. Glerup, *Acta Chem. Scand. 26* (1972) 3775; c) E. Pedersen, *ibid. 26* (1972) 333.

[7] **1**: monoclinic, space group, $P2_1n$ (C_{2h}^5, No. 14) $a = 12.259(9)$ $b = 15.963(9)$, $c = 22.93(1)$ Å, $\beta = 100.48(5)°$, $Z = 4$, $\varrho_{calc} = 1.48$ g/cm^3, AED II (Siemens) diffractometer, ω-scan, graphite monochromator, $Mo_{K\alpha}$ radiation. The structure was solved by Patterson and difference Fourier methods; the Ti,P,O and N atoms were refined with anisotropic temperature factors, and all other atoms with isotropic temperature factors; the positions of the H atoms were calculated: $R = 0.10$, $R_w = 0.081$ for 1424 unique reflections with $I > 2.0\sigma(I)$, $\theta > 20°$. Since only very small crystals were obtainable ($0.1 \times 0.1 \times 0.3$ mm), the data set is very small for 281 refined parameters.—Further details of the crystal structure analysis are available on request from the Fachinformationszentrum Karlsruhe, Gesellschaft für wissenschaftlich-technische Information mbH, D-7514 Eggenstein-Leopoldshafen 2 (FRG), on quoting the depository number CSD-54148, the names of the authors, and the journal citation.

[8] In a complex of $Ti^{IV}(d^0)$ with a $Ti_2^{IV}(\mu\text{-O})(\mu\text{-carboxylato})_2$ framework the Ti···Ti distance is 3.31 Å: N. W. Alcock, P. N. Bartlett, D. Gordon, T. F. Illson, M. G. H. Wallbridge, *J. Chem. Soc. Chem. Commun. 1986*, 614.

[9] The magnetic susceptibility of **1** and **2** was investigated on microcrystalline powders in the temperature range 90–298 K with a Faraday balance.

[10] We thank Prof. *A. X. Trautwein* (Lübeck) and Dr. *J. J. Girerd* for recording the ESR spectra. We thank Dr. *J. J. Girerd* and Dr. *J. Bonviosin* for helpful discussions on the spin-spin coupling in **1**.

[11] The intensity of the signal at $g \approx 2.0$ relative to that of the strong signal at smaller magnetic field is dependent on the sample preparation. In quite fresh samples of **1** the intensity of this signal at $g \approx 2.0$ is very much smaller than shown in Figure 2.

[12] E. Wassermann, L. C. Snyder, W. A. Yager, *J. Chem. Phys. 41* (1964) 1763. The strong signal at small magnetic fields is the "half-field signal"; a maximum of seven weaker signals can also be observed.

[13] A completely similar spin coupling mechanism has been proposed for the complex $[LVO(\mu\text{-OH})_2VOL]^{2\oplus}$; it contains two vanadium(IV) ions with d^1_{xy} electron configuration; a) K. Wieghardt, U. Bossek, K. Volckmar, W. Swiridoff, J. Weiss *Inorg. Chem. 23* (1984) 1387; b) A. Ozarowski, D. Reinen *ibid. 25* (1986) 1704.

Coordination Chemistry of Polyoxomolybdates: The Structure of a Dodecanuclear Molybdate Cage Incorporating Hydrogen Squarate Ligands, $[(C_4H_9)_4N]_4[Mo_{12}O_{36}(C_4O_4H)_4] \cdot 10Et_2O$ **

By *Qin Chen, Shuncheng Liu,* and *Jon Zubieta**

The coordination chemistry of polyoxometalate clusters with organic substrate molecules has received considerable attention in recent years by virtue of the structural relationship of polyoxoanions to solid oxides.[1] The reaction chemistry of polyoxomolybdates with organic compounds containing carbonyl or enolic oxygens has proved particularly fruitful,[2] and we recently demonstrated that rhodizonic acid **1** reacts with octamolybdate **2** to yield **3**, an unusual cyclic octanuclear polyoxomolybdate with an oxalate-occupied cavity,[3] while *Haushalter* und *Lai* have described the aggregate $[Et_4N]_6[Na_{14}Mo_{24}P_{17}O_{97}(OH)_{31}]$, a hollow cluster filled with an H_3PO_4 molecule.[4] This result suggested that the chemistry of other "oxocarbons",[5] compounds in which all of the carbon atoms are bonded to carbonyl or

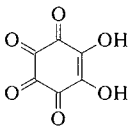

1

$[(n\text{-}C_4H_9)_4N]_4[Mo_8O_{26}]$ **2**

$[(n\text{-}C_4H_9)_4N]_2[Mo_8O_{16}(OCH_3)_8(C_2O_4)]$ **3**

enolic oxygens, with polyoxomolybdate anions would provide further insight into polyoxomolybdate-carbonyl chemistry and into ligand-oxometalate aggregation chemistry. Consequently, we initiated investigations of the chemistry of squaric acid **4** with dimolybdate **5** under a variety of reaction conditions. We have already reported on the struc-

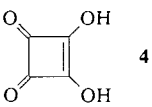

4

$[(n\text{-}C_4H_9)_4N]_2[Mo_2O_7]$ **5**

$[(n\text{-}C_4H_9)_4N]_3[Mo_3O_8(OCH_3)(C_4O_4)_2]$ **6**

$[(n\text{-}C_4H_9)_4N]_4[Mo_4O_8(OCH_3)_2(C_4O_4)_2(C_4O_4H)_2] \cdot CH_3OH$ **7**

tures of the trinuclear complex **6**[6] and the tetranuclear complex **7**,[7] and herein report the characterization of a unique dodecanculear oxomolybdate-hydrogen squarate complex **8**.

$[(n\text{-}C_4H_9)_4N]_4[Mo_{12}O_{36}(C_4O_4H)_4] \cdot 10\ (C_2H_5)_2O$ **8**

The product of the reaction of **4** with **5** is a colorless, crystalline, diamagnetic species of analytical composition

[*] Professor J. Zubieta, Q. Chen, S. Liu,
Department of Chemistry
State University of New York at Albany
Albany, NY 12222 (USA)

[**] This work was supported by a grant from the National Science Foundation (CHE 8815299 to *J. Z.*)

8.[13] The IR spectrum of **8** shows a band at 1630 cm^{-1} associated with C=O stretching vibrations and intense bands at 949 and 919 cm^{-1} attributed to $\nu_s(Mo=O_t)$ and $\nu_{as}(Mo=O_t)$ stretching vibrations (O_t = terminal oxygen), respectively. The band at 812 cm^{-1} establishes the presence of bridging oxo groups (Mo–O_b–Mo). Furthermore, a broad feature at 3440 cm^{-1} may be ascribed to ν(O–H), while the bands at 1382 and 1080 cm^{-1} are assigned to O–H and C–OH bending respectively.

The complex anion of compound **8** (Fig. 1)[8] consists of a dodecanuclear cage of Mo atoms, bridged by oxo groups, producing a cyclic $[Mo_{12}O_{12}]$ framework. Each of the hydrogen squarate ligands bridges six Mo sites, such that two of the oxygen donors adopt bridging modes and two oxygen

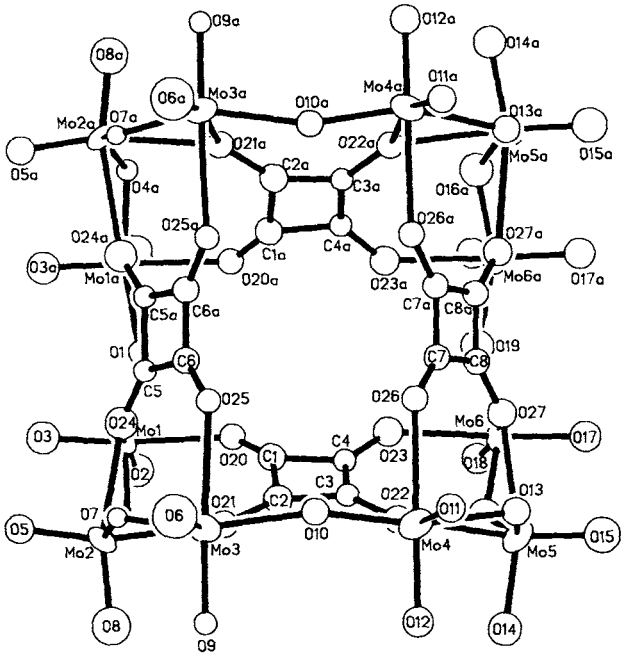

Fig. 1. Structure of the anion of **8**. Selected average bond lengths [Å] and angles [°]: Mo–O_t 1.68(3), Mo–O_b 1.92(3), Mo–O_t (ligand) 2.24(2); Mo–O_s (ligand) 2.37(3), O_t–Mo–O_t 104.9(15), O_b–Mo–O_b 146.8(17). Abbreviations: O_t = terminal oxo-group; O_b = bridging oxo-group; O_s(ligand) = terminally ligated squarate oxygen donor; O_b(ligand) = bridging squarate oxygen donor.

donors assume terminal coordination. In this fashion, each Mo center exhibits distorted octahedral geometry via coordination to two terminal oxo groups, two bridging oxo groups,

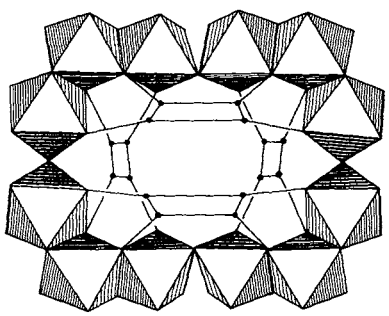

Fig. 2. The structure of the anion of **8** viewed as edge- and corner-sharing $[MoO_6]$ octahedra, with the hydrogen squarate C_4 backbones represented by the tetragons.

and two oxygen donors from the hydrogen squarate ligands. The anion exhibits approximate four-fold inversion symmetry about an axis normal to and passing through the center of the molecule, as illustrated in Figure 1.

Although polyoxomolybdate structures are generally constructed exclusively from edge-shared octahedra,[9] **8** presents both edge- and corner-sharing in the framework, as illustrated in Figure 2. Another unusual feature of the structure is the presence of the organic ligand as the singly deprotonated hydrogen squarate moiety **9**, rather than the commonly observed pseudoaromatic squarate form **10**.[10] The

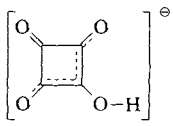

9

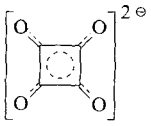

10

protonated ligand form **9** is consistent with the relatively long Mo–O(ligand) distances (2.24(2) Å, average terminal squarate O atom; 2.37(2) Å, average bridging squarate O atom), compared to distances in the 1.95 Å to 2.12 Å range for Mo–O(squarate) bonds with 1,2 bridging structures **11**.[6, 7] A similar trend in bond lengths has been estab-

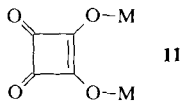

11

lished for structures exhibiting coordinated alcohol moieties [Mo(HOR)] as opposed to coordinated alkoxide [Mo(OR)] where ranges of 1.81 to 1.98 Å[11] and 2.24 to 2.28 Å[3, 12], respectively, have been observed. The quality of the data precluded assignment of the protonation sites, nor did ^{1}H-NMR studies provide resonances attributable to the alkoxy protons, presumably as a consequence of rapid exchange. The observation of a broad O–H stretching band at 3440 cm^{-1} in the IR spectrum of **8** is consistent with some degree of intramolecular H-bonding.

Experimental

A solution of **5** (2.0 g, 2.5 mmol) in CH_2Cl_2 (10 mL) was added to a solution of **4** (0.43 g, 3.8 mmol) in 2-chloroethanol/CH_2Cl_2 (30 mL, 1:1 by volume). After stirring at room temperature for 10 h, the resulting orange-brown solution was filtered and concentrated to 15 mL on a rotary evaporator. After layering this solution with diethyl ether (25 mL) and allowing it to stand for 2 weeks at 4 °C, small greenish crystals were isolated. Recrystallization of these from 2-chloroethanol/diethyl ether afforded colorless transparent crystals of **8** in 70% yield. Upon standing at room temperature, crystals of **8** became waxy and opaque. Removal from the mother liquor likewise resulted in opacity and loss of crystallinity. The analytical data corresponds to a sample which has lost two diethyl ether molecules of crystallization, i.e. $[(n\text{-}C_4H_9)_4N]_4[Mo_{12}O_{36}(C_4O_4H)_4] \cdot 8(C_2H_5)_2O$: calcd. C 35.9, H 6.10, N 1.49; found: C 35.3, H 6.23, N 1.29.

Received: July 21, 1989 [Z 3456 IE]
German version: *Angew. Chem. 102* (1990) 100

[1] V. W. Day, W. G. Klemperer, *Science (Washington, DC) 228* (1986) 533; M. T. Pope: *Heteropoly and Isopoly Oxometalates*, Springer, New York 1983; E. M. McCarron III, R. L. Harlow, *J. Am. Chem. Soc. 105* (1983) 6179; L. Ma, S. Liu, J. Zubieta, *Inorg. Chem. 28* (1989) 723.

[2] R. D. Adams, M. F. Fredrich, W. G. Klemperer, R.-S. Liu, *J. Am. Chem. Soc. 101* (1979) 491; R. D. Adams, W. G. Klemperer, R.-S. Liu, *J. Chem. Soc. Chem. Commun. 1979*, 256; V. W. Day, M. R. Thompson, W. G. Klemperer, R.-S. Liu, *J. Am. Chem. Soc. 102* (1980) 5973; H. Kang, S. N. Shaikh, T. Nicholson, J. Zubieta, *Inorg. Chem. 28* (1989) 920.

[3] Q. Chen, S. Liu, J. Zubieta, *Angew. Chem. 100* (1988), 1792; *Angew. Chem. Int. Ed., English 27* (1988) 1724.
[4] R. C. Haushalter, F. W. Lai, *Angew. Chem. 101* (1989) 802; *Angew. Chem. Int. Ed. Engl. 18* (1989) 743.
[5] R. West: *Oxocarbons*, Academic Press, New York 1980.
[6] Q. Chen, L. Ma, S. Liu, J. Zubieta, *J. Am. Chem. Soc. 111* (1989) 5944.
[7] Q. Chen, S. Liu, J. Zubieta, *Inorg. Chim. Acta, 164* (1989) 115.
[8] Crystal data at 233 K: orthorhombic, space group *Cmc*2 (alternative setting of No. 40, *Ama*2), $a = 25.391(5)$ Å, $b = 28.071(5)$ Å, $c = 26.335(5)$ Å, $V = 18.769.4(19)$ Å^3, $Z = 4$. Structure solution and refinement based on 3973 reflections with $F_0 \geq 4\sigma(F_0)$ ($Mo_{K\alpha}$, $\lambda = 0.71073$ Å); final discrepancy factor, 0.0757. The sample was mounted in a quartz capillary tube in the presence of the mother liquor to prevent loss of diethyl ether and consequent loss of crystallinity. The $[(n\text{-}C_4H_9)_4N]^{\oplus}$ ions and the diethyl ether molecules of crystallization displayed varying degrees of disorder, giving rise to several unreasonable bonding parameters and to large temperature factors. No completely satisfactory disorder model could be deduced, and this was not pursued as the anion was well-ordered. Further details of the crystal structure investigation can be obtained from the Fachinformationszentrum Karlsruhe, Gesellschaft für Wissenschaftlich-technische Information mbH, D-7514 Eggenstein-Leopoldshafen 2 (FRG), by quoting the depository number CSD 54171, the names of the authors, and the journal citation.
[9] A. Goiffon, B. Spinner, *Chim. Minérale 12* (1975) 316.
[10] J. P. Chesick, F. Doany, *Acta Crystallogr. Sect. B 37* (1981) 1076; J. A. C. van Ooijen, J. Reedijk, A. L. Spek, *Inorg. Chem. 18* (1979) 1184; M. Habenscluss, B. C. Gerstein, *J. Chem. Phys. 61* (1974) 852.
[11] M. H. Chisholm, J. C. Huffman, C. C. Kirkpatrick, *Inorg. Chem. 20* (1981) 871; M. H. Chisholm, J. C. Huffman, R. Kelly, *ibid. 19* (1980) 2762.
[12] S. Lincoln, S. A. Koch, *Inorg. Chem. 25* (1986) 1594.

Characterization by Microwave Spectroscopy of a Transient Hydrogen-Bonded Complex of Oxirane and Hydrogen Chloride Isolated in a Pulsed Jet**

By *Anthony C. Legon** and *Christopher A. Rego*

From the experimental standpoint little is known about the mechanism of the reaction in which an oxirane ring is opened by a hydrogen halide HX to give the 2-halogenoethanol. When X = Cl the gas-phase reaction at room temperature has been reported[1] to produce instantaneously a fog of 2-chloroethanol, even when conducted with anhydrous components in a polypropylene vessel to minimize surface effects. An ab initio investigation[2] of the reaction pathway

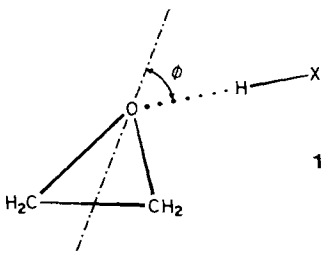

1

for X = F suggests that the first step is the formation of the hydrogen-bonded complex **1** followed by concerted cleavage of the HF bond and an OC bond with synchronous formation of OH and CF bonds. The interaction of HF with the oxygen atom of oxirane in **1** (X = F) was found to lower substantially the energy necessary to break the HF bond. While such a mechanism does not appear to predominate in the relatively slow reaction of oxirane and HF (2-fluoroethanol is a minor product[11]), it might be appropriate for X = Cl when the reaction occurs in aprotic nonpolar solvents (where no evidence for the presence of ions has been adduced[12]) or in the gas phase when surface effects are rigorously excluded. Of course, the ab initio calculation[2] refers to a pair of interacting molecules that are otherwise isolated. Is it possible to investigate experimentally the interaction of an oxirane molecule and a hydrogen chloride molecule under conditions appropriate to the ab initio calculation? In particular, can **1** (X = Cl) be observed and characterized as a stable but reactive species prior to any rapid ring opening reaction?

We report here the first observation and characterization of the hydrogen-bonded complex **1** (X = Cl) in isolation in the gas phase. The rotational spectrum of **1** (X = Cl) has been observed with a pulsed-nozzle, Fourier-transform microwave spectrometer[3] (frequency range 4–18 GHz) which incorporates a mixing nozzle of the type described by *Gutowsky* et al.[4] The essential feature of this nozzle is that the two reactive components do not mix until the point at which they independently expand into the Fabry-Pérot cavity. A gas mixture of ca. 1% oxirane in argon is pulsed through a 0.7 mm orifice in a solenoid valve into a tube which vents into the cavity. This supersonically expanded gas then meets a mixture of ca. 5% hydrogen chloride in helium that issues continously from a concentric, narrow bore (0.3 mm) tube. The time between mixing and the subsequent collisionless expansion of the species thereby formed is thus kept very short ($\lesssim$ a few μs) and hence the complex **1** (X = Cl) is frozen before any rapid ring opening reaction can occur. According to the microwave spectrum no 2-chloroethanol was formed after the mixing process in our experiments.[5] However, a careful search revealed a rotational spectrum that required the presence of both oxirane and hydrogen chloride and that could be attributed to the ground state of **1** (X = Cl).

The observed spectrum was characteristically that of a nearly prolate asymmetric rotor ($\kappa = -0.993$) containing a single Cl($S = 3/2$) nucleus. Quadrupole hyperfine structure arising from the presence of this nucleus allowed the unambiguous assignment of rotational transitions. Analysis of 33 hyperfine components of nine μ_a-transitions in the observed spectrum of the ^{35}Cl-isotopomer of **1** by standard methods yielded the rotational constants A_0, B_0, C_0, the centrifugal distortion constants Δ_J, Δ_{JK}, and δ_J and the ^{35}Cl-nuclear quadrupole coupling constants χ_{aa}, χ_{bb} and χ_{ac} shown in Table 1. Also included in Table 1 is the quantity $P_b = 1/2\,(I_a + I_c - I_b)$ where $I_b = h/(8\pi^2)B_0$, etc.

Table 1. Spectroscopic constants for the ground state of **1** (X = Cl).

$A_0 = 15286(20)$ MHz	$B_0 = 2077.3620(9)$ MHz	$C_0 = 2030.4161(9)$ MHz
$\Delta_J = 4.663(9)$ kHz	$\Delta_{JK} = 11.52(8)$ kHz	$\delta_J = 0.35(1)$ kHz
$\chi_{aa} = -38.518(5)$ MHz	$\chi_{bb} = 25.97(2)$ MHz	$\chi_{ac} = 31.6(4)$ MHz
$P_b = 19.34(2)$ amu Å^2		

The spectroscopic constants in Table 1 allow a preliminary description of the species responsible for the spectrum. Since $P_b = \sum_i m_i b_i^2$ is unchanged from the corresponding quantitiy $P_a = 1/2\,(I_b + I_c - I_a) = \sum_i m_i a_i^2 = 19.432$ amu Å^2 of free

[*] Prof. A. C. Legon, [+] Dr. C. A. Rego
Department of Chemistry, University of Exeter
Stocker Road, Exeter EX4 4QD (UK)
[+] Present address:
Department of Chemistry, University College London
20 Gordon Street, London WC1HOAJ (UK)
[**] This work was supported by the Science and Engineering Research Council through research grants. We thank Dr. *Z. Kisiel* for helpful discussions.

oxirane,[6] there is strong evidence that the inertial plane *ac* of the complex coincides with a vertical symmetry plane (*bc*) of oxirane, that the HCl subunit lies in this plane, and that the geometry of oxirane is not significantly changed on complex formation. Conversely, the other symmetry plane (*ab*) of oxirane has not been preserved, for otherwise A_0 for the complex would be essentially identical with $B_0 =$ 22120.77 MHz for free oxirane.[6] The most likely arrangement of the two subunits consistent with these conclusions is as illustrated in **1** (X = Cl), with HCl forming a hydrogen bond to O in oxirane. Detailed isotopic substitution is necessary to establish this conclusion rigorously and is in progress.

Assuming a linear hydrogen bond O···H–Cl, an unchanged r_s-geometry of oxirane[6] and an unchanged r_0-distance in hydrogen chloride,[7] the geometry of **1** (X = Cl) is defined by the angle ϕ and the distance $r(O\cdots Cl)$. A least squares fit of A_0, B_0 and C_0 then leads to $\phi = 77.08(2)°$ and $r(O\cdots Cl) = 3.112(3)$ Å. We note that ϕ is consistent with some simple rules recently proposed[8] for the rationalization of angular geometries of hydrogen-bonded complexes. These suggest that at equilibrium the HCl subunit should lie along the axis of a nonbonding electron pair on the acceptor atom. Given that the angle between the nonbonding pairs, as conventionally pictured, on oxygen in dimethyl ether is $2 \times 54.5°$, we expect the corresponding angle in oxirane to increase as the angle COC decreases. Hence, the rules predict that ϕ should be greater than 54.5°, as observed.

A property of **1** (X = Cl) of importance in connection with the mechanism of the gas-phase ring opening reaction is the position of the H atom in the HCl subunit. Is **1** (X = Cl) a reactive intermediate in the sense that there is already incipient proton transfer to O and a concomitant weakening of the HCl bond? Qualitatively, a contribution $>\overset{\oplus}{O}H\cdots\overset{\ominus}{Cl}$ to the valence bond description of **1** can be detected from the magnitude of the ^{35}Cl-nuclear quadrupole coupling constant along the direction *z* of the HCl subunit in the complex. For this structure, χ_{zz} is expected to be similar in magnitude to the value $-5.643(4)$ MHz observed[9] for the vapor-phase ion pair $\overset{\oplus}{Na}\overset{\ominus}{Cl}$. In the free $Cl^{\ominus}$ ion, χ is necessarily zero.

The zero-point average value $\chi_{zz} = -53.6$ MHz is readily obtained by diagonalization of the complete Cl-nuclear quadrupole coupling tensor in the principal inertial axis system given in Table 1. Although χ_{zz} is greatly reduced in magnitude from $\chi_0 = -67.62$ MHz in the free HCl molecule,[10] the reduction does *not* arise from a significant ionic contribution. The *z*-component of the electric field gradient at the Cl nucleus due to the oxirane subunit and the zero-point oscillation of the HCl subunit both also act to reduce χ_{zz}. In the related, effectively planar complex $H_2O\cdots H^{35}Cl$, for which there is no evidence of ionic character,[11] these two factors decrease the value of χ_{zz} from -67.62 MHz to -53.4 MHz.[12] If we assume that the two factors have a broadly similar effect in **1** (X = Cl) to that in $H_2O\cdots HCl$, we thus find it unnecessary to invoke an ionic contribution $>\overset{\oplus}{O}H\cdots\overset{\ominus}{Cl}$. A larger ionic contribution might be expected in **1** when X = Br, because of the weaker HBr bond, or when the oxirane is replaced by the stronger base aziridine. We are examining both of these systems experimentally.

Received: July 24, 1989;
revised: September 15, 1989 [Z 3461 IE]
German version: *Angew. Chem. 102* (1990) 76

CAS Registry numbers:
HCl, 7647010; oxirane, 75218.

[1] G. Bellucci, G. Berti, R. Bianchini, G. Ingrosso, A. Moroni, *J. Chem. Soc. Perkin Trans. 2 1981*, 1336.
[2] G. Alagona, E. Scrocco, J. Tomasi, *Theor. Chim. Acta 51* (1979) 11.
[3] A. C. Legon, *Annu. Rev. Phys. Chem. 34* (1983) 275.
[4] T. D. Klots, T. Emilsson, H. S. Gutowsky, *Symp. Mol. Struct. Spectrosc. Ohio, USA 1988*, Abstract TF2.
[5] R. G. Azrak, E. B. Wilson, *J. Chem. Phys. 52* (1970) 5299.
[6] C. Hirose, *Bull. Chem. Soc. Jpn 47* (1974) 976, 1311.
[7] For $H^{35}Cl$, $r_0 = 1.28387$ Å is obtained from B_0 given by F. C. De Lucia, P. Helminger, W. Gordy, *Phys. Rev. A 3* (1971) 1971.
[8] A. C. Legon, D. J. Millen, *Chem. Soc. Rev. 16* (1987) 467.
[9] F. H. de Leeuw, R. van Wachem, A. Dymanus, *Symp. Mol. Struct. Spectrosc. Ohio, USA 1969*, Abstract R5.
[10] E. W. Kaiser, *J. Chem. Phys. 53* (1970) 1686.
[11] A. C. Legon, D. J. Millen, *Proc. R. Soc. London A 417* (1988) 21.
[12] A. C. Legon, L. C. Willoughby, *Chem. Phys. Lett. 95* (1983) 449.

Coupling of an Iridium Vinylidene Complex with Aluminum Alkyls; Carbon-Carbon Bond Formation via Migratory Insertion of a Vinylidene Unit

By *Michael D. Fryzuk,* Neil T. McManus, Steven J. Rettig,* and *Graham S. White*

Very reactive organic fragments can be stabilized by coordination to metal complexes.[1] These include, inter alia, carbenes,[2] benzynes,[3] cyclobutadienes,[4] and thiocarbonyls.[5] Vinylidenes (:C=CHR) are tautomers of terminal acetylenes and have only short lifetimes at normal temperatures;[6] however, they can also be stabilized by coordination to a metal complex. Indeed, much has been reported on the formation of vinylidene-metal complexes and the reactivity of the coordinated vinylidene unit.[7] Depending on the L_nM fragment the α–C atom can be attacked either nucleophilically or electrophilically (cf. **A**, **B**).[8]

Herein we document a new mode of reactivity for a vinylidene ligand that involves carbon–carbon bond formation via coupling with an organoaluminum reagent. The key feature in this type of reactivity is that the metal center is coordinatively unsaturated and this promotes migratory insertions with electrophiles.

The red-orange vinylideneiridium complex **3** was prepared by addition of acetylene to the cyclooctene derivative **1**[9] by way of the transient η^2-acetylene adduct **2**. Although this adduct was only spectroscopically characterized, its identity is unmistakable.[10] The transformation of **2** into the vinylidene complex **3** occurs without observation of any intermediates (by ^{1}H-NMR spectroscopy) over a period of 24 h in benzene or toluene. Diagnostic of the vinylidene complex is the presence of an upfield triplet at $\delta = -3.53$

[*] Prof. Dr. M. D. Fryzuk, Dr. N. T. McManus, Dr. S. J. Rettig,[+] Dr. G. S. White
Department of Chemistry, University of British Columbia
2036 Main Mall, Vancouver, B. C., V6T 1Y6 (Canada)
[+] X-ray structure analysis, UBC Crystallographic Service.
[**] This work was funded by the NSERC (Canada) in the form of an operating grant to *M.D.F.* and a Postdoctoral Fellowship to *G.S.W.* We also thank Johnson-Matthey for the generous loan of $IrCl_3 \cdot x\,H_2O$.

 © *VCH Verlagsgesellschaft mbH, D-6940 Weinheim, 1990* *0570-0833/90/0101-0073 $ 02.50/0*

($^4J_{PH}$ = 3.5 Hz),[11] in accord with other related vinylidene-iridium complexes.[12]

Addition of trimethyl- or triethylaluminum to a solution of **3** in toluene results in the loss of the red color and formation of yellow-orange solutions containing a single product ($^{31}P\{^1H\}$-NMR spectroscopy); crystallization from toluene/hexane affords the new complexes **4a**, **b**[13] in 70–80% yield (Scheme 1).

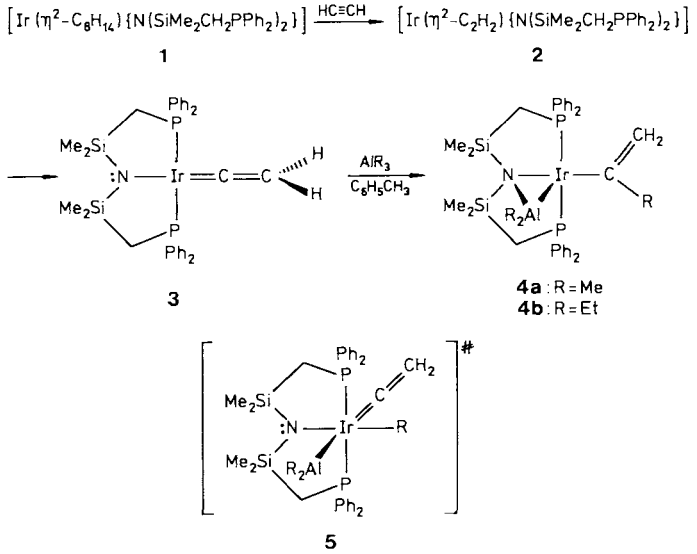

Scheme 1.

The ^{1}H-NMR spectrum of **4a** is very straightforward but structurally ambiguous; resonances are observed that indicate that the $AlMe_3$ reagent has transferred a methyl group to the vinylidene moiety to generate an isopropenyl ligand and that the $AlMe_2$ unit is still bound in some way to the complex. Similar results were obtained with $AlEt_3$, leading to **4b**.[13] To ascertain the mode of binding of the $AlMe_2$ unit to iridium, we carried out an X-ray crystal structure analysis of **4a** (Figure 1).[14]

The aluminum-iridium complex **4a** has a distored square-pyramidal geometry with the isopropenyl ligand in the equatorial plane and an $AlMe_2$ group apical but bent, bridging over to the nitrogen atom of the iridium amide. The Ir–Al bond length of 2.411(2) Å is slightly shorter than the Rh–Al distance of 2.4581(8) Å in $[CpRh(PMe_3)_2(Al_2Me_4Cl_2)]$.[15] The distances in the Ir–N–Al triangle are informative; the Ir–N bond length is 2.373(5) Å and the Al–N distance is 1.970(5) Å, indicative of metal-amine[16] lengths typical for an amide ligand bridging two metals. The nitrogen has a distorted tetrahedral geometry. Also of interest in the solid state structure is the presence of an agostic C–H ··· Ir interaction from an *ortho* hydrogen of one of the phenyl rings to the open site of the square-based pyramid; the Ir–H(32) bond length is 2.68 Å.

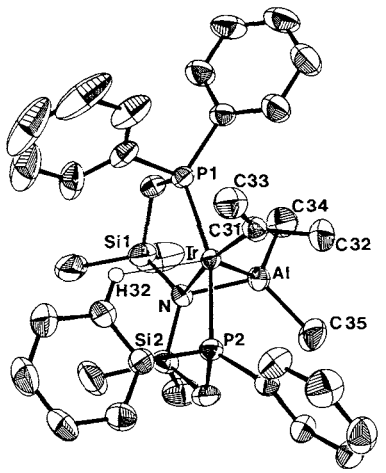

Fig. 1. Crystal structure of **4a**. Important bond lengths [Å] and bond angles [°]: Ir–P1, 2.272(2); Ir–P2, 2.294(2); Ir–N, 2.373(5); Ir–Al, 2.411(2); Ir–C31, 2.014(6); C31–C33, 1.348(9); C31–32, 1.505(8); Al–N, 1.970(5); Al–C34, 1.961(7); Al–C35, 1.979(8); Ir ··· H32, 2.68; P1–Ir–P2, 161.86(5); Ir–C31–C32, 115.8(4); Ir–C31–C33, 125.8(5); C32–C31–C33, 118.4(6); Ir–Al–N, 64.7(1); N–Ir–Al, 48.6(1); Ir–N–Al, 66.7(1); Si1–N–Si2, 119.8(3); C31–Ir–N, 168.8(2).

The formation of the complexes **4a**, **b** probably involves oxidative addition[17] of the AlR_3 monomer to the 16-electron Ir^I-complex **3** to generate a transient species **5** having an AlR_2 ligand, an alkyl ligand and the vinylidene ligand (cf. Scheme 1). Migration of the vinylidene ligand to the Me–Ir bond generates the isopropenyl unit; the proximity of the amide N-atom to the Al-atom undoubtedly facilitates formation of the amide bridge.

For the most part, the reactivity of the coordinated vinylidene fragment has been investigated on systems that are coordinatively saturated at the metal center. While this has allowed a number of new reactivity patterns to be unveiled, systems having unsaturation at the metal site should allow new reaction types to be found. An especially good example of this involves protonation via the metal center to convert a vinylidene unit into a carbyne ligand.[18]

Our particular tridentate ligand combination has allowed for the isolation of an iridium-aluminum adduct with carbon–carbon bond formation. Further work is underway in our laboratory to exploit the migratory insertion capability of both a vinylidene fragment and a methylidene unit[19] coordinated to an unsaturated metal center.

Received: July 10, 1989 [Z 3428 IE]
German version: *Angew. Chem. 102* (1990) 67

CAS Registry numbers:
1, 84074-30-6; **2**, 124462-68-6; **3**, 124462-69-7; **4a**, 124462-70-0; **4b**, 124462-71-1; $AlMe_3$, 75-24-1; $AlEt_3$, 97-93-8.

[1] J. P. Collman, L. S. Hegedus, J. R. Norton, R. G. Finke: *Principles and Applications of Organotransition Metal Chemistry*, University Science Books, Mill Valley, CA, 1987, p. 58.
[2] K. H. Dötz, H. Fischer, P. Hofmann, F. R. Kreissl, U. Schubert, K. Weiss, *Transition Metal Carbene Complexes*. Verlag Chemie, Weinheim 1983.
[3] S. L. Buchwald, R. B. Neilsen, *Chem. Rev. 88* (1988) 1047; M. A. Bennett, H. Schwemlein, *Angew. Chem. 10* (1989) 1349; *Angew. Chem. Int. Ed. Engl. 28* (1989) 1296.
[4] A. Efraty, *Chem. Rev. 77* (1977) 691.
[5] a) I. M. Butler, *Acc. Chem. Res. 10* (1977) 359; b) P. V. Yaneff, *Coord. Chem. Rev. 23* (1977) 183.
[6] R. P. Duran, V. T. Amorebieta, A. J. Colussi, *J. Am. Chem. Soc. 109* (1987) 3154.
[7] a) M. I. Bruce, A. G. Swincer, *Adv. Organomet. Chem. 22* (1983) 59; b) R. S. Iyer, J. P. Selegue, *J. Am. Chem. Soc. 109* (1987) 910; c) A. Mayr, K. C. Schaefer, E. Y. Huang, *ibid. 106* (1984) 1517; d) K. R. Birdwhistell, T. L. Tonker, J. L. Templeton, *ibid. 107* (1985) 4474; e) S. J. Landon, P. M. Shulman, G. L. Geoffroy, *ibid. 107* (1985) 6739; f) B. E. Boland-Lussier, M. R. Churchill, R. P. Hughes, A. L. Rheingold, *Organometallics 1* (1982) 628; g) G. Consiglio, F. Morandini, G. F. Ciani, A. Sironi, *ibid. 5* (1986) 1977; h) R. G. Beevor, M. J. Freeman, M. Green, C. E. Morton, A. G. Orpen, *J. Chem. Soc. Chem. Commun. 1985*, 68; i) G. Consiglio, R. Schwab, F. Morandini, *ibid. 1988*, 25.
[8] a) D. R. Senn, A. Wong, A. T. Patton, M. Marsi, C. E. Strouse, J. A. Gladysz, *J. Am. Chem. Soc. 110* (1988) 6096; b) A. Davison, J. P. Selegue, *ibid. 102* (1980) 2455; c) H. Werner, J. Wolf, R. Zolk, U. Schubert, *Angew. Chem. 95* (1983) 1022; *Angew. Chem. Int. Ed. Engl. 22* (1983) 981; d) J. Wolf, R. Zolk, U. Schubert, H. Werner, *J. Organomet. Chem. 340* (1988) 161.
[9] M. D. Fryzuk, P. A. MacNeil, S. J. Rettig, *Organometallics 4* (1986) 2469.

[10] **2**: ^{1}H NMR (300 MHz, C_6D_6): δ = 0.03 (s; $SiCH_3$), 1.70 (vt; N = 5.4 Hz; PCH_2), 2.40 (s; C_2H_2), 7.08 (m; *p/m*-H), 7.70 (m; *o*-H). $^{31}P\{^1H\}$-NMR (121.4 MHz, C_6D_6): δ = 11.9 (s). IR (KBr): $\tilde{\nu}$ = 1958 cm^{-1} [ν(C≡C)]; see H. Werner, A. Höhn, *J. Organomet. Chem. 272* (1984) 105.

[11] **3**: ^{1}H NMR (300 MHz, C_6D_6): δ = −3.53 (t, ^4J(PH) = 3.5 Hz; $=CH_2$), 0.16 (s; $SiCH_3$), 1.90 (vt; N = 5.3 Hz; PCH_2), 7.08 (m; *p/m*-H), 7.94 (m; *o*-H). $^{31}P\{^1H\}$-NMR (121.4 MHz, C_6D_6): δ = 15.8 (s). ^{13}C NMR (75.4 MHz, C_6D_6): δ = 91.6 (s; β-C), 268.1 (t, ^2J(PC) = 7.0 Hz; α-C). IR (KBr): $\tilde{\nu}$ = 1648 cm^{-1} [ν(C=C)]. Correct C, H, N analysis.

[12] a) A. Höhn, H. Otto, M. Dziallas, H. Werner, *J. Chem. Soc. Chem. Commun. 1987*, 852; b) F. J. Garcia Alonso, A. Höhn, J. Wolf, H. Otto, H. Werner, *Angew. Chem. 97* (1985) 401; *Angew. Chem. Int. Ed. Engl. 24* (1985) 406; c) H. Werner, J. Wolf, G. Müller, C. Krüger, *ibid. 96* (1984) 421 and *23* (1984) 431; d) *J. Organomet. Chem. 342* (1988) 381.

[13] **4a**: ^{1}H NMR (300 MHz, C_6D_6): 0.07 (s; $SiCH_3$), 0.50 (s; $AlCH_3$), 1.91 (dvt, J_{gem} = 14.3, N = 5.2 Hz) and 2.53 (dvt, N = 5.3 Hz; PCH_2), 4.77 and 6.01 (s; $=CH_2$), 7.20 (m; *p/m*-H), 7.92 and 8.03 (m; *o*-H). $^{31}P\{^1H\}$-NMR (121.4 MHz, C_6D_6): δ = 18.0 (s). IR (KBr): $\tilde{\nu}$ = 1590 cm^{-1} [ν(C=C)]. **4b**: ^{1}H NMR (300 MHz, C_6D_6): δ = 0.06 and 0.48 (s; $Si(CH_3)_2$), 1.88 (dvt, J_{gem} = 14.4, N = 5.1 Hz) and 2.53 (dvt, N = 5.3 Hz; PCH_2), 0.61 (m; $AlCH_2CH_3$), 1.46 (t, J = 8.1 Hz), $AlCH_2CH_3$), 2.19 (q, J = 7.4 Hz; CH_2CH_3), 0.98 (t, J = 7.4 Hz; CH_2CH_3), 4.84 and 5.96 (br.s; $=CH_2$), 7.18 (m; *p/m*-H), 7.85 and 7.98 (m; *o*-H). $^{31}P\{^1H\}$-NMR (121.4 MHz, C_6D_6): δ = 17.7 (s). IR (KBr): $\tilde{\nu}$ = 1586 cm^{-1} [ν(C=C)]. Correct C, H, N analysis.

[14] $C_{35}H_{47}AlIrNP_2Si_2$, M_r = 819.08, monoclinic (from toluene/hexane), space group $P2_1/c$, Z = 4, a = 18.823(6) Å, b = 9.701(2) Å, c = 21.359(8) Å, β = 111.78(2)°, V = 3622(2) Å^3, ϱ_{calc} = 1.50 g cm^{-3}, $\mu(Mo_{K\alpha})$ = 38.73 cm^{-1}, $F(000)$ = 1648. 8600 measured reflections (Rigaku AFC6, $Mo_{K\alpha}$, λ = 0.71069 Å), T = 21 °C, $\omega - 2\theta$ scan, maximum 2θ = 55.1°; 8352 independent reflections, empirical absorption correction, heavy atom method, Lorentz and polarization corrections, R = 0.034, R_w = 0.040 ($w = 1/\sigma^2(F_0)$) for 5723 observed reflections ($I > 3.00\sigma(I)$) and 379 parameters, residual electron density (max.) = 1.85 eÅ^{-3}. Further details of the crystal structure analysis may be obtained from the Fachinformationszentrum Karlsruhe, Gesellschaft für wissenschaftlich-technische Information mbH, D-7514 Eggenstein-Leopoldshafen 2 (FRG), by quoting the depository number CSD-54150, the names of the authors, and the journal citation.

[15] J. M. Mayer, J. C. Calabrese, *Organometalics 3* (1984) 1292.

[16] For related iridium–amine bond lengths, see M. D. Fryzuk, P. A. MacNeil, S. J. Rettig, *J. Am. Chem. Soc. 109* (1987) 2803; for typical aluminum nitrogen bond lengths, see M. J. Zaworotko, J. L. Atwood, *Inorg. Chem. 19* (1980) 268.

[17] a) D. L. Thorn, R. L. Harlow, *J. Am. Chem. Soc. 111* (1989) 2575; b) K. Isobe, A. Vazquez de Miguel, A. Nutton, P. M. Maitlis, *J. Chem. Soc. Dalton Trans. 1984*, 929.

[18] A. Höhn, H. Werner, *Angew. Chem. 98* (1986) 745; *Angew. Chem. Int. Ed. Engl. 25* (1986) 737.

[19] M. D. Fryzuk, P. A. MacNeil, S. J. Rettig, *J. Am. Chem. Soc. 107* (1985) 6708.

Application of Titanacycles to Heterocycle Synthesis: Phospha- and Arsacyclobutenes**

By *William Tumas,* Joseph A. Suriano,* and *Richard L. Harlow*

Dedicated to Dr. George Parshall on the occasion of his 60th birthday.

The propensity of early transition metal alkyls to undergo transmetalation reactions with main group halides[1] coupled with the wealth of metallacyclic complexes now available[2] should provide access to novel heterocycles that heretofore have been difficult to prepare. Except for the widely studied phosphetanes,[3] examples of four-membered carbocycles containing a group 15 (5th main group) element are rare.[4, 5] In the course of our search for organometallic routes to main group heterocycles, we have discovered that the bis(cyclopentadienyl)titanacyclobutene **1** reacts rapidly and cleanly with group 15 aryl dichlorides to yield the corresponding heterocyclobutenes, **2** and **3**. Herein, we report the synthesis, and characterization of **2** the first arsacyclobutene (1,2-dihydroarsete); comparisons with the P analog **3** will be drawn.

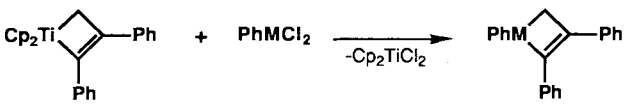

1 **2**: M = As; **3**: M = P

The addition of one equivalent of $PhAsCl_2$ or $PhPCl_2$ to bis(cyclopentadienyl)titanacyclobutene **1**[6] in hydrocarbon solvents results in the immediate precipitation of titanocene dichloride and formation of **2** or **3**,[7] respectively (essentially quantitative by NMR spectroscopy).[8] **2** and **3** were isolated in greater than 50% yield as colorless crystals by filtration of the titanocene dichloride byproduct, removal of solvent, and recrystallization from cold (−20 °C) ether or pentane. NMR[9] and high resolution mass spectral data[10] are consistent with a four-membered ring structure for **2** and **3**. The diastereotopic α-methylene hydrogens appear as doublets (J = 13.3 Hz) at δ = 2.75 and 2.35 in the ^{1}H-NMR spectrum of **2**. The $^1J_{PC}$ of 33.9 Hz for the *ipso* phenyl carbon of **3** (^{13}C NMR) is consistent with reported values for phosphetanes. $^1J_{CH}$ at the α positions of 140–146 Hz (^{13}C NMR) of **2** and **3** are also indicative of a cyclic structure.[11]

The proposed arsacyclobutene structure **2** was confirmed by X-ray crystallography (Fig. 1).[12] The four-membered

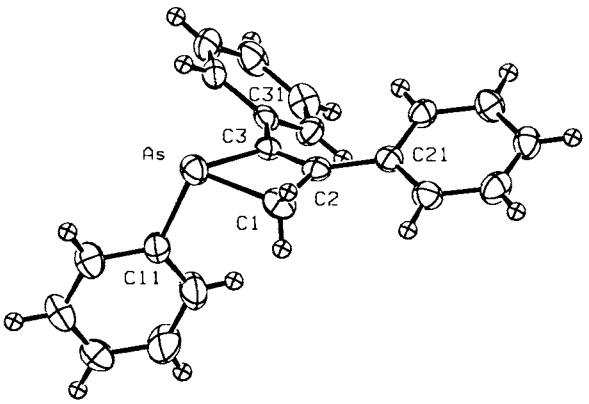

Fig. 1. Structure of **2** in the crystal. For bond lengths and angles see Table 1.

ring is essentially planar with only a slight enveloping; the atoms of the ring deviate from a mean plane by only 0.039, −0.052, 0.073, and −0.059 Å, for As, C1, C2, and C3, respectively. Moreover, the As atom is clearly pyramidal with C–As–C angles of 69.9, 102.3 and 101.7°. For the sake of comparison we also prepared and structurally characterized the isostructural phosphacyclobutene **3**.[7, 13] Pertinent bond lengths and angles for **2** and **3** as well as two previously reported metallacyclobutenes[14] are listed in Table 1. The

[*] Dr. W. Tumas, J. A. Suriano, Dr. R. L. Harlow
Central Research and Development Department
E.I. du Pont de Nemours and Co.
Experimental Station, Wilmington, DE 19880 (USA)

[**] Contribution No. 5275 from the Central Research and Development Department. We thank *F. Davidson* for the ^{13}C NMR spectra, *J. Lazar* for high-resolution mass spectra data, and *W. Marshall* for assistance with the X-ray crystallography.

Table 1. Comparison of X-ray data for heterocyclobutenes.

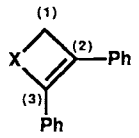

RX	PhAs (2)	PhP (3)	Cp_2Ti (1) [14a]	$Br(PMe_3)_3Ir$ [a]
Bond length [Å]				
X-C1	1.989(6)	1.872(4)	2.122(5)	2.166(6)
X-C3	1.949(4)	1.826(3)	2.104(4)	2.134(5)
C1-C2	1.499(7)	1.510(5)	1.537(6)	1.525(8)
C2-C3	1.358(6)	1.359(4)	1.344(6)	1.344(7)
Bond angle [°]				
C1-X-C3	69.9(2)	73.8(2)	69.3(2)	64.5(2)
X-C1-C2	89.4(3)	88.4(2)	86.0(3)	91.2(3)
X-C3-C2	95.4(3)	95.2(2)	91.8(3)	98.0(4)
C1-C2-C3	104.1(4)	101.3(3)	112.8(6)	106.1(5)
Ph-X-C1	102.3(2)	104.3(2)		
Ph-X-C3	101.7(2)	104.1(2)		

[a] [14b]; this structure is for *p*-tolyl rather than phenyl substituents.

four-membered ring in all these compounds is essentially planar.[15] The X–C bond lengths also reflect the hybridization of the carbon atoms in the ring. As expected, the C1–C2 single bond is considerably longer than the C2–C3 double bond. The double bond in the four-membered ring is, however, slightly longer in the P and As compounds than in the transition metal complexes. It is possible that this difference may be indicative of more delocalization in the main group compounds or may be due to less strain in the transition metal complexes due to bonding through d orbitals.

Both the arsa- and phosphacyclobutenes are surprisingly robust; no appreciable decomposition was observed upon heating toluene solutions in sealed tubes at 100 °C for up to 20 h. Preliminary studies reveal that **2** and **3** are, however, photochemically reactive. We are also investigating a number of other heterocycles prepared by transmetalation reactions of titanacycles.

Received: August 24, 1989 [Z 3519 IE]
German Version: *Angew. Chem. 102* (1990) 89

CAS Registry numbers:
1, 74834-09-6; **2**, 124481-54-5; **3**, 124511-69-9; $PhAsCl_2$, 696-28-6; $PhPCl_2$, 644-97-3.

[1] There is considerable precedent for these transmetalation reactions. The synthesis of a number of heterocycles from zirconacyclopentadienes and -cyclopentenes has recently been reported. P. J. Fagan, W. A. Nugent, *J. Am. Chem. Soc. 110* (1988) 2310. Also see: M. D. Fryzuk, G. S. Bates, C. Stone, *J. Org. Chem. 53* (1988) 4425; M. D. Fryzuk, G. S. Bates, C. Stone, *Tetrahedron Lett. 27* (1986) 1537; B. J. J. van de Heisteeg, G. Schat, O. S. Akkerman, F. Bickelhaupt, *Organometallics 5* (1986) 1749.

[2] a) C. P. Casey, *React. Intermed. (Plenum) 2* (1981) 135; b) J. P. Collman, L. S. Hegedus, J. R. Norton, R. G. Finke: *Principles and Applications of Organotransition Metal Chemistry*, University Science, Mill Valley, CA, USA 1987; c) D. J. Cardin, M. F. Lappert, C. L. Raston: *Chemistry of Organozirconium and -Hafnium Compounds*, Ellis Horwood Limited, Chichester 1986; d) S. L. Buchwald, R. B. Nielsen, *Chem. Rev. 88* (1988) 1047.

[3] a) Review: L. D. Quin: *The Heterocyclic Chemistry of Phosphorus*, Wiley, New York, 1981, Chapter 4 and refs. within; b) S. A. Weissman, S. G. Baxter, *Tetrahedron Lett. 29* (1988) 1219.

[4] There is one report of the synthesis of arsetanes: M. Mickiewicz, S. B. Wild, *J. Chem. Soc. Dalton Trans.* 1977, 704.

[5] Only a few reports on 1,2-dihydrophosphetes exist. For example: a) R. H. Nielson, B. A. Boyd, D. A. DuBois, R. Hani, G. M. Scheide, J. T. Schore, U. G. Wettermark, *Phosphorus Sulfur 30* (1987) 463; b) B. A. Boyd, R. J. Thoma, R. H. Nielson, *Tetrahedron Lett. 28* (1987) 6121; c) A. Marinetti, J. Fischer, F. Mathey, *J. Am. Chem. Soc. 107* (1985) 5001; d) X-ray structure analysis of a metal carbonyl complex of 1,2-dihydrophosphete: N.H. Tran Huy, L. Ricard, F. Mathey, *Organometallics 7* (1988) 1791.

[6] Prepared according to literature methods from the Tebbe reagent and diphenylacetylene in THF and recrystallized from toluene/pentane: F. N. Tebbe, R. L. Harlow, *J. Am. Chem. Soc. 102* (1980) 6149.

[7] While this manuscript was in preparation, *Doxsee* et al. also prepared **3** via this transmetalation route and structurally characterized it; K. M. Doxsee (Eugene, OR, USA), private communication; see G. S. Shen, C. B. Knobler, *J. Am. Chem. Soc. 111* (1989) 9129.

[8] All manipulations were carried out under inert atmosphere either in a drybox (Vacuum Atmospheres) or on a high vacuum line using dry, deoxygenated solvents.

[9] Spectroscopic data: **2**: ^1H NMR (300 MHz, CD_2Cl_2): δ = 7.6, 7.0–7.4 (m = 15H), 2.75 (d, J_{HH} = 13.3 Hz, 1H), 2.35 (d, J_{HH} = 13.3 Hz, 1H).—^{13}C NMR (75.6 MHz, CD_2Cl_2,): δ = 147.0, 144.3, 141.0, 139.0, 137.7, 132.7, 129.3, 128.9, 128.8, 128.6, 128.5, 127.6, 127.5, 126.9, 23.3 (CH_2, J_{CH} = 142.6, 145.5 Hz). **3**: ^1H NMR (300 MHz, CD_2Cl_2): δ = 7.6, 7.45–7.55, 7.2–7.4 (m, 15H), 2.94 (dd, J_{HH} = 14.5, J_{PH} = 10.1 Hz, 1H), 2.55 (dd, J_{HH} = 14.5, J_{PH} = 4.2 Hz, 1H).—^{13}C NMR (75.6 MHz, CD_2Cl_2): δ = 144.7, 143.1 (d, J_{PC} = 7.1 Hz), 138.4 (d, J_{PC} = 33.9 Hz), 137.1 (d, J_{PC} = 4.0 Hz), 136.5 (d, J_{PC} = 10.5 Hz), 132.6 (d, J_{PC} = 19.0 Hz), 129.9 (d, J_{PC} = 1.3 Hz), 128.9, 128.8 (d, J_{PC} = 6.7 Hz, 128.7, 128.6, 127.9 (d, J_{PC} = 1.3 Hz), 127.4 (d, J_{PC} = 5.1 Hz), 127.0, 28.3 (CH_2, d, J_{PC} = 7.1, J_{CH} = 140.1, 143.5 Hz).—^{31}P NMR (121.7 MHz, CD_2Cl_2): δ = −18.0 (relative to external H_3PO_4).

[10] High resolution MS (EI, 70 eV): The molecular ions of both **2** and **3** were observed. **2**: *m/z* 344.0522, ($AsC_{21}H_{17}$, 344.0546 calc.). **3**: *m/z* 300.1062 ($PC_{21}H_{17}$, 300.1068 calc.).

[11] E. Breitmaier, W. Voelter: *Carbon-13 NMR Spectroscopy*, VCH Publishers, Weinheim/New York 1987.

[12] Crystals of **2** suitable for X-ray diffraction were grown from concentrated diethyl ether solutions at ca. −20 °C. Crystal data: $AsC_{21}H_{17}$, parallelepiped, ca. 0.28 × 0.35 × 0.42 mm, monoclinic, space group $P2_1/n$ (No. 14), a = 9.292(4), b = 6.734(1), c = 26.037(9) Å, β = 93.33(2)°, T = −70 °C, V = 1626.4 Å^3, $Mo_{K\alpha}$ radiation (CAD-diffractometer), μ_{calcd}(Mo) = 20.76 cm^{-1}, $\varrho_{calc.}$ = 1.406 g cm^{-3}, Z = 4, FW = 344.29. The structure was solved by direct methods and refined by a full-matrix least squares procedure to residuals of R = 0.042, R_w = 0.041, GOF = 1.34, for 2004 unique reflections with $I \geq 3\sigma$ and 267 variables, including isotropic refinement of all hydrogen atoms. Further details of the crystal structure investigations may be obtained from the Fachinformationszentrum Karlsruhe, Gesellschaft für wissenschaftlich-technische Information mbH, D-7514 Eggenstein-Leopoldshafen 2 (FRG), on quoting the depository number CSD-54274, the names of the authors, and the journal citation.

[13] Crystal data for **3**: $PC_{21}H_{17}$, irregular block, ca. 0.30 × 0.25 × 0.40 mm, monoclinic, space group $P2_1/n$ (No. 14), a = 9.248(2), b = 6.797(1), c = 25.851(6) Å, β = 93.50(1)°, T = −70 °C, V = 1621.9 Å^3, $Mo_{K\alpha}$ radiation, $\mu_{calc.}$(Mo) = 1.58 cm^{-1}, $\varrho_{calc.}$ = 1.230 g cm^{-3}, Z = 4, FW = 300.34. Compound **3** was found to be isostructural with **2** and was refined by a full-matrix least squares procedure to residuals of R = 0.048, R_w = 0.038, GOF = 1.13, for 1485 unique reflections with $I \geq 3\sigma$ and 267 variables, including isotropic refinement of all hydrogen atoms. For full details see reference [12].

[14] a) R. J. McKinney, T. H. Tulip, D. L. Thorn, T. S. Coolbaugh, F. N. Tebbe, *J. Am. Chem. Soc. 103* (1981) 5584; b) J. C. Calabrese, D. C. Roe, D. L. Thorn, T. H. Tulip, *Organometallics 3* (1984) 1223.

[15] The atoms in the four-membered ring of **3** deviate from a mean plane by 0.039, −0.071, 0.071, and −0.061 Å for P, C1, C2, and C3, respectively.

Structure of a 1:1 Adduct of Silyl Chloride and Dimethyl Ether at 100 K

By *Alexander J. Blake,* Stephen Cradock, E. A. V. Ebsworth,* and *Keith C. Franklin*

In the course of an investigation of the Raman and IR spectra of mixtures of dimethyl ether with silyl and germyl halides at low temperatures,[1] we found evidence for the existence of discrete adducts. As there are very few reports of simple adducts involving silyl halides as acceptors,[2,3] and no structural data have been reported except for (chlorosilyl)dimethylamine,[4] (where we have shown that a dimer forms in the crystal, with nitrogen acting as a donor to a five coordinate silicon), we sought more direct evidence for the precise nature of the interactions in the dimethyl ether sys-

[*] Dr. A. J. Blake, Dr. S. Cradock, Prof. E. A. V. Ebsworth, K. C. Franklin
Department of Chemistry, University of Edinburgh,
West Mains Road, GB-Edinburgh EH9 3JJ (Scotland)

tems by diffraction experiments. Noting that an equimolar mixture of silyl chloride and dimethyl ether formed a mass of crystals very readily on cooling or sublimation at low temperatures, this mixture was solidified by cooling on a Stoë STADI-4 four-circle diffractometer equipped with an Oxford Cryosystems low temperature device.[5] The bulk of the solid was melted, leaving only a seed crystal from which a single crystal ($0.5 \times 0.5 \times 0.6$ mm) suitable for X-ray diffraction was grown by cooling at the rate of 1 K min^{-1} to 100 ± 0.1 K, at which temperature data collection was undertaken.[6]

The individual adduct molecules lie on crystallographic mirror planes, with Cl, Si, H(1S) and O all lying in the plane and with the remaining silyl H atoms and the two methyl groups related by it (Fig. 1). The coordination at oxygen is

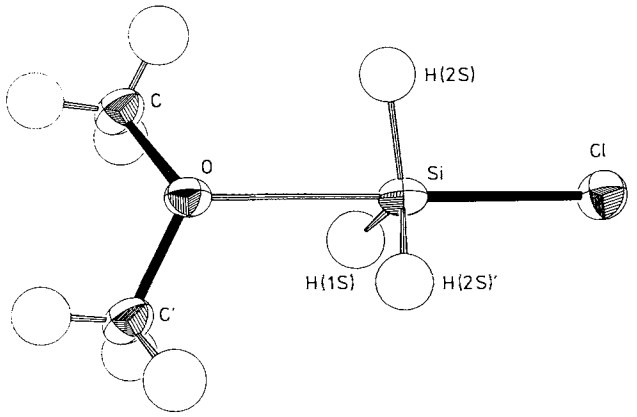

Fig 1. ORTEP plot of the 1:1 adduct of silyl chloride and dimethyl ether, with atom labeling scheme. Some pertinent bond lengths [Å] and angles [°] are: Si-Cl 2.1422(6), Si-O 2.2724(12), C-O 1.4331(20); O-Si-Cl 178.56(4), Cl-Si-H(1S) 101.7(12), Cl-Si-H(2S) 98.3(9), H(1S)-Si-H(2S) 115.4(15), H(2S)-SiH(2S)' 121.3(13), Si-O-C 115.53(9), C-O-C' 111.02(12).

pyramidal, the sum of the bond angles being only 342°. Cl, Si and O are almost colinear, which is consistent with trigonal bipyramidal coordination at Si, where Cl and O are axial. The silyl hydrogens are apparently pushed apart by the donor oxygen, giving HSiH and HSiCl angles which are respectively greater than and less than the tetrahedral value. Fully trigonal bipyramidal coordination at Si is not achieved in this structure, in contrast to the situation in the pentamer of silyldimethylamine,[9] where two equivalent bonds to nitrogen are axial, and the three bonds to hydrogen on each silicon equatorial.

The Si–Cl bond has lengthened over that found in the isolated SiH_3Cl molecule (2.05076(6) Å; gas phase, r_0).[10] This increase is less than that found in the dimer of (chlorosilyl)dimethylamine,[4] where the Si–Cl bond length is 2.231(6) Å, compared with 2.070(1) Å in the monomer (gas phase, r_a). The increase (0.09 Å) is comparable with that between solid and gaseous germyl chloride (0.07 Å).[11] In solid germyl chloride the germanium is essentially five coordinate, with two chlorine atoms in axial positions. Although it is clear from powder diffraction patterns that solid silyl chloride is isostructural with GeH_3Cl, difficulties in obtaining single crystals[12] mean that no Si–Cl bond length in solid SiH_3Cl is available.

The Si–O distance is far too short to be a van der Waals contact (the sum of the van der Waals radii is 3.5 Å), but long for a single bond. The sum of the covalent radii is 1.91 Å, and Si–O bonds are normally shorter than this (1.63–1.70 Å), because of the effects of bond polarity and d-orbital participation on Si. We may therefore compare the distance with other "secondary bonding" contacts in crystals of silyl compounds where we have shown that significant interactions occur between Si and donor atoms in other molecules (Table 1). The Si–O distance in Me_2O–SiH_3Cl is much short-

Table 1. Intermolecular contact distances between Si and first-row atoms in crystals.

Substance	Atom Pair	Distance [Å]	Ref.
$(ClH_2SiNMe_2)_2$	Si–N'	2.054(13)	[4]
Me_2O–SiH_3Cl	Si–O	2.2724(12)	this work
Silyl acetate	Si···O(=C)	2.721(4)	[a]
Methoxysilane	Si···O	2.8470(19)	[b]
Silyl fluoride	Si···F	2.8941(14)	[13]
Disiloxane	Si···O	3.115(5)	[c]
Silyl isocyanate	Si···O	3.303(3)	[d]

[a] M. J. Barrow, S. Cradock, E. A. V. Ebsworth, D. W. H. Rankin, *J. Chem. Soc. Dalton Trans. 1981*, 1988. [b] A. J. Blake, E. A. V. Ebsworth, S. G. D. Henderson, M. Dyrbusch, *Acta Crystallogr. Sect. C44* (1988) 1. [c] M. J. Barrow, E. A. V. Ebsworth, M. M. Harding, ibid. *Sect. B35* (1979) 2093. [d] M. J. Barrow, E. A. V. Ebsworth, M. M. Harding, *J. Chem. Soc. Dalton Trans. 1980*, 1838.

er than any other Si ··· O contact yet characterized; it is also shorter than the Si ··· F contact in solid silyl fluoride[13] or the Si ··· N contact in solid silyl cyanide,[14] both of which form well-defined chains. It is much more like the longer Si–N bond in the dimer of (chlorosilyl)dimethylamine[4] (like the present adduct, formed only in the solid), which at 2.054(13) Å is only 10% shorter.

We may relate these differences crudely to the differing basicities of the donor atoms; it is well known[15] that oxygen bound to Si is much less basic than oxygen in normal alkyl ethers, while nitrogen is intrinsically more basic than oxygen. The weak acceptor power of a silyl group thus allows the formation of distinctly stronger, and shorter, secondary bonds with dimethyl ether than between molecules of disiloxane, and even stronger, shorter bonds to the nitrogen of (chlorosilyl)dimethylamine, even though all these interactions are so weak that they give rise to discrete bonded species only in crystalline solids.

Received: August 7, 1989 [Z 3483 IE]
German version: *Angew. Chem. 102* (1990) 87

[1] S. Cradock, K. C. Franklin, unpublished.
[2] H. J. Campbell-Ferguson, E. A. V. Ebsworth, *J. Chem. Soc A 1966*, 1508; *1967*, 705.
[3] B. J. Aylett and J. Emsley, *J. Chem. Soc A 1967*, 652.
[4] D. G. Anderson, A. J. Blake, S. Cradock, E. A. V. Ebsworth, D. W. H. Rankin, A. J. Welch, *Angew. Chem. 98* (1986) 97; *Angew. Chem. Int. Ed. Engl. 25* (1986) 107.
[5] J. Cosier, A. M. Glazer, *J. Appl. Crystallogr. 19* (1986) 105.
[6] Orthorhombic, space group $Pn2_1m$, $a = 4.5395(5)$, $b = 7.7207(10)$, $c = 8.6532(10)$ Å, $V = 303.28$ Å^3 [from 2θ values of 36 reflections measured at $\pm\omega$ ($2\theta = 30-32°$, $\lambda = 0.71073$ Å)], $M = 112.63$, $Z = 2$ (implying that each adduct molecule lies on a crystallographic mirror plane), m.p. 190 K, $\varrho_{calc} = 1.233$ g cm^{-3}, $T = 100$ K, $\mu(Mo_{K\alpha}) = 0.691$ mm^{-1}. Data collection using $Mo_{K\alpha}$ radiation yielded 1493 data to $2\theta_{max} = 60°$, 768 unique ($R_{merg} = 0.034$), of which 741 with $F > 6\sigma(F)$ were used in all calculations. Automatic direct methods [7] located the non-H atoms, and a difference Fourier synthesis located all H atoms: these were subsequently refined [8] with anisotropic and isotropic thermal parameters respectively. Refinement converged to $R = 0.0203$, $R_w = 0.0264$, $S = 1.173$ for 46 refined parameters and the final ΔF synthesis showed no peak above

0.40 eÅ^{-3}. (In contrast, the alternative polarity gave higher residuals of 0.0307 and 0.0428 respectively and higher uncertainties in all refined parameters.) Atomic coordinates may be obtained from The Director of the Cambridge Crystallographic Data Centre, University Chemical Laboratory, Lensfield Road, GB-Cambridge CB2 1EW. Any request should be accompanied by the full literature citation for this communication.

[7] G. M. Sheldrick, *SHELX86, Program for crystal structure solution*, University of Göttingen, FRG, 1986.

[8] G. M. Sheldrick, *SHELX76, Program for crystal structure refinement*, University of Cambridge, England, 1976.

[9] A. J. Blake, E. A. V. Ebsworth, A. J. Welch, *Acta Crystallogr. Sect. C40* (1984) 895.

[10] J. L. Duncan, J. L. Harvie, D. C. McKean, S. Cradock, *J. Mol. Struct. 145* (1986) 225.

[11] A. J. Blake, E. A. V. Ebsworth, M. Dyrbusch, *Acta Crystallogr. Sect. C43* (1987) 1683.

[12] A. J. Blake, unpublished.

[13] A. J. Blake, E. A. V. Ebsworth, S. G. D. Henderson, A. J. Welch, *Acta Crystallogr. Sect. C41* (1985) 1141.

[14] P. D. Blair, A. J. Blake, R. W. Cockman, S. Cradock, E. A. V. Ebsworth, D. W. H. Rankin, *J. Mol. Struct. 193* (1989) 279.

[15] R. West, L. S. Whatley, K. J. Lake, *J. Am. Chem. Soc. 83* (1961) 761.

Ambident Behavior of the "New Vitamin" Methoxatin (Cofactor PQQ) towards Metals: Coordinative Stabilization of the Pyrrolide Form and the Semiquinone Form**

By *Brigitte Schwederski, Volker Kasack, Wolfgang Kaim,* Eberhard Roth,* and *Jeanne Jordanov*

Following the discovery and characterization of the novel oxidoreductase-coenzyme methoxatin (cofactor PQQ, 4,5-dioxo-4,5-dihydro-1*H*-pyrrolo[2,3-*f*]quinoline-2,7,9-tricarboxylic acid) in methanogenic and other microorganisms,[1] this system was recently established by several research groups as amineoxidase cofactor in bovine serum[2] and even designated as a potential "new vitamin".[3] Biochemical studies have afforded evidence pointing to an important function of the $1e^{\ominus}$-reduced (= *o*-semiquinone) form of methoxatin;[4] also the possibility of the redox behavior being influenced by coordination has been deduced from investigations conducted in the presence of metal ions.[5] On the basis of an ESR spectroscopically detectable ^{14}N-hyperfine structure, complexes of methoxatin[6] with $[Cu^{II}(bpy)]^{2\oplus}$ or $[Cu^{II}(terpy)]^{2\oplus}$[6b] have been described as *N,O*-coordinated; we report here that an O^4,O^5-coordination[7a] with resulting stabilization of the *o*-semiquinone intermediate[7] and of the pyrrole-deprotonated form favored by resonance takes place with the π-back-bonding metal center in $[Ru(bpy)_2]^{2\oplus}$.[7]

Reaction of PQQ with *cis*-$[Ru(bpy)_2Cl_2]$ in ethanol/water (1:5) under reflux affords after 1 h the green *o*-quinone complex **1** with intensive metal-to-ligand charge transfer (MLCT) transitions[7] from occupied d-levels of ruthenium(II) (low spin d^6) to the π* orbitals of the *o*-quinone PQQ and of the 2,2'-bipyridine ligands (Table 1). The comparability of these data with those of *o*-quinone model complexes such as for example of the 4,7-phenanthroline-5,6-dione **2** or of the 9,10-phenanthrenequinone **3**[7a] as well as the absence of the quinonecarbonyl stretching vibration at 1700 cm^{-1} in the IR spectrum confirm the O^4,O^5-coordination.[7] An elemental analysis and a pH titration indicated the neutral form of the isolated complex with double deprotonation of the very acidic[1c, 3a] COOH groups in the 7- and 9-position.

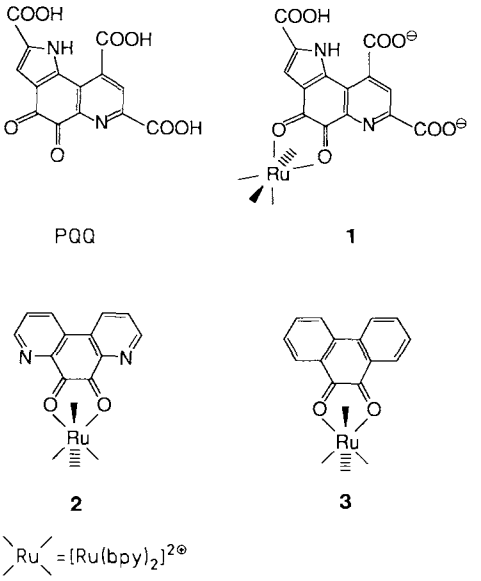

Table 1. Electrochemical, UV/VIS and ESR spectroscopic dat of Ru^{II} complexes of methoxatin and its model compounds.

	1	2	3
Cyclovoltammetry:			
E_1 (semiquinone/catechol)	0.26 V [a]	0.28 V [b]	0.30 V [b]
E_2 (quinone/semiquinone)	0.82 V [a]	0.82 V (irr.) [b]	0.90 V (irr.) [b]
UV/VIS:			
quinone complex			
λ_{max} ($d_{Ru} \rightarrow \pi^*_{bpy}$)	375 nm [c]	386 nm [d, e]	417 nm [d, e]
λ_{max} ($d_{Ru} \rightarrow \pi^*_{quinone}$)	722 nm [c]	748 nm [d, e]	752 nm [d, e]
Semiquinone complex			
λ_{max} ($d_{Ru} \rightarrow \pi^*_{bpy}$)	475 nm [f]	497 nm [d]	509 nm [d]
ESR (semiquinone):			
g_1	2.0210 [g]	2.0212 [h]	2.0287 [h]
g_2	2.0032 [g]	1.9992 [h]	1.9985 [h]
g_3	1.9851 [g]	1.9847 [h]	1.9829 [h]
$\langle g \rangle_{calculated}$	2.0032	2.0018	2.0035
$\langle g \rangle_{solution}$	2.0048 [i]	2.0014 [d]	2.0034 [d]
$\langle g \rangle_{solid}$	–	2.0034 [j]	2.0050 [j]

[a] In acetonitrile, 0.1 M $(Bu_4N)PF_6$, versus SCE. [b] In 1,2-dichloroethane, 0.1 M $(Bu_4N)PF_6$, versus SCE. [c] In 0.1 N $HClO_4$. [d] In 1,2-dichloroethane, 300 K. [e] Oxidized with $AgBF_4$. [f] In acetonitrile. [g] Adsorbed on Al_2O_3, 300 K. [h] In acetone, 4 K. [i] In acetonitrile, 300 K; $a(^{99,101}Ru) = 0.5$ mT. [j] In the solid state, 300 K.

Reduction to the brown *o*-semiquinone complex $\mathbf{1}^{\bullet\ominus}$ takes place in a physiologically easily accessible range at a more positive potential than in the case of free PQQ[3a] (Table 1); the radical shows a low-temperature ESR signal (Fig. 1a), which is identical to that of the reduced model complex $\mathbf{2}^{\bullet\ominus}$ (Fig. 1b) and is also hardly distinguishable from that of the phenanthrene-9,10-semiquinone complex $\mathbf{3}^{\bullet\ominus}$[7a] (Table 1).

[*] Prof. Dr. W. Kaim, Dr. B. Schwederski, Dipl.-Chem. V. Kasack, Dipl.-Chem. E. Roth
Institut für Anorganische Chemie der Universität
Pfaffenwaldring 55, D-7000 Stuttgart 80 (FRG)
Dr. J. Jordanov
Département de Recherche Fondamentale, Service de Physique
Centre d'Etudes Nucléaires, 85X
F-38041 Grenoble, Cédex (France)

[**] This work was supported by the Deutsche Forschungsgemeinschaft and the Deutsche Akademische Austauschdienst (Program PROCOPE). We thank Degussa AG and Ciba AG for generous gifts of chemicals.

As expected, the ESR spectrum of $\mathbf{1}^{\bullet\ominus}$ at room temperature (Fig. 1c) shows no resolution of the ^{1}H-and ^{14}N-hyperfine splitting.[1c] Therefore the particular line shape of the signal could not be reproduced. Nevertheless, the outer lines of the ^{99,101}Ru isotopic coupling (sextet) of 0.5 mT are clearly observable ($I = 5/2$, 30% natural abundance),[8] and can be reproduced by computer simulation (Fig. 1d): satellite lines and main lines appear in a ratio of (30%:6)/70% = 7.14%. From the absence of a strong ^{14}N-superhyperfine coupling in the ESR spectrum,[6b] O^4,O^5-coordination is also concluded at this stage; the basicity of the *o*-quinone oxygen centers should increase to a particularly large extent upon reduction, as also shown by the increase of the d(Ru)→π* excitation energy[7] (Table 1). A second reduction to the diamagnetic catecholate complex takes place at 0.26 V.

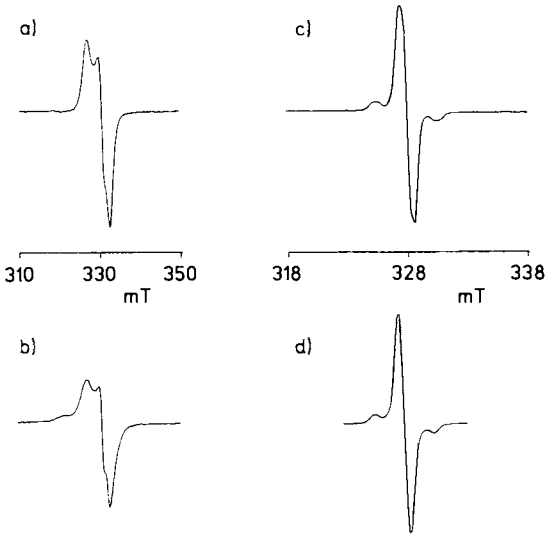

Fig. 1. ESR spectra (X band, measuring frequency $\nu = 9.22$ GHz) of a) complex $\mathbf{1}^{\bullet\ominus}$, adsorbed on Al_2O_3, 300 K; b) complex $\mathbf{2}^{\bullet\ominus}$ in acetone, 4 K; c) complex $\mathbf{1}^{\bullet\ominus}$ in acetonitrile, 300 K. d) Simulation of c) with $a(^{99,101}Ru) = 0.5$ mT, line width = 0.5 mT, gaussian line shape.

The quinone complex can not only be deprotonated at the carboxylic acid groups ($pK_a \leq 2.7$), but, with $pK_a = 8.5$, that is in a physiologically interesting region, at the pyrrole ring of the chromophore. The protonated green form of the complex **1** shows absorption maxima at 722 nm ($d_{Ru} \rightarrow \pi^*_{methoxatin}$) and 375 nm ($d_{Ru} \rightarrow \pi^*_{bpy}$) (Table 1), whereas these values are shifted upon deprotonation to 465 nm and 332 nm. This can

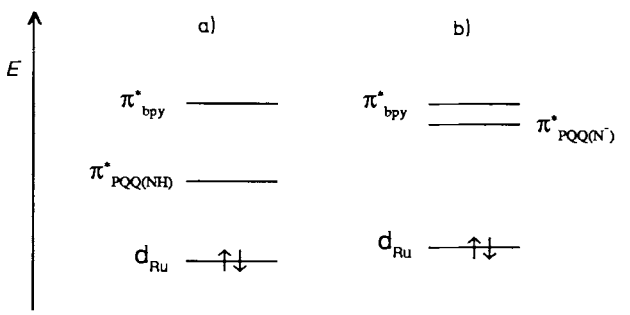

Fig. 2. Orbital energy diagrams of the complex **1** in a) protonated (pH < 7) and b) deprotenated form (pH > 10).

be interpreted in terms of a destabilization of the ruthenium d orbitals with concomitant larger destabilization of the methoxatin π* orbitals, as depicted in Figure 2.

The marked ease of pyrrolide formation (free PQQ has $pK_a \approx 10$)[1c] can be explained in terms of an electron delocalization corresponding to the three resonance forms of the deprotonated chromophore PQQ – $4H^{\oplus}$, whereby, as also in the semiquinone step,[1c, 7b, 9] a substantial part of the negative charge reaches to the metal-coordinating oxygen centers.

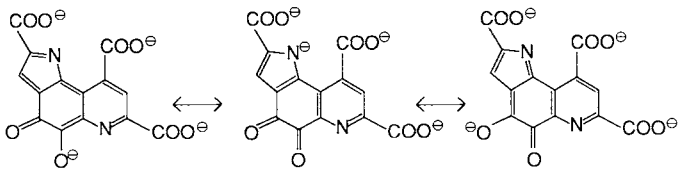

PQQ is thus an "isoambialterdentate" ligand,[10] which can not only coordinate differently to metal clusters with different "hardness", but, in addition, is also strongly influenced in its acid-base and redox behavior.

Experimental

A solution of methoxatin (50 mg, 0.15 mmol) and *cis*-$[Ru(bpy)_2Cl_2]\cdot 2H_2O$(80 mg, 0.15 mmol) in 30 mL of water/ethanol (5:1) was heated under reflux for 1 h. After cooling, the solution was treated with 50 mg of NH_4PF_6; the resulting precipitate was filtered off, washed with ethanol/water, and dried in a vacuum. Recrystallization from acetonitrile/diethyl ether (4:1) afforded the complex **1** in 65% yield (73 mg).

Received: July 19, 1989 [Z 3454 IE]
German version: *Angew. Chem. 102* (1990) 74

[1] a) J. A. Duine, J. Frank, *Trends Biochem. Sci. Pers. Ed. 6* (1981) 278; b) S. A. Salisbury, H. S. Forrest, W. B. T. Cruse, O. Kennard *Nature (London) 280* (1979) 843; c) J. A. Duine, J. Frank, J. A. Jongejan, *Adv. Enzymol. 59* (1987) 169; d) T. Ishida, M. Doi, K. Tomita, H. Hayashi, M. Inoue, T. Urakami, *J. Am. Chem. Soc. 111* (1989) 6822.

[2] a) C. L. Lobenstein-Verbeek, J. A. Jongejan, J. Frank, A. Duine, *FEBS Lett. 170* (1984) 305; b) R. S. Moog, M. A. McGuirl, C. E. Cote, D. M. Dooley, *Proc. Natl. Acad. Sci. USA 83* (1986) 8435; c) M. Ameyama, E. Shinagawa, K. Matsushita, K. Takimoto, K. Nakashima, O. Adachi, *Agric. Biol. Chem. 49* (1985) 3623.

[3] a) P. R. Sleath, J. B. Noar, G. A. Eberlein, T. C. Bruice, *J. Am. Chem. Soc. 107* (1985) 3328; b) J. A. Jongejan, R. A. van der Meer, J. A. Duine, *Trends Biochem. Sci. Pers. Ed. 11* (1986) 511.

[4] C. J. Suckling, *Angew. Chem. 100* (1988) 555; *Angew. Chem. Int. Ed. Engl. 27* (1988) 537.

[5] J. B. Noar, E. J. Rodriguez, T. C. Bruice, *J. Am. Chem. Soc. 107* (1986) 7199.

[6] a) J. A. Jongejan, R. A. van der Meer, G. A. van Zuylen, J. A. Duine, *Recl. Trav. Chim. Pays-Bas 106* (1987) 365; b) S. Suzuki, T. Sakurai, S. Itoh, Y. Ohshiro, *Inorg. Chem. 27* (1988) 592; c) cf. also P. F. Knowles, R. W. Strange, N. J. Blackburn, S. S. Hasnain, *J. Am. Chem. Soc. 111* (1989) 102.

[7] a) S. Ernst, V. Kasack, C. Bessenbacher, W. Kaim, *Z. Naturforsch B42* (1987) 425; b) S. Ernst, P. Hänel, J. Jordanov, W. Kaim, V. Kasack, E. Roth, *J. Am. Chem. Soc. 111* (1989) 1733; c) M. Haga, E. S. Dodsworth, A. B. P. Lever, *Inorg. Chem. 25* (1986) 447.

[8] W. Kaim, S. Ernst, S. Kohlmann, P. Welkerling, *Chem. Phys. Lett. 118* (1985) 431.

[9] a) R. deBeer, D. van Ormondt, M. A. van Ast, R. Banen, A. Duine, J. Frank, *J. Chem. Phys. 70* (1979) 4491; b) E. J. Rodriguez, T. C. Bruice, D. E. Edmondson, *J. Am. Chem. Soc. 109* (1987) 532.

[10] A. von Zelewsky, *Inorg. Chem. 20* (1981) 4448.

Combined Chemoenzymatic Synthesis of *N*-Glycoprotein Building Blocks**

By *Joachim Thiem** and *Torsten Wiemann*

N-Glycoproteins play a central role in processes of biological recognition[1a, b] such as oncogenesis,[1c] bacterial and viral infection,[1d] and uptake of various macromolecular substances. Furthermore, they govern blood-group type[1e] and are responsible for cell–cell recognition, cell growth, and cell differentiation.[1f]

ical synthesis of unprotected heterooligosaccharides is laborious and affords only low yields. Despite several modern and efficient glycosylation procedures, a practical alternative is often the use of enzymes.

With the goal of synthesizing partial structures of *N*-glycoproteins, we have used galactosyltransferase to form the Gal-β(1→4)-GlcNAc bond in the asparagine-linked oligosaccharides **6** and **10** (Scheme 1). The substrates for this enzymatic reaction (**5** and **9**, respectively) were synthesized via a chemical route (Scheme 2). The oligosaccharides **4** and **8**,

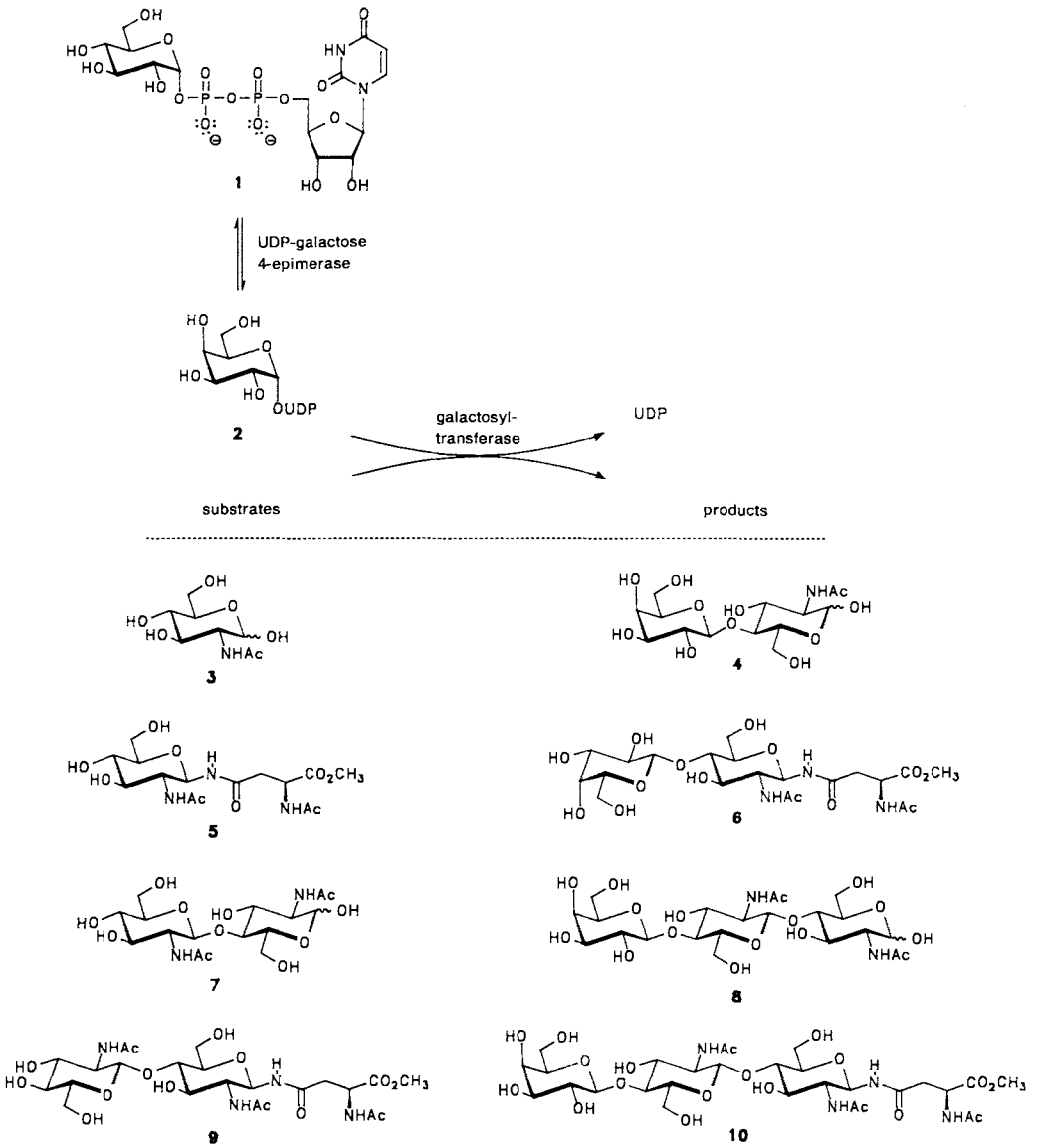

Scheme 1. Galactosylation catalyzed by galactosyltransferase.

The ready availability of reference substances for investigations of these highly specific phenomena is therefore of great importance. The molecular basis of such recognition processes derives from the extremely diverse ways of coupling monosaccharides; however, this also means that chemical synthesis of unprotected heterooligosaccharides is laborious and affords only low yields. Despite several modern and efficient glycosylation procedures, a practical alternative is often the use of enzymes.

With the goal of synthesizing partial structures of *N*-glycoproteins, we have used galactosyltransferase to form the Gal-β(1→4)-GlcNAc bond in the asparagine-linked oligosaccharides **6** and **10** (Scheme 1). The substrates for this enzymatic reaction (**5** and **9**, respectively) were synthesized via a chemical route (Scheme 2). The oligosaccharides **4** and **8**, which are not linked to an amino acid, were also synthesized enzymatically.

The galactosylation was accomplished by a standard procedure. The activated form of galactose required for the transferase reaction, namely, uridine-5′-diphosphate galactose (UDP-Gal, **2**) is very expensive and was therefore generated in situ from UDP-glucose (**1**) in a reaction catalyzed by UDP-galactose 4-epimerase. The galactose transfer from UDP-galactose to the respective acceptor thus occurs with release of UDP.

[*] Prof. Dr. J. Thiem, Dipl.-Chem. T. Wiemann
Organisch-chemisches Institut der Universität
Orléansring 23, D-4400 Münster (FRG)

[**] This work was supported by the Deutsche Forschungsgemeinschaft and the Fonds der Chemischen Industrie.

 © VCH Verlagsgesellschaft mbH, D-6940 Weinheim, 1990 0570-0833/90/0101-0080 $ 02.50/0

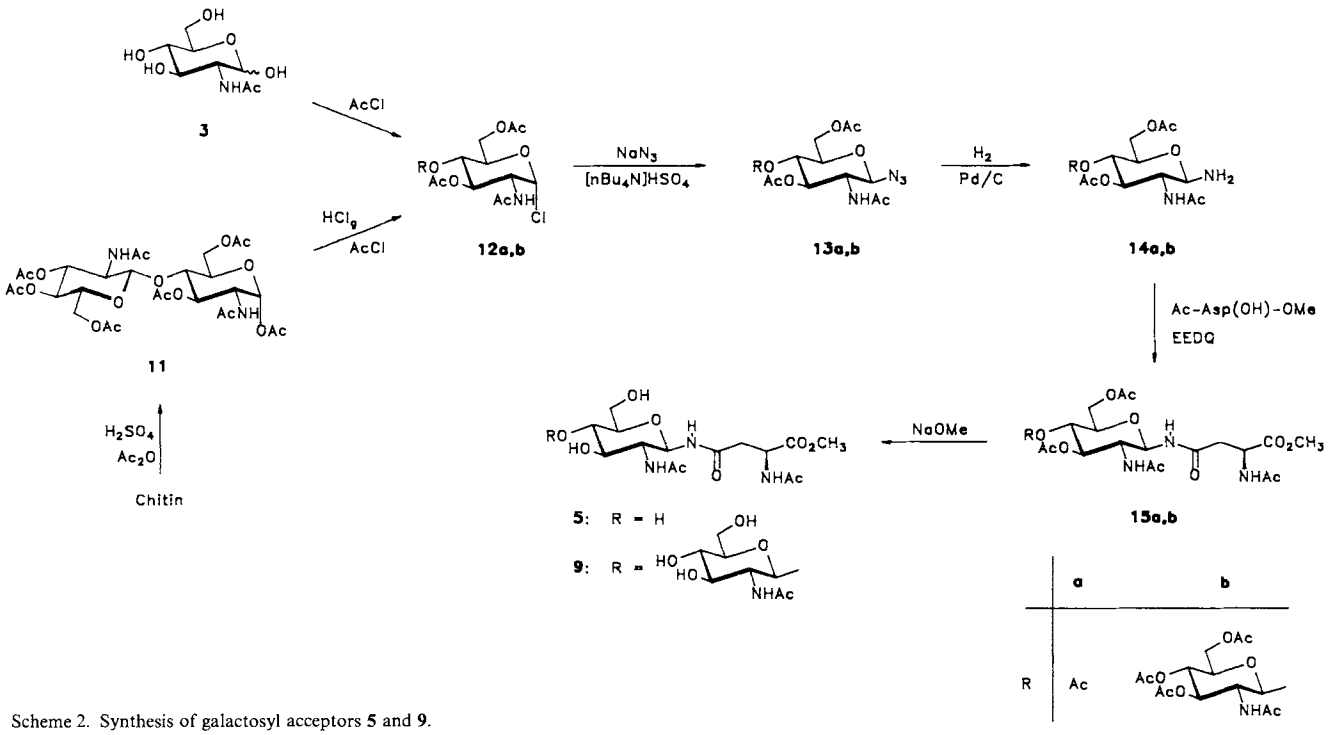

Scheme 2. Synthesis of galactosyl acceptors **5** and **9**.

This two-step galactosylation has also been carried out with immobilized enzymes and applied to other substrates in a synthetic cycle involving cofactor regeneration.[2] The combination of transferase and epimerase in soluble form offers a good compromise between cost on the one hand and preparation time and experimental facility on the other.

Galactosylation of *N*-acetylglucosamine (GlcNAc, **3**; 280 mg, 0.43 mmol) and of *N,N'*-diacetylchitobiose (**7**; 10 mg, 24 μmol) according to the procedure described here affords *N*-acetyllactosamine (**4**; 46 mg, 28%),[3a] the central disaccharide unit of numerous glycoproteins, and trisaccharide **8** (8 mg, 60%),[3b] respectively. Both substances may also be synthesized starting from UDP-Gal;[4] in the case of *N*-acetyllactosamine (**4**), a synthetic cycle involving cofactor regeneration[2] is also possible. The older chemical synthesis of **4** is much more laborious in our opinion, because of the large number of steps.[5]

The glycoconjugate β-D-galactopyranosyl-(1→4)-2-acetamido-1-[(*N*-acetyl-1-methyl-4-L-aspartyl)amino]-2-deoxy-β-D-glucopyranose (**6**) is present in the urine of patients suffering from aspartylglucosaminyluria.[6] The acceptor **5** required for the enzymatic galactosylation step was synthesized chemically by a procedure similar to that of *Hough* et al.[7] (Scheme 2). First, GlcNAc (**3**, 25 g, 113 mmol) was allowed to react with acetyl chloride to give the peracetylated α-chloride **12a**. Its substitution to afford β-azide **13a** was accomplished under phase-transfer catalysis in chloroform/water. Compound **13a** was then reduced to β-amine **14a**, which was coupled with α-methyl *N*-acetyl-L-aspartate in a reaction promoted by ethyl 2-ethoxy-1,2-dihydroquinoline-1-carboxylate (EEDQ). The de-*O*-acetylation with sodium methoxide affords the aspartylglucosamine **5** (20% yield over five steps, based on **3**). Before the galactosylation step, **5** has to be chromatographically purified on Bio-Gel P2. The standard method was again used in the enzymatic galactosylation to **6**, which was obtained in 35% yield (0.1-mmol scale). The expected β(1→4) linkage in **6** was confirmed by ^{1}H NMR spectroscopy.[3c] An earlier chemical synthesis of the completely deprotected form of **6** was accomplished by *Jeanloz* et al. in sixteen steps.[8]

Glycopeptide **10** is probably the receptor site for Robinia lectin on the surface of erythrocytes.[9] The synthesis of the asparagine-linked trisaccharide requires, once again, an initial chemical synthesis; galactosyl acceptor **9** was prepared in analogy to the work of *Jeanloz* et al.[10] and *Kunz* et al.[11] Acetolysis of chitin affords a mixture of oligomers, from which α-octaacetylchitobiose (**11**, 10%) can be isolated by flash chromatography. Octaacetate **11** (4.5 g, 6.7 mmol) was converted into α-chloride **12b**, which, in analogy to the synthesis of **5**, was transformed into β-azide **13b**. Compound **13b** was reduced to **14b**, which, in turn, was coupled with α-methyl *N*-acetyl-L-aspartate in an EEDQ-promoted reaction to give **15b**. After de-*O*-acetylation, the free disaccharide **9** (295 mg, 18% over five steps, based on **11**) was purified on Bio-Gel P2 and then used in the enzymatic galactosylation. The synthesis of the asparagine-linked trisaccharide **10** was accomplished in 28% yield (50-μmol scale).[3d]

Experimental Procedure

Enzymatic galactosylation of **3**, **5**, **7**, and **9**: The reaction was carried out in sodium cacodylate buffer (25 mM, pH 7.7) in the presence of manganese chloride (5 mM). After addition of UDP-glucose (**2**, 13 mM), acceptor (13 mM), and bovine serum albumin (1 mg mL^{-1}), the solution was degassed with nitrogen. Galactosyltransferase (EC 2.4.1.22, 1 U) and UDP-galactose 4-epimerase (EC 5.1.3.2, 10 U) were then added. After two days at 37 °C, the reaction mixture was worked up by anion exchange and the products **4**, **6**, **8**, and **10** were purified by gel chromatography (Bio-Gel P2).

Received: July 13, 1989 [Z 3434 IE]
German version: *Angew. Chem.* *102* (1990) 78

CAS Registry numbers:
3, 7512-17-6; **4**, 32181-59-2; **5**, 123883-46-5; **7**, 35061-50-8; **8**, 72358-28-2; **9**, 123883-47-6; **10**, 123883-48-7; **11**, 7284-18-6; **12a**, 3068-34-6; **12b**, 7531-49-9; **13a**, 6205-69-2; **13b**, 29625-70-5; **14a**, 4515-24-6; **14b**, 29673-51-6; **15a**, 123883-49-8; **15b**, 123883-50-1; Ac-Asp-OMe, 4910-47-8; chitin, 1398-61-4.

[1] a) H. Schachter, *Clin. Biochem. 17* (1984) 3; b) N. Sharon, H. Lis, *Chem. Eng. News 59 (13)* (1981) 21; c) T. Feizi, *Nature (London) 314* (1985) 53; d) J. A. Wilson, J. J. Shekel, D. C. Wiley, *ibid. 289* (1981) 373; e) V. Ginsburg, *Adv. Enzymol. 36* (1972) 131; f) G. E. Edelman, *Sci. Am. 1984* (4) 80; *Spektrum Wiss. 1984 (6)* 62.

[2] a) S. L. Haynie, C.-H. Wong, G. M. Whitesides, *J. Org. Chem. 47* (1982) 5416; b) C. Augé, S. David, C. Mathieu, C. Gautheron, *Tetrahedron Lett. 25* (1984) 1467; c) J. Thiem, W. Treder, *Angew. Chem. 98* (1986) 1100; *Angew. Chem. Int. Ed. Engl. 25* (1986) 1096.

[3] Selected ^{1}H NMR data (300 MHz, D_2O): a) **4**: δ = 5.19 (d, 1H, H-1, $J_{1,2}$ = 2.2 Hz, α form), 4.71 (d, 1H, H-1, $J_{1,2}$ = 7.5 Hz, β-form), 4.46 (d, 1H, H-1′, $J_{1',2'}$ = 7.5 Hz), 2.03 (s, 3H, NAc); b) **8**: δ = 5.20 (d, 1H, H-1, $J_{1,2}$ = 2.7 Hz, α form), 4.71 (d, 1H, H-1, $J_{1,2}$ = 8.1 Hz, β form), 4.62 (d, 1H, H-1′, $J_{1',2'}$ = 7.9 Hz), 4.48 (d, 1H, H-1″, $J_{1'',2''}$ = 7.8 Hz), 2.08 and 2.05 (each s, each 3H, each NAc); c) **6**: δ = 5.06 (d, 1H, H-1, $J_{1,2}$ = 9.4 Hz), 4.49 (d, 1H, H-1′, $J_{1',2'}$ = 7.6 Hz), 2.95 (dd, 1H, β-Asn, $J_{\alpha,\beta}$ = 5.6 Hz, $J_{\beta,\beta'}$ = 17.1 Hz), 2.82 (dd, 1H, β'-Asn, $J_{\alpha,\beta'}$ = 7.6 Hz); d) **10**: δ = 5.09 (d, 1H, H-1, $J_{1,2}$ = 9.6 Hz), 4.62 (d, 1H, H-1′, $J_{1',2'}$ = 8.1 Hz), 4.47 (d, 1H, H-1″, $J_{1'',2''}$ = 7.7 Hz), 2.06, 2.02, 2.01 (each s, each 3H, each NAc).

[4] H. A. Nunez, R. Barker, *Biochemistry 21* (1982) 1421.

[5] R. T. Lee, Y. C. Lee, *Carbohydr. Res. 77* (1979) 270.

[6] R. J. Pollitt, K. M. Pretty, *Biochem. J. 141* (1974) 141.

[7] D. E. Cowley, L. Hough, C. M. Peach, *Carbohydr. Res. 19* (1971) 231.

[8] M. A. E. Shaban, R. W. Jeanloz, *Bull. Chem. Soc. Jpn. 54* (1981) 3570.

[9] A. M. Leseney, R. Bourrillon, S. Kornfeld, *Arch. Biochem. Biophys. 153* (1972) 831.

[10] M. Spinola, R. W. Jeanloz, *J. Biol. Chem. 245* (1970) 4158.

[11] H. Kunz, H. Waldmann, *Angew. Chem. 97* (1985) 885; *Angew. Chem. Int. Ed. Engl. 24* (1985) 883.

Direct Electrical Communication between Graphite Electrodes and Surface Adsorbed Glucose Oxidase/Redox Polymer Complexes

By *Michael V. Pishko, Ioanis Katakis, Sten-Eric Lindquist, Ling Ye, Brian A. Gregg,* and *Adam Heller**

The redox centers of glucose oxidase, like those of most oxidoreductases, are electrically insulated by a protein (glycoprotein) shell. Because of this shell, the enzyme cannot be oxidized or reduced at an electrode at any potential. In an earlier communication it was shown that in homogeneous solutions, water-soluble polycationic poly(vinylpyridine) complexes of $[Os(bpy)_2Cl]^{2\oplus}$ bind to and accept electrons from reduced glucose oxidase, a polyanion.[1] Here we show that the same polycationic redox polymers are strongly adsorbed on graphite; that these modified surfaces adsorb strongly the enzyme; and that the surface adsorbed enzyme/polymer complexes communicate electrically with the electrodes. Electrodes containing these adsorbed complexes are faster and easier to construct than commercially available glucose electrodes.

Poly(4-vinylpyridine) (PVP), as well as *N*-methylated PVP, were shown earlier to be strongly adsorbed on pyrolytic graphite and to yield, with diffusing redox species, long-lived reproducible electrodes.[2, 3] Their electrochemistry is consistent with the physisorption of segments of the macromolecules providing a three-dimensional network into and out of which ions diffuse. Earlier studies of the electrochemistry of small redox proteins that do not have thick insulating shells around their redox centers, (such as cytochrome c, myoglobin, ferredoxin and phycocyanin) have also shown that, even though these proteins are directly electrooxidized/reduced on electrodes, their rates of electron transfer can be enhanced by adsorbed "promoters" (e.g. bipyridine, methyl viologen) that bind and orient the proteins, but do not participate in the redox processes.[4] We now find that pyrolytic carbon and graphite electrode surfaces can be modified with adsorbed polycationic redox polymers that complex glucose oxidase. In these structures, electrons are vectorially transferred from enzyme-bound glucose to the electrode via the redox centers of the enzyme and those of the redox polymer.

Strong adsorption of the redox polymer **1** on graphite is seen in the cyclic voltammetry of the terpolymer of poly(*N*-methyl-4-vinyl pyridinium chloride), 4-aminostyrene, and the PVP complex of $[Os(bpy)_2Cl_2]$ (see Scheme 1); at scan rates from 2 to 200 mV s^{-1}, the peak separation is 30 mV or less. Integration of the cyclic voltammograms at low scan rates (2–5 mV s^{-1}) shows that approximately 1.0×10^{-9} moles cm^{-2} of **1** are electroactive. The polymer does not desorb from rotating disk electrodes even at high angular velocities (2000 rpm), and coulometry shows that less than 10% of the polymer is desorbed from the electrodes after 30 days of storage in a stirred water bath. The polycationic adsorbed polymer **1** strongly binds glucose oxidase. Cyclic voltammograms for the oxidation of glucose by the enzyme–polymer complex are shown in Figure 1. The current response at a constant potential of 0.45 V (vs. SCE) persists for more than 10 hours when electrodes are rotated at 20 rpm in physiological salt solutions that do not contain

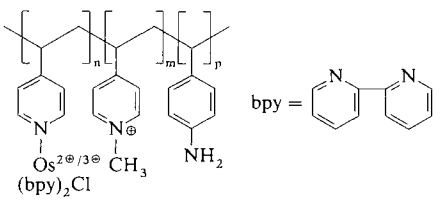

1, n = 0.14, m = 0.81, p = 0.05

Scheme 1. Structure of the quaternized redox terpolymer **1**.

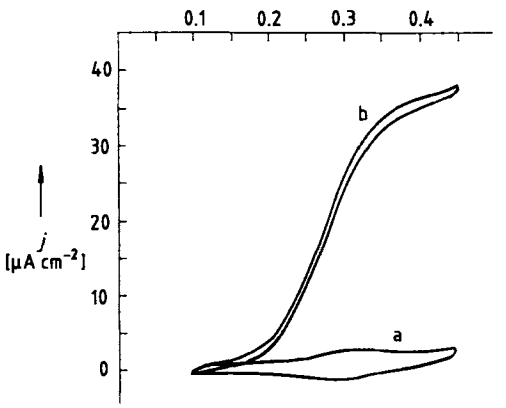

Fig. 1. Cyclic voltammogram of the **1**/glucose oxidase complex in 60 mM glucose, 9.9 units catalase mL^{-1}, 0.15 M sodium (4-(2-hydroxymethyl)-1-piperazineethanesulfonate (NaHEPES) at pH 7. Scan rate: 5 mV s^{-1} a) no glucose, b) 60 mM glucose. Potential Cl vs. SCE; glucose oxidase/**1**/graphite electrode.

[*] Prof. Dr. A. Heller, M. V. Pishko, I. Katakis, Dr. S.-E. Lindquist, L. Ye, Dr. B. A. Gregg
Department of Chemical Engineering, University of Texas at Austin
Austin, TX 78712 (USA)

[**] We wish to thank *Yinon Degani* for his valuable advice on the synthesis of the polymers and *Goran Svensk* for the molar mass determination of the Osmium-containing redox-polymer **1**. This work was supported in part by the Office of Naval Research and the Robert A. Welch Foundation.

any enzyme or polymer, declining approximately 10% over the first hour and 70% after 10 hours. The electrodes were stored in air at room temperature for 30 days with negligible loss in activity. Chronoamperometric measurements in a flow cell show that the current responds to an increase in glucose concentration in less than 1 s (Fig. 2). Response

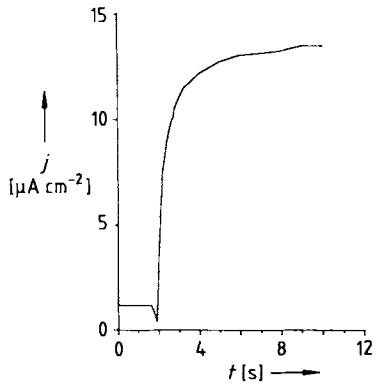

Fig. 2. Electrode response to a change in glucose concentration from 0 to 50 mM glucose in 0.15 M NaHEPES at pH 7.9.9 units catalase mL^{-1}. Flow rate: 193 $cm\,s^{-1}$. Glucose oxidase/**1**/graphite electrode.

times for different flow rates vary from 0.4 s at a linear flow rate of 42 $cm\,s^{-1}$ to 0.2 s at a flow rate of 210 $cm\,s^{-1}$. The glucose concentration dependence of the current at 0.45 V (SCE) is shown in Figure 3. A background current persists at zero glucose concentration. Because the electrodes are simple to construct and the materials cost little, they are likely to be appropriate for use in fast, disposable glucose sensing tips.

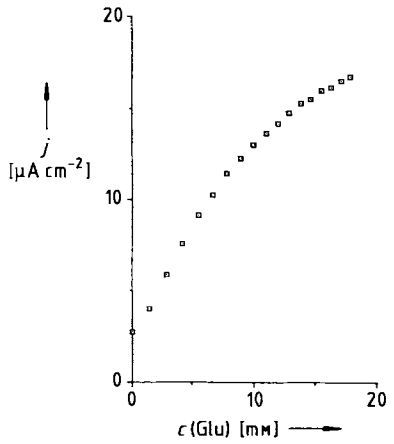

Fig. 3. Glucose concentration dependence of the current density at 0.45 V for the glucose oxidase/**1**/graphite electrode system in 0.15 M NaHEPES at pH 7 and 9.9 units catalase mL^{-1}.

The rate of glucose oxidase adsorption on redox-polymer **1** modified graphite electrode was studied by chronoamperometry. Electrodes were placed in 4 mL solutions of 60 mM glucose and 0.15 M NaHEPES at pH 7 and kept under N_2. 0.9 μg of catalase (44 000 units per mg protein) was added to prevent the deactivation of glucose oxidase by evolved H_2O_2. Approximately 10 μL of a 4 $mg\,mL^{-1}$ solution of glucose oxidase was slowly injected into the electrochemical cell to yield a final glucose oxidase concentration of 10 $\mu g\,mL^{-1}$. The potential was then stepped from 0 V to 0.45 V (SCE). The rise in current upon enzyme-complexing by the redox polymer coating of the electrode is shown in Figure 4.

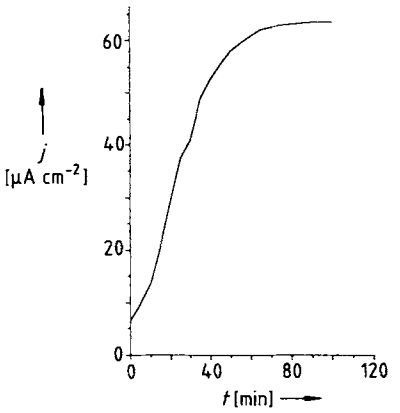

Fig. 4. Chronoamperometric response of a **1**/graphite electrode in 10 $\mu g\,mL^{-1}$ glucose oxidase, 60 mM glucose, 0.15 M NaHEPES at pH 7 with no catalase present.

Investigation of the effect of increasing salt concentration shows that electron transfer ceases at high (> 0.5 M) salt concentration in solutions containing only NaCl and buffer (no enzyme) but recovers upon dilution (to 0.15 M). This indicates that appropriate electrostatic bonding is critical for electron transfer not only in solution,[1] but also in adsorbed layers. The recovery of the current when the ionic strength is decreased shows that even at increased ionic strength, the complex does not dissociate. The loss in current response to glucose at high ionic strength is apparently caused by coiling of the polycationic redox polymer **1**.[1, 5] The coiled polymer no longer penetrates the protein, wherefore electron transfer cannot take place. At physiological ionic strength, the complex of polyanionic glucose oxidase and polycationic redox polymer **1** is, however, an effective electron relay between the enzyme bound substrate and the conductor.

Experimental Procedure

Glucose oxidase (E.C. 1.1.3.4) type X, catalase (E.C. 1.11.1.6) and NaHEPES were purchased from Sigma. $[Os(bpy)_2Cl_2]$ was prepared from K_2OsCl_6 (Aldrich) following a reported procedure. [6] 4-aminostyrene was purchased from Polysciences. Azobisisobutyronitrile (AIBN) and 4-vinylpyridine were purchased from Aldrich. Synthesis of the redox terpolymer **1** was prepared as reported [1]. Graphite (HB pencil leads 0.5 or 0.9 mm diameter) and pyrolytic carbon disks (4 mm diameter) were used as electrodes.

A Pine Instruments AFMSRX Rotator and an MSRX Speed Control were used for the rotating disk electrode (RDE) experiments. The flow cell was similar in design to a reported wall jet system [7].

The electrodes were insulated with a heat-shrinkable polypropylene sleeve. Their tips were then polished with 0.3 μm alumina, sonicated in deionized water for 20 s and blown dry with a stream of N_2. A drop (4 μL) of a solution of **1** (2.6 $mg\,mL^{-1}$ solvent) was applied to the electrode tip, allowed to stand for 4 min and then washed off with deionized water. The enzyme was adsorbed on the terpolymer coated surfaces by placing a 4 μL droplet of glucose oxidase solution (4.5 $mg\,mL^{-1}$) on the electrode surface, contacting for 10 min and rinsing. No containment membrane was used. Electrodes for the RDE experiments were polished and modified with a redox polymer in a similar manner.

Received: August 7, 1989;
supplemented: October 2, 1989 [Z 3485 IE]
German version: *Angew. Chem. 102* (1990) 109

[1] Y. Degani, A. Heller, *J. Am. Chem. Soc. 111* (1989) 2357.
[2] N. Oyama, F. C. Anson, *J. Am. Chem. Soc. 101* (1979) 739, 3450; K. Shigehara, N. Oyama, F. C. Anson, *Inorg. Chem. 20* (1981) 518; N. Oyama, F. C.

Anson, *J. Electrochem. Soc. 127* (1980) 247, 640; N. Oyama, T. Shimomura, K. Shigehara, F. C. Anson, *J. Electroanal. Chem. 112* (1980) 271; N. Scott, N. Oyama, F. C. Anson, *ibid. 110* (1980) 303; T. Shimomura, N. Oyama, F. C. Anson, *ibid. 112* (1980) 265; *J. Am. Chem. Soc. 103* (1981) 2552; N. Oyama, S. Yamaguchi, Y. Nishita, K. Tokuda, H. Matsuda, F. C. Anson, *J. Electroanal. Chem. 139* (1982) 371.

[3] J. Jernigan, N. Surridge, M. Zvanut, M. Silver, R. Murray, *J. Phys. Chem. 93* (1989) 4620; P. Denisovich, H. Abruna, C. Leidner, T. Meyer, R. Murray, *Inorg. Chem. 21* (1982) 2153; J. Calvert, T. Meyer *ibid. 21* (1982) 3978; E. Kober, B. Sullivan, W. Dressiale, J. Caspar, T. Meyer, *J. Am. Chem. Soc. 102* (1980) 7387; J. Facci, R. Schmehl, R. Murray, *ibid. 104* (1982) 4959; J. Facci, R. Murray, *Anal. Chem. 54* (1982) 7721; R. Murray, *Annu. Rev. Mater. Sci. 14* (1984) 145; *Philos. Trans. R. Soc. London A 302* (1981) 253.

[4] P. Yeh, T. Kuwana, *Chem. Lett. 1977*, 1145; E. Bowden, F. Hawkridge, H. Blount, *J. Electroanal. Chem. 161* (1984) 355; D. Reed, F. Hawkridge, *Anal. Chem. 59* (1987) 2334; J. Willit, E. Bowden, *J. Electroanal. Chem. 221* (1987) 265; K. Koller, F. Hawkridge, *ibid. 239* (1988) 291; E. Bowden, F. Hawkridge, H. Blount: "Electrochemical Aspects of Bioenergetics" in S. Srinivasan, Y. Chizmadzhev, J. Bockcis, B. Conway, E. Yeager (Eds.): *Comprehensive Treatment of Electrochemistry, Vol. 10*, Plenum, New York 1985, S. 297–346; J. Frew, H. Hill, *Philos. Trans. R. Soc. London B316* (1987) 95–106; H. Hill, *Pure Appl. Chem. 59* (1987) 743; F. Armstrong, H. Hill, N. Walton, *Acc. Chem. Res. 21* (1988) 407; M. Eddowes, H. Hill, *J. Chem. Soc. Chem. Commun. 1977*, 771; M. Eddowes, H. Hill, K. Uosaki, *J. Am. Chem. Soc. 101* (1979) 4461; *Bioelectrochem. Bioenerg. 7* (1980) 527; A. Cass, M. Eddowes, H. Hill, K. Uosaki, R. Hammond, I. Higgins, E. Plotkin, *Nature (London) 285* (1980) 673; K. Uosaki, H. Hill, *J. Electroanal. Chem. 122* (1981) 321; W. Albery, M. Eddowes, H. Hill, A. Hillman, *J. Am. Chem. Soc. 103* (1981) 3904; M. Eddowes, H. Hill, K. Uosaki, *ibid. 101* (1979) 7113.

[5] I. Nagata, H. Morawetz, *Macromolecules 14* (1981) 87; A. Katchalsky, *Pure Appl. Chem. 26* (1971) 327; H. Eisenberg: *Biological Macromolecules and Polyelectrolytes in Solution*, Clarendon Press, Oxford 1976; S. Carnie, G. Christos, T. Creamer, *J. Chem. Phys. 89* (1988) 6484.

[6] D. Buckingham, F. Dwyer, H. Goodwin, A. Sargeson, *Aust. J. Chem. 17* (1964) 325; P. Lay, A. Sargeson, H. Taube, *Inorg. Synth. 24* (1986) 291–306.

[7] W. Albery, P. Bartlett, A. Cass, D. Creston, B. Haggett, *J. Chem. Soc. Faraday Trans. 1 82* (1986) 1033–1050.

Platinum in the Unusual Oxidation State + 2.75: A Linear Tetranuclear Complex with the Model Nucleobase 1-Methylthymine**

By *Oliver Renn, Alberto Albinati,** and *Bernhard Lippert**

Besides the numerous mixed valence compounds of platinum with polymeric structure, which are stabilized via direct (Pt···Pt) stacking contacts[1] or via axial halogeno bridges,[2, 3] also smaller aggregates have been known for some time. In these tetra- and octanuclear complexes **I** and **II**, which, without exception, can be obtained from *cis*-$[(NH_3)_2Pt^{II}]$ and deprotonated cyclic[4–6] or open chain amides,[7] there are stacked dinuclear units with head-to-head bridging amidate ligands and direct (Pt···Pt) contacts; the average oxidation state is + 2.25[4, 6b, 7] and + 2.5,[5] respectively. A further type (**III**), which so far has only been isolated with M = Pd,[8] has a trinuclear structure with an average oxidation state of + 2.33 for the three metal atoms.

We report here on a new type of chloro-bridged tetranuclear complex (**IV**), in which platinum is present in the formal oxidation state + 2.75.

Mixed valence platinum compounds with the nucleobases uracil, thymine and cytosine ("platinum-pyrimidine blue

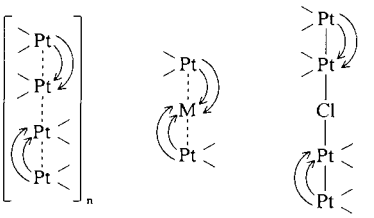

I, n = 1
II, n = 2 **III** **IV**

compounds") are of interest, inter alia, in view of their cancerostatic properties.[9]

In connection with studies on the characterization of such species we have also concerned ourselves with the oxidation behavior of diplatinum complexes which contain two 1-methylthymine anions in head-to-head arrangement as well as ammine- and choro-ligands. We found that diplatinum(II) complexes of type **1** (4 NH_3 ligands) exhibit a different oxidation behavior than **2** (3 NH_3, 1 Cl^-) and **3** (2 NH_3,

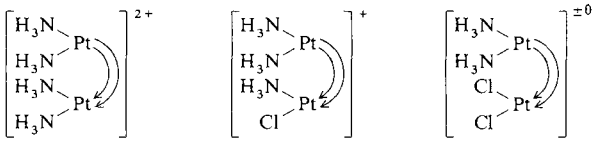

1 **2** **3**

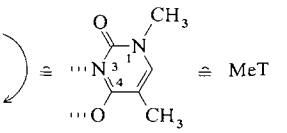

≙ MeT

2 Cl^-). Thus, in the absence of Cl^-, **1** is oxidized by cerium(IV), first to the tetranuclear platinum (2.25) complex **1a** and then to the diplatinum(III) complex **1b**;[10] in the case of **2** and **3**, on the other hand, not only the Pt(2.25) step is inter-

$$2\,[Pt(2.0)]_2 \xrightarrow{-e^\ominus} [Pt(2.25)]_4 \xrightarrow{-3e^\ominus} 2\,Pt(3.0)]_2$$
1 **1a** **1b**

mediary but also further mixed valence complexes, which are also characterized by their intense colors. For example, the $[Pt(2.25)]_4$-compound **2a** ($E^0_{Pt(2.0)/Pt(2.25)}$ = 450 mV, λ_{max} = 740 nm, ε = 16300 $M^{-1}cm^{-1}$) initially formed from **2** is first oxidized with cerium(IV) to one (or two[11]) further compound(s) (**2b**(?), **2c**) which absorbs (absorb) at 480 nm and after further addition of cerium(IV) is (are) finally converted into an orange-yellow diplatinum(III) compound **2d**.

$$2[Pt(2.0)]_2 \xrightarrow{-e^\ominus} [Pt(2.25)]_4 \xrightarrow{-e^\ominus} [Pt(2.5)]_4 \xrightarrow{-e^\ominus} [Pt(2.75)]_4 \xrightarrow{-e^\ominus} 2\,[Pt(3.0)]_2$$
2 **2a** **2b** **2c** **2d**

The preparative synthesis of the cations **2c** and **2d** in the form of the compounds **4** and **5**, respectively, was achieved by oxidation of **[2]**Cl[12] with H_2PtCl_6 in acid (pH 0.3). The structures are confirmed by the elemental and crystal structure analyses.[13] The average oxidation states of the platinum in the cations **2c** and **2d** are 2.75 and 3.0, respectively. With inclusion of all Pt atoms, i.e. also those of the anions,

[*] Prof. Dr. B. Lippert, Dipl.-Chem. O. Renn
Fachbereich Chemie, Lehrstuhl III Anorganische Chemie der Universität
Postfach 50 05 00, D-4600 Dortmund 50 (FRG)
Prof. Dr. A. Albinati
Istituto Chimico Farmaceutico della Università di Milano
Viale Abruzzi, 42, I-20131 Milano (Italy)

[**] This work was supported by the Deutsche Forschungsgemeinschaft and the Fonds der Chemischen Industrie.

the average oxidation numbers are 3.0 and 3.2 for **4** and **5** respectively.

cis-{[$(NH_3)_2Pt(MeT)_2PtCl_2]_2Cl$}$[PtCl_6] \cdot 6\,H_2O$
4 with cation **2c**

cis-$[(H_2O)(NH_3)_2Pt(MeT)_2PtCl_3][PtCl_6]_{0.5} \cdot 3\,H_2O \cdot 0.4\,HCl$ **5**
5 with cation **2d**

In both oxidation products, the NH_3-ligand *cis* to the Cl-ligand of the starting compound **2** has been replaced by a $Cl^{\ominus}$. A similar situation has already been found in a related diplatinum(III) complex of 1-methyluracil (MeU).[14] In **5** the geometry of the cation **2d** closely resembles that of the related MeU complex;[6c] however, a disorder of axial ligands (Cl, H_2O) and Cl^- from HCl is observed. This is the subject of further refinements. The Pt–Pt distance is 2.556(1) Å.

The centrosymmetric $[Pt(2.75)]_4$ cation **2c** consists of two diplatinum units of the composition *cis*-$(NH_3)_2Pt(MeT)_2$-$PtCl_2$ (Fig. 1) bound via a chloro bridge (Fig. 1). The geometry of these units is, in principle, similar to that of the corresponding diplatinum(II) compound **3**,[12] yet they both differ significantly in their Pt–Pt distances: 2.699(1) Å in **2c**, 2.861(1) Å in **3**. The Pt–Cl bonds in the linear chloro bridge (Pt1–Cl1–Pt* 180°) are markedly longer than the equatorial Pt–Cl bonds. The geometry of the $[PtCl_6]^{2\ominus}$ anion is normal. Aside from the hydrogen bonding there are no interactions with the cation. It may be assumed that the linearity of the chloro bridge is crucial for the electronic delocalization along the Pt_4 chain. It is reflected in the golden luster of the compound and in the ESR spectrum, which is typical for axially symmetric, mixed valence Pt-chains ($g_\perp = 2.411$, $g_\parallel = 1.987$).

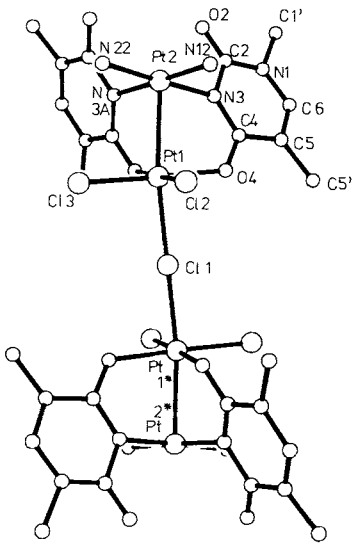

Fig. 1. Structure of the cation **2c** in compound **4**. Selected bond lengths [Å] and angles [°]: Pt1-Pt2 2.699(1), Pt1-Cl1 2.542(3), Pt1-Cl2 2.288(3), Pt1-Cl3 2.283(3), Pt1-O4 2.051(7), Pt1-O4A 2.034(7), Pt2-N3 2.027(8), Pt2-N3A 2.033(7), Pt2-N12 2.057(9), Pt2-N22 2.046(8); Pt2-Pt1-Cl1 167.00(2). Numbering of ring A corresponds to that of the ring shown here.

In contrast to [**2**]Cl and **5** (with the cation **2d**), **4** (with the cation **2c**) is relatively sparingly soluble in water. The cation **2c** ($\lambda_{max} = 430-480$ nm) is unstable in water and exhibits time-dependent changes in the visible spectral region. Reduction of **2d** with $Na_2S_2O_3$ leads to an intense absorption at 463 nm, whose maximum is reached after addition of exactly 0.25 equivalents of $S_2O_3^{2-}$ per Pt and which disappears again upon addition of further $Na_2S_2O_3$.[15] In terms of **2c** an extinction coefficient $\varepsilon \approx 21\,000\ M^{-1}\,cm^{-1}$ is obtained for this absorption.

The title compound **4** with the cation **2c** described here represents the first linear Pt_4-complex in which formally three platinum(III) and one platinum(II) are present.

Experimental

4 with cation **2c**: A solution of [**2**]Cl (44 mg) in 1 N HCl (7.5 mL) was treated dropwise with 0.1 mL of a 25% solution of H_2PtCl_6 in H_2O. After crystallinization at 4 °C in an open dish the supernatant orange solution was pipetted off; the shiny golden cubic crystals were washed with H_2O and acetone. Yield: 20%.

5 with cation **2d**: A solution of [**2**]Cl (44 mg) in 1 N HCl (7.5 mL) was treated with 0.3 mL of a 25% solution of H_2PtCl_6 in H_2O. After crystallization at 4 °C in an open dish, the supernatant orange solution was pipetted off; the red needlelike crystals were washed with H_2O and acetone. Yield 40%. Alternatively, **5** is obtained in comparable yield by reaction of a suspension of **3** in 1 N HCl with H_2PtCl_6.

Received: August 11, 1989 [Z 3494 IE]
German version: *Angew. Chem. 102* (1990) 71

[1] K. Krogmann, *Angew. Chem. 81* (1969) 10; *Angew. Chem. Int. Ed. Engl. 8* (1969) 35.
[2] For example R. J. H. Clark, V. B. Croud, H. M. Dawes, M. B. Hursthouse, *J. Chem. Soc. Dalton Trans. 1986*, 403, and references cited therein.
[3] For example a) R. J. H. Clark, M. Kurmoo, H. M. Dawes, M. B. Hursthouse, *Inorg. Chem. 25* (1986) 409; b) L. G. Butler, M. Heinrichs Zietlow, C.-M. Che, W. P. Schaefer, S. Sridhar, P. J. Grunthaner, B. I. Swanson, R. J. H. Clark, H. B. Gray, *J. Am. Chem. Soc. 110* (1988) 1155.
[4] J. K. Barton, H. N. Rabinowitz, D. J. Szalda, S. J. Lippard, *J. Am. Chem. Soc. 99* (1977) 2827.
[5] K. Matsumoto, K. Fuwa, *J. Am. Chem. Soc. 104* (1982) 897.
[6] a) B. Lippert, D. Neugebauer, *Inorg. Chem. 21* (1982) 451; b) P. K. Mascharak, I. D. Williams, S. J. Lippard, *J. Am. Chem. Soc. 106* (1984) 6428; c) B. Lippert, H. Schöllhorn, U. Thewalt, *Inorg. Chem. 26* (1987) 1736; d) W. Micklitz, J. Riede, B. Huber, G. Müller, B. Lippert, *ibid. 27* (1988) 1979.
[7] K. Sakai, K. Matsumoto, *J. Am. Chem. Soc. 111* (1989) 3074.
[8] W. Micklitz, G. Müller, B. Huber, J. Riede, F. Rashwan, J. Heinze, B. Lippert, *J. Am. Chem. Soc. 110* (1988) 7084.
[9] J. P. Davidson, P. J. Faber, R. G. Fischer, Jr., S. Mansy, H. J. Peresie, B. Rosenberg, L. van Camp, *Cancer Chemother. Rep., Part 1 59* (1975) 287.
[10] E^0 (**1/1a**) 560 mV (vs. Ag/AgCl); E^0 (**1a/1b**) 720 mV. For details of the methods see [6d]: λ_{max} (**1a**) 740 nm, $\varepsilon = 24\,100\ cm^{-1}\,M^{-1}$.
[11] From the shape and width of the 480-nm absorption it can be assumed that this is possibly an overlap of two bands, whereby an absorption in the range 510–520 nm would be expected for a $[Pt(2.5)]_2$ compound. Cf. B. Lippert, *New J. Chem. 12* (1988) 715.
[12] W. Micklitz, O. Renn, H. Schöllhorn, U. Thewalt, B. Lippert, *Inorg. Chem.*, in press.
[13] Crystal structure analysis: CAD-4 diffractometer, $Mo_{K\alpha}$ radiation, room temperature.—**4** with cation **2c**: monoclinic, space group $P2_1/n$, $a = 13.562(2)$, $b = 11.058(3)$, $c = 18.728(3)$ Å, $\beta = 105.60(2)°$, $V = 2705(2)$ Å^3, $Z = 4$, $\omega/2\theta$ scan with $2\theta \leq 50.0°$, 4717 reflections (corrected for absorption and decay), 3298 observed reflections with $F_0^2 \geq 2\sigma(F_0^2)$, Patterson and Fourier methods, anisotropic temperature factors for heavy atoms except water of crystallization oxygen atoms, $R = 0.037$ (observed reflections). Bridge Cl atoms (Cl1) and Pt3 ($PtCl_6^{2-}$ anion of **4**) on crystallographic inversion center (1), therefore only half a tetramer unit and half an anion independent, one H_2O molecule disordered, refined with occupation factors 0.5.—**5** with cation **2d**: monoclinic, space group C_2/c, $a = 23.874(3)$, $b = 19.144$; 4.78(2) Å, $\beta = 123.18(1)°$, $V = 5538(3)$ Å^3, $Z = 8$, $2\theta \leq 45.0°$, 4852 observed reflections with $F_0 \geq 2.5\sigma(F_0)$, heavy atoms refined with anisotropic temperature factors, $R = 0.064$ (observed reflections). Water of crystallization, water bound to Pt, and Cl disordered, possible models for the refinement in progress. Further details of the crystal structure investigations are available on request from the Fachinformationszentrum Karlsruhe, Gesellschaft für wissenschaftlich-technische Information mbH, D-7514 Eggenstein-Leopoldshafen 2 (FRG), on quoting the depository number CSD-54 140, the names of the authors, and the journal citation.
[14] B. Lippert, H. Schöllhorn, U. Thewalt, *Inorg. Chem. 25* (1986) 407.
[15] For comparison: Na_2PtCl_6 is not reduced under the given reaction conditions (pH 3).

A Wagner–Meerwein Rearrangement as Intermediate Step in the Formation of Dihydroindolones from 2-Diazoacetoacetanilides **

By *Gerhard Himbert** and *Martin Ruppmich*

For an intended study of the intramolecular reactivity of arylcarbamoylketenes, we synthesized the *N*-aryl-2-diazoacetoacetamides **1**[1] and attempted to induce them to undergo Wolff rearrangement. Our plan to achieve this by metal-catalyzed decomposition—an unfavorable route in view of our goal—was abandoned when, shortly after the start of our work, *Doyle* et al.[2] reported that this approach[3] (for example, addition of $[Rh_2(OAc)_4]$) could be used to transform 2-diazoacetoacetanilides **1** into 2-hydroxyindoles (type **2**) or the tautomeric dihydroindolones (type **3**).

We found, however, that simple heating of toluene or xylene solutions of **1** without the addition of a metal catalyst also led to the corresponding indole derivatives. Thus, thermolysis of *N*-(4-chlorophenyl)-2-diazo-*N*-methylacetoacetamide (**1a**) and of *N*-benzyl-2-diazo-*N*-(3,5-dimethylphenyl)acetoacetamide (**1b**) gave the 2-hydroxyindole derivative **2** and the tautomeric dihydroindolone derivative **3**, respectively (see Table 1). The formation of these derivatives

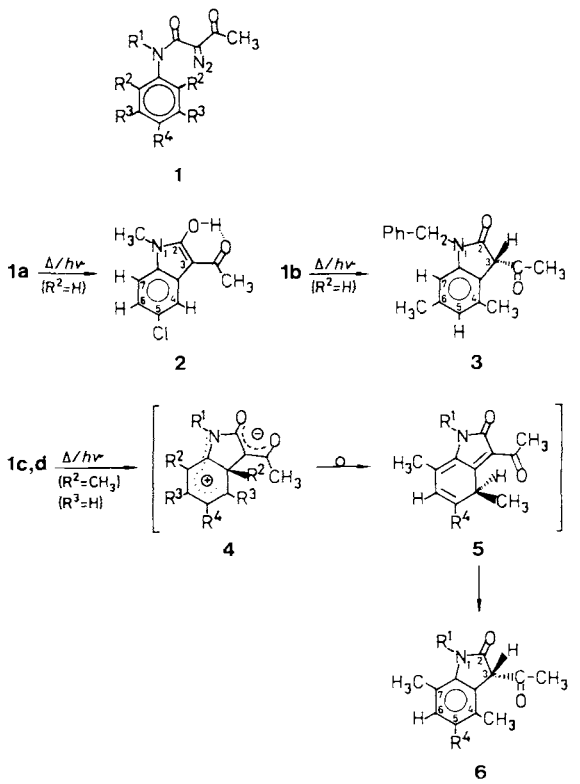

1	R^1	R^2	R^3	R^4	⟶	product
a	CH_3	H	H	Cl	⟶	**2**
b	$CH_2C_6H_5$	H	CH_3	H	⟶	**3**
c	CH_3	CH_3	H	H	⟶	**6a**
d	$CH_2C_6H_5$	CH_3	H	CH_3	⟶	**6b**

[*] Doz. Dr. G. Himbert, Dipl.-Chem. M. Ruppmich
Fachbereich Chemie der Universität
Postfach 3049, D-6750 Kaiserslautern (FRG)

[**] We thank *T. Grub* for his assistence as part of an advanced laboratory course.

can be explained as formally occurring by insertion of the carbene C atom into the *ortho* C–H bonds of aniline.[4]

We were very surprised, therefore, when thermolysis of the diazoacetoacetanilides **1c** and **1d** afforded the dihydroindolones **6a** and **6b**, respectively, as the sole characterizable products.[5] Since both *ortho* positions in the aniline moieties of **1c** and **1d** were blocked by methyl groups, Wolff rearrangement was expected to lead to carbamoylketenes.

The structure of the dihydroindolones **6a** and **6b** is supported by the spectroscopic data, in particular the ^1H NMR evidence that the methine H atom (3-H) is derived from the aryl H atom of **1c,d** (see Table 1). Both **6a** and **6b**, like **3**,

Table 1. Selected physical data for the indole derivatives **2**, **3**, **6a**, and **6b**.

2: Colorless needles with m.p., 120–121 °C in 79% yield after 24 h of heating in xylene. IR (KBr): $\tilde{\nu}$ [cm^{-1}] = 1650, 1630 (C=O/C=C); ^1H NMR (60 MHz, $CDCl_3$): δ = 2.40 (s, 3H, $COCH_3$), 3.30 (s, 3H, NCH_3), 6.78 (d, J_{AB} = 10 Hz, 1H, 7-H), 7.0–7.3 (m, 2H, 4-H, 6-H), 12.5 (s, 1H, OH); ^{13}C NMR (50.28 MHz, $CDCl_3$): δ = 20.57 (q, CH_3), 25.92 (q, NCH_3), 101.28 (s, C-3), 109.77, 119.77, 124.95 (3d, C-7, C-6, C-4), 123.73, 127.66, 137.31, 170.89, 174.47 (5s, C-5, C-7a, C-3a, C-2, C=O)

3: Colorless needles with m.p., 105–107 °C in 32% yield after 12 h of heating in toluene. IR (KBr): $\tilde{\nu}$ [cm^{-1}] = 1720, 1685, 1615 (C=O); ^1H NMR (60 MHz, $CDCl_3$): δ = 2.10, 2.23 (2s, 3H and 6H, 3 CH_3), 4.50 (s, 1H, 3-H), 4.85 (d, AB character, 2H, NCH_2), 6.40, 6.64 (2s, each 1H, 7-H and 5-H), 7.25 (m, 5H, Ph)

6a: Colorless crystals with m.p., 95–96 °C in 30% yield after 12 h of heating in toluene. IR (KBr): $\tilde{\nu}$ [cm^{-1}] = 1690 (C=O); ^1H NMR (90 MHz, $CDCl_3$): δ = 2.11, 2.26, 2.55 (3s, each 3H, 3 CCH_3), 3.50 (s, 3H, NCH_3), 4.43 (s, 1H, 3-H), 6.79, 7.02 (AB signal, J_{AB} = 8 Hz, each 1H, 5-H, 6-H); ^{13}C NMR (50.28 MHz, $CDCl_3$): δ = 18.33, 18.73, 28.28, 29.92 (4q, 4 CH_3), 60.63 (d, ^1J = 136.9 Hz, C-3), 117.69, 123.19, 124.72, 133.05, 133.24, 142.52 (total of 4s, 2d, 6 aryl C), 171.57, 200.17 (2s, 2 C=O)

6b: Colorless crystals with m.p., 122–124 °C in 40% yield after 12 h of heating in toluene. IR (KBr): $\tilde{\nu}$ [cm^{-1}] = 1690–1720 (C=O); ^1H NMR (90 MHz, $CDCl_3$): δ = 2.08, 2.21, 2.34 (3s, 3H, 6H and 3H, 4 CH_3), 4.60 (s, 1H, 3H), 5.18 (s, broad, 2H, NCH_2), 6.80 (s, 1H, 6-H), 7.1–7.4 (m, 5H, Ph)

exist in the keto form. Owing to its steric interaction with the acetyl methyl group, the methyl group in the 4 position prevents formation of the lower energy 2-hydroxyindole form, which has an intramolecular hydrogen bond (cf. **2**; the H atom in the 4 position leaves the acetyl group just enough room to form the planar enol system).

The formation of **6** more or less compells the intermediacy of zwitterion **4**, which arises by electrophilic attack of the carbene center on the *ortho* C atom[6] and whose charges can be optimally delocalized into, on the one hand, an aminosubstituted benzenium system, and, on the other, a bisacyl anion.[7] Since only indole formation occurs (see **2**, **3**, **6**), we are convinced that this electrophilic substitution of an arene does not involve free carbene. Instead, nitrogen elimination is induced by anchimeric participation of the electron-rich arene. In **4**, all prerequisites are present for the 1,2 shift of the "perturbing" methyl group in the neighboring (formerly, *meta*) position; the negative charge of the anionic moiety further promotes this rearrangement. The fully conjugated trienone **5** thereby obtained undergoes rearomatization to the benzene system, perhaps by 1,5-sigmatropic shift of the H atom to the O atom of the acetyl group. The final products, after tautomeric hydrogen shift, are the 3-acetyl-1,3-dihydro-2-indolones **6**.

Experimental Procedure

A solution of diazoacetamide **1a–d** [1] (10 mmol) in 30 mL of toluene or xylene (see Table 1) was refluxed for several hours. The solvent was removed under vacuum and the residue was dissolved in diethyl ether. Cooling of the resulting

solution and scratching of the glass to induce crystallization afforded the crystalline indole derivatives **2**, **3**, **6a**, and **6b** (solvent, reaction times and yields, see examples in Table 1).

Received: August 14, 1989;
supplemented: October 20, 1989 [Z 3499 IE]
German version: *Angew. Chem. 102* (1990) 69

CAS Registry numbers:
1a, 124043-87-4; **1b**, 124043-88-5; **1c**, 124043-89-6; **1d**, 124043-90-9; **2**, 124043-91-0; **3**, 124043-92-1; **6a**, 124043-93-2; **6b**, 124043-94-3.

[1] Synthesis of **1**: 2,2,6-Trimethyl-1,3-dioxin-4-one reacts with secondary amines to afford acetoacetamides (69–96%), which, upon treatment with tosyl azide or mesyl azide in the presence of triethylamine, give the diazo compounds **1** (44–63%).

[2] M. P. Doyle, M. S. Shanklin, H. Q. Pho, S. N. Mahapatro, *J. Org. Chem. 53* (1988) 1017.

[3] Reviews: M. P. Doyle, *Acc. Chem. Res. 19* (1986) 348; *Chem. Rev. 86* (1986) 919; G. Maas, *Top. Curr. Chem. 137* (1987) 75.

[4] Reviews: B. Eistert, M. Regitz, G. Heck, H. Schwall in E. Müller (Ed.): *Methoden der Organischen Chemie* (Houben-Weyl), *Bd. XI/4*, Thieme, Stuttgart 1968, p. 473ff.; M. Regitz, K. Korobizina, L. L. Rodina in F. Zymalkowsky (Ed.): *Methodicum Chimicum, Bd. 6*, Thieme, Stuttgart 1975, p. 253ff.; D. S. Wulfman, G. Linstrumelle, C. F. Cooper in S. Patei (Ed.): *The Chemistry of Diazonium and Diazo Group*, Wiley, New York 1978. p. 764ff.

[5] Also, photolysis of **1c** (10 mmol in 150 mL of benzene, 2.5 h at room temperature; Heraeus TQ 150 laboratory immersion lamp) gives **6a** (22%) as the sole product.

[6] The formation of zwitterion **4** might be preceded by an intramolecular cyclopropanation by the carbene center at the π system between *ipso* and *ortho* C atoms. The resulting norcaradiene, containing a fused β-lactam moiety, should then, for steric reasons, undergo heterolytic bond cleavage at the central σ bond affording **4**.

[7] Zwitterion **4** may also be involved as an intermediate in the formation of indole derivatives **2** and **3**.

Anions Isosteric with CO_3^{2-} in Cs_5SiP_3, Cs_5SiAs_3, Cs_5GeP_3, and Cs_5GeAs_3**

By *Brigitte Eisenmann*,* *Jürgen Klein*, and *Mehmet Somer*

The oxygen ligands in the orthosilicate ion SiO_4^{4-} and in the germanate ion Ge_4^{4-} can be completely replaced by the 5B elements phosphorus and arsenic. The charges of the resulting isosteric Zintl anions SiP_4^{8-} and $SiAs_4^{8-}$ and GeP_4^{8-} and $GeAs_4^{8-}$, respectively, can be compensated by doubly positive cations (E^{II} = Ca,Sr,Ba)[1–3] or by singly (Na) and doubly positive cations (E^{II} = Ca,Sr,Eu)[4] in the ratio 4:2. In contrast to the colorless oxosilicates and oxogermanates, these phosphido- and arsenido-silicates and -germanates are deep-red to black and are highly reflecting.

All attempts to replace the doubly positive cations completely by Na^+ ions have thus far failed. They led instead to the compounds Na_5SiX_3 and Na_5GeX_3 (X = P,As), respectively. These compounds contain oligomeric, binuclear units $[Si_2X_6]^{10-}$ and $[Ge_2X_6]^{10-}$, respectively,[5,6] which are formed from two edge-sharing tetrahedra.

We have now replaced the sodium by the significantly larger cesium and obtained the analogous compounds Cs_5SiX_3 and Gs_5GeX_3 (X = P,As) in the form of metallic, dark colored, extremely air-sensitive crystals. The compounds form an isotypic series: According to complete X-ray structure determinations[7] their crystal structures contain isolated SiP_3^{5-}, $SiAs_3^{5-}$ and GeP_3^{5-}, $GeAs_3^{5-}$ units respectively, in which the central atom is still only threefold coordinated by P and As atoms, respectively. The anions are strictly planar, but not exactly trigonal. The variation in the bond lengths is small; in all four compounds the maximum difference in the bond angles is about 6° (Table 1). The mean bond lengths are significantly shorter than the sum of the single bond radii corrected with regard to the difference in electronegativity.[8] Values between 1.28 ($SiAs_3^{5-}$) and 1.12 (GeP_3^{5-}) are calculated for the bond order according to *Pauling*.[8]

Table 1. Bond lengths d (E^{IV}-E^{III}) and bond angles ∢ (E^{III}-E^{IV}-E^{III}) in the anions [a].

Cpd.	d [pm]	∢ [°]	d_m [pm]	d_1 [pm]	d_2 [pm]	n
Cs_5SiP_3	217.9	116.5	219.0	225.2	205.2	1.22
	218.1	122.0				
	221.0	121.5				
Cs_5SiAs_3	228.2	116.2	229.1	236.8	219.2	1.28
	228.5	122.4				
	230.6	121.4				
Cs_5GeP_3	226.8	115.7	227.3	230.8	210.8	1.12
	227.0	121.8				
	228.2	122.1				
Cs_5GeAs_3	235.6	116.1	236.7	243.8	223.8	1.26
	235.9	121.8				
	238.5	122.1				

[a] d_m = mean bond length; d_1 = single bond lengths corrected with respect to difference in electronegativity according to *Pauling*; d_2 = double bond lengths corrected with respect to difference in electronegativity according to *Pauling*; n = bond order according to *Pauling*.

In the crystal, all atoms lie in the (010) plane at $y = 1/4$ and $y = 3/4$; the SiX_3^{5-} or GeX_3^{5-} groups in these planes are translated relatively to one another referred to the direction of projection [010] of Figure 1. The charge balancing Cs ions encapsule the anions in the form of large distorted trigonal prisms in which the centers of the basal plane edges are each occupied by a further Cs atom. The large prisms can thus also be described as an assemblage of four smaller trigonal prisms coupled face-to-face, each of which form the coordination polyhedron around each atom of the anionic groups. The coupling of the larger prisms via their basal planes leads to the formation of triangular columns parallel to [010], which in turn are each further bonded via two common edges to give puckered layers. Adjacent layers, displaced by 1/2 in b with regard to the anion planes, are so arranged that "free" prism edges of one and coupling edges of the other layer are adjoining.

With regard to their structure the SiX_3^{5-} and GeX_3^{5-} ions fit in the series of 24-valence-electron units BO_3^{3-}, CO_3^{2-} and NO_3^-, that is oxoanions of the first short period. They are the first examples of planar YX_3 anions in the solid state in which central atoms and ligands belong to higher periods. In the case of the PS_3^- ion, a trigonal-planar structure had actu-

[*] Dr. B. Eisenmann, Dipl.-Ing. J. Klein, Dr. M. Somer [+]
Eduard-Zintl-Institut der Technischen Hochschule
Hochschulstrasse 10, D-6100 Darmstadt (FRG)

[+] Permanent address: Max-Planck-Institut für Festkörperforschung
Heisenbergstrasse 1, D-7000 Stuttgart 80 (FRG)

[**] This work was supported by the Deutsche Forschungsgemeinschaft, the Fonds der Chemischen Industrie, and the Vereinigung von Freunden der Technischen Hochschule Darmstadt. We thank Prof. Dr. *R. Kniep* for stimulating discussions.

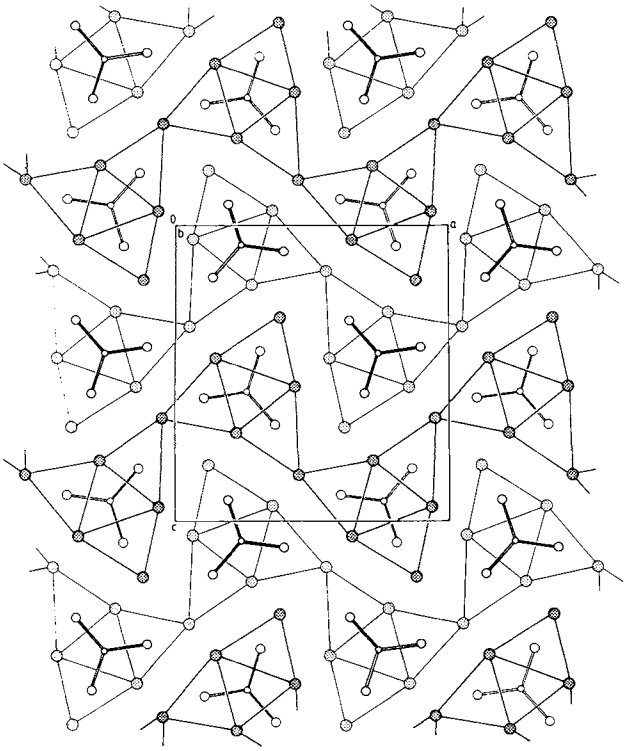

Fig. 1. Projection of the crystal structure of the compounds Cs_5SiP_3, Cs_5SiAs_3, Cs_5GeP_3 and Gs_5GeAs_3 on (010). The Cs atoms are shown as hatched circles, the Si and Ge atoms as small open circles, and the P and As atoms as large open circles; the boldness of the lines indicate the heights of the displacements 1/2 in *b*. The connecting lines between the Cs atoms do not represent bonds but merely serve to outline the polyhedra.

ally been deduced for the gaseous state, but this could not be unequivocally detected in the solid state.[9] Homonuclear trigonal-planar Si_4 clusters are present in $Li_{12}Si_7$.[10] Here, band structure calculations[11] show that largely covalent Li–Si interactions contribute to the stabilization of the clusters.

Experimental

The elements (Cs; Si or Ge; P or As) were weighed out in the ratio 7:1:3 under argon in tantalum ampoules and heated within 4 h to 675 °C, kept at this temperature for 6–8 h, and then cooled to room temperature in 40 h. For the preparation of the phosphorus compounds the elemental phosphorus was replaced by equivalent amounts of Cs_4P_6. The excess Cs was removed by distillation in a high vacuum at 150 °C. According to X-ray powder photographs, the compounds are formed in pure phases. They form dark, shiny metallic, prismatic crystals, which decompose spontaneously to still unidentified products on exposure to moist air.

Received: September 1, 1989 [Z 3533 IE]
German version: *Angew. Chem. 102* (1990) 92

[1] B. Eisenmann, H. Jordan, H. Schäfer, *Angew. Chem. 93* (1981) 211; *Angew. Chem. Int. Ed. Engl. 20* (1981) 197.
[2] B. Eisenmann, H. Jordan, H. Schäfer, *Z. Anorg. Allg. Chem. 475* (1981) 74.
[3] B. Eisenmann, H. Jordan, H. Schäfer, *Mater. Res. Bull. 17* (1982) 95.
[4] H. G. von Schnering, M. Hartweg, H. Kalpen, J. Nuss, W. Hönle, *Z. Kristallogr. 182* (1988) 238.
[5] B. Eisenmann, M. Somer, *Z. Naturforsch. B 40* (1985) 886.
[6] B. Eisenmann, J. Klein, M. Somer, unpublished.
[7] Crystal structure data: measurement: PW 1100 four-circle diffractometer, graphite monochromator, scintillation counter, $5° \le 2\theta/2\theta \le 60°$, $\theta/2\theta$ scan, $Mo_{K\alpha}$ radiation. Determination: SHELX-86, SHELX-76, direct methods, least squares, full matrix, 55 variables in each case.—Cs_5SiP_3: $a = 1414.4(4)$, $b = 599.5(2)$, $c = 1550.0(4)$ pm; space group *Pnma*; $Z = 4$; $R_{aniso} = 0{,}057$ for $N_{(hkl)} = 1938$.—Cs_5SiAs_3: $a = 1446.7(4)$, $b = 604.3(2)$, $c = 1582.0(4)$ pm; space group *Pnma*; $Z = 4$; $R_{aniso} = 0.054$ for $N_{(hkl)} = 1850$.—Cs_5GeP_3: $a = 1431.1(4)$, $b = 599.4(2)$, $c = 1561.8(4)$ pm; space group *Pnma*; $Z = 4$; $R_{aniso} = 0.083$ for $N_{(hkl)} = 1903$.—Cs_5GeAs_3: $a = 1461.5(4)$, $b = 604.5(2)$, $c = 1596.4(4)$ pm; space group *Pnma*; $Z = 4$; $R_{aniso} = 0.077$ for $N_{(hkl)} = 1628$. Further details of the crystal structure investigations are available on request from the Fachinformationszentrum Karlsruhe, Gesellschaft für wissenschaftlich-technische Information mbH, D-7514 Eggenstein-Leopoldshafen 2 (FRG), on quoting the depository number CSD-54182, the names of the authors, and the journal citation.
[8] L. Pauling: *Die Natur der chemischen Bindung*, Verlag Chemie, Weinheim 1962, pp. 210–227; *The Nature of the Chemical Bond*, Cornell University Press, Ithaca 1960.
[9] H. W. Roesky, R. A. Ahlrichs, S. Brode, *Angew. Chem. 98* (1986) 91; *Angew. Chem. Int. Ed. Engl. 25* (1986) 82.
[10] H. G. von Schnering, R. Nesper, J. Curda, C.-F. Tebbe, *Angew. Chem. 92* (1980) 1070; *Angew. Chem. Int. Ed. Engl. 19* (1980) 1033.
[11] M. C. Böhm, R. Ramirez, R. Nesper, H. G. von Schnering, *Phys. Rev. B30* (1984) 4870.

$[H_6As_{10}Mo_{24}O_{90}]^{8\ominus}$, a Heteropolyanion Comprising Two Linked Spherical Fragments, and Reduced Keggin Anions as Its Degradation Products**

By *Achim Müller,* Erich Krickemeyer, Michael Penk, Volker Wittneben,* and *Joachim Döring*

Dedicated to Professor Gerhard Fritz on the occasion of his 70th birthday

We have been interested in V^{IV}/V^V, $As^{III}/V^{IV}/V^V$, $As^{III}/Mo^V/Mo^{VI}$, and $Bi^{III}/Mo^V/Mo^{VI}$ oxygen clusters and polyanions because of their interesting structural chemistry and their importance for catalysis.[1] Examples include a bismuth-molybdate catalyst[1c] for selective oxidations in petrochemistry and the "V_2O_5" catalyst, which contains V^{IV} centers.[1a] Both catalysts are poisoned by As. Of particular interest, for example in analytical chemistry, are reduced heteropolyanions of the Keggin type (cf. Ref. [2]). Very little is known about the corresponding crystalline mixed-valence species, especially about their electronic structures, which are of general importance for understanding the electron-storage function of metal clusters.[2]

We have now synthesized the blue title compound **1**, whose anion may be formally described as $[H_6As^{III}_{10}Mo^V_8Mo^{VI}_{16}O_{90}]^{8\ominus}$. Oxidation of **1** by exposure to air affords the likewise blue salts **2** and **3** containing mixed-valence Keggin-type heteropolyanions (a well-known Keggin anion is $[PMo_{12}O_{40}]^{3\ominus}$),[2] which may be formally regarded as $[H_4As^VMo^V_4Mo^{VI}_8O_{40}]^{3\ominus}$ and $[H_2As^VMo^V_2Mo^{VI}_{10}O_{40}]^{3\ominus}$.

$(HNMe_3)_8[H_6As_{10}Mo_{24}O_{90}] \cdot 9\,H_2O$ **1**
$(HNMe_3)_3[H_4AsMo_{12}O_{40}]$ **2**
$(HNMe_3)_3[H_2AsMo_{12}O_{40}]$ **3**

These species provide textbook examples for structural chemistry; however, their isolation and characterization has been difficult so far.[2] The compounds **1**–**3** were characterized by elemental analysis (including manganometric titration of Mo^V), electrochemical studies (for **1**), thermoanalysis (to determine the amount of crystal water in **1**), IR and

[*] Prof. Dr. A. Müller, E. Krickemeyer, M. Penk, V. Wittneben, J. Döring
Fakultät für Chemie der Universität
Postfach 8640, D-4800 Bielefeld 1 (FRG)

[**] We thank Professor *M. T. Pope*, Washington, D.C., for important suggestions.

electronic absorption spectroscopy, and single-crystal X-ray structure analysis.[3]

The novel 34-nuclear mixed-valence discrete anion of **1** occupies a center of inversion in the crystal lattice and consists of MoO_6 octahedra and AsO_3 pyramids (Fig. 1). For-

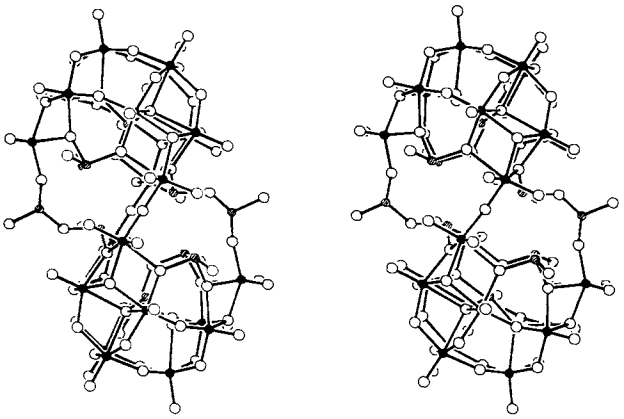

Fig. 1. Stereoview of the structure of the anion in **1** (H atoms omitted; Mo = black, As = hatched, O = white). Interatomic distances [pm] and angles [°]: Mo···Mo (edge-linked 327.6–348.0, Mo···Mo (corner-linked) 363.3–369.1, Mo-O_{term} 165.6–173.1, Mo-(μ-O) 182.4–237.8, As-O_{term} 173.2–181.1, As-(μ-O) 174.9–180.8; O_{term}-Mo-(μ-O) 87.5–104.4, 162.5–170.3, (μ-O)-Mo-(μ-O) 69.5–97.4, 148.1–159.1, O-As-O 93.2–102.5.

mally, it is composed of two $As_4Mo_{12}O_{42}$ spherical fragments of approximate C_{3v} symmetry with a central AsO_3 group. The two units are linked by four bridges in such a way that the openings of the spheres do not lie directly opposite each other. Both halves contain an $AsMo_9$ Keggin fragment (cf. Fig. 1) capped by a ring built up of three AsO_3 and three $Mo^{VI}O_6$ polyhedra (the oxidation states of these three Mo atoms are derived from the significantly higher value of the valence sum[4] and are also supported by the fact that, in polyanions, reduced Mo centers with two terminal O atoms are unknown). This means that, in both halves, four electrons are delocalized over the remaining Mo atoms.

Cluster **1** displays a number of interesting structural features, such as the novel connection of two spherical fragments[5] and the As_2O_5 groups linking the two halves.

The anions of **2** and **3**, formed from **1** by mild oxidative degradation, are both of the Keggin type and each contains one As^V center (Fig. 2; the anions are viewed from a similar perspective as in Fig. 1 in order to highlight the partial structural similarity of the anions). $[H_4AsMo_{12}O_{40}]^{3\ominus}$ (**2**) is a four-electron-reduced β-Keggin anion;[2] disregarding the H atoms, it is isostructural to $[H_6PMo_{12}O_{40}]^{\ominus}$,[2a] the only previously structurally characterized reduced Mo Keggin anion, whose protonated O atoms could not be completely identified. The anion of the further oxidation product **3** formally contains two Mo^V centers and has an α-Keggin structure. (To the best of our knowledge, a twofold reduced Keggin anion has not yet been structurally characterized.) The β isomer of the Keggin anion can formally be formed from the α isomer by rotating one of the four Mo_3O_{13} units by 60° (similar structural changes presumably occur within the bismuth-molybdate catalyst; cf. Ref. [1c]). It is interesting in this connection that the Mo_{12} partial framework of **1** rearranges to the Keggin-type framework of **2** and **3** with retention of the structure of the $AsMo_9$ spherical fragment (cf. Figs. 1 and 2) and that, on going from **1** to **2**, merely As^{III} is oxidized to As^V.

The Mo–Mo distances in the anions are, on average, 335.9 pm in **1** and 347.2 pm in **2** for the edge-linked octahedra and 366.0 pm in **1** and 368.7 pm in **2** for the corner-linked octahedra. An average Mo–Mo distance of 358.2 pm (influenced by the disorder[3]) is found in the anion of **3**. The slight changes in the Mo–Mo distances in comparison to those in nonreduced polymolybdates[2] indicate only weak metal–metal interactions (cf. below).

The number of protons in **1**, **2**, and **3** was derived from a titrimetric determination of the number of Mo^V centers and the charge of the anion. The six terminal O atoms bonded to As in **1** are probably protonated, because the As–O_{term} and As–(μ-O) bonds are of roughly equal length (cf. Fig. 1). In **2**, the positions (cf. Fig. 2a) of the four protonated O atoms can be identified unambiguously owing to the markedly longer Mo–O bonds (210.0 instead of 191.1 pm) and smaller Mo–O–Mo angles (115.9 instead of 126.6°).

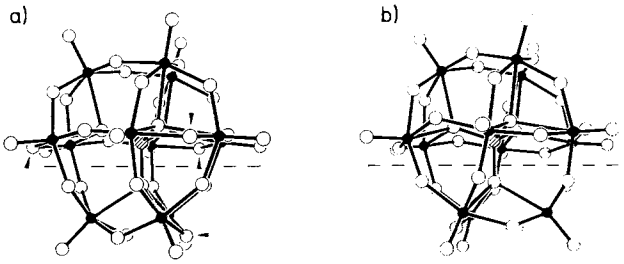

Fig. 2. Comparison of the two Keggin anions (H atoms omitted) of **2** and **3**, which may be transformed into each other by rotating an Mo_3O_{13} group (below the broken line) [3]. The structural moiety above the broken line corresponds to the $AsMo_9$ spherical fragment of **1**. Mo = black, As = hatched, O = white. a) Structure of the β-Keggin anion of **2** (protonated O atoms marked with arrows). Interatomic distances [pm] and angles [°]: Mo···Mo (edge-linked) 341.0–361.3, Mo···Mo (corner-linked) 364.7–371.1, Mo-O_{term} 165.5–171.1, Mo-(μ-O) 187.5–243.0, As-O 165.3–169.1; O_{term}-Mo-(μ-O) 96.9–105.1, 164.8–171.5, (μ-O)-Mo-(μ-O) 69.8–94.2, 149.7–163.2, O-As-O 108.2–111.7. b) Structure of the α-Keggin anion of **3**. The central AsO_4 tetrahedron is shown in only one of the disordered positions (bond lengths and angles are not accurate owing to disorder). Interatomic distances [pm] and angles [°]: Mo···Mo 350.5–379.6, Mo-O_{term} 161.1–167.5, Mo-(μ-O) 176.6–248.0, As-O 165.9–170.7; O_{term}-Mo-(μ-O) 98.9–104.3, 151.6–161.6, (μ-O)-Mo-(μ-O) 56.8–101.8, 154.9–158.9, O-As-O 105.4–112.2.

The electronic spectra of **1**–**3** (measured in H_2O) show characteristic intervalence charge-transfer transitions at ca. 8850 (**1**), 9000 (**2**), and 9100 (**3**) cm^{-1}. In basic solvents (e.g., dimethylformamide (DMF)) deprotonations of the anions lead to marked changes in the electronic spectra, especially for the more intense and complex near-IR bands (presumably also intervalence charge-transfer bands) with a maximum at ca. 12000 cm^{-1}. Magnetic measurements on **1**–**3** indicate very strong spin–spin interactions. Detailed investigations are in progress.

Mixed-valence metal clusters[9] that exist with different electron populations, such as those described here,[10] are also of importance for understanding electron-transfer and electron-storage systems in nature (e.g., ferredoxins, which are very important and ubiquitous in the biosphere) and in catalysis. In the catalysts described at the beginning of this communication, the "turn-over process" results in the delocalization of electrons in the lattice or the metal cluster, whereby HOMO and LUMO have to satisfy certain conditions. Of particular importance is the kind of interaction of the nd valence electrons of the metal atoms, which should not be involved in strong covalent metal–metal bonds. Weak metal–metal interactions have been observed, for example,

in Fe/S clusters (nitrogenases, ferredoxins), in V/O clusters,[1b] and, as described here, in Mo/O clusters (cf. Refs. [6, 7]). For 5d metal centers, for example, tungsten, very strong 5d–5d overlap results in more facile formation of markedly covalent metal–metal bonds (cf. the significant shortening of certain W–W distances in sixfold-reduced $[H_2W_{12}O_{40}]^{12\ominus}$[8] with Keggin-like structure).

Experimental Procedure

Some characteristic main IR absorption bands in the region of framework stretching vibrations (solid, CsI pellet; 1000 to 600 cm^{-1}) are given.

1: All operations were carried out with degassed H_2O under argon atmosphere. $(NH_4)_6[Mo_7O_{24}] \cdot 4\,H_2O$ (2.1 g, 1.7 mmol), As_2O_3 (1.5 g, 7.6 mmol), and NH_4SCN (5.0 g, 66 mmol) were dissolved in 60 mL of H_2O at 95 °C. The solution was allowed to cool to 80 °C and hydrazinium sulfate (0.8 g, 6.1 mmol) was then added, resulting in a sudden change in color from pale yellow to green to dark blue. The resulting mixture was stirred for 3 min at 80 °C and cooled rapidly to 20 °C, and the unreacted As_2O_3 was removed by filtration. The filtrate was treated immediately with a solution of $(HNMe_3)Cl$ (6.0 g, 63 mmol) in 140 mL of H_2O and allowed to stand in a closed vessel for 24 h at 20 °C. The deep blue crystals of **1** that formed were collected by filtration and dried on the filter paper. Yield 1.85 g (73%). IR: $\tilde{\nu}[cm^{-1}] = 964/955$(vs) ($Mo\text{-}O_{term}$); 760(m), 660(m) (As-O; As-O-As, Mo-O-Mo). Potentials [V] versus SCE (solvent DMF; electrolyte $(NBu_4)BF_4$; three-electrode arrangement, Pt, Pt, SCE; scan rate 150 $mV s^{-1}$); −0.06, +0.04, +0.43, +0.54 (cf. [10]).

2: **1** (5.0 g, 1.0 mmol) in 200 mL of H_2O in a 300-mL Erlenmeyer flask (wide-necked, covered with a watch glass (d = 6 cm)) was allowed to stand on a hot plate at 70–75 °C for 20 h without stirring. After separation of the blue precipitate, the filtrate was allowed to stand for 2–3 d without stirring at 70–75 °C. The deep blue crystals of **2** that formed were collected by filtering the hot solution and dried on the filter paper. Yield 1.1 g (28%). IR: $\tilde{\nu}[cm^{-1}] = 968/955$(vs) ($Mo\text{-}O_{term}$), 890(m) (As-O), 854(s), 740(m), 675/660(s) (Mo-O-Mo).

3: **1** (0.5 g, 0.1 mmol) was dissolved in 27.5 mL of H_2O at 70–75 °C and the resulting solution in a 100-mL Erlenmeyer flask (as described for **2**) was allowed to stand on a hot plate at 70–75 °C without stirring. The deep blue crystals of **3** that had formed after 5–6 d were collected by filtering the hot solution and dried on the filter paper. Yield 0.11 g (28%) (clearly, **3** can also be prepared from **2**). IR: $\tilde{\nu}[cm^{-1}] = 968$(vs) ($Mo\text{-}O_{term}$), 884(vs) (As-O), 770(vs) (Mo-O-Mo).

Received: August 30, 1989 [Z 3528 IE]
German version: *Angew. Chem. 102 (1990) 85*

[1] a) E. Bartholomé, E. Biekert, H. Hellmann, H. Ley, W. M. Weigert (Eds.): *Ullmanns Encyklopädie der technischen Chemie, 4. Aufl., Band 13*, Verlag Chemie, Weinheim 1977, p. 530ff; b) A. Müller, M. Penk, E. Krickemeyer, H. Bögge, H.-J. Walberg, *Angew. Chem. 100* (1988) 1787; *Angew. Chem. Int. Ed. Engl. 27* (1988) 1719; A. Müller, J. Döring, *ibid. 100* (1988) 1789 and *27* (1988) 1721; c) J. Haber: *The Role of Molybdenum in Catalysis*, Climax Molybdenum, London 1981.

[2] a) J. N. Barrows, G. B. Jameson, M. T. Pope, *J. Am. Chem. Soc. 107* (1985) 1771; b) M. T. Pope (*Heteropoly Blues*) in D. B. Brown (Ed.): *Mixed-Valence Compounds*, Reidel, Dordrecht 1980; c) M. T. Pope: *Heteropoly and Isopoly Oxometalates (Inorg. Chem. Concepts 8)*, Springer, Berlin 1983.

[3] **1**: $P\bar{1}$: a = 1353.8(2), b = 1381.5(2), c = 1840.1(2) pm, α = 67.77(1), β = 81.66(1), γ = 64.96(1)°, $V = 2886.0 \times 10^6$ pm^3; μ = 54.1 cm^{-1}; Z = 1, ϱ_{calcd} = 2.75 $g\,cm^{-3}$; R = 0.074 for 9511 reflections ($F_o > 3.92\,\sigma(F_o)$). **2**: $Cmc2_1$; a = 1747.5(5), b = 1540.6(4), c = 1575.6(4) pm, $V = 4241.7 \times 10^6$ pm^3, μ = 42.3 cm^{-1}; Z = 4, ϱ_{calcd} = 3.21 $g\,cm^{-3}$; R = 0.059 for 2122 reflections ($F_o > 4\,\sigma(F_o)$); η = 1.0(2) according to D. Rogers, *Acta Crystallogr. Sect. A 37* (1981) 734. **3**: *Pnma*; a = 1605.6(4), b = 1897.7(6), c = 1419.9(4) pm, $V = 4326.6 \times 10^6$ pm^3; μ = 41.2 cm^{-1}; Z = 4, ϱ_{calcd} = 3.08 $g\,cm^{-3}$; R = 0.089 for 3701 reflections ($F_o > 4\,\sigma(F_o)$). Syntex $P2_1$ diffractometer, $Mo_{K\alpha}$ radiation, graphite monochromator. The protons of the anions of **1** and **3** could not be localized. In the crystals of **1**, **2**, and **3**, one cation per formula unit and in **1** a part of the crystal water is disordered. The anion of **3** is disordered over two positions, resulting in approximate apparent O_h symmetry. The disorder could only be solved for the O atoms of the central $AsO_4^{3\ominus}$ group, since the positions of the remaining atoms were only slightly changed by the disorder. The powder diffraction diagrams calculated from the single-crystal data agree with the measured diagrams. Further details of the crystal structure investigation may be obtained from the Fachinformationszentrum Karlsruhe, Gesellschaft für wissenschaftlich-technische Information mbH, D-7514 Eggenstein-Leopoldshafen 2 (FRG), on quoting the depository number CSD-54186, the names of the authors, and the journal citation.

[4] The average valence sum is 6.1 for Mo atoms in the As_3Mo_3 ring and 5.5 for the other Mo atoms; it was calculated as described by I. D. Brown, Kang Kun Wu, *Acta Crystallogr. Sect. B32* (1976) 1957.

[5] In addition to **1**, we were also able to synthesize and characterize preliminarily $[H_xAs_8Mo_{24}O_{88}]^{y\ominus}$ as its ammonium salt containing crystal water. **4**. **4** also contains Mo^V centers and, like **1**, consists of two $As_4Mo_{12}O_{42}$ units. The only difference is the absence of two As-O groups in the bridges of **4**. Two Mo atoms are thereby coordinated by three terminal O atoms in a fashion unusual for heteropolyanions.

[6] A. Müller, V. Wittneben, *J. Mol. Struct. (THEOCHEM)*, in press. In contrast to 3d clusters with classical ligands, in most cases strong metal–metal interactions occur in 4d clusters, for example, Mo_xS_y species (cf. A. Müller, R. Jostes, W. Eltzner, Chong-Shi Nie, E. Diemann, H. Bögge, M. Zimmermann, M. Dartmann, U. Reinsch-Vogell, Shun Che, S. J. Cyvin, B. N. Cyvin, *Inorg. Chem. 24* (1985) 2872).

[7] Relevant in this connection are the results of X_α calculations on model substances ($[Fe_4S_4(SH)_4]^{2\ominus}$, $[VFe_3S_4(SH)_6]^{4\ominus}$, and $[MoFe_3S_4(SH)_6]^{3\ominus}$) for the catalytic centers or cofactors (FeMS cluster, M = Fe, V, Mo) of nitrogenases and of alternative forms in which only weak interactions are present [6].

[8] Y. Jeannin, J. P. Launay, M. A. Seid Sedjadi, *Inorg. Chem. 19* (1980) 2933.

[9] The term is used generally here to refer to species in which metal–metal interactions are present, even if they are weak, as is the case for the ferredoxins (with no covalent metal–metal bonds).

[10] Cluster **1**, which, in DMF, undergoes four quasi-reversible two-electron oxidations in a cyclovoltammetric study, as well as the Keggin anions of **2** and **3** and the corresponding, known $[AsMo_{12}O_{40}]^{3\ominus}$ nonreduced anion.

A Cyclodimeric Silaketenimine**

By *Manfred Weidenbruch,* Brigitte Brand-Roth, Siegfried Pohl,* and *Wolfgang Saak*

Dedicated to Professor Gerhard Fritz on the occasion of his 70th birthday

Despite the great progress made in recent years in the area of unsaturated silicon compounds,[1] compounds containing silicon as part of a cumulated double-bond system have not yet been reported.

Recently, *Arrington* et al.[2] as well as *Pearsell* and *West*[3] investigated the reactions of silanediyls (silylenes) with carbon monoxide in matrices. Whereas reaction of dimethylsilanediyl supposedly forms silaketene **A**,[2] in the case of the dimesitylsilanediyl addition product, for example, both the electronic spectra and the formation of disilenes on thawing of the matrix indicate that Lewis acid–base adducts of type **B** are formed between the silanediyl and CO. Theoretical

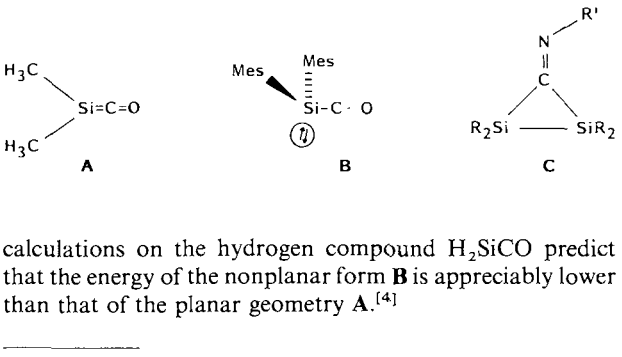

calculations on the hydrogen compound H_2SiCO predict that the energy of the nonplanar form **B** is appreciably lower than that of the planar geometry **A**.[4]

[*] Prof. Dr. M. Weidenbruch, Dipl.-Chem. B. Brand-Roth, Prof. Dr. S. Pohl, Dipl.-Chem. W. Saak
Fachbereich Chemie der Universität
Carl-von-Ossietzky-Strasse 9–11, D-2900 Oldenburg (FRG)

[**] Silicon Compounds with Strong Intramolecular Steric Interactions, Part 38. This work was supported by the Deutsche Forschungsgemeinschaft and the Fonds der Chemischen Industrie. Part 37: M. Weidenbruch, B. Brand-Roth, S. Pohl, W. Saak, *J. Organomet. Chem.*, in press.

We found that the reaction of di-*tert*-butylsilanediyl (**2**) with phosphaalkynes[5] and with nitriles[6] begins with [2 + 1] cycloaddition, resulting in the formation of three- and six-membered rings, respectively. On the other hand, reactions of **2** with isocyanides, which are isolectronic to CO, should lead to compounds of type **A** or **B** or to products derived therefrom.

Indeed, reaction of **2**, generated photolytically from hexa-*tert*-butylcyclotrisilane (**1**),[7] with phenyl isocyanide (**3**) gives a compound, **5**,[8] whose mass spectra and NMR data

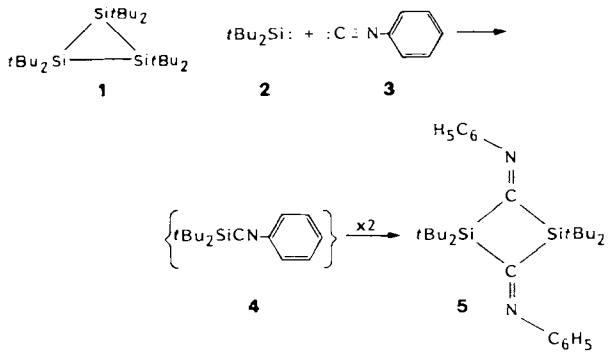

support a cyclodimeric silaketenimine. The X-ray structure analysis[9] (Fig. 1) confirms its structure and clearly reveals that the two phenyl rings are exclusively *trans* to each other in the crystal. The ring atoms, as well as the exocyclic N atoms, lie almost exactly in one plane. Within the ring, the smaller angles are found at the Si atoms, the larger angles at the carbon atoms.

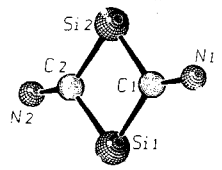

Fig. 1. Molecular structure of **5** (H atoms omitted). Selected bond lengths [pm] and angles [°] (standard deviations): C1-Si1 195.0(3), C2-Si1 192.8(3), C1-Si2 192.9(3), C2-Si2 194.8(3), C1-N1 127.7(3), C2-N2 128.3(3); C1-Si1-C2 = C1-Si2-C2 83.0(1), Si1-C1-Si2 = Si1-C2-Si2 97.0(1).

The most striking feature of **5** is its ruby red color, which is reflected in the absorption at $\lambda_{max} = 520$ nm. This shift of the longest-wavelength band, which is extreme for silyl imines, has only been observed previously for a disilacyclopropanimine (**C**) with $\lambda = 510$ nm, obtained by addition of an isocyanide to a disilene.[10] The rationalization given there for the color of the compound—the effect of ring strain on the transition energy or on an intramolecular Si–Si $\sigma \rightarrow \pi$ charge transfer—should be reconsidered, since the less strained compound **5** exhibits the same phenomenon. Simple MO considerations indicate that the lowering of the excitation energy is more likely due to an adiabatic shift of the excited state in the direction of the ground-state minimum.[11]

To verify that **5** indeed results from dimerization of the silaketenimine of type **4** and not from twofold addition of **3** to tetra-*tert*-butyldisilene formed simultaneously in the photolysis of **1**, we allowed **2** to react with isocyanide **6**,[12] whose bulky ortho-*tert*-butyl groups should disfavor both cyclodimerization and insertion into the Si–Si bond of a possible intermediate of type **C**.

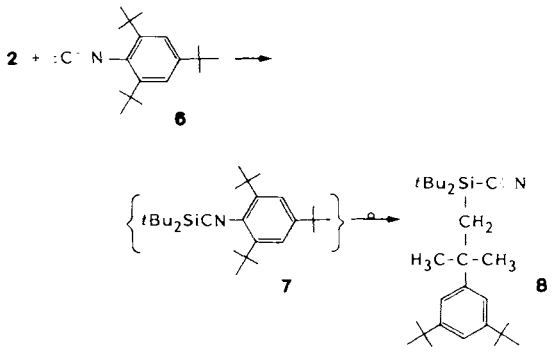

In fact, a monomeric compound, consisting of **2** and **6** in a ratio of 1:1, was isolated. The spectroscopic data indicate, however, that the expected intermediate **7** rearranged to the trialkylsilyl cyanide **8**.[13] Several examples of such aryl–alkyl isomerizations of the 2,4,6-tri-*tert*-butylphenyl group have meanwhile been observed.[14] Their mechanism is still not understood.

To determine whether **8** might result from a precursor of type **5** via a CH activation of the peripheral *tert*-butyl groups, we have also carried out the photolysis of **1** in the presence of 2,4,6-trimethylphenyl isocyanide (mesityl isocyanide). This compound also contains methyl groups capable of undergoing isomerization reactions, but it cannot compete with the steric overloading of **6**. In this case, we isolated a derivative of **5** with mesityl instead of phenyl groups. Although other routes of formation for **5** cannot be definitively ruled out, these reactions support the formation of cyclodimer **5** from **2** and **3** via the monomeric compound **4**.

Experimental Procedures

5: A solution of **1** (0.42 g, 1.0 mmol) and **3** (0.31 g, 3.0 mmol) in 40 mL of petroleum ether (40–60 °C) was irradiated with a medium-pressure Hg lamp for 2 h at 20 °C. Fractional crystallization (*n*-pentane) of the residue remaining after removal of the solvent by distillation gave 0.16 g (65% yield, based on **1**) of **5** as ruby red crystals.

8: Analogously to the synthesis of **5**, reaction of **1** (0.42 g, 1.0 mmol) and **6** (0.82 g, 3.0 mmol) in 70 mL of petroleum ether (40–60 °C) for 6 h at 20 °C gave 0.29 g (70%) of crystalline **8**.

Received: August 25, 1989;
supplemented: October 2, 1989 [Z 3520 IE]
German version: *Angew. Chem. 102* (1990) 93

CAS Registry numbers:
1, 89463-49-0; **2**, 98187-49-6; **3**, 931-54-4; **5**, 124127-38-4; **6**, 69847-28-5; **8**, 124127-37-3.

[1] Review: G. Raabe, J. Michl in S. Patai, Z. Rappoport (Eds.): *The Chemistry of Organic Silicon Compounds, Part 2*, Wiley, Chichester 1989, p. 1015.
[2] C. A. Arrington, J. T. Petty, S. E. Payne, W. C. K. Haskins, *J. Am. Chem. Soc. 110* (1988) 6240.
[3] M.-A. Pearsall, R. West, *J. Am. Chem. Soc. 110* (1988) 7228.

[4] T. P. Hamilton, H. F. Schaefer III, *J. Phys 90* (1989) 1031.
[5] A. Schäfer, M. Weidenbruch, W. Saak, S. Pohl, *Angew. Chem. 99* (1987) 806; *Angew. Chem. Int. Ed. Engl. 26* (1987) 776.
[6] M. Weidenbruch, A. Schäfer, K. Peters, H. G. von Schnering, *J. Organomet. Chem. 314* (1986) 25.
[7] A. Schäfer, M. Weidenbruch, K. Peters, H. G. von Schnering, *Angew. Chem. 96* (1984) 311; *Angew. Chem. Int. Ed. Engl. 23* (1984) 302.
[8] **5**: m.p. 173–178 °C. ^{1}H NMR (300 MHz, C_6D_6): δ = 0.84 (s, 36H), 7.66 bis 7.93 (m, 10H). ^{13}C NMR (75.44 MHz, C_6D_6): δ = 23.84, 30.55, 118.56, 125.52, 129.21, 160.43, 223.65. MS (EI, 70 eV): *m/z* 490 ($M^{\oplus}$,3%), 387 ($M^{\oplus}$ − 103, 100%). IR (KBr): $\tilde{\nu}$ [cm^{-1}] = 1585 (C = N). UV/VIS: λ_{max} [nm] (ε) = 311 (8990), 456 (1060), 520 (530). Correct C,H,N analysis.
[9] **5**: Orthorhombic, space group *Pbca* (No. 61), a = 1665.4(1), b = 1730.1(1), c = 2086.1(1) pm, V = 6010.7 × 10^6 pm^3, Z = 8, P_{calc} = 1.085 g cm^{-3}; 4735 unique reflections, 3544 observed reflections ($I > 2\sigma(I)$), 307 variables, R = 0.050, R_w = 0.047. Further details of the crystal structure investigation may be obtained from the Fachinformationszentrum Karlsruhe, Gesellschaft für wissenschaftlich-technische Information mbH, D-7514 Eggenstein-Leopoldshafen 2 (FRG), on quoting the depository number CSD-54149, the names of the authors, and the journal citation.
[10] H. B. Yokelson, A. J. Millevolte, K. J. Haller, R. West, *J. Chem. Soc. Chem. Commun. 1987*, 1605, and references therein.
[11] R. S. Grev, H. F. Schaefer III, *J. Am. Chem. Soc. 111* (1989) 6137, and references therein.
[12] **6**, m.p. 132–136 °C, was prepared by the phosgene method (see I. Ugi, U. Fetzer, U. Eholzer, H. Knupfer, K. Offermann, *Angew. Chem. 77* (1965) 492; *Angew. Chem. Int. Ed. Engl. 4* (1965) 432) from *N*-(2,4,6-tri-*tert*-butylphenyl)formamide in 86% yield.
[13] **8**: Colorless crystals, m.p. 134 °C. ^{1}H NMR (300 MHz, C_6D_6):δ = 0.84 (s,18H), 1.14 (s, 2H), 1.39 (s, 18H), 1.60 (s, 6H), 7.40 (t, 1H), 7.52 (d, 2H); ^4J = 1.62 Hz. ^{13}C NMR (75.44 MHz, C_6D_6): δ = 19.17, 26.47 (CH_2), 27.94, 31.69, 32.21, 35.13, 37.33, 120.93, 148.34, 150.49. MS (EI, 70 eV): *m/z* 413 ($M^{\oplus}$, 5%); 398 ($M^{\oplus}$ − 15, 17); 356 ($M^{\oplus}$ − 57, 23). IR (KBr): $\tilde{\nu}$ [cm^{-1}] = 2185 (C≡N). Correct C,H,N analysis.
[14] M. Weidenbruch, K. Schäfers, S. Pohl, W. Saak, K. Peters, H. G. von Schnering, *J. Organomet. Chem. 346* (1988) 171; *Z. Anorg. Allg. Chem. 570* (1989) 75.

The Pagodane Route to Dodecahedranes: An Efficient Variant—New Substitution Patterns**

By *Rolf Pinkos, Johann-Peter Melder,* and *Horst Prinzbach**

Our efficient syntheses of 4,9,14,19-tetrasubstituted pagodanes **A**[1] have opened a broad route to dodecahedranes **B** and homologous dodecahedranes **C**, **D**.[2, 3] Beyond an intrinsic aesthetic appeal, the value of this class of carbo- and heterocyclic compounds is determined not least by the possibility of specifically varying the substitution pattern.[4] For the dodecahedranes **B**, the aldol route (starting from **A**, X = $CHCO_2R$, CHCN; Y = C=O) allows the directed functionalization of up to eight framework positions.[1–3]

The S_N2 variant described here (starting from **A**, X = CHA; Y = CHL; cf. "d" in the caption to Scheme 1 in Ref. [2]) permits a significant extension of this synthetic concept[5]—preparatively in the realization of additional substitution patterns (cf. **16, 21**) and thermodynamically unfavorable C–C coupling reactions (cf. **25**),[6] methodologically in that the reaction sequence **I** → **VI** → **VII** → **V** → **II** (Scheme 1) corresponds to the third (C) variant of the originally formulated pagodane → dodecahedrane routes[7] (A,[8] B[9]). For the parent hydrocarbons, the corresponding reaction sequence of hydrogenative C–C bond cleavages and dehydrogenative C–C bond formations had earlier failed at the stage of the kinetically unusually stable species **VI**. A noteworthy feature of this C route is the occurrence of "isododecahedranes"[10, 11] derived from **VII**. In the S_N2 route, however, leaving (L) and acceptor (A) groups have to be incorporated at the pagodane stage (**A**, X = CHA; Y = CHL), and the lateral C–C coupling reactions (X,Y) are only possible after the pagodane four-membered ring (**I**, a) has been opened.[2, 3] Thus, it was necessary to study the effect of the electronegative functionalities on the conditions of four-membered ring opening, that is, on the photochemical addition and elimination of bromine, as well as to determine what kinds of leaving groups are compatible with the drastic reaction conditions required in these reactions.

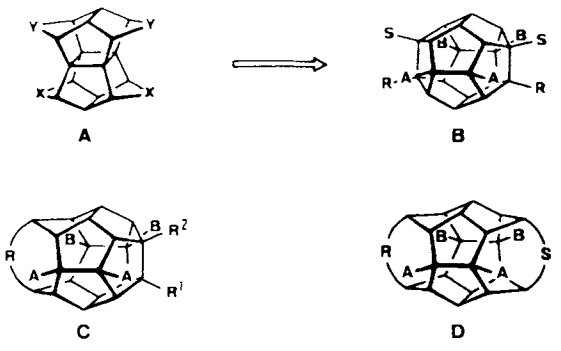

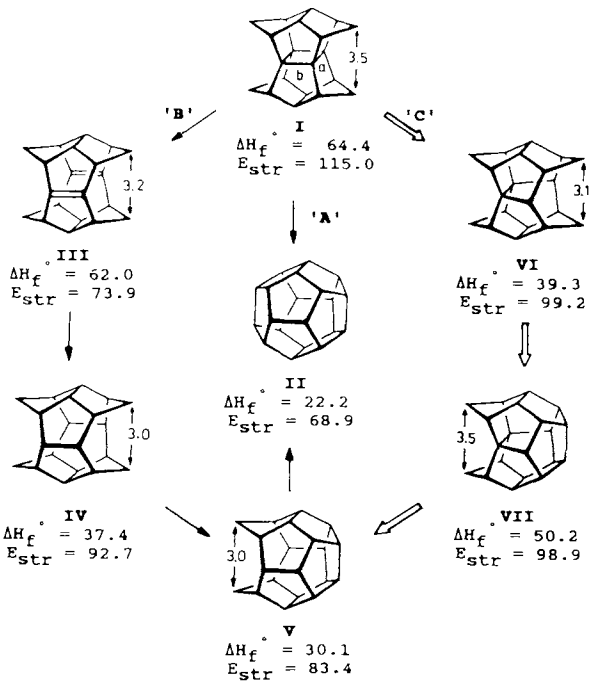

Scheme 1. Alternative pagodane → dodecahedrane routes (A, B, C). MM2-calculated ΔH_f° and E_{str} (strain energy) values [kcal mol^{-1}].

The starting materials for the S_N2 route are pagodanes **4** (cf. **A**) with leaving groups on C-14(19) in *anti* position and acceptor groups on C-4(9) in *syn* position (Scheme 2). After the yield of bislactone **2** obtained from biscarboxamide **1** (R = NH_2), readily accessible via the pagodane synthesis,

[*] Prof. Dr. H. Prinzbach, Dipl.-Chem. R. Pinkos, Dipl.-Chem. J.-P. Melder
Chemisches Laboratorium der Universität,
Institut für Organische Chemie und Biochemie
Albertstrasse 21, D-7800 Freiburg (FRG)

[**] This work was supported by the Deutsche Forschungsgemeinschaft, the Fonds der Chemischen Industrie, and BASF AG. We would like to thank Prof. Dr. *H. Fritz*, Dr. *D. Hunkler*, and Dr. *M. Keller* for NMR analyses, Dr. *J. Wörth* for MS analyses, *M. Lutterbeck*, *G.* and *J. Leonhardt*, and *M. Froom* for starting materials, *G. Fehrenbach* for graphical work, and Dr. *W.-D. Fessner*, Dr. *C. Rücker*, and Dr. *L. Knothe* for helpful discussions.

could be increased from originally 35% to 70%,[3] **2** became the intermediate of choice for the regiospecific introduction of *anti*-Y leaving groups.[1,2] Reaction of **2** with Me_3SiY (Y = Br, I) afforded dibromide **4a** and diiodide **4b**[1,3] in nearly quantitative yield (10-mmol scale). The first (**2** → **3**) and second (**3** → **4**) substitutions are kinetically so different that intermediates **3a, b**, which are useful in other transformations (see below), can be isolated selectively. The four-membered ring opening **4** → **5**, which we planned to accomplish by proven procedures,[3] presented difficulties—as was found for the aldol route[2]—since the photochemical addition of bromine was considerably slowed by the four electronegative substituents. Under the more drastic conditions therefore required, diiodide **4b** underwent halogen exchange to give dibromide **4a**; total conversion unavoidably results in subsequent bromination of **4a** to pentabromide **6** and (to a lesser extent) hexabromide **7** (at room temperature (RT) in $CDCl_3$, rotamers are present according to NMR). Fortunately, the mixture of bromides could largely be transformed into **6** (92% together with **7** (5%), 2-mmol scale); moreover, treatment of **6** with Pt/H_2 led to selective replacement of the bromine substituent at C4 with hydrogen (100% **5**, no cyclization to **8**[6]). The ring closure, which, in the parent framework (**VI** → **VII**), is considerably endothermic and could not be achieved, could be effected by deprotonation in **5** as well as reductively in **6** (**7**). As expected, only the "open" side (d(C4-C14) ca. 3.1 Å) participates in each case. The yields of tri- and tetrabromoisododecahedranedicarboxylic esters **8** and **9**, respectively, were reproducibly better than 85%. Attempts to achieve, via **8** or **9**, C–C bond formation on the "closed" side (d(C10–C19) ca. 3.5 Å) to give the extremely strained dehydrododecahedrane derivative **11** were unsuccessful. The use of various bases or reducing agents led to epimerization of **8** to give **10** and to the formation of a complex mixture of products from **9** (no **11**).

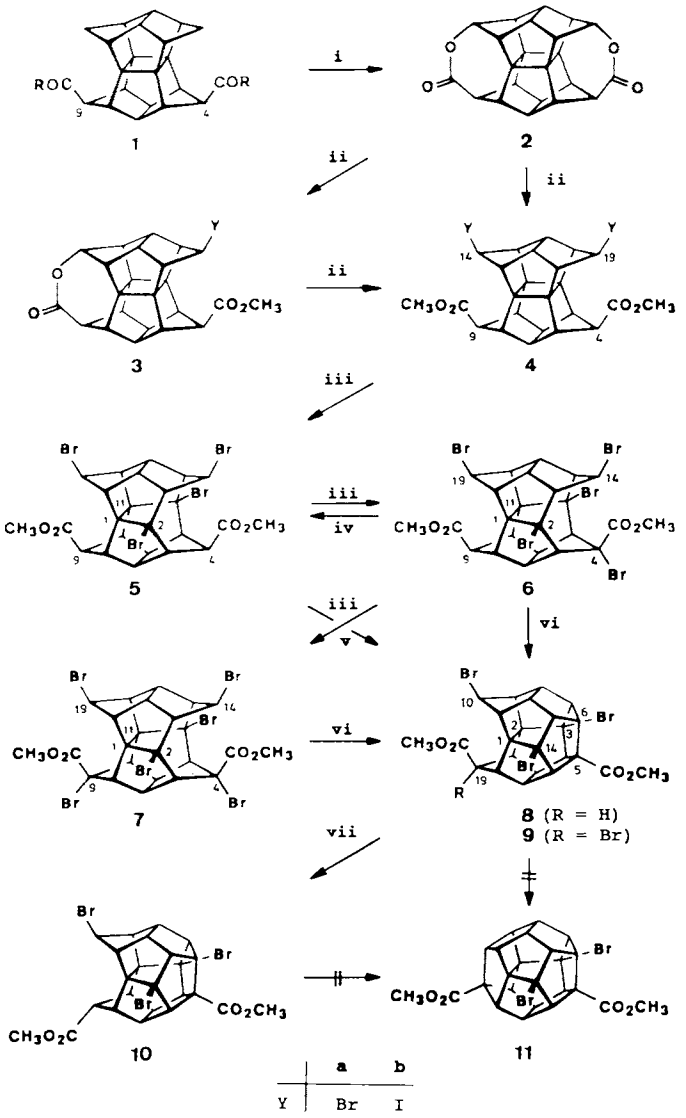

Scheme 2. i: 1. I_2, $Pb(OAc)_4$, CH_2Cl_2, reflux, *hv*; 2. HOAc, HCl, reflux; 3. EtOH, $NaBH_4$; 4. benzene, DMF, $(COCl)_2$. ii: 1. $CHCl_3$, Me_3SiBr (Me_3SiI), reflux; 2. MeOH; 3. CH_2N_2. iii: CH_2Cl_2, Br_2, reflux, *hv*. iv: CH_2Cl_2, PtO_2, H_2. v: THF, NaH (1 equiv.). vi: DMF, Zn, NaI, 100 °C. vii: THF, NaH (5 equiv.).

The preparation of bissecododecahedradiene **12** by 1,4-bromine elimination from **5**—competing reductive recyclization to **4** necessitates high reaction temperatures—was also expected to be problematic owing to the additional bromine substituents. The 58–62% yield of **12** (2% **3a**), obtained after very short treatment (10 s) with $Zn/NaI/Na_2SO_3$ (DMF, 153 °C; ca. 90% conversion), is relatively small, but may be amenable to further improvement. Presumably, the modest yield primarily reflects the instability of this diene; moreover, 1,4-bromine elimination involving the bromine substituent at C19 is a probable side reaction (cf. the high yield with **4** (**5**)[6]). The conversion of pentabromide **6** to seco-diene **13** was carried out in a one-pot reaction at 130 °C under otherwise identical conditions and, after quantitative conversion and chromatography of the reaction mixture, has so far afforded only a ca. 60% yield of **13** together with **8** (ca. 10%). Compound **13** is presumably formed preferentially via the zinc enolate (C3) of **12**; in control experiments, 1,4-bromine elimination from **8** is much slower and much less selective than that from **6**.

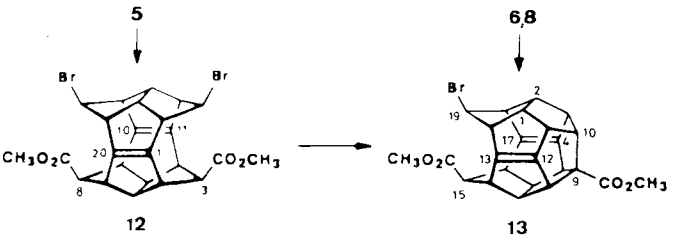

The bisseco-diene **12** (d(C1-C11) ca. 2.7 Å, δ_{C1} = 155.7 ($CDCl_3$)) exhibits the transannular reactivity known for this framework (*Z,Z*- or *E,E*-cyclodeca-1,6-diene subunits): clean [$\pi_2 + \pi_2$] cycloaddition to give **4a** on excitation in the presence of a sensitizer (acetone); clean homo-1,4-addition of bromine to give **5**. The secododecahedradiene framework, isolated here in the form of **13** for the first time, is useful as a "hermaphroditic" model consisting of bissecododecahedradiene (**12**, $d_{\pi\text{-}\pi}$ ca. 2.7 Å) and dodecahedra-1,16-diene ($d_{\pi\text{-}\pi}$ ca. 3.5 Å; cf. **10** in Ref. [6]) skeletal moieties. Transannular interactions in **13** between the CC double bonds, which are coplanar but not parallel (d(C13-C17) = 2.849 Å and d(C4-C12) = 3.195 Å according to X-ray structure analysis[6,14]), are manifested in the UV spectrum (CH_3CN) by a maximum at 263 nm (ε = 25) and by strongly differing pyramidalization of the sp^2 C atoms, as revealed by the ^{13}C NMR shifts of the olefinic carbon atoms (δ = 149.8 (C-13,-17), 172.2 (C-4,-12)). The transannular reactivity of the "hermaphrodite" **13** has not been elucidated in every detail. As in **12**, bromine adds rapidly and regiospecifically in a homo-1,4

fashion, with re-formation of **8**; addition at C13(17) would be much more unfavorable energetically. However, irradiation in acetone does not lead to the $[\pi_2 + \pi_2]$ cycloadduct, a dehydropagodane derivative.

The further modifications of the dodecahedrane sphere made possible by the synthesis of **12** and **13** are closely connected with a stepwise transformation of the CC double bonds and with the reactivity of the corresponding singly unsaturated frameworks ("hyperstable" versus "non-hyperstable"). Clearly, the procedure exemplified here for the saturated dodecahedranes **16** and **21** can be extended to a wide variety of other derivatives. Examples not mentioned in the following communication[6] include the preparation of singly unsaturated analogues of **16** and **21**, which are accessible by single epoxidation or hydrogenation of **12** or **13**.

Dienes **12** and **13** are oxidized quantitatively to the diepoxides **14** and **15**, respectively, by treatment with excess benzoylperoxycarbamic acid (4 equiv., CH_2Cl_2, RT). Ring closure of **14** (d(C3-C14) ca. 3.2 Å)[1] to give **15** and of **15** (d(C3-C11) ca. 3.3 Å) to give **16** (cf. **7** → **14** → **15** in Ref. [2]), a considerably exothermic reaction in each case, occurs quantitatively (ca. 40% based on **1**) by transannular substitution using NaH as base (2 equiv., THF, RT). C_{2v} symmetry of the diepoxydodecahedranedicarboxylic ester **16** (m.p. 280–283 °C) is revealed by five ^{1}H NMR ($J_{10,11}$ = 11.2 Hz) and seven ^{13}C NMR skeletal signals of corresponding intensity (assignment confirmed by COSY, NOE, and selective decoupling experiments). In the mass spectrum of **16** (m/z [%] 404 ($M^{\oplus}$, 100), 344 (40), 285 (21)), loss of the two ester groups gives rise to a remarkably intense signal at m/z 285 (protonated diepoxydodecahedradiene).[6]

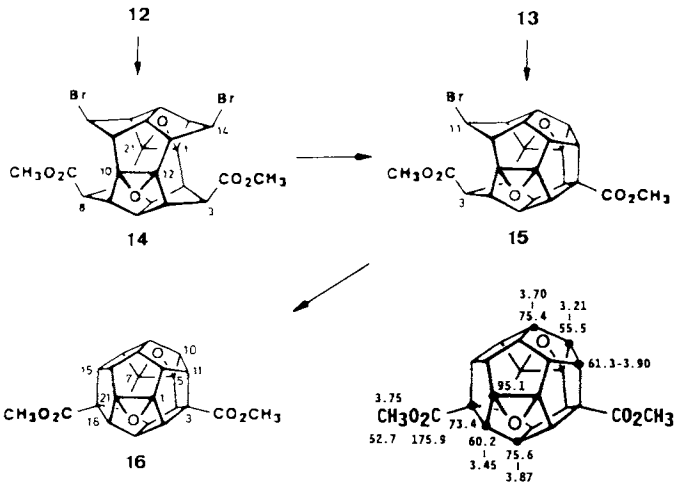

The hydrogenations of **12** and **13** with diimide ($(KOOCN)_2$, HOAc; 26 equiv., CH_2Cl_2/CH_3OH, RT) proceed, as expected, differently (cf. **2** → **3** → **4** in Fig. 1 of Ref. [9] as well as **A** → **B** → **C** and **G** → **H** → **I** in Scheme 1 of Ref. [2]). Bisseco-ene **17** proved to be hyperstable (no **19**); seco-ene **18** rapidly reacts further to give **20**. Compound **20** (d(C15-C19) ca. 3.0 Å) undergoes quantitative cyclization (ca. 45% based on **1**) in the presence of NaH (THF, RT) to the C_{2v} dodecahedrane-1,6-dicarboxylic ester **21** (m.p. 190–192 °C), which was fully characterized by NMR spectroscopy. Its mass spectrum (m/z [%] 376 ($M^{\oplus}$, 14), 344 (10), 316 (100), 257 (58), 256 (34)) also displays relatively intense signals for (protonated) dodecahedradiene (m/z 257, 256).[6]

The value of the S_N2 variant for endothermic transformations is impressively demonstrated by the direct cyclization of dienes **12** and **13** to dodecahedradienes[6] as well as by the cyclization of the homologous seco-diene **24b** to the homologous dodecahedradiene **25** (cf. **A** → **I** ($\Delta\Delta H_f^\circ$ = + 13.5, ΔE_{str} = + 23.3 kcal mol^{-1}) in Scheme 1 of Ref. [3]) and the absence of the corresponding aldol cyclization.[3] Two synthetic routes were used for the precursors **24a, b**: In the dibromobislactone **22**, prepared from **2**, the more highly strained lactone ring on the "closed" side is selectively opened by nucleophiles, for example, by reaction with Me_3SiI (20 equiv., CH_2Cl_2, RT, 12 h). After O–Si cleavage (CH_3OH) and esterification (CH_2N_2), the yield of **23b** was over 95%. The 1,4-bromine elimination in iodide **23b** under conditions that take account of the iodine substituent (NaI, Na_2SO_3, DMF, 153 °C, 30 min) affords diene **24b**, isolated by chromatography, in a relatively low yield of 45% (together with ca. 10% of the known[3] dienebislactone). The alternative offered by the availability of monobromide **3a** might be more economical, since the photochemical addition of bromine to **23a**, which is energetically more favorable, occurs exclusively on its lactone side. Under the conditions used for **14**/**16** and **20**/**21** (NaH, THF, RT), compound **24b** is cleanly converted into **25** (ca. 25% based on **1**). Compound **25** (m.p. 280–283 °C, $\tilde{\nu}_{CO}$ = 1720 cm^{-1}) can be chromatographed, crystallized, and stored as a solid (0 °C); however, it is rapidly attacked by oxygen, particularly in solution.

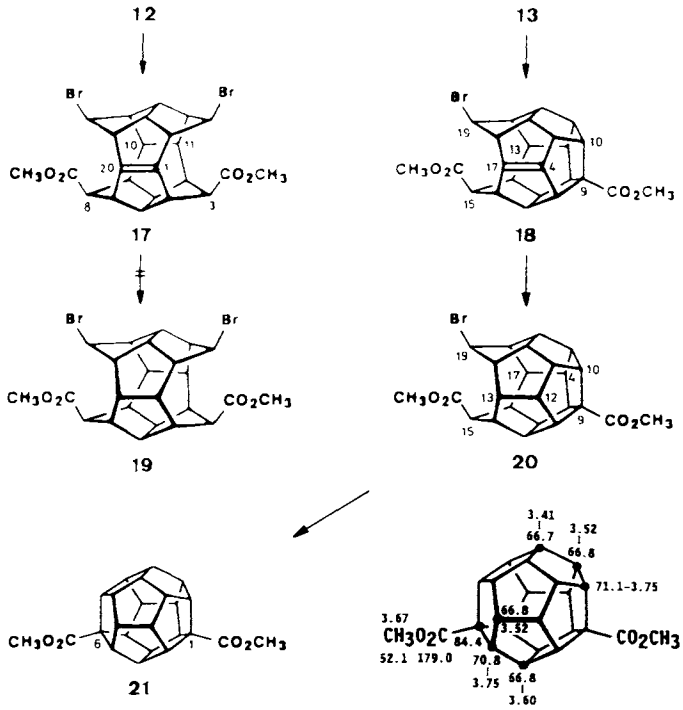

The relative arrangement of the CC double bonds in **25**,[6] a dodecahedradiene enlarged on one side (π–π transannular distances 2.9 and 3.1 Å[3]) and flattened, largely corresponds to that in seco-diene **13**.[14] Characteristic of this structure are the comparatively small vicinal H,H coupling constants (e.g., $J_{1,13}$ = 6.8, $J_{9,10}$ = 7.1 Hz) as well as the strongly, differing ^{13}C NMR shifts of the olefinic centers. Electron impact leads to CH_3CO_2H elimination and formation of an intense (protonated) trienelactone fragment (m/z [%] 358 ($M^{\oplus}$, 100), 298 (64)). As in **13**, bromine adds regiospecifically to the "dodecahedradiene side" (C-3(19)); the hydrogenation with diimide (excess) leads cleanly to the homododecahedrane **26**.

In summary, based on efficient syntheses of the correspondingly substituted starting materials, the S_N2 variant significantly extends the scope of the pagodane → dodecahedrane route. There is good evidence that the efforts re-

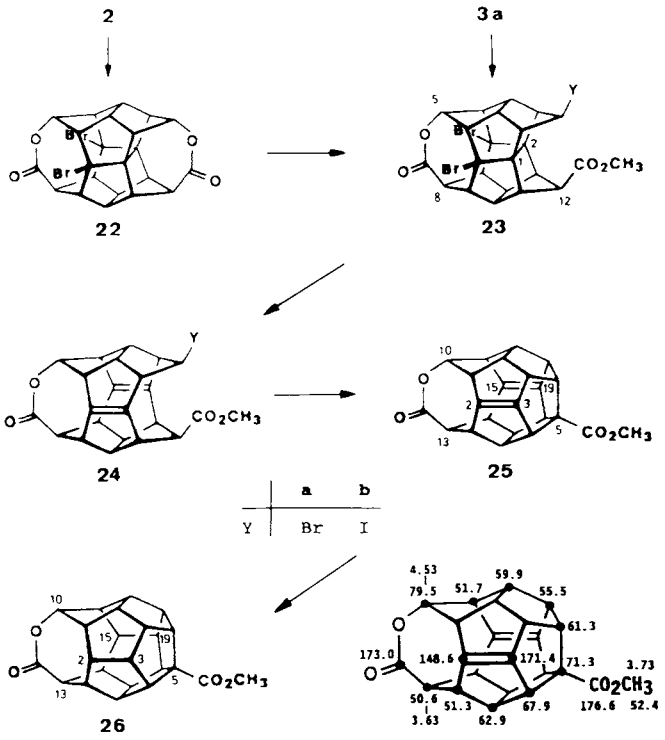

quired to prepare the key intermediates **12** and **13** can be dramatically decreased: Extensive photochemical bromination of the pagodane-*syn,syn*-dicarboxylic ester **1** (R = OCH_3) (2,12-di- → 2,4,12-tri- → 2,4,9,12-tetra- → 2,4,9,12,14-pentabromide, subsequent brominations nonselective), followed by bromination (at C-19) with *N*-bromosuccinimide), at low conversions (25–41%), affords hexabromide **7** with high selectivity and with low material loss. However, conversion of **7** to **12** (**13**) has so far given unsatisfactory results.[15]

Received: August 14, 1989 [Z 3500 IE]
German version: *Angew. Chem. 102* (1990) 102

CAS Registry numbers:
1, 124316-47-8; **2**, 120497-67-8; **3a**, 124316-48-9; **3b**, 124316-63-8; **4a**, 124316-49-0; **4b**, 124316-55-8; **5**, 124316-50-3; **6**, 124316-51-4; **7**, 124316-52-5; **8**, 124316-53-6; **9**, 124316-54-7; **10**, 124377-57-7; **12**, 124316-56-9; **13**, 124316-57-0; **14**, 124316-58-1; **15**, 124316-59-2; **16**, 124316-60-5; **17**, 124316-61-6; **18**, 124316-62-7; **20**, 124316-64-9; **21**, 124316-65-0; **22**, 120523-83-3; **23a**, 124316-70-7; **23b**, 124316-66-1; **24a**, 124316-71-8; **24b**, 124316-67-2; **25**, 124316-68-3; **26**, 124316-69-4.

[1] J.-P. Melder, H. Fritz, H. Prinzbach, *Angew. Chem. 101* (1989) 309; *Angew. Chem. Int. Ed. Engl. 28* (1989) 300; R. Pinkos, G. Rihs, H. Prinzbach, *ibid. 101* (1989) 312 and *28* (1989) 303.

[2] J.-P. Melder, R. Pinkos, H. Fritz, H. Prinzbach, *Angew. Chem. 101* (1989) 314; *Angew. Chem. Int. Ed. Engl. 28* (1989) 305.

[3] R. Pinkos, J.-P. Melder, H. Fritz, H. Prinzbach, *Angew. Chem. 101* (1989) 319; *Angew. Chem. Int. Ed. Engl. 28* (1989) 310.

[4] Mono- and bifunctionalizations were recently described by *Paquette* et al.: L. A. Paquette, J.-C. Weber, T. Kobayashi, *J. Am. Chem. Soc. 110* (1988) 1303; G. A. Olah, G. K. Surya Prakash, T. Kobayashi, L. A. Paquette, *ibid. 110* (1988) 1304.

[5] Taken from the dissertations of *R. Pinkos* and *J.-P. Melder*, Universität Freiburg 1990.

[6] J.-P. Melder, R. Pinkos, H. Fritz, H. Prinzbach, *Angew. Chem. 102* (1990) 105; *Angew. Chem. Int. Ed. Engl. 29* (1990) 95.

[7] W. D. Fessner, *Dissertation*, Universität Freiburg 1986; W.-D. Fessner, Bulusu A. R. C. Murty, H. Prinzbach, *Angew. Chem. 99* (1987) 482; *Angew. Chem. Int. Ed. Engl. 26* (1987) 451.

[8] W.-D. Fessner, Bulusu A. R. C. Murty, J. Wörth, D. Hunkler, H. Fritz, H. Prinzbach, W. D. Roth, P. von R. Schleyer, A. B. McEwen, W. F. Maier, *Angew. Chem. 99* (1987) 452; G. Lutz, D. Hunkler, G. Rihs, H. Prinzbach, *ibid. 101* (1989) 307 and *28* (1989) 298.

[9] P. R. Spurr, Bulusu A. R. C. Murty, W.-D. Fessner, H. Fritz, H. Prinzbach, *Angew. Chem. 99* (1987) 486; *Angew. Chem. Int. Ed. Engl. 26* (1987) 455.

[10] The difficulty in the nomenclature of these complex, in part highly symmetrical polycyclic compounds according to the von Baeyer system lies in the selection of main bridge from the large number of zero bridges. In this communication, the systematic names and numberings were determined by use of the POLCYC program (*G. Rücker* and *C. Rücker*, unpublished; computer version of IUPAC rule A-32 as well as its proposed improvement by CAS). Several earlier names [1–3] were corrected with this computer program: **13**: dimethyl 19-*anti*-bromo-decacyclo[9.9.0.0^{2,18}.0^{3,10}.0^{4,17}.0^{5,9}.0^{6,16}.0^{7,14}.0^{8,12}.0^{8,12}.0^{13,20}]icosa-4(17),12-diene-9,15-*syn*-dicarboxylate. **16**: dimethyl 6,22-dioxatridecacyclo-[10.10.0.0^{1,21}.0^{2,19}.0^{3,11}.0^{4,18}.0^{5,7}.0^{5,10}.0^{7,17}.0^{8,15}.0^{9,13}.0^{14,21}.0^{16,20}]docosane-3,16-dicarboxylate. **25**: methyl 12-oxo-11-oxaundecacyclo-[11.9.0.0^{2,9}.0^{3,7}.0^{4,22}.0^{5,20}.0^{6,18}.0^{8,17}.0^{10,16}.0^{14,21}.0^{15,19}]decosa-2,15-(19)diene-5-carboxylate.

[11] L. A. Paquette, R. J. Ternansky, D. W. Balogh, W. J. Taylor, *J. Am. Chem. Soc. 105* (1983) 5441; L. A. Paquette, T. Kobayashi, M. A. Kesselmayer, J. C. Gallucci, *J. Org. Chem. 54* (1989) 2921, and references therein; cf. a recent review: L. A. Paquette, *Chem. Rev. 89* (1989) 1051.

[12] Also possible and preparatively important is the twofold substitution by C nucleophiles (F. Wahl, H. Prinzbach, unpbulished).

[13] The new compounds were characterized by spectra (400-MHz ^{1}H NMR, 100.6-MHz ^{13}C NMR, IR, MS) and elemental analyses. For example, dimethyl 2,12,14-*anti*,19-*anti*-tetrabromodecacyclo-[9.9.0.0^{1,8}.0^{2,15}.0^{3,7}.0^{5,12}.0^{6,10}.0^{11,18}.0^{13,17}.0^{16,20}]icosane-4-*syn*,9-*syn*-dicarboxylate **5**: m.p. 231–240 °C (dec.). IR (KBr): $\tilde{\nu}$ = 2985, 2940(C–H), 1720(C–O) cm^{-1}. ^{1}H NMR ($CDCl_3$): δ = 4.70≡ (br.s, 14s-H), 4.20 (br.s, 19s-H), 3.85 (s, OCH_3), 3.74 (m, 16-,17-H), 4.20 (br.s, 19s-H), 3.85 (s, OCH_3), 3.76 (s, OCH_3), 3.74 (m, 16-,17-H), 3.69 (m, 3-,5-H), 3.66 (m, 13-,15-H), 3.31 (m, 8-,10-H), 3.14 (m, 18-,20-H), 2.98 (m, 6-,7-H), 2.68 (m, 9a-H), 2.53 (t, 4a-H); $J_{3,4}$ = 5.1 Hz. ^{13}C NMR ($CDCl_3$): δ = 172.3 (CO), 171.7 (CO), 93.1 (C-2,-12), 78.0 (C-1,-11), 61.0 (C-13,-15), 57.0 (C-16,17), 56.6 (C-6,-7), 55.1 (C-14), 54.3 (C-19), 53.8 (C-4), 52.9 (OCH_3), 52.6 (C-18,-20), 52.4 (OCH_3), 52.2 (C-3,-5), 50.7 (C-9), 47.4 (C-8,-10). dimethyl 3,10-*anti*,14-tribromoundecacyclo-[9.9.0.0^{1,14}.0^{2,9}.0^{2,18}.0^{3,7}.0^{4,17}.0^{5,15}.0^{6,13}.0^{8,12}.0^{16,20}]icosane-5,19-*syn*-dicarboxylate **8**: m.p. 220–221 °C. IR (KBr): $\tilde{\nu}$ = 3000, 2975 (C-H), 1730 (C=O) cm^{-1}. ^{1}H NMR ($CDCl_3$): δ = 4.27 (m, 10s-H), 3.85 (t, 6-H), 3.77 (s, OCH_3), 3.72 (s, OCH_3), 3.57 (m, 18-,20-H), 3.54 (m, 8-,12-H), 3.42 (m, 9-,11-H), 3.33 (m, 4-,15-,16-,17-H), 3.21 (m, 7-,13-H), 2.67 (m, 19a-H); $J_{6,7}$ = 10.5, $J_{18,19} \approx 2$, $J_{9,10} \approx 1.5$ Hz. ^{13}C NMR ($CDCl_3$): δ = 174.5(CO) 172.2(CO), 96.8 (C-3,-14), 79.7 (C-1,-2,-5), 67.8 (C-6), 64.7 (C-4,-15), 61.3 (C-16,-17), 60.9 (C-8,-12), 59.7 (C-7,-13), 56.3 (C-9,-11), 54.1 (C-10), 52.7 (OCH_3), 52.1 (OCH_3), 51.3 (C-18,-20), 50.2 (C-19).

[14] G. Rihs, U. Reifenstahl, H. Irngartinger, P. R. Spurr, G. Lutz, R. Pinkos, J.-P. Melder, H. Prinzbach, unpublished.

[15] K. Weber, R. Pinkos, H. Prinzbach, unpublished.

The Pagodane Route to Dodecahedranes: Dodecahedradienes—Unusually "Pyramidalized", Isolable Olefins**

By *Johann-Peter Melder, Rolf Pinkos, Hans Fritz,* and *Horst Prinzbach**

Carbon–carbon double bonds on the surface of regular pentagonal dodecahedrane[1,2] are particularly attractive functionalities[3] (Scheme 1). On the one hand, the rigid[4] spherical framework enforces an unusually strong pyramidalization of the sp^2 centers, that is, *syn* bending of the CC double bonds;[3,5,6] on the other hand, advantageously

[*] Prof. Dr. H. Prinzbach, Dipl.-Chem. J.-P. Melder, Dipl.-Chem. R. Pinkos, Prof. Dr. H. Fritz
Chemisches Laboratorium der Universität,
Institut für Organische Chemie und Biochemie
Albertstrasse 21, D-7800 Freiburg (FRG)

[**] This work was supported by the Deutsche Forschungsgemeinschaft, the Fonds der Chemischen Industrie, and BASF AG. We would like to thank Dr. *D. Hunkler* and Dr. *M. Keller* for NMR analyses, Dr. *J. Wörth* for MS analyses, *M. Lutterbeck, G.* and *J. Leonhardt*, and *M. Froom* for starting materials, *G. Fehrenbach* for graphical work, and Dr. *W.-D. Fessner*, Dr. *C. Rücker*, and Dr. *L. Knothe* for helpful discussions.

placed H atoms should provide an effective steric shielding of these very reactive double bonds against dimerization/polymerization. Indeed, a fourfold substituted pentagonal dodecahedrene (cf. parent compound **A**) proved to be isolable in crystalline form,[7] and the existence of multiply unsaturated dodecahedranes has been inferred from intense signals in mass spectra.[1, 7, 8] Doubly and multiply unsaturated dodecahedranes such as the D_{2h} diene **B**, the C_{2v} triene **C**, and the D_{2h} tetraene **D**, which are per se a challenge because of their structural and energetic particularities, are also of special interest with respect to transannular electron interactions ("σ-homoaromaticity") in the bissecododecahedradiene radical cation[9] and dication.[10] The first results in our quest for diene **B** (≡ **10**) as well as for two- and fourfold substituted derivatives (**12** and **6**, respectively) are presented in this communication.[11]

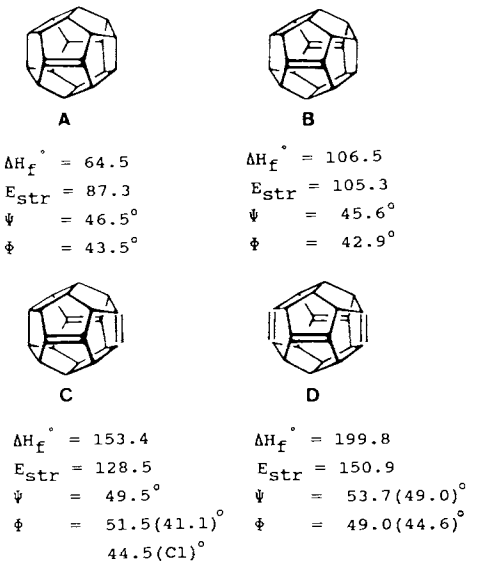

Scheme 1. Dodecahedranes **A**–**D** with double bonds. MM2-calculated ΔH_f^0 and E_{str} (strain energy) values [kcal mol^{-1}]. Ψ, Φ see [6].

Potential routes to the unsubstituted dodecahedradiene **B** (≡ **10**) are twofold β-elimination or Grob fragmentation in 1,6,11,16-tetrasubstituted dodecahedranes **7**[7] and twofold CO_2 elimination from bis-β-lactone **8**. Because of the presumably high sensitivity of **10** toward oxygen and electrophiles/nucleophiles, we first studied the gas-phase thermolysis of **8**, especially since the aldol route (cf. Ref. [1]) provides an efficient access to **8**. Tribromide **2**,[7] prepared selectively from the dioxopagodanedicarboxylic ester **1**, undergoes clean catalytic cleavage of the C4–Br bond (5-mmol scale, >95%), although as a mixture of seco-diene **5a** and bisseco-diene **4**. Reaction of this crude mixture with diimide decahedrane derivative **3** (95%).[15, 16] Of the several methods of 1,4-bromine elimination tested on **3**,[7, 8] the Zn/DMF variant at 120 °C (1–2 h) gave an excellent yield (2-mmol scale, >95%), although as a mixture of seco-diene **5a** and bisseco-diene **4**. Reaction of this crude mixture with diimide ($(KOOCN)_2$, HOAc; 50 equiv., CH_2Cl_2/CH_3OH, **4** → hyperstable dihydro-**4**; **5a** → tetrahydro-**5a**), with CH_3ONa/CH_3OH (2 equiv., dihydro-**4** → dihydro-**5a** → dihydro-**6a**, tetrahydro-**5a** → **7a**), with $Pd/C/H_2$ (50 mg mmol^{-1}, dihydro-**6a** → **7a**), with KOH/CH_3OH (**7a** → **7b**), and with phenylsulfonyl chloride/pyridine (2.25 equiv., RT, 24 h)[18] gave bislactone **8** ($\tilde{\nu}_{C=O}$ = 1820 cm^{-1}; *m/z* (CI, NH_3) 362 ($M^{\oplus}$ + 18), 318 (100, **9** + 18), 274 (48, **10** + 18), 256 (20, **10**)).[19] Compound **8**, isolated from the CH_2Cl_2/pyridine extraction phase, is sufficiently pure for use in subsequent reactions; it can be crystallized (68% based on **1**) from CH_2Cl_2/ethyl acetate (a small amount of pyridine should be added for stabilization) and remains unchanged in the solid state and in degassed solution (toluene) to ca. 220 °C, but decomposes with gas evolution at higher temperatures. Thermolysis of **8** in the gas phase (500 °C, 10^{-2} Torr) and condensation of the product on a cold finger affords up to 70% of the crystalline diene **10** (together with traces of **9** in some cases). The NMR spectra (Fig. 1) reveal D_{2h} symmetry; the mass spectrum (*m/z* [%] 256 ($M^{\oplus}$, 60), 141 (34)) shows the stability of the molecular ion. In degassed, ca. 10^{-2} M solutions and in the solid state (inert atmosphere), **10** is stable at room temperature for hours, but reacts rapidly and unspecifically (no **15a**) with oxygen. After evaporation of degassed THF solutions to dryness, up to ca. 70% of the colorless, crystalline residue is soluble as monomeric **10**.

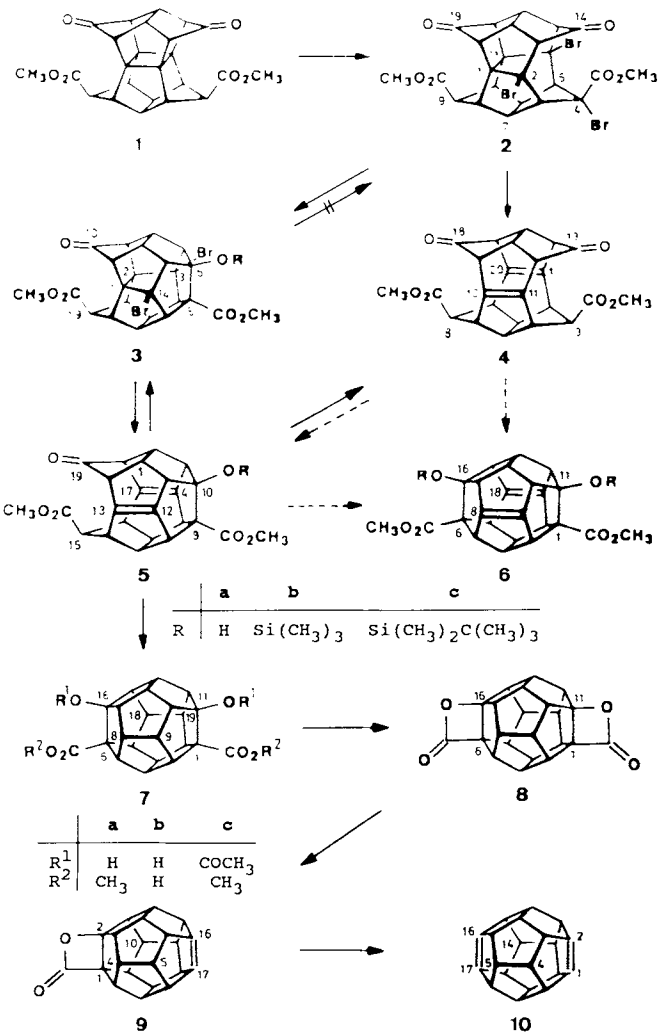

In the course of these investigations, the limits of the aldol variant once more became obvious. Our attempts to prepare the 1,6,11,16-fourfold substituted dodecahedradienes **6** (presumably less reactive than **10**), which, among other things, are of interest as potential intermediates along the route to tetraene **D**, starting from **1** and using the aldol variant via bisseco-diene **4**, had already met with failure (the C–C

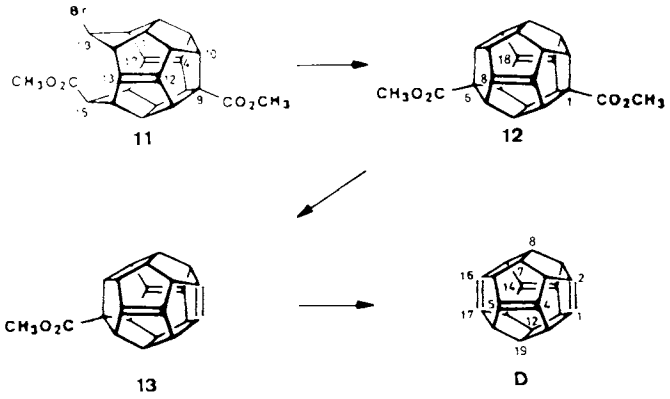

coupling reactions **4a** → **5a** → **6a** are considerably endothermic; cf. **A** → **G** ($\Delta\Delta H_f^\circ = +12.4$ kcal mol^{-1}) and **G** → **N** ($\Delta\Delta H_f^\circ = +5.9$ kcal mol^{-1}) in Scheme 1 of Ref. [7]). The availability of the seco intermediates **5a–c** provides no breakthrough; even under potentially irreversible conditions, no cyclization **5** → **6** could be realized.

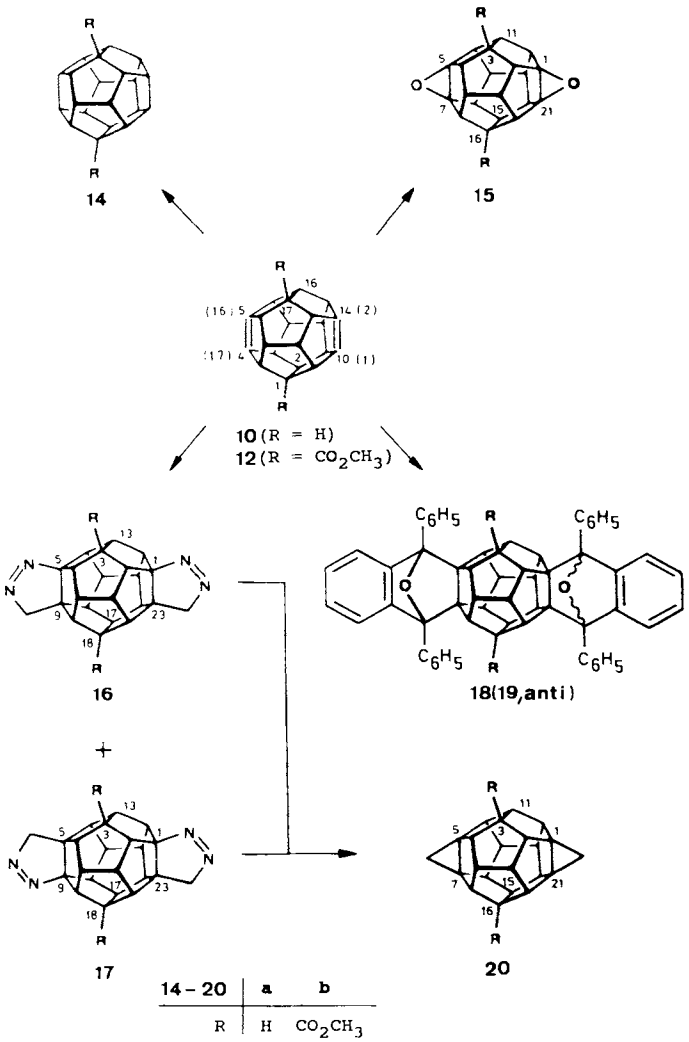

Encouragingly unproblematic, on the other hand, is the preparation of the dodecahedra-8,18-diene-1,6-dicarboxylic ester **12** by the S_N2 variant via the *anti*-bromo seco-diene diester **11** (d(C15-C19) = 3.281 Å) described in the preceding communication.[1] Stirring the degassed THF solution of **11** over NaH (2 equiv., 2 h, RT), followed by filtration and concentration, afforded pure, colorless, crystalline **12**. Compound **12**, like **10**, is very sensitive toward oxygen, readily soluble in benzene, THF, and CH_2Cl_2 (ca. 20 mg in 0.3 mL), and thermally stable (in ca. 10^{-2} M solutions or in the crystalline state, **12** remains unchanged for days in the absence of oxygen). In the qualitatively recorded UV spectrum (CH_3CN), there is no pronounced maximum (no shoulder) along an absorption band that steadily decreases to ca. 260 nm—in contrast to the spectra of **11** or **4/5**. The NMR data of **12** (Fig. 1) are characterized, in particular, by the similarity of the shifts of the olefinic ^{13}C NMR signals with those of C-4(12) in seco-diene **11** and those of C-1(16) in diene **10**. The most striking feature of the mass spectrum (m/z [%] 372 ($M^\oplus$, 56), 312 (100, e.g., **13**), 253 (72), 252 (58, e.g., **D**)) is the intensity of the signals ascribable to multiply unsaturated dodecahedranes.

Common to dienes **10** and **12** is the ease of hydrogenation (Pt, H_2, diimide) of both double bonds (formation of dodecahedranes **14a, b**[11]), their rapid oxidation by benzoylperoxycarbamic acid (5 equiv., CH_2Cl_2, RT, 5 min) to give diepoxides **15a, b**,[1] and the addition of diazomethane (10 equiv., CH_2Cl_2, 10 min) to give ca. 1:1 mixtures of *syn*/*anti*-bis(dihydropyrazoles) **16a, b**/**17a, b** and of diphenylisobenzofuran (5 equiv., RT, immediate reaction) to give ca. 1:1 mixtures of *syn*/*anti*-bisadducts **18a, b**/**19a, b**. Compound **18a** was isolated in pure form by chromatography. Photolysis of dihydropyrazoles **16a**/**17a** ($\lambda_{max} = 310$ nm, benzene, Pyrex photoreactor, high-pressure Hg lamp) gave dicyclopropadodecahedrane **20a** (m/z [%] 284 ($M^\oplus$, 77), 97 (26), 71 (54), 57 (100)). The assignment of the cyclopropane-ring ^{13}C NMR signals (Fig. 1), which differs from that of cyclopropadodecahedrane,[2, 20] was confirmed by DEPT experiments. Addition of bromine to **10** or **12** at room temperature leads to the spontaneous formation of complex mixtures of products, in contrast to the corresponding reactions with bisseco-dienes

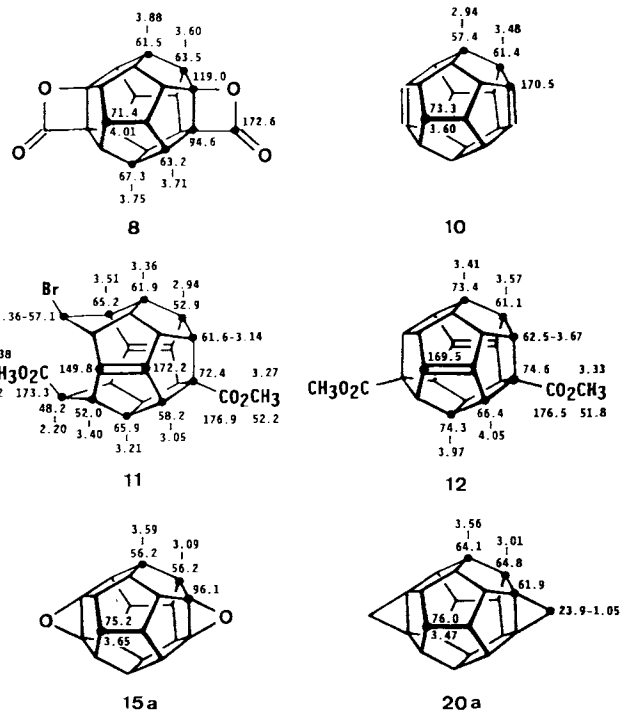

Fig. 1. ^1H and ^{13}C NMR spectroscopic data ($CDCl_3$) of **8**, **10** (C_6D_6), **11**, **12** (C_6D_6), **15a**, and **20a**.

(e.g., **4**) and seco-dienes (e.g., **11**); the homo-1,4 adducts derived analogously from **21a,b** (cf. **11** in Ref. [1]) are extremely unfavorable thermodynamically.

Prospects: The pagodane route provides the prerequisites for the preparation and isolation of singly and doubly unsaturated, variously substituted (stabilized) dodecahedranes. Thus, it becomes possible to test experimentally[21] diverse and in part contradictory thermodynamic predictions (heats of hydrogenation and heats of formation) and to investigate the homoconjugative interactions in dienes **B** and cations of type **21**.[10, 22] Trienes (**C**) and tetraenes (**D**) are important in this context. There is mass spectrometric evidence that they are possibly isolable compounds. The "inner life" of such multiply unsaturated dodecahedranes, for example, homoconjugative/homoaromatic interactions in the potentially "three-dimensionally homoaromatic"[23] dication **22** or in cations/dications such as **23/24** derived from tetraene **D**, is

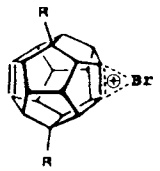

21

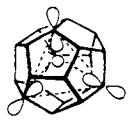

22

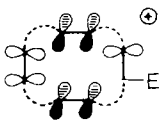

23

a, R = H

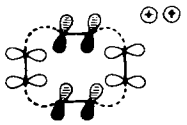

24

just one exciting aspect. The respective transannular p–π and π–π distances clearly touch the limits of such interactions, all the more since decreases in distances due to bonding interactions are severely counteracted by the rigidity of the molecular frameworks.[24] For the same reason, the MM2-calculated structural parameters, in particular the relevant transannular distances and Ψ (Φ) values,[6] should be subject to relatively small error,[25] usually due to underestimate of repulsive π–π interactions.[26] Particularly informative in this respect are the X-ray structure data[27] of seco-diene **11** and diepoxide **25** (Fig. 2). Compound **25** is the best model so far available for the diene framework **B** (**10, 12**); cf. the transannular distances [Å] of the bonds in **25** (Fig. 2), **10** [MM2, 3.52 (1(2)-17(16)), 4.12 (4(5)-10(14)), 4.05 (7(8)-19(12))], and **D** [MM2, 3.59 (1(2)-17(16)), 3.79 (4(5)-10(14)), 4.12(7(8)-19(12))]. Undoubtedly, the unsaturated dodecahedranes will open a further fascinating chapter in the chemistry of this class of compounds.[28]

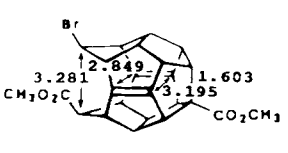

11

Φ: 15.5°; 35.3°

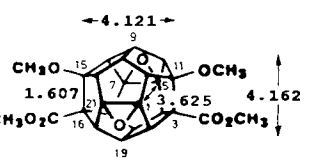

25

Ψ: 47.5°
Φ: 46.5°

Fig. 2. Selected X-ray structure data [Å] for seco-diene **11** and diepoxydodecahedrane **25**. Φ values [6] for C-13(17)/C-4(12) in **11**, Ψ and Φ values for C-1(5,7,21) in **25**.

Received: August 14, 1989 [Z 3501 IE]
German version: *Angew. Chem. 102* (1990) 105

[1] R. Pinkos, J.-P. Melder, H. Prinzbach, *Angew. Chem. 102* (1990) 102; *Angew. Chem. Int. Ed. Engl. 29* (1990) 92.
[2] L. A. Paquette, T. Kobayashi, M. A. Kesselmayer, J. C. Gallucci, *J. Org. Chem. 54* (1989) 2921, and references therein; L. A. Paquette, *Chem. Rev. 89* (1989) 1051.
[3] W. F. Maier, P. von R. Schleyer, *J. Am. Chem. Soc. 103* (1981) 1891; A. B. McEwen, P. von R. Schleyer, *J. Org. Chem. 51* (1986) 4357; W. D. Fessner, *Dissertation*, Universität Freiburg 1986.
[4] O. Ermer, *Angew. Chem. 89* (1977) 431; *Angew. Chem. Int. Ed. Engl. 16* (1977) 411.
[5] A. Greenberg, J. F. Liebmann: *Strained Organic Molecules*, Academic Press, New York 1978, p. 90; G. Szeimies, *React. Intermed. (Plenum) 3* (1983) 299; H.-U. Wagner, G. Szeimies, J. Chandrasekhar, P. von R. Schleyer, J. A. Pople, J. S. Binkley, *J. Am. Chem. Soc. 100* (1978) 1210; M. Toda, K. Okada, M. Oda, *Tetrahedron Lett. 29* (1988) 2329; P. E. Eaton, M. Maggini, *J. Am. Chem. Soc. 110* (1988) 7230.
[6] The "pyramidalization (*syn* bending) is characterized, as in our preceding communications, by Ψ (180° − R–C·C–R torsional angle) and, in the less symmetrical diene **11**, by Φ.

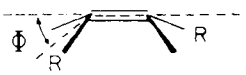

[7] J.-P. Melder, R. Pinkos, H. Fritz, H. Prinzbach, *Angew. Chem. 101* (1989) 314; *Angew. Chem. Int. Ed. Engl. 28* (1989) 305, and references therein.
[8] R. Pinkos, J.-P. Melder, H. Fritz, H. Prinzbach, *Angew. Chem. 101* (1989) 319; *Angew. Chem. Int. Ed. Engl. 28* (1989) 310, and references therein.
[9] H. Prinzbach, Bulusu A. R. C. Murty, W.-D. Fessner, J. Mortensen, J. Heinze, G. Gescheidt, F. Gerson, *Angew. Chem. 99* (1987) 488; *Angew. Chem. Int. Ed. Engl. 26* (1987) 457.
[10] G. K. Surya Prakash, V. V. Krishnamurty, R. Herges, R. Bau, H. Yuan, G. Olah, W.-D. Fessner, H. Prinzbach, *J. Am. Chem. Soc. 110* (1988) 7764; G. K. Surya Prakash, W.-D. Fessner, G. Olah, G. Lutz, H. Prinzbach, *ibid. 111* (1989) 746.
[11] Taken from the dissertations of *J.-P. Melder* and *R. Pinkos*, Universität Freiburg 1990. Compare the experimental and theoretical studies in the homologous series of tricyclic, bicyclo[3.3.0]oct-1(5)-ene-derived alkenes **26** [12, 13] and of planar-parallel dienes of type **27** [14]. The **26** homologue with n = 2 dimerizes in an argon matrix at temperatures as low as 40 K [13].
[12] D. A. Hrovat, W. T. Borden, *J. Am. Chem. Soc. 110* (1988) 4710, zit. Lit.; W. T. Borden, *Chem. Rev. 89* (1989) 1095.
[13] J. G. Radziszewski, T.-K. Yin, F. Miyake, G. E. Renzoni, W. T. Borden, J. Michl, *J. Am. Chem. Soc. 108* (1986) 3544.

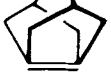

26

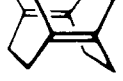

27

[14] R. L. Viavattene, F. D. Greene, L. D. Cheung, R. Majeste, L. M. Trefonas, *J. Am. Chem. Soc. 96* (1974) 4342; K. B. Wiberg, R. D. Adams, P. J. Okarma, M. G. Matturro, B. Segmuller, *ibid. 106* (1984) 2200; K. B. Wiberg, *Chem. Rev. 89* (1989) 975; K. J. Shea, A. C. Greeley, S. Nguyen, P. D. Beauchchamp, D. H. Aue, J. S. Witzemann, *J. Am. Chem. Soc. 108* (1986) 5901; vgl. J. E. McMurry, G. J. Haley, J. R. Matz, J. C. Clardy, G. van Duyne, R. Gleiter, W. Schäfer, D. H. White, *ibid. 108* (1986) 2932.
[15] For nomenclature, see footnote [10] in reference [1]. Several earlier names [7] were corrected with the computer program POLYCYC (**5a, 11** [1], **15b** [1], **25**): **20a**, tridecacyclo[10.10.0.0^{1,21}.0^{2,19}.0^{3,11}.0^{4,18}.0^{5,7}.0^{5,10}.0^{7,17}.0^{8,15}.0^{9,13}.0^{14,21}.0^{14,20}]docosane; **25**, dimethyl 11,15-dimethoxy-6,22-dioxatridecacyclo[10.10.0.0^{1,21}.0^{2,19}.0^{3,11}.0^{4,18}.0^{5,7}.0^{5,10}.0^{7,17}.0^{8,15}.0^{9,13}.0^{14,21}.0^{16,20}]docosane-3,16-dicarboxylate.
[16] The new compounds were characterized by their spectra (400-MHz ^{1}H NMR, 100.6-MHz ^{13}C NMR, IR, MS) and by elemental analyses. For

example, dimethyl 3,14-dibromo-6-hydroxy-10-oxo-undecacyclo[9.9.0.0^{1,14}.0^{2,9}.0^{2,18}.0^{3,7}.0^{4,17}.0^{5,15}.0^{6,13}.0^{8,12}.0^{16,20}.0^{16,20}]icosane-5,19-*syn*-dicarboxylate **3a**: m.p. 265–267 °C. IR (KBr): $\tilde{\nu}$ = 3480 (O-H), 2980 (C-H), 1812 (C=O), 1765 (C=O), 1725 (C=O), 1690 (C=O), 1245 (C-O) cm^{-1}. ^{1}H NMR ($CDCl_3$): δ = 3.83 (s, OCH_3, (ester on C5)), 3.68 (s, OCH_3, (ester on C19)), 3.65 (m, 4-,15-H), 3.60 (m, 8-,12-H), 3.58 (m, 18-,20-H), 3.41 (m, 16-,17-H), 3.24 (m, 7-,13-H), 3.01 (m, 9-,11-H), 2.76 (m, 19-H). ^{13}C NMR ($CDCl_3$): δ = 210.5 (C-10), 172.8 (CO_2R), 109.5 (C-6), 92.9 (C-3,-14), 83.0 (C-5), 80.7 (C-1,-2), 69.6 (C-7,-13), 62.2 (C-4-15), 61.5 (C-16,-17), 55.6 (C-8,-12), 53.1 (OCH_3, ester on C(5)), 52.4 (OCH_3 (ester on C-19)), 51.4 (C-9,-11), 51.0 (C-18,-20), 49.7 (C-19). MS (EI): *m/z* [%] 564 ($M^{\oplus}$, 8), 532(8), 485(98), 483(100), 453(80), 451(78),421(38), 419(36), 372(58), 343(26). Dimethyl 19-oxo-10-trimethylsilyloxydecacyclo[9.9.0.0^{2,18}.0^{3,10}.0^{4,17}.0^{5,9}.0^{6,16}.0^{7,14}.0^{8,12}.0^{13,20}]icosa-4(17),12-diene-9,15-*syn*-dicarboxylate **5b**: m.p. 180–181 °C. IR (KBr): $\tilde{\nu}$ = 2950 (C-H), 1740 (C=O), 1720 (C=O), 1240 (C-O), 1220 (C-O) cm^{-1}. ^{1}H NMR ($CDCl_3$): δ = 3.96 (m, 5-,8-H), 3.86 (m, 14-,16-H), 3.76 (m, 1-,2-H), 3.74 (s, OCH_3), 3.72 (s, OCH_3), 3.64 (m, 6-,7-H), 3.49 (m, 3-,11-H), 3.35 (m, 18-,20-H), 2.66 (t, 15-H; J = 6.0 Hz), 0.14 (s, $Si(CH_3)_3$). ^{13}C NMR ($CDCl_3$): δ = 213.5 (C-19), 175.4 (C-4,-12), 172.9 (CO_2R), 172.0 (CO_2R), 151.8 (C-13,-17), 107.0 (C-10), 81.8 (C-9), 65.7 (C-6,-7), 63.5 (C-3,-11), 58.9 (C-18,-20), 57.7 (C-1,-2), 55.5 (C-5,-8), 52.5 (OCH_3), 51.9 (OCH_3), 51.0 (C-14,-16), 46.9 (C-15), 1.5 ($Si(CH_3)_3$). UV (CH_3CN): $\lambda_{max}(\varepsilon)$ = 270 sh(240), 261 sh(280), 250 sh(420). MS (EI): *m/z* [%]: 476 ($M^{\oplus}$, 58), 361(90), 372(23), 224(17), 73(100). C_{2v} diphenylisobenzofuran bisadduct **18a** (numbering of diene **10**): m.p. > 320 °C. ^{1}H NMR ($CDCl_3$): δ = 7.77 (m, 8H), 7.44 (m, 8H), 7.33 (m, 4H), 7.06 (m, 4H), 6.96 (m, 4H), 3.68 (q, 8-,12-H), 3.36 (q, 7-,19-H), 3.33 (m, 10-,14-H), 3.13 (m, 3-,6-,9-,11-,13-,15-,18-,20-H), 2.46 (m, 4-,5-H); $J_{3,7} = J_{6,7} = J_{7,8} = J^{12,19} = J_{8,9} = J_{8,15}$ = 11.0 Hz. ^{13}C NMR ($CDCl_3$): δ = 147.4 (4C), 139.0 (4C), 128.4 (8C), 127.1 (4C), 126.1 (4C), 126.0 (8C), 120.5 (4C), 95.4 (4C), 94.0 (C-1,-2,-16,-17), 70.8 (C-8,-12), 69.4 (C-10,-14), 67.8 (C-9,-11,-13,-15), 67.5 (C-3,-6,-18,-20), 67.4 (C-7,-19), 64.8 (C-4,-5). MS DCI; NH_3): *m/z* [%] 797 ($M^{\oplus}$, 3), 271 (100).

[17] If alcohol **3a** is converted into ether **3b** (5 equiv., Me_3SiCl/pyridine/CH_2Cl_2, RT, 95%), the competing retro-aldol reaction (**5** → **4**) is precluded and a 92% yield of seco-diene **5b** is obtained. For **5b**, interaction between the CC double bonds (cf. the π-π transannular distances measured for **11**: 2.849 and 3.195 Å, Fig. 2) is revealed in the UV spectrum (CH_3CN) by long-wavelength shoulders (270 nm (ε = 240), 261 (280), 250 (420)).

[18] W. Adam, J. Baeza, J. C. Liu, *J. Am. Chem. Soc. 94* (1972) 2000.

[19] The ^{13}C NMR shifts of **8** (Fig. 1), in particular those of C-8(9,18,19) (δ = 71.4) and of C-10(12,15,17) (δ = 63.5), are surprising compared with those of **7c** (δ = 63.9 and 71.6, respectively); the assignment has been unambiguously confirmed by selective decoupling experiments.

[20] L. A. Paquette, T. Kobayashi, J. C. Gallucci, *J. Am. Chem. Soc. 110* (1988) 1305; L. A. Paquette, I. Kobayashi, M. A. Kesselmayer, *ibid. 110* (1988) 6568.

[21] For diene diester **12**, cyclovoltammetry (CH_2Cl_2, Bu_4NPF_6) [9] revealed two irreversible oxidation potentials of +1.2 and +1.4 eV (vs. Ag/AgCl) (dication **28/29**?) (G. Lutz, *Dissertation*, Universität Freiburg 1990).

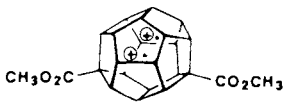

28

29

[22] G. A. Olah, G. K. Surya Prakash, T. Kobayashi, L. A. Paquette, *J. Am. Chem. Soc. 110* (1988) 1304.

[23] M. Bremer, P. von R. Schleyer, K. Schötz, M. Kausch, M. Schindler, *Angew. Chem. 99* (1987) 795; *Angew. Chem. Int. Ed. Engl. 26* (1987) 261.

[24] Calculations at various theoretical levels [20] will be published elsewhere (W.-D. Fessner, J.-P. Melder, H. Prinzbach, unpublished).

[25] For a critical evaluation of MM2 and MM3 calculations, in particular of saturated (seco)dodecahedranes, see N. L. Allinger, H. J. Geise, W. Pykhout, L. A. Paquette, J. C. Gallucci, *J. Am. Chem. Soc. 111* (1989) 1106; cf. O. Ermer, *Angew. Chem. 95* (1983) 251; *Angew. Chem. Int. Ed. Engl. 22* (1983) 251.

[26] C. Jaime, E. Osawa, *Tetrahedron 39* (1983) 2769, and references therein.

[27] G. Rihs, U. Reifenstahl, H. Irngartinger, P. R. Spurr, J.-P. Melder, R. Pinkos, H. Prinzbach, unpublished; cf. J. C. Gallucci, R. T. Taylor, T. Kobayashi, J. C. Weber, J. Krause, L. A. Paquette, *Acta Crystallogr. Sect. C 45* (1989) 893.

[28] The existence of dodecahedrene was recently concluded indirectly from gas-phase ion-molecule reactions, although the molecule was not directly observed: a strain energy (heat of hydrogenation) of 63 ± 3 kcal mol^{-1} was estimated for the CC double bond: J. Kiplinger, F. R. Tollens, A. G. Marshall, T. Kobayashi, D. R. Lagerwall, L. A. Paquette, J. E. Bertmess, *J. Am. Chem. Soc. 111* (1989) 6914.

Synthesis of (−)-Neplanocin A from (*R*,*R*)-Tartaric Acid**

By *Hans Jürgen Bestmann** and *Dieter Roth*

Recently, we reported on the possibility of transforming tartaric acid into optically active cyclopentanediol synthetic building blocks such as **5**.[1] Here we describe the use of **5** to synthesize the naturally occurring carbocyclic nucleoside analogue (−)-neplanocin A (**13**), which exhibits antiviral and antitumor activity.[2]

The synthesis of **5** has meanwhile been improved as shown in Scheme 1. The protected monomethyl tartrate (*R*,*R*)-**1**

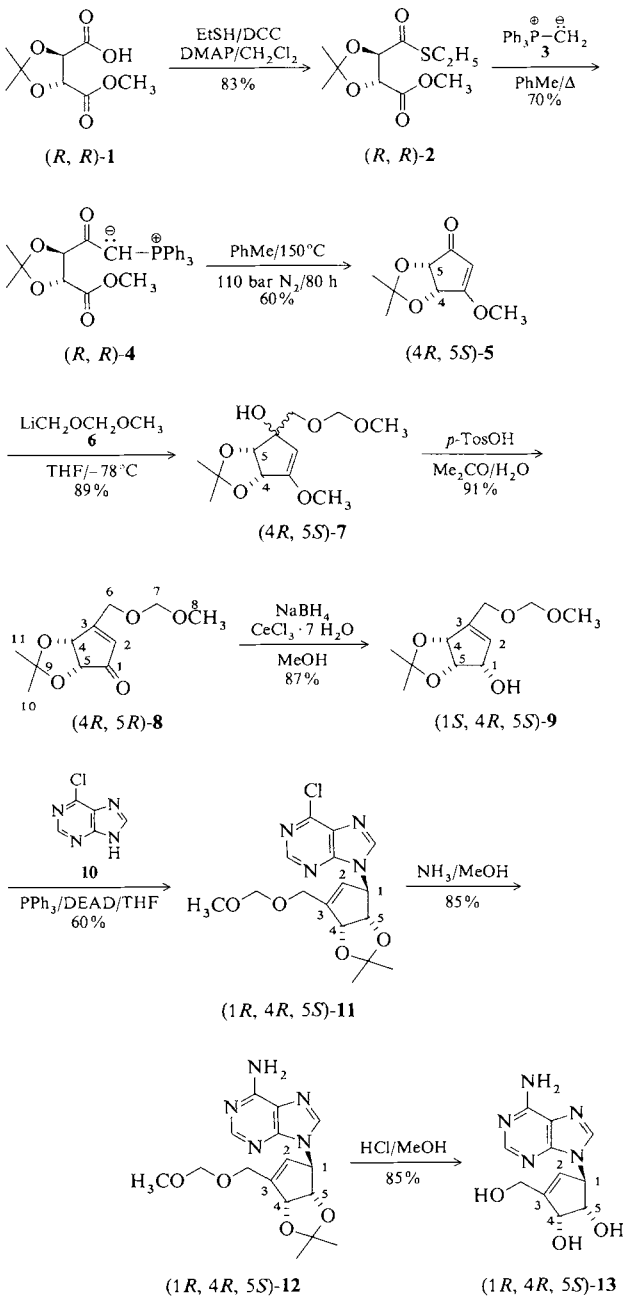

(*R*, *R*)-**1** (*R*, *R*)-**2** (*R*, *R*)-**4** (4*R*, 5*S*)-**5** (4*R*, 5*S*)-**7** (4*R*, 5*R*)-**8** (1*S*, 4*R*, 5*S*)-**9** **10** (1*R*, 4*R*, 5*S*)-**11** (1*R*, 4*R*, 5*S*)-**12** (1*R*, 4*R*, 5*S*)-**13**

Scheme 1. Synthesis of (−)-neplanocin A (**13**).

[*] Prof. Dr. H. J. Bestmann, Dipl.-Chem. D. Roth
Institut für Organische Chemie der Universität Erlangen-Nürnberg
Henkestrasse 42, D-8520 Erlangen (FRG)

[**] We thank Hoechst AG for carrying out studies of the biological activity of **13**.

was converted into the *S*-ester **2** by treatment with ethanethiol and dicyclohexylcarbodiimide (DCC) in the presence of dimethylaminopyridine (DMAP).[3] Compound **2** reacts with methylenetriphenylphosphorane (**3**) to give ylide **4**.[4] We found that the subsequent intramolecular Wittig reaction at the ester carbonyl group[5] proceeded much more smoothly under increased pressure. As described earlier, epimerization occurs during the reaction. Originally, we assumed by analogy that *ent*-**5** of absolute configuration (4*S*,5*R*) had been formed.[1] Using the new procedure of triplet phase measurement, however, we were able to show that the absolute configuration of **5** is, in fact, (4*R*,5*S*);[6] that is, the epimerization takes place at the C atom bearing the C=O ylide group.

Addition of (methoxymethoxy)methyllithium (**6**), generated in situ from *n*-butyllithium and (methoxymethoxy)-methyltributyltin,[7] gives a mixture of the diastereoisomeric α,β-unsaturated alcohols **7**, which, without further purification, were converted into cyclopentenone **8** by acid-catalyzed elimination of methanol accompanied by allylic rearrangement. Diastereoselective reduction[8] of the carbonyl function of **8** affords the optically pure α,β-unsaturated alcohol **9**. The base component of the nucleoside structure was introduced by reaction of **9** with 6-chloropurine (**10**) according to the Mitsunobu procedure (triphenylphosphane/diethyl azodicarboxylate (DEAD)[9]) with inversion at C1 to give **11**. Transformation of the chloropurine ring to the adenine ring (**11** → **12**) was accomplished by a known method[2c] using a methanolic solution of ammonia in a sealed reaction vessel. The subsequent, simultaneous cleavage of both protecting groups in **12** with dilute HCl affords **13**; its physical constants, spectroscopic data (Table 1), and antiviral activity are identical with those of natural neplanocin A. Thus, this natural product is accessible in 11 steps from inexpensive, natural tartaric acid.

If, instead of **6**, other organolithium compounds (**14**) are used in the synthetic route shown in Scheme 1, neplanocin derivatives (**15**) with different side chains R may be prepared.

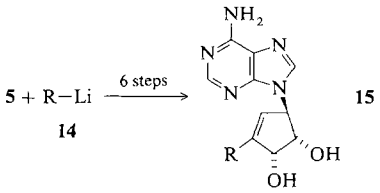

Table 1. Selected physical data for **8**, **9**, and **11**–**13**:

8: b.p. 77–78 °C/0.01 Torr, $[\alpha]_D^{20} = -13.1$ ($c = 1.1$, $CHCl_3$); ^1H NMR (400 MHz, $CDCl_3$): $\delta = 1.36$, 1.37 (each s, 10-, 11-H, each 3H), 3.36 (s, 8-H, 3H), 4.38 (dd, $J_a = 17.7$, $J_b = 1.83$ Hz, 6-H, 1H), 4.47 (d, $J = 5.49$ Hz, 5-H, 1H), 4.52 (dd, $J_a = 17.7$, $J_b = 1.83$ Hz, 6-H, 1H), 4.68 (s, 7-H, 2H), 5.08 (d, $J = 5.49$ Hz, 4-H, 1H), 6.12 (t, $J = 1.83$ Hz, 2-H, 1H)

9: b.p. 74–76 °C/0.02 Torr, $[\alpha]_D^{20} = +36.8$ ($c = 0.8$, $CHCl_3$) (>97:3 after GC, ^1H- and ^{13}C NMR); ^1H NMR (400 MHz, $CDCl_3$): $\delta = 1.22$, 1.26 (each s, 10-, 11-H, each 3H), 2.73 (d, $J = 10.1$ Hz, 1-OH, 1H), 3.38 (s, 8-H, 3H), 4.17 (d, $J = 13.6$ Hz, 6-H, 1H), 4.24 (d, $J = 13.6$ Hz, 6-H, 1H), 4.57 (m, 1-H, 1H), 4.66 (s, 7-H, 2H), 4.77 (t, $J = 5.5$ Hz, 5-H, 1H), 4.97 (d, $J = 5.5$ Hz, 4-H, 1H), 5.78 (br. s, 2-H, 1H)

11: m.p. 56–57 °C, $[\alpha]_D^{20} = -68.8$ ($c = 1.0$, $CHCl_3$) (>99:1 after ^1H- und ^{13}C NMR); ^1H NMR (400 MHz, $CDCl_3$): $\delta = 1.39$, 1.51 (each s, 10-, 11-H, each 3H), 3.42 (s, 8-H, 3H), 4.38 (m, 6-H, 2H), 4.74 (s, 7-H, 2H), 4.78 (d, $J = 5.8$ Hz, 4-H, 1H), 5.46 (d, $J = 5.8$ Hz, 5-H, 1H), 5.70 (br.s, 1-H, 1H), 5.87 (br.s, 2-H, 1H), 8.10, 8.77 (each s, arene-H, each 1H)

12: m.p. 134–135 °C, $[\alpha]_D^{20} = -74.2$ ($c = 0.8$, $CHCl_3$) [according to [2c]: m.p. = 134–136 °C, $[\alpha]_D^{20} = -69.8$ ($c = 1.1$, $CHCl_3$)]; ^1H NMR (400 MHz, $CDCl_3$): $\delta = 1.37$, 1.49 (each s, 10-, 11-H, each 3H), 3.42 (s, 8-H, 3H), 4.35 (m, 6-H, 2H), 4.72 (d, $J = 5.5$ Hz, 4-H, 1H), 4.73 (s, 7-H, 2H), 5.40 (d, $J = 5.5$ Hz, 5-H, 1H), 5.70 (br.s, 1-H, 1H), 5.84 (br.s, 2-H, 1H), 6.20 (br.s, NH_2, 2H), 7.71 8.38 (each s, arene-H, each 1H)

13: m.p. 218–220 °C (dec.), $[\alpha]_D^{20} = -154.5$ ($c = 0.3$, H_2O) [according to [2a]: m.p. = 220–222 °C (dec.), $[\alpha]_D^{23} = -157.0$ ($c = 0.5$, H_2O)]; ^1H NMR (400 MHz, $(D_3C)_2SO$): $\delta = 4.16$ (m, 6-H, 2H), 4.32 (dd, $J_a = 6.7$, $J_b = 5.5$ Hz, 5-H, 1H), 4.44 (t, $J = 5.5$ Hz, 4-H, 1H), 4.93 (t, $J = 5.5$ Hz, 6-OH, 1H), 4.98 (d, $J = 6.1$ Hz, 4-OH, 1H), 5.16 (d, $J = 6.7$ Hz, 5-OH, 1H), 5.35 (br.s, 1-H, 1H), 5.71 (d, $J = 1.8$ Hz, 2-H, 1H), 7.22 (br.s, NH_2, 2H), 8.13, 8.21 (each s, arene-H, each 1H)

Received: July 25, 1989 [Z 3465 IE]
German version: *Angew. Chem. 102* (1990) 95

CAS Registry numbers:
1, 67812-33-3; **2**, 123883-95-4; **3**, 3487-44-3; **4**, 104832-18-0; **5**, 104738-61-2; **6**, 123883-96-5; **7** isomer 1, 123883-97-6; **7** isomer 2, 123932-32-1; **8**, 123883-98-7; **9**, 123883-99-8; **10**, 87-42-3; **11**, 89505-90-8; **12**, 85390-44-9; **13**, 72877-50-0.

[1] H. J. Bestmann, T. Moenius, *Angew. Chem. 98* (1986) 1007; *Angew. Chem. Int. Ed. Engl. 25* (1986) 994.
[2] a) S. Yaginuma, N. Muto, M. Tsujino, Y. Sudata, M. Hayashi, M. Otani, *J. Antibiot. 34* (1981) 359; M. Hayashi, S. Yaginuma, *ibid. 34* (1981) 675; R. T. Borchardt, B. T. Keller, U. Patel-Thombre, *J. Biol. Chem. 259* (1984) 4353; b) M. Jung, G. Offenbächer, J. Rétey, *Helv. Chim. Acta 66* (1983) 1915; c) M. Arita, K. Adachi, Y. Ito, H. Sawai, M. Ohno, *J. Am. Chem. Soc. 105* (1983) 4049; d) M. I. Lim, V. E. Marquez, *Tetrahedron Lett. 24* (1983) 5559; C. K. H. Tseng, V. E. Marquez, *ibid. 26* (1985) 3669; V. E. Marquez, M. I. Lim, C. K. H. Tseng, A. Morcovac, M. A. Priest, M. S. Khan, B. Kaskar, *J. Org. Chem. 53* (1988) 5709; e) J. R. Medich, K. B. Kummen, C. R. Johnson, *Tetrahedron Lett. 28* (1987) 4131.
[3] W. Steglich, B. Neises, *Angew. Chem. 90* (1978) 556; *Angew. Chem. Int. Ed. Engl. 17* (1978) 522.
[4] H. J. Bestmann, B. Arnason, *Chem. Ber. 95* (1962) 1513.
[5] For the intramolecular Wittig reaction, see H. J. Bestmann, D. Schade, H. Lüttke, T. Moenius, *Chem. Ber. 118* (1985) 2640.
[6] H. Burzlaff, K. Hümmer, W. Rothammel, G. Schäfer, E. Weckert, H. J. Bestmann, D. Roth, *Acta Crystallogr. Sect. B45* (1989) 303.
[7] C. W. Still, *J. Am. Chem. Soc. 100* (1978) 1481; J. S. Sawjer, A. Kucerovy, T. L. MacDonald, G. J. Garvey, *ibid. 110* (1988) 842; C. R. Johnson, J. R. Medich, *J. Org. Chem. 53* (1988) 4131.
[8] A. Gamal, J. L. Luche, *J. Am. Chem. Soc. 103* (1981) 5454.
[9] O. Mitsunobu, *Synthesis 1981*, 1; M. Iwakawa, B. M. Pinto, W. A. Szarek, *Can. J. Chem. 56* (1978) 326; W. A. Szarek, C. Depew, H. C. Jarell, J. K. N. Jones, *J. Chem. Soc. Chem. Commun. 1975*, 648.

About the $Li^{\oplus}$ Gegenion Effect on α-Sulfonyl Carbanions**

By *Hans-Joachim Gais,** *Gunther Hellmann*, and *Hans Jörg Lindner*

Characteristic for lithium salts of α-sulfonyl carbanions are monomeric (in THF solution)[1, 2] and dimeric (in the crystal)[1, 3–5] O–Li contact ion pairs (cf. Scheme 1 and

[*] Prof. Dr. H.-J. Gais, Dipl.-Ing. G. Hellmann
Institut für Organische Chemie und Biochemie der Universität
Albertstrasse 21, D-7800 Freiburg (FRG)
Prof. Dr. H. J. Lindner
Institut für Organische Chemie der Technischen Hochschule
Petersenstrasse 22, D-6100 Darmstadt (FRG)

[**] This work was supported by the Deutsche Forschungsgemeinschaft and the Fonds der Chemischen Industrie. We thank Dr. *H. Paulus* (Darmstadt) for the crystallographic data sets, Dr. *W. Bauer* (Erlangen) for the cryoscopic measurements, Dr. *D. Hunkler* for NMR measurements, Dr. *E. Keller* for a version of SCHAKAL-88, and *J. Vollhardt* and *N. Reuter* for the SCHAKAL figures. TMEDA = *N,N,N',N'*-tetramethylethylenediamine.

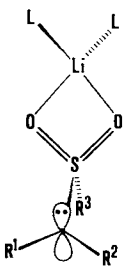

Scheme 1.

Fig. 1) as well as an anion conformation in which the C_α electron pair is *gauche* with respect to both O atoms. This conformation brings about the chirality for an α-sulfonyl carbanion whose anionic C atom bears different groups. The finding that the racemization barrier of lithio*trifluoromethyl*-sulfones (lithiotriflones) is appreciably larger than that of lithio*phenyl*sulfones recently made possible the enantioselective synthesis of a lithiosulfone that was optically stable at low temperatures.[1] It then became of interest to determine how the O-associated $Li^\oplus$ ion (+ ligands) influences the structure and dynamic behavior of an α-sulfonyl carbanion and what importance torsional effects have for the C_α–S rotational barrier of lithiotriflones. Ab initio calculations on the structural aspect of the $Li^\oplus$ gegenion effect, which is still of current interest in carbanion chemistry,[6] have already been performed.[7]

$[PhCH_2C(Ph)\text{–}SO_2R]^\ominus$
$\mathbf{1}^\ominus$, R = CF_3; $\mathbf{2}^\ominus$, R = *t*Bu; $\mathbf{3}^\ominus$, R = Ph

To answer the questions posed above, we have prepared the tetraalkylammonium salt $\mathbf{1}^\ominus/NBu_4^\oplus$, elucidated its crystal structure, and determined the enantiomerization barriers of the salts $\mathbf{1}^\ominus/NBu_4^\oplus$, $\mathbf{1}^\ominus/K^\oplus$, and $\mathbf{2}^\ominus/Li^\oplus$. In addition, we have measured the ^1H NMR and ^{13}C NMR chemical shifts for the *para* position of the α-phenyl ring in $\mathbf{1}^\ominus/NBu_4^\oplus$and $\mathbf{1}^\ominus/Li^\oplus$ as probes for the charge distribution[8] of the anion $\mathbf{1}^\ominus$. A tetraalkylammonium salt of $\mathbf{1}^\ominus$ was chosen because the large $NBu_4^\oplus$ ion, the positive charge of which is distributed over the H atoms,[9] should have a smaller and less specific effect on $\mathbf{1}^\ominus$ than the small, O-associated $Li^\oplus$ ion, which has a high charge density. Tetraalkylammonium salts of other carbanions have long been known,[10] but their crystal structure, apart from a few exceptions,[10e–g] is unknown. The crystal structure of the lithium salt ($\mathbf{1}^\ominus/Li^\oplus \cdot TMEDA)_2$ served as a reference structure;[11] in order to know exactly how the TMEDA ligands structurally influence the anion $\mathbf{1}^\ominus$, however, we determined, in addition, the crystal structure of $(\mathbf{1}^\ominus/Li^\oplus \cdot 2\ THF)_2$—the first of a THF-coordinated monolithiosulfone.[11]

Although, according to cryoscopy, $\mathbf{1}^\ominus/Li^\oplus$ is monomeric in THF solution,[1] it crystallizes as an achiral dimer ($\mathbf{1}^\ominus/Li^\oplus \cdot 2\ THF)_2$[12a] (Fig. 1) with O-associated $Li^\oplus$ ions, similarly to a lithiosulfone containing *chelate* ligands.[1,3,4] The anionic C atoms (sum of bond angles 360 °C) of the anions, which have (*M*) and (*P*) configuration, are coordinated in a planar fashion. There are no fundamental differences in the crystal structures of $(\mathbf{1}^\ominus/Li^\oplus \cdot 2\ THF)_2$ and ($\mathbf{1}^\ominus/Li^\oplus \cdot TMEDA)_2$. The exchange of the ligands has only a small effect on the conformational parameters of $\mathbf{1}^\ominus$ and practically none on its bonding parameters.

Single crystals of the ammonium salt $\mathbf{1}^\ominus/NBu_4^\oplus$ were obtained by deprotonation of (α-benzyl)benzyltriflone with Bu_4NOH and crystallization from *n*-hexane/THF. $\mathbf{1}^\ominus/NBu_4^\oplus$ is less sensitive to moisture than $\mathbf{1}^\ominus/Li^\oplus$ and melts without decomposition. In the crystal of $\mathbf{1}^\ominus/NBu_4^\oplus$[12b] there exist discrete cations and anions (Fig. 2), which are possibly joined through weak C-H···O hydrogen bonds[9,14] between the *n*-butyl and the sulfonyl groups: The distances O1-H281′ and O2-H241 (2.27 and 2.46 Å, respectively) are smaller than the sum of the van der Waals radii of O and H

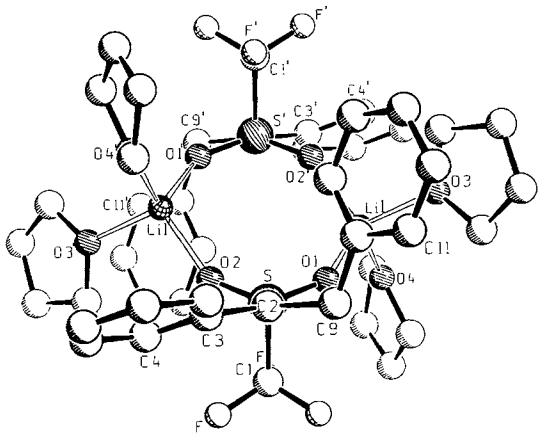

Fig. 1. Molecular structure of $(\mathbf{1}^\ominus/Li^\oplus \cdot 2\ THF)_2$ in the crystal [13]. Selected distances [Å] and angles [°]: S-C2 1.620(3), S-C1 1.859(3), S-O1 1.447(2), S-O2 1.449(2), C2-C3 1.467(3), Li1-O1 1.952(5), Li1-O2′ 1.925(5), Li1-O3 1.944(4), Li1-O4 1.940(5), C2-Li 4.214 (mean value); C3-C2-S 122.6(2), C9-C2-S 117.0(2), C9-C2-C3 120.3(2), O1-S-O2 117.4(1), C1-S-C2 112.6(1), C1-S-C2-C9 − 93.1, C1-S-C2-C3 84.0, S-C2-C3-C4 − 15.4.

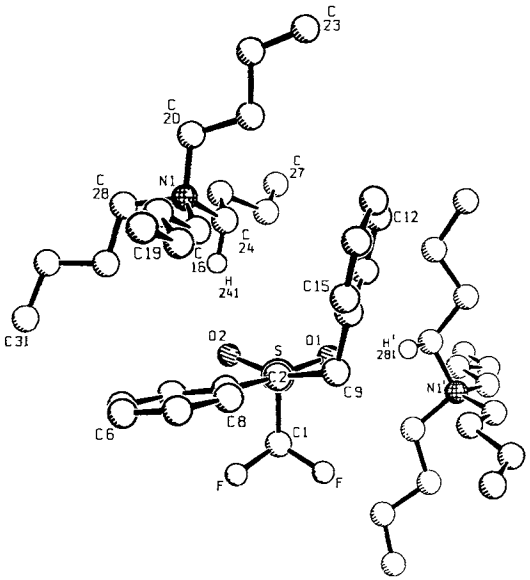

Fig. 2. Molecular structure of $\mathbf{1}^\ominus/NBu_4^\oplus$ including a $NBu_4^\oplus$ ion (symmetry operation $1-x, y-1/2, 1/2-z$) in the crystal [13]. Selected distances [Å] and angles [°]: S-C2 1.638(4), S-C1 1.826(6), S-O1 1.449(3), S-O2 1.443(3), C2-C3 1.468(5), Ni-C16 1.519(4), N1-C20 1.516(4), N1-C24 1.521(5), N1-C28 1.528(5), N1-O1 5.590, N1-O2 4.493, N1-C2 4.813, N1′-O2 6.302, N1′-C2 6.378, N1′-O1 4.124; C3-C2-S 122.7(3), C9-C2-S 116.5(3), C9-C2-C3 120.3(3), O1-S-O2 118.2(2), C1-S-C2 110.6(2), C1-S-C2-C9 − 95.2, C1-S-C2-C3 77.1, S-C2-C3-C4 − 8.5.

(2.70);[15] the angles C28′-H281′ ··· O1 and C24-H241 ··· O2 are 152° and 160°, respectively, and the H atoms of $NBu_4^{\oplus}$ involved are those with the highest positive partial charge.[9] With respect to the partial negative centers of $1^{\ominus}$, the $NBu_4^{\oplus}$ ion (Fig. 2) is positioned more symmetrically than the $Li^{\oplus}$ ions in $(1^{\ominus}/Li^{\oplus} \cdot 2\,THF)_2$ (Fig. 1). The packing diagram of $1^{\ominus}/NBu_4^{\oplus}$ shows a quasi ionic lattice consisting of layers of parallel anion–cation helices (Fig. 3). The (mutually repulsive) CF_3 groups face one another (shortest F–F distance 4.056 Å) within a double layer of $1^{\ominus}$. The anion $1^{\ominus}$ displays

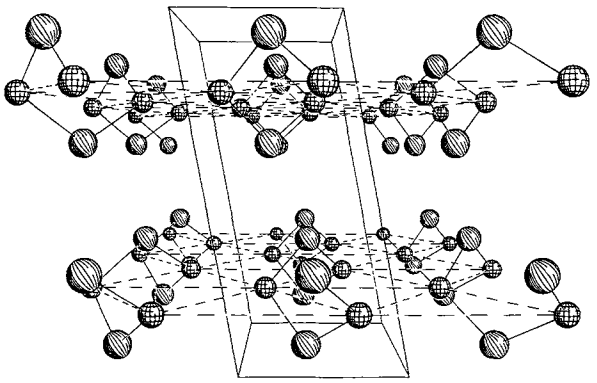

Fig. 3. Crystal packing diagram of $1^{\ominus}/NBu_4^{\oplus}$ [13]. Perspective view along the crystallographic *c* axis. Only the S (large spheres) and N (small spheres) atoms are shown.

the typical chiral conformation of the $Li^{\oplus}$-associated anions of $(1^{\ominus}/Li^{\oplus} \cdot 2\,THF)_2$ as well as a practically planar coordinated α-C atom (sum of bond angles 359°). The α-phenyl ring in $1^{\ominus}/NBu_4^{\oplus}$ (Fig. 2) is somewhat better placed for benzyl resonance than that in $(1^{\ominus}/Li^{\oplus} \cdot 2\,THF)_2$ (Fig. 1). Presumably owing to the thereby resulting repulsion between H4 and O2 (distance 2.162 Å) in $1^{\ominus}/NBu_4^{\oplus}$, the deviation from the ideal *gauche* position of the C_α electron pair (with respect to both O atoms) is slightly larger that in $(1^{\ominus}/Li^{\oplus} \cdot 2\,THF)_2$. Whereas the S–O bonds of $1^{\ominus}/NBu_4^{\oplus}$ and $(1^{\ominus}/Li^{\oplus} \cdot 2\,THF)_2$ are nearly identical in length, the C1–S bond in $1^{\ominus}/NBu_4^{\oplus}$ is 0.033 Å shorter and the C2–S bond 0.018 Å longer than those in $(1^{\ominus}/Li^{\oplus} \cdot 2\,THF)_2$. The lengthening of the C2–S bond can be explained as resulting from the loss of a stronger n_C–$\sigma^*_{SCF_3}$ conjugation and Coulomb interaction due to the O-association of the $Li^{\oplus}$ ion. Ab initio calculations on $[MeSO_2CH_2]^{\ominus}$ and $[MeSO_2CH_2]^{\ominus}Li^{\oplus}$ (with a structure of the type shown in Scheme 1)[7] also revealed that, as a result of the O-association of the $Li^{\oplus}$ ion, the C_α–S bond is shortened (by 0.029 Å); in addition, however, a lengthening (not realized for $1^{\ominus}/NBu_4^{\oplus}$) of the S–O bond by 0.040 Å was found. The effect of the $Li^{\oplus}$ ion on the charge distribution of $1^{\ominus}$ can be probed by NMR spectroscopy in THF solution: In $1^{\ominus}/Li^{\oplus}$, the charge density in the *para* position of the α-phenyl ring is smaller than in $1^{\ominus}/NBu_4^{\oplus}$ (deshielding of the *para* H and *para* C atoms by $\Delta\delta = 0.18$ and 1.1, respectively). If the lack of lengthening of the C1–S bond on going from (α-benzyl)benzyltriflone (1.859 Å) to $(1^{\ominus}/Li^{\oplus} \cdot TMEDA)_2$ (1.853 Å)[1] and also to $(1^{\ominus}/Li^{\oplus} \cdot 2\,THF)_2$ (1.859 Å) was already somewhat surprising in view of the n_C–$\sigma^*_{SCF_3}$ stabilization,[7] even more surprising is the shortening of this bond in $1^{\ominus}/NBu_4^{\oplus}$ (1.826 Å). Whether and to what extent this is due to the repulsion between the CF_3 groups remains to be answered.

The relatively small effect of the O-associated $Li^{\oplus}$ ion (+ ligands) on $1^{\ominus}$ found so far is also reflected in its dynamic properties. The C_α–S rotational barrier of $1^{\ominus}/Li^{\oplus}$ (cf. Scheme 1, L = THF) in THF amounts to $\Delta G^{\ddagger}_{333} = 16.0$ kcal mol^{-1}.[1] For $1^{\ominus}/NBu_4^{\oplus}$ in DMSO *or* THF solution ($c = 10^{-2}$ mol L^{-1}) as well as for $1^{\ominus}/K^{\oplus}$ in DMSO solution ($c = 2 \times 10^{-2}$ to 2×10^{-1} mol L^{-1}), $\Delta G^{\ddagger}_{327}$ values of 15.7 ± 0.2 kcal mol^{-1} were determined by ^{1}H NMR spectroscopy on the basis of the exchange of the nonequivalent methylene protons.[16, 17] This value corresponds to the C_α–S rotational barrier of the gegenion-free anion $1^{\ominus}$, since, in DMSO solution with $K^{\oplus}$[18] and presumably also with $NBu_4^{\oplus}$ as gegenion,[19] ion pairing plays only a minor role. This is supported, for example, by the observation that the ^{1}H and ^{13}C NMR chemical shifts for the *para* position of the α-phenyl ring of $1^{\ominus}/K^{\oplus}$ ($\delta = 6.42$ and 116.3, respectively) in DMSO solution ($c = 2 \times 10^{-1}$ mol L^{-1}) do not change either upon dilution by a factor of 100 or upon addition of one equivalent of [2.2.2]cryptand. The ^{1}H and ^{13}C NMR chemical shifts of $1^{\ominus}$ in DMSO solutions of the salts $1^{\ominus}/K^{\oplus}$ and $1^{\ominus}/NBu_4^{\oplus}$ are practically identical.

The C_α–S rotational barrier of the lithiotriflone $1^{\ominus}/Li^{\oplus}$ is appreciably greater than that of the lithiophenylsulfone $3^{\ominus}/Li^{\oplus}$ ($\Delta G^{\ddagger}_{215} = 9.6$ kcal mol^{-1}, THF).[1] We conclude from the following results that this finding is due *primarily* to the stronger n_C–$\sigma^*_{CF_3}$ conjugation and Coulomb interaction and not to the larger torsional effects:[21] As determined by NMR spectroscopy, the $\Delta G^{\ddagger}_{283}$ value for the enantiomerization of the lithio-*tert*-butylsulfone $2^{\ominus}/Li^{\oplus}$ in THF is "only" 13.5 ± 0.2 kcal mol^{-1} ($c = 2.8 \times 10^{-1}$ mol L^{-1}),[16] despite the still increased steric hindrance to C_α–S rotation, and, as shown by the ^{1}H and ^{13}C NMR spectra, the charge density in the *para* position of the α-phenyl ring is appreciably smaller for $1^{\ominus}/Li^{\oplus}$ than for $2^{\ominus}/Li^{\oplus}$ and $3^{\ominus}/Li^{\oplus}$ [deshielding of the *para* H(C) atoms by $\Delta\delta = 0.33$ (4.5) and 0.21 (3.5), respectively, all in THF]. According to cryoscopic measurements in THF (8.7×10^{-2} mol L^{-1}) at −108 °C, the salt $2^{\ominus}/Li^{\oplus}$ is also monomeric[22] and most likely contains two coordinated THF molecules.

Experimental Procedure

$1^{\ominus}/NBu_4^{\oplus}$: (±)-(α-Benzyl)benzyltriflone (314 mg, 1.0 mmol) was dissolved in 5 mL of Et_2O and the resulting solution was treated dropwise at 0 °C with 10 mL of a 0.1 M solution of Bu_4NOH in *i*PrOH. The reaction mixture was allowed to warm to 25 °C and the volatile components were then removed at 25 °C/10^{-3} Torr. The solid residue, obtained by drying at 40 °C/10^{-3} Torr, was dissolved in 15 mL of *n*-hexane/THF (4:3) by warming to 60 °C under argon. Cooling the solution to 0 °C afforded light yellow needles of $1^{\ominus}/NBu_4^{\oplus}$ within 12 h. The crystals were collected by filtration under argon, washed with *n*-hexane, and dried (25 °C/10^{-3} Torr). Yield 466 mg (84%), m.p. 118–120 °C; correct elemental analysis.

Received: August 18, 1989;
revised version: October 10, 1989 [Z 3511 IE]
German version: *Angew. Chem. 102* (1990) 96

CAS Registry numbers:
1 ($K^{\oplus}$), 124318-18-9; **1** ($Li^{\oplus}$), 121756-21-6; **1** ($NBu_4^{\oplus}$), 124318-19-0; **2** ($Li^{\oplus}$), 124318-20-3.

[1] H.-J. Gais, G. Hellmann, H. Günther, F. Lopez, H. J. Lindner, S. Braun, *Angew. Chem. 101* (1989) 1061; *Angew. Chem. Int. Ed. Engl. 28* (1989) 1025.

[2] M. J. Kaufmann, S. Gronert, D. A. Bors, A. Streitwieser, Jr., *J. Am. Chem. Soc. 109* (1987) 602.

[3] Review on the crystal structures of lithiosulfones: G. Boche, *Angew. Chem. 101* (1989) 286; *Angew. Chem. Int. Ed. Engl. 28* (1989) 277.

[4] Structure and reactivity of lithioallylsulfones with norbornane or norbornene partial frameworks; J. Müller, *Diplomarbeit*, Universität Freiburg 1989; b) H.-J. Gais, J. Müller, S. Braun, H. J. Lindner, unpublished.

[5] A potassiosulfone was found to have a molecular structure in the crystal of the type shown in Scheme 1: H.-J. Gais, J. Vollhardt, C. Krüger, *Angew. Chem. 100* (1988) 1108; *Angew. Chem. Int. Ed. Engl. 27* (1988) 1092.
[6] Recent investigations: P. P. Power, *Acc. Chem. Res. 21* (1988) 147; S. Buchholz, K. Harms, M. Marsch, W. Massa, G. Boche, *Angew. Chem. 101* (1989) 57; *Angew. Chem. Int. Ed. Engl. 28* (1989) 72; B. Becker, V. Enkelmann, K. Müllen, *ibid. 101* (1989) 501 and *28* (1989) 458.
[7] a) D. A. Bors, A. Streitwieser, Jr., *J. Am. Chem. Soc. 108* (1986) 1397; b) S. Wolfe, *Stud. Org. Chem. (Amsterdam) 19* (1985) 133, and references therein.
[8] S. Bradamante, G. A. Pagani, *J. Chem. Soc. Perkin Trans. 2 1986*, 1035.
[9] M. Meot-Ner (Mautner), C. A. Deakyne, *J. Am. Chem. Soc. 107* (1985) 469; G. N. J. Port, H. Pullman, *Theor. Chim. Acta 31* (1973) 231.
[10] a) $[PhCH_2]NMe_4$: W. Schlenk, J. Holtz, *Chem. Ber. 49* (1916) 603; b) $[Ph_3C]NMe_4$: W. Schlenk, J. Holtz, *ibid. 50* (1917) 274; c) [fluorenide]-NMe_4 and $[CH(COOEt)_2]NMe_4$: G. Wittig, M. Heintzeller, M. W. Wetterling, *Justus Liebigs Ann. Chem. 557* (1947) 201; d) [MeCOCHCOMe]-NBu_4: A. Brändström, U. Junggren, *Acta Chem. Scand. 23* (1969) 3585; e) $\{[(NC)_2C=C(CN)]_2CH\}NMe_4$: R. L. Sass, T. D. Nichols, *Z. Kristallogr. 140* (1974) 1; f) $\{[(NC)_2C=C(CN)]_2CiPr\}NMe_4$: J. C. Huffman, *Cryst. Struct. Commun. 5* (1976) 187; g) $[cC_5(COOMe)_5]NMe_4$: M. I. Bruce, P. A. Humphrey, B. W. Skeleton, A. H. White, *Aust. J. Chem. 37* (1984) 2441; h) $[RC(COOR')_2]NBu_4$, $[MeC(CN)_2]NBu_4$ and $[Me_2CNO_2]NBu_4$: M. T. Reetz, T. Knauf, U. Minet, C. Bingel, *Angew. Chem. 100* (1988) 1422; *Angew. Chem. Int. Ed. Engl. 27* (1988) 1373.
[11] Solution and crystal structure of a THF-coordinated dilithiosulfone: H.-J. Gais, J. Vollhardt, H. Günther, D. Moskau, H. J. Lindner, S. Braun, *J. Am. Chem. Soc. 110* (1988) 978.
[12] a) Crystal structure data of $(1^{\ominus}/Li^{\oplus} \cdot 2\,THF)_2$: A single crystal was mounted in a glass capillary under argon. Space group $P\bar{1}$, $a = 12.340(7)$, $b = 11.131(6)$, $c = 10.990(6)$ Å, $\alpha = 62.37(1)$, $\beta = 68.06(1)$, $\gamma = 67.91(1)^\circ$, $V = 1202.18$ Å^3, $Z = 2$, $\varrho_{calcd} = 1.382$ g cm^{-2}, $\mu(Mo_{K\alpha}) = 1.46$ cm^{-1}. Intensity measurements at room temperature with a STOE four-circle diffractometer, graphite monochromator, 4564 reflections ($2^\circ \le \theta \le 25^\circ$), 3521 unique reflections with $|F| \ge 2\sigma$. Structure determination: direct methods, anisotropic refinement with positioned hydrogen atoms of the THF molecules, other hydrogen atoms isotropic, 328 variables, $R = 0.060$, $R_w = 0.065$ (SHELX-76, SHELX-86): b) Crystal structure data of $1^{\ominus}/NBu_4^{\oplus}$: A single crystal was mounted as described in a). Space group $P2_1/c$, $a = 9.580(5)$, $b = 16.391(5)$, $c = 20.671(6)$ Å, $\beta = 100.47(1)$, $V = 3191.83$ Å^3, $Z = 4$, $\varrho_{calcd} = 1.156$ g cm^{-3}, $\mu(Mo_{K\alpha}) = 1.09$ cm^{-1}. Measurement as in a), 3587 reflections ($2^\circ \le \theta \le 20^\circ$) measured, 2567 reflections with $|F| \ge 2\sigma$, anisotropic refinement with positioned hydrogen atoms, 357 parameters, $R = 0.060$, $R_w = 0.065$ (SHELX-76, SHELX-86). Further details of the crystal structure investigation may be obtained from the Fachinformationszentrum Karlsruhe, Gesellschaft für wissenschaftlich-technische Information mbH, D-7514 Eggenstein-Leopoldshafen 2 (FRG), on quoting the depository number CSD-54123, the names of the authors, and the journal citation.
[13] E. Keller, SCHAKAL-88, *A FORTRAN Program for the Graphic Representation of Molecular and Crystallographic Models*, Freiburg 1988.
[14] a) R. Taylor, O. Kennard, *J. Am. Chem. Soc. 104* (1982) 5063; b) Z. Berkovitch-Yellin, L. Leiserowitz, *Acta Crystallogr. Sect. B40* (1984) 159; c) J. A. P. R. Sarma, G. R. Desiraja, *Acc. Chem. Res. 19* (1986) 222; d) P. Seiler, G. R. Weisman, E. D. Glending, F. Weinhold, V. B. Johnson, J. D. Dunitz, *Angew. Chem. 99* (1987) 1216; *Angew. Chem. Int. Ed. Engl. 26* (1987) 1175; e) A. G. Orpen, T. F. Koetzle, *Acta Crystallogr. Sect. C43* (1987) 2084.
[15] A. Bondi, *J. Phys. Chem. 68* (1964) 441.
[16] Estimated at the coalescence point as described by R. J. Kurland, M. B. Rubin, M. B. Wise, *J. Chem. Phys. 37* (1962) 974.
[17] By contrast, a marked dependence of the topomerization barrier on the gegenion was found for $[PhS(O)CH_2]^{\ominus}M^{\oplus}$: G. Chassaing, A. Marquet, J. Corset, F. Froment, *J. Organomet. Chem. 232* (1982) 293.
[18] F. G. Bordwell, *Acc. Chem. Res. 21* (1988) 456, and references therein.
[19] L. A. Avaca, A. Bewick, *Electroanal. Chem. Interfacial Electrochem. 41* (1973) 405.
[20] $1^{\ominus}/NBu_4^{\oplus}$ (cf. Fig. 2); ^1H NMR [400 MHz, [D$_6$]DMSO, 25 °C, [D$_5$]DMSO ($\delta = 2.49$) as standard]: $\delta = 0.92$ (t, $J = 7.3$ Hz, 12H; 19/23/27/31-H), 1.30 (sext., $J = 7.3$ Hz, 8H; 18/22/26/(30-H), 1.46–1.67 (m, 8H; 17/21/25/29-H), 3.04–3.23 (m, 8H; 16/20/24/28-H), 3.50 (d, $J = 17.5$ Hz, 1H; 9-H), 3.86 (d, $J = 17.5$ Hz, 1H; 9-H), 6.41 (m, 1H; 6-H), 6.82 (m, 2H; 5/7-H), 7.00–7.10 (m, 3H; 4/8-H, 13-H), 7.17 (m, 2H; 12/14-H), 7.32 (m, 2H; 11/15-H). ^{13}C NMR [100 MHz, [D$_6$]DMSO, 25 °C, [D$_6$]DMSO ($\delta = 39.5$) as standard]: $\delta = 13.4$ (C-19/23/27/31), 19.1 (C-18/22/26/30), 23.0 (C-17/21/25/29), 35.0 (C-9), 57.5 (C-16/20/24/28), 60.4 (C-2), 116.2 (C-6), 120.7 (C-4/8), 124.8 (C-13), 124.9 (C-1, J(C,F) = 344 Hz), 126.9 (C-5/7), 127.6 (C-12/14), 127.7 (C-11/15), 142.5 (C-3), 144.1 (C-10).
[21] According to ab initio calculations, the C_α—S rotational barrier of $[MeSO_2CH_2]^{\ominus}$ is almost completely governed by such conjugative or non-conjugative effects; torsional effects are practically insignificant [7a].
[22] W. Bauer (Erlangen), personal communication; W. Bauer, D. Seebach, *Helv. Chim. Acta 67* (1984) 1972.

2-Methylene-2*H*-azirines by Photolysis of 1-Azidoallenes**

By *Klaus Banert** and *Manfred Hagedorn*

Although cyclopropenone **1**[1] has been known for several decades, and the first synthesis of the methylenecyclopropene **2**[2] was reported a few years ago, only plausible indications but no unequivocal proof could be found for derivatives of the aza compounds **3**[3] and **4a**.[4, 5] We report here on the first trapping reactions which confirm the existence of 2-methylene-2*H*-azirine **4a** as well as on the methyleneazirine derivatives **4b–d** and their spectroscopic data.

1 **2** **3** **4a**

The recently accessible 1-azidoallenes **5**[6] have proven to be ideal precursors for methyleneazirines. The photolyses[7] of **5b–d** generate **4b** (yield $\le 54\%$), **4c** ($\le 59\%$) and **4d** ($\le 60\%$), respectively. The yield of methyleneazirine is limited by a photochemical secondary reaction leading to the fragments **7** and **8**.[7] Prolonged radiation leads to complete degradation of **4b–d**, with almost quantitative formation of **7b**, **7c** and **7d**, respectively (yields referred to **5**), without any further products being detectable. At room temperature, solutions of **4b** are stable at most for 1 h, while concentrated solutions of **4c** or **4d** are stable for only a few minutes.

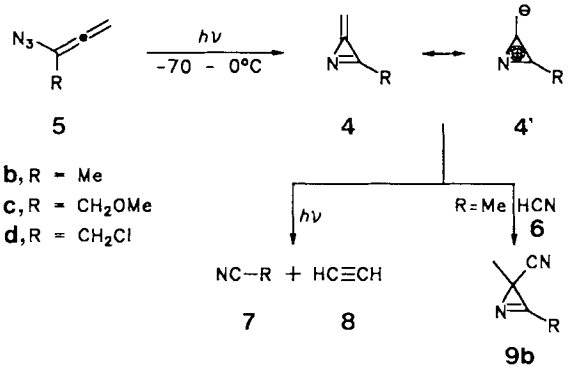

Although the methyleneazirines **4b–d** already polymerize rapidly in solution,[8] their structure can nevertheless be confirmed by spectroscopic data (Table 1). In the region of double-bond stretching vibrations, the IR spectrum of **4b** resembles the spectra of substituted methylenecyclopropenes,[9] whereas the frequency of the C=N stretching vibration is shifted considerably compared to that of simple 2*H*-azirines.[10] A participation of the dipolar mesomer **4'**, which contains an aromatic azirinylium ion[11] as partial structure,

[*] Dr. K. Banert, M. Hagedorn
Fachbereich, 8, Organische Chemie II der Universität-Gesamthochschule Adolf-Reichwein-Strasse, D-5900 Siegen (FRG)

[**] Reactions of Unsaturated Azides, Part 10. This work was supported by the Deutsche Forschungsgemeinschaft. We thank Frau *E. Reissaus* for painstaking assistance. Part 9: [6].

[5] A potassiosulfone was found to have a molecular structure in the crystal of the type shown in Scheme 1: H.-J. Gais, J. Vollhardt, C. Krüger, *Angew. Chem. 100* (1988) 1108; *Angew. Chem. Int. Ed. Engl. 27* (1988) 1092.
[6] Recent investigations: P. P. Power, *Acc. Chem. Res. 21* (1988) 147; S. Buchholz, K. Harms, M. Marsch, W. Massa, G. Boche, *Angew. Chem. 101* (1989) 57; *Angew. Chem. Int. Ed. Engl. 28* (1989) 72; B. Becker, V. Enkelmann, K. Müllen, *ibid. 101* (1989) 501 and *28* (1989) 458.
[7] a) D. A. Bors, A. Streitwieser, Jr., *J. Am. Chem. Soc. 108* (1986) 1397; b) S. Wolfe, *Stud. Org. Chem. (Amsterdam) 19* (1985) 133, and references therein.
[8] S. Bradamante, G. A. Pagani, *J. Chem. Soc. Perkin Trans. 2 1986*, 1035.
[9] M. Meot-Ner (Mautner), C. A. Deakyne, *J. Am. Chem. Soc. 107* (1985) 469; G. N. J. Port, H. Pullman, *Theor. Chim. Acta 31* (1973) 231.
[10] a) $[PhCH_2]NMe_4$: W. Schlenk, J. Holtz, *Chem. Ber. 49* (1916) 603; b) $[Ph_3C]NMe_4$: W. Schlenk, J. Holtz, *ibid. 50* (1917) 274; c) [fluorenide]-NMe_4 and $[CH(COOEt)_2]NMe_4$: G. Wittig, M. Heintzeller, M. W. Wetterling, *Justus Liebigs Ann. Chem. 557* (1947) 201; d) [MeCOCHCOMe]-NBu_4: A. Brändström, U. Junggren, *Acta Chem. Scand. 23* (1969) 3585; e) $\{[(NC)_2C=C(CN)]_2CH\}NMe_4$: R. L. Sass, T. D. Nichols, *Z. Kristallogr. 140* (1974) 1; f) $\{[(NC)_2C=C(CN)]_2CiPr\}NMe_4$: J. C. Huffman, *Cryst. Struct. Commun. 5* (1976) 187; g) $[cC_5(COOMe)_5]NMe_4$: M. I. Bruce, P. A. Humphrey, B. W. Skeleton, A. H. White, *Aust. J. Chem. 37* (1984) 2441; h) $[RC(COOR')_2]NBu_4$, $[MeC(CN)_2]NBu_4$ and $[Me_2CNO_2]NBu_4$: M. T. Reetz, T. Knauf, U. Minet, C. Bingel, *Angew. Chem. 100* (1988) 1422; *Angew. Chem. Int. Ed. Engl. 27* (1988) 1373.
[11] Solution and crystal structure of a THF-coordinated dilithiosulfone: H.-J. Gais, J. Vollhardt, H. Günther, D. Moskau, H. J. Lindner, S. Braun, *J. Am. Chem. Soc. 110* (1988) 978.
[12] a) Crystal structure data of $(1^{\ominus}/Li^{\oplus} \cdot 2\,THF)_2$: A single crystal was mounted in a glass capillary under argon. Space group $P\bar{1}$, $a = 12.340(7)$, $b = 11.131(6)$, $c = 10.990(6)$ Å, $\alpha = 62.37(1)$, $\beta = 68.06(1)$, $\gamma = 67.91(1)^\circ$, $V = 1202.18$ Å^3, $Z = 2$, $\varrho_{calcd} = 1.382$ g cm^{-2}, $\mu(Mo_{K\alpha}) = 1.46$ cm^{-1}. Intensity measurements at room temperature with a STOE four-circle diffractometer, graphite monochromator, 4564 reflections ($2^\circ \le \theta \le 25^\circ$), 3521 unique reflections with $|F| \ge 2\sigma$. Structure determination: direct methods, anisotropic refinement with positioned hydrogen atoms of the THF molecules, other hydrogen atoms isotropic, 328 variables, $R = 0.060$, $R_w = 0.065$ (SHELX-76, SHELX-86): b) Crystal structure data of $1^{\ominus}/NBu_4^{\oplus}$: A single crystal was mounted as described in a). Space group $P2_1/c$, $a = 9.580(5)$, $b = 16.391(5)$, $c = 20.671(6)$ Å, $\beta = 100.47(1)$, $V = 3191.83$ Å^3, $Z = 4$, $\varrho_{calcd} = 1.156$ g cm^{-3}, $\mu(Mo_{K\alpha}) = 1.09$ cm^{-1}. Measurement as in a), 3587 reflections ($2^\circ \le \theta \le 20^\circ$) measured, 2567 reflections with $|F| \ge 2\sigma$, anisotropic refinement with positioned hydrogen atoms, 357 parameters, $R = 0.060$, $R_w = 0.065$ (SHELX-76, SHELX-86). Further details of the crystal structure investigation may be obtained from the Fachinformationszentrum Karlsruhe, Gesellschaft für wissenschaftlich-technische Information mbH, D-7514 Eggenstein-Leopoldshafen 2 (FRG), on quoting the depository number CSD-54123, the names of the authors, and the journal citation.
[13] E. Keller, SCHAKAL-88, *A FORTRAN Program for the Graphic Representation of Molecular and Crystallographic Models*, Freiburg 1988.
[14] a) R. Taylor, O. Kennard, *J. Am. Chem. Soc. 104* (1982) 5063; b) Z. Berkovitch-Yellin, L. Leiserowitz, *Acta Crystallogr. Sect. B40* (1984) 159; c) J. A. P. R. Sarma, G. R. Desiraja, *Acc. Chem. Res. 19* (1986) 222; d) P. Seiler, G. R. Weisman, E. D. Glending, F. Weinhold, V. B. Johnson, J. D. Dunitz, *Angew. Chem. 99* (1987) 1216; *Angew. Chem. Int. Ed. Engl. 26* (1987) 1175; e) A. G. Orpen, T. F. Koetzle, *Acta Crystallogr. Sect. C43* (1987) 2084.
[15] A. Bondi, *J. Phys. Chem. 68* (1964) 441.
[16] Estimated at the coalescence point as described by R. J. Kurland, M. B. Rubin, M. B. Wise, *J. Chem. Phys. 37* (1962) 974.
[17] By contrast, a marked dependence of the topomerization barrier on the gegenion was found for $[PhS(O)CH_2]^{\ominus}M^{\oplus}$: G. Chassaing, A. Marquet, J. Corset, F. Froment, *J. Organomet. Chem. 232* (1982) 293.
[18] F. G. Bordwell, *Acc. Chem. Res. 21* (1988) 456, and references therein.
[19] L. A. Avaca, A. Bewick, *Electroanal. Chem. Interfacial Electrochem. 41* (1973) 405.
[20] $1^{\ominus}/NBu_4^{\oplus}$ (cf. Fig. 2); ^1H NMR [400 MHz, [D$_6$]DMSO, 25 °C, [D$_5$]DMSO ($\delta = 2.49$) as standard]: $\delta = 0.92$ (t, $J = 7.3$ Hz, 12H; 19/23/27/31-H), 1.30 (sext., $J = 7.3$ Hz, 8H; 18/22/26/(30-H), 1.46–1.67 (m, 8H; 17/21/25/29-H), 3.04–3.23 (m, 8H; 16/20/24/28-H), 3.50 (d, $J = 17.5$ Hz, 1H; 9-H), 3.86 (d, $J = 17.5$ Hz, 1H; 9-H), 6.41 (m, 1H; 6-H), 6.82 (m, 2H; 5/7-H), 7.00–7.10 (m, 3H; 4/8-H, 13-H), 7.17 (m, 2H; 12/14-H), 7.32 (m, 2H; 11/15-H). ^{13}C NMR [100 MHz, [D$_6$]DMSO, 25 °C, [D$_6$]DMSO ($\delta = 39.5$) as standard]: $\delta = 13.4$ (C-19/23/27/31), 19.1 (C-18/22/26/30), 23.0 (C-17/21/25/29), 35.0 (C-9), 57.5 (C-16/20/24/28), 60.4 (C-2), 116.2 (C-6), 120.7 (C-4/8), 124.8 (C-13), 124.9 (C-1, J(C,F) = 344 Hz), 126.9 (C-5/7), 127.6 (C-12/14), 127.7 (C-11/15), 142.5 (C-3), 144.1 (C-10).
[21] According to ab initio calculations, the C_α—S rotational barrier of $[MeSO_2CH_2]^{\ominus}$ is almost completely governed by such conjugative or non-conjugative effects; torsional effects are practically insignificant [7a].
[22] W. Bauer (Erlangen), personal communication; W. Bauer, D. Seebach, *Helv. Chim. Acta 67* (1984) 1972.

2-Methylene-2*H*-azirines by Photolysis of 1-Azidoallenes**

By *Klaus Banert** and *Manfred Hagedorn*

Although cyclopropenone **1**[1] has been known for several decades, and the first synthesis of the methylenecyclopropene **2**[2] was reported a few years ago, only plausible indications but no unequivocal proof could be found for derivatives of the aza compounds **3**[3] and **4a**.[4, 5] We report here on the first trapping reactions which confirm the existence of 2-methylene-2*H*-azirine **4a** as well as on the methyleneazirine derivatives **4b–d** and their spectroscopic data.

1 **2** **3** **4a**

The recently accessible 1-azidoallenes **5**[6] have proven to be ideal precursors for methyleneazirines. The photolyses[7] of **5b–d** generate **4b** (yield $\le 54\%$), **4c** ($\le 59\%$) and **4d** ($\le 60\%$), respectively. The yield of methyleneazirine is limited by a photochemical secondary reaction leading to the fragments **7** and **8**.[7] Prolonged radiation leads to complete degradation of **4b–d**, with almost quantitative formation of **7b**, **7c** and **7d**, respectively (yields referred to **5**), without any further products being detectable. At room temperature, solutions of **4b** are stable at most for 1 h, while concentrated solutions of **4c** or **4d** are stable for only a few minutes.

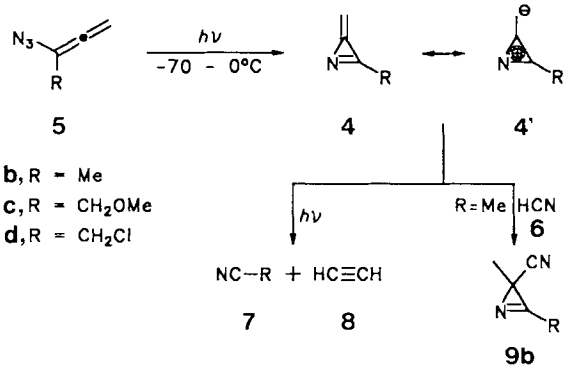

Although the methyleneazirines **4b–d** already polymerize rapidly in solution,[8] their structure can nevertheless be confirmed by spectroscopic data (Table 1). In the region of double-bond stretching vibrations, the IR spectrum of **4b** resembles the spectra of substituted methylenecyclopropenes,[9] whereas the frequency of the C=N stretching vibration is shifted considerably compared to that of simple 2*H*-azirines.[10] A participation of the dipolar mesomer **4'**, which contains an aromatic azirinylium ion[11] as partial structure,

[*] Dr. K. Banert, M. Hagedorn
Fachbereich, 8, Organische Chemie II der Universität-Gesamthochschule Adolf-Reichwein-Strasse, D-5900 Siegen (FRG)

[**] Reactions of Unsaturated Azides, Part 10. This work was supported by the Deutsche Forschungsgemeinschaft. We thank Frau *E. Reissaus* for painstaking assistance. Part 9: [6].

Table 1. Spectroscopic data of **4b–d**, **9b**, and **14** [a].

4b: IR: $\tilde{\nu}$ = 1915 (w), 1855, 1560, 1215. ^{1}H NMR: δ = 2.70 (s, 3H), 4.11 (d, J = 2.0, 1H), 4.34 (d, J = 2.0, 1H). ^{13}C NMR: δ = 14.9 (q, CH_3), 64.6 (t, $J \approx 167$, CH_2), 133.15 (s, C-2), 186.8 (s, C-3). GC-MS: m/z 67 ($M^{\oplus}$, 100%), 66 (22), 41 ([M–C_2H_2]$^{\oplus}$, 96), 26 ([M–MeCN]$^{\oplus}$, 30)

4c: IR: $\tilde{\nu}$ = 1850. ^{1}H NMR: δ = 3.58 (s, 3H), 4.19 (d, J = 2.3, 1H), 4.40 (d, J = 2.3, 1H), 4.88 (s, 2H). ^{13}C NMR (−30 °C): δ = 59.9 (q, $J \approx 143$, CH_3), 65.4 (t, $J \approx 168$, C=CH_2), 68.0 (t, $J \approx 147$, OCH_2), 131.3 (s, C-2), 187.7 (s, C-3)

4d: ^{1}H NMR: δ = 4.23 (d, J = 2.6, 1H), 4.48 (d, J = 2.6, 1H), 4.88 (s, 2H). ^{13}C NMR (−30 °C): δ = 38.5 (t, $J \approx 156$, CH_2Cl), 66.3 (t, $J \approx 168$, $C=CH_2$), 133.5 (s, C-2), 185.5 (s, C-3)

9b: IR (CCl_4): $\tilde{\nu}$ = 2230 (C≡N), 1770 (C=N). ^{1}H NMR: δ = 1.50 (s, CH_3 at C-2), 2.56 (s, CH_3 at C-3). ^{13}C NMR: δ = 12.0 (q, CH_3 at C-3), 20.1 (q, CH_3 at C-2), 20.8 (s, C-2), 121.2 (s, C≡N), 166.4 (s, C-3). GC-MS: m/z 94 ($M^{\oplus}$, 34%), 93 (28), 53 ([M–MeCN]$^{\oplus}$, 56), 42 (100)

14: ^{1}H NMR: δ = 2.21 (s, 1H), 2.64 (s, 3H). ^{13}C NMR: δ = 12.5 (q, aeCH$_3$), 13.7 (d, $J \approx 200$, C-2), 119.3 (s, C≡N), 160.1 (s, C-3). GC-MS: m/z 80 ($M^{\oplus}$, 23%), 79 (9), 54 ([M–CN]$^{\oplus}$, 13), 53 ([M–HCN]$^{\oplus}$, 100)

[a] IR and NMR spectra in $CDCl_3$ (if not otherwise stated); ^{1}H NMR at 80 and 400 MHz, ^{13}C NMR at 100.6 MHz; GC-MS at 70 eV; $\tilde{\nu}$ in cm^{-1}, J in Hz.

is manifested in the ^{13}C-NMR data of the 2-methylene-2*H*-azirines: the signal for C-3 lies extremely downfield, while a relatively small δ value is measured for the sp^2-hybridized methylene carbon. This is demonstrated by a comparison with simple 2*H*-azirines[10] and the heterocycles **10**,[12] **11**,[13] and **12**[14] (Fig. 1). Analogous, but more marked shifts are found for the ^{13}C-NMR signals of **2**[2a] upon comparison with the data for cyclopropene[15] and methylenecyclopropane.[16]

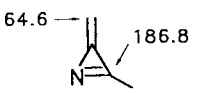

4b

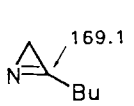

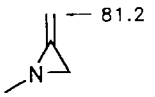

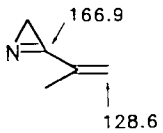

10 **11** **12**

Fig. 1. Selected ^{13}C-NMR data (δ values) of **4b** and of **10**, **11** [13], and **12** (for comparison).

4b reacts with hydrogen cyanide **6** in chloroform to give the azirine **9b** in 84% yield. The same product (**9b**) is obtained upon photolysis of **5b** in the presence of an excess of **6** (74%, based on **5b**). In this case the irradiation must be conducted at 0 °C, because the addition of **6** to **4b** cannot compete with the photochemical decomposition to **7b** and **8** at low temperatures.

Photolysis of the azidoallene **5a** yields the products **6**, **8**, **13** and **14** whose compositions strongly depend upon the temperature (0 to −70 °C) and the concentration of **5a**.[7] Whereas the yield of **8** decreases with increasing temperature (−70 °C 35%, −30 °C ca. 9%, 0 °C 7%), that of **13** (24–30%) remains almost constant. Hydrogen cyanide **6** can be detected only after irradiation at low temperature (ca. 40% at −70 °C). In contrast **14** is rather formed at higher temperatures (2–4% at 0 to −30 °C, traces at −70 °C).

We consider **6**, **8** and **14** as secondary products of the parent compound **4a** ("1-azatriafulvene"). This seems plausible when one compares this reaction with the reactions of **4b–d**. How effectively the formation of **14** from **4a** and **6** can compete with the photoreaction **4a** → **6** + **8** is apparently dependent upon the temperature and the concentration of hydrogen cyanide **6**. When **5a** is photolyzed at 0 to −70 °C in the presence of an excess of added **6** the yield of **14** increases to 54–57%, whereas it hardly changes in the case of **13**, and decreases in the case of **8**. Since a good yield of **14** can also be obtained at −70 °C, the addition **4a** + **6** → **14** presumably proceeds much more rapidly than the analogous reaction **4b** + **6** → **9b**. Acrylonitrile **13** is most likely generated not from **4a**, but via another route from **5a**. This is the reason why the yield of **13** proves to be almost independent of the temperature and of the concentration of **6**.

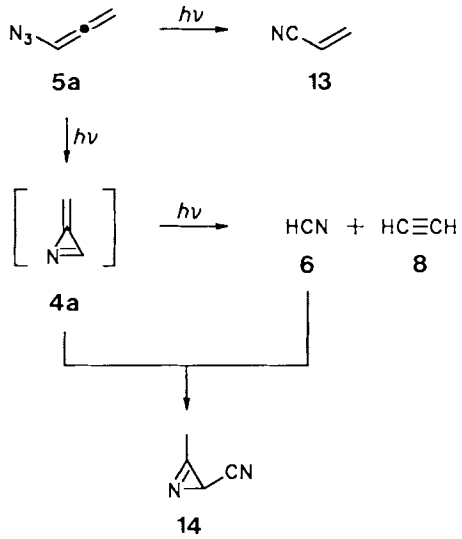

We are presently trying to characterize the, presumably very unstable,[17] compound **4a** spectroscopically at still lower temperatures.

Received: September 7, 1989 [Z 3541 IE]
German version: *Angew. Chem. 101* (1990) 90

CAS Registry numbers:
4a, 110027-86-6; **4b**, 124318-31-6; **4c**, 124318-32-7; **4d**, 124318-33-8; **5a**, 88596-79-6; **5b**, 123625-03-6; **5c**, 123625-04-7; **5d**, 123625-05-8; **8**, 74-86-2; **9b**, 124318-34-9; **13**, 107-13-1; **14**, 124318-35-0.

[1] R. Breslow, G. Ryan, *J. Am. Chem. Soc. 89* (1967) 3073.
[2] a) W. E. Billups, L.-J. Lin, E. W. Casserly, *J. Am. Chem. Soc. 106* (1984) 3698–3699; b) S. W. Staley, T. D. Norden, *ibid. 106* (1984) 3699–3700.
[3] A. Hassner, R. J. Isbister, R. B. Greenwald, J. T. Klug, E. C. Taylor, *Tetrahedron 25* (1969) 1637–1641; A. Padwa, J. K. Rasmussen, A. Tremper, *J. Am. Chem. Soc. 98* (1976) 2605–2614.
[4] E. M. Burgess, J. P. Sanchez, *J. Org. Chem. 38* (1973) 176–178; *39* (1974) 940–948.
[5] The quantum mechanically calculated total energy of **4a** is reported on by E.-U. Würthwein, R. Weigmann, *Angew. Chem. 99* (1987) 918–919; *Angew. Chem. Int. Ed. Engl. 26* (1987) 923–924.
[6] K. Banert, M. Hagedorn, *Angew. Chem. 101* (1989) 1710–1711; *Angew. Chem. Int. Ed. Engl. 28* (1989) 1675–1676.
[7] The photolyses of **5** were carried out in $CDCl_3$, CCl_4, or ether (mercury high-pressure lamps TQ 150 and Q 81, Quarzlampengesellschaft Hanau, Duran NMR tubes). The identification of **6**, **7**, **8** and **13** was achieved via ^{1}H- and ^{13}C-NMR data and partly via analytical gas chromatography; in all cases the samples were compared with authentic samples. All the yields were determined ^{1}H-NMR spectroscopically using an internal standard (e.g. naphthalene). They are always based on starting amount of (not consumed) **5**. Compound **5a** (0.06–0.07 M $CDCl_3$ solution in sealed tubes) was generally irradiated until complete conversion of the starting compound.
[8] The low stability of the methyleneazirines is in complete contrast to the unusually high stability reported for the azirine imines: W. Meyer zu Reckendorf, N. Schultz, *Angew. Chem. 100* (1988) 1094–1096; *Angew. Chem. Int. Ed. Engl. 27* (1988) 1075–1077.

[9] B. Halton, M. G. Banwell in Z. Rappoport (Ed.): *The Chemistry of the Cyclopropyl Group, Part 2*, Wiley, Chichester 1987, pp. 1223–1339, and references cited therein; T. Eicher, J. L. Weber, *Top. Curr. Chem. 57* (1975) 1–109, and references cited therein; D. Wendisch in *Houben-Weyl-Müller: Methoden der Organischen Chemie, Band IV/3*, Thieme, Stuttgart 1971, pp. 749–763, and references cited therein.
[10] V. Nair in A. Hassner (Ed.): *Small Ring Heterocycles, Part 1*, in A. Weissberger, E. C. Taylor (Ed.): *The Chemistry of Heterocyclic Compounds, Vol. 42*, Wiley, New York 1983, pp. 215–332, and references cited therein.
[11] Azirinylium ions have been discussed as intermediates in rearrangement reactions and in the interpretation of mass spectra, and have been investigated by quantum mechanical calculations: G. R. Harvey, K. W. Ratts, *J. Org. Chem. 31* (1966) 3907–3910; J. Ciabattoni, M. Cabell, Jr., *J. Am. Chem. Soc. 93* (1971) 1482–1483; C. U. Pittman, Jr., A. Kress, T. B. Patterson, P. Walton, L. D. Kispert, *J. Org. Chem. 39* (1974) 373–378; A. Padwa, T. J. Blacklock, P. H. J. Carlsen, M. Pulwer, *ibid. 44* (1979) 3281–3287; K. Krogh-Jespersen, *Tetrahedron Lett. 21* (1980) 4553–4556; G. Bouchoux, Y. Hoppilliard, *Org. Mass Spectrom. 16* (1981) 459–464; T. C. Gallagher, R. C. Storr, *Tetrahedron Lett. 22* (1981) 2905–2908; K. Krogh-Jespersen, C. M. Young, R. A. Moss, M. Wlostowski, *ibid. 23* (1982) 2339–2342; D. J. Swanton, G. B. Bacskay, G. D. Willett, N. S. Hush, *J. Mol. Struct. (Theochem) 91* (1983) 313–323.
[12] Measured in $CDCl_3$ at 100.6 MHz; Synthesis: G. Smolinsky, *J. Org. Chem. 27* (1962) 3557–3559.
[13] H. Quast, R. Frank, A. Heublein, E. Schmitt, *Liebigs Ann. Chem. 1980*, 1814–1835.
[14] K. Banert, *Angew. Chem. 97* (1985) 231–232; *Angew. Chem. Int. Ed. Engl. 24* (1985) 216–217.
[15] H. Günther, H. Seel, *Org. Magn. Reson. 8* (1976) 299–300.
[16] H. Günther, W. Herrig, *Chem. Ber. 106* (1973) 3938–3950.
[17] 2*H*-Azirines unsubstituted in position 3 are especially unstable: K. Isomura, M. Okada, H. Taniguchi, *Tetrahedron Lett. 1969*, 4073–4076.

[2.2](4,4')Azobenzenophane

By *Nobuyuki Tamaoki,* Kenichi Koseki,* and *Tsuguo Yamaoka*

In macrocyclic compounds containing two azobenzene units in the skeletal framework the rate of isomerization of the azobenzene unit on one side is dependent on the conformation (*trans* or *cis*) of the other azobenzene unit. According to *Rau* et al. the *cis-trans* isomerization of an azobenzene unit on one side of the [3.3]azobenzenophane **5** occurs 1000 times faster at 25 °C when the other azobenzene unit is *trans* configurated instead of *cis* configurated.[1] The shorter the bridges between the two azobenzene units are, the more significant is the effect of the one azobenzene unit on the rate of isomerization of the other. In the extreme case (direct bonding between the two azobenzenes), a *trans, cis(tc)*-conformation may not exist because of too large a strain.

In this communication we report on a simple synthesis of [2.2](4,4')azobenzenophane **1**, on spectroscopic data which suggest deformed azo linkages in **1** in solution, and on the extremely rapid thermal isomerization of the *tc* form to the *tt* form.

Several azobenzenophanes whose bridges contain more than two atoms each have been synthesized.[1,2] Many [2.2]- and [2.2.2]cyclophanes have also been synthesized, but usually by a method in which the cyclization process is accomplished by "bridge-building".[3] The reaction conditions for "bridge-building", however, seem to be too harsh for azo linkages. We describe here a synthetic route in which the azobenzene chromophores are first formed in the final step, so that the exposure of azo linkages to harsh synthetic conditions can be circumvented.[4,5] A dilute solution of 1,2-bis(4'-nitrophenyl)ethane in dry THF was reduced with

[*] N. Tamaoki, Dr. K. Koseki, Prof. Dr. T. Yamaoka
Department of Image Science and Technology, Chiba University 1–33, Yayoi-cho, Chiba 260 (Japan)

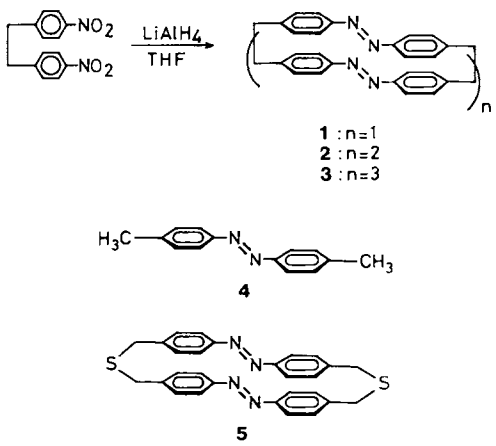

$LiAlH_4$. From this reaction mixture the macrocyclic compounds **1**–**3** were isolated by column chromatography.

The spectroscopic data of the compounds **1**–**3** and of the model compound 4,4'-dimethylazobenzene **4** are summarized in Table 1. The ^{1}H-NMR signals of the aromatic protons shift to higher magnetic field as the number of azobenzene units is decreased. This finding is understandable if one assumes that the azobenzene units are arranged triangularly and quadrilaterally in compounds **2** and **3**, respectively, and face-to-face in **1**. In the macrocycles **1**–**3** the angle between the benzene rings, which are linked by ethylene bridges, grows and the mutual effect of the magnetic anisotropy between benzene units decreases.[6] In the UV/VIS spectra the molecular extinction coefficient (ε) from the $\pi \rightarrow \pi^*$ transition per azobenzene unit becomes smaller as the number of azobenzene units is decreased, while ε for the $n \rightarrow \pi^*$ transition of an azobenzene unit in **1** is exceptionally large. On the basis of CPK models this spectral behavior is most reasonably explained in terms of the bent conformation shown in Figure 1. In this conformation the n orbital of an azo linkage could have better overlap with the π orbital.[7,8]

Table 1. Spectroscopic data of the compounds **1**–**4**.

	$\pi\pi^*$ [a]		$n\pi^*$ [a]		^{1}H NMR [b]	
	$\varepsilon(\lambda_{max}$ [nm])	ε/unit	$\varepsilon(\lambda_{max}$ [nm])	ε/unit	CH_2	arene
1	41300(328)	20700	2400(462)	1200	3.07	6.79, 7.24
2	74600(329)	24900	2200(442)	750	3.08	6.98, 7.53
3	116000(333)	29000	3000(440)	750	3.06	7.03, 7.70
4	24900(339)	24900	880(442)	880	2.38	7.24, 7.76

[a] In benzene. [b] δ value in $CDCl_3$.

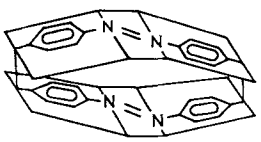

Fig. 1. Bent structure of the azobenzene units of **1**

Upon exposure to 366-nm light, **1** isomerizes like azobenzene to the photostationary state, whereby 88% of the initial absorbance at 328 nm (λ_{max} of the $\pi \rightarrow \pi^*$ transition band) disappears and the absorbance around 440 nm ($n \rightarrow \pi^*$ tran-

sition band) increases. This means that more than 88% of compound **1** in *tt*-form is photochemically isomerized to the *cc*-form. The photostationary state can be reversed by slow thermal reaction or 436-nm irradiation. If the photoisomerization by 366-nm light is arbitrarily interrupted, a small amount of rapid thermal recovery of **1** in the spectrum is also observed. A similar phenomenon observed in the case of **5** was attributed to the thermal isomerization of the *tc*-form to the *tt*-form (*tc* → *tt*).[1] UV/VIS spectroscopically determined thermal isomerization data for *tc* → *tt* and *cc* → *tc* in the case of **1**, and for *c* → *t* in the case of **4** are listed in Table 2. The thermal isomerization *tc* → *tt* in the case of **1** is

Table 2. Rate constants and activation parameters for the thermal isomerization of **1** and **4** in benzene.

	Type of isomerization	k_{298} [s^{-1}]	E_a [kcal mol^{-1}]	$\Delta S^{\neq}_{298}$ [cal K^{-1}]
1	*tc* → *tt*	4.54×10^{-2}	14.0	− 19.8
	cc → *tc*	4.53×10^{-6}	22.2	− 10.5
4	*c* → *t*	4.53×10^{-6} [9]	21.7 [9]	− 12.0 [9]

10000 times faster than *cc* → *tc* for **1** or *c* → *t* for **4** at 25 °C. This difference is 10 times larger than in the case of the [3.3]azobenzenophane **5**. This is mainly due to the extremely low activation energy E_a of the *tc* → *tt* isomerization in **1**. Thus, the shorter the chains which connect the two azobenzene units, the less stable is the *tc* form.

Experimental

A solution of 9.6 g (35 mmol) of 1,2-bis(4′-nitrophenyl)ethane in 240 mL of dry THF was added dropwise in 3 h to a suspension of 6.7 g (180 mmol) of $LiAlH_4$ in 400 mL of dry THF under a nitrogen atmosphere. After 21 hours' stirring, 200 mL of water was carefully added to the reaction mixture. The precipitate was filtered off and the THF was removed from the water/THF mixture by distillation. A further orange solid that precipitated in the water was separated by filtration, and then the solid was extracted by dichloromethane. The dichloromethane solution was washed with water and evaporated down. The residue was purified by column chromatography (silica gel and dichloromethane/chloroform (1:1 v/v)). The fractions with R_f values of 0.90, 0.86 and 0.81 were evaporated down, recrystallized by slow evaporation of dichloromethane solution and identified as **3**, **2** and **1**, respectively, by ^1H NMR, FD-MS and satisfactory elemental analyses [10]. **1**: 22 mg (0.30%); m.p. above 305 °C, $m/z = 416 (M^{\oplus})$. **2**: 38 mg (0.52%); m.p. 286–288 °C, $m/z = 624 (M^{\oplus})$. **3**: 17 mg (0.23%); m.p. above 305 °C, $m/z = 832 (M^{\oplus})$.

Received: July 26, 1989 [Z 3466 IE]
German version: *Angew. Chem. 102* (1990) 66

[1] a) D. Gräf, H. Nitsch, D. Ufermann, G. Sawitzki, H. Patzelt, H. Rau, *Angew. Chem. 94* (1982) 385; *Angew. Chem. Int. Ed. Engl. 21* (1982) 373; b) H. Rau, E. Lüddecke, *J. Am. Chem. Soc. 104* (1982) 1616.

[2] a) H.-W. Losensky, H. Spelthann, A. Ehlen, F. Vögtle, J. Bargon, *Angew. Chem. 100* (1988) 1225; *Angew. Chem. Int. Ed. Engl. 27* (1988) 1190; b) U. Funke, H.-F. Grützmacher, *Tetrahedron 43* (1987) 3787; c) S. Shinkai, Y. Honda, Y. Kusano, O. Manabe, *J. Chem. Soc. Chem. Commun. 1982*, 848.

[3] D. J. Cram, H. Steinberg, *J. Am. Chem. Soc. 73* (1951) 5691; V. Boekelheide, R. A. Hollins, *ibid 92* (1970) 3512.

[4] Similar synthesis of [2.2](4,4′)stilbenophane: D. Tanner, O. Wennerström, *Tetrahedron Lett. 22* (1981) 2313.

[5] Synthesis of cyclic azo compounds by the oxidation of amines. S. Shinkai, T. Minami, Y. Kusano, O. Manabe, *J. Am. Chem. Soc. 105* (1983) 1851.

[6] A similar behavior of the ^1H-NMR chemical shifts has been observed in the [2.2]paracyclophane oligomer series: I. Tabushi, H. Yamada, Y. Kuroda, *J. Org. Chem. 40* (1975) 1946.

[7] In crystalline **5** the atoms of the C–N=N–C moiety do not lie in a plane. G. Sawitzki, H. Rau, *Liebigs Ann. Chem. 1981*, 993.

[8] Conformation of [2.2](4,4′)stilbenophane in the crystal: Y. Ito, S. Miyata, M. Nakatsuka, T. Saegusa, M. Takamoto, Y. Wada, *J. Chem. Soc. Chem. Commun. 1982*, 375.

[9] D. Schulte-Frohlinde, *Liebigs Ann. Chem. 612* (1958) 138.

[10] Elemental analyses and ^1H-NMR spectrum indicate that **2** and **3** contain 1 mole of CH_2Cl_2 per 2 moles of **2** and **3**, respectively.

Oxygen Activation with Transition Metal Complexes: Nickel-Catalyzed Oxidation of a Pentacoordinated Substrate **

By *Albrecht Berkessel,* Jan. W. Bats, and Christine Schwarz*

Selective oxidations, e.g. the epoxidation[1] and dihydroxylation[2] described by *Sharpless* et al. count among the important methods of modern organic synthesis. The ultimate aim in the development of methods for selective oxidation can be seen as the stereoselective functionalization of non-activated substrates with the readiest available oxidant, namely molecular oxygen.

Hydroxylations with microorganisms[3] or with isolated monooxygenases such as cytochrome P-450[4] fulfill the aforementioned requirements, but, on the other hand, are subject to the side effects of enzymatic reactions, e.g. undesired substrate selectivity. An alternative approach is the development of low molecular weight catalysts, which in the ideal case are supposed to make selective reactions possible on any desired substrate ("enzyme models"). Molecular oxygen has already been successfully used as selective oxidizing agent, both with some monooxygenase models[5–7] as well as with model compounds for dioxygenases such as the catechol dioxygenase.[8a–c] We have now extended the principle used by dioxygenases and their models to initiate or steer the oxygen transfer by *coordination of oxygen and substrate to a suitable transition metal ion*,[8,9] to an oxidation reaction without natural precedent and with a metal center ($Ni^{2\oplus}$) as yet unknown for oxygenases.

By reaction of the diamine **1a** with salicylaldehyde and the acetate of $Co^{2\oplus}$, $Ni^{2\oplus}$ or $Cu^{2\oplus}$ the chelate complexes *rac*-**2a–c** were obtained [Eq. (a)], of which *rac*-**2b** and *rac*-**2c** were characterized by X-ray structure analyses.[10]

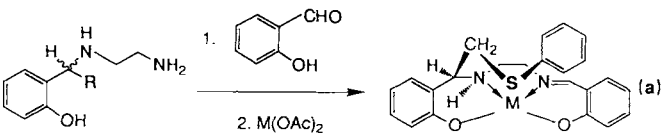

1a: R = CH_2-S-Ph

rac-**2a,b,c** 90–95 %

2a: M = Co
2b: M = Ni
2c: M = Cu

Figure 1 shows the result of an X-ray structure analysis of *rac*-**2b**. The nickel ion is coordinated equatorially to the O and N atoms of the ligand, while the S atom of the thioether side chain occupies an axial position. In the crystal the octahedral coordination of the metal ion is completed by a phenolate O-atom of a second (enantiomeric to the first) molecule (Fig. 1).

In *solution* this sixth coordination site can either be occupied by a solvent molecule or it could coordinate molecular oxygen. Indeed, the complex *rac*-**2b**, which is stable in the crystalline state, reacts rapidly with oxygen in solution (ca. 2–3 h at room temperature, a few minutes in EtOH under reflux) according to Scheme 1 to give the Ni(salen) complex

[*] Dr. A. Berkessel, Dr. J. W. Bats, [†] Dr. C. Schwarz [†·††]
Institut für Organische Chemie der Universität
Niederurseler Hang,
D-6000 Frankfurt am Main 50 (FRG)

[†] X-ray structure analysis.

[††] Present address:
Max-Planck-Institut für Festkörperforschung
Heisenbergstrasse 1, D-7000-Stuttgart 80 (FRG)

[**] This work was supported by the Fonds der Chemischen Industrie.

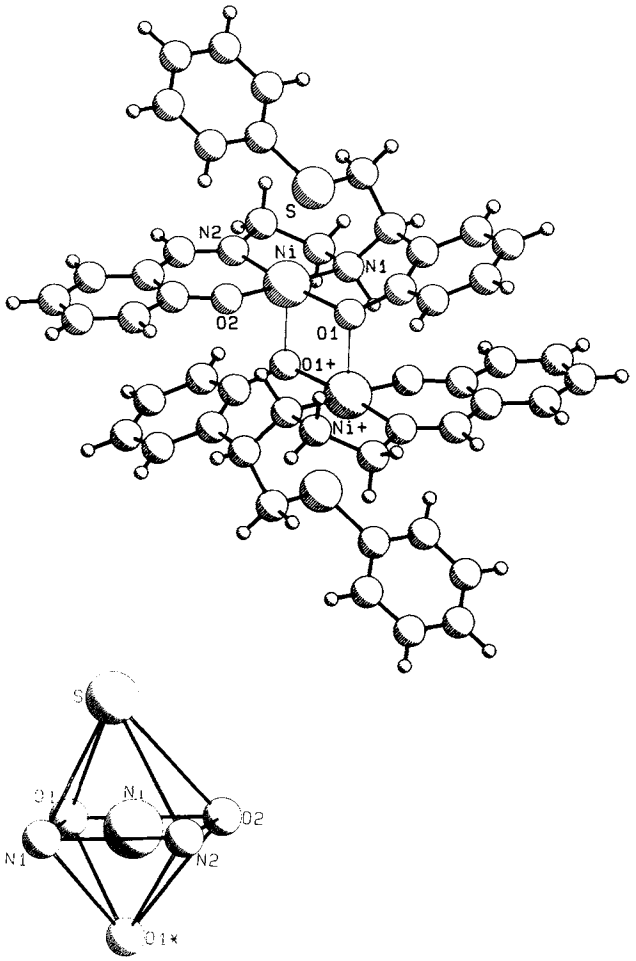

Fig. 1. Top: Structure of *rac*-**2b** in the crystal; intermolecular O–Ni coordination is shown in thin lines. Bottom: Coordination sphere of the nickel ion (PLUTO plot).

4 (H_2salen = bis(salicylidene)ethylenediamine). The thioether side chain of *rac*-**2b** undergoes degradation thereby, to formaldehyde and diphenyl disulfide.

Scheme 1 also contains a mechanistic interpretation of the oxidation beginning with the binding of oxygen to the free axial coordination site at the Ni atom of *rac*-**2b**. *Reversible* binding of molecular oxygen is well documented for a plethora of $Co^{2\oplus}$ chelate complexes,[6,11,12] and the analogous adduct formation of a specific group of macrocyclic $Ni^{2\oplus}$ complexes has also been reported.[13] As follows from ESR and structural data,[6,9,11,12] O_2-adducts such as *rac*-**3** (Scheme 1) can be described as complexes of the superoxide anion with the metal ion in the $(n+1)$ oxidation state. In the case of *rac*-**3** the electron deficit at the metal center can be balanced out by the axially coordinated S-ligand. Radical abstraction of the amine H atom and subsequent homolytic β-cleavage[14] lead to the salen-complex **4** and the ionic fragments **5** and **6**. Their combination to give (phenylthio)methyl hydroperoxide **7** and subsequent intramolecular oxygen transfer afford **8**, the precursor of formaldehyde and diphenyl disulfide. Loss of formaldehyde from **8** leads to formation of benzenesulfenic acid **9** [Eq. (b)].[15] This is not isolable and like numerous other unstable arenesulfenic acids

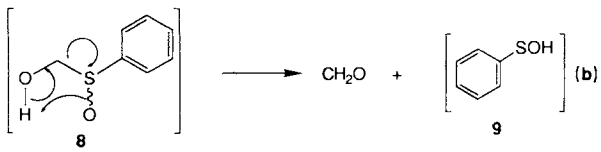

reacts further to give the corresponding diaryl disulfide—along with other disproportionation products.[16,17] Only in exceptional cases can the sulfenic acids be isolated.[16,17]

By deuteration of the methylene group adjacent to the S atom in *rac*-**2b** (Scheme 1) and ^{2}H- and ^{1}H-NMR spectroscopic monitoring of the atmospheric oxidation it could be shown that this CH_2 group is converted *exclusively* into formaldehyde, and that it is the *only* source of formaldehyde.

The assumption that formation of the labile (hydroxymethyl)phenyl sulfoxide **8** occurs in the oxidation of *rac*-**2b** could be substantiated by a control experiment with the stable benzoyl-protected derivative **10**:[18] hydrolysis of **10** with

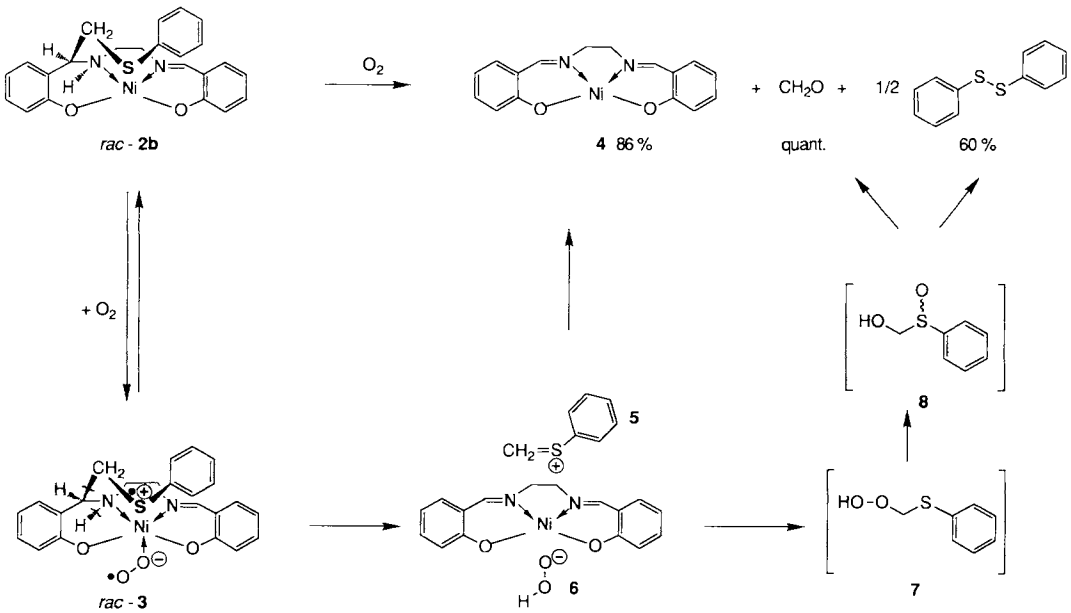

Scheme 1. Mechanistic interpretation of the oxidation of *rac*-**2b**. The yields of diphenyl disulfide and **4** refer to isolated, analytically pure material; the yield of formaldehyde was determined by ^{1}H- and ^{2}H-NMR spectroscopy.

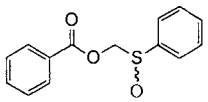

10

potassium hydroxide in methanol afforded formaldehyde (^{1}H-NMR spectroscopically quantitative as $DO-CH_2-OCD_3$ in CD_3OD) and diphenyl sulfide (61%) as the only chromatographically isolable product.[19] The yields of formaldehyde and diphenyl disulfide were thus comparable with those obtained in the atmosheric oxidation of *rac*-**2b** (Scheme 1).

For further examination of the mechanism of oxidation of *rac*-**2b** (Scheme 1) the $Ni^{2\oplus}$ complexes *rac*-**11** and *rac*-**12** were prepared from the corresponding diamines **1b**

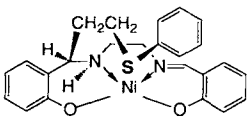

rac-**11**

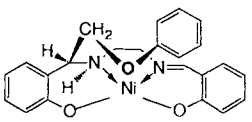

rac-**12**

($R = CH_2CH_2-S-Ph$) and **1c** ($R = -CH_2-O-Ph$) according to Equation (a). Both complexes are stable towards oxygen. In the case of *rac*-**11** the structural requirements for the formation of the sulfonium ion **5** by homolytic β-cleavage[14] (as in the O_2-adduct *rac*-**3**, Scheme 1) are lacking; in the oxygen analogue *rac*-**12**, oxidation of the axially coordinated heteroatom cannot take place.

The Co-complex *rac*-**2a** proved to be oxidizable, as shown by the rapid formation of diphenyl disulfide. In contrast, the Cu-complex *rac*-**2c**, as also the metal-free ligand, was found to be inert towards oxygen. The crystal structure of *rac*-**2c** is essentially the same as that of the Ni-complex *rac*-**2b** (Fig. 1); the distances between the central ion and the axially coordinated heteroatoms, however, are—as to be expected for a d^9 ion—significantly longer (Ni–S: 2.575(2); Cu–S: 2.896(2) Å; Ni–O_{ax}: 2.109(4), Cu–O_{ax}: 2.543(4) Å). These differences, in particular the different M–S distances possibly explain the difference in reactivity. Also, for the same ligand a higher half-wave potential $M^{2\oplus}/M^{3\oplus}$ is found for copper chelate complexes than for the corresponding nickel complexes.[13,20] This property is likewise detrimental to the oxygen coordination[6,11-13] and thus to the overall reaction according to Scheme 1.

Experimental

Preparation of the complexes *rac*-**2a–c, 11, 12**: A solution of 0.50 mmol of the diamine **1** [21] in 5 mL of ethanol was treated with 61.0 mg (0.50 mmol) of salicylaldehyde. The resulting yellow solution was added dropwise with stirring into a solution of 0.50 mmol of the metal acetate in 3 mL of distilled water at ca. 50 °C. The incipient precipitation was completed by addition of 30 mL of H_2O. After filtration and drying over P_2O_5 in vacuo the complexes *rac*-**2, 11, 12** were obtained as microcrystalline powders in 90–95% yield. C,H,N analyses: Δ% < 0.3.

Crystals of *rac*-**2b** and *rac*-**2c** suitable for an X-ray structure analysis were obtained by slow cooling of their solutions in MeOH in the absence of O_2.

Atmospheric oxidation of *rac*-**2b**: The complex (100 mg, 0.223 mmol) was dissolved with stirring in warm ethanol (5 mL); upon contact with oxygen the color of the solution became darker (reddish brown). When no further darkening was observed, the solution was partially evaporated, cooled, and filtered under suction. The Ni(salen) complex was obtained in the form of reddish-brown crystals (62 mg, 86%). Chromatographic separation of the mother liquor on silica gel (elution with dichloromethane/hexane 1/1) furnished 29 mg (60%) of diphenyl disulfide.

For the qualitative detection of formaldehyde, air can be bubbled through a solution of *rac*-**2b** in $CHCl_2$–$CHCl_2$ and fed into a solution of 2,4-dinitrophenylhydrazine or 5,5-dimethyl-1,3-cyclohexanedione (dimedone). For the quantitative NMR spectroscopic determination of formaldehyde (as hemiacetal) the atmospheric oxidation of *rac*-**2b** was carried out in $CDCl_3$ (2% EtOH) (^{1}H-NMR) and that of deuterated *rac*-**2b** in $CHCl_3$ (2% EtOH) (^{2}H-NMR). The yields of formaldehyde determined in this way were quantitative. The 1:1 stoichiometry of the reaction of *rac*-**2b** with oxygen was determined by measured addition of air with concomitant monitoring of the reaction by UV/VIS.

Received: August 14, 1989 [Z 3498 IE]
German version: *Angew. Chem.* 102 (1990) 81

[1] Y. Gao, R. M. Hanson, J. M. Klunder, S. Y. Ko, H. Masamune, K. B. Sharpless, *J. Am. Chem. Soc. 109* (1987) 5765.
[2] E. N. Jacobson, I. Markó, W. S. Mungall, G. Schröder, K. B. Sharpless, *J. Am. Chem. Soc. 110* (1988) 1968.
[3] K. Kieslich: *Microbial Transformations of Non-Steroid Cyclic Compounds*, Thieme, Stuttgart 1976.
[4] a) G. M. Whitesides, C.-H. Wong, *Angew. Chem. 97* (1985) 617; *Angew. Chem. Int. Ed. Engl. 24* (1985) 617; b) H. Fretz, W.-D. Woggon, R. Voges, *Helv. Chim. Acta 72* (1989) 391.
[5] D. Mansuy, *Pure Appl. Chem. 59* (1987) 759.
[6] A. E. Martell, D. T. Sawyer (Eds.): *Oxygen Complexes and Oxygen Activation by Transition Metals*, Plenum, New York 1988.
[7] a) I. Tabushi, K. Morimitsu, *J. Am. Chem. Soc. 106* (1984) 6871; b) I. Tabushi, M. Kodera, M. Yokoyama, *ibid. 107* (1985) 4466; c) Y. Matsuda, S. Sakamoto, H. Koshima, Y. Murakami, *ibid. 107* (1985) 6415; d) E. I. Karasevich, A. M. Khenkin, A. E. Shilov, *J. Chem. Soc. Chem. Commun. 1987*, 731.
[8] a) D. D. Cox, L. Que, Jr., *J. Am. Chem. Soc. 110* (1988) 8085; b) L. Que, Jr., R. C. Kolanczyk, L. S. White, *ibid. 109* (1987) 5373; c) L. Que, Jr., R. B. Lauffer, J. B. Lynch, B. P. Murch, J. W. Pyrz, *ibid. 109* (1987) 5381; d) M. Kumar, G. J. Colpas, R. O. Day, M. J. Maromey, *J. Am. Chem. Soc. 111* (1989) 8323.
[9] G. Henrici-Olivé, S. Olivé, *Angew. Chem. 86* (1974) 1; *Angew. Chem. Int. Ed. Engl. 13* (1974) 29.
[10] X-ray structure analysis: Enraf-Nonius CAD-4 diffractometer, Cu_{K_α} radiation, $2\theta = 100°$; empirical absorption correction based on ψ scans; structure determination by Patterson and Fourier methods; the hydrogen atoms, in part from difference syntheses, in part at calculated positions, were not refined.—*rac*-**2b**: $C_{23}H_{22}N_2O_2SNi$, monoclinic, space group $P2_1/n$, $a = 13.647(9)$, $b = 6.977(2)$, $c = 20.822(8)$ Å, $\beta = 94.79(4)°$, $V = 1976(3)$ Å^3, $Z = 4$, $\varrho_{calcd} = 1.510$ g cm^3; 2027 independent reflections, 1894 with $I > 0.1\,\sigma(I)$ used; $R = 0.055$, $R_w = 0.062$. The residual electron density was less than 0.53 e Å^{-3}.—*rac*-**2c**: $C_{23}H_{22}N_2O_2SCu$, monoclinic, space group $P2_1/n$, $a = 13.778(8)$, $b = 6.931(8)$, $c = 21.08(2)$ Å, $\beta = 93.08(6)°$, $V = 2011(5)$ Å^3, $Z = 4$, $\varrho_{calcd} = 1.499$ g cm^{-3}; 2063 independent reflections, 1897 with $I > 0.1\,\sigma(I)$ used; $R = 0.057$, $R_w = 0.061$, the residual electron density was less than 0.42 e Å^3. Further details of the crystal structure investigations are available on request from the Fachinformationszentrum Karlsruhe, Gesellschaft für wissenschaftlich-technische Information mbH, D-7514 Eggenstein-Leopoldshafen 2 (FRG), on quoting the depository number CSD-54056, the names of the authors, and the journal citation.
[11] a) R. D. Jones, D. A. Summerville, F. Basolo, *Chem. Rev. 79* (1979) 139; b) G. B. Jameson, W. T. Robinson, G. A. Rodley, *J. Chem. Soc. Dalton Trans. 1978*, 191; c) W. P. Schaefer, B. T. Huie, M. G. Kurilla, S. E. Ealick, *Inorg. Chem. 19* (1980) 340.
[12] R. A. Sheldon, J. K. Kochi: *Metal-Catalyzed Oxidations of Organic Compounds*, Academic Press, New York 1981.
[13] a) E. Kimura, A. Sakonaka, R. Machida, M. Kodama, *J. Am. Chem. Soc. 104* (1982) 4255; b) E. Kimura, R. Machida, M. Kodama, *ibid. 106* (1984) 5497.
[14] a) J. K. Kochi (Hrsg.): *Free Radicals*, Wiley, New York 1973; b) K. U. Ingold in [14a], *Vol. 1*, p. 99; c) J. W. Wilt in [14a], *Vol. 1*, p. 398; d) J. K. Kochi, in [14a], *Vol. 2*, p. 665.
[15] In an analogous way arenesulfenic acids and olefins or nitriles are formed on thermolysis of arylalkyl sulfoxides and *N*-alkylidenearene sulfinamides [16, 17].
[16] a) F. A. Davis, L. A. Jenkins, R. L. Billmers, *J. Org. Chem. 51* (1986) 1033; b) F. A. Davis, R. L. Billmers, *ibid. 50* (1985) 2593; c) F. A. Davis, R. H. Jenkins, Jr., S. Q. A. Rizvi, S. G. Yocklovich, *ibid. 46* (1981) 3467; d) F. A. Davis, R. H. Jenkins, Jr., *J. Am. Chem. Soc. 102* (1980) 7967.
[17] a) D. R. Hogg, in D. Barton, W. D. Ollis, D. N. Jones (Eds.): *Comprehensive Organic Chemistry, Vol. 3*, Pergamon, New York 1979, p. 261 (*Sulphenic Acids and Their Derivatives*); b) J. L. Kice, *Adv. Phys. Org. Chem. 17* (1980) 65.
[18] L. Horner, E. Jürgens, *Justus Liebigs Ann. Chem. 602* (1957) 135.
[19] Small amounts of methyl benzoate could also be isolated chromatographically.
[20] P. Zanello, A. Cinquantini, *Transition Met. Chem. 10* (1985) 370.
[21] The diamines **1a–c** were obtained by reductive amination of the corresponding ketones with ethylenediamine/$Na[BH_3(CN)]$ in methanol.

Book Reviews are written by invitation from the editor. Suggestions for books to be reviewed and for book reviewers are welcome. Publishers should send brochures or (better) books to the following address: Redaktion Angewandte Chemie, Postfach 101161, D-6940 Weinheim, Federal Republic of Germany. The editor reserves the right of selecting which books will be reviewed. Uninvited books not chosen for review will not be returned.

Beilstein Handbook of Organic Chemistry. 4th Edition. 5th Supplementary Series. Volumes 17, 18, and 19. Edited by *R. Luckenbach*. Springer, Berlin 1984–1988. 30572 pp., hardcover, DM 90440.00

With the appearance of sub-volume 17/1, the first in the 5th Supplementary Series of the 4th Edition, in 1984 and sub-volume 19/12 in 1988 all the chalcogen-containing heterocycles reported in the period 1960–1979 have now been fully described in "Beilstein".

This is an overwhelming work considering that in 35 sub-volumes and more than 30000 pages 200307 individual compounds have been described. In the accompanying Subject Index to the sub-volumes some 219296 names are listed; however, several compounds are cited more than once under different names. Cumulative Subject Indexes covering the contents of Volumes 17–19 will soon appear and should be completed by 1990.

The contents of Volumes 17–19 cover the oxygen heterocycles. Volumes 17 (11 sub-volumes) and 19 (12 sub-volumes) deal with oxygen heterocycles with one oxygen atom in the ring while Volume 19 (12 sub-volumes) is devoted to the oxygen heterocycles with two or more ring oxygens. Following the traditional Beilstein system, the heterocycles containing higher chalcogens in the ring are dealt with as derivatives of the corresponding oxygen compounds and follow them accordingly. A very useful feature is the inclusion, in each sub-volume, of a short introduction to the Beilstein system. With this even the unpractised user can soon locate the compound sought for. Additional help is available in the form of the booklet "How To Use Beilstein" published by the Beilstein Institute in German, English, and Japanese, and a "German-English Dictionary" containing the most important formulations used in Beilstein. These are both available free of charge. For those who wish to have electronic access to Beilstein the search program "SANDRA" is available. In this respect Beilstein has also managed a smooth transition into modern developments and so fulfilled the needs of all those users to whom date processing is a daily routine.

Use of the sub-volume Subject Index is facilitated by the inclusion of a short introduction to the nomenclature used by Beilstein. In addition, in sub-volumes 17/1, 18/1 and 19/1, a comprehensive list of the prefixes used and a dual language explanation of the stereochemical descriptors has also been included. These are all valuable aids, enabling one, on the one hand, to find compounds easily in Beilstein and, on the other, to name new compounds correctly. It would be a great advantage if the names thus generated were accepted by the primary publications.

On taking a closer look at Volumes 17–19 one finds that industrially important compounds, e.g. ethylene oxide (sub-volume 17/1), ecologically relevant substances, e.g. chlorinated dibenzodioxins (sub-volume 19/2), and natural products, e.g. steroids (sub-volume 19/3) are all represented. The foregoing is only an indication of the wide selection of compounds which are dealt with. Precisely in the case of the dibenzodioxins one becomes aware of the advantages of the Beilstein system. One finds chlorinated compounds containing the dibenzodioxin skeleton, with the chlorine atoms in all possible positions, are dealt with one after the other following the parent compound. This gives the user an overview of related compounds which in practice allows him or her to make a substructure search in a printed medium. In addition, Beilstein enables the user to see the relationships between stereoisomers as they so often occur in natural products. In sub-volume 19/3, for example, there are entries for seven stereoisomeric spirostan-2,3-diols which have been described and assigned their correct stereodescriptors.

The layout of the individual entries follows a well established pattern. Details about the constitution and configuration of a compound, which have often been clarified and corrected by the Beilstein team after taking into consideration the latest available literature, are followed by an account of the natural occurrence, extraction from natural products, preparation, synthesis, and purification. It is worth mentioning that biochemical methods are also dealt with here if they have been used on a preparative scale.

There then comes the factual part, which is the largest and, certainly for the user looking for data, the most important part of the entry. Here the structure and energy parameters as well as the physical properties, including spectroscopic data, are presented. Special mention should be made of the plethora of numerical data in Beilstein, which makes it one of the largest factual databases in the world. It still has not dawned on many chemists that a wealth of information is tucked away in Beilstein. This should be emphasized more strongly in future. As a result of this data collection, Beilstein has become a link between the spectroscopic databases dealing with relatively few compounds and the bibliographic databases of Chemical Abstracts Services (CAS). Due to the method of indexing it is difficult to make a directed search for data in Chemical Abstracts.

The entry continues with a description of the chemical behavior and addition compounds and concludes with an account of the derivatives.

Changing the language in which Beilstein is published from German to English has made further compression in the text of the entries possible. This is particularly noticeable in the descriptions of preparative methods and chemical behavior, which are presented in telegraphic style. For the chemist who is exclusively interested in preparative work this compression – relative to that in the earlier Supplementary Series – may be painful. In exchange, however, he gets an enormous increase in the amount of physico-chemical data: this is to be welcomed. In this area especially, functions have been assumed from which the "classic" Beilstein user can only profit.

The "Beilstein Online Database" must also be viewed in this light. The first part of this database (at the time of writing) contains the heterocycles reported in the period 1830–1959 which were described in Volumes 17–27 of the Main Series and Supplementary Series I–IV. The volumes reviewed here form an extension to the database. Together

the two constitute a valuable supplement to the CAS databases.

In this connection it would be useful if the CAS Registry Numbers were available in the text as well as in the indexes so that one could move more easily from one reference work to the other.

The overall impression of the volumes reviewed is excellent, and how could it be otherwise for this standard work on organic chemistry with its new, up-to-date format? Both the publisher and the Institute have done everything possible to make "Beilstein" attractive to the synthetic chemist. He should make the most of what is offered.

Heinrich Heydt, Manfred Regitz [NB 1033 IE]
Fachbereich Chemie
der Universität Kaiserslautern (FRG)

Non-Metal Rings, Cages and Clusters. By *J. D. Woollins*, Wiley, Chichester 1988. ix, 124 pp., hardcover, £ 25.95. – ISBN 0-471-91592-0

The rapid progress made during the last 25 years in the chemistry of cyclic nonmetal compounds is still not reflected in the contents of most textbooks. This very area, however, is particularly well suited to making students clearly aware, at an early stage, that the chemistry of all nonmetal elements (including carbon) forms a unified whole. Therefore, this introductory book, which originated as the text of a lecture, unquestionably fulfills a real need by serving as an appetizer to this area of chemistry.

After a short presentation of the most important fundamental concepts and synthetic strategies, the following three chapters discuss a series of exemplary nonmetal ring systems, from electron-deficient compounds and classical ("electron-precise") compounds to electron-rich compounds. Understandably, the limited coverage of the book necessitates a somewhat arbitrary selection of compounds or, as the author puts it, the selection "should be regarded as my choice from a very large box of chocolates". However, the limited number of compounds makes it possible to indicate numerous relationships and structural similarities between different classes of compounds. This feature is especially valuable for students, who, all too often, organize their chemical knowledge in separate boxes according to element symbols. In this respect, however, it would have been useful to have included at least some examples of cyclic hydrocarbons.

The chapter on electron-deficient compounds contains a good overview on structures, bonding, syntheses, and properties of boron–hydrogen compounds and metallaboranes. The importance of ^{1}H and ^{11}B NMR spectroscopy for structural elucidation is made clear through several representative spectra. However, the section on polyhedral boron subchlorides is much too short, while the fragmentary treatment of transition-metal clusters could have been omitted in view of the book's title.

The chapter on normal ("electron-precise") compounds covers the most important homo- and heterocyclic ring systems of sulfur, phosphorus, and silicon. The cyclic silicates and metaphosphates are not mentioned, since this would have exceeded the intended coverage of the book. Lacking in the discussion of homocyclic silicon compounds is mention of the three-membered ring as well as of the existence of fused ring systems; this also holds true for the large number of corresponding silazanes. Similarly, the discussion of phosphorus omits mention of the interesting cyclic acid anions with P–P bonds.

The last chapter on electron-rich compounds presents a concise discussion, illustrated by numerous formula schemes, of what is currently known about borazenes, phosphazanes, phosphazenes, sulfur–nitrogen rings and cages, and polychalcogen cations.

The book is directed at undergraduates with the goal of awakening their interest in this area of molecular chemistry. Helpful in this respect is the list of references, in particular key review articles, at the end of each chapter. Furthermore, the two-volume work of *Haiduc-Sowerby* is recommended as a source of additional information.

Not surprisingly, the treatment of such a huge amount of information and the attempt to systematize it leads to some errors. Apart from obvious typographical errors (like the name *Gillespie* on page 5), these can sometimes lead to confusion, especially for students. For example, on page 7, the formation of P_3H_5 from P_2H_4 is not a polymerization. On page 15 (sixth line from the bottom), electron pairs would be correct; on page 49, dichlorodisulphane; on page 54, P_4H_6 and P_7H_3; on page 55 in Fig. 3.11, Li_2P_{16}; and on page 67 in Fig. 3.18, $P_3O_9^{3\ominus}$. The "equation" for the synthesis of P_5H_5 (page 54) is incomprehensible and the formation of P_9Me_3 (page 55) is not a redox reaction with evolution of elemental chlorine. In addition, several references to the literature contain errors.

Despite these privisos, this highly readable book offers an initial, informative overview of the heterogeneous area of cyclic nonmetal compounds and is also suitable as an introduction to those wanting to study nonmetal rings and cages. Moreover, chemists interested in preparative and structural chemistry will find the book highly interesting. The book is excellent in appearance, although somewhat overpriced.

Marianne Baudler [NB 1039 IE]
Institut für Anorganische Chemie
der Universität Köln (FRG)

Industrial Inorganic Chemistry. By *W. Büchner, R. Schliebs, G. Winter* and *K. H. Büchel*. Translated by *D. R. Terrell*. VCH Verlagsgesellschaft, Weinheim/VCH Publishers, New York 1989. 614 pp., hardcover, DM 145.00. – ISBN 3-527-26629-1/0-89573-610-1

This English translation of a 1984 German edition has been updated and supplemented with data from the U.S. industrial inorganic chemicals market. The original authors were all with Bayer AG in 1984, and have produced a book which includes a broad range of "technical chemistry". It is organized into "primary inorganic materials" (H_2, H_2O, peroxides, N-compounds, P-compounds, S-compounds, halogen compounds, metals and their compounds), then into product classes (mineral fertilizers, silicones, zeolites, inorganic fibers, construction materials, ceramics, wear-resistant materials, pigments) as well as nuclear fuel principles and production. The organization by element makes it ideal for lecturers wishing to illustrate an inorganic chemistry course with applications (e.g., video cassettes, optical fibers, microelectronic devices).

The advertising claims that economic aspects, process energy balance and ecological consequences are treated, and that the intended use is not only the classroom (abundant marginal notes repeat central points of the text), but also in business and law. Indeed, there is an abundance of tables of workable terrestrial reserves, of production, and of consumption (e.g., annual asbestos production, by country, to six significant digits!). Ecological matters are treated only

 © VCH Verlagsgesellschaft mbH, D-6940 Weinheim, 1990 0570-0833/90/0101-0110 $ 02.50/0

superficially, however, (e.g., one sentence about asbestos "toxicity"). Since any single topic is treated very briefly, references are crucial for effective non-classroom utilization of such a book. While the book is liberally referenced, these are frequently limited to standard reference encyclopedias of chemical technology and to statistical yearbooks. There are too few references to more current and specialized review articles, especially those describing scientific (or ecological) rather than technological points. Likewise, certain topics are referenced with only older literature (e.g., silicones); a topic as modern as magnetic coatings is only thinly referenced.

It goes without saying that I learned a great deal from this book: the molecular mechanism of chrome tanning of leather, that Norway exceeds the U.S. in production of ferrosilicon, that South Africa possesses the predominant world reserve of chromite ores, "... and the world's dependence thereon can therefore not be overlooked". The book even encourages self-development: I was forced to consult my dictionary to learn the meaning of nacreous.

In addition to all of the above applications, this book will also be useful to the inorganic researcher seeking a bridge into new research areas with problems worthy of his/her attack.

Kenneth G. Caulton [NB 997 IE]
Department of Chemistry, Indiana University
Bloomington, IN (USA)

Bromine Compounds. Chemistry and Applications. Edited by *D. Price, B. Iddon* and *B. J. Wakefield.* Elsevier, Amsterdam 1988. xii, 422 pp., hardcover, HFl 285.00. – ISBN 0-444-42982-4

This volume contains the edited contributions to the First International Conference on the Chemistry and Applications of Bromine and its Compounds, held in September 1986 at the University of Salford, Great Britain. The contents are arranged in 14 chapters. Of the 39 authors 17 are from Great Britain, 17 from Israel, four from the USA and one from Switzerland. Since the majority of them work in industrial laboratories (The Associated Octel Co. Ltd., Bromine Compounds Ltd., Great Lakes Chemical Corporation, and Dow Chemical Europe), the papers deal mainly with problems related to industrial applications.

World production of bromine, which is usually obtained by oxidation of bromides by chlorine, is currently in the region of 4×10^5 t/year. However, the relative shares of the different bromine compounds of technological importance have altered greatly; since 1975, 1,2-dibromoethane, which for the previous 50 years was by far the most important product (being used mainly as a fuel additive in combination with lead tetraethyl, to scavenge the lead that is released by forming the more volatile lead bromide) has come increasingly into disrepute. An alternative market for organobromine compounds which has come into prominence is in fire retardants for polymers (e.g. brominated diphenyl ethers, polypentabromobenzylacrylate, or tetrabromobisphenol-A). In the area of inorganic bromine compounds a market which has become increasingly important is in transporting oil and natural gas, where solutions of bromine salts (calcium and zinc bromides) are used as components of "packer fluid". The book reviewed here provides up-to-date surveys and reports on research relevant to these new applications. Moreover, the chapter on the up and down history of the bromine industry ("Bromine Chemical Industry—Retrospect and Prospect", by *W. R. Merriman* and *H. E. Arkens,* 24 pp., 21 refs.) is an interesting and stimulating account of an important part of the industrial history of the twentieth century.

Now that the standard monograph on bromine chemistry ("Bromine and its Compounds", edited by *Z. E. Jolles,* 1966) is getting on in years, new review articles on bromine compounds are especially welcome. The "Introductory Review" of the present book (120 pp., 459 refs.), written by eight authors from Associated Octel, provides a very good review of recent developments, including the applications of bromine compounds. Other reviews deal with "Brominated Marine Natural Products" (*D. J. Faulkner,* 24 pp., 103 refs.), "Polybromoalkanes—Aspects of Chemistry and Reaction Mechanisms" (*R. Bolton,* 36 pp., 132 refs.), "Brominated Aromatic and Heteroaromatic Compounds" (*B. Iddon* and *B. J. Wakefield,* 71 pp., 323 refs.) and "The Use of Bromine Compounds as Flame Retardants" (*C. F. Cullis,* 31 pp., 66 refs.). The remaining eight chapters deal with special topics and report new research results.

Altogether the book offers a great deal of information. Since it contains review articles as well as research reports from a conference, it has, of course, not been possible to completely avoid some imbalances in emphasis; for example, the numbers of literature references in the individual chapters vary between 459 and 2. Half of the articles include in their references the titles of the original papers, which is very useful in view of the fact that the secondary literature is widely scattered. The inorganic side of bromine chemistry tends to be treated here as subordinate to the organic; for example, silver halide photography, which is still very important, is only touched on briefly, and there is no mention of perbromates or bromine cations, which have stimulated much scientific discussion about the higher oxidation states of bromine. In contrast the organic chemistry and marine biological chemistry of bromine are comprehensively treated. The particular value of this book probably lies in the detailed and up-to-date account of the present and potential future uses of bromine and its compounds in science and technology. The book can be thoroughly recommended; it will be indispensable to all bromine chemists, and useful as a source of information for many others, including chemistry teachers. It is a pity that it is so expensive.

Max Herberhold [NB 1001 IE]
Anorganisch-chemisches Laboratorium
der Universität Bayreuth (FRG)

Copper Oxide Superconductors. By *C. P. Poole, T. Datta* and *H. A. Farach.* Wiley, Chichester 1988. xii, 289 pp., hardcover, £ 22.40. – ISBN 0-471-62342-3

To write a monograph on this subject now is a bold and welcome initiative. It is scarcely possible to review the whole of the flood of published work in this field (about 10000 papers have appeared in three years of research!). Nevertheless the authors have competently surveyed and evaluated the most recent work up to the book's manuscript deadline of July 1988.

Basic concepts, standard techniques and the many different physical and chemical aspects of these materials are covered. Starting from what is known about conventional superconductors, the authors extend the discussion to the various phenomena found with the new oxide type materials. A concise description of the currently accepted basic theories is followed by an experimentally-orientated review of the chemical methods for preparation, including essential advice

regarding the quite considerable toxicity of thallium compounds. Next there comes a detailed account of the structural features of the most important compounds, and of the unique physical and chemical properties which result. In this context the authors also deal with the chemical characterization of the materials. The magnetic behavior, which is of crucial importance in superconductors, is discussed in detail, taking into consideration both the fundamental macroscopic magnetic effects which are important in superconductivity, and phenomena of microscopic origin such as paramagnetism and antiferromagnetism. The magnetic resonance methods which are routinely used to investigate such phenomena are described, with special emphasis on their applications to superconductors. Other features of the solid state such as energy gaps, densities of states, electron-phonon coupling, and the experimental methods used to investigate them, are also covered, and a selection of typical data is included, which is useful for the experimentalist. The concluding chapters are devoted to transport properties and tunneling phenomena, especially in relation to electrical and thermal effects.

It would have been useful to include more detail on real structures, e.g. by discussing results from electron microscopy studies. Also it is surprising that the ionic radii according to *Shannon*, which are nowadays most generally used, have not been applied here. The few small errors which have crept into the work as a consequence of the vast amount of literature to be covered do not significantly diminish the value of the monograph. The book is aimed particularly at readers who are already working in this field, but it also provides a valuable introduction to the very large and complex body of published work for newcomers to the topic.

Reginald Gruehn [NB 974 IE]
Institut für Anorganische und Analytische Chemie
der Universität Gießen (FRG)

Vitamins. By *W. Friedrich*. Walter de Gruyter, Berlin/New York 1988. xii, 1058 pp., hardcover, DM 380.00.—ISBN 3-11-010244-7/0-89925-273-7

This comprehensive monograph is a very welcome revised and translated edition of a recently published book in German by the same author (W. Friedrich: *Handbuch der Vitamine*, Urban & Schwarzenberg, Munich 1987, 657 pp.). This book provides a lucid and authoritative summary of the present state of knowledge in biochemical and medical research on vitamins, and is a rich source of information, especially for readers interested in the medical, pharmaceutical and biochemical aspects. As in the German version, this convenient and attractive book contains a separate comprehensive chapter (thirteen altogether) on each of the vitamins and their derivatives.

The introduction examines in a general way the topic of vitamins. Historical aspects are discussed, and an overview is presented of where vitamins are found, the need for them, and their biological functions. This chapter is enhanced by clear illustrations in color relating to the individual vitamins.

Next come a series of chapters devoted to the individual vitamins and vitamin derivatives. In accordance with the usual sub-division of the topic, the first four chapters deal with the fat-soluble vitamins (1. Vitamin A and its Provitamins; 2. Vitamin D; 3. Vitamin E; 4. Vitamin K). These are followed by nine chapters on the water-soluble vitamins (5. Thiamine, Vitamin B_1, Aneurine; 6. Vitamin B_2: Riboflavin and its Bioactive Variants; 7. Niacin: Nicotinic Acid, Nicotinamide; 8. Vitamin B_6; 9. Folic Acid and Unconjugated Pteridines; 10. Biotin; 11. Pantothenic Acid; 12. Vitamin B_{12}; 13. Vitamin C). These thirteen comprehensive and information-packed chapters on the individual vitamins (each with about 60 to 80 pages of text) all follow a similar construction. Each chapter treats (mainly from a medical and biochemical standpoint) the following aspects: history, nomenclature, stereochemistry and structure, synthesis and chemical reactions, vitamin analogs and antagonists, biosynthesis, stability, physical properties, separation and purification, analysis and standardization, biochemical functions, metabolization, transport and storage in the human body, pathological symptoms of vitamin deficiency, etc. A comprehensive bibliography is provided at the end of each chapter. The clarity of presentation of the information is helped by a well-balanced choice of clearly arranged tables and by carefully prepared figures and chemical formula schemes.

The work is rounded off by a supplement giving references to the more recent literature (1984 to 1986), mainly on medical topics, and a lengthy but clearly arranged subject index.

Like the original German version, this lucidly written book is an excellent and comprehensive source of up-to-date information on the biochemical and physiological aspects of vitamins; it is mainly suitable for use by medical scientists, biologists, biochemists, pharmaceutical chemists, and all chemists with medical or biochemical interests. It also shows that, contrary to what many people think, the subject of vitamins is a highly productive field of research. From the chemist's point of view the work would be even more valuable if it included a more detailed treatment of the chemical aspects of vitamins research (chemical structure, reactivity, synthetic methods); nevertheless the book is highly recommended.

Bernhard Kräutler [NB 992 IE]
Laboratorium für Organische Chemie
der ETH Zürich (Switzerland)

Registered names, trademarks, etc. used in this journal, even when not marked as such, are not to be considered unprotected by law.

© VCH Verlagsgesellschaft mbH, D-6940 Weinheim, 1989. – Printed in the Federal Republic of Germany by Konrad Triltsch Druck- und Verlagsanstalt Würzburg.

All rights reserved (including those of translation into foreign languages). No part of this issue may be reproduced in any form — by photoprint, microfilm, or any other means — nor transmitted or translated into a machine language without written permission from the publishers. Only single copies of contributions, or parts thereof, may be made for personal use. This journal was carefully produced in all its parts. Nevertheless, authors, editors and publisher do not warrant the information contained therein to be free of errors. Readers are advised to keep in mind that statements, data, illustrations, procedural details or other items may inadvertently be inaccurate.

Valid for users in the USA: The appearance of the code at the bottom of the first page of an article (serial) indicates the copyright owner's consent that copies of the article may be made for personal or internal use, or for the personal or internal use of specific clients. This consent is given on the condition, however, that the copier pay stated per-copy fee through the Copyright Clearance Center, Inc. (CCC), for copying beyond that permitted by Sections 107 or 108 of the U.S. Copyright Law. This consent does not extend to other kinds of copying, such as copying, for general distribution, for advertising or promotional purposes, for creating new collective works, or for resale. For copying from back volumes of this journal see 'Permissions to Photo-Copy: Publisher's Fee List' of the CCC.

Editorial office: Postfach 10 11 61, D-6490 Weinheim, Federal Republic of Germany, Telephone (06201) 60 22 55, Telex 465 516 vchwh d, Telefax (06201) 602 328.

Editor: *Peter Gölitz*

Associate editors: *D. J. Loewus, A. Stimson.* **Editorial assistant:** *E. Schweikart*

Publishers: VCH Verlagsgesellschaft mbH. (Managing Director: *Hans Dirk Köhler*), Pappelallee 3, D-6940 Weinheim, Federal Republic of Germany.

Advertising office (Advertising Manager *R. J. Roth*): Postfach 10 11 61, D-6940 Weinheim, Federal Republic of Germany, Telephone (0 62 01) 60 61 30, Telex 4 67 155, Telefax (0 62 01) 606 184.

ANGEWANDTE CHEMIE
International Edition in English
Volume 29 · Number 2
February 1990
Pages 113–222

Fractals and Related Hierarchical Models in Polymer Science

By Alexander Blumen* and Horst Schnörer

Polymer science, an interdisciplinary science well-rooted in organic chemistry and in materials science, encompasses an inordinate number and diversity of substance classes and thus has far-reaching applications. Interestingly, polymers also represent a great challenge to the theoreticians, since their theoretical treatment often necessitates appropriate extensions of the classical methods from solid state physics and from statistical physics. Thus, new concepts often have to be invoked when considering the special properties of polymers. In this review we concentrate on one of the modern concepts in the theory of polymers, namely on scaling. Scaling is closely associated with new developments in the field of fractals and of hierarchical structures. Such concepts are invaluable for the modeling of complex geometries and for describing dynamical processes in polymeric materials. Here, we focus on a presentation of these ideas and we outline examples of recent research in which these concepts have been successfully applied.

1. Introduction

One of the most fascinating aspects of today's polymer science lies in the highly interesting combination of new materials' properties on the one hand and of recent theoretical developments on the other. That polymers are substances with enormous potential in the applied sciences is self-evident; that the same polymers display features making them one of the favorite testing-grounds for new theoretical concepts is not so well known. In the authors' opinion, this underscores the fact that progress in natural sciences occurs historically, by which we mean that formerly, apparently unrelated fields are suddenly perceived as related, and thereafter develop in parallel. Thus, in polymer science theoretical modeling and chemical synthesis are, in fact, much more intimately linked than what one might naively expect. In fact, as we shall now demonstrate, most of the *mathematical* apparatus required for modeling macromolecules as objects sui generis was already available for quite some time; the *need* to use such mathematical techniques, however, increased dramatically with the advent of highly sophisticated devices for monitoring substances usually regarded as complex and irregular (i.e. not fitting simple model concepts of the day).

The basic idea underlying the new theoretical models is that of scaling, which, in its geometrical form is exemplified by the concepts of percolation[1] and of fractals.[2–5] In Sections 2 and 3 we shall remind our readers of these ideas, which, in view of the large number of recent publications,[2–14] may by now be quite familiar (a fact which for some time made us hesitate to write this article). Geometric scaling (self-similarity) is, however, only one part of the story—scaling involves also the dynamical properties of polymers, an aspect often ignored in most of the recent reviews. We will therefore also address questions related to the dynamics of excitation and charge carrier transport in polymeric materials,[10,15–17] topics which require modeling through time fractals[18–21] and through hierarchical energy distributions.[22] First, however, let us discuss the basic ideas.

[*] Prof. Dr. A. Blumen, Dipl. Phys. H. Schnörer
Physikalisches Institut der Universität
and Bayreuther Institut für Makromolekülforschung (BIMF)
Postfach 101251, D-8580 Bayreuth (FRG)

 © VCH Verlagsgesellschaft mbH, D-6940 Weinheim, 1990 0570-0833/90/0202-0113 $ 02.50/0

2. Polymers and Scaling Concepts

In 1979 *de Gennes*[23] published one of the seminal works in the field, underscoring the importance of scaling ideas in deriving the properties of numerous diverse materials. In this brilliant work *de Gennes* demonstrates how scaling, combined with a feeling for the problems at hand, leads to a seemingly effortless derivation of many polymeric features. Of course, many of the foundations underlying *de Gennes*' book were laid in the classical works of *Flory, Rouse, Zimm,* and *Stockmayer*.[24–27]

As perhaps simplest example for scaling let us consider a polymer chain and focus on its mean squared end-to-end distance $<\boldsymbol{R}^2>$. For a chain consisting of N monomers and in the absence of any hindering interactions it is a simple matter to show that $<\boldsymbol{R}^2>$ is proportional to N [Eq. (a)], where L is a (model-dependent) constant.

$$<\boldsymbol{R}^2> = NL^2 \qquad \text{(a)}$$

The result (a) is very general, since it can be traced back to one of the basic theorems of probability theory, the central-limit theorem. In fact many textbooks[24, 28–30] use models based on random walk (Fig. 1a) ideas (the random flight chain, the freely rotating chain, the Gaussian chain) and show that Equation (a) holds true in all these (special) cases. Interestingly, one also learns from these derivations that *local* hindrances (such as fixed bond lengths, limitations of the rotations around the bonds, or *short-ranged* correlations in orientation) do not change the character of Equation (a). Thus, different models only lead to differences in the constant L (L is practically *Kuhn*'s persistence length[31]).

It should also be pointed out, of course, that Equation (a)—as distinct from many of the expressions which we will encounter in the following—does *not* depend on the dimension d of the Euclidean space in which the random walk takes place; Equation (a) is truly very general.

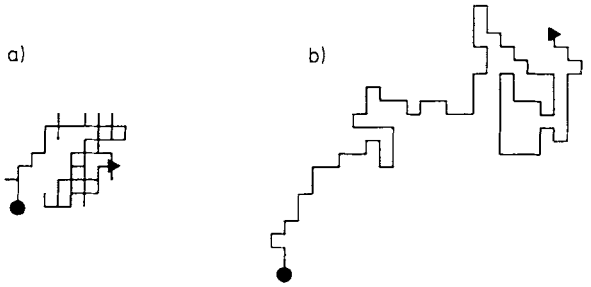

Fig. 1. Random walk (a) and self-avoiding walk (b) with 100 steps each on a square lattice, using the same sequence of random numbers. Starting points and end points are marked with filled circles or triangles, respectively. In case (b) the walker cannot visit occupied sites again ("excluded volume"), which leads to an increase of the spatial extension of the walk.

It is thus very remarkable that the introduction of an excluded volume,[31] i.e. of steric hindrances between the monomers (this results in so-called self-avoiding walks, SAW) leads to a vastly different behavior for $<\boldsymbol{R}^2>$. One has the relationship (b), where ν (the Flory-parameter[32]) is

$$<\boldsymbol{R}^2> \sim N^{2\nu} \qquad \text{(b)}$$

in general a non-integral, dimension-dependent constant. The physical reason for steric hindrances is the short-range repulsion between different monomers, as occurs, for instance, in good solvents. Now we already know that interactions between neighboring monomers *along the chain* do not cause departures from Equation (a). What happens here is that some monomers, which along the chain are quite distant, may come into close contact due to a loop in the chain. The repulsion between such monomers creates (mathematically speaking) *long-range* correlations. As forcefully stressed by *Flory*, this leads to swelling of the polymer in good solvents (see Fig. 1b). A straightforward approximate

Alexander Blumen, born 1948 in Bucharest/Rumania, studied physics at the University of Munich 1966–71. He gained his PhD in theoretical chemistry in 1976 from the Technical University Munich under the guidance of G. L. Hofacker. After a post-doc period in the chemistry department of the Massachusetts Institute of Technology with R. Silbey and J. Ross he obtained his Habilitation in 1982 at the T.U. Munich, where he was appointed Privatdozent in 1983. A Heisenberg stipend was awarded to him by the Deutsche Forschungsgemeinschaft in 1984. He spent a year, starting in 1985, at the Max-Planck-Institute of Polymer Science in Mainz with E. W. Fischer. Since 1986 he has been a member of the Physical Institute of the University of Bayreuth, where he has a C3-Fiebiger professorship. His special interests are the theory of disordered media (glasses, polymers), the dynamics of complex systems, and stochastic processes.

Horst Schnörer, born 1962 in Nankendorf (Bavaria), studied physics at the University of Bayreuth from 1982 to 1987. After an experimental diploma thesis dealing with photoconductivity in polymers, he now aims at his PhD in theoretical physics under the guidance of Alexander Blumen. Central topics of his research are the theory of transport processes on irregular structures and the kinetics of diffusion-limited reactions.

calculation of the free energy for the polymer chains leads to Equation (c).[32] The values obtained from Equation (c) are

$$\nu = 3/(d+2) \tag{c}$$

in remarkable agreement with today's best estimates for SAWs[30] ($\nu = 0.588$ for $d = 3$ and $\nu = 0.750$ for $d = 2$). Furthermore, Equation (c) displays two limiting behaviors: In $d = 1$ a SAW is trivial (being a straight segment of length LN) so that $<\boldsymbol{R}^2> = L^2N^2$, i.e. $\nu = 1$. Moreover, in $d \geq 4$ $\nu = 1/2$, i.e. the SAW behaves as a simple random walk; for this reason the dimension $d = 4$ is marginal.

The expression (b) provides a classical example for a scaling law. First, it relates the mean end-to-end SAW distance $R = \sqrt{<\boldsymbol{R}^2>}$ to the number of monomers N in a highly nontrivial way (d). The exponent $1/\nu$ in (d) is dimension-

$$N \sim R^{1/\nu} \tag{d}$$

dependent [Eq. (c)], and we thus have *qualitatively* different behaviors for different d, while the details of the local interactions are unimportant: the problem displays distinct *universality* classes. Secondly, introduction of the innocuously-looking but fundamental condition of monomer-monomer repulsion causes departures from the central-limit theorem. In later sections we will show that the first point [Eq. (d)] is directly related to (geometric) fractals, whereas the ideas behind the second aspect are echoed in non-Gaussian (Lévy) stable laws and in time fractals.

The linear chain in a good solvent is only one of the many examples for scaling, and we refer the reader to the books by *de Gennes*,[23] by *Doi* and *Edwards*[29] and by *des Cloizeaux* and *Jannink*[30] for an extensive list of scaling relations. To present just a few spectacular examples, we consider the semidilute regime, in which there is a relatively small concentration of chains in a good solvent; the concentration c is, however, high enough, so that chains can mutually interpenetrate. In this regime the osmotic pressure π behaves as in Equation (e)[23, 29] (using $\nu = 3/5$), whereas the averaged

$$\pi \sim c^{3\nu/(3\nu-1)} \sim c^{9/4} \tag{e}$$

end-to-end distance R follows the law (f), i.e. the chains

$$R \sim c^{(2\nu-1)/(2-6\nu)} \sim c^{-1/8} \tag{f}$$

shrink therefore with increasing concentration, a result confirmed by neutron scattering.[33]

A much-discussed scaling relation concerns the viscosity η. At a constant content of polymeric material in concentrated solutions and in melts the viscosity scales with the degree of polymerization N in accord with Equation (g), where the

$$\eta \sim N^{\varepsilon} \tag{g}$$

exponent ε is about 3.4. This behavior is quite universal, independent of temperature and molecular species, and requires only linear, flexible polymers in dense, entangled fluids.[29] Remarkably, the reptation theory by *de Gennes* predicts $\varepsilon = 3$.[23] In recent years, however, several improvements have been proposed for the determination of ε; thus the very recent theories of *Scher, Shlesinger, Weiss* and *Bendler* give $\varepsilon = 10/3$ as exact solution to their models.[34, 35]

3. Theories of Scaling

A fundamental aspect of scaling-laws such as (b) or (d)–(g) is their self-similarity. Take for instance Equation (d), which relates a mesoscopic, i.e. in general fairly large (ca. 1000 Å) length R to the (microscopically determined) degree of polymerization N (average number of monomers per chain). Equation (d) also holds if we group our monomers in pairs (dimers) and relate R to the number $(N/2)$ of dimers. The same is, of course, true if we group λ monomers together, and view R as a function of (N/λ); as long as λ stays much less than N we have $R \sim (N/\lambda)^{1/\nu}$. On the mesoscopic level we are unable to distinguish the microscopic details and a scale change (within reasonable bounds) leads to the same physicochemical situation. Pictorially speaking, we cannot differentiate between the whole system and a (fairly substantial) rescaled part of it—on the mesoscopic scale both look the same.

This idea is the basis of the renormalization group (RG) theory, a very powerful method developed in conjunction with the analysis of phase transitions.[36–38] Here the main observation is that near a critical point the correlation length of the order parameter diverges. We may exemplify the situation by considering a percolation cluster—probably the best means for visualizing a phase transition geometrically. In (site-)percolation, sites on a regular lattice are occupied at random by conducting and insulating elements. Now an electrical current can pass a bond only if both its ends are occupied by conducting elements. The question is: when does a current cross the entire sample? It is evident that for a small concentration of conducting elements no current will be transferred, whereas in the opposite case a current will flow. Interestingly now, such a transition is not very gradual. A detailed analysis shows that (for an infinite sample) below a critical concentration p_c no current will flow at all: the resistivity is infinite. Above p_c there is always a macroscopic current I, whose magnitude scales around p_c. One has for the conductance σ above p_c:

$$\sigma \sim I \sim (p - p_c)^{\bar{t}} \tag{h}$$

where $\bar{t}$ is a universal constant ($\bar{t} \simeq 1.3$ in $d = 2$ and $\bar{t} \approx 2.0$ in $d = 3$ for lattice percolation[11]). This behavior is thus very reminiscent of a second-order phase transition; here the conductance plays the role of an order parameter. These are in fact detailed works which stress the close correspondence between typical features encountered in percolation and the behavior of the thermodynamic parameters in second-order phase transitions.[39, 40]

Furthermore, at p_c the incipient infinite cluster (that set of connected conducting elements which spans the system from one side to the other) scales. Figure 2 illustrates the realization of such a cluster on a square lattice, for which $p_c \approx 0.593$. Note the appearance of voids of all sizes and that one cannot distinguish the random pattern of this cluster from that of a similar enlarged section of another incipient

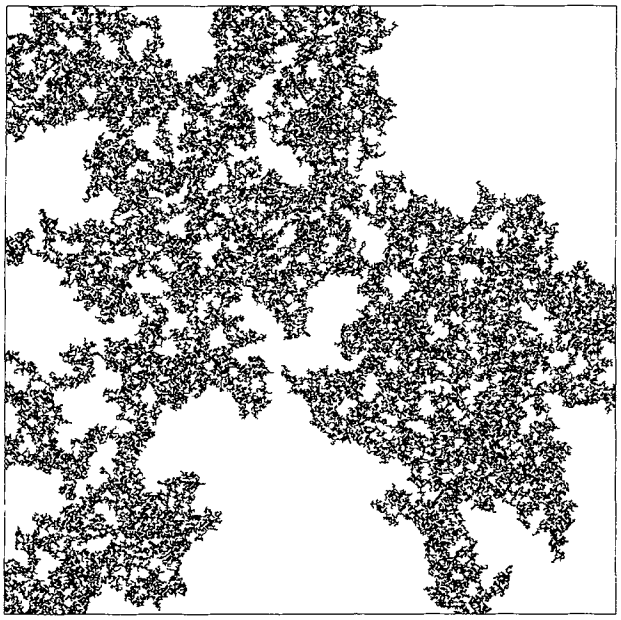

Fig. 2. Percolation cluster on a two-dimensional square lattice at the critical concentration $p_c = 0.593$.

infinite cluster. That such a cluster (barely) conducts current is due to the divergence of its connectivity at p_c, i.e. to a singularity in the correlation length.

Now the renormalization group theory makes use of this observation through judicious use of scaling: Imagine that we were to repeatedly enlarge (renormalize) our scale (or, equivalently, shrink our sample) by a fixed factor. Obviously, finite clusters will then become smaller and smaller at each step, whereas a self-similar infinite cluster would practically stay the same. Hence, the iterated renormalization procedure allows us to get rid of the uninteresting features (finite clusters), while keeping that part of the problem which stays invariant under the transformation. In mathematical terms, the critical variables at the transition show up as fixed-points of the corresponding hamiltonian function under the RG.[36-38]

An early implementation of the RG was suggested by *Kadanoff*:[37,41] it consisted in systematically deleting (decimating) lattice points from a hamiltonian formulated in the site representation and in recalculating the effective interactions between the remaining sites (renormalization of the interactions). For regular lattices (but not for some simple fractals!) this real-space renormalization (RSR) scheme runs into difficulties,[42] because it often alters the structure of the hamiltonian (e.g. it may lead to long-range interactions). Hence, a more successful way to implement the RG procedure is to renormalize in momentum space,[43] also splendidly demonstrated by *Wilson*, who was awarded the Nobel Prize for Physics in 1982 for his work in this field.

The real-space renormalization (RSR) could have been the starting point for fractals. Indeed, one of *Wilson*'s students, the Indian scientist *Dhar*, proceeded along these lines and asked himself what simple lattice-type structures stay invariant under RSR. In this way he created a structure[44,45] which is similar to the Sierpinski-gaskets, which we will discuss in the following section. The historical development followed, however, another course.

3.1. Fractals

The notion of fractals was introduced by *Mandelbrot* in a book in 1975;[46] he stressed that many structures in Nature are self-similar.[2,46] Starting point for a mathematical self-similar description were the works of *Cantor, Sierpinski, Julia,* and *Fatou,* who provided us with classes of patterns which display scale-invariance.[47]

In this section we present several ways of obtaining geometrical patterns which scale with distance. Common to all objects is their underlying self-similarity, which is most easily visualized in terms of dilation. We start thus by discussing the fundamental features in terms of Sierpinski gaskets and continue by describing the general stochastic and deterministic means of creating fractal shapes.

Perhaps the simplest fractal is the Sierpinski gasket[2,48] embedded in the two-dimensional space, as displayed in Figure 3. The structure can be generated by a procedure which

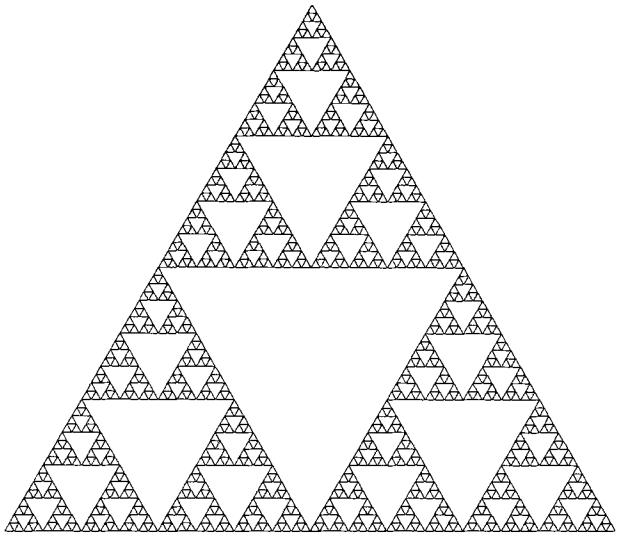

Fig. 3. Sierpinski gasket in $d = 2$ at the sixth stage of iteration.

renders clear the underlying symmetry. One starts with a triangle of side length 2, which includes three smaller, upwards-pointing triangles of side length 1. In the nomenclature introduced by *Mandelbrot*[2] this basic pattern is called a generator. A dilation by a factor of 2 from the upper corner transforms the upper small triangle into the large one, and creates two additional, larger triangles. One may also view the operation as attaching two copies (left and right) below the original pattern. The procedure is then iterated n times, and leads to the structure at its nth stage. As an example, the portion of the Sierpinski gasket depicted in Figure 3 corresponds to the 6th stage of iteration.

Sierpinski gaskets can be generated in embedding spaces of arbitrary dimension d, by starting with the corresponding

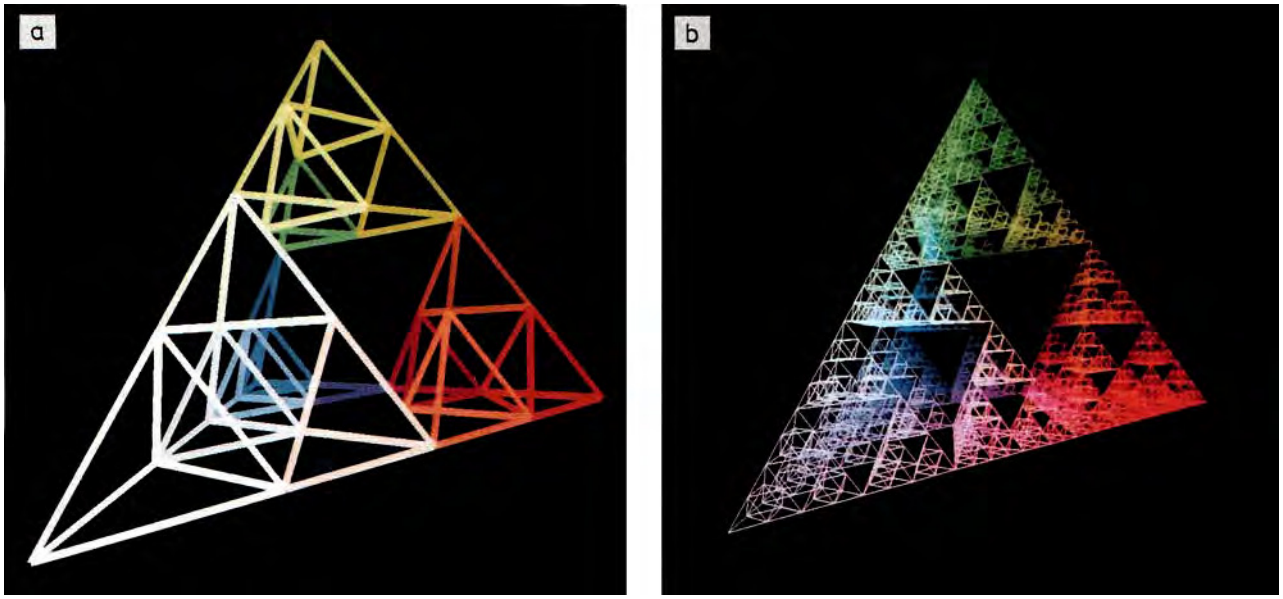

Fig. 4. Sierpinski gasket in $d = 3$ at the second (a) and the fifth (b) stage of iteration.

hypertetrahedrons.[49, 50] Figure 4 shows a Sierpinski gasket in three dimensions at the 2nd and 5th stage of iteration. Also more general patterns can be constructed along the same lines of reasoning.

Properties of fractal objects related to physical quantities (such as mass distribution, density of vibrational states, conductivity and elasticity) are describable by several, not necessarily integral parameters. These parameters play roles similar to that of the spatial dimension. Here we focus on the fractal (Hausdorff) dimension $\bar{d}$ which characterizes the distribution of mass. Denoting by N the number of lattice points inside a sphere of radius R, one has the proportionality (i), where $\bar{d}$ is defined by $\bar{d} = \lim_{R \to \infty} \ln N / \ln R$. Hence,

$$N \sim R^{\bar{d}} \tag{i}$$

for a Sierpinski gasket embedded in the d-dimensional Euclidean space one obtains Equation (j).[2, 51]

$$\bar{d}_s = \frac{\ln (d+1)}{\ln (2)} \tag{j}$$

A comparison of the expressions (i) and (d) shows that a polymer chain in a good solvent has a fractal dimension $\bar{d}$ of $1/\nu$.

Another important parameter which plays a role in connection with the dynamical properties of or on fractals (such as diffusion-controlled reactions and heat conduction) is the spectral (fracton) dimension $\tilde{d}$. Using a scaling argument, *Alexander* and *Orbach*[51] have found that Equation (k) holds for Sierpinski gaskets in d dimensions.

$$\tilde{d}_s = 2 \frac{\ln (d+1)}{\ln (d+3)} \tag{k}$$

As example, for the Sierpinski gasket of Figure 3, (where $d = 2$) one has $\bar{d}_s = 1.584$ and $\tilde{d}_s = 1.365$. In many cases the relation $\tilde{d} < \bar{d} < d$ holds; furthermore, for Sierpinski gaskets $1 < \tilde{d}_s < 2$, as may be seen from Equation (k). It should be emphasized that $\bar{d}$ and $\tilde{d}$ are amenable to experimental observation.[10, 51, 52] For modeling purposes it is therefore desirable to construct deterministic fractals with prescribed $\bar{d}$ and $\tilde{d}$ values.

Based on the systematic construction of the Sierpinski gaskets one can consider modified Sierpinski-type structures. The spectral dimensions $\tilde{d}$ for these structures lie between that of a 2d-Sierpinski gasket, $\tilde{d}_s = 1.36$, and the value 2. In References [49, 50] one took as generators d-dimensional tetrahedrons of side length b filled with N smaller tetrahedrons of unit side length. For such generators the fractal pattern follows by iteration, and one has the relationship (l).

$$\bar{d} = \ln N / \ln b \tag{l}$$

On the other hand, $\tilde{d}$ can be obtained from the long-time behavior of the probability of being at the origin (see References [49, 50] for details) and lies between 1 and 2. Hence such symmetric fractals represent a wide class of lattices which generalize the Sierpinski gaskets.

Not all fractal systems display the strong symmetry of the Sierpinski gaskets, which are 'deterministic' fractals, designated as such since for each point in space it is unambiguously clear whether it belongs to the structure or not. The distribution of points in a fractal pattern may be random, as exemplified through the previously discussed percolation clusters. A related model is that of photopolymerization of multifunctional monomers. Here the procedure is to pick at random at each step a monomer adjacent to the boundary of the growing cluster, and to attach it to the cluster. This so-called Eden model is a special case of epidemic growth, where, in a more general version, a fresh cell at the boundary of an infected cluster either gets infected with probability p (and hence joins the cluster) or becomes immune. The general version is identical to percolation;[1] for p smaller than the

critical concentration p_c the growth of the cluster always terminates, while for $p \geq p_c$ infinite clusters may be formed. Models similar to epidemic growth have also been developed in conjunction with the spread of forest fires.[1, 53, 54]

A wide variety of fractal patterns is encountered in the investigation of kinetic growth models. Here (see reviews [6] and [12]) it is customary to distinguish the models according to the mass transport and to accretion. Mass transport describes the way in which the reactants come in close contact: in solvents the reactants diffuse towards each other, so that one has Brownian motion; more rarely also ballistic aggregation may occur, in which case the reactants approach each other along linear trajectories. Accretion may occur at first encounter (the growth is then motion-limited) or several encounters of the reactants may happen before a bond is created (the growth is then reaction-limited). Furthermore, one may allow only monomers to attach themselves to the already existing polymer cluster (monomer-cluster aggregation, MC) or the clusters may also combine (cluster-cluster aggregation, CC). An example for a MC diffusion-limited aggregate (DLA) is given in Figure 5. As a rule, CC leads to more ramified clusters than MC, and the density of clusters increases from diffusion-limited to ballistic to reaction-limited. Model calculations[112] lead to the following fractal dimensions $\bar{d}$ for clusters grown in $d = 3$: a) MC: diffusion-limited $\bar{d} = 2.50$, ballistic $\bar{d} = 3.00$, reaction-limited (Eden model) $\bar{d} = 3.00$; b) CC: diffusion-limited: $\bar{d} = 1.80$, ballistic $\bar{d} = 1.95$, reaction limited $\bar{d} = 2.09$. All these patterns are encountered in polymeric systems, and examples will be provided in Section 4, where we will discuss the experimental techniques used to monitor the fractal dimensions. First, however, let us turn to scaling aspects in dynamical processes.

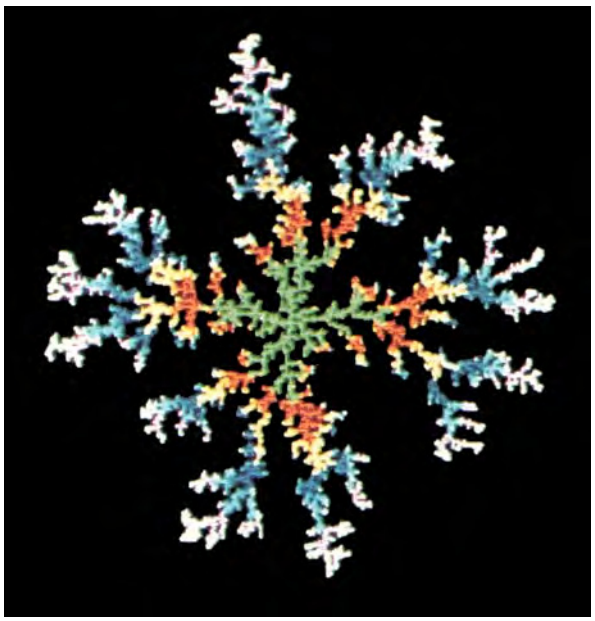

Fig. 5. Cluster of monomers grown by diffusion-limited monomer–cluster aggregation on a square lattice. The different colors show different stages of evolution.

3.2. Time-Fractals and Ultrametric Spaces

A major field of application of scaling ideas in the time domain is photoconductivity.[115, 116] As pointed out in a recent review article[117] the use of polymeric photoconductors in printing and copying techniques represents one of the most sophisticated applications for organic materials. In fact organic photoconductors have been improved in the last two decades to the extent that they are nowadays at least equivalent (if not even superior) to their inorganic counterparts.

From the theoretical viewpoint, the issue at stake in amorphous photoconductors is the dispersive transport, as contrasted to the familiar diffusive, Gaussian behavior. Diffusive motion, in its many facets, ranging from the transfer of heat (macroscopic) to Brownian motion (microscopic) is a well-understood phenomenon and may be modeled using the mathematical theory of Markov processes, in which the system keeps no memory of past events. Typical discrete examples are random walks on regular lattices—first introduced by *Bachelier* at the turn of the century for monitoring the fluctuations of the stock market[55]—which nowadays comprise a vast mathematical literature.[56] Simple random walks on regular lattices for arbitrary dimensions lead to a time-independent diffusion coefficient, or, expressed differently, in the absence of a biasing field, to a linear increase in the mean squared displacement as a function of time.

In amorphous photoconductors the situation is different, since one encounters dispersive transport: the motion of the carriers through a sample becomes slower and slower with the passage of time, so that no diffusion constant in the usual sense can be defined. Here the diffusion coefficient D displays an algebraic dependence on time [(m) with $\gamma < 1$];

$$D(t) \sim t^{\gamma - 1} \qquad \text{(m)}$$

with a similar finding for the current $I(t)$ flowing in a biasing field. Such behavior is incompatible with the usual diffusion equation. Note, however, the nontrivial scaling behavior of D with respect to t.

Progress in the advancement of theoretical models for dispersive transport was slow, due to the Gaussian character of most of the probability distribution functions put forward. Here again the central-limit theorem of probability theory plays an important role. One should recall that under very general conditions, a sum of random variables will tend to form a normal (Gaussian) distribution when the number of elements in the sum increases. The position vector of a particle may be viewed as a sum of distance increments due to past events, say collisions. If energies, directions etc., are randomized after such events, most distributions will lead to regular diffusion. Hence, for a successful modeling of dispersive transport in such a framework one has to look for the (relatively rare) distributions for which the central-limit theorem does not hold.

The basic theoretical problem in modeling the transport of light-generated charge carriers through an amorphous medium is to take care of the broad distribution of stepping times. One models the motion of individual carriers which move under the influence of an external electric field through hopping. Here it is important that the probability for performing a step per unit time is not exponential, but decays much more

slowly. Physically this may be pictured as arising from the fact that an amorphous material has rather irregular lattice spacings (geometrical disorder), which lead to large variations in stepping times (temporal disorder).

Mathematically, the most important parameter characterizing the transport is the distribution of waiting-times between subsequent carrier jumps. A theoretical breakthrough occurred here through the works of *Scher, Lax,* and *Montroll,* who showed that long tails in the waiting-time distribution $\psi(t)$ between the microscopic events can qualitatively describe the dispersive transport,[57, 58] when one assumes the relationship (n) with $0 < \gamma < 1$,

$$\psi(t) \sim t^{-1-\gamma} \tag{n}$$

so that the zeroth but not the first moment of the distribution $\psi(t)$ exists. Such distributions lead to Lévy processes, a field which was long considered to be a domain of mathematical curiosities only.[2, 59] The main technical point in investigating random walks in continuous time (CTRW) with such distributions, was the realization that the basic CTRW framework (as formulated ten years earlier by *Montroll* and *Weiss,*[60] could readily incorporate these, less usual, $\psi(t)$-forms. However, although the theory developed in References [57, 58] was successful in providing a scheme for the qualitative understanding of dispersive transport, one could at the time only speculate on the nature of the microscopic parameters leading to $\psi(t)$.

Today we know that this approach is only one of the possible was of obtaining algebraic time dependences for $D(t)$, and that the key ingredient in the CTRW framework is the idea of temporal scaling, or of time fractals, as formulated by *Shlesinger.*[18-21, 61]

As pointed out in Reference [21], scaling has a long history in probability theory. As early as 1713 the work of *N. Bernoulli* was reported, who analyzed a game of chance with infinite average winning (the Petersburg paradox). Furthermore, scaling also shows up in a function introduced by *Weierstrass* [Eq. (o)]. $W(k)$ is everywhere continuous but

$$W(k) = (1-a)\sum_{n=0}^{\infty} a^n \cos(b^n k) \tag{o}$$

$(a < 1,\ b > a^{-1})$

nowhere differentiable. For our purposes, an expression related to Equation (o) provides an excellent means to obtain the asymptotic behavior given by Equation (n).[10, 21]

$$\psi(t) = \frac{1-a}{a}\sum_{n=1}^{\infty} a^n b^n \exp(-b^n t) \tag{p}$$

It is a rather straightforward matter to verify that at large values for t Equation (p) scales: From (p) one has $ab\psi(bt) = \psi(t) - (1-a)\mathrm{b}\exp(-\mathrm{b}t)$, so that for slowly decaying (slower than exponential) $\psi(t)$ one finds at longer times: $\psi(t) \approx ab\psi(bt)$, i.e. scaling behavior. From the last expression one obtains γ of Equation (n) to be equal to $\ln a/\ln b$. Expression (p) is very valuable, since it allows one to investigate the behavior of several dynamical quantities near their marginal dimensions; notice that we can, through a judicious choice of a and b, get any preassigned value of γ. Some examples concerning photocurrents and excitation depolarization in polymeric materials will be presented in Sections 5 and 6.

One physical reason for such broad distributions of waiting times is energy disorder. The motion of particles through an amorphous solid as well as relaxation in glassy materials can be described in terms of dynamical processes in multidimensional random potentials with valleys and barriers of different heights.[10, 62] The microscopic motion over the barriers is in many ways similar to *Eyring*'s ideas of the activated complex in chemical reactions.[63]

There are several models which are simplified variants of the random potential, e.g. the random valley and random barrier models[64] (see Fig. 6). Random valley models consider a random distribution of valley depths with barriers at equal top level. A similar model, in which charge carriers in the conduction band get captured by and released from traps of various depth (multiple trapping) was formulated by *Schmidlin.*[65] The multiple trapping model was shown to correspond to the CTRW-theory.[16, 66]

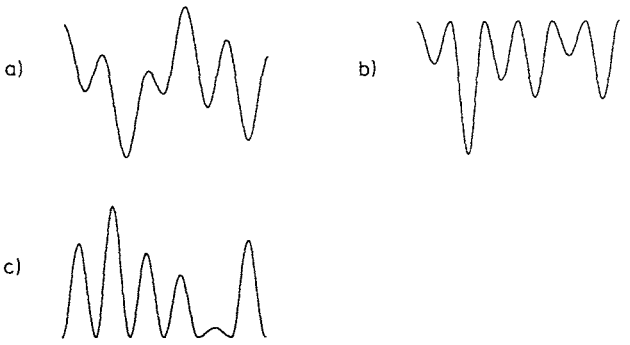

Fig. 6. (a) Random potential, (b) random valley, and (c) random barrier models.

In random barrier models the valleys are at equal level. These structures are amenable to hierarchical modeling through so-called ultrametric spaces.[10, 22] In these models sites are separated by energy barriers with random heights. Thus, a particle positioned on a certain site needs thermal energy to surmount the surrounding barriers. A given activation energy lets the particle visit only a subset (cluster) of sites around the starting point. One may then classify the sites through the energy required to reach them:[67] To such a classification corresponds an ultrametric space (UMS).

As examples, Figure 7 shows the regularly multifurcating ultrametric spaces Z_2 and Z_3. Note that only the points on the baseline belong to the UMS and that the structure above the baseline documents barrier heights and intersite connections. The height $d(x,y)$ of the barrier between sites x and y may be used as a generalized 'distance': It may be easily verified that Equation (q) holds for all UMS sites. Equation

$$d(x,y) \leq \max(d(x,w),\ d(y,w)) \tag{q}$$

(q) is the 'strong' triangle inequality which leads to the name 'ultra'metric. Z_2 and Z_3 have branching ratios $z = 2$ and

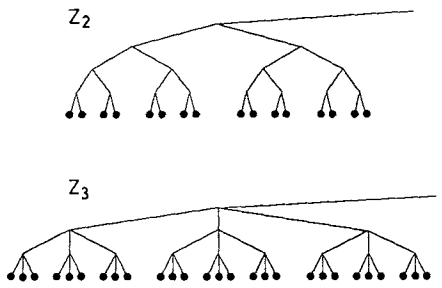

Fig. 7. The ultrametric spaces Z_2 and Z_3.

$z = 3$, respectively, and, for simplicity, we have taken the barrier heights to be hierarchically arranged, so that all consecutive energy levels differ by Δ. Now, it may be shown that several dynamical parameters scale with $\delta = kT \ln z/\Delta$. We refrain, however, from continuing with this topic and we refer the interested reader to References [10, 22, 68] and works cited therein for further details.

4. Geometrical Aspects of Disordered Systems

In this section we focus on the determination of the geometric scaling aspect for aggregates. The basic quantity here is the fractal dimension $\bar{d}$, which was defined in Equation (i). Since the total mass M of the aggregate is directly proportional to N, the number of monomers involved, the expression (i) may be replaced by (r).

$$M \sim R^{\bar{d}} \tag{r}$$

Objects that obey Equation (r) are named "mass-fractals".[12] Distinct from these, one also encounters "surface fractals", i.e. aggregates which are uniformly dense ($d = 3$), while having a rough surface S, for which the relationship (s) holds, where $\bar{d}_f$ is the surface fractal dimension.

$$S \sim R^{\bar{d}_f} \tag{s}$$

The methods of choice for investigating fractal objects include, in particular, scattering techniques. The intensity profile I of a scattered beam (light, neutrons, X-rays) is in such cases algebraically dependent upon the scattering wave vector $\boldsymbol{k}$ in accordance with (t),[12] where $-2\bar{d} + \bar{d}_f$ is the

$$I \sim k^{-2\bar{d}+\bar{d}_f} \tag{t}$$

so-called Porod slope. *Schaefer* et al. have investigated whole classes of substances and have demonstrated that, in general, many structures can be distinguished by their Porod slopes; they find that aggregates formed by polymer precursors give rise to scattering curves whose slopes lie between -1 and -3, whereas rough colloids yield slopes between -3 and -4 and smooth colloids slopes of -4. The methods even allow one to differentiate between substances grown by monomer-cluster (MC) and cluster-cluster (CC) aggregation; we refer the reader to Reference [12] for a summary of recent results.

Another method of choice in measuring the fractal dimension, advocated by *Avnir* et al.,[13] makes extensive use of adsorption techniques. It consists in determining the monolayer capacity $N(\sigma)$ of adsorbed molecules of cross section σ required to cover the surface to be investigated. For a fractal surface one expects as a function of the cross section the relationship (u).[69]

$$N(\sigma) \sim \sigma^{-\bar{d}_f/2} . \tag{u}$$

Such behavior was reported by *Avnir, Pfeifer* et al.[69-72] in their study of crushed glass, carbon black, charcoal, and of porous silica gels. The adsorbates that they use include N_2, alkanes and polycyclic arenes and alcohols.

This approach, however, has its problems: adsorption is an intricate process, in which the local interactions of the molecules with the surface are complex and may mask the geometric details.[73] It appears that both the measurements of the monolayer capacity and the calculations of the molecular cross sections are quite delicate. Recent molecular-size-dependent experiments on porous silica gels[74] led to values of $\bar{d}_f$ even larger than 3, a clearly very problematic result.

Another method which provides morphological information (including the fractal dimension of self-similar objects) centers on the direct transfer of electronic excitations. This method, which monitors the *fractal* dimension and which was proposed by us,[75] is now of widespread use. Furthermore, the *spectral* dimension can be monitored through reaction-diffusion processes as propagated by us[75] and by *Kopelman*.[76] For newer developments on the spectral dimension see References [77, 78].

Let us now consider the direct energy transfer (ET), which takes place from donor molecules to acceptor molecules, and assume that donors and acceptors occupy substitutionally sites on a regular lattice. In this classical problem[79, 80] one considers an excited donor molecule surrounded by acceptors which occupy some of the sites of the structure. The transfer rates $w(\boldsymbol{r})$ depend on the mutual distance r between each donor-acceptor pair. An often encountered form for $w(\boldsymbol{r})$ which holds for isotropic multipolar interactions is Equation (v).[79] The parameter s equals 6 for dipole-dipole,

$$w(\boldsymbol{r}) = ar^{-s} \tag{v}$$

8 for dipole-quadrupole and 10 for quadrupole-quadrupole interactions. For regular, d-dimensional lattices one obtains the decay function $\Phi(t)$ according to (w), where A is a constant and B is the reciprocal intrinsic lifetime of the donor in the absence of acceptors.

$$\Phi(t) = \exp(-At^{d/s} - Bt) \tag{w}$$

Let us now focus on optical properties related to fractals. From Equation (w) we see that the Förster-type decays are determined by the spatial dimension d of the region accessible to acceptors. Thus, the extension of Equation (w) to fractal objects gives (x) (see Ref. [10] for a detailed derivation).

$$\Phi(t) = \exp(-At^{\bar{d}/s} - Bt) \tag{x}$$

Since $\bar{d} < s$, the long-time decay is governed by intramolecular processes. This, on the other hand, also limits the

spatial range in which the ET method can probe the structure of the underlying material. Typically, this range is of the order of 100 Å, which is also the region amenable to the small angle X-ray scattering technique. Hence, in this region these two methods give complementary information.

The ET method, as proposed in Reference [75], was first used by *Even* et al.[81] for the investigation of the pore structure of Vycor glass. They studied the kinetics of the ET between rhodamine B and malachite green in solution inside the glass. Using Equation (x), *Even* et al. found $\bar{d} = 1.74$. This result has recently been questioned with regard to its compatibility with light and X-ray scattering data.[82, 83] Similar experiments have been conducted by *Rojanski* et al.[84] on a porous silica gel; they obtained $\bar{d}_f = 3$ for the silica gel surface, a result also corroborated by adsorption and by X-ray scattering. These findings were later questioned by *Levitz* and *Drake*[85] and by *Levitz* et al.[86] who asserted that this type of silica gel is characterized by a smooth surface on the molecular scale ($\bar{d}_f = 2$). As shown by *Levitz* et al.[86] it is problematic to claim that a structure is fractal based only on results compatible with Equation (x).

Yang et al. performed computer simulations;[87] they considered the ET among particles located on pores of spherical or cylindrical shape, whose radii are of the order of the typical transfer distance; the calculated kinetics show fractal-like decays. Similar geometrical restrictions for ET have been studied by *Baumann* and *Fayer*[88] and by ourselves.[89, 90]

ET processes have been studied for polymeric systems. Singlet ET mechanisms in anthracene-loaded copolymers of vinylnaphthalene show complicated temporal behaviors, which are thought to be partly due to fractal-like distributions of naphthalene and anthracene molecules.[91] Triplet ET kinetics in doped polymer films has been investigated by *Lin, Nelson,* and *Hanson*.[92] Their data fit their model better when fractal structures are taken into account. Further discussions of polymeric systems in terms of fractals are given in References [93 and 94].

We close this section by mentioning that the ET model has also initiated new ideas; thus, fractals have been considered in the discussion of the energy migration and trapping among cationic porphyrins adsorbed on anionic vesicle surfaces.[85] Furthermore, a stretched exponential modulation model has been proposed for simulating vibrational dephasing in locally amorphous media.[96] Finally, hierarchical and fractal concepts have been used in the analysis of time-resolved spectra of mixed crystals of dichlorobenzene and dibromobenzene.[97]

5. Dynamical Aspects of Disordered Systems

We will now turn our attention to dynamical aspects for which the ideas of scaling in time play an important role. The dominant feature, distinct from the topics of the previous section, is that here we focus on changes in dynamics brought about by irregular objects, rather than on the geometrical aspects. Important problems in this field are (macroscopically) liquid flows through porous systems and (microscopically) charge and excitation transfer through polymeric samples.

A flow through a porous system, as any motion through a fractal space, may show dispersion, i.e. the diffusion is in general governed by Equation (m). This field has recently been well reviewed by *Po-Zen Wong*,[98] so we shall contend ourselves here with a summary of the results. The ionic conductivity of rocks σ_r scales with their porosity φ, following *Archie*'s law,[99] $\sigma_r \sim \varphi^{-m}$, where m is around 2. This result corresponds to the 'shrinking tube' model, which is analogous to percolation,[1] see for instance Equation (h), with $p_c = 0$.[99] An extension of the model leads to the 'grain consolidation' model, obtained from random sphere packing.[100] This model again leads to *Archie*'s law over much of the range of practical interest.[100]

Special topics of attention in flows in random systems involve problems which arise when two (or more) liquids are present at the same time, e.g. the question of how oil and water displace each other. Here one encounters 'viscous fingering' aspects, and 'invasion percolation'.[101] The latter model ensures that the invader flows along a continuous path while the defender may form trapped clusters. For details on these models we refer the reader to the literature.[98]

Another field of research in which temporal scaling and the CTRW scheme play an important role is charge carrier transport in amorphous materials, especially in polymeric photoconductors. A technique which is often applied for investigating the properties of amorphous photoconductors is the time-of-flight method. Charge carriers, generated by a short light pulse near the top surface of a thin film of the photoconductive material, drift under the influence of an external electric field through the sample and give rise to a transient photocurrent in the external circuit. In many inorganic and organic amorphous materials the shapes of the photocurrents $I(t)$ show dispersive behavior, i.e. the current decreases monotonically without exhibiting a regime with constant current, which one would expect if all charge carriers moved with the same mean velocity through the sample.

As also noted in Section 4, *Scher* and *Montroll*[58] applied the CTRW-theory to this problem and using the algebraic waiting-time distribution of the form (n) derived expressions for the asymptotic decay of the current. Two regimes have to be distinguished. In the time regime before the so-called transit time t_T (the time when the fastest carriers passed through the sample) the current decays according to (y),

$$I \sim t^{-1+\gamma} \tag{y}$$

whereas in the time range $t > t_T$ the current decays according to (z).

$$I \sim t^{-1-\gamma} \tag{z}$$

The results (y) and (z) mean that here the temporal aspect dominates the dynamics. As an example for which Equations (y) and (z) provide the right description for experimental data we present in Figure 8 the transient photocurrent in polysiloxanes with pendant carbazole groups.[102] Note that both axes are logarithmic, leading to an algebraic decay of the form $t^{-\beta}$ appearing as a straight line with slope $-\beta$. The experimental curve (1) and the theoretical curve (2), calculated with $\gamma = 0.58$, coincide over a period of four decades in

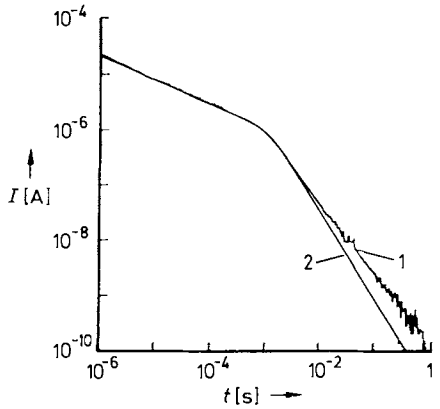

Fig. 8. Transient photocurrent in polysiloxane (1) and theoretical curve, calculated from an algebraic $\psi(t)$ with $\gamma = 0.58$ (2), double logarithmic plot.

time. Therefore, also in photoconductivity we obtain in many instances scaling behavior (see Ref. [15]).

However, the behavior of the photocurrents in polymeric systems is manifold. In the next section we will show some limitations of the idea of temporal scaling and we will also present crossover effects.

Let us now turn to percolative aspects in photoconductivity, an aspect more akin to geometric scaling. Percolation is important, if the substrate consists of impurity centers embedded in an inert matrix. In a recent investigation[1103] a benzotriazole derivative embedded in a polycarbonate matrix was used. In such a situation, especially at relatively low impurity concentrations, the fluctuations in the intersite distances become very drastic. As a result, the influence of the geometric disorder becomes dominant, and percolation, as described in Section 3, prevails. As discussed there, one has a critical concentration p_c, below which no current can flow. Slightly above p_c the current depends on the impurity concentration p, according to the expression (h), where p_c is nonuniversal while t is a universal constant (which depends mainly on the dimension). Figure 9 shows the carrier mobilities μ_T found for the benzotriazole–polycarbonate system. The experimental data appear to agree fairly well with the percolation picture.

To close this section let us consider the problem of electronic energy transfer in substitutionally disordered molecular and ionic crystals. Here the general interest has focused on the diffusion coefficient, which is related to the mean-squared distance traveled by the excitation, or on the decay of the excitation, due to trapping and annihilation.[10, 104–106] In the case of dipolar interactions, a less direct but experimentally very versatile method to test the transport consists in performing depolarization measurements.[107, 108] For randomly oriented molecules already a single-step transfer depolarizes very efficiently, so that in the long run the memory of the original polarization is lost, *except* for those excitations which are (still or again) on the originally excited sites. Thus depolarization measurements probe $P_0(t)$, the probability that an originally excited site is excited at time t. As we will show, $P_0(t)$ scales with time.

We have treated this problem in the framework of the previously described CTRW theory,[57, 58, 109] incorporating the local disorder in the waiting-time distribution $\psi(t)$, for which we used the time fractal Weierstrass-form Equation (p). Now for a simple random walk in $d = 3$ the relationship (A) holds true, and for general dimension d the relationship (B). Here the geometry of the lattice plays an important role.

$$P_0(t) \sim t^{-3/2} \quad \text{(A)}$$
$$P_0(t) \sim t^{-d/2} \quad \text{(B)}$$

On the other hand, when we perform a continuous-time random walk with an algebraic $\psi(t) \sim t^{-1-\gamma}$ we find that the long-time $P_0(t)$ expression is a direct reflection of the waiting-time distribution $\psi(t)$, as long as this distribution is broad, while for sufficiently narrow waiting-time distributions the classical random-walk behavior [Eq. (B)] for $P_0(t)$ is recovered. The decay behavior follows Equation (C)

$$P_0(t) \sim \begin{cases} t^{-\gamma} & \text{for } 0 < \gamma < 3/2 \\ t^{-3/2} & \text{for } \gamma \geq 3/2 \end{cases}, \quad \text{(C)}$$

(see also Fig. 10). Equation (C) is an example for the interplay between temporal and spatial aspects of excitation transport, the temporal aspect being dominant for small γ (high dispersion, wide distribution of jump times).

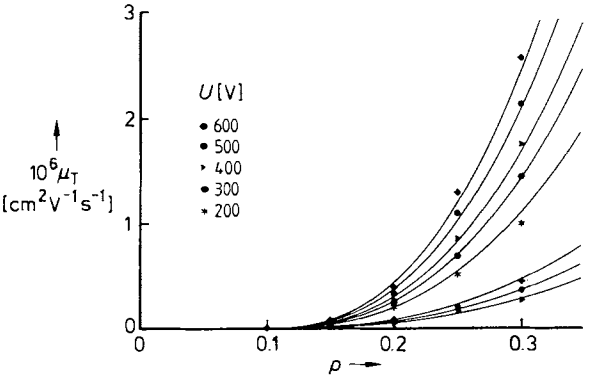

Fig. 9. Effective charge carrier mobilities μ_T of polycarbonate matrices containing different concentrations p of benzotriazole. The μ_T data were measured at the U-values given in the inset (sample thickness ca. 10 μm) at two different temperatures (293 K and 333 K). All curves are fitted to the percolation model [(h), with $p_c = 0.1$ and $\bar{t} = 2.5$].

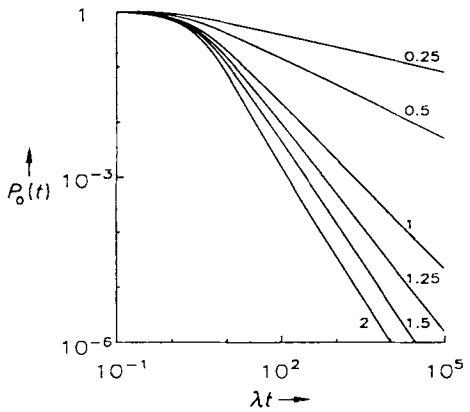

Fig. 10. Decay behavior of $P_0(t)$ for a bcc lattice under CTRW with $0.25 \leq \gamma \leq 2$, plotted on log–log scales. The γ-values are as indicated. λ is a scaling factor with the dimension s^{-1}.

In summary, in this section we have shown that the ideas of temporal and geometrical scaling (exemplified by the CTRW and by the percolation scheme) are fruitful methods for describing transport phenomena in disordered systems like polymers. In the next section we will outline some limitations of these methods.

6. Concluding Remarks

In a real physical system one cannot expect to have an infinite hierarchy of temporal or spatial scales. There always exist maximal and minimal cut-offs, like the size of the system or the distances between atoms, where the hierarchy of scales ends. Therefore, it depends on the range of the experimental parameters, whether the idea of scaling is fully applicable. Moreover, a more subtle limitation for scaling occurs when one works in the marginal regime for the critical parameters; in this regime one must be careful, since crossover effects (which may lead to a transition to normal behavior) may have to be taken into account. In such transition regions scaling is attainable only at exceedingly long times, possibly far outside the experimentally interesting range.

In order to illustrate this comment let us consider a very transparent model: we focus on a particle (charge carrier) diffusing under the influence of an external bias (electric field) on a linear chain and take the sites (traps) to have different energy levels ε with a distribution $\varrho(\varepsilon)$ (Fig. 11).

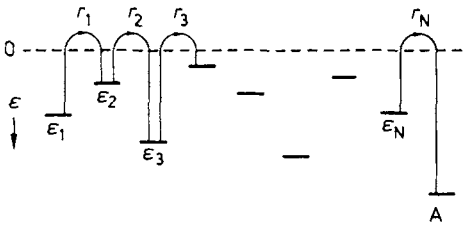

Fig. 11. Charge carrier hopping on a linear chain of equidistant sites with different trap energies ε_i and transition rates r_i. The ε_i are randomly chosen for a distribution $\varrho(\varepsilon)$. A = absorber.

Assuming thermal activation, we readily calculate the transition rates and, after averaging over the distribution $\varrho(\varepsilon)$, we get the corresponding waiting-time distribution $\psi(t)$.[110] This leads, like in the CTRW theory, to the current $I(t)$. The analysis shows that for a finite mean waiting-time $\tau = <t> = \int_0^\infty t\psi(t)\,dt$, a crossover from dispersive behavior for $t < \tau$ to nondispersive behavior for $t \gg \tau$ occurs. This is illustrated in Figure 12, which shows the current I for a Gaussian distribution of energy levels. Depending on the length N of the chain, the regime of normal transport (constant I) is more or less pronounced.

The situation is quite different for exponential energy distributions of the form (D). These lead to $\psi(t) \sim t^{-1-\gamma}$, just as considered in Section 3.

$$\varrho(\varepsilon) = \gamma e^{-\gamma\varepsilon} \qquad \text{(D)}$$

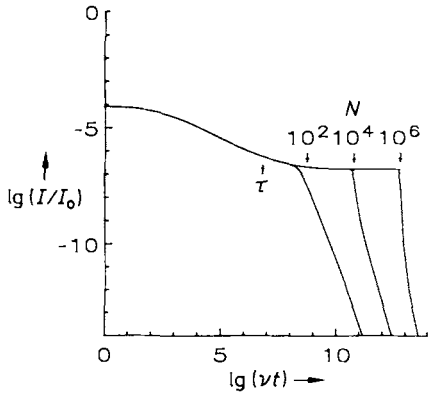

Fig. 12. Current curves for a Gaussian distribution $\varrho(\varepsilon)$ with $\varepsilon_0 = 12.5$ and $\sigma = 2.5$ for different chain lengths N. The arrows mark τ and $N\tau$, respectively. ν is a scaling factor.

For $\gamma > 1$ there exists a mean waiting-time $\tau = \gamma/(\gamma-1)$ and thus in the long-time limit the transport behavior is nondispersive. As long as γ is less than unity, the resulting current decays asymptotically as $I(t) \sim t^{-1+\gamma}$. These findings are illustrated in Figure 13. Now we have a crossover from dispersive to nondispersive behavior depending on the parameter γ. Note, however, and this is the important point here, that the time to reach the asymptotic regime diverges as γ approaches the marginal value 1. Thus, if γ is around unity, the asymptotic behavior may well be of no experimental significance.

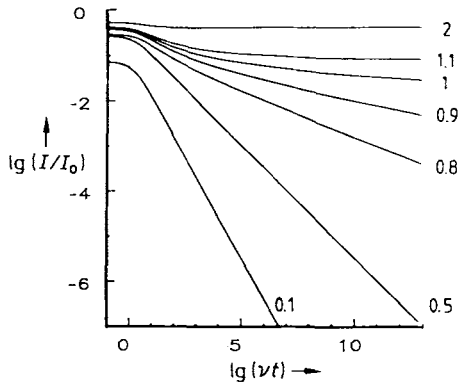

Fig. 13. Current curves for an infinite chain with an exponential distribution $\varrho(\varepsilon)$. The parameters γ are as indicated.

This example shows that the ideas of scaling are quite useful if one is well inside the range of validity of the critical parameters. However, in a marginal regime one has to be aware that a simple asymptotic scaling analysis may not be sufficient and that crossover effects have to be taken into account.

In conclusion, there is no doubt that ideas based on scaling, such as fractals and related hierarchical models have entered into almost all scientific disciplines. Scaling concepts are becoming increasingly standard for physicists and chemists, and such concepts are ideally suited for the analysis of polymers. Nevertheless, on a note of caution, it must be emphasized that not all irregular structures are ultimately

fractals; furthermore, switching now to the time scale, it must be pointed out that not all irregular time evolutions are indicative of scaling. In applications one has to be aware of crossover effects and of the fact that self-similarity is generally bounded by lower and upper cut-offs, a feature that renders the interpretation of experimental data delicate and which requires care in order to attain a sound physicochemical understanding.

The support of this work by the Deutsche Forschungsgemeinschaft (SFB 213), by the Fonds der Chemischen Industrie (grant of an IRIS-workstation) and by grants of computer time from the Hochschulrechenzentrum Bayreuth is gratefully acknowledged. We have greatly benefited from discussions with our friends and colleagues, Professors D. Haarer, J. Friedrich, J. Klafter and G. Zumofen, who have callaborated with us on many of the here-mentioned articles. Many thanks are also due to Dr. G. Zumofen for providing us with Figures 1 to 3 and 5.

Received: May 3, 1989 [A 747 IE]
German version: *Angew. Chem. 102* (1990) 158

[1] D. Stauffer: *Introduction to Percolation Theory*, Taylor and Francis, London and Philadelphia 1985.
[2] B. B. Mandelbrot: *The Fractal Geometry of Nature*, W. H. Freeman, San Francisco 1982.
[3] J. Feder: *Fractals*, Plenum Press, New York 1988.
[4] A. Amann, L. Cederbaum, W. Gans: *Fractals, Quasicrystals, Chaos, Knots and Algebraic Quantum Mechanics* (NATO ASI Ser. C235 (1988)).
[5] H. O. Peitgen, P. H. Richter: *The Beauty of Fractals*, Springer, Berlin 1986.
[6] R. Jullien, R. Botet: *Aggregation and Fractal Aggregates*, World Scientific, Singapore 1987.
[7] H. E. Stanley, N. Ostrowsky: *On Growth and Form*, M. Nijhoff, Dordrecht 1986.
[8] L. Pietronero, E. Tosatti: *Fractals in Physics*, North-Holland, Amsterdam 1986.
[9] R. Pynn, A. Skjeltorp: *Scaling Phenomena in Disordered Systems* (NATO ASI Ser. B133 (1986)).
[10] A. Blumen, J. Klafter, G. Zumofen in I. Zschokke (Ed.): *Optical Spectroscopy of Glasses*, Reidel, Dordrecht 1986, p. 199.
[11] A. Amann, W. Gans, *Angew. Chem. 101* (1989) 277; *Angew. Chem. Int. Ed. Engl. 28* (1989) 268.
[12] D. W. Schaefer, *Science (Washington) 243* (1989) 1023.
[13] D. Avnir: *The Fractal Approach to Heterogeneous Chemistry*, Wiley, New York 1989.
[14] J. Klafter, J. M. Drake: *Molecular Dynamics in Restricted Geometries*, Wiley, New York 1989.
[15] J. Mort, D. M. Pai: *Photoconductivity and Related Phenomena*, Elsevier, Amsterdam 1976.
[16] G. Pfister, H. Scher, *Adv. Phys. 27* (1978) 747.
[17] D. Haarer, A. Blumen, *Angew. Chem. 100* (1988) 1252; *Angew. Chem. Int. Ed. Engl. 27* (1988) 1210.
[18] M. F. Shlesinger, B. D. Hughes, *Physica A 109* (1981) 597.
[19] B. D. Hughes, E. W. Montroll, M. F. Shlesinger, *J. Stat. Phys. 30* (1983) 273.
[20] M. F. Shlesinger, E. W. Montroll, *Proc. Natl. Acad. Sci. USA 81* (1984) 1280.
[21] M. F. Shlesinger, *Annu. Rev. Phys. Chem. 39* (1988) 269.
[22] R. Rammal, G. Toulouse, M. A. Virasoro, *Rev. Mod. Phys. 58* (1986) 765.
[23] P. G. de Gennes: *Scaling Concepts in Polymer Physics*, Cornell University Press, Ithaca, NY, USA 1979.
[24] P. J: Flory: *Statistical Mechanics of Chain Molecules*, Wiley Interscience, New York 1969.
[25] P. E. Rouse, *J. Chem. Phys. 21* (1953) 1272.
[26] B. H. Zimm, *J. Chem. Phys. 24* (1956) 269.
[27] W. H. Stockmayer in R. Balian, G. Weill (Eds.): *Molecular Fluids*, Gordon and Breach, New York 1976.
[28] H. Yamakawa: *Modern Theory of Polymer Solutions*, Harper and Row, New York 1971.
[29] M. Doi, S. F. Edwards: *The Theory of Polymer Dynamics*, Clarendon Press, Oxford 1986.
[30] J. des Cloizeaux, G. Jannink: *Les Polymères en Solution: Leur Modelisation et Leur Structure*, Editions de Physique, Les Ulis 1987.
[31] W. Kuhn, *Kolloid Z. 68* (1934) 2.
[32] P. J. Flory, *J. Chem. Phys. 17* (1949) 303.
[33] M. Daoud, J. P. Cotton, P. Farnoux, G. Jannink, G. Sarma, H. Benoit, R. Duplessis, C. Picot, P. G. de Gennes, *Macromolecules 8* (1975) 804.
[34] H. Scher, M. F. Shlesinger, *J. Chem. Phys. 84* (1986) 5922.
[35] G. H. Weiss, J. T. Bendler, M. F. Shlesinger, *Macromolecules 21* (1988) 521.
[36] K. G. Wilson, *Rev. Mod. Phys. 47* (1975) 773.
[37] L. P. Kadanoff, W. Götze, D. Hamblen, R. Hecht, E. A. S. Lewis, V. V. Paloiauskas, M. Reyl, J. Swift, D. Aspnes, J. Kane, *Rev. Mod. Phys. 39* (1967) 395.
[38] S. K. Ma: *Modern Theory of Critical Phenomena*, Benjamin/Cummings, London 1976.
[39] J. M. Zimm: *Models of Disorder*, Cambridge University Press, Cambridge, MA, USA 1979.
[40] R. Zallen: *The Physics of Amorphous Solids*, Wiley, New York 1983.
[41] L. P. Kadanoff, *Physics 2* (1966) 263.
[42] T. W. Burkhardt, J. M. J. van Leeuwen: *Real Space Renormalization*, Springer, Berlin 1982, p. 1.
[43] K. G. Wilson, *Phys. Rev. B 4* (1971) 3174, 3184.
[44] D. Dhar, *J. Math. Phys. 18* (1977) 577.
[45] D. Dhar, *J. Math. Phys. 19* (1978) 5.
[46] B. B. Mandelbrot: *Les objects fractale: forme, hasard et dimension*, Flammarion, Paris 1975.
[47] See apart from Refs. [2] and [46] also P. Urysohn, *Verh. K. Ned. Akad. Wet. Afd. Natuurkd. Reeks 1* 13 (1927) 1.
[48] W. Sierpinski, *R. Hebd. Seances Acad. Sci. 160* (1915) 302; *ibid. 162* (1916) 629; in S. Hartman: *Oeuvres Choisies*, Editions Scientifiques, Warsaw 1974.
[49] R. Hilfer, A. Blumen, *J. Phys. A 17* (1984) L537, L783.
[50] R. Hilfer, A. Blumen in Ref. [8], p. 33.
[51] s. Alexander, R. Orbach, *J. Phys. Lett. (Orsay, Fr.) 43* (1982) L625.
[52] R. Rammal, G. Toulouse, *J. Phys. Lett. (Orsay, Fr.) 44* (1983) L13.
[53] G. Mackay, M. Jan, *J. Phys. A 17* (1984) L757.
[54] W. von Niessen, A. Blumen, *J. Phys. A 19* (1986) L289; *Can. J., For. Res. 18* (1988) 805.
[55] L. Bachelier, *Ann. Sci. E.N.S. III-17* (1900) 21 (Théorie de la spéculation).
[56] F. Spitzer: *Principles of Random Walk*, Springer, Berlin 1976.
[57] H. Scher, M. Lax, Phys. Rev. B 7 (1973) 4491, 4502.
[58] H. Scher, E. W. Montroll, *Phys. Rev. B 12* (1975) 2455.
[59] B. V. Gnedenko, A. N. Kolmogorov: *Limit Distribution for Sums of Independent Random Variables*, Addison-Wesley, Reading 1954.
[60] E. W. Montroll, G. H. Weiss, *J. Math. Phys. 6* (1965) 167.
[61] M. F. Shlesinger, *J. Stat. Phys. 36* (1984) 639.
[62] P. W. Anderson in R. Balian, R. Maynard, G. Toulouse (Eds.): *Ill-Condensed Matter*, North-Holland, Amsterdam 1983.
[63] See for instance K. J. Laidler: *Chemical Kinetics*, McGraw-Hill, New Delhi 1982.
[64] J. W. Haus, K. W. Kehr, *Phys. Rep. 150* (1987) 263.
[65] F. W. Schmidlin, *Phys. Rev. B 16* (1977) 2362.
[66] J. Noolandi, *Phys. Rev. B 16* (1977) 4466.
[67] A. D. Gordon: *Classification*, Chapman and Hall, London 1981.
[68] A. Blumen, G. Zumofen, J. Klafter in Ref. [4], p. 21.
[69] P. Pfeifer, D. Avnir, *J. Chem. Phys. 79* (1983) 3558.
[70] D. Avnir, P. Pfeifer, *J. Chem. Phys. 79* (1983) 3566.
[71] D. Avnir, D. Farin, P. Pfeifer, *Nature (London) 308* (1984) 261.
[72] P. Pfeifer in Ref. [8], p. 47.
[73] J. J. Kipling: *Adsorption from Solutions of Non-Electrolytes*, Academic Press, London 1965.
[74] J. M. Drake, P. Levitz, S. Sinha, *Mater. Res. Soc. Symp. Proc. 73* (1986) 305.
[75] J. Klafter, A. Blumen, *J. Chem. Phys. 80* (1984) 875.
[76] R. Kopelman, P. W. Klymko, J. S. Newhouse, L. W. Anacker, *Phys. Rev. B 29* (1984) 3747.
[77] R. Kopelman, *J. Stat. Phys. 42* (1986) 185.
[78] R. Kopelman, S. Parus, J. Prasad, *Phys. Rev. Lett. 56* (1986) 1742.
[79] T. Förster, *Z. Naturforsch. A 4* (1949) 321.
[80] D. L. Dexter, *J. Chem. Phys. 21* (1953) 836.
[81] U. Even, K. Rademann, J. Jortner, N. Manor, R. Reisfeld, *Phys. Rev. Lett. 52* (1984) 2164.
[82] D. W. Schaefer, B. C. Bunker, J. P. Wilcoxon, *Phys. Rev. Lett. 58* (1987) 284.
[83] D. W. Schaefer in H. E. Stanley, N. Ostrowsky (Eds.): *Fluctuations and Pattern Formation*, Nijhoff, Kluwer Academic, Boston 1988.
[84] D. Rojanski, D. Huppert, H. D. Bale, X. Dacai, P. W. Schmidt, D. Farin, A. Seri-Levy, D. Avnir, *Phys. Rev. Lett. 56* (1986) 2505.
[85] P. Levitz, J. M. Drake, *Phys. Rev. Lett. 58* (1987) 686.
[86] P. Levitz, J. M. Drake, J. Klafter, *J. Chem. Phys. 89* (1988) 5224.
[87] C. L. Yang, P. Evesque, M. A. El-Sayed, *J. Phys. Chem. 89* (1985) 3442.

[88] J. Baumann, M. D. Fayer, *J. Chem. Phys. 85* (1986) 4087.
[89] J. Klafter, A. Blumen, *J. Lumin. 34* (1985) 77.
[90] A. Blumen, J. Klafter, G. Zumofen, *J. Chem. Phys. 84* (1986) 1397.
[91] F. Bai, C.-H. Chang, S. W. Weber, *Macromolecules 19* (1986) 2484.
[92] Y. Lin, M. C. Nelson, D. M. Hanson, *J. Chem. Phys. 86* (1987) 1586.
[93] D. R. Coulter, A. Gupta, A. Yavrouian, G. W. Scott, D. O'Connor, O. Vogl, S.-C. Li, *Macromolecules 19* (1986) 1227.
[94] H. F. Kauffmann, B. Mollay, W.-D. Weixelbaumer, J. Bürbaumer, M. Riegler, E. Meisterhofer, F. R. Aussenegg, *J. Chem. Phys. 85* (1986) 3566.
[95] A. Takami, N. Mataga, *J. Phys. Chem. 91* (1987) 619.
[96] W. G. Rothschild, M. Perrot, F. Guillaume, *Chem. Phys. Lett. 128* (1986) 591.
[97] T. Kirski, J. Grimm, C. von Borczyskowski, *J. Chem. Phys. 87* (1987) 2062.
[98] Po-Zen Wong, *Phys. Today 41* (1988) No. 12, p. 24.
[99] G. E. Archie, *Trans. Am. Inst. Min. Metall. Eng. 146* (1942) 54.
[100] J. N. Roberts, L. M. Schwartz, *Phys. Rev. B31* (1985) 5990.
[101] R. Lenormand in J. R. Banavar, J. Koplik, K. W. Winkler (Eds.): *Physics and Chemistry of Porous Media II (AIP Conf. Proc. 154* (1987) 243).
[102] H. Schnörer, H. Domes, A. Blumen, D. Haarer, *Philos. Mag. Lett. 58* (1988) 101.
[103] H. Domes, R. Leyrer, D. Haarer, A. Blumen, *Phys. Rev. B36* (1987) 4522.
[104] R. Silbey in V. M. Agranovich, R. M. Hochstrasser (Eds.): *Spectroscopy and Excitation Dynamics of Condensed Molecular Systems,* North Holland, Amsterdam 1983, p. 1.
[105] R. Kopelman in Ref. [104], p. 139.
[106] A. I. Burshtein, *Sov. Phys. Usp. (Engl. Transl.) 27* (1986) 579.
[107] H. Kellerer, A. Blumen, *Biophys. J. 46* (1984) 1.
[108] J. Knoester, J. E. van Himbergen, *J. Chem. Phys. 84* (1986) 2990.
[109] H. Schnörer, A. Blumen, J. Singh, A. Thilagam, *Chem. Phys. Lett. 160* (1989) 80.
[110] H. Schnörer, D. Haarer, A. Blumen, *Phys. Rev. B38* (1988) 8097.

Highly Reactive Intermediates from the Cocondensation Reactions of Iron, Cobalt and Nickel Vapor with Arenes**

New Synthetic Methods (80)

By Ulrich Zenneck*

In 1969, *P. L. Timms* reported the first preparative cocondensation reactions of metal vapors with organic and inorganic substrates. The use of this technique in preparative chemistry soon spread rapidly, but in recent years there has been less activity in this sector. If metal atom reactions are not utilized primarily for the formation of new products, but for the synthesis of highly reactive intermediates, a new synthetic strategy may be developed. Our aims are reaction sequences which, based on an effective cocondensation reaction, lead gradually and selectively to new substance classes. This principle can be illustrated by the example of the cocondensation products of arenes and iron, cobalt, or nickel vapor, which decompose between −70 and −50 °C. The classes of products accessible by this method extend from clusters, through π-complexes, organophosphorus and organoboron cage compounds to pure organic cycloaddition products.

1. Introduction

Many chemical reactions require an activation process. In the case of a transition metal complex, this can mean that a coordination site is opened up in a preceding reaction. The substrate molecule can then directly attack at the center. On the other hand, thermal or photochemical excitation of the central particle gives rise to a highly energetic state, which is particularly reactive. A special type of excitation is the production of free atoms by the vaporization of nonvolatile elements. These exhibit enhanced reactivity since:

- They are free of ligands, which could kinetically hinder any reaction; substrate molecules encounter atoms with each collison.
- The atoms possess a high potential energy, so that reactions are mostly exothermic.

The combination of both of these factors suggests that the reaction of free atoms with ligands should be carried out at low temperature, and this is generally the case. In practice, the region between −100 and −196 °C has proved to be the best for preparative work.

The first work of this kind was carried out in 1963 by *Skell* et al. on the vaporization products of graphite.[1] In 1969, *Timms* cocondensed transition metal vapors with organic substrates for the first time.[2] This initiated a rapid increase in the amount of work being carried out in this field, which appeared in several reviews[3] and monographs.[4, 5]

Neglecting the certain, gradual coupling of ligands to a free metal atom, the simplified energetic course of a metal atom reaction can be represented by Figure 1.

The vaporization of metals requires a relatively high vaporization enthalpy. In the case of transition metals, this energy is, on the whole, higher than for the C–C bond.[6] If an atom is introduced into a cooled matrix or solution of substrate molecules, there are two reaction pathways available to it. Either the desired reaction with the ligand results, with formation of the monomeric complex ML_n, or the metal atoms react with each other to give clusters M_xL_y, which often then aggregate to a metallic state.[7] Cluster formation is generally the kinetically and thermodynamically favored process.[3e] Thus, to obtain noticeable yields of the monomeric complex, it is necessary to use large excesses of the ligand molecules (at least 10:1, better 50:1). Therefore, this method is limited to ligands which are readily available and easily vaporized or highly soluble at low temperature. The complex forming reactions are mostly strongly exothermic, due to the high potential energies of the metal atoms. A clear tendency to give side reaction results, as can be seen in the example of transition metal atom/alkyne reactions.[8] This is not such a problem if, first of all, a highly reactive intermediate complex is generated in a metal atom reaction, and then allowed to react in situ to give the desired complex. This simultaneously results in an increase in the usefulness of metal atom reactions which can be worked with on a stoi-

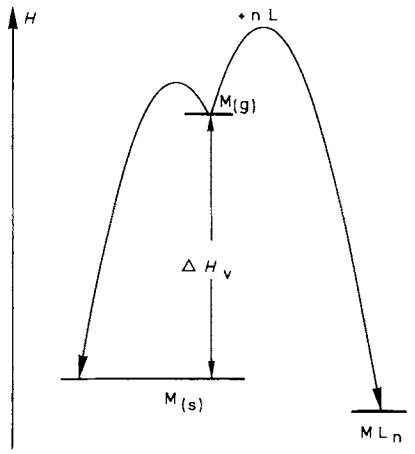

Fig. 1. Simplified representation of the energetic course of a metal atom reaction (arbitrary units) ΔH_v = vaporization enthalpy.

[*] Priv.-Doz. Dr. U. Zenneck
Anorganisch-Chemisches Institut der Universität
Im Neuenheimer Feld 270, D-6900 Heidelberg (FRG)

[**] Reactive π-Complexes of Electron-rich Transition Metals, Part 10.—Part 9: D. Hu, H. Schäufele, H. Pritzkow and U. Zenneck, *Angew. Chem. 101* (1989) 929; *Angew. Chem. Int. Ed. Engl. 28* (1989) 900.

 © VCH Verlagsgesellschaft mbH, D-6940 Weinheim, 1990 0570-0833/90/0202-0126 $ 02.50/0

chiometric basis at the second stage. The simplified energy diagram of this reaction pathway is shown in Figure 2.

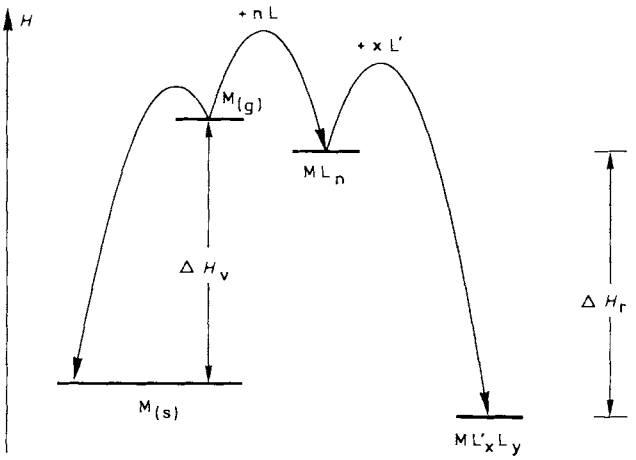

Fig. 2. Energy diagram of a two step synthesis involving a metal atom reaction and a highly reactive intermediate (arbitrary units) ΔH_r = reaction enthalpy of the second step.

The first examples of this type again came from the research groups of *Skell* and *Timms*, who allowed bis(arene)-iron[2] to react at about $-60\,^{\circ}C$ with PF_3. The result was the simple substitution of an arene ligand with formation of $[(\eta^6\text{-arene})Fe(PF_3)_2]$.[9, 10]

A systematic exploitation of the high energy available in the intermediate step is only possible, however, if the pathway outlined in Figure 2 is broadened. The aim of the resultant reaction of the cocondensation product ML_n (ML_n = reactive intermediate step **A**) should preferably not be a thermodynamically stable product, but another reactive particle which thermally decomposes below room temperature. Thus, from the partially extremely unstable cocondensation products **A**, one can obtain new, reactive, isolable intermediates **B** which can be optimized to the requirements of the desired synthetic aim. This step may be repeated, such that further reactive but more easily handled complexes **C** are synthesized from the isolable intermediates **B**. In the end, a cascade **A** → **B** → **C** → **D** etc. of slightly exothermic reactions results from metal atom product **A**. Thereby emerged the following hypotheses:

- If the energy changes between the single steps are small, then the reactions can be carried out selectively.
- The more intermediate steps, **A, B, C, D** etc. that can be carried out, the greater is the variability of the resulting chemistry.

In principle, this concept contains no limitations with respect to the metal or substrate which can be used.

The present review is intended to show some of the possibilities, for instance, of cocondensation products of iron, cobalt and nickel vapor with arenes. We are particularly interested in the cyclization reactions of unsaturated organic molecules in the coordination sphere of reactive metal complexes. By using new intermediates, we are looking for novel aspects of this reaction type, as compared with the known systems.

2. Areneiron Complexes

The first reaction of iron atoms with an arene was reported in the very first communication on metal atom chemistry by *Timms* in 1969.[2] The resulting bis(benzene)iron **1a** exploded at about $-50\,^{\circ}C$. As has already been described in Sec-

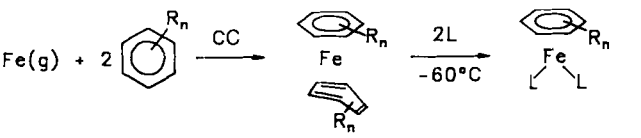

1a-e

1a: R_n = H **1b**: R_n = Me **1c**: R_n = 1,4-Me_2
1d: R_n = CF_3 **1e**: R_n = 1,4-F_2

tion 1, the thermally labile arene/iron cocondensation products can react with ligands at ca. $-60\,^{\circ}C$ to give stable complexes of the type $[(\eta^6\text{-arene})FeL_2]$. Ligands which have been added by this route are: PF_3,[9, 10] $P(OR)_3$, PR_3, diolefins, cycloheptatriene, 1,3,5,7-cyclooctatetraene[11] and 2,2'-bipyridyl (CC = metal-ligand cocondensation).[12]

The structures of the cocondensation products of iron atoms with arenes were disputed for a long time, for the results of the investigations are dependent on the concentra-

Ulrich Zenneck was born in 1946 in Clausthal-Zellerfeld/West Germany. After professional training as a dairyman and four years service in the federal border police, he studied chemistry at the Universities of Clausthal und Marburg. In 1980 he received his Ph.D. from the University of Marburg, under the supervision of Christoph Elschenbroich. He left Marburg for postdoctoral studies with P. L. Timms in Bristol (UK) (1980/81) and moved to the University of Heidelberg thereafter, where he finished his habilitation in 1988. He is now teaching there. His scientific interests are centered on preparative organometallic chemistry, starting with metal vapors, and redox reactions of transition metal complexes. His investigations of redox processes involve the utilization of electrochemical and ESR and NMR spectroscopical characterization of paramagnetic redox products.

tions of the species involved, as well as on the reaction temperature. In principle, 1:1 and 2:1 complexes, as well as clusters can be postulated. In the case of the 2:1 complexes η^6:η^6-, η^6:η^4- and η^4:η^4-structures have been discussed.[13-18] The requirements of preparative metal atom chemistry clearly favor the η^6:η^4-structure type for benzene and toluene.[16,17] In contrast to this, the stable bis(hexamethylbenzene)iron has an η^6:η^6-structure, and can be prepared by classical methods.[19]

In a number of cases, a three component reaction of Fe(g) with arenes and ligands L has proved to be an alternative for the formation of [(arene)FeL_2] complexes.[11] This is particularly true for benzene, since **1a** usually gives only low yields in substitution reactions with ligands.

2.1. Synthesis of Novel, Highly Reactive Areneiron Complexes

Olefinic ligands can be rapidly substituted well below room temperature in the case of cyclopentadienylbis(olefin)cobalt and tricarbonylbis(olefin)iron complexes, which are isoelectronic with areneiron complexes.[20,21] Thus, (η^6-arene)bis(alkene)iron complexes seemed to be promising candidates for novel reactive intermediates. On the other hand, there was the opportunity to replace the (η^4-arene)-ligands of bis(arene)iron by naphthalene derivatives. This can offer additional bonding energy via better π-conjugation of the uncoordinated naphthalene ring. Accordingly an (η^6-arene)(η^4-naphthalene)iron complex of type **3** should be more stable than an (η^6-arene)(η^4-arene)iron complex of type **1**. But it can still be assumed that the η^4-bonded naphthalene may be substituted by other ligands as also (η^6-naphthalene)-ligands can easily be exchanged.[22] Until now, structurally confirmed (η^4-naphthalene)metal complexes have been confined to only two examples with one 4d- and one 5d-metal respectively.[23,24,25] Naphthaleneiron complexes have thus far only been obtained by matrix isolation in spectroscopic quantities.[17] Earlier reports of a [(naphthalene)$Fe(CO)_3$] complex[26] were soon questioned.[27]

Bis(toluene)iron **1b**, freshly prepared by cocondensation, is stirred in the temperature range −80 to −40 °C under an atmosphere of ethene. A 56% yield of bis(ethene)-tolueneiron **2** is obtained, calculated from the amount of iron which is vaporized.[28] Since it is impossible to direct all of the metal vapor produced into the cocondensation zone,[5] only about two-thirds of the metal atoms can react with the toluene. The remainder form a metal layer on exposed surfaces of the apparatus. Thus, the chemical yield of the reaction is in excess of 80%. We usually vaporize 5–10 g of iron, or other 3d-metals, over a period of 1–2 hours in our "home-made" apparatus, thus obtaining 10–20 g of **2** in less than a day.[28] Other complexes described herein are also attainable in similar quantities. Cocondensation apparatus of comparable efficiency are also commercially available. **2** decomposes in solution above −20 °C, and as crystals at 0 °C. Long term stability can be obtained by storage at −78 °C under ethene. Decomposition products are the ligands and metallic iron. Despite its instability, **2** could be characterized spectroscopically and by crystal structure analysis.[28]

Reaction of 1-methylnaphthalene and **1b** in the temperature range −80 to −40 °C, furnishes orange-brown (η^4-1-methylnaphthalene)(η^6-toluene)iron as a mixture of two isomers, **3a** and **3b**, in the ratio 5:3.[29]

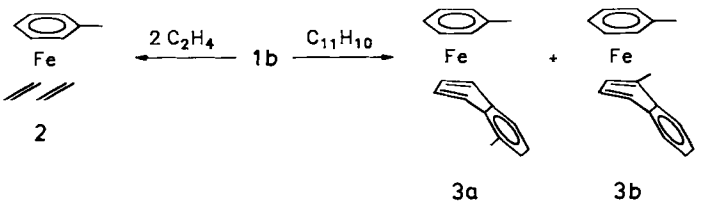

3a and **3b** can be subjected to work-up by normal chromatographic techniques at −30 °C. However, a successful separation cannot be achieved by column chromatography. Apart from their NMR spectra, there are no noticeable differences between **3a** and **3b**. They both decompose at ca. 0 °C, to the ligands toluene and 1-methylnaphthalene, and metallic iron.

The (1,4-dimethylnaphthalene)(*p*-xylene)iron derivatives **4a** and **4b** are analogous to **3**, and also have very similar properties. They are most conveniently synthesized in a three component reaction between iron atoms and the ligands. Again, the 5–8-η-isomer **4a** is predominant over the 1-4-η-

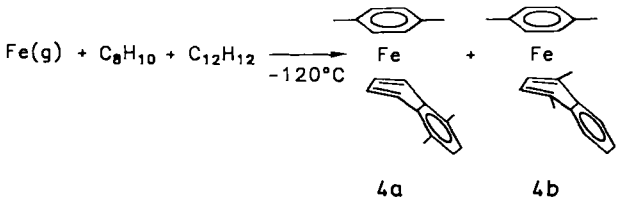

complex **4b**, but, in this case, the two isomers can be partially separated by chromatography. (5–8-η-1,4-Dimethylnaphthalene)tris(trialkylphosphite)iron **5** (orange) is obtained from 1,4-dimethylnaphthalene, the relevant trialkylphosphites and iron vapor. Neither in **5a** nor in **5b** have the 1–4-η-derivatives been observed. Unlike **3** and **4**, both **5a** and **5b** are stable up to almost 150 °C, although they are far more sensitive to oxidation.

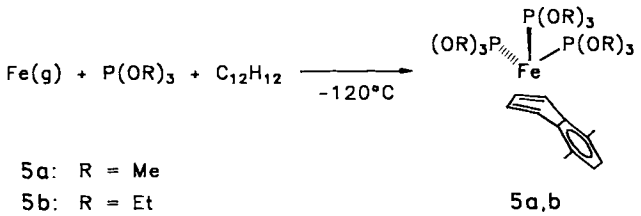

Reaction of **2** with 2-butyne and naphthalene affords the brown complex (η^6-hexamethylbenzene)(η^4-naphthalene)iron **6**, which is stable up to room temperature.[30]

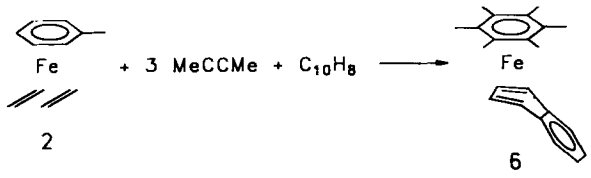

As with the other η^4-naphthalene complexes,[24, 25, 29] the bicyclic moiety in **6** is bent along the C1–C4 axis (Fig. 3). The properties of this class of substances can best be understood if one accepts that there is a very extensive decoupling of the

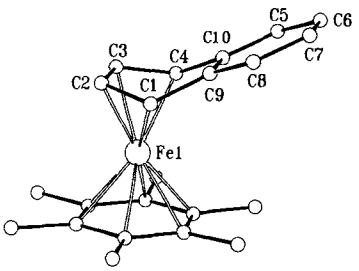

Fig. 3. Molecular structure of hexamethylbenzene(naphthalene)iron **6** in the crystalline state.

complexed π^4-system from the free π^6-system. The substances behave, both NMR-spectroscopically and in structural terms, about the same as would be expected for benzoannelated 1,3-cyclohexadiene complexes. Thus, the dihedral angle in the partly coordinated six-membered ring is $40 \pm 2°$ in the naphthalene complexes **5a** and **6**, as well as in the cyclohexadiene complex **31b** (see Section 2.3). Also, the ^{1}H- and ^{13}C-NMR shifts for the corresponding nuclei of the ligands of both substance types lie close to one another,[11, 29] and the free rings of the bicyclic moieties are influenced little by the metal.

Upon stirring a mixture of **1b** and 1,3,5,7-cyclooctatetraene (COT) variable amounts of the known complex cyclooctatetraene(η^6-toluene)iron[11] and the dinuclear complex μ-cyclooctatetraenebis[(η^6-toluene)iron] **7** are formed, depending on the concentration ratios used. **7** is obtained as a mixture of different structural isomers.[31]

Using an excess of **1b** gives **7** as the major product. Red solutions of **7** stored at $-78\,°C$ in aliphatic solvents, quantitatively decompose overnight to give cyclooctatetraene(η^6-toluene)iron and metallic iron. Solutions in toluene or benzene are stable up to 20 °C, and then slowly form metallic mirrors. Crystals of **7** are stable up to 70 °C, and then decompose in the same way as in solution.

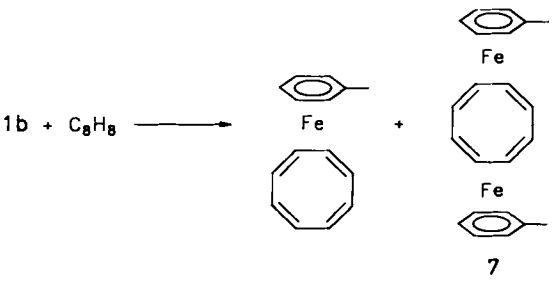

2.2. Substitution Reactions with Unsaturated Boron-Containing Heterocycles

As with **1**, the initial product of the cocondensation of arenes with iron, the novel reactive areneiron complexes **2, 3, 4, 6** and **7** also give substitution reactions at temperatures below room temperature with ligands such as phosphanes, phosphites, diphosphanes, dienes and CO. These always form complexes of the type [(arene)FeL_2] in the first step.[28–31] If one disregards the more easily handleable complexes which have been used here as educts, the reactions do not, in principle, differ from the well-known analogous reactions of derivatives of **1**.[9–12]

Since boron heterocycles possess a number of interesting ligand properties,[32] we decided to check whether the reactive complexes accessible from cocondensation reactions would allow, should the situation arise, a route to areneiron sandwich complexes with unsaturated boron-containing heterocycles as second ligand.

On allowing 3,4-diethyl-2,5-dihydro-2,5-dimethyl-1,2,5-thiadiborole **8** to react with **1a–1e** or **2**, the red compounds (η^6-arene)(η^5-dihydrothiadiborole)iron **9a–9e** are obtained as substitution products,[33] while 2,3-diethyl-1,4-dimethyl-1,4-diboracyclohex-2-ene **10**[34] and **1b** form the orange-red sandwich complex **11** containing an (η^6-diboracyclohexadiene) ligand by dehydrogenative complexation.[35]

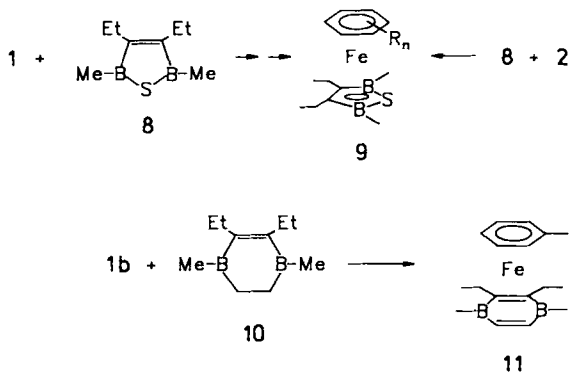

The reaction of the tetraethyl(methyl) derivative **12a** of 2,3-dihydro-1*H*-1,3-diborole with **1b** follows a complex pathway.[36] The desired substitution product, (η^5-tetraethyl(methyl)dihydrodiborole)(η^6-toluene)iron **13a** (orange-red), can actually be obtained. What is particularly interesting is the reaction of the thermally labile intermediate **15** with concentrated HCl, which is unusual in organometallic chemistry. Without this reaction, the only stable iron complex isolated from **1b** and **12a** is the hydrogenation product **16**. X-ray and neutron diffraction experiments carried out on single crystals of **13a**[32, 36] show that in this complex, a pentacoordinated carbon atom (C-2) exists which has enhanced reactivity—similarly to the electronically isovalent cyclopentadienyl cobalt complex of **12a**.[37] Thus, **13a** can be deprotonated at C-2, quantitatively forming the corresponding complex anion.

The reactivity of the C2–H bond of complex **13a** allows a rapid and effective reaction with **1b** at low temperatures which is much faster than the reaction of **1b** with **12a**, but

leads to the same result. The combination of electrochemical[38] and ESR-spectroscopical measurements on the reaction mixtures of **1b** with **12a** or **1b** with **13a**, furnishes results from which a reaction hypothesis might be derived.

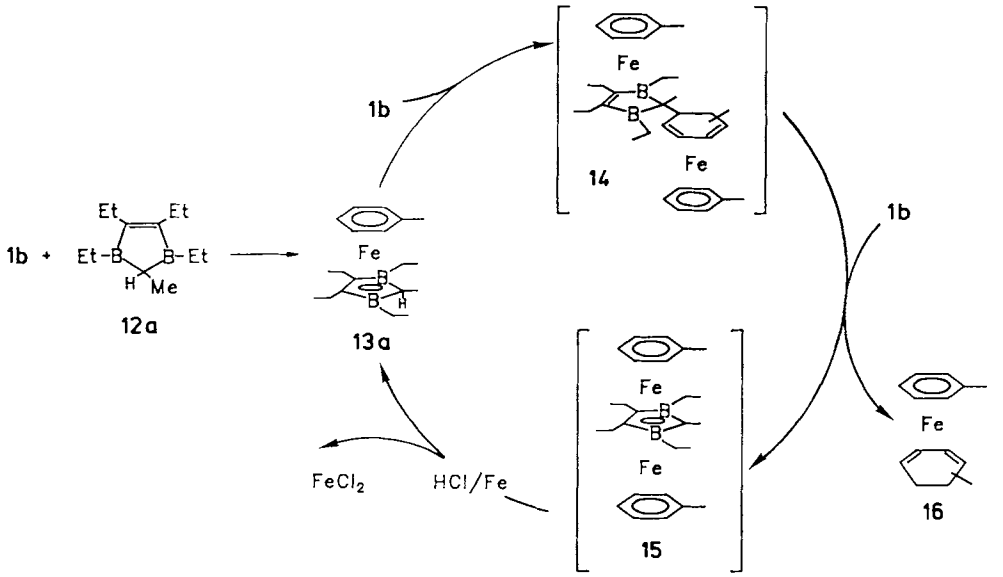

From the measurements it emerges that the end product **13a** is concomitantly the first intermediate of the reaction sequence. A large number of oligodecker sandwich complexes containing the (μ,η^5-dihydrodiborolyl)(η^6-toluene)iron unit can be synthesized from **13a** and its deprotonated product,[32,39] thus confirming the structures proposed for **14** and **15** on the basis of spectroscopic data.

Unlike **1b**, **3** does not react with **12a**, while reaction of **2** with **12a** gives only small amounts of the substitution product **13a**, along with the (η^6-toluene)iron complex of a product formed by ethene insertion into **12a**. An alternative route to derivatives of **13** is the reaction of **2** with the diborafulvene **17**[41] under an atmosphere of hydrogen. In this reaction, a molecule of hydrogen is added across the exocyclic double bond, whereupon the diborafulvene is transformed into a 2-isopropyldihydrodiborole derivative, and forms the sandwich complex **13b**.[42]

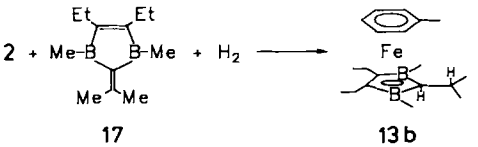

2.3. Substitution of Arene Ligands

In benzenebis(trimethylphosphane)iron **18**,[11] either the arene, the phosphane, or the entire ligand sphere can be substituted at room temperature, depending on the choice of substrate. This is contrary to the reactions described in Section 2.2. Typical examples of the numerous products accessible from **18** are complexes of the type [(benzene)FeL_2] **19**, [(indenyl)FeL_2H] **20** (or analogous cyclopentadienyliron complexes), as well as CC-coupling products such as the bridged ferrocene derivative **21**.[43]

18 has proved to be a versatile reagent for these reactions, and is rapidly accessible on a 20 g-scale, like **2** and **3**, in a three component reaction of iron vapor with the ligands.[43]

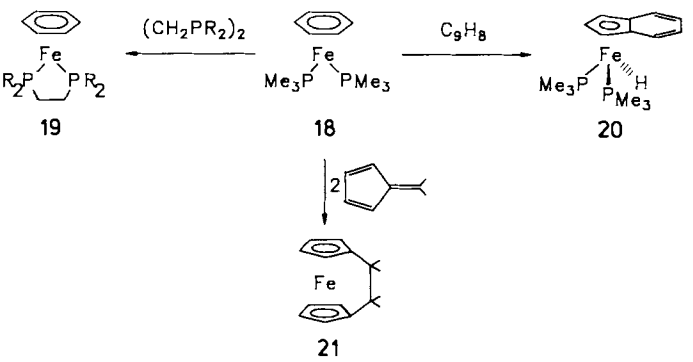

Arenebis(trimethyl phosphite)iron **22** is obtained almost quantitatively from **1**,[11] **2** or **3**[29] by ligand exchange with trimethyl phosphite. If it is allowed to react with additional trimethyl phosphite and organic chloro compounds, it will also lose its arene ligand.[44]

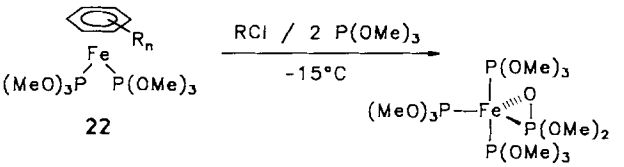

RCl = $CHCl_3$, $CDCl_3$, $MeCCl_3$, $PhCH_2Cl$

R_n = H, Me, 1,4-Me_2, 1,3,5-Me_3

The formation of the dark green, paramagnetic iron complex **23** requires a Michaelis-Arbusov reaction, in which a methyl group is removed, as well as an exchange of the arene for additional phosphite ligands. According to the ^{31}P-hyperfine structure observed in the ESR spectrum ($a_1 = 2.69$, $a_2 = 3.06$, $a_3 = a_4 = 3.63$ mT; $<g> = 2.063$), the dimethylphosphonate ligand cannot be σ-bonded;[45] rather, it suggests an η^2-coordination, which otherwise is only known in thiophosphonate ligands.[46] It shows good correlation with the ESR data of 17-valence electron (VE) complexes of the type $[(\eta^3\text{-allyl})[P(OMe)_3]_3Fe]$.[47]

2.4. Reactions with Alkynes

Alkynes belong to the most important group of substances for cycloaddition reactions in the coordination sphere of transition metals. The opportunity presented itself to investigate their reactivity with areneiron complexes.

A number of alkynes have been cyclotrimerized by the complexes described in Section 2.1, in some cases at temperatures lower than room temperature.[31] These catalytic reactions can be of use as an effective source of further, reactive areneiron complexes, which can be converted into new alkyne complexes.[48]

Reaction of **2** with alkynes at −20 °C, followed by addition of trialkyl phosphite to the reaction mixture at less than 0 °C, leads to the the intensely blue-violet alkynetris(trialkyl phosphite)iron complexes **24a**–**24f** in fairly good yields.

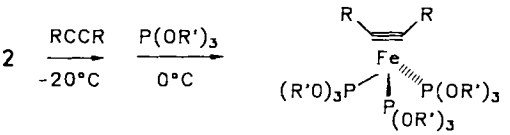

24a-f

	R	R'
24a:	Ph	Me
24b:	Ph	Et
24c:	COOMe	Me
24d:	COOMe	Et
24e:	$SiMe_3$	Me
24f:	$SiMe_3$	Et

Hitherto, **24a** and **24b** were only available in small amounts by another route.[49] Both the ^{13}C-NMR signals for this series of complexes ($\delta(^{13}C)$ for the sp carbons lies between 178 and 206, cf. Ref. [50]) as well as the results of the crystal structure analysis of **24a** (Fig. 4) indicate that the alkynes in these compounds use all four π-electrons in their bonding to the metal.[44] Thus, they can be viewed as 18VE complexes, which is reflected in their thermal stability.

Reaction of bis(trimethylsilyl)acetylene with **2** affords the two bis(μ-alkyne)Fe_2 clusters tetrakis[bis(trimethylsilyl)acetylene]diiron(*Fe=Fe*) **25** (dark brown)[51] and tris[bis(trimethylsilyl)acetylene]bis(trimethyl phosphite)diiron **26** (deep violet).[31] While diamagnetic **25** can be synthesized just as well from **3**, paramagnetic **26** (two unpaired electrons) is

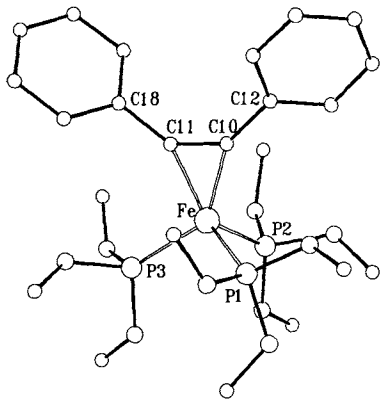

Fig. 4. Molecular structure of tolantris(trimethyl phosphite)iron **24a** in the crystal. Selected bond lengths [Å]: Fe–C10 1.896(5); Fe–C11 1.850(6).

only accessible via the route using **2**, since the trimethyl phosphite must be added at between −20 and 0 °C.

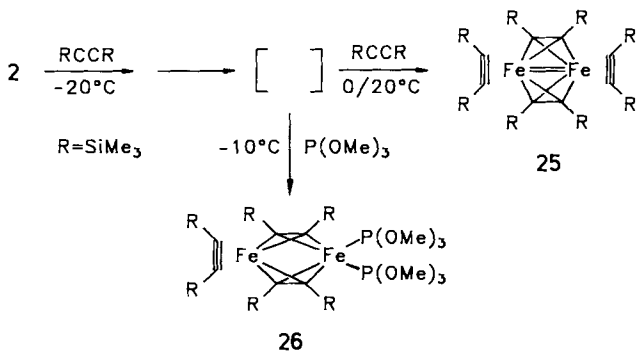

26

Since both dinuclear complexes are electronically isovalent (the terminal alkyne ligands of **25** and **26** function as π^4 ligands as in **24**), the structural (Fe–Fe distance: **25**, 2.46 Å;[51] **26**, 3.08 Å[52]) and magnetic[53] differences between them are noteworthy.

25 is the first, structurally characterized, homoleptic alkyne metal cluster. The practically quantitative route from **2** or **3**, directly illustrates the great advantage of a "roundabout" approach to the synthesis using reactive intermediates. The product formed by the direct cocondensation of iron atoms with bis(trimethylsilyl)acetylene has been de-

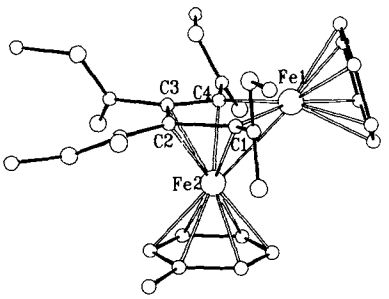

Fig. 5. Molecular structure of {(η^6-toluene)[η^5-1-(η^6-toluene)-2,3,4,5-tetrakis(methoxycarbonyl)ferrole]}iron **28b** in the crystal. The toluene ligand of Fe1 is rotationally disordered.

scribed as a non-stoichiometric substance,[54] which also obviously contains some of **25**.

The C–C linkage of two alkynes in the catalytic cyclotrimerization by areneiron complexes leads presumably first of all to ferrole complexes of the type **27**. The likely existence of these can be demonstrated by allowing an excess of **1b** to react with an alkyne. Dark green, complex-stabilized ferroles **28** are formed (Fig. 5). Tetraphenylcyclobutadiene(toluene)iron **29** (Fig. 6), which is a σ-π rearrangement

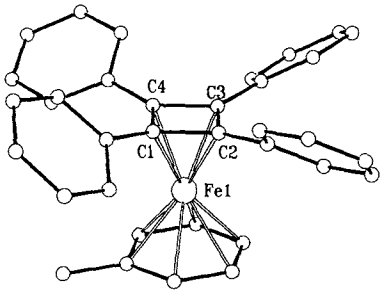

Fig. 6. Molecular structure of (η^4-tetraphenylcyclobutadiene)(η^6-toluene)iron **29** in the crystal. Selected bond lengths [Å]: Fe–C(C_4R_4) 2.002–2.050; Fe–C-(toluene) 2.036–2.138.

product of the ferrole, and the hydrogen addition product tetraphenylbutadiene(toluene)iron (**30**, Fig. 7) are formed together from **1b** and tolan.[48] The origin of the hydrogen for the formation of **30** has not been explained in this instance. Hydrogen addition reactions have also been observed with other derivatives of **1**.[55]

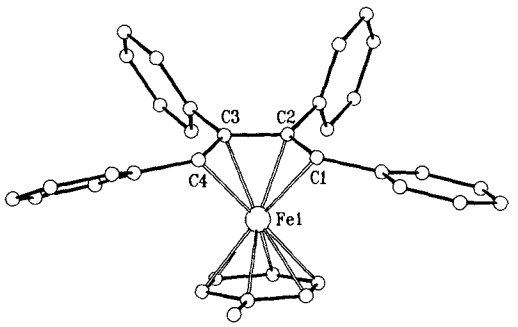

Fig. 7. Molecular structure of (η^4-tetraphenylbutadiene)(η^6-toluene)iron **30** in the crystal. Selected bond lengths [Å]: Fe–C($C_4R_4H_2$) 2.060–2.113; Fe–C-(toluene) 2.007–2.115.

29 and **30** form a pair of electronically isovalent complexes. The Fe–C distances differ only very little, while other properties are markedly different. Thus, for example, **29** can be reversibly oxidized and reduced, which is very unusual for a mononuclear areneiron complex, and it only starts to thermally decompose at about 500 °C.[44] **30**, however, like most other (arene)FeL_2 complexes, is air sensitive and decomposes at 210 °C.

The important synthetic value of reactions of reactive areneiron complexes with alkynes is shown by the [2+2+2]-cycloaddition of two alkynes with one olefin. Here, 1,3-cy-

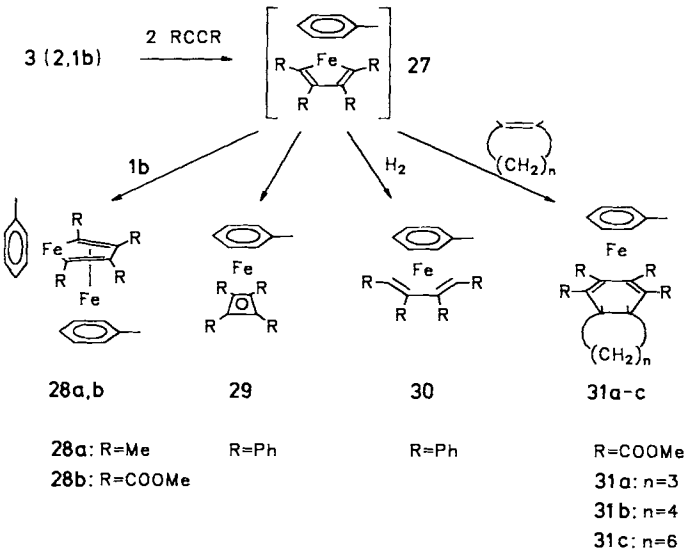

clohexadienes are formed in the coordination sphere of the metal, and bound as ligands, as in the analogous reactions of cyclopentadienylcobalt complexes.[56] However, contrary to the cobalt system, the reaction of the iron complexes (**3** is most suitable in this case) is strictly stereoselective. For example, upon addition of cyclic mono- or diolefins, the olefinic ring inserted into complexes of the type arene(cyclohexadiene)iron **31** are always found in the *exo*-position.[48] The *endo*-isomers cannot be detected NMR spectroscopically. A reason for the higher stereoselectivity of the iron complexes could primarily be the low reaction temperatures used—maximally room temperature—while for the cobalt complexes more than 70 °C is required.[56] Decomplexation of the ring bound to the metal in **31** and other related complexes is simple. After addition of $Fe^{3\oplus}$-salts to solutions of the complexes, the ligands can be almost quantitatively isolated.

The cyclotrimerization products of alkynes have also been fixed directly as complex ligands, and the reaction using 1,5-cyclooctadiene (COD) affords arene(cyclooctadiene)-iron derivatives **32** in high yield.[44]

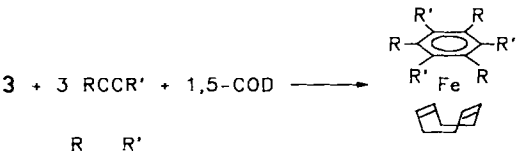

	R	R'
32a:	H	H
32b:	Me	Me
32c:	Et	Et
32d:	H	*t*Bu

In this case, the entire ligand sphere of the iron has been exchanged. Hence, for formation of benzene-, 1,3,5-trialkylbenzene- or hexaalkylbenzene-complexes, one can also start with tolueneiron complexes **2** or **3**, both of which are readily accessible. Hexamethylbenzene(naphthalene)iron **6** (see Section 2.1) offers the additional possibility of carrying out such a synthesis stepwise. Firstly, the areneiron fragment is formed from **2** and the alkyne between −20 and +20 °C,

and then the naphthalene is slowly replaced at room temperature by the desired ligands.

2.5. Reactions with *tert*-Butyl Phosphaacetylene

tert-Butylphosphaacetylene **33**[57] was first used in metal-catalyzed cycloaddition reactions in 1986.[58] Since then its chemistry has developed exceedingly quickly.[59, 60] Since the ligand sphere of the reactive areneiron complexes can be completely exchanged for alkynes, we hoped that addition of phosphaalkyne **33** would lead to formation of larger oligomers at the iron center.

The reaction of **3** with **33** in molar ratios from 1:2 to 1:5 between 0 and 20 °C yields the cyclodimer of **33**, which is bound as a ligand in 1,3-diphosphete(toluene)iron **34** (orange) and the sandwich complexes **35** (olive), **36** (green), and **37** (green)[61, 62] containing 1,3-diphospholyl- and 1,2,4-triphospholyl ligands. The formation of these ligands must also involve cleavage of the P–C triple bond in **33**.

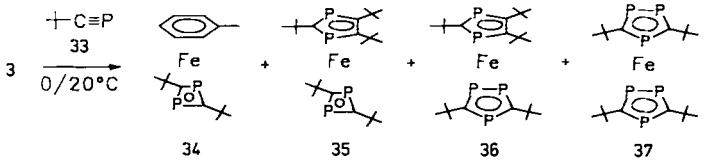

34 is a diphosphorus analogue of the cyclobutadiene complex **29**; the properties of the two complexes manifest their close relationship. **36** and **37** can be regarded as penta- and hexaphosphaferrocene derivatives respectively. However one should distinguish **36** from the similarly green pentaphosphaferrocene derivative containing a *cyclo*-P_5 ligand, which has recently been described by *Scherer* et al.[63]

Although one must accept that **36** is formed via an exceedingly complex reaction pathway, nevertheless five complete molecules of **33** react with one molecule of **3** in the formation of both five-membered rings. For **35** and **37**, things are more complicated. In these compounds, the ratio of the P/C units of the phosphaalkyne is not 1:1. In **35**, there are four phosphorus atoms and five C–R fragments, while for **36** the ratio is 6:4. This has to be interpreted in terms of an intermolecular exchange of these groups, at least in the early stages of the isolated complexes.

By using a very large excess of phosphaalkyne in the reaction of **3** with **33** (which offers no problems, due to its improved accessibility[64]), the consumption of about 9 moles of **33** per mole of **3** is observed in less than a day at room temperature.[65]

Aside from **34** to **37**, which are present in lower proportions than when using smaller amounts of **33**, a product mixture is now obtained which was shown by medium pressure chromatography to contain at least ten other iron-containing fractions. After repeated MPLC of this mixture, the complexes $(PCCMe_3)_6Fe$ **38** (dark brown, paramagnetic), $(PCCMe_3)_7Fe$ **39** (olive brown, paramagnetic), and $P_8(CCMe_3)_7HFe$ **40** (red, diamagnetic) were isolated in small quantities and characterized.[65, 66]

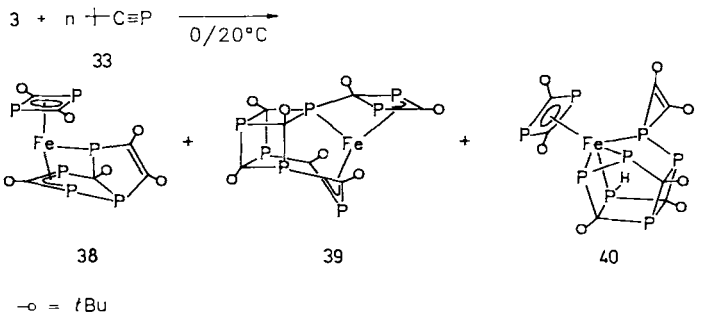

38[66] and **39** are thermally stable 16VE complexes, which are clearly distinguishable in this respect from other 16VE complexes of iron.[67] In **38** (Fig. 8), as in **34** and **35**, there is

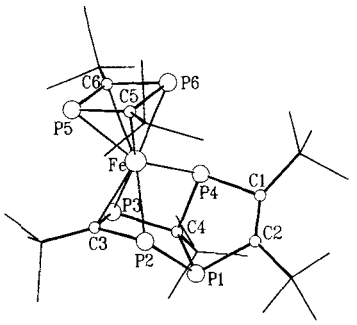

Fig. 8. Molecular structure of $(PCCMe_3)_6Fe$ **38** in the crystal.

a diphospheteiron fragment which is bound to a bicyclic tetramer of **33** in a complex. The interaction of the tetramer with iron takes place via a 1,3-diphosphaallyl grouping and a P–Fe σ bond. In **39** (Fig. 9), the ligand is formed by a

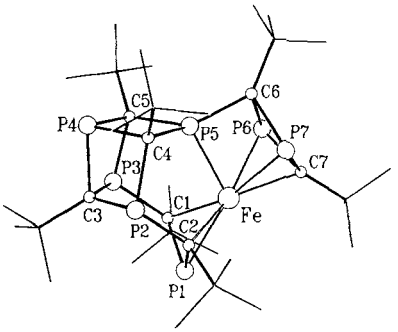

Fig. 9. Molecular structure of $(PCCMe_3)_7Fe$ **39** in the crystal.

polycyclic heptamer of **33**. Again, there is a coordinating $P_2(CCMe_3)_2$ ring, but this is joined to a $(PCCMe_3)_5$ cage via a σ-bond between C6 and P5, and is bound as a 1,3-diphosphaallyl ligand. The cage is bound to the metal by a 2-phosphaallyl on the one side, and on the other side a coordination site is occupied by the free electron pair of the phosphorus atom P5. The skeletal framework of **40** can be described as a ferrahexaphosphapentaprismane derivative (Fig. 10),[66] in which the $P_6(CCMe_3)_5H$ moiety behaves as a tetradentate

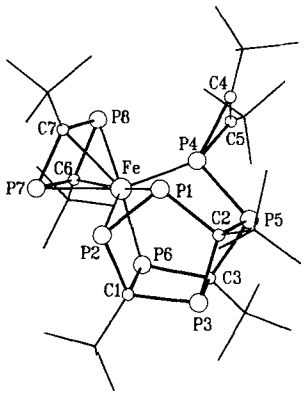

Fig. 10. Molecular structure of $P_8(CCMe_3)_7HFe$ **40** in the crystal.

P_4 ligand. In contrast to **38** and **39**, **40** has a closed shell, 18VE structure. The phosphirene ring[68] P4C4C5, which juts out of the molecule, is only bound via P4 to the framework and the metal. Thus, reaction of a larger excess of **33** with the iron complex **3** can lead to up to seven units of the phosphaalkyne being coupled around the metal to give novel types of cage structures. All attemps at the direct removal of the organophosphorus skeletal frameworks from the complexes have thus far proved unsuccessful. However, heating of the reaction mixture under vacuum at 100 °C, on completion of the above-mentioned reaction met with some success. Thus, aside from the iron complexes 38 to 40, small amounts of metal-free organophosphorus skeletal compounds can also be obtained.

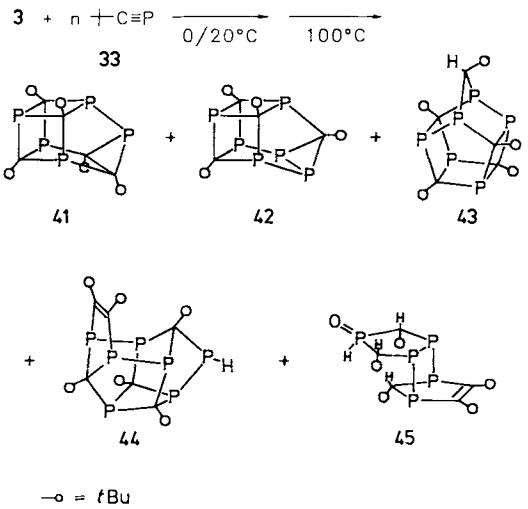

$(PCCMe_3)_5$ **41** is a polycyclic pentamer of **33**,[65] the structure of which can be derived from that of the tetraphosphacubane[69] by replacing one corner by a three-membered ring, formed by insertion of a $PCCMe_3$ unit. A structurally analogous hydrocarbon is known,[70] but not an organophosphorus compound or a polyphosphide. $P_6(CCMe_3)_4$ **42** (Fig. 11) belongs to the same structural group.[66] $P_6(CCMe_3)_5H$ **43**[65] is a heteroanalogue of homopentaprismane.[71] Like **40**, which also has a pentaprismane structure, **43** contains an additional hydrogen atom. $P_7(CCMe_3)_6H$ **44**

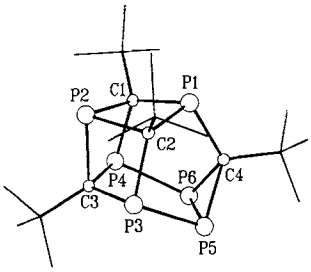

Fig. 11. Molecular structure of $P_6(CCMe_3)_4$ **42** in the crystal.

is formally derived from **43**, which has been enlarged by an additional unit of **33**. The structural form of **44** is, to our knowledge, new. Parts of the framework have similarities with organopolyphosphanes of the type P_7R_3.[72]

Tricyclic $(PCCMe_3)_5H_4O$ **45** (Fig. 12)[66] has far less internal bonding than the compounds **41**–**44**. Here, we are dealing with an oxidation product, which has, in addition, incorporated four hydrogen atoms. The pentaphosphaferrocene derivative **36**, in particular, could be considered to be an educt of **45**. Not only is the number of $PCCMe_3$ units the same in each, but also the relative orientation of the two five-membered rings. Similar correlations can be drawn between **39** and **41**, as well as **40** and **43**. In both cases, only one diphosphete-iron fragment has to be removed from the complexes, such that on formation of the new structures, the remaining frameworks can be stabilized in their most saturated and closed conformations. An explanation to this problem has been sought just as intensively as the principal question, of how these systems organize themselves around the metal center.

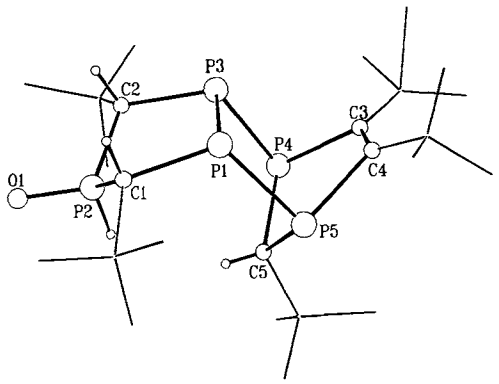

Fig. 12. Molecular structure of $(PCCMe_3)_5H_4O$ **45** in the crystal.

3. Arenecobalt Complexes

Arene/cobalt condensates have already proved useful in the formation of bis(2,2'-bipyridyl)cobalt,[73] of reactive organometallic slurries[74] and of catalytically active solutions.[75] However, up till now, it has not proved possible to attach the arenes as π-ligands to the cobalt atoms, to form cobalt complexes.

Reaction of the cocondensates **46a** to **46e** (arene = benzene, toluene, *p*-xylene, trifluoromethylbenzene 1,4difluorobenzene) in the temperature range −100 to −20 °C with alkynes [2-butyne, bis(trimethylsilyl)acetylene] yields both alkyne(arene)cobalt **47** (green, paramagnetic) and μ-alkynebis(arenecobalt) **48** (red, diamagnetic) in variable ratios, dependent on the type and concentration of the educts used.[76]

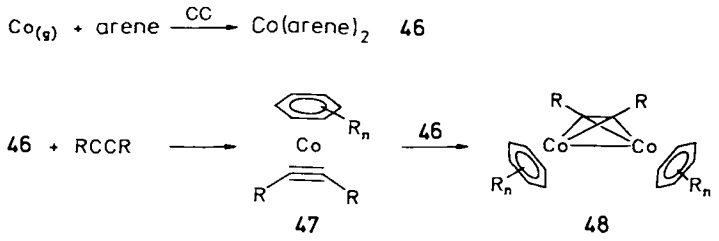

47, 48	R	R_n
a	Me	H
b	Me	Me
c	Me	1,4-Me_2
d	Me	CF_3
e	Me	1,4-F_2
f	$SiMe_3$	Me

The benzene complex **46a** reacts with 2-butyne to give **47a**. For the toluene/butyne system, the formation of **48b** is strongly favored. Addition of excess butyne to **46b** increases the amount of **47b**, so that the reaction path outlined in the scheme is assumed. In the case of toluene/$C_2(SiMe_3)_2$, the formation of **47f** is favored, and **48f** is formed in trace amounts only. As in the toluene system, the dinuclear complex **48d** is again favored in the trifluoromethylbenzene/butyne system, and the corresponding mononuclear complex **47d** can only be identified spectroscopically. In the reactions of butyne with *p*-xylene and with 1,4-difluorobenzene, the respective derivatives of **47c** and **47e**, respectively, can be observed by ESR spectroscopy. Separation of the reaction products is achieved by fractional vacuum sublimation. It must be accepted that certain losses arise during this process (**47a**–**47f** slowly decompose above room temperature).

While the dinuclear complexes **48** are analogous to $[CO_2(CO)_6(\mu\text{-alkyne})]$ clusters,[77] there was, at first, no other example comparable to complex **47**.[78] The crystal structure analysis of **47a** (Fig. 13), and interpretation of the ESR data for the series of compounds,[76] afforded unequivocable proof of the alkynes using all four π-electrons in their bonding with the metal.

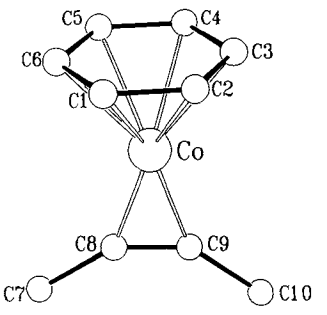

Fig. 13. Molecular structure of (η^6-benzene)(2-butyne)cobalt **47a**. Selected bond lengths [Å]: Co–C8 1.885(4); Co–C9 1.901(5).

Chemical and electrochemical oxidation experiments on **47a** and **47f**, to form **47a**$^{\oplus}$ and **47f**$^{\oplus}$, have, up till now, been unsuccessful. The lifetime of the predicted 18 VE cationic complex **47**$^{\oplus}$ is so short, even at −60 °C, that only clean, irreversible oxidations are observed.

Thermal decomposition of the mononuclear butyne complexes affords hexamethylbenzene, together with small amounts of the corresponding dinuclear complexes. These also yield the cyclotrimer of 2-butyne at higher temperatures.

Reaction of **46b**, not with alkynes, but with the N–C triple bond of acetonitrile, leads to formation of small amounts of the dark red trimetallatetrahedrane (μ_3-benzylidyne)tris(toluenecobalt) **49**,[76] and much metallic cobalt. **49** is not observed in the thermal decomposition of **46b**.

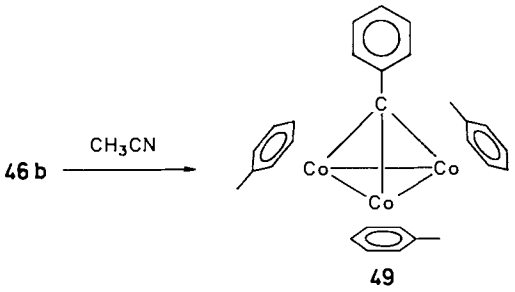

49 is closely related to **48**, and results from the formal replacement of a C–R fragment by an isolobal arenecobalt unit.

4. Arenenickel Complexes

Arene/nickel cocondensates also behave similarly to the corresponding iron and cobalt compounds **1** and **46**, respectively.[3e, 4, 5] Upon thermal decomposition of (toluene)$_2$Ni **50**[79] at about −50 °C, very finely divided nickel with a hydrocarbon coated surface is obtained, which can be used for a number of reactions.[80]

When the decomposition of **50** is allowed to take place in the presence of phosphites, $[P(OR)_3]_4Ni$ is formed.[79] In the presence of ethene, $(C_2H_4)_3Ni$ **51a**[81] is obtained, which is also accessible via classical routes.[82] Owing to the small amount of time required, and the use of very simple chemicals, together with the availability of a cocondensation apparatus, the route to derivatives of **51** via **50** is an interesting alternative to the synthesis of **51a** from cyclododecatrienenickel.

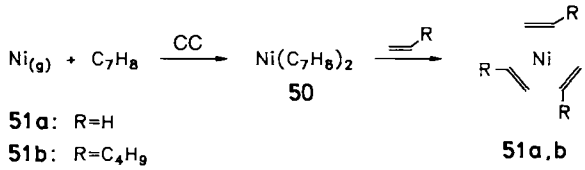

The synthesis of **51a** from **50** is complete in less than one working day, analogously to the synthesis of **2** from **1b**. Even

the yields and amounts synthesized correlate very well (10–20 g per run). Reaction of **50** with hex-1-ene instead of ethene furnishes tris(hexene)nickel **51b**, which thermally decomposes above −30 °C. The characterization of **51b** has not yet been completed.

Reaction of **51b** with the dihydrodiborole derivative **12a** (cf. Section 2.2) in a ratio of greater than 1:1 in the presence

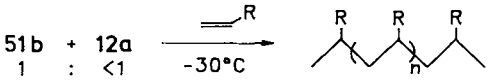

of free hexene led to rapid polymerization of the hexene above −30 °C. Ethene polymerization can also be observed in reactions of the ethene complex **51a** with **12a** or **12b** in a molar ratio greater than 1:1 below room temperature. However, the yields of polymers are clearly lower than with hexene.[83] This may be caused by the olefin concentration, since the reaction was conducted at normal pressure.

Reaction of **51a** and **12b** in a ratio of 1:1.5 at room temperature for several hours leads to formation of the novel green compound bis(diethyltrimethyl-2,3,5-tricarbahexaboranyl)nickel **52**,[84] the parent compound of a series of oligodecker sandwich complexes **53a** to **53c**, which are obtained in only small amounts via this reaction route.

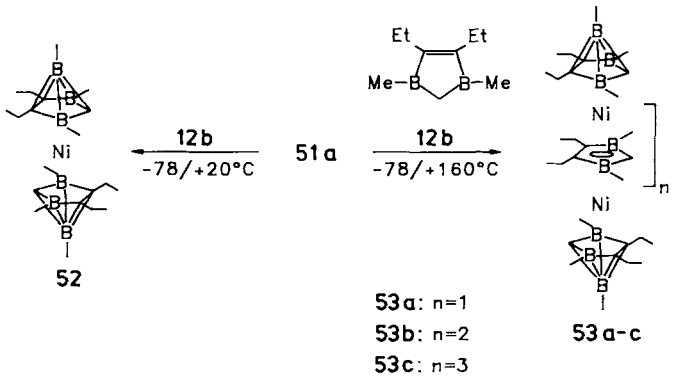

The same reaction can be optimized with regard to the yield of the known tripledecker **53a**.[85] The educts, in a ratio of 1:3, are heated to over 160 °C, without solvent, at which point, a little air is introduced to initiate partial oxidation.[86] The higher oligodeckers **53b** and **53c** can be detected, although their amounts are still small. Qualitative MO considerations show that the η^5-1,3,5-tricarbahexaboranyl ligands can be regarded as being isolobal with cyclopentadienyl ligands. **52** would then be a nickelocene analogue. In fact, all of the properties which are related to the electronic structure of the molecule can easily be understood in terms of this hypothesis.[84] This holds true, for instance, for the magnetism—which shows Curie-Weiss behavior of two unpaired electrons for both compounds and for the electrochemistry.[88] However the ESR data for the reversibly formed 19 VE-cation $\mathbf{52}^{\oplus}$ are clearly different from that for the nickelocenium ion.[89] The reason for this lies in the Jahn-Teller activity of the nickelocenium, which does not appear in **52** for reasons of symmetry.

5. Conclusion

The areneiron system, in particular, has proved its versatility in the results which have been presented and summed up in this review. The initially formulated aim to convert a few highly reactive cocondensation products gradually and selectively via further reactive, but isolable intermediates into a number of novel compound classes, could, in some cases, be achieved. For example, in the reaction sequence $Fe_{(met)} \rightarrow Fe_{(g)} \rightarrow \mathbf{1b} \rightarrow \mathbf{2} \rightarrow \mathbf{25}$, a total yield of 50% can be obtained (calculated from the amount of iron vaporized); 20 g of **25** can be prepared in two days from elemental iron. Pieces of nail or waste sheet steel have proved to be a far better source of iron for metal vaporization than pure metal powder, which tends to liberate too much gas when heated under vacuum.

The intermediates are so reactive that in several cases the entire coordination sphere of the metal complex is exchanged, even under mild conditions. Thus, novel types of structures with an organoelement framework can be built around a metal, using the appropriately reactive educts.

On searching through the literature of metal atom reactions conducted on a preparative scale and the corresponding matrix spectroscopy, it would seem that stable primary products are in the minority. Thus, we feel confident that we have revealed a much broader scope of application for highly reactive cocondensation products in systematic syntheses, than was hitherto ever thought possible.

I would like to thank my co-workers Dr. A. Funhoff, D. Hu, Dr. H. Schäufele, C. Tolxdorff, and Dr. L. Vasquez for their care, commitment and enthusiasm shown in carrying out this work. The assignment of particular projects was as indicated in the literature. Dr. H. Pritzkow performed all of the crystal structure analyses which appear in this review. Reactions involving boron heterocycles were the result of strong collaboration with Professor Dr. W. Siebert, Heidelberg, and his co-workers Dr. G. Brodt, Dr. D. Büchner, Dr. L. Suber, Dr. J.-K. Uhm, and Dr. J. Zwecker. I would like to thank them all for their outstanding cooperation, and in particular Prof. Dr. W. Siebert for giving me all the necessary support for such a project. Finally, I am most grateful to the Stiftung Volkswagenwerk, the Land Baden-Württemberg, and the Deutsche Forschungsgemeinschaft (SFB 247) for their generous financial support of this work.

Received: July 20, 1989;
supplemented: September 18, 1989 [A 748 IE]
German version: *Angew. Chem. 102* (1990) 171

[1] P. S. Skell, L. D. Wescott, Jr., *J. Am. Chem. Soc. 85* (1963) 1023; P. S. Skell, L. D. Wescott, Jr., J. P. Goldstein, R. R. Engel, *ibid. 87* (1965) 2829.
[2] P. L. Timms, *Chem. Commun. 1969*, 1033.
[3] a) P. L. Timms, *Adv. Inorg. Chem. Radiochem. 14*, (1972) 121; b) P. S. Skell, J. J. Havel, M. J. McGlinchey, *Acc. Chem. Res. 6* (1973) 97; c) K. J. Klabunde, *Acc. Chem. Res. 8* (1975) 393; d) P. L. Timms, M. Moskovits, G. A. Ozin in M. Moskovits, G. A. Ozin (Eds.): *Cryochemistry*, Wiley-Interscience, New York, 1976; e) P. L. Timms, T. W. Turney, *Adv. Organomet. Chem. 15* (1977) 53; f) G. A. Ozin, S. A. Mitchell, *Angew. Chem. 95* (1983) 706; *Angew. Chem. Int. Ed. Engl. 22* (1983) 674.
[4] J. R. Blackborrow, D. Young: *Metal-Vapor Synthesis in Organometallic Chemistry*, Spinger, Heidelberg 1979.
[5] K. J. Klabunde: *Chemistry of Free Atoms and Particles*, Academic Press, New York 1980.
[6] *Handbook of Chemistry and Physics*, 59th Edit. CRC, Cleveland, OH 1986.
[7] a) A. J. L. Hanlan, G. A. Ozin, *Inorg. Chem. 16* (1977) 2848; 2857; b) M. Moskovits, J. E. Hulse, *J. Chem. Soc. Faraday Trans. 1977*, 471; c) M.

Moskovits, J. E. Hulse, *J. Chem. Phys. 66* (1977) 3988; d) K. J. Klabunde, B. B. Anderson, M. Bader, L. J. Radonovich, *J. Am. Chem. Soc. 100* (1978) 1313.
[8] R. W. Zoellner, K. J. Klabunde, *Chem. Rev. 84* (1984) 545, and references cited therein.
[9] D. L. Williams-Smith, L. R. Wolf, P. S. Skell, *J. Am. Chem. Soc. 94* (1972) 4042.
[10] R. Middleton, J. R. Hull, S. R. Simpson, C. H. Tomlinson, P. L. Timms, *J. Chem. Soc. Dalton Trans. 1973*, 120.
[11] S. D. Ittel, C. A. Tolman, *J. Organomet. Chem. 172* (1979) C47; *Organometallics 1* (1982) 1432.
[12] L. J. Radonovich, M. W. Eyring, T. J. Groshens, K. J. Klabunde, *J. Am. Chem. Soc. 104* (1982) 2816.
[13] H. F. Efner, D. E. Tevault, W. B. Fox, R. R. Smardzewksi, *J. Organomet. Chem. 146* (1978) 45.
[14] L. K. Beard, Jr., M. P. Silvon, P. S. Skell, *J. Organomet. Chem. 209* (1981) 245.
[15] G. A. Ozin, C. G. Francis, H. X. Huber, M. Andrews, L. Nazar, *J. Am. Chem. Soc. 103* (1981) 2453.
[16] S. F. Parker, C. H. F. Peden, *J. Organomet. Chem. 272* (1984) 411.
[17] P. D. Morand, C. G. Francis, *Organometallics, 4* (1985) 1653.
[18] D. W. Ball, Z. H. Kafafi, R. H. Hauge, J. L. Margrave, *J. Am. Chem. Soc. 108* (1986) 6621.
[19] E. O. Fischer, F. Röhrscheid, *Z. Naturforsch. B 17* (1962) 483.
[20] H. Fleckner, F.-W. Grevels, D. Hess, *J. Am. Chem. Soc. 106* (1984) 2027.
[21] K. Jonas, E. Deffense, D. Habermann, *Angew. Chem. 95* (1983) 729; *Angew. Chem. Int. Ed. Engl. 22* (1983) 716; *Angew. Chem. Suppl. 1983*, 1005.
[22] C. Elschenbroich, R. Möckel, *Angew. Chem. 89* (1977) 908; *Angew. Chem. Int. Ed. Engl. 16* (1977) 870; E. P. Kündig, P. L., Timms,. *J. Chem. Soc. Chem. Commun. 1977*, 912; *J. Chem. Soc. Dalton Trans. 1980*, 991.
[23] E. L. Muetterties, J. R. Bleake, E. J. Wucherer, T. A. Albright, *Chem. Rev. 82* (1982) 499.
[24] J. W. Hull, W. L. Gladfelter, *Organometallics 3* (1984) 605.
[25] J. O. Albright, L. D. Brown, S. Datta, J. K. Kouba, S. S. Wreford, B. M. Foxman, *J. Am. Chem. Soc. 99* (1977) 5518; J. O. Albright, S. Datta, B. Dezube, J. K. Kouba, D. S. Marynick, S. S. Wreford, B. M. Foxman *ibid. 101* (1979) 611.
[26] R. J. Harper, *US Pat.* 3 073 855 (January 15, 1963), Ethyl Corporation.
[27] T. A. Manuel, *Inorg. Chem. 3* (1964) 1794.
[28] U. Zenneck, W. Frank, *Angew. Chem. 98* (1986) 806; *Angew. Chem. Int. Ed. Engl. 25* (1986) 831.
[29] H. Schäufele, D. Hu, H. Pritzkow, U. Zenneck, *Organometallics 8* (1989) 396.
[30] C. Tolxdorff, H. Pritzkow, U. Zenneck, unpublished.
[31] A. Funhoff, H. Schäufele, U. Zenneck, *J. Organomet. Chem. 345* (1988) 331.
[32] W. Siebert, *Angew. Chem. 97* (1985) 924; *Angew. Chem. Int. Ed. Engl. 24* (1985) 943.
[33] U. Zenneck, L. Suber, H. Pritzkow, W. Siebert, *Chem. Ber. 119* (1986) 971.
[34] J.-K. Uhm, H. Römich, H. Wadepohl, W. Siebert, *Z. Naturforsch. B 42* (1988) 306.
[35] J.-K. Uhm, H. Pritzkow, U. Zenneck, W. Siebert, unpublished.
[36] D. Büchner, *Dissertation,* Universität Heidelberg 1986; H. Fuess, P. Schweiss (Frankfurt am Main), H. Pritzkow (Heidelberg), unpublished.
[37] J. Edwin, M. C. Böhm, N. Chester, D. M. Hofman, R. Hoffmann, H. Pritzkow, W. Siebert, K. Stumpf, H. Wadepohl, *Organometallics 2* (1983) 1666.
[38] J. Zwecker, *Dissertation,* Universität Heidelberg 1986.
[39] D. Büchner, T. Kuhlmann, G. Brodt, W. Siebert, unpublished.
[40] A. Funhoff, U. Zenneck, W. Siebert, unpublished.
[41] V. Schäfer, H. Pritzkow, W. Siebert, *Chem. Ber. 122* (1989) 467.
[42] G. Brodt, *Dissertation,* Universität Heidelberg 1988.
[43] M. L. H. Green, L.-L. Wong, *J. Chem. Soc. Chem. Commun. 1984*, 1442; *J. Chem. Soc. Dalton Trans. 1987*, 411; M. L. H. Green, D. O'Hare, L.-L. Wong, *ibid. 1987*, 2031.
[44] H. Schäufele, *Dissertation,* Universität Heidelberg 1989.
[45] B. Walther, *Coord. Chem. Rev. 60* (1984) 67; H. Neukomm, H. Werner, *J. Organomet. Chem. 108* (1976) C26; H. Werner, R. Feser, *Z. Anorg. Allg. Chem. 458* (1979) 301; W. Kläui, *Z. Naturforsch. B 34* (1979) 1403; Q.-B. Bao, T. B. Brill, *Organometallics 6* (1987) 2588.
[46] D. H. M. W. Thewissen, *J. Organomet. Chem. 192* (1980) 115; H. P. M. M. Ambrosius, J. H. Noordik, G. J. A. Ariaans, *J. Chem. Soc. Chem. Commun. 1980*, 832.
[47] S. D. Ittel, P. J. Krusic, P. Meakin, *J. Am. Chem. Soc. 100* (1978) 3264.
[48] D. Hu, H. Pritzkow, H. Schäufele, C. Tolxdorff, U. Zenneck in H. Werner, G. Erker (Eds.): *Organometallics in Organic Synthesis, Vol. 2*, Springer, Heidelberg 1989, p. 45.
[49] T. V. Harris, J. W. Rathke, E. L. Muetteries, *J. Am. Chem. Soc. 100* (1978) 6966.
[50] J. L. Tempelton, B. C. Ward, *J. Am. Chem. Soc. 102* (1980) 3288.
[51] H. Schäufele, H. Pritzkow, U. Zenneck, *Angew. Chem. 100* (1988) 1577; *Angew. Chem. Int. Ed. Engl. 27* (1988) 1519.
[52] J. Roziere (Montpellier), unpublished EXAFS-results.
[53] L. Vasquez, *Dissertation,* Universität Heidelberg 1988; J. Ensling, P. Gütlich (Mainz), unpublished.
[54] J. R. Blackborrow, unpublished results cited as Ref. [65b] in [8].
[55] P. L. Timms, *Angew. Chem. 87* (1975) 295; *Angew. Chem. Int. Ed. Engl. 14* (1975) 273.
[56] Y. Wakatsuki, O. Nomura, K. Kitaura, K. Marokuma, H. Yamazaki, *J. Am. Chem. Soc. 105* (1983) 1907; Y. Wakatsuki, H. Yamazaki, *J. Organomet. Chem. 139* (1977) 169; M. B. Gomes de Lima, J. E. Guerchais, F. J. Le Floch-Pérennou, P. L. L'Haridon, F. Y. Pétillon, J. Talarmin, *Organometallics 6* (1987) 1930; D. W. Macomber, A. V. Verma, R. D. Rogers, *ibid. 7* (1988) 1241.
[57] G. Becker, G. Gresser, W. Uhl, *Z. Naturforsch. B 36* (1981) 16.
[58] P. B. Hitchcock, M. J. Maah, J. F. Nixon, *J. Chem. Soc. Chem. Commun. 1986*, 737; P. Binger, R. Milczarek, R. Mynott, M. Regitz, W. Rösch, *Angew. Chem. 98* (1986) 645; *Angew. Chem. Int. Ed. Engl. 25* (1986) 644.
[59] M. Regitz, P. Binger, *Angew. Chem. 100* (1988) 1541; *Angew. Chem. Int. Ed. Engl. 27* (1988) 1484, and references cited therein.
[60] J. F. Nixon, *Chem. Rev. 88* (1988) 1327, and references cited therein.
[61] M. Driess, D. Hu, H. Pritzkow, H. Schäufele, U. Zenneck, M. Regitz, W. Rösch, *J. Organomet. Chem. 334* (1987) C35.
[62] **36** and **37** are also accessible via another route: R. Bartsch, P. B. Hitchcock, J. F. Nixon, *J. Chem. Soc. Chem. Commun. 1987*, 1146.
[63] O. J. Scherer, T. Brück, *Angew. Chem. 99* (1987) 59; *Angew. Chem. Int. Ed. Engl. 26* (1987) 59; O. J. Scherer, T. Brück, G. Wolmershäuser, *Chem. Ber. 121* (1988) 935.
[64] W. Rösch, U. Hees, M. Regitz, *Chem. Ber. 120* (1987) 1645.
[65] D. Hu, H. Schäufele, H. Pritzkow, U. Zenneck, *Angew. Chem. 101* (1989) 929; *Angew. Chem. Int. Ed. Engl. 28* (1989) 900.
[66] D. Hu, H. Schäufele, H. Pritzkow, U. Zenneck, unpublished.
[67] H. Hoberg, K. Jenni, K. Angermund, C. Krüger, *Angew. Chem. 99* (1987) 141; *Angew. Chem. Int. Ed. Engl. 26* (1987) 153.
[68] See also: A. Marinetti, F. Mathey, J. Fischer, A. Mitschler, *J. Am. Chem. Soc. 104* (1982) 4484; *J. Chem. Soc. Chem. Commun. 1984*, 182.
[69] T. Wettling, J. Schneider, O. Wagner, C. G. Kreiter, M. Regitz, *Angew. Chem. 101* (1989) 1035; *Angew. Chem. Int. Ed. Engl. 28* (1989) 1013.
[70] E. L. Allred, B. R. Beck, *J. Am. Chem. Soc. 95* (1973) 2393.
[71] E. C. Smith, J. C. Barborak, *J. Org. Chem. 41* (1976) 1433; A. P. Marchand, T.-C. Chou, J. D. Eckstrand, D. van der Helm, *ibid. 41* (1976) 1438; P. E. Eaton, L. Cassar, R. A. Hudson, R. H. Deng, *ibid. 41* (1976) 1445.
[72] M. Baudler, *Angew. Chem. 99* (1987) 429; *Angew. Chem. Int. Ed. Engl. 26* (1987) 419; H. G. von Schnering, W. Hönle, *Chem. Rev. 88* (1988) 243, and references cited therein.
[73] T. G. Groshens, B. Henne, D. E. Bartok, K. J. Klabunde, *Inorg. Chem. 20* (1981) 3629.
[74] K. J. Klabunde, D. Ralston, R. Zoellner, H. Hattori, Y. Tanaka, *J. Catal. 55* (1978) 213.
[75] G. Vitulli, S. Bertozzi, M. Vignali, R. Lazzaroni, P. Salvatori, *J. Organomet. Chem. 326* (1987) C33.
[76] L. Vasquez, H. Pritzkow, U. Zenneck, *Angew. Chem. 100* (1988) 705; *Angew. Chem. Int. Ed. Engl. 27* (1988) 706.
[77] R. D. W. Kemmit, D. R. Russell in G. Wilkinson, F. G. A. Stone (Eds.): *Komprehensive Organometallic Chemistry Vol. 5*, Pergamon, Oxford, 1982, p. 195.
[78] A second route to this class of substances has ben reported recently: P. Biagini, T. Funaioli, G. Fachinetti, F. Laschi, P. F. Zanazzi, *J. Chem. Soc. Chem. Commun. 1989*, 405.
[79] K. J. Klabunde, H. F. Efner, T. O. Murdock, R. Ropple *J. Am. Chem. Soc. 98* (1976) 1021.
[80] K. J. Klabunde, H. F. Efner, *J. Fluorine Chem. 4* (1974) 114; J. H. Sinfelt, *J. Catal. 29* (1973) 308; K. J. Klabunde, S. Davis, H. Hattori, Y. Tanaka, *ibid. 54* (1978) 254.
[81] R. M. Atkins, R. Mackenzie, P. L. Timms, T. W. Turney, *J. Chem. Soc. Chem. Commun. 1975*, 764.
[82] K. Fischer, K. Jonas, G. Wilke, *Angew. Chem. 85* (1973) 620; *Angew. Chem. Int. Ed. Engl. 12* (1973) 595.
[83] W. Herter, *Dissertation,* Universität Heidelberg 1984.
[84] J. Zwecker, H. Pritzkow, U. Zenneck, W. Siebert, *Angew. Chem. 98* (1986) 1129; *Angew. Chem. Int. Ed. Engl. 25* (1986) 1099.
[85] T. Kuhlmann, H. Pritzkow, U. Zenneck, W. Siebert, *Angew. Chem. 96* (1984) 994; *Angew. Chem. Int. Ed. Engl. 23* (1984) 371.
[86] J. Zwecker, T. Kuhlmann, H. Pritzkow, W. Siebert, U. Zenneck, *Organometallics 7* (1988) 2316.
[87] H. P. Fritz, K. E. Schwarzhans, *J. Organomet. Chem. 1* (1964) 208; E. O. Fischer, R. Jira, *Z. Naturforsch. B 8* (1953) 217; P. Prins, J. D.- van Voorst, C. J. Schinkel, *Chem. Phys. Lett. 1* (1967) 54.
[88] J. L. Robbins, N. Edelstein, B. Spencer, J. C. Smart, *J. Am. Chem. Soc. 104* (1982) 1882.
[89] M. V. Rajasekharan, R. Bucher, E. Deiss, L. Zoller, A. K. Salzer, E. Moser, J. Weber, J. H. Ammeter, *J. Am. Chem. Soc. 105* (1983) 7516.

Starburst Dendrimers: Molecular-Level Control of Size, Shape, Surface Chemistry, Topology, and Flexibility from Atoms to Macroscopic Matter**

By Donald A. Tomalia,* Adel M. Naylor, and William A. Goddard III

In memoriam Piero Pino

Starburst dendrimers are three-dimensional, highly ordered oligomeric and polymeric compounds formed by reiterative reaction sequences starting from smaller molecules—"initiator cores" such as ammonia or pentaerythritol. Protecting group strategies are crucial in these syntheses, which proceed via discrete "Aufbau" stages referred to as generations. Critical molecular design parameters (CMDPs) such as size, shape, and surface chemistry may be controlled by the reactions and synthetic building blocks used. Starburst dendrimers can mimic certain properties of micelles and liposomes and even those of biomolecules and the still more complicated, but highly organized, building blocks of biological systems. Numerous applications of these compounds are conceivable, particularly in mimicking the functions of large biomolecules as drug carriers and immunogens. This new branch of "supramolecular chemistry" should spark new developments in both organic and macromolecular chemistry.

1. Introduction

Over 300 years ago, the notion of "a universe within a universe" became a well documented and vivid concept in the work of *Jonathan Swift*.[1] A more contemporary version of this concept may be seen in the fractal geometry of *Mandelbrot*[80, 81] (Fig. 1). Each of these analogies serves well in dimensionally relating atoms to "pointlike" covalent molecules and to biomacromolecules, which are so quintessential of life (cf. Fig. 3). Although the first Lilliputian organic molecules were discovered some 150 years ago, molecular biologists and synthetic chemists are just now beginning to understand how nature bridges this dimensional gap.[2] Recent results[3] indicate that a dimensional hierarchy can also exist in abiotic systems. Within metals or partitioned water, for example, clusters of specific "mesoscopic" dimensions exhibit unique properties which differentiate them from single atoms or molecules or from higher-dimensioned macroscopic matter.

Are there abiotic synthetic strategies which allow covalent entry to such mesoscopic systems? More specifically, are there viable synthetic schemes which allow a systematic molecular morphogenesis from atoms to (microscopic) pointlike organic molecules and ultimately to (mesoscopic) biomorphic/receptor-like molecules and assemblies (cf. Fig. 3)? The latter question has been asked from a multitude of perspectives.[4]

This article offers partial answers to these questions and describes our efforts to develop, characterize, and predict three-dimensional organizations of ordered, covalent connectivity around various microscopic reference points (i.e., pointlike organic molecules referred to as initiator cores). The resulting covalent architecture can be systematically controlled by stepwise reiterative reaction sequences (generations). This process (cf. Fig. 2) involves the following steps:

1. Start with an initiator core ① possessing N_c reactive sites (e.g., $N_c = 3$ for ammonia).

Fig. 1. Computer-generated enlargement of a boundary site in a Mandelbrot set (generated in a Graphiklabor "Dynamische Systeme" by *Heinz-Otto Peitgen, P. H. Richter*, and *D. Saupe*, Universität Bremen).

[*] Dr. D. A. Tomalia
Applied Organic and Functional Polymers Research
The Dow Chemical Company
Midland, MI 48674 (USA)
and (please send inquiries to this address)
Michigan Molecular Institute
1910 W. St. Andrews Road
Midland, MI 48640 (USA)
Dr. A. M. Naylor [+], Prof. W. A. Goddard III
Arthur Amos Noyes Laboratory of Chemical Physics
California Institute of Technology
Pasadena, CA 91125 (USA)
[+] Current address:
Merck, Sharp & Dohme Research Laboratories
Molecular Systems Department
West Point, PA 19486 (USA)

[**] STARBURST is a registered trademark of The Dow Chemical Company.

2. Choose a reaction sequence so that each of the N_c reactive sites adds a reactant B_1 possessing N_b ($N_b > 1$) new reactive sites, which introduce multiplicity, to obtain dendrimer[70] D_0 of generation 0. With ammonia as initiator core, a β-alanine derivative ($N_b = 2$) might be chosen as reactant.
3. Use protection/deprotection strategies to ensure that B_1 reacts with all reactive sites of ①, but that no reactions occur at the new reactive sites on B_1 of dendrimer D_0.
4. Define an iterative sequence involving addition of new reactants B_{i+2} to the molecule D_i of generation i to form a new dendrimer D_{i+1} of generation i + 1.

In this fashion, it is possible to control size, shape, topology, flexibility, and surface chemistry, referred to as critical molecular design parameters (CMDPs), at the molecular level. Such space-filling, terminally functionalized molecular organizations have been coined starburst dendrimers.[70] One can grow predictable, stoichiometric structures up to a self-limited dimension (generation), which is determined by N_c and N_b as well as by the dimensions of the structural components.

The branching implicit in $N_b > 1$ leads to geometric growth in the number of atoms for each generation. For example, the number of β-alanine monomers for starburst polyamidoamines (PAMAMs) with ammonia as initiator core is 3, 9, 21, 45, 93, 189, 381, 765, and 1533 for generations 0–8, respectively. Since the overall size can only grow linearly because of the constraints of the covalent bonds, these systems eventually become congested and change from an open, starfish-shaped molecule to a ball-shaped structure. This is illustrated in Figure 2 (generations 0–7) for PAMAM (molecular dynamics simulations).

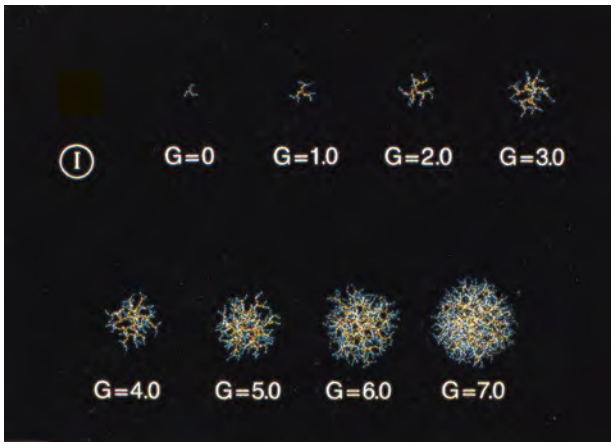

Fig. 2. Computer-simulated molecular graphics (wireframe) using POLYGRAF [97b] for starburst polyamidoamines (PAMAMs) as a function of generation. Initiator core ① (ammonia), red; interior, yellow; surface units, blue. Here, the dendrimer core is generation 0.

2. Dimensional Hierarchy in the Evolution of Organic Matter and Life

In order to comprehend the complex architectures obtainable by controlling a few critical molecular design parameters, we will consider some aspects of life processes from the perspective of these parameters.

2.1. Critical Molecular Design Parameters Involved in Life Processes

The most plausible current models for the origin and evolution of life revolve around self-assembling molecular systems: "Order begot order from chaos."[5, 6] These models have the following features:[5, 6c]

1. Small pointlike molecules were assembled into more complex, "intelligent" biomacromolecules and assemblies possessing ordered, retrievable molecular information for specialized functions.
2. Successful molecular evolution required very faithful transfer of molecular information. This was possible only by exquisite molecular-level control of size, shape, topology, flexibility, and surface chemistry. In this context, these five parameters are referred to as critical molecular design parameters (CMDPs).
3. Control of these CMDPs allowed the development of features and functions inherent in all living systems; namely, their ability to reproduce, to pass on genetic information (i.e., a prototype blueprint) to their progeny, to perform various specialized functions, and finally to grow to prespecified limited dimensions, usually with some characteristic morphology.

These very simple principles, together with natural selection processes, have led to an incredibly rich array of life forms. Figure 3 illustrates a hierarchy which describes the

Donald Tomalia was born in Owosso, Michigan, in 1938. He received a B.A. in chemistry from the University of Michigan (Flint College) in 1961 and joined the Dow Chemical Company as a research chemist in 1962. He progressed to the level of research manager while receiving a Ph.D. from Michigan State University in physical-organic chemistry (1968). His major activities from 1965 to 1975 were in the area of synthetic polymer chemistry; his discovery of the cationic polymerization of 2-oxazolines led to the receipt of two national industrial research awards (IR-100 Awards) for creative research in 1978 and 1986. Presently, he holds the positions of Research Scientist at The Dow Chemical Company (Agricultural Discovery Synthesis) and Adjunct Professor at the Michigan Molecular Institute. D. A. Tomalia holds 78 U.S. patents and has published extensively in the areas of carbonium ion chemistry, reactive heterocyclic monomers, and new polymer architectures. His main research interests include molecular recognition, enzyme inhibition, molecular self-organization, controlled delivery systems, and precision design of macromolecules.

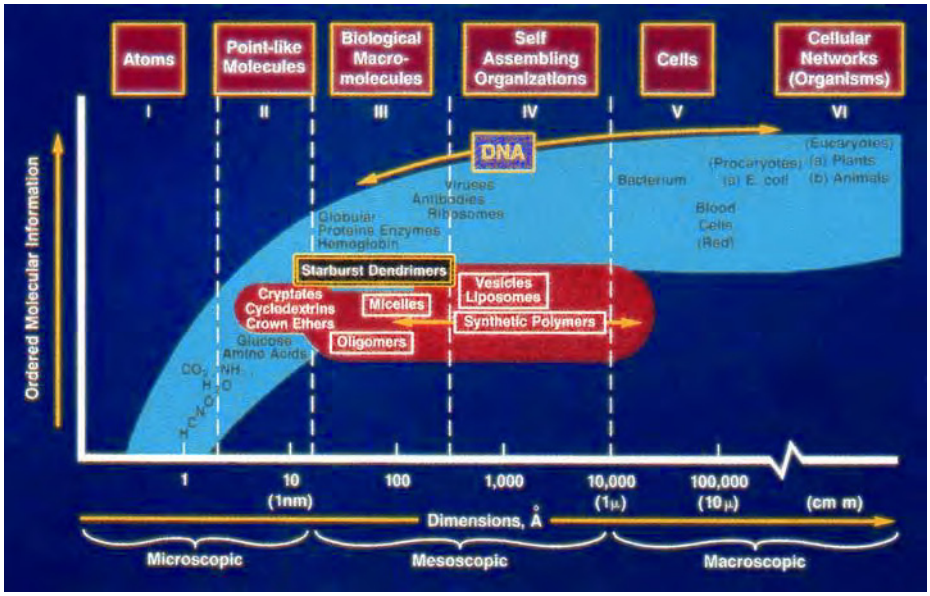

Fig. 3. Dimensional hierarchy of atoms, covalent matter, assemblies, and biological cells as a function of ordered molecular information.

advancement of atomic- and molecular-level entities (I, II) along various biological pathways to biomacromolecules (III) and higher-ordered molecules and assemblies such as IV–VI. Advancement from atoms (I) to pointlike molecules and subsequently to biocellular networks (VI) can generally be related to the amount of ordered molecular information possessed by the entities II–VI as well as to their relative dimensions. Superseding and in fact directing the assembly and function of many members of categories III–VI is the fundamental template of life, deoxyribonucleic acid (DNA). Because of its relatively high aspect ratio, one may think of DNA as a one-dimensional template which transmits molecular information through a cascade of intermediates (m-, t-, and rRNAs, ribosomes, etc.). Ultimately, this genetic (molecular) information becomes translated into one-dimensional protein sequences. The size of these proteins is determined by the length of the polypeptide chain, whereas the shape, interior topology, and surfaces result from foldings and convolutions determined by the sequence and the side chains of the amino acids.[7] Thus, the initial one-dimensional molecular information is ultimately translated into a three-dimensional message. Precise control of the CMDPs is the foundation upon which evolution chemistry has advanced and reached its present state of development.

2.2. Comparison of Synthetic with Evolutionary Strategies for Controlling Critical Molecular Design Parameters

Over the last 150 years, organic chemists have learned how to synthesize highly complex compounds as they have explored the options for precisely controlling the CMDPs of pointlike organic molecules (category II, Fig. 3). More recent attention has been directed toward the synthesis of larger, yet structurally defined macromolecules. For example, such molecules have been the subject of intense interest over the past 20 years as "endo-receptors" for the examination of guest–host relationships. Their design has been derived largely from macrocyclic[8] or macropolycyclic[9] structures as well as from acyclic architecture (podands).[10] The selectivity achieved by such endo-supramolecular chemistry[9c, 11–13] has been compared with that of binding substrates in the cavities (active sites) of larger proteins (enzymes).[14] Currently, these synthetic constructions depend largely on low-aspect-ratio, three-dimensional architecture for their endo-receptor design. Most notable are the cavitands and carcerands, whose interiors are large enough to enclose covalent guest molecules. They have been referred to recently by *Cram* in his Nobel lecture[12c] as synthetic molecular cells.

In contrast, biological protein synthesis involving one-dimensional sequences of amino acids is the fundamental theme of evolution chemistry in the construction of biomacromolecules (category III, Fig. 3). This one-dimensional polymerization strategy, which involves specific sequences of just 20 naturally occurring amino acids, leads to proteins with an enormous variety of possible shapes and sizes. The control of their chemical reactivity, provided by the juxtaposition of electrostatic and hydrogen-bonding "scenarios" at their surfaces, governs the CMDPs of living systems. By this means, very "intelligent", information-laden protein structures (i.e. bio-morphic/receptor molecules) have evolved to fulfill intricate molecule-recognition roles in biological membranes. In other instances, these CMDPs have been used to create microdomains (cavities) suitable for the amazingly selective substrate binding and catalytic chemical transformation carried out by enzymes. The cavity and cleft dimensions required for these important life processes generally seem to necessitate globular proteins with around 300 amino-acid units and molecular dimensions of the order of 25–200 Å in order to provide adequate scaffolding and tertiary-structure development.[15]

On the other hand, a completely different strategy is used for constructing biological compartments and assemblies such as micelles, liposomes, viruses, protein coats, and biological cells. Here, the game plan is *organization* and *aggregation* of either pointlike molecules or biomacromolecules,

whereby *self-assembly* processes are involved. Very precise control of size, shape, topology, flexibility, and surface chemistry (CMDPs) is the primary function and role these entities display in various life processes. These self-assembling systems use weaker interactions such as van der Waals forces and hydrophobic associations to produce precise three-dimensional structures.

Since the days of *Staudinger*[16] and the birth of polymer science early in this century, vast arrays of oligomers and high-molar-mass synthetic polymers have been produced with coil dimensions well over 10 Å.[17] Although many advances have been made in defining classical polymerizations as a function of types, mechanisms, and processes, substantial progress will be necessary to approach the control of CMDPs that Mother Nature has mastered in the production of biomacromolecules and assemblies (categories III und IV, Fig. 3). Considering only size, for example, most globular proteins are obtained as monodispersed products with $M_w/M_n = 1.00$, whereas classical random coil polymers are usually polydispersed with $M_w/M_n \gg 1.00$. Only recently has significant progress been made in producing such monodispersed synthetic polymer systems[18,19] without the use of protection/deprotection strategies. At best these methods offer reproducible control of one-dimensional lengths without necessarily controlling ultimate three-dimensional features such as shape, surface chemistry, or topology.

Without a doubt, the solid-phase peptide synthesis (Merrifield method) remains a preferred method for controlling all five critical molecular design parameters (size, shape, topology, flexibility, and surface chemistry) by precisely producing amino-acid sequences in a stepwise fashion. The scope and limitations of this approach have been reviewed[20a] and widely recognized.[20b] These solid-phase syntheses with protection/deprotection procedures are used routinely to produce numerous polypeptides and polynucleotides which were previously unattainable.[20c,d] Perhaps one of the ultimate synthetic efforts in the control of CMDPs was the total synthesis by *Khorana* et al.[21] of a DNA molecule in the 1960s.

In spite of these accomplishments, no synthetic strategy has successfully matched the diversity or the precise molecular morphogenesis which Mother Nature has mastered in the successful evolutionary development from simple pointlike organic molecules to more complex biomacromolecules and assemblies. It is in this quest that we sought not necessarily total solutions but at least new synthetic strategies for producing such *bio-morphic/receptor mimetics*.[22] This adventure has led us not only to new insights into the molecular-level control of size, shape, topology, flexibility, and surface chemistry, but has also demonstrated some remarkable parallels between higher-ordered biocellular networks (organisms) and information transfer in abiotic molecular-level networks (cf. Section 10).

2.3. Mimicking Macroscopic Ordered Branching Networks at the Molecular Level—A New Strategy

The belief that molecular-level prototypes can be constructed to imitate familiar macroscopic objects has been the inspiration for many intensive and successful synthetic efforts.[23–29] Molecular-level construction of Platonic solids such as the tetrahedron,[26] the cube,[27] and the dodecahedron,[28] as well as non-Euclidian objects such as molecular knots,[29a] Möbius strips,[29b] and even molecular machinery[29d] exemplifies such efforts. Synthetic organic chemists have developed a rich legacy in this area as described in more detail by *Nickon* and *Silversmith*.[29c]

Inspired by the beauty and efficiency with which nature "controls" macroscopic three-dimensional space by use of branching networks in trees,[30] coral,[83] and physiological structures,[31,32] one of us (*D.A.T.*) sought to mimic such branched assemblies at the molecular level. Analysis of parameters involved in synthetically mimicking such branching included the following hypothetical steps (see Fig. 4):

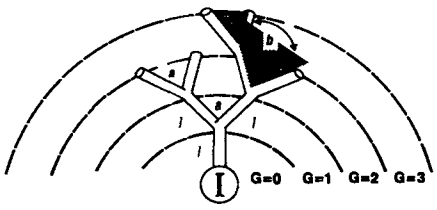

Fig. 4. Illustration of construction parameters involved in controlling macroscopic or microscopic space. l = branch-segment length; a = branching angle, b = rotational angle.

1. Construction and control of branch-segment lengths l.
2. Control and development of branch multiplicities m.
3. Development of a reiterative growth process which would allow concentric construction of branches upon branches around an initiator core ⓘ, which specifies the direction of growth.

The branching angles a are determined by the chemical nature (geometry) of the branch juncture, whereas the rotational angles b are influenced by secondary-structure parameters such as steric effects and hydrogen bonding. These parameters contribute significantly to the development of excluded volume around the branch juncture. Reiteration of these branching patterns in an ideal, tiered manner (G = 0,1,2,3...) should lead to highly ordered macromolecular domains ("microdomains"). The ultimate interplay of all the above parameters would be expected to produce near total control of size, shape, and disposition of chemical moieties, both in the interior and on the exterior surface of these microdomains.

This hypothesis for producing a low-aspect-ratio, three-dimensional molecular prototype can be contrasted with nature's one-dimensional protein synthesis strategy for molecular morphogenesis. Beginning with a reference carbon (Fig. 5), one can use its tetravalency to construct a wide variety of pointlike molecules. In this molecular category, one can find molecules which may function as initiators as well as monomers. Mother Nature elected to use α-amino acids with various side chains (R) for this function. In this case, polymerization involves unidirectional accumulation of α-amino-acid units in a one-dimensional mode. The ultimate size of this one-dimensional protein is controlled by the degree of polymerization n. Its shape, however, is deter-

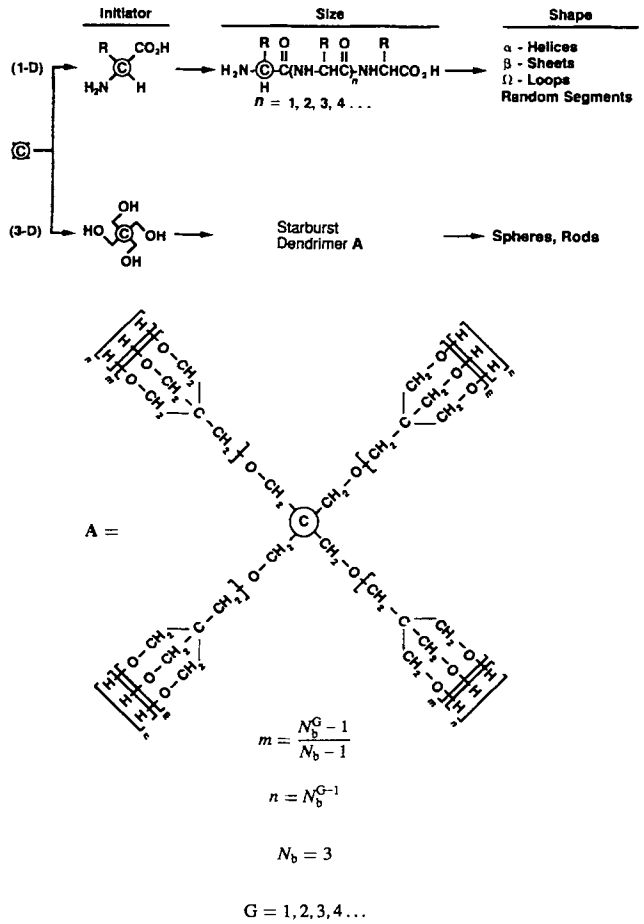

Fig. 5. Molecular morphogenesis: one-dimensional versus three-dimensional strategy for controlled construction of macromolecules.

mined by the sequence of the R groups, which, of course, produces a variety of secondary shapes connected by random sequences; these secondary structures include α-helices, β-sheets, and Ω-loops. These domains then self-assemble into three-dimensional shapes, the tertiary protein structures. Our three-dimensional approach, in contrast, involves the use of a multifunctional initiator (e.g., pentaerythritol) which can accumulate monomer units as branch cells (see Section 3, Fig. 7) in a radial, exponential fashion by forming branches upon branches to produce a starburst topology. This results in the development of entities with low aspect ratios, wherein the degree of branch-cell polymerization m, and hence the size, is defined by the following relation:

$$m = \left[\frac{N_b^G - 1}{N_b - 1}\right]$$

N_b is the branch-juncture multiplicity ($N_b = 3$ for pentaerythritol) and G the generation. The size and shape are clearly influenced by the nature of the initiator core. In addition, the degree of surface congestion caused by the summation of the excluded volumes for the branched monomer units might affect both the shape and the packing density of the surface. Should this be true, this morphogenesis strategy differentiates itself from that used by nature to control CMDPs. Although clearly different molecular arrangements are involved, the CMDPs of these highly branched synthetic macromolecules might be controlled and designed to mimic the CMDPs of naturally occurring biomacromolecules and assemblies. Success in this quest would give rise to a new molecular realm of mesoscopic building blocks, which we refer to as *bio-morphic/receptor mimetics*.[22]

2.4. Why Should We Want to Mimic Bio-Morphic/Receptor Structures and Assemblies Found in Nature?

Human fascination with the mysteries of biological processes has been going on since the origins of man. Molecular-level examination and probing of these processes is a relatively recent development. Led by intense efforts in molecular biology, biophysics, and biochemistry, a rudimentary understanding of these phenomena is beginning to evolve. More recently, however, this understanding has been used in the development of molecular-level, synthetic prototypes to mimic these entities and phenomena. Most notable are the efforts of *Lehn*,[9] *Cram*,[12] and *Pedersen*,[8] whose studies on molecular recognition in guest–host systems involving organic and inorganic compounds are viewed as initial steps toward mimicking highly specific recognition reactions commonly found in biological systems.[9c, 10, 33–36] In a similar manner, extensive efforts by *Ringsdorf*,[37] *Fendler*,[38] *Kunitake*,[39] *Fuhrhop*,[40] and others[41, 153] have been directed toward the use of liposomes as a means for mimicking the organization, surface recognition, and dynamics of biological membranes (cells). Although these efforts were initially

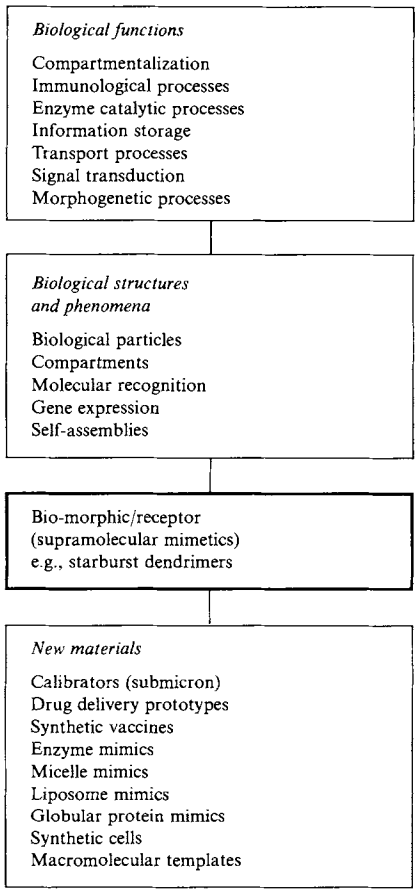

Fig. 6. Potential new materials resulting from bio-morphic/receptor supramolecular mimicking of biological structures and phenomena.

driven by sheer intellectual curiosity, it is becoming apparent that they will ultimately lead to the development of many new prototypes and materials which will constitute a new field of materials science for which *Fendler* has coined the term membrane mimetics.[42] By our own approach, we hope to discover new and useful materials which will contribute not only to materials science but also to a better understanding of biological structure and phenomena.[163] Figure 6 (left side) describes just a few of the potential new materials that may arise in the efforts to develop such biomorphic and bioreceptor mimetics (see also Section 14).

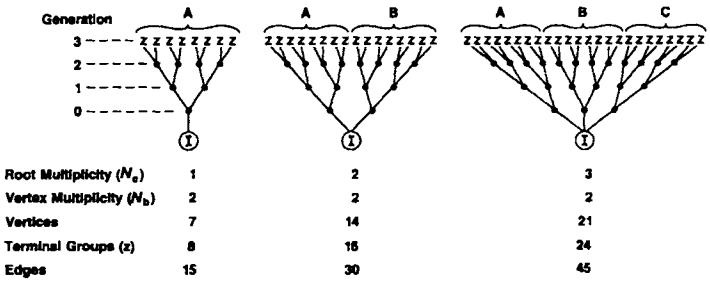

Fig. 8. Chemical graphs for a monodendron (A), a didendron (A-B), and a tridendron, (A-B-C).

3. Historical Background

The origins of the present three-dimensional molecular-level branching concepts can be traced back to the initial introduction of infinite network theory by *Flory*[43-46] and *Stockmayer*.[47,48] In 1943, *Flory* introduced the term network cell, which he defined as the most fundamental unit in a molecular network structure.[49] To paraphrase the original definition, it is the recurring branch juncture in a network system as well as the excluded volume associated with this branch juncture. *Graessley*[50,51] took the notion one step further by describing ensembles of these network cells as micronetworks. Taken out of the context of *Flory*'s and *Graessley*'s statistical treatment of Gaussian-coil networks, analogous species that are part of an open, branched organization have been coined branch cells and branch-cell assemblies, respectively (Fig. 7).

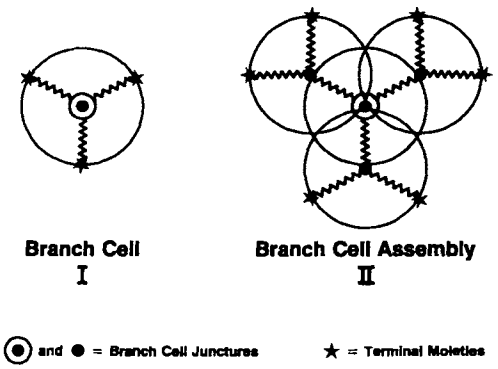

Fig. 7. Two-dimensional projections of branch cells (I) and a branch-cell assembly (II).

Subsequent statistical modeling by *Gordon* et al.[52a-e] and others[52d,e] reduced such branched species to graph theory designed to mimic the morphological branching of trees (Fig. 8). These dendritic models were combined with "cascade theory"[53a,b] mathematics to give a reasonable statistical treatment for network-forming events at that time.

Since these species were conceptual, there were no well-characterized synthetic examples of such regular architecture. Although *Meyer*[56] proposed such symmetrical, ordered architecture for amylopectin, subsequent work by *Erlander* and *French*,[57] as well as by *Burchard* et al.,[58] showed that amylopectin and glycogen are not so regular; instead, they are random f-functional polycondensates possessing a large, highly branched dextrin core as shown in Figure 9.

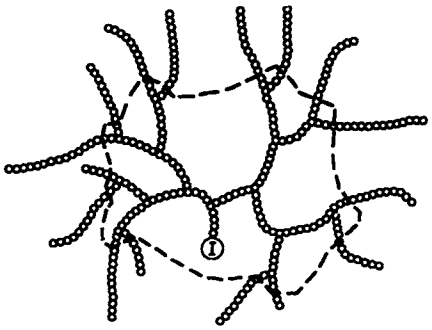

Fig. 9. Dendritic branching topology of amylopectin.

It was not until 1978 that *Vögtle* et al.[59] reported a single, isolated example of a protection/deprotection scheme involving the idea of assembling branches upon branches. The scheme consisted of a sequence of reactions involving Michael addition of an amine to acrylonitrile, followed by reduction of the nitrile group to an amino group. Perhaps due to the difficulties and disappointing yields in the reduction step, no subsequent reports on this work could be found. In any case, the idea of "cascade synthesis" was first introduced to the literature at this time. Essentially concurrent with these activities, we began our work at the Dow Laboratories in Midland, Michigan (USA), on the synthesis of starburst dendrimers.[70] In 1979, we discovered that a variety of amines could be added to methyl acrylate and the products subsequently amidated with α,ω-diaminoalkanes to give "cascade products" (Section 5). With this chemistry, controlled concentric "starburst growth" could be produced around various initiator cores. This growth could be dramatically influenced by both the geometry and multiplicity of the initiator core, as well as by the reiterative chemistry. Subsequent synthetic effort at Dow (1981–1984) showed that, much as anticipated from the macroscopic tree and coral branching analogies, these starburst systems offered a wide range of synthetic options for controlling size, shape, interior topology, flexibility, and surface chemistry at the molecular level.[60-67]

In 1983, mathematical predictions by *de Gennes* et al.[68] showed that a starburst dendrimer series should reach a so-

called starburst limited generation beyond which branching can no longer occur in an ideal fashion. More recent studies have shown that advancement to higher-generation dendrimers ultimately leads to a new critical branching state which is referred to as starburst dense packing.[67-69] At this critically branched generation, an apparent surface association occurs to yield solvent-filled spheroids[69, 101] which are reminiscent of "unimolecular cells".[12b, 69, 71] Such morphologies were suggested in a theoretical paper by *Maciejewski*[72] in 1982, where he referred to them as "shell topologies".

At that time, an isolated, yet related, dendrimer example appeared in the patent literature. *Denkewalter* et al.[73] reported that highly monodispersed macromolecular products were produced by a stepwise linking of α,ω-protected diamino acids (e.g., lysine). Using protection/deprotection methods of polypeptide chemistry, these workers synthesized a series of dendrimers possessing unsymmetrical branch lengths. Although the precise nature of the branch cells and the chemical structures has not been established, subsequent work by *Aharoni* et al.[74] and us[67] showed that they differed dramatically from the present symmetrical starburst dendrimers in certain important physical properties. Unlike starburst dendrimers, they were found to be constant density, nonhollow macromolecules with "nondraining" character and may constitute a subclass to the present dendritic series.

Since 1985, *Newkome* and co-workers[75-77] have reported the synthesis of related symmetrically branched macromolecules which they refer to as "arborols". These macromolecules are highly branched dendrimers which are not amenable to size control as a function of generation in that reiterative chemistry for advancing concentric growth has not been reported. These prototypes have been used successfully for controlling molecular shape and, in some cases, surface moieties. To date, examples of uni-, di- and tridirectional arborols have been reported[75-77] (see Section 5).

4. Starburst Topology and Branching Concept

4.1. Mathematical and Geometrical Precedence

Mathematicians such as *Cantor* and *Koch*[78, 79] and, more recently, *Mandelbrot*[80] have partitioned dimensionality in a variety of ways. *Cantor* started with a simple line, removed the middle third of the line segment, repeated this process on the two remaining segments, and so on to produce increasingly more segments (Fig. 10a). Connecting the midpoints of the segments produces a branching pattern which remains confined in width to the original length of the line. Hence, the connectivity pattern becomes more congested as a function of generation. Subsequently, the Swedish mathematician *Helge von Koch* (1904) partitioned two-dimensional triangles in an analogous fashion to produce the well-known Koch snowflakes (Fig. 10b). This reiterative process produces triangular-edged Koch curves, whose shapes depend on the generation. These curves enclose areas which are less than but approach the limiting area of the circumscribed circle around the curve.[82] In a similar manner, one may envision the partitioning of three-dimensional space by conceptualizing a "spherical universe within a universe" as a series of nesting spheres[31a] (Fig. 10c).

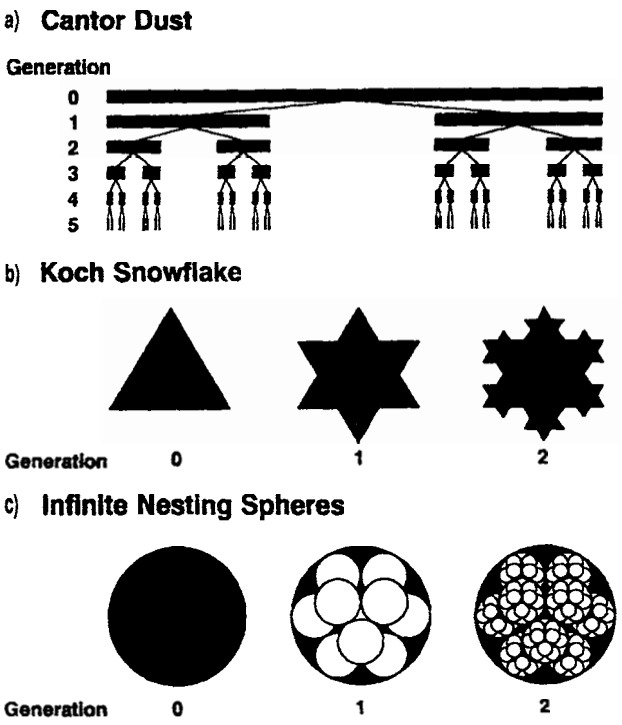

Fig. 10. a) Bifurcation of a line segment with connectivity paths to define Cantor dust. b) Bifurcation of a triangle (two-dimensions) to define Koch snowflakes. c) Fitting of a sphere (three-dimensions) to define a series of infinite nesting spheres (see also Fig. 56).

These three cases are classical examples of fractal curves and dimensions as pioneered by *Mandelbrot*[80, 81] for macroscopic objects. They suggested to us possible extensions for the creation and analysis of unique spatial organizations of atoms within monomer repeat units within branch cells within dendrons within a dendrimer to give molecular-level surfaces in three dimensions.

4.2. Molecular-Level Perspective of Cubic Space

The present dendritic branching concept uses these mathematical/geometrical notions in the context of partitioning or occupying three-dimensional molecular-level space around a reference point, with atoms, chemical bonds, repeating chemical units, and branch cells as the construction parameters. The dendritic branching of coral,[32] Bryozoan colonies,[83] trees,[30] and physiological networks[31] provided prototypes to mimic at the molecular level. The resulting branch-cell assemblies were referred to as possessing starburst topology, and the molecular entities, constructed by reiterative synthetic steps, were coined starburst dendrimers.[70a] Two-dimensional projections of these dendrimers (A–E, Fig. 11) illustrate the concentric assembly of branches upon branches to produce radial arrays of branch

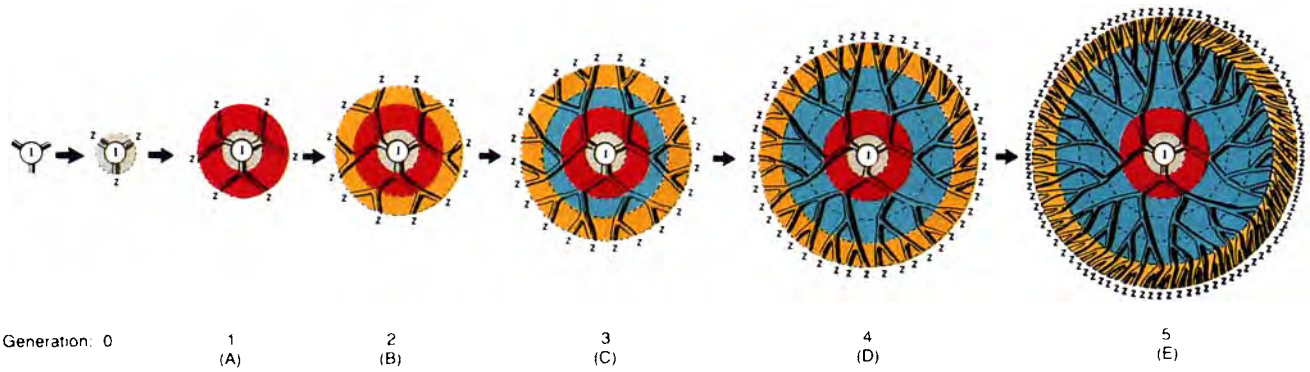

Fig. 11. Two-dimensional projections of an initiator core ($N_c = 3$), a core cell, and tridendron dendrimers ($N_b = 2$).

junctures and terminal functionality (Z) around a reference point or initiator core, ①.[70b]

In a geometrical context, the treelike structures A–E are recognized by physicists and mathematicians as Bethe lattices or Cayley trees. According to graph theory,[70c] dendrimers in this series may be viewed as triads of symmetrical trees rooted to a common initiator core ①. Each of these trees is referred to as an ideal dendron. Such a dendron consists of a root, ①, with connectivity to vertices (branch junctures) through edges (branch segments) which expand symmetrically according to a geometric progression to produce generations containing predictable numbers of vertices and edges.

4.2.1. Effect of Core and Branch-Juncture Multiplicity on Molecular Structure

Both the initiator-core multiplicity N_c and the branch-juncture multiplicity N_b directly affect the number of terminal groups, the number of repeating units (branch segments), and the molar mass of the dendrimers as a function of generation. These values can be predicted mathematically for ideal systems according to the following expressions:

Number of dendrimer terminal groups $z = N_c N_b^G$

Number of dendrimer repeat units (degree of polymerization) $N_{RU} = N_c\left(\dfrac{N_b^{G+1} - 1}{N_b - 1}\right)$

Number of dendrimer branch cells $N_{BC} = N_c\left(\dfrac{N_b^{G} - 1}{N_b - 1}\right)$

Theoretical molar mass of dendrimer $M = M_c + N_c\left[M_{RU}\left(\dfrac{N_b^{G+1} - 1}{N_b - 1}\right) + M_t N_b^{G+1}\right]$

$$M = M_c + N_c\left[M_{BC}\left(\frac{N_b^{G} - 1}{N_b - 1}\right) + M_t N_b^{G}\right]$$

M_c, M_{RU} or M_{BC}, and M_t are the molar masses of the initiator core, repeat units or branch cells, and terminal units, respectively. A general structural notation for a homogeneous dendrimer with core multiplicity N_c and branch-juncture multiplicity N_b may be represented in empirical form as follows:

$$[\text{core}]\left[\text{repeating unit}_{\left[\frac{N_b^{G+1} - 1}{N_b - 1}\right]}\text{terminal unit}_{[N_b^{G+1}]}\right]_{N_c}$$

From a molecular perspective, dendrimers are simply assemblies of dendrons attached to a common initiator core, ①, or a variety of initiator cores in the same molecule. Beginning with ①, these branched assemblies are developed by growing dendrons in a stepwise, radial manner according to multiplicity rules. Figure 11 shows an example of dendrimer growth for $N_c = 3$ and a branch-juncture multiplicity of $N_b = 2$. A wide range of multiplicities N_c are possible, varying from mono- to polydendron assemblies. The size, shape, and initiator-core multiplicity dramatically influence the ultimate CMDPs of the dendrimer.

4.3. Structural Aspects

4.3.1. Dendrimer Branch-Cell Hierarchy

Dendrimers possess three distinguishing architectural features: (1) an initiator-core region, (2) interior zones containing cascading tiers of branch cells with radial connectivity to the initiator core, and (3) an exterior or surface region of terminal moieties attached to the outermost generation. Even in an ideal, homologous dendrimer series there exists a hierarchy of branch cells that are differentiated not only by their topological positions, but also by structural features. This is illustrated in Figure 12, where a fully developed dendrimer is grown in four stages from an initiator core, ①, with $N_c = 3$.

The initiator core ① may be as small as an atom or as large as a molecule. It may be homogeneous with the other dendrimer components or it may contain special design features (e.g., metal atoms, chromophores, etc.) which make it heterogeneous.

Synthetic elaboration to create the first tier of terminal functionality or branch junctures defines a microdomain referred to as the *core cell* (gray-green in Fig. 12). In situ construction of branch junctures or coupling partially masked, branch-cell reagents ($N_b \geqq 2$) gives the first three surface cells (orange-yellow), each of which possesses two reactive surface groups (Z). On progressing from dendrimer A to B, the three surface cells become initiator cells (red) and six new

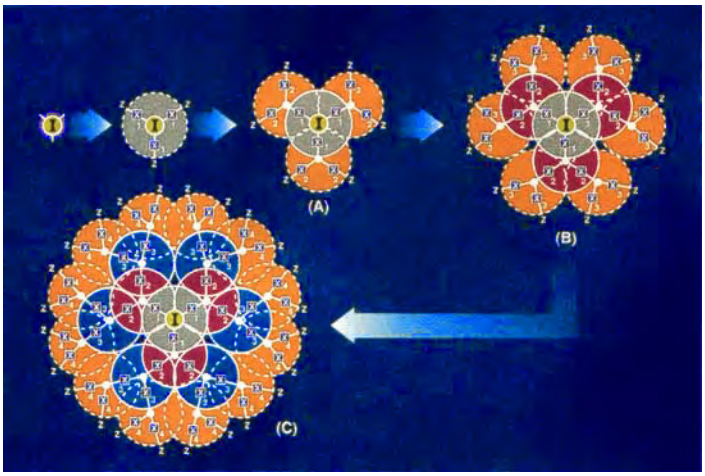

Fig. 12. Construction of a dendrimer of generation 3 (the numbers 1 to 4 in the circles should be replaced by 0 to 3) and its dendrimer branch-cell hierarchy. Color coding: green-gray, core cell (G = 0) red, initiator cells (G = 1); blue, interior cells (G = 2); yellow-orange, surface cells (G = 3).

surface cells are added. Advancement from B to dendrimer C leads to complete development of the cell hierarchy, which consists of one initiator core cell, three initiator cells, six interior cells (blue), and twelve surface cells with a total surface stoichiometry of twenty-four Z groups. Owing to these surface groups, the dendrimer should function as an exo-receptor.[9c]

If the branch junctures or the coupling junctures are heteroatoms or contain designed moieties amenable to reaction or chelation, the dendrimer should exhibit endo-receptor characteristics.[9c] Each of these bonding features has been observed experimentally (for experimental examples, see Section 9).

4.3.2. *Dendrimer Branch-Cell Symmetry Properties*

The symmetry properties of the interior branch cells can dramatically affect the physical and perhaps chemical properties of a dendrimer. For example, symmetrical interior and surface cells, such as those in Figures 11 and 12, exhibit identical connectivity paths from the initiator core to the termini. The equal radii place the terminal groups on a sphere or a segment of a sphere, thus making these dendrimers ideal models of functionalized submicron spheres.

In contrast, the polylysine dendrimers described by *Denkewalter* et al.[73] have unsymmetrical branch cells with either three or seven bonds between branch points. If one considers the paths of connectivity from initiator core to termini of a single dendritic branch, it can be seen that no two paths are identical. In fact, every possible permutation of the sequences of the two given linear segments is present in the branch. If the two segment lengths are given values of s and l, and the number of tiers in the branch is N, the number of different paths, X, is given by the relation $X = 2^N$. Since the paths are constructed from all possible combinations of the two given segment lengths, the number of paths of a given length follows a binominal distribution. Thus, the number of paths composed of a short segments and b long segments (in a molecule consisting of $a + b$ tiers) is given by the following relation:

$$X_{a+b} = (a + b)!/(a!\, b!)$$

For example, a molecule with three tiers of branching has eight terminal groups. There is one path consisting of three short segments, three paths consisting of two short and one long segment, three paths consisting of one short and two long segments, and one path consisting of three long segments (see Fig. 13).

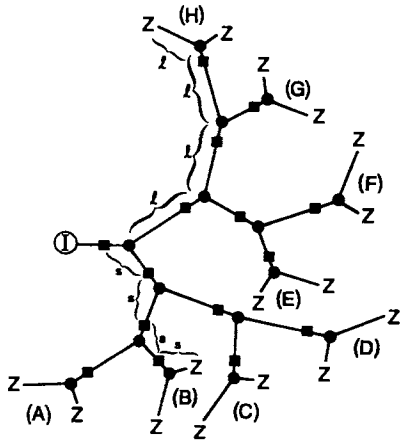

Fig. 13. Two-dimensional projection of a monodendron with unsymmetrical branch junctures (Denkewalter topology) and surface branch cells (A–H). s and l are the lengths of the short and long segments, respectively.

The different lengths of these paths mandate that some terminal groups will be tethered closer to the center of the branched assembly than others and be subject to more steric interactions. This suggests that this dendrimer class has surfaces with higher fractal dimensions[80–82, 84] and interior branching zones which are less ordered than those of the starburst dendrimers (Fig. 14).

These two classes differ substantially in certain physical properties.[67] Although it has not been demonstrated, one might expect the various terminal groups in the Denkewalter dendrimers to show a range of chemical reactivities based on different steric environments. These clefted, highly fractal

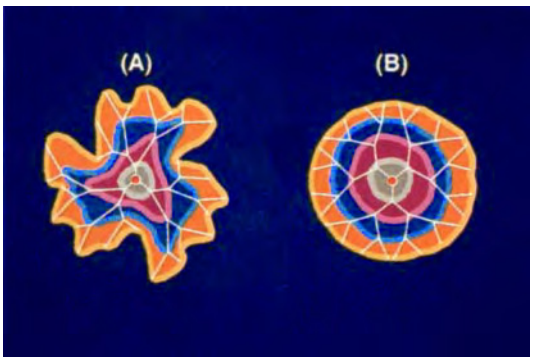

Fig. 14. Two-dimensional projection of a tridendron dendrimer ($N_c = 3$; $N_b = 2$) with unsymmetrical branch junctures (A) compared with one possessing symmetrical branch junctures (B).

surfaces are not unlike microenvironments usually associated with enzymes. This issue as well as other topological questions will, no doubt, provide ample reason for wanting to characterize and gain a deeper understanding of dendrimer infrastructure and surfaces.

5. Dendrimer Syntheses

Classical, random coil, functional macromolecules are substrates upon which it is often difficult to perform high-yield, efficient reactions. Their coiled configurations frequently lead to inaccessible buried functionality that can frustrate even the most patient synthetic chemist. Unlike these situations, the radial orientation of starburst topology presents the terminal functionality in a very favorable fashion, accessible to incoming reagents and media. For this reason, essentially any reaction that proceeds well on a pointlike organic molecule can be expected to occur equally well on a dendrimer surface, at least in the earlier generations. As surface congestion develops, however, reaction kinetics and stoichiometry would be expected to change dramatically (cf. Section 9).

Considering the intricacies of the dendrimer assembly steps, one can conceive of a variety of defects that could lead to divergence from ideality. Broadly speaking, they are of two types: those involving intra-dendrimer events and those leading to inter-dendrimer bridging or looping. The former defects decrease branching ideality, whereas the inter-dendrimer bridging events lead to more polydispersed systems. These defects have been minimized or eliminated by both process optimization and synthetic strategy optimization. Figure 15 illustrates some flawed structures.[85]

Defects such as **1** and **2** lead to abnormal cell development within the dendrimers and can dramatically affect the surface stoichiometry if they become extensive. Branch defects

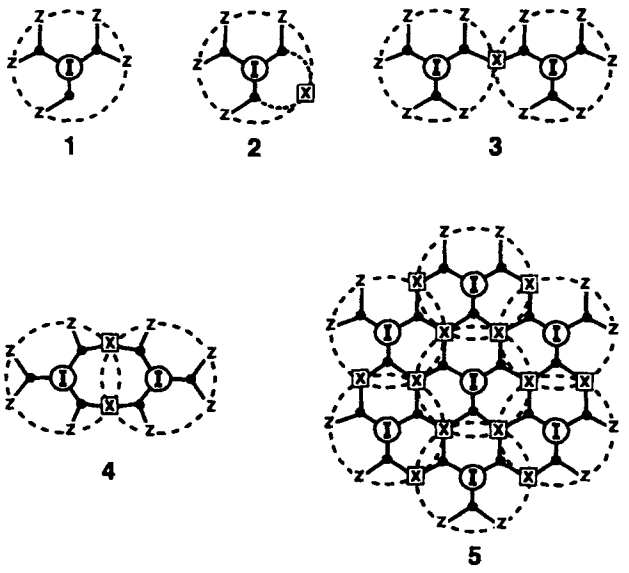

Fig. 15. Two-dimensional projections of various branch-cell defects which may lead to divergence from ideal dendrimer development. Branch defective dendrimer, **1**; intra-dendrimer looping, **2**; inter-dendrimer bridging, **3**; inter-dendrimer looping, **4**; dendrimer cluster (bridged/looped), **5**.

such as **1** may be due to (1) incomplete reactions resulting from surface-group deactivation or inappropriate reaction conditions, (2) branch-juncture fragmentation, (3) abnormal branch-juncture development, or (4) sterically induced stoichiometry (SIS, see Section 9). Both this type of defect and intramolecular cyclization lead to reduced surface stoichiometry and may affect ultimate symmetry properties of the dendrimer.

Intermolecular events leading to bridged or looped structures such as **3**, **4**, and **5** are the chief contributors to increased polydispersity. Other factors that can cause polydispersity include (1) incomplete removal of reagents (which may function as initiator cores) and (2) dendrimer fragmentation (to produce molecular entities which may subsequently become initiator species).

In general, successful synthetic strategies allowing the assembly of branch cells into ideal open-branched assemblies (i.e., dendrons, dendrimers) have involved the following steps:

1. Selection of a suitable initiator that can be converted in high yield into a reactive initiator core cell.
2. Definition of an iterative reaction sequence that allows presentation of the reactive initiator core cell to appropriate reagents or other reactive branch cells (partially protected), resulting in high-yield conversions to a branched assembly with specific molecular surfaces.
3. Reiteration of these step-growth or chain-growth sequences to produce dendrimers possessing concentric generations of repeating units and branch junctures. These parameters define the number of branch cells which accumulate exponentially within these generation zones. A geometric consequence of this reiterative step-growth propagation is that the covalent connectivity paths (i.e., the radial summation of branch-cell diameters) from the initiator core to the dendrimer surface increases linearly, whereas the microvolumes occupied by the dendrimer surface cells accumulate exponentially as a function of generation. Because of the "tethering effect" on these exponentially greater numbers of surface cells, one eventually reaches a "starburst limited generation" as predicted by *de Gennes* et al.[68] This defines a self-limiting size (generation) for any given dendrimer series, which is based on its branch-segment lengths, core/juncture multiplicities, and surface-group dimensions. Penultimate to this generation, certain reaction rate digressions and stoichiometry aberrations are observed.

Specific synthetic approaches may be divided into two major categories: Controlled step-growth propagation and uncontrolled chain-growth propagation.

5.1. Initiator Cores and Dendrimer Profiles

The selection or synthesis of the initiator core is of great importance. It is the fundamental unit to which the dendrons are tethered; thus, its size, shape, multiplicity, and specialized function will clearly influence the dendrimer throughout its construction. Core-cell design may range from simple attachment of one dendron to the use of "starbranched", multiarmed functionalized entities,[86] or even multifunc-

tionalized, polymeric substrates. Synthetic design of these core cells may include introduction of chromophores, chelating groups, metals, molecular recognition moieties, or hydrophilic/hydrophobic domains for desired guest–host properties. Enclosure or molecular encapsulation of these core cells is initiated in the next step of the dendrimer construction. Introduction of branch junctures (see Figs. 11, 12) may involve either "in situ" construction, coupling of preformed branch cells, or chain propagation of functionally differentiated branched monomers to produce the first tier of branch cells.

Considering the present starburst polyamidoamine family derived from an ammonia core and $-CH_2CH_2CONHCH_2CH_2N$ units, such dendrimer compositions may be expressed in the following way:

$$N[(-CH_2CH_2CONHCH_2CH_2N<)_x(H)_y]_{N_c}$$

$$x = \left(\frac{N_b^{G+1} - 1}{N_b - 1}\right), \quad y = N_b^{G+1},$$

In this case, $N_c = 3$ and $N_b = 2$.

The first three generations have the following compositions:

$$G = 0: N(CH_2CH_2CONHCH_2CH_2NH_2)_3$$

$$G = 1: N[CH_2CH_2CONHCH_2CH_2N(CH_2CH_2CONHCH_2CH_2NH_2)_2]_3$$

$$G = 2: N[CH_2CH_2CONHCH_2CH_2N(CH_2CH_2CONHCH_2CH_2N[CH_2CH_2CONHCH_2CH_2NH_2]_2)_2]_3$$

$$G = 3: N[CH_2CH_2CONHCH_2CH_2N(CH_2CH_2CONHCH_2CH_2N[CH_2CH_2CONHCH_2CH_2N(CH_2CH_2CONHCH_2CH_2NH_2)_2]_2)_2]_3$$

Since one has the option of continuing homogeneous dendrimer development or changing chemistry to produce differentiated generations, it is important to define a dendrimer profile for describing a branched assembly composition. We propose the use of cross-sectional descriptions, as illustrated here for a hypothetical heterogeneous starburst polyamidoamine dendrimer. This second-generation polyamidoamine dendrimer derived from an ammonia initiator core, with a 50% hexamethylenediamine component in the first generation and hydroxyl terminal groups, may be expressed as follows:

$$N[CH_2CH_2CONHCH_2CH_2\text{-}N\begin{pmatrix}CH_2CH_2CONH[CH_2]_6\text{-}N[CH_2CH_2CONHCH_2CH_2OH]_2\\ CH_2CH_2CONHCH_2CH_2\text{-}N[CH_2CH_2CONHCH_2CH_2OH]_2\end{pmatrix}_2]_3$$

Examination of such dendrimer profiles allows one to identify the initiator core, core cells, initiator cells, interior cells, and surface cells as illustrated in Figures 11, 12, and 16.

5.2. Controlled Step-Growth Propagation

5.2.1. *In Situ Construction of Branch Cells*

Dendrimer construction with this synthetic strategy requires very high yield/conversion syntheses as well as efficient workup procedures for separation of the dendrimers from the reagents. A variety of polypeptide synthesis methods were used successfully for this approach. They included (1) protection/deprotection methods, (2) solid-phase synthesis and (3) excess reagent methods. Either ultrafiltration or preparative HPLC techniques were used for workup and purification. A major advantage offered by this approach is that the steric bulk of the reagents is usually much lower than that of branched-reagent coupling synthons.

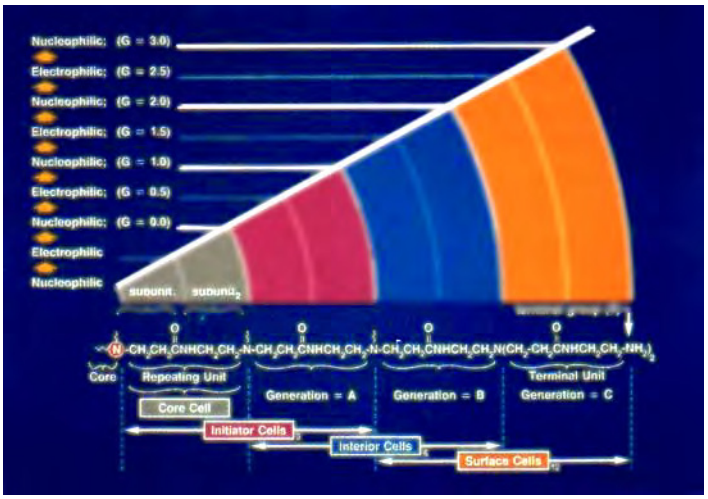

Fig. 16. Cross-sectional view of PAMAM dendron (generation 3) illustrating repeating branch segments, branch-cell hierarchy (for color coding see Fig. 12) and surface electron density features as a function of generation.

Starburst Polyamidoamine (PAMAM) Dendrimers

Starburst polyamidoamine (PAMAM) synthesis may begin with either a nucleophilic or an electrophilic core. In the case of a nucleophilic core such as ammonia or amine, step A in Scheme 1 involves exhaustive Michael addition to methyl acrylate. This addition occurs very rapidly and in high yield with essentially complete selectivity and no amidation at room temperature. Step B requires addition of this triester intermediate to a large excess of ethylenediamine at room temperature (formation of "subunit$_2$", Fig. 16) to produce the terminal triamine core cell shown in Scheme 1. Repeating the sequence of steps A and B leads, via a hexaester (generation = 0.5), to a hexaamine (generation = 1.0). Continuing the sequence of steps A and B (Scheme 1) produces increasingly higher generations. Dendrimer growth beyond generation 3 simply introduces more concentric tiers of interior cells which provide scaffolding for surface cells whose number follows a geometric progression. Ideal branching

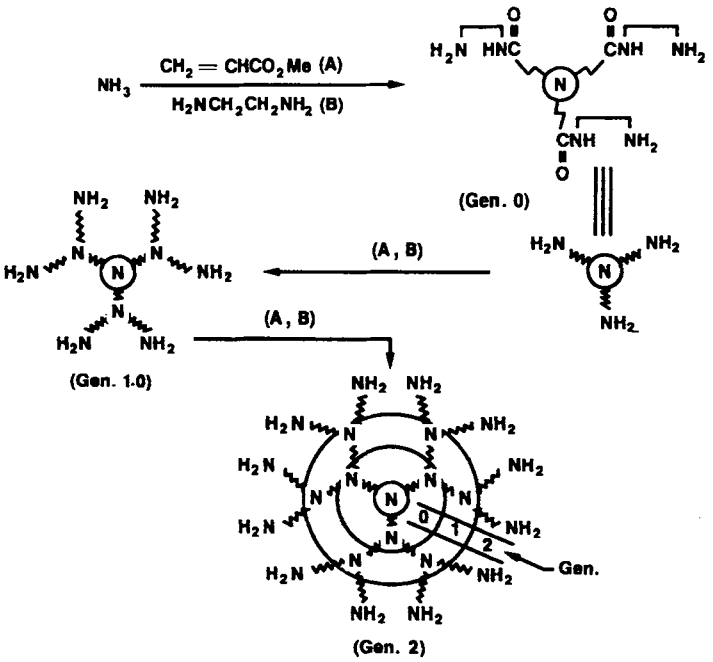

Scheme 1. Synthetic scheme for starburst PAMAM dendrimers.

growth would produce dimensionally precise surfaces with a defined number of surface groups (see Table 1).

Table 1. Relative molar mass M_r, number of monomer units, number of terminal amino groups, predicted diameters (CPK models), and hydrodynamic diameter (determined by size exclusion chromatography) for starburst (PAMAM dendrimers as a function of generation).

Generation	M_r	Monomer units	Terminal groups	Diameters [Å] CPK [a]	SEC
0	359	3	3	9.6 (19.2)	10.8
1	1043	9	6	12.8 (28.8)	15.8
2	2411	21	12	17.6 (41.6)	22.0
3	5147	45	24	24.1 (51.2)	31.0
4	10619	93	48	30.6 (65.6)	40.0
5	21563	189	96	38.5 (81.6)	53.0
6	43451	381	192	47.5 (91.2)	67.0
7	87227	765	384	61.8 (104.0)	80.0
8	174779	1533	768	78.0 (117.0)	92.0
9	349883	3069	1536	98.0 (130.0)	105.0
10	700091	6141	3072	123.0 (143.0)	124.0

[a] CPK = Corey–Pauling–Koltun; the first value refers to a three-dimensional contracted model, the value in parentheses to a three-dimensional extended model.

The present tridendron PAMAM dendrimer series increases its diameter by approximately 10 Å per generation, evolving from a disklike shape (generations 0–2) to an oblate spheroid (generations 3, 4) to a nearly symmetrical spheroid at generations 5 and higher[111] (cf. also Section 10). A Corey–Pauling–Koltun (CPK) model of generation 5 is shown in Figure 17. Successful syntheses of ideal highly branched PAMAM dendrimers through generation 9 have been completed.

Alternatively, initiator cores have been tethered to solid supports (Merrifield resins). Using protein synthesis procedures that avoid the workup difficulties involved in handling large excesses of reagents, one can readily control dendrimer growth. Unfortunately, only noncleavable linkers have been examined to date for these PAMAM dendrimers. The use of initiator cores possessing cleavable linkers should make dendrimer synthesis and isolation very facile. This was demonstrated for starburst polylysines by *Tam* et al.[129–131] (see Section 9.2.6).

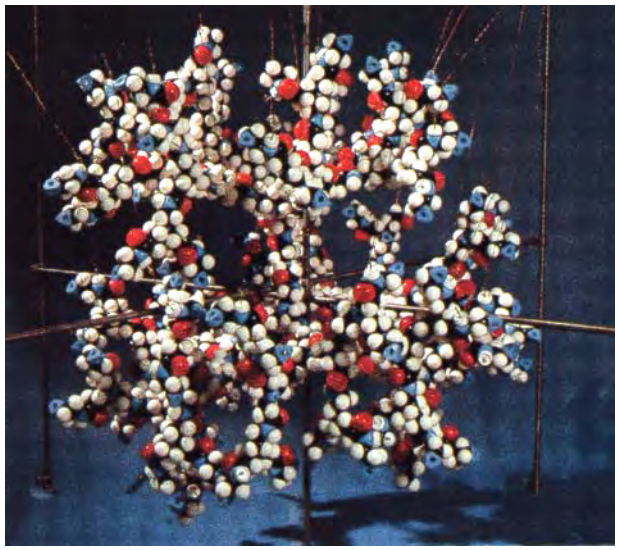

Fig. 17. CPK model of a starburst PAMAM dendrimer of generation 5.

A variety of mono-, di-, tri-, tetra-, and polydendron PAMAMs have been synthesied from simple amines as well as linear polyamine cores.[62–67] Linear polyethylenimines with core multiplicities N_c of ca. 300–400) have been shown to produce high-aspect-ratio, rodlike dendrimers at generation 3 or 4.[87] Their length is determined by the degree of polymerization (n) of the initiator core and their diameter is derived from the number of generations (see Scheme 2).

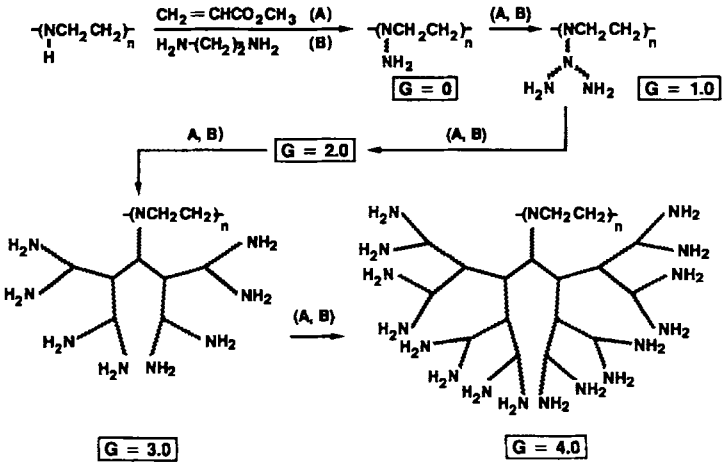

Scheme 2. Synthetic scheme for starburst PAMAM rodlike dendrimers.

Starburst Polyethylenimine (PEI) Dendrimers

Polyethylenimine (PEI) has been examined extensively both in its classical random branched topology[88] and in its

linear form.[89] Here we describe the first example of this polymer system as an ideal highly branched molecular assembly. Synthesis of a tridendron polyethylenimine dendrimer derived from an ammonia core involved first the selective alkylation of diethylenetriamine (DETA) with aziridine to produce a symmetrical core cell, namely, tris-(2-aminoethyl)amine. Subsequent exhaustive alkylations of the terminal amino moieties with activated aziridines,[88] such as *N*-tosyl- or *N*-mesylaziridine gave very good conversions to the first-generation protected starburst PEI (SPEI) dendrimer (see Scheme 3). Deprotection by acid hydrolysis

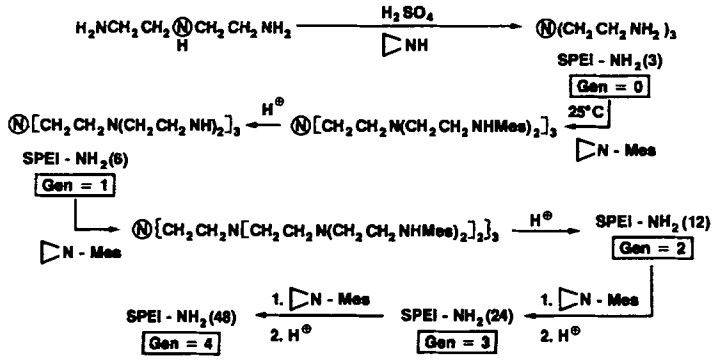

Scheme 3. Synthetic scheme for starburst polyethylenimine (SPEI) dendrimers.

yielded the demasked first-generation dendrimer. The higher generations were obtained by simply repeating these sequences. These SPEIs are described by the following general notation:

$$N[(CH_2CH_2N<)_x(H)_y]_{N_c}$$

$$x = \left(\frac{N_b^{G+1} - 1}{N_b - 1}\right),\ y = N_b^{G+1},\ N_c = 3,\ N_b = 2$$

The defect levels become progressively higher and divergence from branch ideality becomes substantial as one approaches generations 3 and 4 and especially generation 5.[90]

These dendrimers have branch-segment lengths which are approximately one-half that of the PAMAM series (5 Å versus 10 Å) and possess chemical linkages which have much greater chemical and physical stability. A comparison of theoretical molar masses, number of terminal groups, CPK-predicted diameters, and measured diameters (size exclusion chromatography, SEC) as a function of generation is shown in Table 2.

Table 2. Relative molar mass M_r, number of terminal amino groups, predicted diameter (CPK models), and hydrodynamic diameter (SEC) for starburst dendrimers as a function of generation.

Generation	M_r	Terminal groups	Diameter [Å] CPK [a]	SEC
0	146	3	7.2 (8.8)	7.9
1	398	6	11.2 (15.6)	15.1
2	917	12	13.6 (19.2)	20.0
3	1949	24	18.2 (24.8)	–
4	3968	48	23.0 (29.0)	–
5 [b]	–	–	–	–

[a] The first value refers to a three-dimensional contracted model, the value in parentheses to a three-dimensional extended model. [b] Forbidden molecular structure.

CPK models of generations 0–5 (Fig. 18) show that these SPEIs are much more congested and compact than the starburst PAMAMs. These models indicate that ideally branched generation 5 is forbidden due to starburst dense packing as described and predicted by *de Gennes* and others.[64, 68, 69]

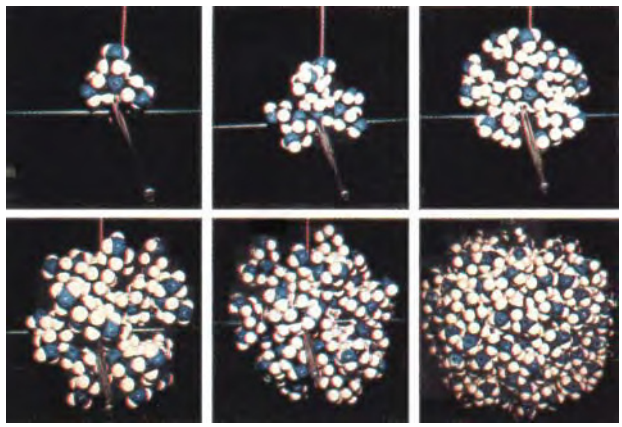

Fig. 18. CPK models of starburst PEI dendrimers of generations 0–5.

Hydrocarbon Dendrimers (Iptycenes)

A unique class of structures referred to as iptycenes has recently been reported by *Hart* et al.[91, 92] These architectures may represent the first examples of all-hydrocarbon dendrimer prototypes. Starting with either benzene or triptycene as the initiator core, branch junctures were constructed in situ by Diels–Alder adduct formation to give the heptaiptycene and the nonaiptycene (tritriptycene) **7**, respectively (Fig. 19). The tritriptycene derivative possesses molecular

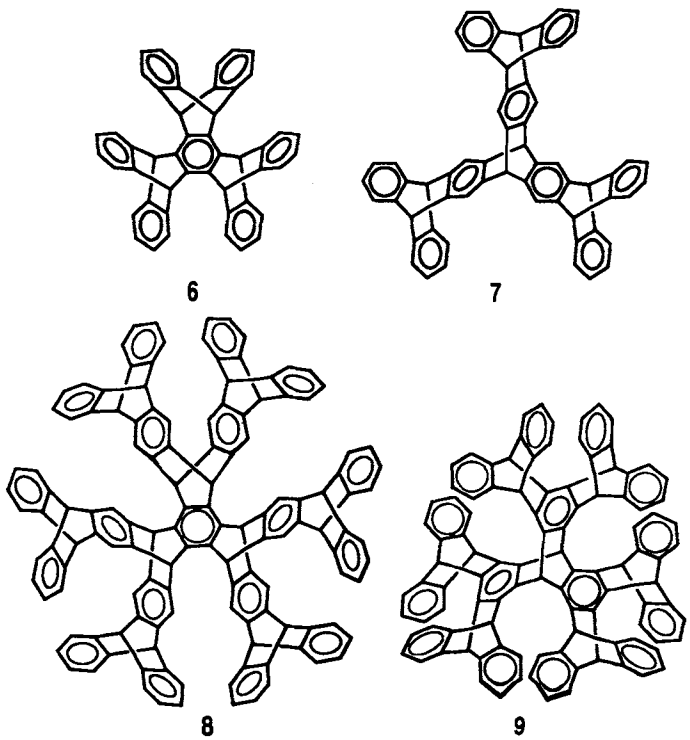

Fig. 19. Hydrocarbon dendrimers (iptycenes): heptaiptycene, **6**; nonaiptycene, **7**; nonadecaiptycene, **8**; supertriptycene, **9**.

clefts defined by parallel benzene moieties ca. 9 Å apart. These U-shaped cavities defined by the arene planes accommodate acetone to form a 1:1 crystalline complex which was verified by X-ray structure studies. More recently, *Hart* et al.[93] have successfully added six more 9,10-dihydroanthracene moieties to **6** to give the $C_{132}H_{78}$ hydrocarbon **8** (nonadecaiptycene). Similar reactions led to **9** (supertriptycene).

5.2.2. *Coupling of Partially Masked or Differentiated Branch-Cell Reagents*

The use of protection/deprotection methods or highly differentiated, branched reagents allows selective coupling without bridging or looping side reactions. Table 3 summarizes the branched reagents used successfully so far.

Table 3. Various branched reagents used to introduce branch cells with $N_b = 2$ or 3.

$N_b = 2$	Ref.	$N_b = 3$	Ref.
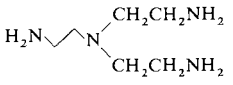	[138]	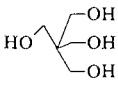	[94]
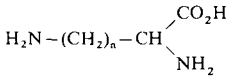	[73]	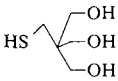	[95]
n = 1-3,5		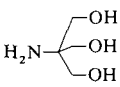	[75-77]
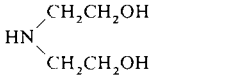	[138]		
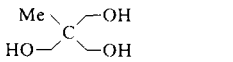	[94]	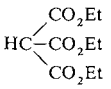	[75-77]
		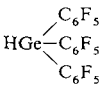	[97]
		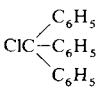	[138]

Starburst Polyether Dendrimers

This dendritic series includes examples of the most highly branched, as well as the shortest-branch, segmented dendrimers produced to date.[65] The high initiator core multiplicity ($N_c = 4$), combined with high branch multiplicity ($N_b = 3$), produces very compact, highly congested microdomains which possess, at most, only very small internal voids. This homologous series has the following general notation:

$$[C(CH_2O)_4][([CH_2C(CH_2O)_3]_x[CH_2C(CH_2OH)_3]_y)_{N_c}$$

$$x = \left(\frac{N_b^G - 1}{N_b - 1}\right),\ y = N_b^G,\ N_c = 4,\ N_b = 3$$

Standard synthetic methods are used to couple partially protected pentaerythritol to the core cell and subsequent dendrimer surfaces.[65] Synthesis of the first generation involves displacement of bromide from $C(CH_2Br)_4$ with a masked pentaerythritol (bicyclic orthoester). One obtains

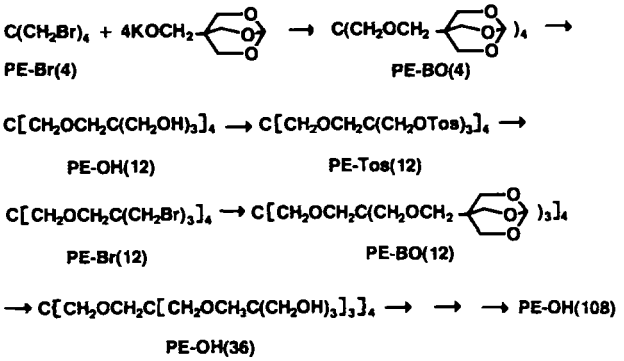

Scheme 4. Synthetic scheme for starburst polyether (PE) dendrimers.

three hydroxyl groups per terminal group after deprotection (Scheme 4; see also Fig. 5, bottom). Therefore, a series that triples both its surface hydroxyl groups and its molar mass is obtained (see Table 4).

Table 4. Relative molar mass M_r, number of terminal hydroxyl groups, predicted diameters (CPK models), and hydrodynamic diameter (SEC) for starburst polyether dendrimers as a function of generation.

Generation	M_r	Terminal groups	Diameter [Å] CPK [a]	SEC
0	136	4	– –	–
1	606	12	10.4 (12.0)	9.8
2	2024	36	16.2 (18.4)	18.6
3	–	108	22.4 (24.0)	25.0
4 [b]	–	–	–	–

[a] The first value refers to a three-dimensional contracted model, the value in parentheses to an extended model. [b] Forbidden molecular structure owing to surface congestion.

Molecular dynamics simulations (Section 6) clearly demonstrate that these tetradendron prototypes assume spheroidal shapes early in their development. Synthetic efforts revealed that branching defects became progressively higher as one advanced from generation 2 to generation 3. The simulations indicate that the fourth-generation dendrimer possessing 324 hydroxyl surface groups is a highly constrained, rigid system with essentially no internal voids or channels (see Figs. 20, 24 and 25). Starburst dense packing appears to occur between generations 3 and 4.

Starburst Polythioether Dendrimers

This series was synthesized according to Scheme 4 as described for the polyethers, with the exception that a mercapto-functionalized, bicyclic orthoester was used for the coupling step.[94] This produced a dendrimer series containing thioether linkages in the interior with hydroxyl surface groups as described by the following general notation:

$$[C(CH_2O)_4][([CH_2C(CH_2O)_3]_x[CH_2C(CH_2OH)_3]_y)_{N_c}$$

$$x = \left(\frac{N_b^G - 1}{N_b - 1}\right),\ y = N_b^G,\ N_c = 4,\ N_b = 3$$

In contrast to the polyether series, the number of hydroxyl surface groups in the thioether series did not triple upon

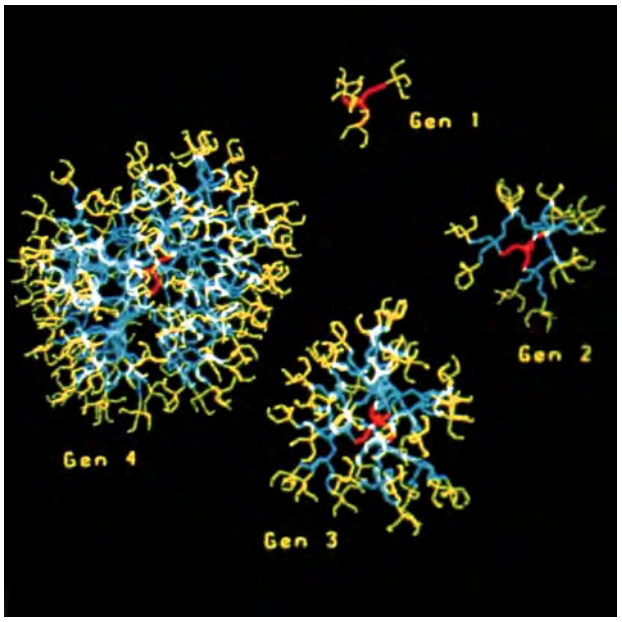

Fig. 20. Computer-simulated molecular graphics (wireframe) using POLYGRAF [97b] for starburst polyether dendrimers of generations 1–4.

attempted advancement from generation 2 to generation 3. This suggests that sterically induced stoichiometry effects are occurring one generation earlier than in the polyether series.

Polyamide Dendrimers (Denkewalter Dendrimers)

Denkewalter et al.[73] reported the synthesis of monodendron polyamides through generation 10. The scheme involved protection/deprotection methods commonly used by polypeptide chemists. Dendrimer construction started with benzhydrylamine as the initiator core and an activated ester of amino-protected L-lysine as the branching reagent (Scheme 5).

N,N'-Bis(*tert*-butoxycarbonyl)-L-lysine nitrophenyl ester was the branching monomer used in the stepwise propagation. The dendrimer surfaces initially possessed hydrophobic Boc units and then, after deblocking, hydrophilic amine moieties. Although the dendrimer structures were not rigorously verified, subsequent work by *Aharoni* et al.[74] showed that they were quite monodispersed and behaved as "nondraining" spheres. *Tam* and co-workers[129–131] produced these dendrimers on a Merrifield resin followed by surface functionalization with various antigenic polypeptide sequences (see Section 9.2.6). A comparison of molar mass, number of terminal groups, and dimensions as a function of generation for the Denkewalter dendrimer is shown in Table 5. Unlike all the other dendrimer examples reported, the branch junctures in this system are constructed from unequal branch-segment lengths.

Table 5. Relative molar mass M_r, number of monomer units (lysine), number of terminal amino groups, and hydrodynamic diameters for starburst polyamide dendrimers as a function of generation.

Generation	M_r	Monomer units	Terminal groups	Diameter [Å] [a]	Diameter [Å] SAXS [b]
0	511	1	2	11.8	–
1	967	3	4	14.6	–
2	1900	7	8	18.2	16.0
3	3700	15	16	22.8	20.0
4	7300	31	32	28.6	25.8
5	14600	63	64	36.0	–
6	29200	127	128	45.2	39.8
7	58400	255	256	57.0	59.2
8	116800	511	512	71.8	–
9	233600	1023	1024	90.6	86.8

[a] By measurement of intrinsic viscosity [74]. [b] By small-angle X-ray scattering.

Polyamido Alcohol Dendrimers (Arborols)

This dendrimer class is a special example of a heterogeneous series. It possesses branch cells derived from the branched reagents triethyl methanetricarboxylate and aminotris(hydroxymethyl)methane. In the present case, a tridendron dendrimer with $N_c = 3$ and $N_b = 3$ is obtained by advancement through an alkylation stage and an amidation step (Scheme 6). The resulting hydroxyl-functionalized dendrimers from these "cascade" syntheses have been coined "arborols" by *Newkome* and co-workers.[75–77] They described the synthesis of mono-, di-, and tridendron proto-

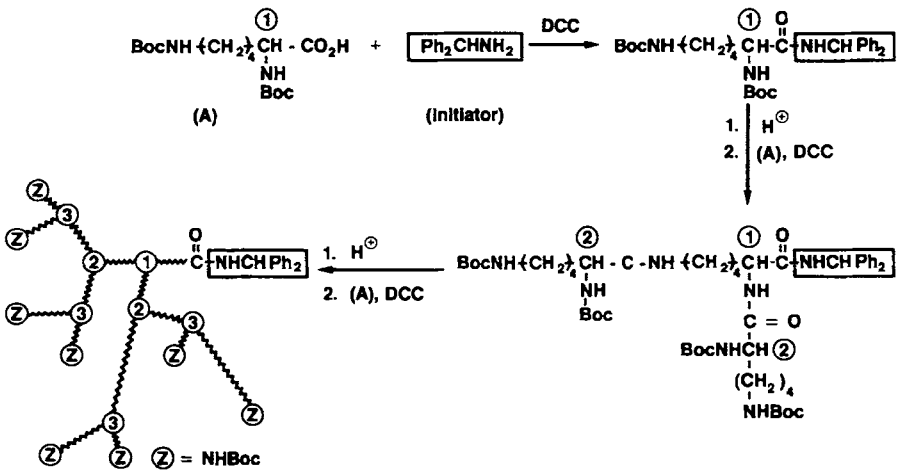

Scheme 5. Synthetic scheme for Denkewalter dendrimers.

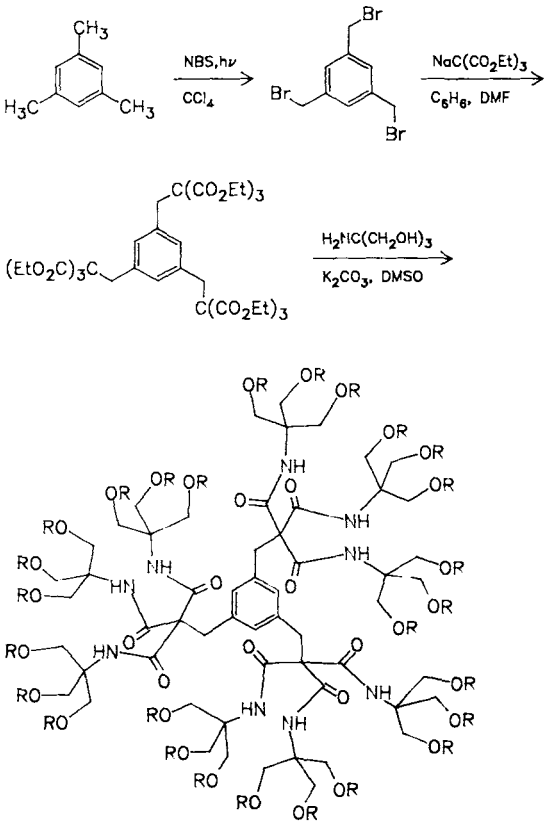

Scheme 6. Synthetic scheme for arborols [75–77]. NBS = *N*-Bromosuccinimide, DMSO = dimethyl sulfoxide; R = H, COC_6H_5.

types, with the following general structural notation ($N_b = 3$);

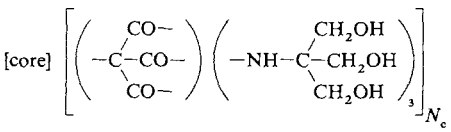

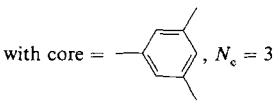

with core = , $N_c = 3$

with core = , $N_c = 2$
with core = C_nH_{2n+1} ($n = 1-9$), $N_c = 1$

Certain didendron prototypes that possess hydrocarbon interiors having "barbell-like" architecture self-assemble into rod-type nanostructures (see Section 13).[77]

This method leads to very compact, highly branched dendrimers possessing as many as 27 surface groups. Reiterative chemistry, which would allow advancement to higher generations, has not been reported yet.

Polyarylamine Dendrimers

Hall et al.[54] produced a low-molar-mass series of polyarylamine dendrimers by using a protection/deprotection scheme involving the protected, branched reagent 2,4-dinitrofluorobenzene. Using various anilines as initiator cores, the reiteration scheme involved fluoride displacement by the anilines, reduction of nitro groups to amino groups, and subsequent reaction with 2,4-dinitrofluorobenzene.

5.3. Uncontrolled Chain-Growth Propagation

Flory[46] first suggested the possibility of forming highly branched, treelike networks by polymerization of a differentiated monomer such as A-R-B_n, where n is greater than one and functional group A can react with B. Very early reports on these systems described them as polycondensates, consisting of broad molar-mass distributions with randomly branched topologies. The methods of synthesis included Friedel–Crafts coupling of benzyl alcohols[55a] and the polymerization of 2,5,6-tribromophenol by aryl ether formation.[55b] In addition, natural carbohydrate polymers, such as amylopectin, dextrin, and glycogen have been extensively studied.[56–58]

Very recently, Russian workers[95] have reported studies on organometallic analogues of these systems. Their work describes the formation of spheroidal, treelike topologies, which appear to approach a self-limiting molecular-mass range, by uncontrolled, anionic chain polymerizations.

Similarly, *Webster* and *Kim*[96] have reported the synthesis of "hyperbranched" polyphenylenes by aryl–aryl coupling reaction of differentiated, branched aryl monomers.

5.3.1. Chain Propagation of Differentiated, Branched Monomers

Bochkarev et al.[95] have recently described the anionic polymerization of $HM(C_6F_5)_3$, M = Ge, Si, or Sn ($N_c = 1$, $N_b = 3$). Most noteworthy is the germanium system, where they have obtained self-limiting molecular-mass ranges of approximately 100000–170000, in spite of the mode of preparation. These workers hypothesize that deprotonation at germanium produces anions that nucleophilically displace fluorine atoms in *para* positions to produce a dendrimer structure of the following general formula:

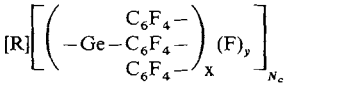

$$x = \left(\frac{N_b^G - 1}{N_b - 1}\right), \quad y = N_b^G; \quad N_c = 1, \quad N_b = 3$$

Structural verification is based on viscosity data (indicating Einstein spheroid characteristics), elemental analyses, light-scattering experiments, and direct observation of individual dendrimers by electron microscopy.

The self-limiting molar-mass ranges correspond to approximately 38 branch-cell propagations (three tiers) around a germanium initiator core. Furthermore, analysis of molecular models indicates that further propagation is precluded owing to "steric screening". This appears to be the first example of a self-limiting *polymerization* to form a densely packed starburst polymer.

6. Molecular Structure of Dendrimers

Although the same types of dendrimer have the same composition and topology for a given generation, they can exhibit an enormous number of possible configurations. In the condensed phase, therefore, each dendrimer is expected to

have a configuration different from the next, so that there is no long-range order. Thus, X-ray diffraction may not be the most effective method for obtaining the molecular-level structure of dendrimers. Consequently, we have resorted to the methods of molecular dynamics to provide these data.

The parameters (force constants, bond distances, etc.) used in these calculations are those of the AMBER force field (optimized for proteins).[97a] The atoms of the dendrimer and solvent (water or methanol) are treated explicitly and used to evaluate the forces on *all* the atoms. Using these forces, we have solved Newton's equations to predict the dynamics of motion for the dendrimer at room temperature. Such calculations, referred to as molecular dynamics, were carried out with the program POLYGRAF.[97b] The polymer-building facilities of POLYGRAF were also used to simulate the dendrimers, generation by generation. At each generation the structures were equilibrated and sampled periodically to obtain average properties.

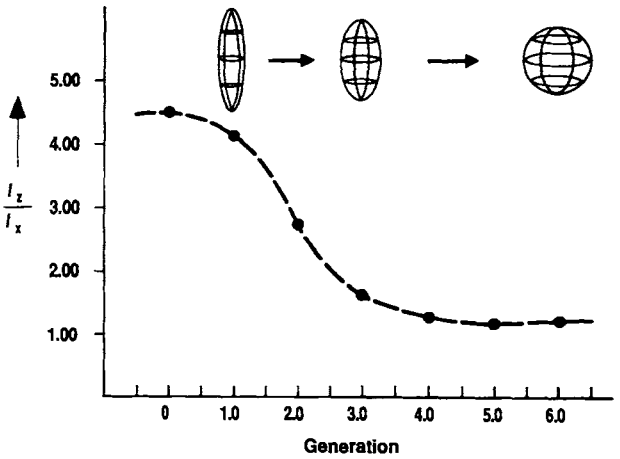

Fig. 22. Comparison of change in starburst PAMAM dendrimer morphology (aspect ratios, I_z/I_y) as a function of generation.

6.1. Starburst Polyamidoamine (PAMAM) Dendrimers

Figure 2 shows wireframe structures of generations 0 through 7 for PAMAM. Through generation 3 the dendrimer resembles a starfish. However, by generation 5 it is already a tangled mass. Better definition of the structure is presented in Figure 21, where dots at the van der Waals

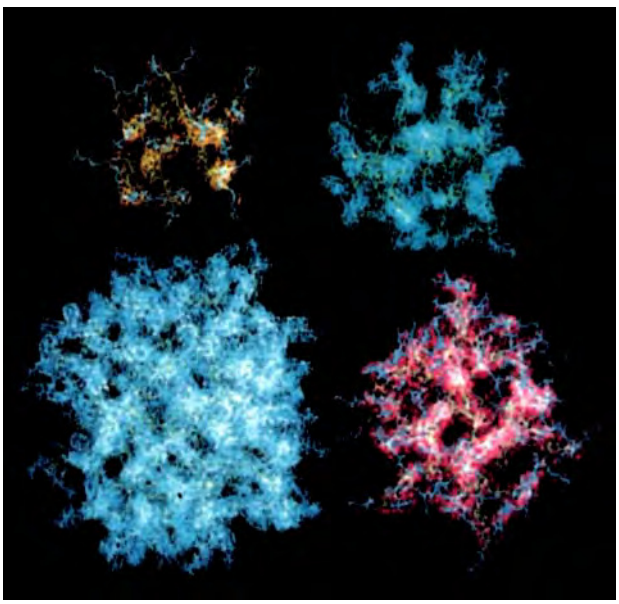

Fig. 21. Computer-simulated molecular graphics (POLYGRAF) for PAMAM dendrimers of generations 3–6 (clockwise). Dots represent van der Waals radii of dendrimer atoms.

radius of each atom define the outside of the molecule. The early generations are somewhat amorphous in shape, but the latter ones are clearly spherical. This transition to a spheroidal form is clearly illustrated by the aspect ratio of the largest to smallest principal moment (I_z/I_x) for various generations (Fig. 22). The aspect ratio decreases from 4.5 for generation 0 to 1.3 for generations 5 and 6.

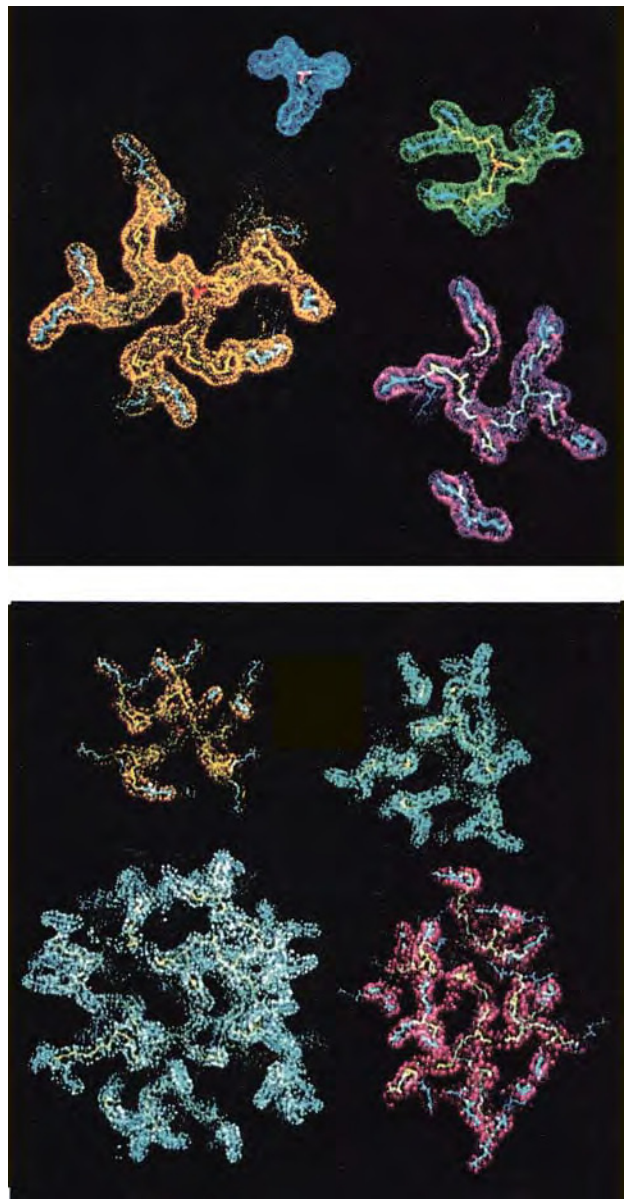

Fig. 23. Computer-simulated molecular graphics (POLYGRAF) of infrastructure of starburst PAMAM dendrimers by graphical slabbing. Top half: generations 0–3. Bottom half: generations 3–6 (clockwise in each case).

These views from the dendrimer exterior give little clue as to the internal character of these systems. This internal structure is illustrated in Figure 23, where graphical "slabbing" is used to display only a section from the middle portion of the macromolecule. Already by generation 4, there are substantial nooks and crannies, which, by generation 6, have evolved into a labyrinth of channels and cavities. These later generations clearly display well-defined internal structures.

6.2. Starburst Polyether Dendrimers

Since the initiator-core and branch-juncture multiplicities in the polyether system ($N_c = 4$, $N_b = 3$) are higher than in the PAMAM system, the polyether system quickly becomes congested and has little in the way of internal cavities (see Figs. 20, 24 and 25).

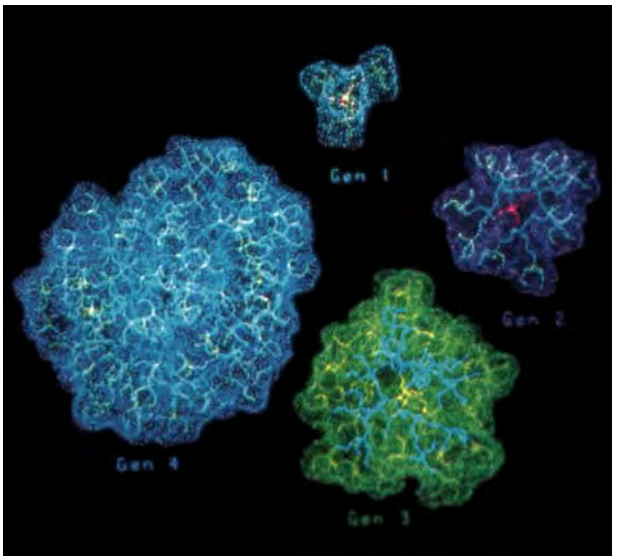

Fig. 24. Computer-simulated molecular graphics (POLYGRAF) of starburst polyether dendrimers of generations 1–4. Dots represent van der Waals radii of dendrimer atoms.

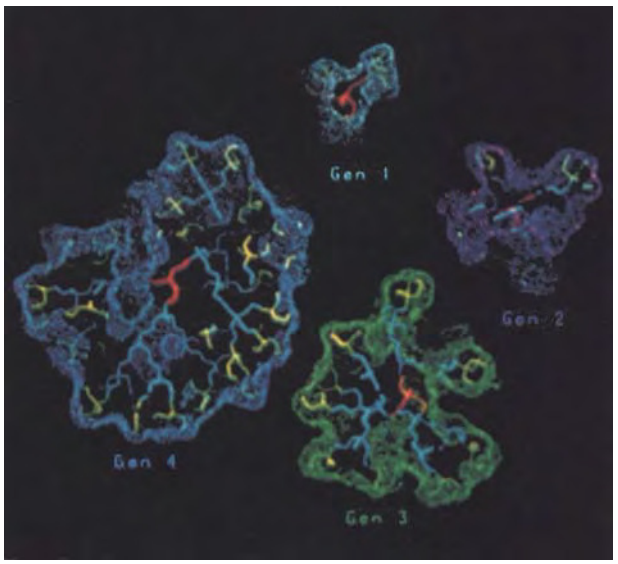

Fig. 25. Computer-simulated molecular graphics (POLYGRAF) of starburst polyether dendrimers of generations 1–4, exposing infrastructure by graphical slabbing.

6.3. Internal Surfaces and Volumes

The PAMAM dendrimers have a great deal of internal surface area and solvent-filled volume (see Fig. 23), whereas the polyether dendrimers have very little. A quantitative comparison can be made by using the concept of solvent-accessible surface (SAS).[98] The SAS is obtained by "rolling" a sphere of radius p (the probe radius) around the van der Waals surface of the molecule, where p represents the effective radius of the solvent (e.g., $p = 1.4$ Å for H_2O). The SAS is then composed of the locus of the probe-sphere midpoints. The program GEPOL87[99] has been used to calculate the SAS and its associated volume as a function of probe radius (see Fig. 26).

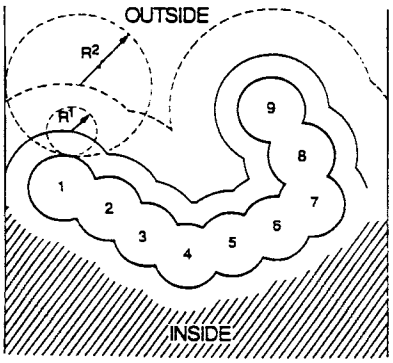

Fig. 26. Schematic representation of the solvent accessible surface (SAS) concept. A section through part of the van der Waals envelope of a dendrimer is shown with the atomic centers numbered 1–9. The SAS is mapped out by the center of various-sized probe spheres.

Consider, for example, the surface of an ideal, spherical body containing no internal voids. For such a system, the surface area is defined as follows:

$$A_{SAS} = 4\pi(R + p)^2$$

R is the radius of the spherical body and p is the radius of the probe. For spherical macromolecules, a plot of $\sqrt{A_{SAS}}$ versus p would be linear with a slope of $2\sqrt{\pi}$ and intercept proportional to the radius R.

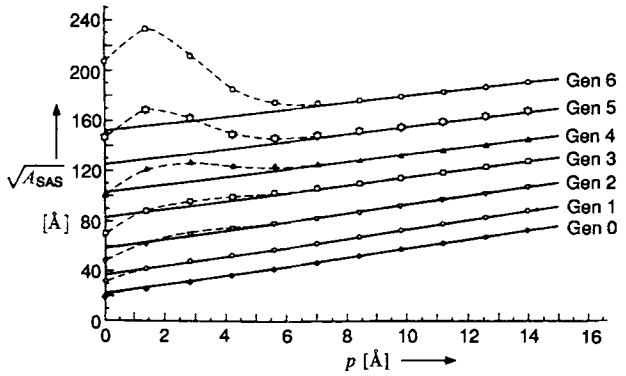

Fig. 27. Plots of $\sqrt{A_{SAS}}$ as a function of probe radius p for PAMAM dendrimers of generations 0–6. Solid lines represent linear regression fits ($p \geq 7.0$ Å); dashed lines connect the calculated values from GEPOL 87 analysis.

The PAMAM and polyether dendrimers are not ideally spheroidal, but they can, to a first approximation, be treated as such. Figures 27 and 28 contain plots of $\sqrt{A_{SAS}}$ as a function of probe radius p for the various PAMAM and polyether dendrimers simulated. Indeed, for large values of

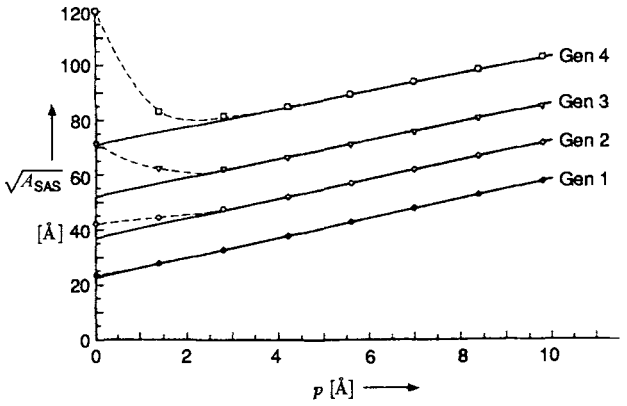

Fig. 28. Plots of $\sqrt{A_{SAS}}$ as a function of probe radius p for polyether dendrimers of generations 1–4. Solid lines represent linear regression fits ($p \geq 4.2$ Å); dashed lines connect the calculated values from GEPOL 87 analysis.

the probe radius, a linear curve is obtained with a slope approximating $2\sqrt{\pi}$. However, for small probe radii, a deviation from linearity is observed owing to the extra surface area associated with the interior regions of the polymer. Linear regression analysis of these SAS areas indicates both the amount of any internal surface area and the size of the macromolecule (see Table 6). For the PAMAM series, the fraction of internal surface is only 1.4% at generation 3 but rises to 29% by generation 4, 69% by generation 5, and 124% by generation 6. Thus, at generation 6, there is more internal surface area than external surface area! In contrast, for the polyether dendrimers, the internal surface area peaks at approximately 20% for generations 3 and 4.

A measure of the volume associated with the internal cavities of the PAMAM dendrimers is achieved by analysis of the volume contained within the calculated SASs (as a function of probe radius). Returning to the example of an ideal sphere devoid of internal cavities, the volume contained within the sphere's SAS is given by the following relation:

$$V_{SAS} = 4/3\,\pi(R + p)^3$$

A plot of $\sqrt[3]{V_{SAS}}$ versus p should be linear with a slope of $\sqrt[3]{4/3\,\pi}$ and an intercept proportional to the radius R. Indeed, this relationship is satisfied for large probe radii (see Figs. 29 and 30), but there is a deficit of volume for small

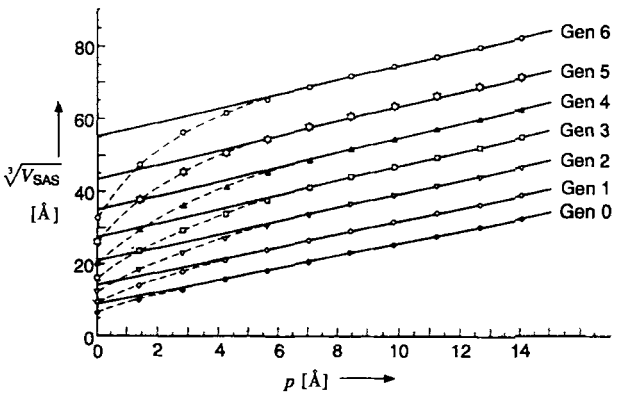

Fig. 29. Plots of $\sqrt[3]{V_{SAS}}$ as a function of probe radius p for PAMAM dendrimers.

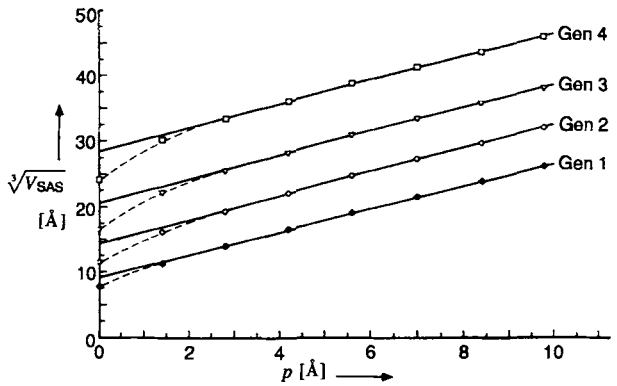

Fig. 30. Plots of $\sqrt[3]{V_{SAS}}$ as a function of probe radius p for polyether dendrimers.

Table 6. Calculated [a] and experimentally determined [b] diameters [Å] as well as internal dendrimer surface areas and volumes [c] of PAMAM and polyether dendrimers as a function of generation.

Gen.	$d_{exp.}$	d_{max}	$d(R_g)$	$d(A_{SAS})$	$A_{int.}$ [%]	$d(V_{SAS})$	$V_{int.}$ [%]
PAMAM dendrimers							
0	11	13	15	12	–	11	–
1	16	24	25	21	–	17	–
2	24	35	35	33	–	25	–
3	31	47	41	47	1.4	34	106
4	40	57	49	58	29	43	103
5	56	68	56	70	69	54	86
6	66	80	70	86	124	68	121
Polyether dendrimers							
1	19	13	13	13	1	11	12
2	19	21	20	21	11	18	16
3	26	30	27	29	22	26	12
4	–	40	37	40	20	35	8

[a] For simulation methods see text. [b] Determined by size exclusion chromatography (solvent H_2O). [c] Based on the outer surfaces and the "outer volumes", respectively.

probes owing to the presence of the internal cavities and channels (see Table 6). The dramatic difference between the PAMAM and polyether series is once again quite evident.

6.4. Diameters

Molecular simulations were used to estimate sizes (diameter d) of both the polyamidoamine and polyether dendrimer families as a function of generation (see Table 6 as well as Figs. 31 and 32). The following four simulation procedures were used.

1. d_{max}, the maximal end-to-end distance between terminal heteroatoms (nitrogens for the PAMAM series and oxy-

gens for the polyethers), was determined periodically and averaged over the entire set of trajectories. This value should provide an upper bound since it emphasizes any dangling arms protruding out of the dendrimer.

2. d_{R_g} is an equivalent diameter determined from the radius of gyration of the polymer, with mass weighting for all atoms.
3. $d_{A_{SAS}}$ is the diameter determined from the linear regression fits of the probe radius versus $\sqrt{A_{SAS}}$, assuming an ideal sphere.
4. $d_{V_{SAS}}$ is the diameter determined from the linear regression fits of the probe radius versus $\sqrt[3]{V_{SAS}}$ assuming an ideal sphere.

All four of these values, plus those obtained from size exclusion chromatography (SEC) studies (d_{exp}, see Section 7), are plotted in Figures 31 and 32 for the PAMAM and

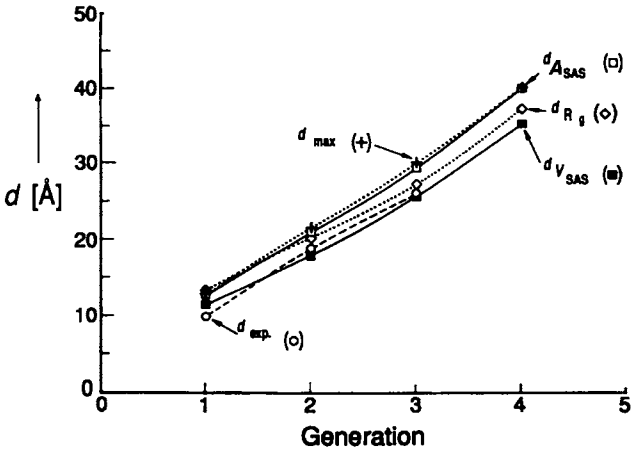

Fig. 31. Plot of calculated and experimental diameters d of PAMAM dendrimers as a function of generation (see text).

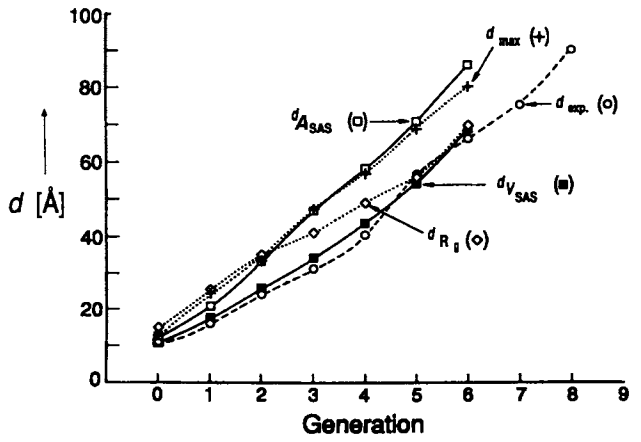

Fig. 32. Plot of calculated and experimental diameters d of polyether dendrimers as a function of generation (see text).

PE dendrimers, respectively. Generally speaking, there is very good agreement between the calculated diameters and those deduced from the experiments. The d_{max} values do indeed provide an upper bracket to the experimental and the other calculated diameters.

7. Characterization of Dendrimers

The structural subtleties represented in these dendrimer topologies require a variety of analytical methods for unequivocal characterization. The following dendrimer features were studied by these methods:

1. *Elemental composition:* C, H, N analyses; mass spectrometric fragmentation patterns.
2. *Molar mass versus generation:* low-angle laser light scattering (LALLS), CI and FAB mass spectrometry; vapor-phase osmometry.
3. *Homogeneity:* size exclusion chromatography (SEC) coupled with low-angle laser light scattering (SEC-LALLS); electron microscopy.
4. *Interior and end groups:* IR spectroscopy; ^{15}N, ^{13}C, and ^{1}H NMR spectroscopy; titration.
5. *Structures:* ^{13}C and ^{1}H NMR spectroscopy (T_1 relaxation times, signal intensity ratio versus generation); rheology studies; electron microscopy; computer-assisted molecular simulations, comparison to CPK models.
6. *Dimensions:* Electron microscopy; intrinsic viscosity measurements; size exclusion chromatography; computer-assisted molecular simulations; comparison with CPK models.

These methods were used extensively for structure verification of starburst PAMAM,[62-66,85] polyether,[65] and polyethylenimine dendrimers.[100] In many cases, small-molecule model systems were used for process optimization, defect identification, and stoichiometry studies.

In the case of PAMAMs, dendrimer bridging and branching defects were identified and minimized by process optimization and/or special purification techniques. Initial work indicated that it would be difficult to prepare dendrimers beyond generations 4 and 5 without bridging.[85] More recent work[101,102] has shown that generations 0–9 can be obtained in very monodispersed form with branching "idealities" of 95 mol% or greater.

7.1. Branching Ideality

^{13}C NMR spectroscopy has served as the best method for appraising branch defects. The symmetry of ideally branched dendrimers produces discrete resonances which are well separated from branch-defect signals (Fig. 33). The branch defects occur when acrylate alkylations are incomplete. The result of such a defect is to give lower molar-mass and surface-group values than theoretically expected. Secondary amine groups resulting from branch defects may become alkylated during advancement to the next generation. The consequence of such an event is that the progeny of such defects are one generation retarded in branch-cell development compared to the rest of the molecule.

7.2. Polydispersity

Very precise appraisals of polydispersities due to branch defects can be made by HPLC fractionation and mass-spectral analyses of the components. The molecular-mass and

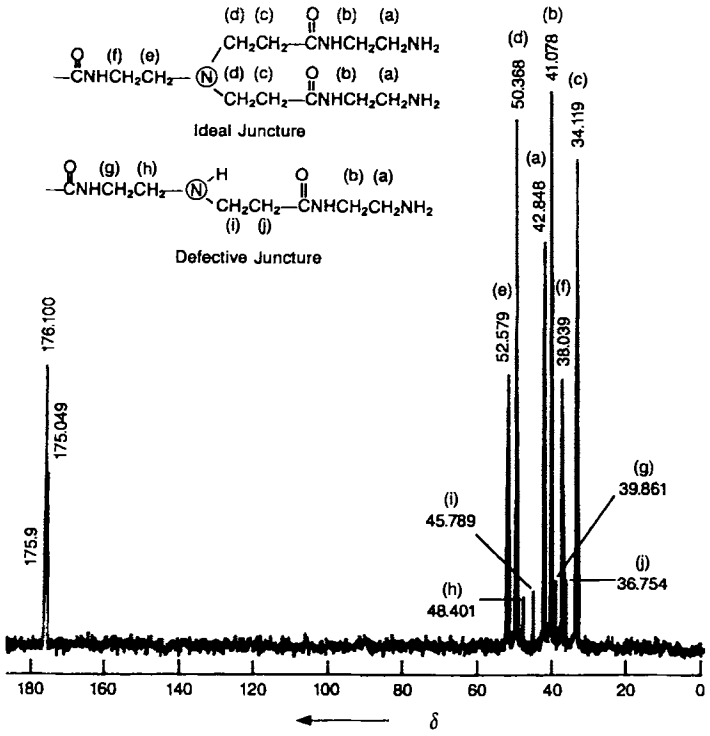

Fig. 33. ^{13}C NMR spectrum of starburst PAMAM dendrimers of generation 7 with assignments for ideal and defective branches (defective branch level ca. 5 mol%).

polydispersity values thus obtained corroborate branch-defect ranges determined by high-field ^{13}C NMR spectroscopy.

Although branch defects may contribute in a minor way to dendrimer polydispersities, inter-dendrimer bridging/looping and extraneous starburst growth derived from unremoved propagating reagents are the major contributors. PAMAM dendrimers may be obtained as very monodispersed samples, if propagating reagents and bridged forms can be removed at each stage. This is accomplished by ultrafiltration with appropriate pore-size membranes. With this technique, polydispersities of 1.01–1.08 were obtained for generations 0–9. Molecular masses, polydispersities, and hydrodynamic diameters are routinely determined by use of size exclusion chromatography (SEC), low-angle laser light scattering (LALLS), and intrinsic viscosity measurements ([η]).

Figure 34 shows an LALLS-monitored SEC chromatogram of a ninth-generation PAMAM dendrimer. In such an experiment, the polymer is injected onto a chromatographic column which separates the sample on the basis of size. Elution of the sample is monitored by two detectors in series. One detector monitors concentration and the other monitors light scattered from the sample. Response from the latter detector depends on the product of concentration and molar mass. By combining the data from both detectors, the molar mass of that portion of the distribution eluting at any instant in time can be determined. In this way, the molar-mass distribution of the entire polymer sample can be determined. For a typical polydisperse sample, the peak profiles for the detector responses will be dramatically different. Since higher-molar-mass components elute first, the LALLS detector will exhibit a larger response at early elution times (and a smaller response at later times) than the concentration detector. On the other hand, for a truly monodisperse sample, the two peaks will coincide since every molecule in the sample has the same molar mass. Figure 34 shows the latter to be essentially

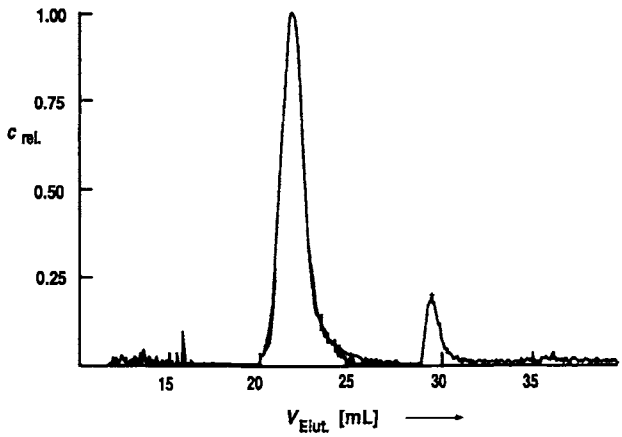

Fig. 34. SEC/LALLS curve for starburst PAMAM dendrimers of generation 9 (* = salt peak). M_w = 351000, M_r = 345000, M_{calcd} = 350338; polydispersity = 1.02. $c_{rel.}$ = relative concentration, $V_{elut.}$ = elution volumes.

the case for this ninth-generation material. Only a small amount of bridged material is present as evidenced by the slight difference between the two profiles of the rising and falling edges. The polydispersity index was determined to be 1.02 for this sample. The absolute molar masses at the peak of the distributions for generations 3–8 are given in Table 7 and compared with the theoretical values. The agreement is well within the experimental error of the light-scattering technique.

Table 7. Comparison of experimental molar masses determined by low-angle laser light scattering (LALLS), theoretical calculations, and hydrodynamic diameters d_{SI} and d_{SEC} (intrinsic viscosity and calibrated SEC) for starburst polyamidoamine dendrimers as a function of generation.

Gen.	M_r (theor.)	M_r (exp.)	d_{SI} [Å]	d_{SEC} [Å]
0	360	– [a]	11	11
1	1044	– [a]	17	16
2	2070	– [a]	22	24
3	5154	5200	31	31
4	10633	10700	40	40
5	21591	21600	53	56
6	43503	44000	67	66
7	87341	88000	76	75
8	175006	174000	90	90

[a] The relative molar mass is too low to be determined by this method.

The hydrodynamic diameter of the dendrimers has been determined by two methods. Both involve application of an equation developed by *Hester* and *Mitchell*.[103] This equation relates the molar mass, the intrinsic viscosity, and the molecular (hydrodynamic) diameter.

$$d = (240/\pi N_A)^{1/3} (M[\eta])^{1/3}$$

d = hydrodynamic diameter (in cm)
N_A = Avogadro number
M = molar mass
$[\eta]$ = intrinsic viscosity (in dL g^{-1})

As mentioned, the factor that determines the elution volume of a polymer from an SEC column is its size. Chemical composition, molar mass, etc. are relevant only to the extent that they determine the hydrodynamic diameter of the polymer in the chromatographic eluent. With this in mind, the SEC columns were calibrated using polyethyleneoxide standards of known molecular mass and intrinsic viscosity. Hydrodynamic diameters of the dendrimers were then determined from their elution volumes by comparison to these standards. They were also determined by measuring intrinsic viscosities. These values and the measured molar masses were used in the Hester–Mitchell equation. The two methods yield diameters which are in very close agreement (see Table 7).

The increase in hydrodynamic diameters as a function of generation in this series may be analyzed by comparing with values obtained from molecular simulations (see Figs. 31 and 32 as well as Table 6). The agreement is excellent. When the surfaces of these dendrimers are charged (e.g., $Z = -CO_2^{\ominus}Na^{\oplus}$), they exhibit hydrodynamic diameters that are dramatically expanded and approach the upper limit. This is no doubt due to Coulombic repulsion on the surface of the dendrimers as well as to an increased solvent cage associated with the charged system.

8. Critical Features and Physical Properties of Dendrimers

8.1. Dendrimer Genealogy

Starburst dendrimers possess three major architectural components: an initiator core/core cell, an interior, and an exterior (see Fig. 35). By definition or construction, these three components are interdependent and reflect a unique molecular genealogy. As one progresses from the initiator-core stage to an advanced dendrimer stage (e.g., generation 3.0), this molecular genealogy manifests itself in a variety of ways (see Figs. 12 and 16).

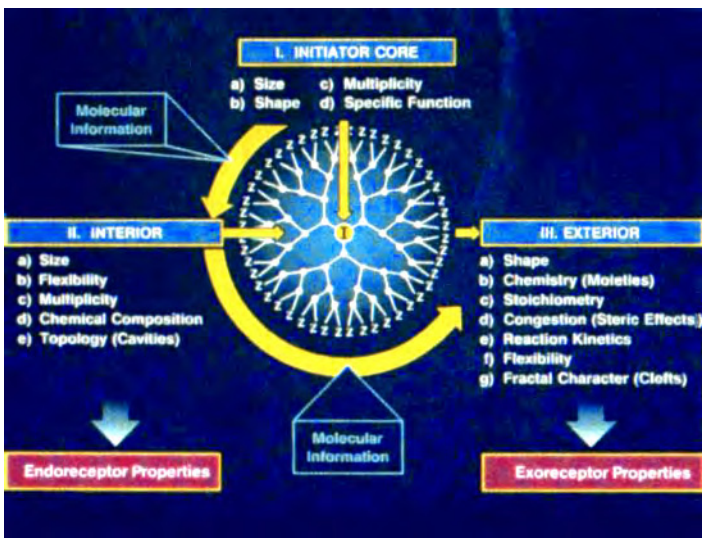

Fig. 35. Dendrimer architectural components with molecular genealogy associated with CMDPs that contribute to endo- and exo-receptor properties.

Just as one can trace ancestry and lineage in higher organisms, so can one observe a molecular-level parallel by thinking of these transformations in the context of (1) stored molecular information at each dendrimer stage and (2) molecular information transferred (transcribed) to the progeny dendrimer surface at each transformation. For example, the initiator core may be thought of as a primitive abiotic gene.[132–134] Beginning with the initiator core, molecular details are sequentially transcribed and stored to produce interior and ultimately exterior (surface) features which are characteristic of that dendrimer family (phenotype). In this fashion, interior features such as size, chemical composition, flexibility, and topology (cavities) are developed and manifested as stored molecular information, which may exhibit convergent recognition[12] or endo-receptor properties.[9c] Important biological analogies to these microenvironments may be found in the active binding sites of enzymes. The interior of a dendrimer consists of a scaffolding upon which surface properties such as shape, reactivity (functionality), stoichiometry, congestion, special kinetic features, flexibility, and "fractal" character (clefts) can be generated and controlled. These surface features govern divergent recognition and as such may be expected to exhibit exo-receptor properties.[9c] Significant biological analogies include antibody–antigen interfaces involved in immunological recognition processes[104–106] as well as most protein–protein interactions and exo-recognition at membranes or cell walls[38, 107, 108] (see also Section 11).

8.2. Topology, Branch-Cell Differentiation, and Surfaces

8.2.1. Initiator-Core and Core-Cell Effects

As mentioned earlier (see also Fig. 35), the initiator core/core cell is the primary template. As such, very important molecular information such as size, shape, multiplicity (N_c), and specific function can be introduced. For example, introduction of a specific function such as a chromophore or metal chelator in the initiator core represents stored information which will become buried by subsequent generations. In contrast, parameters such as size, shape, and multiplicity will be transcribed and displayed (translated) throughout the dendrimer development. These variables can have dramatic effects on the ultimate shape, the interior topology, and the exterior surface properties (congestion) of the developing dendrimer.

8.2.2. Interior Development

In addition to size, chemical composition, multiplicity, and flexibility, the interior of a dendrimer may be characterized by branch-cell differentiation, topology, and the evolution of a branch-cell hierarchy. Branch-cell differentiation, in particular, can dramatically change not only the interior topology but also the gross exterior surface of a dendrimer. Symmetrical branch junctures appear to favor "shell topology" formation if they have adequate branch-segment lengths l and the N_c and N_b values are not too high. Asymmetrical

branch junctures, as represented by Denkewalter dendrimers (Figs. 13 and 14) exhibit a more classical relationship between density and molecular mass[67] (Fig. 36). Presumably, this is due to more effective interior packing of the asymmetrical branch cells.

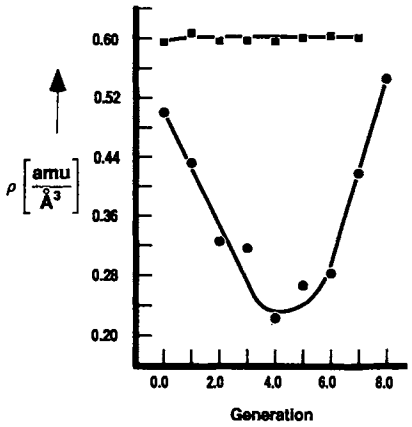

Fig. 36. Dependence of density ϱ on generation for symmetrically branched and asymmetrically branched dendrimers. amu = atomic mass unit. ■, Denkewalter dendrimers (unsymmetrical branch cells); ●, starburst PAMAM dendrimers (symmetrical branch cells).

Such subtleties are difficult to analyze in most homogeneous, classically branched, random-coil macromolecules in that these systems generally lack suitable internal reference points. An exception to this is the generic class referred to as starbranched macromolecules.

8.2.3. Comparison of Starburst Dendrimers to Starbranched Systems

The topology of starbranched macromolecules has certain similarities to that of starburst dendrimers, such as an initiator core, radial branches, and, in some cases, even telechelic functionality.[150] Beyond these comparisons and according to the Daoud–Cotton model,[109, 110] there are dramatic differences between the two systems. In the starbranched model, there are radial cell-like differentiations referred to as blobs. Most notable, however, is the fact that the branch-segment densities of many-armed starbranched polymers are inverse to those of symmetrically branched starburst dendrimers. As found in the two-dimensional projections of the Daoud–Cotton model (Fig. 37) and in computer-simulated models of many-armed starbranched systems (Fig. 38), the branch-segment densities are greatest near the initiator core and decrease in a concentric, radial fashion. In contrast, starburst dendrimer models possessing symmetrical branch cells and shell topologies predict increased branch-segment densities (congestion) as one advances to higher generations (cf. Fig. 11). By contrast, asymmetrically branched starburst dendrimers (cf. Figs. 14 and 36) exhibit constant branch-segment densities as a function of generation.[67]

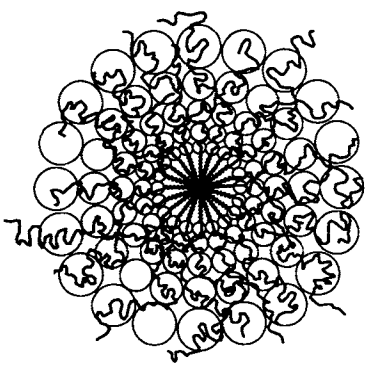

Fig. 37. A two-dimensional projection of a Daoud–Cotton model for starbranched polymers.

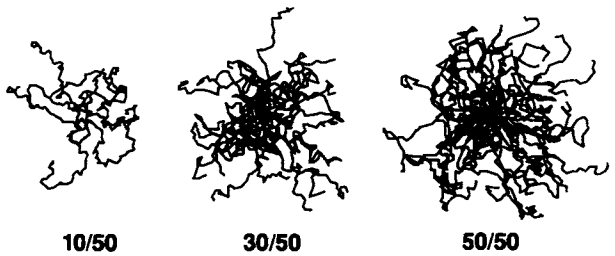

Fig. 38. Computer-simulated models of starbranched systems with 10, 30, and 50 arms. Each arm consists of 50 monomer units.

8.2.4. Starburst Dense Packing—A Critical Branched State?

Mathematically, one can appraise dendrimer surface congestion, as a function of generation, from the following relation:

$$A_Z = \frac{A_D}{N_z} \propto \frac{r^2}{N_c N_b^G}$$

A_Z is the surface area per terminal group Z, A_D the dendrimer surface area, and N_Z the number of surface groups Z per generation. From this relation, it can be seen that at higher generations G, the surface area per Z group should become increasingly smaller and experimentally approach the cross-sectional area or van der Waals dimensions of the surface groups Z. The generation G thus reached is referred to as the starburst dense-packed generation. As predicted by *de Gennes* and *Hervet*,[68] ideal starburst growth without branch defects is possible only for those generations preceding this dense-packed state. This critical dendrimer property gives rise to self-limiting starburst dimensions, which are a function of the branch-segment length l, the core multiplicity N_c, the branch-juncture multiplicity N_b, and the steric dimensions of the terminal group Z. Since the dendrimer radius r in the expression above is dependent on the branch-segment lengths l, larger l values will delay this congestion, whereas larger N_c and N_b values and larger Z dimensions will dramatically hasten it.

As early as 1983, *de Gennes* et al.[68] derived a simple equation from fundamental principles, which was proposed to predict the starburst limited or dense-packed generation m_l for PAMAM dendrimers. Based on ideal starburst growth, with tertiary amine branch junctures connected by

linear, flexible branch segments P, this equation relates m_1 to the branch-segment length l or P:

$$m_1 \approx 2.88\ (\ln P + 1.5)$$

With this equation and based on branch-segment lengths described for PAMAMs (see Section 5), the dense-packed generation m_1 was predicted to occur between generations 9 and 10. This appears to have been experimentally verified.

Clearly, this proposed congestion at the critical branched state M_1 should exhibit (1) sterically inhibited reaction rates, (2) sterically induced stoichiometry, and, quite possibly, (3) a critical phase change due to surface cooperativity (association). These phenomena have been observed experimentally for the starburst PAMAM dendrimers and may prove to be diagnostic probes for this critical branched state in other dendrimer families.

Computer-assisted molecular modeling has shown that starburst PAMAM dendrimers progress through a continuum of morphologies ranging from open hemispherical domes to closed spheroids (see Fig. 22).[111] The simulations indicate that the closed spheroids possess well-developed internal hollows and channels beyond generations 4 and 5. These morphological changes are paralleled by monotonic decreases in the spin–lattice relaxation times T_1 when various guest molecules (e.g. acetylsalicylic acid or 2,4-dichlorophenoxyacetic acid) are present. Presumably, this finding indicates a multiple guest–host relationship. Guest:host stoichiometries as high as 4:1 (by weight) and 3:1 (based on molar comparison of the interior tertiary amino groups of the dendrimer to the carboxylic acid moieties of the guest) were observed for generations 1.5 to 4.5.

Calculation of dendrimer exterior surface areas, assuming spherical geometry, allows the determination of surface area per Z group, A_Z, as a function of generation (Fig. 39). The

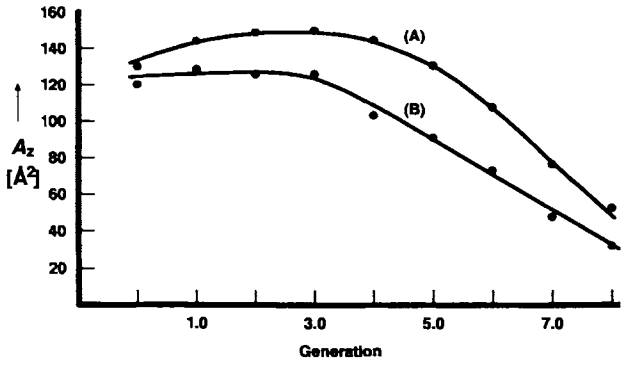

Fig. 39. Plot of surface area per terminal Z group, A_z, as a function of generation for starburst PAMAM dendrimers. Curves A and B assume 95% and 100%, respectively of the theoretical number of surface groups.

curves show that A_Z values remain relatively constant (ca. 100–120 Å^2 per Z group) for generations 0–3 and then decline to a minimum value of ca. 33 Å^2 per Z group at generation 8. These experimental data are supported by computer-assisted simulations and surface areas derived from these calculations.

These effects all contribute to the differentiation of dendrimer branch cells as one advances to higher generations (Fig. 40). A comparison of T_1 values for dendrimer interior carbons and surface carbons shows that although the T_1 values for interior carbons remain relatively constant with increasing generation, the T_1 values for the surface carbons decrease dramatically.[102]

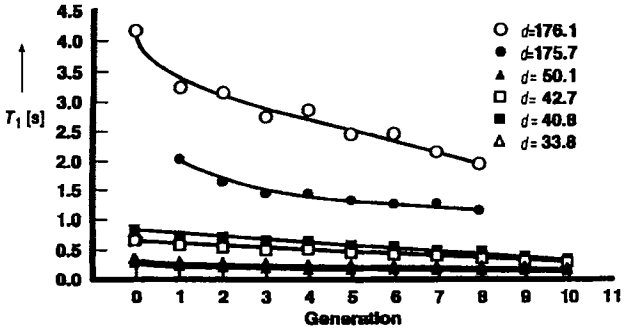

Fig. 40. Plot of spin–lattice relaxation times T_1 for interior and surface carbons versus generation.

Additional physical evidence that supports the anticipated development of congestion as a function of generation is shown in the composite comparison in Figure 41. The plots of intrinsic viscosity [η], density ϱ, surface area per Z group (A_Z), and refractive index n as a function of generation clear-

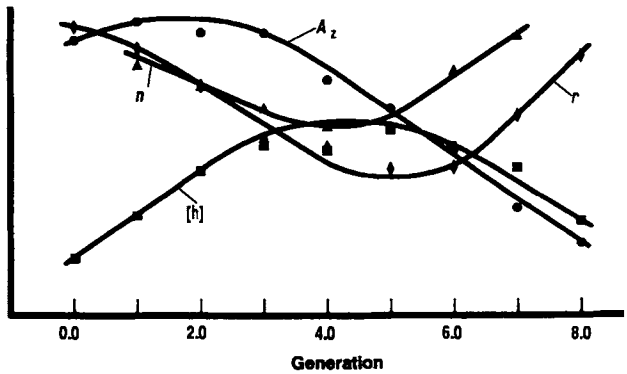

Fig. 41. Variation of surface area per terminal group (A_z), refractive index n, density ϱ, and intrinsic viscosity [η] for starburst PAMAM dendrimers as a function of generation. The units along the ordinate are arbitrary.

ly show maxima or minima at generations 3–5 which parallel computer-assisted molecular-simulation predictions. The intrinsic viscosities [η] increase in a very classical fashion as a function of molar mass (generation) and then decline beyond generation 4, presumably owing to surface congestion, which would reduce optimum surface–solvent interactions. In effect, the dendrimer is beginning to act more like an Einstein spheroid beyond generation 4. The dendrimer density ϱ (atomic mass units per unit volume) clearly minimizes between generations 4 and 5 and then begins to increase owing to the increasingly larger exponential accumulation of surface groups as a function of generation. Since refractive indices are directly related to density parameters,[112] their

values should minimize and parallel the above density relationship.

Less certain, however, is the necessary inducement of a critical phase change. Penultimate induction of branch defects would be expected to lead to unordered, heterogeneous surfaces which would not likely exhibit any special surface cooperativity or association. For this reason, it was surprising to observe physical change, which suggested a critical phase change for starburst PAMAM dendrimers at generation 8.0. Upon attempted removal of solvent from this generation, it was found that the dendrimer assembled into colorless sheets which precipitated from the solution. These sheets were separated, frozen (liquid N_2), thin-sliced, and stained with OsO_4 to produce a reverse-contrast electron micrograph (Fig. 42, left). The electron micrograph is self-consistent, if one compares an apparent isolated dendrimer at the sample edge to the ordered rows in the sample interior. A possible explanation invokes desolvation of the surface amino groups, thus leading to both intramolecular two-dimensional surface association and inter-dendrimer association to produce the assembly shown in Figure 42.[116]

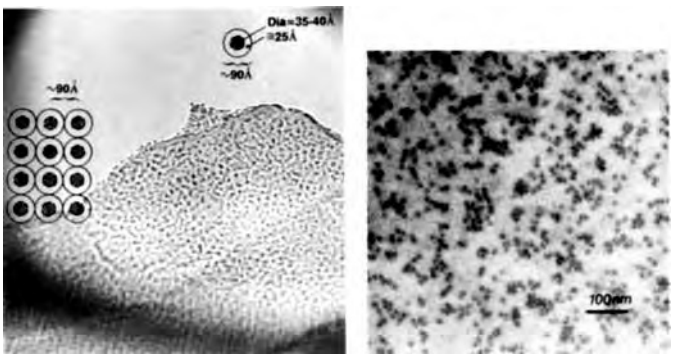

Fig. 42. a) Electron micrograph of thin-sliced films of starburst PAMAM dendrimers of generation 8. Stain: osmium tetraoxide (reverse contrast). b) Electron micrograph of individual starburst PAMAM dendrimers: core = NH_3; surface = $NH_3^{\oplus}{}^{\ominus}O_2C$-polystyrene; generation = 9; diameter = 107–110 Å; stained with RuO_4 vapor, normal contrast. (Courtesy of Prof. D. Meier and Y. Zou, Michigan Molecular Institute.)

Stain was taken in the outer congested dendrimer cells to give the observed reverse-contrast effect. This should be compared to Figure 42b, where starburst PAMAM dendrimers (generation = 9.0) have been treated with carboxylated polystyrene to give hydrocarbon-soluble dendrimers. Individual, dispersed dendrimers are observed by staining with RuO_4 (normal contrast) to produce hollow spheroids approximately 107 Å in diameter.

In either case, it is apparent that physical differentiation of the dendrimer branch cells has occurred to give what appears to be a unique example of *unimolecular encapsulation.*

9. Dendrimer Surface Reactions

In biological systems, the size and shape of smaller components is often controlled (morphogenesis) to produce self-assemblies, such as cellular vesicles, viruses, and phages. As noted by *Stryer*[113] and others,[114] many of these biological assemblies are either spheres, rods, or combinations of these shapes. Analogous molecular-level morphogenesis from pointlike organic molecules to well-defined covalent macromolecular entities has rarely been observed until the present.[9c] The ability to construct starburst dendrimers with similar shapes, sizes, and well-defined surfaces is no doubt of considerable importance in the effort to mimic the CMDPs and biomorphic features of these fundamental biological entities.

It is well known that small viruses possess many identical protein subunits symmetrically arranged around their RNA, which both provide protection and fulfill targeting functions. Similarly, the self-assembling polyhedral clathrin surfaces on cellular vesicles have recently been shown[115] to play important roles in mediating uptake of biological cell-surface receptors. Topologically, dendrimers may be viewed as analogues of the surfaces of these biological particles. The dendrimer surface cells would be expected not only to provide steric protection to its interior, but also function in primary molecular recognition of external reagents and solvents. This has indeed been observed in dendrimer protonation modes[62] as well as in the solubility characteristics of well-developed dendrimers. Solubilities are determined by the hydrophilic–hydrophobic characteristics of the surface cells (groups) of dendrimers. For example, dendrimers with very hydrophobic interiors and hydrophilic surfaces are water-soluble (e.g., starburst polyethers), whereas dendrimers such as starburst PAMAMs with hydrophilic interiors and hydrophobic surfaces are hydrocarbon-soluble.

Starburst dendrimers may be functionalized with either reactive or passive surface cells. It is implicit that all dendrimers involved in reiterative starburst growth schemes possess reactive surface groups; however, there are occasions where reactivity needs to be reduced or suppressed altogether.

In either case, the homogeneity of symmetrical, branch-junctured dendrimer surfaces provides unique opportunities to study the effect of congestion on surface stoichiometry, reaction kinetics, surface cooperativity,[164] and surface charge repulsion. Physical evidence for surface congestion was noted in Section 8.2.4. A constriction in the surface area per Z group due to the dendrimer tethering effect does not occur until approximately generation 4.0. This congestion is manifested in the higher generations by dramatically decreased surface reactivity as one approaches the starburst dense-packed generation.

9.1. Sterically Induced Aberrations due to Dendrimer Tethering Effect

9.1.1. Sterically Induced Stoichiometry and Reaction Rates

Examination of Figure 39 shows that, at generation 8, the surface area per Z group in PAMAM dendrimers approaches the cross-sectional area of the amine-terminated branch segment (ca. 33 $Å^2$) of the surface cell. Curve B assumes quantitative reactions and 100% branching ideality at each stage. Since our present analytical methods assure branching-ideality detection limits of no more than 95%, curve A may more nearly approximate experimental congestion levels.

Thus, sterically induced stoichiometry (SIS) is manifested whenever the summation of dendrimer surface-group volumes ® and incoming reagent volumes ® approaches available exterior volume surrounding the reactive dendrimer surface groups Z. This concept is illustrated in Figure 43. As

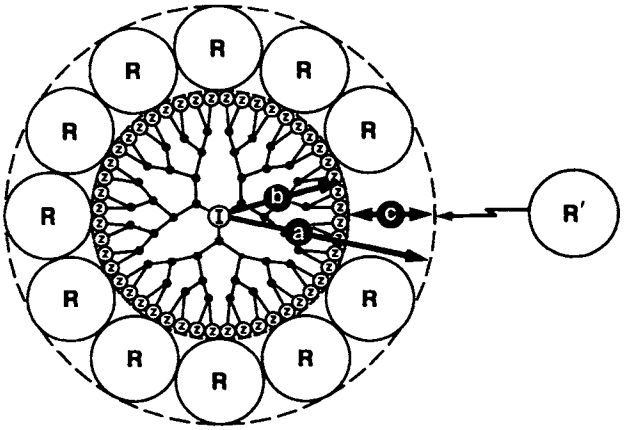

Fig. 43. Sterically induced stoichiometry (SIS).

long as the summation of the volumes ® and ® involved in bond formation with Z remains much less than $4/3\,\pi(r_a^3-r_b^3)$, ideal starburst surface stoichiometry should be expected. Large increases in the volume ® relative to the surface groups Z can be used as a means for controlling or, in fact, dramatically reducing surface stoichiometry at a particular generation. Preliminary evidence for this phenomenon was observed when advanced-generation starburst PAMAM dendrimers (where $Z = CO_2CH_3$) were combined with a large excess of a dendrimer with volume ® and NH_2 surface functionality. As much as 70% of the CO_2CH_3 groups remained unreacted in the bridged dendrimer adducts, although less sterically hindered model systems indicated the amidation was nearly quantitative under the same conditions.

Similarly, in the starburst polythioether system,[94] the surface stoichiometry was approximately one-third of the anticipated amount when attempting to advance from generation 2.0 (PTE-OH(36)) to generation 3.0 (PTE-OH(108)). This is one generation earlier than in the starburst polyether series.

9.2. Surface Chemistry

Dendrimer surface chemistry has been used to introduce both reactive and passive chemical moieties for a wide variety of interior or exterior design functions, which include:

1. chelation
2. dendrimer stratification (heterogeneous generations)
3. optically active groups
4. molecular-level templating (antigenic surfaces)
5. modification of dendrimer stoichiometry
6. modification of dendrimer solubility

In view of the ordered, nonrandom proximities of functional groups either inside or on the dendrimer surfaces, one should expect to observe time-dependent reaction rate "constants" referred to as fractal kinetics by *Kopelman*.[117] This area is still unexplored.

9.2.1. Protonation

Analyses of NH_2-terminated PAMAM dendrimers by titration and concurrent ^{13}C NMR monitoring of carbons attached to primary and tertiary amino groups were very interesting. Usually, it is assumed that tertiary amines are more basic than primary amines. With the present prototypes, the opposite was true. Titrations with hydrochloric acid showed that neutralizations occurred to give rather sharp breaks at pH ≈ 6.85 and pH ≈ 3.86 (Fig. 44), which

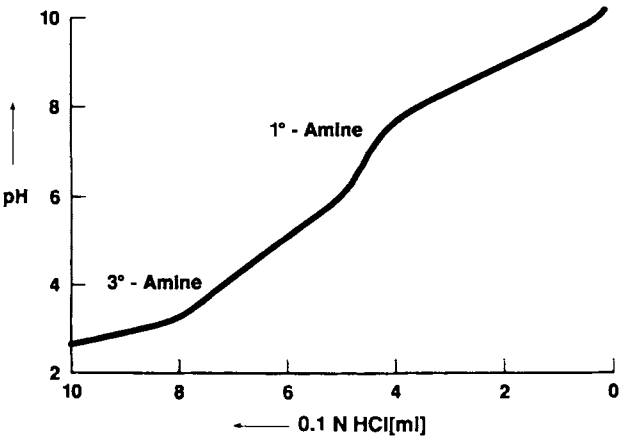

Fig. 44. Titration curve for starburst PAMAM dendrimers of generation 1 with endpoints observed for tertiary and primary amino groups.

were in very close agreement with theoretical values for terminal primary amino groups and interior tertiary amino groups, respectively.[62] The distinctive endpoints exhibited by these dendrimers are quite different from those observed for classical amino macromolecules, such as polyethylenimine.[88,89]

A wide variety of crystalline derivatives have been prepared by allowing various NH_2-terminated dendrimers to react with either inorganic or organic acids. One such intermediate was implicated in the development of lyotropic phases[118] when octanoic acid was combined with starburst polyethylenimine (generation 3).

9.2.2. Chelation to Endo- and Exo-Receptor Sites

The construction of starburst dendrimers can be controlled by appropriate choices of N_c, N_b, and branch-segment lengths l, as well as the flexibilities and shapes of the branch segments. A qualitative overview of how N_c and N_b may affect interior topology is provided by the two-dimensional projections shown in Figure 45. Because of the variety of possible heteroatoms or functional groups, it is easy to conceptualize many new endo-receptor microenvironments, which would resemble multiarmed entities described by *Vögtle* and *Weber*,[119] *Suckling*,[120] and *Menger*[121] or pseudo-macrocyclic (cryptate-like) prototypes.[9,13,34-36]

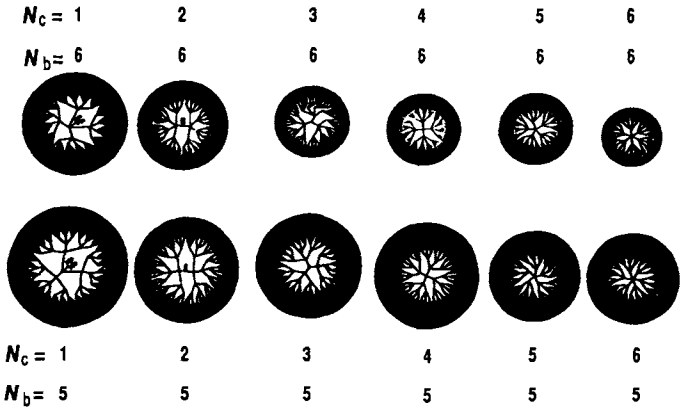

Fig. 45. Two-dimensional projections of various starburst dendrimers (symmetrical branch junctures) as a function of N_c and N_b.

Very little is known about these dendrimer properties, although it has been noted that ester-terminated PAMAM dendrimers form deep blue complexes with $CuSO_4$ solutions, whereas NH_2-terminated homologues produce deep purple solutions.[62] The well-known coordination properties of the amide bond, which lead to the formation of metal-ion complexes,[122] should make this a very rich area for further investigation.

PAMAM dendrimers develop molecular clefts[111] on their surfaces. This may be visualized from *de Gennes'* starburst dendrimer model (Fig. 46).[68] *de Gennes*[68] hypothesizes

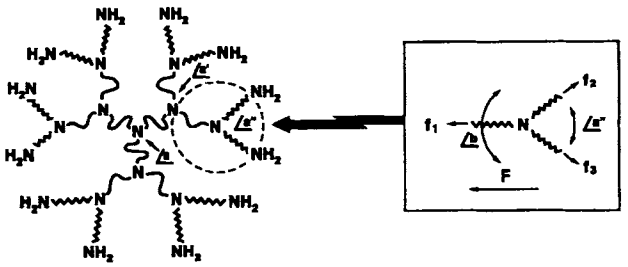

Fig. 46. The de Gennes model for self-consistent force field operating on a dendrimer branch cell.

that the starburst structures should be quite flexible in the early generations, whereas the surface branch cells should become substantially more rigid and constrained as one approaches the starburst dense-packed limit. This would be expected to affect the branching angles $\measuredangle a$ of the branch cells or dendrons as well as their rotational angles $\measuredangle b$. Suppressed spin–lattice relaxation times for dendrimer surface cells in advanced generations appear to support this notion, as do apparent enhanced complexation constants for advanced generations.

The most facile entry into surface complexation involved hydrolysis of ester-terminated dendrimers, derived from Michael additions of surface NH_2 groups to methyl acrylate, with stoichiometric amounts of alkali-metal hydroxides. In this manner, salts of $Na^{\oplus}$, $K^{\oplus}$, $Cs^{\oplus}$, or $Rb^{\oplus}$ were readily obtained (Scheme 7) as white hygroscopic powders. Dilute solutions of the sodium salts allowed direct observation of the individual dendrimer molecules by scanning transmission electron microscopy without the use of staining techniques.[62–64] Elemental analyses showed that essentially stoichiometric exchanges with divalent cations such as $Ca^{2\oplus}$ could be performed.[123]

Alternatively, $N(CH_2CO_2^{\ominus})_2$ salts were prepared by the reaction of starburst PAMAM or PEI NH_2-terminated dendrimers with methyl bromoacetate, followed by hydrolysis. Each of the above dendrimer carboxylate families readily formed complexes with such metals as $Fe^{3\oplus}$, $Gd^{3\oplus}$, $Mn^{2\oplus}$, $Pr^{3\oplus}$, and $Y^{3\oplus}$. In general, the $N(CH_2CO_2^{\ominus})_2$ complexes were more stable than the $N(CH_2CH_2CO_2^{\ominus})_2$ complexes. Within the latter series, it was found that the complexes were considerably more stable (e.g., toward $OH^{\ominus}$ attack) for the higher generations (6, 7) than for the lower generations (2, 3). For example, a multimetal chelate with the empirical formu-

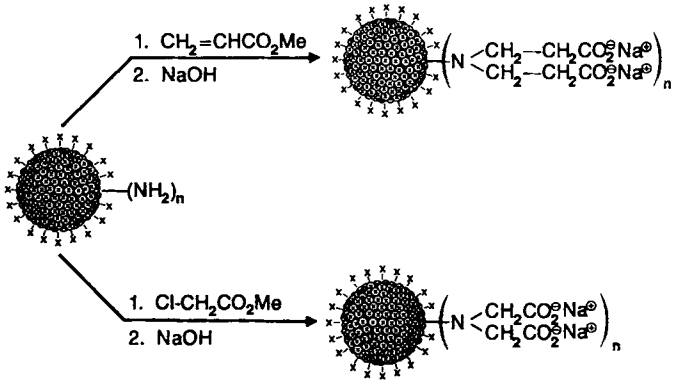

Scheme 7. Synthetic scheme for surface complexation of dendrimers.

la $[Na_5H_{127}Fe_{20}][C_{1521}H_{2469}N_{379}O_{573}]$ was readily formed from $FeCl_3$ and a starburst PAMAM dendrimer (96 $N(CH_2CH_2CO_2^{\ominus})_2$ groups).[124,128] An orange complex containing approximately 60 iron atoms was obtained from the next-generation dendrimer possessing 192 $N(CH_2–CH_2–CO_2^{\ominus})_2$ groups. These two complexes were stable up to pH 9–10, whereas ferric hydroxide precipitated from lower-generation homologues at pH 5.

Sub-stoichiometric yttrium complexes of starburst PAMAMs with $N(CH_2CH_2CO_2^{\ominus})_2$ surface groups displayed intramolecular exchange reactions as determined by ^{13}C NMR spectroscopy and ^{90}Y tracer experiments.[125] These and other complexation properties may serve as useful probes for the systematic characterization of dendrimer surfaces.

9.2.3. *Reactions with Electrophilic and Nucleophilic Reagents*

Table 8 lists a small sampling of surface reactions which have been successfully carried out. Reactions 1–3, 8, 9, 13–17, and 19–22 have been used in reiterative starburst propagation schemes. They are generally very high yield, quantitative processes, unless one is close enough to the starburst limited generation. Reactions 1–3 and 14–17 have been used in various combinations to create stratified dendrimers with differentiated generations possessing different segment lengths, different branch-juncture multiplicities, and varied hydrophobicity. Reaction 17 is of special interest in combi-

Table 8. Dendrimer surface reactions with various electrophiles and nucleophiles.

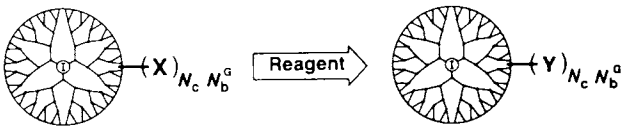

Reaction	Type of dendrimer [a]	X	Gen.	Reagent	Y	Ref
1	S-PAMAM	NH_2	0–10	$CH_2=CHCO_2Me$	$N(CH_2CH_2CO_2Me)_2$	[60, 67, 85, 101]
2	S-PAMAM	NH_2	0–4	$BrCH_2CO_2Me$	$N(CH_2CO_2Me)_2$	[124, 125, 128]
3	S-PEI	NH_2	0–3	$CH_2=CHCO_2Me$	$N(CH_2CH_2Me)_2$	[100]
4	S-PAMAM	NH_2	0–10	$CH_2-\overset{*}{C}HR-O$ [b]	$N(CH_2\overset{*}{C}H(OH)R)_2$ [b]	[138]
5	S-PEI	NH_2	0–3	$CH_2-\overset{*}{C}HR-O$ [b]	$N(CH_2\overset{*}{C}H(OH)R)_2$ [b]	[138]
6	S-PAMAM	NH_2	0–6	RCOCl/VNaOH [c]	NHCOR [c]	[123]
7	S-PAMAM	NH_2	0–4	Aryl-CH_2Cl	$NHCH_2Aryl$	[123]
8	S-PEI	NH_2	0–4	CH_2-CH_2-NR [d]	$N(CH_2CH_2NHR)_2$ [d]	[100]
9	S-PE	OH	0–3	Tosyl-Cl	Tosyl	[65]
10	Arborol	OH	2	Aryl-COCl	OCO-Aryl	[75–77]
11	S-PEI	NH_2	0–2	HCHO	$N(Me)_2$	[138]
12	S-PA	NH_2	0–9	$tBuOCO_2tBu$	NHBoc	[73]
13	S-PA	NH_2	0–9	$RO_2C-\underset{\underset{NHBoc}{|}}{CH}-(CH_2)_5NHBoc$		[73]
14	S-PAMAM	CO_2Me	0–10	$H_2N-(CH_2)_2-NH_2$	$CONH(CH_2)_n-NH_2$	[60–67, 85]
15	S-PAMAM	CO_2Me	0–3	$H_2N-(CH_2)_6-NH_2$	$CONH(CH_2)_n-NH_2$	[101, 138]
16	S-PAMAM	CO_2Me	0–3	$N(CH_2CH_2NH_2)_3$	$CONH(CH_2)_2-N((CH_2)_2-NH_2)_2$	[138]
17	S-PAMAM	CO_2Me	0–4	$H_2N(CH_2)_2NH(CH_2)_2OH$	$CONH(CH_2)_2-NH-(CH_2)_2-OH$	[138]
18	Arborol	CO_2Me	1	$H_2N-C(CH_2OH)_3$	$CONHC-(CH_2OH)_3$	[75–77]
19	S-PAMAM	CO_2Me	0–9	$NH_2CH_2CH_2OH$	$CONHCH_2CH_2OH$	[102, 138]
20	S-PE	Tosyl	0–3	NaBr	Br	[65]
21	S-PE	Br	0–3	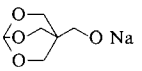	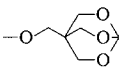	[65]
22	S-PTE	Br	0–2	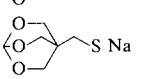	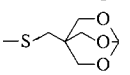	[94]

[a] S = starburst. [b] R = H, alkyl, aryl; asterisk indicates a potentially stereogenic C atom. [c] R = C_4 to C_{18}-Alkyl. [d] R = mesyl, tosyl. [e] R = *p*-nitrophenyl.

nation with reactions 1–3 in that it can be used to produce linear nonbranched dendrimer segments which possess interior OH groups. Since the OH groups do not participate in Michael addition reactions, these hydroxylated segments can be subsequently functionalized.

Reactions 1–3 produce intermediates which can be hydrolyzed to give dendrimers with anionic surfaces. Intermediates derived from reaction 11 yield cationic surfaces after quaternization. Dendrimers possessing chiral surfaces were readily prepared from optically active epoxides, as in reaction 4.

Hydrophobic surfaces result from reactions 4–10, 11, and 20–22. Thus, the resulting dendrimers are soluble in organic solvents, although their interiors might be quite hydrophilic. Conversely, water-soluble dendrimers are obtained from reactions 1–3 (after hydrolysis), 4 (R = H), 14, and 16–19.

9.2.4. Comparison of Dendrimers to Regular and Inverse Micelles

Very recently, both starbranched macromolecules[151a–c] and starburst[64] dendrimers have been compared to micelle systems both as synthetic models and for theoretical purposes. Theoretically, a micelle may be viewed as two concentric spherical regions: an inner core consisting of close-packed, solvent-incompatible, amphiphilic components and an outer corona of solvent-compatible (swollen) moieties. In the starburst case, the analogy is good for a number of critical parameters. First, the dendrimer dimensions (10–200 Å) are of the right order, the spherical shape is appropriate, and the number of head groups as a function of generation can be compared to well-known, discrete aggregation numbers.[126,127] A closer examination reveals that the surface area per head group can vary from about 100 $Å^2$ to 33 $Å^2$ (cf. Fig. 39), thus simulating surface-group proximity effects ranging from those in spherical micelles to those noted for liposomes or bilayers.[126] For these reasons, certain star-

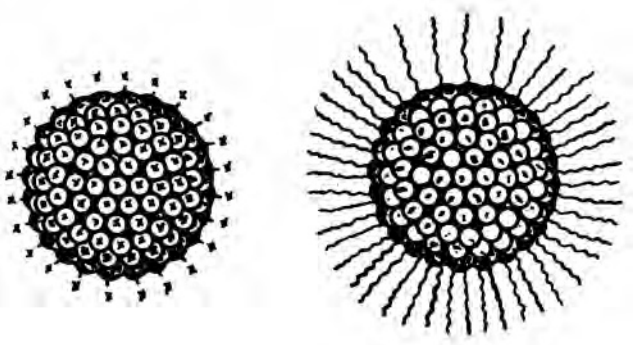

Fig. 47. Hydrophilic (left) and hydrophobic (right) surface-functionalized dendrimers viewed as mimics of reverse and inverse micelles.

burst dendrimer families may be thought of as covalently fixed microdomains, which mimic either regular or inverse micelles, depending on the compatibility of the dendrimer surface with water[164] (Fig. 47).

Appropriate dendrimer surface and interior design offers many possibilities for unimolecular mimicry of micelles. With this approach, the head-group multiplicity is determined by synthesis, in contrast to the self-adjusting micelle systems, where aggregation numbers (head groups) are determined by free-energy minimization[126] and/or head-to-tail packing ratios.[127]

9.2.5. *Starburst Dendrimers as Models for Liposomes*

The sequestering of small molecules such as dopamine in the channels of PAMAM dendrimers (cf. Section 6.1) has been studied by use of molecular dynamics calculations.

Dopamine, which is important pharmacologically, possesses both the hydrogen-bond donor and acceptor sites necessary for favorable binding interactions with the dendrimer's interior carbonyl, amide, and amino groups. Potentially advantageous in various areas of cardiovascular therapy are the ability to selectively deliver dopamine to peripheral kidney receptors without eliciting complications due to the existence of dopamine receptors in the central nervous system and the ability to maintain a supply of non-metabolized dopamine.

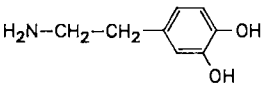

Dopamine

A dendrimer of generation 6 should have a hosting capacity for 10–20 molecules of dopamine. Molecular simulations were carried out with ten dopamine guest molecules sequestered in the channels of a PAMAM host dendrimer of generation 6. Initially, the dendrimer matrix was treated as a rigid entity while the small molecules optimized their positions within the interior regions. Subsequent calculations then allowed both polymeric host and dopamine guest to relax and equilibrate. After 1.5 and 3.0 ps of simulation time, the environment of the heteroatom units of the ten encapsulated dopamine molecules was examined (Fig. 48). Of the dopamine amino groups, 75% were involved in hydrogen bonding to dendrimer interior components while the remaining 25% occupied sites distant enough from these moieties to be accessible to the solvent. For the hydroxyl groups, 90% were involved in hydrogen bonds with the dendrimer interior while only 10% were free from dendrimer interaction to hydrogen bond with solvent.

The dimensions of the higher-generation β-alanine dendrimers (Fig. 49) are such that these dopamine–dendrimer complexes should not readily cross the blood–brain barrier.

A potential advantage of this strategy is the modification of the dendrimer surface to allow targeted delivery to a desired site. Thus, adding catechol units to the terminal amino groups leads effectively to dopamine-like surface features on the dendrimer. These modified surfaces should recognize

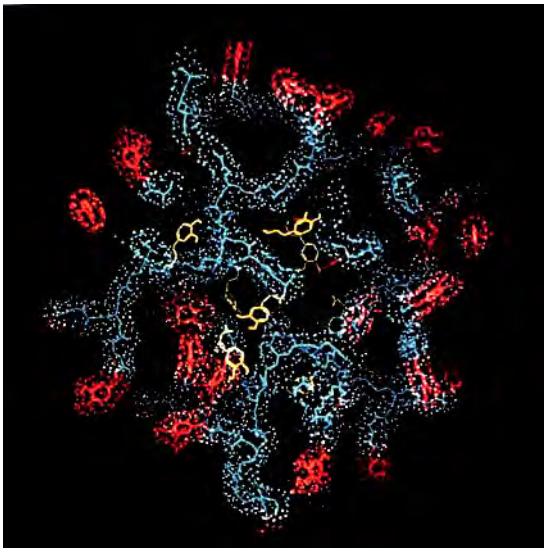

Fig. 48. Computer simulation (POLYGRAF) of a complex formed from a dendrimer (interior, light blue) containing catechol units (red) on its surface and dopamine (yellow).

dopamine receptor sites and bind sufficiently well to help increase the concentration of ligand near these sites. However, this composite dendrimer should be displaceable by dopamine as it diffuses out of the dendrimer. This concept has not yet been verified experimentally.

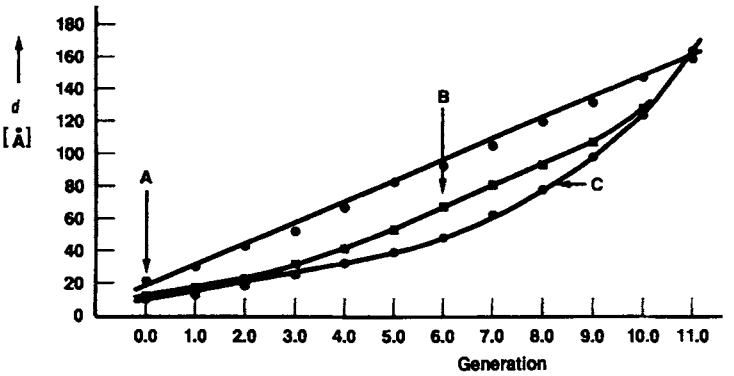

Fig. 49. Plot of the diameter d of starburst PAMAM dendrimers as a function of generation. A: extended CPK diameters. B: hydrodynamic diameters (measured by SEC). C: contracted CPK diameters.

9.2.6. *Dendrimers with Antigenic Surfaces*

The ability to conjugate starburst dendrimers to monoclonal antibodies and subsequently deliver these antibodies to desired sites is of special interest for both therapeutic and diagnostic purposes.[128]

Recently, *Tam* and co-workers[129–131] have demonstrated the unique properties of polylysine dendrimers as scaffolding for the presentation of certain antigen structures. This approach, which could lead to new synthetic vaccine strategies, involves growing appropriate polypeptide sequences upon a dendrimer scaffold. These prototypes have been referred to as multiple antigen peptide (MAP) systems. Dendrimer matrices used to date include those shown in

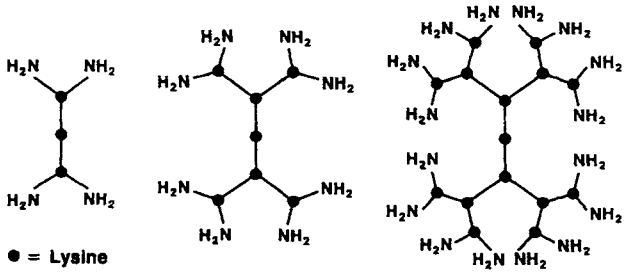

Fig. 50. Two-dimensional projections of dendrimer matrices (scaffolding) used for multiple antigen peptide (MAP) systems.

Figure 50. The octameric MAP (Fig. 51) was highly immunogenic in mice and rabbits, thus allowing production of both polyclonal and monoclonal antibodies. Most significant was the fact that no antibodies were raised against the

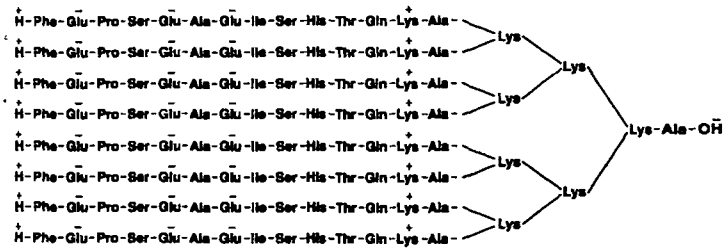

Fig. 51. An octameric multiple antigen peptide (MAP) system.

lysine dendrimer core. This indicates that the dendrimer matrix (core) is effectively and uniformly covered by the antigenic surface. Such behavior is dramatically different from conventional peptide-carrier conjugates composed of large protein substrates and low-density peptide antigen structures randomly distributed along the support matrix. It will be of considerable interest to determine the type of dendrimer and the dendrimer generation levels most effective in supporting antigen structures.

10. Biological Analogies

10.1. Dendrimers as Templates

As early as 1926, the American geneticist *H. J. Muller* and others proposed that the first organisms were simply naked genes. At least 25 years before the role of DNA was defined, Muller described genetic material as "any substance which, in given surroundings—protoplasmic or otherwise—is capable of causing the reproduction of its own specific composition, but which can nevertheless change repeatedly—'mutate'— and yet retain the property of reproducing itself in its various forms."[133] Subsequently, *Cairns-Smith*[132] proposed inorganic genes based on clays as the earliest templates, predating nucleic acids and proteins.

More recently, *Dawkins*[134] has shown that computer simulations involving reiterations of branched structures, which are actually two-dimensional projections of our dendrimer prototypes, can be used to demonstrate a variety of evolutionary principles. For example, such notions as gene expression, selection, and mutations were introduced to produce a rich array of structural entities which he referred to as biomorphs.

This suggests that there may be very primitive, abiotic, molecular examples of gene expression, transcription, translation, and self-replication which may mimic the more elaborated and ubiquitous biological examples. For comparison to our system, a generalized, conceptual overview of eukaryotic biocellular network development[168] is shown in Figure 52.

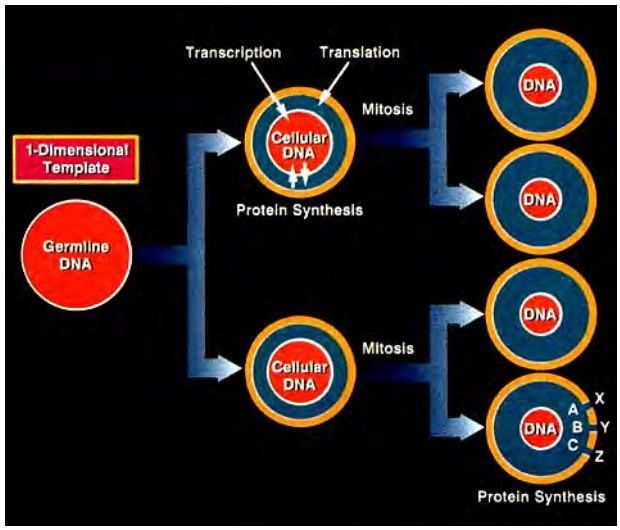

Fig. 52. Biocellular network development involving genetic transcription, translation, and protein synthesis.

Molecular information from the germ-line DNA is transferred to somatic DNA, where it is subsequently transcribed and translated into proteins. It is estimated that an average cell synthesizes 10^3-10^4 different proteins,[135] thus allowing transfer of both intra- und intercellular information, designated as A–C and X–Z, respectively, in Figure 52. This molecular information determines cellular size, shape, and surface features. No doubt this information is also involved in intercellular communication for defining the ultimate architecture, morphology, development, and growth of the biocellular network (organism).

With this as a conceptual reference, let us examine the degree of mimicry offered by the more simplistic starburst dendrimer systems. First, dendrimer branch-cell growth (for $N_b = 2$) may be viewed as an abiotic molecular-level analogue of biological cell division, where the growth numbers in each case follow a geometric progression (2^{gen}).[149]

Second, the dendrimer initiator core (i.e., NH_3) may be regarded as an abiotic analogue of the germ-line gene. The sequence of transcription, translation, and ultimately, somatic branch-cell self-replication results in the construction of a starburst polyamidoamine dendrimer (Fig. 53).

Below each of these stages is listed the molecular information which is transcribed to the dendrimer surface at that particular stage. As observed in biological systems, abiotic

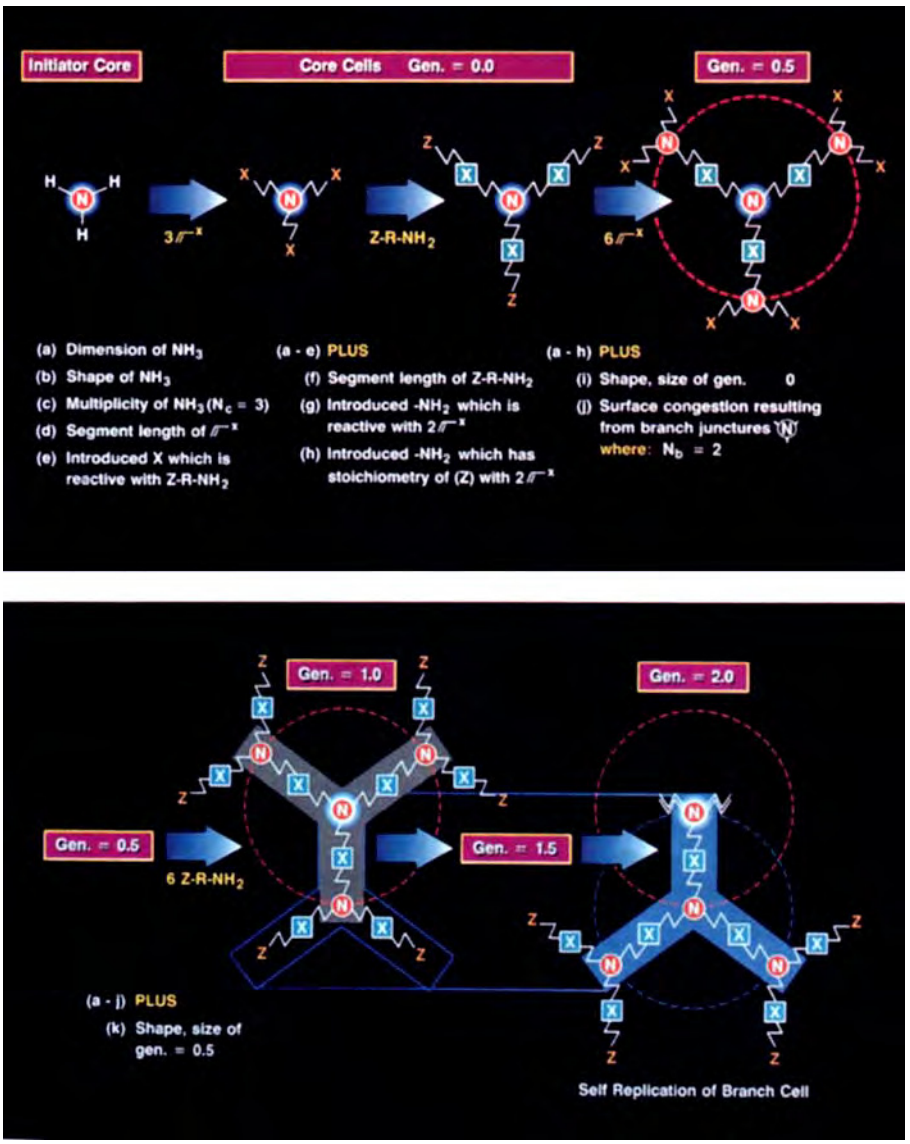

Fig. 53. Molecular information transferred from the initiator core NH_3 to the surface of starburst PAMAM dendrimers as a function of generation.

growth defects may be induced by introducing non-reiterative X or Z groups. A branch defect (missing arm) may manifest itself as an abnormal branch cell. Similar events are observed in biological systems during embryonic development and may account for many of the morphological variations in both the plant[136] and animal[137] kingdoms.

We have shown that fragments of a dendrimer that possess X or Z groups may function as "genetic" material to produce new dendrimer species which are compositionally altered ("mutated") relative to the original idealized dendrimer series.[85, 138] Preliminary work has shown that "cross-breeding" various dendrimer morphologies (e.g., spheres with rods or various-sized spherical dendrimers) yields new molecular organizations (templates) which may function as "abiotic molecular genes".[138]

Of course, it is very risky to compare such primitive abiotic prototypes to the highly elaborated, sophisticated examples nature has produced over billions of years of evolution. Hopefully, deeper insights into these issues will shed additional light upon our evolutionary origins.

10.2. In Quest of the Unimolecular Synthetic Cell

Nature teaches us that compartmentalization and self-organization of lipids into bilayers is quintessential of life. For that reason, considerable effort has been expended in the past several decades to mimic these organizations and their functions. The polymolecular assembly approach, referred to as membrane mimetics,[38] has been the central theme in this strategy.

More recently, *Cram*[139] posed a very interesting synthetic challenge, directed at unimolecular synthetic cells, by raising the following questions:

"Can cavitands be prepared with 'pores' in their 'skins' that allow the entrance and departure of certain guests from their interior, but forbid passage to others?"

"In other words, can cavitands be made that resemble cells?"

"What types of synthetic strategies are required to bring such cavitands to hand and to make their solubility properties manipulable?"

Within five years, *Cram*'s group had synthesized the first unimolecular synthetic cell (Scheme 8), which he refers to as a cacerand.[12c] Their approach involved the covalent coupling of two cavitand molecules, rim to rim, much like two soup bowls in a kettle of stew, in an effort to capture guest species in the kettle. Although these prototypes satisfy many of the criteria initially raised, *Cram* concedes that their physical and chemical usefulness will become apparent only after their design renders them soluble and separable.

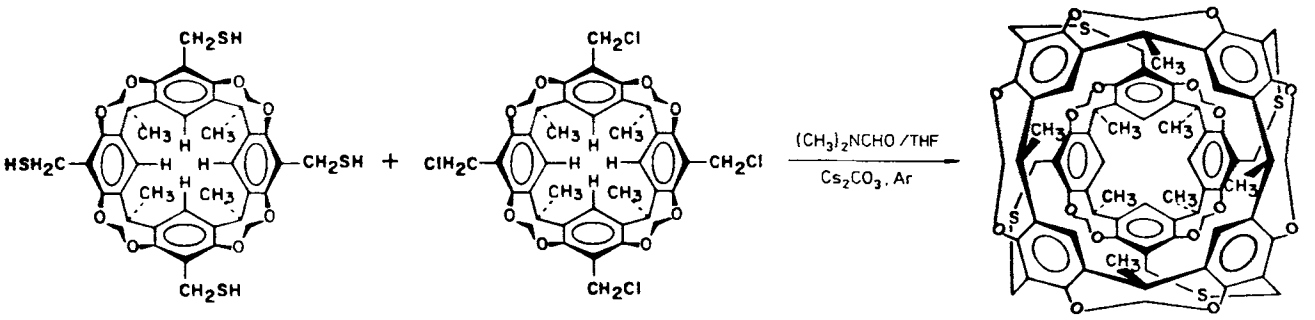

Scheme 8. Synthetic scheme for cacerands (unimolecular synthetic cells).

Although our objectives are much the same, our approach to producing unimolecular synthetic cells involves a closer mimicry of biological cells by systematically developing a substructure (cytoskeleton). It was anticipated that, upon approaching the starburst limiting generation, a tridendron dendrimer (see Fig. 12) with appropriate dimensions and flexibility would force a geometric and steric closure of the surface. One would visualize a variety of surface modifications for further biological cell mimicry. These might include templating groups for organizing lipid layers[164] or bilayers as well as the introduction of channels or pores for controlling entry and exit of guest molecules. Designing appropriate interiors to encourage guest entry may already have been accomplished.[111]

The cytoskeletal organizations and substructures, which are currently the object of extensive investigations in biological cells,[140] provide a clearer vision and offer further incentives for continuing the above dendrimer approach toward construction of new unimolecular synthetic cells.

11. Dendrimers as Bio-Morphic/Receptor (Supramolecular) Mimetics

As stated by *Lehn*,[9c] "Molecular chemistry, the chemistry of the covalent bond, is concerned with uncovering and mastering the rules that govern the structures, properties, and transformations of molecular species." According to him, "Supramolecular chemistry may be defined as 'chemistry beyond the molecule', bearing on the organized entities of higher complexity that result from the association of two or more chemical species held together by intermolecular forces ... to form supermolecules possessing features as well defined as those of molecules themselves." He aptly states that "supermolecules are to molecules and the intermolecular bond what molecules are to atoms and the covalent bond." This latter analogy makes dimensionality an explicit component in the definition of supramolecular chemistry and supermolecules. Driven by evolution, biological systems manifest a very efficient use of molecular space in the supramolecular domain for molecular recognition, transformation, and translocation, thus allowing one to make qualitative correlations between stored molecular information and dimensionality (see Fig. 3 in Section 2).

Recent articles by *Lehn*[9c] and *Ringsdorf*[37] have described synthetic supramolecular chemistry as being divided into two broad, overlapping categories: (1) well-defined *oligo*molecular species resulting from intermolecular association of a receptor (usually an endo-receptor) with a substrate, giving rise to supermolecules; (2) polymolecular assemblies resulting from spontaneous association of amphiphilic molecules into a specific phase having well-defined microscopic organization and macroscopic behavior (e.g., micelles, vesicles, membranes, layers). Certain of these latter prototypes may possess both exterior and interior surfaces (e.g., liposomes).

To place starburst dendrimers in an appropriate supramolecular perspective, we would like to enlarge and build upon these earlier definitions. Examination of the biological hierarchy of supramolecular chemistry reveals a broad category of macromolecular bio-morphic/receptors (e.g., enzymes, globular proteins, antibodies) which exhibit colloidlike dimensionality in addition to well-defined endo- and exo-receptor sites; however, their structures are governed by specific sequences as well as noncovalent forces (e.g. electrostatic forces, hydrogen bonding, van der Waals forces), which are not unlike those involved in the polymolecular, supramolecular assemblies (category 2) described above. Starburst dendrimers may be viewed as synthetic models for this third, broad category of bio-morphic/receptors. They also possess the supramolecular features of category 1 (i.e., endo-receptor properties) and category 2 (i.e., morphogenetic-type exo-receptor properties).

The demonstrated mimicry of gross properties such as dimensionality, surface area, morphology, and topology is readily apparent. For example, the diameter (ca. 58 Å) and spherical shape of a fifth-generation starburst polyamidoamine dendrimer are almost identical to the diameter (ca. 55 Å) and shape of hemoglobin[113] (Fig. 54, top).

Starburst polyethers, polyethylenimines, and early-generation polyamidoamines exhibit exterior surface areas similar to those involved in antigen–antibody complexes. *Amit* et al.[106] have shown that surface areas of 600–1000 Å^2 are

involved in these supramolecular complexes (cf. Fig. 54, bottom). Perhaps this similarity plays an important role in the successful use of dendrimers for the presentation of antigen moieties as reported by *Tam* et al.[129–131]

Fig. 54. Top: Structural model of hemoglobin (taken from [113]). Bottom: Structural model of antigen–antibody complexes. The H and L chains of the Fab D1.3 antibody are shown in blue and yellow, respectively; lysozyme (antigen) is shown in green and the L-glutamate moieties crucial for binding in red (taken from [106]).

One can envision many surface modifications which would allow the design of dendrimers having shapes, sizes, and cleft/concavity features similar to those of biological exo-receptors as well as of substrates, inhibitors, and cofactor mimetics.

Histones are ubiquitous DNA-binding proteins in plants and animals. The structures of histones are reminiscent of those of dendrimers, whose shapes (spheres, cylinders), dimensions (40–125 Å), and charge-modifiable surfaces suggest their use as templates for presenting DNA in a variety of replication and transcription experiments. A review of these possibilities has recently been published.[141]

The topology and dimensions of IgM antibodies[142] are remarkably similar to those of starburst dendrimers (Fig. 55, top). These biological assemblies are pentamers of the basic four-chain antibody structural units (e.g., IgG type). A high multiplicity and radial distribution of their variable regions (binding sites) no doubt accounts for their very high binding affinity to microorganisms (e.g., viruses). Their ability to activate macrophages suggests the possible design and use of starburst dendrimers for this purpose.

Finally, recent work on the topology of central neurons in mammals[143] reveals the involvement of distal dendritic tree configurations, which are reminiscent of a monodendron dendrimer (Fig. 55, bottom). Although this biological example is orders of magnitude larger than the dendrimer molecular assemblies, it suggests that these connectivity patterns may be mimicked by molecular-level computer prototypes.

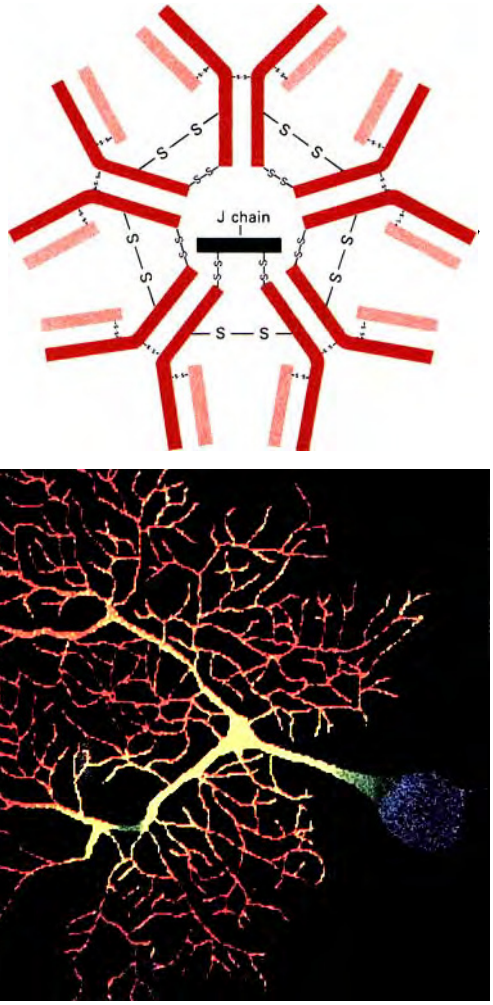

Fig. 55. Top: Pentameric structure of an IgM antibody (taken from [137a]). Bottom: Neuronal network (taken from [143].

Hopefully, these comparisons and the suggested potentials of dendrimers for developing systems based on molecular recognition will stimulate and encourage further investigations.

12. Nanostructures, Nanotechnology, and Supramolecular Devices

The biological world is replete with examples of self-organizing supramolecular assemblies: the double helix of DNA, the assembly of protein coat to form viruses, the self-organization of lipids to produce cellular membranes and vesicles, and the aggregation of α- and β-tubulin to form biological nanostructures[152] exhibiting specialized functions. These nanostructures may function as molecular receptors, catalysts, or carriers/transporters.

In the past, substantial effort has been expended to mimic these functions. Such terms as membrane mimetics or supramolecular devices have been coined to describe this synthetic mimicry. Successful pioneering efforts by *Ringsdorf*,[37] *Fendler*,[38] *Kunitake*,[39] and others[40, 155] have led to a better understanding of how lipids assemble to form membranes and how transport through membranes occurs. Investigators such as *Lehn, Cram, Vögtle, Breslow, Tabushi, Diederich, Rebek, Stoddart*, and others[154] have established sound foundations for the comprehension of molecular recognition, receptors, and catalysts.

The statement by *Pauling*[155] that "the elaboration of macromolecular structure may be necessary to stabilize transition states" is indeed prophetic[14b] in view of recent successes by *Lerner* et al.[144] and *Schultz* et al.[145] with "abzymes". Macromolecular architecture may provide further guidance for other efforts to develop not only synthetic models of biological structures, but also self-assembling synthetic organizations not found in nature.

Such assemblies include macromolecular dendrimer species shaped like "barbells", which have been reported by *Newkome* et al.[77] to exhibit unusual micellar- and gelation-type properties. Slight changes in the microscopic architecture of these prototypes can dramatically alter their macroscopic (gelation) properties. Perhaps the relationship of head group to hydrophilic tail dimensions (morphology) as described by *H. Hoffmann* et al.[156] and others[126, 127] may play an important role in this behavior.

Other self-assembling nanostructures referred to as helicates have recently been reported by *Lehn* et al.[148] These oligomeric bipyridine ligands develop rodlike configurations with metal ions, giving lengths that appear to be limited only by the molecular mass (length) of the organic ligand.

Lubensky and *Piscus*[146] have noted that colloid-sized particles up to 1000 Å act like atoms or molecules as they assemble to form supramolecular chains, periodic lattices, and entities with fractal geometries. These mesoscopic systems, which possess properties between those of single atoms or molecules and bulk materials, may assemble into macroscopic systems. Such mesoscopic behavior has been noted for metal clusters,[147] various microclusters,[170] and microdomains of water held between lipid bilayers, wherein they act as binary systems in association with macroscopic matter.[3]

We propose that this analogy might be made for our covalent dendrimer assemblies. One need only examine dendrimers and their architectural components as part of a self-similar assembly hierarchy or unimolecular fractal organized around an initiator core. For simplicity, one may visualize these scaled, self-similar organizations as a series of nesting spheres (Fig. 56), starting with atoms and proceeding dimensionally upward to macroscopic matter. *Mazur* has organized atoms (elements of the periodic table) in a similar fashion with period cones stretched in a vertical display.[157] Preliminary results[158] show that dendrimers can be dimensionally advanced from the mesoscopic range to the macroscopic region (infinite networks) as shown in Figure 42 as well as by use of other covalent bridging schemes. These bridged dendrimers are referred to as starburst polymers.

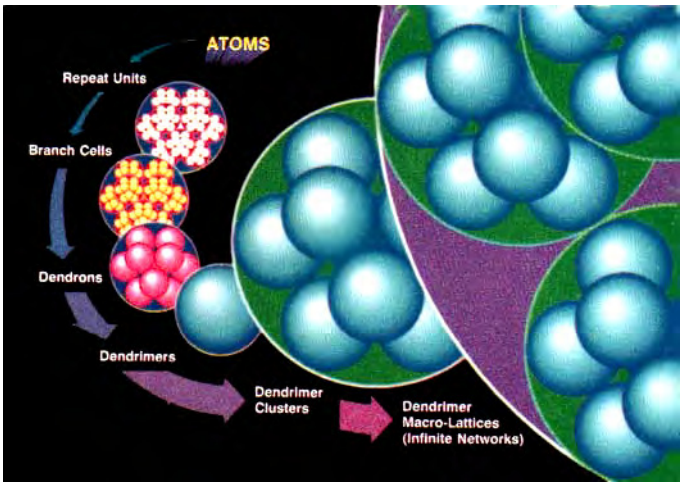

Fig. 56. Finite series of nesting spheres representing atoms, repeat units, branch cells, dendrons, dendrimers, dendrimer clusters, and dendrimer macrolattices (ordered infinite networks).

13. Starburst Dendrimers and Polymers in Relation to Classical Polymer Science

In the 1930s, *Staudinger* launched the present polymer science era by demonstrating that monomers (X–Z) can be covalently organized to produce Gaussian distributions of one-dimensional macromolecules referred to as random-coil polymers. Their well-known molar mass distributions ($M_w/M_n \gg 1$) result from largely uncontrolled processes, which produce molecular species spanning the entire continuum from microscopic to macroscopic sizes. Those species found in the mesoscopic region are often referred to as oligomers. This entire area is commercially recognized as the basis for thermoplastics technology (cf. Fig. 57).

Nearly a decade later, *Flory* and *Stockmayer* demonstrated that copolymerization of monomers containing several reactive groups with normal X–Z monomers produces three-dimensional macromolecules. Once again, the uncontrolled nature of these processes generally leads to broad molar-mass distributions. The vast array of species found in the mesoscopic range are referred to as pre-gel sols, reactive colloids, microgels, etc. This area has been the subject of intensive investigation for the past five decades.[159] The commercial importance of these infinite network systems is well recognized as the basis for thermoset/elastomer technologies (Fig. 57).

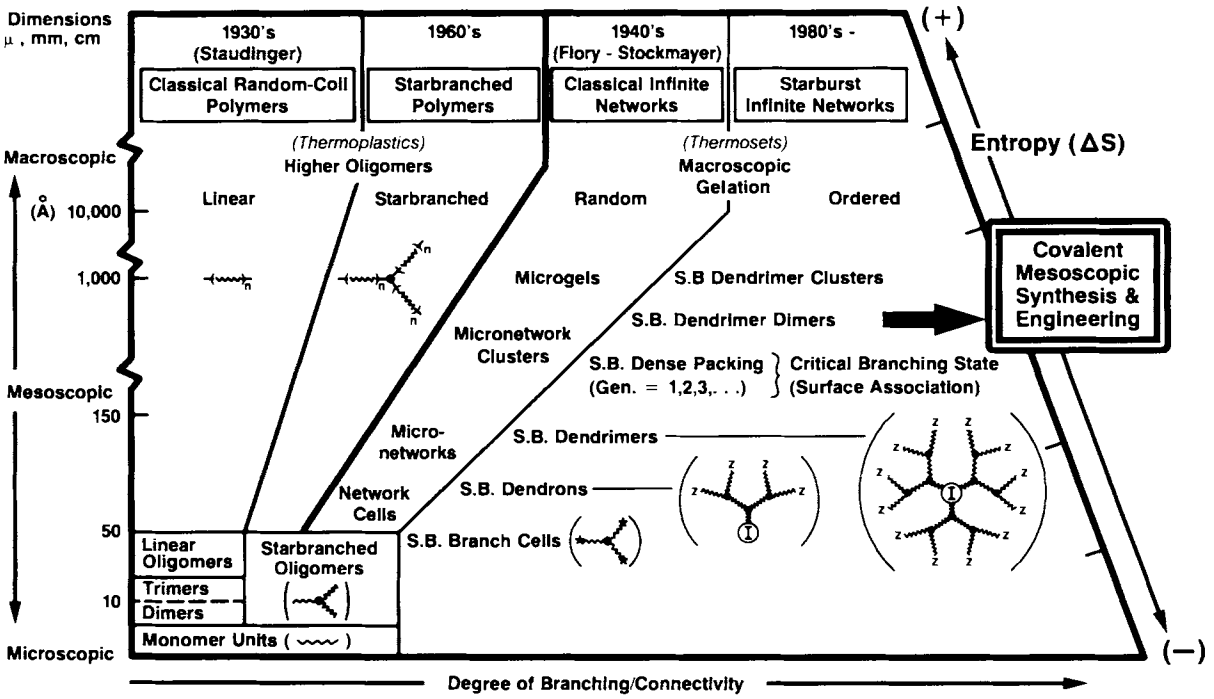

Fig. 57. Developments in polymer science

The present starburst dendrimer chemistry differs from either of these classical areas in that it teaches the systematic construction of three-dimensional, ordered, covalent organizations (dendrimers), which permit complete control of CMDPs as one progresses from microscopic to mesoscopic molecular species. This synthetic control (monomer repeat units → branch cells → dendrons → dendrimers) produces very unique mesoscopic building blocks, which have many of the attributes of atomic species and should allow the creation of new, higher-ordered covalent systems.

Figure 57 shows a comparison of the infinite network of starburst dendrimers to classical random-coil (thermoplastic) and infinite-network (thermoset) systems as a function of dimensions, degree of branching and covalent connectivity, and relative entropy. Without a doubt, the more highly organized dendrimer assemblies would be expected to be higher-energy, lower-entropy systems compared to their less-ordered classical counterparts.

14. Synthesis, Engineering, and Applications of Covalent Mesoscopic Compounds

During the past 150 years, history has witnessed a steady and sometimes dramatic progress in covalent microscopic synthesis. The field has been generally referred to as classical organic chemistry. Since the days of *Staudinger*,[16] *Flory*,[43] and *Stockmayer*,[47] macromolecular chemistry has also evolved into a flourishing area of chemical research and commerce.[160] We refer to this field as covalent macroscopic synthesis. Between these two extremes lies the more or less neglected area of covalent mesoscopic synthesis, which in a classical sense deals with reactive oligomers, teleomers, colloids, microgels, latexes etc.[169] Systematic development of covalent order and structure in this region has been hampered by the absence of reactive entities which possess controllable CMDPs (size, shape, topology, surface chemistry, and flexibility).[166] Starburst dendrimers set the stage for such progress. However, there are still technical hurdles to be dealt with, if one wishes to use dendrimers as building blocks for ordered, mesoscopic systems. One might consider dividing a dendrimer sphere into quadrants with different functionalities and reactivities (in analogy to tetrahedral sp^3 C atoms; cf. Fig. 58a). Such strategies may involve classical protection/deprotection schemes and/or SIS-type (see Section 9.1.1) protection. Such an approach has allowed us to produce a number of monodendrons possessing various masked functionalities on the initiator core. Subsequent coupling of these differentiated monodendrons to external tetradirectional anchoring reagents possessing differentiated or partially protected functionality is expected to give dendrimers with differentiated quadrants or hemispheres.

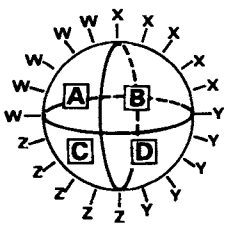

Fig. 58. a) Differentiation of dendrimer quadrants with various dendron surface moieties (A, B, C, D); b) Differentiated initiator core I–(A, B, C, D).

Perhaps a more simple demonstration might involve hemispherical functionalization.[167] Such differentiation could involve dendrimer growth on a polymeric support.[161] Linear coupling of such dendrimers would be expected to lead to

rod-type assemblies. Such condensations may mimic the polymerization of G actin to F actin.[162]

Combining various dendrimer morphologies (e.g., spheres and rods) would give rise to a wide variety of construction components and combinations. Reaction of dendrimers with classical telechelic polymers or oligomers[150] would produce novel networks with dendrimer branch junctures, whereas hydrophobic functionalization of dendrimer rods might be expected to yield unique self-assembling rod clusters with applications as artificial channels. Covalent linking of dendrimers to important bioactive entities should allow targeted delivery of therapeutic or diagnostic amounts of metals or radionuclides[125, 128]

Mesoscopic engineering offers diverse applications, such as producing submicron calibrators, abiotic templates, catalytic/chromatographic supports, synthetic membranes, molecular encapsulation devices, synthetic enzymes, biosensors, molecular electronic devices, chemical amplifiers, and photographic imagery. Clearly, mesoscopic systems have broad implications in such fields as materials research, biophysics, and microelectronics, as well as medical diagnostics and therapy.

15. Conclusion

A living organism has the astonishing gift of concentrating a stream of order on itself and thus escaping decay into atomic chaos.

Erwin Schrödinger, 1947

Just as nature has derived "order out of chaos" by evolving and using biotemplates (RNA and DNA),[79, 165] so may there be similar promise in the synthetic materials science area. Abiotic templates as simple as "initiator cores" and a branching strategy based on starburst dendrimers may provide the appropriate covalent synthetic organizations necessary for deriving ordered complexity and covalent control from atoms to macroscopic matter.

I ascribe to nature neither beauty, deformity, order nor confusion. It is only from the viewpoint of our imagination that we say that things are beautiful or unsightly, orderly or chaotic.

Baruch Spinoza, 1665

We wish to express sincere thanks to numerous colleagues both past and present who have contributed so much to the work cited in this paper. We are especially grateful for useful discussions with Professors P. de Gennes (Collège de France), G. Newkome (University of South Florida), N. Turro (Columbia University), H. Hall (University of Arizona), D. Tirrell (University of Massachusetts), and D. Meier (Michigan Molecular Institute), as well as Dr. D. M. Hedstrand and Dr. L. R. Wilson (Dow Chemical Company). Generous support for one of us (D.A.T.) from the Michigan Molecular Institute and the New Energy and Technology Development Organization (NEDO) of the Ministry of International Trade and Industry of Japan (MITI) assisted significantly in certain critical synthetic and theoretical efforts. The computer simulations were funded by a contract from Energy Conversion and Utilization Technologies Program of the Department of Energy (USA). The computer equipment used was funded by a contract (No. N00014-86-K-0735) from Defense Advanced Research Projects Agency, Office of Naval Research, and by a grant (No. DMR-94-21119) from the Division of Materials Research of the National Science Foundation, Materials Research Groups (USA).

Received: February 3, 1989 [A 746 IE]
German version: *Angew. Chem. 102* (1990) 119

[1] J. Swift: *Gulliver's Travels* (1726), Nal Penguin Inc., New York; *Gullivers Reisen* (Insel Taschenbuch 58), Insel Verlag, Frankfurt am Main 1974.
[2] a) R. J. Leatherbarrow, A. R. Fersht, *Protein Eng. 1* (1986) 7; b) J. R. Knowles, *Science (Washington) 236* (1987) 1252.
[3] a) G. Nimtz, P. Marquardt, D. Stauffer, W. Weiss, *Science (Washington) 242* (1988) 1671; b) Z. Cai, C. R. Martin, *J. Am. Chem. Soc. 111* (1989) 4138; c) R. N. Barnett, U. Landman, D. Scharf, J. Jortner, *Acc. Chem. Res. 22* (1989) 350; d) J. Koutecky, P. Fantucci, *Chem. Rev. 86* (1986) 539.
[4] a) E. T. Kaiser, *Angew. Chem. 100* (1989) 945; *Angew. Chem. Int. Ed. Engl. 27* (1988) 913; E. T. Kaiser, H. Mihara, G. A. Laforet, J. W. Kelly, L. Walters, M. A. Findeis, T. Sassaki, *Science (Washington) 243* (1989) 187; b) M. Mutter, *Angew. Chem. 97* (1985) 639; *Angew. Chem. Int. Ed. Engl. 24* (1985) 639; M. Mutter, S. Vuilleumier, *ibid. 101* (1989) 551 and *28* (1989) 535.
[5] a) H. Kuhn, J. Waser, *Angew. Chem. 93* (1981) 435; *Angew. Chem. Int. Ed. Engl. 20* (1981) 500; b) H. Haken: *Erfolgsgeheimnisse der Natur – Synergetik: Die Lehre vom Zusammenwirken*, Deutsche Verlagsanstalt, Stuttgart 1986; c) B. O. Küppers (Ed.): *Ordnung aus dem Chaos, Prinzipien der Selbstorganisation und Evolution des Lebens*, Piper, München 1987; d) F. Cramer, *Chaos und Ordnung. Die komplexe Struktur des Lebendigen*, Deutsche Verlagsanstalt, Stuttgart 1988.
[6] a) M. Eigen, *Naturwissenschaften 10* (1971) 465; b) M. Eigen, W. Gardiner, P. Schuster, R. Winkler-Oswatitch in J. M. Smith (Ed.): *Evolution Now*, Freeman, New York 1982, p. 11; c) I. Prigogine, *Phys. Today 25* (1972) No. 12, p. 38.
[7] C. B. Anfinsen, *Science (Washington) 181* (1973) 223; R. Jaenicke, *Angew. Chem. 96* (1984) 285; *Angew. Chem. Int. Ed. Engl. 96* (1984) 395.
[8] C. J. Pedersen, *J. Am. Chem. Soc. 89* (1967) 7017; C. J. Pedersen, H. K. Frensdorff, *Angew. Chem. 84* (1972) 16; *Angew. Chem. Int. Ed. Engl. 11* (1972) 16; C. J. Pedersen, *ibid. 100* (1989) 1053 and *27* (1988) 1029.
[9] a) J. M: Lehn, *Struct. Bonding (Berlin) 16* (1973) 1; *Acc. Chem. Res. 11* (1978) 49; b) P. G. Potvin, J. M. Lehn in R. M. Izatt, J. J. Christensen (Eds): *Synthesis of Macrocycles: The Design of Selective Complexing Agents (Prog. Macrocyclic Chem. 3*, Wiley, New York 1987, p. 167; c) J. M. Lehn, *Angew. Chem. 100* (1988) 91; *Angew. Chem. Int. Ed. Engl. 27* (1988) 89.
[10] F. Vögtle, E. Weber, *Angew. Chem. 91* (1970) 813; *Angew. Chem. Int. Ed. Engl. 18* (1979) 753.
[11] J. Rebek, Jr., *Acc. Chem. Res. 17* (1984) 258; *Science (Washington) 235* (1987) 1478; *Angew. Chem. 102* (1990) No. 3; *Angew. Chem. Int. Ed. Engl. 29* (1990) No. 3.
[12] a) D. J. Cram, J. M. Cram, *Acc. Chem. Res. 11* (1978) 8; b) D. J. Cram, *Angew. Chem. 98* (1986) 1041; *Angew. Chem. Int. Ed. Engl. 25* (1986) 1039; c) *ibid. 100* (1988) 104 and *27* (1988) 109; *Science (Washington) 240* (1988) 760.
[13] a) I. Tabushi, *Acc. Chem. Res. 15* (1982) 66; b) C. D. Gutsche, *ibid. 16* (1983) 161; c) F. Diederich, *Angew. Chem. 100* (1988) 372; *Angew. Chem. Int. Ed. Engl. 27* (1988) 362.
[14] a) F. A. Jurnak, A. McPherson (Eds.): *Biological Macromolecules and Assemblies*, Wiley, New York 1987; b) J. Kraut, *Science (Washington) 242* (1988) 533; c) G. M. Whitesides, C.-H. Wong, *Angew. Chem. 97* (1985) 617; *Angew. Chem. Int. Ed. Engl. 24* (1985) 617.
[15] R. F. Doolittle, *Sci. Am. 253* (1985) No. 10, p. 74; *Spektrum Wissensch. 1985*, No. 12, p. 78.
[16] a) E. Jostkleigrewe (Ed.): *Makromolekulare Chemie – Das Werk Hermann Staudingers in seiner heutigen Bedeutung*, Schnell und Steiner, München 1967; b) H. Morawetz, *Angew. Chem. 99* (1987) 95; *Angew. Chem. Int. Ed. Engl. 26* (1987) 93.
[17] H. Morawetz: *Polymers. The Origin and Growth of a Science*, Wiley, Chichester, England 1985.
[18] a) O. W. Websater, W. R. Hertler, D. Y. Sogah, W. B. Farnham, T. V. Rajan Baba, *J. Am. Chem. Soc. 105* (1983) 5706; b) M. T. Reetz, *Angew. Chem. 100* (1988) 1026; *Angew. Chem. Int. Ed. Engl. 27* (1988) 994.
[19] a) T. Higashimura, S. Aoshima, M. Sawamoto, *Makromol. Chem. Macromol. Symp. 13/14* (1988) 457; b) *ibid. 13/14* (1988) 513; c) M. Zsuga, R. Faust, J. P. Kennedy, *Polym. Bull. 21* (1989) 273.
[20] a) R. B. Merrifield, G. Barany in E. Gross, J. Meienhofer (Eds.): *The Peptides, Vol. 2*, Academic Press, New York 1980; b) R. B. Merrifield,

Angew. Chem. 97 (1985) 801; *Angew. Chem. Int. Ed. Engl. 24* (1985) 799; c) M. Bodanzky: *Principles of Peptide Synthesis,* Springer, New York 1984; d) M. Bodanzky, A. Bodanzky: *The Practics of Peptide Synthesis,* Springer, New York 1984.
[21] H. G. Khorana in *Nobel Lectures: Physiology or Medicine 1963–1970,* American Elsevier, New York 1973, p. 341; *Angew. Chem. 81* (1969) 1027.
[22] A term coined to denote synthetic mimicry of biological supramolecular structures with self-assembling or covalent fixed architectures.
[23] N. Turro, *Angew. Chem. 98* (1986) 872; *Angew. Chem. Int. Ed. Engl. 25* (1986) 882.
[24] J. H. Fendler, *Acc. Chem. Res. 13* (1980) 7.
[25] F. H. Kohnke, A. M. Z. Slawin, J. F. Stoddart, D. J. Williams, *Angew. Chem. 99* (1987) 941; *Angew. Chem. Int. Ed. Engl. 26* (1987) 892; siehe auch F. H. Kohnke, J. P. Mathias, J. F. Stoddart, *Angew. Chem. Adv. Mater. 101* (1989) 1129; *Angew. Chem. Int. Ed. Engl. Adv. Mater. 28* (1989) 1103; *Adv. Mater. 1* (1989) 275.
[26] G. Maier, S. Pfriem, U. Schäfer, R. Matusch, *Angew. Chem. 90* (1978) 552; *Angew. Chem. Int. Ed. Engl. 17* (1978) 520.
[27] P. E. Eaton, T. W. Cole, *J. Am. Chem. Soc. 86* (1964) 3157.
[28] a) L. A. Paquette, *Chem. Rev. 89* (1989) 1051; b) J. P. Melder, R. Pinkos, H. Fritz, H. Prinzbach, *Angew. Chem. 101* (1989) 314; *Angew. Chem. Int. Ed. Engl. 28* (1989) 305.
[29] a) C. O. Dietrich-Buchecker, J.-P. Sauvage, *Angew. Chem. 101* (1989) 192; *Angew. Chem. Int. Ed. Engl. 28* (1989) 189; b) D. M. Walba, *Tetrahedron 41* (1985) 3161; c) A. Nickon, E. F. Silversmith: *Organic Chemistry: The Name Game,* Pergamon Press, New York 1987; K. Mislow, *Chemtracts-Org. Chem. 2* (1989) 151.
[30] K. J. Niklas, *Sci. Am. 254* (1986) No. 3, p. 78.
[31] a) B. J. West, A. L. Goldberger, *Am. Sci. 75* (1987) 354; b) N. MacDonald: *Trees and Networks in Biological Models,* Wiley, New York 1983.
[32] D'Arcy W. Thompson: *On Growth and Form,* Cambridge University Press, Cambridge, England 1961.
[33] J. M. Lehn: *Science (Washington) 227* (1985) 849.
[34] F. Vögtle, H.-G. Löhr, J. Franke, D. Worsch, *Angew. Chem. 97* (1985) 721; *Angew. Chem. Int. Ed. Engl. 24* (1985) 727.
[35] F. Vögtle, E. Weber (Eds.): *Host Guest Complex Chemistry I–III (Top. Curr. Chem. 98* (1981), *101* (1982), *121* (1984).
[36] F. Vögtle, E. Weber (Eds.):*Biomimetic and Bioorganic Chemistry I–III (Top. Curr. Chem. 128* (1985), *132* (1986), *136* (1986)).
[37] H. Ringsdorf, B. Schlerb, J. Venzmer, *Angew. Chem. 100* (1988) 118; *Angew. Chem. Int. Ed. Engl. 27* (1988) 113.
[38] J. H. Fendler: *Membrane Mimetic Chemistry,* Wiley, New York 1982.
[39] T. Kunitake, Y. Okashata, *J. Am. Chem. Soc. 99* (1977) 3860.
[40] J.-H. Fuhrhop, J. Mathieu, *Angew. Chem. 96* (1984) 124; *Angew. Chem. Int. Ed. Engl. 23* (1984) 100.
[41] D. Y. Takigawa, D. A. Tirrell, *Macromolecules 18* (1985) 338.
[42] J. H. Fendler, *Chem. Rev. 87* (1987) 877.
[43] P. J. Flory, *J. Am. Chem. Soc. 63* (1941) 3083, 3091, 3096.
[44] P. J. Flory, *Ann. N.Y. Acad. Sci. 57* (1953) No. 4, p. 327.
[45] P. J. Flory, *J. Am. Chem. Soc. 74* (1952) 2718.
[46] P. J. Flory: *Principles of Polymer Chemistry,* Cornell University Press, Ithaca, NY, USA 1953.
[47] W. H. Stockmayer, *J. Chem. Phys. 11* (1943) 45; *12* (1944) 125.
[48] B. Zimm, W. H. Stockmayer, *J. Chem. Phys. 17* (1949) 1301.
[49] P. J. Flory, J. Rehner, *J. Chem. Phys. 11* (1943) 512.
[50] W. W. Graessley, *Macromolecules 8* (1975) 185
[51] W. W. Graessley, *Macromolecules 8* (1975) 865.
[52] a) M. Gordon, G. N. Malcolm, *Proc. R. Soc. (London) A 295* (1966) 29; b) M. Gordon, S. B. Ross-Murphy, *Pure Appl. Chem. 43* 1; c) M. Gordon, G. R. Dobson, *J. Chem. Phys. 43* (1975) 35; d) K. Dusak, *Makromol. Chem. Suppl. 2* (1979) 35; e) W. Burchard, *Adv. Polym. Sci. 48* (1988) 1.
[53] a) I. J. Good, *Proc. Combridge Phil. Soc. 45* (1948) 360; b) *Proc. R. Soc. (London) A 263* (1963) 54.
[54] H. K. Hall, Jr., D. W. Polls, *Polym. Bull. 17* (1987) 409.
[55] a) R. A. Jacobson, *J. Am. Chem. Soc. 54* (1932) 1513; b) W. H. Hunter, G. H. Woolett, *ibid. 43* (1921) 135.
[56] C. O. Beckman, *Ann. N.Y. Acad. Sci. 57* (1953) 384.
[57] S. Erlander, D. French, *J. Polym. Sci. 20* (1956) 7.
[58] a) W. Burchard, *Macromolecules 5* (1972) 604; b) W. burchard, I. Kranztz, B. Pfannenmüller, *Makromol. Chem. 150* (1971) 63.
[59] E. Buhlein, W. Wehner, F. Vögtle, *Synthesis 1978,* 155.
[60] D. A. Tomalia, *1st Society Polymer Science, Japan, Int. Polym. Conf.,* August 1984, Kyoto, Japan.
[61] D. A. Tomalia, *6th Biennial Carl S. Marvel Symp.,* 19 March 1985, Tucson, AZ, USA.
[62] D. A. Tomalia, H. Baker, J. R. Dewald, M. Hall, G. Kallos, S. Martin, J. Roeck, J. Ryder, P. Smith, *Polym. J. (Tokyo) 17* (1985) 117.
[63] D. A. Tomalia, H. Baker, J. R. Dewald, M. Hall, G. Kallos, S. Martin, J. Roeck, J. Ryder, P. Smith, *Macromolecules 19* (1986) 2466.
[64] D. A. Tomalia, V. Berry, M. Hall, D. M. Hedstrand, *Macromolecules 20* (1987) 1164.
[65] H. Hall, A. Padias, R. McConnell, D. A. Tomalia, *J. Org. Chem. 52* (1987) 5305.
[66] D. A. Tomalia, J. R. Dewald, US Pat. 4507466 (1985); US Pat. 4558120 (1985); US Pat. 4568737 (1986); US Pat. 4587329 (1986); US Pat. 4631337 (1986); US Pat. 4694064 (1987); US Pat 4713975 (1987); US Pat. 4737550 (1988); US Pat. 4871779 (1989); US Pat. 4857599 (1989).
[67] D. A. Tomalia, M. Hall, D. M. Hedstrand, *J. Am. Chem. Soc. 109* (1987) 1601.
[68] P. G. de Gennes, H. J. Hervet, *Phys. Lett. (Paris) 44* (1983) 351.
[69] D. A. Tomalia, Bürgenstock Conf., May 3, 1987, Bürgenstock, Switzerland. See *Nachr. Chem. Tech. Lab. 35* (1987) 693.
[70] a) This term was coined in deference to their branched (dendritic = treelike) as well as their oligomeric nature. b) The dendrimer generation numbering system used in earlier work [62–64, 67, 111] designated the first starbranched species derived from the initiator core as generation 1. The present system is preferred wherein that starbranched intermediate is designated generation 0, thus making it consistent with the geometric progression (cf. Section 4.2.1). c) R. E. Merrifield, H. E. Simmons (Eds.): *Topological Methods in Chemistry,* Wiley, New York 1989.
[71] D. Cram, *Science (Washington) 238* (1987) 612.
[72] M. Maciejewski, *J Macromol. Sci. Chem. A 17* (1982) 689.
[73] R. G. Denkewalter, J. F. Kolc, W. J. Lukasavage, US Pat. 4410688 (1983); *Chem. Abstr. 100* (1984) 103907p.
[74] a) S. M. Aharoni, C. R. Crosby III, E. K. Walsh, *Macromolecules 15* (1982) 1093; b) S. M. Aharoni, N. S. Murthym, *Polym. Commun. 24* (1983) 132.
[75] G. R. Newkome, Z.-q. Yao, G. R. Baker, V. K. Gupta, *J. Org. Chem. 50* (1985) 2003.
[76] G. R. Newkome, Z.-q. Yao, G. R. Baker, V. K. Gupta, P. S. Russo, M. J. Saunders, *J. Am. Chem. Soc. 108* (1986) 849.
[77] G. R. Newkome, G. R. Baker, M. J. Saunders, P. S. Russo, V. K. Gupta, Z.-q. Yao, J. E. Miller, K. Bouillion, *J. Chem. Soc. Chem. Comm. 1986,* 752.
[78] G. Cantor, *Contributions to Transfinite Numbers,* Dover Press, London 1915.
[79] J. Gleick: *Chaos: Making a New Science,* Viking Penguin, New York 1987, p. 99.
[80] B. B. Mandelbrot: *Fractals: Form, Chance and Dimensions,* W. H. Freeman, New York 1977; *The Fractal Geometry of Nature,* W. H. Freeman, New York 1982.
[81] B. H. Kaye: *A Random Walk Through Fractal Dimensions,* VCH Verlagsgesellschaft/VCH Publishers, Weinheim/New York 1989.
[82] See also the following communication in this issue: A. B. Blumen, H. Schnörer, *Angew. Chem. 102* (1990) 158; *Angew. Chem. Int. Ed. Engl. 29* (1990) 113.
[83] A. Cheetham, K. McCormick (Smithsonian Institution, Washington, D.C., USA), personal communication.
[84] M. Lewis, D. C. Rees, *Science (Washington) 230* (1985) 163.
[85] P. B. Smith, S. J. Martin, M. J. Hall, D. A. Tomalia in J. Mitchell, Jr., (Ed.): *Applied Polymer Analysis and Characterization,* Hanser, München/New York 1987, p. 357.
[86] F. M. Menger, *Top. Curr. Chem. 136* (1986) 1.
[87] D. A. Tomalia, P. Kirchoff, D. Downing, unpublished results.
[88] O. C. Dermer, G. E. Ham: *Ethyleneimine and Other Aziridines,* Academic Press, New York 1969.
[89] D. A. Tomalia, G. Killat ("Alkyleneimine Polymers") in *Encyclopedia of Polymer Science and Engineering, 2nd ed. Vol. 1,* Wiley, New York 1985.
[90] D. M. Hedstrand, P. Meister, D. A. Tomalia, unpublished results.
[91] A. Bashir-Hashemi, H. Hart, D. L. Wart, *J. Am. Chem. Soc. 108* (1986) 6675.
[92] H. Hart, A. Bashir-Hashemi, J. Luo, M. Meador, *Tetrahedron 42* (1986) 1641.
[93] H. Hart, personal communication.
[94] A. Padias, H. Hall, D. A. Tomalia, *Polym. Prepr. Am. Chem. Soc. Div. Polym. Chem. 30* (1989) 119.
[95] M. N., Bochkarev, *Organomet. Chem. (USSR) 1* (1988) 115.
[96] Y. H. Kim, O. W. Webster, *Polym. Prep. Am. Chem. Soc. Div. Polym. Chem. 29* (1988) 310.
[97] a) S. J. Weiner, P. A. Kollman, D. A. Case, U. C. Singh, C. Ghio, G. Alagona, S. Profeta, Jr., P. Weiner, *J. Am. Chem. Soc. 106* (1984) 765; b) POLYGRAF is an interactive molecular mechanics/graphics program available from Molecular Simulations, Inc. Pasadena, CA, USA. All simulations were performed on DEC Vax 8650 and Alliant FX8/8 computers. Structures were displayed on Evans & Sutherland PS330 and PS390 series graphics systems.
[98] F. M. Richards, *Annu. Rev. Biophys. 6* (1977) 151.
[99] J. L. Pascual-Ahuir, E. Silla, *QCPE Program No. 554,* Quantum Chemistry Program Exchange Center, Bloomington, IN, USA.
[100] D. A. Tomalia, S. Edwards, D. M. Hedstrand, P. Meister, unpublished results.
[101] L. R. Wilson, D. A. Tomalia, *Polym. Prepr. Am. Chem. Soc. Div. Polym. Chem. 30* (1989) 115.

[102] a) D. Meltzer, D. A. Tirell, unpublished results. b) P. Smith, unpublished results.
[103] R. D. Hester, P. H. Mitchell, J. Polym. Sci. Chem. Ed. 18 (1980) 1729.
[104] C. Milstein, *Angew. Chem. 97* (1985) 819; *Angew. Chem. Int. Ed. Engl. 24* (1985) 816.
[105] A. Nurnen, S. Demotz, G. Corradin, H. Binz, H. R. Bosshard, *Science (Washington) 235* (1987) 780.
[106] A. G. Amit, R. A. Mariuzza, S. E. V. Phillips, R. J. Poljak, *Science (Washington) 233* (1986) 747.
[107] M. Lewis, D. C. Rees, *Science (Washington) 230* (1985) 1163.
[108] J. F. Leszczynski, G. D. Rose, *Science (Washington) 234* (1986) 849.
[109] a) M. Daoud, J. P. Cotton, *J. Phys. (Paris) 43* (1982) 531; b) T. M. Birshtein, E. B. Zhulina, *Polymer 25* (1984) 1453.
[110] A. Miyake, K. F. Freed, *Macromolecules 16* (1983) 1228.
[111] A. M. Naylor, W. A. Goddard III, G. Keifer, D. A. Tomalia, *J. Am. Chem. Soc. 111* (1989) 2339.
[112] a) S. S. Kurtz, Jr., A. L. Ward, *J. Franklin Inst. 222* (1936) 563; *ibid. 224* (1937) 583, 697; b) A. L. Ward, S. S. Kurtz, Jr., W. H. Fuleveiler in A. E. Dunstan, A. W. Nash, B. T. Brooks, N. T. Tizard (Eds.): *Science of Petroleum, Vol. 2,* Oxford University Press, London 1938, p. 1172; c) S. S. Kurtz, Jr., A. Sankin in A. Farkas (Ed.): *Physical Chemistry of Hydrocarbons, Vol. 2,* Academic Press, New York 1953.
[113] L. Stryer: *Biochemistry,* 2nd ed., W. H. Freeman, New York 1981, p. 724.
[114] J. W. Erickson, A. M. Silva, M. R. N. Muthy, I. Fita, M. G. Rossman, *Science (Washington) 229* (1985) 625.
[115] F. M. Brodsky, *Science (Washington) 242* (1988) 1396.
[116] It is well known that classical systems of particles with purely repulsive two-body interactions freeze into an ordered crystalline-like phase if they are sufficiently dense. a) M. Ross, *Contemp. Phys. 12* (1971) 333; b) M. N. V. Temperleg, J. S. Rowlinson, G. S. Rushbrooke (Eds): *Physics of Simple Liquids,* North-Holland, Amsterdam 1968.
[117] R. Kopelman, *Science (Washington) 241* (1988) 1620.
[118] S. E. Friberg, M. Podzimek, D. M. Hedstrand, D. A. Tomalia, *Mol. Cryst. Liq. Cryst. 164* (1988) 157–165.
[119] F. Vögtle, E. Weber, *Angew. Chem. 86* (1974) 896; *Angew. Chem. Int. Ed. Engl. 13* (1974) 814.
[120] C. J. Suckling, *J. Chem. Soc. Chem. Commun. 1982,* 661.
[121] See [86], particularly chapters 2–4.
[122] H. Sigel, R. B. Martin, *Chem. Rev. 82* (1982) 385.
[123] B. Helmer, D. A. Tomalia, unpublished results.
[124] D. S. Edwards, C. W. Jung, D. A. Tomalia, unpublished results.
[125] I. A. Tomlinson, M. J. Fazio, unpublished results.
[126] C. Tanford: *The Hydrophobic Effect: Formation of Micelles and Biological Membranes,* 2nd ed., Wiley-Interscience, New York 1980.
[127] D. J. Mitchell, B. W. Ninham, *J. Chem. Soc. Faraday Trans. 2 1981,* 601.
[128] D. A. Tomalia, D. A. Kaplan, J. W. Kruper, R. C. Cheng, I. A. Tomlinson, M. J. Fazio, D. M. Hedstrand: *PCI Int. Appl. WO8801, 178; Chem. Abstr. 110* (1989) 150378x.
[129] J. P. Tam, *Proc. Natl. Acad. Sci. USA 85* (1988) 5409.
[130] K. J. Chang, W. Pugh, S. G. Blanchord, J. McDermed, J. P. Tam, *Proc. Natl. Acad. Sci. USA 85* (1988) 4929.
[131] D. N. Posnett, H. McGrath, J. P. Tam, *J. Biol. Chem. 264* (1988) 1719.
[132] A. G. Cairns-Smith: *Sci. Am. 253* (1985) No. 6, p. 90; *Spektrum Wiss. 1985,* No. 8, p. 82.
[133] A. G. Cairns-Smith: *Genetic Takeover and the Mineral Origins of Life,* Cambridge University Press, Cambridge, England 1982.
[134] R. Dawkins, *New Scientist 25* (1986) 24.
[135] K. Verner, G. Shatz, *Science (Washington) 241* (1988) 1307.
[136] W. J. Gehring, *Sci. Am. 253* (1985) No. 10, p. 153; D. R. Kaplan, *ibid 249* (1983) No. 7, p. 98.
[137] a) J. Darnell, H. Lodish, D. Baltimore: *Molecular Cell Biology,* Scientific American Books, New York 1986, chapt. 22, pp. 987ff.; b) I. G. David, T. D. Sargent, *Science (Washington) 240* (1986) 1443.
[138] D. A. Tomalia et al., unpublished results.
[139] D. J. Cram, *Science (Washington) 219* (1983) 1177.
[140] J. L. Marx, *Science (Washington) 222* (1983) 1109.
[141] J. H. White, N. R. Cozzarelli, W. R. Bauer, *Science (Washington) 241* (1988) 323.
[142] See [137a], p. 1086.
[143] D. W. Tank, M. Sugimori, J. A. Connor, R. R. Llinás, *Science (Washington) 242* (1988) 773.
[144] R. A. Lerner, K. D. Janda, D. Schloeder, S. J. Benkovic, *Science (Washington) 241* (1988) 323.
[145] Review: P. G. Schultz, *Angew. Chem. 101* (1989) 1336; *Angew. Chem. Int. Ed. Engl. 28* (1989) 1283.
[146] T. C. Lubensky, P. A. Pincus, *Phys. Today 37* (1984) No. 10, p. 44.
[147] T. P. Martin, *Angew. Chem. 98* (1986) 197; *Angew. Chem. Int. Ed. Engl. 25* (1988) 197.
[148] J. M. Lehn, A. Rigault, *Angew. Chem. 100* (1988) 1121; *Angew. Chem. Int. Ed. Engl. 27* (1988) 1095, and references therein.
[149] Spheroidal cancer tumor growth is analyzed in this fashion and exhibits strong analogies to spherical dendrimers. W. Duchting, T. Vogelsaenger, *Bio Systems 18* (1985) 79; R. M. Sutherland, *Science (Washington) 240* (1988) 177.
[150] E. J. Goethals (Ed.): *Telechelic Polymers: Synthesis and Applications,* CRC Press, Boca Raton, FL, USA 1989.
[151] a) A. Halperin, *Macromolecules 20* (1987) 2943; b) C. Marques, J. F. Joanny, L. Leibler, *ibid. 21* (1988) 1051; c) A. Halperin, *ibid. 22* (1989) 3806.
[152] See [137a], pp. 774ff.
[153] J.-H. Fuhrhop, H.-H. David, J. Mathieu, U. Liman, H.-J. Winter, E. Boekema, *J. Am. Chem. Soc. 108* (1986) 1785.
[154] a) C. D. Gutsche, L.-G. Lin, *Tetrahedron 42* (1986) 1633; b) E. T. Jarvi, H. W. Whitlock, *J. Am. Chem. Soc. 104* (1982) 7196.
[155] L. Pauling, *Chem. Eng. News 24* (1946) 1375; *Am. Sci. 36* (1948) 51.
[156] H. Hoffmann, G. Ebert, *Angew. Chem. 100* (1988) 933; *Angew. Chem. Int. Ed. Engl. 27* (1988) 902.
[157] E. G. Mazur: *Graphic Representation of the Periodic System During One Hundred Years,* The University of Alabama Press, AL, USA 1974; I. Hargittai, M. Hargittai: *Symmetry Through the Eyes of a Chemist,* VCH, Weinheim/New York 1986, pp. 5f.
[158] D. A. Tomalia, D. M. Hedstrand, L. R. Wilson in *Encyclopedia of Polymer Science and Engineering, 2,* Wiley, New York, 1990, pp. 46–92.
[159] A. A. Berlin, N. G. Matveyeva, *J. Polym. Sci. Macromol. Rev. 12* (1977) 1; *15* (1980) 107.
[160] P. J. Flory, *Br. Polym. J. 17* (1985) 96.
[161] P. Hodge, D. C. Sherrington (Eds): *Polymer Supported Reactions in Organic Synthesis,* Wiley, New York 1980.
[162] See [137a], pp. 816f.
[163] S. Borman, *Chem. Eng. News 67* (1989) No. 15 (April 10, 1989), p. 25.
[164] a) Cationic surfactants have been successfully organized and characterized on the surfaces of anionically functionalized dendrimers. A "cooperative effect" was noted for higher-generation PAMAM dendrimers (generations 4.5–9.5) according to photoluminescence probe techniques. b) Generation-dependent morphologies consistent with [111] were corroborated by probing with photoinduced electron-transfer reactions on the dendrimer surfaces: N. D. Turro, G. Caminati, D. A. Tomalia, *Macromolecules* (1990), in press.
[165] J. P. Crutchfield, J. D. Farmer, N. H. Packard, R. S. Shaw, *Sci. Am. 255* (1986) No. 1, p. 46.
[166] One might argue that artificial protein synthesis as described by *M. Mutter* [4b] is one of the first efforts in this direction.
[167] This has been demonstrated for micron-sized particles referred to as Janus beads: a) E. Raphael, *C.R. Acad. Sci. Paris 307* (1988) 12; b) C. Casagrande, M. Veyssie, *ibid. 306* (1988) 1423.
[168] M. Maclean, S. P. Gregory, R. A. Flavell (Eds.): *Eukaryotic Genes, Their Structure, Activity and Regulation,* Butterworth & Co., London/Boston 1983.
[169] W. Ostwald, M. H. Fischer (Eds.): *Theoretical and Applied Colloid Chemistry: "The World of Neglected Dimensions",* Wiley 1917.
[170] M. A. Duncan, D. H. Rouvray, *Sci. Am.,* No. 12 (1989), p. 110.

Communications may be submitted in English *or* in German. Further details regarding the submission of communications can be found in the "Notice to Authors" reproduced in the January issue of the journal. Copies thereof may be obtained from the editorial office upon request.

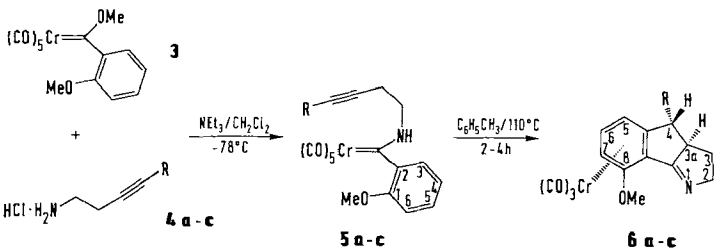

Scheme 1. **a**, R = CH_3; **b**, R = C_2H_5; **c**, R = $SiMe_3$

Synthesis of Nitrogen Heterocycles by Diastereoselective Intramolecular Aminocarbene Annelation**

By *Karl Heinz Dötz,* Thomas Schäfer*, and *Klaus Harms*

Reaction of alkoxycarbene-carbonyl complexes of chromium with alkynes results in regioselective alkyne/carbene/CO coupling to give $Cr(CO)_3$-coordinated 4-alkoxyphenols **1**.[1] By contrast, the corresponding aminocarbene complexes undergo five-membered ring annelation to give **2**;[2] however, the higher temperatures required often lead to loss of the metal complex fragment, so that the planar chirality is no longer present as an important stereogenic element in the product. Since the $Cr(CO)_3$ fragment in either the arene ligand or the aryl side chain should offer an effective means of stereocontrol in subsequent reactions,[3] we have attempted to suppress decomplexation of the annelation product by using milder reaction conditions. A possible approach—besides the use of carbene chelate complexes[4]—is an *intra*molecular annelation.

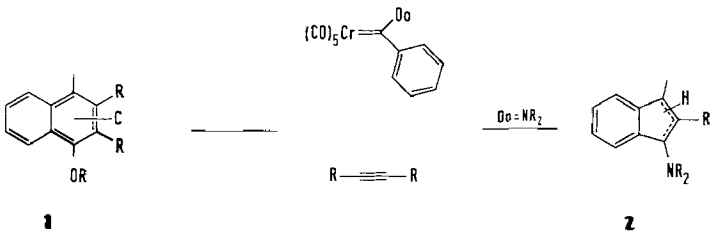

1 **2**

To examine this concept, we have investigated the alkynylaminocarbene complexes **5a–c** (Scheme 1). They are accessible from **3** and the amine hydrochlorides **4a–c** in the presence of a base in yields of 85–95% by modification of the known aminolysis reaction. On heating these complexes in refluxing toluene, annelation of the aryl substituents occurs to give the tetrahydroindeno[1,2-*b*]pyrrole complexes **6a–c**, which have three new stereogenic elements. The cyclization proceeds with high diastereoselectivity: ^1H and ^{13}C NMR spectroscopy reveal only a single diastereomer. The relative configuration of the two neighboring stereocenters in the central five-membered ring (3a-C, 4-C) was determined for **6a** by an ^1H NOE experiment. Irradiation of the 3a-H absorption resulted in an increase in intensity by 5.2% for 4-H and by 5.9% and 8.3% for the two 3-H atoms; these latter increases in intensity serve as internal standard for the interaction with vicinal *trans* and *cis* H atoms, respectively. Accordingly, 3a-H and 4-H are arranged *trans* to each other. On the other hand, only the X-ray structure analysis[5] of **6a** (Fig. 1) showed unambiguously that the $Cr(CO)_3$ fragment and the substituent R, originally the alkyne substituent, are *cis* to each other and thus bonded to the same side of the ring system as 3a-H. The resulting steric interaction in **6c** between the trimethylsilyl group and the metal fragment explains the ready decomplexation of this tricyclic compound.

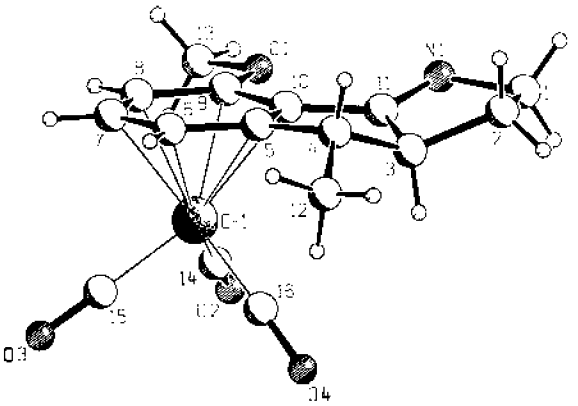

Fig. 1. Molecular structure of **6a** (the C atoms are only labeled with numbers). Selected bond lengths [Å] and angles [°]: C5-C10 1.429(7), C10-C11 1.452(7), **C3-C11 1.497(7), C3-C4 1.526(7), C4-C5 1.510(8), C11-N1 1.281(6), C1-N1** 1.491(7); C10-C11-C3 108.5(4), C3-C11-N1 118.1(5), N1-C11-C10 132.8(5), C3-C4-C5 102.7(4), C1-N1-C11 105.2(4); Torsional angle [°]: C3-C4-C5-C10 − 20.3(6), C3-C11-N1-C1 0.8(7), C11-C3-C4-C5 27.2(5), C1-C2-C3-C11 − 25.4(5), C5-C10-C11-N1 − 156.6(6).

The diastereoselective carbene annelation may be explained as follows (Scheme 2): After thermally induced decarbonylation, the alkyne is coordinated intramolecularly and then inserted into the metal–carbene bond by alkyne/carbene coupling.[6] Electrophilic addition of the metal complex fragment (16-electron species) to the arene followed by reductive elimination leads to formation of the central five-membered ring, with the complex fragment and the C_{sp^3} H atom lying on opposite sides of the ring. The six-membered ring can undergo rearomatization by a suprafacial sigma-

[*] K. H. Dötz, T. Schäfer, K. Harms
Fachbereich Chemie der Universität
Hans-Meerwein-Strasse, D-3550 Marburg (FRG)

[**] Reaction of Complex Ligands, Part 40. This work was supported by the Deutsche Forschungsgemeinschaft and the Fonds der Chemischen Industrie. Part 39: K. H. Dötz, R. Noack, K. Harms, G. Müller, *Tetrahedron*, in press.

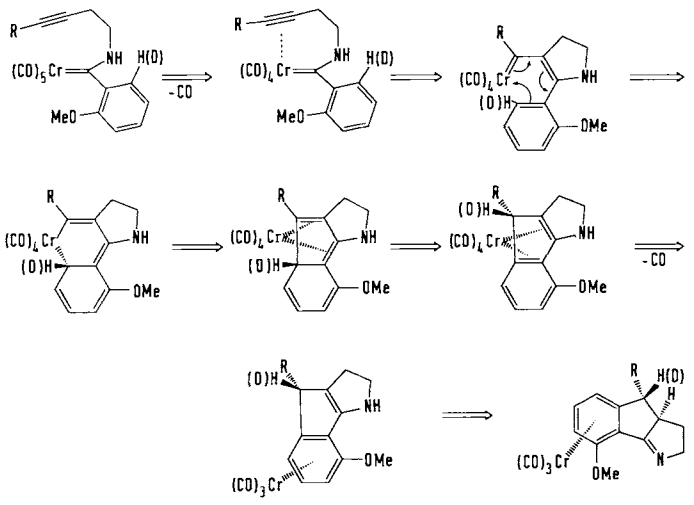

Scheme 2. Proposed mechanism for the transformation of **5** to **6**.

tropic 1,5-H shift in the five-membered ring and then coordinate the metal carbonyl fragment. This step also establishes the *cis* configuration of R and the complex fragment. Thus, whereas the chiral center 4-C and the planar chirality arise during the diastereoselective, metal-induced carbene annelation, the configuration of the stereocenter 3a-C presumably results from a thermodynamically controlled enamine/imine tautomerization.[7] The mechanism proposed in Scheme 2 is supported by a labeling study, which showed that deuterium introduced at the 3-position of the aryl substituent of **5a** is incorporated exclusively as *trans* 4-D in **6a**.

Metal-induced aminocarbene annelation thus offers a novel diastereoselective entry to arene–$Cr(CO)_3$ complexes, which may be further functionalized in a controlled fashion by metalation and nucleophilic addition.[8]

Experimental Procedures

Typical aminolysis: 5-Amino-2-pentyne hydrochloride, **4a** (0.70 g, 5.85 mmol), was added to a solution of pentacarbonyl[methoxy(1-methoxy-2-phenyl)carbene]chromium, **3** (1.65 g, 4.82 mmol), and 4 mL of triethylamine in 10 mL of dichloromethane at −78 °C. After 30 min, the solvent was removed under high vacuum. Column-chromatographic workup (0 °C, petroleum ether/dichloromethane 2/1) afforded **5a** as a yellow-brown oil (1.63 g, 86%. ^{1}H NMR (300 MHz, $CDCl_3$): δ = 9.43 (s, br, 1H, NH), 7.21 (m, 1H, 5-H_{aryl}), 7.00 (m, 1H, 4-H_{aryl}), 6.89 (d, J = 8.3 Hz, 1H, 6-H_{aryl}), 6.74 (m, 1H, 3-H_{aryl}), 3.82 (s, 3H, OCH_3), 3.25 (m, 2H, NCH_2), 2.39 (m, 2H, $\equiv CCH_2$), 1.86 (t, J = 2.5 Hz, 3H, CH_3). ^{13}C NMR (75 MHz, $CDCl_3$): δ = 280.2 (Cr=C), 223.6 (CO_{cis}), 217.3 (CO_{trans}), 148.7 (1-C_{aryl}), 138.0 (2-C_{aryl}), 128.2 (C_{aryl}), 120.9 (3-C_{aryl}), 120.8, 110.8 (2 C_{aryl}), 80.6 ($C\equiv C$-CH_3), 73.7 ($\equiv C$-CH_3), 55.3 (OCH_3), 48.5 (NCH_2), 19.3 ($\equiv CCH_2$), 3.3 (CH_3). IR (CH_2Cl_2): $\tilde{\nu}$ = 2060, 1975, 1930 cm^{-1} [$Cr(CO)_5$]. EI-MS: m/z 393 ($M^{\oplus}$, 4%).

Typical carbene annelation: A solution of **5a** (0.26 g, 0.65 mmol) in 20 mL of toluene was heated at 110 °C for 2 h. After removal of the solvent under high vacuum and chromatography on silica gel (− 30 °C, dichloromethane containing 2% methanol), **6a** was obtained as a yellow powder (0.11 g, 50%). ^{1}H NMR (300 MHz, $CDCl_3$): δ = 5.69 (t, J = 6.5 Hz, 1H, H_{aryl}), 5.05 (d, J = 6.7 Hz, 1H, H_{aryl}), 4.96 (d, J = 6.2 Hz, 1H, H_{aryl}), 4.38 (m, 1H, 2-H), 4.18 (m, 1H, 2-H), 3.89 (s, 3H, OCH_3), 3.18 (m, 1H, 3a-H), 2.86 (m, 1H, 4-H), 2.30 (m, 1H, 3-H), 1.62 (m, 1H, 3-H), 1.48 (d, J = 6.8 Hz, CH_3). ^{13}C NMR (75 MHz, $CDCl_3$): δ = 232.1 [$Cr(CO)_3$], 180.4 (C=N), 140.4 (8-C), 129.9 (C_{aryl}), 94.3 (C_{aryl}), 86.6 (C_{aryl}), 81.0 (C_{aryl}), 73.0 (C_{aryl}), 67.5 (2-C), 58.5 (OCH_3), 56.4 (3a-C), 40.7 (4-C), 30.5 (3-C), 15.6 (CH_3). EI-MS: m/z 337 ($M^{\oplus}$, 5%). IR (CH_2Cl_2): $\tilde{\nu}$ = 1961, 1897 [$Cr(CO)_3$], 1654 cm^{-1} (C=N).

Starting from 6-deutero-2-methoxybenzoic acid [9], the alkoxycarbene complex [D]**3** was accessible via the acid chloride [10]. Aminolysis of [D]**3** gave [D]**5**, which was cyclized to [D]**6a**. [D]**5a**: δ = 9.43 (s, br, 1H, NH), 7.21 (m, 1H, 5-H_{aryl}), 7.00 (m, 1H, 4-H_{aryl}), 6.89 (d, J = 8.3 Hz, 1H, 6-H_{aryl}), 6.74 (m, 90% D, 3-H_{aryl}), 3.82 (s, 3H, OCH_3), 3.25 (m, 2H, NCH_2), 2.39 (m, 2H, $\equiv CCH_2$), 1.86 (t, J = 2.5 Hz, 3H, CH_3). ^{13}C NMR (75 MHz, $CDCl_3$): δ = 280.1 (Cr=C), 223.5 (CO_{cis}), 217.2 (CO_{trans}), 148.6 (1-C_{aryl}), 137.9 (2-C_{aryl}), 128.2 (C_{aryl}), 120.8 (3-C_{aryl}, decreased intensity), 120.7, 110.7 (2 C_{aryl}), 80.5 ($C\equiv C$-CH_3), 73.6 ($\equiv C$-CH_3), 55.2 (OCH_3), 48.4 (NCH_2), 19.2 ($\equiv CCH_2$), 3.2 (CH_3). [D]**6a**: influenced signals δ (^{1}H) = 3.18 (m, 1H, 3a-H), 2.86 (m, 90% D, 4-H), 1.48 (s, 3H, CH_3); δ (^{13}C) = 40.7 (4-C, decreased intensity).

Received: October 3, 1989 [Z 3578 IE]
German version: *Angew. Chem. 102* (1990) 188

[1] Reviews: K. H. Dötz, *Angew. Chem. 96* (1984) 573; *Angew. Chem. Int. Ed. Engl. 23* (1984) 587; W. D. Wulff in L. Liebeskind (Ed.): *Advances in Metal-Organic Chemistry, Vol. 1*, JAI Press, Greenwich 1989, p. 206; K. H. Dötz in H. tom Dieck, A. de Meijere (Eds.): *Organometallics in Organic Synthesis: Aspects of a Modern Interdisciplinary Field*, Springer, Berlin 1988.

[2] A. Yamashita, *Tetrahedron Lett. 27* (1986) 5915; K. H. Dötz, D. Grotjahn, K. Harms, *Angew. Chem. 101* (1989) 1425; *Angew. Chem. Int. Ed. Engl. 28* (1989) 1384.

[3] M. F. Semmelhack, G. R. Clark, J. L. Garcia, J. J. Harrison, Y. Thebtarantonth, W. D. Wulff, A. Yamashita, *Tetrahedron 37* (1981) 3957; G. Jaouen in H. Alper (Ed.): *Transition Metal Organometallics in Organic Synthesis*, Academic Press, New York 1978.

[4] K. H. Dötz, H. G. Erben, K. Harms, *J. Chem. Soc. Chem. Commun. 1989*, 692.

[5] a) Crystallographic data for **6a** ($C_{16}H_{15}CrO_4N$, M = 337.29): monoclinic, space group $P2_1/c$, a = 8.854(2), b = 13.399(1), c = 25.919(6) Å, β = 95.83(1)°, Z = 8 (two molecules per asymmetric unit, which differ by slightly different positions of the tricarbonylchromium groups), ϱ_{calcd} = 1.465 g cm^{-3}, $\mu(Cu_{K\alpha})$ = 64.0 cm^{-1}. Measurement with an ENRAF-NONIUS CAD4 diffractometer ($Cu_{K\alpha}$ radiation, λ = 1.5418 Å, graphite monochromator, room temperature); 7934 measured reflections, 3581 unique (R_{int} = 0.026), 3050 with $F_o > 4\sigma(F_o)$ were considered as observed. Solution by direct methods [5b], refinement [5c] to R = 0.054, R_w = 0.041 ($w = 1/\sigma^2$), all non-hydrogen atoms anisotropic, H atoms at calculated positions with groupwise common isotropic temperature factors, 413 parameters. Empirical absorption corrections in the ENRAF-NONIUS SDP SYSTEM. All calculations were performed on a Micro-Vax II [5d–f]; b) G. M. Sheldrick, SHELXS-86, Program for Crystal Structure Solution, Universität Göttingen, 1986; c) G. M. Sheldrick, SHELX-76, Program for Crystal Structure Determination, Cambridge 1976; d) A. L. Spek, Platon 89, Program for Geometrical Analysis of Crystal Structures, Utrecht 1989; e) E. Keller, SCHAKAL-88 B, A FORTRAN Program for the Graphic Representation of Molecular and Crystallographic Models, Freiburg 1988; f) Further details of the crystal structure investigation may be obtained from the Fachinformationszentrum Karlsruhe, Gesellschaft für wissenschaftlich-technische Information mbH, D-7514 Eggenstein-Leopoldshafen 2 (FRG), on quoting the depository number CSD-320027, the names of the authors, and the journal citation.

[6] P. Hofmann, M. Hämmerle, *Angew. Chem. 101* (1989) 940; *Angew. Chem. Int. Ed. Engl. 28* (1989) 908.

[7] B. Jeso, J. C. Pommier, *J. Chem. Soc. Chem. Commun. 1977*, 65; B. A. Shainyan, A. N. Mirskova, *Russ. Chem. Rev. 48* (1979) 107.

[8] A. Solladié-Cavallo in L. Liebeskind (Ed.): *Advances in Metal-Organic Chemistry, Vol. 1*, JAI Press, Greenwich 1989, p. 99.

[9] W. J. S. Lockley, *Tetrahedron Lett. 23* (1982) 3819.

[10] M. F. Semmelhack, G. R. Lee, *Organometallics 6* (1987) 1839.

Hexaalkynyltriphenylene: A New Type of Nematic-Discotic Hydrocarbon**

By *Klaus Praefcke,** *Bernd Kohne*, and *Dirk Singer*

Hydrocarbons are rarely found in the group of non-calamitic, disc-shaped liquid crystals.[1–4] Large, highly unsaturated, centrosymmetric hydrocarbons, as well as analogous heteroatom-containing compounds, with unusual liquid crystalline properties, have now become available for the first time by a simple one-pot reaction involving repeated

[*] Prof. Dr.-Ing. K. Praefcke, Dr. B. Kohne, Dipl.-Chem. D. Singer
Institut für Organische Chemie, C3, der Technischen Universität
Strasse des 17. Juni 135, D-1000 Berlin 12

[**] Liquid Crystalline Compounds, Part 52. This work was supported by the Deutsche Forschungsgemeinschaft (Sfb 335, Teilprojekt C3), E. Merck (Darmstadt), and the Technische Universität Berlin (UP, K, and PA 1). We thank *S. Völzke* for technical assistance. Part 51: [12a].

Pd-catalyzed alkynylation of brominated arenes with variously substituted arylacetylenes.[1-4]

Particularly noteworthy are the favorable nematodiscogenic properties of these novel mesogens.[1-4] Of great interest, furthermore, are the electrooptic field effects[3-5] recently found in the surprisingly low-viscosity N_D phases of some representatives of this class of compounds. Similar results are also expected for structurally varied multi(phenylethynyl)arenes, such as hydrocarbons of the series **1** and **2**, and potential applications are conceivable.

We synthesized the seven new hydrocarbons presented here, **1a–c, 2a, b,** and two only hexaalkynyl-substituted triphenylene derivatives (see *Experimental Procedure*), by C–C coupling[1-4] reaction of (4-alkylphenyl)acetylenes and 1-alkynes with hexabromobenzene and the relatively recently prepared 2,3,6,7,10,11-hexabromotriphenylene,[6] respectively. Whereas the alkylethynyl derivatives of triphenylene, unlike hexaalkynylbenzenes,[1] do not exhibit liquid crystalline phases, the yellow hydrocarbons **1a–c** and **2a, b,** which emit blue fluorescence in solution (e.g., in $CHCl_3$), are monothermomesomorphic and, in fact, nematic-discotic, with the phase transition data given in the *Experimental Procedure*.

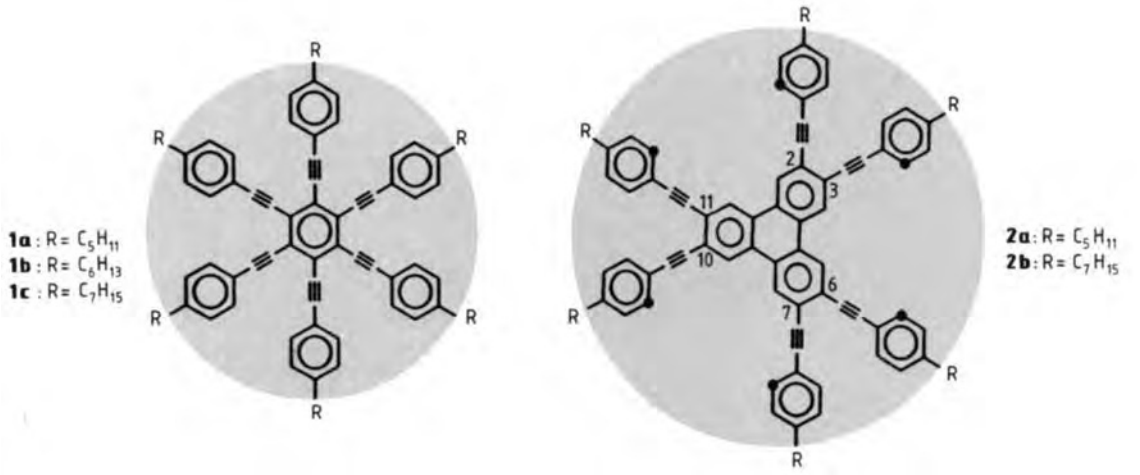

When the mesogens **1a–c** and **2a, b** are heated above their melting points and examined under a polarization microscope, one observes in each case only an N_D phase displaying the typical fluidity, strong thermal fluctuations, and schlieren or marbled texture;[2,4,7] such a phase has been very seldom found for noncalamitic mesogens.[1,2] This characterization is corroborated by the fact that these N_D phases are miscible with those of two hexa(phenylethynyl)benzene derivatives, which were shown to be nematic-discotic by X-ray structure investigations.[4] On slow cooling of the isotropic melts of mesogens **1** and **2** below the clearing temperatures or after annealing their N_D phases, nonbirefringent, pseudoisotropic regions are formed as a result of homeotropic orientation of the large molecules parallel to the surfaces of the glass slides.

Like other multi(phenylethynyl)arenes with N_D phases,[1-4] the new nematic-discotic compounds **1a–c** and **2a, b** exhibit strikingly small transition enthalpies $\Delta H_{N_D \rightarrow I}$ (approximately 0.2 kJ mol^{-1}) for the clearing processes ($N_D \rightarrow I$), as determined by differential scanning calorimetry (DSC).[8]

The stable mesophase regions (ΔT_{N_D}) observed for **2a, b** (80 and 54 K, respectively) are appreciably broader than those found (16 and 32 K, respectively) for the hexakis(phenylethynyl)benzenes **1a, c** with the same R groups. In contrast to **1a–c**, compounds **2** display three "bays", each roughly 8.5 Å[9] wide, between the carbon atoms marked with solid circles in the formula and assumed to lie in the same plane. If this difference in the surface features of the "core" region is ignored, the width of the N_D phases of the two classes of liquid crystals can be regarded as a function of the diameter of their superdisc-like[10] mesogen cores (gray background). Whereas the core diameter of **1a–c** is about 19.5 Å, the mesogen core[11] of **2a, b** has a diameter of about 24 Å.[9]

The significance of the core size and geometry for the liquid crystalline behavior of noncalamitic mesogens is made still clearer by comparison of the N_D-phase-forming monomesomorphic hexaynes **1a, c** and of **2a, b**, which contain benzene and triphenylene, respectively, as centers of the mesogen cores, with analogous naphthalenes containing alkyne substituents at positions 1–3 and 5–7.[2] The latter mesogens are ellipsoidal in structure and therefore biaxial with "superdisc core" diameters of about 19.5 and 21.7 Å, respectively.[2,9] These naphthalene derivatives are multimesomorphic with inverse phase sequence $K \rightarrow N_D \rightarrow D_r \rightarrow D_h \rightarrow I$; the D phases vanish when the alkyl groups are lengthened.[2]

Like the naphthalene derivatives, the triphenylene derivatives **2a, b** also readily form complexes with numerous functionalized carbocyclic compounds (e.g., cyclohexyl chloride, chloro- and nitrobenzene), whereby the type of mesophase changes (transformation of N_D phases into columnar mesophases!).[3] Further doping effects with typical acceptor molecules (e.g., 2,4,7-trinitrofluoren-9-one) on both low-molecular-weight and polymeric liquid crystals have been reported recently.[12]

Because of their enantiotropic N_D phases and their strongly unsaturated character, hydrocarbons **1a–c** and, even more (owing to their larger core diameters), those of type **2** are potential model substances[1,13] for the study of the "carbonaceous" mesophases described as occurring in pitches and pyrolysis products.[14]

Experimental Procedure

The seven new hexaalkynylarene derivatives were prepared on a 2-mmol scale from hexabromobenzene and 2,3,6,7,10,11-hexabromotriphenylene [6], respectively, and an excess (e.g., 20 mmol for **1a, b** and 36 mmol for **2a, b**) of monosubstituted ethynes following a proven C–C coupling principle [1–4]. Reaction conditions: 100–120 °C bath temperature, 25–180 h, argon atmosphere (e.g.,

for **2a, b**, 38 h at 100 °C in 30 mL of NEt_3 with 250 mg of $(Ph_3P)_2PdCl_2$, 250 mg of CuI, and 500 mg of Ph_3P; for **1a, c**, 180 and 43 h, respectively, in 20 mL of NEt_3 with 100 mg of $(Ph_3P)_2PdCl_2$, 100 mg of CuI, and 250 mg of Ph_3P). Workup was performed by treating the reaction mixture with petroleum ether (PE, b.p. 30–70 °C) or ether, followed by filtration. The filtrate was washed with 2 M hydrochloric acid as well as with saturated aqueous sodium chloride solution, dried over magnesium sulfate, filtered, and evaporated to dryness under vacuum. Products **1a–c** were purified by flash chromatography on 100 mL of silica gel 60 (E. Merck, 230–400 mesh; eluent PE/ethyl acetate (EE) 100/1) and repeated crystallization from acetone and heptane. The triphenylenehexaynes **2a, b** were each purified by column chromatography on 400 mL of silica gel 60 (E. Merck, 70–230 mesh; eluent PE/EE 100/1) and subsequent recrystallization (**2a**, 2 × from acetone, 1 × from heptane, 3 × from acetone containing 30% 1,2-dichlorobenzene, and 6 × from acetone; **2b**, 1 × from acetone containing 30% 1,2-dichlorobenzene and 20 × from acetone). The phase transition data were obtained by polarizing microscopy (PM, Leitz Laborlux 12 Pol with a Mettler FP 82 hot stage, usual rate of heating 1 K min^{-1}) and by DSC (Mettler TA 3000/DSC 30 S and GraphWare TA 72, usual heating rate 5 K min^{-1}).

The hexaynes **1** and **2** described here are multimorphic in the solid phase with reproducible solid/solid transitions and/or form—depending on the thermal history of the sample—metastable modifications. The value given as the melting point refers in each case to the highest-melting crystal modification; if necessary, this modification was obtained by suitable thermal pretreatment of the samples (e.g., annealing or a second heating). K = crystalline, N_D = nematic-discotic, I = isotropic phase.

Hexakis[(4-pentylphenyl)ethynyl]benzene **1a** ($C_{84}H_{90}$, M_r = 1099.7): Yield 46%, yellow crystals from heptane, m.p. (K → N_D) = 169.5 °C (PM), 170.4 °C (DSC, ΔH = 44.1 kJ mol^{-1}), clearing point (N_D → I) ≈ 187 °C (PM, owing to the strong tendency of this compound to decompose, only an approximate transition temperature could be measured; after determining the rough transition temperature, a fresh sample was placed in the hot stage at a temperature just below this value and the sample was heated at 10 K min^{-1}), 184.9 °C (DSC, ΔH = 0.2 kJ mol^{-1}, heating rate 10 K min^{-1}). IR (CCl_4): $\tilde{\nu}$ [cm^{-1}] = 2220 (C≡C). UV/VIS (Cary 118, hexane): λ_{max} [nm] (lg ε) = 373 (sh, 4.946), 350 (5.199). ^1H NMR partial spectrum (Bruker WH 400, $CDCl_3$): δ = 7.6 and 7.2 (2 d, $^3J(H,H) \approx 8$ Hz each; phenyl H *ortho* and *meta* to C≡C); 2.6 (t, $^3J(H,H) \approx 7.5$ Hz; α-CH_2), 1.7 (tt, $^3J(H,H) \approx 7.5$ Hz each; β-CH_2). ^{13}C NMR (Bruker AM 270, off resonance, $CDCl_3$): δ = 143.89 (s; phenyl *C*-CH_2), 131.83 and 128.48 (2 d; 2 × phenyl CH each), 127.37 and 120.66 (2 s; 2 × phenyl *C*-C≡C), 99.42 and 87.20 (2 s; C≡C), 35.99, 31.50, 30.88, 22.52, and 13.98 (4 t, 1 q; pentyl C). **1b, c** were obtained analogously; their spectra are in good agreement with those of **1a**.

Hexakis[(4-hexylphenyl)ethynyl]benzene **1b** ($C_{90}H_{102}$, M_r = 1183.8): Yield 57%, yellow crystals from acetone, m.p. (K → N_D) = 123.7 °C (PM), 124.4 °C (DSC, ΔH = 38.9 kJ mol^{-1}), clearing point (N_D → I) = 142.0 °C (PM), 142.9 °C (DSC, ΔH = 0.2 kJ mol^{-1}).

Hexakis[(4-heptylphenyl)ethynyl]benzene **1c** ($C_{96}H_{114}$, M_r = 1268.0): Yield 52%, yellow crystals from acetone, m.p. (K → N_D) = 98.2 °C (PM), 99.0 °C (DSC, ΔH = 44.4 kJ mol^{-1}), clearing point (N_D → I) = 131.2 °C (PM), 132.6 °C (DSC, ΔH = 0.4 kJ mol^{-1}).

2,3,6,7,10,11-Hexakis[(4-pentylphenyl)ethynyl]triphenylene **2a** ($C_{96}H_{96}$, M_r = 1249.7): Yield 35%, bright yellow crystals from acetone, m.p. (K → N_D) = 156.2 °C (PM), 156.8 °C (DSC, ΔH = 36.7 kJ mol^{-1}), clearing point (N_D → I) = 236.6 °C (PM, owing to the strong tendency of this compound to decompose, only an approximate transition temperature could be measured; after determining the rough transition temperature, a fresh sample was placed in the hot stage at a temperature just below this value and the sample was heated at 10 K min^{-1}), 237.1 °C (DSC, ΔH = 0.1 kJ mol^{-1}). IR(CCl_4): $\tilde{\nu}$ [cm^{-1}] = 2220 (C≡C). UV/VIS (heptane): λ_{max} [nm] (lg ε) = 367 (sh, 5.176), 345.0 (5.370), 314.0 (sh, 5.001). ^1H NMR partial spectrum: δ = 8.6 (s; triphenylene H), 7.6 and 7.2 (2 d, $^3J(H,H) \approx 8$ Hz each; phenyl H *ortho* and *meta* to C≡C), 2.6 (t, $^3J(H,H) \approx 7.8$ Hz; α-CH_2), 1.7 (tt, $^3J(H,H) \approx 7.5$ Hz each; β-CH_2). ^{13}C NMR: δ = 143.18 (s; phenyl *C*-CH_2), 131.99 and 128.30 (2 d; 2 × phenyl CH each), 127.97 and 124.77 (2 s; inner and outer triphenylene C without assignment, 126.67 (d; triphenylene CH), 120.79 (s; phenyl *C*–C≡C), 94.62 and 88.41 (2 s; C≡C), 36.04, 31.68, 30.99, 22.64, and 14.13 (4 t, 1 q; pentyl C). Compound **2b** was obtained analogously; its spectra are in good agreement with those of **2a**.

2,3,6,7,10,11-Hexakis[(4-heptylphenyl)ethynyl]triphenylene **2b** ($C_{108}H_{120}$, M_r = 1418.2): Yield 23%, bright yellow needles from acetone, m.p. (K → N_D) = 121.3 °C (PM), 122.0 °C (DSC, ΔH = 41.1 kJ mol^{-1}), clearing point (N_D → I) = 174.8 °C (PM), 176.6 °C (DSC, ΔH = 0.1 kJ mol^{-1}).

2,3,6,7,10,11-Hexakis(1-heptynyl)triphenylene ($C_{60}H_{72}$, M_r = 793.2): Yield 14–20%, bright yellow, partly crystalline oil. IR (CCl_4): $\tilde{\nu}$ [cm^{-1}] = 2235 (C≡C). ^1H NMR partial spectrum: δ = 8.5 (s; triphenylene H), 2.5 (t, $^3J(H,H) \approx 7$ Hz; C≡C-CH_2) 1.7 (tt, $^3J(H,H) \approx 7$ Hz each; β-CH_2). ^{13}C NMR: δ = 127.96 and 125.35 (2 s; inner and outer triphenylene C without assignment), 126.99 (d; triphenylene CH), 95.12 and 79.65 (2 s; C≡C), 31.19, 28.55, 22.31, 19.77, and 14.01 (4 t, 1 q; pentyl C).

2,3,6,7,10,11-Hexakis(1-decynyl)triphenylene ($C_{78}H_{108}$, M_r = 1045.7): Yield 13%, bright yellow crystals after flash column chromatography (silica gel 60, heptane/ethyl acetate 150/1), m.p. (K → I) ≈ 37 °C (PM), 41.0 °C (DSC, ΔH = 63.0 kJ mol^{-1}). IR ($CHCl_3$): $\tilde{\nu}$ [cm^{-1}] = 2235 (C≡C). ^1H NMR partial spectrum: δ = 8.5 (s; triphenylene H), 2.5 (t, $^3J(H,H) \approx 7$ Hz; C≡C-CH_2), 1.7 (tt, $^3J(H,H) \approx 7$ Hz each; β-CH_2). ^{13}C NMR: δ = 127.96 and 125.37 (2 s; inner and outer triphenylene C without assignment) 126.96 (d; triphenylene CH), 95.12 and 79.66 (2 s; C≡C), 31.91, 29.25, 29.07, 28.69, 22.68, 19.82, and 14.09 (6 t, 1 q, aliphatic CH_2 and CH_3).

Received: August 29, 1989 [Z 3527 IE]
German version: *Angew. Chem. 102* (1990) 200

[1] B. Kohne, K. Praefcke, *Chimia 41* (1987) 196, and papers of other authors cited therein.
[2] K. Praefcke, B. Kohne, K. Gutbier, N. Johnen, D. Singer, *Liq. Cryst. 5* (1989) 233.
[3] K. Praefcke, B. Kohne, unpublished results. D. Singer, *Diplomarbeit FB 5*, Technische Universität Berlin 1989.
[4] M. Ebert, D. A. Jungbauer, R. Kleppinger, J. H. Wendorff, B. Kohne, K. Praefcke, *Liq. Cryst. 4* (1989) 53.
[5] G. Heppke, H. Kitzerow, F. Oestreicher, S. Quentel, A. Ranft, *Mol. Cryst. Liq. Cryst. Lett. Sect. 6* (1988) 71.
[6] R. Breslow, B. Jaun, R. Q. Kluttz, C.-Z. Xia, *Tetrahedron 38* (1982) 863.
[7] D. Demus, L. Richter: *Textures of Liquid Crystals*, Verlag Chemie, Weinheim 1978.
[8] For a discussion of further interesting results on the phase transition N_D → I for compounds having the same type of core as in **1** in comparison to the N → I transition of calamitic/rod-shaped liquid crystals, see [4].
[9] A measure according to Dreiding models: the distance between the centers of the first elements of the aliphatic side chains lying in the disc plane (with respect to **1a–c** as well as **2a, b**, cf. formula).
[10] B. Kohne, K. Praefcke, *Chem.-Ztg. 109* (1985) 121.
[11] For known cores in noncalamitic, disc-shaped and thermomesomorphic compounds, see [1, 2] and references therein.
[12] a) H. Ringsdorf, R. Wüstefeld, M. Ebert, J. H. Wendorff, K. Praefcke, B. Kohne, *Adv. Mater. 2* (1990), in press; b) H. Ringsdorf, R. Wüstefeld, E. Zerta, M. Ebert, J. H. Wendorff, *Angew. Chem. 101* (1989) 934; *Angew. Chem. Int. Ed. Engl. 28* (1989) 914.
[13] Compare the following excerpt—which supports our opinion—from J.-C. Dubois, J. Billard in A. C. Griffin, J. F. Johnson (Eds.): *Liquid Crystals and Ordered Fluids, Bd. 4*, Plenum Press, New York 1984, p. 1054: "Interest in the D_F phase (Note: $D_F \equiv N_D$) as a model for the carbonaceous mesophases [H. Gasparoux, C. Destrade, G. Fug, *Mol. Cryst. Liq. Cryst. 59* (1980) 109; 5×10^8 tons per year] is understood [C. J. Atkinson, J. R. Landes. H. Marsh, *Br. Polym. J. 13* (1981) 1], but until now no pure discogenic hydrocarbon has been made. This void will be filled later."
[14] J. D. Brooks, G. H. Taylor, *Carbon 3* (1965) 185; J. E. Zimmer, J. L. White, *Mol. Cryst. Liq. Cryst. 38* (1977) 177; S. Otami, *ibid. 63* (1981) 249.

Asymmetric Nucleophilic Acylation via Metalated Chiral Amino Cyanides: Enantioselective Synthesis of 3-Substituted 4-Oxoesters by Asymmetric Michael Addition**

By *Dieter Enders,** *Peter Gerdes,* and *Helmut Kipphardt*

Since the pioneering work of *Hauser* et al.[1] in the early 1960s, metalated amino cyanides **A**[2] have been used as d^1 synthons[3] for umpolung of the classical a^1 reactivity of carbonyl compounds[4] and amines.[5] Examples include the syntheses of α-hydroxy ketones,[6] amino alcohols,[7] and α-amino ketones.[8] Compounds **A** are of particular synthetic value as equivalents of acyl carbanions **B**, especially since conjugate additions of **A** to 1,4-unsaturated ketones,[1b, 9] cyanides,[10, 11a, b] and esters[1b, 9c, 11] have been developed

[*] Prof. Dr. D. Enders, Dipl.-Chem. P. Gerdes, Dr. H. Kipphardt
Institut für Organische Chemie der Technischen Hochschule
Professor-Pirlet-Strasse 1, D-5100 Aachen (FRG)

[**] This work was supported by the Fonds der Chemischen Industrie. We thank Boehringer Mannheim GmbH, BASF AG, Bayer AG, and Hoechst AG for donation of chemicals.

to prepare 1,4-dicarbonyl compounds.[12] Numerous applications of optically active amino cyanides have been published in recent years.[13–23] Surprisingly, however, their synthetic potential for asymmetric nucleophilic acylation has

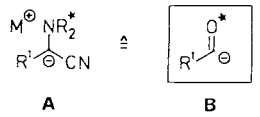

A B

hardly been exploited so far. Here we report an efficient enantioselective synthesis of 3-substituted 4-oxoesters by asymmetric Michael addition of lithiated chiral amino cyanides to α,β-unsaturated esters (Scheme 1).

In this approach, aldeydes **1** are first allowed to react with the enantiomerically pure secondary amine (*S,S*)-**3**[24] [(*S,S*)-**3** · HCl, KCN, H_2O, 0 °C; 1.3 equivalents R^1CHO, 0 °C → room temperature, 3–14 h, 90–98 %] to give the epimeric amino cyanides (*S,S,R/S*)-**4**, which are then metalated with lithium diisopropylamide in ether. Addition of the α,β-unsaturated ester (*E*)-**2** at −100 °C results in formation of the partially crystalline, highly diastereomerically pure Michael adducts (*S,S,R,R*)-**5**, which, as crude products, are hydrolyzed without racemization by addition of saturated copper sulfate solution and tetrahydrofuran as cosolvent. Distillative or chromatographic workup affords the 3-substituted 4-oxoesters (*R*)-**6** in good overall yields (47–71 %) and with high enantiomeric excesses (*ee* = 90 to ≥ 96 %; Table 1). Up to 91 % of the chiral auxiliary reagent (*S,S*)-**3** may be recovered from the aqueous phase, after basification, by extraction with ether.

Table 1. Oxoesters (*R*)-**6** of high enantiomeric purity prepared by conjugate nucleophilic acylation.

6	R^1	R^2	Overall yield [%]	α_D^{23} [°] (neat)	*ee* [%] [a]	Configuration [b]
a	CH_3	CH_3	69	+ 57.2	93	(*R*)
a	CH_3	CH_3	65	− 56.6	92	(*S*) [c]
b	C_2H_5	n-C_4H_9	47	+ 51.9	≥ 95	(*R*)
c	n-C_3H_7	C_2H_5	51	+ 47.2	≥ 95	(*R*)
d	p-C_6H_4Cl	CH_3	66	+ 28.7	≥ 95	(*R*)
e	2-furyl	n-C_4H_9	61	+ 62.6	90	(*R*)
f	p-C_6H_4F	CH_3	71	+ 18.25	≥ 96	(*R*)

[a] Determined by ^1H NMR shift experiments with $Eu(hfbc)_3$. [b] The absolute configurations are based on an X-ray structure analysis of a crystalline adduct, **5**, as well as on polarimetric measurement after chemical correlation with compounds of known configuration [25]. [c] (*R,R*)-**3** was used as chiral auxiliary.

As exemplified for **6f** ($R^1 = p$-C_6H_4F, $R^2 = CH_3$), the enantiomeric excesses may be determined in a facile and relatively exact fashion from the ^1H NMR shift of the sharp methoxy singlet of the ester function (Fig. 1). The racemic oxoester *rac*-**6**, required as a reference compound, was prepared in each case by a route analogous to that in Scheme 1 with achiral pyrrolidine instead of (*S,S*)-**3**. The optical antipodes (*S*)-**6** are correspondingly obtained by using the enantiomeric auxiliary (*R,R*)-**3** [for example, (*R*)-**6a**/(*S*)-**6a**].

The absolute configurations given here are supported by an X-ray structure analysis of a crystalline adduct, **5g** ($R^1 = p$-$H_3COC_6H_4$, $R^2 = CH_3$), and by polarimetric measurement after chemical correlation with known compounds as well as by the assumption of a uniform reaction mechanism.[25]

This new procedure of conjugate nucleophilic acylation of enoates with metalated amino cyanides, which occurs with

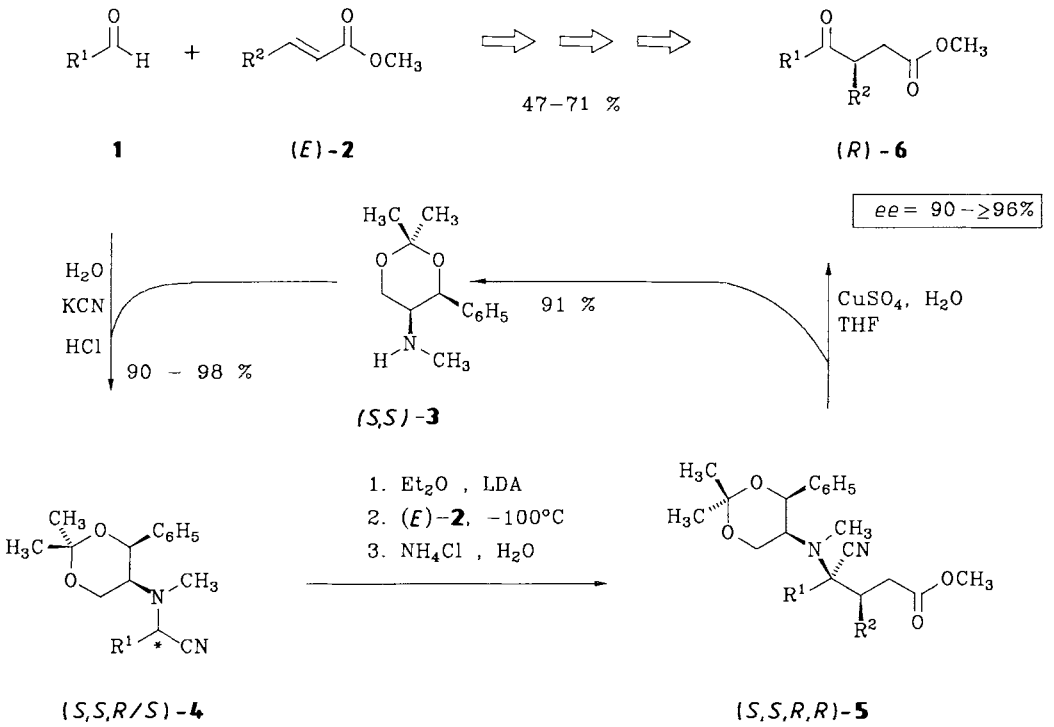

Scheme 1.

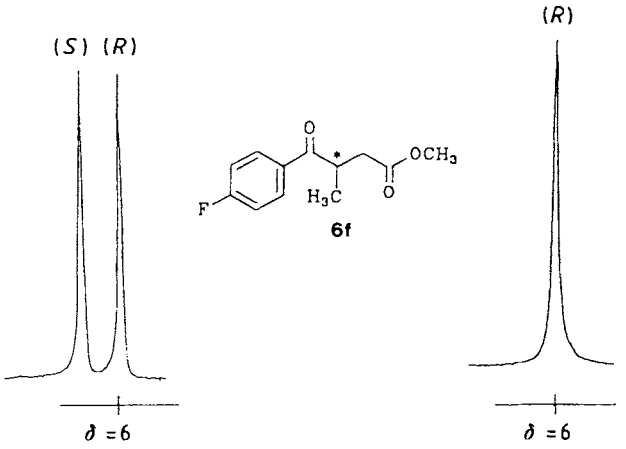

Fig. 1. Determination of the enantiomeric excess by ^{1}H NMR shift experiments (methoxy singlet). Samples: 50 mg **6f** + 200 mg Eu(hfbc)$_3$ in 1 mL $CDCl_3$. Left: *rac*-**6f**, *ee* = 0%. Right: (*R*)-**6f**, *ee* ≥ 96%.

high asymmetric induction, opens a simple route to 3-substituted 4-oxoesters **6**[26, 27] of high enantiomeric purity. Preliminary investigations with other Michael acceptors, such as α,β-unsaturated phosphonates and sulfones, show that the new method has a wide scope of application.[25b]

Experimental Procedure

6: A solution of (*S,S,R/S*)-**4** (10 mmol) in 75 mL of ether was added dropwise to a stirred solution at −78 °C of lithium diisopropylamide (11.0 mmol; prepared from 6.9 mL of a 1.6 N solution of butyllithium in *n*-hexane and 1.1 g of diisopropylamine in 25 mL of ether at 0 °C). The reaction mixture was allowed to warm over 0.5 h to 0 °C and then cooled to − 100 °C. (*E*)-**2** (10 mmol) was slowly added to the vigorously stirred solution, which was then stirred for an additional 1 h, allowed to warm over 2–3 h to − 20 °C, and worked up with 20 mL of saturated NH_4Cl solution and 30 mL of ether. The organic phase was separated, washed with 2 × 10 mL of saturated NaCl solution, dried over Na_2SO_4, and evaporated under vacuum. The crude Michael adducts **5** were hydrolyzed with 20 mL of saturated $CuSO_4$ solution and 40 mL of THF as cosolvent by stirring at room temperature (2–16 h, TLC monitoring; **5d–f**, 3 h, reflux). Ether (150 mL) was then added and the aqueous phase was separated and extracted with 2 × 50 mL of ether. The combined organic phases were washed with 2 × 10 mL of saturated NaCl solution and dried over Na_2SO_4. After removal of the solvent, the oxoesters (*R*)-**6** were purified by kugelrohr distillation or flash chromatography (petroleum ether:ether 1:1). The chiral auxiliary (*S,S*)-**3** can be recovered (2.0 g, 91%) by addition of 3 g of K_2CO_3 to the aqueous phase followed by extraction with 3 × 50 mL of ether.

Received: September 19, 1989 [Z 3552 IE]
German version: *Angew. Chem. 102* (1990) 226

[1] a) C. R. Hauser, H. M. Taylor, T. G. Ledford, *J. Am. Chem. Soc. 82* (1960) 1786; b) H. M. Taylor, C. R. Hauser, *ibid. 82* (1960) 1790, 1960; c) C. R. Hauser, G. F. Morris, *J. Org. Chem. 26* (1961) 4740.
[2] Reviews: a) J. D. Albright, *Tetrahedron 39* (1983) 3207; b) T. A. Hase (Ed.): *Umpoled Synthons*, Wiley, New York 1987.
[3] For d/a nomenclature, see D. Seebach, *Angew. Chem. 91* (1979) 259; *Angew. Chem. Int. Ed. Engl. 18* (1979) 239.
[4] Reviews: a) D. Seebach, *Angew. Chem. 81* (1969) 690; *Angew. Chem. Int. Ed. Engl. 8* (1969) 639; b) *Synthesis 1969*, 17; c) D. Seebach, M. Kolb, *Chem. Ind. (London) 1974*, 687; d) O. W. Lever, Jr., *Tetrahedron 32* (1976) 1943; e) D. Seebach, B.-T. Gröbel, *Synthesis 1977*, 357; f) P. Beak, D. B. Reitz, *Chem. Rev. 78* (1978) 275.
[5] D. Seebach, D. Enders, *Angew. Chem. 87* (1975) 1; *Angew. Chem. Int. Ed. Engl. 14* (1975) 15.
[6] V. Reutrakul, P. Ratananukul, S. Nimgirawath, *Chem. Lett. 1980*, 71.
[7] G. Stork, R. M. Jacobson, R. Levitz, *Tetrahedron Lett. 1979*, 771.
[8] D. Enders, H. Lotter, *ibid. 23* (1982) 639, and references therein.
[9] a) E. Leete, *J. Org. Chem. 41* (1976) 3438; b) G. Sork, A. A. Ozario, A. Y. W. Leong, *Tetrahedron Lett. 1978*, 5175; c) H. Ahlbrecht, H.-M. Kompter, *Synthesis 1983*, 645; d) M. Zervos, L. Wartski, J. Seyden-Penne, *Tetrahedron 42* (1986) 4963; e) M. Zervos, L. Wartski, *Tetrahedron Lett. 27* (1986) 2985.
[10] a) E. Leete, M. R. Chedekel, G. B. Bodem, *J. Org. Chem. 37* (1972) 4465; b) W. Müller, R. Preuß, E. Winterfeldt, *Angew. Chem. 87* (1975) 385; *Angew. Chem. Int. Ed. Engl. 14* (1975) 357; c) E. Leete, G. B. Bodem, *J. Am. Chem. Soc. 98* (1976) 6321.
[11] a) J. D. Albright, F. J. McEvoy, D. B. Moran, *J. Heterocycl. Chem. 15* (1978) 881; b) F. J. McEvoy, J. D. Albright, *J. Org. Chem. 44* (1979) 4597; c) W. E. McEven, A. V. Grossi, R. J. McDonald, A. P. Stamegna, *ibid. 45* (1980) 1301; d) H. Schick, F. Theil, H. Jablokoff, S. Schwarz, *Z. Chem. 21* (1981) 68; e) O. Tsuge, K. Ueno, S. Kanemasa, K. Yorozum *Bull. Chem. Soc. Jpn. 60* (1987) 3347.
[12] For the use of 2-(*N*-methylanilino)acrylonitrile as a doubly "umpoled" acetaldehyde, see H. Ahlbrecht, K. Pfaff, *Synthesis 1980*, 413; H. Ahlbrecht, M. Ibe, *ibid. 1988*, 210, and references therein.
[13] a) K. Weinges, G. Graab, D. Nagel, B. Stemmle, *Chem. Ber. 104* (1971) 3594; b) K. Weinges, B. Stemmle, *ibid. 106* (1973) 2291; c) K. Weinges, G. Gries, B. Stemmle, W. Schrank, *ibid. 110* (1977) 3098; d) K. Weinges, G. Brune, H. Droste, *Liebigs Ann. Chem. 1980*, 212; e) K. Weinges, H. Blackholm, *Chem. Ber. 113* (1980) 3098; f) K. Weinges, H. Brachmann, P. Stahnecker, H. Rodewald, M. Nixdorf, H. Irngartinger, *Liebigs Ann. Chem. 1985*, 566; g) K. Weinges, U. Reinel, W. Maurer, N. Gässler, *ibid. 1987*, 833.
[14] S. Yamada, S. Hashimoto, *Chem. Lett. 1976*, 921.
[15] K. Hiroi, K. Nakazawa, *ibid. 1980*, 1077.
[16] a) D. Enders in H. Nozaki (Ed.):, *Current Trends in Organic Synthesis*, Pergamon Presss, Oxford 1983, p. 151; b) D. Enders, H. Lotter, N. Maigrot, J.-P. Mazaleyrat, Z. Welvart, *Nouv. J. Chim. 8* (1984) 747.
[17] D. M. Stout, L. A. Black, W. L. Martier, *J. Org. Chem. 48* (1983) 5369.
[18] a) N. Maigrot, J.-P. Mazaleyrat, Z. Welvart, *J. Chem. Soc. Chem. Commun. 1984*, 40; b) *J. Org. Chem. 50* (1985) 3916.
[19] a) H. Kunz, W. Sager, *Angew. Chem. 99* (1987) 595; *Angew. Chem. Int. Ed. Engl. 26* (1987) 557; b) H. Kunz, W. Sager, W. Pfrengle, D. Schanzenbach, *Tetrahedron Lett. 29* (1988) 4397.
[20] a) J. L. Marco, J. Royer, H.-P. Husson, *Tetrahedron Lett. 26* (1985) 3567; b) *Synth. Commun. 17* (1987) 669; c) D. J. Aitken, J. Royer, H.-P. Husson, *Tetrahedron Lett. 29* (1988) 3315.
[21] D. Döpp, M. Pies, *J. Chem. Soc. Chem. Commun. 1987*, 1734.
[22] A. Delgado, D. Mauleon, *Synth. Commun. 18* (1988) 823.
[23] E. Zeller, D. S. Grierson, *Heterocycles 27* (1988) 1575.
[24] (4*S*,5*S*)-(+)-2,2-Dimethyl-5-methylamino-4-phenyl-1,3-dioxane [(*S,S*)-**3**] may be prepared from commercially available (4*S*,5*S*)-(+)-5-amino-2,2-dimethyl-4-phenyl-1,3-dioxane in molar amounts by a two-step reaction (1) HCO_2CH_3, reflux, 3d; crystallization (Et_2O); (2) $LiAlH_4$, THF, reflux; overall yield 84%: b.p. 77–80 °C/0.05 Torr, $\alpha_D^{20} = +61.8°$ (neat) $[\alpha]_D^{20} = +46°$ (*c* = 1.5, benzene). (*R,R*)-**3** may be obtained analogously: H. Lotter, *Dissertation*, Universität Bonn 1985.
[25] a) G. Boche, D. Enders, P. Gerdes, K. Harms, M. Marsch, H. Ahlbrecht, H. Sommer, unpublished; b) P. Gerdes, *Dissertation*, Technische Hochschule Aachen 1989.
[26] Alternatively, the oxoesters **6** may be obtained with high enantiomeric excess by α-alkylation of (*S*)/(*R*)-aminomethoxymethylpyrrolidine hydrazones (SAMP-/RAMP-hydrazones) with $BrCH_2CO_2R$: D. Enders, U. Baus, P. Müller, unpublished; U. Baus, *Dissertation*, Universität Bonn 1985.
[27] All new compounds gave correct elemental analyses and suitable spectra (IR, NMR, MS).

Synthesis of Tetrachloroammonium Hexafluoroarsenate, $NCl_4^{\oplus}AsF_6^{\ominus}$ **

By *Rolf Minkwitz,* Dirk Bernstein,* and *Wolfgang Sawodny*

The chemistry of binary haloamines[1, 2] is characterized by striking contrasts. Only NF_3 is thermodynamically stable ($\Delta H^\circ = -31.44$ kcal mol^{-1} [3]); even with elemental fluorine, it reacts in the presence of Lewis acids only when energy is supplied[4] to give $NF_4^{\oplus}$ salts. Pure NCl_3 ($\Delta H^\circ = +54.7$ kcal mol^{-1} [5]), on the other hand, violently explodes

[*] Prof. Dr. R. Minkwitz, Dipl.-Chem. D. Bernstein
Fachbereich Chemie, Anorganische Chemie, der Universität
Postfach 50 05 00, D-4600 Dortmund 50 (FRG)
Prof. Dr. W. Sawodny
Abteilung Anorganische Chemie der Universität
Oberer Eselsberg, D-7900 Ulm (FRG)

[**] This work was supported by the Deutsche Forschungsgemeinschaft and the Fonds der Chemischen Industrie.

upon warming or during phase transitions. This behavior is so pronounced for NBr_3 that it has so far eluded spectroscopic identification.[6] Finally, NI_3 can be stabilized in the solid state in the presence of diverse nitrogen bases; these substances are mostly nonexplosive and consist of a polymeric network of chains composed of NI_4 tetrahedra.[7] This coordination is presumably responsible for the kinetic stability of NI_3 derivatives. This observation motivated us to attempt the synthesis of $NCl_4^{\oplus}AsF_6^{\ominus}$ (**1**).

In order to determine whether the $NCl_4^{\oplus}$ ion can indeed exist, an ab initio calculation, using the force-field method[8, 9] and a basis set already employed for other NCl compounds,[10] was carried out for the isolated species. An energy minimum was found for a tetrahedral configuration with an N–Cl distance of 176.4 pm, only slightly longer than known N–Cl distances.[13]

Since it was expected that $NCl_4^{\oplus}$ salts would be stable only at low temperatures, we chose the oxidative chlorination of NCl_3 with Cl_2/AsF_5 in SO_2 as the route of synthesis [Eq. (a)].

$$2\,NCl_3 + Cl_2 + 3\,AsF_5 \xrightarrow{SO_2} \underset{\mathbf{1}}{2\,NCl_4^{\oplus}AsF_6^{\ominus}} + AsF_3 \qquad (a)$$

The reaction was carried out at −78 °C, usually in a Raman cuvette, and is dependent on the solvent. All components except for **1** were then removed at this temperature under dynamic high vacuum. This procedure avoids the necessity of working directly with the potentially explosive substance in subsequent reactions.

$NCl_4^{\oplus}AsF_6^{\ominus}$ is a colorless, moisture-sensitive solid, which is stable at −40 °C for ca. 14 days and at −78 °C indefinitely. In contrast to NCl_3, the salt is not explosive. Subsequent explosions that sometimes occurred were clearly due to residual NCl_3. Compound **1** decomposes in melting H_2O to short-lived NCl_3, which can be observed by Raman spectroscopy. The identity of **1** is also established by the reactions given in Equations (b) to (f). The $NH_4^{\oplus}AsF_6^{\ominus}/Cl_2$ ratio in Equation (b) is 1:4.12. The amount of $NH_4^{\oplus}AsF_6^{\ominus}$ was determined gravimetrically and that of Cl_2 iodometrically.

$$\mathbf{1} + 4\,HCl \longrightarrow NH_4^{\oplus}AsF_6^{\ominus} + 4\,Cl_2 \qquad (b)$$

$$\mathbf{1} + 4\,CH_3Cl \not\longrightarrow \qquad (c)$$

$$\mathbf{1} + 4\,CH_3Br \longrightarrow N(CH_3)_4^{\oplus}AsF_6^{\ominus} + 4\,BrCl \qquad (d)$$

$$2\,\mathbf{1} + CF_3SCl \longrightarrow SCl_3^{\oplus}AsF_6^{\ominus} + CF_4 + 2\,NCl_3 + AsF_5 \qquad (e)$$

$$\mathbf{1} \xrightarrow{\Delta} NCl_3 + AsF_5 + SiF_4 \text{ (from ClF + glass)}$$
$$\text{(isolated in an } N_2 \text{ matrix)} \qquad (f)$$

The vibrational absorption spectra in Figure 1 show, besides the signals of the cation, those of the anion (O_h) [IR: $\tilde{\nu}$ = 690 s, 399 m cm^{-1}; Raman: $\tilde{\nu}$ = 681(100), 573(32), 377(62) cm^{-1}]. From the isotope data for the cation (Table 1), a force field having the following values was calculated for $NCl_4^{\oplus}$: A_1: $F_{11} = 3.812 \times 10^2$ Nm^{-1}; E: $F_{22} = 1.154$ aJrad^{-2}; F_2: $F_{33} = 2.544 \times 10^2$ Nm^{-1}, $F_{34} = 0.803 \times 10^{-8}$ $Nrad^{-1}$, $F_{44} = 1.107$ aJrad^{-2}. These values give an NCl valence force constant of 2.86×10^2 Nm^{-1}, which is somewhat larger than that of NCl_3.[10] Compared with CCl_4, the $NCl_4^{\oplus}$ ion exhibits lower frequencies with the exception of the deformation vibration of type E and, accordingly, a smaller valence force constant (3.35×10^2 Nm^{-1} for CCl_4[11]). The valence force constants of $NF_4^{\oplus}$ are also smaller, by about 15%,[12] than those of CF_4.[13] This is certainly due to increased ligand repulsion in the arrangement around the small N atom.

Table 1. Raman wavenumbers $\tilde{\nu}$ of $NCl_4^{\oplus}$ in **1** [cm^{-1}].

$^{14}NCl_4^{\oplus}$ measured	calcd	$^{15}NCl_4^{\oplus}$ measured	calcd	$\Delta\tilde{\nu}(^{14}N, ^{15}N)$ calcd	Assignment
635(50	634.9	618(50)	618.1	16.8	ν_{as} (F_2)
430.3(90)	430.1	430(90)	430.1	0	ν_s (A_1)
283.3(95)	283.1	281.8(20)	281.9	1.2	δ_{as} (F_2)
233.3(70)	232.4	231.5(70)	232.4	0	δ_s (E)

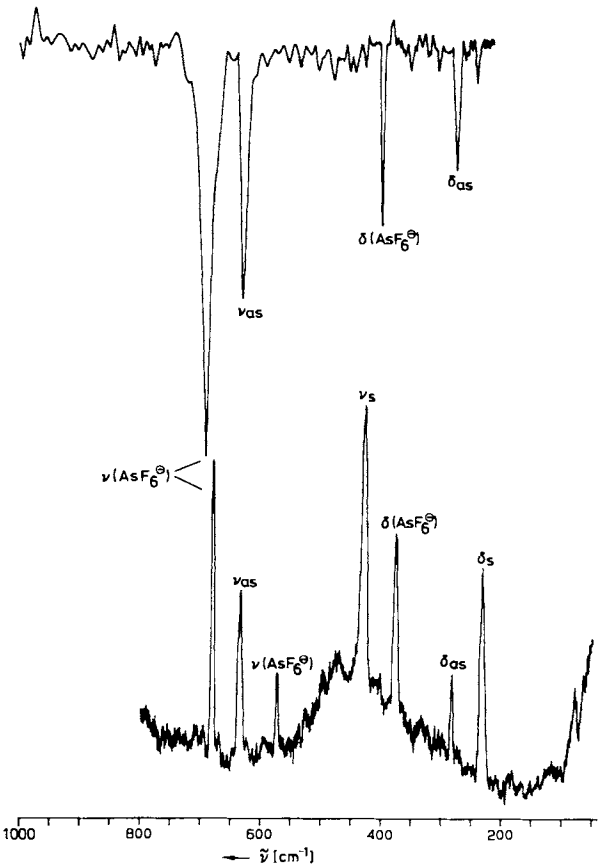

Fig. 1. IR and Raman spectrum of $^{14}NCl_4^{\oplus}AsF_6^{\ominus}$, measured at −78 °C for pure solid in each case.

Experimental Procedure

NCl_3 was prepared by bubbling Cl_2 gas through 4 mL of a 2 M NH_4Cl solution. The NCl_3/Cl_2 gas mixture leaving the solution was passed through a $CaCl_2$ drying tower, pretreated with this mixture, and then bubbled over 3 h into a solution of AsF_5 (375 mg, 2.1 mmol) in 1.5 mL of SO_2 at −78 °C. The reaction vessel was then sealed and kept for 14 h at this temperature. The solution turned dark red to brown during this period. The solvent and starting materials were removed within 48 to 60 h under dynamic vacuum. This time is required in order to quantitatively remove simultaneously formed $AsF_5 \cdot SO_2$ adduct (the presence of the adduct is revealed by an intense Raman line at 721 cm^{-1}). Colorless **1** (ca. 150 mg) remains as residue.

Received: July 14, 1989;
supplemented: October 23, 1989 [Z 3439 IE]
German version: *Angew. Chem. 102* (1990) 185

CAS Registry numbers:
1, 124604-83-7; NCl_3, 10025-85-1; Cl_2, 7782-50-5; AsF_5, 7784-36-3; HCl, 7647-01-0; CH_3Br, 74-83-9; CF_3SCl, 421-17-0; $NH_4^{\oplus}AsF_6^{\ominus}$, 23377-90-4; $N(CH_3)_4^{\oplus}AsF_6^{\ominus}$, 16893-80-4; $SCl_3^{\oplus}AsF_6^{\ominus}$, 27075-96-3.

[1] P. Martlet in *Gmelin: Handbook of Inorganic Chemistry, Vol. 5 (4)*, Springer, Berlin 1986, p. 171 ff.
[2] J. Jander, U. Engelhardt in C. B. Colburn (Ed.): *Developments in Inorganic Nitrogen Chemistry, Vol. 2*, Elsevier, Amsterdam 1973, p. 70.

[3] G. C. Sinke, *J. Phys. Chem. 71* (1967) 359.
[4] K. O. Christe, W. W. Wilson, C. J. Schack, R. D. Wilson, *Inorg. Synth. 24* (1986) 39.
[5] L. H. Long, *Q. Rev. Chem. Soc. 7* (1953) 155.
[6] J. Jander, J. Knackmuss, K. U. Thiedemann *Z. Naturforsch. B 30* (1975) 464.
[7] J. Jander, *Adv. Inorg. Chem. Radiochem. 19* (1976) 1.
[8] P. Pulay, *Mol. Phys. 17* (1969) 197.
[9] P. Pulay in H. F. Schaefer III (Ed.): *Modern Theoretical Chemistry, Vol. 4*, Plenum Press, New York 1977.
[10] W. Sawodny, H. Härtner, R. Minkwitz, D. Bernstein, *J. Mol. Struct. 213* (1989) 145.
[11] H. J. Becher: *Z. Phys. Chem. (München) NF81* (1972) 225.
[12] K. O. Christe, *Spectrochim. Acta A 36* (1980) 921.
[13] H. Siebert: *Anwendung der Schwingungsspektroskopie in der anorganischen Chemie*, Springer, Berlin 1966.

Experimental and Theoretical IR Spectra of the 2-Norbornyl Cation**

By *Wolfram Koch,* Bowen Liu, Douglas J. DeFrees, Dionis E. Sunko,** and *Hrvoj Vančik*

Koch et al.[1] were recently able to conduct a systematic, high-level quantum-chemical investigation of the vibrational spectrum of the 2-norbornyl cation, which unequivocally showed that the 2-norbornyl cation assumes a nonclassical geometry in the gas phase,[2] in line with earlier theoretical studies.[3,4] Not included in that paper was the complete set of harmonic frequencies and IR intensities which were obtained at high levels of ab initio theory, including electron correlation effects. At the same time, *Sunko* and *Vančik*[5] developed a new experimental technique, which allows the study of short-lived reactive intermediates like carbocations and carbocation-like species in cryogenic SbF_5 matrices by IR spectroscopy.[6] In this communication we wish to present a comparison of the experimental IR spectrum of the matrix-generated 2-norbornyl cation with the theoretically predicted spectrum.

2-Chloronorbornane and SbF_5 were codeposited on the CsI window according to the previously described technique[5] and the IR spectrum recorded (Figs. 1a, 2a). On allowing the temperature to rise to 150 K, the IR bands of the chloride start to decrease with the appearance of new signals corresponding to the 2-norbornyl cation. This spectrum remains unchanged up to 200 K. The final spectrum of the matrix-generated carbocation (Figs. 1b, 2b, Table 1) is significantly different from the spectrum of the precursor chloride. The deformation region below 1500 cm^{-1} clearly shows bands not present in the chloride. Particularly eye-catching is the region between 1440 and 1340 cm^{-1}. Here the 2-chloronorbornane spectrum shows hardly any peak while the IR spectrum of the cation exhibits bands of strong intensity.[7] Subsequent quenching of the deposited material afforded *exo*-2-norborneol.

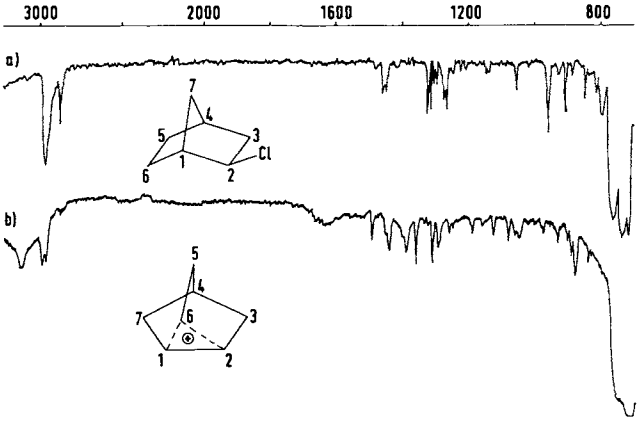

Fig. 1. IR spectra of (a) 2-chloronorbornane and (b) the cation generated from 2-chloronorbornane.

The structure of the nonclassical 2-norbornyl cation was optimized in C_s symmetry by using analytical gradient techniques. A standard 6-31G* basis set was used.[8] The effects of dynamical electron correlation were included through second-order Moller–Plesset perturbation theory (MP2).[8] The vibrational frequencies at this MP2/6-31G* level were then obtained by numerical differentiation of analytical gradients, which consisted of more than 60 MP2/6-31G* analytical gradient computations, possibly one of the largest calculations ever done for a molecule of this size. All calculations were performed using the vectorized IBM version of the Gaussian 86 program[9] installed on an IBM 3090 with Vector Facility computer at the IBM Science and Engineering National Support Center in Dallas, Texas. The results of the calculations are presented in Table 1.

It is well documented in the recent literature that harmonic frequencies computed at the MP2/6-31G* level of approximation in general tend to overestimate the experimental, anharmonic frequencies by 4–7%.[10–13] This is due to the combined effect of the neglect of anharmonicity and the insufficiency of the theoretical method. Therefore, a uniform scaling factor was applied to the theoretical frequencies to achieve better agreement with the experimental spectrum (Table 1). However, it should be noted that this uniform scaling of all frequencies with only a single scaling factor may even worsen the agreement with the experimental frequencies for some modes. Known examples are multiple bond stretching and out-of-plane deformation modes for which the computed, unscaled frequencies are sometimes even *smaller* than the experimental frequencies.[10,12] The same pertains for high-frequency in-plane stretching modes, which typically have a larger anharmonicity.[12] The recent review by *Hess* et al.[14] describes many examples where the comparison of theoretically determined harmonic frequencies with the experimental IR spectra has been successfully applied to aid structure identification and to decide between structural possibilities.[15] The assignment of the experimental to the computed frequencies in Table 1 is based on the best numerical match of the two sets of frequencies and intensities. Figure 2 shows a graphical representation on the

[*] Dr. W. Koch
IBM Heidelberg Scientific Center,
Institute for Supercomputing and Applied Mathematics
D-6900 Heidelberg (FRG)
Prof. Dr. D. E. Sunko, Dr. H. Vančik
Department of Chemistry, Faculty of Science
University of Zagreb, 41000 Zagreb (Yugoslavia)
Dr. B. Liu
IBM Almaden Research Center
San Jose, CA 95120-6099 (USA)
Dr. D. J. DeFrees
Molecular Research Institute
Palo Alto, CA 94304 (USA)

[**] The work in Zagreb was supported by the Research Council of Croatia and the National Science Foundation (USA), grants JPF 545 and 841. We thank *D. Gerson* of the IBM Dallas Engineering and Scientific National Support Center for making available computing resource and facilitating our calculations. *W. K.* thanks *M. D. Miller* for helpful discussions.

Table 1. Computed unscaled and scaled (by 0.96) and experimentally observed frequencies and IR intensities for the 2-norbornyl cation.

No.	Symmetry	Unscaled frequency [cm^{-1}]	Scaled frequency [cm^{-1}]	Calculated intensity [km mol^{-1}]	Exp. frequency [cm^{-1}][a]	Exp. IR intensity [b]
48	A′	3276	3145	7.0	3110	s
47	A″	3262	3131	6.2		
46	A′	3214	3086	0.0		
45	A″	3214	3085	0.0		
44	A′	3198	3070	0.9		
43	A″	3198	3070	1.2		
42	A″	3174	3047	18.0	2990	vs
41	A′	3150	3024	0.6		
40	A′	3134	3009	20.9	2980	vs
39	A″	3116	2991	0.1		
38	A′	3112	2988	3.7	2875	m
37	A′	1569	1506	6.9		
36	A′	1550	1488	0.2		
35	A′	1528	1467	18.3	1490	s
34	A″	1522	1461	19.1	1445	s
33	A′	1488	1428	27.1	1435	vs
32	A″	1412	1355	10.1	1380	m
31	A′	1368	1314	10.9	1348	s
30	A′	1350	1296	11.9	1305	vs
29	A″	1334	1281	0.1		
28	A′	1314	1262	3.5	1288	s
27	A″	1305	1252	4.2	1280	s
26	A″	1250	1200	0.4		
25	A′	1226	1178	1.0		
24	A′	1207	1159	1.8	1160	w
23	A″	1204	1156	0.5		
22	A″	1168	1122	6.5	1120	m
21	A′	1141	1095	0.0		
20	A″	1104	1060	0.2		
19	A′	1087	1043	3.5	1056	m
18	A′	1064	1022	1.6	1040	m
17	A″	1017	976	2.8	970	w
16	A′	1011	970	0.3		
15	A″	989	950	0.1		
14	A′	972	933	0.3		
13	A″	962	923	2.8	928	m
12	A′	930	893	4.1	900	w
11	A″	924	887	5.0	890	m
10	A′	912	875	18.0	878	vs
9	A′	822	789	0.7		
8	A″	790	757	0.0		
7	A″	683	656	16.0		
6	A′	650	624	0.5		
5	A′	484	464	8.4		
4	A″	452	434	3.1		
3	A′	415	398	0.0		
2	A″	291	279	24.4		
1	A″	255	244	9.1		

[a] The assignment of the experimental frequencies to the computed ones is based purely on the best numerical match. [b] w, weak; m, medium; s, strong; vs, very strong.

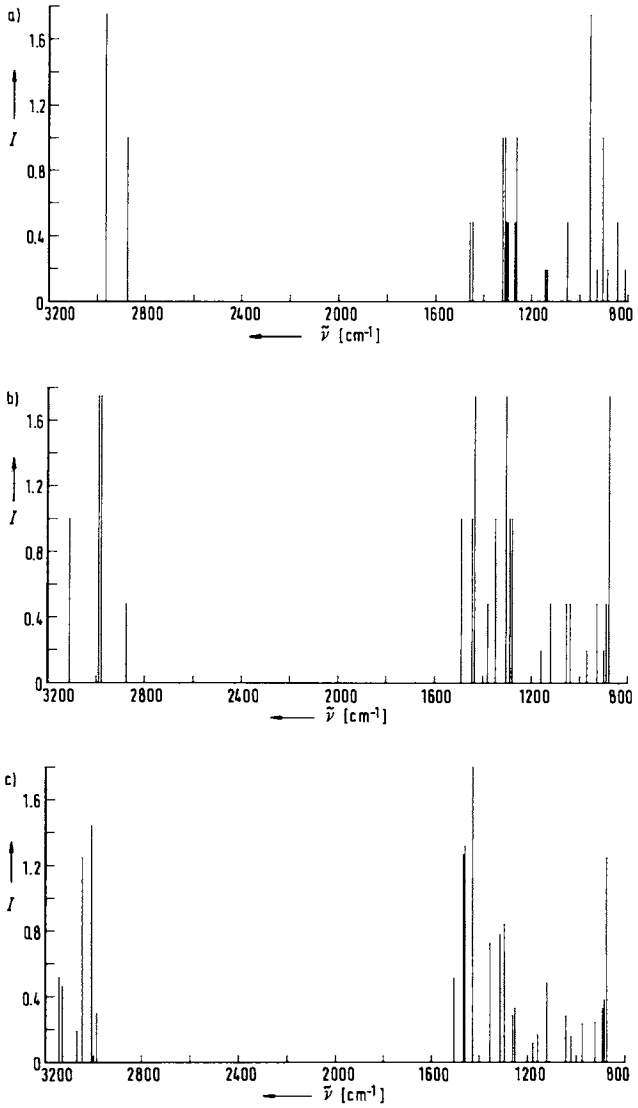

Fig. 2. Bar representation of (a) the IR spectrum of 2-chloronorbornane, (b) the experimentally observed IR spectrum of the 2-norbornyl cation, and (c) the calculated IR spectrum of the 2-norbornyl cation, computed at the MP2/6-31G* level for the nonclassical, bridged structure (scaled by a factor of 0.96).

same scale of the experimental spectrum and the scaled, computed spectrum to allow an easy comparison of the two spectra. The overall agreement of the two spectra (Fig. 2b, c) is reasonably good if one bears in mind that experimentally we are not dealing with an isolated cation in the gas phase but with ion pairs which obviously may have a slightly different spectrum.

In the CH stretching region we experimentally observe four bands at 3110(s), 2990(vs), 2980(vs), and 2875(m) cm^{-1}. The corresponding computed bands, after scaling, are at 3145 and 3131(s), 3047(vs), 3009(vs), and 2988(m) cm^{-1}, respectively. Before scaling, the computed frequencies in this region differ from the experimental ones by 5.2–8.2% (average 6.2%), which is very similar to the 6.5% average difference reported for CH and NH stretches in heterocyclic arenes by *Simandiras* et al. using a comparable level of approximation.[12] However, more significant than the CH stretching region, which can be expected to show similar frequencies for most carbocations, is the lower-frequency region of the spectrum. Here, below 1600 cm^{-1}, the agreement is even more satisfactory, in particular when bands with strong and very strong intensity are considered. The very strong bands in the experimental spectrum occur at 1435, 1305, and 878 cm^{-1}, while their computed counterparts (after scaling) are at 1428, 1296, and 875 cm^{-1}, respectively.

The agreement of the computed and experimental spectra supports all previously reported evidence that antimony pentahalide complexes of the 2-norbornyl cation have a bridged, nonclassical structure. This was inferred by *Yannoni* et al.[16] from the ^{13}C cross-polarization magic-angle-spinning (CP-MAS) spectra of a fluoroantimonate of the 2-norbonyl cation as well as by *Laube*[17] and by *Montgomery* et al.[18] from the X-ray structure of a fluoroantimonate of the 1,2,4,7-tetramethylnorborn-2-yl cation and of 2-methoxy-1,7,7-trimethylbicyclo[2.2.1]hept-2-ylium fluoroborate, respectively. Similar conclusions were reached by *Saunders*

and *Kates*[19] based on the deuterium isotopic perturbation effect. An additional factor that supports this conclusion can be found by analyzing further the CH stretching region. In the hypothetical classical 2-norbornyl cation, the hyperconjugative interaction of the C(3)–H bonds with the formally empty p orbital at C(2) should exert a significant stabilizing effect. This would lead to a weakening of the C(3)–H bonds, which should be reflected in a sizeable decrease in the frequencies of the corresponding CH stretching modes. Such a shift was recently demonstrated for the 1-methylcyclopentyl cation,[5] where strong hyperconjugative interaction of the C(2)–H bonds with the cationic center at C(1) caused a decrease in the frequency of the C(2)H stretch of about 220 cm^{-1} to 2775 cm^{-1}, in perfect agreement with accurate calculations for the parent cyclopentyl cation.[20] In a delocalized, bridged structure ascribed to the 2-norbornyl cation, such an interaction should be small and the only bonds that could contribute to a hyperconjugative stabilization are C(3)–H and C(7)–H. The normal mode analysis of the computed spectrum shows that the modes corresponding to the two lowest CH stretching modes, computed at 2991 and 2987 cm^{-1}, indeed involve hydrogens at C(3) and C(7). The absence of a significant hyperconjugative decrease in the stretching frequencies is additional, albeit negative, evidence for the bridged structure of the cation. The same conclusion was reached some twenty years ago[21] on the basis of secondary kinetic isotope effect measurements in solvolysis of 2-norbornyl brosylates.[22]

Received: September 20, 1989 [Z 3556 IE]
German version: *Angew. Chem. 102* (1990) 198

CAS Registry number:
2-Norbornyl cation, 24321-81-1.

[1] W. Koch, D. J. De Frees, B. Liu, *J. Am. Chem. Soc. 111* (1989) 1527.
[2] Recent reviews on the 2-norbornyl cation: a) C. A. Grob, *Acc. Chem. Res. 16* (1983) 426; b) H. C. Brown, *ibid. 16* (1983) 432; c) G. A. Olah, G. K. S. Prakash, M. Saunders, *ibid. 16* (1983) 440; d) C. Walling, *ibid. 16* (1983) 448; e) H. C. Brown (with comments by P. v. R. Schleyer): *The Non-Classical Ion Problem* Plenum, New York 1077; f) P. A. Vogel: *Carbocation Chemistry* Elsevier, New York 1985, Chapter 7.8.6 (p. 281).
[3] K. Raghavachari, R. C. Haddon, P. von R. Schleyer, H. F. Schaefer, III, *J. Am. Chem. Soc. 105* (1983) 5915.
[4] M. Yoshimine, A. D. McLean, B. Liu, D. J. DeFrees, J. S. Binkley, *J. Am. Chem. Soc. 105* (1983) 6185.
[5] H. Vančik, D. E. Sunko, *J. Am. Chem. Soc. 111* (1989) 3742.
[6] *M. Saunders* et al. recently reported a similar matrix isolation technique. They used IR spectroscopy to monitor the formation of acyl cations from the corresponding acyl chlorides: R. M. Jarret, Ny Sin, T. Ramsey, M. Saunders, *J. Phys. Org. Chem. 2* (1989) 51.
[7] Further evidence that the 2-norbornyl cation has indeed been generated stems from the fact that the cation generated from 7-chloronorbornane is the same species (identical spectra) as the one formed from the 2-chloronorbornane. It is known that solutions of 7-chloronorbornane in SbF_5/SO_2 mixtures rearrange rapidly, yielding, after quenching, 94% of 2-*exo*-norborneol: see P. v. R. Schleyer, W. E. Watts, R. C. Fort, Jr, M. B. Comisarow, G. A. Olah, *J. Am. Chem. Soc. 86* (1964) 5679. Details on this work will be published in a forthcoming paper dealing with various Wagner–Meerwein rearrangements and hydride shifts in a cryogenic matrix.
[8] For a description of the basis set and Moller–Plesset perturbation theory, see W. Hehre, L. Radom, P. von R. Schleyer, J. A. Pople: *Ab initio Molecular Orbital Theory*, Wiley Interscience, New York 1986, chapter 4.
[9] M. J. Frisch, J. S. Binkley, H. B. Schlegel, K. Raghavachari, C. F. Melius, R. L. Martin, J. J. P. Stewart, F. W. Bobrowicz, C. M. Rohlfing, L. R. Kahn, D. J. DeFrees, R. Seeger, R. A. Whiteside, D. J. Fox, E. M. Fluder, J. A. Pople, Gaussian 86, Carnegie-Mellon Quantum Chemistry Publishing Unit, Pittsburgh, PA, USA, 1984.
[10] R. F. Hout, B. A. Levy, W. J. Hehre, *J. Comput. Chem. 3* (1982) 234.
[11] D. J. DeFrees, A. D. McLean, *J. Chem. Phys. 82* (1985) 333.
[12] E. D. Simandiras, N. C. Handy, R. A. Amos, *J. Phys. Chem. 92* (1988) 1739.
[13] See also the detailed discussion in chapter 6.3 (p. 226) of [8].
[14] B. A. Hess, L. J. Schaad, P. Carsky, R. Zahradnik, *Chem. Rev. 86* (1986) 709.
[15] For a recent application, see G. Maier, H. P. Reisenauer, W. Schwab, P. Carsky, B. A. Hess, L. J. Schaad, *J. Am. Chem. Soc. 109* (1987) 5183.
[16] C. S. Yannoni, V. Macho, P. C. Myhre, *J. Am. Chem. Soc. 104* (1982) 907, 7380.
[17] T. Laube, *Angew. Chem. 99* (1987) 580; *Angew. Chem. Int. Ed. Engl. 26* (1987) 560.
[18] L. K. Montgomery, M. P. Grendze, J. C. Huffman, *J. Am. Chem. Soc. 109* (1987) 4749.
[19] M. Saunders, M. R. Kates, *J. Am. Chem. Soc. 105* (1983) 3571.
[20] P. von R. Schleyer, J. W. de M. Carneiro, W. Koch, K. Raghavachari, *J. Am. Chem. Soc. 111* (1989) 5475.
[21] J. M. Jerkunica, S. Borcic, D. E. Sunko, *Chem. Commun. 1967*. 1302.
[22] For a summary of subsequent uses of isotope effects in this system, see p. 203 in [2e].

Peptides as Conformational Switch: Medium-Induced Conformational Transitions of Designed Peptides **

By *Manfred Mutter** and *René Hersperger*

The design of peptides adopting predetermined secondary and tertiary conformations is of utmost interest in structure–function studies as well as in protein de novo design.[1, 2] Empirical predictive schemes[3] and experimental studies on synthetic model peptides[4] have allowed the delineation of design principles for the construction of peptides which exhibit tailor-made conformational properties.[5] More recently, the amphiphilicity of secondary structures has been used as a powerful design principle for the stabilization of helical and β-sheet conformations in solution and for the design of self-associating peptides in the de novo design of tertiary structures.[2, 6, 7]

We have now used these design principles to construct peptides which exhibit solvent-induced conformational transitions. Most notably, this type of peptide may serve as a "conformational switch", the predetermined change in the configurational properties being intimately related to changes in the physicochemical and biological properties. To this end, three different primary sequences of the same overall composition (4 A, 4 L, 3 E, 3 K) were designed (Fig. 1).

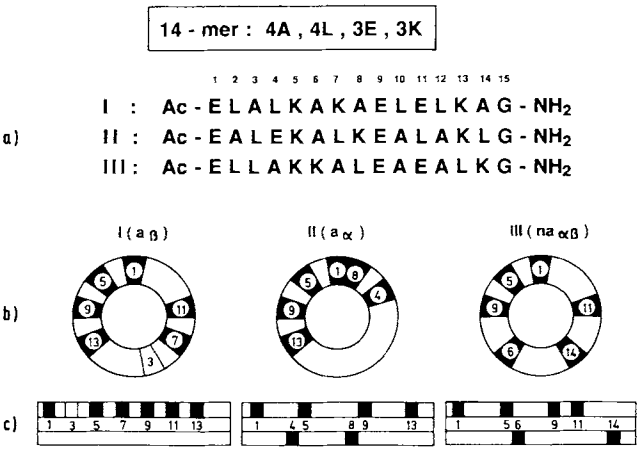

Fig. 1. Design of three tetradecapeptides (with an additional C-terminal glycine). a) Primary sequences of peptides **I**–**III** (A = alanine, L = leucine, E = glutamic acid, K = lysine). In the "helical wheel" [9] and β-sheet representation, the hydrophilic residues (E, K) are indicated by the sequence number and a black square.

[*] Prof. Dr. M. Mutter, Dr. R. Hersperger
Séction de chimie de l'Université Lausanne
Rue de la Barre 2, CH-1005 Lausanne (Switzerland)

[**] This work was supported by the Swiss National Science Foundation.

Residues with high potential for secondary-structure formation were chosen;[3, 4a] in order to achieve maximum flexibility in the design of amphiphilic structures, we used L as hydrophobic residue, E and K as hydrophilic residues, and A as a "neutral" building block. The chain length of 14 residues (the C-terminal G was attached for synthetic reasons) corresponds to the critical size for helix formation in solution.[4b] The periodicity of hydrophilic and hydrophobic residues was chosen so as to obtain one of the following conformations:

1. an amphiphilic β-sheet[8] (a_β = peptide **I**)
2. an amphiphilic α-helix[9] (a_α = peptide **II**)
3. a peptide sequence which is nonamphiphilic with respect to α-helix or β-sheet formation ($na_{\alpha,\beta}$ = peptide **III**)

The CD spectra of **I**–**III** (Fig. 2a) show that the three peptides adopt a helical conformation in the helix-supporting solvent 2,2,2-trifluoroethanol (TFE), as expected from the high potential for helix formation of the individual residues. The values of $<P_\alpha>$ and $<P_\beta>$ for the three peptides according to the Chou–Fasman predictive algorithm[3] are 1.31 and 0.87, respectively; that is, all three peptides are much more likely to occur in an α-helical than in a β-sheet conformation. It is very interesting that despite the difference in their amino acid sequences and their Coulombic interactions along the helical cylinder,[10] all three peptides exhibit a comparable degree of helix formation in TFE (Fig. 2a). On going from TFE to H_2O, the CD spectra reveal dramatic differences in the preferred conformation of peptides **I**–**III** (Fig. 2b). The CD spectrum of peptide **I** is consistent with the adoption of a fully established β-sheet conformation.[11a] The solvent-induced conformational transition (Fig. 2c) of the type $\alpha \rightleftharpoons \beta$ occurs for a mixture of 55% H_2O and 45% TFE. On the other hand, peptides **II** and **III** show only partially helical structures. Interestingly, the amphiphilic peptide **II** exhibits a substantially higher helix content than the nonamphiphilic peptide **III** in H_2O.

As shown schematically in Figure 3, the self-association of amphiphilic peptide blocks provides the major free energy contribution ("hydrophobic interaction") for the formation of a specific secondary structure. For example, despite the low intrinsic β-sheet potential of peptide **I**, the formation of an energetically favorable bilayer structure, in which two pleated sheets assemble to form a hydrophobic pocket and a hydrophilic surface, will increase the tendency of this peptide to form an amphiphilic β-sheet in H_2O. Similarly, the amphiphilic helical cylinder of peptide **II** shows a high tendency to self-associate to a multimeric bundle structure[6a] (as verified by gel permeation chromatography (GPC) studies[11b]); the helical conformation is thereby stabilized. The different conformational features of peptides **I**–**III** in aqueous solution are also preserved in the solid state as indicated by IR data (Fig. 4): the amide I absorptions[12] are observed at 1655 cm^{-1} for peptides **II** and **III** (α-helix or random coil) and at 1630 cm^{-1} for peptide **I** (β-sheet). The observed conformational features of peptides **I**–**III** are also reflected in their membrane activity.[13]

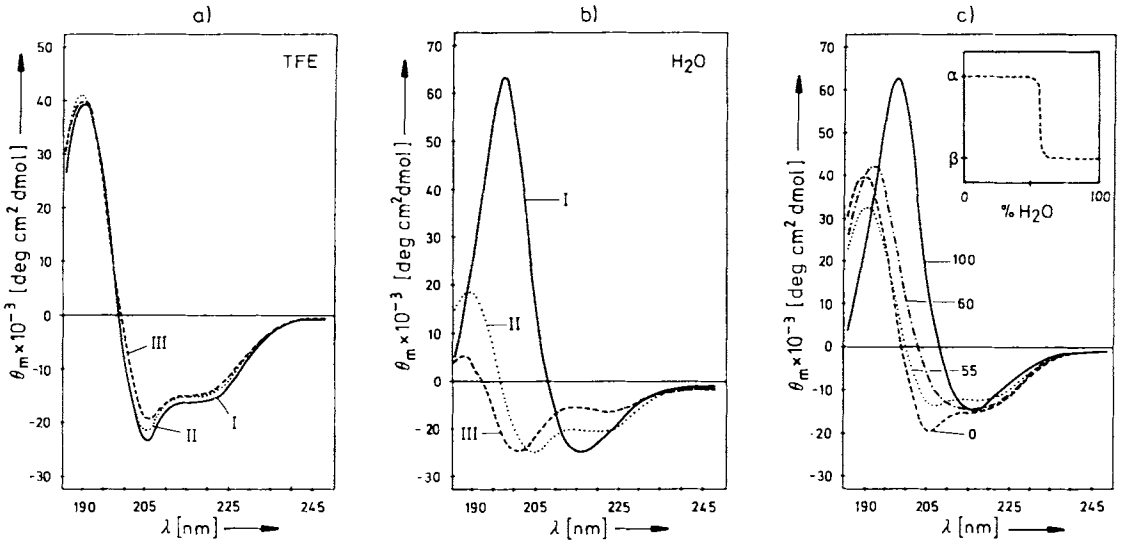

Fig. 2. Circular dichroism (CD) spectra of peptides **I**–**III** (1 mg mL^{-1}) in (a) 2,2,2-trifluoroethanol (TFE) and in (b) H_2O, pH 7; (c) CD spectra of peptide **I** (1 mg mL^{-1}) in H_2O/TFE systems. The numbers indicate the percentage of H_2O in TFE (vol%). The insert shows the cooperative transition from a α-helix (TFE) to a β-sheet (H_2O) conformation at 55% H_2O.

The question of the preferred conformation of peptides containing the same amino acids but different amino acid sequences has been addressed in earlier studies.[4b, 6d] For example, *Brack* and *Spach* have demonstrated that alternating copolymers of K and L are capable of adopting a β-sheet conformation in salt-containing aqueous solutions, whereas

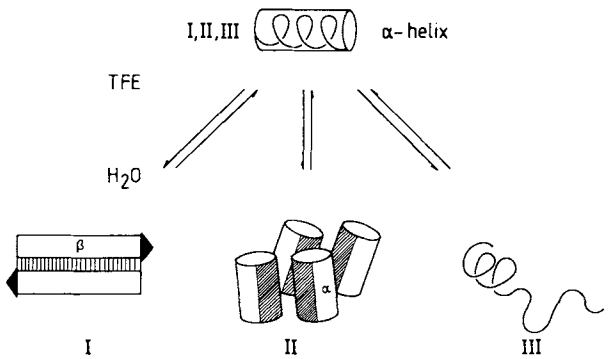

Fig. 3. Schematic representation of the conformational states of peptides **I**–**III** in TFE (α-helix) and in H_2O. **I**, bilayer; **II**, helix bundle; **III**, unordered conformation (see text).

 © VCH Verlagsgesellschaft mbH, D-6940 Weinheim, 1990 0570-0833/90/0202-0186 $ 02.50/0

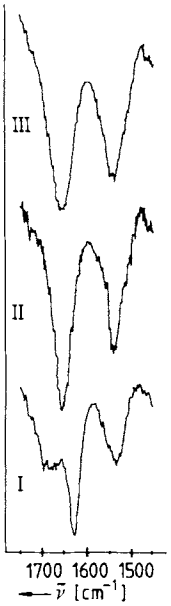

Fig. 4. IR absorption spectra in the amide I region of peptides **I**–**III** (KBr pellets).

statistical copolymers of the same composition favor a helical conformation under the same experimental conditions. In contrast to the peptides investigated in the present study, these copolymers contain only two different amino acids and have molecular weights greater than 5000; moreover, owing to the statistical distribution of the hydrophilic and hydrophobic residues, the nonalternating homologues are not able to adopt a helical conformation with well-defined amphiphilic character. In contrast, *DeGrado* and *Lear*[6d] studied the conformational properties of smaller peptides with the sequences $(LKKLLKL)_2$ and LKLKLKL. In analogy to the results of *Brack* and *Spach*, they found that the peptide with the alternating sequence of K and L residues formed a β-structure in aqueous solution; at low peptide concentration, $(LKKLLKL)_2$ did not exhibit any ordered conformation, but high peptide or salt concentrations resulted in the formation of an amphiphilic helical structure. It is important to note that these α-helix- and β-structure-forming peptides are of different chain length; thus, the conformational behavior of these isocompositional peptides is substantially different from the reversible $\alpha \rightleftharpoons \beta$ transition observed for peptide **I** in this study.

In summary, the data presented here clearly show that the self-association of peptide blocks (releasing solvation entropy) represents a major driving force for secondary structure formation. Whenever the sequence of a peptide allows the adoption of an ordered conformation which is amphiphilic with respect to the spatial orientation of hydrophobic and hydrophilic residues, this particular conformation will be the preferred state in aqueous solution. This finding can be used for the design of peptides that exhibit reversible conformational transitions, thus acting as "conformational switch". For example, a pronounced relationship between conformation and physicochemical properties of the peptides **I**–**III** was found;[14] whereas the three peptides show excellent solubility in TFE (helical conformation), the transition of peptide **I** to a β-sheet structure in H_2O results in a considerable decrease in its solubility. On the other hand, the postulated helical-bundle structure of peptide **II** and the predominantly unordered (monomeric) structure of peptide **III** guarantee good solubility of these peptides in H_2O. The design principles emerging from these observations are presently being used in the construction of template-assembled synthetic proteins (TASP).[7]

Experimental Procedures

The peptides were synthesized by the solid-phase method [15] on a trialkoxybenzhydrylamine resin [16] (1% cross-linked polystyrene); the 9-fluorenylmethoxycarbonyl (Fmoc) group was used for temporary protection of the α-amino function and the *tert*-butyl and *tert*-butoxycarbonyl (Boc) groups for side-chain protection of glutamic acid and lysine, respectively. Reaction with a 3.5-fold excess of the symmetrical anhydride of the corresponding Fmoc-amino acid in DMF for 1 h in each case gave complete reaction as monitored by the quantitative ninhydrin test. Removal of the Fmoc group was achieved by double treatment of the peptide resin (3 and 15 min) with 20% piperidine in DMF. After the last deprotection step, the terminal amino group was blocked by treatment with an excess of a 1:1 mixture of acetic anhydride and pyridine in DMF (30 min). After cleavage from the resin with 2% trifluoroacetic acid (TFA) in dichloromethane (1 h, room temperature) and subsequent final deprotection with TFA/*m*-cresol (9:1; 1 h, 0 °C), the crude peptides were desalted and purified by gel filtration chromatography (Sephadex LH 20, methanol/80% acetic acid (1:1)) and HPLC (C_{18} reversed-phase column, 0.05% aqueous TFA and 0.05% TFA in acetonitrile). The peptides proved to be pure according to TLC, HPLC, and amino acid analysis.

Received: August 17, 1989;
supplemented: October 27, 1989 [Z 3507 IE]
German version: *Angew. Chem. 102* (1990) 115

CAS Registry numbers:
I, 124686-61-9; **II**, 124686-62-0; **III**, 124686-63-1.

[1] T. E. Creighton: *Proteins*, Freeman, New York 1983.
[2] a) R. Moser, S. Frey, K. Münger, T. Hehlgans, S. Klauser, H. Langen, E. L. Winnacker, R. Merz, B. Gutte, *Protein Eng. 1* (1987) 339; b) C. G. Unson, B. W. Erickson, D. C. Richardson, J. S. Richardson, *Fed. Proc. Fed. Am. Soc. Exp. Biol. 43* (1984) 1837; c) J. S. Richardson, D. C. Richardson, *Trends Biochem. Sci.* 14 (1989) 304; d) D. Eisenberg, W. Wilcox, S. M. Eshita, P. M. Pryciak, S. P. Ho, W. F. DeGrado, *Proteins: Struct., Funct., Genet. 1* (1986) 16; e) L. Regan, W. F. DeGrado, *Science (Washington, D.C.) 241* (1988) 976; f) J. S. Richardson, D. C. Richardson in D. L. Oxender, C. F. Fox (Eds.): *Protein Engineering*, A.R. Liss, New York 1987, p. 149; g) M. Mutter in G. R. Marshall (Ed.): *Peptides, Chemistry and Biology*, ESCOM, Leiden 1987, p. 349; h) M. Mutter, E. Altmann, K.-H. Altmann, R. Hersperger, P. Koziej, K. Nebel, G. Tuchscherer, S. Vuilleumier, H.-U. Gremlich, K. Müller, *Helv. Chim. Acta 71* (1988) 835; i) W. F. DeGrado, Z. R. Wasserman, J. D. Lear, *Science (Washington, D.C.) 243* (1989) 622.
[3] P. Y. Chou, G. D. Fasman, *Adv. Enzymol. 47* (1978) 45.
[4] a) M. Goodman, C. Toniolo, F. Naider in E. R. Blout, F. A. Bovey, M. Goodman, N. Lotan (Eds.): *Peptides and Proteins*, Wiley, New York 1974, p. 308; b) F. Maser, K. Bode, V. N. R. Pillai, M. Mutter, *Adv. Polym. Sci. 65* (1984) 177; c) M. Sueki, S. Lee, S. P. Powers, J. B. Denton, Y. Konishi, H. A. Scheraga, *Macromolecules 17* (1984) 148; d) A. Brack, G. Spach, *J. Am. Chem. Soc. 103* (1981) 6319.
[5] M. Mutter, *Angew. Chem. 97* (1985) 639; *Angew. Chem. Int. Ed. Engl. 24* (1985) 639.
[6] a) S. P. Ho, W. F. DeGrado, *J. Am. Chem. Soc. 109* (1987) 6751; b) E. T. Kaiser, *J. Biol. Chem. 261* (1986) 13167; c) E. T. Kaiser, F. J. Kezdy, *Annu. Rev. Biophys. Chem. 16* (1987) 561; d) W. F. DeGrado, J. D. Lear, *J. Am. Chem. Soc. 107* (1985) 7684.
[7] M. Mutter, S. Vuilleumier, *Angew. Chem. 101* (1989) 551; *Angew. Chem. Int. Ed. Engl. 28* (1989) 535.
[8] D. G. Osterman, E. T. Kaiser, *J. Cell. Biochem. 19* (1985) 57.
[9] M. Schiffer, A. B. Edmundson, *Biophys. J. 7* (1967) 121.
[10] K. R. Shoemaker, P. S. Kim, E. J. York, J. M. Stewart, R. L. Baldwin, *Nature (London) 326* (1987) 563.
[11] a) S. Brahms, J. Brahms, *J. Mol. Biol. 11* (1980) 149; b) R. Hersperger, M. Mutter, unpublished.
[12] a) T. Miyazawa in G. D. Fasman (Ed.): *Poly-α-Amino Acids*, Dekker, New York 1967, p. 69; b) S. Krimm, J. Bandekar, *Adv. Protein Chem. 38* (1986) 181.
[13] A. Seelig, L. Kürz, M. Mutter, unpublished.
[14] a) M. Mutter, V. N. R. Pillai, H. Anzinger, E. Bayer, C. Toniolo in K. Brunfeldt (Ed.): *Pept. Proc. Eur. Pept. Symp. 16th 1980*, Scriptor, Copenhagen 1981, p. 660; b) V. N. R. Pillai, M. Mutter, *Acc. Chem. Res. 14* (1981) 122.
[15] G. Barany, R. B. Merrifield in E. Gross, J. Meienhofer (Eds.): *Peptides: Analysis, Synthesis, Biology, Vol. 2*, Academic Press, New York 1980, p. 3.
[16] H. Rink, *Tetrahedron Lett. 28* (1987) 3787.

X-Ray Structure Analysis of an Iminium Ion Generated by Grob Fragmentation**

By *Sandro Hollenstein* and *Thomas Laube**

Grob fragmentation,[1] which is generally carried out under solvolytic conditions, can lead to formation of carbocations as intermediates, which, depending on their subsequent reactions, afford various solvolysis products. Heterolysis of the well-investigated γ-haloalkylamines gives unfragmented γ-aminoalkyl cations or, for synchronous fragmentation, iminium ions and olefins. To investigate the electronic interaction of the iminium C=N bond with the olefin C=C bond (which, in the extreme case, may be regarded as a hyperconjugation), we have determined the structure of the iminium ion **2**, formed as an intermediate upon solvolysis of 1-bromo-3-dimethylamino-5,7-dimethyladamantane (**1**),[2] by carrying out an X-ray structure analysis[3] of the corresponding triflate (prepared by reaction of **1** with silver triflate).[4] The asymmetric unit consists of three ion pairs (Fig. 1), for which

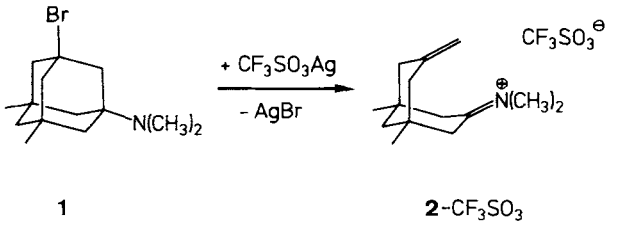

1 **2**-CF_3SO_3

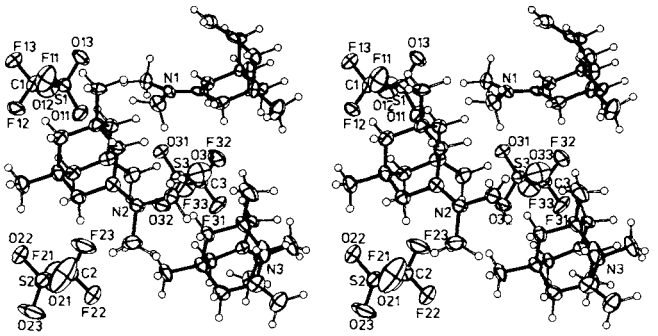

Fig. 1. Stereoplot (ORTEP) of the asymmetric unit of **2**-CF_3SO_3 (three ion pairs). The ellipsoids are drawn at the 50% probability level; the hydrogen atoms are represented by spheres with a radius of 0.1 Å (complete numbering of the atoms in the cation is given in Fig. 2).

there is no evidence of covalent bonding between cations and anions.[5, 6] All cations belong approximately to point group C_s (cations 1 and 3 display a slight torsion of ca. 3° around the Cx03=Nx bonds) and have similar conformations[7] (see Table 1).

Equally oriented rotations of the C=C and C=N systems around the Cx06–Cx08 and Cx04–Cx02 axes, respectively, reveal a certain degree of flexibility for ion **2** (Fig. 2). The mean distance Cx03···Cx10 (ca. 3.26 Å) is only slightly smaller than the sum of the van der Waals radii of the two C atoms (3.40 Å). Thus, the iminium ion structure **2** provides a largely accurate description of the structure of the cation in the crystal; that is, the contribution of the adamantyl cation resonance formula **2'** is small[8, 9] (the experimentally determined structure of **2** is similar to the calculated structure[10] of ketone **3**[6]). Nonetheless, the pyramidalizations at Cx03 and Cx07 in all three ions are in the direction expected for **2'**.[11] Furthermore, the fact that force-field calculations[10] on ketone **3** reveal no pyramidalization for the olefinic bond and only very weak pyramidalization in the expected direction ($\Delta C_{C=O}$ = 0.015 Å) for the carbonyl double bond indicates the existence of an electronic interaction. The weak correlation of the lengthening of the two double bonds with the conformational change (represented as a change in the angle between the planes: see Table 1; x, 3 → 2 → 1), the

Table 1. Selected structural data for cation **2** (distances in Å, angles and torsional angles in °). *P*(n,···) is the best plane through the atoms Cx0n, ...; Mx is the midpoint of the axis through Cx07 and Cx10; *p*A is a point on that part of the symmetry axis of the p-like orbital on atom A that passes through the larger lobe of the orbital; ΔA is the distance of atom A from the plane defined by its three bonding partners.

	Cation No. (x)		
	1	2	3
Cx03–Nx	1.301(8)	1.275(9)	1.274(9)
Cx07–Cx10	1.35(1)	1.32(1)	1.32(1)
Cx03–Cx02	1.487(9)	1.508(9)	1.482(9)
Cx03–Cx04	1.50(1)	1.501(9)	1.488(9)
Cx03···Cx10	3.22(1)	3.28(1)	3.27(1)
Cx03···Cx07	2.86(1)	2.894(9)	2.85(1)
|ΔCx03|	0.05	0.06	0.04
|ΔCx07|	0.02	0.03	0.03
|ΔNx|	0.02	0.01	0.01
P(2,3,4),*P*(1,2,4,5)	150.2(8)	147.0(7)	141.7(7)
P(6,7,8),*P*(1,5,6,8)	129.9(8)	131.9(7)	134.1(9)
Nx–Cx03···Cx10	94.0(4)	93.3(4)	86.1(4)
Nx–Cx03···Mx	105.7(4)	104.4(4)	97.1(4)
*p*Cx03–Cx03–Nx–*p*Nx	−2.9	+0.8	−177.3

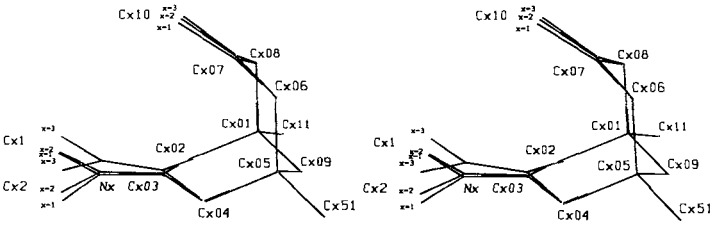

Fig. 2. Stereodrawing of the superposition of the three crystallographically independent cations **2** (x, which refers to the number of the cations, can have the values 1, 2, and 3). The least-squares adjustment was carried out with a hundredfold weighting for Cx01, Cx02, Cx04, Cx05, Cx06, Cx08, Cx09, Cx11, and Cx51 in comparison with the other atoms.

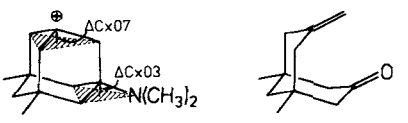

2' **3**

[*] Priv.-Doz. Dr. T. Laube, Dipl.-Chem. S. Hollenstein
Laboratorium für Organische Chemie
der Eidgenössischen Technischen Hochschule
ETH-Zentrum, Universitätstrasse 16, CH-8092 Zürich (Switzerland)

[**] Taken from the Diplomarbeit of *S. H.* We thank Prof. *D. Seebach* and Prof. *J. D. Dunitz* for financial support. *T. L.* thanks the Fonds der Chemischen Industrie for a Dozentenstipendium

shortening of the distance Cx03···Cx10, and the increase in the angle Nx–Cx03···Cx10 indicate an increasing interaction in the sense of a nucleophilic attack of the C=C on the C=N$^{\oplus}$ bond (which would lead to **2'**).[12]

Received: August 25, 1989;
supplemented: November 8, 1989 [Z 3521 IE]
German version: *Angew. Chem. 102* (1990) 194

CAS Registry numbers:
1, 124686-11-9; **2**·$CF_3SO_3^{\ominus}$, 124686-13-1.

[1] C. A. Grob, *Angew. Chem. 88* (1976) 621–627; *Angew. Chem. Int. Ed. Engl. 15* (1976) 569–575; *ibid. 81* (1969) 543–555 and *8* (1969) 535–546.

[2] The adamantane derivative **1** was synthesized starting from commercially available 3,5-dimethyladamantan-1-ol as follows: bromination with HBr/glacial acetic acid (W. Fischer, C. A. Grob, H. Katayama, *Helv. Chim. Acta 59* (1976) 1953–1962) and Koch–Haaf reaction and bromination with $Br_2/AlBr_3$ (F. N. Stepanov, Yu. I. Srebrodol'skii, *Zh. Org. Khim. 2* (1966) 1612–1615; *J. Org. Chem. USSR Engl. Transl. 2* (1966) 1590–1592) to give 3-bromo-5,7-dimethyladamantane-1-carboxylic acid, followed by conversion to the amide, Hofmann degradation to a urethane (from which ketone **3** is obtainable by refluxing in aqueous sodium hydroxide) in analogy to H. Stetter, P. Tacke, *Chem. Ber. 96* (1963) 694–698, and, finally, hydrolysis and *N*-methylation (formalin and catalytic hydrogenation) in analogy to C. A. Grob, W. Schwarz, *Helv. Chim. Acta 47* (1964) 1870–1878.

[3] Enraf–Nonius CAD4 diffractometer, $Mo_{K\alpha}$ radiation, graphite monochromator, measurement temperature −80 °C, space group $Pna2_1$, a = 14.98(1), b = 14.76(1), c = 23.678(9) Å, V = 5237(6) Å^3, ϱ_{calcd} = 1.352 g cm^{-3}, Z = 12, 4721 measured reflections (Θ < 25°), 3640 with $I > 3\sigma_I$. The structure was solved by direct methods (SHELXS 86; G. Sheldrick, Universität Göttingen); the non-hydrogen atoms were refined isotropically with SHELX 76 and anisotropically (first unweighted, then with $w = 1/\sigma_F^2$) with the UCLA version (Nov. 1985) of SHELX 76. Most of the H atoms were refined at calculated positions by using the riding model; for 15 H atoms, U_{iso} = 0.08 Å^2 was fixed and not varied (a total of 708 optimized parameters); R = 0.052, R_w = 0.047. (The structure could not be solved in the space group *Pnma*, which also fits the systematic absences.) Further details of the crystal structure investigation are available from the Director of the Cambridge Crystallographic Data Centre, University Chemical Laboratory, Lensfield Road, GB-Cambridge CB2 1EW (UK), on quoting the names of the authors and the full journal citation.

[4] **2**-SbF_6 was synthesized by reaction of **1** with $AgSbF_6$; however, the crystal studied showed orientational disorder of the cations and anions. The analogously prepared tosylate of **2** crystallized only after the solution had been allowed to stand for weeks; the perchlorate of **2** formed no crystals.

[5] In principle, a trifluoromethanesulfonate ester might also have been formed. For the structure of a bromobenzenesulfonate ester of a tertiary alcohol, see B. L. Barnett, J. D. Yordy, *J. Cryst. Mol. Struct. 5* (1975) 113–119.

[6] ^1H and ^{13}C NMR measurements in solution confirm that **1** is a covalent compound, whereas the data for **2** (largely independent of the counterion (triflate, tosylate, $SbF_6^{\ominus}$) and the solvent (CD_2Cl_2, CD_3NO_2)) are similar to those obtained for ketone **3** and are therefore only in agreement with an iminium ion (see also G. A. Olah, P. Kreienbühl, *J. Am. Chem. Soc. 89* (1967) 4756–4759).

[7] The mean bond lengths of the C=N fragment in **2** do not deviate significantly from those of known iminium ions substituted with four sp^3 C atoms (Cambridge Structural Database: F. H. Allen, O. Kennard, R. Taylor, *Acc. Chem. Res. 16* (1983) 146–153).

[8] Formulas **2** and **2'** may be regarded as resonance formulas in the sense of a hyperconjugation (see also T. Laube, *Angew. Chem. 98* (1986) 368–369; *Angew. Chem. Int. Ed. Engl. 25* (1986) 349–350).

[9] The slight shortening of the Cx03–Cx02 and Cx03–Cx04 bonds (mean value: 1.494(4) Å) compared with the C_{sp^3}–C_{sp^3} bonds of ketones (1.511 Å; F. H. Allen, O. Kennard, D. G. Watson, L. Brammer, A. G. Orpen, R. Taylor, *J. Chem. Soc. Perkin Trans. 2* (1987) S1–S19) might be due to an increased hyperconjugative interaction of the cationic center with the α-CH_2 groups.

[10] MM2(85) in the program MacroModel, version 1.5 (W. C. Still, Columbia University, New York, USA).

[11] Similar pyramidalizations are found for the carbonyl groups of ketones that have a C=C bond lying above the C=O bond; see, e.g., W. B. Schweizer, J. D. Dunitz, R. A. Pfund, G. M. Ramos Tombo, C. Ganter, *Helv. Chim. Acta 64* (1981) 2738–2740; M. A. Gómez-Rodríguez, M. Martínez-Ripoll, S. García-Blanco, *Acta Crystallogr. Sect. C42* (1986) 894–896.

[12] All effects observed here are similar to those found for structures that can be interpreted in the sense of an attack of O or N nucleophiles on carbonyl groups; e.g., H. B. Bürgi, J. D. Dunitz, E. Shefter, *Acta Crystallogr. Sect. B30* (1974) 1517–1527; M. Kaftory, J. D. Dunitz, *ibid. B32* (1976) 1–4.

Alkyltechnetium Oxides: First Examples and Reactions**

By *Wolfgang A. Herrmann,* Roger Alberto, Paul Kiprof,* and *Franz Baumgärtner*

Methyltrioxorhenium(VII) (**2**) is an excellent catalyst for the epoxidation of even nonactivated olefins with hydrogen peroxide.[1] Still not understood, however, was why the valence-isoelectronic analogue osmium tetraoxide (**4**), in view of the parallels in its structural and coordination chemistry,[2] does not react with olefins to give epoxides, but instead directly affords so-called osmate esters (e.g., $O_2Os(-OCH_2CH_2O)$) and is therefore the only catalyst widely used so far for the *cis* hydroxylation of olefins.[3] A better understanding of the difference in reactivity of CH_3ReO_3 (**2**) and OsO_4 (**4**) was expected from the investigation of hitherto unknown alkyltechnetium oxides.

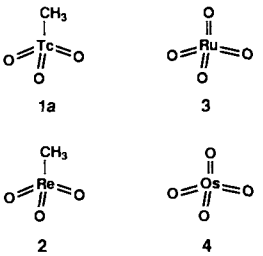

Treatment of Tc_2O_7 with tetramethyltin at approximately 10 °C (Scheme 1) yields methyltrioxotechnetium(VII) (**1a**) together with the stannyl ester **1c** of pertechnetium acid. Heating to temperatures above 20 °C leads to formation of larger amounts of reduced products, especially the likewise new,

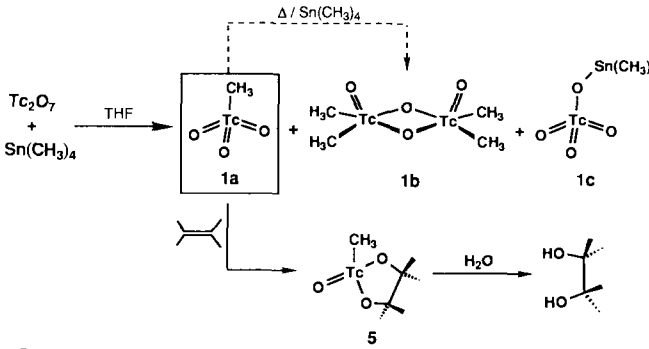

Scheme 1.

paramagnetic, sublimable Tc^{VI} complex **1b**, whose molecular and crystal structure[4] we determined by X-ray diffraction analysis (Fig. 1). Separation of the mixture of compounds proved to be very simple, since **1a** can be rapidly distilled

[*] Prof. Dr. W. A. Herrmann, Dr. R. Alberto, P. Kiprof
Anorganisch-chemisches Institut der Technischen Universität München
Lichtenbergstrasse 4, D-8046 Garching (FRG)
Prof. Dr. F. Baumgärtner
Institut für Radiochemie der Technischen Universität München
Am Coulombwall, D-8046 Garching (FGR)

[*] Multiple Bonds between Main-Group Elements and Transition Metals, Part 75. This work was supported by the Alexander von Humboldt Foundation (*R. A.*), the Deutsche Forschungsgemeinschaft, and the Fonds der Chemischen Industrie. We thank the Paul-Scherrer-Institut in Würenlingen (Switzerland) for supplying ^{99}Tc. Part 74: J. Takacs, P. Kiprof, J. Riede, W. A. Herrmann, *Organometallics*, in press.

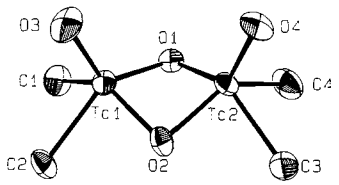

Fig. 1. Structure of bis[dimethyl(μ-oxo)oxotechnetium(VI)] (**1b**) in the crystal (ORTEP plot, hydrogen atoms omitted). The thermal ellipsoids are drawn at the 50% level. The coordination sphere of the Tc atom is best described as distorted square-pyramidal (Tc=O unit apical). The TcTc distance of 256.17(3) pm appears to support the assumption of a (single) bond, but the paramagnetism of the compound (no ^{99}Tc NMR signal) indicates that there is no bonding. Further distances [pm] and angles [°]: Tc1-C1 213.3(2), Tc1-C2 212.9(3), Tc1-O1 190.6(2), Tc1-O2 192.5(2), Tc1-O3 166.6(2), Tc2-C4 212.8(3), Tc2-C3 208.6(3), Tc2-O1 191.2(2), Tc2-O2 190.0(2), Tc2-O4 164.7(2); O1-Tc1-O2 88.77(8), C1-Tc1-C2 79.5(2), Tc1-O1-Tc2 84.28(6), O1-Tc2-O2 89.37(8), C3-Tc2-C4 79.9(1), Tc1-O2-Tc2 84.06(7). Further details of the crystal structure investigation may be obtained from the Fachinformationszentrum Karlsruhe, Gesellschaft für wissenschaftlich-technische Information mbH, D-7514 Eggenstein-Leopoldshafen 2 (FRG), on quoting the depository number CSD-54298, the names of the authors, and the journal citation.

from the mixture at 0 °C under oil-pump vacuum; **1b** (yellow) can be extracted with nonpolar solvents (e.g., *n*-pentane) and **1c** (colorless), the most polar and least volatile component, with tetrahydrofuran. The titanium(IV) reagent $CH_3Ti(O\text{-}i\text{-}C_3H_7)_3$, which is suitable for the methylation of metal oxides,[5] may be used instead of tetramethyltin.

Although methyltrioxotechnetium(VII) (**1a**) is obtainable as yellowish, centimeter-long, fine crystalline needles and is stable when stored at ca. 0 °C, it decomposes above ca. 20 °C to form primarily **1b**. In addition, **1a** is sensitive to moisture. By contrast, the rhenium analogue **2** is stable even at temperatures up to 200 °C and also, to a certain extent, in aqueous solution; in alkaline solution, however, it decomposes quantitatively according to Equation (a).[6a]

$$CH_3ReO_3 + OH^{\ominus} \longrightarrow CH_4 + [ReO_4]^{\ominus} \qquad (a)$$

Presumably, CH_3TcO_3 is a much stronger Lewis acid than CH_3ReO_3 ($pK_a \approx 6.9$ for **2**[7]), since it reacts even with water to give pertechnetium acid. Unlike **2**,[6b] moreover, **1a** does not form stable adducts with amines, not even with 2,2'-bipyridine or quinuclidine.

Taking into consideration the large difference in atomic masses (^{99}Tc versus ^{186}Re), the IR investigations indicate that the title compound **1a** has appreciably weaker metal–oxygen bonds (νTcO 1002 m, 948 cm^{-1} vs; CS_2) than the rhenium analogue **2** (ν ReO 1002 m, 967 cm^{-1} vs; CS_2).

In other reactions, the two alkylmetal oxides differ not only in degree but fundamentally. Thus, olefins such as cyclohexene add to **1a** as shown in Scheme 1 to form glycolate complexes **5** (Tc^V), which, in the presence of water and acids, decompose with liberation of the 1,2-diol and disproportionation to $TcO_2 \cdot xH_2O$ and $[TcO_4]^{\ominus}$; as observed for osmium tetraoxide, this reaction sequence occurs catalytically and leads, in the case of cyclohexene, to formation of *cis*-1,2-cyclohexanediol in a stereospecific fashion. The complex $[TcO_3Cl(2,2'\text{-bpy})]$ also adds olefins, which may then be functionalized and released (although noncatalytically) as *cis* diols;[8a] the analogous rhenium(VII) complex does not react with olefins.[8b]

Apart from the finding that alkyltechnetium oxides are in principle isolable compounds,[9–12] the results described here show that the oxidizing strength and apparently the Lewis acidity of Tc^{VII} derivatives are far greater than those of the Re^{VII} analogues. The importance of the "double-bond structure" **A** in describing the ground state of CH_3TcO_3 (**1a**)

$$M{=}\ddot{O} \leftrightarrow \overset{\ominus}{M}{\equiv}\overset{\oplus}{O}$$
A **B**

appears to be responsible for its ability to add to olefins to give 1,2-glycolate complexes. We draw particular attention to this relationship between technetium and osmium. Accordingly, the still more powerful, olefin-cleaving oxidizing agent RuO_4 (**3**) should correspond to "CH_3MnO_3", which has so far eluded all synthetic efforts. CH_3MnO_3 should be unstable, in agreement with theoretical studies,[13] so long as the strong decrease in thermal stability on going from CH_3ReO_3 to CH_3TcO_3 is continuous.

Experimental Procedure

Important Notice: The isotope ^{99}Tc used in the synthesis is a low-energy β emitter ($E_{max} \approx 0.29$ MeV) with a very long half-life (2.1×10^5 a) and without nuclide-specific γ radiation. Owing to the high volatility of **1a**, special precautions were necessary to avoid contamination.

All preparative procedures were carried out in a glove box. The total radioactivity used was at most 370 MBq. The whole-body exposure outside the glove box was 2 μSv/h, the hand exposure < 25 μSv/h.

1a: The reaction vessel should be equipped with an acetone/dry ice cold finger. Particular care must be taken to exclude moisture. Tc_2O_7 (127 mg, 0.41 mmol) was treated with a solution of $Sn(CH_3)_4$ (81 mg, 0.45 mmol) in 7 mL of precooled THF and the reaction solution was stirred for 2 h at 0 °C; it turned initially green then yellow. After warming to room temperature, the mixture was stirred until the color had vanished (ca. 10 h). A dark precipitate contained only 5–7% of the radioactivity. THF was removed under oil-pump vacuum. Once the residue was free of solvent, it was cooled *immediately* to − 50 °C and sublimed onto the cold finger. Despite these precautions, losses of up to 25% occurred on sublimation. Compound **1a** can also be extracted from the residue with *n*-pentane. If the extraction residue is then sublimed (see above), the losses can be kept smaller. Yield in solution > 90%, after sublimation 46 mg (68%). Colorless crystals, ^{99}Tc content: 60.70% (calcd 61.10%). EI-MS: *m/z* 162 (molecular ion). IR (CS_2): $\tilde{\nu}$ = 1002 m, 948 vs cm^{-1} (νTcO); 2922 w, 2850 w cm^{-1} (νCH). ^{1}H NMR (C_6D_6, 28 °C): δCH_3 = 1.55 [s]. ^{99}Tc NMR ([D$_8$]THF/C_6D_6, 28 °C): δTc = 433 (vs. $[TcO_4]^{\ominus}$).

1c: The extraction residue (see above) was dissolved in 7 mL of THF. After filtration and evaporation of the filtrate under oil-pump vacuum at − 50 °C, 119 mg of **1c** was obtained as a colorless, microcrystalline substance (89%), ^{99}Tc content: 30.90% (calcd 30.28%). EI-MS: *m/z* 313 (35%, $[M-CH_3]^{\oplus}$), 283 (20%; $[M-3\ CH_3]^{\oplus}$), 165 (100%; $[Sn(CH_3)_3]^{\oplus}$). IR (KBr): $\tilde{\nu}$ = 920 vs 908 vs cm^{-1} (νTc=O). ^{1}H NMR ([D$_8$]THF, 28 °C): $\delta(CH_3) = 0.66$ [s; $^2J(^1H,^{117}Sn) = 64.6$ Hz; $^2J(^1H,^{119}Sn) = 67.2$ Hz]. ^{99}Tc NMR ([D$_8$]THF/C_6D_6, 28 °C): δTc = − 1.16 (vs. $[TcO_4]^{\ominus}$).

1b: Same amounts as for **1a**, but 2 h at reflux temperature. After evaporation of the black-brown solution under oil-pump vacuum (− 50 °C), **1b** was sublimed at 65 °C, affording orange crystals. ^{99}Tc content: 59.94% (calcd 61.46%). EI-MS: *m/z* 322 (molecular ion). IR (KBr): $\tilde{\nu}$ = 1006 s, 986 cm^{-1} vs (νTcO). ^{1}H NMR (C_6D_6, 28 °C): $\delta(CH_3) = 2.40$ [broad].

Received: October 10, 1989 [Z 3588 IE]
German version: *Angew. Chem. 102* (1990) 208

[1] W. A. Herrmann, D. W. Marz, J. G. Kuchler, G. Weichselbaumer, W. Wagner, R. W. Fischer, GP 3902357.5 (Jan 27, 1989), Hoechst AG, and [2b].

[2] Reviews: a) W. A. Herrmann, *Angew. Chem. 100* (1988) 1269; *Angew. Chem. Int. Ed. Engl. 27* (1988) 1297; b) *J. Organomet. Chem. 382* (1990) 1.

[3] a) Reviews: M. Schröder, *Chem. Rev. 80* (1980) 187; b) recent work: J. S. M. Wai, I. Marko, J. S. Svendsen, M. G. Finn, E. N. Jacobsen, K. B. Sharpless, *J. Am. Chem. Soc. 111* (1989) 1123.

[4] **1b**: Obtained from *n*-pentane as yellow-orange, long platelets; size not measured; systematic absences: *h0l* ($h + l = 2n + 1$); monoclinic, space group *Pn* (No. 7); lattice constants refined by the least-squares method from 50 reflections at high diffraction angles: a = 601.1(1), b = 844.1(1), c = 922.4(2) pm, β = 94.12(2)°, $V = 467 \times 10^6$ pm^3; $C_4H_{12}O_4Tc_2$ (322.1); Z = 2; $F_{(000)}$ = 308; ϱ_{calcd} = 2.277 g cm^{-3}; Enraf-Nonius CAD-4, $Mo_{K\alpha}$ radiation (λ = 71.073 pm), graphite monochromator; T = − 50 ± 3 °C; $2.0° \leq \Theta \leq 25.0°$; ω scan; scan width: $(1.00 + 0.30 \cdot \tan\Theta)°$ ± 25% before and after each reflection to determine background; t_{max} = 60 s; 3235 measured reflections ($\pm h$, $\pm k$, $\pm l$), 1619 unique reflections, three reflections (1,0,−1; −1,0,1; 1,0,3) suppressed; 230 parameters, full-matrix least-squares refinement; $R = \sum\|F_o| - |F_c\|/\sum|F_o| = 0.023$; $R_w = [\sum w(|F_o| - |F_c|)^2/\sum w|F_o|^2]^{1/2} = 0.028$; GOF = $[\sum w(|F_o| - |F_c|)^2/(NO - NV)]^{1/2} = 4.46$ mit $w = 1/\sigma^2(F_o)$. Structure solution: The Tc atomic positions are identical with the Re positions of the isostructural rhenium

compound, difference Fourier technique; empirical absorption correction, $\mu = 28.6\ cm^{-1}$, nine reflections; − 4.2% decomposition in 29.5 h for three control reflections, not corrected; extinction not corrected. H-atom positions: four successive positions taken from difference Fourier syntheses, eight calculated for ideal geometry (d(C–H) 95 pm) and included per C atom with collective isotropic temperature factor in the structure factors. H atoms were not refined; anomalous dispersion was taken into consideration. Shift/error, <0.01 in the last refinement cycle; residual electron density, + 1.32 $e_0^{-1}\ Å^{-3}$ and − 1.55 $e_0^{-1}\ Å^{-3}$ next to the heavy atom. The refinement in the enantiomorphic arrangement does not result in a significant change in the R values.

[5] Examples: Synthesis of $(CH_3)_4OsO$ from OsO_4 (cf. [7]) and of $(CH_3)_4Re_2O_4$ from Re_2O_7 (K. A. Jung, W. A. Herrmann, unpublished results).

[6] a) W. A. Herrmann, J. G. Kuchler, G. Weichselbaumer, E. Herdtweck, E. Kiprof, *J. Organomet. Chem. 372* (1989) 351; b) W. A. Herrmann, G. Weichselbaumer, E. Herdtweck, *ibid. 372* (1989) 371.

[7] S. J. Eder, *Diplomarbeit*, Technische Universität München 1989.

[8] a) R. M. Pearlstein, A. Davison, *Polyhedron 7* (1988) 1981; b) W. A. Herrmann, J. G. Kuchler, unpublished results.

[9] A polymeric ^{99}Tc complex, $[(\eta^5\text{-}C_5Me_5)Tc_2O_3]_n$, was recently reported [10]. The argumentation used in that communication is not convincing in our opinion: (1) The position of the ν(TcO) bands (909, 880 cm^{-1}) is characteristic of terminal oxo ligands for *all* known Re and Tc complexes. (2) The TcTc distance (186.7 pm) is surprisingly short, about 27 pm shorter than the quadruple bond in $[Tc_2Cl_8]^{2\ominus}$ [11]! For "$Tc(\mu\text{-}O)_2Tc$" systems with formal TcTc triple bonds, on the other hand, distances of 235 pm have been found [12]. (3) The still unsatisfactorily solved crystal structure of $(\eta^5\text{-}C_5Me_5)ReO_3$ shows comparable cell constants to those of "$[(\eta^5\text{-}C_5Me_5)Tc_2O_3]_n$": 594.6/869.7/1063.0 and 592.6/865.1/1059.1 pm. The isomorphism of the analogous Tc and Re complexes, as observed here for **1b**, indicates that compound described in [10] is in fact $(\eta^5\text{-}C_5Me_5)TcO_3$.

[10] B. Kanellakopulos, B. Nuber, K. Raptis, M. L. Ziegler, *Angew. Chem. 101* (1989) 1055; *Angew. Chem. Int. Ed. Engl. 28* (1989) 1055.

[11] F. A. Cotton, L. Daniels, A. Davison, C. Orvig, *Inorg. Chem. 20* (1981) 3051.

[12] H. B. Bürgi, G. Anderegg, P. Bläuenstein, *Inorg. Chem. 20* (1981) 3829.

[13] T. Szyperski, P. Schwerdtfeger, *Angew. Chem. 101* (1989) 1271; *Angew. Chem. Int. Ed. Engl. 28* (1989) 1228.

Catalytic Cyclophanes: A Porphyrin-Bridged Cyclophane as a Model for Cytochrome P-450 Enzymes**

By *David R. Benson, Robert Valentekovich,* and *François Diederich**

Cytochrome P-450 enzymes represent an extraordinarily versatile class of biological oxidation catalysts.[2] In their function as monooxygenases, they are responsible for the metabolism of endogenous as well as exogenous lipophilic substrates. Prominent examples for the mode of action of P-450 enzymes are the hydroxylation of steroids and the epoxidation of unsaturated fatty acids, the first steps in the metabolism of these compounds. The hydroxylation of alkanes and arenes represents the predominant mechanism for enzymatic detoxification of these materials in humans. Substrates include disease-targeted drugs and environmental pollutants. However, with some polycyclic aromatic hydrocarbons, such as benzo[*a*]pyrene, the same transformation can also lead to the formation of extremely potent carcinogens.[3]

A large body of biochemical studies[2] and recent X-ray crystal structure analyses[4] have made enormous contributions to the understanding of the structure and mode of action of the P-450 cytochromes. Three structural features are highly characteristic for these enzymes: (1) An iron porphyrin forms one side of the oxygen and substrate binding site, which is deeply buried in the protein and, therefore, of pronounced hydrophobic character. (2) No additional catalytically active groups can be found at this hydrophobic active site. (3) A cysteinyl ligand, located on the porphyrin side opposite to the binding site, acts as a sixth axial ligand of the heme-bound iron.[5] For monooxygenase activity, molecular oxygen is bound by the heme iron(II). In a sequence of redox processes, the bound oxygen is cleaved with formation of water and a high-valent iron oxo complex ("oxenoid") believed to be $Porph^{\bullet\oplus}Fe^{IV}=O$. This iron oxo complex subsequently transfers its oxygen atom to the complexed substrate.

In many elegant studies in recent years, the mechanism and the synthetic potential of olefin epoxidations and alkane hydroxylations catalyzed by simple cytochrome P-450 model systems have been explored.[6] High catalytic turnovers and remarkable regio- and stereoselectivity have been reported. In the majority of these studies, the natural process of oxygen activation has been circumvented, and the catalytically active iron oxo intermediate has been generated by direct reaction of iron(III) porphyrinates with oxygen-transfer agents like iodosobenzene.[7]

Interestingly, the hydroxylation of aromatic hydrocarbons has not been at the center of interest in studies with P-450 model compounds. Therefore, we planned the synthesis of the porphyrin-bridged cyclophane **1**, having an efficient apolar binding site for arene complexation in close proximity to a porphyrin ring.[8, 9] Detailed studies of arene hydroxylation in complexes of the iron-containing host **3** were intended to focus specifically on the dependence of the redox potential and the spin state of **3** on substrate binding.[4b, 10, 11] Furthermore, the possibility of developing new homogeneous catalysts for synthetically useful arene hydroxylations added additional interest to the projected studies with **3**. Here, we describe the synthesis and complexation properties of **1** and **3** as well as first studies of the catalytic properties of the iron complex **3**.

For the synthesis of **1**, the activated ester **4**[12] was prepared in three steps starting from salicylaldehyde. Alkyl-

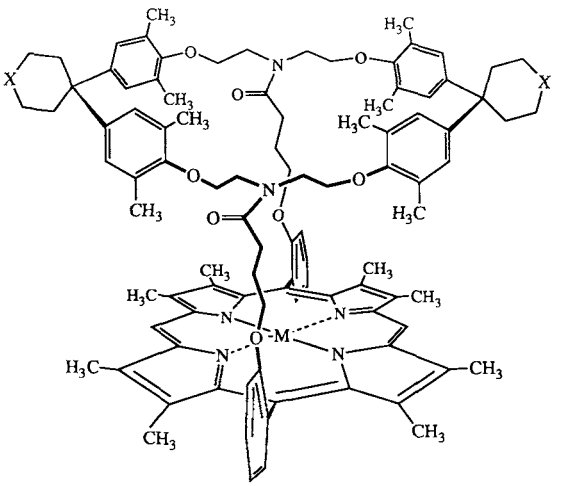

1, M = 2 H, X = EtN
2, M = Zn, X = EtN
3, M = Fe-Br, X = $EtHN^{\oplus}Br^{\ominus}$

[*] Prof. F. Diederich, D. R. Benson, R. Valentekovich
Department of Chemistry and Biochemistry
University of California
Los Angeles, CA 90024-1569 (USA)

[**] Catalytic Cyclophanes, Part 5. We are grateful to the Office of Naval Research for generously supporting this research. *R.V.* thanks the National Science Foundation for a Summer Undergraduate Fellowship. Part 4: [1].

ation of salicylaldehyde with ethyl 4-bromobutanoate (DMF, K_2CO_3) gave **5**,[12] which was hydrolyzed (MeOH, 2 N, KOH) to **6**,[12] followed by esterification (dioxane, *N*-hydroxysuccinimide, *N,N'*-dicyclohexylcarbodiimide) to **4** (see Table 1 for yields and physical data of the new compounds). The reaction of the macrocyclic tetramine **7**[13] with

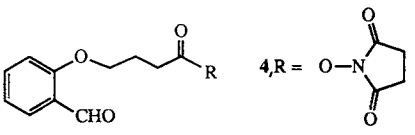

5,R = OCH_2CH_3

6,R = OH

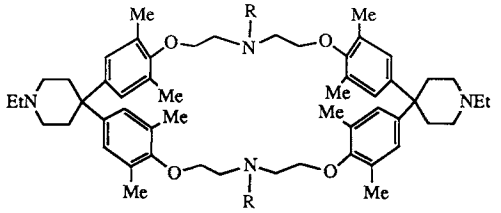

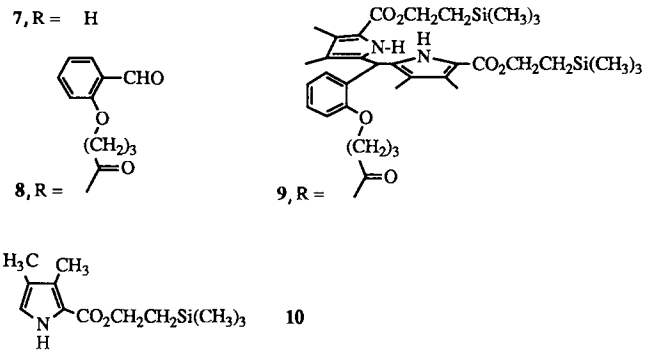

Table 1. Selected physical data of new compounds.

1: quantitative yield; m.p. 220 °C, dec. ^{1}H NMR (500 MHz, [D$_{10}$]*p*-xylene, T = 393 K): $\delta = -1.56$ (br, s, 2H), 0.5–0.6 (m, 4H), 1.05 (*t*, J = 7.1 Hz, 6H), 1.4–1.5 (m, 2H), 1.55–1.65 (m, 10H), 1.76 (br. s, 24H), 2.1–2.25 (m, 8H), 2.28 (q, J = 7.1 Hz, 4H), 2.3–2.6 (m, 16H), 2.77 (s, 12H), 3.54 (s, 12H), 4.04 (t, J = 6.4 Hz, 4H), 6.76 (s, 8H), 7.23 (ddd, J = 7.5, 7.5 and 1.2 Hz, 2H), 7.36 (dd, J = 8.3 and 1.2 Hz, 2H), 7.55 (dd, J = 7.5 and 1.6 Hz, 2H), 7.67 (ddd, J = 8.3, 7.5 and 1.6 Hz, 2H), 10.21 (s, 2H) UV/VIS (CH_2Cl_2): λ_{max} (lg ε) = 628 (3.10), 576 (3.78), 541 (3.69), 507 (4.16), 409 (5.25), 338 (sh, 4.20), 277 (sh, 4.04), 271 (4.05) [14a]. MS (FAB, *m*-nitrobenzyl alcohol): *m/z* 1589 ($M^{\oplus}$ + 2H, 38%), 1588 ($M^{\oplus}$ + H, 82%), 1587 ($M^{\oplus}$, 100%)

2: 7–10% yield; m.p. 247 °C, dec. UV/VIS (CH_2Cl_2): λ_{max} (lg ε) = 575 (3.95), 539 (4.20), 502 (3.49), 411 (5.47) [14a]. MS (FAB, *m*-nitrobenzyl alcohol): *m/z* 1651 ($M^{\oplus}$ + 2H, 97%), 1650 ($M^{\oplus}$ + H, 100%), 1649 ($M^{\oplus}$, 32%)

3: M.p. 277 °C, dec. UV/VIS (CH_2Cl_2): λ_{max} (lg ε) = 652 (3.45), 589 (sh, 3.40), 540 (sh, 3.81), 507 (3.94) 394 (4.97) [14a]. MS (FAB, *m*-nitrobenzyl alcohol): *m/z* 1644 ($M^{\oplus}$ – HBr – 2Br, 54%), 1643 ($M^{\oplus}$ – 2HBr – Br, 100%), 1642 ($M^{\oplus}$ – 3HBr, 75%)

4: 87% yield; m.p. 119–121 °C

5: 93% yield; colorless oil

6: 85% yield; m.p. 91–92.5 °C

8: 75% yield; colorless foam

9: 75% yield; pale-yellow foam

10: 78% yield; m.p. 68–69 °C

four equivalents of **4** in dioxane at 80 °C afforded the dialdehyde **8**.[12] For the construction of the porphyrin according to the procedure of *Baldwin* et al.,[14] the β-(trimethylsilyl)ethyl ester **10**[12] was prepared by allowing ethyl 3,4-dimethylpyrrole-2-carboxylate[15] to react with 2-trimethylsilylethanol in the presence of sodium methoxide. The tetrapyrrole derivative **9**[12] was obtained by heating **8** with four equivalents of **10** in absolute ethanol in the presence of 2.1 equivalents of methanesulfonic acid. Fourfold β-elimination with tetra-*n*-butylammonium fluoride in THF led to formation of ethylene, trimethylsilyl fluoride, and the free tetra(2-pyrrolecarboxylic acid) derived from **9**. This was treated in situ in dichloromethane with trimethyl orthoformate and trichloroacetic acid in the presence of zinc acetate dihydrate (48 h, 20 °C) to give the zinc-containing porphyrin.[14] Two atropisomers are formed, interconvertible by rotation about the bond from the porphyrin to the *meso*-phenyl ring, and these could be separated by flash chromatography. The desired atropisomer **2**[12] with an open, preorganized cavity was isolated in 7–10% yield and spectroscopically unambiguously identified as a zinc-containing octamethyl-*meso*-diphenylporphyrin derivative. Upon short stirring of **2** in methanol/conc. HCl (1:1), the free porphyrin cyclophane **1**[12] was obtained. At the free porphyrin stage, heating of the atropisomer mixture in toluene led to the quantitative conversion of the undesired into the desired atropisomer **1**. According to examination of CPK models, the atropisomer with the bridges to the cyclophane on opposite sides of the porphyrin is sterically disfavored. The iron(III) porphyrinate **3**[12] was prepared by treating **1** with anhydrous $FeBr_2$ at reflux in THF, washing with 2% HBr, and subsequent crystallization from CH_2Cl_2/EtOAc.

^{1}H NMR binding studies (500 MHz, 293 K) demonstrated the formation of inclusion complexes between **1** and aromatic hydrocarbons in [D$_4$]methanol/D_2O/[D$_4$]acetic acid (95:4.85:0.15 v/v). The ^{1}H NMR binding titrations were evaluated by nonlinear least-squares curve fitting. Table 2 gives the association constants and the free energies of formation for the 1:1 arene complexes. Figure 1 shows the remarkably large upfield shifts calculated for saturation binding for those guest proton resonances which could be evaluated in the binding titrations.[16] The upfield complexation shifts of the guest resonances in complexes of **1** are considerably larger than in the complexes of similar cyclophanes[9] that are not bridged by a porphyrin. In the complexes of **1**, the aromatic substrates are exposed not only to the shielding cyclophane cavity but also to the strongly shielding region of the porphyrin ring. According to computer modeling studies using the MM2 force field in the Macromodel program,[17] acenaphthylene and phenanthrene come

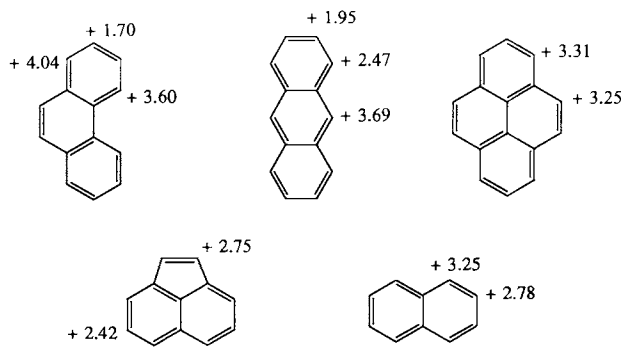

Figure 1. Calculated upfield complexation shifts ($\Delta\delta$ values) of observable guest proton resonances in complexes of **1** at saturation binding; for experimental details, see Table 2.

 © VCH Verlagsgesellschaft mbH, D-6940 Weinheim, 1990 0570-0833/90/0202-0192 $ 02.50/0

within van der Waals distance of the porphyrin ring upon energetically favorable incorporation deep into the cyclophane cavity of **1**.

Preliminary investigations of the catalytic properties of the iron(III) porphyrinate **3** were undertaken in homogeneous solution in 2,2,2-trifluoroethanol with the strongly binding acenaphthylene as substrate (Table 2) and iodosobenzene as the oxygen-transfer reagent.[18] The GC-MS and ^{1}H NMR spectroscopic analysis showed that acenaphthylene is exclusively attacked at the C1–C2 bond, which is intermediate between an aromatic and an olefinic C=C bond in its reactivity towards epoxidizing agents.[19] In all runs, acenaphthen-1-one was the major isolable product. Thus, stirring a mixture of **3** (0.48 mM), acenaphthylene (10.5 mM), and iodosobenzene (11 mM) for four hours with rigorous exclusion of oxygen afforded a 65% yield of acenaphthen-1-one, isolated by column chromatography. This yield corresponds to a turnover number (moles of substrate converted per mole of catalyst) of ca. 14. The initial reaction is extremely fast as evidenced by thin layer chromatograms recorded directly after the reaction had started. The reaction of iodosobenzene with acenaphthylene in the absence of catalyst leads to less than one percent conversion. 2,2,2-Trifluoroethanol was chosen as solvent since it provides homogeneous reaction conditions and represents an extraordinarily good solvent for promoting apolar complexation processes, second only to water.[20] Furthermore, this solvent, in contrast to methanol, is not subject to oxidation by the catalytically active, high-valent iron oxo intermediate.[21] The evaluation of UV/VIS titrations, in which the decrease in intensity of the Soret band was monitored as a function of increasing guest concentration, gave an association constant of $K_a = 39\,500\ \mathrm{L\,mol^{-1}}$ for the high-spin **3**–phenanthrene complex in 2,2,2-trifluoroethanol at 293 K. Support for supramolecular catalysis is provided by the inhibition of the acenaphthen-1-one formation by phenanthrene, an arene of low reactivity, presumably as a result of strong but unproductive binding. Upon addition of phenanthrene (9.9 mM) to the catalytic run described above, the isolated yield of acenaphthen-1-one is reduced to 55%. According to computer modeling, phenanthrene highly prefers an axial inclusion geometry which orients the reactive C9–C10 double bond away from the catalytic center and, under the above-mentioned conditions, phenanthrene shows very low reactivity (conversion to products: ca. 1%). The elucidation of the structure of the catalytically active complex and of the mechanism of the **3**-mediated oxidation of acenaphthylene to acenaphthen-1-one are currently the subject of intensive investigations.

Table 2. Association constants K_a and free binding energies $-\Delta G^\circ$ for the arene complexes of the porphyrin cyclophane **1** in [D$_4$]methanol/D$_2$O/[D$_4$]acetic acid (95:4.85:0.15 v/v), $T = 293$ K.

Guest	K_a[L mol^{-1}] [a]	$-\Delta G^\circ$[kcal mol^{-1}]
Phenanthrene	1330	4.19
Acenaphthylene	1050	4.05
Anthracene [b]	460	3.57
Naphthalene	330	3.38
Pyrene	160	2.95

[a] Accuracy of the K_a values: ± 10%. [b] In [D$_4$]methanol/[D$_6$]Me$_2$SO/D$_2$O/[D$_4$]acetic acid (90:5:4.85:0.15 v/v).

Received: October 2, 1989;
supplemented: November 24, 1989 [Z 3572 IE]
German version: *Angew. Chem. 102* (1990) 213

CAS Registry numbers:
1, 124856-14-0; **1**-phenanthrene complex, 124890-57-9; **1**-acenaphthylene complex, 124856-22-0; **1**-anthracene complex, 124856-23-1; **1**-naphthalene complex, 124890-58-0; **1**-pyrene complex, 124890-59-1; **2**, 124856-24-2; **3**, 124856-25-3; **3** (high-spin) phenanthrene complex, 124856-28-6; **4**, 124856-15-1; **5**, 124856-16-2; **6**, 124856-17-3; **7**, 92787-66-1; **8**, 124856-18-4; **9**, 124856-19-5; **10**, 124856-20-8; tetra(2-pyrrolecarboxylic acid), 124856-21-9; salicylaldehyde, 90-02-8; ethyl 4-bromobutyrate, 2969-81-5; ethyl 3,4-dimethylpyrrole-2-carboxylate, 938-75-0; cytochrome P-450 enzyme, 9035-51-2; acenaphthylene, 208-96-8; acenaphthen-1-one, 2235-15-6.

[1] F. Diederich, H.-D. Lutter, *J. Am. Chem. Soc. 111* (1989) 8438.
[2] a) P. R. Ortiz de Montellano (Ed.): *Cytochrome P-450*, Plenum, New York 1986; b) F. P. Guengerich, T. L. MacDonald, *Acc. Chem. Res. 17* (1984) 9; c) S. D. Black, M. J. Coon, *Adv. Enzymol. Relat. Areas Mol. Biol. 60* (1987) 35; d) J. H. Dawson, *Science (Washington D.C.) 240* (1988) 433.
[3] C. Heidelberger, *Annu. Rev. Biochem. 44* (1975) 79.
[4] a) T. L. Poulos, B. C. Finzel, I. C. Gunsalus, G. C. Wagner, J. Kraut, *J. Biol. Chem. 260* (1985) 16122; b) R. Raag, T. L. Poulos, *Biochemistry 28* (1989) 917.
[5] Model systems with thiolate ligands: a) B. Stäubli, H. Fretz, U. Piantini, W.-D. Woggon, *Helv. Chim. Acta 70* (1987) 1173; b) A. R. Battersby, W. Howson, A. D. Hamilton, *J. Chem. Soc. Chem. Commun. 1982*, 1266; c) J. P. Collman, S. E. Groh, *J. Am. Chem. Soc. 104* (1982) 1391.
[6] a) T. C. Bruice, *Proc. Robert A. Welch Found. Conf. Chem. Res. 31* (1987) 37; b) J. T. Groves, *J. Chem. Educ. 62* (1985) 928; c) J. P. Collman, T. Kodadek, J. I. Brauman, *J. Am. Chem. Soc. 108* (1986) 2588. d) T. G. Traylor, F. Xu, *ibid. 110* (1988) 1953. e) B. Meunier, *Bull. Soc. Chim. Fr. 1986*, 578; f) D. Mansuy, *Pure Appl. Chem. 59* (1987) 759.
[7] J. T. Groves, T. E. Nemo, R. S. Myers, *J. Am. Chem. Soc. 101* (1979) 1032.
[8] Review on bridged porphyrins: B. Morgan, D. Dolphin, *Struc. Bonding (Berlin) 64* (1987) 115. Synthetic porphyrin receptors: a) M. C. Gonzalez, A. C. Weedon, *Can. J. Chem. 63* (1985) 602; b) A. D. Hamilton, J.-M. Lehn, J. L. Sessler, *J. Am. Chem. Soc. 108* (1986) 5158; c) J. T. Groves, R. Neumann, *ibid. 111* (1989) 2900; d) J. S. Lindsey, P. C. Kearney, R. J. Duff, P. T. Tjivikua, J. Rebek, Jr., *ibid. 110* (1988) 6575; e) Y. Aoyama, A. Yamagishi, M. Asagawa, H. Toi, H. Ogoshi, *ibid. 110* (1988) 4076; f) R. Breslow, A. B. Brown, R. D. McCullough, P. W. White, *ibid. 111* (1989) 4517; g) Y. Kuroda, T. Hiroshige, T. Sera, Y. Shiroiwa, H. Tanaka, H. Ogoshi, *ibid. 111* (1989) 1912; h) T. Sasaki, E. T. Kaiser, *ibid. 111* (1989) 380; i) I. O. Sutherland, *Pure Appl. Chem. 61* (1989) 1547; j) H. L. Anderson, C. A. Hunter, J. K. M. Sanders, *J. Chem. Soc. Chem. Commun. 1989*, 226; k) K. Eshima, Y. Matsushita, E. Hasegawa, H. Nishide, E. Tsuchida, *Chem. Lett. 1989*, 381.
[9] F. Diederich, *Angew. Chem. 100* (1988) 372; *Angew. Chem. Int. Ed. Engl. 27* (1988) 362.
[10] a) K. Korzekwa, W. Trager, M. Gouterman, D. Spangler, G. H. Loew, *J. Am. Chem. Soc. 107* (1985) 4273. b) C. K. Chang, F. Ebina, *J. Chem. Soc. Chem. Commun. 1981*, 778; c) J. R. L. Smith, P. R. Sleath, *J. Chem. Soc. Perkin Trans. II 1982*, 1009.
[11] M. T. Fisher, S. G. Sligar, *J. Am. Chem. Soc. 107* (1985) 5018.
[12] Elemental analysis (C,H,N), and spectroscopic data (IR, 500-MHz, ^{1}H NMR, UV/VIS, EI-MS, and FAB-MS) support the structures proposed for all new compounds; see also Table 1. The bis(hydrobromide) **3** was analyzed as the dihydrate.
[13] F. Diederich, K. Dick, D. Griebel, *J. Am. Chem. Soc. 108* (1986) 2273.
[14] a) J. E. Baldwin, M. J. Crossley, T. Klose, E. A. O'Rear III, M. K. Peters, *Tetrahedron 38* (1982) 27; b) G. P. Arsenault, E. Bullock, S. F. MacDonald, *J. Am. Chem. Soc. 82* (1960) 4384.
[15] G. M. Badger, R. A. Jones, R. L. Laslett, *Aust. J. Chem. 17* (1964) 1157.
[16] The concentration ranges for the ^{1}H NMR titrations were chosen to provide approximately 20–90% complexation of the arene present at constant total concentration. The resonances of the guest protons marked in Figure 1 were evaluated, and the binding data in Table 2 are averaged data. Example: [**1**] = 1.16–15.9 mM and [acenaphthylene] = 5.01 mM. 1-H: $\Delta\delta_{max/obs.} = 2.51$, $\Delta\delta_{sat/calcd} = 2.75$: $K_a = 1029$, 4-H: $\Delta\delta_{max/obs.} = 2.22$, $\Delta\delta_{sat/calcd} = 2.42$: $K_a = 1075$. K_a (average) = 1052 L mol^{-1}.
[17] Macromodel Version 2.6, Professor *W. C. Still*, Columbia University, New York.
[18] In 2,2,2-trifluoroethanol (ROH), iodosobenzene presumably is present as PhI(OH)OR: see T. G. Traylor, J. C. Marsters, Jr., T. Nakano, B. E. Dunlap, *J. Am. Chem. Soc. 107* (1985) 5537.
[19] The Hückel bond order of the C1–C2 bond in acenaphthylene (0.7956) is intermediate between that of the C–C bonds in benzene (0.6666) and ethylene (1.000); E. Heilbronner, P. A. Straub: *Hückel Molecular Orbitals*, Springer, Berlin 1966.
[20] D. B. Smithrud, F. Diederich, *J. Am. Chem. Soc. 112* (1990) 339.
[21] Prof. *T. G. Traylor*, University of California, San Diego, personal communication.

High-Pressure NMR Studies of $[(\eta^3\text{-}C_5H_5)(\eta^5\text{-}C_5H_5)Cr(CO)_2]$. Evidence for Concerted Ring Interchange

By *John M. Millar, Rodney V. Kastrup, Suzanne Harris,** and *István T. Horváth**

Dedicated to Professor György Bor on the occasion of his 65th birthday

Reversible ring slippage of coordinatively saturated sandwich and half-sandwich complexes is a possible path to accommodate ligand activation in homogeneous catalytic reactions.[1] The reversible reaction of $[(\eta^5\text{-}C_5H_5)_2Cr(CO)]$ (**1**) with CO at elevated pressure has recently been studied [Eq. (a)].[2] On the basis of high-pressure IR spectral data, the formation of the ring-slipped species $[(\eta^3\text{-}C_5H_5)(\eta^5\text{-}C_5H_5)Cr(CO)_2]$ (**2**), analogous to the structurally characterized complex $[(\eta^3\text{-}C_5H_5)(\eta^5\text{-}C_5H_5)W(CO)_2]$,[3] was suggested. We now wish to report that **2** undergoes concerted ring interchange, with an activation barrier of 13.5 ± 1.0 kcal mol^{-1}, which does not involve CO-elimination-induced $\eta^3 \rightarrow \eta^5$ ring slippage or CO-addition-induced $\eta^5 \rightarrow \eta^3$ ring slippage.

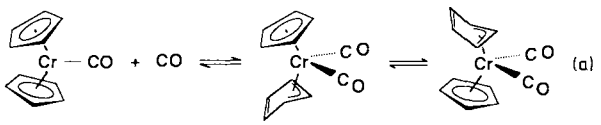

1 **2**

Reaction of $[(\eta^5\text{-}C_5H_5)_2Cr]$ with CO at 1.5 atm resulted in the formation of **1**.[4] The ^{13}C NMR spectrum of **1** at room temperature shows a resonance at $\delta = 75.9$ for the C_5H_5 ligands and another at $\delta = 263.1$ for the carbonyl ligand (Fig. 1, top), while the ^1H NMR spectrum shows a singlet at $\delta = 4$ for the C_5H_5 ligands. When the CO pressure was increased to 130 atm, the intensity of the peak at $\delta = 75.9$ in the ^{13}C NMR spectrum decreased and a new singlet appeared at $\delta = 96.9$ (Fig. 1, middle). Similarly, the ^1H NMR spectrum showed a new singlet at $\delta = 5.2$, while the intensity of the peak at $\delta = 4$ decreased. The new resonances are due to the formation of **2**, which at room temperature undergoes ring interchange. Surprisingly, there was only one resonance in the carbonyl region at $\delta = 259.4$, slightly shifted from the value observed for **1**. The ratio of its intensity to the combined intensity of the signals for the C_5H_5 ligands in **1** and **2**, however, clearly indicates that the former resonance is due to the carbonyls of both **1** and **2**.

On cooling to 0 °C, the peak at $\delta = 75.9$ disappeared, as expected from the temperature dependence of equilibrium (a),[2] and only **2** is present in the solution. Upon further cooling, the peak at $\delta = 96.9$ broadened and coalesced at -15 °C. Two singlets of equal intensity at $\delta = 89.0$ and 102.7 were resolved on cooling to -70 °C (Fig. 1, bottom). Although this proves the presence of two different C_5H_5 ligands in **2**, rotation of the η^3- and η^5-C_5H_5 ligands renders the ring carbon atoms equivalent even at -140 °C in a 1:1 mixture of $[D_8]$toluene and CD_2Cl_2. Simulations of the ^{13}C NMR spectrum at various temperatures give 76000 s^{-1} as the rate of exchange of the two C_5H_5 ligands at

[*] Dr. I. T. Horváth, Dr. R. V. Kastrup, Dr. J. M. Millar, Dr. S. Harris
Corporate Research Science Laboratories
Exxon Research and Engineering Company
Annandale, NJ 08801 (USA)

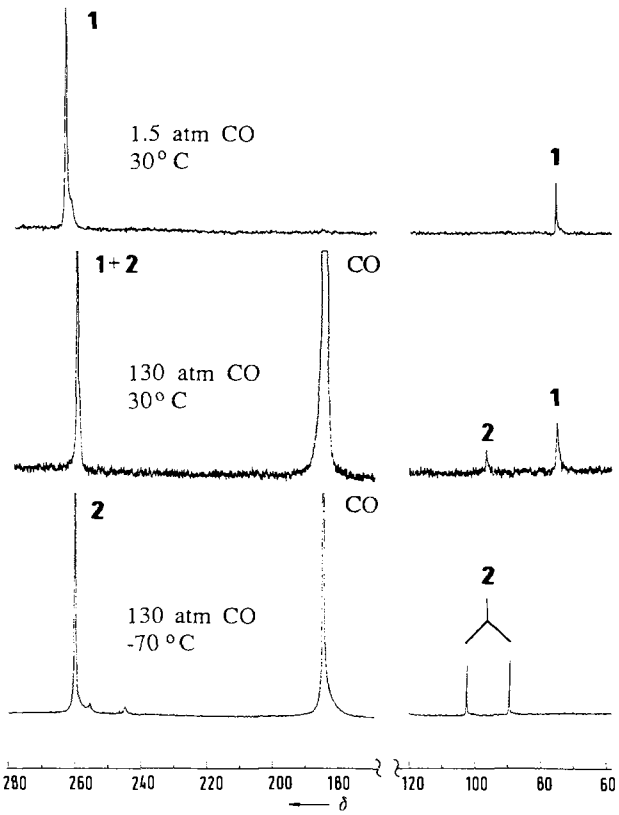

Fig. 1. ^{13}C NMR spectra of $[(C_5H_5)_2Cr]$ under 1.5 atm of ^{13}CO at 30 °C and under 130 atm of ^{13}CO at 30 °C and -70 °C. The extremely weak signals at $\delta = 256$ and 245 are due to $[(\eta^5\text{-}C_5H_5)_2Cr_2(CO)_6]$, which is formed above 0 °C under CO pressure [2].

room temperature and an energy of activation of 13.5 ± 1 kcal mol^{-1} (Fig. 2). As expected from the variable-temperature ^{13}C NMR results, two different rings are resolved in the low-temperature ^1H NMR spectrum as well.

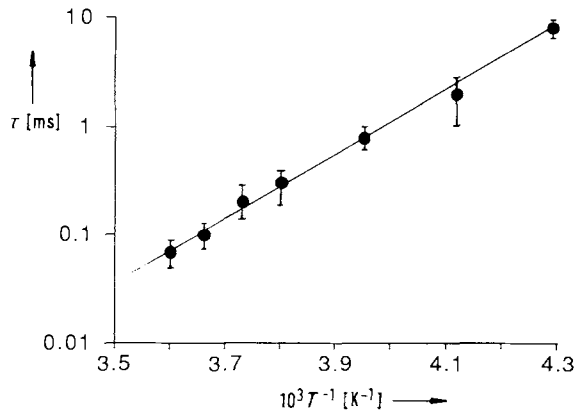

Fig. 2. Arrhenius plot for the concerted η^3/η^5 ring interchange in $[(\eta^3\text{-}C_5H_5)(\eta^5\text{-}C_5H_5)Cr(CO)_2]$ (**2**).

Saturation-transfer experiments do not show any evidence for exchange between the coordinated CO ligands in **2** and free CO. Our measurements indicate an upper limit of 10 s^{-1} for this process at room temperature. Mechanistically, it is clear that **2** undergoes concerted ring interchange, which does not involve CO-elimination-induced $\eta^3 \rightarrow \eta^5$ ring slip-

page followed by CO-addition-induced $\eta^5 \rightarrow \eta^3$ ring slippage. An examination and comparison of the electronic structures of $[(\eta^5\text{-}C_5H_5)_2M(CO)_2]$ and $[(\eta^3\text{-}C_5H_5(\eta^5\text{-}C_5H_5)M(CO)_2]$ complexes suggest why and how a ring interconversion not requiring loss of a CO ligand occurs in **2**. Strong M-to-CO π back-donation is generally observed in 18-electron $[(\eta^5\text{-}C_5H_5)_2M(CO)_x]$ complexes,[6, 7] and we find that this π back-donation becomes even more important in a complex such as **2**.

Recent calculations for $[(C_5H_5)_2M(CO)_2]$, M = Ti, Zr, show that the ordering of the lower-energy metal-based orbitals is as shown in Figure 3a.[7] The HOMO in the 18-electron (d^2) Ti and Zr complexes is an a_1 orbital which facilitates back-donation from the metal to the CO π^* orbitals lying in the plane of the CO ligands. The two lowest-energy unoccupied orbitals are the b_1 and a_2 orbitals. These orbitals are antibonding between the metal and C_5H_5 orbitals (this interaction is not shown in Fig. 3), but are stabilized by bonding interactions with the CO π^* orbitals which are perpendicular to the plane of the two CO ligands. The addition of two more electrons in $[(C_5H_5)_2M(CO)_2]$, M = Cr, Mo, W, leads to a formally 20-electron complex, and the unusual bent, rather than merely slipped, η^3-C_5H_5 configuration observed for one of the C_5H_5 rings in $[(\eta^3\text{-}C_5H_5)(\eta^5\text{-}C_5H_5)W(CO)_2]$ is usually associated with the attainment of a formally 18-electron complex. In order to better understand the effects of this bent C_5H_5 ring, Fenske–Hall[8] MO calculations were carried out for $[(\eta^3\text{-}C_5H_5)(\eta^5\text{-}C_5H_5)W(CO)_2]$. The results of these calculations show that the bending of the C_5H_5 ring and the resulting C_s symmetry lead to a loss of most of the M–C_5H_5 antibonding character in the b_1 (now a') orbital (Fig. 3b). As a result, this orbital is

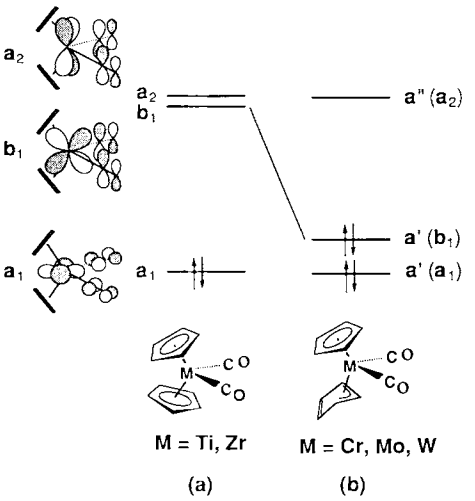

Fig. 3. Lowest-energy metal-based orbitals for $[(C_5H_5)_2M(CO)_2]$ complexes in which (a) both C_5H_5 rings are bound to the metal via a normal η^5-coordination mode and (b) one of the C_5H_5 rings binds to the metal via the unusual bent η^3-coordination mode.

significantly stabilized in the W complex (and presumably in the Mo and Cr complexes) and becomes the HOMO. The occupation of this orbital in the W, Mo, or Cr complex leads to increased back-donation to the CO π^* orbitals, which in turn stabilizes the complex. Both sets of CO π^* orbitals now accept charge from the metal. The significant degree of back donation is consistent both with the CO vibrational frequencies in **2** (the average of the two CO stretching frequencies in **2** is close to the single CO stretching frequency in **1**)[2] and with the similar ^{13}C NMR chemical shifts for the carbonyl ligands in **1** and **2**.

In light of the strong M–CO back-donation observed in the dicarbonyl complex **2**, it is perhaps not surprising that the concerted ring interchange does not involve elimination or addition of a CO ligand. Interconversion of the two rings (the bent η^3 and the flat η^5 rings) presumably occurs through a simultaneous straightening and bending of the two rings. The intermediates involved in such a conversion would continue to be stabilized by π back-donation, since even though the a' (b_1) orbital would be somewhat destabilized during the process, this orbital would remain occupied and serve to remove charge from the metal throughout the whole process.

Received: September 12, 1989 [Z 3548 IE]
German version: *Angew. Chem. 102* (1990) 216

CAS Registry number:
2, 123892-90-0.

[1] J. M. O'Connor, C. P. Casey, *Chem. Rev. 87* (1987) 307.
[2] E. U. van Raaij, H. H. Brintzinger, *J. Organomet. Chem. 356* (1988) 315.
[3] G. Huttner, H. H. Brintzinger, L. G. Bell, P. Friedrich, V. Bejenke, D. Neugebauer, *J. Organomet. Chem. 145* (1978) 329.
[4] Compound **1** was prepared in situ in a high-pressure sapphire NMR tube [5] by allowing 0.1 g of chromocene (Strem) in 3 mL of $[D_8]$toluene/CD_2Cl_2 (1/1) (or in 3 mL of $[D_8]$toluene) to react with ^{13}CO (99.9% isotopic purity, Isotech Inc.) at 1.5 atm pressure. After the formation of **1** was confirmed, the tube was charged with 130 atm ^{13}CO at room temperature. Variable-temperature NMR spectra were obtained on Bruker MSL 300 and Varian XL 300 instruments operating at 75 MHz for carbon.
[5] D. C. Roe, *J. Magn. Reson. 63* (1985) 388.
[6] J. W. Lauher, R. Hoffmann, *J. Am. Chem. Soc. 98* (1976) 1729.
[7] M. Casarin, E. Ciliberto, A. Gulino, I. Fragala, *Organometallics 8* (1989) 900.
[8] M. B. Hall, R. F. Fenske, *Inorg. Chem. 11* (1972) 768.

Mixed Kolbe Electrolyses with Sugar Carboxylic Acids**

By *Andreas Weiper* and *Hans J. Schäfer**

Dedicated to Professor Christoph Rüchardt on the occasion of his 60th birthday

Carboxylic acids can be decarboxylated to give radicals and/or carbocations by anodic oxidation. Dimers or the products of addition to double bonds are accessible via the radical pathway (Kolbe electrolysis).[1] The cationic pathway (non-Kolbe electrolysis) can give esters, ethers, acetals, and olefins as well as fragmentation and rearrangement products.[1c, 2] The pathway taken is determined not only by the reaction conditions (pH of the electrolyte, kind of electrode material, added salts, current density) but also, to a large extent, by the structure of the carboxylic acid. For example, carboxylic acids bearing hydrogen atoms or electron-withdrawing substituents on the α-carbon atom preferentially afford dimers, whereas carboxylic acids bearing alkyl or aryl groups or electron-donating substituents on the α-carbon atom give primarily or exclusively products arising from

[*] Prof. Dr. H. J. Schäfer, Dipl.-Chem. A. Weiper
Organisch-chemisches Insitut der Universität
Corrensstrasse 40, D-4400 Münster (FRG)

[**] Electroorganic Synthesis, Part 46. This work was supported by the Bundesministerium für Forschung und Technologie and by the Fonds der Chemischen Industrie. Part 45: R. Schneider, H. J. Schäfer, *Synthesis 1989*, 742.

Table 1. Coelectrolysis of sugar carboxylic acids with substituted and unsubstituted alkanoic acids.

Sugar carboxylic acid **1**	Coacid **2** [a]	Product **3** [b] (Yield)
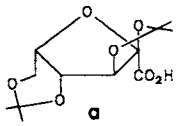 **a**	$HO_2C-(CH_2)_3-OAc$ **a**	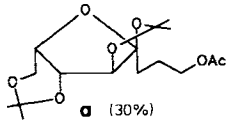 **a** (30%)
a	$HO_2C-(CH_2)_2-CO_2Me$ **b**	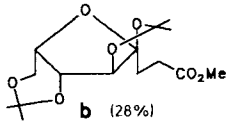 **b** (28%)
a	$HO_2C-C_7H_{15}$ **c**	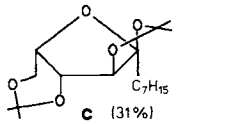 **c** (31%)
a	$HO_2C-C_{11}H_{23}$ **d**	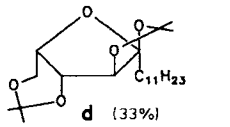 **d** (33%)
a	$HO_2C-(CH_2)_{10}-Br$ **e**	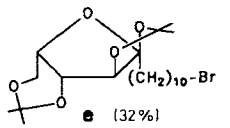 **e** (32%)
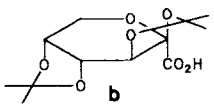 **b**	$HO_2C-C_7H_{15}$ **c**	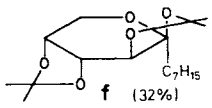 **f** (32%)
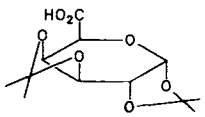 **c**	$HO_2C-C_7H_{15}$ **c**	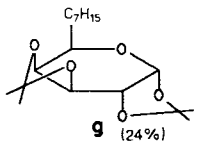 **g** (24%)
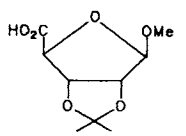 **d**	$HO_2C-C_7H_{15}$ **c**	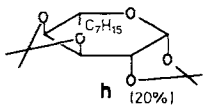 **h** (20%)
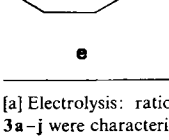 **e**	$HO_2C-C_7H_{15}$ **c**	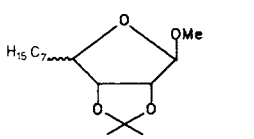 **i** (40% [c]) 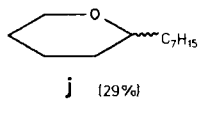 **j** (29%)

[a] Electrolysis: ratio sugar carboxylic acid/coacid = 1/10. [b] Compounds **3a–j** were characterized unequivocally by elemental analysis, ^1H NMR spectroscopy, and mass spectrometry. [c] Isomeric mixture: 1/2.04.

cations. Thus, in the anodic decarboxylation of sugar carboxylic acids and of tetrahydropyran-2-carboxylic acids, acetals were isolated but no coupling products.[3]

We have now found that, in the presence of coacids (ratio 1:10), sugar carboxylic acids can be coupled to give satisfactory yields of unsymmetrical coupling products (Table 1).

In addition, the reaction gives products in which the carboxyl group is replaced by a methoxy group and which presumably are formed from cationic intermediates. Coupling of **1a** in the absence of coacid to give a symmetrical dimer has only been accomplished in yields of less than 5%. Electrolysis of **1a** at a graphite anode affords **4** in 85% yield. By contrast, electrolysis of **1c** in the presence of octanoic acid as coacid gives, in addition to **3g** and **3h**, two further products in 43% and 9% yield, respectively, which were shown to be probably **5** and the dimer of **1c**, respectively.

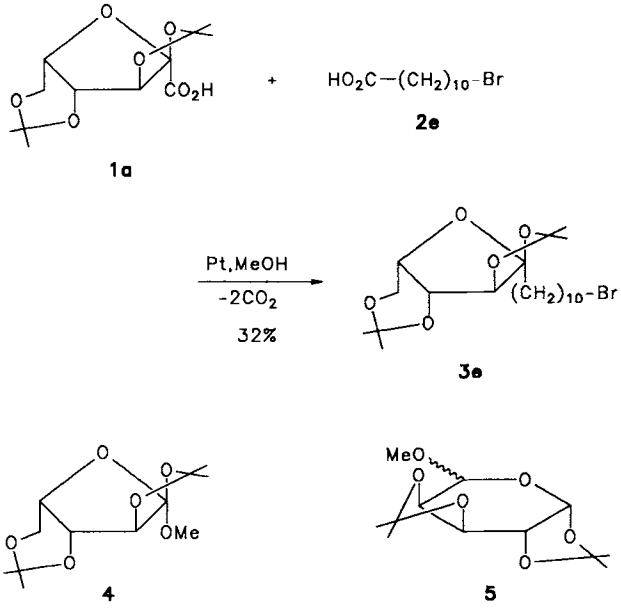

The occurrence of radical coupling despite the favorable conditions for a cationic pathway appears to be due, at least in part, to the simultaneous decarboxylation of the coacids. The alkyl radicals thereby formed apparently couple with part of the α-alkoxymethylene radicals, before these can be further oxidized to cations. In the absence of coacids, radical reactions play only a minor role.

The sugar carboxylic acids are accessible in a one-step reaction from the corresponding protected sugars by oxidation at a nickel hydroxide electrode.[4] The reaction described here offers a simple route for CC coupling of substituted alkyl moieties with carbohydrates.

Experimental Procedure

Preparation of 1,2:3,4-di-*O*-isopropylidene-6-deoxy-6-*n*-hexyl-D-galactopyranose (**3g**) and 1,2:3,4-di-*O*-isopropylidene-6-deoxy-6-*n*-hexyl-L-altropyranose (**3h**): Octanoic acid (2.88 g, 20 mmol) and **1c** (548 mg, 2 mmol) were dissolved in 30 mL of methanol, neutralized to 10% with potassium methoxide, and electrolyzed in a glass-beaker cell [5] at Pt electrodes with a current density of 200 mA cm^{-2} at 40 °C (current consumption: 1.2 F mol^{-1}). The electrolyte was concentrated to about 10 mL and added to 100 mL of saturated $NaHCO_3$ solution. The resulting solution was saturated with NaCl and then extracted with ether (5 × 30 mL). The organic phases were combined and dried ($MgSO_4$), and the solvent was evaporated. The remaining mixture of products was separated by flash chromatography (eluent: petroleum ether/ether, 20/1 and 10/1) to give 128 mg (20%) of **3h** and 153 mg (24%) of **3g**. GC-MS indicated that compound **5** (ca. 43% based on **1c**) and the dimer of **1c** (ca. 9% based on **1c**) were also present. **3g**: ^1H NMR (300 MHz, $CDCl_3$): δ = 0.8 (t, ^3J = 6.7 Hz, 3H; 12-H), 1.16–1.70 (m, 24H), 3.64 (m, 1H; 5-H), 4.06 (dd, $J_{3,4}$ = 7.9, $J_{4,5}$ = 1.7 Hz, 1H; 4-H), 4.22 (dd, $J_{1,2}$ = 5.1, $J_{2,3}$ = 2.3 Hz, 1H; 2-H), 4.51 (dd,

1H; 3-H), 5.47 (d, 1H; 1-H). GC-MS (70 eV): m/z 328 ($M^{\oplus}$, 0.5%), 313 (M-CH_3, 22), 282(3), 255(4), 195(12), 167(10), 113(60), 100(100). $[\alpha]_D^{20} = -77.8$ ($c = 1.24$ in $CHCl_3$). **3h**: ^{1}H NMR (300 MHz, $CDCl_3$): $\delta = 0.8$ (t, $^3J = 6.6$ Hz, 3H; 12-H), 1.19–1.70 (m, 24H), 3.07 (m, 1H; 5-H), 3.81 (dd, $J_{3,4} = 5.4$, $J_{4,5} = 9.6$ Hz, 1H; 4-H), 4.14 (d, $J_{1,2} = 2.5$ Hz, 1H; 2-H), 4.43 (d, 1H; 3-H), 5.14 (d, 1H; 1-H). GC-MS (70 eV) as for **3g**. $[\alpha]_D^{20} = -50.2$ ($c = 0.96$ in $CHCl_3$).

Received: September 19, 1989 [Z 3555 IE]
German version: *Angew. Chem. 102* (1990) 228

[1] a) L. Eberson, J. H. P. Utley in M. M. Baizer (Ed.): *Organic Electrochemistry* 2nd ed., Dekker, New York 1983, p. 435; b) H. J. Schäfer, *Angew. Chem. 93* (1981) 978; *Angew. Chem. Int. Ed. Engl. 20* (1981) 911; c) H. J. Schäfer, *Top. Curr. Chem. 152* (1990) 91.
[2] S. Torii: *Electroorganic Syntheses, Methods and Applications, Pt. 1: Oxidations*, VCH, Weinheim 1985.
[3] a) M. Yoshikawa, T. Kamigauchi, Y. Ikeda, I. Kitagawa, *Chem. Pharm. Bull. 29* (1981) 2571, 2582; *Heterocycles 15* (1981) 349; b) P. G. M. Wuts, C. Sutherland, *Tetrahedron Lett. 23* (1982) 3987.
[4] a) P. Seiler, P. M. Robertson, *Chimia 36* (1982) 305; b) R. Schneider, H. J. Schäfer, unpublished.
[5] H. J. Schäfer, *Kontakte (Darmstadt) 1987*, No. 2, p. 17.

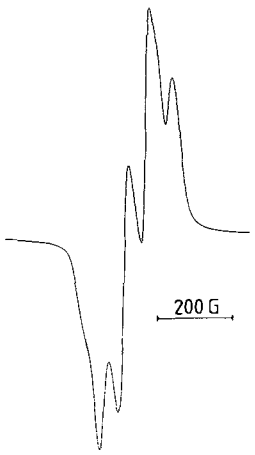

Fig. 1. ESR spectrum of $[Au([9]aneS_3)_2]^{2\oplus}$ in CH_3CN at 77 K.

Bis(1,4,7-trithiacyclononane)gold Dication: A Paramagnetic, Mononuclear Au^{II} Complex**

By *Alexander J. Blake, John A. Greig, Alan J. Holder, Timothy I. Hyde, Anne Taylor,* and *Martin Schröder**

We have shown previously that the potentially six-electron donor macrocycle [9]aneS$_3$ (1,4,7-trithiacyclononane), which prefers to bind metal ions facially,[1,2] is capable of modifying its coordination to accommodate a range of transition-metal stereochemistries.[3] As part of a study of third-row transition-metal complexes of [9]aneS$_3$,[3b] we report herein the preparation of $[Au([9]aneS_3)_2]^{2\oplus}$, the first structurally characterized mononuclear Au^{II} complex.

Reaction of $KAuCl_4$ with two molar equivalents of [9]aneS$_3$ in refluxing aqueous HBF_4(40%)/MeOH affords a reddish brown solution, which was extracted with CH_3NO_2 after addition of water. The CH_3NO_2 solution was filtered, the solvent removed in vacuo, and the residue taken up in CH_3CN. Vapor diffusion with diethyl ether afforded the complex $[Au([9]aneS_3)_2](BF_4)_2$ in 50% yield. $[Au([9]aneS_3)_2]^{2\oplus}$ shows characteristic UV/VIS absorption bands at $\lambda_{max} = 398$ ($\varepsilon = 7990$), 234 nm ($\varepsilon = 15000\ M^{-1}\ cm^{-1}$) and a strong signal in the ESR spectrum at $g_{av} = 2.010$ (77 K). Hyperfine coupling to ^{197}Au ($I = 3/2$, 100%) is observed clearly with $A_{av} = 57.3$ G (Fig. 1).

Crystals of $[Au([9]aneS_3)_2](BF_4)_2 \cdot 2CH_3CN$ suitable for X-ray diffraction were grown from CH_3CN/Et_2O. The single-crystal X-ray structure[4] of the complex (Fig. 2) confirms unequivocally its assignment as a genuine, mononuclear d^9 Au^{II} species: in the centrosymmetric cation, Au^{II} is bound to six thioether donors in a tetragonally elongated stereochemistry (Au-S1 2.839(5), Au-S4 2.462(5), Au-S7 2.452(5) Å). The two [9]aneS$_3$ macrocycles therefore encapsulate the d^9 Au^{II} center to give a Jahn–Teller-distorted octahedral stereochemistry. Interestingly, the related d^9 complex cation $[Cu([9]aneS_3)_2]^{2\oplus}$ also shows an octahedral stereochemistry, although in this case the tetragonal elongation is less than in the Au^{II} analogue (Cu-S1 2.419(3), Cu-S4 2.426(3), Cu-S7 2.459(3) Å[1]).

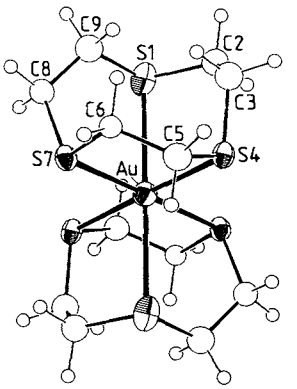

Fig. 2. Structure of the cation $[Au([9]aneS_3)_2]^{2\oplus}$.

$[Au([9]aneS_3)_2]^{2\oplus}$ is air-stable in the solid state. It can be reduced in MeOH or more slowly in CH_3CN to a colorless d^{10} Au^{I} species, $[Au([9]aneS_3)_2]^{\oplus}$ ($E_{pc} = +0.10$ V vs $Fc^{\oplus}$/Fc, Fc = ferrocene), and can be oxidized to the corresponding d^8 Au^{III} complex $[Au([9]aneS_3)_2]^{3\oplus}$ ($E_{\frac{1}{2}} = +0.46$ V vs $Fc^{\oplus}$/Fc).[3b] When the oxidation of Au^{II} to Au^{III} ($\lambda_{max} = 334$ ($\varepsilon = 19765$), 246 nm ($\varepsilon = 20265\ M^{-1}\ cm^{-1}$)) is monitored by UV/VIS spectroscopy, isosbestic points ($\lambda_{iso} = 372$, 208 nm) are observed. The chemical synthesis of $[Au([9]aneS_3)_2]^{2\oplus}$ depends on control of these redox reactions. Isolation of the Au^{II} species from electrosynthesis experiments is hampered by problems associated with removing the base electrolyte and purifying the complex.

Very few examples of mononuclear Au^{II} species have been reported in the literature. Most of these examples are transient or intermediate species or involve significant charge delocalization onto the ligands (e.g., $[Au(mnt)_2]^{2\ominus}$, mnt = 2,3-dimercapto-2-butanedinitrile[5]). The ligand [9]aneS$_3$ is redox-inactive up to +0.99 V (vs $Fc^{\oplus}$/Fc),[2] suggesting that delocalization of the positive charge in $[Au([9]aneS_3)_2]^{2\oplus}$ onto the thioether donors will be limited. The coordination about the Au center in $[Au([9]aneS_3)_2]^{2\oplus}$ is fully consistent with that of a d^9 transition-metal center and reflects the ability of [9]aneS$_3$ to encapsulate and stabilize an otherwise highly reactive metal radical center. Interestingly, we have found that the hexathia ligand [18]aneS$_6$ is also capable

[*] Dr. A. J. Blake, J. A. Greig, Dr. A. J. Holder, Dr. T. I. Hyde, A. Taylor, Dr. M. Schröder
Department of Chemistry, University of Edinburgh
West Mains Road, GB-Edinburgh EH9 3JJ (Scotland)

[**] We thank the British Science and Engineering Research Council (SERC) for support and Amersham International Plc and SERC for a CASE Award to JAG.

of stabilizing Au^{I}, Au^{II} and Au^{III} centers in the complexes $[Au([18]aneS_6)]^{\oplus/2\oplus/3\oplus}$, respectively.

Received: September 4, 1989 [Z 3536 IE]
German version: *Angew. Chem. 102* (1990) 203

[1] R. S. Glass, W. N. Setzer, C. A. Ogle, G. S. Wilson, *Inorg. Chem. 22* (1983) 266.

[2] K. Wieghardt, H.-J. Küppers, J. Weiss, *Inorg. Chem. 24* (1985) 3067; H.-J. Küppers, A. Neves, C. Pomp, D. Ventur, K. Wieghardt, B. Nuber, J. Weiss, *ibid. 25* (1986) 2400.

[3] a) M. Schröder, *Pure Appl. Chem. 60* (1988) 517, and references therein; M. N. Bell, A. J. Blake, R. O. Gould, A. J. Holder, T. I. Hyde, A. J. Lavery, G. Reid, M. Schröder, *J. Inclusion Phenom. 5* (1987) 169; b) A. J. Blake, R. O. Gould, J. A. Greig, A. J. Holder, T. I. Hyde, M. Schröder, *J. Chem. Soc. Chem. Commun. 1989*, 876.

[4] Structure determination of $[Au([9]aneS_3)_2]^{2\oplus} \cdot 2BF_4^{\ominus} \cdot 2CH_3CN$: An orange-red column-shaped crystal ($0.55 \times 0.3 \times 0.2$ mm), bathed in mother liquor, was sealed in a Lindemann capillary tube and cooled to 173 ± 0.1 K on a Stoe STADI-4 four-circle diffractometer equipped with an Oxford Cryosystems low-temperature device [6]. $M_r = 813.28$, orthorhombic, space group *Pcab*, $a = 8.6921(13)$, $b = 14.823(3)$, $c = 21.5687(23)$ Å, $V = 2779.0$ Å^3 [from 2Θ values of 42 reflections measured at $\pm\omega(2\Theta = 24 \rightarrow 26°$, $\lambda = 0.71073$ Å)], $T = 173$ K, $\varrho_{calcd} = 1.944$ g cm^{-3}, $Z = 4$, $\mu(Mo_{K\alpha}) = 5.781$ mm^{-1}, $T = 173$ K, $\omega - 2\Theta$ scans, 2715 reflections measured ($2\Theta_{max} = 45°$), 1586 unique ($R_{int} = 0.022$), initial correction for absorption by means of ψ scans, giving 1146 data with $F \geq 4\sigma(F)$. Intensity statistics indicated the position of the Au atom on an inversion center and, using this information, DIRDIF [7] located the S atoms. Iterative rounds of least-squares refinement and difference Fourier synthesis [8] then located all other non-H atoms. At isotropic convergence, final corrections for absorption were made using DIFABS [9]. Some disorder in the $BF_4^{\ominus}$ anion required modeling. H atoms were included in fixed, calculated positions [8]. At final convergence, $R, R_w = 0.0663$ and 0.0859, respectively, for 123 parameters, $S = 1.209$. The maximum and minimum residues in the final ΔF syntheses were $+1.50$ and -1.21 eÅ^{-3} respectively. Further details of the crystal structure investigation are available on request from the Director of the Cambridge Crystallographic Data Centre, University Chemical Laboratory, Lensfield Road, Cambridge CB2 1EW (UK), on quoting the full journal citation.

[5] R. J. Puddephatt in G. Wilkinson, R. D. Gillard, J. A. McCleverty (Eds): *Comprehensive Coordination Chemistry, Vol. 5*, Pergamon Press, Oxford 1987, chapter 54, p. 861; A. MacCragh, W. S. Koski, *J. Am. Chem. Soc. 87* (1965) 2496; J. H. Waters, H. B. Gray, *ibid. 87* (1965) 3534; I. F. Warren, M. F. Hawthorne, *ibid. 90* (1968) 4823; J. H. Waters, T. J. Bergendahl, S. R. Lewis, *J. Chem. Soc. Chem. Commun. 1971*, 834; R. Kirmse, B. Lorenz, W. Windsch, E. Hoyer, *Z. Anorg. Allg. Chem. 384* (1971) 160; T. J. Bergendahl, E. M. Bergendahl, *Inorg. Chem. 11* (1972) 638; R. L. Schlupp, A. H. Maki, *ibid. 13* (1974) 44; J. G. M. Rens, M. P. A. Viegers, E. de Boer, *Chem. Phys. Lett. 28* (1974) 104; T. J. Bergendahl, J. H. Waters, *Inorg. Chem. 14* (1975) 2556; W. S. Crane, H. Beall, *Inorg. Chim. Acta 31* (1978) L469, and references therein.

[6] J. Cosier, A. M. Glazer, *J. Appl. Crystallogr. 19* (1986) 105.

[7] DIRDIF: P. T. Beurskens, W. P. Bosman, H. M. Doesbury, T. E. M. van den Hark, P. A. J. Prick, J. H. Noordik, G. Beurskens, R. O. Gould, V. Parthasarathia, *Applications of Direct Methods to Difference Structure Factors*, University of Nijmegen, Netherlands, 1983.

[8] SHELX76: G. M. Sheldrick, *Program for Crystal Structure Determinations*, University of Cambridge 1976.

[9] DIFABS: N. Walker, D. Stuart, *Program for Empirical Absorption Corrections, Acta Crystallogr. Sect. A 39* (1983) 158.

$[H_2Ru_6(CO)_{16}(\mu\text{-}C_6H_4O)]$: Binding of Five Metal Atoms to a Phenol Molecule**

By *D. Scott Bohle*, and *Heinrich Vahrenkamp**

Alcohols, esters and similar compounds belong to the important products of metal-catalyzed CO hydrogenation, e.g. in the Fischer-Tropsch reaction or the synthesis of methanol.[1] Since, as end products of such reactions they form only moderately stable carbonylmetal complexes, they are seldom investigated as ligands.[2] With the aim of also testing the soundness of the cluster-surface analogy[3] on them with regard to structure and reactivity we turned our attention to the cluster chemistry of organic OH-compounds. Here, some important bond types are known,[4] but also the observation that one synthesizes $Os_3(CO)_{12}$ in alcohol,[5] and the comment about $Ru_3(CO)_{12}$, "the corresponding reactions with alcohols are complex and will be reported later".[6]

Twenty years and one publication[7] later we now find that the complexation of organic oxo compounds with carbonylruthenium compounds can be controlled on a preparative scale. To demonstrate this, we present the title complex $[H_2Ru_6(CO)_{16}(\mu\text{-}C_6H_4O)]$, which is formed in almost 30% yield upon heating $Ru_3(CO)_{12}$ and an excess of phenol in boiling cyclohexane.[8]

The structure analysis (cf. Fig. 1[9]) gives a good indication of the course of the reaction: In the first step the oxidative addition of the phenol could lead to a complex $[Ru_3(CO)_{10}(\mu\text{-H})(\mu\text{-OR})]$,[7] which is still recognizable here in the form of the Ru1–Ru2–Ru3–O unit. The second Ru_3-unit could then be attacked in the sense of an *ortho*-metalation at the β-C atom of the phenol,[4b] opened by η^6-coordination of the phenol ring to Ru4, and condensed to the first Ru_3 unit via four new metal–metal bonds (Ru1–Ru4, Ru1–Ru5, Ru2–Ru5, Ru2–Ru6). This results in a highly puckered "raft" arrangement[10] of the ruthenium atoms, of which only Ru3 is not coupled to the phen-yl-olate ligand. Alternatively, the C_6H_4O–Ru_5 fragment can be regarded as a doubly *C*-metalated derivative of cyclohexadienone, even though the uniformity of the C–C bond lengths in the ring [139–144(1) pm] and the C–O distance of 136(1) pm, which corresponds to that in the free phenol, do not support this. The bridging Ru–O and Ru–C bonds (Ru1–O 217(1), Ru2–O 213(1), Ru5–C 234(1), Ru6–C 221(1) pm) of the phen-yl-olate ligand lie in the known range;[2,4] however, the asymmetry of the Ru5–C–Ru6 bridge and the very long Ru5–C distance are striking. The two hydride ligands are presumably over the two longest edges least shielded by CO groups, namely Ru2–Ru3 (308 pm) and Ru2–Ru5 (311 pm); the remaining Ru–Ru bonds have lengths of 277–304 pm.

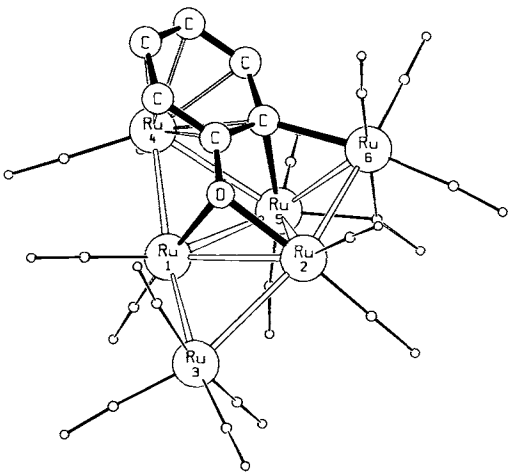

Fig. 1. Structure of $[H_2Ru_6(CO)_{16}(\mu\text{-}C_6H_4O)]$ in the crystal (schematic).

The C_6H_4O ligand counts as a 10-electron donor (6 e from the aromatic π-system, 1 e from the *ortho* metalation and 3 e

[*] Prof. Dr. H. Vahrenkamp, Dr. D. S. Bohle
Institut für Anorganische und Analytische Chemie der Universität
Albertstrasse 21, D-7800 Freiburg (FRG)

[**] This work was supported by the Volkswagen Foundation, the Fonds der Chemischen Industrie, and the Rechenzentrum der Universität Freiburg.

from the μ-OR unit). Together with the electrons of the 2 H- and 16 CO-ligands, the raft-shaped R_6-unit has 44 ligand electrons, two more than would be required to fulfill the 18-electron rule for all ruthenium ions. An electron excess of this kind has already been observed and theoretically justified in earlier works for structures of this type.[11]

The three bonding modes of the C_6H_4O fragment (η^6 of the arene, M–C–M three-center bonding, and μ-OR coordination) are each in themselves not unusual in Ru- and Os-complexes.[2] However, they are found together for the first time in the title complex. They demonstrate, on the one hand, how far the "loading" of such a simple molecule as phenol with metal atoms can go, and on the other, how multiple coordination can stabilize the very open metal atom arrangement. In the context of the cluster-surface analogy they draw attention to the possibility of multiple functionalization of the substrate (here of the phenol) and the deformability of the surface by attachment of the substrate.

Received: September 15, 1989 [Z 3550 IE]
German version: *Angew. Chem. 102* (1990) 202

CAS Registry numbers:
$H_2Ru_6(CO)_{16}(\mu\text{-}C_6H_4O)$, 124620-65-1; $Ru_3(CO)_{12}$, 15243-33-1; phenol, 108-95-2.

[1] R. A. Sheldon: *Chemicals from Synthesis Gas*, D. Reidel, Dordrecht 1983.
[2] Cf. for the most abundant carbonylmetal compounds G. Wilkinson, F. G. A. Stone, E. W. Abel (Eds.): *Comprehensive Organometallic Chemistry, Vol. 4*, Pergamon, Oxford 1982.
[3] E. L. Muetterties, T. N. Rhodin, E. Band, C. F. Brucker, W. R. Pretzer, *Chem. Rev. 79* (1979) 91.
[4] a) B. F. G. Johnson, J. Lewis, P. A. Kilty, *J. Chem. Soc. A 1968*, 2859; b) K. A. Azam, A. J. Deeming, I. P. Rothwell, M. B. Hursthouse, L. New, *J. Chem. Soc. Chem. Commun. 1978*, 1086.
[5] B. F. G. Johnson, J. Lewis, *Inorg. Synth. 13* (1972) 92.
[6] G. R. Crooks, B. F. G. Johnson, J. Lewis, I. G. Williams, *J. Chem. Soc. A 1969*, 797.
[7] S. Aime, M. Botta, R. Gobetto, D. Osella, F. Padovan, *J. Chem. Soc. Dalton Trans. 1987*, 253.
[8] 0.50 g (0.78 mmol) of $Ru_3(CO)_{12}$ and 0.74 g (7.8 mmol) of phenol, 4 d in 20 mL of boiling cyclohexane. After removal of C_6H_{12} and C_6H_5OH in vacuo, chromatography with hexane/CH_2Cl_2 (10:1 to 4:1) on silica gel. After separation of 0.20 g (40%) of $Ru_3(CO)_{12}$, 0.13 g (29%) of $[H_2Ru_6(CO)_{16}(\mu\text{-}C_6H_4O)]$ could be recovered. Black crystals, m.p. 180 °C (decomp.); IR (CH_2Cl_2): $\tilde{\nu}$ = 2122 w, 2083 m, 2051 vs, 2031 m, 1983 sh, 1957 m, 1791 w cm^{-1}; ^{1}H NMR ($CDCl_3$, int. TMS) ABCD pattern with signal centers at δ = 3.63, 4.27, 6.06 and 6.87, hydride signals at −11.78 and −21.72.
[9] Structural data: monoclinic, $C2/c$, a = 3686.5(5), b = 905.2(5), c = 1827.5(4) pm, β = 102.23(3)°, Z = 8, 3165 reflections, R = 0.038. Further details of the crystal structure investigation are available on request from the Fachinformationszentrum Karlsruhe, Gesellschaft für wissenschaftlich-technische Information mbH, D-7514 Eggenstein-Leopoldshafen 2 (FRG), on quoting the depository number CSD-54069, the names of the authors, and the journal citation.
[10] J. R. Goutsmith, B. F. G. Johnson, J. Lewis, P. R. Raithby, K. H. Whitmire, *J. Chem. Soc. Chem. Commun. 1982*, 640; *ibid. 1983*, 246.
[11] P. Sundberg, *J. Chem. Soc. Chem. Commun. 1987*, 1307; D. G. Evans, D. M. P. Mingos, *Organometallics 2* (1983) 435.

A Carbonyliron Complex of an Amino-9-fluorenylideneborane with Coordination at a Borabutadiene Unit

By *Sreelatha Channareddy, Gerald Linti,* and *Heinrich Nöth**

Alkylideneboranes, compounds of two-coordinate boron containing a B=C double bond, are kinetically stabilized by sterically demanding substituents.[1] In alkylidene(amino)-boranes an electronic component also contributes to the stability.[2] Nevertheless, 9-fluorenylidene(tetramethylpiperidino)borane **1**,[2a, b] is highly reactive due to the presence of a dicoordinated boron atom. Thus, **1** adds covalent metal and nonmetal halides, forming B–C metal/nonmetal bonds, and boron-containing heterocycles result from [2+2]- and [2+3]-cycloadditions.[2a, 3, 4] **1** can also function as an η^5- or η^2-ligand. Typical examples are $[(\eta^5\text{-tmpBClCR}_2)TiCl_3]$ and $[(\eta^2\text{-tmpBCR}_2)Fe(CO)_4]$[3a, 5] (tmp = 2,2,6,6-tetramethylpiperidino, CR_2 = 9-fluorenylidene). We have now observed an unusual behavior of **1** towards pentacarbonyliron.

Prolonged UV-irradiation of **1** in the presence of $Fe(CO)_5$ does not afford $[(\eta^2\text{-tmpBCR}_2)Fe(CO)_4]$ but the tricarbonyliron complex **2** [Reaction (1)]. Its carbonyl groups are equivalent on the NMR time scale at room temperature.[6] At 210 K, however, the ^{13}C-NMR spectrum shows three signals in a 1:1:1 ratio. In addition, there are four ^{1}H- and four ^{13}C-NMR signals for the methyl groups of the tetramethylpiperidino substituent as well as twelve ^{13}C-NMR signals for the fluorenylidene group. The fluorenylidene C-atom bound to boron is not observed due to quadrupolar broadening. These findings and the presence of three ν(CO) stretching bands in the IR spectrum are consistent with an asymmetric coordination of the $Fe(CO)_3$ unit to the ligand **1**.

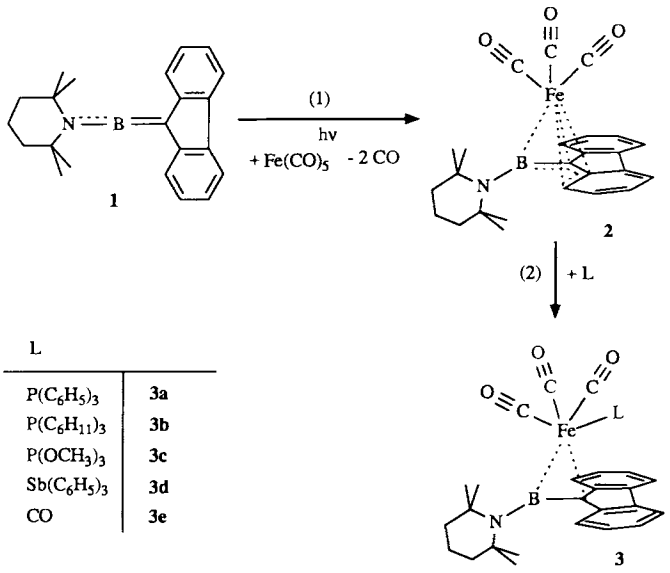

L	
$P(C_6H_5)_3$	**3a**
$P(C_6H_{11})_3$	**3b**
$P(OCH_3)_3$	**3c**
$Sb(C_6H_5)_3$	**3d**
CO	**3e**

This conclusion is further supported by the X-ray structure of **2**[7] (cf. Fig. 1). It demonstrates that the $Fe(CO)_3$ group is coordinated to a "borabutadiene" unit, B=C–C=C,[8] of the fluorenylideneborane moiety of **1**. This occupies two basal sites in the slightly distorted tetragonal pyramid, as is well established in other conjugated diene-metal complexes.[9] The B–C1 and C2–C3 bonds are 0.08 and 0.10 Å longer, while the C1–C2 bond is 0.04 Å shorter than in uncomplexed **1**;[4] this is indicative of a delocalization of electron density in the borabutadiene moiety. Such a bonding would imply the loss of aromaticity in the benzene ring to which the coordinated C=C-bond belongs. This is indeed reflected in the rest of the C–C bond lengths of this ring. On the other hand, the bond lengths in the uncoordinated benzene ring of **2** are normal.[10] Significant is also the fact that the Fe–C bond lengths vary considerably. The distances of

[*] Prof. Dr. H. Nöth, Dr. S. Channareddy, Dipl.-Chem. G. Linti
Institut für Anorganische Chemie der Universität München
Meiserstrasse 1, D-8000 München 2 (FRG)

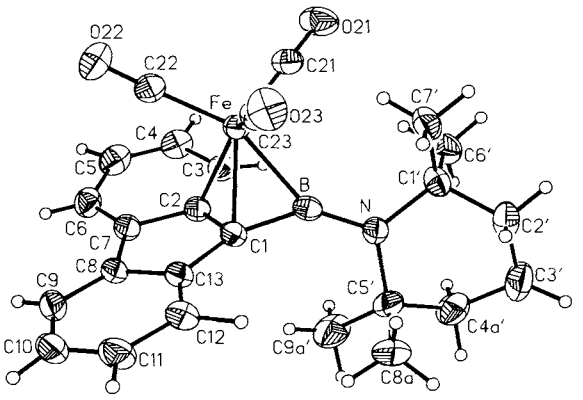

Fig. 1. ORTEP-Plot of **2**. Thermal ellipsoids are shown at the 30% probability level. Selected bond lengths [Å] and angles [°]: B-Fe 2.080(4), Fe-C1 2.072(4), Fe-C2 2.138(4), Fe-C3 2.330(4), B-C1 1.504(7), C1-C2 1.432(6), C2-C3 1.393(6), C1-C3 1.484(6), C11-C12 1.381(7), C10-C11 1.375(9), C9-C10 1.367(7), C8-C9 1.307(7), C8-C13 1.415(7), C2-C3 1.393(6), C3-C4 1.427(7), C4-C5 1.345(8), C5-C6 1.413(7), C6-C7 1.354(7), C2-C7 1.434(6), C7-C8 1.458(6), Fe-C21 1.774(5), Fe-C22 1.808(5), Fe-C23 1.735(5), B-N 1.370(6); Fe-B-N 149.3(3), C21-Fe-C22 104.4(2), C21-Fe-C22 100.7(2), C22-Fe-C23 92.3(2), B-Fe-C21 153.1(2), C3-Fe-C23 165.0(2), C3-Fe-C22 96.6(2). B-Fe-C21 102.5(2), B-Fe-C21 83.0(2), C2-Fe-C22 91.9(2), C1-Fe-C21 138.9(2), C2-Fe-C21 124.4(2).

2.072(4) and 2.138(4) Å compare favorably with the literature values,[11] and although the Fe–C3 bond (2.330(4) Å) is longer it has still to be considered as a bonding distance. The Fe–B bond length is almost equal to the Fe–C1 bond distance, despite the fact that the atomic radius of boron exceeds that of carbon. This may be explained by the π-acceptor character of the boron atom.[12] The electron demand of the boron atom is also satisfied by BN-π-bonding, as evidenced by the short B–N bond. Consistent with this conclusion, the C1′/C5′/N/B plane is almost parallel to the Fe/B/C1 plane, the angle between the normals being only 11.2°.[13]

2 is thus one of the few organometallic complexes in which η^4-complexation is achieved at the expense of the aromaticity of a ligand.[14] It was, therefore, to be expected that **2** would react with donor molecules to produce η^2-complexes of the ligand **1**. Triphenylphosphane, tricyclohexylphosphane, trimethylphosphite and triphenylstibane, indeed, readily form complexes of type **3** [Reaction (2)]; CO reacts in the same way to give the known **3e**.[5] **3a–d** are also obtained by the addition of the ligands to the complex **2** prepared in situ. The ^{13}C-NMR spectra of the complexes **3 a–d** reveal symmetrical bonding of the $Fe(CO)_3L$ group in **1**, since only six signals are observed for the fluorenylidene unit. The CO groups are equivalent on the NMR time scale at ambient temperature. However, at 210 K two signals appear in a 1:2 ratio as doublets in the phosphite complex **3c** and as singlets in **3d**. The IR spectra show three bands for the carbonyl groups shifted to lower wave numbers as compared to those in **2**. Moreover, the 1718 cm^{-1} band of **1** is missing in all complexes of type **3**, indicative of an η^2-complex.[5]

This binding of ligand **1** is confirmed by the X-ray structure of **3c** (see Figure 2).[15] The stereochemistry of this compound can be described either as distorted trigonal bipyramidal or as distorted tetragonal pyramidal.[12, 16] However, due to the low symmetry of **3c**, neither of the two is unambiguous. Assuming the latter alternative, both the σ-donor and the B=C-ligand would occupy a basal position.[17] Due to the presence of the bulky phosphite ligand as well as the steric requirements of **1** the angle between the apical CO and the basal CO group reduces from 151.2° in $[(CO)_4Fe(\eta^2\text{-}\mathbf{1})]$ to 141.3° in **3c**. The BC bond length in **3c** is increased by 0.11 Å relative to **1**. The C1′/N/C5′ plane of the tetramethylpiperidino group is almost coplanar with the Fe/B/C1 plane (angle between the normals of these planes: 7.2°). In consonance with **3e**[5], the Fe–B bond distance in **3c**

Table 1. Spectroscopic data of **2** and **3a–d**. 90-MHz ^{1}H-, 64.186-MHz ^{11}B-, 50.323-MHz ^{13}C-, and 81.015-MHz ^{31}P-NMR spectra in $CDCl_3$, toluene, $CDCl_3$ (except in the case of **3d**) and toluene/$CDCl_3$, respectively; 70 eV mass spectra.

2: IR (CCl_4, cm^{-1}): $\tilde{\nu}$ = 2028, 1967, 1945; NMR (δ-values); ^{1}H: 0.79, 1.57, 1.69, 1.98, 1.69–1.82 (4 s, m, 18H, tmp-unit), 4.72 (d, ^3J(HH) = 5.86 Hz, H-atom an C13), 7.24–8.00 (3 m, 7H, $C_{13}H_8$-unit); ^{11}B: 55.4; ^{13}C (298 K, atom numbering here and for the following compounds as in Fig. 1 and 2, resp.): 15.8 (C3′), 31.2, 33.5, 34.9, 36.3 (C6′–C9′), 37.5, 38.0 (C2′, C4′), 56.6, 57.7 (C1′, C5′), 71.3 (C3), 122.0, 122.3 (C6, C9), 123.1, 124.0 (C4, C11), 128.0 (double intensity, C5, C10), 134.4 (C12), 111.7, 148.9 (C12, C13), 134.8, 140.3 (C8, C7); no signal for C1; at 210 K (CO region): 219.9, 215.5, 202.6 (1:1:1); MS: no molecular ion; *m/z* 427 ($M-CO^{\oplus}$, 11%), 399 ($M-2CO^{\oplus}$, 17%), 372 ($M-3CO^{\oplus}$, 8%), 164 ($C_{13}H_8^{\oplus}$, 100%)

3a: IR (cm^{-1}): $\tilde{\nu}$ = 1986, 1916, 1889; NMR (δ values): ^{1}H: 0.72, 1.40, 1.60 (2 s, m; 18H, tmp-unit) 7.11–7.91 (3 m, 23H, $C_{13}H_8$- and C_6H_5-unit); ^{11}B: 60.4; ^{13}C: 16.0 (C3′), 32.6, 32.7 (C6′–C9′), 39.0, 39.3 (C2′, C4′), 57.6, 61.3 (C1′, C5′), 119.6 (C6, C9), 122.9 (C3, C12), 123.9 (C4, C11), 125.5 (C5, C10), 138.1 (C7, C8), 156.3 (C2, C13), 134.4 (d, ipso-C, $^1J(^{31}P^{13}C)$ = 46.2 Hz), 128.3 (d, *o*-C, $^2J(^{31}P^{13}C)$ = 10.5 Hz), 133.2 (d, *m*-C, $^3J(^{31}P^{13}C)$ = 9.4 Hz), 130.3 (d, *p*-C, $^4J(^{31}P^{13}C)$ = 2.1 Hz), 201.6 (CO); ^{31}P: 75.6

3b: IR (Nujol, cm^{-1}): $\tilde{\nu}$ = 1983, 1878; NMR (δ values): ^{1}H: 0.69, 2.08 (2 s, 12H, CH_3), 1.24–1.83 (m, 39H, CH_2 groups), 7.11–7.89 (3 m, 8H, $C_{13}H_8$); ^{11}B: 58.9; ^{13}C: 16.1 (C3′), 29.5, 29.6 (C6′–C9′), 32.7, 33.7 (C2′, C4′), 58.0, 61.3 (C1′, C5′), 119.4 (C6, C9), 122.7 (C3, C12), 123.7 (C4, C11), 125.5 (C5, C10), 138.2 (C7, C8), 156.5 (C2, C13), 39.2 (d, ipso-C, $^1J(^{31}P^{13}C)$ = 27.4 Hz), 38.2 (d, *o*-C, $^2J(^{31}P^{13}C)$ = 19 Hz), 27.7 (d, *m*-C, $^3J(^{31}P^{13}C)$ = 10 Hz), 26.2 (d, *p*-C, $^4J(^{31}P^{13}C)$ = 1 Hz) – C atoms of the C_6H_{11} group –, 213.1 (d, CO, $^2J(^{31}P^{13}C)$ = 25 Hz); ^{31}P: 46.3

3c: IR: 2005, 1914, 1905. NMR (δ values): ^{1}H: 0.80, 1.98, 1.74, 1.92 (2 s, 2 m, 18H, tmp group), 3.61 (d, 9H, $^3J(^{31}P^{13}C)$ = 11.7 Hz, $POCH_3$), 7.1–7.9 (m, 8H, $C_{13}H_8$); ^{11}B: 59.0; ^{13}C: 16.7 (C3′), 33.3, 33.6 (C6′–C9′), 39.4, 40.1 (C2′, C4′), 58.9, 61.6 (C1′, C5′), 53.25 (d, $^2J(^{31}P^{13}C)$ = 6 Hz, OCH_3), 120.0 (C6, C9), 123.2 (C3, C12), 123.7 (C4, C11), 125.7 (C5, C10), 138.0 (C7, C8), 156.0 (C2, C13), 210.7 (d, $^2J(^{31}P^{13}C)$ = 38 Hz, CO); at 210 K in CD_2Cl_2: 211.6, 210.3 (2 d, intensity 1:2, $^2J(^{31}P^{13}C)$ = 24, 46 Hz); ^{31}P: 176.4); MS: 579 ($M^{\oplus}$, 5.7%), 523 ($M-2CO^{\oplus}$, 37.3%), 495 ($M-3CO^{\oplus}$, 100%)

3d: IR: 1984, 1916, 1881; NMR (δ values): ^{1}H: 0.75, 1.81, 1.51, 1.75 (2 s, 2 m, 18H, tmp group), 7.0–7.65 (m, 23H, aromatic protons); ^{11}B: 62.1; ^{13}C: 16.4 (C3′), 33.3, 34.2 (C6′–C9′), 39.0, 39.6 (C2′, C4′), 58.2, 61.2 (C1′, C5′), 120.7 (C6, C9), 123.7 (C3, C12), 123.2 (C4, C11), 126.1 (C5, C10), 138.5 (C7, C8), 156.4 (C2, C13), 132.1 (ipso-C), 135.6 (*m*-C), 130.3 (*p*-C), 129.6 (*o*-C), 212.7 (CO); at 210 K in CD_2Cl_2: 214.5, 209 (1:2)

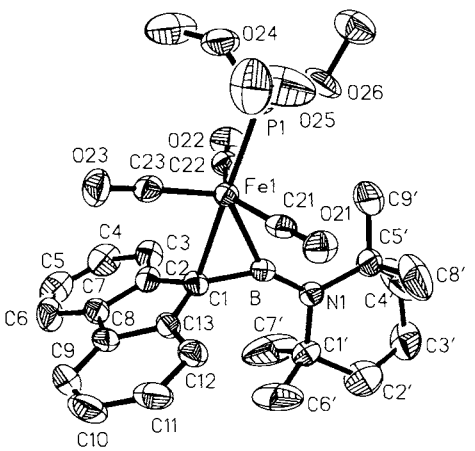

Fig. 2. ORTEP-Plot of one of the two independent molecules of **3c**. Thermal ellipsoids at the 25% probability level. Selected bond lengths [Å] and angles [°]: Fe1-P1 2.180(3), Fe1-C21 1.773(9), Fe1-C22 1.762(9), Fe1-C23 1.796(9). Fe1-C1 2.182(8). Fe1-B 2.109(9), B-N1 1.366(10); P1-Fe1-C23 95.0(3), C21-Fe1-C22 141.3(4), P1-Fe1-C1 179.7(3), P1-Fe1-B 138.0(3), C1-B-N1 141.8(8), C23-Fe1-C1 85.2(3), C23-Fe1-B 126.7(4), C23-Fe1-C22 109.8(4), C23-Fe1-C21 108.5(4).

is considerably shorter than the Fe–C1 bond length, indicating that the boron atom plays a dominant role in accepting π-electron density from the metal atom,[12] as is the case in many other metal π-complexes of unsaturated organoboranes.[18]

Experimental

2: A mixture of **1** (2.17 g, 6.9 mmol) and $Fe(CO)_5$ (0.96 g, 6.9 mmol) in toluene (100 mL) was irradiated for 3 h using a Hg-lamp, Hanau Q150. In this period ca. 13 mmol of CO gas was liberated. The resulting dark red-brown solution was filtered, concentrated in vacuo to about 10 mL and layered with 20 ml of pentane. On cooling to −20 °C for one week, dark red microcrystalline **2** separated. When the reaction was carried out in hexane solution, the product separated from the solution at −20 °C within 24 h as well formed crystals. Yield: 60–65%, m.p. 160–165 °C (decomp.).

3a: A solution of **2** (1.1 g, 2.4 mmol) in toluene (5 ml) was stirred with an equimolar amount of $P(C_6H_5)_3$ (0.63 g, 2.4 mmol) for 2 h at ambient temperature. **3a** separated as a yellow powder; this was recrystallized from a hot toluene/hexane mixture (1:2). Yield: 53%, m.p. 200–205 °C.

3b: Addition of $P(C_6H_{11})_3$ (0.90 g, 3.2 mmol) to an irradiated mixture of 1.02 g (3.2 mmol) of **1** and 0.4 g (3.2 mmol) of $Fe(CO)_5$ in 40 mL of toluene yielded a yellow orange powder after 3 h. Recrystallization from a mixture (1:2) of hot toluene and hexane. Yield: 57%, m.p. 185 °C (decomp.).

3c: Analogously to **3b**, from 0.6 ml (5 mmol) of $P(OCH_3)_3$, 1.6 g (5 mmol) of **1** and 0.86 mL (6 mmol) of $Fe(CO)_5$. Yield: 66%, orange crystals, m.p. 175 °C (decomp.).

3d: Analogously to **3a**, from 1.62 g (4.6 mmol) of $Sb(C_6H_5)_3$ and 2.0 g (4.6 mmol) of **2**. Yellow orange crystals from toluene/hexane. Yield: 52%, m.p. 169–172 °C.

3e: Dry CO gas was bubbled through a solution of 1.5 g of **2** dissolved in 20 mL of toluene. The color of the solution changed from red to brown. Removal of the solvent, dissolution of the residue in a minimum amount of toluene, and layering with 10 mL of hexane afforded light-brown crystals of **3e**. The yield was not determined; m.p. 137 °C (dec.). Identity checked by comparison with an authentic sample[5].

Received: August 11, 1989 [Z 3495 IE]
German version: *Angew. Chem. 102* (1990) 222

CAS Registry numbers:
1, 96097-03-9; **2**, 124891-80-1; **3a**, 124891-81-2; **3b**, 124891-82-3; **3c**, 124891-83-4; **3d**, 124891-84-5; **3e**, 116725-86-1.

[1] P. Jutzi, *Angew. Chem. 87* (1975) 269; *Angew. Chem. Int. Ed. Engl. 14* (1975) 232; G. Maier, J. Henkelmann, H. P. Reisenauer, *ibid. 97* (1985) 1061 and *24* (1985) 1065; H. Klusik, A. Berndt, *ibid. 95* (1983) 895 and *22* (1983) 877, H. Lukasch, G. Schmidt-Lukasch, U. Lippold, A. Berndt, *ibid. 100* (1988) 959 and *27* (1988) 960.

[2] a) B. Glaser, H. Nöth, *Angew. Chem. 97* (1985) 424; *Angew. Chem. Int. Ed. Engl. 24* (1985) 416; b) B. Glaser, E. Hanecker, H. Nöth, H. Wagner, *Chem. Ber. 120* (1987) 659; c) R. Boese, P. Paetzold, A. Tapper, *ibid. 120* (1987) 1069.

[3] S. W. Helm, *Dissertation*, Universität München 1988; C. Euringer, *Dissertation*, Universität München 1988.

[4] a) B. Glaser, H. Nöth, *Chem. Ber. 119* (1986) 3856; b) B. Glaser, *Dissertation*, Universität München 1985; c) E. P. Mayer, *Dissertation*, Universität München 1989.

[5] S. W. Helm, H. Nöth, *Angew. Chem. 100* (1988) 1378; *Angew. Chem. Int. Ed. Engl. 27* (1988) 1331.

[6] L. Kruczynski, L. K. K. LiShin Man, J. Takats, *J. Am. Chem. Soc. 96* (1974) 4006; H. Angermund, F. W. Grevels, R. Moser, R. Benn, C. Krüger, M. Romao, *Organometallics 7* (1988) 1994; J. W. Faller, *Adv. Organomet. Chem. 16* (1977) 211.

[7] a) $C_{25}H_{26}BFeNO_3$, M_r = 455.1, crystal size 0.25 × 0.3 × 0.5 mm³, triclinic, a = 8.372(4), b = 11.599(4), c = 12.025(4) Å, α = 79.38(3), β = 83.22(3), γ = 79.51(3)°, V = 1124.2(7) Å³, space group $P\bar{1}$, Z = 2, $\varrho_{calc.}$ = 1.345 g cm⁻³, $\mu(Mo_{K\alpha})$ = 6.94 cm⁻¹, ω-2θ scan, 2θ = 2–50° in h +/ −k +/ −l, 4042 reflections measured, 3767 unique, internal consistency 0.0408, 3081 reflections observed with $I > 3\sigma(I)$. Structure solved by direct methods (SHELXTL program package), nonhydrogen atoms refined anisotropically, H atoms isotropically, final R = 0.058, R_w = 0.067 for 331 variables, $1/w = \sigma^2(F) + 0.0045(F)^2$. Highest residual electron density = 0.33 e/Å³. The tetramethylpiperidino group showed disorder at the atoms C15, C19, C20 (split model used with occupancy factor 0.5); b) Further information on the crystal structure investigations can be obtained from the Fachinformationszentrum Karlsruhe, Gesellschaft für wissenschaftlich-technische Information mbH, D-7514 Eggenstein-Leopoldshafen 2 (FRG), on quoting the deposit number CSD 54103, the names of the authors, and the literature citation.

[8] Examples of π-bonded borabutadiene groups containing tricoordinate boron atoms in the ligand are reported by G. E. Herberich, E. Raabe, *J. Organomet. Chem. 309* (1986) 143.

[9] H. W. Quinn, J. H. Tsai, *Adv. Inorg. Chem. Radiochem. 12* (1969) 217; M. R. Churchill, R. Mason, *Adv. Organomet. Chem. 5* (1967) 93; F. A. Cotton, V. W. Day, B. A. Frenz, K. I. Hardcastle, J. M. Troup, *J. Am. Chem. Soc. 95* (1973) 4522.

[10] J. W. Johnson, P. M. Treichel, *J. Am. Chem. Soc. 99* (1977) 1477.

[11] C. Krüger, Yi H. Tsay, *Angew. Chem. 83* (1971) 250; *Angew. Chem. Int. Ed. Engl. 10* (1971) 261; M. Mathews, G. J. Palenik, *Inorg. Chem. 11* (1972) 2809.

[12] P. Hofmann, Technische Universität München, private communication, 1988; results will be published in a joint paper.

[13] Details of bonding will be described elsewhere.

[14] R. E. Davis, R. Pettit, *J. Am. Chem. Soc. 92* (1970) 716; R. B. King, A. Fronzaglia, *ibid. 88* (1966) 709; R. Victor, , R. Ben-Shoshan, S. Sarel, *Chem. Commun. 1970*, 1680.

[15] $C_{28}H_{35}BFeNO_6P$, M_r = 579.2, crystal size 0.35 × 0.3 × 0.45 mm³, triclinic, a = 11.223(4), b = 16.355(5), c = 16.965(5) Å, α = 84.88(2), β = 72.63(2), γ = 86.09(3)°, V = 2957(1) Å³, space group $P\bar{1}$, Z = 4, $\varrho_{calc.}$ = 1.301 g cm⁻³, $\mu(Mo_{K\alpha})$ = 6.0 cm⁻¹, ω-2θ-scan, 2θ-range: 2–50° in h +/ −k +/ −l, 9303 measured reflexions, 8610 unique, internal consistency 0.033, 5877 relexions observed with $I > 3\sigma(I)$. Structure solved by direct methods, non-hydrogen atoms refined anisotropically, final R = 0.086, R_w = 0.089, $1/w = \sigma^2(F) + 0.00484(F)^2$, for 679 variables; highest residual electron density 0.67 e/Å³. One of the two independent molecules showed disorder of its tetramethylpiperidino group. Calculations using a split atom model. Good convergence was then achieved inspite of the fact that the standard deviations in the disordered part of this molecule remained high. For further information see Ref. [7b].

[16] For structure and bonding of [Fe(CO)$_3$L(olefin)] complexes, which are related to **3** see M. Rosi, A. Sgamellotti, C. Floriani, *Inorg. Chem. 26* (1987) 3805.

[17] We are indebted to one of the referees for pointing out some arguments in favor of the tetragonal pyramidal arrangement. In the trigonal pyramidal configuration both the B=C unit and the P atom would occupy an equatorial position; the latter would be electronically less favorable. A. R. Rossi, R. Hoffmann, *Inorg. Chem. 14* (1975) 365; M. V. R. Stainer, J. Takats, *ibid. 21* (1982) 4044.

[18] W. Siebert, *Adv. Organomet. Chem. 18* (1980) 301; G. E. Herberich, H. Ohst, *ibid. 25* (1986) 199.

Tetrasilylmethane, $C(SiH_3)_4$, the Si/C-Inverse of Tetramethylsilane, $Si(CH_3)_4$**

By *Rudolf Hager, Oliver Steigelmann, Gerhard Müller, Hubert Schmidbaur,* Heather E. Robertson,* and *David W. H. Rankin*

Hydrogen-containing amorphous silicon (a-Si:H) is of great interest as a semiconductor material, particularly because the inclusion of other elements allows desired variations in photoelectric properties to be achieved in a simple manner. Besides the elements of the third and fifth main groups the group IV elements carbon and germanium in particular can also be used for doping; the band gap of the amorphous semiconductor (a-Si:H) can be increased by carbon, whereas with germanium (a-SiGe:H) the band gap is decreased. These layers are usually prepared by Plasma

[*] Prof. Dr. H. Schmidbaur, Dipl.-Chem. R. Hager,
Dipl. Chem. O. Steigelmann,[+] Priv.-Doz. Dr. G. Müller,[+]
Anorganisch-chemisches Institut der Technischen Universität München
Lichtenbergstrasse 4, D-8046 Garching (FRG)
Dr. H. E. Robertson,[++] Dr. D. W. H. Rankin
Department of Chemistry, University of Edinburgh
West Mains Road, Edinburgh EH9 3JJ (UK)

[+] X-ray structure analysis.

[++] Electron diffraction analysis.

[**] This work was supported by the Organisation der Europäischen Gemeinschaft [EN3 S-0059-D(B)], the Deutsche Forschungsgemeinschaft (Leibniz-Programm), the Fonds der Chemischen Industrie, and Wacker-Chemie, Burghausen (donations of chemicals).

Enhanced Chemical Vapor Deposition (PE-CVD) of mixtures of SiH_4 and CH_4 or GeH_4, respectively. In contrast to the a-SiGe:H and pure a-Si:H films, the a-SiC:H films obtained in this way show much poorer optoelectrical properties, especially if the carbon content is high.[1]

Numerous investigations in recent years have shown that, because of the relatively high stability of the CH bond, the use of methane results in the inclusion of carbon predominantly in the form of CH_3 groups, so that carbon itself makes hardly any contribution to the formation of the amorphous network; indeed it tends to loosen it.[2] In order to prepare a-Si:H films with larger band gaps—an "optical gap" of at least 2 eV is of special interest for applications in the area of solar cells[3]—which nevertheless have satisfactory electronic properties, the carbon atoms must be included in the Si network in an efficient manner, preferably substituent-free. One possible method for doing this is to use as sources of carbon (feedstock gases) those organosilanes which possess few or no CH functions, such as the last members of the series of silylmethanes $(H_3Si)_xCH_{4-x}$ (x = 1, 2, 3 or 4). Only modest success was achieved at first with methylsilane, H_3SiCH_3,[4] but the deposition of a-SiC:H films with the desired high photoconductivity, with a large "optical gap", was achieved soon afterwards in several laboratories with disilylmethane, $(H_3Si)_2CH_2$.[5] The properties are apparently also determined by the abundance of quasi-crystalline domains.[6] Investigations with trisilylmethane, $(H_3Si)_3CH$, are in progress.[7]

Tetrasilylmethane, $(H_3Si)_4C$, was hitherto unknown even though its use has already been patented.[5b] We now report the first synthesis of tetrasilylmethane. Several convenient methods for the preparation of disilylmethane[8] have been reported recently.[9] However, in the case of trisilylmethane[9a,10] there are already considerable preparative difficulties, and it has only recently been possible to develop a really efficient method for the synthesis of this compound.[11] As pointed out in the cited work, a similar route should be suitable for the preparation of tetrasilylmethane.

Chlorophenylsilane, an easily accessible, stable compound[11,12] can, with the use of magnesium metal and tetrahalogenomethanes under conditions described earlier by *Merker* and *Scott* for similar systems,[13] be converted into tetrakis(phenylsilyl)methane **1** in ca. 50% yield [Eq. (a)].

$$CBr_4 + 4\,PhSiH_2Cl + 4\,Mg \rightarrow \underset{\mathbf{1}}{C(SiH_2Ph)_4} + 4\,MgClBr \qquad (a)$$

$$HCBr_3 + 3\,PhSiH_2Cl + 3\,Mg \rightarrow \underset{\mathbf{2}}{HC(SiH_2Ph)_3} + 3\,MgClBr \qquad (b)$$

$$H_2CBr_2 + 2\,PhSiH_2Cl + 2\,Mg \rightarrow \underset{\mathbf{3}}{H_2C(SiH_2Ph)_2} + 2\,MgClBr \qquad (c)$$

As well as the desired precursor **1** the less silyl-rich homologues tris(phenylsilyl)methane **2** and bis(phenylsilyl)methane **3**, are also obtained in not inconsiderable yields (20% and 10% respectively) [Eq. (b), (c)]; presumably transmetalation reactions are responsible for this. **2** and **3** can be separated from the reaction mixture by distillation and can be usefully converted into tri- or disilylmethanes.[11] Colorless crystals (m.p. = 46 °C) separate at − 78 °C from hexane solutions of the residue from the distillation, the ^{1}H-NMR spectrum of which shows almost exclusively the signals expected for **1**. The structure of this product has been established by, inter alia, single crystal X-ray structure analysis.[14] As shown in Figure 1 the central carbon atom is surrounded tetrahedrally by four silicon atoms.

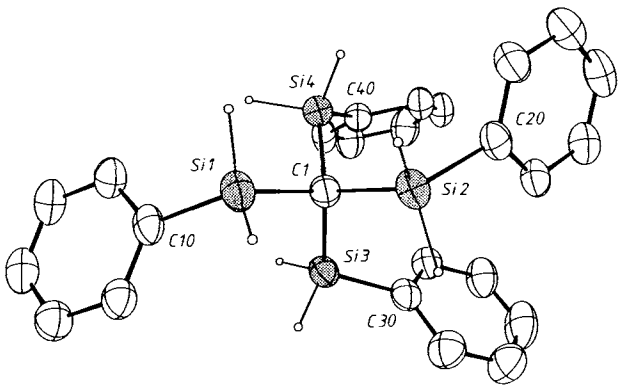

Fig. 1. Molecular structure of compound **1** in the crystal (ORTEP 50%). Important distances [Å] and angles [°]: C1–Si1 1.889(2), C1–Si2 1.892(2), C1–Si3 1.876(2), C1–Si4 1.884(2); Si1–C10 1.876(2), Si2–C20 1.873(2), Si3–C30 1.872(2), Si4–C40 1.865(2); Si1–C1–Si2 103.1(1), Si1–C1–Si3 109.3(1), Si1–C1–Si4 105.9(1); Si2–C1–Si3 11.5(1), Si2–C1–Si4 105.9(1), Si3–C1–Si4 113.5(1); C1–Si1–C10 117.6(1), C1–Si2–C20 115.0(1), C1–Si3–C30 115.5(1), C1–Si4–C40 117.2(1).

The phenyl groups in **1** can be removed as benzene by treatment with liquid hydrogen bromide at − 78 °C[15] [Eq. (d)].

$$\underset{\mathbf{1}}{C(SiH_2Ph)_4} + 4\,HBr \rightarrow \underset{\mathbf{4}}{C(SiH_2Br)_4} + 4\,C_6H_6 \qquad (d)$$

In contrast to the phenylsilylmethanes **2** and **3**, where the reaction to the corresponding bromosilylmethanes proceeds in nearly quantitative yield in a relatively short time (3 h and 10 h respectively), the removal of the phenyl groups in **1** is not complete even after several days. The ^{1}H-NMR spectrum of the product mixture clearly shows in the HSi region the singlet ($\delta = 4.52$) with ^{29}Si satellites ($^1J(H, Si) = 253.6$ Hz) which is expected for tetrakis(bromosilyl)-methane **4**. In addition, however, there are several other groups of signals. Presumably the long reaction times lead to isomerization and to bromination of the SiH functions. Nevertheless the whole reaction mixture can be converted with $LiAlH_4$ into the title compound **5** without prior purification [Eq. (e)].

$$\underset{\mathbf{4}}{C(SiH_2Br)_4} \xrightarrow{LiAlH_4} \underset{\mathbf{5}}{H_3Si-\overset{\displaystyle SiH_3}{\overset{|}{\underset{|}{C}}}-SiH_3} \qquad (e)$$
$$\qquad\qquad\qquad

86.5 °C and freezes at 5 °C; the yield is 15% based on the amount of **1** used. The spectroscopic data for **5** are as expected. For example, in the high resolution ^{1}H-NMR spectrum a singlet is observed at 3.84 ppm, which, because of the magnetic inequivalence of the protons on the ^{29}Si and ^{28}Si nuclei, shows satellites at a larger distance with decet fine structure (^1J(H, Si) = 205.7 Hz, ^4J(H, H) = 0.6 Hz; 5% intensity relative to the central singlet) and at a smaller distance satellites with quartet structure (^3J(H, Si) = 4.6 Hz; 15%).

The structure of compound **5** has been determined by electron diffraction.[18] In principle, the molecule adopts the expected tetrahedral structure, but the idealized T_d symmetry is reduced to point group T through a silyl twist (dihedral angle Si–C–Si–H = 20.04°).[19, 20] All other dimensions are in the expected range (Fig. 2). The structure of tetramethylsilane has been determined previously.[21]

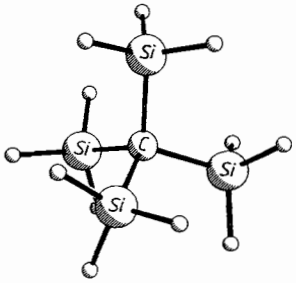

Fig. 2. Molecular structure of **5** in the gas phase. Important distances [Å] and angles [°]: Si–C 1.8751(7), Si–H 1.486(4), Si–C–Si 109.47 (fix.), C–Si–H 108.5(6), Si–C–Si–H 20.0(10), SiH_3(tilt) 0.00(fix.).

Details of photoelectron spectroscopic studies,[22] and CVD experiments will be reported later.

Experimental

1: A mixture of 56.7 g (0.40 mol) of $PhSiH_2Cl$ and 10.6 g (0.44 mol) of Mg turnings in 200 mL of THF was first treated at 60 °C with a solution of 33.2 g (0.10 mol) of CBr_4 in 200 mL of THF over a period of 6 h and then heated to boiling for a further 4 h. The whole reaction mixture was poured onto ice and neutralized with $NaHCO_3$. The organic phase was separated and, after addition of 100 mL of *n*-hexane, washed three times with 100-mL portions of water, and dried over $MgSO_4$. After removal of the hexane, the bright yellow crude oil was fractionally distilled at a pressure of 0.1 torr through a short Vigreux column at a temperature of 220 °C to achieve the separation and isolation of **2** (b.p. 96 °C/0.2 torr) and **3** (b.p. 190 °C/0.2 torr). The residue from the distillation (21.7 g, containing at least 20 g of **1**, corresponding to a crude product yield of 45%) was dissolved in 75 mL of *n*-hexane and stored for 4 weeks over dry ice. The majority of the material separated again as an oil, but in addition 0.6 g of **1** was obtained as a colorless crystalline solid (m.p. 46 °C).—^{1}H NMR (400 MHz, C_6D_6, 25 °C, TMS int.): δ = 4.90 (s, 8 H; SiH_2), 7.19 (m, 20 H; C_6H_5); ^{13}C NMR (100.4 MHz, C_6D_6, TMS): δ = − 19.78 (non, ^2J(C, H) = 6.7 Hz, ^1J(C, Si) = 30.5 Hz; CSi_4), 128.07 (dd; C2/6), 130.29 (dt; C4), 131.13 (m; C1), 136.91 (dm; C3/5), $^1J(C_{ar}, H)$ ca. 159 Hz, $^2J(C_{ar}, H)$ ca. 7 Hz; ^{29}Si NMR (79.4 MHz, C_6D_6, TMS): δ = − 29.84 (tm, ^1J(Si, H) = 202.6 Hz); IR (Nujol, [cm^{-1}]): 2132 (*v* SiH); MS (70 eV): *m/z* 440 ($M^{\oplus}$, 3%), 282 ($Ph_2CSi_4H_4$, 100).

4: 19.0 g (0.043 mol) of **1** (oily fraction) was transferred to a Schlenk tube and covered with an excess of anhydrous HBr (31 g, 0.383 mol) by condensation at − 196 °C. After warming to − 78 °C, the mixture, which was largely homogeneous after a few hours, was stirred for three days at this temperature. The excess HBr was evaporated off by warming to room temperature and the resulting benzene (9.5 g, 71%) was removed at a pressure of 1 torr.—^{1}H NMR: δ = 4.52 (s, ^1J(Si, H) = 253.6 Hz; SiH_2), together with other signals.

5: A solution of 18.3 g of the oily product mixture **4** (obtained from the reaction with HBr) in 50 mL of tetrahydronaphthalene (THN) was added dropwise to a suspension of 9.2 g (0.24 mol) $LiAlH_4$ and 1.9 g (8.3 mmol) of benzyltriethylammonium chloride in 200 mL of THN. The reaction mixture was first stirred for 3 days at room temperature and then for a further 5 h at 60 °C. The volatile products were then condensed at this temperature at a pressure of 10^{-1} torr into a nitrogen cold trap through a gas cooler (helix length ca. 2.5 m) which was connected to the reaction flask. *Caution*: on thawing the cold trap, a not inconsiderable amount of SiH_4 undergoes spontaneous combustion at the exit of the Hg vent connected to the apparatus! The remaining colorless liquid (1.9 g) contains **5**, **6**, THN and $PhSiH_3$ as the main components. By further HBr treatment of the reaction residue (after filtration and removal of the solvent by distillation), followed by hydrogenation in an analogous manner to above, a further 2 g of crude product was obtained. From the combined product mixture 0.85 g of **5** (14.5% based on **1**) can be isolated as a colorless liquid by repeated trap-to-trap condensation and fractional distillation (b.p. 86.5 °C, m.p. ca. 5 °C).—^{1}H NMR: δ = 3.84 (s, ^1J(H, Si) = 205.7 Hz, ^3J(H, Si) = 4.6 Hz, ^4J(H, H) = 0.6 Hz; SiH_3); ^{13}C NMR (pure, C_6D_6 ext.): δ = − 38.99 (tredecet, ^1J(C, Si) = 31.3 Hz, ^2J(C, H) = 5.5 Hz); ^{29}Si NMR (pure, TMS ext.): δ = − 47.78 (qdec); IR (Film [cm^{-1}]): 2155 s (*v* SiH), 916 s, 883 m (δ SiH_3), 798 vw (vSiC); MS (70 eV): *m/z* 136–124 [CSi_4H_x], 106–96 [CSi_3H_x], 74–69 [CSi_2H_x], 32–28 [SiH_x].

Received: September 1, 1989 [Z 3534 IE]
German version: *Angew. Chem. 102* (102) 204

CAS Registry numbers:
1, 124462-66-4; **2**, 121232-83-5; **3**, 26799-07-5; **4**, 124462-67-5; **5**, 5675-86-5; **6**, 4335-85-7; $PhSiH_2Cl$, 4206-75-1; CBr_4, 558-13-4.

[1] W. Paul, D. K. Paul, B. von Roedern, J. Blake, S. Oguz, *Phys. Rev. Lett. 46* (1981) 1016; A. Morimoto, T. Miura, M. Kumeda, T. Shimizu, *Jpn. J. Appl. Phys. 20* (1981) L833.
[2] W. Beyer, *J. Non-Cryst. Solids 97–98* (1987) 1027; J. Sotiropoulos, G. Weiser, *ibid. 92* (1987) 95.
[3] Y. Tawada, K. Tsuge, M. Kondo, H. Okamoto, Y. Hamakawa, *J. Appl. Phys. 53* (1982) 5273.
[4] D. P. Tanner, G. R. Johnson, M. D. Sefcik, *Solar Energy Mater. 3* (1980) 533; A. Matsuda, T. Yamaoka, S. Wolff, M. Koyama, Y. Imanishi, H. Kataoka, H. Matsuura, K. Tanaka, *J. Appl. Phys. 60* (1986) 4025; A. Bubenzer, M. Gorn, N. Kniffler, K. Thalheimer, G. Winterling, in R. Urban (Ed.): *Status Report 1987 – Photovoltaic*, PBE-Kernforschungsanlage Jülich 1988, p. 349.
[5] a) W. Beyer, R. Hager, H. Schmidbaur, G. Winterling, *Appl. Phys. Lett. 54* (1989) 1666; b) C. R. Dickson, Eur. Pat. Appln. 0.233.613 (1987), Solarex Corporation.
[6] B. Goldstein, C. R. Dickson, I. H. Campbell, P. M. Fauchet: *Photovoltaic Solar Energy Conference, Proceedings of the International Conference, Florence 1988*, Kluwer Academic Publishers, Dordrecht 1988, p. 969.
[7] W. Beyer, R. Hager, H. Schmidbaur, G. Winterling, unpublished results.
[8] A. D. Petrov, V. A. Ponomarenko, *Dokl. Akad. Nauk SSSR 90* (1953) 387; G. Fritz, *Angew. Chem. 79* (1967) 657; *Angew. Chem. Int. Ed. Engl. 6* (1967) 677; J. A. Morrison, J. M. Bellama, *J. Organomet. Chem. 92* (1975) 163.
[9] a) H. Schmidbaur, J. Ebenhöch, *Z. Naturforsch. 41* (1986) 1527; b) B. F. Fieselmann, C. R. Dickson, *J. Organomet. Chem. 363* (1989) 1.
[10] E. Amberger, H. D. Boeters, *Chem. Ber. 97* (1964) 1999.
[11] R. Hager, O. Steigelmann, G. Müller, H. Schmidbaur, *Chem. Ber. 122* (1989) 2155.
[12] N. S. Hosmane, S. Cradock, E. A. V. Ebsworth, *Inorg. Chim. Acta 72* (1983) 181.
[13] R. L. Merker, M. J. Scott, *J. Org. Chem. 29* (1964) 953.
[14] **1**: $C_{25}H_{28}Si_4$, M_r = 440.85, tetragonal, space group $P4_1$, $a = b$ = 13.176(1), c = 14.619(2) Å, V = 2537.96 Å^3, Z = 4, ϱ_{calcd} = 1.154 g cm^{-3}, $\mu(Mo_{K\alpha})$ = 2.4 cm^{-1}, Enraf-Nonius CAD4 diffractometer, $Mo_{K\alpha}$-Radiation, λ = 0.71069 Å, T = − 60 °C. 4444 independent reflections, of which 4133 are considered "observed" with $F_0 \geq 4.0\,\sigma(F_0)$. Solution by direct methods (SHELXS-86), $R(R_w)$ = 0.028 (0.027), $w = 1/\sigma^2(F_0)$ for 293 refined parameters (C, Si anisotropic, Si–H isotropic, remaining H constant, SHELX-76). $\Delta\varrho_{fin}$ (max/min) = + 0.33/− 0.29 e/Å^3. Further details of the crystal structure investigation are available on request from the Fachinformationszentrum Karlsruhe, Gesellschaft für wissenschaftlich-technische Informationen mbH, D-7514 Eggenstein-Leopoldshafen 2 (FRG), on quoting the depository number CSD-54289, the names of the authors, and the journal citation.
[15] G. Fritz, D. Kummer, *Z. Anorg. Allg. Chem. 308* (1961) 105.
[16] H. Schmidbaur, C. Dörzbach, J. Ebenhöch, R. Hager, J. Rott; unpublished results 1985–89.
[17] V. N. Gevorgyan, L. M. Ignatovich, E. Lukevics, *J. Organomet. Chem. 284* (1985) C31.
[18] For the general experimental procedure see Ref. [19]; R_g = 0.087, R_d = 0.069, R_m/C = 0.083 for measurements at two different plate distances: 285.9/128.2 mm; Δs 0.2/0.4 nm^{-1} (s_{min} 2/4, sw_1 4/8, sw_2 12.2/29.6, s_{max} 14.4/34.8), Correlation parameter 0.4839/0.4468; Scaling factor 0.727(8)/0.715(16), electron wavelength λ 0.05661/0.05663 Å.
[19] D. G. Anderson, D. W. H. Rankin, H. E. Robertson, C. M. F. Frazao, H. Schmidbaur, *Chem. Ber. 122* (1989) 2213.
[20] H. Schmidbaur, G. Blaschke, B. Zimmer-Gasser, U. Schubert, *Chem. Ber. 113* (1980) 1612.
[21] B. Beagley, J. J. Monaghan, T. G. Hewitt, *J. Mol. Struct. 8* (1971) 401.
[22] H. Schmidbaur, R. Hager, H. Bock, unpublished.

 © *VCH Verlagsgesellschaft mbH, D-6940 Weinheim, 1990* *0570-0833/90/0202-0203 $ 02.50/0*

Novel S-Heteroquinoid Electron Acceptors. Synthesis of 2,5-Bis(cyanoimino)-2,5-dihydrothieno-[3,2-*b*]thiophenes (DCNTTs) and Conductive Charge Transfer Complexes**

By *Erhard Günther, Siegfried Hünig,* Karl Peters, Harald Rieder, Hans Georg von Schnering, Jost-Ulrich von Schütz, Svante Söderholm, Hans-Peter Werner,* and *Hans C. Wolf*

The discovery of highly conductive charge transfer (CT) complexes of tetracyanoquinodimethane (TCNQ) **1** and tetrathiafulvalene (TTF)[1] initiated an intensive search for further CT complexes with high conductivity. The skeletal framework in the donor TTF was kept intact, while the substitution pattern and the heteroatoms (S, Se, Te) were varied extensively.[2] In the case of TCNQ on the other hand, so far the $=C(CN)_2$ terminal groups have been kept intact and only a few variations of the quinoid skeleton have been examined. Some good conducting CT complexes were recently synthesized with the thieno[3,2-*b*]thiophene system **2**.[3]

In the meantime the *N,N'*-dicyanoquinone diimines (DCNQIs) **3** have been described as novel acceptors, accessible

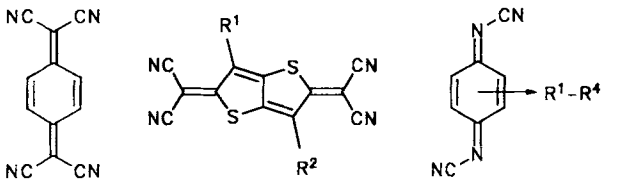

1 **2**: R = H, Br **3**

with widely different substituents from the corresponding quinones, bis(trimethylsilyl)carbodiimide and $TiCl_4$ in dichloromethane at 0–25 °C.[4, 5] These DCNQIs act as efficient acceptors in CT complexes[6] and especially in highly conductive radical anion salts.[7]

The question now arose as to how far these properties are retained when the =N–CN groups bracket a heteroquinoid system. As first examples of such compounds we describe the DCNTTs **4** mentioned in the title, which were obtained from the corresponding quinones **5** via the route previously developed for **3**.[8, 9] However, the standard conditions which have proven satisfactory for DCNQIs do not apply in this instance. Conversion of the largely unreactive **5** into **4** [Eq. (a)] was first achieved in 1,2-dichlorobenzene at 60 °C; the small yields of **4b, c** and **f** (cf. Table 1) are due to the sensitivity towards $TiCl_4$.

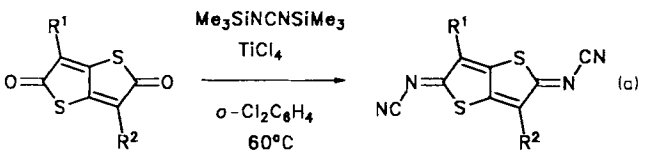

5 **4** (a)

The compounds **4a–g** (Table 1) behave as two-step, reversible redox systems; the radical anions are, according to the lgK_{SEM} values, thermodynamically equally as stable as those of the DCNQIs. The redox potentials can be varied within wide limits by suitable substituents R^1 and R^2.

Table 1. Yields, melting points, and electrochemical data of the 2,5-bis(cyanoimino)-2,5-dihydrothieno[3,2-*b*]thiophenes **4a–g**.

4	R^1	R^2	Yield [%] [a]	M.p. [°C]	E_1 [V] [b]	E_2 [V] [b]	lgK_{SEM}
a	CH_3	CH_3	42	230	−0.46	−0.05	7.03
b	CH_3	H	16	165	−0.42	+0.01	7.20
c	H	H	5	195	−0.33	+0.10	7.34
d	CH_3	Cl	30	192	−0.32	+0.12	7.34
e	CH_3	Br	59	237	−0.32	+0.12	7.34
f	Br	H	4	226	−0.23	+0.21	7.51
g	Br	Br	49	272	−0.14	+0.31	7.46

[a] Correct C,H,N analyses. [b] In CH_2Cl_2, nBu_4NPF_6 as supporting electrolyte; Pt electrodes versus Ag/AgCl in CH_3CN.

The compounds **4e, g** react with various donors to form complexes exhibiting considerable conductivity (Table 2). **4g** · TMTSeF is one of the best conducting CT complexes with TMTSeF as donor.

The crystal structure of **4g** · TTF[10] suggests the presence of a two-stack conductor array: Figure 1 shows separated,

Table 2. CT complexes from **4e** and **4g** with TTF derivatives (TM = tetramethyl, TSeF = tetraselenafulvalene, TTT = tetrathiatetracene, BEDT = bisethylenedithio).

Complex [a]	M.p. [°C] [b]	Conductivity [Scm^{-1}] σ_p [c]	σ_s
4g · TTF	200	7×10^{-2}	25 [d]
4g · TMTSeF	200	2×10^{-2}	200 [e]
4g · TMTTF	164	1.2	–
4g · TTT (5:2)	208	5×10^{-2}	–
4g · BEDT-TTF	184	2×10^{-5}	–
4e · TMTTF	182	2.0	–

[a] Composition determined by elemental analysis. [b] Determined by differential thermoanalysis. [c] Powder conductivity, measured on pressed powder. [d] Single crystal conductivity, two-contact measurement. [e] Single crystal conductivity, four-contact measurement.

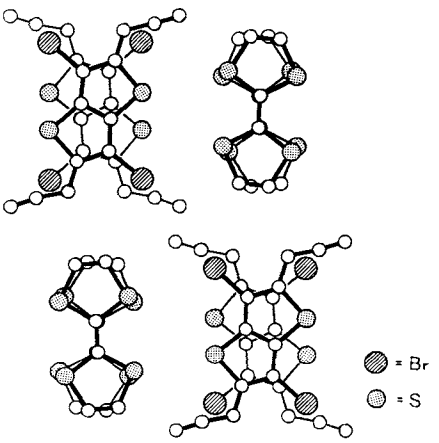

Fig. 1. *a,b*-Projection of the structure of **4g** · TTF in the crystal.

[*] Prof. Dr. S. Hünig, Dipl.-Chem. E. Günther
Institut für Organische Chemie der Universität
Am Hubland, D-8700 Würzburg (FRG)
Dipl.-Phys. H. Rieder, Dr. J.-U. von Schütz, Dr. S. Söderholm, Dr. H.-P. Werner, Prof. Dr. H. C. Wolf
3. Physikalisches Institut der Universität
Pfaffenwaldring 57, D-7000 Stuttgart 80 (FRG)
Dr. K. Peters, Prof. Dr. H. G. von Schnering
Max-Planck-Institut für Festkörperforschung
Heisenbergstrasse 1, D-7000 Stuttgart 80 (FRG)

[**] This work was supported by the Volkswagen Foundation, the Fonds der Chemischen Industrie, and BASF AG. Part of the work was already presented in a lecture at the "Naurod Meeting", Wiesbaden-Naurod, May 1898.

straight stacks of planar donor and acceptor units which are almost equidistant at room temperature (stack separation 348 pm).

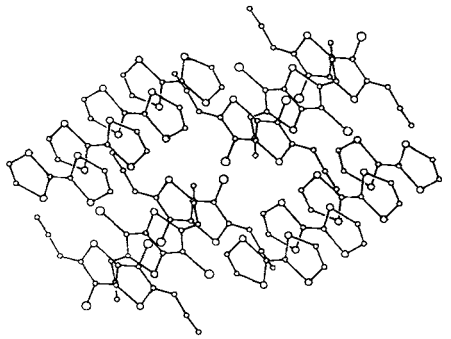

Fig. 2. Perspective view of the unit cell of **4g** · TTF.

According to Figure 3c the conductivity of the complex **4g** · TFF increases slightly with decreasing temperature down to a phase transition temperature of $T_c = 160$ K and then decreases down to 77 K, corresponding to a transition from metal to semiconductor.

The complex shows a broad ESR signal ($\Delta B_{pp} = 4.5$–8.5 mT) and a spin concentration of ca. 9×10^{22} s mol^{-1} (Fig. 3b) above room temperature. Also these values, as well as the susceptibility (Fig. 3a), first change below ca. 160 K.

According to the above results it can be expected that also other heteroquinoid systems containing =N–CN terminal groups as acceptors will be suitable for the production of conductive materials. The radical anion salts of the DCNTTs will be reported on elsewhere.

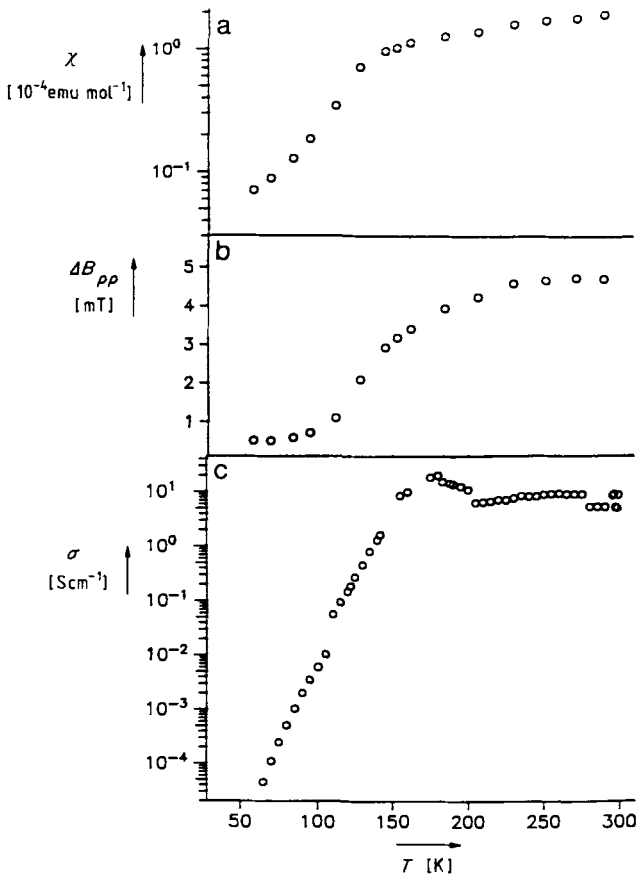

Fig. 3. Temperature dependence a) of the susceptibility, b) of the ESR line width, and c) of the conductivity of the CT complex **4g** · TFF. The steps in the curve (c) are due to cracks (jogs) in the crystal upon cooling.

Received: October 5, 1989 [Z 3583 IE]
German version: *Angew. Chem. 102* (1990) 220

[1] a) J. Ferraris, D. O. Cowan, V. Walatka, Jr., J. H. Perlstein, *J. Am. Chem. Soc. 95* (1973) 948; b) L. B. Coleman, M. J. Cohen, D. J. Sandman, F. G. Yamagishi, A. F. Garito, A. J. Heeger, *Solid State Commun. 12* (1973) 1125.

[2] E. Fanghänel, G. Schukat, A. M. Richter, *Sulfur Rep. 7* (1987) 155–240.

[3] a) K. Yui, H. Ishida, Y. Aso, T. Otsubo, F. Ogura, *Chem. Lett. 1987*, 2239–2342; b) *ibid. 1988*, 1069–1072; c) K. Yui, H. Ishida, Y. Aso, T. Otsubo, F. Ogura, A. Kawamoto, J. Tanaka, *Bull. Chem. Soc. Jpn. 62* (1989) 1547–1555.

[4] A. Aumüller, S. Hünig, *Liebigs Ann. Chem. 1986*, 142, 165.

[5] A. Aumüller, S. Hünig, *Angew. Chem. 96* (1984) 437–438; *Angew. Chem. Int. Ed. Engl. 23* (1984) 447.

[6] A. Aumüller, P. Erk, H. Meixner, J.-U. von Schütz, H.-P. Werner, *Liebigs. Ann. Chem. 1987*, 997–1006.

[7] a) A. Aumüller, P. Erk, G. Klebe, S. Hünig, J.-U. von Schütz, H.-P. Werner, *Angew. Chem. 98* (1986) 759–761; *Angew. Chem. Int. Ed. Engl. 25* (1986) 740–741; b) A. Aumüller, P. Erk, H. Meixner, J.-U. von Schütz, H. J. Gross, U. Langohr, H.-P. Werner, H. C. Wolf, C. Burschka, G. Klebe, K. Peters, H. G. von Schnering, *Synth. Met. 27* (1988) B181–188.

[8] The procedure given in the literature for **5a–c** [G. F. Pedulli, P. Zanirato, A. Alberti, M. Guerra, M. Tiecco, *J. Chem. Soc. Perkin Trans. 2* (1976) 946–952] has been modified somewhat. **5d–f** were obtained by halogenation of **5b** and **5c** with SO_2Cl_2 in chlorobenzene and Br_2 in acetic acid, respectively. **5c** was recently synthesized via another route (K. Kobayashi, ISNA Conference, Osaka, August 1989).

[9] a) Preparation of the 2,5-bis(cyanoimino)-2,5-dihydrothieno[3,2-*b*]thiophenes, as for example **4a**: A solution of $TiCl_4$ and bis(trimethylsilyl)carbodiimide in 1,2-dichlorobenzene was treated with a solution of 3,6-dimethyl-2,5-dihydrothieno[3,2-*b*]thiophene-2,5-dione **5a** in anhydrous 1,2-dichlorobenzene (10 equivalents of $TiCl_4$ and bis(trimethylsilyl)carbodiimide per equivalent of **5a**). After 48 hours' stirring at 60 °C the mixture was poured onto ice, extracted with CH_2Cl_2, and the organic phase dried over $MgSO_4$. After removal of CH_2Cl_2 by distillation the mixture was treated with pentane. The resulting precipitate was filtered off (suction) and chromatographed on silica gel (CH_2Cl_2, Kieselgel Woehm, 0.063–0.200). The product was then recrystallized from CH_3CN. b) Preparation of the CT complex: donor and acceptor components were combined in the ratio 1:1 in acetonitrile at the boiling point. On cooling, black needles or a microcrystalline powder separated out.

[10] **4g** · TFF: orthorhombic, *Pccn*, $a = 1382.4(8)$, $b = 1918.8(11)$, $c = 697.0(3)$ pm, $V = 1849(2) \times 10^6$ pm^3, $Z = 4$, $\varrho_{calcd} = 2.085$ gm cm^{-3}, $Mo_{K\alpha}$ radiation (graphite monochromator), 1931 reflections, 1176 measured with $F > 3\sigma(F)$, $R = 0.052$, $R_w = 0.038$. Further details of the crystal structure investigation are available on request from the Fachinformationszentrum Karlsruhe, Gesellschaft für wissenschaftlich-technische Information mbH, D-7514 Eggenstein-Leopoldshafen 2 (FRG), on quoting the depository number CSD-54131, the names of the authors, and the journal citation.

[11] K. Yakushi, S. Nishimura, T. Sugano, H. Kuroda, I. Ikemoto, *Acta Crystallogr. Sect. B 36* (1980) 358.

Optically Active Bipyridines in Asymmetric Catalysis**

By *Carsten Bolm,* Margareta Zehnder,* and *Daniel Bur*

Owing to their good chirality transferring properties, optically active phosphanes are of special importance in enan-

[*] Dr. C. Bolm
Institut für Organische Chemie der Universität
St.-Johanns-Ring 19, CH-4056 Basel (Switzerland)
Priv.-Doz. Dr. M. Zehnder [†], Dr. D. Bur [†]
Institut für Anorganische Chemie der Universität
Spitalstrasse 51, CH-4056 Basel (Switzerland)

[†] X-ray structure analysis.

[**] This work was supported by the Volkswagen Foundation. *C.B.* thanks the Fonds der Chemischen Industrie for a Liebig fellowship and Prof. Dr. *B. Giese* for his support.

tioselective catalysis with transition metal complexes.[1] The use of this homogeneous catalysis is, however, limited in that the frequently strongly reducing reaction conditions (e.g. in hydrogenations or hydroformylations) can lead to rupture of the phosphorus-carbon bond and thus to destruction of the catalyst.[2] Optically active chelate-forming nitrogen compounds are therefore finding increasing interest in preparative chemistry[3, 4] and increasing use as ligands of transition metals in asymmetric catalysis.[4, 5] Although the complex forming properties of bipyridine and phenanthroline derivatives have been well investigated,[6] only a few optically active compounds of this class of substances have thus far been described.[4]

Herein we report the enantioselective synthesis of the homochiral C_2-symmetric bipyridines **6** and **7**, the X-ray structure analysis of a complex of (*R*,*R*)-**7** and cobalt(II) chloride, and the first investigations of the use of these optically active bipyridines in enantioselective catalysis.

For the synthesis of the enantiomerically pure bipyridine (−)-(*R*,*R*)-**6** (Scheme 1) we used the optically active alcohol

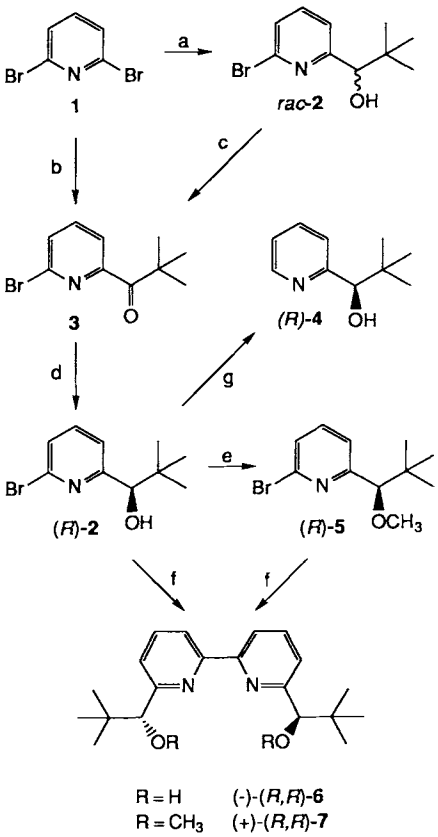

Scheme 1. a) BuLi, *t*BuCHO, THF, −78 °C to room temperature (RT), 3 h (79%). b) BuLi, $tBuCO_2CH_3$, THF, −78 °C to RT, 3.5 h (80%). c) Pyridinium chlorochromate, CH_2Cl_2, RT, 16 h (74%). d) 1) (−)-*B*-chlorodiisopinocampheylborane (1.2 equiv.) neat, RT, 2 d; 2) iminodiethanol (3.6 equiv.), ether, 3 h (59%): (*R*)-**2**:(*S*)-**2** = 95:5. e) NaH, CH_3I, THF, 0 °C to RT, 1.5 h (85%). f) $NiCl_2 \cdot 6H_2O$ (1.2 equiv.), Zn (1.3 equiv.), PPh_3 (4.8 equiv.), DMF, 72 °C, 3.5 h (**6**: 55%, **7**: 65%). g) Bu_3SnH, AIBN, toluene, 90 °C, 3 h (72%).

(*R*)-**2**, which is accessible in a two-step reaction from 2,6-dibromopyridine (**1**); two molecules of (*R*)-**2** were coupled by a nickel(0)/triphenylphosphane-mediated reaction.[7, 8] (*R*)-**2** and (*S*)-**2** were obtained in the ratio 95:5 by asymmetric reduction of the ketone **3** with (−)-*B*-chlorodiisopino-campheylborane.[9] The enantiomeric excess can be determined NMR spectroscopically on the camphanates; the absolute configuration is found by correlation with the known alcohol (*R*)-**4**.[10]

It could be shown via the camphanic acid diester of **6**, whose methine protons in the α-position to the *tert*-butyl group give rise to separate signals in the ^{1}H-NMR spectrum (400 MHz), that the chromatographically purified sample of the optically active bipyridine (*R*,*R*)-**6** was an *enantiomerically* pure compound.

Two molecules of the optically active methyl ether (*R*)-**5** can be coupled with nickel(0)/triphenylphosphane to give the bipyridine (*R*,*R*)-**7**. *rac*-**2** and *rac*-**5** each form two diastereomers (*rac*-**6**/*meso*-**6** and *rac*-**7**/*meso*-**7**, respectively) in the ratio 1:1, which can be separated by column chromatography.[11]

From the characteristic downfield shift of the NMR signals of the 3,3′-protons ($\delta = 8.31$ for (*R*,*R*)-**6**, $\delta = 8.26$ for (*R*,*R*)-**7**, a *transoid* arrangement must be assumed for the nitrogen atoms in solution.[12] Complexation with a metal converts the molecule into the *cisoid* form.

Deep-blue crystals of the composition (*R*,*R*)-**7** · $CoCl_2$ could be obtained from a solution of (*R*,*R*)-**7** and $CoCl_2 \cdot 6H_2O$ in the molar ratio 1:1 in acetonitrile/methanol. The X-ray structure analysis (Fig. 1) confirms the C_2 symmetry

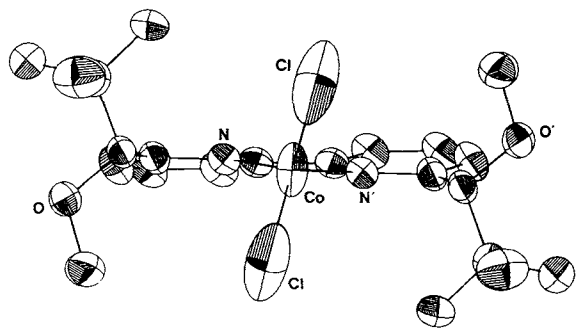

Fig. 1. Structure of (*R*,*R*)-**7** · $CoCl_2$ in the crystal (hydrogen atoms not shown).

of the metal complex; the cobalt is surrounded tetrahedrally by the two nitrogen atoms of the bipyridine ligand and the two chlorine atoms.[13] Coordinative bonding of an ether oxygen atom to the metal center, as observed in $CoCl_2$ complexes with bipyridine crown ethers,[14] does not take place.

High asymmetric induction has been achieved in additions of diethylzinc to aldehydes in the presence of catalytic amounts of optically active amino alcohols.[15] (*R*,*R*)-**6** has

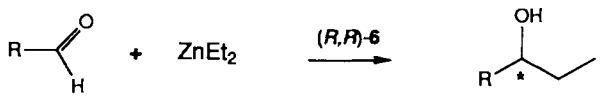

also proven to be an efficient enantioselective catalyst for this reaction. With only 5 mol-% of this optically active bipyridine, alcohols are formed in good yields and with high enantiomeric excess (up to 97%) (Table 1).

A lowering of the reaction temperature leads to an increase of asymmetric induction in the reaction with benzaldehyde (No. 1–3); however, the product is still obtained with high enantiomeric excess even at room temperature (Table 1). A doubling of the amount of catalyst from 5 to 10 mol-% has only little effect on the enantioselectivity (No. 2, 93 and 94% *ee*, respectively). Both the reactivity as

Table 1. Enantioselective addition of diethylzinc to aldehydes, catalyzed by 5 mol-% (*R,R*)-**6**.

No.	R	Solvent	*T* [°C]	*t* [h]	Yield [%] [a]	$[\alpha]_D$ [°] [b]	*ee* [%] [c]
1	C_6H_5	toluene	−25	48	94	+44.1	97(92)
2	C_6H_5	toluene	0	3	83	+42.3	93(86)
3	C_6H_5	toluene	+22	0.5	90	+41.6	91(84)
4	C_6H_5	hexane	0	3	92	+42.9	94(88)
5	C_6H_5	acetonitrile	[d]	[d]	71	+36.1	79(70)
6	*p*-ClC_6H_4	toluene	0	3	65	+26.7	93(90)
7	*p*-$MeOC_6H_4$	toluene	0	9.5	96	+30.4	90(80)
8	*n*-C_6H_{13}	toluene	0	3	≈75 [e]	≈ − 5.2 [e]	≈54 [e] (70)

[a] By column chromatography. [b] All products are of *R*-configuration. [c] According to rotation value [15b]; in brackets: determined ^{1}H- (No. 1–7) or ^{13}C-NMR spectroscopically (No. 8) after esterification with (−)-3,3,3-trifluoro-2-methoxy-2-phenylacetyl chloride ((−)-MPTA chloride). [d] 0 °C/9.5 h, then RT/37 h. [e] The product was not analytically pure.

well as the asymmetric induction is lower in acetonitrile than in toluene or hexane (No. 1–5). The methylated compound (*R,R*)-**7** and the cobalt complex (*R,R*)-**7** · $CoCl_2$ show only slight catalytic activity and lead to products with lower enantiomeric excesses.[16]

Further investigations should prove whether the optically active bipyridines presented here can also act as enantioselective catalysts in other reactions.

Received: September 28, 1989;
revised: October 31, 1989 [Z 3568 IE]
German version: *Angew. Chem. 102* (1990) 206

[1] a) H. B. Kagan in J. D. Morrison (Ed.): *Asymmetric Synthesis, Vol. 5*, Academic Press, Orlando, FL (USA) 1985, pp. 1–39; b) H. B. Kagan in G. Wilkinson, F. G. A. Stone, E. W. Abel (Eds.): *Comprehensive Organometallic Chemistry, Vol. 8*, Pergamon, Oxford 1982, pp. 463–498; c) H. Brunner, *Synthesis 1988*, 645–654.

[2] a) P. E. Garrou, *Chem. Rev. 85* (1985) 171–185; b) J. V. Ortiz, Z. Havlas, R. Hoffmann, *Helv. Chim. Acta 67* (1984) 1–17.

[3] a) A. A. Watson, D. A. House, P. J. Steel, *Inorg. Chim. Acta 130* (1987) 167–176; b) D. A. House, P. J. Steel, A. A. Watson, *Aust. J. Chem. 39* (1986) 1525–1536.

[4] a) S. Gladiali, G. Chelucci, F. Soccolini, G. Delogu, *Appl. Organomet. Chem. 2* (1988) 227–231; b) C. Botteghi, G. Chelucci, G. Chessa, G. Delogu, S. Gladiali, F. Soccolini, *J. Organomet. Chem. 304* (1986) 217–225.

[5] a) H. Brunner, U. Obermann, *Chem. Ber. 122* (1989) 499–507; b) H. Nishiyama, H. Sakaguchi, T. Nakamura, M. Horihata, M. Kondo, K. Itoh, *Organometallics 8* (1989) 846–848; c) A. Pfaltz in R. Scheffold (Ed.): *Modern Synthetic Methods, Vol. 5*, Springer, Berlin 1989, pp. 199–248.

[6] a) D. E. McKenzie, *Coord. Chem. Rev. 6* (1971) 187–216; b) W. A. E. McBryde: *IUPAC Chemical Data Series, No. 17*, Pergamon, Oxford 1978, pp. 1–78; c) W. R. McWhinnie, J. D. Miller, *Adv. Inorg. Chem. Radiochem. 12* (1969) 135–215.

[7] M. Tiecco, L. Testaferri, M. Tingoli, D. Chianelli, M. Montanucci, *Synthesis 1984*, 736–738.

[8] The α,α-disubstituted pyridine analogous to **6** was synthesized as a diastereomeric mixture; the enantiomers could be separated by fractional crystallization with dibenzoyl tartrate: a) J. M. Hawkins, J. C. Dewan, K. B. Sharpless, *Inorg. Chem. 25* (1986) 1501–1503; b) J. M. Hawkins, K. B. Sharpless, *Tetrahedron Lett. 28* (1987) 2825–2828.

[9] a) H. C. Brown, J. Chandrasekharan, P. V. Ramachandran, *J. Org. Chem. 51* (1986) 3394–3396; b) J. Chandrasekharan, P. V. Ramachandran, H. C. Brown, *ibid. 50* (1985) 5446–5448.

[10] A. Ohno, J.-i. Nakai, K. Nakamura, T. Goto, S. Oka, *Bull. Chem. Soc. Jpn. 54* (1981) 3482–3485.

[11] All new compounds have been characterized by spectra [^{1}H NMR (300, 400 MHz), ^{13}C NMR (75, 100 MHz), IR, MS] and elemental analyses.

[12] a) G. R. Newkome, A. Nayak, F. Fronczek, T. Kawato, H. C. R. Taylor, L. Meade, W. Mattice, *J. Am. Chem. Soc. 101* (1979) 4472–4477; b) T. McL. Spotswood, C. I. Tanzer, *Aust. J. Chem. 20* (1967) 1227–1242; c) S. Castellano, H. Günther, S. Ebersole, *J. Phys. Chem. 12* (1965) 4166–4176.

[13] Crystal data for (*R,R*)-**7** · $CoCl_2$: monoclinic space group C_2 (No. 5), $a = 14.620(2)$, $b = 8.602(1)$, $c = 10.120(3)$ Å, $\beta = 105.48(2)°$, $V = 1226.6$ Å^3, $Z = 2$, $\varrho_{calcd} = 1.093$ g cm^{-3}, $F(000) = 506$, $\mu(Mo_{K\alpha}) = 8.77$ cm^{-1}, 1583 unique reflections, 974 observed, ($F > 2\sigma(F)$), 143 refined parameters, $R = 0.062$, $R_w = 0.067$, weighting scheme: $1.08/(\sigma^2(F) + 2.08 \times 10^{-3} F^2)^{-1}$, diffractometer: Enraf Nonius CAD 4, $Mo_{K\alpha}$ ($\lambda = 0.71069$ Å). Futher details of the crystal structure investigation are available on request from the Director of the Cambridge Crystallographic Data Center, University Chemical Laboratory, Lensfield Road, Cambridge CB2 1EW (UK) on quoting the full journal citation.

[14] a) G. R. Newkome, H. C. R. Taylor, F. R. Fronczek, V. K. Gupta, *J. Org. Chem. 51* (1986) 970–974; b) G. R. Newkome, D. K. Kohli, F. Fronczek, *J. Chem. Soc. Chem. Commun. 1980*, 9–11.

[15] For example a) M. Kitamura, S. Suga, K. Kawai, R. Noyori, *J. Am. Chem. Soc. 108* (1986) 6071–6072; b) K. Soai, A. Ookawa, T. Kaba, K. Ogawa, *ibid. 109* (1987) 7111–7115; c) M. Kitamura, S. Okada, S. Suga, R. Noyori, *ibid. 111* (1989) 4028–4036, and references cited therein.

[16] For (*R,R*)-**7**: 52 h at 0 °C: 93% yield, 28% *ee* (*R*); for (*R,R*)-**7** · $CoCl_2$: 52 h at 0 °C: 7% yield, 19% *ee* (*R*).

Alkyne Cleavage as a Novel Route to Low-Valent Carbyne-Metal Complexes**

By *Alexander C. Filippou,* Christian Völkl, Walter Grünleitner,* and *Paul Kiprof*

The compounds *trans*-$X(CO)_4M{\equiv}CR$ (X = halogen; M = Cr, Mo, W; R = alkyl, aryl) containing a metal–carbon triple bond were first reported on in 1973 by *E. O. Fischer*.[1] Such complexes and their carbonyl-containing substitution products obtainable by successive CO exchange exhibit a versatile reaction behavior which has been well documented in numerous works.[2] In contrast, the reactivity of low-valent, carbonyl-free carbyne complexes has been the subject of very few studies.[2a, 2b, 3]

We recently reported on a novel acid-induced carbyne–isocyanide coupling reaction, the reaction of the carbyne complex **1** with HBr to give the aminoalkyne complex **2** (Scheme 1).[4] This type of reaction was previously postul-

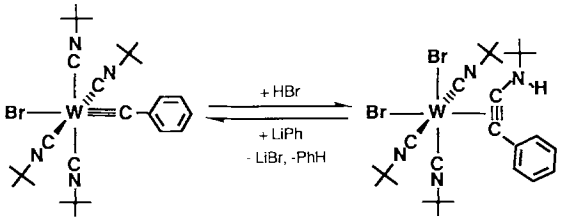

1 **2**

Scheme 1. Acid-induced CC coupling in **1**—base-induced CC cleavage in **2**.

ated as the elementary step of CC bond formation in the reductive coupling of two isocyanide ligands in sevenfold coordinated complexes of Mo^{II} and W^{II}, but could not be experimentally verified.[5] We have now successfully carried out the converse of this carbyne–isocyanide coupling: reaction of the *alkyne* complex **2** with LiPh affords the *carbyne* complex **1** (Scheme 1). This base-induced reaction is to our knowledge the only hitherto known example for the cleavage

[*] Dr. A. C. Filippou, Dipl.-Chem. C. Völkl,
Dipl.-Chem. W. Grünleitner, Dipl.-Chem. P. Kiprof
Anorganisch-chemisches Institut der Technischen Universität München
Lichtenbergstr. 4, D-8046 Garching (FRG)

[**] This work was supported by the bayerischen Staatsministerium für Wissenschaft und Kunst and by the Volkswagenwerk Foundation. We thank Prof. Dr. *E. O. Fischer* and Prof. Dr. *W. A. Hermann* for support.

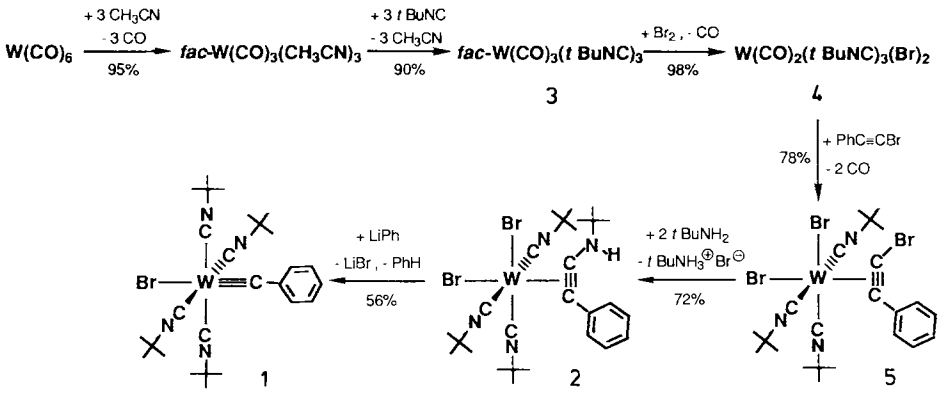

Scheme 2. New synthetic route to **1** from $W(CO)_6$ via alkyne complexes.

of an alkyne to C_1 fragments at a transition metal center.[6] On the basis of this reaction we have developed a new synthetic route to low-valent carbyne complexes starting from $(W(CO)_6$; the strategy is presented here, outlining the synthesis of **1** as example (Scheme 2).

$W(CO)_6$ is converted in two steps via *fac*-$W(CO)_3(CH_3CN)_3$[7a] into the triisocyanide-substituted complex **3**,[7b] which is oxidatively decarbonylated with Br_2 to the sevenfold coordinated W^{II} complex **4**. Thermal substitution of the two remaining CO ligands by $PhC\equiv CBr$ then leads to the bromoalkyne complex **5**,[8] which is finally converted with tBuNH$_2$ into the structurally related aminoalkyne complex **2**. This can then be converted by reaction with phenyllithium into **1**. Some data for the complexes **1**–**5** are collected in Table 1.

Table 1. Spectroscopic data of the complexes **1**–**5** [a, b].

1: IR: $\tilde{\nu}$[cm^{-1}] = 2156w, 2097s, 2064m [ν(C≡N*t*Bu)]; ^{1}H-NMR: δ = 1.52 (s, 36H; Me_3C), 7.06–7.15 (m, 5H; Ph); ^{13}C-NMR: δ = 31.3 (*Me*$_3$C), 57.1 (Me$_3$*C*), 124.7–152.4 (C_6H_5), 165.4 (Me$_3$CN*C*), 260.5 (W≡*C*).

2: IR: $\tilde{\nu}$[cm^{-1}] = 3394w [ν(NH)], 2173m, 2135vs, 2060m,sh [ν(C≡N*t*Bu)], 1685m [ν(C=N)]; ^{1}H-NMR: δ = 1.14 (s, 9H; *Me*$_3$CNH), 1.38 (s, 9H; Me_3C), 1.45 (s, 18H; 2 × Me_3C), 6.18 (s, 1H; NH), 6.88 (m, 2H), 7.16 (m, 1H) and 7.36 (m, 2H) (*m*-, *p*- and *o*-H of Ph); ^{13}C-NMR: δ = 29.7 (*Me*$_3$CNH), 31.1 (2 × *Me*$_3$C), 31.3 (*Me*$_3$C), 56.5 (Me$_3$*C*NH), 57.6 (2 × Me$_3$*C*), 60.0 (Me$_3$*C*), 124.0–149.8 (C_6H_5), 157.6 (2 × Me$_3$CN*C*), 175.1 (Me$_3$CN*C*), 193.5, 194.3 (*C*≡*C*).

3: IR: $\tilde{\nu}$[cm^{-1}] = 2155m, 2108m, 2065w,sh [ν(C≡N*t*Bu)], 1929vs, 1858s [ν(C≡O)]; ^{1}H-NMR: δ = 1.47 (s, 27H; Me_3C); ^{13}C-NMR: δ = 31.1 (*Me*$_3$C), 56.1 (Me$_3$*C*), 149.1 (Me$_3$CN*C*), 205.6 (*CO*).

4: IR: $\tilde{\nu}$[cm^{-1}] = 2175s, 2160s,sh [ν(C≡N*t*Bu)], 1975s, 1912s [ν(C≡O)]; ^{1}H-NMR: δ = 1.54 (s, 27H; Me_3C); ^{13}C-NMR: δ = 30.3 (*Me*$_3$C), 58.7 (Me$_3$*C*), 143.0 (Me$_3$CN*C*), 231.9 (*CO*).

5: IR: $\tilde{\nu}$[cm^{-1}] = 2187w,sh, 2158vs, 2133m,sh [ν(C≡N*t*Bu)]; ^{1}H-NMR: δ = 1.35 (s, 9H; Me_3C), 1.64 (s, 18H; 2 × Me_3C), 7.42–7.61 (m, 5H; Ph); ^{13}C-NMR: δ = 31.0 (*Me*$_3$C), 31.1 (2 × *Me*$_3$C), 57.9 (Me$_3$*C*), 59.7 (2 × Me$_3$*C*), 128.5–138.3 (C_6H_5), 152.8 (2 × Me$_3$CN*C*), 157.5 (Me$_3$CN*C*), 188.5 (Br*C*≡), 204.9 (Ph*C*≡).

[a] Correct elemental analyses and isotopically correct mass spectra for all compounds. [b] IR spectrum: ν(C≡N*t*Bu), ν(C≡O) and ν(C=N) in CH_2Cl_2, ν(NH) of **2** in KBR (Nicolet FT-5 DX spectrometer); NMR spectra in CD_2Cl_2 at 20 °C, values referred to the solvent (Jeol FT-GX-400 spectrometer).

The positions of the signals of the alkyne C atoms in the ^{13}C-NMR spectra ($\delta \approx 200$) of **2** and **5** are consistent with the presence of a 4e-donor alkyne ligand.[9a] The tungsten(II) center thus achieves noble gas configuration, like other d^4 metals in alkyne complexes.[9a] In agreement with earlier findings, no C≡C stretching vibration is observed for the 4e-donor alkyne ligands in **2** and **5**.[4a, 9a] In the series of carbyne complexes $Br(CO)_{4-n}(t$BuNC$)_n$W≡CPh (n = 0–4) the carbyne-C signal in the ^{13}C-NMR spectrum is shifted upfield with increasing n.[3b, 4a, 9b]

The assignment of the structure of the carbyne complex **1** was confirmed for the solid state by a single crystal X-ray structure analysis (Fig. 1).[10] For low-valent carbyne-tungsten complexes, striking features of the structure of **1** are the remarkably short W≡C (176.4(6) pm) distance and the long W–Br distance (275.62(6) pm.[11] The atomic sequence Br–W≡C–C is almost linear. Four equatorial *tert*-butyl isocyanide ligands complete the distorted octahedron (Fig. 1).

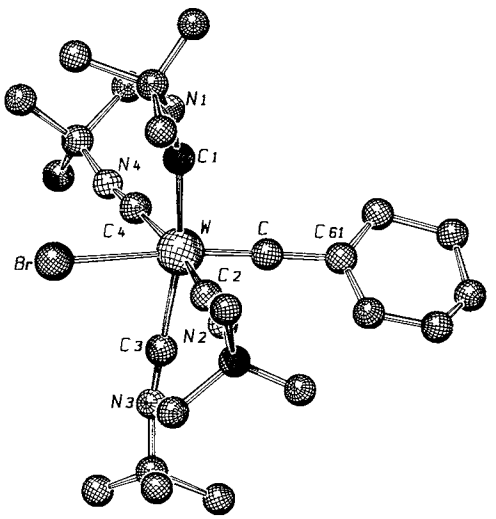

Fig. 1. Molecular structure (SCHAKAL) of the carbyne complex **1** in the crystal. Selected bond lengths [pm] and angles [°]: W–C 176.4(6), W–Br 275.62(6) W–C1 211.4(7), W–C2 209.1(6), W–C3 204.8(7), W–C4 210.9(5); W–C–C61 172.9(4), Br–W–C 171.0(1), Br–W–C1 80.5(1), Br–W–C2 82.1(1), Br–W–C3 85.5(2), Br–W–C4 88.4(1).

The newly developed synthetic route to the low-valent carbyne complex **1** from $W(CO)_6$ is not only an equally good alternative to the hitherto only known route via carbonyl-containing carbyne complexes,[3b, 4a] but, owing to its adaptability to alkyne complexes of other metals isoelectronic with W^{II}, (e.g. Ta^{I}), it opens up new perspectives in the chemistry of the low-valent carbon–metal multiple-bond systems. The key step of this new route, the base-induced CC-cleavage in

2 to give **1** is directly connected with the catalytic activity of carbyne-metal complexes in alkyne metathesis.[2c]

Experimental

All experiments were carried out in the absence of air and moisture. **4**: A solution of **3** (0.34 g, 0.66 mmol) in CH_2Cl_2 (20 mL) was treated at $-80\,^{\circ}C$ with a solution of Br_2 (0.105 g, 0.034 mL, 0.66 mmol) in CH_2Cl_2 (20 mL). The color of the reaction solution turned from pale to intense yellow. Finally, the solution was allowed to warm to room temperature, the solvent removed by evaporation, and the resulting residue reprecipitated from Et_2O/pentane; yield 0.42 g (98%), yellow solid, m.p. 115 °C (decomp.).

5: A solution of **4** (0.30 g, 0.46 mmol) in toluene (40 mL) was treated with PhC≡CBr (0.142 g, 0.097 mL, 0.78 mmol) and heated at 70 °C for 1 h. The color of the solution changed from yellow to green. After cooling to room temperature, the solvent was removed by distillation, and the resulting residue chromatographed on Al_2O_3 silica gel at 0 °C. **5** was eluted with CH_2Cl_2/Et_2O (1/5); yield 0.28 g (78%), green solid after reprecipitation from Et_2O/pentane, m.p. 66 °C.

2: A solution of **5** (0.48 g, 0.62 mmol) in THF (50 mL) was treated with tBuNH$_2$ (0.223 g, 0.32 mL, 3.05 mmol) and heated under reflux for 1.5 h. The color of the solution changed from green to blue. After removal of the solvent the residue was chromatographed on silica gel at 0 °C. **2** was eluted with Et_2O; yield 0.34 g (72%), blue, microcrystalline solid after reprecipitation from Et_2O/pentane, m.p. 144 °C.

1: A solution of **2** (0.32 g, 0.42 mmol) in THF (40 mL) was treated at $-80\,^{\circ}C$ with 1.10 mL of a 0.49 M solution of LiPh in Et_2O (0.54 mmol LiPh), warmed to room temperature, and stirred for 1.5 h. The color of the reaction solution changed from blue to brown-red. After removal of solvent, the residue was chromatographed on Al_2O_3 at 0 °C, and **1** was eluted with Et_2O/CH_2Cl_2 (2/1); yield 160 mg (56%), red, microcrystalline solid after reprecipitation from Et_2O/pentane, m.p. 122 °C (decomp.).

Received: September 22, 1989 [Z 3563 IE]
German version: *Angew. Chem. 102* (1990) 224

CAS Registry numbers:
1, 124618-91-3; **2**, 124618-92-4; **3**, 42401-95-6; **4**, 102258-54-8; **5**, 124650-70-0; PhC≡CBr, 932-87-6; tBuNH$_2$, 75-64-9; LiPh, 591-51-5.

[1] Summary: E. O. Fischer, Nobel lecture, Stockholm, December 11, 1973; *Angew. Chem. 86* (1974) 651.
[2] a) F. G. A. Stone, *Angew. Chem. 96* (1984) 85; *Angew. Chem. Int. Ed. Engl. 23* (1984) 89; b) H. P. Kim, R. J. Angelici, *Adv. Organomet. Chem. 27* (1987) 51; c) H. Fischer, P. Hofmann, F. R. Kreissl, R. R. Schrock, U. Schubert, K. Weiss: *Carbyne Complexes*, VCH, Weinheim 1988.
[3] a) A. C. Filippou, E. O. Fischer, *J. Organomet. Chem. 365* (1989) 317; b) *ibid. 383* (1990) 179.
[4] a) A. C. Filippou, W. Grünleitner, *Z. Naturforsch. B, 446* (1989) 1023; b) A. C. Filippou in U. Schubert (Ed.): *Advances in Metal Carbene Chemistry*, Kluwer Academic Publishers, Dordrecht 1989, p. 101; c) A. C. Filippou, *Polyhedron*, in press.
[5] S. Warner, S. J. Lippard, *Organometallics 8* (1989) 228.
[6] M. L. Listemann, R. R. Schrock, *Organometallics 4* (1985) 74.
[7] a) D. P. Tate, W. R. Knipple, J. M. Augl, *Inorg. Chem. 1* (1962) 433; b) M. O. Albers, E. Singleton, N. J. Coville, *J. Chem. Edu. 63* (1986) 444.
[8] Only a few halogenoalkyne complexes of this kind are known: a) R. G. Beevor, M. Green, A. G. Orpen, I. D. Williams, *J. Chem. Soc. Chem. Commun. 1983*, 673; b) C. Löwe, H.-U. Hund, H. Berke, *J. Organomet. Chem. 371* (1989) 311.
[9] a) J. L. Templeton, *Adv. Organomet. Chem. 29* (1989) 1; b) E. O. Fischer, G. Kreis, *Chem. Ber. 109* (1976) 1673.
[10] **1**: red, oblong plates from n-pentane/ether; systematic absences: OkO ($k = 2n + 1$); space group $P2_1$ (No. 4); lattice constants from a least squares refinement of 44 reflections at high diffraction angles; $a = 1160.3(5)$, $b = 1019.8(6)$, $c = 1329.6(4)$ pm, $\beta = 91.67(4)°$; $V = 1573 \times 10^6$ pm^3; empirical formula: $C_{27}H_{41}BrN_4W$ ($M_r = 685.4$), $Z = 2$, $\varrho_{calcd} = 1.447$ g cm^{-3}; $F_{000} = 680$; Enraf-Nonius CAD4, $Mo_{K\alpha}$ radiation, $\lambda = 71.073$ pm, graphite monochromator; $T = -50 \pm 3\,^{\circ}C$; measurement range: $1.0° \le \theta \le 25°$; ω scan; $t_{max} = 60$ s; 5533 measured reflections ($+h$, $\pm k$, $\pm l$); numerical absorption correction (6 faces), $\mu = 50.9$ cm^{-1}; decomposition: in 86.8 hours recording time -16.3%, corrected; structure solution: Patterson methods, difference Fourier technique; 5096 unique reflections, 4965 with $I > 0.5\sigma(I)$ used for the refinement; 249 parameters refined; $R = \sum (\|F_o| - |F_c\|)/\sum|F_o| = 0.041$; $R_w = [\sum w(|F_o| - |F_c|)^2/\sum wF_o^2]^{1/2} = 0.032$; GOF $= [\sum w(|F_o| - |F_c|)^2/(NO-NV)]^{1/2} = 2.96$ ($w = 1/\sigma^2[F_o]$); shift error < 0.01 in the last refinement cycle; $\Delta e_o/Å^3 = +2.05$ (besides the heavy atom tungsten); the refinement of the enantiomorph yields poorer agreement values; hydrogen positions calculated for ideal geometry ($d_{C\,H} = 95$ pm) and incorporated with collective isotropic displacement parameters per C atom in the structure factor calculation, but not refined, anomalous dispersion taken into account. Further details of the crystal structure investigation are available on request from the Fachinformationszentrum Karlsruhe, Gesellschaft für wissenschaftlich-technische Information mbH, D-7514 Eggenstein-Leopoldshafen 2 (FRG), on quoting the depository number CSD-54283, the names of the authors, and the journal citation.
[11] a) G. Huttner, A. Frank, E. O. Fischer, *Isr. J. Chem. 15*(1976/77) 133; b) D. Neugebauer, E. O. Fischer, N. Q. Dao, U. Schubert, *J. Organomet. Chem. 153* (1978) C41; c) F. A. Cotton, W. Schwotzer, *Inorg. Chem. 22* (1983) 387.

Lithium Bis(di-*tert*-butylfluorosilyl)amide as Contact Ion Pair with Linear Si–N$^{\ominus}$–Si Unit and as Ion Pair without Li$^{\oplus}$-Anion Contact**

By *Ursula Pieper, Simone Walter, Uwe Klingebiel,** and *Dietmar Stalke*

Structure investigations on lithium organo(fluorosilyl)-amides have repeatedly furnished astonishing results: the structural types found so far include tri-(**I**),[1] bi- (**IIa, IIb**),[2, 3] and monocyclic (**III**)[4] compounds containing an LiF contact, as well as LiF adducts (**IV**) of iminosilanes.[5]

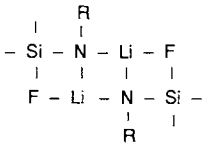

I[1]

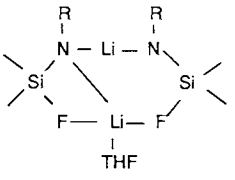

IIa[2]

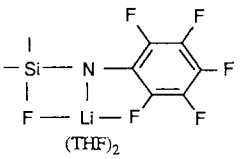

IIb[3]

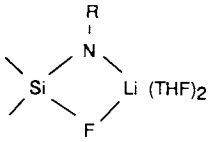

III[4]

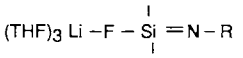

IV[5]

Essentially three factors determine the structural make up of the lithium derivatives:

1) A common feature of all compounds is that the Lewis acid strives to bind lithium, while the Lewis base strives to bind fluorine.
2) The LiF contact is influenced by bases which coordinate lithium.

[*] Prof. Dr. U. Klingebiel, U. Pieper, S. Walter, Dr. D. Stalke
Institut für Anorganische Chemie der Universität
Tammannstrasse 4, D-3400 Göttingen (FRG)

[**] This work was supported by the Fonds der Chemischen Industrie. We thank Prof. Dr. *P. von R. Schleyer* and Dr. *M. Bremer* for their help with the ab initio calculations.

3) The decreasing basicity of the nitrogen in the series of lithium derivatives with R = alkyl, silyl, aryl finally leads to rupture of the Li–N bond.

In the present communication we describe the syntheses and crystal structures of the first lithium bis(fluorosilyl) amide in various donor solvents.

Starting from $t\mathrm{Bu_2SiFNH_2}$ and $t\mathrm{Bu_2SiF_2}$ we isolated bis-(tri-*tert*-butylfluorosilyl)amine **1** [6] (Table 1). **1** was lithiated with BuLi, and, after treatment with the donor reagent THF, TMEDA, or [12]crown-4, the amides **2, 3** and **4**, respectively, were isolated and characterized (Table 1). **4** is also formed on using only one equivalent of the crown ether.

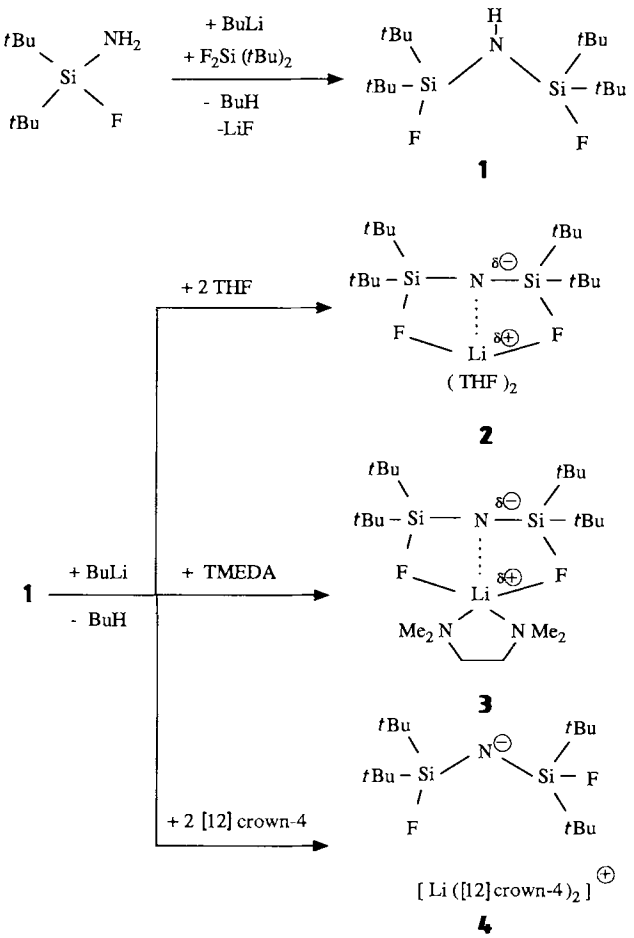

Table 1. NMR data of the compounds **1**–**4**. All measurements at 25 °C with a 250-MHz spectrometer (except ^{19}F: 80-MHz apparatus). Standard for ^{1}H, ^{13}C and ^{29}Si NMR: TMS int., for ^{19}F NMR C_6F_6 ext., for ^{7}Li NMR: LiCl ext.

1 (all measurements in CH_2Cl_2/C_6D_6: ^{1}H NMR: $\delta = 1.08$ (d, ^4J(H,F) = 0.6 Hz, 36H; *t*Bu); ^{13}C NMR: $\delta = 20.6$ (d, ^2J(C,F) = 15.8 Hz, 4C; CC_3), 27.7 (d, ^3J(C,F) = 0.9 Hz, 12C; CC_3); ^{19}F NMR: $\delta = 1.58$ (d, ^3J(H,F) = 8.61 Hz); ^{29}Si NMR: $\delta = 2.60$ (d, ^1J(Si,F) = 305.8 Hz, 2 Si)

2: ^{1}H NMR (C_6D_6): $\delta = 1.32$ (36H; *t*Bu), 1.3 (8H; $O(CH_2CH_2)_2$), 3.5 (8H; $O(CH_2CH_2)_2$); ^{13}C NMR (C_6D_6): $\delta = 22.5$ (d, ^2J(C,F) = 21.7 Hz, 4C; CC_3), 29.7(12C; CC_3), 68.2 (4C; $O(C_2C_2)$); ^{19}F NMR (C_6D_6): $\delta = 11.7$; ^{29}Si NMR (hexane/THF: $\delta = -12.3$ (d, ^1J(Si,F) = 272.5 Hz); ^{7}Li NMR (toluene/THF: $\delta = 0.17$ (t, ^1J(Li, F) = 15.0 Hz)

3 (all measurements in C_6D_6): ^{1}H NMR: $\delta = 1.36$ (36H; tBu), 1.9 (12H; TMEDA); ^{13}C NMR: $\delta = 22.07$ (d, ^2J(C,F) = 22.7 Hz; 4C; CC_3), 29.72 (12C; CC_3), 46.2 (4C; TMEDA); ^{19}F NMR: $\delta = 13.1$; ^{29}Si NMR: $\delta = -12.0$ (d, ^1J(Si,F) = 271.4 Hz)

4 (all measurements in C_6D_6/THF): ^{1}H NMR: $\delta = 1.02$ (36H; *t*Bu); 3.5 (32H; [12]crown-4); ^{13}C NMR: $\delta = 22.0$ (d, ^2J(C,F) = 23.7 Hz; d, ^4J(C,F) = 2.3 Hz, 4C; CC_3), 29.93 (12C; CC_3), 68.93 (16C, [12]crown-4); ^{19}F NMR: $\delta = -22.5$ (d, ^1J(Si,F) = 295.2 Hz); ^{7}Li NMR: $\delta = -1.34$

Lithiated bis(di-*tert*-butylfluorosilyl)amine crystallizes from THF as the monomeric amide **2** (Fig. 1). According to the results of an X-ray structure analysis [7] the coordination sphere of the lithium is made up of the two fluorine atoms, the nitrogen atom, and two THF molecules. The lithium thus brackets the Si_2NF_2 skeleton to form a planar six-membered ring. This geometry enforces the *tert*-butyl groups into an eclipsed position. Despite this steric compression the nitrogen atom is shifted, as a result of electrostatic interaction, towards the lithium atom. The six-membered ring contains an almost linear Si–N$^{\ominus}$–Si unit (Si–N–Si = 176.7°), the first time that this has been observed. Alkali-metal compounds of bis(trimethylsilyl)amine have Si–N–Si angles of 125 to 136°.[8] The amide **2** is thus structurally analogous to the isoelectronic siloxane (Ph_3Si–O–$SiPh_3$).[9] The widening of the Si–N–C angle in **II b** to 140.1° continues towards linearity in **2**. The Si–N distances in **2** (163.6 pm) lie in the range typical for Si–N double bonds. The ^{7}Li-NMR spectrum already shows a triplet at $\delta = 0.17$ with $J_{LiF} = 15$ Hz at room temperature, i.e. the lithium atom is also coordinated to fluorine in solution. From the similarity of their NMR data it can be concluded that **2** and **3** have analogous molecular structures.

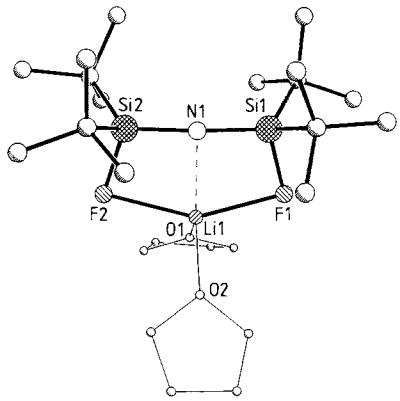

Fig. 1. Molecular structure of **2** in the crystal. Selected bond lengths [pm] and angles [°]: Si1–N1 163.6(6), Si–N1 163.6(6), Si1–F1 165.9(4), Si2–F2 165.3(4), Li1–F1 212.3(15), Li1–F2 220.5(13), Li1–N1 211.5(13), mean Li–O 193.9; Si1–N1–Si2 176.7(4), F1–Li1–F2 149.5(6), N1–Si1–F1 104.2(2), N1–Si2–F2 104.3(2).

If, however, the stronger donor [12]crown-4 is used for coordination saturation of the Lewis acid lithium, free ions are formed instead of a contact pair like **2** (Fig. 2). It follows

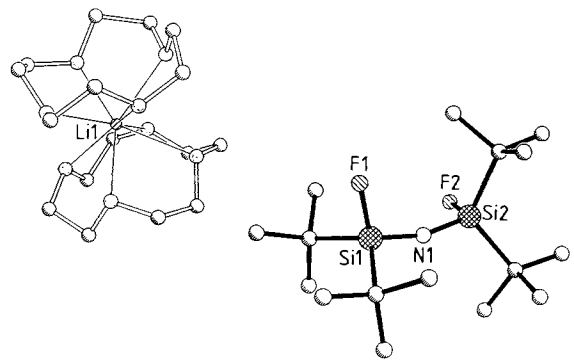

Fig. 2. Molecular structure of the amide **4** in the crystal. Selected bond lengths [pm] and angles [°]: Si1–N1 160.6(7), Si2–N1 163.0(6), Si1–F1 164.4(5), Si2–F2 163.7(5), mean Li–O 236.5; Si1–N1–Si2 162.6(5).

from the crystal structure analysis of **4**[10, 11] that interaction between the ions ceases upon coordination of two crown ether molecules to the lithium ion. Lithium is formally eightfold coordinated. Since the lithium atom no longer brackets the two fluorine atoms of the anion, the *tert*-butyl groups become staggered, and steric compression thus minimized. The Si–N–Si angle in **4** is reduced by 14.1° compared to that in **2** to 162.6°, and is thus ca. 8° larger than in the $[Ph_3SiNSiPh_3]^{\ominus}$ system.[12]

The model system $(H_3Si)_2N^{\ominus}$ was computed with GAUSSIAN 88[13] using the basis set 6–31 + G*.[14] The starting value for the Si–N–Si angle was optimized from 120° to 180°. The calculated Si–N bond length is 162.4 pm. The experimental data of the structure analysis of **2** and **4** are thus in good agreement with the ab initio calculated data.[13–15] The $Si–N^{\ominus}–Si$ system bent at an angle of 120° at the nitrogen atom is only 25 kJ mol^{-1} more energetic than the system with optimized geometry.

Experimental

1: A solution of 0.01 mol (1.77 g) of tBu_2SiFNH_2 in 50 mL of hexane was treated with 0.01 mol of BuLi (15% in hexane). The lithium salt that was formed was brought into solution by addition of ca. 50 mL of THF. After subsequent addition of 0.01 mol of tBu_2SiF_2, the reaction mixture was heated under reflux for ca. one week. The reaction was monitored ^{19}F-NMR spectroscopically. **1** was purified by distillation. Yield 3.0 g (90%).

2 and **3**: A solution of 0.01 mol (3.37 g) of **1** in 25 mL of hexane was treated with 0.01 mol of BuLi (15% in hexane). The resulting slurry was brought into solution by addition of THF. The solvent was then removed in vacuo and the crude product was crystallized from hexane (**2**) or TMEDA (**3**). Yield: 95% of **2** and 95% of **3**, respectively.

4: A solution of 0.01 mol (3.37) of **1** in 50 mL of THF was treated with 0.01 mol of BuLi (15% in hexane). After addition of 0.02 mol (1.76 g) of [12]crown-4, the crude product was recrystallized from THF. Yield: 85%.

Received: September 4, 1989;
revised: November 15, 1989 [Z 3535 IE]
German version: *Angew. Chem. 102* (1990) 218

CAS Registry numbers:
1, 124686-71-1; **2**, 124686-74-4; **3**, 124686-75-5; **4**, 124686-73-3; TMEDA, 110-18-9; tBu_2SiFNH_2, 83312-30-5; tBu_2SiF_2, 558-63-4; [12]crown-4, 294-93-9.

[1] D. Stalke, N. Keweloh, U. Klingebiel, M. Noltemeyer, G. M. Sheldrick, *Z. Naturforsch. B42* (1987) 1237.
[2] D. Stalke, U. Klingebiel, G. M. Sheldrick, *J. Organomet. Chem. 344* (1988) 37.
[3] D. Stalke, U. Klingebiel, G. M. Sheldrick, *Chem. Ber. 121* (1988) 1457.
[4] D. Stalke, *Dissertation*, Universität Göttingen 1987.
[5] R. Boese, U. Klingebiel, *J. Organomet. Chem. 315* (1986) C17.
[6] **1**: b.p. 72 °C/0.01 mbar; MS (70 eV): *m/z* 337 ($M^{\oplus}$, 2%); IR (neat): $\tilde{\nu}$ [cm^{-1}] = 3360 (N–H).
[7] **2**: $C_{24}H_{52}LiNO_2F_2Si_2$, monoclinic *C*2/*c*, a = 3495.3(7), b = 991.3(2), c = 1774.2(4) pm, β = 101.13(2)°, V = 6.030 nm^3, ϱ_{calcd} = 1.1 g cm^{-3}, Z = 8, $\mu(Mo_{K\alpha}$, graphite monochromator) = 0.14 mm^{-1}, 5475 reflections collected, 3912 unique and 2295 observed with $F \geq 3\sigma F$, $2\Theta_{max}$ = 45°, refinement of 289 parameters, R = 0.0988, R_w = 0.0704, $w^{-1} = \sigma(F) + 0.0001\,F^2$, residual electron density ± 4.2 × 10^2 nm^{-3} [11].
[8] T. Fjeldberg, P. B. Hitchcock, M. F. Lappert, A. J. Thorne, *J. Chem. Soc. Chem. Commun. 1984*, 822; R. Grüning, J. L. Atwood, *J. Organomet. Chem. 137* (1977) 101; A. M. Domingos, G. M. Sheldrick, *Acta Crystallogr. Sect. B30* (1974) 517; F. Pauer, D. Stalke, M. Wedler, F. T. Edelmann, unpublished.
[9] C. Glidewell, D. C. Liles, *J. Chem. Soc. Chem. Commun. 1977*, 632.
[10] **4**: $C_{32}H_{68}LiNO_8F_2Si_2$, monoclinic, $P2_1/n$, a = 1014(7(2), b = 2474.2(7), c = 1645.5(5) pm, β = 91.88(3)°, V = 4.129 nm^3, ϱ_{calcd} = 1.12 g cm^{-3}, Z = 4, $\mu(Mo_{K\alpha}$, graphite monochromator) = 0.13 mm^{-1}, 6205 reflections collected, 5331 unique and 2577 observed with $F \geq 3\sigma F$, $2\Theta_{max}$ = 45°, refinement of 295 parameters, R = 0.0933, R_w = 0.0699, $w^{-1} = \sigma(F) + 0.0005\,F^2$, residual electron density ± 4.7 × 10 e nm^{-3}.
[11] Data collection for both structures on a Stoe-Siemens AED at −85°, solution of structure and refinement with SHELX 86; in **2** all non-hydrogen atoms, in **4** only the non-hydrogen atoms of the anion and the lithium atom were refined anisotropically. All hydrogen atoms placed at ideal geometric positions and incorporated in the calculations as a rigid group using a riding model with fixed temperature factors. Further details of the structure investigations are available on request from the Fachinformationszentrum Karlsruhe, Gesellschaft für wissenschaftliche-technische Information mbH, D-7514 Eggenstein-Leopoldshafen 2 (FRG), on quoting the depository number CSD-54192, the names of the authors, and the journal citation.
[12] H. Chen, R. A. Bartlett, H. V. R. Dias, M. M. Olmstead, P. P. Power, *J. Am. Chem. Soc. 111* (1989) 4338.
[13] GAUSSIAN 88: M. J. Frisch, M. Head-Gordon, H. B. Schlegel, K. Raghavachari, J. S. Binkley, C. Gonzalez, D. J. Defrees, D. J. Fox, R. A. Whiteside, R. Seger, C. F. Melius, J. Baker, L. R. Kahn, J. J. P. Stewart, E. M. Fluder, S. Topiol, J. A. Pople, GAUSSIAN Inc., Pittsburgh, PA (USA).
[14] P. J. Hehre, L. Radom, P. von R. Schleyer, J. A. Pople: *Ab initio Molecular Orbital Theory*, Wiley, New York 1986.
[15] C. Glidewell, C. Thomson, *J. Comput. Chem. 3* (1982) 495.

Vinylogous Cyanine-like Dications of Tetrakis(dimethylamino) Compounds**

By *Karin Elbl-Weiser, Claus Krieger,* and *Heinz A. Staab**

The dications **1**–**3** can be regarded as a vinylogous series in which two cyanine-like mesomeric π-bond systems are coupled by one, two and three single bonds, respectively. The dication **1** derived from tetrakis(dimethylamino)ethene was already studied in detail by *Wiberg* and *Buchler*[1] in the sixties; its spatial structure, however, was still unknown.[2] An X-ray structure analysis of **1** $(PF_6^{\ominus})_2$[3] confirmed the above formulation: the two cyanine-like substructures show a hitherto unexpected[1b] strong twisting of ca. 72° about the central C–C bond, which, according to its length of 151.1(5) pm, is a single bond. We already reported in 1986 on the synthesis of 1,2,4,5-tetrakis(dimethylamino)benzene and on the formation and structure of the dication **2** derived therefrom.[4] The two mesomeric substructures in **2** are also twisted (≮ 49°) against each other, leading to a correspondingly distinct twist form of the six-membered ring; on the basis of their lengths the C(1), C(2) and C(4)–C(5) bonds can be regarded as single bonds, whereas the C–N bonds at C(1), C(2), C(4), and C(5) have double bond character corresponding to the formulation **2**. In continuation of this series, the species **3**, whose π-subsystems are to be formally seen as vinylogous to **2**, was of special interest.[5]

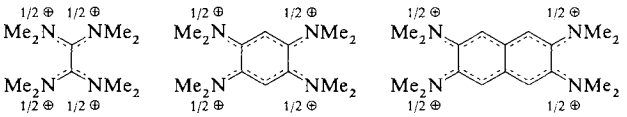

For the synthesis of 2,3,6,7-tetrakis(dimethylamino)naphthalene **4** the diaminonaphthalene **5**[6] was converted by reaction with *N*-bromosuccinimide (1,4-dioxane, 3 h, 20 °C, under argon) and subsequent treatment with tin in the pres-

[*] Prof. Dr. H. A. Staab, Dr. K. Elbl-Weiser, C. Krieger
Abteilung Organische Chemie
Max-Planck-Institut für medizinische Forschung
Jahnstrasse 29, 6900 D-Heidelberg (FRG)

[**] Electron Donor-Acceptor Compounds, Part 47.—Part 46: H. A. Staab, C. Krieger, P. Wahl, K.-Y. Kay, *Chem. Ber. 120* (1987) 551.

ence of glacial acetic acid (18 h reflux)[7] into **6** (76% yield; m.p. 229–230 °C).[8] Reductive *N*-methylation of **6** (formaldehyde, sodium cyanotrihydroborate, acetonitrile/glacial acetic acid)[9] afforded **7** (93% yield; m.p. 51–52 °C).[8] Subsequent halogen-metal exchange (*n*-butyllithium, tetrahydrofuran/*n*-hexane, 20 min, −78 °C), reaction with diphenyl azidophosphate (tetrahydrofuran, −78 °C), and immediate reduction with sodium bis(2-methoxyethoxydihydridoaluminate (toluene, −78 °C to 0 °C)[10] furnished **8**, which was converted by reductive methylation (see above) into **4** (13% yield; m.p. 170–171 °C)[8] [^{1}H NMR (360 MHz, CD_2Cl_2):

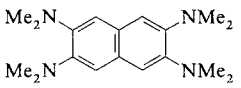

4

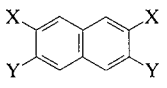

5: X = NH_2, Y = H
6: X = NH_2, Y = Br
7: X = NMe_2, Y = Br
8: X = NMe_2, Y = NH_2

δ = 2.83 (s, 24H), 7.02 (s, 4H); MS: *m/z* 300 ($M^{\oplus}$, base peak)]. Figure 1 shows (above) the molecular structure of **4**[11] viewed onto the naphthalene plane and (below) a side view perpendicular to the C(2)–C(3) bond.

Despite the steric interaction between the two pairs of vicinal dimethylamino groups (N···N distances between neighboring dimethylamino groups: 285.2 pm) the C–N bonds at C(2), C(3), C(2i) and C(3i) do not deviate out of the naphthalene plane; striking, however, is the lengthening of the bond between the substituted ring atoms C(2)–C(3) and C(2i)–C(3i), resp., to 143.8 pm.

Compound **4** differs markedly from its benzene analogue in its much weaker electron donor strength. Whereas the first two oxidation steps in the latter, which lead to the formation of **2**, cannot be separated cyclovoltammetrically (E_{ox} = −0.266 V),[4] in the case of **4** one finds, under the same conditions, a first oxidation step corresponding to donation of *one* electron with E_{ox} = +0.08 V, followed by a second oxidation step, which likewise corresponds to a *one*-electron transfer with E_{ox} = +0.16 V (the potentials of higher oxidation steps were not determinable, owing to irreversible processes under the conditions employed).[12] Consistent with these results is the finding that **4** forms a more stable radical cation than 1,2,4,5-tetrakis(dimethylamino)benzene, the ESR and ENDOR investigations of which will be reported elsewhere.[13] With oxidizing agents

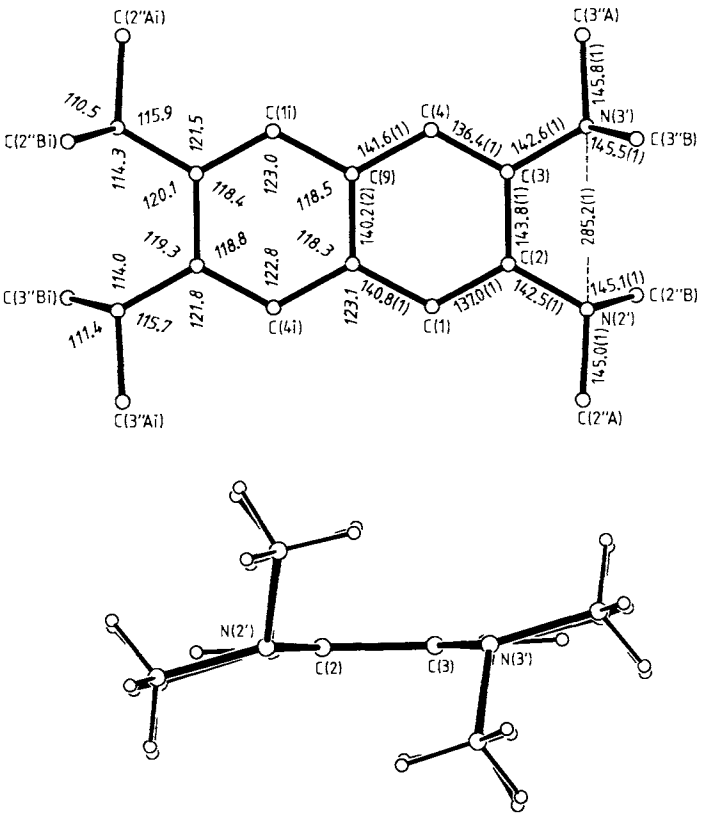

Fig. 1. Molecular structure of **4**; above: view onto the naphthalene plane with bond lengths [pm] and bond angles [°]; below: side view in the direction of the longitudinal axis of the naphthalene plane [11].

such as iodine or 2,3-dichloro-5,6-dicyanobenzoquinone (DDQ), **4** forms green to black products which we have so far been unable to fully characterize; with tetracyanoquinodimethane (TCNQ) a crystalline complex [black prisms, m.p. 207 °C (decomp.)] was actually isolable, but its analytical data provided no confirmatory evidence for the presence of the dication **3**. Also an attempt to detect **3** spectroscopically in a dilute solution of **4** in dichloromethane after addition of two equivalents of bromine did not lead to an unequivocally informative result. We attribute the striking difference in the stability of the vinylogous dications **2** and **3** to the following steric factors: whereas in the case of **2** a high degree of planarity is possible within the two cyanine subunits including the terminal Me_2N groups by the above-

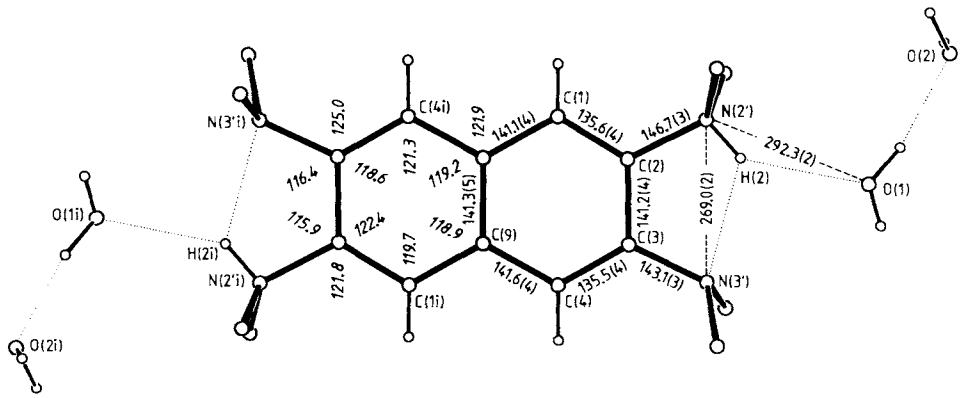

Fig. 2. Partial structure of **4** · dihydrobromide tetrahydrate viewed onto the naphthalene plane, with bond lengths [pm] and bond angles [°] [16].

mentioned twist arrangement of the six-membered ring, in the case of **3** the bicyclic framework is so strongly planarized by threefold coupling that steric interaction between the neighboring Me_2N groups hinders a planar arrangement of the mesomeric cyanine systems.

Although the N···N distance between the neighboring dimethylamino groups in **4** is only a few pm greater than in typical "proton sponges",[14] **4** does not display the special properties of these compounds. In **4**, both the destabilization of the base by repulsive interaction of the dimethylamino groups as well as the stabilization of the protonated form are less, since the lone pairs of the nitrogen atoms are not directed towards each other due to steric factors, and strong linear N···H···N hydrogen bonds cannot be formed. However, in analogy to the "proton sponges", **4** is not protonated fourfold but only twofold in the presence of excess acid. Reaction with aqueous hydrobromic acid affords the dihydrobromide of 4, which crystallizes as the tetrahydrate.[8] Figure 2 shows the structure of diprotonated **4** with incorporated molecules of water of crystallization. It is immediately apparent that in each case the subunits of two neighboring dimethylamino groups are singly protonated and that unsymmetric strongly bent N–H···N hydrogen bonds are present which are "bifurcated" due to interaction with the molecules of water of crystallization. This structure resembles that of the dihydrobromide dihydrate of 1,2,4,5,-tetrakis(dimethylamino)benzene.[15]

Received: August 28, 1989;
revised: November 3, 1989 [Z 3525 IE]
German version: *Angew. Chem. 102* (1990) 183

CAS Registry numbers:
1·2$PF_6^\ominus$, 7163-17-9; **3**, 124604-82-6; **4**, 124604-75-7; **4**·TCNQ, 124604-79-1; **4**·2HBr·4H_2O, 124604-80-4; $4^{\bullet\oplus}$, 124604-81-5; **5**, 613-76-3; **6**, 124604-76-8; **7**, 124604-77-9; **8**, 124604-78-0.

[1] a) N. Wiberg, J. W. Buchler, *Chem. Ber. 96* (1963) 3223; b) N. Wiberg, *Angew. Chem. 80* (1968) 809; *Angew. Chem. Int. Ed. Engl. 7* (1968) 766.
[2] After submission of the original version of this communication we were informed by the editors that structural analyses of **1** ($X^\ominus$)$_2$ with X = Cl and Br had been submitted for publication: H. Bock, K. Ruppert, K. Merzweiler, D. Fenske, H. Goesmann, *Angew. Chem. 101* (1989) 1715; *Angew. Chem. Int. Ed. Engl. 28* (1989) 1684. With regard to the structure of the cation **1** they are consistent with the structural analysis of **1**($PF_6^\ominus$)$_2$ carried out by us. We have therefore waived a detailed description of our structure analysis in this revised version of our communication.
[3] a) Crystallographic data of **1**($PF_6^\ominus$)$_2$: colorless prisms, m.p. 284–285 °C (decomp.) from acetonitrile/ether (2:1); orthorhombic, space group Pbca; a = 2131.1(3), b = 1534.3(3), c = 1221.2(3) pm; Z = 8, ϱ_{calc} = 1.631 g cm^{-3}; 3497 measured reflections, 1903 regarded as observed with $I \geq 3.0\,\sigma(I)$; solution by direct methods (MULTAN), R = 0.058. b) Further details of the crystal structure investigation are available on request from the Fachinformationszentrum Karlsruhe, Gesellschaft für wissenschaftlich-technische Information mbH, D-7514 Eggenstein-Leopoldshafen 2 (FRG), on quoting the depository number CSD-54188, the names of the authors, and the journal citation.
[4] K. Elbl, C. Krieger, H. A. Staab, *Angew. Chem. 98* (1986) 1024; *Angew. Chem. Int. Ed. Engl. 25* (1986) 1023; related compounds have been reported by R. Gompper and H.-U. Wagner [*Angew. Chem. 100* (1988) 1492; *Angew. Chem. Int. Ed. Engl. 27* (1988) 1437].
[5] Cf. also the calculations by A. Mehlhorn, J. Fabian, *J. Mol. Struct. 109* (1984) 27; J. Fabian, R. Zahradnik, *Angew. Chem. 101* (1889) 693; *Angew. Chem. Int. Ed. Engl. 28* (1989) 677; J. Fabian, private communication.
[6] E. Bamberger, W. J. Schieffelin, *Ber. Dtsch. Chem. Ges. 22* (1889) 1374.
[7] This reaction provides the selective debromination in the 1-position of the initially formed tribromo product.
[8] Elemental analyses and spectroscopic data confirm the proposed structures.
[9] See R. F. Borch, A. I. Hassid, *J. Org. Chem. 37* (1972) 1673.
[10] Analogous to S. Mori, T. Aoyama, T. Shioiri, *Tetrahedron Lett. 25* (1984) 429.
[11] Crystal structure data of **4**: monoclinic, space group $P2_1/n$: a = 1100.2(2), b = 738.4(2), c = 1207.1(2) pm, β = 116.28(1)°; Z = 2, ϱ_{calcd} = 1.135 g cm^{-3}; 2219 measured reflections, 1964 observed with $I \geq 3.0\sigma(I)$, solution by direct methods (MULTAN); R = 0.043; for further details cf. [3b].
[12] Cyclovoltammetry in acetonitrile/0.1 M tetrabutylammonium perchlorate, glassy carbon electrode versus Ag/$Ag^\oplus$; ferrocene correction.
[13] K. Elbl-Weiser, F. A. Neugebauer, H. A. Staab, *Tetrahedron Lett. 30* (1989) 6161.
[14] Review: H. A. Staab, T. Saupe, *Angew. Chem. 100* (1988) 895; *Angew. Chem. Int. Ed. Engl. 27* (1988) 865.
[15] H. A. Staab, K. Elbl, C. Krieger, *Tetrahedron Lett. 27* (1986) 5719.
[16] Crystal data of 4 · 2 HBr · 4H_2O: monoclinic, space group $P2_1/n$; a = 704.1(2), b = 2276.4(4), c = 796.5(2) pm, β = 102.71(1)°; Z = 2, ϱ_{calcd} = 1.425 g cm^{-3}; 2964 measured reflections, 1964 observed with $I \geq 3.0\sigma(I)$, solution by direct methods (MULTAN); R = 0.040; for further details cf. [3b].

Structure and Color of Substituted Pentaphenylbismuth **

By *Arno Schmuck, Pekka Pyykkö,* and *Konrad Seppelt* *

The deep violet complex $Bi(C_6H_5)_5$, first described by Wittig in 1952, has an almost regular square pyramidal structure[1] quite like that of solvate-free $Sb(C_6H_5)_5$,[2] but in complete contrast to that of $P(C_6H_5)_5$ and $As(C_6H_5)_5$, both of which have trigonal-bipyramidal stereochemistry.[3] In the solid state $Bi(C_6H_5)_5$ is dichroic. The aim of this investigation was to establish, by experimental and theoretical work, how the structure of the molecule and its derivatives affects their chromophoric properties.

$Bi(C_6H_5)_3(2\text{-}F\text{-}C_6H_4)_2$ **1** $Bi(4\text{-}H_3C\text{-}C_6H_4)_3(2\text{-}F\text{-}C_6H_4)_2$ **2**

All previously investigated pentaphenylbismuth derivatives are colored and have a square-pyramidal structure,[4, 5] an unusual feature in main group chemistry. The fluoro-derivative **1** is violet and dichroic in the solid state also, and has a square-pyramidal structure (Fig. 1a). In solution, however, it has a reddish color (see Fig. 2), but again forms purple crystals. The very similar methylfluoro-derivative **2** has the same color in solution (see Fig. 2), but forms *orange* crystals. Its structure is the first in which five (substituted) phenyl groups surround bismuth in a trigonal-bipyramidal array (Fig. 1b).

It is clear from the colors in solution that both structures involved in the Berry pseudorotation mechanism are present. The ratio of the absorption intensities does not change, even with large variations in temperature. It follows, therefore, that the difference between the energies of the trigonal-bipyramidal and square-pyramidal arrangements must be close to zero and that the solid state structure is determined by lattice forces. Ligand exchange cannot be frozen-out even at the lowest achievable temperature (^{19}F NMR); this result also points to a low energy barrier between the two structures ($\Delta G < 20$ kJ mol^{-1}).

[*] Prof. Dr. K. Seppelt, Dipl.-Chem. A. Schmuck
Institut für Anorganische und Analytische Chemie der Freien Universität
Fabeckstrasse 34–36, D-1000 Berlin 33
Prof. P. Pyykkö
Department of Chemistry, University of Helsinki
Et Hesperiankatu 4, 00100 Helsinki (Finland)

[**] This work was supported by the Deutsche Forschungsgemeinschaft and the Fonds der Chemischen Industrie. We thank Prof. Dr. *G. Huttner* and his co-workers, Heidelberg, for help with the recording of the low-temperature UV/VIS spectra.

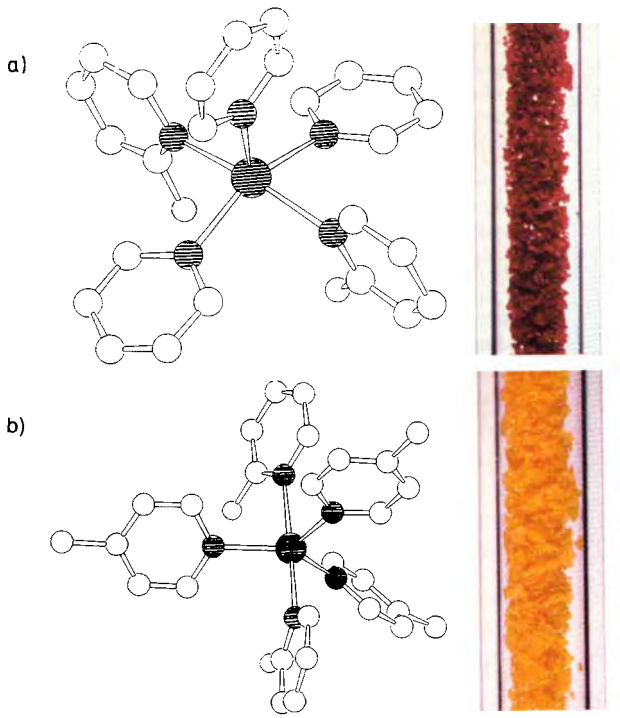

Fig. 1. a) Crystal structure of **1** (violet); section, original color. The skeletal atoms are hatched. Stoe four-circle Diffractometer −40°; $Mo_{K\alpha}$, graphite monochromator, ω-2θ scan, DIFABS absorption correction, XTAL, full matrix, all atoms anisotropic, without H atoms. $P\bar{1}$, $a = 981.0(7)$, $b = 1026.9(14)$, $c = 1324.3(27)$ pm, $\alpha = 110.06(1)$, $\beta = 95.2(1)$, $\gamma = 97.4(1)°$, $V = 1252 \times 10^6$ pm^3, $Z = 2$. Reflections: 3677 measured, 3085 independent, 2851 with $I \geq 3\sigma(I)$ within $2 \leq \theta \leq 25°$. $R = R_w = 0.025$. Bi–C(ax) 221.6(5). Bi–C (basal) 234.6(4), 328.5(7), 228.4(7), 236.3(5) pm; C(basal)–Bi–C(basal) 169.2(2), 150.0(2)°. $\Delta = 19.2°$ corresponding to the definition in Ref. [4], $\Delta = 0°$ for ideal square pyramids.—b) Crystal structure of **2** (orange); section: original color. The skeletal atoms are hatched. For technical data and calculations see Fig. 1a, $P2_1/n$, $a = 1029.3(2)$, b = 2262.8(5), $c = 1214.1(3)$ pm, $\beta = 101.32(2)°$, $V = 2773 \times 10^6$ pm^3, $Z = 4$. Reflections: 3097 measured, 2845 independent, 2538 with $I \geq 2\sigma(I)$ within $2 \leq \theta \leq 20°$, $R = 0.44$, $R_w = 0.050$. Bi–C(ax) 242.33(16), 235.8(16), Bi–C(eq) 213.4(15), 220.1(13), 221.7(16) pm; C(ax)–Bi–C(ax) 176.3(5), C(eq)–Bi–C(aq) 118.9(6), 130.6(6), 110.4(5)°. $\Delta = 45.4°$ corresponding to the definition in Ref. [4], $\Delta = 60°$ for ideal trigonal bipyramids.—Further details of the crystal structure investigations are available on request from the Fachinformationszentrum Karlsruhe, Gesellschaft für wissenschaftlich-technische Information mbH, D-7514 Eggenstein-Leopoldshafen 2 (FRG), on quoting the depository number CSD-54259, the names of the authors, and the journal citation.

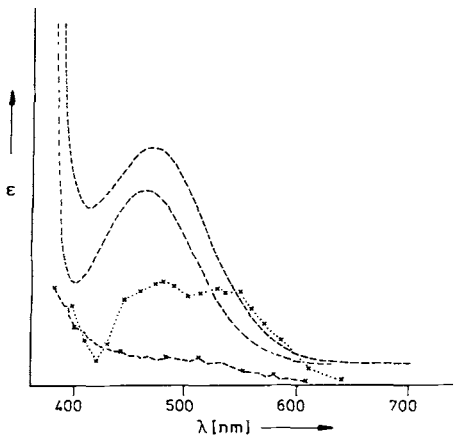

Fig. 2. UV/VIS spectra for **1** and **2**. (——) above: **1** in THF solution −40 °C; (——), below: **2** in THF solution, −40 °C. The two curves are almost identical, but the absorption of **2** is weaker (solubility!). (x···x): **1**, crystalline, +25 °C; (x–––x): **2**, crystalline, +25 °C. Solid state UV measurements: Carl Zeiss UMSP-80 microphotometer. Because of the intense light the substances have only a short lifetime; this explains the poor quality of the spectra. The eye is the better spectrometer in this instance.

Extended Hückel calculations with relativistic corrections show a very different MO diagram for the hypothetical molecule BiH_5 in the case of ideal D_{3h} and C_{4v} symmetry.[6] The reduced HOMO-LUMO separation in the latter is very striking. The HOMO is predominantly a (non-bonding) ligand orbital in the basal plane, while the LUMO has mainly Bi-6p$_z$ character, i.e. it points into the vacant coordination site (Fig. 3). Such a qualitative difference between the MO diagrams for the two geometries has already been calculated for the hypothetical PH_5,[7] which, even if it existed, however, should be trigonal-bipyramidal. The optical transition in the bismuth compounds corresponds to charge transfer from the basal ligand to bismuth. This electronic excitation is actually forbidden; and the ε values of the absorption are correspondingly small.

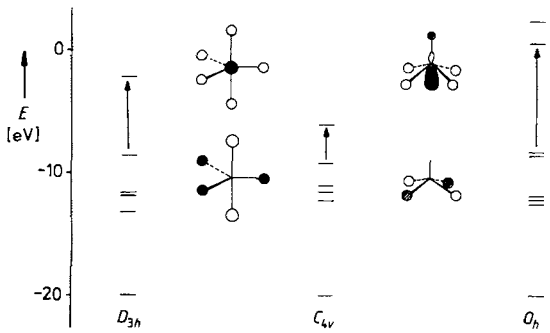

Fig. 3. MO diagram for BiH_5 with trigonal-bipyramidal geometry (D_{3h}) and square-planar (C_{4v}) geometry, and for $BiH_6^{\ominus}$ (O_h), corrected for relativistic effects. The HOMO–LUMO excitation is symbolized by an arrow. Alongside: presentation of HOMO and LUMO by population analyses. Since the HOMO has practically no Bi-orbital participation, whereas the LUMO has a large one, only the LUMO is drastically lowered by lanthanoids and relativistic contraction. The occupation of the sixth coordination site in the C_{4v} model leads to an octahedral $BiH_6^{\ominus}$ with particularly large HOMO–LUMO splitting (right). The unstable anion $Bi(C_6H_5)_6^{\ominus}$ is pale yellow [11].

The bonding in the excited molecule is comparable to that of a trivalent square-pyramidal bismuth compound, e.g. $BiCl_5^{2\ominus}$. Because of the poor shielding by the 4f electrons and through the relativistic contraction, s-orbitals participate less in bonding than in the lighter homologues; hence the preference for the square-pyramidal structure. Moreover, the highly bismuth-centered LUMO in particular is considerably lowered by the above mentioned effects, so that the absorption is centered in the visible region of the spectrum. To our knowledge this is the first demonstration of the influence of the relativistic effect on an excited state. Extended Hückel calculations without relativistic correction for BiH_5 in both geometries give a qualitatively similar diagram with smaller HOMO-LUMO splitting for the C_{4v} model. The HOMO-LUMO splitting changes by about 27%, however, on applying the relativistic correction for C_{4v}, but only by about 14% for D_{3h}. That is, "non-relativistic" pentaphenylbismuth would not be violet.

It is possibly worthwhile pointing out that bismuth behaves similarly in oxidic superconductors: a Bi^{III}-Bi^{IV} redox process coupled with a square-pyramidal/octahedral vibrational transition can be assumed.[8] In addition, common to both phenomena is that they are only observed within a narrow set of boundary conditions.

Since the intensity of color of the pentaphenylbismuth derivatives correlates with the weakness and ease of excitation of the basal Bi–C bonds, compounds with even weaker Bi–C bonds, which would be expected to be more deeply

colored, may no longer be stable at room temperature. In the case of the pentaphenylantimony derivatives, corresponding phenomena should be observable in the UV, except that the weak absorption will be masked by strong phenyl ring π-π^* transitions.

Experimental

A solution of 6 mmol of 2-F-C_6H_4Li (freshly prepared from 1-bromo-2-fluorobenzene and *n*BuLi at $-78\,^{\circ}C$) in anhydrous Et_2O was fed through a small Teflon tube into a stirred suspension of 3 mmol of triarylbismuth dichloride [9, 10] in 20 mL of anhydrous Et_2O cooled to $-78\,^{\circ}C$. The colored suspension was then warmed with stirring to room temperature. After decanting from deposited LiCl, the clear red-violet solution was carefully evaporated. Crystallization at $0\,^{\circ}C$ and $-25\,^{\circ}C$, respectively, afforded the substituted pentaarylbismuth compounds **1** and **2**, which are readily soluble in diethyl ether, insoluble in pentane, and sensitive to hydrolysis.

1: 45%, violet dichroic crystals, m.p. 103 °C (decomp.); ^{19}F NMR (84.25 MHz, THF, $CFCl_3$ ext.): $\delta = -94.1$; FIR (Nujol): $\tilde{\nu} = 530, 452, 444, 434, 282, 231, 195, 175, 126, 109\ cm^{-1}$; UV (THF): $\lambda_{max} = 487$ nm.

2: 39%, orange colored crystals, m.p. 122 °C (decomp.); ^{19}F NMR (84.25 MHz, THF, $CFCl_3$ ext.): $\delta = -94.0$; FIR (Nujol): $\tilde{\nu} = 564, 534, 523, 488, 480, 473, 435, 303, 285, 260, 220, 212, 192, 173, 152, 125, 109\ cm^{-1}$; UV (THF): $\lambda_{max} = 475$ nm.

Received: September 21, 1989;
revised: November 2, 1989 [Z 3560 IE]
German version: *Angew. Chem. 102* (1990) 211

CAS Registry numbers:
1, 124652-37-5; **2**, 124652-38-6; 2-F-C_6H_4Li, 348-53-8; $(C_6H_5)_3BiCl_2$, 594-30-9; $(4\text{-}CH_3\text{-}C_6H_4)_3BiCl_2$, 6729-64-2; BiH_3 (trigonal-bipyramidal), 124652-39-7; BiH_5 (square-planar), 124752-07-4; 1-bromo-2-fluorobenzene, 1072-85-1.

[1] A. Schmuck, J. Buschmann, J. Fuchs, K. Seppelt, *Angew. Chem. 99* (1987) 1206; *Angew. Chem. Int. Ed. Engl. 26* (1987) 1180.
[2] P. J. Wheatley, *J. Chem. Soc. 1964*, 3718; A. L. Beauchamp, M. J. Bennett, F. A. Cotton, *J. Am. Chem. Soc. 90* (1968) 6675.
[3] P. J. Wheatley, G. Wittig, *J. Chem. Soc. 1962*, 251; P. J. Wheatley, *ibid. 1964*, 2206.
[4] A. Schmuck, K. Seppelt, *Chem. Ber. 122* (1989) 803.
[5] A. Schmuck, S. Wallenhauer, D. Leopold, K. Seppelt, *Chem. Ber.*, in press.
[6] Programm ITEREX-87, P. Pykkö, *Methods Comput. Chem. 2* (1988) 137. Parameter: $r_{Bi-H} = 185$ pm for all bonds, angles 90° and 120°, $a_H = -10$ eV.
[7] R. Hoffmann, J. M. Howell, E. L. Muetterties, *J. Am. Chem. Soc. 94* (1972) 3047.
[8] A. Simon, *Angew. Chem. 99* (1987) 602; *Angew. Chem. Int. Ed. Engl. 26* (1987) 579; A. W. Sleigh, J. L. Gibson, P. E. Bierstedt, *Solid State Commun. 17* (1975) 27.
[9] A. Michaelis, A. Polis, *Ber. Dtsch. Chem. Ges. 20* (1887) 54.
[10] A. Michaelis, A. Marquardt, *Justus Liebigs Ann. Chem. 251* (1889) 323.
[11] D. Hellwinkel, G. Kilthau, *Justus Liebigs Ann. Chem. 705* (1967) 66.

unusual physical or catalytic properties[1, 2] and as building blocks for new polymers.[3, 4] The metallacumulene species $M=(C=)_4CR_2$ is still a hypothetical transient species, although a few examples of allenylidene-metal complexes $M=(C=)_2CR_2$ have been described,[5, 6] (arene)-$Ru=(C=)_2CR_2$ intermediates were obtained from propargyl alcohol derivatives, and they readily underwent further reaction to give 2-propenylidene ruthenium complexes,[6]; we have therefore considered the possibility of generating metallacumulenes (arene)$Ru=(C=)_4CR_2$ by reaction of H-$(C\equiv C)_2CR_2OY$ derivatives with ruthenium(II) complexes to give highly unsaturated complexes. We now describe the first example of a 2,3,4-pentatrienylidene-metal complex and its transformation into a novel 3-oxo-1,4-pentadienyl-ruthenium derivative.[7]

Reaction of the Ru-complex **1a** with $NaPF_6$ and 1,1-diphenylpenta-2,4-diyn-1-ol **2a** in methanol led, via a violet intermediate, to formation of orange crystals (48%) of **3a**. Similarly, the complex **1a** and the diynol derivative **2b** afforded 56% of **4a**. Analogous complexes **3b** and **4b** were obtained by reaction of **1b** with **2a** and **2b**, respectively (Scheme 1).

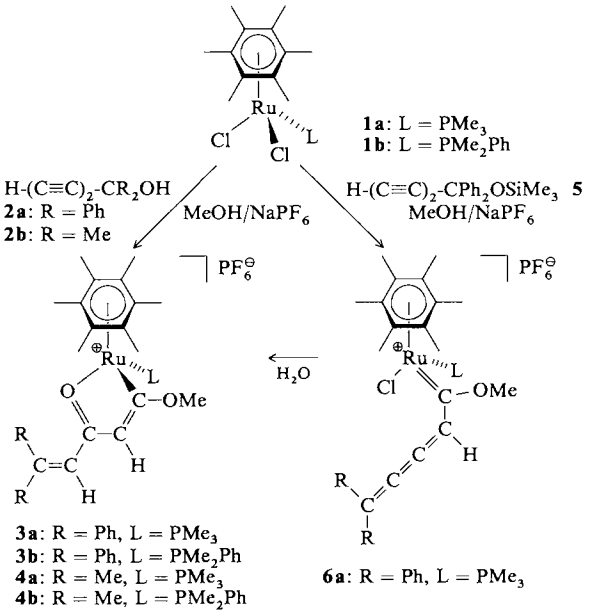

Scheme 1.

Ruthenium-containing Cumulenes: Generation of 2,3,4-Pentatrienylidene- and 3-Oxo-1,4-pentadienyl-Complexes**

By *Antonio Romero, Angel Vegas,* and *Pierre H. Dixneuf**

Polyunsaturated organometallic complexes are scarce, in spite of their interest for access to novel compounds with unusual physical or catalytic properties[1, 2] and as building blocks for new polymers.[3, 4] The metallacumulene species $M=(C=)_4CR_2$ is still a hypothetical transient species, although a few examples of allenylidene-metal complexes $M=(C=)_2CR_2$ have been described,[5, 6] (arene)-$Ru=(C=)_2CR_2$ intermediates were obtained from propargyl alcohol derivatives, and they readily underwent further reaction to give 2-propenylidene ruthenium complexes,[6]; we have therefore considered the possibility of generating metallacumulenes (arene)$Ru=(C=)_4CR_2$ by reaction of H-$(C\equiv C)_2CR_2OY$ derivatives with ruthenium(II) complexes to give highly unsaturated complexes. We now describe the first example of a 2,3,4-pentatrienylidene-metal complex and its transformation into a novel 3-oxo-1,4-pentadienyl-ruthenium derivative.[7]

Reaction of the Ru-complex **1a** with $NaPF_6$ and 1,1-diphenylpenta-2,4-diyn-1-ol **2a** in methanol led, via a violet intermediate, to formation of orange crystals (48%) of **3a**. Similarly, the complex **1a** and the diynol derivative **2b** afforded 56% of **4a**. Analogous complexes **3b** and **4b** were obtained by reaction of **1b** with **2a** and **2b**, respectively (Scheme 1).

A single-crystal X-ray structural analysis of **3a**[8] (Fig. 1) confirms that the activation of the diynol **2a** by **1a** results in the unprecedented formation of a novel 3-oxo-1,4-pentadienyl-ruthenium derivative.[9] The structure of the product **3a**, and the fact that (arene)RuC_2CPh_2 moieties exist,[6] suggest formation of an "RuC_4CPh_2" intermediate followed by addition of methanol at C1 and of the released water at C3 of the ligand. To gain an insight into the formation of complexes **3** and **4** an attempt to isolate the violet intermediate was undertaken. The complex **1a** was allowed to react with one equivalent of the silyloxypentadiyne **5** in dry methanol. A violet product was isolated in 40% yield and was identified as complex **6a**. This compound shows one strong absorption in the IR spectrum at $2080\ cm^{-1}$, which can be assigned to the [C=C=C=C] group.[1] In the ^{13}C-NMR spectra, a signal is observed at $\delta = 295.13$, characteristic for a ruthenium-bound carbene carbon atom,[6]; a signal at

[*] Prof. Dr. P. H. Dixneuf, Dr. A. Romero
Département de chimie, URA CNRS D0415
Campus de Beaulieu, Université de Rennes
F-35042 Rennes (France)
Dr. A. Vegas
Instituto de Quimica Fisica 'Rocasolano'
CSIC, Serrano 119, E-28006 Madrid (Spain)

[**] This work was supported by the CNRS. We thank the Consejo Superior de Investigaciones Cientificas (Spain) for a postdoctoral fellowship for *A.R.* and an X-ray structural analysis.

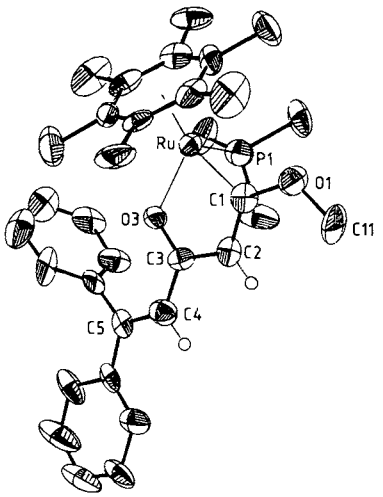

Fig. 1. Molecular structure of **3a** (ORTEP, 50% probability thermal motion ellipsoids). Selected bond lengths [Å] and angles [°]: Ru-C1 1.99(2), C1-C2 1.36(3), C2-C3 1.38(2), C3-O3 1.30(2), Ru-O3 2.09(1), Ru-P 2.32(1), C3-C4 (1.49(2), C4-C5 1.35(2); Ru-C1-C2 116(1), C2-C3-O3 119(2), C3-O3-Ru 112(1), O3-Ru-C1 78.0(6).

109.79 ($^1J_{C,H}$ = 172 Hz) can be assigned to the HC=C= group, and three singlets at δ = 166.88, 148.83 and 148.42 stem from the $(C=)_3$ skeleton.

Compound **6a** reacts with water at room temperature to give **3a** quantatively after 3 h. This demonstrates that complexes of type **3** and **4** are formed on addition of water to the C(3) carbon of the butatrienyl group of intermediate **6**.

Since the addition of methanol to the $Ru=(C=)_2CR_2$ moieties leads to 2-propenylidene-ruthenium complexes,[6] the metallacumulene $Ru=(C=)_4CPh_2$ is likely to be the key intermediate in the reaction of the diynes **2** or **5** with the complexes **1** to afford complex **6** by addition of methanol.

Experimental

3a: **2a** (0.24 g, 1 mmol) was added to a solution of **1a** (0.41 g, 1 mmol) and $NaPF_6$ (0.18 g, 1 mmol) in 20 mL of dry methanol. The solution turned violet after a few minutes and then progressively dark red. The mixture was stirred for 20 h at room temperature. The solvent was removed in vacuo and the red solid was dissolved in 20 mL of THF. The solution was filtered, and crystallization from a THF/*n*-hexane (2/1) solution afforded 0.36 g (48%) of **3a** as orange crystals.

3a: IR (KBr): $\tilde{\nu}$ = 1615 [s, ν(C=O)], 855 [s, ν(P-F)] cm^{-1}; ^{1}H NMR (300.13 MHz, $CDCl_3$): δ = 6.77 (s, 1H; *HC*=C), 5.57 (d, 1H, ^4J(P, H) = 0.8 Hz; *HC*=C), 3.76 (s, 3H; OMe), 1.99 (s, 18H; C_6Me_6), 1.15 (d, 9H, ^2J(P, H)) = 10.1 Hz; PMe_3). ^{31}P NMR: δ = 3.55 (s, PMe_3), −144.39 (sept; $PF_6^{\ominus}$). ^{13}C NMR: δ = 254.82 (d, ^2J(P, C) = 20.4 Hz; RuCOMe), 199.60 (s; C=O), 153.48 (s; =*C*Ph$_2$), 121.92 (^1J(C, H) = 156.6 Hz, H*C*=CPh$_2$), 111.09 (^1J(C, H) = 162.4 Hz; *HC*=C(OMe). Correct elemental analysis (C, H).

3b and **4a, b** were prepared analogously to **3a** and isolated in 52%, 56% and 58%, respectively. ^{13}C-NMR data for Ru-*C*OMe (75.469 MHz, $CDCl_3$): δ = (^2J(C, P) = 255.29/18.9 Hz (**3b**), 253.11/20.2 Hz (**4a**), 253.76/20.3 Hz (**4b**): δ = ^1J(C, H) = 112.25/162.4 Hz (**3b**), 110.79/161 Hz (**4a**), 111.38/161 Hz (**4b**).

6a: **1a** (0.30 g, 0.73 mmol) and $NaPF_6$ (0.13 g, 0.77 mmol) were dissolved in 20 mL of dry methanol and treated with 0.225 g, 0.73 mmol of 5,5-diphenyl-5-(trimethylsiloxy)penta-1,3-diyne **5**. The mixture was stirred at room temperature for 1 h. Half of the solvent was removed in vacuo. The red-violet product was filtered and crystallized from dichloromethane/ether (20 mL/10 mL); Yield: 0.22 g (40%) of a violet powder of **6a**. Correct elemental analysis (C, H).

6a: IR (KBr): $\tilde{\nu}$ = 2080 [s, ν(C=C=C=C)]; 855 [vs, ν(P-F)] cm^{-1}, ^{31}P NMR (121.49 MHz, CD_2Cl_2): δ = 10.54 (s; PMe_3), −143.45 (sept., $PF_6^{\ominus}$); ^{1}H NMR (300.13 MHz, CD_2Cl_2), δ = 7.69–7.47 (m, 10H; Ph), 7.29 (s, 1H; =C=*CH*), 4.51 (s, 3H; OMe); 2.06 (d, 18H; ^4J(P, H) = 0.7 Hz; C_6-*Me*$_6$), 1.40 (d, 9H; ^2J(P, H) = 10.6 Hz; PMe_3). ^{13}C NMR (75.469 MHz, CD_2Cl_2): δ = 295.13 (^2J (C, P) = 21.2 Hz; Ru=*C*-OMe), 166.88, 148.83 and 148.42 (=*C*=*C*=*C*Ph$_2$), 109.79 (^1J(C, H) = 172 Hz; H*C*=C=), 106.47 (C_6Me$_6$), 67.43 (OMe), 16.41 (C_6*Me*$_6$), 16.05 (^1J(C, P) = 34.6 Hz; PMe_3). The conformation of the carbene ligand is based on an NOE experiment.

Received: October 2, 1989 [Z 3569 IE]
German version: *Angew. Chem. 102* (1990) 210

CAS Registry numbers:
1a, 80298-82-4; **1b**, 110800-51-6; **2a**, 4945-70-4; **2b**, 763-12-2; **3a**, 124686-52-8; **3b**, 124686-54-0; **4a**, 124686-56-2; **4b**, 124686-58-4; **5**, 124686-50-6; **6a**, 124686-60-8.

[1] a) P. J. Stang, A. K. Datta, V. Dixit, L. G. Wistrand, *Organometallics 8* (1989) 1020; b) P. J. Stang, A. K. Datta, *ibid. 8* (1989) 1024.
[2] T. J. Katz, S. M. Hacker, E. D. Kendrick, C. S. Yannoni, *J. Am. Chem. Soc. 107* (1985) 2182.
[3] M. Bertault, J. Canceill, A. Collet, L. Toupet, *J. Chem. Soc. Chem. Commun. 1988*, 163.
[4] D. Macomber, M.-H. Hung, M. Liang, A. G. Verma, P. Madhukar, *Macromolecules 21* (1988) 1189.
[5] a) E. O. Fischer, H.-J. Kalder, A. Frank, F. H. Köhler, G. Huttner, *Angew. Chem. 88* (1976) 683; *Angew. Chem. Int. Ed. Engl. 15* (1976) 623; b) H. Berke, *Chem. Ber. 113* (1980) 1370; c) H. Berke, P. Harter, G. Huttner, J. von Seyerl, *J. Organomet. Chem. 219* (1981) 317; d) J. Selegue, *Organometallics 1* (1982) 217.
[6] H. Le Bozec, K. Ouzzine, P. H. Dixneuf, *J. Chem. Soc. Chem. Commun. 1989*, 219.
[7] Presented at the international symposium "Interfaces in Metal Complex Chemistry", July 10–14, 1989, Rennes, France.
[8] Crystals for X-ray analysis were obtained from a THF/ether (1/2) solution. **3a** crystallizes in the space group $P2_1/n$ with a = 13.788(5), b = 13.328(5), c = 18.457(6) Å, β = 100.21(3)°, Z = 4, V = 3338 Å^3, ϱ_{calcd} = 1.488 g cm^{-3}, crystal dimensions 0.50 × 0.20 × 0.10 mm. The diffraction data were collected with a single-crystal diffractometer CAD-4 (graphite monochromator, $Mo_{K\alpha}$-radiation, (θ – 2θ scan) at 293 K. 5855 reflections were obtained in the range 3° < 2θ < 50°, 1831 with $I > 3\sigma(I)$ considered as observed. The structure was solved by the heavy atom method and refined by full-matrix least-squares calculations and unit weights, using absorption correction data; all calculations were carried out with the program system 'X RAY-70'. The fluorides of the hexafluorophosphate ion showed extremely high temperature factors and some unresolved disorder and they were fixed at the position of the maxima in the Fourier map. Anisotropic treatment of the non-hydrogen atoms, except the $[PF_6]^{\ominus}$ ion, gave R = 0.064 for the observed reflections. Further details of the crystal structure investigation are available on request from the Fachinformationszentrum Karlsruhe, Gesellschaft für wissenschaftlich-technische Information mbH, D-7514 Eggenstein-Leopoldshafen 2 (FRG), on quoting the depository number CSD-54350, the names of the authors, and the journal citation.
[9] E. Carmona, E. Gutierrez-Puebla, A. Monge, J. M. Marin, M. Paneque, M. Poveda, *Organometallics 8* (1989) 967.

An Intramolecularly Lewis-Base-Stabilized Ge=N-Compound and a Related Ge-Fe Complex

By *Michael Veith,* Sabine Becker,* and *Volker Huch*

We have recently demonstrated that a germanium–sulfur double bond can be stabilized by intramolecular addition of bases to the germanium atom. The bonds in the polycyclic azasilagermane **1** can be formally described in terms of the resonance structures **1a** and **1b**.[1]

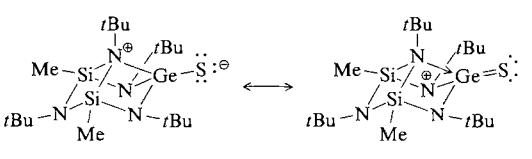

1a **1b**

[*] Prof. Dr. M. Veith, Dipl.-Chem. S. Becker, Dr. V. Huch
Institut für Anorganische Chemie der Universität
D-6600 Saarbrücken 11 (FRG)

We have now considered the question of whether germanediylamines (germanimines) and germanediyl-transition-metal complexes analogous to **1** can also be prepared, i.e. whether the sulfur in **1** can be replaced by a nitrene, e.g. $Me_3Si-\ddot{N}$, or an isolobal complex fragment such as $Fe(CO)_4$. Stable germanediylamines have only recently been isolated and spectroscopically characterized,[2] while germanediyl complexes of the transition metals have been known for some time.[3] Some X-ray structure analyses of silanediylamines (silanimines) and base-stabilized silanediylamines have been carried out independently by others.[4]

The target compounds **3** and **4** are obtained in high yields upon reaction of the germanediyl **2** with nonacarbonyldiiron and trimethylsilylazide respectively at room temperature. The reactions proceed in accord with Scheme 1, with elimination of pentacarbonyliron and dinitrogen, respectively.

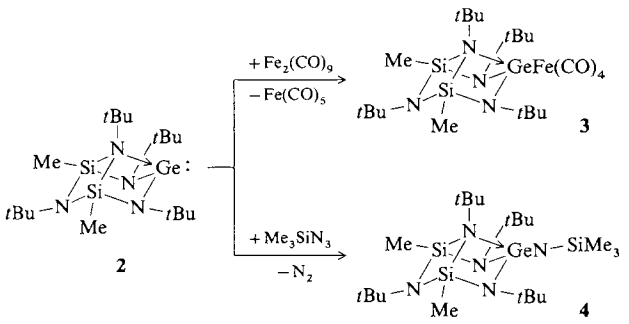

Scheme 1. Synthesis of **3** and **4**.

The ^{1}H-NMR spectra of **3** and **4** in solution[5] differ primarily in that three signals are observed for the *tert*-butyl groups in the case of **3**, whereas only two signals are observed in the case of **4**. Thus, in **3** the donor bond from the nitrogen to the germanium atom is closed on the ^{1}H-NMR time scale, whereas in the case of **4** (like in **1**[1]) a bond fluctuation occurs (see also the ^{13}C-NMR spectrum of **4**[5]). The $\Delta G^{\ddagger}$ value of **4** derived from the temperature dependence of the ^{1}H-NMR spectra is 56(9) kJ mol^{-1} at 298 K and is thus 8 kJ mol^{-1} smaller than that of **1**. The marked difference in the activation entropies of **1** and **4** ($\Delta S^{\ddagger}$(**1**) = − 51(5), $\Delta S^{\ddagger}$(**4**) = − 95(9) J mol^{-1} K^{-1}) is apparently associated with the additional trimethylsilyl groups in **4**.

The results of the X-ray structure analyses of **3** and **4** are collected in Figure 1.[6] In the solid state, both compounds are present as isolated molecules with only van-der-Waals contacts. **3** contains a crystallographic mirror plane, whereas **4** loses its point symmetry C_s(m) in the crystal. In both molecules the germanium atom is incorporated in a seconor-cubane-like Si_2N_4Ge cage by bonding to three nitrogen atoms. The fourth coordination site of the germanium atom is taken up in an $Fe(CO)_4$ and $N(SiMe_3)$ group, respectively. The nitrogen atom N5 in **4** is only twofold coordinated; the Ge–N5–Si3 angle is 151.2(7)°.

The germanium atoms in **3** and **4** are *not* in a tetrahedral environment but lie almost in a plane together with the bond partners N1,N1′ and Fe or N2,N3 and N5 (sum of angles at Ge in **3**: 354.7°, in **4**: 357.7°). The fourth bond to a further nitrogen atom of the polycycle forms an angle of 49 and 57°, respectively, to this plane. From a comparison of the Ge–N bond lengths it follows that this fourth interaction is the weakest (**3**: Δ(N3–Ge/N1–Ge) = 0.144 Å; **4**: Δ(N1–Ge/N(2,3)–Ge = 0.156 Å).

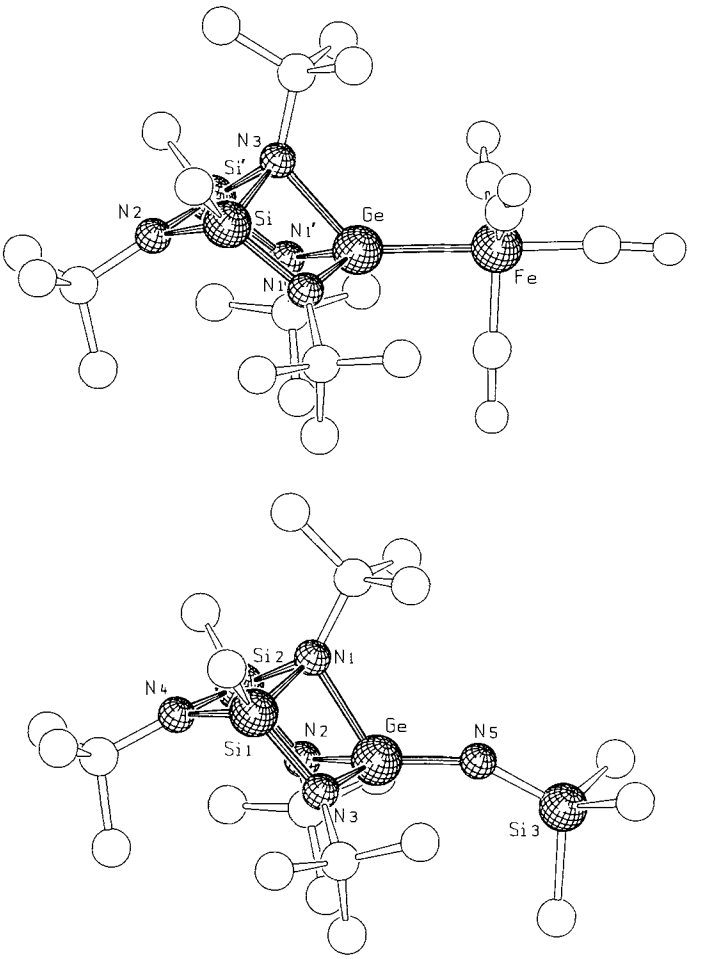

Fig. 1. The crystal structures of **3** (top) and **4** (bottom) (Schakal drawings, the carbon atoms are not shown). Some important bond lengths [Å] and angles [°]: **3**: Ge–Fe 2.348(1), Ge-N1 1.916(3), Ge-N3 2.060(4), Si-N1 1.718(3), Si-N2 1.735(3), Si-N3 1.821(3); N3-Ge-Fe 130.6(1), N1-Ge-Fe 122.8(1), N1-Ge-N1′ 109.1(1), N1-Ge-N3 78.8(1). **4**: Ge-N1 2.045(7), Ge-N2 1.896(7), Ge-N3 1.882(7), Ge-N5 1.688(9), Si1-N1 1.819(7), Si1-N3 1.710(7), Si2-N1 1.803(7), Si2-N2 1.697(8), Si3-N5 1.648(9); N1-Ge-N5 122.6(4), N2-Ge-N3 108.3(3), N2-Ge-N5 125.8(4), N3-Ge-N5 123.6(4), N2-Ge-N1 78.5(3), N3-Ge-N1 79.5(3), Ge-N5-Si3 151.2(7).

The Ge–N bond lengths for the three different nitrogen atoms in **4** (N1 quadruply, N2 and N3 each triply, and N5 only doubly coordinated) correlate as usual with the coordination numbers.

Of special interest are the Ge–Fe and the Ge–λ^2-N bond lengths. They have to be assessed differently! The value found for Ge–Fe corresponds approximately to the sum of the single bond radii of the two elements (2.39 Å,[7a] 2.37 Å[7b]). The Ge–N5 distance is very much smaller than expected for a single bond (1.86 Å[7b]) and on taking into account the larger atomic radius of germanium is comparable with the Si–λ^2-N distances (1.57–1.60 Å) in free and base-stabilized silanedylamines.[4] The bond shortening relative to the standard single bond is 9% in the case of Ge–λ^2-N in **4**, whereas it is noticeably smaller (7%) in the case of Ge–S in **1** (Ge–λ^1-S = 2.063(3),[1] Ge–λ^2-S = 2.21[7b]). The Si3–N5 bond length and the Ge–N5–Si3 angle in **4** resemble the corresponding bond length and bond angle in (thf) $Me_2Si{=}N{-}SitBu_3$ (N–Si 1.66 Å, Si = N–Si 161.3°[4]).

As quintessence for the description of the bonding in **3** and **4**, it follows from the experimental data that:

1) The germanium–iron bond in **3** is analogous to the bonding of a classical two-electron donor to a transition

metal. A back-bonding of the metal to the germanium cannot be ruled out, but if present does not lead to a drastic bond shortening. The addition of the $Fe(CO)_4$ fragment to **2** leads to a strengthening of the donor bond N3 → Ge, as can be deduced from the different ^{1}H-NMR spectra[1] (in the case of **3** no coalescence of the nonequivalent *tert*-butyl groups is observed up to 90 °C).

2) In **4**, the plane in which the N2,N3 and N5 atoms lie and the plane through the atoms Ge, N5 and Si3 are orthogonal. Hence, a p_π–p_π bond between Ge and N5 can be ruled out on geometric grounds, independently of the coordination number of Ge.

3) The donor bond N1 → Ge in **4** competes, similarly as in the case of **1**[1] in solution, with the N4 → Ge bond. This bond fluctuation has a highly negative activation entropy (ca. -96 J mol^{-1} K^{-1}), which could be explained in terms of a threefold and symmetrically coordinated germanium atom in the transition state.

4) Of the resonance structures **A**–**C**, **A** best reproduces the polar portions. Thus seen, **4** can in the broadest sense be

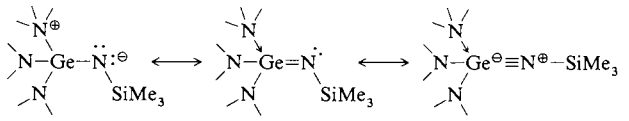

A **B** **C**

referred to as a neutral pendant to a germylsilylamide or disilylamide ion.[8] The stabilization of negative partial charges on N by electropositive Si has already been pointed out on a number of occasions.[9] However, the coordination geometry found at the germanium atom is not satisfactorily explained in terms of the resonance structure **A**.

The resonance structure **B** takes into account possible d_π–p_π bonds between Ge and N5 and must, by all means, also be taken into consideration besides the structure **A**. The observed Ge–N–Si angle suggests a resonance between **B** and **C**, but details of the structure would indicate that the widening of the angle is largely of steric origin.

Experimental

A solution of **2** (217 mg, 0.49 mmol) **1** in benzene (5 mL) was treated at room temperature, either dropwise with a solution of trimethylsilylazide (59 mg, 0.49 mmol) in benzene (2 mL) or with 178.2 mg (0.49 mmol) of $Fe_2(CO)_9$. The resulting solution, or suspension, was stirred for 12 h and the solvent removed by distillation. Subsequent sublimation at 80 °C/0.001 torr or crystallization from toluene, afforded 185 mg (71%) of **4** and 291 mg (97%) of **3** (yellow crystals), respectively.

Received: September 4, 1989 [Z 3537 IE]
German version: *Angew. Chem. 102* (1990) 186

CAS Registry numbers:
2, 124686-70-0; **2** (salt), 124686-67-5; **3**, 124686-68-6; **4**, 124686-69-7; $Fe_2(CO)_9$, 15321-51-4; Me_3SiN_3, 4648-54-8.

[1] M. Veith, S. Becker, V. Huch, *Angew. Chem. 101* (1989) 1287; *Angew. Chem. Int. Ed. Engl. 26* (1989) 1237.
[2] a) C. Glidewell, D. Lloyd, K. W. Lumbard, J. S. McKechnie, M. B. Hursthouse, R. L. Short, *J. Chem. Soc. Dalton Trans. 1987*, 2981; b) J. Pfeiffer, W. Maringgele, M. Noltemeyer, A. Meller, *Chem. Ber. 122* (1989) 245.
[3] a) W. Petz, *Chem. Rev. 86* (1986) 1019; b) P. B. Hitchcock, M. F. Lappert, S. A. Thomas, A. J. Thorne, A. J. Carty, N. J. Taylor, *J. Organomet. Chem. 315* (1986) 27.
[4] G. Reber, J. Riede, N. Wiberg, K.Schurz, G. Müller, *Z. Naturforsch. B 44* (1989) 786.
[5] ^{1}H-NMR (80 MHz, C_6D_6, TMS as standard): **3** (307 K): $\delta = 0.48$ (s, 6H, $SiCH_3$), 1.07 (s, 9H, $NC(CH_3)_3$), 1.28 (s, 9H, $NC(CH_3)_3$), 1.43 (s, 18H, $NC(CH_3)_3$). No coalescence of the signals at $\delta = 1.07$ and 1.28 up to 363 K. **4** (307 K): $\delta = 0.50$ (s, 6H, $SiCH_3$), 0.61 (s, 9H, $Si(CH_3)_3$), 1.22 (s, 18H, $NC(CH_3)_3$), 1.46 (s, 18H, $NC(CH_3)_3$). **4** (217 K): $\delta = 0.48$ (s, 6H, $SiCH_3$), 0.59 (s, 9H, $Si(CH_3)_3$), 1.13 (s, 9H, $NC(CH_3)_3$), 1.31 (s, 9H, $NC(CH_3)_3$), 1.51 (s, 18H, $NC(CH_3)_3$). Coalescence temperature $T_c = 237$ K. $^{13}C\{^1H\}$-NMR (20 MHz, 307 K): **4**: $\delta = 2.6$ ($SiCH_3$), 6.0 ($Si(CH_3)_3$), 31.8 ($NC(CH_3)_3$), 33.6($NC(CH_3)_3$), 52.5($NC(CH_3)_3$), 59.3($NC(CH_3)_3$).
[6] Crystallographic data: **3**: orthorhombic, *Pnma*, $a = 19.07(1)$, $b = 14.629(7)$, $c = 10.611(7)$ Å, $V = 2961$ Å^3, $Z = 4$; 1936 reflections, 217 as not observed ($F_0 \leq 2\sigma_F$), 197 parameters $R = 0.037$.—**4**: orthorhombic, *Pbca*, $a = 17.52(1)$, $b = 17.52(1)$, $c = 20.11(2)$, $V = 6170$ Å^3; $Z = 8$; 3325 reflections, 1090 as not observed ($F_0 \leq \sigma_F$), 303 parameters, $R = 0.066$.—Further details of the crystal structure investigations are available on request from the Fachinformationszentrum Karlsruhe, Gesellschaft für wissenschaftlich-technische Information mbH, D-7514 Eggenstein-Leopoldshafen 2 (FRG), on quoting the depository number CSD-54918, the names of the authors, and the journal citation.
[7] a) J. E. Huhey: *Anorganische Chemie—Prinzipien von Struktur und Reaktivität*, Walter de Gruyter, Berlin 1988; b) V. Schomaker, D. P. Stevenson, *J. Am. Chem. Soc. 63* (1941) 37.
[8] R. A. Bartlett, P. P. Power, *J. Am. Chem. Soc. 105* (1987) 6509.
[9] P. von R. Schleyer, P. D. Stout, *J. Chem. Soc. Chem. Commun. 1986*, 1373.

Book Reviews are written by invitation from the editor. Suggestions for books to be reviewed and for book reviewers are welcome. Publishers should send brochures or (better) books to the following address: Redaktion Angewandte Chemie, Postfach 101161, D-6940 Weinheim, Federal Republic of Germany. The editor reserves the right of selecting which books will be reviewed. Uninvited books not chosen for review will not be returned.

Vom Radiothor zur Uranspaltung. Eine wissenschaftliche Selbstbiographie. (Reprint of the 1st Edition). By *O. Hahn*. F. Vieweg & Sohn, Braunschweig/Wiesbaden 1988. xvi, 160 pp., hard cover, DM 78.00.—ISBN 3-528-08413-8

Of the many books on the life and work of *Otto Hahn* this one, published in 1962 in his 84th year, was the first, and it is probably the only one written entirely by him. The re-publication of the book on the fiftieth anniversary of the discovery of nuclear fission is therefore greatly to be welcomed. The description of it as a "reprint" is to be interpreted literally, as *Otto Hahn*'s text has remained completely unaltered. Even the few printing errors have not been corrected. Also unaltered are the three appendices, which are facsimiles of papers on nuclear fission: *Otto Hahn* and *Fritz Strassmann*'s "second" paper in the 1939 volume of Naturwissenschaften reporting the famous radioactive indicator experiments, and two review articles from the Abhandlungen der Preußischen Akademie der Wissenschaften for 1941 and 1944. The illustrations section has, however, been revised; the editor *Dietrich Hahn*, grandson of the author, has approximately doubled their number to 40. Also new are a preface by the editor and an introduction by *Kurt Starke*, who worked with *Hahn* from 1935 to 1940 as a graduate student and scientific collaborator.

The book is first and foremost a *scientific* autobiography; personal details are only included in special circumstances. However, it is not written in a scientific style with the customary self-effacement on the part of the author. On the contrary, *Hahn*'s temperament and his style of working become clearly apparent after only a few pages. In a relaxed and unpretentious way he describes his early youth, student days and teaching days with much anecdotal background—his famous "cock tales"—even when the point of the story is at his expense. A lucky accident—and in this book luck is often mentioned—had the effect of diverting him from a planned career as an industrial organic chemist towards radioactivity instead. Having gone to London in order to learn English, he achieved his first scientific success in 1904 in *William Ramsey*'s laboratory, in a way that was typical of him: while separating radium from barium salts by fractional crystallization the mother liquor was unexpectedly found to be still weakly radioactive afterwards. This "residue effect" led him to discover a new member of the natural radioactive decay series, radiothorium (thorium-228). This earned him a place in *Ernest Rutherford*'s laboratory in Montreal, and eventually, in 1906, in that of *Emil Fischer* in the chemistry department of Berlin University. There he made his next important discovery, that of mesothorium-1 (radium-228), which was soon greatly in demand for radiotherapy as an alternative to the considerably more expensive radium. However, the greatest discovery escaped him: despite the fact that he had made more unsuccessful attempts than *Frederick Soddy* at separating closely similar "radioelements" (p. 46), it was *Soddy* rather than *Hahn* who arrived at the concept of isotopes which was the key to this problem.

In 1907 he gained his Habilitation under *Fischer*. In the same year there began the collaboration with the physicist *Lise Meitner*, which was excellent both scientifically and from a personal standpoint. *Hahn* had access to nearly all the known radioelements, and they now undertook a systematic study of all their radiations. While once more investigating a "residue effect", they discovered radioactive recoil. *Lise Meitner* gradually made a reputation for herself in this environment, in which the attitude towards women was one of disapproval. In 1912 the two moved to the new Kaiser-Wilhelm-Institut für Chemie, which was another stroke of luck, since *Otto Hahn* had scarcely any prospects for a university career in his field of work; he was regarded by chemists as a physicist, whereas to physicists he was a chemist. He turned his attention to the radioactivity of the elements potassium and rubidium; out of this work was developed, twenty years later, the rubidium-strontium method for determining the age of geological samples. The laborious studies of radioactive decay series, interrupted by *Hahn*'s and *Meitner*'s war service, reached their high point in 1918 with the discovery of element 91, protactinium. Once again it was a "residue effect" in protactinium-234 which led to *Hahn*'s discovery in 1922 of the first example of nuclear isomerism, although it was not fully understood until many years later.

The paths of *Otto Hahn* and *Lise Meitner* now diverge. Although *Hahn* continued to provide support for *Lise Meitner*'s detailed studies of radioactive emissions, which eventually led *Wolfgang Pauli* to the discovery of the neutrino, *Hahn* himself now turned, with the help of his now numerous collaborators, to applied radiochemistry. He used radioactive isotopes to investigate chemical problems such as the chemistry of substances in extremely small quantities, or—by using his "emanation method"—the modification of surfaces, the structures of solids, and solid-state chemical reactions. In 1933 he gave a series of lectures at Cornell University, Ithaca, which subsequently appeared in the form of a book. Worried about political developments and about the fate of Jewish friends and colleagues, he cut short his stay there. In January 1935 he courageously gave the keynote address at the remarkable memorial service for *Fritz Haber*. From a scientific point of view this was the least productive period in *Hahn*'s life. At that time, as *Kurt Starke* describes it, the younger research collaborators felt that nothing more remained to be discovered in radiochemistry.

However, that verdict was premature. In the spring of 1934 *Enrico Fermi* and his collaborators reported the discovery of the first transuranic element, number 93, resulting from the irradiation of uranium with neutrons. Nevertheless there were objections to this: might not the element be protactinium instead? *Lise Meitner* and *Otto Hahn*, acknowledged authorities on matters related to protactinium, resumed their work together, and were soon joined by the young *Fritz Strassmann*. The results became more and more complex; it emerged that there were two decay series of transuranic elements which extended as far as element 96. For thorium too several isomeric decay series were found, but in this case they corresponded to known elements, begin-

ning with radium. In the summer of 1938 events took a dramatic turn: *Lise Meitner* was forced to flee the country, while *Irène Curie* and *Paul Savitch* in Paris discovered a transuranic element whose chemical properties certainly did not fit into the scheme of the Berlin team. *Hahn* and *Strassmann* at first identified this activity as due to radium, but after further work aimed at rigorously verifying this surprising result they revised their verdict and identified barium—thus uranium fission was discovered. A hesitant first communication was followed soon by the second paper which is reprinted here, providing certain confirmation through a whole series of brilliant radiochemical indicator experiments. In the fractional crystallization of barium salts the activity obtained from uranium became uniformly distributed through all the fractions, whereas natural radium added at the same time became selectively concentrated in the top fractions. These fractionations were the same as those which *Hahn* had performed in his student days in *Ramsey*'s laboratory, and the most important indicator for radium was mesothorium-1, *Hahn*'s own discovery. In this remarkable way the nearly sixty-year-old scientist had thus returned to the starting-point of his researches.

Otto Hahn does not discuss the further developments leading to the atomic bomb, since the team at the Kaiser-Wilhelm-Institut was not involved in this aspect. Nor do we learn anything about the German "uranium club". The political tensions in the Institute receive equally little attention. The fact that *Hahn* was under extraordinary pressure at that time can be best only be inferred between the lines: the anecdotal detail no longer appears, the tone becomes more serious. He summarizes the work of chemically unravelling the complex mixture of fission products, and the results thus obtained. He relates with satisfaction how, using primitive resources, they identified 100 products, and speculates about which of the fission products might have been mistaken for "transuranics". From the pre-war research only uranium-239 remains as having been unambiguously identified as such by *Hahn, Meitner* and *Strassmann*. However, its decay product, element 93, proved very difficult to find in Berlin. The final chapter is brief: a few sentences about *Hahn*'s internment in England, the Nobel Prize for Chemistry in 1944, the presidency of the Max-Planck-Gesellschaft.

The illustrations section has grown in size compared with the first edition, as *Dietrich Hahn* has chosen to include some photographs relevant to the period. Some of these are of great interest, such as the "Sofabild" of 1920 (p. 88), showing *Lise Meitner* and *Otto Hahn* with their circle of friends—*Herta Sponer, Einstein, Grotrian, Westphal,* the *Francks, Otto von Baeyer, Peter Pringsheim, Haber, Hertz*. What a remarkable élite was gathered there!—and what happened to them? However, some changes in the selection of photographs will be a cause of regret. For example, Kaiser *Wilhelm* the second arriving in uniform at the formal opening of the Chemie-Institut, followed by *Adolf von Harnack* and *Emil Fischer* wearing top-hats, is so typical of the period that one would have liked to see this photograph (1st Edition, p. 61) still included.

Kurt Starke evokes the atmosphere in *Hahn*'s research institute from the viewpoint of a young member of the team. One gains an impression of the rather simple way in which the laboratory was furnished, and of the strict safety precautions against radioactive contamination; one senses the cordial atmosphere, but also the clear division between the leader's immediate team and the younger members. For the latter, the first news of the successful experiments carried out around the turn of the year in 1938/39 came when the work was published.

Otto Hahn's book ends with a backward look, in which he represents his scientific career as a succession of lucky events. This probably has something to do with his Rhineland-Hessen temperament, which always looks at the positive side of a situation. The fact that there were also low points, such as the propagation over several years of the transuranic elements, which eventually faded away, is not apparent from the book, but only from the correspondence between *Hahn* and *Meitner*. Nevertheless, *Hahn* and *Strassmann* were able to correct their error by making a discovery of even greater importance. Of course there are many questions that remain unanswered: what prompted *Hahn* and *Strassmann* to carry out the apparently superfluous radioactive indicator experiments?—how were tasks distributed, and what was the nature of the interactions, in the *Hahn-Meitner-Strassmann* team?—and many more. However, one can learn a great deal from this book without necessarily wishing to go into radioactive phenomena in greater depth: concerning, for example, how science advances not by logical steps in an orderly sequence, but by circuitous and often strange routes; how the most experienced research groups can continue for years with experiments and theories which miss the point; how, on the other hand, they can be set on the right track by a lucky stroke of intuition; and how a scientist may return, decades later, to something which he worked on as a novice. One therefore hopes that this book will be read especially by young scientists. Some will look here for some comments on nuclear energy by the man who has often been called the "father of the atomic era". *Otto Hahn* devotes only half a sentence in the foreword to this topic—it seems that he did not see himself in that role.

Günter Herrmann [NB 989 IE]
Institut für Kernchemie
der Universität Mainz (FRG)

Nitrosamines. Toxicology and Microbiology. (Ellis Horwood Series in Food Science and Technology). Edited by *M. J. Hill*. VCH Verlagsgesellschaft, Weinheim/VCH Publishers, New York/Ellis Horwood, Chichester 1988. 169 pp., hardcover, DM 180.00—ISBN 3-527-26708-5/0-89573-605-0; ISSN 0930-3332

Many nitrosamines are highly toxic, carcinogenic and genetically harmful. Owing to their organ-specific carcinogenic properties and their occurrence in foodstuffs, cosmetics and tobacco smoke, and in work-places, together with the fact that they can be formed endogenously in the human body, there has been widespread interest in this class of compounds in experimental cancer research and in environmental health studies.

The main emphasis in this book is on the importance of nitrosamines in relation to human health. The eight chapters by various authors cover methods for detecting *N*-nitroso compounds in biological samples, the chemistry of *N*-nitrosylation reactions, mechanisms of endogenous *N*-nitrosylation, the occurrence of *N*-nitroso compounds in the human environment, the toxicology of *N*-nitroso compounds, and the role of these compounds in inducing human cancers. A further chapter suggests ways in which the risks of nitrosamine-induced cancers can be minimized.

Impressive characteristics of the book are the systematic and well-disciplined structure of the individual chapters, and the detailed references to original publications (extending up to 1988 in some parts). The book deals with all important aspects of the topics treated, and the reader is enabled to

quickly locate the relevant original papers. Another feature likely to be useful to the non-specialist is that gaps in current knowledge are clearly pointed out.

To summarize, the book is a sound introduction to and overview of this subject for all chemists with an interest in nitrosamines, and for foodstuff and pharmaceutical chemists, biologists and medical scientists; it can be unreservedly recommended.

Manfred Metzler [NB 994 IE]
Institut für Lebensmittelchemie und Umwelttoxikologie
der Universität Kaiserslautern (FRG)

The Chemistry of Organic Silicon Compounds. Parts 1 and 2. Edited by *S. Patai* and *Z. Rappoport*. Wiley, Chichester 1989. Part 1: pp. 1–892; Part 2: pp. 893–1668, hardcover, £ 350.00.—ISBN 0-471-91441-X (Pt. 1)/0-471-91992-6 (Pt. 2)/0-471-91993-4 (set)

In the preface to the two latest volumes in the series "The Chemistry of Functional Groups" the editors write: "The chemistry of organic silicon compounds is one of the fastest growing fields in organic chemistry". In 25 chapters the 32 authors of these volumes, most of whom are very eminent, offer proof of this statement. Such a comprehensive treatment of organosilicon chemistry was long overdue; as well as the classic works in this field, such as *C. Eaborn*'s "Organosilicon Compounds" of 1960, the 1968 article by *C. Eaborn* and *R. W. Bott* in "Organometallic Compounds of the Group IV Elements" (edited by *A. G. McDiarmid*), and the seven-volume "Handbook of Organosilicon Compounds" (edited by *V. Bažant, V. Chvalovský* and *J. Rathouský*, published in 1965 and 1973, and mainly arranged under individual compounds), there are also numerous annual reviews and monographs on particular compound classes, but no comprehensive and up-to-date treatment of the whole field.

The recent blossoming of organosilicon chemistry owes much to the unsaturated compounds, most of which were isolated or proved to exist only in the last few years, and which keep reappearing under different topics like a red thread running through many of the articles. The editors have nevertheless managed to avoid too much overlapping of subject matter, resulting in a well-integrated and up-to-date treatment of this aspect.

The introductory chapter, in which carbon and silicon are compared (*J. Y. Corey*, 56 pp.), reads in some parts like a summary of the articles which follow. Next there is a brilliant account of the theoretical treatment of organosilicon compounds (*Y. Apeloig*, 170 pp.). Embedded in two useful reviews dealing with structural chemistry (*W. S. Sheldrick*, 38 pp.) and thermochemistry (*R. Walsh*, 21 pp.) is a description of the dynamic stereochemistry of silicon compounds (*R. J. P. Corriu, C. Guerin* and *J. J. E. Moreau*, 66 pp.). Although a similar article by the same authors appeared not long ago in another series (*Top. Stereochem. 15* (1984) 43), a definitive article of this sort is worth reading for a second time, especially as it has been updated and expanded. Regrettably, the same does not apply to the article on the analysis of organosilicon compounds (*T. R. Crompton*, 52 pp.), which has been repeated virtually unaltered from Volume 2 of the series "Chemical Analysis of Organometallic Compounds", published in 1974 (!). Nowadays it seems strange that only gas chromatography and IR spectroscopy are discussed in detail as modern instrumental methods.

In the exemplary way expected of these authors, *H. Schwarz* deals with the gas phase ionic chemistry of organosilicon compounds (64 pp.), while *H. Bock* and *B. Solouki* describe their photoelectron spectra (98 pp.). The latter article is a pleasure to read because of the many clear illustrations and the critical comments that are interspersed. Between these two articles there is a short contribution on ^{1}H, ^{13}C and ^{29}Si NMR spectroscopy (*E. A. Williams*, 44 pp.).

The central item in previous monographs on organosilicon compounds, namely a discussion of methods for forming Si–C bonds, here reappears in a less obvious form as Chapter 10 (106 pp.), in which *L. Birkofer* and *O. Stuhl* collect together methods for the preparation of organosilanes, including compounds which contain SiN, SiO, SiS, SiSe and SiTe functional groups. After a digression into synthetic applications of various organosilanes (*G. L. Larson*, 46 pp.), *A. R. Bassindale* and *P. G. Taylor* deal with the acid-base and complex-forming properties of organosilanes (30 pp.). The same authors have also written the chapter on the mechanisms of nucleophilic attack at silicon atoms (54 pp.), and that on activating and directing effects of silicon (71 pp.), which is perhaps of particular interest to the preparative organic chemist.

The contributions by *A. G. Brook* on photochemistry (42 pp.), *R. Tacke* and *H. Linoh* on organosilicon compounds in biochemistry (64 pp.), and *R. West* on polysilanes (34 pp.) are, as one expects from these authors, competently written and highly topical. The chapter by *G. Raabe* and *J. Michl* on multiple bonding to silicon (128 pp.) was awaited with some anticipation, since at the end of 1985 the same authors published an article on the same subject in *Chemical Reviews*, which was not merely long but of high quality. By leaving out aspects which have been treated in other chapters of this book, thus shortening it (!), and by updating it, the authors have again produced an excellent critical evaluation of the literature on this topic.

Although the notion of "hypervalence" is not universally accepted, *R. J. P. Corriu* and *J. C. Young* give, under this title, a review of penta- and hexacoordinated silicon compounds (48 pp.) which is well worth reading. In the short chapter (8 pp.) by *J. B. Lambert* and *W. J. Schulz* on trivalent silyl ions, the opportunity to explain the reasons for the considerable error and confusion which has arisen regarding the evidence for $R_3Si^{\oplus}$ ions in solution is unfortunately allowed to slip by; this would have provided an understanding of the definite proof now emerging for the existence of such ions.

Silicones, whose annual production in the western world has now reached a value of around $ 3 billion, receive a due amount of attention in the contribution by *T. C. Kendrick, P. Parbhoo* and *J. W. White* on siloxane polymers and copolymers (80 pp.); this includes the manufacture of silicones and their present and potential applications, and also those of the organofunctional polysiloxanes which are still relatively new.

After two short articles by *D. A. Armitage* on phosphorus, arsenic, antimony and bismuth derivatives (32 pp.), and on SiS, SiSe and SiTe compounds, there is a more extensive review of transition metal-silyl derivatives by *T. D. Tilley* (63 pp.). The text part of the book then ends with an informative chapter on hydrosilylation reactions (*I. Ojima*, 48 pp.).

At the end of the second volume are a name index of cited authors and an index of compounds. Difficulties can sometimes arise when using the compounds index, due to the fact that the nomenclature is not always consistent, but the name

index is pleasingly free of errors. However, this reviewer was surprised to find that a well-known Munich chemist seemed to have acquired an aristocratic title.

The two volumes are well produced, and the structural formulas are clear and easy to read. Some occasional instances where an R has been omitted from a formula or silicon has apparently become sulfur are almost unavoidable. Errors that one notices instantly are few. Examples of such are on page 1343, where the hydrosilylation mechanism has been incorrectly taken from the original paper, and on pages 659–660, where a synthetic route is given for tetracyclohexylsilane which was refuted as long ago as 1966.

The literature coverage is claimed to extend to mid-1987, and sometimes to the beginning of 1988. This has been achieved in most, though not all, cases.

The editors indicate in the preface that the originally intended chapters on "Silyl radicals, silylenes and rearrangements" and on "Silicon-nitrogen bonds" could not be included. This is regrettable, since considerable advances have been made in these areas especially in the last few years. Thus, for example, it has proved possible to isolate a large number of silanediyls (silylenes) in matrices. Trapping reactions of these intermediates have yielded various novel cyclic and open-chain compounds.

These two volumes are definitely a must for all university libraries. There is some confusion regarding the price information given by the publishers, since a large international book supplier in West Germany quoted a price of more than DM 1700 for the two volumes!

Manfred Weidenbruch [NB 991 IE]
Fachbereich Chemie
der Universität Oldenburg (FRG)

Application of Pattern Recognition to Catalytic Research. By *I. I. Ioffe*. Research Studies Press, Letchworth/Wiley, Chichester 1988. viii, 188 pp., hard cover, £ 30.50. – ISBN 0-86380-069-6/0-471-91907-1

In this monograph the author presents a survey of quantitative methods for the optimization of heterogeneous catalysts. The methods described, which belong to the category called "pattern recognition", are based on searching for correlations between the activity and selectivity of catalysts and their chemical composition and properties. Properties such as the specific surface area and density of the catalyst, and the electron affinities, lowest ionization potentials and ionic radii of the elements present, together with many other variables, have a major role in determining the catalytic activity. Since in many cases there is not a simple linear relationship between these properties and the activity and selectivity of the catalyst, statistical methods are used to analyze the data. The required data must either be taken from the literature or determined by experiment. It is important to base the analysis on a large number of catalysts for the reaction being investigated.

The first stage is to classify the catalysts into three groups with high, medium and low selectivities, and to correlate these with the properties of the catalysts concerned. On the basis of the properties that show the best correlations, one can now allocate new catalysts, which have not yet been investigated, between these three groups. Finally, experiments must be carried out to test whether or not the method of classification is appropriate. The purpose of such a study is to reduce, by appropriate preselection, the number of experiments that are needed to evaluate new catalysts. The questions of how reliable this classification is, and whether it is likely to result in an active catalyst being rejected too soon because of wrong classification, is determined, among other factors, by the quality of the data used and of the computer model. Accordingly, the greater part of the book is devoted to a discussion of the various models for heterogeneous catalysts with one or more components. The capabilities and limitations of the method are illustrated by examples such as the aromatization of dodecane, the oxidation of arenes, and the synthesis of isoprene from formaldehyde.

The monograph makes easy reading, and gives an insight into the relationships between the molecular properties of catalysts and their activities. However, those wishing to learn about the technique in greater depth so as to apply it in their own research will need to consult the original papers. Most of these are only available in Russian, as can be seen from the references listed. Consequently the book is of only limited value to the experimentalist in his day-to-day work. It is aimed more especially at readers who are involved in the theoretical aspects of catalysts, or who are engaged in long-term development work on large-scale chemical processes and need to evaluate large amounts of data.

Jochem Henkelmann [NB 1006 IE]
BASF AG, Ludwigshafen (FRG)

Registered names, trademarks, etc. used in this journal, even when not marked as such, are not to be considered unprotected by law.

© VCH Verlagsgesellschaft mbH, D-6940 Weinheim, 1990. - Printed in the Federal Republic of Germany by Konrad Triltsch Druck- und Verlagsanstalt Würzburg.

All rights reserved (including those of translation into foreign languages). No part of this issue may be reproduced in any form — by photoprint, microfilm, or any other means — nor transmitted or translated into a machine language without written permission from the publishers. Only single copies of contributions, or parts thereof, may be made for personal use. This journal was carefully produced in all its parts. Nevertheless, authors, editors and publisher do not warrant the information contained therein to be free of errors. Readers are advised to keep in mind that statements, data, illustrations, procedural details or other items may inadvertently be inaccurate.

Valid for users in the USA: The appearance of the code at the bottom of the first page of an article (serial) indicates the copyright owner's consent that copies of the article may be made for personal or internal use, or for the personal or internal use of specific clients. This consent is given on the condition, however, that the copier pay stated per-copy fee through the Copyright Clearance Center, Inc. (CCC), for copying beyond that permitted by Sections 107 or 108 of the U.S. Copyright Law. This consent does not extend to other kinds of copying, such as copying, for general distribution, for advertising or promotional purposes, for creating new collective works, or for resale. For copying from back volumes of this journal see 'Permissions to Photo-Copy: Publisher's Fee List' of the CCC.

Editorial office: Postfach 10 11 61, D-6490 Weinheim, Federal Republic of Germany, Telephone (06201) 60 22 55, Telex 465 516 vchwh d, Telefax (06201) 602 328.

Editor: *Peter Gölitz*

Associate editors: *D. I. Loewus, A. Stimson.* **Editorial assistant:** *E. Schweikart*

Publishers: VCH Verlagsgesellschaft mbH. (Managing Director: *Hans Dirk Köhler*), Pappelallee 3, D-6940 Weinheim, Federal Republic of Germany.

Advertising office (Advertising Manager *R. J. Roth*): Postfach 10 11 61, D-6940 Weinheim, Federal Republic of Germany, Telephone (0 62 01) 60 61 30, Telex 4 67 155, Telefax (0 62 01) 606 156.

ANGEWANDTE CHEMIE
International Edition in English
Volume 29 · Number 3
March 1990
Pages 223–328

Active MgH_2–Mg Systems for Reversible Chemical Energy Storage

By Borislav Bogdanović,* Alfred Ritter, and Bernd Spliethoff

Dedicated to Professor Günther Wilke on the occasion of his 65th birthday

An overview of the importance of and methods available for heat storage in the form of sensible and latent heat is followed by a discussion of the advantages and disadvantages of reversible thermochemical energy storage compared to conventional energy sources such as fuels, i.e. irreversible chemical energy carriers. Of the reversible metal-hydride–metal systems, the MgH_2–Mg system is particularly attractive as a hydrogen and a high-temperature heat storage material because of its high hydrogen content and the high energy content of the Mg–H bond. The advances made in this area over the past few years, namely in catalytic hydrogenation and the doping of magnesium powders, have led to the development of "active MgH_2–Mg systems" for energy storage. The first experimental results on high-temperature heat storage (also with cooling) by coupling a MgH_2–Mg storage system with a low-temperature metal hydride storage system are presented.

1. Introduction

For thousands of years—ever since the discovery of fire—mankind has conveniently satisfied its energy needs by burning wood or fossil fuels, thus liberating, in the form of high grade heat, solar energy which had been stored chemically for years (or millions of years) by photosynthesis. The energy problem currently facing us primarily arises from an incorrigible disparity between the storage of solar energy in nature and our energy consumption, which will lead, on the one hand, to a serious shortage of fossil fuels and, on the other, most probably to a climatic change through a build-up of carbon dioxide in the atmosphere ("greenhouse-effect"). This problem may be resolved, however, by: 1) reduction of the use of fossil fuels in favor of other energy sources, such as nuclear power, water power and wind power; 2) intelligent, more economical energy consumption;[1] 3) the search for, and use of energy storage systems which obtain their energy from a primary energy source, e.g. from the sun, and whose energy transformations occur in a closed cycle and hence are environmentally unobjectionable.[2] The following review article describes, inter alia, an experimental chemical contribution to the last of these three possibilities.

[*] Prof. Dr. B. Bogdanović, Dipl.-Ing. B. Spliethoff
Max-Planck-Institut für Kohlenforschung
Kaiser-Wilhelm-Platz 1, D-4330 Mülheim an der Ruhr 1 (FRG)
Dr. A. Ritter
Max-Planck-Institut für Strahlenchemie
Stiftstrasse 34–36, D-4330 Mülheim an der Ruhr 1 (FRG)

2. The Importance of Energy and Heat Storage, especially of High-Temperature Heat Storage[3]

The necessity of energy storage in general, and of heat storage in particular, arises from the fact that there is a temporal and intensity mismatch and also a spatial separation between the energy supply from an available energy source and our need or consumption of energy. Energy storage can offset this incongruity, improve the efficiency of an

 © VCH Verlagsgesellschaft mbH, D-6940 Weinheim, 1990 0570-0833/90/0303-0223 $ 02.50/0

energy supply system and hence reduce the energy costs. Consequently, energy storage is a major factor in energy saving and conservation. The storage of energy from a periodic or intermittent energy source, such as the sun, is of prime importance.

The type and magnitude of the mismatch between energy supply and need are exemplified in Figure 1.[4] Figure 1 (a) shows the case of constant energy supply with, however, a brief peak load which must be covered by energy storage. In case (b), the energy supply is periodic (solar energy), while the energy requirement remains constant; a significant part of the energy must, therefore, be stored during daytime in order to cover the needs at any time. Finally, when energy supply and demand are out of phase, as in (c), the total energy requirement must be stored (e.g., nocturnal indoor heating via solar heat).

The potential significance of heat storage, is impressively demonstrated by the fact that sufficient solar energy could be collected on the roof of a building during the summer for covering the heating requirements of the building during the winter (Fig. 2). In the case of a typical one-family house *in Germany* with a roof surface of 100 m^2—either facing south or oriented horizontally (flat roof)—an average incident solar radiation of 10^5 kWh[5] could be collected per year. This energy is sufficient to produce an amount of warm water equivalent to that requiring approximately 10000 L of heating oil, i.e., an amount which is more than adequate for heating a household during the winter. If one could make use of this energy in all of the households in the FRG, then up to ca. 40% of the currently consumed primary energy could be saved.

The amount of warm water whose energy content on cooling from, e.g., 90° to 40 °C corresponds to that of 10000 L of heating oil has however, in the ideal case, i.e. without heat storage loss, a volume of 1724 m^3. This is far larger than the volume of an average one-family house. Because of the unavoidable heat losses which constantly occur due to insulation problems, the volume of the warm-water storage tank would have to be substantially larger. Thus, it is immediately apparent that the, as yet, unsolved problem of *seasonal heat storage* is the main reason why solar radiation can presently play only an insignificant role as a source of energy, particularly in more northerly latitudes.[5,6]

An important aspect in connection with the amount of stored heat, namely the quality of the energy, or the so-called "exergy", should not be overlooked. Heat energy can be converted into other forms of energy with good Carnot efficiency, e.g. mechanical or electrical energy, but only above

Borislav Bogdanović was born in 1934 in Novi Sad, Yugoslavia and studied chemistry at the University of Belgrade. He gained his doctorate in 1962 under the supervision of G. Wilke at the Technische Hochschule Aachen. Since 1960 he has been working at the Max-Planck-Institut für Kohlenforschung in Mülheim an der Ruhr, where he is now head of a catalysis department. Bogdanović habilitated in 1974 at the Universität Bochum where he was awarded a professorship in 1976. His research interests center on organometallic chemistry and catalysis and its applications in organic and inorganic synthesis; in 1986 he was awarded the Ruhrpreis für Kunst und Wissenschaft der Stadt Mülheim an der Ruhr for his more recent works on the storage of energy with the MgH_2–Mg system.

Alfred Ritter was born in 1928 in Rottweil am Neckar and studied chemistry at the Technische Hochschule Stuttgart (where he gained his doctorate under L. Birkofer). Thereafter he worked as a scientific assistant at the Universität Köln and was engaged in research on organosilicon reactions in organic synthesis. In 1963 he was awarded a fellowship grant by the Dow Corning Corporation (Midland, Michigan) for research with L. H. Sommer at the Pennsylvania State University. Since 1964 he has been in charge of a research group at the Max-Planck-Institut für Strahlenchemie in Mülheim an der Ruhr. His current interests center on the radiation chemistry of organosilicon compounds and reversible chemical reactions for the storage of solar energy.

Bernd Spliethoff was born in 1953 in Oberhausen and completed his training as a laboratory technician at the Max-Planck-Institut für Kohlenforschung in Mülheim an der Ruhr. In 1971 he won the Bundeskanzler's Prize for young scientists in the open competition "Jugend forscht". Since completing his studies in engineering science at the Gesamthochschule Essen in 1975 he has been working at the Max-Planck-Institut für Kohlenforschung. He has participated right from the beginning in the development of active MgH_2–Mg systems as energy storers; he has developed measuring instruments and measuring techniques for the characterization of their storage properties.

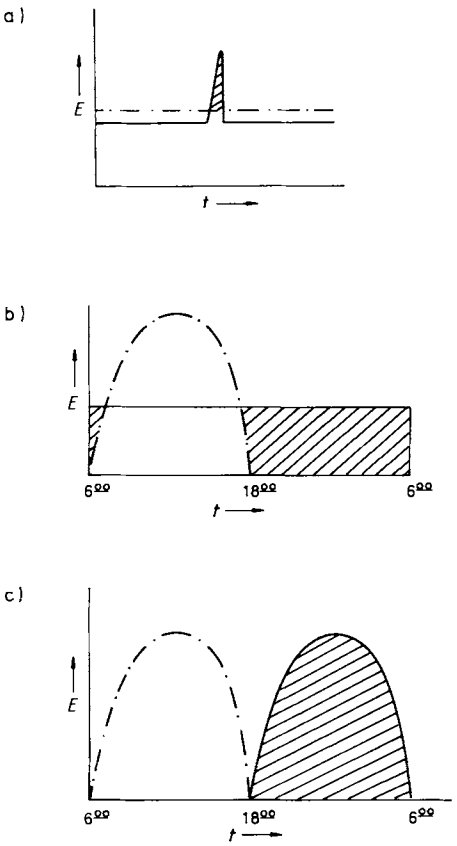

Fig. 1. Energy available from store ▨, which balances out the mismatch between energy supply (· – ·) and need (—): a) constant energy supply, short peak period; b) constant energy requirement, variable (periodic) energy supply during a half-day cycle; c) phase shift between energy supply and need; the entire energy need is covered by stored energy [3a] (reproduced by kind permission of Kluwer Academic Publishers).

300–400 °C. Consequently, energy storage systems must be developed, not only for low-temperature heat (LT) but also for high-temperature heat (HT).

An example of the *spatial* separation between energy supply and need, is provided by electrical power plants, which produce large amounts of low-grade waste heat, but owing to the distances between supply and consumer, often only part of this heat can be economically used for domestic heating ("power-heat-coupling").

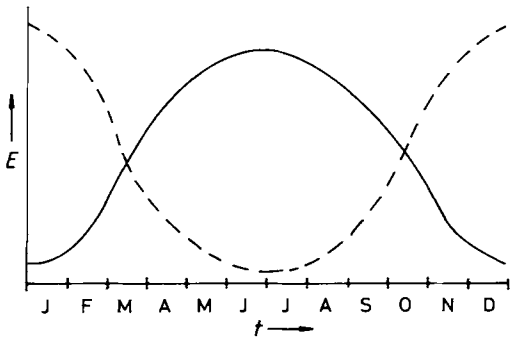

Fig. 2. Utilizable solar energy and heating energy needs in summer and winter: —— rooftop solar energy, – – – heating energy need.

3. Methods of Heat Storage

The oldest and simplest method used in everday life, as in industry, is to store heat in the form of sensible (perceptible) heat using materials having a high specific heat c. The materials most commonly used, and their heat capacities, are listed in Table 1.

Table 1. Frequently used liquid and solid materials for the storage of sensible heat [3a, b].

	M.p. [°C]	Temperature range [°C]	ϱ [g/cm³]	c [kJ kg⁻¹ K⁻¹]
Water	0	0–100	0.98 [a]	4.19
Thermo-oils	−70/−10	up to 350 [b]	0.87 [a]	2.1
53 KNO_3/40 $NaNO_2$/ 7 $NaNO_3$ [c]	142	up to 450	1.85 [a]	1.3
Na	98	– –	0.84	1.26
Cast iron	1150–1300	– –	7.2 [d]	0.54
Aluminum	660	– –	2.7 [d]	0.92
Fire-clay	–	– –	2.1–2.6 [d]	1.0
Al_2O_3	1700	– –	3.0 [d]	1.0
MgO	1700	– –	3.0 [d]	1.0
Stone	–	– –	1.9–2.6 [d]	0.8–0.9
Concrete	–	– –	–	0.9

[a] Average density in the temperature range given. [b] Some thermo-oils can be used up to 390 °C. [c] Wt.%. [d] At room temperature.

A further basic method for reversible heat storage consists in storing the heat evolved in a solid–liquid phase transition process in the form of latent heat. The advantage over the storage of sensible heat is the higher energy density and that the temperature remains constant during the heat storage and heat recovery processes. In contrast to the systems for the storage of sensible heat, those for the storage of latent heat are still at an early stage of development. A list of possible materials for this purpose is given in Table 2.

Table 2. Data for several potential latent heat stores [3a, b].

	M.p. [°C]	Heat of fusion [kJ kg⁻¹]
Salt hydrates	0–150	100–300
Paraffins	20–65	150–200
LiOH	471	1080
LiF	848	1050
48 NaCl/52 $MgCl_2$ [a]	450	431
67 LiF/33 MgF_2 [a]	741	900
67 NaF/33 MgF_2 [a]	832	618
24.5 NaCl/20.5 KCl/55 $MgCl_2$ [a]	385–393	410

[a] Wt.%.

The demand for high energy content per unit weight and volume especially in the case of mobile energy carriers,[7] as well as high exergetic quality and constant temperature, together with an unlimited storability of the stored energy, usually can only be satisfied by chemically stored energy, i.e., by fuels and not by sensible heat. An advantage of chemically stored energy is its direct transformability not only into heat, but also into other forms of energy with high efficiency (e.g., into electrical energy via fuel cells). The basic proce-

dures for transforming heat energy into chemical energy are dealt with in the following section.

4. Energy Storage from the Chemist's Viewpoint; Reversible and Irreversible Chemical Energy and Heat Storage

A list of the best-known fuels and their energy densities is given in Table 3. In general, the energy densities of the conventional energy carriers are much higher than those of the potential reversible chemical energy storage systems (Table 4). One should, however, take into consideration that these high energy densities arise from the fact that the combustion process generally occurs in an open system in the presence of oxygen from the environment, and this oxygen is not taken into account in the energy density calculation.[8] If the combustion were to take place in a closed system and if the amount of the consumed oxygen were to be considered in the calculation of the energy density, then, e.g., in the case of hydrogen as a rocket propellant the energy density would drop to 14×10^3 kJkg^{-1} and in the case of gasoline to 10×10^3 kJkg^{-1}.

Table 3. Most common fuels and their energy densities.

Fuel	Energy density [kJ kg^{-1}]
Hydrogen	125×10^3
Methane	48×10^3
Petrol	44.5×10^3
Heating oil	39.6×10^3
Coal	29.9×10^3
Wood	15.1×10^3
Ethanol	28.8×10^3
Methanol	21.6×10^3

A major disadvantage, both in the case of conventional energy sources and of hydrogen[9] (Table 3) is the practical irreversibility of the combustion reaction. The combustion processes occur at temperatures much lower than those at which the combustion products CO_2 and H_2O are in thermodynamic equilibrium with fuels and oxygen. This means that the regeneration of the combustion products CO_2 and/or water in fuels and O_2 by direct thermochemical pathways is not feasible because of the extremely high temperatures which would be required. The indirect thermochemical[10] procedures for achieving this for water are presently being intensively investigated, while the photochemical methods[11] are still at an early stage of development.

In the following, we will concentrate on the problems of heat storage. Its importance becomes immediately apparent through the fact that, apart from the fossil energy sources, the major remaining primary energy sources—nuclear energy and solar energy—deliver their energy in the form of high-quality heat or in the form of electromagnetic radiation which can immediately be converted into high-quality heat.

Independent of the fact, whether nuclear or solar energy is the primary energy source, it is necessary to search for new, reversible (i.e., closed), ecologically compatible cycles for heat storage. These should preferentially be reversible chemical systems, as mentioned in the previous section. This poses the question: How can heat be reversibly transformed into chemical energy?

In the reversible thermochemical[12] storage of energy the heat of a reversible chemical reaction is stored in the form of chemical energy. Thus, a compound of, e.g., type A–B can, by take up of heat (positive ΔH, endothermic process, heat storage), dissociate reversibly into the components A and B (molecules or atoms) and hence transform the heat energy ΔH into the chemical energy of the system A + B [Eq. (a)]. If the reverse reaction of A + B to A–B is prevented by

$$\text{A–B} + \Delta H \underset{\text{heat recovery}}{\overset{\text{heat storage}}{\rightleftharpoons}} \text{A} + \text{B} \qquad \text{(a)}$$

separating A from B, or by the absence of a catalyst in the case of a catalytic reaction, then the amount of heat ΔH stored in chemical form can be stored without any loss. On combining A and B or on catalysis, the reaction proceeds in the opposite sense liberating the amount of heat ΔH[13] (exothermic process, heat recovery). If A–B and A + B are in chemical equilibrium, then displacement of the equilibrium in favor of A + B or A–B will depend on the amount of heat added to or withdrawn from the system ("self-regulating systems", "chemical heat buffer").

Two thermodynamically based criteria must be fulfilled by potential chemical reactions for heat storage: for high energy density a high heat of reaction ΔH is required; for technical reasons the reaction must be reversible in a temperature region adjusted to that of the heat source. The temperatures should not be too high (for instance, above 1000 °C), because of material and heat insulation problems.[14] As will be shown in the following, high energy densities can generally only be achieved in reactions which have high turning temperatures T^*.[15] In other words: The reversibility of a chemical reaction at an acceptably low temperature can only be achieved by loss of energy density, i.e. compared to the case of irreversible heat storage (fuels), compromises concerning the energy densities must be accepted.

For a chemical reaction at equilibrium, Equation (b) holds true.

$$\Delta F = \Delta H - T\Delta S = 0 \qquad \text{(b)}$$

According to this the turning temperature is, to a first approximation,[15] given by Equation (c).

$$T^* = \frac{\Delta H}{\Delta S} \qquad \text{(c)}$$

It therefore follows that the turning temperature T^* does not exceed a certain value, and high energy densities (cf. ΔH) can only be achieved if the reaction proceeds with large entropy changes (ΔS).[8, 16] The highest entropy changes occur in dissociation reactions with gaseous reaction products and with large differences in the number of moles of starting materials and reaction products [see, e.g., Eq. (d)].[16]

$$NH_4HSO_4\ (\text{liq.}) \rightleftharpoons NH_3\ (g) + H_2O\ (g) + SO_3\ (g) \qquad \text{(d)}$$

According to *Alefeld*,[17] the so-called heterogeneous vaporization reactions (i.e. reactions of type (e)) are especially suitable for heat storage.

$$\text{A–B (solid or liquid)} + \Delta H \underset{\text{heat recovery}}{\overset{\text{heat storage}}{\rightleftharpoons}} \text{A (solid or liquid)} + \text{B (gaseous)} \qquad \text{(e)}$$

In these reactions the turning temperature T^* is relatively low and in addition the different aggregation states allow simple separation of A from B. The thermodynamical and technical advantages of heterogeneous vaporization are counterbalanced by the disadvantage of the considerable increase in volume, which lowers the volumetric energy density of the total system (for a solution of this problem in the case of the MgH_2–Mg system, see Section 6).

The energetic and thermodynamic factors are not the sole factors which are important for the choice of reactions for reversible heat(energy)storage. Other criteria such as the following may also be important or even decisive:

- complete reversibility of the reaction over a large number of cycles, i.e., no side reactions and hence no loss of storage capacity;
- excellent kinetics of the heat storage and recovery processes; long stability and activity of the catalyst in the case of catalytic reactions;
- possibility of stopping or controlling the heat producing process by separation of the components from each other or from the catalyst;
- minimal heat loss by thermal radiation;
- heat storage and recovery in desired temperature ranges;
- as constant and controllable as possible a temperature during the heat recovery process;
- simple realization and low processing costs;
- no (or only minor) hysteresis effects; low temperature differences between storage and recovery, i.e., minimal exergy loss;
- excellent heat transport to and from the reaction bed;
- availability of the storage material in large amounts and at low costs;
- no environmental or fire risks on handling the storage material and carrying out the storage reaction; low toxicity or corrosiveness of the materials used.

In view of the many criteria, it is obvious that the choice of the reactions must involve compromises.

Some examples of the best-known types of reactions which have been suggested for reversible thermochemical heat storage or which are presently being investigated are given in Table 4. Of the catalytic gas dissociation reactions, the dissociation of SO_3 to SO_2 and O_2 (Solchem process) and the dissociation of NH_3 to give N_2 and H_2 have been particularly well investigated or considered as reversible reactions for the storage of solar energy. The technically mature NH_3 dissociation (catalysis of forward and reverse reaction, separation of the reactants, corrosiveness and toxicity) is considered to be less problematic than that of SO_3 dissociation.[18] The thermal dissociation of NH_4HSO_4 is a potential candidate for energy storage because of the high energy density and relatively low reaction temperature. The Eva-Adam process now being operated on a pilot-plant scale at the nuclear research center Jülich (West Germany) is based on the known steam reforming of methane to CO and H_2. This process was developed for the transportation of nuclear reactor heat to distant users according to the principle of the chemical heat pipe.[19]

Because of the necessity of complete reversibility, i.e., absence of side reactions, the organic chemical reactions that were considered, apart from the methane reforming reaction, included only the reversible catalytic dehydrogenations of cyclohexane, methyl cyclohexane, and ethane to benzene, toluene, and ethene, respectively.[20]

All of the remaining reactions in Table 4 belong to the category of heterogeneous vaporization reactions. Of the

Table 4. Several potential reversible reactions for the thermochemical energy storage [3a, b].

Type of reaction	Examples	Temperature range [°C]	Energy density [kJ kg^{-1}]
Catalytic or thermal dissociation	$SO_3 \overset{Cat.}{\rightleftharpoons} SO_2 + 1/2\ O_2$ [a]	520–960	1235
	$NH_4HSO_4 \rightleftharpoons NH_3 + H_2O + SO_3$	927–427	2011
Steam reformation of methane (Eva–Adam)	$CH_4 + H_2O \overset{Cat.}{\rightleftharpoons} CO + 3H_2$	480–1195	6053
Dehydrogenation of ethane or cyclohexane	$C_2H_6 \overset{Cat.}{\rightleftharpoons} C_2H_4 + H_2$	–	–
	$C_6H_{12} \overset{Cat.}{\rightleftharpoons} C_6H_6 + 3H_2$	–	–
Dehydration of metal hydroxides, salt hydrates, acids and zeolites	$Ca(OH)_2 \rightleftharpoons CaO + H_2O$	572–402	1415
	$MgCl_2 \cdot 6H_2O \rightleftharpoons MgCl_2 \cdot 4H_2O + 2H_2O$	–	3180
	$H_2SO_4/H_2O \rightleftharpoons H_2SO_4 + H_2O$	–	–
	zeolite/$H_2O \rightleftharpoons$ zeolite + H_2O	50–150	974–1370
NH_3-elimination from salt ammoniates	$CaCl_2 \cdot 8NH_3 \rightleftharpoons CaCl_2 \cdot 4NH_3 + 4NH_3$	32–100	745
Thermal dissociation of metal carbonates	$CaCO_3 \rightleftharpoons CaO + CO_2$	–	1780
	$MgCO_3 \rightleftharpoons MgO + CO_2$	427–327	1200
Thermal deoxygenation of metal oxides	$Na_2O_2 \rightleftharpoons Na_2O + 1/2\ O_2$	650–975	1537
	$2KO_2 \rightleftharpoons K_2O + 1\ 1/2\ O_2$	300–800	2148
	$BaO_2 \rightleftharpoons BaO + 1/2\ O_2$	300–825	528
Thermal dehydrogenation of metal hydrides	see Section 5 and Table 5		

[a] Solchem process.

dehydration reactions, slaked lime, $Ca(OH)_2$, has been particularly well investigated for the storage of solar heat, as have also the salt hydrates (e.g., $MgCl_2 \cdot 6\,H_2O$) and H_2SO_4, in addition to the reversible *adsorption* of water on zeolites.[21] In contrast, the thermal dissociation of metal carbonates and the reversible thermal dissociation of several metal oxides and peroxides ("reversible oxidation") have hardly been investigated for heat storage purposes. Apart from the advantage of easy separation of the gaseous reaction products from the solids, positive aspects in the dehydration and in the thermal dissociation of ammoniates and carbonates include the easy condensation of water vapor, NH_3 and CO_2, which means that large spaces for interim gas storage are not required. A particular advantage of "reversible oxidation" compared to other reversible reactions would be the possibility of storing heat in an open system.[8]

Apart from very few exceptions (Eva–Adam process,[19] the $Na_2S \cdot H_2O$ system[22]) the reactions mentioned have thus far only been investigated on a laboratory scale. In many cases, the suitability of the proposed reactions was only estimated on the basis of available physicochemical data, while chemical investigations of the systems under conditions relevant for heat storage and recovery or tests during various cycles have not been carried out. It is thus obvious why all of the present large-scale solar thermal storage systems are based only on sensible heat.[23]

5. Metal Hydrides as Reversible Chemical Energy Stores

Numerous metal-hydride–metal systems fulfill many of the criteria required for reversible thermochemical heat storage.[24] A special feature of the reversible metal-hydride–metal reactions compared to other heterogeneous vaporization reactions (cf. Table 4) is that the hydrogen liberated during the thermal loading is the chemical fuel having the highest energy density (cf. Table 3), and it is considered as the possible future clean secondary energy source.[9]

$$MH_n + \Delta H \underset{\text{heat recovery}}{\overset{\text{heat storage}}{\rightleftharpoons}} M + n/2\,H_2 \qquad \text{(f)}$$

M = metal, metal alloy, intermetallic compound

Since the reversible reaction of many metals, metal alloys and intermetallic compounds with hydrogen [Eq. (f), right to left] is being intensively investigated, inter alia, as a method for the safe *storage of hydrogen* with a high hydrogen density per unit weight and volume (Table 5) for the transport of hydrogen and as a fuel for motor vehicles, fuel cells etc.,[24,25] the metal-hydride–metal systems should be regarded as reversible energy stores in a double sense, namely as hydrogen stores *and* as heat stores. A fundamental difference between the use of metal hydrides as heat stores and hydrogen stores is that, in the former case, the heat of reaction of the hydride formation can be used as heat while retaining the hydrogen in a closed system during many heat storage cycles, whereas in the latter case the hydrogen is liberated from the hydride in an open system and is burned irreversibly to give water. The reversibly stored chemical energy in the case of the metal hydrides used as heat storage systems is naturally smaller than that of hydrogen as irreversible energy carrier, but it can be up to one third of the energy of the hydrogen bound in the hydride, as in the case of the MgH_2–Mg system.

The properties of many metal-hydride–metal systems as reversible hydrogen storage materials are well-known and have been thoroughly tested through many hydrogen charging and discharging cycles; such systems have already been used commercially for preparing high purity hydrogen[25] and are used technically as inherently safe hydrogen stores.[25] Their use as materials for thermochemical heat pumps and for air conditioners, has already been tested on a large scale but has not yet been commercialized.[26]

On the basis of the temperature T_d, at which the decomposition pressure reaches values of $P_{H_2} \geq 1$ bar, *Buchner*[24a] subdivided metal hydrides into low ($50 \geq T_d \geq -30\,^\circ C$ or lower) middle ($200 \geq T_d \geq 100\,^\circ C$) and high temperature hydrides ($T_d \geq 200\,^\circ C$). A list of some typical metal-hydride–metal systems used for hydrogen storage together with characteristic data is given in Table 5. The low-temperature hydrides are characterized by relatively low hydrogen contents (1.3–2.0 wt%) and low heats of hydrogenation; they thus have low energy densities as hydrogen and heat storage materials. Liberation of hydrogen from these hydrides is already achieved with small amounts of low-temperature heat (environmental heat). The low-temperature hydrides are therefore suitable, e.g., for heat pumps, air conditioners, and refrigerators (see Section 6). Disadvantageous, however, are the relatively high costs of the alloys. In the case of high-temperature hydrides, hydrogen contents of 3.8 (Mg_2NiH_4) to 7.6 wt.-% (MgH_2) are achieved. Because of the high stability of their metal–hydrogen bonds, they have high heats of hydrogenation. All of these hydrides have in common a high hydrogen storage density per unit volume of the storage material; in all cases it exceeds that in liquid hydrogen (0.075 g/cm³ at 20 K).

Table 5. Data for several energy stores used as reversible metal hydride–metal systems.

Metal hydride–Metal system	H_2 content [wt.%]	g H_2 per cm³ hydride [a]	H_2-dissociation pressure of the hydride/T	ΔH [kJ per mol H_2]	Energy density as heat store [kJ kg^{-1}]	Energy density as H_2 store [kJ kg^{-1}]
$FeTiH_{1.93}$–FeTi	1.8	0.1	3.5 bar/20 °C	28 [b]	~ 300	2200
$LaNi_5H_6$–$LaNi_5$	1.4	0.09	2 bar/20 °C	32	200	1700
Mg_2NiH_4–Mg_2Ni	3.8	0.08	1 bar/245 °C	65	1260	4600
MgH_2–Mg	7.6	0.1	1 bar/284 °C	75	3079	9000

[a] Density of the hydride calculated from X-ray structure analyses. [b] Valid for the reaction $FeTiH_{1.0}$–$FeTiH_{0.1}$.

6. Magnesium Hydride as an Energy Store; Generation and Possible Applications of Active MgH_2–Mg Systems as Hydrogen and High-Temperature Heat Stores

Since magnesium is the lightest of the metals or metal alloys which can be considered for hydrogen storage, MgH_2 has the highest hydrogen content[27] and hence the highest energy density (9 MJ/kg Mg) of all the hydrides used for this purpose. Further principle advantages of MgH_2 as an energy storage material are the low costs of magnesium metal, the wide distribution of magnesium in nature[28] and its environmental compatibility. Furthermore, hydrogen storage in the form of MgH_2 is much safer than the conventional storage technology using containers under pressure.

The disadvantage of magnesium hydride as a *hydrogen* store, is that a relatively large amount of energy [75 kJ mol^{-1}, Eq. (g)] at a high temperature level is needed

$$MgH_2 + 75\ kJmol^{-1} \rightleftharpoons Mg + H_2 \qquad (g)$$

capacity for heat storage: 0.9 kWh (3 MJ) per kg Mg

to displace the hydrogen, but this is advantageous for the MgH_2–Mg system when used as a *heat* store because, in principle, 75 kJ per mol of heat or 0.9 kWh per kg Mg can be stored at a hydrogen pressure (1 to >100 bar) dependent temperature level between 300 and about 500 °C (Table 6,

Table 6. Temperature-dependent hydrogen dissociation pressure of magnesium hydride p_{H_2}.

T [°C]	p_{H_2} [bar] [a]	T [°C]	p_{H_2} [bar] [b]
280	0.9	400	19.4
290	1.2	410	23.9
300	1.6	420	29.2
310	2.2	430	35.5
320	2.8	440	43.0
330	3.7	450	51.8
340	4.8	460	62.0
350	6.2	470	74.0
360	7.9	480	87.8
370	10.0	490	103.7
380	12.5	500	121.9
390	15.6		

[a] Own measurements. [b] Extrapolated values based on own measurements.

Fig. 3). Hence, an extremely interesting temperature range is made available for possible technical uses of heat storage. Heat energy at this temperature level can be efficiently transformed into other forms of energy, in particular into mechanical energy (steam turbines, Stirling motors) and electrical energy or via thermovoltaic cells directly into electrical energy. There are no equally suitable thermochemical systems in this temperature region. Therefore, heat stores based on sensible or latent heat (Tables 1 and 2) are currently used to store high-temperature heat between 300–500 °C. In comparison with conventional heat storage materials in the same temperature range, magnesium hydride has the advantages of an energy density which is an order of magnitude higher (c.f., Table 1), and the chemically stored heat is free from losses for any length of time. In contrast to sensible heat

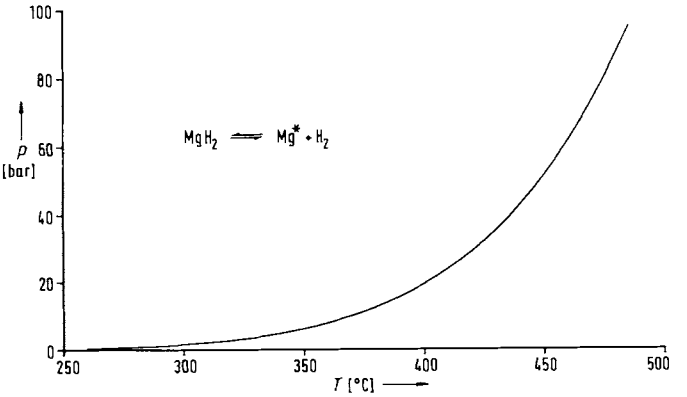

Fig. 3. Temperature dependence of the hydrogen dissociation pressure of magnesium hydride.

stores in which the temperature and hence the exergetic quality of the stored energy continually decreases during the heat discharge process (see Section 3), in the case of the MgH_2–Mg systems the exergetic quality remains constant because of the horizontal plateau of the concentration–pressure isotherm (Fig. 4) during the hydrogenation as long as the

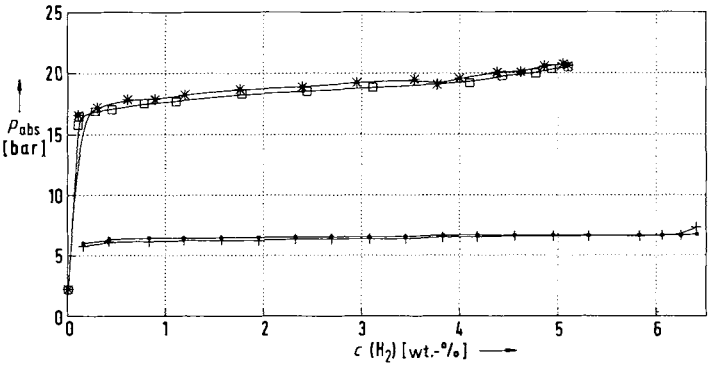

Fig. 4. Concentration-pressure isotherm for the MgH_2–Mg system (nickel-doped, 270 mesh Mg powder) at 352° (■ absorption, + desorption) and 402 °C (• absorption, □ desorption).

hydrogen pressure above the magnesium remains constant. By regulating the H_2-pressure the desired temperature level of heat generation can be maintained because each hydrogen pressure corresponds to a precisely fixed equilibrium temperature (cf. Table 6). Furthermore, the steep gradient of the hydrogen pressure in the range of 300–500 °C (Fig. 3) makes it suitable for heat transformations (raising heat to a higher temperature level) and for hydrogen compression.[26d]

The disadvantages of the hydride heat stores in comparison to heat stores based on sensible heat, are their cost, which cannot be estimated at present (no plant of this type is in operation, as yet), and the necessity of interim storage of the hydrogen liberated from the hydride. The heat conductivities are comparable with those of conventional heat storage systems or, in certain cases, even better. The intermediate storage of the liberated hydrogen in another metal–metal-hydride system which has different thermodynamic properties can be very advantageous, since the coupling of two metal hydride storage systems represents a chemical heat

pump and hence can be used for heat transformation and for cooling (see below).[26, 29]

The synthesis of MgH_2[30] from the elements was first described in 1951 by *Wiberg* and *Bauer*.[31] Ever since *Alefeld*[17] first proposed the MgH_2–Mg system as a possible candidate for heat storage because of its favorable thermodynamic properties, its use has been the subject of continued discussion. A technical evaluation concluded that there were no economic benefits over heat stores based on sensible heat,[32] mainly because of the estimated low heat conductivity of the MgH_2–Mg reaction bed and inadequate reaction kinetics. The reason for the lack of experiments in this direction is probably due to the known poor chemical reactivity of the pure MgH_2–Mg system.[33] Our own experiments have shown that the above-mentioned shortcomings do not apply to the active MgH_2–Mg systems.

Reilly and *Wiswall*[34] showed that the intermetallic compound Mg_2Ni and also magnesium that is alloyed with metallic nickel exhibit a higher hydrogenation-dehydrogenation rate than pure magnesium. This finding led to numerous experiments involving the formation of alloys of magnesium with other metals[33, 35] in order to improve the kinetics of the hydrogen charging and discharging processes. A magnesium/nickel alloy with ca. 10 wt.-% Ni[35, 36] has been considered as a hydrogen storage material for hydrogen-powered vehicles, but it could only be used in combination with a low-temperature metal hydride store or an additional heat source, since the energy content of the exhaust gases did not suffice in order to obtain the necessary high-temperature heat for displacing hydrogen gas from the store.[37]

Our chemical research on energy storage is mainly concerned with improving the kinetics of the dehydrogenation and hydrogenation steps of the active MgH_2–Mg systems. The work began with the so-called homogeneous catalytic[38] synthesis of magnesium hydride.[39] The superior kinetics of the dehydrogenation of magnesium hydride which had been prepared by homogeneous catalysis (referred to as MgH_2^* from here on), and the hydrogenation of the active magnesium (Mg*)[33, 40] obtained from it, prompted our investigations on their use as energy stores. Furthermore, MgH_2^* and Mg* found useage as reagents in organic and inorganic syntheses because of their high reactivity.[41] They have also been employed for the preparation of intermetallic compounds and their hydrides and carbides via non-metallurgic routes.[42] In the following, we shall review more recent developments in the area of energy storage (for earlier work, see Ref. [33]).

The high chemical reactivity of MgH_2^* is considered to be due to its generation in an inert atmosphere in the form of microcrystals (0.05 μm) with an oxide-free and high specific surface area (70–180 $m^2 g^{-1}$).[41] Other possible reasons for the superior dehydrogenation–rehydrogenation kinetics of MgH_2^* include the defects in the crystal lattice caused by impurities such as MgO and $MgCl_2$ and the catalytic effect of the transition metals (Ti, Cr)[43] resulting from the tetrahydrofuran-soluble hydrogenation catalysts which remain in the solid. In order to test this effect, the influence of doping MgH_2^* with small amounts of transition metals was studied using the transition metals in the form of soluble organometallic complexes or compounds and assessing the effect on the dehydrogenation–rehydrogenation. It was found that both the rate and the degree of the dehydrogenation–rehydrogenation could be improved considerably by adding small amounts (0.5–3 wt.-%) of transitional metal complexes, especially nickel complexes, to the MgH_2^*.[44]

MgH_2^*, as an energy storage material, has the disadvantages of being highly pyrophoric and of being relatively difficult to prepare. It therefore seemed obvious to use the above-described method of catalytic doping to improve the properties of the commercially available magnesium powders. This led to the development of various, relatively simple methods for the preparation of storage materials based on magnesium powders.[44]

The doping generally consists of treating finely ground magnesium powders (preferentially 270 mesh or finer) or magnesium hydride with a solution of a suitable transition metal complex, if necessary in the presence of hydrogen. In this way, the transition metal is deposited in an extremely finely divided form on the surface of the Mg or MgH_2 particles and it assumes the role of the catalyst in the hydrogenation and dehydrogenation processes. The advantages of this method are that small amounts of the deposited transition metal already have a strong catalytic effect and that the so *doped* magnesium powders become air-stable. A typical procedure consists of doping the Mg powder with a solution of bis(1,5-cyclooctadiene)nickel (cod_2Ni)[45] in toluene by passing hydrogen into the solution at room temperature under normal pressure. The nickel complex is autocatalytically hydrogenated to cyclooctane and nickel which is deposited in very fine distribution on the surface of the Mg particles [Eq. (h)].

$$\text{Mg powder (excess)} + cod_2Ni + 4\,H_2 \xrightarrow[-2c\text{-}C_8H_{16}]{20\,^\circ C} Mg(Ni) \qquad \text{(h)}$$

The Mg powder (270 mesh) doped with 2 wt.-% of nickel and obtained in this way proved to be suitable as a hydrogen and heat storage material in numerous tests and it is used at the present time as a standard material in our experiments described below. The standard material has the following properties:

- reversible hydrogen contents of 6–6.5 wt.-%,
- satisfactory and complete display of the kinetics after the first hydrogenation,
- stability over a long period, demonstrated by extended testing in a closed system through 1800 cycles,
- very little absorption–desorption hysteresis[46] and an almost horizontal plateau in the concentration-pressure isotherm (cf. Fig. 4),
- relatively good heat conductivity of the solid MgH_2–Mg storage bed during the hydrogenation and dehydrogenation (Fig. 5).[47]

A further improvement of the H_2-storage capacity and of the long term stability as well as the economic optimization of the storage material production are currently being attempted.[48]

Our present research in the area of energy storage is focused on the use of active MgH_2–Mg systems as high temperature heat stores.[8, 29] A heat store based on MgH_2, operating on the principle shown in Equation (g), consists essentially of a pressure-proof container interconnected with a second container for the intermediate storage of the de-

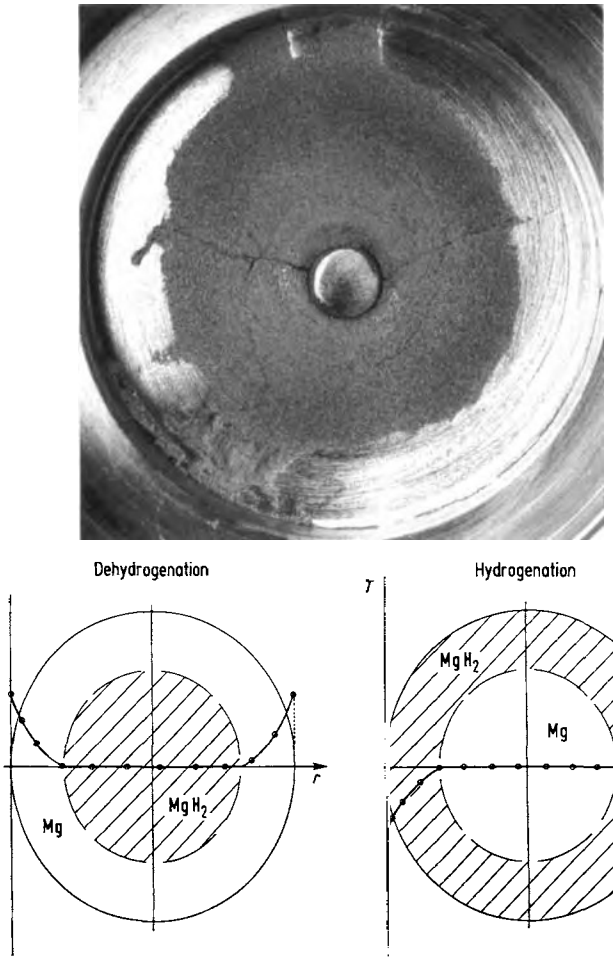

Fig. 5. Top: opened cylindrical MgH_2–Mg experimental heat store with an internal diameter of 70 mm which can be heated or cooled externally. During the dehydrogenation, which proceeds from the outside to the inside, as does the heat flow, the reaction was stopped, so that two cylindrical zones were present in the store. The slightly abraded material clearly shows an outside metallic shining ring made of magnesium, and an inner ring consisting of MgH_2. The middle of the store has a sinter metal pipe for delivering and withdrawing hydrogen. The irregularities within the outer ring are due to the difficulties encountered while abrading the brittle material. By measuring the dynamic temperature curves during the hydrogenation and dehydrogenation at various depths in the hydride bed, the "average effective total heat conductivity" of the MgH_2–Mg system during the chemical reaction can be determined when using an empirical formula. This is characterized by the various single conductivities of the MgH_2–Mg material combinations which are formed from the initially pure educts MgH_2 or Mg, respectively, and which are separated by the reaction zone which always moves from the outside to the inside. Bottom: From the narrow width of the reaction zone and the temperature jump which occurs there, it can be concluded that the chemical reaction rate must be greater than the rate of the heat transportation. In the inverse case, the reaction zone should be spread over the entire width of the tube filling [47].

sorbed hydrogen. A valve regulates the flow of hydrogen between the two containers. The intermediate storage of the desorbed hydrogen can be achieved in three ways: 1) storage in a gas container under normal pressure; 2) storage under the decomposition pressure of the magnesium hydride in a pressure-proof container; 3) storage in the form of a low-temperature metal hydride. The latter two possiblities have been realized and tested by us on a laboratory scale.[29]

The third possibility of intermediate storage of hydrogen is based on the use of a suitable metal alloy, which on taking up hydrogen yields a low-temperature hydride by delivering heat to the environment. This hydride must be able to release the chemically bound hydrogen by taking up environmental heat to cover the reaction enthalpy. This approach is of particular interest for the following reasons:

- The absorption of hydrogen yielding the low-temperature metal hydride releases low-temperature heat, which constitutes 30–40% of the high-temperature heat of reaction and can be used, for example, for chemical heat pump processes.
- The desorption of hydrogen from the low-temperature metal hydride results in cooling, which can be used to produce ice or for air-conditioning purposes.
- The large temperature difference, which occurs in the combined metal hydride systems during the reverse reaction of magnesium to magnesium hydride can be used advantageously for improving the efficiency of thermodynamic machines such as Stirling motors or thermovoltaic cells.
- By supplying low-temperature heat, e.g., waste heat from industrial processes, into the low-temperature part of a combined metal hydride system, the hydrogen pressure can be increased, hence leading to a temperature increase in the high-temperature section (heat transformation).
- The volume of the intermediate hydrogen storage tank is much smaller than that of either of the alternative storage variants.

The apparatus shown in Figure 6 was used in order to study the processes mentioned. Section A (HT heat store)

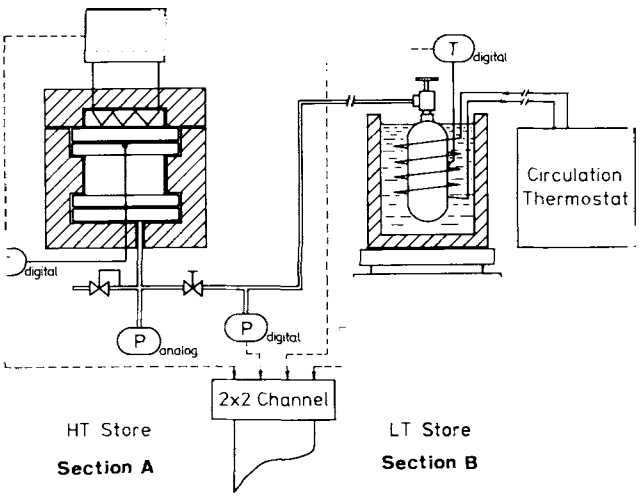

includes a thermally insulated cylindrical stainless steel container which is filled with 1054 g of nickel-doped magnesium powder (standard material).[44] Heat was transferred via the upper horizontal plate of this container to the magnesium hydride bed using an electrically heated hot plate.

Section B (LT heat store) shows the commercially available[49] low-temperature metal hydride container (hydrogen storage capacity 1 m^3), which contains the alloy Code 5800 ($Ti_{0.98}$ $Zr_{0.02}$ $V_{0.43}$ $Fe_{0.09}$ $Cr_{0.05}$ $Mn_{1.2}$). This is immersed in a water or water/glycol bath which is kept at the desired

constant temperature using a thermostat. The two containers are interconnected via a copper tube in order to allow hydrogen exchange in both directions. A high precision digital balance serves for the gravimetric determination of the absorbed/desorbed hydrogen in and from the low-temperature metal hydride container.

The experimental set up shown in Figure 6 was used to carry out the following experiments, the results of which are summarized in Table 7. In all of the experiments, the rate of heating (405 $K\,h^{-1}$) of the magnesium hydride container from room temperature to the final temperature of 425 °C

Table 7. Experimental results during high-temperature heat storage and recovery (for experimental setup see Fig. 6).

Temp. of the LT-metal hydride [°C]	Amount of H_2 desorbed from MgH_2 [g]	Max. rate of H_2-desorption [gh^{-1}]	Amount of H_2 resorbed by Mg [g]	Heat performance of the MgH_2 container [kW]	Heat capacity of the MgH_2 container [kWh]
+10	69	40.4	69(6.0 h)	0.26(2.5 h)	0.71
+20	69.4	33.6	69(6.0 h) [a]	0.3(2.5 h)	0.71
+30	60.6	26.0	62.6(6.0 h)	0.33(2.0 h)	0.65
+40	36.4	24.0	37.6(6.0 h)	0.33(1.2 h)	0.38

[a] 60 g after 2.5 h.

was constant. This temperature was maintained for an additional 5 h. The temperature at which the liberated hydrogen was absorbed by the low-temperature alloy was varied at 10 °C intervals between 10 and 40 °C.

The amount of absorbed hydrogen in the low-temperature metal alloy, i.e. the amount of hydrogen desorbed from MgH_2, was determined by weighing the relevant container on a high-precision balance (columns 2 and 3 of Table 7). During the heat recovery, the heating plate is removed so that the heat can be delivered to the surroundings via the upper plate of the autoclave. The amounts of hydrogen desorbed from the low-temperature metal hydride (which become reabsorbed by Mg) are listed in column 4 of Table 7. The plot of the experiment carried out at 20 °C (Fig. 7) shows

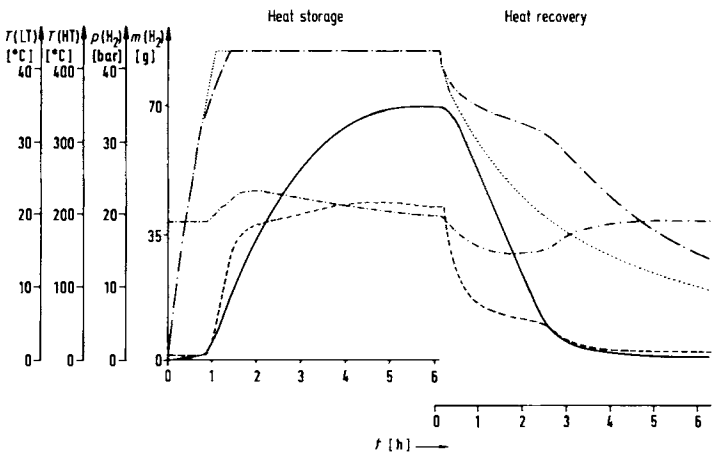

Fig. 7. Plot of the heat storage and recovery cycle using the setup shown in Figure 6: —— weight increase or decrease of the low-temperature hydride store, - - - temperature of the high-temperature heat store, – · – · – temperature of the low-temperature heat store, – – – H_2-pressure, · · · heating and cooling curves of the high-temperature heat store with closed valve.

that the hydrogen displacement from the MgH_2 store was complete after about 4 h, and that the resorption required approximately 3 h at a practically constant rate. The values in column 4 of Table 7 apply only to the case where the heat of hydrogen sorption in the magnesium container is vented to the atmosphere by thermal radiation and natural convection via its thermally uninsulated upper horizontal plate. A remarkable increase of hydrogen sorption is recorded when this plate is covered with a pot containing cold water, which after a short time starts boiling.

Also the data in Table 7, column 5 for the heat output during regeneration of the magnesium hydride only apply when the high-temperature reaction heat is given off under the conditions described above. In an experiment carried out at 10 °C on the low-temperature side of the system, the heat output could be doubled by using cold water for the heat transfer.

The used heat capacity of the magnesium hydride container (Table 7, column 6), like the maximum amount of H_2 desorbed and reabsorbed by Mg per hour, decreases with increasing temperature of the low-temperature metal hydride container (Table 7, column 3).

In order to realize the heat recovery during a reaction cycle, one must know the lowest preheating temperature in the magnesium container at which the hydrogen resorption begins. On the basis of two experiments, during which the low-temperature metal hydride container was kept at 10 and 20 °C, respectively, it could be demonstrated that the magnesium container had to be heated to 150 °C in order to initiate the heat recovery process.

The most interesting application of the storage unit shown in Figure 6 is the simultaneous production of ice with the low-temperature metal hydride container and of high-temperature heat by resorption of hydrogen in the magnesium container with reformation of magnesium hydride.

To demonstrate this double effect, the container with the low-temperature metal alloy was cooled to 0 °C and kept at this temperature level using a water/ice bath until the hydrogen transfer from the magnesium hydride container was completed. Under these conditions, 67.2 g of hydrogen gas are taken up within 3 h at a maximum delivery rate of 46.0 $g\,h^{-1}$ by the low-temperature metal alloy, leading to formation of the corresponding metal hydride.

After completion of this step, the low-temperature metal hydride container was immersed in a water-bath at 0 °C and the magnesium container was heated to the preheat temperature, as mentioned above. After 3 h, 59.0 g of the hydrogen is resorbed by the magnesium bed and 2.5 g more after a further two hours. This corresponds to a heat capacity of 0.64 kWh for the magnesium container. The heat performance is almost constant over a period of 2.3 h and amounts to 0.23 kW. At the end of the reaction, 1.9 kg of ice had formed around the low-temperature metal hydride container. This is equivalent to a cooling capacity of 0.18 kWh (28 % of the high-temperature heat capacity) and a cooling performance of 0.076 kW. The temperature at the hot plate of the magnesium container was 315 °C during this period of ice production (Table 8).

The system shown in Figure 6 can also be used as a heat transformer, as can be verified by the following experiment: The magnesium hydride in the container is thermally decom-

Table 8. Simultaneous production of ice and high-temperature heat (for experimental setup, see Fig. 6).

Cooling capacity of the LT-metal hydride container:	0.18 kWh (28% of the high-temperature heat capacity)
Cooling performance of the LT-metal hydride container:	0.076 kW
Operation temperature of the HT-heat store during the cooling process:	315 °C
Amount of ice produced at the end of the experiment:	1.9 kg

posed by heating from 20 to 349 °C within 45 min, and the desorbed hydrogen (76 g) is absorbed in the container with the low-temperature metal alloy, which is kept at −20 °C, corresponding to a final hydrogen pressure in the system of 4.3 bar.

The reverse reaction is allowed to take place at 29 °C in the low-temperature metal hydride container. The hydrogen pressure in the system rose from the initial 4.3 bar to 24.3 bar.

The temperature in the insulated magnesium container, from which heat can only be emitted in accord with the degree of insulation, rapidly rises from the initial 350 °C to 373 °C, and remains at this temperature for two hours. After a further 2 h, the temperature drops to 340 °C. The result of this experiment shows that the initial temperature increase of 49 K in the low-temperature metal hydride container leads to an upgrading of high-temperature heat in the magnesium container of 23 K, whereby the considerable hysteresis of the low-temperature hydride has an adverse influence.

7. Summary and Outlook

The experimental results presented in Section 6 demonstrated, for the first time, the use of a high-temperature metal hydride based on a pure metal and not an alloy, for the storage of high-temperature heat. Further development work on active MgH_2–Mg systems as high-temperature heat stores is currently being carried out at the two Max-Planck-Institutes in Mülheim an der Ruhr (FRG) in cooperation with BOMIN-SOLAR, Lörrach (FRG) (project leader: Dipl.-Phys. *J. Kleinwächter*) and the Institut für Kernenergetik und Energiesysteme (IKE) der Universität Stuttgart (FRG) (project leader: Prof. Dr.-Ing. *M. Groll*) with financial support of the German Federal Ministry for Research and Technology, (BMFT). A major aim of this project is to build and test the first thermochemical energy store with about 100 kg MgH_2 for solar and other energy supply systems on the basis of MgH_2–Mg.[50]

From a chemist's point of view, it is still an urgent and rewarding task to develop new and inexpensive reversible metal hydrides with high energy densities on both the high and low temperature sides, and also to search for other reversible thermochemical energy storage systems.

We would like to thank Professor Dr. G. Wilke for his generous support of the work described above. One of us, (B.B.), would like to thank his co-workers, mentioned in the references, for their valuable contributions to this work. We are grateful to the Federal Ministry for Research and Technology, for financial support.

Received: August 21, 1989 [A 749 IE]
German version: *Angew. Chem. 102* (1990) 239
Translated by Dr. *W. Dahlhoff*, Mülheim an der Ruhr (FRG)

[1] In this context, the energy saving homes, which require only 10% of the average heating energy, should be mentioned: H. Erhorn, 13th National Passive Solar Conference, Cambridge, Mass. (USA), June 20–24, 1988, *Conference Proceedings*, p. 3.
[2] C.-J. Winter, *Phys. Bl. 45* (1989) 264, and references cited therein.
[3] a) H. P. Garg, S. C. Mullick, A. K. Bhargava, *Solar Thermal Energy Storage*, D. Reidel, Dordrecht 1985; b) G. Beckmann, P. V. Gilli, *Thermal Energy Storage*, Springer, Vienna 1984; c) M.A.K. Lodhi, *Int. J. Hydrogen Energy 14* (1989) 379; d) P. Kesselring, *VDI-Ber. 288* (1977) 87; e) R. E. West, *NATO ASI Ser., Ser. E 129* (1987) 490.
[4] See [3a], p. 3.
[5] a) A Committee of the European Community publication: *Atlas über die Sonnenstrahlung Europas*, Verlag TÜV Rheinland (1984); b) Report on the joint meeting of the Swiss Union for Solar Energy and the German Solar Energy Society *Heizen mit Sonne/Part 3.: Speicherung*, Freiburg i. B. 1977.
[6] The storage and transport of heat by sea water has an important influence on the climate in our geographical latitude (Gulf Stream).
[7] For stationary use the volumetric energy density is decisive.
[8] A. Ritter in M. Becker, K.-H. Funken (Eds.): *Solarchemische Technik, Vol. 1. Grundlagen der Solarchemie*, Springer, Berlin 1989, p. 157.
[9] a) M. Fischer, *Chem. Ing.-Tech. 61* (1989) 124, and references cited therein; b) *VDI-Ber. 725*, (1989) 37; c) R. Weber, *IZE-Reportagen*, 1988.
[10] a) K.-F. Knoche, *VDI-Ber. 725* (1989) 235; b) A. Aochi, T. Tadakoro, K. Yoshida, H. Kameyama, M. Nobue, T. Yamaguchi, *Int. J. Hydrogen Energy 14* (1989) 421.
[11] D. Behrens (Ed.): *Hydrogen Technology*, Dechema Study, Frankfurt 1986, p. 40.
[12] In contrast to *photochemical* energy storage, which includes photosynthesis; c.f., T. J. Meyer, *Acc. Chem. Res. 22* (1989) 163.
[13] Reduced by the amount of heat required to heat up A and B to reaction temperature.
[14] With this aim, chemists are trying, e.g., to obviate the high dissociation temperature of water by dividing the reaction $H_2O \rightarrow H_2 + 1/2\,O_2$ into several single thermochemical steps [10].
[15] $T^* = \Delta H^\circ_{T_0}/\Delta S^\circ_{T_0}$, where $C_p = 0$, $K = 1$. For exact derivation of the turning temperature, see [3a], pp. 298–299.
[16] See [3a], p. 301.
[17] G. Alefeld, *Wärme 81* (1975) 89; *Energie 27* (1975) 180.
[18] See [3a], pp. 336–337.
[19] L. Kugeler, *Nucl. Eng. and Design 34* (1975) 65, 129.
[20] a) See [3a], p. 361; b) M. Taube, D. Rippin, W. Knecht, D. Hakimfard, B. Milisavljević, N. Gruenenfelder, *J. Int. J. Hydrogen Energy 10* (1985) 595, Figure 1.
[21] a) See [3a], chapters 4.3, 4.5 and 4.7, and references cited therein; b) E. Lävemann, R. Schneewind, R. Sizmann in W. H. Bloss, F. Pfisterer (Eds.): *Advances in Solar Energy Technology*, Pergamon Press, Oxford 1988, p. 2622.
[22] See [3a], p. 394.
[23] M. Geyer, H. Klaiss, R. Tamme, *VDI Ber. 704* (1988) 73.
[24] a) H. Buchner: *Energiespeicherung in Metallhydriden*, Springer, Wien 1982; b) R. G. Barnes (Ed.): *Materials Science Forum*, Vol. 31, Trans. Tech. Publications, Aedermannsdorf, Switzerland 1988.
[25] O. Bernauer, *Int. J. Hydrogen Energy 13* (1988) 181.
[26] a) M. Groll, W. Supper, R. Werner: *Dynamic Pressure-Concentration Isotherms and Their Impact on Metal Hydride Machine Design*, Int. Symp. on Metal-Hydrogen Systems, Stuttgart, September 4–9, 1988; b) See [24b], p. 1; c) S. Suda, *Int. J. Hydrogen Energy 12* (1987) 323; d) G. Alefeld, *Top. Appl. Phys. 29* (1978) 1.
[27] LiH (12.6%) and AlH_3 (10.0%) have higher H_2-contents but are not suited for H_2-energy stores since their thermodynamic stabilities are too high and too low, respectively.
[28] E. G. Rochow: *Silicon and Silicones*, Springer, New York 1987, pp. 58–59.
[29] a) B. Bogdanović, A. Ritter, B. Spliethoff, *Int. Symp. on Metal Hydrogen Systems*, Stuttgart, September 4–9, 1988, *Z. Phys. Chem. 164* (1989) 1497; b) *VDI Ber. 725* (1989) 37; c) B. Bogdanović, A. Ritter, B. Spliethoff, DBP 3639545 (1988), Studiengesellschaft Kohle mbH.
[30] P. Jolibois, *C.R. Acad. Sci. 155* (1912) 353.
[31] E. Wiberg, H. Goeltzer, R. Bauer, *Z. Naturforsch. B6* (1951) 394.
[32] a) W. Rummel, *Siemens Forsch. Enwicklungsber. 7* (1978) 44; b) W. Rummel, DOS 2800903 (1979), Siemens AG.
[33] B. Bogdanović, *Angew. Chem. 97* (1985) 253; *Angew. Chem. Int. Ed. Engl. 24* (1985) 262.
[34] J. J. Reilly, R. H. Wiswall, *Inorg. Chem. 7* (1968) 2254.

[35] P. Selvam, B. Viswanathan, C. S. Swamy, V. Srinavasan, *Int. J. Hydrogen Energy 11* (1986) 169.
[36] a) H. Buchner, O. Bernauer, W. Straub, in T. N. Veziroglu, W. Seifritz (Eds.): *Hydrogen Energy System; Proc. 2nd World Hydrogen Energy Conf., Vol. 3*, Pergamon, New York 1978, p. 1677; b) J. Töpler, O. Bernauer, H. Buchner, *J. Less-Common Met. 74* (1980) 385; c) G. M. Friedlmeier, J. C. Bolcich, *Int. J. Hydrogen Energy 13* (1988) 467; d) I. Ischido, S. Ono, J. Akiba, *J. Less-Common Met. 120* (1986) 168.
[37] See [24a], p. 165.
[38] Homogeneous catalytic—since the catalyst is homogeneously dissolved in the organic solvent (tetrahydrofuran).
[39] B. Bogdanović, S. Liao, M. Schwickardi, P. Sikorsky, B. Spliethoff, *Angew. Chem. 92* (1980) 845; *Angew. Chem. Int. Ed. Engl. 19* (1980) 818; B. Bogdanović, G. Koppetsch, M. Schwickardi, U. Westeppe in R. B. King, J. J. Eisch (Eds.): *Organometallic Syntheses, Vol. IV*, Elsevier, Amsterdam 1988, pp. 399, 404; c) B. Bogdanović, Eur. Pat. 3564 (1979), Studiengesellschaft Kohle mbH.
[40] E. Bartmann, B. Bogdanović, N. Janke, S. Liao, K. Schlichte, B. Spliethoff, J. Treber, U. Westeppe, U. Wilczok, *Chem. Ber.*, in press.
[41] B. Bogdanović, *Acc. Chem. Res. 21* (1988) 261.
[42] B. Bogdanović, S. C. Huckett, U. Wilczok, A. Rufińska, *Angew. Chem. 100* (1988) 1569; *Angew. Chem. Int. Ed. Engl. 27* (1988) 1513; B. Bogdanović, S. C. Huckett, B. Spliethoff, U. Wilczok, *Zeitschr. f. Phys. Chemie N.F. 162* (1989) 191.
[43] U. Westeppe, *Dissertation*, Universität Bochum 1985.
[44] B. Bogdanović, B. Spliethoff, *Int. J. Hydrogen Energy 12* (1988) 863; B. Bogdanović, US-Pat. 4 554 152 (1985), Studiengesellschaft Kohle mbH.
[45] B. Bogdanović, M. Kröner, G. Wilke, *Justus Liebigs Ann. Chem. 699* (1966) 1.
[46] Hysteresis in metal hydrides: a) S. Qian, D. O. Northwood, *Int. J. Hydrogen Energy 13* (1988) 25; b) T. B. Flanagan, C. N. Park, D. H. Everett, *J. Chem. Educ. 64* (1987) 944.
[47] B. Bogdanović, A. Ritter, K. Strassburger, unpublished.
[48] Part of the project sponsored by the German Federal Ministry for Research and Technology: "Development, construction and testing of a thermochemical energy store based on MgH_2–Mg for solar and other energy systems", 1989.
[49] HWT, Gesellschaft für Hydrid- und Wasserstofftechnik mbH, 4330 Mülheim an der Ruhr (FRG).
[50] J. Kleinwächter, B. Bogdanović, B. Spliethoff, A. Ritter in W. H. Bloss, F. Pfisterer (Eds.): *Advances in Solar Energy Technology*, Vol. 3, Pergamon Press, Oxford 1988, p. 3029.

Nickel: An Element with Wide Application in Industrial Homogeneous Catalysis

By Wilhelm Keim*

Dedicated to Professor Günther Wilke on the occasion of his 65th birthday

The efficiency and future development of the chemical industry are closely linked to catalysis. It has been estimated, for example, that 60 to 70% of all industrial chemicals have involved the use of a catalyst at some point during their manufacture. In the past two decades the share of the market credited to homogeneous transition metal catalysis increasead to 10–15%. Besides cobalt, which is used mainly in hydroformylation reactions, nickel is the most frequently used metal. Many carbon–carbon bond formation reactions can be carried out with high selectivity if catalyzed by organonickel complexes. Such reactions include, inter alia, carbonylation reactions, cyclic and linear oligomerization and polymerization reactions of monoenes and dienes, and hydrocyanation reactions. It was *Reppe* and *Wilke* who pioneered and shaped the field of homogeneous nickel catalysis. Great impetus was also given to the development of organonickel chemistry by *Wilke* and his students. Research in this area has contributed immensely towards an understanding of the reactions involved in catalysis.—This review is primarily concerned with nickel-catalyzed reactions which are of interest both preparatively and industrially; some mechanistic aspects are also dealt with.

1. Introduction

In the 16th century, miners working in the neighborhood of Annaberg in Sachsen tried to recover copper from a reddish ore which in fact contained only nickel and arsenic. They never suspected that this "enchanted copper", copper-nickel, contained a new element that would later play a significant role in industrial catalysis. Nickel, meaning "bad partner (boy)" in the German language, was later isolated in pure form from this "enchanted rock" by *Cronstedt* in 1754. More than a further hundred years were to pass before Mond, in 1888, discovered the first carbonylnickel complex, $Ni(CO)_4$. This discovery initiated a vigorous development of organonickel chemistry. A metal, which existed in the gas phase and which could be isolated in pure form in this way fascinated Mond's contemporaries, one of whom even wrote: "Mond gave wings to a metal".

In 1906, *Sabatier* reported the nickel-catalyzed hydrogenation of carbon monoxide to methane, a reaction which is still used today on an industrial scale to remove carbon monoxide from a stream of hydrogen gas, as, e.g., in the production of ammonia. The reverse reaction, the cleavage of methane (steam reforming), also proceeds via nickel-based catalysis. *Sabatier*'s biggest contribution to chemistry was the recognition of these hydrogenation properties, thus paving the way for catalysis. One of the oldest hydrogenation catalysts is Raney-nickel, which was first used industrially in 1925, and which subsequently became one of the most important catalysts. In more recent times, however, dissatisfaction with the pyrophoric properties of Raney-nickel led to the development of Ziegler systems,[1] in which, for instance, nickel salts are reduced with alkylaluminum compounds. The nature of these catalysts has not been studied in great detail, and the "solutions" obtained after the reduction appear to be homogeneous to the eye. A process developed by Rhône Poulenc for the hydrogenation of benzene to cyclohexane using this catalyst is used on a large scale by many companies.

Many inherent drawbacks of highly dispersed nickel catalysts can be avoided by supporting nickel salts on various carriers. In this connection, particular mention must be made of the nickel catalysts used for hydrogenating fats and those used, in the form of $Ni \cdot Mo/Al_2O_3$ and Ni/Al_2O_3, in crude oil conversions and hydrogenations. Among the industrial applications, the processes for the hydrogenation of carbon-carbon double bonds are the most widely used, followed by those for the hydrogenation of carbonyl groups, with those for the hydrogenation of nitrogen-containing compounds third.

The development of homogeneous nickel catalysis began over fifty years ago with the pioneering work of *Reppe*.

2. Nickel in Reppe Chemistry

On searching for possible applications of carbon monoxide, produced as a byproduct in the manufacture of acetylene, *Reppe* discovered a series of homogeneous catalytic reactions called carbonylations [Eq. (a)–(c)].[2–5] Reaction (a)

$$HC{\equiv}CH + CO + HY \xrightarrow{[Ni]} H_2C{=}CH{-}\overset{\overset{O}{\|}}{C}{-}Y \qquad (a)$$

$$H_2C{=}CH_2 + CO + HY \xrightarrow{[Ni]} H_3C{-}CH_2{-}\overset{\overset{O}{\|}}{C}{-}Y \qquad (b)$$

$$R{-}CH_2OH + CO \xrightarrow{[Ni]} R{-}CH_2{-}\overset{\overset{O}{\|}}{C}{-}OH \qquad (c)$$

$Y = OH, OR, NR_2, RS, O_2CR$

[*] Prof. Dr. W. Keim
Institut für Technische Chemie
und Petrolchemie der Technischen Hochschule
Worringerweg 1, 5100 Aachen (FRG)

represented the most important route used for acrylic acid production until the end of the 1960's. Depending upon the amount of $Ni(CO)_4$ used in the reaction, distinction was made between a stoichiometric, a modified, and a catalytic variant, the latter of which is still used today by BASF. New methods of acrylic acid synthesis, however, favor a route via propene oxidation.

The use of ethylene [Eq. (b)] leads to propionic acid, a process employed by BASF which produces about 50,000 tons per year.

The carbonylation of alcohols [Eq. (c)], especially that of methanol in the synthesis of acetic acid, has developed into one of the most important industrial processes. Originally, nickel was used as catalyst; in the first industrial plant at BASF, however, cobalt complexes were used as catalyst. Later the Monsanto Process, using rhodium catalysts, proved superior, and it is currently the preferred process for acetic acid synthesis.

The carbonylation of esters yields acid anhydrides, a reaction which is used by Tennessee Eastman for the synthesis of acetic acid anhydride.[7, 8] Rhodium catalysts are also used in this homogeneous process. Numerous efforts are being made in industry, however, to replace rhodium by the more economical nickel, and these efforts appear very promising in the case of the latter process. The variety of potential applications of Equations (a)–(c) is immense, the fundamental "building blocks" are inexpensive, and the process technology is well worked out. It can be anticipated that many further uses of carbonylation reactions may evolve in the future, especially if the raw materials derived from crude oil should be replaced by coal, natural gas, or biomass in the manufacture of synthesis gas. For instance, processes for the manufacture of ethylene from acetic acid, which in the final analysis originates from synthesis gas, are already known; two steps are involved, namely hydrogenation, yielding ethanol, followed by dehydration.

One of the most impressive reactions discovered by *Reppe* is perhaps the tetramerization of acetylene to cyclooctatetraene.[10] Although this reaction has not, as yet, found commercial application, it has nevertheless played a decisive role in the development of theoretical chemistry. The planar $C_8H_8^{2\ominus}$ dianion with its 10 π-electrons and its numerous complexes have stimulated a plethora of fundamental theoretical investigations.[11]

The element nickel, especially $Ni(CO)_4$, heralded the beginning of homogeneous transition metal based catalysis. *Reppe* himself wrote: "It became evident throughout these investigations that it was a lucky choice using nickel carbonyl as a starting material from the beginning of this work."[84]

3. Nickel in Wilke Chemistry[12–16]

Up to now, one of the most important discoveries in chemistry in our century has been that of *Holzkamp*, who, in 1952, observed that nickel salts can alter the AlR_3-catalyzed "growth reaction" of ethylene to α-olefins in such a way that only dimers (butenes) are formed, a phenomenon referred to in the literature as the "nickel effect".[16] This observation consequentially led to the discovery of "Ziegler catalysis", a reaction which is of utmost importance, both in industry and in academic research for the production of a variety of polymers.

In 1959, *Wilke* studied the possibility of using Ziegler catalysts prepared from nickel acetylacetonate and $AlEt_2OEt$ for the polymerization of butadiene. A mixture of products was obtained: (*E,E*)-1,5-cyclooctadiene (COD) (25%), 4-vinylcyclohexene (VCH) (10%), and (*E,E,E*)-1,5,9-cyclododecatriene (CDT) (65%). Had *Wilke* tried only the Ziegler system $NiCl_2/Et_2AlCl$, which produces polybutadiene, an exciting area of organonickel chemistry might have been overlooked. Cyclic compounds containing large ring systems were in great demand by preparative chemists, and the synthesis, especially of eight- and twelve-membered ring derivatives, was an exceptional challenge. Following *Wilke*'s discovery, various ring systems could be produced economically and quite elegantly. Not long after, *Wilke* observed that the ratio of COD:CDT:VCH could be altered by addition of R_3P-ligands (see Table 1).[16] One of *Wilke*'s greatest accomplishments was to have recognized for the first time the route to controlling the distribution of oligomers by ligand varia-

Table 1. Reaction of butadiene with nickel acetylacetonate and $AlEt_2OEt$; control of oligomerization using R_3P ligands. Conditions: 30 °C, 5 bar.

Product	$(c\text{-}C_6H_{11})_3P$ [%]	$(o\text{-}Ph\text{-}C_6H_4O)_3P$ [%]	without [%]
4-Vinylcyclohexene (VCH)	39.6	3.1	10
1,5-Cyclooctadiene (COD)	41.2	96.5	25
1,5,9-Cyclododecatriene (CDT)	14.4	0.2	65
Higher oligomers	4.8	0.2	–

Wilhelm Keim was born in Oberhausen in 1934. He studied chemistry at the Universities of Münster and Saarbrücken before moving to the Max-Planck-Institut für Kohlenforschung in Mülheim an der Ruhr, where he obtained his doctorate under the supervision of Professor G. Wilke. After one year as a postdoc with Professor T. Katz at the Columbia University, New York, he joined the Shell Development Company in Emeryville, CA. In 1967 he was promoted to leader of the petrochemistry research group, in 1969 to leader of the Department of Petrochemistry, and, finally, in 1972 to leader of Basic Research. In 1973 he accepted an appointment as Professor and Director of the Institut für Technische Chemie und Petrolchemie der RWTH Aachen. Wilhelm Keim is, among other things, a member of the board of the Deutsche Gesellschaft für Mineralölwissenschaften und Kohlechemie, Gesellschaft Deutscher Chemiker, and the Deutsche Gesellschaft für Chemisches Apparatewesen, Chemie Technik und Biotechnologie. He also is a member of the supervisory board of Degussa AG.

tion. This so-called "ligand tailoring" is of considerable importance to all scientists working in this area of chemistry. The ligands are often precisely "tailored" to the process envisaged. Two noteworthy examples of industrial uses are: Shell's hydroformylation reaction for converting olefins into linear alcohols,[18] and Du Pont's hydrocyanation of butadiene to adipodinitrile (see Section 4.5).

Over the years, *Wilke* and his co-workers have studied the syntheses of the above ring systems quite extensively. Scheme 1 shows examples of the various possibilities. De-

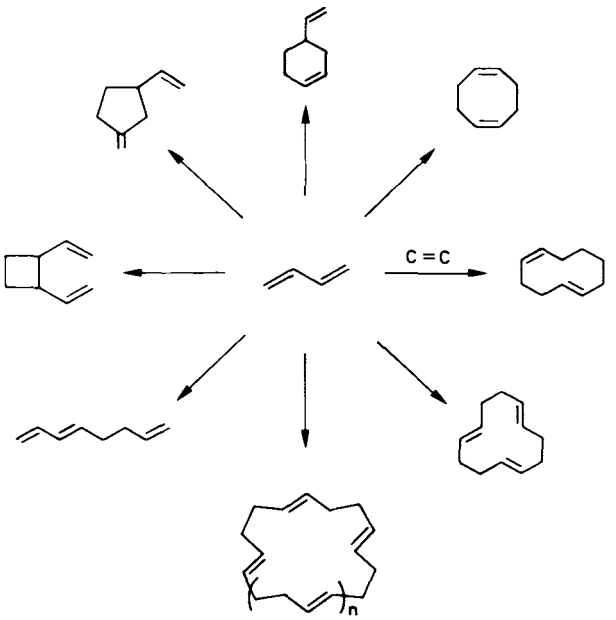

Scheme 1. Ring syntheses from butadiene.

pending on the reaction conditions, linear and/or cyclic compounds are obtainable, whereby cyclooctadiene and cyclododecatriene are of special industrial importance. Fundamental investigations leading to an understanding of the impact of various ligands on controlling product selectivity go back to the work of *Heimbach*.[17]

Cyclododecatriene is used for the preparation of Nylon-12. Scheme 2 outlines this synthesis as practiced by Hüls AG (18,000 tons per year) and Du Pont.[19] Valuable textiles are produced from Du Pont's Qiana®. Owing to its stability of shape, corrosive resistance, and low-temperature properties, Vestamid®, manufactured by Hüls AG, has numerous applications in compression cylinders for brakes in automobiles, in fuel pressure lines, in the soles of sports shoes, in cable coverings, in anti-corrosive coatings (coatings for wires, steel pipe construction units) and in the linings of jackets and coats. Hüls AG also manufactures the special rubber Vestenamer® from cyclooctadiene, [Eq. (d)]. Characteristic features of Vestenamer are its partial crystallinity and its relatively low molecular weight. The crystallinity is dependent on the number of *trans* double bonds present. In blends with other rubbers, Vestenamer improves the viscosity and is thus of great help in complicated production procedures, such as those of brake hoses from EPDM (ethylene-propene-diene elastomer), corrugated bellows from polychloroprene, tooth

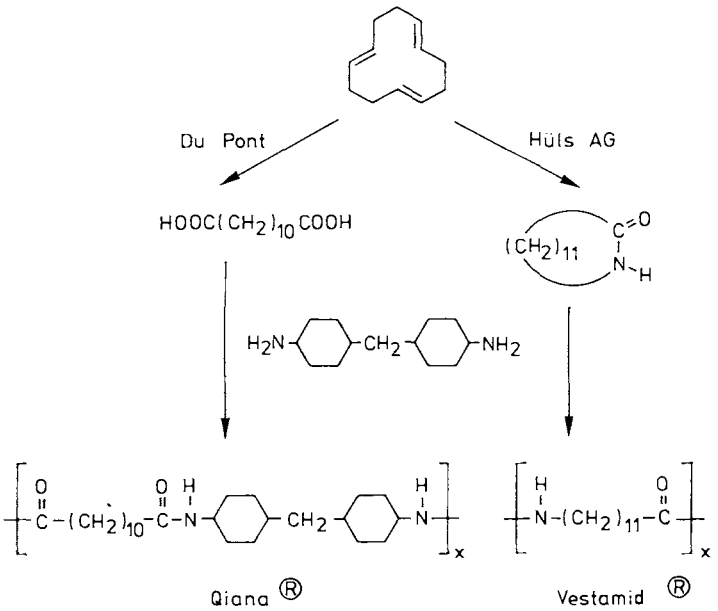

Scheme 2. Nylon-12 derivatives from cyclododecatriene.

crowns from hard plastics, and printing molds from nitrile rubber.

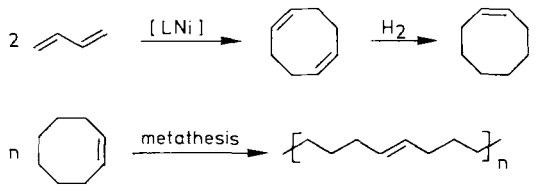

Shell produces a selection of industrially interesting olefins based on cyclooctadiene and cyclododecatriene by the Feast Process, [Eqs. (e)–(g)].[20]

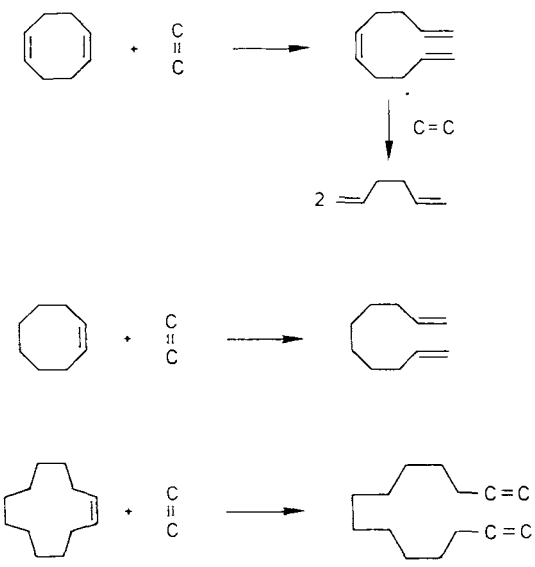

The successful reactions of organonickel complexes with dienes automatically led to an extension of their range of

application by including reactions with monoenes. One of the most impressive examples of ligand-nickel-control, the dimerization of propene, was first reported by *Bogdanović* and *Wilke* et al.[16, 21, 23] With trialkyl- or arylphosphane-modified nickel systems, hexenes, 2-methylpentenes, or 2,3-dimethylbutenes can be produced depending upon the substituent on the phosphorus (see Table 2). The catalytic activity is exceptionally high, and even at low temperatures good turnover numbers can be obtained. It should be noted, however, that the selectivity leading to 2,3-dimethylbutene in the case of *tert*-butyldiisopropylphosphane can be increased to 96.4% at −70 °C. A mixture rich in branched dimers has proven useful for increasing the octane number in gasoline, and is used in the Dimersol process (see Section 4.4.1). 2,3-Dimethylbutene has also attracted some industrial attention since it can be dehydrogenated to 2,3-dimethylbutadiene, a potential monomer for polymerization. The oxidation of 2,3-dimethylbutenes could provide a route to pinacol.

Table 2. Dimerization of propene with $C_3H_5NiCl/AlClEt_2$. Influence of the ligand R_3P on the selectivity. Conditions: 25 °C, 10 bar.

R_3P	Hexenes [%]	2-Methylpentenes [%]	2,3-Dimethylbutenes [%]
Ph_3P	21.6	73.9	4.5
Me_3P	9.9	80.3	9.8
iPr_2tBuP	0.1	19.0	80.9
$iPrtBu_2P$	1.0	81.5	17.5

It is not surprising that the possibilities for controlling carbon-carbon linkages via nickel-phosphane ligand systems have also led to the investigation of enantioselective syntheses with organonickel complexes.[22] The catalysts consist of 1:1 adducts of η^3-allylnickel halides and optically active phosphanes. For instance, as depicted in Equation (h), *ee* values of 80% could be achieved for **1**. Racemic **1** is of interest as third component ("diene") in EPDM. A noteworthy example of "ligand tailoring" is displayed by the enantioselective dimerization of styrene with ethylene; (*R*)-(−)-3-phenyl-1-butene is formed with *ee* values greater than 95%.[16] In this context, also *Pino*'s work on the asymmetric oligomerization of propylene is of interest.[23]

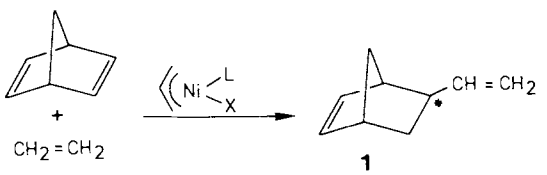

Almost exclusively monoenes and dienes are used in the aforementioned C–C linkage reactions. The inclusion of functionalized olefins would considerably expand the scope of application of homogeneous nickel catalysis. *Wilke* and co-workers have also attempted to include functionalized olefins in their catalytic investigations. In this connection, the linear dimerization of acrylic acid, which leads to starting materials for the production of nylon, is worth mentioning. Acrylic acid methyl ester dimerizes smoothly with complex **2** to yield monounsaturated esters of adipic acid.[16] In general, such a dimerization of functionalized olefins with Ziegler catalysts is difficult because in most cases the catalysts will react with the functionalizing group. Unfortunately, the turnover numbers achieved so far using complexes of type **2** are too low for this synthesis to be applied industrially.

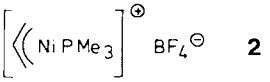

2

Other pioneering contributions by *Wilke* and his co-workers include their mechanistic investigations related to organonickel chemistry, which have greatly improved our understanding of the reactions involved in the catalysis. A large variety of complexes could be isolated which are considered to be reactive intermediates. For the mechanism of the cyclotrimerization of butadiene, it could be shown that π-complexes and $\eta^1\eta^3$-allyl systems play a crucial role in the reaction pathways. Scheme 3 illustrates this for cyclododecatriene synthesis. Using bis(η^3-allyl)nickel as starting complex, three molecules of butadiene orient themselves coordinatively around a "naked" nickel atom with displacement of 1,5-hexadiene. The nickel atom with its six possible coordination sites can coordinate up to three molecules of butadiene, bound either as η^4- or η^2-coordinated ligands. Two butadiene molecules combine via a carbon–carbon linkage to yield complex **3**, in which a C_8-chain with two η^3-allyl

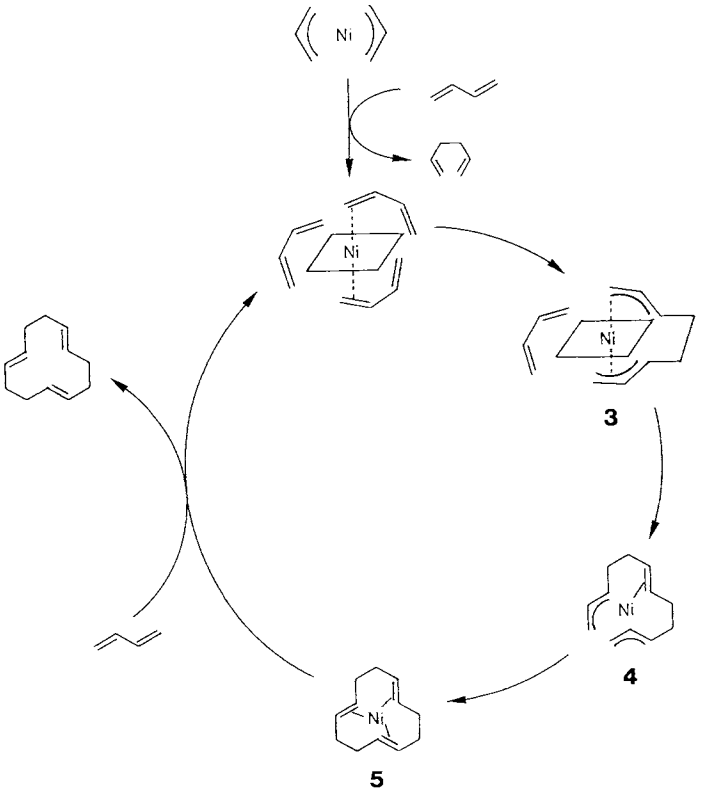

Scheme 3. Mechanism of cyclododecatriene synthesis.

ligands is bonded to the nickel atom. Formation of an additional C–C linkage leads to complex **4**, in which a C_{12}-chain is arranged around the nickel atom. In this stepwise mechanism the intermediate **5** is formed via a third C–C linkage. Butadiene displaces the nickel atom from **5**; cyclododecatriene is formed and "naked" nickel is liberated and reacts again with butadiene, thus completing the catalytic cycle. The complexes **4** and **5** could be isolated, and their structures have been determined by X-ray crystallography.[22]

If phosphane ligands are added to the system (see Table 1), coordination sites for butadiene are blocked and the intermediates **6**–**8** are formed, in which the nickel atom is so modified that only two butadiene molecules fit into the coordination sphere of the nickel (see Scheme 4). Cyclooctadiene, divinylcyclobutane, and vinylcyclohexene are easily derived from complexes **6**–**8**.

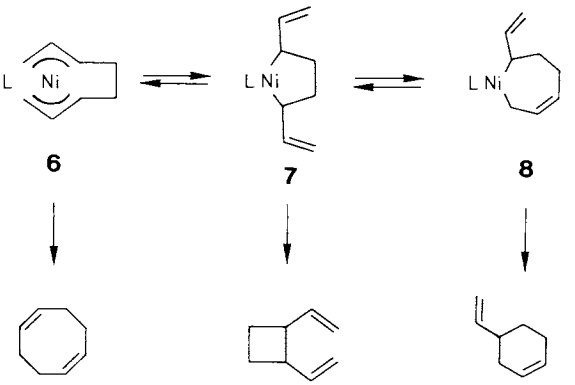

Scheme 4. Product distribution in the dimerization of butadiene in dependence of phosphane addition $L = R_3P$ (see Table 1).

Several important criteria, first recognized and postulated by *Wilke*, emerge from the catalytic cycles described in Schemes 3 and 4:

- η^1- and η^3-allyl complexes are reactive intermediates from which C–C linkages can be derived. A continual change in the formal oxidation state occurs through oxidative addition and reductive elimination.
- "naked" metal atoms or ligand-metal systems facilitate a "pre-orientation" of the reactants, thus influencing the stereochemistry (selectivity) and consequently the type of product formed. The necessary free coordination sites are created as a result of ligand dissociation via η^1- and η^3-allyl equilibria.
- isolated, well characterized organometallic complexes can be used as precursor complexes leading to the "true" catalyst.

The complex chemistry of η^1- and η^3-allyl systems as we know it today goes back to the fundamental work carried out at the Max-Planck-Institut für Kohlenforschung. Numerous allyl complexes were synthesized, and their reaction behavior monitored in detail in a series of systematic investigations.[24–26] In this connection, the numerous X-ray structure analyses performed by *Krüger* deserve special mention, for they impressively support formation of the various reaction intermediates proposed for the catalytic cycles.

The expression "naked" nickel was introduced by *Wilke* in order to describe one of the most important principles of catalysis, namely that of the necessity of free coordination sites. There is a very close relationship here to heterogeneous catalysis which requires free sites for chemisorption—a phenomenon which had already been postulated by *Taylor* and is illustrated in **9**[27]. Some 60 years ago *Taylor* put forward the theory that single nickel atoms stick out randomly from the metal surface, and thus form the "free" sites for the chemisorption (coordination) of molecules.

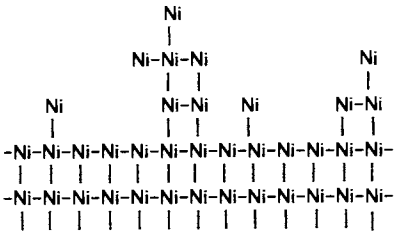

9

The ongoing studies of *Wilke*'s η^1,η^3-allyl systems led to numerous "one component catalysts", which are far less complex than Ziegler catalysts. These studies opened up a new area of research, mainly focused on the use of organometallic compounds as precursor complexes in homogeneous catalysis, and thus leading to new reactions which provide a better understanding of catalysis.

4. Further Examples of Homogeneous Nickel Catalysts Used in Industrial Processes

4.1. Dimerization and Oligomerization of Monoolefins[28]

With *Wilke*'s discoveries, a new era of chemistry developed based on organometallic chemistry applied to homogeneous transition metal catalysis. There are first of all the students of *Wilke* who provided a rapid transfer of technological knowhow to industry. But there are also other research groups who—inspired by *Wilke*'s publications—have developed their own ideas and concepts.

4.1.1. Dimersol Technology

One of the earliest works on propene dimerization, and following the *Wilke* tradition, goes back to *Ewers*.[29] Also *Chauvin* from the Institut Français du Pétrole (IFP) developed nickel catalysts ($Ni^{2\oplus}/AlEtCl_2$) that dimerize propene and/or *n*-butene.[30–32] These systems are highly active, hence the recycling of catalyst can be dispensed with. The propene dimers are used extensively, especially in the USA, for improving the octane number in gasoline and to provide heptenes and octenes for plasticizers. Since the first plant was established in the USA in 1977, IFP have given about 45 licences, which include the following variants: in the Dimersol G process, propene, produced by catalytic cracking, is dimerized to yield C_6-olefins useful in octane-number improvements (about 20 plants). The Dimersol X variant has found application in the dimerization of butene or codimer-

ization of propylene/butene for the preparation of plasticizers. In the Dimersol E process, high-octane gasoline is prepared form FCC-based olefins (FCC = fluid catalytic cracking process for the processing of crude oil).

In this context, the Hüls Octol process must be mentioned.[33] 1-Butene is first separated off from the corresponding C_4-fraction, and the remaining 2-butene/*n*-butane mixture is converted into (remarkably linear) octenes on a supported nickel catalyst. Two commercial processes underline the importance of this new technology, which is in direct competition with the homogeneous Dimersol route.

Other recent examples include the replacement of oxygen by sulfur in acetylacetonate ligands to give dithio-β-diketonate species. Nickel complexes of the dithio ligand give rise to extremely active olefin oligomerization catalysts.[34]

4.1.2. Shell Higher Olefin Process (SHOP)

While employed at the Shell Oil Company in 1965, the author was given the task of converting ethylene into value added chemicals such as α-olefins. As a former student of *Wilke* familiar with the background of ligand tailoring the author used the model shown in Scheme 5 for tackling the

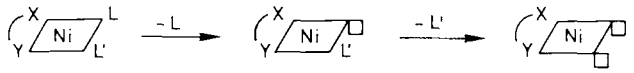

Scheme 5. Proposed model for the formation of free coordination sites □.

problem. Chelates $\widehat{XY}$ were chosen since they favor square-planar structures with potentially free coordination sites for formation of an octahedral system.[35] The atoms X and Y should behave as an electron donor and acceptor, respectively. Finally, it should be possible to exchange the ligands L and L′ for ethylene. In the course of the investigations, this concept led to the Shell Higher Olefin Process (SHOP),[36–39] which, with approximately a one million ton capacity in 1990, is one of the largest applications of homogeneous catalysis by a transition metal, especially nickel.

Figure 1 shows the X-ray structure of complex **10**, which fulfills all of the requirements in Scheme 5.[40] Indeed, when

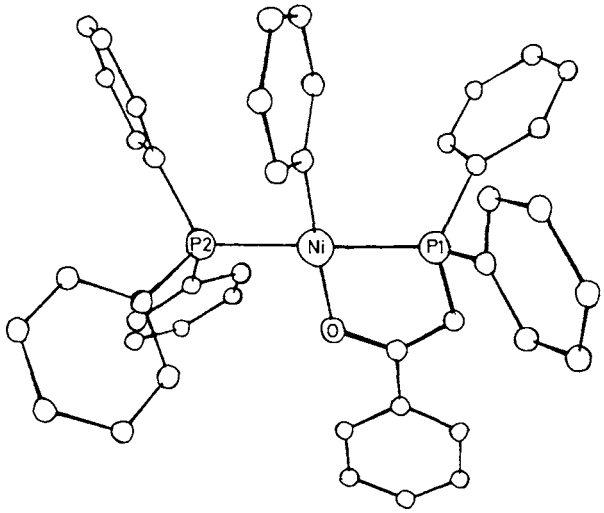

Fig. 1. Molecular structure of complex **10** in the crystal [see Eq. (k)].

10 is dissolved in toluene and allowed to react with ethylene, oligomers are produced which are up to 99% linear, of which about 98% are formed as α-olefins. The olefins up to C_{30}, and present in geometric distribution, were isolated by gas chromatography. Activities of 6000 moles of ethylene per mole of complex **10** have been observed. If, however, the reactions are carried out with complex **10** suspended in *n*-hexane, linear polyethylene is produced. The directly marketable α-olefins produced in the oligomerization part of Shell's SHOP-process are separated by distillation. The remaining, unmarketable α-olefins are isomerized and converted in a third step by metathesis reactions into linear olefins with internal double bonds. An overview of the products manufactured by Shell is given in Scheme 6. By com-

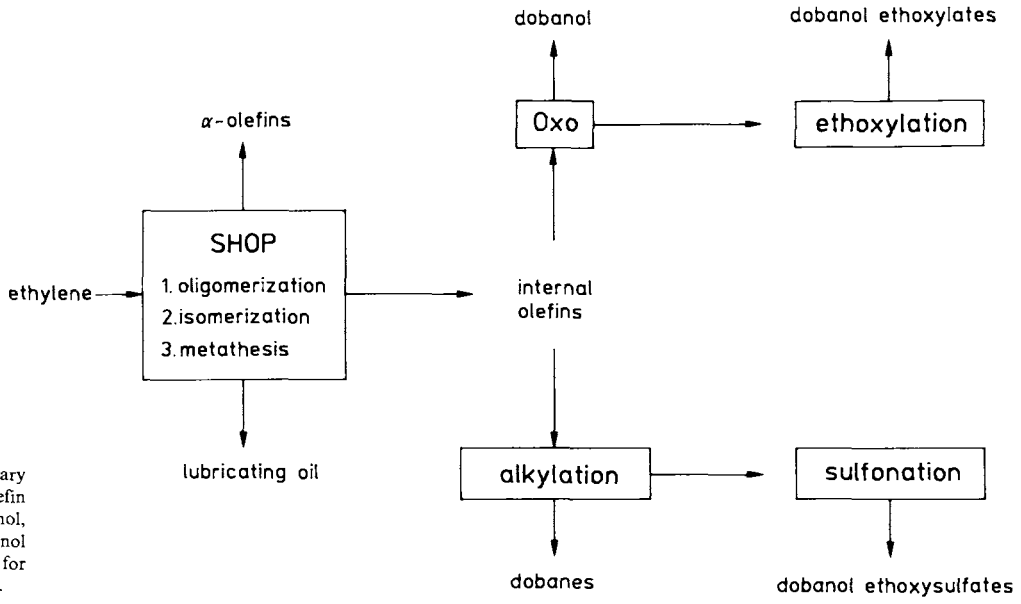

Scheme 6. Products and secondary products of the Shell Higher Olefin Synthesis (SHOP). Dobane, dobanol, dobanol ethoxylate and dobanol ethoxysulfate are Shell tradenames for surface active products (detergents).

bining oligomerization, isomerization, and metathesis, a high degree of flexibility in producing linear olefins of any carbon chain length is possible.

To gain a better insight into the reaction mechanism of the SHOP-process, our research group at Aachen synthesized a number of $\widehat{PO}$ nickel chelate complexes and tested them as catalytic precursors.[41] In general, it may be stated that: all complexes active in the SHOP-process consist of a chelate moiety and an organyl ligand part, as in Figure 2. The organo part only stabilizes the complex, while the chelate ligand controls the catalytic activity and selectivity.[42, 43]

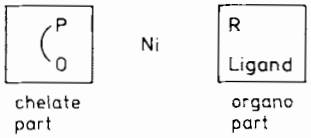

Fig. 2. General form of precursor complexes leading to catalysts.

Assuming that nickel hydride complexes are the active catalysts, the reactions (i)–(k) offer a plausible explanation for Ni–H formation, starting from various complexes as catalyst precursors. In reaction (i) temperatures of 130 °C are needed for the insertion of ethylene into the cyclopentadienyl group and formation of a nickel hydride, whereas the nickel-crotyl complex in reaction (j) readily yields a nickel hydride through butadiene elimination at 40 °C, and, finally, in reaction (k) ethylene inserts into the nickel-phenyl group followed by elimination of styrene. All the reactions (i)–(k) outlined could be verified chemically. As predicted, the complexes **10**–**12** only become active for ethylene oligomerization at the temperatures needed for nickel hydride formation as depicted in (i)–(k).

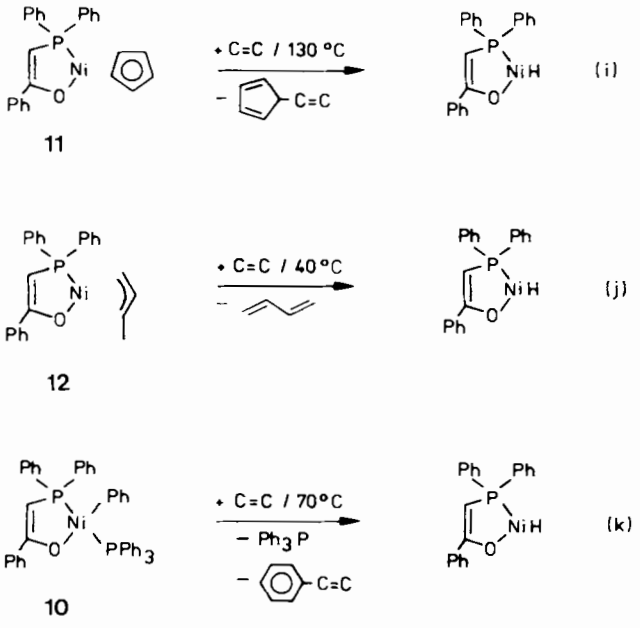

Scheme 7 presents a postulated mechanism for ethylene oligomerization, using complex **13** as a catalyst precursor

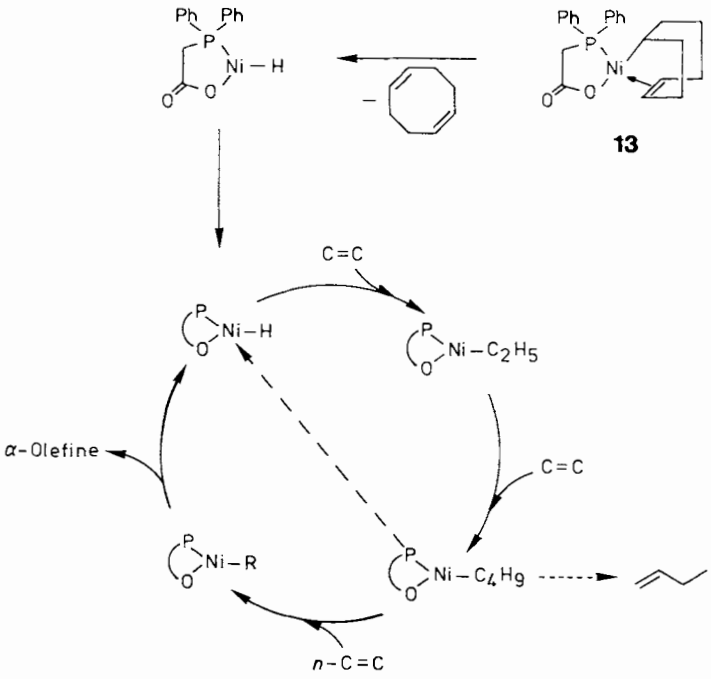

Scheme 7. Postulated mechanism of ethylene oligomerization.

complex. In the case of complex **13**, only in situ NMR studies indicated that a nickel hydride is produced,[44] while the nickel hydride **14** (Fig. 3) could be trapped by using

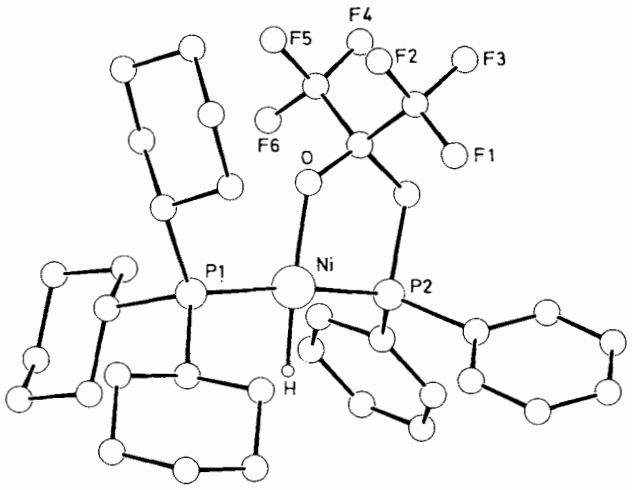

Fig. 3. Molecular structure of the Ni-H complex **14** in the crystal.

$Ph_2PCH_2C(CF_3)_2OH$ as a ligand.[45] It was also possible to isolate the corresponding ethyl complex of **14**, formed by an ethylene insertion into the nickel hydride bond. On heating, the nickel-ethyl complex splits off ethylene to give complex **14** again. A variety of nickel hydrides are reported in the literature that can be considered as additional support for the postulated mechanism.[15, 16, 46]

The success with $\widehat{PO}$ chelate ligands suggested the use of other ligands of this type to be included in a systematic study. The chelate complex **15** catalyzes the linear oligomerization

of α-olefins.[35,47] To our knowledge, this is the only complex (catalyst) that produces highly linear dimers (> 80%), but unfortunately, until now, the turn over numbers are too low for an industrial application.[48] In this context, also the work of *Cavell* and *Masters* concerning olefin oligomerization deserves mentioning.[34]

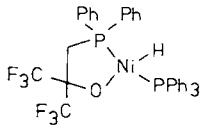

14

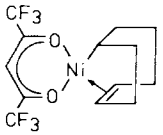

15

4.2. Monoolefin Polymerization

The formation of polyethylene using nickel catalysts was already reported in a patent in 1953.[49] Also, *Bogdanović* and *Wilke* reported the formation of polyethylene on using the catalyst η^3-$C_3H_5NiX/AlX_3/P(tC_4H_9)_3$.[16] In our investigations with various chelate ligands, e.g. derivatives of 1,3-diphosphapropene[50] or $(C_6H_{11})_2PCH_2COOH$,[51] we frequently observed polyethylene formation, especially when a solvent was used in which the complex was insoluble.[40] Until now, no general predictions can be made as to what ligand properties are needed to synthesize either oligomeric olefins or polyethylene, respectively. Generally, it can be said that starting from a nickel hydride, growth occurs via ethylene insertion and β-elimination leading to the α-olefins as shown in Scheme 7, thus giving rise to a geometric distribution (Schulz-Flory distribution) of products.[28] In agreement with this, and under the assumption that no chain transfer occurs, the product pattern can consist predominantly of dimers, higher oligomers or even polymers.

Following our work, and in an attempt to react functionalized monoolefins such as acrylic esters, *Klabunde* also employed complexes of the type shown in Figure 2 in polymerization and copolymerization reactions.[52,53]

Of *Klabunde*'s investigations, the formation of polyketones from ethylene and carbon monoxide using complex **10** should be emphasized.[54] We were able to demonstrate that the ligand **16** in combination with $(cod)_2Ni$ also yielded

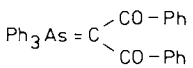

16

polyketones from ethylene and carbon monoxide. Such polyketones have potential application as novel industrial polymers. Also worth noting in this connection are the works of *Sen*[57], *Nozaki*[58] and *Drent*[59] of Shell, who have used palladium instead of nickel in their catalytic studies aimed at the production of polyketones from ethylene and carbon monoxide.

By reacting amino-bis(imino)phosphorane **17**, $(cod)_2Ni$ and ethylene acording to Equation (l), a system results which catalyzes a novel ethylene polymerization (2,ω-polymerization).[60] According to *Fink*, who has thoroughly investigat-

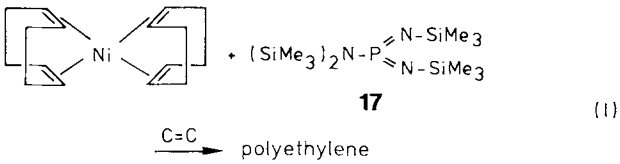

17

(l)

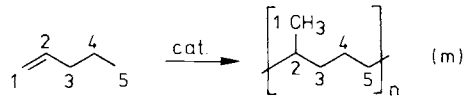

(m)

ed and interpreted this system,[61] polymers with methyl-branches arranged at regular intervals are formed [Eq. (m)]. The methyl groups of the polymer chain are formed from the C(1)-atom of the α-olefins. This can be explained in terms of a 1,2-hydride shift with concommitant migration of the catalytically active nickel atom along the carbon chain. It should be emphasized that this type of polymerization—in contrast to that with Ziegler catalysts—is carried out with aluminum-free systems.

4.3. Dimerization and Oligomerization of Dienes

The success of the trimerization of butadiene to cyclododecatriene led a number of research groups to further investigations with other 1,3-dienes such as, for example, isoprene.[4,13,28] Until now, however, poor selectivities have precluded larger industrial applications. An example of an industrial use is the trimerization of isoprene to 1,5,9-trimethyl-1,5,9-cyclododecatriene reported by the Takasago Perfumery Company.[62]

The nickel-catalyzed codimerization of butadiene with ethylene leading to 1,4-hexadiene, which is useful for the manufacture of EPDM, has been thoroughly investigated.[28,63] Here, rhodium catalysts proved to be superior for industrial production.[64]

4.4. Polymerization of Dienes

A large variety of nickel complexes used for the polymerization of butadienes has been reported.[17,64,65] Depending on the nature of the nickel starting salt, *cis*-1,4-, *trans*-1,4- or 1,2-polybutadienes and/or mixtures are formed. An explanation for the stereoselectivity may rest on the *syn* and *anti* forms of the η^3-allyl system [Eqs. (n, o)]. The choice of anion

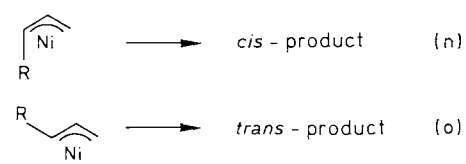

(n)

(o)

also plays a crucial role; e.g. with η^3-C_3H_5NiI, 1,4-*trans*-polybutadiene is obtained. *Teyssié* et al.[65] contributed to a better understanding of the observed selectivities, by show-

ing that variation of X in η^3-allylnickel-X leads to a dramatic change in activity in the series $X = CH_3COO^{\ominus} < CCl_3COO^{\ominus} < CF_3COO^{\ominus}$.[66]

The Goodyear Tire and Rubber Company introduced a nickel-BF_3 system for the synthesis of 1,4-*cis*-polybutadiene.[67]

Bunawerke Hüls markets, "Polyöl Hüls", a low molecular weight 1,4-*cis*-butadiene polymer. This oligomer is prepared by a nickel-catalyzed reaction and is used as an anticorrosion agent and as an adhesive material.[68]

4.5. Hydrocyanation

The nickel-catalyzed addition of hydrocyanic acid to mono- and di-olefins is an elegant method for the synthesis of alkyl nitriles, which are important starting materials for the production of amides, amines, and acids. Hydrocyanation, first reported by *Taylor*,[69] was used by *Drinkard* of Du Pont for the reaction with butadiene according to Equations (p) and (q).[70, 71] This reaction is currently used at three

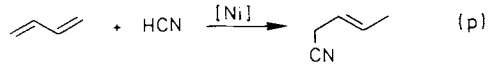

(p)

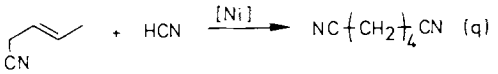

(q)

plants by Du Pont for producing the starting materials for nylon. It may be assumed that the primary amines supplied by Du Pont are produced likewise via α-olefin hydrocyanation. Complexes such as NiL_4 (L = aryl phosphite) are employed as catalysts for the hydrocyanation. An explanation of the reaction mechanism goes back to the work of *Tolman*, who thoroughly investigated this process.[72–74] The proposed mechanism is shown in Scheme 8. HCN reacts with

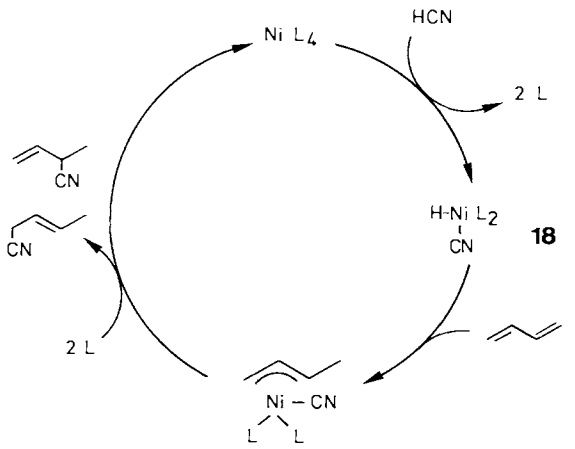

Scheme 8. Proposed mechanism of butadiene hydrocyanation. L = $P(OC_6H_5)_3$.

NiL_4 with dissociation of two phosphite ligands to yield **18**, which can be isolated.[73] Reaction of **18** with butadiene yields an η^3-nickel complex, from which butene carbonitriles are released through reductive elimination with re-initiation of the catalytic cycle. This reaction is another example of ligand control. By using Ph_3P instead of $(PhO)_3P$, the reaction path changes [Eq. (r)], and no nickel hydride is formed; $(Ph_3P)_2Ni(CN)_2$ precipitates, and leads to "catalyst death".[75]

$$(Ph_3P)_4Ni + 2HCN \xrightarrow{-2\,Ph_3P} (Ph_3P)_2Ni(CN)_2 + H_2 \qquad (r)$$

4.6. Telomerization[6, 13, 28, 76]

A reaction studied in great detail is that of 1,3-dienes with nucleophiles HY, as shown for butadiene in Equation (s). The telomer **19** or octatriene is formed. Although these reactions lead to a wide range of products, their use on an industrial scale has not yet been reported.

$$2C=C-C=C + HY \xrightarrow{[Ni]} \underset{\mathbf{19}}{Y-C-C=C-C-C-C-C=C}$$

$$\xrightarrow{[Ni]} HY + C=C-C=C-C-C-C=C \qquad (s)$$

5. Outlook

Aside from cobalt, which is used mainly in hydroformylation reactions, nickel is probably the most frequently used metal in homogeneous transition metal catalysis. This is undoubtedly due, on the one hand, to its economical price,[77] and, on the other, to the abundant and diverse reaction possibilities and selectivities. In the present article, primarily only industrial processes have been considered. About 15% of the established catalytic processes used in the chemical industry can be ascribed to homogeneous transition metal catalysis, and many products can be obtained only by these processes. Nickel plays an important role in this area which may even increase in the future. Generally, one can expect that homogeneous transition metal catalysis will attract increasing interest as value added chemicals grow in importance in the chemical industry.[78, 79] Considering the potential in the area of specialty chemicals, many uses of nickel catalysts may be foreseen. Organonickel complex chemistry is progressing at a considerable rate, and this could provide the nutrient for many future applications. Of course, the question may be raised: "Is the current importance of the element nickel in catalysis due to its nature or due to the amount of work which has been undertaken in organonickel complex chemistry?"

Homogeneous catalysis by nickel began with the work of *Reppe*, and it is to *Wilke*'s great merit to have introduced organonickel chemistry and its application into catalysis. By isolating model compounds, he was able to gain insights into the mechanistic pathways of homogeneous catalysis and catalytic cycles. The areas of homogeneous transition metal catalysis and organonickel chemistry are greatly indebted to both *Reppe* and *Wilke*. In conclusion it would not be amiss to quote Max Planck:[83]

"During the stormy development of all branches of science, it has become apparent that the progress of science rests first of all upon the success of the individual scientist".

Received: September 14, 1989 [A 751 IE]
German version: *Angew. Chem. 102* (1990) 251

[1] S. J. Lapporte, W. R. Schuett, *J. Org. Chem. 28* (1963) 1947.
[2] A. Mullen in J. Falbe (Ed.): *New Syntheses with Carbon Monoxide*, Springer, Berlin 1980, pp. 243–308.
[3] G. N. Schrauzer, *Adv. Organomet. Chem. 2* (1964) 1–45.
[4] a) G. Wilkinson, F. G. A. Stone, E. W. Abel (Eds.): *Comprehensive Organometallic Chemistry*, Pergamon, Oxford 1982; b) P. W. Jolly in [4a], *Vol. 8*, pp. 773–796.
[5] T. Ohara, T. Sato, N. Shimizu in: *Ullmann's Encyclopedia of Industrial Chemistry, Vol. A 1*, VCH Verlagsgesellschaft, Weinheim 1985, pp. 161–174.
[6] a) A. Mortreux, F. Petit (Eds.): *Industrial Applications of Homogeneous Catalysis*, Reidel, Dordrecht 1988; b) M. Röper in [6a], pp. 1–15.
[7] S. W. Polichnowski, *J. Chem. Educ. 63* (1986) 206.
[8] W. Keim in D. R. Fahey (Ed.): *Industrial Chemicals via C_1-Processes, ACS Symp. Ser. 328* (1987) 1–16.
[9] W. Keim (Ed.): *Catalysis in C_1 Chemistry*, Reidel, Dordrecht 1983.
[10] J. P. Collman, L. S. Hegedus, J. R. Norton, R. G. Finke: *Principles and Applications of Organotransition Metal Chemistry*, University Science Books, Mill Valley 1987, pp. 613–615.
[11] M. A. Bennett, *Adv. Organomet. Chem. 4* (1966) 375–384.
[12] P. W. Jolly, G. Wilke: *The Organic Chemistry of Nickel, Vol. 1*, Academic Press, New York 1971.
[13] P. W. Jolly, G. Wilke: *The Organic Chemistry of Nickel, Vol. 2*, Academic Press, New York 1975.
[14] P. W. Jolly in [4a], *Vol. 8*, pp. 615–709.
[15] P. W. Jolly in [4a], *Vol. 6*, pp. 3–223.
[16] a) G. Wilke, *Angew. Chem. 100* (1988) 190; *Angew. Chem. Int. Ed. Engl. 27* (1988) 185; b) G. Wilke in M. Tsutsui (Ed.): *Fundamental Research in Homogeneous Catalysis, Vol. 3*, Plenum, New York 1979, pp. 1–24.
[17] a) P. Heimbach, R. Traunmüller: *Metall-Olefin-Komplexe*, Verlag Chemie, Weinheim 1970; b) P. Heimbach, T. Bartik: *An Ordering Concept on the Basis of Alternative Principles in Chemistry*, Springer, Berlin 1989.
[18] L. H. Slaugh, R. D. Mullineaux, US-Pat. 3 239 569 (1966), Shell Oil Co.
[19] K. Weissermel, H. J. Arpe: *Industrielle Organische Chemie*, VCH Verlagsgesellschaft, Weinheim 1988, pp. 94, 259–260, 279–282.
[20] R. Streck, *J. Mol. Catal. 46* (1988) 305.
[21] B. Bogdanović, *Adv. Organomet. Chem. 17* (1979) 105–137.
[22] B. Bogdanović, B. Henc, B. Meister, H. Pauling, G. Wilke, *Angew. Chem. 84* (1972) 1070; *Angew. Chem. Int. Ed. Engl. 11* (1972) 1023.
[23] P. Pino, P. Cioni, M. Galimberti, J. Wei, N. Piccolrovazzi in W. Kaminsky, H. Sinn (Eds.): *Olefin Polymerization*, Springer, Berlin 1988, pp. 269–279.
[24] G. Wilke, B. Bogdanović, P. Borner, H. Breil, P. Hardt, P. Heimbach, G. Hermann, H.-J. Kaminsky, W. Keim, M. Kröner, H. Müller, W. Oberkirch, E. W. Müller, J. Schneider, J. Stedefeder, K. Tanaka, K. Weyer, *Angew. Chem. 75* (1963) 10; *Angew. Chem. Int. Ed. Engl. 2* (1963) 105.
[25] G. Wilke, B. Bogdanović, P. Hardt, P. Heimbach, W. Keim, M. Körner, W. Oberkirch, K. Tanaka, E. Steinrücke, D. Walter, H. Zimmermann, *Angew. Chem. 78* (1966) 157; *Angew. Chem. Int. Ed. Engl. 5* (1966) 151.
[26] G. Wilke, *J. Organomet. Chem. 200* (1980) 349.
[27] H. S. Taylor, *J. Phys. Chem. 30* (1926) 150.
[28] W. Keim, A. Behr, M. Röper in [4a], *Vol. 8*, pp. 372–429.
[29] J. Ewers, *Angew. Chem. 78* (1966) 593; *Angew. Chem. Int. Ed. Engl. 5* (1966) 584.
[30] Y. Chauvin, J. F. Gaillard, D. V. Quang, J. W. Andrews, *Chem. Ind. (London) 1974*, 375.
[31] a) Y. Chauvin, J. F. Gaillard, J. Leonard, P. Bonnifay, J. W. Andrews, *Hydrocarbon Process. 1982*, 110; b) J. Leonard, J. G. Gaillard, *Hydrocarbon Process. 1981*, 99.
[32] B. Bogdanović, B. Henc, H.-G. Karmann, H.-G. Nüssel, D. Walter, G. Wilke, *Ind. Eng. Chem. 62* (1970) 34.
[33] R. H. Friedlander, D. J. Ward, F. Obenaus, F. Nierlich, J. Neumeister, *Hydrocarbon Process. 1986*, 31.
[34] a) K. J. Cavell, A. F. Masters, *J. Chem. Res. Synop. 3* (1983) 72; b) A. F. Masters, K. J. Cavell, US Pat. 4 533 651 CSIRO (1985); c) K. J. Cavell in D. M. Bibley, C. D. Chang, R. F. Howe, S. Yurahak (Eds.): *Studies in Surface Science and Catalysis, Vol. 36*, Elsevier, Ansterdam 1988, pp. 523.
[35] W. Keim, B. Hoffmann, R. Lodewick, M. Peuckert, G. Schmitt, J. Fleischhauer, U. Meier, *J. Mol. Catal. 6* (1979) 79.
[36] M. Peuckert, W. Keim, *Organometallics 2* (1983) 594.
[37] W. Keim, *Chem.-Ing.-Tech. 56* (1984) 850.
[38] E. R. Freitas, C. R. Gum, *Chem. Eng. Prog. 75* (1979) 73.
[39] A. Behr, W. Keim, *Arabian J. Sci. Eng. 10* (1984) 377.
[40] W. Keim, F. H. Kowaldt, R. Goddard, C. Krüger, *Angew. Chem. 90* (1978) 493; *Angew. Chem. Int. Ed. Engl. 17* (1978) 466.
[41] W. Keim, A. Behr, B. Gruber, B. Hoffmann, F. H. Kowaldt, U. Kürschner, B. Limbäcker, F. P. Sisting, *Organometallics 5* (1986) 2356.
[42] W. Keim, *J. Mol. Catal. 52* (1989) 19.
[43] W. Keim, *New J. Chem. 11* (1987) 531.
[44] W. Keim in D. W. Slocum, W. R. Moser (Eds.): *Catalytic Transition Metal Hydrides, Ann. N.Y. Acad. Sci. 415* (1983) 191.
[45] U. Müller, W. Keim, C. Krüger, P. Betz, *Angew. Chem. 101* (1989) 1066; *Angew. Chem. Int. Ed. Engl. 28* (1989) 1011.
[46] D. M. Roundhill, *Adv. Organomet. Chem. 13* (1975) 274–354.
[47] W. Keim, A. Behr, G. Kraus, *J. Organomet. Chem. 251* (1983) 377.
[48] U. Freudenberg, W. Keim, *Chem.-Ing.-Tech. 60* (1988) 1058.
[49] E. F. Peters, A. Zletz, B. L. Evering, *Ind. Eng. Chem. 49* (1957) 1879.
[50] W. Keim, R. Appel, S. Gruppe, F. Knoch, *Angew. Chem. 99* (1987) 1042; *Angew. Chem. Int. Ed. Engl. 26* (1987) 1012.
[51] W. Keim, S. Murata, unpublished results.
[52] U. Klabunde, S. D. Ittel, *J. Mol. Catal. 41* (1987) 123.
[53] U. Klabunde, R. Mulhaupt, T. Herskovitz, A. H. Janowicz, J. Calabrese, S. D. Ittel, *J. Polym. Sci. Polym. Phys. Ed. 25* (1987) 1989.
[54] U. Klabunde, T. H. Tulip, D. C. Roe, S. D. Ittel, *J. Organomet. Chem. 334* (1987) 141.
[55] W. Keim, A. Behr, B. Limbäcker, C. Krüger, *Angew. Chem. 95* (1983) 505; *Angew. Chem. Int. Ed. Engl. 22* (1983) 503.
[56] W. Keim, B. Driessen, unpublished results.
[57] A. Sen, *CHEMTECH 1986*, 48.
[58] K. Nozaki, US-Pat. 3 689 460 (1972), Shell Oil Co.
[59] E. Drent US-Pat. 4 740 625 (1988), Shell Oil Co.
[60] W. Keim, R. Appel, A. Storeck, C. Krüger, R. Goddard, *Angew. Chem. 93* (1981) 91; *Angew. Chem. Int. Ed. Engl. 20* (1981) 116.
[61] V. M. Möhring, G. Fink, *Angew. Chem. 97* (1985) 982; *Angew. Chem. Int. Ed. Engl. 24* (1985) 1001.
[62] Jpn. Pat. 7 531 138 (1975) Takasago Perfumery Co.; *Chem. Abstr. 84* (1976) 164 281; Shell Catalog "Shell Fine Chemicals" 1986, 39.
[63] A. C. L. Su, *Adv. Organomet. Chem. 17* (1979) 269.
[64] G. W. Parshall: *Homogeneous Catalysis*, Wiley, New York 1980, p. 63.
[65] M. Julémont, P. Teyssié, *Aspects Homogeneous Catal. 4* (1981) 99–141.
[66] J. P. Durand, F. Dawans, P. Teyssié, *J. Polym. Sci. Part A 1, 8* (1970) 979.
[67] M. C. Throckmorton, F. S. Farson, *Rubber Chem. Technol. 45* (1972) 268.
[68] R. Streck im GDCh-Kurs Organische Synthesen durch Metallkomplex-Katalyse, RWTH Aachen 1988; B. Schleimer, H. Weber, *Angew. Makromol. Chem. 16/17* (1971) 253.
[69] B. W. Taylor, H. E. Swift, *J. Catal. 26* (1972) 74.
[70] C. A. Tolman, *J. Chem. Educ. 63* (1986) 199.
[71] B. R. James in [4a], *Vol. 8*, pp. 285–369.
[72] J. C. Draliner, A. D. English, J. P. Jesson, P. Meakin, C. A. Tolman, *J. Am. Chem. Soc. 98* (1976) 2156.
[73] C. A. Tolman, *Chem. Rev. 77* (1977) 313.
[74] W. Keim, A. Behr, H.-O. Lühr, J. Weisser, *J. Catal. 78* (1982) 209.
[75] W. Keim, A. Behr, J. P. Bioul, J. Weisser, *Erdöl Kohle, Erdgas, Petrochem. 35* (1982) 436.
[76] A. Behr, *Aspects Homogeneous Catal. 5* (1984) 5–61.
[77] G. W. Parshall, W. A. Nugent, *CHEMTECH 1988*, 314.
[78] W. Keim in [6a], pp. 335–349.
[79] W. Keim in M. Graziani, M. Giongo (Eds.): *Fundamental Research in Homogeneous Catalysis, Vol. 4*, Plenum, New York 1984, pp. 131–141.
[80] P. W. Jolly in [4a], *Vol. 8*, pp. 713–772.
[81] G. P. Chiusoli, G. Salerno, *Adv. Organomet. Chem 17* (1979) 195–243.
[82] R. Baker, *Chem. Rev. 73* (1973) 487.
[83] Max Planck, opening speech at the 100th anniversary of the Gesellschaft Deutscher Chemiker und Ärzte, Leipzig 1922.
[84] W. Reppe: Neue Entwicklungen auf dem Gebiet der Chemie des Acetylens und Kohlenoxyds, Springer, Berlin 1949.

Molecular Recognition with Model Systems

By Julius Rebek, Jr.*

How structures fit together is the principal domain of molecular recognition, and current studies are evolving from the host–guest chemistry of ions to interactions between two molecules. Recent advances in the synthesis of sizable concave molecules, especially those featuring convergent functional groups, make it possible to bind smaller convex structures with considerable selectivity. One result is that hydrogen bonding can be addressed in model systems. The present review emphasizes the use of cleftlike structures as a means of probing the forces involved in nucleic acid recognition. The application of such molecules to the catalysis of chemical reactions, particularly those involved in self-replicating systems, is also described. Some implications for future pharmaceutical agents are suggested as a result of access to synthetic receptors for biologically relevant targets.

1. Introduction

The study of intermolecular forces is one of the paradigms of current bioorganic chemistry. With good reason. The biochemical phenomena that inspire much of the work in the area all owe their origins to such forces. Regulation, recognition, transport, and catalysis are some of the specific phenomena and they have captured the attention of model builders during the 1980s. These terms have added charms for the adventuresome; they have no structural content. It is up to the investigator to guess which structural features are required to express the given behavior. Our own work has followed the path from regulation[1] to recognition, and in the present review we relate efforts to bridge the gap between recognition and catalysis, that is, bring these two events *closer together in space and time.*

In 1984 we introduced molecules of a cleftlike shape to bioorganic chemistry.[2] This was, and may still be regarded as, heresy in a field so dominated by macrocyclic structures, but the peculiar advantages of such structures justified the apostasy. One significant advantage was the convergence of useful functional groups, particularly carboxylic acids. It permitted the use of hydrogen-bonding interactions rather than the ion–dipole interactions that are the principal forces offered by crown ethers[3] or the hydrophobic interactions of cyclodextrins[4] and cyclophanes.[5] Directionality in binding was the result, and structures bearing basic sites could be considered targets for recognition studies.

The unique shapes of the molecules arise from the use of Kemp's triacid,[6] a molecule in which the triaxial conformation of three carboxyls forces a U-shaped relationship between any two of them. Its condensation with diamines (Scheme 1) leads to molecules which fold back upon themselves, structures in which the carboxylic acid can be oriented with respect to other parts of the molecule. The concave shape of the overall structure is due to the passive effects of the methyl groups. Those α to the carboxyls prevent epimerizations, while those *ortho* to the imides prevent rotations to divergent conformations. In macrocyclic structures, the concavity of the interior is due to the existence of the ring itself. The new structures, particularly those involving the convergence of carboxylic acids, have been useful in exploring stereoelectronic effects at carboxyl oxygen (see Section 2).

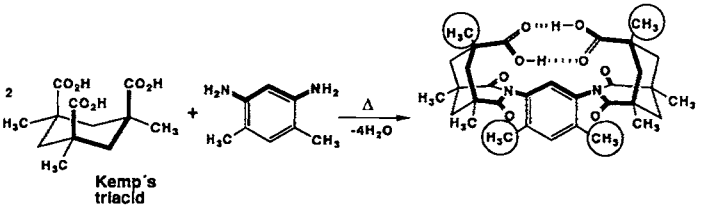

Scheme 1.

Another advantage that accelerated our explorations was the facile, modular assembly of cleftlike molecules of different sizes and shapes. For example, using the inexpensive dye acridine yellow and a technique resembling a mixed melting point determination, excellent yields of a new dicarboxylic acid could be obtained[7] (Scheme 2). Such structures are capable of binding molecules of the size of small biological targets, for example, amino acids,[8] heterocyclic amines,[9] and diketopiperazines.[10] These structures, with their relatively few degrees of rotational freedom, make attractive frameworks for computational chemistry. Recent calculations by *Jorgensen* et al.[11] and by *Lipkowitz* et al.[12] have elaborated the dynamics and multipoint contacts available

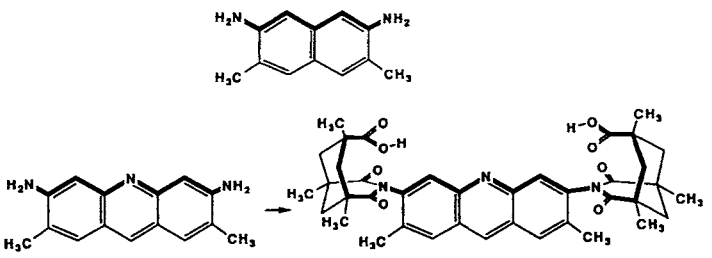

Scheme 2.

[*] Prof. J. Rebek, Jr.
Department of Chemistry
Massachusetts Institute of Technology
Cambridge, MA 02139 (USA)

in complexations involving the clefts. Kemp's triacid is commercially available and it is conveniently prepared on an 80-gram scale in the laboratory.[9]

2. Stereoelectronic Effects at Carboxyl Oxygen

Because we had a franchise on molecules featuring convergent carboxyl functions, we felt obliged to examine the consequences. Nearly a decade has passed since *Gandour*[13] drew attention to the consistent orientation of carboxyl groups at enzyme active sites. It had been known that the basicities of the in-plane lone pairs of a carboxylate were different, so much so that approximately 5 kcal mol^{-1} separate the two forms of a carboxylic acid.[4] Recent calculations[15] indicate that the energy difference can be even greater. What *Gandour* pointed out was that, in enzyme active sites, the more basic *syn* lone pair is invariably directed toward the substrate (Scheme 3). For example, in aspartic

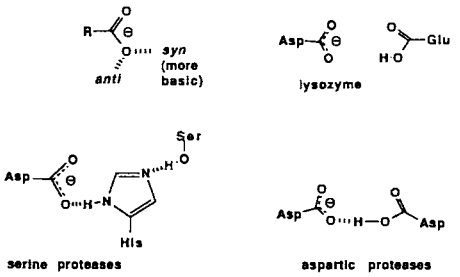

Scheme 3.

proteases or lysozyme, it is the convergence of two carboxyl functions that creates the active site. In zinc proteases,[16] a carboxyl is likewise directed toward the substrate, and, even in serine proteases, the more basic *syn* lone pair of the aspartate is directed toward the proton relay apparatus of the catalytic triad. Since Nature incorporates this feature of carboxyl groups, it was inevitable that we would attempt some experimental measures of these effects with our model systems.

Our first qualitative evidence on these effects was the rather unusual behavior of the dicarboxylic acid in Scheme 1, which reacted *slowly* with diazomethane. With other alkylating agents (e.g., Meerwein salts) slow and clean monoalkylation occurred.[7] Remarkably, the peracid derivatives showed selective epoxidation of *cis* versus *trans* olefins.[17] In acyl transfer reactions, however, the diacids showed normal behavior. For example, they could be converted into their acid chlorides, from which methyl esters or amides could be made without event. This behavior can be understood from the point of view of reaction trajectories; in acyl transfer reactions, nucleophiles enter and depart along a line (Scheme 4) where there is not much of an opportunity for them to interact with the distal carboxyl group. In electrophilic reactions, particularly when the more basic *syn* lone pairs are involved, the electrophile must wedge between the two carboxyl functions. The slow reactions with electrophilic reagents were one of the first expressions of this effect.

Another result has been the observation of direct proton exchange within hydrogen-bonded amides.[18] These studies involved the detection of different rates for exchange in the diamide of Scheme 4. H_Z exchanges with solvent some 30 times slower than H_E under basic conditions.

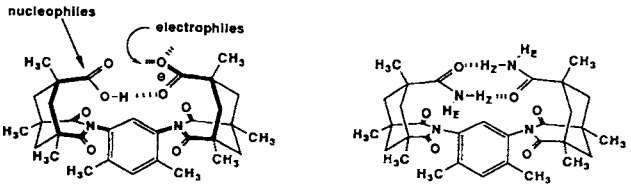

Scheme 4.

We have attempted to evaluate this effect in a number of settings (Scheme 5) but are on the verge of despair concerning a quantitative measure of it. The problem is merely staging a fair comparison between a system involving the *syn* lone pair and a corresponding one with the *anti* lone pair. It has been nearly impossible for us to obtain two molecules that differ in that respect, yet have the same degrees of rotational freedom as well as the same rigidity, distance, etc. To be sure, unfair comparisons are quite easy to arrange, but as we have pointed out,[7] one of the problems of physical organic chemistry is that there are no continuities of structure. Even the insertion of a single methylene into a system changes not only the distance, but the conformation as well. Some of the settings that we have studied are shown in Scheme 5.

Julius Rebek, Jr., was born in Hungary in 1944 and lived in Austria from 1945 to 1949. He and his family then settled in the USA in Kansas. He completed his undergraduate education at the University of Kansas in 1966 and obtained the Ph.D. degree from the Massachusetts Institute of Technology in 1970 for studies in peptide chemistry with Professor D. S. Kemp. As an Assistant Professor at the University of California at Los Angeles (1970–1976), he developed the "three-phase test" for reactive intermediates. In 1976 he moved to the University of Pittsburgh, where he rose to the rank of Professor of Chemistry and Chairman of the Organic Division. In 1989 he returned to the Massachusetts Institute of Technology as Professor of Chemistry. He has been awarded NSF, Alfred P. Sloan, J. S. Guggenheim, and Alexander von Humboldt Fellowships. His current research interests are in mechanistic organic chemistry, enzyme models, oxidation reagents, and molecular recognition.

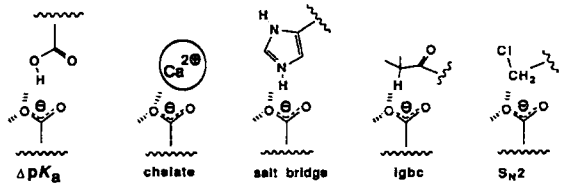

Scheme 5. igbc = intramolecular general base catalysis.

The extraordinary difference in the first and second pK_a of the dicarboxylic acids, namely, six units, is probably the most dramatic observation,[19] and the very high affinity of these new chelating agents to divalent metals[20] must also reflect these stereoelectronic effects. Perhaps one of the best comparisons we have staged is in the carboxylate–imidazolium salt bridge.[21] The difference in pK_a's of our model system and dihydrourocanic acid indicate that most of the requirements of distance, flexibility, lack of strain, etc. are met (Scheme 6). Here, we see that the *syn* lone pair is approximately one order of magnitude more basic than the *anti* lone pair.[22] However, many of these situations are dominated by electrostatic components, where distance rather than orientation is the greatest consideration and stereoelectronics can be whelmed. Accordingly, we have looked at a system involving intramolecular general base catalysis. In enolization reactions,[23] about an order of magnitude (relative to the reference) is observed. Even in such a system, it was not possible to avoid strains in trying to arrange the perfect transition structure. *Houk* et al.[24] have computed that these strains can mask the effects to some yet unknown extent.

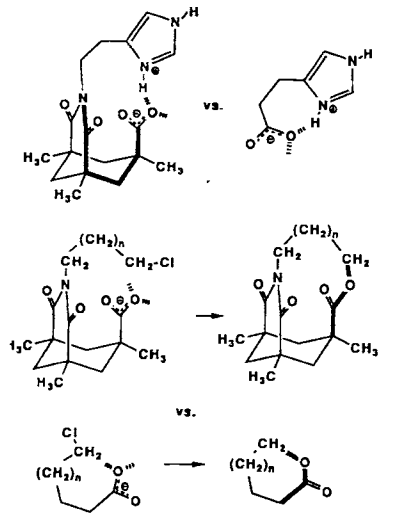

Scheme 6.

Most recently, we have studied a lactonization reaction in which some larger, directional (covalent) component could be expected. In direct comparisons between the cyclization to the *Z* ester (Scheme 6) and that involved in valerolactone, the rates are found to be quite comparable; that is, no effect is apparent.[25] Is this the bottom line, then? Who knows? Again, there may exist subtle strains or torsional effects in our molecule worth a few kilocalories per mole that could confuse the issue. Moreover, it has been suggested[26] that the *syn* lone pairs are more heavily solvated than the *anti* lone pairs. If so, their intrinsic reactivity in protic solvents is inevitably at a disadvantage. Only in proton transfers from solvent (i.e., basicity) or in enzyme interiors, where water has been squeezed out, will this effect be of any magnitude. Whether it is from misplaced optimism or sheer stubbornness, we intend to continue these studies with our model systems.

3. Other Stereoelectronic Effects

One spin-off of these investigations concerns the active sites of enzymes and the stereoelectronics of proton transfer reactions. We begin with the assumption that *every structural detail is important*. For example, phenomena such as the leucine zipper[27] have recently emerged and the subtle difference between aspartate and glutamate in enzyme active sites[28] also underscores the importance of details; every side chain of every amino acid is laden with this information, whether or not it has been brought to light.

Consider the side chain of histidine, which is frequently found at active sites. The pK_a of the imidazolium ion, ca. 7, permits significant concentrations of both acidic and basic forms to exist near neutrality. There is another attribute of the structure, namely, its ability to transfer protons in a variety of directions.[29] By anchoring the imidazole at C-5, the acidity (or basicity) can be reoriented by rotations about the C5–Cβ bond. These are represented by the circles of Scheme 7. The significance of this motion may be expressed in the action of the serine proteases.

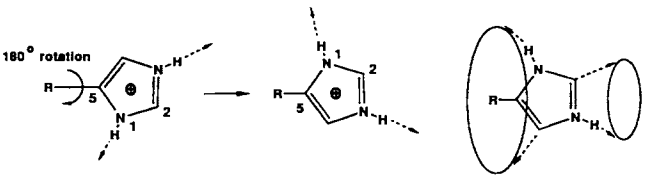

Scheme 7.

The generally accepted sequence of events for this type of enzyme (Scheme 8) involves the formation of a tetrahedral intermediate.[30] The departing nitrogen must become protonated before breakdown of the tetrahedral intermediate can occur. This could be accomplished by rotation around the single bond indicated. The hydrogen-bonding network is temporarily disrupted during the rotation but is recovered as the system is poised for the breakdown of the intermediate. A reversal of the sequence, with water entering as a nucleophile on the serine ester, leads ultimately to deacylation. There is some evidence that the protease and esterase activities of chymotrypsin involve different nitrogen atoms of the imidazole ring.[31] This would support the mechanism of proton transfers described above. At any rate, we suggest that the shape of histidine may be as important as its pK_a for its function at the active sites of enzymes.

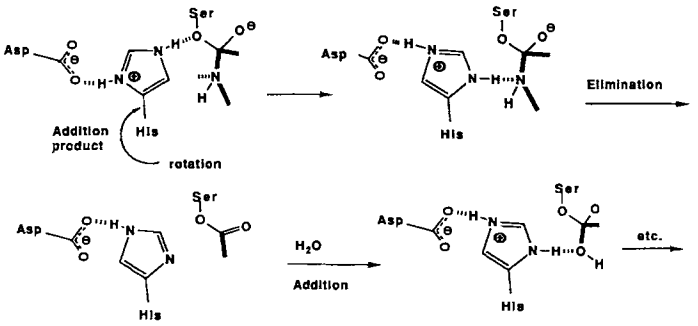

Scheme 8.

4. Base-Pairing and Stacking Interactions

Among the more attractive recent targets of molecular recognition have been the heterocyclic bases of nucleic acids. They are small and rigid and they present a wealth of basic sites that are unattractive to receptors with more conventional linings. The hydrogen-bonding aspects have been well-established[32] using the relatively noncompeting solvent $CHCl_3$. In water, stacking associations dominate the interactions.[33] The U-turn inherent in derivatives of Kemp's triacid permitted us to construct molecules in which hydrogen-bonding and aryl-stacking interactions (Scheme 9) could

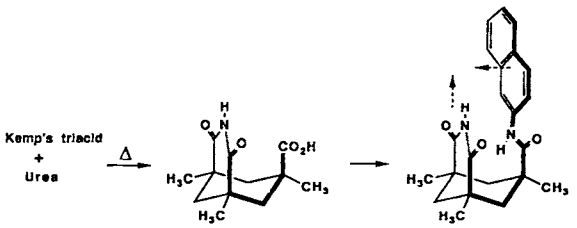

Scheme 9.

be evaluated simultaneously.[34] Organic solvents, which have a polarity between the fierce competitions in aqueous media and the calculational simplicity of the gas phase, provide a magnifying glass with which to observe these principal forces that stabilize double-stranded nucleic acids.

Merely heating Kemp's triacid with urea gives the imide, which presents a hydrogen-bonding surface similar to that of thymine. We were able to attach a number of molecular surfaces, including a series from methyl to anthracyl, and measure the association constants by NMR titration methods.[35] These gave the results shown (Scheme 10) in which it can be seen that about 400 cal mol^{-1} separate adjacent pairs of the series. The overall effect of a large polarizable aryl surface is worth about 1.2 kcal mol^{-1}, corresponding to nearly an order of magnitude in binding affinity at room temperature. These are not hydrophobic effects; rather, they represent the polarizability that an anthracyl surface experiences when the dipole of adenine is brought up against it. In other systems, progress has been made in understanding ion–dipole effects[36] and the intrinsic nature of hydrophobic effects.[37] Both of these advances have been made using macrocyclic structures in aqueous media.

Geometric considerations lead to the conclusion that the aryl–aryl interactions in these systems are of the face-to-face sort rather than the edge-to-face sort observed in protein interiors by *Petsko* et al.[38] There may even be the possibility that the stacking directly enhances the hydrogen bonding in such systems.[39] Even so, we were surprised to find that the aromatic surface not only increased overall binding, but could contribute to the *orientation* of the components. Experiments involving nuclear Overhauser enhancement (NOE) measurements established that, with small surfaces, roughly equal amounts of Watson–Crick and Hoogsteen base pairing (and their reverse counterparts) were involved in the complexation. Heteronuclear NOE experiments revealed that even bifurcated hydrogen bonding was present in these systems.[40] But the Hoogsteen/Watson–Crick ratio was affected by the length and shape of the aromatic surface. For example, with the extended anthracyl surface, the Watson–Crick base-pair mode, involving extensive overlap between the π systems, is favored (Scheme 10). On the other

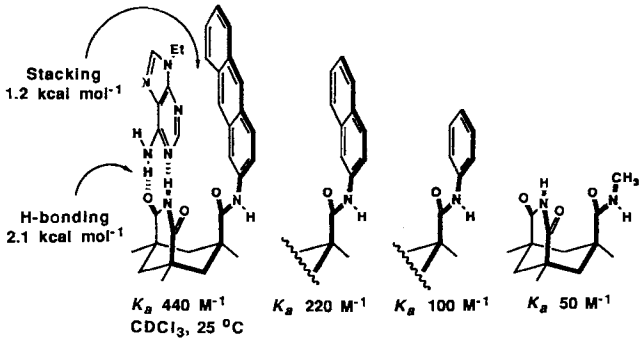

Scheme 10.

hand, it was possible to use remote steric effects to enforce Hoogsteen base pairing.[41] Specifically, the *tert*-butyl derivative of the naphthyl ester (Scheme 11) can accommodate the aryl-stacking interaction best in the Hoogsteen mode; the Watson–Crick mode causes destabilizing steric interactions between the side chains of the receptor and adenine components.

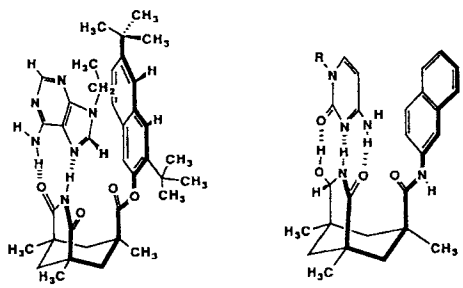

Scheme 11.

The pattern of hydrogen bonds and their significance in recognition could be explored by tailoring the edges of such structures. For example, the imides bind adenines over cy-

tosines by a factor of >20. Merely reducing the imide to the hydroxy lactam (Scheme 11) alters the acid–base patterns; cytosine is bound >10 times better than adenine.[42] At first glance, an *apparently* singular change alters the recognition pattern. However, because these forces act over such short distances, an isolated change is not possible. This reflects a frequently encountered problem in physical organic chemistry: *changes can rarely be made one at a time*. The influence of the change extends beyond the immediate atom or functional group and causes disruptions elsewhere. Interpretations become, accordingly, ambiguous.

We have recently been successful in preparing acylated amidine derivatives for the recognition of guanines.[43] These are prepared by treating the imide nitriles with amides such as $NaNH_2$ (Scheme 12, top). Association constants for the binding of guanines to such surfaces are greater than $10^4\ M^{-1}$. These again parallel earlier observations and bear out the more recent predictions of *Jorgensen* et al.[44] concerning the secondary interactions involved in hydrogen-bonding patterns. In parallel studies with macrocyclic frameworks, *Hamilton*'s group has been able to observe hydrogen-bonding and aryl-stacking interactions in the complexation of such nucleic acid components.[45]

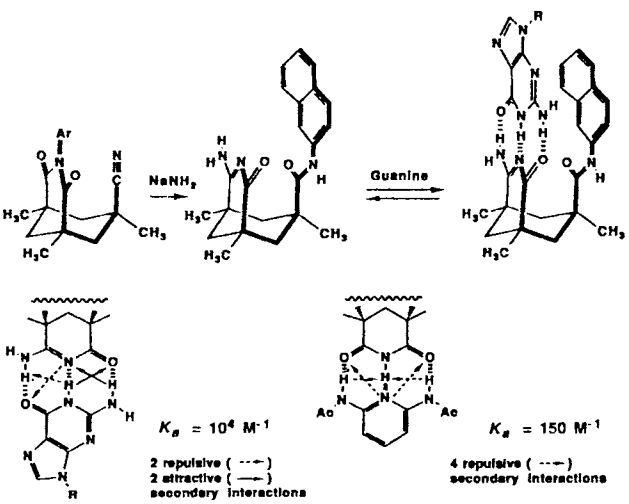

Scheme 12. Ar = aryl.

The triple helices that have been recently developed for sequence-specific DNA recognition[46] could also be modeled by these simple structures. By merely combining two imides with proper orientation on a single naphthyl surface, structures with extraordinary affinity for adenines resulted (Scheme 13). Adenine and even carbohydrate derivatives—adenosine and deoxyadenosine—could be extracted from aqueous solution and transported across organic liquid membranes by such materials.[47] We are currently developing systems for similar recognition and transport of nucleotides, using the guanidinium functions developed by *de Mendoza* et al.[48] and *Schmidtchen* et al.[49] (see also Section 9).

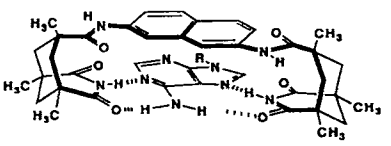

Scheme 13.

5. Recognition and Replication

Another dividend, perhaps even a distraction, resulting from our research in nucleic acid recognition has been the development of self-replicating systems. The premise was quite simple, even tautological; covalent attachment of an adenine to a receptor for adenine must lead to a molecule that can recognize itself. Provided that the orientation, flexibility, and spacing of the binding surfaces are appropriate, the molecule might collapse through intramolecular folding, it might dimerize, or even higher molecular assemblies might be organized (Scheme 14). In any event, such a molecule is self-complementary.

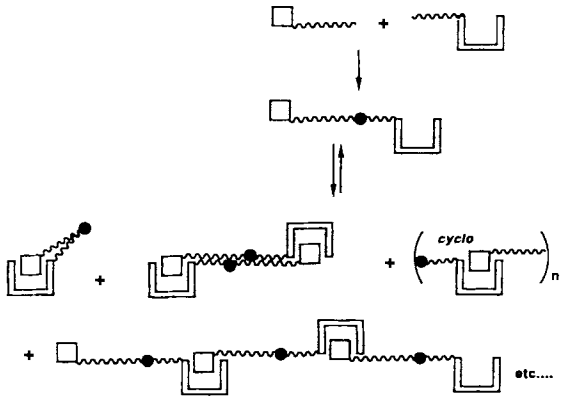

Scheme 14.

This simple notion has led us into swampy terrain or even the prebiotic soup. The simple aminolysis of the adenosine derivative with the imide bearing a phenyl spacer shows template-assisted behavior. That is, base-pairing precedes acyl transfer (Scheme 15). This is easily demonstrated; merely placing an *N*-methyl group on the imide reduces the coupling rate sixfold, a factor that can hardly be attributed to steric effects at a site so remote from the acyl-transfer reaction. The product with the phenyl spacer is self-complementary in an

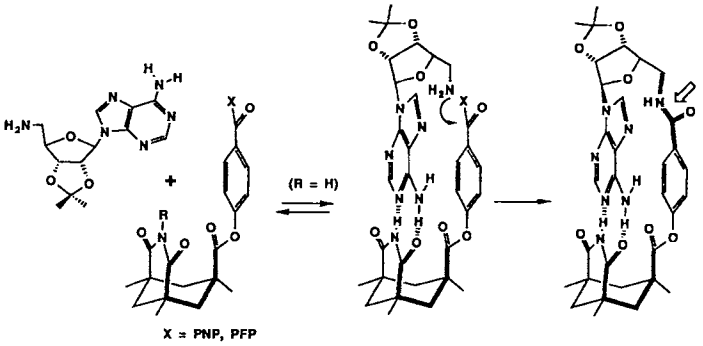

Scheme 15. PNP = *p*-nitrophenyl; PFP = *p*-fluorophenyl.

intramolecular sense and it remains "folded shut". This is because a short phenyl spacer can accommodate a perfectly stable *trans* amide bond in the coupled product.

We next examined the consequences of using a longer naphthalene spacer. Again, template effects are operating and simple inhibition experiments can be used to demonstrate this. For example, other imides, as well as diacylamino pyridine, compete for the reaction surfaces and slow the coupling reaction. But now, when intramolecular acyl transfer does take place, the initial product is a *cis* amide. Once this material is formed, it can relax to the *trans* amide by a "jackknife" motion (Scheme 16). This exposes the complementary hydrogen-bonding surfaces and leads to dimerization (Fig. 1). The association constant observed for dimerization is somewhat less than would be expected for four reasonable hydrogen bonds and suggests that some steric effects are operating at the bulges in the middle of the dimer.

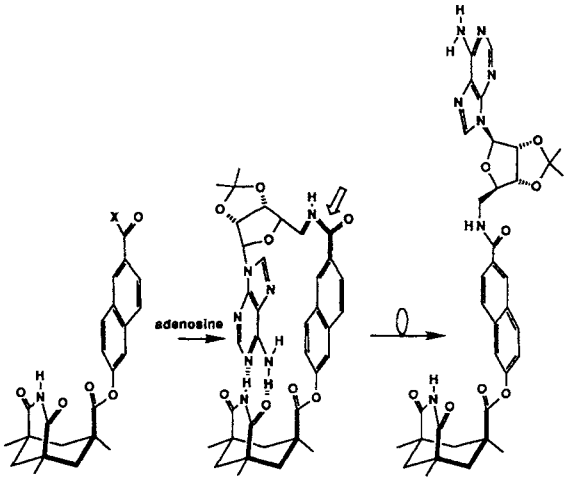

Scheme 16.

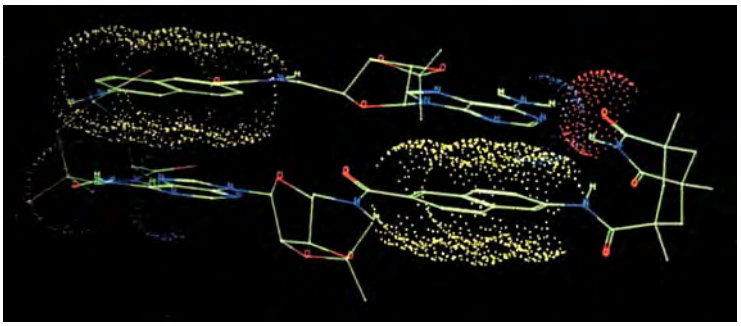

Fig. 1. Hydrogen-bonding (red/blue) and aryl-stacking interactions (yellow) stabilize a self-complementary and self-replicating system.

This system, however, shows a very astonishing feature of catalysis. *The product catalyzes its own formation,* and this is a primitive sign of a living system.[50] Addition of various amounts of product to coupling mixtures is observed to increase the initial coupling rates. One interpretation (yet unproven) is that in this case a third type of reaction leads to

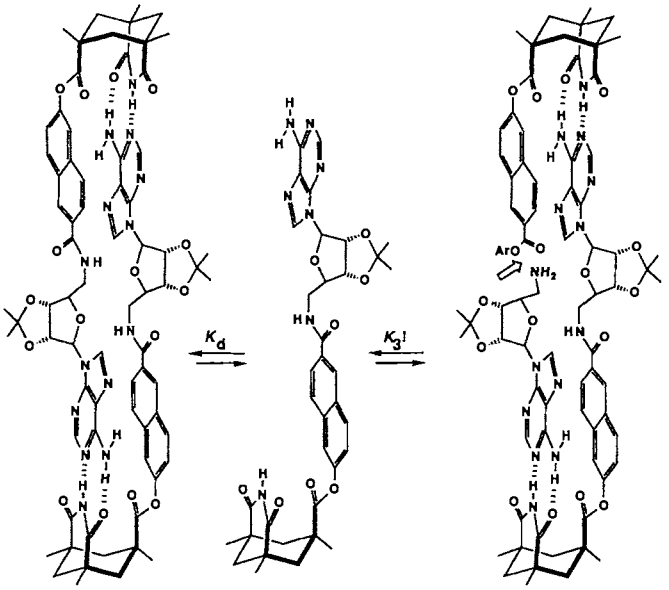

Scheme 17. Ar = aryl.

coupled product. The likely process involves a termolecular complex (Scheme 17 and Fig. 2) in which electrophile and nucleophile are brought together on the product's surface acting as a template.[51] This reaction must be quite efficient, since it can be calculated from the known association constants that the termolecular species represents only a few

Fig. 2. Electrophile and nucleophile are brought together on a template through hydrogen-bonding (red, blue) and aryl-stacking (yellow) forces. Autocatalysis is observed in this self-replicating system.

percent of the reaction mixture. We are now refining the system to reduce the number of nonproductive complexes and thereby further increase the efficiency of autocatalysis. In the meantime, we draw attention to an exceptionally beautiful template-catalyzed system devised by *Kelly* et al.[52] for a substitution reaction.

6. Catalysis

Using base pairing to enhance acyl-transfer reactions is an example of bringing recognition and catalysis closer together in time. The ultimate goal in model systems would be to recognize transition states as is defined by the Pauling princi-

ple.[53] Many groups have been concerned with the development of such synthetic catalysts and a number of excellent examples exist in the chemistry of cyclophanes,[54] cyclodextrins,[55] and crown ethers.[56] In most bioorganic model systems, the general endeavor involves fitting a substrate into the host species, then placing catalytically useful functional groups nearby. The advantage of cleftlike molecules having rigid spacers is that both acidic and basic components can coexist without collapsing upon one another (Scheme 18). Convergence again is the key. Functional groups arranged in

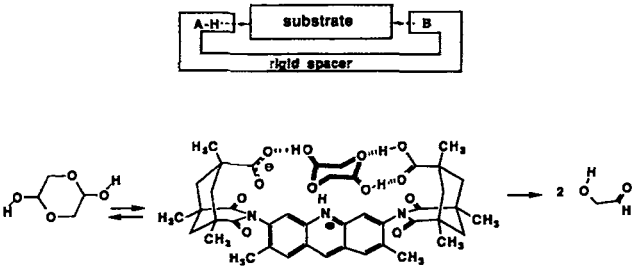

Scheme 18.

a divergent sense could annihilate one another in intermolecular interactions, but arrangement in a convergent sense, that is, on concave surfaces[57] with rigid spacers, allows the two groups to communicate only through solvent. Accordingly, concerted or general acid-base catalysis[58] is ideally suited for study with such molecular scaffolds.

Our first success with these was in the cleavage of a hemiacetal (Scheme 18).[59] This molecule just fits within the cleft and, once bound, a constellation of acids and bases can focus on the reacting centers. At the present time, the identity of the participating acid and base components is unknown. The carboxylic acid itself could act in the manner of a conventional mutarotation catalyst. Alternatively, the protonated acridine nitrogen and the carboxylate could act on the substrate from perpendicular directions.

We have permissive evidence for the latter sort of catalysis in the enolization of ketones. Stereoelectronic considerations indicate that the ideal arrangement for acid and base components in a concerted or "push-pull" mechanism involves the approach of such components from perpendicular directions (Scheme 19). This follows from the early observations of

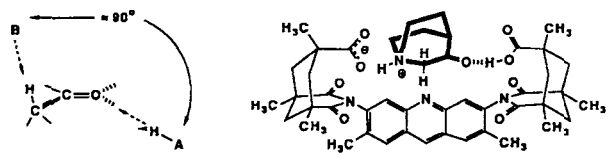

Scheme 19.

Corey and *Sneen*[60] and the recent NMR characterization[61] of simple enols in solution. The quinuclidinone shown fits within the cleft, and, in the complex, acids and bases are poised in the proper geometry. Catalysis of α-hydrogen exchange occurs.[62]

In the two previous examples, a substrate can be tailored to fit within the cleft, but it is a much more difficult proposition to design a catalyst for a given substrate or even type of reaction. Nonetheless, we cannot help but think that the efficient synthesis of cleftlike molecules and the richness of shapes, sizes, and functionality that they provide will offer solutions. In this we are responding to the message provided by naturally occurring molecules. They generally present *concave* surfaces: clefts, pockets, folds, and even grooves that are lined with a variety of chemical functions.

It may also be important to bring the recognition and the catalysis events closer in *space* as well as in time. The significance of this point stems from the difficulty in controlling conformations over considerable distances. Systems that fold back upon themselves can reduce the distance between functional groups and enhance their efficacy. The remarkable progress made recently with catalytic antibodies presents an urgent challenge. The combining sites of antibodies are unrivaled in selectivity and versatility. If catalytically useful functionality can be introduced, as has been achieved in some cases by *Lerner* et al.[63] and *Schultz* et al.,[64] model systems such as ours may become the dinosaurs of the 1990s.

7. New Sizes and Shapes

We have already reported on the uses and limitations of rigid aromatic spacers represented by the series benzene, naphthalene, and acridine.[9] We report now on progress with some newer spacers. Tetraarylporphyrins provide very large aromatic surfaces and a tetracarboxylic acid was readily synthesized (Scheme 20) by the procedure recently devel-

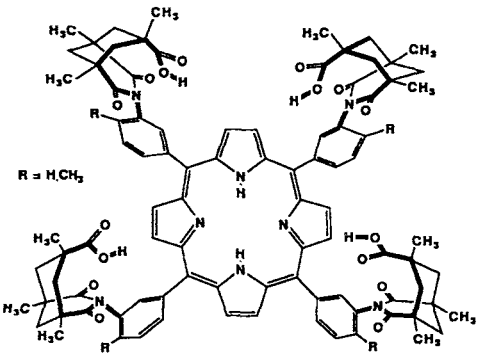

Scheme 20.

oped by *Lindsey* et al.[65] In this molecule, the space is appropriate for the complexation of 4,4′-bipyridine derivatives. A 2:1 complex is formed, since one bipyridine can be held above the porphyrin plane by two carboxylic acids while a second is held beneath, perpendicular to the first.[66] It should be possible to develop metal-ion derivatives of these molecules in which the reactive metal center is brought to the middle of an α,ω-diamine grasped at both ends by the carboxyls. Within macrocyclic frameworks, this notion is being explored by *Lehn*'s group[67] and *Sutherland*'s group.[68]

Spacers with three arms have also been obtained. For example, the *tris* imide in Scheme 21 shows an extraordinary

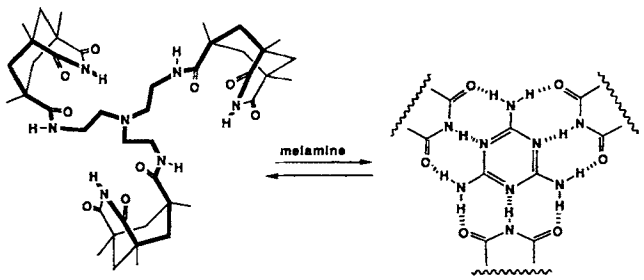

Scheme 21.

affinity for melamine.[66] This material forms 1:1 complexes (Fig. 3) and features slow exchange at room temperature. Dilution studies put the lower limit on the dissociation constant in the micromolar range.

Rigid spacers with three arms are also available. Condensation of acetophenone derivatives leads to triarylbenzenes (Scheme 22). These have been used in molecular recognition

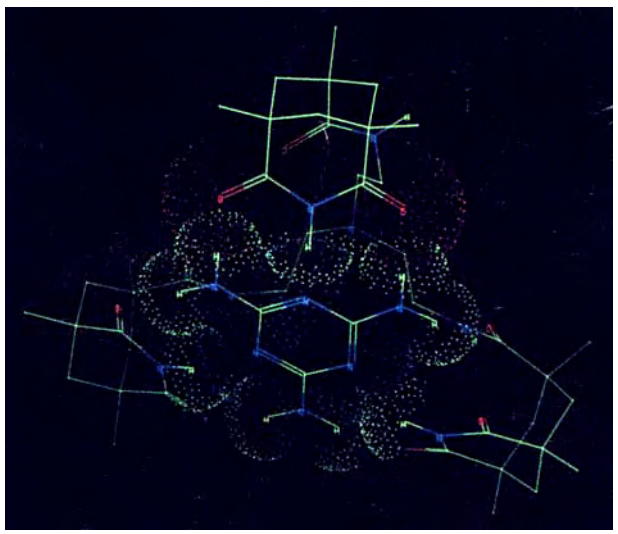

Fig. 3. Three imide functions converge to provide a complementary hydrogen-bonding surface to melamine. Convergent functional groups tailored for small, biorelevant targets are a key feature of model systems for molecular recognition.

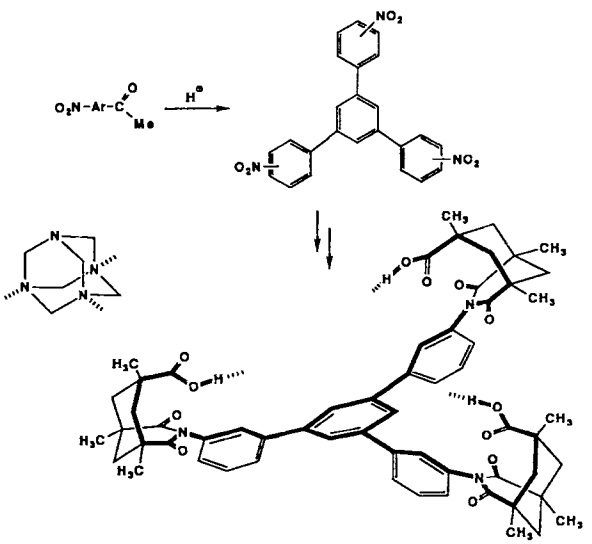

Scheme 22. Ar = C_6H_4.

studies by *Vögtle* et al.[69] We have also prepared the Kemp triacid derivatives of these systems. For example, the *meta*-substituted compound binds hexamethylenetetramine quite nicely; at low temperature, the exchange process can be frozen out. A larger cleft, represented by the *para*-substituted compound, is also easily prepared.[70] Macrocyclic compounds have also been devised recently by *Still*'s group for complexation of heterocycles.[71] These studies have led to the discovery of the effects of solvent size on complexation phenomena.[72]

8. Asymmetry and Auxiliaries

Asymmetric recognition has been a long-standing endeavor in complexation chemistry, and, for reasons that are not at all clear, most synthetic receptors, both macrocyclic and cleft-shaped,[73] feature C_2 symmetry. As we have pointed out, there is no advantage of this shape for recognition of a single asymmetric center.[74] Rather, as in *Pirkle*'s systems,[75] three contact points appear to be the minimal requirement. Whether such points of contact are attractive or steric in nature, they are much better suited in shape for recognizing a single asymmetric center than are more symmetrical shapes. The Kemp triacid may be regarded as a tripod on which three groups—large, medium, and small—can be placed on a single face of the molecule (Scheme 23), and we have found such structures useful for asymmetric recognition.

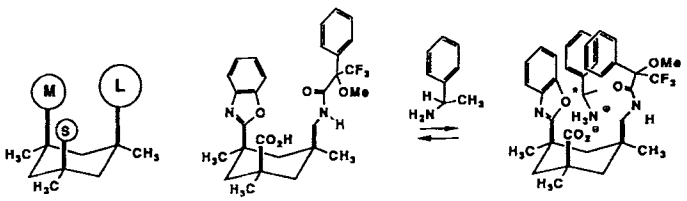

Scheme 23.

More recently, we have developed sandwiching (Scheme 23). Aromatic amines are bound initially by the acid–base interaction; then the two aryl surfaces of the receptor surround the amine as shown.[76] In these systems as well as others we have explored, acidity is directed toward an asymmetric microenvironment. This can be contrasted with conventional carboxylic acids in which acidity is directed *away* from the nearest asymmetry (usually at the α-carbon).

We have now developed these findings into some chiral proton sources. The tricyclic lactam shown in Scheme 24 is quite efficient in this regard. It is prepared in simple steps and it protonates the test system developed by *Hünig* et al.[77] in $\geq 98\%$ enantiomeric excess. From studies of other diastereomers it is clear that both the asymmetric center and the sense of molecular asymmetry of the cyclohexane ring are involved.[78]

Derivatives of this structure are also quite effective as chiral auxiliaries. For example, acyl derivatives can be prepared as shown in Scheme 25 and their enolates show high diastereofacial selectivity in complementary alkylation reac-

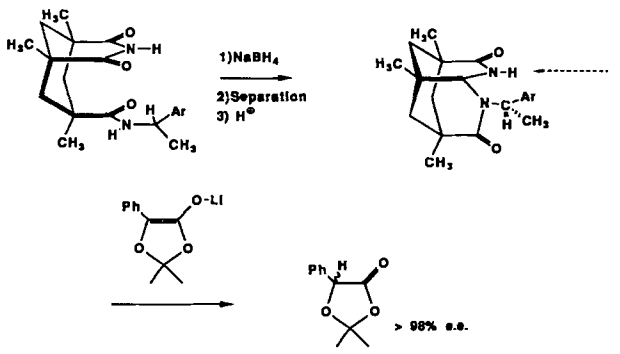

Scheme 24. Ar = aryl.

tions.[79] The selectivity extends to other types of reactions as well. *Curran* et al.[80] have shown that acryl derivatives, as well as other derivatives, feature high selectivities in cycloadditions with nitrile oxides. The extended shelf beneath the

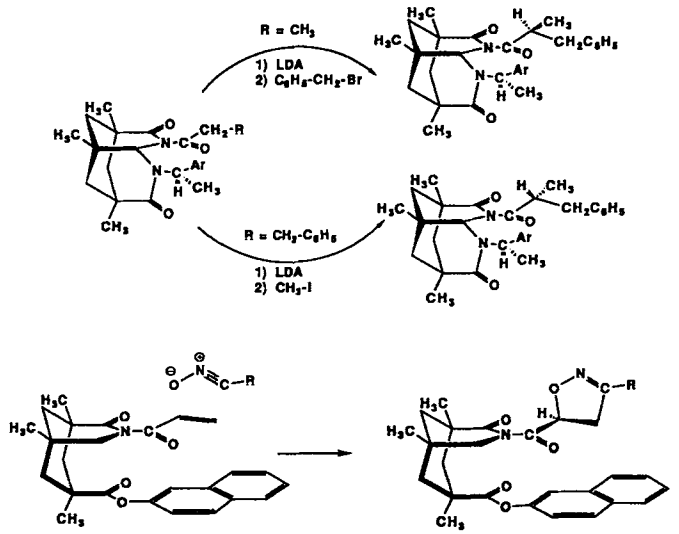

Scheme 25. Ar = 2-naphthyl. LDA = lithium diisopropylamide.

structure prevents approach of the notoriously unselective nitrile oxide from the bottom. Removal of the auxiliary can be accomplished by, among other methods, selectride reduction.

9. Newer Cleft Systems

It would be negligent of me to overlook the rapid progress being made elsewhere in the area of molecular recognition, particularly as many of the new systems involve cleftlike structures. A large number of these feature acidic sites that converge: NH bonds, OH bonds, and even metal-ion empty orbitals.[81] The slow development of these systems reflects the greater difficulty in arranging convergent Lewis acidic sites versus Lewis basic sites; that is, it has always been easier to complex cations than anions.

Two new cleftlike systems have appeared for complexation of adenine derivatives (Scheme 26). Remote steric barriers enforce the concave shapes of these structures, and they show unprecedented affinity for adenine derivatives. *Zimmerman* et al.[82] report a system that features a carboxyl group deep within the cleft with low accessibility to solvents. *Wilcox* et al.[83] have a system that features convergent carboxylic acid at a distance appropriate for simultaneous Watson–Crick and Hoogsteen binding. This latter structure has added versatility; rotation about the carboxyl group leads to hydrogen-bonding patterns complementary to, for example, trimethylene urea.

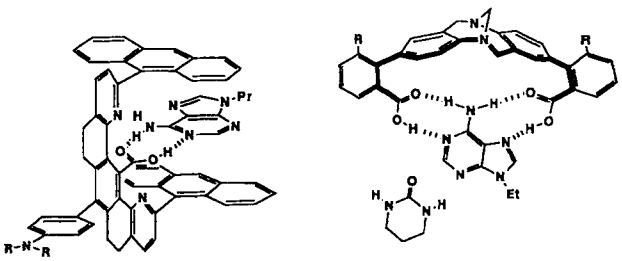

Scheme 26.

Another recent development is the synthesis of "two-dimensional" systems for the complexation of flat substrates (Scheme 27, left). *Bell* et al.[84] have developed a naphthyridine-derived system which binds urea. It should be possible to enhance binding by incorporating acidic sites for the carbonyl oxygen. *Kelly* et al.[85] have prepared complexing agents for uric acid derivatives (Scheme 27, right). The gentle curvature imparted by the central five-membered ring provides the complementary functions for the convex shape of the substrate. The inflexibility of such systems places a high premium on arranging an exact match between host and guest. Systems with a little adjustability (and corresponding "promiscuity") are usually easier to synthesize. The ideal design for artificial receptors is still a matter of some debate.

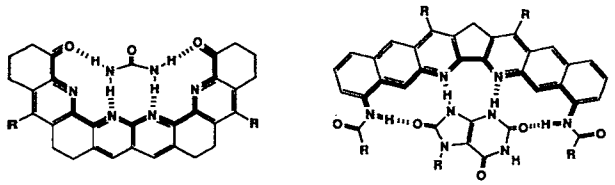

Scheme 27.

Systems for the binding of carboxylates have also been developed, and a cleftlike strategy has been useful to arrange additional contacts between host and guest. Since initial encounter of the carboxylate is with its *syn* lone pairs, a U-turn must be built into the receptor to arrange contacts beyond the α-carbon of the acid. One system, prepared by *de Mendoza* et al.[48] involves a guanadinium derivative (Scheme 28) in which aryl-stacking interactions provide the additional contact. The second system, due to *Schmidtchen* et al.,[49] also uses the guanadinium function and a well-placed hydroxyl group to provide an additional hydrogen bond. By using highly lipophilic derivatives of this receptor, valine can

be extracted as the anion from aqueous solution into $CHCl_3$. Both of these systems have excellent potential for asymmetric recognition.

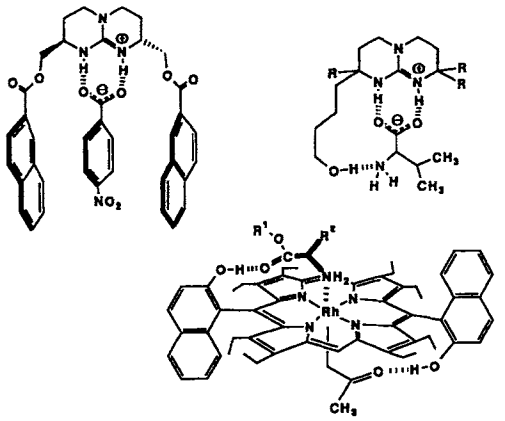

Scheme 28.

Finally, a porphyrin derivative has been developed by *Aoyama* et al.[86] for the recognition and extraction of amino acids and their derivatives. The metal ion in the porphyrin complexes the amine, and hydroxyl groups on the periphery stabilize the carboxyl by hydrogen bonding.

Excitement continues in macrocyclic host–guest chemistry as well. Molecular belts and collars[87] and molecules within molecules[88] define the leading edge of this field. Self-assembling structures are also emerging,[89] but are beyond the scope of the present review.

10. Perspective

As the discussion above indicates, most of the activity in model systems for molecular recognition is concerned with the design of host species for small, convex, biorelevant targets. In addition to the amino acid and nucleic acid components, carbohydrates[90] and dicarboxylates[91] have become accessible targets and synthetic drugs such as barbiturates[92] can also be complexed. The sequestration of small endogenous intermediates is the first step in what may become a new pharmaceutical tactic. Biochemical cycles could be interrupted by either removing these intermediates, or processes could be enhanced by delivering them to the requisite sites more effectively. Their sequestration requires access to medium-sized molecules with concave surfaces such as described in this review.

Why has Nature not availed itself of this type of intervention? One reason may be stoichiometry. When the targets are biological macromolecules such as receptors, enzymes, or nucleic acids, the low concentrations of such molecules require only small "doses". But in at least in one case, Nature has availed itself of concave agents. The vancomycin antibiotics are of the size of structures discussed here and involve a concave surface lined with hydrogen-bonding arrays complementary to a dipeptide terminus. With access to molecules of intermediate size, such as antibody-combining sites, synthetic peptides, and synthetic nucleotides, the tactic offered by the concave medicinal agent may become an attractive one in the future.

I am grateful to the outstanding group of young men and women who have been associated with this project; their names appear on the publications cited. The National Institutes of Health and the National Science Foundation provided financial support of this research.

Received: September 22, 1989 [A 752 IE]
German version: *Angew. Chem. 102* (1990) 261

[1] J. Rebek, Jr., *Acc. Chem. Res. 17* (1984) 258.
[2] J. Rebek, Jr., L. Marshall, R. Wolak, J. McManis, *J. Am. Chem. Soc. 106* (1984) 1170.
[3] D. J. Cram, *Angew. Chem. 100* (1988) 1041; *Angew. Chem. Int. Ed. Engl. 27* (1988), 1009; J.-M. Lehn, *Angew. Chem. 100* (1988) 91; *Angew. Chem. Int. Ed. Engl. 27* (1988) 89.
[4] G. Trainor, R. Breslow, *J. Am. Chem. Soc. 103* (1981) 154; V. T. D'Souza, M. L. Bender, *Acc. Chem. Res. 20* (1987) 146.
[5] H. Stetter, E.-E. Roos, *Chem. Ber. 88* (1955) 1390; K. Odashima, A. Itai, Y. Iitaka, K. Koga, *J. Am. Chem. Soc. 102* (1980) 2504; S. P. Miller, H. W. Whitlock, Jr., *ibid. 106* (1984) 1492; J. Winkler, E. Coutouli-Argyropopoulou, R. Leppkes, R. Breslow, *ibid. 105* (1983) 7198; F. Diederich, *Angew. Chem. 100* (1988) 372; *Angew. Chem. Int. Ed. Engl. 27* (1988) 362; C. D. Gutsche, *Acc. Chem. Res. 16* (1983) 161; H.-J. Schneider, T. Blatter, *Angew. Chem. 100* (1988) 1211; *Angew. Chem. Int. Ed. Engl. 27* (1988) 1163; A. Collet, *Tetrahedron 43* (1987) 5725.
[6] D. S. Kemp, S. K. Petrakis, *J. Org. Chem. 46* (1981) 5140.
[7] J. Rebek, Jr., L. Marshall, R. Wolak, K. Parris, M. Kolloran, B. Askew, D. Nemeth, N. Islam, *J. Am. Chem. Soc. 107* (1985) 7476.
[8] J. Rebek, Jr., B. Askew, D. Nemeth, K. Parris, *J. Am. Chem. Soc. 109* (1987) 2432.
[9] J. Rebek, Jr., B. Askew, M. Killoran, D. Nemeth, F.-T. Lin, *J. Am. Chem. Soc. 109* (1987) 2426.
[10] J. Rebek, Jr., *Science 235* (1987) 1478.
[11] W. L. Jorgensen, S. Boudon, T. B. Nguyen, *J. Am. Chem. Soc. 111* (1989) 755.
[12] K. B. Lipkowitz, R. Zegarra, *J. Comput. Chem. 10* (1989) 595.
[13] R. Gandour, *Bioorg. Chem. 10* (1981) 169.
[14] R. Meyer, T. K. Ha, H. S. Guntnard, *Chem. Phys. 9* (1975) 393.
[15] K. B. Wiberg, K. E. Laidig, *J. Am. Chem. Soc. 109* (1987) 5935.
[16] D. W. Christianson, R. S. Alexander, *J. Am. Chem. Soc. 111* (1989) 6419; D. W. Christianson, W. N. Lipscomb, *Acc. Chem. Res. 22* (1989) 62.
[17] J. Rebek, Jr., L. Marshall, J. McManis, R. Wolak, *J. Org. Chem. 51* (1986) 1649.
[18] C. L. Perrin, *Acc. Chem. Res. 22* (1989) 268; C. L. Perrin, T. J. Dwyer, J. Rebek, Jr., R. J. Duff, *J. Am. Chem. Soc.*, in press.
[19] J. Rebek, Jr., R. J. Duff, W. E. Gordon, K. Parris, *J. Am. Chem. Soc. 108* (1986) 6068.
[20] L. Marshall, K. Parris, J. Rebek, Jr., S. V. Luis, M. I. Burguete, *J. Am. Chem. Soc. 110* (1988) 5192.
[21] J. Huff, B. Askew, R. J. Duff, J. Rebek, Jr., *J. Am. Chem. Soc. 110* (1988) 5908.
[22] S. C. Zimmerman, K. D. Cramer, *J. Am. Chem. Soc. 110* (1988) 5906.
[23] B. M. Tadayoni, K. Parris, J. Rebek, Jr., *J. Am. Chem. Soc. 111* (1989) 4503.
[24] Y. Li, K. N. Houk, *J. Am. Chem. Soc. 111* (1989) 4505.
[25] M. B. Tadayoni, J. Rebek, Jr., unpublished observations.
[26] R. Gandour, personal communication.
[27] W. H. Landschulz, P. F. Johnson, S. L. McKnight, *Science 240* (1988) 1759; but see also E. K. O'Shea, R. Rutkowski, P. S. Kim, *ibid. 243* (1989) 538.
[28] R. T. Raines, E. L. Sutton, D. R. Straus, W. Gilbert, J. R. Knowles, *Biochemistry 25* (1986) 7142.
[29] J. Rebek, Jr., *Struct. Chem. 1* (1990) 129.
[30] K. S. Ventkatasubban, R. L. Schowen, *Crit. Rev. Biochem. 17* (1984) 1. For alternatives to the charge-relay interpretation, see W. W. Bachovchin, *Biochemistry 25* (1986) 775; A. Warshel, G. Naray-Szabo, F. Sussman, J.-K. Hwang, *ibid. 28* (1989) 3629.
[31] J. B. West, J. Scholten, N. J. Stolowich, J. L. Hogg, A. I. Scott, C.-H. Wong, *J. Am. Chem. Soc. 110* (1988) 3709.
[32] Y. Kyogoku, R. G. Lord, A. Rich, *Proc. Natl. Acad. Sci. USA, 57* (1967) 250; J. Pitha, R. N. Jones, P. Pithova, *Can. J. Chem. 44* (1966) 1045; N. G. Williams, L. D. Williams, B. R. Shaw, *J. Am. Chem. Soc. 111* (1989) 7205, and references cited therein.

[33] S. I. Chan, M. P. Schweitzer, P. O. P. Ts'o, G. K. Helmkamp, *J. Am. Chem. Soc. 86* (1964) 4182.
[34] J. Rebek, Jr., B. Askew, P. Ballester, C. Buhr, S. Jones, D. Nemeth, K. Williams, *J. Am. Chem. Soc. 109* (1987) 5033.
[35] B. Askew, P. Ballester, C. Buhr, K.-S. Jeong, S. Jones, K. Parris, K. Williams, J. Rebek, Jr., *J. Am. Chem. Soc. 111* (1989) 1082; K. Williams, B. Askew, P. Ballester, C. Buhr, K.-S. Jeong, S. Jones, J. Rebek, Jr., *J. Am. Chem. Soc. 111* (1989) 1090.
[36] T. J. Shepodd, M. A. Petti, D. A. Dougherty *J. Am. Chem. Soc. 110* (1988) 1983.
[37] S. B. Ferguson, E. W. Seward, F. Diederich, E. M. Sanford, A. Chou, P. Inocencio-Szweda, C. B. Knobler, *J. Org. Chem. 53* (1988) 5593.
[38] S. K. Burley, G. Petsko, *Science 229* (1985) 23; S. K. Burley, G. Petsko, *J. Am. Chem. Soc. 108* (1986) 7995.
[39] See, for example, R. Osman, S. Topiol, L. Rubenstein, H. Weinstein, *Mol. Pharmacol. 32* (1987) 699.
[40] J. Rebek, Jr., B. Askew, P. Ballester, C. Buhr, A. Costero, S. Jones, K. Williams, *J. Am. Chem. Soc. 109* (1987) 6866.
[41] J. Rebek, Jr., K. Williams, K. Parris, P. Ballester, K. S. Jeong, *Angew. Chem. 99* (1987) 1297; *Angew. Chem. Int. Ed. Engl. 26* (1987) 1244.
[42] K. S. Jeong, J. Rebek, Jr., *J. Am. Chem. Soc. 110* (1988) 3327.
[43] J. Rebek, Jr., J. Schroeder, T. Park, unpublished results.
[44] W. Jorgensen, J. Pranata, *J. Am. Chem. Soc.*, in press. We thank Prof. *Jorgensen* for sharing his results prior to publication.
[45] A. D. Hamilton, D. Van Engen, *J. Am. Chem. Soc. 109* (1987) 5035; A. V. Muehldorf, D. Van Engen, J. C. Warner, A. D. Hamilton, *ibid. 110* (1988) 6561.
[46] For recent developments in DNA triple-helix formation, see: L. J. Maher, B. Wold, P. B. Dervan, *Science 245* (1989) 725; D. Praseuth, L. Perrouault, T. L. Doan, M. Chassignol, N. Thuong, C. Helene, *Proc. Natl. Acad. Sci. USA 85* (1988) 1349.
[47] T. Benzing, T. Tjivikua, J. Wolfe, J. Rebek, Jr., *Science 242* (1988) 266.
[48] A. Echaverren, A. Galan, J.-M. Lehn, J. de Mendoza, *J. Am. Chem. Soc. 111* (1989) 4994.
[49] F. P. Schmidtchen, A. Gleich, A. Schummer, *Pure Appl. Chem. 61* (1989) 1535; G. Müller, J. Riede, F. P. Schmidtchen, *Angew. Chem. 100* (1988) 1574; *Angew. Chem. Int. Ed. Engl. 27* (1988) 1516.
[50] T. Tjivikua, P. Ballester, J. Rebek, Jr. *J. Am. Chem. Soc. 112* (1990) 1249.
[51] For template-directed nucleotide synthesis, see P. M. Pitha, J. Pitha, *Nature New Biol. 98* (1972) 78; G. von Kiedrowski, *Angew. Chem. 98* (1986) 932; *Angew. Chem. Int. Ed. Engl. 25* (1986) 932; J. Visscher, C. G. Bakker, R. van der Woerd, A. Schwartz, *Science 244* (1989) 329.
[52] T. R. Kelly, C. Zhao, G. J. Bridger, *J. Am. Chem. Soc. 111* (1989) 3744.
[53] L. Pauling, *Chem. Eng. News 24* (1946) 1375.
[54] H. D. Lutter, F. Diederich, *Angew. Chem. 96* (1986) 1125; *Angew. Chem. Int. Ed. Engl. 25* (1986) 1125; L. Jimenez, F. Diederich, *Tetrahedron Lett. 30* (1989) 2759, and references therein.
[55] E. Anslyn, R. Breslow, *J. Am. Chem. Soc. 111* (1989) 5972.
[56] D. J. Cram, P. Y.-S. Lam, S. P. Ho, *J. Am. Chem. Soc. 108* (1986) 839; J.-M. Lehn, C. Sirlin, *J. Chem. Soc. Chem. Commun. 1978,* 949.
[57] For the development of this notion in macrocyclic contexts, see R. E. Sheridan, H. W. Whitlock, *J. Am. Chem. Soc. 110* (1988) 4071 and earlier work by this group.
[58] C. G. Swain, J. F. Brown, *J. Am. Chem. Soc. 74* (1952) 2534, 2538.
[59] J. Wolfe, D. Nemeth, A. Costero, J. Rebek, Jr., *J. Am. Chem. Soc. 110* (1988) 983.
[60] E. J. Corey, R. A. Sneen, *J. Am. Chem. Soc. 78* (1956) 6279.
[61] B. Capon, A. K. Siddhanta, C. Zucco, *J. Org. Chem. 50* (1985) 3580; B. Capon, A. K. Siddhanta, *ibid. 49* (1984) 255.
[62] J. Wolfe, unpublished observations; for a discussion, see also J. Rebek, Jr., *J. Inclusion Phenom. 7* (1989) 7.
[63] K. D. Janda, D. Schloeder, S. J. Benkovic, R. A. Lerner, *Science 241* (1988) 1188.
[64] E. Baldwin, P. G. Schultz, *Science 245* (1989) 1104; Review: P. G. Schultz, *Angew. Chem. 101* (1989) 1336; *Angew. Chem. Int. Ed. Engl. 28* (1989) 1283.
[65] J. S. Lindsey, I. C. Schreiman, H. C. Hsu, P. C. Kearney, A. M. Marguerattaz, *J. Org. Chem. 52* (1987) 827.
[66] J. S. Lindsey, P. C. Kearney, R. J. Duff, P. T. Tjivikua, J. Rebek, Jr., *J. Am. Chem. Soc. 110* (1988) 6575.
[67] A. D. Hamilton, J.-M. Lehn, J. L. Sessler, *J. Am. Chem. Soc. 108* (1986) 5158.
[68] I. O. Sutherland, *Pure Appl. Chem. 61* (1989) 1547.
[69] F. Ebmeyer, F. Vögtle, *Angew. Chem. 101* (1989) 95; *Angew. Chem. Int. Ed. Engl. 28* (1989) 79 and references therein.
[70] J. Huff, unpublished observations.
[71] J. D. Kilburn, A. MacKenzie, W. C. Still, *J. Am. Chem. Soc. 110* (1988) 1307.
[72] K. T. Chapman, W. C. Still, *J. Am. Chem. Soc. 111* (1989) 3075.
[73] C. S. Wilcox, L. M. Greer, V. Lynch, *J. Am. Chem. Soc. 109* (1987) 1865.
[74] J. Rebek, Jr., B. Askew, M. Doa, P. Ballester, *J. Am. Chem. Soc. 109* (1987) 4119.
[75] W. H. Pirkle, T. C. Pochapsky, *Chem. Rev. 89* (1989) 347.
[76] J. Rebek, Jr., P. Ballester, unpublished observations. For similar sandwiching of carboxylic acids, see A. Echevarren, A. Galan, J.-M. Lehn, J. de Mendoza, *J. Am. Chem. Soc. 111* (1989) 4994.
[77] V. Gerlach, S. Hünig, *Angew. Chem. 99* (1987) 1323; *Angew. Chem. Int. Ed. Engl. 26* (1987) 1283; for other asymmetric protonations, see L. Duhamel, S. Fouquay, J.-C. Plaquevent *Tetrahedron Lett. 27* (1986) 4975; C. Fehr, J. Galindo, *J. Am. Chem. Soc. 110* (1988) 6909.
[78] K. Williams, unpublished observations.
[79] K. S. Jeong, K. Parris, P. Ballester, J. Rebek, Jr., *Angew. Chem. 102* (1990), in press; *Angew. Chem. Int. Ed. Engl.* 29 (1990), in press.
[80] D. P. Curran, K.-S. Jeong, T. A. Heffner, J. Rebek, Jr. *J. Am. Chem. Soc. 111* (1989) 9238.
[81] See, for example P. K. Coughlin, S. J. Lippard, *J. Am. Chem. Soc. 106* (1984) 2328.
[82] S. C. Zimmerman, W. Wu, *J. Am. Chem. Soc. 111* (1989) 8054.
[83] J. C. Adrian, Jr., C. S. Wilcox, *J. Am. Chem. Soc. 111* (1989) 8055.
[84] T. W. Bell, J. Liu, *J. Am. Chem. Soc. 110* (1988) 3673. For macrocyclic structures for binding urea, see C. J. van Staveren, D. E. Fenton, D. N. Reinhoudt, J. van Eerden, S. Harkema, *J. Am. Chem. Soc. 109* (1987) 3456.
[85] T. R. Kelly, M. P. Maguire, *J. Am. Chem. Soc. 109* (1987) 6549.
[86] Y. Aoyama, A. Yamagishi, M. Asagawa, H. Toi, H. Ogoshi, *J. Am. Chem. Soc. 110* (1988) 4076; see also Y. Aoyama, T. Motomura, H. Ogoshi, *Angew. Chem. 101* (1989) 922; *Angew. Chem. Int. Ed. Engl. 28* (1989) 921.
[87] F. H. Kohnke, J. F. Stoddart, *Pure Appl. Chem. 61* (1989) 1581; F. H. Kohnke, J. P. Mathias, J. F. Stoddart, *Angew. Chem. 101* (1989) 1129; *Angew. Chem. Int. Ed. Engl. 28* (1989) 1103; *Adv. Mater. 1* (1989) 275.
[88] J. C. Sherman, D. J. Cram, *J. Am. Chem. Soc. 111* (1989) 4527.
[89] J.-M. Lehn, A. Rigault, *Angew. Chem. 100* (1988) 1121; *Angew. Chem. Int. Ed. Engl. 27* (1988) 1095; A. Schepartz, J. P. McDevitt, *J. Am. Chem. Soc. 111* (1989) 5976.
[90] Y. Aoyama, Y. Tanaka, S. Sugahara, *J. Am. Chem. Soc. 111* (1989) 5397.
[91] M. W. Hosseini, J.-M. Lehn, *J. Am. Chem. Soc. 104* (1982) 3525, R. Breslow, R. Rajagopalan, J. Schwartz, *ibid. 103* (1981) 3041, J. Rebek, Jr., D. Nemeth, P. Ballester, F.-T. Lin, *ibid. 109* (1987) 3474.
[92] S.-K. Chang, A. D. Hamilton, *J. Am. Chem. Soc. 110* (1988) 1318.

On the Conformation and Structure of Organometal Complexes in the Solid State: Two Studies Relevant to Chemical Synthesis

By Soroosh Shambayati, William E. Crowe, and Stuart L. Schreiber *

Dedicated to Professor Jack Dunitz

Conformational preferences of two classes of organometal complexes have been surveyed by inspecting the Cambridge Structural Database (CSD). Lewis acid carbonyl complexes demonstrate a variety of coordination geometries, depending on the electronic and steric requirements of the carbonyl ligands and the nature of the Lewis acid. Similarly, the solid-state conformation of various π-bonding ligands in metal acyl, metal nitrosyl, metal acetylene, and metal imido complexes is revealed. These insights have stimulated the development of a conformational model that is based on considerations of π-bond hybridization and frontier molecular orbital theory. The analyses are relevant to the mechanism and transition structures of many synthetically important transformations. A deeper understanding of the conformational properties of organometal complexes, based on accurate structural information, will likely expedite the design and improvement of metal-mediated processes.

1. Introduction

Soon after the advent of X-ray crystallography, it became clear that crystal structures can uncover more than just a simple picture of the covalent connectivity of molecular entities.[1] The realization of the potential of X-ray crystallography in providing information regarding two central questions in chemistry—namely, reactivity and the three-dimensional conformation of molecules—rapidly led to the foundation of the powerful field of structural chemistry.[2] In organic chemistry, perceptions of bonding and reactivity have benefited from this structural approach enormously. Although many of the important questions remain unanswered, many of the ground-state physicochemical properties of molecules can be predicted fairly reliably by the structural theory of organic chemistry. At first, it seemed implausible that static, crystalline species could reveal any information regarding the dynamics of transition states. However, the pioneering work of *Dunitz, Bürgi,* and coworkers in the early 1970s showed that, in certain instances, even these parameters can be derived from the inspection of a family of crystal structures.[3] Hence, this approach came to be known as the "structure–reactivity correlation" method.[4]

Today, largely due to the efforts of the Cambridge Crystallographic Data Centre[5] and partly due to the ready availability of powerful and efficient computing machines, thorough searches of more than 70000 crystal structures of organic, inorganic, and organometallic compounds can be achieved with reasonable ease and speed. Attracted by the wealth and accuracy of the information provided by crystal structure analyses, an ever-growing number of organic chemists now utilize this powerful tool to infer mechanistic and conformational hypotheses based on structural data.[6] This approach has been particularly fruitful in the study of weak interactions such as hydrogen bonding[7] and donor–acceptor interactions of Lewis acid–Lewis base pairs.[8]

In this review we shall describe how analyses of crystal structures led to the formulation of principles and hypotheses regarding the conformational preferences of two classes of organometal complexes. First, we report on recent insights into carbonyl–Lewis acid complexation. Next, the influence of π bonding on the conformation of a variety of ligands attached to transition metals will be addressed. In both instances the original search of the Cambridge Structural Database (CSD) was prompted by a simple question regarding the conformation of a complex or an intuitive hunch about the origins of an unusual observation. Unfortunately, even after careful inspection of numerous crystal structures, the answers to the original questions were not altogether transparent. However, during this exercise many important lessons were learned and some of the missing links in the context of the more general problem were pinpointed. It is hoped that these observations will not only lead to a better understanding of the conformational properties of organometal complexes, but also guide future efforts in related areas of research.

2. Carbonyl–Lewis Acid Complexation

A Lewis basic carbonyl group can be activated through coordination to a metal-centered Lewis acid, with profound reactivity and stereochemical consequences. In the context of asymmetric synthesis, many of the Lewis acid–mediated reactions are known to proceed with improved stereoselectivities as compared to their non-catalyzed counterparts, and, most recently, a variety of chiral Lewis acids have been used as remarkably efficient catalysts for carbonyl addition processes.[9] Although the origins of many of the effects brought about by Lewis acids are still poorly understood, it is clear that the conformational preferences of the Lewis acid carbonyl complex are ultimately responsible for determining the stereochemical course of Lewis acid–mediated reactions. In

[*] Prof. S. L. Schreiber, S. Shambayati
Department of Chemistry, Harvard University
Cambridge, MA 02138 (USA)
Dr. W. E. Crowe
Department of Chemistry, Massachusetts Institute of Technology
Cambridge, MA 02139 (USA)

 © VCH Verlagsgesellschaft mbH, D-6940 Weinheim, 1990 0570-0833/90/0303-0256 $ 02.50/0

Sections 2.1–2.3, some of the crystallographic studies on the complexes of Lewis acids with organic carbonyl ligands will be discussed. The relevance of the crystallographic data to the general conformational biases of such complexes will be the focus of this discussion.

2.1. Conformational Issues

Factors that may influence the reactivity and conformation of Lewis acid carbonyl complexes can be classified broadly into three categories. The primary question in analyzing a Lewis acid carbonyl complex concerns the mode of coordination. Both η^1 (σ) bonding and η^2 (π) bonding of Lewis acids to carbonyl ligands are observed (Fig. 1), and, as will be seen, crystallographic studies seem to provide fairly straightforward rules for the prediction of each mode of coordination.

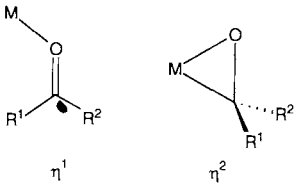

Fig. 1. σ (left) vs. π (right) bonding in Lewis acid carbonyl complexes.

Second, the exact location of the Lewis acid with respect to its carbonyl ligand is of interest. Specifically, knowledge of the range and limits of several parameters, such as the Lewis acid–oxygen distance r and the angles θ and ϕ in Figure 2, is an obvious requirement for the prediction of the structure of these complexes.

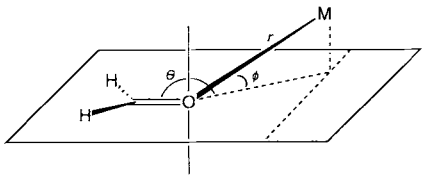

Fig. 2. Definition of the parameters r, θ and ϕ.

Third, the effect of Lewis acid coordination on the inherent conformational preferences adjacent to the carbonyl group should be considered. In particular, how is the s-*cis*–s-*trans* equilibrium of α,β-unsaturated carbonyls or the energy

Stuart Lee Schreiber was born in 1956 and raised in Virginia. His undergraduate studies were at the University of Virginia in Charlottsville from 1973 to 1977. It was at Virginia, in the laboratory of Professor Richard J. Sundberg, that he first discovered the excitement of organic chemical research. He spent the following years (1977–81) at Harvard University in the Chemistry Department, where he received his doctorate with Professors R. B. Woodward and Yoshito Kishi. His first appointment, as Assistant Professor, was at Yale University (1981), where he was promoted to Associate Professor (1984) and then Professor (1986) of Chemistry. In 1988, he returned to Harvard to accept a position in the Chemistry Department as Professor of Chemistry. His research interests include the synthesis and conformational analysis of complex systems, including complexes of ligands and their biological receptors.

Soroosh Shambayati was born in Tehran, Iran, on December 8, 1964. After receiving his secondary education in Sweden, he moved to the United States in 1982. He studied chemistry at Occidental College under the direction of Professor Donald Deardorff, before joining Professor Schreiber's research group at Yale University in 1986. In 1987 he followed Professor Schreiber to Harvard University, where he is now a fourth-year graduate student.

William E. Crowe was born in Salem, Massachusetts, on May 31, 1960. He received a B.S. degree from the California Institute of Technology and earned his Ph.D. under Professor Stuart Schreiber at Yale University. Currently, Dr. Crowe is an NIH postdoctoral fellow at the Massachusetts Institute of Technology under the direction of Professor Richard Schrock.

profile for the rotation about the CO–C_α bond of nonconjugated carbonyls affected by Lewis acid complexation (Fig. 3)?

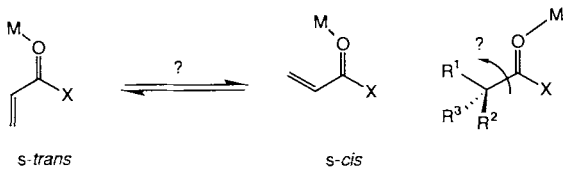

Fig. 3. How is rotation about the CO–C_α bond of carbonyls influenced by Lewis acid coordination?

2.2. Crystal Structures of Lewis Acid Carbonyl Complexes

2.2.1. *Cationic Alkali-Metal Lewis Acids*

Some of the earliest inquiries into such questions were performed by *Dunitz, Seebach,* and co-workers. In their report of the crystal structure of the LiBr–acetone complex, these researchers discussed the conformational biases of alkali–metal carbonyl complexes.[10] In particular, the LiBr–acetone complex assumes a dimeric form in the solid state, in which each lithium ion is coordinated by two molecules of acetone through the carbonyl lone-pair electrons with a bent, planar geometry in a tetrahedral environment (Fig. 4). The

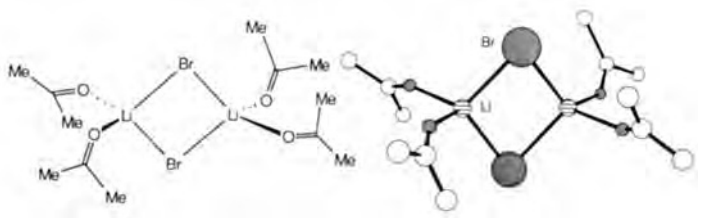

Fig. 4. Crystal structure of LiBr–acetone complex [10].

Li–O bond length is 2.0 Å, the Li–O–C angle 145°. In order to determine the generality of these observations in other alkali-metal carbonyl complexes, the researchers also conducted a general search of the Cambridge Structural Database. Of the nine crystal structures that were analyzed in this study, six contained $Li^\oplus$, two $Na^\oplus$, and one $K^\oplus$ as the Lewis acid bound to the carbonyl ligands. The coordination angle θ for $Li^\oplus$ (cf. Fig. 2) was consistently found to be less than 180° (120–156.3°), but large distortions from planarity ($\phi \neq 0°$) seemed to occur randomly. Furthermore, the Li–O bond distance showed no linear dependence on the Li–O–C–X dihedral angle.

The crystal structures of $Na^\oplus$ complexes, however, showed that linear and bent geometries are equally accessible and bending out of the plane of the carbonyl was once again observed (Fig. 5).[11]

The researchers concluded that the potential energy surface for carbonyl coordination to alkali metals is likely to be fairly flat with respect to changes in the M–O–C angle and the M–O–C–X dihedral angle.

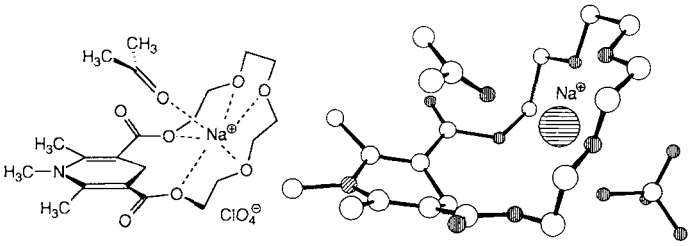

Fig. 5. Linear complexation of a $Na^\oplus$–acetone complex [11].

A more recent search of the CSD for crystal structures of alkali-metal carbonyl complexes also confirmed these results.[12] The average Li–O bond length and the Li–O–C bond angle were found to be 1.99 ± 0.07 Å and 139 ± 3°, respectively. Of the 23 examples found, 9 exhibited coordination by more than 10° out of the plane of the carbonyl group.

Thus, cationic alkali-metal Lewis acids do not exhibit any strong directional preferences upon coordination to carbonyls. In particular, bending toward the π cloud of the carbonyl ($\phi \neq 0$) with no significant lengthening of the M–O bond is commonly observed. Coordination seems to occur from the direction that best satisfies the cation's electron demand and minimizes steric interactions. These, in turn, depend on the coordination number of the cation, the relative size and electronic properties of the ligands, and, in the solid state, on crystal packing forces.

Two remarkable examples of the diversity of $Li^\oplus$–carbonyl coordination can be found in the crystal structures of $Li^\oplus$ bound to the cyclic decapeptides antamanide and perhydroantamanide, reported by *Karle*.[13,14] In the $Li^\oplus$–antamanide complex (Fig. 6), for instance, lithium was found to

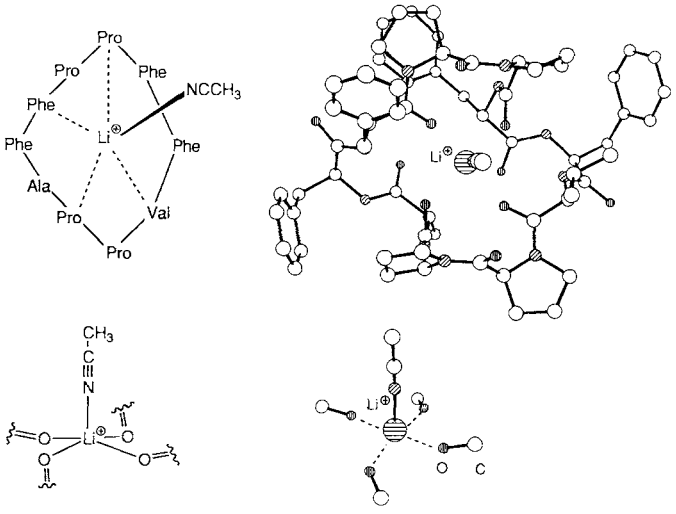

Fig. 6. Crystal structure of $Li^\oplus$–antamanide complex [13].

be pentacoordinated to four carbonyl oxygens and the nitrogen atom of an acetonitrile solvent molecule in a pseudo-square-pyramidal arrangement. In this structure, the Li–O bond lengths and Li–O–C bond angles are similar to the values discussed previously and are consistent with the principles of the foregoing discussion.

It is interesting to note that ab initio, gas-phase calculations on the $Li^{\oplus}$–carbonyl complexes predict a strong preference for the linear, planar geometry ($\theta = \phi = 0°$), wherein the main source of metal–carbonyl interaction is electrostatic ion–dipole attraction.[15, 16] This discrepancy with the experimental observations may be an artifact of either the assumption of in vacuo conditions or the restriction of 1:1 stoichiometry. Thus, bent geometries may have been predicted had solvent molecules or additional carbonyl ligands been included in these calculations.

2.2.2. *Main-Group and Early-Transition-Metal Lewis Acids*

Relative to alkali-metal cations, neutral Lewis acids seem to perform much more consistently. The crystal structure of the BF_3–benzaldehyde complex may serve as a representative example (Fig. 7).[17] Here the Lewis acid is placed 1.59 Å

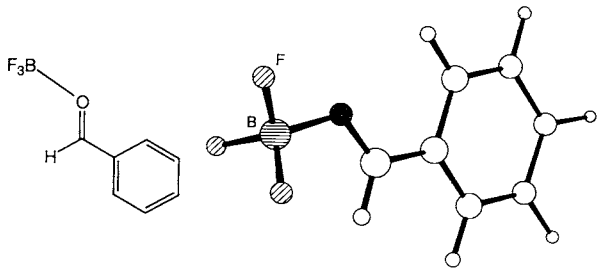

Fig. 7. Crystal structure of BF_3–benzaldehyde complex [17].

from the carbonyl oxygen, along the direction of the oxygen lone pair and *anti* to the larger phenyl substituent.[18]

Although crystal structures of other bimolecular complexes of carbonyls with boronic Lewis acids have not been reported, a number of intramolecular chelates have been detected in the solid state.[19–21] In all these cases boron is found to lie in the direction of the carbonyl lone pair with no more than an 11° distortion (ϕ) away from the best plane of the carbonyl group. The average B–O bond length (r) is 1.581 ± 0.019 Å and the B–O–C angle lies between 112 and 119°.

A search of the CSD files for the Al–O=C substructure revealed thirty such interactions with Lewis acidic aluminum atoms from 23 crystal structures.[13] Mean values for the Al–O distances (r) and Al–O–C bond angles were found to be 1.88 ± 0.09 Å and 136 ± 4°, respectively, and aluminum was found to lie within 18° (ϕ) of the carbonyl plane.

The crystal structure of the $AlCl_3$–tetramethylurea (TMU) complex shows a 1:1 adduct (Fig. 8) in which aluminum binds to the carbonyl lone-pair electrons at an angle of 132.5° and at a distance of 1.78 Å.[22] The C–O bond length (1.239 Å) is approximately 0.06 Å longer than that of unbound TMU and 0.03 Å longer than in the corresponding Me_2SnCl_2–TMU complex. The Lewis acid is slightly out of the plane of the carbonyl, although the dimethylamino group *syn* to aluminum is completely twisted out of conjugation to avoid steric interactions.

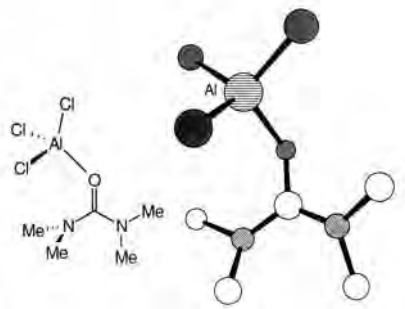

Fig. 8. Crystal structure of $AlCl_3$–TMU complex [22].

Based on the average values revealed in the CSD searches (see above), it may be reasonable to propose that the structure in Figure 8 reflects the "idealized" or low-energy mode of coordination to carbonyls for aluminum-centered Lewis acids. It would be interesting to see how distortions away from such an arrangement may come about. Imposition of steric congestion through bulky substituents is one way to address this question. The crystal structure of the complex formed between (2,6-di-*tert*-butyl-4-methyl)phenoxydiethylaluminum and methyl *p*-toluate was recently reported by *Ittel* et al. (Fig. 9).[23] In this structure a pseudo-tetrahedrally

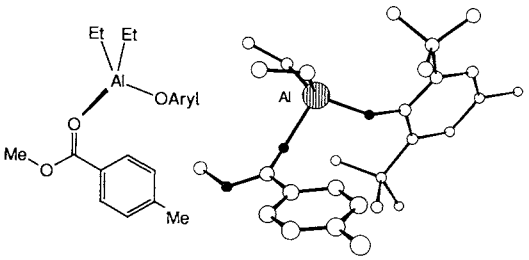

Fig. 9. Crystal structure of $Et_2Al(OAryl)$–methyl *p*-toluate complex [23]. Aryl = 2,6-tBu$_2$-4-Me-C_6H_2.

coordinated aluminum is positioned 1.89 Å from the carbonyl ligand. The Al–O–C angle of 145.6° is on the more linear end of the Al–O–C angle spectrum, but, more interestingly, the Al–O–C–C torsion angle (49.9°) shows considerable bending toward the π plane. Clearly, this distortion from the idealized structure is a result of the unusually bulky di-*tert*-butylphenoxide ligand on the Lewis acid, coupled with the fact that in *Z* aromatic esters both sp^2 lone pairs are fairly hindered. Notice that other available mechanisms for relief of steric strain were not employed. Either twisting of the phenyl substituent or alteration of an idealized *Z*-ester conformation could have accommodated a more planar Lewis acid complex, but neither occurs to any considerable extent (τ(O-C-C-C) = 12.1°, τ(O-C-O-C) = 4.1°). Furthermore, a linear Lewis acid complex would also avoid steric interactions with the carbonyl substituents, but this mode of coordination seems to be excluded as well. These results suggest that the energetic barrier for out-of-plane bending of the Lewis acid is less steep and probably lower than the barrier for either *E*/*Z* ester isomerization, rotation about the phenyl–carbonyl C–C bond, or *in-plane distortion to a linear structure*. The latter proposition is in sharp contrast to theoretical predictions.[24]

Ittel's crystal structure (Fig. 9) also supports a model proposed by *H. Yamamoto* et al. for the complexation of bulky aluminum Lewis acids to carbonyls.[25] These researchers have attributed the preponderance of axial attack of nucleophiles on cyclohexanones such as **1** (formation of **3**), in the

presence of the Lewis acid MAD, to out-of-plane complexation (**2**), as depicted in Figure 10.

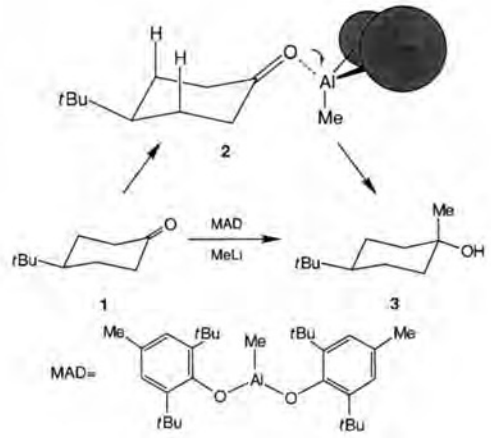

Fig. 10. Out-of-plane complexation of MAD to carbonyls leads to axial attack of nucleophiles on cyclohexanones such as **1** [25].

When a Lewis acid possesses two empty coordination sites, another degree of complexity is added to the structural issues discussed above. Titanium(IV) Lewis acids, for example, show a strong preference for a six-coordinate, octahedral arrangement. Thus, the acid:carbonyl stoichiometry for these complexes is often 1:2 or, when only a single equivalent of the carbonyl base is present, dimeric structures with bridging ligands are observed. The crystalline 1:1 adduct of $TiCl_4$ and ethyl acetate, for example, contains dimeric units of two octahedrally coordinated titaniums with bridging chlorine atoms (Fig. 11).[26] The 2.03-Å-long Ti–O bond is almost

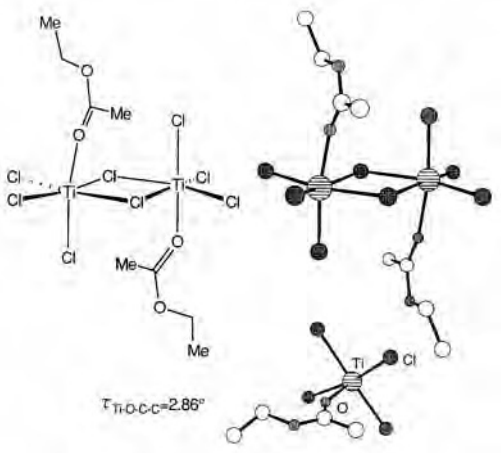

Fig. 11. Crystal structure of $TiCl_4$–ethyl acetate complex [26]. Bottom right: Side view of in-plane titanium coordination.

coplanar with the carbonyl group (τ(Ti-O-C-C) = 2.86°) and the Ti–O–C angle is 152°.

These values agree well with the average Ti–O bond lengths and Ti–O–C bond angles derived from searches of the CSD files (mean Ti-O = 2.14 ± 0.07 Å), though the Ti–O–C angle is on the wider side of the observed range (mean Ti-O-C = 125 ± 12°).[12] The *Z* conformation of the ester is retained (τ(O-C-O-C) = 2.6°) due to *syn* coordination of the Lewis acid to the methyl substituent.

In line with the behavior of aluminum-centered Lewis acids, deviations from the idealized conformation are observed when steric congestion is imposed on the structure. This point is illustrated in the crystal structure of the $TiCl_4$–ethyl anisate complex (Fig. 12).[27] Although at first glance

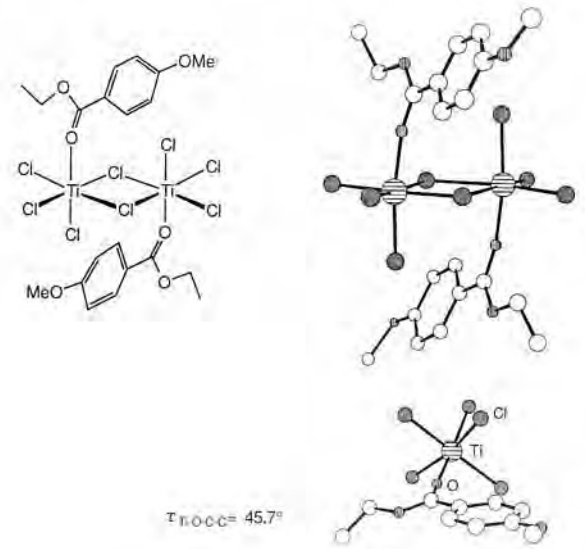

Fig. 12. Crystal structure of $TiCl_4$-ethyl anisate complex [27]. Bottom right: Side view of out-of-plane titanium coordination.

the main features of this complex (dimeric complex, octahedral titanium, etc.) are very similar to those of the $TiCl_4$–ethyl acetate structure, out-of-plane bonding to the carbonyl clearly distinguishes the two structures. The Ti–O–C–C dihedral angle is 45.7° and the Ti–O–C angle has now opened up to 168.7°. The *Z* conformation of the ester is still intact (τ(O-C-O-C) = 1.4°), and the Lewis acid is bound more or less *syn* to the phenyl substituent, which, in turn, is twisted out of conjugation and away from the Lewis acid by 13.0°. These structural features are very similar to those of the bulky aluminum Lewis acid complex (Fig. 9) and one may expect them to be quite general in similar systems. Interestingly, distortions from the idealized structures are more prominent for the titanium complex, which may suggest that, in the dimeric form, $TiCl_4$ is in fact even larger than the aryloxyaluminum reagent or that π distortion occurs more readily for Ti than for Al.

Extreme out-of-plane bonding is observed in the crystalline complex of $TiCl_4$ and acryloylmethyl lactate (Fig. 13).[28] In this structure Ti is bound by two ester car-

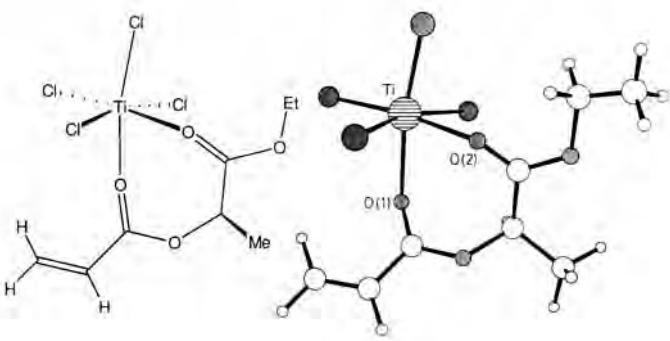

Fig. 13. Crystal structure of $TiCl_4$–acryloylmethyl lactate complex [28].

bonyls in a seven-membered ring chelate. Both carbonyls are bound out-of-plane with τ(Ti-O(1)-C-C) = 63.6° and τ(Ti-O(2)-C-C) = − 132.2°. Both esters, however, remain very close to planarity (τ_1 = 8.8°, τ_2 = 4.1°) and in the preferred *Z* conformation. Furthermore, due to the presence of a chelate ring, the Lewis acid is *anti* to the acrylate double bond and the enoate adopts an s-*cis* geometry. It is difficult to rationalize out-of-plane bonding in this case since direct steric interactions appear to be unimportant. Moreover, out-of-plane bonding cannot be the result of chelation, since crystal structures of $TiCl_4$ chelated by acetic anhydride (Fig. 14, left)[29] or 3,3-dimethyl-2,4-pentanedione[30] show no evidence for π bonding. Even the seven-membered ring

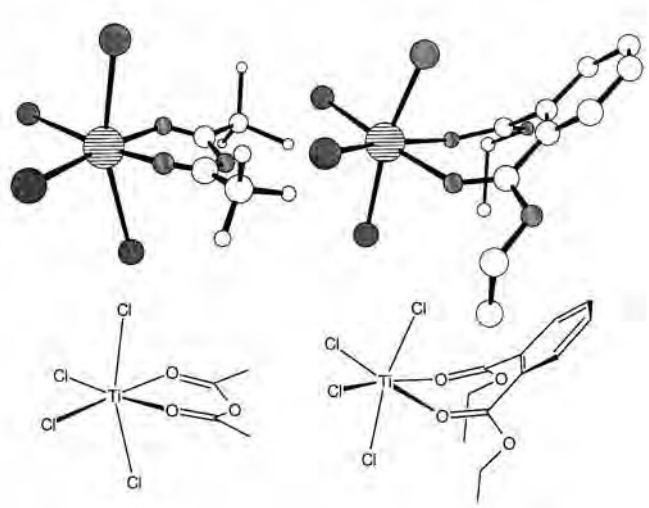

Fig. 14. Crystal structure of two $TiCl_4$ chelates [29, 31].

diester chelate of $TiCl_4$ with diethyl phthalate (Fig. 14, right) has the Lewis acid coplanar with the carbonyl ligands.[31] Another noticeable feature of the chelated structures is that they are all monomeric, probably due to the ability of the bidentate ligands to satisfy titanium's desire for hexacoordination and octahedral geometry.

The crystal structures of titanocene cations containing coordinated dimethylformamide (DMF) also support the idea of loose angle dependence of carbonyl coordination to titanium Lewis acids. For example, the $[Cp^*_2TiCl]^{\oplus}$–DMF complex displays a near-linear Ti–O–C angle of 167.0° and a Ti–O–C–N dihedral angle of − 140.2° (Fig. 15).[32] Similar semilinear η^1 bonding is also observed for the $[Cp^*_2Ti]^{2\oplus}$–$(DMF)_2$ complex.[32] In this structure the two Ti–O–C angles are 148.1° and 158.2° and the respective dihedral angles 163.6° and 174.2°.

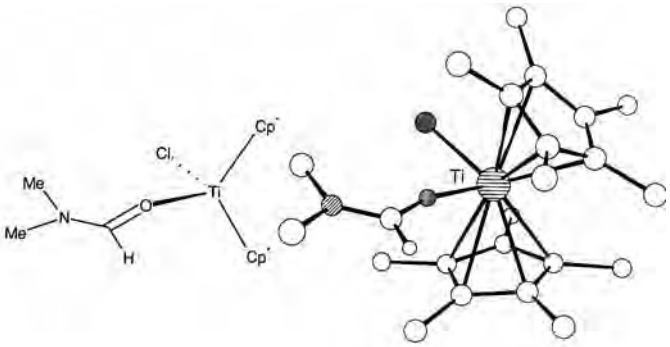

Fig. 15. Crystal structure of $[Cp^*_2TiCl]^{\oplus}$–DMF complex [32].

Zirconocene complexes with ketone and aldehyde ligands show yet another interesting variety of coordination chemistry. In the solid state, carbonyl-bound zirconocenes are often found η^2-coordinated and in dimeric units. The structure of the zirconocene–benzophenone complex is illustrative (Fig. 16).[33] In this structure the observed Zr–O–C geometry, the benzophenone C–O bond lengths (1.425 and 1.419 Å), and the Zr–C distances (2.346 and 2.35 Å) indicate a π-bonded metallaoxirane conformation. The fundamentally different modes of coordination for the related zirconocene and titanocene structures are doubtless a result of the electronic requirements of the Lewis acid. Thus, η^2 bonding seems to be the preferred mode of coordination for the more electron-rich zirconium complexes, while η^1 complexation is observed with the more highly oxidized titanocene cations (also see Section 2.2.3).

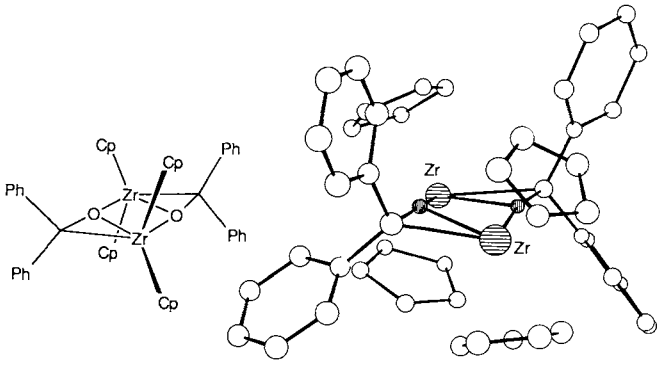

Fig. 16. Crystal structure of the Cp_2Zr–benzophenone dimer [33].

NMR spectroscopic studies indicate that in solution tin-derived Lewis acids, like titanium, prefer to form 1:2 acid:carbonyl or 1:1 chelated adducts.[34] Consistent with these findings, the crystal structure of $SnCl_4$–4-*tert*-butylbenzaldehyde shows a 1:2 stoichiometry with two nonequivalent aromatic aldehydes *cis* to one another around the octahedrally coordinated tin atom (Fig. 17).[34]

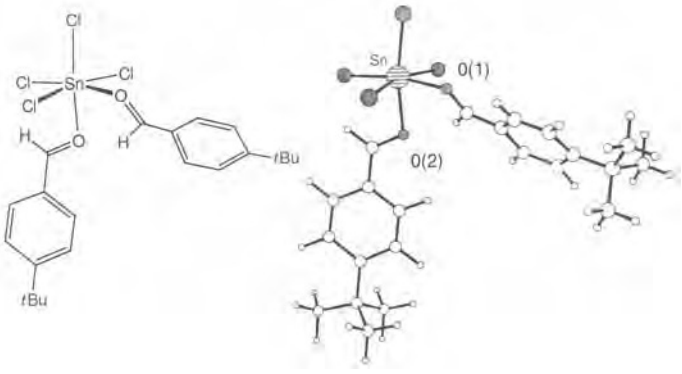

Fig. 17. Crystal structure of the $SnCl_4$–4-*tert*-butylbenzaldehyde complex [34].

Similar to the BF_3–benzaldehyde complex (Fig. 7), tin lies within the carbonyl plane with respect to both aldehydes (τ_1 = 2°, τ_2 = 4°), in the direction of sp^2-hybridized lone

pairs (Sn-O(1)-C = 128°, Sn-O(2)-C = 126.2°) and *anti* to the aromatic ring.

These measurements and the Sn–O bond lengths (2.23 Å) are close to the average values of Sn–carbonyl bond angles and bond lengths found in the CSD files (Sn-O = 2.3 ± 0.1 Å; Sn-O-C = 127 ± 10°).[12] However, the 1:2 stoichiometry and the *cis* relationship of the carbonyl ligands are not universal. Only slight alterations in the nature of the Lewis acid or its ligands are necessary to alter this arrangement. For example, an X-ray analysis of the Ph_2SnCl_2–*p*-dimethylaminobenzaldehyde complex shows a monomeric 1:1 complex with a trigonal-bipyramidally pentacoordinated tin atom (Fig. 18).[35] Although neither the Sn–O bond

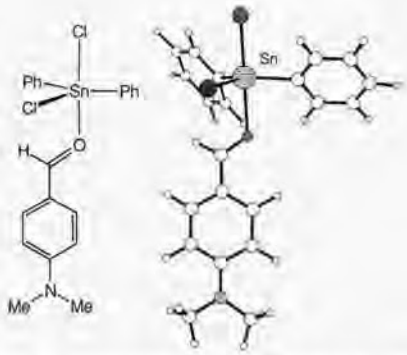

Fig. 18. Crystal structure of Ph_2SnCl_2–*p*-NMe_2-C_6H_4-CHO complex [35]

length (2.3 Å), nor the bond angles (Sn-O-C = 121°, τ(Sn-O-C-C) = 4°), nor the *anti* geometry of coordination have changed significantly, compared to the $SnCl_4$ complex (Fig. 17), the environment about the Sn atom is clearly different. It is likely that these changes are caused by the substitution of chlorines for aryl groups on the Lewis acid. Thus, crystal structures of Ph_3SnCl–TMU,[36] Me_2SnCl_2–TMU,[37] Me_3SnCl–diacetonetriphenylphosphorane,[38] and Me_2SnCl_2–salicaldehyde[39] all feature pentacoordinated, trigonal-bipyramidal 1:1 adducts, while $SnX_4 \cdot 2\,L$ (X = Cl, Br, I; L = urea or thiourea) complexes contain *cis*-octahedrally coordinated tin centers.[40] The *cis* and *trans* stereochemistry of the octahedral complexes seems to depend on the size and the basicity of the base, as well as on the nature of the Lewis acid. Me_2SnCl_2–DMU[37] and $SnCl_4$–ethyl cinnamate[41] are both *trans*-octahedral 1:2 complexes. The latter complex is particularly relevant to the discussion of the conformational preferences of α,β-unsaturated carbonyl complexes (Fig. 19). Here the ligand adopts a *Z*-s-*trans* conformation with tin coordinated *syn* to the double bond. The Sn–O–C–C dihedral angle of 21° indicates some out-of-plane bonding although not as much as in the titanium complexes.

Crystal structures of chelated tin Lewis acids have also been obtained. Recently, X-ray analysis of two five-membered chelates of $SnCl_4$ were reported by *Reetz* et al.[42] $SnCl_4$ complexes of 2-benzyloxy-3-pentanone and methoxyacetophenone are both 1:1 monomeric chelates with distorted octahedral geometry (Fig. 20). In the former complex (Fig. 20, left), tin is apparently coplanar with the carbonyl plane (10° puckering of the stannacycle) at a distance of

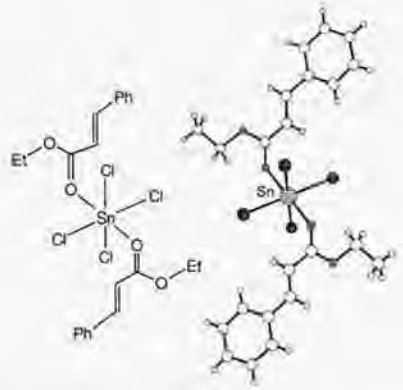

Fig. 19. Crystal structure of $SnCl_4$–ethyl cinnamate complex [41].

2.184(3) Å away from the carbonyl oxygen. More importantly, the ether group is planar and the ether oxygen seems to coordinate to the Lewis acid through an sp^2-like lone pair. This observation lends credence to the proposal of *Keck* et al. for $A^{1,3}$-like interactions between the oxygen protecting group and a second β-substituent in chelation of β-alkoxy aldehydes.[43] Methoxyacetophenone chelates $SnCl_4$ in much the same way (Fig. 20, right).[42] There are, however,

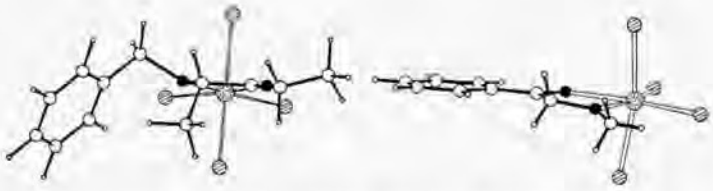

Fig. 20. Crystal structures of two $SnCl_4$ chelates [42]. Left: With 2-benzyloxy-3-pentanone. Right: With methoxyacetophenone. ◎ = Sn, ◍ = Cl, ● = O.

two distinct conformations about the ether oxygen in these crystals. In one conformer, the ether group is planar with sp^2-like donation to the Lewis acid, while in the second conformer (not shown) the ether oxygen is better described as sp^3-hybridized and pseudo-tetrahedral.

2.2.3. Late-Transition-Metal Lewis Acids

Despite the focus of the previous section on the most commonly utilized Lewis acids in organic synthesis, a much larger body of data regarding the structure of donor–acceptor complexes of late transition metals with carbonyls exists. Although a comprehensive treatment of this subject is beyond the scope of the present discussion, it is nonetheless worthwhile to consider the structural features of some of these complexes briefly, since many demonstrate novel and unusual interactions with the carbonyl group.[44]

To begin with, one can consider those high-valent transition metals that seem to behave analogously to the Lewis acids discussed thus far. The crystal structure of a cationic iridium complex, $[IrH_2(Me_2CO)_2PPh_3]BF_4$, shows *cis* coordination of two acetone ligands to an octahedrally coordinated iridium atom (Fig. 21).[45] Iridium is coordinated to the lone pairs of the acetone ligands and is coplanar with the

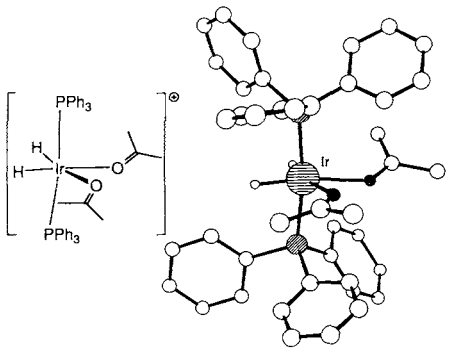

Fig. 21. Crystal structure of $[IrH_2(Me_2CO)_2PPh_3]BF_4$ [45] (anion omitted).

carbonyl groups at an Ir–O–C angle of 133.1° for one acetone ligand and 134.9° for the other. Aside from the interest in this complex due to its role as an active dehydrogenation catalyst,[46] one can also regard it as an effective Lewis acid towards acetone, since it seems to possess all the necessary structural characteristics.

Dicarbonylcyclopentadienyliron cation, $[CpFe(CO)_2]^{\oplus}$ ($\{Fp\}^{\oplus}$), is another reactive Lewis acid. This 16-electron complex is known to coordinate ethers, nitriles, and various carbonyl-containing compounds quite effectively and with 1:1 stoichiometry. The resulting 18-electron complexes are often stable, crystalline compounds and the crystal structures of a few of them have been solved.[12, 47, 48]

X-ray analysis of $[\{Fp\}(cyclohexenone)]PF_6$, for instance, shows iron σ-bonded in the plane of the carbonyl ligand (τ(Fe-O-C-C) = 3.7(9)°) with an Fe–O–C angle of 132.81(4)° (Fig. 22).[12, 47] Interestingly, iron is coordinated

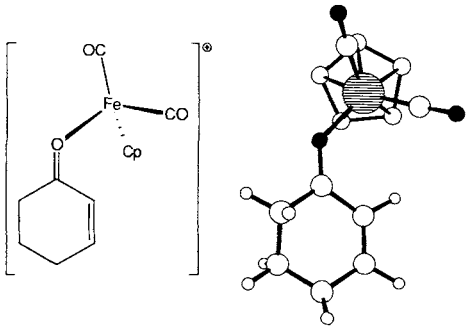

Fig. 22. Crystal structure of $[\{Fp\}(cyclohexenone)]PF_6$ [12, 47] (anion omitted).

syn to the C–C double bond, which could be explained by steric or electronic arguments. Sterically, coordination next to the smaller methine, as opposed to the methylene, α to the carbonyl should be favored. A similar preference may be expected if the enone moiety is envisioned in an enol ether resonance structure (cf. Fig. 23). Thus, the known preference of enol ethers to adopt a *Z* conformation may be extended to this case to explain the observed result. The latter, electronic argument, however, does not appear to override steric factors in an aldehyde complex. Preliminary results from a crystal structure of $[\{Fp\}(cinnamaldehyde)]PF_6$ indicate metal coordination *cis* to the aldehydic hydrogen and *trans* to the enal double bond.[12]

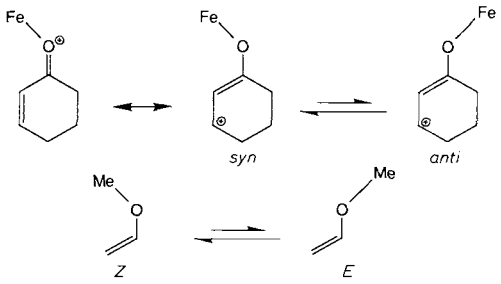

Fig. 23. Is there an analogy between *E*/*Z* enol ethers and *syn*/*anti* Lewis acid complexes with α,β-unsaturated carbonyl compounds?

It is also noteworthy that the observed conformation of the Lewis acid–bound cyclohexenone is fully consistent with the transition structure **5** (Fig. 24) of *Corey, Hannon* et al. for the asymmetric 1,4-addition of alkyl cuprates to cyclohexenone (**4**).[49]

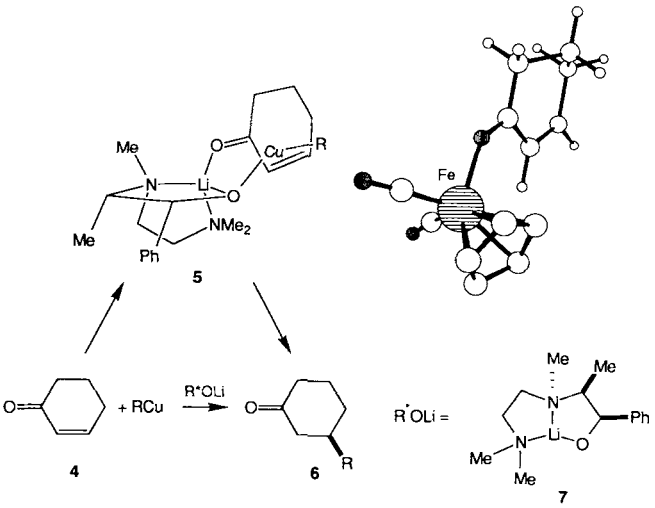

Fig. 24. The Corey–Hannon model for the asymmetric Michael reaction of alkylcopper reagents with cyclohexenone (**4**) in the presence of chiral Li salts such as **7** to give cyclohexanones (**6**). [49].

$[\{Fp\}(4\text{-methoxy-3-butenone})]BF_4$ also shows coordination *syn* to the C–C double bond, s-*trans* geometry, and no evidence for π bonding (Fig. 25, τ(Fe-O-C-C) = 0(1)°).[12] $[\{Fp\}(tropone)]BF_4$ is yet another complex whose crystal structure has been solved.[48] In this case, the complex is particularly stable due to the high basicity of the tropone ligand and the crystal shows very similar structural features to other $\{Fp\}^{\oplus}$ complexes of carbonyl compounds.

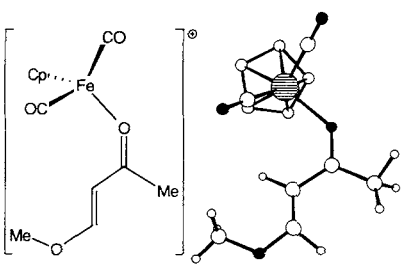

Fig. 25. Crystal structure of $[\{Fp\}(4\text{-methoxy-3-butenone})]BF_4$ [12] (anion omitted).

A tungsten Lewis acid, $[(Me_3P)(CO)_3(NO)W]SbF_6$, was recently reported to catalyze diene polymerization and Diels–Alder reactions.[50] A crystal structure of the acrolein-bound complex (Fig. 26) shows tungsten σ-coordinated

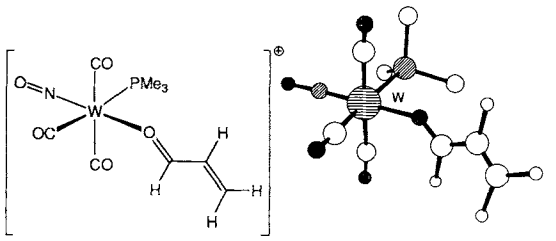

Fig. 26. Crystal structure of $[(Me_3P)(CO)_3(NO)W]SbF_6$–acrolein complex [50] (anion omitted).

(τ(W-O-C-C) = 180°), *syn* to hydrogen, at an angle of 137.1°. In line with ab initio predictions,[51] acrolein adopts an s-*trans* conformation, despite the absence of any obvious steric interactions in the s-*cis* conformer. It is apparent from this crystal structure that the tungsten complex behaves similarly to classical Lewis acids, and its structure can be predicted based on the same principles.

Gladysz's cationic complex $[(\eta^5\text{-}C_5H_5)(PPh_3)(NO)Re]^{\oplus}$ (**A**) is capable of binding carbonyls either η^2, through the π system, or η^1 through the lone-pair electrons.[52, 53] Crystal structures of **A**–phenylacetaldehyde (Fig. 27, right) and **A**–acetophenone (Fig. 27, left) clearly show the two different

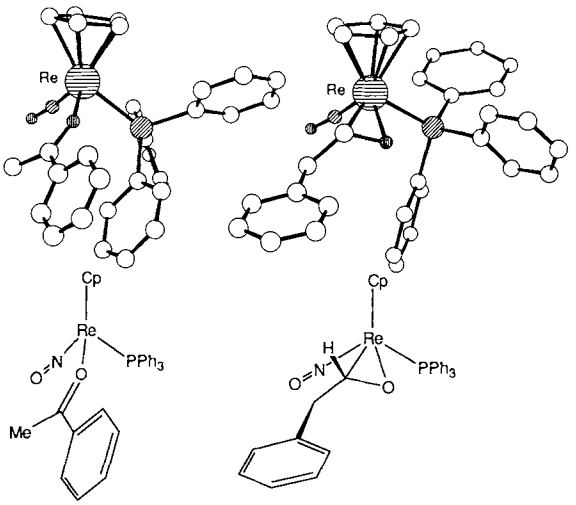

Fig. 27. η^1 (left) and η^2 (right) bonding for $[Cp(Ph_3P)(NO)Re]^{\oplus}$ (**A**) [52, 53].

modes of complexation. The authors attributed the difference in binding to increased steric bulk and lower π acidity of ketones as compared to aldehydes. No crystal structures of $\{Fp\}^{\oplus}$–aldehyde complexes are available in order to determine whether $\{Fp\}^{\oplus}$ has a similar "amphichelic" binding property, but $[(Ph_3P)(CO)_2Fe^0]$ binds cinnamaldehyde in an η^4 fashion.[54, 55] Additionally, it is worth noting that both of the rhenium complexes shown here are chiral and it has been shown that in the enantiomerically pure form, they undergo nucleophilic additions to the carbonyls with high enantioselectivities.[52, 53] Finally, the significance of the phenylacetaldehyde crystal structure should not escape attention. This is the first crystal structure of a nonchelated, α-substituted complex formed between a Lewis acid and an aldehyde. Despite the unusual, η^2 bonding in this complex there may be direct implications for the conformational preferences of complexes formed between Lewis acids and α-chiral aldehydes. Remarkably, the phenyl ring lies nearly perpendicular to the plane of the carbonyl at a dihedral angle of τ(C-C-C-O) = 94°, which is reminiscent of the Felkin–Anh proposal for the reactive conformation of α-substituted carbonyl systems.[56] However, it also seems reasonable to argue that the phenyl group occupies the sterically least congested area of space, and that the observed conformation is merely an artifact of the steric requirements of this particular complex, rather than a general, electronic phenomenon.

η^2 Bonding appears to occur with electron-rich metals and electron-deficient carbonyls. This combination allows for better back-bonding from the metal to the carbonyl π* orbital and disfavors competitive η^1 coordination by lowering the carbonyl lone-pair basicity. Hexafluoroacetone, for example, is η^2-bound to $[Ir(Ph_3P)_2(CO)Cl]$[57] (cf. also Ref. [45]), and electron-rich Ni^0 complexes show π bonding to both aldehydes[58] and ketones.[59] The crystal structure of $[(tmeda)Ni(C_2H_4)(H_2CO)]$, for example, shows formaldehyde bound in a metallaoxirane structure in which the C–O bond has lengthened to 1.311 Å (Fig. 28).[60] Similarly, a

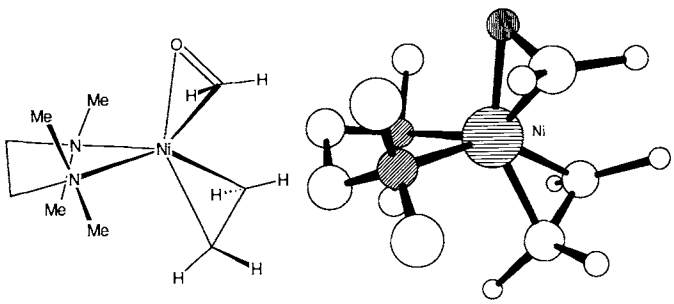

Fig. 28. Crystal structure of $[(tmeda)Ni(C_2H_4)]$–formaldehyde complex [60].

molybdenum Lewis acid bound to benzaldehyde shows η^2 bonding and a C–O bond length of 1.333 Å.[61] Acetone bound to pentaammineosmium(II) (C-O = 1.322 Å) has also been detected in the solid state, and π bonding is observed in this case as well.[62]

The structure of these η^2-bound carbonyl–Lewis acid complexes, especially those of Ni, may be relevant to the Au^I-catalyzed aldol reaction of isocyanoacetates with aldehydes to give the heterocycles **9**, discovered by *Ito, Sawamura,* and *Hayashi*.[63] It is reasonable to expect that the isoelectronic Ni^0–aldehyde complexes and the presumed Au^I–aldehyde intermediate in this reaction would exhibit similar structural features. Thus, **8** can be proposed as a transition-state model (Fig. 29), although the presence of other potential ligands in the reaction mixture (i.e., isocyanates, tertiary amines) may lead to other, structurally distinct, Au^I complexes as well.

Finally, carbonyls can bind two metals at once. The crystal structure of a complex containing bridging μ-η^2-bound acetaldehyde, for example, shows the carbonyl coordinated

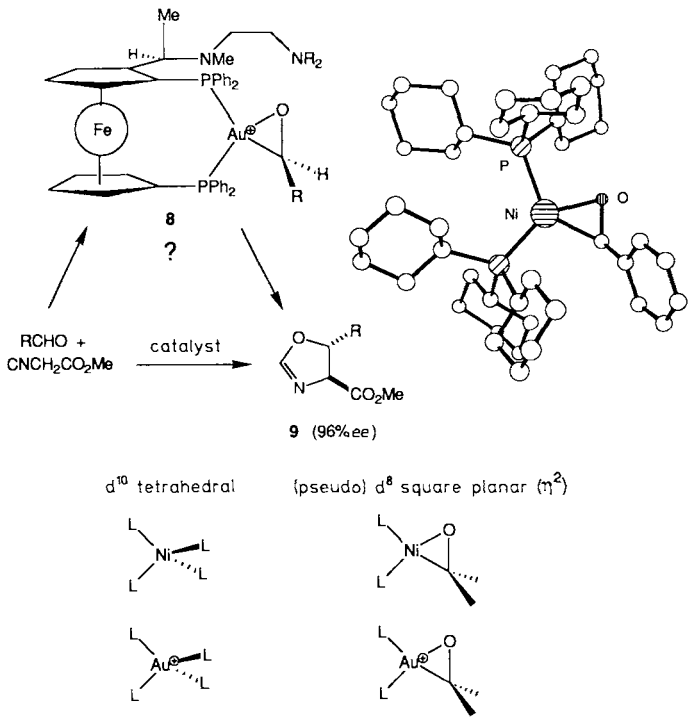

Fig. 29. A Ni^0–aldehyde complex as model for the transition state of Au^I-catalyzed aldol reaction of cyanoacetoacetates and aldehydes [58, 63].

to two molybdenum atoms (Fig. 30).[64] It appears that in this structure the carbonyl utilizes its π as well as its lone-pair electrons to bond to the two metal centers. Conceptually, one can think of this molybdenum complex as a bidentate Lewis acid that chelates the carbonyl group.

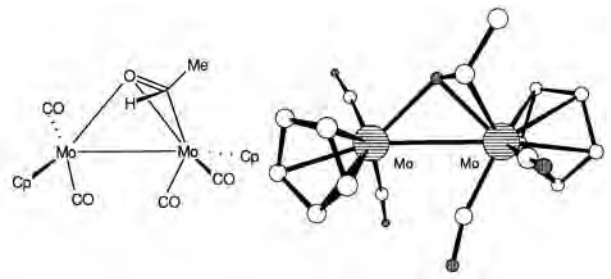

Fig. 30. Crystal structure of $[(\eta^2\text{-}\mu\text{-}CH_3CHO)Cp_2(CO)_4Mo_2]$ [64].

2.3. Discussion

It is now appropriate to summarize a few general points that can be made, based on the structural information in Sections 2.2.1–2.2.3, regarding the complexation of the carbonyl group to various Lewis acids. It is fairly clear that alkali-metal cations do not show a strong directional preference for binding to carbonyls and, for these complexes, coordination numbers and coordination geometries vary greatly. Boron, aluminum, titanium, and tin Lewis acids all accept electron density from sp^2 lone pairs of a carbonyl ligand at an angle of ca. 130–140°, but, in the presence of steric interactions, they easily distort from their optimal geometry. For aluminum, titanium, and tin complexes there is fairly strong evidence that, contrary to theoretical predictions, these distortions are invariably out of plane, toward the π cloud of the carbonyl group rather than the linear, in-plane geometry. This may also suggest a mechanism for *syn–anti* isomerization of the Lewis acid, although this point is less clear. Electron-rich metals and electron-deficient carbonyls prefer η^2 bonding. Thus, many of the late transition metals bind carbonyls through the π cloud.[65]

The stoichiometry of complexation is ordinarily 1:1 (acid:carbonyl) for boron- and aluminum-centered Lewis acids, which give pseudo-tetrahedral complexes, and 1:2 for octahedral Ti^{IV} complexes. Sn^{IV} Lewis acids can form either 1:2 octahedral or 1:1 trigonal-bipyramidal complexes, depending on the nature of their ligands and on the carbonyl base. For late transition metals the stoichiometry is often predicted by the 18-electron rule.

η^1-Bound Lewis acids prefer to lie *syn* to the smaller substituent of the carbonyl: for example, *syn* to H for aldehydes, *anti* to -OR for simple alkyl esters. In α,β-unsaturated systems, Lewis acid coordination *syn* to the C–C double bond favors the s-*trans* conformation, but in two crystal structures, where coordination *anti* to the olefin occurs, s-*cis* complexes are observed.[28, 66] Finally, chelation with titanium and tin occurs readily and yields stable, crystalline complexes.

Some of the difficulties encountered in obtaining structural data on Lewis acid carbonyl complexes should also be noted here. One of the most common challenges in X-ray crystallographic analyses is the task of obtaining suitable, X-ray-diffracting crystals. This task is made even more formidable for the highly reactive and often unstable Lewis acid carbonyl complexes. Most of the crystal structures discussed in Sections 2.2.1 and 2.2.2 were obtained by crystal growth and data collection at low temperatures, under inert atmospheres. Some of the late-transition-metal complexes, however, seem to be exceptional in this respect. Many of the systems discussed in Section 2.2.3 exhibit exceptional robustness, stability, and a propensity to form crystalline complexes. This would facilitate the task of crystallization and structural analysis, and one can imagine that transition-metal complexes could be used as structural probes of carbonyl–Lewis acid interactions.

3. π-Bond Hybridization in Transition-Metal Complexes[67]

Numerous theoretical[68] and structural[69] studies point to the fact that π bonding plays an important role in determining the geometry of transition-metal complexes. Conformational preferences of π-bonding ligands are often rationalized by simple consideration of the relative energies of the metal d orbitals which can overlap with the ligand in question. In d^8 trigonal-bipyramidal complexes, for example, π-acid ligands favor equatorial positions and adopt geometries which allow π overlap with the $d_{x^2-y^2}$ or d_{xy} orbitals (metal-centered HOMOs) lying in the equatorial plane. Likewise, d^6 octahedral and pseudo-octahedral complexes possessing a single carbonyl (or nitrosyl) ligand have a well-defined metal-centered HOMO lying in the plane perpendicular to the carbonyl (or nitrosyl) ligand (Fig. 31, left). *Gladysz* et al.

have shown that stereoelectronic interactions involving the metal-centered HOMO in [CpRe(NO)(PPh_3)R] complexes dramatically influence the structure and reactivity in a wide variety of these chiral molecules (Fig. 31, middle and right).[70] Thus, electronic interactions involving ligand π

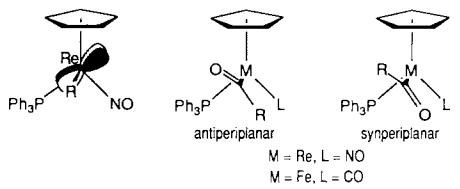

Fig. 31. Alternative acyl ligand conformations that maximize primary stereoelectronic interactions in d^6 complexes containing a single carbonyl (or nitrosyl) ligand. Left: Metal-centered HOMO.

orbitals and metal-centered HOMOs and LUMOs, which we will term primary stereoelectronic interactions, are often reliable predictors of ligand conformation.[71]

Ordinarily, assessment of primary stereoelectronic interactions plays a key role in the conformational analysis of transition-metal complexes. Nevertheless, ligand alignment is seldom uniquely determined by primary stereoelectronic interactions since there are often two ligand alignments that maximize π bonding or primary stereoelectronic interaction (see Fig. 31). Considering the chiral metal acyl complexes studied by *Gladysz* et al.,[72] *Davies* et al.[73] and *Liebeskind* et al.,[74] we note that the observed alignment of the acyl carbonyl antiperiplanar to the π-bonding CO (or NO) ligand maximizes π back-bonding to the acyl ligand from the metal-centered HOMO. However, alignment of this acyl carbonyl *syn* to the CO (or NO) ligand also maximizes π back-bonding. This raises the question: What forces govern the preferred antiperiplanar orientation of the acyl carbonyl?

The influence of steric interactions on the *syn–anti* isomerism of acyl ligands in [CpFe(CO)(PPh_3)(RC=O)] and [CpRe(NO)(PPh_3)(RC=O)] complexes (see Fig. 31) has been argued persuasively by *Davies*.[75] While steric interactions are certainly important in these systems, there are some trends which indicate that *syn–anti* isomerism in these complexes is not adequately rationalized by consideration of steric interactions alone. Notably, formyl complexes (R = H) show the same antiperiplanar conformational preference as acyl complexes possessing bulky alkyl (e.g., R = *sec*-butyl) substituents (see Section 3.1.2).

Since a number of metal acyl complexes with *cis* π-bonding ligands show a preference for alignment of the acyl oxygen antiperiplanar to the π-bonding ligand, and since evaluation of steric interactions does not adequately explain this alignment in all of the cases, we sought another explanation for the phenomenon. In Section 3.1 we discuss how examination of crystallographic data led to the proposal that *syn–anti* isomerism in transition-metal acyl complexes possessing *cis* π-bonding ligands is influenced by *secondary* stereoelectronic interactions. Secondary stereoelectronic interactions result from the mixing of metal-centered d and p orbitals, which occurs during π bonding. This dp mixing leads to hybridization of π-bonding molecular orbitals toward the π-bonding ligand. Interaction of the C–O σ* orbital of the acyl ligand with the π-bonding orbitals of the *cis* CO (or NO) ligand leads to a stereoelectronically preferred antiperiplanar orientation of the acyl ligand.

Secondary stereoelectronic interactions may also influence the alignment of *cis* π-bonding ligands in systems other than the acyl complexes mentioned above. Based on the presence of orbital interactions similar to those found for acyl complexes, we also propose that ligand orientations that place a ligand acceptor orbital (e.g., σ*) *syn* or a ligand donor orbital (e.g., heteroatom lone pair) *anti* to a *cis* π-bonding ligand are stereoelectronically favored (Fig. 32).

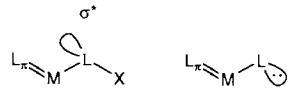

Fig. 32. Ligand conformation favored by secondary stereoelectronic interactions in complexes containing a *cis* π-bonding ligand. Left: Ligand acceptor, orbital (σ*) *syn* to L_π. Right: Lone-pair donor orbital *anti* to L_π. See sections 3.2.1–3.2.3.

The theoretical basis for the conformational model depicted in Figure 32 has been presented elsewhere.[67] Here, we consider the structural data which lend credence to this model.

3.1. *Syn–Anti* Isomerism in Metal Acyl Complexes

3.1.1. Steric Interactions in Metal Acyl Complexes: The Seeman–Davies Model

Certain reactions of organic ligands attached to stereogenic transition-metal centers in complexes of the type $CpML_3$ have been shown to proceed with a remarkable degree of asymmetric induction. Prompted by this observation, *Seeman* and *Davies* recently published conformational models for alkyl and acyl complexes containing the organometallic fragment [CpFe(CO)(PPh_3)].[76] Their models were based on the results of extended Hückel and ab initio calculations on model systems where PPh_3 was replaced with simpler ligands. Their principal conclusions were that iron serves primarily as a template for the ligands and that alkyl or acyl ligand conformation is governed by steric interactions with the PPh_3 ligand.

3.1.2. Acyl Ligand Conformations Not Explained by the Seeman–Davies Model

If Seeman–Davies-type steric interactions are the only forces responsible for the observed conformational preferences for metal acyl complexes, then formyl complexes should—due to the smaller size of H versus O on the formyl ligand—show a preference for alignment of the acyl oxygen *syn* to the M–CO bond. *This is not the case.*

The solid-state structure of [CpRe(NO)(PPh_3)(CHO)] (**10**) has been determined by *Gladysz* et al.[77] and this formyl complex has the formyl oxygen oriented antiperiplanar ($N–Re–C_{acyl}–O_{acyl}$ torsional angle = 176°) to the M–NO bond (Fig. 33). This conformation is not predicted by the Seeman–Davies model. *Gladysz* has noted that the observed conformation allows for a stabilizing electronic interaction between the highest occupied d orbital on the rhenium and the π^*_{CO} orbital on the acyl ligand. Complex **10** also shows a very short $Re–C_{formyl}$ bond (2.06 Å) and a low formyl car-

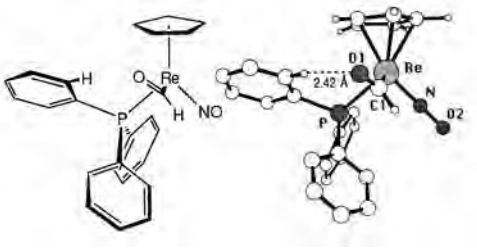

Fig. 33. Structure of **10** [77].

bonyl stretching frequency (ν_{CO} = 1558 cm^{-1}); both of these observations are in accord with a substantial amount of Re-to-formyl electron donation. However, synperiplanar orientation of the formyl ligand would allow for the same electronic stabilization. There are no obvious intramolecular steric interactions between the other ligands and the formyl ligand; in fact, the triphenylphosphane conformation is as observed by *Davies* and *Seeman* in iron acyl complexes. Intermolecular steric interactions (crystal packing forces) are unlikely to play a major role in determining the formyl ligand conformation due to the smallness of this ligand relative to other ligands on the complex. Clearly, some other force must be acting to align the formyl ligand in the observed antiperiplanar orientation.

Based on the examination of some other metal acyl complexes with *cis* CO ligands that do not possess Seeman–Davies-type steric interactions (Figs. 34–36), it is tempting to speculate that there is an intrinsic electronic preference for alignment of the acyl oxygen *anti* to the CO ligand. In *Herndon*'s iron acetyl complex **11** (Fig. 34)[78] the bulky

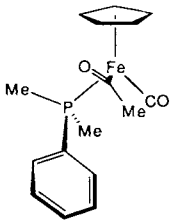

Fig. 34. Solid-state geometry of [CpFe(CO)(PMe_2Ph)COMe] (**11**) [78].

triphenylphosphane ligand central to the Seeman–Davies model is replaced by the smaller dimethylphenylphosphane ligand. Although there is no steric interaction between the acyl ligand and the *ortho* C–H bond of a phenyl group, the acetyl ligand adopts an antiperiplanar alignment (C_{CO}–Fe–C_{acyl}–O_{acyl} torsional angle = − 163°). The methoxycarbonyl ligand in *Albano*'s octahedral iridium complex **12** (Fig. 35)[79] certainly is in a very different steric environment

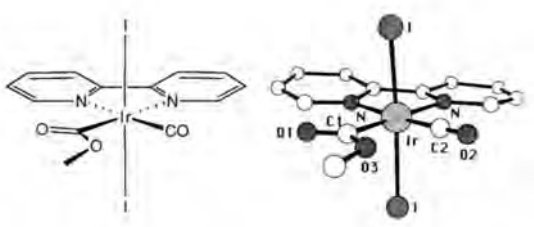

Fig. 35. Structure of [Ir(bpy)I_2(CO)CO_2Me] (**12**) [74].

than that found in pseudo-octahedral complexes of the type [CpFe(CO)(PPh_3)(COR)], yet the carbonyl oxygen is aligned antiperiplanar to the CO ligands (C_{CO}–Ir–C_{acyl}–O_{acyl} torsional angle = 176°).

Berke's octahedral rhenium complex **13**[80] (Fig. 36) is another example of a rhenium formyl complex where the formyl oxygen is aligned *anti* to the *cis* π-bonding ligand (cf. *Gladysz*'s complex, Fig. 33) despite steric interactions which should favor the *syn* alignment.

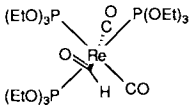

Fig. 36. Solid-state geometry of [$Re(CO)_2${$P(OEt)_3$}$_3$CHO] (**13**) [80].

Electronic interactions that lead to preferential stabilization of the antiperiplanar rotational isomer of the metal acyl complexes discussed above are depicted in Figure 37. Primary stereoelectronic interaction is optimized when the acyl ligand is coplanar with the M–CO bond, since this allows for maximum overlap of the π^*_{CO} orbital of the acyl ligand with the metal-centered HOMO (cf. Fig. 31). Secondary stereoelectronic interactions are optimized when the acyl ligand is antiperiplanar to the M–CO bond, since this allows for max-

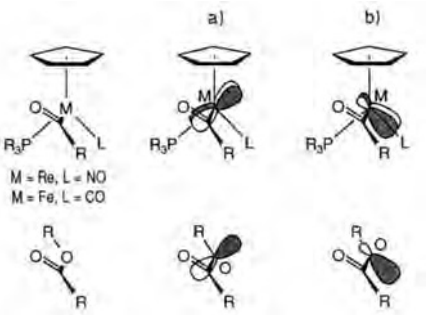

Fig. 37. Stereoelectronic interactions in metal acyl complexes and carboxylic esters. a) Primary stereoelectronic effect; b) secondary stereoelectronic effect.

imum overlap of the σ^*_{CO} orbital of the acyl ligand with the M–CO π-bonding orbital, which is metal-centered *and hybridized toward the CO ligand.* Similar electronic effects have been invoked to explain the stability of the *Z* conformation of carboxylic esters (Fig. 37, bottom).[81, 82] In this description of π bonding, the polarized metal-centered d orbitals are similar to the lone pair of the oxygen heteroatom.

Despite the plausibility of these arguments in a qualitative sense, it is extremely difficult to assess the exact energetic worth of secondary stereoelectronic interactions. However, a general sense of the energetic contributions of secondary stereoelectronic effects may be derived from the consideration of factors that can override these preferences. We close this section with a discussion of some metal acyl complexes with *cis* CO ligands where the acyl ligands are not oriented antiperiplanar to CO ligands.

Ruthenium formyl complex **14** (Fig. 38), prepared by *Nelson* et al.,[83] has a C_{CO}–Ru–C_{formyl}–O_{formyl} torsional angle of − 28°. However, this complex possesses several unusual structural features, including an exceptionally short C–O

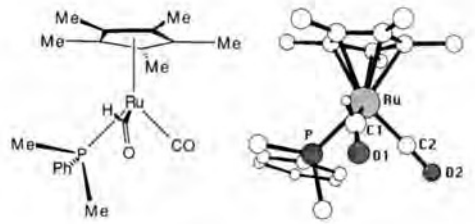

Fig. 38. Structure of [Cp*Ru(CO)(PMe_2Ph)CHO] (**14**) [83].

bond length (1.106 Å) and a large Ru–C–O bond angle (140°) for the formyl ligand—the C–O bond of the formyl ligand is shorter than that of the carbonyl ligand present in the same complex (C-O = 1.134 Å for the carbonyl ligand). The reasons for the unusual structural features present in **14** are unclear. However, a comparison between *Nelson*'s ruthenium formyl complex **14** ($C\text{-}O_{formyl}$ = 1.11 Å, $\tilde{\nu}_{CO}$ = 1601 cm^{-1}) and *Gladysz*'s rhenium formyl complex **10** ($C\text{-}O_{formyl}$ = 1.22 Å, $\tilde{\nu}_{CO}$ = 1554 cm^{-1}) indicates that there is substantially less back-bonding to and hence less electronic stabilization of the formyl ligand in the ruthenium complex **14**. In *Nelson*'s complex, the stereoelectronic preference for antiperiplanar alignment of the formyl ligand is presumably overridden by the steric demand of the bulky pentamethylcyclopentadienyl ligand.

Polar groups such as the CO group in metal acyl complexes are often involved in electrostatic interactions. Figure 39

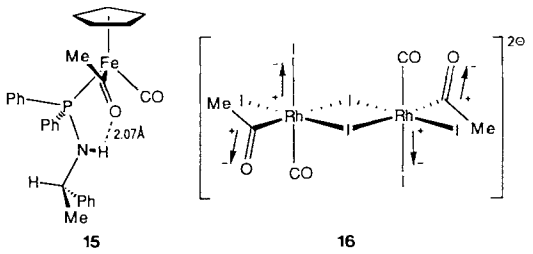

Fig. 39. Structures of [CpFe(CO)($PPh_2NHCHMePh$)COMe] (**15**) [84] and $[RhI_3(CO)COMe]_2^{2\ominus}$ (**16**) [85], where electrostatic interactions determine acyl ligand conformation.

shows two acyl complexes whose solid-state structures may be influenced by electrostatic interactions. The orientation of the acetyl ligand in iron complex **15** is controlled by a strong hydrogen bond to the NH group attached to the phosphane ligand.[84] The orientation of acetyl ligands in the binuclear rhodium complex **16**[85] may be determined by dipole–dipole interactions, since the observed conformation leads to the most favorable alignment of $Rh^{\delta\oplus}$–$I^{\delta\ominus}$ and $(C^{\delta\oplus}\text{–}O^{\delta\ominus})_{acyl}$ dipoles.

3.2. *Syn–Anti* Isomerism of Ligands other than η^1-Acyl

3.2.1. *Bent Nitrosyl Ligands*

X-ray crystal structures of the bent nitrosyl complexes **17**[86] and **18**[87] are shown in Figures 40 and 41. In both cases the bent nitrosyl ligand adopts the stereoelectronically preferred conformation (Scheme 1) that places its lone pair antiperiplanar to the *cis* π-bonding ligand.

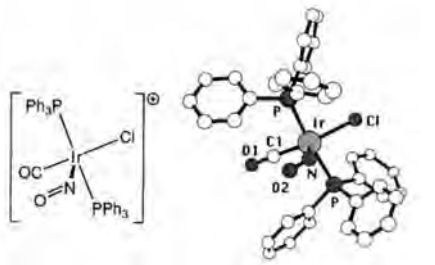

Fig. 40. Structure of $[Ir(PPh_3)_2(CO)(NO)Cl]BF_4$ (**17**) (anion omitted). The C–Ir–N–O torsional angle is − 5° [86].

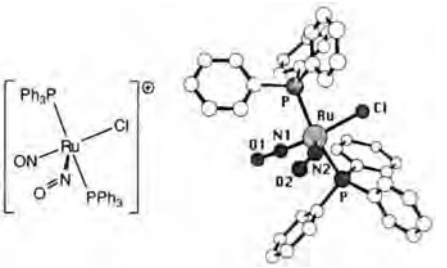

Fig. 41. Structure of $[Ru(PPh_3)_2(NO)_2Cl]PF_6$ (**18**) (anion omitted). The N_{linear}–Ir–N_{bent}–O torsional angle is 2° [87].

Scheme 1. Conformations of the nitrosyl ligand (cf. Fig. 32).

Bent nitrosyl complexes are related to acyl complexes by the isoelectronic substitution of N for CR. As this substitution replaces the C–R bond with a nitrogen lone pair, the stereoelectronically preferred alignment of the nitrosyl N=O bond is different from that of the acyl C=O bond [Eq. (a)]. Since the metal-centered M–CO π cloud ("lone

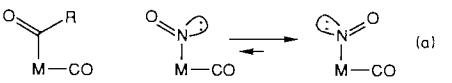

(a)

pair") is concentrated along the M–C bond, the lone pair of the bent nitrosyl can minimize "lone pair–lone pair" repulsion in the *syn* conformation.

It is interesting to compare bent nitrosyl and acyl complexes to their organic analogues: nitrite and carboxylic esters. Since nitrite esters are related to carboxylic esters by the same isoelectronic substitution (N for CR), the stereoelectronically preferred alignment of the nitrite N=O bond should be different from that of the carboxylic C=O bond. In fact, this appears to be the case: In both methyl nitrite[88] and methyl formate[89] the *Z* conformer is preferred, but to a very different extent [Eqs. (b) and (c)].

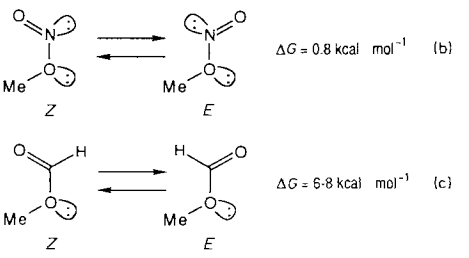

ΔG = 0.8 kcal mol^{-1} (b)

ΔG = 6.8 kcal mol^{-1} (c)

This difference is understood if the forces governing these conformational preferences are viewed as a superposition of electrostatic (dipolar) and stereoelectronic interactions (Fig. 42). Electrostatic forces favor the *Z* conformation for

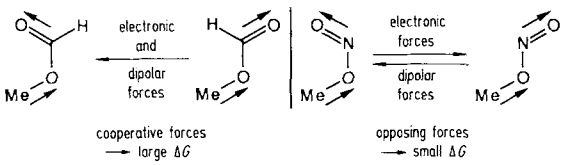

Fig. 42. The influence of electronic and dipolar forces on the preferred conformations of carboxylic esters (left) and nitrite esters (right).

both nitrite and carboxylic esters. Stereoelectronic forces, however, favor the *Z* conformation for carboxylic esters and the *E* conformation for nitrite esters. In the case of methyl formate stereoelectronic and electrostatic forces act in unison to produce an energetically substantial conformational preference, whereas in the case of methyl nitrite these forces largely cancel out to produce a small conformational preference.

3.2.2. *Acetylene Ligands*

Figures 43–45 show some ynolate and ynol ether complexes of tungsten (**19**–**21**) which are derived from carbyne–

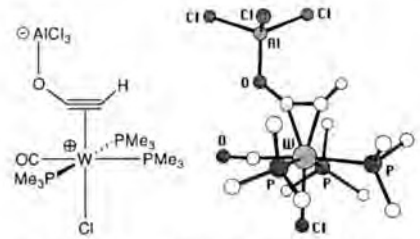

Fig. 43. Structure of [W(HC≡COAlCl$_3$)(CO)(PMe$_3$)$_3$Cl] (**19**) [90a].

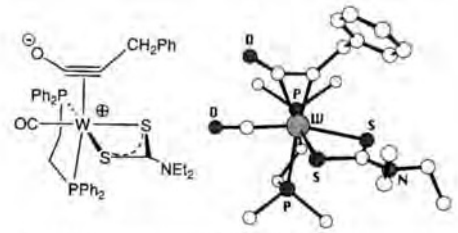

Fig. 44. Structure of [W(PhCH$_2$C≡CO)(CO)(Ph$_2$PCH$_2$CH$_2$PPh$_2$)(S$_2$CNEt$_2$)] (**20**) [90b].

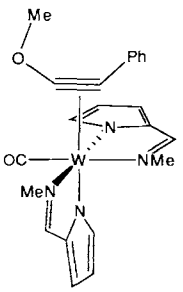

Fig. 45. Solid-state structure of [W(PhC≡COMe)(CO)(2-MeNCH-pyrrole)$_2$] (**21**) [90c].

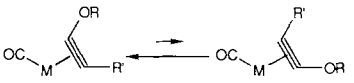

Scheme 2. Conformations of alkyne ligands (see also Fig. 46).

ic interactions that cause the alkyne ligands to be parallel to the carbonyl ligand have been discussed at length by *Templeton* et al.[91] The alkyne is thus aligned so that it may receive electron density from a filled tungsten-centered orbital and donate electron density to an empty one. The *syn* orientation of the oxygen substituent, however, is not explained by these interactions. The π^*_{CC} orbital of an ynolate or ynol ether is hybridized toward the carbon bearing the oxygen substituent and the filled metal-centered orbital with which it interacts is polarized toward the carbonyl ligand (Fig. 46).[92] Thus, the observed conformation of the alkynes is that which maximizes the overlap between these two orbitals.

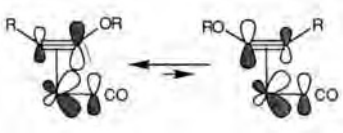

Fig. 46. Preferred alkyne alignment for maximum π back-bonding in complexes **19**–**21**.

3.2.3. *Bent Imido Ligands*

X-ray crystal structures of the bis-imido complexes **22**[93] and **23**[94] are shown in Figures 47 and 48. In both cases the bent imido ligand adopts the stereoelectronically preferred conformation that places its lone pair antiperiplanar to the

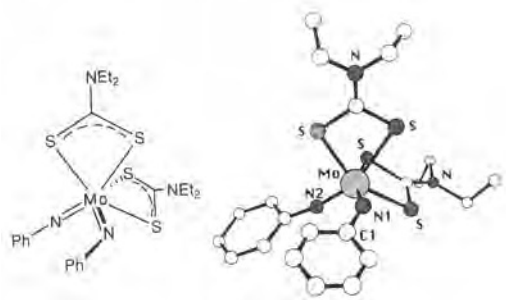

Fig. 47. Structure of [Mo(S$_2$CNEt$_2$)$_2$(NPh)$_2$] (**22**). The N_{linear}–Mo–N_{bent}–C torsional angle is −5° [93].

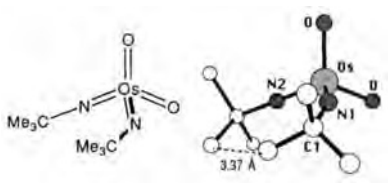

Fig. 48. Structure of [OsO$_2$(N-*t*Bu)$_2$] (**23**). The N_{linear}–Os–N_{bent}–C torsional angle is 0° [94].

metal–nitrogen triple bond of the linear imido ligand (Scheme 3). Here, the stereoelectronic preference is probably governed by donation of the lone pair of the bent amido

Scheme 3. Conformations of imido ligands (cf. Fig. 32).

ligand into a metal-centered non-bonding orbital.[82c] Of course, avoidance of "lone-pair"–π interactions in the antiperiplanar arrangement may also contribute to a bias for the observed conformation.

Interestingly, both **22** and **23** adopt conformations which place the imido substituent in a sterically more hindered environment. Thus, in these cases secondary stereoelectronic effects seem to override steric preferences.

4. Summary and Outlook

The examples presented in this article demonstrate a few of the many ways that useful conformational conjectures can be made using the Cambridge Structural Database. Synthetic and design applications aside, the development of further mechanistic studies that would verify the validity of these conjectures should be emphasized. In particular, systematic structural analyses of a family of related complexes—where only a few parameters change in going from one complex to another—would be highly informative. In the absence of systematic studies, care should be taken to avoid overinterpretation of single structures and invalid generalizations. Generally, statistical analyses of a larger number of crystal structures can be used to distinguish the ordinary from the unusual. In unusual systems, crystal packing forces may be the cause of deviations from the norm, and it is always important to take this factor into consideration.

In the complexation of Lewis acids to carbonyls—a process of great interest in organic synthesis—definite structural trends were observed. The more unexpected observations included the widespread occurrence of out-of-plane bonding and the diversity of coordination geometries for very similar Lewis acids (e.g., $L_nX_{4-n}Sn$ Lewis acids). Of the unanswered questions, the conformational preferences of Lewis acid–bound, α-chiral carbonyls seem to attract the most immediate attention.

In organometal complexes with π-bonding ligands, the presence of secondary stereoelectronic interactions is strongly implicated by the structural data. Considerations of molecular orbital theory also support this notion. Notably, the cases where stereoelectronic *syn–anti* preferences override clear steric preferences (complexes **10, 13, 22,** and **23**) occur for metals (Re, Mo, and Os) that have been noted to show a predilection for forming metal–ligand multiple bonds. It may be that stereoelectronic interactions (primary and secondary) are more important for these metals than for metals, such as Fe, which do not show a tendency to form multiple bonds. A more definitive answer, however, is likely to come from future X-ray analyses and the test of our ability to predict the conformation of these complexes.

Another way to gain insights from the structure of molecules is through the structure–reactivity correlation method.[1, 3, 4] Recently, for example, the question of the structure and basicity of silyl ethers was probed using the CSD.[95] A search for the $Si–O–C_{sp^3}$ fragment revealed an unusually wide average Si–O–C angle (134.2°) and a negative correlation between the Si–O bond length and the Si–O–C bond angle (Fig. 49; correlation factor − 0.68). The latter observation contradicts the steric arguments previously presented for the occurrence of wide Si–O–C angles.

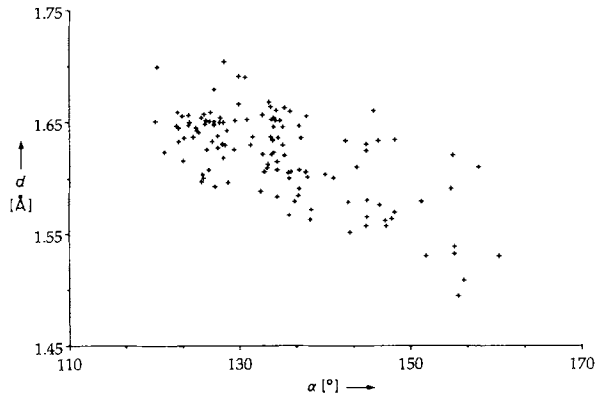

Fig. 49. Correlation of the Si–O bond length and the Si–O–C angle in acyclic silyl ethers [95].

An alternative explanation, based on Si–O π interactions, on the other hand, is consistent with the observed results.[96] Subsequently, calculations of *Jorgensen* et al.[95] at the 6-31G* level reproduced the same contrasteric trend and presented a theoretical basis for these observations. Although these findings do not yield any direct information on the features of a transition structure, they can account for the relatively low basicity of silyl ethers and also for the inability of α- and β-siloxy carbonyls to chelate Lewis acids.[96]

Finally, it should be recalled that "chemical reactivity depends on many factors besides purely conformational ones; an exclusive preoccupation with the geometric aspects of molecular structure can sometimes prevent us from recognizing other factors that might be important or even decisive in influencing the rate of a reaction."[97] Future work in this area will focus not only on the refinement of the conformational models, but also on the uncovering of the "other factors" that influence the reactivity of organometal complexes.

We are grateful to Kurtis MacFerrin for the implementation of CSD on a VAXstation 3500 computer. Financial support for this project was provided by NIH, NSF, and Pfizer Inc., to whom we express our deep appreciation.

Received: September 1, 1989 [A 750 IE]
German version: *Angew. Chem. 102* (1990) 273

[1] J. D. Dunitz: *X-ray Analysis of the Structure of Organic Molecules*, Cornell University Press, Ithaca, NY, USA 1979.
[2] L. Pauling: *The Nature of the Chemical Bond*. 3rd. ed., Cornell University Press, Ithaca, NY, USA 1960.
[3] a) H.-B. Bürgi, J. D. Dunitz, E. Shefter, *J. Am. Chem. Soc. 95* (1973) 5065; b) H.-B. Bürgi, *Angew. Chem. 87* (1975) 461; *Angew. Chem. Int. Ed. Engl. 14* (1975) 460.

[4] H.-B. Bürgi, J. D. Dunitz, *Acc. Chem. Res. 16* (1983) 153.
[5] a) O. Kennard, D. Watson, F. H. Allen, W. Motherwell, W. Town, J. Rodgers, *Chem. Br. 11* (1975) 213; b) F. H. Allen, O. Kennard, R. Taylor, *Acc. Chem. Res. 16* (1983) 146.
[6] For two excellent reviews on the use of structural data in gaining a better understanding of organic reactions see: a) D. Seebach, *Angew. Chem. 100* (1988) 168; *Angew. Chem. Int. Ed. Engl. 27* (1988) 1624; b) G. Boche, ibid. 101 (1989) 286 and *28* (1989) 277.
[7] a) R. Taylor, *J. Mol. Struct. 73* (1981) 125; b) C. Ceccarelli, G. A. Jeffrey, R. Taylor, *ibid. 70* (1981) 255; c) R. Newton, G. A. Jeffrey, S. Takagi, *J. Am. Chem. Soc. 101* (1979) 1997.
[8] P. Chakrabarti, J. D. Dunitz, *Helv. Chim. Acta 65* (1982) 1482.
[9] D. A. Evans, *Science (Washington) 240* (1988) 420.
[10] a) R. Armstutz, J. D. Dunitz, T. Laube, W. B. Schweizer, D. Seebach, *Chem. Ber. 119* (1986) 434 (CSD Refcod: DEXCEO01) b) For reviews of organoalkali-metal crystal structures see: W. N. Setzer, P. von R. Schleyer, *Adv. Organomet. Chem. 24* (1985) 353; *ibid. 27* (1987) 169.
[11] R. H. van der Veen, R. M. Kellogg, A. Vos, T. J. van Bergen, *J. Chem. Soc. Chem. Commun. 1978*, 923 (CSD Refcod: XZCNAP).
[12] S. Shambayati, unpublished results.
[13] I. L. Karle, *J. Am. Chem. Soc. 96* (1974) 4000 (CSD Refcod: ANTAML01).
[14] I. L. Karle, *Proc. Natl. Acad. Sci. USA 82* (1985) 155.
[15] P. Russegger, P. Schuster, *Chem. Phys. Lett. 19* (1973) 254.
[16] D. J. Raber, N. K. Raber, J. Chandrasekhar, P. von R. Schleyer, *Inorg. Chem. 23* (1984) 4076.
[17] M. T. Reetz, M. Hüllman, W. Massa, S. Berger, P. Rademacher, P. Heymanns, *J. Am. Chem. Soc. 108* (1986) 2405.
[18] Heteronuclear NOE experiments provided evidence for the *anti* geometry in solution. Enhancement at the aldehydic (but not the phenyl) proton absorption was observed upon irradiation of the fluorine atoms [17].
[19] A. J. Baker, C. M. Lukehart, *J. Organometal. Chem. 254* (1983) 149.
[20] R. C. F. Jones, G. E. Peterson, *Tetrahedron Lett. 24* (1983) 4757.
[21] S. J. Rettig, J. Trotter, *Can. J. Chem. 54* (1976) 1168.
[22] A. Bittner, D. Männig, H. Nöth, *Z. Naturforsch. B41* (1986) 587.
[23] A. P. Shreve, R. Mülhaupt, W. Fultz, J. Calabrese, W. Robbins, S. D. Ittel, *Organometallics 7* (1988) 409.
[24] T. J. LePage, K. B. Wiberg, *J. Am. Chem. Soc. 110* (1988) 6642.
[25] K. Maruoka, T. Itoh, H. Yamamoto, *J. Am. Chem. Soc. 107* (1985) 4573.
[26] L. Brun, *Acta Crystallogr. 1966*, 20739 (CSD Refcod: TICLEA).
[27] I. W. Bassi, M. Calcaterra, R. Intrito, *J. Organomet. Chem. 127* (1977) 305 (CSD Refcod: TITEAN).
[28] T. Poll, J. O. Metter, G. Helmchen, *Angew. Chem. 97* (1985) 116; *Angew. Chem. Int. Ed. Engl. 24* (1985) 112 (CSD Refcod: CUZXIE).
[29] B. Viard, M. Poulain, D. Grandjean, J. Anandrut, *J. Chem. Res. 1983*, 850 (CSD Refcod: BUDHIR).
[30] G. Maier, U. Seipp, *Tetrahedron Lett. 28* (1987) 4515 (CSD Refcod: FOSMOP).
[31] J. Utka, P. Sobota, T. Lis, *J. Organomet. Chem. 334* (1987) 341 (CSD Refcod: FOTBIZ).
[32] B. Honold, U. Thewalt, *J. Organomet. Chem. 316* (1986) 291 (CSD Refcod: FEXFIX).
[33] G. Erker, U. Dorf, P. Czisch, J. L. Petersen, *Organometallics 5* (1986) 668 (CSD Refcod: DUBDAF).
[34] S. E. Denmark, B. R. Henke, E. Weber, *J. Am. Chem. Soc. 109* (1987) 2512 (CSD Refcod: FEJDAZ).
[35] C. Mahadevan, M. Seshasayee, A. S. Kothiwal, *Cryst. Struct. Commun. 11* (1982) 1725 (CSD Refcod: BUHKEU).
[36] S. Calogero, G. Valle, U. Russo, *Organometallics 3* (1984) 1205.
[37] G. Valle, S. Calogero, U. Russo, *J. Organomet. Chem. 228* (1982) C79.
[38] J. Buckle, P. G. Harrison, T. J. King, J. A. Richards, *J. Chem. Soc. Dalton 1975*, 1552.
[39] D. Cunningham, T. Donek, M. J. Frazer, M. McPartlin, J. D. Matthews, *J. Organomet. Chem. 90* (1975) C23.
[40] For an extensive discussion of this subject cf. [36].
[41] F. D. Lewis, J. D. Oxman, J. C. Huffman, *J. Am. Chem. Soc. 106* (1984) 466 (CSD Refcod: CEJDAW).
[42] M. T. Reetz, K. Harms, W. Reif, *Tetrahedron Lett. 29* (1988) 5881.
[43] a) G. E. Keck, S. Castellino, *J. Am. Chem. Soc. 108* (1986) 3847; b) G. E. Keck, S. Castellino, M. R. Wiley, *J. Org. Chem. 51* (1986) 5478.
[44] For a recent review of transition-metal carbonyl complexes see Y.-H. Huang, J. A. Gladysz, *J. Chem. Educ. 65* (1988) 299.
[45] R. H. Crabtree, G. G. Hatky, C. P. Parnell, B. E. Segmüller, P. J. Uriarte, *Inorg. Chem. 23* (1984) 354 (CSD Refcod: CEXLUM).
[46] R. H. Crabtree, M. F. Mellea, J.-M. Milhelcic, J. Quirk, *J. Am. Chem. Soc. 104* (1982) 107.
[47] The crystal structure of 3-methylcyclohexenone has also been reported: B. M. Foxman, P. T. Klemarczyk, R. E. Liptrot, M. Rosenblum, *J. Organomet. Chem. 187* (1980) 253.
[48] P. Boudjouk, J. B. Woell, L. J. Radonovich, M. W. Eyring, *Organometallics 1* (1982) 582.
[49] a) E. J. Corey, R. Naef, F. J. Hannon, *J. Am. Chem. Soc. 108* (1986) 7114; b) E. J. Corey, F. J. Hannon, *Tetrahedron Lett. 28* (1987) 5233.
[50] a) R. V. Honeychuck, P. V. Bonnesen, J. Farahi, W. H. Hersh, *J. Org. Chem. 52* (1987) 5293 (CSD Refcod: FUCGAL); b) P. V. Bonnesen, C. L. Puckett, R. V. Honeychuck, W. H. Hersh, *J. Am. Chem. Soc. 111* (1989) 6070.
[51] R. J. Loncharich, T. R. Schwartz, K. N. Houk, *J. Am. Chem. Soc. 109* (1987) 14.
[52] J. M. Fernández, K. Emerson, R. D. Larsen, J. A. Gladysz, *J. Am. Chem. Soc. 108* (1986) 8268.
[53] J. M. Fernández, K. Emerson, R. D. Larsen, J. A. Gladysz, *J. Chem. Soc. Chem. Commun. 1988*, 37 (CSD Refcod: FUVWAU).
[54] M. Sacerdotti, V. Bertolasi, G. Gilli, *Acta Crystallogr. Sect. B36* (1980) 1061.
[55] NMR spectroscopic studies of [{Fp}(cinnamaldehyde)]PF_6 complex in CD_2Cl_2 indicate η^1 bonding in solution [12].
[56] a) N. T. Anh, O. Eisenstein, *Nouv. J. Chim. 1* (1977) 61; b) M. Cherset, H. Felkin, N. Prudent, *Tetrahedron Lett. 1968*, 2199.
[57] B. Clark, M. Green, R. B. L. Osborn, F. G. A. Stone, *J. Chem. Soc. A 1968*, 167.
[58] M. Sacerdoti, V. Bertolasi, G. Gilli, *Acta Crystallogr. Sect. B36* (1980) 1061.
[59] T. T. Tsou, J. C. Huffman, J. K. Kochi, *Inorg. Chem. 18* (1979) 2311.
[60] W. Schröder, K. R. Pörschke, Y.-H. Tsay, C. Krüger, *Angew. Chem. 99* (1987) 953; *Angew. Chem. Int. Ed. Engl. 26* (1987) 919 (CSD Refcod: FONNEB).
[61] H. Brunner, J. Wachter, I. Bernal, M. Creswick, *Angew. Chem. 91* (1979) 920; *Angew. Chem. Int. Ed. Engl. 18* (1979) 861.
[62] W. D. Harman, D. P. Fairlie, H. Taube, *J. Am. Chem. Soc. 108* (1986) 8223.
[63] a) Y. Ito, T. Sawamura, T. Hayashi, *J. Am. Chem. Soc. 108* (1986) 6405; b) *Tetrahedron Lett. 28* (1987) 6215; c) For recent studies on the role of central chirality in these reactions see: S. D. Pastor, A. Togni, *J. Am. Chem. Soc. 111* (1989) 2333; d) For a crystal structure of the bisphoshane ligand in **8** bound to a π-allyl palladium complex see: T. Hayashi, A. Yamamoto, Y. Ito, E. Nishioka, H. Miura, K. Yanagi, *ibid. 111* (1989) 6301.
[64] H. Adams, N. A. Bailey, J. T. Gauntlett, M. J. Winter, *J. Chem. Soc. Chem. Commun. 1984*, 1360 (CSD Refcod: COCKIO).
[65] Two crystal structures reported by *Floriani* and co-workers also support these contentions. Formaldehyde binds to the vanadium(II) complex Cp_2V in an η^2 fashion (S. Gambarotta, C. Floriani, A. Chiesi-Villa, C. Guastini, *J. Am. Chem. Soc. 104* (1982) 2019), while the more oxidized $Cp_2V^{\oplus}$ is η^1-bound to acetone (S. Gambarotta, M. Pasquali, C. Floriani, A. Chiesi-Villa, C. Guastini, *Inorg. Chem. 20* (1981) 1173). We thank one of the referees for bringing these structures to our attention.
[66] W. Oppolzer, I. Rodriquez, J. Blagg, G. Bernardinelli, *Helv. Chim. Acta 72* (1989) 123.
[67] Taken in part from the *Ph.D. Thesis* of William E. Crowe, Yale University 1988, New Haven, CT, USA.
[68] a) T. A. Albright, *Acc. Chem. Res. 15* (1982) 149; b) B.E.R. Schilling, R. Hoffmann, J. W. Faller, *J. Am. Chem. Soc. 101* (1979) 592; c) N. M. Kostic, R. F. Fenske, *Organometallics 1* (1982) 974; d) *J. Am. Chem. Soc. 104* (1982) 3879; e) M. B. Hall, R. F. Fenske, *Inorg. Chem. 11* (1972) 768; f) A. K. Rappé, W. A. Goddard III, *J. Am. Chem. Soc. 104* (1982) 448, 3287; g) E. A. Carter, W. A. Goddard III, *ibid. 108* (1986) 4746.
[69] a) W. A. Nugent, J. M. Mayer: *Metal-Ligand Multiple Bonds*, Wiley Interscience, New York 1988; b) R. R. Schrock, *Acc. Chem. Res. 12* (1979) 98; c) J. L. Templeton, P. B. Winston, B. C. Ward, *J. Am. Chem. Soc. 103* (1981) 7713.
[70] S. Georgiou, J. A. Gladysz, *Tetrahedron 42* (1986) 1109.
[71] Since the evolution of the frontier orbitals that participate in primary stereoelectronic interactions is fairly well understood and has been discussed at length elsewhere (see, for example [68 a]), it will not be considered further here.
[72] G. S. Bodner, A. T. Patton, D. E. Smith, S. Georgiou, W. Tam, W.-K. Wong, J. A. Gladysz, *Organometallics 6* (1987) 1954.
[73] S. G. Davies, I. M. Dordor-Hedgecock, K. H. Sutton, J. C. Walker, *Tetrahedron 42* (1986) 5123.
[74] L. S. Liebeskind, M. E. Welker, R. W. Fengl, *J. Am. Chem. Soc. 108* (1986) 6328.
[75] a) B. K. Blackburn, S. G. Davies, M. Whittaker in I. Bernal (Ed.): *Stereochemistry of Organometallic and Inorganic Compounds, Vol. 3*, Elsevier, Amsterdam 1988; b) B. K. Blackburn, S. G. Davies, K. H. Sutton, M. Whittaker, *Chem. Soc. Rev. 7* (1988) 147.
[76] a) J. I. Seeman, S. G. Davies, *J. Chem. Soc. Chem. Commun. 1984*, 1019; b) *J. Am. Chem. Soc. 107* (1985) 6522; c) S. G. Davies, I. M. Dordor-Hedgecock, K. H. Sutton, M. Whittaker, *ibid. 109* (1987) 5711.
[77] W.-K. Wong, W. Tam, C. E. Strouse, J. A. Gladysz, *J. Chem. Soc. Chem. Commun. 1979*, 530 (CSD Refcod: FMCPRE).
[78] J. W. Herndon, C. Wu, H. L. Ammon, *J. Org. Chem. 53* (1988) 2873.
[79] V. G. Albano, P. L. Bellon, M. Sansoni, *Inorg. Chem. 8* (1969) 298 (CSD Refcod: ICOIRP).
[80] C. Sontag, O. Orama, H. Berke, *Chem. Ber. 120* (1987) 559.
[81] P. DesLongchamps: *Stereoelectronic Effects in Organic Chemistry*, Pergamon, Oxford 1983, Chapter 3.

[82] Evaluation of the orbital mixing that occurs when a π-bonding ligand interacts with a transition-metal center requires the assessment of second-order mixing which takes place when two or more orbitals on the same fragment (i.e., metal d and p orbitals) overlap with the same orbital of an interacting ligand (i.e., ligand p orbital). The result of this second-order mixing is that bonding and antibonding orbitals are hybridized toward the ligand involved in the bonding interaction, and nonbonding orbitals are hybridized away from the ligand. This is illustrated in Scheme 4 for the

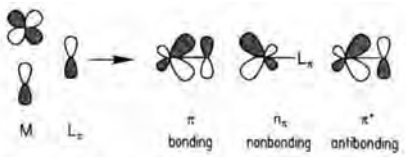

Scheme 4. Orbital mixing leading to π-bond hybridization.

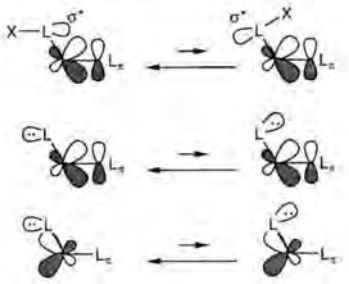

Scheme 5. Possible stereoelectronic interactions in complexes consisting of a σ-bound ligand L and a complex fragment M-L_n, where L and L_n are *cis*. The X–L–M–L_n dihedral angle is 180° on the left and 0° on the right.

interaction of a π-bonding ligand with a transition-metal center. There are three types of stereoelectronic interactions that could influence the *syn–anti* isomerism of a ligand bound *cis* to a π-bonding ligand: (1) π↔acceptor (e.g., σ*)—a stabilizing two-center two-electron interaction (Scheme 5, top); (2) π↔π′ donor (e.g., lone pair)—a destabilizing two-center four-electron interaction (Scheme 5, middle); (3) n_π↔donor (e.g., lone pair)—a stabilizing two-center two-electron interaction (Scheme 5, bottom). The relative importance of the three types of stereoelectronic interactions depicted above will, of course, depend on the nature of the metal–L_n bonding interaction [70]. In all cases, however, ligand conformations that place a ligand acceptor orbital *syn* or a donor obital *anti* to a metal ligand π bond are stereoelectronically favored. For a complete discussion of the theoretical basis of second-order mixing see ref. [67].

[83] G. O. Nelson, C. E. Sumner, *Organometallics 5* (1986) 1983 (CSD Refcod: CIMXAX).
[84] J. D. Korp, I. Bernal, *J. Organomet. Chem. 220* (1981) 355.
[85] G. W. Adamson, J. J. Daly, D. Forster, *J. Organomet. Chem. 71* (1974) C17.
[86] a) D. J. Hodgson, J. A. Ibers, *Inorg. Chem. 7* (1968) 2345; b) *ibid. 8* (1969) 1282 (CSD Refcod: CNOPIR).
[87] C. G. Pierpont, D. G. Van Derveer, W. Durland, R. Eisenberg, *J. Am. Chem. Soc. 92* (1970) 4760 (CSD Refcod: TPNORU10).
[88] P. H. Turner, M. J. Corkill, A. P. Cox, *J. Phys. Chem. 83* (1979) 1473.
[89] a) S. Ruschin, S. H. Bauer, *J. Phys. Chem. 84* (1980) 3061; b) C. E. Blom, H. H. Günthard, *Chem. Phys. Lett. 84* (1981) 267.
[90] a) M. R. Churchill, H. J. Wasserman, S. J. Holmes, R. R. Schrock, *Organometallics 1* (1982) 766 (CSD Refcod: BILKEM); b) K. R. Birdwhistell, T. L. Tonker, J. L. Templeton, *J. Am. Chem. Soc. 107* (1985) 4474 (CSD Refcod: DAKVOA); c) A. Mayr, G. A. McDermott, A. M. Dorries, D. Van Engen, *Organometallics 6* (1987) 1503.
[91] a) [69c]; b) K. Tatsumi, R. Hoffmann, J. L. Templeton, *Inorg. Chem. 21* (1982) 466; c) P. B. Winston, S. J. N. Burgmayer, J. L. Templeton, *Organometallics 2* (1983) 167.
[92] This model was first proposed by *Templeton* et al.. See: D. C. Brower, K. R. Birdwhistell, J. L. Templeton, *Organometallics 5* (1986) 94.
[93] B. L. Haymore, E. A. Maatta, R. A. D. Wentworth, *J. Am. Chem. Soc. 101* (1979) 2063 (CSD Refcod: PNTCMO).
[94] W. A. Nugent, R. L. Harlow, R. J. McKinney, *J. Am. Chem. Soc. 101* (1979) 7265 (CSD Refcod: ADOOSB).
[95] S. Shambayati, S. L. Schreiber, J. F. Blake, S. G. Wierschke, W. L. Jorgensen, *J. Am. Chem. Soc. 112* (1990) 697.
[96] a) G. E. Keck, S. Castellino, *Tetrahedron Lett. 28* (1987) 281; b) G. E. Keck, E. P. Boden, *ibid. 25* (1984) 265; c) S. D. Kahn, G. E. Keck, W. J. Hehre, *ibid. 28* (1987) 279.
[97] [1], p. 312.

Communications may be submitted in English *or* in German. Further details regarding the submission of communications can be found in the "Notice to Authors" reproduced in the January issue of the journal. Copies thereof may be obtained from the editorial office upon request.

The Preparation of Finely Divided Metal and Alloy Powders

By *Helmut Bönnemann,* Werner Brijoux,* and *Thomas Joussen*

Dedicated to Prof. Günther Wilke on the occasion of his 65th birthday

Finely divided powders of metals and alloys are of great interest in industrial powder technology[1] and as catalysts.[2] Newer methods for the preparation of metals in the form of very fine powders are metal evaporation,[3] electrolytic processes,[4] and the reduction of metal salts, either with naphthalene-activated alkali metals[5] or with anthracene-activated magnesium.[6] We report here a process for preparing finely divided powders of metals and alloys by reducing metal salts in organic phases. The salts are kept in solution using organoboron complexing agents BR_3 or $BR_n(OR')_{3-n}$ (R,R' = alkyl or aryl; $n = 0, 1, 2$) in the form of hydroorganoborates[7] of the general formula $M'H_v \cdot (BR_3)_v$ or $M'H_v[BR_n(OR')_{3-n}]_v$ (M' = alkali or alkaline earth metal, $v = 1, 2$).

Elements of groups 6–12 and 14 of the periodic table can be prepared as pure powders by treating their metal salts with hydroorganoborates in THF or hydrocarbons at temperatures between −20 °C and 67 °C. Since the ate complexes formed by reaction of hydroxides, alkoxides, cyanides, cyanates and thiocyanates with the organoboron complexing agents are highly soluble in organic solvents, the metal powders can be isolated according to Equation (a) ($u = 1, 2$) by simple filtration (Table 1). The organoboron complexing agent can be regenerated by treatment with acid. Thus, HCl/THF liberates 98% of the triethylborane from $Na(BEt_3)OH$.

$$uMX_v + vM'(BR_3H)_u \xrightarrow{THF} uM\downarrow + vM'(BR_3X)_u + uv/2\ H_2\uparrow \quad (a)$$

M = metal powder,

M' = alkali or alkaline earth metal,

R = C_1-C_6-alkyl;

X = OH, OR, CN, OCN, SCN

M' halides do not generally form stable ate complexes, but, in many cases, remain with the BR_3 in solution in the organic solvent [Eq. (b)]. This is true in particular in the case of LiCl, LiBr, LiI, and NaI in THF. To simplify the regeneration, the cation in the hydride is chosen so that the corresponding halide is soluble in organic solvents. If the M' halide (e.g., NaCl) precipitates, it must be separated from the metal powder by washing with water.

[*] Prof. Dr. H. Bönnemann, Dr.-Ing. W. Brijoux, Dipl.-Chem. T. Joussen
Max-Planck-Institut für Kohlenforschung
Postfach 101353, D-4330 Mülheim a.d. Ruhr (FRG)

Table 1. Preparation of microcrystalline to amorphous metal powders from MX_v in THF with formation of soluble borates $(BR_3X)^{\ominus}$ [Eq. (a)].

No.	Educt metal salt	Reducing agent	Conditions t [h]	Conditions T [°C]	Product Metal content [%]	Product Boron content [%]
1	$Fe(OEt)_2$	$NaBEt_3H$	16	67	96.8	0.16
2	$Co(OH)_2$	$NaBEt_3H$	2	23	94.5	0.40
3	$Co(CN)_2$	$NaBEt_3H$	16	67	96.5	0.20
4	$Ni(OH)_2$	$NaBEt_3H$	2	23	94.7	0.13
5	$Ni(OEt)_2$	$NaBEt_3H$	16	67	91.4	0.58
6	CuCN	$LiBEt_3H$	2	23	97.3	0.0
7	CuSCN	$NaBEt_3H$	16	67	95.0	0.23
8	$Pd(CN)_2$	$NaBEt_3H$	16	67	95.5	1.38
9	AgCN	$Ca(BEt_3H)_2$ [a]	2	23	89.6	0.20
10	$Cd(OH)_2$	$NaBEt_3H$	2	23	97.9	0.22
11	$Pt(CN)_2$	$NaBEt_3H$	16	67	87.5	0.93
12	AuCN	$NaBEt_3H$	2	23	97.5	0.0

[a] Solvent: diglyme

$$uMX_v + vM'(BR_3H)_u \xrightarrow{THF} uM\downarrow + vM'X_u + vBR_3 + uv/2\ H_2\uparrow \quad (b)$$

X = halogen

The reduction of metal halides can also be achieved using a "catalytic amount" of BR_3, since the organoboron complexing agents liberated according to Equation (b) react in situ with further $M'H_v$ [Eq. (c), Table 2, Nos. 5 and 23).

$$uMX_v + vM'H_u \xrightarrow{BR_3,\ THF} uM\downarrow + vM'X_u + uv/2\ H_2\uparrow \quad (c)$$

X = halogen

The line widths in the X-ray diffractograms reveal that the metal powders prepared in this way are microcrystalline to amorphous. The line widths of the strongest reflection ($Co_{K\alpha}$ radiation, Fe filter)[8] allowed an initial rough estimate of ca. 5 nm for the grain size of the base metals Fe, Co and Ni. According to scanning electron microscope studies,[8] the particle size lies between 10 and 100 nm.

In analogy to Equations (a) and (b), the simple co-reduction of salts of different metals affords alloys of two and more metals. This method corresponds to a "cold powder technology". The alloy powders, which are shown by X-ray diffraction measurements to be practically amorphous, can be generated on support materials; this is of particular interest in catalytic applications. Co-reduction of $FeCl_3$ and $CoCl_2$ according to Equation (b) yields a boron-free Fe/Co powder with a particle size of ca. 100 nm (Table 3, No. 3). In the diffractogram,[8] only the diffuse strongest reflection at a scattering angle 2θ of 52.5° and a reciprocal lattice distance D of 2.02 Å can be discerned (Fig. 1a, bottom). The line

Table 2. Preparation of microcrystalline to amorphous metal powders from metal halides in THF [Eq. (b)]; Py = pyridine, COD = 1,5-cyclooctadiene.

No.	Educt Metal salt	Reducing agent	Conditions t [h]	T [°C]	Product Metal content [%]	Boron content [%]
1	$CrCl_3$	$NaBEt_3H$	2	23	93.3	0.3
2	$MnCl_2$	$LiBEt_3H$	1	23	94.0	0.42
3	$FeCl_3$	$LiBEt_3H$	2	23	97.1	0.36
4	CoF_2	$NaBEt_3H$	16	67	96.9	0.0
5	$CoCl_2$	LiH + 10% BEt_3	16	67	95.8	0.0
6	$CoBr_2$	$LiBEt_3H$	2	23	86.6	0.0
7	$NiCl_2$	$NaBEt_3H$	16	67	96.9	0.0
8	$CuBr_2$	$LiBEt_3H$	2	23	94.9	0.0
9	$CuCl_2$	$Na(Et_2BOMe)H$	2	23	94.7	0.1
10	$ZnCl_2$	$LiBEt_3H$	12	67	97.8	0.0
11	$RuCl_3$	$NaBEt_3H$	16	67	95.2	0.52
12	$RhCl_3 \cdot 3\,H_2O$	$NaBEt_3H$	2	23	98.1	0.10
13	$RhCl_3$	$LiBEt_3H$	2	23	96.1	0.66
14	$PdCl_2$	$NaBEt_3H$	16	67	98.0	0.29
15	AgF	$NaB(OMe)_3H$	2	23	94.1	0.05
16	AgI	$NaBEt_3H$	2	23	95.3	0.02
17	$CdCl_2$	$LiBEt_3H$	2	23	99.4	0.0
18	$ReCl_3$	$LiBEt_3H$	2	23	95.4	0.0
19	$OsCl_3$	$NaBEt_3H$	2	23	95.8	0.0
20	$IrCl_3 \cdot 4\,H_2O$	$NaBEt_3H$	2	23	77.1	0.16
21	$IrCl_3$	$KBPr_3H$	16	67	94.7	0.08
22	$PtCl_2$	$NaBEt_3H$	2	23	98.2	0.21
23	$PtCl_2$	LiH + 10% BEt_3	5	67	98.8	0.0
24	$PtCl_2$	$LiBEt_3H$	12	67	99.0	0.0
25	$PtCl_2$	$LiBEt_3H$	4	0	99.0	0.0
26	$SnCl_2$	$LiBEt_3H$	2	23	96.7	0.0
27	$SnBr_2$	$LiBEt_3H$	2	23	87.1	0.0
28	$Pt(NH_3)_2Cl_2$	$NaBEt_3H$	2	23	97.1	0.32
29	$Pt(Py)_2Cl_2$	$LiBEt_3H$	2	23	97.1	0.02
30	$Pt(Py)_4Cl_2$	$LiBEt_3H$	2	23	97.5	0.01
31	$CODPtCl_2$	$NaBEt_3H$	2	60	97.9	0.58

width reveals that weakly crystalline to amorphous phases are present in the Fe/Co powder. After the sample has been heat treated (2 h, 400 °C), one observes that the line becomes sharper (Fig. 1 a, top). Since scanning electron microscopy[8] shows that the particle size is unchanged by the heat treatment, the sharpening of the peak indicates that the grain size has increased.

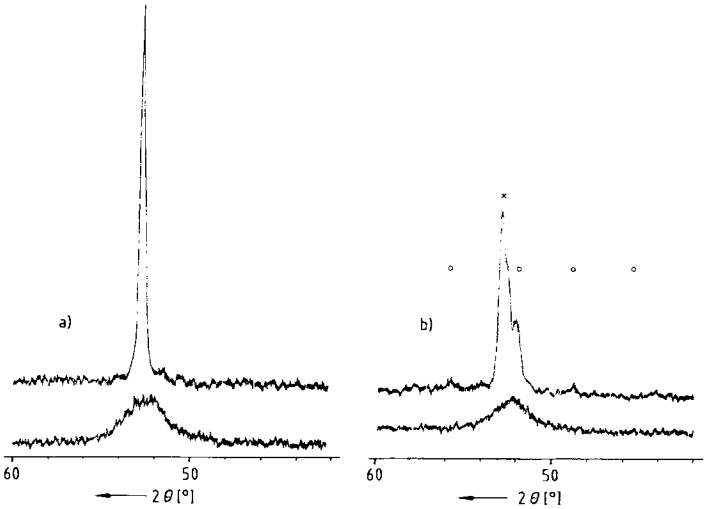

Fig. 1 a) Strongest reflection in the diffractogram of the Fe/Co alloy (Table 3, No. 3); bottom: untreated original sample; top: after 2 h at 400 °C ($Co_{K\alpha}$-radiation with Fe filter). b) Strongest reflection in the diffractogram of an Fe/Co mixture; bottom: untreated original sample; top: after 2 h at 400 °C. x = Fe, o = Co ($Co_{K\alpha}$ radiation with Fe filter).

A comparison of the diffractograms of the alloys with that of a mixture of amorphous iron and cobalt powders (Fig. 1 b, bottom) demonstrates that the Fe/Co alloy is formed at the stage of the co-reduction (under thermodynamic control[9]) and not as a result of the subsequent heat treatment: after the tempering, the diffractogram of the Fe/Co mixture (Fig. 1 b, top) is, in contrast to that of the alloy, a superimposition of two sets of lines for Fe and Co.

Table 3. Preparation of microcrystalline to amorphous alloys by co-reduction of metal salts in THF

No.	Educt Metal salt	Reducing agent	Conditions t [h]	T [°C]	Products Metal [%]	Boron [%]	DIF [a] 2θ [b] [°]	D [c] [Å]	Comments
1	$CO(OH)_2$ $Ni(OH)_2$	$NaBEt_3H$	7	67	Co: 48.3 Ni: 45.9	0.25	51.7	2.05	single phase microcrystalline
2	$FeCl_3$ $CoCl_2$	LiH + 10% BEt_3	6	67	Fe: 47.0 Co: 47.1	0.0	52.7	2.02	single phase microcrystalline
3	$FeCl_3$ $CoCl_2$	$LiBEt_3H$	5	23	Fe: 54.8 Co: 24.5	0.0	52.5 99.9	2.02 1.17	single phase microcrystalline
4	$CoCl_2$ $PtCl_2$	$LiBEt_3H$	7	67	Co: 21.6 Pt: 76.3	0.0	55.4 47.4	1.93 2.23	single phase
5	$RhCl_3$ $PtCl_2$	$LiBEt_3H$	5	67	Rh: 26.5 Pt: 65.5	0.04	40.2 46.3	2.24 1.96	single phase
6	$RhCl_3$ $IrCl_3$	$LiBEt_3H$	5	67	Rh: 33.5 Ir: 62.5	0.15	42.3	2.14	single phase + traces $IrCl_3$
7	$PdCl_2$ $PtCl_2$	$LiBEt_3H$	5	67	Pd: 33.6 Pt: 63.4	0.04	40.1 46.3	2.25 1.96	single phase
8	$PtCl_2$ $IrCl_3$	$NaBEt_3H$	12	67	Pt: 50.2 Ir: 48.7	0.15	40.0 46.5	2.25 1.95	single phase microcrystalline
9	$CuCl_2$ $SnCl_2$	$LiBEt_3H$	4	67	Cu: 49.6 Sn: 47.6	0.0	30.2 53.5	2.96 1.80	Cu_6Sn_5 + Cu + Sn
10	$FeCl_3$ $CoCl_2$ $NiCl_2$	$LiBEt_3H$	1.5	23	Fe: 30.1 Co: 31.4 Ni: 30.9	0.0			single phase microcrystalline

[a] X-ray diffractogram, $Co_{K\alpha}$ irradiation, Fe filter. [b] Strongest reflection(s). [c] Reciprocal lattice distance.

 © VCH Verlagsgesellschaft mbH, D-6940 Weinheim, 1990 0570-0833/90/0303-0274 $ 02.50/0

The fact that an alloy had been prepared as a result of the co-reduction was finally proved by recording a Mössbauer spectrum (source: $^{57}Co/Pt$, 27 °C)[10] of the sample before heat treatment. The spectrum shows the characteristic six resonance lines for metallic iron. The total splitting (i.e., the distance between the outer lines) is 36 T, a value which has been found for comparable alloys formed by melting but which is 3 T larger than for pure iron.

Therefore the co-reduction of metal salts in organic solvents with hydroorganoborates provides a method of preparing single-phase, almost amorphous alloys of two or more components (Table 3).

The redox potential of sodium hydrotriethylborate in THF (supporting electrolyte: NBu_4PF_6) was determined electrochemically to be -0.77 V, corresponding to -0.62 V in H_2O.[11] Thus, the reaction between the metal salt and the hydride proceeds either as a reduction or as a metathesis depending on the particular metal involved. The findings described above can be rationalized on the basis of the HSAB concept.[12] The metal ions $M^{\oplus}$ act as soft acids and compete with the moderately hard acid BR_3[13] for the soft basic hydride ion to form **1**. If $M^{\oplus}$ is a softer acid than BR_3, the hydride is transferred to $M^{\oplus}$, the resulting MH then decomposes spontaneously to metal and hydrogen [Eq. (d)].

$$MX + M'(BR_3H) \xrightarrow{-M'X} \underset{\mathbf{1}}{(M\cdots H\cdots BR_3]} \longrightarrow [MH] + BR_3 \xrightarrow{-BR_3} M\downarrow + 1/2\ H_2\uparrow \qquad \text{(d)}$$

Experimental

Preparation of an iron/cobalt alloy from $FeCl_3$, $CoCl_2$ and $LiBEt_3H$ in THF: A solution of 9.1 g (56 mmol) of $FeCl_3$ and 3.1 g (24 mmol) of $CoCl_2$ in 2.5 L of THF was added dropwise to a stirred 1.7 M (255 mmol) solution of $LiBEt_3H$ in THF over 5 h at 23 °C. After stirring overnight, the iron/cobalt alloy was separated from the clear reaction solution and washed twice with 200 mL portions of THF. The product was then stirred with 300 mL of ethanol and subsequently with a mixture of 200 mL of ethanol and 200 mL of THF until the evolution of gas ceased. Finally, the product was washed again with 2×200 mL of THF. The yield of alloy powder after drying in a high vacuum (10^{-3} mbar) was 5.0 g (Table 3, No. 3); Particle size according to scanning electron microscopy: 10–100 nm.

Received: October 25, 1989 [3607 IE]
German version: *Angew. Chem. 102* (1990) 324

[1] a) R. Kieffer, F. Benesovsky, *Ullmanns Encykl. Techn. Chem. 4th Edit. Vol. 19*, pp. 563; b) K. H. Roll, *Kirk-Othmer, Encycl. Chem. Technol., 3rd Edit. Vol. 19*, pp. 28.
[2] R. Krabetz, W. D. Mross, *Ullmanns Encykl. Techn. Chem. 4th Edit. Vol. 13*, pp. 517.
[3] S. C. Davis, K. J. Klabunde, *Chem. Rev. 82* (1982) 152–208.
[4] N. Ibl, *Chem. Ing.-Tech. 36* (1964) 601–609.
[5] R. D. Rieke, *Organometallics 2* (1983) 377.
[6] H. Bönnemann, B. Bogdanović, DOS 3541633 (May 27, 1989), Studiengesellschaft Kohle mbH.
[7] R. Köster, *Methoden Org. Chem. (Houben-Weyl), 4th Edit. Vol. XII/3b*, pp. 798.
[8] We thank Dr. *G. Block* and *E. Schauf*, Gesellschaft für Systemtechnik mbH, Münchener Strasse 100, D-4300 Essen 1 (FRG), for the measurement and interpretation of the X-ray diffractograms and for the scanning electron microscope studies.
[9] E. A. Moelwyn-Hughes: *Physikalische Chemie*, Thieme, Stuttgart 1970, pp. 325.
[10] We acknowledge the help of Prof. Dr. *W. Keune* and Dipl.-Ing. *U. von Hörsten*, Laboratorium für Angewandte Physik, Universität-Gesamthochschule Duisburg, for recording and interpreting the Mössbauer spectra.
[11] We thank Prof. Dr. *U. Kölle*, Institut für Anorganische und Elektrochemie, Technische Hochschule Aachen, for providing us with these results.
[12] HSAB (Hard and Soft Acids and Bases): R. G. Pearson, *Surv. Prog. Chem. 5* (1969) pp. 1–52.
[13] L. Kolditz (Ed): *Anorganikum, Teil 1*, VEB Deutscher Verlag der Wissenschaften, Berlin 1981, pp. 474.

Ketenimine Complexes from Metal Isocyanides and Diazoalkanes**

By *Beate Strecker* and *Helmut Werner**

Dedicated to Professor Günther Wilke on the occasion of his 65th birthday

Carbene-metal complexes react with isocyanides under mild conditions to give ketenimine–metal compounds which are useful building blocks for the synthesis of four-, five-, and six-membered carbo- and N-heterocycles.[1] With regard to the converse reaction, namely addition of a free carbene to a metal isocyanide, so far the only example has been the synthesis of the nickel complex $Ni[\eta^2\text{-}N,C\text{-}(t\mathrm{Bu})N{=}C{=}C(CN)_2](CN t\mathrm{Bu})_2$.[2]

As part of a study of [2+2]- and [2+3]-cycloadditions of cobalt isocyanide complexes $[(C_5H_5)Co(CNR)(PMe_3)]$,[3] we have found that their reactions with carbene sources, as for instance diaryldiazomethanes, opens up a facile entry to ketenimine complexes. This formal [2+1]-cycloaddition of a carbene to a M=C=NR moiety reinforces our recently developed method of adding a nitrene to an M=C=CHR unit, which leads to an N,C-bound ketenimine ligand.[4]

The cobalt compounds **1** and **2** react with Ph_2CN_2, $(p\text{-Tol})_2CN_2$, and 9-diazofluorene in acetone at -78 to 20 °C to give the dark-colored, slightly air- and moisture-sensitive complexes **3**–**6**.[5] The "side-on" coordination (π-bond) of the ketenimine ligand which is expected for electron-rich ligand–metal fragments[1] is clearly demonstrated by the IR and NMR spectroscopic data.[6] Moreover, these data confirm that in **3** and **4** the ketenimine is coordinated via the C=C bond, whereas in complexes **5** and **6** it is bound via the C=N bond. Supporting evidence for the two types of bonding is provided by: 1) the difference in the NCC stretching frequencies in the IR (ca. 1695 cm^{-1} for **3** and **4** in contrast to ca. 1625 cm^{-1} for **5** and **6**); 2) the different chemical shift and coupling constants of the signal of the NCH_3 protons in the ^{1}H-NMR spectra; and 3) the considerable difference in the chemical shift of the signals of the C_α and C_β atoms in the ^{13}C-NMR spectra of **3**, **4** and **5**, **6**.[6]

$$[(C_5H_5)Co(CNR)(PMe_3)] + R'_2CN_2 \xrightarrow[-N_2]{} [(C_5H_5)Co(RN{=}C{=}CR'_2)(PMe_3)]$$

1, R = Me
2, R = (*S*)-CHMePh

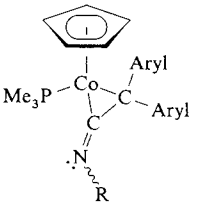

3, **4**

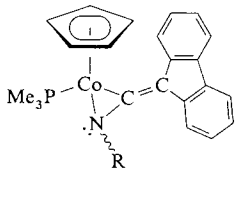

5, **6**

3, R = Me, $CR'_2 = CPh_2$
4, R = Me, $CR'_2 = C(p\text{-Tol})_2$
5, R = Me, $CR'_2 = C(C_{12}H_8)$
6, R = CHMePh, $CR'_2 = C(C_{12}H_8)$

[*] Prof. H. Werner, Dipl. Chem. B. Strecker
Institut für Anorganische Chemie der Universität
Am Hubland, 8700 Würzburg (FRG)

[**] This work was supported by the Volkswagen Foundation and the Fonds der Chemischen Industrie. We thank Prof. *P. L. Pauson*, University of Strathclyde, Glasgow for helpful discussions and *P. Schwab* for experimental assistance.

The proposed structure of **3** and **4** is further supported by a comparison of the ^{13}C-NMR data with those of the rhodium complexes $[(C_5H_5)Rh(\eta^2\text{-}C,C\text{-}RN{=}C{=}CHPh)(PiPr_3)]$ ($R = p\text{-}SO_2C_6H_4Me$, $o\text{-}C_6H_4NO_2$)[4b] and $[(C_5H_5)Rh(\eta^2\text{-}CH_2{=}C{=}CHR)(PiPr_3)]$ (R = H, Me, Ph),[7] in which the respective heteroallene and allene ligands are also coordinated via a C=C bond. The reaction of **2** with 9-diazofluorene affords, as expected, two diastereomers, which can be easily discerned by the duplicate sets of signals in both the ^{1}H- and ^{13}C-NMR spectra of **6**.[6]

By adding an equimolar amount of iodine to toluene solutions of complexes **3**–**6**, the corresponding ketenimines **7**–**10** are formed. $C_5H_5Co(PMe_3)I_2$ is obtained as by-product.[8] Compounds **7**–**10** are soluble in most organic solvents and can be isolated in good yields as yellow, partially oily materials. Compound **7** had previously been described and was spectroscopically characterized;[9] **8**–**10** are, to our knowledge, new compounds not yet reported in the literature. In the IR spectra, very intense bands are found at ca. 2020 to 2030 cm^{-1}, which are characteristic for ketenimines;[10] this is also the range expected for IR bands typical of cumulenes.[11]

R/CR'$_2$ see **3**–**6** (above)

Since both cobalt complexes of the type $[(C_5H_5)Co(L)(CNR)]$[12] as well as diaryldiazoalkanes are easily accessible, we assume that other novel ketenimines, similar to **8**–**10**, can also be prepared in two steps in this way. It is predicted that isocyanide complexes, like carbene complexes,[1, 13] will establish themselves as useful building blocks for the synthesis of various heterocyclic compounds.

Received: August 28, 1989 [Z 3523 IE]
German version: *Angew. Chem. 102* (1990) 310
Publication delayed at authors' request

[1] R. Aumann, *Angew. Chem. 100* (1988) 1512; *Angew. Chem. Int. Ed. Engl. 27* (1988) 1456, and references cited therein.

[2] D. J. Yarrow, J. A. Ibers, Y. Tatsuno, S. Otsuka, *J. Am. Chem. Soc. 95* (1973) 8590.

[3] a) H. Werner, B. Heiser, C. Burschka, *Chem. Ber. 115* (1982) 3069; b) H. Werner, B. Heiser, H. Otto, *ibid. 118* (1985) 3932; c) review: H. Werner in A. de Meijere, H. tom Dieck (Eds.): *Organometallics in Organic Synthesis*, Springer, Heidelberg 1987, p. 51.

[4] a) A. Höhn, H. Werner, *Chem. Ber. 121* (1988) 881; b) U. Brekau, *Dissertation*, Universität Würzburg 1989.

[5] a) Experimental procedure for **3**: A solution of Ph_2CN_2 (1.0 mmol) in acetone (5 mL) was added at −78 °C to a solution of **1** (1.0 mmol) in acetone (15 mL). The reaction mixture was stirred and allowed to warm to room temperature (3.5 h). The solvent was then removed in vacuo and the residue extracted with 20 mL of ether. On cooling the extract to −78 °C, red needles were formed; yield 63%; m.p. 135 °C (dec.); b) **4**: recrystallization from benzene/pentane (1:1); red-brown crystals; yield 54%; m.p. 130 °C (dec.); c) **5**: work-up directly after warming to room temperature; recrystallization from benzene/pentane (1:1); dark green crystals; yield 68%, m.p. 45 °C (decomp.); d) **6**: work-up directly after warming to room temperature; dark green crystals from ether at −78 °C; yield 63%; m.p. 47 °C (dec.). Satisfactory elemental analyses (C,H,N) were obtained for all compounds.

[6] Spectroscopic data. **3**: M_r = 407 (MS); IR (KBr): ν(NCC) = 1700 cm^{-1}; ^{1}H NMR (90 MHz, C_6D_6): δ = 7.36 (m, C_6H_5), 4.25 (d, J_{PH} = 0.9 Hz, C_5H_5), 3.97 (d, J_{PH} = 0.9 Hz, NCH_3), 0.32 (d, J_{PH} = 8.9 Hz, PMe_3); ^{13}C NMR (22.5 MHz, C_6D_6): δ = 207.1 (d, J_{PC} = 18.6 Hz, =C=), 152.4, 146.5, 128.2, 127.1, 125.3, 122.9 (all s, C_6H_5), 84.9 (d, J_{PC} = 1.7 Hz, C_5H_5), 46.2 (d, J_{PC} = 2.6 Hz, NCH_3), 19.4 (d, J_{PC} = 28.2 Hz, PMe_3), 11.0 (d, J_{PC} = 2.6 Hz, $=CPh_2$).—**4**: M_r = 435 (MS); IR (KBr): ν(NCC) = 1690 cm^{-1}; ^{1}H NMR (90 MHz, C_6D_6): δ = 7.55 (d, J_{HH} = 8.0 Hz, C_6H_4), 6.94 (d, J_{HH} = 8.0 Hz, C_6H_4), 4.31 (d, J_{PH} = 0.8 Hz, C_5H_5), 4.00 (d, J_{PH} = 0.6 Hz, NCH_3), 2.05 (s, $C_6H_4CH_3$), 2.02 (s, $C_6H_4CH_3$), 0.38 (d, J_{PH} = 8.9 Hz, PMe_3); ^{13}C NMR (50.3 MHz, C_6D_6): δ = 207.9 (d, J_{PC} = 17.8 Hz, =C=), 149.4, 143.7, 134.5, 131.8 (all s, C_6H_4), 84.9 (s, C_5H_5), 46.2 (d, J_{PC} = 2.8 Hz, NCH_3), 21.1 (s, $C_6H_4CH_3$), 20.9 (s, $C_6H_4CH_3$), 19.0 (d, J_{PC} = 27.8 Hz, PMe_3), 10.7 (s, br, $=C(p\text{-tol})_2$).—**5**: M_r = 405 (MS); IR (KBr): ν(NCC) = 1625 cm^{-1}; ^{1}H NMR (90 MHz, C_6D_6): δ = 9.05 (d, br, J_{HH} = 7.5 Hz, C_6H_4), 7.73 (m, C_6H_4), 4.54 (d, J_{PH} = 0.5 Hz, C_5H_5), 2.66 (s, NCH_3), 0.46 (d, J_{PH} = 10.2 Hz, PMe_3); ^{13}C NMR (50.3 MHz, C_6D_6): δ = 175.2 (d, J_{PC} = 18.7 Hz, =C=), 142.8, 137.9, 136.8, 134.2, 125.7, 125.5, 122.7, 122.3, 121.5, 120.4, 120.1, 118.9 (all s, C_6H_4), 101.9 (s, $=C(C_{12}H_8)$), 83.8 (s, C_5H_5), 45.0 (s, NCH_3), 16.4 (d, J_{PC} = 28.3 Hz, PMe_3).—**6**: IR (KBr): ν(NCC) = 1626 cm^{-1}; ^{1}H NMR (90 MHz, C_6D_6): δ = 9.11 (d, br, J_{HH} = 8.2 Hz, C_6H_4), 7.19 (m, br, C_6H_4 and C_6H_5), 5.03 (q, J_{HH} = 6.6 Hz, C*H*MePh), 4.80 (q, J_{HH} = 6.9 Hz, C*H*MePh), 4.39 (d, J_{PH} = 0.6 Hz, C_5H_5), 4.27 (d, J_{PH} = 0.5 Hz, C_5H_5), 1.56 (d, J_{HH} = 6.8 Hz, $CH(CH_3)Ph$), 1.01 (d, J_{HH} = 6.6 Hz, $CH(CH_3)Ph$), 0.44 (d, J_{PH} = 10.1 Hz, PMe_3), 0.43 (d, J_{PH} = 10.2 Hz, PMe_3); ^{13}C NMR (50.3 MHz, C_6D_6): δ = 162.9 (d, J_{PC} = 18.9 Hz, =C=), 160.4 (d, J_{PC} = 17.5 Hz, =C=), 145.8, 144.6, 143.1, 142.6, 138.5, 138.0, 135.7, 135.5, 134.0, 133.7, 128.3, 127.8, 127.7, 127.1, 126.8, 126.6, 125.5, 125.3, 125.2, 121.7, 121.5, 121.1, 120.5, 120.2, 116.6, 116.5 (all s, C_6H_4 and C_6H_5), 97.7 (s, $=C(C_{12}H_8)$), 96.7 (s, $=C(C_{12}H_8)$), 82.8 (s, C_5H_5), 82.7 (s, C_5H_5), 58.1 (s, *C*HMePh), 56.2 (s, *C*HMePh), 21.7 (s, $CH(CH_3)Ph$), 17.7 (s, $CH(CH_3)Ph$), 16.4 (d, J_{PC} = 27.8 Hz, PMe_3), 16.2 (d, J_{PC} = 27.9 Hz, PMe_3).

[7] J. Wolf, R. Zolk, U. Schubert, H. Werner, *J. Organomet. Chem. 340* (1988) 161.

[8] H. Werner, B. Juthani, *Z. Anorg. Allg. Chem. 473* (1981) 107.

[9] a) C. L. Stevens, J. C. French, *J. Am. Chem. Soc. 76* (1954) 4398; b) S. Otsuka, A. Nakamura, T. Yoshida, *J. Organomet. Chem. 7* (1967) 339.

[10] Spectroscopic data. **8**: IR (C_6H_6): ν(N=C=C) = 2018 cm^{-1}.—**9**: IR (C_6H_6): ν(N=C=C) = 2030 cm^{-1}; ^{1}H NMR (200 MHz, C_6D_6): δ = 7.48 (m, C_6H_4), 2.74 (s, NCH_3); ^{13}C NMR (50.3 MHz, C_6D_6): δ = 176.0 (s, =C=), 138.8, 135.8, 126.5, 125.2, 121.7, 120.8 (all s, C_6H_4), 71.3 (s, $=C(C_{12}H_8)$), 37.6 (s, NCH_3).—**10**: IR (C_6H_6): ν(N=C=C) = 2020 cm^{-1}; ^{1}H NMR (90 MHz, C_6D_6): δ = 7.31 (m, C_6H_4), 4.62 (q, J_{HH} = 6.6 Hz, C*H*MePh), 1.36 (d, J_{HH} = 6.6 Hz, $CH(CH_3)Ph$); ^{13}C NMR (22.5 MHz, C_6D_6): δ = 177.2 (s, =C=), 142.1, 138.7, 135.9, 129.0, 127.7, 126.6, 126.4, 125.3, 121.6, 120.8 (all s, C_6H_4), 73.1 (s, $=C(C_{12}H_8)$), 63.6 (s, *C*HMePh), 24.4 (s, $CH(CH_3)Ph$).

[11] G. R. Krow, *Angew. Chem. 83* (1971) 455; *Angew. Chem. Int. Ed. Engl. 10* (1971) 435.

[12] a) H. Werner, S. Lotz, B. Heiser, *J. Organomet. Chem. 209* (1981) 197; b) B. Heiser, H. Werner, *Synth. React. Inorg. Met.-Org. Chem. 16* (1986) 527; c) B. Strecker, *Diplomarbeit* Universität Würzburg 1987.

[13] K. H. Dötz, *Angew. Chem. 96* (1984) 573; *Angew. Chem. Int. Ed. Engl. 23* (1984) 587.

Cycloaddition Reactions of CpCo-Stabilized Cyclobutadiene Derivatives**

By *Rolf Gleiter** and *Detlef Kratz*

Dedicated to Professor Paul von Ragué Schleyer on the occasion of his 60th birthday

The reaction of alkynes to form arenes using homogenous transition metal catalysts is described in the literature in terms of catalytic loops as depicted in scheme 1.[1, 2] The formation of cobalt-stabilized cyclobutadiene derivatives **B** is usually considered as an unwanted side reaction and as a pathway constituting a dead end of [2+2+2]-cyclotrimerization reactions to arenes **D** with catalysts of the type $CpCoL_2$.

These complexes **B** withdraw the catalytically active species, the CpCo-fragment, from the trimerization cycle and

[*] Prof. Dr. R. Gleiter, Dipl. Chem. D. Kratz
Organisch-chemisches Institut der Universität
Im Neuenheimer Feld 270, D-6900 Heidelberg (FRG)

[**] This work was supported by the Deutsche Forschungsgemeinschaft (SFB 247), the Volkswagenwerk-Stiftung, the Fonds der Chemischen Industrie, and BASF Aktiengesellschaft. *D.K.* thanks the Studienstiftung des Deutschen Volkes for a postgraduate grant.

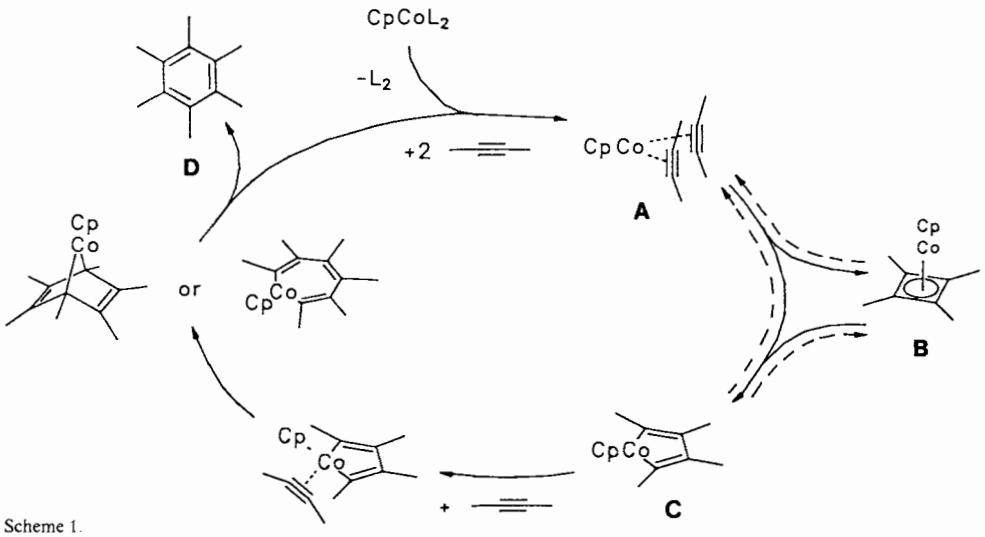

Scheme 1.

are excluded as possible intermediates on the following grounds: firstly, the formation of **B** requires a higher activation energy than the formation of a cobaltacyclopentadiene **C** (cobaltole);[3, 4] secondly, they are considered to be inert and to show resistance to further cycloaddition reactions; and thirdly, an equilibrium between the primary dialkyne complex **A**, the CpCo-cyclobutadiene complex **B** and the cobaltacyclopentadiene **C** has not, as yet, been unequivocally substantiated.[5, 6] In the present communication we show that complexes of type **B** are by no means entirely inert and may react with triple bonded species X≡Y to yield arenes.

Our research focussing on the reactivity of the cobalt complexes **5** and **10** was initiated by the following observations: To our surprise the reaction (a) of cyclodeca-1,6-diyne **1** with

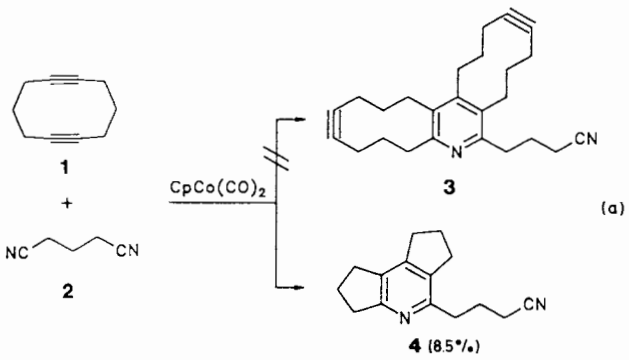

glutaronitrile **2** in xylene in presence of catalytic amounts of $CpCo(CO)_2$ did not afford the "intermolecular" 2:1 pyridine derivative **3**, that we had hoped for; apart from the already known CpCo-cyclobutadiene complexes,[7] only the "intramolecular" 1:1 pyridine derivative **4** was detected. When the reaction of **1** was carried out in the absence of a nitrile it was also possible to isolate, inter alia, the CpCo-cyclopentadienone derivative **13** (Table 1). In both products a formal cleavage of one of the triple bonds in **1** has occurred. Furthermore, the results of X-ray investigations[8] on tricylic CpCo-cyclobutadiene complexes such as **5** clearly indicate bond alternance,[8] whereas the bonds in the four-membered ring of CpCo-cyclobutadiene complexes are normally equalized out.[9]

It seemed reasonable to conclude that **5** could behave as a diene towards further species with triple bonds. In fact we were able to transform **5** into the 6π-systems **4**, **8** and **9** (Table 1).

Table 1. Some spectral data of the compounds **4, 8, 9, 11,** and **13**.

4: ^{1}H NMR ([D$_6$]-acetone, 300 MHz): δ = 2.7–2.9 (m, 10H), 2.41 (t, 2H), 1.99–2.13 (m, 6H); ^{13}C NMR ([D$_6$]-acetone, 75.46 MHz): δ = 17.0, 23.8, 25.2, 25.3, 29.6, 30.9, 31.8, 34.4, 34.6, 120.7, 131.3, 135.9, 150.0, 153.8, 163.6; UV/VIS (CH_2Cl_2): λ_{max} (lg ε) = 225 nm (4.51), 275 nm (4.67); MS (EI): *m/z* (%) = 226(13), 225(11), 186(25), 173(100), 172(34), 85(26), 71(42), 57(74), 43(68), 41(40).

8: ^{1}H NMR ($CDCl_3$, 200 MHz): δ = 2.69–2.86(m), 1.96–2.11(q), 1.62(br.), 1.34(broad), 1.23(s) (integration is not clear-cut as trimeric cyclooctyne is present); ^{13}C NMR ($CDCl_3$, 50.32 MHz): δ = 24.95, 26.34, 28.5, 29.69, 31.49, 31.5, 134.45, 136.9, 140.4; GC-MS (EI): *m/z* [%] = 240(82), 211(41), 197(100), 185(40), 171(43), 155(27), 128(20), 115(17), 77(9), 41(15).

9: ^{1}H NMR (CD_2Cl_2, 200 MHz): δ = 7.16 (m, 5H), 4.01 (s, 2H), 2.73–2.93 (m, 8H), 1.94–2.14 (m, 4H); ^{13}C NMR (CD_2Cl_2, 50.32 MHz): δ = 23.49, 24.96, 29.5, 30.9, 31.5, 34.2, 42.5, 126.2, 128.5, 129.1, 131.2, 135.8, 140.5, 150.1, 153.6, 163.2; UV/VIS (CH_2Cl_2): λ_{max} (lg ε) = 212 nm (4.03), 277 nm (3.82); GC-MS (EI): *m/z* [%] = 249(50), 248(100), 221(6), 172(2), 170(3), 115(3), 91(4), 65(2).

11: ^{1}H NMR (CD_2Cl_2, 300 MHz): δ = 7.12–7.26 (m, 5H), 4.05 (s, 2H), 2.83 (br. 2H), 2.54 (q, 6H), 1.83 (q, 4H), 1.7 (m, 4H); ^{13}C NMR (CD_2Cl_2, 75.46 MHz): δ = 22.8, 23.0, 23.5 (2×), 25.7, 26.5, 26.6, 33.4, 41.9, 126.2, 128.3, 128.6, 128.7, 129.1, 140.6, 145.2, 153.1, 155.3; UV/VIS (CH_2Cl_2): λ_{max} (lg ε) = 212 nm (4.09), 272 nm (3.60); GC-MS (EI): *m/z* [%] = 277(72), 276(100), 262(14), 248(5), 218(2), 186(8), 115(3), 91(5), 65(2).

13: ^{1}H NMR ($CDCl_3$, 200 MHz): δ = 4.74 (s, 5H), 2.84 (br. 2H, H_2O), 1.83–2.42 (m, 12H), ^{13}C NMR (DEPT spectrum) ($CDCl_3$, 50.32 MHz): δ = 25.39 (CH_2), 25.86 (CH_2), 28.8 (CH_2), 83.11 (CH), 92.97 (C), 94.5 (C), 149.0 (CO); UV/VIS (CH_2Cl_2): λ_{max} (lg ε) = 212 nm (4.09), 283 nm (4.29), 358 nm (3.43), 420 nm (2.93); MS (EI): *m/z* [%] = 284(57), 255(68), 189(100), 187(23), 129(46), 128(35), 124(73), 115(22), 91(27), 59(76), 40(38); IR ($CDCl_3$): $\tilde{\nu}$ = 3684(m), 3150(w), 2952(m), 2846(w), 2254(m), 2208(m), 1599(s), 1548(s), 1261(vs), 804(vs).

In choosing **10** as a diene component we wanted to test a cyclobutadiene complex containing bonds of almost equal length in its four-membered ring (cf. Scheme 3). This compound also led to cycloaddition reactions under more vigorous conditions[10] to afford the aromatic compounds **11** (Table 1) and **12**.[11]

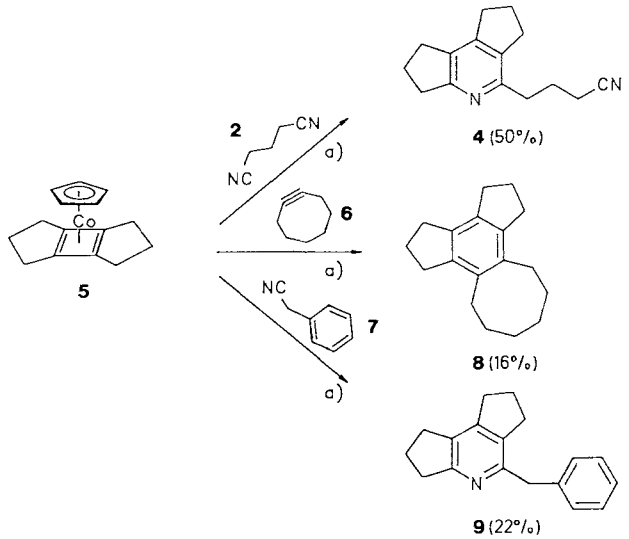

Scheme 2. a) In xylene under reflux.

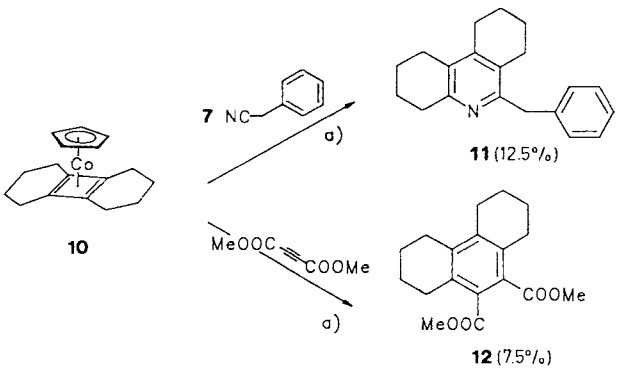

Scheme 3. a) 200 °C, without solvent.

These results suggest that certain (steric) restrictions may influence the reaction in a manner such that the "cyclobutadiene path" in cobalt-catalyzed [2+2+2]-cyclotrimerizations cannot be excluded from the start. To explain the formal cleavage of the triple bond of **1** in reaction (a) we postulate a mechanism that includes the cyclobutadiene derivative **II** as a plausible intermediate (Scheme 4).

Thus, the cobaltacyclopentadiene **I** is in equilibrium with its isomer cobaltacyclopentadiene **III** via the CpCo-cyclobutadiene complex **II**. This isomerization is the decisive step in order to explain the course of the reaction. The equilibrium **I** $\rightleftharpoons$ **II** $\rightleftharpoons$ **III** corresponds to an alkyne metathesis reaction, for which cyclobutadienes stabilized by transition metal fragments have been invoked as potential intermediates.[12] The "cycloaddition" of a further triple bond X$\equiv$Y may then proceed directly on **II** or by primary coordination of the 16e-species **III** and subsequent cyclization. A Dewar-benzene derivative may occur as an intermediate that is formed with concomitant liberation of the CpCo-fragment. However, under the reaction conditions this intermediate is unstable and will rearrange to the corresponding 6π-system. An analogous reaction of **I** would lead to the highly strained [3]paracyclophane skeleton and does not seem feasible on energetic grounds; the extremely labile [4]paracyclophane has been observed to undergo Wagner-Meerwein rearrangement to yield an *ortho*-substituted benzene under acid catalyzed conditions.[13]

The simultaneously released 14e-transition metal fragment (CpCo) may now become catalytically active as in reaction (a), and either induce further formation of **4** from the cyclic dialkyne **1** and dinitrile **2**, or react with the "dienophile" component and thus lead to numerous side reactions. Therefore, depending on the X$\equiv$Y-component present we observe the formation of cyclooctyne-trimer,[14] dimeric or trimeric products of benzyl cyanide, or mellitic acid hexamethyl ester in varying amounts. The catalyst is, however, prone to reduction and may decompose to form a cobalt mirror in the reaction flask.

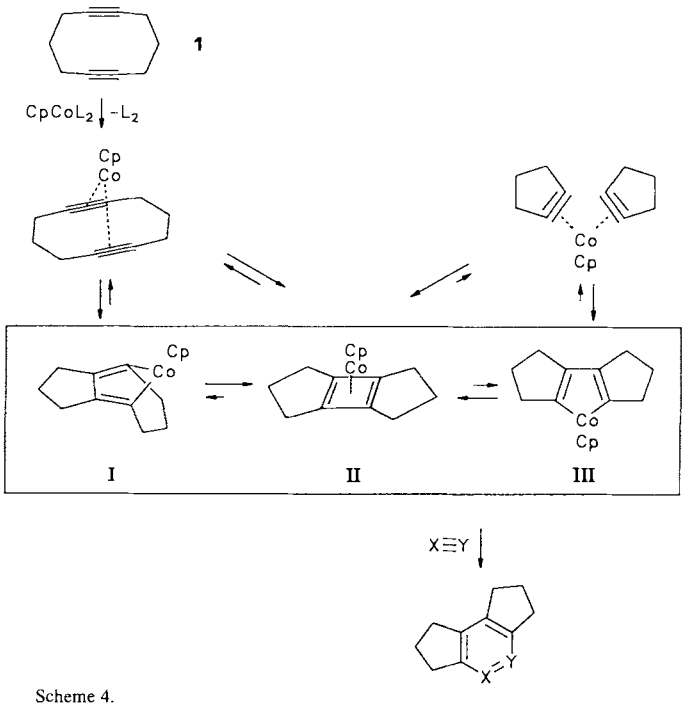

Scheme 4.

If the same mechanism is presumed to operate in the formation of **13** (a mechanism via CpCo(CO)-dimers or -clusters is also conceivable), the final cleavage of the triple bond is caused by "end-on" addition of carbon monoxide. This may be preceded by a "side-on" coordination, as this mode of reaction has already been observed in reactions of CpCo complexes with ketones and aldehydes.[15]

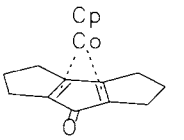

13

Received: October 20, 1989 [Z 3599 IE]
German version: *Angew. Chem. 102* (1990) 304

[1] D. R. McAllister, J. E. Bercaw, R. G. Bergman, *J. Am. Chem. Soc. 99* (1977) 1666; H. Bönnemann, *Angew. Chem. 97* (1985) 264; *Angew. Chem. Int. Ed. Engl. 24* (1985) 248; K. P. C. Vollhardt, *ibid. 96* (1984) 525 and *23* (1984) 539, and references cited therein.
[2] J. P. Colman, L. S. Hegedus: *Principles and Applications of Organotransition Chemistry*, University Science Books, Mill Valley, CA 1987.
[3] Y. Wakatsuki, O. Nomura, K. Kitaura, K. Morokuma, H. Yamazaki, *J. Am. Chem. Soc. 105* (1983) 1907.

[4] F. D. Mango, J. H. Schachtschneider, *J. Am. Chem. Soc. 91* (1969) 1030.
[5] R. L. Hillard III, K. P. C. Vollhardt, *J. Am. Chem. Soc. 99* (1977) 4058; G. A. Ville, K. P. C. Vollhardt, M. J. Winter, *ibid. 103* (1981) 5267; G. A. Ville, K. P. C. Vollhardt, M. J. Winter, *Organometallics 3* (1984) 1177.
[6] K. P. C. Vollhardt, R. G. Bergman, *J. Am. Chem. Soc. 96* (1974) 4996.
[7] R. Gleiter, M. Karcher, M. L. Ziegler, B. Nuber, *Tetrahedron Lett. 28* (1987) 195.
[8] The bond lengths of the cyclobutadiene fragments of **5** and **10** are shown below. They stem from X-ray analyses performed by *B. Nuber* and *M. L. Ziegler*, Heidelberg.

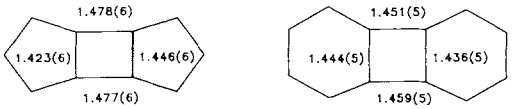

[9] A. Efraty, *Chem. Rev. 5* (1977) 691.
[10] The lower reactivity of **10** becomes evident in the reaction of cyclododeca-1,7-diyne with 1,4-dicyanobutane using catalytic or equimolar amounts of $CpCo(CO)_2$. No pyridine derivative and only **10** itself is formed. Furthermore, **10** will only react if the dienophile itself is used as solvent.
[11] Data are identical to those in the literature: P. Courtot, J.-C. Clement, *Bull. Soc. Chim. France* (1973) 2121.
[12] J. R. Fritch, K. P. C. Vollhardt, *Angew. Chem. 91* (1979) 439; *Angew. Chem. Int. Ed. Engl. 18* (1979) 409.
[13] G. B. M. Kostermans, M. Bobeldijk, W. H. de Wolf, F. Bickelhaupt, *J. Am. Chem. Soc. 109* (1987) 2471.
[14] G. Wittig, P. Fritze, *Justus Liebigs Ann. Chem. 712* (1968) 79.
[15] R. Gleiter, V. Schehlmann, *Tetrahedron Lett. 30* (1989) 2893; D. F. Harvey, B. M. Johnson, C. S. Ung, K. P. C. Vollhardt, *Synlett.* 1 (1989) 15.

Stereo- and Regioselectivity of Chiral, Alkyl-substituted *ansa*-Zirconocene Catalysts in Methylalumoxane-activated Propene Polymerization**

By *Werner Röll, Hans-Herbert Brintzinger,* Bernhard Rieger,* and *Ralf Zolk*

Dedicated to Professor Dr. Günther Wilke on the occasion of his 65th birthday

The isotactic polymerization of α-olefins by methylalumoxane-activated, chiral *ansa*-zirconocene catalysts has recently been studied in considerable detail. With very few exceptions,[1, 2] however, studies on the stereochemical course of these reactions have been limited to ring-bridged bis(indenyl)- and bis(tetrahydroindenyl)zirconium complexes (see, e.g., Refs. [3–6, 10–14]). Since further insights into the factors governing the stereoselectivity of these reactions[3–5] can only be gained from a more widely varying range of complexes, we have studied the course of methylalumoxane-activated propene polymerization by a series of differently substituted, axially symmetric *ansa*-zirconocenes, **1**–**4**.[7]

[*] Prof. Dr. H. H. Brintzinger, Dr. W. Röll
Fakultät für Chemie der Universität
D-7750 Konstanz (FRG)
Dr. B. Rieger, Dr. R. Zolk
BASF AG
D-6700 Ludwigshafen (FRG)

[**] ansa-Metallocene Derivatives, Part 19. This work was supported by the Deutsche Forschungsgemeinschaft and the Fonds der Chemischen Industrie. We wish to thank Frau E. Barsties (Universität Konstanz), Dr. W. Ball, Dr. Merthes and Dr. P. Simak (BASF AG) for the polymer analyses, BASF AG for gifts of chemicals, and Prof. *J. E. Bercaw* (California Institute of Technology) and one of the referees for valuable comments. Part 18: P. Burger, H. U. Hund, K. Evertz, H. H. Brintzinger, *J. Organomet. Chem. 378* (1989) 153.

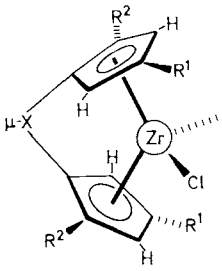

1, R^1 = *t*Bu, R^2 = H, μ-X = $Me_2\overset{t}{C}-\overset{t}{C}Me_2$
2, R^1 = *t*Bu, R^2 = H, μ-X = Me_2Si
3, R^1 = *t*Bu, R^2 = Me, μ-X = Me_2Si
4, R^1 = *i*Pr, R^2 = Me, μ-X = Me_2Si

Polymerization reactions with the tetramethylethano-bridged zirconocene complex **1**, with the dimethylsilano-bridged zirconocene complexes **2**–**4**, and, for comparison, with the ethano-bridged bis(tetrahydroindenyl)zirconium complex **5**[6] were studied at 50 °C, a propene pressure of 2 bar and an Al/Zr ratio of 300:1. The yields and properties of the polymers thus obtained are collected in Table 1.

Table 1. Yields and properties of the polypropylene (PP) polymers obtained with the complexes **1**–**5** after activation with methylalumoxane (Al/Zr = 300/1) at 50 °C under 2 bar of propene.

Catalyst	**1**	**2**	**3**	**4**	**5**
Reaction time [min]	120	120	185	45	50
Polymer yield [g]	9	36	79	114	95
Productivity [kg(PP)/(h mol(Zr) p)]	85	355	505	3000	2250
Melting point [°C]	103	128	149	107	85
M_w [a]	775	1981	9190	4958	3153
M_w/M_n	1.8	2.4	2.5	3.0	2.9
Isotacticity [% mmmm Pentads]	62	77	94	73	49
n-Propyl- ends [b]	3.5	2	0.6	1.5	1.5
2-Propenyl ends [b]	1.5	2	0.5	0.8	1.5
1-3-Misinsertions [b]	1.5	1.5	0.4	–	1.5

[a] Absolute values with uncertainties of ±20%. [b] Intensities of the ^{13}C-NMR signals in percent of main signals; besides the signals for 2-propenyl end groups, another set of signals with varying intensity occurs at δ = 17.9, 25.7, 129.1, and 132.2.

Under the reaction conditions employed, the catalysts **1**–**4** all yield more highly isotactic polymers than the "classical" catalyst **5**. Of the *t*Bu-substituted zirconocenes, the Si-bridged complex **2** is distinctly superior to its C_2-bridged analogue **1** in terms of stereoselectivity, probably due to its higher stereorigidity.[8] An even higher degree of isotacticity, with an mmmm pentad intensity of greater than 90%, is obtained with the Si-bridged complex **3**, which contains at each ring ligand, in addition to the *t*Bu group in the 4(β) position, a methyl group in the 2(α) position. The decreased stereoselectivity of the catalyst **4** with *i*Pr instead of β-*t*Bu substituents demonstrates the importance of steric bulk in the β position of both rings for a stereochemically uniform olefin insertion.

A remarkable effect of α-methyl substituents is the suppression of 1–3 misinsertions, which arise from a tail-to-tail (2–1) insertion of the α-olefin into the metal–polymer bond and subsequent isomerization of the ensuing species with a secondary alkyl ligand.[9] These misinsertions occur in the polymers obtained with **1** and **2** with a frequency of ca. 1.5%, i.e. about as often as in polymers obtained with the catalyst **5**.[10–13] In polymers produced with the α-methyl-substituted complexes **3** and **4**, however, these regio-irregularities are suppressed to levels close to or below the detec-

tion limit. In this respect, the performance of the α-methyl substituted catalysts approaches that of heterogeneous Ziegler catalysts, in which these regio-irregularities are not observed.

The molecular weights of the polymers obtained with the catalysts **1**–**4** show a surprising correlation with the respective stereo- and regio-regularities of the catalysts: Complex **3** produces by far the longest and most isotactic, complex **1** the shortest and least isotactic polymer chains. This unexpected observation can be explained based on structural models for the reactive zirconocene alkyl olefin cation[15]: The β-agostic binding required for chain termination by β-H transfer places the polymer chain (Pl) of a stereoregular unit into that ligand sector (Fig. 1a) which is occupied by the ring substituent R^1. If R^1 is sufficiently large, chain termination will therefore be largely suppressed except in those cases where the positions of the polymer and CH_3 substituents at the β-carbon are inverted, i.e. in a stereo-irregular unit, or where the β-carbon carries two H atoms, as in a regio-irregular unit.

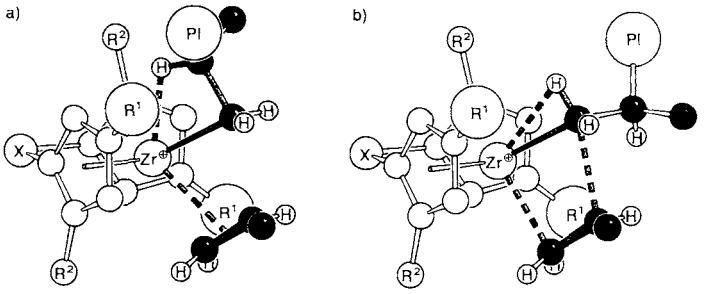

Fig. 1. a) β-agostic Zr-H interaction as prerequisite for the β-H transfer and thus chain termination; b) α-agnostic Zr-H interaction leads to stereoregular olefin insertion.

Stereoregular olefin insertion on the other hand might proceed via agostic binding of that one of the two α-H atoms[16] which places the polymer chain in an open sector of the ligand framework (Fig. 1b): The entering olefin will then be steered into the correct enantiofacial orientation both by repulsive interaction with the ring substituent R^1 and by the preferred *trans* configuration of the CH_3 and $CH(CH_3)Pl$ groups in the four-center transition state. Simple models of this kind might prove useful for the development of working hypotheses for more far-reaching, rational modifications of these metallocene polymerization catalysts.

Experimental

The propene polymerizations were carried out under N_2 in solutions of methylalumoxane (0.45 g, 7.6 mmol CH_3AlO) (Schering AG, mean molecular weight 1300 g/mol) in 400 mL of dry toluene containing 2.5×10^{-2} mmol (10–12 mg) of the respective racemic *ansa*-zirconocene dichloride, under 2 bar of propene (BASF AG). After draining the reaction mixture into CH_3OH/HCl, the precipitated polymer was filtered, washed with CH_3OH, and dried in vacuo. The molecular weights were determined by gel permeation chromatography, the melting points by differential scanning calorimetry. ^{13}C-NMR spectra were measured at 120 °C in solutions containing 120–150 mg of polymer in 0.4 mL of $C_2D_2Cl_4$, on a Bruker AC-250 FT spectrometer and analyzed by known methods [10–14].

Received: November 3, 1989 [Z 3619 IE]
German version: *Angew. Chem. 102* (1990) 339

[1] S. Miya, T. Yoshimura, T. Mise, H. Yamazaki, *Polym. Prepr. Jpn. 37* (1988) 285; T. Mise, S. Miya, H. Yamazaki, *Chem. Letters* (1989) 1853.
[2] M. Antberg, L. L. Böhm, V. Dolle, H. Lüker, J. Rohrmann, W. Spalek, A. Winter, 44th South-West Reg. Meet. Am. Chem. Soc. 1988, Abstract No. 48.
[3] P. Pino, P. Cioni, J. Wei, *J. Am. Chem. Soc. 109* (1987) 6189.
[4] P. Corradini, G. Guerra, M. Vacatello, V. Villani, *Gazz. Chim. Ital. 118* (1988) 173.
[5] W. Kaminsky, A. Ahlers, N. Möller-Lindenhof, *Angew. Chem. 101* (1989) 1304; *Angew. Chem. Int. Ed. Engl. 28* (1989) 1216.
[6] W. Kaminsky, K. Külper, H. H. Brintzinger, F. R. W. P. Wild, *Angew. Chem. 97* (1985) 507; *Angew. Chem. Int. Ed. Engl. 24* (1985) 507; W. Kaminsky, *Angew. Makromol. Chem. 145/146* (1986) 149.
[7] S. Gutmann, P. Burger, H. U. Hund, J. Hofmann, H. H. Brintzinger, *J. Organomet. Chem. 369* (1989) 343; H. Wiesenfeldt, A. Reinmuth, E. Barsties, K. Everts, H. H. Brintzinger, *ibid. 369* (1989) 359.
[8] Propene polymerization with 93% mmmm pentads has been reported for **2** at 30 °C and Al/Zr = 10000/1 in Ref. [1].
[9] As reported for **5** in Refs. [10, 11], weak sets of m-configurated head-to-head insertion signals were observed in polymers obtained with **2** at 0 °C; at 50 °C, isomerization to 1–3 units appears to be faster than head-to-head insertion.
[10] K. Soga, T. Shiono, S. Takemura, W. Kaminsky, *Makromol. Chem. Rapid Commun. 8* (1987) 305.
[11] A. Grassi, A. Zambelli, L. Resconi, E. Albizzati, R. Mazzocchi, *Macromolecules 21* (1988) 617; A. Grassi, P. Amendola, P. Longo, E. Albizzati, L. Resconi, R. Mazzocchi, *Gazz. Chim. Ital. 118* (1988) 539.
[12] T. Tsutsui, A. Mizuno, N. Kashiwa, *Makromol. Chem. 190* (1989) 1177.
[13] B. Rieger, J. C. W. Chien, *Polymer Bull. 21* (1989) 159; B. Rieger, X. Mu, D. T. Mallin, J. C. W. Chien, *J. Am. Chem. Soc.*, in press.
[14] J. A. Ewen, *J. Am. Chem. Soc. 106* (1984) 6355; in T. Keii, K. Soga (Eds.): *Catalytic Polymerisation of Olefins*, Kohdansha Elsevier, Tokyo 1986, p. 271.
[15] R. F. Jordan, R. E. LaPointe, C. S. Bajgur, S. F. Echols, R. Willet, *J. Am. Chem. Soc. 109* (1987) 4111; R. F. Jordan, P. K. Bradley, N. C. Baenziger, R. E. LaPointe, *ibid. 112* (1990) 1289.
[16] M. Brookhart, M. L. H. Green, *J. Organomet. Chem. 250* (1983) 395; M. Brookhart, M. L. H. Green, L. Wong, *Prog. Inorg. Chem. 36* (1988) 1.

A New Type of Double Calix[4]arenes by Linkage via the Phenolic Hydroxy Groups

By *M. Anthony McKervey,* Michael Owens, Hans-Rolf Schulten, Walter Vogt,* and *Volker Böhmer**

Calixarenes are macrocyclic molecules in which phenolic units (normally four, six or eight) are linked via methylene bridges.[1] In addition to their easy accessibility,[2] these compounds have the great advantage that they can be chemically modified in various ways.[3] We and others have demonstrated that calix[4]arene esters, amides, and ketones are very efficient and selective receptors for alkali metal cations. The potential importance of these ligands ranges from purely analytical applications (ion-selective electrodes, ion-selective field effect transistors) via medical problems (complexes with a long lifetime) to applications in the decontamination of industrial waste water, including nuclear wastes.

We recently reported the first examples of double calixarenes in which the two calix[4]arene moieties are linked via their *para* positions by one, two or four aliphatic chains.[4] An alternative way of combining calixarenes into larger molecular assemblies having potentially new receptor properties consists in linking two or more units via the phenolic positions. The tetraethyl ester **1** can be very selectively hy-

[*] Prof. Dr. M. A. McKervey, M. Owens
Department of Chemistry, University College Cork (Ireland)
Prof. Dr. H.-R. Schulten
Fachhochschule Fesenius
Dambachtal 20, D-6200 Wiesbaden (FRG)
Prof. Dr. W. Vogt, Dr. V. Böhmer
Institut für Organische Chemie, Johannes Gutenberg Universität
J.-J.-Becher-Weg 34, D-6500 Mainz (FRG)

drolyzed by trifluoroacetic acid in chloroform to give the triester monoacid **2**.[5] Thus, a subsequent coupling of two molecules of **2** via amide or ester links is possible. We describe here the first examples of this new type of double calix[4]arenes.[6]

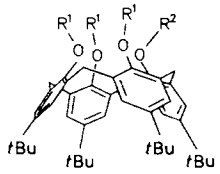

1: $R^2 = CH_2-COOEt$
2: $R^2 = CH_2-COOH$
3: $R^2 = CH_2-COCl$

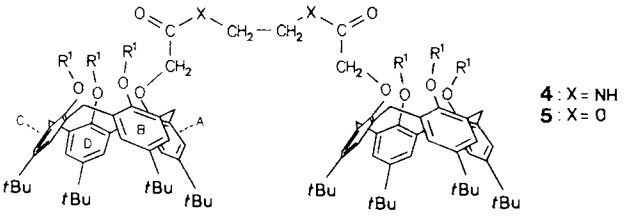

4: X = NH
5: X = O

$R^1 = CH_2-COOEt$

Treatment of the acid **2** with thionyl chloride afforded the acid chloride **3**, which, without further purification, was treated with 1,2-diaminoethane in benzene in the presence of triethylamine. The product thus obtained in 41% yield was unequivocally identified from its ^{1}H-NMR spectrum as the double calix[4]arene **4**[7]. The signals for NH- ($\delta = 8.687$) and N-$(CH_2)_2$-N ($\delta = 3.638$) have the correct intensity ratio to those of the other protons. For the aromatic protons as well as for the *tert*-butyl groups, three signals are observed (ratio 1:2:1), corresponding to the different phenolic units A, B/D and C. Also in the case of the ethyl groups the correct ratio 1:2 is observed in the region for CH_2-protons. Two quartets superimpose to give a multiplet with intensities in the ratio 2:6:7:5:3:1. Characteristic for the molecular structure are the O–CH_2–CO protons. Two singlets (units A and C), and especially the two doublets of the AB-system of the diastereotopic protons at the phenolic units B and D, provide convincing evidence in support of structure **4**. Two superimposed AX-systems for the two different types of Ar-CH_2-Ar protons (A/B, D/A and B/C, C/D) show that the two calix[4]arene moieties are still fixed in the cone conformation.

The structure of **4** was further confirmed by mass spectrometry. The molecular peak $M^{\oplus}$, $m/z = 1953$, can already be detected with a relative abundance of ca. 8% in the electron impact spectrum. With the field ionization technique[8] (FIMS) the molecular peak is obtained as the base peak under optimum conditions. Peaks at 976.5 (for $M^{2\oplus}$, and 1867 (for $M^{\oplus} - 86$) are in agreement with the postulated structure. The distribution of isotopes found for the molecular ion corresponds to that expected theoretically.

In the field desorption mass spectrum[8] (FDMS) intense signals for the ions $M^{\oplus}$ ($m/z = 1953$) and $M^{\oplus}$ + Na ($m/z = 1976$) provide unequivocal proof of the molecular weight. In addition, peaks are observed at $m/z = 1867$ and 1890 at higher emitter temperature, which again indicate the loss of one CH_3COOEt group. Interestingly, no signal is observed for the ion $M^{2\oplus}$ + 2 Na, although such a complex is formed in solution (see below).

When a solution of NaSCN in CD_3OD is added portionwise to a solution of **4** in $CDCl_3$, initially additional signals for the $Na^{\oplus}$-complex are observed in the ^{1}H-NMR spectrum. This spectrum becomes simpler again after a total amount of 2 moles of NaSCN has been added per mol of **4**, and then does not change further. The same spectrum is obtained after a solution of **4** is shaken with solid NaSCN. The spectral changes are similar to those observed earlier with the tetraester **1** and NaSCN.[9] Particularly striking is the downfield shift of the aromatic protons ($\delta = 7.04-7.07$) and the upfield shift of the O–CH_2–CO protons and the A part of the Ar–CH_2–Ar protons ($\delta \approx 4.5$). In contrast, the B part is shifted to lower field (3.31 and 3.29, respectively). These results show that, under these conditions, kinetically stable complexes are formed in which obviously both calix[4]arene moieties independently take up a $Na^{\oplus}$ ion.[9]

Similarly to **4**, the double calixarene **5** with a diester bridge was formed upon reaction of **3** with ethylene glycol. Extended bridging with three or four calixarene subunits in a linear arrangement should also be possible using the recently described *1,3*-derivatives of calix[4]arenes.[10] Furthermore, the synthesis of double calixarenes, in which two calix[4]arene units are linked by more than one ester and/or amide bridge, is presently under investigation. The latter type of bridged calixarene should be highly preorganized for cation reception. Thus, new host molecules with higher affinity and improved selectivity for metal ions could be obtained on the basis of the readily available calix[4]arenes.

Experimental:

2: A solution of **1** (5.01 g, 5.05 mmol) in chloroform (100 mL) was treated with trifluoracetic acid (0.2 mL), and the mixture stirred at room temperature for 24 h. The solution was washed with water, dried, and evaporated to dryness. The white, solid residue was recrystallized from ethanol/water, furnishing 4.3 g (88%) of **2** as colourless crystals, m.p. 166–169 °C. Correct elemental analysis.

3: A solution of **2** (3.86 g, 4 mmol) was treated with 25 mL of thionyl chloride and the mixture heated under reflux in a nitrogen atmosphere for 2.5 h. Subsequent removal of excess thionyl chloride at reduced pressure furnished a yellow solid, which was used without further purification.

4: To a stirred solution of 3 g (3 mmol) of the acid chloride **3** in 100 mL of dry benzene under nitrogen was added dropwise at room temperature a solution of 0.1 mL (0.09 g, 1.5 mmol) of ethylenediamine and 1 mL (0.72 g, 7.0 mmol) of triethylamine in 200 mL of dry benzene. The mixture was stirred for 24 h and then was filtered to remove triethylammonium chloride. Concentration of the filtrate at reduced pressure furnished a white solid, which was purified by column chromatography over silica gel with methanol/ethyl acetate (2:3) followed by recrystallization from acetone to yield 1.21 g (41%) of **4** as white crystals, m.p. 250–253 °C. Correct elemental analysis.

Received: November 13, 1989 [Z 3629 IE]
German version: *Angew. Chem. 102* (1990) 326

[1] For reviews on calixarenes see: C. D. Gutsche, *Top. Curr. Chem. 123* (1984) 1; *Prog. Macrocyclic Chem. 3* (1987) 93; C. D. Gutsche in J. F. Stoddart (Ed.): *Calixarenes, Monographs in Supramolecular Chemistry, Vol. 1*, The Royal Society of Chemistry, London 1989.

[2] Procedures for the synthesis of calix[4]-, calix[6]-, and calix[8]arenes have been submitted for publication: C. D. Gutsche, *Org. Synth.*, in press.

[3] The *tert*-butyl group in the readily available *tert*-butylcalixarenes may be replaced by different substituents such as SO_3H (S. Shinkai, S. Mori, H. Koreishi, T. Tsubaki, O. Manabe, *J. Am. Chem. Soc. 108* (1986) 2409), NO_2 (S. Shinkai, K. Araki, T. Tsubaki, T. Arimura, O. Manabe, *J. Chem. Soc. Perkin Trans. 1, 1987*, 2297), N=N-C_6H_4-R (S. Shinkai, K. Araki, J. Shibata, O. Manabe, *ibid. 1989*, 195), CH_2-CH_2-NH_2 (C. D. Gutsche, K. C. Nam, *J. Am. Chem. Soc. 110* (1988) 6153), and CH_2-CH_2-COOH (C. D. Gutsche, I. Alam, *Tetrahedron 44* (1988) 4689). Reactions at the phenolic hydroxy groups lead, e.g., to esters (F. Arnaud-Neu, E. M. Collins, M. Deasy, G. Ferguson, S. J. Harris, B. Kaitner, A. J. Lough, M. A. McKervey, E. Marques, B. H. Ruhl, M.-J. Schwing, E. M. Seward, *J. Am. Chem. Soc. 111* (1989) 8681), ketones (G. Ferguson, B. Kaitner, M. A. McKervey, E. M. Seward, *J. Chem. Soc. Chem. Commun. 1987*, 587), and amides (A. Arduini, E. Ghidini, A. Pochini, R. Ungaro, G. D. Andreetti, G. Calestani, F. Ugozzoli, *J. Inclusion Phenom. 6* (1988) 119) with complexation selectivities toward certain alkali cations. Macrobicyclic derivatives like calixcrowns (C. Alfieri, E. Dradi, A. Pochini, R. Ungaro, G. D. Andreetti, *J. Chem. Soc. Chem. Commun. 1983* 1075) or

calixspherands (D. N. Reinhoudt, D. J. Dijkstra, P. J. A. in't Veld, K. E. Bugge, S. Harkema, R. Ungaro, E. Ghidini, *J. Am. Chem. Soc. 109* (1987) 4761) should be mentioned too. Finally, the methylene groups may also be converted, e.g., into keto groups by oxidation (G. Görmar, K. Seiffarth, M. Schulz, J. Zimmermann, G. Flämig, *Makromol. Chem.*, in press). These few examples demonstrate the wide variety of possibilities.

[4] V. Böhmer, H. Goldmann, W. Vogt, J. Vicens, Z. Asfari, *Tetrahedron Lett. 30* (1989) 1391.

[5] V. Böhmer, W. Vogt, S. J. Harris, R. G. Leonard, E. M. Collins, M. Deasy, M. A. McKervey, M. Owens, *J. Chem. Soc. Perkins Trans. 1*, in press.

[6] Other types of host molecules have been combined in a similar way to ditopic receptor molecules, e.g. crown ethers (G. W. Gokel, S. H. Korzeniowski, *Macrocyclic Polyether Synthesis*, Springer, Berlin 1982, p. 34), quarternary-ammonium cages (F. P. Schmidtchen, *J. Am. Chem. Soc. 108* (1986) 8249), cyclophanes (C.-F. Lai, K. Odashima, K. Koga, *Tetrahedron Lett. 26* (1985) 5179), and cyclodextrins (R. Breslow, N. Greenspoon, T. Guo, R. Zarzycki, *J. Am. Chem. Soc. 111* (1989) 8296).

[7] ^{1}H NMR (400 MHz, $CDCl_3$): **3**: δ = 7.143 (s, 2H; Ar-H), 7.133 (s, 2H; Ar-H), 6.621 (d, J_{AB} = 2.4 Hz, 2H; Ar-H), 6.526 (d, J_{AB} = 2.4 Hz, 2H; Ar-H), 4.939 (s, 2H; O-CH_2-CO), 4.859 (d, J_{AB} = 15.7 Hz, 2H; O-CH_AH_B-CO), 4.574 (s, 2H; O-CH_2-CO), 4.350 (d, J_{AB} = 15.7 Hz, 2H; O-CH_AH_B-CO), 4.963 (d, J_{AB} = 12.8 Hz, 2H; Ar-CH_AH_B-Ar), 4.589 (d, J_{AB} = 12.5 Hz, 2H; Ar-CH_AH_B-Ar), 3.248 (d, J_{AB} = 12.8 Hz, 2H; Ar-CH_AH_B-Ar), 3.187 (d, J_{AB} = 12.9 Hz, 2H; Ar-CH_AH_B-Ar), 4.251 (q, J = 7.2 Hz, 4H; O-CH_2-CH_3), 4.208 (q, J = 7.2 Hz, 2H; O-CH_2-CH_3), 1.300 (t, J = 6.7 Hz, 6H; O-CH_2-CH_3), 1.285 (t, J = 7.5 Hz, 3H; O-CH_2-CH_3, disturbed by superposition with *tert*-butyl), 1.316 (s, 9H; $C(CH_3)_3$), 1.305 (s, 9H; $C(CH_3)_3$), 0.815 (s, 18H; $C(CH_3)_3$).

4: 8.687 (br. s, 2H; -NH-), 6.789 (s, 4H; ArH), 6.766 (s, 8H; ArH), 6.695 (s, 4H; ArH), 5.012 (d, J_{AB} = 16.2 Hz, 4H; O-CH_AH_B-CO), 4.632 (d, J_{AB} = 16.2 Hz, 4H; O-CH_AH_B-CO), 4.698 (s, 4H; O-CH_2-CO), 4.536 (s, 4H; O-CH_2-CO), 4.735 (d, J_{AB} = 13.1 Hz, 4H; Ar-CH_AH_B-Ar), 4.702 (d, J_{AB} = 13.3 Hz, 4H; Ar-CH_AH_B-Ar), 3.226 (d, J_{AB} = 13.3 Hz, 4H; Ar-CH_AH_B-Ar), 3.207 (d, J_{AB} = 13.1 Hz, 4H; Ar-CH_AH_B-Ar), 4.214 (q, J = 7.1–7.4 Hz, 8H; CH_2-CH_3), 4.177 (q, J = 7.1–7.4 Hz, 4H; CH_2-CH_3), 3.638 (br. s, 4H; CH_2-CH_2), 1.238 (t, J = 7.1 Hz, 18H; CH_2-CH_3), 1.087 (s, 18H; $C(CH_3)_3$), 1.056 (s, 36H; $C(CH_3)_3$), 1.014 (s, 18H; $C(CH_3)_3$).

5: 6.753 (s, 8H; ArH), 6.750 (s, 4H; ArH), 6.744 (s, 4H; ArH), 4.822 (s, 4H; O-CH_2-CO), 4.773 (s, 8H; O-CH_2-CO), 4.764 (s, 4H; O-CH_2-CO), 4.846 (d, J_{AB} = 13.1 Hz, 4H; Ar-CH_AH_B-Ar), 4.806 (d, J_{AB} = 12.7 Hz, 4H; Ar-CH_AH_B-Ar), 4.323 (s, 4H; CH_2-CH_2), 4.177 (q, J = 6.9 Hz, 4H; CH_2-CH_3), 4.160 (q, J = 7.0 Hz, 8H; CH_2-CH_3), 3.169 (d, J_{AB} = 13.0 Hz, 4H; Ar-CH_ACH_B-Ar), 3.161 (d, J_{AB} = 12.9 Hz, 4H; Ar-CH_ACH_B-Ar), 1.254 (t, J = 7.1 Hz, 6H; CH_2-CH_3), 1.241 (t, J = 7.1 Hz, 12H; CH_2-CH_3), 1.052 (s, 36H; $C(CH_3)_3$), 1.046 (s, 36H; $C(CH_3)_3$).

[8] The experimental conditions for FI and FDMS are described in detail by H. D. Beckey, H.-R. Schulten, *Angew. Chem. 87* (1975) 425; *Angew. Chem. Internat. Edit. 14* (1975) 403; H.-R. Schulten, *Int. J. Mass. Spectrom. Ion Phys. 32* (1979) 97. Methanol was used as solvent for the FDMS of **4**.

[9] Compare the spectra of the tetra-*tert*-butyl ester derivates: A. Arduini, A. Pochini, S. Reverberi, R. Ungaro, G. D. Andreetti, F. Ugozzoli, *Tetrahedron 42* (1986) 2089. The X-ray structure of the $K^{\oplus}$-complex of a tetraamide derivative (A. Arduini, E. Ghidini, A. Pochini, R. Ungaro, G. D. Andreetti, G. Calestani, F. Ugozzoli, *J. Inclusion Phenom. 6* (1988) 119) shows the $K^{\oplus}$ ion in a highly symmetrical polar cavity surrounded by eight oxygen atoms (ether and carbonyl groups). A similar structure may be assumed for these complexes in solution.

[10] E. M. Collins, M. A. McKervey, S. J. Harris, *J. Chem. Soc. Perkin Trans. 1*, 1989, 372.

Carbonylation of Doubly Lithiated *N*-Pivaloylanilines. A Novel Approach to Dioxindoles via Intramolecular Trapping of Aromatic Acyllithiums**

By *Keith Smith** and *Gareth J. Pritchard*

Doubly lithiated *N*-pivaloylanilines react smoothly with carbon monoxide at 0 °C and atmospheric pressure to give, following protonation during workup, good yields of 3-*tert*-butyldioxindoles. The reactions were undertaken in order to investigate whether intramolecular trapping of intermediate acyllithiums might lead to more convenient and more generally useful synthetic procedures than those currently available for acyllithiums. The results bear out the validity of the hypothesis and the reactions provide an interesting new access to indole derivatives.

Whereas reactions of organolithium compounds with carbon dioxide are widely used for the synthesis of carboxylic acids, reactions with carbon monoxide are almost never used in synthetic organic chemistry. This latter fact presumably results from the instability and high reactivity of acyllithiums, which can decompose, dimerize, take up further carbon monoxide, or in other ways lead to products other than those derived by simple electrophilic trapping.[1] To circumvent this problem, organic chemists have devised a range of acyl carbanion equivalents with which to effect nucleophilic acylation reactions.[2] Useful though these reagents are, however, they necessitate the use of additional steps to unmask the carbonyl functionality, lack the appeal of genuine acyllithiums, and preclude the use of isotopically substituted carbon monoxide for introduction of an isotopic label. Thus, there is still much to be gained by direct carbonylation of organolithium reagents.

Seyferth et al. have shown that it is possible to trap acyllithiums formed via carbonylation of alkyllithium reagents provided that the temperature is kept very low (preferably ca. −130 °C) and the trapping electrophile can be used in situ.[3] These conditions are extremely restrictive, however, and in any case are reported generally to be unsuccessful in the case of aryllithiums.[4]

Against this background we wondered if intramolecular trapping of intermediate acyllithiums might provide a more generally applicable synthetic approach for carbonylation reactions of organolithium reagents. As a first attempt to investigate this idea, we undertook the direct carbonylation of doubly lithiated *N*-pivaloylaniline (**1**)[5] and were extremely gratified to discover that carbon monoxide was smoothly taken up, even at room temperature (Scheme 1). Protonation and workup of the reaction mixture gave a substantial yield of a crystalline product, identified as 3-*tert*-butyldioxindole (**2**).[6] The yield was even better (77% after purification) when the carbonylation was carried out at 0 °C.

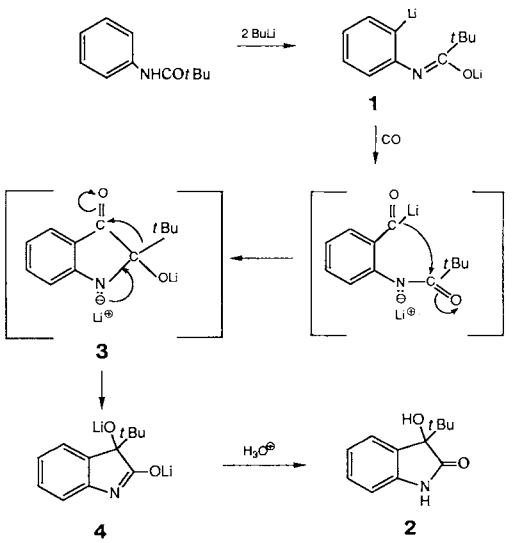

Scheme 1.

[*] Prof. Dr. K. Smith, G. J. Pritchard
Department of Chemistry
University College of Swansea
GB-Swansea, SA2 8PP (UK)

[**] We thank the University College of Swansea for providing the studentship to *G. J. P.* which enabled this work to be carried out.

In order to test the generality of the method for the synthesis of substituted 3-*tert*-butyldioxindoles **6**, a range of ring-substituted *N*-pivaloylanilines **5** was subjected to identical reaction conditions without optimization of individual cases. The yields of isolated products were good (Table 1). It is known that dioxindoles such as **2** and **6** can be reduced to the corresponding indoles.[9, 11]

Table 1. Synthesis of 3-*tert*-butyldioxindoles **5** from *N*-pivaloylanilines **6**.

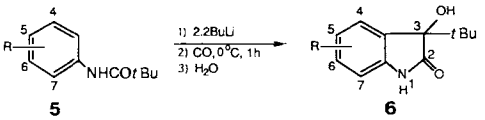

5 **6**

5/6	R	M.p. of **6** [°C]	Yield of **6** [%] [a]
a	7-CF_3	149	80
b	5-Cl	280–285 (dec.)	82
c	5-Me	263 [b]	61
d [c]	4-OMe	194–195	78

[a] Yield of isolated, purified product based on **5**. [b] Ref. [8] 260–261 °C. [c] The structure of **6d** has been verified by X-ray crystallography [12].

We have not investigated the mechanism of the reaction leading to **2**, but Scheme 1 shows a plausible pathway. There is literature precedent for the rearrangement of 2-*tert*-butyldioxindole **2** under basic conditions,[7, 8, 13] which adds credence to the intermediacy of species **3** and **4**. Furthermore, when the reaction of **5b** was carried out with ^{13}CO, the product **6b** had the label at position 3, as evidenced by ^{13}C NMR.

This reaction appears to be the first generally applicable carbonylation reaction of aryllithiums which allows trapping of the acyllithium intermediate without incorporating a second aryl group from the original reagent. It also demonstrates the value of intramolecular trapping of intermediate acyllithiums even when the trapping center is a weakly electrophilic amide anion. The ease of incorporation of carbon monoxide into the indole nucleus holds out the prospect that such reactions might be applicable to reactions of ^{11}C carbon monoxide ($t_{1/2}$ = 20 min), which could present opportunities for use in positron emission tomography (PET).[14] The method also nicely complements *Wender*'s recent method for the regiocontrolled synthesis of indoles.[15] Finally, it appears likely that other ring systems can be synthesized via carbonylation of appropriately substituted organolithium reagents.

Typical Experimental Procedure

A solution of **5b** (1.00 g, 4.7 mmol) in THF (20 mL) was stirred at 0 °C under nitrogen for 2 h with *n*BuLi (6.5 mL, 1.6 M, 10.4 mmol). A balloon filled with carbon monoxide (ca. 500 mL) was fitted to a needle and CO was allowed to bleed into the reaction mixture. After 1 h the solution was poured into saturated NH_4Cl solution (40 mL) and extracted with ethyl acetate (60 mL). The organic layer was washed with water, dried ($MgSO_4$), and evaporated. The solid obtained was recrystallized from ethyl acetate to give **6b** (0.92 g, 82%), as a white solid. ^1H NMR ([D$_6$]DMSO, 250 MHz): δ = 0.94 (s, 9H, *t*Bu), 5.82 (s, 1H, OH), 6.76 (d, J = 8 Hz, 1H, H-7), 7.18 (d, J = 2 Hz, 1H, H-4), 7.22 (dd, J = 2, 8 Hz, 1H, H-6), 10.26 (br. s, 1H, NH). ^{13}C NMR ([D$_6$]DMSO, 62.9 MHz): δ = 179.05, (s, C-2), 141.2 (s, C-7a), 133.5 (s, C-3a), 128.3 (d, C-6), 125.5 (d, C-4), 124.8 (s, C-5), 110.4 (d, C-7), 80.0 (s, C-3, enriched in reactions utilizing ^{13}CO), 36.7 (s, $C(CH_3)_3$), 23.8 (q, $C(CH_3)_3$). MS (ammonia CI, % intensity): m/z 259 (33), 257 (100, $M + NH_4^{\oplus}$), 242 (23), 240 (84, $M + H^{\oplus}$); accurate mass of $M + H^{\oplus}$ ion 240.0791 (calcd for $C_{12}H_{15}{}^{35}ClNO_2$ = 240.0791).

Received: June 6, 1989;
revised: November 21, 1989 [Z 3380 IE]
German version: *Angew. Chem. 102* (1990) 298

[1] L. S. Trzupek, T. L. Newirth, E. G. Kelly, N. E. Sharbati, G. M. Whitesides, *J. Am. Chem. Soc. 95* (1973) 8118; for a recent review of carbonylation reactions of organometallic reagents, see C. Narayama, M. Periasamy, *Synthesis 1985*, 253.
[2] Selected reviews of this topic: D. Seebach, *Angew. Chem. 81* (1969) 690; *Angew. Chem. Int. Ed. Engl. 8* (1969) 639; O. W. Lever, Jr., *Tetrahedron 32* (1976) 1943; P. Beak, D. R. Reitz, *Chem. Rev. 78* (1978) 275; S. F. Martin, *Synthesis 1979*, 633; J. D. Albright, *Tetrahedron 39* (1983) 3207; T. A. Hose (Ed.): *Umpoled Synthons. A Survey of Sources and Uses in Synthesis*. John Wiley, New York 1987; for a novel type of acyl carbanion equivalent, see M. Ashwell, R. F. W. Jackson, *J. Chem. Soc. Perkin Trans. 1 1989*, 835.
[3] D. Seyferth, R. M. Weinstein, *J. Am. Chem. Soc. 104* (1982) 5534; D. Seyferth, R. M. Weinstein, W.-L. Wang, *J. Org. Chem. 48* (1983) 1144, 3367; D. Seyferth, R. M. Weinstein, W.-L. Wang, R. C. Hui, *Tetrahedron Lett. 24* (1983) 4907; D. Seyferth, R. C. Hui, *Organometallics 3* (1984) 327.
[4] D. Seyferth, W.-L. Wang, R. C. Hui, *Tetrahedron Lett. 25* (1984) 1651.
[5] W. Fuhrer, H. W. Gschwend, *J. Org. Chem. 44* (1979) 1133.
[6] M.p. 224–225 °C (dec.) (Lit. 220 °C [7]; 222 °C [8]; 224–226 °C [9]; 225–227 °C [10]). The isomeric 2-*tert*-butyldioxindole melts at 85 °C [7].
[7] E. Brandeau, S. David, J.-C. Fischer, *Tetrahedron 30* (1974) 1445.
[8] F. Piozzi, M. Cecere, *Atti. Accad. Naz. Lincei, Cl. Sci. Fis. Mat. Nat. Rend. 28* (1960) 639; *Chem. Abstr. 55* (1961) 9372d.
[9] M.-C. Battembourg, S. David, *Bull. Soc. Chim. Fr. 1962*, 772.
[10] M. A. Colle, S. David, *Compt. Rend. 250* (1960) 2226; *Chem. Abstr. 55* (1961) 23490f.
[11] R. Menicagli, C. Malanga, L. Lardicci, *Chem. Ind. (Milan) 59* (1977) 652; *Chem. Abstr. 88* (1978) 50588k.
[12] We thank Prof. *M. B. Hursthouse* and the SERC X-ray crystallography service for carrying out the structure determination.
[13] M. A. Sukari, J. M. Vernon, *J. Chem. Soc. Perkin Trans. 1 1983*, 2219.
[14] V. W. Pike in J. R. Jones (Ed.): *Isotopes: Essential Chemistry and Applications. R. Soc. Chem. Spec. Publ. 68* (1988) 1.
[15] P. A. Wender, A. W. White, *Tetrahedron 39* (1983) 3767.

Mesolytic Cleavage of C–C Bonds. Comparison with Homolytic and Heterolytic Processes in the Same Substrate**

By *Przemyslaw Maslak** and *Javier N. Narvaez*

Mechanistic information on cleavage of C–C bonds leading to formation of two fragments containing three-valent carbon atoms has been limited for a long time to homolytic reactions.[1] Only recently have examples of heterolytic scission[2] been found and investigated in detail. Carbon–carbon bond cleavage may also be induced by one-electron reduction[3, 4] or oxidation[5–7] of molecules. In such cases, unimolecular fragmentation of the resulting radical ions leads to radicals and ions in a process that may be viewed as homolytic or heterolytic depending on electron apportionment to the fragments.[8] To reflect this mechanistic duality we propose to call such processes mesolytic. Here we provide the first kinetic and thermodynamic comparison of four different C–C bond cleavage modes in the same molecule. The study illustrates the tremendous accelerations obtainable in mesolytic processes. We show that this acceleration is due to thermodynamic factors, and, most importantly, that almost all of the thermodynamic advantage is expressed in the lowering of the transition-state energy, even for weakly endergonic processes.

When **1** was heated to 110–140 °C in perdeuterio-*o*-xylene in the presence of thiophenol (Scheme 1), a first-or-

[*] Prof. P. Maslak, J. N. Narvaez
Department of Chemistry
The Pennsylvania State University
University Park, PA 16802 (USA)

[**] This work was supported by a grant from the National Science Foundation and by the New Faculty Award from the Camille and Henry Dreyfus Foundation.

der reaction was observed, resulting in the formation of 3-(4′-nitrophenyl)pentane (87%) and 3-(4′-dimethylaminophenyl)pentane (91%) as the major products. The half-life for disappearance of **1** at 130 °C was 11 min. The observed products and kinetic parameters are consistent with the homolytic cleavage of the central C–C bond. The kinetic data for the homolysis of **1** (Table 1) are almost identical to those reported by *Rüchardt* et al. for homolysis[9] of the hydrocarbon analogue of **1**. The characteristically large entropy of activation is due largely to release of rotational degrees of freedom in the side chains. Based on the studies of *Rüchardt* et al.,[9] it might be assumed that, even in these sterically crowded molecules, radical recombination has only a small barrier, mostly due to entropic effects. Thus, the activation energy measured for this process may serve as a good estimate of the free energy change in this process ($\Delta G^{\neq}(\mathbf{1}) \approx \Delta G(\mathbf{1})$).

In a polar solvent ($(CD_3)_2SO$, 80–110 °C), **1** underwent a clean unimolecular heterolysis of the C–C bond with $t_{1/2} = 7$ min at 100 °C. The major products were 3-(4′-nitrophenyl)pentane (78%) and 3-(4′-dimethylaminophenyl)-pent-2-ene (93%), apparently formed via proton transfer from $\mathbf{3}^{\oplus}$ to $\mathbf{2}^{\ominus}$ (Scheme 1). The dramatically different activation parameters—as compared to those observed in the nonpolar solvent—attest to the change of cleavage mechanism. When this reaction was run in the presence of sodium azide, the rate was unchanged. In addition to 3-(4′-dimethylaminophenyl)pent-2-ene (48%), 3-azido-3-(4′-dimethylaminophenyl)pentane (47%) was observed, indicating involvement of the corresponding benzylic cation ($\mathbf{3}^{\oplus}$).

The radical anion of **1** decayed in a clean first-order fashion[4] with a half-life of 21 min at 20 °C in Me_2SO. The rate constant was independent of the counterion ($Li^{\oplus}$, $Na^{\oplus}$, $K^{\oplus}$). One of the products, anion $\mathbf{2}^{\ominus}$, could be observed directly by NMR. After quenching the reaction mixture with O_2/MeOH/H_2O, the major products of this *aniomesolytic* fragmentation of the C–C bond included 3-(4′-nitrophenyl)-pentan-3-ol (60%), 3-(4′-nitrophenyl)pentane (25%), 3,4-diethyl-3,4-bis(4′-dimethylaminophenyl)hexane (30%), and 4′-dimethylaminophenyl)pentan-3-ol (50%).

The *catiomesolytic* cleavage of $\mathbf{1}^{\bullet\oplus}$ was very rapid even at −95 °C ($t_{1/2} = 3.0$ min, CH_2Cl_2/MeOH (10%), $SbCl_6^{\ominus}$ counterion).[7] The isolated products included 3-(4′-nitrophenyl)-3-methoxypentane (30%), 3-(4′-nitrophenyl)pent-3-ene (65%), 3-(4′-dimethylaminophenyl)-3-methoxypentane (20%), and 3-(4′-dimethylaminophenyl)pent-3-ene (24%). Apparently, $\mathbf{2}^{\bullet}$ is oxidized by $\mathbf{1}^{\bullet\oplus}$ to the corresponding cation, and both cations ($\mathbf{2}^{\oplus}$ and $\mathbf{3}^{\oplus}$) are trapped by methanol. The styrenes are products of thermal decomposition of the ethers.[7]

The data in Table 1 illustrate the dramatic acceleration of C–C bond scission obtainable by addition or removal of an electron. The difference between the homolytic and catiomesolytic fragmentations spans nearly twenty powers of ten when expressed in half-lives of the species undergoing cleavage, or more than 24 kcal mol^{-1} in activation energy. The aniomesolytic process is 10^8 times faster than homolysis. Of course, to fully evaluate these cleavage processes, thermodynamic data must also be considered. The primary products of the other three modes of cleavage are derived from $\mathbf{2}^{\bullet}$ and $\mathbf{3}^{\bullet}$ by one-electron redox processes. Therefore, the knowledge of redox potentials of these radicals and **1** would make thermodynamic comparison of all these processes possible via appropriate thermodynamic cycles[10] (Scheme 1). The required reversible redox potentials for $\mathbf{2}^{\ominus}/\mathbf{2}^{\bullet}$, $\mathbf{3}^{\oplus}/\mathbf{3}^{\bullet}$, and $\mathbf{1}/\mathbf{1}^{\bullet\oplus}$ or $\mathbf{1}/\mathbf{1}^{\bullet\ominus}$ may be obtained using cyclic voltammetry (CV)[11] or second-harmonic ac voltammetry (SHAC)[12] (Scheme 1).

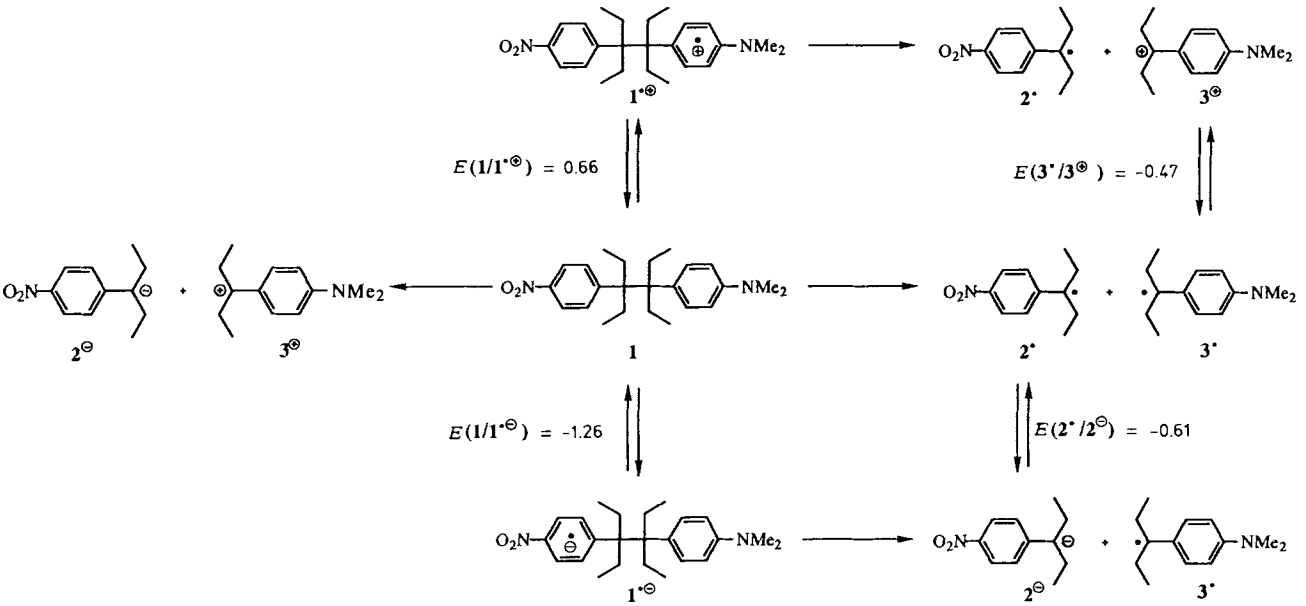

Scheme 1. Fragments derived from **1** and its radical ions as well as the corresponding redox potentials in V vs. SCE.

Interestingly, the estimated free-energy change in heterolysis ($\Delta G(\mathbf{1}\pm)$) is 11 kcal mol^{-1} higher than the activation energy measured for this process. This discrepancy can be accounted for if ion pairs, and not free ions, are the primary products. There is evidence[13] that Coulombic attraction may stabilize such ion pairs by as much as 27 kcal mol^{-1}. A plausible description of the products may involve an ion sandwich solvated on the outside, but with no solvent

Table 1. Kinetic data of four alternative modes of C–C bond cleavage in **1** ($T = 300$ K) [a].

Mode of cleavage	$t_{1/2}$ [b] [min]	$\Delta H^{\neq}$ [kcal mol^{-1}]	$\Delta S^{\neq}$ [cal K^{-1} mol^{-1}]	$\Delta G^{\neq}_{300}$ [kcal mol^{-1}]	ΔG_{300} [c] [kcal mol^{-1}]
Homolytic	1.7×10^{9}	45.6	38	34.2	34
Heterolytic	8.2×10^{3}	22.5	−13	26.4	37
Aniomesolytic	2.0×10^{1}	22.2	2	21.6	20
Catiomesolytic	2.0×10^{-11}	7.0	−10	10.0	8

[a] The estimated errors of enthalpies and entropies of activation for homolysis and heterolysis are ± 2 kcal mol^{-1} and ± 5 cal K^{-1} mol^{-1}. The corresponding estimates for mesolyses are ± 1 kcal mol^{-1} and ± 3 cal K^{-1} mol^{-1}. [b] Estimated. The actual values measured in the experimentally accessible range are reported in the text. [c] Estimated from redox data (± 2 kcal mol^{-1}).

molecules between the aromatic rings. The transition state very likely resembles such an ion pair. Therefore, the observed highly negative $\Delta S^{\neq}$ of heterolysis might be due in part to the compactness of the transition structure. It has to be stressed that **1** is biased by substitution to favor a heterolytic process. A rate increase such as that observed in this case (in comparison to homolysis) is not expected to be a universal phenomenon.

In contrast, the thermodynamically driven acceleration of mesolytic processes is general since radicals undergo oxidation or reduction easier than the corresponding neutral precursors.[14] As our data indicate, all the scission reactions have activation energies that are only slightly higher than the free-energy changes accompanying the reactions. This is not surprising for the highly endergonic homolysis, but quite remarkable for mesolytic cleavages. In the latter cases, almost all of the thermodynamic advantage gained by electron removal or addition is exhibited in the transition state, even for the very weakly endergonic reaction of $\mathbf{1}^{\bullet\oplus}$. This observation is of particular significance for designing low-activation-energy processes for fragmentation of C–C bonds. Not only can the cleavage be carried out in a selective manner[15] under mild conditions, but the energy supplied to the system in order to generate the reactive radical ions is likely to result in the largest possible lowering of the activation energy.

Received: October 16, 1989 [Z 3592 IE]
German version: *Angew. Chem. 102* (1990) 302

CAS Registry numbers:
1, 125379-43-3; **2**, 38896-06-9; **3**, 96558-51-9; 3-(4′-dimethylaminophenyl)-pent-(2)-ene, 125379-44-4; 3-(4′-nitrophenyl)propan-3-ol, 62558-06-9; 3,4-diethyl-3-4-bis(4′-di-3-(4′-nitrophenyl)pentane, 125379-45-5; (4′-dimethylaminophenyl)propan-3-ol, 85665-76-5; 3-(4′-nitrophenyl)-3-methoxypropane, 65288-75-7; 3-(4′-nitrophenyl)prop-(3)-ene, 25798-60-1; 3-(4′-dimethylaminophenyl)-3-methoxypropane, 125379-46-6; 3-(4′-dimethylaminophenyl)prop-(3)-ene, 92146-61-7.

[1] Reviews: a) C. Rüchardt, H.-D. Beckhaus, *Angew. Chem. 92* (1980) 417; *Angew. Chem. Int. Ed. Engl. 19* (1980) 429; b) *ibid. 97* (1985) 531 and *24* (1985) 529; c) *Top. Curr. Chem. 130* (1986) 1.
[2] a) Review: E. M. Arnett, K. E. Molter, *Acc. Chem. Res. 18* (1985) 339; compare also b) E. M. Arnett, K. E. Molter, E. C. Marchot, W. H. Donovan, P. Smith, *J. Am. Chem. Soc. 109* (1987) 3788; c) K. Komatsu, S. Aonuma, K. Takeuchi, K. Okamoto, *J. Org. Chem. 54* (1989) 2038.
[3] T. D. Walsh, *J. Am. Chem. Soc. 109* (1987) 1511.
[4] For the method of generation of $\mathbf{1}^{\bullet\ominus}$ and the kinetic technique used, see P. Maslak, J. N. Narvaez, *Chem. Commun. 1989*, 138.
[5] Reviews of C–C bond cleavage in photogenerated radical cations: a) A. M: Fox, M. Chanon, (Eds.): *Photoinduced Electron Transfer*, Elsevier, Amsterdam 1988; b) H. D. Roth, *Acc. Chem. Res. 20* (1987) 343.
[6] a) D. M. Camaioni, J. Franz, *J. Org. Chem. 49* (1984) 1607; b) L. A. Deardurff, M. S. Alnajjar, D. M. Camaioni, *ibid. 51* (1986) 3686; c) E. Baciocchi, D. Bartoli, C. Rol, R. Ruzziconi, G. Sebastiani, *ibid. 51* (1986) 3587.
[7] For the method of generation of $\mathbf{1}^{\bullet\oplus}$ and kinetic technique used, see P. Maslak, S. L. Asel, *J. Am. Chem. Soc. 110* (1988) 8260.
[8] P. Maslak, R. D. Guthrie, *J. Am. Chem. Soc. 108* (1986) 2628, 2637.
[9] a) G. Krat, H.-D. Beckhaus, H. J. Lindner, C. Rüchardt, *Chem. Ber. 116* (1983) 3235; b) G. Krat, H.-D. Beckhaus, C. Rüchardt, *ibid. 117* (1984) 1748.
[10] The cycles used: $\Delta G(\mathbf{1}) - \Delta G(\mathbf{1}\pm) = 23.06\ [E(\mathbf{2}^{\bullet}/\mathbf{2}^{\ominus}) - E(\mathbf{3}^{\bullet}/\mathbf{3}^{\oplus})]$; $\Delta G(\mathbf{1}) - \Delta G(\mathbf{1}^{\bullet\ominus}) = 23.06\ [E(\mathbf{2}^{\bullet}/\mathbf{2}^{\ominus}) - E(\mathbf{1}/\mathbf{1}^{\bullet\ominus})]$; $\Delta G(\mathbf{1}) - \Delta G(\mathbf{1}^{\bullet\oplus}) = 23.06\ [E(\mathbf{1}/\mathbf{1}^{\bullet\oplus}) - E(\mathbf{3}^{\bullet}/\mathbf{3}^{\oplus})]$.
[11] All quoted potentials are versus SCE. For use of CV to obtain reversible potentials, see a) R. J. Klingler, J. K. Kochi, *J. Am. Chem. Soc. 104* (1982) 4186; b) S. Fukuzumi, S. Koumitsu, K. Hironaka, T. Tanaka, *ibid. 109* (1987) 305.
[12] For an example of similar use of SHAC, see E. M. Arnett, N. G. Harvey, K. Amarnath, J.-P. Cheng, *J. Am. Chem. Soc. 111* (1989) 4143.
[13] Reviews: a) P. Suppan, *Chimia 42* (1988) 320; b) G. J. Kavarnos, N. J. Turro, *Chem. Rev. 86* (1986) 401.
[14] This statement applies to removal of bonding electrons or addition of electrons to antibonding orbitals of the precursor molecules.
[15] The increased selectivity (as compared to homolysis) is due to the fact that substitution and solvent influence ion stability more strongly than radical stability.

The Ammonium Salt Route to Oligomeric Lanthanum Salt Complexes: Synthesis and X-Ray Crystal Structure of $La(NCS)_3 \cdot 4\,HMPA$**

By *Donald Barr, Alan T. Brooker, Michael J. Doyle, Simon R. Drake, Paul R. Raithby,* Ronald Snaith,* and *Dominic S. Wright*

Donor complexes of alkali and alkaline-earth metal salts, $(MX \cdot xL)_n$ and $(MX_2 \cdot xL)_n$, respectively (e.g., M = Li, Na, K, Ca, Sr, Ba; X = Cl, Br, I, SCN; L = HMPA, TMEDA; x = 1–4), can be obtained by reactions of solid ammonium salts with metal sources (*n*BuLi solution, MH or MH_2, the metals themselves) in toluene containing stoichiometric amounts (x) of Lewis bases (L) ("ammonium salt route").[1, 2] Here we report extensions of this synthetic method (but using the metal only, not its hydride or an organometallic compound) to complexes of salts of similarly electropositive non-main-group metals, namely lanthanum (in particular), yttrium, europium, and manganese; the crystal structure of one product so obtained, $La(NCS)_3 \cdot 4$ HMPA (**1**), is also described. In related previous work,[3a, b] ammonium salts have been employed in the syntheses of (uncomplexed) organolanthanoid and -actinoid salts by reacting them with cyclopentadienyl organometallic compounds. For example, NH_4X salts (X = F, Cl, NO_3, BPh_4) react with $(C_5H_5)_4U$ in benzene or tetrahydrofuran to give $(C_5H_5)_3UX$ salts,[3a] and $(C_5Me_5)_2ThMe_2$ reacts with $[R_3NH][BPh_4]$ (R = Me or Et) in toluene to give $[(C_5Me_5)_2Th(Me)][BPh_4]$.[3b]

$La(NCS)_3 \cdot 4$ HMPA **1**

In a typical procedure, a mixture of La metal, solid NH_4NCS, and HMPA (1:3:3 molar ratios) in toluene was treated with ultrasound and heated at 90 °C for up to 1 day (see *Experimental Procedure*). Such conditions caused gas

[*] Dr. P. R. Raithby, Dr. D. Barr, A. T. Brooker, M. J. Doyle, Dr. S. R. Drake, Dr. R. Snaith, Dr. D. S. Wright
University Chemical Laboratory
Lensfield Road, GB-Cambridge, CB2 1EW (UK)

[**] This work was supported by the Associated Octel Co. Ltd., ICI, the UK Science and Engineering Research Council, and St. John's College, Cambridge. HMPA = hexamethylphosphoramide; TMEDA = *N,N,N′,N′*-tetramethylethylenediamine.

evolution and dissolution of most of the solids. After filtration, chilling of the colorless solution afforded colorless crystals of **1**. The complex has a relatively low melting point and moderate solubility in benzene or toluene, properties indicative of a monomeric or oligomeric (ionically bonded) structure rather than of a continuously latticed one. Reaction of La metal with NH_4Br, under similar conditions, affords the complex $LaBr_3 \cdot 4$ HMPA.[4] All such processes can best be rationalized in terms of $NH_4^{\oplus}$ behaving as a protic acid (pK_a of $NH_4^{\oplus}$: 9.24) towards the metal, so leading to its oxidation (compare reactions of electropositive metals with organic acids such as PhOH, pK_a 10.0).[5]

This ammonium salt route to such complexes has several advantageous features. First, the parent (uncomplexed) lanthanum salts themselves are not too easy to make; for example, the halides LaX_3 are all formed from high-temperature reactions of La metal with HX or X_2 vapors,[6] and the rare-earth trichlorides, in particular, have been obtained (8–97% yields) by allowing the metal oxides to react with $AlCl_3$ at temperatures of 310–500 °C.[7] In contrast, the ammonium salt route assembles LaX_3 species under mild, solution or suspension conditions. Second, although some lanthanoid (Ln) salts will dissolve directly in donor solvents (e.g. $PrCl_3$ dissolves on heating in ethanolic HMPA to give $PrCl_3 \cdot 4$ HMPA[8]), such dissolution is often incomplete; in some cases, of course, where lattice energy factors outweigh complexation energy ones, it does not occur at all. Again in contrast, an infinite lattice $(LnX_3)_\infty$ is not necessarily allowed to form in the ammonium salt route since association of initially generated LnX_3 monomers can be prevented (or at least limited) by the small donor molecules (L) present. Finally, even when direct dissolution works, the parent $(LnX_3)_\infty$ salts are extremely hygroscopic (even deliquescent);[6] it is difficult to obtain these salts as fully anhydrous materials, so that H_2O often appears as a coligand (with L) in complexes. This difficulty is avoided in the ammonium salt route since the precursors are not generally hygroscopic.

The solid-state structure of **1** (Fig. 1)[9] has been solved by X-ray diffraction. As its physical properties indicated, **1** is monomeric. The La atom has a geometry in which the three $NCS^{\ominus}$ ligands occupy positions which are pseudo-*trans* to O atoms of three of the four HMPA ligands. The three La–N distances average 2.581(14) Å; the three La–O distances pseudo-*trans* to the La–N bonds average 2.436(10) Å, the fourth La–O distance being slightly shorter, 2.385(9) Å. The La center thus has a relatively unusual (low) coordination number, seven; eight-coordination seems most common for lanthanoid species, though much higher coordination numbers are well documented for these highly ionic systems.[6]

Similar reactions of NH_4X salts (X = SCN, Br) with the lanthanoid and transition elements Eu, Y, and Mn in toluene containing various donors (TMEDA, HMPA, and DMPU (DMPU = $MeN\overline{C(=O)NMe(CH_2)_2CH_2}$) have afforded, in yields of up to 80%, complexes such as $Eu(NCS)_3 \cdot 2$ TMEDA, $Y(NCS)_3 \cdot 3$ HMPA, and $MnBr_3 \cdot 3$ DMPU.[10] All such low-melting, oligomeric complexes (and others derived from NH_4NO_3, such as $La(NO_3)_3 \cdot 3$ HMPA[10, 11]) are being examined as possible precursors for vapor-phase deposition of metal oxide films, while the reactions of the halide complexes (which are soluble in organic solvents) in solution with RLi and ROLi reagents are being studied as possible routes to organometallic and metal alkoxide complexes.

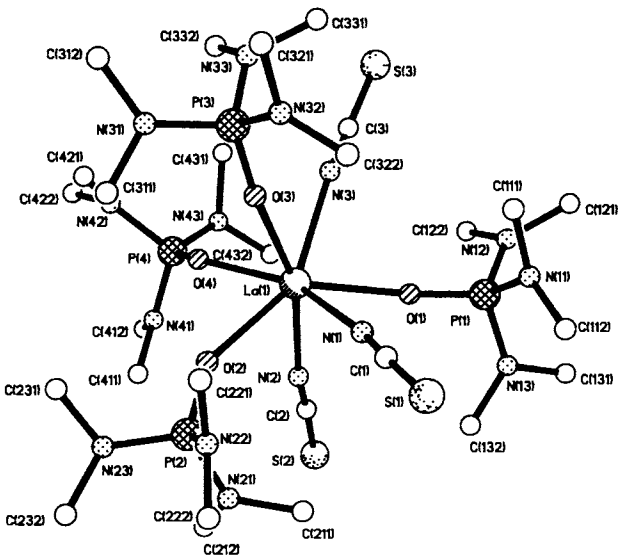

Fig. 1. The molecular structure of **1**. Hydrogen atoms have been omitted for clarity. Key bond lengths [Å]: La(1)-O(1) 2.385(9), La(1)-O(2) 2.450(8), La(1)-O(3) 2.418(8), La(1)-O(4) 2.441(8), La(1)-N(1) 2.581(12), La(1)-N(2) 2.576(12), La(1)-N(3) 2.587(11).

Experimental Procedure

1: A mixture of powdered La metal (0.32 g, 2.3 mmol), solid NH_4SCN (0.52 g, 6.9 mmol), and HMPA (1.24 g, 6.9 mmol) in toluene (10 mL) was first treated with ultrasound for 1 h. No reaction was apparent at this stage, but, on heating to 90 °C, gas evolution (H_2 and NH_3, confirmed by gas chromatography) was observed. Such evolution continued over 24 h, most of the solids dissolving. Extra toluene (10 ml) was added and the mixture filtered hot; cooling of the resulting colorless solution afforded colorless crystals characterized, after filtration and drying in vacuo, as **1** (first-batch yield, 0.84 g, 49%, m.p. 183–185 °C; correct C, H, N, P analysis. ^1H NMR (C_6D_6, 80 MHz, 20 °C): $\delta = 2.51/2.63$ (HMPA doublet).

Single crystals of **1** suitable for X-ray crystallography were sealed under N_2 in Lindemann capillary tubes prior to data collection.

Received: August 7, 1989 [Z 3486 IE]
German version: *Angew. Chem. 102* (1990) 300

[1] a) D. Barr, R. Snaith, D. S. Wright, R. E. Mulvey, K. Wade, *J. Am. Chem. Soc. 109* (1987) 7891; b) D. Barr, M. J. Doyle, R. E. Mulvey, P. R. Raithby, R. Snaith, D. S. Wright, *J. Chem. Soc. Chem. Commun. 1988*, 145; c) D. Barr, M. J. Doyle, S. R. Drake, P. R. Raithby, R. Snaith, D. S. Wright, *ibid. 1988*, 1415; d) *Polyhedron 8* (1989) 215; e) D. Barr, M. J. Doyle, R. E. Mulvey, P. R. Raithby, D. Reed, R. Snaith, D. S. Wright, *J. Chem. Soc. Chem. Commun. 1989*, 318; f) D. Barr, M. J. Doyle, S. R. Drake, P. R. Raithby, R. Snaith, D. S. Wright, *Inorg. Chem. 28* (1989) 1767; g) D. Barr, A. T. Brooker, M. J. Doyle, S. R. Drake, P. R. Raithby, R. Snaith, D. S. Wright, *J. Chem. Soc. Chem. Commun. 1989*, 893.

[2] The ammonium salt route to alkali-metal complexes is the subject of a patent (Eur. Pat. Appl. 88309913.7) filed by the Associated Octel Co. Ltd. A patent application field (U. K. Pat. Appl. 8915531.1) concerns extensions of the route to complexes of the alkaline-earth, lanthanoid, and transition metals.

[3] a) E. Dornberger, R. Klenze, B. Kanellakopulos, *Inorg. Nucl. Chem. Lett. 14* (1978) 319; b) Z. Lin, J.-F. Le Marechal, M. Sabat, T. J. Marks, *J. Am. Chem. Soc. 109* (1987) 4127.

[4] For $LaBr_3 \cdot 4$ HMPA: reaction of La, NH_4Br, and HMPA (1:3:3 molar equivalents) required ultrasound treatment for 12 h at 40 °C, then heating for 4 h at 90 °C. The resulting solution, on cooling, gave the product, in a first-batch yield of 55%; m.p. 178–180 °C.

[5] A. Streitwieser Jr., C. H. Heathcock: *Introduction to Organic Chemistry*, 3rd ed., Macmillan, New York 1985, pp. 62, 195; *Organische Chemie*, VCH Verlagsgesellschaft, Weinheim 1986.

[6] N. N. Greenwood, A. Earnshaw: *Chemistry of the Elements*, Pergamon Press, Oxford 1984: see Chapter 20, pp. 1102–1110, and Chapter 30, especially pp. 1433–1436, pp. 1439–1441, and pp. 1445–1447; *Chemie der Elemente*, VCH Verlagsgesellschaft, Weinheim 1988.

[7] H. Gunsilius, W. Urland, R. Kremer, *Z. Anorg. Allg. Chem. 550* (1987) 35.

[8] L. J. Radonovich, M. D. Glick, *J. Inorg. Nucl. Chem. 35* (1973) 2745.

[9] 1. Crystal data: $C_{27}H_{72}LaN_{15}O_4P_4S_3 \cdot 0.5\ (C_6H_5CH_3)$, $M_r = 1069$, monoclinic, space group $P2_1/n$, $a = 11.179(3)$, $b = 21.922(7)$, $c = 22.432(7)$ Å,

$\beta = 91.40(2)^\circ$, $V = 5496(3)$ Å^3, $Z = 4$, $\varrho_{calcd} = 1.29$ g cm^{-3}, $F(000) = 2228$, $Mo_{K\alpha}$ radiation, $\lambda = 0.71073$ Å, $\mu = 1.05$ mm^{-1}. The structure was determined by Patterson and Fourier difference techniques and refined from 5070 unique observed reflections measured at room temperature with a Nicolet R3mV diffractometer ($2\Theta_{max} = 45.0^\circ$), with anisotropic thermal parameters, and with isotropic H atoms in calculated positions; $R = 0.082$, $R_w = 0.099$, $S = 1.71$ for 512 parameters. The crystals examined (sealed in tubes without prior vacuum drying) contained disordered toluene solvate molecules, hence the high-weighted R factor; attempts to grow crystals without solvent failed. Further details of the crystal structure investigation can be obtained from the Director of the Cambridge Crystallographic Data Centre, University Chemical Laboratory, Lensfield Road, Cambridge, CB2 1EW (England) on quoting the full journal citation.

[10] The four complexes mentioned were obtained in a similar way to **1**. Typically, the mixture of metal and NH_4X salt in L/toluene was first ultrasonicated for 1 h, then heated at 80–110 °C for 12 h. Most of all of the solids dissolved over this period to give, after filtration, colorless (for Eu, Y, La) or green (Mn) solutions. Refrigeration then afforded the crystalline products: $Eu(NCS)_3 \cdot 2$ TMEDA, yield 64%, m.p. 127–131 °C; $Y(NCS)_3 \cdot 3$ HMPA, yield 80%, m.p. 177–179 °C; $MnBr_3 \cdot 3$ DMPU, yield 44%, m.p. 125–127 °C; $La(NO_3)_3 \cdot 3$ HMPA, yield 76%, m.p. 213–214 °C. Product identities were established by satisfactory elemental analyses (C, H, N; P and Br in the appropriate cases). No evidence (from analyses, IR spectra) was found for the presence of coordinated NH_3 in the products. For the europium complex, the presence of $Eu^{3\oplus}$ was confirmed by cyclic voltammetry.

[11] X-ray crystallography shows $La(NO_3)_3 \cdot 3$ HMPA to be monomeric, with bidentate $NO_3^{\ominus}$ ligands and thus nine-coordinate lanthanum.

Ethynyl(phenyl)iodonium Triflate, $[HC\equiv ClPh][OSO_2CF_3]$: Preparation, Spectral Properties, Mechanism of Formation and X-Ray Molecular Structure**

By *Peter J. Stang,* Atta M. Arif,* and *Charles M. Crittell*

Dedicated to Professor Paul von Ragué Schleyer on the occasion of his 60th birthday

The newest members of the family of polycoordinated iodine species, alkynyl(phenyl) iodonium salts **1**, have rapidly become valuable reagents in organic chemistry.[1] They serve as precursors to novel alkynyl esters such as alkynyl sulfonates,[2] alkynyl carboxylates,[3] and alkynyl phosphates,[4] as well as to microbicides.[5] Vinylcopper reagents stereoselectively couple with **1** to give conjugated enynes with stereodefined double-bond geometries.[6] Alkynyliodonium salts **1** undergo efficient cyclopentene annulations[7] and serve as a progenitor of a unique vinyliodinane species.[8]

$R{-}C{\equiv}C{-}\overset{\oplus}{I}{-}PhX^{\ominus}$ (**1**) $H{-}C{\equiv}C{-}\overset{\oplus}{I}{-}Ph\ \ CF_3SO_3^{\ominus}$ (**2**)

In spite of the surging interest in alkynyl(phenyl)iodonium salts **1**, the parent member of the family, **2**, remains unknown and little is known about the mechanism of formation of these species. Current methods of preparation of **1** employ either terminal alkynes[2, 9] or silylalkynes,[10, 11] neither of which are applicable for the formation of the parent, unsubstituted, ethynyl(phenyl)iodonium salt. In this communication we wish to report the preparation, spectral properties, X-ray structure, and mechanism of formation of **2**, the simplest member of the family of alkynyliodonium salts **1**.

[*] Prof. P. J. Stang, Dr. A. M. Arif, C. M. Crittell
Department of Chemistry, The University of Utah
Salt Lake City, UT 84112 (USA)

[**] This work was supported by the National Cancer Institute of the NIH (ROCA16903).

Reaction of Zefirov's reagent,[12] **5**, readily prepared[13] in situ by the reaction of iodosobenzene (**3**) with triflic anhydride (**4**), with tri-*n*-butylstannylacetylene gave, upon workup, the desired species **2** in 56% isolated yield (Scheme 1). Compound **2** is a stable, off-white, microcrystalline solid.

$$2\,PhIO\ (\mathbf{3}) + (CF_3SO_2)_2O\ (\mathbf{4}) \xrightarrow[0\,^\circ C]{CH_2Cl_2} PhI(OTf)-O-IPh(OTf)\ (\mathbf{5})$$

$$2\,nBu_3SnC{\equiv}CH + \mathbf{5} \xrightarrow[0\,^\circ C,\ 30\ min]{CH_2Cl_2} 2\,HC{\equiv}\overset{\oplus}{C}IPh\ \overset{\ominus}{O}Tf\ (\mathbf{2}) + (nBu_3Sn)_2O$$

Scheme 1. Tf = CF_3SO_2.

Its IR spectrum shows absorptions at 3285 cm^{-1} and at 2047 cm^{-1} characteristic of the terminal acetylenic C–H stretch and the C–C triple bond, respectively, as well as at 1174, 1232, 1251, 1276, and 634 cm^{-1} due to ionic triflate absorptions.[14] The ^{1}H NMR spectrum of **2** displays a singlet at $\delta = 3.75$ due to the acetylenic hydrogen and aromatic signals at $\delta = 7.65$, 7.83, and 8.24. The relatively low-field position of these signals is in accord with the strong electron-withdrawing effect and concomitant deshielding by the $PhI^{\oplus}$ moiety. Likewise, the ^{13}C NMR spectrum has signals at $\delta = 27.3$ and 98.3 due to the α and β acetylenic carbons, respectively, at $\delta = 117.6$, 134.2, 134.8, and 136.4 for the four different aromatic carbons, and at $\delta = 121.6$ (q, $J_{FC} = 319.1$ Hz) due to the triflate carbon. The very low field absorption of the β carbon ($\delta = 98.3$ vs. 71.9 for acetylene[15] itself) is indicative of a considerable amount of positive charge on this carbon, due to the importance of the resonance structures $HC{\equiv}C{-}\overset{\oplus}{I}Ph$ and $H\overset{\oplus}{C}{=}C{=}IPh$. Analogous low-field ^{13}C absorptions have been observed in the case of alkynyl phosphonium salts.[16] The ^{19}F NMR signal of the triflate is at $\delta = -77.6$.

A suitable single crystal of **2**, grown from $CHCl_3$, was subjected to standard X-ray analysis (Fig. 1). The data indicate a distorted pseudo-trigonal-bipyramidal or T-shaped geometry for **2** in accord with the 10–I–3 nature[17] of **2**. Particularly noteworthy are the I–O1 and I–O2 distances of 2.620 and 2.915 Å, well outside the computed covalent I–O single-bond length of 1.99 Å, along with the three nearly identical S---O bond lengths of 1.424 ± 0.023 Å, which are indicative of the strongly ionic nature of this salt. The unusually short C≡C bond (1.145 ± 0.006 Å) is also interesting. It represents one of the shortest acetylenic bonds known; the average C≡C bond length[18] is 1.181–1.183 Å for 350 acetylenes for which structures have been determined[17] and only a few C≡C bonds are shorter than 1.167 Å.[17] In contrast, the gross features of **2** are in accord with the known[2, 19] structural features of other tricoordinate iodine species such as $PhICl_2$ and $PhI(OAc)_2$.

The mechanism of formation of **2** is deserving of attention. In general, the preparation[2, 9–11] of alkynyliodonium salts **1** must involve the electrophilic addition of an iodonium species to an alkyne and initial formation of a vinyl cation.[20] The high energy[20] of the parent vinyl cation accounts for the lack of reactivity of acetylene itself and hence the fact that the parent species **2** was previously unknown. It is well established[21, 22] that Si substitution destabilizes α-cations but stabilizes β-cations ($Me_3SiC\text{-}\overset{\oplus}{C}$). Yet, we found $Me_3SiC{\equiv}CH$ still too unreactive to give **2**. However,

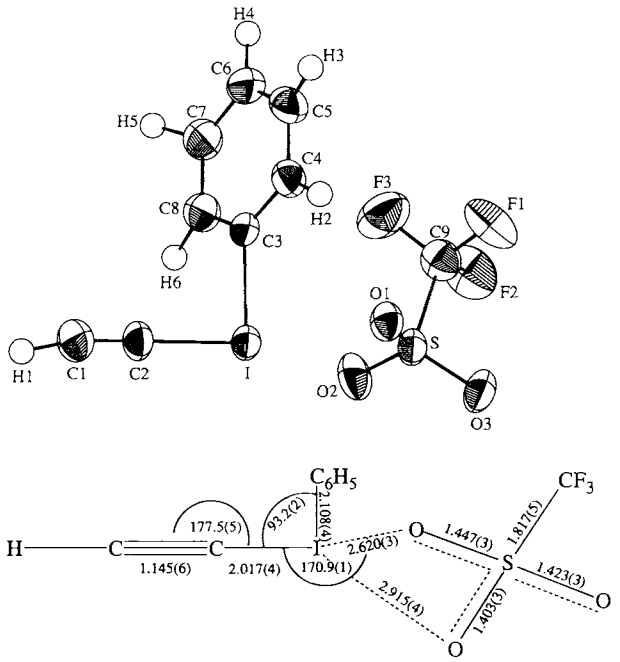

Fig. 1. Top: Molecular structure (ORTEP) of **2**. Bottom: Relevant structural data such as bond lengths [Å] and angles [°]. Crystallographic data: space group $P2_1/n$ (No. 1014); monoclinic, $a = 12.744(4)$, $b = 6.993(2)$, $c = 14.164(6)$ Å, $\beta = 101.79(3)°$, $V = 1235.58$, $Z = 4$; crystal dimensions $0.29 \times 0.25 \times 0.15$ mm^3, $\varrho_{calcd} = 2.032$ g cm^{-3}, $Mo_{K\alpha}$ radiation (0.71073 Å), 2234 measured reflections, 2054 unique; $2.50 < 2\Theta < 48°$, $\Theta/2\Theta$ scan. $I < 3.00\sigma(I)$, 1602 observed reflections, 154 variables; $R = 0.0214$, $R_w = 0.0238$. Further details of the crystal structure investigations are available on request from the Director of the Cambridge Crystallographic Data Centre, University Chemical Laboratory, Lensfield Road, Cambridge CB2 1EW (UK), on quoting the full journal citation.

recently *Lambert* and co-workers[23] demonstrated that a β-stannyl substituent stabilizes a cation some $10^{20}-10^{35}$ times better than a β-silyl group. Hence, our use of nBu$_3$SnC≡CH and the highly ionic (therefore strongly electrophilic) Zefirov reagent results in the formation of **2** (Scheme 2).

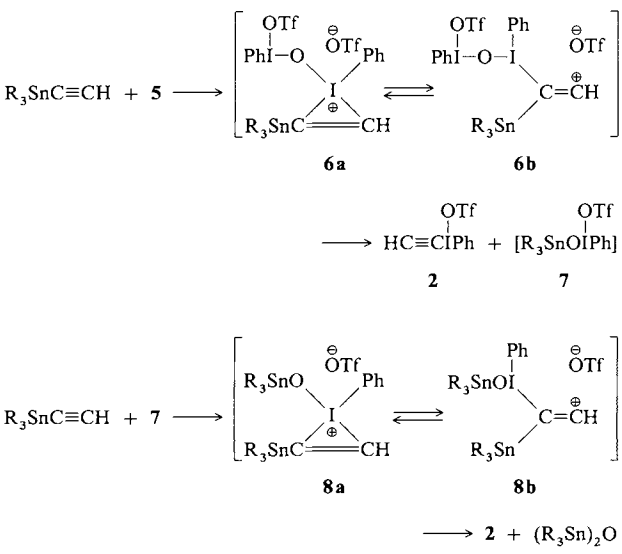

Scheme 2. R = nBu.

Electrophilic addition of Zefirov's reagent, **5**, to nBu$_3$SnC≡CH results in the β-tin-stabilized vinyl-cation ion pair **6**, which forms **2** upon loss of the iodonium compound **7**. Species **7** adds to a second molecule of nBu$_3$SnC≡CH to form the β-tin-stabilized vinyl-cation ion pair **8**, which gives a second mole of the desired salt **2** and one mole of the stannyl ether **9** (Scheme 2). This mechanism nicely accounts for the overall stoichiometry of the reaction, the observed formation of **9**, and, most importantly, why only the stannylacetylene yields the desired parent ethynyliodonium salt **2**. The ions **6a** and **6b** need the powerful stabilizing effect of the β-stannyl group to be readily accessible.

Owing to the powerful electron-withdrawing iodonium group, the acetylene derivative **2** should be among the strongest known carbon acids. *Kresge* et al.[24] recently determined the pK_a of HC≡CCN to be 8. Based upon this value, the pK_a for **2** should be in the range of 2–5 or comparable to carboxylic acids and approaching that of HF with a pK_a of 3.2.[25]

Received: August 22, 1989 [Z 3516 IE]
Publication delayed at authors' request
German version: *Angew. Chem. 102* (1990) 307

[1] Reviews: a) R. M. Moriarty, O. Prakash, *Acc. Chem. Res. 19* (1986) 244; b) A. Varvoglis, *Synthesis 1984*, 709; c) G. F. Koser in S. Patai, Z. Rappoport (Eds.): *The Chemistry of Functional Groups, Supplement D*, Wiley, New York 1983, Chapter 25, pp. 1265–1351; d) G. A. Olah, *Halonium Ions*, Wiley, New York 1975; e) D. F. Banks, *Chem. Rev. 66* (1966) 243.
[2] P. J. Stang, B. W. Surber, Z. C. Chen, K. A. Roberts, A. G. Anderson, *J. Am. Chem. Soc. 109* (1987) 228.
[3] P. J. Stang, M. Boehshar, H. Wingert, T. Kitamura, *J. Am. Chem. Soc. 110* (1988) 3272.
[4] P. J. Stang, T. Kitamura, M. Boehshar, H. Wingert, *J. Am. Chem. Soc. 111* (1989) 2225.
[5] A. J. Margida, G. F. Koser, *J. Org. Chem. 49* (1984) 4703; C. S. Carman, G. F. Koser, *ibid. 48* (1983) 2534.
[6] P. J. Stang, T. Kitamura, *J. Am. Chem. Soc. 109* (1987) 7561.
[7] M. Ochiai, M. Kunishima, Y. Nagao, K. Fuji, M. Shiro, E. Fujita, *J. Am. Chem. Soc. 108* (1986) 8281.
[8] P. J. Stang, H. Wingert, A. M. Arif, *J. Am. Chem. Soc. 109* (1987) 7235.
[9] L. Rebrovic, G. F. Koser, *J. Org. Chem. 49* (1984) 4700; G. F. Koser, L. Rebrovic, R. H. Wettach, *ibid. 46* (1981) 4324.
[10] T. Kitamura, P. J. Stang, *J. Org. Chem. 53* (1988) 4105.
[11] M. Ochiai, M. Kunishima, K. Sumi, Y. Nagao, E. Fujita, M. Arimoto, H. Yamaguchi, *Tetrahedron Lett. 26* (1985) 4501.
[12] N. S. Zefirov, V. V. Zhdankin, Y. V. Dan'kov, A. S. Koz'min, *J. Org. Chem. USSR (Engl. Transl.) 20* (1984) 401. *Zh. Org. Khim. 20* (1984) 446; J. Gallos, A. Varvoglis, N. W. Alcock, *J. Chem. Soc. Perkin Trans. 1 1985*, 757.
[13] T. R. Hembre, C. P. Scott, J. R. Norton, *J. Org. Chem. 52* (1987) 3650.
[14] G. A. Lawrance *Chem. Rev. 86* (1986) 17.
[15] G. C. Levy, R. L. Lichter, G. L. Nelson: *Carbon-13 Nuclear Magnetic Resonance Spectroscopy*, 2nd ed., Wiley-Interscience, New York 1980.
[16] H. J. Bestmann, L. Kisielowski *Chem. Ber. 116* (1983) 1320.
[17] J. C. Martin, *Science (Washington, DC) 221* (1983) 509.
[18] F. H. Allen, O. Kennard, D. G. Watson, L. Brammer, A. G. Open, R. Taylor, *J. Chem. Soc. Perkin Trans. 2 1987*, S1–S19.
[19] N. W. Alcock, R. M. Countryman, S. Esperas, J. F. Sawyer, *J. Chem. Soc. Dalton Trans 1979*, 854; C. K. Lee, T. C. W. Mak, W. K. Li, J. F. Kirner, *Acta Crystallogr. 39* (1974) 2812; E. M. Archer, T. G. D. Van Schalkwyk, *ibid. 6* (1953) 88; D. G. Naae, J. Z. Gougoutas, *J. Org. Chem. 40* (1975) 2129; E. Shafter, W. Wolf, *Nature (London) 203* (1964) 512.
[20] P. J. Stang, Z. Rappoport, M. Hanack, L. R. Subramanian: *Vinyl Cations*, Academic Press, New York 1979.
[21] M. D. Schiavelli, D. M. Jung, A. K. Vaden, P. J. Stang, T. E. Fisk, D. S. Morrison, *J. Org. Chem. 46* (1981) 92, and references therein.
[22] J. B. Lambert, G. T. Wang, R. B. Finzel, D. H. Terommura, *J. Am. Chem. Soc. 109* (1987) 7838 and references therein.
[23] J. B. Lambert, G. T. Wang, D. H. Teramura, *J. Org. Chem. 53* (1988) 5422; J. B. Lambert, G. T. Wang, *Tetrahedron Lett. 21* (1988) 2551.
[24] T. Aroella, C. H. Arrowsmith, M. Hojatti, A. J. Kresge, M. F. Powell, Y. S. Tang, C. H. Wang, *J. Am. Chem. Soc. 109* (1987) 7198.
[25] D. D. Perrin: *Ionization Constants of Inorganic Acids and Bases in Aqueous Solution*, 2nd Edit., Pergamon Press, Oxford 1982.

Restricted Rotation of an Unsubstituted η^5-Cyclopentadienyl Group in Solution Demonstrated by ^{13}C NMR Spectroscopy

By *Richard Mynott,* Herbert Lehmkuhl, Eva-Maria Kreuzer,* and *Eckhard Joussen*

Dedicated to Professor Günther Wilke on the occasion of his 65th birthday

The barrier to rotation of η^5-cyclopentadienyl groups about the ring–transition-metal axis, which has been studied both in solution and the solid by a number of methods,[1–7] is generally considered to be very low. The activation energy $\Delta G^{\ddagger}_{300}$ in solution for rotation of the unsubstituted cyclopentadienyl ring in $[(\eta^5\text{-}C_5H_5)(\eta^5\text{-}C_5H_4R)Fe]$ (R = CMe_2Et, *n*Bu) has been determined from ^{13}C NMR T_1 measurements to be 8.3 and 8.6 kJ mol^{-1}, respectively.[2] Low-temperature solid-state NMR studies on substituted ferrocenes using the temperature dependence of the second moments of the ^1H lines[3] and ^{13}C spin–lattice relaxation times in $CpTiCl_3$, $[CpMo(CO)_3]_2$, and Cp_2TiS_5[4] have demonstrated similarly low barriers. Despite many attempts to observe restricted rotation of unsubstituted η^5-cyclopentadienyl groups in the NMR spectra of transition-metal complexes in solution at low temperature, to our knowledge no such case has been reported.[1] Indeed, examples are rare even where the Cp ring carries bulky substituents such as *tert*-butyl groups.[7] We have now found that in cationic $[Cp(Ph_3P)_2(\eta^2\text{-olefin})M]^{\oplus}$ (M = Ru, Os) complexes with sterically demanding olefin ligands, the barrier to rotation of an unsubstituted η^5-Cp group can be high enough to give rise to splitting of the Cp signal in the ^{13}C and ^1H NMR spectra in solution at low temperature.

The cationic $[(\eta^5\text{-Cp})(R_3P)_2(\eta^2\text{-olefin})M]^{\oplus}$ complexes **1–3** were prepared from the corresponding $[(\eta^5\text{-Cp})(R_3P)_2MHal]$ compounds according to Scheme 1 by methods based upon known syntheses.

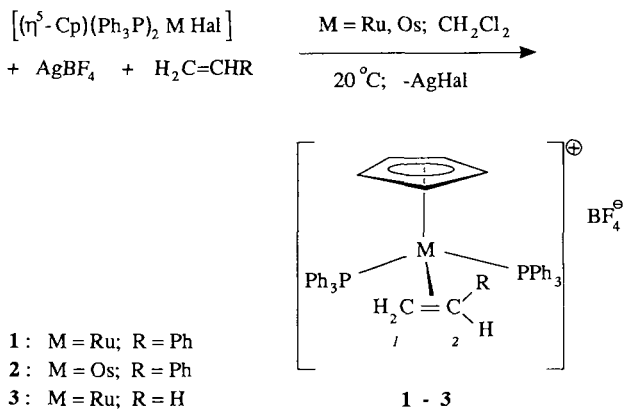

1: M = Ru; R = Ph
2: M = Os; R = Ph
3: M = Ru; R = H

Scheme 1. Synthesis of the cationic complexes **1–3** as $BF_4^{\ominus}$ salts.

At 40 °C the signals in the ^{31}P and ^{13}C NMR spectra of **1** dissolved in CD_2Cl_2 are broadened by dissociation and exchange of the phosphane ligands. The sample was therefore examined at lower temperature in order to obtain well-resolved spectra. In the 75.5-MHz ^{13}C NMR spectrum at −30 °C the cyclopentadienyl resonance ($\delta_C = 90.0$) was sharp. However, while all the other resonances had become narrow at −80 °C, the line width of the Cp signal had increased to 400 Hz. On cooling the sample to −100 °C, this line then split into four signals in the intensity ratio 1:2:1:1 (Fig. 1). Their weighted average chemical shift ($\delta_C = 89.4$) is

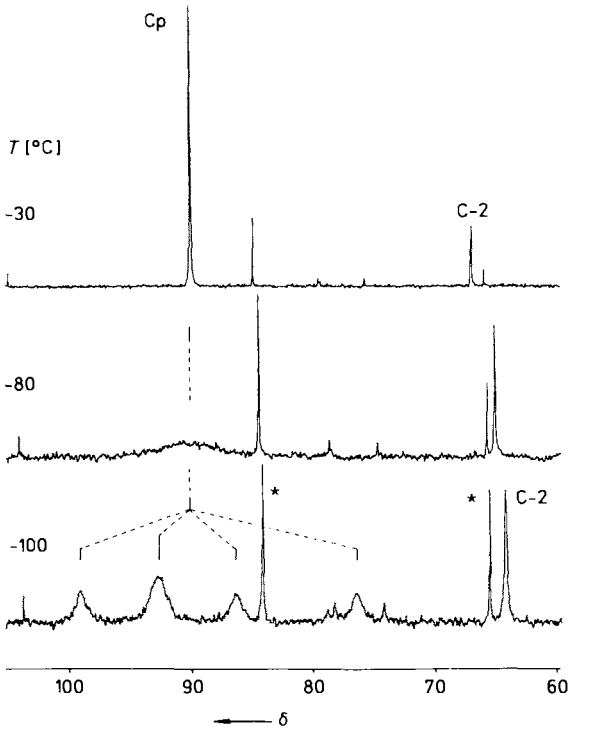

Fig. 1. The η^5-C_5H_5 region of the 75.5-MHz ^{13}C NMR spectrum of **1** in CD_2Cl_2 at −30 °C, −80 °C, and −100 °C. The signal intensities at −100 °C are 1:2:1:1; two of the Cp resonances are unresolved. The corresponding spectrum of **2** is very similar, except that all five Cp signals are resolved. The impurity (*) in the spectrum of **1** is $[Cp(Ph_3P)_2RuCH_2CH_2Ph]$ [8]. The two unresolved ^{13}C NMR resonances of the Cp group in **1** can just be separated in $CD_2Cl_2/CFCl_3$ at −110 °C.

the same within experimental error as that of Cp at higher temperatures (see Table 1). Analogous behavior was observed in the 400-MHz ^1H NMR spectrum. The Cp resonances of **1** dissolved in $CD_2Cl_2/CFCl_3$ ($\delta_H = 4.37$ at −80 °C) split into five signals of equal intensity at −120 °C.

Since the ^{31}P NMR spectrum and the single resonances for the olefinic carbon atoms of the coordinated styrene in the ^{13}C NMR spectrum indicate that (with the exception of a small amount of $[(\eta^5\text{-Cp})(Ph_3P)_2RuCH_2CH_2Ph]$[8] as an impurity) the sample contained just one compound, it can be ruled out that these observations are due to the presence of different compounds, isomers, or rotamers.

The NMR spectra of **2** show similar behavior, except that all five cyclopentadienyl signals of equal intensity were resolved in the ^{13}C NMR spectrum at −110 °C.

The NMR spectra of **1** and **2** are consistent with the rotation of the η^5-Cp ring about the Cp–metal axis becoming slow on the NMR time scale at −100 °C. The molecules possess no elements of symmetry (C-2 in the styrene ligand is a chiral center). Therefore, the η^5-Cp group should give rise to five NMR signals in the limit of slow exchange. The

[*] Dr. R. Mynott, Prof. Dr. H. Lehmkuhl, Dipl.-Chem. E.-M. Kreuzer, Dipl.-Chem. E. Joussen
Max-Planck-Institut für Kohlenforschung
Kaiser-Wilhelm-Platz 1, D-4330 Mülheim an der Ruhr (FRG)

Table 1. ^{31}P and ^{13}C NMR data for **1**–**3** in CD_2Cl_2.

	T [°C]	δ_P	J(P,P) [Hz]	δ_C C-1 (η^2-olefin)	C-2	η^5-Cp	δ_H η^5-Cp
1	− 30	42.2, 40.4	30.6	48.2	66.9	90.0	
	−100	43.1, 40.8	30.4	47.0	64.2	99.0, 92.7 [a], 86.2, 76.5 [b]	5.71, 4.57, 4.38, 3.95, 3.24 [c]
2	− 30	−1.3, − 11.1	18.1	33.9	46.9	87.2	
	−110			32.6	44.6	97.1, 90.4, 89.8, 81.6, 73.2 [d]	5.83, 4.83, 4.69, 4.08, 3.65 [c]
3	− 95	42.8		42.0		87.0	

[a] Intensity = 2. [b] Weighted average of the η-C_5H_5 signals: δ = 89.4. [c] In $CD_2Cl_2/CFCl_3$ at −120 °C. [d] Weighted average of the η^5-C_5H_5 signals: δ = 86.4.

barrier to rotation $\Delta G^{\neq}_{183}$ of the Cp group in **1** was estimated from the ^{13}C NMR spectra by line-shape analysis to be 34.2 ± 1.5 kJ mol^{-1}.[9] This unusually large value apparently results largely from steric crowding: when the styrene ligand in **1** is replaced by ethylene to give **3**, no significant broadening of the Cp resonance in the ^{13}C NMR spectrum is observed at temperatures down to −95 °C, even though the appearance of three sets of phenyl resonances shows that the phenyl groups on each phosphorus become inequivalent as a result of the slowing of the rotation of the phosphane ligands about the Ru–P bonds.

Complexes **1** and **2** are probably pseudo-tetrahedral with the axis of the C–C double bond parallel to the plane of the Cp ring and with the phenyl group of the styrene on the same side as the Cp ring (see Scheme 1), similar to the X-ray structure of **4**, which has less bulky phosphorus ligands.[10]

$[(\eta^5\text{-Cp})\{P(OMe)_3\}_2(CH_2{=}CHPh)Fe]BF_4$ **4**

It appears that the crowding in **1** and **2** forces the Cp group and the phenyl substituent in the stryrene ligand close to one another and that the phenyl groups on phosphorus and in the styrene mesh well with the cyclopentadienyl ligand.[6]

The Cp resonances of these compounds at low temperature cover unexpectedly large ranges (**1**, ^{13}C 22.5, ^1H 2.47; **2**, ^{13}C 23.9, ^1H 2.18 ppm; see Table 1). While this suggests that the bonding between the metal and the individual carbon atoms of the cyclopentadienyl ring varies considerably (e.g., by ring tilting[11]), the ^{13}C NMR chemical shifts show that all the ring carbons must be complexed. Thus, while we attribute the high rotational barrier mainly to steric factors, it cannot be ruled out that electronic factors may also contribute to the barrier in **1** and **2**. We are examining compounds related to **1** to establish more about the nature of the barrier.

Experimental Procedure[12]

The ^{13}C and ^{31}P NMR spectra were measured on a Bruker WM-300 NMR spectrometer at 75.5 and 121.4 MHz, respectively (δ_P relative to 85% aqueous phosphoric acid). The ^1H NMR spectra were recorded on Bruker AM-200 and WH-400 spectrometers.

1: A solution of $[Cp(Ph_3P)_2RuCl]$ (3.99 g, 5.49 mmol), $AgBF_4$ (1.07 g, 5.49 mmol), and styrene (0.63 mL, 5.49 mmol) in 50 mL of CH_2Cl_2 was kept at 20 °C for 15 min. After filtration, the solution was evaporated to 20 mL and, on addition of 200 mL of ether, 4.62 g (5.24 mmol; 95%) of **1** was precipitated as a yellow solid. ^1H NMR (200 MHz, CD_2Cl_2, 27 °C): δ = 7.8–6.8 (Ph), 4.42 (s, Cp), 4.37 (m, partly obscured by Cp signal, H-2 (styrene)), 3.65 (m, H-1(*Z*)), 2.36 (m, H-1(*E*)). For ^{13}C and ^{31}P NMR data, see Table 1.

2: A solution of $[Cp(Ph_3P)_2OsBr]$ (1.0 g, 1.16 mmol) in 20 mL of CH_2Cl_2 was added dropwise to $AgBF_4$ (0.23 g, 1.16 mmol) and styrene (1 mL, 8.73 mmol) in 10 mL of CH_2Cl_2. Immediately afterwards, the AgBr that had precipitated was filtered off, the filtrate was evaporated to ca. 5 mL, and 50 mL of Et_2O was added. The light yellow precipitate that had formed was filtered off, washed with Et_2O, and dried in vacuo to yield 1.1 g (1.13 mmol; 97%) of **2**. ^1H NMR (200 MHz, $CDCl_3$, 27 °C): δ = 7.8–7.0 (m, Ph), 4.66 (s, Cp), 3.77 (m, H-2 (styrene)), ^3J(H-2,H-1(*Z*)) = 10.7, ^3J(H-2,H-1(*E*)) = 8.4, J(P,H) = 10.1 Hz), 3.21 (m, H-1(*Z*), ^2J(H-1(*E*),H-1(*Z*)) = 1.8, J(P,H) = 7.1, 4.5 Hz), 2.74 (m, H-1(*E*), J(P,H) = 13.0, ca. 1 Hz). For ^{13}C and ^{31}P NMR data see Table 1.

3: Prepared similarly to **1** and **2**, except that ethylene was passed through the solution. From 2.05 g (2.82 mmol) of $[Cp(Ph_3P)_2RuCl]$ and 0.55 g (2.83 mmol) of $AgBF_4$ in 150 mL of CH_2Cl_2, 1.94 g (2.41 mmol; 85%) of **3** was obtained as a yellow solid. ^1H NMR (200 MHz, CD_2Cl_2, 27 °C): δ = 7.48 (*o*-H (Ph)), 7.33 (m, *p*-H (Ph)), 6.89 (m, *m*-H (Ph)), 4.85 (s, Cp), 3.12 (t, $H_2C{=}CH_2$). For ^{13}C and ^{31}P NMR data, see Table 1.

Received: May 26, 1989;
revised: November 30, 1989 [Z 3358 IE]
German version: *Angew. Chem. 102* (1990) 314

[1] B. E. Mann in G. Wilkinson, F. G. A. Stone, E. W. Abel (Eds.): *Comprehensive Organometallic Chemistry, Vol. 3*, Pergamon, Oxford 1982, p. 111, and references therein.

[2] B. E. Mann, C. M. Spencer, B. F. Taylor, P. Yavari, *J. Chem. Soc. Dalton Trans. 1984*, 2027.

[3] L. N. Mulay, A. Attalla, *J. Am. Chem. Soc. 85* (1963) 702; M. K. Makova, E. V. Leonova, Yu. S. Karimov, N. S. Kochetkova, *J. Organomet. Chem. 55* (1973) 185.

[4] D. F. R. Gilson, G. Gomez, *J. Organomet. Chem. 240* (1982) 41.

[5] Other studies include line-shape analysis of solid-state ^{13}C NMR spectra of $(\eta^5\text{-}C_5Me_5)_2Fe$: D. E. Wemmer, D. J. Ruben, A. Pines, *J. Am. Chem. Soc. 103* (1981) 28. The activation energies in $[(\eta^5\text{-}C_5H_5)PtR_3]$ (R = Me, Et, or Ac] have been estimated by mechanical spectroscopy to lie between 20.5 and 25.9 kJ mol^{-1}: A. Eisenberg, A. Shaver, T. Tsutsui, *J. Am. Chem. Soc. 102* (1980) 1416. Electron diffraction studies on ferrocene in the gas phase indicate a barrier of 3.8 kJ mol^{-1}: A. Haaland, J. E. Nilsson, *Acta Chem. Scand. 22* (1968) 2653. The dynamics of ring rotation have also been studied by incoherent quasi-elastic neutron scattering (IQENS): e.g., A. B. Gardner, J. Howard, T. C. Waddington, R. M. Richardson, J. Tomkinson, *Chem. Phys. 57* (1981) 453. A very low rotational barrier for Cp has been calculated for $CpML_3$ complexes: T. A. Albright, P. Hofmann, R. Hoffmann, *J. Am. Chem. Soc. 99* (1977) 7546.

[6] E. Maverick, J. D. Dunitz, *Mol. Phys. 62* (1987) 451; they analyzed atomic displacement parameters from X-ray diffraction data to estimate the barrier to ring rotation in cyclopentadienyl complexes. They report that the barrier to rotation of the Cp rings in ferrocene is considerably greater in the orthorhombic modification (e.g., 33 ± 16 kJ mol^{-1} for one of the rings) than in the triclinic or monoclinic forms, showing that steric interactions in a suitable packing can cause a high rotational barrier. The authors thank one of the referees for bringing their attention to this observation.

[7] W. Hofmann, W. Buchner, H. Werner, *Angew. Chem. 89* (1977) 836; *Angew. Chem. Int. Ed. Engl. 16* (1977) 795; W. D. Luke, A. Streitwieser, *J. Am. Chem. Soc. 103* (1981) 3241; G. Erker, T. Mühlenbernd, R. Benn, A. Rufińska, Y.-H. Tsay, C. Krüger, *Angew. Chem. 97* (1985) 336; *Angew. Chem. Int. Ed. Engl. 24* (1985) 321.

[8] H. Lehmkuhl, J. Grundke, G. Schroth, R. Benn, *Z. Naturforsch. B39* (1984) 1050.

[9] D. S. Stephenson, G. Binsch: DNMR5, Program 365 Quantum Chemistry Program Exchange, Indiana University 1978. Ring rotation in steps of $2\pi/5$ was assumed. Further studies, including 2D ^{13}C NMR exchange spectroscopy, have been carried out on these compounds and will be reported in a later publication.

[10] H. Lehmkuhl, T. Wildt, C. Krüger, unpublished; T. Wildt, *Dissertation*, Universität-Gesamthochschule Essen 1987.

[11] For discussion of distortion of the cyclopentadienyl ring and associated changes in the bonding with the metal, see: P. J. Fitzpatrick, Y. Le Page, J. Sedman, I. S. Butler, *Inorg. Chem. 20* (1981) 2852; J. M. O'Connor, C. P. Casey, *Chem. Rev. 87* (1987) 307.

[12] Modification of the preparation of $[(\eta^5\text{-Cp})(PPh_2CH_2CH_2PPh_2)(L)Ru]PF_6$ (L: $H_2C{=}CH_2$, $H_2C{=}CHCH_3$, $H_2C{=}CHPh$) described by S. G. Davies, F. Scott, *J. Organomet. Chem. 188* (1980) C41. See also: M. I. Bruce, F. S. Wong, *ibid. 210* (1981) C5; G. Consiglio, P. Pregosin, F. Morandini, *ibid. 310* (1986) C66.

Solid-Phase Synthesis of Glycopeptide Amides under Mild Conditions: Morphiceptin Analogues**

By *Eduard Bardají, Josep L. Torres,* Pere Clapés, Fernando Albericio, George Barany,* and *Gregorio Valencia*

The crucial role of membrane glycoproteins in many biological processes has stimulated the efforts of peptide chemists to develop methods for the synthesis of glycopeptides.[1] This is an especially difficult task due to the sensitivity of the glycosidic bond to acids and bases.[2] Under basic conditions, *O*-glycosyl-β-hydroxycarboxylic acid derivatives (e.g., glycosylserine or -threonine) undergo β-elimination.[3] The sugar moiety of glycopeptides may also be cleaved[4] or anomerized[5] by acids.

Many synthetic opioid derivatives are *C*-terminal amides.[6] One of our laboratories has recently shown that incorporation of sugar moieties into the fifth position of an enkephalinamide results in very active antinociceptive analogues,[7] and we have described a versatile solution-phase route to prepare large amounts of such glycopeptides.[8] These promising results make it important to find a facile procedure for the rapid preparation under mild conditions of a series of glycopeptide amide analogues for pharmacological testing; a solid-phase approach[9] would have obvious advantages in this regard.

The standard Boc/MBHA strategy[9] for synthesis of *C*-terminal amides relies on final cleavage with anhydrous hydrogen fluoride and is therefore unsuitable for solid-phase synthesis of glycopeptide amides. An attractive alternative procedure may use N^{α}-9-fluorenylmethoxycarbonyl (Fmoc) protection[10] in conjunction with appropriate resin-linkage agents.[11] Unfortunately, a literature procedure[12] involving cleavage of a 4-hydroxymethylbenzoic acid linker with ammonia–methanol is liable to result in β-elimination of the glycosyl moiety.

The recent result from one of our laboratories[13, 14] that *C*-terminal peptide amides can be successfully prepared by Fmoc chemistry, with final acidolytic cleavage, suggested an answer to our synthetic problem. Here we describe the incorporation of 5-[4-(Fmoc-aminomethyl)-3,5-dimethoxyphenoxy]valeric acid (PAL, **1**) onto aminomethyl-polystyrene and subsequent synthesis of the glycosyl derivatives $O^{1,4}$-(β-D-galactopyranosyl) [Hyp^4]-morphiceptin (**2**) and $O^{1,4}$-(β-D-glucopyranosyl) [Hyp^4]-morphiceptin (**3**).

[*] Dr. E. Bardají, Dr. J. L. Torres, Dr. P. Clapés, Dr. G. Valencia
Unit for Peptide Chemistry and Biochemistry, C.I.D.-C.S.I.C.
Jordi Girona 18–26, E-08034-Barcelona (Spain)
Dr. F. Albericio
Department of Organic Chemistry, University of Barcelona
E-08028-Barcelona (Spain) and
Department of Chemistry, University of Minnesota
Minneapolis, MN 55455 (USA)
Dr. G. Barany
Department of Chemistry, University of Minnesota
Minneapolis, MN 55455 (USA)

[**] This work was supported by the Comisión Interdepartamental para la Ciencia y la Tecnología (BI088-0694), the Biotechnology Action Programme (BAP.0412.E (JR)), the National Institutes of Health (GM 28934 and 42722), and NATO (Collaborative Research Grant 0841/88). We thank *E. Crusi* (University of Barcelona) for the NMR data and Dr. *J. Rivera* and *M. Guerra* (Laboratory of Mass Spectrometry, C.I.D.-C.S.I.C., Barcelona) for the FAB-MS analyses. Abbreviations: Boc, *tert*-butoxycarbonyl; DCC, *N,N'*-dicyclohexylcarbodiimide; DMF, *N,N*-dimethylformamide; FAB-MS, fast atom bombardment mass spectrometry; Fmoc, 9-fluorenylmethoxycarbonyl; galac, galactopyranosyl; glcp, glucopyranosyl; HOBt, 1-hydroxybenzotriazole; HPLC, high-performance liquid chromatography; Hyp, hydroxyproline; MBHA, *p*-methylbenzhydrylamine; PAL, 5-[4-(9-fluorenylmethoxycarbonyl-aminomethyl)-3,5-dimethoxyphenoxy]valeric acid; Su, *N*-hydroxysuccinimidyl; TFA, trifluoroacetic acid.

For the synthesis of glycosylmorphiceptins, the linker **1** (2 equiv.) was attached to an aminomethyl-polystyrene (1% cross-linked, 200–400 mesh, 0.65 m equiv. aminomethyl groups per gram resin) by DCC/HOBt coupling in DMF. After removal of the Fmoc group from **1** with piperidine-DMF (1:4), the syntheses of tetrapeptides **2** and **3** proceeded smoothly using the corresponding building blocks **4** and

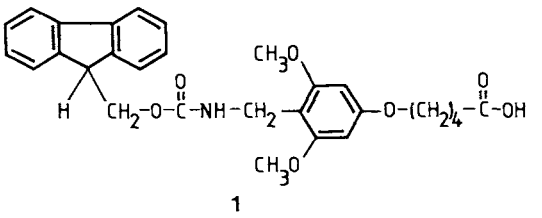

1

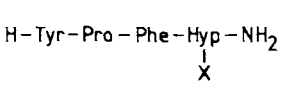

2, X = Galac
3, X = Glcp

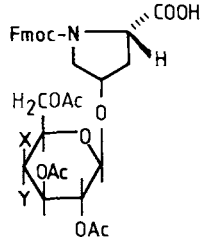

4, X = OAc, Y = H (Galac)
5, X = H, Y = OAc (Glcp)

5[15] via their HOBt esters, performed in situ with DCC in CH_2Cl_2. The remaining Fmoc-amino acids were incorporated by the same procedure.[16] Upon completion of chain assembly, the Fmoc group was removed with piperidine–DMF (1:4), and the acetyl protecting groups for the sugar moiety were best removed with hydrazine–methanol *while the peptide remained anchored to the resin.* Thus, excess hydrazine was simply eliminated by washings with methanol and CH_2Cl_2. Deacetylation with hydrazine–methanol (4:1) was complete after 2 h at 25 °C.[17–19] Acidolytic cleavage from the support was achieved by treatment with TFA–CH_2Cl_2 (7:3) for 2.5 h at 25 °C with concomitant formation of the *C*-terminal amide and deprotection of the *tert*-butyl side chain on tyrosine. This procedure provided glycopeptide amide analogues **2** and **3** in nearly quantitative yields for the cleavage[20] and initial purities of 90% and 75%, respectively. Both compounds were purified by reversed-phase semipreparative HPLC to obtain, in 85 and 70% recovery, final products of >99% purity as shown by analytical HPLC. The FAB MS was correct.[21, 22]

In conclusion, we have successfully applied the recently described PAL handle **1**[13] to the synthesis of glycopeptide amides. The cleavage conditions do not cause damage to the glycosidic bond, and *C*-terminal amides are smoothly obtained in good yields. Moreover, the described solid-phase synthesis allows deprotection of the sugar moiety to be carried out on the resin. These results provide the first examples for the synthesis of glycopeptide amides by the solid-phase procedure.

Received: October 2, 1989
supplemented: November 27, 1989 [Z 3570 IE]
German version: *Angew. Chem. 102* (1990) 311

CAS Registry numbers:
1, 115109-65-4; (*cis*)-**2**, 125281-19-8; (*trans*)-**2**, 125355-38-6; (*cis*)-**3**, 125355-36-4; (*trans*)-**3**, 125355-39-7; (*cis*)-**4**, 125281-20-1; (*trans*)-**4**, 125355-40-0; (*cis*)-**5**, 125355-37-5; (*trans*)-**5**, 125355-41-1.

[1] H. Kunz, *Angew. Chem. 99* (1987) 297; *Angew. Chem. Int. Ed. Engl. 26* (1987) 294.
[2] K. Wakabayashi, W. Pigman, *Carbohydr. Res. 35* (1974) 3.
[3] R. Kuhn, I. Löw, *Ber. Dtsch. Chem. Ges. B 74* (1941) 219.
[4] H. G. Garg, R. W. Jeanloz, *Carbohydr. Res. 52* (1976) 246.
[5] H. Kunz, *Nachr. Chem. Tech. Lab. 32* (1984) 11.
[6] P. E. Hansen, B. A. Morgan in S. Udenfriend, J. Meienhofer (Eds.): *The Peptides, Vol. 6*, Academic Press, New York 1984, p. 269.
[7] J. L. Torres, I. Haro, G. Valencia, F. Reig, J. M. García-Antón, *Experientia 45* (1989) 574; R. E. Rodríguez, F. D. Rodríguez, M. P. Sacristán, J. L. Torres, G. Valencia, J. M. García-Antón, *Neurosci. Lett. 101* (1989) 89.
[8] J. L. Torres, I. Haro, E. Bardají, G. Valencia, J. M. García-Antón, F. Reig, *Tetrahedron 44* (1988) 6131.
[9] G. Barany, R. B. Merrifield in E. Gross, J. Meienhofer (Eds.): *The Peptides. Analysis, Synthesis, Biology, Vol. 2*, Academic Press, New York 1979, p. 1.
[10] L. A. Carpino, G. Y. Han, *J. Org. Chem. 37* (1972) 3404.
[11] Other groups (B. Scolaro, L. Biondi, F. Filira, E. Peggion, R. Rochi in G. Jung, E. Bayer (Eds.): *Peptides 1988, Proceedings of the 20th European Peptide Symposium*, de Gruyter, Berlin 1989, p. 322; H. Paulsen, G. Merz, U. Weichert, *Angew. Chem. 100* (1988) 1425; *Angew. Chem. Int. Ed. Engl. 27* (1988) 1365) reported on glycopeptide acids made by Fmoc chemistry, with final cleavage of a *p*-alkoxybenzyl ester anchoring linkage achieved under relatively mild conditions with TFA–CH_2Cl_2. Furthermore, *Kunz* et al. (H. Kunz, B. Dombo, *Angew. Chem. 100* (1988) 732; *Angew. Chem. Int. Ed. Engl. 27* (1988) 711) have recently reported on glycopeptide syntheses using allyl-based handles.
[12] E. Atherton, C. J. Logan, R. C. Sheppard, *J. Chem. Soc. Perkin Trans. 1 1981*, 538.
[13] F. Albericio, G. Barany, *Int. J. Peptide Protein Res. 30* (1987) 206; F. Albericio, N. Kneib-Cordonier, S. Biancalana, L. Gera, R. I. Masada, D. Hudson, G. Barany, *J. Org. Chem.*, in press.
[14] The recent literature (P. Sieber, *Tetrahedron Lett. 28* (1987) 2107; H. Rink, *ibid. 28* (1987) 3787; G. Breipohl, J. Knolle, W. Stüber, *ibid. 28* (1987) 5651; S. Funakoshi, E. Murayama, L. Guo, N. Fujii, H. Yajima, *Collect. Czech. Chem. Commun. 53* (1988) 2791; B. Penke, L. Nyerger, N. Klenk, K. Nagy, A. Asztalos in B. Penke, A. Török (Eds.): *Peptides. Chemistry, Biology, Interactions with Proteins*, de Gruyter, Berlin 1988, p. 121) describes several other acid-labile linkers for peptide amides. Presumably, some of these can also be applied to the synthesis of glycopeptide amides.
[15] The building blocks **4** and **5** were prepared from Z-Hyp-OBzl and the corresponding per-*O*-acetyleted sugar using $BF_3 \cdot Et_2O$ as catalyst (G. Magnusson, G. Noori, J. Dahmen, T. Frejd, T. Lave, *Acta Chem. Scand. B 35* (1981) 213), followed by catalytic hydrogenolysis to remove the Z and Bzl groups and finally introduction of the Fmoc group with Fmoc-OSu (P. B. W. Ten Kortenaar, B. G. Van Dijk, J. M. Peeters, B. J. Raaben, P. J. H. M. Adams, G. I. Tesser, *Int. J. Peptide Protein Res. 27* (1986) 398). Compounds **4** and **5** were each found to be anomerically pure by ^{13}C NMR (only two peaks in $CDCl_3$ for C1 at $\delta = 99.7$ and 99.3, corresponding to *cis* and *trans* conformations of hydroxyproline): E. Breitmaier, W. Voelter: *^{13}C-NMR Spectroscopy*, Verlag Chemie, Weinheim 1974, Chapter 5.4; J. M. Lacombe, A. A. Pavia, J. M. Rocheville, *Can. J. Chem. 51* (1981) 473).
[16] The incorporation of protected Fmoc-amino acids was carried out using previously described deprotection/coupling protocols [13], featuring DCC/HOBt coupling.
[17] P. Schultheiss-Reiman, H. Kunz, *Angew. Chem. 95* (1983) 64; *Angew. Chem. Int. Ed. Engl. 22* (1983) 62; *Angew. Chem. Suppl.* (1982) 39.
[18] The absence of peptide in the filtrates from hydrazine–methanol treatments was proved by HPLC.
[19] Despite the fact that glycosylhydroxyproline does not undergo β-elimination under basic conditions, we opted for a mild treatment so that it could be generalized in the future to the solid-phase synthesis of more labile glycopeptide amides.
[20] After cleavage, no peptide was detected on the resin by amino-acid analysis.
[21] Analytical HPLC of **2** and **3**: $t_R = 11.6$ min, $k = 3.5$. Conditions: 4.6 × 250-mm C_{18} column, 10 μm, elution with 0.1% aqueous TFA – 0.1% TFA in a CH_3CN gradient from 10% to 100% organic solvent over 30 min (flow rate 0.9 mL min^{-1}, $\lambda = 215$ nm). FAB MS of **2** and **3**: *m/z* 700 ($M + 1$), 722 ($M + Na$).
[22] No destruction of the glycosydic bond occurred as proved by the absence of nonglycosylated peptides. These compounds were prepared by the same procedure and used as HPLC standard ($t_R = 12.9$ min, $k = 3.9$, under the same conditions stated in [21]). This test was performed before cleavage of the glycopeptide from the resin.

A Bicyclic Isomer of the *closo*-Carbaborane $(CH)_2(BR)_4$**

By *Albrecht Krämer, Hans Pritzkow*, and *Walter Siebert**

Dedicated to Professor Paul von Ragué Schleyer on the occasion of his 60th birthday

The prediction of *Schleyer* et al.[1] that the puckered 1,3-dihydro-1,3-diborete **1** should be more stable than the planar 1,2-dihydro-1,2-diborete **2** (R = R′ = H) was followed by the successful synthesis of substituted derivatives of **1**[2–4] and of a derivative of **2**.[5] A comparison of the calculated structure of **1** for R′ = H and R = H, NH_2[1,6] with the results of the X-ray structure analyses[2] showed remarkably good agreement. Compounds **1** can be reduced to dianions $\mathbf{1}^{2\ominus}$,[7,8] which could in principle react with diborane(4) derivatives XRB–BRX (X = Cl) to give 2,3,5,6-tetraborabicyclo[2.1.1]hexane derivatives **6**; however, this has not yet been achieved. Here we report on the synthesis and structure of the boron-rich organoborane **6** (R = N*i*Pr$_2$), the predicted classical isomer of *closo*-carbaboranes **3** and **4**. Compound **6** (R = H) was postulated by *Lipscomb* et al.[9] as an intermediate in the rearrangement of **3** to **4**; our results corroborate the PRDDO calculations, which indicated that electron-donor substituents on boron should stabilize the organoborane structure. In the case of the fluorine-substituted derivative, **6** (R = F) is 130 and 134 kcal mol^{-1} more stable than **3** and **4**, respectively.[9] This is also supported by an example of destabilization of a *nido*-C_4B_2 carbaborane by amino substituents on boron, resulting in formation of the bicyclic organoborane.[10]

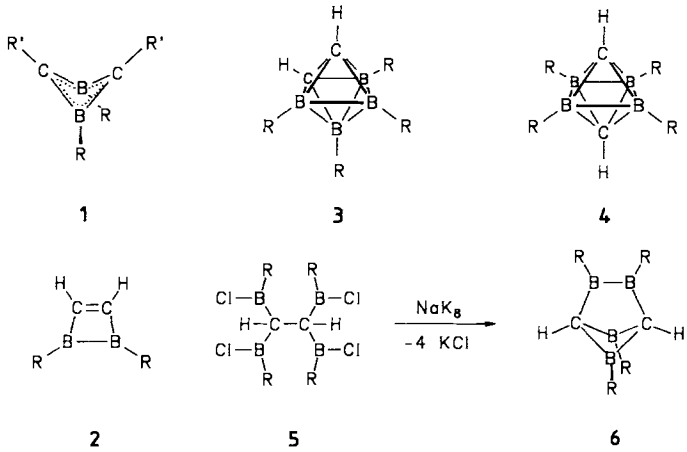

Starting from 1,1,2,2-tetrakis(dichloroboryl)ethane (**5**, R = Cl),[11] partial amination with HN*i*Pr$_2$ gives 1,1,2,2-tetrakis[chloro(diisopropylamino)boryl]ethane (**5**, R = N*i*Pr$_2$) in 83% yield. Its dehalogenation with Na/K in refluxing benzene affords **6** (R = N*i*Pr$_2$) in 73% yield.

The X-ray structure analysis[12] of **6** (R = N*i*Pr$_2$) confirms the presence of a 1,3-diboretane derivative bridged at the 2,4-positions with a 1,2-diborane(4)diyl unit (Fig. 1a). The bicyclic compound does not have the expected C_{2v} symmetry in the crystal, but rather approximate C_2 symmetry. The

[*] Prof. Dr. W. Siebert, Dr. A. Krämer, Dr. H. Pritzkow
Anorganisch-chemisches Institut der Universität
Im Neuenheimer Feld 270, D-6900 Heidelberg (FRG)

[**] This work was supported by the Deutsche Forschungsgemeinschaft, the Fonds der Chemischen Industrie, and BASF AG.

B2B3 bridge does not lie symmetrically over the diboretane, but instead has a zigzag structure (Fig. 1 b). This deviation is clearly revealed in the different angles B2C2B1/B2C2B4 and B3C1B1/B3C1B4 as well as, to a lesser extent, in the B–C distances in the 1,3-diboretane.

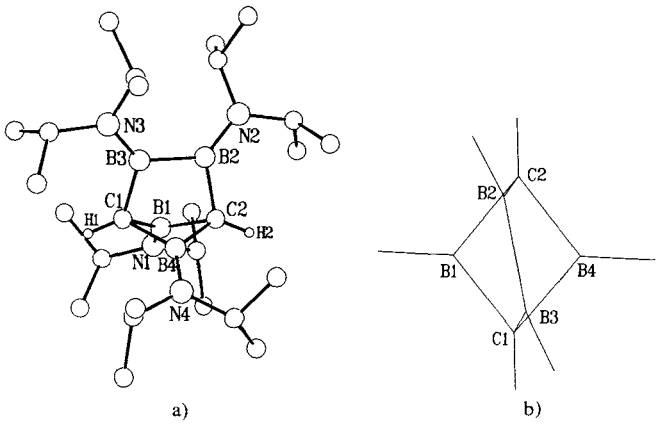

Fig. 1. a) Molecular structure of **6** (R = N*i*Pr$_2$) in the crystal. Selected distances [Å] and angles [°] (±0.007 Å and ±0.3°; values for the two independent molecules): C1-B1 1.561/1.566, C2-B4 1.589/1.576, C1-B4 1.605/1.594, C2-B1 1.611/1.612, C1-B3 1.562/1.563, C2-B2 1.566/1.557, B2-B3 1.749/1.738, B1-B4 1.934/1.918, B1-N1 1.396/1.391, B4-N4 1.376/1.387, B2-N2 1.413/1.416, B3-N3 1.413/1.411; B1-C1-B4 75.3/74.7, B1-C2-B4 74.4/74.0, C1-B1-C2 95.3/94.6, C1-B4-C2 94.5/94.9, B3-C1-B1 101.8/102.3, B2-C2-B4 103.1/104.0, B3-C1-B4 94.0/94.8, B2-C2-B1 93.3/92.5. b) Framework of **6** (R = N*i*Pr$_2$). Projection along the (approximate) twofold axis of the molecule.

Noteworthy is the very short transannular B1–B4 distance (1.93 Å), which likewise confirms the weak, nonbonding boron–boron interaction predicted by the MO calculations.[9b] In **6** (R = N*i*Pr$_2$) the 1,3-diboretane ring is more strongly puckered (angle E1(C1,B1,C2)/E2(C1,B4,C2) 53°, E3(B1,C1,B4)/E4(B1,C2,B4) 44°) than in the nonbridged 1,3-diboretane derivative[8] $(CH_2)_2(BN{i}Pr)_2$ (E1/E2 39°, E3/E4 34°) (R = N*i*Pr$_2$).

Compound **6** displays temperature-dependent ^{1}H NMR spectra. At 293 K, the diisopropyl groups give rise to three septets in the ratio 1:2:1, two doublets, and two broad signals; at 183 K, four septets and eight, partly overlapping doublets are observed. At 363 K, however, two overlapping septets and two doublets are found. A singlet is observed for the ring protons. The splitting of the signal pattern into four septets and eight doublets is in agreement with the crystal structure. At room temperature, vibration of the B2–B3 bridge results in averaging of the signals at N1 and N4; at increased temperature, we expect a rotation around the B–N bond, so that the diisopropylamino groups only give rise to two septets and two doublets. A broad ^{11}B NMR signal is found at $\delta = 46$ ($T = 298$ K) with a half-width of 1.2 kHz; this signal is in agreement with the presence of a diborane(4) derivative with alkyl and dialkylamino substituents or of a dialkylamino(organo)borane. In the mass spectrum, the molecular-ion peak appears at $m/z = 470$ (81.8%) with the isotope distribution expected for four boron atoms.

Experimental Procedure

5 (R = N*i*Pr$_2$): HN*i*Pr$_2$ (15.9 mL, 114.4 mmol) was slowly added dropwise to a solution of **5** (R = Cl; 5.0 g, 14.3 mmol) [11] in 120 mL of petroleum ether 60/70. The reaction mixture was then refluxed for 2 h, filtered, and washed three times with petroleum ether 60/70. The solvent was removed from the combined filtrates under high vacuum and the residue was recrystallized from *n*-pentane. Yield: 7.24 g (11.9 mmol, 83%), m.p. 213.5 °C. ^{1}H NMR (200 MHz, $CDCl_3$): $\delta = 1.12$(d$_a$, 24H), 1.34(d$_b$, 12H), 1.36(d$_b$, 12H), 1.92(s, 2H), 3.31(sept$_b$, 4H), 4.13(sept$_a$, 4H), $^3J_a = 7.0$ Hz, $^3J_b = 6.6$ Hz. ^{11}B NMR (28.75 MHz, $CDCl_3$): $\delta = 40$. ^{13}C NMR ($CDCl_3$, 50 MHz): $\delta = 20.83$(q, NCH*C*H$_3$), 21.64(q, NCH*C*H$_3$), 23.2(q, NCH*C*H$_3$), 23.31(q, NCH*C*H$_3$), 29(br, B*C*), 45.97(d, N*C*HCH$_3$), 50.51(d, N*C*HCH$_3$). MS (EI): m/z 610 ($M^{\oplus}$, 1%), 595 ([M–Me]$^{\oplus}$, 23), 510 ([M – N*i*Pr$_2$]$^{\oplus}$, 5.9), 429 ([M – BClN*i*Pr$_2$ – Cl]$^{\oplus}$, 60), 386 ([M – BClN*i*Pr$_2$ – *i*Pr – Cl]$^{\oplus}$, 100).

6 (R = N*i*Pr$_2$): **5** (R = N*i*Pr$_2$) (2.3 g, 3.75 mmol) and NaK$_8$ (640 mg, 1.91 mmol) were allowed to react in 60 mL of refluxing benzene for 24 h. The reaction mixture was then filtered, the solvent was removed under high vacuum, and the residue was recrystallized from *n*-pentane. Yield 1.29 g (2.74 mmol, 73%); m.p. 136.5 °C (dec.). ^{1}H NMR (293 K, [D$_8$]toluene): $\delta = 1.05$(br, 12H), 1.10(d, 12H), 1.20(d, 12H), 1.39(br, 12H), 2.83(s, 2H), 3.20(m, 2H), 3.50(sept, 4H), 3.82(m, 2H); 193 K: $\delta = 1.0$–1.25[br, m, (5d)], 1.33(d, 6H), 1.42(d, 6H), 1.44(d, 6H), 2.90(sept, 2H), 2.95(s, 2H), 3.14(sept, 2H), 3.93(sept, 2H), 4.08(sept, 2H); 363 K: $\delta = 1.11$(d, 24H), 1.20(d, 24H), 2.81(s, 2H), 3.51(m, 8H). ^{11}B NMR ([D$_8$]toluene): $\delta = 46$(br, half-width = 1.2 kHz). ^{13}C NMR(C_6D_6, 293 K): $\delta = 22.9$(br, NCH*C*H$_3$), 23.91(NCH*C*H$_3$), 23.97(NCH*C*H$_3$), 25.7(br,NCH*C*H$_3$), 44.7(br,N*C*HCH$_3$), 48.9(br,N*C*HCH$_3$), 55.2(br,N*C*HCH$_3$), 62(br, B*C*). MS (EI): m/z 470($M^{\oplus}$, 81.8%), 455([M-Me]$^{\oplus}$, 100), 427([M-*i*Pr]$^{\oplus}$, 93.2), 369([M-HN*i*Pr$_2$]$^{\oplus}$, 37.2).

Received: November 8, 1989 [Z 3625 IE]
German version: *Angew. Chem. 102* (1990) 333

[1] K. Krogh-Jespersen, D. Cremer, J. D. Dill, J. A. Pople, P. von R. Schleyer, *J. Am. Chem. Soc. 103* (1981) 2589.
[2] M. Hildenbrand, H. Pritzkow, U. Zenneck, W. Siebert, *Angew. Chem. 96* (1984) 371; *Angew. Chem. Int. Ed. Engl. 23* (1984) 371; A. Krämer, *Dissertation*, Universität Heidelberg 1989.
[3] R. Wehrmann, C. Pues, H. Klusik, A. Berndt, *Angew. Chem. 96* (1984) 372; *Angew. Chem. Int. Ed. Engl. 23* (1984) 372.
[4] S. M. van der Kerk, P. H. M. Budzelaar, A. van der Kerk-van Hoof, G. J. M. van der Kerk, P. von R. Schleyer, *Angew. Chem. 95* (1983) 61; *Angew. Chem. Int. Ed. Engl. 22* (1983) 48.
[5] M. Hildenbrand, H. Pritzkow, W. Siebert, *Angew. Chem. 97* (1985) 769; *Angew. Chem. Int. Ed. Engl. 24* (1985) 759.
[6] P. von R. Schleyer, P. H. M. Budzelaar, D. Cremer, E. Kraka, *Angew. Chem. 96* (1984) 374; *Angew. Chem. Int. Ed. Engl. 23* (1984) 374; P. H. M. Budzelaar, K. Krogh-Jespersen, T. Clark, P. von R. Schleyer, *J. Am. Chem. Soc. 107* (1985) 2773.
[7] G. Schmid, G. Baum, W. Massa, A. Berndt, *Angew. Chem. 98* (1986) 1123; *Angew. Chem. Int. Ed. Engl. 25* (1986) 1111.
[8] P. Hornbach, M. Hildenbrand, H. Pritzkow, W. Siebert, *Angew. Chem. 98* (1986) 1121; *Angew. Chem. Int. Ed. Engl. 25* (1986) 1112; G. Karger, P. Hornbach, A. Krämer, H. Pritzkow, W. Siebert, *Chem. Ber. 122* (1989) 1881.
[9] a) R. N. Camp, D. S. Marynick, G. D. Graham, W. N. Lipscomb, *J. Am. Chem. Soc. 100* (1978) 6781; b) *ibid.* Reference [16]. Ab initio calculations: M. L. McKee, *ibid. 110* (1988) 5317.
[10] G. E. Herberich, H. Ohst, H. Meyer, *Angew. Chem. 96* (1984) 975; *Angew. Chem. Int. Ed. Engl. 23* (1984) 969.
[11] C. Chambers, A. K. Holliday, S. M. Walker, *Proc. Chem. Soc. 1964*, 286; F. Kuhlmann, *Diplomarbeit*, Universität Heidelberg 1987.
[12] Space group $P2_1/n$, $a = 25.91(2)$, $b = 10.141(9)$, $c = 26.26(2)$ Å, $\beta = 103.97(7)°$, $V = 6697$ Å^3, $Z = 8$ (two independent molecules); $R = 0.048$ and $R_w = 0.045$ for 4251 reflections (four-circle diffractometer, Mo$_{K\alpha}$ radiation, ω scan); B,C,N anisotropic, H atoms in calculated positions or as rigid CH$_3$ groups with common isotropic temperature factors. Further details of the crystal structure investigation may be obtained from the Fachinformationszentrum Karlsruhe, Gesellschaft für wissenschaftlich-technische Information mbH, D-7514 Eggenstein-Leopoldshafen 2 (FRG), on quoting the depository number CSD-54343, the names of the authors, and the journal citation.

$Te_8^{2\oplus}$, a New Tellurium Polycation

By *Johannes Beck* *

The elements sulfur, selenium, and tellurium are capable of forming homo- and heteronuclear polycations. Of the tellurium-containing cations, $Te_4^{2\oplus}$ [1] and $Te_6^{4\oplus}$,[2] as well as

[*] Dr. J. Beck
Institut für Anorganische Chemie der Universität
Engesserstrasse, D-7500 Karlsruhe (FRG)

$[Te_2Se_2]^{2\oplus}$,[3] $[Te_3Se]^{2\oplus}$,[3], $[Te_2Se_4]2^{\oplus}$[4], $[Te_3S_3]^{2\oplus}$,[4] $[Te_2Se_6]^{2\oplus}$,[5] and $[Te_2Se_8]^{2\oplus}$,[5] have so far been structurally characterized. These ions are obtained from the elements by oxidation with oleum, AsF_5, or SbF_5 or in $AlCl_3$ melts with $TeCl_4$ as oxidizing agent. The species $Te_8^{2\oplus}$, analogous to the known homonuclear cations of sulfur and selenium, $S_8^{2\oplus}$[6] and $Se_8^{2\oplus}$,[7] has not yet been reported.

During attempts to synthesize the first ternary compounds in the system W-Te-halogen, I found that WCl_6 is also a suitable oxidizing agent for the synthesis of tellurium polycations. WCl_6 is reduced by tellurium to the hexachlorotungstate(v). Reaction of WCl_6 and two equivalents of tellurium in an evacuated, sealed glass ampoule at 170–200 °C gives $Te_4[WCl_6]_2$, a compound containing the square-planar $Te_4^{2\oplus}$ cation.[8] Even the use of an excess of tellurium does not reduce WCl_6 beyond oxidation state +5. Reaction of WCl_6 with four equivalents of tellurium results in formation of $Te_8[WCl_6]_2$ (**1**). This reaction is carried out in an evacuated, sealed glass ampoule at 150 °C and the yield, after three weeks, is quantitative.[9] Compound **1** is obtained as blue-black crystals, which are transported to the coolest side of the ampoule. In the presence of moist air, the crystals slowly hydrolyze. Above 280 °C, **1** decomposes to the starting materials, elemental tellurium and liquid WCl_6, the latter of which can be removed by distillation. When the temperature is lowered again to 150 °C, **1** is re-formed.

The structure determination[10] shows that **1** consists of $Te_8^{2\oplus}$ cations and $[WCl_6]^{\ominus}$ anions. The $Te_8^{2\oplus}$ ion can be described as a bicyclic framework made up of two five-membered rings in envelope conformation (Fig. 1). A crystallographic twofold axis passes through the cation, resulting in point-group symmetry C_2. The Te–Te distances in the eight-membered ring range from 270.4 to 278.3 pm. These values correspond to twice the covalent radius of tellurium (274 pm)[11] and are found in compounds with Te–Te single bonds. For example, the Te–Te distances in diphenyl telluride are 271.2 pm[12] and the Te–Te distance in the $Te_2^{\ominus}$ anion of $MgTe_2$ is 274.0 pm.[13] In addition, there is a transannular interaction between Te1 and Te1^{I} in $Te_8^{2\oplus}$. The Te1–Te1^{I} distance (299.3 pm) is longer than a single bond, but still markedly shorter than the Te–Te bonds (312 pm) in the trigonal-prismatic $Te_6^{4\oplus}$ cation along the edges of the prism.[2] All angles in $Te_8^{2\oplus}$ lie between 84.3° and 100.0°, smaller than the angle of 103.1° in the helical tellurium chain in the structure of the element.[14] Such an angle contraction relative to the element has so far been observed for all chalcogen cations. The structure of $Te_8^{2\oplus}$ thus displays clear differences with those of its homologues $S_8^{2\oplus}$ and $Se_8^{2\oplus}$, which exhibit approximate mirror symmetry (C_s) and only weak transannular interactions.

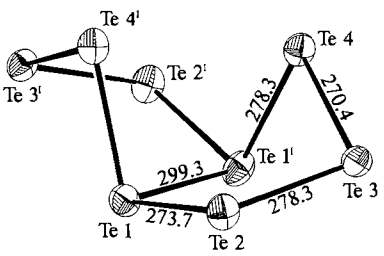

Fig. 1. Structure of the $Te_8^{2\oplus}$ ion in the crystal of $Te_8[WCl_6]_2$ (**1**). The thermal elipsoids are drawn at the 70% probability level. The bond lengths are given in pm (standard deviation: 0.1 pm). Bond angles [°]: Te2-Te1-Te4^{I} 97.7(1), Te2-Te1-Te1^{I} 98.3(1), Te1^{I}-Te1-Te4^{I} 90.7(1), Te1-Te2-Te3 99.8(1), Te2-Te3-Te4 100.0(1), Te3-Te4-Te1^{I} 84.3(1).

An association of the $Te_8^{2\oplus}$ ions occurs in **1**, as shown more clearly in Figure 2 by a larger section of the structure. The

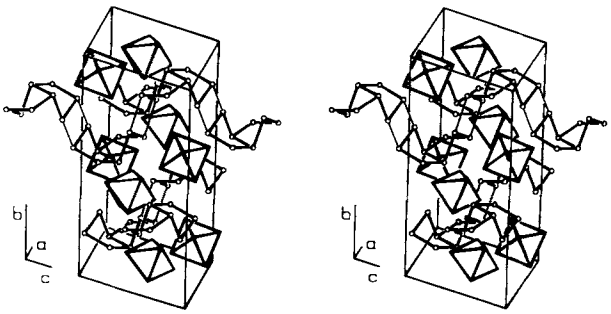

Fig. 2. Stereoscopic drawing of the unit cell of **1**. The $WCl_6^{\ominus}$ ions are drawn as octahedra. Bond lengths [pm] and angles [°]: W-Cl 226.7(2) to 235.8(2), Cl-W-Cl 88.1(1) to 92.1(1) and 176.4(2) bis 179.3(2).

edges Te3-Te4 and Te3^{I}-Te4^{I} of each $Te_8^{2\oplus}$ ion form a rectangular, planar Te_4 ring with the corresponding edges of the neighboring ion. The Te–Te distances to the neighboring cation (342.4 pm) lie in the range of weak bonding; they are much shorter than the sum of the van der Waals radii (440 pm[11]) and also shorter than the Te–Te bond of bond order 2 in the element (349.1 pm[14]). The tellurium partial structure in **1** can therefore be regarded as a one-dimensional, undulating, band-shaped tellurium polycation $[Te_n]^{n/4\oplus}$. No association of the ions has been observed in tellurium cations so far investigated; the homologous ions $S_8^{2\oplus}$ and $Se_8^{2\oplus}$ in $S_8[AsF_6]_2$[6] and $Se_8[AlCl_4]_2$[7] are also isolated. In the structure of $Se_8[AlCl_4]_2$, however, one interionic Se–Se contact less than the van der Waals distance has been found and may point to the increasing tendency of the heavy main-group elements to assume higher coordination numbers.

The $WCl_6^{\ominus}$ ions in **1** form distorted octahedra, whose W–Cl bond lengths (226.7 to 235.7 pm) differ significantly. The average W–Cl distance of 232.1 pm, however, is in good agreement with that in $Te_4[WCl_6]_2$ (232.2 pm[8]) and that in $CsWCl_6$ (232.5 pm[15]).

The distortion of the $WCl_6^{\ominus}$ ion is due to strong interactions of the chlorine atoms with the $Te_8^{2\oplus}$ ions. The shortest Te–Cl distances are 316.5 and 331.4 pm; overall, the atoms Te1 to Te4 display distances to 15 Cl atoms that are shorter than the sum of the van der Waals radii (400 pm[11]). Short chalcogen–halogen distances are typical of halometalates of chalcogen cations and are regarded as the cause for the generally observed distortion of the ions.[1–3, 7, 16]

Received: November 6, 1989 [Z 3622 IE]
German version: *Angew. Chem. 102* (1990 301

[1] T. W. Couch, D. A. Lokken, J. D. Corbett, *Inorg. Chem. 11* (1972) 357; G. Cardinal, R. J. Gillespie, J. F. Sawyer, J. E. Vekris, *J. Chem. Soc. Dalton Trans. 1982*, 765; M. J. Collins, R. J. Gillespie, J. W. Kolis, J. F. Sawyer, *Acta Crystallogr. C43* (1987) 2033.
[2] R. C. Burns, R. J. Gillespie, W.-C. Luk, D. R. Slim, *Inorg. Chem. 18* (1979) 3086.
[3] P. Boldrini, I. D. Brown, M. J. Collins, R. J. Gillespie, E. Maharajh, D. R. Slim, J. F. Sawyer, *Inorg. Chem. 24* (1985) 4302.
[4] R. J. Gillespie, W.-C. Luk, E. Maharajh, D. R. Slim, *Inorg. Chem. 16* (1977) 892.

[5] M. J. Collins, R. J. Gillespie, J. F. Sawyer, *Inorg. Chem. 26* (1987) 1476.
[6] C. Davies, R. J. Gillespie, J. J. Park, J. Passmore, *Inorg. Chem. 10* (1971) 2781.
[7] R. K. McMullan, D. J. Prince, J. D. Corbett, *Inorg. Chem. 10* (1971) 1749.
[8] J. Beck, *Z. Naturforsch.*, in press.
[9] *Experimental Procedure:* $WOCl_4$-free WCl_6 (2 g) and finely powdered tellurium (2.57 g) were placed in a glass ampoule of 20-cm length and 1.5-cm diameter. The ampoule was sealed under vacuum and heated for two days at 180 °C with as little temperature gradient as possible. The temperature was then reduced to 150 °C. At the start of the reaction, it is advantageous to make the contents of the ampoule homogeneous by strongly tapping it several times. The tellurium reacts completely within several weeks and **1** is formed as blue-black crystals up to 5 mm in size.
[10] Crystal structure analysis of **1**: Lattice constants $a = 1192.5(3)$, $b = 2080.0(9)$, $c = 1186.0(4)$ pm, $\beta = 116.87(1)°$, monoclinic space group $C2/c$, $Z = 4$, 2215 unique reflections with $I > 1\sigma(I)$, 100 parameters, numerical absorption correction, $R = 0.025$. Further details of the crystal structure investigation may be obtained from the Fachinformationszentrum Karlsruhe, Gesellschaft für wissenschaftlich-technische Information mbH, D-7514 Eggenstein-Leopoldshafen 2 (FRG), on quoting the depository number CSD-54348, the name of the author, and the journal citation.
[11] L. Pauling, *Die Natur der chemischen Bindung*, Verlag Chemie, Weinheim 1968; *The Nature of the Chemical Bond*, Cornell University Press 1960.
[12] G. Llabres, O. Dideberg, L. Dupont, *Acta Crystallogr. B28* (1972) 2438.
[13] S. Yanagisawa, M. Tashiro, S. Anzai, *J. Inorg. Nucl. Chem. 31* (1969) 943.
[14] C. Adenis, V. Langer, O. Lindqvist, *Acta Crystallogr. C45* (1989) 941.
[15] W. Eichler, H.-J. Seifert, *Z. Anorg. Allg. Chem. 431* (1977) 123.
[16] M. J. Collins, R. J. Gillespie, J. W. Kolis, J. P. Sawyer, *Acta Crystallogr. C43* (1987) 2033.

$Si[(Me_2P)_2C(SiMe_3)]_2$, a Stable σ-Bonded Compound Containing Divalent Silicon**

By *Hans H. Karsch,* Ursula Keller, Siegfried Gamper,* and *Gerhard Müller*

Divalent silicon compounds should lead to novel silicon chemistry because of their high synthetic potential. Only one such compound,[1] $(C_5Me_5)_2Si$, which contains π-bonded ligands (silicocene),[2] has so far proven stable under normal conditions. Upon derivatization, however, its monomeric Si^{II} structure is lost.[3] Stable silicon(II) compounds containing σ-bonded ligands have not yet been reported.

Although silanediyls, SiR_2, which are isoelectronic to carbenes, have been intensively investigated as short-lived species,[4] no stable monomers, even those containing bulky substituents, have been isolated so far. Dimesitylsilanediyl, for example, dimerizes even at low temperatures to give disilenes.[5]

Donor ligands increase the stability only slightly: the adducts decompose even at temperatures < -70 °C.[6] Only when the lone pair on silicon is deactivated by complex formation are such "Si^{II}" compounds ("donor-stabilized silanediyl complexes") stable.[7] However, in these complexes the oxidation state is hardly more than a mere formalism.

The most promising route to unstable silicon(II) compounds appeared to be via *intramolecular* donor stabilization exploiting the chelate effect. Earlier results with the corresponding germanium(II) and tin(II) compounds (cf. **1**, **2**) indicated that diphosphinomethanides should be particularly suitable as ligands.[8, 9]

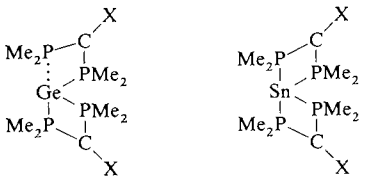

1 **2**

a, X = PMe_2; **b**, X = $SiMe_3$

Because the coordinated phosphane donors shield the negative charge of the carbanion from electron-rich, low-valent coordination centers, a high ionic bonding component and thus the attainment of higher coordination numbers is ensured and the compounds are thereby stabilized. Simultaneously, this carbanion nature leads to increased chemical reactivity, which can be exploited to carry out ligand exchange reactions without changing the oxidation state. Moreover, unlike many other monoanionic chelate ligands, phosphinomethanides are stable toward reduction. Accordingly, it should also be possible to stabilize silicon(II) with phosphinomethanide ligands. Indeed, in the presence of $Li[C(PMe_2)_2(SiMe_3)]$, Si_2Cl_6 is smoothly reduced to **3** [Eq. (a)].

$$Si_2Cl_6 + 4\,Li[C(PMe_2)_2(SiMe_3)] \xrightarrow{a,\,b} \underset{\mathbf{3}}{2\,Si[(Me_2P)_2\,C(SiMe_3)]_2} \qquad (a)$$

a, Mg/THF; b, Li-naphthalide/THF.

The bright yellow, air-sensitive crystals of **3**, like those of **1a,b** and **2a,b**, are readily soluble in hydrocarbons. An X-ray structure analysis[10] shows that, in the crystal, **3**, like **1a** and **2a**, has a (distorted) pseudo-trigonal-bipyramidal (ψ-tbp) structure in which silicon, as a spiro center, is surrounded by four phosphorus atoms[12] (Fig. 1). A common

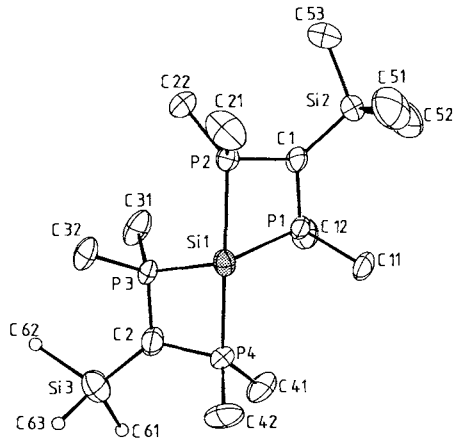

Fig. 1. Molecular structure of **3** (ORTEP, displacement ellipsoids 50%; H atoms omitted; only one alternative is shown for the disordered methyl C atoms at Si3). Important distances [Å] and angles [°]: Si1-P1 2.271(4), Si1-P2 2.514(4), Si1-P3 2.269(4), Si1-P4 2.609(4), C1-P1 1.72(1), C1-P2 1.76(1), C1-Si2 1.82(1), C2-P3 1.73(1), C2-P4 1.67(1), C2-Si3 1.89(1); P1-Si1-P2 68.4(1), P3-Si1-P4 67.3(1), P1-Si1-P3 111.6(1), P2-Si1-P4 154.2(1), P2-Si1-P3 98.0(1), P1-Si1-P4 96.3(1), P1-C1-P2 101.8(5), P3-C2-P4 106.1(6); sum of angles at C1, 359.8; at C2, 359.9.

feature of the three compounds is also the marked difference between axial and equatorial element–phosphorus bond lengths. For **3**, the latter agree with the expected value for

[*] Prof. Dr. H. H. Karsch, Dipl.-Chem. U. Keller, S. Gamper, Priv.-Doz. Dr. G. Müller
Anorganisch-chemisches Institut der Technischen Universität München
Lichtenbergstrasse 4, D-8046 Garching (FRG)

[**] This work was supported by the Deutsche Forschungsgemeinschaft and the Fonds der Chemischen Industrie. We thank Prof. *H. Schmidbaur* for institutional support, Prof. *F. R. Kreissl* for recording the mass spectrum, and Prof. *B. Wrackmeyer* for recording the complicated NMR spectra.

Si–P single bonds (although no data is available for Si^{II}). A bond shortening, which would be expected for an ylide formalism, is not observed. On the other hand, the relatively short P–C1/2 bonds are evidence supporting such an ylide component.[13]

One equatorial position within the tbp structure remains unoccupied and can formally be assigned to the lone pair on silicon. Thus, **3** is the first silicon(II) compound containing σ-bonded ligands and the first with a formal electron "decet".

Interestingly, the structure of the silicon compound **3** more strongly resembles that of the tin compound **2a** than that of the germanium derivative **1a**.[14] Compounds **2a** and **3** are tetracoordinated; the two axial M–P bond lengths in each molecule differ only slightly (**2a**, 0.04 Å; **3**, 0.1 Å). By contrast, these bond lengths differ markedly in **1a** (0.38 Å), thus indicating a transition from tetracoordination to tricoordination, as is also typically observed for carbon (see below). Since the values for **3** are subject to large errors due to the poor quality of the crystal, more detailed structural comparison must await a new measurement.

Compounds **3** and **2b** behave similarly in solution. Whereas the pseudorotation of the germanium compound **1b**, that is, the equilibration of axial and equatorial PMe_2 groups, can be frozen out at low temperature, this is not possible for either **2b** or **3**; between 50 and −100 °C, only a singlet is observed in the ^{31}P NMR spectrum of **3**.[15] In principle, the structural units $R_3P \rightarrow E$:, such as those in **1–3**, may be regarded as phosphorus ylides and are thus comparable to phosphane-donor-stabilized carbenes, R_3P–CX_2. Accordingly, they may be compared structurally with, for example, **4**,[16] whose planar carbanion is stabilized by three phosphonium centers (alternatively, **4** may be viewed as a triphosphane adduct of $:C^{2\oplus}$).

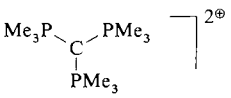

4

However, the high tendency to expand their coordination and the low tendency to undergo hybridization clearly distinguishes the higher homologues from the phosphorus ylides.

Experimental Procedure

3: All operations were performed under nitrogen. First $Li[C(PMe_2)_2(SiMe_3)]$ (1.6 g, 7.47 mmol) [13] and then Si_2Cl_6 (0.32 mL, 1.86 mmol) was added to a solution of naphthalene (0.57 g, 4.48 mmol) and lithium (0.03 g, 4.48 mmol) in 40 mL of THF at −78 °C. The reaction solution was allowed to warm to 0 °C, the solvent was removed under vacuum, and the residue was dissolved in 60 mL of pentane. After filtration, the pentane was removed under vacuum and the naphthalene was removed by sublimation (40 °C, 10^{-2} Torr, 8 h). Recrystallization of the residue from pentane afforded bright yellow needles, 1.27 g (77%).

M.p. 95–98 °C; MS(EI, 70 eV, 20 °C): m/z = 442 ($M^{\oplus}$, 5.6%), 235 ($M^{\oplus}$ − $C(PMe_2)_2(SiMe_3)$, 23), 147 ($CH(PMe_2)(SiMe_3)$, 7), 73 ($SiMe_3$, 100); NMR (C_6D_6, 20 °C, TMS or H_3PO_4 ext.): δ (^1H) = 1.33 (pseudo-quint; PCH_3), 0.28 (s; $SiCH_3$); δ (^{13}C) = 21.5 (s; PCH_3), 4.4 (s; $SiCH_3$); δ (^{31}P) = −5.2(s).

Received: October 20, 1989 [Z 3600 IE]
German version: *Angew. Chem. 102* (1990) 297

[1] Although formally low-valent silicon compounds containing bipyridyl ligands have been described, these ligands make determination of the oxidation state of silicon problematical. Such compounds are therefore not considered here. Most recent key publication: M. Weidenbruch, A. Schäfer, H. Marsmann, *J. Organomet. Chem. 345* (1988) C12.

[2] P. Jutzi, D. Kanne, C. Krüger, *Angew. Chem. 98* (1986) 163; *Angew. Chem. Int. Ed. Engl. 25* (1986) 164.

[3] P. Jutzi, U. Holtmann, H. Bögge, A. Müller, *J. Chem. Soc. Chem. Commun. 1988*, 305.

[4] a) W. P. Neumann, *Nachr. Chem. Tech. Lab. 30* (1982) 190; b) P. P. Gaspar, D. Holten, S. Konieczny, *Acc. Chem. Res. 20* (1987) 329; c) R. West, *Angew. Chem. 99* (1987) 1231; *Angew. Chem. Int. Ed. Engl. 26* (1987) 120; d) P. P. Gaspar, *React. Intermed. (Wiley) 3* (1985) 335.

[5] a) R. West, M. J. Fink, J. Michl, *Science (Washington DC) 214* (1981) 1343; b) The most stable free silylene so far (half-life of 1 h at 238 K) was recently identified in solution: D. B. Puranik, M. J. Fink, *J. Am. Chem. Soc. 111* (1989) 5951.

[6] a) C. A. Arrington, J. T. Petty, S. E. Payne, W. C. K. Haskins, *J. Am. Chem. Soc. 110* (1988) 6240; b) M.-A. Pearsall, R. West, *J. Am. Chem. Soc. 110* (1988) 7229; c) G. H. Noren, R. West, *Organometallics 8* (1989) 487; d) W. Ando, S. Sekiguchi, K. Hagiwara, A. Sakakibara, H. Yoshida, *ibid. 7* (1988) 558; e) G. Levin, P. K. Das, C. L. Lee, *ibid. 7* (1988) 1231; f) T. Akasaka, S. Nagase, A. Yabe, W. Ando, *J. Am. Chem. Soc. 110* (1988) 6270.

[7] a) C. Zybill, *Nachr. Chem. Tech. Lab. 37* (1989) 248; b) K. Ueno, H. Tobita, M. Schimoi, H. Ogino, *J. Am. Chem. Soc. 110* (1988) 4092.

[8] H. H. Karsch, A. Appelt, G. Müller, *Organometallics 5* (1986) 1664.

[9] H. H. Karsch, B. Deubelly, J. Riede, G. Müller, *J. Organomet. Chem. 344* (1988) 153.

[10] Crystal structure data: $C_{16}H_{42}P_4Si_3$, M_r = 442.666, triclinic, space group $P\bar{1}$ (Nr. 2), a = 6.511(1), b = 9.335(1), c = 24.114(3) Å, α = 87.29(1), β = 86.74(1), γ = 71.21(1)°, V = 1383.9 Å^3, Z = 2, ϱ_{calcd} = 1.062 g cm^{-3}, $\mu(Mo_{K\alpha})$ = 3.9 cm^{-1}, T = −50 °C. 4341 unique reflections, 3505 observed with $F_o \geq 4.0\sigma(F_o)$; Lp but no absorption correction (hkl range: ±7, +10, ±27, $(\sin\vartheta/\lambda)_{max}$ = 0.573 Å^{-1}, $Mo_{K\alpha}$ radiation, λ = 0.71069 Å, graphite monochromator, Syntex $P2_1$ diffractometer). Solution by direct methods (SHELXS-86). $R(wR)$ = 0.112(0.130) (unit weights) for 217 refined parameters (anisotropic, C at Si3 isotropic in three alternatives, SHELX-76). $\Delta\varrho_{fin}$(max/min) = 1.30/−1.45 e Å^{-3} [11].

[11] Further details of the crystal structure investigation may be obtained from the Fachinformationszentrum Karlsruhe, Gesellschaft für wissenschaftlich-technische Information mbH, D-7514 Eggenstein-Leopoldshafen 2 (FRG), on quoting the depository number CSD-54286, the names of the authors, and the journal citation.

[12] Fourfold P coordination is not completely new for silicon: a) tetrahedral in $Si[P_2tBu_2]_2$: M. Baudler, T. Poutzen, *Z. Anorg. Allg. Chem. 491* (1982) 27; b) octahedral in $Cl_2Si[C(PMe_2)_2(SiMe_3)]_2$: H. H. Karsch, B. Deubelly, U. Keller, G. Müller, unpublished; cf. B. Deubelly, *Dissertation*, Technische Universität München 1988.

[13] a) H. H. Karsch, B. Deubelly, G. Müller, *J. Organomet. Chem. 352* (1988) 47; b) H. H. Karsch, A. Appelt, B. Deubelly, K. Zellner, J. Riede, G. Müller, *Z. Naturforsch. B43* (1988) 1416.

[14] The possible influence of the exocyclic groups PMe_2 in **1a** and **2a** compared with $SiMe_3$ in **3** has not been considered.

[15] The Si1 atom is represented by ^{29}Si satellites: $^1J(^{29}Si^{31}P)$ = 89.8 Hz.

[16] H. H. Karsch, B. Zimmer-Gasser, D. Neugebauer, U. Schubert, *Angew. Chem. 91* (1979) 519; *Angew. Chem. Int. Ed. Engl. 18* (1979) 484.

Preparation of an Enantiomerically Enriched Allyllithium Derivative by Deprotonation with Kinetic Resolution of Enantiomers**

By *Oliver Zschage, Jan-Robert Schwark*, and *Dieter Hoppe**

Dedicated to Professor Paul von Ragué Schleyer on the occasion of his 60th birthday

Chiral allylmetal derivatives with a uniformly configurated metal-bearing carbon atom—for example, boronates **1**,[1] stannanes **2**,[2] silanes,[3] or titanates **3**[4]—have proven useful in the enantioselective and diastereoselective synthesis of homoallyl alcohols **6**; they add to aldehydes with nearly complete transfer of chirality from C-1 to C-3 and with high enantiofacial differentiation at the carbonyl group. The corresponding secondary (1-lithio-2-alkenyl)carbamates **5a** have so far been the only alkali-metal allyl derivatives found to be configurationally stable to a preparatively useful de-

[*] Prof. Dr. D. Hoppe, Dipl.-Chem. O. Zschage, Dipl.-Chem. J.-R. Schwark
Institut für Organische Chemie der Universität
Olshausenstrasse 40–60, D-2300 Kiel 1 (FRG)

[**] This work was supported by the Deutsche Forschungsgemeinschaft and the Fonds der Chemischen Industrie.

gree.[4] They are obtained by "stereoretentive" deprotonation of optically active carbamates such as **4a**.[4] The lithium compound (*R*)-**5b** was obtained from the prochiral precursor **4b** by asymmetric lithiation in the presence of the diamine (−)-sparteine (**7**); here, the stereochemical course is governed by a second-order asymmetric transformation.[5]

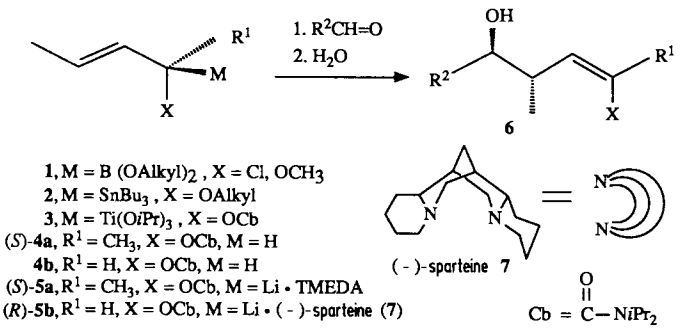

1, M = B (OAlkyl)$_2$, X = Cl, OCH_3
2, M = $SnBu_3$, X = OAlkyl
3, M = $Ti(OiPr)_3$, X = OCb
(*S*)-**4a**, R^1 = CH_3, X = OCb, M = H
4b, R^1 = H, X = OCb, M = H
(*S*)-**5a**, R^1 = CH_3, X = OCb, M = Li • TMEDA
(*R*)-**5b**, R^1 = H, X = OCb, M = Li • (-)-sparteine (7)

Here we report on the first generation of nonracemic, chiral lithium derivatives by enantiomer-differentiating deprotonation. A solution of *rac*-**4a**[6] and 0.5 equiv. of (−)-sparteine (**7**) in pentane was treated with 0.5 equiv. of *n*-butyllithium at −78 °C and, after 10 h, with methoxycarbonyl chloride (**9**). Ester **10** was obtained in 36% yield with 82% *ee*[7] together with the γ-adducts (*E*)- and (*Z*)-**11** (13%)[8] and a 46% yield of (*R*)-**4a** with 80% *ee*.[4] The

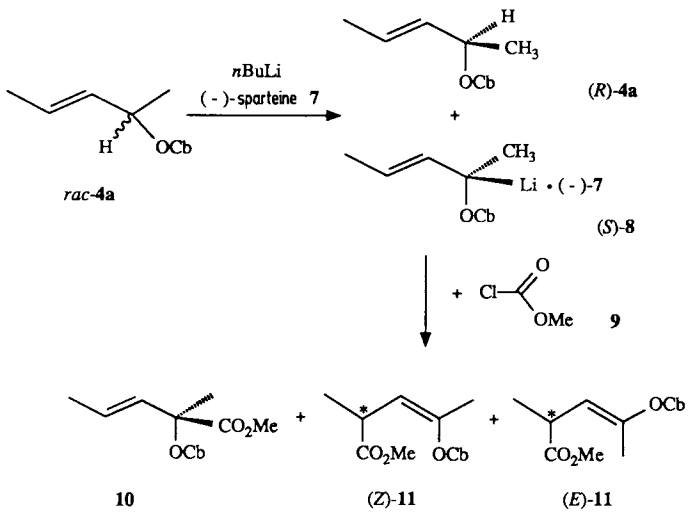

yields are based on *rac*-**4a**. Even the use of 1.1 equiv. of *n*-butyllithium and 1.1 equiv. of (−)-**7** (4 h at −78 °C)—that is, an amount of base that should be sufficient for complete deprotonation of (*R*)-**4a** as well—gave the same result.[9] Under the reaction conditions, therefore, (*S*)-**4a** is rapidly deprotonated to give (*S*)-**8**, but (*R*)-**4a** reacts only very slowly.

Reaction of a solution enriched in (*S*)-**8** with tri-*n*-butyltin chloride (**12**) leads to a mixture of stannanes[10,11] (*S*,*Z*)- and (*R*,*E*)-**13** in an 87:13 ratio (96% yield based on **7**); this configuration, as well as the enantiomeric purity of >80% *ee*, was determined by a recently developed reaction sequence:[4c] reaction of **13** with 2-methylpropanal (**15**) and

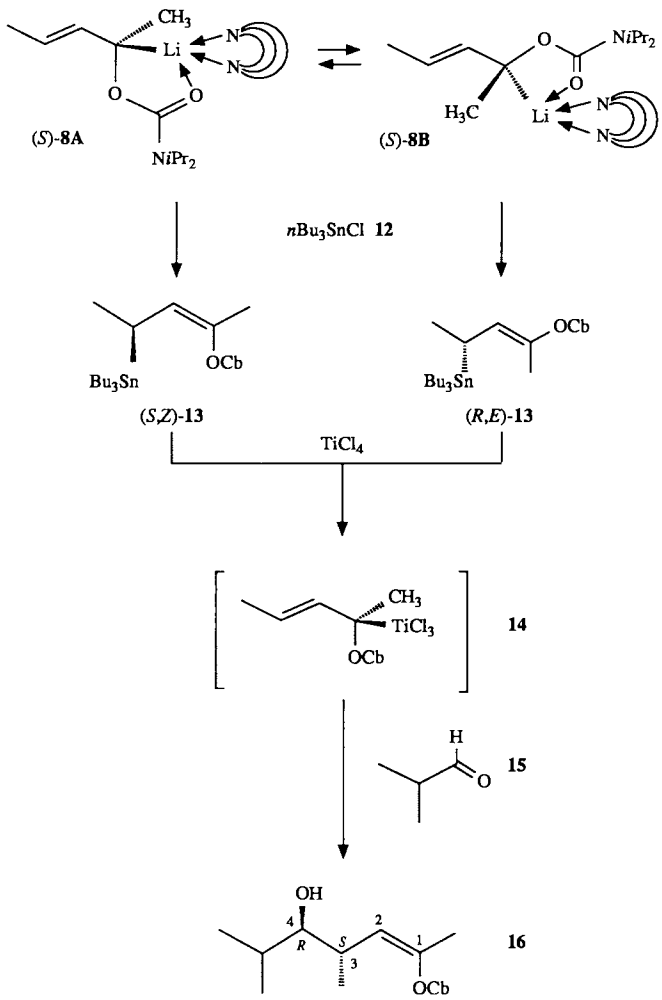

$TiCl_4$ gave the homoaldol adduct (1*Z*,3*S*,4*R*)-**16** in 74% yield and with 80% *ee*.[10,12]

Thus, the trichlorotitanium intermediate **14** has (*R*) configuration and, since the tin–titantium exchange proceeds via a *syn*-S_E2' mechanism,[4c] the two stannanes **13** have the configuration shown. The stereodivergence of their formation from conformers (*S*)-**8A** and (*S*)-**8B** is "neutralized" by the stereoconvergent transformation to (*R*)-**14** and is therefore unimportant in preparative applications. In a control experiment, the enantiomerically pure (*Z*)-carbamate (*S*)-**17**[13] was lithiated with *n*-butyllithium/TMEDA[4c] and converted, by reaction with **12**, into the stannanes (*S*,*Z*)- and (*R*,*E*)-**13**, which were then allowed to react with **15**/$TiCl_4$. The homoaldol adduct thereby obtained in 82% yield exhibits 83% *ee*.

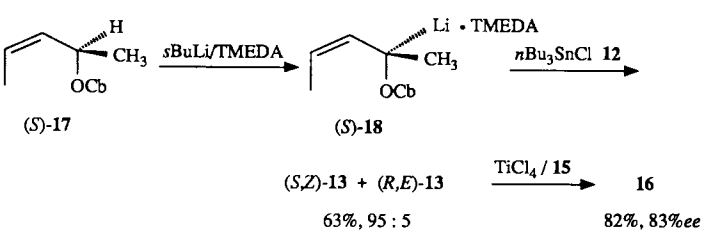

Overall, the kinetic resolution of enantiomers with chiral allyllithium complexes offers a novel route to nonracemic

allylmetal derivatives, the efficiency of which extends to the deprotonation of enantiomerically pure precursors.

Experimental Procedure

A ca. 1.6 M solution of *n*-butyllithium (2.2 mmol) was added to a solution of 4 mmol of (*E*)-1-methyl-2-butenyl-*N*,*N*-diisopropylcarbamidate (*rac*-**4a**)[6] and 2 mmol of (−)-sparteine (**7**) in 10 mL of pentane cooled in a dry ice–acetone bath. After 10 h, 15 mmol of methoxycarbonyl chloride (**9**) or 2.4 mmol of tributyltin chloride (**12**), both precooled, were added dropwise. After 10 min, the solution was allowed to warm to room temperature and then treated with 2 N hydrochloric acid and ether (20 mL each) and worked up as usual. Purification was accomplished by flash chromatography on silica gel with ether/pentane (1:8 or 1:10).

Received: November 28, 1989 [Z 3657 IE]
German version: *Angew. Chem. 102* (1990) 336

[1] R. W. Hoffmann, K. Ditrich, G. Köster, R. Stürmer, *Chem. Ber. 122* (1989) 1783, and references therein.
[2] V. J. Jephcote, A. J. Pratt, E. J. Thomas, *J. Chem. Soc. Perkin Trans. I 1989*, 1529, and references therein.
[3] T. Hayashi, Y. Matsumoto, T. Kiyoi, Y. Ho, *Tetrahedron Lett. 29* (1988) 5667, and references therein.
[4] a) D. Hoppe, T. Krämer, *Angew. Chem. 98* (1986) 171; *Angew. Chem. Int. Ed. Engl. 25* (1986) 160; b) T. Krämer, D. Hoppe, *Tetrahedron Lett. 28* (1987) 5149; c) T. Krämer, J.-R. Schwark, D. Hoppe, *ibid. 30* (1989) 7037.
[5] D. Hoppe, O. Zschage, *Angew. Chem. 101* (1989) 67; *Angew. Chem. Int. Ed. Engl. 28* (1989) 69.
[6] D. Hoppe, R. Hanko, A. Brönneke, F. Lichtenberg, E. van Hülsen, *Chem. Ber. 118* (1985) 2822.
[7] **10**: $[\alpha]_D^{20} = -2.5$ (MeOH, $c = 1.5$) ^{1}H NMR ($CDCl_3$): $\delta = 1.24$ [d, $J = 6.8$ Hz, NCH(CH_3)$_2$], 1.67 (s, 1-CH_3), 1.74 (d, $J = 5.0$ Hz, 4-H_3), 3.72 (s, OCH_3), 3.26 and 4.05 (each m, NCH_3), 5.76 (dd, $J_{3,4} = 5.0$ Hz, $J_{3,2} = 15.6$ Hz, 3-H), 5.84 (d, $J = 15.6$ Hz, 2-H). ^{13}C NMR ($CDCl_3$): $\delta = 17.87$ (4-C), 23.37 (1-CH_3), 21.2 [NCH(CH_3)$_2$], 46.08 (NCH), 52.11 ($COOCH_3$), 79.32 (1-C), 126.53 (3-C), 130.98 (2-C), 153.99 (NCO), 172.50($COOCH_3$). The *ee* value was determined by ^{1}H NMR spectroscopy with 23 mol% tris[(3-heptafluoropropylhydroxymethylene)-D-camphorato]europium(III) [Eu(hfpc)$_3$] in ca. 0.2 M $CDCl_3$ solution on the basis of the 1-CH_3 signal ($\Delta\delta_s = 0.2$). The absolute configuration shown for **10** is based on the assumption that the substitution by C-electrophiles (as observed for alkylation [10] and hydroxyalkylation [4a]) proceeds with retention.
[8] The isomeric γ-adducts (*E*)- and (*Z*)-**11** were not separated and checked for their enantiomeric purity. Gas-chromatographic analysis gave a diastereomeric ratio of 58:42. (*E*)- and (*Z*)-**11**: ^{1}H NMR ($CDCl_3$): $\delta = 1.24$ (d, $J = 7.3$ Hz, 4-H_3), 1.25 [d, $J = 6.4$ Hz, NCH(CH_3)$_2$], 1.91 and 1.92 (each d, $J = 1.1$ Hz, 1-CH_3), 3.35 (dq, $J_{3,2} = 9.1$ Hz, $J_{3,4} = 7.3$ Hz, 3-H), 3.20 and 4.05 (each m, NCH), 3.66 and 3.70 (each s, OCH_3), 5.07 (dd, $J_{2,3} = 9.1$ Hz, $J_{2,1\text{-Me}} = 1.1$ Hz, 2-H). ^{13}C NMR ($CDCl_3$): $\delta = 17.93$ (4-C), 19.84 and 21.13 (1-CH_3), 20.53 [NCH(CH_3)$_2$], 36.78 (3-C), 46.21 (NCH), 51.73 and 52.62 ($COOCH_3$), 114.22 and 115.33 (2-C), 146.50 and 147.56 (1-C), 152.57 (NCO), 175.15 ($COOCH_3$).
[9] Compounds **4a** (10 mmol) and **7** (10 mmol) were dissolved in 20 mL of pentane and stirred with 11 mmol of a ca. 1.6 M solution of *n*-butyllithium in hexane for 4 h at −78 °C to −70 °C. Compound **9** (50 mmol) was then added and, after 30 min, the reaction mixture was worked up as described. (*R*)-**4a** was obtained in 47% yield with 79% *ee* together with **10** (34% yield, 80% *ee*) and **11** (8% yield).
[10] T. Krämer, *Dissertation*, Universität Kiel 1989.
[11] (*E*)-**13**: ^{1}H NMR ($CDCl_3$): $\delta = 0.7$–1.6 [m, $SnCH_2$, CH_2CH_3, NCH(CH_3)$_2$, 4-H_3, CH_2CH_3,$SnCH_2CH_2$], 1.85 (d, $J = 1.1$ Hz, 1-CH_3), 2.14 (dq, $J_{3,2} = 12.0$ Hz, $J_{3,4} = 7.2$ Hz, 3-H), 5.16 (dq, $J_{2,3} = 12.1$ Hz, $J_{2,1\text{-Me}} = 1.1$ Hz, 2-H). ^{13}C NMR ($CDCl_3$): $\delta = 8.89$ ($SnCH_2$), 13.63 (CH_2CH_3), 15.85 (1-CH_3), 18.72 and 18.99 (3-C and 4-C), 21.08 [NCH(CH_3)$_2$], 27.52 and 29.28 (CH_2CH_3 and $SnCH_2CH_2$), 46.01 (NCH), 122.99 (2-C), 139.71 (1-C), 153.11 (C=O). (*Z*)-**13**: ^{1}H NMR ($CDCl_3$): $\delta = 0.82$–0.90 (m, $SnCH_2$, CH_2CH_3), 1.24 [d, $J = 6.7$ Hz, NCH(CH_3)$_2$], 1.25 (d, $J = 7.3$ Hz, 4-H_3), 1.25–1.35 (m, CH_2CH_3), 1.40–1.45 (m, $SnCH_2CH_2$), 1.87 (d, $J = 1.1$ Hz, 1-CH_3), 2.27 (dq, $J_{3,2} = 11.6$ Hz, $J_{3,4} = 7.3$ Hz, 3-H), 3.81 and 4.04 (each m, NCH), 4.94 (dq, $J_{2,1\text{-Me}} = 1.1$ Hz, $J_{2,3} = 11.6$ Hz, 2-H). ^{13}C NMR ($CDCl_3$): $\delta = 8.80$ ($SnCH_2$), 13.71 (CH_2CH_3), 18.19 (3-C), 18.34 (4-C), 19.69 (1-CH_3), 21.12 [NCH(CH_3)$_2$], 27.54 (CH_2CH_3), 29.29 ($SnCH_2CH_2$), 46.01 (NCH), 122.46 (2-C), 139.48 (1-C), 153.14 (C=O).
[12] (1*Z*,3*S*,4*R*)-**16**, 82% *ee*: $[\alpha]_D^{20} = +5.1$ (MeOH, $c = 2.0$), see [4b, c].
[13] J.-R. Schwark, D. Hoppe, *Synthesis 1990*, No. 4.

On a (1,4-Diazabutadiene)bis(ethene)nickel(0) Complex and Related Compounds**

By *Werner Bonrath, Klaus R. Pörschke,** and *Stephan Michaelis*

Dedicated to Professor Günther Wilke on the occasion of his 65th birthday

Tetracoordinated 18-electron Ni^0 complexes containing ethene as ligand have so far been isolated only in the form of $[(Me_2PC_2H_4PMe_2)(R_3P)Ni(C_2H_4)]$ (R = Me, *cyclo*-C_6H_{11}, Ph; dec. −20 °C)[1] and $[(Me_2NC_2H_4NMe_2)Ni(C_2H_4)(H_2C=O)]$ (dec. −10 °C).[2] Apparently, their formation strongly depends on the coordination of the bidentate chelate ligand to nickel(0) to give a five-membered ring ("five-membered ring effect"). Although they readily decompose, the complexes have been characterized by, among other methods, crystal structure analysis. A "$[(Ph_3P)_2Ni(C_2H_4)_2]$" complex, however, has remained speculative.[3] Here we report on the synthesis and reactivity of the first 18-electron Ni^0 complex containing two ethene ligands and on related compounds.

Deep violet, fine cubes of **1** (81%) crystallized from a solution of tris(ethene)nickel(0)[4] and an equimolar amount of 1,4-bis(2,6-diisopropylphenyl)-1,4-diazabutadiene (iPr$_2$Ph)$_2$-dad[5] in pentane at −78 °C.[6] Under argon, **1** is only stable to −5 °C, but under ethene atmosphere it is stable to 20 °C. The complex is readily soluble in cold pentane as well as in other solvents. It shows an extremely high reactivity starting at −100 °C. In the ^{1}H NMR spectrum (400 MHz) recorded at −80 °C, the ethene protons of **1** give rise to two signals ($\delta_H = 2.62$, 2.22; AA'BB') and, in the ^{13}C NMR spectrum (75.5 MHz), the ethene C atoms to one signal ($\delta_C = 64.9$; sharp to −105 °C). Assuming that the Ni^0 atoms are tetrahedrally coordinated by the dad N atoms and the ethene ligands, the NMR spectra are consistent with an idealized parallel orientation of the C=C bonds with respect to the N–N axis, resulting in magnetically equivalent ethene C atoms and magnetically different geminal ethene protons. Upon raising the temperature, the signals of the ethene protons coalesce owing to rotation of the ligands around the bond axis to the Ni^0 atom ($\Delta G^{\ddagger}_{200K} \approx 40$ kJ mol^{-1}). The phenyl rings of the 2,6-diisopropylphenyl substituents are either perpendicular to the plane of the dad-Ni five-membered ring or they are able to rotate freely around their bond to the N atom, even at low temperature.

A solution of Ni(cdt)[7] (cdt = all-*trans*-1,5,9-cyclododecatriene) in 1,5-hexadiene at 20 °C affords the yellow complex Ni(η-C_6H_{10})$_2$.[8a] Addition of an equimolar amount of

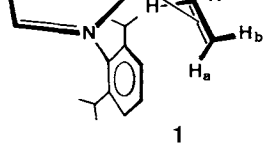

1

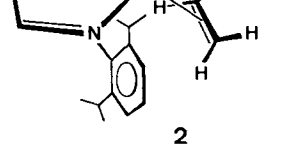

2

[*] Priv.-Doz. Dr. K. R. Pörschke, Dr. W. Bonrath, Dipl.-Chem. S. Michaelis
Max-Planck-Institut für Kohlenforschung
Postfach 10 13 53, D-4330 Mülheim an der Ruhr 1 (FRG)

[**] We thank *Barbara Gabor, Gerhard Schroth,* and *Richard Mynott* for the NMR studies.

(iPr$_2$Ph)$_2$-dad dissolved in pentane results in the formation of a deep red reaction solution, which yields dark crystals of **2** (91%) at −78 °C. This method allows the preparation of numerous, in part thermally labile $L_nNi(\eta\text{-}C_6N_{10})$ complexes (n = 1,2; L,L$_2$ = phosphanes, phosphites, 2,2′-bipyridyl, 1,4-diazabutadienes).[8] Complex **2**, like **1**, shows good solubility; it is stable at room temperature (m.p. 142 °C) and exhibits its reactivity above about −30 °C. Presumably, the complex geometry of **2** is similar to that of **1**; owing to the C_2H_4 bridging of the two vinyl groups, however, the C_2 axis is no longer present. In the low-temperature ^{1}H NMR (400 MHz, −30 °C) and ^{13}C NMR spectra (75.5 MHz, −30 °C), therefore, **2** shows one set of signals for the hexadiene ligand and two sets of signals for the nonequivalent halves of the (iPr$_2$Ph)$_2$-dad ligands. The mass spectrum of **2** displays the molecular ion peak at m/z 516 (for ^{58}Ni); the molecular ion undergoes fragmentation with loss of hexadiene.

Complexes **1** and **2** are appreciably more reactive than **3**, preparable from Ni(cod)$_2$[7] (cod = 1,5-cyclooctadiene) and (iPr$_2$Ph)$_2$-dad (36%),[5] in which the macrocyclic effect[9] of the cod ligand contributes to the stabilization of the complex. The order of stability is also reflected in the increasing thermodynamic reactivity of the compounds. Thus, reaction of **1** with 1,5-hexadiene affords **2** and reaction of **1** or **2** with cod affords **3** (60%); the backward reactions are not observed (e.g., **3** dissolved in 1,5-hexadiene does not reconvert into **2**). Complexes **1** and **2** react with one equivalent of (iPr$_2$Ph)$_2$-dad to give the reddish-brown complex **4** (X-ray structure analysis), which is not accessible from **3**[5] and which we will describe elsewhere.[10]

[{(iPr$_2$Ph)$_2$-dad}Ni(cod)] **3** [{(iPr$_2$Ph)$_2$-dad}$_2$Ni] **4**

Compounds **1** and **2** in pentane, on addition of cyclooctatetraene (cot) at −78 to −30 °C, afford red reaction solutions and, at −78 °C, cubes of **5a** slowly crystallize (94%). Complex **5a** has been synthesized via a different route before, but could not be isolated in pure form.[11] Crystalline **5a** may be kept at 20 °C for several days without noticeable decomposition. The substance is readily soluble in THF, but less soluble in ether and pentane; in solution at 20 °C, **5a** slowly dimerizes with loss of a cot ligand to form **5b**.

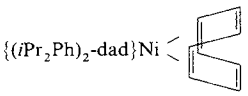

5a

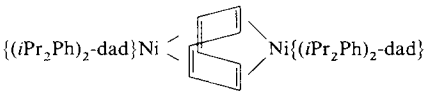

5b

The IR spectrum of **5a** contains stretching bands for free and for complexed C=C bonds ($\tilde{\nu}$ = 1620 and 1512 cm^{-1}). NMR spectroscopy revealed a dynamic process for **5a**. In the 200-MHz ^{1}H NMR spectrum at −30 °C, signals of equal intensity were observed at δ_H = 5.38 and 3.79 for the protons of the free and coordinated double bonds, respectively; at 27 °C, a coalescence signal, due to rapid exchange, was observed at δ_H = 4.59. As in [(Me$_3$P)$_2$Ni(1:2,5:6-η-cot)] (X-ray structure analysis),[12] a cod-like coordination of the cot at nickel is presumed for **5a**. Reaction of **1**–**3** with cot at 20 °C in pentane affords a violet solution, from which needles of the dinuclear complex **5b** (58%) crystallize (cot, δ_H = 3.81). In the mass spectrum, the molecular ion of **5a** ($M^{\oplus}$ 538) fragments by loss of cot and that of **5b** ($M^{\oplus}$ 972) by loss of [(iPr$_2$Ph)$_2$-dad]Ni (transformation to **5a**$^{\oplus}$).

Complex **1** reacts with ethyne at −100 °C (!) immediately and **2** at −30 °C within only a few minutes to give a blue solution (**3**: several hours at 20 °C), from which dark crystals of the dinuclear complex **6** slowly crystallize in up to 70% yield. Extensive spectroscopic investigations and an X-ray crystal structure analysis of **6** revealed the presence of a butadienediyl group, formed by coupling of two ethyne molecules.[13] The (iPr$_2$Ph)$_2$-dad complexes **1**–**3** thus differ in their reactivity from the analogous bipyridyl complexes (e.g., [bipyNi(C$_2$H$_4$)$_2$][14] at −78 °C), which decompose on addition of ethyne.

[{[(iPr$_2$Ph)$_2$-dad]Ni}$_2$(μ-C$_4$H$_4$)] **6**

On thermal decomposition of **1**, the ethene ligands do not couple with nickel(0) to form a nickelacyclopentane complex, as reported for the system PPh$_3$/Ni(0)/C$_2$H$_4$;[3b] instead, **4** is formed. In the presence of **1**, ethene under pressure (60 bar) at 40 °C reacts to form polyethylene.[8b,16]

Experimental Procedure

1: A yellow solution of Ni(C$_2$H$_4$)$_3$ in 30 mL of pentane was prepared from Ni(cdt) (1.17 g, 5.0 mmol; 95%, some cocrystallized cdt) and ethene and then treated at −30 °C with a solution of (iPr$_2$Ph)$_2$-dad (1.88 g, 5.0 mmol) in 20 mL of pentane. The reaction solution immediately turned violet and, on cooling to −78 °C, afforded fine, violet, crystalline cubes. These were freed of mother liquor with a capillary, washed twice with cold pentane, and dried under oil-pump vacuum at −30 °C. Yield 1.99 g (81%); correct elemental analysis.
MS: The compound cannot be vaporized without decomposition. ^{1}H NMR (400 MHz, [D$_8$]THF, −100 °C): δ = 8.08 (2H; CH=N), 7.28 (6H; Ph), 2.96 (4H; CHMe$_2$), 1.30, 1.06 (each 12H; CH$_3$, dad), 2.62, 2.22 (each 4H; C$_2$H$_4$). ^{13}C NMR (75.5 MHz, [D$_8$]THF, −80 °C): δ = 152.2 (s, 2C), 140.3 (s, 4C), 126.0 (d, 2C), 123.7 (d, 4C; each Ph), 144.8 (dd, 2C, ^1J(CH) = 174 Hz; CH=N), 28.2 (d, 4C; CHMe$_2$), 26.4, 23.5 (each q, 4C; CH$_3$, dad), 64.9 (t, 4C; C$_2$H$_4$).

2: A yellow solution of Ni(cdt) (1.17 g, 5.0 mmol) in 5 mL of 1,5-hexadiene (nonisolable Ni(η^2,η^2-C$_6$H$_{10}$)$_2$ is presumably present) was treated with a solution of (iPr$_2$Ph)$_2$-dad (1.88 g, 5.0 mmol) in 30 mL of pentane, whereby the color turned deep red. On cooling the reaction solution from −30 to −78 °C, red crystals formed; these were isolated as described above and dried at 20 °C. Yield 2.35 g (91%); correct elemental analyses; m.p. 142 °C. The substance tends to retain small amounts of solvent.
MS (70 eV, 110 °C): m/z 516 ($M^{\oplus}$, 8%), 434 ($M^{\oplus}$ − C$_6$H$_{10}$, 100). UV/VIS (benzene): λ_{max} = 495 nm (ε_{max} = 9212 Lmol^{-1}cm^{-1}). ^{1}H NMR (400 MHz, [D$_8$]THF, −30 °C): δ = 8.04, 8.03 (each s, 1H; CH=N and CH′=N), 7.25, 7.20 (each 3H; Ph and Ph′), 3.15 (4H; CHMe$_2$ and CH′Me$_2$), 1.35, 1.32, 1.10, 1.00 (each d, 6H; CH$_3$, dad), 4.06 (2H; C=CH–), 2.44, 2.34 (each 2H; H$_2$C=), 2.16, 1.21 (each 2H, partially overlapped; CHH′, alkene; at 27 °C, the signals are broadened. ^{13}C NMR (75.5 MHz, [D$_8$]THF, −30 °C): δ = 154.25 (s, 1C), 153.5 (s, 1C), 140.1 (s, 2C), 139.9 (s, 2C), 125.9 (d, 1C), 125.7 (d, 1C), 123.55 (d, 2C), 123.5 (d, 2C; each Ph), 143.3, 142.1 (each dd, 1C, ^1J(CH) = 171 Hz; CH=N), 28.3, 28.25 (each d, 2C; CHMe$_2$), 26.5–23.0 (4 signals q, 2C; CH$_3$, dad), 89.8 (d, 2C; C=CH–), 67.3 (t, 2C; H$_2$C=), 32.3 (t, 2C; CH$_2$, each alkene).

3: Synthesis from Ni(cod)$_2$ and (iPr$_2$Ph)$_2$-dad [5] or from **1** (or **2**) and cod in pentane; from brown reaction solution (20 °C), dark brown crystals obtained at −78 °C; m.p. 131 °C.
MS: The substance cannot be vaporized without decomposition. UV/VIS (benzene): λ_{max} = 476 nm (ε_{max} = 8223 Lmol^{-1}cm^{-1}) [5]. ^{1}H NMR (200 MHz, [D$_8$]THF, 27 °C): δ = 7.97 (s, 2H; CH=N), 7.22 (m, 6H; Ph), 3.21 (sept, 4H; CHMe$_2$), 1.33, 1.04 (each d, 12H; CH$_3$, dad); 3.70 (4H; –CH=), 2.39, 1.49 (each m, 4H; –CH$_2$–, cod); see also [5]. ^{13}C NMR (75.5 MHz, [D$_8$]THF, 38 °C): δ = 154.8 (s, 2C), 140.2 (s, 4C), 125.7 (d, 2C), 123.4 (d, 4C; each Ph), 142.3 (dd, 2C, ^1J(CH) = 170 Hz; CH=N), 28.4 (d, 4C; CHMe$_2$), 26.5, 23.1 (each q, 4C; CH$_3$, dad), 89.3 (d, 4C; –CH=), 30.9 (t, 4C; –CH$_2$–, cod).

5a: Reaction of **2** and cot in pentane at $-30\,^{\circ}C$ afforded a red solution, from which red cubes (94%) crystallized at $-78\,^{\circ}C$; correct elemental analysis; m.p. 261 °C.
MS (70 eV, 90 °C): *m/z* 538 ($M^{\oplus}$, 20%), 434 ($M^{\oplus}-C_8H_8$, 100). UV/VIS (benzene): $\lambda_{max} = 498$ nm ($\varepsilon_{max} = 5280\ Lmol^{-1}cm^{-1}$). ^1H NMR (200 MHz, [D$_8$]THF, $-30\,^{\circ}C$): $\delta = 8.19$ (s, 2H; CH=N), 7.23 (m, 6H; Ph), 3.32 (sept., 4H; $CHMe_2$), 1.30, 1.08 (each d, 12H; CH_3, dad), 5.38 (4H; $-CH=_{free}$), 3.79 (4H; $-CH=_{compl.}$, cot). ^{13}C NMR (75.5 MHz, [D$_8$]THF, $-80\,^{\circ}C$): $\delta = 153.3$ (s, 2C), 140.1 (s, 4C), 125.9 (d, 2C), 123.6 (d, 4C; each Ph), 143.3 (dd, 2C, $^1J(CH) = 173$ Hz; CH=N), 28.3 (d, 4C; $CHMe_2$), 26.3, 23.3 (each q, 4C; CH_3, dad), 134.1 (d, 4C; $-CH=_{free}$), 94.4 (d, 4C; $-CH=_{compl.}$, cot).

5b: Reaction of **2** and cot at 20 °C gave a violet solution, from which dark violet needles formed at $-30\,^{\circ}C$; correct elemental analyses; m.p. 266 °C.
IR (KBr, Nujol): no bands from 1700 to 1480 cm^{-1}. MS (70 eV, 200 °C): *m/z* 972 ($M^{\oplus}$, 45%), 538 (**5a**$^{\oplus}$, 10). UV/VIS (benzene): $\lambda_{max} = 525$ nm ($\varepsilon_{max} = 17872\ Lmol^{-1}cm^{-1}$). ^1H NMR (200 MHz, [D$_8$]THF, 27 °C): $\delta = 7.94$ (s, 4H; CH=N), 7.10 (m, 12H; Ph), 3.17 (sept., 8H; $CHMe_2$), 1.15, 0.97 (each d, 24H; CH_3, dad), 3.81 (s, 8H; $-CH=$, cot). ^{13}C NMR (75.5 MHz, [D$_8$]THF, 38 °C): $\delta = 154.1$ (s, 4C), 140.3 (s, 8C), 125.8 (d, 4C), 123.5 (d, 8C; each Ph), 141.8 (dd, 4C, $^1J(CH) = 170$ Hz; CH=N), 28.2 (d, 8C; $CHMe_2$), 25.7, 23.5 (each q, 8C; CH_3, dad), 98.2 (d, 8C; $-CH=$, cot).

Received: September 19, 1989 [Z 3554 IE]
German version: *Angew. Chem. 102* (1990) 295

[1] K. R. Pörschke, R. Mynott, C. Krüger, M. J. Romao, *Z. Naturforsch. B 39* (1984) 1076.
[2] W. Schröder, K. R. Pörschke, Y.-H. Tsay, C. Krüger, *Angew. Chem. 99* (1987) 953; *Angew. Chem. Int. Ed. Engl. 26* (1987) 919.
[3] a) R. H. Grubbs, A. Miyashita, *J. Chem. Soc. Chem. Commun. 1977*, 864; *J. Am. Chem. Soc. 100* (1978) 1300; b) *ibid. 100* (1978) 7416; *Fundam. Res. Homogeneous Catal. 3* (1979) 151.
[4] K. Fischer, K. Jonas, G. Wilke, *Angew. Chem. 85* (1973) 620; *Angew. Chem. Int. Ed. Engl. 12* (1973) 565.
[5] H. tom Dieck, M. Svoboda, T. Greiser, *Z. Naturforsch. B 36* (1981) 823; M. Svoboda, *Dissertation*, Universität Frankfurt 1978.
[6] W. Bonrath, *Dissertation*, Universität Bochum 1988.
[7] B. Bogdanović, M. Kröner, G. Wilke, *Justus Liebigs Ann. Chem. 699* (1966) 1.
[8] a) K. R. Pörschke, unpublished; b) S. Michaelis, unpublished.
[9] F. A. Cotton, G. Wilkinson, *Advanced Inorganic Chemistry*, 5th ed., Wiley, New York 1988, pp. 47f.
[10] W. Bonrath, K. R. Pörschke, R. Mynott, C. Krüger, unpublished.
[11] R. Diercks, *Dissertation*, Universität Hamburg 1984, S. 73.
[12] K. R. Pörschke, G. Wilke, K. Angermund, C. Krüger, unpublished.
[13] W. Bonrath, S. Michaelis, K. R. Pörschke, B. Gabor, R. Mynott, C. Krüger, unpublished.
[14] W. Mayer, K. R. Pörschke, unpublished; C. Krüger, single-crystal structure analysis, unpublished; see W. Schröder, K. R. Pörschke, *J. Organomet. Chem. 322* (1987) 385.
[15] Concerning the failure of an ethene coupling reaction with (2,2'-bipyridyl)(alkene)nickel complexes, see P. Binger, M. J. Doyle, C. Krüger, Y.-H. Tsay, *Z. Naturforsch. B 34* (1979) 1289.
[16] In the condensate of the reaction solutions, no cyclobutane and only traces of 1- and 2-butene were found by gas chromatography.

Synthesis and Structure of a Dimeric Lithium Diphenylcuprate: $[\{Li(OEt)_2\}(CuPh_2)]_2$**

By *Nis Peter Lorenzen* and *Erwin Weiss**

Dedicated to Professor Alfred Schmidpeter on the occasion of his 60th birthday

Lithium organocuprates, particularly lithium diorganocuprates (Gilman reagents) find many applications in organic syntheses, e.g. in the Corey-Posner reaction[1] and in the stereospecific 1,4-addition of alkyl, alkenyl or aryl groups to α,β-unsaturated carbonyl compounds.[2] In many cases they are superior to the traditional Grignard and organolithium reagents in such reactions. Since they are thermolabile, however, very little information is available concerning their structure.[3]

Lithium di*alkyl*cuprates are particularly unstable. They are generated at low temperatures according to the overall equation (a) by reaction of organolithium compounds with

$$2\ LiR + CuX \xrightarrow[\text{or THF}]{Et_2O} LiCuR_2 + LiX \qquad (a)$$

suspensions of Cu^I-halides or better with soluble Cu^I compounds, and are used in situ for the reactions.

So far it has still not been possible to isolate even any of the simpler lithium di*alkyl*cuprates in a form suitable enough for an X-ray crystallographic characterization. Consequently, structural investigations have been limited, inter alia, to those performed in solution (NMR methods[4] and molecular weight determinations). Depending on the molar ratio LiR/CuX, not only different species were detected (e.g. $LiCuMe_2$, $LiCu_2Me_3$, Li_2CuMe_3[4a–c]), but also complicated equilibria, e.g. $Li_2CuMe_4 \rightleftharpoons LiMe + LiCu_2Me_3$.[5]

Dimers of the type $Li_2Cu_2R_4$ had already been discussed more than a decade ago.[6] According to EXAFS investigations on the dissolved methyl compound $Li_2Cu_2Me_4$ **1**,[6] a cyclic structure as in $[Cu(CH_2SiMe_3)]_4$ **2a**[7] or $[Cu(OCMe_3)]_4$ **2b**[8] (planar eight-membered ring) appeared more likely than a tetrahedral structure resembling that of $(LiCH_3)_4$.[9]

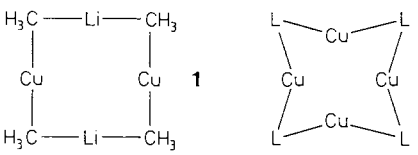

2a, L = CH_2SiMe_3
2b, L = $OCMe_3$

In this connection, we should also mention recent investigations in which salts with *isolated* diorganocuprate ions have been prepared and X-ray crystallographically characterized for the first time. Such salts are obtained either by using sterically bulky residues such as in $[Cu(dppe)_2][Cu(C_6H_2Me_3\text{-}2,4,6)_2]$[10] (dppe = bis(diphenylphosphino)ethane) and $[Li(thf)_4][Cu\{C(SiMe_3)_3\}_2]$[11] or by complexation of the Li ions with crown ethers, e.g. as in the compounds obtained from $[Li([12]crown\text{-}4)_2]^{\oplus}$ and the monomeric linear anions $[CuMe_2]^{\ominus}$, $[CuPh_2]^{\ominus}$, and $[Cu(Br)CH(SiMe_3)_2]^{\ominus}$.[12]

The thermally somewhat more stable lithium *aryl*cuprates have likewise been insufficiently studied regarding their structure. Since 1966, lithium phenylcuprates of various stochiometries have been obtained from the reaction of CuBr with LiPh.[13] Later NMR spectroscopic[14] and especially X-ray crystallographic investigations revealed, inter alia, the formation of polynuclear (lithium-)cuprate ions such as $[Cu_5Ph_6]^{\ominus}$,[15a] $[LiCu_4Ph_6]^{\ominus}$,[15b] and $[Li_2Cu_3Ph_6]^{\ominus}$.[16a] The latter can be described as trigonal-bipyramidal metal clusters in which the equatorial positions are always occupied by the Cu, the axial by Li and Cu; the Ph groups form bridges between axial and equatorial metal atoms. Noteworthy, is the recently determined structure of $[Li_3Cu_2Ph_5(SMe_2)_4]$;[16b] the $[Cu_2Ph_5]^{3\ominus}$ anion contained

[*] Prof. Dr. E. Weiss, Dr. N. P. Lorenzen
Institut für Anorganische und Angewandte Chemie der Universität
Martin-Luther-King-Platz 6, D-2000 Hamburg 13 (FRG)

[**] Metal-Alkyl and Metal-Aryl Compounds, Part 42. This work was supported by the Deutsche Forschungsgemeinschaft and the Fonds der Chemischen Industrie.—Part 41: K. Gregory, M. Bremer, W. Bauer, P. von R. Schleyer, N. P. Lorenzen, J. Kopf, E. Weiss, *Organometallics*, in press.

herein can be imagined as consisting of $[CuPh_2]^{\ominus}$ and $[CuPh_3]^{2\ominus}$ units.

On using aromatic ligands with chelating amino groups in the *o*-position, e.g. [2-(dimethylamino)methyl]phenyl, *dimers* with a cyclic structure, $[(Li_2Cu_2(C_6H_4CH_2NMe_2\text{-}2)_4]$ **3** and related compounds, could already be unequivocally characterized earlier, at first NMR spectroscopically,[17] and later also X-ray crystallographically.[18] By way of analogy, such a structure has also been proposed for $[Li_2Cu_2(4\text{-tolyl})_4(Et_2O)_2]$.[19]

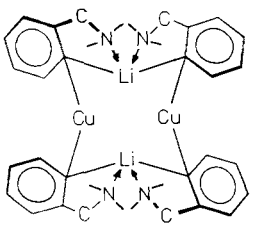

3

Undoubtedly the N-donor substituents play an important role in determining the structure of the cuprates containing amino-substituted phenyl groups. Hence, a direct structural comparison with simple methyl- or unsubstituted phenyl cuprates, as are present in the preparatively interesting compounds remains an open question.

Lithium phenylcuprates are usually obtained by reaction of a phenyllithium-solution with a suspension or solution of the Cu^{I} starting compound in Et_2O, THF, or *n*-hexane at lower temperatures. Instead of using the pure copper(I) halides, it is far more advantageous to use their soluble solvates. In our attempts to synthesize lithium phenylcuprates[20] it emerged that not only the reaction temperature but also the solvent composition is an important reaction parameter. With CuI · P*n*Bu$_3$ as starting compound and ether/hexane mixtures as reaction medium we were able to isolate the title compound **4** in crystalline form according to Equation (b).

$$2\,CuI \cdot PnBu_3 + 4\,LiPh \xrightarrow[-2\,PnBu_3]{\substack{n\text{-Hexan/}Et_2O\\ -78\,^{\circ}C}} \underset{\mathbf{4}\,(38\,\%)}{[\{Li(OEt_2)\}(CuPh_2)]_2} + \frac{2}{n}[LiI(Et_2O)]_n \quad (b)$$

4 is also formed in smaller yield from CuBr · SMe_2 (0.05 M in pure Et_2O) under otherwise similar reaction conditions. When the reaction (b) was carried out with CuI · P*n*Bu$_3$ and LiPh in a ratio other than 2:4, other products were obtained.

The structure analysis of **4** revealed the following:[21a] the unit cell contains four dimers, two of which form the asymmetric unit (molecules 1 and 2). Only one of these (molecule 1) is shown in Figure 1. The molecules 1 and 2 are virtually mirror images of each other, but their atomic distances and angles are significantly different. The differences are best explained in terms of a packing effect.

Each dimer consists of two almost linear $CuPh_2$ units (C–Cu–C 163.3 to 168.0°), which are bound by solvated Li ions to give a distorted eight-membered ring. To our knowledge, **4** is the first example of an X-ray crystallographically characterized lithium cuprate dimer as have been suggested to exist in ether solutions. The two diphenylcuprate moieties in the ring are strongly bent towards each other, but only very weak Cu–Cu interactions have been reported (Cu–Cu 286.5 and 307.5 pm; cf. **2a** (241.7 pm), **2b** (264.6(2)–277.1(3) pm), **3** (266.60(8) pm), and Ref. [23]. The four-membered ring formed by the Cu and Li atoms is also not planar, but noticeably folded at the Cu atoms (154.3° in molecule 1, 140.6° in molecule 2). The Cu–C_{ipso} distances (av. 191.8 pm) are similar to those also found in other phenylcuprates, and similar-

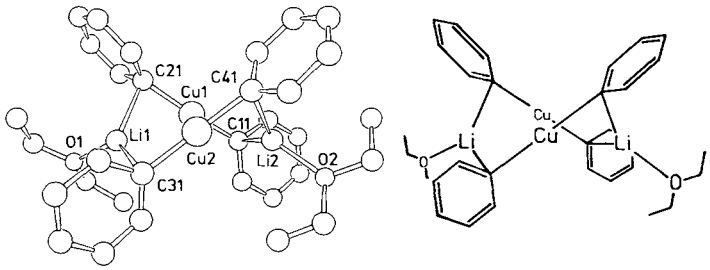

Fig. 1. SCHAKAL plot and line drawing of **4** (molecule 1). Important bond lengths [pm] and angles [°] (the values in square brackets refer to molecule 2): Cu1-Cu2 286.5(2) [307.5(3)], Cu1-C11 192.2(7) [192.8(7)], Cu1-C21 190.6(5) [191.5(7)], Cu2-C31 192.8(7) [192.3(7)], Cu2-C41 191.4(6) [191.2(6)], Li1-C21 221.6(11) [227.8(11)], Li1-C31 226.4(10) [224.9(11)], Li2-C11 225.4(10) [228.2(13)], Li2-C41 221.3(12) [221.1(12)], Li1-O1 192.6(9) [192.6(10)], Li2-O2 191.5(10) [188.9(11)]; C11-Cu1-C21 167.7(3) [165.2(3)], C31-Cu2-C41 168.0(2) [163.3(3)], C21-Li1-C31 123.6(4) [118.0(5)], C11-Li2-C41 121.9(5) [126.4(5)].

ly, the Li–C_{ipso} distances (av. 225.2 pm) are comparable with those in $[PhLi(tmeda)]_2$ (av. 224.3 pm)[24] and other organolithium compounds. The planes of the two phenyl groups in each $CuPh_2$ moiety are twisted through about 88° with respect to each other as a result of Li–C interactions. The additional solvation by ether molecules leads to a trigonal-planar coordination with bond angles deviating only slightly from 120°, a rare coordination geometry for Li.

A comparison of **4** with the above mentioned homo- and heteronuclear (lithium-)phenylcuprate clusters shows close structural relationships. Thus, the skeletal framework of **4** can be derived from that of $Li_2Cu_3Ph_6$ by removal of $[CuPh_2]^{\ominus}$; the resulting vacant coordination sites are occupied by two ether molecules. Since $[Li_2Cu_3Ph_6]^{\ominus}$ (and similarly also $[LiCu_4Ph_6]^{\ominus}$) consists of three $CuPh_2$ units, which are held together by Li (and Cu) ions, all the phenylcuprates known so far contain, in end effect, the $CuPh_2$ unit as building block.

In the synthesis of lithium phenylcuprates, equilibria can be assumed from which various products can be isolated depending on the reaction conditions (concentrations, solvent, temperature). Almost all previously characterized lithium phenylcuprates are consequently built up from the basic units CuPh, $CuPh_2$, and LiPh. From these, a model for the formation of the various products can be developed (Scheme 1).

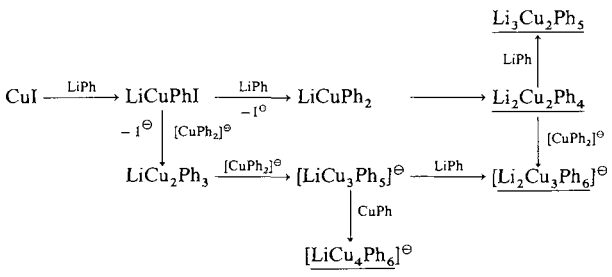

Scheme 1. Model for the formation of lithium phenylcuprates; products characterized by X-ray structure analysis are underlined; solvate ligands are not shown.

Experimental

4: A cooled (CO_2, −78 °C) solution of phenyllithium (1.4 g, 16.8 mmol) [25] in 30 mL of diethyl ether was treated dropwise with stirring and continuous cool-

ing within 90 min with a solution of CuI · $PnBu_3$ [26] (3.3 g, 8.4 mmol) in 90 mL of *n*-hexane. The temperature of the reaction mixture must not in any case exceed − 60 °C. After completion of the addition the mixture was stirred for a further 3 h at − 75 °C, and the finely crystalline pale yellow percipitate was filtered off (max. temp. − 30 °C), washed portionwise with a total of 90 mL *n*-hexane (− 30 °C), and dried at − 30 °C. Yield 0.94 g (38%); golden yellow, extremely air-sensitive rhombs, stable in the dry state at room temperature but not in solution (decomposition with separation of Cu). Readily soluble in hexane and benzene. Correct analytical values for Cu, Li, C, H, O. Crystals suitable for an X-ray structure analysis were obtained from the yellow filtrate after prolonged storage at − 30 °C.

Received: October 30, 1989 [Z 3613 IE]
German version: *Angew. Chem. 102* (1990) 322

CAS Registry number:
4, 125303-71-1.

[1] E. J. Corey, G. H. Posner, *J. Am. Chem. Soc. 89* (1967) 3911; G. H. Posner: *An Introduction to Synthesis Using Organocopper Reagents*, Wiley, New York 1980.
[2] a) H. O. House, W. L. Respess, G. M. Whiteside, *J. Org. Chem. 31* (1966) 3128; b) H. O. House, *Acc. Chem. Res. 9* (1976) 59.
[3] G. van Koten, J. G. Noltes in G. Wilkinson (Ed.): *Comprehensive Organometallic Chemistry, Vol. 4*, Pergamon, New York 1982, pp. 709–63, and references cited therein.
[4] a) E. C. Ashby, J. J. Watkins, *J. Am. Chem. Soc. 99* (1977) 5312; b) J. San Filippo, Jr., *Inorg. Chem. 17* (1978) 275; c) E. C. Ashby, J. J. Lin, J. J. Watkins, *J. Org. Chem. 42* (1977) 1099; d) G. Hallnemo, T. Ollson, C. Ullenius, *J. Organomet. Chem. 282* (1985) 133; e) G. Hallnemo, C. Ullenius, *Tetrahedron Lett. 27* (1986) 395; f) H. Bertz, R. A. J. Smith, *J. Am. Chem. Soc. 111* (1989) 8276.
[5] B. H. Lipshutz, J. A. Kozlowski, C. M. Breneman, *J. Am. Chem. Soc. 107* (1985) 3197.
[6] R. G. Pearson, C. D. Gregory, *J. Am. Chem. Soc. 98* (1976) 4098.
[7] J. A. J. Jarvis, R. Pearce, M. F. Lappert, *J. Chem. Soc. Dalton Trans. 1977*, 999.
[8] T. Greiser, E. Weiss, *Chem. Ber. 109* (1976) 3142.
[9] a) E. Weiss, E. A. C. Lucken, *J. Organomet. Chem. 2* (1964) 197; b) E. Weiss, T. Lambertsen, B. Schubert, J. K. Cockcroft, A. Wiedenmann, *Chem. Ber. 123* (1990) 79.
[10] P. Leoni, M. Pasquali, C. A. Ghilardi, *J. Chem. Soc. Chem. Commun. 1983*, 240.
[11] C. Eaborn, P. B. Hitchcock, J. D. Smith, A. C. Sullivan, *J. Organomet. Chem. 263* (1984) C23.
[12] H. Hope, M. M. Olmstead, P. P. Power, J. Sandell, X. Xu, *J. Am. Chem. Soc. 107* (1985) 4337.
[13] G. Costa, A. Camus, L. Gatti, N. Marsich, *J. Organomet. Chem. 5* (1966) 568.
[14] S. H. Bertz, G. Dabbagh, *J. Am. Chem. Soc. 110* (1988) 3668.
[15] a) P. G. Edwards, R. W. Gellert, M. W. Marks, R. Bau, *J. Am. Chem. Soc. 104* (1982) 2072; b) S. I. Khan, P. G. Edwards, H. S. H. Yuan, R. Bau, *ibid. 107* (1985) 1682.
[16] a) H. Hope, D. Oram, P. P. Power, *J. Am. Chem. Soc. 106* (1984) 1149; b) M. M. Olmstead, P. P. Power, *ibid. 111* (1989) 4135.
[17] a) G. van Koten, J. G. Noltes, *J. Chem. Soc. Chem. Commun. 1972*, 940; b) G. van Koten, J. G. Noltes, *J. Organomet. Chem. 174* (1979) 367.
[18] G. van Koten, J. T. B. H. Jastrzebski, F. Muller, C. H. Stam, *J. Am. Chem. Soc. 107* (1985) 697.
[19] G. van Koten, J. T. B. H. Jastrzebski, J. G. Noltes, *J. Organomet. Chem. 140* (1977) C23.
[20] N. P. Lorenzen, *Dissertation*, Universität Hamburg 1989.
[21] a) Crystal structure analysis of **4**: $2 \times C_{32}H_{40}O_2Li_2Cu_2$, monoclinic space group $P2_1/c$, $Z = 2$, $a = 1352.8(9)$, $b = 3063.6(17)$, $c = 1662.4(17)$ pm, $\beta = 112.10(8)°$, $V = 6384(9) \times 10^6$ pm^3, ϱ_{calcd} 1.244 g cm^{-3}, crystal dimensions $0.5 \times 0.4 \times 0.6$ mm^3, 293 K, $Cu_{K\alpha}$, Enraf-Nonius CAD4, measurement range $2.25° < \theta < 66.6°$, 6370 significant reflections ($|F| > 4\sigma(|F|)$), solution of structure by direct methods (SHELXS [21b]), 674 refined parameters, $R = 0.063$, $R_w = 0.069$ ($[\sigma^2(F) + 0.0003\,F^2]^{-1}$), all non-H atoms with anisotropic temperature factors, H atoms in calculated positions with isotropic temperature factors; same in the case of the C atoms of one of the four Et_2O molecules (disorder) [22]. b) G. M. Sheldrick, *SHELXS 86. Programs for Crystal Structure Solution*, Universität Göttingen 1986.
[22] Further details of the crystal structure investigation are available on request from the Fachinformationszentrum Karlsruhe, Gesellschaft für wissenschaftlich-technische Information mbH, D-7514 Eggenstein-Leopoldshafen 2 (FRG), on quoting the depository number CSD-54288, the names of the authors, and the journal citation.
[23] P. K. Mehrotra, R. Hoffmann, *Inorg. Chem. 17* (1978) 2187.
[24] D. Thönnes, E. Weiss, *Chem. Ber. 111* (1978) 3157.
[25] M. Schlosser, V. Ladenberger, *J. Organomet. Chem. 8* (1967) 193.
[26] G. B. Kauffman, L. A. Teter, *Inorg. Synth. 7* (1963) 9.

The First Monomeric Diorgano(pyrazolyl)borane: A Nonclassical Boronium Ion in Solution?**

By *Mohamed Yalpani,* Roland Köster, Roland Boese,** and *Waldemar A. Brett*

Dedicated to Professor Günther Wilke on the occasion of his 65th birthday

Aminoboranes **I** exhibit a tendency toward self-association.[1] The tetrasubstituted members generally occur as monomers.[2] The diorgano(pyrazolyl)boranes, however, exist exclusively in the form of the unusually stable dimers **II**.[3,4] Here we report the synthesis and structure of a number of these donor–acceptor molecules which remain monomeric even in the solid state.

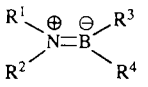

I

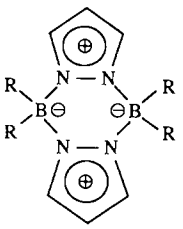

II

Reaction of the sterically very demanding 3,5-di- and 3,4,5-trisubstituted pyrazoles **1a–c** with the similarly bulky and rigid bis(9*H*-9-borabicyclo[3.3.1]nonane), $(9H\text{-9-BBN})_2$, in a 2:1 ratio in refluxing toluene for 18–24 h gave the diorgano(pyrazolyl)boranes **2a–c**, respectively, in nearly quantitative yields.

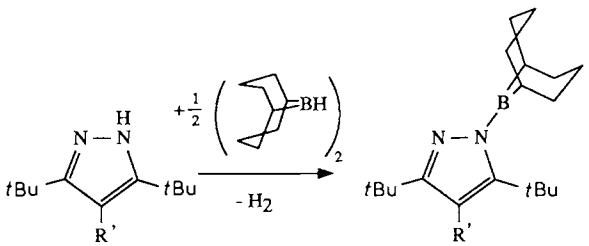

1a-c **2a-c**

a, R' = H ; **b**, R' = CH_3 ; **c**, R' = C_2H_5

Compounds **2a–c** were obtained as crystalline low-melting solids. The low-field ^{11}B NMR signals at $\delta = 63.0$ for **2a**, $\delta = 64.2$ for **2b**,[5] and $\delta = 65.3$ for **2c** strongly suggest the presence of monomeric species in solution. Both the room-temperature 200.1-MHz ^{1}H NMR and 50.3-MHz ^{13}C NMR spectra show only one set of signals for the two *t*Bu groups

[*] Prof. Dr. M. Yalpani, Prof. Dr. R. Köster
Max-Planck-Institut für Kohlenforschung
Kaiser-Wilhelm-Platz 1, D-4330 Mülheim an der Ruhr (FRG)
Dr. R. Boese, Dipl. Chem. W. A. Brett
Institut für Anorganische Chemie der Universität
Universitätsstrasse 5–7, D-4300 Essen (FRG)

[**] We are grateful to one of the referees, Prof. Dr. *P. von R. Schleyer*, for suggestions and valuable discussions.

in **2a–c** and for each of the sets of α, β, and γ carbon atoms of the 9-BBN skeleton.[6] The ^{13}C NMR spectra of **2a–c** obtained at −50 °C show no significant changes, suggesting a continued rapid exchange of the boryl group between the two nitrogen atoms of the pyrazolyl groups. Further cooling of the probe of **2a** to −80 °C resulted in partial line broadening and, at −100 °C, the ^{13}C NMR spectrum (75.5 MHz) shows resolved sharp peaks for the two *t*Bu groups and for the C 3,5 atoms of the pyrazolyl group. For the carbon atoms (2α, 4β, 2γ) of the 9-BBN skeleton only three broadened peaks are observed. This shows that, while the fluctuation of the 9-BBN group has become relatively slow, its rotation about the N–B bond remains fast. In the limiting structures shown, two separate signals for each of the two α and four β carbon atoms of the 9-BBN group should be expected.

In the ^{13}C NMR spectrum of **2b** obtained at −110 °C, the sharp lines for only one type of *t*Bu group and for the other relevant carbon atoms are retained. This suggests either the continued rapid fluctuation of the 9-BBN group or the presence of the unique intermediate structure **4**, in which the boron atom is partially and simultaneously bonded to both nitrogen atoms of the pyrazolyl group. Such a structure, as deduced from the solid-state structure of **2a** and **2c** (see below), could be stabilized by the severe spatial interactions of the 9-BBN skeleton with the neighboring *t*Bu groups.

The X-ray structure analysis of **2c**[7] (Fig. 1) shows, as inferred from its low-temperature ^{13}C NMR spectrum, that

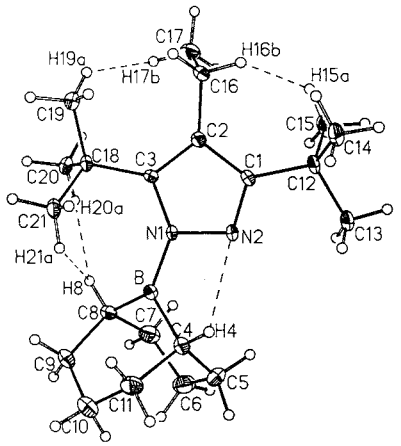

Fig. 1. Molecular structure of **2c**. Selected bond lengths [Å] and angles [°]: B-N1 1.466(4), N2-C1 1.314(3), C1-C2 1.431(4), C2-C3 1.384(3), C3-N1 1.387(4); B-N1-N2 110.3(2), N1-B-C4 119.4, N1-B-C8 128.2(2), B-N1-C3 139.4(2). Broken lines: very short intramolecular nonbonded distances.

the boron atom is bonded to only one of the nitrogen atoms of the pyrazole. The presence of severe steric interactions is clearly revealed by the extremely short H8···H20a, H8···H21a, H15a···H16b, and H17b···H19a distances (Fig. 1, broken lines). A consequence of these interactions is the distortion of the interplanar angle between the planes C1-C2-C3-N1-N2 and C4-B-C8 by 15.6° in **2a**[8] and by 44.3° in **2c** (torsion angle C8-B-N1-C3 = −19.8° in **2a** and 44.1° in **2c**), causing a severe decrease of optimal π overlap between the boron and the nitrogen atoms. As a result, the B–N bond (1.466 Å) is significantly longer than that calculated[9] and commonly found in amino(diorgano)boranes.[10]

Molecular models show that these strains can significantly decrease when the 9-BBN group is rotated by 90°, placing the vacant p_z orbital of boron orthogonal to the nonbonded electron pair of the adjacent nitrogen atoms [stucture **3** (**3'**)]. In this conformation a pendular motion of the 9-BBN group between the two equivalent structures, with partially developed B–N single bonds, is largely unhindered. This interconversion presumably proceeds via species **4** involving a nonclassical boronium ion.

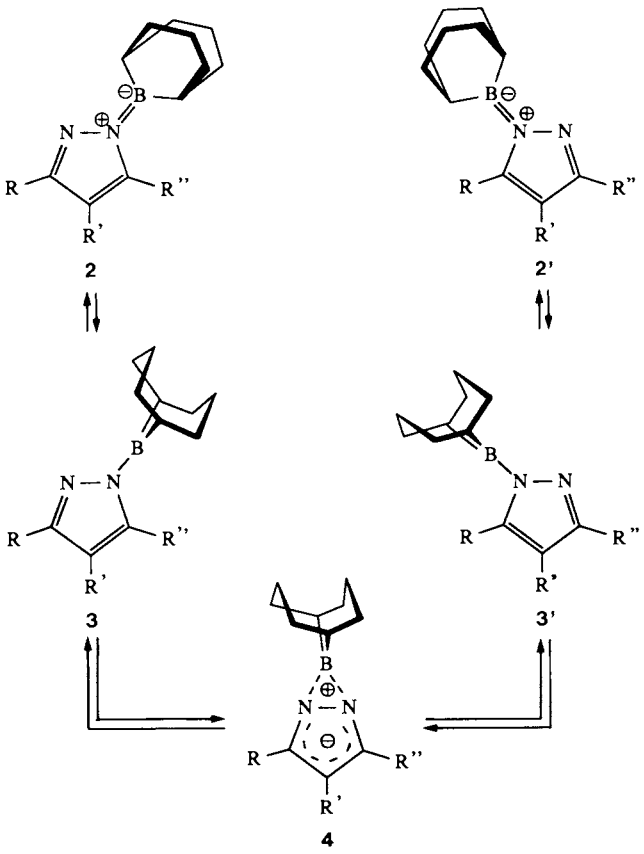

Conversion of **2** to an intermediate of type **3** should not only reduce the intramolecular steric interactions, but also decrease the dipolar character of the molecule and shift its electronic absorption maximum to lower wavelengths. Conversely, the conversion of **2** to the symmetrical intermediate **4** should increase the dipole character and shift the absorption maximum to higher wavelengths. The observed ultraviolet spectra do in fact show a progressive shift of the main absorption band to higher wavelengths as the bulkiness of the substituents increases.[11]

To estimate the viability of **4** as a relatively stable intermediate, we carried out extensive MNDO calculations[12, 13] on the limiting acyclic and the proposed intermediate cyclic structures for **2a–c**[14] and for **2d**, the analogue of **2a** with Me instead of *t*Bu groups, in order of increasing bulkiness of their substituents. The result of introducing such substituents is a progressive decrease in the calculated differences of the enthalpies of formation between the acyclic and the cyclic structures (Fig. 2). The corresponding energy barriers between the two structures increase: for **2c**, $\Delta H_f^{SCF}(\max) - \Delta H_f^{SCF}(\text{cyclic}) = 14.4\ \text{kJ mol}^{-1}$.

Even if the most crowded pyrazolylborane presently available, **2c**, should, on further experimental scrutiny, prove to possess an acyclic structure in solution, the considerations presented above suggest an enhancement in both the kinetic

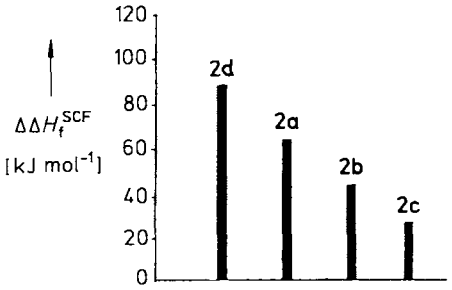

Fig. 2. Dependence of the differences in the enthalpy of formation $\Delta\Delta H_f^{SCF}$ (ΔH_f^{SCF}(cyclic) − ΔH_f^{SCF}(acyclic)) on the substituents of the pyrazolyl groups of boranes **2a–d**.

and thermodynamic stability of species **4** relative to the corresponding acyclic structure (**3**/**3'**) upon further increase in the internal crowding of the molecule. Hitherto, all attempts to introduce a substituent substantially larger than a methyl or ethyl group have failed at the β-diketone, starting material stage.

Experimental Procedure

2a: A solution of **1a** (1.5 g, 8.3 mmol) and (9*H*-9-BBN)$_2$ (1.0 g, 4.15 mmol) dissolved in 10 mL of toluene was heated to reflux for 18 h, during which time 200 mL of H_2 gas evolved. The solvent was removed in vacuo and the solid residue recrystallized from hexane by slow cooling to −78 °C. Crystalline **2a**: 2.4 g (96%). m.p. 89–90 °C. MS: *m/z* 300 ($M^{\oplus}$, B_1, 90%), 285 (45), 271 (45), 257 (65), 243 (100). ^{11}B NMR (64.2 MHz, $CDCl_3$): δ = 63.1 ($h_{1/2}$ = 350 Hz). ^{1}H NMR (200.1 MHz, $CDCl_3$): δ = 6.09 (s, 1H), 2.33 (br, 2H), 1.88 (m, 12H), 1.26 (s, 18H). ^{13}C NMR (50.3 MHz, $CDCl_3$, *T* = 311 K): δ = 162.8 (s, 2C), 106.5 (d, 1C), 33.6 (t, 4C), 30.5 (q, 6C), 30.0 (s, 2C), 28.5 (br., d, 2C), 22.8 (t, 2C). ^{13}C NMR (75.5 MHz, C_7D_8, *T* = 173 K): δ = 165.1 (s, 1C), 161.9 (s, 1C), 108.0 (d, 1C), 33.9 (t, 4C), 32.8 (s, 1C), 32.5 (s, 1C), 31.4 (q, 3C), 29.9 (q, 3C), 28.4 (br., d, 2C), 23.5 (t, 2C).

2b: (9*H*-9-BBN)$_2$ (0.53 g, 2.2 mmol) and **1b** (0.84 g, 4.3 mmol) were allowed to react as above for 24 h to give 1.3 g (94%) of a colorless solid. Purified by sublimation in vacuum; m.p. 70–71 °C. MS: *m/z* = 314 ($M^{\oplus}$, B_1, 80%), 299 (20), 285 (40), 257 (100). ^{11}B NMR (64.2 MHz, $CDCl_3$). δ = 64.2 ($h_{1/2}$ = 500 Hz). ^{1}H NMR (200.1 MHz, $CDCl_3$): δ = 1.95 (s, br., 12H); 1.27 (s, 3H); 1.39 (s, 20H). ^{13}C NMR (50.3 MHz, CD_2Cl_2, *T* = 311 K): δ = 157.4 (s, 2C), 115.8 (s, 1C), 33.8 (t, 4C), 32.9 (s, 2C), 30.1 (br., d, 2C), 29.9 (q, 6C), 22.8 (t, 2C), 12.7 (q, 1C). ^{13}C NMR (75.5 MHz, C_4D_8O, *T* = 163 K): δ = 158.5 (s, 2C), 117.3 (s, 1C), 34.7 (t, 4C), 33.9 (s, 2C), 31.2 (d, 2C), 30.3 (q, 6C), 24.0 (t, 2C), 13.6 (q, 1C).

2c: (9-H-9-BBN)$_2$ (0.84 g, 3.4 mmol) and **1c** (1.36 g, 6.5 mmol) were allowed to react as above for 24 h to give 1.9 g (88%) of a colorless solid. Purified by sublimation in vacuum; m.p. 82–83 °C. MS: *m/z* = 328 ($M^{\oplus}$, B_1, 100%), 285 (65), 271 (85), 245 (85), 232 (90). ^{11}B NMR (64.2 MHz, $CDCl_3$): δ = 65.3 ($h_{1/2}$ = 550 Hz). ^{1}H NMR (200.1 MHz, $CDCl_3$): δ = 2.67 (q, 2H), 1.95 (br., 2H), 1.88 (m, 12H), 1.36 (s, 18H), 1.14 (t, 3H). ^{13}C NMR (50.3 MHz, $CDCl_3$, *T* = 311 K): δ = 157.9 (s, 2C), 122.3 (s, 1C), 33.8 (t, 4C), 33.2 (s, 2C), 30.8 (q, 6C), 30.0 (br., d, 2C), 22.8 (t, 2C), 17.8 (t, 1C), 16.5 (q, 1C).

Received: October 2, 1989;
revised: December 14, 1989 [Z 3571 IE]
German version: *Angew. Chem. 102* (1990) 318

CAS Registry numbers:
1a, 1132-14-5; **1b**, 18712-47-5; **1c**, 125281-21-2; **2a**, 125303-72-2; **2b**, 125281-22-3; **2c**, 125281-23-4; (9*H*-9-BBN)$_2$, 21205-91-4.

[1] K. Beeker in: *Gmelin Handbuch der Anorganischen Chemie, 22. Ergänzungswerk, Borverbindungen, Teil 4*, Springer, Berlin 1975, p. 99ff.
[2] A. Meller in: *Gmelin Handbook of Inorganic Chemistry, B 3rd Suppl. Vol. 3, Boron Compounds*, Springer, Berlin 1988, p. 148.
[3] K. Niedenzu in J. F. Liebmann, A. Greenberg (Eds.): *Molecular Structure and Energetics, Vol. 5*, VCH Verlagsgesellschaft, Weinheim 1988, p. 357.
[4] Monomeric diamino(pyrazolyl)boranes of the type $PzB(NR_2)_2$ are known [F. Alam, K. Niedenzu, *J. Organomet. Chem. 243* (1983) 19]; in these, however, the participation of lone-pair electrons of the three neighboring nitrogen atoms in π bonding with the boron atom largely eliminates the Lewis acidity of the latter.
[5] B. Wrackmeyer, R. Köster in: *Houben-Weyl-Müller, Methoden der Organischen Chemie, Vol. XIII/3c*, 4th ed., Thieme, Stuttgart 1984, p. 493.
[6] M. Yalpani, R. Boese, R. Köster, *Chem. Ber. 122* (1989) 19.
[7] **2c**: Monoclinic $P2_1/n$, a = 9.698(2), b = 23.753(4), c = 9.869(2) Å, β = 118.55°, V = 1996.8(7) Å^3, Z = 4, ϱ_{calcd} = 1.092 g cm^{-3}, μ = 0.06 mm^{-1}, $Mo_{K\alpha}$ radiation (graphite monochromator), 3–50° in 2Θ, 3532 unique intensities, 2664 observed [$(F_0 \geq 4\sigma(F))$], R = 0.059, R_w = 0.065, 257 refined parameter, T = 115 K. Further information on the crystal structure investigation is available on request from the Fachinformationszentrum Karlsruhe, Gesellschaft für wissenschaftlich-technische Information mbH, D-7514 Eggenstein-Leopoldshafen 2 (FRG), on quoting the depository number CSD-320069, the names of the authors, and the journal citation.
[8] M. Yalpani, R. Köster, R. Boese, unpublished.
[9] The calculated B–N bond length in Me_2NBMe_2 is 1.422 Å: M. J. S. Dewar, M. L. McLee, *J. Am. Chem. Soc. 99* (1977) 5231.
[10] For Me_2NBMe_2 the observed B–N bond length is 1.40 and 1.43 Å for the two independent molecules found in the crystal: J. Bullen, N. H. Clark, *J. Chem. Soc. A 1977*, 992.
[11] **2d**, λ_{max} = 220 ($\varepsilon = 1.5 \times 10^3$); **2a**, λ_{max} = 240 (3.1×10^3); **2b** = **2c**, λ_{max} = 255 nm (2.8×10^3).
[12] Program MOPAC, Version 3.12, QCPE No 455.
[13] The version of this manuscript submitted on October 10, 1989 also included an MNDO calculation for the hypothetical unsubstituted parent compound of **4**. The results led to an intermediate (activated complex) structure with C_s geometry (interplanar N_2B/N_2C_3 angle 37.1°) with bond lengths and energies of similar magnitudes as are reported by *Schleyer* et al. [15] using ab initio methods. Since our results evoked the criticism of one of the referees, who insisted on a C_{2v} geometry, we omitted their discussion in the present version of this communication. Finally, since the IGLO NMR calculations in [15] do not take account of the severe intermolecular interactions present in the real molecules **2a–c**, their relevance to the values actually found is open to question.
[14] The calculated structural data (bond distances and angles) are in good agreement with the experimental values found by X-ray diffraction.
[15] P. von R. Schleyer, M. Bühl, *Angew. Chem. 102* (1990) 320; *Angew. Chem. Int. Ed. Engl. 29* (1990) 304.

On the Nature of Pyrazolylborane. An Ab Initio/IGLO/NMR Study**

By *Paul von Ragué Schleyer** and *Michael Bühl*

Dedicated to Professor Dr. Günther Wilke on the occasion of his 65th birthday

As described in the preceding communication by *Yalpani* et al., diorgano(pyrazolyl)boranes substituted with bulky groups undergo degenerate fluxional isomerization in solution.[1] Although the available crystal structures show the BR_2 group to be classically bonded to a single nitrogen (but with varying degrees of twist), the possibility was considered that a symmetrical structure might be present in solution. This species would involve simultaneous bonding between the boron and both nitrogens. We were intrigued by this novel system, and also by the possibility of using the combined ab initio/IGLO/NMR chemical shift method[2, 3] to probe the nature of the highly substituted species in solution. This new combination of methods, which involves comparison of chemical shifts calculated for several structural models with experimental data, is quite successful for the elucidation of structural problems.[3]

We calculated the structural parameters of **1–3**, three basic forms of the parent pyrazolylborane, at reasonably sophisticated ab initio levels.[4] The geometries were optimized with the polarized split valence 6-31G* basis set; key parameters are included in Figure 1. One set of single point

[*] Prof. P. von R. Schleyer, Dipl.Chem. M. Bühl
Institut für Organische Chemie der Universität Erlangen-Nürnberg
Henkestrasse 42, D-8520 Erlangen (FRG)

[**] This work was supported by the Deutsche Forschungsgemeinschaft, the Fonds der Chemischen Industrie, Convex Computer Incorporated and the Volkswagenstiftung. We thank the Kernforschungsanstalt Jülich for a grant of computer time, and are indebted to Prof. *W. Kutzelnigg* and his group for the development of the IGLO program. *M. Schindler* for the Convex version, and *U. Fleischer* for discussions. We thank Prof. *Yalpani* and his associates for discussions and for additional experimental information.

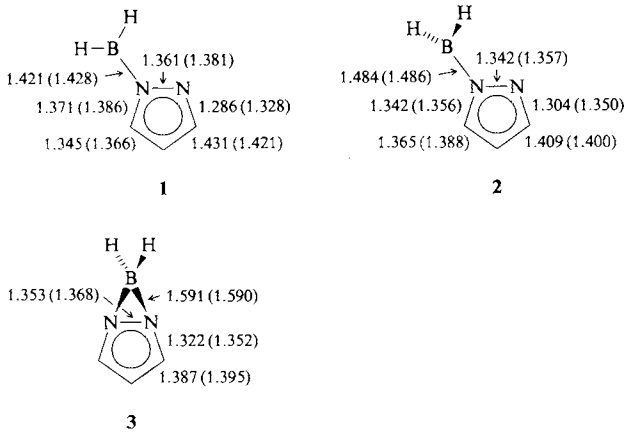

Fig. 1. The 6-31G* optimized geometries of **1**–**3** (C_s symmetry). The MP2(FU)/6-31G* parameters are given in parentheses.

energies were obtained with a larger basis set, 6-31+G*, which adds a set of diffuse s and p functions on the non-hydrogen atoms, and includes electron correlation at the second order Møller-Plesset (MP2) level using the frozen core (FC) approximation. Electron correlation favors the bridged structure (**3**) preferentially and lowers its relative energy below that of **2** (Table 1). The effect of correlation results from the more delocalized character of the bonding in **3** with its three-membered ring. Consequently, **1**–**3** were reoptimized at the MP2(FU)/6-31G* correlated level (FU = full). This changed the geometries only slightly (see Fig. 1, MP2 values are given in parentheses). Our final relative energies (Table 1) include the zero point (ZPE) corrections, calculated at 6-31G*. At MP2(FU)/6-31G*//MP2(FU)/6-31G*+ZPE(6-31G*), **3** lies 12.4 kcal mol^{-1} above **1** and the energy of **2** is a little higher (18.1 kcal mol^{-1}).

Frequency calculations at 6-31G* indicate both **1** and **3** to be minima. Transition state **2** is involved in BH_2 rotation, while **3** is an intermediate in the interconversion between **1** and its degenerate counterpart. The barrier we calculate for the parent species (our best value is at least 12.4 kcal/mol) is in line with the experimental observations on the more crowded derivatives in solution.[1] The bulky substituents lower the barrier and, as indicated from the crystal structures, twist the borane moieties from the preferred coplanar arrangement (**1**) to intermediate conformations tending towards **2**. The geometries shown in **1** and **2** are in reasonable agreement with the X-ray data,[1] when one takes the expected repulsions due to the substituents into account.

Table 1. Absolute [a] and relative [b] energies for **1**–**3**.

Level of theory	**1** (C_s, planar)	**2** (C_s, perpend.)	**3** (C_s, bridged)
6-31G*//6-31G*	250.08825 (0.0)	250.05479 (21.0)	250.04713 (25.8)
6-31+G*//6-31G*	250.09526 (0.0)	250.06238 (20.6)	250.05336 (26.3)
MP2(FC)/6-31+G*//6-31G*	250.87806 (0.0)	250.84647 (19.8)	250.85594 (13.9)
MP2(FU)/6-31G*//6-31G*	250.89061 (0.0)	250.85815 (20.4)	250.87280 (13.0)
MP2(FU)/6-31G*//MP2(FU)/6-31G*	250.89375 (0.0)	250.86200 (19.9)	250.87280 (13.1)
ZPE(6-31G*) [c]	49.8	48.0	49.1
Final [d]	0.0	18.1	12.4

[a] In a.u. [b] In parentheses, kcal mol^{-1}. [c] Zero point energy, kcal mol^{-1}, scaled by 0.89 as recommended in reference [4]. [d] Relative energies in kcal mol^{-1} at MP2(FU)/6-31G*+ZPE.

We now address the two principal questions which were posed by the experimental results, but remained unanswered. Even though **3** is inherently less stable than **1**, could it be possible that the bulky substituents result in a preference for the symmetrical form in solution? If this symmetrical form be present, what is its electronic structure? This second question can be answered by examining an ab initio wave function, but the calculated geometry (see **3**) also is revealing. Since the C–C and C–N bond lengths in the pyrazole ring in **3** have about the averaged values of those in **1** and **2**, there is no indication of any significant change in the basic 6π aromatic character of the pyrazole ring. The B–N bond lengths in **3**, 1.590 Å at 6-31G* (the MP2/6-31G* lengths are nearly the same), are about 0.2 Å longer than the single B–N distance in **2**, but are ca. 0.1 Å shorter than the dative[5] N → B bond length, 1.690 Å, calculated at the same level for H_3NBH_3.[4] Hence, the geometry of **3** indicates a classical three-membered ring arrangement. When the B–N–N angle is decreased, the nitrogen lone pair electrons in **2** interact with the vacant p-orbital on boron and a three-membered ring structure for **3** results.

Natural population analysis[6] confirms this picture. As expected, B–N bond order (0.88) is highest in **1**, because of the double bond character. The partial ionic nature of the bonding reduces the bond order, as calculated using *Wiberg*'s definition.[7] The B–N bond order of 0.71 in **2** represents the value for a single B–N bond given by this method of analysis. The B–N bond order of 0.54 in **3** is only slightly smaller despite the three-membered ring structure and partial dative character. The natural charge[6] on boron is largest in **2** (+0.81); the lower value +0.64 in **1** results from the π back donation from the ring nitrogen to boron. The boron charge (+0.49) in **3** is lowest of all. Note that the sign is positive, despite the formal negative charge which one would write classically for a tetravalent borate ion. This is general behavior. When the atoms involved differ in electronegativity (as do B and N in the present case), the formal charges which satisfy Lewis octet requirements are not consistent with charges derived from quantum mechanics wave functions.[8] (See below for an example.)

The IGLO ^{11}B-NMR chemical shifts, calculated for **1**–**3** using the MP2/6-31G* geometries, showed large variations with structure. These IGLO calculations employed a double zeta (DZ) basis set for most of the atoms,[2] but a more sophisticated triple zeta + polarization basis for boron. This better description of the nucleus in question employing "locally dense basis sets" has been proposed by *Chestnut*.[9] While perfect agreement with the experimental values obtained on substituted derivatives cannot be expected, the general accord is pleasing. Thus, $\delta(^{11}B)$ (vs. $BF_3 \cdot OEt_2$) for planar **1** (47.6) and for perpendicular **2** (62.0) may be compared with the values (63.1, 64.2) found experimentally for twisted structures.

The IGLO ^{11}B-NMR chemical shift calculated for **3**, $\delta = 19.3$, effectively rules out symmetrically bridged structures as candidates for the species present in solution. None of the experimentally observed ^{11}B-NMR chemical shifts[1] approach this IGLO value. However, there is good agreement between the IGLO result for **3** and that for numerous other tetracoordinated boron analogues which involve the simultaneous attachment of two nitrogen substituents to boron.[10] A simple experimental example, $[(CH_3)_2B(NH_3)_2]Br$ with $\delta(^{11}B) = 13.9$,[10, 11] is representative. The IGLO $\delta(^{11}B)$ value is 11.5 for $[(CH_3)_2B(NH_3)_2]^{\oplus}$ using the 6-31G*-optimized geometry. The computed B–N length is 1.657 Å

 © VCH Verlagsgesellschaft mbH, D-6940 Weinheim, 1990 0570-0833/90/0303-0305 $ 02.50/0

and the Wiberg bond order is 0.67. The natural charges are +0.87 on B and −1.00 on N (vide supra, note signs).

We conclude that the diorgano(pyrazolyl)boranes have similar geometries in solution and in the solid phase. Although symmetrical structures like **3** are involved in the degenerate rearrangement, they are not present in significant concentration in solution. Both the electronic structure and the ^{11}B-NMR chemical shift of **3** are normal.[12] That is, the pyrazole ring in the hypothetical **3** retains its 6π aromatic character and the B–N bonding is intermediate between single B–N and dative N → B arrangements.

Received: December 20, 1989 [Z 3695 IE]
German version: *Angew. Chem. 102* (1990) 320.

CAS Registry number:
pyrazolylborane, 62427-83-2.

[1] M. Yalpani, R. Köster, R. Boese, W. A. Brett, *Angew. Chem. 102* (1990) 318; *Angew. Chem. Int. Ed. Engl. 29* (1990) 302, the authors did extensive MNDO calculations; M. Yalpani, private communication.
[2] W. Kutzelnigg, *Isr. J. Chem. 19* (1980) 193. M. Schindler, W. Kutzelnigg, *J. Chem. Phys. 76* (1982) 1919. Review: W. Kutzelnigg, U. Fleischer, M. Schindler, *NMR Basic Princ. Prog.*, in press.
[3] See, e.g. applications to carbocations: a) M. Schindler, *J. Am. Chem. Soc. 109* (1987) 1020; b) M. Bremer, P. von R. Schleyer, K. Schötz, M. Kausch, M. Schindler, *Angew. Chem. 99* (1987) 795; *Angew. Chem. Int. Ed. Engl. 26* (1987) 761; c) P. von R. Schleyer, K. E. Laidig, K. B. Wiberg, M. Saunders, M. Schindler, *J. Am. Chem. Soc. 110* (1988) 300; d) M. Saunders, K. E. Laidig, K. B. Wiberg, P. von R. Schleyer, *ibid. 110* (1988) 7652; e) P. von R. Schleyer, J. W. de M. Carneiro, W. Koch, K. Raghavachari, *ibid. 111* (1989) 5475; f) M. Bremer, P. von R. Schleyer, *ibid. 111* (1989) 1147; g) M. Bremer, K. Schötz, P. von R. Schleyer, U. Fleischer, M. Schindler, W. Kutzelnigg, P. Pulay, *Angew. Chem. 101* (1989) 1063; *Angew. Chem. Int. Ed. Engl. 28* (1989) 1042; h) P. von R. Schleyer, W. Koch, B. Liu, U. Fleischer, *J. Chem. Soc. Chem. Commun. 1989*, 1089; Application to boron NMR chemical shifts: P. von R. Schleyer, M. Bühl, U. Fleischer, W. Koch, *Inorg. Chem. 29* (1990) 153.
[4] The Gaussian series of programs with standard procedures and basis sets were employed. See W. J. Hehre, A. Radom, P. von R. Schleyer, and J. A. Pople: *Ab Initio Molecular Orbital Theory*, Wiley-Interscience, New York 1986.
[5] A. Haaland, *Angew. Chem. 101* (1989) 1017; *Angew. Chem. Int. Ed. Engl. 28* (1989) 992.
[6] Review: A. E. Reed, L. A. Curtis, F. Weinhold, *Chem. Rev. 88* (1988) 899.
[7] K. Wiberg, *Tetrahedron 24* (1968) 1083.
[8] A. Greenberg, R. Winkler, B. L. Smith, J. Liebman, *J. Chem. Educ. 59* (1982) 367.
[9] D. B. Chestnut, K. D. Moore, *J. Comput. Chem. 10* (1989) 648.
[10] H. Nöth, B. Wrackmayer: *Nuclear Magnetic Resonance Spectroscopy of Boron Compounds*, Springer, Berlin 1978.
[11] K. Maier, *Dissertation*, Universität Marburg 1971.
[12] We also examined two planar symmetrially-bridged C_{2v} structures like **3**, with perpendicular and with coplanar BH_2 groups. The latter was 85 kcal mol^{-1} higher in energy than **1** at 6-31G*//6-31G* and possessed three imaginary frequencies. The perpendicular form was a transition state for the degenerate interconversion of **3**, and was 2.4 kcal mol higher in energy than the latter at our final level.

Switching Reaction Mechanism by Monolayer Compression: An Ester Hydrolysis

By *Jamil Ahmad** and *Kenneth Brian Astin**

Monolayers provide a novel opportunity to examine the reactivity of molecules constrained to a plane, where the geometrical requirements of transition states may be inferred from the reactivity of films at varying surface pressures (or areas per molecule). The method is suitable for the investigation of neighboring group and proximity effects.[1–3]

[*] Prof. Dr. J. Ahmad, Prof. Dr. K. B. Astin,
Department of Chemistry, University of Bahrain
P.O. Box 32038, Isa Town (Bahrain)

For example, the rates of the acid-catalyzed cyclization of nerol[1] and the acid-catalyzed dehydration of 1,1-diphenyl-1-octadecanol[2] are strongly affected by surface pressure changes, since these reactions require the involvement of remote functionalities, i.e. the remote double bond in nerol and the β-hydrogens in the 1,1-diphenyl-1-octadecanol, for reaction. High surface pressures disfavor this participation and the rate is correspondingly lowered. By contrast, reactions taking place at a single center, e.g. the chromic acid oxidation of 1-phenyl-1-hexadecanol[3] and the base-catalyzed hydrolysis of an octadecyl ester,[4] are not significantly affected by surface pressure changes. We report here the effect of surface pressure on the mechanism of the acid-catalyzed hydrolysis of 1-phenylhexadecyl ethanoate **1** to 1-phenyl-1-hexadecanol **2** in monolayers at an air/sulfuric acid interface.

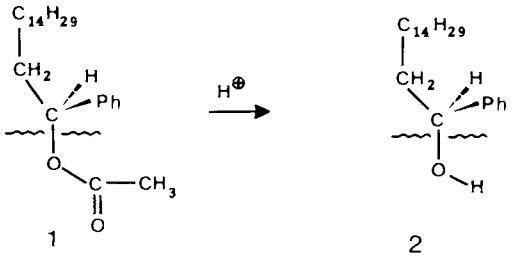

1 2

The investigation of reactions in monolayers requires that the substrate forms films stable within the time scale of the experiment. The monolayer film of 1-phenylhexadecyl ethanoate amply satisfies this requirement. Compressed films ($\pi > 15.0$ mN m^{-1}) over water produce negligible reduction in π (< 5%) over a 30 min period. The surface pressure-area (π-A) isotherm (Fig. 1) is characteristic of amphipatic systems; the limiting area (obtained by extrapolating the π-A isotherm to $\pi = 0$) of 0.85 nm^2 is larger than for simple alkyl chains such as octadecanoic acid, where the limiting area is 0.21 nm^2,[5] because of the phenyl group inhibiting further compression. 1,1-Diphenyl-1-octadecanol has a limiting area of 0.72 nm^2.[2] Interestingly, the surface pressure-area isotherm in Figure 1 exhibits a just discernible plateau region

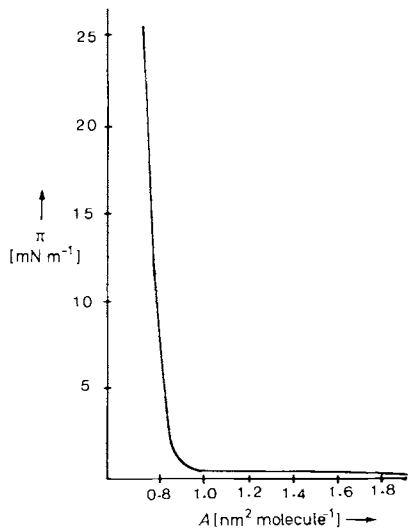

Fig. 1. π-A isotherm of 1-phenylhexadecyl acetate at 25 °C over water, using a Wilhelmy balance (initial film area 300 cm^2, final area 70 cm^2, compression rate 24 cm^2 min^{-1}).

suggesting a liquid type film between ca. 0.9 nm^2 and ca. 1.6 nm^2. In this film type the hydrophobic chains are believed to be interacting and orientated away from the surface, but are less ordered than in the solid type film observed at higher π. The gaseous type film at larger area/molecule consists of molecules which are essentially independent.[5]

The experiments were performed on a modified Langmuir trough, consisting of a thermostated multicompartment PTFE trough with Wilhelmy plate balance.[2, 6] The films were formed by spreading a calculated volume (ca. 2–20 μL) of a hexane solution of the ester onto a trough area to give the desired area/molecule. After a given time at constant area (surface pressure in the compressed films also remained essentially constant since the major product of the reaction 1-phenyl-1-hexadecanol is also surface active with a limiting area of ca. 0.55 nm^2[3]), the monolayer was swept into a reservoir containing hexane, where the reaction mixture dissolved. Typical recoveries exceeded 90%, even at the longest reaction times studied.

Despite the low qualities of material in the monolayer film the reaction mixture could be readily analyzed by HPLC using a Supercosil LC-8 5 μm column. Both ester and products were detected in the UV at 210 nm at 0.02 absorbance units full scale (AUFS): the peaks were integrated electronically and the concentrations determined using molar response factors calculated from standard solutions. The kinetics of hydrolysis were pseudo-first-order and a plot of the rate constant k against concentration of H_2SO_4 is shown in Figure 2.

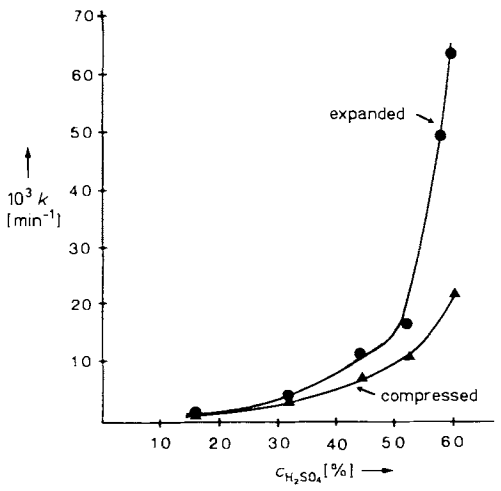

Fig. 2. Plot of the pseudo-first-order rate constant versus sulfuric acid concentration [%] for compressed (0.8 nm^2 $molecule^{-1}$) and expanded (3.8 nm^2 $molecule^{-1}$) film types at 25.0 ± 0.1 °C.

The dramatic difference in behavior between compressed (0.8 nm^2 $molecule^{-1}$) and expanded (3.8 nm^2 $molecule^{-1}$) films is apparent from the plot. At low acid concentrations the rates of hydrolysis are essentially independent of film type. This behavior is typical for reactions taking place at a single center, i.e. one not involving proximate or neighboring functionalities.[3, 4] Increasing the acid concentration produces enhanced reaction rates in the expanded films; this is strongly suggestive of the incursion of a new mechanistic pathway.[7] If the increased reactivity of the expanded film had been due to a neighboring group effect,[1, 2] parallel curves would have been expected in Figure 2 since the enhanced reactivity of the expanded film would then be evident at all acid concentrations.

The two most probable acid-catalyzed mechanisms[8] are outlined in Scheme 1. The bimolecular $A_{AC}2$ mechanism is the one generally observed in dilute acid solution and we suggest the major pathway in the compressed film. At higher acid concentration the unimolecular $A_{AL}1$ mechanism involving alkyl-oxygen fission and the formation of the secondary 1-phenylhexadecyl cation becomes competitive. The increased curvature of the compressed film rate profile could reflect imperfection in the film, allowing a component of the $A_{AL}1$ mechanism to take place even in the compressed film. An alternative unimolecular mechanism $A_{AC}1$ involving acyl-oxygen fission is considered highly unlikely since it would involve the formation of an acylium ion and is only observed at high acid concentrations (> 90% H_2SO_4).[9]

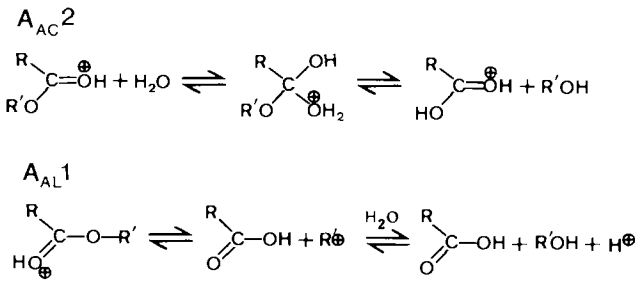

Scheme 1.

This analysis is supported by the elegant work of *Yates*[9] on bulk phase ethanoate ester hydrolysis in aqueous sulfuric acid. With Type II ethanoates (i.e. those with secondary alkyl, benzyl or allyl residues), increasing acid concentration affords an initial rate increase followed by a drop, reflecting the $A_{AC}2$ mechanism, catalyzed by acid but requiring the less available free H_2O as a nucleophile. This is followed by a further dramatic rate increase as the $A_{AL}1$ mechanism takes over; this mechanism does not require the nucleophilic participation of water.

The observation of small quantities (maximally 8% at 60% H_2SO_4 usually 3–6%) of the alkene product[10] 1-phenyl-1-hexadecene, from the reaction of expanded films at higher acid concentrations is, unfortunately, not unequivocal support for the $A_{AL}1$ mechanism, since the alkene can also be formed from the dehydration of the alcohol product **1**.[10] Control experiments with the expanded alcohol over sulfuric acid gave similar, although slightly lower, amounts of alkene than the corresponding ester films.

To obtain further insight into the mechanism, the reactivity of the ester film over 58% H_2SO_4 was studied as a function of area/molecule, (Fig. 3). The sigmoid nature of the curve is reminiscent of that obtained for the acid-catalyzed dehydration of 1,1-diphenyl-1-octadecanol;[2] however, in the present study the rate increase is less dramatic and occurs at a smaller area/molecule (1.5 instead of 2.5 nm^2).[2]

This suggests that a gaseous film type is not required for the ester hydrolysis and that the $A_{AL}1$ mechanism can occur at relatively small areas/molecule. It is clear that neighboring group effects are inoperative here and that the absence of the $A_{AL}1$ mechanism in the compressed film can be traced to a simpler geometric factor, namely, that the alkyl group is forced out of the subphase at high surface pressures and the alkyl–oxygen fission and concomitant cation ion formation thereby disfavored. Only a modest reduction in surface pres-

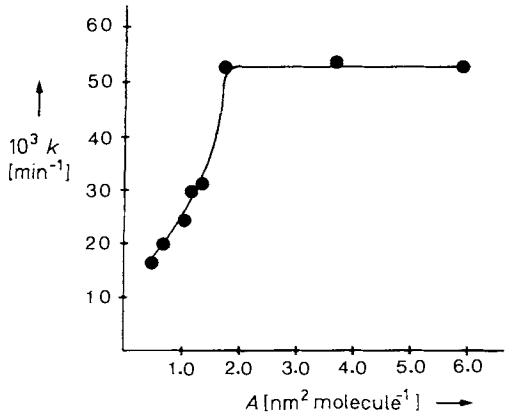

Fig. 3. Plot of the pseudo-first-order rate constant versus area/molecule over 58% sulfuric acid at 25.0 ± 0.1 °C.

sure is required to allow the alkyl–oxygen bond into the subphase where fission and solvation of the cation can take place.

Received: October 19, 1989 [Z 3597 IE]
German version: *Angew. Chem. 102* (1990) 337

CAS Registry number:
125520-15-2.

[1] J. Ahmad, K. B. Astin, *J. Am. Chem. Soc. 108* (1986) 7434.
[2] J. Ahmad, K. B. Astin, *J. Am. Chem. Soc. 110* (1988) 8175.
[3] J. Ahmad, K. B. Astin, *Langmuir 4* (1988) 780.
[4] S. J. Valenty, *J. Am. Chem. Soc. 101* (1979) 1.
[5] A. W. Adamson: *Physical Chemistry of Surfaces;* Wiley, New York 1982, pp. 124–133.
[6] P. Fromherz, *Rev. Sci. Instrum. 46* (1975) 1380.
[7] The shape of the plot is notably similar to the classic plot of acetolysis rates of *threo*-3-aryl-2-butyl brosylates against σ (Hammett): H. C. Brown, C. J. Kim, C. J. Lancelot, P. von R. Schleyer, *J. Am. Chem. Soc. 92* (1970) 5244. This plot also results from two distinct mechanistic pathways.
[8] The mechanisms are schematic and do not show initial and final proton transfer that may occur in the intermediates.
[9] K. Yates, *Acc. Chem. Res. 4* (1971) 136.
[10] This alkene is observed as a single peak on HPLC and capillary GC and exhibits the same chromatographic behavior as an authentic sample of (*Z*)-1-phenyl-1-hexadecene.

[*n*BuLi · LiO*t*Bu]$_4$, Solid-State Structure of an *n*-Butyllithium–Lithium *tert*-Butoxide Complex **

By *Michael Marsch, Klaus Harms, Lubomir Lochmann,* and *Gernot Boche* *

Dedicated to Professor Paul von Ragué Schleyer on the occasion of his 60th birthday

Complexes [RLi · LiOR] formed from organolithium compounds RLi and lithium alkoxides LiOR, which are expected to be formed, for example, during addition of RLi to an aldehyde or ketone, have long been known.[1–4] The properties of the starting materials change upon complex formation, as exemplified in the addition of *n*BuLi to a C=O[5] or C=C[6] bond. Anionic polymerization is also affected by LiOR,[7–9] and, in the presence of LiOR, organolithium compounds are less thermally stable.[10, 11]

During NMR spectroscopic investigations of *n*BuLi in the presence of lithium *n*-butoxide or lithium *tert*-butoxide in THF, complexes of structure $n\mathrm{Bu}_x\mathrm{Li}_4(\mathrm{OBu})_{4-x}$ ($x = 1-4$) were observed, whereby one or two LiOR ligands acted to stabilize the structure.[4] The complex *n*BuLi · LiO*t*Bu[2] forms a tetramer, **1**, in benzene (degree of aggregation $\alpha = 3.7$).[12]

$[CH_3(CH_2)_3Li \cdot LiOC(CH_3)_3]_4$

1

A Weissenberg photograph (of little informative value)[13] has been recorded for *n*BuLi · LiO*t*Bu.[2] Here we report on the X-ray structure analysis of this compound, which crystallizes from hexane as tetramer **1** (Fig. 1). The elucidation of its structure interested us because solid-state structures are unknown either for a complex of the type [RM · MOR'] (M = Li, Na, K) or for *n*BuLi and LiO*t*Bu.

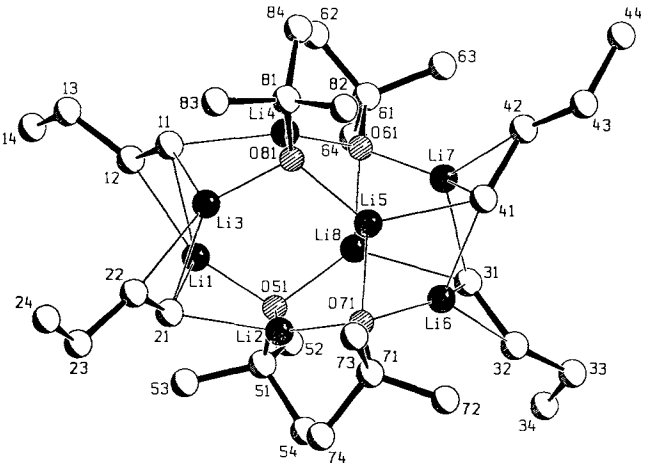

Fig. 1. Molecular structure [14] of **1** (hydrogen atoms omitted). Important bond lengths and distances [pm]: Li1-C11 215(1), Li1-C12 236(1), Li1-C21 219(1), Li1-O51 185(1), Li1-H121 197(5), Li1-H122 280(5), Li3-C21 215(1), Li3-C22 234(1), Li3-C11 222(1), Li3-O81 185(1), Li3-H221 264(5), Li3-H222 213(5), Li6-C31 217(1), Li6-C32 234(1), Li6-C41 225(1), Li6-O71 182(1), Li6-H321 252(5), Li6-H322 203(6), Li7-C41 215(1), Li7-C42 236(1), Li7-C31 226(1), Li7-O61 184(1), Li7-H421 208(5), Li7-H422 256(5), Li2-C21 218(1), Li2-O51 190(1), Li2-O71 186(1), Li4-C11 221(1), Li4-O61 187(1), Li4-O81 192(1), Li5-C41 225(1), Li5-O71 189(1), Li5-O81 186(1), Li8-C31 222(1), Li8-O51 186(1), Li8-O61 192(1).

As revealed by Figure 1, two kinds of differently bonded Li atoms are present. Li1, Li3, Li6, and Li7 are each bonded to two *n*Bu α-C atoms (e.g., for Li3: Li3-C11 222(1) pm; Li3-C21 215(1) pm) and one O atom (Li3-O81 185(1) pm). Unusual are the short distances to the *n*Bu β-C atoms (Li3-C22 234(1) pm) as well as to one of the two β-hydrogen atoms (Li3-H222 213(5) pm; Li3-H221 264(5) pm). Figure 2 shows the typical structure of the *n*-butyl groups.

The β-H atoms H222 and H221, which are tilted toward Li3, are reminiscent of agostic hydrogen atoms.[20] The $^6Li^1H$ HOESY NMR spectrum of $(n\mathrm{BuLi})_4$ in THF reveals

[*] Prof. Dr. G. Boche, M. Marsch, Dr. Klaus Harms
Fachbereich Chemie der Universität
Hans-Meerwein-Strasse, D-3550 Marburg (FRG)
Dr. L. Lochmann
Institute of Macromolecular Chemistry,
Czechoslovakian Academy of Sciences
CS-16206 Prague 6 (Czechoslovakia)

[**] This work was supported by the Deutsche Forschungsgemeinschaft. We thank Professor *C. Krüger*, Max-Planck-Institut für Kohleforschung, Mülheim-Ruhr, for helpful discussion.

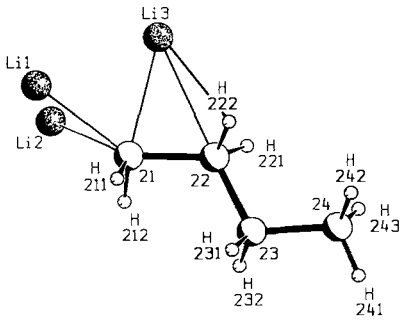

Fig. 2. Section of the crystal structure of **1**, showing the bonding of a typical *n*Bu group; bond lengths [pm]: Li1-C21 219(1), Li2-C21 218(1), Li3-C21 215(1), Li3-C22 234(1), Li3-H211 272(5), Li3-H212 300(5), Li3-H222 213(5), Li3-H221 264(5), C21-C22 151.4(9) [24].

an interaction between Li and the β-H atoms.[21] At the same time, the *n*-butyl groups were assumed to have a conformation largely corresponding to that found for **1**.[21] However, whereas the cross peaks to the β-H atoms are smaller than those to the α-H atoms in the $^6Li^1H$ HOESY spectrum of $(n\text{BuLi})_4$,[21] the Li–H distances in **1** are always smaller for the β-H atoms than for the α-H atoms (see caption to Fig. 2).

The second kind of Li, namely, Li2, Li4, Li5, and Li8, has two Li–O contacts (e.g., Li2-O71 186(1) pm and Li2-O51 190(1) pm) and only one Li–α–C contact (Li2-C21 218(1) pm), whereas the fourth coordination site of Li remains unoccupied, presumably owing to steric hindrance by the O*t*Bu groups (Fig. 1).

When RLi is mixed with Na(K,Rb,Cs)OR, superbases such as *n*BuLi + KO*t*Bu are obtained; the formation of these species, which are extremely useful synthetically, is also assumed to proceed via complexes.[22, 23] Since nothing is known about the structure of these complexes, the structure of **1** offers possible clues (although any conclusions drawn therefrom can only be speculative owing to the different sizes of Li and, e.g., K). The fourfold coordination of Li1, Li3, Li6, and Li7 might resemble the bonding of the K atoms, while the more strongly O-bonded threefold coordinated atoms Li2, Li4, Li5, and Li8 should instead correspond to the Li atoms. The formation of *n*BuK and LiO*t*Bu as well as the reaction with RH to give RK could involve such a complex.[22, 23]

Received: August 29, 1989 [Z 3526 IE]
Publication delayed at authors' request
German version: *Angew. Chem. 102* (1990) 334

[1] T. L. Brown, J. A. Ladd, G. M. Newman, *J. Organomet. Chem. 3* (1965) 1.
[2] L. Lochmann, J. Pospíšil, J. Vodňanský, J. Trekoval, D. Lím, *Collect. Czech. Chem. Comm. 30* (1965) 2187.
[3] M. Y. Darensbourg, B. Y. Kimura, G. E. Hartwell, T. L. Brown, *J. Am. Chem. Soc. 92* (1970) 1236.
[4] J. F. McGarrity, C. A. Ogle, *J. Am. Chem. Soc. 107* (1985) 1805.
[5] J. F. McGarrity, C. A. Ogle, Z. Brich, H.-R. Loosli, *J. Am. Chem. Soc. 107* (1985) 1810.
[6] L. Lochmann, R. Lukáš, D. Lím, *Collect. Czech. Chem. Commun. 37* (1972) 569.
[7] L. Lochmann, M. Rodová, J. Trekoval, *J. Polymer Sci. Polym. Chem. Ed. 12* (1974) 2091.
[8] J. E. L. Roovers, S. Bywater, *Trans. Faraday Soc. 62* (1966) 1876.
[9] H. L. Hsieh, *J. Polym. Sci. A-1 8* (1970) 533.
[10] W. H. Glaze, G. M. Adams, *J. Am. Chem. Soc. 88* (1966) 4653.
[11] R. A. Finnegan, H. W. Kutta, *J. Org. Chem. 30* (1965) 4138.
[12] V. Halaška, L. Lochmann, *Collect. Czech. Chem. Commun. 38* (1973) 1780.
[13] K. Huml, *Czech. J. Phys. B15* (1965) 699.
[14] Crystal structure data of **1**, $C_{32}H_{72}O_4Li_8$, $M = 576.44$: **1** forms monoclinic crystals, space group $P2_1/n$, $a = 11.024(6)$, $b = 23.659(9)$, $c = 16.377(18)$ Å, $\beta = 101.83(3)°$, $Z = 4$, $\varrho_{calcd} = 0.916\ g\,cm^{-3}$, $\mu(Mo_{K\alpha}) = 4.1\ cm^{-1}$. 4949 reflections are measured on an ENRAF-NONIUS CAD4 diffractometer ($Mo_{K\alpha}$ radiation, graphite monochromator, $T = -48\,°C$); 3615 of these were unique ($R_{int} = 0.016$), 2517 with $F_0 > 4\sigma(F_0)$ were considered as observed. Solution by direct methods (SHELXS-86 [15]), refinement (SHELX-76 [16]) to $R = 0.076$, $wR = 0.040$, $w = 1/\sigma^2(F_0)$; non-hydrogen atoms anisotropic; H atoms on C atoms without Li contacts were refined with fixed isotropic temperature factors at calculated positions. The positions of the H atoms on the C atoms with Li contacts (C1 and C2 of the *n*-butyl anions) were localized and refined with a common temperature factor. 446 parameters. All calculations were performed on a Micro-VAX II [17–19].
[15] G. M. Sheldrick, *SHELXS-86, Program for Crystal Structure Solution*, Göttingen 1986.
[16] G. M. Sheldrick, *SHELX-76, Program for Crystal Structure Determination*, Cambridge 1976.
[17] A. L. Spek, *Platon 89, Program for Geometrical Analysis of Crystal Structures*, Utrecht 1989.
[18] E. Keller, *SCHAKAL-88B, A FORTRAN Program for the Graphic Representation of Molecular and Crystallographic Models*, Freiburg 1988.
[19] Further details on the crystal structure investigation may be obtained from the Fachinformationszentrum Karlsruhe, Gesellschaft für wissenschaftlich-technische Information mbH, D-7514 Eggenstein-Leopoldshafen 2 (FRG), on quoting the depository number CSD-320021, the names of the authors, and the journal citation.
[20] Agostic H atoms are actually those bonded covalently to a C atom and a transition-metal atom: M. Brookhart, M. L. H. Green, *J. Organomet. Chem. 250* (1983) 395.
[21] "The conformation of the *n*-butyl group is assumed to be the most favorable energetically": W. Bauer, T. Clark, P. von R. Schleyer, *J. Am. Chem. Soc. 109* (1987) 979.
[22] a) L. Lochmann, J. Pospíšil, D. Lím, *Tetrahedron Lett. 1966*, 257; b) L. Lochmann, J. Trekoval, *Collect. Czech. Chem. Commun. 53* (1988) 76; c) L. Lochmann, *J. Organomet. Chem.*, in press.
[23] a) M. Schlosser, *J. Organomet. Chem. 8* (1967) 9; b) M. Schlosser, S. Strunk, *Tetrahedron Lett. 25* (1984) 741; c) M. Schlosser, *Pure Appl. Chem. 60* (1988) 1627.

Note added in proof (February 28, 1990): In a theoretical work (J. P. Ritchie, S. M. Bachrach, *J. Am. Chem. Soc. 109* (1987) 5909), which has only recently come to our attention the authors agreed, in the case of 1,3-dilithiocyclobutane, upon a "bond path connecting a methylenic carbon to lithium, in addition to the bond paths connecting lithium to the anionic carbons." This unexpected bond path appears to have been demonstrated experimentally for the first time in structure **1**.

Lewis-Acid-Induced Transformation of a Terminal Carbonyl Ligand: Synthesis and Structure of the Alkyne-Cluster-Analogue $[(\mu\text{-H})_3Os_3(CO)_9\{\mu_3,\eta^2\text{-}C(OBC_8H_{14})B(Cl)\}]$**

By *David P. Workman, Hai-Bin Deng,* and *Sheldon C. Shore**

Lewis acids have been shown to activate the BCO fragment of the boron-triosmium cluster $[(\mu\text{-H})_3Os_3(CO)_9(\mu_3\text{-BCO})]$ **1**[1] by electrophilic addition at its oxygen atom.[2] Reaction of **1** with $BH_3 \cdot THF$ leads to reduction of the unique carbonyl to a methylene group with formation of the vinylidene analogue $[(\mu\text{-H})_3Os_3(CO)_9(\mu_3,\eta^2\text{-}BCH_2)]$ **2**.[4] In contrast, reaction of **1** with BCl_3 leads to formation of **3**, a structurally different type of vinylidene comlex analogue[5]

[*] Prof. S. G. Shore, Dr. D. P. Workman, H.-B. Deng
Department of Chemistry
The Ohio State University
Columbus, OH 43210 (USA)

[**] This work was supported by the National Science Foundation (Grants CHE 88-00515 and CHE 84-11630). The spectroscopic data were recorded at The Ohio State University Campus Chemical Instrument Center (funded in part by NSF Grant 79-10019 and NIH Grant 1 S10 PRO145128-O1A).

$[(\mu\text{-}H)_3Os_3(CO)_9(\mu_3\text{-}CBCl_2)]$ **3**

in which the transformation is believed to occur via an intramolecular rearrangement of the boron and carbon atom positions. Such a mechanistic scheme requires halogen atom transfer from the BCl_3 to the cluster boron. We report here the first structurally characterized product formed by the electrophilically induced shift of a terminal carbonyl in a neutral carbonyl cluster.[6]

The reaction of **1** with the electrophilic reagent 9-chloro-9-borabicyclo[3.3.1]nonane (9-Cl-9-BBN),[7] provides direct evidence for such a halogen atom transfer. Electrophilic activation of the BCO unit of **1** results in a shift of the carbonyl group from a terminal position to a face capping site, leading to formation of **4** [Eq. (a)]

$$\underset{\mathbf{1}}{[(\mu\text{-}H)_3Os_3(CO)_9(\mu_3\text{-}BCO)]} + \text{9-Cl-9-BBN} \rightarrow \underset{\mathbf{4}}{[(\mu\text{-}H)_3Os_3(CO)_9\{\mu_3,\eta^2\text{-}C(OBC_8H_{14})B(Cl)\}]} \quad (a)$$

The initial step in the formation of **4** (Scheme 1) involves addition of the boron of 9-Cl-9-BBN to the oxygen of the

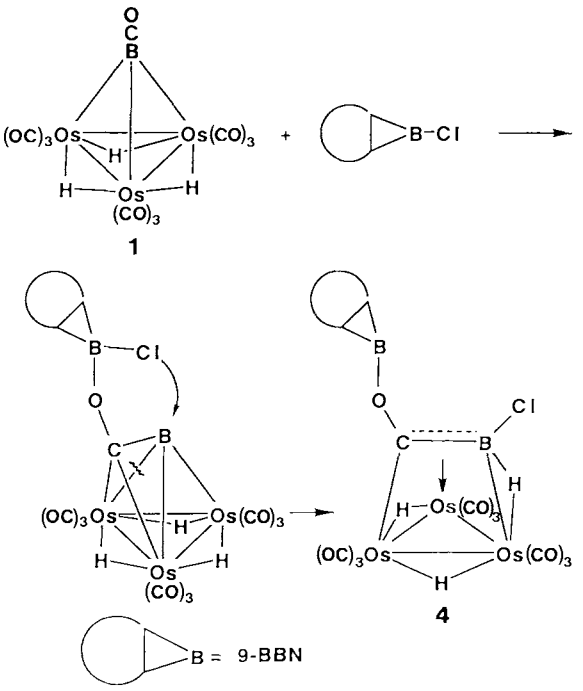

Scheme 1. Proposed mechanism for Reaction (a).

boron-bound carbonyl group in **1**.[2] The resulting reduction of the CO bond order induces a shift of the carbonyl carbon to a μ_3 position,[8] thereby exposing the boron vertex which allows the chlorine atom to transfer to it.

The molecular structure of **4** (Fig. 1) was determined by a single crystal X-ray diffraction study.[10] It consists of a triangle of osmium atoms bound to the boron and carbon atoms of a triply bridging ligand derived from the BCO unit of **1**. The carbonyl has been shifted to occupy a bridge site between two osmiums and the boron atom. The 9-BBN group is bound to the oxygen atom of the carbonyl group

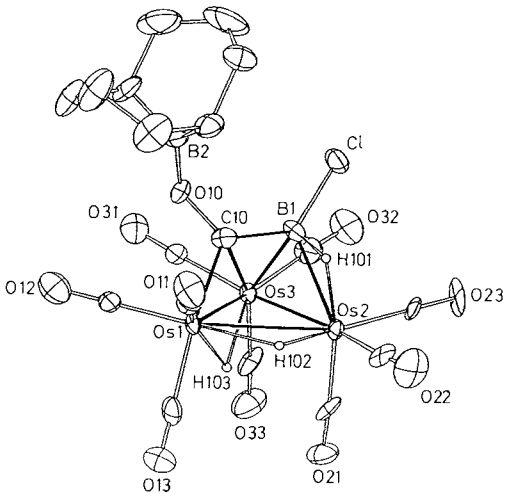

Fig. 1. Structure of **4** in the crystal (ORTEP plot with 50% probability ellipsoids). Selected distances [Å]: Os1-Os2 3.0454(6), Os1-Os3 2.8532(6), Os2-Os3 2.7974(5), Os1-C10 2.13(1), Os3-C10 2.24(2), Os2-B1 2.38(1), Os3-B1 2.36(1), B1-Cl 1.81(1), B1-C10 1.46(2), C10-O10 1.40(1), B2-O10 1.36(1).

[B2-O10 1.36(2) Å], while the chlorine atom from the 9-Cl-9-BBN unit now resides on the boron vertex, [B1-Cl 1.82(1) Å]. The C10-O10 distance of 1.40(1) Å, (single bond[12]) is larger than the corresponding distance in **1** (1.145(15) Å). The B1-C10 distance of 1.46(2) Å is comparable with the corresponding B-C distances in **1**,[1,3] **3**,[5] and in the ditungstenalkyne complex analogue $[W_2(\mu\text{-MeCB(H)Et})(CO)_4(\eta^5\text{-}C_5H_5)_2]$[11] (1.469(15) Å, 1.47(2) Å, and

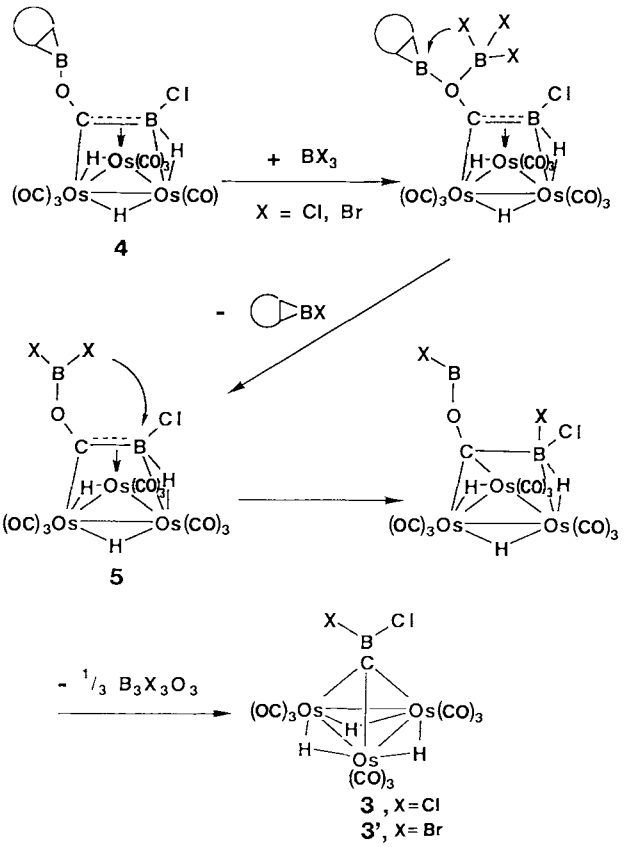

Scheme 2. **4** as model for the postulated intermediate **5** in the synthesis of **3** from **1**.

1.46(2) Å, respectively). These bonds are considered to have boron–carbon partial double bond character. They are longer than the boron–carbon double bond distance of 1.361(4) Å reported by *Paetzold* et al.,[13] but shorter than B–C single bonds (ca. 1.6 Å[14]). The "short" B–C distances found in **1**, **2**, and **3** suggest that a strong boron–carbon interaction is maintained throughout the transformation of **1** into **3**, supporting an intramolecular process.

Compound **4** is a model compound for the proposed intermediate in the transformation of **1** into **3**. The availability of only one chlorine atom in Reaction (a) halts the conversion of **1** into **3** and allows isolation of **4**. The intermediacy of **4** is revealed by treating it with BX_3 to produce **3** (X = Cl) or the mixed halo derivative **3'** (X = Br) and the boroxine $B_3X_3O_3$, (Scheme 2). This completes the conversion of **1** into **3**. Scheme 2 is based on ^{11}B-NMR studies which indicate initial formation of the 9-BBN halide, which would produce the intermediate **5** proposed for the reaction of **1** with BCl_3 when X = Cl.

Compound **4** can also be considered to be an alkyne complex analogue. The B–C fragment adopts a μ_3,η^2 bonding mode and is oriented nearly parallel to the Os1–Os2 bond. The B–C unit along with the hydrogen atom bridging Os2–B1, donate four electrons to the cluster.[15] Two electrons are donated to Os3 through a π-interaction and the two remaining electrons are distributed between a σ-bond to Os1 and a hydrogen bridged bond to Os2.

Experimental

A CH_2Cl-solution (6 ml) of 9-Cl-9-BBN (74.3 mg, 0.474 mmol) was transferred to a flask containing 82.1 mg, 0.095 mmol of **1**. The reaction mixture was stirred at room temperature for one hour, and the volatile components were then removed leaving an oily yellow residue, which, on washing with pentane, furnished pale yellow **4**: yield 72.5 mg (0.071 mmol, 75%). IR (ν_{CO}, CH_2Cl_2): $\tilde{\nu}$[cm^{-1}] = 2010 m(sh), 2035s, 2075s, 2095s, 2117w cm^{-1}. Satisfactory H,C-analysis. MS (EI): *m/z* 1027 ($M^{\oplus}-1$). 250.1-MHz ^{1}H-NMR (CD_2Cl_2, 30 °C): δ = 1.90(m), 1.82(m), 1.39(m), −11.75 (br. s), −16.18(s), −21.87(s), −21.87(s). 80.3-MHz ^{11}B NMR (CD_2Cl_2, 30 °C): δ = 58.8 (br. s), 18.5(s). 69.9 MHz ^{13}C{^{1}H}NMR (CD_2Cl_2, 30 °C): δ = 138.0 (br.s, C-B), 175.03, 174.42, 172.75, 169.06, 168.26, 167.95, 166.06, 165.93, 162.51 (each CO), 33.79, 33.57, 24.96 (br. s), 23.42 (9-BBN C-atoms).

Received: October 25, 1989 [Z 3610 IE]
German version: *Angew. Chem. 102* (1990) 328

CAS Registry numbers:
1, 86727-98-2; **3**, 109801-61-8; **3**, 125454-99-1; **4**, 125454-97-9; 9-Cl-9-BBN, 22086-34-6.

[1] S. G. Shore, D.-Y. Jan, W.-L. Hsu, L.-Y. Hsu, *J. Am. Chem. Soc. 105* (1983) 5923.
[2] Fenske-hall calculations [3] have shown that this is the most negative oxygen in the molecule.
[3] R. D. Barreto, T. P. Fehlner, L.-Y. Hsu, D.-Y. Jan, S. G. Shore, *Inorg. Chem. 25* (1986) 3572.
[4] D.-Y. Jan, S. G. Shore, *Organometallics 6* (1987) 428.
[5] D.-Y. Jan, L.-Y. Hsu, D. P. Workman, S. G. Shore, *Organometallics 6* (1987) 1984.
[6] a) Previously reported examples involve reactions of anionic ketenylidene clusters with electrophiles; b) J. A. Hriljac, D. F. Shriver, *J. Am. Chem. Soc. 109* (1987) 6010; c) M. J. Went, M. J. Sailor, P. L. Bogdan, C. P. Brock, D. F. Shriver, *ibid. 109* (1987) 6023.
[7] G. W. Kramer, H. C. Brown, *J. Organomet. Chem. 73* (1973) 1.
[8] The ability of a Lewis acid to induce a shift of a carbonyl ligand from a terminal to a bridge site was first observed by *Shriver* et al. [9].
[9] a) J. S. Kristoff, D. F. Shriver, *Inorg. Chem. 13* (1974) 499; b) A. Alich, N. J. Nelson, D. Stroppe, D. F. Shriver, *ibid. 11* (1972) 2976.
[10] Crystals were grown at −40 °C in CH_2Cl_2. Structure analysis at −50 °C: space group $P\bar{1}$, a = 9.362(9), b = 11.586(4), c = 12.574(3) Å, α = 90.70(2)°, β = 91.40(5)°, γ = 112.50(4)°, V = 1259.4 Å^3, ϱ_{calcd} = 2.692 g cm^{-1} for M = 1021.01, Z = 2, μ = 152.753 cm^{-1} for $Mo_{K\alpha}$. Diffraction data were collected with an Enraf-Nonius CAD4 diffractometer. All data were corrected for Lorentz and polarization effects. An empirical absorption correction was made. Crystallographic computations were carried out on a PDP11/44 computer using the SDP (*S*tructure *D*etermination *P*ackage). The structure was solved by the direct method MULTAN 11/82 and difference Fourier syntheses. Hydrogen atoms were located and refined. R = 0.038 and R_w = 0.048 (319 parameters refined) for 2695 unique reflections ($I \geq 3\,\sigma(I)$) of 3519 reflection collected in the range of $4 \leq 2\theta \leq 45°$. Further details of the crystal structure investigation are available on request from the Fachinformationszentrum Karlsruhe, Gesellschaft für wissenschaftlich-technische Information mbH, D-7514 Eggenstein-Leopoldshafen 2 (FRG), on quoting the depository number CSD-54377, the names of the authors and the journal citation.
[11] D. D. A. Barratt, S. J. Davies, G. P. Elliott, J. A. K. Howard, D. B. Lewis, F. G. A. Stone, *J. Organomet. Chem. 325* (1987) 185.
[12] L. Pauling: *The Nature of the Chemical Bond*, 3rd edit., Cornell University Press, Ithaca, NY, USA 1960, p. 229.
[13] R. Boese, P. Paetzold, A. Tapper, R. Ziembinski, *Chem. Ber. 122* (1989) 1057.
[14] a) D. J. Saturnino, M. Yamauchi, W. R. Clayton, W. R. Nelson, S. G. Shore, *J. Am. Chem. Soc. 97* (1975) 6063; b) L.-Y. Hsu, J. F. Mariategui, K. Niedenzu, S. G. Shore, *Inorg. Chem. 26* (1987) 143.
[15] a) Alkynes adopting the μ_3, η^2 bonding mode donate four electrons to the cluster through two σ bonds and a π interaction. b) E. Sappa, A. Tiripicchio, P. Braunstein, *Chem. Rev. 83* (1983) 203, and references therein.

Formation of Tetranuclear Chelate(4-) Ions of Divalent Metals (Mn, Co, Ni) with Idealized *T* Symmetry by Spontaneous Self-assembly

By *Rolf W. Saalfrank,* Armin Stark, Matthias Bremer,* and *Hans-Ulrich Hummel*

Dedicated to Professor Paul von Ragué Schleyer on the occasion of his 60th birthday

The structures of enolates and their reactivity are currently of great interest.[1] The same holds true for polynuclear metal complexes.[2] Since a tetranuclear manganese cluster constitutes the active center in photosystem II, which carries out photooxidation of water in green plants and algae, tetranuclear manganese chelate complexes might serve as models for the elucidation of this fundamental biological process.

Earlier we obtained the tetranuclear magnesium chelate complex **3b** in 85% yield by reaction of diethyl malonate (**1b**), methylmagnesium iodide, and oxalyl chloride (**2**) in a molar ratio of 1:1:0.25 at −78 °C in tetrahydrofuran followed by workup in aqueous ammonium chloride solution.[3] We were convinced that, in addition to magnesium, other divalent metals would also undergo such "*spontaneous self-assembly*"[4] to form similar "adamantanoid" chelate complexes. However, the alkylmetal chlorides of manganese, cobalt, and nickel are less readily available.[6] We have therefore modified our synthetic procedure for **3b** and now use methyllithium/magnesium chloride instead of methylmagnesium iodide. The advantage of this approach lies not only in the slight improvement in yield of **3b** from 85% to 90% but also in the simpler experimental procedure. Much more important than the more facile preparation of **3b** is the fact that mere replacement of magnesium chloride by the chlorides of manganese, cobalt, and nickel allows the

[*] Prof. Dr. R. W. Saalfrank, Dipl.-Chem. A. Stark, Dr. M. Bremer [+]
Institut für Organische Chemie der Universität Erlangen-Nürnberg
Henkestrasse 42, D-8520 Erlangen (FRG)
Priv. Doz. Dr. H.-U. Hummel [++]
Institut für Anorganische Chemie der Universität Erlangen-Nürnberg

[**] "Adamantanoid" Chelate Complexes, Part 2. This work was supported by the Deutsche Forschungsgemeinschaft and the Fonds der Chemischen Industrie. Part 1: [3].

[+] Single-crystal X-ray structure analysis of the Co complex.
[++] Single-crystal X-ray structure analysis of the Mn complex.

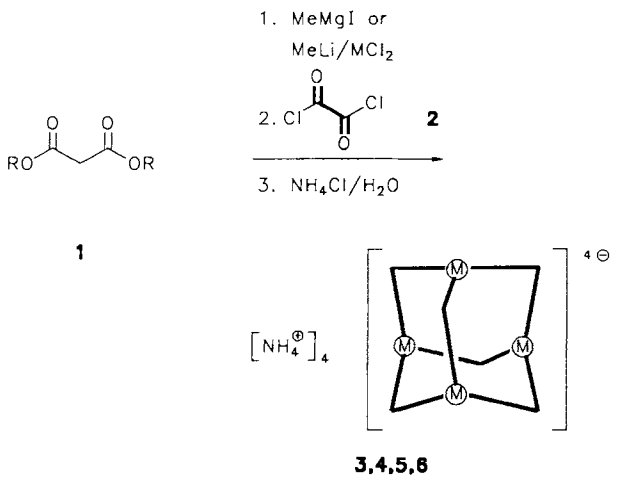

1,3–8	a	b
R	Me	Et

Ⓜ	3	4	5	6
	$Mg^{2\oplus}$	$Mn^{2\oplus}$	$Co^{2\oplus}$	$Ni^{2\oplus}$

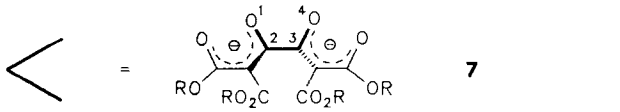

corresponding tetranuclear complexes **4**, **5**, and **6**, respectively, to be easily synthesized in good yields (80 to 87%).[7] The doubly bidentate bridging ligand **7** is formally obtained by *template coupling* of two malonate ester monoanions with oxalyl chloride (**2**) to give the tetraalkyl 2,3-dihydroxy-1,3-butadiene-1,1,4,4-tetracarboxylate **8** followed by spontaneous double deprotonation of **8**.

Under appropriate conditions, the 2,3-dihydroxy-1,3-butadienes **8** may be isolated. Hydrolysis of **6a** under mild conditions (pH ≈ 5, 20 °C, 2 min ultrasonication) affords **8a** (keto–enol equilibrium; yield 46%, m.p. 77 °C). Compound **8a** reacts with bromotrimethylsilane/pyridine to give tetramethyl 2,3-bis(trimethylsiloxy)-1,3-butadiene-1,1,4,4-tetracarboxylate (**9**; oil, yield 82%, dec. ≈50 °C). Reaction of **9** with benzoyl chloride in the presence of a catalytic amount

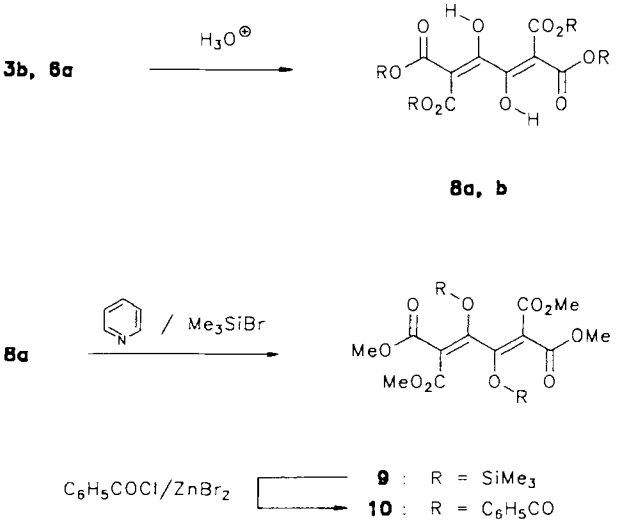

of zinc bromide results in formation of tetramethyl 2,3-bis(benzoyloxy)-1,3-butadiene-1,1,4,4-tetracarboxylate (**10**; yield 44%, m.p. 139 °C).

The ^1H and ^{13}C NMR spectra of **4**, **5**, and **6** (electron configurations: $Mn^{2\oplus}$, d^5; $Co^{2\oplus}$, d^7; $Ni^{2\oplus}$, d^8; paramagnetism) do not unambiguously establish the structure of these compounds. Therefore, we chose[8] to carry out X-ray structure analyses of **4a** and **5a**.[9] The two compounds are present as tetraammonium salts in the crystal. The counterions are the fourfold negatively charged, "adamantanoid",[10] complex tetramanganate(4-) $\mathbf{4a}^{4\ominus}$ and tetracobaltate(4-) $\mathbf{5a}^{4\ominus}$, respectively. Complexes **4a** and **5a** are the first of this type.[11] Complex **5a** was chosen for graphical presentation (Figs. 1–3). The core of the complex tetra-

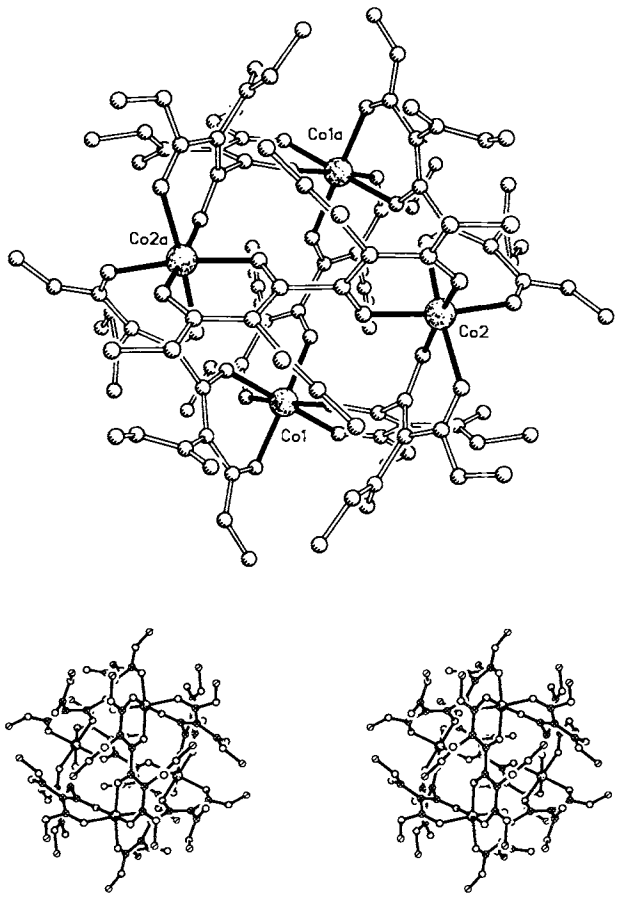

Fig. 1. Top: Structure of the tetracobaltate(4-) chelate ion $\mathbf{5a}^{4\ominus}$ in the crystal along the crystallographic C_2 axis. Bottom: Stereoview of $\mathbf{5a}^{4\ominus}$ along the crystallographic C_2 axis. ○ = O, ⊗ = C, ∅ = CH_3.

cobaltate(4-) ion $\mathbf{5a}^{4\ominus}$ is a distorted tetrahedron composed of four cobalt(II) ions [Co–Co distances: Co1-Co1a 660.6, Co1-Co2a and Co2-Co1a 660.9, Co1-Co2 and Co1a-Co2a 669.6, Co2-Co2a 675.6 pm]; these ions are linked along each of the six edges of the tetrahedron by a doubly bidentate tetramethyl 2,3-dioxobutane-1,1,4,4-tetracarboxylato(2-) bridge (**7a**), so that each of the four cobalt(II) ions is octahedrally coordinated by six oxygen atoms[12] [the torsional angles O1-C2-C3-O4 are 65.1, 73.9, 93.2, and 101.5°].

The tetracobaltate(4-) chelate ion $\mathbf{5a}^{4\ominus}$ has exact C_2 symmetry in the crystal. Viewed ideally (the Co–Co distances differ by less than 2.3%); however, the anion can be regarded as having nearly T symmetry (characterized by three C_2

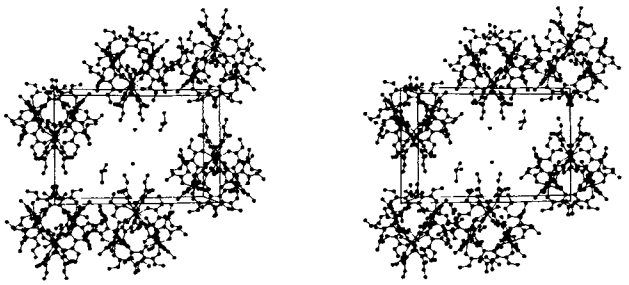

Fig. 2. Stereoview of the crystal packing of **5a**. For clarity, the hydrogen atoms, the crystal water, and the $\mathbf{5a}^{4\ominus}$ ions lying at the center in front of and behind the plane of the figure are not shown. The ammonium ions are shown as points, the chloroform molecules as three-pointed stars.

Fig. 3. Space-filling model of **5a** (cocrystallized chloroform and water are also shown) as viewed along the crystallographic C_2 axis. White, H atoms; black, C atoms; violet, N atoms outside the "adamantanoid" chelate anion; red, O atoms; green, Cl atoms; blue, Co atoms inside the "adamantanoid" chelate anion.

and four C_3 axes).[13] Accordingly, the tetracobaltate(4-) ion $\mathbf{5a}^{4\ominus}$ should be dissymmetric and thus chiral. The dissymmetry of this tetranuclear anion results from the atropisomerism[14] of ligands **7a**. The six chelate bridges **7a** linking the four $Co^{2\oplus}$ centers are twisted in the same sense and have nearly C_2 symmetry. The chiral subgroups of the point symmetry groups of the regular tetrahedron T_d are C_2, C_3, D_2, and T. Whereas numerous examples of molecules with C_2 symmetry are known, there are only a few organic molecules having the higher point-group symmetries (C_3,[15] D_2,[16] T[17]). Only relatively complicated molecules can have T symmetry. One of the reasons for the rarity of the higher-symmetry chiral compounds is that the required geometric prerequisites, all of which have to be simultaneously fulfilled, make a non-directed formation improbable. All the more surprising, therefore, is the high degree of symmetry obtained by "*spontaneous self-assembly*".

Experimental Procedure

4a, 5a, 6a: 30 mmol of a 1.6 M solution of methyllithium in diethyl ether was added to a solution of **1a** (4.0 g, 30 mmol) in 50 mL of dry THF (under N_2, $-78\,^\circ C$). The reaction mixture was stirred for 1 h at $-78\,^\circ C$ followed by addition of 30 mmol of previously dried MCl_2 (**4a**, $MnCl_2$; **5a**, $CoCl_2$; **6a**, $NiCl_2$). After stirring for 1 h, the mixture was treated dropwise with oxalyl chloride (**2**; 0.9 g, 7.5 mmol) in 20 mL of THF over 30 min, then allowed to warm over 18 h to 20 °C, and finally worked up with aqueous ammonium chloride solution.

4a: yield 2.2 g (80%), colorless prisms from $CHCl_3$/hexane, dec. $\approx 185\,^\circ C$. IR (KBr): $\tilde{\nu} = 1685$ (C=O), 1625 cm^{-1} (C=C).

5a: yield 2.4 g (87%), violet prisms from $CHCl_3$/hexane, dec. $\approx 193\,^\circ C$. IR (KBr): $\tilde{\nu} = 1690$ (C=O), 1625 cm^{-1} (C=C).

6a: yield 2.4 g (87%), green prisms from $CHCl_3$/hexane, dec. $\approx 160\,^\circ C$. IR (KBr): $\tilde{\nu} = 1685$ (C=O), 1620 cm^{-1} (C=C).

8a: **6a** (1.1 g, 0.5 mmol) was suspended in 100 mL of water and treated with a solution of 15 g of aluminum sulfate in 50 mL of water. After ultrasonication of the reaction mixture for 2 min, the aqueous phase was extracted with 3×100 mL of dichloromethane. The extracts were dried over sodium sulfate and the solvent was removed. The remaining yellow oil was crystallized from chloroform/diethyl ether. Yield: 0.4 g (46%), colorless crystals, m.p. 77 °C. IR (KBr): $\tilde{\nu} = 1725$ (C=O), 1650 cm^{-1} (C=C). The ^1H and ^{13}C NMR spectra contained many signals (keto–enol equilibrium). MS (70 eV): m/z 318 ($M^{\oplus}$).

9: **8a** (1.0 g, 3 mmol) was dissolved in 40 mL of dry THF (under N_2) and treated with pyridine (0.5 g, 6 mmol) and bromotrimethylsilane (1.9 g, 13 mmol). The reaction mixture was stirred for 1 h at 20 °C and then filtered. The solvent was removed and all volatiles were removed from the silyl enol ether at 20 °C under high vacuum. Yield: 1.2 g (82%). Dec. $\approx 50\,^\circ C$. IR (neat): $\tilde{\nu} = 1730$ (C=O), 1635 cm^{-1} (C=C). ^1H NMR (400 MHz, $CDCl_3$): $\delta = 0.16$ (s, 18H; $2Si(CH_3)_3$), 3.58 and 3.67 (each s, 12H; $4CH_3$). ^{13}C NMR (100.5 MHz, $CDCl_3$): $\delta = 0.15$ ($2Si(CH_3)_3$), 51.83 ($4CH_3$, two coincidentally overlapping signals), 112.37 (2 =C), 157.46, 163.95 and 164.28 (2 =C–O and 4 O–C=O). MS (70 eV): m/z 434 ($M^{\oplus} - 28$).

10: **9** (1.0 g, 2 mmol) was dissolved in 20 mL of dry dichloromethane (under N_2) and treated with benzoyl chloride (0.6 g, 4 mmol) and previously dried $ZnBr_2$ (0.1 g). After 18 h, the mixture was worked up with 20 mL of a saturated aqueous solution of sodium hydrogen carbonate. The organic layer was dried over sodium sulfate and the solvent removed. The remaining oil was crystallized from diethyl ether. Yield: 0.5 g (44%), colorless crystals, m.p. 139 °C. IR (KBr): $\tilde{\nu} = 1750$ and 1720 (C=O), 1640 cm^{-1} (C=C). ^1H NMR (400 MHz, $CDCl_3$): $\delta = 3.56$ and 3.71 (each s, 12H; $4CH_3$), 7.49, 7.64 and 8.08 (each m_c, 10H; $2C_6H_5$). ^{13}C NMR (100.5 MHz, $CDCl_3$): $\delta = 52.77$ and 52.90 ($4CH_3$), 120.81 (2 =C), 127.71 ($2\,C_{ipso}$), 128.70, 130.49 ($4\,C_{ortho}$ and $4\,C_{meta}$, respectively), 134.33 ($2\,C_{para}$), 149.77 (2 =C–O), 162.03, 162.15, and 162.84 (6 O–C=O). MS (70 eV): m/z 526 ($M^{\oplus}$).

Correct elemental analyses for **4a**, **5a**, **6a**, **8a**, and **10**.

Received: September 22, 1989 [Z 3562 IE]
German version: *Angew. Chem. 102* (1990) 292

[1] D. Seebach, *Angew. Chem. 100* (1988) 1685; *Angew. Chem. Int. Ed. Engl. 27* (1988) 1624.

[2] K. Wieghardt, *Angew. Chem. 101* (1989) 1179; *Angew. Chem. Int. Ed. Engl. 28* (1989) 1153. We thank Prof. Dr. *K. Wieghardt* for a preprint of this work; W. F. Beck, J. Sears, G. W. Brudvig, R. J. Kulawiec, R. H. Crabtree, *Tetrahedron 45* (1989) 4903.

[3] R. W. Saalfrank, A. Stark, K. Peters, H. G. von Schnering, *Angew. Chem. 100* (1988) 878; *Angew. Chem. Int. Ed. Engl. 27* (1988) 851.

[4] Formation of the thermodynamically most stable product, having a special structure, under appropriate conditions (concentration, temperature, solvent) from labile, mononuclear metal complexes, multidentate ligands, and bridging ligands [2, 5].

[5] J.-M. Lehn, A. Rigault, *Angew. Chem. 100* (1988) 1121; *Angew. Chem. Int. Ed. Engl. 27* (1988) 1095; L. A. Ibers, R. H. Holm, *Science 209* (1980) 223.

[6] C. Eaborn, P. B. Hitchcock, J. D. Smith, *J. Chem. Soc. Chem. Commun. 1985*, 535.

[7] The use of sodium hydride/metal chloride has so far given ca. 15% lower yields. The multistep process used, for example, in the synthesis of the corresponding zinc chelate complex [3] cannot compete with these one-pot procedures. In this process, hydrolysis of the magnesium chelate complex **3b** initially yields the tetraethyl ester **8b**. Reaction of **8b** with sodium hydride/zinc bromide proceeds via the free doubly bidentate chelate anion **7b** to afford, after workup with aqueous ammonium chloride solution, the "adamantanoid" zinc chelate complex, but only in yields of ca. 66% (based on **3b**).

[8] In addition to **4a,b**, **5a,b**, and **6a,b**, the corresponding complexes with R = *tert*-butyl or benzyl were also synthesized. In all cases, beautiful crystalline compounds were obtained, although only the methyl-substituted derivatives (**a** series) were suitable for X-ray analysis.

[9] **4a**: $C_{72}H_{72}O_{60}Mn_4\,(NH_4)_4$, colorless prisms from chloroform/hexane. The compound crystallizes with two equivalents of chloroform and water. Single crystals, $0.3 \times 0.5 \times 0.5\ mm^3$; monoclinic, space group $C2/c$ (No. 15), $a = 2607.6(5)$, $b = 1747.3(3)$, $c = 2303.4(5)$ pm, $\beta = 101.43(7)^\circ$, $V = 10287 \times 10^6\ pm^3$, $Z = 4$; Philips PW1100 diffractometer, graphite monochromator, $Ag_{K\alpha}$ radiation, $\lambda = 0.55943$ Å, SHELXS-86 and SHELX-76 program systems, 16300 reflections measured ($4 < 2\Theta < 40^\circ$, ω scan with scan width $[1.2 + 0.2\tan\Theta]^\circ$. Averaged data set: 4082 reflections, 2288 "observed" reflections with $F > 6\sigma(F)$. $R = 0.077$. $R_w = 0.080$; 328 parameters refined block-diagonally. **5a**: $C_{72}H_{72}O_{60}Co_4\,(NH_4)_4$, violet parallelepipeds from chloroform/hexane. The compound crystallizes with two equivalents of chloroform and water. Single crystal, $0.5 \times 0.4 \times 0.4\ mm^3$; monoclinic, space group $C2/c$ (No. 15), $a = 2568.8(6)$, $b = 1729.9(4)$, $c = 2276.0(6)$ pm, $\beta = 101.33(2)^\circ$, $V = 9916 \times 10^6\ pm^3$, $Z = 4$; Nicolet R3m/V diffractometer, graphite monochromator, $Mo_{K\alpha}$ radiation, $\lambda = 0.71073$ Å, SHELXTL PLUS program system, 11371 reflections measured ($4 < 2\Theta < 54^\circ$, ω scan with $3-15^\circ\ min^{-1}$ in

ω). Averaged data set: 9748 reflections, 7382 "observed" with $F > 6\sigma(F)$. $R = 0.059$, $R_w = 0.063$; 708 refined parameters. Further details of the crystal structure investigation may be obtained from the Fachinformationszentrum Karlsruhe, Gesellschaft für wissenschaftlich-technische Information mbH, D-7514 Eggenstein-Leopoldshafen 2 (FRG), on quoting the depository number CSD-54193, the names of the authors, and the journal citation.

[10] Schematic representation.

[11] The band patterns and characteristics of the IR spectra indicate that compounds **4b**, **5b**, and **6a**, **b** and the corresponding complexes with R = *tert*-butyl or benzyl have the same structures as **4a** and **5a**.

[12] Concerning the topology of the tetranuclear chelate anions $\mathbf{4a}^{4\ominus}$ and $\mathbf{5a}^{4\ominus}$ (bridgeheads: $M^{2\oplus}$ ions), compare the relationships in spherical tricycles (bridgeheads: N atoms): J. M. Lehn, *Angew. Chem. 100* (1988) 91; *Angew. Chem. Int. Ed. Engl. 27* (1988) 89; *Pure Appl. Chem. 49* (1977) 857; E. Graf, J. M. Lehn, *J. Am. Chem. Soc. 97* (1975) 5022; E. Weber, F. Vögtle, *Kontakte (Darmstadt) 1981*, No. 1, p. 24; E. Weber: *Phase Transfer Catalysts, Properties and Applications* (Merck-Schuchardt 1987), p. 33; F. P. Schmidtchen, *Angew. Chem. 89* (1977) 751; *Angew. Chem. Int. Ed. Engl. 16* (1977) 720; *Nachr. Chem. Tech. Lab. 36* (1988) 8.

[13] R. S. Cahn, C. K. Ingold, V. Prelog, *Angew. Chem. 78* (1966) 413; *Angew. Chem. Int. Ed. Engl. 5* (1966) 385; G. Haas, V. Prelog, *Helv. Chim. Acta. 52* (1969) 1202.

[14] Cf. M. Rösner, G. Köbrich, *Angew. Chem. 86* (1974) 775; *Angew. Chem. Int. Ed. Engl. 13* (1974) 741; R. W. Saalfrank, W. Paul, P. Schierling, *Chem. Ber. 118* (1985) 2150; G. Becher, A. Mannschreck, *ibid. 116* (1983) 264.

[15] A. de Meijere, O. Schallner, *Angew. Chem. 85* (1973) 400; *Angew. Chem. Int. Ed. Engl. 12* (1973) 399; S. Nishigaki, K. Aida, K. Senga, F. Yoneda, *Tetrahedron Lett. 1969*, 247; R. C. Fort, W. L. Semon, *J. Org. Chem. 32* (1967) 3685.

[16] K. Mislow, M. A. W. Glass, H. B. Hopps, E. Simon, G. H. Wahl, Jr., *J. Am. Chem. Soc. 86* (1964) 1710; M. Nakazaki, K. Naemura, Y. Kondo, *J. Org. Chem. 41* (1976) 1229; H. J. Bestmann, W. Schaper, *Tetrahedron Lett. 1975*, 3511; H. Irngartinger, *Chem. Ber. 106* (1973) 761, 2796; M. Nakazaki, K. Yamomoto, S. Tanaka, *J. Chem. Soc. Chem. Commun. 1972*, 433; D. J. Cram, K. C. Dewhirst, *J. Am. Chem. Soc. 81* (1959) 5963.

[17] H. Irngartinger, A. Goldmann, R. Jahn, M. Nixdorf, H. Rodewald, G. Maier, K.-D. Malsch, R. Emrich, *Angew. Chem. 96* (1984) 967; *Angew. Chem. Int. Ed. Engl. 23* (1984) 993.

[4+2]-Cycloadditions of Phosphinodiazoalkanes: Synthesis of 1,2,4-λ^5-Diazaphosphinines**

By *Thomas Facklam, Oliver Wagner, Heinrich Heydt,* and *Manfred Regitz**

Dedicated to Professor Alfred Schmidpeter on the occasion of his 60th birthday

There is no reaction which so compellingly characterizes aliphatic diazo compounds as 1,3-dipolar cycloaddition. This behavior has been documented in numerous reactions with double- and triple-bonded systems, and has been used for the synthesis of heterocycles.[1] It is all the more surprising that the phosphinodiazoalkanes first reported a few years ago[2] undergo either [3+2]- or even, as presented here, [4+2]-cycloadditions, depending on the cycloaddition partners.

As model substances, we have used the phosphinodiazoalkanes **1a** and **1b**,[3] which are readily accessible by electrophilic diazoalkane substitution[4] of lithium 1-diazo-2,2-dimethylpropane with the corresponding chlorophosphane. Their reaction with the phosphaalkyne **2**,[5] which possesses an electron-rich triple bond, still proceeds "normally": the regiospecific [3+2]-cycloaddition step leading to the 3*H*-1,2,4-diazaphospholes **3a, b** is followed by spontaneous sigmatropic [1,5]-shift of the R_2P residue to give the isomers **4a, b**.[6] Since $^1J_{PP}$ couplings are absent in the ^{31}P-NMR spectra, and since the ^{13}C-NMR spectrum of **4a** shows only sp^2 ring carbon atoms with comparably large phosphorus couplings (δ = 189.2, 199.2, $^1J_{PC}$ = 59.1 and 63.0 Hz), the phosphino substituent must be bound to one of the nitrogen atoms.[7]

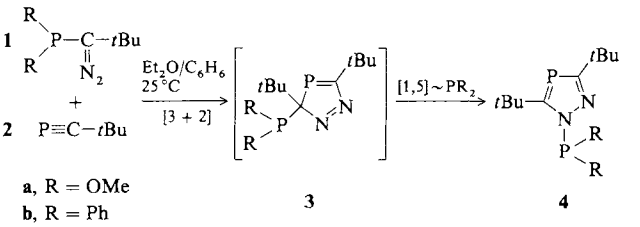

In contrast **1a, b** react quite differently, and in the sense of a [4+2]-cycloaddition, with the electron-deficient alkynes **5a, b**: the previously unknown 1,2,4-λ^5-diazaphosphinines **7a–d** are formed in good yields. The special role played by the phosphino residue in this reaction is best expressed in terms of a nucleophilic attack at the alkyne carbon atom (→ **6**), followed by a 1,6-ring closure leading to **7**.

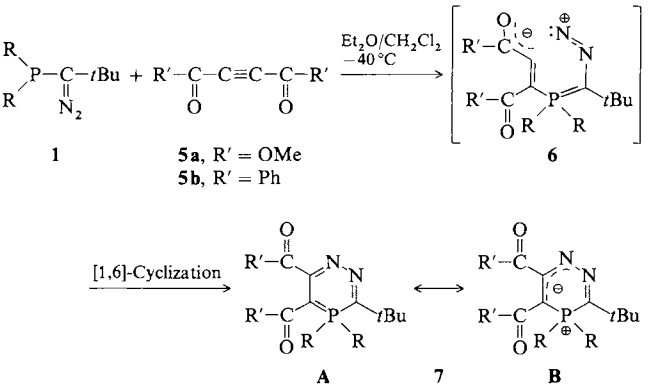

In general, the transition **1** → **7** is characterized by an upfield shift of the ^{31}P-NMR resonance signal, which is especially striking upon methoxy substitution at the phosphorus (cf. Ref. [3] and Table 1). In the ^{13}C-NMR spectra of **7a–d**, the ylidic character of C-5 is indicated by the high-field resonances at δ = 65.1–104.0 ($^1J_{PC}$ = 95.6–131.8 Hz) (**7A** ↔ **7B**);[8] C-3 is clearly identifiable by the unmistakable broadening of its signal in the ^{1}H-decoupled ^{13}C-NMR spectrum (small ^3J(H,C)-coupling). That the six-membered ring is no longer planar is immediately evident from the presence of two magnetically different P-methoxy groups for **7a** and **7b**, only one of which, however, shows a distinct ^3J(P,H) coupling in the ^{1}H-NMR spectrum (see Table 1).

The crystal structure analysis carried out on **7c** shows that the heterocycle has a distorted boat conformation[9] (Fig. 1); λ^5-phosphinines without further heteroatoms, on the other hand, are planar.[10]

The deviations from the least squares plane for the atoms N2, C3, C5, C6 are −0.038, 0.040, 0.044 and −0.047 Å, respectively. The angles between this plane and the P–C3–C5 and N1–N2–C6 planes are 22.67 and 10.77°, respectively.

[*] Prof. Dr. M. Regitz, Dr. T. Facklam, Dr. O. Wagner, Dr. H. Heydt
Fachbereich Chemie der Universität
Erwin-Schrödinger-Strasse, D-6750 Kaiserslautern (FRG)

[**] Diazo Compounds, Part 71. This work was supported by the Deutsche Forschungsgemeinschaft and the Fonds der Chemischen Industrie.—Part 70: M. Regitz, M. Böhshar, S. Arenz, H. Heydt, *Chem. Ber. 122* (1989) 565.

Table 1. Characteristic data of the 1,2,4-λ^5-diazaphosphinines **7a**, R = R′ = OMe; **7b**, R = OMe, R′ = Ph; **7c**, R = Ph, R′ = OMe; and **7d**, R = R′ = Ph [a].

7a: 67%, m.p. = 106 °C (decomp. colorless). ^{1}H NMR[b]: δ = 1.37 (s, *t*Bu), 3.60 (s, OMe), 3.78 (d, ^3J(P,H) = 12.4 Hz, P-OMe), 3.80 (s, OMe), 4.96 (s, OMe); ^{13}C NMR: δ = 29.0 [q, ^1J(C,H) = 127.3 Hz, C(CH_3)$_3$], 39.6 [d, ^2J(P,C) = 13.3 Hz, C(CH_3)$_3$], 44.5 (q, ^1J(C,H) = 142.2 Hz, OCH_3), 52.0 (q, ^1J(C,H) = 148.3 Hz, OCH_3), 52.7 (dq, ^2J(P,C) = 7.0, ^1J(C,H) = 147.4 Hz, P-OCH_3), 53.3 (q, ^1J(C,H) = 148.3 Hz, OCH_3), 93.1 (d, ^1J(P,C) = 131.8 Hz, C-5), 150.3 (s, C-6), 161.7 (d, ^1J(P,C) = 104.9 Hz, C-3), 162.4 (d, J(P,C) = 9.7 Hz, CO), 165.1 (s, CO); ^{31}P NMR: δ = −1.5

7b: 50%, m.p. = 123 °C (decomp. colorless). ^{1}H NMR[b]: δ = 1.35 (s, *t*Bu), 3.26 (d, ^3J(P,H) = 11.4 Hz, P-OMe), 3.52 (s, P-OMe), 7.3–8.0 (m, arene-H); ^{13}C NMR: δ = 29.1 [q, ^1J(C,H) = 127.5 Hz, C(CH_3)$_3$], 39.4 [d, ^2J(P,C) = 12.4 Hz, C(CH_3)$_3$], 44.7 (q, ^1J(C,H) = 135.0 Hz, P-OCH_3), 52.3 (dq, ^2J(P,C) = 5.5, ^1J(C,H) = 135.0 Hz, P-OCH_3), 104.0 (d, ^1J(P,C) = 127.6 Hz, C-5), 127.7–139.5 (m, arene-C), 154.6 (s, C-6), 161.7 (d, ^1J(P,C) = 101.5 Hz, C-3), 189.2 (d, J(P,C) = 7.3 Hz, CO), 192.2 (s, CO); ^{31}P NMR: δ = 0.3

7c: 57%, m.p. = 204 °C (decomp. yellow). ^{1}H NMR: δ = 1.07 (s, *t*Bu), 3.45, 4.90 (each s, OMe), 7.5–8.9 (m, arene-H); ^{13}C NMR: δ = 30.0 [q, ^1J(C,H) = 126.4 Hz, C(CH_3)$_3$], 41.7 [d, ^2J(P,C) = 18.1 Hz, C(CH_3)$_3$], 50.8, 52.10 (each q, ^1J(C,H) = 146.8 Hz, OCH_3), 65.1 (d, ^1J(P,C) = 102.6 Hz, C-5), 123.7–133.6 (m, arene-C), 137.1 (d, ^1J(P,C) = 31.5 Hz, C-3), 151.6 (s, C-6), 165.8 (d, ^3J(P,C) = 7.4 Hz, CO), 167.3 (d, J(P,C) = 10.9 Hz, CO); ^{31}P NMR: δ = −27.4

7d: 61%, m.p. = 176 °C (decomp. yellow). ^{1}H NMR: δ = 1.16 (s, *t*Bu), 7.0–8.1 (m, arene-H); ^{13}C NMR: δ = 29.9 [q, ^1J(C,H) = 127.6 Hz, C(CH_3)$_3$], 41.7 [d, ^2J(P,C) = 17.9 Hz, C(CH_3)$_3$], 74.8 (d, ^1J(P,C) = 95.6 Hz, C-5), 121.5–139.8 (m, arene-C, C-3), 154.3 (s, C-6), 192.8, 192.9 (each s, CO); ^{31}P NMR: δ = −32.0

[a] 90-MHz ^{1}H-, 50.32-MHz ^{13}C-, and 80.8-MHz ^{31}P-NMR spectra in CD-Cl_3 TMS (int.) or 85% H_3PO_4 (ext.). [b] Note that only one P–OMe residue shows the expected $^3J_{PH}$ coupling.

The ylidic character of **7c** is immediately recognizable from the distances between the phosphorus atom and its neighboring carbon atoms P–C3 1.811(4), P–C5 1.744(4) Å; The P–C5 distance corresponds almost exactly to the P–C distance

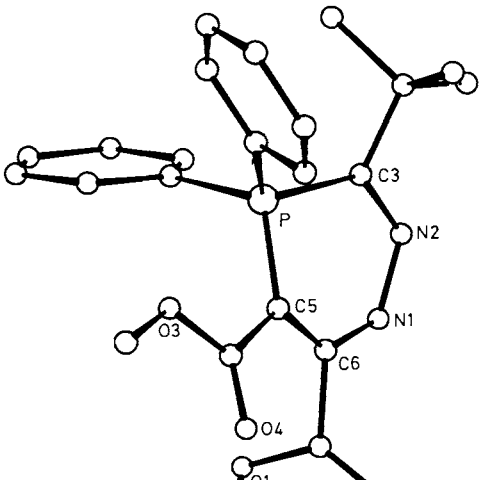

Fig. 1. Structure of **7c** in the crystal [11]. Selected bond lengths [Å] and angles [°]: P-C3 1.811(4), P-C5 1.744(4), N1-N2 1.373(5), N1-C6 1.321(5), N2-C3 1.284(5), C5-C6 1.373(5); C3-P-C5 99.3(2), N2-N1-C6 118.9(3), N1-N2-C3 126.5(3), P-C3-N2 120.9(3), P-C5-C6 116.3(3), N1-C6-C5 129.6(4).

in acceptor-substituted 1λ^5,3λ^5-diphosphetes.[2b] Shortening of the C5-C6 bond [1.373(5) Å] and lengthening of the N1–C6 distance are consistent with an electron distribution as in **7B**. In comparison to the case in λ^5-phosphinines,[10] the internal angle at the phosphorus atom is compressed, while the internal angles at N2 and N6 are markedly widened.

Experimental

7a–d: a solution of **1a** and **1b** (2.5 mmol) in diethylether/dichloromethane 1/1 (100 mL) was treated with stirring at −40 °C with 2.5 mmol of **5a** or **5b**, and the respective mixture allowed to thaw, prior to evaporating down at 25 °C/10^{-1} mbar. Subsequent chromatography on 40 g of silica gel with the same solvent mixture furnished, after evaporation to dryness and cooling to −30 °C, **7b** or **7d**; in the case of **7a** and **7c**, chromatographic purification was unnecessary.

Received: October 24, 1989 [Z 3604 IE]
German version: *Angew. Chem. 102* (1990) 316

[1] H. Heydt, M. Regitz in A. Padwa (Ed.): *1,3-Dipolar Cycloaddition Chemistry, Vol. 1*, Wiley, New York 1984, pp. 393.
[2] a) A. Baceiredo, G. Bertrand, G. Sicard, *J. Am. Chem. Soc. 107* (1985) 4781; b) H. Keller, G. Maas, M. Regitz, *Tetrahedron Lett. 27* (1986) 1903.
[3] **1a**: yellow oil; IR (NaCl): $\tilde{\nu}$ = 2005 cm^{-1}; 50.32 MHz ^{13}C-NMR (CD-Cl_3): δ = 52.1 (d, $^1J_{PC}$ = 58.7 Hz, C-N_2); 80.8 MHz ^{31}P-NMR ($CDCl_3$): δ = 150.6. **1b**: orange colorless oil; IR (NaCl): $\tilde{\nu}$ = 2020 cm^{-1}; 50.32 MHz ^{13}C-NMR ($CDCl_3$): δ = 48.5 (d, $^1J_{PC}$ = 41.7 Hz, C-N_2); 80.8 MHz ^{31}P-NMR ($CDCl_3$): δ = −19.7.
[4] Review: M. Regitz, G. Maas: *Diazo Compounds – Properties and Synthesis*, 1st Edit., Academic Press, Orlando, FL, USA 1986, pp. 436.
[5] G. Becker, G. Gresser, W. Uhl, *Z. Naturforsch. B36* (1981) 16; modified procedure: W. Rösch, U. Hees, M. Regitz, *Chem. Ber. 120* (1987) 1645.
[6] Review: M. Regitz, P. Binger, *Angew. Chem. 100* (1988) 1541; *Angew. Chem. Int. Ed. Engl. 27* (1988) 1484.
[7] Further data for **4**, **4a**: 65% colorless oil; 80.8-MHz ^{31}P NMR ($CDCl_3$): δ = 82.4 (phosphole-P), 115.6 (phosphino-P) **4b**: 46%, colorless crystals; 80.8-MHz ^{31}P NMR ($CDCl_3$); δ = 62.8 (phosphino-P), 84.6 (phosphole-P).
[8] H. Kalinowski, S. Berger, S. Braun: *^{13}C-NMR-Spektroskopie*, Thieme, Stuttgart 1984, pp. 199, 213, and 530.
[9] This also applies for the sterically demanding substituted methyl 2,4,5,6-tetra-*tert*-butyl-λ^3-phosphinine-3-carboxylate; here however, the bow/stern deviation is even greater: G. Maas, J. Fink, H. Wingert, K. Blatter, M. Regitz, *Chem. Ber. 120* (1987) 819.
[10] U. Thewalt, *Angew. Chem. 80* (1969) 783; *Angew. Chem. Int. Ed. Engl. 8* (1969) 769; T. Debaerdemaeker, *Cryst. Struct. Commun. 8* (1979) 309.
[11] $C_{23}H_{25}N_2O_4P$: $P2_1/n$, a = 9.033(3), b = 26.280(8), c = 10.025(4) Å, α = 90.00, β = 110.83, γ = 90.00°, T = 20 °C, Z = 4, ϱ_{calcd} = 1.27 g cm^{-3}, μ = 1.483 cm^{-1}. Enraf-Nonius four-circle diffractometer CAD4; 3067 measured reflections, anisotropic refinement with 1804 reflections ($I > 3.00\,\sigma(I)$; R = 0.047, R_w = 0.048 for 271 parameters). Further details of the crystal structure investigation are available on request from the Fachinformationszentrum Karlsruhe, Gesellschaft für wissenschaftlich-technische Information mbH, D-7514 Eggenstein-Leopoldshafen 2 (FRG), on quoting the depository number CSD-54117, the names of the authors, and the journal citation.

trans-1,2-Difluoro-1,2-bis[(tetracarbonyl)cobaltio]-ethene, a Difluoroethyne Complex with μ_2-η^1-η^1-Coordination**

By *Dieter Lentz** and *Dagmar Preugschat*

So far, only a few complexes containing dihaloethyne ligands have been described in the literature.[1,2] We recently reported the synthesis of the first difluoroethyne complex $[Cp^*CoFe_3(CO)_9(\mu_4\text{-}\eta^2\text{-}FC{\equiv}CF)]$[2] by C–C linkage of two fluoromethylidine ligands. Since free difluoroethyne is extremely unstable[3] and thus inaccessible for direct reactions, we searched for further possibilities of synthesizing difluoroethyne complexes via an indirect route.

[*] Priv.-Doz. Dr. D. Lentz, D. Preugschat
Institut für Anorganische und Analytische Chemie der Freien Universität Fabeckstrasse 34–36, D-1000 Berlin 33

[**] This work was supported by the Fonds der Chemischen Industrie and the Deutsche Forschungsgemeinschaft. We thank Prof. Dr. *J. Fuchs* for his help with the crystal structure investigations.

Reaction of difluorofumaric dichloride **1** or difluoromaleic dichloride with the tetracarbonylcobaltate **2** seemed a promising strategy. First of all, reactions of difluoromalonic dichloride with $[Co(CO)_4]^{\ominus}$ and $[Mn(CO)_5]^{\ominus}$ enabled a systematic synthesis of difluoromethylene-bridged metal complexes,[4] and secondly the alkynecobalt complexes $[Co_2(CO)_6(\mu_2\text{-}\eta^2\text{-}RC{\equiv}CR)]$ are very stable.[5]

By reaction of **2** with difluorofumaric dichloride **1**, we have now been able to synthesize the difluoroethyne complex **4**,[6] in which the difluoroethyne ligand bridges two tetracarbonylcobalt fragments in the very unusual μ_2-η^1-η^1 coordination. The formation of **4** presumably proceeds via the bis(acyl)-complex **3**.

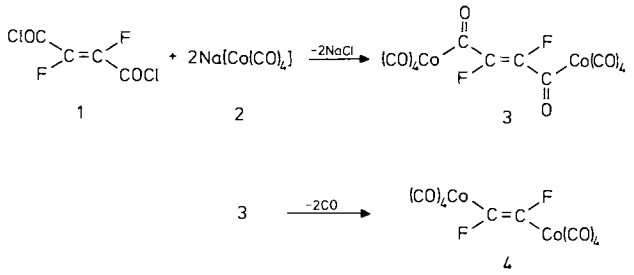

The structure of **4** is confirmed by its spectroscopic data[6] and a crystal structure analysis (Fig. 1).[7] Each of the two cobalt atoms is trigonal-bipyramidally coordinated by four carbonyl ligands and the μ_2-η^1-η^1-difluoroethyne ligand, which occupies the axial position. The distance from the

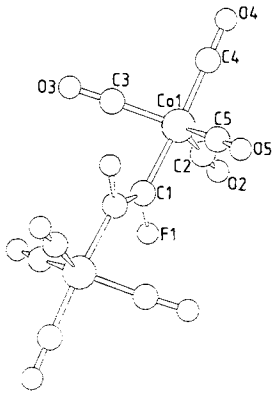

Fig. 1. Structure of **4** in the crystal. Selected bond lengths [pm] and angles [°]: Co1-C1 197.3(3), C1-F1 138.3(3), Co1-C2 181.8(3), Co1-C3 179.1(3), Co1-C4 181.4(3), Co1-C5 180.6(3), C1-C1 132.3(5), C-O 112.4(4)–113.2(4); C1-Co1-C2 91.3(1), C3-Co1-C5 125.9(2), C1-Co1-C3 82.6(1), C4-Co1-C5 93.7(1), C1-Co1-C4 173.5(1), C1-Co1-C5 83.7(1), C2-Co1-C3 116.3(2), C2-Co1-C4 95.2(1), C2-Co1-C5 116.1(1), C3-Co1-C4 94.3(1), Co1-C1-F1 115.5(2).

cobalt atom to the carbon atom C1 of the difluoroethyne ligand corresponds to a cobalt–carbon σ-bond. The bond angle (F–C1–Co) at the carbon atom is 115.5(2)°, so that the carbon atom is largely sp^2 hybridized. The atoms of the difluoroethene ligand and the two cobalt atoms lie in a plane (max. deviation 0.3 pm) and the C–C distance (132.3(5) pm) corresponds to that of a C=C double bond. Consequently, **4** is best described as 1,2-difluoro-1,2-dicobaltio-ethene. There are very few examples for such a μ_2-η^1-η^1-coordination of an ethyne to transition metals. Thus, *Wilkinson* et al. obtained a compound of the composition $K_6[Co_2(CN)_{10}C_2H_2]\cdot 4\,H_2O$, for which they formulated a *trans*-dimetallioethene structure on the basis of IR spectroscopic data.[8] A crystal structure analysis of the derivative $K_6[Co_2(CN)_{10}(H_3COOC\text{-}C{\equiv}C\text{-}COOCH_3)]\cdot 6\,H_2O$ has already been reported,[9] which confirms the μ_2-η^1-η^1-*trans*-configuration. $[(CH_3)_3PAu(CF_3)C{=}C(CF_3)Au(CF_3)_2\text{-}P(CH_3)_3]$[10] is likewise *trans*-configurated. However, in further structurally characterized examples such as $[(C_6H_5)_3PAu(F_3C)C{=}C(CF_3)AuP(C_6H_5)_3]$[11], $[\{(C_6H_5)_3P\}_2(NO)_2Ir_2(\mu_2\text{-}\eta^1\text{-}\eta^1\text{-}F_3C\text{-}C{\equiv}C\text{-}CF_3)_2]$[12], $[(\eta\text{-}C_5H_5)_2Rh_2(CO)_2(\mu_2\text{-}\eta^1\text{-}\eta^1\text{-}F_3C{\equiv}C\text{-}CF_3)]$[13], $[(\eta\text{-}C_5H_5)_2Rh_2(CO)(C_9H_9N)(\mu_2\text{-}\eta^1\text{-}\eta^1\text{-}F_3C{\equiv}C\text{-}CF_3)]$[14] and $[Re_2(CO)_{10}(\mu_2\text{-}\eta^1\text{-}\eta^1\text{-}C_4O_2)]$[15] a *cis*-configuration is observed.

The synthesis via difluoromaleic dichloride has thus far failed. On attempting to prepare the difluoromaleic dichloride, only difluoromaleic anhydride was obtained. This is not particularly surprising in view of the extremely questionable existence of maleic dichloride.[16] A substance described on several occasions as dichloromaleic dichloride has proven to be a γ-lactone of tetrachloro-4-hydroxybut-2-enic acid.[17]

Received: October 27, 1989 [Z 3614 IE]
German version: *Angew. Chem. 102* (1990) 308

CAS Registry numbers:
1, 125641-85-2; **2**, 14878-28-5; **4**, 125641-86-3; difluorofumaric acid, 2714-32-1.

[1] G. Varadi, G. Palay, *Inorg. Chim. Acta 20* (1976) L33; K. Stahl, U. Müller, K. Dehnicke, *Z. Anorg. Allg. Chem. 527* (1985) 7; K. Stahl, A. El-Kholi, U. Müller, K. Dehnicke, *J. Organomet. Chem. 316* (1986) 95; A. El-Kholi, K. Stahl, U. Müller, K. Dehnicke, *ibid. 317* (1986) C9; K. Stahl, F. Weller, K. Dehnicke, *Z. Anorg. Allg. Chem. 533* (1986) 73.

[2] D. Lentz, H. Michael, *Angew. Chem. 100* (1988) 871; *Angew. Chem. Int. Ed. Engl. 27* (1988) 845.

[3] W. J. Middleton, US-Pat. 2831835 (1958); *Chem. Abstr. 52* (1958) 14658f.; J. Heicklen, V. Knight, *J. Phys. Chem. 69* (1965) 2484; L. Kevan van, P. Hamlet, *J. Chem. Phys. 42* (1965) 2255; G. Bieri, J.-P. Stadelmann, F. Thommen, J. Vogt, *Helv. Chim. Acta 61* (1978) 357; G. Bieri, A. Schmelzer, L. Asbrink, M. Jonsson, *Chem. Phys. 49* (1980) 213.

[4] W. Schulze, H. Hartl, K. Seppelt, *Angew. Chem. 98* (1986) 189; *Angew. Chem. Int. Ed. Engl. 25* (1986) 185.

[5] R. D. W. Kemmitt, D. R. Russel in G. Wilkinson, F. G. A. Stone, E. Abel: *Comprehensive Organometallic Chemistry, Vol. 5*, Pergamon, Oxford 1982, pp. 192, and references cited therein.

[6] *Experimental procedures.* Difluorofumaric dichloride **1**: A suspension of difluorofumaric acid[18] (8.8 g, 57 mmol) in dichloromethane (50 mL) was treated portionwise with 28.5 g (136 mmol) of phosphorus pentachloride at room temperature and the mixture heated under reflux for 2 h. Distillation on a spinning band column furnished 5.3 g (49%) of **1** as colorless crystals. M.p. 53 °C. MS (80 eV): *m/z* 188 ($M^{\oplus}$), 153 ($M^{\oplus}$–Cl), 125 ($M^{\oplus}$–COCl), 90 ($C_3F_2O_3^{\oplus\oplus}$), 62 ($C_2F_2^{\oplus\oplus}$), 43 ($C_2F^{\oplus}$); IR (Nujol): $\tilde{\nu}$ = 1764(s), 1245(s), 1228(m), 1077(s), 633(m) cm^{-1}; ^{19}F NMR ($CDCl_3$, $CFCl_3$ as ext. standard): $\delta = -131.4$; ^{13}C NMR ($CDCl_3$, δ ($CDCl_3$) = 77.1 as standard): δ = 142.75 (CF; in combination with the ^{13}C-satellites of the ^{19}F-NMR spectrum, the spectrum can be simulated as an ABX system [19], whereby the different chemical shifts of the fluorine atoms induced by the ^{13}C nucleus must be taken into account. $J_{AX} = {}^1J_{CF} = -287.4$, $J_{BX} = {}^2J_{CF} = 34.4$, $J_{AB} = {}^3J_{FF} = -134.7$ Hz, $\Delta\delta_{Fa} = -0.097$, $\Delta\delta_{Fb} = -0.045$), 158.5 (COCl, $J_{AX} = {}^2J_{CF} = 41.1$, $J_{BX} = {}^3J_{CF} = -8.8$, $J_{AB} = {}^3J_{FF} = -134.7$ Hz, $\Delta\delta_{Fa} = -0.013$, $\Delta\delta_{Fb} = -0.0$). *trans*-1,2-Difluoro-1,2-bis[(tetracarbonyl)cobaltio]ethene **4**: A solution of **1** (500 mg, 2.7 mmol) in diethyl ether (50 mL), prepared under an atmosphere of argon, was treated dropwise at −78 °C with a solution of 5.3 mmol of $Na[Co(CO)_4]$ **2** in 50 mL of diethyl ether. The reaction mixture was stirred for 3 d at −78 °C and then allowed to warm to 10 °C within 12 h. After addition of 30 mL of water, the organic phase was separated off, dried over sodium sulfate, and evaporated to dryness under reduced pressure. Sublimation in vacuo (10^{-2} mbar) onto a cold finger (−30 °C) gave 30 mg (2.8 %) of **4** in the form of yellow crystals. M.p. 86–87 °C. MS (80 eV): *m/z* 404 ($M^{\oplus}$), 376 ([*M*−CO]$^{\oplus}$), 348 ([*M*−2 CO]$^{\oplus}$), 320 ([*M*−3 CO]$^{\oplus}$), 292 ([*M*−4 CO]$^{\oplus}$), 264 ([*M*−5 CO]$^{\oplus}$), 236 ([*M*−6 CO]$^{\oplus}$), 208 ([*M*−7 CO]$^{\oplus}$), 180 ([*M*−8 CO]$^{\oplus}$); IR (*n*-pentane): $\tilde{\nu}$ = 2109(s), 2053(vs), 2045(vs), 2013(w) cm^{-1}; ^{19}F NMR ($CDCl_3$): $\delta = -87.3$; ^{13}C NMR ($CDCl_3$): δ = 142.55 (simulation as ABX system gave $J_{AX} = {}^1J_{CF} = -324.4$, $J_{BX} = {}^2J_{CF} = 70.4$, $J_{AB} = {}^3J_{FF} = -125.2$ Hz, $\Delta\delta_{Fa} = -0.097$, $\Delta\delta_{Fb} = -0.045$).

[7] A crystal suitable for the crystal structure analysis of **4** was obtained by sublimation in vacuo. Monoclinic, $P2_1/c$, $a = 654.6(5)$, $b = 963.1(6)$, $c = 1171.1(5)$ pm, $\beta = 103.52(5)^\circ$, $\varrho_{calcd} = 1.88\ g\,cm^{-3}$. $R = 0.029$, $R_w = 0.029$ ($Mo_{K\alpha} = 71.069$ pm), 1256 crystallographically independent reflections, 1142 with $F_0 > 3\sigma(F_0)$, anisotropic temperature factors, starting coordinates by Patterson methods (SHELXS-86) [20], full-matrix least squares refinement (SHELX-76) [21], 100 refined parameters, max. shift/error 0.002, residual electron density 0.29 $eÅ^{-3}$, empirical absorption with the Program DIFABS by *D. Stuart* and *N. Walker* [22]. Further details of the crystal structure investigation are available on request from the Fachinformationszentrum Karlsruhe, Gesellschaft für wissenschaftlich-technische Information mbH, D-7514 Eggenstein-Leopoldshafen 2 (FRG), on quoting the depository number CSD-54273, the names of the authors, and the journal citation.
[8] W. P. Griffith, G. Wilkinson, *J. Chem. Soc. 1959*, 1629.
[9] K. D. Grande, A. J. Kunin, L. S. Stahl, *Inorg. Chem. 22* (1983) 1791.
[10] J. A. J. Jarvis, A. Johnson, R. J. Puddephatt, *J. Chem. Soc. Chem. Commun. 1973*, 373.
[11] C. J. Gilmore, P. Woodward, *J. Chem. Soc. (D) 1971* 1233; C. Mitchel, F. G. A. Stone, *Chem. Commun. 1970*, 1263.
[12] J. Cleemens, M. Green, M.-C. Kuo, C. J. Fritchie Jun., J. T. Mague, F. G. A. Stone, *J. Chem. Soc. Chem. Commun. 1972*, 53.
[13] R. S. Dickson, S. H. Johnson, H. P. Kirsch, D. J. Lloyd, *Acta Crystallogr. Sect. B33* (1977) 2057.
[14] J. W. Bixler, A. M. Bond, R. S. Dickson, G. D. Fallon, R. S. Nesbit, H. Pateras, *Organometallics 6* (1987) 2508.
[15] W. Beck, M. Schweiger, G. Müller, *Chem. Ber. 120* (1987) 889.
[16] R. Anschütz, Q. Wirtz, *Ber. Dtsch. Chem. Ges. 18* (1885) 1947; W. H. Perkin, *ibid. 14* (1881) 2540.
[17] H.-D. Scharf, H.-J. Knops, H.-G. Fitzky, *Chem. Ber. 109* (1976) 1163, and references cited therein.
[18] M. S. Rasch, R. E. Miegel, J. E. Castle, *J. Am. Chem. Soc. 81* (1959) 2678.
[19] A. A. Bothner-By, S. M. Castellano *(LAOCN3, A Program for Computer Simulation of Complex NMR Spectra)* in D. F. de Tar (Ed.): *Computer Programs for Chemistry, Vol. 1*, New York 1968; MS-DOS version for IBM Personal Computer: M. Clark, J. S. Thrasher, The University of Alabama, Tuscaloosa, USA.
[20] G. M. Sheldrick: *SHELXS-86, A Program for Crystal Structure Solution*, Göttingen 1986.
[21] G. M. Sheldrick: *SHELX-76, A Program for Crystal Structure Determination*, Göttingen 1976.
[22] N. Walker, D. Stuart, *Acta Crystallogr. Sect. A39* (1983) 158.

Borole Dianions: Metalation of 1-(Dialkylamino)-2,5-dihydro-1*H*-boroles and the Structure of $Li_2(C_4H_4BNEt_2) \cdot TMEDA$ **

By *Gerhard E. Herberich,* Martin Hostalek, Ralf Laven,* and *Roland Boese*

Borole dianions (dihydroborolediides) are,[1] as boracarbocyclic 6π-electron systems, isoelectronic with the cyclopentadienide ion (Scheme 1). We report here on the synthesis of some dilithium 1-(dialkylamino)dihydroborolediides and on the structure of one of their TMEDA adducts.

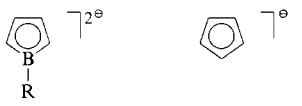

Scheme 1.

[*] Prof. Dr. G. E. Herberich, Dr. M. Hostalek, Dr. R. Laven
Institut für Anorganische Chemie der Technischen Hochschule
Professor-Pirlet-Strasse 1, D-5100 Aachen (FRG)
Dr. R. Boese
Institut für Anorganische Chemie der Universität-Gesamthochschule
Universitätsstrasse 3-5, D-4300 Essen 1 (FRG)

[**] Derivatives of Borole, Part 15. This work was supported by the Deutsche Forschungsgemeinschaft and the Fonds der Chemischen Industrie.—Part 14: G. E. Herberich, I. Hausmann, B. Hessner, M. Negele, *J. Organomet. Chem. 362* (1989) 259.

As a rule 1-(Dialkylamino)-2,5-dihydro-1*H*-boroles **1**[2] are quaternized by organolithium compounds LiR′ to borates **2**.[2] Borate formation can be suppressed only by steric hindrance at the boron atom and at the basic center of LiR′: **1c** reacts with Li*t*Bu to give the lithiation product **3c**.[1b]

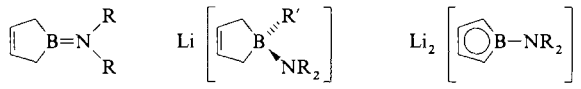

1 **2** **3**

a, R = Me; **b**, R = Et; **c**, R = *i*Pr

Quaternization usually also occurs with lithium amides: from **1a**/$LiNMe_2$, **1b**/$LiNEt_2$ and from **1a**/$LiNiPr_2$ or **1c**/$LiNMe_2$ the corresponding bis(dialkylamido)borates **4a, b, d** are formed, recognizable in the NMR experiment by

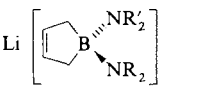

4a, R = R′ = Me
4b, R = R′ = Et
4c, R = R′ = *i*Pr
4d, R = Me, R′ = *i*Pr

a shift of the ^{11}B signal from $\delta \approx 51$[2] to $\delta \approx 5$.[3] The oily borate **4a** was converted with tetramethylethylenediamine (TMEDA) into a crystalline adduct **5**.[4] At 60 °C, borate formation is reversible; metalation (25 h) of **1a, b** leads to formation of the dihydroborolediides **3a, b** with $\delta(^{11}B) = 25-27$.[3] In the case of **1c**/$LiNiPr_2$ the formation of the borate **4c** is blocked because of double steric hindrance, and at 60 °C **1c** isomerizes very slowly (7 d)[3] to the known 1-(diisopropylamino)-4,5-dihydro-1*H*-borole.[2]

With the sterically demanding lithium 2,2,6,6-tetramethylpiperidide (LiTMP), borate formation does not take place. Here, the metalation of **1a, b** to **3a, b** already occurs at room temperature, and the troublesome problems of ether cleavage do not arise. In contrast, **1c** does not react with LiTMP at 20 °C.

$Li_2(C_4H_4BNR_2) \cdot TMEDA$
6a, R = Me
6b, R = Et
6c, R = *i*Pr

The lithium derivates **3a–c** are powdery solids which form well crystallized derivatives **6a–c** with TMEDA. The determination of the structure of a dihydroborolediide was possible for the first time with the diethylamino compound **6** (Fig. 1).[5, 6]

6b is a centrosymmetric dimer containing a phane-like $(C_4H_4BNEt_2 \cdot Li)_2$ ring and two external Li(TMEDA) groups. Both Li atoms of a dihydroborolediide unit are pentahapto bound, and the higher coordinated Li1 atom of the Li(TMEDA) group is expectedly weaker than the Li2 atom of the Li–NEt_2 group. The π-coordination of the Li atom and the formation of a dimer with the help of N-donor atoms of the metalated ring are known structural patterns in the case of organolithium compounds.[7]

The C_4B ring is planar (maximum deviation 0.5 pm for the B atom). The bond pattern in the ring is that of a delocalized 6π-electron system and impressively reflects the occupation of the borole LUMO (B–C1, B–C4 and C2–C3 shortened,

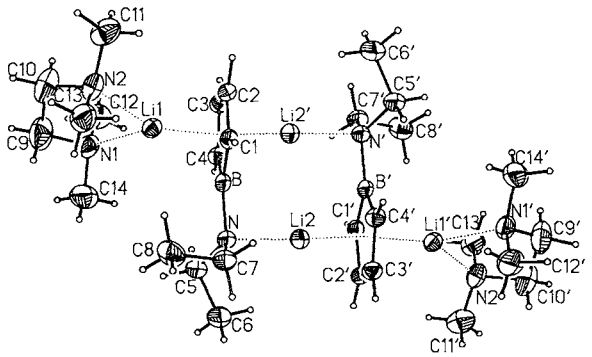

Fig. 1. Structure of **6** in the crystal. Selected bond lengths [pm]: Li1-C1 227.2(4), Li1-C2 218.4(4), Li1-C3 217.1(4), Li1-C4 226.9(3), Li1-B 234.1(3), Li1-C_4B-ring 186.9, Li2'-C1 220.2(4), Li2'-C2 212.3(3), Li2'-C3 213.2(4), Li2'-C4 219.5(4), Li2'-B 227.5(4), Li2'-C_4B-ring 179.5, Li1-N1 215.0(4), Li1-N2 216.9(3), Li2-N 202.8(3); in the C_4B-ring: B-C1 152.2(3), C1-C2 143.4(3), C2-C3 139.9(3), C3-C4 144.0(3), C4-B 152.0(3); B-N 151.5(3).

C1–C2 and C3–C4 lengthened). The π-interaction with the exocyclic amino group is also greatly weakened: the B–N bond (151.5 pm) is about 10 pm longer than that typically found in (dialkylamino)boranes (141–142 pm[8]), and the amino group is no longer planar (sum of angles at the N atom 344.7° vs. 328.5° in the case of the regular tetrahedron).

Dihydroborolediides are interesting synthetic building blocks, as has already been demonstrated in the case of the diisopropylamino compound **3c**.[9] However, in the numerous transition metal complexes of **3c**, substitution at the B atom has thus far proven impossible.[9b] We shall shortly show elsewhere that this limitation does not arise in the case of complexes of **3a, b**:[3b, 10] borole complexes with quite different substituents at the B atom can be prepared via the 1-(dimethylamino)- and 1-(diethylamino)borole complexes by substitution reactions.

Experimental

3a: a solution of LiTMP [11] (18.0 g, 122 mmol) in THF (60 mL) was treated at −78 °C with 6.4 g (59 mmol) of **1a** [2] and the mixture stirred for 12 h at 20 °C. Concentration of the solution, addition of 200 mL of pentane and double crystallization at −78 °C furnished colorless needles of **3a** · THF, which on drying in vacuo (10^{-6} bar) yielded 5.0 g (70%) of powdery **3a**. M.p. >250 °C, extremely sensitive towards air and moisture [12]. ^{1}H NMR (80 MHz, [D$_8$]THF, int. TMS): δ = 5.35 (m; H-3,4), 4.03 (m; H-2,5), $N = {}^3J_{2,3} + {}^4J_{2,4}$ = 7.4 Hz, 2.27 (s; NMe_2); ^{11}B NMR (32.08 MHz, [D$_8$]THF, ext. $BF_3 \cdot Et_2O$): δ = 27 (halfwidth 280 Hz); ^{13}C NMR (67.88 MHz, 213 K, [D$_8$]THF, int. TMS): δ = 98.9 (d, J = 151 Hz; C3,4), 82.8 (d, J = 140 Hz; C2,5), 44.5 (q, J = 129 Hz; NMe_2).

3b: synthesis as in the case of **3a** afforded a colorless powder of **3b** (71%). M.p. 126 °C, no decomposition up to 250 °C, extremely sensitive towards air and water [12].—^{1}H NMR (80 MHz, [D$_8$]THF, int. TMS): δ = 5.37 (m; H-3,4), 3.95 (m; H-2,5), $N = {}^3J_{2,3} + {}^4J_{2,4}$ = 7.3 Hz, 2.70 (q, J = 7.1 Hz; 2 CH_2), 0.96 (t, J = 7.1 Hz; 2 Me); ^{11}B NMR (32.08 MHz, [D$_8$]THF, ext. $BF_3 \cdot Et_2O$): δ = 25 (halfwidth, 400 Hz).

4a: $LiNMe_2$ (1.0 g, 20 mmol) was treated at 0 °C with 2.1 g (19.3 mmol) of **1a** [2] and the mixture stirred for 3 h at 20 °C. Removal of the solvent in vacuo (10^{-2} bar) furnished **4a** as a highly viscous oil (97%), which could not be brought to crystallization from, e.g., Et_2O/pentane at −70 °C; soluble in THF, insoluble in pentane.—NMR data: [3b]; see also **5** [13].

5: a solution of **4a** (1.5 g, 9.4 mmol) in THF (20 mL) was treated with 1.2 g (10 mmol) of TMEDA. Concentration of the solution, layering with pentane, and cooling to −78 °C furnished 2.4 g (93%) of white crystals of **5**. M.p. 53 °C, decomp. 110 °C, sensitive towards air and moisture [12]. ^{1}H NMR (80 MHz, [D$_8$]THF, int. TMS): δ = 5.55 (m, H-3,4), 0.92 (s br; H-2,5), 2.33 (s, 2 NCH_2), 2.18 (s; 2 + 2 NMe_2); ^{11}B NMR (32.08 Mhz, [D$_8$]THF, ext. $BF_3 \cdot Et_2O$): δ = 5.0 (halfwidth, 49 Hz); ^{13}C NMR (67.88 MHz, 300 K, [D$_8$]THF, int. TMS): δ = 134.0 (d, J = 153 Hz; C3,4), 26.3 (t, J = 132 Hz; C2,5), 44.5 (q, J = 133 Hz; 2 NMe_2); TMEDA: 58.3 (t, J = 129 Hz; 2 NCH_2), 46.1 (q, J = 134 Hz; 2 NMe_2).

6a: a solution of **3a** (1.0 g, 8.3 mmol) in THF (30 mL) was treated with 1.2 g (10 mmol) of TMEDA. Evaporation of the reaction solution to a half of its volume and crystallization at −78 °C furnished 1.9 g (97%) of clustered crystals of **6a**. M.p. >250 °C, extremely sensitive towards air and moisture [12].—NMR data: [3b, 13].

6b: synthesis as in the case of **6a** yielded colorless rectangular crystals of **6b** (94%). M.p. 166 °C, decomp. 210 °C (black coloration), extremely sensitive towards air and moisture [12].—NMR data: [3b, 13].

6c: synthesis from **3c** [1b] as in the case of **6a** afforded colorless rectangular crystals of **6c** (97%). M.p. 193 °C, no decomposition up to 250 °C, extremely sensitive towards air and moisture [12].—NMR data: [3b, 13].

Received: October 23, 1989 [Z 3602 IE]
German version: *Angew. Chem. 102* (1990) 330

[1] a) $K_2[C_4BPh_5]$: G. E. Herberich, B. Buller, B. Hessner, W. Oschmann, *J. Organomet. Chem. 195* (1980) 253; J. J. Eisch, J. E. Galle, S. Kozima, *J. Am. Chem. Soc. 108* (1986) 379; b) **3c**: G. E. Herberich, H. Ohst, *Z. Naturforsch. B38* (1983) 1388; c) $K_2[C_4BEt_3Me_2]$ in THF: B. Wrackmeyer, *Organometallics 3* (1984) 1.

[2] G. E. Herberich, W. Boveleth, B. Hessner, M. Hostalek, D. P. J. Köffer, H. Ohst, D. Söhnen, *Chem Ber. 119* (1986) 420.

[3] a) R. Laven, *Diplomarbeit*, Technische Hochschule Aachen 1987; b) *Dissertation*, Technische Hochschule Aachen 1990.

[4] Such amidoborates are rare; cf. R. Köster in *Houben-Weyl-Müller: Methoden der Organischen Chemie, Bd. 13, Teil 3b*, Thieme, Stuttgart 1983, pp. 854, 860–862.

[5] The same type of structure was found X-ray crystallographically in the case of **6c**; the crystals however, were disordered.

[6] Nicolet R3m/V, $Mo_{K\alpha}$ radiation, measurement temperature 125 K. **4b**: $P2_1/n$ (No. 14), a = 1014.4(2), b = 1142.6(2), c = 1517.0(3) pm, β = 103.91(2)°; V = 1.7522(6) nm^3; Z = 4/2; ϱ_{calcd} = 0.967 g cm^{-3}; 2271 independent reflections with $F_0 \geq 4\sigma(F)$; non-hydrogen atoms refined anisotropically, H atoms placed at calculated positions and their isotropic temperature factors refined groupwise: 220 parameters, extinction correction, R = 0.55, R_w = 0.076 with $w^{-1} = \sigma^2(F_0) + 0.00179\,F_0^2$. Further details of the crystal structure investigation are available on request from the Fachinformationszentrum Karlsruhe, Gesellschaft für wissenschaftlich-technische Information mbH, D-7514 Eggenstein-Leopoldshafen 2 (FRG), on quoting the depository number CSD-320068, the names of the authors, and the journal citation.

[7] W. N. Setzer, P. von R. Schleyer, *Adv. Organomet. Chem. 24* (1984) 353; α-lithio-2,6-dimethylpyridine-TMEDA dimer: P. von R. Schleyer, R. Hacker, H. Dietrich, W. Mahdi, *J. Chem. Soc. Chem. Commun. 1985*, 622.

[8] P. Paetzold, *Adv. Inorg. Chem. 31* (1987) 123.

[9] a) G. E. Herberich, H. Ohst, H. Mayer, *Angew. Chem. 96* (1984) 975; *Angew. Chem. Int. Ed. Engl. 23* (1984) 969; G. E. Herberich, H. Ohst, *Chem. Ber. 118* (1985) 4303; G. E. Herberich, B. Hessner, H. Ohst, I. Raap, *J. Organomet. Chem. 348* (1988) 305; b) H. Ohst, *Dissertation*, Technische Hochschule Aachen 1984.

[10] G. E. Herberich, M. Hostalek, unpublished.

[11] M. Fieser, L. F. Fieser: *Reagents for Organic Synthesis, Vol. 4*, Wiley Interscience, New York 1974.

[12] Correct C, H analyses.

[13] The NMR spectra of **5** and **6a–c** show no significant differences from those of the TMEDA-free compounds apart from the additional signals of the TMEDA.

Synthesis and Structure of the Novel μ_2-Carbido Complex [(TPP)Fe=C=Re(CO)$_4$Re(CO)$_5$]**

By *Wolfgang Beck,* Wolfgang Knauer,* and *Christian Robl*

Dedicated to Professor Günther Wilke on the occasion of his 60th birthday

Of the organometallic compounds with multiple bonds between substituent-free main group elements and transition

[*] Prof. Dr. W. Beck, Dipl.-Chem. W. Knauer, Dr. habil. C. Robl [+]
Institut für Anorganische Chemie der Universität
Meiserstr. 1, D-8000 München (FRG)

[+] X-ray structure analysis.

[**] Hydrocarbon-Bridged Complexes, Part 16. This work was supported by the Deutsche Forschungsgemeinschaft and the Fonds der Chemischen Industrie. We thank Professor Dr. *W. Herrmann* and Dr. *E. Herdtweck*, Technische Universität München, for valuable discussions.—Part 15: [18].

metal atoms,[1] dinuclear complexes with a single carbon atom between two metal atoms appear especially interesting. To our knowledge the dimetalla-allenes **1** (L = tetraphenylporphyrinate,[2] phthalocyaninate[3]) and the C-metalated carbyne complex **2**[4] have thus far been isolated and structurally characterized.

$[LFe=C=FeL]$ **1** $[(Me_3CO)_3W\equiv C\text{-}Ru(CO)_2Cp]$ **2**

$[L_2Pt\{\text{-}C\equiv W(OR)_3\}_2]$ **3** $[(OC)_4Fe=Si=Fe(CO)_4]\cdot 2\,HMPT$ **4**

$[L(OC)_2Mn=E=Mn(CO)_2L]$ **5**

Pt–C≡W compounds, e.g. **3**, have been mentioned as intermediates.[5] μ-Carbido complexes are of interest as model systems for surface carbides.[1,4] Of the compounds of the homologues of carbon, **4**[6] and **5** (E = Ge,[7] Sn,[8] Pb[9]; L = C_5H_5 or C_5Me_5) are known. In the course of our studies on the directed synthesis of hydrocarbon-bridged complexes using carbonylmetalates[10] we found a simple entry to heterometallic μ_2-carbido complexes. Reaction of the dichlorocarbene complex **6**[11] with pentacarbonylrhenate(-*I*) affords the trinuclear compound **7** with 1,3-dimetalla-allene system[12] (TPP = tetraphenylporphyrinate).

$$[(TPP)Fe=CCl_2] \xrightarrow[CO,\ 2\,Cl^{\ominus}]{2\,Re(CO)_5^{\ominus}} [(TPP)Fe=C=Re(CO)_4Re(CO)_5]$$

6 **7**

Compound **7**, which is moderately soluble in dichloromethane and stable in the solid state, is extremely thermostable (decomposition above 260 °C). In the ^{13}C-NMR spectrum of **7**, the "carbide" C-atom is shifted upfield by about $\Delta\delta = 13$ compared to that of **6**.

Upon adding *n*-hexane to a CH_2Cl_2 solution of **7**, shiny deep-violet crystals suitable for an X-ray structure analysis were obtained. The structure of **7** in the crystal (Fig. 1) shows an almost linear Fe–C–Re grouping (172.8(4)°). The Fe–C distance (1.605(13) Å) is very short; it is shorter than in **1**, L = tetraphenylporphyrinate (1.67 Å),[2b] and also shorter than in carbynemetal complexes.[13] The Re–C(carbide) bond in **7** (1.957(12) Å) is somewhat longer than the axial Re–C(carbene) bond of the carbene complex **8** (1.85(3) Å)[14] and of about the same length as found in an allylidene-rhenium complex.[15] In **9**, Ru–C and C≡W distances of 2.09(2) and 1.75(2) Å, respectively, have been established.[4] The Re–Re bond in **7** is of a similar length to that found in the Fischer carbene complexes **10**[14] (3.052(1) Å) and **11**[14] (3.091(2) Å) and in $Re_2(CO)_{10}$ (3.041(1) Å).[16]

$[\{Ph_3Si(EtO)C=\}(OC)_4Re\text{-}Re(CO)_4\{=C(OEt)SiPh_3\}]$ **8**

$[Cp(OC)_2Ru\text{-}C\equiv W(OCMe_3)_3]$ **9** $[Re_2(CO)_9\{C(OR)SiPh_3\}]$ **10**

$[Re_2(CO)_8\{C(OEt)SiPh_3\}_2]$ **11**

Figure 1b shows quite impressively the twisting of the porphyrin ligand in **7**.

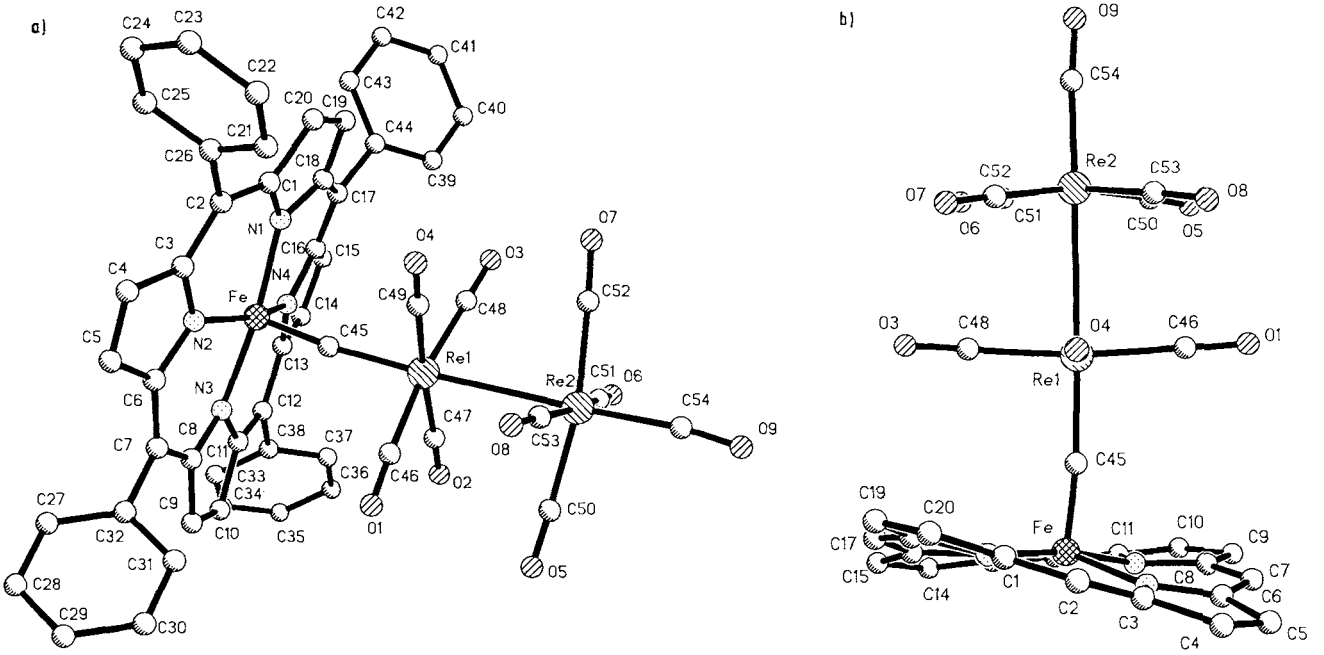

Fig. 1. a) Structure of $C_{54}H_{28}N_4O_9FeRe_2$ **7** in the crystal at 22 °C. H atoms not shown. b) Side view of **7**, without phenyl groups and H atoms.—Siemens R3m/V diffractometer, space group $P\bar{1}$ (No. 2), $a = 12.626(5)$, $b = 14.121(4)$, $c = 14.860(4)$ Å, $\alpha = 77.17(2)$, $\beta = 67.65(3)$, $\gamma = 72.46(3)°$, $V = 2319.0(1.3)$ Å^3, $Z = 2$. $\varrho_{calcd} = 1.87$ g cm^{-3}, $F(000) = 1256$, $\mu = 56.5$ cm^{-1} ($Mo_{K\alpha}$), numerical absorption correction. ω-Scan, $\theta_{max} = 25°$, measuring rate 2.44–14.65 grad min^{-1}, scan width 1.40°. 8870 reflections measured, 8116 symmetry independent, $R_{inf} = 0.011$; 6429 reflections with $F > 3\sigma F$. 585 parameters, $R = 0.081$, $wR = 0.036$, $w = 1/\sigma^2 F$. Phenyl rings and H atoms positioned geometrically. Calculations with SHELXTL-PLUS. Selected bond lengths [Å] and angles [°]: Re1-Re2 3.043(1), Re1-C45 1.957(12), Fe-C45 1.605(13), Fe-N1 1.990(9), Fe-N2 1.973(11), Fe-N3 1.995(8), Fe-N4 1.972(11); Fe-C45-Re1 173.3(9), C45-Re1-Re2 176.8(3), N1-Fe-N2 90.1(4), N1-Fe-N3 172.8(4), N1-Fe-N4 89.2(4), N2-Fe-N3 89.1(4), N2-Fe-N4 161.5(4), N3-Fe-N4 89.3(4). Further details of the crystal structure determination are available on request from the Fachinformationszentrum Karlsruhe, Gesellschaft für wissenschaftlich-technische Information mbH, D-7514 Eggenstein-Leopoldshafen 2 (FRG), on quoting the depository number CSD-54270, the names of the authors, and the journal citation.

The equatorial CO ligands of the two $Re(CO)_4$ groups are staggered and as in $Re_2(CO)_{10}$,[16] **12**,[17] and **13**,[18] are bent towards each other.

$[(OC)_5Re\text{–}CH_2CH_2\text{–}Re(CO)_5]$ **12**

$[(OC)_5Re\text{–}C\equiv C\text{–}Re(CO)_5]$ **13**

Experimental

All operations were carried out in anhydrous solvent under nitrogen.

7: A clear orange-colored solution (20 °C) of $Na[Re(CO)_5]$ (prepared from 185 mg (0.285 mmol) of $Re_2(CO)_{10}$ and sodium amalgam in 5 mL of THF) was added with stirring to the violet suspension of **6** [11] (150.3 mg, 0.2 mmol) in 10 mL of THF (−78 °C). After 1 h at −78 °C, the mixture was warmed to 30 °C, stirred for a further 60 min, and the solvent removed in vacuo. The residue was taken up in CH_2Cl_2, centrifuged, and the solvent again removed in vacuo. Subsequent washing of the residue with hexane (three times) and cold MeOH (once) followed by drying in vacuo furnished **7** as a reddish-brown powder. *Yield*: 135 mg (51%). Crystals from CH_2Cl_2/hexane.

IR (KBr): $\tilde{\nu}$[cm^{-1}] = 3050–3020 (w, CH); 2104(m), 2053(m), 2005(s), 1975(s) (CO); 1595 (m, C=C). IR (CH_2Cl_2): νCO[$Re(CO)_5$] = 2109 (m, A_1), 2003 (s, E), 1970 (s, A_1); νCO[$Re(CO)_4$] = 2054 (s, E).—^{1}H NMR (270 MHz; $CDCl_3$, 25 °C, $CDCl_3$ as standard): δ = 7.73 (m, 12H), 8.11, 8.36 (m, 8H); 8.86 (s, 8H). —^{13}C NMR (67.89 MHz; $CDCl_3$, 25 °C, $CDCl_3$ as standard): δ = 120.8, 121.8, 126.8, 127.7, 132.1, 133.6, 141.7, 145.6 (TPP); 178.9 (CO); 211.7 (carbene-C).

Received: October 20, 1989 [Z 3598 IE]
German version: *Angew. Chem. 102* (1990) 331

[1] Review: W. A. Herrmann, *Angew. Chem. 98* (1986) 57; *Angew. Chem. Int. Ed. Engl. 25* (1986) 56.
[2] a) D. Mansuy, J.-P. Lecomte, J.-C. Chottard, J.-F. Bartoli, *Inorg. Chem. 20* (1981) 3119; b) V. L. Goedken, M. R. Deakin, L. A. Bottomley, *J. Chem. Soc. Chem. Commun. 1982*, 607; c) D. R. English, D. N. Henrickson, K. S. Suslick, *Inorg. Chem. 22* (1983) 367.
[3] G. Rossi, V. L. Goedken, C. Ercolani, *J. Chem. Soc. Chem. Commun. 1988*, 46; E. N. Bakshi, C. D. Delfs, K. S. Murray, B. Peters, H. Homborg, *Inorg. Chem. 27* (1988) 4318;
[4] S. L. Latesky, J. P. Selegue, *J. Am. Chem. Soc. 109* (1987) 4731.
[5] R. J. Blau, M. H. Chisholm, K. Folting, R. J. Wang, *J. Am. Chem. Soc. 109* (1987) 4552.
[6] C. Zybill, D. L. Wilkinson, G. Müller, *Angew. Chem. 100* (1988) 574; *Angew. Chem. Int. Ed. Engl. 27* (1988) 583.
[7] W. Gäde, E. Weiss, *J. Organomet. Chem. 213* (1981) 451; D. Melzer, E. Weiss, *ibid. 263* (1984) 67; J. D. Korp, I. Bernal, R. Hörlein, R. Serrano, W. A. Herrmann, *Chem. Ber. 118* (1985) 340; W. A. Herrmann, H.-J. Kneuper, E. Herdtweck, *ibid. 122* (1989) 433.
[8] W. A. Herrmann, H.-J. Kneuper, E. Herdtweck, *Chem. Ber. 122* (1989) 437.
[9] W. A. Herrmann, H.-J. Kneuper, E. Herdtweck, *Angew. Chem. 97* (1985) 1060; *Angew. Chem. Int. Ed. Engl. 24* (1985) 1062; *Chem. Ber. 122* (1989) 445.
[10] Review: W. Beck, *Polyhedron 7* (1988) 2255; W. Beck, B. Niemer, J. Breimair, J. Heidrich, *J. Organomet. Chem. 372* (1989) 79.
[11] D. Mansuy, M. Lange, J.-C. Chottard, P. Guerin, P. Morliere, D. Brault, M. Rougee, *J. Chem. Soc. Chem. Commun. 1977*, 648; D. Mansuy, M. Lange, J.-C. Chottard, J. F. Bartoli, B. Chevrier, R. Weiss, *Angew. Chem. 90* (1978) 828; *Angew. Chem. Int. Ed. Engl. 17* (1978) 781; D. Mansuy, *Pure Appl. Chem. 52* (1980) 681; review on dihalocarbene complexes: P. J. Brothers, W. R. Roper, *Chem. Rev. 88* (1988) 1293.
[12] Compound **6** was also allowed to react with the carbonylmetalates $Mn(CO)_5^{\ominus}$, $Fe(CO)_4^{2\ominus}$ and $Cr(CO)_5^{2\ominus}$. The manganese compound can, according to the IR spectrum [νCO [cm^{-1}] (CH_2Cl_2): 2095(m), 2033(s), 2004(s), 1970(m)], be assigned a structure analogous to **7**. Analytical and IR data of the products obtained from **6** and $Fe(CO)_4^{2\ominus}$ and $Cr(CO)_5^{2\ominus}$ are consistent with the formation of (TPP)Fe=C=$Fe(CO)_4$ and (TPP)Fe=C=$Cr(CO)_5$, respectively.
[13] H. Fischer, P. Hofmann, F. R. Kreissl, R. R. Schrock, U. Schubert, K. Weiss: *Carbyne Complexes*, VCH Verlagsgesellschaft, Weinheim 1988.
[14] U. Schubert, K. Ackermann, P. Rustemeyer, *J. Organomet. Chem. 231* (1982) 323.
[15] W. A. Herrmann, R. A. Fischer, E. Herdtweck, *Angew. Chem. 99* (1987) 1286; *Angew. Chem. Int. Ed. Engl. 26* (1987) 1263.
[16] L. F. Dahl, E. Ishishi, R. E. Rundle, *J. Chem. Phys. 26* (1957) 1750; M. R. Churchill, K. N. Amoh, H. J. Wasserman, *Inorg. Chem. 20* (1981) 1609.
[17] K. Raab, U. Nagel, W. Beck, *Z. Naturforsch. B38* (1983) 1466.
[18] J. Heidrich, M. Steimann, M. Appel, W. Beck, J. R. Phillips, W. C. Trogler, *Organometallics*, in press.

Dependence of Anomeric Stabilization on Structure in Acetals**

By *Hans-Dieter Beckhaus, Barbara Dogan, Sergej Verevkin, Johannes Hädrich*, and *Christoph Rüchardt**

Dedicated to Paul von Ragué Schleyer on the occasion of his 60th birthday

The anomeric effect[1] is a well known example of a synergetic interaction of geminal substituents on a saturated carbon atom. According to this concept the two alkoxy groups in acetals **1** contribute more to the stabilization of the molecule than would correspond to a purely additive effect.[1c] Although this extra stabilization is thought to be responsible for a number of phenomena, e.g. the conformational preference and reactivity of glucosides,[1e] very few quantitative experimental data are available[2, 3] on the extent of anomeric stabilization and its variation by substituents on the anomeric carbon atom. The generally accepted model[1d] of "negative hyperconjugation" suggests that alkyl and aryl residues on the central C-atom could alter the anomeric stabilization.

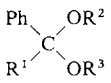

1a: R^1 = H, R^2 = R^3 = Me
1b: R^1 = R^2 = R^3 = Me
1c: R^1 = H, R^2, R^3 = $-CH_2CH_2-$
1d: R^1 = Me, R^2, R^3 = $-CH_2CH_2-$
1e: R^1 = H, R^2, R^3 = $-CH_2CMe_2CH_2-$
1f: R^1 = Me, R^2, R^3 = $-CH_2CMe_2CH_2-$

We report here on thermochemical measurements with the aromatic acetals **1a–f**. The standard enthalpies of formation ΔH_f^0 (g) were obtained from the enthalpies of combustion ΔH_c (l) and vaporization ΔH_v[4] (Table 1). The results of earlier measurements on aliphatic acetals[3] were used in the calculations.

We determined the extra, anomeric stabilization by comparison of the increments in enthalpy of formation of alkyl and alkoxy groups with acetal groups. That is, we did not use the enthalpy of formation of an individual compound in the otherwise usual process of the isodesmic reaction,[5] but group increments,[2] which were calculated from several homologous structures. The result then has a broader experimental basis. We used the known increments ΔH_{alkyl} for alkanes[6a] and alkylbenzenes[6b] (Table 2) and determined the remaining increments according to the least squares method. Firstly, the increments for the alkoxy groups ΔH_{oxy} were calculated from the ΔH_f^0 (g) values of dialkyl ethers.[7] The division into the ether group O[2C] and the groups with C as key atom and an O atom as neighbor CH_2[O,C], CH[O,2C], and C[O,3C] was done by defining the methyl group: ΔH_f^0 (g) of CH_3[O] = ΔH_f^0 (g) of CH_3[C] = −10.05 kcal mol^{-1}. Finally, the increments for the alkyl groups with two

[*] Prof. Dr. C. Rüchardt, Dr. H.-D. Beckhaus, Dr. B. Dogan, Dr. J. Hädrich
Institut für Organische Chemie und Biochemie der Universität
Albertstrasse 21, D-7800 Freiburg (FRG)
Dr. S. Verevkin
Kuibyshew Politechnisches Institut, Kuibyschew (UdSSR)

[**] Geminal Substituent Effects, Part 2. This work was supported by the Deutsche Forschungsgemeinschaft and the Fonds der Chemischen Industrie. S.V. thanks the Deutscher Akademischer Austauschdienst (DAAD) for an exchange grant.—Part 1: [4c].

Table 1. Combustion enthalpies $\Delta H_c(l)$, vaporization enthalpies ΔH_v and standard enthalpies of formation ΔH_f^0 of **1a–f**, as well as calculated values from group increments $\Delta H_{f,calcd}$ [kcal mol^{-1}].

	$\Delta H_c(l)$	ΔH_v	$\Delta H_f^0(l)$	$\Delta H_f^0(g)$	$\Delta H_{f,calc}$ [a, b]	$\Delta\Delta H$ [c]
1a	−1176.42 ±0.39	14.21 ±0.17	−79.93 ±0.39	−65.72 ±0.42	−64.62	1.10
1b	−1328.31 ±0.42	13.15 ±0.30	−90.41 ±0.42	−77.26 ±0.52	−76.94	0.32
1c	−1120.26 ±0.33	15.72 ±0.23	−67.77 ±0.33	−52.05 ±0.39	−52.92	−0.87
1d	−1267.03 ±0.53	19.57 ±0.12	−83.37 ±0.53	−63.80 ±0.54	−65.24	−1.44
1e	−1578.90 ±0.30	16.04 ±0.19	−91.79 [d] ±0.30	−75.75 ±0.36	−76.32	−0.57
1f	−1733.76 ±0.55	13.63 ±0.28	−103.74 ±0.55	−90.11 ±0.62	−88.64	1.47

[a] Group increments, see Table 2. [b] Ring strain (7.5 kcal mol^{-1} in the case of dioxacyclopentane, 2.5 in the case of all other oxacycles) and repulsion of geminal methyl groups at the quaternary C-atom (2.0 kcal mol^{-1}) were taken into consideration as additive terms. [c] $\Delta\Delta H = \Delta H_{f,calcd} - \Delta H_f^0(g)$. [d] $\Delta H_m = 4.44$.

O-atoms as neighbors (ΔH_{dioxy}) were calculated from the enthalpies of formation of the acetals (Table 1).[8] The goodness of fit is seen from the small differences $\Delta\Delta H$ (see Table 1) between the calculated value $\Delta H_{f,calcd}^0$, i.e. the sum of the increments including the strain enthalpy, and $\Delta H_f^0(g)$.

The increments ΔH_{oxy} for α-CH_2, α-CH and α-C atoms in ethers are clearly smaller than the corresponding ΔH_{alkyl} values in alkanes (Table 2). Since we have allotted the same

Table 2. Increments in enthalpy of formation [kcal mol^{-1}] for alkyl (ΔH_{alkyl}), alkoxy (ΔH_{oxy}) and acetal groups (ΔH_{dioxy}) [8].

	ΔH_{alkyl} [6]	ΔH_{oxy} [7]	ΔH_{dioxy} aliphatic [8]		ΔH_{dioxy} aromatic [b]
CH_3	[C] −10.05	[O] ≡ −10.05		–	–
CH_2	[2C] −5.13	[O,C] −8.0	[2O] −14.1	–	
CH	[3C] −2.16	[O,2C] −6.3	[2O, C] −15.6	[2O, C_{Ph}]	−18.9
C	[4C] −0.30	[O,3C] −4.7	[2O, 2C] −17.9	[2O, C, C_{Ph}]	−21.2

[a] Neighboring atoms of CH_2 in square brackets; C_{Ph} signifies phenyl-C atom and C an sp^3-C-atom. [b] From the acetals of Table 1.

values to the methyl groups CH_3[O] as to the CH_3[C] groups, it follows that C atoms are more strongly stabilized by a neighboring C-atom. The extent of this stabilization corresponds to the differences $\Delta H_{oxy} - \Delta H_{alkyl}$ and $\Delta H_{dioxy} - \Delta H_{oxy}$ (Table 3). In ethers, this oxygen effect is similar for all groups ($\Delta H_{oxy} - \Delta H_{alkyl} = -2.8$ to -4.4 kcal mol^{-1}). The stabilization on going from the ether to the acetal, on the other hand, strongly depends on the degree of substitution of the C-atom; $\Delta H_{dioxy} - \Delta H_{oxy}$ varies from -6.1 to -16.5 kcal mol^{-1}.

The extra, anomeric stabilization $\Delta\Delta H_{anomer}$, i.e. the additional energy gained on introduction of the second oxygen atom in comparison to the first is given by the difference $(\Delta H_{dioxy} - \Delta H_{oxy}) - (\Delta H_{oxy} - \Delta H_{alkyl})$ (Table 3). Aliphatic acetals containing the C[2O,2C] group are stabilized by $\Delta\Delta H_{anomer} = -8.8$, aliphatic acetals containing the CH[2O,C] group by -5.1, and formaldehyde acetals by only -3.3 kcal mol^{-1}. The anomeric effect increases by 2–4 kcal mol^{-1} on substitution of the anomeric carbon atom by an alkyl. On replacing an alkyl group by a phenyl group with the ability to undergo π conjugation the molecule is stabilized by a further 3.3 kcal mol^{-1}. The acetal of an alkyl phenyl ketone containing the C[2O,C,C_{ph}] group exhibits

Table 3. Anomeric stabilization $\Delta\Delta H_{anomer}$ of aliphatic and aromatic acetals from the difference in group increments (cf. Table 2) [kcal mol^{-1}].

	ΔH_{oxy} [a] $-\Delta H_{alkyl}$ [c]	ΔH_{dioxy} [b] $-\Delta H_{oxy}$ [a]		$\Delta\Delta H_{anomer}$ [d]	
C_{Ph} present [e]		no	yes	no	yes
$CH_2[O_x, C_{2-x}]$	−2.8	−6.1	–	−3.3	–
$CH[O_x, C_{3-x}]$	−4.2	−9.3	−12.6	−5.1	−8.4
$C[O_x, C_{4-x}]$	−4.4	−13.2	−16.5	−8.8	−12.1

[a] Number of neighboring O atoms x = 1. [b] Number of neighboring O atoms x = 2. [c] Number of neighboring O atoms x = 0. [d] $\Delta\Delta H_{anomer} = (\Delta H_{dioxy} - \Delta H_{oxy}) - (\Delta H_{oxy} - \Delta H_{alkyl})$. [e] To differentiate the pure aliphatic acetals with $CH_y[2O,C_{2-y}]$ groups from aromatic compounds with $CH_y[2O,C_{1-y}C_{Ph}]$ groups.

the highest anomeric stabilization (-12.1 kcal mol^{-1}) detected so far. Current investigations should show whether a further phenyl group (in benzophenone acetals) would increase the anomeric effect further, and whether an analogous phenyl effect is effective in benzyl ethers.[9]

Received: October 26, 1989 [Z 3611 IE]
German version: *Angew. Chem. 102* (1990) 313

CAS Registry numbers:
1a, 1125-88-8; **1b**, 4316-35-2; **1c**, 936-51-6; **1d**, 3674-77-9; **1e**, 776-88-5; **1f**, 5406-58-6.

[1] a) A. J. Kirby: *The Anomeric Effect and Related Stereoelectronic Effects at Oxygen*, Springer, Berlin 1983, and references cited therein; b) R. W. Franck, *Tetrahedron 39* (1983) 3251; c) P. von R. Schleyer, E. D. Jemmis, G. W. Spitznagel, *J. Am. Chem. Soc. 107* (1985) 6393; d) P. von R. Schleyer, A. J. Kos, *Tetrahedron 39* (1983) 1141; e) H.-G. Korth, R. Sustmann, K. S. Gröninger, M. Leisung, B. Giese, *J. Org. Chem. 53* (1988) 4364.

[2] S. W. Benson: *Thermochemical Kinetics*, Wiley, New York 1976, p. 274.

[3] a) J. B. Pedley, R. D. Naylor, S. P. Kirby: *Thermochemical Data of Organic Compounds*, Chapman and Hall, London 1986; b) J. D. Cox, G. Pilcher: *Thermochemistry of Organic and Organometallic Compounds*, Academic Press, London 1970.

[4] a) Synthesis of **1a–f**: J. Hädrich, *Dissertation*, Universität Freiburg 1989; b) combustion in a Lund isoperibolic calorimeter: S. Sunner, M. Manson: *Combustion Calorimetry, Vol. 1*, Pergamon Press, Oxford 1979; c) measurement of the enthalpy of vaporization: K. Fritzsche, B. Dogan, H.-D. Beckhaus, C. Rüchardt, *Thermochim. Acta*, in press.

[5] a) W. J. Hehre, R. Ditchfield, L. Radom, J. A. Pople, *J. Am. Chem. Soc. 92* (1970) 4796; b) P. George, M. Trachtman, A. M. Brett, C. W. Bock, *J. Chem. Soc. Perkin Trans. 2 1977*, 1036.

[6] a) P. von R. Schleyer, J. E. Williams, K. P. Blanchard, *J. Am. Chem. Soc. 92* (1970) 2377; b) H.-D. Beckhaus, *Chem. Ber. 116* (1983) 86.

[7] The $\Delta H_f^0(g)$ values [3] of the following alkyl ethers enter into the calculation of the group increments ΔH_{oxy} (Table 2): methoxymethane, 1-methoxyethane, 1-methoxypropane, 1-methoxybutane, 2-methoxypropane, 2-methoxy-2-methylpropane (1.4 kcal mol^{-1}), 1-ethoxyethane, 1-ethoxypropane, di-*n*-propyl ether, diisopropyl ether (0.5), di-*n*-butyl ether, diisobutylether (0.5) and di-*tert*-butyl ether (6.6). The respective steric strains taken into account in the calculations are quoted in brackets. They were determined from the structurally analogous alkanes, obtained by replacing O by CH_2. O[2C] = −23.8 kcal mol^{-1}.

[8] The group increments for aliphatic acetals in Table 2 were derived from 1,3-dioxolane ($\Delta H_f^0(g) = -71.10$ kcal mol^{-1}), 1,3-dioxane (−80.86), 1,3,5-trioxacyclohexane (−111.32), 1,3,5,7-tetraoxacyclooctane (−148.24), 1,3,5,7,9-pentaoxacyclodecane (−186.38), 2-methoxytetrahydropyran (−95.50), dimethoxymethane (−83.27), 1,1-dimethoxyethane (−93.26), 2,2-dimethoxypropane (−101.89), diethoxymethane (−99.14), 1,1-diethoxyethane (−108.39), 2,2-diethoxypropane (−121.08), and dibutoxymethane (−119.81) [3].

[9] $\Delta H_f^0(g)$ values for alkyl benzyl and dibenzyl ethers have not yet been listed [3].

First Coupling of a Metal Atom with Four Ethene Molecules to give a Metallaspiroalkane**

By *Klaus Jonas,** *Günter Burkart, Christian Häselhoff, Peter Betz,* and *Carl Krüger*

Dedicated to Professor Günther Wilke on the occasion of his 65th birthday

Up to now, only a few examples of transition metal complexes with more than two ethene ligands are known. Tris(ethene)nickel(0),[1] the first homoleptic transition-metal-ethene-complex, was reported in 1973, and two years later *Stone* et al. described the analogous platinum compound **2**.[2] There are only the iridium compound **3**[3] and the alkali metal-transition metal complexes **4** and **5** containing one more ethene ligand. **4** and **5** are accessible from cobaltocene and ferrocene, respectively, by reductive five-membered ring ligand removal[4].

$Ni(C_2H_4)_3$ $Pt(C_2H_4)_3$ $ClIr(C_2H_4)_4$

1 **2** **3**

$M_A[Co(C_2H_4)_4]$, $Li_2[Fe(C_2H_4)_4]$

4, M_A = Li,K **5**

First findings on the reactivity of ethene towards low-valent manganese have already been briefly reported in a review article.[4] In the case of the reaction of manganese(II) cyclopentadienide (Cp_2Mn) with naphthalenepotassium (molecular ratio 1:3) in ethene-saturated tetrahydrofuran (THF) mentioned therein, we have now found that exactly 3 moles of C_2H_4 are taken up per mole of Mn at $-65\,^{\circ}C$. All the Cp precipitates as KCp, and the markedly thermolabile manganese compound **6**, which must contain potassium and manganese in the molar ratio 1:1, remains in solution [Eq. (a)]. As yet we have been unable to isolate and fully characterize **6**. Consequently, it is also still an open question whether the manganese in **6** is present as manganese(-I) (with three π-bound ethene molecules) or whether the oxidation state of the manganese increases with uptake of the ethene (**6** as a metallacyclopentane[4, 5] or as a hydridovinyl compound[6]).

$$Cp_2Mn + 3\,K[C_{10}H_8] + 3\,C_2H_4 \xrightarrow[-65\,^{\circ}C]{THF} 2\,KCp\downarrow + x\,C_{10}H_8 + K[C_6H_{12}Mn(C_{10}H_8)_{3-x}] \quad (a)$$

6

When Cp_2Mn is reduced with naphthalenelithium (again in the ratio 1:3) and the ethene is replaced by trimethylphosphane [Eq. (b)], then, after substitution of the tetrahydrofuran bound to lithium by tetramethylethylenediamine (TMEDA), the novel manganese(-I) compound **7**, which is stable at room temperature, can be isolated (yield: 65%).

According to an X-ray structure analysis of the diamagnetic complex **7**,[7] three coordination sites of the pentacoordinated manganese are occupied by PMe_3 ligands, while the other two are occupied by an η^4-coordinated naphthalene molecule.

$$Cp_2Mn + 3\,Li[C_{10}H_8] + 3\,PMe_3 \xrightarrow[78\,^{\circ}C\ldots+20\,^{\circ}C]{THF}$$

$$2\,LiCp + 2\,C_{10}H_8 + [Li(thf)_x][Mn(\eta^4\text{-}C_{10}H_8)(PMe_3)_3]$$

$$\downarrow TMEDA \quad THF \quad (b)$$

$$[Li(tmeda)_2][Mn(\eta^4\text{-}C_{10}H_8)(PMe_3)_3]$$

7

We intended to convert complex **6**, which is obtained in THF solution according to equation (a), to a more thermally stable manganate. Decisive for the success of the synthesis of the novel potassium manganese compound **8** from **6**, ethene and pyridine [Eq. (c)] was the observation that the color of the ethene-saturated THF solution of **6** changes from red to brownish-yellow on warming to $-35\,^{\circ}C$. Orange **8** is isolated if pyridine is added and the solution subsequently warmed to room temperature (yield: 68%).

$$\mathbf{6}\text{ in THF (ethene)} \xrightarrow[-65\,^{\circ}C\ldots-35\,^{\circ}C]{} \text{brownish-yellow solution} \xrightarrow[-35\,^{\circ}C\ldots+20\,^{\circ}C]{pyridine} [K(py)_2][(py)Mn(C_4H_8)_2] \quad (c)$$

8

In the solid state, **8** contains two crystallographically independent ion pairs. Figure 1 shows both pairs in comparable orientation. With almost identical bond lengths they differ in the orientation of the pyridine ligands, both at the distorted square-pyramidally coordinated manganese atom as well as at the potassium. In the unit cell the latter forms ion pair contacts of unequal length to the butanediyl ligands of adjacent anions (K-C_α 3.09–3.33 Å). Correspondingly, the arrangements of the pyridine ligands bound to potassium (N–K (av) 2.787(3) Å) are not linear; the N–K–N angle is 139.0(1) and 147.0(1)°, respectively. The C–C bond lengths and the angles of the C_4H_8 ligands correspond within the limits of error to the values expected for $C(sp^3)$–$C(sp^3)$ bonds. The average Mn–N distance is 2.354(2) Å, while the average Mn–$C(sp^3)$ distance is 2.128(10) Å.

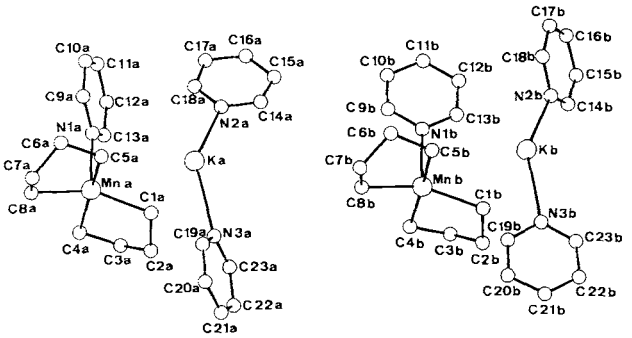

Fig. 1. Structure of **8** in the crystal (two crystallographically independent ion pairs, see text). $P2_1/a$, $a = 17.092(8)$, $b = 15.482(6)$, $c = 17.959(6)$ Å, $\beta = 108.32(3)°$, $V = 4511.4$ Å^3, $T = -173\,^{\circ}C$, $Z = 8$, $\varrho_{calcd} = 1.31$ g cm^{-3}, $\lambda = 0.71069$ Å, $\mu = 7.59$ cm^{-1}, $R = 0.052$, $R_w = 0.045$. 13127 independent reflections, 8538 observed ($I > 2\sigma(I)$), 505 refined parameters, residual electron density 0.51 eÅ^{-3}. Hydrogen atoms localized, but not refined [13].

[*] Prof. Dr. K. Jonas, Dr. G. Burkart, Dipl.-Chem. C. Häselhoff, Dr. P. Betz [+], Prof. Dr. C. Krüger [+]
Max-Planck-Institut für Kohlenforschung
Kaiser-Wilhelm-Platz 1, D-4330 Mülheim a. d. Ruhr (FRG)

[+] Crystal structure analysis.

[**] This work was supported by the Deutsche Forschungsgemeinschaft (stipendium for *P.B.*).

The synthesis and elucidation of the structure of **8** confirm once again that ring closure reactions of metal atoms with ethene to give metallacyclopentanes are to be expected, especially of the transition elements on the left of the 8th subgroup in the periodic system.[4, 8] That butanediyl ligands formed by the coupling of two ethene molecules can also occupy bridge positions was first demonstrated with the dinuclear complex $CpV(\mu\text{-}C_4H_8)_2VCp$.[9] Here we report on the new finding in metallacyclic chemistry[10, 11] that the ring closure with ethene leading to formation of a five-membered ring can also take place twice at a metal atom. The result is a metallaspirononane in which the transition metal functions as spiroatom.

Experimental

A THF-solution of naphthalenelithium (prepared from lithium (0.6 g, 86.5 mmol), naphthalene (10.98 g, 85.7 mmol) and THF (150 mL) at −15 °C) was treated with 10 mL (ca. 100 mmol) of PMe_3 at −78 °C and then with 5.28 g (28.5 mmol) of solid Cp_2Mn. After 1.5 hours' stirring at −78 °C, the mixture was allowed to warm to room temperature, and the resulting deep-red solution was evaporated to dryness; uncomplexed naphthalene was then removed by sublimation (20 °C, high vacuum). The residue remaining was taken up in 250 mL of Et_2O, filtered to remove LiCp, and the filtrate treated with 20 mL of TMEDA. On cooling to −30 °C, dark-red crystals of **7** separated out; these were washed with a little ether at −78 °C and dried in vacuo (oil-pump) at 20 °C (yield 12.10 g, 65%). Correct elemental analysis.

8: A solution of naphthalene (18.25 g, 142.4 mmol) in THF (400 mL) was treated with 5.63 g (144.0 mmol) of potassium pellets [12] and the mixture stirred for 1.5 h at −15 °C. Following subsequent cooling to −65 °C, saturation with ethene, and addition of solid Cp_2Mn (8.87 g, 47.9 mmol) the mixture was stirred under an atmosphere of ethene for a further 16 h and allowed to warm to −35 °C within 8 h. After a further 16 h at −78 °C, the KCp that separated out was removed by filtration, the filtrate treated with 15 mL (186.2 mmol) of pyridine and the mixture warmed to 20 °C. After evaporation to dryness, the naphthalene was removed at 20 °C by sublimation in vacuo. The residue was then taken up in 400 mL of ether, filtered, and the filtrate evaporated down in vacuo until **8** began to separate. By warming to 30 °C, **8** was brought into complete solution again and the solution stored at −30 °C. **8** separated as brownish-orange crystals. The crystals were washed with pentane and dried at 20 °C in vacuo (oil-pump). Yield: 14.45 g, 68%; correct elemental analysis.

Received: August 31, 1989 [Z 3531 IE]
German version: *Angew. Chem. 102* (1990) 291

CAS Registry numbers:
7, 125281-25-6; **8**, 125281-27-8; Cp_2Mn, 73138-26-8.

[1] K. Fischer, K. Jonas, G. Wilke, *Angew. Chem. 85* (1973) 620; *Angew. Chem. Int. Ed. Engl. 12* (1973) 565.
[2] M. Green, J. A. K. Howard, J. L. Spencer, F. G. A. Stone, *J. Chem. Soc. Chem. Commun 1975*, 3; *Dalton Trans. 1977*, 271.
[3] A. L. Onderdelinden, A. van der Ent, *Inorg. Chim. Acta 6* (1972) 420.
[4] K. Jonas, *Angew. Chem. 97* (1985) 292; *Angew. Chem. Int. Ed. Engl. 24* (1985) 295, and references cited therein.
[5] G. Erker, U. Dorf, A. L. Rheingold, *Organometallics 7* (1988) 138, and references cited therein.
[6] C. K. Ghosh, J. K. Hoyano, R. Krentz, W. A. G. Graham, *J. Am. Chem. Soc. 111* (1989) 5480, and references cited therein.
[7] Disorder in the region of the TMEDA moiety of the cation precluded a detailed discussion of the molecular geometry of **7**. $P2_1/c$, $a = 9.249(2)$, $b = 27.715(8)$, $c = 15.311(3)$ Å, $\beta = 101.84(1)°$, $Z = 4$, $R = 0.094$, $R_w = 0.089$. 8623 independent reflections [13].
[8] M. L. Steigerwald, W. A. Goddard III, *J. Am. Chem. Soc. 107* (1985) 5027.
[9] K. Jonas, W. Rüsseler, C. Krüger, E. Raabe, *Angew. Chem. 98* (1986) 902; *Angew. Chem. Int. Ed. Engl. 25* (1986) 925.
[10] a) G. Wilke, *Angew. Chem. 100* (1988) 189; *Angew. Chem. Int. Ed. Engl. 27* (1988) 185, and references cited therein. b) G. Wilke, *Pure Appl. Chem. 50* (1978) 677, and references cited therein.
[11] S. D. Chapell, D. J. Cole-Hamilton, *Polyhedron 1* (1982) 739.
[12] K. Jonas, E. Deffense, D. Habermann, *Angew. Chem. 95* (1983) 729; *Angew. Chem. Int. Ed. Engl. 22* (1983) 716; *Angew. Chem. Suppl. 1983*, 1005.
[13] Further details of the crystal structure analyses are available on request from the Fachinformationszentrum Karlsruhe, Gesellschaft für wissenschaftlich-technische Information mbH, D-7514 Eggenstein-Leopoldshafen 2 (FRG), on quoting the depository number CSD-54065, the names of the authors, and the journal citation.

BOOK REVIEWS

Book Reviews are written by invitation from the editor. Suggestions for books to be reviewed and for book reviewers are welcome. Publishers should send brochures or (better) books to the following address: Redaktion Angewandte Chemie, Postfach 101161, D-6940 Weinheim, Federal Republic of Germany. The editor reserves the right of selecting which books will be reviewed. Uninvited books not chosen for review will not be returned.

Supramolekulare Chemie. By *F. Vögtle*. Teubner, Stuttgart 1989. 447 pp., paperback, DM 42.00. – ISBN 3-519-03502-2

This book meets a need arising from the growth of interest in supramolecular chemistry, especially since the award of a Nobel Prize to *Pedersen, Lehn* and *Cram* for their work in the area. The twelve chapters (whose lengths vary from six to 135 pages) describe both older and more recent aspects of supramolecular chemistry. Molecular recognition mechanisms of a purely biochemical nature are not included, nor are membrane and polymer chemistry. Instead the book concentrates mainly on the now almost classical chemistry of the complexation of charged and uncharged guest molecules by host molecules of widely differing structures. In addition, however, it contains separate chapters on liquid crystals and inclusion complexes in the solid state. These are followed by chapters on organic switches, organic conductors, molecular electronics and the light-induced decomposition of water, which indicate future perspectives in supramolecular chemistry.

Following an introductory chapter, host molecules for cations and anions are described (Chapter 2). Here, after a thorough treatment of bipyridyl-containing molecules, Section 2.2 discusses in detail the differences and common features of various open-chain podands, macrocyclic coronands and macrobicyclic cryptands, and describes the wide variety of molecules and applications (e.g., in phase transfer catalysis or in analysis). In the chapter on podands, however, it is surprising that the EDTA molecule is not included. After a detailed treatment of iron-complexing siderophores and descriptions of some cyclophane complexes (metal ion complexes; the neutral complexes of cyclophanes are treated in Chapter 4), this chapter concludes with the catenanes.

The separation of Chapters 3 and 4, on bioinorganic and bioorganic model compounds, from Chapter 2 seems rather arbitrary. In these two chapters host–guest complexes are

grouped together from a different viewpoint (keyword: model enzymes). Beginning with the chemistry of the cyclodextrins, the discussion is concerned mainly with the bonding of neutral guest molecules in host systems such as cyclophanes and cryptophanes, though some ionic guest molecules are also discussed. Chapter 4 ends with an account of the host–guest chemistry of non-macrocyclic molecular pincers.

Chapters 5 and 6 are devoted to inclusion complexes in the solid state and their applications. Chapter 7 describes systems that can function as molecular switches, beginning with those based on azobenzenes. Chapter 8 gives a very detailed treatment of liquid crystal systems, from the physico-chemical fundamentals through LCDs to the latest applications in polymer chemistry. The book concludes with short chapters on surface-active agents, micelles and vesicles (Chapter 9), organic conductors (Chapter 10), molecular electronics (Chapter 11), and light-induced decomposition of water (Chapter 12); these describe new developments, mainly those based on supramolecular chemistry.

The division of such a new field as supramolecular chemistry into separate sub-areas is very difficult, and the author addresses this problem in the preface. Thus, for example, the photoactive cryptands (Chapter 2, Section 2.2.2.6) seem rather out of place in the section on multinuclear host–guest complexes (2.2.2), as also do the catenanes (Section 2.5) in Chapter 2, which is on host–guest chemistry involving cations and anions.

Excellent and detailed descriptions of synthetic methods are given for some host molecules and supramolecular structures, e.g. *Collet*'s synthesis for cryptophanes, *Corey*'s total synthesis of enterobactin, *Schill*'s method for catenanes, and *Sauvage*'s for catenands. Unfortunately the policy of making each chapter self-contained results in some repetition, e.g. the separation of the enantiomers of cyclotriveratrylene derivatives appears on pages 173 and 217.

Last but not least, thanks to the 48 pages of literature references (up to 1988) the book provides a good guide to published work in many different areas of supramolecular chemistry, especially in the author's own fields of research. However, the provision of references varies greatly between individual topics. In Section 2.2 the introduction alone has 94 references, whereas there is only one reference for the whole of Chapter 6. The collecting together of all the references at the end of the book is a good feature. However, it does not entirely eliminate repeated searching, since in each chapter the references begin again with [1].

Whereas most of the sections are written in such a way that a knowledge at undergraduate level is enough to understand them, Section 2.3 goes into great depth, and Table 1 contains many abbreviations which are incomprehensible without a familiarity with the original literature. The book contains few spelling mistakes, although there are some which occur repeatedly (e.g. *Allcook* instead of *Allcock*). On page 191 the impression is given that *Whitlock* did not begin his researches until after 1985. The modern German names Benzen and Toluen are used; on the other hand, the pressure unit atm (atmosphere) still finds its way into this book (p. 271). The structural diagrams are clear and consistent, which is a considerable achievement in view of the fact that some of the three-dimensional structures are very complicated.

It has, of course, not been possible to include in this book all that is known about supramolecular chemistry. For example, a few readers may notice the absence of some particularly effective host structures such as molecular boxes, collars or belts. Syntheses also could have been given a further section, as the "dilution principle" and the "template effect" have received insufficient attention. The coverage of historical aspects could also have been extended: the first macrocyclic polyethers were reported by *Lüttringhaus* 30 years earlier than *Pedersen*, and even the chemistry of the cyclam macrocycles has been known for many years.

Reactions, including those of a catalytic nature, that can be carried out using supramolecular systems are treated rather too briefly. Perhaps it will be possible in a future edition to devote a separate chapter to these applications. The desirability of publishing an English translation of the work has already been mentioned at the 1989 Conference on Macrocyclic Chemistry.

In summary, this is a very interesting book on the many different aspects of supramolecular chemistry, which provides both a good introduction to the topic, through the comprehensive introductory sections included in each of the chapters, and a good starting point for reading the original literature (with 48 pages of references). It is also a valuable source of new ideas, especially in the last few chapters. However, two facts in particular stand out: the book is written in the *German* language, and each page costs less than ten pfennigs!

Ulrich Lüning [NB 1009 IE]
Institut für Organische Chemie und Biochemie
der Universität Freiburg (FRG)

Pesticide Chemistry. (Series: Studies in Environmental Science, Vol. 32). Edited by *Gy. Matolcsy, M. Nádasy* and *V. Andriska*. Elsevier, Amsterdam 1988. 800 pp., hardcover, HFl 495.00. – ISBN 0-444-98903-X

The last comprehensive review of the chemistry of plant protection chemicals appeared about ten years ago. On the other hand there are numerous excellent and up-to-date monographs on individual topics which have been well cataloged. It is to be welcomed, therefore, that *Gy. Matolcsy, M. Nádasy* and *V. Andriska*, as they indicate in the preface to this new review of the field, have set out to devote particular attention to the most recent developments in plant protection chemistry, and on products which exemplify interesting new trends. The expert will immediately think in this context of keywords such as pyrethroids, azoles, sterol biosynthesis inhibitors, sulfonylureas, imidazolinones, ALS inhibitors, chlorotics and photosynthesis inhibitors, and will be glad to learn that at last a compact treatment of these topics, which has long been needed, has arrived. However, the expectation will be dampened to some extent on glancing through the contents list of this bulky volume. The reader will find only nine pages on pyrethroids, as a sub-section in a chapter on "Insecticides of Natural Origin", whereas a little later on, no less than 43 pages are allocated to the older chlorinated hydrocarbons. The triazoles, which are now probably the most important and intensively studied single class of fungicides, are dealt with in eight pages, and the sulfonylureas, which have set new standards in the area of herbicides, are given only three pages. This apparent lack of topical emphasis can perhaps be explained by the book having been a long time in preparation. From an analysis of the literature citations, which are very numerous in all the chapters, one can conclude that the manuscript deadline was in 1984. The delay in publication is regrettable, expecially as the authors have been exceptionally thorough and careful in summarizing the published material up to that date; the coverage is considerably wider than in the earlier reviews, especially as regards mechanisms of action, metabolism and the effects of

residues, aspects which have been given more space for every class of compounds where the information was available.

Within each of the six large chapters on insecticides, acaricides, nematicides, rodenticides, fungicides and herbicides, the material is arranged strictly according to chemical classes. Of course this is reasonable, but it makes it more difficult to recognize the characteristic behaviour of each of the various classes of compounds, which in practical use as well as in research are determined by their common mechanisms of action or activity spectra. The clarity of presentation within the individual chapters would have benefited greatly from a consistent and more visibly obvious division into the recurring sections dealing with chemistry, spectrum of biological activity, mechanism of action, metabolism and toxicology, together with a greater use of tables to summarize the information.

The chapter on insecticides is clearly dominated by the conventional classes of compounds. The pyrethroids, for example, are definitely under-represented. Compared with the space devoted to other compound classes one notices the absence here not only of some of the newer products such as Cyfluthrin and Fenpropathrin, but, more importantly, of any impression of the considerable chemical research activity in this field that was already under way in the late 1970s. For example, although there is a description of one of the enantiospecific, but commercially quite insignificant, syntheses of chrysanthemum dicarboxylic acid, one searches in vain for one of the more commercially important permethrin acid syntheses, which was the subject of a brilliant research project. Again under phosphoric acid esters some important, and even quite old, products such as Azodrin® (Monocrotophos), Counter® (Terbufos), Miral® (Isazofos) and Nemacur® (Fenamifos) are not included. The last two are also missing from the appropriate part of the chapter on nematicides.

In contrast the section on insect growth regulators is excellent. On the basis of the literature up to 1984, the theoretical studies that have been carried out in this area with the aim of developing highly specific insecticides with favorable toxicological properties are reviewed. The chemistry and synthesis of these compounds and the insect physiological aspects are discussed in detail. Research along these lines has so far failed to yield products of wide applicability, despite some limited successes in narrow areas, and the accurate assessment given here still remains appropriate now.

On the other hand, the chapter of acaricides, the section on triazoles, and some parts of the chapter on herbicides are considerably diminished in value by the rapid further developments in these areas during the long time that it has taken to complete the book. For example, it has not been possible to include the new standards in acaricides that were introduced into the market between 1983 and 1985, namely Hexythiazox (Nissorun®), and Clofentezine (Apollo®), nor to convey an impression of the wide-ranging developments and many new products in the triazoles area. The mechanism whereby these act as sterol biosynthesis inhibitors is only briefly mentioned as a literature reference.

However, the chapter on herbicides, which is the longest in the book (300 pp.), is a very detailed and comprehensive account of these classes of compounds. Particularly noteworthy are the sections on phenoxyalkanecarboxylic acids, phenoxyethanols and dinitroanilines. The chapter includes a detailed review of structure-activity relationships and of the biodecomposition of phenoxyacetic acids, a discussion of the TCDD problem, and a comprehensive account of the research on 2,4-dichlorophenoxyethanol (DCPE) and on Buvinol® (pp. 533–541). Here, as also in many other parts of the book, one gains an interesting impression of plant protection research in Eastern Europe and of the products developed from it; this does not emerge to the same extent from books published in the West. The photochemical decomposition of Trifluralin is described in detail, and alternative routes are given in the two schemes on pages 608 and 609; however, the difference between these is only one of emphasis, and this illustrates that there are many points where the material could be tightened up and presented more concisely. In the case of the sulfonylureas there is regrettably no mention of the results published in 1984 on the mechanism of action of this group of compounds as acetolactate-synthase inhibitors, nor of the intensive worldwide chemical research, leading to a flood of patents, that has occurred since the appearance of the first examples of these compounds.

From today's standpoint the book definitely does not justify the claim to present current trends and synthetic methods of modern plant protection chemistry; furthermore, some of the obsolete plant protection chemicals that are discussed in detail here, such as the organomercury fungicides and the chlorinated hydrocarbon insecticides, need to be differently evaluated nowadays. Nevertheless, despite the fact that other more up-to-date books exist, the considerable amount of material which this book contains, and the special attention that is given to biochemical, toxicological and ecological aspects, make it a valuable addition to the existing review literature. It will therefore be a useful source book for those engaged in research or applications who need rapid access to comprehensive information, and a guide to the original publications on particular classes of compounds that are or have been important in plant protection. The high price means that it will not be easy for individuals to commit themselves to buying it, but the book will find a place in well-equipped departmental libraries.

Joachim Weißmüller [NB 999 IE]
Bayer AG, Agrochemical Division
PF-Zentrum Monheim (FRG)

Modern Supercritical Fluid Chromatography. Edited by *C. M. White*. Dr. Alfred Hüthig Verlag, Heidelberg 1988. xii, 239 pp., hardcover, DM 98.00. – ISBN 3-7785-1569-1

Supercritical fluid chromatography (SFC), in which a supercritical gas is used as the mobile phase, has established a place as a third technique intermediate between gas chromatography and liquid chromatography. Rapid strides are being made in the development of this method and of commercially available instruments. In the book reviewed here *Curt M. White* provides an up-to-date account of the development of SFC.

The editor has been successful in enlisting a number of eminent authors as collaborators. The eleven chapters, dealing with such varied and topical themes as an introduction to the mechanisms producing gradients in SFC, the advantages and disadvantages of packed columns in SFC, the solubility of modifiers in CO_2, interfacing SFC to mass spectrometry and FTIR, applications of SFC in petrochemicals analysis, and restrictor properties, are all written by scientists with many years of experience in these fields.

The individual contributions are self-contained rather than forming a sequence of interdependent chapters. A few of the authors preface their contributions by short introductions to the essentials of SFC, but the inclusion of a general introductory overview would have given the book a better defined structure, and would undoubtedly have made it useful to a wider readership.

The contributions are written in the style of review articles, giving both an insight into the authors' own research and an up-to-date survey of the current state of knowledge. The literature references, varying from 20 to 59 in number for the individual contributions, enable the reader to find more detailed information on the topics covered. Scientists who already follow the current literature on SFC will gain little new knowledge from the book. However, for readers who are only familiar with the basics of SFC the book offers an opportunity to rapidly absorb a thorough knowledge of current developments. The chapters on column techniques and on SFC-MS interfacing are especially valuable in that respect. The numerous examples of separations of oligomers, polymers and polymer additives, pesticides, dyestuffs, detergents and petroleum fractions provide readers with a good survey of the many varied areas to which SFC can be applied. From this point of view the book well fulfills the promise of its title. However, it is less suitable for complete novices and for students, as some of the chapters require quite a sound knowledge of the fundamentals of SFC in order to understand them.

The numerous, and often very detailed, figures are an excellent feature of the book; this applies especially to the chapter on SFC-MS interfacing. Equally impressive are the typography and the quality of production. The text and the many tables are easy and convenient to read; good quality paper, stitched binding and a substantial cover combine to make this a serviceable book.

Wolfgang Kleiböhmer [NB 1000 IE]
Anorganisch-chemisches Institut
der Universität Münster (FRG)

Strategies and Tactics in Organic Synthesis. Vol. 2. Edited by *T. Lindberg*, Academic Press, San Diego 1989. 469 pp., hardcover, \$ 75.00. – ISBN 0-12-450-281-4

The book describes various case histories of organic syntheses, originating from 13 prominent academic laboratories of the United States. Unlike Volume 1, which also featured the synthesis of two unnatural products (dodecahedrane and superphane), changing views on research funding probably dictate that the present volume deals with the synthesis of natural products, which are of intrinsic structural and also of special medicinal interest. Ideas and false starts, spin-offs and setbacks, changes of direction and key experimental problems are often chronicled, and this makes the recorded efforts human and the book interesting to read.

Cycloaddition methodology plays an important role in at least five chapters. In Chapter 1 (*D. L. Boger*: synthetic quinoline-5,8-quinones, antitumor antibiotics of the streptonigrin and lavendamycin types) the intramolecular, inverse-electron demand Diels–Alder addition of azadienes is developed and utilized, and one may gather that the synthetic endeavors had something to do with the appearance of a recent useful book in this general area.[1] In Chapter 7 *M. E. Jung* describes a concise synthesis of the bottom half of ivermectin. The combination of the electron-rich 3,4-dibenzoxyfuran (as 2π component) and an electron-deficient coumalic ester (α-pyrone as 4π component) turns out to be a key reaction. In Chapter 9 *S. F. Martin* deals with the synthesis of indole alkaloids of the yohimbine and corynanthe family, including reserpine: intramolecular Diels–Alder additions of nitrogen-linked trienes and heterotrienes are used to build up the D/E ring fragments. Chapter 12 by *D. D. Sternbach* describes the synthesis of a linearly fused triquinane ($\Delta^{9(12)}$-capnellene) and of an angularly fused triquinane (silphinene). Again, intramolecular Diels–Alder reactions of substituted cyclopentadienes are used to approach the triquinanes.

Retigeranic acid, a member of the comparatively rare class of sesterpenes (C_{25}) has a tricyclic fragment resembling silphinene, with a trans-perhydroindane fused to it. *E. J. Corey* and *T. A. Engler* (Ch. 3) develop an intramolecular cycloaddition of a ketene to an olefin to assemble an advanced pentacyclic intermediate. As a beginner in synthesis one is often given the advice: "Don't use known chemistry. Choose the target so that you have to invent new chemistry. Otherwise you only reinvent the wheel". At its best, science is, of course, often iconoclastic. The crossed cycloaddition of ketenes to electron-rich olefins is a very old reaction which, in its intermolecular form, goes back to *Staudinger* and the turn of the century. Who could have foreseen – or why did it take so long to realize – that given the optimum three-atom tether, the intramolecular variant can be so spectacularly successful, even with simple unactivated olefins, for building up a variety of four-membered rings within complex polycyclic frameworks?[2, 3]

S. D. Burke (Chapter 2) describes the synthesis of (+)-phyllantocin, which is the sesquiterpene aglycone of biologically active phyllantoside, and also the synthesis of (±)-quadrone, a compact tetracyclic ketolactone. Quadrone has also been a target of *P. Helquist* (Chapter 5), who shows clearly that the development of new chemistry can often become more important and probably have greater impact than the synthesis of the target itself. In fact, quadrone appears to have been synthesized by at least 15 groups up to now,[4] yet this does not detract from the work accomplished.

In Chapter 4 *Fraser-Reid* and *Tsang* continue to demonstrate that carbohydrate chemistry has become an active part of mainstream organic chemistry. Further strategies for preparing carbocycles from carbohydrates are introduced, where the carbocycle is built "around" the sugar and advantage is elegantly taken of the natural stereochemistry of the sugar.

Saxitoxin (Chapter 6 by *P. A. Jacobi*), one of the most toxic of the non-protein poisons known, is a non-crystalline diiminium salt. Plenty of heteroatoms dictate the synthetic strategy (or is it tactics?), which features electrophilic activations with, e.g. Meerwein salt, and intramolecular 1,3-dipolar cycloadditions. The route developed is remarkably efficient, giving the key saxitoxin precursor on a 0.5–1.0 g scale without any chromatographic separation. In Chapter 8 *A. P. Kozikowski* and *M. N. Greco* tackle the mycotoxic cyclopiazonic acids which belong to the category of substituted tetramic/tetronic acids. In the course of this work a novel C-glycoside synthesis is developed, using *O,S*-acetals and dimethylzinc.

Olivomycin A (Chapter 10) was originally chosen by *W. R. Roush* as a target to learn about two important areas of contemporary research, i.e. (i) acyclic diastereoselective techniques and (ii) carbohydrate chemistry. Both premises turned out to be entirely correct. With respect to (i), allylboronate chemistry proved to be most useful. (−)-Casbene and (−)-bertyadionol are two diterpenes that have yielded to total synthesis by the group of *A. B. Smith* (Chapter 11), who, like *E. J. Corey*, had also contributed a chapter to Volume 1. Finally, the synthesis of pseudomonic acid C (*D. R. Williams*, Chapter 13) provides an exercise of stereocontrol in tetrahydropyran chemistry and also requires attachment of two appendages, one of which is chiral.

If the case for organic synthesis needs to be restated,[5, 6] the present volume, like Volume 1, helps to focus that case.

There is a great deal in this book that the attentive reader and student may learn, also by reading between lines. Organic chemistry without synthesis is hard to imagine. Conversely and even more cogently, organic synthesis remains the essence of organic chemistry.

H. Martin R. Hoffmann [NB 1002 IE]
Institut für Organische Chemie
der Universität Hannover (FRG)

[1] D. L. Boger, S. M. Weinreb, *Hetero Diels-Alder Methodology in Organic Synthesis*, Academic Press 1987.
[2] D. Bellus, B. Ernst, *Angew. Chem. 100* (1988) 820; *Angew. Chem. Int. Ed. Engl. 27* (1988) 797.
[3] B. B. Snider, *Chem. Rev. 88* (1988) 793.
[4] R. S. Liu et al., *Can. J. Chem. 66* (1988) 528.
[5] Chapter 2 of this volume, refs. [88a–d].
[6] R. Scheffold, *Chimia 43* (1989) 37–38.

Metalloproteins, Chemical Properties and Biological Effects. (Series: Bioactive Molecules, Vol. 8). Edited by *C. I. Otsuka* and *T. Yamanaka*. Elsevier, Amsterdam 1988. xiv, 572 pp., hardcover, HFl 450.00. – ISBN 0-444-98887-4

This book is the result of the combined efforts of 54 authors. As one expects from the title, it contains chapters on metalloproteins and metalloenzymes containing one or more of the metals magnesium, calcium, vanadium, manganese, iron, cobalt, nickel, copper, zinc, molybdenum, tungsten and selenium; in addition there are chapters on flavines and metal ions, complexes formed by nucleosides and nucleotides with metal ions, carcinogenicity of metal ion, and antitumor activity of metal compounds. Finally, there is a chapter on affinity fractionation using metal chelates.

The book is mainly suitable as a work of reference, since much of the information which it contains is presented in the form of useful tables. However, this only applies to the older literature; results from the last four years receive little coverage or are treated only superficially, sometimes only by a "note added in proof". The individual chapters are very varied in quality. For example, the sections on molybdoenzymes and nickel enzymes are hardly up to the standard of a good textbook treatment. Nowhere is there a critical discussion of the historical significance of particular topics, e.g. of the discovery of nickel in urease. These failings detract appreciably from the value of this otherwise interesting book.

Rudolf Kurth Thauer [NB 1003 IE]
Fachbereich Biologie
der Universität Marburg (FRG)

Houben-Weyl. Methoden der Organischen Chemie. Band E13, Teil 1 und 2: Organische Peroxo-Verbindungen. 4th Edition. Edited by *H. Kropf*. Thieme, Stuttgart 1988. Part 1: xliv, pp. 1–990, hardcover, ISBN 3-13-218304-0; Part 2: xx, pp. 991–1768, hardcover, ISBN 3-13-218304-0; price for Parts 1 and 2: DM 2200.— (subscription and pre-ordered price: DM 1980.—)

The fourth edition of "Houben-Weyl" began to appear in 1952 with Volume VIII and the article "Herstellung und Umwandlung von Peroxyden", by *R. Criegee*. The topic which could then be reviewed in 74 pages by one author has now grown to a two-volume work whose contents list alone consists of 57 pages. In this connection it is interesting to read in the preface which *E. Müller* wrote for Volume VIII: "It is planned to complete the new work, consisting of about 14 volumes of 700 pages each, over a four-year period." Evidently it was not then foreseen that in 34 years time there would be 67 volumes, together with indexes and supplementary volumes.

Despite the large number of contributors to Volume E13 (30 authors), the editor *H. Kropf* has managed to achieve a very uniform style of presentation which is in keeping with the high quality of this standard work. The new volumes are also commendably up-to-date: the literature up to 1987 has been covered, and even some 1988 references are included (the volumes appeared on 1 December 1988). The nomenclature is mainly in accordance with the IUPAC rules. Alongside the physical data in SI units the values in older units have also been included in some cases; this unnecessarily increases the size of the tables, for example where all the energy data are given both in kJ and (in parentheses) in kcal. However, listing distillation pressures in kPa could lead to mistakes in converting to more familiar units, resulting in delayed boiling or other accidents, and in this case, therefore, all the values have been given in torr (with the SI units, kPa, in parentheses in this case).

The arrangement of the subject matter essentially follows the usual pattern adopted in "Houben-Weyl". The first volume, which is the larger of the two, contains an introductory chapter and preparative methods (Part A). The second volume contains transformations of peroxides into other compounds (Part B), peroxy compounds as reagents (Part C), and analysis (Part D). The whole work is rounded off by a general section (classification, structure, thermochemical data, naturally occurring substances, safety aspects and toxicology), which precedes Part A, and a comprehensive index at the end of Volume 2.

The classification of peroxy compounds given in the introductory chapter contains a degree of arbitrariness. According to this, peroxy compounds contain the characteristic group -O-O-, which, in organic peroxides, is attached through at least one carbon atom (or through a heteroatom X bonded to a carbon atom). As a result of this definition, carbonyl oxides are not counted as peroxides, and they are not covered. However, organo-heteroelement peroxides are included only in cases where the carbon is σ-bonded. Consequently the important metalla-dioxiranes are not covered (p. 956). On the other hand, the dioxiranes which are analogous to metallacycles are included, even though these are isomeric with the carbonyl oxides (and related to them in chemical properties). A somewhat more pragmatic definition of peroxides would definitely have helped here.

In the first, introductory, chapter the newer methods of "experimental computer chemistry" are treated too briefly, even for a work in which the emphasis is on preparative methods. A sentence such as "Theoretical calculations gave values ranging from 80 to 180°, depending on the method of calculation (CNDO, INDO, MINDO, MNDO, ab initio, 4–31 G)..." certainly does not do justice to the enormous power of modern theoretical methods. In the area of peroxides especially, there are many instances where structures first arrived at by calculation have later been confirmed in an impressive way by experimental results.

Notable features of the general section are the newly revised thermochemical tables, and the chapter on safety aspects. This short and lucidly written chapter should be on display in every laboratory where peroxides are used.

Part A which follows, dealing with methods of preparation, is the core of the whole work. In the familiar style of

"Houben-Weyl" it details a wealth of general and specialized preparative methods, including yields, melting or boiling points, and information about the properties of the compounds. This section is a mine of information, and in looking up a particular compound or experimental recipe one is continually tempted to browse on adjacent pages. Part A is arranged according to compound classes, starting with alkylhydroperoxides and continuing through to organotrioxides and -tetroxides. A detailed index enables one to easily find individual compounds, and the arrangement under compound classes also makes it possible to quickly locate functional groups, in cases where one is concerned with variations in the peroxide group. In a work as large as "Houben-Weyl", however, it would be useful to have an index in the form of a computer data base (as in Beilstein), which would allow one to search for particular structural units. The general section of the subject index is quite pathetic. Under heading F, "General terms, named reactions, compound classes, trivial names", we find a more or less arbitrary selection of terms, consisting of only eight pages of the lengthy 176-page subject index. Important reactions such as the Criegee rearrangement and the Sharpless epoxidation are not included in this section, for example.

Part B deals with reactions whereby peroxides are converted into non-peroxide containing products. The topic is treated under nine reaction type headings: thermal reactions, catalytic reactions (catalysis by metals, bases and acids), photolytic and radiolytic reactions, rearrangements, reductions, oxidations and lastly a short separate chapter on organohydrotrioxides in the ozonolysis of C—H sp^3 bonds. After discussing the general mechanisms, specific examples are given, often in the form of tables. The treatment of rearrangements in a separate chapter leads to some overlapping with material in other chapters of Part B, but in view of the importance of many of these reactions (e.g. the Hock and Criegee rearrangements) this is justified. However, one searches in vain here for the Baeyer-Villiger reaction; instead this has been banished to a half-page paragraph on page 862.

The many different methods whereby peroxy compounds are used as reagents in organic chemistry are described in Part C. This part is a continuation of Section 1a (Peroxy Compounds as Oxidizing Agents) in Volume IV of the Handbook, published in 1981, and it therefore covers only the more recent literature. However, as the arrangement of the topics is identical to that in the 1981 treatment, it is easy to refer back to the earlier literature. The reactions described here range from the use of "exotic" peroxides such as the dioxiranes for the hydroxylation of unactivated CH bonds to some very detailed chapters on the use of transition metal catalysts. In particular the enantioselective Sharpless epoxidations have been given a considerable amount of space in view of their importance.

Volume E13 concludes with the excellent Part D, which has the simple title "Analysis". Everyone who has ever searched through the literature for spectroscopic data on a group of compounds will appreciate the value of the tables and the large compilation of data given here. All the analytical methods that are important for elucidating the structures of peroxides are represented, from IR spectroscopy through NMR spectroscopy (^1H, ^{13}C, ^{17}O) to mass spectrometry. Wet chemical methods for quantitative analysis and chromatographic methods are also described.

Volume E13 of Houben-Weyl will have a place in every well-equipped chemistry library. Critical reviews of the literature on specialist topics such as this make an important contribution towards maintaining a perspective over the tide of publications which continues to grow exponentially. Good workmanship has its price, and when one considers how often Houben-Weyl is referred to, there can be no doubt that it is a worthwhile purchase for every library.

Wolfram Sander [NB 996 IE]
Organisch-chemisches Institut
der Universität Heidelberg (FRG)

Registered names, trademarks, etc. used in this journal, even when not marked as such, are not to be considered unprotected by law.

© VCH Verlagsgesellschaft mbH, D-6940 Weinheim, 1990. – Printed in the Federal Republic of Germany by Konrad Triltsch Druck- und Verlagsanstalt Würzburg.

All rights reserved (including those of translation into foreign languages). No part of this issue may be reproduced in any form — by photoprint, microfilm, or any other means — nor transmitted or translated into a machine language without written permission from the publishers. Only single copies of contributions, or parts thereof, may be made for personal use. This journal was carefully produced in all its parts. Nevertheless, authors, editors and publisher do not warrant the information contained therein to be free of errors. Readers are advised to keep in mind that statements, data, illustrations, procedural details or other items may inadvertently be inaccurate.

Valid for users in the USA: The appearance of the code at the bottom of the first page of an article (serial) indicates the copyright owner's consent that copies of the article may be made for personal or internal use, or for the personal or internal use of specific clients. This consent is given on the condition, however, that the copier pay stated per-copy fee through the Copyright Clearance Center, Inc. (CCC), for copying beyond that permitted by Sections 107 or 108 of the U.S. Copyright Law. This consent does not extend to other kinds of copying, such as copying, for general distribution, for advertising or promotional purposes, for creating new collective works, or for resale. For copying from back volumes of this journal see 'Permissions to Photo-Copy: Publisher's Fee List' of the CCC.

Editorial office: Postfach 10 11 61, D-6490 Weinheim, Federal Republic of Germany, Telephone (06201) 60 22 55, Telex 465 516 vchwh d, Telefax (06201) 602 328.

Editor: *Peter Gölitz*

Associate editors: *D. I. Loewus, A. Stimson.* **Editorial assistant:** *E. Schweikart*

Publishers: VCH Verlagsgesellschaft mbH. (Managing Director: *Hans Dirk Köhler*), Pappelallee 3, D-6940 Weinheim, Federal Republic of Germany.

Advertising office (Advertising Manager *R. J. Roth*): Postfach 10 11 61, D-6940 Weinheim, Federal Republic of Germany, Telephone (0 62 01) 60 61 30, Telex 4 67 155, Telefax (0 62 01) 606 156.

ANGEWANDTE CHEMIE
International Edition in English
Volume 29 · Number 4
April 1990
Pages 329–438

The Quartz Microbalance: A Novel Approach to the In-Situ Investigation of Interfacial Phenomena at the Solid/Liquid Junction

New Analytical Methods (40)

By Rolf Schumacher*

When *Archimedes* was asked by King Hiero of Syracuse to prove whether a handcrafted crown really consisted of pure gold and not of gold with a proportion silver, he immersed the crown and an equal weight of pure gold, both attached to a beam balance, into a vessel of water. We all know that according to Archimedes's principle the scale beam rose on the side the crown was attached proving that the goldsmith had intermingled some silver. In spite of the simplicity of this experiment, the result convincingly demonstrates the physical integrity of this classical approach which is based on a weighing procedure. The mass sensitive technique we shall report on in this article is based on the principle that a shift in the resonance frequency of an oscillating AT-cut quartz disk can be correlated quantitatively with a change in mass in the nanogram range. One side of the quartz disk is in contact with a liquid, while the other side remains exposed to the atmosphere. The changes in weight involved in testing Hiero's crown were probably several hundred grams which corresponds to about 10^{25} water molecules. By applying the quartz microbalance, e.g., to solvent migration through thin films, one can sense entrapment of water with a resolution down to 10^{14} molecules per unit surface area. If adsorbate layers are in question, fractional coverages down to 0.02 monolayers can be monitored, which only goes to prove the capability of this instrument for investigating interfacial processes on a microscopic level. The option of recording charge flux and interfacial capacitance along with the mass change makes this instrument a powerful in-situ tool for scientific and technological applications in many fields.

1. Introduction

In the past few years, some novel techniques have been developed which enable the in-situ detection and monitoring of interfacial phenomena on a microscopic level.[1] One such approach involves the use of quartz crystals, which can be made to oscillate in a liquid environment.[2–8] The quartz microbalance has demonstrated its extraordinary sensitivity for monitoring accurately mass changes of several nanograms even when applied in-situ for the investigation of interfacial phenomena at a solid/liquid junction.[3–8]

The monitoring of a surface process on the basis of a change in weight is a classical but not very specific approach. However, a coupling of the in-situ microbalance with the recording of the differential capacity and charge flux enables an assignment of the measured data to specific processes in the region of the phase boundary. Furthermore, the three measurements can, in part, be carried out concomitantly. This decisive extension determines the character and uniqueness of the information which can be obtained with this methodological approach.

Since their introduction to in-situ interfacial research about half a decade ago, quartz oscillators have gained immense importance and broad acceptance as highly informative measuring devices. In this article, we present an overview

[*] Priv.-Doz. Dr. Rolf Schumacher
Schering AG, Research Division GT
Müllerstrasse 170–178, D-1000 Berlin 65

 © VCH Verlagsgesellschaft mbH, D-6940 Weinheim, 1990 0570-0833/90/0404-0329 $ 02.50/0

of the characteristic features and broad applicability of this technique with special emphasis on the uniqueness of the information that can be drawn from such measurements. It also outlines some concepts developed for describing the changes in frequency observed upon contact of a resonator surface with a liquid. These concepts are related to the physical and chemical nature of the interfacial environment. The article focuses on the state of the art of this area of research with the in-situ microbalance and reflects a currently fast changing situation.

In Figure 1 some fundamental principles associated with oscillating quartz resonators brought into contact with a

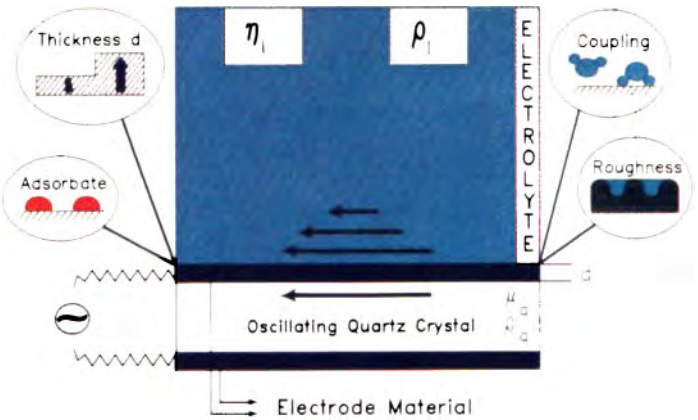

Fig. 1. Schematic presentation of the principles of a quartz microbalance which operates in solution. The arrow size and direction indicates the shear wave oscillations at the solid/liquid junction sustained by an electronic driver (~). Some interfacial phenomena which affect the resonant frequency of the quartz resonator are indicated in the insets. The bulk properties of the electrolyte such as viscosity and density are denoted as η_l and ϱ_l, respectively; μ_q and ϱ_q are the shear modulus and the density of quartz.

fluid are illustrated along with some typical interfacial processes. The damped propagation of shear oscillations[2] perpendicular to the resonator surface is symbolized by the decreasing arrow length on the liquid side of the junction. It is obvious that not only the viscosity η_l and density ϱ_l of the liquid but also the degree of coupling between the two phases will determine the extent to which these viscous oscillations penetrate into the liquid before they are damped out. The penetration represents the thickness of the liquid layer which is dragged along while the oscillator vibrates; this layer behaves like a rigidly attached liquid deposit and gives rise to a characteristic lowering of the resonant frequency f_0. Other processes of importance on the solid side of the junction, e.g., growth,[3, 5-7, 9-10] decay,[5, 7-8, 17-19] and content[11-16, 20-21] of solid thin films, adsorbate formation[5, 22-27] on a submonolayer range, passivity[4, 6, 7, 28-30] and roughness effects[4, 7, 28-30] etc., are presented in supermagnified images inside the circled areas of Figure 1. As illustrated in the lower right circled area, some water is confined in valleys of the roughened surface and is dragged along while the oscillator vibrates, thus giving rise to significant changes in weight which are related to the roughness pattern.[4, 30]

The present article deals firstly with some requirements of importance for designing an operating system, and then with frequency changes which can be ascribed to physical effects such as solid and liquid deposition, surface roughness and stress etc. Finally, the influence of chemically induced interfacial processes on the resonance frequency of quartz oscillators is discussed.

2. Some Experimental Requirements and Setups to Sustain Stable Shear Wave Oscillations of Quartz Resonators in Liquids

Figure 2 gives a schematic presentation of an experimental setup for recording in-situ changes of frequency of shear wave oscillations on quartz resonators immersed with one face in a liquid. Several groups have independently developed their own technical approaches and instrumentation, details of which are given elsewhere.[5-8, 28] Here are some useful principal requirements: The quartz oscillators used were AT-cuts which operate in the shear mode (the abbreviation AT signifies the lines of the quartz cut relative to the crystal axis). Both oscillator faces are covered with conducting layers (thickness d typically 1000 Å), which are electrically connected to an electronic driver device to sustain stable oscillating shear motions. To affix various noble and less noble metals onto the quartz surface, standard surface cleaning procedures such as sputtering with argon and/or seeding with chromium or silicon were used. The face exposed to the liquid serves as working electrode if this setup is used as an electrochemical device. The function generator of the potentiostatic control unit allows repetetive potential scanning at various rates and provides a fast potential step technique, which, inter alia, is essential for recording complex plane impedance spectra in conjunction with the Fourier transform method.[30, 31] For experiments which are carried out

Rolf Schumacher, born 1943, studied chemistry from 1968 to 1973 at Bonn University, where he also gained his doctorate under the supervision of R. N. Schindler for physicochemical work, the experimental part of which was performed at the KFA Jülich. From 1978 to 1979 (Research Fellowship) and 1984 to 1985 (Visiting Scientist) he worked as postdoc in the USA at the Research Centers of General Electric, Schenectady (L. A. Harris, R. N. Wilson) and IBM, San Jose (J. G. Gordon, K. K. Kanazawa). Following his research activities at KFA Jülich and the Universities of Essen and Kiel in 1987 he joined the GT Research Staff of the Schering AG in Berlin. In 1989 he habilitated as a Faculty Member for Physical Chemistry at the University of Kiel. His research activities are focused on the kinetics of gas phase reactions and interfacial electrochemical phenomena at the solid/liquid junction.

under potentiostatic/galvanostatic control, commercial systems can be used if these instruments operate with a grounded working electrode. This instrumental arrangement is needed to match the design of the driver electronics, the requirement of which is that the grounded resonator face is exposed to the liquid while its opposite hot face is free from the electrolyte. In case the electrochemical arrangement is operated without any external potential/current control, the potential of the working electrode can adjust dynamically to the electrolyte conditions.

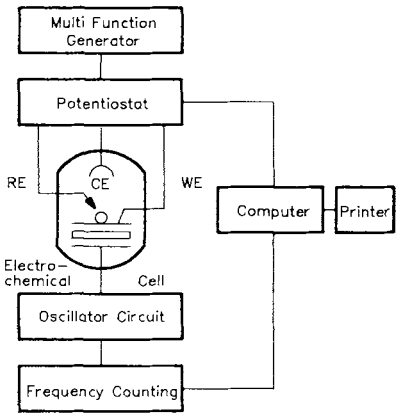

Fig. 2. Experimental setup for sustaining and recording frequency changes of a quartz resonator immersed in a fluid [8]. RE, CE, WE = reference electrode, counter electrode and working electrode, respectively.

Recently, a dynamic technique was suggested in which a galvanostatically controlled deposition process is perturbed with a small sinusoidal current oscillation. The analysis of the frequency data is performed with a transfer function analyzer which allows a simultaneous registration of impedance data. The observed mass-voltage transfer function is expected to reveal information on, e.g., the nature and kinetics of intermediary processes of the electrochemical surface process.[32]

Two different experimental concepts were put forward for the exploitation of the extraordinary sensitivity of shear wave oscillations toward a mass load. The first concept is based on the stationary arrangement;[3-8] the immersed quartz housing is kept at a fixed position and does not make any movement in the cell. This is the most common technique and is used in the meantime in many laboratories around the globe. Recently, an elegant variant was developed in which the resonator disk rotates and still operates effectively as a mass-sensitive tool.[20] This type of device provides defined hydrodynamic conditions suitable for the suppression of polarization, e.g., in experiments with dilute solutions.

The design of a quartz housing which allows a quick and easy oscillator change presents its own problems. On the one hand, the resonator plates have to be mounted without incurring any strain, which, of course, would affect the resonance conditions, and, on the other, the liquid must be prevented from penetrating into the housing, which requires a certain amount of stress to be applied to effectively seal the crucial contacts. Suggestions, which meet these opposing needs are based on a sandwich model.[7, 8] One of the historical proposals for solving this problem is given in Figure 3. A bent glass tube houses the electronic driver circuit. The quartz resonator is pressed against the tube opening and sealed with silicone adhesive.[3, 4]

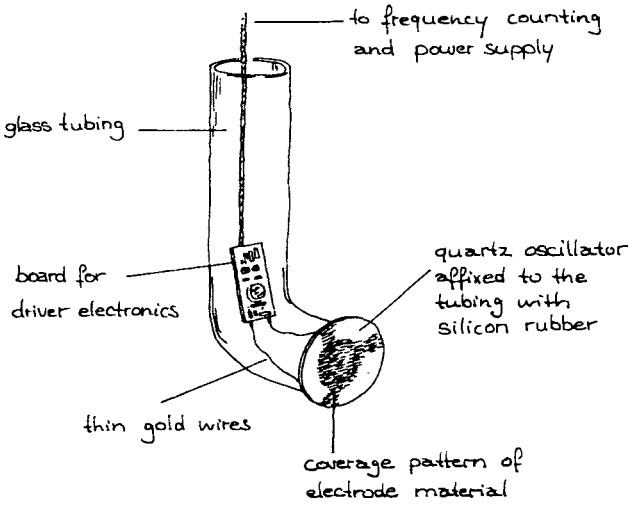

Fig. 3. Early assemblage of a quartz microbalance for operation in solution.

The layout of the electronic driver circuits to sustain stable oscillating shear motions on resonators with one face in contact with a liquid is based on the conventional type of driver devices such as those proposed by *Pierce-Miller, Colpitz* etc.[33] But devices which are operated with a differential video type amplifier,[3, 4, 8, 28, 29, 34] have also been used. The electronic modifications suggested account for the viscous damping at the liquid/solid junction. The resulting losses can be compensated, e.g., with a positive feedback which enhances the amplification characteristic of the driver.

3. Shear Stress Oscillations at the Solid/Liquid Interface

3.1. Influence of Solid Deposits on the Resonance Frequency of Quartz Oscillators

The relationship which quantitatively correlates a change in frequency Δf with a change in mass Δm [Eq. (a)] was first derived by *Sauerbrey*.[35] In this relationship, with μ_Q the

$$\Delta f = -[2 f_0^2 (A \sqrt{\mu_Q \varrho_Q})^{-1} \Delta m] \qquad \text{(a)}$$

shear module of quartz, ϱ_Q its density and A the geometric surface area of the deposits, Δf is linearly related to Δm; this has been verified experimentally for thin rigid overlayers exposed to vacuum or to ambient pressure conditions. In these cases, the physical properties of the deposits such as mechanical stress and damping[36] do not affect the material constants of the quartz μ_Q and ϱ_Q significantly, so that Δf changes linearly with Δm. When the overlayers are thick, this relationship becomes nonlinear, a behavior for which corrections have been developed. Today, this technique is used

routinely in vacuum systems, e.g., in thin film technology.[36]

The evaluation of Equation (a) for reduced and ambient pressure conditions was achieved by varying the amount and nature of the foreign mass deposited. The results reveal that the relationship between Δf and Δm is no longer linear when the coverages exceed a value of roughly 0.5% with respect to the weight of the uncovered quartz resonator. Thus, for a 5-MHz resonator weighing about 100 mg, the linearity of Equation (a) ranges up to a point corresponding to a deposit of about 0.5 mg of foreign material.[36]

The negative sign on the right hand side of Equation (a) indicates that a loss in mass causes an increase in frequency and vice versa.

The interesting question whether this linear mass-frequency relationship holds also for resonators with one face exposed to a fluid was explored on 5-MHz, 6-MHz and 10-MHz crystals operated in their fundamental oscillation modes.[5-9] The experimental procedure used was based on the electrochemical dissolution of copper and silver from various thick deposits to determine the relevant quotient $(\Delta f/\Delta m)$ A. By recording Δf and the corresponding charge flux Δq in-situ and simulataneously, this quotient can be calculated with the help of Equation (a) and Faraday's law. A comparison of the experimental data obtained with theoretical expectations according to Equation (a) are shown in Figure 4 for the resonators used. In this figure both

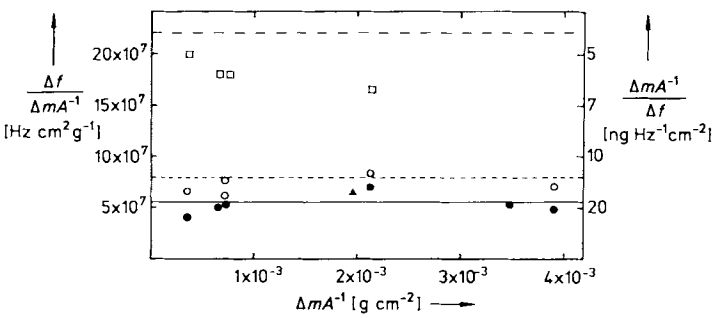

Fig. 4. Sensitivity of a quartz microbalance in a liquid environment. Dependence of the integrated sensitivity $(\Delta f/\Delta m)A$ and its reciprocal $(\Delta m/\Delta f A)$ on the amount and nature of foreign deposits $\Delta m/A$. 5 MHz: Cu(●), Ag(▲); 6 MHz: Cu(○); 10 MHz; Cu(□). The data points represent experimentally determined values, while the predicted sensitivities for 5 MHz (—), 6 MHz (....) and 10 MHz (---) resonators according to Equation (f) are given as horizontal lines [8].

$(\Delta f/\Delta m)$ A and its reciprocal $(\Delta m/\Delta f$A) are given as a function of the amount of metal deposited $\Delta m A^{-1}$. According to these data, there is a satisfactory agreement between experiment and theory; the deviation from theory does not exceed 20% in the range of investigations, regardless of whether one face is attached to a liquid. Thus, for a 5-MHz crystal a change in frequency of 1 Hz corresponds to a mass change of about 18 ng, which corresponds to a fractual coverage of about 0.06 monolayers of copper. The same frequency change on a 10-MHz crystal corresponds to 4.5 ng or about 0.02 monolayers of copper. These data are related to a unit surface area and correspond to investigations which were carried out under reduced pressure.[36]

3.2. Influence of a Total Immersion of One Resonator Face in a Liquid on the Resonance Frequency

The change in resonant frequency that occurs upon coupling one face of a resonator to a liquid has been ascribed to the liquid density,[37] to combinations of density/conductivity,[38] density/viscosity,[39] and to the mass of a solid deposit as outlined in the previous chapter. The response of shear wave oscillations to a liquid-like deposit,[40-42] as treated in recent papers, does not describe the case where one face of the resonator plate is totally immersed in a viscous environment. As outlined by *Kanazawa* et al.,[2] the case at hand can be analyzed in terms of a simple physical model which treats the quartz resonator as a lossless elastic solid and the liquid as a purely viscous medium. The resulting change in frequency upon immersion arises from the coupling of the standing shear wave of the oscillating resonator to the liquid. The result is a damped propagating shear wave that travels normal to the surface in the viscous medium. According to the definition of the coordinates[2] the fluid velocity v_x describes the movement of the liquid parallel to the surface and can be described with the differential Equation (b), in which ϱ_l and

$$\frac{\partial^2 v_x(z,t)}{\partial z^2} = \frac{\varrho_l}{\eta_l}\frac{\partial v_x(z,t)}{\partial t} \tag{b}$$

η_l are the density and viscosity of the bulk liquid, respectively. Equation (b) is based on the assumption that the first layer of fluid is rigidly attached to the oscillator surface and that η_s, the interfacial viscosity, is identical with η_l, the bulk viscosity. The explicit solution of this equation in terms of v_x yields Equation (c), where z is the coordinate normal to the surface, L the thickness of the oscillator, v_0 the velocity of the quartz surface, ω the fundamental frequency, and k_l the propagation constant.

$$v_x(z-L,t) = v_0 e^{-k_l(z-L)} e^{j[k_l(z-L)-\omega t]} \tag{c}$$

The latter quantity is given by Equation (d) and describes

$$k_l = \sqrt{\frac{\omega \varrho_l}{2\eta_l}} \tag{d}$$

shear waves traveling normal to the surface with extremely heavy damping. Their velocity profiles $\bar{v}$ normal to the surface are shown in Figure 5. These snapshots represent three different times, corresponding to: a) peak surface velocity, b) intermediate surface velocity, and c) zero surface velocity.[2]

The reciprocal of k_l is the characteristic decay length σ of the envelope function which indicates that the oscillating crystal resonator does not drive the entire bulk of liquid. The decay length σ represents the effective thickness of a rigidly bound liquid deposit, which in the case of water is ca. 2500 Å. Since σ increases with increasing viscosity, the added mass Δm_σ of this liquid deposit increases as well [Eq. (e)].

$$\Delta m_\sigma = A\sqrt{\frac{2\varrho_l\eta_l}{\omega}} \tag{e}$$

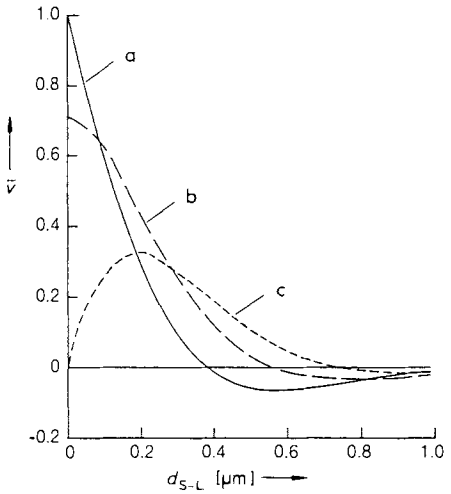

Fig. 5. Distribution profiles of the fluid velocity $\bar{v}$ normal to the surface d_{S-L}. The profiles (a–c) for pure water represent three different times: a) time of peak velocity at the surface; b) intermediate time; c) time of zero velocity at the surface [2].

The change in frequency Δf due to the total contact of one resonator face[2] with a viscous fluid can, under the assumption that the transverse velocity of the quartz surface is identical to that of the adjacent fluid layer, also be evaluated from Equation (b).[2] The solution is expressed in terms of Equation (f).

$$\Delta f = -f_0^{3/2}\sqrt{\frac{\eta_l \varrho_l}{\pi \mu_Q \varrho_Q}} \qquad \text{(f)}$$

Several attempts have been made at the verification of Equation (f). The results are not consistent and, in the following, are subjected to a critical evaluation: *Kanazawa* et al.[2] have tested several systems such as glucose–water and ethanol–water mixtures and found a satisfactory agreement between theory [Eq. (f)] and experiment. Figure 6

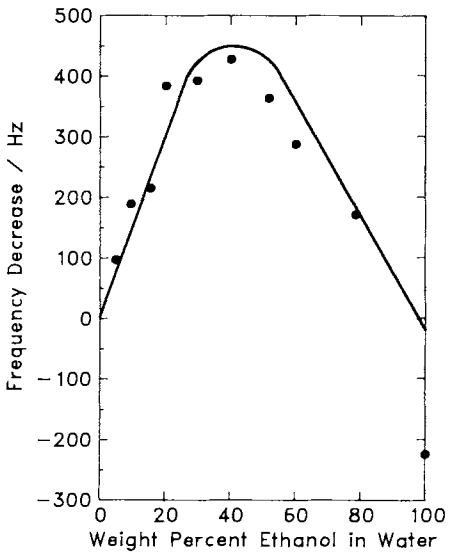

Fig. 6. Influence of water:ethanol ratio in a water/ethanol mixture on the resonance frequency of an immersed quartz oscillator. The solid line represents predictions according to Equation (f), while the data points correspond to a relative frequency shift with respect to pure water [2].

shows the frequency response of various mixtures with respect to pure water. A good agreement between theory and experiment was also found for a saccharose–water mixture.[38] Equation (f) does not apply, however, in the case of some organic fluids,[43] as can be seen from Figure 7, in which the comparison of calculated and experimentally ob-

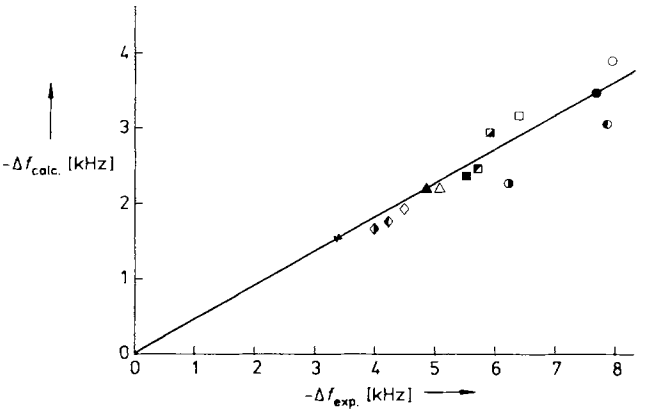

Fig. 7. Observed decrease in frequency upon immersion of one resonator face in various organic fluids [43] versus the predicted frequency decrease according to Equation (f): (×): hexane; (◪): cyclohexane; (◆): acetonitrile; (◑): acetone; (□): ethanol; (▲): methanol; (△): 4-methyl-2-pentanone; (◇): 2-butanone; (■): toluene; (◩): benzene; (○): dioxane; (●): 1,2-dichloroethane; (◑): carbon disulfide; (◐): chloroform.

served data fits to a straight line which passes through the origin of the coordinate system. The slope is about 0.45, indicating that the predicted data are generally smaller by roughly a factor of 2 than the experimentally determined data. This observation is in accord with an early study by *Haardt*:[44] on using a 5-MHz oscillator he obtained, from the observed changes in frequency, viscosity data which are clearly higher than the calculated data. In his explanation, he adopted a model which claims that the viscosity of water close to the surface, η_s, is much higher, than of the bulk, η_l. Using the relation η_s/η_l he calculated a value of 4.2, which is in excellent agreement with *Pechel*'s experimental results. To investigate the interfacial viscosity of liquids[45,46], these authors used thin, fused silica disks, which were allowed to approach each other along their common central axis under the influence of a given force.

In a more recent paper, *Pittermann* and *Weil* et al.[47] likewise observed deviations between data calculated with *Kanazawa*'s formula and their experimental results obtained in various concentrated LiCl solutions. Their results reveal, that these deviations might be related to the electronic circuits used to drive the crystal. Upon immersion, the measured decrease in frequency Δf with a 4.9-MHz resonator connected to a Pierce-Miller circuit is roughly a factor of 3 larger than that predicted according to Equation (f). A lowering of Δf by a factor of roughly 1.5 compared to the theoretical value was found for a 9.4-MHz resonator with integrated circuit (IC). Both crystals were operated in their fundamental modes. On the other hand, a good agreement between theory and experiment was found for the 3rd harmonic of a 5-MHz crystal driven with a Pierce-Miller circuit. Finally, a good agreement was found for all three types of

circuits provided the frequency was determined with reference to the real impedance. This was demonstrated on a 5-MHz crystal operated in its fundamental and 3rd harmonic modes as well as for a driver circuit based on an IC. To explain this finding the authors pointed out that the readout of the frequency counter must not be necessarily identical with the resonance frequency of the quartz oscillator calculated from the maximum of the real impedance. Coincidence of both frequencies might occur, however, for a driver circuit which uses a video type amplifier with a positive feedback to ensure that the oscillation occurs near the zero-phase condition.

3.3. Influence of Surface Roughness on the Resonance Frequency

As shown by *Schumacher* et al.,[4, 28–30] surface roughness can also drastically affect the resonant frequency f_0. As outlined schematically in Figure 8, liquid confined in surface cavities is dragged along while the crystal surface oscillates. This leads to a frequency shift, which correlates with the mass of the liquid confined. This amount of liquid can be determined and related to the mean cavity size ε which makes up the roughness pattern.

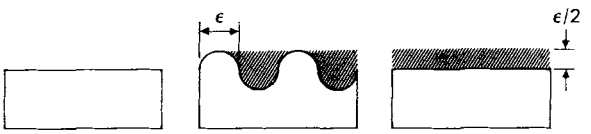

Fig. 8. Electrode cross section to illustrate liquid enclosures in an ideally roughened surface. Left: smooth surface; center: roughened surface made up from hemicylinders with liquid entrapments (hatched area); right: equivalent rigidly attached liquid layer on the smooth surface [4].

To illustrate this procedure, we refer to the electrochemical oxidation/reduction of polycrystalline gold electrodes in neutral and alkaline solutions. Figure 9 shows the cyclovoltammogram and potentiodynamic recording of the frequency at a gold electrode in an alkaline environment. It can be seen that the onset potentials for charge flux and frequency change coincide, indicating the formation and decay of an oxide adlayer. The change in surface roughness is clearly shown by SEM micrographs taken before and after the oxidative/reductive cycle and on samples emersed and examined after their electrochemical oxidation (cf. Fig. 10A, B). These pictures definitely show that the oxidized surface is rougher. The metallic surface remaining after the reduction process is comparable in roughness with an untreated surface (Fig. 10C). Interestingly, the surface layers deposited in alkine medium (Fig. 10B) are visibly rougher than those which are formed in a neutral environment (Fig. 10A).

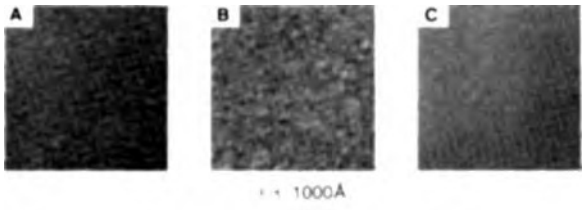

Fig. 10. Scanning electron micrographs on gold surfaces. Micrograph C: surface structure before and after the redox cycle. A and B: surface structure after electrochemical oxidation in neutral and basic media, respectively [4].

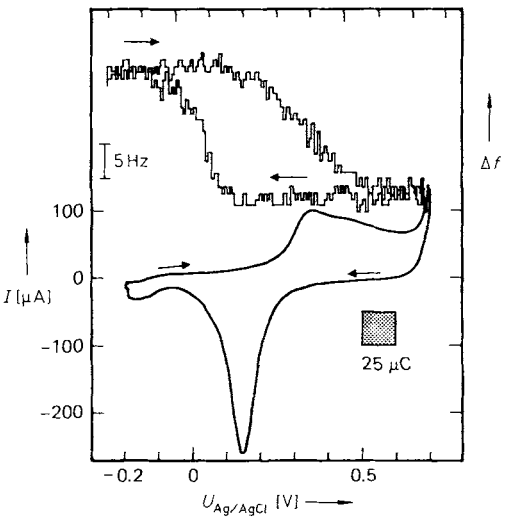

Fig. 9. Potentiodynamic recordings of current and frequency for a freshly prepared gold sample in an alkaline environment [4].

The mass, Δm_1, of liquid confined in cavities of the roughened, oxidized gold electrode can be determined by substracting, Δm_q, the weight gain due to oxide formation, from Δm_f, the total apparent weight gain as measured with the microbalance. Δm_q is determined from Δq, the total charge measured during oxidation, by applying Faraday's law. In order to estimate the degree of surface roughness, the surface was assumed to be corrugated, as illustrated in Figure 8, with a hemicylindrical corrugation of diameter ε.

The amount of liquid carried along in the valleys according to this simplified model is equal to that in uniform layer of thickness $\varepsilon/2$ rigidly attached to a smooth surface. By modification of Equation (a) the mean diameter ε can be estimated from Δm_1 and the density ϱ_1 of the liquid [Eqs. (g) and (h)]. The value obtained for sample A (Fig. 10A) is ca.

$$\Delta f = -[2f_0^2(A\sqrt{\mu_Q \varrho_Q})^{-1}\,\Delta m_1] \qquad \text{(g)}$$

$$\Delta m_1 = \varrho_1 A\,\varepsilon/2 \qquad \text{(h)}$$

30 Å, that for sample B (Fig. 10B) ca. 62 Å. Estimations based on the respective SEM micrographs however give ε-values of 250 ± 100 Å. This difference is not surprising, since it is unlikely that the water confined in surface pockets will behave completely rigidly at this frequency. On the other hand, one cannot determine the depth accurately from SEM; it is possible that the real roughness pattern of samples A, B in Figure 10 can be described only approximately by a hemispherical model and that the observed features are flattened spheroids with a depth shallower than their width. It is interesting to note, that the surface roughness generated in an alkaline environment (cf. Fig. 10B) due to oxidation is approximately twice as large as that created in a neutral environment (cf. Fig. 10A). This is also indicated by the Δm_1 values which were found to be 140 ng for sample A and

310 ng for sample B. Thus, roughly 80% of the observed frequency shifts are caused by roughness effects, while the remainder are due to oxide formation. This analysis definitely demonstrates the uniqueness of information which can be gained from these measurements and underlines the formation of a distinctly different roughness pattern upon oxidation of gold in various electrolytes.

3.4. Influence of Surface Stress on the Resonance Frequency

When one face of a quartz resonator is immersed in a liquid while the opposite face remains exposed to the atmosphere internal strains arise due to the hydrostatic pressure. The magnitude of this pressure depends on how deep the crystal is immersed into the liquid. As outlined by *Heusler* et al.[48] these strains cause a frequency shift that depends on the hydrostatic pressure and on the mass rigidly deposited on the quartz faces. This effect is not to be confused with the change in resonance frequency that occurs if both faces of the resonator are in contact with the liquid. Such frequency changes are found to depend linearly on the hydrostatic pressure, but occur at much higher pressure values.[44]

In Figure 11, the effects described by *Heusler* et al. are schematically presented in a frequency/pressure diagramm.

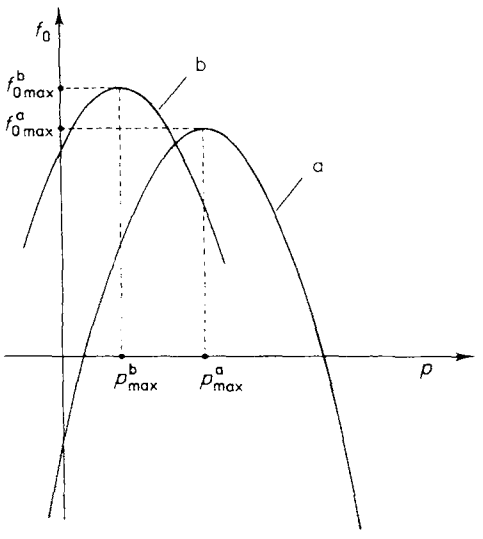

Fig. 11. Parabolic dependence of the resonant frequency f_0 on the pressure p between the *im*mersed and the *e*mersed oscillator face. The superscript *max* refers to the maximum of the parabolic curves with mass loads a and b (a > b) [48].

The curves a and b describe the situation for different mass loads. Contrary to the postulate of *EerNisse*,[49] who claims a linear frequency/pressure behavior, the curves are parabolic and can be expressed by the relationship (i).

$$f_0 - f_{0max} = A(p - p_{max})^2 \qquad \text{(i)}$$

The absolute values $|f^a_{0max} - f^b_{0max}|$ and $|p^b_{max} - p^a_{max}|$ are related to the increase in mass Δm and to the increase in compressive surface stress γ. For the quantitative determination of $\Delta\gamma$ one measures the pressure difference, Δp_{max}, at f^b_{0max} and f^a_{0max}. With the help of equation (j), which was worked out by *Heusler* et al.[48] one can determine $\Delta\gamma$ for that face

$$\frac{\Delta\gamma}{\Delta p_{max}} = \frac{R^3}{4 r_e d}\,[(7 + \nu)(1 - \nu)]^{1/2} \qquad \text{(j)}$$

which encounters stress changes. In this equation, ν is Poisson's number; R and r_e describe the overall radius and effective radius of the electrode surface, respectively.

The first in-situ investigations on the measurement of surface stress $\Delta\gamma$ were carried out on a polycrystalline gold substrate covered with a monolayer of lead.[48] For this type of measurement a special apparatus was designed which allows compensation of the hydrostatic pressure to determine Δp_{max}. From these data the surface stress change was estimated to be $3(\pm 2)$ N m^{-1}, indicating that this type of measurement is, in principle, possible and valuable, but the reproducibility of the measured results leaves much to be desired.

The important question of whether the strains caused by the hydrostatic pressure and their consequent effects lead to a falsification of the results measured by the quartz microbalance can be unequivocally ruled out, since the resonators are typically kept just below the liquid surface, where the hydrostatic pressure effect is negligible. However, strain effects which occur as a result of an increase in film thickness etc. can seriously affect the mass–frequency relation discussed above.[8, 36]

4. Usage of Oscillating Quartz Resonators to Investigate Interfacial Processes on the Solid/Liquid Junction

4.1. Growth and Decay of Solid Thin Films

4.1.1. Metallic Layers

So far, most of the investigations performed with oscillating quartz crystals have been concerned with the dissolution and deposition of various metallic films. In some cases it could be demonstrated that the dissolution and deposition rate, which is proportional to $\Delta\dot{f}$, is constant with time, as expected under galvanostatic control.[7, 9] By combining *Sauerbrey*'s equation [Eq. (a)] with Faraday's law, it has also been shown that, under certain conditions, the current efficiency ξ is close to 1, while in other cases values of $\xi < 1$ were determined. As described above, the former conditions were usually applied to calibrate frequency and mass changes (see Fig. 4). The change in ξ was observed to occur as a function of the applied current density or could be related to a simultaneously occurring competitive reaction which uses up additional charge.[9]

Dissolution experiments under potentiostatic control were performed on nickel[7] and nickel-phosphorus[18] films fixed to polycrystalline gold substrates. As shown in Figure 12, a plot of the anodic dissolution of electrochemically deposited nickel films as a function of the applied voltage exhibits two distinct current maxima at roughly -250 mV and -120 mV (reference potential: saturated calomel electrode, SCE). Since the observed current flux represents the mass

change associated with it, the dissolution rate, $> \Delta\mathring{f}$, is expected to follow this current pattern as well. The occurrence of two maxima correlates with *Fleischmann*'s[50] postulated concept that the nickel films consist of two different nickel

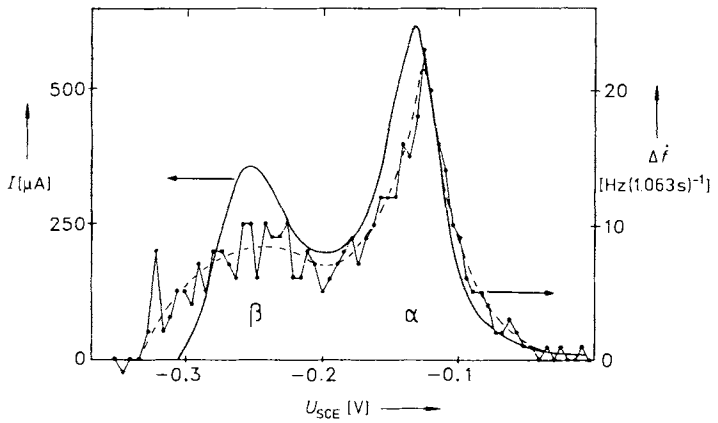

Fig. 12. Anodic dissolution of a nickel film presented in terms of current I and $\Delta\mathring{f}$ as function of the applied voltage U [7].

hydrogen NiH_x phases α and β which dissolve anodically in different potential regions in accord with Equation (k).

$$NiH_x \rightarrow Ni^{2\oplus} + 2e^{\ominus} + \tfrac{x}{2}H_2 \qquad (k)$$

By comparing the observables frequency response and current flux upon anodic dissolution, informative results could also be gained on the composition of nickel-phosphorus films. Here again, two distinctly separate anodic processes were identified. In order to avoid an atmospheric contact of galvanically deposited Ni–P films (composition $Ni_{100-x}P_x$; $8 \leq x \leq 30$) an apparatus was developed which enabled a rapid electrolyte exchange. Using the resulting data in conjunction with Equation (l) the compositional vari-

$$Ni_{100-x}P_x \rightarrow (100-x)\ Ni^{2\oplus} + x P^{z\oplus} + [2(100-x) + xz]\ e^{\ominus} \qquad (l)$$

able x can now be calculated. If one takes $z = 5$ as a basis, it can be concluded from the mass to charge ratio that two Ni–P structures with different composition are present. This result is consistent with the Ni–P phase diagram and electron diffraction experiments on the Ni–P system. The phosphorus content of the electrochemically more noble phase is higher than that of the electrochemically less noble phase. The less noble phase corresponds to supersaturated cubic face centered nickel, while the more noble phase corresponds to a nickel-phosphorus glass.

Investigations on the corrosion[17] and electroless deposition[3] of copper with the in-situ quartz microbalance likewise furnished interesting information. These investigations were carried out without potentiostatic/galvanostatic control, so that the potential of the working electrode could adjust itself according to the electrolytic conditions. In both cases the change in mass was monitored as a function of time. The data were analyzed according to formal kinetic rules. The results underscore the importance of surface reactions that occur on the submonolayer range for the dissolution and deposition of copper films.

Figure 13 shows that the frequency of resonators with copper films[17] in a sulfuric acid electrolyte enriched with various amounts of dissolved oxygen increases with time and is determined by corrosion. The data measured suggest that surface reactions with $Cu^{\oplus}$, O_2, $H^{\oplus}$ with formation of $HO_2^{\ominus}$ and $Cu^{2\oplus}$ are important steps in the dissolution of metallic

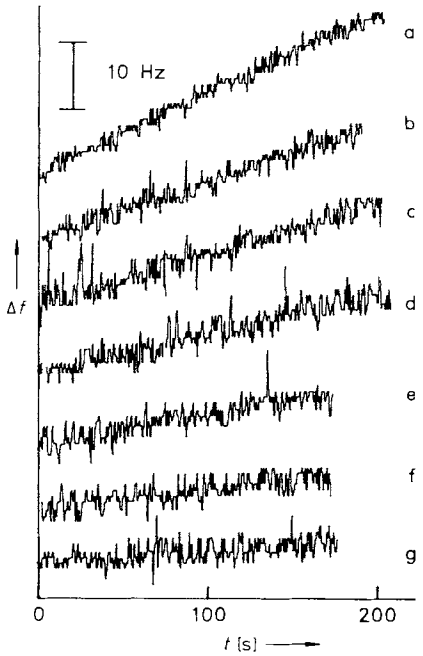

Fig. 13. Dissolution of a copper film presented as a frequency increase vs time plot in oxygenated sulfuric acid solution for various oxygen contents [μg/cm³]. a: 1.6; b: 6.5; c: 5.5; d: 4.3; e: 3.2; f: 2.2; g: 1.6 [17].

copper in oxygenated sulfuric acid according to the overall reaction given in Equation (m).

$$Cu + O_2 + 2H^{\oplus} \rightarrow Cu^{2\oplus} + H_2O_2 \qquad (m)$$

The observation, that the H_2O_2 concentration in an electrolyte does not exceed the millimole range under these conditions suggests that a simultaneous decomposition of dissolved H_2O_2 which may be catalyzed either homogeneously with cupric solution ions or heterogeneously on the copper surface.[51]

As shown by *Schumacher* et al.[3] the electroless deposition of copper with formaldehyde as reducing agent occurs via participation of adsorbed methanediol anions (MDA). The proportionality between $\Delta\mathring{f}$ and the concentration for formaldehyde in the electrolyte is consistent with a formal first order reaction. It also demonstrates that the degree of coverage of the copper surface with the active surface species MDA is proportional to the concentration of the formaldehyde under stead-state conditions and thus reflects a general principle that, at low adsorbent concentrations, the adsorption isotherm increases practically linearly with the concentration of the adsorbent. In the case of electroless deposition of copper the degree of surface coverage with MDA under steady-state conditions was estimated from measurements with the quartz microbalance to be 0.07. As proven in experiments with deuterated formaldehyde, the rate-determining

step for the deposition of copper is the cleavage of the carbon–hydrogen bond of the adsorbed MDA species to give formate.[3]

Weil et al.[10] have carried some fast solution exchange experiments on the same system. They observed anodic and cathodic current transients after removal of cupric ions and/or formaldehyde from the electrolyte; the current-time diagrams are shown in Figure 14. The broken lines represent the corresponding partial currents recalculated from the deposition rate, which was recorded with the microbalance before solution exchange. From the data these authors concluded that the oxidation of formaldehyde is accelerated by the concomitant reduction of cupric ions. On the other hand, formaldehyde does not donate electrons exclusively to cupric ions for their reduction. It was suggested that a surface catalyst is formed, probably chemisorbed methanediol anions. These conclusions were confirmed recently.[52] They are not in accord, however, with the principle of *Wagner* and *Traud*[53] who claimed independence for the simultaneously occurring oxidation and reduction processes at the mixed potential.[53]

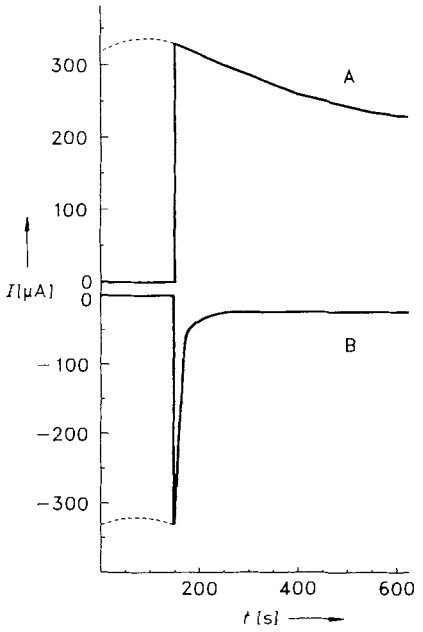

Fig. 14. Fast solution exchange experiments on an electroless copper electrolyte. The current transients occur at the mixed potential due to removal of cupric ions (A) or formaldehyde (B) from a complete electrolyte. The broken lines in (A) and (B) represent the currents recalculated from the deposition rate before solution exchange [10].

4.1.2. Viscoelastic Layers

As concluded by *Crane* and *Fischer*[41] the application of nonmetallic coatings to quartz resonators may cause large errors since these films may behave viscoelastically rather than rigidly. A general theoretical treatment of viscoelastic films which experience shear stress oscillations has not yet been addressed. However, as outlined by *Kanazawa* et al.,[19] thin films with viscoelastic properties can be regarded as rigid if $d \ll 1/k$, where k is a constant for viscoelastic waves propagating through a film of thickness d. This concept holds true for resist films of type AZ 4620 coated on quartz oscillators: the frequency changes observed after the coating agree well with the values predicted according to *Sauerbrey*'s equation.[19] Furthermore, the observed frequency response for long-chain, multilayer systems prepared according to the Langmuir-Blodgett technique was also in accord with *Kanazawa*'s prediction. As demonstrated by *Bruckenstein* et al.[54] a linear relationship is found between the recorded increase in mass and the number of layers deposited on the oscillator. *Buttry* et al.[11] were able to show that polymer films formed by electropolymerization of aniline on metalated quartz oscillator surfaces are also to be regarded as rigid up to a layer thickness of approximately 300 nm. This finding forms the basis for extensive investigations of the growth of polymer films with the quartz microbalance. Some examples are discussed in the following.

The growth of polymer films on metallic substrates has been monitored, both at constant potential as well as potentiodynamically, and evaluated by means of the recorded frequency shifts Δf and the simultaneously recorded charge flux Δq. The linear relationship Δf versus charge Δq as found in potentiodynamic investigations of the formation of thin polymer films such as polypyrrole PP,[55] diheptylviologen bromide DHV,[56] polyvinylferrocene PVF,[12] polyaniline PA,[11,16] and polydithiophene PT[15] indicates that mass transport is not rate-determining.[55] As has been demonstrated[55] for a PP electrode, the film behaves like a dynamically growing electrode, suggesting that the polymer is maintained at an oxidation state which is high enough to sustain growth. It is thought, that this film is able to directly oxidize additional monomers which then react with and add to the end of the polymer chain. In the polymerization of 2,6-dimethylaniline Δf and Δq are independent of each other.[16] This finding is attributed to side reactions such as, e.g., the diffusing-out of oligomeric compounds. In the initial stage, the layer thickness increases linearly with the logarithm of time, which is consistent with a growth law for insulating oxides and inhibitor films.[57] The growth kinetics observed at a constant potential for the electropolymerization of PA reveals that the mass increase below 1000 seconds is negligibly small. In this induction period adsorption and oligomerization take place. Above 1000 seconds nucleation takes place, followed by autocatalytic polymerization, leading to a very rapid increase in film thickness.[16]

An illustrative example for a photochemically-induced film decay is presented in Figure 15. This picture demonstrates, on the one hand, the technological applicability of oscillating quartz resonators as rate monitors (e.g. in microlithography), and, on the other, it reveals some interesting physical features of thin, light-absorbing films.[19] The photochemically induced film dissolution is shown for a Microposit 1470 resist which was in contact with an aqueous Microposit developer and irradiated with light of wavelength 436 nm. The rate of dissolution depends on the light intensity (which was varied between 80 and 160 mJ cm^{-2}), while the unexposed film remains practically unaffected by the developer solution. The modulation in the dissolution rate reflects the interference pattern for thin light-absorbing films and was used to assure the accuracy of thickness data that were determined in-situ with the quartz microbalance.[58]

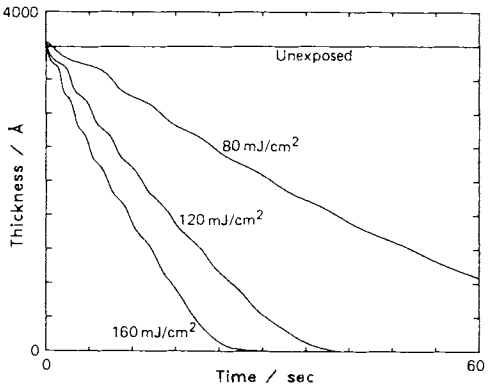

Fig. 15. Photochemical dissolution at $\lambda = 436$ nm of a Microposit 1470 resist which contacts an aqueous Microposit developer [19].

4.2. Ion and Solvent Population in Grown Thin Film Coatings

The contact of a solid with a liquid phase leads, in many cases, to a partial material exchange in both directions. This process is diffusion controlled and leads to an alteration of the bulk properties of the phases involved. The intrinsic transport of ion and solvent molecules in thin films grown on noble metal substrates in a liquid environment by electropolymerization, electrocrystallization etc. strongly depends on their redox state. Ion expulsion and insertion takes place during oxidation and reduction and the resulting mass changes were found to be intrinsic to the electrochemistry of these films. In some cases, solvent exchange at the solid/liquid junction was also observed. The monitoring of these migration processes by means of oscillating quartz resonators furnished detailed information on the distribution of mass and charge in the boundary layers. The various films studied span from pure inorganic materials such as manganese dioxide, tungsten trioxide, and prussian blue films to organic polymer films like polypyrrole PP,[59] polyaniline PA,[11, 14] polythiophene PT,[15] polyvinylferrocene PVF,[12] polycarbonate PC,[60] and polyvinyl chloride PVC.[60]

Using rotating quartz resonators coated with manganese dioxide *Heusler* et al.[20] were able to investigate the migration of manganese ions and the migration of oxygen ions separately under equilibrium conditions. It emerged that the manganese ions are transported without a water sheath, while the oxygen ions are transported together with water molecules. It therefore follows that the exchange current for the naked manganese ions is much larger than for the corresponding oxygen ions. Moreover, it was established that water migrates into the manganese oxide film independent of the ion migration. The incorporation of water in tungsten trioxide films could likewise be demonstrated by in-situ microweighing during coloring-bleaching cycles. The results reveal an aging effect associated with water entrapment.[61]

Mass change measurements during reduction and reoxidation of prussian blue films indicate a change in mass of the films that depends on the electrolyte cation. As shown by *Melroy* et al.[21] reduction of prussian blue films results in the incorporation of alkali metal cations, while oxidation results in alkali metal cation expulsion. For bulky immobile cations, probably proton expulsion occurs. These observations are consistent with a lattice reconstruction upon initial reduction of such films; this can be expressed in terms of Equation (n),

$$Fe_4[Fe(CN)_6]_3 \cdot 6H_2O \xrightarrow[+3M^{\oplus}]{-Fe^{3\oplus},\ -6H_2O} 3MFe_2(CN)_6 \qquad (n)$$

which shows that the net mass changes of the prussian blue film correlates with the mass of the cations $M^{\oplus}$ in the electrolyte.

A thin polyaniline PA electrode is suitable, for demonstrating ion and solvent migration through polymer films. As shown by *Buttry* et al.[11] and confirmed by *Heitbaum* et al.,[14] proton expulsion and anion insertion take place upon oxidation of PA in a moderately acidic solution, thus indicating partial protonation of PA amine nitrogens in the reduced form. Experiments in a strongly acidic environment which were not carried out under steady-state conditions led to a change in solvent content (number of molecules of solvent in the film) during oxidation; this affects the electrochemical response of PA, as is demonstrated in Figure 16, where current A and frequency B responses during potential

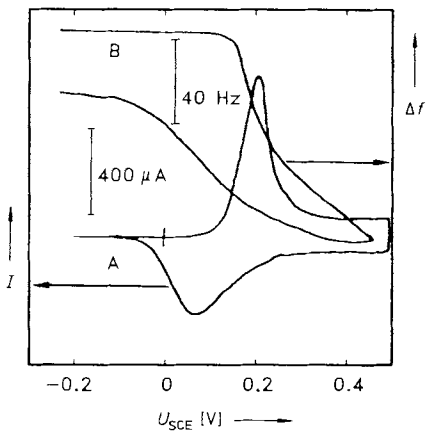

Fig. 16. Electrochemical behavior of a polyaniline PA film in 10 M sulfuric acid in terms of current (A) and frequency (B) [11].

cycling are shown. The frequency changes are much larger than those recorded under steady-state conditions, and the observed slow regain of the frequency to its initial value after the cycle indicates a solvent transport of ca. 500 ng. This is thought to be associated with the dehydrating nature of the electrolyte, in this case concentrated sulfuric acid. This explanation is in accord with the observed positive shift of the anodic peak by 110 mV with respect to the steady state scan. Such effects have been attributed to low solvent levels in the reduced films.

Bimolecular reactions between PVF films and solution species were investigated under open circuit conditions by *Ward*.[13] The observed mass gains on oxidation of the film material with $I_2/I_3^{\ominus}$ are attributed to the formation of PVF-I_3, while the mass losses observed on reduction with $[Fe^{II}(CN)_6]^{4\ominus}$ and $[Ru(NH_3)_6]^{2\oplus}$ are ascribed to the expulsion of counterions.

The technique of in-situ microgravimetry has also been applied to the interesting but complicated biologically related issue of the binding of immunoglobulin IgG and anti-IgG

to silver electrodes in phosphate-buffered electrolytes.[62] The results of this investigation are in accord with the model concepts developed by *Steengard* et al.[63] for this system. Combined microgravimetric and coulometric experiments showed that the composition of IgG/anti-IgG complexes changes from more soluble to an insoluble form which saturates on the silver electrode when the IgG : anti-IgG ratio is 27 : 1.

The isotherms for the adsorption of bovine serum albumin on polysulfone surfaces have been described by *Laatikainen* et al.[64] These authors were able to demonstrate by in-situ microweighing in solution and vacuum that during equilibration of bovine serum albumin with the exposed hydrophilic polysulfone surface, co-deposition of water takes place with formation of a hydrated protein adlayer.

4.3. Processes Associated with Formation and Decay of Adsorbate Adlayers

Heterogeneous surface reactions are often strongly influenced by adsorbate layers. In the classical electrochemical oxidations of formaldehyde and methanol these reactions are catalyzed by under potentially deposited (UPD) layers of lead and tin on platinum electrodes.[65-67] The UPD monolayers are formed by deposition of the corresponding ions which were added to the electrolyte in small amounts.

The formation and decay of adlayers on solid substrates cause a change in surface concentration Γ_{ad}, and, in the case of involvement of charged species, a corresponding change in surface charge q_m is observed. Both quantities are directly measureable, i.e. in-situ and simultaneously, with the oscillating quartz resonator technique and can be used for the calculation of the thermodynamic parameters of the monolayers.[68-72] The electrosorption valency γ of adlayers formed at a constant potential U_{ad} is described by Equation (o), in which the Faraday constant is denoted as F.

$$\left(\frac{\partial q_m}{\partial \Gamma_{ad}}\right)_{U_{ad}} = -\gamma F \qquad \text{(o)}$$

The significance of the thermodynamic quantity γ in the case of the surface dipole moment μ_{ad} of adsorbed species was recently demonstrated by *Schmickler*.[73] It turned out that μ_{ad} values are much smaller than the corresponding values in the bulk phase, indicating that the charge q_m on the adsorbed species is apparently shielded by liquid molecules and surface electrons of the metallic substrate.[73]

Table 1 lists some γ values determined by the quartz oscillator method. The data were measured for both anions and cations on polycrystalline gold substrates. Furthermore, the adsorption of lead and of silver on gold in acetonitrile and of mercury on gold in sulfuric acid were also investigated. The results were not used, however, for determining thermodynamic data.[5, 27]

For comparison we refer to a paper by *Schultze* et al.,[74] who presents a collection of thermodynamic data obtained by various techniques and in different solvent environments.

Model examples for the adsorption/desorption process of ionic species on/from metal surfaces are sulfate and palladium adsorbate formation and decay on polycrystalline gold surfaces.[24, 25] These processes were monitored potentiodynamically using the in-situ microbalance technique (Figs. 17, 18). During the adsorption/desorption process of the sulfate ions on/from the gold surface the differential capacity and the resonance frequency change within the same potential range (Fig. 17). The interesting point, however, is the observed irreversibility of the adsorption and desorption of this anion. As demonstrated by the hatched areas in the cyclic voltammogram the charge fluxes involved during adsorption/desorption are comparable, while frequency and capacitance clearly reveal that adsorption and desorption are inherently different. The reported frequency shift due to adsorption correspondes to about 13 ng and is roughly twice as much as found during desorption. These observations indicate that, upon reduction, only half of the sulfate ions desorb, while the remainder stay adsorbed on the surface, and this in turn would suggest a fairly strong interaction between sulfate anions and the substrate.

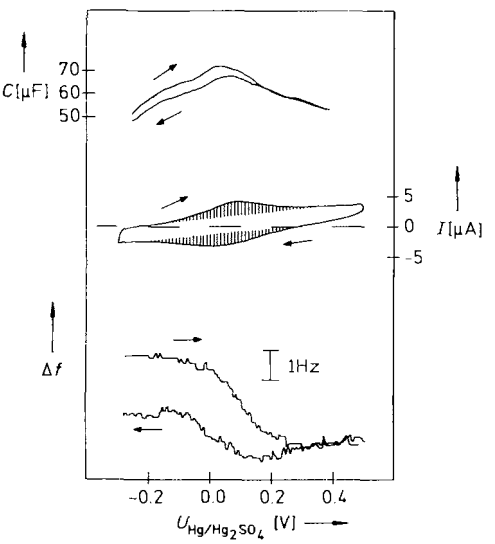

Fig. 17. Formation/decay of a sulfate adlayer on a polycrystalline gold electrode: Potentiodynamic recordings of capacitance, current, and frequency response [24].

A strong anion/adsorbate interaction might also explain the observations shown in Figure 18, which clearly reveal an interference of surface sulfate anions with the adsorption/desorption of palladium ions. Interestingly, the onset potentials for dissolution of under potentially deposited UPD palladium from the gold substrate and for the deposition of sulfate ions are practically identical. The reverse processes, palladium adsorption and sulfate desorption occur under comparable conditions. All these processes occur, as can be seen in Figures 17 and 18, at a potential of around 0.1 V. In

Table 1. Electrosorption valencies $-\gamma$ determined with oscillating quartz resonators by recording charge and mass changes in-situ and simultaneously (polycrystalline gold electrodes).

$-\gamma$: Anions: $Cl^{\ominus}$ 0.06 [24], $Br^{\ominus}$ 0.34 [24], 0.39 [23], $I^{\ominus}$ 1.01 ± 0.05 [23], $SO_4^{2\ominus}$ 0.5 [24]
$-\gamma$: Cations: $Cu^{2\oplus}$ 1.4 [22], $Pd^{2\oplus}$ 1.8 [25], $Cd^{2\oplus}$ 1.6–2.0 [22], $Pb^{2\oplus}$ 2.08 ± 0.1 [26], 2.0 [22], $Bi^{3\oplus}$ 2.7 [22]

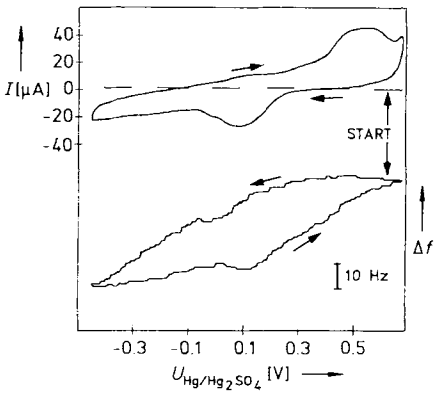

Fig. 18. Formation/decay of a palladium adlayer on a polycrystalline gold electrode: Potentiodynamic recordings of current and frequency in a sulfuric acid solution containing 10^{-4} mol/L of palladium ions [25].

the absence of palladium ions the observed current and frequency pattern are due to the adsorption/desorption of sulfate anions as shown in Figure 17.

A strong interaction of sulfate anions with a copper substrate was recently discussed on the basis of an in-situ EXAFS study.[75, 76] The observed Cu–O distance of 2.08 Å is indicative of sulfate ions which are in direct contact with the copper surface.

4.4. Electrochemical Passivation of Metals

Surface processes associated with the formation and decay of oxidic overlayers on metal electrodes can be characterized cyclovoltammetrically.[77, 78] Oxidation/reduction processes which occur in the intermediate potential range between oxygen and hydrogen evolution appear as pronounced anodic/cathodic current waves. Since, however, the non-specific observable current does not allow discrimination between the growth/decay of oxide adlayers and other surface related processes, the extraordinary mass sensitivity of shear stress oscillations provides further insights into these processes. If an oxide adlayer is formed, oxygen containing species are expected to diffuse into the surface, and thus to increase its weight. The reverse reductive process leads to a loss of weight, since these species diffuse out of the solid. The weight changes are recorded as frequency changes in the oscillating crystals, and are expected to coincide with the onset potentials for anodic/cathodic current fluxes. This does, in fact, occur on a gold electrode in contact with an alkaline electrolyte, as shown in Figure 9. On the other hand, no frequency changes are observed in the intermediate potential range between oxygen and hydrogen evolution if the gold electrode is immersed in an acid environment.[8] Interestingly, the current response still shows pronounced waves, indicating some surface related chemistry. This observation is a clear indication that anodic/cathodic surface processes on gold in an acidic medium and in the intermediate potential range are not related to formation and decay of oxide adlayers since otherwise a parallel mass change would have to be indicated. It seems feasible that, in an acidic environment, adsorbed water molecules are oxidized to hydroxide and vice versa. A loss or gain of one hydrogen atom per adsorbed molecule is probably too small to be detected. For instance, a monolayer of hydrogen accounts for a frequency shift of less than 1 Hz with respect to a 5-MHz oscillator. The results described here for gold electrodes are conclusive and explain the formation and decay of oxide layers on gold in various electrolytic environments. They are in accord with ex-situ spectroscopic investigations and investigations with the Kelvin probe.[79, 80]

Figure 19 shows an interesting experimental result concerning the passivation of metal surfaces: the response of current and frequency on a copper electrode to a variation of

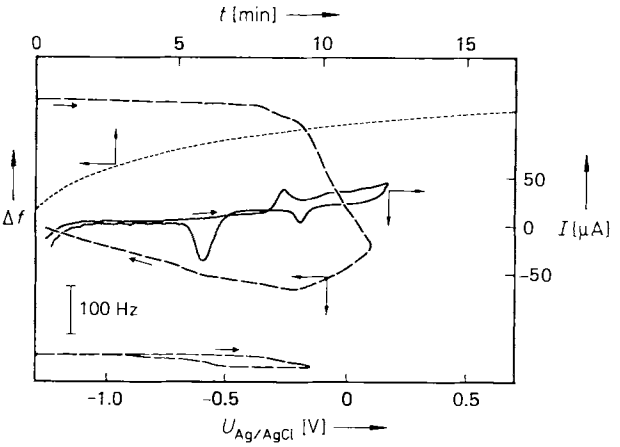

Fig. 19. Potentiodynamic recordings of current and frequency on a polycrystalline copper electrode in the region of oxide formation and dissolution. The regain in frequency with time upon reduction is indicated by a dotted line [28, 29].

potential in alkaline medium.[28, 29] As expected, the two oxidative and reductive current waves which are related to the formation and decay of cuprous- and cupric-oxide films, are paralleled with the frequency response of the oscillator. As shown in the lower part of this diagram, formation and decay of cuprous oxide is reversible in terms of mass changes. But the drastic frequency changes observed in the potential range of cupric oxide formation do not disappear upon reduction. This observation underscores the irreversible nature of processes involved on the time scale of cycling. Interestingly, however, the frequency reaches its starting value again within about 20 minutes, indicating that some time is needed to re-establish the initial state of the surface. The agreement of this frequency–time feature with *Tammann*'s law[81] supports the idea that the oxidized surface needs some relaxation time to rearrange itself after the reduction. *Tammann*'s law relates the mass transport in annealed surface layers to diffusion processes. Since the increase in mass Δm_q (derived from the charge flux) is much smaller than the total mass increase Δm_f (derived from the frequency decrease) an incorporation of water into the oxide layer is postulated. Thus, it is most likely the out-diffusion of these water molecules, after the oxide film is reduced, that determines the rearranging period. A similar result is observed on silver electrodes; however, the degree of surface roughness which goes along with the formation and decay of oxide adlayers is, for this material, much more pronounced.[28, 29]

The electrochemical passivation of titanium[30] and aluminum[34] has also been investigated in terms of frequency

and current changes using the in-situ microbalance. The results for titanium electrodes are shown in Figure 20. By comparing mass changes evaluated from charge fluxes Δm_q with those obtained from frequency shifts Δm_f, it is found that $\Delta m_q \gg \Delta m_f$, which contradicts the results reported for gold, copper and silver electrodes.[4, 28, 29] From the plot Δm_q vs Δm_f it can be estimated that only one third of the

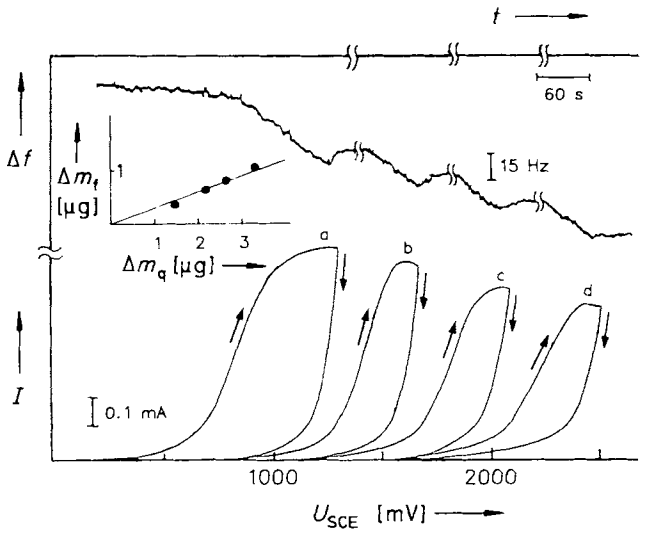

Fig. 20. Electrochemical passivation of a titanium electrode. The current waves a–d represent a consecutive growing oxide film which leads to a frequency decrease as shown in the upper part of the diagram. The evaluation of these data in terms of a mass gain according to charge flux, Δm_q, and frequency response, Δm_f, is given in the inset [30].

charge transported is used in the passivation of the metal surface. The remainder probably leads to the formation of oxygen, which diffuses into the electrolyte. This estimation neglects water entrapment in surface pockets (cf. Section 3.3), although according to the impedance pattern a certain roughness is indicated. The semicircles representing Z_r and Z_i (real and imaginary parts of the impedance, respectively) are twisted clockwise and decrease with increasing thickness of the passive layer. These observations could be recalculated on the basis of a fractal structured surface pattern.[30]

4.5. Surface Sites and Their Influence on the Degree of Electrode/Electrolyte Coupling

In the previous sections we have discussed cases in which the amount of a liquid deposit according to Equations (d) and (e) does not change, so that the frequency responses obtained could be related to mass changes which occur on the solid side of the solid/liquid junction. In this type of experiment, the coupling of shear stress oscillations of the resonator surface to the viscous liquid remains unaffected. However, this requirement does not hold for cases where surface processes are involved that affect the coupling of shear stress oscillations of the resonator surface to the first liquid layer.

A convincing example which demonstrates that the degree of resonator–liquid coupling is affected by the formation/decay of effective surface sites is presented in Figure 21. In this diagram the observables frequency response and current flux are shown under potentiodynamic conditions for a platinum electrode in contact with an acid medium. Interesting is the region of adsorption/desorption of hydrogen atoms and protons, respectively, at potentials below 0.5 V. In this potential region a drastic increase in frequency of ca. 120 Hz occurs, which corresponds to a mass change of ca. 2.5 μg. This change in mass is much larger than changes in weight associated with the formation and decay of a hydrogen monolayer that occurs in this potential region. As has already been mentioned, the frequency changes associated with the formation and decay of a hydrogen monolayer are less than 1 Hz for a 5-MHz resonator. To explain these drastic changes in frequency we refer to a recent study by *Benzinger* et al.[82] who investigated emersed platinum electrodes by means of surface IR spectroscopy. From their results they concluded, in agreement with *Bewick* et al.,[83] the formation of chemisorbed surface sites **A** in the hydrogen region. They

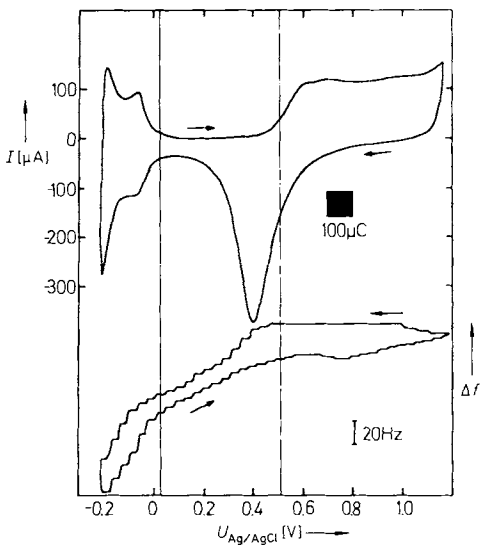

Fig. 21. Potentiodynamic recordings of current and frequency on a polycrystalline platinum electrode in contact with a sulfuric acid solution [8].

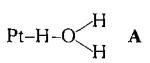

A

are formed in the region of hydrogen adsorption/desorption with participation of water molecules. Consistent with this is that the surface is hydrophilic in this potential range. On the other hand, the surface was found to be hydrophobic in the double layer region, for which a featureless infrared spectrum was observed. These hydrophilic-hydrophobic transitions may create an interfacial slip which changes the coupling between electrode and electrolyte. This, of course, affects the characteristic decay length k_1 for shear waves traveling normal to the surface. As a consequence, the thickness of the attached liquid layer changes and a drastic frequency shift is observed which is much larger than the changes in weight associated with the surface chemistry involved.

A similar result was obtained with titanium oxide electrodes which were investigated in an alkaline environment.[30] The observed strong frequency changes expressed in terms of $\Delta f/\Delta t$ (cf. Fig. 22), which occur under potential

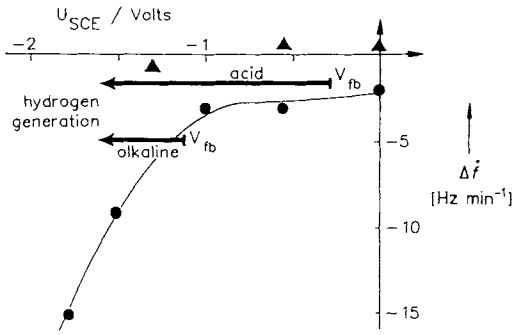

Fig. 22. Decrease in frequency with time Δf for some potentials on an electrochemically passivated titanium electrode. The points represent data measured in acid (▲) and alkaline (●) media. The potential region of hydrogen generation in marked by arrows [30].

conditions where hydrogen atoms are generated on the surface, are related to a surface species **B** which mediates the

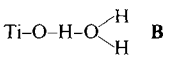

B

coupling between electrode and electrolyte. These sites are formed from $TiO^{\ominus}$ surface species, protons, and water molecules. The protons were either generated by a solid-state reaction of hydrogen atoms and the titanium oxide electrode or they originated from the electrolyte. The former mechanism is based on the diffusion of hydrogen atoms into the solid oxide,[84–86] which in the case of n-type semiconductors like titanium oxide occurs at potentials below the flat band potential V_{fb}. The potential region in which hydrogen atoms are generated at the surface depends on the pH and is indicated in Figure 22 for a strong acid and a strong alkaline solution. Once inside the oxide these hydrogen atoms donate their electrons to the conduction band, leaving behind surface protons $H_s^{\oplus}$ which either diffuse into the solid bulk or equilibrate with $TiO^{\ominus}$ surface sites to form TiOH.[87] These newly formed TiOH sites couple with water molecules, as was observed for a platinum surface in the hydrogen region. How densely the oxide surface is populated with species **B**, depends on the number of $TiO^{\ominus}$ sites and on the $H_s^{\oplus}$ concentration. This of course depends on the generation rate of hydrogen atoms which is potential controlled. As a consequence, in alkaline solutions the coupling changes with the potential as shown in Figure 22.

The insignificant frequency shifts observed upon variation of the potential in an acidic environment (cf. Fig. 22) are also consistent with this interpretation. At low pH the presence of a high electrolyte proton concentration will yield protonated surface groups, so that the surface density of TiOH sites in an acidic solution is independent of $H_s^{\oplus}$ formation. Thus, the frequency shifts remain unaffected by the potential, regardless of the generation of $H_s^{\oplus}$ below 0.5 V.

5. Summary and Outlook

The technique of in-situ microweighing with oscillating quartz resonators immersed in a fluid has proven capable of sensing interfacial processes on a microscopic level. This novel approach has also testified its applicability to a variety of surface related processes; these are summerized in Table 2.

Table 2. In-situ applications of the quartz microbalance at the solid/liquid junction.

Application	Information
Rate monitor	– deposition [3, 10–12, 15–16, 55–56] dissolution [17, 19]
Surface weighing	adsorbate formation [22–26, 64] – mass transport through thin films [11–15, 20, 59–61] – passivation [4, 29–30] – roughness [4, 29]
Surface stress	– adsorbate formation [48]
Coupling	physical/chemical nature of the surface [8, 30]

The information obtained is unique and undoubtedly provides new insights into the complicated mechanisms of interfacial processes. In contrast to the results obtained for the solid/vacuum interface the data observed for the solid/liquid junction are less straightforward. It turned out for the latter case, that recorded changes in the resonance frequency of the oscillating quartz disks are not necessarily associated with a change in mass on the solid side of the solid/liquid junction. It would seem that the state of the surface and its interaction with the bulk liquid (electrolyte) can cause dramatic frequency shifts. These shifts probably reflect a change in thickness of a liquid deposit which moves parallel to the vibrating surface. The results indicate that special surface sites mediate the coupling of the two phases. But also surface roughness and surface stress account for frequency shifts which can accumulate to about 80% of the total frequency shift involved.

As already mentioned in the introductory section the specifity of weight changes, even when they are recorded with nanogram resolution, is inherently insufficient. However, as has been demonstrated, a noticeable improvement is made by recording charge flux and interfacial capacitance simultaneously. This observation suggests the implementation of further specific surface sensitive techniques which can be used along with microgravimetry and can be applied in-situ. A good choice might be spectroscopic in-situ techniques such as surface IR spectroscopy, surface enhanced Raman spectroscopy, EXAFS, etc. A powerful combination would be microgravimetry and scanning tunneling microscopy.

Since our understanding of the fundamental principles associated with the coupling of an oscillator surface to a fluid is still in a poor state, further theoretical work on the treatment of viscoelastic overlayers is called for. And finally, the influence of driver electronics on changes in the resonance frequency requires further investigation.

The author is indebted to Ms. G. Cordes and to HGS for designing and preparing the graphic artwork.

Received: June 2, 1989 [A 754 IE]
German version: *Angew. Chem. 102* (1990)

[1] D. M. Kolb, *Ber. Bunsenges. Phys. Chem. 92* (1988) 1175; H. Gerischer, *ibid. 92* (1988) 1436.
[2] K. Kanazawa, J. Gordon, *Anal. Chem. 57* (1985) 1771; *Anal. Chim. Acta 175* (1985) 99.
[3] R. Schumacher, J. Pesek, O. Melroy, *J. Phys. Chem. 89* (1985) 4338.
[4] R. Schumacher, G. Borges, K. Kanazawa, *Surf. Sci. 163* (1985) L 621.
[5] S. Bruckenstein, S. Swathirajan, *Electrochim. Acta 30* (1985) 851.
[6] S. Bruckenstein, M. Shay, *Electrochim. Acta 30* (1985) 1295; *J. Electroanal. Chem. Interfacial Electrochem. 188* (1985) 138.
[7] M. Benje, M. Eiermann, U. Pittermann, K. G. Weil, *Ber. Bunsenges. Phys. Chem. 90* (1986) 435.
[8] W. Stöckel, R. Schumacher, *Ber. Bunsenges. Phys. Chem. 91* (1987) 345.
[9] U. Pittermann, *Z. Naturforsch. A 42* (1987) 1366.
[10] H. Wiese, K. G. Weil, *Ber. Bunsenges. Phys. Chem. 91* (1987) 619.
[11] D. Orata, D. Buttry, *J. Am. Chem. Soc. 109* (1987) 3574.
[12] P. Varineau, D. Buttry, *J. Phys. Chem. 91* (1987) 1292.
[13] M. Ward, *J. Phys. Chem. 92* (1988) 2049.
[14] B. Schreck, J. Heitbaum, *DECHEMA Monogr. 112* (1988) 49.
[15] B. Krische, W. Stöckel, R. N. Schindler, 39. Bunsenkolloquium: *Anwendung von Quarzoszillatoren in der Elektrochemie*, Clausthal-Zellerfeld 1988.
[16] A. Hochfeld, R. Kessel, J. W. Schultze, A. Thyssen, *Ber. Bunsenges. Phys. Chem. 92* (1988) 1406.
[17] R. Schumacher, A. Müller, W. Stöckel, *J. Electroanal. Chem. Interfacial Electrochem. 219* (1987) 311.
[18] M. Benje, U. Hofmann, U. Pittermann, K. G. Weil, *Ber. Bunsenges. Phys. Chem. 92* (1988) 1257.
[19] W. Hinsberg, C. Willson, K. Kanazawa, *J. Electrochem. Soc. 133* (1986) 1448; *Proc. SPIE Int. Soc. Opt. Eng. (Adv. Resist Technol. Processing II) 539* (1985) 6.
[20] A. Grzegorzewski, K. Heusler, *J. Electroanal. Chem. Interfacial Electrochem. 228* (1987) 455.
[21] B. Feldman, O. Melroy, *J. Electroanal. Chem. Interfacial Electrochem. 234* (1987) 213.
[22] M. Deakin, O. Melroy, *J. Electroanal. Chem. Interfacial Electrochem. 239* (1987) 321.
[23] M. Deakin, T. Li, O. Melroy, *J. Electroanal. Chem. Interfacial Electrochem. 243* (1988) 343.
[24] W. Stöckel, R. Schumacher, *Ber. Bunsenges. Phys. Chem. 93* (1989) 600.
[25] W. Stöckel, R. Schumacher, *Ber. Bunsenges. Phys. Chem. 93* (1989) 606.
[26] O. Melroy, K. Kanazawa, J. Gordon, D. Buttry, *Langmuir 2* (1986) 697.
[27] M. Shay, S. Bruckenstein, *Langmuir 5* (1989) 280.
[28] R. Schumacher, *DECHEMA Monogr. 102* (1986) 107.
[29] R. Schumacher, J. Gordon, O. Melroy, *J. Electroanal. Chem. Interfacial Electrochem. 216* (1987) 127.
[30] A. Müller, M. Wicker, R. Schumacher, R. N. Schindler, *Ber. Bunsenges. Phys. Chem. 92* (1988) 1395.
[31] J. Ühlken, R. Waser, H. Wiese, *Ber. Bunsenges. Phys. Chem. 92* (1988) 730.
[32] S. Bourkane, C. Gabrielli, M. Keddam, *J. Electroanal. Chem. Interfacial Electrochem. 256* (1988) 471.
[33] Fachverband Bauelemente der Elektronik im ZEVI-Zentralverband der Elektrotechnischen Industrie: *Schwingquarze, ein unverzichtbares Bauelement in der Elektronik*, Tagungsdokumentation Quarz Symposium '85, VISTAS Verlag, Berlin 1985.
[34] M. R. Deakin, O. Melroy, *J. Electrochem. Soc. 136* (1989) 349.
[35] G. Sauerbrey, *Z. Phys. 155* (1959) 206.
[36] C. Lu (Ed.): *Applications of Piezoelectric Quartz Crystal Microbalances, Vol. 7*, Elsevier, Amsterdam 1984.
[37] P. L. Konash, G. J. Bastiaans, *Anal. Chem. 52* (1980) 1929.
[38] T. Nomura, A. Minemura, *Nippon Kagaku Kaishi 1980*, 1261.
[39] Yao Shouzhou, Zhou Tiean, *Human Daxue Xuebao 15* (1988) 1.
[40] A. P. M. Glassford, *J. Vac. Sci. Technol. 15* (1978) 1836.
[41] R. A. Crane, G. Fischer, *J. Phys. D 12* (1979) 2019.
[42] V. Mecea, R. V. Bucur, *Thin Solid Films 60* (1979) 73.
[43] T. Nomura, M. Okuhara, *Anal. Chim. Acta 142* (1982) 281.
[44] H. Haardt, *Dissertation*, Universität Kiel 1971.
[45] K. H. Adlfinger, G. Pechel, *Ber. Bunsenges. Phys. Chem. 74* (1970) 347.
[46] G. Pechel, K. H. Adlfinger, *Ber. Bunsenges. Phys. Chem. 74* (1970) 351.
[47] R. Beck, U. Pittermann, K. G. Weil, *Ber. Bunsenges. Phys. Chem. 92* (1988) 1363.
[48] K. E. Heusler, A. Grzegorzewski, L. Jäckel, J. Pietrucha, *Ber. Bunsenges. Phys. Chem. 92* (1988) 1218.
[49] E. P. EerNisse in C. Lu A. Czanderna (Eds.): *Methods and Phenomena, Vol. 7*, Elsevier Sequoia, Lausanne 1984.
[50] M. Fleischmann, A. Saraby-Reintjes, *Electrochim. Acta 29* (1984) 69.
[51] T. Anderson, M. Ghandehari, H. Eyring, *J. Electrochem. Soc. 122* (1975) 1580.
[52] B. J. Feldmann, O. Melroy, *J. Electrochem. Soc. 136* (1989) 640.
[53] C. Wagner, W. Traud, *Z. Elektrochem. Angew Phys. Chem. 44* (1938) 391.
[54] R. R. McCaffrey, S. Bruckenstein, P. N. Prasad, *Langmuir 2* (1986) 228.
[55] C. K. Baker, J. R. Reynolds, *Polym. Prep. Am. Chem. Soc. Div. Polym. Chem. 28* (1987) 284.
[56] G. S. Ostrom, D. A. Buttry, *J. Electroanal. Chem. Interfacial Electrochem. 256* (1988) 411.
[57] J. W. Schultze, R. Rolle, *Makromol. Chem. Macromol. Symp. 8* (1987) 335.
[58] M. Nakao, R. Schumacher, R. N. Schindler, *J. Electrochem. Soc. 133* (1986) 2308.
[59] J. H. Kaufman, K. Kanazawa, B. Street, *Phys. Rev. Lett. 53* (1984) 2461.
[60] B. Schreck, *Diplomarbeit*, Universität Bonn 1986.
[61] H. Masuda, H. Tanaka, N. Baba, *Hyomen Kagaku 9* (1988) 388.
[62] E. S. Grabbe, R. Buck, O. Melroy, *J. Electroanal. Chem. Interfacial Electrochem. 223* (1987) 67.
[63] J. Steengard, A. S. Johansen, C. Jacobsen, *Immunology 38* (1979) 697; J. Steengard, J. R. Frich, *ibid. 26* (1979) 279.
[64] M. Laatikainen, M. Lindström, *J. Colloid Interface Sci. 125* (1988) 610.
[65] W. Vielstich, *DECHEMA Monograph. 102* (1986) 329.
[66] E. Schwarzer, W. Vielstich, *Chem. Ing. Tech. 45* (1973) 201.
[67] R. R. Adzic, *Adv. Electrochem. Electrochem. Eng. 13* (1984) 159.
[68] K. J. Vetter, J. W. Schultze, *Ber. Bunsenges. Phys. Chem. 76* (1972) 920.
[69] K. J. Vetter, J. W. Schultze, *Ber. Bunsenges. Phys. Chem. 76* (1972) 927.
[70] J. W. Schultze, K. J. Vetter, *J. Electroanal. Chem. Interfacial Electrochem. 44* (1973) 63.
[71] K. J. Vetter, J. W. Schultze, *J. Electroanal. Chem. Interfacial Electrochem. 53* (1974) 67.
[72] H. D. Sedlmaier, W. J. Plieth, *J. Electroanal. Chem. Interfacial Electrochem. 180* (1984) 219.
[73] W. Schmickler, *Berl. Bunsenges. Phys. Chem. 92* (1988) 1203.
[74] J. W. Schultze, F. D. Koppitz, *Electrochim. Acta 21* (1976) 327.
[75] L. Blum, H. D. Abruna, J. White, J. Gordon, G. Borges, M. G. Samant, O. Melroy, *J. Chem. Phys. 85* (1986) 6732.
[76] O. Melroy, M. G. Samant, G. Borges, J. Gordon, L. Blum, J. White, M. J. Albarelli, M. McMillan, H. Abruna, *Langmuir 4* (1988) 728.
[77] F. G. Will, C. A. Knorr, *Z. Elektrochem. 64* (1960) 258.
[78] F. G. Will, C. A. Knorr, *Z. Elektrochem. 64* (1960) 270.
[79] M. Peuckert, F. P. Coenen, H. P. Bonzel, *Surf. Sci. 141* (1984) 515.
[80] G. W. Piller, R. Schumacher, *Ber. Bunsenges. Phys. Chem. 92* (1988) 545.
[81] G. Wedler: *Lehrbuch der Physikalischen Chemie*, VCH, Weinheim 1985, pp. 804.
[82] J. Benziger, F. Pascal, S. Bernasek, M. Soriaga, T. Hubbard, *J. Electroanal. Chem. Interfacial Electroden 198* (1986) 65.
[83] A. Bewick, J. Russel, *J. Electroanal. Chem. Interfacial Electrochem. 132* (1982) 329.
[84] L. A. Harris, R. Schumacher, *J. Electrochem. Soc. 127* (1980) 1186.
[85] R. Schumacher, *Ber. Bunsenges. Phys. Chem. 84* (1980) 642.
[86] E. Serwicka, R. N. Schindler, R. Schumacher *Ber. Bunsenges. Phys. Chem. 85* (1981) 192.
[87] G. W. Simons, B. C. Beard, *J. Phys. Chem. 91* (1987) 1143.

[7] M. Bianchi, U. Matteoli, P. Frediani, F. Piacenti, U. Nardelli, G. Pelizzi, *Chim. Ind. (Milan) 63* (1981) 475.
[8] Crystal structure data: The structure was determined with a Stoe-Siemens AED2 four-circle diffractometer ($Mo_{K\alpha}$, graphite monochromator, $\lambda = 0.71073$ Å) using SHELXS-86 [9] and refined with SHELX-76 [10]. **5**: space group *R*3, three independent molecules A, B and C per asymmetric unit; the crystal contains randomly distributed uncoordinated MeCN molecules $a = 17.544(1)$, $b = 17.544(1)$, $c = 62.005(5)$ Å, $\alpha = \beta = 90°$, $\gamma = 120°$, $V = 16528.1$ Å^3, $Z = 9$, $\varrho_{calcd} = 1.500$ g cm^3, $\mu = 11.5$ cm^{-1}, $\theta_{max} = 25°$; 6016 independent reflections, only Lp correction; index limits h: −18/18, k: 0/20, l: 0/73; 4833 reflections with $F_0 > 5\sigma(F_0)$; hydrogen atoms of the OH groups could not be located; refinement with weighted anisotropic temperature factors by the least squares method gave $R = 0.051$, $R_w = 0.050$ with $w^{-1} = \sigma^2(F_0) + 0.0094(F_0^2)$. Residual density in the last difference map 1.12(max) in the neighborhood of the CH_3 carbon atoms of an uncoordinated MeCN molecule, −0.62 (min) Å^{-3}. Further details of the crystal structure investigation are available on request from the Director of the Cambridge Crystallographic Data Centre, University Chemical Laboratory, Lensfield Road, Cambridge CB2 1EW (UK), on quoting the complete literature citation.
[9] G. M. Sheldrick, "SHELXS-86". Program for Crystal Structure Determination, Universität Göttingen 1986.
[10] G. M. Sheldrick, "SHELX-76". Program for Crystal Structure Determination, University of Cambridge (UK) 1976.
[11] W. D. S. Motherwell, W. Clegg, "Pluto". Program for Plotting Molecular and Crystal Structures, University of Cambridge (UK) 1978.

Multiple 1,2-*O*,*O*-Shift of *tert*-Butyldiphenylsilyl Groups in Polyols

By *Johann Mulzer** and *Bernd Schöllhorn*

tert-Butyldimethylsilyl (TBDMS) and *tert*-butyldiphenylsilyl (TBDPS) groups are standard protecting groups for OH functions.[1] The *O*,*O* silyl migration to be expected in polyols was hitherto chiefly observed in the case of the less stable TBDMS unit.[2] In the case of the TBDPS group two examples have been described in the literature, namely a 1,3-shift[3] and 1,2-shift.[4] We now report a multiple 1,2-*O*,*O* migration of TBDPS groups in the polyol derivatives **1**, **2**, **4**–**6**, **8**, **9** and **13**.[5]

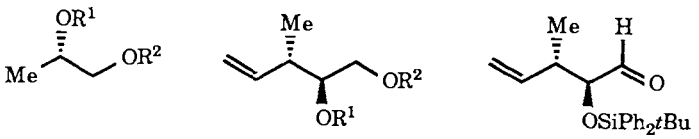

1 **2** **3**

a, $R^1 = t\text{BuPh}_2\text{Si}$, $R^2 = H$
b, $R^1 = H$, $R^2 = t\text{BuPh}_2\text{Si}$

The silyl migration requires base catalysis (standard conditions: potassium carbonate in methanol, 22 °C). **1a** and **2a** then isomerize completely to **1b** and **2b**, respectively. Under neutral or acid conditions the TBDPS group is stable towards migration. Reduction of the aldehyde **3** with lithium aluminum hydride in diethyl ether therefore leads uniformly to **2a**, whereas that with sodium tetrahydroborate in methanol yields **2b** quantitatively. During the reaction **2a** is detectable as intermediate.

Under standard conditions, the triol derivative **4a** forms an 87:7:6 equilibrium mixture (HPLC analysis) of **4c**, **4b** and **4a** in 20 min, from which **4b** can be separated and used again. After 15 min, the same product ratio as from **4a** is obtained, thus proving that the silyl migration proceeds reversibly in both directions. Responsible for the equilibrium

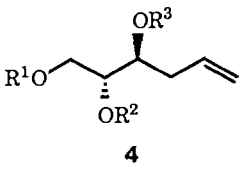

4

4	R^1	R^2	R^3
a	H	H	$t\text{BuPh}_2\text{Si}$
b	H	$t\text{BuPh}_2\text{Si}$	H
c	$t\text{BuPh}_2\text{Si}$	H	H

position is the preference of the bulky TBDPS group for the primary position, which is favored by ca. 8–9 kJ mol^{-1} compared to the secondary positions, but, because of the reversibility of the migration step, is only reached by trial and error. The establishment of equilibrium therefore takes longer the larger the number of the participating OH functions.

The pentol **5a** derived from D-mannitol isomerizes to **5b**, which, because of the C_2 symmetry of the unprotected mol-

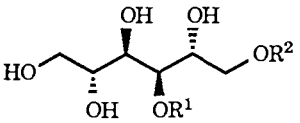

5

5	R^1	R^2
a	$t\text{BuPh}_2\text{Si}$	H
b	H	$t\text{BuPh}_2\text{Si}$

ecule, can be formed by two- or threefold *O*,*O* migration. Both routes are possible, as demonstrated by the uniform formation of **7** from **6a** and **6b**. The *syn*- or *anti*-position of the OH functions to be traversed, and thus the conformational strain in the postulated intermediate **Z**,[2b] apparently have no influence on the product pattern. This experiment also proves that the silyl migration—consistent with **Z**—proceeds with retention at the carbinol centers, since **7** would otherwise be epimerized differently compared to the precursors **6a/b**.

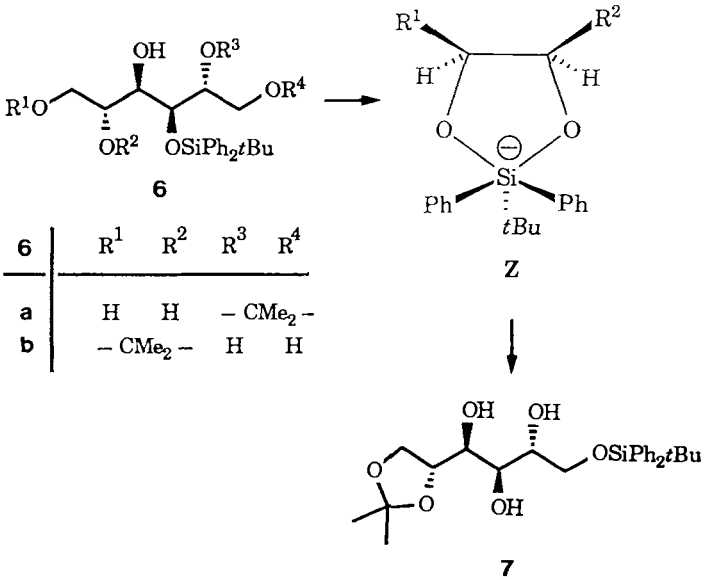

6

6	R^1	R^2	R^3	R^4
a	H	H	$-CMe_2-$	
b	$-CMe_2-$		H	H

Z

7

[*] Prof. Dr. J. Mulzer, Dipl.-Chem. B. Schöllhorn
Institut für Organische Chemie der Freien Universität
Takustrasse 3, D-1000 Berlin 33.

By incorporation of a methyl branch, the migration in the direction of this branching is prevented: under standard conditions derivative **8a** affords only **8b**; of the two monoacetals **9**, **9a** remains unchanged, whereas **9b** quantitatively forms **10**, which furnishes **8b** again upon cleavage of the acetal. A 1,3 shift[3] apparently does not take place. To further check this finding the 1,3-diol **11a** was investigated. Under standard conditions it does not isomerize to **11b**; only concentrated methanolate enforces this reaction, albeit with a small conversion over several days.

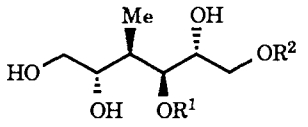

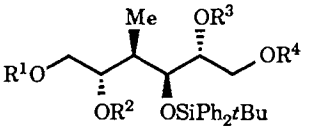

8	R^1	R^2
a	tBuPh$_2$Si	H
b	H	tBuPh$_2$Si

9	R^1	R^2	R^3	R^4
a	H	H	$-CMe_2-$	
b	$-CMe_2-$		H	H

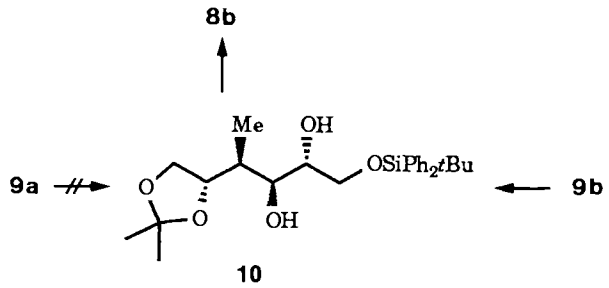

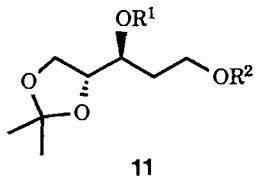

11	R^1	R^2
a	tBuPh$_2$Si	H
b	H	tBuPh$_2$Si

The silyl group migrates intramolecularly. This follows from the fact that di- or desilylation have never been observed under standard conditions. Also diol **12** added to **4a** is recovered unsilylated after establishment of the equilibrium of **4**, despite the two primary OH functions.

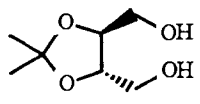

The structures of the products mentioned so far are unequivocally confirmed via the ^{1}H-NMR spectrum; primary OH functions are recognized by the OH multiplet, secondary OH functions by the OH doublet.[5]

Also cyclic 1,2-diols display the phenomenon of TBDPS migration. Thus, the glucose derivative **13a** is silylated with TBDPS chloride under kinetic conditions to give a 94:6 mixture of the monosilyl ethers **13b** and **13c**. Under our standard conditions, however, a 2:1 mixture of **13c** and **13b** is formed within a few minutes. Thus, kinetic and thermodynamic control afford extremely different results.

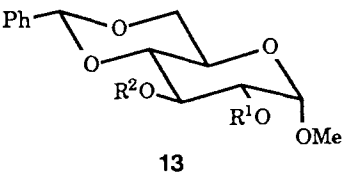

13	R^1	R^2
a	H	H
b	tBuPh$_2$Si	H
c	H	tBuPh$_2$Si

These findings can be exploited preparatively, on the one hand to obtain terminally monosilylated polyols such as **5b** or **8b** without having to deal with the relatively strongly hydrophilic and thus difficultly handleable free polyols; small amounts of secondary silyl ethers can be readily separated by column chromatography. On the other hand, two primary terminal groups can be easily differentiated via this migration. Thus, **7** is readily accessible from **6**, and its free secondary OH functions can then be benzylated together. Finally, the terminal protecting groups can be removed, separately. The same is also accomplished with the methyl derivatives **8** and **9**, so that such large monosaccharides blocks can be used in "ex-chiral pool syntheses".

General Procedure

A mixture of TBDPS-protected polyol (1.0 g in 10 mL of methanol) and saturated methanolic potassium carbonate solution was stirred at 22 °C for 10 min to 12 h (TLC control). The mixture was then neutralized with saturated ammonium chloride solution, evaporated down (rotary evaporator), taken up in dichloromethane, washed with water, dried over magnesium sulfate, and chromatographed on silica gel with hexane/ethyl acetate or ethyl acetate/methanol (**5b**/**8b**). By using a few drops of methanolic sodium methanolate solution instead of potassium carbonate the rate of migration of the silyl group could be increased considerably.

Received: December 4, 1989 [Z 3671 IE]
German version: *Angew. Chem. 102* (1990) 433

CAS Registry numbers:
1a, 125803-66-9; **1b**, 125803-68-1; **2a**, 125803-67-0; **2b**, 125803-69-2; **3**, 125803-70-5; **4a**, 125803-71-6; **4b**, 125803-72-7; **4c**, 125803-73-8; **5a**, 125803-74-9; **5b**, 125803-75-0; **6a**, 125803-76-1; **6b**, 125803-77-2; **7**, 125803-78-3; **8a**, 125803-79-4; **8b**, 125803-80-7; **9a**, 125827-91-0; **9b**, 125803-81-8; **10**, 125803-82-9; **11a**, 125827-92-1; **12**, 86992-57-6; **13a**, 57701-27-6; **13b**, 112669-90-6; **13c**, 125803-0.

[1] E. J. Corey, A. Venkateswarlu, *J. Am. Chem. Soc. 94* (1972) 6190, T. Greene: *Protective Groups in Organic Synthesis*, Wiley, New York 1981, p. 47.
[2] a) G. H. Dodd, B. T. Golding, P. V. Iounnou, *J. Chem. Soc. Perkin Trans. 1 1976*, 2273; S. S. Jones, C. B. Reese, *ibid. 1979*, 2762; K. K. Ogilvie, S. L. Beaucage, A. L. Schifman, N. Y. Theriault, K. L. Sadana, *Can. J. Chem. 89* (1981) 203; b) W. Köhler, W. Pfleiderer, *Liebigs Ann. Chem. 1979*, 1855.
[3] U. Peters, W. Bankova, P. Welzel, *Tetrahedron 43* (1987) 3803.
[4] J. Jurczak, S. Pikul, K. Ankner, *Pol. J. Chem. 61* (1987) 767.
[5] We shall report on the synthesis, properties, and preparative use of the compounds **2**, **4**–**9** and **10** in a separate communication.

Reductive Alkylation of Enamines with Chloromethyl *p*-Tolyl Sulfone via a Radical Chain Process**

By *Philippe Renaud** and *Serge Schubert*

In the past few years, the addition of radicals to olefins by chain processes has emerged as a very valuable alternative to ionic reactions for the formation of carbon–carbon bonds.[1] For intermolecular reactions, the use of activated olefins is usually necessary. In most reported cases, activation is performed by lowering the LUMO of the olefins by introduction of electron withdrawing groups in order to favor their reaction with nucleophilic radicals. A few reports have been in connection with the reverse process,[2, 3] i.e. the use of olefins with high energy HOMO (electron-rich olefins) and electrophilic radicals.[4] Surprisingly, enamines have never been used for performing such reactions in a preparative way.[5] However, their use should allow the development of new strategies for the synthesis of nitrogen-containing compounds. We report here a method for the reductive alkylation of enamines with chloromethyl sulfones via a radical chain process. Particular attention has been given to the stereochemical course of the reaction[6] together with factors influencing the reaction rate.

The chloromethyl sulfone **1** reacts in the presence of tributyltinhydride and azobis(isobutyronitrile)(AIBN), with enamines which, like **2** and **3** are not substituted in the β-position, to give the products of reductive alkylation **4** and **5** in 55% and 75% yield respectively [Eq. (1)]. In the absence of AIBN no reaction takes place, and thus an ionic mechanism for these reactions can be ruled out. *cis*-*N*-(1-Propenyl)-aziridine **6** and *N*-(2-methyl-1-pro-penyl)morpholine **7** failed to react under these conditions and the product of direct reduction (methyl *p*-tolyl sulfone) was isolated in quantitative yield.

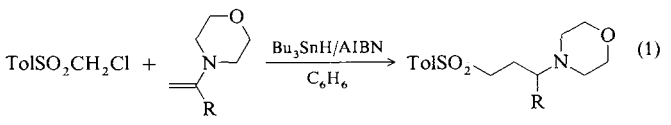

(1)

1 **2**: R = *t*Bu; **3**: R = Ph **4**: R = *t*Bu; **5**: R = Ph

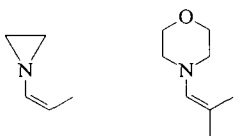

6 **7**

Under the same reaction conditions, **1** reacts with cyclic enamines derived from morpholine (**8**, **9**), pyrrolidine (**10**) and azetidine (**11**) [Eq. (2), Table 1]. The major products all possess the *cis* configuration, the selectivity being especially high in the formation of the cyclohexane derivatives **13** and **14** (>95% *cis*) and somewhat lower for the cyclopentane derivative **12** (84% *cis*). The relative configurations were determined ^{1}H-NMR spectroscopically from the coupling constants and in the case of **12** and **14** by reduction with sodium amalgam[7] to the known[8] *cis*-4-[(2-methyl)cyclopentyl]morpholine and *cis*-1-[(2-methyl)cyclohexyl]pyrrolidine respectively.

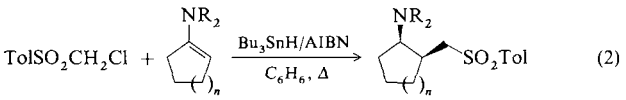

(2)

1 **8–11** **12–15**

Table 1. Reductive alkylation of cyclic enamines **8–11** with chloromethyl p-tolyl sulfone **1** [Eq. (2)].

Enamine	*n*	NR_2	Product	Yield [a]	*cis*:*trans* [b]
8	1	O N—	**12**	54%	84:16
9	2	O N—	**13**	62%	96:4
10	2	N—	**14**	57%	97:3
11	2	N—	**15**	10%	>95:5[c]

[a] Purified *cis* product; [b] Determined by GC and ^{1}H-NMR analysis of the crude products; [c] After crystallization.

Rationalization of these results in the case of the cycohexane derivatives is depicted in Figure 1. The radical adduct may exist in conformations **A** and **B**. We believe that the very high selectivity observed for the formation of **13** and **14** arises from the fact that only **A** is involved in the transition state (reaction of **B** should be less stereoselective). Kinetically, the formation of conformer **A** is favored for the same stereoelectronic reasons which govern the alkylation of

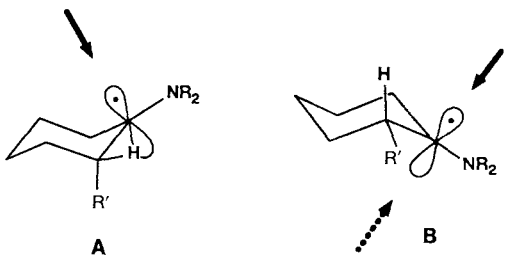

Fig. 1. Model for stereoselective H-atom transfer. Preferred and possible attacks are shown with unbroken and broken arrows, respectively. R' = CH_2SO_2Tol.

enamines.[9] The assumption that **A** is also the more stable conformer may be supported by the existence of steric interactions between the *p*-tolylsulfonylmethyl and the NR_2 groups which destabilize **B**. But even then, if **B** is the more stable conformer, the ring flip may be slower than reaction with Bu_3SnH and thus only **A** is present at the time of the reaction. A simple estimation of the interconversion rate shows that under our reaction conditions this is the case for energy barriers ≥ 12 kcalmol^{-1} (we have used an estimated value of 5×10^5 L mol^{-1} s^{-1} for the hydrogen abstraction rate constant of the radical adducts **A** and **B**.[10]) In the cyclopentane derivative **12**, the conformational changes of the radical adduct are much faster than for cyclohexane derivatives and about 16% *trans* isomer is formed.

On the basis of competition experiments, it was possible to show that the reaction of the radical generated from **1** with 1-cyclohexenylpyrrolidine (**10**) was occurring at a rate (k_a) similar to that found for hydrogen abstractions from Bu_3SnH (k_H). Since no value for k_H has been specifically reported for primary sulfonylated radicals, we assumed that

[*] Dr. P. Renaud, S. Schubert
Institut de Chimie Organique de l'Université
2, rue de la Barre, CH-1005 Lausanne (Switzerland)

[**] We thank the Swiss Science Foundation for generous financial support.

it is of the same order of magnitude as for primary alkyl radicals[11] ($k_H = 2 \times 10^6$ L mol^{-1}s^{-1}.[12,13] A k_a value of about 10^6 L mol^{-1} s^{-1} may be deduced, indicating that the addition process is very fast. For comparison, this rate constant is similar to the one for the classical addition of a primary alkyl radical to acrylonitrile. Such a high rate constant can be, caused by two factors: a) by the stabilization of the radical intermediate via spin delocalization to the nitrogen atom,[14] and b) by the strong electron donor character of pyrrolidine enamines. The first point is important only if the addition is a late transition state process, which is usually not the case for radical additions to olefins.[15] Moreover, this contribution is similar for the different enamines. The second point plays a crucial role and has been quantified by measuring the oxidation peak potential of the enamines in acetonitrile (Table 2). Values for the first ionization potential, when found in the literature, are also reported and are in agreement with the oxidation peak potentials we have determined. Pyrrolidine enamines are easier to oxidize than morpholine enamines; this is consistent with the observation that in direct competition **10** reacts about 20 times faster than **9**. We can now explain why *cis-N*-(1-propenyl)aziridine **6** does not react: **6** is a very weak electron donor, as shown by its very high oxidation potential ($> +1.50$ V vs. Ag/Ag$^{\oplus}$). Such a behavior is characteristic for unactivated alkenes. This confirms the calculations of *Müller* and *Previdoli*[16] which predict that **6** may exist in a *trans*-bisected conformation with no possibility for n–π delocalization. As expected for radical additions,[15] steric effects also play an important role in determining the reactivity of enamines. Although the reaction of **7** with radicals is favored by electronic effects, this enamine does not react because of steric hindrance by the two methyl substituents in the β-position.

Table 2. Oxidation peak potential OP [V] vs. Ag/Ag$^{\oplus}$ (cyclic voltammetry, glassy carbon electrode, CH_3CN, 0.2 M $LiClO_4$) and first ionization potential IP_1 [eV] [17] of enamines **6**–**11**.

	6	7	**8**	**9**	**10**	**11**
OP [a]	$> +1.50$	+0.19	+0.19	+0.18	−0.05	−0.05
IP_1	8.50	–	7.60	7.67	7.10	7.46

[a] Irreversible oxidation (100 mVs^{-1}).

In conclusion, we have developed a new method of reductive alkylation of enamines based on a radical chain process. High diastereoselectivities have been observed with cyclic enamines. Moreover, the rate of addition of sulfinylated and sulfonylated carbon centered radicals to enamines is high enough to make the method widely applicable in inter- and intramolecular reactions.

Experimental

1 was prepared from chloromethyl p-tolylsulfoxide[18] by oxidation with 1 equivalent of *m*-chloroperbenzoic acid in CH_2Cl_2. The enamines **2**[19], **3**[20], **6**[21], 7[19] and **11**[21] were prepared by known methods. **8**–**10** are commercially available and were distilled prior to use. The new compounds were characterized by ^{1}H NMR (250 MHz), ^{13}C NMR (62.5 MHz), IR, MS and elemental analysis.

Typical procedure: A solution of 1 mmol of **1** in benzene (15 mL) was treated with 4 mmol of enamine, 0.6 mmol of Bu_3SnH and 10 mg of AIBN and the mixture heated under reflux. After 1 h, a further 0.6 mmol of Bu_3SnH and a further 10 mg of AIBN were added and reflux continued for 5 h. The reaction mixture was poured into Et_2O/toluene (1:1) and extracted with 1M HCl. The aqueous phase was treated with an excess 3 M NaOH and extracted with CH_2Cl_2. The crude product was purified by recrystallization or flashchromatography.

4: colorless oil. ^{1}H NMR ($CDCl_3$): 0.89 (s, 9H); 1.80–1.95 (m, 2H); 2.12 (dd, J = 4.0, 10.0 Hz, 1H); 2.42 (s, 3H); 2.65–2.75 (m, 4H); 3.05–3.19 (m, 1H); 3.25–3.40 (m, 1H); 3.45–3.58 (m, 4H); 7.38 (m, 2H); 7.80 (m, 2H).

5: colorless oil. ^{1}H NMR ($CDCl_3$): 1.96–2.13 (m, 1H); 2.20–2.40 (m, 5H); 2.45 (s, 3H); 2.95 (A part of an ABXY system, J_{AB} = 14.0, J_{AX} = 10.5, J_{AY} = 5.0 Hz, 1H); 3.10 (B part of an ABXY system, J_{AB} = 14.0, J_{BX} = 5.5, J_{BY} = 11.0 Hz); 3.32 (t, J = 7.0 Hz, 1 Hz); 3.60–3.68 (m, 4H); 7.05–7.12 (m, 2H); 7.20–7.40 (m, 5H); 7.72 (m, 2H).

12: m.p. 114–115.5 °C; ^{1}H NMR ($CDCl_3$): 1.10–1.28 (m, 1H); 1.60–1.88 (m, 5H); 2.20–2.40 (m, 5H); 2.45 (s, 3H); 2.50–2.60 (m, 1H); 2.70 (dd, J = 10.0, 13.0 Hz, 1H); 3.55–3.65 (m, 5H); 7.35 (m, 2H); 7.78 (m, 2H).

13: m.p. 110–111 °C; ^{1}H NMR ($CDCl_3$): 0.70–0.90 (dq, J = 3.5, 12.5 Hz, 1H); 1.10–1.55 (m, 4H); 1.70–1.85 (m, 2H); 1.95–2.10 (m, 2H); 2.20–2.35 (m, 4H); 2.45 (s, 3H); 2.52–2.62 (m, 1H); 3.08 (dd, J = 10.5, 14.0 Hz, 1H); 3.52 (m, 4H); 3.62 (d, J = 14.0 Hz, 1H); 7.37 (m, 2H); 7.80 (m, 2H).

14: m.p. 110–111 °C; ^{1}H NMR ($CDCl_3$): 0.90–1.50 (m, 5H); 1.53–1.80 (m, 6H); 1.88–2.00 (m, 1H); 2.03–2.12 (m, 1H); 2.25–2.38 (m, 4H); 2.42 (s, 3H); 2.50–2.60 (m, 1H); 3.12 (dd, J = 11.0, 14.0 Hz, 1H); 3.54 (d, J = 14.0 Hz, 1H); 7.32 (m, 2H); 7.80 (m, 2H).

15: m.p. 108–110 °C; ^{1}H NMR ($CDCl_3$): 0.60–1.00 (m, 1H); 1.10–2.20 (m, 10H); 2.30–2.45 (m, 1H); 2.46 (s, 3H); 2.85–3.05 (m, 4H); 3.04 (dd, J = 10.5, 14.5 Hz, 1H); 3.44 (d, J = 14.5 Hz, 1H); 7.35 (m, 2H); 7.80 (m, 2H).

Received: November 6, 1989 [Z 3621 IE]
German version: *Angew. Chem. 102* (1990) 416

CAS Registry numbers:
1, 7569-26-8; **2**, 22502-84-7; **3**, 7196-01-2; **4**, 125803-50-1; **5**, 125803-51-2; **6**, 80839-91-4; 7, 2403-55-6; **8**, 936-52-7; **9**, 670-80-4; **10**, 1125-99-1; **11**, 7326-44-5; **12** *cis*-isomer, 125803-52-3; **12** *trans*-isomer, 125803-56-7; **13** *cis*-isomer, 125803-53-4; **13** *trans*-isomer, 125803-57-8; **14** *cis*-isomer, 125803-54-5; **14**-*trans*-isomer, 125803-58-9; **15** *cis*-isomer, 125803-55-6; **15** *trans*-isomer, 125803-59-0.

[1] Recent reviews on this topic: B. Giese: *Radicals in Organic Synthesis: Formation of Carbon–carbon Bonds*, Pergamon, Oxford 1986; M. Ramaiah, *Tetrahedron 43* (1987) 3541. W. P. Neumann, *Synthesis 1987*, 665. D. P. Curran, *ibid. 1988*, 417, 489.
[2] B. Giese, H. Horler, M. Leising, *Chem. Ber. 119* (1986) 444.
[3] K. Riemenschneider, H. M. Bartels, R. Dornow, E. Drechsel-Grau, W. Eichel, H. Luthe, Y. M. Matter, W. Michaelis, P. Boldt, *J. Org. Chem. 52* (1987) 205; G. J. Gleicher, B. Mahiou, A. J. Aretakis *ibid. 54* (1989) 308.
[4] Polar effects in radical reactions: a) B. Giese, J. He, W. Mehl, *Chem. Ber. 121* (1988) 2063; b) I. Beranek, H. Fischer in F. Minisci (Ed.): *Free Radicals in Synthesis and Biology*, Kluwer, Dordrecht 1989, p. 303.
[5] Enamines have been used for the study of radical reactivity by *Giese* et al. ([2], [4a]).
[6] Review about stereoselectivity in radical reactions: B. Giese, *Angew. Chem. 101* (1989) 993; *Angew. Chem. Int. Ed. Engl. 28* (1989) 969.
[7] B. M. Trost, H. C. Arndt, P. E. Strege, T. R. Verhoeven, *Tetrahedron Lett. 1976*, 3477.
[8] R. O. Hutchins, W.-Y. Su, R. Sivakumar, F. Cistone, Y. P. Stercho, *J. Org. Chem. 48* (1983) 3412.
[9] P. Deslongchamps: *Stereoelectronics Effects in Organic Chemistry*, Pergamon, Oxford 1983, p. 282.
[10] We were not able to detect a change of the stereoselectivities with low concentrations of Bu_3SnH or by using tris(trimethylsilyl)silane which is a less reactive hydrogen donor.
[11] Sufonyl groups do not stabilize radicals: E. Block: Reactions of Organosulfur Compounds, Academic, New York 1978, p. 196.
[12] K. A. Gupta, A. K. Saxena, P. C. Jain, *J. Indian Chem. Soc. 21 B* (1982) 228.
[13] A value of 6.3×10^6 L mol^{-1}s^{-1} was estimated for a tertiary, sulfonylated C-radical: B. Vacher, A. Samat, A. Allouche, A. Laknifli, A. Baldi, M. Chanon, *Tetrahedron 44* (1988) 2925.
[14] S. F. Nielsen in J. K. Kochi (Ed.): *Free Radicals*, Vol II, Wiley, New York 1973, p. 527.
[15] B. Giese, *Angew. Chem. 95* (1983) 771; *Angew. Chem. Int. Ed. Engl. 22* (1983) 753.
[16] K. Müller, F. Previdoli, *Helv. Chim. Acta 64* (1981) 2508.
[17] K. Müller, F. Previdoli, H. Desilvestro, *Helv. Chim. Acta 64* (1981) 2497.
[18] T. Satoh, T. Oohara, Y. Ueda, K. Yamakawa, *Tetrahedron Lett. 29* (1988) 313.
[19] R. Carlson, R. Phan-Tan-Luu, D. Mathieu, F. S. Ahouande, A. Babadjamian, J. Metzger, *Acta Chem. Scand. B32* (1978) 335.
[20] R. Noyori, K. Yokoyama, Y. Hayakawa, *Org. Synth. 58* (1978) 56.
[21] E. Previdoli, Dissertation 6707, ETH Zürich 1980.

Book Reviews are written by invitation from the editor. Suggestions for books to be reviewed and for book reviewers are welcome. Publishers should send brochures or (better) books to the following address: Redaktion Angewandte Chemie, Postfach 101161, D-6940 Weinheim, Federal Republic of Germany. The editor reserves the right of selecting which books will be reviewed. Uninvited books not chosen for review will not be returned.

Comprehensive Organic Transformations. By *R. C. Larock*. VCH Publishers, Inc., New York/VCH Verlagsgesellschaft, Weinheim 1989. xxxiv, 1160 pp., hardcover, $55.00.— ISBN 0-89573-710-8/3-527-26953-3

This monograph represents a most courageous attempt by a lone author to provide in a single volume a comprehensive, highly condensed, systematic collection of literature references designed to allow for the most effective selection of a protocol for accomplishing a specific organic transformation. The outcome is an especially useful reference book that makes available at one's fingertips a wealth of information concerning a broad range of reaction types. Its nonannotated format causes it to stand apart from the Wagner and Zook compilation of the 1950s, the Buehler and Pearson two-volume set of the 1970s, and the popular Fieser series of the last two decades. The organization is based on the functional group being synthesized, each subsection focusing on a specific aspect of methodology. The innumerable reagent combinations and accompanying literature citations that are found on every page are a mine of information. The author is to be congratulated on meeting his challenging objectives so successfully.

The book treats with great thoroughness the present state of knowledge surrounding the synthesis of alkanes and arenes, alkenes, alkynes, halides, amines, ethers, alcohols and phenols, aldehydes and ketones, nitriles, and carboxylic acids and their derivatives. No attempt has been made to cover less important functional groups unless they impact indirectly on the above. Although it is possible to quarrel with the author's subjective exclusions, the wealth of topics included and their coordination have to be regarded as highly commendable.

It is relevant to deal explicitly with two chapters in order to transmit the scholarly approach taken by the author. The second chapter (Alkenes) contains ten sections, each detailing specifically a type of synthetic method useful for gaining access to this class of compounds. Under the topic of elimination can be found 51 subsections, each identifying a different precursor type (37 pages in all). Although not as lengthy, the coverage of the Wittig and allied reactions, metal-promoted couplings, and alkyne/diene addition reactions is vast and very densely referenced. The chapter dealing with aldehydes and ketones begins immediately with the topic of carbonyl transposition. Rearrangement processes are given extensive attention as are condensation, cyclization, annulation, carbonylation, and acylation schemes, to include only a few.

The literature coverage extends through 1987. A special attempt has been made to highlight reviews and significant publications separately. For this purpose, each chapter begins with a listing of general references. Although the table of contents is very adequately detailed, an extensive transformation index spanning 160 pages has been included at the rear of the book to provide additional assistance in locating citations central to the transformation in question.

In light of the rapidity of computer searches and the availability of software packages dedicated to entirely similar objectives, one might argue that such a text is superfluous today. While this reviewer does not deny the advantages of computer technology, which he profits from regularly, it is important to recognize that this book is hard copy and, as such, brings with it the many benefits associated with textual material. These benefits include the capability to scan quickly across reaction types, to browse, and to encounter relevant reactions that were not included in the initial search menu. The book presents synthetic organic transformations in a visually receptive manner and contains much of what every synthetic chemist is interested in. The density of information is unrivaled. All in all, we have in this book a manifold demonstration of the power of synthetic methodology.

This monograph will be especially useful to those who are engaged in laboratory work, since discussion and comparative analysis are nonexistent. The possibility exists for developing a course around the text, but extensive "fleshing out" would be required on the part of the instructor. The attractive price of this large volume should allow it to be purchased by all who are serious about synthesis. The possibility is real that the author has compiled during 25 years of diligent effort a reference book destined to become a classic of its time.

Leo A. Paquette [NB 1058 IE]
Evans Chemical Laboratories
The Ohio State University
Columbus, OH (USA)

The Logic of Chemical Synthesis. By *E. J. Corey* and *Xue-Min Cheng*. Wiley, Chichester 1989, 436 pp., hardcover, £ 19.15.— ISBN 0-471-50979-5

The importance of synthesis for the development of organic chemistry can hardly be overestimated. The number of compounds synthesized, whether natural products or substances which have not yet been detected in nature, has increased considerably. One of the factors which has contributed to this rapid development is the formulation of rules for systematically analyzing a synthetic problem. An important additional motivation was the development of computer programs for retrosynthetic analysis.

In view of this, it is fortunate that one of the most important organic chemists who has made major contributions to the synthesis of natural products and to the development of computer programs for the planning of syntheses has taken the time to join in the writing of a book on the synthesis of natural products. The book is divided into three parts. In the first part, in six chapters, the concepts of retrosynthetic analysis are introduced. After a short historical overview there follows a discussion on the importance of the different types of reactions, and the nomenclature used to describe retrosyn-

thetic analyses is introduced. The following four chapters describe different strategies for retrosynthesis. The mix of general rules and theoretical considerations on the one hand, with the discussion of specific examples on the other, is very effective. Chapter 2 deals with the Diels-Alder reaction, the Claisen rearrangement and the Sharpless expoxidation as examples of key transformations. Chapter 3 discusses examples of the analysis of a synthetic problem starting from the educt, and the rules for the analysis of complex ring systems. These rules have here been summarized in a clear and perceptive way, relieving the reader of the laborious task of extracting them from the literature. The synthesis of diastereomerically and enantiomerically pure compounds is the subject of Chapter 4. Here there is less emphasis on systematically treating the various theoretical concepts than on specific examples of diastereoselective and enantioselective syntheses. Chapter 5 treats the synthesis of carbon skeletons using functional group transformations. Especially noteworthy are the examples of coupled transformations. Finally, in the last chapter of this part the retrosynthetic analysis of seven natural products is discussed.

The second part (six chapters) describes syntheses (with flow schemes) of over 140 compounds, mainly natural products, which have been synthesized in the laboratory of the principal author (*Corey*) during the last 30 years. The syntheses have been arranged according to the structural types of the natural products. If the reader, instead of following this sequence, reads the synthetic schemes in chronological order, he or she will gain a very good insight into the extraordinary progress of organic synthetic methodology during this period. This, together with the discussions of well chosen examples of new reactions which have been developed by *Corey*'s group to solve specific problems, gives the reader a fascinating insight into the process which the authors have called "Synthesis in Action". The chapters on prostaglandins and leucotrienes are especially well done. Several generations of synthetic approaches are discussed and compared. This well illustrates the evolutionary process, which also applies to synthetic strategies. In the other chapters one sometimes misses such comparisons with syntheses carried out in other laboratories.

Part 3 balances and complements the first two sections of the book. A compilation of some 600 structures is given, together with references to the original literature on successful chemical syntheses. In each case the structural formula and the name of the compound are followed by the principal author and the literature reference. The aim is to provide as complete as possible a review of total syntheses carried out up to 1988. The diversity of compounds which have been synthesized by nature and later by chemists is impressive. It is also interesting to see how many complex naturally occurring molecules have already been synthesized by more than one group. It is not uncommon to find ten or even more reported syntheses of one natural product within only a few years. However, it is not easy for the student to find the necessary information on these syntheses. For the inexperienced it is difficult to choose from the numerous structures and literature references, and to decide which of the reported syntheses are worth studying when planning a new synthesis.

Finally, who are the readers whom one should recommend to buy this book? In the blurb on the jacket of the book the main aim is stated to be: "to help students and research workers in chemistry to master the analysis of complex synthetic problems and the planning of syntheses". All those who are concerned with the synthesis of natural products, either as teachers or in their own research, should buy the book. Even though the first part is rather difficult to read because a special vocabulary has been introduced, the compilation of the rules for developing synthetic strategies and the illustration of these by examples are always interesting. The second section, which traces the story of the natural products synthetic work by *Corey*'s group, is full of stimulating examples. During the period covered here, natural products synthesis has developed from something of an art carried on only at a few places into a skilled craft successfully used by many groups throughout the world. In "The Logic of Chemical Synthesis" the development and applications of the concept of retrosynthesis from the standpoint of *Corey*'s group have been traced in an attractive manner. We can only hope that a paperback version will follow soon, so that undergraduate and post-graduate students too can afford to buy it. However, work on the synthesis of natural products has been pursued in many other laboratories besides that at Harvard, and it is therefore to be hoped that other eminent synthetic chemists will be stimulated to describe their work in an equally attractive manner for the benefit of the chemical community.

Reinhard Neier [NB 1045 IE]
Institut de Chimie Organique
Université de Fribourg (Switzerland)

Chemiluminescence and Photochemical Reaction Detection in Chromatography. Edited by *J. W. Birks*. VCH Verlagsgesellschaft, Weinheim/VCH Publishers, New York 1989. X, 291 pp., hardcover, DM 138.00.—ISBN 3-527-26782-4/0-89573-281-5

Chemiluminescence and photochemical detectors for both gas (GC) and high pressure liquid (HPLC) chromatography are the subjects of this slim volume. There are seven chapters, which include an introduction to photochemistry, chemiluminescence detection for GC, GC detectors based on the reaction between NO and O_3, a general discussion of chemiluminescent detection in HPLC, HPLC detection based on the chemiluminescent reaction of peroxyoxalates, a general discussion of photochemical HPLC detectors, and photochemical HPLC detection based on singlet oxygen sensitization.

In the preface, the editor states that the book is "addressed to the adventurous analytical chemists who are willing to try something a little out of the ordinary to solve their analysis problems and to those researchers who would like to contribute to this very fertile field." The book appears to succeed in achieving this purpose.

Although compressed, Chapter 1 gives the novice the important aspects of photochemistry and adequate exposure to the terminology to understand the remainder of the book. Chapter 2 describes GC detection based on several chemiluminescent reactions. These reactions involve active nitrogen (an excited state produced in a discharge); a variety of reactions of ozone, including those with NO; a sulfur-specific detector based on reaction with F_2; a similar detector which uses atomic F (both detectors use microwave discharge decomposition of SF_6); a halocarbon detector that uses sodium vapor; and additional sulfur detectors that use a reaction with ClO_2 or a combination of combustion and ozone addition. These methods all require the combination of the GC effluent with the reagent in a post column mixer, where the luminescence is observed. None of these methods appears to surpass the FID in sensitivity; specificity is the attraction, particularly when the analytes are in a complex matrix.

 © VCH Verlagsgesellschaft mbH, D-6940 Weinheim, 1990 0570-0833/90/0404-0436 $ 02.50/0

Chapter 3 discusses detectors based on the reaction of NO with ozone. A post column reactor is used to generate NO by a reaction of the analyte; ozone is then added downstream and the chemiluminescent emission measured. The first such system is specific for N-nitroso compounds which undergo catalyzed pyrolysis to form NO. Specificity for nitrogen compounds is obtained by catalytic oxidation of the effluent with O_2, since only nitrogen compounds form NO. A general detector is obtained by use of NO_2 as a reagent, which reacts with most analytes on a hot gold surface to yield NO.

HPLC detection based on solution-phase chemiluminescence is discussed in Chapter 4. Systems include luminol, lucigenin, peroxyoxalates, tris(2,2'-bipyridine)ruthenium(II), electroluminescence, and luciferin. One, or sometimes two, post-column reagent-introduction systems are used. The analytes may be catalysts which stimulate emission, or catalyst suppressors which lower emission levels. Labeling the analytes with, for example, luminol is also discussed. The entirety of Chapter 5 is devoted to the peroxyoxalate chemiluminescence reaction; the mechanism and kinetics of the process are reviewed. Hydrogen peroxide reacts with one of several aryl oxalate esters to produce an energetic intermediate, which then reacts with an acceptor (fluorophore) from which the actual light emission occurs. Hydrogen peroxide and certain classes of organic fluorophores can be detected.

Photochemical reaction HPLC detection is reviewed lucidly in Chapter 6. The introductory sections of this chapter present the limitations of HPLC detectors currently in use, the rationale for use of photochemical detectors of generally greater complexity, and the effect of post-column reactors on chromatography. This may be the best chapter in the book for the scientist unfamiliar with this field since it clearly delineates why anyone would bother with these rather complex systems and gives a good overview of their limitations as well as their advantages.

Chapter 7 discusses the use of singlet oxygen sensitization, by which the authors mean analyte-induced photooxidation of a singlet oxygen acceptor which has been spiked into the HPLC mobile phase. Here, the change in UV absorption caused by the photooxidation reaction is monitored. In favorable cases, detection limits are improved by 10–100 fold over usual UV detection.

The book is attractively produced, thoroughly referenced, and appears to be free of errors. It is recommended to anyone interested in the subject matter.

Wilson M. Gulick, Jr. [NB 1050 IE]
College of Engineering
Michigan Technological University
Houghton, MI (USA)

Ion and Cluster Ion Spectroscopy and Structure. Edited by *J. P. Maier*. Elsevier, Amsterdam 1989. xiv, 484 pp., hardcover, DFl. 330.00.–ISBN 0-444-87283-3

This book provides the reader with in depth and up to date knowledge concerning various aspects of the physics and chemistry of ions (including cluster ions). In particular this book, written by several leaders in their respective fields, aims to cover the subject of photon-ion interaction (spectroscopy, photodissociation and photodetachment). In addition, Coulomb explosion, high pressure mass spectrometry and metastable fragmentations are discussed as methods to elucidate the structure of ions. Some of the chapters are written very well, are based on a large basis of new and interesting findings and constitute hoped-for first competent reviews on these subjects.

The book starts with a chapter (*Z. Vager, R. Naaman, E. P. Kanter*) describing a new approach to the study of molecular structure—Coulomb Explosion Imaging—and its application to systems where classical spectroscopic methods are limited, i.e. non rigid molecules and molecular ions. This is followed by a chapter (*R. C. Woods*) on recent advances in microwave spectroscopy, including details of (22) molecular ions studied so far and their detection in interstellar space by radioastronomy. Chapter 3 (*P. Botschwina*) provides a review on spectroscopic properties obtained by the author for molecular ions with up to 7 nuclei. Special emphasis is given to effects of vibrational anharmonicity. Chapter 4 (*H. F. Schaefer III*) and Chapter 5 (*J. V. Coe, R. J. Saykally*) demonstrate the profitable alliance between a theoretical and an experimental group in order to unravel the infrared spectra of 6 polyatomic molecular ions (H_3O^+, NH_4^+, H_2CH^+, HCO_2^+, HN_2O^+, $C_2H_2^+$). Besides a brief chronology *Saykally* et al. describe several new developments in the field of high resolution infrared laser molecular ion spectroscopy. Chapter 6 (*D. M. Neumark*) discusses high resolution photodetachment studies, including both direct photodetachment and autodetachment spectra of molecular negative ions. Chapter 7 (*J. P. Maier*) consists of current progress in the characterization of open-shell cations by means of their electronic transitions. As an example, the $\tilde{B}^4\Sigma_u^- - \tilde{X}^4\Sigma_g^-$ transition of C_2^+ is discussed in detail, demonstrating the first successful probing of a fragment ion.

Chapter 8 through 13 deal with the rapidly growing field of cluster ions. This part of the book starts with a Chapter (*R. A. Kennedy, C. Y. Kung, T. A. Miller*) describing a prototype instrument in which cluster ions are analysed by time of flight mass spectrometry after spectroscopic probing by laser induced fluorescence. Chapter 9 (*M. T. Bowers*) gives a comprehensive overview on the photodissociation dynamics of small cluster ions (21 dimers and trimers). These studies yield information on the location and nature of the electronic excited states, on product branching ratios and product energy disposal. Chapter 10 (*R. G. Keesee, A. W. Castleman, Jr.*) summarizes the importance of thermochemical data for inferring structural information of solvated cluster ions and demonstrates the supportive role of adequate calculations concerning cluster ion stability. Moreover, this chapter also contains new results from photodissociation, unimolecular and collision induced dissociation of cluster cations. Chapter 11 (*N. Heinrich, H. Schwarz*) contains an essay demonstrating the intriguing gas phase chemistry of metastable cations of some keto/enol tautomers using recent experimental and theoretical data. It is postulated that loosely bound H-bridged ion/dipole complexes have to be seen as central intermediates in the low energy metastable ion decomposition of these ions. The remaining two chapters by *R. E. Smalley* and coworkers and *K. H. Bowen* and coworkers deal with the recent development of cluster anion photodetachment spectroscopy, using pulsed cluster ion sources and continuous cluster ion sources, respectively. These methods permit the study of ultraviolet photoelectron spectra of virtually any cluster of any element or combination of elements.

This book constitutes a valuable source of reference in the rapidly expanding topic of ion physics and chemistry and appears to be a must for every scientist working in the field of molecular and cluster ions.

T. D. Märk [NB 1025 IE]
Institut für Ionenphysik
Universität Innsbruck (Austria)

Organometallics. A Concise Introduction. By *C. Elschenbroich* and *A. Salzer*. VCH Verlagsgesellschaft, Weinheim/VCH Publishers, New York 1989. 479 pp., softcover, DM 58.00.—ISBN 3-527-27817-6/0-89573-868-6

Although courses in organometallic chemistry are now offered by nearly all chemistry departments that grant graduate degrees, there are only a handful of books that are suitable as texts. The new book by *Elschenbroich* and *Salzer* on Organometallics is an attention-getting and innovative addition to this genre. As befits its moderate length (479 pp), this richly illustrated text constitutes both a dynamic and tractable choice for a ten- to fifteen-week course.

The most striking feature of this book, and one that is lacking in its chief competitors, is the extensive coverage of main group organometallic chemistry. These sections, which comprise nearly half of the book, are organized by groups of the periodic table. Admirably, the authors do far more than simply outline preparative methodology and descriptive chemistry. For example, structural features of most classes of compounds are detailed. These are frequently accompanied by MO analyses.

In the same vein, a variety of spectroscopic techniques are covered (^{6}Li, ^{7}Li, ^{11}B, ^{119}Sn NMR; Mössbauer spectroscopy), usually in the context of brief digressions entitled "excursions". As might be expected, only selected group 15 (As, Sb, Bi) and group 16 (Se, Te) elements are treated. Overall, the descriptive chemistry within the main group sections is refreshingly modern. For example, mention is made of recent work with optically active boron reagents for enantioselective organic synthesis, as well as syntheses and properties of molecules with Si=Si, Ge=Ge, and As=As bonds.

The sections on transition metal organometallic chemistry begin, predictably, with the eighteen electron rule and electron counting. Both commonly used protocols ("closed shell" and "neutral ligand" methods) are presented, but without endorsement or extensive exemplification. Hence, some supplementation may be appropriate in a course.

The subsequent chapters are organized, in contrast to the main group portion of the book, by ligand type: σ donor ligands, σ donor/π acceptor ligands, and σ,π donor/π acceptor ligands. Preparative routes to and fundamental reactions of dozens of types of ligands are systematically outlined over the course of nearly 200 pages. In common with the main group portion of the book, there are frequent and informative digressions into structural, MO, and spectroscopic topics. The authors, for reasons noted in their preface, deliberately underemphasize mechanism. One consequence is a greater "breadth of exposure" for the reader.

The book concludes with chapters on metal–metal bonds/clusters, and catalysis. The former includes an extended discussion of *Hoffmann*'s isolobal analogy. The latter focuses on homogeneous systems, and is the most mechanistically oriented portion of the text. In addition, the authors touch upon several interfaces of organometallic chemistry and biology throughout the book.

Mention should also be made of the nice historical overview of organometallic chemistry and related introductory material that is provided at the beginning of the text. However, direct literature citations are not generally given, which limits the utility of the book as a desktop reference source. Nonetheless, many key discoveries are designated by a year and the name of the principal investigator. An extensive bibliography is provided at the end of the text. The book is well indexed. However, as with most competitive texts, student homework problems are not given.

In summary, *Elschenbroich* and *Salzer* have written the textbook of choice for graduate or senior-level courses that place an equal emphasis on main group element and transition metal organometallic chemistry. They and the publisher are to be further commended for the moderate price of the softcover edition. Hence, this book can be unequivocally recommended to any teacher or student of organometallic chemistry.

John A. Gladysz [NB 1043 IE]
Department of Chemistry
University of Utah
Salt Lake City, CA (USA)

Registered names, trademarks, etc. used in this journal, even when not marked as such, are not to be considered unprotected by law.

© VCH Verlagsgesellschaft mbH, D-6940 Weinheim, 1990. – Printed in the Federal Republic of Germany by Konrad Triltsch Druck- und Verlagsanstalt Würzburg.

All rights reserved (including those of translation into foreign languages). No part of this issue may be reproduced in any form — by photoprint, microfilm, or any other means — nor transmitted or translated into a machine language without written permission from the publishers. Only single copies of contributions, or parts thereof, may be made for personal use. This journal was carefully produced in all its parts. Nevertheless, authors, editors and publisher do not warrant the information contained therein to be free of errors. Readers are advised to keep in mind that statements, data, illustrations, procedural details or other items may inadvertently be inaccurate.

Valid for users in the USA: The appearance of the code at the bottom of the first page of an article (serial) indicates the copyright owner's consent that copies of the article may be made for personal or internal use, or for the personal or internal use of specific clients. This consent is given on the condition, however, that the copier pay stated per-copy fee through the Copyright Clearance Center, Inc. (CCC), for copying beyond that permitted by Sections 107 or 108 of the U.S. Copyright Law. This consent does not extend to other kinds of copying, such as copying, for general distribution, for advertising or promotional purposes, for creating new collective works, or for resale. For copying from back volumes of this journal see 'Permissions to Photo-Copy: Publisher's Fee List' of the CCC.

Editorial office: Postfach 10 11 61, D-6490 Weinheim, Federal Republic of Germany, Telephone (06201) 60 22 55, Telex 465 516 vchwh d, Telefax (06201) 602 328.

Editor: *Peter Gölitz*

Associate editors: *D. I. Loewus, A. Stimson.* **Editorial assistant:** *E. Schweikart*

Publishers: VCH Verlagsgesellschaft mbH. (Managing Director: *Hans Dirk Köhler*), Pappelallee 3, D-6940 Weinheim, Federal Republic of Germany.

Advertising office (Advertising Manager *R. J. Roth*): Postfach 10 11 61, D-6940 Weinheim, Federal Republic of Germany, Telephone (0 62 01) 60 61 30, Telex 4 67 155, Telefax (0 62 01) 606 156.

ANGEWANDTE CHEMIE
International Edition in English
Volume 29 · Number 5
May 1990
Pages 439–564

Two-Dimensional Model Networks

By Heinz Rehage* and Madeleine Veyssié*

This article is concerned with the structure and dynamic properties of thin films that have been chemically stabilized by polymerization and cross-linking reactions. By using different types of monomers it is possible to construct networks with rubber-like elasticity or with glassy properties, or temporary networks, in the interfacial region between oil and water. The systematic study of these ultrathin membranes offers new insights into aspects of current research, and opens up a wide range of potential new applications.

1. Introduction

Monolayers of surface active compounds have properties resembling those of biological membranes. Such monomolecular films stabilize the boundary layer and control the exchange of material between the media on either side. Films formed from commonly used surface active agents are usually in a two-dimensional phase analogous to a gas or a liquid. Structures of this kind are by their nature very unstable, and can easily be broken down by external forces. Questions relating to stability are crucially important in technological applications. There has therefore been much interest in techniques for transferring such films onto solid materials such as mica, glass, silicates, metals, or even semiconductors (Langmuir–Blodgett films). The strength of the membranes can thereby be greatly increased due to the reinforcing effect of the solid support, and this opens up a wide range of new applications.

Polymerization and cross-linking reactions offer an alternative method of stabilization (Fig. 1) which is completely different in nature. The most detailed studies carried out up to now on the mechanisms of the reactions involved have been concerned with the water-air interface. A detailed discussion of recent developments and current topics of interest in this area can be found in the comprehensive review article by *Ringsdorf* et al.[1] During surface polymerization the conformations and spatial arrangement of the monomers alter,

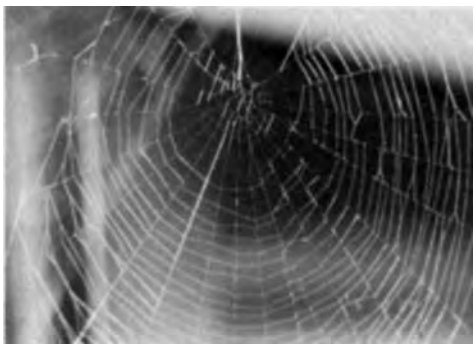

Fig. 1. A fiber net as a simple example of a "two-dimensional cross-linked" system. The thickness is practically constant ("invariance"), whereas the other two dimensions are not fixed. Two parameters are therefore sufficient to describe the dimensions.

[*] Dr. H. Rehage
Institut für Physikalische Chemie I
Universitätsstrasse 30, D-8580 Bayreuth (FRG)
Prof. Dr. M. Veyssié
Collège de France
F-75231 Paris Cedex 5 (France)

 © VCH Verlagsgesellschaft mbH, D-6940 Weinheim, 1990 0570-0833/90/0505-0439 $ 02.50/0

in a way similar to that in three-dimensional polymerization. This usually leads to experimental difficulties caused by contraction or (surface) dilatation of the film. In extreme cases this can completely prevent the formation of a continuous film. At the interface between water and air these processes can be controlled; the equilibrium distance between the molecules is continuously monitored during the polymerization by measuring the surface pressure, and the reaction variables are adjusted as necessary.[1] This can be achieved by using a film balance or by other experimental techniques. In this way one can obtain orientated macromolecular layers of high stability. Films of this kind often exist in a solid two-dimensional phase, and their properties have been intensively studied, especially in the case of diacetylenes.[2, 3]

Similar problems due to shrinkage processes during polymerization arise in the case of the oil-water interface. However, these effects can be more effectively controlled than at the water-air interface, and even automatic correction is possible. In this case the monomers are soluble in one of the two phases of different polarities, resulting in a large excess concentration in that phase. If film defects then occur during the polymerization, diffusion of monomer molecules from the adjacent phase brings about a repair process, leading to an intact network structure. Comparable repair mechanisms are only possible at the water-air interface by using monomers that are to some extent soluble in water. However, most macromolecular compounds are hydrophobic, and can only be converted into water-soluble compounds by attaching strongly polar groups. Nevertheless, the monomer should not possess too much surface-active character, since that would lead to the formation of aggregates (micelles) in which the molecules are tightly packed. Under these circumstances the surface polymerization is also accompanied by chemical reactions occurring within the micelles, leading to further complications. For this reason one aims to have a system in which only single monomer molecules are in solution in the water phase. With a suitable choice of conditions at the interface one can arrange that the average distance between the reacting molecules in the solvent is very large, whereas the molecules at the interface are densely packed owing to adsorption. Under these conditions the polymerization and cross-linking reactions are confined to the interfacial region itself. The adjacent phase acts only as a reservoir, supplying new monomer molecules as required for the formation of the network. Mechanisms of this type are especially easy to control at the water-oil interface. After polymerization and crosslinking one obtains stable films, leading to a number of interesting technological applications, such as microlithography, dialysis, ultrafiltration, reverse osmosis, separation of gases, and desalination of sea-water. As well as industrial applications there are many potential applications in biological fields. The functions and importance of two-dimensional networks in living organisms have been thoroughly reviewed in two articles by *Burchard*.[4, 5]

In interfacial polymerization one is not restricted to flat surfaces; the methods based on it can also be used with curved phase boundaries. Oil droplets suspended in water can be encapsulated in thin network structures by polymerization of surface active molecules. The cross-linked films on the surfaces of the droplets have an appreciable stabilizing effect on the spherical shape. Such emulsions represent a new kind of microencapsulation. As in the case of living cells, the deformation of the droplets depends on the elasticity of the surrounding membrane. In a flow field one observes quite marked deformations and orientation processes similar to those occurring in red blood cells (erythrocytes) and other living cells. The encapsulated oil droplets have a very simple structure, and therefore represent a suitable model system for studying these phenomena. Microcapsules of this kind are also suitable for controlled release of active substances stored in either the oil or the water phase. The network of the surrounding membrane acts as a semipermeable barrier, allowing only a limited diffusional flow though the boundary layer. Thus it is possible, for example, to release drugs in a controlled manner over long periods. Because of these numerous areas of application, there is now worldwide interest in synthesizing new types of polymer films, and the microscopic and macroscopic properties of these substances are the subject of extensive studies ranging from fundamental problems to technological products.

2. Monomer Systems

Cross-linked membranes can be divided into two classes according to the nature and strength of the bonding forces. In so doing one is essentially making a distinction between temporary and permanent networks. When the bonding between the molecules is a result of chemical reactions, the structures are always of the permanent type. The strength of covalent bonds between carbon atoms is of the order of 100 to 400 kJ mol^{-1}, resulting in very high stability of the corresponding structures. The opposite extreme occurs when the linking arises from entanglements, i.e. frictional interactions

Heinz Rehage was born in 1952 in Aachen, FRG. He studied chemistry at the universities of Clausthal-Zellerfeld (Vordiplom in 1976), Göttingen (Diplom in 1979) and Bayreuth, where he earned his Ph. D. under the supervision of Prof. H. Hoffmann (1983). He spent one year as a postdoctoral fellow at the Collège de France in Paris (Physique de la matière condensée), where he started his work on two-dimensional model networks in cooperation with Prof. P. G. de Gennes and Prof. M. Veyssié. After his Habilitation in 1989 he was appointed to his current position as "Privatdozent" in the department of physical chemistry at the University of Bayreuth. His research interests include rheology, surfactants, ultrathin organic films and microcapsules. He has been awarded the "Dozentenstipendium" of the Fonds der Chemischen Industrie.

and mechanical interferences between the molecules. For small external forces and over short periods these attachments act in a similar way to permanent linkages, and confer elastic properties on the structures. However, under greater external forces and longer loading times these mechanical linkages can become broken by diffusional motion of the molecules, resulting in a reduction in the number of cross-linking sites. These dynamic molecular rearrangement processes, referred to as relaxation phenomena, ultimately result in the external stresses decaying to zero. In the ideal case the behavior of the system after a long period is characteristic of a liquid. Thus, networks in which the contacts between the molecules arise solely from mechanical attachments exhibit both elastic and viscous properties. The fundamental physical properties show a marked dependence on the duration of the measurements or on the frequency, a type of behavior well described by the expression "temporary network".

A wide variety of other types of bonding, lying between the two extreme cases of chemical and physical network forming mechanisms, are now known. Most of these are physical contact mechanisms, and include hydrogen bonding, complex formation, coulombic interactions and dipolar forces. It is usually possible to break these types of bonds by heating or adding suitable solvents giving non-cross-linked systems which can be reversibly restored to the gel state by cooling. Systems with these special properties are described as "thermoreversible". The bond energies for physical contacts are low in comparison with those for covalent bonds, usually being of the same order as the thermal energy kT. For this reason only a small fraction of the maximum possible cross-linking sites usually contributes to the stability of the gel. Thus a thermodynamic equilibrium is established between the points of attachment and other sites that are potential linkage points but still remain free. In the equilibrium condition the number of new cross-links formed per unit time is constant, and is exactly equal to the number of existing linkages broken during the same interval. Consequently, on a time-averaged basis no change is observed in the concentration of cross-linking sites.

However, there are positional variations, which occur as a result of kinetic effects (Fig. 2). When the period of observation is appreciably shorter than the average lifetime of a point of attachment, a gel of this type appears to be fully cross-linked. However, over longer periods variations appear, and some of the linkages that are subjected to mechanical forces become broken. As a result those molecules that are under stress have more degrees of freedom and can undergo diffusional motions which have the effect of relieving the forces. Consequently any external work applied to the system becomes completely dissipated after a time, i.e. it is converted irreversibly into heat. Under these conditions the viscous properties of the temporary cross-linked structure are dominant. Thus, in contrast to permanent networks, the dynamics and kinetics of temporary gels play a considerable role, with the result that the structures show quite different behavior patterns depending on the time scale of the observations.

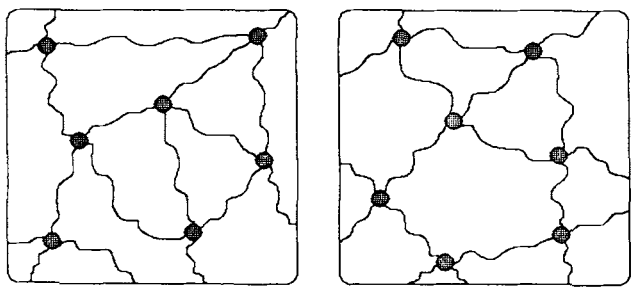

Fig. 2. Diagrammatic representation of the fluctuations in a dynamic network. Both figures contain the same number of cross-linking sites, but these are in different positions.

In order to synthesize two-dimensional networks with this temporary character, monomers with certain properties are needed. In addition to a functional group which can form linkages to neighboring molecules, hydrophilic and hydrophobic chains are essential to give the molecules the required amphiphilic character. Stabilization mechanisms depending on hydrogen bonding are very common in nature. Phenomena of the same kind can readily be recognized in the behavior of surface active agents, in circumstances where the polar head-group of the molecule has access to a large number of free hydroxyl groups. This is the case for "sugar-type" surface active agents, a class of compounds obtained by the esterification of various polysaccharides with long-chain fatty acids. The elasticity of the corresponding films is only noticeable in observations on a short time scale. When a force is applied for a longer period such films begin to flow, and the molecules rearrange to form new structures with quite different properties. When the external forces are removed the original condition starts to reestablish itself by kinetic processes, and the intact structure is restored. Thus, films of this type show "self-repairing" behavior, which opens up interesting possibilities for new technological applications.

For chemically cross-linked systems, other types of reactive groups which can form bonds to neighboring molecules are needed. Those reported in the literature up to now are various classes of surface active monomers, often related to naturally occurring lipid molecules. A detailed review of these is given in the article by *Ringsdorf* et al.[1] As well as conventional surface active agents such as dialkylmethylammonium salts, the types of compounds investigated have included phospholipids, diacetylenes and esters of various acids. All the experiments carried out have been concerned with the water-air interface, and the measurements have usually been made using a film balance. Surprisingly, there have been few studies of the rheological properties of the polymerized films. For the oil-water interface the choice of suitable monomers is determined not only by the criteria of reactivity and surface activity, but also by solubility considerations. The nature and mechanism of the two-dimensional polymerization reaction raise further questions that need to be considered when synthesizing the network. In principle, one can prepare macromolecular membranes using the same methods as are already used to form three-dimensional networks. Among the most important of these reactions are typical synthetic methods of macromolecular chemistry, such as polycondensations and free radical polymerizations.

The best known heterogeneous polycondensation reaction carried out at the oil-water interface is a variant of the Schot-

ten-Baumann reaction, in which a dicarboxylic acid dichloride is reacted with the appropriate diamine or diol.[6-9] A graphic demonstration of this, which is also suitable for illustrating a lecture, is the following experiment: 3 mL of sebacyl dichloride (1,8-octanedicarboxylic acid dichloride) is dissolved in 100 mL of carbon tetrachloride, and a solution of 4.4 g hexamethylenediamine in 50 mL of water is carefully added to form a top layer; an ultrathin film then forms at the interface, and this can easily be lifted off using a fine glass tube ("nylon rope trick").[7] This process is technologically important in the manufacture of polycarbonates, and can be used to synthesize polymers with high molecular mass. However, detailed studies of the polymerization kinetics, in particular by *Enkelmann* and *Wegner*,[8, 9] have shown that reactions of this type are largely diffusion-controlled. The hydrated diamine molecules are also slightly soluble in the oil phase, and can therefore diffuse through the film at the interface and react at their non-polar ends with further acid chloride. This leads to the formation of stable films whose thickness increases as the reaction continues.[8, 9] By using solutions of different concentrations the growth of the thin films can be controlled over a wide range. However, this gives structures whose thicknesses are not very well defined, and their use for investigating true two-dimensional phenomena is therefore somewhat limited.

Free radical polymerizations at the interface between two liquids can be performed using relatively simple techniques. Unlike the situation with polycondensations, only one chemically active component is needed, and the reaction can be initiated very easily using UV irradiation. This gives simple systems which can be studied under well-defined conditions. By controlling the light intensity and choosing suitable wavelengths one can vary the radical concentration over a wide range, giving complete control over the growth of the network.

The simplest monomers capable of undergoing photopolymerizations of this kind are bifunctional esters such as diacrylates, dimethacrylates or diallyl esters. Depending on the molecular structure and rigidity of the hydrocarbon chain, molecules of this kind can be used to prepare cross-linked membranes with either rubber-like or glassy properties. The special properties of such structures will be briefly described in the following sections.

3. Experimental Techniques

3.1. Synthetic Methods

Many of the amphiphilic compounds capable of forming cross-linked films at an interface are commercial products available from a variety of chemical manufacturers, and can therefore be obtained relatively cheaply in large quantities. An example of such a compound is Span 65, a trioctadecanyl ester of sorbic acid, which forms temporarily cross-linked membranes even at relatively low concentrations. Chemically stabilized neworks, on the other hand, can be prepared using unsaturated diesters such as tetramethylene diacrylate or bisphenol-A dimethacrylate. Some of these compounds are obtainable in commercial quantities, and others can easily be synthesized in the laboratory by reacting acid chlorides with the appropriate diols. However, in order to form network structures that are as perfect as possible, careful purification of all the monomers used, including solvents, is essential. It has been found that even the minutest amounts of contaminants can interfere with the formation of the film, and the requirements with regard to the purity of the substances involved are therefore extremely stringent. These difficulties can be avoided by using chromatographic separation methods such as MPLC (medium pressure liquid chromatography) or HPLC (high performance liquid chromatography); the efficiency of these methods has reached remarkable levels in the last few years. It is now possible, by using these techniques, to quickly and reliably purify even quite large quantities of substances.

3.2. Apparatus

The first requirement for synthesizing two-dimensional networks is a knowledge of the adsorption behavior of the monomers. This is obtained by measuring the surface tension at the interface, which is related to the characteristic properties of the film. Various measuring techniques are available for precisely determining the fundamental quantities; these include the ring method, the stirrup method, and the pendant drop method. Details of the execution of such experiments and the calculation of results from the experimental data can be found in the literature.[10, 11]

The physical properties at an interface are different from those of the three-dimensional phases on either side of the boundary. The elastic and rheological properties of the film are determined using special instruments called surface rheometers or interfacial rheometers which are described in the literature. The measuring probe consists of a thin disk or platinum ring which is precisely positioned in the interface. This device then undergoes either a sinusoidal or a square-wave deformation, and one measure the torque which this motion produces. Full details of the apparatus and the method of carrying out the measurements are described in a number of review articles.[12-28]

The flow properties of encapsulated emulsion droplets can be determined by using sensitive capillary rheometers or rotating viscometers.[29, 30] The deformations of the droplets are investigated using a flow cell which is incorporated into a microscope. In this way one can study rheological phenomena at high optical magnifications.[28, 31, 32]

4. Adsorption Properties

Thermodynamic arguments indicate that the higher concentrations of amphiphilic monomers which occur in the interfacial layer between oil and water are associated with a lowering of the interfacial tension. For dilute solutions and under conditions in which there are no interactive forces between the molecules, this process can be described by the Szyskowski equation [Equation (a)].[33]

$$\gamma = \gamma_0 - RT\Gamma_0^{\infty} \ln(1 + cB^{-1}) \qquad \text{(a)}$$

In this equation Γ_0^{∞} is the saturation concentration of the film (maximum number of molecules per m^2) and γ is the

interfacial tension. The thermodynamic properties of the pure oil-water interface are represented by the symbol γ_0. c is the monomer concentration in one of the adjacent three-dimensional phases. The quantity B is a constant which is specific to the particular monomer, and is related to the chemical adsorption potential $\Delta\mu_0$ as shown in Equation (b).

$$B = 55.4 \exp[\Delta\mu_0^\sigma (RT)^{-1}] \quad \text{(b)}$$

The Szyskowski equation is obtained by combining the Langmuir adsorption isotherm with the Gibbs adsorption law. These two fundamental equations are only valid under ideal conditions in which there are no interactions, and in which the adsorption process is limited to the formation of monomolecular layers. The Szyskowski equation can therefore only be applied to simple systems. The special importance of this relationship lies in the fact that it gives a complete description of the experimental data. By performing a dual parameter fit one obtains the characteristic saturation concentration for the film and the chemical adsorption potential. From these two quantities the excess Γ of the surface active component can be calculated (Langmuir adsorption isotherm, Equation (c)).

$$\Gamma^\sigma = \Gamma_0^\sigma c(B + c)^{-1} \quad \text{(c)}$$

The quantity Γ^σ specifies the degree of enrichment of the amphiphilic molecules in the surface layer. Monomer molecules are also present in the adjacent solvent phase, and the term Γ^σ thus gives the excess of adsorbed molecules compared with the concentration in the solvent. For low monomer concentrations Γ^σ is a measure of the packing density of the molecules (number of molecules per m^2 of surface). The area occupied by one monomer molecule is given by Equation (d).

$$F = (\Gamma^\sigma)^{-1} \quad \text{(d)}$$

The quantity F is related to the conformation and dynamic properties of the monomer molecule. With the help of suitable computer models it is possible to deduce important information about the adsorption process from the value of F.

Some typical results from measurements of the interfacial tension of octamethylenediacrylate **1** as a function of the ester concentration are shown in Figure 3. In this experiment

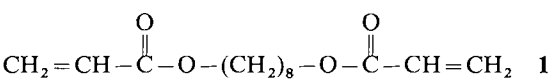

the monomer **1** under investigation has two terminal double bonds and therefore readily forms cross-linked membranes. For very low ester concentrations the interfacial tension between water and *trans*-decalin was found to be 5.12×10^{-2} Nm^{-1}, which agrees with the literature value for the pure oil-water interface. With increasing ester concentration the interfacial tension between the two liquids becomes smaller. The downward trend of the curve is related to the formation of a monomolecular film. It can be seen from Figure 3 that there is good agreement between the results obtained by the different experimental methods. The continuous line is the theoretical curve for the values $\Gamma_0^\sigma = 1.1 \times 10^{18}$ m^{-2} and $\Delta\mu_0^\sigma = -25$ kJ mol^{-1} (dual parameter least squares fit). From these two values one can calculate further properties of the surface active molecules. If it is assumed that each electron lone pair of the oxygen atoms can form not more than one hydrogen bond, with an average bond energy of 4 kJ mol^{-1}, the observed value of $\Delta\mu_0^\sigma$ indicates that there are about six bonds per molecule. As the octamethylene diacrylate molecule has a symmetrical structure, it appears on energetic grounds that both head-groups take part in the same type of adsorption. According to this only even hydration numbers occur. When the ester molecule is adsorbed the chain conformation alters, and on grounds of symmetry it must be concluded that instead of the low-energy *trans* conformation there are now three *cis* or *gauche* conformations. For this to occur requires an energy contribution of approximately 3 kJ mol^{-1} per chain segment. Thus the observed value of 25 kJ mol^{-1} is in excellent agreement with a symmetrical arrangement of the molecules in the interfacial layer, with all the electron lone pairs of the oxygen atoms fully hydrated. From the saturation value Γ_0^σ one obtains a value of 0.9 nm^2 for the area occupied by each molecule. From this one can calculate the molecular arrangement of the adsorbed diester molecules at the interface (Fig. 4). Here the value of 0.9 nm^2 for the interfacial area per molecule corresponds to a molecular arrangement in which the two polar head-groups are anchored in the aqueous phase, while the octamethylene chains form an arc across the molecule. If we assume that there is free rotational motion, the

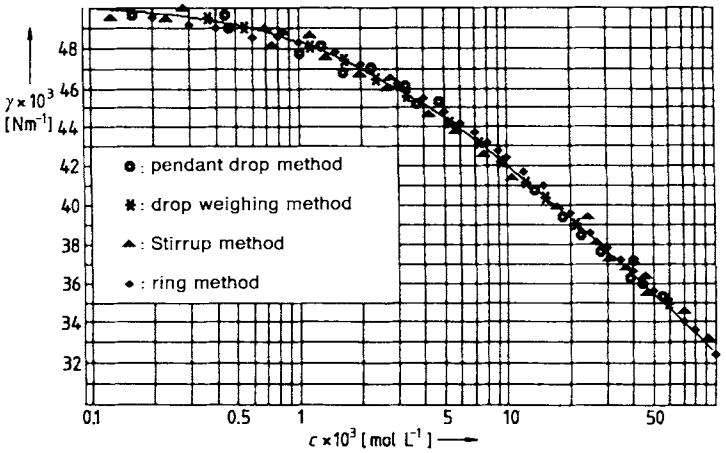

Fig. 3. The interfacial tension of octamethylene diacrylate as a function of ester concentration. Interface: water-*trans*-decalin, $T = 20$ °C.

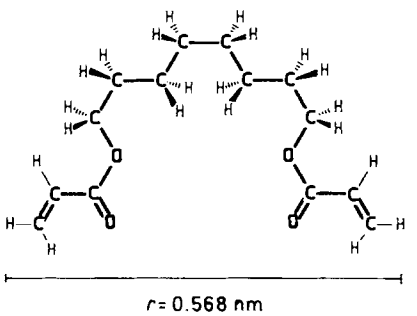

Fig. 4. Conformation of octamethylene diacrylate at the oil-water interface ($T = 20$ °C).

observed surface requirement per molecule gives an average molecular radius $r \simeq 0.54$ nm, in fairly good agreement with the theoretical value of 0.568 nm. Similar conformations have also been found for monolayers of other diesters,[28, 34–36] The theoretical relationships discussed here can therefore be applied in a similar way to other related systems.

5. Films with Rubberlike Elasticity

Diesters with flexible hydrocarbon chains form membranes with rubber-like elasticity when the polymerization is complete. This behavior is visible even with the unaided eye, and can be shown by the following simple experiment, which is also suitable as a lecture demonstration.

Some water in a glass beaker is covered by adding a 0.01 molar solution of hexamethylene diacrylate in dodecane, and this is then irradiated for about 4 h with a low pressure mercury vapor lamp (wavelength 253.7 nm). After allowing about 8 h for the reaction to proceed, a fully cross-linked film is obtained. The highly elastic nature of this membrane can be shown by scattering tracer particles (paper or metal filings) on the interface and deflecting the film mechanically with a needle. On removing the pressure the film springs back sharply, as is seen from the motion of the tracer particles. This simple experiment can also be shown to a large audience by placing the beaker on an overhead projector and thus observing the motions of the tracer particles.

The polymerization and cross-linking of the adsorbed molecules can easily be followed by monitoring the rheological properties of the film as a function of time. Some typical results on the kinetics of network growth are shown in Figure 5. The curve shows the increase of the two-dimensional modulus of elasticity as a function of the reaction time t. The irradiation was stopped after 250 min; the growth of the network was allowed to continue, and this resulted after 460 min in a transition from a sol to a gel. Below this transition point the polymer consists mainly of linear chains, whereas above it cross-linked chains predominate. The gel point is defined in terms of the coherence of the system, and is the critical point at which a single "infinitely" large molecule is formed. The two-dimensional phase transition can be described mathematically using percolation theory.[37, 38] If the number of chemical bonds formed is assumed to be proportional to the reaction time, the relationship shown in Equation (e) is obtained.[16, 36, 39–41]

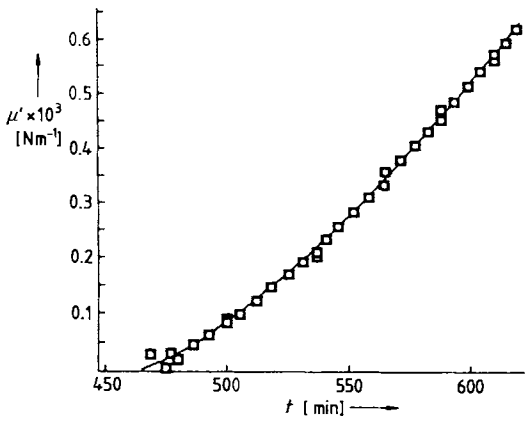

Fig. 5. The two-dimensional elastic modulus as a function of reaction time in the photopolymerization of octamethylene diacrylate at the interface between water and *trans*-decalin ($T = 20$ °C, UV wavelength 254 nm, radiation intensity 5×10^{19} photons m^{-2} s^{-1}, duration of irradiation: 250 min, $c = 5$ mmol L^{-1}, deformation = 0.15%).

$$\mu' \approx C(t - t_{gel})^x \qquad \text{(e)}$$

A simple analysis by *de Gennes* shows that x is approximately equal to the two-dimensional exponent for the electrical conductivity.[16, 37, 42] This number is of the order of 4/3.[37, 38] According to this, one expects to find a steep increase in the elastic modulus after passing the gel point. The individual squares in Figure 5 correspond to the experimental data, and the continuous line shows the result of fitting these to the theoretical equation (e). From the dual parameter fit one obtains a value $x = 1.4 \pm 0.1$ for the critical exponent. The gel time is $t_{gel} = 460 \pm 5$ min. Experiments with different conditions still give values of the same order of magnitude for the exponent, and the average value from several experiments[16, 28, 36, 41] is $x = 1.4 \pm 0.1$. It is interesting to note that the same value for the exponent has also been found for cross-linked membranes of the glassy type.[28, 41] Thus Equation (e) is a universal relationship which is independent of the type of network. However, more detailed considerations force one to recognize that the analogy between elasticity and electrical conductivity rests on simplified assumptions, which are not always valid in practice. In particular, the effects of ring closures, entanglements and the free ends of chains are matters which continue to provoke further discussion. Kinetic processes such as diffusion and relaxation phenomena can also cause departures from the simple theory. It has recently become possible to study these types of phenomena by Monte-Carlo computer simulation methods, but owing to the large amounts of computer time needed such calculations have only been carried out for a few cases. However, in view of the rapid progress in the field of digital electronics one can expect that calculations of this kind will become increasingly important in the next few years. Also of interest are other theoretical approaches concerned with analyzing network formation by means of fractals. Cross-linked membranes are suitable models for all these fields of study, and can therefore be used in a variety of ways for testing theories.

Percolation theories only describe the formation of the network in the regime near to the sol-gel transition. A generalized description of two-dimensional polymerization can be derived from kinetic theories based on the fundamental studies by *Flory*.[28, 36, 44]

Four reaction stages are distinguished, as described in Equations (f) to (i).

$$\text{Chain initiation:} \quad M \xrightarrow{UV} R \qquad \text{(f)}$$

$$\text{Chain growth:} \quad R + M \xrightarrow{k_p} P_1 \qquad \text{(g)}$$

$$\text{Cross-linking:} \quad P_1 + R \xrightarrow{k_p} P_v \qquad \text{(h)}$$

$$\text{Termination:} \quad R + R \xrightarrow{k_a} R - R,\ R_1 + R_2 \qquad \text{(i)}$$

A fraction of the monomer molecules are converted by the UV radiation into reactive radicals. These can then grow into linear chains with the rate constant k_p. Linear chains and free radicals then react further to give a cross-linked polymer. If two radicals collide this results in a chain-terminating reaction, which has the rate constant k_a.

From Equations (f) to (i) one can derive a simple relationship describing the increase in elastic modulus [Equation (j)].[26]

$$\mu'(t) = \mu'(\infty)\{1 - \exp(-k_p[R](t - t_{gel}))\}^2 \quad (j)$$

In this equation [R] is the free radical concentration and t_{gel} is the time to gel formation. $\mu'(\infty)$ is the final elastic modulus attained by the network. By applying Equation (j) it is possible to obtain more detailed information about the polymerization mechanism. Figure 6 shows a comparison between theoretical calculations and experimental results.

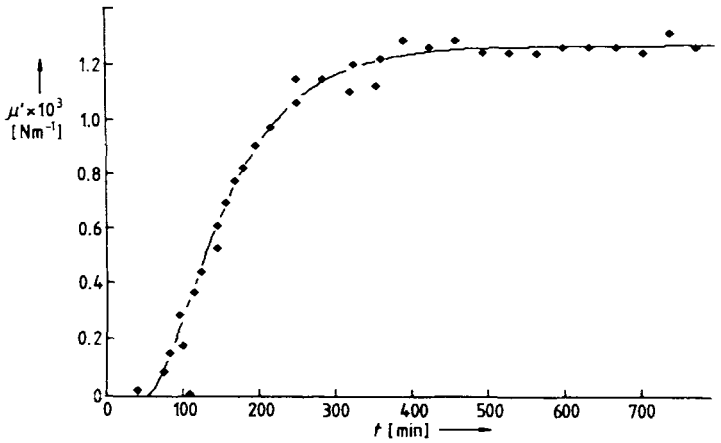

Fig. 6. The two-dimensional storage modulus as a function of reaction time in the photopolymerization of octamethylene diacrylate at the water-dodecane interface ($T = 20\,^{\circ}C$, UV wavelength 254 nm, radiation intensity 8.5×10^{19} photons $m^{-2}\,s^{-1}$, duration of irradiation 150 min, $c = 5$ mmol L^{-1}).

The individual points correspond to the experimental data, and the curve was obtained by fitting Equation (j), with a value k_p [M] $= 2 \times 10^{-4}\ s^{-1}$ for the network growth rate. The four-stage reaction model (Equations (f)–(i)) thus appears to represent a good approximation. As predicted by the theory, the formation of the coherent network begins only when the gel point ($t = 50$ min) is passed. In this region the elastic modulus increases rapidly, as predicted by the kinetic equations and also by percolation theories. At longer reaction times a constant final value is reached. In this region all the chemical reactions have ceased and the two-dimensional structure is fully formed.

The final value of each of the elastic properties that can be measured is unaffected by the growth parameters. If the rheological properties are measured at different frequencies, constant values are obtained for the moduli, showing no evidence of relaxation processes. By analogy with three-dimensional systems, the behavior is described as showing a rubber-like elasticity plateau. The elastic modulus remains constant up to quite large deformations, and evidence of a breakdown of the structure only begins to appear at about 60% elongation. If one assumes that the diester molecules are in a symmetrical arrangement (Fig. 5), this strain value corresponds to a situation in which the monomer molecules are stretched into the all-*trans* conformation. Thus the elastic properties of the cross-linked membranes are a direct consequence of molecular motion mechanisms. The "source" of the elastic behavior must therefore be sought within the monomer unit, and the rheological phenomena can be attributed, in the simplest cases, to mechanisms involving deformations of the hydrocarbon chain. Under these ideal circumstances one expects to find a simple relationship between the final elastic modulus $\mu'(\infty)$ and the number of adsorbed monomer molecules Γ^{σ}. Applying the theory of rubber elasticity to two-dimensional systems gives the simple relationship shown in Equation (k).[28, 36, 43]

$$\mu'(\infty) = A\Gamma^{\sigma}kT \quad (k)$$

The proportionality constant A is called the structural factor. It depends on the type of network and on the functionality of the linkage. For three-dimensional systems proportionality factors of the order of 1/3 to 1 are found, and similar values are expected to apply for cross-linked membranes. However, the exact form of the relationship between network structure and the proportionality factor A is not yet known, for either the three- or the two-dimensional case.

According to Equation (k) the final elastic modulus of the cross-linked membrane is determined essentially by the surface concentration of the adsorbed molecules. Ring closures, entanglements and free chain ends have initially been disregarded in deriving this expression, and if necessary they must be taken into account by including additional terms. Thus, Equation (k) is valid only under ideal conditions, but these are quite easy to achieve in the two-dimensional case. Since both $\mu'(\infty)$ and Γ^{σ} can be determined quite well by rheological experiments and measurements of the interfacial tension, there are a number of ways whereby theoretical predictions can be tested. For all the rubbery elastic networks that we have investigated so far, Equation (k) has been shown to be valid, the proportionality factor A being of the order of 1.[28, 36, 45] Thus the cross-linked membranes behave as ideal networks and obey the elasticity relationships that apply for rubbery materials.

6. Membranes with Glassy Properties

Diesters which contain rigid hydrocarbon chains form, on completion of photopolymerization, networks that exist in a glass-like state. This phenomenon can also be observed easily with the unaided eye. It can be demonstrated by the following simple experiment.

Some water in a glass beaker is covered by a 0.005 M solution of bisphenol-A dimethacrylate in dodecane, and this is irradiated for 4 h with a low-pressure mercury vapor lamp (wavelength 253.7 nm, or better still the 365 nm line). After a reaction time of 24 h the cross-linked film is obtained. The strength of the structure can be demonstrated by scattering tracer particles (paper fragments or metal filings) onto the interface and carefully deflecting the film with a

needle. In contrast to the rubbery elastic films, no elastic recovery is observed; instead there is only a viscous resistance caused by the cross-linked membrane.

During the photopolymerization of such a glassy film one observes phenomena similar to those seen for rubbery elastic structures. The sol-gel transition can be fully described by percolation theories, and the growth of the network is subject to the same kinetic relationships.[28,41] As well as monomolecular films it is possible, at high ester concentrations, to form multilayer films. This can be seen from Figure 7, which clearly shows the stepped form of the network growth process.

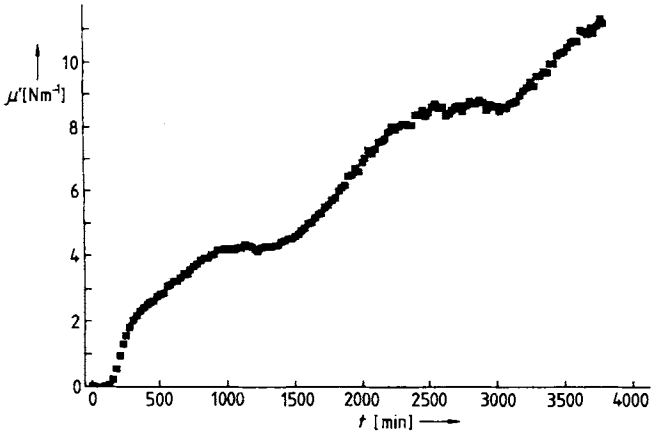

Fig. 7. The two-dimensional storage modulus as a function of reaction time in the photopolymerization of bisphenol-A dimethacrylate at the water-dodecane interface ($T = 20\,^{\circ}C$, UV wavelength 254 nm, duration of irradiation: 180 min, $c = 12$ mmol L^{-1}, angular frequency $\omega = 0.01\ s^{-1}$, radiation intensity 4.1×10^{18} photons $m^{-2}\ s^{-1}$).

With increasing ester concentration one expects to find that polymer molecules are also formed in the solvent. However, the highest ester concentrations occur at the oil-water interface, and it can be assumed that this is where the radical chain reaction is initiated.

Evidently the growth of the network takes place in several stages. The UV irradiation was switched off after 180 min. This period of time corresponds to that needed to reach the sol-gel transition. At about $t = 1300$ min a cross-linked membrane is formed, and this acts as the seed for the further growth processes that follow. Evidently, new layers can form on top of this basic structure, and the first of these is complete at about 2800 min. The (two-dimensional) elastic modulus now has twice the value found for the original film. As the reaction proceeds more of these networks are added, until eventually the polymerization ceases as a result of chain-terminating radical reactions. The tendency to form multiple layers increases with the ester concentration and the duration of UV irradiation. True monomolecular films are only obtained when the values of both these variables are small.

The main difference between the rubbery elastic membranes and the glassy cross-linked films is in the order of magnitude of the rheological constants. The first thing one notices is that the networks formed by rigid monomer molecules already suffer irreversible damage when subjected to deformations as small as 0.1%. The (two-dimensional) shear modulus is of the order of 5 Nm^{-1}. Since the film has a uniform thickness of 10^{-9} m, this corresponds to a three-dimensional "equivalent shear modulus" of $5 \times 10^{9}\ Nm^{-2}$. For normal polymers in the glassy range the shear modulus is between 10^{9} and $10^{11}\ Nm^{-2}$, and the two-dimensional structure therefore resembles a phase with frozen segmental mobility. From the threshold strain value (0.1%) and the equivalent shear modulus one obtains a yield stress of $5 \times 10^{6}\ Nm^{-2}$. The tensile strength of three-dimensional glassy polymers is of the order of $10^{7}\ Nm^{-2}$. These simple comparisons show that there are clear parallels with the three-dimensional glassy state.

7. Temporary Films

To prepare films that are physically cross-linked one requires molecules with polar head-groups that are capable of forming hydrogen bonds. Sugar-type surface active compounds are well suited for this purpose, as they have active centers with free hydroxyl groups. A typical surface active agent with these special properties is sorbitol trioctadecanate, which is commercially available under the name Span 65.

If some water in a glass beaker is covered with a 5×10^{-4} M solution of Span 65 in dodecane, a cross-linked film is formed. The strength of the structure can be shown by scattering tracer particles onto the interface and carefully deflecting the membrane with a needle. A viscous resistance is observed, and this is easily seen if the motions are rapid. For slow deformations, however, there is no noticeable hindrance to the motion.

The rheological properties of such membranes indicate the existence of temporary cross-linking points. This can be seen from Figure 8, which gives an insight into the structural

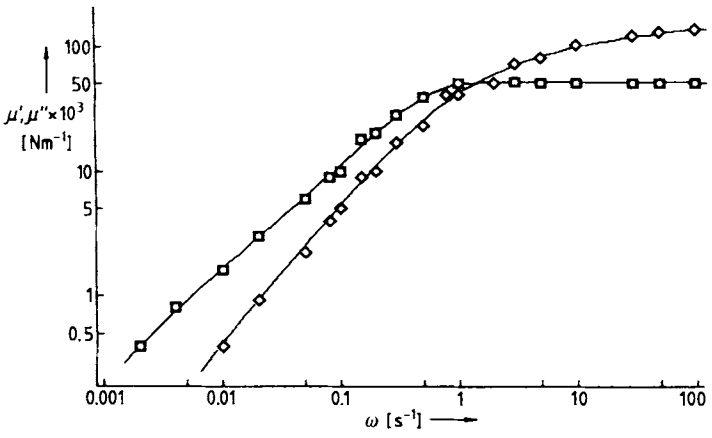

Fig. 8. The two-dimensional storage modulus μ' and two-dimensional loss modulus μ'' as functions of the angular frequency for a temporarily cross-linked film of Span 65 at the water-dodecane interface (deformation 0.2%, $T = 20\,^{\circ}C$, $c = 0.5$ mmol L^{-1}).

dynamics. In this experiment the two-dimensional storage modulus and the two-dimensional loss modulus were measured as functions of the angular frequency ω; μ' is propor-

tional to the elasticity of the film and μ'' is related to the dissipated energy, and thus to the viscosity. From the results we can recognize the characteristic behavior of such films.

At high frequencies μ' reaches a plateau value. Under these conditions the elastic properties of the film are dominant, and it is capable of storing mechanical energy. For monomolecular films the shear modulus is of the order of 0.1 Nm^{-1}.[28] If we compare this value with the concentration of the ester molecules at the interface we find the interesting relationship shown in Equation (l).[28]

$$\mu' = 15\Gamma^{\sigma}kT \qquad (l)$$

One molecule of sorbitol trioctadecanate has a total of 16 electron lone pairs on its oxygen atoms, and it can therefore form this number of hydrogen bonds. The observed proportionality factor of 15 indicates that each bond contributes an energy of about 1 kT.

At low frequencies the storage modulus is reduced and the viscous properties are dominant. In this region relaxation processes occur, and the film behaves like a liquid. The behavior in the intermediate frequency range shows a dual character, and both elastic and viscous phenomena are observed.

The rheological data show that the film has properties that are characteristic of temporary networks. Since the polar head-groups of the surface active molecules have free hydroxyl groups, it is possible for the linking of the molecules to occur by hydrogen-bonding. However, our experiments indicate that viscoelastic films are only obtained when the surface active molecule also has several hydrocarbon chains. Thus Span 60, which, unlike Span 65, has only one alkyl chain, does not form cross-linked membranes, despite the fact that the molecular structure of the head-group is the same in both compounds. (In fact, Span 60 should in principle be capable of forming even more hydrogen bonds than Span 65.) The three alkyl chains result in a greater oil solubility, and it therefore seems possible that the head-group of Span 65 is partly drawn into the non-polar phase. Under these conditions hydrogen bonds can form between the polar centers within the oil phase. It is also possible that in some cases the molecules need to have a particular orientation at the interface in order for cross-linking to occur. The value of 0.4 nm^2 for the area occupied by each molecule, as determined from interfacial tension measurements, indicates a high degree of anisotropy and molecular ordering in the adsorbed layer.

It thus appears possible that the surface active monomer molecules need to have a particular orientation to form temporary contacts.

8. Outlook

Ultrathin polymer networks are of great interest for many technological applications, and they can also be used, for example, to produce emulsions with exceptionally high stability. Oil droplets that are encapsulated by a network of this kind are thereby stabilized. Since the elastic properties of the surrounding membrane can be adjusted by chemical means, such encapsulated oil droplets provide simple model systems for studying complex biological processes. The topics that have so far been investigated in this way are material transport through membranes and the deformation of such droplets in a flow field. The first of these problems concerns the density of cross-linking in the covering layer; obviously the size of the mesh is the crucial factor in the controlled release of active substances (permeability barriers). Information about the density of cross-linking can be obtained from rheological measurements or, very elegantly, from ESR experiments.[46, 47] In this latter method spin-labeled species of different molecular sizes, soluble in both the oil and water phases, are allowed to diffuse through the membrane. The changes in concentration with time are then measured, and from this one can calculate the resistance of the membrane to the diffusional flow. This quantity is of crucial importance in relation to the use of such membranes for separation processes or for controlled release of substances.

The second area of study is concerned with the deformational behavior of the stabilized oil droplets in a flow field. This is of interest in relation to fundamental problems that arise in many biological systems, but are difficult to study in those systems because of their complexity. It has long been known that red blood corpuscles are able to flow through vessels that are very much narrower than the average diameters of the erythrocytes. This can be clearly seen in the conjunctive tissue of the human eye with the help of a strong magnifying lens. In these very fine capillaries the blood cells are severely deformed, and the question arises as to what is the hydrodynamic cause of this behavior.

Human blood has interesting properties. When stationary it is quite glutinous and has a high viscous flow resistance. However, when it is brought into a flowing condition the viscosity rapidly falls, and the blood then circulates much more easily. If the flow properties of blood are measured as a function of flow velocity, a falling viscosity curve is obtained. Several different factors contribute to this behavior. In the quiescent state the erythrocytes arrange themselves in a sort of superlattice structure resembling a network, resulting in high viscosity and elastic modulus. In the flowing state these "supermolecular" structures begin to break down, leading to a drastic reduction of the viscous resistance. At high shear rates practically all the aggregates are broken down, and the blood cells undergo reorientations and deformations. It would be interesting to discover the exact relationship between the elastic properties of the membrane and the deformation behavior, since this would open up the possibility of using simple viscosity measurements to diagnose blood diseases which involve abnormal changes in the flexibility of the membrane. A number of theoretical studies have already been made in relation to this problem, but experimental confirmation of the equations has not yet been possible, owing to the lack of suitable model systems.[48–50] Microencapsulated oil droplets now offer a possible solution to this problem, and afford an insight into basic processes which are of fundamental importance for biological systems.

Figure 9 illustrates this by a simple example. This shows the flow-induced deformation of oil droplets. Processes of this kind can be studied by means of an optical rheometer built into an inverse microscope giving a high magnification.[28] The image is recorded by means of a special video system which feeds into an electronic image processor.[28]

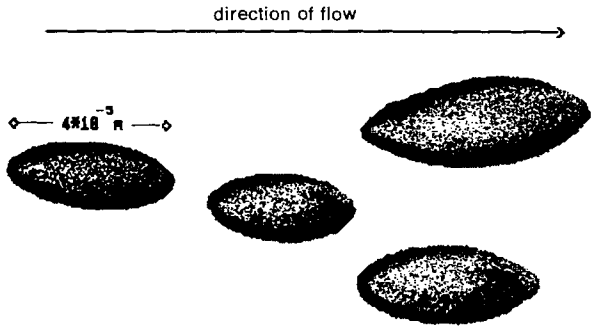

Fig. 9. Shear-induced deformation of oil droplets in a flow field ($T = 20\,^{\circ}C$, shear rate: $80\ s^{-1}$).

The droplet on the left of the figure is about 40 μm in length, and the dimensions of the other droplets can easily be calculated by means of an electronic scaling system. It can be seen that the larger droplets are much more severely distorted than the smaller ones. This behavior is predicted by the theory; in the ideal case the distortion should show a quadratic dependence on the droplet radius.[48-50] There is now particular interest in studying the deformations for membranes with different elastic moduli, as this has direct relevance to problems of medical importance. The experimental technique described here also offer a simple way of studying the flow behavior of clusters and aggregates, thus enabling one to investigate the two main types of blood rheological phenomena in isolation from each other. This has great advantages for developing a theoretical description of such systems, as it opens up the possibility of breaking down complex processes into simple stages that can be more easily analyzed. In this area and many others there exist innumerable possibilities for new applications, and two-dimensional networks thus open up a large new field of research for industrial and academic laboratories.

We thank the Deutsche Forschungsgemeinschaft for financial support of this work. We also thank Professor P. G. de Gennes and Professor H. Hoffmann for their very generous support of these studies, and for many valuable discussions that have stimulated interesting new experiments.

Received: October 18, 1989 [A 759 IE]
German version: *Angew. Chem. 102* (1990) 497
Translated by Dr. *J. K. Becconsall*, Pwllheli, U.K.

[1] H. Bader, K. Dorn, B. Hupfer, H. Ringsdorf, *Adv. Polym. Sci. 69* (1985) 1.
[2] H. Koch, H. Ringsdorf, *Makromol. Chem. 182* (1981) 255.
[3] D. Day, H. H. Hub, H. Ringsdorf, *Isr. J. Chem. 18* (1979) 325.
[4] W. Burchard, *Chem. Unserer Zeit 23* (1989) 37.
[5] W. Burchard, *Chem. Unserer Zeit 23* (1989) 69.
[6] H. G. Elias: *Makromoleküle*, Hüthig & Wepf, Basel 1981.
[7] B. Vollmert: *Grundriß der Makromolekularen Chemie 2*, E. Vollmert Verlag, Karlsruhe 1985.
[8] V. Enkelmann, G. Wegner, *Makromol. Chem. 157* (1972) 303.
[9] V. Enkelmann, G. Wegner, *Appl. Polym. Symp. 26* (1975) 365.
[10] A. W. Adamson: *Physical Chemistry of Surfaces*, 4th ed., Wiley, New York 1982.
[11] M. J. Schick, *Nonionic Surfactants – Physical Chemistry 23*, Dekker, New York 1987.
[12] M. Joly, *Surf. Colloid Sci. 5* (1972) 1.
[13] B. M. Abraham, K. Miyano, S. Q. Xu, J. B. Ketterson, *Rev. Sci. Instrum. 54* (1983) 213.
[14] B. M. Abraham, K. Miyano, J. B. Ketterson, *Ind. Eng. Chem. Prod. Res. Dev. 23* (1984) 245.
[15] B. M. Abraham, K. Miyano, S. Q. Xu, J. B. Ketterson, *Phys. Rev. Lett. 49* (1982) 1643.
[16] K. Miyano, M. Veyssié, *Phys. Rev. Lett. 52* (1984) 1318.
[17] R. J. Mannheimer, R. S. Schechter, *J. Colloid Interface Sci. 32* (1970) 225.
[18] R. J. Mannheimer, R. S. Schechter, *J. Colloid Interface Sci. 32* (1970) 195.
[19] R. J. Mannheimer, R. S. Schechter, *J. Colloid Interface Sci. 32* (1970) 212.
[20] H. A. Waterman, *J. Colloid Interface Sci. 101* (1984) 377.
[21] A. R. Deemer, J. D. Chen, M. G. Hedge, J. C. Slattery, *J. Colloid Interface Sci. 78* (1980) 87.
[22] A. J. Pinta, A. B. Israel, D. T. Wasan, *J. Colloid Interface Sci. 37* (1971) 52.
[23] W. Lifshutz, M. G. Hedge, J. C. Slattery, *J. Colloid Interface Sci. 37* (1971) 73.
[24] S. S. Jiang, J. D. Chen, J. C. Slattery, *J. Colloid Interface Sci. 96* (1983) 7.
[25] P. B. Briley, A. R. Deemer, J. C. Slattery, *J. Colloid Interface Sci. 56* (1976) 1.
[26] S. G. Oh, J. C. Slattery, *J. Colloid Interface Sci. 67* (1978) 516.
[27] N. W. Tschoegl, *J. Colloid Sci. 13* (1958) 500.
[28] H. Rehage, *Habilitation Thesis*, Universität Bayreuth 1988.
[29] H. Chmiel, E. Walitza in W. M. Kulicke (Ed.): *Fließverhalten von Stoffen und Stoffgemischen*, Hüthig & Wepf, Basel 1986.
[30] G. B. Thurston, *Biorheology 13* (1976) 191.
[31] H. Schmid-Schönbein, R. Wells, *Science (Washington, D.C.) 165* (1969) 288.
[32] H. Schmid-Schönbein, J. von Gosen, J. Heinrich, L. Klose, H. J. Volger, *Microvasc. Res. 6* (1973) 366.
[33] B. von Szyskowski, *Z. Phys. Chem. Stoechiom. Verwandtschaftsl. 64* (1908) 385.
[34] C. Casagrande: *Processus de polymérisation bidimensionelle linéaire et réticulante à l'interface eau-air, Dissertation*, Paris 1981.
[35] J. T. Davies, *Trans. Faraday Soc. 44*, (1948) 909.
[36] H. Rehage, E. Schnabel, M. Veyssié, *Makromol. Chem. 189* (1988) 2395.
[37] P. G. de Gennes: *Scaling Concepts in Polymer Physics*, Cornell University Press, Ithaca, 1979.
[38] D. Stauffer, A. Coniglio, M. Adam, *Adv. Polym. Sci. 44* (1982) 105.
[39] M. Rehage, M. Veyssié, *Ber. Bunsenges. Phys. Chem. 89* (1985) 1166.
[40] H. Rehage, M. Veyssié, *Progress and Trends in Rheology II, Suppl. Rheol. Acta 26* (1988) 200.
[41] H. Rehage, M. Veyssié, *Advances in Rheology, X. International Congress on Rheology 2*, Sydney 1988, p. 199.
[42] K. W. Yu, P. M. Chaikin, R. Orbach, *Phys. Rev. 28* (1983) 4831.
[43] P. J. Flory: *Principles of Polymer Chemistry*, Cornell University Press, Ithaca 1975.
[44] A. Dubault, C. Casagrande, M. Veyssié, *J. Phys. Chem. 79* (1975) 2254.
[45] H. Rehage, M. Veyssié, *Ber. Bunsenges. Phys. Chem. 89* (1985) 1166.
[46] M. Bredimas, M. Veyssié, D. Barthès-Biesel, V. Chhim, *J. Colloid Interface Sci. 93* (1983) 513.
[47] R. Wagner, M. Schwoerer, unpublished.
[48] D. Barthès-Biesel, V. Chhim, *Int. J. Multiphase Flow 7* (1981) 493.
[49] D. Barthès-Biesel, *J. Fluid Mech. 100* (1980) 831.
[50] D. Barthès-Biesel, A. Acrivos, *Int. J. Multiphase Flow 1* (1973) 1.

Boron-Phosphorus Compounds and Multiple Bonding

By Philip P. Power*

Boron-phosphorus compounds have not been as thoroughly studied as their boron-nitrogen counterparts. Until recently many classes of B-P compounds that had been well established in B-N chemistry were either unknown or poorly characterized. This statement is particularly true for compounds involving possible multiple bonding between boron and phosphorus. For example, detailed structural information on simple monomeric phosphino-boranes, $R_2BPR'_2$, did not become available until 1986 even though the isoelectronic SiC double bonded species, the silenes, had already been reported. However, new work has shown that it is possible to prepare and characterize several novel types of boron-phosphorus compounds with varying degrees of multiple B–P bonding. These include not only monomeric phosphinoboranes but also phosphanediylborates (borylphosphides), three- and four-membered rings (diphosphadiboretanes), boron phosphorus analogues of borazine, B-P skeletal analogues of allyl cations and anions, butadiene and cage compounds. Structural, spectroscopic (mainly NMR) and theoretical studies reveal some important differences between B-P and B-N compounds which in many cases can be traced to the presence of a high inversion barrier at phosphorus that reduces the π interaction. This usually causes compounds such as $R_2BPR'_2$ to associate through σ bonding between B and P. Supporting evidence for this view comes from species that involve phosphorus and nitrogen in competitive π bonding with a boron p orbital in which the dative interaction between B and N is dominant and the phosphorus center remains pyramidal. Recently published work has shown that steric and electronic factors can be used to favor π bonding and give an approximately planar $\geq$B–P$\leq$ system. Furthermore, theoretical studies reveal that p–p π overlap in a planar B-P system is of similar efficiency to its B-N analogue. Good examples are seen in the phosphanediyl borates, the boron-phosphorus analogues of borazine and the π-allyl cations, whose molecular configurations and B–P bond lengths support strong boron–phosphorus π bonding.

1. Introduction

Since the discovery of borazine by *Stock* et al. in 1926[1] boron-nitrogen compounds have enjoyed continued popularity.[2] The widespread interest in such compounds stems, in large measure, from their isoelectronic relationship to carbon species. Interest in compounds having boron bonded to the heavier main group 5 elements P,As,Sb or Bi has been much slower to develop.[3] One reason for this has been the much greater tendency of simple units such as $R_2BPR'_2$ to associate through donation of the lone pair on phosphorus to an empty p orbital on boron. This usually results in highly stable, generally cyclic, oligomeric, σ-bonded species with low reactivity in which boron and phosphorus are invariably four-coordinate (e.g., **1**).[3] Other species involving four-coordination are the donor-acceptor adducts of formula $R_3BPR'_3$, **2**, which also exhibit high thermal stability.

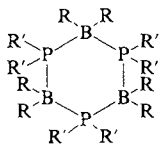

1

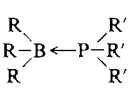

2

In contrast, well-characterized compounds involving bonding between boron and phosphorus centers that are three-coordinate have proved much more elusive. Unlike the four-coordinate compounds the coordination number three (or lower) allows for the possibility of π bonding between the boron and phosphorus p orbitals and this review is primarily concerned with compounds that involve varying degrees of B–P π bonding.

Early cryoscopic measurements on the compounds **3**–**5**

Ph_2BPPh_2 **3** $(Ph_2B)_2PPh$ **4** $PhB(PPh_2)_2$ **5**

(and related derivatives) showed that they were monomeric in benzene at concentrations of about one wt.%.[4, 5] In addition it was concluded, on the basis of dipole moment and infrared measurements, that phosphinodiarylboranes were unassociated, not because of π bonding to phosphorus, but because the boron center undergoes π bonding with its aryl substituents. Prior work, using isopiestic molecular weight measurements, had indicated that Me_2BPH_2 was monomeric in ether but polymerized over a period of days.[6] Furthermore, the synthesis of the interesting cyclic diphosphadiboretane species **6**[5] was claimed but it was only characterized on the basis of molecular weight measurements. Other work postulated the existence of the species **7**[7] and a mixture of compounds of formula **8**.[8] None were sufficient-

$(PhBPPh_2)_2$ **6** $PhB[P(Ph)BPhCl]_2$ **7** $(PhBPPh)_{3\text{ or }4}$ **8**

[*] Prof. P. P. Power
Department of Chemistry
University of California
Davis, California 95616 (USA)

 © VCH Verlagsgesellschaft mbH, D-6940 Weinheim, 1990 0570-0833/90/0505-0449 $ 02.50/0

ly characterized to enable structures to be assigned. In addition, it was reported that molecular orbital calculations indicated that analogues of borazine with P instead of N might exist as stable compounds.[9] In view of these encouraging results it is surprising to note that it was not until 1986 that the first compound having B–P multiple bond character was structurally characterized.[10] In fact, until recently there were little structural or spectroscopic, i.e. ^{1}H,^{11}B and ^{31}P NMR, data on any compounds involving bonding between three-coordinate boron and phosphorus. Rare exceptions were the compounds **9**,[11] the first diphosphadiboretanes to be spectroscopically characterized, and the three-membered ring compound **10**,[12] whose X-ray crystal structure (vide infra) was the first such report for a compound involving bonding between three-coordinate boron and phosphorus centers. It is of significant interest that the last five years have seen an exciting series of papers from a number of groups that have described the first structurally characterized phosphanediylborates (also to be formulated as borylphosphide

$(RBPSiMe_3)_2$, R = NMe_2, Ph $Et_2NB(PtBu)_2$

9 **10**

anions),[10,13–15] 1,2-[16] and 1,3-[13,14,17–20] diphosphadiboretanes, the B-P analogues of borazines (compounds of type **34**),[20] a large number of heterocycles with boron–phosphorus bonds in addition to other atoms (see Sections 4.3, 5.1, 6), monomeric phosphinoboranes,[17,21] B-P skeletal analogues of the allyl cation,[22,23] anion,[22,23] butadiene,[24] and cage compounds.[25] These results have already yielded much new information on B–P multiple bonding and they represent the beginning of what should prove to be a rich vein of chemistry.

A feature common to a number of these recently characterized compounds is the presence of relatively short (1.8–1.9 Å) B–P bonds.[10,20–23] This has given rise to considerable speculation on the strength of the bonding arising from the overlap of the empty boron p orbital and the phosphorus lone pair. This aspect of the structures is also of considerable current interest in the context of multiple bonding in the main group elements owing to the isoelectronic relationship of the pairs BP, CSi and AlN. It is, perhaps, because of such analogies and the implications for other main group 3–5 species, involving pairs such as Ga-As, Al-P, and In-P, that B-P compounds are currently enjoying a revival in interest.

2. B–P Bonding

A key parameter in the discussion of bond order is bond length. Numerous other factors such as coordination number, type of substituent, molecular configuration and the presence of delocalization also affect the length of a bond. Any proposal for the existence of multiple bonding due to π overlap has to be considered in the light of these influences. Addition of the covalent radii of phosphorus (1.11 Å) and boron (0.82 Å) suggests that a boron–phosphorus single bond involving three-coordinate boron and phosphorus should be about 1.93 Å long.[26] It is thus instructive to consider this prediction in the light of theoretical studies on the hypothetical molecules H_2BPH_2 and the related compound H_2BNH_2. Experimental results on the various substituted derivatives of H_2BPH_2 will be discussed in Section 4.

The theoretical data clearly illustrate the large influence that the molecular conformation can have on the length of the B–P bond in H_2BPH_2.[27] Calculations have been carried out on four different states of this molecule (Fig. 1). In the

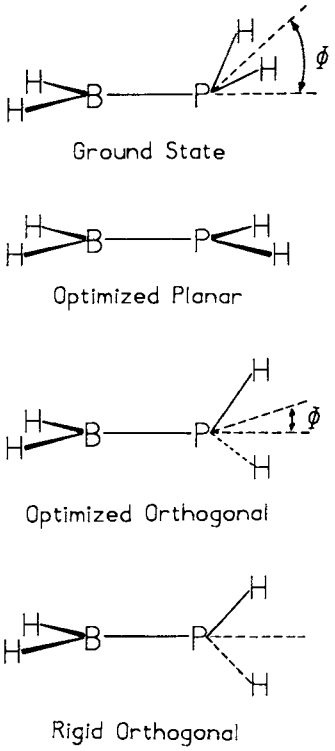

Fig. 1. Schematic drawings of four possible configurations of H_2BPH_2 [27].

lowest energy (or ground) state the phosphorus center is pyramidal (although it is somewhat flattened in comparison to PH_3) and the B–P distance is 1.91 Å. In the optimized planar and orthogonal forms the B–P bond lengths are 1.83 Å and 1.98 Å. It is clear from the calculations that B-P compounds do not show the same ability to form planar species as B-N compounds. Furthermore, this is very probably a reflection of the high inversion barrier at phosphorus (36.7 kcal mol^{-1} for PH_3)[28] rather than inherently poor and inefficient overlap between the boron and phosphorus p orbitals. The inversion barrier at phosphorus is, in fact, reduced to only 8.14 kcal mol^{-1} in H_2BPH_2 which indicates that there is strong conjugation in the planar form.[27] The energy difference between the optimized planar form and the non-optimized orthogonal form was calculated to be 40.4 kcal mol^{-1}. This is only 2.2 kcal mol^{-1} less than that in H_2BNH_2. In addition, the results of population analyses are in agreement with these calculations. For example, the total and π overlap populations in the planar form of H_2BPH_2 are 0.99 and 0.29, respectively, in comparison to 0.70 and 0.30 for H_2BNH_2. During rotation from planar to the non-optimized orthogonal form, the electron population in the vacant p orbital on boron is reduced from 0.29 to 0.01 in H_2BPH_2 whereas in H_2BNH_2 it is reduced from 0.29 to 0.04.

In short, the conjugation in planar H_2BPH_2 is predicted to be about the same as H_2BNH_2. However, non-planarity at P is favored because of the fairly high inversion barrier at the phosphorus center.

A further important consideration for the bonding in boron-phosphorus compounds is the polarity of the B-P pair. The electronegativity difference between boron and phosphorus is very small (B = 2.01; P = 2.06, cf. N = 3.07).[29] Thus, a purely σ-bonded boron-phosphorus pair would possess only a small partial charge separation. In a multiply bonded boron-phosphorus system charge is transferred from phosphorus back to boron via the π interaction so that the σ and π bond polarities tend to cancel each other. Thus, it is possible to argue that the B-P pair could be significantly less polarized than the corresponding B-N system. Such differences may become important when the aromaticity or reactivity of B-P systems is considered.

3. Synthetic Strategies

The major synthetic approaches to the title compounds involve either the use of sterically crowding groups or electron-rich substituents to reduce or prevent association of the boron and phosphorus centers. Since boron is considerably smaller than phosphorus it requires less highly hindering substituents to block access of σ donors to the empty boron p orbital. It has been shown in a number of laboratories that two mesityl substituents on boron are generally sufficient to restrict its coordination number to three.[30] In a different context, the Mes_2B group has found use in the stabilization of carbanions,[30, 31] and the reactions of these ions display many of the characteristics of ylides.[32] Presumably, a similar restriction in access to the boron center could be obtained with most substituents that are similar in size or configuration to the mesityl group. It should be emphasized that the kinetic stabilization of the boron center is primarily due to steric effects, and any reduction in the Lewis acidity of the boron p orbital by interaction with the ring π electrons of the mesityl substituents must necessarily be small or non-existent because of the high dihedral angle between the mesityl rings and the boron plane.[31]

An alternative method of preventing association of boron-phosphorus compounds involves the use of π-bonding substituents on boron. The most commonly used group to date has been the 2,2,6,6-tetramethylpiperidino ligand (tmp).[13, 14, 17, 18] This species forms a π bond through a side-on overlap of the nitrogen lone pair in a p orbital with the empty p orbital on boron. This effectively reduces the Lewis acid character of boron so that it is no longer very susceptible to attack by other donors. Although tmp is a large group, its effectiveness is primarily a result of the π bonding to boron. The multiple nature of the boron–nitrogen bond in the tmp derivatives implies that when phosphorus substituents are included in the molecule they are, in effect, competing with nitrogen for the boron p orbital. The evidence to date shows that nitrogen is more effective than phosphorus in this process.[13, 17, 18] Presumably, this is due mainly to the lower barrier to inversion at nitrogen. The use of other electron donating groups, such as –OR[23] or –SR, to reduce boron Lewis acidity is also possible. This aspect of the boron-phosphorus compounds has been little investigated to date.

Various synthetic pathways for the formation of B–P bonds are outlined in Equations 1–6.

$$R_{3-n}BX_n + n\,LiPR'_2 \longrightarrow R_{3-n}B(PR'_2)_n + n\,LiX \quad (1)$$
n = 1,2 or 3; R and R′ = large group

$$R_2BX + LiPHR' \xrightarrow{-LiX} R_2BPHR' \xrightarrow{n\text{BuLi}} R_2BP(Li)R' \quad (2)$$
R and R′ = large group

$$RBX_2 + 2\,LiPHR' \longrightarrow 1/n\,(RBPR')_n + 2\,LiX + H_2PR' \quad (3)$$
n = 2 or 3; R and R′ = large group

$$RBX_2 + LiP(SiMe_3)R' \xrightarrow{-LiX} RB(X)P(SiMe_3)R' \xrightarrow{-Me_3SiX} 1/2\,(RBPR')_2 \quad (4)$$

$$RBX_2 + LiPHR' \xrightarrow{-LiX} RB(X)PHR' \xrightarrow[\text{or } NaN(SiMe_3)_2]{n\text{BuLi}} 1/2\,(RBPR')_2 \quad (5)$$

$$R_2NBX_2 + 2\,LiP(SiMe_3)_2 \xrightarrow{-2\,LiX} R_2NB\{P(SiMe_3)_2\}_2 \xrightarrow{-P(SiMe_3)_3} 1/2\,(R_2NBPSiMe_3)_2 \quad (6)$$

The simplest route involves the reaction between boron halide derivatives and alkali metal salts of the phosphorus precursors. This is currently the method of choice in the synthesis of phosphinoboranes (Eq. 1),[21] the B-P allyl analogues (Eq. 1),[22, 23] phosphanediylborates (Eq. 2)[10] and the boron-phosphorus analogues of benzene and cyclobutadiene (Eq. 3).[20] In the case of the latter ring compounds the reaction involves the elimination of a primary phosphane. Synthetic pathways involving either the elimination of Me_3SiCl, from adjacent $=PSiMe_3$ and $=BCl$ moieties (Eq. 4)[13, 14, 17, 18, 25] or HCl from $=P-H$ and $=BCl$ groups in the presence of various bases (Eq. 5)[13, 14, 17, 18] or disproportionation reactions with the elimination of $P(SiMe_3)_3$ (Eq. 6)[11] have also proved extremely effective.

4. Structural Data

4.1. Phosphinoboranes

Detailed structural information on a range of three-coordinate boron-phosphorus compounds did not become available until recently. In addition to the structural report on a three-membered ring in 1981,[12] the first X-ray crystal structures of several types of boron-phosphorus compounds only appeared in 1986.[10, 13, 17, 18, 21] The simplest compounds are derivatives of the parent phosphinoborane (H_2BPH_2).[14, 17, 21] These are the species **11**[14, 17] (Fig. 2) and **12**[21] (Fig. 3) which are accessible by addition of lithium

(tmp)ClBP(H)Mes Mes_2BPPh_2

11 **12**

phosphide to the substituted boron halide [cf. Eq. (1)]. Both compounds are monomeric and feature a planar three-coordinate boron center and phosphorus geometries that have different degrees of pyramidicity. Three further monomeric phosphinoborane structures have also been determined[33, 34] and the important structural data for the five compounds are presented in Table 1. The most notable feature of the data is the good correlation between the pyra-

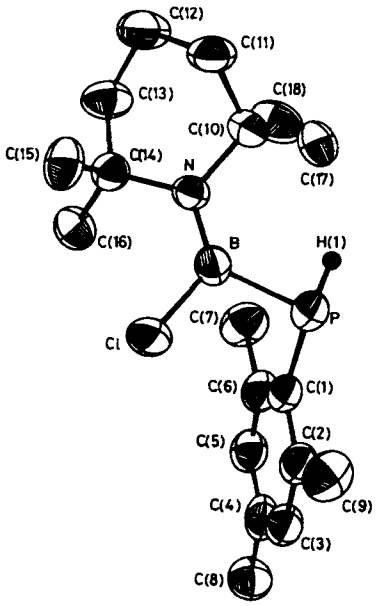

Fig. 2. A thermal ellipsoidal plot of (tmp)ClBP(H)Mes **11** [17]. The B–P distance is 1.948(3) Å and the sum of the angles at P is 307.1°.

midicity at phosphorus and the B–P bond lengths. There is also remarkably good agreement with the theoretical predictions. When planarity is forced upon phosphorus by using bulky mesityl substituents[33] a bond length as short as 1.839(8) Å is observed (vs. 1.83 Å predicted for the planar form of H_2BPH_2). At the other extreme, a long boron–phosphorus distance of 1.948(3) Å is seen when there is a nitrogen substituent on boron. The structure in Figure 2 neatly illustrates the dominance of the nitrogen lone pair interaction with the boron p orbital. Not only is the B–P distance long, the angles at phosphorus are typical of trivalent phosphanes and the B–N distance is 1.380(3) Å which is indicative of a strong dative π interaction. The structure of **15**[34] perhaps most closely resembles the ground state of H_2PBH_2 (B–P = 1.91 Å) and again the agreement between theory and experiment is good. The inversion barriers in **12** and **15**, measured by variable temperature ^{1}H NMR, are near 10 and 11.4 kcal mol^{-1} [33] (slightly higher than the value calculated for H_2BPH_2).

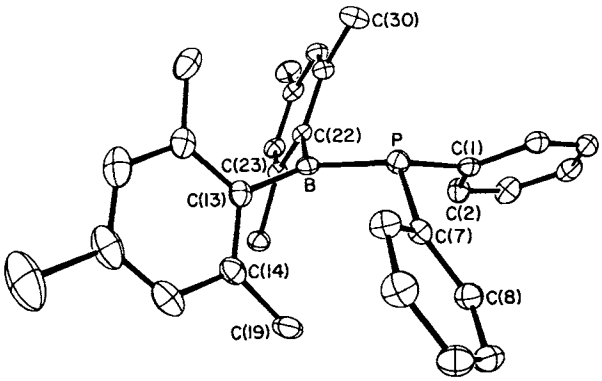

Fig. 3. A thermal ellipsoidal plot of Mes_2BPh_2 **12** [21]. The B–P distance is 1.859(3) Å and the sum of the angles at P is 339.4°.

Table 1. Important structural parameters of phosphinoboranes.

	Bond length B-P [Å]	Sum of angles at P [°]	Φ[°][a]	Ref.
Mes, Mes, B–P, Mes, Mes **13**	1.839(8)	≈360	≈0	[33]
Mes, Mes, B–P, *t*Bu, *t*Bu **14**	1.844(6)	356	3	[33]
Mes, Mes, B–P, Ph, Ph **12**	1.859(3)	339.4	40	[21]
Mes, Mes, B–P, H, 1-Ad **15**	[b] 1.897(3)	315	61	[34]
tmp, Cl, B–P, H, Mes **11**	1.948(3)	307.1	71	[17]
H, H, B–P, H, H	[c] 1.91	306.7	70	[27,35]

[a] Φ = out-of-plane angle at P, see formula **A**. [b] 1-Ad = 1-adamantyl. [c] Calculated values.

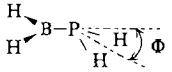

A

4.2. Phosphanediylborates (or Borylphosphides)

The phosphinoboranes above are of further interest because when there is a hydrogen substituent on phosphorus it can easily be removed with *n*BuLi to give lithium salts having the phosphanediylborate (or borylphosphide) anion $[R_2BPR']^{\ominus}$. The structures of the salts **16a–c** and **17–20** have been determined.[10] **20** features a naked $[PMesBMes_2]^{\ominus}$ ion. The structure of **16b**[10a] is illustrated in Figure 4. When [12]crown-4 is added to **16a, b, d** to remove the $Li^{\oplus}$ion, salts like **20** with anions of the type illustrated in Figure 5 are obtained. In contrast to the neutral phosphinoborane precursors, the deprotonated phosphorus centers are planar at phosphorus. Furthermore, the dihedral angles between the boron and phosphorus planes are small (usually $<10°$). The B–P distances are short and vary from 1.810(4) to 1.836(2) Å. These features indicate considerable multiple bond character in the B–P bond. The planarity at P is probably due to an enhanced π interaction owing to a greater electron density at the phosphorus atom. Recent, more sophisticated calculations[35] on the molecules Li[H_2BPH] and $[H_2BPH]^{\ominus}$ are in close agreement with experimental findings and indicate essential double bond character in these planar molecules and also in the planar configuration

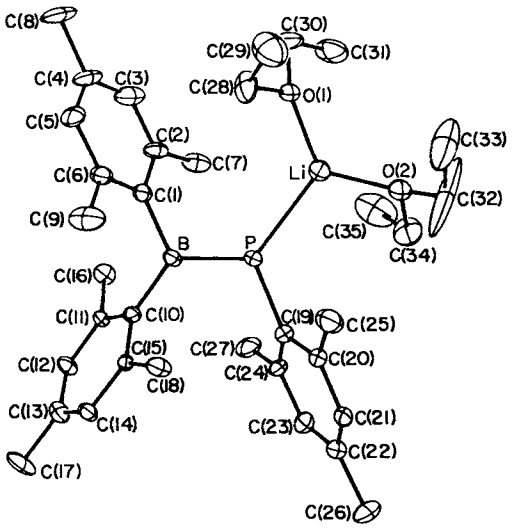

Fig. 4. Structure of $[Li(Et_2O)_2][Mes_2BPMes]$ **16b** [10a]. The B–P distance is 1.823(7) Å.

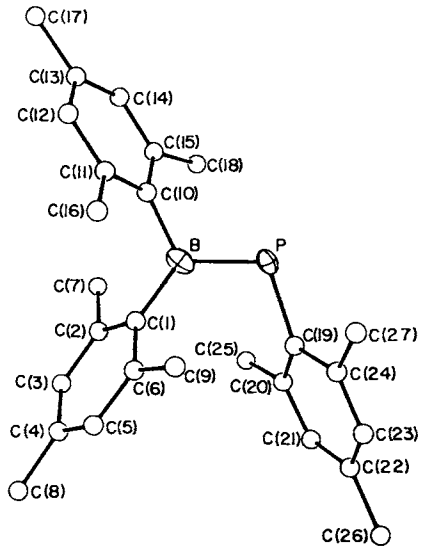

Fig. 5. Structure of the anion $[Mes_2BPMes]^{\ominus}$ of **20**, obtained by treating the lithium salt in Figure 4 with [12]crown-4. The B–P distance is 1.835(13) Å.

of H_2BPH_2. For example, calculations of the bond order in $[H_2BPH]^{\ominus}$ using two different approaches[36,37] indicate B–P bond orders of 1.83 and 2.01, respectively. Treatment of the chloroborylphosphane **21** with *t*BuLi also gives the anion **23**.

$[Li(Et_2O)_2][Mes_2BPR]$ **16**
a, R = *cyclo*-C_6H_{11}; **b**, R = Mes; **c**, R = 1-Ad; **d**, R = Ph

$[Li(Et_2O)_2][Trip_2BPtBu]$ **17**
Trip = 2,4,6-$iPr_3C_6H_2$

$[Li(thf)_3][Mes_2BPSiMe_3]$ **18**

$[Li(Et_2O)_2][Mes(H)PB(Trip)PMes]$ **19**

$[Li([12]crown\text{-}4)_2][Mes_2BPMes]$ **20**

An interesting feature of this reaction is the concomitant formation of the ring compound **24**. This has led to the B=P species **22** being postulated as intermediate.[14] This intermediate was reported to be detectable by mass spectroscopy of the dimer which apparently dissociates at high temperature.[13,14]

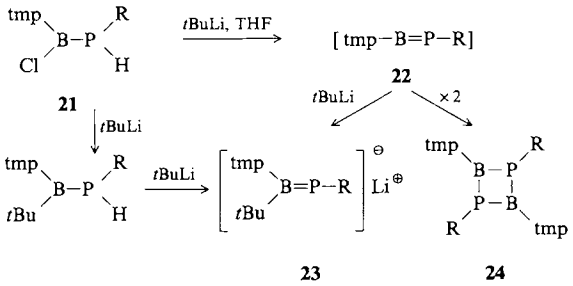

R = 2,4,6-$tBu_3C_6H_2$

4.3. B–P Ring and Cage Compounds

The first diphosphadiboretanes to be characterized by NMR and mass spectroscopy data and elemental analysis were reported in 1977.[11] These were the compounds **9**, which were synthesized by the thermolysis of **25** at 150 °C [see Eq. (6)].[11] The synthesis and X-ray structure of the related three-membered ring compound **10** were reported in 1981.[12] This was the first X-ray crystal structure report of a compound with bonding between three-coordinate boron and phosphorus centers (Fig. 6). The B–P distances average

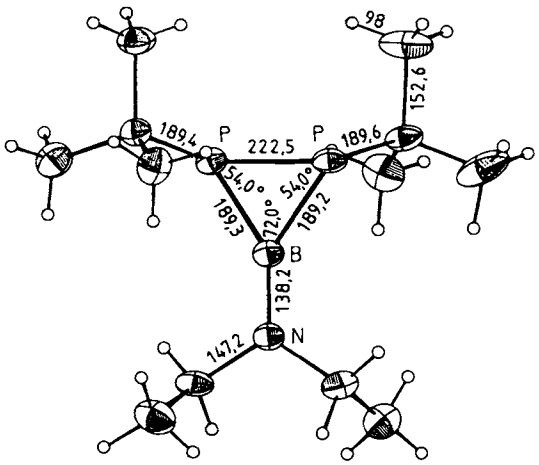

Fig. 6. A thermal ellipsoidal plot of the diphosphaborirane $Et_2NB(PtBu)_2$ **10** [12].

1.893(2) Å and the B–N distance is 1.382(3) Å. Although the B–P bond is somewhat shortened relative to a single bond it is notable that the B–N bond is consistent with considerable

$RB[P(SiMe_3)_2]_2 \xrightarrow{\Delta} 1/2\,(RBPSiMe_3)_2$
25 **9**
R = NMe_2, Ph

$Et_2NB(PtBu)_2$ **10**

B–N π bonding. The first X-ray structures of diphosphadiboretanes, involving the compounds **24**,[13] **26**,[17] (Fig. 7), and **27a**,[18] were reported in 1986. They were synthesized

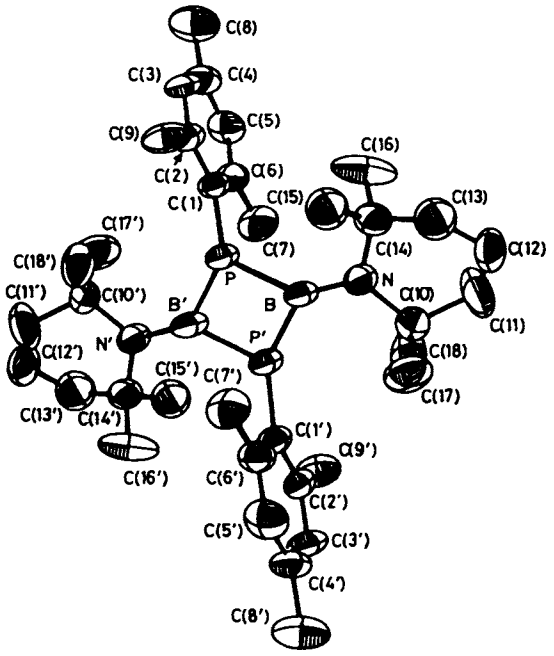

Fig. 7. Structure of the diphosphadiboretane $(tmpBPMes)_2$ **26** [17]. The B–P bond length is 1.916(3) Å.

$(tmpBPMes)_2$	$(tmpBPCEt_3)_2$	$(tmpBNtBu)_2$
26	**27a**	**28**

by reaction of $tmpBCl_2$ with $LiP(SiMe_3)R$ (→**24**), with one equiv. of a 1:1 mixture of LiPHMes and Li_2PMes (→**26**) or with $LiPHCEt_3$ (→**27a**) followed by elimination of Me_3SiCl or HCl in the second step [see Eq. (4)]. These featured a planar B_2P_2 core. The phosphorus centers are pyramidal and trigonal planar geometries were observed at both boron and nitrogen with B–N distances of 1.38 Å–1.431 Å. The B–P distances are 1.916(3) Å, 1.96(2) Å and 1.925 Å (av.), and the sum of the angles at P are 329.0° and 339.9°. Accordingly, there is little evidence for dative P → B π bonding. It is also notable that the exocyclic π bonding in these compounds is stronger than that in the diazadiboretane **28** ($B–N_{exo}$ = 1.465(3) Å) where the ring nitrogens compete for the boron p orbital.[38] However, the B–N distance in **27a**,[18] 1.431(2) Å, is unusually long, although it remains consistent with significant B–N π bonding. These data also support the calculations (see Section 5.2)[27, 35] which indicate a reluctance of the phosphorus center to participate in delocalization. Several other diphosphadiboretanes involving amino substituents on boron have been reported, and three different synthetic methods have been described.[18b] Three of the products, the compounds **29**–**31**, have been structurally characterized[18b] and reveal features that are broadly similar to those that had already been reported.[13, 17, 18] Long

$(tBu_2NBPTrip)_2$	$(tBu_2NBPSiMe_3)_2$	$(tmpBPSiMe_3)_2$
29	**30**	**31**

B–P bonds were observed in the compounds **30** and **31** [1.947(4)–1.969(12) Å]. This shows that increased steric congestion increases the B–P bond length, as already observed in **24**.[13, 17] It is notable that these B–P bond lengths approach those found in four-coordinate B-P compounds. This trend suggests that it should be possible to induce dissociation of the ring to give the interesting monomeric species R_2NBPR' by increasing the steric hindrance further. However, it is notable that the barrier for dimerization of the hypothetical $H_2N–B=PMe$ to $(H_2N–BPMe)_2$ has been calculated (by MNDO III) to be only 5 kcal mol^{-1}.[18b]

It has also proved possible to obtain diphosphadiboretane compounds without amine substituents on boron.[20b, 33, 34] The absence of competition for the boron p orbital allows its tendency for interaction with the phosphorus lone pair to be more accurately gauged. Alkyl- or aryl-substituted diphosphadiboretanes can be readily synthesized by treatment of an organodihaloborane with two equiv. of LiPHR [see Eq. (3)]. Two examples are $(ThexylBPMes)_2$[20b] and (1-AdPB-

$(ThexylBPMes)_2$	$(MesBP(1\text{-}Ad))_2$
32, Thexyl = CMe_2CHMe_2	**33**

$Mes)_2$[33, 34] (Fig. 8). The B_2P_2 ring is planar and the phosphorus centers are pyramidal. The observed ^{11}B NMR

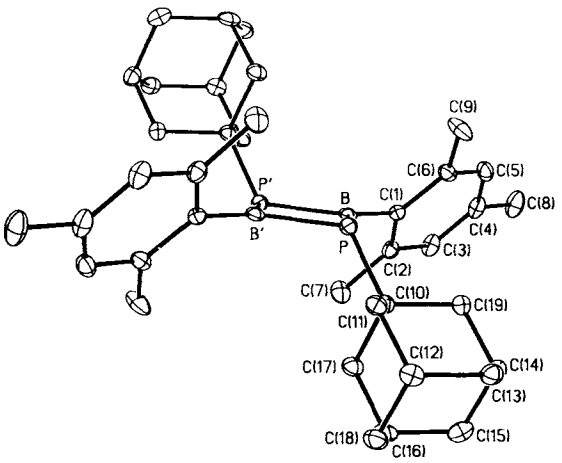

Fig. 8. Structure of the diphosphadiboretane $(MesBP(1–Ad))_2$. The B–P distance averages 1.900(2) Å. The sum of the angles at phosphorus is 328.9° [33, 34].

chemical shifts are consistent with three coordinate boron whereas the ^{31}P NMR δ values (ca. −70) are well upfield. The latter values are, in fact, more than $\Delta\delta = 100$ upfield of those (see Table 2 below) observed in the delocalized six-

Table 2. ^1H and ^{31}P NMR data (δ values) of selected B-P compounds.

	Compound	^{31}P	^1H [a]		Δ
			o	*p*	(*o*–*p*)
34a	$(MesBPPh)_3$	42.5	2.36	1.94	0.42
34b	$(MesBPcyclo\text{-}C_6H_{11})_3$	51.9	2.63	2.17	0.46
34c	$(MesBPMes)_3$	60.5	2.52	1.84	0.68
			2.47	1.72	0.75
34d	$(PhBPMes)_3$	14.5	2.45	1.93	0.52
33	$(MesBP(1\text{-}Ad))_2$	−69.8	2.49	2.16	0.33
15	$Mes_2BP(H)1\text{-}Ad$	0.45	2.24	2.0	0.24
12	Mes_2BPPh_2	26.7	2.28	2.02	0.26
14	$Mes_2BP(tBu)_2$	75.0	2.56	2.14	0.42
	$PMesH_2$	−153.9	2.20	2.08	0.12
	$BMesBr_2$	–	2.76	2.66	0.10

[a] Protons of the methyl groups of the mesityl substituents.

membered ring $(RBPR')_3$ compounds which emphasizes the very different bonding in the ring systems. The sums of the angles at phosphorus are 331.3° and 328.9°, respectively, and the B–P bond lengths are 1.897(6) Å and 1.899(2) Å.[20b, 33] These bonds are somewhat shorter than those usually observed in B_2P_2 rings with $-NR_2$ groups on boron. A shortening is certainly predicted in the absence of competition from the amino groups on boron. However, in view of the large substituents on B and P a more planar phosphorus configuration might be expected. These results can be explained by regarding the species in Figure 8 as a substituted cyclobutadiene analogue. In this case delocalization of the phosphorus lone pairs onto the borons offers little energy advantage since two of these electrons would occupy non-bonding π-energy levels. The energy gain (if any) upon delocalization is probably insufficient to overcome the inversion barrier at

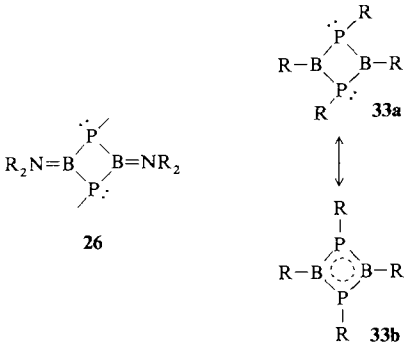

Fig. 9. Schematic drawings of an amino-substituted diphosphadiboretane **26** (cf. Fig. 7) and two resonance forms **a** and **b** of an organo-substituted diphosphadiboretane **33** (cf. Fig. 8).

phosphorus. The bonding in the compounds in Figures 7 and 8 is illustrated schematically in Figure 9. In the amino-substituted compound **26** there is no delocalization and B–P single bonding and B–N π bonding is observed. Although structure **33a** most closely represents the bonding of the molecule in Figure 8, it may be that structure **33b** also makes a small contribution owing to the shorter B–P bonds and the flattened geometry at phosphorus.

Other interesting four-membered ring systems involving BP_2N or AsB_2N rings have also been reported.[39] Examples are **35a** and **35b** (Fig. 10). These involve long B–P and B–As

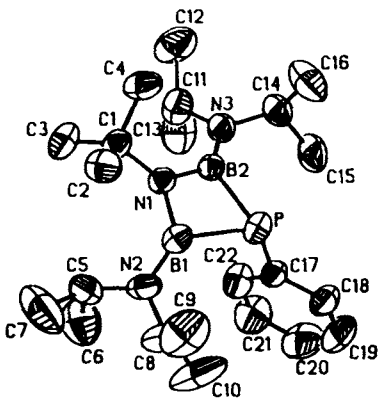

Fig. 10. Structure of the azaphosphadiboretane **35a** with B-P distances averaging 1.955(3) Å. The nitrogen center is planar, the sum of the angles at phosphorus is 280.7° [39].

distances which average 1.955(3) Å and 2.066(4) Å as the boron atoms are substituted by exocyclic NR_2 groups. Even longer B–P distances 1.97(1) Å were observed in the more encumbered ring system **36**[40]. Interestingly, the nitrogen

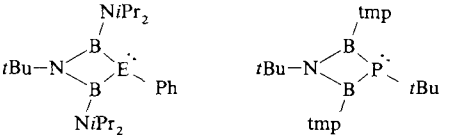

a, E = P; **b**, E = As

centers in all these rings are essentially planar whereas the P (or As) centers are very pyramidal.

Details of other rings systems involving boron–phosphorus bonds have also appeared. Three-membered BP_2 rings with various amino substituents on boron have been known since 1981.[12] These were synthesized by the reaction of the bis(alkali metal) salt of a diphosphane with the aminoboron dihalide. More recent results[41] have extended the range of these compounds to three-membered ring species involving various combinations of B,N,Si and P and their reactions with a variety of reagents. Fused three-membered boron-phosphorus ring systems **37** can be prepared by the photolysis of the four-membered ring precursor **27**.[42] The structure

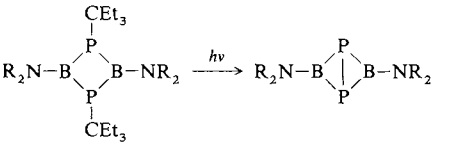

27 **37**

a, NR_2 = tmp; **b**, NR_2 = N*t*Bu$_2$

of the product **37a** is illustrated in Figure 11.[42] The B–P distances average 1.906(6) Å and the P–P distance, 2.349(2) Å, is extremely long indicating, perhaps, considerable ring

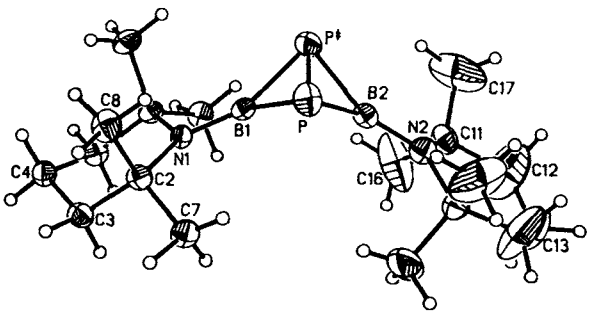

Fig. 11. A thermal ellipsoidal plot of the bicyclic system **37a** featuring two three-membered BP_2 rings [42]. Some details are given in the text.

strain. The B–N distances averaging 1.383(8) Å are indicative of an undiminished B-N π interaction. Another interesting ring system is the five-membered phosphadiborole derivative **38**.[43] Here the sum of the angles at phosphorus is

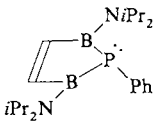

38

295.9° and the B–P distance is 1.949(2) Å. The inversion barrier at phosphorus was estimated at 10–15 kcal mol^{-1} on the basis of variable temperature ^{1}H NMR spectroscopy. Other notable B-P ring systems have also been reported recently. However, they involve either pentavalent[44] or four-coordinate[45] phosphorus and thus do not fall within the scope of this review.

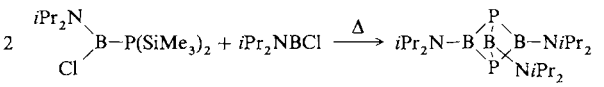

39 40 41

Reaction of the phosphinoborane **39** with the borane **40** at 160 °C affords the bicycle **41** (Fig. 12), the first example of a cage compound involving three-coordinate boron and phosphorus.[25] It has a trigonal bipyramidal B_3P_2 framework. The B–P distance 1.969(8) Å is slightly longer than those found in the four-membered ring compounds. The B–N distance 1.34(2) Å is consistent with a high degree of B-N overlap which precludes B–P multiple bonding.

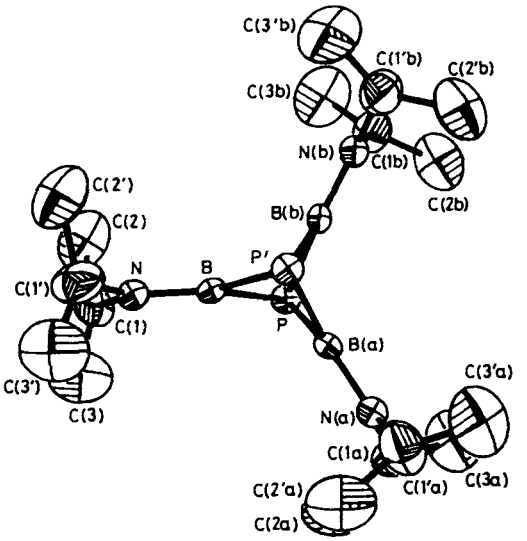

Fig. 12. Structure of the first cage compound **41** involving three-coordinate boron and phosphorus [25].

5. Possible Aromaticity in Delocalized B-P Rings and Acyclic Systems

5.1. Benzene or Borazine Analogues

The foregoing discussion has shown that, with a few notable exceptions, the majority of currently known ring compounds with *endo*-B–P bonds also involve boron bonding to an exocyclic $-NR_2$ group which, for the most part, effectively prevents delocalization or dative π bonding between phosphorus and boron. In the two cases that involved no amino substituents on boron it was argued that delocalization did not occur because of the energetically unfavorable anti-aromatic cyclobutadiene structure of the molecule.[20b, 33, 34] Conversely, a six-membered ring with alternate three-coordinate B and P atoms should show extensive delocalization since three of the π-molecular orbitals would be bonding in this case. It was found that, if the substituents on boron and phosphorus in reaction (7) were of suitable size, good yields

$$RBX_2 + 2LiPHR' \rightarrow 1/3(RBPR')_3 + H_2PR' + 2LiX \quad (7)$$

34

of these six-membered rings of type **34** could be obtained.[20] One of the products is illustrated in Figure 13.

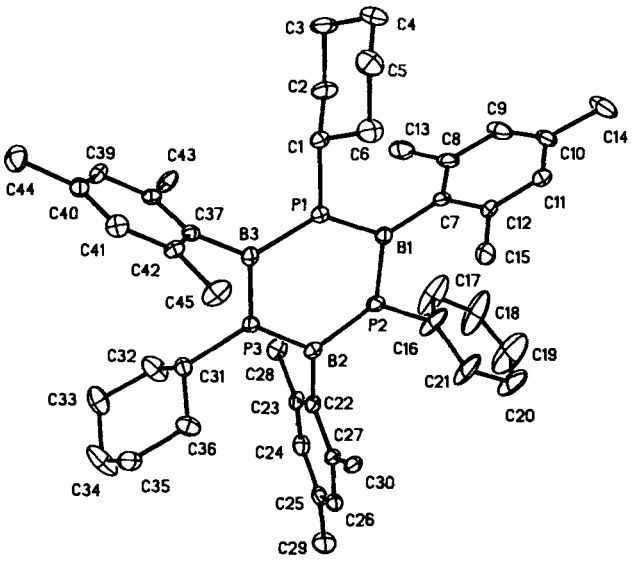

Fig. 13. Structure of the borazine analogue (MesBP*cyclo*-C_6H_{11})$_3$ **34b** [20]. The B–P bonds are all equal and about 1.84 Å long.

The most important features of the rings are: a) the B_3P_3 array and the six *ipso*-carbon atoms of the substituent groups are coplanar; b) all the B–P distances are essentially equal; c) the B–P bonds are short and about 1.84 Å in length. These structural data clearly suggest considerable delocalization of the phosphorus lone pairs over the six-membered ring system.

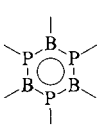

34

The structural differences between these systems and the organo-substituted four-membered rings[20b, 33, 34] discussed in Section 4.3 are striking. In the latter compounds the phosphorus centers are pyramidal and the B–P bonds are

about 1.9 Å long. Important spectroscopic differences were also observed. For example, the data in Table 2 indicate that in the ^{31}P NMR spectra there are large chemical shift differences between the four- and six-membered rings. The ^{1}H NMR data also show interesting differences. In acyclic boron and phosphorus compounds and the four-membered ring species the differences in chemical shift between the *ortho*- and *para*-methyl protons tend to average ca. 0.2 ppm. In contrast, larger differences of 0.42–0.75 ppm were observed for the benzene-like compounds. One possible explanation is that a ring current induced in the B_3P_3 π system as depicted in Figure 14 may account for the observed differences. With regard to the possible aromatic character of the

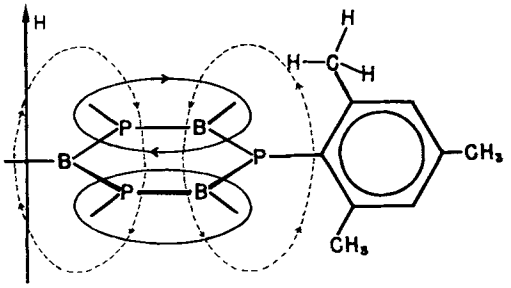

Fig. 14. Schematic drawing of the possible origin of the anomalously large difference in chemical shift between the *ortho*- and *para*-methyl protons of the mesityl groups.

B_3P_3 array it should be borne in mind that the B–P bonds are not very polar. Thus, the low polarity in the B_3P_3 ring should facilitate ring current. However, proof of the aromatic character of these molecules awaits more sophisticated spectroscopic studies and theoretical calculations.

5.2. Acyclic Delocalized Systems

Further extended π-bonded systems involving B-P skeletons have also been synthesized. Several analogues of both the π-allyl cation and anion featuring B_2P or BP_2 arrays with a variety of substituents have been reported.[22, 23] Examples are **42** (Fig. 15) and **43**, which were synthesized by simple salt elimination procedures.[22] They may be regarded as ana-

$(Mes_2B)_2PPh$ **42** $MesB(PPh_2)_2$ **43**

logues of the allyl cation and anion, respectively. The allyl cation analogue **42** features a twofold rotation axis along the P–C bond. The CPB_2 center is therefore planar but the planarity also extends to the two *ipso* carbon atoms on each boron. There is also a wide BPB angle of 133°. Although planar three-coordinate phosphorus is a common feature of the structure of numerous phosphanediyl-metal complexes of the type $RP[M(CO)_n]_2$,[47] the phosphorus in **42** differs fundamentally from these because its valence shell possesses four electron pairs. Three are used for σ bonding to one carbon and two boron atoms. The remaining pair is available for π donation to the empty boron p orbitals. Conversely, in the bridging metal-phosphanediyls the phosphorus be-

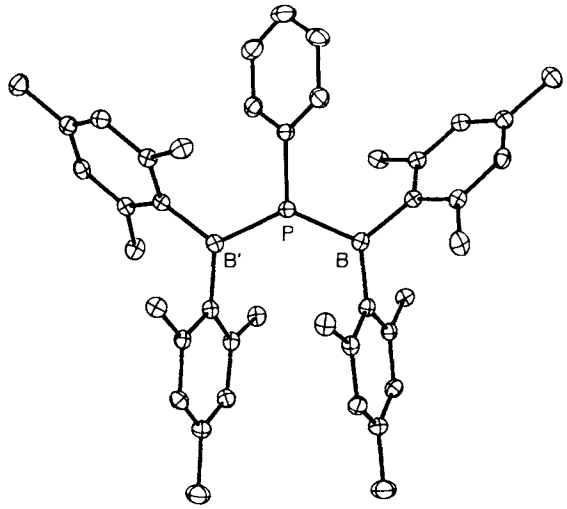

Fig. 15. Structure of the allyl-cation analogue $PPh(BMes_2)_2$ **42** [22]. The $B_2PC(ipso)_2$ array is planar and the B–P bond is 1.871(2) Å and the BPB angle is 131.0(2)°.

haves as a π acceptor. The planar nature of the B_2PC_5 array is good evidence for π bonding in the BPB moiety, which is maximized by having all three p orbitals parallel to each other even at the expense of considerably greater steric congestion caused by the coplanarity of the five organo groups and the short B–P distance of 1.87 Å

In **43** the boron is planar with B–P distances 1.89 Å. However, the phosphorus centers in this case are pyramidal. There is a slight asymmetry in the B–P distances which is reflected in slightly differing degrees of pyramidicity.[22] The almost equal B–P distances in both compounds are consistent with the π-molecular orbital picture of the allyl group since the extra pair of electrons is accommodated in a nonbonding orbital. This is also consistent with the slightly longer B–P distance (1.89 vs. 1.87 Å) on the basis of increased interelectronic repulsion. The preparation and structures of the compounds **44** and **45**[23] show that the electronic properties of the boron substituent exert considerable influence on the degree of multiple P → B bonding. In the case of **44** with Br as substituent (–I effect, Fig. 16) the B–P distances average 1.83 Å, whereas in the OEt (+I) derivative **45** the B–P distances average 1.93 Å in length.

$XB(PMes_2)_2$

44, X = Br; **45**, X = OEt

Other B–P analogues of carbon compounds are also possible. For example, during reactions of **16** (a phosphido ligand precursor with reduced bridging tendency owing to the P → B effect) with some transition metal halides it was found that the phosphido group could be oxidized to give the 1,2-diboryldiphosphanes **46**.[24] These compounds constitute

$[Li(Et_2O)_2][Mes_2BPR]$ **16** $Mes_2B–PR–PR–BMes_2$ **46**, **a**, R = 1-Ad; **b**, R = Mes

a new class of diphosphanes with a number of unusual features (Fig. 17). The most notable are the short P–P bond

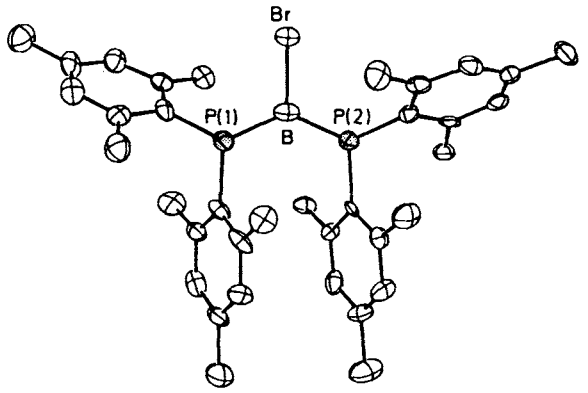

Fig. 16. Structure of the allyl-anion analogue $BrB(PMes_2)_2$ **44** [23]. The B–P distances of ca. 1.83 Å are quite short owing to the –I effect of the halogen.

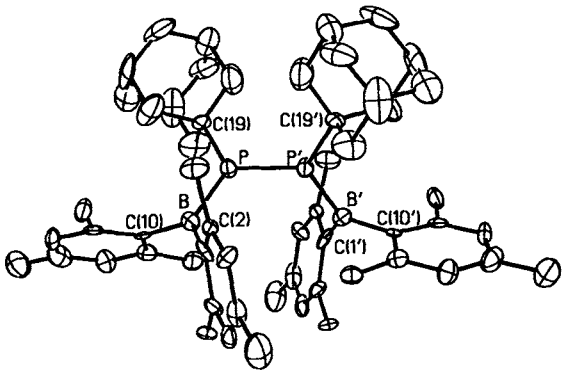

Fig. 17. A thermal ellipsoidal plot of the butadiene analogue $[P(1\text{-Ad})BMes_2]_2$ **46a** [24]. The P–P single bond of ca. 2.1 Å is extremely short.

distances, ca. 2.11 Å, and the planar phosphorus and boron centers. Clearly, an analogy could be drawn between these compounds and butadiene. However, the twist angle between the two phosphorus planes is ca. 70° so that there is little conjugative interaction between the two B-P π systems. The short P–P bonds may be due to the changes in hybridization at phosphorus which now has $\sim sp^2$ hybridized orbitals. Overlap of these sp^2 hybrids may result in shorter P–P bonds than those in normal diphosphanes, where the P–P distances are about 2.22–2.23 Å. In the latter, the hybridization of the bonding orbitals is less than sp^3 (between sp^3 and pure p) since the angles at phosphorus are generally less than tetrahedral values. Interestingly, the "mixed" diphosphane, **47**,

$Mes_2BP(1\text{-Ad})PPh_2$

47

with one normal P-bound phosphorus atom and one sp^2-hybridized B-bound phosphorus atom has a P–P bond length of 2.173(2) Å,[33] which is close to that predicted by interpolation of the 2.11 and 2.22–2.23 Å P–P values. These structural data imply that about half of the contraction observed in P–P double bonds (ca. 2.02 Å long) is due to the rehybridization, the remainder being due to p–p π overlap. This is in contrast to doubly bonded carbon compounds where only 25–30% of the shortening can be traced to rehybridization.

6. Reactivity Studies

Since many of the compounds described in the preceding sections have only been recently discovered the investigation of their chemistry is in the preliminary stage. In many cases the boron-phosphorus compounds are sensitive to air and moisture. However, the quasi-aromatic compounds described in Section 5.1 react only slowly (several days in "wet" THF) with water to give a primary phosphane and various boron-oxygen compounds.[20] The ring systems also react rapidly with Br_2 to give $RPBr_2$ and $RBBr_2$ products. The four-membered 1,3-diphosphadiboretanes have been shown to undergo an interesting photolysis reaction to give fused ring systems as in **37a** (Fig. 11).[42] The related four-membered 1,3,2,4-azaphosphadiboretane skeleton has also been investigated.[40] Addition of methyl iodide led to formation of the methylphosphonium salt **48**, which was characterized by ^1H, ^{11}B, ^{13}C and ^{31}P NMR spectra and by an elemental analysis.[40] The phosphorus lone pair may also form

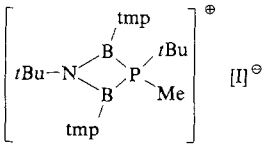

48

a bond to $W(CO)_5$. With selenium the P(*t*Bu) moiety is displaced from the ring and a cyclic four-membered ring involving NB_2Se is produced instead. The three-membered ring system **49** also undergoes a variety of reactions, e.g. with $M(CO)_6$, S, Se or MeI.[41] These facile reactions clearly

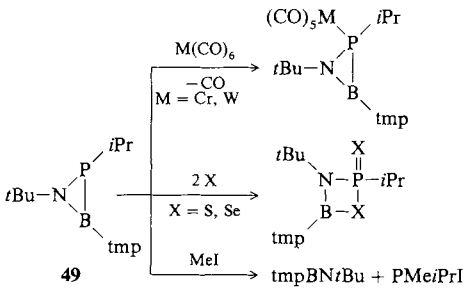

49

demonstrate the ready availability of the phosphorus lone pair in **49** and its almost negligible involvement with the boron p orbital in this case.

Compounds involving bonding between four-coordinate boron and phosphorus are generally very stable. However, when coordinative unsaturation is introduced rearrangement and elimination reactions may occur. For example, the attempted synthesis of Br_2BPMes_2 led instead to the novel heterocycle **50**, which presumably arose from the activation

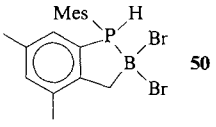

50

of the C–H bond on one of the *ortho*-CH_3 groups of a mesityl substituent.[23] Activation of C–H has also been observed during the attempted synthesis of the phosphinoborane **51**; in this case the dimer **52** was isolated.[47] The proposed reaction sequence which led to this unexpected compound is believed to involve a double elimination (retro-hydroboration) of isobutene followed by an anti-Markovnikov hydroboration and dimerization to give the product **52**.

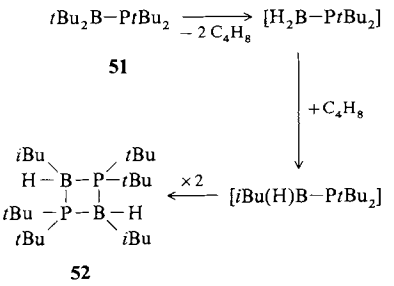

7. Outlook

Several decades after the first phosphinoboranes and borane–phosphane adducts were reported, the first compounds involving multiple boron–phosphorus bonding are being investigated. It is ironic to note that exotic compounds involving isoelectronic carbon–silicon double bonded systems were isolated and structurally characterized some years before their simple boron–phosphorus counterparts the phosphinoboranes. Similarly, the synthesis of the boron-phosphorus counterparts of borazines involved nothing more complicated than the addition of two equivalents of LiPHR to $R'BHal_2$. The initial findings suggest that there are many exciting discoveries to be made. The synthesis of stable B-P analogues of the iminoboranes, RBPR', remains an obvious goal. The coordination chemistry of the compounds already synthesized and the synthesis of a large variety of boron-phosphorus cage compounds are areas of considerable potential. A striking feature of the work already published is the very large effect that the boron substituents can have on B–P multiple bonding and in most cases where nitrogen is bonded to boron little or no multiple bonding to phosphorus is observed. On the other hand, when there is an electron-withdrawing substituent on boron enhanced multiple bonding to phosphorus is seen. It should therefore be possible to control boron–phosphorus multiple bonding very accurately with the appropriate substituent.

Note added in proof (April 3, 1990): Species involving two-coordinate boron and boron–phosphorus multiple bonds have now appeared. The Zintl anions $[BP_2]^{3\ominus}$ and $[BAs_2]^{3\ominus}$ were crystallized as their $K^{\oplus}$ salts from the reaction of the elements at 1000–1100 K. The bond lengths are B-P = 1.767 Å and B-As = 1.868 Å. These short distances are in line with earlier predictions[10] and with the two-coordination and sp hybridization at boron.[49]

The author is grateful to his many coworkers named in the bibliography who carried out many of the experiments described with skill and enthusiasm. The financial assistance of the National Science Foundation and the A. P. Sloan Foundation are also gratefully acknowledged.

Received: September 12, 1989 [A 758 IE]
German version: *Angew. Chem. 102* (1990) 527

[1] A. Stock, E. Pohland, *Ber. Dtsch. Chem. Ges. 59* (1926) 2215.
[2] K. Niedenzu, J. W. Dawson: *Boron-Nitrogen Compounds*, Springer, Berlin 1965.
[3] J. R. Wasson in *Gmelin Handbuch der Anorganischen Chemie, Ergänzungswerk zur 8. Aufl. Bd. 19, Borverbindungen, Teil 3*, Springer, Berlin 1975, p. 93.
[4] G. E. Coates, J. G. Livingstone, *J. Chem. Soc.* 1961, 1000.
[5] G. E. Coates, J. G. Livingstone, *J. Chem. Soc.* 1961, 5053.
[6] A. B. Burg, R. I. Wagner, *J. Am. Chem. Soc. 75* (1953) 3872; A. B. Burg in J. F. Liebman, A. Greenberg, R. E. Williams (Eds.): *Advances in Boron and the Boranes*, VCH Verlagsgesellschaft, Weinheim, 1988, p. 1.
[7] A. D. Tevebaugh, *Inorg. Chem. 3* (1964) 302.
[8] W. D. English, *Chem. Abstr. 57* (1962) 11 239. US Pat. 3 035 095.
[9] D. A. Brown, C. G. McCormack, *J. Chem. Soc. 1964*, 5385.
[10] a) R. A. Bartlett, X. Feng, P. P. Power, *J. Am. Chem. Soc. 108* (1986) 6817; b) R. A. Bartlett, H. V. R. Dias, X. Feng, P. P. Power, *ibid. 111* (1989) 1306.
[11] G. Fritz, W. Hölderich, *Z. Anorg. Allg. Chem. 431* (1977) 61.
[12] a) M. Baudler, A. Marx, *Z. Anorg. Allg. Chem. 474* (1981) 18; b); M. Fehér, R. Frölich, K.-F. Tebbe, *ibid. 474* (1981) 31.
[13] A. M. Arif, J. E. Boggs, A. H. Cowley, J.-G. Lee, M. Pakulski, J. M. Power, *J. Am. Chem. Soc. 108* (1986) 6083.
[14] C. Courét, J. Escudié, B. Garrigues, M. Lazraq, J. Satgé, *Can. J. Chem. 65* (1987) 1230.
[15] R. A. Bartlett, X. Feng, M. M. Olmstead, P. P. Power, *Phosphorus Sulfur, 20* (1987) 245.
[16] M. Baudler, M. Hintze, *Z. Anorg. Allg. Chem. 522* (1985) 184.
[17] A. M. Arif, A. M. Cowley, M. Pakulski, J. M. Power, *J. Chem. Soc. Chem. Commun. 1986*, 889.
[18] a) P. Kölle, H. Nöth, R. T. Paine, *Chem. Ber. 119* (1986), 2681; b) P. Kölle, G. Linti, H. Nöth, G. L. Wood, C. K. Narula, R. T. Paine, *ibid. 121* (1988) 871.
[19] J. Escudie, C. Couret, M. Lazraq, B. Garrigues, *Synth. React. Inorg. Met.-Org. Chem.* (1987) 379.
[20] a) H. V. R. Dias, P. P. Power, *Angew. Chem. 99* (1987) 1320; *Angew. Chem. Int. Ed. Engl. 26* (1987) 1270; b) *J. Am. Chem. Soc. 111* (1989) 144.
[21] X. Feng, M. M. Olmstead, P. P. Power, *Inorg. Chem. 25* (1986) 4616.
[22] R. A. Bartlett, H. V. R. Dias, P. P. Power, *Inorg. Chem. 27* (1988) 3919.
[23] H. H. Karsch, G. Hanika, B. Huber, K. Mundl, S. König, C. Krüger, G. Müller, *J. Chem. Soc. Chem. Commun. 1989*, 373.
[24] D. C. Pestana, P. P. Power, *J. Am. Chem. Soc. 111* (1989) 6887.
[25] G. L. Wood, E. N. Duesler, C. K. Narula, R. T. Paine, H. Nöth, *J. Chem. Soc. Chem. Commun. 1987*, 496.
[26] The radius of boron is the subject of some controversy [10a], much of which can be resolved by consideration of the coordination number for boron. The value 0.82 Å appears to be a reasonable one for three-coordinate boron. For example, compounds involving three-coordinate boron-carbon bonds usually have B–C bond distances of *ca.* 1.58–1.60 Å [26a]. If the usually accepted carbon radius (0.77 Å) is subtracted, a value of 0.81–0.83 Å is obtained for boron. Longer distances are observed when boron is four-coordinate. Typical B–P distances for such compounds are about 2.0 Å or an effective radius of 0.9 Å for four-coordinate boron.
[27] O. Gropen, *J. Mol. Struct. 36* (1977) 111. Other more recent calculations are to be found in: E. Magnusson, *Tetrahedron 41* (1985) 5235; *Aust. J. Chem. 39* (1986) 735; J. A. Baban, B. P. Roberts, *J. Chem. Soc. Perkin Trans. II 1987* 487.
[28] J. M. Lehn, B. Munsch, *Mol. Phys. 23* (1972) 91. However, the presence of substituents such as silyl groups can have a dramatic effect on the inversion barrier e.g. 18.9 kcal mol^{-1} in the silylphosphane $Me_3SiPPh(iPr)$, see R. D. Baechler, K. Mislow, *J. Am. Chem. Soc. 92* (1970) 4759 and A. Rauk, J. D. Andose, W. G. Frick, R. Tang, K. Mislow. *ibid. 93* (1971) 6507. The studies show that there is a strong correlation between substituent electronegativity and the inversion barrier. Presumably, some of the lowering of the barrier in phosphinoboranes is due to the low electronegativity of the boryl group. However, it is notable that the calculated and experimental inversion barriers in these compounds (8–11 kcal mol^{-1}) are very much lower than those in the silyl compounds, whereas the electronegativity of boron (2.01) is greater than silicon (1.74) [29].
[29] A. L. Allred, E. G. Rochow, *J. Inorg. Nucl. Chem. 5* (1958) 264.
[30] H. C. Brown, V. H. Dodson, *J. Am. Chem. Soc. 79* (1957) 2302; J. W. Wilson, *J. Organomet. Chem. 186* (1980) 297; A. Pelter, B. Singaram, L. Williams, J. W. Wilson, *Tetrahedron Lett. 24* (1983) 620.
[31] R. A. Bartlett, P. P. Power, *Organometallics, 5* (1986) 1916; M. M. Olmstead, P. P. Power, K. J. Weese, R. J. Doedens, *J. Am. Chem. Soc. 109* (1987) 2541.

[32] A. Pelter, B. Singaram, J. W. Wilson, *Tetrahedron Lett. 24* (1983) 635.
[33] D. C. Pestana, P. P. Power, unpublished results.
[34] H. V. R. Dias, D. C. Pestana, M. Petrie, P. P. Power, *Phosphorus Sulfur*, in press.
[35] T. L. Allen, A. C. Scheiner, H. F. Schaefer, III, *Inorg. Chem.*, unpublished.
[36] I. Mayer, *Chem. Phys. Lett. 97* (1983) 270; *110* (1984) 440; *Int. J. Quantum Chem. 29* (1986) 73.
[37] M. A. Natiello, J. A. Medrano, *Chem. Phys. Lett. 105* (1984) 180; *ibid. 110* (1984) 445.
[38] P. Paetzold, *Adv. Inorg. Chem. Radiochem. 31* (1987) 123.
[39] K.-H. van Bonn, P. Schreyer, P. Paetzold, R. Boese, *Chem. Ber. 121* (1988) 1045.
[40] P. Kölle, H. Nöth, R. T. Paine, W. Rattay, *Z. Naturforsch. B43* (1988) 1439.
[41] P. Kölle, H. Nöth, R. T. Paine, *Chem. Ber. 122* (1989) 423.
[42] P. Kölle, G. Linti, H. Nöth, K. Polborn, *J. Organomet. Chem. 355* (1988) 7.
[43] M. Driess, H. Pritzkow, W. Siebert, *Angew. Chem. 99* (1987) 789; *Angew. Chem. Int. Ed. Engl. 26* (1987) 781.
[44] D. Gudat, E. Niecke, M. Nieger, P. Paetzold, *Chem. Ber. 121* (1988) 565.
[45] H. Nöth, *Z. Anorg. Allg. Chem. 555* (1987) 79.
[46] M. Driess, H. Pritzkow, W. Siebert, *Angew. Chem. 100* (1988) 410; *Angew. Chem. Int. Ed. Engl. 27* (1988) 399.
[47] G. Huttner, K. Evertz, *Acc. Chem. Res. 19* (1986) 406.
[48] H. H. Karsch, G. Hanika, B. Huber, J. Riede, G. Müller, *J. Organomet. Chem. 361* (1989) C25–C29.
[49] H.-G. von Schnering, M. Somer, M. Hartweg, K. Peters, *Angew. Chem. 102* (1990) 63; *Angew. Chem. Int. Ed. Engl. 29* (1990) 65.

The Chemistry of Vitamin A and Vision

By Robert R. Rando*

Vision is initiated in the retina by the photochemical isomerization of an 11-*cis*-retinal Schiff base to its all-*trans* counterpart in the photosensitive protein rhodopsin. All-*trans*-retinal is released, reduced to form all-*trans*-retinol (vitamin A), and finally esterified. In order for vision to proceed an 11-*cis*-retinoid must be regenerated in the eye. *Kühne* observed in the 1870s that the pigment epithelium must be in place behind the retina in order for rhodopsin to form. And indeed it was in the pigment epithelium that an isomerase system was recently discovered that can produce 11-*cis*-retinol from added vitamin A. *Pauling* predicted in the 1930s that certain *cis* double bonds in carotenoids and retinoids, including 11-*cis*-retinoids, should be quite unstable with respect to their all-*trans* congeners. This prediction is borne out by experiment, but leaves open the crucial question as to where the energy comes from to drive the isomerization process in the eye. This question was answered by the demonstration that the energy is found in the membrane phospholipids. The fact that membranes may serve as an energy source reveals a previously unsuspected biological function of membranes. The chemistry of the novel energy-linked isomerization process is explored in this review.

1. Introduction

The chemistry of the visual cycle provides the crucial link between the physical phenomenon of light and the biological act of perception. Since at least the 1870s it has been understood that light causes the rhodopsin in the retina to bleach from red to white when we see.[1] This bleaching destroys the chromophore and is the first event of the visual cycle. The rest of the cycle is the recovery from vision, the preparation to see again, as the rhodopsin is reformed. Only recently has the second half of the visual cycle begun to be understood in detail.

An analogy is often made between a camera and the human eye. Each has a lens system, and the iris of the eye, like the aperture of the camera, governs the amount of light that enters. The retina, like the film, is "exposed" by the light. But like all other animal–machine analogies, this one, too, is imperfect and does not nearly describe the complexity and beauty of the biological system. For example, the retina is considerably more versatile than camera film. Certainly, both camera film and the retina contain photosensitive materials. The retina contains photosensitive proteins, called rhodopsins, in organelles known as rods and cones. However, this is where the analogy ends. Two major differences are that the retina can adjust its sensitivity to match the strength of the ambient light and, most importantly, that the photosensitive pigments of the retina are renewable. That is, the pigmented material is continually renewed after transformation by light so that new images can be formed on it. The capacity of the retina to adjust its sensitivity to low light levels and the renewability of rhodopsin depend on the latter's ability to be altered to a non-visible-light-absorbing form by light and then to be reconstituted in the dark. In this way light itself may adjust the sensitivity of the retina to its ambient level by titrating the amount of pigment in the retina.

[*] Prof. R. R. Rando
Department of Biological Chemistry and Molecular Pharmacology
Harvard Medical School
240 Longwood Ave., Boston, MA 02115 (USA)

Rhodopsin is a holoprotein consisting of 11-*cis*-retinal, as the chromophore, and opsin, which is transparent. A particularly vexing problem in visual science has been the thermal mechanism by which 11-*cis*-retinal is biosynthesized in the vertebrate eye. The eye is the only organ in the body in which this isomeric form of retinoid is found to a significant extent. *Wald*[2] showed that the exposure of rhodopsin to light transforms the 11-*cis*-retinal of rhodopsin into all-*trans*-retinal. Subsequently it was reported[3, 4] that soluble isomerase enzymes can act on all-*trans*-retinal from homogenized eye tissue to regenerate 11-*cis*-retinal, thereby completing the visual cycle. Further experimentation, however, has shown these latter two reports to be in error. Upon reexamination, it was found that, under the reported conditions, nonphysiological 9-*cis*-retinal and isorhodopsin (the adduct of 9-*cis*-retinal and opsin) were formed, rather than 11-*cis*-retinal and rhodopsin.[5, 6] The lability of all-*trans*-retinal towards chemical isomerization, coupled with the extreme difficulty of separating the various retinoid isomers prior to the advent of HPLC, has cast into doubt any earlier report on the isomerase problem. As of 1986, no system capable of forming 11-*cis*-retinoids in vitro in darkness had yet been confirmed.

How then does the biosynthesis of 11-*cis*-retinal occur in the eye? It is the purpose of this review article to illuminate the nature of this process and to explore its chemical basis as revealed by recent findings.

2. Vitamin A and Vision

Since proteins do not absorb visible light, it was clear that an organic chromophore must be in some way involved. It was known in antiquity that night blindness could have a dietary etiology.[7] The ancient Egyptians discovered that fresh liver contained a material that could combat this problem. It was not until much later, however, that the material was identified as vitamin A and its role in vision elucidated. The absence of vitamin A from the diet will produce night blindness. Eventually, if the deficiency is not treated, permanent total blindness will result.[8] Even today, vitamin A

deficiency is the single greatest cause of blindness, occurring primarily in Third World countries.

Vitamin A, or all-*trans* retinol (Fig. 1), is a diterpene derived from β-carotene by an oxidative mechanism which

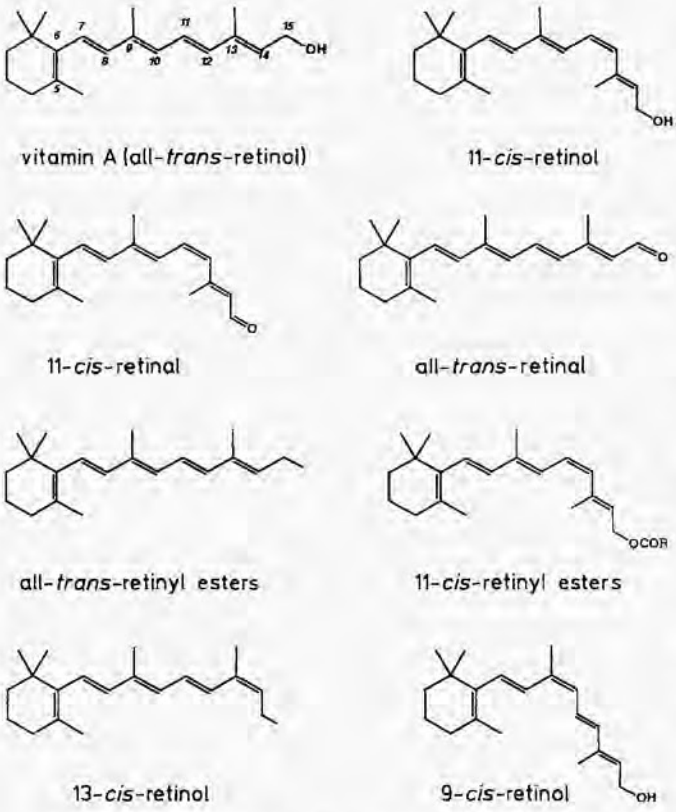

Fig. 1. Structures of vitamin A and other retinoids important in vision

to this day remains somewhat of a puzzle. Nevertheless, the β-carotene is certainly cleaved in the gut, producing all-*trans*-retinal, which is then enzymatically reduced and esterified, thus producing retinyl esters, which are carried to the liver, hydrolyzed to all-*trans*-retinol, and then distributed to various tissues, including the eye. In the eye the retinol is delivered to the retinal pigment epithelium (PE), which sits directly behind the retina and is intimately associated with it (Fig. 2). It has been known for years that the PE is important for the maintenance of a healthy retina. The separation of

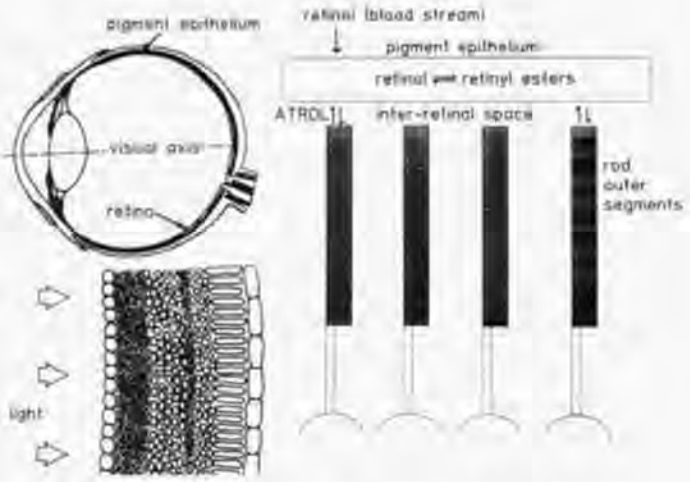

Fig. 2. The retina and pigment epithelium. Schematic views of the retina and pigment epithelium at different levels of resolution. In the upper left, a cross-section of an eye is shown with the retina and pigment epithelium labeled. Below the eye, a blowup of the retina and the pigment epithelium is shown. The rightmost rectangular shaped cells represent the pigment epithelium and to its immediate left are the rod outer segments. Finally, the cartoon on the right half of the figure shows the pigment epithelium and the rod outer segments in close apposition. The flux of retinoids between the two cell types is also indicated. ATROL is all-*trans*-retinol.

the retina from the PE produces a detached retina, which can lead to blindness if not treated. One important role of the PE is to supply the retina with retinoids, the precursors to the visual chromophore.

In the 1930s, the knowledge that vitamin A or some product derived from it is critical in vision led *George Wald* and others to formulate the idea that it was 11-*cis*-retinal, one of the products derived from vitamin A, that was the crucial component of rhodopsin.[2] Since 11-*cis*-retinal absorbs light maximally at approximately 380 nm and rod rhodopsin absorbs maximally at approximately 500 nm, the protein needs to significantly perturb the 11-*cis*-retinal chromophore. It was shown that 11-*cis*-retinal readily formed a Schiff base with the protein opsin to form rhodopsin (Fig. 3).[9] This adduct, in the protonated form, is the actual chromophore of the visual pigments. It should be noted that 11-*cis*-retinoids exist only in the eyes of sighted animals and are not otherwise dietary constituents. Of further interest is the fact that the three phyla with sight—the vertebrates, the arthropods, and the molluscs—all utilize 11-*cis*-retinal as their visual chromophore.

Dr. Rando was born in New York City in 1941. He received a doctorate in physical organic chemistry with Professor William von E. Doering in 1966 at Yale University. He then studied with Professor Konrad Bloch in the Department of Chemistry, Harvard University, where he investigated the mechanism of action of β-hydroxydecanoyl thioester dehydrase. He also carried out mechanistic studies on the first mechanism-based irreversible enzyme inhibitor, 3-decynoyl-N-acetyl cysteamine. Dr. Rando has worked on the development of new kinds of mechanism-based inhibitors and also discovered natural products which follow this mechanistic paradigm. His recent work has involved a study of biochemical mechanisms in vertebrate vision and membrane biochemistry. Dr. Rando is currently the Gustavus Adolphus Pfeiffer Professor of Biological Chemistry and Molecular Pharmacology at Harvard Medical School.

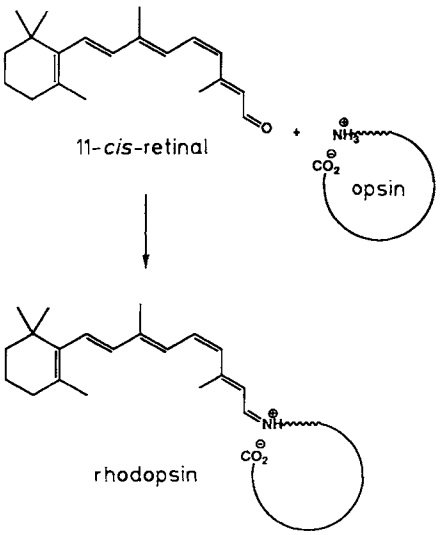

Fig. 3. Formation of rhodopsin from the protein opsin and 11-*cis*-retinal.

3. A Photochemical *cis*-to-*trans* Isomerization Initiates Vision

The isolation of rhodopsin immediately reveals its great light sensitivity. The integral membrane protein rapidly loses its red color when exposed to light, in a process called bleaching (Fig. 4). The products of this light exposure are all-*trans*-retinal and the protein component opsin. In the dark, there is no measurable tendency for 11-*cis*-retinal to form when rhodopsin is in an isolated retina or when it is in a detergent solution. The photochemical isomerization of rhodopsin occurs with a high quantum efficiency of approximately 0.67.[10] This is about 100-fold higher than that of a protonated retinal Schiff base by itself.[10] This photochemical *cis*-to-*trans* conversion occurs within picoseconds and is the only process where light is involved in the visual response.[11] As will be shown in Section 5.2, 11-*cis*-retinoids are approximately 4 kcal mol^{-1} higher in energy than their all-*trans* congeners. Thus, unlike other photochemical processes where light energy is used to drive thermodynamically unfavorable reactions, in the visual process light initiates an otherwise exothermic reaction.

The photochemical isomerization of the chromophore in rhodopsin leads to a series of intermediates, ending in the hydrolysis of the all-*trans*-retinyl Schiff base to produce all-*trans*-retinal and opsin as shown in Figure 5.[9] The isomerization itself is largely complete by the time the first well-established intermediate, bathorhodopsin, is formed.[12] It is interesting to note that bathorhodopsin retains a substantial portion of the energy of the incident photon.[13] A mole of photons at 500 nm carries 57 kcal with it. Photomicrocalorimetric measurements determined that bathorhodopsin is approximately 35 kcal mol^{-1} higher in energy than rhodopsin.[13] Possible ways this energy might be retained include strain energy in the chromophore, and charge separation, induced by the isomerization reaction, between the protonated Schiff base and its protein-bound counterion[14] as shown in Figure 6.

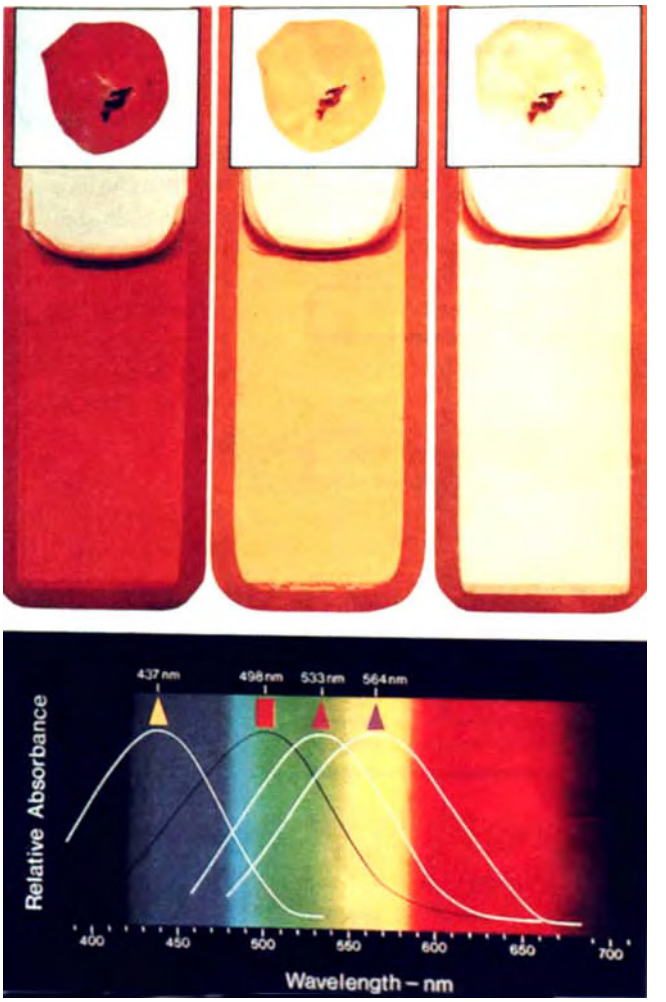

Fig. 4. Top: The bleaching of rhodopsin by light in the retina and in detergent solution [21]. Bottom: The absorption characteristics of rod rhodopsin and the cone rhodopsins. The latter rhodopsins are responsible for color vision [21]. The retina and extracts were prepared by *P. K. Brown* and *J. E. Dowling*. The inset was prepared by *P. K. Brown*. (Taken from [21] with permission).

The remaining intermediates in the visual cascade have also been studied in some detail.[11] Presumably, these spectroscopically defined intermediates reflect conformational alterations in the protein which are induced by the photoisomerization. Of great interest is metarhodopsin II, because it is the intermediate (R*) that transmits the information that light has been absorbed. Unlike the other intermediates, metarhodopsin II contains a deprotonated Schiff base.[14] Abolishing the possibility of deprotonation by monomethylating the active-site lysine of rhodopsin prevents the formation of metarhodopsin II, and hence the R* stage is never reached.[15, 16] Thus, Schiff base deprotonation is obligate in the biochemical activation of rhodopsin. It is also clear that major conformational changes in the rhodopsin molecule accompany the formation of metarhodopsin II, and these alterations are transmitted to the next molecular entity in the visual cascade, the retinal G-protein.

The interaction of R* with its G-protein partner has been well studied.[17] This interaction results in catalysis of the exchange of GDP for GTP at the active site of the G-protein. When GTP is bound to the active site of the G-protein, the

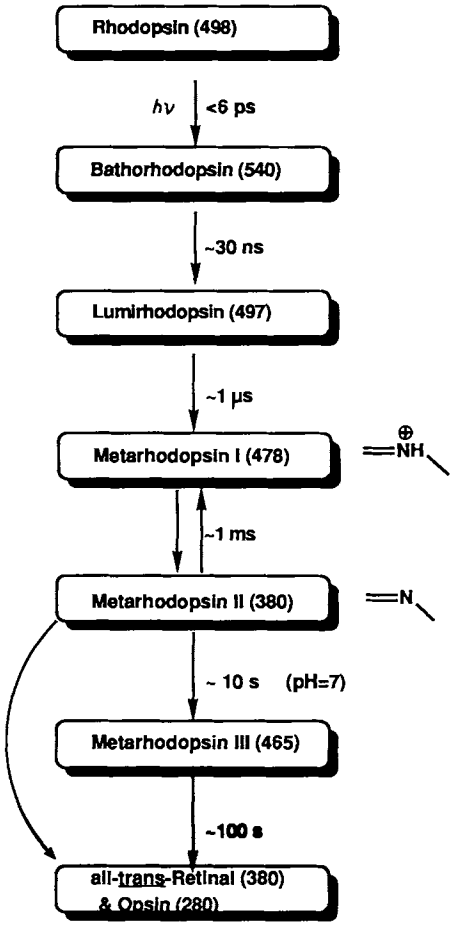

Fig. 5. Photochemistry of rhodopsin. The bleaching of rhodopsin results in the formation of the spectroscopically defined intermediates shown in the above figure. The λ_{max} values for the different intermediates are given in parentheses and their half-lives at room temperature are provided adjacent to the arrows.

latter becomes activated, enabling it to free from inhibition the rod outer-segment phosphodiesterase specific for cyclic-GMP (cGMP). And when this enzyme in turn is activated, it can hydrolyze cGMP at the diffusion-controlled limit.[18] This hydrolysis is thought to lower the free concentration of this effector. Since the sodium ion permeability of the rod outer-segment sodium channels is gated by cGMP,[19] hydrolysis of the latter results in the hyperpolarization of the rod outer segments. This change in membrane potential is signaled to other nerve cells in the retina and communicated to the brain, where the visual image can then be constructed.

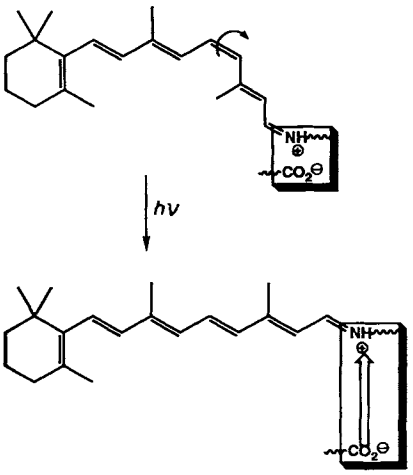

Fig. 6. Possible mechanism for charge separation caused by the *cis*-to-*trans* photoisomerization of the 11-*cis*-retinal protonated Schiff base. The carboxylate ion in the figure is part of the polypeptide backbone.

Subsequent to the formation of metarhodopsin II, its direct hydrolysis can occur to provide all-*trans*-retinal and opsin.[17] Metarhodopsin III can also be produced from metarhodopsin II, and the former intermediate may serve as a storage form for the latter physiologically active conformer.[17]

The fact that all-*trans*-retinal is liberated as a consequence of bleaching requires that a physiological mechanism be in place for the regeneration of 11-*cis*-retinal. Otherwise, vision would have the character of a once-in-a-lifetime event. The reason why vertebrate vision operates via a bleaching mechanism is presumably related to the role that bleaching plays in visual adaptation.[20] Sensory adaptation, including of course visual adaptation, refers to the ability of a sensing system to alter its sensitivity to match the strength of the ambient signal. This ability can be prodigious, for in the case of vision the eye must be able to distinguish between light intensities differing from the background by only a few percent over a range of approximately 10^{10} in ambient light intensity.[21] Although this process is multifactorial, one important aspect of it, namely, dark adaptation, is importantly controlled by the amount of rhodopsin in the rods. Dark adaptation is usually experienced when we move from a well-lit environment to a darkened one, such as a theater. Initially our sense of vision is quite limited, but it improves slowly with time. This slow phase of dark adaptation is described by a rate which is congruent with the overall rate of 11-*cis*-retinal regeneration.[21] This rate is characteristic for a given species; for humans, $t_{1/2}$ is 5 min, while for amphibians and rats it is 30 min and 40 min, respectively.[21, 22] Since there is a logarithmic relationship observed between the amount of rhodopsin and visual sensitivity,[21] an alteration in the level of rhodopsin will have a marked effect on visual sensitivity. The immense sensitivity of human vision, which can operate at the single photon level,[23] is partly a reflection of the exceedingly high concentration of rhodopsin in the rod outer segments (10^9 rhodopsin molecules per rod).[21] To decrease the inherent sensitivity of this system requires that the amount of pigment be modulated by the bleaching–regeneration cycles.

4. The Regeneration of Rhodopsin

4.1. The Visual Cycle

More than a half-century before it was understood that a vitamin A derivative is the photosensitive chromophore in vision, the great German physiologist *Kühne* had already achieved substantial insights into the visual process. For example, he had understood that the retina contained a photosensitive material that turned white (i.e., bleached) when it was exposed to light.[1] Furthermore, he discovered that the red color would not return in an isolated retina but required

the close apposition of the retinal pigment epithelium (PE) in order to regenerate its red color. This discovery was of great importance and has stood the test of time; in all the years since *Kühne*'s work—more than a century—no one has convincingly demonstrated rhodopsin rgeneration in an isolated retina.

The discovery of the role of vitamin A in vision led to analysis of the bleaching–regeneration cycle on a molecular level. It was quickly understood that the enzymological processing of vitamin A was at the heart of these transformations. The all-*trans*-retinal liberated by the bleaching of rhodopsin was shown to be rapidly reduced enzymatically in the retina by specific nicotinamide-linked retinol dehydrogenases to produce vitamin A.[24] The vitamin A is then transported to the pigment epithelium, where it is esterified, largely to long-chain saturated fatty acid esters, such as those in the palmitate and stearate series. For each of the three all-*trans*-retinoids, there is a corresponding 11-*cis*-retinoid (see Fig. 7), and the totality of biochemical reactions required to interconvert these six molecules comprises the classical and oversimplified visual cycle (Fig. 7). Thus, the double-bond isomerization reaction could potentially occur with any of three substrates and produce any of the three corresponding products, and it could occur either in the pigment epithelium or in the retina. After isomerization has occurred, the 11-*cis*-retinoid, in either the alcohol or the aldehyde form, must be transported back to the rod outer segments, by means of specific binding proteins,[25–28] where it can be used for rhodopsin regeneration (after oxidation, if 11-*cis*-retinol is transported back).

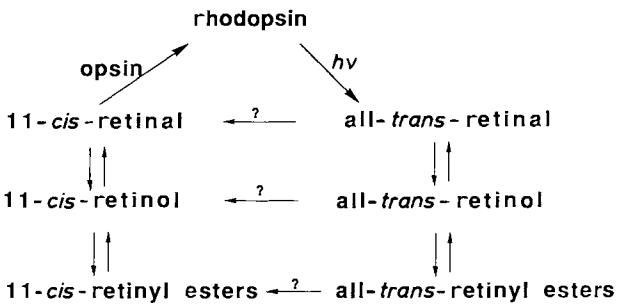

Fig. 7. The classical visual cycle.

The dynamic nature of the visual cycle can be understood from experiments designed to measure the amounts of the various retinoids during dark and light adaptation in living animals.[29, 30] In the albino rat, there is only a slight excess of retinoids; that is, all the opsin is bound to retinoids and there is only a small amount of retinoids left over. In this simple case, a striking flow of retinoids from the retina to the PE can be observed in the light, with the reverse occurring in the dark (Fig. 8).[21] In higher vertebrates and in amphibians there is an approximately threefold excess of retinoids over opsin. In these cases, the excess retinoids are stored in the PE as esters.[29] In the dark, the retinoid pool in an animal such as the frog can consist of up to 75% 11-*cis*-retinoids, of which 11-*cis*-retinal bound to opsin in the retina and 11-*cis*-retinyl esters in the pigment epithelium are the major components.[29, 31] In the light, there is a major shift to the all-*trans*-retinoid congeners, with the esters being the predominant form. Dark adaptation reverses this shift.[29, 31] Since none of the enzymes of the visual cycle has as yet been completely purified or characterized, possible elements of control remain unidentified.

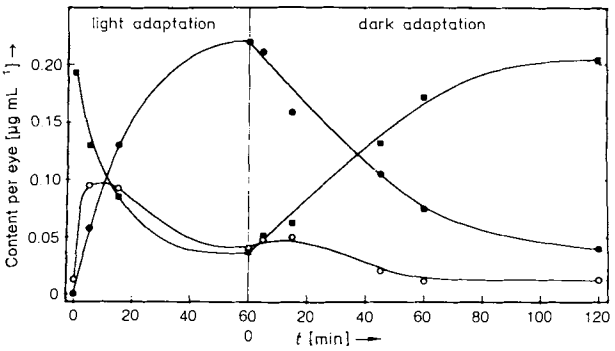

Fig. 8. Retinoid fluxes between the retina and pigment epithelium of the rat in the dark and in the light [29]. In the light the rhodopsin is bleached and the retinal is reduced and transported to the PE. The process is reversed in the dark. ▪-▪, retinal in retina; o-o, vitamin A in retina; •-•, vitamin A in pigment epithelium. (Taken from [29] with permission.)

4.2. A Thermal Isomerization Completes the Visual Cycle

In considering the nature of the isomerization process which provides the required 11-*cis*-retinoids in vision, it must first be determined if the reaction is photochemical or thermal in nature. It is quite clear that 11-*cis*-retinoids are regenerated in the dark from all-*trans*-retinoids. Furthermore, the rates of rhodopsin regeneration in dim light are independent of the wavelength of light that the animal is being exposed to.[32] These two facts support the idea that, unlike the bleaching process, the physiologically relevant reverse *trans*-to-*cis* isomerization phenomenon is purely thermal in nature. Although this presents chemical difficulties, there are clear teleological advantages in the process being a thermal enzymatic one. Two major advantages are that a thermal regeneration process will be independent of the wavelength and intensity of the ambient light and that an enzymatic process can be subjected to efficient control mechanisms unavailable in a photochemical process.

5. The Isomerization Problem

5.1. Introduction

Uncovering the nature of the isomerization reaction presents many nontrivial difficulties. One must determine both the substrate and the product of the isomerization reaction. As mentioned in Section 4.1, retinoids are found as retinols, retinals, and retinyl esters in the visual system (Fig. 9). Any one of the three all-*trans*-retinoids might be the substrate and any one of the three 11-*cis*-retinoids might be the isomerization product. A second crucial issue, which turns out to be inextricably linked to the nature of the substrate, is con-

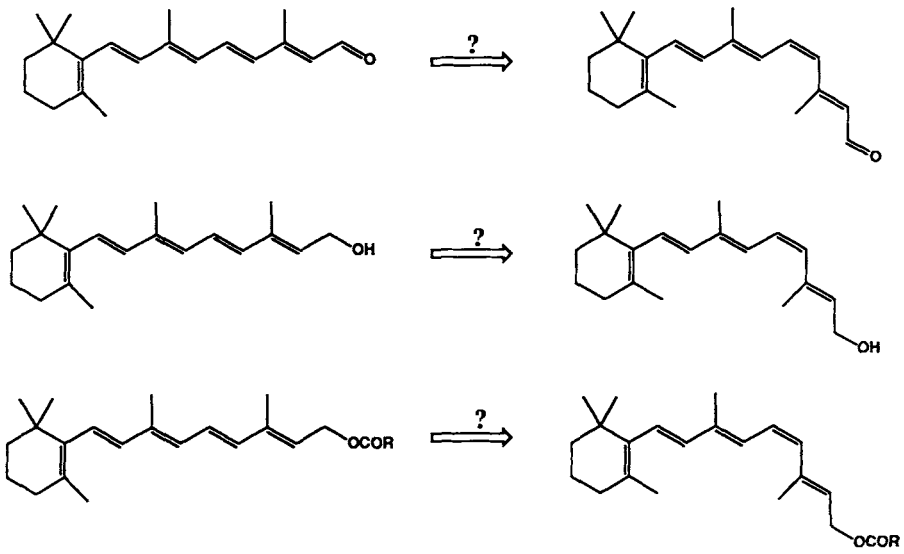

Fig. 9. Possible isomerization substrates.

cerned with where the energy comes from to drive the *trans*-to-*cis* isomerization reaction.

5.2. Thermodynamic Considerations

This thermodynamic issue was first pointed out in the 1930s by *Pauling*, who was considering carotenoid structures at the time.[33, 34] *Pauling* deduced from structural principles that certain *cis* double bonds should be unstable with respect to their all-*trans* counterparts (Fig. 10). In retinols, planar double bonds would cause the methyl groups to overlap with the hydrogen atoms indicated in Figure 10 if the polyene system as a whole remained planar. *Pauling* predicted large energetic differences between the sterically strained *cis* isomers and their *trans* counterparts due to the loss of resonance stabilization caused by a steric retreat from planarity. For example, he predicted that dividing an all-*trans*-carotenoid containing eleven double bonds into three noninteracting fragments containing three or five conjugated double bonds would raise the energy of the system by 16.1 kcal mol^{-1}.[34] As applied to the retinals, it could be estimated that 11-*cis*-retinal should be 8–9 kcal mol^{-1} higher in energy than all-*trans*-retinal.[35] It was assumed that relatively small deviations from planarity would eliminate conjugative interactions and thus resonance stabilization. Furthermore, although 7-*cis*-retinal would be predicted to be unstable, both 9-*cis*- and 13-*cis*-, as well as 9-*cis*,13-*cis*-retinal should be relatively stable (cf. Fig. 10). The 7-*cis*-retinal suffers from severe steric crowding, whereas the other isomers are relatively free of this problem.

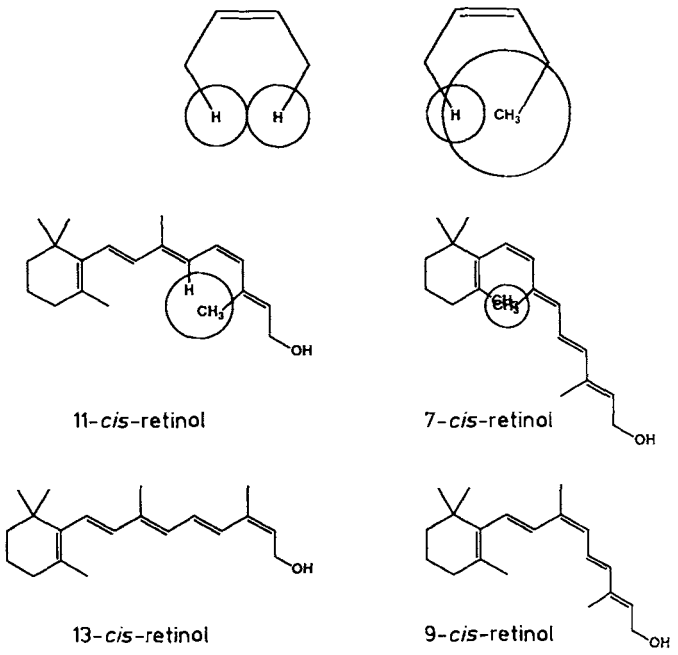

Fig. 10. Methyl–hydrogen repulsion as a source of strain in 11-*cis*-retinoids.

Early equilibrium measurements on the retinals were incorrect and greatly overestimated the stability of 11-*cis*-retinoids.[36] NMR measurements on retinal in trifluoroacetic acid showed none of the typical olefinic C–H resonances attributable to the 11-*cis* double bond, suggesting that 11-*cis*-retinal was not a major contributor at equilibrium.[37] These experiments were confirmed by HPLC measurements.[38] Furthermore, when the various isomers of the retinals and retinyl esters were brought into equilibrium with either iodine or trifluoroacetic acid, it was found that 11-*cis*-retinoids accounted for approximately 0.1 % of the equilibrium mixture.[39] The same results are obtained when the retinols are brought into equilibrium with iodine. There is a difference of 4.1 kcal mol^{-1} between 11-*cis*-retinal and its all-*trans* counterpart, with similar differences being observed between the other retinoid congeners. Since the destabilizing interaction involves intramolecular steric repulsion between the hydrogen at C10 and the methyl group at C13 (or the C13 vinyl moiety when the molecule is in the 12-s-*cis* form), the nature of the substitution at C15 does not have a marked effect on the equilibrium position. Thus, *Pauling*'s brilliant structural hypothesis is qualitatively correct. Quantitatively, it somewhat missed the mark, largely because it was not understood at the time that resonance interactions between conjugated double bonds were still possible even when the double bonds were not completely coplanar.

The three-dimensional structure of 11-*cis*-retinal has been determined by X-ray analysis and is in accord with *Pauling*'s hypothesis, because rotation about the C12–C13 bond is obvious in comparison to the structure of all-*trans*-retinal (Fig. 11).[40] In the crystalline state there is a large torsion

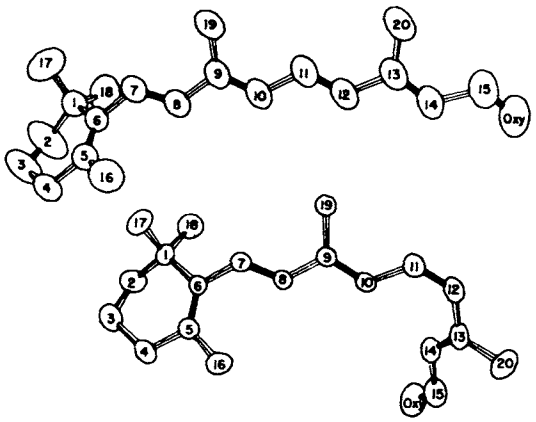

Fig. 11. X-ray structures of 11-*cis* and all-*trans*-retinal [40]. (Taken from [40] with permission.)

about the C12–C13 bond such that the C12 to O moiety is no longer coplanar with the rest of the molecule.[40] In addition, the bond angles at C11 and C12 are 127.3 and 130.3°, respectively, and the 12-s-*cis* conformer is favored.[40] Furthermore, as expected, 11-*cis* isomers are major contributors at equilibrium in both 13-desmethylretinal and the C11-substituted retinal shown in Figure 12.[41,42] In the former compound, removal of the methyl group at C13 abolishes the destabilizing steric interaction, and in the latter molecule the substituent at C11 destabilizes the all-*trans* but not the 11-*cis* configuration. It should be emphasized that destabilization of the 11-*cis*-retinoid configuration by an intramolecular steric interaction means that solvent perturbations should have little or no effect on the equilibrium position. This view has been confirmed in hydrocarbons, chlorinated hydrocarbons, and alcohols as solvents.[43] In addition, the equilibrium position is not measurably perturbed by phospholipid-based vesicles prepared from egg-yolk lecithin containing *cis*-unsaturated fatty acid esters.[44] Therefore, we can be reasonably certain that the equilibrium constraints measured in vitro will be quite relevant to the situation in vivo, and hence an energy source will have to be identified to account for the preponderance of the 11-*cis*-retinoid configuration in the eye.

5.3. Catalysis of Isomerization in Model Systems

Another concern, in addition to the thermodynamic considerations, relates to the mechanisms by which the isomerization of retinoids may be catalyzed. It is of interest to consider the thermochemistry of the uncatalyzed isomerization reactions. Here only the retinals have been seriously investigated, and then largely the conversion of 11-*cis*-retinal to all-*trans*-retinal.[36] The activation energy E_A for the purely thermal conversion is 25 kcal mol^{-1}.[36] This number is far below the bond energy of a π bond of approximately 64 kcal mol^{-1}. This means that the presumed diradical centers are strongly stabilized by the flanking double bonds—a result that is expected based on what is known about the isomerization of conjugated olefins.[45] The E_A value of 25 kcal mol^{-1} is interesting, because it means that a relatively small decrease in the E_A of approximately 5 kcal mol^{-1} would allow the reaction to occur at a significant rate at physiological temperatures. In principle, this decrease might be achieved by extending the conjugation of the polyene system even further by Schiff base formation with an aromatic amine (Fig. 13).[46] This could have biological relevance, because aromatic amines abound in nature. In fact, however, aromatic Schiff bases of the kind shown in Figure 13 actually thermally isomerize more slowly than their retinal precursors.[46]

There have been several studies on the catalyzed isomerizations of retinoids and carotenoids. Much of the early literature on this subject was concerned with free-radical-induced isomerization reactions of the carotenoids and retinoids, with iodine as the usual catalyst.[47] Clearly, the retinoids can be brought into equilibrium by free radicals, almost certainly via addition–elimination processes, but these kinds of mechanisms are probably not relevant to the biological situation.

Although Schiff base formation with the retinals in and of itself will not catalyze the isomerization reaction, protonated Schiff bases readily isomerize.[46] It is likely that base catalysis is also involved, because the isomerization rates are markedly affected by the nature of the counterions.[46] For example, the first-order rate (25 °C) of isomerization of the *N*-butylamine Schiff base of 11-*cis*-retinal catalyzed by HCl

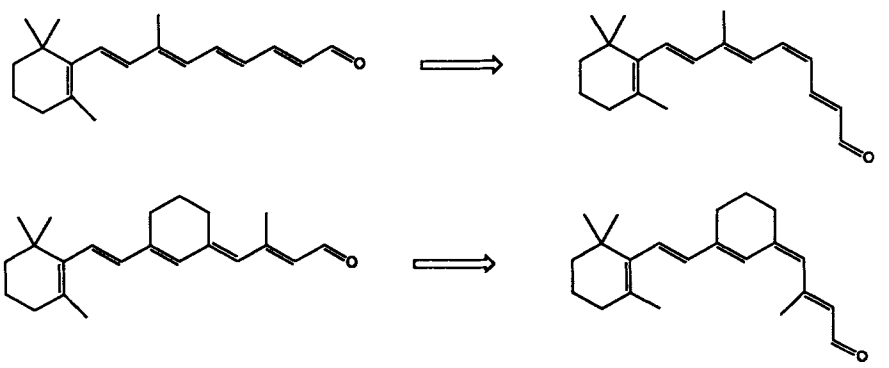

Fig. 12. Retinals in which the 11-*cis* isomer is relatively stable compared to the all-*trans* congener.

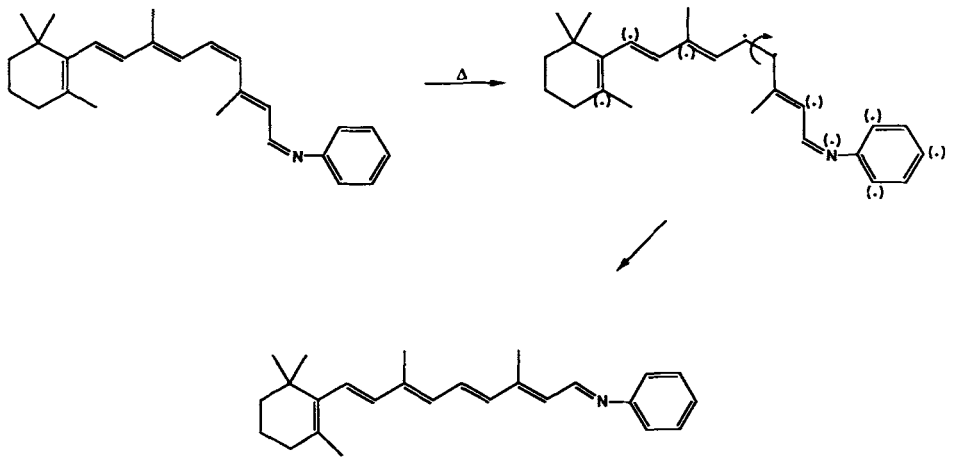

Fig. 13. Thermal isomerization of an aromatic amine Schiff base of 11-*cis*-retinal.

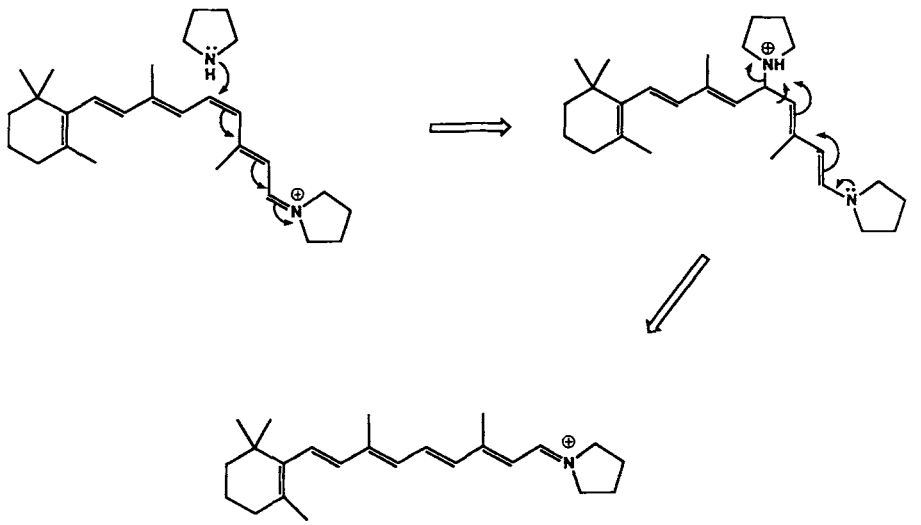

Fig. 14. Secondary amine catalysis of the isomerization of 11-*cis*-retinal.

is $2 \times 10^{-2}\ s^{-1}$, whereas, under the same conditions, it is only $2.6 \times 10^{-6}\ s^{-1}$ with trifluoroacetic acid.[46]

To explore the base-catalyzed mechanism, Schiff bases formed with secondary amines such as piperidine were studied.[46] The difficulty with protonated primary amine Schiff bases is that strong bases cannot be used as catalysts, because they will simply deprotonate the protonated Schiff base. When 11-*cis*-retinal was treated with an equivalent of piperidine hydrogen perchlorate and a catalytic amount of piperidine, the rate-limiting step in the isomerization pathway turned out to be Schiff base formation (Fig. 14).[46] Therefore, it appears that acid-base catalysis markedly enhances the rates of isomerization of retinal Schiff bases. These kinds of reactions can also occur under physiological conditions. The retinals can be isomerized both by reduced flavins[48] and by phosphatidylethanolamines.[49] Both isomerization reactions are thought to require Schiff base formation prior to the actual isomerization reaction. For catalysis by phosphatidylethanolamine, it is possible that a phosphate oxygen acts as the base.[49]

Although several model isomerization studies have been performed on the retinals, no substantial studies have been reported on the retinols or retinyl esters. Both series of compounds would be expected to form carbonium ions easily, and these could then isomerize. The reason why model isomerization studies have not been reported on these molecules might have to do with their propensities to undergo elimination reactions. At least with the retinols, it has been found that their treatment with HCl produces anhydroretinols as the major product (Fig. 15).[50]

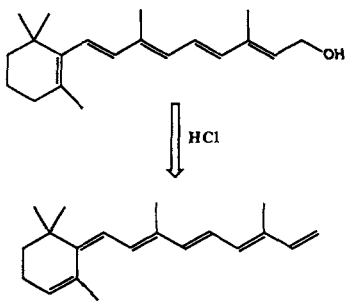

Fig. 15. Acid-catalyzed formation of an anhydroretinol from all-*trans*-retinol.

6. The Nature of the Isomerase Reaction

6.1. The Energy Source Cannot Be a Binding Protein

The key issue in approaching the isomerase question is to understand the nature of the energy source that drives the

thermodynamically uphill process. Superficially one might argue that the availability of opsin can serve as the thermodynamic sink to drive the isomerization process towards 11-*cis*-retinal formation. This could be possible in instances where there are equivalent amounts of vitamin A and opsin, but not where there are excess amounts of vitamin A, as in humans, where 11-*cis*-retinoids build up in the eye in the dark even after rhodopsin synthesis has already been completed. Another possibility for an energy source might be specific binding proteins that could recognize the 11-*cis*-retinoid moiety. Indeed, several retinoid binding proteins have been identified in the visual system, although only one of them is reported to be specific for the 11-*cis* linkage.[25] Ths binding protein, however, is only found in amounts of about 10–20% relative to vitamin A levels in the eye and hence can probably be discounted as a possible energy source. It would have to be found in at least stoichiometric amounts to be useful. Furthermore, 11-*cis*-retinyl esters, which are the major 11-*cis*-retinoid storage form, are known to exist in the pigment epithelium in an uncomplexed form in oil droplets, at least in amphibians.[51] Nevertheless, it was possible that hitherto undescribed retinoid binding proteins might be important, and it was critical to determine whether this mode of energy transduction was possible. The use of aromatic amines that "short-circuit" the visual cycle provided an unanticipated solution to this problem.

We had found that retinotoxic aromatic amines of the type shown in Figure 16 were capable of depleting previously

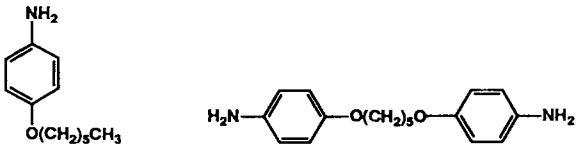

Fig. 16. Retinotoxic aromatic amines.

formed 11-*cis*-retinoids in the dark.[52–54] These molecules were capable of engaging in Schiff base formation with 11-*cis*-retinal in vitro and rapidly catalyzing its exothermic isomerization to all-*trans*-retinal in phosphatidylcholine-based vesicles (Fig. 16).[53, 54] These same Schiff bases were also found to be present in vivo after the administration of these amines. This led to the hypothesis that these aromatic amines depleted 11-*cis*-retinoids in vivo, in essence short-circuiting the visual cycle by depleting the 11-*cis*-retinal as it was formed.[53] This mechanism has important consequences for the operation of the visual cycle. First, it demonstrates that a non-energy-linked retinal isomerase cannot exist, because that is what the aromatic amines are, and their effects are entirely destructive. Second, it shows that the enzymes of the visual cycle are active in the dark. Third, it demonstrates a general mechanism of toxicity in the retina. Finally, and most importantly, it shows that specific 11-*cis*-retinoid binding proteins cannot be important as an energy source to produce these retinoids in vivo. If specific 11-*cis*-retinoid binding proteins were present, then the aromatic amines should not have depleted the endogenous 11-*cis*-retinoids.

6.2. The Nature of the Substrate in Vivo

The results described in Section 6.1 show that simple stabilization mechanisms are not in and of themselves sufficient to favor the production of 11-*cis*-retinoids. In order to begin to address the issue of the energy source, it was important first to gain some understanding of the nature of the isomerase substrate. At the time these experiments were performed, no in vitro system capable of carrying out the *trans*-to-*cis* isomerization reaction had yet been uncovered. To approach the issue of substrate, the in vivo double-labeling experiment diagrammed in Figure 17 was performed.[55] The idea behind this experiment is straightforward. A racemic mixture of [(15*S*)-^{3}H]- and [(15*R*)-^{3}H]-all-*trans*-retinol plus [15-^{14}C]-all-*trans*-retinol was administered to either rats or frogs.[55] From previous experiments we knew that this mixture would be incorporated into the visual systems of the animals. If isomerization occurs at the aldehyde level of oxidation, then one-half of the ^{3}H should be lost in the initially formed 11-*cis*-retinol (ester), whereas ^{3}H should be retained if isomerization occurs at the alcohol level of oxidation.

In an in vivo double-labeling experiment such as this, a number of implicit assumptions must be made if the results are to be interpretable. These assumptions and their conse-

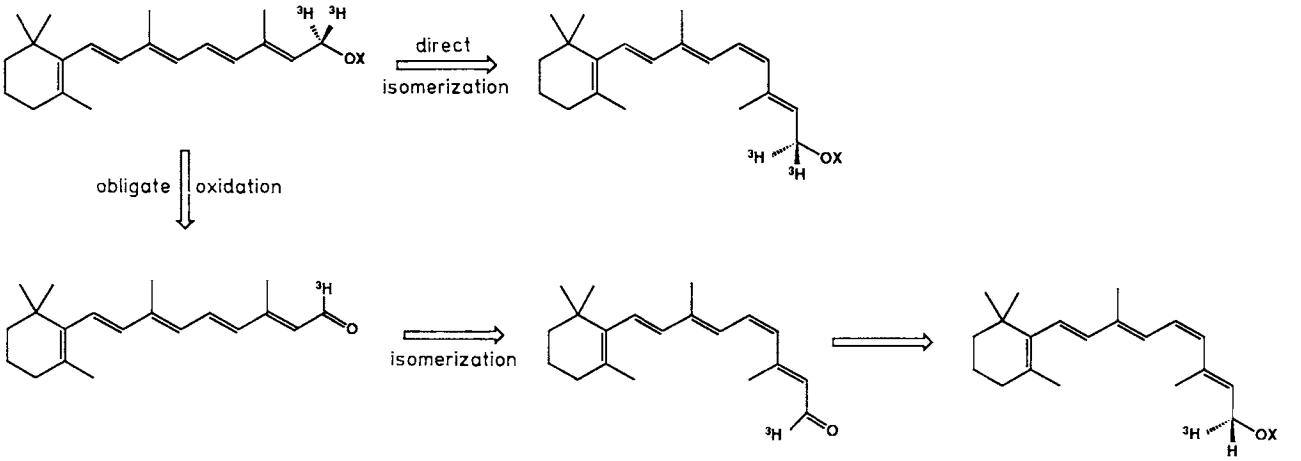

Fig. 17. Double-labeling experiment designed to determine if isomerization occurs at the alcohol or aldehyde oxidation state.

quences are as follows: (1) Nonspecific (i.e., nonenzymatic) loss of ^3H is minimal in vivo. If it were substantial, then ^3H loss might exceed the 50% limit, and the loss would be observed to continue over time. However, this type of loss is unlikely, since the ^3H label in retinol is quite resistant to exchange in protic solvents. (2) Kinetic isotope effects that would alter $^3H/^{14}C$ ratios from expected values are assumed to be small. Neither a primary ^{14}C isotope effect nor a secondary ^3H isotope effect would be expected to decrease reaction rates by even 10%. Because the ^3H label is released during oxidation, a primary ^3H isotope effect on product formation is not possible. Hence, the $^3H/^{14}C$ ratios in retinal will not be affected by possible primary isotope effects. $^3H/^{14}C$ ratios of the reactants in an oxidation reaction could be increased by a primary ^3H isotope effect, but only if the reaction had gone substantially to completion; this situation would not be expected in the experiments described here where low conversions occurred. (3) It is important that redox reactions of the retinols mediated by retinol dehydrogenases should not be too rapid relative to the isomerization time scale. However, these reactions can be slowed with retinol dehydrogenase inhibitors.

Given these assumptions, the double-labeling experiments, as performed on the rat, produced unequivocal results.[55] Approximately 70% of the ^3H of the starting material was retained in the initially formed 11-*cis*-retinyl esters, and this number could be increased to greater than 80% by the inclusion of 4-methylpyrazole, a well-known inhibitor of the retinol dehydrogenases.[55] After a long period of incubation (24 h), the ^3H loss for all of the retinoids was approximately 50%, a result that shows that only stereospecific loss of ^3H occurred. (The issue of the stereochemistry of the dehydrogenases will be further addressed in Section 6.4.) Thus, isomerization must occur at the alcohol level of oxidation; that is, all-*trans*-retinal cannot be the substrate. Although these experiments still leave both ester and alcohol as possible substrates, they favor the former, because, under all conditions, the recovered all-*trans*-retinol had lost 50% of its ^3H and hence could not easily have served as an isomerase substrate, given that the products retained substantially greater than 50% ^3H. The all-*trans*-retinyl esters, on the other hand, retained approximately 90% of their ^3H and hence could be isomerase substrates.

6.3. 11-*cis*-Retinoid Regeneration in Vitro

As mentioned in Section 4, *Kühne*[1] demonstrated that a bleached frog retina would not regenerate its visual pigment unless it was placed in contact with its pigment epithelium. The usual experience of subsequent investigators was that 50–85% pigment regeneration occurs in these in vitro preparations after a single strong bleaching.[29, 56–58]

However, even this degree of regeneration might be accounted for by the use of endogenous, preformed 11-*cis*-retinoids for rhodopsin regeneration, without any de novo biosynthesis of these retinoids prior to regeneration, especially if the preparations had not been adequately bleached to deplete stores of 11-*cis*-retinyl esters in the pigment epithelium. This possibility, along with the repeated failures to demonstrate a retinal isomerase or, for that matter, any retinoid isomerase, led to a hypothesis that perhaps the biosynthesis of 11-*cis*-retinoids does not occur outside the living organism, either because a necessary efferent neural input controlling dark adaptation is disrupted when the optic nerve is severed, or perhaps because the in vitro culture systems are inadequate to maintain tissue viability.

Initial investigation of this problem proved that efferent neural control of rhodopsin regeneration does not occur, because, when the optic nerve was severed unilaterally in living frogs, both of the animal's eyes regenerated rhodopsin at an identical rate.[59] When amphibian eyecup preparations (in which there is an intact retina and pigment epithelium) were placed in an amphibian tissue culture medium, clear evidence for the de novo biosynthesis of 11-*cis*-retinoids was obtained.[59] Rhodopsin regeneration occurred after repeated bleaching–regeneration cycles, and unambiguous data for the de novo biosynthesis of 11-*cis*-retinyl esters in these eyecup preparations was also obtained.[59]

Based on the experiments described above, it was of interest to simplify this in vitro 11-*cis*-retinoid biosynthetic system to facilitate its eventual characterization and purification. A $600 \times g$ supernatant membrane preparation from amphibian retina/pigment epithelium proved capable of converting added all-*trans*-retinol into a mixture of 11-*cis*-retinol, 11-*cis*-retinal, and 11-*cis*-retinyl palmitate.[60] All-*trans*-retinyl palmitate and all-*trans*-retinal were also generated by these membranes. A time-dependent, approximately linear increase in the absolute amount of [^3H]-11-*cis*-retinol formed was found, while, in the absence of eye tissue, none was produced.[60] In Figure 18A, data are shown for the relative amounts of the various isomers of [^3H]retinol present as a function of time in an incubation with eye tissue. It is clearly shown that [^3H]-13-*cis*-retinol, a retinol isomer of no known visual function, is not formed in substantial amounts. Figure 18B gives the results of a control experiment in which retina/pigment epithelium supernatant was not included. A small amount of nonspecific isomerization of all-*trans*-retinol to 13-*cis*-retinol was observed, but a measurable amount of 11-*cis*-retinol was not formed. As would be expected of a biologically significant process, the membrane-bound 11-*cis*-retinoid biosynthetic activity proved to be heat sensitive.[60] Intact protein and membrane are required, because activity was abolished by treatment with proteinase K or phospholipase C.[61]

Great care was taken not to misidentify the 11-*cis*-retinoids produced by the membrane system, since this has been a source of serious errors in the past. The 11-*cis*-retinoids described were identified by both chromatographic and chemical means.[60] When biosynthetically formed 11-*cis*-retinol was chromatographically purified and either isomerized with iodine or esterified with palmitoyl chloride, it behaved identically to authentic material.[60]

The results described above unequivocally demonstrate the presence of an 11-*cis*-retinoid biosynthetic activity which was able to produce substantial quantities of 11-*cis*-retinoids. For example, 11-*cis*-retinol could constitute up to 40–50% of the isolated retinol pool, a figure far removed from the equilibrium value. It was of interest to determine whether the isomerase activity is located in the retina or the pigment epithelium and to determine the precise nature of the substrate for isomerization. Studies on the amphibian

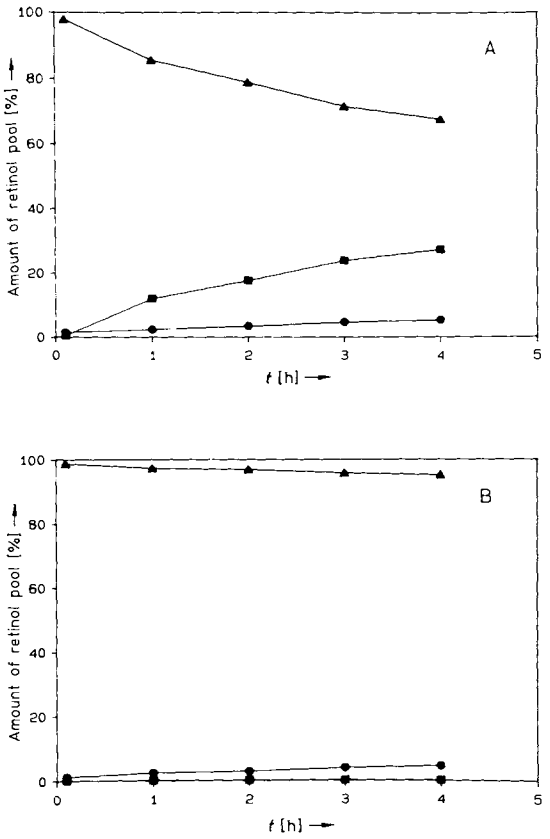

Fig. 18. Isomeric distribution of [^{3}H]retinol during in vitro incubation [60]. 1.0 mL of 600 × g supernatant from light-adapted retina pigment epithelium of two frog eyes (A) or 1.0 mL of phosphate buffer (B) was incubated in the dark with 50 μL of 10% bovine serum albumin and 4 μCi of [11,12-^{3}H]-all-*trans*-retinol in 4 μL of ethanol. Hexane extraction and HPLC analysis of [^{3}H]retinol isomers were performed hourly on 200-μL samples. ■-■, [^{3}H]-11-*cis*-retinol; ●-●, [^{3}H]-13-*cis*-retinol; ▲-▲, [^{3}H]-all-*trans*-retinol. (Taken from [60] with permission.)

showed that the isomerization activity was almost entirely located in the membranes of the pigment epithelium.[60] The trivial amount of activity found in the retinal fraction was almost certainly due to contamination by a small amount of adherent pigment epithelium. The isomerization activity has also been observed in the bovine system, where a more complete separation of the retina from the pigment epithelium is possible, and there the activity was found only in the pigment epithelium membranes.[62]

These results explain why previous attempts to obtain pigment regeneration by adding various all-*trans*-retinoids to isolated retinas were negative.[63, 64] On the other hand, they are in conflict with two published reports in which it was claimed that pigment epithelium tissue and homogenates derived from it were incapable of transforming added all-*trans*-retinol into any 11-*cis*-retinoids.[65, 66] However, these reports are now known to be in error because the all-*trans*-retinol was added in 2–4% ethanol in the absence of any carrier protein. The membrane-bound isomerization system is denatured under these conditions.[60, 61] The successful demonstration of isomerase activity in the pigment epithelium membranes depended on the use of very low ethanol levels, 0.5% bovine serum albumin as carrier, and the detection and confirmation of the 11-*cis*-retinol product.[60] Recently, it has been demonstrated that added all-*trans*-retinol is processed into 11-*cis*-retinoids by intact pigment epithelium cultures.[67, 68]

6.4. Substrate Specificity of the Isomerase

Since labeled all-*trans*-retinol can be converted into all-*trans*-retinal, all-*trans*-retinyl palmitate, and the three 11-*cis* congeners by the pigment epithelium membrane preparation described in Section 6.3, it cannot be assumed that all-*trans*-retinol is the substrate for the isomerase system or that 11-*cis*-retinol is the direct product of the isomerase action. The possibility that all-*trans*-retinal is the isomerization substrate was easily ruled out. Both unwashed membranes and membranes thoroughly washed to remove nicotinamide-based cofactors were able to isomerize added all-*trans*-retinol equally well.[60] However, only the unwashed membranes, in which redox reactions occur, substantially processed all *trans*-retinal. In the bovine system, isolated pigment epithelium membranes will not isomerize all-*trans*-retinal to 11-*cis*-retinal.[62] The proposition that free all-*trans*-retinal cannot be the isomerization substrate was directly demonstrated by the finding that [15-^{3}H,15-^{14}C]-all-*trans*-retinol is processed to 11-*cis*-retinol by the native frog and bovine pigment epithelium membranes with complete retention of the tritium label (Fig. 19).[61] This result is completely consistent with the in vivo variant of the double-labeling experiment described in Section 6.2[55] and rules out the possibility that free all-*trans*-retinal is the isomerase substrate, since tritium would be lost if the retinol were oxidized before isomerization.

The experiments described above show that retinal cannot be the substrate, but they do not distinguish between retinol and retinyl palmitate as possible substrates. When all-*trans*-retinol is processed by bovine pigment epithelium membranes that have been irradiated with UV light and washed, virtually all of the retinol is esterified to form retinyl esters (Fig. 20 A).[69] Subsequently, 11-*cis*-retinol is produced concomitant with a decrease in the amount of all-*trans*-retinyl esters. Furthermore, when all-*trans*-retinyl palmitate is processed by these membranes, 11-*cis*-retinol is produced, as shown in Figure 20 B.[69] Other retinyl esters, such as the oleate and decanoate esters, are also processed to 11-*cis*-retinol, but not to their corresponding 11-*cis*-retinyl esters.[70] Although these experiments taken together do not prove the point unequivocally, they strongly suggest that retinyl esters are the actual isomerase substrates and that the esters are directly converted into 11-*cis*-retinol. The ramifications of this kind of process will be discussed in Section 7.1, when energetic questions are addressed.

The specificity of the isomerase system towards particular retinol isomers is considerable. In washed pigment epithelium membranes, added 9-*cis*- and 13-*cis*-retinol are efficiently esterified; however, neither is isomerized to a significant extent.[61] Methylated analogues of all-*trans*-retinol such as the *O*-methyl and 15-methyl derivatives have been studied. The *O*-methyl ether derivative is completely inactive, whereas the 15-methyl derivative is an exceedingly weak substrate for the isomerase.[71] Thus, the isomerase system appears to be highly specific for all-*trans*-retinoids.

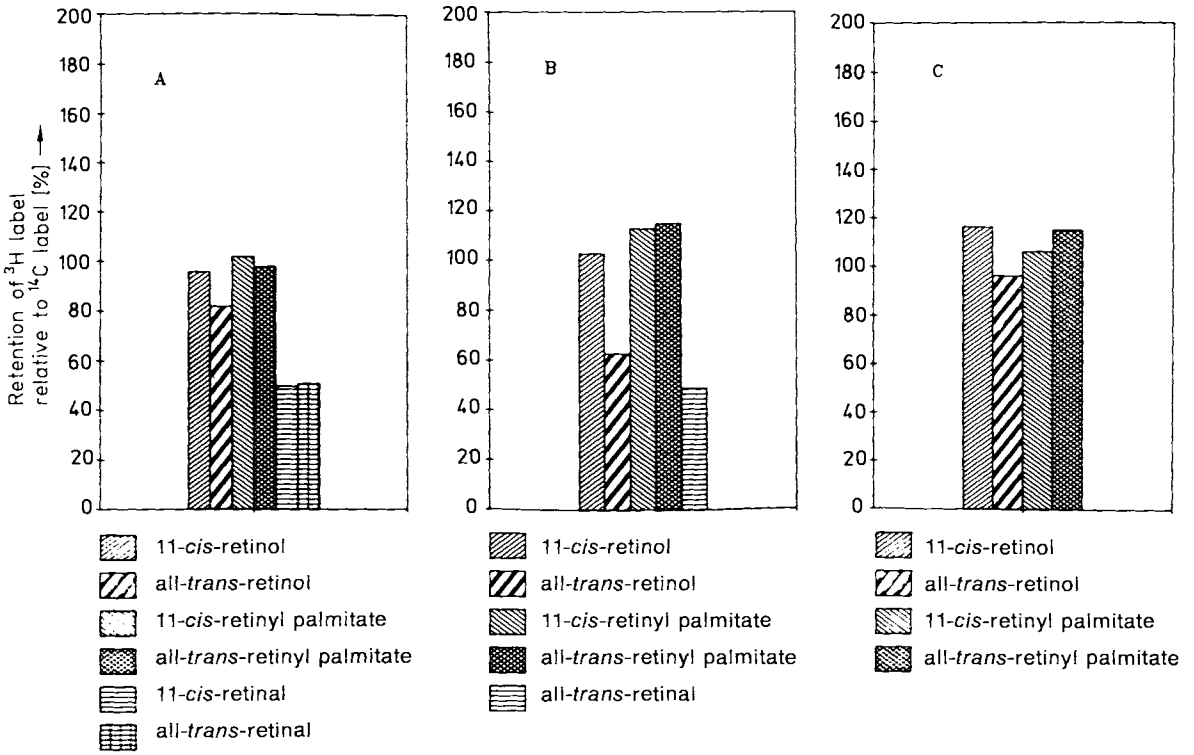

Fig. 19. Double-labeling experiments on frog epithelium 600 × g supernatant (A), on frog retina pigment epithelium washed 600 × g particulate fraction (B), and on bovine pigment epithelium 150000 × g particulate fraction (C) [61]. A) A mixture of [15-^{3}H]- and [15-^{14}C]-all-*trans*-retinol containing 0.1 μCi of ^{3}H (^{3}H:^{14}C = 5.2:1) was incubated with 4 mL of retina pigment epithelium 600 × g supernatant from four light-adapted *Rana pipiens* frogs and 100 μL of 10% bovine serum albumin for 3 h at room temperature. The retinoids were analyzed by standard methods. B) The washed 600 × g particulate fraction was prepared by two successive pelletings of the 600 × g supernatant at 50000 g for 20 min at 4 °C, followed by resuspension each time in the original volume of buffer. A mixture of [15-^{3}H]- and [15-^{14}C]-all-*trans*-retinol containing 0.1 μCi of ^{3}H (^{3}H:^{14}C = 5.2:1) was incubated with 4 mL of retina pigment epithelium washed 600 × g particulate fraction from four light-adapted *Rana pipiens* frogs at room temperature for 3 h. The retinoids were analyzed by standard methods. No appreciable radioactivity associated with 11-*cis*-retinal was found. C) The same amount of [^{3}H]- and [^{14}C]-labeled all-*trans*-retinol in 100 μL of 10% bovine serum albumin (as retinol carrier) was incubated with 3 mg of protein from bovine pigment epithelium suspended in 4 mL of 50 mM phosphate buffer (pH 7.2) at 35 °C for 1 h. The retinoids were analyzed by standard methods. This homogenate preparation is essentially free of redox activity since appreciable quantities of 11-*cis*- and all-*trans*-retinal were not formed. All four retinoid isomers analyzed completely retained their ^{3}H label. (Taken from [61] with permission.)

The specificity of the isomerase described above needs to be reconciled with the observed lack of stereospecificity found in vivo.[72] It is a fact that the intraocular injection of [15-^{14}C]-13-*cis*-retinol and [11,12-^{3}H]-all-*trans*-retinol leads to the incorporation of both isotopes into rhodopsin with roughly equal efficiency.[72] This in vivo result can also be reproduced in vitro under appropriate conditions. For example, with unwashed pigment epithelium membranes, 13-*cis*-retinol appears to be isomerized to 11-*cis*-retinoids approximately as rapidly as all-*trans*-retinol itself.[61]

These results can be reconciled when it is realized that unwashed membranes contain nicotinamide-based cofactors along with the enzymes necessary to oxidize the added 13-*cis*-retinol to 13-*cis*-retinal. Nonenzymatic isomerization of 13-*cis*-retinal gives all-*trans*-retinal, which is then reduced to all-*trans*-retinol. The kinetically facile and thermodynamically favorable isomerization of 13-*cis*-retinal to all-*trans*-retinal has previously been shown to occur in the presence of phosphatidylethanolamine or lipids derived from the retina.[49] Indeed, the retinals are readily isomerized by various primary and secondary amines (cf. Section 5.3).[46] The possible physiological significance of this "chemical" isomerization pathway remains to be determined, although it would explain why 13-*cis*-retinoids are not normally found in the eye. The rapid chemical and non-isomerase-mediated isomerization of 13-*cis*-retinal to all-*trans*-retinal, followed by the reduction of the latter to the isomerase system precursor, all-*trans*-retinol, could rapidly utilize any 13-*cis* retinoids present and would act as a form of salvage pathway.

Structure–activity studies were also performed on a variety of dihydroretinols (Fig. 21).[73] None of the dihydro isomers was substantially processed into its 11-*cis* counterpart, although vitamin A_2 (3,4-didehydro-all-*trans*-retinol) was. Thus, an intact polyene chain is essential if a molecule is to be an isomerase substrate.[73] The mechanistic ramifications of this will be discussed in Section 8. It is interesting to note that vitamin A_2 is an important visual chromophore in early amphibian development and, as mentioned, was processed by the isomerase system.[73]

6.5. Biochemical Characterization of the Isomerase System

As already mentioned in Section 6.3, the isomerase system is membrane bound. The isomerase activity can be removed from the supernatant by centrifugation, with the concomitant appearance of the activity in the pellet.[60] The isomer-

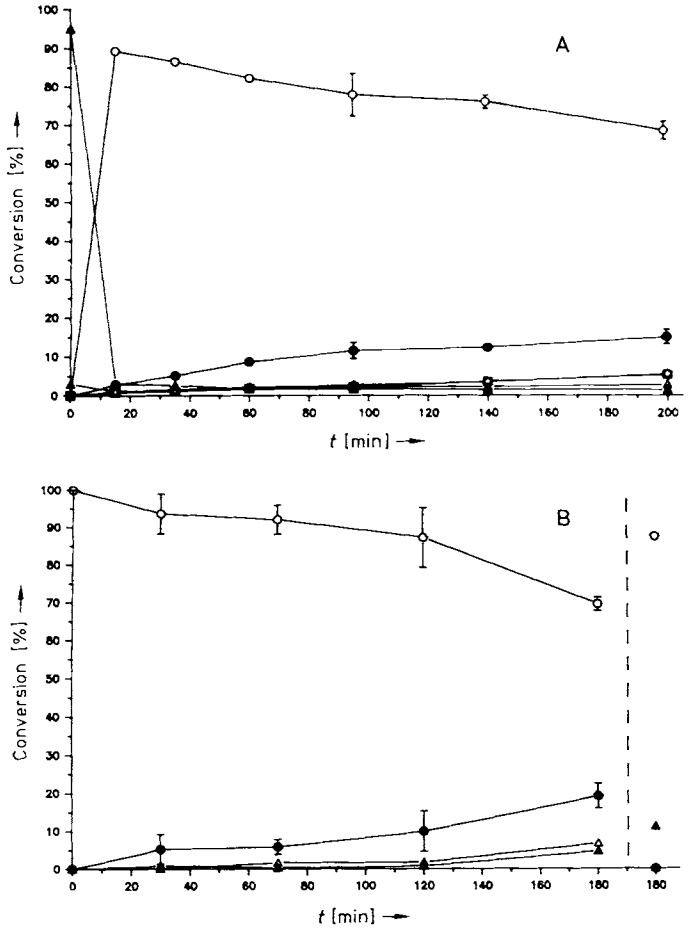

Fig. 20. Processing of vitamin A (A) and all-*trans*-retinyl palmitate (B) by irradiated pigment epithelial membranes [69]. A) Bovine pigment epithelial membranes were irradiated and washed. The membranes (2 mg mL^{-1}) were incubated with 0.05 μM of [11,12-$^3H_2$]-all-*trans*-retinol (50 Ci mM^{-1}, Amersham) and bovine serum albumin. In the absence of membranes no 11-*cis*-retinol was formed. At the indicated times, the retinoids were extracted with methanol–hexane and analyzed by HPLC. Individual experiments were run in duplicate and repeated several times. Small amounts of the retinals (<5%) were also found after incubation. B) Membranes were incubated with synthetic [^{3}H]-all-*trans*-retinyl palmitate (0.3 μM, 5 Ci mM^{-1}). At the indicated times samples were removed, and the retinoids were analyzed as in A. Control incubations in the absence of membranes showed substantially larger amounts of all-*trans*-retinol formed (approximately 10% of the total radioactivity at end of incubation) than in the case where membranes were added. ○-○, retinyl esters; ●-●, 11-*cis*-retinol; △-△, 13-*cis*-retinol; ▲-▲, all-*trans*-retinol. (Taken from [61] with permission.)

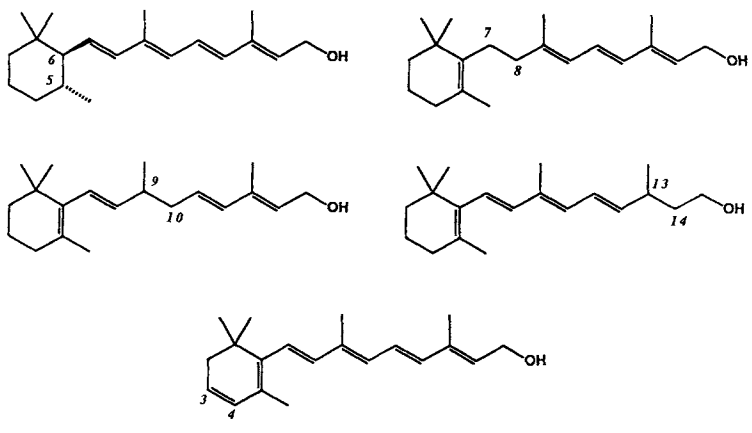

vitamin A_2

Fig. 21. Dihydroretinoids and vitamin A_2 as isomerase substrates.

ization activity also appears to distribute, without great preference, throughout the various membrane fractions, as determined by centrifugation studies.[62] These studies are complicated by the large amount of ester synthetase activity that appears to comigrate with the isomerase activity.[60, 62] However, extensive sonication of amphibian PE membranes produced a 100 000 × g supernatant of light membranes so strongly depleted in their ability to process all-*trans*-retinol by routes other than isomerization that less than 8% of the added retinol was esterified.[61] The isomerase activity in these membranes was saturable upon addition of all-*trans*-retinol, as required of a biologically significant process, and showed an apparent V_{max} of 5 pmol h^{-1} per milligram of protein and an apparent K_M of 0.8 μM. The origin of this low V_{max} value is discussed below. The pH optimum is 8.0.[61] In a less purified 600 × g supernatant, it is estimated that the V_{max} is 100 pmol h^{-1} per eye. This value is a lower limit, because a substantial portion (approximately one-half) of the isomerase activity remains in the 600 × g pellet, and activity is lost during homogenization. In living *Rana pipiens* frogs, the rate of 11-*cis*-retinoid synthesis during dark adaptation is 1–2 nmol h^{-1} per eye, and 11-*cis*-retinyl palmitate is formed during prolonged darkness about one tenth as fast.[29, 31] Therefore, even in the absence of any unknown rate-limiting cofactors, the in vitro rate of 11-*cis*-retinoid formation is substantial and comparable to the physiological rate.

In a 600 × g supernatant from bovine pigment epithelia, the V_{max} for isomerization is approximately 1 nmol h^{-1} per milligram of protein. The low V_{max} described above in the amphibian case was measured in a system that had purposefully been depleted of ester synthetase activity. Later experiments demonstrated that the esters are obligate intermediates in the isomerization process. This explains the much higher rates found with crude membranes compared to membrane preparations that had been depleted of their ester synthetase activity.

Although the isomerase and ester synthetase activities are quite easily destroyed by a wide range of detergents, it has recently proven possible to find adequate detergents for their solubilization and further purification.[74]

6.6. Detergent Solubilization and Partial Purification of the Isomerase and Ester Synthetase

The isomerase and ester synthetase enzymes are readily denatured by a wide variety of detergents.[61] However, we have recently been able to solubilize both activities successfully in the zwitterionic detergent Zwittergent-3,14 [3-(*N*,*N*-dimethyl-*N*-tetradecylammonio)-1-propanesulfonate].[75] Using ion exchange and gel filtration chromatography, the ester synthetase was purified approximately 200-fold.[74] The isomerase was purified approximately 10–14-fold after anion exchange chromatography.[74]

Several interesting observations were made on the enzymes as a consequence of these purification studies. As previously mentioned (Section 6.4), PE membranes are capable of producing retinyl esters from added retinols in the absence of added acylating agents, such as fatty acyl CoA derivatives. This was first discovered by *Krinsky*[75] and sug-

gests that the membranes themselves contain the acyl donors. Solubilization and substantial purification of the retinyl ester synthetase readily revealed the source of the acyl donor. It is the membrane constituent lecithin (phosphatidylcholine), and the transfer occurs from the 1-position of the phospholipid to the retinol, producing a retinyl ester and a 2-acyl lysophospholipid (Fig. 22).[74] Hence, the enzyme is a lecithin:retinol acyltransferase (LRAT). Similar

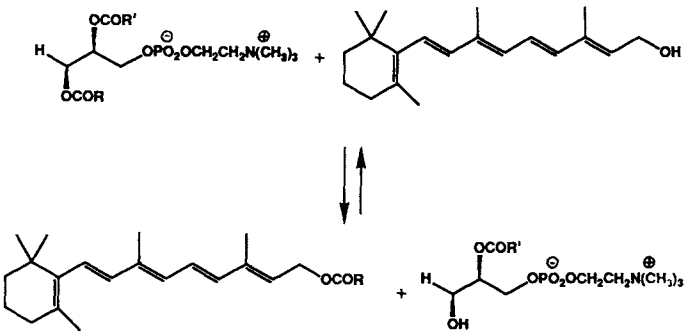

Fig. 22. Transesterification of retinol with phosphatidylcholine (lecithin) catalyzed by the enzyme lecithin:retinol acyltransferase (LRAT).

conclusions were drawn by *Saari* et al. working with crude membrane fractions.[76] Thus, the retinyl ester synthetase operates by a transesterification route similar to that found in the liver.[77] Of interest is the fact that this reaction is reversible and could liberate retinol from a retinyl ester by a back transesterification without hydrolysis in vivo. This would obviously save energy because, when retinol is required, it can be formed without, in effect, requiring the hydrolysis of a phospholipid. A second point of interest is that the isomerase and ester synthetase activities copurified after anion exchange and gel filtration chromatography, suggesting the possibility of a multienzyme complex or some other functional linkage.[74]

7. Finding the Energy Source

7.1. Retinyl Esters Are the Isomerase Substrates

As stated in Section 6.3, pigment epithelium membranes are capable of processing added vitamin A into 11-*cis*-retinoids in the absence of added energy sources. The fact that thorough washing of the membranes did not seem to affect isomerase activity suggests that it is not a soluble energy source that provides the needed energy. Indeed, the addition of high-energy compounds, such as MgATP, MgGTP, or palmitoyl CoA, to the preparations did not stimulate isomerase activity.[61] An issue of some interest relates to the energization mechanism. In vivo experiments with aromatic amine isomerization catalysts would appear to rule out the possibility that hitherto undescribed binding proteins provide the necessary energy. Other mechanistic possibilities must be entertained to explain the energy-requiring isomerization process. The possibility that an irreversible process might provide the energy was eliminated when it was shown that all of the reactions of the visual cycle are reversible.[69] Thus, another type of energy source must be considered.

The intriguing relationship existing between endogenous retinyl ester synthesis and isomerization provides the key.[62] Thus far, studies on the membrane localization of the isomerase and of the ester synthetase activities have shown that the two activities cannot be dissociated from one another either by differential or density gradient centrifugation studies. As mentioned in Section 6.6, the solubilized enzymatic activities also copurify. Finally, chemically diverse reagents, such as ethanol, hydroxylamine, and *p*-hydroxymercuribenzoate, all appear to inhibit both activities in a roughly parallel manner.[62] Ethanol can denature enzymes. Hydroxylamine is an agent known to inhibit retinyl ester synthesis, presumably because it can react with a high-energy acyl intermediate.[75] The observation that both ester synthetase and retinoid isomerase activities are inhibited to approximately the same degree by pretreatment with hydroxylamine suggests a linkage between the two enzymatic processes. The results with *p*-hydroxymercuribenzoate, an alkylating agent specific for sulfhydryl groups, are equally striking.[62] This reagent affects both activities in a roughly parallel, multiphasic fashion, implying that the two activities are linked in a fundamental way.

Recent studies using all-*trans*-retinyl α-bromoacetate as a specific inhibitor of retinyl ester synthesis by the pigment epithelial membranes bear importantly on the issue of the actual substrate of the isomerase.[78] In the pigment epithelial system, all-*trans*-retinyl α-bromoacetate does not inactivate the synthetase, but rather, at micromolar concentrations, is an exceedingly potent inhibitor of it. When pigment epithelial membranes are pretreated with this molecule and then with all-*trans*-retinol, there is virtually no ($< 5\%$) conversion of the vitamin to retinyl esters and no 11-*cis*-retinoids are generated. However, when the membranes were first treated with all-*trans*-retinol, producing largely all-*trans*-retinyl esters, and then were treated with inhibitor, 11-*cis*-retinol production proceeded close to control levels (i.e., with no added inhibitor). These experiments leave little doubt that it is an all-*trans*-retinyl ester and not all-*trans*-retinol that is processed to 11-*cis*-retinol and that retinyl ester formation is an obligate part of the isomerase pathway. Had a direct isomerization of all-*trans*-retinol to 11-*cis*-retinol occurred, then pretreatment of the membranes with all-*trans*-retinyl α-bromoacetate should have enhanced the isomerization, since less substrate would have been lost to ester formation. Furthermore, it was also found that, in the presence of inhibitor, all-*trans*-retinyl esters were processed into 11-*cis*-retinol without the formation of 11-*cis*-retinyl esters. This experiment eliminates an ester–ester isomerization route from consideration.

Why might the linkage of ester synthesis to isomerization be of interest? Esters are "high-energy" compounds and are hydrolyzed with free energies of hydrolysis of around $-5\ \text{kcal mol}^{-1}$.[79] If the free energy of hydrolysis of an ester could be coupled to the isomerization process, more than enough energy would be provided to drive the latter process. The free energy of any complex chemical reaction can be calculated if it can be formally broken down into

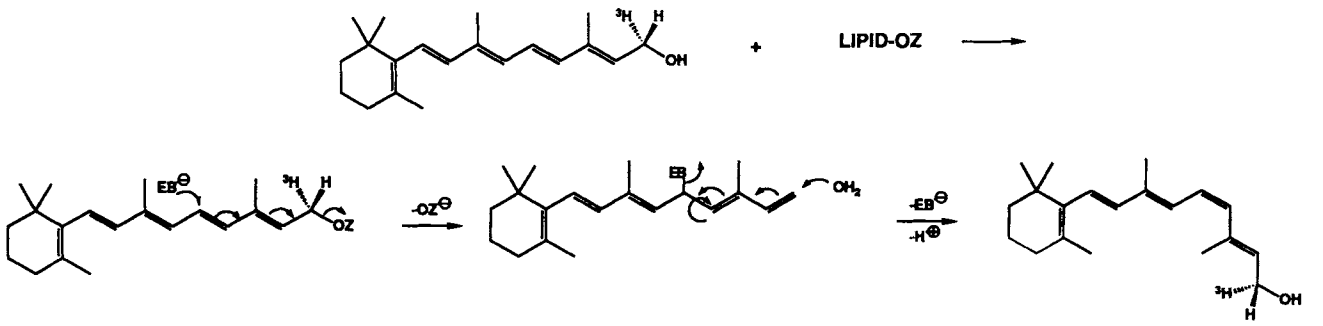

Fig. 23. A coupled reaction can drive the thermodynamically unfavorable isomerization reaction [69]. $EB^{\ominus}$ = enzyme active-site nucleophile; $OZ^{\ominus}$ = carboxylate.

all-*trans*-retinyl ester + H_2O	→ all-*trans*-retinol	$\Delta G^0 \approx -5$ kcal mol^{-1}
all-*trans*-retinol	→ 11-*cis*-retinol	$\Delta G^0 \quad +4$ kcal mol^{-1}
all-*trans*-retinyl ester + H_2O	→ 11-*cis*-retinol	$\Delta G^0 \quad -1$ kcal mol^{-1}

simpler chemical reactions whose free energy changes are known. As applied here, the energies sum as shown in Figure 23 to yield a possible mechanism by which ester hydrolysis could be linked to isomerization.[69] Here, the substrate would be an all-*trans*-retinyl ester, and the product, 11-*cis*-retinol. The enzyme catalyzing the isomerization reaction is actually an "isoesterase" rather than a simple isomerase. The isomerization reaction is here broken down into two independent reactions. The overall free energy change is the sum of the free energy changes of the two component reactions, resulting in an exothermic isomerization. It is important to note that these two reactions do not occur independently of one another. Most interestingly, the energy to drive the reaction would originate in the membrane phospholipids, since retinyl esters arise by a transesterification reaction with lecithin. In this case, therefore, the phospholipids would act as an ATP surrogate.

That an all-*trans*-retinyl ester is the substrate for isomerization is consistent with previous observations. As already mentioned in Section 6.4, added all-*trans*-retinol is rapidly processed to all-*trans*-retinyl esters prior to the formation of 11-*cis*-retinol.[60, 69] In addition, all-*trans*-retinyl esters are processed to form 11-*cis*-retinol by the isomerase-containing membranes.[69] Finally, the in vivo double-labeling experiments using [(15*S*)-^{3}H]- and [(15*R*)-^{3}H]-all-*trans*-retinol plus [15-^{14}C]-all-*trans*-retinol showed that only the all-*trans*-retinyl esters were of high enough specific activity to serve as 11-*cis*-retinoid precursors.[55] The mechanism shown in Figure 23 also makes understandable the structure–activity studies performed on the dihydroretinoids. Finally, the experiments with the retinyl ester synthetase inhibitor all-*trans*-retinyl α-bromoacetate described above are also fully consistent with this mechanism.

7.2. C–O Bond Cleavage Accompanies Isomerization

The mechanism shown in Figure 23 allows experimentally testable predictions. One prediction is that C–O bond cleavage accompanies isomerization. Furthermore, this cleavage could have an effect on the stereochemistry of suitably labeled retinoids at C15, since the prochiral center becomes symmetrical at the intermediate state. The prediction of C–O bond cleavage was readily testable by studying the fate of the ^{18}O of [15-^{18}O]-all-*trans*-retinol after enzyme-catalyzed isomerization in $H_2{}^{16}O$-containing buffer using field desorption mass spectrometry.[69] This experiment demonstrated unequivocally that the 11-*cis*-retinol product formed contained only ^{16}O (Fig. 24).[69] Hence, complete cleavage and replacement of the C–O bond accompanies isomerization.

7.3. Stereochemical Course of the Reactions Catalyzed by the Isomerase and Related Enzymes

The ^{18}O release experiments (Fig. 24) are consistent with the type of mechanism shown in Figure 23. Since this mechanism proposes that C15 undergoes an sp^3-to-sp^2 conversion during isomerization, it is possible to probe this process with stereochemical experiments. It was of interest to determine whether retention or inversion occurs at C15 as a consequence of the isomerization reaction (Fig. 25).

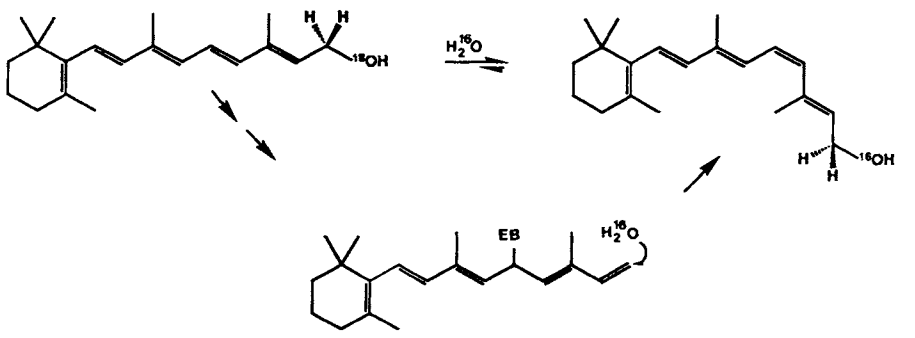

Fig. 24. The isomerization reaction occurs with C–O bond cleavage.

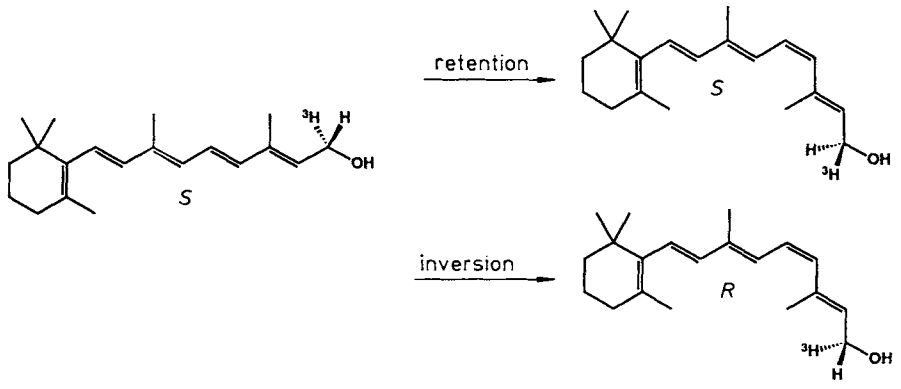

Fig. 25. Isomerization can occur with retention or inversion of stereochemistry at the C15 prochiral center of vitamin A.

To this end, stereochemical experiments were performed using chirally labeled [(15*R*)-^{3}H]- and [(15*S*)-^{3}H]-all-*trans*-retinol.[80] [(15*S*)-^{3}H]-all-*trans*-Retinol was prepared by the reduction of [15-^{3}H]-all-*trans*-retinal with horse liver alcohol dehydrogenase (HLADH) and NADH.[80] [(15*R*)-^{3}H]-all-*trans*-Retinol was prepared by incubation of all-*trans*-retinol with [α-^{3}H]benzyl alcohol, HLADH, and NAD. The labeled retinols, along with [15-^{14}C]-all-*trans*-retinol, were incubated with either amphibian or bovine pigment epithelial membranes.[80] At the end of the incubation period, the retinols and retinyl esters were collected and analyzed. The analyses of the isolated retinols and retinyl esters were performed as indicated in Figure 26. The enzymatically formed 11-*cis*-retinol was isomerized with I_2, which is without effect on the stereochemistry at C15, to produce all-*trans*-retinol. The retinyl esters were hydrolyzed to produce the corresponding retinols. Then, using HLADH, it could readily be decided if inversion or retention of absolute configuration had occurred.[80]

The results were striking in that, within experimental error, complete inversion of configuration had occurred as a consequence of isomerization in both the bovine and amphibian cases.[80] This result can be interpreted mechanistically with the addition of two further pieces of information to the fact that the C–O bond is cleaved during isomerization. First, isomerization must occur at the alcohol oxidation state, and, second, it is highly improbable that there is a mechanism by which enzyme-bound all-*trans*-retinol is oxidized to retinal followed by isomerization and reduction at the opposite face to produce 11-*cis*-retinol, because no evidence for any isotope effect has been found. This kind of mechanism would predict a primary isotope effect that would be extremely large, since it would be the product of two separate isotope effects. Furthermore, added all-*trans*-retinal is not isomerized.

The stereochemical inversion result is readily understandable in terms of the mechanism shown in Figure 23 and supports this mechanistic interpretation. The inversion of stereochemistry during isomerization allowed us to determine that the isomerase acts in reverse.[69] Chirally labeled 11-*cis*-retinol is processed by the isomerase to produce all-*trans*-retinol of the opposite absolute stereochemistry.[69] 11-*cis*-Retinol is relatively unstable with respect to isomerization, but it isomerizes to all-*trans*-retinol with the expected retention of absolute configuration at C15.

In chemical reactions in solution it is possible to interpret the result of a stereochemical experiment mechanistically. In the case of enzymes, however, a straightforward interpretation is often not possible. It is of interest to consider further the inversion result obtained here. Because of the approxi-

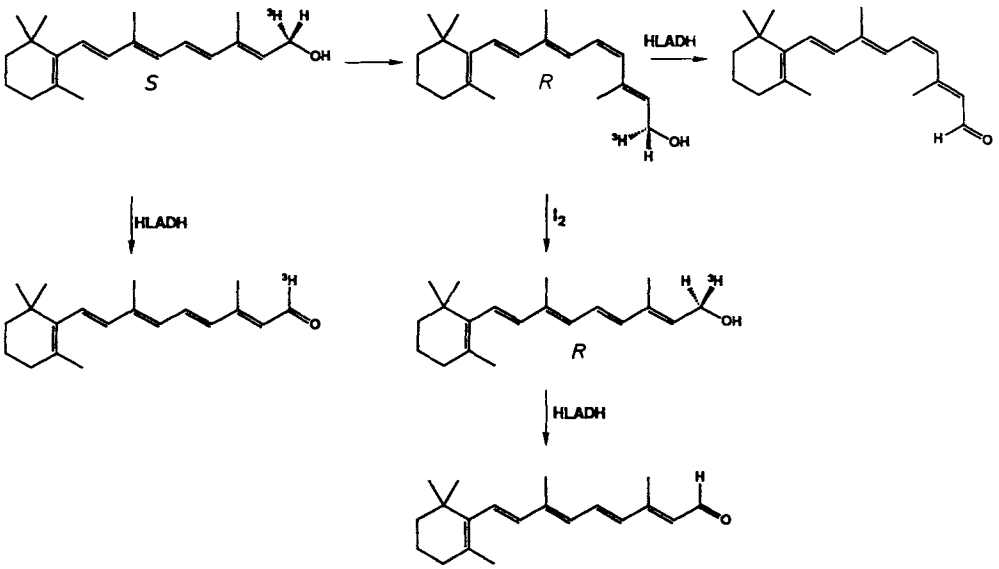

Fig. 26. Analysis of the stereochemical outcome of the isomerization reaction.

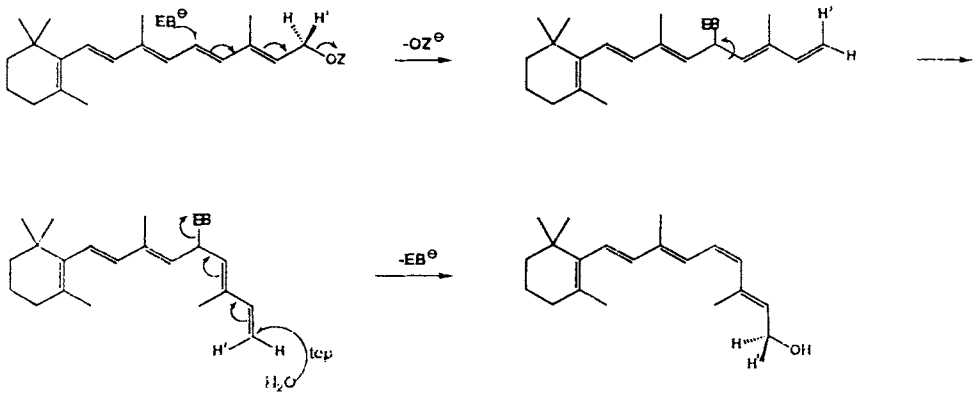

Fig. 27. Same-face C–O bond cleavage and reformation can result in apparent stereochemical inversion.

mately 180° rotation about the C11–C12 bond during the isomerization reaction, an inversion result could be obtained even though C–O bond cleavage and formation occurred from the same face of the molecule with respect to the active site of the enzyme (Fig. 27).

The inversion of stereochemistry at C15 must be reconciled with the fact that a maximum of 50% loss of ^3H from [15-^3H]-all-*trans*-retinol was found in the various retinoids after administration of the labeled retinol to rats.[55] Since the retinols were either *R* or *S* (they were prepared by NaB^3H_4 reduction of all-*trans*-retinal), stereochemical inversion and oxidation by retinol dehydrogenases of the same specificity with respect to the hydrogen removed would result in the eventual complete washout of ^3H from the retinoids. It was found that HLADH has the same stereospecificity towards 11-*cis*-retinol as it does towards all-*trans*-retinol, which is assumed to be pro-*R* specific by analogy with other alcohol substrates of this enzyme.[80, 81] However, it was also found that the ocular all-*trans* and 11-*cis*-retinol dehydrogenases showed opposite stereochemistries with respect to substrates.[80, 82] With respect to the NAD cofactors, the situation is quite clear in the amphibian, where the multiple all-*trans*-retinol dehydrogenases found in the bovine case do not exist. In the amphibian, the 11-*cis*-retinol dehydrogenase is again pro-*S* specific with respect to NAD, whereas the opposite stereochemistry is obtained with the all-*trans*-retinol dehydrogenase.[82]

In the bovine case, the 11-*cis*-retinol dehydrogenase again proved to be pro-*S* specific with respect to cofactor.[82] The all-*trans*-retinol dehydrogenases, both from the rod outer segment and from the pigment epithelium, were pro-*R* selective, although substantial processing of the pro-*S* hydrogen also occurred.[82] In light of the fact that the redox potentials for all-*trans* and 11-*cis*-retinol are the same, it is not apparent what mechanistic significance the stereochemistry of these redox reactions might have.[82] With respect to the cofactors, *Bernhard* et al.[83] have suggested that opposite chiral specificity of dehydrogenases with respect to the C4 H of NADH means that the cofactors are transferred directly from one dehydrogenase active site to another.

8. Possible Mechanisms for the Isomerization Reaction

The stereochemical and isotopic release studies described above entirely support the kind of mechanism shown in Figure 23, as do the structure–activity experiments conducted with the dihydroretinoids. In Figure 23, an S_N2' mechanism is drawn for simplicity's sake, although other mechanistic possibilities must be considered (Fig. 28). Many different mechanisms are possible, as long as they postulate intermediates higher in energy than 11-*cis*-retinol. For example, in Figure 28, three other categories of mechanisms are shown. Carbonium ion mechanisms (Fig. 28 A) are certainly possible given the polyene nature of the retinols. C–H abstraction mechanisms (Fig. 28 B) are also attractive candidates, especially if a C–H bond of the C9 methyl group is cleaved. C–H abstraction at the C13 methyl would not affect the C11–C12 double bond and abstraction at the C5 methyl or at the cyclohexyl ring would produce very stable intermediates. The last mechanism (Fig. 28 C) involves purely thermal reactions in which the ester moiety "walks" down the polyene backbone. Although we cannot at present distinguish among the different mechanisms, further structure–activity studies with various retinoids bear on this issue (Fig. 29).[84] All of the retinoids shown are processed to all-*trans*-retinyl esters prior to any possible isomerization reaction. Of the C–H abstraction mechanisms, only C–H abstraction at the C9 methyl group is viable at this time, since 9-desmethyl-all-*trans*-retinol (**3**) was not isomerized after esterification. The fact that vitamin A_2 (Fig. 21), 5-desmethyl-all-*trans*-retinol (**4**), and 13-desmethyl-all-*trans*-retinol (**2**) are all isomerase substrates (after esterification) eliminates other possible C–H abstraction mechanisms. There is currently no information that would rule in or out the other mechanisms shown (Fig. 28 A and C).

9. The Membrane as an Energy Source

Although it is possible to speculate on the exact nature of the isomerization mechanism, the broad outlines are clear. Most importantly, all of the mechanisms shown provide a solution to the issue concerning the nature of the energy source used to drive the isomerization reaction. The energy is provided by the free energy of hydrolysis of the retinyl esters. Since the retinyl esters are formed by a transesterification reaction with membrane phospholipids, it is the membrane itself that provides the energy to drive the uphill isomerization reaction (Fig. 30).

The group-transfer strategy used here is similar to cases where ATP, which has a free energy of hydrolysis of

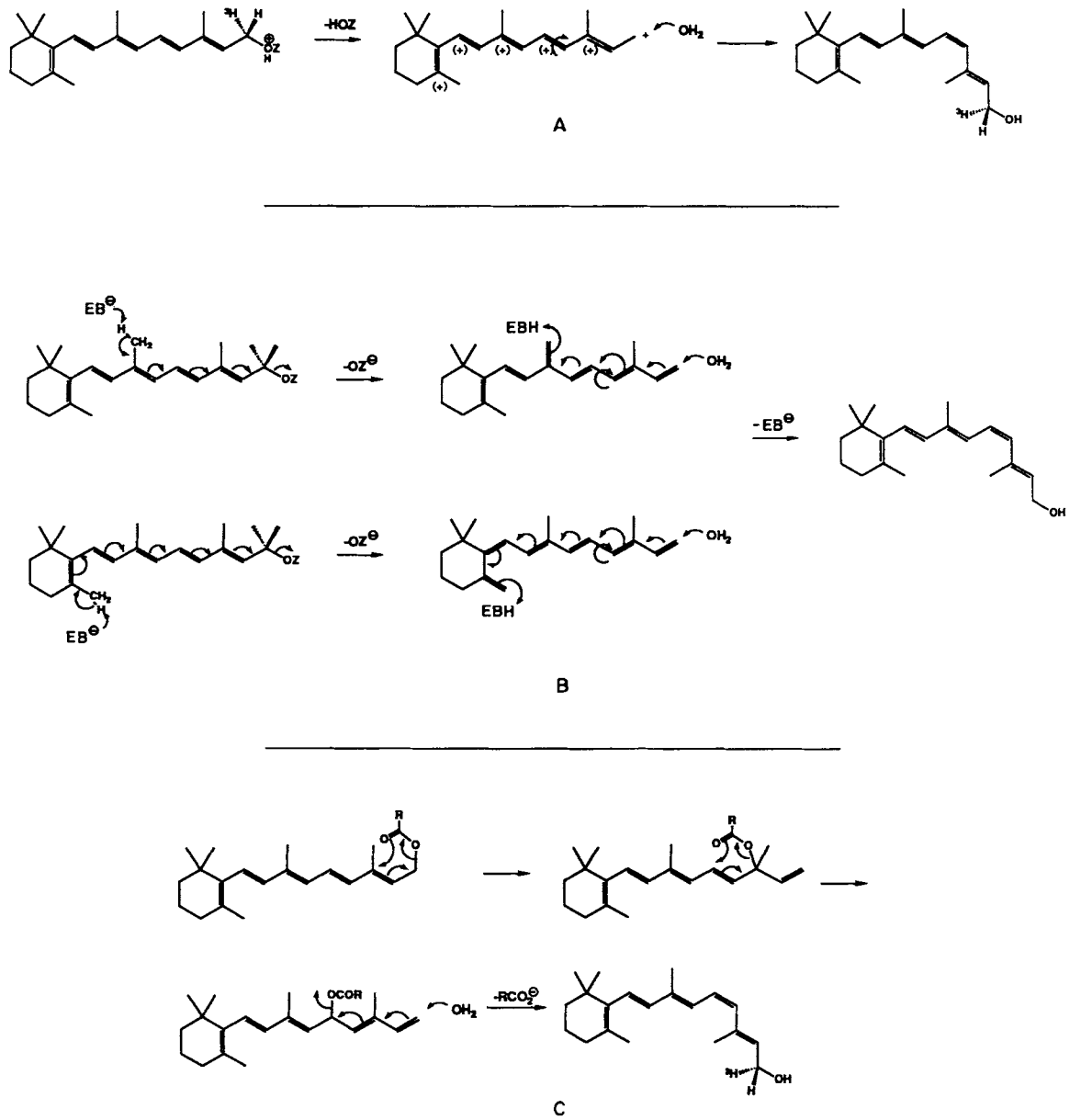

Fig. 28. Possible isomerase mechanisms. A) Carbonium ion mechanism; B) C–H abstraction mechanism; C) thermal reaction.

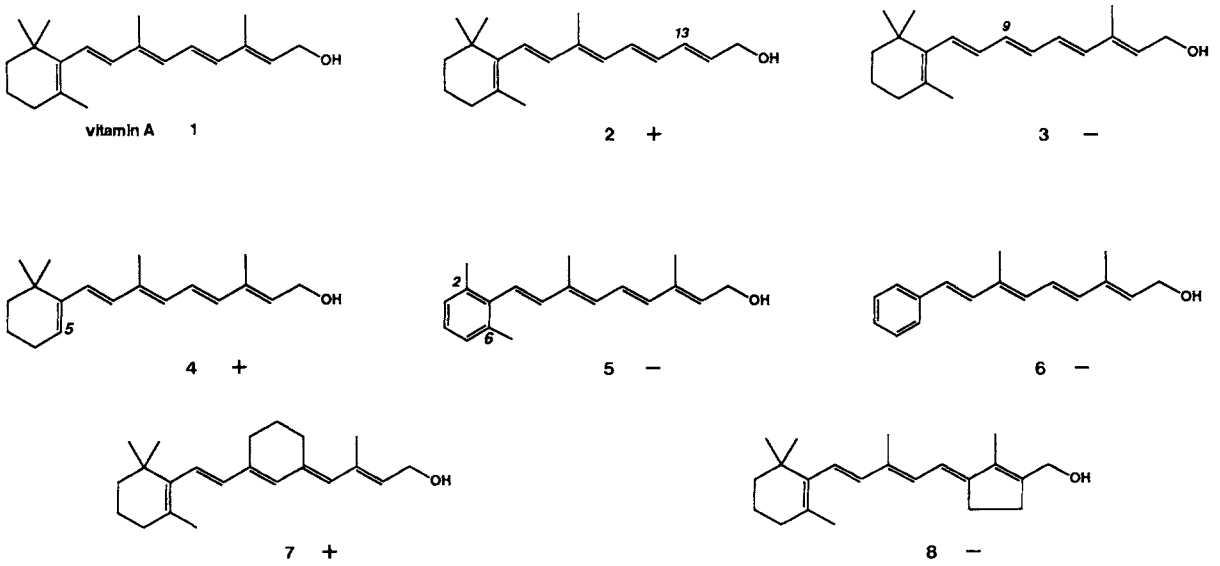

Fig. 29. Structure–activity studies on the isomerase. +, active; −, inactive.

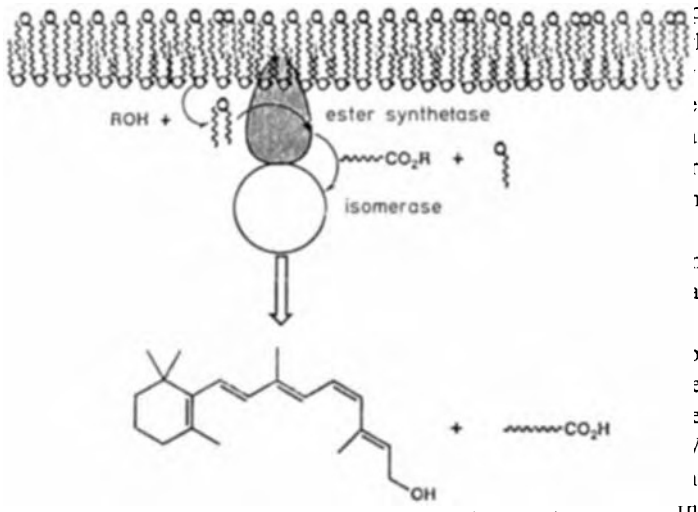

Fig. 30. The biosynthesis of 11-*cis*-retinol showing the involvement of membrane phospholipids.

$-7.3\ \text{kcal mol}^{-1}$, is utilized as the energy source to drive otherwise thermodynamically unfavorable reactions. In many of these cases, such as the biosynthesis of sucrose from fructose and glucose, phosphorylation of a hydroxyl group occurs followed by displacement reactions which occur sequentially rather than in a concerted fashion. Nevertheless, in terms of driving force, these mechanisms are very similar to the proposed isomerase mechanism. This latter mechanism could be of general interest as a new mechanism of energy transduction in membranes with phospholipids being used as an energy source. This also provides a hitherto unsuspected role for membranes.

Finally, coming back to the visual cycle itself, our current understanding is depicted in Figure 31. The idea that the

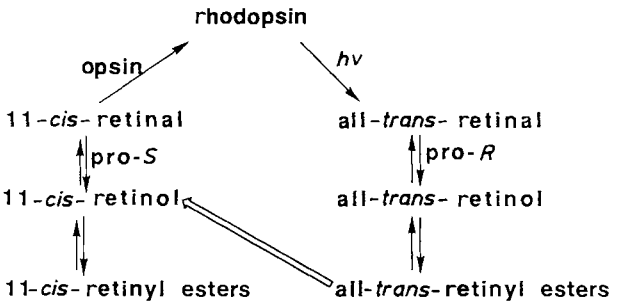

Fig. 31. Current model of the visual cycle (cf. Fig. 7).

retinyl esters play a mere passive role as a storage form of retinol must be discarded and replaced with a vision of them in a critical dynamical role as the precursors of the 11-*cis*-retinoid chromophores.

10. Summary and Outlook

The studies described here provide a brief survey of the molecular mechanisms of 11-*cis*-retinoid biosynthesis in the eye. Interestingly, the solution depended on strictly chemical approaches. That is, the work began with the question of where the energy comes from to drive the thermodynamically uphill isomerization of all-*trans*-retinoids to 11-*cis*-retinoids. Simple solutions to the problem, such as that enabled in the retinal isomerase conjecture, could not be and are not correct because they do not provide a mechanism for energy transduction. Unlike retinol, retinal does not contain a group that can be activated by a group-transfer reaction and, hence, retinal cannot be activated in a thermodynamically fruitful way.

Many intriguing questions remain to be solved. With respect to the isomerization process, it will be important to determine what the actual mechanism of the isomerase is. Several mechanistic possibilities have been considered. Which if any of these possibilities apply will have to be determined. Moreover, the exact relationship that holds between the ester synthetase and the isomerase needs to be elucidated, as does the relationship among the remaining enzymes of the visual cycle. The isomerase, or perhaps more properly, the "isoesterase", and ester synthetase will have to be purified and sequenced to determine their possible relationships to other known enzymes. Knowing the primary sequences of these enzymes will be important in determining whether any of the important diseases of vision might find an etiology in mutations in these enzymes.

Perhaps of greatest importance biologically is to determine if the group-transfer mechanisms described here involving membrane phospholipids are general. Although ATP has been singled out as the energy currency of the cell, the studies described here show that other possibilities exist and will need careful consideration.

I wish to gratefully acknowledge the important contributions of Dr. Robert Barry, Dr. Paul S. Bernstein, Dr. Francisco J. Cañada, Dr. Andrew Chang, Dr. Peter Deigner, Dr. Brian S. Fulton, Dr. Wing C. Law, and John Lichtman to the research described here. The work from the author's laboratory was supported by U.S. Public Health Service Research Grant EY 04096 from the National Institutes of Health.

Received: October 23, 1989 [A 761 IE]
German version: *Angew. Chem. 102* (1990) 507

[1] W. Kühne, *Unters. Physiol. Inst. Heidelberg 1* (1878) 341.
[2] G. Wald, *Annu. Rev. Biochem. 22* (1953) 497.
[3] S. Amer, M. Ahktar, *Nature New Biol. 237* (1972) 266.
[4] R. Hubbard, *J. Gen. Physiol. 39* (1956) 935.
[5] J. P. Rotmans, F. J. M. Daemen, S. L. Bonting, *Biochim. Biophys. Acta 267* (1972) 583.
[6] J. J. Ostapenko, V. V. Furajev, *Nature New Biol. 243* (1973) 185.
[7] G. Wolf, *Am. J. Clin. Nutr. 31* (1978) 290.
[8] J. E. Dowling, G. Wald, *Proc. Natl. Acad. Sci. (USA) 44* (1958) 648.
[9] R. R. Birge, *Annu. Rev. Biophys. Bioeng. 10* (1981) 315.
[10] R. R. Birge, L. M. Hubbard, *Biophys. J. 34* (1981) 517.
[11] K. S. Peters, M. L. Applebury, P. M. Rentzepis, *Proc. Natl. Acad. Sci. (USA) 74* (1977) 3119.
[12] R. Mathies, *Methods Enzymol. 88* (1982) 633–643.
[13] A. Cooper, *Nature (London) 282* (1979) 531.
[14] A. G. Dougas, B. Aton, R. H. Callender, T. G. Ebrey, *Biochemistry 17* (1978) 2430.
[15] C. Longstaff, R. R. Rando, *Biochemistry 24* (1985) 8137.
[16] C. Longstaff, R. D. Calhoon, R. R. Rando, *Proc. Natl. Acad. Sci. (USA) 83* (1986) 4209.
[17] K. P. Hofmann, *Photobiochem. Photobiophys. 13* (1986) 309.
[18] L. Stryer, *Annu. Rev. Neurosci. 9* (1986) 87.
[19] E. E. Fesenko, S. S. Kolesnikov, A. L. Lyubarsky, *Nature (London) 313* (1985) 310.

[20] G. W. R. Weinstein, R. Hobson, J. E. Dowling, *Nature (London) 215* (1967) 134.
[21] J. E. Dowling: *The Retina*, Harvard University Press, Cambridge 1987, Chapter 7.
[22] H. Davson: *Physiology of the Eye*, 4th ed., Academic Press, New York 1980, p. 232.
[23] S. Hecht, C. Haig, A. M. Chase, *J. Gen. Physiol. 20* (1937) 831.
[24] P. Julia, J. Farres, X. Pares, *Exp. Eye Res. 42* (1986) 305.
[25] J. C. Saari, A. H. Bunt-Milan, D. L. Bredberg, G. G. Garwin, *Vision Res. 24* (1984) 1595.
[26] D. Bok, *Invest. Ophthalmol. Visual Sci. 26* (1985) 1659.
[27] A. J. Adler, C. D. Evans, *Prog. Clin. Biol. Res. 190* (1985) 65.
[28] G. J. Chader, B. Wiggert, Y.-L. Lai, L. Lee, R. T. Fletcher, *Prog. Retinal Res. 2* (1983) 163–184.
[29] J. E. Dowling, *Nature (London) 188* (1960) 114.
[30] A. Knowles, H. J. A. Dartnall in H. Davson (Ed.): *The Eye, Vol. 2B*, Academic Press, New York 1977, Chapter 10.
[31] C. D. B. Bridges, *Exp. Eye Res. 22* (1976) 435.
[32] W. A. H. Rushton, *J. Gen. Physiol. 41* (1957) 419.
[33] L. Pauling, *Fortschr. Chem. Org. Naturst. 3* (1939) 203.
[34] L. Pauling, *Helv. Chim. Acta 32* (1949) 2241.
[35] R. Hubbard, G. Wald in A. Rich, N. Davidson (Eds.): *Structural Chemistry and Molecular Biology*, W. H. Freeman, San Francisco 1968, pp. 545–554.
[36] R. Hubbard, *J. Biol. Chem. 24* (1966) 1814.
[37] D. J. Patel, *Nature (London) 224* (1969) 799.
[38] W. Sperling, P. Carl, C. N. Rafferty, N. A. Dencher, *Biophys. Struct. Mech. 3* (1977) 79.
[39] R. R. Rando, A. Chang, *J. Am. Chem. Soc. 105* (1983) 2879.
[40] R. Gilardi, I. L. Karle, J. Karle, W. Sperling, *Nature (London) 232* (1971) 187.
[41] Y. Schichida, A. Kropf, T. Yoshizawa, *Biochemistry 20* (1981) 1962.
[42] A. Albeck, M. Friedman, M. Sheves, M. Ottolenghi, *J. Am. Chem. Soc. 108* (1986) 4614.
[43] A. Chang, B. Fulton, R. R. Rando, unpublished results.
[44] L. Boni, R. R. Rando, unpublished results.
[45] W. von E. Doering, W. R. Roth, *Angew. Chem. 75* (1963) 27; *Angew. Chem. Int. Ed. Engl. 2* (1963) 115.
[46] D. Lukton, R. R. Rando, *J. Am. Chem. Soc. 106* (1984) 4525.
[47] L. Zechmeister, *Chem. Rev. 34* (1944) 267.
[48] S. Futterman, M. H. Rollins, *J. Biol. Chem. 248* (1973) 7773.
[49] G. W. T. Groenendijk, C. W. M. Jacobs, S. L. Bonting, F. J. M. Daemen, *Eur. J. Biochem. 106* (1980) 119.
[50] R. A. Auerbach, M. F. Granville, B. E. Kohler, *Biophys. J. 25* (1979) 443.
[51] H. Davson: *Physiology of the Eye*, 4th ed., Academic Press, New York 1980, pp. 218–219.
[52] P. S. Bernstein, J. R. Lichtman, R. R. Rando, *Proc. Natl. Acad. Sci. (USA) 83* (1986) 1632.
[53] P. S. Bernstein, B. S. Fulton, R. R. Rando, *Biochemistry 25* (1986) 3370.
[54] B. S. Fulton, R. R. Rando, *Biochemistry 26* (1987) 110.
[55] P. S. Bernstein, R. R. Rando, *Biochemistry 25* (1986) 6473.
[56] M. Zewi, *Acta Physiol. Scand. 1* (1941) 271.
[57] T. Reuter, *Vision Res. 6* (1966) 15.
[58] C. D. B. Bridges in H. Lauger (Ed.): *Biochemistry and Physiology of Visual Pigments*. Springer, New York 1973, pp. 115–121.
[59] P. S. Bernstein: "Biochemistry and Pharmacology of Rhodopsin Regeneration in the Vertebrate Eye", *Ph.D. Thesis*, Harvard University 1987.
[60] P. S. Bernstein, W. C. Law, R. R. Rando, *Proc. Natl. Acad. Sci. (USA) 84* (1987) 1849.
[61] P. S. Bernstein, W. C. Law, R. R. Rando, *J. Biol. Chem. 262* (1987) 16848.
[62] B. S. Fulton, R. R. Rando, *Biochemistry 26* (1987) 7938.
[63] D. R. Pepperberg, R. H. Masland, *Brain Res. 151* (1978) 194.
[64] J. I. Perlman, B. R. Nodes, D. R. Pepperberg, *J. Gen. Physiol. 80* (1982) 885.
[65] M. T. Flood, C. D. B. Bridges, R. A. Alvarez, W. S. Blaner, P. Gouras, *Invest. Ophthalmol. Visual Sci. 24* (1983) 1227.
[66] S.-L. Fong, C. D. B. Bridges, R. A. Alvarez, *Vision Res. 23* (1983) 47.
[67] S. R. Das, P. Gouras, *Biochem. J. 250* (1988) 459.
[68] J. G. Flannery, W. O'Day, J. Horwitz, D. Bok in T. Hara (Ed.): *Molecular Physiology of Retinal Proteins*, Proc. of the Yamada Conference, Yamada Science Foundation, Japan 1988, pp. 261–266.
[69] P. S. Deigner, W. C. Law, F. J. Cañada, R. R. Rando, *Science (Washington, DC) 244* (1989) 968.
[70] F. J. Cañada, R. R. Rando, unpublished results.
[71] W. C. Law, R. R. Rando, unpublished results.
[72] P. S. Bernstein, J. R. Lichtman, R. R. Rando, *Biochemistry 24* (1985) 487.
[73] W. C. Law, R. R. Rando, S. Canonica, F. Derguini, K. Nakanishi, *J. Am. Chem. Soc. 110* (1988) 5915.
[74] R. J. Barry, F. J. Cañada, R. R. Rando, *J. Biol. Chem. 264* (1989) 9231.
[75] N. I. Krinsky, *J. Biol. Chem. 232* (1958) 881.
[76] J. C. Saari, D. L. Bredberg, *J. Biol. Chem. 264* (1989) 8636.
[77] P. N. MacDonald, D. E. Ong, *Biochem. Biophys. Res. Commun. 156* (1988) 157.
[78] A. Trehan, F. J. Cañada, R. R. Rando, *Biochemistry 29* (1990) 309.
[79] W. P. Jencks in H. A. Sober (Ed.): *CRC Handbook of Biochemistry and Molecular Biology*, 3rd ed., Chemical Rubber Co., Cleveland 1970, p. J183.
[80] W. C. Law, R. R. Rando, *Biochemistry 27* (1988) 4147.
[81] F. Loewus, F. H. Westheimer, B. Vennesland, *J. Am. Chem. Soc. 75* (1953) 5018.
[82] W. C. Law, S. Kim, R. R. Rando, *J. Am. Chem. Soc. 111* (1988) 793.
[83] D. K. Srivastava, S. A. Bernhard, R. Langridge, J. A. McClarin, *Biochemistry 24* (1985) 629.
[84] W. C. Law, F. J. Cañada, R. R. Rando, S. Canonica, F. Derguini, K. Yamamoto, K. Nakanishi, unpublished results.

Five Decades Ago: From the "Transuranics" to Nuclear Fission**

By Günter Herrmann*

The discovery of nuclear fission is one of the most outstanding episodes in the history of chemistry: It starts in the spring of 1934 when *Enrico Fermi* and his group irradiate uranium with neutrons and seem to succeed in going beyond uranium, the then heaviest known element, reaching the first transuranic element; it continues with *Otto Hahn, Lise Meitner* and *Fritz Strassmann* who believe to have found additional transuranic elements; with *Irène Curie* and *Paul Savitch* who observe an activity which somehow does not fit into that scheme; again with *Otto Hahn* and *Fritz Strassmann* who first identify this activity as radium but then on the 17th of December 1938 after rigorous chemical tests realize that the activity is instead barium, thus discovering the fission of the uranium atom into two lighter nuclei; and with *Lise Meitner* and *Otto Robert Frisch* who explain nuclear fission on the basis of an already known nuclear model; *Otto Robert Frisch* finally performs a physical experiment on the 13th of January 1939 which corroborates the fission of uranium. This discovery of nuclear fission is not only an event of historic dimensions, it is also an excellent example of how science evolves, not by successive logical steps but rather through strange detours.

1. The "Transuranic Elements"

1.1. Rome 1934: Element 93, Eka-Rhenium?

When *Enrico Fermi* and his group irradiate uranium with neutrons in the spring of 1934 they do not figure at all on fissioning uranium into two medium sized nuclei. Their intention is quite different: They want to go beyond the heaviest naturally occurring element in the periodic table, uranium (atomic number $Z = 92$) and to reach element 93, the first transuranic element. This became feasible after *Fermi* and co-workers succeeded in obtaining radioactive isotopes of a number of elements by irradiation with neutrons, which had been discovered only shortly before. In contrast to α-particles, which were previously used to induce nuclear transformations, the uncharged neutrons attach very easily to the positively charged atomic nuclei, even in heavy elements.[1, 2] In this case one obtains isotopes of the starting element[2, 3] which subsequently undergo β^--decay. In β^--decay the isotope emits an electron from the nucleus and is transformed into the element with the next higher atomic number. The stable silver isotope 109 ($Z = 47$), for example, captures a neutron to form silver-110 which decays by β^--emission with a 24s half-life into the stable cadmium-110 [Reaction (1)].

$$^{109}_{47}\mathrm{Ag} + {}^{1}_{0}\mathrm{n} \longrightarrow {}^{110}_{47}\mathrm{Ag} \xrightarrow[24\mathrm{s}]{\beta^-} {}^{110}_{48}\mathrm{Cd} \qquad (1)$$

If the same kind of reaction could be induced also with uranium, one would expect formation of element 93 [Reaction (2)].

$$^{238}_{92}\mathrm{U} + {}^{1}_{0}\mathrm{n} \longrightarrow {}^{239}_{92}\mathrm{U} \xrightarrow{\beta^-} {}^{239}93 \qquad (2)$$

This element should be radioactive and, if it is again a β^--emitter, might even decay into another transuranic element, 94 [Reaction (3)].

$$^{239}93 \xrightarrow{\beta^-} {}^{239}94 \qquad (3)$$

This concept seems indeed to be correct: In several publications[2, 4, 6-8] *Fermi* et al. report on at least five β^--emitters with half-lives of 10 s, 40 s, 13 min, 40 min and about 1 d which are observed in their Rome laboratory after the irradiation of uranium with neutrons.

It is not sufficient, however, to simply rely on the detection of β^--emitters. One has to prove the formation of the new elements in a more direct way which can only be achieved by chemical methods. For this purpose one relies on similarities between the elements of the periodic table: One attempts to prove that the activities,[*] which are ascribed to the transuranic elements, behave chemically in a way which is expected according to their location in the periodic table. This concept is shown in Figure 1.

The task of element identification is quite difficult, because the β^--emitters are produced in tiny amounts which are neither visible nor weighable. The only means of identification is their radioactivity which allows one to detect even single atoms. These problems, however, did not appear for the first time, because some of the naturally occurring radioactive elements were also found in such small quantities. Therefore, as early as at the end of the last century, radiochemists had to find out when trace amounts start to behave chemically in the same way as macroscopic quantities.[9] Radium, for example, is co-deposited with a number of insoluble barium compounds, because its corresponding salts are also insoluble. Later, when radioelements were accessible

[*] Prof. Dr. G. Herrmann
Institut für Kernchemie der Universität
Fritz-Strassmann-Weg 2, D-6500 Mainz (FRG), and
Gesellschaft für Schwerionenforschung
Planckstrasse 1, D-6100 Darmstadt (FRG)

[**] Based on a paper "Discovery and Confirmation of Fission" presented at the conference "Fifty Years Research in Nuclear Fission" in Berlin on April 4, 1989.

[*] In the historical context we use the then common word "activity" or "body" to name a radioactive species; the more modern expressions are "nuclide" or "isotope". We also use the old nomenclature of isotopes even though it is somewhat misleading. Mesothorium 1 (MsTh 1), for example, is not a thorium but a radium isotope. We will, however, usually add today's nomenclature with element symbol, mass number, and often also the half-life; for example: Mesothorium 1, 5.8-y radium-228.

 © VCH Verlagsgesellschaft mbH, D-6940 Weinheim, 1990 0570-0833/90/0505-0481 $ 02.50/0

in visible amounts, these findings obtained with unweighable quantities were confirmed. On occasions, however, irregular chemical behavior had also been noticed.

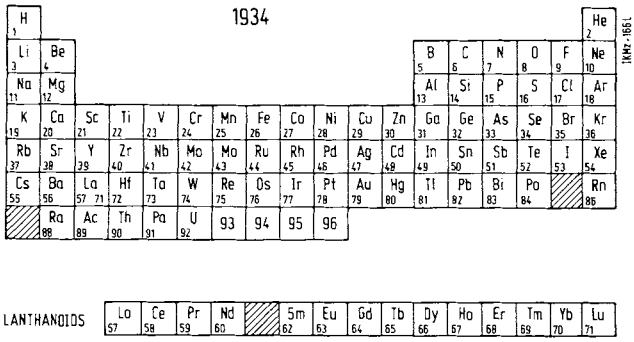

Fig. 1. The periodic table of the elements in 1934. Missing elements at that time are shown as shaded boxes. The present symbols for the elements are used, except for masurium (43).

Thus, for the activities ascribed to transuranic elements it has to be shown that they behave in the same way as their homologous elements during characteristic chemical operations. For these tests *Fermi* et al., and all other groups who perform experiments with transuranic elements, rely on two assumptions which seem to be justified by both theory and experiment but which later turn out to be wrong: First, as a result of nuclear reactions—whether they occur spontaneously during radioactive decay or whether they are induced by particle irradiation—the atomic number changes only slightly. Thus, only elements in the vicinity of the initial element can be formed. Second, in the periodic table thorium, protactinium, and uranium are placed in the 4th, 5th and 6th group of transition elements; therefore, the sought after element 93 should belong to the 7th group of transition elements, it would be eka-rhenium, and the elements 94 through 96 would be eka-platinum metals. Therefore, one has to prove chemically that elements to the right of uranium are formed and that elements in its close vicinity to the left can be excluded.

All experimental facts known until then[3] suggest that the products of nuclear reactions are confined to the vicinity of the original nucleus; a differing phenomenon had never been observed. This view is also reflected in a then introduced illustrative description of nuclear reactions.[10] But also theory corroborates this view. According to *Gamow*'s theory of α-decay,[12] one of the early triumphs of quantum mechanics, even the α-particle with its two nuclear charges can hardly tunnel through the electrostatic Coulomb barrier of the nucleus; for larger fragments this barrier increases rapidly and tunneling becomes extremely unlikely.[13] This reasoning is indeed correct; only decades later is the extremely rare emission of carbon-13 nuclei from radium-223 discovered.[14] The crucial point is, however, that the breakup of a heavy nucleus into two fragments of similar size should not be treated as a tunneling process. Quantum mechanics was more of an obstacle than a help for the discovery of fission.

In the periodic table thorium is so closely related to hafnium, protactinium to tantalum, and uranium to tungsten that an ordering different from the one shown in Figure 1 is not seriously considered, even though a second series of f-elements similar to the rare earths have repeatedly been postulated since *Niels Bohr*'s Nobel talk in 1922;[15] however, this series is suspected as being rather to the right than to the left of uranium.[16–19] In contrast, *A. von Grosse*[20] explicitly argues again in the early thirties that the elements 93 and 94 might have properties completely different from eka-rhenium and eka-osmium.

The presumption that element 93 is eka-rhenium is not easy to integrate into chemical separation procedures, because one has to work with the least familiar group of the periodic table. The two homologous elements 43 and 75, masurium (later technetium) and rhenium, were discovered just a few years earlier by *Walter Noddack, Ida Tacke* (who later married *Noddack*) and *Otto Berg*.[21,22] Even though the properties of rhenium have not yet been well understood it is already available in small quantities, in contrast to masurium of which hardly anything is known. For the eka-platinum metals a complicated chemistry has to be expected as well, as is obvious from their homologues.

Therefore, in order to chemically prove the identity of element 93, *Fermi* and his coworkers focus their attention on manganese. As a characteristic reaction they choose the precipitation of manganese dioxide in strong nitric acid by adding chlorate; this is not a fortunate choice, because the precipitate has a large surface and all kinds of elements get attached to it. Initially, however, their concept seems to be correct: the 13-min activity, which for such experiments is the best suited one of the new activities, is found in the

Günter Herrmann was born in 1925 in Greiz (Thüringen). From 1946 until 1956 he studied chemistry at the University of Mainz where he received his doctorate for work on nuclear fission under the supervision of Fritz Strassmann. In 1962 he habilitated and became privatdocent at Mainz. In 1967 he was offered but did not take up an appointment as full professor at the Kansas State University in Manhattan. Since 1968 Herrmann has been full professor and Director of the Institut für Kernchemie an der Universität Mainz, and, since 1970 he has in addition been directing a nuclear chemistry research department of the Gesellschaft für Schwerionenforschung Darmstadt. His main fields of interest are: rapid methods of chemical separation, nuclear fission and reactions between heavy atom nuclei, exotic atomic nuclei, the search for superheavy elements, radionuclides in the environment. The honors conferred on him include, inter alia: since 1984 corresponding member of the Academie der Wissenschaften und der Literatur zu Mainz; 1987 Miller guest professor at the University of California in Berkeley; 1988 Nuclear Chemistry Award of the American Chemical Society.

precipitate, in contrast to uranium and the lighter elements down to lead, as is verified with radioisotopes.[2, 4, 6–8] The 13-min activity also coprecipitates with rhenium sulfide in strong hydrochloric acid;[2, 6–8] this is a reaction by far more specific than the precipitation of manganese dioxide. The 90-min activity chemically behaves very similarly to the 13-min activity. The conclusion that elements heavier than uranium have been found, is presented by *Fermi*[7] only reluctantly, however, as is obvious from the title of the publication; he is not content with the more definite public statements of his mentor *Carbino*.[23]

1.2. Objections and Their Consequences

Objections are being raised. *Von Grosse* and *Agruss*[25–27] ascribe *Fermi*'s activity to element 91, protactinium, which they succeed in coprecipitating completely with manganese dioxide and to a large extent with rhenium sulfide. Also *Fermi* et al. meet some problems in connection with protactinium and its coprecipitation with manganese dioxide.[2, 4, 8] Being aware of this controversy, *Otto Hahn* and *Lise Meitner* feel challenged, since they are the ones who found the only protactinium isotope which in nature is available in weighable quantities, the 3.3×10^4-y protactinium-231,[28] and who had also named the element. Moreover, *Hahn*[29] had discovered with protactinium-234 the phenomenon of nuclear isomerism, namely the existence of two nuclei with the same numbers of protons and neutrons but with different half-lives of 1.17 min for the metastable (m) and 6.75 h for the ground state (g). *Lise Meitner* is immediately attracted[30, 31] by *Fermi*'s neutron-induced nuclear reactions; she persuades[32, 34] *Otto Hahn* to resume their collaboration after twelve years of interruption and to focus attention on the transuranic elements.

In a first note[35] they present evidence in favor of *Fermi*'s interpretation: the 13-min and the 90-min activities can be separated from protactinium in two ways. First, both activities can be coprecipitated with platinum sulfide, with protactinium remaining completely dissolved. The second procedure is just the opposite, where the new activities remain dissolved if protactinium is co-precipitated with zirconium phosphate. To obtain these results the transuranic activities are mixed with natural 6.7-h protactinium-234g and in the course of the subsequent separation the distribution of the three activities among different fractions is determined. The two transuranic elements are more similar to platinum than to rhenium and they might be chemically different,[35] the 13-min activity could possibly be element 93, the 90-min activity element 94. *Fermi* et al.[36, 37] obtain similar results and presume the decay of the 13-min into the 90-min activity. This was the last word from Rome with respect to the "uranium case"; they leave it to those who are more experienced in radiochemistry[38] and turn to an exciting new problem, the intense reaction of slow neutrons with atomic nuclei, a phenomenon which is also discovered in Rome.

Ida Noddack's criticism[39] is of a more conceptual nature. In an article[40] dealing with yet unknown elements in the periodic table she conjectures that the transuranic elements, with increasing atomic number, should tend to be more and more short-lived and rare, with the even numbered elements 94 and 96 possibly still within the realm of being found; apparently she is speaking of a search in nature. In a Supplementary note[39] she discusses two discoveries of element 93. The first case,[41] a natural element 93 in the Joachimsthal pitch-blende, is closed quickly because she does not detect element 93 in the original samples either chemically or by X-ray spectroscopy. In the second case, namely *Fermi*'s[7] element 93, she objects that only the heaviest known elements were excluded; *Fermi* ought to have compared his new element with *all* the known elements. According to her own studies, a large number of ordinary elements are being coprecipitated with manganese dioxide; in her opinion the coprecipitation with rhenium sulfide is not a strong proof either. *Ida Noddack* notes:[39][*] "Es wäre denkbar, daß bei der Beschießung schwerer Kerne mit Neutronen diese Kerne in mehrere *größere*[**] Bruchstücke zerfallen, die zwar Isotope bekannter Elemente, aber nicht Nachbarn der bestrahlten Elemente sind".

Can this statement be taken as the prediction of nuclear fission, as it is done sometimes?[42, 43] Not really, because *Ida Noddack* herself does not consider her proposition of a new and surprising nuclear reaction to be that meaningful to test it experimentally. She seems more concerned, according to contemporaries, to render the detection of element 93 as inconclusive; her objection is not relevant for the future developments.[44] She may plan herself to search for eka-rhenium in nature, since the 7th group of transition elements is already well known to her. Her objection is hardly noticed in Rome[45] and Berlin;[46] *Strassmann* even calls it a chance coincidence.[48] This ignorance is certainly influenced by *Noddack*'s dubious and irreproducible discovery of the natural element 43.[45, 50, 51] When *Ida Noddack* later complains about this attitude in a note,[52] *Hahn* and *Strassmann* refrain from submitting an already formulated harsh reply[50] and leave it to the editors to react.[53] The relationship between the *Noddacks* and *Hahn* and *Meitner* remains reserved, also caused by political controversies,[50] even though—or maybe because—they work in the same city.

1.3. Berlin 1935–1938: Elements 94 through 96, the Eka-Platinum Elements?

From now on further studies of the transuranic elements are mainly carried out by *Otto Hahn* and *Lise Meitner*; they soon ask the much younger *Fritz Strassmann* to join them in their efforts, since he has shown a talent for difficult chemical separations. No photograph exists from that time showing all three together, so one has to combine two separate photographs—Figure 2—or use a later common one—Figure 3. The experiments are performed in three different rooms on the ground-floor of the Kaiser-Wilhelm-Institut für Chemie[***] in Berlin-Dahlem, the plan of which is depicted in Figure 4.

---

[*] "It is conceivable that during the irradiation of heavy nuclei with neutrons these nuclei may disintegrate into a number of *larger* [**] fragments which are isotopes of known elements but not necessarily neighbors of the elements irradiated originally.

[**] Emphases as in the original.

[***] The Kaiser-Wilhelm-Institut für Chemie is heavily damaged by bombs in February 1944. The institute and its members temporarily move to Tailfingen in Württemberg. After the war the institute finds a new home in Mainz and is called the Max-Planck-Institut für Chemie. The Berlin building, after reconstruction, now serves as the Otto-Hahn-Bau of the Freie Universität.

Fig. 2. *Otto Hahn* (1879–1968) and *Lise Meitner* (1878–1968) at an institute outing, ca. 1934/35, and *Fritz Strassmann* (1902–1980), Berlin, ca. 1936 (after [48]).

The equipment is very simple. Near the front of the table depicted in Figure 5 two brick-like lead blocks can be seen in which the counters are housed in order to reduce the radiation background. In the right block, which is open, one sees a cylindrical Geiger-Müller counter. The samples to be measured are glued on "boat-shaped" lead holders and placed underneath the counters; samples, lead holders, and absorber foils can be found between the two blocks. The counters are made of a 0.01 cm thick aluminum tube of 6 cm length and 2 cm diameter, the two ends of which are closed with rubber plugs and gas-tightened with pizein wax. The central counting wire, made of a piano string, is fixed in the same way, as is also a glass tube which is used for pumping and filling the counter with an argon-ethanol-mixture 10:1 at a pressure of about 10 kPa. The wire is at a positive potential of about 1500 volts, to collect the electrons which are created by β^--rays ionizing the counting gas; to increase the signal height the electrons are accelerated in the strong electric field of the counter forming an electron avalanche.

In the center of the table one sees two amplifiers with two amplifier tubes each; to the left of both amplifiers is a mechanical counting unit which registers the number of electrical pulses. Each counting unit is equipped with a stop-watch, which is not shown on the table.[48] The counters are coupled to the amplifiers via high-impedance resistors, which can be seen to the right of the tubes; the resistors consist[56] of a glass tube filled with toluene and imbedded in paraffin. The power supplies producing the necessary voltages are located at the back of the table; the voltages for the counters are supplied by a chain of anode batteries underneath the table.

Neutrons are produced according to Reaction (4) by irradiating beryllium with α-particles from natural radioisotopes.

$$^{9}_{4}\mathrm{Be} + {}^{4}_{2}\alpha \longrightarrow {}^{12}_{6}\mathrm{C} + {}^{1}_{0}\mathrm{n} \qquad (4)$$

The neutron sources which consist of six brass tubes of about 6 cm length can be seen in the upper right part of Figure 5. Each one is made of a fused glass tube containing beryllium powder and either about 100 mg of radium sulfate or short-lived radon gas, which is freshly obtained once a week by separation from radium performed in a separate hut in the institute's yard.[56] If slow neutrons are to be used for irradiation, the sources are installed in a cyclindrical paraffin block (upper right) on top of which the sample is to be placed. The flux of thermal neutrons is about 10^4 neutrons per $cm^2 \cdot s$.

Fig. 3. *Fritz Strassmann*, *Lise Meitner*, and *Otto Hahn* (from left to right) 1956 in Mainz at the inauguration of the Max-Planck-Institut für Chemie (from [54]).

Finally, a filter flask is to be seen in the lower right of Figure 5; this is used for rapid filtration of radioactive precipitates in the so crucial radiochemical experiments. Below the filter flask one sees the historical note-book "Chem. II".

As experiments are performed at quite different levels of activity, strict precautions have to be followed in order not to accidentally spread radioactivity, as this would make sensitive measurements impossible in the long run. Toilet paper is affixed to the doors of coffee rooms, rest rooms, and corridors and is supposed to be used when touching door handles. In the lecture hall and the library one finds light and dark colored chairs for those working with "strong" and "weak" radioactivities. One does not shake hands either; if practiced at all, greetings are reduced to the touching of each others little finger tips. Laboratory tables are covered with absorbent paper; for this purpose waste paper from the printing office of the Reichsbahn[*] is well suited and is available cheaply. On the other hand, the institute has quite an advanced local telephone system to facilitate communication without direct contact.

The natural radioactivity of uranium creates a severe problem. To obtain statistically significant count rates of the artificial activities—about a hundred pulses per minute—using the weak neutron sources ten- to hundred-gram samples of uranium have to be irradiated. These sources contain

[*] National Railway.

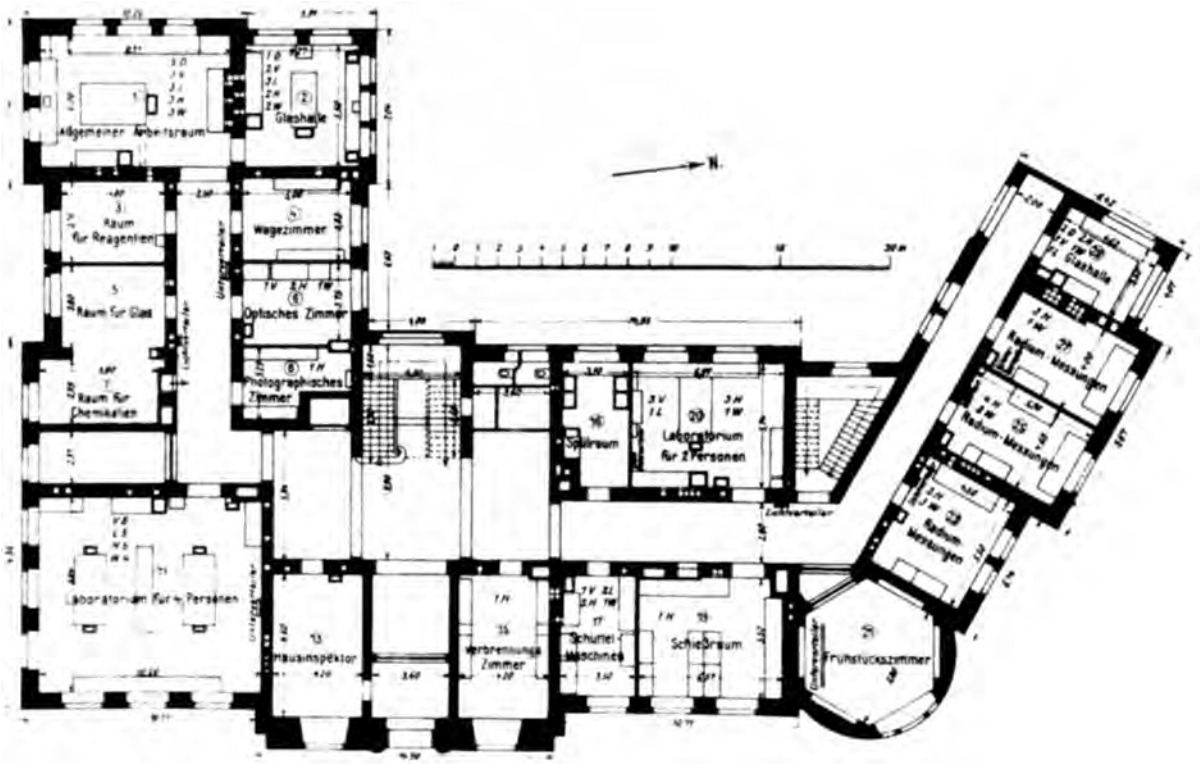

Fig. 4. Kaiser-Wilhelm-Institut für Chemie at Berlin-Dahlem, plan of the ground-floor. Irradiations with neutron sources were carried out in room 29, *Hahn*'s "private laboratory"—room 20—was used for the chemistry, and in room 23 the radioactivity was measured; *Lise Meitner*'s office was located between rooms 7 and 11, *Otto Hahn*'s office was on the first floor (from [55]).

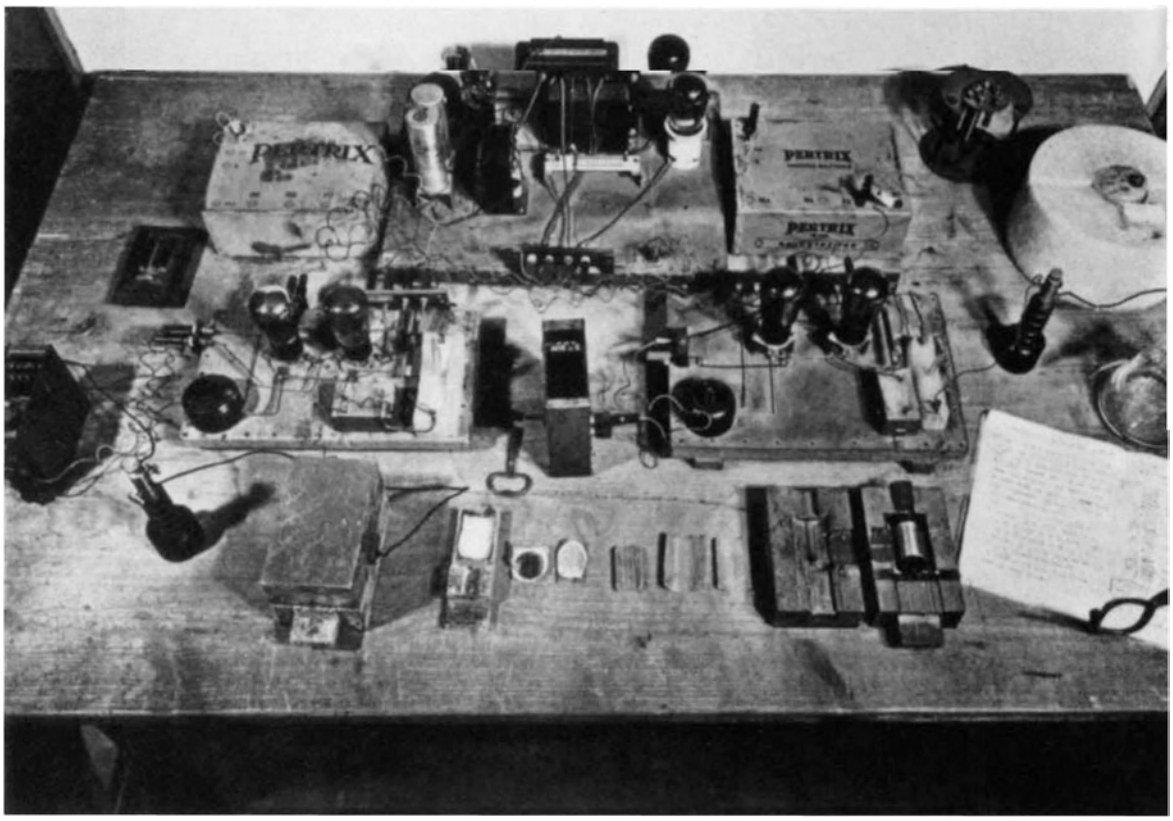

Fig. 5. Some of the Berlin team's instruments, now in the Deutsches Museum in München: Geiger-Müller counters (front part), pulse amplifiers and mechanical counters (middle part), high voltage supply (rear part), neutron source and paraffin block (upper right); additional details in the text. The instruments shown here were located in the rooms 20, 23, and 29 of Figure 4.

four to five orders of magnitude more activity in the decay chain (5).

$$^{238}_{92}\mathrm{U} \xrightarrow[4.5\times10^{9}\,\mathrm{y}]{\alpha} {}^{234}_{90}\mathrm{Th} \xrightarrow[24.1\,\mathrm{d}]{\beta^-} {}^{234m}_{91}\mathrm{Pa} \xrightarrow[1.17\,\mathrm{min}]{\beta^-} {}^{234}_{92}\mathrm{U} \xrightarrow[2.5\times10^{5}\,\mathrm{y}]{\alpha} {}^{230}_{90}\mathrm{Th} \quad (5)$$

The energetic β^--rays of 1.17-min protactinium-234m pass through the aluminum tube of the counters. It is certainly possible to chemically separate protactinium-234 and its precursor thorium-234 from uranium; however, both activities are growing continuously from the decaying uranium, which therefore must be purified immediately before the irradiation.[57] For this purpose uranium is precipitated with a mixture of ammonia and ammonium carbonate in the presence of some iron and is dissolved again as a complex uranyl carbonate; thorium- and protactinium-234 remain attached to the precipitated iron hydroxide. From the filtrate, ammonium diuranate is precipitated; this is usually used for the irradiation.

The more the Berlin group progresses with the radiochemical analysis of the uranium-born activities and with refining the separation techniques, the more puzzling are the results. During the next three years new transuranic activities are discovered;[58, 59] and the respective formation reactions,[57, 60, 61] decay properties,[62] and chemical behavior are studied.[63] In May 1937 the results are presented in detail in two publications.[61, 63] A few days before *Lise Meitner*'s escape from Germany the last joint note[64] which includes a new activity, the 60-d eka-iridium, is submitted.

The scheme of transuranic elements now looks as depicted in Figure 6. Three β^--emitters are assigned to uranium. Two

$_{92}$U	$_{93}$Eka-Re	$_{94}$Eka-Os	$_{95}$Eka-Ir	$_{96}$Eka-Pt	$_{97}$Eka-Au
10 sec	→ 2,2 min	→ 59 min	→ 66 h	→ 2,5 h	→ ?
40 sec	→ 16 min	→ 5,7 h	→ 60 d	→ ?	
23 min	→ ?				

Fig. 6. Decay chains of uranium and of the transuranic elements produced by irradiation of uranium with neutrons; situation as of June 1938 according to the last joint publication by *O. Hahn, L. Meitner*, and *F. Strassmann* [64].

are the origin of two long β^--decay chains with seven transuranic activities; one chain ends with element 95, eka-iridium, the second extends even to element 96, eka-platinum. No decay product is found for the strongest activity, the third uranium isotope with 23-min half-life, even though it is clearly identified chemically as uranium and shown to be a β^--emitter by using a cloud chamber;[57] thus, it must decay into element 93. As even in pure samples of this activity no decay product is found, *Hahn* et al. presume it to be a long-lived eka-rhenium.[63] Finally,[61] all uranium activities are ascribed to the same isotope, uranium-239. However, such a triple nuclear isomerism which even continues in the decay products is difficult to understand; this is certainly realized by *Meitner, Hahn*, and *Strassmann*.[61] Another peculiarity is the stability against α-decay in the chains approaching a region where α-decay should increasingly dominate. However, no α-emitters are observed among the transuranic elements.[65] This stability is theoretically explained[66] by the assumption that transuranic nuclei might be elongated rather than spherical. The nuclei in that region are indeed elongated, as is found much later. The same results and an additional product with a 17-h half-life[65] are obtained at the Berkeley cyclotron, which has a neutron flux larger by many orders of magnitude. Several β^--emitters are also produced[67] when uranium is bombarded with energetic neutrons.

The scheme of parallel decay chains is based on a number of different arguments, which, taken together, make up a reasonable picture. First of all one has the cloud chamber experiments[57, 62] which prove that β^--emitters are formed. Genetic relationships within the chains are obtained by chemically isolating one of the activities and by tracing its decay into another activity; for example, 16-min eka-rhenium decays into 5.7-h eka-osmium[61] and 66-h eka-iridium into 2.5-h eka-platinum.[63] Even in cases where such relationships are difficult to establish, those activities already present after a short irradiation time should be near the beginning of a decay chain; they cannot be formed from the decay of later members. Using this argument the 10-s, 40-s, 2.2-min, and 16-min activities are ascribed to either uranium or eka-rhenium.[61] An additional criterion is the influence of the neutron energy on the production of the activities. The two long decay chains can be produced with either thermal, slow, or fast neutrons without any noticeable difference, the 23-min activity, however, only by resonance capture of neutrons with 25 electron volts energy.[61] The production cross-sections obtained for the three chains seem to be only compatible with uranium-238 as the primary nucleus rather than with the much less abundant uranium isotopes 235 and 234.[61] Thus, the conclusion is that all three chains emerge from uranium-239. During experiments which focus more on aspects of nuclear physics chemical methods are also used for disentangling the reaction mixture.

The main emphasis in identifying the unknown activities is, however, placed on their chemical properties, still with the assumption that one is dealing with uranium, eka-rhenium, and eka-platinum elements. A large variety of methods is used in these chemical studies,[63] either based on group separations which focus on all four transuranic or all three eka-platinum elements, or on methods which are very specific for individual elements. In the case of the first and the last members of the chains, the chemical studies are quite straightforward. The 16-min, 23-min, and 59-min activities dominate after a short irradiation and are still long-lived enough to allow for more complicated chemical operations. If, on the other hand, one carries out the irradiation and then waits for a long time, only the 66-h activity and its 2.5-h decay product remain. The treatment of the intermediate products is more problematic due to the complex mixture of decaying and growing activities. It also seems easier to distinguish between uranium, eka-rhenium, and the group of all eka-platinum elements rather than between the individual eka-platinum elements.

The almost quantitative coprecipitation of all transuranic elements with platinum sulfide in medium-strong hydrochloric acid is thought to be a very characteristic reaction; in this way, transuranic elements can be separated from large amounts of uranium and strong activities of natural decay products.[63] In the framework of the periodic table of that time, this sulfide formation is considered to be the most

striking difference between the transuranic elements on the one hand and uranium and the cisuranic elements on the other. The 23-min activity can be isolated[63] from the filtrate of such a sulfide precipitate together with the insoluble sodium uranyl acetate, which is characteristic of uranium. If the precipitation from the bulk of the irradiated uranium is performed quicker, a shorter-lived activity is noticeable; thus, also the 40-s activity seems to be a uranium isotope[63] according to this nice early example of fast radiochemical separations of complex mixtures.

As expected, eka-rhenium is found electrochemically to be the least noble transuranic element; in contrast to the eka-platinum elements it is not deposited on noble metal foils placed in solutions nor can it be reduced to the metal state with bismuth as carrier. With some reagents the transuranic elements can even be sequenced. In a precipitation of uranium by sodium hydroxide the following order of coprecipitation is obtained: eka-Os > eka-Ir > eka-Re > eka-Pt. If precipitation is performed with rhenium sulfide in strong hydrochloric acid the order is eka-Os > eka-Re ≥ eka-Ir > eka-Pt. In contrast to uranium and the cisuranic elements the transuranic elements have in common that they are volatile at medium and higher temperatures. If a sulfide precipitate is heated under aerobic conditions, the volatility increases in going from eka-rhenium to eka-platinum; if it is treated with aqua regia to form chlorides before heating, the sequence is reversed. Finally, two very specific reactions seem to corroborate this scheme: eka-rhenium coprecipitates with nitron perrhenate and eka-platinum with ammonium platinum hexachloride; thus, element 93 obviously forms a species analogous to perrhenate while element 96 forms one analogous to platinum hexachloride.

Hahn, Meitner and *Strassmann*[63] finish their article about the chemistry of the transuranic elements by discussing similarities to and differences from rhenium and the platinum metals. The similarities prevail and the trends seem to continue plausibly. There should no longer be any doubts about their place in the periodic table and, above all, their difference from all other known elements is firmly established.[63] This conclusion, however, is premature; what one could not imagine was that a complex mixture of lighter elements could simulate these results.

The Berlin team refrains from suggesting names for the transuranic elements. The group in Rome instead feels confident enough to start using the names ausonium for 93 and hesperium for 94.[3, 68] *Enrico Fermi*, too, uses them when he receives the Nobel Prize on December 10, 1938, partly for the synthesis of new elements. In the published version of his lecture[69] he adds a footnote, noble indeed, that after the discovery of nuclear fission—a few days after the lecture—all transuranic elements should be reexamined because they might in fact be fission products. *Fermi* does not return to Italy. Shortly before, a detailed review article appears dealing with the transuranic elements.[70] Even the discovery of element 93 in nature by X-ray-spectroscopy is again reported.[71, 72]

1.4. Interlude: Radium from Thorium?

Not only uranium, but also thorium is especially interesting regarding activation by neutrons. In this case the focus is not on transuranic elements which should not be accessible from thorium; still there is some connection with our topic, as we shall see later. Radiochemists were fascinated,[73, 74] instead, by the possibility of reaching the long sought 4n + 1 decay series via reactions like (6) and (7).

$$^{232}_{90}\mathrm{Th} + {}^{1}_{0}\mathrm{n} \longrightarrow {}^{233}_{90}\mathrm{Th} + \gamma \qquad (6)$$

or

$$^{232}_{90}\mathrm{Th} + {}^{1}_{0}\mathrm{n} \longrightarrow {}^{229}_{88}\mathrm{Ra} + {}^{4}_{2}\alpha \qquad (7)$$

For the three radioactive decay series starting with uranium-238, uranium-235, and thorium-232 the mass numbers of all members of the respective chains can be divided by either 4n + 2, 4n + 3, or 4n. Therefore, a 4n + 1 series is postulated which, however, is not found in nature.

Upon irradiation of thorium one has to cope with all nine members of the 4n decay series.[75] Even when thorium samples are used which have been repeatedly purified from decay products over many years[76] so that these have almost disappeared, one still has to perform cumbersome purifications and additional test experiments.[73, 75, 78]

Fermi and his co-workers[2, 8] are again the first ones to start with experiments; they find two β^--emitters with half-lives of 1 min and 15 min, respectively. The latter is soon corrected to a value of 24 min.[36, 37] This activity has the characteristic chemical properties of thorium. It coprecipitates with thorium fluoride and thorium peroxide and can be separated from all other elements between lead and uranium.[37] *Hahn* and *Meitner*[73] confirm the two activities and also identify the longer-lived one as being thorium-like. As the short-lived activity is produced with fast neutrons they assign it to radium-229, which is formed by an (n,α)-reaction according to Equation (7); they argue that an additionally observed 11-min activity might be its actinium decay product.

But soon the situation becomes more complex, as in the case of uranium. In Paris, *Irène Curie, Hans von Halban* and *Pierre Preiswerk* first find four,[74] then a total of five[79] β^--emitters with half-lives of[80] 1 min, 2.5 min, 12 min, 25 min, and 3.5 h, respectively. They assign them all to thorium and its neighbors, for example the 3.5-h activity to actinium, because it coprecipitates with lanthanum fluoride.[80] Finally, a 42-h actinium is added.[78] It remains controversial whether the 4n + 1 series is believed to have been found first in Berlin or in Paris; this may be the reason why the Berlin group remains quite reserved[10] towards the following work of the group in Paris.

The mixture of activites, however, becomes more and more puzzling. *Lise Meitner, Fritz Strassmann* and *Otto Hahn*[75] show that 23-min thorium is formed via a resonance capture (n,γ)-process (6) and correctly conclude that it must be thorium-233. They identify its decay product—again correctly—as 27-d protactinium-233. With fast neutrons they even find three β^--emitting radium isotopes (Fig. 7), one of them with a 0.8 min half-life; all three are chemically identified as radium and can be connected with three actinium isotopes. They are presumed to be formed by a Th(n,α)Ra reaction (7), although (n,α)-reactions have up to then been observed only for light elements;[3] the instability of thorium against α-particle emission, apparent in its

$^{232}Th\ (n,\alpha) \longrightarrow {}^{229}Ra \xrightarrow[<1\ Min.]{\beta} {}^{229}Ac \xrightarrow[\sim 18\ Min.]{\beta} Th?$

$^{232}Th\ (n,\alpha) \longrightarrow {}^{229}Ra \xrightarrow[15\ Min.]{\beta} {}^{229}Ac \xrightarrow[\sim 3{,}5\ Std.]{\beta} Th?$

$^{232}Th\ (n,\alpha) \longrightarrow {}^{229}Ra \xrightarrow[\sim 4\ Std.]{\beta} {}^{229}Ac \xrightarrow[20\ bis\ 30\ Std.]{\beta} Th?$

Fig. 7. Three isomeric decay chains for radium and actinium formed by irradiation of thorium with fast neutrons; after *L. Meitner, F. Strassmann,* and *O. Hahn* [75], May 1938.

natural decay, is taken as an argument for this explanation.[75] It seems to be further corroborated by a note[81] dealing with energetic α-particles which appear during the irradiation of thorium with neutrons; in *Meitner*'s group, however, a search for these prompt α-particles is not successful.[82] The activities of the Berlin group are confirmed by using much stronger neutron sources, and a new decay product, 24-h thorium-231, is added.[83] Since natural thorium mainly consists of thorium-232, all three radium activities have to be assigned to radium-229 and its decay products to actinium-229 (Fig. 7). This triple nuclear isomerism is, however, difficult to understand,[75] as is already the case with uranium (Fig. 6).

Today, the $4n+1$ series[84] is known to start with neptunium-237, which, due to its half-life of 2.14×10^6 y, does not exist in nature any more; neither does the rest of the decay series. Among the nuclides which are correctly assigned in these early experiments, 27.0-d protactinium-233 is indeed a member of the chain, but not 22.3-min thorium-233.

1.5. Paris 1937–1938: The 3.5-hours Activity

Let us now go back to the artificial activities produced from uranium. The cumbersome purification of uranium prior to irradiation can be omitted if the energetic β^--rays of the natural decay product, protactinium-234m, are discriminated by covering the sample with a copper foil through which these β^--rays cannot pass. Then, naturally only those activities can be detected whose β^--rays are even more energetic. *Irène Curie* and *Paul Savitch*,[85] in the summer of 1937, decide to proceed thus in dealing with the artificial uranium-born activities. In addition to the known 40-s, 2-min and 16-min components they find[86] a new activity with 3.5 h half-life as depicted in Figure 8. The 3.5-h activity appears without absorber foil, too, if the activity of irradiated and non-irradiated uranium is followed with a compensation method. It is not noticed, however, that a very similar activity appears also upon irradiation of thorium with neutrons.[80] The 3.5-h activity does not coprecipitate with sulfides in acid solution[85] and can be separated this way from the transuranic elements reported until then. It seems to follow the natural decay product of uranium, thorium-234. This assignment to thorium from the reaction (8) cannot

$$^{238}_{92}U + {}^{1}_{0}n \longrightarrow {}^{235}_{90}Th + {}^{4}_{2}\alpha \qquad (8)$$

be confirmed in Berlin, however, where again—as already before[61]—thorium is not found. A letter is written to the researchers in Paris suggesting the withdrawal of these results.[87]

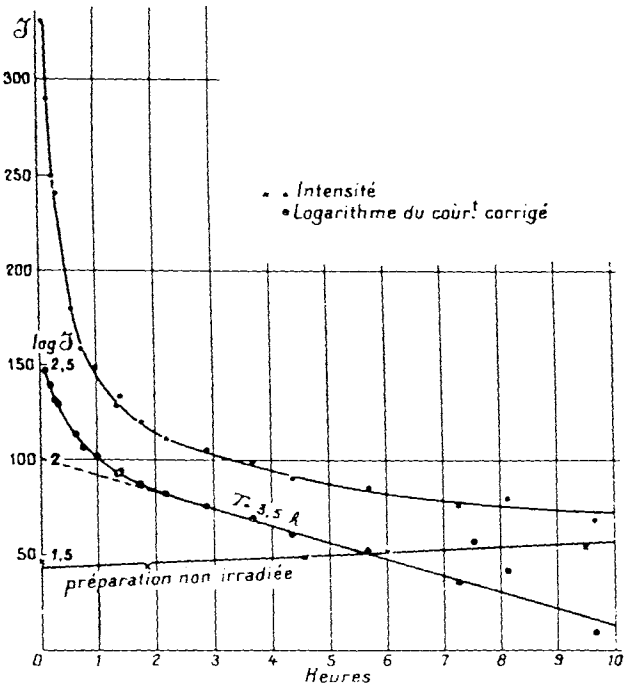

Fig. 8. The 3.5-h activity found in uranium irradiated by neutrons and measured directly as published by *I. Curie* and *P. Savitch* [86] in Paris, July 1938. Upper curve: activity measured with the sample covered by a copper foil of 0.48 g · cm^{-2} thickness, depicted linearly as a function of time; lower curve: build-up of natural decay products in uranium, also depicted linearly; middle curve: difference between the two measurements in semilogarithmic representation with 16-min "eka-rhenium" at the beginning followed by a pure decay with 3.5 h half-life.

A following note by *I. Curie* and *P. Savitch*[88] is indeed modified with regard to this after they succeed in chemically separating the 3.5-h activity from thorium and protactinium. What they further find is even more remarkable: the chemical properties of the activity are similar to those of the lanthanoids; it is likely that it is either actinium, the heavier homologue of this group of elements, or a new transuranic element with properties completely different from eka-rhenium or the eka-platinum elements. In the next note[89] additional lanthanoid properties are ascribed to the 3.5-h activity, for example its coprecipitation with fluorides and oxalates. As they are able to separate the 3.5-h activity chemically from actinium *I. Curie* and *Savitch* favor the hypothesis of a new transuranic element, even though they find it difficult to understand. For this separation the activity is isolated with lanthanum as a carrier. Natural radio-actinium is added followed by a fractional precipitation of lanthanum oxalate. The 3.5-h activity is found in the head fraction and actinium—as expected—in the tail fraction.

All these results along with some others are presented in detail in the following publication[86] which is supplemented by a note[90] about the maximum β^--energy of the 3.5-h activity, 3.2 MeV. *I. Curie* and *Savitch* present additional chemical evidence against actinium. The similarity to the lanthanoids is summarized:[86] "Dans l'ensemble, les propriétés de $R_{3,5h}$ sont celles du lanthane, dont il semble jusqu'ici qu'on ne puisse le séparer que par fractionnement".[*] One is

[*] "On the whole the properties of $R_{3.5h}$ are those of lanthanum, from which, it seems so far, it can be separated only by fractionation."

tempted to think that if *I. Curie* and *Savitch* had simply omitted the second half of the sentence the puzzle would have been solved; the observation of fractionation, however, is correct, as we will see below. According to a later remark[91] *I. Curie* and *Savitch* even consider uranium breaking into lighter elements; yet, they reject this explanation because the 3.5-h activity as well as the transuranic elements, represented by the 16-min eka-rhenium, show the same behavior with respect to different neutron energies[86] and thus seem to be related. In conclusion, albeit with some hesitation, they favor the hypothesis of a transuranic element with completely different properties and probably being at the beginning of this series of elements:[86] "On pourrait imaginer, par exemple, que ce corps a le nombre atomique 93 et que les corps étudiés par *Hahn, Meitner* et *Strassmann* ont des nombres atomiques de 94 à 97"[*] This, of course, is a challenge for the group in Berlin. At last, enough details are known to critically test the foundation of these results. In Berlin one is sceptical, as *Otto Hahn* tells *Frédéric Joliot—Irène Curie*'s husband—when they meet in May 1938 during a congress in Rome.[10, 92] In Berlin, somewhat jokingly, one speaks of "*Curio*sum".[76]

2. Alkaline Earth Metals from Uranium

2.1. Berlin, Autumn 1938: the "Radium" Activities

As soon as the detailed publication by *I. Curie* and *Savitch*[86] appears in the third week of October 1938, *Hahn* and *Strassmann* are able to reproduce the 3.5-h activity.[93] The best method, as recommended in Paris, to chemically isolate the activity is its coprecipitation with sparingly soluble potassium lanthanum sulfate. *Strassmann* immediately notices[48] that if radium should be present it would coprecipitate as sulfate and later during fractionation appear in the head fraction, as prescribed for the 3.5-h activity. Radium could be formed if thorium from a U(n,α)Th reaction disintegrates by α-decay [Reaction (9)].

$$^{238}_{92}\mathrm{U} + {}^{1}_{0}\mathrm{n} \longrightarrow {}^{4}_{2}\alpha + {}^{235}_{90}\mathrm{Th} \xrightarrow{\alpha} {}^{231}_{88}\mathrm{Ra} \xrightarrow{\beta^-} {}^{231}_{89}\mathrm{Ac} \qquad (9)$$

Finally, actinium could result from β^--emitting radium. An α-emitting thorium may well not have been noticed before. This hypothesis would serve to trace back the puzzling chemical properties of the 3.5-h activity to a mixture of already known elements. Of these elements, radium can be identified more easily than a lanthanum-like element. *Strassmann* suggests,[76, 94] not to coprecipitate radium as usual with barium sulfate, which has a large surface, but with barium chloride instead; this salt crystallizes from concentrated hydrochloric acid as beautiful, colorless, and particularly pure needles and can easily be reprecipitated after having been dissolved in water. With this elegant method radium can quickly and unambiguously be identified; it is accompanied only by barium.

Within a matter of days *Hahn* and *Strassmann* obtain their first important results, as *Hahn* notes on October 25, 1938 in a letter to *L. Meitner*.[93] The "countdown" for the discovery of nuclear fission has started; it is documented in the laboratory notebook "Chem. II",[96] a plain booklet bound in wax-paper of about 18 × 24 cm format and 94 pages.[*] We are well informed about the subsequent events by a series of letters exchanged between *Otto Hahn* and *Lise Meitner*, which were edited under somewhat different aspects.[97, 98] Whatever seems important to one of them is written down and the answer often arrives within two days. It is especially informative to read the scientific part of the letters and the laboratory notes in chronological order.[98] *Hahn* urgently asks for explanations of these unexpected results, *Lise Meitner* for more information. All this occurs in quite a troubled period of time, as one notices clearly from *Hahn*'s autobiographic notes of 1945[76] and, in a more condensed and dramatic way, from his pocket-book of 1938.[99] Even when *Lise Meitner* is still with him, *Hahn* has already isolated

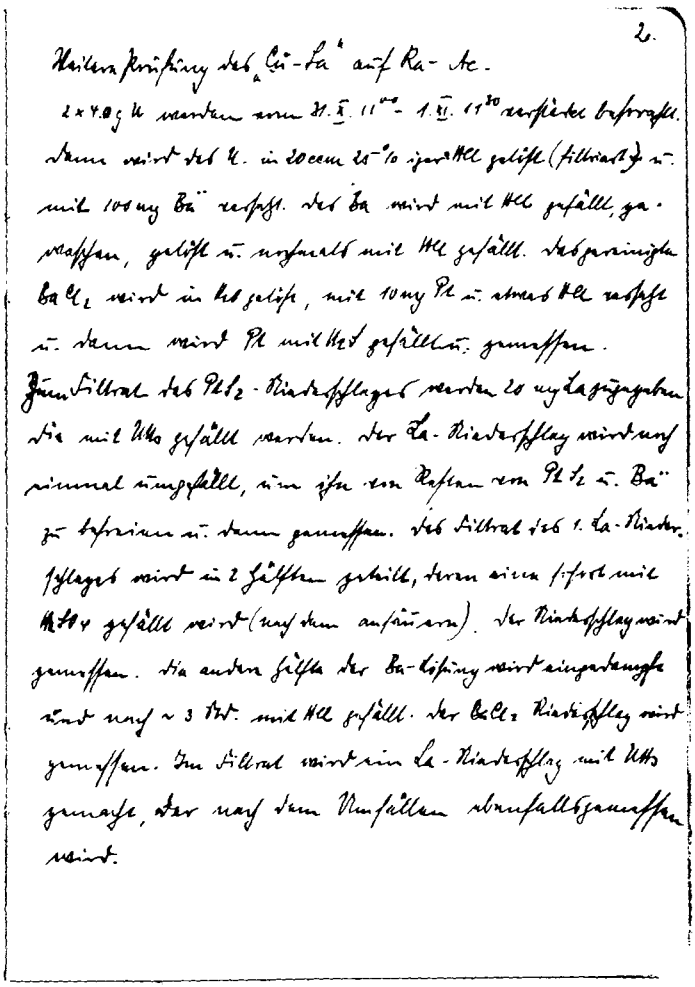

Fig. 9. Beginning of the note-book "Chem. II" by *O. Hahn* and *F. Strassmann* [103]: Chemical separation for "Weitere Prüfung des "Cu-Sa" auf Ra-Ac" ("Further tests of "Cu-Sa" for Ra-Ac") on November 1, 1938, written by *F. Strassmann*; separation of a radium fraction from irradiated uranium by precipitation of barium chloride from strong hydrochloric acid. "Cu-Sa" represents the 3.5-h activity of *I. Curie* and *P. Savitch* [86].

[*] "One could imagine, for example, that this body has the atomic number 93 and that the bodies investigated by *Hahn, Meitner*, and *Strassmann* have the atomic numbers 94 to 97."

[*] The author is indebted to *Ernst Berninger* for a copy of the booklet "Chem. II". A previous note-book "Chem. I" seems to have been lost. The subsequent books starting with "Chem. III" and the corresponding larger decay-curve drawings are stored in the Landeshauptarchiv Koblenz, legacy *Fritz Strassmann*.

himself completely;[101] no one else in the institute is told what is about to happen. It is the time of the Reichskristallnacht. Some of the institute's senior scientists are fanatic supporters of the "National Socialists" (Nazis), others, like *Fritz Strassmann*, succeed in remaining aloof though it meant facing disadvantages. A potential successor for *Hahn*, who is considered politically unreliable, is already in the institute. In this atmosphere the problem of safeguarding *Lise Meitner*'s property has to be solved. *Hahn*'s wife *Edith* starts to suffer from a mental disease and *Hahn* also feels completely exhausted at times. The exciting results with uranium distract him and save this extremely difficult situation.[76] The secluded *Fritz Strassmann*, whom he also trusts politically, cares for the continuous progress of the experiments.

"Chem. II" starts on November 1, 1938, with a note[103] shown in Figure 9. To verify whether "Cu-Sa", the 3.5-h activity of *I. Curie* and *Savitch*, might be radium or actinium, the respective homologous elements barium and lanthanum are separated from the bulk of irradiated uranium and accompanying "transuranic elements" are then removed with platinum sulfide. To this purpose 8 g of uranium are irradiated with slow neutrons for one day, dissolved in hydrochloric acid, and barium chloride is precipitated from the resulting solution. After reprecipitating barium chloride and dissolving it again, platinum is separated as sulfide and lanthanum as hydroxide. One half of the barium–radium fraction is immediately processed to yield a sulfate, the remaining half is put aside to allow for actinium to be formed and is later separated into a barium–radium fraction and a lanthanum–actinium fraction.

The barium–radium fractions are especially active. The decay curves indicate the presence of even three radium isotopes, having half-lives of about 25 min, 110 min, and several days; they seem to be related to three actinium decay-products, as shown in Figure 10. *Hahn* and *Strassmann* soon

$$^{231}_{88}\mathrm{Ra}_1 \xrightarrow[\sim 25\ \mathrm{Min.}]{\beta} {}_{89}\mathrm{Ac}_1 \xrightarrow[\sim 40\ \mathrm{Min.}]{\beta} {}_{90}\mathrm{Th}?$$

$$_{88}\mathrm{Ra}_2 \xrightarrow[\sim 110\ \mathrm{Min.}]{\beta} {}_{89}\mathrm{Ac}_2 \xrightarrow[\sim 4\ \mathrm{Std.}]{\beta} {}_{90}\mathrm{Th}?$$

$$_{88}\mathrm{Ra}_3 \xrightarrow[\text{mehrere Tage}]{\beta} {}_{89}\mathrm{Ac}_3 \xrightarrow[\sim 60\ \mathrm{Std.}]{\beta} {}_{90}\mathrm{Th}?$$

Fig. 10. Three radium isomers and their respective actinium decay products in the barium fraction of neutron-irradiated uranium; note by *O. Hahn* and *F. Strassmann* [104], November 1938.

describe these findings in a note.[104] All three radium activities are ascribed to radium-231; thus, as already in the case of the activities isolated from thorium and ascribed to radium-229, an inherited triple isomerism is assumed. It is obviously not recognized that the half-lives are quite similar in both cases, probably because different radium isotopes are postulated. Strangely enough, the (n,α)-reaction (9) of uranium already occurs with slow neutrons;[104] this effect is observed for the first time.

In the following publication which is submitted to "Naturwissenschaften" on December 22, 1938, *Hahn* and *Strassmann*[105] present details of these activities. The editor, *Paul Rosbaud*, realizes the significance of some of the results reported at the end and has the publication appear already in the next issue on January 6, 1939. However, four out of the five printed pages deal with interesting but not really spectacular results. At first, one only notices that the title speaks of "alkaline earth metals" instead of "radium" as in the case of the preceding note. In the text it again says "radium", mostly in quotation marks, as well as in the decay chains (Fig. 11) which are now supplemented. Proof is shown of all

$$\text{„Ra I"}? \xrightarrow[<1\ \mathrm{Min.}]{\beta} \mathrm{Ac\ I} \xrightarrow[<30\ \mathrm{Min.}]{\beta} \mathrm{Th}?$$

$$\text{„Ra II"} \xrightarrow[14 \pm 2\ \mathrm{Min.}]{\beta} \mathrm{Ac\ II} \xrightarrow[\sim 2{,}5\ \mathrm{Std.}]{\beta} \mathrm{Th}?$$

$$\text{„Ra III"} \xrightarrow[86 \pm 6\ \mathrm{Min.}]{\beta} \mathrm{Ac\ III} \xrightarrow[\sim \text{mehrere Tage?}]{\beta} \mathrm{Th}?$$

$$\text{„Ra IV"} \xrightarrow[250\text{–}300\ \mathrm{Std.}]{\beta} \mathrm{Ac\ IV} \xrightarrow[<40\ \mathrm{Std.}]{\beta} \mathrm{Th}?$$

Fig. 11. The decay chains of Figure 10 in the detailed publication by *O. Hahn* and *F. Strassmann* [105] from December 22, 1938, in a more complete form and with the radium symbols in quotation marks.

activities by decay curves which are obtained after different irradiation and separation times; Figure 12 presents an example. The chemical separation is discussed in detail and it is stressed that the activity precipitated with the barium salts can only stem from radium, "wenn man das Barium selbst als allzu unwahrscheinlich vorerst außer Betracht läßt[105]",[*] as it still says in the beginning of the text.

2.2. Berlin, December 17, 1938: Radiochemical Detection of Barium

The big surprise comes only at the end of the paper;[105] one hardly suspects it in a publication entitled "Über den Nachweis und das Verhalten der bei der Bestrahlung des Urans mittels Neutronen entstehenden Erdalkalimetalle".[**] *Hahn* and *Strassmann* report on some recent investigations which they only publish with hesitation. They have decided to prove more rigorously the occurrence of radium. Since *Marie Curie*'s time it has been known how to achieve this:[106] Upon fractional crystallization of certain barium salts, for example the chloride, radium becomes enriched in the head fractions and, after many repetitions, can even be obtained in pure form. *Hahn* became acquainted with these methods during his time with *Ramsay* in London[76, 107] and discovered his first radioactive species this way,[109] the 1.9-y thorium-229, then called radiothor. Until the thirties, the study of such coprecipitation reactions was one of his main research interests.[9]

Presumably these control experiments are motivated by some doubts which theorists raised against the inherited isomerism.[13] Already then nuclear isomerism is correctly

[*] "if one does not consider the quite unlikely candidate barium for the time being."

[**] "On the identification and behavior of the alkaline earth metals formed upon irradiation of uranium with neutrons"

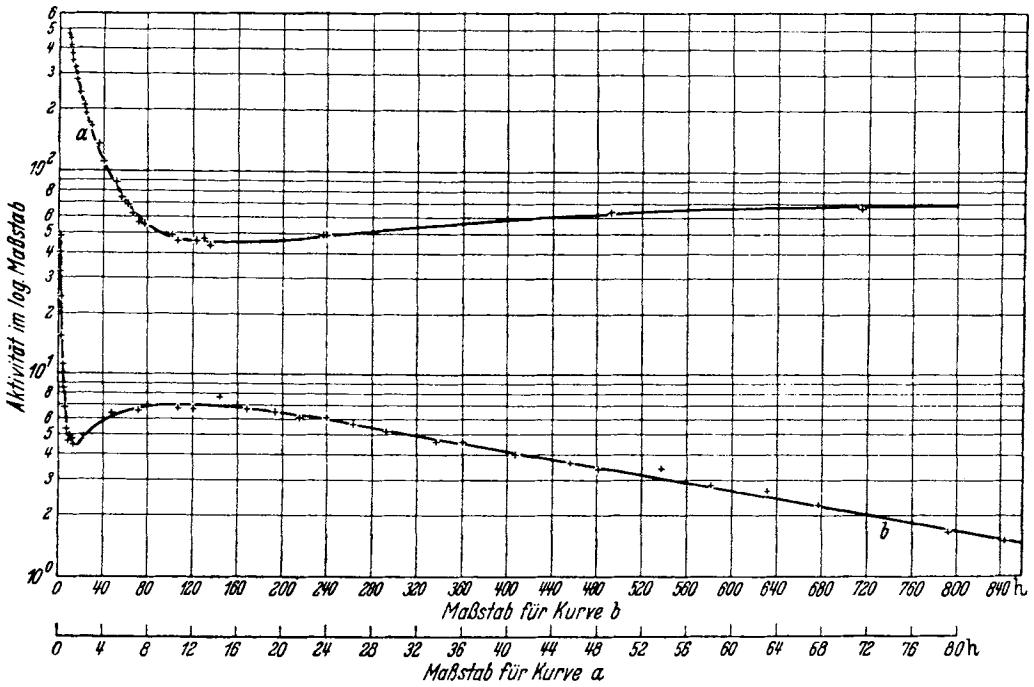

Fig. 12. One of the decay curves from the same publication [105] as Figure 11: The three radium isotopes after four days of irradiation. The measured activity is depicted logarithmically versus time (lower curve), its initial decrease with a ten-times extended time axis (upper curve). The initial decrease is mainly due to 86-min "Ra III", the subsequent rise is caused by the 40-h "Ac IV", the decay product of the long-lived 12-d "Ra-IV", which dominates the final decrease.

understood as an effect of nuclear spin[110]—large spin differences hinder the transition from excited nuclear states to the ground states; but it is thought to be very unlikely that such an effect is preserved in a decay chain. Therefore, starting with the idea of deformed transuranic nuclei,[66] another kind of isomerism is suggested,[111] namely the possibility of nuclei having the same numbers of protons and neutrons but with different deformations and, in turn, differences in half-lives. Much later, this shape isomerism is indeed found for the real transuranic elements[112–115] via their spontaneous nuclear fission. The formation reaction is a second point which raises scepticism;[116] it is understood by many to be a very peculiar, successive detachment of two α-particles[13, 117] [cf. (10)], although *Hahn* and *Strassmann*[104]

$$^{238}_{92}\mathrm{U} + {}^{1}_{0}\mathrm{n} \longrightarrow {}^{231}_{88}\mathrm{Ra} + 2\,{}^{4}_{2}\alpha \qquad (10)$$

explicitly point to one or more α-emitting thorium isotopes as intermediate products. But *Hahn* also sometimes speculates about an (n,2α)-reaction.[48, 116] For *Hahn*[76, 117] the most substantial doubts are probably the ones that he hears in Copenhagen on November 13–14, 1938, when he visits *Niels Bohr* to give a talk; on this occasion he also meets[99] *Lise Meitner* and her nephew *Otto Robert Frisch*, who works as an experimental physicist in *Bohr*'s institute. In the Berlin institute, too, doubts are being raised,[118] some based on theoretical arguments, others because prompt α-particles from an (n,α)-reaction are not observed[82] upon irradiation of uranium with neutrons.

Later, however, *Hahn* mentions also a more trivial reason for the fractionations:[46, 94, 117] Due to the thickness of the barium samples the β-rays of especially the most long-lived new activities are strongly absorbed. Therefore, by enrichment of radium in a smaller portion of barium the counting efficiency is to be improved. This is crucial for the long-lived 12-d component in Figure 12 which is only evident by growth of its 40-h daughter substance.

The first fractionation is performed on November 25, 1938. Figure 13 depicts the notes of this amazingly simple experiment.[119] 8.5 g of uranium are irradiated over night, dissolved in strong hydrochloric acid, and barium ions (1 g) are added to the solution. Barium is precipitated as chloride, the precipitate, in turn, is dissolved in water, and hydrochloric acid is added again; after cooling, barium chloride is precipitated in several portions. The barium precipitates are measured one after the other and, as can be read at the end of the protocol, are converted into barium carbonate after about two hours. In addition, further elements are isolated, which we will not discuss, however.

The data of the first measurement of each of the three barium chloride precipitates are collected in Figure 14. The corrected count rates are placed in the next to the last column. They develop continuously within error limits when switching from one fraction to the next. The half-life turns out to be about 40 minutes; thus, mainly the short-lived species "radium" II and III are present. No sudden decrease can be perceived between the first and second and between the second and third fractions. In contrast to what was expected originally, "radium" is not enriched in the first fraction. No comment on that is found in the notes; in the headline, however, "Ra" is put in inverted commas—Figure 13—whereas in the following notes and in the letters of *Hahn-Meitner* it is not.

The next fractionation is attempted on November 28, this time with 86-min "Ra III" and by using barium bromide,[120] in which radium is enriched to a larger extent than

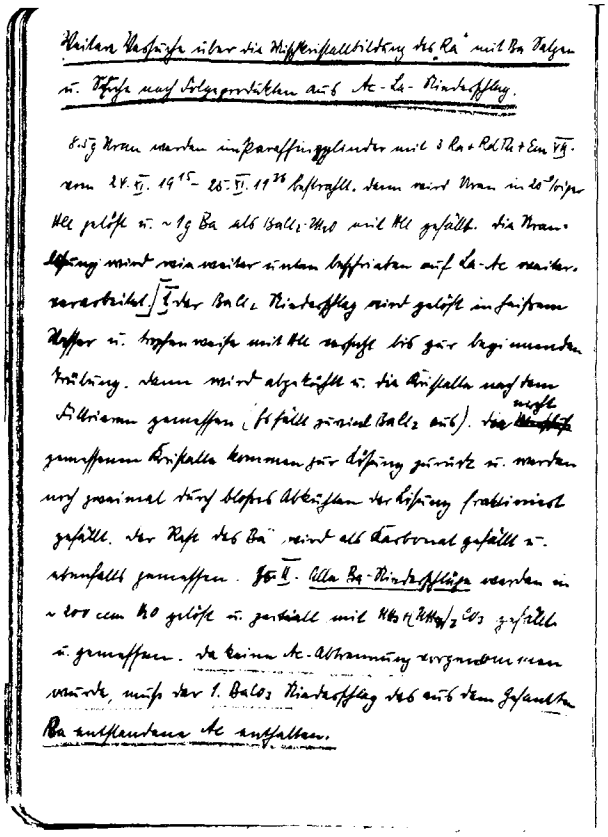

Fig. 13. First chemical fractionation of the radium activity from irradiated uranium with barium as carrier element, November 25, 1938 [119]: Beginning of the chemistry protocol concerning "Weitere Versuche über die Mischkristallbildung des "Ra" mit Ba Salzen u. Suche nach Folgeprodukten aus Ac-La-Niederschlag" ("Further experiments about the formation of mixed crystals of "Ra" with Ba salts and search for decay products from Ac-La precipitate"), written by *F. Strassmann*. The irradiated uranium is dissolved in hydrochloric acid. Barium chloride is precipitated from the solution, dissolved again in water, and, after cooling, precipitated in fractions. After a quick measurement the precipitates are converted into barium carbonate. Note the quotation marks for Ra in the title.

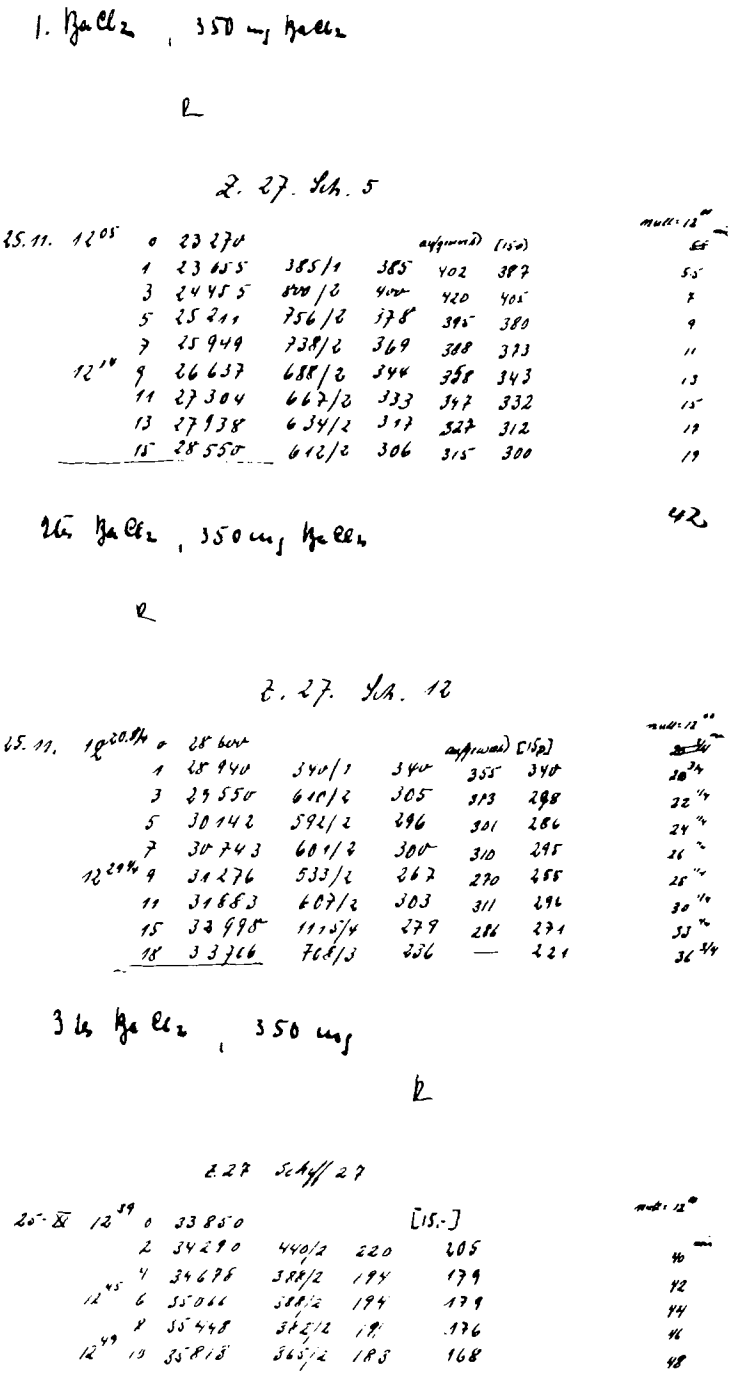

Fig. 14. Some of the data of the fractionation experiment from November 25, 1938 [119]: First indication that the "radium" isotopes from uranium do not behave like radium because they are not enriched in the head fraction. The first measurements of each of the three successive barium chloride fractions are depicted; the samples were placed on different holders (Sch) and measured with the same counter (Z.27). The columns represent from left to right: 1 date, 2 time, 3 elapsed time, 4 counts on the meter, 5 difference between the counts and duration of the measurement in minutes, 6 count rate in counts per minute, 7 count rate corrected for counting losses, 8 count rate after subtraction of the background of 15.0 counts/min, 9—on the right—normalized elapsed time. During these 43 min, the activity—a mixture of "radium" II and III—decreases continuously over all three fractions without the sudden decrease between successive fractions that is expected for radium. Remarks concerning the chemistry were written by *Hahn*, other notes by *Irmgard Bohne*, *Clara Lieber*, and *F. Strassmann*.

in the chloride. Due to the longer half-life the fractions can now be measured alternately and thus, the count rates can be compared better. Again, the activity is distributed equally among four fractions. The third attempt, from December 6 to 8, again makes use of the bromide but is performed with the long-lived "Ra IV"; the results are the same as before.[121]

In a first hypothesis the unexpected behavior of radium is assumed to be caused by its extremely low concentrations, much lower than at the time when the fractionation of radium was studied with radiation detectors which were far less sensitive. In the "active" laboratory on the 1st floor *Hahn*[76] starts to fractionate radium in amounts which were common earlier. When switching to the small amounts typical of artificial isotopes no difference is observed—the behavior is as usual.[46, 76]

Now there is only one more consequent step left: The chemical behavior of the artificial and the natural radium isotopes has to be compared directly—the famous indicator experiment by *Otto Hahn* and *Fritz Strassmann* on December 17, 1938, a Saturday.[122] 86-min "radium" obtained from uranium is compared with natural radium-228, mesothorium 1. This long-lived radium isotope, half-life 5.8 y, decays into the short-lived 6.1-h actinium-228, mesothorium 2. The discovery of radium-actinium-228 was *Hahn*'s first important achievement in Berlin.[123–125] The

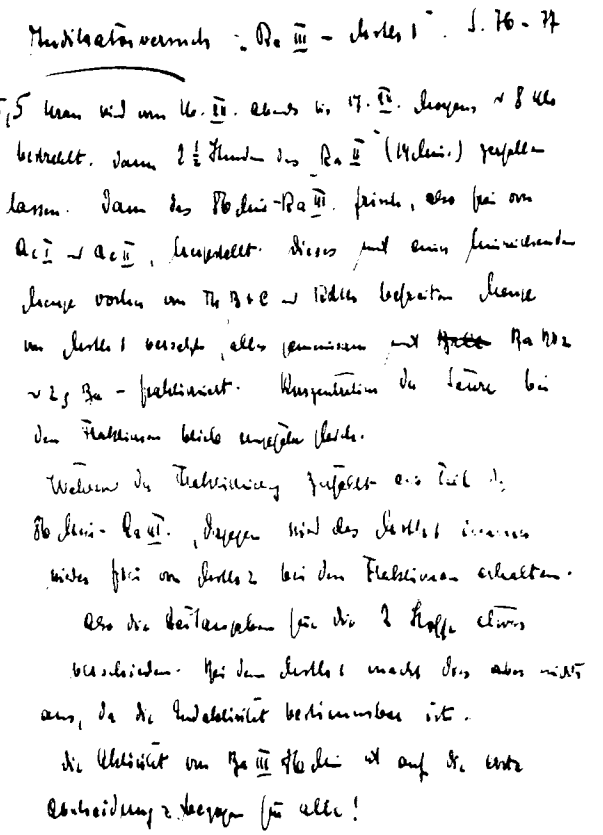

Fig. 15. Discovery of nuclear fission at Berlin on December 17, 1938: The indicator experiment "Ra III–Msth 1"; comparison of the behavior of artificial and natural radium in the fractional crystallization of barium bromide. Eight lines are sufficient for *Otto Hahn* to describe the chemical procedure [126]: "15,5 [g] Uran wird am 16. XII. abends bis 17. XII. morgens ≈ 8 Uhr bestrahlt. Dann 2 1/2 Stunden das "Ra II" (14 Min.) zerfallen lassen. Dann das 86 Min-Ra III frisch, also frei von Ac I und Ac II, hergestellt. Dieses mit einer hinreichenden Menge vorher von Th B + C und Rdth befreiten Menge von Msth 1 [= 5.8-a Radium-228] versetzt, alles gemeinsam mit $BaBr_2$ [−] ≈ 2 g Ba-fraktioniert. Konzentration der Säure bei den Fraktionen blieb ungefähr gleich". (15.5 [g] of uranium was irradiated from the evening of Dec. 16 until the morning of Dec. 17 ≈ 8 a.m. Then "Ra II" (14 min) was allowed to decay for 2 1/2 h. Then the 86-min Ra III freshly prepared, viz. free of Ac I and Ac II. To this a sufficiently large amount of Msth 1 [= 5.8-y radium-228] was added from which Th B+C and Rdth had been removed beforehand; the complete mixture was fractionated with $BaBr_2$ [−] ≈ 2 g Ba. The concentration of acid for the fractions remained approximately constant".)

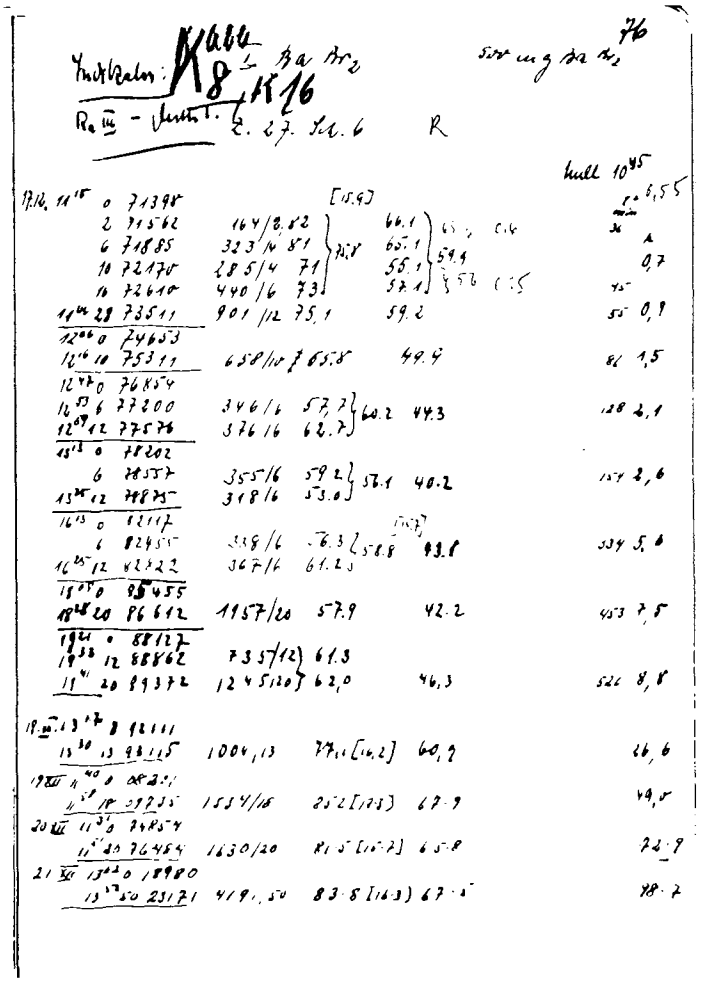

Fig. 16. Counting data for the first of three barium bromide fractions from the indicator experiment radium III–mesothorium 1 using 500 mg $BaBr_2$, measured on December 17, 1938 from 11:15 h until 20:01 h; measurements of the growth of mesothorium 2 from mesothorium 1 until December 21 are included [127]. The columns represent from left to right: 1 date, 2 time, 3 elapsed time in minutes, 4 meter counts, 5 difference between the meter counts and counting time in minutes, 6 count rate in counts per minute, 7 count rate after subtraction of the background, 8 elapsed time in minutes and in hours. "K 8, K 16" are remarks added later concerning the corresponding sheets with decay curves. The notes were taken by *I. Bohne, O. Hahn, C. Lieber*, and *F. Strassmann*.

experiment is simple in principle and the record of the chemical part is correspondingly short;[126] it is reproduced in Figure 15. As before, barium bromide is precipitated in fractions.

By the evening of the same day the artificial radium in the three fractions of barium bromide has already decayed; for several days the growth of actinium-228 is being measured until it is in equilibrium with its "mother substance" radium-228. In Figure 16 the data[127] for the first fraction of 500 mg barium bromide is depicted; facsimiles of the two remaining data sheets can be found elsewhere.[128] The conclusion[129]—Figure 17—is drawn by *Hahn* at the end of the data sheet for the third barium bromide fraction and even more concisely in his note-book:[99] "Indikatorversuch Msth 1 + unser Ra III. Ra III reichert sich nicht an. Msth 1 stark!!".[*]

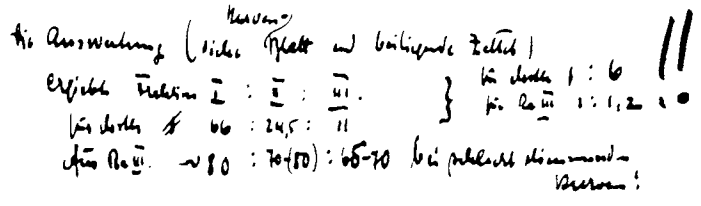

Fig. 17. *Otto Hahn*'s conclusion from the indicator experiment radium III–mesothorium 1 of December 17, 1938, at the end of the data sheet of the third barium bromide fraction [129].
„Die Auswertung (siehe Kurven-Blatt und beiliegende Zettel)
ergibt Fraktion I : II : III } für Msth 1:6
für Msth 66:24,5 :11 } für Ra III 1:1,2
für Ra III ≈80:70(−80):65–70 bei schlecht stimmenden Kurven!"
("The evaluation (see decay-curve sheet and attached paper)
yields fraction I : II : III } for Msth 1:6
for Msth 66:24,5 :11 } for Ra III 1:1,2
for Ra III ≈80:70(−80):65–70 for curves not well matching!")

On the evening of the following Monday, December 19, he informs *Lise Meitner*:[130] "Zwischendurch arbeite ich, soweit ich dazu komme, und arbeitet Straßmann unermüdlich an den Urankörpern, unterstützt von Lieber und

[*] "Indicator experiment Msth 1 + our Ra III. Ra III is not enriched. Msth 1 strongly!!"

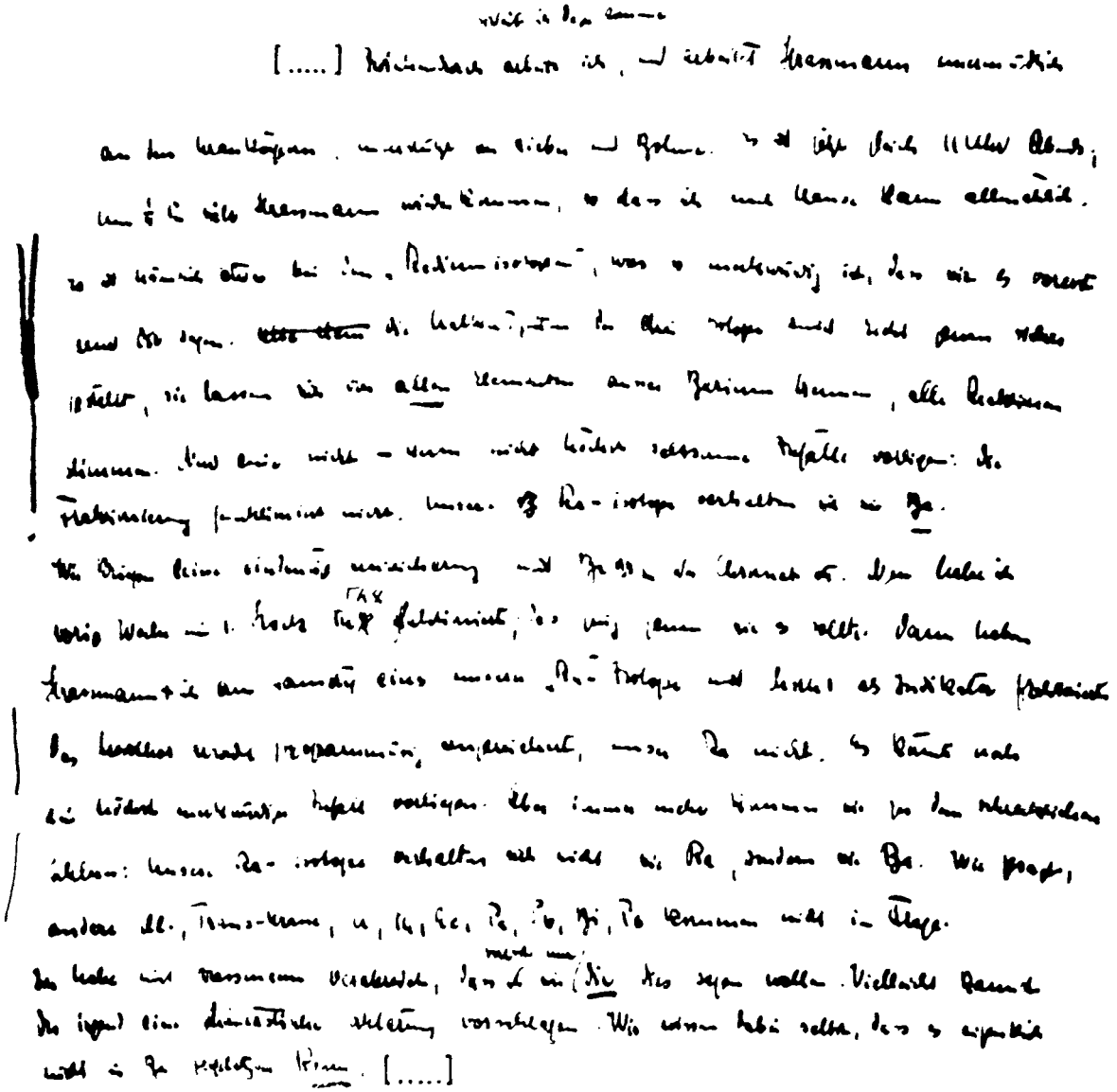

Fig. 18. *Otto Hahn* informs *Lise Meitner* on the evening of December 19, 1938, about the detection of barium in irradiated uranium; excerpt from page 2 of the letter [130], transcription in the text.

Bohne. Es ist jetzt gleich 11 Uhr abends; um 1/4 12 will Straßmann wiederkommen, so daß ich nach Hause kann allmählich. Es ist nämlich etwas bei den "Radium-Isotopen", was so merkwürdig ist, daß wir es vorerst nur Dir sagen. Die Halbwertszeiten der drei Isotope sind recht genau sichergestellt; sie lassen sich von *allen* Elementen außer Barium trennen; alle Reaktionen stimmen. Nur eine nicht— wenn nicht höchst seltsame Zufälle vorliegen: Die Fraktionisierung funktioniert nicht. Unsere Ra-Isotope verhalten sich wie *Ba*. Wir kriegen keine eindeutige Anreicherung mit $BaBr_2$ oder Chromat etc. Nun habe ich vorige Woche im 1. Stock ThX [$=^{224}$Ra] fraktioniert; das ging genau, wie es sollte. Dann haben Straßmann + ich am Samstag eines unserer "Ra"-Isotope mit Msth 1 als Indikator fraktioniert. Das Mesothor wurde programmäßig angereichert, unser Ra nicht. Es könnte noch ein höchst merkwürdiger Zufall vorliegen. Aber immer mehr kommen wir zu dem schrecklichen Schluß: Unsere Ra-Isotope verhalten sich nicht wie Ra, sondern wie Ba. Wie gesagt, andere Ele[mente], Trans-Urane, U, Th, Ac, Pa, Pb, Bi, Po kommen nicht in Frage. Ich habe mit Straßmann verabredet, daß wir vorerst nur *Dir* dies sagen wollen. Vielleicht kannst Du irgendeine phantastische Erklärung vorschlagen. Wir wissen dabei selbst, daß es eigentlich nicht in Ba zerplatzen *kann*".[*] This part of the

[*] "Whenever I have the time I do some work and Strassmann works tirelessly on the uranium bodies, assisted by Lieber and Bohne[**]. It is almost 11 p.m.; at 11:15 h Strassmann will return, so I can go home at last. You know, there is something so strange about the "radium isotopes" that for the time being we only want to tell it to you. The half-lives of the three isotopes are quite well determined; they can be separated from *all*[***] elements except barium; all reactions are fine. Except one—unless there are some really odd coincidences: The fractionation does not work. Our Ra-isotopes behave as *Ba*. We do not obtain an unambiguous enrichment using $BaBr_2$ or chromate etc. Last week I fractionated ThX [$=^{224}$Ra] on the 1st floor; this worked exactly as it should. Then, on Saturday, Strassmann + I fractionated one of our "Ra"-isotopes with Msth 1 as indicator. Mesothor was enriched as expected, not so our Ra. All this may still be due to a very peculiar coincidence. But more and more we come to the frightening conclusion: Our Ra-isotopes do not behave like Ra but like Ba. As I said, other ele[ments], trans-uranics, U, Th, Ac, Pa, Pb, Bi, Po are ruled out. I agreed with Strassmann that we only tell *you* about all this for now. Maybe you can suggest some phantastic explanation. We know ourselves that it *cannot* really break into Ba."

[**] *Clara Lieber* was an American guest scientist, *Irmgard Bohne* was a technician at the Kaiser-Wilhelm-Institut für Chemie.

[***] Emphases as in the original.

Über den Nachweis und das Verhalten der bei der Bestrahlung des Urans mittels Neutronen entstehenden Erdalkalimetalle.

O. Hahn und F. Strassmann

22. Dezember 1938

Nun müssen wir aber noch auf einige neuere Untersuchungen zu sprechen kommen, die wir der seltsamen Ergebnisse wegen nur zögernd veröffentlichen. Um den Beweis für die chemische Natur der mit dem Barium abgeschiedenen und als „Radiumisotope" bezeichneten Anfangsglieder der Reihen über jeden Zweifel hinaus zu erbringen, haben wir mit den aktiven Bariumsalzen fraktionierte Kristallisationen und fraktionierte Fällungen vorgenommen, in der Weise, wie sie für die Anreicherung (oder auch Abreicherung) des Radiums in Bariumsalzen bekannt sind.

Bariumbromid reichert das Radium bei fraktionierter Kristallisation stark an, Bariumchromat bei nicht zu schnellem Herauskommen der Kristallchen noch mehr. Bariumchlorid reichert weniger stark an als das Bromid, Bariumkarbonat reichert etwas ab. Entsprechende Versuche, die wir mit unseren von Folgeprodukten gereinigten aktiven Bariumpräparaten gemacht haben, verliefen ausnahmslos negativ: *Die Aktivität blieb gleichmäßig auf alle Bariumfraktionen verteilt*, wenigstens soweit wir dies innerhalb der nicht ganz geringen Versuchsfehlermöglichkeiten angeben können. Es wurden dann ein paar Fraktionierungsversuche mit dem Radiumisotop ThX und mit dem Radiumisotop $MsTh_1$ gemacht. Sie verliefen genau so, wie man aus allen früheren Erfahrungen mit dem Radium erwarten sollte. Es wurde dann die „Indikatorenmethode" auf ein Gemisch des gereinigten langlebigen „Ra IV" mit reinem, radiumfreien $MsTh_1$ angewandt: das Gemisch mit Bariumbromid als Trägersubstanz wurde fraktioniert kristallisiert. *Das $MsTh_1$ wurde angereichert, das „Ra IV" nicht*, sondern seine Aktivität blieb bei gleichem Bariumgehalt der Fraktionen wieder gleich. Wir kommen zu dem Schluß: Unsere „Radiumisotope" haben die Eigenschaften des Bariums; als Chemiker müßten wir eigentlich sagen, bei den neuen Körpern handelt es sich nicht um Radium, sondern um Barium; denn andere Elemente als Radium oder Barium kommen nicht in Frage.

Schließlich haben wir auch einen Indikatorversuch mit unserem rein abgeschiedenen „Ac II" (H.Z. rund 2,5 Stunden) und dem reinen Actiniumisotop $MsTh_2$ gemacht. Wenn unsere „Ra-Isotope" kein Radium sind, dann sind die „Ac-Isotope" auch kein Actinium, sondern sollten Lanthan sein. Nach dem Vorgehen von Mme Curie[1] haben wir eine Fraktionierung von Lanthanoxalat, das die beiden aktiven Substanzen enthielt, aus salpetersaurer Lösung vorgenommen. Das $MsTh_2$ fand sich, wie von Mme Curie angegeben, in den Endfraktionen stark angereichert. Bei unserem „Ac II" war von einer Anreicherung am Ende nichts zu merken. In Übereinstimmung mit Curie und Savitch[2] über ihren allerdings nicht einheitlichen 3,5-Stunden-Körper finden wir also, daß das aus unserem aktiven Erdalkalimetall durch β-Strahlenemission entstehende Erdmetall kein Actinium ist. Den von Curie und Savitch angegebenen Befund, daß sie die Aktivität im Lanthan anreicherten, der also gegen eine Gleichheit mit Lanthan spricht, wollen wir noch genauer experimentell prüfen, da bei dem dort vorliegendem Gemisch eine Anreicherung vorgetäuscht sein könnte.

[1] Mme Pierre Curie, J. Chim. physique etc. 27, 1 (1930).
[2] I. Curie u. P. Savitch, C. r. Acad. Sci. Paris 206, 1643 (1938).

Ob die aus den „Ac-La-Präparaten" entstehenden, als „Thor" bezeichneten Endglieder unserer Reihen sich als Cer herausstellen, wurde noch nicht geprüft.

Was die „Trans-Urane" anbelangt, so sind diese Elemente ihren niedrigeren Homologen Rhenium, Osmium, Iridium, Platin zwar chemisch verwandt, mit ihnen aber nicht gleich. Ob sie etwa mit den noch niedrigeren Homologen Masurium, Ruthenium, Rhodium, Palladium chemisch gleich sind, wurde noch nicht geprüft. Daran konnte man früher ja nicht denken. Die Summe der Massenzahlen Ba + Ma, also z. B. 138 + 101, ergibt 239!

Als Chemiker müßten wir aus den kurz dargelegten Versuchen das oben gebrachte Schema eigentlich umbenennen und statt Ra, Ac, Th die Symbole Ba, La, Ce einsetzen. Als der Physik in gewisser Weise nahestehende „Kernchemiker" können wir uns zu diesem, allen bisherigen Erfahrungen der Kernphysik widersprechenden, Sprung noch nicht entschließen. Es könnten doch noch vielleicht eine Reihe seltsamer Zufälle unsere Ergebnisse vorgetäuscht haben.

Es ist beabsichtigt, weitere Indikatorenversuche mit den neuen Umwandlungsprodukten durchzuführen. Insbesondere soll auch eine gemeinsame Fraktionierung der aus Thor durch Bestrahlen mit schnellen Neutronen entstehenden, von Meitner, Strassmann und Hahn untersuchten Radiumisotope mit unseren aus dem Uran entstandenen Erdalkalimetallen versucht werden. An Stellen, denen starke künstliche Strahlenquellen zur Verfügung stehen, könnte dies allerdings wesentlich leichter geschehen.

Zum Schlusse danken wir Frl. Cl. Lieber und Frl. I. Bohne für ihre wirksame Hilfe bei den sehr zahlreichen Fällungen und Messungen.

[1] L. Meitner, F. Strassmann u. O. Hahn, l.c.

Die Naturwissenschaften Heft 1. 6. 1. 1939

Fig. 19. Last three columns of the first historical publication by *Otto Hahn* and *Fritz Strassmann* [105] where nuclear fission is still announced hesitatingly; it was submitted to "Naturwissenschaften" on December 22, 1938, and appeared on January 6, 1939. The figures not belonging to this part of the text are taken out and the layout is slightly modified. Emphases by the author. The "vorerst" (earlier in the text, see end of Sect. 2.1) and the paragraph "Was die ... ergibt 239!" were added by *Hahn* on December 27, 1938, upon correction of the proofs [139]; in the paragraph "Als Chemiker ... vorgetäuscht haben" the expression "Gesetze" ("laws") was replaced by "Erfahrungen" ("experiences"), since (natural) laws were not encountered.

letter is depicted in Figure 18. *Hahn* mentions that they want to check whether the "actinium" isotopes growing from "radium" behave like lanthanum.

When the letter is written this experiment[132] is already being carried out. The 40-h "actinium IV" is obtained from the long-lived "radium IV", which is still present in the samples of December 17, and is mixed with natural actinium-228 and lanthanum carrier. Upon fractionation of lanthanum oxalate in nitric acid solution natural actinium, as is expected, becomes strongly enriched in the tail fraction whereas "actinium IV" from uranium is distributed uniformly: it is lanthanum.

All these results are presented in the last three columns of *Hahn* and *Strassmann*'s first historical publication;[105] they are depicted in Figure 19. The authors still hesitate in the often quoted passage "Als Chemiker ... als Kernchemiker"[*] to replace radium, actinium, and thorium by the elements barium, lanthanum, and cerium. The results about these fission products, however, are surprisingly good; comparing the decay chains in Figure 11 with today's situation, Figure 20, one notices that everything was determined correctly; only chain II later had to be divided into two similar chains. Soon it is realized in Berlin that the barium activities emerge from short-lived cesium and xenon precursors.

It is probably quite unique that a result of such significance was presented so indirectly and with that much understatement. This may explain why some of the later publications by others sound as if *Hahn* and *Strassmann* had not really noticed what they had found. Also recently it is argued[134] that it was only after *Lise Meitner*'s positive comment that *Hahn* was encouraged to formulate more explicitly the breakup into two nuclei. However, already in his letter of December 19 (Figure 18) he speaks of "Zerplatzen".

The peculiar presentation of the discovery of nuclear fission can, however, be accounted for by the hurry in which this manuscript[105] was written. As *Hahn* explains later,[135] he starts with an almost finished text about the radium isotopes, a more detailed publication of what was reported previously[104] in a note. The results of the indicator experiments are added at the end. The mention of "barium" in the title is considered instead of the initially chosen "radium", but then the whole manuscript would have to have been rewritten; the choice of "alkaline earth metals" is a way

[*] "As chemists ... as nuclear chemists".

out.[135] There is no time for major modifications because on December 21 all the personnel go on a 2-week Christmas vacation; in view of the competition with the Paris group it seems to be risky to wait this long. The evidence for barium instead of radium is written down on December 21–22 and the manuscript is picked up[99] by *Rosbaud* on the evening of the 22nd for publication in "Naturwissenschaften". The hurry does not allow for a careful checking or for detailed arguments. Thus, strange inconsistencies remained unnoticed: The printed text says that the indicator experiments were carried out with "langlebigen RaIV"[*] and with "AcII (H. Z. rund 2,5 Stunden)",[**] as one can read in Figure 19; what was used in fact was 86-min "Radium III" (as is obvious from the protocol, Figures 15 through 17) and[132] 40-h "Actinium IV". This inconsistency is never commented on later.

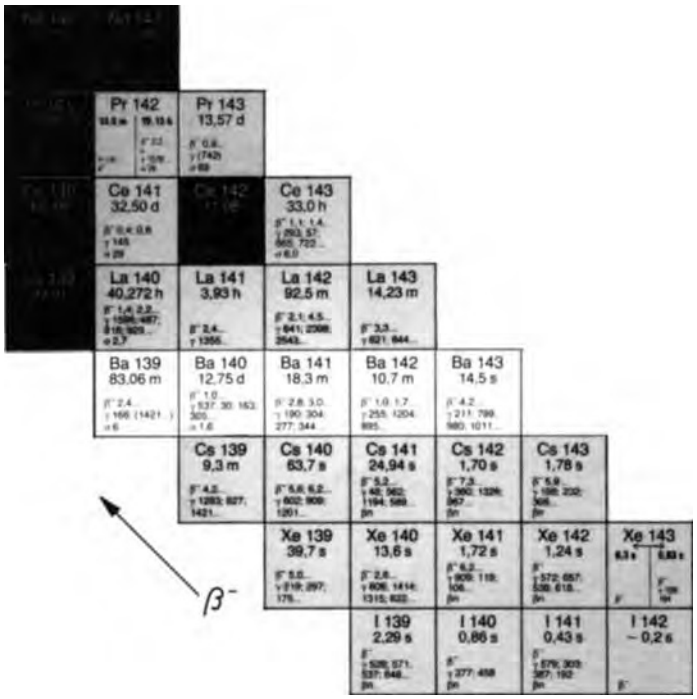

Fig. 20. The historical barium–lanthanum decay chains and the respective precursor nuclides today [133]. "Ra III" is Ba-139 and "Ra-Ac IV" are Ba-La-140, "Ra-Ac-II" later turned out to be complex, namely Ba-La-141 mixed with Ba-La-142; the presence of a very short-lived "Ra I" was also realized correctly. The β^--decay proceeds diagonally from the lower right to the upper left with constant mass number; stable nuclides are shown in black.

On December 21 *Hahn* informs *Lise Meitner* about his intention to publish quickly and writes that he is sending a copy of the manuscript to her.[136] He submits the paper without waiting for *Lise Meitner*'s comment on his letter of December 19 with the unexpected results. He receives her reply[137] on December 23;[138] she writes that the assumption of such a drastic breakup appears difficult for her to understand but that in nuclear physics there have been so many surprises that one cannot really call anything impossible. During the many years of collaboration *Lise Meitner* became acquainted with the accuracy of radiochemical methods in such a classic system like radium–barium; therefore, she is more inclined to give up nuclear-physics dogma rather than to question the results.[34] She also asks for the transuranic elements which may have caused *Hahn* on the same day to formulate a short paragraph "Was die ... ergibt 239!"[*] when modifying[99] the manuscript somewhat; upon correction on December 27 this paragraph is added to the text.[139] There he indicates, Figure 19, that the transuranic elements might be lighter rather than heavier homologues of rhenium and the platinum metals, because the sum of the mass numbers of barium and masurium is 239, the initial mass. Thus, a breakup into two large nuclei rather than a breakup into many nuclei is clearly referred to here. *Hahn* realizes,[139] however, that the argument is problematic, since not the sum of masses but the sum of the nuclear charges instead is of importance: krypton, element 36, is the complementary fragment of barium, element 56, rather than "masurium", element 43. The suspicion, however, that the transuranic elements might in fact be lighter homologues, for example element 43 instead of eka-rhenium, is correct.

The decay curves of the indicator experiment of December 17 are presented in the second historical publication by *Otto Hahn* and *Fritz Strassmann*,[140] which is submitted on January 28, 1939. This time the title clearly indicates the main theme: "Nachweis der Entstehung aktiver Bariumisotope aus Uran und Thorium durch Neutronenbestrahlung."[**] Chemistry and data are described and discussed in detail for the correct isotopes. In part A of Figure 21 the radioactivity of the three barium bromide fractions is shown to decrease first, followed by an increase towards plateaus of different height; curve I depicts the data from the protocol, Figure 16. Part B indicates how this increase of actinium-228 in the radium indicator radium-228 is corrected for. After subtracting this contribution the resulting decrease is shown in part C: The data points for the three fractions fall on one single decay curve for 86-min barium III. The reason why *Hahn* is not completely satisfied with the curves, as he mentioned in the note book—Figure 17—, is obvious: the last data points for fractions I and III in part C are clearly above the decay curve.

The contents, however, of this publication are even more profound: "The experiments described in *Hahn* and *Strassmann*'s "second" paper rank among the most careful and unambiguous ever carried out in radiochemistry."[141] *Hahn* and *Strassmann* now demonstrate the whole range of their radiochemical virtuosity; between January 4, when work is resumed at the Kaiser-Wilhelm-Institut,[142] and the formulation of this second manuscript a wealth of results is obtained. The fractionations are repeated with other activities and other barium salts: 86-min barium III is mixed with natural thorium X, 3.7-d radium-224, and fractionated as chromate; this works extremely well, since natural radium is enriched in the first fraction by a factor 19.5 with respect to

[*] long-lived Ra IV

[**] AcII (half-life about 2.5 hours)

[*] "As to ... yields 239!"

[**] "Proof of the formation of active barium isotopes from uranium and thorium by neutron irradiation."

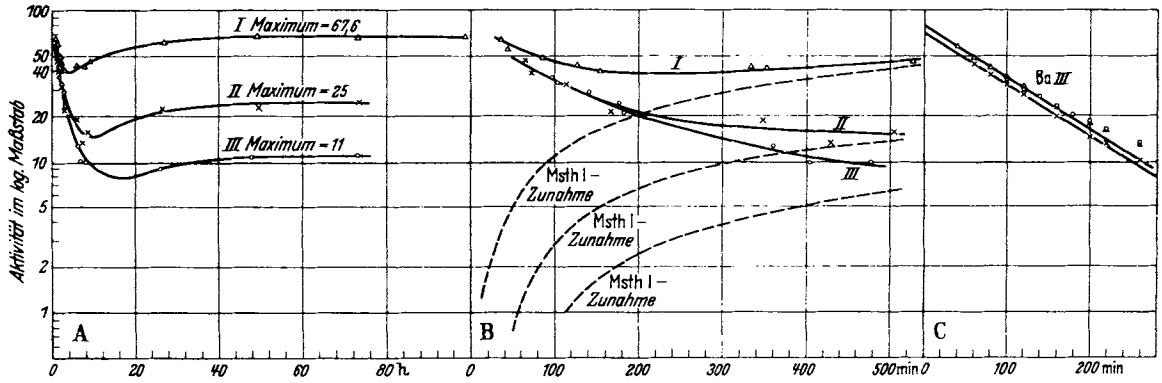

Fig. 21. Decay curves of the radioactivity in the three barium bromide fractions I,II,III from the indicator experiment barium III–mesothorium 1 of December 17, 1938; they were published in the second historical paper by *Otto Hahn* and *Fritz Strassmann* [140] on January 28, 1939. The count rate is displayed logarithmically as a function of time. The raw data are depicted in part A, compare the protocol of fraction 1 in Figure 16. The initial decrease is followed by an increase until radioactive equilibrium is established between the indicator mesothorium 1, 5.8-y radium-228, and its decay product mesothorium 2, 6.1-h actinium-228, in this section the decay curves differ appreciably, because the radium indicator is enriched in the order fraction I > II > III. Part B shows, how this growth is subtracted. Then, part C results with three practically identical decay curves for the initial portion, the barium III, 86-min barium-139. In contrast to natural radium, its activity is distributed equally among the three fractions. The conclusion shown in Figure 17 is based on these curves.

the second whereas the barium activities remain unchanged. The same procedure is performed for long-lived barium IV and radium-224. Finally, for barium IV a cyclic experiment is performed, namely a successive preparation of barium compounds: chloride, succinate, nitrate, carbonate, again chloride, iron(III) mannite, and again chloride; the activity of equal amounts of barium is again constant for all samples. Joy in experimenting and not—as is alleged[134]—lack of certainty is the likely reason for these variations. This is reflected in *Lise Meitner*'s comment:[143] "Euere Versuche stellen eine wunderbar geschlossene Beweiskette dar und es ist fabelhaft, was Ihr in diesen kurzen Wochen alles gemacht habt."[*]

The 15-min and 4-h "radium" from thorium, Figure 7, are also identified as barium by fractionation as barium chromate using radium-224 as indicator; thus thorium fissions too.[140] At last the "radium" decay-chains emerging from thorium are interpreted correctly. The right mass number 139 is assigned to barium III from uranium, for barium IV the mass number 140 is assumed. It is still left open whether the barium isotopes from uranium and thorium are identical, even though the half-lives are quite similar.

The main focus is, however, on the search for complementary fragments of uranium in the vicinity of krypton[140] which, via β^--decay, might turn into rubidium, strontium, and yttrium; this important aspect is also underlined by *Lise Meitner* and *Otto Robert Frisch*,[144] of which *Hahn* is informed by a preprint when the corresponding radiochemical experiments have just started.[145] By precipitation of the nicely crystallizing strontium nitrate using fuming nitric acid, strontium is isolated, from which yttrium is separated; both are active. A radioactive noble gas is found which decays into an alkaline metal that is active as well; it is temporarily left open whether the two are krypton and rubidium or xenon and cesium. When uranium breaks into two fragments of equal size palladium, element 46, should be formed; however, neither palladium nor the neighboring element silver are found among the fission products. For the first time the strange asymmetry of uranium fission, namely the breakup into a lighter and a heavier fragment, is thus apparent—a fact which will raise questions for both experimentalists and theorists for years to come. Only later[146] are products of symmetric fission into fragments of equal size detected after irradiation with energetic neutrons.

Naturally, the question as to what to think of the earlier transuranic elements is also discussed. In the course of the intensifying correspondence between *Hahn* and *Meitner*[97, 98] this problem is raised again and again with changing points of view—and not without some ill feeling between the two. For *Lise Meitner* this point is especially important,[134] because if all the transuranic elements were in fact fission products her work during the last years would be lost without her having the opportunity to participate in a discovery of even greater significance. After additional chemical experiments and some reflection, the suspicion[105] that the transuranic elements are lighter homologues of rhenium and the platinum elements is dismissed for the time being; it is expressed instead that the transuranic elements continue to exist.[140] We will come back to this later.

3. Confirmation of Nuclear Fission

3.1. Physical Experiments and Theoretical Explanations

Through letters and a copy of the manuscript *Lise Meitner* and *Otto Robert Frisch* know what has happened; the scientists at the institute in Berlin, however, are informed only[13, 118] on returning from their Christmas vacation at the beginning of January 1939 when the "first" publication appears. *Lise Meitner* meets *Otto Robert Frisch* at Christmas 1938 in Kungälv on the western shore of Sweden.[34, 147] When walking together out in the snow they come upon a very simple explanation[144] of this unexpected nuclear reaction. The separation of large fragments from heavy nuclei should not be viewed as a quantum-mechanical tunnel process;[12] another concept[148] which describes nuclei as liquid

[*] "Your experiments are a beautifully consistent series of proofs and it is marvellous how much you could achieve during these few weeks".

drops has to be applied. Nuclei, too, have a surface tension which protects them from disintegrating due to the repulsive electrical forces between the protons. For the uranium nucleus, however, this protection has almost vanished. Thus, after capture of a neutron, such a nucleus first starts to vibrate strongly, then elongates, and finally divides into two nuclei. These two fragments repel each other electrostatically with a kinetic energy of about 200 MeV, as can be estimated from the nuclear radii and charges. This energy is indeed available, since two nuclei of medium size are bound stronger than uranium just by this amount. Thus, energetically this process is possible; due to its similarity to the fission of cells they call it "fission",[144] after a suggestion by the biochemist *W. A. Arnold*.[147] *Meitner* and *Frisch*[144] express their ideas in a publication whose essential paragraph is depicted in Figure 22.

Disintegration of Uranium by Neutrons: a New Type of Nuclear Reaction

It seems therefore possible that the uranium nucleus has only small stability of form, and may, after neutron capture, divide itself into two nuclei of roughly equal size (the precise ratio of sizes depending on finer structural features and perhaps partly on chance). These two nuclei will repel each other and should gain a total kinetic energy of c. 200 Mev., as calculated from nuclear radius and charge. This amount of energy may actually be expected to be available from the difference in packing fraction between uranium and the elements in the middle of the periodic system. The whole 'fission' process can thus be described in an essentially classical way, without having to consider quantum-mechanical 'tunnel effects', which would actually be extremely small, on account of the large masses involved.

LISE MEITNER.

Physical Institute,
Academy of Sciences,
Stockholm.

O. R. FRISCH.

Institute of Theoretical Physics,
University,
Copenhagen.
Jan. 16.

Fig. 22. Interpretation of nuclear fission in the framework of the liquid drop model of atomic nuclei by *Lise Meitner* and *Otto Robert Frisch* according to their ideas developed in Kungälv. Part of the publication submitted on January 16, 1939 [144].

In addition, krypton is thought[144] to be the complementary fragment and the activities previously ascribed to the transuranic elements are rather considered to be related with lighter homologues of rhenium and the platinum metals; this would make the isomeric chains superfluous. The similarity is realized between the "radium-actinium" chains from thorium, Figure 7, and the activities identified as barium-lanthanum, with the conclusion that thorium is fissile, too. At the end they discuss the 24-min uranium; its existence, they argue, demonstrates that not all vibrations of the uranium nucleus would lead to fission.[144]

Back in Copenhagen, *Frisch* informs *Bohr* in detail on January 3, 1939 and on the next day *Hahn* in a brief letter.[149] *Bohr*'s reaction is drastic:[147] "Oh what fools we have been! We ought to have seen that before". Presumably he had not been taking the liquid-drop model that seriously[150] because it was initially developed to describe static nuclear properties like the nuclear masses without paying much attention to its dynamic aspects. On the telephone, *Meitner* and *Frisch* then prepare[147] a note which is drafted by *Frisch* on January 6 and modified after a discussion with *Bohr*; on January 7, with *Bohr* already at the railway station ready to depart for the U.S.A. by train and ship, *Frisch* gives him the first two pages of the note.[151] *Bohr* promises not to release anything before the note is published.[150]

Meanwhile *Hahn* and *Strassmann*'s "first" publication has appeared. *Frisch* discusses the new phenomenon with *G. Placzek* who is very sceptical about it.[151] This motivates[147] *Frisch*, who at first had not intended to perform an experiment, to think of a possibility of physically detecting the fast fission fragments. In a gas they should create an unusually large number of ions, by far more than α-particles for example; this should yield extraordinarily large signals. The corresponding experiment is very simple[147] taking only two days, January 13 and 14, 1939. In Figure 23 the important part of the protocol[152] is shown, in Figure 24 its author. The note about the interpretation of fission[144] is not submitted until *Frisch*, on January 16, is able to report on his experiment also:[154] "By means of a uranium-lined ionization chamber, connected to a linear amplifier, I have succeeded in demonstrating the occurrence of such bursts of ionization". Using an oscilloscope he observes large pulses above the background of α-particles from uranium which he concludes are caused by nuclei of at least a mass number of 70. Thorium produces the same effect.

Frisch does not show a picture of the fission-fragment pulses; the picture in Figure 25 is taken during the first detection[155, 157, 158] of nuclear fission on the American continent in New York on January 25, 1939. The most direct way of identifying the fission fragments escaping in opposite directions is to use a cloud chamber. One of the first two of such exposures[159, 160] is shown in Figure 26.

The notes by *Meitner* and *Frisch* "Disintegration of Uranium by Neutrons: a New Type of Nuclear Reaction"[144] and by *Frisch* "Physical Evidence for the Division of Heavy Nuclei under Neutron Bombardment"[154] do not appear until February 11 and 18, 1939, respectively; they had not insisted on rapid publishing.[34] Meanwhile, however, the phenomenon of nuclear fission has become known through *Hahn* and *Strassmann*'s first publication.[105] The first ones to react in Berlin are the theoreticians;[66, 111] they develop ideas similar to the ones of *Meitner* and *Frisch* discussing[161] the energetics of the process and reasons for the formation of just barium.

Within a short time the huge pulses of fission fragments are observed at several places, in New York,[155] Berkeley,[162] Baltimore,[163] Washington,[164] and Vienna;[165] in Berlin the experimental physicists react somewhat later.[166] Two quite different groups of fragment energies are found, which correspond to the light and heavy fragment; their mean kinetic energies are already determined surprisingly well by *W. Jentschke* and *F. Prankl*[165] to be 61 and 98 MeV, resulting in a kinetic energy release of altogether about 160 MeV.

F. Joliot[167] in Paris chooses another way for a physical detection of the fission process; he had learned early of the

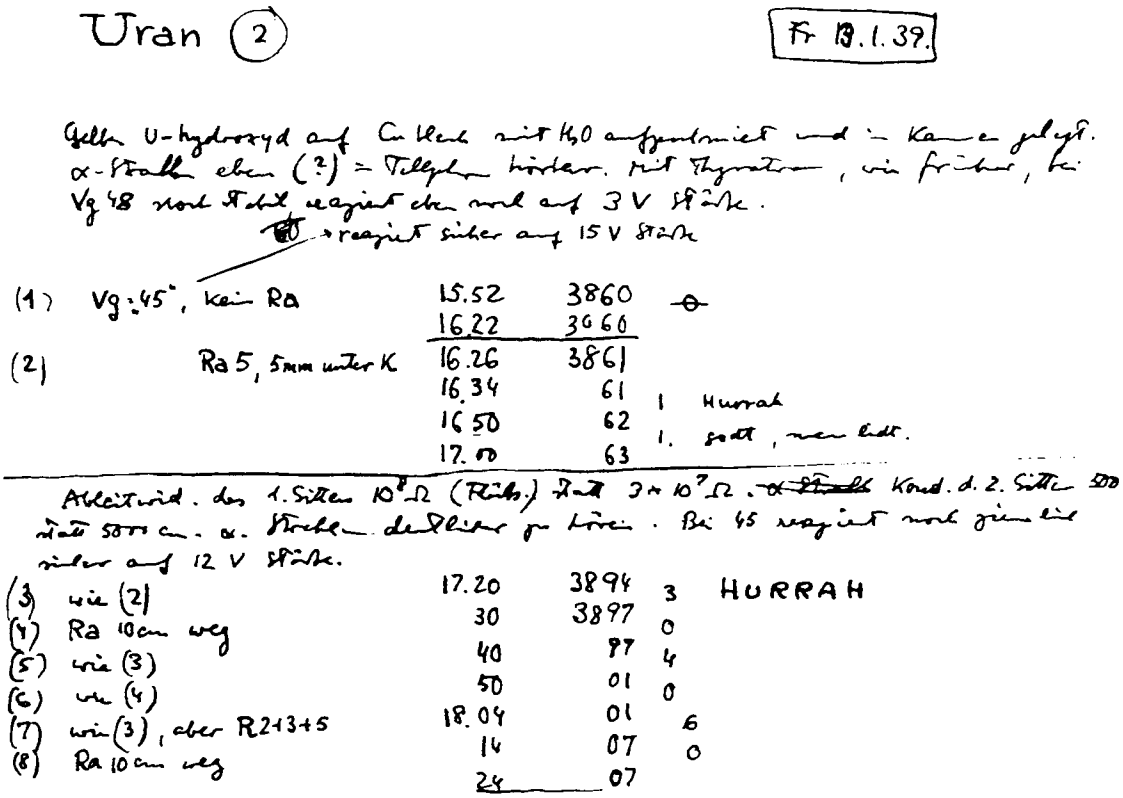

Fig. 23. The first physical detection of nuclear fission by *Otto Robert Frisch* in Copenhagen on January 13, 1939; upper half of the protocol sheet "Uran 2" [152]. A uranium sample is installed inside a hydrogen-filled ionization chamber of 1 cm depth and 3 cm diameter and is irradiated with neutrons from a radium-beryllium source, 100 mg Ra. The electrical pulses are transmitted by a thyratron, whose threshold voltage rejects pulses of the natural α-particles and only accepts larger pulses. The upper line of the text says: "Gelbes U-hydroxid auf Cublech mit H_2O aufgeschmiert und in Kammer gelegt". ("Yellow U-hydroxide smeared on Cu-plate with H_2O and put into the chamber".) The subsequent lines at the top and in the middle contain information about the eletronics used. Readings are alternately taken without (1,4,6,8) and with the neutron source "Ra" (2,3,5,7). The numbers of the third column represent the time, those of the fourth column the meter rating, and those of the fifth column the number of registered pulses. The first fission event between 16:34 and 16:50 h is welcomed with "Hurrah". Pulses only appear with the neutron source installed.

Fig. 24. *Otto Robert Frisch* (1904–1975) around the time of the "Frisch-experiment" [153].

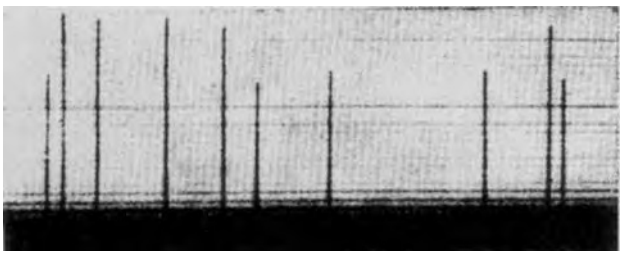

Fig. 25. Oscilloscope picture of the strongly ionizing fission fragments obtained with an ionization chamber during the irradiation of uranium with neutrons; a background of natural α-rays from uranium-238 can be seen [156]. The picture was taken upon the first observation of nuclear fission on the American continent by *H. L. Anderson, E. T. Booth, J. R. Dunning, E. Fermi, G. N. Glasoe*, and *F. G. Slack* in New York on January 25, 1939 [155].

Berlin results through a letter from *O. R. Frisch* addressed to his friend *H. von Halban* who works with *Joliot*; it is not possible to establish[168,169] exactly when this happened. For his experiment on January 26, 1939[170] *Joliot* makes use of the pronounced recoil of fission fragments caused by their large kinetic energy. Uranium or thorium is spread onto the surface of a hollow cyclinder which contains a neutron source. Within 3 mm distance from the surface a bakelite cylinder is mounted concentrically; on the latter, radioactive products are found after irradiation which could have reached there only by recoil. *Joliot*'s work "Preuve expérimentale de la rupture explosive des noyaux d'uranium et de thorium sous l'action des neutrons"[167][*] is reported to the

[*] "Experimental proof of the explosive rupture of uranium and thorium nuclei caused by neutrons."

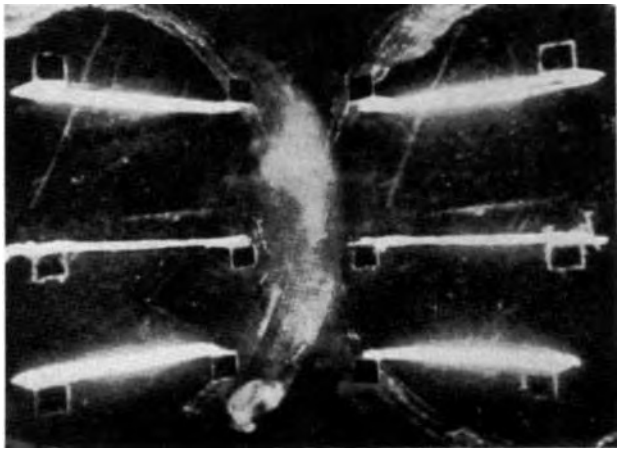

Fig. 26. One of the first photographs of the detection of nuclear fission using a cloud chamber with three pairs of fission fragments flying in opposite directions. The stereo picture was taken at Berkeley [159]; it consists of two halves, left and right.

French Academy of Sciences on January 30, 1939, even before *Meitner* and *Frisch*'s publications[144, 154] appear. The experiment by *E. McMillan*[171] at Berkeley is quite similar; he already determines the penetration depth of fission fragments in aluminum foils and cigarette paper which corresponds to 2.2 cm if converted to air at normal pressure. This is less than for α-particles even though the kinetic energy is far larger; fission fragments carry a much higher charge and therefore interact with matter more strongly.

In the U.S.A. the situation is dramatic.[150, 172] On the journey *Bohr* is accompanied by *L. Rosenfeld*, a theoretical physicist with whom he has intense discussions. He does not tell him, however, of the obligation to be silent. Thus, on January 16 the physicists at Princeton, *Rosenfeld*'s first stop, learn of the big news.[173] When on January 20 *Bohr* still does not know whether *Frisch*'s interpretation[144] has been accepted—he has no idea of *Frisch*'s intermittent experiments—and after having seen *Hahn* and *Strassmann*'s publication at Princeton he submits a note,[174] which describes the fission process in the framework of the liquid drop model. Not until January 22 does he receive news from *Frisch*. *Bohr* departs to attend a theory conference in Washington; on January 25 he stops by in New York and talks to *H. L. Anderson*, a student of *Fermi*, who immediately starts preparing the experiment furnishing Figure 25. On January 26 the conference is opened with *Bohr* and *Fermi* reporting the spectacular news, the main event of the conference.[175] A number of groups immediately start to carry out experiments similar to the one by *Frisch* and thus, on January 28 the conference is closed with positive results being presented;[155, 163, 164] the local group can even demonstrate to *Bohr* and *Fermi* the fission phenomenon.[158, 164] Newspapers report on it.[172, 176] *Bohr* has some trouble defending the priority of *Meitner* and *Frisch* with regard to the physical results.

Literally a flood of studies on fission and fission products is set in motion. The rare uranium isotope 235, with its 0.72% abundance only discovered a few years before,[178] is recognized by *Bohr*[177] to be that component of uranium which is fissile with thermal neutrons. A quantitative formulation[111, 179, 180] of the concept of a fissioning liquid drop is developed; it forms the basis of *Bohr* and *Wheeler*'s[181] pioneering theoretical study, which appears at the beginning of the second world war. As first step towards a chain reaction the neutrons are found that are being released in the course of fission.[182, 183] *Flügge*[184] is the first to clearly announce the feasibility of an energy producing "uranium machine" and of a nuclear explosion. About one year after the discovery, *L. A. Turner*[44] completes the first review article which is based on close to one hundred publications. Almost all important aspects are already mentioned. As early as December 2, 1942, *Enrico Fermi* and his team[185] succeed in Chicago in carrying out the first chain reaction. Only much later is the public informed about this result because very soon almost everything that deals with fission is kept secret.

Not the slightest doubt is raised against the phenomenon, yet there is some trouble for the discoverers which is expressed in the letters between *Hahn* and *Meitner*.[97, 98] A number of publications—for example *Bohr*'s first notes[174, 177]—sound as if it was not *Hahn* and *Strassmann* who had realized the significance of the process but only *Meitner* and *Frisch*. Elsewhere,[182] this realization is even ascribed to *Joliot* as well as *Meitner* and *Frisch* without even mentioning *Hahn* and *Strassmann*; interestingly enough, the respective publication is immediately followed by another one[186] which starts with the names of *Hahn* and *Strassmann*. At times[167, 187] the story is told in such a way as if *Hahn* and *Strassmann* had simply confirmed results by *I. Curie* and *Savitch*; in one case, upon intervention by *Hahn*, a correction[188] is made. Quite likely the peculiar style of *Hahn* and *Strassmann*'s "first" publication has to some extent provoked this confusion: Upon taking a brief look at the article, hardly anybody would anticipate the discovery of nuclear fission hiding behind the "alkaline earth elements"[105] mentioned in the title—Figure 19. Even a reader who has become more inquisitive will, after reading a few paragraphs, no doubt put aside the detailed radiochemical report about radium from uranium. And those who finally make their way through and even realize the significance of the chemical fractionations will again be made helpless by the famous ambivalent paragraph "Als Chemiker—als Kernchemiker" which *Strassmann* would have formulated not as undecidedly.[48] In contrast, the subsequent physical articles[144, 154, 167] with their imaginative titles are much more readable. Today, however, some reader may discover a particular attraction just in the style of the "first" publication.

3.2. Missed Opportunities

Before moving on to some of the later results we want to look back wondering why nuclear fission had not been discovered earlier, since it is so simple to observe fission fragments with an ionization chamber. Experiments similar to the one by *Frisch*[154] are at that time being performed in a number of laboratories. They are designed to search for energetic α-particles from an (n, α)-process [cf. Reaction (8, 9)], which may occur when uranium or thorium are irradiated with neutrons, and thus to corroborate the production of "radium" activities from uranium or thorium. Such experiments are being carried out at Berkeley,[189] Berlin,[82] Cambridge,[190] Heidelberg,[191] Rome,[38, 192] Zürich,[81] and

presumably elsewhere, too. To this purpose the disturbing background of natural α-particles, visible in Figure 25, is suppressed by absorber foils and not by electronics, as in *Frisch*'s experiment; in this way, however, the fission fragments are suppressed, too. As soon as fission is discovered, the foils have only to be removed in order to see the fragments. "But who can say whether even *Fermi* would have recognized them for what they were if he had seen them?"[192] Although perceived at times, they are ignored as being electrical noise;[190] this is *von Droste*'s opinion in Berlin[118] and presumably also that of researchers in Zürich, since an announced[81] detailed article on prompt α-particles is never published.

P. Abelson, a graduate student at Berkeley, has also come very close. Using a strong sample he measures the energies of the characteristic X-rays of 66-h eka-iridium—Figure 6—in a crystal spectrometer; while the exposure is taken, *Abelson*[193] reads the news from Berlin in a newspaper. He immediately modifies the experiment to measure the absorption of the radiation, which works faster, and finds the characteristic K-X-rays of iodine emitted after the β^--decay of its mother substance 66-h eka-iridium. The latter is thus identified as an isotope of tellurium, as is reported in a note[194] of nine lines length; later *Abelson*[195] presents details. Nuclear fission is thus again corroborated by detection of a fission product.

The Berlin group, too, could have arrived at fission as early as 1936 had only some night-time playful chemistry by *Fritz Strassmann*[196] been taken more seriously. In order to find a fast chemical separation for 16-min eka-rhenium he attempts to coprecipitate it with barium sulfate. Potassium permanganate gets incorporated into crystals of barium sulfate. The homologous eka-rhenium might behave the same way if present in a modification corresponding to perrhenate. The precipitate is active; however, the activities are not those of the 16-min species. *Strassmann* has to admit to *Lise Meitner* that adsorption effects cannot be ruled out. In turn, she rejects the results, in a friendly manner but quite firmly.[196]

It is difficult to judge from *I. Curie*'s short remark[91] how close she came to seeing the lighter elements. In the fall of 1939 she tells[34, 151] *G. von Hevesy* that at times she thinks the whole periodic table is in the irradiated uranium samples. In spite of intensive discussions during seminars no one finds a solution to the puzzle, as a participant recalls.[197] Also in Berlin lighter elements are being considered but this idea is not pursued because of the seemingly insurmountable Coulomb barrier.[118]

In contrast to a recent suggestion,[43] element 43, the masurium of *Walter* and *Ida Noddack*,[21, 22] should not be considered as one of the missed opportunities. All isotopes of this element are short-lived having already decayed since the heavy elements were synthesized in the interior of stars. On the other hand, element 43 is continuously being produced on the Earth by the spontaneous nuclear fission of uranium, which we will discuss below. Its quantity, however, is minute. In order to detect this amount and thus to—unconsciously—observe fission the *Noddack*'s X-ray fluorescence spectroscopy would have had to be five orders of magnitude more sensitive than according to their own claim; there are no arguments in favor of this.[198]

3.3. Further Fission Products

What is left now of the uranium-transuranium decay chains of Figure 6 and what is the story behind the "transuranic elements"? It has just been mentioned that *Abelson*[194, 195] identifies the 66-h eka-iridium as a tellurium isotope and thus the daughter substance 2.5-h eka-platinum as iodine. His result is confirmed[199] by the same method, namely X-ray absorption, and by *Hahn* and *Strassmann*[200] who investigate in detail the chemical properties of this eka-iridium. In these experiments they find a second activity with a quite similar half-life which they correctly identify as molybdenum. They discuss how the 2.5-h iodine could have been taken for a platinum metal: The crystallization of ammonium hexachloroplatinate[63] was thought to be a selective reaction for platinum. The possibility that iodine would precipitate as the analogous ammonium hexaiodoplatinate was not taken into account since fission was not envisaged. In the platinum sulfide precipitate 2.5-h iodine appears, because it is formed from the coprecipitating 66-h tellurium. Additional experimental studies concerning the transuranic elements are not published, even though they were announced[200] by *Hahn* and *Strassmann*.

Instead of looking at individual activities of "transuranic elements", *Meitner* and *Frisch*[186] examine the complete mixture coprecipitated with platinum sulfide as a whole. To this purpose recoiling fission fragments emitted from irradiated uranium are collected in a water layer from where they are coprecipitated with platinum sulfide. The decay curve is compared with a precipitate of platinum sulfide which is directly isolated from irradiated uranium without exploiting the recoil effect. The two decay curves match perfectly. Therefore, the "transuranic elements" are fission products, which are the only species having such a high recoil energy. In the same way fission products of thorium are identified;[201] thus, similar products result from the fission of uranium and thorium. Using such recoil experiments, other authors[202, 203] reach similar conclusions.

In his autobiography[204] *Hahn* reflects, on the basis of comments by *Strassmann*,[205] on what might have simulated the other "transuranic elements". Later, this problem is also approached experimentally[206] with high-resolution γ-ray spectroscopy by examining precipitates of platinum sulfide and other transuranic fractions produced according to *Hahn, Meitner* and *Strassmann*. These components are found to be complex, too. One half of the historically most important activity, the 16-min eka-rhenium, consists of technetium-101, the remaining half is a mixture of molybdenum-101, antimony-130g, antimony-131, and tellurium-131g. The 55-min activity is dominated by iodine-134, with some tellurium-134 and tin-128, and the 5.5-h activity by ruthenium-105, with some antimony-129 and iodine-133. The 16-min activity precipitating with manganese dioxide, which was considered by *Fermi* et al. to be element 93, is also complex; mainly molybdenum-101 is precipitated, from which technetium-101 is formed.[207]

With respect to the 3.5-h activity of *I. Curie* and *Savitch* it is soon realized[44] that it is related to 3.5-h yttrium-92; its 3.6 MeV β^--radiation is much more energetic than that of natural protactinium-234m with 2.3 MeV. In addition, contributions are to be expected by 3.90-h lanthanum-141, 93-

min lanthanum-142, and, in the chemically unprocessed mixture, by 76-min krypton-87. Now it is understandable, with yttrium-92 as the main constituent, that the 3.5-h activity can be fractionated from lanthanum; thus, this finding turns out to be correct. Since *I. Curie* and *Savitch* isolate this activity directly from irradiated uranium, their lanthanoid fraction always contains yttrium-92. *Hahn* and *Strassmann*, on the other hand, do not obtain the lanthanoid elements directly but only as decay products of "radium"-barium; this way they exclude yttrium because its mother substance strontium is not contained in their barium fraction.

The fission products prove to be an extremely complicated mixture of elements with several isotopes each. They form long β^--decay chains, often branching out into different isomers. Some of them are depicted in Figure 20. During the subsequent years the small group at Berlin, which has been joined by *H. J. Born*, *H. Götte*, and *W. Seelmann-Eggebert*, is busy unravelling these chains, at least to the extent it is possible in a war-time situation that is becoming more and more difficult. These experiments are all published. As *Hahn* reports in his Nobel Prize lecture,[46] in the beginning of 1945 about 100 products of 25 elements have been found.[208] Around this time the corresponding American results are released which have been obtained by *Charles Coryell*[209] at "Met Lab" under superior conditions; they first appear in tabulated form,[210] later in more detail.[211] Here, 170 products of 37 elements are listed. Very few of the products observed in Berlin are not contained in these American tables; focusing on some of the unsettled cases, work is resumed by *Fritz Strassmann* and his students as soon as it is possible after the war.[212]

In Berlin, only the first steps[213] towards quantitative measurements of the abundance of individual fission products are made which would indicate into what kind of fragments the uranium nucleus tends to fission predominantly. For this aspect the American groups can already present a complete distribution as a function of the mass number.[210, 211] The mass distribution is chosen, because the mass number does not change during β^--decay; if one waits for β^--decay to reach the long-lived final members of the decay chains, the total yield of all members of a chain is summed up in quite a natural way. The element distribution, however, continuously changes with time due to β^--decay. The initial distribution just after the breakup of the uranium nucleus is more difficult to establish experimentally because—as can be seen from some examples in Figure 20—the fission products at the beginning of the decay chains are usually very short-lived. In order to establish the initial abundance of individual elements the yields of all the respective isotopes have to be determined and added. Data of this kind have only been obtained in more recent times. The abundance of elements formed by fission of uranium-235[214] is shown in Figure 27. The lighter and the heavier fragment from the asymmetric fission process can be seen with five elements each created predominantly, krypton to zirconium and tellurium to barium. *Hahn* and *Strassmann*'s barium isotopes are mainly formed indirectly via β^--decay of short-lived xenon and cesium nuclei, which are close to the center of the heavy fragment wing.

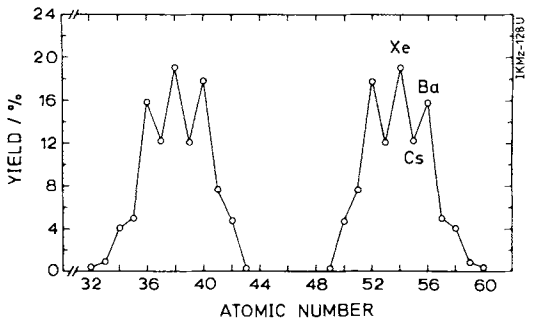

Fig. 27. Element distribution in the fission of uranium-235 by thermal neutrons: primary abundance in percent as a function of the atomic number. The asymmetry of fission into a smaller and a larger fragment is evident; xenon, cesium, and barium, key elements for the discovery, are located in the heavy branch. After [214].

4. Transuranic Elements Again

4.1. Element 93, Neptunium

We are left with one member of the decay chains of Figure 6, the 23-min uranium-239, which is chemically[63] verified to be uranium and whose assignment to mass number 239 is established physically[61] in uranium-238. As a β^--emitter it must decay into the isotope 239 of element 93. The detection of this decay product, however, proves to be very difficult. *E. McMillan*[171] takes a first decisive step. When measuring the range of fission products in cigarette paper he examines the thin uranium layer as well and notices two strong activities: one with a 23-min half-life, which he ascribes to uranium-239, and one with about a 2 d half-life, which is strong compared to the activities of fission products of similar half-life. Even the natural activity of uranium is negligible compared to this. This hint[171] causes a reader—was it *Hahn* himself?—at the Berlin institute to put a large exclamation mark at the edge of the publication which is still nicely visible today; the much superior means of the American competitors start to take effect.

Is this the sought after element 93, whose recoil energy is expected to be so small not to recoil out of the uranium target? Based on decay curves, *E. Segrè*[215] first draws the conclusion that the 2.3-d activity does not emerge from 23-min uranium-239; at this point he is misled[216] by its low β-energy. He then attempts to chemically identify the long-lived activity again assuming element 93 to have the properties of eka-rhenium. As one of the discoverers[217] of element 43 he already had experience with chemical studies in the 7th group of transition elements. *Segrè* finds, however, that the 2.3-d activity does not coprecipitate with rhenium sulfide but rather behaves like a lanthanoid element: it coprecipitates with lanthanum fluoride and oxalate, with potassium lanthanum sulfate and other typical precipitates and it can be separated from actinium by fractionation of lanthanum oxalate. Segrè[215] ascribes the 2.3-d activity to a lanthanoid fission product and concludes that 23-min uranium should decay into a long-lived element 93 which has not yet been found. Also other experiments[218] where element 93 was to be isolated with rhenium sulfide from highly enriched samples of 23-min uranium end with negative results.

After one year *E. McMillan* resumes his studies[171] applying a larger neutron flux which allows the use of a thinner uranium layer. Even then the 2.3-d activity remains inside uranium and can be completely separated from fission products this way. It is obtained with resonance neutrons just as well as the 23-min uranium-239. *P. Abelson*, who is now at Washington, observes that the 2.3-d activity does not always behave like a lanthanoid. The two start working together at Berkeley and within five days[193] they find the solution:[219] In a strongly oxidizing medium, bromate in strong acid, the 2.3-d activity does not coprecipitate with cerium fluoride; however, in a reducing medium, sulfite, it precipitates quantitatively. After oxidation the activity co-precipitates with sodium uranyl acetate, and after reduction it accompanies thorium iodate and peroxide. Properties typical of rhenium, like the sulfide precipitation, are not observed. Obviously, like uranium the finally discovered element 93 has two main oxidation states, four and six, the lower state being the more stable one, in contrast to uranium. *McMillan* and *Abelson*[219] presume a new series of related elements starting with uranium. Uranium is also the basis for the "astronomical" name of element 93: neptunium.

With these chemical results *McMillan* and *Abelson*[219] are able to prove that the 2.3-d activity is the daughter of 23-min uranium. This experiment is depicted in Figure 28. Every 20

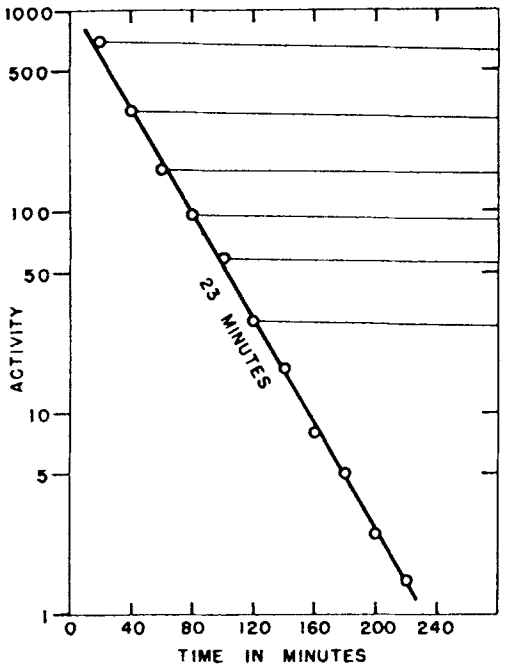

Fig. 28. Discovery of element 93, neptunium, by *E. McMillan* and *P. Abelson* at Berkeley [219]: Proof of the genetic relationship between the 23-min uranium-239 and its 2.3-d decay product. The initial count rates of the 2.3-d activity are measured in cerium fluoride precipitates obtained upon successive precipitations from the same solution of uranium-239. When depicted logarithmically as a function of time these count rates decrease with the half-life of uranium-239, 23 min. Thus, uranium-239 decays into the 2.3-d activity which is therefore identified as neptunium-239.

minutes cerium fluoride is precipitated from a reducing solution of the 23-min activity; thus, each time the 2.3-d activity continuously formed from 23-min uranium-239 is "milked" from its parent. The initial intensities of these samples decrease with a half-life of 23 minutes if displayed as a function of the time of precipitation, as is shown in Figure 28. According to the laws of radioactive decay, this proves that the 2.3-d activity arises from 23-min uranium and thus must be neptunium-239. Neptunium-239 has soft β^--rays of only 0.47 MeV energy. A decay product, element 94, is sought after but not found.[219]

In Berlin, following *McMillan*'s first publication,[171] one does not succeed in observing the 2.3-d activity, even in samples which have been more strongly irradiated[220] at the Copenhagen high voltage facility. The explanation is simple: the activity is not contained in a platinum sulfide precipitate; in the uranium fraction it is only weakly produced from 23-min uranium. In addition, the activity is difficult to detect due to the strong absorption of its low energy radiation. Therefore, in Berlin special enrichment procedures have to be developed for 23-min uranium. This is achieved by *K. Starke*[221, 222] based on a Szilard-Chalmers-separation.[223] This technique exploits the fact that atoms having become radioactive as a result of nuclear reactions may be transformed into a chemical state different from the one of the irradiated species. If uranium is irradiated as uranyl benzoyl acetonate, 23-min uranium-239 becomes partly converted into an inorganic species and can thus be concentrated from a large bulk of uranium. In strongly enriched uranium-239 samples of this kind *Starke*[224, 225] finds the 2.3-d activity even before the paper of *McMillan* and *Abelson*[219] arrives at Berlin[226] at the end of August 1940. Due to the war, however, *Starke*'s results are published later.[221, 222, 224, 225]

Hahn and *Strassmann* also start working on element 93; again they encounter some difficulties in finding the 2.3-d activity[227] and therefore construct a counter with a thin entrance window. They develop a chemical procedure to isolate element 93 directly from large amounts of uranium and perform a detailed study[228] of the chemistry of element 93. Properties already described[215, 219] are partly confirmed and new ones are added. They all point at a discontinuity in the periodic table: Element 93 has nothing in common with eka-rhenium.

4.2. Eka-Rhenium, Element 107

Now starts the era of nuclear chemical element syntheses. The periodic table extends more and more and takes a course different from the one originally expected: The series of actinoids is recognized, first by *Seaborg*.[229] It extends as far as lawrencium, 103, and then returns to the transition elements with element 104, presently reaching up to element 109.[230] Today's periodic table is shown in Figure 29.

Element 107 is placed below rhenium, and it takes almost four decades until this eka-rhenium is finally produced by *Gottfried Münzenberg, Peter Armbruster*, and the SHIP-group[231] at the heavy-ion accelerator UNILAC in Darmstadt by nuclear fusion of chromium-54 with bismuth-209 [Reaction (11)].

$$^{54}_{24}Cr + {}^{209}_{83}Bi \longrightarrow {}^{262}107 + {}^{1}_{0}n \qquad (11)$$

Its detection is again based on the genetic connection with decay products: The isotope 262 decays with 8.2 msec half-

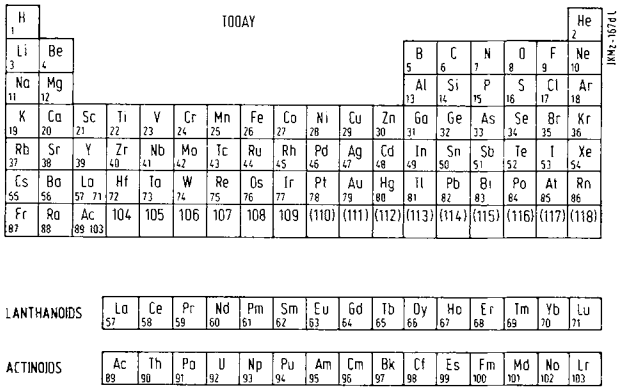

Fig. 29. The periodic table of the elements today. The atomic numbers of unknown elements are given in brackets.

life via α-emission into the known isotope 258 of element 105 and its well-known decay chain; an example for the decay chain of an individual atomic nucleus is depicted in Figure 30.

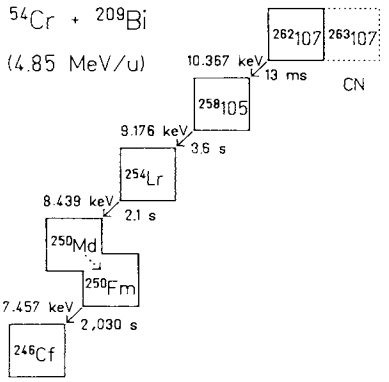

Fig. 30. Discovery of element 107, eka-rhenium, by the SHIP-group at Darmstadt [231]: one of five observed decay chains of a short-lived α-emitter which decays into the known nuclide 105–258 and its known decay products; the α-emitter therefore has to be assigned to the isotope 262 of element 107. This element 107 is produced by nuclear fusion of chromium-54, element 24, with bismuth-209, element 83.

Nothing is known as yet about the chemistry of eka-rhenium; thus, it is not clear whether the extrapolations of chemical properties will eventually be correct. Due to short half-lives and extremely low production rates, studies of this kind are not feasible for the time being. Chemical experiments with transactinoids have been performed up to element 105 and are described in review articles[232–234] and several more recent publications[236–238].

5. Nuclear Fission in Nature

The fission of uranium is a natural process; uranium already fissions spontaneously without an additional energy input. This spontaneous fission is discovered in 1940 by *G. N. Flerov* and *K. A. Petrzhak*,[239, 240] who use a large ionization chamber where about 10 g of uranium is spread to a thin layer. They observe about six fission events per hour and estimate the half-life of uranium-238 with respect to spontaneous fission to be in the range of 10^{16} to 10^{17} years,[239, 241] already the right order of magnitude. For the transuranic elements spontaneous fission becomes an important decay mechanism which in the end limits the periodic table.[230]

But also the chain reaction has occurred in nature. The possibility of a natural nuclear reactor is discussed early[184, 242] but is first dismissed with the argument that in such a case uranium deposits should not exist; later this question is raised again and it is realized[243] that a natural chain reaction is possible. A natural nuclear reactor is indeed discovered due to minute deviations of the uranium-235 concentration of some uranium delivered to France, namely[243] 0.7171% as compared to the usual value of 0.7202%. This deviation was caused by a uranium ore from Oklo, Gabon; at the respective mining site samples are found with uranium-235 depleted down to a concentration of 0.29%. About 1.8 billion years ago the reactor was operating for about 600 000 years and has released roughly 10 000 megawatt-years of energy, the amount delivered by a large power reactor within about three years; upon operation 4 tons of uranium-235 were consumed.[245, 246] It is interesting to note that the fission products formed have not migrated from the site during this long time interval.[245, 246]

6. Conclusion

The discovery of nuclear fission has given access to the energy hidden in atomic nuclei intensively discussed for several decades.[172] Not only was the discovery itself exciting but also the way in which it came about: The breakup of the uranium nucleus was not observed directly, but only some resulting secondary products. Looking back, however, this was probably the most straightforward path towards this discovery; there was no way to circumvent the barium in the Berlin beakers: "It was good solid chemistry that got things on the right track."[147] *Otto Hahn* and *Fritz Strassmann* and their predecessors had intended to pursue a different goal. This, however, does not make the discovery of nuclear fission a chance happening; they did not simply stumble on it, instead it was the fruit of many years of intensive work in radiochemical analysis. To think of chances may be more appropriate when imagining how strongly the events described here depend on minor fluctuations of the nuclear binding energy, which is, however, governed by subtle quantum mechanical effects. These fluctuations cause the asymmetry of the fission process with a heavy fragment just in the region that *Hahn* and *Strassmann* studied in their search for radium. On the other hand, such local fluctuations cause the β^--decay of neptunium-239 to be of an unusually low energy; for this reason, *Otto Hahn*, *Lise Meitner*, and *Fritz Strassmann* could not find element 93, even though it is formed from uranium with an abundance one order of magnitude greater than that of the strongest fission products. Thus, to *Hahn*'s disappointment,[247] whereas protactinium, the neighbor to the left of uranium in the periodic table, was found in Berlin, the corresponding neighbor to the right escaped discovery.

The history of nuclear fission tells us of how science often evolves, not by successive logical steps but rather through strange detours; how for many years the most experienced groups miss the central point in their experiments and in their thinking because they remain attached to seemingly well founded but erroneous concepts; how in the end they intuitively find the right track; and how after decades a scientist returns to the kind of work he pursued as a beginner.

The author thanks Peter Brix, Hans Otto Denschlag, Helmut Folger, Jens-Volker Kratz, Klaus Lützenkirchen, Chaturvedula Sastri, Matthias Schädel and Norbert Trautmann who have critically read this article, and Karl-Heinz Gläsel, Ursula Othmer and Annette Zauner, who have helped to prepare the manuscript.

Received: September 21, 1989;
Supplemented: December 5, 1990 [A 760 IE]
German version: *Angew. Chem. 102* (1990) 469
Translated by Dr. *Klaus Lützenkirchen*, Mainz (FRG)

Note: In the case of some works the date received for publication is quoted.

[1] E. Fermi, "Radioactivity Induced by Neutron Bombardment," *Nature (London) 133* (1934) 757 (April 10, 1934).
[2] E. Fermi, E. Amaldi, O. D'Agostino, F. Rasetti, E. Segrè, "Artificial Radioactivity Produced by Neutron Bombardment," *Proc. Roy. Soc. London 146* (1934) 483–500 (July 25, 1934).
[3] E. Amaldi, "Künstliche Radioaktivität durch Neutronen," *Phys. Z. 38* (1937) 692–734 (August 2, 1936).
[4] E. Amaldi, O. D'Agostino, E. Fermi, F. Rasetti, E. Segrè, "Radioattività "beta" provocata da bombardamento di neutroni III," *Ric. Scient. 5(1)* (1934) 452–453 (May 10, 1934). English translation in [5], p. 677–678.
[5] E. Fermi: *Note e Memorie (Collected Papers), Vol. I*, Accademia Nazionale dei Lincei, Roma 1962.
[6] E. Fermi, F. Rasetti, O. D'Agostino, "Sulla possibilità di produrre elementi di numero atomico maggiore di 92", *Ric. Sci. 5(1)* (1934) 536–537 (June 6, 1934).
[7] E. Fermi, "Possible Production of Elements of Atomic Number Higher than 92," *Nature (London) 133* (1934) 898–899 (appeared June 16, 1934).
[8] E. Amaldi, O. D'Agostino, E. Fermi, F. Rasetti, E. Segrè, "Radioattività provocata da bombardamento di neutroni V," *Ric. Scient. 5(2)* (1934) 21–22 (June 12, 1934). English translation in [5], p. 681–682.
[9] O. Hahn: *Applied Radiochemistry*, Cornell University Press, Ithaca 1936.
[10] S. R. Weart, "The Discovery of Fission and a Nuclear Physics Paradigm," in [11], p. 91–133.
[11] W. R. Shea (Ed.): *Otto Hahn und the Rise of Nuclear Physics*, Reidel, Dordrecht 1983.
[12] G. Gamow, "Zur Quantentheorie des Atomkerns," *Z. Phys. 51* (1928) 204–212.
[13] S. Flügge, "Zur Entdeckung der Uranspaltung vor zehn Jahren," *Z. Naturforsch. 4a* (1949) 82–84.
[14] H. J. Rose, G. A. Jones, A New Kind of Natural Radioactivity, *Nature (London)* 307 (1984) 245–247.
[15] N. Bohr, "The Structure of the Atom," *Nature (London) 112* (1923) 30–44.
[16] G. T. Seaborg, "Electronic Structure of the Heaviest Elements," in G. T. Seaborg, J. J. Katz, W. M. Manning (Eds.): *The Transuranium Elements*, McGraw-Hill, New York 1949, p. 1492–1524.
[17] G. T. Seaborg, "Place in the Periodic System and Electronic Structure of the Heaviest Elements," *Nucleonics 5(5)* (1949) 16–36.
[18] M. Haissinsky, "The Position of the Cis- and Transuranic Elements in the Periodic System: Uranides or Actinides?," *J. Chem. Soc. (London)* 1949, S241–S243.
[19] M. Haissinsky, "La place des éléments transuraniens dans le système périodique," *Experientia 9* (1953) 117–120.
[20] A. v. Grosse, "The Chemical Properties of Elements 93 and 94," *J. Am. Chem. Soc. 57* (1935) 440–441 (December 11, 1934).
[21] W. Noddack, I. Tacke, O. Berg, "Zwei neue Elemente der Mangangruppe," *Sitzungsber. Preuss. Akad. Wiss. Phys.-Math. Kl. 19* (1925) 400–409.
[22] W. Noddack, I. Tacke, O. Berg, "Die Ekamangane", *Naturwissenschaften 13* (1925) 567–574.
[23] E. Amaldi, in [24], p. 275.
[24] E. Amaldi, "From the Discovery of the Neutron to the Discovery of Nuclear Fission," *Phys. Rep. 111* (1984) 1–332.
[25] A. v. Grosse, M. S. Agruss, "The Chemistry of Element 93 and Fermi's Discovery," *Phys. Rev. 46* (1934) 241 (July 7, 1934).
[26] A. v. Grosse, M. S. Agruss, "Fermi's Element 93," *Nature (London) 134* (1934) 773 (October 12, 1934).
[27] A. v. Grosse, M. S. Agruss, "The Identity of Fermi's Reactions of Element 93 with Element 91," *J. Am. Chem. Soc. 57* (1935) 438–439 (December 11, 1934).
[28] O. Hahn, L. Meitner, "Die Muttersubstanz des Actiniums, ein neues radioactives Element von langer Lebensdauer," *Phys. Z. 19* (1918) 208–218.
[29] O. Hahn, "Über das Uran Z und seine Muttersubstanz," *Z. Phys. Chem. 103* (1923) 461–480.
[30] L. Meitner, "Über die Erregung künstlicher Radioaktivität in verschiedenen Elementen," *Naturwissenschaften 22* (1934) 420 (appeared June 1, 1934).
[31] L. Meitner, "Über die Umwandlung der Elemente durch Neutronen," *Naturwissenschaften 22* (1934) 759 (October 1934).
[32] L. Meitner, Letter to M. von Laue of September 4, 1944, reproduced in [33], p. 128–129; under the erroneous date of September 4, 1941.
[33] J. Lemmerich: *Die Geschichte der Entdeckung der Kernspaltung*, Catalogue for the Exhibition at the Deutsches Museum München, University Library of the Technische Universität Berlin, Berlin 1988.
[34] L. Meitner, "Wege und Irrwege zur Kernenergie," *Naturwiss. Rundsch. 16* (1963) 167–169; English Version: "Right and Wrong Roads to the Discovery of Nuclear Energy," *Adv. Sci. 1963*, 363–365.
[35] O. Hahn, L. Meitner, "Über die künstliche Umwandlung des Urans durch Neutronen," *Naturwissenschaften 23* (1935) 37 (December 22, 1934).
[36] E. Amaldi, O. D'Agostino, E. Fermi, B. Pontecorvo, F. Rasetti, E. Segrè," Artificial Radioactivity Produced by Neutron Bombardment II," *Proc. R. Soc. London 149* (1935) 522–558 (February 15, 1935).
[37] E. Amaldi, O. D'Agostino, E. Fermi, B. Pontecorvo, E. Segrè, "Radioattività indotta da bombardamento di neutroni IX, *Ric. Sci. 6(1)* (1935) 435–437 (April 3, 1935). English translation in [5], p. 693–696.
[38] E. Amaldi, in [24], p. 278.
[39] I. Noddack, "Über das Element 93," *Angew. Chem. 47* (1934) 653–655 (September 10, 1934).
[40] I. Noddack, "Das Periodische System der Elemente und seine Lücken," *Angew. Chem. 47* (1934) 301–305 (April 25, 1934).
[41] O. Koblic, "Bohemium," *Chemiker Ztg. 58* (1934) 581.
[42] H. G. Graetzer, D. J. Anderson: *The Discovery of Fission, a Documentary History*, Van Nostrand, New York 1971, p. 15.
[43] P. H. M. Van Assche, "The Ignored Discovery of the Element Z = 43," *Nucl. Phys. A 480* (1988) 205–214.
[44] L. A. Turner, "Nuclear Fission," *Rev. Mod. Phys. 12* (1940) 1–29 (completed December 6, 1939).
[45] E. Amaldi, in [24], p. 277.
[46] O. Hahn, "Von den natürlichen Umwandlungen des Urans zu seiner künstlichen Zerspaltung," Nobel-Prize Lecture on December 13, 1946, reprinted in [47], p. 247–267.
[47] O. Hahn: *Mein Leben*, Bruckmann, München 1968.
[48] F. Strassmann: *Kernspaltung—Berlin Dezember 1938*, private printing, Mainz 1978, Text without pictures also in [49], p. 203–211.
[49] F. Krafft: *Im Schatten der Sensation—Leben und Wirken von Fritz Strassmann*, Verlag Chemie, Weinheim 1981.
[50] F. Krafft, in [49], p. 314–322.
[51] K.-E. Zimen, "Die Saga des Urans und der Januskopf des Fortschritts," *Atomwirtschaft 1988*, 578–584.
[52] I. Noddack, "Bemerkung zu den Untersuchungen von O. Hahn, L. Meitner und F. Strassmann über die Produkte, die bei der Bestrahlung von Uran mit Neutronen entstehen," *Naturwissenschaften 27* (1939) 212–213. (March 10, 1939).
[53] Editors remark with respect to [52], *Naturwissenschaften 27* (1939) 213.
[54] I. Strassmann, M. Strassmann, *In Memoriam Fritz Strassmann*, private printing, Mainz 1980.
[55] F. Krafft, in [49] p. 219.
[56] W. Seelmann-Eggebert, "Über die Entdeckung der Kernspaltung—ein historischer Rückblick," *Chimia 33* (1979) 275–282.
[57] O. Hahn, L. Meitner, F. Strassmann, "Neue Umwandlungs-Prozesse bei Neutronen-Bestrahlung des Urans; Elemente jenseits Uran," *Ber. Dtsch. Chem. Ges. 69* (1936) 905–919 (March 14, 1936).
[58] O. Hahn, L. Meitner, "Über die künstliche Umwandlung des Urans durch Neutronen II," *Naturwissenschaften 23* (1935) 230–231 (March 2, 1935).
[59] O. Hahn, L. Meitner, F. Strassmann, "Einige weitere Bemerkungen über die künstlichen Umwandlungsprodukte beim Uran," *Naturwissenschaften 23* (1935) 544–545 (July 15, 1935).
[60] L. Meitner, O. Hahn, "Neue Umwandlungsprozesse bei Bestrahlung des Urans mit Neutronen," *Naturwissenschaften 24* (1936) 158–159 (February 10, 1936).
[61] L. Meitner, O. Hahn, F. Strassmann, "Über die Umwandlungsreihen des Urans, die durch Neutronenbestrahlung erzeugt werden," *Z. Phys. 106* (1937) 249–270 (May 14, 1937).
[62] L. Meitner, "Über die β- und α-Strahlen der Transurane," *Ann. Phys. 29* (1937) 246–250 (April 15, 1937).
[63] O. Hahn, L. Meitner, F. Strassmann, "Über die Transurane und ihr

chemisches Verhalten," *Ber. Dtsch. Chem. Ges. 70* (1937) 1374–1392 (May 15, 1937).
[64] O. Hahn, L. Meitner, F. Strassmann, "Ein neues langlebiges Umwandlungsprodukt in den Trans-Uranreihen," *Naturwissenschaften 26* (1938) 475–476 (July 12, 1938).
[65] P. Abelson, "Neutron Produced Activities in Uranium," *Phys. Rev. 53* (1938) 211–212 (abstract of a talk on December 17, 1937).
[66] W. Wefelmeier, "Ein Modell der Transurane," *Naturwissenschaften 27* (1939) 110–111 (January 28, 1939).
[67] M. L. Pool, J. M. Cork, R. L. Thornton, "A Survey of Radioactivity Produced by High Energy Neutron Bombardment," *Phys. Rev. 52* (1937) 239–240 (July 3, 1937).
[68] O. M. Corbino, "Il radio artificiale: l'Ausonio e l'Esperio," *Nuova Antologia 71* (1936) 454–456, quoted after [24], p. 284.
[69] E. Fermi, "Artificial Radioactivity Produced by Neutron Bombardment," in: The Nobel Foundation (Ed.): *Les Prix Nobel en 1938*, Norsted, Stockholm 1939, p. 1–8.
[70] L. L. Quill, "The Transuranium Elements," *Chem. Rev. 23* (1938) 87–155 (June 27, 1938).
[71] H. Hulubei, Y. Cauchois, "Existence probable de l'élément 93 à l'état naturel," *C.R. Hebd. Séances Acad. Sci. 207* (1938) 333–335 (August 1, 1938).
[72] H. Hulubei, Y. Cauchois, "Nouvelles recherches sur l'élément 93 naturel," *C.R. Hebd. Séances Acad. Sci 209* (1939) 476–479 (September 4, 1939).
[73] O. Hahn, L. Meitner, "Die künstliche Umwandlung des Thoriums durch Neutronen: Bildung der bisher fehlenden radioaktiven 4n+1 Reihe," *Naturwissenschaften 23* (1935) 320 (May 2, 1935).
[74] I. Curie, H. von Halban, P. Preiswerk, "Sur la création artificielle des éléments d'une famille radioactive inconnue, lors de l'irradiation du thorium par les neutrons," *C.R. Hebd. Séances Acad. Sci. 200* (1935) 1841–1843 (May 27, 1935).
[75] L. Meitner, F. Strassmann, O. Hahn, "Künstliche Umwandlungsprozesse bei Bestrahlung des Thoriums mit Neutronen: Auftreten isomerer Reihen durch Abspaltung von α-Strahlen," *Z. Phys. 109* (1938) 538–552 (May 16, 1938).
[76] O. Hahn: *Erinnerungen 1901–1945*, written in June 1945 and reprinted in [77], p. 15–73.
[77] D. Hahn (Ed.): *Otto Hahn, Erlebnisse und Erkenntnisse*, Econ, Düsseldorf 1975.
[78] E. Rona, E. Neuninger," Weitere Beiträge zur Frage der künstlichen Aktivität des Thoriums durch Neutronen," *Naturwissenschaften 24* (1936) 491 (July 1, 1936).
[79] I. Curie, H. von Halban, P. Preiswerk, "Sur les éléments radioactifs formés lors de l'irradiation du thorium par les neutrons," *C.R. Hebd. Séances Acad. Sci. 200* (1935) 2079–2080 (June 17, 1935).
[80] I. Curie, H. von Halban, P. Preiswerk, "Sur la création artificielle d'éléments appartenant à une famille radioactive inconnue, lors de l'irradiation du thorium par les neutrons," *J. Phys. Radium (7)6* (1935) 361–364 (July 15, 1935).
[81] A. Braun, P. Preiswerk, P. Scherrer, "Detection of α-Particles in the Disintegration of Thorium," *Nature (London) 140* (1937) 682 (August 31, 1937).
[82] G. v. Droste, "Über Versuche eines Nachweises von α-Strahlen während der Bestrahlung von Thorium und Uran mit Radium + Beryllium-Neutronen," *Z. Phys. 110* (1938) 84–94 (May 25, 1938).
[83] Y. Nishina, T. Yasaki, K. Kimura, M. Ikawa, "Artificial Production of Uranium Y from Thorium," *Nature (London) 142* (1938) 874 (September 13, 1938).
[84] G. Friedlander, J. W. Kennedy, E. S. Macias, J. M. Miller: *Nuclear and Radiochemistry*, Wiley, New York 1981, p. 13–14.
[85] I. Curie, P. Savitch, "Sur les radioéléments formés dans l'uranium irradié par les neutrons," *J. Phys. Radium (7)8* (1937) 385–387 (August 1, 1937).
[86] I. Curie, P. Savitch, "Sur les radioéléments formés dans l'uranium irradié par les neutrons II," *J. Phys. Radium (7)9* (1938) 355–359 (July 12, 1938).
[87] L. Meitner, O. Hahn, Letter to I. Curie of January 20, 1938, Archives of the Institut Curie, Paris; the author is indebted to *Monique Bordry* for clarifying this point as well as some others.
[88] I. Curie, P. Savitch, "Sur le radioélément de période 3,5 heures formé dans l'uranium irradié par les neutrons," *C.R. Hebd. Séances Acad. Sci. 206* (1938) 906–908 (March 21, 1938).
[89] I. Curie, P. Savitch, "Sur la nature du radioélément de période 3,5 heures formé dans l'uranium irradié par les neutrons," *C.R. Hebd. Séances Acad. Sci. 206* (1938) 1643–1644 (May 30, 1938).
[90] I. Curie, P. Savitch, A. Marques da Silva, "Sur le rayonnement du corps de période 3,5 heures formé par irradiation de l'uranium par les neutrons," *J. Phys. Radium (7)9* (1938) 440 (July 20, 1938).
[91] I. Curie, P. Savitch, "Sur les radioéléments formés dans l'uranium et le thorium irradiés par les neutrons. *C.R. Hebd. Séances Acad. Sci. 208* (1939) 343–346 (January 30, 1939).
[92] P. Biquard: *Frédéric Joliot-Curie et l'Énergie Atomique*, Seghers, Paris 1961, quoted after [24], p. 285–286.
[93] O. Hahn, Letter to L. Meitner of October 25, 1938, in [49], p. 236.
[94] O. Hahn: *Die Auffindung der Uranspaltung, FIAT Review of German Science 1939–1946, Nuclear Physics and Cosmic Rays, Part 1*, Dieterich, Wiesbaden 1948, p. 171–178, reprinted in [95], p. 304–311.
[95] H. Wohlfarth (Ed.): *40 Jahre Kernspaltung—Eine Einführung in die Originalliteratur*, Wissenschaftliche Buchgesellschaft, Darmstadt 1979.
[96] O. Hahn, F. Strassmann, Note book "Chem. II", November 1, 1938—January 14, 1939, Deutsches Museum, München; commented transcription of the text without the counting data in [49], p. 234–280.
[97] D. Hahn (Ed.): *Correspondence with Lise Meitner November 1938—April 1939*, in [77], p. 75–129.
[98] F. Krafft (Ed.): *Correspondence Otto Hahn—Lise Meitner August 11, 1938—March 25, 1945*, in [49], p. 74–135 and 228–337.
[99] O. Hahn, Pocket book 1938, reproduced in [100], partly as facsimile.
[100] P. Brix, "Die folgenreiche Entdeckung der Uranspaltung—und wie es dazu kam," *Phys. Bl. 45* (1989) 1–10; *Naturwiss. Rundsch. 42* (1989) 1–9.
[101] L. G. Cook, "Personal Reminiscences of the Kaiser Wilhelm Institute, Berlin, 1937/38, and of the Nuclear Project in Canada, 1944/45," in [102], p. 69–72.
[102] J. W. Behrens, A. D. Carlson (Ed.): *50 Years with Nuclear Fission*, 2 Vols., American Nuclear Society, La Grange Park, Illinois, 1989.
[103] "Chem. II" [96], p. 2v.
[104] O. Hahn, F. Strassmann, "Über die Entstehung von Radiumisotopen aus Uran durch Bestrahlen mit schnellen und verlangsamten Neutronen," *Naturwissenschaften 26* (1938) 755–756 (November 8, 1938).
[105] O. Hahn, F. Strassmann, "Über den Nachweis und das Verhalten der bei der Bestrahlung des Urans mittels Neutronen entstehenden Erdalkalimetalle," *Naturwissenschaften 27* (1939) 11–15 (December 22, 1938).
[106] [M.] S. Curie: *Untersuchungen über die radioaktiven Substanzen*, German Edition, 3rd Edit., Vieweg, Braunschweig 1904, p. 29–33.
[107] O. Hahn, in [108], p. 15–19.
[108] O. Hahn: *Vom Radiothor zur Uranspaltung—Eine wissenschaftliche Selbstbiographie*, Reprint of the 1st Edit. 1962 (D. Hahn, Ed.), Vieweg, Braunschweig 1989.
[109] O. Hahn, "Ein neues radioaktives Element, das Thorium-Emanation aussendet," *Ber. Dtsch. Chem. Ges. 38* (1905) 3371–3375.
[110] C. F. von Weizsäcker, "Metastabile Zustände der Atomkerne," *Naturwissenschaften 24* (1936) 813–814 (November 28, 1936).
[111] C. F. von Weizsäcker, "Zum Wefelmeierschen Modell der Transurane," *Naturwissenschaften 27* (1939) 133 (February 9, 1939).
[112] S. M. Polikanov, V. A. Druin, V. A. Karnaukhov, V. L. Mikheev, A. A. Pleve, N. K. Skobelev, V. G. Subbotin, G. M. Ter-Akopian, V. A. Fomichev, "Spontannoe delenie s anomalno korotkim periodom poluraspada," *Zh. Eksperim. Teor. Fiz. 42* (1962) 1464–1471; "Spontaneous Fission with Anomalously Short Period," *Sov. Phys. JETP 15* (1962) 1016–1021.
[113] V. M. Strutinsky, "Shell Effects in Nuclear Masses and Deformation Energies," *Nucl. Phys. A 95* (1967) 420–442.
[114] S. M. Polikanov, "Spontanno deljaschtschiesja isomery," *Usp. Fiz. Nauk 94* (1968) 43–62; "Spontaneously Fissioning Isomers," *Sov. Phys. Usp. 11* (1968) 22–33.
[115] S. M. Polikanov, "Jadernye isomery formy," *Usp. Fiz. Nauk 107* (1972) 685–704; "Nuclear Shape Isomers," *Sov. Phys. Usp. 15* (1973) 486–496.
[116] O. Hahn, Letter to N. Feather of June 2, 1939, in [49], p. 330–331.
[117] O. Hahn, "Die 'falschen' Transurane," *Naturwiss. Rundsch. 15* (1962) 43–47.
[118] S. Flügge, "How Fission Was Discovered," in [102], p. 26–29.
[119] "Chem. II" [96], p. 40r–42r.
[120] "Chem. II" [96], p. 48r–50r.
[121] "Chem. II" [96], p. 64v, 68r–70v.
[122] "Chem. II" [96], p. 75r–77v.
[123] O. Hahn, "Ein neues Zwischenprodukt im Thorium," *Ber. Dtsch. Chem. Ges. 40* (1907) 1462–1469.
[124] O. Hahn, "Ein kurzlebiges Zwischenprodukt zwischen Mesothor und Radiothor," *Phys. Z. 9* (1908) 246–248.
[125] O. Hahn, in [108], p. 39–44.
[126] "Chem. II" [96], p. 75r.
[127] "Chem. II" [96], p. 76v.
[128] F. Krafft, in [49], p. 262.
[129] "Chem. II" [96], p. 77v.
[130] O. Hahn, Letter to L. Meitner of December 19, 1938, facsimile from [131], p. 152; transcription in [77], p. 77–79, and [49], p. 263–265.
[131] D. Hahn (Ed.): *Otto Hahn—Begründer des Atomzeitalters*, List, München 1979.
[132] "Chem. II" [96], p. 79r–81v.
[133] W. Seelmann-Eggebert, G. Pfennig, H. Münzel, H. Klewe-Nebenius: *Karlsruher Nuklidkarte*, 5th Edit., Gersbach, München 1981.
[134] R. L. Sime, "Lise Meitner and the Discovery of Fission," *J. Chem. Educ. 66* (1989), 373–376.
[135] O. Hahn, in [108], p. 131–132.
[136] O. Hahn, Letter to L. Meitner of December 21, 1938, in [77], p. 80–82, and [49], p. 265.
[137] L. Meitner, Letter to O. Hahn of December 21, 1938, in [77], p. 79–80, and [49], p. 264–265.

[138] O. Hahn, Letter to E. von Bahr-Bergius of December 23, 1938, in [49], p. 267.
[139] Based on [49], p. 254, 267; indications of further corrections can be found therein; see also the letter by O. Hahn to L. Meitner of December 28, 1938, in [49], p. 267.
[140] O. Hahn, F. Strassmann, "Nachweis der Entstehung aktiver Bariumisotope aus Uran und Thorium durch Neutronenbestrahlung; Nachweis weiterer aktiver Bruchstücke bei der Uranspaltung," *Naturwissenschaften 27* (1939) 89–95 (January 28, 1939).
[141] E. K. Hyde: *The Nuclear Properties of the Heavy Elements, Vol. III, Fission Phenomena*, Prentice-Hall, Englewood Cliffs 1964, p. 4.
[142] "Chem. II" [96], p. 81r.
[143] L. Meitner, Letter to O. Hahn of February 5, 1939, in [77], p. 98–100, and [49], p. 295.
[144] L. Meitner, O. R. Frisch, "Disintegration of Uranium by Neutrons: a New Type of Nuclear Reaction," *Nature (London) 143* (1939) 239–240 (January 16, 1939).
[145] O. Hahn, Letter to L. Meitner of January 24, 1939, in [77], p. 94, and [49], p. 282–283.
[146] Y. Nishina, T. Yasaki, H. Ezoe, K. Kimura, M. Ikawa, "Fission of Thorium by Neutrons," *Nature (London) 144* (1939) 547–548 (July 29, 1939).
[147] O. R. Frisch, "The Discovery of Fission: How It All Began," *Phys. Today 20(11)* (1967) 43–48.
[148] G. Gamow, Mass Defect Curve and Nuclear Constitution, *Proc. Roy. Soc. London A 126* (1930) 632–644.
[149] O. R. Frisch, Letters to L. Meitner of January 3, 1939, in [150], and to O. Hahn of January 4, 1939, in [49], p. 271–272.
[150] R. H. Stuewer, "Bringing the News of Fission to America," *Phys. Today 38(10)* (1985) 49–51.
[151] O. R. Frisch, Letter to L. Meitner of January 8, 1939, in [33], p. 179, 182.
[152] O. R. Frisch, Laboratory protocol of January 13, 1939, sheet 2, upper part, from [33], p. 181; therein the sheets "Uran 1" and "Uran 2" are reproduced completely.
[153] From [33], p. 174.
[154] O. R. Frisch, "Physical Evidence for the Division of Heavy Nuclei under Neutron Bombardment," *Nature (London) 143* (1939) 276 (January 16, 1939).
[155] H. L. Anderson, E. T. Booth, J. R. Dunning, E. Fermi, G. N. Glasoe, F. G. Slack, "The Fission of Uranium," *Phys. Rev. 55* (1939) 509–510 (February 16, 1939); Figure 25 is not depicted there but in [156].
[156] S. Glasstone: *Sourcebook on Atomic Energy*, 3rd Edit., Van Nostrand, New York 1967, p. 477.
[157] H. L. Anderson, "The Legacy of Fermi and Szilard," *Bull. At. Scientists 30(9)* (1974) 56–62.
[158] M. A. Tuve, "Droplet Fission of Uranium and Thorium Nuclei," *Science (Washington DC) 89* (1939) 202–203.
[159] D. R. Corson, R. L. Thornton, "Disintegration of Uranium," *Phys. Rev. 55* (1939) 509 (February 15, 1939).
[160] F. Joliot, "Observation par la méthode de Wilson des trajectoires de brouillard des produits de l'explosion des noyaux d'uranium," *C.R. Hebd. Seances Acad. Sci. 208* (1939) 647–649 (February 27, 1939).
[161] S. Flügge, G. v. Droste, Energetische Betrachtungen zu der Entstehung von Barium bei der Neutronenbestrahlung von Uran," *Z. Phys. Chem. B 42* (1939) 274–280 (January 22, 1939).
[162] G. K. Green, L. W. Alvarez, "Heavily Ionizing Particles from Uranium," *Phys. Rev. 55* (1939) 417 (January 31, 1939).
[163] R. D. Fowler, R. W. Dodson, "Intensely Ionizing Particles Produced by Neutron Bombardment of Uranium and Thorium," *Phys. Rev. 55* (1939) 417–418 (February 3, 1939).
[164] R. B. Roberts, R. C. Meyer, L. R. Hafstad, "Droplet Fission of Uranium and Thorium Nuclei," *Phys. Rev. 55* (1939) 416–417 (February 4, 1939).
[165] W. Jentschke, F. Prankl, "Untersuchung der schweren Kernbruchstücke beim Zerfall von neutronenbestrahltem Uran und Thorium," *Naturwissenschaften 27* (1939) 134–135 (February 14, 1939).
[166] G. v. Droste, Über die Energieverteilung der bei Bestrahlung von Uran mit Neutronen entstehenden Bruchstücke, *Naturwissenschaften 27* (1939) 198 (March 17, 1939).
[167] F. Joliot, "Preuve expérimentale de la rupture explosive des noyaux d'uranium et de thorium sous l'action des neutrons," *C.R. Hebd. Séances Acad. Sci. 208* (1939) 341–343 (January 30, 1939).
[168] P. Radvanyi, M. Bordry: *La radioactivité artificielle et son histoire*, Seuil/CNRS, Paris 1984, p. 149.
[169] P. Radvanyi, personal communication, November 1989.
[170] S. R. Weart: *Scientists in Power*, Harvard University Press., Cambridge 1979, p. 64.
[171] E. McMillan, "Radioactive Recoils from Uranium Activated by Neutrons," *Phys. Rev. 55* (1939) 510 (February 17, 1939).
[172] L. Badash, E. Hodes, A. Tiddens, "Nuclear Fission: Reaction to the Discovery in 1939," *Proc. Am. Philos. Soc. 130* (1986) 196–231.
[173] J. A. Wheeler, "Fission in 1939: The Puzzle and the Promise," in [102], p. 45–52; also in *Annu. Rev. Nucl. Part. Sci. 39* (1989) XIII–XXVIII.
[174] N. Bohr, "Disintegration of Heavy Nuclei," *Nature (London) 143* (1939) 330 (January 20, 1939).
[175] C. F. Squire, F. G. Brickwedde, E. Teller, M. A. Tuve, "The Fifth Washington Conference on Theoretical Physics," *Science (Washington, DC) 89* (1939) 180–182.
[176] "Atom Explosion Frees 200,000,000 Volts—New Physics Phenomenon Credited to Hahn," New York Times of January 28, 1939, reprinted in [108], p. 145.
[177] N. Bohr, "Resonance in Uranium and Thorium Disintegrations and the Phenomenon of Nuclear Fission," *Phys. Rev. 55* (1939) 418–419 (February 7, 1939).
[178] A. J. Dempster, "Isotopic Constitution of Uranium," *Nature (London) 136* (1939) 180 (July 12, 1935).
[179] E. Feenberg, "On the Shape and Stability of Heavy Nuclei," *Phys. Rev. 55* (1939) 504–505 (February 14, 1939).
[180] J. Frenkel, "On the Splitting of Heavy Nuclei by Slow Neutrons," *Phys. Rev. 55* (1939) 987 (March 12, 1939).
[181] N. Bohr, J. A. Wheeler, "The Mechanism of Nuclear Fission," *Phys. Rev. 56* (1939) 426–450 (June 28, 1939).
[182] H. von Halban, F. Joliot, L. Kowarski, "Liberation of Neutrons in the Nuclear Explosion of Uranium," *Nature (London) 143* (1939) 470–471 (March 8, 1939).
[183] H. L. Anderson, E. Fermi, H. B. Hanstein, "Production of Neutrons in Uranium Bombarded by Neutrons," *Phys. Rev. 55* (1939) 797–798 (March 16, 1939).
[184] S. Flügge, "Kann der Energieinhalt der Atomkerne technisch nutzbar gemacht werden?," *Naturwissenschaften 27* (1939) 402–410 (appeared June 9, 1939).
[185] E. Fermi, "Experimental Production of a Divergent Chain Reaction," *Am. J. Phys. 20* (1952) 536–558.
[186] L. Meitner, O. R. Frisch, "Products of the Fission of the Uranium Nucleus," *Nature (London) 143* (1939) 471–472 (March 6, 1939).
[187] N. Feather, "Fission of Heavy Nuclei: a New Type of Nuclear Disintegration," *Nature (London) 143* (1939) 877–879 (appeared May 27, 1939).
[188] N. Feather, "Fission of Heavy Nuclei," *Nature (London) 143* (1939) 1027 (appeared June 17, 1939).
[189] L. W. Alvarez: *Alvarez—Adventures of a Physicist*, Basic Books, New York 1988, p. 75.
[190] S. Curran, quoted in G. N. Walton, "Nuclear Fission," *Q. Rev. Chem. Soc. (London) 15* (1961) 74.
[191] H. Maier-Leibnitz (1937), quoted after A.-L. Edingshaus: *Heinz Maier-Leibnitz—Ein halbes Jahrhundert experimentelle Physik*, Piper, München 1986, p. 66.
[192] E. Segrè, "Fermi and Neutron Physics," *Rev. Mod. Phys. 27* (1955) 257–263.
[193] P. H. Abelson, "Products of Neutron Irradiation," *J. Chem. Educ. 66* (1989) 364–366.
[194] P. Abelson, "Cleavage of the Uranium Nucleus," *Phys. Rev. 55* (1939) 418 (February 3, 1939).
[195] P. Abelson, "An Investigation of the Products of the Disintegration of Uranium by Neutrons," *Phys. Rev. 56* (1939) 1 (May 11, 1939).
[196] F. Strassmann, personal communication to the author, ca. 1950, and hand-written note 1969, in [49], p. 221.
[197] B. Goldschmidt: *Pionniers de l'atome*, Stock, Paris 1987, p. 39–40.
[198] G. Herrmann, "Technetium or Masurium—a Comment on the History of Element 43," *Nucl. Phys. A 505* (1989) 352–360.
[199] N. Feather, E. Bretscher, "Atomic Numbers of the So-called Transuranic Elements," *Nature (London) 143* (1939) 516 (March 9, 1939).
[200] O. Hahn, F. Strassmann, "Zur Frage nach der Existenz der "Trans-Urane". I. Endgültige Streichung von Eka-Platin und Eka-Iridium," *Naturwissenschaften 27* (1939) 451–453 (June 19, 1939).
[201] L. Meitner, "New Products of the Fission of the Thorium Nucleus," *Nature (London) 143* (1939) 637 (March 26, 1939).
[202] E. Bretscher, L. G. Cook, "Transmutations of Uranium and Thorium Nuclei by Neutrons," *Nature (London) 143* (1939) 559–560 (March 11, 1939).
[203] V. G. Khlopin, M. A. Pasvick-Khlopina, N. F. Volkov, "Division of Uranium Nuclei under the Action of Neutrons and the Problem of the Existence of Transuraniums," *C. R. (Dokl.) Acad. Sci. URSS 24* (1939) 118–121 (May 9, 1939).
[204] O. Hahn, in [108], p. 144–149.
[205] F. Strassmann, Letter to O. Hahn of October 5, 1960, based on a study of the author, in [49], p. 228–232.
[206] H. Menke, G. Herrmann, "Was waren die 'Transurane' der dreissiger Jahre in Wirklichkeit?," *Radiochim. Acta 16* (1971) 119–123.
[207] F. Baroncelli, "Che cosa erano i 'Transuranici' studiati a Roma nel 1934," *Atti Accad. Naz. Lincei Cl. Sci. Fis. Mat. Nat. 78* (1985) 29–33.
[208] W. Seelmann-Eggebert, F. Strassmann, "Über die bei der Uranspaltung noch zu erwartenden Bruchstücke," *Z. Naturforsch. 2a* (1947) 80–86 (October 31, 1946).
[209] E. P. Steinberg, "Radiochemistry of the Fission Products," *J. Chem. Educ. 66* (1989) 367–372.
[210] J. M. Siegel (Ed.), "Nuclei Formed in Fission: Decay Characteristics,

Fission Yields, and Chain Relationships," *J. Am. Chem. Soc. 68* (1946) 2411–2442 (August 29, 1946); simultaneously in *Rev. Mod. Phys. 18* (1946) 513–544.
[211] C. D. Coryell, N. Sugarman (Ed.): *Radiochemical Studies: The Fission Products*, 3 Vols., McGraw-Hill, New York 1951.
[212] G. Herrmann, Über einige Strontiumisotope in der Uranspaltung, *Z. Elektrochem. 58* (1954) 626–629.
[213] O. Hahn, F. Strassmann, "Weitere Spaltprodukte aus der Bestrahlung des Urans mit Neutronen," *Naturwissenschaften 27* (1939) 529–534 (July 22, 1939).
[214] A. C. Wahl, "Nuclear Charge Distribution in Fission," in N. Metropolis, D. M. Kerr, G.-C. Rotta (Eds.): *New Directions in Physics*, Academic Press, New York 1987, p. 163–189.
[215] E. Segrè, "An Unsuccessful Search for Transuranic Elements," *Phys. Rev. 55* (1939) 1104–1105 (May 10, 1939).
[216] E. Segrè, "The Discovery of Nuclear Fission," *Phys. Today 42(7)* (1989) 38–43.
[217] C. Perrier, E. Segrè, "Some Chemical Properties of Element 43," *J. Chem. Phys. 5* (1937) 712–716.
[218] J. W. Irvine, "Concentrating the Uranium Isotope of Twenty-Three-Minute Half-Life," *Phys. Rev. 55* (1939) 1105 (May 16, 1939).
[219] E. McMillan, P. H. Abelson, "Radioactive Element 93," *Phys. Rev. 57* (1940) 1185–1186 (May 27, 1940).
[220] O. Hahn, Letters to Lise Meitner of May 10 and 16, 1939, in [49], p. 307.
[221] K. Starke, "Abtrennung des Elements 93," *Naturwissenschaften 30* (1942) 107–108 (January 19, 1942).
[222] K. Starke, "Anreicherung des künstlich radioaktiven Uran-Isotops $^{239}_{92}U$ und seines Folgeprodukts $^{293}93$ (Element 93)," *Naturwissenschaften 30* (1942) 577–582 (appeared September 18, 1942).
[223] L. Szilard, T. A. Chalmers, "Chemical Separation of the Radioactive Element from its Bombarded Isotope in the Fermi Effect," *Nature (London) 134* (1934) 462.
[224] K. Starke, "Transuranium Research in Germany 1939 to 1945," *Atomkernenergie 41* (1982) 264–266.
[225] K. Starke, "Zur Frühgeschichte des Neptuniums," *Isotopenpraxis*, in press.
[226] O. Hahn, Letter to L. Meitner of August 31, 1940, in [49], p. 125–126.
[227] O. Hahn, Letters to L. Meitner of September 16 and October 17, 1940, in [49], p. 126.
[228] F. Strassmann, O. Hahn," Über die Isolierung und einige Eigenschaften des Elements 93," *Naturwissenschaften 30* (1942) 256–260 (April 2, 1942).
[229] G. T. Seaborg, "The Chemical and Radioactive Properties of the Heavy Elements," *Chem. Eng. News 23* (1945) 2190–2193 (December 10, 1945).
[230] G. Herrmann, "Synthese schwerster chemischer Elemente—Ergebnisse und Perspektiven," *Angew. Chem. 100* (1988) 1471–1491; "Synthesis of the Heaviest Chemical Elements—Results and Perspectives," *Angew. Chem. Int. Ed. Engl. 27* (1988) 1417–1436.
[231] G. Münzenberg, S. Hofmann, F. P. Hessberger, W. Reisdorf, K. H. Schmidt, J. H. R. Schneider, P. Armbruster, C. C. Sahm, B. Thuma, "Identification of Element 107 by α Correlation Chains, *Z. Phys. A 300* (1981) 107–108.
[232] E. K. Hulet, "Chemistry of the Elements Einsteinium through Element 105," *Radiochim. Acta 32* (1983) 7–23.
[233] O. L. Keller, "Chemistry of the Heavy Actinides and Light Transactinides," *Radiochim. Acta 37* (1984) 169–180.
[234] R. J. Silva, "Transeinsteinium Elements," in [235], Vol. 2, p. 1086–1117.
[235] J. J. Katz, G. T. Seaborg, L. R. Morss (Eds.): *The Chemistry of the Actinide Elements*, 2nd Edit., Chapman and Hall, New York 1986.
[236] K. E. Gregorich, R. A. Henderson, D. M. Lee, M. J. Nurmia, R. M. Chasteler, H. L. Hall, D. A. Bennett, C. M. Gannett, R. B. Chadwick, J. D. Leyba, D. C. Hoffman, G. Herrmann, "Aqueous Chemistry of Element 105," *Radiochim. Acta 43* (1988) 223–231.
[237] J. V. Kratz, H. P. Zimmermann, U. W. Scherer, M. Schädel, W. Brüchle, K. E. Gregorich, C. M. Gannett, H. L. Hall, R. A. Henderson, D. M. Lee, J. D. Leyba, M. J. Nurmia, D. C. Hoffman, H. Gäggeler, D. Jost, U. Baltensperger, Ya Nai-Qi, A. Türler, Ch. Lienert," Chemical Properties of Element 105 in Aqueous Solutions: Halide Complex Formation and Anion Exchange into Triisooctyl Amine," *Radiochim. Acta 48* (1989) 121–133.
[238] B. L. Zhuikov, Yu. T. Chuburkov, S. N. Timokhin, Kim U Jin, I. Zvara, "Is Element 104 (Kurchatovium) a p-Element?," *Radiochim. Acta 46* (1989) 113–116.
[239] [G. N.] Flerov, [K. A.] Petrjak [Petrzhak]," Spontaneous Fission of Uranium," *Phys. Rev. 58* (1940) 89 (June 14, 1940).
[240] K. A. Petrzhak, G. N. Flerov, "Über die spontane Teilung von Uran," *C. R. (Dokl.) Acad. Sci. URSS 28* (1940) 500–501 (June 15, 1940).
[241] G. N. Flerov, K. A. Petrzhak, "Spontaneous Fission of Uranium," *J. Phys. 3* (1940) 275–280, reprinted in [95], p. 196–204.
[242] O. R. Frisch: *What Little I Remember*, Cambridge University Press, Cambridge 1979, p. 118.
[243] P. K. Kuroda, "On the Nuclear Physical Stability of the Uranium Minerals," *J. Chem. Phys. 25* (1956) 781–782.
[244] H. Bouzigues, R. J. M. Boyer, C. Seyve, P. Teulières (1972), in [245], p. 237–243.
[245] Le Phénomène D'Oklo, Comptes Rendus d'un Colloque, Libreville, 23 au 27 Juin 1975, Int. Atomic Energy Agency, Wien 1975.
[246] M. Maurette, "Fossil Nuclear Reactors," *Annu. Rev. Nucl. Sci. 26* (1976) 319–350.
[247] O. Hahn, in [108], p. 122–123.

Communications may be submitted in English *or* in German. Further details regarding the submission of communications can be found in the "Notice to Authors" reproduced in the January issue of the journal. Copies thereof may be obtained from the editorial office upon request.

Kinetic Isotope Effects as a Mechanistic Tool for the Elucidation of the Rate-Determining Step(s) in the Transition-Metal-Ion-Mediated Activation of CH/CC Bonds. Ethylene Loss from Metastable 4-Octyne/$M^{\oplus}$ Complexes in the Gas Phase**

By *Christian Schulze* and *Helmut Schwarz**

Dedicated to Professor Wolfgang R. Roth on the occasion of his 60th birthday

While there exist quite a number of case studies in which the mechanistic details of CH/CC bond activation by transition-metal complexes in solution were uncovered by using kinetic isotope effects,[1] analogous investigations in the gas phase are scarce as far as the elucidation of the rate-determining step(s) (RDS) is concerned.[2, 3] Here we report a study of the transition-metal-ion-mediated generation of ethylene from metastable 4-octyne/$M^{\oplus}$ complexes (M = Cr, Mn, Fe, Co, Ni, Cu) in the gas phase.[4–6] It will be demonstrated that, depending on $M^{\oplus}$, three distinct cases can be distinguished: (1) The rate-determining step corresponds to the activation of a CH bond, (2) the olefin detachment is rate-determining, and (3) the hydrogen transfer and the loss of ethylene are associated with kinetic isotope effects.

The analysis of the data displayed in Table 1 is straightforward. For all metal ions, except $Mn^{\oplus}$,[5] the reaction involves exclusively the C1/C2 positions of the substrate. Hydrogen exchange reactions do not take place. In addition, the reactions **2** → **3** and **4** → **3**[7] are strictly irreversible. Thus, **3** is more likely to dissociate than to revert to the intermediates involved in its formation (Scheme 1).

A further analysis of the isotope distribution reveals the following: (1) Comparison of the data for the $Cr^{\oplus}$ and $Cu^{\oplus}$ complexes **1a** and **1b** clearly demonstrates that the ligand detachment **3** → **5** is *not* associated with a kinetic isotope effect (C_2H_4 and $C_2H_2D_2$ are eliminated to the same extent from **1b**). Rather, for these metal-ion complexes it is the CH bond activation step **2** → **3** (or **1**-$M^{\oplus}$ → **4**) which constitutes the RDS. The fact that this primary isotope effect is relatively small (1.38 for $Cr^{\oplus}$ and 1.94 for the $Cu^{\oplus}$ system) points to bent transition structures,[8] which may indicate that the reaction actually proceeds via the route **1**-$M^{\oplus}$ → **2** → **3**. (2) In distinct contrast, for $M^{\oplus} = Fe^{\oplus}$ it is the loss of $C_2H_{4-x}D_x$ which is affected by isotopic substitution. If the C–H bond activation constituted the RDS, one should observe a primary kinetic isotope effect discriminating against loss of $C_2H_2D_2$ versus C_2H_4 from **1a**-$Fe^{\oplus}$ relative to **1b**-$Fe^{\oplus}$. This is not the case. Rather, both isotopomers give exactly the same isotope distribution from which we obtain a value of $k_H/k_D = 1.22$ (or of 1.10 per deuterium). This value is in line with what one would expect for secondary isotope effects caused by rehybridization $sp^x \rightarrow sp^2$ ($x > 2$) of the carbon

Table 1. Ethylene loss from the metastable 4-octyne/$M^{\oplus}$ complexes [a, b] **1a**, $CD_3CH_2CH_2C{\equiv}CC_3H_7$; **1b**, $CH_3CD_2CH_2C{\equiv}CC_3H_7$; **1c**, $CH_3CH_2CD_2C{\equiv}CC_3H_7$; **1d**, $CD_3CD_2CH_2C{\equiv}CC_3H_7$.

Substrate	$C_2H_{4-x}D_x$	$Cr^{\oplus}$	$Mn^{\oplus}$ [c]	$Fe^{\oplus}$	$Co^{\oplus}$	$Ni^{\oplus}$	$Cu^{\oplus}$
1a	C_2H_4	58	55	55	58	60	66
	C_2H_3D						
	$C_2H_2D_2$	42	45	45	42	40	34
	C_2HD_3						
	k_H/k_D	1.38	–	1.22	1.38	1.50	1.94
1b	C_2H_4	50	45	55	55	55	51
	C_2H_3D		10				
	$C_2H_2D_2$	50	45	45	45	45	49
	k_H/k_D	1.00	–	1.22	1.22	1.22	1.04
1c	C_2H_4	100	82	100	100	100	100
	C_2H_3D		13				
	$C_2H_2D_2$		5				
1d	C_2H_4	57	45	59	61	62	66
	C_2H_3D		2				
	$C_2H_2D_2$		2				
	C_2HD_3		8				
	C_2D_4	43	43	41	39	38	34
	k_H/k_D	1.32	–	1.44	1.56	1.63	1.94

[a] Intensities are normalized to $\sum C_2H_{4-x}D_x = 100\%$: the reproducibility of the data is better than ±3%. [b] Elimination of ethylene (% total ion fragment current) from metastable 4-octyne/$M^{\oplus}$ amounts to: 15% ($Cr^{\oplus}$), 40% ($Mn^{\oplus}$), 98% ($Fe^{\oplus}$), 94% ($Co^{\oplus}$), 98% ($Ni^{\oplus}$), and 84% ($Cu^{\oplus}$). [c] For $Mn^{\oplus}$, due to the partial scrambling between C2 and C3, no k_H/k_D data are given.

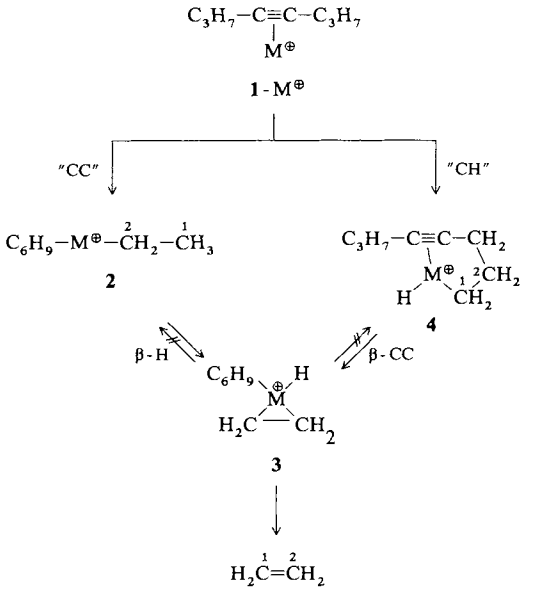

Scheme 1.

[*] Prof. Dr. H. Schwarz, Dr. C. Schulze [+]
Institut für Organische Chemie der Technischen Universität
Strasse des 17. Juni 135, D-1000 Berlin 12

[+] Present address: Department of Chemistry, University of Oslo
P.O. Box 1033 Blindern, N-0315 Oslo 3 (Norway)

[**] We are grateful to the Volkswagen-Stiftung, the Fonds der Chemischen Industrie, and the Deutsche Forschungsgemeinschaft for financial support.

atoms in the step $\mathbf{3} \rightarrow \mathbf{5}$.[1a, b, 9] (3) It is obvious from Table 1 that for the $Co^{\oplus}$ and $Ni^{\oplus}$ complexes of 4-octyne both steps, i.e., C–H bond activation *and* ligand detachment, are subject to a kinetic isotope effect. For the ligand detachment $\mathbf{3} \rightarrow \mathbf{5}$ the data for **1b** and **1d** permit the estimation of an isotope effect $k_H/k_D = 1.10$ (per deuterium) for either $Co^{\oplus}$ or $Ni^{\oplus}$. The C–H bond activation step $\mathbf{2} \rightarrow \mathbf{3}$ (or, less likely, $\mathbf{1}\text{-}M^{\oplus} \rightarrow \mathbf{4}$) is associated with slightly differing k_H/k_D values of 1.25 and 1.36 for $Co^{\oplus}$ and $Ni^{\oplus}$, respectively.[10] *Obviously, the various transition-metal ions cause a switching in regard to the bottleneck of the multistep event* which is shown in Scheme 1 in a simplified manner.

As indicated in Figure 1, a quite remarkable *inverse* relationship exists between the magnitude of the kinetic isotope

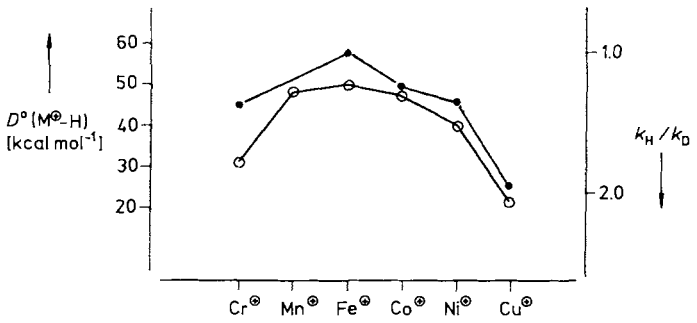

Fig. 1. Qualitative relationship between $D°(M^{\oplus}\text{-H})$ (-○-○-○-) and kinetic isotope effects (-●-●-●-) for C–H bond activation ($\mathbf{2} \rightarrow \mathbf{3}$ or $\mathbf{1}\text{-}M^{\oplus} \rightarrow \mathbf{4}$). The data for $D°(M^{\oplus}\text{-H})$ are taken from [11]. For $Mn^{\oplus}$ no accurate k_H/k_D value can be given (see text).

effect of the oxidative addition of a CH bond to a metal-ion center and the strength of the $M^{\oplus}$–H bond, $D°(M^{\oplus}\text{-H})$, to be formed.[11] In a qualitative sense the *data suggest that weaker and stronger $M^{\oplus}$–H bonds cause larger and smaller isotope effects, respectively*. The origin of this relationship remains to be established through further experimental and theoretical studies.

Received: January 8, 1990 [Z 3725 IE]
German version: *Angew. Chem. 102* (1990) 566

CAS Registry numbers:
Cr, 7440-47-3; Mn, 7439-96-5; Fe, 7439-89-6; Co, 7440-48-4; Ni, 7440-02-0; Cu, 7440-50-8; atomic deuterium, 16873-17-9; 4-octyne, 1942-45-6.

[1] Selected references: a) W. D. Jones, F. J. Feher, *Acc. Chem. Res. 22* (1989) 91; b) P. O. Stoutland, R. G. Bergman, *J. Am. Chem. Soc. 110* (1988) 5732; c) F. R. Hartley, S. Patai, (Eds.): *The Chemistry of the Metal-Carbon Bond*, Vol. 1, 2, Wiley, New York 1985; d) R. H. Crabtree, *Chem. Rev. 85* (1985) 245.

[2] a) G. Czekay, T. Drewello, H. Schwarz, *J. Am. Chem. Soc. 111* (1989) 4561.

[3] a) N. Steinrück, H. Schwarz, *Organometallics 8* (1989) 759; b) C. Schulze, T. Weiske, H. Schwarz, *ibid. 7* (1988) 898.

[4] Preliminary results were previously described for $M^{\oplus} = Fe^{\oplus}$, $Cr^{\oplus}$: a) C. Schulze, T. Weiske, H. Schwarz, *Chimia 40* (1986) 362; b) C. Schulze, H. Schwarz, D. A. Peake, M. L. Gross, *J. Am. Chem. Soc. 109* (1987) 2368; c) [3b].

[5] In the present study $Mn^{\oplus}$ is not included in the discussion on the grounds that, in contrast to the other transition-metal ions, ethylene loss is preceded by exchange processes involving the CH bonds at positions C2 and C3 of the substrate (see Table 1). This fact prevents a reliable determination of the kinetic isotope effects. See also: a) C. Schulze, H. Schwarz, *J. Am. Chem. Soc. 110* (1988) 67; b) [3b].

[6] The 4-octyne/$M^{\oplus}$ complexes were generated in the ion source of a VG Instruments ZAB-HF-3F by reacting 4-octyne with $M^{\oplus}$; the latter ions were generated by either 100-eV electron impact ionization of a suitable organometallic compound or by fast atom bombardment of appropriate transition-metal salts. The complexes thereby formed were accelerated to 8 keV kinetic energy, mass selected by means of $B(1)E$ (B stands for magnetic and E for electric field) at a resolution sufficient to separate isobaric species, and the unimolecular dissociations occurring in the field-free region between E and $B(2)$ recorded by scanning of $B(2)$. Averaging techniques were employed to significantly improve the signal-to-noise ratios such that the intensity measurements were better than ±3%. For a full description of the apparatus and the techniques used, see: a) [3, 5a]; b) H. Schwarz, *Acc. Chem. Res. 22* (1989) 282; c) C. Schulze, *Ph.D. Thesis, Technische Universität Berlin, 1989*.

[7] The description of **3** as a metallacyclopropane derivative is somewhat arbitrary; of course, the species could also correspond to an η^2-olefin complex.

[8] a) F. H. Westheimer, *Chem. Rev. 61* (1961) 265; For other examples of isotope effects in β-hydrogen transfers in organometallic systems, see: b) [3, 6b]; c) D. S. Bomse, R. L. Woodin, J. L. Beauchamp, *J. Am. Chem. Soc. 101* (1979) 5503.

[9] A. Streitwieser, R. H. Jagow, R. C. Fahey, S. Suzuki, *J. Am. Chem. Soc. 80* (1958) 2326.

[10] Since two factors determine the experimental value, the calculations include a deconvolution to separate both effects. For details of the procedure, see [6c].

[11] The $D°(M^{\oplus}\text{-H})$ data are taken from: P. B. Armentrout, J. L. Beauchamp, *Acc. Chem. Res. 22* (1989) 315.

Rhodium-Catalyzed Synthesis of Trisubstituted Olefins from Ethene Derivatives and Diazoalkanes**

By *Justin Wolf, Lutz Brandt, Arno Fries,* and *Helmut Werner**

During attempts to prepare square-planar carbene metal complexes of type **1**, we discovered a new catalytic reaction for forming C–C bonds. The vinylidene rhodium and iridium complexes *trans*-$[MCl(=C=CRR')(PiPr_3)_2]$, which are structurally related to **1**, are known[1] and (for M = Ir) have been used for the synthesis of the cationic carbyne complexes *trans*-$[MCl(\equiv C\text{-}CHRR')(PiPr_3)_2]^{\oplus}$.[2]

trans-$[MCl(=CRR')(PiPr_3)_2]$ **1**, M = Rh, Ir

$[RhCl(PiPr_3)_2]$ **2**

trans-$[RhCl(=CH_2)(PiPr_3)_2]$ **3**

The monomeric three-coordinate rhodium compound **2** (Scheme 1), used as starting material for the preparation of the vinylidene complex *trans*-$[RhCl(=C=CH_2)$-

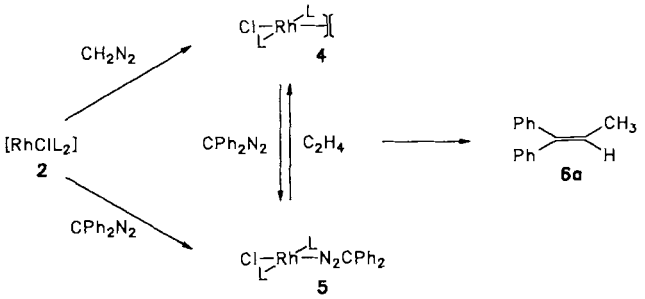

Scheme 1. L = $PiPr_3$.

[*] Prof. Dr. H. Werner, Dr. J. Wolf, L. Brandt, A. Fries
Institut für Anorganische Chemie der Universität
Am Hubland, D-8700 Würzburg (FRG)

[**] This work was supported by the Deutsche Forschungsgemeinschaft, the Commission of the European Communities, and the Fonds der Chemischen Industrie.

$(PiPr_3)_2]$,[1a,c] reacts with diazomethane in ether to give mainly the ethene complex **4**[3] instead of the carbene complex **3**. Whether **3** is formed as an intermediate is unclear. Similarly, the reaction of **2** with diphenyldiazomethane does not lead to a carbene complex but to the diazoalkane complex **5**,[4] which is stable at room temperature under argon. The position of the N-N stretching frequency at 1940 cm^{-1} in the IR spectrum of **5** suggests an end-on coordination of the CPh_2N_2 ligand.[5] Similar iridium compounds with the general composition *trans*-$[IrCl(\eta^1\text{-}N_2CR_2)(PPh_3)_2]$ with conjugatively stabilized diazoalkanes such as $N_2C_5X_4$ (X = Cl, Br) or $N_2C(COPh)_2$ have been described by *Ibers* et al.[6] and *Cowie* et al.[7] The compound containing $N_2C_5Cl_4$ as a ligand was characterized by X-ray structural analysis.[6]

Attempts to use complex **5** for cyclopropanation reactions have failed. On treatment of **5** (in benzene) with ethene at room temperature, an equilibrium between **4** and **5** is reached, which in ethene atmosphere lies mainly on the side of the ethene complex. In a *catalytic* reaction addition of excess diphenyldiazomethane and warming to ca. 40 °C unexpectedly produces 1,1-diphenylpropene **6a** (Scheme 1), which is formally built up by the linking of the $:CPh_2$ fragment of the diazoalkane with the ethene isomer $:CHCH_3$.[8] Turnover numbers of ca. 30 have been observed for **6a** at 35–40 °C in acetone, benzene, or toluene solution, after which deactivation of the catalyst occurs.

The iridium analogue of **5** cannot be obtained from the reaction of CPh_2N_2 with *trans*-$[IrCl(C_8H_{14})(PiPr_3)_2]$, which is generated in situ from $[IrCl(C_8H_{14})_2]_2$ and $PiPr_3$ and is used in the synthesis of organoiridium compounds.[1a,b,9] The main product in this reaction, as well as in the reaction of the Ir complex **7** with CPh_2N_2, is the dinitrogen complex *trans*-$[IrCl(N_2)(PiPr_3)_2]$.[10] If, however, the chloro ligand in **7** is displaced by CH_3 and the resulting methyl derivative **8** (Scheme 2) is treated with CPh_2N_2 under mild conditions in

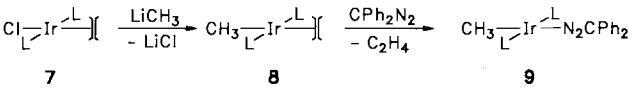

7 **8** **9**

Scheme 2. L = $PiPr_3$.

ether, the corresponding diphenyldiazomethane complex **9** is formed in almost quantitative yield.[11] Complex **9** is completely inert toward ethene even if it is stirred at 60 °C in an ethene atmosphere. On treatment of **7** with excess CPh_2N_2 in toluene at 60 °C, only small amounts of **6a** (ca. 10% yield with regard to **7**) can be detected.

The iridium complex **11** and the rhodium analogue **12** (Scheme 3) are significantly more reactive than **7** and **8** toward mixtures of ethene and the diaryldiazomethanes **10a–d**.[12] **12** is particularly reactive for it allows a *catalytic* synthesis of trisubstituted olefins. With 3 mg of **12** in 15 mL of toluene, turnover numbers of 125, 460, 515, and 105 for **6a–d** are observed after 6 h at 50 °C. If propene or styrene is used instead of ethene, the ethene derivatives **13a–d** and **14a–d** are formed. In this case, however, the yield of the olefinic product is lower than in the reactions with ethene. The trisubstituted olefins are separated from the metal-containing species by column chromatography (Al_2O_3, activity grade III) using pentane as solvent; they were identified by mass spectrometry and ^1H NMR spectroscopy.

Treatment of 9-diazofluorene with ethene, propene, or styrene as parent olefin gives the compounds **15–17**. After the catalytic reaction leading to the olefins is nearly finished, the formation of cyclopropane derivatives such as 1,1,2-triphenylcyclopropane (from **10a** and styrene) can also be detected. In addition, thermal cyclopropanation of styrene with **10a** is possible but has not been observed in the absence of **12** under the conditions employed in our experiments.

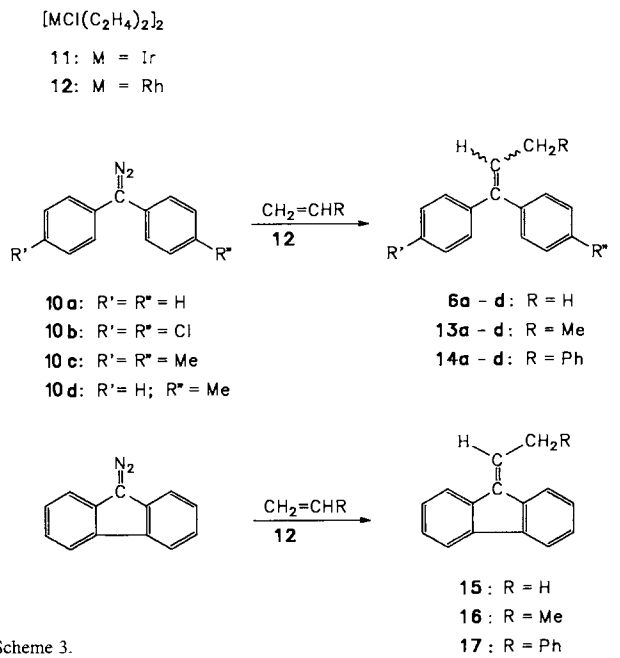

Scheme 3.

The turnover numbers for the formation of **6a–d** do not depend on the solvent; they remain almost the same regardless whether a nonpolar solvent such as benzene or toluene or a polar solvent such as acetone is used. In methanol, the reaction of ethene with **10a** affords not only **6a** but also the insertion product $MeOCHPh_2$.

The new method for forming C–C bonds can also be applied to diazoketones and to olefins containing a functional group (Scheme 4). For example, the reaction of ethene with diazodiphenylethanone (**18**) gives the α,β-unsaturated carbonyl compound **19**, whereby only the *Z* stereoisomer is obtained. At 50 °C in toluene, the turnover number is ca. 15. Treatment of **20a,b** with CPh_2N_2 (**10a**) leads to the unsaturated alcohols **21a** and the previously unknown **21b**.

Concerning the mechanism of this new olefin synthesis, it is important to note that **6a** is obtained from **4** and CPh_2N_2 as well as from **5** and C_2H_4. We therefore assume that in the initial stage of the reaction *both* substrates, the olefin and the

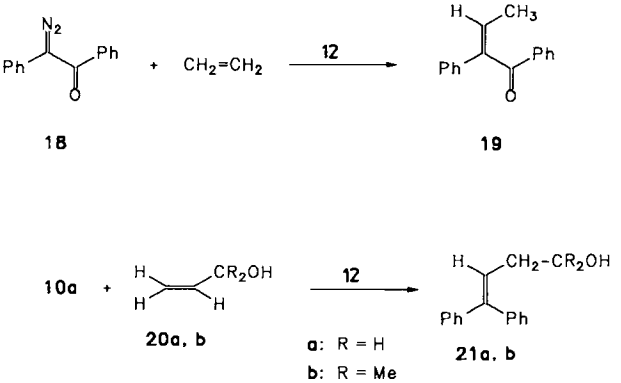

Scheme 4.

diazoalkane, are coordinated to the metal and form an MN_2C_3 six-membered ring via a cycloaddition reaction promoted by the metal center. After elimination of N_2, a metallacyclobutane derivative may be generated, from which an η^3-allylhydrido intermediate is obtained by a β-H shift. Finally, migration of the hydride ligand to a terminal carbon of the allyl group can lead to the product olefin, thus reforming the catalytically active species. We are currently trying to prepare independently metallacyclobutane derivatives related in structure to the intermediate in the catalytic cycle to find out whether they can generate the observed olefin.

Received: December 27, 1989 [Z 3705 IE]
German version: *Angew. Chem. 102* (1990) 584

[1] a) F. J. Garcia Alonso, A. Höhn, J. Wolf, H. Otto, H. Werner, *Angew. Chem. 97* (1985) 401; *Angew. Chem. Int. Ed. Engl. 24* (1985) 406; b) A. Höhn, H. Otto, M. Dziallas, H. Werner, *J. Chem. Soc. Chem. Commun. 1987*, 852; c) H. Werner, F. J. Garcia Alonso, H. Otto, J. Wolf, *Z. Naturforsch. B 43* (1988) 722; d) A. Höhn, H. Werner, *J. Organomet. Chem., 382* (1990) 255.

[2] A. Höhn, H. Werner, *Angew. Chem. 98* (1986) 745; *Angew. Chem. Int. Ed. Engl. 25* (1986) 737.

[3] C. Busetto, A. D'Alfonso, F. Maspero, G. Perego, A. Zazzetta, *J. Chem. Soc. Dalton Trans. 1977*, 1828.

[4] Procedure for **5**: A solution of 335 mg (0.73 mmol) **2** in 20 mL of ether was treated at room temperature with a solution of 142 mg (0.73 mmol) CPh_2N_2 in 5 mL of ether. An immediate color change from violet to green was observed. After the solution was stirred for 10 min, it was concentrated to ca. 5 mL, and 30 mL of pentane was added. Cooling to −78 °C gave a green, air-sensitive solid; yield 368 mg (77%); m.p. = 94 °C (dec). IR (KBr): $\tilde{\nu}(N_2CPh_2)$ = 1940 (br) cm^{-1}; ^1H NMR (90 MHz, C_6D_6): δ = 7.2 (m; C_6H_5), 2.35 (m; PCH), 1.26 (dvt, N = 13.3 Hz, J(HH) = 7.1 Hz; $PCHCH_3$); ^{13}C NMR (50.3 MHz, C_6D_6): δ = 129.5, 128.9, 125.1, 124.3 (4 × s; phenyl C atoms), 78.7 (s, br; CN_2), 23.6 (vt, N = 18.2 Hz; $PCCH_3$), 20.0 (s; $PCCH_3$).

[5] For reviews on $M(N_2CR_2)$ complexes see: a) A. Albini, H. Kisch, *Top. Curr. Chem. 65* (1976) 105; b) W. A. Herrmann, *Angew. Chem. 90* (1978) 855; *Angew. Chem. Int. Ed. Engl. 17* (1978) 800.

[6] K. D. Schramm, J. A. Ibers, *Inorg. Chem. 19* (1980) 1231, 2435.

[7] M. Cowie, S. J. Loeb, J. R. McKeer, *Organometallics 5* (1986) 854.

[8] A similar isomerization of ethene occurs on treatment of the ketene complex $[(\eta^4\text{-}Ph_2C{=}C{=}O)Fe(CO)_3]$ with C_2H_4; in this reaction, the compound $[(\eta^4\text{-}Ph_2C{=}CHMe)Fe(CO)_3]$ is formed as one of the products; yield 24%: W. A. Herrman, J. Weichmann, B. Balbach, M. L. Ziegler, *J. Organomet. Chem. 231* (1982) C69.

[9] M. Schulz, *Diploma Thesis*, University of Würzburg 1988.

[10] H. Werner, A. Höhn, *Z. Naturforsch. B 39* (1984) 1505.

[11] **9** (preparation similar to that of **5**): yield 83%; dark green, air-sensitive crystals. IR (KBr): $\tilde{\nu}(N_2CPh_2)$ = 2040 (s) cm^{-1}; ^1H NMR (200 MHz, C_6D_6): δ = 7.15 (m; C_6H_5), 2.45 (m; PCH), 2.03 (t, J(PH) = 7.4 Hz; $IrCH_3$), 1.27 (dvt, N = 12.9 Hz, J(HH) = 7.1 Hz, $PCHCH_3$); ^{31}P NMR (36.2 MHz, C_6D_6): δ = 26.1 (s); ^{13}C NMR (50.3 MHz, C_6D_6): δ = 128.0, 125.9, 125.3, 122.7 (4 × s, phenyl C atoms), 69.1 (s; CN_2), 23.7 (vt, N = 24.0 Hz; $PCCH_3$), 19.9 (s; $PCCH_3$), -7.1 (t, J(PC) = 8.1 Hz; $IrCH_3$).

[12] R. Cramer, *Inorg. Synth. 15* (1974) 14.

[13] G. W. Griffin, A. F. Marcantonio, H. Kristinsson, R. C. Petterson, C. S. Irving, *Tetrahedron Lett. 1965*, 2951.

Enantioselective Catalysis with a New Zirconium Trichloride Lewis Acid Containing a "Dibornacyclopentadienyl" Ligand**

By *Gerhard Erker** and *Adolphus A. H. van der Zeijden*

Important aldol-type C–C coupling reactions are catalyzed by Lewis acids.[1] Enantioselectivity is usually achieved by the use of stoichiometric amounts of chiral auxiliaries.[2] Only in a few exceptional cases have chiral Lewis acids recently been employed in stoichiometric amounts or as catalysts.[3] Here we describe the synthesis of the new organometallic Lewis acid **6a**, which contains a "dibornacyclopentadienyl" ligand, and its use as an effective catalyst for the enantioselective C–C coupling of pyruvic esters with a reactive arene.

The "chiral pool" synthesis of the dibornacyclopentadienyl ligand started from (+)-camphor (**1**),[4] which was converted, via Shapiro reaction, into 2-bornen-2-yllithium (**2**).[5] Reaction of **2** with ethyl formate in a 2:1 molar ratio afforded, under optimal conditions, bis(2-bornen-2-yl)methanol (**3**) in nearly quantitative yield (spectroscopically clean). Cyclization of **3** with $KHSO_4$ at 100–150 °C gave the cyclopentadiene system **4**[6] (80%, m.p. 87 °C, two isomers in a 75:25 ratio, presumably H *endo* (**4a**) and *exo* (**4b**) at C3').[7] Deprotonation of **4** with *n*-butyllithium in ether gave **5**. Subsequent reaction of **5** with zirconium tetrachloride in toluene (molar ratio 1:1) afforded **6a** (40%). The analogous sequence of reactions with $HfCl_4$ led to the corresponding hafnium compound **6b** (40% based on **4**).[7]

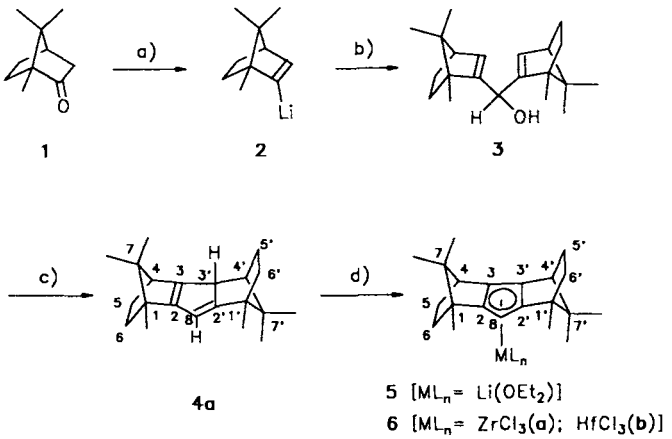

Scheme 1. a) 1. 2,4,6-$iPr_3C_6H_2SO_2NHNH_2$, 2. *s*BuLi; b) HCO_2Et; c) $KHSO_4$, 100–150 °C; d) 1. *n*BuLi, Et_2O, 2. $ZrCl_4$ ($HfCl_4$) toluene.

Pharmacologically interesting 2-(2-hydroxyaryl)lactic esters can be prepared from pyruvic esters and hydroxyarenes in a reaction catalyzed by Lewis acids.[8] For example, reaction of 1-naphthol (**7**), as its Li salt, with ethyl pyruvate (**8a**) in the presence of 1 molar equivalent of $AlCl_3$ affords ethyl 2-(1-hydroxy-2-naphthyl)lactate (**9a**) as a racemate. To synthesize optically active **9a**, for example, (−)-menthyl-O-(Et)AlCl was used in stoichiometric amount.[8a] Asymmetric catalysis of this C–C coupling reaction proceeds under mild reaction conditions with the chiral Lewis acid **6a** ($[\alpha]_D$ = +51°). Reaction of **7** with **8a** at room temperature in the presence of a catalytic amount of **6a** (ratio **7**:**8a**:**6a** ≈ 100:100:1, catalyst concentration ca. 3 mmol L^{-1}) affords **9a** (70% after 2 h) with 27% *ee*. The enantiomeric excess was determined by ^1H NMR spectroscopy after complete conversion of ester **9a** to mixtures of the diastereomeric amides **10**/**11** by treatment with enantiomerically pure (*R*)- or (*S*)-1-phenyl-ethylamine in excess[9] and then checked independently and confirmed by ^1H NMR spectroscopy using the shift reagent $Eu(hfc)_3$. Use of catalyst **6a**, which has (1*R*,4*S*,1'*R*,4'*S*) configuration and is dextrorotatory, gives an excess of product **9a** with (*R*) configuration. This assign-

[*] Prof. Dr. G. Erker, Dr. A. A. H. van der Zeijden
Institut für Organische Chemie der Universität,
Am Hubland, D-8700 Würzburg (FRG)

[**] This work was supported by the Fonds der Chemischen Industrie, the Bundesminister für Forschung und Technologie, and the Alfried Krupp von Bohlen und Halbach-Stiftung. Dr. *van der Zeijden* thanks the Alexander von Humboldt-Stiftung for a fellowship.

ment is based on ^1H NMR analysis of the resulting diastereomeric carboxamides (**10**/**11**) according to the method of *Helmchen* et al.[10] and on the reduction of the isolated product **9a** (84% *ee*, $[\alpha]_D = +118°$) to the enantiomer **12** ($[\alpha]_D = +26°$) of the known compound (*S*)-2-(1-hydroxy-2-naphthyl)propane-1,2-diol ($[\alpha]_D = -28.8°$).[8a]

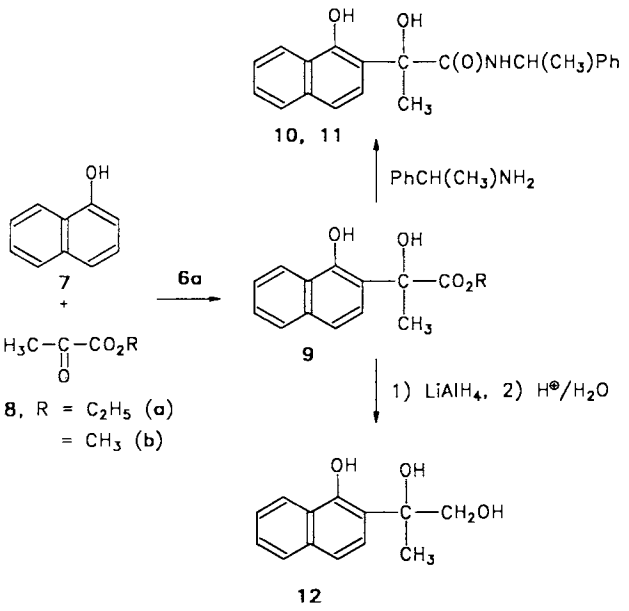

Initial attempts to optimize the enantioselective formation of (*R*)-**9a** showed that a lowering of the reaction temperature to $-10\,°C$ under otherwise identical conditions (**7**:**8a**:**6a** = 100:100:1, CH_2Cl_2, reaction time 24 h) leads to an increase in *ee* (20 °C, 21% *ee*; 0 °C, 32% *ee*; −5 °C, 46% *ee*; −10 °C, 54% *ee*). Further lowering of the temperature did not result in higher enantioselectivity. At −10 °C, the selectivity decreases markedly with increasing conversion (reaction time 2 h, 40% conversion, 78% *ee*; 5 h, 65% conversion, 70% *ee*; 24 h, 75% conversion, 54% *ee*; 48 h, 85% conversion, 49% *ee*). Changing the solvent (with the exception of coordinating solvents like THF) and variation of the $RCOCO_2R'$ components (R = methyl, isopropyl; R′ = methyl, ethyl, isopropyl, cyclohexyl) have little effect on the stereochemistry of the catalyzed C–C coupling process. An increase in the concentration of 1-naphthol appears to have a negative effect on the selectivity (**7**:**8a**:**6a** = 500:100:1, CH_2Cl_2, −10 °C: 2 h, 50% conversion, 53% *ee*; 5 h, 70% conversion, 42% *ee*; 24 h, 90% conversion, 32% *ee*). Presumably, under the acidic reaction conditions, catalyst **6a** is not stable over long periods but, instead, gradually loses the dibornacyclopentadienyl ligand to form an achiral, though still catalytically active, species. In agreement with this interpretation, an increase in the concentration of **8**, as well as the use of more catalyst **6a**, leads to considerably higher enantioselectivity, even for complete conversion of the limiting component **7** (e.g., **7**:**8a**:**6a** = 100:500:5, CH_2Cl_2, −10 °C; 2 h, 70% conversion, 80% *ee*; 5 h, 85% conversion, 80% *ee*; 24 h, quantitative conversion, 72% *ee*).

The addition of small amounts of water has a surprisingly positive effect. We have reproducibly obtained increases of about 10% in enantiomeric excess (e.g., molar ratio **7**:**8a**:**6a**:H_2O = 100:500:5:27, CH_2Cl_2, −10 °C; 2 h, 55% conversion, 89% *ee*; 5 h, 70% conversion, 89% *ee*; 24 h, 90% conversion, 84% *ee*).

It is known that the achiral organometallic Lewis acid (η-cyclopentadienyl)zirconium trichloride (**13**)[11] forms adducts with many organic carbonyl compounds as well as with HO-containing substrates.[12] We were unable to obtain a defined adduct of **13** with the individual components 1-naphthol (**7**) or pyruvic esters (**8**). However, if a mixture of **7** *and* **8b** is added to $CpZrCl_3$, then the addition product **14b** of the C–C coupling product of the organic starting materials can be isolated in 59% yield[13] (Scheme 2). Compounds

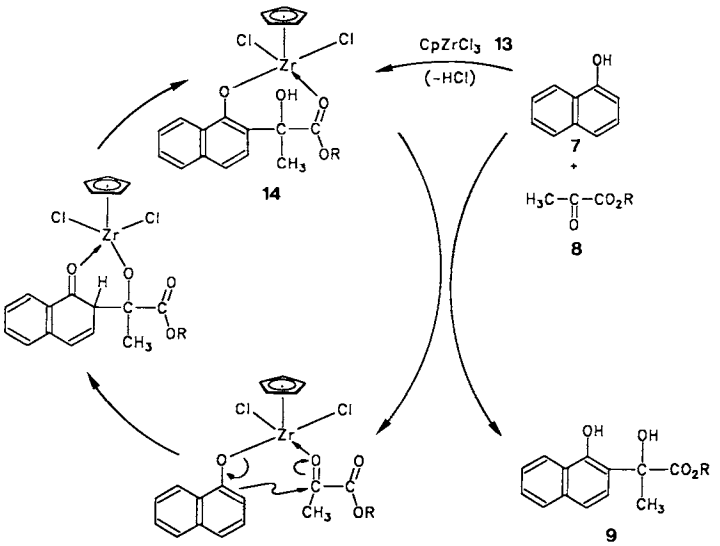

Scheme 2. **a**, R = C_2H_5; **b**, R = CH_3.

14 [R = C_2H_5 (**a**), CH_3 (**b**)] catalyze the reaction of **7** with **8** to give **9**. The enantioselective C–C coupling reaction involving the chiral organometallic Lewis acid **6a** presumably proceeds according to a similar reaction scheme. We hope to elucidate the details of this catalytic process, such as the surprising role of small amounts of water,[12b] by studying model reactions, based on the achiral $CpZrCl_2X$ system, of the isolated intermediate **14** of the catalytic cycle.

Experimental Procedure

Synthesis of ethyl (*R*)-2-(1-hydroxy-2-naphthyl)lactate (**9a**) with **6a** as catalyst: 1-Naphthol (**7**) (0.94 g, 6.53 mmol), ethyl pyruvate (**8a**) (2.5 mL, 23 mmol), and water (30 mg, 1.7 mmol) were added to a solution of catalyst **6a** (154 mg, 0.38 mmol) in 26 mL of CH_2Cl_2 at −60 °C. The reaction mixture was stirred for 24 h at −10 °C and then worked up as usual [8] to give 0.95 g (56%) of **9a**, m.p. 47 °C. Correct elemental analysis; $[\alpha]_D = +118°$ (corresponds to 84% *ee*). This value was confirmed independently by an ^1H NMR experiment with the shift reagent tris[3-((heptafluoropropyl)hydroxymethylene)-d-camphorato]europium as well as by reaction with enantiomerically pure 1-phenylethylamine.

Received: January 4, 1990 [Z 3720 IE]
German version: *Angew. Chem. 102* (1990) 543

CAS Registry numbers:
3, 126035-89-0; *endo*-**4a**, 126035-88-9; *exo*-**4a**, 126108-08-5; **5**, 126035-92-5; **6a**, 126035-93-6; **6b**, 126035-95-8; **7**, 90-15-3; **8a**, 617-35-6; **8b**, 600-22-6; (*R*)-**9a**, 113322-82-0; *rac*-**9a**, 126108-09-6; **10**, 126035-90-3; **11**, 126035-91-4; **12**, 126061-74-3; **13**, 34767-44-7; **14a**, 126035-94-7; **14b**, 126035-96-9; $PhCH(CH_3)NH_2$, 98-84-0; $ZrCl_4$, 10026-11-6; $HfCl_4$, 13499-05-3.

[1] D. A. Evans, J. V. Nelson, D. J. Taber, *Top. Stereochem. 13* (1982) 1; C. H. Heathcock in J. D. Morrison (Ed.): *Asymmetric Synthesis, Vol. 2*, Academic Press, New York 1983, S. 111.

[2] Recent examples: Siegel, E. R, Thornton, *J. Am. Chem. Soc. 111* (1989) 5723; C. Gennari, F. Molinari, P. Cozzi, A. Oliva, *Tetrahedron Lett. 30* (1989) 5163; T. Basile, S. Biondi, G. P. Boldrini, E. Tagliavini, C. Trombini, A. Umani-Ronchi, *J. Chem. Soc. Perkin Trans 1* (1989) 1025; R. O. Duthaler, P. Herold, W. Lottenbach, K. Oertle, M. Riediker, *Angew. Chem. 101* (1989) 490; *Angew. Chem. Int. Ed. Engl. 28* (1989) 495; D. Enders, B. B. Lohray, *ibid. 100* (1988) 594 bzw. *27* (1988) 581; Übersicht: R. W. Hoffmann, *ibid. 99* (1987) 503 bzw. *26* (1987) 489.

[3] Selected examples: K. Mikami, M. Terada, T. Nakai, *J. Am. Chem. Soc. 111* (1989) 1940; S. Kobayashi, T. Sano, T. Mukaiyama, *Chem. Lett. 1989*, 1319; S. Kobayashi, T. Mukaiyama, *ibid. 1989*, 297; I. Paterson, J. M. Goodman, *Tetrahedron Lett. 30* (1989) 997; Y. Ito, M. Sawamura, H. Hamashima, T. Emura, T. Hayashi, *ibid. 30* (1989) 4681; K. Maruoka, Y. Hoshino, T. Shirasaka, H. Yamamoto, *ibid. 29* (1988) 3967; M. T. Reetz, A. E. Vougioukas, *ibid. 28* (1987) 793; M. T. Reetz, F. Kunish, P. Heitmann, *ibid 27* (1986) 4721.

[4] Syntheses of similarly substituted Cp ligands: L. A. Paquette, K. J. Moriarty, P. Meunier, B. Gautheron, C. Sornay, R. D. Rogers, A. L. Rheingold, *Organometallics 8* (1989) 2159; L. A. Paquette, K. J. Moriarty, J. A. McKinney, R. D. Rogers, *ibid. 8* (1989) 1707; L. A. Paquette, K. J. Moriarty, R. D. Rogers, *ibid. 8* (1989) 1506, 1512; L. A. Paquette, K. J. Moriarty, P. Meunier, B. Gautheron, V. Crocq. *ibid. 7* (1988) 1873; J. C. Gallucci, B. Gautheron, M. Gugelchuk, P. Meunier, L. A. Paquette, *ibid. 6* (1987) 15; L. A. Paquette, M. Gugelchuk, M. L. McLaughlin, *J. Org. Chem. 52* (1987) 4732; M. L. McLaughlin, J. A. McKinney, L. A. Paquette, *Tetrahedron Lett. 27* (1986) 5595; R. L. Haltermann, K. P. C. Vollhardt, *Organometallics 7* (1988) 883; *Tetrahedron Lett. 27* (1986) 1461; R. L. Haltermann, K. P. C. Vollhardt, M. E. Welker, *J. Am. Chem. Soc. 109* (1987) 8105.

[5] A. R. Chamberlin, J. E. Stemke, F. T. Bond, *J. Org. Chem. 43* (1978) 147; A. R. Chamberlin, E. L. Liotta, F. T. Bond, *Org. Synth. 61* (1983) 141.

[6] Synthetic principle: R. S. Threlkel, J. E. Bercaw, *J. Organomet. Chem. 136* (1977) 1; R. S. Threlkel, J. E. Bercaw, P. F. Seidler, J. M. Stryker, R. G. Bergman, *Org. Synth. 65* (1987) 42.

[7] **4a** (major isomer): ^{1}H NMR ($CDCl_3$, 200 MHz), numbering as in Scheme 1: δ = 3.51 (3'-H), 2.36, 2.52 (4,4'-H), 0.5–2.1 (5,5',6,6'-H), 5.39 (8-H), 0.67, 0.88, 0.90, 1.02, 1.04, 1.05 (1,1',7,7'-CH_3). ^{13}C NMR ($CDCl_3$, 50 MHz, ^1J(CH) in Hz): δ = 11.8, 15.4 (1,1'-CH_3), 18.6, 19.9, 20.2, 20.8 (7,7'-CH_3), 27.5 (134) and 29.8 (128; 5,5'), 33.6 (131) and 35.7 (137; 6,6'), 48.2 (137) and 49.3 (138; 4,4'), 50.5, 52.4 (double intensity), 53.8 (1,1',7,7'), 74.2 (121; 3'), 112.2, 146.7, 146.9, 164.4 (2,2',3,8). **4b** (minor isomer): ^{1}H NMR ($CDCl_3$, 200 MHz): δ = 3.03 (3'-H), 2.31 (double intensity, 4,4'-H), 0.5–2.1 (5,5',6,6'-H), 5.52 (8-H), 0.34, 0.73, 0.76, 0.96 (1,1',7,7'-CH_3, two signals beneath those of the main isomer). ^{13}C NMR ($CDCl_3$, 50 MHz): δ = 12.0, 13.9 (1,1'-CH_3), 18.5, 19.6, 20.4, 21.2 (7,7'-CH_3), 24.7, 25.9 (5,5'), 35.7, 39.9 (6,6'), 47.5, 49.2 (4,4'), 51.3, 51.6, 56.0, (1,1',7,7', one signal beneath those of the main isomer), 73.7 (3'), 116.6, 122.7, 134.5, 144.2 (2,2',3,8). **5a**: ^{1}H NMR ([D_6]benzene, 200 MHz): δ = 2.78, 2.96 (4,4'-H), 0.6–2.5 (5,5',6,6'-H), 5.52 (8-H), 0.85, 1.02 (double intensity), 1.08, 1.40, 1.44 (1,1',7,7'-CH_3), 0.74 and 2.82 (Et_2O-coordinated). ^{13}C NMR ([D_6]benzene, 50 MHz): δ = 13.8, 14.4 (1,1'-CH_3), 20.8, 21.2, 21.7 (double intensity) (7,7'-CH_3), 30.9, 32.0, (5,5'), 37.6, 38.5 (6,6'), 50.2, 51.3 (4,4'), 51.3, 52.0, 55.5, 63.1 (1,1',7,7'), 84.4 (8) (2,2',3,3' not observed). **6a**: ^{1}H NMR ($CDCl_3$, 200 MHz): δ = 2.73, 3.05 (4,4'-H), 0.8–1.0, 1.8–2.2, 2.68 (5,5',6,6'-H), 6.11 (8-H), 0.26, 0.92, 0.93, 0.95, 1.19, 1.46 (1,1',7,7'-CH_3). ^{13}C NMR ($CDCl_3$, 50 MHz, ^1J(CH) in Hz): δ = 11.6, 12.5 (1,1'-CH_3), 19.8, 20.6 (double intensity), 29.8 (7,7'-CH_3), 25.8 (122) and (125; 5,5'), 32.1 (131) and 38.5 (137; 6,6'), 50.5, (149) and 51.6 (147; 4,4'), 55.8 (triple intensity), 68.6 (1,1',7,7'), 106.4 (173; 8), 144.9, 146.9, 152.7, 159.7, 159.2 (2,2',3,3'). **6b**: $[\alpha]_D$ = +34°, correct elemental analysis (C, H). ^{1}H NMR ($CDCl_3$, 200 MHz): δ = 2.73, 3.06 (4,4'-H), 0.7–1.0, 1.7–2.2, 2.65 (5,5',6,6'-H), 5.96 (8-H), 0.26, 0.91, 0.92, 1.00, 1.18, 1.43 (1,1',7,7'-CH_3). ^{13}C NMR ($CDCl_3$, 50 MHz, ^1J(CH) in Hz): δ = 11.7, 12.4 (1,1-CH_3), 20.0, 20.7 (double intensity), 28.6 (7,7'-CH_3), 26.2 (128) and 29.0 (125; 5,5'), 32.5 (132) and 39.2 (138; 6,6°), 50.3 (145) and 51.4 (148; 4,4'), 55.3, 55.5, 55.6, 69.7 (1,1',7,7'), 104.1 (173; 8), 142.0, 145.4, 150.3, 156.4 (2,2',3,3').

[8] a) G. Casiraghi, F. Bigi, G. Casnati, G. Sartori, P. Soncini, G. G. Fava, M. F. Belicchi, *J. Org. Chem. 53* (1988) 1779; b) G. Casiraghi, G. Sartori, G. Casnati, F. Bigi, *J. Chem. Soc. Perkin Trans. 1 1983*, 1649; M. Cornia, G. Casiraghi, *Tetrahedron 45* (1989) 2869; O. Piccolo, L. Filippini, L. Tinucci, E. Valoti, A. Citterio, *Helv. Chim. Acta 67* (1984) 739; A. Citterio, M. Gandolfi, O. Piccolo, L. Filippini, L. Tinucci, E. Valoti, *Synthesis 1984*, 761; c) cf. K. Mikami, M. Terada, T. Nakai, *J. Am. Chem. Soc. 111* (1989) 1940; J. K. Whitesell, K. Nabona, D. Deyo, *J. Org. Chem. 54* (1989) 2258.

[9] The diastereomeric compounds **10** (*R,R* or *S,S*) and **11** (*R,S* or *S,R*) show markedly different ^{1}H NMR signals ($CDCl_3$, 200 MHz, +27 °C) for the following groups: -NHCHPhCH_3, δ = 1.39 (**10**), 1.48 (**11**). Naphth.-C(OH)CH_3, δ = 1.84 (**10**), 1.89 (**11**) as well as the signal of protons (one each) on the naphthol moiety at δ = 7.62 (**10**), 7.52 (**11**).

[10] G. Helmchen, R. Ott, K. Sauber, *Tetrahedron Lett. 37* (1972) 3873.

[11] G. Erker, K. Berg, L. Treschanke, K. Engel, *Inorg. Chem. 21* (1982) 1277; G. Erker, K. Berg, C. Sarter, *Organomet. Synth. 3* (1987) 29.

[12] a) G. Erker, C. Sarter, S. Dehnicke, C. Krüger, E. Raabe, R. Schlund, R. Benn, A. Rufińska, R. Mynott, *J. Organomet. Chem. 382* (1990) 89; b) G. Erker, C. Sarter, S. Werner, C. Krüger, *ibid. 377* (1989) C55.

[13] **14a** (R = C_2H_5): 71% isolated, correct elemental analysis (C, H). IR (KBr): ν(C=O) = 1641 cm^{-1}. ^{1}H NMR ($CDCl_3$, 200 MHz): δ = 2.04 (s, 3H; Ar-C(CH_3)OH-), 4.36 and 1.25 (OCH_2CH_3), 6.76 (s, 5H; Cp), 5.8 (OH), 7.21 (1H) 7.31 (1H), 7.50 (2H), 7.71 (1H), 8.26 (1H; naphthyl). ^{13}C NMR ($CDCl_3$, 50 MHz): δ = 22.6 (ArC(*C*H_3)OH), 81.4 (Ar*C*(CH_3)OH), 178.3, 67.3, 13.5 (-CO-OC_2H_5), 118.1 (Cp), 121.8, 123.6, 125.6, 126.7, 127.2, 127.6 (naphthyl-CH), 158.1 (naphthyl-CO), 114.2, 126.7, 135.7 (naphthyl-*ipso*-C); the structural assignment is supported by ^{1}H NMR NOE spectra [irradiation of Ar-C(CH_3)OH-, for example, leads to NOEs at Ar-C(CH_3)O*H* (15%) and the 3-H of the aromatic ring (24%)]. **14b** (R = CH_3): 59% isolated, correct elemental analysis (C, H). IR (KBr): ν(C=O) = 1643 cm^{-1}. 1H/^{13}C NMR spectra similar to those of **14a**.

What Are the Structures of Fenestin A and Fenestin B?**

By *Ulrich Schmidt,* Albrecht Lieberknecht, Uli Kazmaier,* and *Ernst Haslinger*

Dedicated to Professor Wolfgang Lüttke on the occasion of his 70th birthday

Numerous linear and cyclic peptides and peptolides have been isolated in recent years from lower marine organisms.[1–8] They consist in part of (*R*)-amino acids, didehydroamino acids, and nonribosomal amino acids. Two natural products were recently isolated from the sponge *Leucophloeus fenestrata* and were assigned structures **1** (fenestin A) and **2** (fenestin B), the rings of which contain exclusively (*S*)-amino acids.[9]

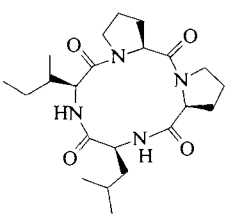

1

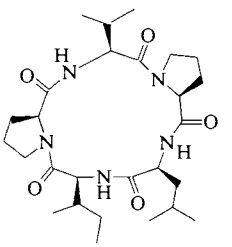

2

We questioned these structural proposals for the following reasons:

1. Except for bottromycin,[6] tentoxin,[7] and dihydrotentoxin,[8] the few known natural cyclotetrapeptides contain at least one (*R*)-amino acid. Tentoxin consists of an alternating arrangement of two tertiary and two secondary amide groups.[10] This allows a stable *cis–trans–cis–trans* conformation of the amide bonds, since the *cis* and *trans* conform-

[*] Prof. Dr. U. Schmidt, Dr. A. Lieberknecht, Dr. U. Kazmaier
Institut für Organische Chemie, Biochemie und
Isotopenforschung der Universität
Pfaffenwaldring 55, D-7000 Stuttgart 80 (FRG)
Prof. Dr. E. Haslinger
Institut für Organische Chemie der Universität
Am Birkengut, D-8580 Bayreuth (FRG)

[**] Amino Acids and Peptides, Part 73. This work was supported by the Fonds der Chemischen Industrie, the Deutsche Forschungsgemeinschaft, and BASF AG. Part 72: U. Schmidt, R. Meyer, V. Leitenberger, A. Lieberknecht, *Angew. Chem. 101* (1989) 946; *Angew. Chem. Int. Ed. Engl. 28* (1989) 929.

ers of tertiary amides differ in energy by only a small amount. Bottromycin is a special case insofar as it contains three amide bonds and one amidine bond.[11] The structure proposed for fenestin A contains exclusively (*S*)-amino acids and neighboring tertiary amide bonds; this type of structure has not been found so far in naturally occurring compounds.

2. For fenestins A and B, the ^{1}H NMR signals of the α-protons of the amino acid units range from $\delta = 3.9$ to 4.09, near the limit of the region where the α-H signals of peptides are usually found.[12] In all cyclopeptides we have studied, these signals ranged from $\delta = 4.0$ to 4.6.

We therefore decided to reexamine these structural proposals by synthesizing **1** and **2**. The linear precursors were prepared in an unambiguous way according to Schemes 1 and 2. We accomplished the ring closure by catalytic hydro-

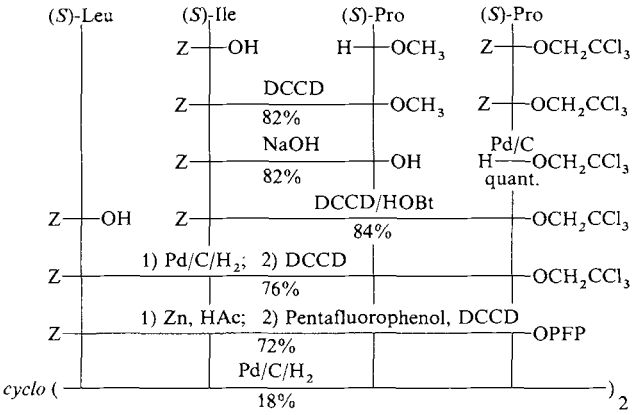

Scheme 1. Synthesis of **1** (dimer). Z = benzyloxycarbonyl, DCCD = dicyclohexylcarbodiimide, HOBt = hydroxybenzotriazole, PFP = pentafluorophenyl.

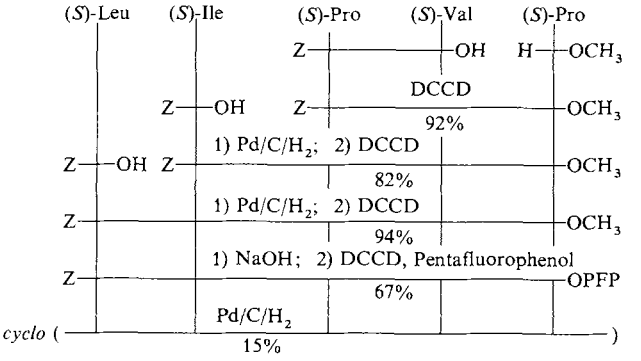

Scheme 2. Synthesis of **2**.

genation of the ω-benzyloxycarbonyl pentafluorophenyl ester.[13] Monomeric fenestin A was thereby formed not at all or only in very small amounts (<5%). A cyclooctapeptide (fenestin A dimer) was isolated in 18% yield (Table 1). Monomeric fenestin B was obtained in 15% yield (Table 1). Large differences were found between the NMR and mass spectra of natural fenestin B and the synthetic product. As expected, the ^{1}H NMR spectrum shows the α-H signals of the amino acid units in both the synthetic cyclopentapeptide and the cyclooctapeptide in the region of $\delta = 4.0-4.65$. The signals of the δ-H atoms of the two proline residues of **2** are found at $\delta = 3.5-3.7$, the NH signals at $\delta = 5.64$, 6.37, and 7.56 (see Table 1). The latter are markedly split by coupling with the α-H atoms. The ^{1}H NMR data published for the natural product differ considerably from this spectrum, especially with respect to the position of the α-H signals of the amino acid units (3.9–4.09). The ^{13}C signals of the two compounds are overall in good agreement. Large differences in the region of $\delta = 2.7-4.8$ occur particularly for resonances assigned to the proline carbon atoms of the natural product. This also holds true for the valine between the proline residues. The previously assigned structure of fenestin B is therefore wrong and that of fenestin A appears questionable.

Table 1. Physical data for compounds **1** (dimer) and **2**. The NMR spectra were recorded with a Bruker AM 500, the mass spectra with an MAT 8500 (LSIMS, ionization with cesium).

1 (dimer): ^{1}H NMR (500 MHz, $CDCl_3$): $\delta = 0.83-0.98$ (sh, 12H), 1.25–2.20 (sh, 11H), 2.30 (m, 1H), 3.45–3.70 (sh, 4H), 3.89 (dt, $J = 9.7$, 7.0 Hz, 1H), 4.20 (dd, $J = 8.8$, 6.0 Hz, 1H), 4.30 (m, 1H), 4.43 and 4.56 (t each, $J = 8.0$ Hz, 1H), 4.61 (dd, $J = 10.3$, 8.1 Hz, 1H), 4.73 (m, 1H), 5.42 (d, $J = 6.6$ Hz, 0.3H), 7.17 (d, $J = 7.2$ Hz, 0.7H), 7.40 (d, $J = 10.3$ Hz, 0.7H), 7.81 (d br, $J = 9.4$ Hz, 0.3H). ^{13}C NMR (125 MHz, $CDCl_3$, decoupled): $\delta = 11.58$, 12.19, 14.43, 15.88, 20.86, 21.86, 22.98, 23.36, 24.67, 24.75, 25.35, 25.40, 25.44, 25.59, 25.92, 26.08, 27.44, 27.77, 29.04, 29.42, 35.38, 36.39, 40.86, 41.50, 46.58, 46.72, 46.99, 47.62, 51.06, 53.59, 54.46, 58.44, 62.12, 62.84, 64.27, 169.10, 169.15, 171.10, 171.21, 171.49, 172.60, 172.78, 173.70. *m/z*: 843, 842 ($M^{\oplus}_{dim}$), 631, 535, 534, 421 ($M^{\oplus}$), 393, 379, 369, 325, 317, 308, 277, 275, 242, 225, 211, 186, 183, 167, 165, 133.

2: ^{1}H NMR (500 MHz, $CDCl_3$): $\delta = 0.82$ (d, $J = 6.7$ Hz, 3H), 0.85 (t, $J = 7.4$ Hz, 3H), 0.94 (d, $J = 6.8$ Hz, 6H), 0.99 (d, $J = 6.9$ Hz, 3H), 1.02 (d, $J = 6.8$ Hz, 3H), 1.24 (m, 1H), 1.43 (m, 1H), 1.48–1.56 (sh, 2H), 1.64 (m, 1H), 1.74–2.02 (sh, 7H), 2.13–2.25 (sh, 2H), 2.32 (m, 1H), 3.47–3.55 (sh, 2H), 3.64–3.71 (sh, 2H), 3.99 (dd, $J = 6.8$, 3.4 Hz, 1H), 4.16 (t, $J = 9.0$ Hz, 1H), 4.42 (dd, $J = 8.7$, 2.2 Hz, 1H), 4.46 (dd, $J = 8.5$, 3.0 Hz, 1H), 4.63 (dddd, $J = 13.5$, 11.5, 9.7, 4.0 Hz, 1H), 5.64 (d br, $J = 3.1$ Hz, 1H), 6.37 (d br, $J = 8.8$ Hz, 1H), 7.56 (d br, $J = 9.4$ Hz, 1H). ^{13}C NMR (125 MHz, $CDCl_3$, decoupled): $\delta = 11.41$, 15.40, 18.33, 19.15, 21.61, 22.52, 22.55, 23.43, 24.78, 25.16, 30.94, 32.16, 32.26, 37.74, 39.55, 46.87, 47.24, 52.38, 56.94, 57.66, 60.53, 61.36, 169.42, 171.26, 171.65, 171.79, 171.84. *m/z*: 521, 520 ($M^{\oplus}$), 407, 369, 324, 317, 275, 242, 225, 211, 197, 183, 167, 149, 133.

Received: December 14, 1989 [Z 3688 IE]
German version: *Angew. Chem. 102* (1990) 562

CAS Registry numbers:
1, 118984-46-6; **1** (dimer), 126134-57-4; **2**, 118984-47-7; Z-Ile-OH, 3160-59-6; H-Pro-OCH_3, 2577-48-2; Z-Leu-OH, 2018-66-8; Z-Ile-Pro-OCH_3, 40296-70-8; Z-Ile-Pro-OH, 13211-37-5; Z-Pro-OCH_2CCl_3, 111110-78-2; H-Pro-OCH_2CCl_3, 126134-58-5; Z-Ile-Pro-Pro-OCH_2CCl_3, 126134-59-6; Z-Pro-Val-Pro-OCH_3; 51782-86-6; Z-Leu-Ile-Pro-Pro-OCH_2CCl_3, 126134-60-9; Z-Leu-Ile-Pro-Pro-OPFP, 126134-61-0; Z-Pro-Val-OH, 21285-27-8; Z-Ile-Pro-Val-Pro-OCH_3, 126134-62-1; Z-Leu-Ile-Pro-Val-Pro-OCH_3, 126134-63-2; Z-Leu-Ile-Pro-Val-Pro-OPFP, 126134-64-3.

[1] A. Closse, R. Huguenin, *Helv. Chim. Acta 57* (1974) 533.
[2] M. Kawai, D. H. Rich, J. D. Walton, *Biochem. Biophys. Res. Commun. 111* (1983) 398.
[3] S. Takayama, A. Isogai, M. Nakata, H. Suzuki, A. Suzuki, *Agric. Biol.* (1982) 3261.
[4] A. Hirota, A. Suzuki, K. Aizawa, S. Tamura, *Agric. Biol. Chem. 37* (1973) 955.
[5] K. Umehara, K. Nakahara, S. Kiyoto, M. Iwami, M. Okamoto, H. Tanaka, M. Kohsaka, H. Aoki, H. Imanaka, *J. Antibiot. 36* (1983) 478.
[6] a) J. M. Waiswisz, M. G. van der Hoeven, J. van Peppen, W. C. M. Zwennis, *J. Am. Chem. Soc. 79* (1957) 4520; b) J. M. Waiswisz, M. G. van der Hoeven, J. F. Hölscher, B. Te Nijenhuis, *ibid. 79* (1957) 4522; c) J. M. Waiswisz, M. G. van der Hoeven, B. Te Nijenhuis, *ibid. 79* (1957) 4524.
[7] G. E. Templeton, *Microb. Toxins 8* (1972) 160.
[8] Y. Kono, J. M. Gardner, S. Takeuchi, *Agric. Biol. Chem. 50* (1986) 2401.
[9] S. Omar, L. Tenenbaum, L. V. Manes, P. Crews, *Tetrahedron Lett. 29* (1988) 5489.
[10] D. H. Rich, P. Mathiaparanam, *Tetrahedron Lett. 1974*, 4037.
[11] D. Schipper, *J. Antibiot. 36* (1983) 1076.
[12] K. Wüthrich: *NMR in Biological Research, Peptides and Proteins*, Elsevier, Amsterdam 1976, p. 51.
[13] U. Schmidt, A. Lieberknecht, H. Griesser, J. Talbiersky, *J. Org. Chem. 47* (1982) 3261.

5-Methyl-1,1,3,3-tetraphenyl-1λ⁵,3λ⁵-diphosphabenzene**

By *Hubert Schmidbaur,* Christos Paschalidis, Oliver Steigelmann*, and *Gerhard Müller*

Ever since their discovery,[1, 2] phosphabenzenes (phosphinines), with λ⁵-P atoms, have attracted considerable attention. In particular, the chemistry of monophosphabenzene has developed into an important area of heterocyclic chemistry.[3, 4] Little is known, however, about the chemistry of *poly*phosphabenzenes. Although *Märkl* obtained evidence suggesting the existence of 1λ⁵,3λ⁵-diphosphabenzenes as early as 1963, adequate characterization was not provided by these initial studies.[5] It was not until recently that *Fluck* et al. were able to synthesize a 1,3-diphosphinine, with a special substitution pattern, and also characterize its structure.[6] 1λ⁵,4λ⁵-Diphosphinines were described in 1970 and 1972,[7, 8] but very little work has been carried out on this class of compounds. Finally, 1,3,5-triphosphabenzenes have also only recently been obtained, the few known representatives containing at least one λ³-P atom in the molecule.[9]

As a continuation of our earlier studies on open-chain and cyclic double ylides ("carbodiphosphoranes")[10, 11] and phosphoniopropenides,[12, 13] we now report a simple, high-yield synthetic route for the title compound **4**, which opens up many new preparative possibilities.

The dication of **2**,[12] obtained by double quaternization of 1,1-bis[(diphenylphosphino)methyl]ethene (**1**) with dihalomethanes, can be treated with one equivalent of *n*-butyllithium or triethylethylidenephosphorane (as a transylidation reagent) to give, for X = I, the semi-ylidic quaternary salt **3**. The addition of a second equivalent of base surprisingly does not result in the conjugated double ylide **5** or in the cumulated double ylide **5'**, but leads directly to the formation of the title compound **4** in high yields (by-products: LiI and Et_4PI, respectively), although numerous analogues of **5** and **5'** with saturated ring systems have already been characterized.[10, 11]

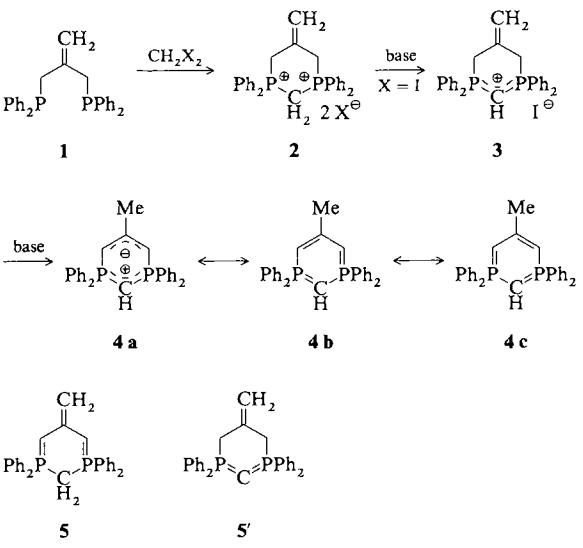

Scheme 1. X = Cl,Br,I.

It appears that the reaction includes a proton transfer from an endocyclic to an exocyclic methylene group leading to formation of a methallyl anion moiety $[CHC(Me)CH]^{\ominus}$, which couples the P atoms of $[Ph_2PCHPPh_2]^{\oplus}$. This resonance form is depicted in formula **4a**, whereas **4b** and **4c** represent the corresponding cyclic "ylene forms".[14]

Elemental analyses and mass spectra confirm the composition of **4**. The NMR spectra are compatible with C_{2v} symmetry of the framework in solution. The chemical shifts of the equivalent P, C, and H atoms of the (MeC)-*CH*-*P* groups and the corresponding coupling constants are indicative of the partially ylidic character of these units. The same result holds for the PCHP unit, for which numerous precedents are available.[10, 11] The yellow color of **4** is consistent with *Märkl*'s observations.[5]

The X-ray structure analysis[15] of **4** revealed the absence of crystallographic symmetry in the solid state, but the molecule is found to at least approach the expected C_{2v}(or C_s) symmetry (Fig. 1). The ring system is almost planar (with a maximum deviation from planarity for C4 of 0.03 Å). Accordingly, the sum of the angles at C3 is exactly 360.0°, and the sum of the angles at the ring atoms is 719.9° (the corresponding inner angles at C1–C4 are significantly larger than 120°, and those at P1 and P2 significantly smaller). The P1–C1 and P2–C1 distances (average 1.697 Å) as well as the P1–C4 and P2–C2 distances (average 1.726 Å) reflect the ylidic character of **4**, as also suggested by the P-phenyl distances (average 1.827 Å).

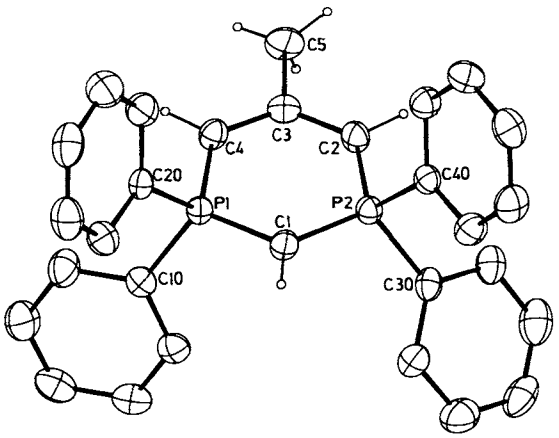

Fig. 1. Structure of **4** in the crystal (ORTEP, vibration ellipsoids at the 50% probability level, phenyl H atoms not shown); atomic numbering *not* consistent with the numbering used for the nomenclature. Selected bond distances [Å] and angles [°]: P1-C1 1.699(3), P2-C1 1.695(3), P1-C4 1.729(3), P2-C2 1.724(3), C2-C3 1.393(4), C3-C4 1.387(4), C3-C5 1.516(4); P1-C1-P2 123.1(2), C1-P1-C4 110.2(1), C1-P2-C2 110.4(1), P2-C2-C3 124.2(2), C2-C3-C4 127.8(3), P1-C4-C3 124.2(2), C2-C3-C5 116.0(2), C4-C3-C5 116.2(2), C10-P1-C20 102.4(1), C30-P2-C40 101.3(1). The rings at C10, C20, C30, and C40 form dihedral angles of 70.1, 106,7, 130.2, and 71.0° with the heterocycle, respectively.

The C3–C5 distance [1.516(4) Å] indicates the presence of a C–C single bond, as opposed to the double bond value of **1** (1.307(5) Å.[16] The methyl hydrogen atoms could also be located by crystallography (and confirmed by the ^1H-coupled ^{13}C NMR spectrum). The C2–C3 and C3–C4 distances

[*] Prof. Dr. H. Schmidbaur, Dipl.-Chem. C. Paschalidis, Dipl.-Chem. O. Steigelmann [+], Priv.-Doz. Dr. G. Müller [+], Anorganisch-chemisches Institut der Technischen Universität München Lichtenbergstrasse 4, D-8046 Garching (FRG)

[+] X-ray structure analysis

[**] This work was generously supported by the Deutsche Forschungsgemeinschaft (Leibniz Programm), by the Fonds der Chemischen Industrie, and by Hoechst AG. We thank Mr. *J. Riede* for supplying the crystallographic data set.

with their average value of 1.390 Å are in agreement with the methallyl anion character of the corresponding structural unit.

Theoretical studies on λ^5-phosphabenzenes[2, 17] and related phosphazenes have shown that the four-coordinate λ^5-phosphorus atom acts as a "conjugation barrier". The model can be adopted for $1\lambda^5,3\lambda^5$-diphosphabenzenes. **4** is best represented by the zwitterionic resonance structure **4a** with two "regions of conjugation". Rather than an aromatic system, the π systems of the methallyl anion and the diphosphoniomethanide cation are sufficient to account for the high tendency of formation of the molecule.

Experimental Procedure

3: 0.42 mL of a 4.02 M solution of *n*-butyllithium in hexane was added at −78 °C to a stirred suspension of **2** (X = I, 1.18 g, 1.70 mmol) in 70 mL of tetrahydrofuran (THF). After 6 h the yellow suspension was filtered, and the precipitate washed with cold water and THF. Yield: 0.90 g (94%), **3**, m.p. 205 °C, correct elemental analysis. $^{31}P\{^1H\}$ NMR ($CDCl_3$): $\delta = 15.5$; $^{13}C\{^1H\}$ NMR ($CDCl_3$): $\delta = -3.49$ (t, $J(PC) = 107.9$ Hz, CHP_2), 33.18 (d, $J(PC) = 58.7$, CH_2P), 121.0 (t, $J(PC) = 9.9$, $H_2C=$), 128.6 (t, $J(PC) = 9.5$, C=), 127.6, 132.0, 129.3, 133.0 (m, phenyl-C); ^1H NMR ($CDCl_3$): $\delta = 1.35$ (t, $J(PH) = 3.8$ Hz, 1H, CHP_2), 3.87, (AXX', $N = 16.8$ Hz, 4H, CH_2), 5.03 (t, $J(PH) = 3.8$, 2H, $=CH_2$), 7.48–7.79 (m, 20H, phenyl-H).

4: A suspension of **2** (X = I, 0.58 g, 0.84 mmol) in 50 mL of THF at −78 °C was treated with a solution of $Et_3P{=}CHMe$ (0.25 g, 1.68 mmol) in 25 mL of THF. After warming to 20 °C the reaction mixture was stirred for another 10 min. The precipitate was separated (0.40 g Et_4PI), and the filtrate evaporated in vacuo and cooled until crystallization of **4** started (at −25 °C). Yellow crystals, yield: 0.32 g (87%), m.p. 115 °C (dec.).—$^{31}P\{^1H\}$ NMR (C_6D_6): $\delta = 7.1$; $^{13}C\{^1H\}$ NMR (C_6D_6): $\delta = -3.0$ (t, $J(PC) = 109.1$ Hz, PCHP), 30.46 (t, $J(PC) = 17.9$, CH_3), 51.79 (AXX', $N = 120.54$ Hz, CHP), 159.52, (t, $J(PC) = 6.9$, CCH_3), 139.3, 131.2, 128.0, 129.7 (m, phenyl-C); ^1H NMR (C_6D_6): $\delta = 1.15$ (br. s, 1H, PCHP), 2.26 (t, $J(PH) = 1.5$ Hz, 3H, CH_3), 3.40 (br. s, 2H, CHP), 7.0–7.7, (m, 20H, phenyl-H).

Received: January 4, 1990 [Z 3722]
German version: *Angew. Chem. 102* (1990) 569

CAS Registry numbers:
2 (X = I), 123775-77-9; **3** (X = I), 125995-75-7; **4**, 125995-74-6.

[1] G. Märkl, *Angew. Chem. 75* (1963) 669; *Angew. Chem. Int. Ed. Engl. 2* (1963) 47.
[2] K. Dimroth, *Acc. Chem. Res. 15* (1982) 58.
[3] K. Dimroth in *Houben-Weyl-Müller: Methoden der Organischen Chemie, Bd. E1*, Thieme, Stuttgart 1982, p. 783.
[4] J. Emsley, D. Hall: *The Chemistry of Phosphorus*, Harper & Row, London 1976.
[5] G. Märkl, *Z. Naturforsch. B15* (1963) 1136.
[6] E. Fluck, B. Neumüller, G. Heckmann, *Chem.-Ztg. 111* (1987) 309; E. Fluck, G. Heckmann, W. Plass, P. G. Jones, *New J. Chem. 13* (1989) 383.
[7] M. A. Shaw, J. C. Tebby, R. S. Ward, D. H. Williams, *J. Chem. Soc. C 1970*, 504.
[8] M. Davies, A. N. Hughes, S. W. S. Jafry, *Can. J. Chem. 50* (1972) 3625.
[9] E. Fluck, G. Becker, B. Neumüller, R. Knebl, G. Heckmann, H. Riffel, *Angew. Chem. 98* (1986) 1018; *Angew. Chem. Int. Ed. Engl. 25* (1986) 1002; *Z. Naturforsch. B 42* (1987) 1213; A. R. Barron, A. H. Cowley, *Angew. Chem. 99* (1987) 956; *Angew. Chem. Int. Ed. Engl. 26* (1987) 907.
[10] H. Schmidbaur, T. Costa, *Chem. Ber. 114* (1981) 3063; *Z. Naturforsch. B 37* (1982) 677; H. Schmidbaur, T. Costa, B. Milewski-Mahrla, *ibid. 114* (1981) 1428; H. Schmidbaur, T. Costa, B. Milewski-Mahrla, U. Schubert, *Angew. Chem. 92* (1980) 557; *Angew. Chem. Int. Ed. Engl. 19* (1980) 555.
[11] H. Schmidbaur, G. Hasslberger, U. Deschler, U. Schubert, C. Kappenstein, A. Frank, *Angew. Chem. 91* (1979) 437; *Angew. Chem. Int. Ed. Engl. 18* (1979) 408; U. Schubert, C. Kappenstein, B. Milewski-Mahrla, H. Schmidbaur, *Chem. Ber. 114* (1981) 3070; H. Schmidbaur, U. Deschler, *ibid. 114* (1981) 2491; *ibid. 116* (1983) 1388.
[12] H. Schmidbaur, C. Paschalidis, O. Steigelmann, G. Müller, *Angew. Chem. 101* (1989) 1739; *Angew. Chem. Int. Ed. Engl. 28* (1989) 1700; *Chem. Ber. 122* (1989) 1851.
[13] H. Schmidbaur, W. Malisch, D. W. H. Rankin, *Chem. Ber. 104* (1971) 145.
[14] G. Wittig, *Angew. Chem. 68* (1956) 505.
[15] Crystal structure data of compound **4**: $C_{29}H_{26}P_2$ (436.48), triclinic, $a = 7.557(1)$, $b = 11.354(2)$, $c = 15.306(2)$ Å, $\alpha = 113.83(1)$, $\beta = 94.96(1)$, $\gamma = 96.39(1)°$, space group $P\bar{1}$, $V = 1181.3$ Å^3, $Z = 2$, $\varrho_{calc} = 1.227$ g cm^{-1}. $\mu(Mo_{K\alpha}) = 1.57$ cm^{-1}, $F(000) = 460$ e$^{\ominus}$, $T = -50$ °C, Syntex $P2_1$, ω-scan, scan width 0.8 ω, *hkl*-range 8, +13, +17; 3909 measured independent reflections, 3204 observed. Solution of structure by direct methods ($R_{int} = 0.00$); 295 parameters; 25 H atoms localized, one calculated; $R/R_w = 0.046/0.046$; $\Delta\varrho_{fin}(max/min) = +0.33/-0.32$. Further details of the crystal structure investigation may be obtained from the Fachinformationszentrum Karlsruhe, Gesellschaft für wissenschaftlich-technische Information mbH, D-7514 Eggenstein-Leopoldshafen 2 (FRG), on quoting the depository number CSD-54502, the names of the authors, and the journal citation.
[16] H. Schmidbaur, C. Paschalidis, O. Steigelmann, G. Müller, *Chem. Ber. 122* (1989) 1851.
[17] W. Schäfer, A. Schweig, K. Dimroth, H. Kanter, *J. Am. Chem. Soc. 98* (1976) 4410, and references cited therein.

Unraveling Overlapping Multiplets in Two-Dimensional NMR Correlation Spectra by Selective Inversion of Coupling Partners**

By *Lyndon Emsley, Peter Huber*, and *Geoffrey Bodenhausen**

Two-dimensional NMR correlation spectroscopy (COSY) is a widely used, simple and efficient technique for identifying systems of coupled spins.[1] The coupling networks that can be determined from such spectra contain information about the number of spins, magnetic or chemical equivalence, and magnitudes and signs of scalar couplings.[2–4] In many cases, a large portion of a spin system can be identified from a low-resolution survey spectrum that can be acquired in less than an hour, preferably with the double-quantum filtered COSY experiment.[5] In order to confirm a hypothesis regarding the network of coupled spins, it may be necessary to study the fine-structure of the multiplets by increasing resolution. One should then take recourse to more informative spectra such as E.COSY,[6, 7] PE.COSY[8] or *z*-COSY.[9, 10] Very often, however, it is not really necessary to subject the entire two-dimensional spectrum to such a detailed investigation. Typically, only one or two multiplets in a low-resolution survey spectrum present problems for interpretation, and in such cases it is much more time efficient to "zoom in" on the multiplets of interest, which can be done by pseudo-COSY[11] or by soft-COSY[12] and related experiments.

These methods can greatly enhance the resolution of a chosen multiplet, but they fail to exploit all the information available to the spectroscopist. Typically, when confronted with a difficult multiplet in COSY, one does not only know the shifts Ω_{A1} and Ω_{A2} of the *active spins* (i.e., spins A_1 and A_2 that carry the transverse magnetization in the evolution and detection periods t_1 and t_2 of the experiment), but one usually has at least an idea about the shifts Ω_{P_i} of the *passive spins* (i.e., spins P_i that are coupled to the active spins in the evolution and/or detection periods). Such coupling partners should give rise to cross-peak multiplets in other parts of the two-dimensional spectrum, though in systems with many degeneracies among the shifts this evidence is perhaps not unequivocal. Nevertheless, a hypothesis regarding the existence and chemical shifts of coupling partners is likely to be available, not only in manual analysis, but also as a result of a computer-supported analysis of a survey spec-

[*] L. Emsley, P. Huber, Prof. Dr. G. Bodenhausen
Section de Chimie, Université de Lausanne
Rue de la Barre 2, CH-1005 Lausanne (Switzerland)

[**] This research was supported in part by Spectrospin AG, Fällanden, Switzerland, by the Swiss National Science Foundation, and by the Commission pour l'Encouragement de la Recherche Scientifique (CERS).

trum.[3,4,13-15] This typically yields various proposals of *fragments* of the coupling network.[3,4,15] Usually, there are too many proposals of this type, often mutually exclusive, and even if they can be ranked by some sort of likelihood function,[3,4,15] it is not easy to discriminate proposals that are reasonable from those that are not. In this communication, we present a variant of soft-COSY that allows one not merely to focus on a multiplet of interest, but also to test a hypothesis about the identity of one or more passive spins. The method is shown to be particularly powerful when multiplets belonging to different coupling networks (e.g., to different isomers or different amino acid residues) partly or completely overlap.

Figure 1a shows the pulse sequence suitable for a soft-COSY experiment,[12] which may be regarded as a selective version of *z*-filtered COSY.[9,10] The sequence comprises three semiselective Gaussian 270° pulses which affect the magnetization of one multiplet (or set of overlapping multiplets) at a time. The first two of these pulses, which precede and follow the evolution interval t_1, are centered at the carrier frequency Ω_{A1}. The third pulse, which precedes the detection period t_2, is applied at Ω_{A2}. These three pulses achieve a similar effect as in selective two-dimensional exchange spectroscopy (soft-NOESY),[16,17] except that the

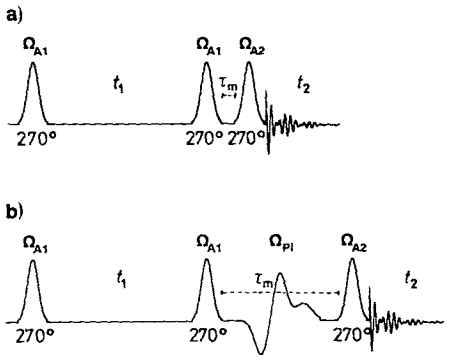

Fig. 1a. Pulse sequence for normal soft-COSY using three self-refocusing 270° Gaussian pulses.[17] The first two pulses are applied at the frequency Ω_{A1} and the last at Ω_{A2}. b) The sequence for soft-COSY with selective inversion of a passive coupling partner P_i (selectively-inverted-soft-COSY, or SIS-COSY), where a G^3 Gaussian pulse cascade[19] has been inserted in τ_m at frequency Ω_{Pi}. The G^3 cascade is a pulse of duration t_p having an envelope consisting of a superposition of three Gaussians with maxima at 28.7, 50.8 and 79.5% t_p, half-height widths of 18.9, 18.3 and 24.3% t_p and relative amplitudes of $-1:1.37:0.49$. The total amplitude of the cascade was adjusted to obtain an overall on-resonance flip-angle of 180°. In both sequences (a & b) the phase of the first pulse is alternated through 0 and 180° in conjunction with addition and subtraction of the signals.

interval τ_m between the last two pulses is so short that no significant relaxation effects can occur. An important advantage of this technique is that there can be no signal contributions from zero-quantum coherences,[17] which is a major disadvantage of normal *z*-COSY.[9,10] The Gaussian envelope and 270° on-resonance flip angle of the pulses allow one to obtain good frequency selectivity with much reduced phase errors when compared to an experiment using soft 90° pulses.[17,18] If even better selectivity and phase properties are required, a more sophisticated pulse, such as a "G^4 cascade",[19] should be used. Although such longer pulses make the experiment more sensitive to relaxation, the sequences are nevertheless still short compared to typical transverse relaxation times, and in the limit where relaxation is so fast as to obliterate the fine structure of the multiplet there is no need for a soft COSY experiment in any case. So far, we have not encountered any problems with relaxation in this type of experiment.

The basic cross-peak pattern in all COSY-type spectra consists of a square spanned by two positive and two negative peaks (filled and open symbols in Fig. 2) separated by the active coupling J_{A1A2} in both frequency domains. If the spin system contains a passive spin P_i that is coupled to both active spins A_1 and A_2, and provided that the polarization of P_i is not affected in the pulse sequence, one obtains two basic patterns displaced with respect to each other by a vector $\boldsymbol{J}_{Pi} = (J_{A1Pi}, J_{A2Pi})$. If both components of this displacement vector are non-vanishing, we speak of a *common* passive coupling partner. If there are N passive spins, there are 2^N basic patterns. Figure 2a shows a typical cross-peak multiplet in a four-spin system, with couplings corresponding to the A^{cis}-X^{cis} cross-peak of *cis* 2-phenylcyclopropanecarboxylic acid methyl ester *cis*-**1** (R = $COOCD_3$, R′ = C_6H_5).

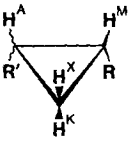

1

The four basic patterns are displaced with respect to each other by $\boldsymbol{J}_M = (J_{AM}, J_{XM}) = (7.7, 9.2\ \text{Hz})$ and $\boldsymbol{J}_K = (J_{AK}, J_{XK}) = (7.5, -5.1\ \text{Hz})$. It is possible to change the apparent sign of the second (horizontal) component of the displacement vector by selectively inverting a passive spin during the interval τ_m. This allows one to manipulate the pattern of the multiplet. If all of the passive spins are inverted one obtains a pattern like in complementary E.COSY[7] or anti-*z*-COSY[9] with displacement vectors $\boldsymbol{J}'_M = (J_{AM}, -J_{XM})$ and $\boldsymbol{J}'_K = (J_{AK}, -J_{XK})$. If, on the other hand, only the passive M proton is inverted selectively, one expects the multiplet shown in Figure 2b with displacement vectors $\boldsymbol{J}'_M$ and $\boldsymbol{J}_K$, while inversion of the passive K proton leads to the multiplet in Figure 2c with displacement vectors $\boldsymbol{J}_M$ and $\boldsymbol{J}'_K$. In effect these new experiments allow us to explore the energy-level diagram and the connectivity diagram[4] of the spin system systematically. In a normal *z*-COSY experiment we observe only correlations between transitions that share common energy-levels, while in anti-*z*-COSY we observe only remotely connected transitions.[9] If only selected coupling partners are inverted we are able to correlate transitions that are remote with respect to the inverted passive spins and connected for the other spins.

Figure 1b shows a pulse sequence suitable for achieving the multiplet manipulations described above. We have inserted a cascade of Gaussian pulses (a so-called "G^3 cascade") in interval τ_m of Figure 1a in order to invert the magnetization over a well-defined rectangular frequency window.[19] The performance of an ordinary Gaussian 180° pulse was found to be insufficient in this experiment, since it was not possible to achieve complete inversion without affecting the other multiplets. The carrier frequency of the pulse cascade is adjusted to a trial frequency Ω_T which should correspond to the chemical shift of a spin that is suspected of playing a passive role. If inversion leads to a new pattern, this provides evidence that Ω_T is indeed the frequency Ω_{Pi} of the passive spin P_i, and the resulting pattern can be analyzed to obtain the magnitudes and relative signs of the passive coupling constants J_{A1Pi} and J_{A2Pi}. If no effect is observed, then the spin with the shift Ω_T can be excluded as a common

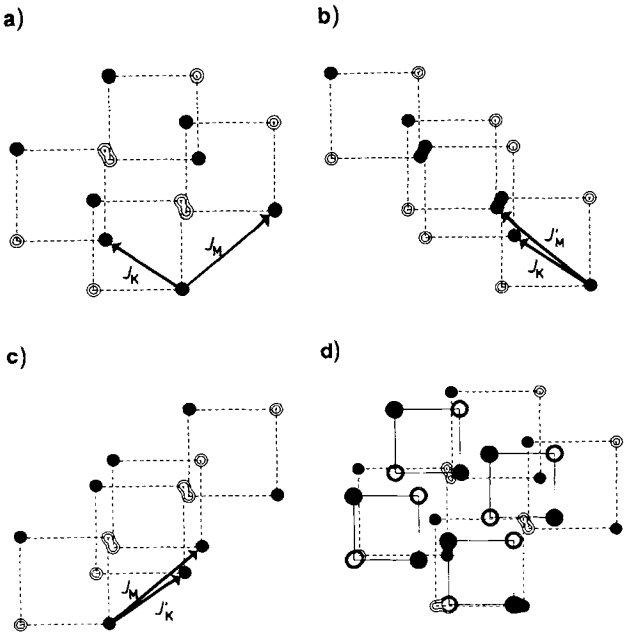

Fig. 2. Simulated A–X multiplets corresponding to *cis* and *trans* isomers of **1**. Protons A and X are coupled to both M and K in each isomer. The shifts of the active spins are pairwise nearly degenerate $\Omega_{Acis} \approx \Omega_{Atrans}$, $\Omega_{Xcis} \approx \Omega_{Xtrans}$, and the active and passive couplings are all in the range of -5.1 to $+10$ Hz. a) Simulated A^{cis}–X^{cis} multiplet as obtained with the sequence of Figure 1a. b) Simulated multiplet, corresponding to selective inversion of the passive spin M^{cis} in the sequence of Figure 1b. c) Simulated multiplet corresponding to selective inversion of the passive spin K^{cis}. The displacement vectors J_M and J_K are affected as described in the text. d) Simulation corresponding to the superposition of the two cross-peak multiplets A^{cis}-X^{cis} and A^{trans}-X^{trans} with relative intensities of 1:3.

passive spin. Note that if P_i is coupled to only one of the active spins, selective inversion will not affect the pattern. This corresponds to the case where J_{Pi} has one component equal to zero.

Figure 2d shows a simulation of the superposition of two A–X cross-peaks arising from a 1:3 mixture of the *cis* and *trans* isomers of the same compound. Neither of the two patterns has been manipulated by selective inversion. Clearly, such a superposition is very difficult to analyze. However, the new experiment presented above provides a simple and effective procedure for separating overlapping multiplets. Figures 3a and b illustrate how overlapping experimental multiplets are modified if one of the passive spins (of the minor *cis* isomer in these examples) is inverted using the sequence shown in Figure 1b. Of course, the multiplet belonging to the major *trans* isomer remains invariant, so that the difference spectrum shown in Figure 3c features *only* a multiplet of the minor *cis* isomer. This latter multiplet contains two sets of four basic square patterns, half of which have opposite phase to the usual situation of Figure 2a. It may be appreciated that the multiplet in the difference spectrum of Figure 3c possesses C_{2v} symmetry, unlike the C_2 symmetry of ordinary multiplets in E.COSY or *z*-COSY.[14] In our experimental example, no residual peaks from the *trans* isomer were left after subtraction, but any misleading residual could have been removed by C_{2v} symmetrization.

The difference procedure illustrated in Figure 3c is of course not restricted to four-spin systems. It can be used to extract a partly or completely hidden multiplet of an arbitrary fragment, provided it contains at least one *common* passive spin (i.e., coupled to *both* active spins), and provided the chemical shift of this passive spin is not accidentally degenerate with that of a passive spin belonging to other fragments that give rise to overlapping cross-peaks in the same region. These constraints do not appear to be too restrictive, so that the new selectively inverted soft COSY (SISCOSY) technique should be useful in many practical situations. The new method is not only useful to unravel overlapping multiplets, but also to verify a hypothesis about the identity of one or more passive spins. The procedure

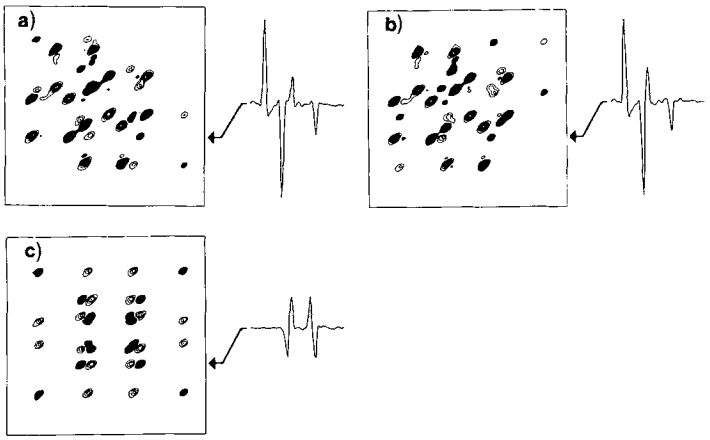

Fig. 3. Experimental multiplets corresponding to a 1:3 mixture of *cis* and *trans* isomers of **1**. a) Multiplets obtained with selective inversion of the passive spin M^{cis} using the sequence of Figure 1b. b) Multiplets obtained with selective inversion of the passive spin K^{cis}. c) Difference of (a) and (b), leading to a multiplet of the minor *cis* isomer only. Cross-sections show the amplitudes of the signals due to the major *trans* and minor *cis* isomers. The multiplets were all obtained using a Bruker AM 400 spectrometer equipped with an Oxford Research Systems Selective Excitation Unit. The 270° pulses were all 40 ms in duration and the inversion pulses had a duration of 110 ms. The matrices consisted of 100 × 1024 data points before and 512 × 1024 data points after zero filling and Fourier transformation; no weighting functions were applied to the data. The spectral widths in the ω_1 and ω_2 domains were 40 and 250 Hz, only a section of 35 × 35 Hz is shown in the figures.

allows one to record routine survey COSY spectra with much reduced resolution, and the time saved can be used to investigate selected areas in detail if required. Typically the spectrum of a single multiplet can be recorded in only 2–20 minutes, depending on the relaxation time and the desired degree of resolution.

Received: November 20, 1989 [Z 3641 IE]
German version: *Angew. Chem. 102* (1990) 576

[1] W. P. Aue, E. Bartholdi, R. R. Ernst, *J. Chem. Phys 64* (1976) 2229; R. R. Ernst, G. Bodenhausen, A. Wokaun: *Principles of Nuclear Magnetic Resonance in One and Two Dimensions*, Clarendon, Oxford 1987.
[2] L. Braunschweiler, G. Bodenhausen, R. R. Ernst, *Mol. Phys. 48* (1983) 535.
[3] P. Pfändler, G. Bodenhausen, *J. Magn. Reson. 79* (1988) 99.
[4] P. Pfändler, G. Bodenhausen, *J. Magn. Reson. 87* (1990), in press.
[5] U. Piantini, O. W. Sørensen, R. R. Ernst, *J. Am. Chem. Soc. 104* (1982) 6800; A. J. Shaka, R. Freeman, *J. Magn. Reson. 51* (1983) 169; M. Rance, O. W. Sørensen, G. Bodenhausen, G. Wagner, R. R. Ernst, K. Wüthrich, *Biochem. Biophys. Res. Commun. 117* (1983) 479.
[6] C. Griesinger, O. W. Sørensen, R. R. Ernst, *J. Am. Chem. Soc. 107* (1985) 6394.
[7] C. Griesinger, O. W. Sørensen, R. R. Ernst, *J. Chem. Phys. 85* (1986) 6837.
[8] L. Müller, *J. Magn. Reson. 72* (1987) 191.
[9] H. Oschkinat, A. Pastore, P. Pfändler, G. Bodenhausen, *J. Magn. Reson. 69* (1986) 559.
[10] P. Pfändler, G. Bodenhausen, *J. Magn. Reson. 72* (1987) 475.

[11] J. Friedrich, S. Davies, R. Freeman, *J. Magn. Reson. 75* (1987) 390; S. Davies, J. Friedrich, R. Freeman, *ibid. 75* (1987) 540; H. Kessler, H. Oschkinat, C. Griesinger, *ibid. 70* (1986) 106; R. Freeman, J. Friedrich, S. Davies, *Magn. Reson. Chem. 26* (1988) 903.
[12] R. Brüschweiler, J. C. Madsen, C. Griesinger, O. W. Sørensen, R. R. Ernst, *J. Magn. Reson. 73* (1987) 380; J. Cavanagh, J. P. Waltho, J. Keeler, *ibid. 74* (1987) 386.
[13] P. Pfändler, G. Bodenhausen, B. U. Meier, R. R. Ernst, *Anal. Chem. 57* (1985) 2510.
[14] B. U. Meier, Z. L. Mádi, R. R. Ernst, *J. Magn. Reson. 74* (1987) 565; M. Nović, G. Bodenhausen, *Anal. Chem. 60* (1988) 582.
[15] P. Pfändler, G. Bodenhausen, *Magn. Reson. Chem. 26* (1988) 888.
[16] H. Oschkinat, W. Bermel, *J. Magn. Reson. 81* (1989) 220.
[17] L. Emsley, G. Bodenhausen, *J. Magn. Reson. 82* (1989) 211.
[18] L. Emsley, G. Bodenhausen, *Magn. Reson. Med. 10* (1989) 273; *J. Magn. Reson. 87* (1990), in press.
[19] L. Emsley, G. Bodenhausen, *Chem. Phys. Lett. 165* (1990) 469.

Synthesis of (±)-Phyllanthocin via a Metal-Catalyzed Cycloreduction**

By *Barry M. Trost** and *Eric D. Edstrom*

The novel molecular architecture and promising biological activity of phyllanthoside[1] has made its aglycone, phyllanthocin (**1**),[2] an attractive synthetic target.[3] The development of a cycloisomerization[4] and of a reductive cyclization[5] of enynes under very mild conditions suggested a convenient convergent strategy from two relatively simple building blocks of about equal size (cf. Scheme 1). The failure of many transition-metal-catalyzed reactions with more elaborate structures led us to test the feasibility of such processes for the construction of oxygen heterocycles in general[6] and to assess the feasibility of its applicability for complex molecule construction by undertaking a synthesis of (±)-phyllanthocin (**1**).

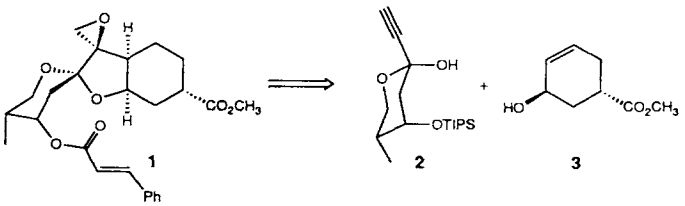

Scheme 1.

The known cyclohexenol **3**[7] is conveniently available from the *cis*-diastereomer[8] in 85% yield by application of the Mitsunobu reaction (Scheme 2).[9]

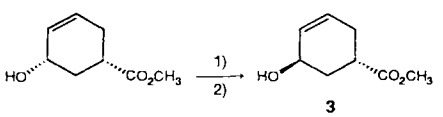

Scheme 2. Synthesis of the cyclohexenol component **3**. 1) PPh_3, DEADCAT ($C_2H_5O_2CN{=}NCO_2C_2H_5$), HCO_2H, THF; 2) $KHCO_3$, CH_3OH.

[*] Professor B. M. Trost, Dr. E. D. Edstrom
Department of Chemistry, Stanford University
Stanford, CA 94305-5080 (USA)

[**] This work was supported by the National Institutes of Health (NIH), Institute of General Medical Sciences. Mass spectra were provided by the Mass Spectrometry Facility, University of California-San Francisco, supported by the NIH Division of Research Resources.

The lactol **2** is available in four steps from the known (2*R**,3*S**)-2-methyl-1-(phenylmethoxy)hex-5-en-3-ol (**4**)[10] (Scheme 3). The choice of protecting group proved crucial owing to the ease of β-elimination during nucleophilic additions to lactone **7**. The triisopropylsilyl protecting group (TIPS) proved efficacious both in terms of its introduction and removal, as well as in terms of its chemical stability in subsequent transformations.[11] Oxidative olefin cleavage proceeded efficiently with buffered potassium permanganate under phase transfer conditions[12] or, for this particular substrate, using the *Lemieux* and *von Rudloff* protocol.[13] Hydrogenolysis of the benzyl ether **6** followed by acidification produces the lactone **7**.[14] Maintaining the acetylide addition at −78 °C followed by quenching with methanol:acetic acid (10:1) prevents the undesired β-elimination. In this way, the lactol **2**[14] is available in 68% overall yield from olefin **4**.

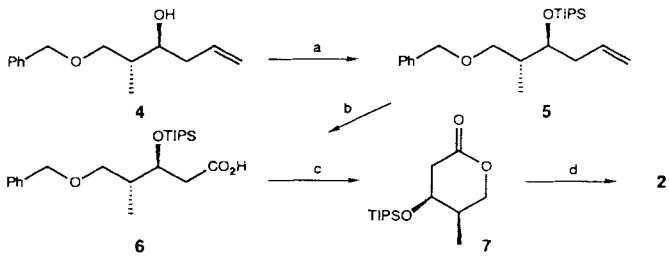

Scheme 3. Synthesis of the lactol component **2**. a) TIPS-OSO_2-CF_3, 2,6-lutidine, CH_2Cl_2, 99%. b) $NaIO_4$, $KMnO_4$ (cat.), *tert*-C_4H_9OH, H_2O, RT, pH 7. c) H_2, 10% Pd/C, C_2H_5OH, directly thereafter pyridinium *p*-toluenesulfonate, 5 Å molecular sieve, benzene, 74% overall yield referred to **5**. d) $(CH_3)_3SiC{\equiv}CLi$, THF, −78 °C, 93%. TIPS = $[(CH_3)_2CH]_3Si$.

The glycosidic coupling event entails treating a solution of the lactol **2** with 2 equivalents of hydroxy ester **3** in benzene (0.3 M) containing K 10 montmorillonite clay[15] and powdered 5 Å molecular sieves at room temperature (75% yield). Due to the fact that our starting materials are racemic, a mixture of **8a**[14] and **9a** is produced which cleanly separates after desilylation to **8b**[14] and **9b**[14] (K_2CO_3, CH_3OH, 0 °C) (Scheme 4). The production of such a mixture does not

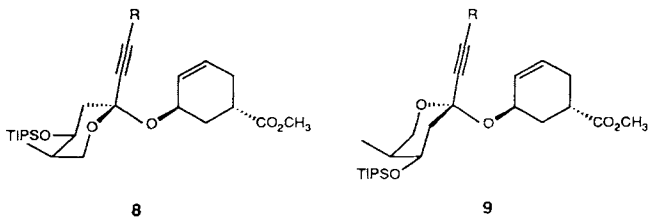

Scheme 4. Products of the reaction of **2** with **3**. **a**, R = $(CH_3)_3Si$; **b**, R = H.

constitute a shortcoming of the synthesis since it can be totally avoided simply by using enantiomerically pure building blocks **2** and **3**.[16] For our purposes, exploring the cyclization of both isomers (**8b** and **9b**) is desirable. Using carefully defined catalytic conditions with proper choice of silane effects (Scheme 5) excellent yields (86% and 78% of **10a**[14] and **11a**,[14] respectively) of the requisite polyhydrobenzofurans. For characterization, **10a** and **11a** were

were completely replaced within 1 h by a new set of signals attributable to the expected selenepine **1c** without evidence of other products (see Table 1). When the solution was allowed to warm to room temperature, **1c** extruded selenium to give diethyl 4,5-di-*tert*-butylphthalate (**9**) quantitatively; this reaction is consistent with the structure of **1c**. Nonetheless, attempted isolation of pure **1c** met with failure due to contamination with **9** even at low temperature. This provides a striking contrast to the pronounced thermal stabilities of 2,7-di-*tert*-butylthiepine and its derivatives.[5]

The clean extrusion of selenium from **1c** to give **9** obeys first-order kinetics in the temperature range 15–35 °C (^{1}H-NMR monitoring in $CDCl_3$).[8] An Arrhenius plot of the data gives the following approximate activation parameters: $\Delta H^{\neq} = 26$ kcal mol^{-1}, $E_a = 26$ kcal mol^{-1}, $\Delta S^{\neq} = 9.3$ J K^{-1}.

The corresponding activation parameters for the sulfur extrusion reaction of ethyl 2,7-di-*tert*-butyl-5-methyl-4-thiepinecarboxylate (**10**) are $\Delta H^{\neq} = 22.4 \pm 3.4$ kcal mol^{-1}, $E_a = 23.3 \pm 3.4$ kcal mol^{-1}, and $\Delta S^{\neq} = -26.9 \pm 3.7$ J K^{-1}.[9] Most conspicuous is the large difference in the activation entropies. The large negative $\Delta S^{\neq}$ value for the thiepine can be attributed to severe nonbonding interaction between two *tert*-butyl groups in a thianorcaradiene intermediate.[10] On the other hand, the selenium extrusion reaction of the selenepine **1c** presumably proceeds via incipient fission of a C–Se bond, whereby the bulky *tert*-butyl groups at the 2- and 7-positions do not play a decisive role. The detailed pathway of the selenium-extrusion reaction must await further study. Nonetheless, our work clearly shows that, although detailed studies on selenophene have confirmed its striking similarity to thiophene, the thermal stability of the vinylogous selenepine is markedly different from that of thiepine.

Received: November 7, 1989 [Z 3623 IE]
German version: *Angew. Chem. 102* (1990) 450

[1] Selected reviews: a) A. R. Katritzky (Ed.): *Comprehensive Heterocyclic Chemistry, Vol. 4–6*, Pergamon Press, Oxford 1984; b) D. R. Hogg (Ed.): *Organic Compounds of Sulfur, Selenium and Tellurium, Vol. 2* (1972), *Vol. 3* (1975), *Vol. 4* (1977), *Vol. 6* (1981), Chem. Soc., London.

[2] M. Renson in S. Patai, Z. Rappoport (Ed.): *The Chemistry of Selenium and Tellurium Compounds, Vol. 1*, Wiley, New York 1986, pp. 399–516.

[3] K. Sindelar, J. Metysova, M. Protiva, *Collect. Czech. Chem. Commun. 34* (1969) 3801; J. Jilek, K. Sindelar, J. Metysova, J. Metys, J. Pomykaek, M. Protiva, *ibid. 35* (1970) 3721.

[4] Attempted detection of a 2,7-diisopropylthiepine derivative: S. Yano, K. Nishino, K. Nakasuji, I. Murata, *Chem. Lett. 1978*, 723.

[5] a) K. Nishino, S. Yano, Y. Kohashi, K. Yamamoto, I. Murata, *J. Am. Chem. Soc. 101* (1979) 5059; b) I. Murata, K. Nishino, S. Yano, Y. Kohashi, K. Yamamoto, *Croat. Chem. Acta 53* (1980) 615; c) K. Yamamoto, S. Yamazaki, Y. Kohashi, A. Matsukawa, I. Murata, *Chem. Lett. 1982*, 1843; K. Yamamoto, S. Yamazaki, Y. Kohashi, I. Murata, Y. Kai, N. Kanehisa, K. Miki, N. Kasai, *Tetrahedron Lett. 23* (1982) 3195; d) K. Yamamoto, A. Matsukawa, I. Murata, *Chem. Lett. 1985*, 1119.

[6] K. Yamamoto, S. Yamazaki, H. Osedo, I. Murata, *Angew. Chem. 98* (1986) 639; *Angew. Chem. Int. Ed. Engl. 25* (1986) 635.

[7] M. R. Detty, J. W. Hassett, B. J. Murray, G. A. Reynolds, *Tetrahedron. 41* (1985) 4853; M. R. Detty, B. J. Murray, M. D. Seidler, *J. Org. Chem. 47* (1982) 1968.

[8] The disappearance of **1c** and the appearance of **9** were monitored by NMR integration. The first-order rate constants are $k^{293} = 2.00 \times 10^{-5}$ s^{-1}, $k^{303} = 9.10 \times 10^{-5}$ s^{-1}, $k^{308} = 2.03 \times 10^{-4}$ s^{-1}, and $k^{313} = 4.12 \times 10^{-4}$ s^{-1}.

[9] The disappearance of **10** and the appearance of ethyl 4,5-di-*tert*-butyl-2-methylbenzoate were monitored by NMR integration. The first-order rate constants in [D_{18}]decalin are $k^{407} = 1.07 \times 10^{-5}$ s^{-1}, $k^{413} = 1.56 \times 10^{-5}$ s^{-1}, $k^{425} = 3.29 \times 10^{-5}$ s^{-1}, and $k^{434} = 6.66 \times 10^{-5}$ s^{-1}.

[10] R. Gleiter, G. Krennrich, D. Cremer, K. Yamamoto, I. Murata, *J. Am. Chem. Soc. 107* (1985) 6874.

Facile Synthesis of a β(1-3)-Linked gal-galactal Disaccharide and Its Use in *N*-Iodosuccinimide-Activated *O*-Glycopeptide Synthesis **

By *Horst Kessler*,* *Andreas Kling*, and *Matthias Kottenhahn*

α-*O*-Glycopeptides with gal-β(1-3)-gal*N*Ac disaccharide building blocks are widespread in Nature.[1] The disaccharide gal-β(1-3)-gal*N*Ac forms the core A of many *O*-glycopeptides, and, moreover, has been identified as the immune-determining structural unit of a tumor associated antigen, of the so-called T-antigen (*T*homson-Friedenreich antigen).[2] Since T-specific immunoreactive structural units have been detected in certain types of carcinoma but not in healthy tissues, the T/anti-T system could prove useful in the diagnostics of cancerous diseases.[3] The keen interest being shown in T-antigen structures is evident from the numerous works on the synthesis of the core A disaccharide[4] and corresponding *O*-glycopeptides.[5]

In our investigations of the synthesis of 2-deoxyglycopeptides by *N*-iodosuccinimide(NIS)-activated addition of amino acids and peptides as glycosyl acceptors to glycals[6, 7] we therefore also checked the addition of amino acid derivatives to the gal-β(1-3)-galactal building block **1** (Fig. 1).

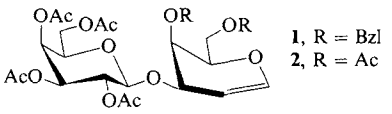

Fig. 1. Protected gal-β(1,3)-galactal disaccharide.

A twelve-step synthesis of the disaccharide **2** (11.5–14% overall yield) has already been described by *Bencomo, Jacquinet* and *Sinay*.[4b] This route appeared to us to be too tedious for such a small overall yield. Therefore, the strategy employed in our synthesis of the disaccharide glycal **1** is based on another concept (Scheme 1).

First, the 3-OH-unprotected galactal derivative **5** is generated by selective benzylation of the 4-OH and 6-OH functions of galactal **4**. Subsequently, **5** and **3** are coupled under Koenigs-Knorr conditions to give the disaccharide glycal **1**.

The selective introduction of protecting groups into **4** constitutes the major problem of this synthetic concept. According to *Kinzy* and *Schmidt*[8] a selective silylation of the 4-OH and 6-OH functions of galactal **4** is not possible; also in the benzoylation of **4** it emerged that the allylic 3-OH function is clearly more reactive than the 4-OH function;[9] according to *Holla*,[10] a selective enzymatic deacetylation of peracetylgalactal is, other than in the case of the glucal analogue, likewise not possible. In contrast, selective benzylation of the 4-OH and 6-OH functions can be achieved, as shown in Scheme 1. The byproduct of this reaction is the perbenzylated galactal.

Flowers[11] had already demonstrated with methylgalactopyranosides that the 4-OH group is more reactive in the benzylation, and, in 1983, *Bovin* et al.[12] described a possible

[*] Prof. Dr. H. Kessler, Dr. A. Kling
Organisch-chemisches Institut der Technischen Universität München
Lichtenbergstrasse 4, D-8046 Garching (FRG)
Dr. M. Kottenhahn
Degussa AG, ZN Wolfgang-FCO
Rodenbacher Chaussee 4, D-6450 Hanau 1/Wolfgang (FRG)

[**] This work was supported by the Deutsche Forschungsgemeinschaft and the Fonds der Chemischen Industrie. *M. K.* thanks the Fonds der Chemischen Industrie for a postgraduate study grant.

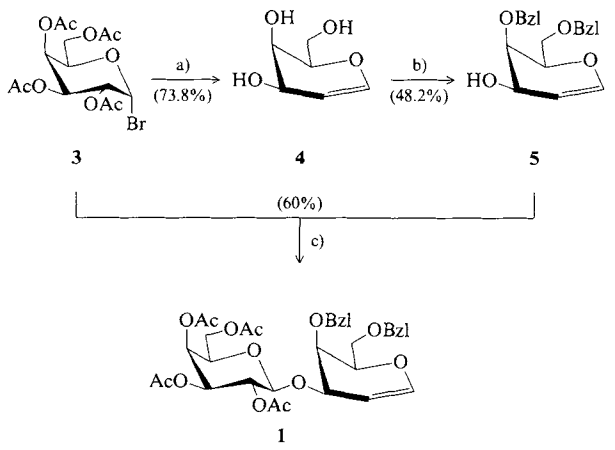

Scheme 1. Synthesis of the disaccharide glycal 2',3',4',6',-tetra-*O*-acetyl-D-galactopyranosyl-β(1-3)-4,6-di-*O*-benzyl-D-galactal **1** in 21.3% overall yield in four steps. a) 1) Zn/glacial acetic acid (90%); 2) KCN/methanol (82%). b) Dimethylformamide (DMF), 2.2 equiv. NaH, 0 °C, 2 h; 2.2 equiv. benzyl bromide BzLBr, 0 °C, 3 h. c) 1.8 equiv. Ag_2CO_3/0.2 equiv. Ag-triflate, 2.7 equiv. **3**, CH_3NO_2, RT, 2 h.

synthesis of 4,6-di-*O*-benzyl-D-galactal by reaction of galactal with NaH/benzyl bromide, but attached little importance to this fact, for they synthesized the glycal **5** in eleven steps with 13.5% overall yield via another route. The entry to **5** according to Scheme 1 seems distinctly superior to such a complex synthesis.

The coupling of **5** and **3** under Koenigs-Knorr conditions to give **1** necessitates a careful choice of catalyst. The allylic enol-acetal structure of the product can easily lead in the presence of nucleophiles and catalytic amounts of Lewis acid to side reactions in which complex mixtures of disaccharides are formed. The combination of reagents quoted in the caption to Scheme 1 have proven to be the most suitable for the synthesis (Table 1); they afforded **1** in ca. 21% overall yield.

The disaccharide glycal **1** was now allowed to react under conditions of NIS activation[6, 14] with the amino acid building block Fmoc-Ser-OBzl. Thereby it showed the expected high reactivity (83.5% overall yield). However, the almost complete α-diastereoselectivity observed in the addition to monosaccharide glycals[6] could not be achieved. Besides the desired 1,2-*trans*-α-product **6** (250 MHz ^{1}H-NMR: $^3J(1, 2) = 2.7$ Hz), both the 1,2-*trans*-β-product **7** (270 MHz ^{1}H-NMR: $^3J(1, 2) = 9$, $^3J(2, 3) = 7.4$ Hz) as well as the 1,2-cis-α-product **8** (270 MHz ^{1}H-NMR: $^3J(1, 2) = 3.78$, $^3J(2, 3) = 11.2$ Hz) were formed (Fig. 2). Because of the increased reactivity of the enolic double bond[12] *both* possible iodonium structures are formed, thus explaining formation of the products **6**–**8**. Owing to the high electron density of the arene substituents on C-4 and C-6, respectively, an opening of the α-iodonium intermediate to give the C-1 carbocation can result, whereby formation of the 1,2-*cis* product **8** is possible. **6** and **8** furnish the same 2-deoxy-α-O-glycosylamino acid after deiodination.

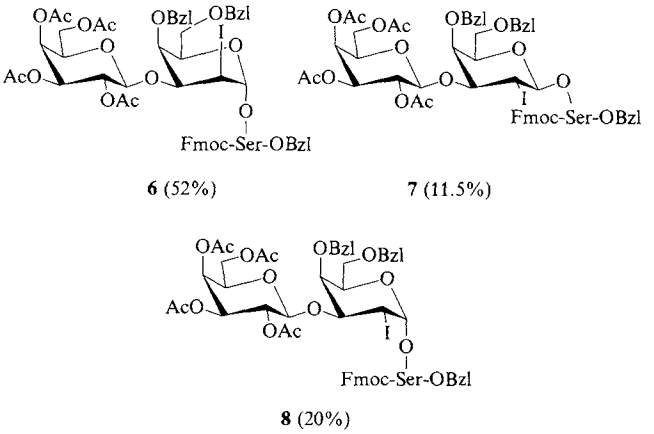

Fig. 2. Products and yields in the NIS-activated addition of Fmoc-Ser-OBzl to disaccharide glycal **1**.

In immunological tests it could be shown that a partial structure of asialoglycophorin A with the amino acids 43–48 exhibits a strong T-antigen activity.[15] After *Paulsen* et al.[5c] had synthesized the linear diglycohexapeptide we directed our attention to the synthesis of the corresponding cyclic peptide analogue cyclo(Val^{43}-Ser-Glu(OBzl)-Ile-Ser-D-Val^{48}) **9** and its conversion into the 2-deoxy-analogue of the T-antigen by direct glycosidation according to the NIS method.

The linear hexapeptide was obtained in a convergent synthesis according to the classical methods of peptide chemistry. Subsequent azide cyclization[16] and HPLC purification afforded the cyclic hexapeptide **9** in 37% yield.[17]

Reactions leading to *O*-glycopeptides according to the NIS method proceed with distinctly better yields at higher temperatures; nevertheless, the glycosidation of **9** could only

Table 1. Yields and reaction conditions for the reaction of **3** with **5** to give **1**. Optimal parameters given in bold print.

5:3	Catalyst [a]	Solvent	*T*	*t*	Yield of **1**
1:1	Ag_2CO_3	CH_2Cl_2/toluene	0 °C → RT	1 d	25.8%
1:1	Et_4NCl	CH_2Cl_2/toluene	0 °C → RT	2 d	no reaction
1:1	NaH	DMF/CH_2Cl_2	0 °C → RT	1 d	?
1:1	AgO	CH_3NO_2	0 °C → RT	2 d	no reaction
1:1	HgO/$HgBr_2$	CH_3NO_2	0 °C → RT	1 d	25%
1:1	$(Bu_3Sn)_2O$ [13]	CH_3NO_2	0 °C → RT	2 d	no reaction
1:1.1	Ag-triflate/collidine	CH_2Cl_2	−40 °C → RT	1 d	25–30%
1:1.1	1.1 equiv. Ag-triflate	CH_3NO_2	RT	5 h	decomposition
1:2	0.9 equiv. Ag_2CO_3/ 0.1 equiv. Ag-triflate	CH_3NO_2	RT	4 h	47%
1:2.7	1.8 equiv. Ag_2CO_3/ 0.2 equiv. Ag-triflate	CH_3NO_2	RT	1 h	47.3%
1:2.7	**1.8 equiv. Ag_2CO_3/ 0.2 equiv. Ag-triflate**	**CH_3NO_2**	**RT**	**2 h**	**60%**
1:2.7	1.8 equiv. Ag_2CO_3/ 0.2 equiv. Ag-triflate	CH_3NO_2	RT	3 h	47.5%

[a] Equivalents w.r.t. **5**.

be carried out at room temperature because of its thermolability. The crude product obtained (33% yield) after work-up[6] and silica gel filtration ($CHCl_3$/acetone 4/1, subsequent elution of the product with 2-propanol) shows exclusively the molecular peak for a monoglycosidation product ($M + Na^{\oplus} = 1509$) in the FAB mass spectrum. Investigations concerning the exact structure are currently under way.

Herein we have described a simple synthesis of the versatile disaccharide glycal **1** and its use in *O*-glycopeptide synthesis. In the case of the addition to Fmoc-Ser-OBzl using the NIS method, a diastereomeric mixture is formed which also contains an unexpected *cis*-addition product. The desired α-epimer, however, is formed in appreciable excess.

Experimental

5 (M = 326.39, $C_{20}H_{22}O_4$): A stirred solution of **4** (8.9 mmol) in 14 mL of anhydrous DMF under argon was treated at 0 °C with 19.58 mmol of NaH (60% in mineral oil). After 2 h at 0 °C the mixture (suspension) was treated dropwise and rapidly with 19.58 mol of BzlBr and then allowed to stand for 3 h at 0 °C. The mixture solidified. It was then thawed out, treated with 50 mL of benzene, washed with 20 mL of water, the aqueous phase back extracted with 3 × 15 mL of benzene and the combined organic phases finally evaporated to dryness in a vacuum (water pump). The residue was purified by chromatography on silica gel with ethyl acetate/isohexane 3/5. The main fraction contained (1.4 g = 48.2%) of **5**. One secondary fraction (39%) contained perbenzylated **4**, a further secondary fraction (8%) another dibenzylated **4**. Oily **5** crystallized out on cooling the main fraction and could be recrystallized from isohexane. M.p. = 65 °C (68 °C [14]), $[\alpha]_D^{20} = 12.06$ ($c = 0.6$ in $CHCl_3$) ($[\alpha]_D = -17$ [14]) (no details of temperature and solvent); the rotation quoted by us was reproduced several times). $R_f = 0.64$ (ethyl acetate/isohexane 1/1), 0.37 (ethyl acetate/isohexane 1/2).—250 MHz ^{1}H-NMR ([D$_6$]DMSO): $\delta = 7.15-7.4$ (m, 10H, H_{phenyl}), 6.27 (dd, 1H, H-1, $^3J(1,2) = 6.19$, $^4J(1,3) = 1.75$ Hz), 4.86 (d, 1H, OH-3, $^3J(OH,3) = 5.83$), 4.85, 4.5 (je d, 2H, Ph-CH_2), 4.46 (d, 2H, Ph-CH_2), 4.63 (ddd, 1H, H-2, $^4J(2,4) = 1.39$ Hz), 4.35 (m, 1H, H-3), 4.14 (m, 1H, H-5), 3.72 (dd, 1H, H-4), 3.7–3.53 (m, 2H, H-6).—75 MHz-^{13}C NMR ($CDCl_3$): $\delta = 144.2$ (C-1), 137.7 (quarternary C_{phenyl}), 127.8–128.6 (C_{phenyl}), 102.9 (C-2), 75.2 (C-5), 74.2, 73.5 (Ph-CH_2), 73.2 (C-4), 68.1 (C-6), 62.8 (C-3).

1 (M = 656.68, $C_{34}H_{40}O_{13}$): A suspension of 300 mg of molecular sieve, 100 mg of calcined $CaSO_4$ and 0.55 mmol of Ag_2CO_3/0.061 mmol Ag-triflate in 5 mL of nitromethane was prepared in a pre-heated dark glass flask and stirred for 1 h at room temperature. 0.826 mmol of **3** co-evaporated with toluene was subsequently dissolved in 5 mL of nitromethane and added to the catalyst suspension at room temperature. After 15 min, solid **5** (0.306 mmol) was added and the mixture stirred for 2.0–2.5 h. The reaction mixture was now filtered through celite into an excess of toluene. After evaporation to dryness in a Rotavapor (35 °C) the residue was extracted with diethyl ether/water. The residue remaining after evaporation of the diethyl ether phase was chromatographed on silica gel with diethyl ether/isohexane 4/1. 120 mg of of colorless oil = 60%, $[\alpha]_D^{20} = -42.5$ ($c = 1.3$ in $CHCl_3$), $R_f = 0.23$ (diethyl ether/isohexane 4/1).—250 MHz ^{1}H-NMR ($CDCl_3$, interner standard TMS): $\delta = 7.2-7.4$ (m, 10H, H_{phenyl}), 6.37 (dd, 1H, H-1, $^3J(1,2) = 6.4$, $^4J(1,3) = 1.9$ Hz), 5.4 (dd, 1H, H-4', $^3J(4',5') = 1.5$ Hz), 5.27 (dd, 1H, H-2', $^3J(2',3') = 10.45$ Hz), 5.03 (dd, 1H, H-3', $^3J(3',4') = 3.53$ Hz), 4.9, 4.56 (each d, 2H, Ph-CH_2), 4.70 (m, 1H, H-2, $^3J(2,3) = 7.9$ Hz), 4.63 (d, 1H, H-1', $^3J(1',2') = 7.97$ Hz), 4.54 (m, 1H, H-3), 4.42 (dd, 2H, Ph-CH_2); 4.14, 4.15 (m, 3H, H-5, H-6', superposed), 3.91, 3.92 (m, 2H, H-5', H-4, superposed) 3.52–3.68 (m, 2H, H-6), 1.95–2.15 (4 × s, 12H, CO-CH_3).—62.9 MHz-^{13}C NMR ($CDCl_3$): $\delta = 169.1-170.3$ (CO-CH_3), 144.8 (C-1), 137.9–138.5 (quarternary C_{phenyl}), 127.5–128.3 (C_{phenyl}), 99.5 (C-1'), 98.4 (C-2), 75.75 (C-5), 73.2 (Ph-CH_2), 71.0, 70.8 (C3, C4, C3', C5'), 68.8 (C-2'), 68.4 (C-6), 67.0 (C-4'), 61.2 (C-6'), 20.5–20.6 (4 × CO-CH_3).

Received: November 14, 1989 [Z 3631]
German version: *Angew. Chem. 102* (1990) 452

CAS Registry numbers:
1, 125827-94-3; **3**, 3068-32-4; **4**, 21193-75-9; **4** perbenzylated deriv., 80040-79-5; **5**, 81928-98-5; **6**, 125803-97-6; **7**, 125874-74-0; **9**, 125874-75-1; Fmoc-Ser-OBzl, 125803-96-5.

[1] J. Montreuil in A. Neuberger, L. L. van Deenen (Eds.): *Comprehensive Biochemistry, Vol 19 BII*, Elsevier, Amsterdam 1989, p. 1–189.
[2] a) S. Hakomori, *Annu. Rev. Immunol. 2* (1984) 103–126; b) P. Vaith, G. Uhlenbruck, *Z. Immunitätsforsch. 154* (1978) 1–14.
[3] a) G. F. Springer, *Bull. Inst. Pasteur (Paris) 81* (1983) 127–158; b) G. F. Springer, S. Murthy, P. R. Desai, W. A. Fry, H. Tegtmeyer, E. F. Scanlon, *Klin. Wochenschr. 60* (1982) 121–131.
[4] a) H. Paulsen, M. Paal, *Carbohydr. Res. 135* (1984) 71–84; b) V. V. Bencomo, J.-C. Jacquinet, P. Sinay, *Carbohydr. Res. 110* (1982) C9–C11.
[5] a) H. Paulsen, M. Schultz, J. D. Klamann, B. Waller, M. Paal, *Liebigs Ann. Chem. 1985*, 2028–2048; b) H. Paulsen, M. Schultz, *ibid. 1986*, 1435–1447; c) H. Paulsen, M. Schultz *Carbohydr. Res. 159* (1987) 37–52; d) B. Ferrari, A. Pavia, *Tetrahedron 41* (1985) 1939–1349; e) H. Kunz, S. Birnbach, *Angew. Chem. 98* (1986) 354–355; *Angew. Chem. Int. Ed. Engl. 25* (1986) 360; f) W. Kinzy, R. R. Schmidt, *Carbohydr. Res. 166* (1987) 265–267.
[6] H. Kessler, M. Kottenhahn, A. Kling, C. Kolar, *Angew. Chem. 99* (1987) 919–921; *Angew. Chem. Int. Ed. Engl. 26* (1987) 888–890.
[7] H. Kessler, M. Kottenhahn in G. Jung, E. Bayer (Eds.): *Peptides 1988 (Proc. 20th Eur. Pept. Symp)*, W. de Gruyter, Berlin 1989, S. 331–333.
[8] W. Kinzy, R. R. Schmidt, *Tetrahedron Lett. 28* (1987) 1981–1984.
[9] M. Kottenhahn, *Dissertation*, Universität Frankfurt 1989.
[10] W. Holla, *Angew. Chem. 101* (1989) 222–223; *Angew. Chem. Int. Ed. Engl. 28* (1989) 220.
[11] H. M. Flowers, *Carbohydr. Res. 39* (1975) 245–251.
[12] N. V. Bovin, S. E. Zurabyau, A. Korlin, *J. Carbohydr. Chem. 2* (1983) 249–262.
[13] J. C. Jacquinet, P. Sinay, *Tetrahedron 35* (1979) 365–371.
[14] J. Thiem, H. K. Schwentner, J. Schwentner, *Synthesis 1978*, 696–698; J. Thiem, M. Gerken, G. Snatzke, *Liebigs Ann. Chem. 1983*, 448–461.
[15] F. G. Hanisch, G. H. Farrar, R. Schmalisch, G. Uhlenbruck, *Immunobiology (Stuttgart) 165* (1983) 147–160.
[16] Y. S. Klausner, M. Bodanszky, *Synthesis 1974*, 549–559.
[17] A. Kling, *Dissertation*, Universität Frankfurt 1989.

Permethyl-β-cyclodextrin, Chemically Bonded to Polysiloxane: a Chiral Stationary Phase with Wider Application Range for Enantiomer Separation by Capillary Gas Chromatography**

By *Peter Fischer,* Reiner Aichholz, Uwe Bölz, Markus Juza* and *Sigfried Krimmer*

Dedicated to Professor Franz Effenberger on the occasion of his 60th birthday

The use of *O*-derivatized cyclodextrins as chiral stationary phases in capillary gas chromatography has attracted increasing interest in recent years.[1–3] So far, capillary columns have been described which are statically coated with differently derivatized cyclodextrins[1,3] (these are also commercially available), as well as columns where a physical mixture of polysiloxane and cyclodextrin is employed as stationary phase (e.g. OV-1701 with 10% permethyl-β-cyclodextrin[2]). Some spectacular GLC enantiomer separations have been achieved with these phases; unfortunately, individual separation problems frequently require a specially tailored derivatization of the cyclodextrins (e.g. tripentyl-, dipentyl/acetyl- etc.).[3] Pure cyclodextrin phases present the additional disadvantage that the inevitably polar chiral selector is also used for building the phase backbone, which thence obtains an unnecessarily polar character.

We have attempted, therefore, to utilize the building principle of chiral amide phases, such as Chirasil-val,[4] also for cyclodextrin phases, and to likewise *chemically* bond this chiral selector to a polysiloxane backbone. Thus, more generally applicable, perhaps even thermally and chemically

[*] Priv.-Doz. Dr. P. Fischer, Dipl.-Ing. R. Aichholz, Dipl.-Chem. U. Bölz, M. Juza, Dipl.-Chem. S. Krimmer
Institut für Organische Chemie der Universität
Pfaffenwaldring 55, D-7000 Stuttgart 80 (FRG)

[**] Chiral Recognition in Capillary Gas Chromatography, Part 3. For generous support of this work, we are indebted to Carlo Erba Instruments. D-6238 Hofheim (FRG). – Part 2: R. Aichholz, U. Bölz, P. Fischer, *HRC CC J. High Resolut. Chromatogr. Chromatogr. Commun. 13* (1990), in press.

more stable cyclodextrin phases should obtain. In this communication, we report first results with a chiral phase, derived from poly(dimethylsiloxane) which has been modified with ca. 5% of permethyl-β-cyclodextrin (PMCD) as chiral side chain (Scheme 1).

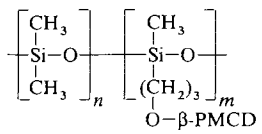

Scheme 1. Structure of the poly(dimethylsiloxane)-cyclodextrin phase; $m:n = 1:20$, i.e. ca. 5% chiral side chain.

The synthesis of this material starts with the reaction of allyl bromide with β-cyclodextrin.[5] Allyloxy groups are formed from ca. 30% of the OH groups in the 6-position. The remaining free OH groups are subsequently subjected to exhaustive methylation (NaH in Me_2SO/CH_3I). The *O*-allylpermethyl-β-cyclodextrin thus obtained is bonded *via* hydrosilylation (catalyst H_2PtCl_6)[6] to a polysiloxane, containing 7% Me-Si-H besides 93% Me_2Si groups. Unconsumed Si-H is alkylated in a final step. The crude phase material is purified by repeated reprecipitation, and statically coated onto an appropriately silylated glass surface. A capillary column, prepared in this manner, may be used, with temperature programming, up to 280 °C without either serious bleeding or notable racemization, even though the stationary phase is neither cross-linked nor chemically bonded to the glass surface.

The enantiomeric resolution potential of the new phase is demonstrated in Figure 1 for a series of alkanediols. The diols were analyzed as a batch, *without* derivatization (4°/min temperature program). The chromatogram shows baseline, or at least 90% valley separation for all *R*/*S* pairs. So far, gas chromatographic separation of enantiomeric diols required trifluoroacetylation[3g] and/or recording under isothermal conditions.[7] The weak tailing of all the diol peaks, despite two free OH groups, bears witness to the inertness of the column and the new phase.[8]

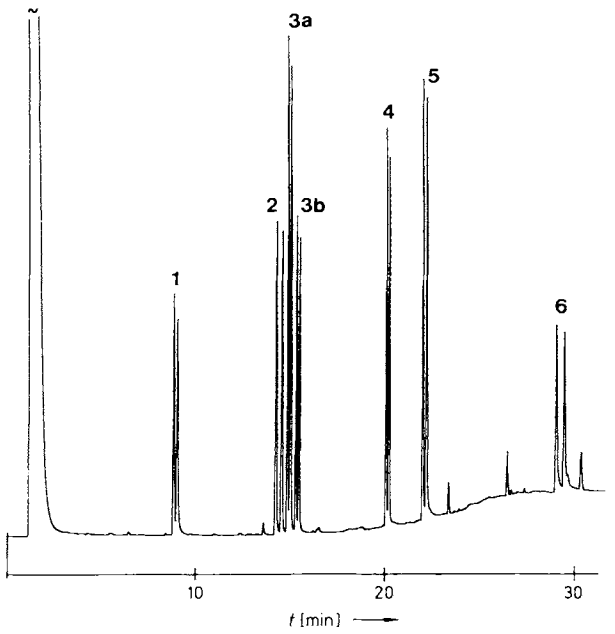

Figure 1. Enantiomer separation of alkanediols: 30 m × 0.3 mm glass capillary, statically coated with poly(dimethylsiloxane), modified with 5% trimethylenoxypermethyl-β-cyclodextrin side chain (see text); 0.8 bar H_2; 100–220 °C; 4°/min; FID detection. **1** = 1,2-pentanediol; **2** = *trans*-1,2-cyclohexanediol; **3a,b** = 2-cetyl-1,3-hexanediol (pair of diastereoisomers); **4** = 1-cyclohexyl-1,2-ethanediol; **5** = 1-phenyl-1,2-ethanediol; **6** = 1-(4-chlorophenyl)-1,2-ethanediol.

Excellent chiral resolution is likewise obtained for the methyl esters of α-hydroxycarboxylic and dicarboxylic acids (without α-OH derivatization; see Table 1, Fig. 2a). Even α-bromomethylcarboxylates are baseline-separated (Fig. 2b).[9] The separation factors (α-values, see Table 1) naturally decrease rapidly with increasing distance between the stereogenic center and the COOR function; however, 4-bromomethylhexanoate, is still clearly separated.

The new phase likewise resolves optically active alkanoic acids, in free, underivatized form, into the enantiomers (Fig. 2c). Even compounds lying more or less at extremes of

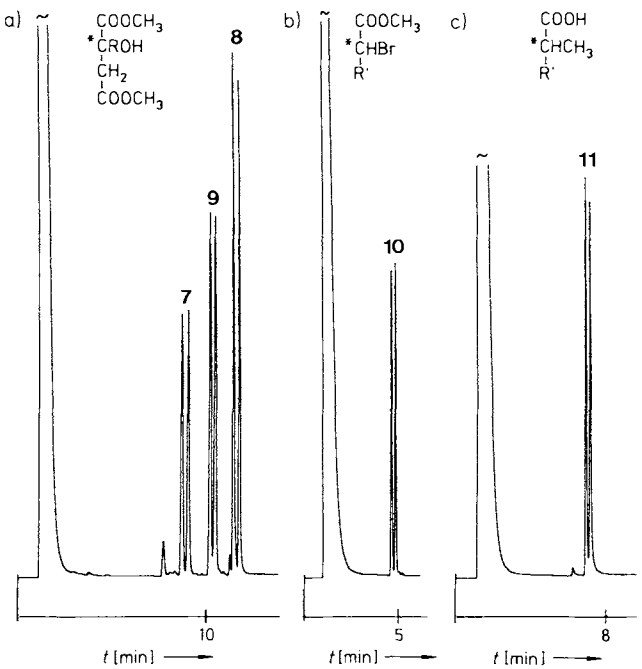

Figure 2. Enantiomer separation on the chiral phase glass capillary, described in Figure 1 of a) malic, 2-ethylmalic acid methyl esters and 2-methylmalic (citramalic), **7** (R = H), **8** (R = Et) and **9** (R = Me), respectively; b) methyl-2-bromohexanoate **10** (R' = *n*Bu); c) 2-methylhexanoic acid, underivatized, **11** (R' = *n*Bu); **7** (R = H), **8** (R = Et) and **9** (R = Me), respec.; conditions as given in Figure 1.

the polarity range, such as chiral alkanes and, for example, methyl-*N*-acetylprolinate, are fully *R*/*S*-resolved in one run on the same column (see Table 1).

A further advantage of the new material is that, if derivatization is required, acetylation suffices, as demonstrated by the separation of the cyanohydrins (Table 1).[10] The chiral resolution for *R*- and *S*-benzaldehydecyanohydrin ($\alpha = 1.3$) lies at the upper limit of all gas-chromatographic enantiomer separations reported so far. The extraordinarily high basic resolution in the case of the structural unit, -C*H(OH)CN enables the smooth resolution of other cyanohydrins, and even of the *o*-chlorobenzaldehyde derivative (see Table 1).

So far, only amines and amino alcohols have proven problematical. Most likely, these classes of compounds require

Table 1. Gas-chromatographic data for enantiomer separations at permethyl-β-cyclodextrin, chemically bonded to poly(dimethylsiloxane) [5].

Class of Compounds and Compounds	T [°C]	Separation factor α [a]
Alkanediols (underivatized)		
2,3-Butanediol	100	<1.010
1,2-Pentanediol	125	1.049
trans-1,2-Cyclohexanediol	145	1.057
2-Cetyl-1,3-hexanediol	145	1.035
(pair of diastereoisomers)		1.037
1-Cyclohexyl-1,2-ethanediol	170	1.028
1-Phenyl-1,2-ethanediol	170	1.034
1-(4-Chlorophenyl)-1,2-ethanediol	200	1.044
2-*Hydroxycarboxylic acids (as methyl esters)*		
2-Hydroxy-3-methylbutyric acid	100	1.021
2-Hydroxyhexanoic acid	100	1.132
2-Hydroxy-4-methylhexanoic acid	100	1.046
2-Hydroxyoctanoic acid	120	1.045
Mandelic acid	140	<1.010
3-Phenyllactic acid	140	1.077
2-*Hydroxydicarboxylic acids (as methyl esters)*		
Malic acid	125	1.075
Citramalic acid (2-methylmalic acid)	125	1.069
2-Ethylmalic acid	125	1.074
Substituted hexanoic acids (as methyl esters)		
2-Bromohexanoic acid	110	1.133
4-Bromohexanoic acid	110	1.050
5-Bromohexanoic acid	110	<1.010
2-Dimethylaminohexanoic acid	110	<1.010
3-Dimethylaminohexanoic acid	110	<1.010
2-Bromo-6-methoxyhexanoic acid	130	1.106
6-Bromo-2-methoxyhexanoic acid	130	1.019
2,6-Dimethoxyhexanoic acid	130	<1.010
Alkanecarboxylic acids (underivatized)		
2-Methylhexanoic acid	130	1.065
2-Ethylhexanoic acid	140	1.037
Cyanohydrins (O-acetylated) of		
Benzaldehyde	140	1.290
Vanillin	190	1.112
Piperonal	190	1.079
o-Chlorobenzaldehyde	165	1.021
m-Chlorobenzaldehyde	165	1.189
p-Chlorobenzaldehyde	165	1.173
Amino acids (as N-acetyl methyl esters)		
Leucine	130	<1.010
Proline	150	1.034
Alkanes		
2,2,4,4,6,8,8-heptamethylnonane	120	1.111

[a] α-Values <1.010 designate that there is no observable chromatographic resolution.

special functionalization of the OH groups in the chiral selector, even in the case of phase-bonded cyclodextrins.

Received: December 4, 1989 [Z 3664 IE]
German version: *Angew. Chem. 102* (1990) 439

CAS Registry numbers:
(±)(*R**,*R**)-[MeCH(OH)]$_2$, 6982-25-8; (±)-PrCH(OH)CH$_2$OH, 91049-43-3; (±)(*R**,*S**)-PrCH(OH)CH(CH$_2$OH)(CH$_2$)$_{15}$Me, 125803-24-9; (±)(*R**,*R**)-PrCH(OH)CH(CH$_2$OH)(CH$_2$)$_{15}$Me, 125803-25-0; (±)-*c*-C$_6$H$_{11}$CH(OH)CH$_2$OH, 125874-67-1; (±)-(*trans*)-*c*-C$_6$H$_{11}$(OH)$_2$-1,2, 54383-22-1; (±)-PhCH(OH)CH$_2$OH, 7138-28-5; (±)-*p*-ClC$_6$H$_4$CH(OH)CH$_2$OH, 125803-26-1; (±)-*i*-PrCH(OH)CO$_2$Me, 21632-23-5; (±)-BuCH(OH)CO$_2$Me, 108740-83-6; (±)-*i*-BuCH(OH)CO$_2$Me, 21632-24-6; (±)-Me(CH$_2$)$_5$CH(OH)CO$_2$Me, 125874-68-2; (±)-PhCH(OH)CO$_2$Me, 4358-87-6; (±)-PhCH$_2$CH(OH)CO$_2$Me, 21632-25-7; (±)-MeO$_2$CCH(OH)CH$_2$CO$_2$Me, 38115-87-6; (±)-MeO$_2$CCH$_2$C(OH)(Me)CO$_2$Me, 125874-69-3; (±)-MeO$_2$CCH$_2$C(OH)(Et)CO$_2$Me, 125874-70-6; (±)-BuCH(Br)CO$_2$Me, 70288-61-8; (±)-EtCH(Br)(CH$_2$)$_2$-CO$_2$Me, 78019-66-6; (±)-MeCH(Br)(CH$_2$)$_3$CO$_2$Me, 125803-27-2; (DL)-BuCH(NMe$_2$)CO$_2$Me, 125803-28-3; (±)-PrCH(NMe$_2$)CH$_2$CO$_2$Me, 125803-29-4; (±)-MeO(CH$_2$)$_4$CH(Br)CO$_2$Me, 125803-30-7; (±)-Br(CH$_2$)$_4$-CH(OMe)CO$_2$Me, 125803-31-8; (±)-MeO(CH$_2$)$_4$CH(OMe)CO$_2$Me, 125803-32-9; (±)-BuCH(Me)CO$_2$Me, 118628-17-4; (±)-BuCH(Et)CO$_2$Me, 125803-33-0; (±)-PhCH(OAc)CN, 119718-87-5; (±)-3,4-(OMe)(OH)C$_6$H$_3$CH-(OAc)CN, 125803-34-1; (±)-*o*-ClC$_6$H$_4$CH(OAc)CN, 125803-35-2; (±)-*m*-ClC$_6$H$_4$CH(OAc)CN, 125803-36-3; (±)-*p*-ClC$_6$H$_4$CH(OAc)CN, 125803-37-4; (DL)-AcLeuOMe, 57289-25-5; (DL)-AcProOMe, 18800-83-4; (±)-*t*-BuCH$_2$-C(Me)$_2$CH$_2$CH(Me)CH$_2$Bu-*t*, 125803-38-5; (±)-*o*-acetylcyanohydrin heliotropin, 119798-32-2.

[1] D. W. Armstrong, T. J. Ward, R. D. Armstrong, T. E. Beesley, *Science (Washington) 232* (1986) 1132.
[2] a) V. Schurig, H. P. Nowotny, *J. Chromatogr. 441* (1988) 155; b) V. Schurig, H. P. Nowotny, D. Schmalzing, *Angew. Chem. 101* (1989) 785; *Angew. Chem. Int. Ed. Engl. 28* (1989) 736.
[3] a) J. Ehlers, W. A. König, S. Lutz, G. Wenz, H.tom Dieck, *Angew. Chem. 100* (1988) 1614; *Angew. Chem. Int. Ed. Engl. 27* (1988) 1566; b) W. A. König, S. Lutz, G. Wenz, E. von der Bey, *HRC CC J. High Resolut. Chromatogr. Chromatogr. Commun. 11* (1988) 506; W. A. König, S. Lutz, C. Colberg, N. Schmidt, G. Wenz, E. von der Bey, A. Mosandl, C. Günther, A. Kustermann, *ibid. 11* (1988) 621; d) W. A. König, S. Lutz, P. Mischnick-Lübecke, B. Brassart, *J. Chromatogr. 447* (1988) 193; e) W. A. König, S. Lutz, M. Hagen, R. Krebber, G. Wenz, K. Baldenius, J. Ehlers, H.tom Dieck, *HRC CC J. High Resolut. Chromatogr. Chromatogr. Commun. 12* (1989) 35; f) W. A. König, *Nachr. Chem. Tech. Lab. 37* (1989) 471; g) W. A. König, *Carbohydr. Res. 192* (1989) 51.
[4] H. Frank, G. J. Nicholson, E. Bayer, *Angew. Chem. 90* (1978) 396; *Angew. Chem. Int. Ed. Engl. 17* (1978) 363.
[5] U. Bölz, *Diplomarbeit*, Universität Stuttgart 1989.
[6] J. S. Bradshaw, S. K. Aggarwal, C. A. Rouse, B. J. Tarbet, K. E. Markides, M. L. Lee, *J. Chromatogr. 405* (1987) 169.
[7] B. Koppenhoefer, H. Allmendinger, G. J. Nicholson, *Angew. Chem. 97* (1985) 46; *Angew. Chem. Int. Ed. Engl. 24* (1985) 48.
[8] K. Grob, G. Grob, K. Grob, Jr., *J. Chromatogr. 219* (1981) 13.
[9] E. Koch, G. J. Nicholson, E. Bayer, *HRC CC J. High Resolut. Chromatogr. Chromatogr. Commun. 7* (1984) 398, report on the enantiomer separation of α-chloro- and α-bromocarboxylic acids after transformation into the respective *tert*-butylamides.
[10] Enantiomer separation of cyanohydrins in the form of their *O*-trifluoroacetyl derivatives has been reported on one occasion [3f].

Organometallic Macrocycles: Synthesis and Molecular Structure of Trimeric Tartratodiruthenium Complexes**

By *Georg Süss-Fink,* Jean-Luc Wolfender, Frank Neumann,* and *Helen Stoeckli-Evans*

It has been known since 1969 that dodecacarbonyltriruthenium reacts with carboxylic acids to give carboxylato complexes containing the $Ru_2(CO)_4(\mu\text{-}OOCR)_2$ structural unit.[1] In the solid state, these complexes form polymer chains in which the dinuclear building blocks are coupled via Ru–O bonds;[2, 3] in solution, the chains depolymerize with uptake of two-electron ligands.[1] The X-ray structure analysis of the bis(tri-*tert*-butylphosphane) derivative **1** shows a molecule with a characteristic saw-horse structure.[4] Of the dicarboxylic acid derivatives, complex **2**, which has been described as a polymer,[5] and the dinuclear complex **3** have already been reported.[6] The X-ray crystallographic investigation of a glutaratotributylphosphane compound of composition **4** revealed that $Ru_2(CO)_4$ units are coupled intramolecularly via glutarato ligands.[7]

$[Ru_2(CO)_4(\mu\text{-}OOCPr)_2(PtBu_3)_2]$ **1**
$[Ru_2(CO)_4\{\mu\text{-}OOC(CH_2)_nCOO\}]_m$, n = 0–4 **2**
$[Ru_2(CO)_4\{\mu\text{-}OOC(CH_2)_4COO\}(3,5\text{-}MeC_3HN_2)_2]$ **3**
$Ru_4(CO)_8\{\mu\text{-}OOC(CH_2)_3COO\}_2(PBu_3)_4$ **4**

[*] Prof. Dr. G. Süss-Fink, J.-L. Wolfender, F. Neumann,
Prof. Dr. H. Stoeckli-Evans
Institut de Chimie, Université de Neuchâtel
Avenue de Bellevaux 51, CH-2000 Neuchâtel (Switzerland)

[**] This work was supported by the Fonds der National Suisse de la Recherche Scientifique and the Volkswagen-Stiftung.

We have now found that trimeric tartratodiruthenium complexes, which can be regarded as organometallic macrocycles, are accessible with tartaric acid. The compounds **5**–**7** are formed upon reaction of $Ru_3(CO)_{12}$ with tartaric acid (*R,R*, *S,S*, and *R,S*) in a pressure Schlenk tube, and can be obtained as acetonitrile adducts in the form of yellow crystals. These are unstable in air and in vacuo and lose both coordinated and uncoordinated acetonitrile. Therefore, in the ^{1}H-NMR spectra integrals that are always too small are found for the CH_3 groups of **5**–**7**. Substitution of the

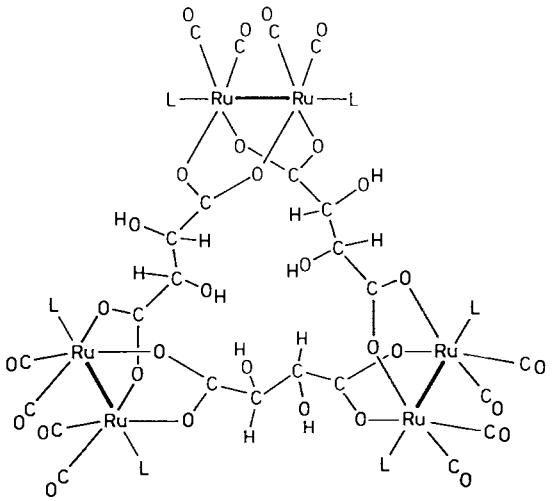

5: all-(*R,R*), L = MeCN; **6**: all-(*S,S*), L = MeCN

7: all-(*R,S*), L = MeCN; **8**: all-(*S,S*), L = PPh_3

acetonitrile ligand in **6** by PPh_3 provided access to the air-stable triphenylphosphane derivative **8**, for which a satisfactory elemental analysis was obtained.

A solid-state structural investigation of the complex **5** revealed the trimeric macrocyclic structure of the compound, in which three $Ru_2(CO)_4$ units are coupled via tartrato bridging ligands to give a tricycle.[8] With acetonitrile, **5** forms hexagonal crystals containing three symmetry-independent molecules A, B and C per asymmetric unit. The crystals contain randomly distributed uncoordinated acetonitrile molecules. The molecular structure of the independent molecule A is shown in Figure 1; the differences with respect to B and C are small. A C_3 axis is the only symmetry element of the chiral compound. Each Ru atom is surrounded almost octahedrally by its ligands. The Ru–Ru distance of 2.6545(13) Å is only slightly shorter than in other carboxylato complexes containing an Ru–Ru single bond such as **1** (2.728(1) Å)[4] or **9** (2.734(3) Å).[7] The planes through the atoms Ru1, Ru2, C1 and Ru1, Ru2, C4 are almost orthogonal to each other (80°), with the accompanying oxygen atoms O1, O2 and O3, O4 located at an average of 0.327 Å above and below the respective planes. Such a twisting of the carboxylato groups is also known, for example, in the case of **10**.[3] The positions of the carbonyl groups and of the acetonitrile ligands are likewise similar to those in monomeric carboxylato complexes. The six OH groups of the macrocycle are all located on one side of the plane through Ru1, Ru1a and Ru1b and are alternately bent towards and away from the C_3 axis.

$[Ru_2(CO)_4\{\mu\text{-}OOC(CH_2)_3COO\}(PBu_3)_2]_2$ **9**

$[Ru_2(CO)_6(\mu\text{-}OOCPh)_2]$ **10**

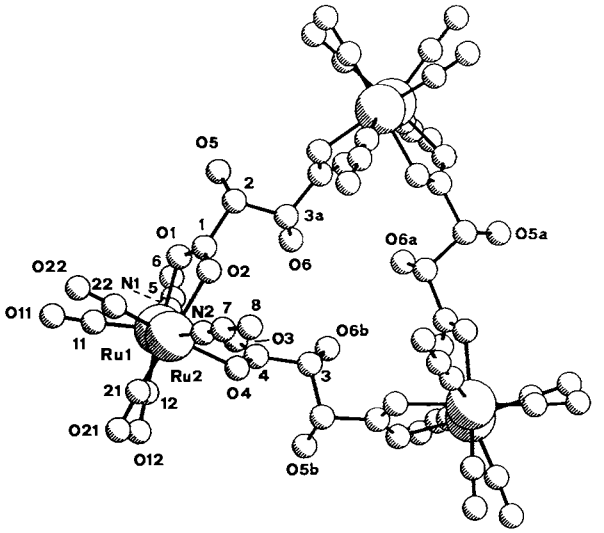

Fig. 1. Structure of **5**, molecule A, in the crystal (Pluto plot [11]), selected bond lengths [Å] and angles [°]: Ru1-Ru2 2.6545(13), Ru1-N1 2.182(12), Ru2-N2 2.202(13), Ru1-O1 2.125(8), Ru1-O3 2.150(13), Ru2-O2 2.143(8), Ru2-O4 2.131(13); Ru2-Ru1-N1 162.8(4), Ru1-Ru2-N2 160.6(4), Ru2-Ru1-O1 84.5(3), Ru2-Ru1-O3 82.1(3), Ru1-Ru2-O2 82.4(2), Ru1-Ru2-O4 83.8(3), N1-Ru1-O1 81.8(4), N2-Ru2-O2 82.3(3), O1-Ru1-O3 82.5(4), O2-Ru2-O4 83.5(4), O1-C1-O2 128.3, O3-C4-O4 126.7.

Experimental

All operations were carried out under nitrogen in anhydrous N_2-saturated solvents.

Synthesis of **5**–**7**: A solution of $Ru_3(CO)_{12}$ (320 mg, 0.50 mmol) in THF (50 mL) was treated with 113 mg (0.75 mmol) of *R,R*- or (*S,S*)-tartaric acid (in the case of **5** and **6**, resp.) or 126 mg (0.75 mmol) of (*R,S*)-tartaric acid monohydrate (in the case of **7**) in a pressure Schlenk tube and the mixture heated to 120 °C and magnetically stirred (**5**, **6**: 15 h; **7**: 13 h). To avoid a back reaction, the gases evolved (CO and presumably H_2) were drawn off from time to time. On completion of reaction the clear orange-colored solutions were evaporated to dryness and the residues heated with acetonitrile until a clear solution was obtained. After storage for several days at 2 °C, **5**–**7** were obtained in crystalline form. **5**: (331 mg, 81%); IR (CH_2Cl_2): ν(CO) = 2045(s), 1995(m), 1963(vs); IR (KBr): ν(OCO) = 1592(s), 1422(m), ν(OH) = 3468(m) cm^{-1}; ^{1}H NMR ([D$_6$]DMSO, 200 MHz): δ = 2.06 (s, <18H, CH_3), 4.13 (d, 6H, J_{HH} = 8 Hz, CH), 5.30 (s, 6H, J_{HH} = 8 Hz, OH).—**6**: (326 mg, 80%); IR (CH_2Cl_2): ν(CO) = 2043(s), 1992(m), 1963(vs); IR (KBr): ν(OCO) = 1592(s), 1422(m), ν(OH) = 3469(m); ^{1}H-NMR ([D$_6$]DMSO, 200 MHz): δ = 2.05 (s, <18H, CH_3), 4.13 (d, 6H, J_{HH} = 8 Hz, CH), 5.30 (d, 6H, J_{HH} = 8 Hz, OH). —**7**: (311 mg, 76%); IR (CH_2Cl_2): ν(CO) = 2042(s), 1989(m), 1966(vs); IR (KBr): ν(OCO) =
1597(m), 1420(m), ν(OH) = 3451(m); ^{1}H NMR ([D$_6$]DMSO, 200 MHz): δ = 2.06 (s, <18H, CH_3), 3.81 (d, 6H, J_{HH} = 4 Hz, CH), 5.54 (d, 6H, J_{HH} = 4 Hz, OH).

Synthesis of **8**: A solution of **6** (272 mg, 0.17 mmol) in THF (50 mL was treated with 262 mg (1.00 mmol) of PPh_3 and the mixture magnetically stirred for 1 h at room temperature. The clear yellow solution was evaporated to dryness, and the resulting residue was dissolved in a little dichloromethane and purified by thin-layer chromatography (eluent cyclohexane/dichloromethane 2/1). Evaporation of the eluent to dryness in vacuo furnished **8** as a yellow solid (281 mg, 57%). IR (CH_2Cl_2): ν(CO) = 2024(s), 1983(m), 1952(vs); IR (KBr): ν(OCO) = 1597(m), 1421(m), ν(OH) = 3524(m); ^{1}H NMR ($CDCl_3$, 200 MHz): δ = 2.30 (s, br. 6H, CH), 3.61 (s, br, 6H, OH), 7.15 and 7.43 (each m, 90 H, C_6H_5); ^{31}P{^{1}H} NMR ($CDCl_3$, 81.03 MHz): δ = 16.8 (s, 6P, PPh_3).

Received: December 11, 1989 [Z 3680 IE]
German version: *Angew. Chem. 102* (1990) 447

[1] G. R. Crooks, B. F. G. Johnson, J. Lewis, I. G. Williams, G. Gamlen, *J. Chem. Soc. 1969*, 2761.
[2] G. Süss-Fink, G. Herrmann, P. Morys, J. Ellermann, A. Veit, *J. Organomet. Chem. 284* (1985) 263.
[3] M. Spohn, T. Vogt, J. Strähle, *Z. Naturforsch. B41* (1986) 1373.
[4] H. Schumann, J. Opitz, J. Pickardt, *J. Organomet. Chem. 128* (1977) 253.
[5] M. Bianchi, P. Frediani, U. Matteloi, G. Menchi, F. Piacenti, G. Petrucci, *J. Organomet. Chem. 259* (1983) 207.
[6] F. Neumann, G. Süss-Fink, *J. Organomet. Chem. 367* (1989) 175.

[7] M. Bianchi, U. Matteoli, P. Frediani, F. Piacenti, U. Nardelli, G. Pelizzi, *Chim. Ind. (Milan) 63* (1981) 475.
[8] Crystal structure data: The structure was determined with a Stoe-Siemens AED2 four-circle diffractometer ($Mo_{K\alpha}$, graphite monochromator, $\lambda = 0.71073$ Å) using SHELXS-86 [9] and refined with SHELX-76 [10]. **5**: space group *R*3, three independent molecules A, B and C per asymmetric unit; the crystal contains randomly distributed uncoordinated MeCN molecules $a = 17.544(1)$, $b = 17.544(1)$, $c = 62.005(5)$ Å, $\alpha = \beta = 90°$, $\gamma = 120°$, $V = 16528.1$ Å^3, $Z = 9$, $\varrho_{calcd} = 1.500$ g cm^3, $\mu = 11.5$ cm^{-1}, $\theta_{max} = 25°$; 6016 independent reflections, only Lp correction; index limits h: −18/18, k: 0/20, l: 0/73; 4833 reflections with $F_0 > 5\sigma(F_0)$; hydrogen atoms of the OH groups could not be located; refinement with weighted anisotropic temperature factors by the least squares method gave $R = 0.051$, $R_w = 0.050$ with $w^{-1} = \sigma^2(F_0) + 0.0094(F_0^2)$. Residual density in the last difference map 1.12(max) in the neighborhood of the CH_3 carbon atoms of an uncoordinated MeCN molecule, −0.62 (min) Å^{-3}. Further details of the crystal structure investigation are available on request from the Director of the Cambridge Crystallographic Data Centre, University Chemical Laboratory, Lensfield Road, Cambridge CB2 1EW (UK), on quoting the complete literature citation.
[9] G. M. Sheldrick, "SHELXS-86". Program for Crystal Structure Determination, Universität Göttingen 1986.
[10] G. M. Sheldrick, "SHELX-76". Program for Crystal Structure Determination, University of Cambridge (UK) 1976.
[11] W. D. S. Motherwell, W. Clegg, "Pluto". Program for Plotting Molecular and Crystal Structures, University of Cambridge (UK) 1978.

Multiple 1,2-*O*,*O*-Shift of *tert*-Butyldiphenylsilyl Groups in Polyols

By *Johann Mulzer** and *Bernd Schöllhorn*

tert-Butyldimethylsilyl (TBDMS) and *tert*-butyldiphenylsilyl (TBDPS) groups are standard protecting groups for OH functions.[1] The *O*,*O* silyl migration to be expected in polyols was hitherto chiefly observed in the case of the less stable TBDMS unit.[2] In the case of the TBDPS group two examples have been described in the literature, namely a 1,3-shift[3] and 1,2-shift.[4] We now report a multiple 1,2-*O*,*O* migration of TBDPS groups in the polyol derivatives **1**, **2**, **4**–**6**, **8**, **9** and **13**.[5]

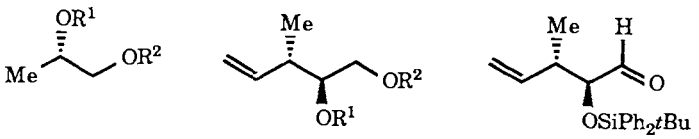

1 **2** **3**

a, $R^1 = t\text{BuPh}_2\text{Si}$, $R^2 = H$
b, $R^1 = H$, $R^2 = t\text{BuPh}_2\text{Si}$

The silyl migration requires base catalysis (standard conditions: potassium carbonate in methanol, 22 °C). **1a** and **2a** then isomerize completely to **1b** and **2b**, respectively. Under neutral or acid conditions the TBDPS group is stable towards migration. Reduction of the aldehyde **3** with lithium aluminum hydride in diethyl ether therefore leads uniformly to **2a**, whereas that with sodium tetrahydroborate in methanol yields **2b** quantitatively. During the reaction **2a** is detectable as intermediate.

Under standard conditions, the triol derivative **4a** forms an 87:7:6 equilibrium mixture (HPLC analysis) of **4c**, **4b** and **4a** in 20 min, from which **4b** can be separated and used again. After 15 min, the same product ratio as from **4a** is obtained, thus proving that the silyl migration proceeds reversibly in both directions. Responsible for the equilibrium

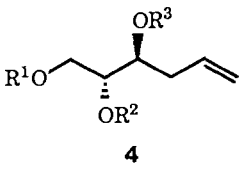

4

4	R^1	R^2	R^3
a	H	H	$t\text{BuPh}_2\text{Si}$
b	H	$t\text{BuPh}_2\text{Si}$	H
c	$t\text{BuPh}_2\text{Si}$	H	H

position is the preference of the bulky TBDPS group for the primary position, which is favored by ca. 8–9 kJ mol^{-1} compared to the secondary positions, but, because of the reversibility of the migration step, is only reached by trial and error. The establishment of equilibrium therefore takes longer the larger the number of the participating OH functions.

The pentol **5a** derived from D-mannitol isomerizes to **5b**, which, because of the C_2 symmetry of the unprotected mol-

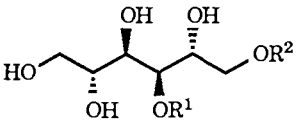

5

5	R^1	R^2
a	$t\text{BuPh}_2\text{Si}$	H
b	H	$t\text{BuPh}_2\text{Si}$

ecule, can be formed by two- or threefold *O*,*O* migration. Both routes are possible, as demonstrated by the uniform formation of **7** from **6a** and **6b**. The *syn*- or *anti*-position of the OH functions to be traversed, and thus the conformational strain in the postulated intermediate **Z**,[2b] apparently have no influence on the product pattern. This experiment also proves that the silyl migration—consistent with **Z**—proceeds with retention at the carbinol centers, since **7** would otherwise be epimerized differently compared to the precursors **6a/b**.

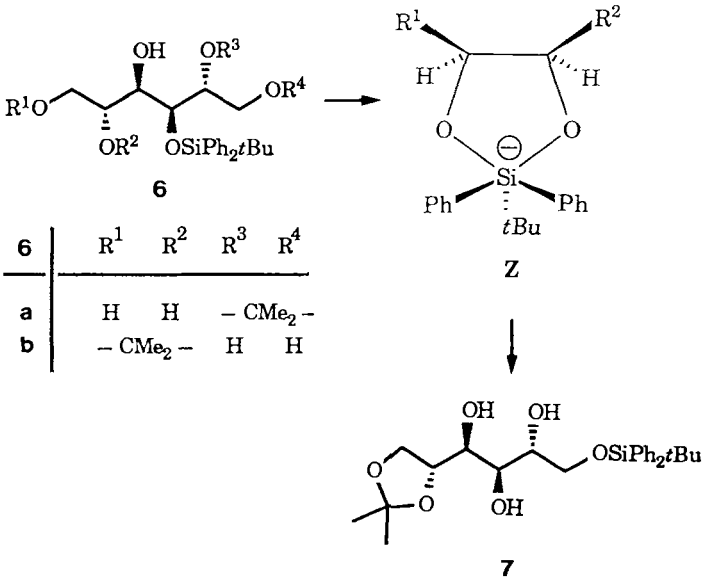

6

6	R^1	R^2	R^3	R^4
a	H	H	$-CMe_2-$	
b	$-CMe_2-$		H	H

Z

7

[*] Prof. Dr. J. Mulzer, Dipl.-Chem. B. Schöllhorn
Institut für Organische Chemie der Freien Universität
Takustrasse 3, D-1000 Berlin 33.

Carbonyl Oxides: Zwitterions or Diradicals?

By Wolfram Sander*

Over the last few years new experimental and theoretical methods have made it possible to gain a more detailed insight into the chemistry of short-lived reaction intermediates. In 1949 *Criegee* postulated the intermediacy of carbonyl oxides in the mechanism of ozonolysis, and since then these species have become the goal of much research effort. Even though the formation of "Criegee zwitterions" during ozonolysis and carbene oxidations was proven by scavenger experiments, the electronic structure—zwitterion or diradical—of this short-lived species is still a subject of debate. To date no stable carbonyl oxide has been found to exist under "normal" laboratory conditions, although by using matrix isolation and laser spectroscopy, it has been possible to obtain highly resolved IR and UV/VIS spectra of carbonyl oxides as well as to determine their dipole moments experimentally. The influence of substituents, exact kinetic data on modes of formation, and the subsequent reactions of carbonyl oxides as well as their photochemistry complete the picture. In accordance with ab initio calculations carbonyl oxides are best viewed as polar diradicals. The zwitterionic state lies at higher energies and should be stabilized by π donors.

1. Introduction

Carbonyl oxides **1** and their isomeric form, the dioxiranes **2**, have become an intensively studied species over the last few years owing to their role in oxygen-transfer reactions. The occurrence of **1** and **2** as short-lived reaction intermediates has been discussed for combustion processes,[1] many "organic" oxidations (ozonolysis, Baeyer–Villiger reaction),[2–5] and enzymatic processes.[6] Furthermore, the use of **1** and **2** in selective oxidations is becoming increasingly important.[3,4,7] The introduction of appropriate substituents causes these species to react with substrates by transfer of O atoms, either in a nucleophilic or electrophilic manner. In contrast to the extremely labile **1**, which has so far only been characterized indirectly or spectroscopically, a number of derivatives of **2** have been isolated in solution or in their pure form at room temperature.[3,4,7]

Carbonyl oxides **1** were first postulated as intermediates in the ozonolysis of olefins by *Criegee* in 1949[2,8] and are also referred to as Criegee zwitterions in the literature. Since then the many experimental and theoretical studies in this area have on the whole substantiated the postulated mechanism in Section 2 [Eq. (2)] in its key points. Nonetheless, a direct proof of the existence of a carbonyl oxide was not achieved until 1983.[9] To prove the existence of **1**, the application of relatively new experimental procedures such as matrix isolation and time-resolved laser spectroscopy was necessary.

Carbonyl oxides are also interesting species from a theoretical point of view. Their isomeric form, the dioxiranes, are molecules with a complete valence shell and are thus easily described in theoretical terms;[10,11] the electronic structure of carbonyl oxides, on the other hand, is still a subject of debate. In most of the experimental work the description as an ylide, **1A** and **1B** [Eq. (1)], originally introduced by *Criegee*, has been invoked. Quite a few important reactions of carbonyl oxides such as 1,3-dipolar cycloaddition, dimerization, and addition to alcohols may be explained in terms of this species. Some of the semiempirical calculations that have been performed postulate a zwitterionic ground state,[12] while ab initio[13–15] and other semiempirical calculations[16,17] predict a diradical ground state **1C**. Experimental evidence also favors a diradical ground state.[12] In a review on ozonolysis in 1975, *Criegee* wrote:[2]

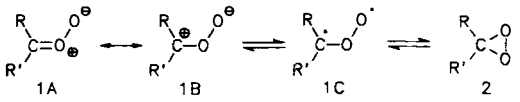

(1)

> Can the view recently expressed by *Goddard* that the so-called carbonyl oxides are singlet diradicals also in solution be confirmed or disproved? Solution of this problem will be of crucial importance for our understanding of the events occurring during the ozonolysis of olefins.

From 1980 onward the development of new experimental and theoretical methods has led to an enormously increased interest in carbene oxidations, carbonyl oxides, and dioxiranes. The use of these new methods in the field of carbonyl oxides is the focus of discussion in this article.

2. The Criegee Zwitterion in Ozonolysis

In the three-step mechanism [Eq. (2)] describing ozonolysis,[2] the initial step involves the 1,3-dipolar cycloaddition of ozone to an olefin, resulting in the formation of a 1,2,3-trioxolane (**3**; "primary" ozonide). In the second step, **3** decomposes to afford a carbonyl compound and **1**. These components react in a further cycloaddition to yield a 1,2,4-trioxolane (**4**; "molozonide"), which may often be isolated from the reaction mixture. The great importance of ozonolysis in

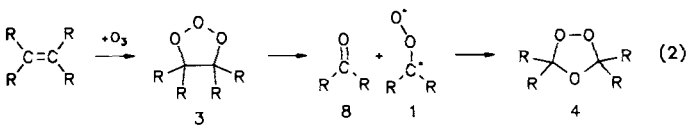

(2)

[*] Priv.-Doz. Dr. W. Sander
Organisch-chemisches Institut der Universität
Im Neuenheimer Feld 270, D-6900 Heidelberg (FRG)

organic chemistry and recently also in the chemistry of the upper atmosphere is reflected in the large number of publications and reviews covering this area.[18-20]

It was possible to confirm the Criegee mechanism by detecting cross products, by carrying out trapping and isotopic labeling experiments, and, finally, by direct detection of the unstable primary ozonides **3**.[2, 18, 19] Recently, the parent compound **3** was detected by microwave spectroscopy as one of the products in the ozonolysis of ethylene.[21] A weak point of the Criegee mechanism is the observed stereoselectivity of ozonolysis: If the proposed three-step mechanism is to operate, *cis* and *trans* olefins should give the same ratio of stereoisomeric molozonides **4** and thus lead to loss of stereochemical information. In fact, *trans* and *cis* olefins with bulky substituents lead mainly to the *trans* and *cis* forms of **4**, respectively. According to a proposal by *Bailey*, the observed stereoselectivity can be explained by a modified mechanism, which rests upon the following points: the cleavage of **3** is presumed to be a concerted process and **1** exists as *syn* or *anti* isomer, the two of which do not equilibrate at room temperature.[14b, 20, 22, 23] With these refinements, the stereochemistry of ozonolysis is determined by the conformation of the primary ozonides **3** and is dependent on the configurational stability of **1**.

In some cases the products of ozonolysis are 1,2,4,5-tetroxanes **5**, which can be viewed as dimers of **1**.[18] Performing the ozonolysis in the presence of alcohols affords alkoxy hydroperoxides **6**, which are formed by addition, no definite spectroscopic evidence exists so far for the alcohol to **1** [Eq. (3)].[18] Apart from these indirect indications, no definite spectroscopic evidence exists so far for the existence of **1** as a reactive intermediate during ozonolysis.

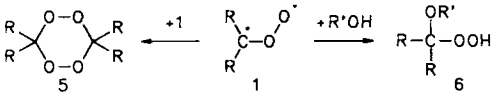

5 1 6 (3)

Suenram and *Lovas* were able to detect the unstable dioxirane **2a**[*] during the gas-phase reaction between ethylene and ozone. Its structure was determined by microwave spectroscopy.[24] Presumably, the thermal relaxation of the "hot" formaldehyde oxide **1a**, formed in the gas phase, is too slow to inhibit the rearrangement to **2a**. Ozonolysis in solution does not produce dioxiranes **2**.

[*] The substituents are given in Scheme 1 (Section 4.2).

3. Oxidation of Diazo Compounds and Carbenes in Solution

Apart from ozonolysis, there are two alternative methods for the preparation of **1** and **2**: the direct reaction of free carbenes **7** with triplet oxygen ($^3O_2$, "triplet path") and the oxidation of diazo compounds **9** with singlet oxygen ($^1O_2$, "singlet path"[25]). A formal "end-on" addition would result in **1**, a "side-on" addition in **2** [Eq. (4)].

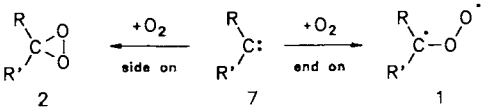

2 7 1 (4)

Kirmse et al. were the first to conduct a selective study in this field.[26] The photooxidation of diphenyldiazomethane (**9b**) in a variety of solvents yielded up to 73% of benzophenone (**8b**); no other products containing oxygen could be detected. It was postulated that the primary adduct arising from photooxidation is benzophenone *O*-oxide, which, in the following step, transfers its terminal O atom to a further molecule of carbene **7b** or diazomethane **9b**.

Bartlett and *Traylor* studied the photooxidation of **9b** with $^{16}O_2$ and $^{18}O_2$ in solid chlorobenzene at $-78\,^{\circ}C$.[27] Under these reaction conditions it was possible to isolate 15% of the tetroxane **5b**, a dimer of **1b**. From their experiments with mixtures of $^{16}O_2$ and $^{18}O_2$, *Bartlett* and *Traylor* were able to conclude that the elimination of O_2 from two molecules of **1b** does not proceed to a significant extent.[27] More recent results by *Girard* and *Griller* show that, if no trapping reagents are present, the extrusion of O_2 from two separate molecules of **1b** can become the main reaction pathway for **1b**, and the formation of **5b**—at least in solution at room temperature—does not occur [Eq. (5)].[28] The activation barrier for this reaction amounts to only 1.8 kcal mol^{-1}.

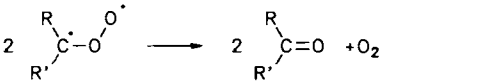

1 8 (5)

Apart from **8** and **5**, other oxidation products that arise from the reaction of **9** are esters (or lactones) **10**. The mechanism of ester formation was elucidated in a number of pub-

Wolfram Sander was born in 1954 in Heidelberg. From 1973 to 1979 he was a student at the Universität Heidelberg, where he subsequently received his Ph.D. in 1982 under R. Gleiter and completed his Habilitation in 1989. He was introduced to the matrix isolation technique as a postdoc with O. L. Chapman in Los Angeles (1982 to 1984). His interests include the characterization of reactive intermediates, oxidation reactions with molecular oxygen, and effect of electron spin on chemical reactivity. In 1988 he was awarded the Karl-Freundenberg-Preis of the Heidelberger Akademie der Wissenschaften, and in 1990 he received a Heisenberg-Stipendium and a Winnacker-Stipendium.

lications by *Sawaki* et al.[29] At first, the formation of **10** was thought to proceed through an intramolecular rearrangement of **2**.

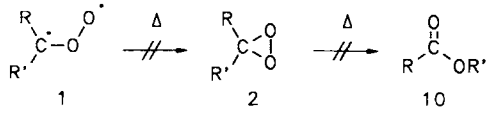

1 2 10 (6)

Since mixed isotopomers of **10** with one atom of ^{16}O and ^{18}O each are formed when mixtures of $^{16}O_2$ and $^{18}O_2$ are used, two molecules of O_2 must participate to form **10**. This excludes **2** as the direct precursor of **10**.[29a] *Sawaki* et al. proposed an alternative explanation in which they presume the presence of **1** as an intermediate. Species **1** reacts with a further molecule of O_2 and then decomposes via different peroxidic species to yield **10** [Eq. (7)].[29a]

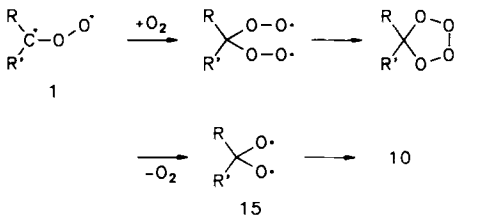

1 15 10 (7)

However, this mechanism is also incompatible with the experimental findings, since the yield of **10** is nearly independent of O_2 pressure. In recent work a radical chain mechanism seems to give a plausible explanation.[29b] According to these results, ester **10** is formed by radical oxidation of a diazo compound (**9**) and not of a free carbene (**7**). The ^{18}O labeling experiments also showed that the rearrangement **1** → **2** is not a thermal process [Eq. (6)].

In the reaction of difluoromethylene (**7s**) with O_2, *McKee* et al. found a species that transfers O atoms stereospecifically onto alkenes.[30] This species was not characterized in detail, yet ab initio calculations make formation of **2s** from the primarily formed compound **1s** plausible.

Besides mechanistic studies, much research has been directed toward the use of the intermediates resulting from the oxidation of **9** as reagents for oxidation. Predominantly the formation of **1** is presumed in these complex reaction mixtures. The most important reactions are the transfer of oxygen onto alkanes,[12] alkenes,[12, 31, 32] sulfides and sulfoxides,[33a, 33b, 34] and aromatic compounds.[35, 36] In the presence of H donors, **1** can react to form autoxidation products.[12] Furthermore, cycloadditions with carbonyl compounds[37, 38] and olefins[39–41] have been reported. The inherent instability of **1** makes it difficult to exclude the possibility that the oxidation proceeds through other peroxidic species, expecially **2**. *Adam* et al. developed an elegant method to distinguish between oxygen-transfer reagents by examining their different nucleophilicities.[33] Thianthrene 5-oxide (**11a**) is prone to nucleophilic oxidation at the sulfoxide S atom, but is oxidized in an electrophilic manner at the sulfide S atom [Eq. (8)].

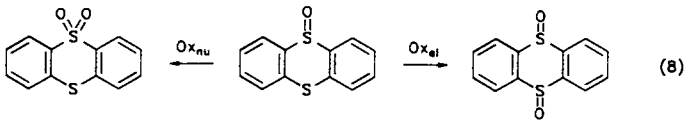

11 11a 12 (8)

From the relative amounts of thianthrene 5,5-dioxide (**11**) and thianthrene 5,10-dioxide (**12**), an X_{Nu} scale ($X_{Nu} = 0$ for electrophiles, $X_{Nu} = 1$ for solely nucleophilic reagents) was developed.[3, 33] Generally, dioxiranes **2** are less nucleophilic ($X_{Nu} \approx 0.7$) than carbonyl oxides **1** ($X_{Nu} > 0.8$). Typical electrophilic oxygenation reagents have even smaller values on the X_{Nu} scale (*m*-chloroperbenzoic acid in CH_2Cl_2, for instance, has $X_{Nu} = 0.36$). According to *Murray*,[4] the nucleophilic properties of dioxiranes are definitely smaller than indicated by an X_{Nu} value of 0.7 and, therefore, the difference to the carbonyl oxides is larger.

From sulfide oxidations[34] and oxidations of naphthalene[42] with a number of *p*-substituted arylcarbonyl *O*-oxides, *Agarwal* and *Murray* obtained positive Hammett constants and came to the conclusion that these oxidations are electrophilic in character. *Ogata* et al. also obtained positive Hammett constants for the oxidation of diphenyl sulfoxide, which indicates the presence of an electrophilic O-transfer process.[12] Obviously, the properties of carbonyl oxides depend strongly on the experimental conditions. Therefore, it became necessary to employ direct spectroscopic methods to come closer to an understanding of the electronic properties and bonding of carbonyl oxides.

4. Spectroscopic Identification of Carbonyl Oxides

To date, all spectroscopically identified carbonyl oxides have been generated by oxidation of free carbenes or diazo compounds. Two techniques—matrix isolation and time-resolved laser spectroscopy—have played an important part in the detection of short-lived species. In both methods the free carbenes are generated by photolysis of either a diazo compound (**9**) or a diazirine (**14**). In contrast to the matrix technique, where the carbene is produced under conditions at which it is stable (low temperature, inert media), the method used by time-resolved spectroscopy is fast detection (μs to ps) under normal laboratory conditions (room temperature, organic solvents). Thus, the two methods go hand in hand.

4.1. Matrix Isolation Technique

Pimentel et al.[43] and *Norman* and *Porter*[44] were the first to use inert-gas matrices to study reactive intermediates. In contrast to organic glasses, which react more or less quickly with free carbenes, the noble gases used in this technique, such as Ne, Ar, Kr, and Xe or nitrogen, are all inert. Through matrix isolation in inert gases it is possible to record highly resolved IR, UV/VIS, luminescence, and ESR spectra and thus to carry out an extensive characterization of reactive intermediates.

A prerequisite for the practicability of the matrix technique as a method to be used extensively in organic chemis-

try was the development of closed-cycle helium cryostats. They allow temperatures as low as 10 K to be attained on a routine basis.[45, 46]

Photolysis of **9** and **14** in a matrix (usually Ar or N_2 at 10 K) generates carbenes **7**, which are stable if they satisfy the following requirements: (1) They do not rearrange intramolecularly. This is why simple alkyl-substituted carbenes that rearrange by a 1,2-shift to give olefins cannot be isolated in a matrix. (2) They are stable to the irradiation that is necessary to photolyze the precursor. Many carbenes are photolabile (phenylmethylene, for instance, easily rearranges photochemically to cycloheptatetraene[47]); therefore, the photolysis should be carried out using the longest wavelength possible and irradiating monochromatically in order to inhibit these side reactions.

The temperature of the matrix influences diffusion processes in a complicated manner[48]. To induce the reaction of **7** with O_2, the matrix is first doped with O_2 (0.2–5%) and then annealed (30–45 K). As long as the matrix is kept at 10 K, even a large excess of O_2 will not lead to a reaction. Once 35 K is reached, however, the oxidation is complete within a few minutes.[49–52] An argon matrix containing small molecules is shown schematically in Figure 1.

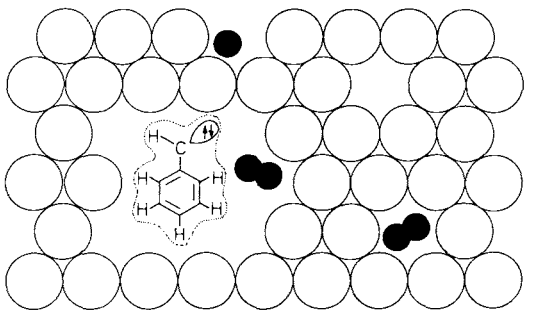

Fig. 1. Schematic representation of an Ar matrix. Open circles, argon atoms; dark circles, small molecules such as N_2 or O_2. At 10 K, diffusion of O_2 is so slow that, even after hours, no oxidation products of carbenes are formed. At 35 K, on the other hand, oxidation is complete within a few minutes.

4.2. Laser Spectroscopy

The great advantage of time-resolved spectroscopy is that it allows the measurement of absolute kinetics; its disadvantage is that the spectroscopic possibilities for structural determination are restricted to the near-UV and visible range with relatively low resolution.[53] Recently, the range has been extended to cover the infrared as well.[54–57] In time-resolved laser spectroscopy, carbonyl oxides **1** are easily detected by observation of their strong band in the visible part of the spectrum, whereas their photoproducts with absorption maxima below 300 nm cannot be monitored.

In order to study carbene oxidations in solution, time resolution in the ns range will suffice. The sample (generally a solution at room temperature) is photolyzed by a short laser pulse, the time resolution being defined by the length of the pulse. The nitrogen (337 nm) and excimer (249 or 308 nm) lasers usually employed have pulse lengths of 5–10 ns.[53] The detection system consists of a source of intense white light and a photomultiplier (for single-channel detection) or an array of diodes (for multichannel detection).

Scheme 1 provides a summary of the carbonyl oxides for which spectroscopic or theoretical data are available.

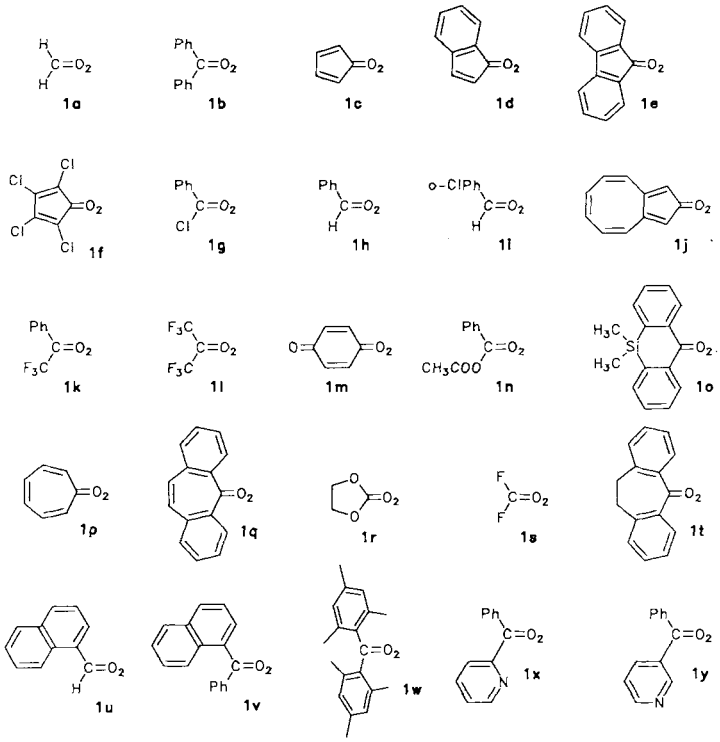

Scheme 1.

4.3. Cyclopentadienone *O*-Oxide

Independently of one another, *Chapman* et al.[58–60] and *Dunkin* et al.[49, 52a] reported the formation of cyclopentadienone *O*-oxide (**1c**) from the matrix oxidation of cyclopentadienylidene (**7c**). *Chapman*'s group studied the photooxidation (irradiation with light at $\lambda > 418$ nm) of diazocyclopentadiene (**9c**) in matrices with high O_2 content (20%). They discovered a product which was assigned structure **1c** owing to its intense IR bands at 1395, 1385, 895, and 741 cm^{-1}.[60]

On the other hand, *Dunkin* et al. described the formation of a different product with IR bands at 1398, 1321, 888, and 758 cm^{-1}. This species, generated by monochromatic irradiation ($\lambda = 296$ nm) of **9c** isolated in a matrix in the presence of 10% O_2, was also assigned structure **1c**.[49] The same IR spectrum was observed when a matrix doped with 1% O_2 and containing carbene **7c** was warmed to 35 K[49] [Eq. (9)].

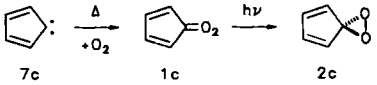

(9)

In a later publication *Dunkin* et al. showed that **1c** is extremely photolabile and that the molecule described by *Chapman* et al. must be an isomer of **1c**, the dioxirane **2c**.[52a] To prove the differing symmetry of **1c** (C_s) and **2c** (C_{2v}),

isotopic labeling with ^{18}O was used.[52a] These experiments indicate clearly that **1c** contains equivalent and **2c** nonequivalent O atoms. A further proof for the structure of **2c** is that, on UV irradiation ($\lambda > 220$ nm), it rearranges to α-pyrone.[46, 52a]

The largest ^{18}O isotopic shifts in **1c** are found for the bands at 1014 (−28) and 947(−22) cm^{-1} (Table 1).[49] These bands lie in a region typical for stretching modes of single bonds and can approximately be assiged to O–O or C–O stretching vibrations. In the region of visible light the spectrum shows an intense absorption with a maximum at 420 nm (Table 1).[61a]

Table 1. Characteristic IR and UV spectroscopic data for some carbonyl oxides **1**.

	ν(O-O) [cm^{-1}] [a] Matrix	Δ [b] [cm^{-1}]	Matrix	π → π* [nm] [c] Laser	Calculation
1b	896 s	−35 (3.9)	422 [d]	410 [e]	455 [f]
1c	1014 m	−28 (2.8)	420 [g]		424 [f]
	947 m	−22 (2.3)			
1d	912 m	–	445 [h, i]		
1e	898 m	–	460 [h, i]	450 [j]	489 [f]
1f			395 [i]		
1g	890 s	−50 (5.6)	400 [k]		
1h	915 m	−30 (3.3)	387 [l]		427 [f]
	890 s	−21 (2.4)			
1i	901 s	−30 (3.3)	406 [m]		
	931 m	−41 (4.4)			
1j	931 s	−42 (4.5)	582 [n]		
		−49 (5.3)			
1k	1009 s	−20 (2.0)	378 [o]		
	943 s	−35 (3.7)			
1l	1049 m	−18 (1.7)	– [o]		
	997 s	−35 (3.5)			
1m	1045 m	−60 (5.7)	462 [p]		468 [f]
	1034 vs	−57 (5.5)			
1n				410 [q]	
1o				425 [r]	
1p					546 [f]
1q					493 [f]
1r					504 [f]
1t				401 [e]	
1u				435 [s]	
1v				405 [e]	
1w				390 [e]	
1x				428 [e]	
1y				418 [e]	

[a] O–O stretching vibration. [b] ^{16}O–^{18}O isotopic shift; in brackets, relative shift in %. [c] Absorption maxima. [d] Ref. [51]. [e] Ref. [68]. [f] Ref. [17]. [g] Ref. [52a]. [h] Ref. [52b]. [i] Ref. [61a]. [j] Ref. [62]. [k] Ref. [65]. [l] Ref. [51]. [m] Ref. [64]. [n] Ref. [73]. [o] Ref. [50]. [p] Ref. [72]. [q] Ref. [71]. [r] Ref. [9]. [s] Ref. [70].

Dunkin et al. also studied indenone *O*-oxide (**1d**),[52b, 61a] fluorenone *O*-oxide (**1e**),[52b, 61a] and tetrachlorocyclopentadienone *O*-oxide (**1f**).[61] The strongest IR bands for **1d** are observed at 912 cm^{-1} and for **1e** at 898 cm^{-1}.[52b] Even though no ^{18}O labeling experiments were performed with **1d** and **1e**, comparison with other carbonyl oxides **1** (see below) convincingly shows that these bands can best be interpreted as O–O stretching modes (Table 1).

Carbonyl oxides **1c**–**1f** show strong absorptions in the visible part of the spectrum between 395 and 460 nm (Table 1).[61a] Absorption in this region is characteristic for **1** and can be used to detect such species in laser photolysis experiments. Of the variety of substituted cyclopentadienone *O*-oxides, only **1e** has been characterized in laser photolysis experiments by *Scaiano* et al.[62] To generate the carbonyl oxide **1e**, diazofluorene (**9e**) was either irradiated in solution at room temperature in the presence of $^3O_2$ (triplet path) or allowed to react with $^1O_2$ (singlet path). Independent of the method of generation, both paths led to a transient species with an absorption maximum at 450 nm.[62] The half-life is strongly dependent on the solvent used and ranges from > 800 μs in benzene to only 9 μs in CH_2Cl_2. On the basis of the kinetic data and the observed absorption maximum, structure **1e** was proposed for the transient species. The above results are in accordance with the data obtained in a matrix and show that the same reactive species is formed both in solution at room temperature and in an inert gas at 10 K. Just as *Criegee* had postulated, **1e** is quickly trapped by reaction with aldehydes.[2] At large enough concentrations of aldehyde, pseudo-first-order kinetics with rate constants between 107 and 109 $mol^{-1}\,s^{-1}$ (in Freon-113) are observed.[62]

4.4. Benzophenone *O*-Oxide and Other Arylcarbonyl Oxides

The chemistry of benzophenone *O*-oxide (**1b**) is well established by trapping experiments in solution, but has also been studied by IR and UV spectroscopy in matrices and with the aid of laser photolysis. In the thermal reaction of diphenylmethylene (**7b**), isolated in a matrix containing $^3O_2$ (Ar, 30–40 K), **1b** is produced in high yield. The product was characterized by UV/VIS and IR spectroscopy as well as by its subsequent photochemistry (Scheme 2).[63, 51] In agreement with the findings from laser photolysis experiments, an intense broad band with $\lambda_{max} = 422$ nm was observed in the visible region of the spectrum (Table 1).[63] This can be taken as proof for the existence of the same products in solution at room temperature and in a matrix at cryogenic temperatures.

The structure of **1b** has been further elucidated by carrying out IR experiments in connection with isotopic labeling analysis. The reaction of [1-^{12}C]-**7b** and [1-^{13}C]-**7b** with $^{16}O_2$ and $^{18}O_2$ leads to four isotopomers of **1b**, thereby

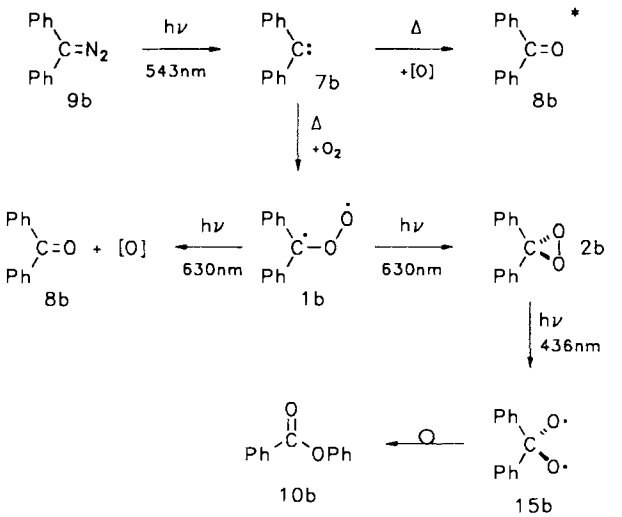

Scheme 2.

allowing a nearly complete assignment of the IR bands.[51] The most intense band in the spectrum is observed at 896 cm^{-1} and exhibits an ^{18}O isotopic shift of 35 cm^{-1} (Table 1). Because of the small shift on labeling of the carbonyl C atom with ^{13}C, one can conclude that this band arises from the O–O stretching vibration. The O–O deformation mode is a weak band at 550 cm^{-1}; in the region typical for the carbonyl vibration, no band is observed.

Like all other carbonyl oxides that have been matrix isolated to date, **1b** is extremely photolabile. Irradiation with light far to the long-wavelength side of the absorption band ($\lambda > 630$ nm) leads to rearrangement (main reaction) to afford diphenyldioxirane (**2b**) or results in cleavage of O atoms (side reaction) to form **8b** (Scheme 2). Presumably, there exists a long-wavelength band of weak intensity that has not been detected so far.[17]

Under these conditions, dioxirane **2b** is stable. On short-wavelength irradiation ($\lambda > 400$ nm), however, it rearranges to the phenyl benzoate (**10b**). On oxidation of **7b** in the matrix, one can also detect an intense chemiluminescence that has been identified as the phosphorescence of **8b**.[51]

Two further carbonyl oxides with absorption maxima at about 400 nm are benzaldehyde *O*-oxide (**1h**)[51] and *ortho*-chlorobenzaldehyde *O*-oxide (**1i**).[64] The absorption spectra of both compounds exhibit distinct vibrational fine structure; for **1i**, ^{18}O isotopic labeling experiments indicate that the vibrational progression corresponds to the O–O stretching mode of its electronically excited state.[64] The vibrational frequency of 901 cm^{-1} in the ground state (Table 1) is reduced to 790 cm^{-1} in the excited state.

Other arylcarbonyl oxides that have been characterized in the matrix are benzoyl chloride *O*-oxide (**1g**)[65] and the CF_3-substituted carbonyl oxides **1k** and **1l**.[50] Whereas the chloro substituent in **1g** hardly has any effect on the characteristic spectroscopic data, the strongly electron-withdrawing CF_3 groups in **1k** and **1l** bring about an increase in the O–O stretching mode—an effect attributed to a strengthening of the O–O bond. On top of that, the UV/VIS absorption maximum is shifted to shorter wavelength (Table 1)[50] in the latter two compounds. The reaction of **7g** with $^3O_2$ is a formally "spin-forbidden" process, because the carbene **7g** has a singlet ground state. As expected, the oxidation proceeds considerably slower than that of triplet carbenes.[65, 64]

Scaiano et al. were able to generate **1b** by laser photolysis in solution at ambient temperatures, via both the triplet-path[66] and the singlet-path.[67] Its existence as a short-lived intermediate was proven by the observation of an intense absorption at 410 nm.[66, 67] If no special trapping reagent is present, **1b** will react according to second-order kinetics.[68] A similar result was obtained by *Girard* and *Griller* with the aid of optical modulation spectroscopy (this method can achieve time resolution into the μs range).[28] Just like *Scaiano*, they found that **1b** disappears in a reaction with bimolecular kinetics, yet they were not able to isolate the dimer **5b**. This observation was made plausible by an alternative reaction path of two molecules of **1b** to yield **8b** and O_2 [Eq. (5)].

Like **1e**, species **1b** is rapidly trapped by aldehydes. The rate constants of the pseudo-first-order reaction in acetonitrile amount to about 10^6 $mol^{-1}\,s^{-1}$[68] and are thus considerably smaller than the corresponding values for **1e**.[62]

Using time-resolved dielectric-loss spectroscopy, *Fessenden* and *Scaiano* estimated the dipole moments of **1b** and **1t** to be 4.0 D and 3.8 D, respectively.[69] These dipole moments are larger than expected for a diradical but considerably smaller than anticipated for a zwitterion, and they give an indication of the complex electronic structure of carbonyl oxides.

Scaiano et al. later studied the absorption spectra and kinetic data of a series of substituted arylcarbonyl *O*-oxides (Table 1).[62, 68, 70] With the exception of **1e**, all absorption maxima fall into the range of 410 ± 20 nm and are hardly dependent on the solvent used. Because of steric interaction, the formation of **1w** from **7w** and $^3O_2$ proceeds more slowly, and the lifetime of **1w** is longer than that of the other carbonyl oxides.[68]

Itoh et al. studied the photooxidation of methyl α-diazophenylacetate (**9n**) and were able to generate carbonyl oxide **1n**.[71] The reaction of **1n** with an excess of methanol was pseudo first order; without methanol, bimolecular kinetics were observed.

4.5. Other Carbonyl Oxides and Analogous Compounds

By laser photolysis of the diazo compound **9o** at room temperature in cyclohexane, *Iwamura* et al. obtained 10,10-dimethyl-10-silaanthracene-9(10*H*)-ylidene (**7o**), which has a lifetime of 870 ns.[9] If the photolysis was carried out in the presence of O_2, carbonyl oxide **1o** was produced, which has a lifetime of 45 μs and exhibits an absorption maximum at 425 nm [Eq. (10)].[9]

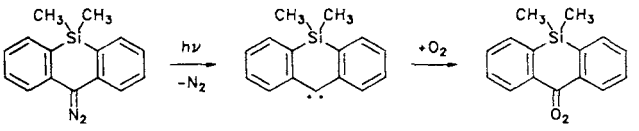

9o 7o 1o (10)

Another cyclic carbonyl oxide that has been monitored in a matrix is *para*-benzoquinone *O*-oxide (**1m**).[72] Since **1m** not only contains a carbonyl group but also a carbonyl oxide functionality, a direct comparison of these two functional groups becomes possible. The O–O stretching mode at 1034 cm^{-1} shows an intensity similar to that of the C–O stretching vibration of the carbonyl group and exhibits an ^{18}O isotopic shift of 57 cm^{-1}. This large isotopic shift indicates that little coupling with other vibrations occurs, so that a force constant corresponding to an O–O single bond may be taken as a good estimate.[72] In contrast to **1m** with its π-acceptor group, bicyclo[6.3.0]undeca-2,4,6,8,11-pentaen-10-one *O*-oxide (**1j**) contains a π-donor group.[73] This effects a strong redshift of the $\pi \rightarrow \pi^*$ band (see Section 5.3.2). The photochemistry of **1m** and **1j** is analogous to that of other carbonyl oxides (Scheme 4): long-wavelength irradiation (630 nm for **1m** or 480 nm for **1j**) yields the spirodioxiranes **2m** and **2j**, respectively. These compounds rearrange to the lactones **10m** and **10j** if irradiation is continued at shorter wavelength (436 nm for **2m** or 350 nm for **2j**).[72, 73]

The reaction of methylene (**7a**) with O_2 in an Ar matrix was studied by *Lee* and *Pimentel*.[74] They were not able to detect **1a** or **2a**, but found formic acid as the main product, which in part is produced in an electronically excited state.

In contrast to the reaction of carbenes **7**, little is known about the reaction of silanediyls ("silylenes") **16** with O_2.[75] The formation of an adduct of dimesitylsilanediyl (**16a**) and O_2 was described by *Ando* et al. (Scheme 3).[76] On the basis of isotopic labeling experiments and ab initio calculations, the adduct was assigned the structure of dimesitylsilanone *O*-oxide (**17a**). Compound **17a** is photolabile, but the photoproducts were not characterized. In contrast to **16a**, the thermal reaction of dimethylsilanediyl (**16b**) with O_2 leads to the formation of dimethyldioxasilirane (**18b**) as the sole product, which on irradiation rearranges to methoxymethylsilanone (**19**) [Eq. (12)].[77a]

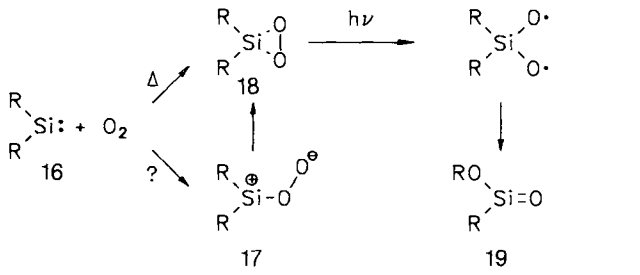

Scheme 3.

The halogenated silanediyls **16c** and **16d** do not react thermally with O_2 in the gas phase or in the matrix to an appreciable extent, yet on irradiation they are photooxidized to the dioxasiliranes **18c** and **18d**, which are stable towards UV irradiation.[77b]

5. Formation and Properties of Carbonyl Oxides

5.1. Mechanism of Carbene Oxidation

Carbenes **7** formed by photolysis of **9** or **14** are primarily generated in the singlet state; in the case of triplet carbenes the triplet ground state is reached through fast intersystem crossing (ISC). Thermal reactions in the matrix generally occur from the ground state, whereas, in reactions in solution at room temperature, low-lying excited states may play an important part (Scheme 4).[78]

The reaction of triplet carbenes (T-7) with $^3O_2$ is an extremely fast process (controlled by diffusion); the formally "spin-forbidden" reaction of singlet carbenes, on the other hand, is very slow[64,65] and cannot be detected by time-resolved spectroscopy in solution.[79]

Since the reaction of **7** with O_2 is very exothermic (for the formation of **1a**, ca. 47 kcal mol^{-1}),[15] the primary products of carbene oxidations, carbonyl oxides **1**, are generated in vibrationally excited states. Their stabilization occurs either through relaxation to the thermal ground state (internal

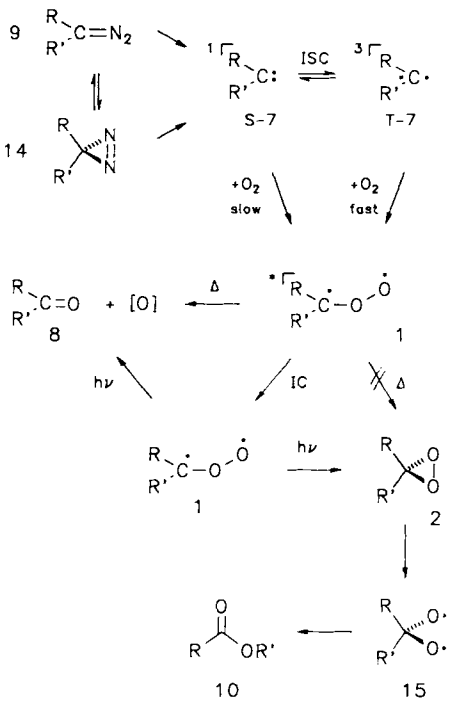

Scheme 4.

conversion, IC) or by extrusion of an O atom and subsequent formation of a carbonyl compound (**8**, Scheme 4). The ratio of **1** to **8** is strongly dependent on the substituents at the carbene center. Especially in the case of H atoms as substituents (**1h**, **1i**), the extrusion of O atoms predominates and **1** is formed only in low yields.[51,80]

According to ab initio calculations (MP2/6-31G*) performed by *Cremer* et al., the rearrangement **1a** → **2a** shows an activation barrier of 22.8 kcal mol^{-1} and is exothermic by 34.5 kcal mol^{-1} (according to *Kafafi* et al., 44.1 kcal mol^{-1}[15]) (Fig. 2).[14d] The activation barrier depends on

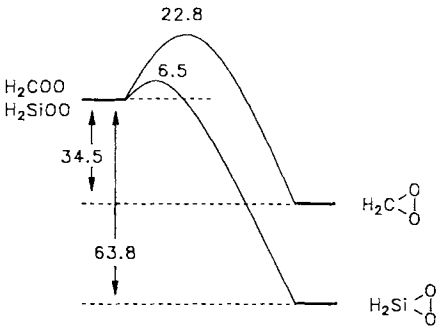

Fig. 2. MP2/6-31G*-calculated barrier of activation and reaction energies [kcal mol^{-1}] for the rearrangements **1a** → **2a** (Ref. [14d]) and **17** → **18**, R = H (Ref. [77a]).

the substituents and is diminished by π-donor ligands. In agreement with these findings, the thermal rearrangement does not occur in solution or in the matrix. In contrast, the rearrangement of silanone *O*-oxides **17** to dioxasiliranes **18** exhibits an activation barrier of only 6.5 kcal mol^{-1} and, consequently, the formation of the three-membered ring **18** is observed.[77a]

Since **1** reacts quickly with alcohols[71] and aldehydes,[68] an important step in the Criegee mechanism of ozonolysis could be verified by direct observation. A reaction competing with the formation of trapped species is that of **1** with itself to yield **5** or **8** and O_2.[27,28]

Irradiation of **1** with red light (presumably into an $n \rightarrow \pi^*$ transition) will either lead to the rearranged species **2** or to the formation of **8** with concomitant extrusion of O atoms. The ratio of **2** to **8** is again influenced by the substituent on **1**. For example, **1m** rearranges completely to **2m**, whereas the aldehyde *O*-oxides (**1h** and **1i**) afford mainly **8**. Therefore, one can selectively generate either **1**, **2**, or free O atoms just by choosing the appropriate substituents and reaction conditions. O atoms in their $O(^3P)$ state (ground state) are only detected indirectly in the matrix. A reaction easily monitored by IR spectroscopy is the oxidation of arylaldehydes to carboxylic acids. This insertion presumably proceeds via intermediate formation of benzoyl and hydroxyl radicals, which recombine instantly to yield carboxylic acids. The activation barrier for the reaction of $O(^3P)$ with acetaldehyde was determined in molecular beam experiments (gas phase) to be 2.4 kcal mol^{-1} by *Kleinermanns* and *Luntz*.[81] In analogy to the H-atom abstraction reactions of free carbenes at cryogenic temperatures[82] described by *Platz*, these H-atom abstractions may also be explained by invoking a quantum-mechanical tunneling effect.

Dioxiranes **2** are much more photostable than carbonyl oxides **1**, so that irradiation with blue or UV light is necessary to form **10**. The rearrangement proceeds by primary cleavage of the weak O–O bond (activation barrier 12–15 kcal mol^{-1})[15] and subsequent migration of a substituent R (Scheme 4). An extrusion of O atoms from **2** and formation of **8** was not observed.

5.2. Chemiluminescence

An interesting phenomenon in carbene oxidations, discovered by *Trozzolo* et al., is chemiluminescence.[83] On warming a solution of carbene **7b** (generated by photolysis of **9b**) in an organic glass in the presence of O_2, an intense blue light is emitted. A similar phenomenon was observed by *Wasserman* et al. when bis(trifluoromethyl)diazomethane (**9l**) was photooxidized.[84] In both cases the chemiluminescence spectra match the phosphorescence spectra of the corresponding carbonyl compounds **8b** and **8l**. *Turro* et al. were able to show that chemiluminescence is a general occurrence in the reaction of arylcarbenes with organic glasses as long as the corresponding carbonyl compound **8** also shows phosphorescence.[85] To explain these observations, a mechanism involving the transfer of a terminal O atom of **1** onto a molecule of O_2 was proposed [Eq. (14)], although it was not possible to detect ozone and **1** in these experiments.[85]

An alternative explanation for this chemiluminescence was provided by *Sawaki* and *Iwamura*.[29a] They proposed that the decomposition of cyclic peroxides [Eq. (7)] may be the cause of chemiluminescence. However, their hypothesis was not substantiated by any experiments.

In all cases the chemiluminescence spectrum is equivalent to the phosphorescence spectrum of the carbonyl compound generated by carbene oxidation. It should be noted that for aryl ketones spin inversion (ISC) of the electronically excited singlet state to the triplet state is extremely effective, so that, on excitation with light, only phosphorescence and no fluorescence is emitted.[86] Therefore, the observation of phosphorescence does not prove that the carbonyl compound is formed directly in the triplet state. Considering the case of bis(trifluoromethyl)methylene (**7l**), where, on oxidation, the chemiluminescence corresponds solely to the phosphorescence of **8l** (on excitation with light, both fluorescence and phosphorescence are observed),[87] one can conclude that hexafluoroacetone (**8l**)—and most probably also the other ketones—is formed directly in its triplet state.[50]

Possible reaction sequences that can lead to triplet carbonyl compounds—and thus to chemiluminescence—are listed in Equations (11)–(14). Reactions (11)–(13) are examples of the transfer of O atoms from a variety of sources onto a free carbene. Reaction (14) corresponds to the mechanism proposed by *Turro* et al.[85]

$$RR'C: + {}^3O_2 \longrightarrow {}^3RR'C{=}O + [O] \quad (11)$$

$$RR'C: + O(^3P) \longrightarrow {}^3RR'C{=}O \quad (12)$$

$$RR'C: + O_2{=}CRR' \longrightarrow {}^3RR'C{=}O + O{=}CRR' \quad (13)$$

$$RR'C{=}O_2 + {}^3O_2 \longrightarrow {}^3RR'C{=}O + O_3 \quad (14)$$

In the matrix, chemiluminescence occurs immediately after warming to temperatures above 10 K. At temperatures lower than 25 K, even the diffusion of small molecules such as O_2 is slow.[48] The observation of chemiluminescence at temperatures below 20 K cannot be explained by reactions (11), (13), and (14). Reaction (14) can also be excluded on other grounds. First, ozone is formed only as a byproduct at high O_2 concentrations, whereas reaction (14) requires the formation of equimolar amounts. Second, chemiluminescence already commences at temperatures below 20 K, when no carbonyl oxide has been formed in the matrix yet, and subsides after only a few minutes at 30 K, even though plenty of carbonyl oxide is now present in the matrix and the mobility of O_2 is very large.[50,51,64]

To exclude O_2 as a reaction component, the rate of formation of carbonyl oxides (a reaction in which O_2 participates) was compared to the rate at which the intensity of chemiluminescence decreases at constant temperature. It could be shown that chemiluminescence decreases four times as fast as carbonyl oxides are formed. It seems reasonable to conclude that the occurrence of chemiluminescence arises from diffusion of a species smaller than O_2.[51] Finally, reaction (11) is endothermic according to thermochemical estimates—at least for **7h**—and may also be excluded.[51]

The best explanation for all of the observations made is the presumption that the reaction of an O atom with **7** is the cause of chemiluminescence [Eq. (12)]. The multiplicity of the carbene (triplet or singlet) does not have much influence on this reaction and the carbonyl compounds are formed directly in their triplet states.

5.3. Influence of Substituents

5.3.1. IR Spectra

A characteristic feature of the IR spectrum of **1** is its intense bands between 890 and 1050 cm^{-1}, which show a large ^{16}O–^{18}O isotopic shift (30–60 cm^{-1}) and are assigned to O–O stretching modes (Table 1). In some cases, a splitting of the bands into two components is observed. This can be attributed either to Fermi resonance or to matrix cage effects. When **1** is unsymmetrically substituted, the occurrence of two bands could also be caused by the existence of *syn* and *anti* isomers. However, there is no experimental evidence for this suggestion.

According to the simple model for a diatomic harmonic oscillator, the highest possible isotopic shift for the O–O vibration amounts to 5.7% if both ^{16}O atoms are replaced by ^{18}O atoms. This maximum value is almost reached by the values monitored for **1g** (5.6%) and **1m** (5.5% and 5.7%; Table 1). These carbonyl oxides exhibit nearly pure O–O vibrations without coupling with other vibrations. For **1b** with its isotopic shift of 3.9% for the band at 896 cm^{-1}, the calculated contribution of the O–O vibration is 68%. The estimated force constant is typical for O–O single bonds.[72] Therefore, O–O bonds in **1** should best be described as single bonds.

The relationship between the position of the O–O stretching mode and the substituents of **1** becomes evident from Table 1. Electron-withdrawing groups shift the bands to higher frequencies. Compared to a phenyl group, a CF_3 group induces a shift of 50 cm^{-1}. Even more effective is the dienone moiety as π acceptor in the quinone **1m**: here, the band is shifted by 138 cm^{-1} to higher frequencies as compared to **1b**. On the other hand, replacing a phenyl group by an H or Cl atom hardly influences the O–O vibration at all. The O–O bond is stabilized by electron acceptors, π acceptors giving rise to larger effects than σ-acceptors.

A weak IR band in the region between 550 and 740 cm^{-1} also shows a marked ^{16}O–^{18}O isotopic shift (0.7–1.9%) and is assigned to an O–O deformation vibration.[51, 72]

Whereas the O–O stretching vibration of **1** is a characteristic group frequency, it is difficult to unequivocally assign the C–O stretching vibration to any of the observed bands. In the "carbonyl region" no absorptions are registered. The C–O stretching vibration is strongly coupled with other vibrations, is of low intensity, and—in comparison to C=O vibrations of carbonyl compounds—is shifted to lower wave numbers. Thus, the electronic structure of a carbonyl oxide group is characterized by a C–O bond of low polarity and a C–O bond order of less than 1.5 and is fundamentally different from that of a normal carbonyl group.

To verify the assignments mentioned above, a comparison of the experimental data with quantum-mechanical calculations seems in order. Unfortunately, the calculation of IR spectra by exact ab initio methods can only be achieved through great computational effort, so that, to date, only calculations on **2a** have been performed on this scale (Table 2).[14c] The comparison with the experimental data for **1m** indicates that not only the position but also the amount of the isotopic shift of the O–O stretching mode and the O–O deformation vibration is well reproduced by the calculations.

Table 2. Comparison of MP2/6-31G* vibrational frequencies of **1a** with experimental frequencies of **1m**.

Assignment	**1a** ν(O-O) [a] [cm^{-1}]	Δ [b] [cm^{-1}]	**1m** ν(O-O) [c] [cm^{-1}]	Δ [b] [cm^{-1}]
ν_4/δ(COO)	1222 (7)	−32 (2.6)	1241 (m)	−6 (0.5)
ν_5/ν(CO)	1116 (52)	−22 (2.0)	1327 (w)	−16 (1.2)
ν_6/ν(OO)	1028 (100)	−49 (4.8)	1034 (vs)	−57 (5.5)
ν_7/δ(COO)	522 (1.2)	−18 (3.4)	570 (w)	−11 (1.9)

[a] Ab initio frequencies of **1a** scaled by 0.93; in brackets, relative intensities. [b] ^{16}O–^{18}O isotopic shift; in brackets, relative shift in %. [c] Experimental data for **1m**; in brackets, relative intensities.

5.3.2. UV Spectra

In the near-UV and visible region of the spectrum of **1** (λ = 380–460 nm) one observes intense and broad absorptions that, in some cases, also exhibit fine structure (Table 1). For **1i** the fine structure is caused by the O–O stretching vibration of the COO group.[64] Owing to this absorption in the visible region of the spectrum, carbonyl oxides isolated in a matrix are yellow to orange, except for **1j**, which is blue.

In order to calculate the UV/VIS transitions, the semiempirical CNDO/S method[88] is appropriate, since it is ideally suited to compute $\pi \rightarrow \pi^*$ and $n \rightarrow \pi^*$ transitions (Table 1). According to the CNDO/S calculations, one expects two characteristic absorptions for carbonyl oxides in the visible region of the spectrum: a very strong $\pi \rightarrow \pi^*$ transition and a weak $n \rightarrow \pi^*$ transition.[17]

The $\pi \rightarrow \pi^*$ transition with $\lg \varepsilon \approx 4$ is the strongest transition in the spectrum and is situated between 378 and 582 nm depending on the substituents (Table 1). Because of the strong intensity and the favorable position of this band in the spectrum, it is especially important for the detection of carbonyl oxides. The comparison of the calculated data with experimental results derived from matrix and laser photolysis studies (Table 1) reveals an excellent agreement between theory and experiment. The largest discrepancy in the calculated and experimental maxima is observed for **1b** (33 nm).

The position of the $\pi \rightarrow \pi^*$ transition depends on the size of the π system and the electronic properties of the substituents (π donor or π acceptor). Large conjugated π systems such as those in **1e**, **1c**, **1m**, or **1p** induce a redshift when compared to **1a**. However, a large redshift is found for **1r**, which features only a small π system (Table 1). Consequently, π donors (like the O atoms in **1r**) also lead to a redshift of the $\pi \rightarrow \pi^*$ transition. The opposite is true for electron acceptors: the $\pi \rightarrow \pi^*$ transition of shortest wavelength is observed at 378 nm for **1k**.

The influence of the π system becomes evident from the comparison of **1c** and **1p** with their benzoannelated derivative **1e** and **1q** (Table 1).[17] Compared to **1a**, the tropylidene group (a π donor) in **1p** induces a redshift of 162 nm. In contrast, the cyclopentadienyl group in **1c** shifts the band into the red by only 40 nm. Benzoannelation leads to reverse effects in both compounds: in **1p** to a blueshift (from 546 nm in **1p** to 493 nm in **1q**) and in **1c** to a redshift (from 424 nm in **1c** to 489 nm in **1e**). This can be explained by the larger π systems in the benzoannelated derivatives, in that they can delocalize the charge more effectively and consequently reduce the influence of the tropylidene or cyclopentadienyl group on the COO moiety. The calculated redshift of the

$\pi \rightarrow \pi^*$ transition induced by π donors[17] was impressively verified by experiment: the carbonyl oxide **1j**, which contains the bicyclo[6.3.0]undecapentaenyl framework as a π donor, is blue and exhibits the highest long-wavelength absorption, with a maximum at 582 nm.[73]

The calculated, extremely weak $n \rightarrow \pi^*$ transitions are situated in the red part of the spectrum (598–895 nm) and have not actually been measured up to now. An indirect indication of their existence is the photochemistry carried out at long wavelengths. The rearrangement of **1** to **2** on irradiation at wavelengths lying far from the $\pi \rightarrow \pi^*$ transition can best be explained by a long-wavelength transition of low intensity.

5.3.3. *Calculations*

Whereas only a few simply substituted carbonyl oxides have been subject to calculation by ab initio methods (**1a**[13, 14a, 14d, 15, 89, 90] and **1s**[14d, 30] as well as some alkyl-substituted derivatives[14a, 14d, 15]), the semiempirical MINDO/3 method[91, 92] allows the inclusion of larger substituents.[17] Nonetheless, just as in the ab initio methods, the semiempirical calculations require that one exceed the RHF level and perform 2X2 CI[16] or UHF calculations.[17, 93]

The calculated spin densities indicate that in π-substituted carbonyl oxides—like **1b** and **1h** or the cyclic carbonyl oxides **1m**, **1c**, and **1p**—the wave functions have diradical character.[17] The spin polarization of the π system and the O–O bond length (Table 3) are influenced by the substituent only to a minor extent. The influence of the phenyl group largely manifests itself in the extension of the π system and transfer of some π-electron density onto the COO group. The result is an enhanced p_π–p_π repulsion in the 3-center 4π-electron system and thus a lengthening of the C1–O1 and O1–O2 bond.

Table 3. Ground-state properties of some carbonyl oxides, calculated with the MINDO/3-UHF procedure (bond lengths R, bond angles, atomic charges, p_π-spin densities).

	R(CO) [Å]	R(OO) [Å]	<COO [°]	Atomic charge C(1)	O(1)	O(2)	N_π [a]	p_π-Spin densities [b] C(1)	O(1)	O(2)
1a	1.281	1.269	124.0	0.074	0.183	−0.331	4.000	0.653	−0.253	−0.400
1b	1.313	1.280	124.9	0.124	0.087	−0.298	4.004	0.640	−0.289	−0.497
1c	1.305	1.280	122.9	0.203	0.084	−0.256	3.928	0.528	−0.278	−0.582
1e	1.305	1.280	124.0	0.150	0.090	−0.281	3.969	0.576	−0.286	−0.521
syn-**1h**	1.298	1.279	125.2	0.113	0.118	−0.296	4.006	0.619	−0.285	−0.491
1m	1.325	1.278	123.0	0.167	0.069	−0.232	3.928	0.528	−0.278	−0.582
1p	1.329	1.279	123.9	0.127	0.071	−0.273	4.038	0.549	−0.312	−0.536
1q	1.321	1.277	130.0	0.126	0.065	−0.285	4.010	0.585	−0.302	−0.521
1r	1.348	1.293	125.5	0.769	−0.056	−0.282	4.276	0.026	−0.015	−0.006
1s	1.294	1.270	132.6	1.015	−0.123	−0.111	4.202	0.044	−0.034	−0.008

[a] Number of π electrons in the COO group. [b] Positive values correspond to an excess of α-spin density, negative values to an excess of β-spin density.

In the cyclic carbonyl oxides the π-electron density in the COO group can either be enhanced (ring as π donor as in **1p** or **1g**) or diminished (ring as π acceptor as in **1e**, **1c**, or **1m**); π donors effect a lengthening of the C1–O2 bond, π acceptors a reduction. The stabilization of the COO group by π acceptors and its destabilization by π donors is not reflected by the calculated O1–O2 bond lengths, which are almost constantly calculated at 1.28 Å (Table 3) but is in agreement with the experimental results. The O–O stretching vibration is shifted to higher wavelengths by electron acceptors, which indicates a stabilization of the O1–O2 bond.

A more dramatic influence on the wave function is calculated for electronegative elements such as O in **1r** and F in **1s**. In these cases only a small amount of spin polarization of the π system remains and the UHF result is identical to the RHF result to a high degree; the wave function is that of a zwitterion. Carbon atom C1 bears a large positive charge in **1r** and **1s** (Table 3).

From the MINDO/3 calculations some general conclusions can be drawn:

1. π acceptors lead to a transfer of π-electron density from the COO group onto the substituent. In consequence, the COO group is stabilized.
2. π donors lead to a transfer of π-electron density of the substituent onto the COO group. Thus, the COO group is destabilized.
3. The C–O bond length is more strongly influenced by substituents than the O–O bond length.
4. Strong σ-acceptors (e.g., O or F) can compensate for the π-electron effects and, in particular, may lead to a more stable zwitterionic state.

On comparing theoretical and experimental results it is important to consider the influence of solvent effects. Polar solvents can stabilize zwitterionic states more strongly than diradical states and can therefore counteract the substituent effects discussed above.[13]

6. Conclusion and Outlook

The experimental and theoretical research discussed in this review gives a relatively consistent picture of the electronic structure of carbonyl oxides. Thus, carbonyl oxides in the ground state in the matrix are polar diradicals. This form should not be mistaken with a zwitterionic state, which lies at higher energy. the O–O bond is best described in terms of a polar single bond, while the C–O bond is less polar and exhibits a bond order of ca. 1.5. Considering that the absorption spectra of carbonyl oxides are very similar in the matrix and in solution at room temperature (Table 1) and that the absorption maxima are only slightly influenced by the polarity of the solvent, it can be concluded that, also in solution, the ground state is best described as a diradical species. Once π-electron donors are introduced (e.g., as in **1r**) carbonyl oxides with a zwitterionic ground state should arise. The experimental verification of a carbonyl oxide with such a zwitterionic ground state has yet to be achieved.

I thank my co-workers G. Bucher, A. Patyk, and A. Runge, whose particular dedication—often at unearthly times of the day—made a completion of our work in the field of matrix spectroscopy possible. My thanks are also due to Prof. Dr. R. Gleiter for generous support over the last years, Dr. P. Bischof for assistance in theoretical matters, Prof. Dr. D. Cremer for excellent cooperation on the calculation of the properties of carbonyl oxides, and Prof. Dr. B. Giese for his help concerning instrumental aspects.—This work was supported by the

Deutsche Forschungsgemeinschaft ("Noncovalent Interactions" and SFB 247), the Stiftung Volkswagenwerk, and the Fonds der Chemischen Industrie.

Received: October 11, 1989 [A757 IE]
German version: *Angew. Chem. 102* (1990) 362

[1] J. A. Miller, G. A. Fisk, *Chem. Eng. News 65* (1987), No. 35 from August 31, 1987, p. 22.
[2] R. Criegee, *Angew. Chem. 87* (1975) 765; *Angew. Chem. Int. Ed. Engl. 14* (1975) 745.
[3] W. Adam, R. Curci, J. O. Edwards, *Acc. Chem. Res. 22* (1989) 205.
[4] R. W. Murray, *Chem. Rev. 89* (1989) 1187.
[5] R. W. Murray, V. Ramachandran, *Photochem. Photobiol. 30* (1979) 187.
[6] T. A. Dix, S. Benkovic, *Acc. Chem. Res. 21* (1988) 101.
[7] R. W. Murray, *Mol. Struct. Energ. 6* (1988) 311.
[8] R. Criegee, G. Wenner, *Justus Liebigs Ann. Chem. 564* (1949) 9.
[9] T. Sugawara, H. Iwamura, H. Hayashi, A. Sekiguchi, W. Ando, M. T. H. Liu, *Chem. Lett. 1983*, 1261.
[10] D. Cremer, M. Schindler, *Chem. Phys. Lett. 133* (1987) 293.
[11] W. Adam, Y. Y. Chan, D. Cremer, J. Gauss, D. Scheutzow, M. Schindler, *J. Org. Chem. 52* (1987) 2800.
[12] Y. Sawaki, H. Kato, Y. Ogata, *J. Am. Chem. Soc. 103* (1981) 3832.
[13] L. B. Harding, W. A. I. Goddard, *J. Am. Chem. Soc. 100* (1978) 7180.
[14] a) D. Cremer, *J. Am. Chem. Soc. 101* (1979) 7199; b) *ibid. 103* (1981) 3627; c) J. Gauss, D. Cremer, *Chem. Phys. Lett. 133* (1987) 420; d) D. Cremer, T. Schmidt, J. Gauss, T. P. Radhakrishnan, *Angew. Chem. 100* (1988) 431; *Angew. Chem. Int. Ed. Engl. 27* (1988) 427.
[15] S. A. Kafafi, R. I. Martinez, J. T. Herron, *Mol. Struct. Energ. 6* (1988) 283.
[16] L. A. Hull, *J. Org. Chem. 43* (1978) 2780.
[17] D. Cremer, T. Schmidt, W. Sander, P. Bischof, *J. Org. Chem. 54* (1989) 2515.
[18] R. L. Kuczkowski (*Ozone and Carbonyl Oxides*) in A. Padwa (Ed.): *1,3-Dipolar Cycloaddition Chemistry*, Wiley, London 1984, Chapter 11.
[19] P. S. Nangia, S. W. Benson, *J. Am. Chem. Soc. 102* (1980) 3105.
[20] P. S. Bailey: *Ozonation in Organic Chemistry*, Academic, New York 1982.
[21] J. Z. Gillies, C. W. Gillies, R. D. Suenram, F. J. Lovas, *J. Am. Chem. Soc. 110* (1988) 7991.
[22] P. S. Bailey, A. Rustaiyan, T. M. Ferrell, *J. Am. Chem. Soc. 98* (1976) 638.
[23] D. Cremer, *Angew. Chem. 93* (1981) 934; *Angew. Chem. Int. Ed. Engl. 20* (1981) 888.
[24] R. D. Suenram, F. J. Lovas, *J. Am. Chem. Soc. 100* (1978) 5117.
[25] D. P. Higley, R. W. Murray, *J. Am. Chem. Soc. 96* (1974) 3330.
[26] W. Kirmse, L. Horner, H. Hoffmann, *Chem. Ber. 614* (1958) 19.
[27] P. D. Bartlett, T. G. Traylor, *J. Am. Chem. Soc. 84* (1962) 3408.
[28] M. Girard, D. Griller, *J. Phys. Chem. 90* (1986) 6801.
[29] a) K. Ishiguro, K. Tomizawa, Y. Sawaki, H. Iwamura, *Tetrahedron Lett. 26* (1985) 3723; b) K. Ishiguro, Y. Hirano, Y. Sawaki, *J. Org. Chem. 53* (1988) 5397.
[30] M. Rahman, M. L. McKee, P. B. Shevlin, R. Sztyribicka, *J. Am. Chem. Soc. 110* (1988) 4002.
[31] W. A. Pryor, C. K. Govindan, *J. Am. Chem. Soc. 103* (1981) 7681.
[32] T. A. Hinrichs, V. Ramachandran, R. W. Murray, *J. Am. Chem. Soc. 101* (1979) 1282.
[33] a) W. Adam, W. Haas, G. Sieker, *J. Am. Chem. Soc. 106* (1984) 5020; b) W. Adam, H. Dürr, W. Haas, B. Lohray, *Angew. Chem. 98* (1986) 85; *Angew. Chem. Int. Ed. Engl. 25* (1986) 101.
[34] S. K. Agarwal, R. W. Murray, *Isr. J. Chem. 23* (1983) 405.
[35] S. Kumar, R. W. Murray, *J. Am. Chem. Soc. 106* (1984) 1040.
[36] R. W. Murray, S. Kumar (*Oxidation of Phenanthrene with a Carbonyl Oxide*) *Polynucl. Aromat. Hydrocarbons: Int. Symp. 7th, 1982*, Butterworth, Boston, USA 1983, pp. 575–581.
[37] W. H. Bunnelle, E. O. Schlemper, *J. Am. Chem. Soc. 109* (1987) 612.
[38] K. Griesbaum, W. Volpp, R. Greinert, *J. Am. Chem. Soc. 107* (1985) 5309.
[39] H. Keul, R. L. Kuczkowski, H.-S. Choi, *J. Org. Chem. 50* (1985) 3365.
[40] M. Mori, M. Nojima, S. Kusabayashi, *J. Am. Chem. Soc. 109* (1987) 4407.
[41] P. R. Story, J. R. Burgess, *J. Am. Chem. Soc. 89* (1967) 5726.
[42] S. K. Agarwal, R. W. Murray, *Photochem. Photobiol. 35* (1982) 31.
[43] E. Whittle, D. A. Dows, G. C. Pimentel, *J. Chem. Phys. 22* (1954) 1943.
[44] I. Norman, G. Porter, *Nature 174* (1954) 508.
[45] A. J. Barnes, W. J. Orville-Thomas, A. Müller, R. Gaufres: *Matrix Isolation Spectroscopy: Nato Advanced Study Institutes Series, Series C, Vol. 76*, Reidel, Dordrecht 1981.
[46] B. Meyer: *Low Temperature Spectroscopy*, American Elsevier, New York 1971.
[47] R. J. McMahon, C. J. Abelt, O. L. Chapman, J. W. Johnson, C. L. Kreil, J. P. LeRoux, A. M. Mooring, P. R. West, *J. Am. Chem. Soc. 109* (1987) 2456.
[48] G. C. Pimentel (*Radical Formation and Trapping in the Solid Phase*) in A. M. Bass, H. P. Broida (Eds.): *Formation and Trapping of Free Radicals*, Academic, New York 1960, pp. 69–115.
[49] G. A. Bell, I. R. Dunkin, *J. Chem. Soc. Chem. Commun. 1983*, 1213.
[50] W. Sander, *J. Org. Chem. 53* (1988) 121.
[51] W. Sander, *J. Org. Chem. 54* (1989) 333.
[52] a) I. R. Dunkin, C. J. Shields, *J. Chem. Soc. Chem. Commun. 1986*, 154; b) I. R. Dunkin, G. A. Bell, *Tetrahedron 41* (1985) 339.
[53] D. Griller, A. S. Nazran, J. C. Scaiano, *Acc. Chem. Res. 17* (1984) 283.
[54] E. P. Wasserman, R. G. Bergman, C. B. Moore, *J. Am. Chem. Soc. 110* (1988) 6076.
[55] M. A. Young, G. C. Pimentel, *Appl. Opt. 28* (1989) 4270.
[56] E. Weitz, *J. Phys. Chem. 91* (1987) 3945.
[57] a) H. Hermann, F.-W. Grevels, A. Henne, K. Schaffner, *J. Phys. Chem. 86* (1982) 5151; b) K. Schaffner, F.-W. Grevels, *J. Mol. Struct. 173* (1988) 51.
[58] O. L. Chapman, *Pure Appl. Chem. 51* (1979) 331.
[59] T. C. Hess: *Low-Temperature Photochemistry: Photooxidation of Ketenes and Diazo Compounds Isolated in Oxygen Doped Argon Matrices at 10 K*, Ph.D. Thesis, University of California 1978.
[60] O. L. Chapman, T. C. Hess, *J. Am. Chem. Soc. 106* (1984) 1842.
[61] a) G. A. Bell, I. R. Dunkin, C. J. Shields, *Spectrochim. Acta, Part A 41A* (1985) 1221; b) I. R. Dunkin, G. A. Bell, F. G. McCleod, A. McCluskey, *ibid. 42A* (1986) 567.
[62] H. L. Casal, M. Tanner, N. H. Werstiuk, J. C. Scaiano, *J. Am. Chem. Soc. 107* (1985) 4616.
[63] W. Sander, *Angew. Chem. 98* (1986) 255; *Angew. Chem. Int. Ed. Engl. 25* (1986) 255.
[64] W. W. Sander, *Spectrochim. Acta, Part A 43A* (1987) 637.
[65] G. A. Ganzer, R. S. Sheridan, M. T. H. Liu, *J. Am. Chem. Soc. 108* (1986) 1517.
[66] N. H. Werstiuk, H. L. Casal, J. C. Scaiano, *Can. J. Chem. 62* (1984) 2391.
[67] H. L. Casal, S. E. Sugamori, J. C. Scaiano, *J. Am. Chem. Soc. 106* (1984) 7623.
[68] J. C. Scaiano, W. G. McGimpsey, H. L. Casal, *J. Org. Chem. 54* (1989) 1612.
[69] R. W. Fessenden, J. C. Scaiano, *Chem. Phys. Lett. 117* (1985) 103.
[70] R. L. Barcus, L. M. Hadel, L. J. Johnston, M. S. Platz, T. G. Savino, J. C. Scaiano, *J. Am. Chem. Soc. 108* (1986) 3928.
[71] Y. Fujiwara, Y. Tanimoto, M. Itoh, K. Hirai, H. Tomioka, *J. Am. Chem. Soc. 109* (1987) 1942.
[72] W. Sander, *J. Org. Chem. 53* (1988) 2091.
[73] S. Murata, H. Tomioka, T. Kawase, M. Oda, unpublished.
[74] Y.-P. Lee, G. C. Pimentel, *J. Chem. Phys. 74* (1981) 4851.
[75] P. P. Gaspar, D. Holten, S. Konieczny, *Acc. Chem. Res. 20* (1987) 329.
[76] T. Akasaka, S. Nagase, A. Yabe, W. Ando, *J. Am. Chem. Soc. 110* (1988) 6270.
[77] a) A. Patyk, W. Sander, J. Gauss, D. Cremer, *Angew. Chem. 101* (1989) 920; *Angew. Chem. Int. Ed. Engl. 28* (1989) 898; b) A. Patyk, W. Sander, J. Gauss, D. Cremer, *Chem. Ber. 123* (1990) 89.
[78] D. Griller, A. S. Nazran, J. C. Scaiano, *Tetrahedron 41* (1985) 1525.
[79] I. R. Gould, N. J. Turro, J. J. Butcher, C. J. Doubleday, N. P. Hacker, G. F. Lehr, R. A. Moss, D. P. Cox, W. Guo, R. C. Munjal, L. A. Perez, M. Fedorynski, *Tetrahedron 41* (1985) 1587.
[80] W. Sander, *Angew. Chem. 97* (1985) 964; *Angew. Chem. Int. Ed. Engl. 24* (1985) 988.
[81] K. Kleinermanns, A. C. Luntz, *J. Chem. Phys. 77* (1982) 3774.
[82] M. S. Platz, *Acc. Chem. Res. 21* (1988) 236.
[83] A. M. Trozzolo, R. W. Murray, E. Wasserman, *J. Am. Chem. Soc. 84* (1962) 4990.
[84] E. Wasserman, L. Barash, W. A. Yager, *J. Am. Chem. Soc. 87* (1965) 4974.
[85] N. J. Turro, J. A. J. Butcher, G. J. Hefferon, *Photochem. Photobiol. 34* (1981) 517.
[86] R. S. Becker: *Theory and Interpretation of Fluorescence and Phosphorescence*, Wiley, New York 1969.
[87] A. Gandini, K. O. Kutschke, *Proc. R. Soc. A. 306* (1968) 511.
[88] J. Del Bene, H. H. Jaffé, *J. Chem. Phys. 48* (1968) 1807.
[89] G. Karlström, S. Engström, B. Jönsson, *Chem. Phys. Lett. 67* (1979) 343.
[90] K. Yamaguchi, S. Yabushita, T. Fueno, S. Kato, K. Morokuma, S. Iwata, *Chem. Phys. Lett. 71* (1980) 563.
[91] R. C. Bingham, M. J. S. Dewar, *J. Am. Chem. Soc. 97* (1975) 1285.
[92] D. F. V. Lewis, *Chem. Rev. 86* (1986) 1111.
[93] P. Bischof, *J. Am. Chem. Soc. 98* (1976) 6844.

Enzymic Reaction Selectivity by Negative Catalysis or How Do Enzymes Deal with Highly Reactive Intermediates?

By János Rétey*

Our current understanding of enzyme catalysis is dominated by the hypothesis of transition-state binding launched by *Linus Pauling* in 1946. Transition-state binding and the interplay of properly positioned, catalytically active functional groups can largely explain both the acceleration and specificities of many enzymic reactions for which chemical analogy exists. Here it is postulated that, for chemically "difficult" or "improbable" reactions, enzymes may resort to an additional device. Using cofactors of potentially high energy (such as coenzyme B_{12}), stabilized radicals, or light, they can transform the bound substrate into a highly reactive (i.e., unstable) intermediate. Selectivity is now achieved by *negative catalysis*, that is, by preventing the "hot" intermediate from undergoing reactions that would occur in solution or in the gas phase and thus prolonging its lifetime. The highly reactive intermediate may then undergo reactions whose activation energy is relatively high and which would therefore be suppressed without negative catalysis. Reaction selectivity is thus achieved by preventing undesired reactions rather than by facilitating the target ones. The high reactivity may be transferred reversibly if its source is, for instance, coenzyme B_{12} or irreversibly if it is generated by light or ATP. Highly reactive intermediates are often radicals but can also be other unstable species. In this article a number of enzymic reactions are discussed that seem to support the above postulate.

1. Introduction

Although the real nature of enzyme catalysis is still elusive, many important details of enzyme structure and enzyme–substrate interaction have been uncovered in the last decades. As a result, some general conclusions may be drawn and it is possible to identify principles that make enzyme action possible. Substrate binding is the first and obligatory step in all enzymic reactions. Although this step is essential, it is not sufficient for catalysis. However, as pointed out by *Linus Pauling* in 1946,[1] the binding site of enzymes is complementary to the transition state rather than to the substrate. Put another way, the lower energy barrier for the enzymic reaction (compared with the uncatalyzed one) results from destabilization of the ground state of the substrate and from concomitant stabilization of the transition-state–enzyme complex. Strictly speaking, this dissection is not completely correct, since, after substrate binding, the whole complex should be treated as a single entity. Allowing for such "sloppiness", one can argue that the measurable binding energy is much less than the intrinsic one, since a portion thereof is "used up" to force the substrate toward the transition-state structure. This may involve locking the substrate into an unfavorable but reactive conformation, desolvation, a change in polarization, or covalent binding to the enzyme. Here it is important to emphasize the role of the nonreacting part of the substrate or of the coenzyme molecule. The binding energy associated with this portion may be used to force the reacting moiety into an "unwelcoming" hole.[2] In many cases (e.g., acyl-CoA, SAM, $NAD^{\oplus}$, and FAD[**]) such a nonreacting portion is attached to the substrate or to the reactive part of the coenzyme. Such a device may serve a double role: for example, it can allow both chemical activation as thioester or sulfonium ion and strong binding by interaction with a complementary site of the enzyme (e.g., the adenosine binding portion). Similar effects can be achieved by phosphorylation or pyrophosphorylation, as in pyridoxal phosphate or thiamine pyrophosphate, which might be bound partly by ionic interactions. A portion of the binding energy can be used not only to destabilize the substrate but also for conformational and structural changes of the enzyme.

A further consequence of *Pauling*'s postulate is the very tight binding of the so-called transition-state analogues to enzymes. These are compounds whose structure resembles that of the putative transition state of the enzymic reaction. Such transition-state analogues have been used as powerful inhibitors and potential drugs and, more recently, in the preparation of catalytic antibodies.[3,4] It is natural that most investigators have focused their efforts on enzymic reactions that are relatively simple and chemically plausible. These include proton transfers, such as tautomerizations, epimerizations, and racemizations as well as hydrolytic reactions such as those of esters and amides.[5–7] Even so, some problems are still unsolved. Since most enzymic reactions consist of several elementary steps, the following question arises: Which is the step whose transition state is relevant for binding-site complementarity? Is it the rate-determining step, or is the enzyme capable of producing complementary binding sites for several transition states following each other in a reaction sequence by subtle and rapid conformational changes?

It is also customary to estimate the rate acceleration that an enzyme is able to achieve by comparing the enzyme-catalyzed reaction with the uncatalyzed reaction. Such an acceleration is said to be roughly equal to the ratio of the dissociation constants for the enzyme–substrate and the

[*] Prof. Dr. J. Rétey
Lehrstuhl für Biochemie im Institut für Organische Chemie der Universität
Richard-Willstätter-Allee, D-7500 Karlsruhe 1 (FRG)

[**] CoA = coenzyme A, SAM = *S*-adenosylmethionine, NAD = nicotinamide adenine dinucleotide, FAD = flavin adenine dinucleotide.

 © *VCH Verlagsgesellschaft mbH, D-6940 Weinheim, 1990* *0570-0833/90/0404-0355 $ 02.50/0*

enzyme–transition-state complexes, K_S and K_T, respectively [Eq. (a)].[8]

$$\frac{k_e}{k_n} = \frac{K_S}{K_T} \qquad (a)$$

Rate accelerations of between 10^{10} and 10^{20} have been estimated. Still another outstanding property of enzymes is their very high specificity. Their substrate specificities and stereospecificities have been demonstrated and discussed on numerous occasions.[9–12] Let us focus here on their reaction specificity; that is, more than one enzyme can act on the same substrate but each will catalyze only one specific reaction yielding only one specific product. Of course, this follows from *Pauling*'s theory of transition-state binding. In other words, many enzymes work according to the following strategy: They select one reaction and lower its energy barrier by stabilizing the corresponding transition state. Other possible reactions cause no problem since their activation energies are and remain high (i.e., the substrate is stable).

There are, however, an increasing number of known enzymic reactions that are neither simple nor chemically plausible. Their enzymic rate acceleration is virtually infinite since the rate of the uncatalyzed reaction is zero. How can enzymes make possible such chemically improbable reactions? Can transition-state binding theory also provide a full explanation for these reactions? To convey to the bound substrate sufficiently high reactivity, enzymes can resort to "energy-rich" agents such as ATP, radical-generating species (e.g., the combination of iron complexes with radical-forming agents like tyrosine or coenzyme B_{12}), or even light. In the case of coenzyme B_{12}, homolysis of the cobalt–carbon bond can generate a highly reactive radical that is able to abstract a hydrogen atom from a nonactivated position of the substrate. The latter, thus destabilized, is now prone to undergo spontaneous reactions. The main task of the enzyme is to prevent stabilization reactions that are typical for free radicals in solution. Such "negative catalysis" may be achieved by isolating the reactive intermediate from groups that might react with it and by preventing conformations from which undesired reactions could occur. This allows the radical intermediate to undergo atypical reactions such as rearrangements involving 1,2 migrations.

In other words, reaction selectivity can be achieved by specific acceleration of a certain reaction or, alternatively, by producing, under energy input, a highly reactive intermediate that is prevented from undergoing undesired reactions. If the lifetime of the highly reactive intermediate is prolonged in this way, unusual transformations can follow. In contrast to ATP, light, or other energy sources, the energy spent by coenzyme B_{12} must be regained at the end of the catalytic cycle.

What is the experimental support for such an alternative or, better, additional principle of reaction selectivity and what is its importance in the realm of enzymic reactions?

2. Rearrangements Catalyzed by Coenzyme-B_{12}-Dependent Enzymes

About a dozen coenzyme-B_{12}-dependent rearrangements are known and they are remarkable in several respects. Coenzyme B_{12} and some of its derivatives are the only bona fide natural products containing a covalent metal–carbon bond. The thermal stability of this bond, particularly in aqueous solution, is also noteworthy. Its homolysis energy has been reported to be about 30 kcal mol^{-1};[13, 14] its photolysis is fast but probably of no relevance for the enzymic reactions. Even more astonishing are the rearrangements. They consist of an interchange of a hydrogen atom and a variable group between adjacent carbon atoms [Eq. (b)].

(b)

If R is an organic residue such as the groups -COSCoA, $-C(H)(NH_2)COOH$, or $C(=CH_2)COOH$, then we talk of carbon-skeleton rearrangements, as in the case of methylmalonyl-CoA, glutamate, and methylene glutarate mutases. All these cases involve attack at a nonactivated methyl group. If, on the other hand, R is an "inorganic" group such as OH or NH_2, then we talk of dioldehydratases or ammonia lyases or amino mutases. An example of the latter is β-lysine mutase.

Whereas the migration of R is strictly intramolecular,[15, 16] that of the H atom is partially intermolecular.[17–20] In 1966, *Frey* and *Abeles*[18] discovered that the migrating H atom scrambles with those of the cobalt-bound methylene group. They concluded that the reaction involves transient cleavage of the cobalt–carbon bond and the intermediacy of 5′-deoxyadenosine. As a further consequence, one has to assume another chemically difficult step, namely, the attack at a nonactivated methyl group of 5′-deoxyadenosine, which is necessary to regenerate the catalyst. Such a minimal mechanism is depicted in Scheme 1.

János Rétey, born in 1934 in Szeged (Hungary), studied chemistry between 1957 and 1960 at ETH Zürich and finished his Ph.D. work on the stereospecificity of oxidoreductases in 1963 with V. Prelog. After postdoctoral years with F. Lynen (Munich, 1963–1965) and D. Arigoni (ETH Zürich, 1965–1968), he became "Oberassistent" and lecturer at ETH Zürich. Since 1972 he has been professor of biochemistry at the University of Karlsruhe. In 1971 he received the Alfred Werner prize of the Swiss Chemical Society. His fields of interest are the mechanism and stereospecificity of enzyme action, synthetic enzyme models, bioorganic and bioinorganic chemistry, and the investigation of enzyme structures by molecular biological methods.

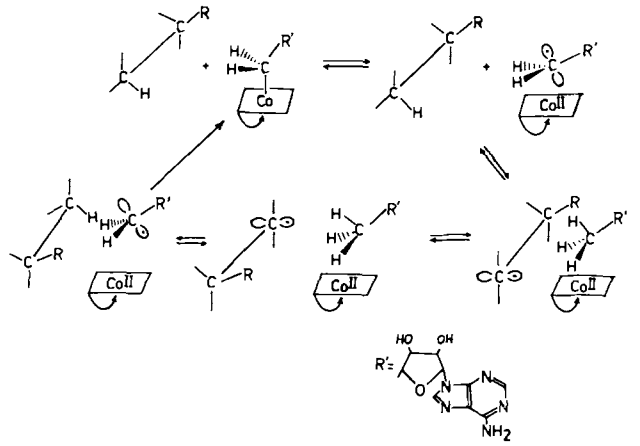

Scheme 1.

The postulated cleavage of the cobalt–carbon bond is likely to be homolytic. Not only is this the mode of cleavage requiring the least energy, but in some cases experimental support (ESR, UV) exists for the intermediacy of a paramagnetic Co^{II} species and an organic radical.[21 - 29] A highly reactive organic radical also has the potential to attack a nonactivated methyl group, for example in reactions involving methylmalonyl-CoA,[30] isobutyryl-CoA,[31] or methylaspartate.[32] Whereas direct evidence for radical intermediates in these carbon-skeleton rearrangements has not yet been provided, ESR spectra of enzyme–substrate complexes with ethanolamine ammonia lyase,[21, 23, 24] dioldehydratase, [25 - 27] and ribonucleotide reductase[28] have been published. They suggest that the paramagnetic Co^{II} center and the 5'-methylene radical of the adenosine moiety are 10–12 Å apart during catalysis. It is tempting to postulate that substrate binding triggers a conformational change of the enzyme that pulls the two moieties apart. The substrate may penetrate into the space created by such a movement. Exact positioning of the methylene radical and substrate is probably required for specific abstraction of the migrating hydrogen atom.

2.1. Dioldehydratase and Ethanolamine Ammonia Lyase

Many interesting and surprising stereochemical details have been revealed in the reactions catalyzed by dioldehydratase and ethanolamine ammonia lyase. In both reactions a pair of homologous substrates can be processed in a similar but stereochemically distinct way [Eqs. (c) and (d)].

$$R{-}\underset{\displaystyle OH}{\underset{|}{CH}}{-}CH_2OH \longrightarrow R{-}CH_2{-}CHO + H_2O \qquad (c)$$

R = H, CH_3

$$R{-}\underset{\displaystyle NH_2}{\underset{|}{CH}}{-}CH_2OH \longrightarrow R{-}CH_2{-}CHO + NH_3 \qquad (d)$$

R = H, CH_3

The results and their consequences for the relevant mechanisms have been reviewed.[11, 12] They support the occurrence of radical intermediates previously indicated by ESR spectra.[21 - 29] In particular, the racemization consistently observed when a reaction proceeds via a methylene radical, indicates that the radical rotates rapidly around the C–C bond, thereby making the homotopic faces indistinguishable [Eq. (e)].

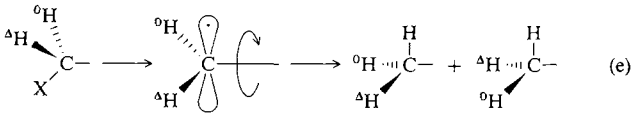

(e)

Replacing one of the hydrogens by a methyl group either prevents rotation at the binding site as in the case of dioldehydratase[33] or, for a low rotational barrier, it renders the two faces of the trigonal center *distinguishable* for the enzyme as in the case of ethanolamine ammonia lyase[34] [Eq. (f)]. Experimentally, a uniform steric course (e.g., inversion) is observed in the first case, and a non-uniform stereospecificity, independent of the substrate configuration, in the second case.

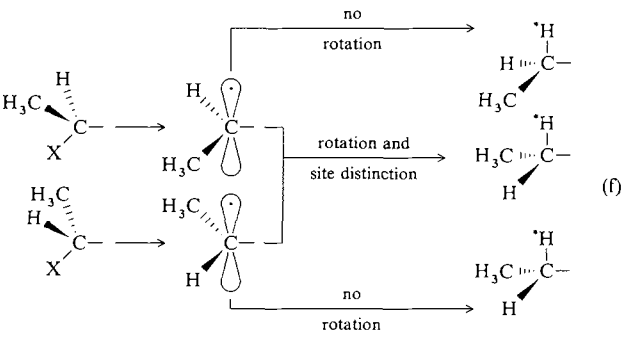

(f)

Thus, stereochemical analysis of enzymic reactions is an excellent probe for the occurrence of methylene radical intermediates. Anionoid methylene groups, such as those implicated in the condensation reactions involving acetyl-CoA, have a high barrier of rotation and are handled by enzymes throughout stereospecifically.[35 - 38]

Enzymic processes where methylene cations might be surmised are rare. In terpene biosynthesis during condensation of the biological isoprene units, isopentenyl and dimethylallyl diphosphate, the putative intermediate is an allylic cation (see **1**).

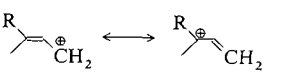

1

The use of stereospecifically labeled substrates showed complete selectivity for the enantiotopic methylene faces, which points to a high rotational barrier in **1**.[39]

2.2. Methylmalonyl-CoA Mutase

Among the coenzyme-B_{12}-dependent carbon-skeleton rearrangements, the methylmalonyl-CoA mutase reaction [Eq. (g)] has been investigated the most thoroughly.

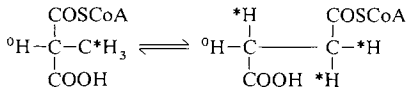

(g)

The steric course of the substitutions at the migrating centers was elucidated using deuterium as a label[40,41] or the substrate analogue ethylmalonyl-CoA.[42] The substitutions occur at both centers mainly but not exclusively with retention. Furthermore, starting from monodeuterated [2-$^2H_1$]-methylmalonyl-CoA, the product succinyl species contained unlabeled and dideuterated molecules, 15–20% of each.[40,41] Because enzymes were thought to be strictly stereospecific, these results were first attributed to impure enzyme preparations or experimental errors. Only 20 years later, when HPLC-purified enzyme preparations were available and high-resolution NMR spectrometers allowed enzymic reactions to be monitored directly in the NMR tube, could it be shown that the surprising deuterium distribution arose not from experimental error but as a consequence of the reaction mechanism.[43,44] Especially clear-cut results were obtained using the carba(dethia)coenzyme A (CH_2CoA) analogue of methylmalonyl-CoA.[45] This is almost as good a substrate as the natural thioester but has the advantage of complete stability to hydrolysis. Thus, in contrast to succinyl-CoA, which is hydrolyzed easily under physiological conditions, the production and deuteration of succinyl-CH_2CoA could be monitored for a day or so in the NMR tube.

The kinetic NMR study[45] confirmed the surprising scrambling of the "nonmigrating" deuterium among the succinyl species produced. Thus, instead of the expected "100%" monodeuterated product molecules, only about 60% were formed, the remainder being unlabeled or geminally dideuterated. In the presence of methyl-malonyl-CoA epimerase, any unlabeled methylmalonyl-CH_2CoA produced in the backward reaction instantly incorporated deuterium into its α-position from the solvent. Repeated rearrangements led once more to some unlabeled product, which was consistently deuterated at the methylmalonyl stage. This process constituted a leak in the system which allowed a continuous deuterium incorporation from the solvent into the product and could be monitored by ^{1}H NMR spectroscopy during a longer period of time.[45] In the strict absence of methylmalonyl-CoA epimerase, the scrambling reached a stationary phase with a statistical distribution of unlabeled, monodeuterated, and geminally dideuterated (1 : 1 : 1) species.[46]

Since the deuterium scrambling occurs before equilibrium is reached, it cannot be explained by lack of stereospecificity in the backward reaction, that is, incomplete distinction between the two diastereotopic 3-methylene hydrogen atoms of the succinyl moiety. Furthermore, in experiments with the natural thioester substrate in deuterium oxide, the monodeuterated succinyl-CoA was about 90% optically pure.[40,47] A mechanism that takes account of all these facts is summarized in Scheme 2.

In Scheme 2 it is assumed that, after homolytic cleavage of the cobalt–carbon bond, the paramagnetic Co^{II} center has the role of a "spectator" only. The adenosine 5′-radical is positioned in a way that it can abstract a methyl hydrogen atom from the substrate, whereby it becomes itself a nonactivated methyl group. After migration of the carbonyl-XCoA group (X = S or CH_2), the product radical **2** can reabstract a hydrogen atom from the 5′-methyl group of adenosine, affording the expected stereospecifically deuterated product. To explain the presence of unlabeled and doubly labeled species, one can assume a 1,2 hydrogen shift which is stereoelectronically favored and may take place in competition with the "intermolecular" H abstraction. The configuration at the "front" center is thereby inverted so that deuterium comes within reach of the 5′-methylene radical.

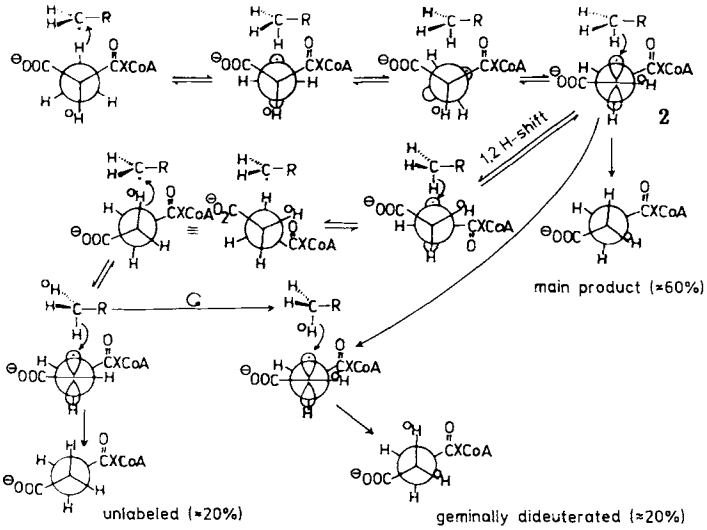

Scheme 2.

The latter is regenerated after hydrogen transfer to the "rear" center and is now able to abstract deuterium from the front center of the bound product. Since methyl groups have a low torsional barrier even at the enzyme's active site, back-transfer of an H atom may lead to unlabeled succinyl-CH_2CoA with concomitant deuterium incorporation into the 5′-methylene group of the coenzyme. In the next catalytic cycle, such a deuterated coenzyme may deliver deuterium to the monodeuterated radical intermediate **2**, affording the observed geminally dideuterated succinyl product.

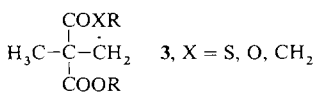

3, X = S, O, CH_2

When the postulated methylmalonyl thioester radical **3** is generated in nonenzymic model systems, relatively low yields of 1,2-migration products are observed.[48–53] Stabilization by direct hydrogen abstraction usually prevails. The migra-

tory aptitude of the groups decreases in the following order: -COR > -COSR > -CN > -COOR.[48, 51, 52, 54] A bona fide 1,2-migration of H atoms in organic radicals has not yet been reported.

It has been noted[51] that the methylmalonyl-CoA mutase reaction is relatively slow compared with the lifetimes of free radical species generated in model studies. This indicates that the enzyme prolongs the lifetime of the free radical intermediates by preventing stabilization pathways typically occurring in solution.

3. Radical Enzymic Reactions Independent of Coenzyme B_{12}

During the last few years more and more enzymic reactions have become known in which radical intermediates have been postulated. Most of them involve unusual chemical transformations that cannot be explained by conventional or ionic mechanisms. Although the postulated mechanisms are not strictly proven, a review of them should illustrate and support the ideas developed in this paper.

Pyruvate formate lyase catalyzes the reversible cleavage of pyruvate to formate and acetyl-CoA [Eq. (h)]. In contrast to

$$H_3C{-}\overset{O}{\overset{\|}{C}}{-}COOH + CoASH \rightleftharpoons H_3C\overset{O}{\overset{\|}{C}}SCoA + HCOOH \qquad (h)$$

the oxidative decarboxylation of pyruvate, the pyruvate formate lyase reaction is independent of thiamine pyrophosphate.[55] *Knappe* et al.[56] found the purified enzyme to contain a radical of unknown nature and postulated[57] independently from others[58] the mechanism depicted in Scheme 3. The key step is the abstraction of a hydrogen atom

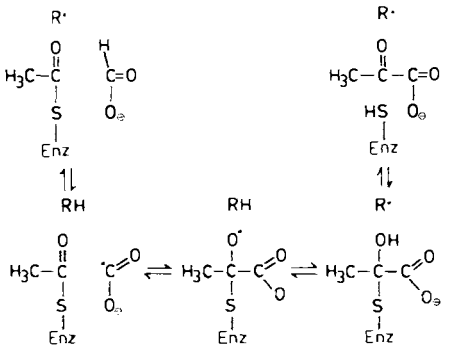

Scheme 3.

from the thiohemiketal intermediate in the forward reaction and from formate in the reverse reaction. The cleavage/formation of the C–C bond is of radical nature, thus avoiding the difficulty of bond formation between two carbon atoms polarized in the same sense. As in the coenzyme-B_{12}-catalyzed reactions, the high reactivity is only "borrowed" by the substrate and must be returned to the catalyst at the end of each catalytic cycle.

Lysine 2,3-aminomutase from *Clostridium* species catalyzes the migration of an amino group in lysine from position 2 to 3 [Eq. (i)].[59] The enzyme is dependent on pyridoxal phosphate and *S*-adenosyl-methionine (SAM) as cofactors. *Frey* and co-workers found a tritium transfer from the 5′-position of the adenosine moiety of SAM to position 2 of β-

$$H_2N{-}(CH_2)_3{-}CH_2{-}\underset{NH_2}{CH}{-}COOH \longrightarrow H_2N{-}(CH_2)_3{-}\underset{NH_2}{CH}{-}CH_2COOH \qquad (i)$$

lysine.[60, 61] This is reminiscent of coenzyme-B_{12}-dependent mutases, and the authors proposed a mechanism in which some elementary steps are very similar (Scheme 4).

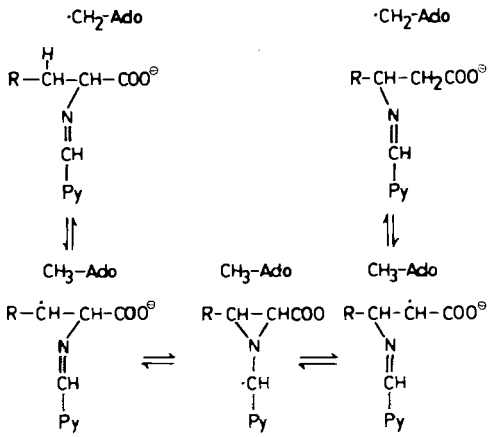

Scheme 4.

In analogy to coenzyme-B_{12}-dependent reactions, they postulate a homolytic cleavage of the sulfur–carbon bond to form a 5′-adenosyl radical which is able to abstract a hydrogen atom from the unreactive 3-position of lysine. The radical thus formed attacks the neighboring imino nitrogen atom of the Schiff base between lysine and pyridoxal phosphate. The resulting new radical is stabilized by both the aromatic ring and the aziridine ring. Rearrangement finally leads to a radical α to the carboxylic group, which is then stabilized by H-atom transfer from the 5′-deoxyadenosine bound to the active site. *Aberhart* et al. carried out an independent investigation using deuterium as a label.[62, 63] They were not able to demonstrate deuterium transfer from the 5′-position of SAM to α- or β-lysine and came to a conclusion different from that of *Frey* and co-workers. Different conditions and enzyme preparations may be the cause of this discrepancy.[61]

One of the best characterized enzymes containing a "stabilized" radical is the ribonucleoside diphosphate reductase from *E. coli*.[64] This was the first case in which a tyrosyl radical "stabilized" by a neighboring binuclear iron(III) complex was identified.[65] It is intriguing that the corresponding enzyme in *Lactobacillus leichmannii* is coenzyme B_{12} dependent. Indeed, it has been postulated[66] that in both cases the different radical-forming centers have similar roles and abstract hydrogen atoms from SH groups and/or from the 3′-position of the nucleotide (Scheme 5).[67] The surprising participation of 3′-H in the reaction is indicated by a substantial deuterium kinetic isotope effect. This mechanism

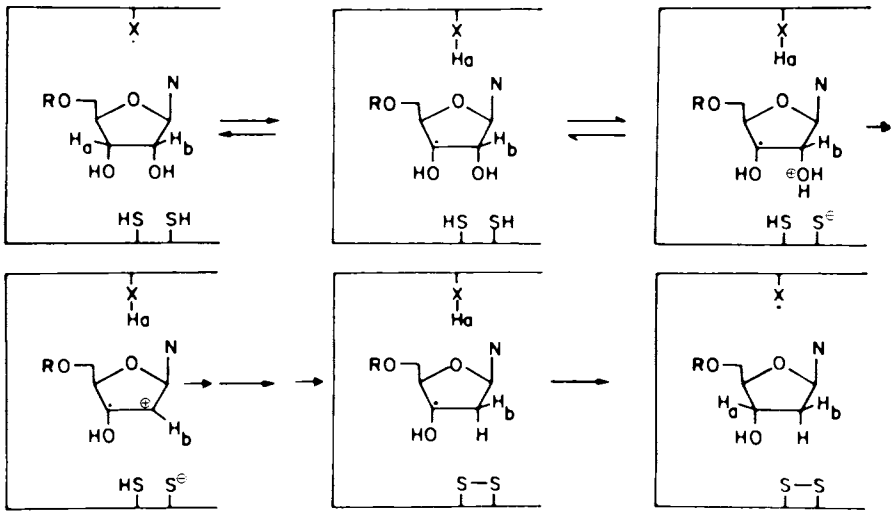

Scheme 5.

shows an interesting analogy to the methylmalonyl-CoA mutase reaction in which a seemingly nonparticipating hydrogen atom is also involved in the rearrangement.[45,46]

There are a great number of other enzymic processes in which highly reactive intermediates, mostly radicals, are implicated. Among them are various oxidations catalyzed by flavoenzymes as well as cytochrome P-450 enzymes and other iron-containing enzymes. In all these cases an important task of the enzyme is to prevent the highly reactive intermediate from undergoing unwanted reactions. Such a control by *negative catalysis* may be equally important as *positive catalysis* when the enzyme deals with unreactive substrate species or intermediates.

In photosynthesis, in which enormous progress has recently been made, negative catalysis may play a role, too. In the thylakoid membrane, electrons are promoted to a higher energy level by light absorption. In most model systems they fall back, dissipating their energy in some useless form. In the chloroplast, enzymes and membranes prevent the electron from doing so and channel it to ferredoxins, NADP, etc., that is, an electron transport chain that is coupled with ATP formation. In contrast to coenzyme-B_{12}, light is an energy donor and not an energy "lender".

4. Conclusions

Highly reactive intermediates are involved in many organic reactions. The unusual outcome of some enzymic reactions can be explained by the control of such highly reactive intermediates in the enzyme-bound state. By suppressing typical stabilization reactions, such intermediates may undergo unexpected rearrangements or group transfers. The mechanisms of some enzymic radical reactions, dependent on or independent of coenzyme B_{12}, show how such chemically improbable conversions become feasible.

The cartoon shows an anthropomorphic view of coenzyme-B_{12}-dependent rearrangements. The potential energy of the cofactor is used to generate a high-energy intermediate which, after rearrangements but without substantial energy loss, returns the borrowed energy to the cofactor. One of the most important tasks of the protein is to prevent the high-energy intermediate from falling down to a lower energy level. The uncatalyzed reaction is symbolized by a man climbing over a wall.

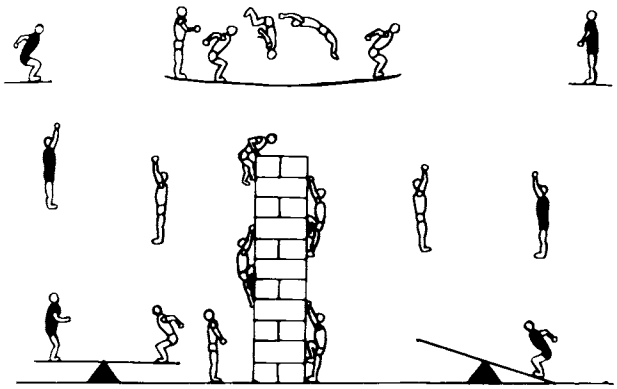

I thank my younger colleagues whose contributions are cited and provided the basis for the ideas described in this paper. The paper was written during a visiting professorship at the Technion-Israel Institute of Technology sponsored by the Swiss Technion Society. I thank the colleagues at Haifa for their kind hospitality and for stimulating discussions, particularly with Professor A. Halevi. The experimental work in the author's laboratory has been supported by the Deutsche Forschungsgemeinschaft, the Fonds der Chemischen Industrie, and the Land Baden-Württemberg.

Received: August 28, 1989 [A 755 IE]
German version: *Angew. Chem. 102* (1990) 373

[1] L. Pauling, *Chem. Eng. News 24* (1946) 1375.
[2] a) M. I. Page, A. Williams (Eds.): *Enzyme Mechanisms*, Royal Society of Chemistry, London 1987 b) M. I. Page in [2a], p. 9.
[3] A. Tramontano, K. D. Janda, R. A. Lerner, *Science 234* (1986) 1566–1570; S. J. Pollack, J. W. Jacobs, P. G. Schultz, *ibid. 234* (1986) 1570–1573.
[4] Review: P. G. Schultz, *Angew. Chem. 101* (1989) 1336; *Angew. Chem. Int. Ed. Engl. 28* (1989) 1283.
[5] W. P. Jencks, *Adv. Enzymol. 43* (1975) 219–402.
[6] R. J. Leatherbarrow, A. R. Fersht in [2a] pp. 79–96.
[7] R. Wolfenden, L. Frick in [2a] pp. 97–122.
[8] J. Kraut, *Science 242* (1988) 533–540.
[9] R. Bentley: *Molecular Asymmetry in Biology, Vol. I, II*, Academic Press, New York 1969.

[10] W. L. Alworth; *Stereochemistry and its Application in Biochemistry*, Wiley-Interscience, New York 1972.
[11] J. Rétey, J. A. Robinson: *Stereospecificity in Organic Chemistry and Enzymology*, Verlag Chemie, Weinheim 1982.
[12] J. Rétey in C. Tamm (Ed.): *Stereochemistry (New Comprehensive Biochemistry, Vol. 3)*, Elsevier Biomedical Press, Amsterdam 1982, pp. 249–282.
[13] B. P. Hay, R. G. Finke, *J. Am. Chem. Soc. 108* (1986) 4820–4829.
[14] J. Halpern, S. H. Kim, T. W. Leung, *J. Am. Chem. Soc. 106* (1984) 8317–8319.
[15] R. W. Kellenmeyer, H. G. Wood, *Biochemistry 1* (1962) 1124–1131.
[16] E. F. Phares, M. V. Long, S. F. Carson, *Biochem. Biophys. Res. Commun. 8* (1962) 142–146.
[17] R. H. Abeles, B. Zagalak, *J. Biol. Chem. 241* (1966) 1245–1246.
[18] P. A. Frey, R. H. Abeles, *J. Biol. Chem. 241* (1966) 2732–2733.
[19] J. Rétey, D. Arigoni, *Experientia 22* (1966) 783-784.
[20] G. J. Cardinale, R. H. Abeles, *Biochim. Biophys. Acta 132* (1967) 517–518.
[21] B. M. Babior, T. H. Moss, D. C. Gould, *J. Biol. Chem. 247* (1972) 4389–4392.
[22] M. R. Hollaway, H. A. White, K. N. Joblin, A. W. Johnson, M. F. Lappert, O. C. Wallis, *Eur. J. Biochem. 82* (1978) 143–154.
[23] B. M. Babior, T. H. Moss, W. H. Orme-Johnson, H. Beinert, *J. Biol. Chem. 249* (1974) 4537–4544.
[24] O. C. Wallis, R. C. Bray, S. Gutteridge, M. R. Hollaway, *Eur. J. Biochem. 125* (1982) 299–303.
[25] S. A. Cockle, H. A. O. Hill, R. J. P. Williams, S. P. Davies, M. A. Foster, *J. Am. Chem. Soc. 94* (1972) 275–277.
[26] T. H. Finlay, J. Valinsky, A. S. Mildvan, R. H. Abeles, *J. Biol. Chem. 248* (1973) 1285–1290.
[27] K. L. Schepler, W. R. Dunham, R. H. Sands, J. A. Fee, R. H. Abeles, *Biochim. Biophys. Acta 397* (1975) 510–518.
[28] G. R. Buettner, R. E. Coffman, *Biochim. Biophys. Acta 480* (1977) 495–505.
[29] J. R. Boas, P. R. Hicks, J. R. Pilbrow, T. D. Smith, *J. Chem. Soc. Faraday Trans. 274* (1978) 417–431.
[30] J. Rétey in D. Dolphin (Ed.): *Vitamin B_{12}, Vol. 2*, Wiley-Interscience, New York 1982, pp. 357–379.
[31] G. Brendelberger, J. Rétey, D. M. Ashworth, K. Reynolds, F. Willenbrock, J. A. Robinson, *Angew. Chem. 100* (1988) 1122–1124; *Angew. Chem. Int. Ed. Engl. 27* (1988) 1089–1090.
[32] H. A. Barker, F. Susuku, A. A. Iodice, V. Rooze, *Ann. N. Y. Acad. Sci. 112* (1964) 644.
[33] J. Rétey, A. Umani-Ronchi, D. Arigoni, *Experientia 22* (1966) 72–73.
[34] P. Diziol, H. Haas, J. Rétey, S. W. Graves, B. M. Babior, *Eur. J. Biochem. 106* (1980) 211–224.
[35] J. W. Cornforth, J. W. Redmond, H. Eggerer, W. Buckel, C. Gutschow, *Nature 221* (1969) 1212.
[36] J. Lüthy, J. Rétey, D. Arigoni, *Nature 221* (1969) 1213.
[37] H. Eggerer, W. Buckel, H. Lenz, P. Wunderwald, G. Gottschalk, J. W. Cornforth, C. Donninger, R. Mallaby, J. W. Redmond, *Nature 226* (1970) 517–519.
[38] J. Rétey, J. Lüthy, D. Arigoni, *Nature 226* (1970) 519–521.
[39] J. W. Cornforth, R. H. Cornforth, C. Donninger, G. Popjak, *Proc. Roy. Soc. B. 163* (1966) 492.
[40] M. Sprecher, M. S. Clark, D. B. Sprinson, *J. Biol. Chem. 241* (1966) 872–877.
[41] J. Rétey, cited by D. Arigoni, E. L. Eliel, *Top. Stereochem. 4* (1969) 147–243.
[42] J. Rétey, E. H. Smith, B. Zagalak, *Eur. J. Biochem. 83* (1978) 437–451.
[43] K. Wölfle, M. Michenfelder, A. König, W. E. Hull, J. Rétey, *Eur. J. Biochem. 156* (1986) 545–554.
[44] M. Michenfelder, W. E. Hull, J. Rétey, *Eur. J. Biochem. 168* (1987) 659–667.
[45] W. E. Hull, M. Michenfelder, J. Rétey, *Eur. J. Biochem. 173* (1988) 191–201.
[46] M. Kunz, W. E. Hull, J. Rétey, unpublished.
[47] J. Rétey, unpublished.
[48] J. Rétey, in B. Zagalak, W. Friedrich (Eds.): *Vitamin B_{12}* de Gruyter, Berlin 1979, pp. 439–460.
[49] P. Dowd, M. Shapiro, *J. Am. Chem. Soc. 98* (1976) 3724–3725.
[50] A. I. Scott, K. Kang, *J. Am. Chem. Soc. 99* (1977) 1997–1999.
[51] S. Wollowitz, J. Halpern, *J. Am. Chem. Soc. 110* (1988) 3112–3120.
[52] W. M. Best, D. A. Widdowson, *Tetrahedron 45* (1989) 5943–5954.
[53] U. Aeberhard, R. Keese, E. Stamm, V. R. Vögeli, W. Lau, J. K. Kochi, *Helv. Chim. Acta 66* (1983) 2740–2759.
[54] M. Tada, T. Nakamura, M. Matsumoto, *J. Am. Chem. Soc. 110* (1988) 4647–4652.
[55] J. Knappe, H. P. Blaschkowski, P. Gröbner, T. Schmitt, *Eur. J. Biochem. 50* (1974) 253–263.
[56] J. Knappe, F. A. Neugebauer, H. P. Blaschkowski, M. Gänzler, *Proc. Natl. Acad. Sci. USA 81* (1984) 1332–1335.
[57] W. Plaga, R. Frank, J. Knappe, *Eur. J. Biochem. 178* (1988) 445–450.
[58] E. J. Brush, K. A. Lipsett, J. W. Kozarich, *Biochemistry 27* (1988) 2217–2222.
[59] T. P. Chirpich, V. Zappia, R. N. Costilow, H. A. Barker, *J. Biol. Chem. 245* (1970) 1778–1789.
[60] M. Moss, P. A. Frey, *J. Biol. Chem. 262* (1987) 14859–14862.
[61] J. Baraniak, M. L. Moss, P. A. Frey, *J. Biol. Chem. 264* (1989) 1357–1360.
[62] D. J. Aberhart, *J. Chem. Soc. Perkin Trans. 1 1988*, 343–350.
[63] D. J. Aberhart, J. A. Dotting, *J. Chem. Soc. Perkin Trans. 1 1988*, 2119–2122.
[64] P. Reichard, A. Ehrenberg, *Science 221* (1983) 514-519.
[65] A. Larsson, B.-M. Sjöberg, *EMBO J. 5* (1986) 2037–2040.
[66] G. W. Ashley, G. Harris, J. Stubbe, *J. Biol. Chem. 261* (1986) 3958–3964.
[67] J. Stubbe, *Biochemistry 27* (1988) 3893–3899.

Chemiluminescence Techniques for the Characterization of Materials

New Analytical Methods (41)

By G. David Mendenhall*

Photons are emitted at low levels from a wide variety of organic materials at wavelengths ranging from the visible to infrared. This light emission accompanies free-radical autoxidation and charge-recombination processes and is particulary useful in assessing thermal oxidation and radiation damage as well as polymer curing reactions. IR chemiluminescence, which offers advantages because of reduced self-absorption, has been shown to mark the end of induction periods in inhibited systems. With the introduction of sensitive solid-state devices, the chemiluminescence technique has been extended to two-dimensional imaging and presentation.

1. Introduction

The progressive replacement of metal and ceramic materials with organic-based polymers and composites has created a practical interest in slow oxidation rates which may determine the lifetime of the replacements. Weak light emission is associated with peroxidic oxidation products of organic materials and with certain physical processes described below. Chemiluminescence is a very attractive way to measure oxidation in real time because of the large molar gain factor $N_{av}\Phi_{em}$ (Avogadro number times the quantum yield for emission) coupled with the availability of sensitive and reliable photon-counting systems.

I reviewed a number of empirical applications of chemiluminescence (CL) from condensed-phase materials in 1977.[1] Since that time, advances in the field have been arithmetic rather than exponential, although a considerable body of information on the technique exists as arcana with various industries. Most studies in this area consist of the effects of temperature and atmosphere on CL as a function of sample composition and history. The purpose of this article is to present updated theories on the origin of light emission, some recent, rather successful applications, and technological advances which promise to make the technique more widely used in the future.

2. Experimental Aspects

The apparatus for CL measurement is fundamentally simple, since no resonant conditions, or high- or low-temperature extremes are involved. The most important requirements are the exclusion of extraneous light and the reproducible placement of the samples with respect to the device for light detection.

Liquids at temperatures below about 90 °C may be examined conveniently in a glass or quartz cell jacketed with circulating water at a constant temperature. For higher temperatures an insulated metal block with heating elements (Fig. 1a) is preferable to baths of silicone and other traditional oils, which themselves give abundant chemiluminescence at elevated temperatures.

Luminescence from solids at near-ambient temperatures and light-stimulated luminescence may be measured reproducibly with the apparatus in Figure 1 b.[2] Light from solids at elevated temperatures may be measured in a heated oven (see, e.g., Ref. [3]) or with fiber-optic techniques and a small sample container in a hot block or bath.[4]

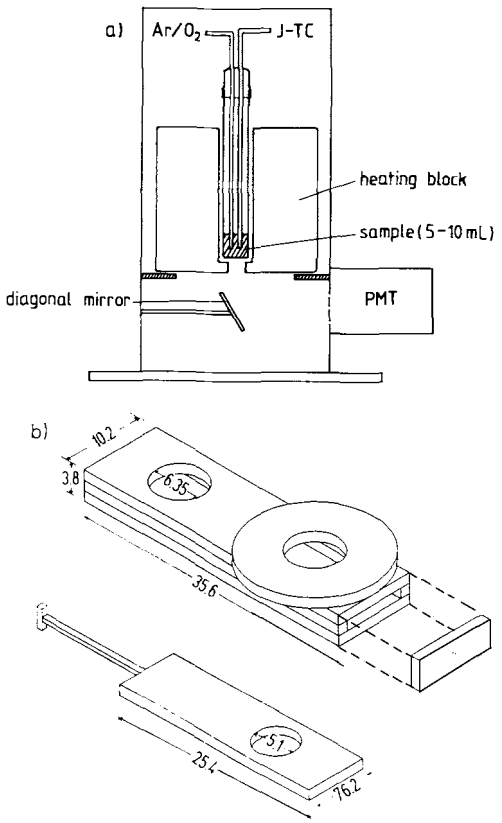

Fig. 1. a) CL apparatus for liquid samples (see also [36]). J-TC = thermocouple b) Apparatus for solids and for study of delayed luminescence (measurements in cm) [2]. The photomultiplier tube (PMT) and constant-temperature housing are placed over the hole with the large flange, and samples contained in a small dish in the sliding insert may be irradiated through the hole at left.

In most of our work, a cooled housing containing a 2"-diameter photomultiplier tube is connected to each apparatus as required. The data acquistition is usually carried out in the single-photon mode with a frequency counter whose output is stored in the memory of a small computer.

[*] Prof. G. D. Mendenhall
Department of Chemistry and Chemical Engineering
Michigan Technological University
Houghton, MI 49931 (USA)

The sensitivity limits of any system are determined by the precision with which the sample emission and background noise can be measured and are subject to the usual statistical relations concerning collection times and signal-to-noise levels. A standard deviation of $\pm$ 2 Hz with a noise level of 5–20 Hz is typical for a cooled, 2″ tube under favorable conditions with samples at ambient temperature and with collection times of 40–120 s. Frequency counters with compensating devices, signal chopping, and selection of low-noise tubes or tubes with smaller active areas can reduce background signals even further. The difficulty with CL, however, is usually not signal strength but in devising suitable experimental protocols to study the wide variety of organic materials that are amenable to the technique and in divining trends from the resulting data.

Chemiluminescence can be enhanced from solids and liquids by addition of highly fluorescent molecules which can accept energy from less emissive excited states. The most commonly used fluorescent substances, 9,10-dibromoanthracene and 9,10-diphenylanthracene, can be destroyed by free-radical attack, especially at elevated temperatures.[5] This can sometimes complicate the interpretation of changes in CL with time.[6]

3. Mechanisms of CL

At present there appear to be at least three sources of adventitious photon emission from condensed-phase organic materials. Two mechanisms involve peroxy radicals, the other is due to charge recombination.

3.1. Peroxy Radicals

Peroxy–peroxy reactions via a tetroxide [Eq. (a)] have long been regarded on kinetic and thermochemical grounds as a major source of excited states when organic materials are heated in air. In the condensed phase the excited-state

$$2\,R^1R^2CHOO^{\cdot} \rightarrow R^1R^2CHOOOOCHR^1R^2 \rightarrow\rightarrow R^1R^2CO(S_0, S_1, T_0) + R^1R^2CHOH + O_2 \quad (a)$$

$$R^1R^2CO^*(S_1, T_0) \rightarrow R^1R^2CO(S_0) + h\nu$$

R^1, R^2 = alkyl, H

products appear to be primarily triplet aldehydes and ketones.[7, 8] Interaction of 2-propylperoxy radicals in the gas phase gives rise, interestingly, to CL with rotational fine structure ascribed to the emission from the $^1\Sigma_g$ state of molecular oxygen.[9]

Thermolysis of peroxides in which an alkyl group has an α-hydrogen can give rise to excited states [Eq. (b)]. The simplest example of this reaction is the decomposition of methyl peroxide to give excited formaldehyde. This exothermic reaction sequence can proceed explosively in the gas phase and produces an easily visible blue glow from formaldehyde fluorescence.[10] Triplet formaldehyde emission can also be observed from methoxy radical self-reactions ($2\,CH_3O^{\cdot} \rightarrow CH_2O + CH_3OH$) in the absence of oxygen.[11]

$$R^1R^2CHOOR \rightarrow [R^1R^2CHO^{\cdot}\ {}^{\cdot}OR]_{cage} \rightarrow R^1R^2CO^*(S_0, S_1, T_0)$$
$$R^1R^2CO^* \rightarrow R^1R^2CO + h\nu \quad (b)$$

In any given system the two mechanisms [Eqs. (a) and (b)] may appear simultaneously depending on the temperature and the concentrations of peroxidic species. For instance, saturated aliphatic hydrocarbon radicals or the radical $R^1R^2CHO^{\cdot}$ can produce a peroxy radical $ROO^{\cdot}$ by H abstraction from any ROOH present. The $ROO^{\cdot}$ radicals can also arise from other radicals by several other mechanisms in the presence of oxygen. The peroxy radicals so formed, even in the absence of oxygen, can give light emission via reaction (a). They can also give peroxides and subsequently excited ketones via reaction (b), by either a Vaughan-type termination step [Eq. (c)] or coupling with carbon radicals to form a chemiluminescence peroxide [Eq. (d)].

$$2\,R^1R^2CHOO^{\cdot} \rightarrow O_2 + R^1R^2CHOOCHR^1R^2 \rightarrow R^1R^2CO^* \rightarrow h\nu \quad (c)$$

$$R^1R^2CHOO^{\cdot} + R^{\cdot} \rightarrow R^1R^2CHOOR \rightarrow ROH + R^1R^2CO^* \rightarrow h\nu \quad (d)$$

3.2. Recombination Luminescence

The third source of light from materials is a delayed emission that is usually ascribed to charge-recombination luminescence.[2, 12–15] This is actually a physical phenomenon, but it is very frequently observed with the sensitive apparatus that investigators use to measure chemiluminescence. A regular, crystalline lattice is not a requirement. Examples of some typical decay curves from our work are given in Figure 2, although most workers have studied the phenomenon at much shorter time scales.

The current portrayal of the process (see, e.g., Ref. [15]) involves formation of an electronically excited chromophore in a material which can eject an electron to give a cation–electron pair. In the absence of an applied electric field, this

G. David Mendenhall received a B. S. degree in chemistry from the University of Michigan in 1966 and a Ph. D. in physical organic chemistry from Harvard University in 1971 under the supervision of Prof. Paul Bartlett. He also attended the Universität Freiburg in 1965. After postdoctorate positions at the National Research Council of Canada (Ottawa) and Stanford Research Institute, he worked at a contract research firm for six years before joining the Department of Chemistry and Chemical Engineering, Michigan Technological University, in 1980, where he is now Professor of Chemistry. He has taught part-time at Otterbein College, worked on drug synthesis at Parke-Davis & Company (Ann Arbor), and carried out consulting work with a number of companies.

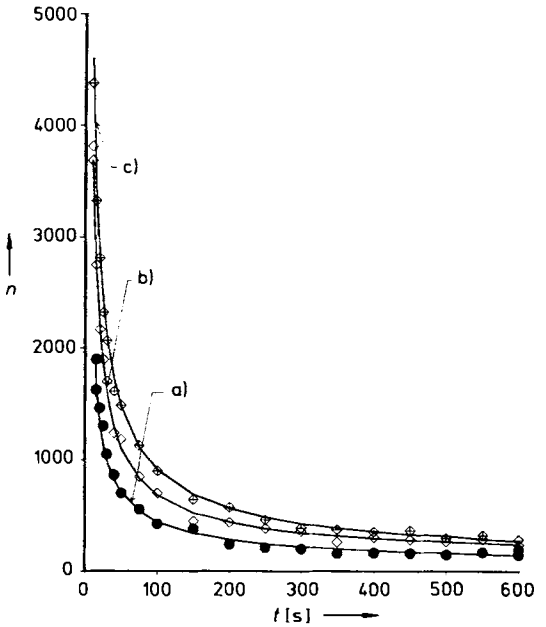

Fig. 2. Delayed emission from polymers fitted to Equation (e). Selected data points and the fitted curve are shown [2]. a) Wheat starch; b) polycarbonate; c) styrene maleic anhydride. n = counts per 5-s interval.

solid-state ionization is usually rather inefficient. Thermal motions in the solid result in a diffusive hopping of the charge through the material, where it resides in potential wells of various depths. Eventually charge recombination occurs with a finite probability of excited-state formation, followed by reionization, radiationless decay, or emission of light. The motion of the charges through the solid is initially rapid, but becomes progressively slower as the charges encounter deeper potential wells. Both electrons and cationic sites, or "holes", can migrate in this fashion, although sometimes only one may do so in a given material.

Such charge-recombination luminescence can be recognized by its dependence on a stimulus (overhead fluorescent room lights were traced as the source in our original discovery), a nonexponential, hyperbolic decay, often extending to tens of minutes, and a small temperature dependence of the recombination rate. Several theoretical treatments[12-16] of the time dependence of the emission have been carried out which lead to a power function [Eq. (e)] as an approximation ($t > 0$; $0.6 < m < 2.0$; B = intensity of background signal; A = preexponential factor).

$$I(t) \equiv \mathrm{d}\,h\nu/\mathrm{d}t = At^{-m} + B \qquad \text{(e)}$$

The cited limits on m are those that we and others have observed empirically. It is important to note in the application of Equation (e) that zero time is not arbitrary.

Some polymers that we studied and their derived values of $\lg A$ and m for delayed emission lasting up to 10 min are given in Table 1. In none of 98 polymers examined did the stimulated emission fit a simple exponential function,[2] although some undoubtedly would if examined at conventional, very short times after excitation.

The decay curves obtained in this manner, however, can also be fitted to a stretched exponential ($I = Ae^{-kt^{\beta}}$) or to a sum of two or three exponential terms.[16] The assignment of a mechanism based on charge-recombination to curves of this sort may not be correct in every case. For instance, the decay of luminescence from solid, tryptophan-containing proteins follows a power function.[17] *Strambini* and *Gabellieri* have interpreted this behavior in terms of phosphorescence from molecules in the matrix with a distribution of first-order decay times (cf. Refs. [16, 18]). Unequivocal proof of a mechanism is not necessarily straightforward, since the chemiluminescence apparatus can respond to light from either radicals or hole–electron pairs that are well below the ESR detection limit, and perturbation of the emission from solids with an applied electric field is characteristic of both correlated radical-ion pairs and localized excited states.[19]

Table 1. Parameters for Equation (e) for commercial polymers stimulated by incandescent light [2].

Polymer	lg A [a]	m [a]
Sodium alginate	4.92	0.924
Methyl cellulose	4.95	0.846
Nylon 6/6	4.43	1.02
Nylon 6/9	4.52	0.942
Nylon 11	4.91	0.973
Nylon 12	5.12	0.943
Poly(*N*-vinylcarbazole) (PVK)	7.81	1.792
Polycaprolactone	6.07	1.059
Poly(phenylene sulfide)	5.33	0.981
Vinylidene chloride/20% acrylonitrile	5.02	0.876
Soluble starch	3.30	0.680
Starch, wheat powder	3.49	0.682
Albumin, egg powder	4.51	0.932
Poly(α-methylstyrene)	4.37	0.600

[a] Variables fitted to the equation $\lg(I\Delta t) = \lg A - m \lg(t/\Delta t)$, with $\Delta t = 5$s and I = counts per time interval Δt.

We concluded from a survey of commercial polymers with incandescent stimulation that nonextractable impurities played a major role in their charge-recombination luminescence.[2] We could stimulate luminescence that decayed according to Equation (e) in a nonemissive (under our conditions) polymer, Nylon 6, by adding a fluorescent, orange dye, Hoechst 3400, which is bound strongly by polyamides.

An aspect of this phenomenon which we have not explored is its possible role in causing polymer photodegradation, especially since wavelengths throughout the visible region of the spectrum are often active.[2]

In the earlier review[1] the delayed emission after incandescent stimulation was ascribed to slow termination of free radicals followed by light production according to Equation (a). This non-steady-state process has been reported in liquids,[20] but the kinetic expressions such as Equation (f) that can be derived to describe the time dependence of the decay of emission do not in our experience usually fit the long-lived

$$t = \frac{1}{\text{constant}} \ln \frac{(I_{\infty}^{1/2} + I_t^{1/2})(I_{\infty}^{1/2} - I_0^{1/2})}{(I_{\infty}^{1/2} - I_t^{1/2})(I_{\infty}^{1/2} + I_0^{1/2})} \qquad \text{(f)}$$

stimulated luminescence from solids. The lack of fit of Equation (f) to the data was recognized at the time of my first review,[1] but dismissed with the very incorrect assumption that the delayed luminescence from a manufactured item, of complicated and often nonhomogeneous composition, could not be expected to obey simple rate expressions.

Under some circumstances, irradiation of samples with UV light does give complicated decay curves due to the simultaneous production of free-radical and charge-recombination luminescence.[21] Inorganic materials also sometimes give luminescence which decays according to Equation (e). Equations similar to (f) have been derived to treat the decay of CL from autoxidizing polymers after changing to an inert atmosphere.[22] Free-radical oxidation of most organic materials would be expected to produce a collection of $RO_2^{\cdot}$ radicals with different R groups, so that the CL may arise simultaneously by way of a number of termination reactions. The rate constants derived from such kinetic methods may therefore represent averaged quantities.

3.3. Other Mechanisms

Other sources of CL from materials, such as acyl radical recombination to give luminescent states,[23] may be important under certain circumstances. 1,2-Dioxetanes are among the most luminescent class of peroxides, but there is no conclusive evidence for their formation during autoxidation of simple hydrocarbons. The autoxidation of α-phenylpropionaldehyde has been proposed to give acetophenone through a dioxetane intermediate[24] and dioxetanes are responsible for the luminescence in air of tetrakis(dimethylamino)ethylene.[25] Chemiluminescent dioxetanes are also produced in the enzymic oxidation of specialized organic substrates.[26]

4. Models for Charge-Recombination Luminescence

We have also studied delayed luminescence from poly(*N*-vinylcarbazole) (PVK), alone and containing 2,4,7-trinitrofluorenone (TNF) as a simulated impurity.[27] This pair is very well known and was a component of one of the first commercial photocopiers.[28] The photoejection of electrons from the PVK–TNF complex (or from more modern substitutes) discharges the surface of an electrified drum in the photocopier and is thus an integral part of the reproduction process. We found that PVK displayed the strongest delayed luminescence of any substance we have ever examined, with the emission in each case following Equation (e). The emission from purer lots of material was greatly reduced, but was enhanced upon addition of TNF, reaching a maximum at a (monomer) mole fraction of 10^{-4} of TNF (Fig. 3). This strong *increase* in charge-recombination luminescence with TNF stands in contrast to its ability to *quench* the prompt fluorescence emission of PVK.[29] The increase in delayed emission is caused by increased absorption of the incandescent light because of the appearance of "charge-transfer" bands in the visible region in the presence of TNF, augmented by the ability of the electronegative TNF to facilitate charge separation.

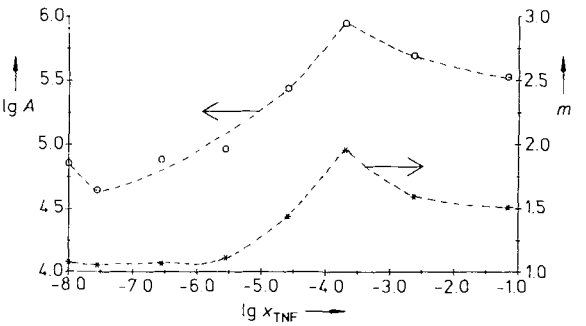

Fig. 3. Values of m and A (per gram of substance) in Equation (e) for light-stimulated PVK films as a function of added TNF. The films were evaporated from PVK–TNF solutions in $CHCl_3$ onto quartz and examined as described in [2, 24].

5. Applications of CL to Polyolefins

5.1. Measurement of Effects of Heat and Ionizing Radiation

Chemiluminescence was recognized in early work (cited in Ref. [1]) as a convenient way to monitor oxidation even in inhibited systems, where most of the peroxy radicals are intercepted by an added reagent [Eq. (g)].

$$\begin{aligned} &ROO^{\cdot} + AH\ (\text{phenol, aromatic amine}) \rightarrow ROOH + A^{\cdot} \\ &A^{\cdot} + ROO^{\cdot} \rightarrow ROOA \end{aligned} \qquad (g)$$

The complete consumption of an inhibitor by reaction (g) at elevated temperatures is often marked by a sudden increase in the chemiluminescence emission due to the resumption of reaction (a), but frequently the level of emission in the preinduction period is significant and proportional to the induction period itself. Polypropylene (PP) appears to be an especially favorable substrate for chemiluminescence studies. Experiments with γ-irradiated, formulated sheets[4] have shown a rough correlation between the light emitted at ambient temperature a week after irradiation (Fig. 4, bottom) and the impact strengths of the sheets measured at the same temperature (Fig. 4, top). Although the apparatus for this work was designed to measure photocurrent, which is converted to a digital display,[30] the lower levels of light emission that we (Fig. 4, bottom) measured correspond to only about 100 photons per second from a sample 1″ in diameter.

A dramatic change in the order of stability of the same formulated polypropylene samples occurred when they were stored at 60 °C (Fig. 4, middle) rather than 25 °C (Fig. 4, top). The sulfide inhibitor is effective at the elevated temperature, but appears to be rather inert at ambient temperatures. The relative chemiluminescence emission from the samples at 150 °C in air, on the other hand, leads to the same ranking of the stabilities of the samples as the results of impact tests at 60 °C. Anomalous behavior of CL from sulfide-stabilized polymers has been noted by others as well.[31]

When powdered polypropylene containing low levels of a phenolic processing stabilizer was irradiated at low dosages with γ-rays from a ^{60}Co source and the chemiluminescence measured immediately after removing the sample from the radioactive source, we observed[32] a slow decay of luminescence that fit a power function fairly well (Fig. 5a). Polypropylene freed from antioxidant by extraction showed similar behavior. When phenolic inhibitor was added to the extracted polymer, the luminescence decay after irradiation changed to a first-order process (Fig. 5b).

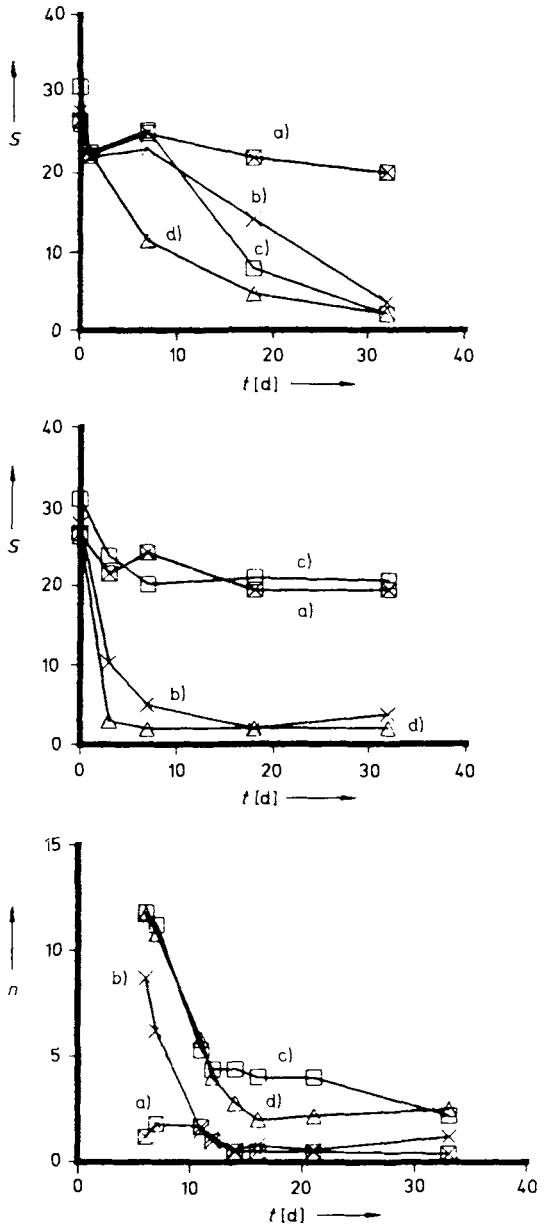

Fig. 4. Top and middle: Loss of impact strength S [inch-1 b] of polypropylene, irradiated to 5 mrd versus storage time at 25 and 60 °C, respectively. Bottom: Ambient chemiluminescence from γ-irradiated (5 mrd) polypropylene samples versus subsequent storage time at 25 °C [4]. a)–c) A "comb" sample contained 0.030% Goodrite 3114 (Phenol) *and* 1.0% of di-*n*-dodecyl 2,2'-dithiodipropionate (Thia). Other samples had just one stabilizer. See Ref. [4]. d) pure PP. n = counts per 2-min interval.

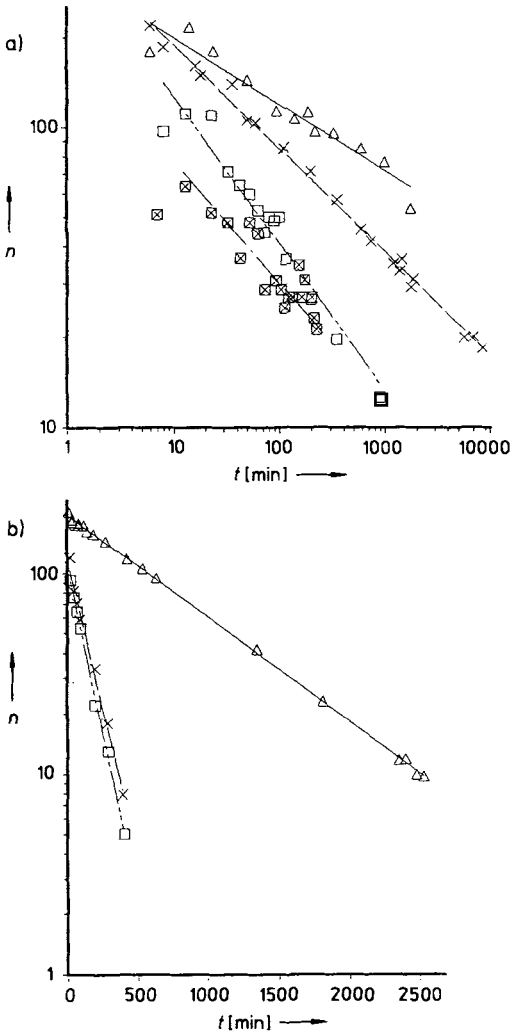

Fig. 5. Chemiluminescence from isotactic polypropylene powder containing 0.73%, 9,10-dibromoanthracene. n = counts per 1-min interval. a) Irradiated to different extents without inhibitor: △ 0.148 mrd, X 0.136 mrd, □ 0.034 mrd, ⊠ 0.006 mrd; b) γ-irradiated to 0.136 mrd in the presence of various amounts of inhibitor. Irganox 1010: △, 0.005%; X, 0.013%; □, 0.040%.

$$P_pOO^{\bullet} + P_tOO^{\bullet} \xrightarrow{k_t} h\nu + \text{termination}$$

$$P_pOO^{\bullet} + AH \xrightarrow{k_i} P_pOOH + A^{\bullet}$$

$$A^{\bullet} + P_tOO^{\bullet} \dashrightarrow \text{termination (fast)}$$

$$dh\nu/dt \equiv I = \Phi k_t[P_pOO^{\bullet}][P_tOO^{\bullet}]$$

$$d[P_pOO^{\bullet}]/dt = -k_t[P_pOO^{\bullet}][P_tOO^{\bullet}] - k_i[P_pOO^{\bullet}][AH]$$

Scheme 1. Possible explanation for first-order decay curves. Φ = quantum yield per $RO_2^{\bullet}$ pair.

The antioxidant in the experiment described above had been added to the sample by evaporation of a slurry containing the polymer and a solution of antioxidant. We suspected that the antioxidant had been deposited principally on the surface, and, indeed, when an unirradiated sample of this same preparation was fused unter nitrogen and then ground to a powder at 77 K, the chemiluminescence after irradiation (all at 25 °C) once again decayed according to a power function. When a relatively large amount of antioxidant (0.4%) was added to another polypropylene sample by fusing and cryogrinding, the subsequent ^{60}Co-stimulated luminescence reverted to an exponential.

There are a number of possible explanations for the kinetic laws that describe these decay curves. A power function may be derived as a limiting case for several sets of initial conditions. Factors such as inhomogeneous distributions of peroxy radicals may play a role in determining the shapes of the decay curves.[33]

The first-order decay curves, on the other hand, may be explained by the sequence in Scheme 1, where AH is a phenolic antioxidant and P_p and P_t are nontertiary and tertiary alkyl sites on the polymer chain, respectively.

If $[P_tOO^{\bullet}]$ and [AH] are nearly constant during the decay of light emission, Equation (h) is obtained.

$$[P_pOO^{\bullet}] \cong [P_pOO^{\bullet}]_0 e^{-k't} \qquad (h)$$
$$k' = k_t[P_tOO^{\bullet}] + k_i[AH]_x$$

Substituting Equation (h) in the rate law of Scheme 1, we obtain Equation (i) and, identifying I_0 as the emission at $t = 0$ we, have Equation (j).

$$I = \Phi[P_tOO^{\cdot}][P_pOO^{\cdot}]_0 \, e^{-k't} \quad (i)$$

$$I = I_0 e^{-k't} \quad (j)$$

The exponential decay constant k' is expected to be a function of the antioxidant concentration and the concentration of tertiary peroxy radicals. The decay rates of CL are indeed faster with higher starting concentrations of AH (Fig. 5b). This simple derivation neglects interconversion of $P_pOO^{\cdot}$ and $P_tOO^{\cdot}$, among other steps, and should be viewed as an approximation.

Recent experiments in our laboratory with formulated samples of PP and higher dose rates have revealed chemiluminescence behavior within the first few minutes after γ-irradiation that sometimes follows neither an exponential nor a power law, probably due in part to sample heating during the irradiation. *Fisher*[34] has shown with CL techniques that rates of oxygen diffusion into polyethylene are comparable to rates of radical production during irradiation of the polymer with an electron beam. Japanese workers[35] have shown a monotonic relation between CL under certain conditions and γ-dosages with several polyolefins, also at high dose rates. Applications of CL to the study of irradiated foodstuffs would appear to be a promising area.

5.2. IR Laser Heating

With γ-irradiated polypropylene again as a substrate, we examined the chemiluminescence in samples heated very rapidly in the apparatus shown in Figure 6.[32] A few milligrams of the powdered polymer were contained in an evacuated, sealed melting point capillary. The IR beam from a continuous, 4-W CO_2 laser passed through a germanium window (which blocked wavelengths in the visible) and heated the tube rapidly above the melting point of the polymer.

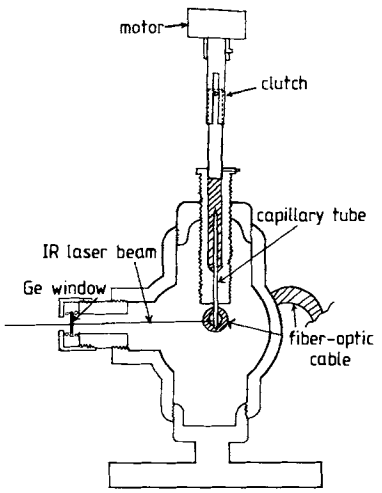

Fig. 6. Apparatus for heating samples with a 10.6-μm laser beam for measurement of CL.

To obtain reproducible results it was necessary to draw the capillary containing the sample slowly through the fixed laser beam. The light was collected with fiber optics and measured in the usual way. The emission from γ-irradiated polypropylene was linearly proportional to γ-dosage and to the peroxide value (POV, equivalents of peroxide per kilogram of material) of the sample, although the proportionality constants were dependent on the polymer formulations.[32]

6. Other Applications

Long-lived recombination luminescence appears to be useful to monitor the formation of chromophores on natural or artificial weathering of polymers, as suggested by an experiment with Nylon 6 (Fig. 7). A number of proprietary examples exist which show that the decay parameters are sensitive to composition and processing conditions of organic materials. A typical result is shown in Figure 8.

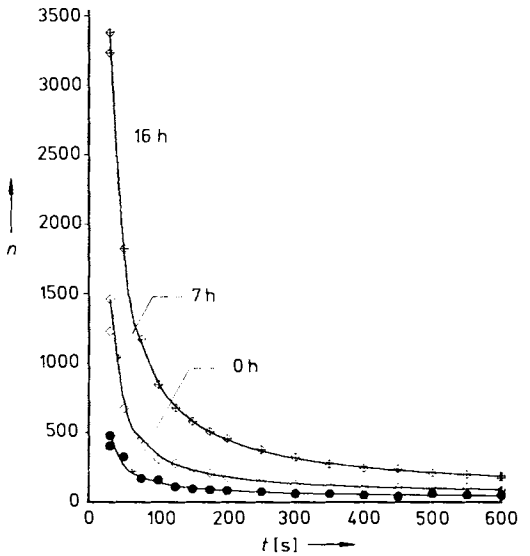

Fig. 7. Charge-recombination luminescence from Nylon 6 immediately after incandescent stimulation from samples that had previously been heated in air at 100 °C for 16, 7, and 0 h [2]. n = counts per 5-s interval.

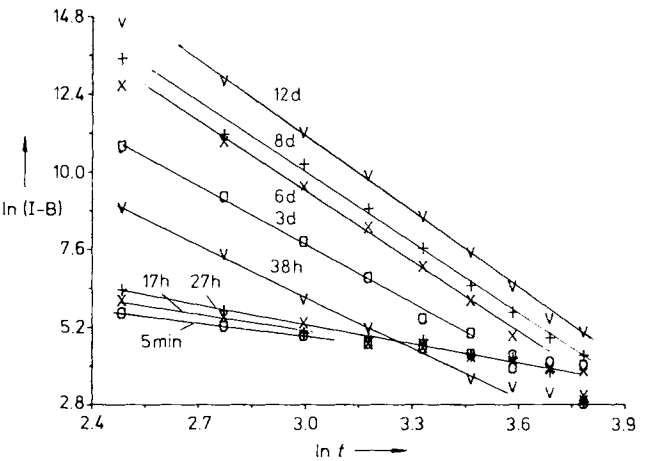

Fig. 8. Charge-recombination luminescence from epoxy cement (TRA-CON BB-2101) plotted in accord with Equation (e) (X. Guo, unpublished work). I − B = signal minus background; time at 25 °C since mixing of the components; t in seconds.

Chemiluminescence under an inert atmosphere can give information on the extent of oxidation in a more sensitive way than conventional methods. The IR-laser approach is one example of this. A second example appears in Figure 9, where the POV of samples was nearly constant within error in the early stages of oxidation while the CL from samples at corresponding times showed significant increases (inset in Fig. 9b).

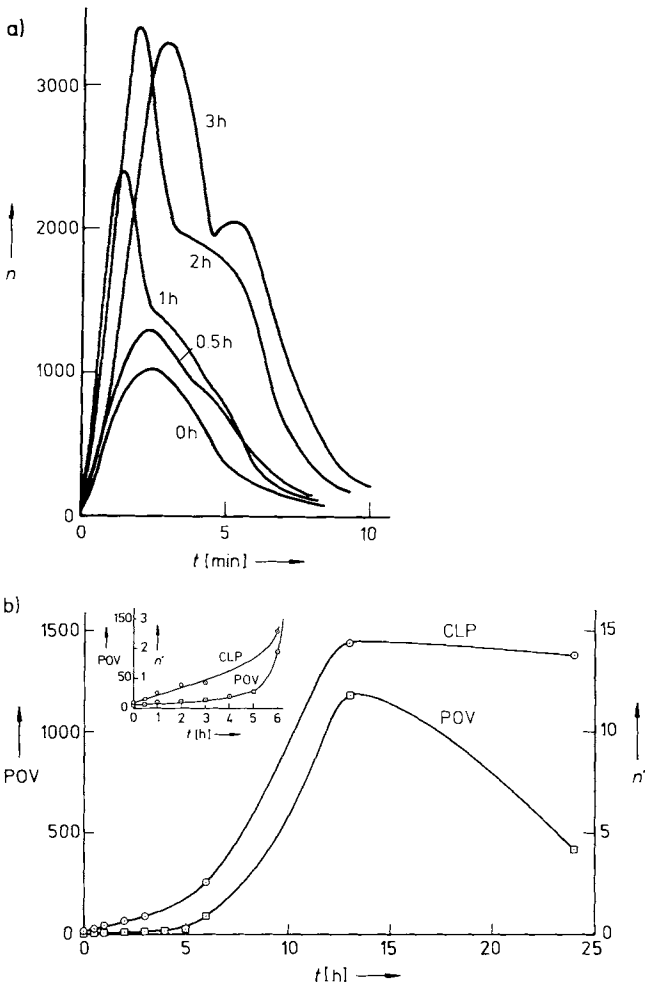

Fig. 9. a) Chemiluminescence from samples of peanut oil, previously oxidized at 100 °C in air for 0 to 3 h Aliquots containing 10^{-3} M 9,10-diphenylanthracene were flushed with N_2 and placed in a preheated oven at 200 °C to generate the curves shown. n = counts per 1-s interval. b) Values of total CL (areas under curves of Fig. 9a; CLP = *CL* on *P*yrolysis) and POV from the aliquots. $n' = 10^{-6}$/CL (number of photons). The inset shows an enlargement of the curve during the first six hours.

The fine structure in the plots of the more oxidized aliquots in Figure 9b is an indication of peroxidic species with differing thermal stabilities. It is noteworthy that the POV drops in the highly oxidized oil whereas the total CL values remain at high levels (Fig. 9b). Plots of this sort with other hydrocarbon substrates may not always show these features, however.[21]

Spilners reported a good correlation between chemiluminescence from a series of lubricating oils and their stabilities as measured by ASTM and other time-consuming procedures.[36] This work has been extended recently by others.[37, 38]

An interesting result was obtained from a sample of paper upon cycling the humidity above the sample (Fig. 10). The CL response was ascribed to free radicals produced by stresses incurred by the absorption and desorption of water.[39]

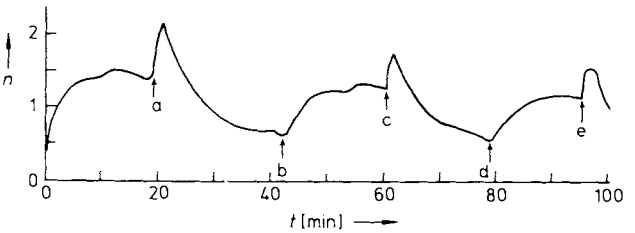

Fig. 10. Effects of cycling between moist and dry air on CL emission from treated Kraft paper at 70 °C [39]. At t = 0, the sample was placed in dry air. At a, c, and e, the dry air was replaced by moist air. At b and d, the moist air was replaced by dry air.

The practice by curators of storing book collections at constant humidity as well as constant temperature would appear to be justified.

7. Wavelength Distribution of CL

Conventional spectrometers are usually not practical for measurement of the spectral distribution of chemiluminescence emitted from materials at temperatures at which the autoxidation is comparatively slow, because of the weakness of the signal. A spectrometer with a 12″ mirror has been constructed for oxidation studies,[40] but most workers in the field have created histograms from the fractions of the light passing through a set of cutoff or interference filters[41, 42] or through a variable interference filter.[43] Using a number of physical and mathematical techniques we attempted to devise an inexpensive alternative[44] with a cell of adjustable thickness containing colored solutions (Fig. 11a). For instance, we could cut off in a progressive manner the wavelengths of light reaching a detector from a source of CL by increasing the optical path of the cell (Fig. 11b). If we obtained data with a perfect step-function cutoff filter, the spectrum could be reconstructed in principle by differentiating the resulting curve of total transmitted intensity versus filter thickness. Although our variable filter itself was more reliable than an expensive commercial one we originally purchased, the applications were not entirely successful because (1) a sharp cutoff was necessary for the computer programs to converge in the subsequent data analysis, even when the input data were calculated from the measured spectra of the dye solutions and an artificial emission spectrum, (2) solutions that showed a sharp cutoff did so over a limited range in wavelengths, so that a series of dye solutions was necessary to cover the visible region, (3) satisfactory spectra could be reconstructed only from extremely precise input data, a requirement not compatible with the nature of the source, and (4) thick dye solutions showed significantly decreased transmittance even at wavelengths where no absorption bands were present. This is apparently a scattering phenomenon and was not due to dust in the solutions.

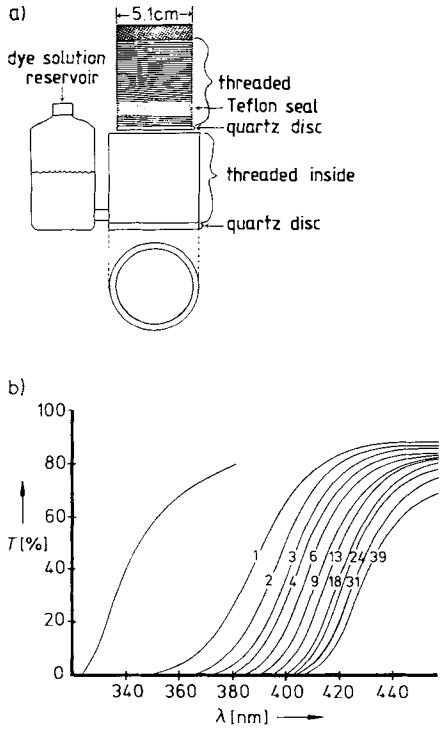

Fig. 11. a) Variable-path filter [44]. The threaded portions were of brass and the dye reservoir of plastic. b) Experimental transmission curves of *m*-nitrophenol in water (ca. 4 g l^{-1}). The numbers refer to the turns from the closed position (0.94 mm per turn). The curve at the extreme left is the transmission curve of a Corning filter No. 3-74.

8. Does Chemiluminescence Arise from the Surface?

This question is asked more frequently than any other when I have given talks on the subject. Imagine a sample of chemiluminescent material of uniform composition and consider only a volume element $1 \times 1 \times dx$ cm with its face normal to the detector (Fig. 12).

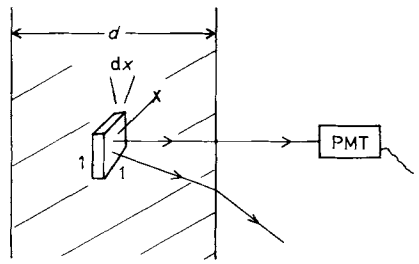

Fig. 12. Absorbed, transmitted, and refracted rays from a volume element in a chemiluminescent material of thickness *d*. PMT = photomultiplier tube.

Consider the case where an absorber is present with concentration C_a and molar absorptivity ε at wavelength λ. The light from a section at distance x from the surface will be attenuated by a factor of $e^{-\varepsilon C_a x}$. The net attenuation for the entire sample is given by integrating from the front surface to the back [Eq. (k), N_{av} = Avogadro number, C_e = emitter concentration, k' = rate constant of the light emission times detection efficiency].

$$I_{det} = \int_{x=0}^{x=d} (N_{av} C_e k'/1000)\, e^{-\varepsilon C_a x}\, dx = (N_{av} C_e k'/1000)\,[1 - e^{-\varepsilon C_a d}] \quad (k)$$

Dividing this result by the light that would have been detected without self-absorption (I), we obtain Equation (l).[45]

$$I_{det}/I = (1 - e^{-\varepsilon C_a d})/\varepsilon C_a d \quad (l)$$

Since the term $\varepsilon C_a d$ is the absorbance of the entire sample along d, the expression can be simplified further. Values of the fractional absorption for various total absorbances appear in Table 2. It can be seen that for absorbances (A) less than 0.2, over 90% of the emission escapes, and for high values of A, the correction factor approaches 1/A.

Table 2. Fractional emission of homogeneously emitted light for various absorbances A.

A	$(1-e^{-A})/A$	A	$(1-e^{-A})/A$
0.05	0.975	1.0	0.63
0.10	0.95	2.0	0.43
0.20	0.906	3.0	0.32
0.50	0.79	10.0	0.10

In general terms, we infer from this calculation that with transparent or translucent materials (lightly colored oils, thin polymer films, biological suspensions, etc.), chemiluminescence will be detected from the surface and interior and will be proportional to sample mass, provided that the initial assumptions are correct. For opaque materials (most edible substances, filled or dyed rubbers, dark liquids, composites, light-scattering polymers), chemiluminescence will be proportional to the area exposed to the detector. For this reason, most of our sample holders for weakly emitting solids are wide and shallow. The CL of light-absorbing substances is maximized and made reproducible merely by filling the container with an opaque layer of material.

The correction factor in Table 2 is usually not applied to the data because (1) a separate factor would usually be required at each wavelength, (2) the absorbance of many relatively opaque or powdered materials of interest is not easily measured, (3) a rigorous treatment would require additional corrections for internal reflections at the air–sample interface, and, (4) since one is invariably comparing samples of different composition or history, the relative values of CL are normally sufficient. Significant spectral differences between samples can be detected in a simple and relatively rapid fashion by measurement of changes in the fraction of light transmittted by a given cutoff filter (f value[3]).

It might be noted that if CL is measured from a translucent sample in a rectangular cell normal to two different faces, the corresponding absorbance of the sample can be calculated from the data by applying the integrated equation (l). The absorbance can also be determined from two measurements with a sample in a cell with reflecting versus absorbing backings.[45]

If the chemiluminescence emission and the sample absorption spectra overlap, only in exceptional cases will chemiluminescence that is emitted homogeneously show the same spectral distribution as the emission in the absence of self-absorption. A reported[46] shift in wavelengths for stretched versus static polymers may have arisen in an analogous manner, if the same excited states were generated at different depths from the surface under the two conditions. With static samples, it is a simple matter to check for surface versus bulk emission by ablating the surface and remeasuring the chemiluminescence, although the treatment itself may generate light emission from mechanochemically produced free radicals.

9. Surface Oxidation

Equation (l) was derived under the assumption that the chemiluminescent species was distributed homogeneously in the sample, which is generally true in liquids but less generally so in solids. For instance, *Carlsson* and *Wiles*[47] established that conventionally extruded polypropylene fiber contains a highly oxidized surface layer. We have measured[48] chemiluminescence from fibers extruded at different rates through a die orifice. The fibers were wound as a monolayer around a mandril (Fig. 13a). The similarity in the curves was

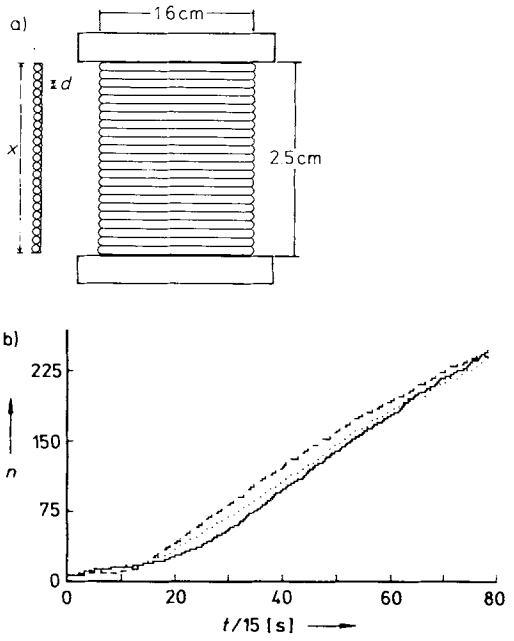

Fig. 13. a) Mandril with a length of 2.5 cm for examination of CL from fibers (air, 150 °C). b) CL from unstabilized polypropylene fiber. Solid line, $d = 0.41$; broken line, $d = 0.66$; dotted line, $d = 1.3$ mm [48]. Unit of $n = 1000$ photons per 15-s interval.

interpreted as a demonstration that CL arose from their similar exposed surface areas πxl ($l = 1.6$ cm, n = number of fibers) which are independent of d, rather than the total exposed mass of the sample $\pi xdl/4$, which increases with d. This result may have important implications for the interpretation of CL from stabilized polypropylene in the preinduction period. *Shard*[49] concluded from an early study of this polymer that CL at elevated temperatures arose from the surface, since the intensity did not change significantly as the film thickness was varied by a factor of ten.

10. Infrared CL at 1.27 μm

The autoxidation process produces singlet molecular oxygen, whose phosphorescence emission appears as a narrow band around 1.27 μm.[50] We have recently measured induction times for systems containing free-radical initiators and phenolic antioxidants (Fig. 14). The appearance of the 1.27 μm emission marks the complete consumption of antioxidant according to Equation (g) and production of $^1O_2$ by the termination reaction (a). The emission equation does not appear in samples with conventional amounts of diphenylamines because (1) the oxidation products of diphenylamines, in contrast to the phenols, are themselves good antioxidants and (2) a portion of the amine is converted into the corresponding nitroxide, which is a good quencher for singlet oxygen.

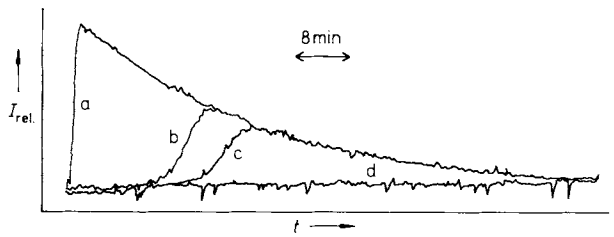

Fig. 14. a) IR CL at 1.27 μm from oxygen-saturated diphenylmethane at 70.6 °C initially containing 0.030 M di-*tert*-butylhyponitrite. b)–d) The solutions contained initially 0.010 M, and 0.012 M 2.6-di-*tert*-butyl-4-methylphenol, respectively. Only the rising portions of curves b) and c) are shown (Q. Niu, unpublished work).

IR chemiluminescence from singlet oxygen is an attractive way to monitor autoxidation because the emission is from a single, well-defined molecule. Scattering and self-absorption of light of this long wavelength is expected to be generally less as well. The principal disadvantages are the larger contribution of thermal (black-body) noise at IR wavelengths and the lower inherent sensitivity of IR detectors.

11. Biological Oxidation

A number of workers have reported weak light emission from both plant and animal sources.[51, 52] Light emission from plant roots has been suggested as a way to monitor oxygen transport.[53] One of the more interesting of the earlier studies resulted in a tabulation of CL from the body organs of a 24-year-old Russian who died of gunshot wounds.[54] Updated versions of the experiment have been reported recently with live rats.[55] The CL emission of the rodents increased after they were injected with halomethanes. A very popular approach among biochemists in recent years has been to monitor enzymatic or whole-cell free-radical generation with luminol, which reacts with oxygenated

radicals in the cells to produce light with high efficiency. The latter subject has also been reviewed recently[56] (see also Ref. [57]).

12. Chemiluminescence Imaging and Other Developments

Recently there have been a number of significant advances in imaging technology at both visible and IR wavelengths. The commercial availability of intensified channel-plate detectors has enabled scientists to obtain conventional spectra and 2D "self-portraits" from materials with comparative ease and in reasonable times. An image of a piece of autoxidizing polybutadiene is shown in Figure 15 along with a

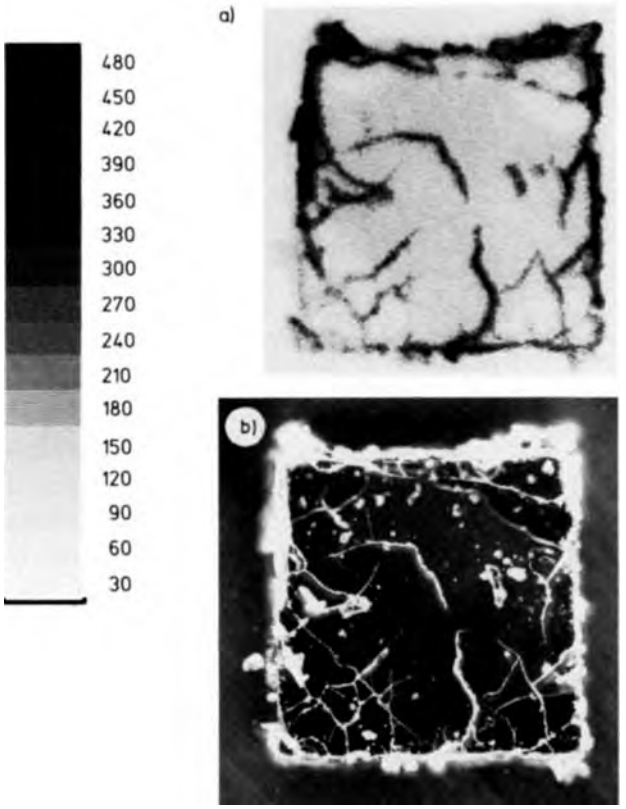

Fig. 15. a) Chemiluminescence image (20-min collection time, 92 °C) and b) conventional photograph of a 1-cm² sample of *trans*-1,4-polybutadiene [58]. The numbers 30–480 on the left signify number of photons per pixel.

photograph of the same sample under ambient lighting conditions. The images are quite similar. The accentuation of CL from cracks and edges in this particular sample is probably an optical scattering phenomenon rather than an indication of enhanced oxidation. Two-dimensional data obtained from emission measurements at two temperatures can be manipulated to give images constructed from spatially resolved values of apparent activation energy and A factor.[58]

Dickenson and co-workers[59] have used a monochromator with an image intensifier to obtain spectra of light simultaneously at all wavelengths emitted from fractured or separated surfaces. When adhesive tape is peeled from its backing, it shows light emission corresponding to bands from molecular nitrogen, which is ionized by sparks in contact with air. The separation of charges with stress is a general phenomenon, and it is not surprising that, when samples of some polymers are crushed, the light that is emitted shows a hyperbolic decay with time that is entirely reminiscent of charge-recombination curves (Fig. 16). Although these phenomena are not due to CL, they are commonly observed in our apparatus and it is appropriate to mention them.

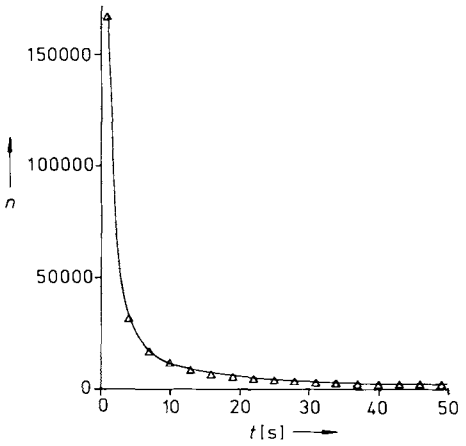

Fig. 16. CL from crushed sample of amorphous PVK (H. K. Agarwal, unpublished work). n = counts per 1-sec interval.

Three-dimensional plots with two time axes are a convenient way to condense data from a series of experiments (Fig. 17). One time axis represents the aging of the sample during storage, and the other the much shorter time of examination at elevated temperature.[4]

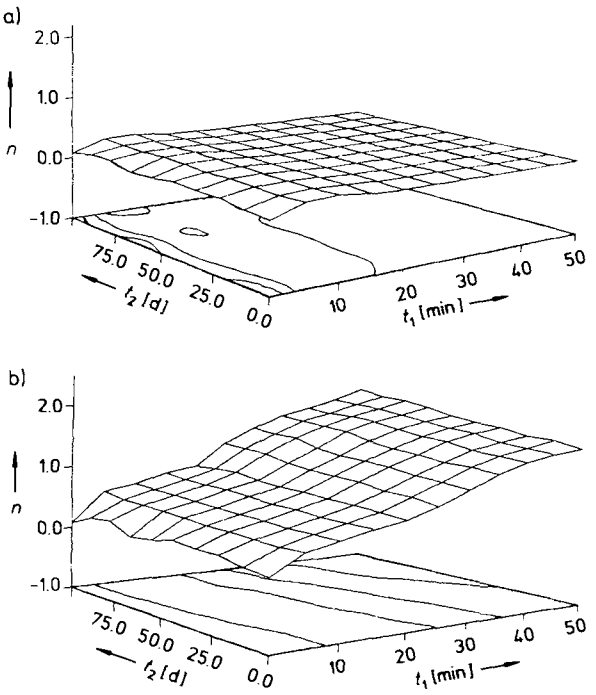

Fig. 17. Plots of CL in air at 150 °C versus storage time at 25 °C from end of irradiation [4]. n = counts per 10^4 s interval. a) Thia, b) Phenol (see Fig. 4).

Oscillating CL at visible wavelengths from oxidizing samples of polypropylene[60] and hydrocarbon liquids[61] has been reported.

Chemiluminescence measured from samples under non-isothermal conditions with photon counting can be analyzed in a manner similar to DSC experiments, to give values of the activation parameters E_a und lg A directly.[62]

13. Conclusions

In our experience, the general approaches for examining CL and other weak light emission from bulk organic materials may be summarized as follows:

1. Heating O_2-free samples above 200 °C rapidly decomposes all peroxidic groups and gives a total CL emission that is proportional to peroxide content, although the proportionality usually varies with the nature of the hydrocarbon.
2. CL from air-saturated samples at any temperature is proportional to the rate of oxidation. The best correlations between CL and a material property are usually obtained when a single organic substrate (which itself may be a complicated mixture) is being tested with small concentrations of additives, especially antioxidants. Direct comparison of CL data from different base stocks of oils or from polymers of different structural types, on the other hand, can be less rewarding. In favorable cases, well-defined induction periods are observed which are not particularly dependent on the nature of the material.
3. Delayed luminescence after *incandescent* stimulation, which decays according to Equation (e) is useful for monitoring material composition as well as changes in materials resulting from heat or photochemical aging. Polyolefins do not usually show delayed emission but aromatic polymers and polyamides, as well as natural materials, usually do (e.g., dry tea leaves, paper, and cereals, but not lettuce).

The application of chemiluminescence techniques to oxidative changes in materials is difficult because the outcome is a dynamic measure of a complicated radical chain reaction followed by excited-state reactions, modified by the optical properties of the bulk sample. The convolution of all of these factors actually is very useful in some cases (e.g., quality control), but it renders the interpretation of results less straightforward in comparison say with IR or NMR spectroscopy.

Familiar measurements, however, such as oxygen uptake and peroxide value also reflect complicated reaction sequences and mixtures of species. As progress is made in unraveling the steps of the autoxidation process in condensed media, and the nature of the reactions giving excited states is better established, investigators will use the technique with increasing confidence. The essential simplicity of the technique is always appealing.

It would be helpful also if academic reviewers for applied journals would bear in mind that empirical analytical procedures, as in medicine, are useful and of interest to people with real-world problems even when the mechanistic details of the analysis are not completely clear.

The work described here was generously supported by the U.S. Army Research Office, 3M Co., Himont USA, Exxon Chemical Co., and numerous other organizations. Indispensable contributions by graduate students Kelly Flaherty, Hamender Agarwal, Honsik Byun, Su-Hua Lee, Xiaoping Guo, Qingshan Niu, and Xiaoning Sheng, and colleagues Drs. Craig A. Ogle, John R. Nixon, and Joel M. Cooke are also gratefully acknowledged. We thank the late Mr. George Turner for loan of an apparatus in earlier stages of the work and Dr. Stephen E. Bialkowski for discussions of techniques for spectral resolution.

Received: November 23, 1988 [A 753 IE]
German version: *Angew. Chem. 102* (1990) 380

[1] G. D. Mendenhall, *Angew. Chem. 89* (1977) 220; *Angew. Chem. Int. Ed. Engl. 16* (1977) 225.
[2] G. D. Mendenhall, H. K. Agarwal, *J. Appl. Polym. Sci. 33* (1987) 1259.
[3] G. D. Mendenhall, R. A. Nathan, M. A. Golub in E. G. Brame, Jr. (Ed.): *Applications of Polymer Spectroscopy*, Academic Press, New York 1978, Chapter 8.
[4] G. D. Mendenhall, H. K. Agarwal, J. M. Cooke, T. S. Dziemianowicz in P. P. Klemchuk (Ed.): *Polymer Stabilization and Degradation (ACS Symp. Ser. 280* (1985) 373).
[5] A. M. Turner, W. A. Waters, *J. Chem. Soc. 1956*, 879.
[6] a) W. R. Jones, Jr. (NASA-Lewis), personal Communication; b) W. R. Jones, Jr., M. A. Meador, W. Morales, *ASLE Trans. 30* (1987) 211.
[7] a) V. A. Belyakov, R. F. Vassil'ev, *Photochem. Photobiol. 6* (1967) 35; b) M. Hofert, *ibid. 9* (1969) 427.
[8] X. C. Sheng, G. D. Mendenhall, unpublished.
[9] D. J. Bogan, F. Celii, R. S. Sheinson, R. A. Coveleskie, *J. Photochem. 25* (1984) 409.
[10] a) J. R. Henderson, M. Muramoto, *J. Chem. Phys. 43* (1965) 1215; b) D. J. Bogan, W. A. Sanders, H. T. Wang, R. S. Sheinson, *Chem. Phys. Processes Combust. 1984*, 4.
[11] D. J. Bogan, W. A. Sanders, H. T. Wang, *190th Am. Chem. Soc. Mtg.* (Chicago, IL 1985), Abstr. ORG 199.
[12] P. Debye, J. O. Edwards, *J. Chem. Phys. 20* (1952) 236.
[13] W. H. Hamill, *J. Phys. Chem. 82* (1978) 2073.
[14] H. Scher, E. W. Montroll, *Phys. Rev. B. 12* (1975) 2455.
[15] a) H. Bassler, *Phys. Status Solidi B 107* (1981) 9; b) B. Ries, H. Bassler, *J. Mol. Electron. 3* (1987) 15.
[16] W. Siebrand, T. A. Wildman, *Acc. Chem. Res. 19* (1986) 238.
[17] G. B. Strambini, E. Gabellieri, *Photochem. Photobiol. 39* (1984) 725.
[18] J. T. Randall, M. H. F. Wilkins, *Proc. R. Soc. London 184* (1945) 390.
[19] R. O. Loutfy, J. H. Sharp, *J. Phys. Chem. 83* (1979) 1208.
[20] A. A. Vichutinskii, *Nature (London) 206* (1965) 292.
[21] N. C. Burlingame, Toronto (Canada), personal communication; paper presented at the *3rd Chem. Conf. North Am.* 1988.
[22] G. A. George, *Polymer Degradation and Stability*, **1** (1979) 217.
[23] a) J. De La Fuente, E. A. Lissi, *Bol. Soc. Chil. Quim. 31* (1986) 123; b) H. W. Holden, K. O. Kutschke, *Can. J. Chem. 39* (1961) 1552.
[24] R. A. Howell (Central Michigan University), personal communication.
[25] A. N. Fletcher, C. A. Heller, *J. Phys. Chem. 71* (1967) 1507.
[26] a) N. Duran, R. C. DeBaptista, G. Cilento, *Photochem. Photobiol. 30* (1979) 101; b) A. Thompson, W. H. Biggley, G. H. Posner, J. R. Lever, H. H. Seliger, *Biochim. Biophys. Acta 882* (1986) 210.
[27] X. Guo, *Masters Thesis*, Michigan Technological University 1988.
[28] H. Hoegl, O. Süs, W. Neugebauer, DBP 1 068 115 (1957), Kalle and Co. Akt.-Ges.
[29] a) W. Klopffer, *Ber. Bunsenges. Phys. Chem. 73* (1969) 864; b) H. Hoegl, G. Barchietto, D. Tar, *Photochem. Photobiol. 16* (1972) 335.
[30] G. K. Turner in K. Van Dyke (Ed.): *Bioluminescence and Chemiluminescence: Instruments and Applications Vol. II*, CRC Press, Boca Raton, FL, USA 1985, Chapter 3.
[31] M. P. Shard, *Polym. Eng. Sci.* 5 (1965) 246.
[32] G. D. Mendenhall, H. Byun, J. M. Cooke in R. B. Seymour, T. Cheng (Eds.): *Advances in Polyolefins*, Plenum, New York 1987, p. 405.
[33] T. V. Pokholok, O. N. Karpukhin, V. Ya. Shlyapintokh, *J. Polym. Sci. 13* (1975) 525.
[34] W. K. Fisher, *J. Ind. Irradiat. Technol. 3* (1985) 167.
[35] F. Yoshii, T. Sasaki, K. Makuuchi, N. Tamura, *J. Appl. Polym. Sci. 30* (1985) 3339.
[36] I. J. Spilners, J. F. Hedenburg, *Ind. Eng. Chem. Prod. Res. Dev. 24* (1985) 442.
[37] P. A. Benoy, S. F. Murray, *J. Am. Soc. Lubr. Eng. 43* (1987) 370.
[38] P. Pei, S. M. Hsu, S. Weeks, R. Lawson, *J. Soc. Tribol. Lubr. Eng. 45* (1989) 10.

[39] G. B. Kelly, J. C. Williams, G. D. Mendenhall, C. A. Ogle in R. K. Eby (Ed.): *Durability of Macromolecular Materials (ACS Symp. Ser. 95* (1979) 117).
[40] R. F. Vassil'ev, *Prog. React. Kinet. 4* (1967) 305.
[41] L. Matislova-Rychla, J. Rychly, M. Vavredova, *Eur. Polym. J. 14* (1978) 1033.
[42] R. E. Barker, Jr., J. H. Daane, P. M. Rentzepis, *J. Polym. Sci. 3* (1965) 2033.
[43] J. P. Hamman, W. H. Biggley, H. H. Seliger, *Photochem. Photobiol. 30* (1979) 519.
[44] K. R. Flaherty, *Masters Thesis*, Michigan Technological University 1982.
[45] S. Stieg, T. A. Nieman, *Anal. Chem. 50* (1978) 401.
[46] D. L. Fanter, R. L. Levy, *ACS Symp. Ser.* (1979) 2118.
[47] D. J. Carlsson, D. M. Wiles, *Macromolecules 4* (1971) 179.
[48] K. R. Flaherty, W. M. Lee, G. D. Mendenhall, *J. Polym. Lett. 22* (1984) 665.
[49] M. P. Schard, C. A. Russell, *J. Appl. Polym. Sci. 8* (1964) 985.
[50] a) J. A. Howard, K. U. Ingold, *J. Am. Chem. Soc. 90* (1968) 1056; b) J. R. Kanofsky, *J. Org. Chem. 51* (1986) 3386.
[51] F. B. Abeles, *Physiol. Plant. 71* (1987) 127.
[52] D. Slawinska, J. Slawinska in J. Burr (Ed.): *Chemi- and Bioluminescence*, Marcel Dekker, New York 1985, Chapters 13 and 14.
[53] B. B. Vartapetian, L. P. Agapova, A. A. Averianov, V. A. Veselovsky, *Nature (London) 249* (1974) 269.
[54] A. I. Zhuravlev, Yu. N. Filippov, V. V. Simonov, *Biofizika 9* (1964) 671.
[55] a) A. Boveris, *Contrib. Cient. Tecnol. Numbero Espec.* (1985) 65; b) E. J. Dowling, A. M. Symons, D. V. Parke, *Agents Actions 19* (1986) 203; c) S. Imaizumi, T. Kayama, J. Suzuki, *Stroke (Dallas) 15* (1984) 1061.
[56] P. S. Rao, J. M. Luber, J. Milinowicz, P. Lalezari, H. S. Mueller, *Biochem. Biophys. Res. Commun. 150* (1988) 39.
[57] K.-D. Gundermann, F. McCapra: *Chemiluminescence in Organic Chemistry*, Springer, Berlin 1987.
[58] a) R. H. Fleming (Charles Evans and Associates, Redwood City, CA), personal communication; b) Final Report, US Government NSF-SBIR Award ISI-8660531, 1987.
[59] a) J. T. Dickinson, M. H. Miles, W. L. Elban, R. G. Rosemeier, *J. Appl. Phys. 55* (1984) 3994; b) M. Zhenyi, F. Jiawen, J. T. Dickinson, *J. Adhes. 25* (1988) 63.
[60] J. Rychly, L. Matislova-Rychla, I. Spilda, *Eur. Polym. J. 6* (1979) 565.
[61] a) J. Rychly, L. Matislova-Rychla, M. Lazar, *J. Polym. Sci. Polym. Symp. 57* (1976) 139; b) J. D. Druliner, E. Wasserman, *J. Am. Chem. Soc. 110* (1988) 5270.
[62] G. D. Mendenhall, J. C. Tauschek, C. A. Ogle, *Int. J. Chem. Kinet. 13* (1981) 1217.

Modern NMR Pulse Experiments: A Graphical Description of the Evolution of Spin Systems

By Urs Eggenberger and Geoffrey Bodenhausen*

Many modern methods designed to enhance the power of NMR spectroscopy have been widely adopted by the scientific community. Some of the best known among these techniques are one-dimensional methods for polarization enhancement and spectral editing ("INEPT" and "DEPT") and various two-dimensional experiments such as correlation spectroscopy ("COSY") and nuclear Overhauser spectroscopy ("NOESY"). Most of these methods cannot be described in terms of classical magnetization vectors, and although they can be understood with the help of the density operator formalism, this approach remains difficult for many users, in part because of its cumbersome notation, which prevents one from recognizing the important features at a glance. In this paper, a set of graphical conventions is described which allows one to represent the effect of sequences of radio-frequency pulses on spin systems in a variety of experiments. The graphs provide a concise description of the network of spins that are coupled through scalar and dipolar interactions, of the state of a spin system expressed in terms of products of operators, and, most importantly, of the transformations from one state to another due to the effect of radio-frequency pulses, chemical shifts, and scalar couplings. The graphical approach also allows one to represent the effect of phase-cycling and multiple-quantum filtration, cross-relaxation (Overhauser effects) and cross-correlated relaxation.

1. Introduction

In the last decade or so, high-resolution nuclear magnetic resonance has undergone a remarkable development, which is largely due to the extensive use of sophisticated pulse sequences in conjunction with one- and multi-dimensional Fourier transforms. In the early days of what is sometimes called "modern" NMR spectroscopy, a variety of more or less formal approaches were used to describe these experiments, ranging from semiclassical vector models to cumbersome density-matrix transformations. In recent years, the discussion of modern NMR experiments has been increasingly unified with the help of new descriptive tools: product operators[1-4] and coherence transfer pathways.[5-7] It has been shown that calculations can not only be considerably simplified but also made much more intelligible if the density operator is expanded into a superposition of products of angular momentum operators.[1-4] In former days, before the advent of modern NMR spectroscopy, it was customary (and indeed sufficient for most purposes) to speak of "longitudinal M_z magnetization" or of the "M_x component of transverse magnetization". The language has undergone such a development in recent years that one now tends to speak in terms of "longitudinal $\boldsymbol{I}_z$ polarization", of "in-phase $\boldsymbol{I}_x$ coherence", of "antiphase $2\boldsymbol{I}_x\boldsymbol{S}_z$ coherence", and of "multiple-quantum coherence $2\boldsymbol{I}_x\boldsymbol{S}_x$", to name but a few examples. The shift in language corresponds to a transition from a semiclassical discussion to a more fundamental approach which is rooted in the accurate density-operator formalism. While the new language does not appear to meet much resistance and is widely accepted, the notation that is used for product operators remains cumbersome, involving unwieldy symbols overloaded with indices, which are required to label the cartesian components ($\boldsymbol{I}_x$, $\boldsymbol{I}_y$, $\boldsymbol{I}_z$) and the relevant spins (for example $\boldsymbol{I}^A$, $\boldsymbol{I}^M$, $\boldsymbol{I}^X$, unless one chooses to use different symbols for angular momentum, e.g. $\boldsymbol{I}$, $\boldsymbol{R}$, $\boldsymbol{S}$). In order to describe the development of the system under shifts and couplings, one has to specify coefficients which are usually products of trigonometric functions with arguments like $\Omega_A t_1$ or $\pi J_{AM} t_1$. These trigonometric terms have to be carried over from one equation to the next, so that one tends to be confronted with very complex expressions which not only demand a time-consuming book-keeping, but also represent an obstacle to anyone who wishes to get a simple physical picture of the experiment.

In parallel with the development of the product operator formalism, the description of phase-cycles and multiple-quantum phenomena has been greatly simplified by the introduction of coherence transfer pathways.[5-7] The strength of this formalism hinges on a graphical convention, which does not require any unwieldy symbols overloaded with lots of indices. Since a simple graphical convention has brought so much clarification to phase-cycling prescriptions, it seems legitimate to ask whether one could not invent a graphical approach that would make the world of product operators more transparent. It is indeed the ambition of the present paper to define a set of graphical conventions for this purpose. Our graphs, if wisely used, achieve the dual purpose of simplifying the notation and of providing a physical picture of the evolution of product operators. The graphs also reveal important features regarding the phases of the signals (absorption or dispersion), which turn out to be related to symmetry relationships between the evolution and detection periods of two-dimensional experiments.

We assume that the reader is acquainted with some of the basic ideas of modern one- and two-dimensional NMR experiments, and that he is familiar with the practical aspects of the product operator formalism, for example at the introductory level discussed by *Kessler, Gehrke* and *Griesinger*.[8] We hope that our graphical approach can help to foster some intuition for the way in which various terms

[*] Prof. Dr. G. Bodenhausen, Dipl. Chem. U. Eggenberger
Section de Chimie, Université de Lausanne
Rue de la Barre 2, CH-1005 Lausanne (Switzerland)

describe the essential features of a particular experiment. It is only by practice that one can gain a "working knowledge" of the product operator formalism, and for a newcomer to the field it is probably necessary to proceed by trial and error to see which terms should be considered, e.g. which terms can lead to coherence transfer, which terms can contribute to the observable signal, etc. We hope that our graphical representation will allow one to facilitate this learning process, and we are confident that the process should be much less strenuous than if one uses the traditional algebraic notation, although we should warn the reader that we have made no concessions in terms of accuracy, so that full density operator formalism remains valid in all its rigor.

In this paper, we shall discuss applications of our graphical approach to describe correlation spectroscopy ("COSY"), nuclear Overhauser effect spectroscopy ("NOESY"), double- and triple-quantum filtered COSY ("DQF-COSY" and "TQF-COSY"), and triple-quantum filtered NOESY ("TQF-NOESY"). We also illustrate applications to relaxation-allowed coherence transfer due to correlated dipolar interactions,[9, 10] to the so-called INADEQUATE double-quantum technique[11, 12] and to a heteronuclear relayed magnetization transfer experiment.[13]

2. Pulse Sequences and Coupling Networks

All illustrations in this paper follow the general pattern of the operator evolution graph of Figure 1. The pulse sequence is drawn horizontally along the bottom; as usual, the durations of the pulses and delays do not necessarily give a realistic picture of the timing of the events. Unless otherwise specified, narrow and wide pulses represent flip angles of 90° and 180°. The RF phases in the rotating frame are indicated for the basic experiment, i.e. for the first step in a phase-cycle. We tend to prefer pulses applied along the y-axis, unless of course the experiment demands different RF phases. In the left margin of the figure, drawn vertically before the first pulse, a simple graph represents the coupling network, i.e., the set of spins subjected to the pulse sequence. These graphs are drawn using the following conventions:

1. The spins I_k are represented by circles. The labels k, l, m ... of the spins may be written into these circles if desired.

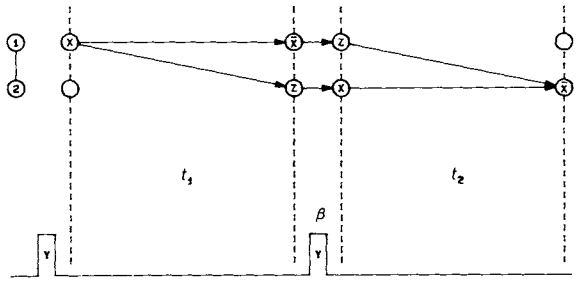

Fig. 1. Operator evolution graph showing a typical sequence of transformations of a two-spin system in the course of a COSY pulse sequence. Only the pathway that contributes to cross-peak signals is shown. The symbols are explained in the text.

2. Non-vanishing scalar couplings J_{kl} are indicated by solid lines. If known, the values of the coupling constants may be written along these lines.
3. Dipolar interactions D_{kl} that are relevant to the sequence of events are indicated by dotted lines.
4. If scalar and dipolar interactions occur simultaneously and if they are both relevant to the experiment, two parallel lines are drawn, one solid and one dotted.

In this paper, dipolar interactions D_{kl} are understood to be averaged by molecular motion, so that they give rise to relaxation effects but not to resolved splittings. Our conventions are somewhat different from those used by *Levitt* et al.[14] and by *Radloff* et al.[15]

3. Density Operator Terms

At various points in time, indicated by vertical dashed lines (see Fig. 1), selected density operator terms are described, again using circles, but with labels x, y or z that indicate if spin I_k is associated with an angular momentum component I_{kx}, I_{ky} or I_{kz}. An open circle indicates that the operator product formally involves a unity operator. Negative signs are symbolized by overbars. In Figure 1, the four pairs of circles drawn above the pulse sequence represent, in chronological order from left to right, the following terms: I_{1x}, $-2I_{1x}I_{2z}$, $2I_{1z}I_{2x}$, and $-I_{2x}$. The normalization factors are not indicated explicitly; one should remember that these factors depend on the number of terms in the product, i.e., $N = 2^{(q-1)}$ for a product containing q terms.

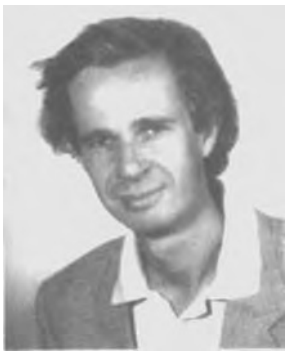

Geoffrey Bodenhausen was born on May 7th, 1951 in The Hague, Netherlands. On completion of his school education in the Netherlands and in Geneva in Switzerland he studied chemistry at the ETH Zürich (1970–1974) and then as post-graduate under Professor Ray Freeman at the Physical Chemistry Laboratory of Oxford University (1975–1977), where he gained his D.Phil. After post-doctoral studies with Robert L. Vold and Regitze R. Vold at the University of California at San Diego, 1978, he joined the research staff of the Francis Bitter National Magnet Laboratory, Massachusetts Institute of Technology, 1979–1980. He then worked as assistant, later senior assistant, in Richard R. Ernst's group in the Laboratory for Physical Chemistry at the ETH Zürich. In 1984 he was Privatdozent for physical chemistry at the ETH. Since 1985 he has been Professeur associé in the Department of Chemistry at the University of Lausanne. Professor Bodenhausen is married and has two daughters (born 1977 and 1979).

4. Transformations of Operator Terms

Transformations under RF pulses are represented symbolically by short, solid arrows, as drawn above the symbol β in Figure 1.

For y-pulses with $\beta = 90°$, the transformations are:[2]

$$z \rightarrow x \rightarrow \bar{z} \rightarrow \bar{x} \tag{1}$$

For x-pulses with $\beta = 90°$, the transformations are:[2]

$$z \rightarrow \bar{y} \rightarrow \bar{z} \rightarrow y \tag{2}$$

It is understood implicitly that each short horizontal arrow is associated with a trigonometric term $\sin\beta$, where β is the flip angle of the RF pulse. In some cases, one must focus attention on a component of the density operator which remains in its initial state in spite of the RF pulse. For example, if a y-pulse is applied to an operator I_{kz}, a fraction $\cos\beta$ of the I_{kz} component remains invariant. This "non-transformation" is rendered graphically by a short dotted horizontal arrow, which is understood implicitly to be associated with a term $\cos\beta$. Finally, if a pulse leaves an operator term invariant (e.g. a y-pulse applied to an operator I_{ky}), there is no need for drawing an arrow.

Transformations under the combined effects of shifts and couplings are illustrated in Figure 2. In weakly-coupled systems, the relevant Hamiltonians commute, which implies that one may consider their effect separately and in arbitrary sequence. If both shifts and couplings are operating in a given interval, it is sometimes convenient to define a virtual state, drawn arbitrarily in the middle of the interval, and represented by dashed circles, which symbolize the state of the system resulting from the effect of one of the interactions, say, of the shift alone. We shall see that in practice one can usually skip the explicit representation of such virtual states, by concatenating the effects of several interactions into one overall transformation. The left-hand side of Figure 2 shows the effects of shifts and couplings drawn separately in two sequential steps involving virtual states, while the right-hand side of Figure 2 shows equivalent diagrams where the virtual states have been skipped for simplicity.

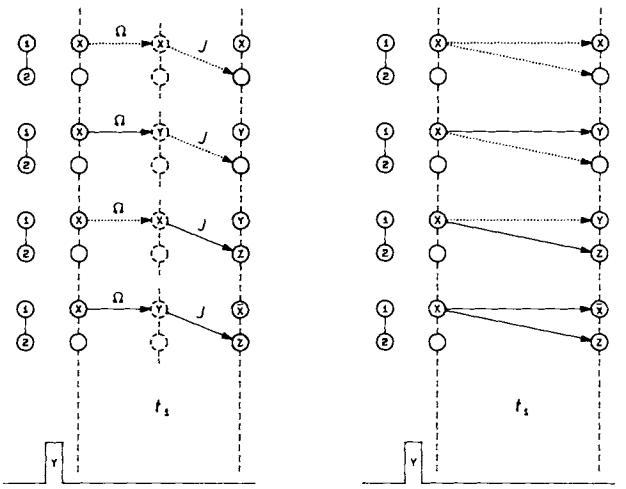

Fig. 2. Representation of the effects of chemical shifts and couplings in a two-spin system. The graphs on the left involve "virtual states" that represent the system after considering the effect of the chemical shift taken in isolation; those on the right represent the overall effect of shifts and couplings.

Transformations under chemical shifts are represented in Figure 2 by long horizontal arrows, which may be labeled for clarity with the symbol Ω representing the offset Ω_k of the spin I_k that appears on the left of the figure. In practice, these labels may often be dropped for simplicity. The shift is represented by a solid arrow if a transformation of the density operator under the effect of the chemical shift is required to obtain a new term that is relevant for the subsequent chain of events. In this case, a trigonometric term $\sin\Omega_k t$ must be included. The signs obey the usual rules:[2]

$$x \rightarrow y \rightarrow \bar{x} \rightarrow \bar{y} \tag{3}$$

The shift is represented by a dotted arrow if such a transformation is not required. In this case, a trigonometric term $\cos\Omega_k t$ must be included.

Transformations under scalar couplings are represented in Figure 2 by sloping arrows, which are solid if the coupling is active, and dotted if it is passive. These arrows may be labeled with the symbol J representing the coupling J_{kl} between the spins I_k and I_l that appear on the left of the figure. Solid sloping arrows (active couplings) imply that a trigonometric term $\sin\pi J_{kl} t$ must be included. The following rules determine the signs of the terms:[2]

$$x \rightarrow yz \rightarrow \bar{x} \rightarrow \bar{y}z \tag{4}$$

$$y \rightarrow \bar{x}z \rightarrow \bar{y} \rightarrow xz \tag{5}$$

Dotted sloping arrows (passive couplings) are intended to remind the reader that a transformation under a coupling has failed to occur, and that a modulation term $\cos\pi J_{kl} t$ must therefore be included. Note that these arrows point at empty circles, so that they might give the impression of a somewhat artificial construct. It is important to remember however that each scalar coupling (i.e., each solid line appearing in the networks drawn on the left-hand side of the figures) must be represented by a sloping arrow, which may be either solid or dotted depending on the transformation that one wishes to represent in the operator evolution graph. The only exceptions to this rule occur if refocusing pulses are employed (see Section 11).

Transformations due to relaxation processes are represented by wavy arrows. To describe cross-relaxation (Overhauser effects), a wavy arrow is used to indicate a partial conversion $I_{iz} \rightarrow I_{jz}$. In the initial rate approximation, the extent of the conversion is expressed by a coefficient $-\sigma_{ij}\tau_m$, where σ_{ij} is the cross-relaxation rate in *Solomon*'s notation, and τ_m the duration of the relaxation interval. Since $\sigma_{ij} = (W_2^{ij} - W_0^{ij})$, σ_{ij} is negative for large molecules, so that $-\sigma_{ij}\tau_m > 0$ in this case, while the opposite situation applies to small molecules in the extreme narrowing limit.[7] The decay of a Zeeman term (i.e., the partial loss in the process $I_{iz} \rightarrow I_{iz}$) can be represented by a dotted wavy arrow. In the initial rate approximation, the extent of this decay is expressed by a factor $(1 - \varrho_i\tau_m)$, where the spin-lattice relaxation rate ϱ_i is defined as positive.[7]

In systems with three or more spins where the time-dependencies of different dipolar interactions are correlated,[16] wavy arrows can be used to represent the conversion of Zeeman order into longitudinal three-spin order (e.g., $\mathbf{I}_{1z} \rightarrow 4\boldsymbol{I}_{1z}\boldsymbol{I}_{2z}\boldsymbol{I}_{3z}$). In the initial rate approximation, the extent of this conversion, which is due to the correlation of the dipolar interactions D_{12} and D_{13}, is represented by a factor $\delta_{1213}\tau_m$. The cross-correlation rate δ_{1213} depends, inter alia, on the angle subtended by the internuclear vectors $\boldsymbol{r}_{12}$ and $\boldsymbol{r}_{13}$.[16] As discussed in Section 9, the appearance of longitudinal three-spin order can be monitored experimentally by triple-quantum filtered NOESY.[17-19]

In a similar fashion, wavy arrows can be used to represent the conversion of Zeeman order into longitudinal two-spin order (e.g., $\boldsymbol{I}_{1z} \rightarrow 2\boldsymbol{I}_{1z}\boldsymbol{I}_{2z}$). In this case, the initial rate factor is denoted $\delta_{112}\tau_m$, and the conversion is due to the correlation of the chemical shift anisotropy of spin $\boldsymbol{I}_1$ and the dipolar interaction D_{12}.[20, 21] The build-up of longitudinal two-spin order can be monitored by double-quantum filtered NOESY.[22]

The decay of longitudinal two- or three-spin order, i.e. the partial losses in the processes $2\boldsymbol{I}_{iz}\boldsymbol{I}_{jz} \rightarrow 2\boldsymbol{I}_{iz}\boldsymbol{I}_{jz}$ or $4\boldsymbol{I}_{iz}\boldsymbol{I}_{jz}\boldsymbol{I}_{kz} \rightarrow 4\boldsymbol{I}_{iz}\boldsymbol{I}_{jz}\boldsymbol{I}_{kz}$, can also be represented by dotted wavy arrows. In the initial rate approximation, the extent of these decay processes is expressed by factors $(1 - \varrho_{ij}\tau_m)$ and $(1 - \varrho_{ijk}\tau_m)$, respectively, in analogy to the decay of Zeeman order.[19, 22]

Finally, wavy arrows can be used to denote the conversion of in-phase transverse magnetization into doubly-antiphase coherence (e.g., $\boldsymbol{I}_{1x} \rightarrow 4\boldsymbol{I}_{1x}\boldsymbol{I}_{2z}\boldsymbol{I}_{3z}$), which can occur in systems with correlated dipolar interactions. We shall denote the extent of such a conversion, which is generally a multi-exponential function of time that depends on the correlation of the dipolar interactions D_{12} and D_{13}, by a function $f_{1213}(t)$. Explicit expressions for these functions can be found elsewhere.[10]

5. The COSY Pulse Sequence

Figure 3 shows five distinct operator evolution graphs for a two-spin system in two-dimensional correlation spectroscopy (COSY). We assume that in the detection period the receiver picks up the magnetization along the x-axis of the rotating frame. This amounts to focusing on the in-phase terms $\boldsymbol{I}_{1x}$ and $\boldsymbol{I}_{2x}$. With the conventions of dotted and solid arrows defined above, it is immediately clear that the five diagrams (a) to (e) in Figure 3 represent the following terms:

$$\sigma^{(a)}(t_1, t_2) = +\boldsymbol{I}_{1x} \cos\Omega_1 t_1 \cos\pi J_{12} t_1 \cos\beta \cos\Omega_1 t_2 \cos\pi J_{12} t_2 \quad (6)$$

$$\sigma^{(b)}(t_1, t_2) = -\boldsymbol{I}_{1x} \sin\Omega_1 t_1 \cos\pi J_{12} t_1 \sin\Omega_1 t_2 \cos\pi J_{12} t_2 \quad (7)$$

$$\sigma^{(c)}(t_1, t_2) = -\boldsymbol{I}_{1x} \cos\Omega_1 t_1 \sin\pi J_{12} t_1 \cos\beta \cos\Omega_1 t_2 \sin\pi J_{12} t_2 \quad (8)$$

$$\sigma^{(d)}(t_1, t_2) = +\boldsymbol{I}_{1x} \sin\Omega_1 t_1 \sin\pi J_{12} t_1 \cos^2\beta \sin\Omega_1 t_2 \sin\pi J_{12} t_2 \quad (9)$$

$$\sigma^{(e)}(t_1, t_2) = -\boldsymbol{I}_{2x} \sin\Omega_1 t_1 \sin\pi J_{12} t_1 \sin^2\beta \sin\Omega_2 t_2 \sin\pi J_{12} t_2 \quad (10)$$

It is important to realize that these terms result from processes that may occur simultaneously. The first four terms contribute to the diagonal multiplet centered at $(\omega_1, \omega_2) = (\Omega_1, \Omega_1)$, while the fifth term gives rise to a cross-peak multiplet centered at $(\omega_1, \omega_2) = (\Omega_1, \Omega_2)$. The first two terms lead to an in-phase doublet structure in both dimensions (modulation in $\cos\pi J_{12} t$), the latter three terms to an antiphase doublet structure (modulation in $\sin\pi J_{12} t$).

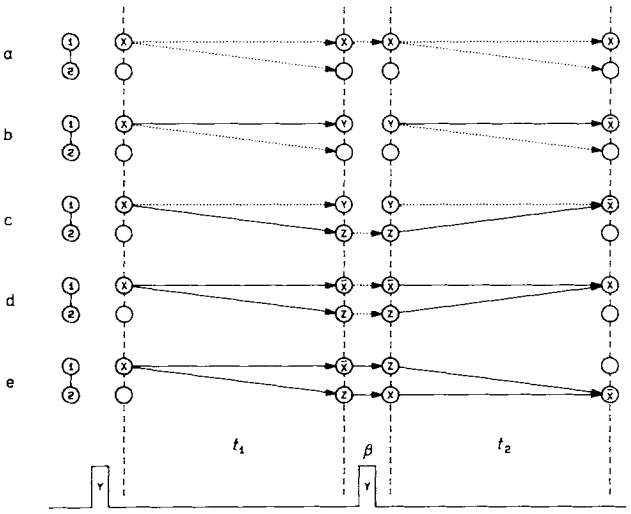

Fig. 3. Set of five operator evolution graphs relevant to the description of signals of a two-spin system in a COSY pulse sequence. Graph (e) is reproduced from Figure 1.

The graphs also inform us about the phases of the signals. If a cosine Fourier transform is used with respect to both t_1 and t_2, the signals will be in absorption if the modulation factor contains an even number of sine terms (even number of solid lines) in both t_1 and t_2 intervals.[7] Thus graphs (a), (d) and (e) correspond to signals that are in absorption in both frequency domains, while the graphs (b) and (c) describe two-dimensional dispersive contributions. For $\beta = 90°$, only the terms (b) and (e) survive, while the pathways (a), (c) and (d), which contain short dotted arrows symbolizing $\cos\beta$, have vanishing intensities. For $\beta = 90°$, we therefore obtain a pure absorption antiphase cross-peak multiplet from term (e) and a pure dispersion in-phase diagonal multiplet from term (b). These rules have of course been established before,[7] but so far it has not been possible to derive them by mere inspection of a set of simple graphs.

To describe the fate of a two-spin system in a COSY experiment, the complete list of all possible pathways that start with the term $\boldsymbol{I}_{1x}$ would consist of no less than 30 operator evolution graphs, and another 30 graphs start with $\boldsymbol{I}_{2x}$. Fortunately, there is no need for such an exhaustive description, since we can easily discard all pathways that do not lead to in-phase magnetization $\boldsymbol{I}_{1x}$ or $\boldsymbol{I}_{2x}$. In particular, we may ignore pathways that yield antiphase terms like $2\boldsymbol{I}_{1x}\boldsymbol{I}_{2z}$ or products like $2\boldsymbol{I}_{1x}\boldsymbol{I}_{2x}$ and pathways that yield longitudinal terms $\boldsymbol{I}_{1z}$ and $2\boldsymbol{I}_{1z}\boldsymbol{I}_{2z}$. It is therefore a simple matter to select the five graphs of Figure 3 that are relevant to the understanding of COSY.

6. The NOESY Pulse Sequence

Figure 4 shows the operator evolution graph relevant to the description of cross-peaks in two-dimensional exchange or nuclear Overhauser spectroscopy (NOESY). We consider a two-spin system which, for the sake of illustration, is as-

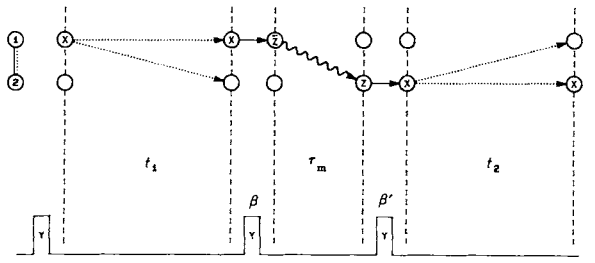

Fig. 4. Evolution of a two-spin system having both scalar and dipolar couplings in a NOESY pulse sequence. Only the pathway that contributes to cross-peak signals arising from cross-relaxation (Overhauser effect) is shown.

sumed to have a resolved coupling J_{12} in addition to a dipolar interaction D_{12}. If we start with the term I_{1x} and focus on the term I_{2x} in the detection period, we can immediately read the following factors from the graph:

$$\sigma(t_1,t_2) = I_{2x}\cos\Omega_1 t_1 \cos\pi J_{12} t_1 \sin\beta(-\sigma_{12}\tau_m) \times \sin\beta' \cos\Omega_2 t_2 \cos\pi J_{12} t_2 \quad (11)$$

In this example, the transformation expressed by the wavy line is associated with a change in sign ($I_{1z} \rightarrow -I_{2z}$) since $-\sigma_{12}$ is negative, a characteristic feature of small molecules with short correlation times $\tau_c < 1/\omega_0$. The opposite sign would be obtained for slowly-tumbling macromolecules.[7]

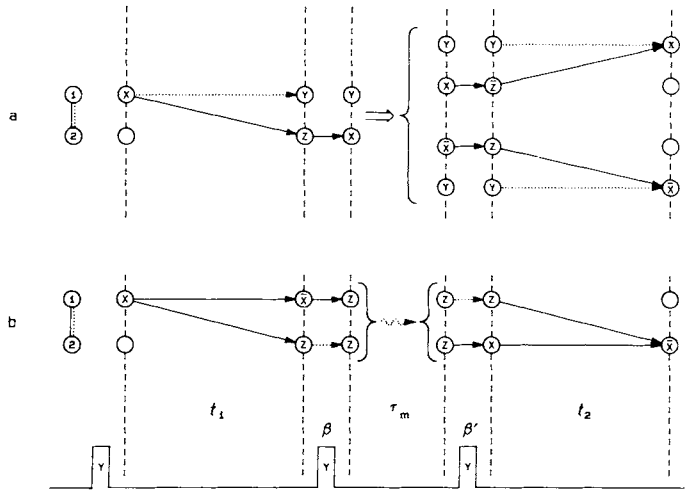

Fig. 5. Pathways that give rise to undesirable signals in NOESY spectra of a two-spin system with dipolar and scalar couplings. a) Two pathways involving zero-quantum coherences, where the double arrow (⇒) represents the effect of the phase cycle; b) pathway involving longitudinal two-spin order.

In view of the tremendous popularity of the NOESY method, it is important to be aware of the fact that serious artifacts may occur in systems with scalar couplings. Figure 5a shows what happens if an antiphase term $2I_{1y}I_{2z}$ is converted into $2I_{1y}I_{2x}$ by the second pulse (β). The term $2I_{1y}I_{2x}$ consists of a superposition of zero- and double-quantum coherences.[2] The phase-cycle used in NOESY, which amounts to a filter that retains only populations and zero-quantum coherences in the τ_m period, causes a split-up of $2I_{1y}I_{2x}$ into $\frac{1}{2}(2I_{1y}I_{2x} - 2I_{1x}I_{2y})$, as discussed in more detail in Section 7. The two resulting pathways shown in Figure 5a give rise to misleading contributions to the diagonal and cross-peak multiplets respectively.[23] The latter contribution has the following form:

$$\sigma(t_1,t_2) = -I_{2x}\cos\Omega_1 t_1 \sin\pi J_{12} t_1 \sin\beta \times \tfrac{1}{2}\sin\beta' \cos\Omega_2 t_2 \sin\pi J_{12} t_2 \quad (12)$$

The factor $\frac{1}{2}$ arises from the split-up into two terms due to the phase cycle. If one uses a cosine/cosine transform so that the desirable pathway of Figure 4 leads to pure two-dimensional absorption, the zero-quantum multiplets due to the pathways of Figure 5a will be dispersive in both dimensions. The precession of the zero-quantum coherence in the τ_m interval under the effect of the chemical shifts is not included in Equation (12). As discussed in Section 12, this would lead to a factor $\cos(\Omega_1 - \Omega_2)\tau_m$.

Another potentially important source of artifacts in NOESY spectra of systems with scalar couplings is illustrated in Figure 5b. The antiphase term $-2I_{1x}I_{2z}$ can be transformed unwittingly into longitudinal two-spin order $2I_{1z}I_{2z}$, which can be subsequently converted into $2I_{1z}I_{2x}$. This leads to a contribution of the form

$$\sigma(t_1,t_2) = -I_{2x}\sin\Omega_1 t_1 \sin\pi J_{12} t_1 \sin\beta\cos\beta(1-\varrho_{12}\tau_m) \times \cos\beta' \sin\beta' \sin\Omega_2 t_2 \sin\pi J_{12} t_2 \quad (13)$$

where the factor $(1 - \varrho_{12}\tau_m)$ represents the fraction of the two-spin order that has not decayed in the τ_m interval. Clearly, accurate calibration of the pulses to $\beta = \beta' = 90°$ (or, preferably, the use of suitable composite pulses) leads to the suppression of these undesirable pathways.[24]

7. Double-Quantum Filtered COSY

In double-quantum filtered COSY (Fig. 6), a term $2I_{1y}I_{2x}$ is generated at the beginning of the Δ interval. The phase cycle selects the double-quantum coherences contained in this $2I_{1y}I_{2x}$ term, thus leading to a transformation symbolically represented by a short double arrow (⇒):

$$2I_{1y}I_{2x} \Rightarrow \tfrac{1}{2}(2I_{1y}I_{2x} + 2I_{1x}I_{2y}) \quad (14)$$

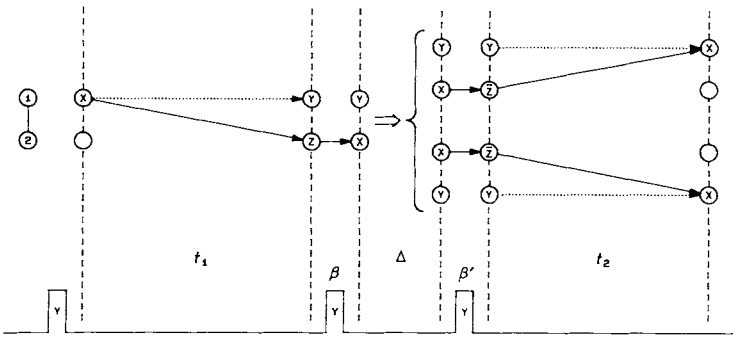

Fig. 6. Evolution of a two-spin system in double-quantum filtered COSY. The two pathways give rise to a diagonal peak and a cross peak. The double arrow (⇒) represents the effect of the phase cycle.

This transformation can easily be verified by expanding the cartesian operators into linear combinations of shift operators, $I_{1y} = -i\frac{1}{2}(I_1^+ - I_1^-)$ and $I_{2x} = \frac{1}{2}(I_2^+ + I_2^-)$, deleting the zero-quantum components $I_1^+ I_2^-$ and $I_1^- I_2^+$ from the product to retain only the double-quantum terms $I_1^+ I_2^+$ and $I_1^- I_2^-$, and transforming the remaining shift operators back into cartesian operators [cf. Eq. (118) of *Sørensen* et al.[2]].

The split-up of one term into two products implied in Equation (14) is represented symbolically in Figure 6. The upper pathway leads to a diagonal peak, the lower pathway to a cross-peak. Both pathways are obviously associated with similar trigonometric modulation terms. This symmetry explains why diagonal and cross-peak multiplets have identical phases and multiplet structures in double-quantum filtered COSY spectra of two-spin systems, in contrast to the situation that arises in conventional COSY (Fig. 3).

The form of the cross-peak multiplet is determined by modulation terms that can be read directly from the lower pathway in Figure 6:

$$\sigma(t_1, t_2) = I_{2x} \cos\Omega_1 t_1 \sin \pi J_{12} t_1 \sin\beta \tfrac{1}{2} \sin\beta' \times \cos\Omega_2 t_2 \sin \pi J_{12} t_2 \quad (15)$$

Note the factor $\frac{1}{2}$ which arises from the split-up into two terms. The experienced reader will recognize a cross-peak multiplet which is in antiphase with respect to the coupling J_{12} in both frequency dimensions. If one uses a cosine/cosine transformation, the multiplet is dispersive in both frequency dimensions. Pure two-dimensional absorption can be obtained by switching to a sine/sine transform or by using a 90° phase correction in both ω_1 and ω_2. Alternatively, one could shift the phase of the first pulse from y to x, so as to start with $-I_{1y}$, which is then converted into $2 I_{1y} I_{2z}$ in the evolution period with a modulation $\sin\Omega_1 t_1 \sin \pi J_{12} t_1$. At the same time, one could observe the y rather than the x component in the detection period. In this case, one obtains two solid arrows in both t_1 and t_2, and hence pure two-dimensional absorption with a cosine/cosine transform, as we have seen above.

Equation (14) and related transformations due to double-quantum filtration can be written in shorthand notation:

$$yx \Rightarrow \tfrac{1}{2}(yx + xy) \quad (16)$$
$$xy \Rightarrow \tfrac{1}{2}(xy + yx) \quad (17)$$
$$xx \Rightarrow \tfrac{1}{2}(xx - yy) \quad (18)$$
$$yy \Rightarrow \tfrac{1}{2}(yy - xx) \quad (19)$$

It is interesting to compare these transformations with those induced by zero-quantum filtration, as employed in the mixing time τ_m of the NOESY experiment and in a variety of experiments involving so-called z-filters. The effect of such filters can be predicted by replacing the cartesian operators by shift operators, deleting the double-quantum components $I_1^+ I_2^+$ and $I_1^- I_2^-$, and transforming the remaining terms $I_1^+ I_2^-$ and $I_1^- I_2^+$ back into cartesian operators:

$$yx \Rightarrow \tfrac{1}{2}(yx - xy) \quad (20)$$
$$xy \Rightarrow \tfrac{1}{2}(xy - yx) \quad (21)$$
$$xx \Rightarrow \tfrac{1}{2}(xx + yy) \quad (22)$$
$$yy \Rightarrow \tfrac{1}{2}(yy + xx) \quad (23)$$

Such transformations can easily be represented graphically in the manner of Figures 5a and 6. In all cases, the effect of the phase cycle is symbolically represented by a short double arrow (⇒).

8. Triple-Quantum Filtered COSY

The pathways relevant to triple-quantum filtered COSY are slightly more involved, as shown in Figure 7. The net effect of triple-quantum filtration can be predicted by substituting the cartesian operators using the relations $I_{1y} = -i\frac{1}{2}(I_1^+ - I_1^-)$ and $I_{2x} = \frac{1}{2}(I_2^+ + I_2^-)$, by deleting from the product all terms except the triple-quantum coherences $I_1^+ I_2^+ I_3^+$ and $I_1^- I_2^- I_3^-$, and by transforming these back into cartesian operators. This procedure leads to the transformation (24).

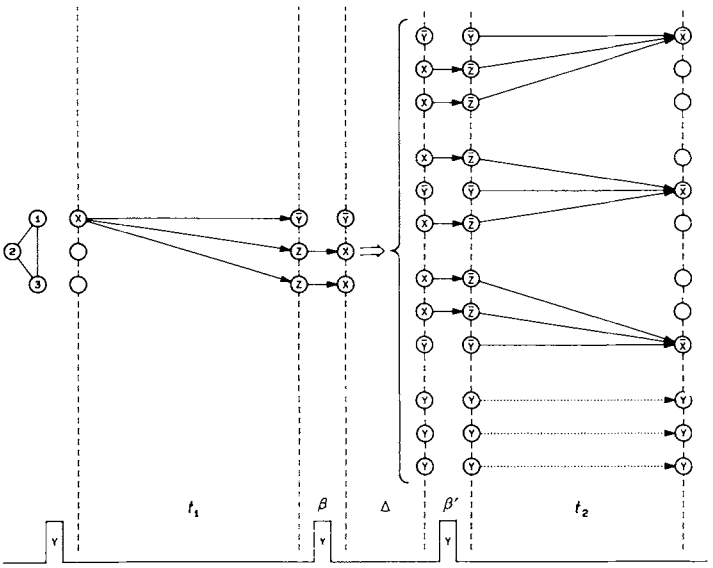

Fig. 7. Evolution of a three-spin system in a triple-quantum filtered COSY experiment.

$$4 I_{1y} I_{2x} I_{3x} \Rightarrow \tfrac{1}{4}(4 I_{1y} I_{2x} I_{3x} + 4 I_{1x} I_{2y} I_{3x} + 4 I_{1x} I_{2x} I_{3y} - 4 I_{1y} I_{2y} I_{3y}) \quad (24)$$

The split-up of one term into four operator products is shown in Figure 7. Although the signs in the Figure are opposite to those in Equation (24), the order of the terms is retained for clarity. The first pathway leads to a diagonal multiplet, while the second and third pathways lead to two distinct cross-peak multiplets. The fourth pathway cannot lead to any observable magnetization, since it yields a superposition of triple-quantum coherence and three-spin single-quantum coherences. The second pathway in Figure 7 is associated with the following modulation terms:

$$\sigma(t_1, t_2) = -I_{2x} \sin\Omega_1 t_1 \sin \pi J_{12} t_1 \sin \pi J_{13} t_1 \sin^2\beta \times \tfrac{1}{4} \sin^2\beta' \sin\Omega_2 t_2 \sin \pi J_{12} t_2 \sin \pi J_{23} t_2 \quad (25)$$

One recognizes a multiplet structure which is in antiphase with respect to J_{12} and J_{13} in ω_1 and in antiphase with respect

to J_{12} and J_{23} in ω_2. The symmetry of the three upper pathways in Figure 7 (three solid arrows in each case) indicates that the multiplet structures and the phases of the diagonal and cross-peak signals are the same. If one uses a sine/sine transform, all signals appear in pure two-dimensional absorption.

In shorthand notation, transformations of the type shown in Equation (24), which describe the effect of triple-quantum filtration, may be written as follows:

$$\mathrm{xxx} \Rightarrow \tfrac{1}{4}(\mathrm{xxx} - \mathrm{xyy} - \mathrm{yxy} - \mathrm{yyx}) \quad (26)$$
$$\mathrm{yxx} \Rightarrow \tfrac{1}{4}(\mathrm{yxx} + \mathrm{xyx} + \mathrm{xxy} - \mathrm{yyy}) \quad (27)$$
$$\mathrm{xyx} \Rightarrow \tfrac{1}{4}(\mathrm{xyx} + \mathrm{xxy} + \mathrm{yxx} - \mathrm{yyy}) \quad (28)$$
$$\mathrm{xxy} \Rightarrow \tfrac{1}{4}(\mathrm{xxy} + \mathrm{yxx} + \mathrm{xyx} - \mathrm{yyy}) \quad (29)$$
$$\mathrm{yyx} \Rightarrow \tfrac{1}{4}(\mathrm{yyx} + \mathrm{xyy} + \mathrm{yxy} - \mathrm{xxx}) \quad (30)$$
$$\mathrm{yxy} \Rightarrow \tfrac{1}{4}(\mathrm{yxy} + \mathrm{yyx} + \mathrm{xyy} - \mathrm{xxx}) \quad (31)$$
$$\mathrm{xyy} \Rightarrow \tfrac{1}{4}(\mathrm{xyy} + \mathrm{yxy} + \mathrm{yyx} - \mathrm{xxx}) \quad (32)$$
$$\mathrm{yyy} \Rightarrow \tfrac{1}{4}(\mathrm{yyy} - \mathrm{yxx} - \mathrm{xyx} - \mathrm{xxy}) \quad (33)$$

Such transformations can readily be represented graphically in the manner of Figure 7, using a double arrow (⇒) to represent the net effect of the phase cycle.

9. Triple-Quantum Filtered NOESY

Recently, we have shown[18, 19] that it is possible to obtain evidence about correlated dipolar relaxation by combining the normal NOESY sequence with triple-quantum filtration. The basic phenomenon that we wish to highlight is the spontaneous conversion of Zeeman order into longitudinal three-spin order, a process which occurs whenever the time-dependencies of the two dipolar interactions D_{12} and D_{13} are correlated.[16–19] This conversion is represented by the wavy arrow in Figure 8. The term $-4\,I_{1z}I_{2z}I_{3z}$ is transformed into $-4\,I_{1x}I_{2x}I_{3x}$ by the third RF pulse. The net effect of triple-quantum filtration is given by Equation (26), and is represented by a double arrow (⇒) in Figure 8. The terms are drawn in the same order as in Equation (26), but they have opposite signs. It can clearly be seen from the figure that the last pulse in the sequence must be about the x-axis, otherwise none of the four terms that make up the triple-quantum coherence can be converted into observable magnetization.[17, 19] Of the four pathways in Figure 8, the second and fourth lead to cross-peak multiplets and the third to a diagonal multiplet. The fourth pathway for example is associated with the modulation pattern (34).

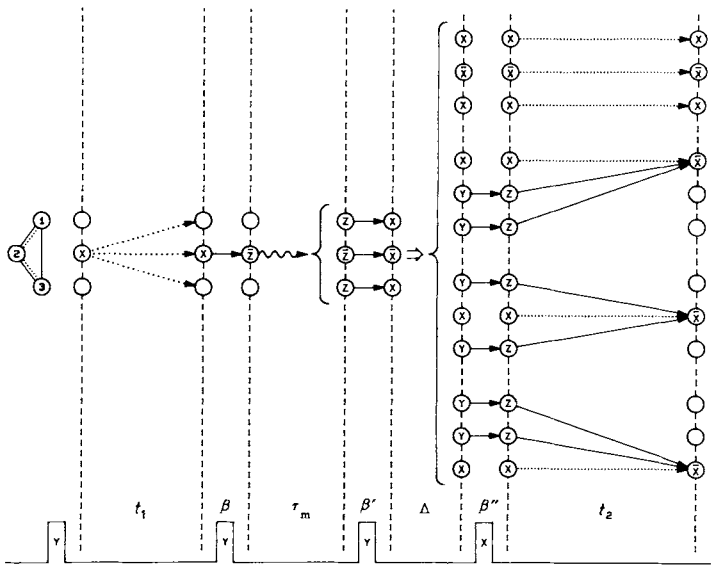

Fig. 8. Evolution of a three-spin system with three scalar couplings and two partly correlated dipolar interactions D_{12} and D_{23} in a triple-quantum filtered NOESY sequence. The double arrow (⇒) represents the effect of the phase-cycle.

$$\sigma(t_1, t_2) = -I_{3x}\cos\Omega_2 t_1 \cos\pi J_{12} t_1 \cos\pi J_{23} t_1 \sin\beta\, \delta_{1223}\tau_m \sin^3\beta' \times \tfrac{1}{4}\sin^2\beta'' \cos\Omega_3 t_2 \sin\pi J_{13} t_2 \sin\pi J_{23} t_2 \quad (34)$$

The amplitude is proportional to the cross-correlation rate δ_{1223}. The measurement of this rate may provide information about the angle subtended by the internuclear vectors r_{12} and r_{23}.[19] One recognizes an in-phase multiplet structure in the ω_1 domain and a doubly-antiphase structure in ω_2. Note the symmetry of the three lower pathways of Figure 8. All signals are in pure two-dimensional absorption if we use a cosine/cosine transform, since all pathways contain an even number of solid arrows in both intervals t_1 and t_2.

10. Relaxation-Allowed Coherence Transfer

Ordinarily, it is assumed that correlation spectra ("COSY") merely provide information about the presence or absence of scalar couplings: if a cross-peak is observed,

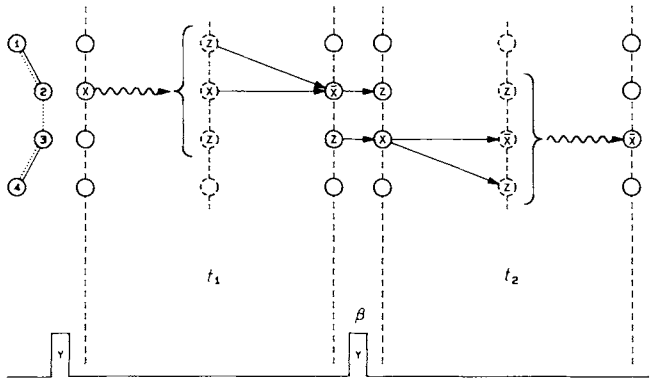

Fig. 9. Evolution of a four-spin system with two scalar couplings and three partly correlated dipolar interactions in the conventional COSY sequence. A pathway is shown that gives rise to cross peaks between spins 2 and 3 although there is no scalar coupling between these spins. The virtual states discussed in the text are represented by dashed circles.

this is taken as evidence that the corresponding spins must be scalar coupled. Under certain circumstances however, it may be possible to observe cross-peaks in COSY spectra between spins that are *not* scalar coupled. Figure 9 shows a four-spin system with three dipolar couplings D_{12}, D_{23} and D_{34} in addition to two scalar couplings J_{12} and J_{34}. If the time-dependencies of the D_{12} and D_{23} interactions are correlated, a coherence I_{2x} can be partly converted into doubly antiphase coherence $4\,I_{1z}I_{2x}I_{3z}$.[9, 10] Subsequent evolution under the

combined effects of the shift Ω_2 and the coupling J_{12} can convert this into $-2\,I_{2x}I_{3z}$, which is partly transformed into $2\,I_{2z}I_{3x}$ by the RF mixing pulse of flip angle β. This term develops into $-4\,I_{2z}I_{3x}I_{4z}$, and is finally converted into $-I_{3x}$ under the effect of correlated relaxation involving the D_{23} and D_{34} interactions. Figure 9 allows one to determine the coefficients:

$$\sigma(t_1,t_2) = -I_{3x}f_{1223}(t_1)\sin\Omega_2 t_1 \times \sin\pi J_{12}t_1\,\sin^2\beta\,\sin\Omega_3 t_2\,\sin\pi J_{34}t_2 f_{2334}(t_2) \quad (35)$$

where the functions $f_{1223}(t_1)$ and $f_{2334}(t_2)$ describe the conversion of in-phase magnetization into antiphase coherence and vice-versa due to correlated relaxation.[10] In both intervals t_1 and t_2 of Figure 9 we show as two sequential steps, the effects of relaxation on the one hand, and of the chemical shifts and couplings on the other, drawing "virtual states" in the middle of the intervals, in analogy to Figure 2. This is justified because the (super)operators relevant to relaxation and free precession commute. Of course, the virtual states represented by dashed circles need not be drawn explicitly. Relaxation, chemical shifts and couplings act throughout the entire durations of these intervals.

The modulation term of Equation (35) describes a cross-peak multiplet centered at the chemical shifts of spins I_2 and I_3, i.e. $(\omega_1,\omega_2) = (\Omega_2,\Omega_3)$, with an antiphase structure due to the couplings J_{12} in ω_1 and J_{34} in ω_2. On superficial inspection such a cross peak might seem to indicate that $J_{23} \neq 0$, but in this case coherence transfer can occur despite the fact that J_{23} vanishes. The appearance of misleading cross peaks in this context may be referred to as the "Wimperis effect".[9, 10]

11. Refocusing

If refocusing pulses are used in pulse sequences, the following rules must be observed:

1. Refocusing pulses eliminate the effects of chemical shifts, so one should not draw any horizontal arrows (neither solid nor dotted) in the relevant intervals.
2. Refocusing pulses do not eliminate the effects of homonuclear couplings, so for each homonuclear coupling a solid or dotted sloping arrow must be drawn, depending on whether the coupling plays an active or a passive role in the interval.
3. Heteronuclear couplings J_{IS} are refocused by 180° pulses applied to either I or S spins. Neither solid nor dotted sloping arrows should be drawn for these couplings.
4. Heteronuclear couplings J_{IS} do play a role if 180° pulses are applied to both I and S spins. These couplings should therefore be represented either by solid or dotted sloping arrows.

Examples of pulse sequences where these rules must be applied are discussed in the next two sections.

12. Multiple-Quantum Evolution

In the preceding sections, we have discussed experiments where multiple-quantum coherences appear only in a transient fashion in brief intervals. If these coherences are allowed to evolve however, their precession under the effects of chemical shifts are described by Equation (90) of *Sørensen* et al.[2] or by Equation (5.3.38) of *Ernst* et al.[7] For double-quantum coherences we have

$$\tfrac{1}{2}(xx - yy) \rightarrow \tfrac{1}{2}(xy + yx) \rightarrow -\tfrac{1}{2}(xx - yy) \rightarrow -\tfrac{1}{2}(xy + yx) \quad (36)$$

or in symbolic notation:

$$\begin{Bmatrix} xx \\ \bar{y}y \end{Bmatrix} \rightarrow \begin{Bmatrix} xy \\ yx \end{Bmatrix} \rightarrow \begin{Bmatrix} \bar{x}x \\ yy \end{Bmatrix} \rightarrow \begin{Bmatrix} \bar{x}y \\ \bar{y}x \end{Bmatrix} \quad (37)$$

The transformations are represented graphically by horizontal arrows (Fig. 10). To avoid confusion with the precession of single spins under the effect of chemical shifts, these arrows are labeled with the frequencies $(\Omega_i + \Omega_j)$ corresponding to the sums of the chemical shifts. Plain arrows correspond to modulation factors $\sin(\Omega_i + \Omega_j)t$, dotted arrows represent factors $\cos(\Omega_i + \Omega_j)t$.

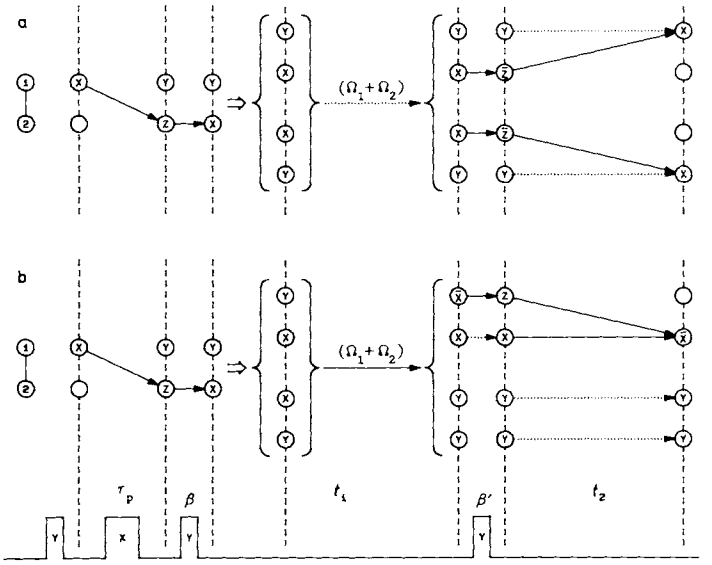

Fig. 10. Evolution of a two-spin system in a double-quantum experiment (INADEQUATE pulse sequence). The double arrows (⇒) represent the effect of the phase cycle. T modulation factors of the transformations are a) $\cos(\Omega_1 + \Omega_2)t_1$ and b) $\sin(\Omega_1 + \Omega_2)t_1$.

Figure 10 illustrates two possible operator evolution graphs that may occur in INADEQUATE (Incredible Natural Abundance DoublE-QUAntum Transfer Experiment), which has proven useful for correlating the signals of neighboring carbon-13 sites.[11, 12] The second pathway from the top in Figure 10 leads to a component

$$\sigma(t_1,t_2) = I_{2x}\sin\pi J_{12}\tau_p\sin\beta\tfrac{1}{2}\cos(\Omega_1 + \Omega_2)t_1 \times \sin\beta'\cos\Omega_2 t_2\,\sin\pi J_{12}t_2 \quad (38)$$

On the other hand, the third pathway from the top in Figure 10 leads to a component

$$\sigma(t_1,t_2) = -I_{2x}\sin\pi J_{12}\tau_p\sin\beta\tfrac{1}{2}\sin(\Omega_1 + \Omega_2)t_1 \times \sin\beta'\cos\beta'\sin\Omega_2 t_2\,\sin\pi J_{12}t_2 \quad (39)$$

Clearly, this latter pathway, which is modulated as a function of $\sin(\Omega_1 + \Omega_2)t_1$, can only play a role if $\beta' \neq 90°$.[12]

For zero-quantum coherences, free precession obeys the following rules:[2]

$$\tfrac{1}{2}(xx + yy) \rightarrow \tfrac{1}{2}(yx - xy) \rightarrow -\tfrac{1}{2}(xx + yy) \rightarrow -\tfrac{1}{2}(yx - xy) \tag{40}$$

or in symbolic notation:

$$\begin{Bmatrix} xx \\ yy \end{Bmatrix} \rightarrow \begin{Bmatrix} yx \\ \bar{x}y \end{Bmatrix} \rightarrow \begin{Bmatrix} \bar{x}x \\ \bar{y}y \end{Bmatrix} \rightarrow \begin{Bmatrix} \bar{y}x \\ xy \end{Bmatrix} \tag{41}$$

In this case, solid and dotted arrows correspond to modulation factors $\sin(\Omega_i - \Omega_j)t$ and $\cos(\Omega_i - \Omega_j)t$ respectively.

With regard to scalar couplings, it is important to remember that interactions between active spins are ineffective, since the coupling Hamiltonians commute with the multiple-quantum coherences. Scalar couplings between active spins should therefore not appear in the graphs (neither solid nor dotted sloping arrows). Scalar couplings to passive spins lead to transformations given by Equation (94) of *Sørensen* et al.[2] or by Equation (5.3.39) of *Ernst* et al.[7]

13. Relayed Proton–Proton–Carbon Transfer

To conclude, we shall give an example of a "relayed" experiment involving a homonuclear transfer of coherence from one proton to another, followed by a transfer to a ^{13}C-nucleus. The pulse sequence of Figure 11 was recently

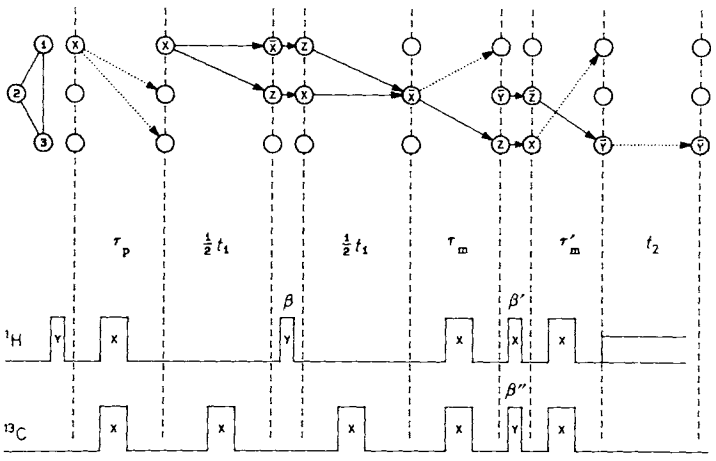

Fig. 11. Evolution in a heteronuclear spin system consisting of a remote proton I_1, a neighboring proton I_2 and a C^{13}-spin I_3. The pulse sequence is designed to bring about relayed coherence transfer $I_1 \rightarrow I_2 \rightarrow I_3$. Only the pathway that gives rise to relayed signals is shown.

developed to facilitate automated analysis of molecular fragments by pattern recognition.[13] The coupling network consists of a "remote" proton spin I_1, a "neighboring" proton spin I_2, and a carbon spin I_3. The pathway shown starts off with transverse magnetization I_{1x} of the remote proton, and ends up with $-I_{3y}$ coherence of the ^{13}C-spin. This pathway is associated with the modulation pattern (42).

$$\begin{aligned}\sigma(t_1, t_2) = & -I_{3y} \cos \pi J_{12} \tau_p \cos \pi J_{13} \tau_p \sin \Omega_1 \tfrac{1}{2} t_1 \\ & \times \sin \pi J_{12} \tfrac{1}{2} t_1 \sin^2 \beta \sin \Omega_2 \tfrac{1}{2} t_1 \\ & \times \sin \pi J_{12} \tfrac{1}{2} t_1 \cos \pi J_{12} \tau_m \sin \pi J_{23} \tau_m \\ & \times \sin \beta' \sin \beta'' \cos \pi J_{13} \tau'_m \sin \pi J_{23} \tau'_m \cos \Omega_3 t_2\end{aligned} \tag{42}$$

In deriving the trigonometric functions from the figure, we have made use of rules (1) to (4) of Section (11):

1. Because of refocusing of the chemical shifts, no horizontal arrows appear in the intervals τ_p, τ_m, and τ'_m.
2. The homonuclear coupling J_{12} is represented by sloping arrows in the intervals τ_p, $\frac{1}{2}t_1$, and τ_m because it is not refocused.
3. The heteronuclear couplings J_{13} and J_{23} are refocused by the 180° pulses applied to the ^{13}C-spins in the middle of the two halves of the evolution period. As a result, neither J_{13} nor J_{23} have any effect in these intervals (neither solid nor dotted sloping arrows).
4. The heteronuclear couplings J_{13} and J_{23} appear as dotted or solid sloping arrows in the intervals τ_p, τ_m, and τ'_m because they are not refocused.

Finally, it is obvious that heteronuclear interactions are ineffective when the proton decoupler is switched on, so that the couplings J_{13} and J_{23} do not appear in t_2.

The pathway illustrated in Figure 11 is only one of many possibilities, most of which give rise to undesirable artifacts in the spectra. It is the bewildering variety of pathways in this experiment which provided the incentive for developing the graphical conventions discussed in this paper. However, the detailed discussion of relayed coherence transfer is beyond the scope of the present work.

14. Recapitulation

At this point, it may be helpful to briefly recapitulate the essential conventions used in the graphs:

1. A short solid horizontal arrow represents a rotation under an RF pulse (coefficient $\sin\beta$). The relevant transformations of the terms are given in Equations (1) and (2).
2. A short dotted horizontal arrow represents a lack of rotation under the influence of an RF pulse (coefficient $\cos\beta$).
3. The absence of a short horizontal arrow indicates that the term is invariant under influence of an RF pulse (coefficient 1).
4. A long solid horizontal arrow represents a rotation under the effect of a chemical shift (coefficient $\sin\Omega_i t$). The relevant transformations of the terms are given in Equation (3).
5. A long dotted horizontal arrow represents a lack of rotation under the effect of a chemical shift (coefficient $\cos\Omega_i t$).
6. The absence of a long horizontal arrow indicates that the chemical shift has been refocused (coefficient 1).
7. A long solid sloping arrow represents a rotation under a scalar coupling (coefficient $\sin\pi J_{ij} t$). The relevant transformations of the terms are given in Equations (4) and (5).

8. A long dotted sloping arrow represents the lack of rotation under a scalar coupling (coefficient $\cos \pi J_{ij} t$).
9. The absence of a long sloping arrow indicates that the scalar coupling has been refocused (coefficient 1).
10. Wavy arrows represent transformations due to various relaxation processes, as discussed in Section 4.
11. A short double arrow ($\Rightarrow$) represents a transformation due to phase-cycling, which amounts to the selection of multiple-quantum coherences of specified order. The relevant transformations are given in Equations (16)–(19), (20)–(23) and (26)–(33).

15. Conclusions and Prospects

It appears that our graphical conventions can be useful to rationalize the mechanism of a wide variety of pulse sequences. The graphs allow one to gain a "feeling" for the relevant terms, i.e., for terms that undergo certain coherence transfer processes and contribute to the observable signals. It is an easy matter to sketch a few pathways to check whether they can give rise to interesting signal contributions or not. The operator evolution graphs can be used not only for qualitative discussions, but also yield the trigonometric functions that determine the time-domain modulation terms, and hence the frequency-domain multiplet patterns and phases of the signals. In fact, the graphs ensure that relevant terms are not accidentally left out, and that the trigonometric terms are correctly accounted for.

We are not aware of any serious limitations, except of course that the use of product operators should preferably be limited to weakly-coupled systems (complications arising in strongly-coupled systems have recently been discussed elsewhere).[25] Another difficulty arises if one attempts to describe the evolution of p-quantum coherences in systems with more than p spins. In such cases, the use of sloping arrows to depict the effect of couplings to passive spins tends to become somewhat confusing, and it might be advisable to define special symbols for the x and y components of multiple-quantum coherences and for their antiphase counterparts. Although we have refrained from introducing such symbols in this paper, it appears that Figure 10 might have been simplified, for example by drawing a rectangular box around the spins that actively participate in the double-quantum coherence. Other graphs could be drawn to depict the fate of shift operators, polarization operators, and irreducible tensor operators.[7] Of course, the meaning of various arrows would have to be defined from case to case.

The figures shown in this paper were drawn with a computer program designed to position various symbols and interconnecting arrows in suitable locations. In principle, it would be possible to incorporate the rules that govern the transformations into this program, although it might be wiser to leave some initiative to the spectroscopist. We hope that these graphs may be helpful not only for teaching but also to pave the way for developing further novel experiments.

The authors gratefully acknowledge useful comments by Dr. Nicolau Beckmann of the Biozentrum of the University of Basel. This research was supported in part by Spectrospin AG, Fällanden, Switzerland, by the Swiss National Science Foundation, and by the Commission pour l'Encouragement de la Recherche Scientifique.

Received: October 16, 1989;
supplemented: January 15, 1990 [A 756 IE]
German version: *Angew. Chem. 102* (1990) 392

[1] U. Fano, *Rev. Mod. Phys. 29* (1957) 74.
[2] O. W. Sørensen, G. W. Eich, M. H. Levitt, G. Bodenhausen, R. R. Ernst, *Prog. Nucl. Magn. Reson. Spectrosc. 16* (1983) 163.
[3] F. J. M. van de Ven, C. W. Hilbers, *J. Magn. Reson. 54* (1983) 512.
[4] K. J. Packer, K. M. Wright, *Mol. Phys. 50* (1983) 797.
[5] A. D. Bain, *J. Magn. Reson. 56* (1984) 418.
[6] G. Bodenhausen, H. Kogler, R. R. Ernst, *J. Magn. Reson. 58* (1984) 370.
[7] R. R. Ernst, G. Bodenhausen, A. Wokaun: *Principles of Nuclear Magnetic Resonance in One and Two Dimensions*, Clarendon Press, Oxford 1987.
[8] H. Kessler, M. Gehrke, C. Griesinger, *Angew. Chem. 100* (1988) 507; *Angew. Chem. Int. Ed. Engl. 27* (1988) 490.
[9] S. Wimperis, G. Bodenhausen, *Chem. Phys. Lett. 140* (1987) 41.
[10] S. Wimperis, G. Bodenhausen, *Mol. Phys. 66* (1989) 897.
[11] A. Bax, R. Freeman, S. P. Kempsell, *J. Am. Chem. Soc. 102* (1980) 4849.
[12] T. H. Mareci, R. Freeman, *J. Magn. Reson. 48* (1982) 158.
[13] U. Eggenberger, G. Bodenhausen, *Anal. Chem. 61* (1989) 2298.
[14] M. H. Levitt, R. R. Ernst, *J. Chem. Phys. 83* (1985) 3297.
[15] C. Radloff, R. R. Ernst, *Mol. Phys. 66* (1989) 161.
[16] P. E. Fagerness, D. M. Grant, K. F. Kuhlmann, C. L. Mayne, R. B. Parry, *J. Chem. Phys. 63* (1975) 2524.
[17] T. E. Bull, *J. Magn. Reson. 72* (1987) 397.
[18] C. Dalvit, G. Bodenhausen, *J. Am. Chem. Soc. 110* (1988) 7924.
[19] C. Dalvit, G. Bodenhausen, *Adv. Magn. Reson. 14* (1990) in press.
[20] M. Goldman, *J. Magn. Reson. 60* (1984) 437.
[21] G. Jaccard, S. Wimperis, G. Bodenhausen, *Chem. Phys. Lett. 138* (1987) 601.
[22] C. Dalvit, G. Bodenhausen, *Chem. Phys. Lett. 161* (1989) 554.
[23] S. Macura, Y. Huang, D. Suter, R. R. Ernst, *J. Magn. Reson. 43* (1981) 259.
[24] G. Bodenhausen, G. Wagner, M. Rance, O. W. Sørensen, K. Wüthrich, R. R. Ernst, *J. Magn. Reson. 59* (1984) 542.
[25] I. Burghardt, L. Di Bari, A. Bonvin, G. Bodenhausen, *J. Magn. Reson.*, in press.

Communications may be submitted in English *or* in German. Further details regarding the submission of communications can be found in the "Notice to Authors" reproduced in the January issue of the journal. Copies thereof may be obtained from the editorial office upon request.

Radiation-Induced Copolymerization of *cis*-$[PdCl_2\{CN(CH_2)_3\text{-}OC(O)\text{–}CH=CH_2\}_2]$: A Novel Route to Organometallic Cross-linked Copolymers Useful for Catalytic Applications

By *Benedetto Corain,* Marco Zecca, Felix Okon Sam, Giancarlo Palma*, and *Silvano Lora*

The copolymerization of organometallic monomers with other conveniently chosen comonomers may be a procedure for the synthesis of macromolecular materials containing homogeneously distributed and chemically well-defined organometallic groups. Such polymers may be useful as hybrid catalysts,[1] tailored precursors of highly dispersed metal catalysts, or designable organometallic materials potentially useful for diverse applications.[2] The radical-initiated copolymerization of organometallic monomers in which alkenyl residues are connected to η^5- or η^6-coordinated aromatic ligands, albeit somewhat troublesome, is well documented.[3]

We have now found that the bifunctional organometallic monomer **1** can be copolymerized under γ-ray irradiation

cis-$[PdCl_2\{CN(CH_2)_3OC(O)\text{–}CH=CH_2\}_2]$ **1**

with dimethylacrylamide (DMAA) in the presence of *N,N'*-methylenebisacrylamide (MBAA), as a cross-linking agent, to give a solid polymer, "Pd-Pol".

Complex **1** is obtained in high yield as a white microcrystalline powder[4] from $[PdCl_2(NCPh)_2]$ and 3-isocyanopropyl acrylate in $C_2H_4Cl_2$ at room temperature.[5] No monoisocyano intermediate is observed in this reaction. Complex **1** is air-stable and melts at 72–73 °C in argon atmosphere, giving rise to a phase which is stable up to 180 °C (DSC control). At 180–240 °C the molten phase undergoes polymerization ($\Delta H \cong -39$ kcal mol^{-1}). The most prominent feature in the IR spectrum of **1** is a double absorption band centered at 2265 cm^{-1} (maxima at 2271 and 2256 cm^{-1}), which is attributed to a *cis*-$[Pd(CNR)_2]$ moiety.[6] The X-ray single-crystal diffraction analysis of **1** was prevented by X-ray-induced polymerization of the sample.

Complex **1** undergoes γ-ray-induced copolymerization with DMAA at −78 °C in the presence of water; the product separates as microcrystals[7] and an overall polymerization conversion of 95% is attained. Similar results are obtained by employing *cis*-$[PdCl_2(PPh_3)(CN(CH_2)_3OC(O)\text{-}CH=CH_2)]$[8] as monomer. The presence of the doublet centered at about 2216 cm^{-1} in the IR spectrum of Pd-Pol strongly suggests the maintenance of the *cis*-$[Pd(CNR)_2]$ moiety in the copolymer.

The bathochromic shift ($\Delta\tilde{\nu} = 49$ cm^{-1}) is similar to that observed on going from $[Pd(NCCH_3)_4]^{2\oplus}$ to $[Pd(NC\text{-}Ⓟ)_4]^{2\oplus}$.[9] Pd-Pol is obtained in the form of beads which are about 0.2 mm in diameter and exhibit a moderately porous structure. It swells appreciably in methanol, dichloromethane, water, and acetone (equilibrium swelling degree around 100%), but to a very limited extent in diethyl ether and tetrahydrofuran. X-ray microprobe analysis reveals a fairly uniform metal distribution inside the polymer beads. The low Pd content in Pd-Pol is explained either by assuming that **1** is substantially less reactive than other comonomers or, more likely, that it partially separates from the reaction mixture when the latter is cooled to the temperature at which polymerization is carried out.[7]

Pd-Pol has been tested as a catalyst in the hydrogenation of phenylacetylene, styrene, and nitrobenzene in methanol under ambient conditions. It shows good activity, is easily separated from the reaction mixture, and may be reused. Turnover numbers of 500 to 900 (not optimized) are obtained after 24 h.

After the first catalytic run, the IR spectrum of Pd-Pol reveals the complete disappearance of the Pd(CNR) unit, which suggests the reduction of Pd^{II} to Pd^0. This is confirmed by a test in which the reduction of **1** to palladium metal is found to take place in methanol under hydrogen under the same experimental conditions after a comparable reaction time.

The reaction mixtures recovered after catalytic runs do not exhibit any catalytic activity in accordance with negligible metal leaching. In view of the general high reactivity of isocyanides with metal complexes[10, 11] and, in particular, with metal halides, our approach is quite likely to be extendible to many different metal centers in various oxidation states.

Experimental Procedure

Synthesis of the monomer: To a solution of $[PdCl_2(NCPh)_2]$ (1.3 g, 3.4 mmol) in dichloroethane (5 mL), a solution of 3-isocyanopropyl acrylate (1.43 g, 10.3 mmol) in the same solvent (5 mL) was added under vigorous stirring. An immediate color change from brownish-yellow to yellow was observed. The solution was stirred for 15 min. The volume of the solvent was then reduced to about 5 mL and 40 mL of diethyl ether was slowly added to the stirred solution. The resulting yellow precipitate (1.97 g) was collected, dissolved in a small amount of dichloroethane, and recrystallized from diethyl ether to give a white microcrystalline powder (overall yield 75%).

Synthesis of Pd-Pol: A mixture of **1** (0.18 g), DMAA (0.79 g), MBAA (0.05 g), and water (0.56 g) was injected dropwise (ca. 1 mL min^{-1}) by means of a syringe (needle inner diameter ca. 0.45 mm) into a cylindrical Pyrex vial (outer diameter 2.5 cm) containing an excess volume of petroleum ether maintained at −78 °C[7]. The system was then irradiated with γ-rays from a ^{60}Co source at a rate of 0.50 Gy s^{-1} for 17 h. Beadlike polymer particles were recovered, washed with ethanol and diethyl ether, and finally dried under vacuum.

Catalytic runs: The reactions were carried out in 100-mL cylindrical vials under vigorous magnetic stirring. The reaction mixtures, prepared volumetrically and degassed by three freezing-thawing cycles, were finally saturated with H_2 at atmospheric pressure, supplied from a large reservoir. The reactions were monitored by gas chromatography $\tilde{\nu}_{NC} = 2237$ (w), 2200 (w, sh). Elemental

[*] Prof. Dr. B. Corain, Dr. M. Zecca, Dr. F. O. Sam
Centro di Studio sulla Stabilita' e Reattivita'
dei Composti di Coordinazione, C.N.R.
Dipartimento di Chimica Inorganica, Metallorganica ed Analitica
Universita' di Padova
Via Marzolo 1, I-35131 Padova (Italy)
Prof. Dr. G. Palma
Dipartimento di Chimica Fisica, Universita' di Padova
Dr. S. Lora
Istituto Fotochimica e Radiazioni di Alta Energia,
C.N.R., Sezione di Legnaro
I-35020 Legnaro (Italy)

 © VCH Verlagsgesellschaft mbH, D-6940 Weinheim, 1990 0570-0833/90/0404-0384 $ 02.50/0

analysis: C, 49.20 (56.10); H, 7.93 (8.05); N, 11.07 (12.92); Pd, 2.5 (4.10); Cl, 1.51% (2.76%). The values in parentheses were calculated from the composition corresponding to complete conversion of the reacting comonomers. The reaction mixture after standing for 30 min was easily separated via cannulation from the catalyst, which was then washed with methanol.

Received: June 30, 1989;
revised: December 28, 1989 [Z 3416 IE]
German version: *Angew. Chem. 102* (1990) 404

[1] G. Parshall: *Homogeneous Catalysis*, Wiley, New York 1980.
[2] C. U. Pittmann, Jr., C. E. Carraher, *Appl. Polym. Proc. Am. Chem. Soc. Symp. O.A. Battista. Appl. Polym. Sci. 1987*, Plenum, New York 1988.
[3] F. R. Hartley: *Supported Metal Complexes*, Reidel, Dordrecht 1985.
[4] FT-IR: $\tilde{\nu}$(cm^{-1}) = 2271, 2256 (m, s, *cis*-Pd(CNR)$_2$). 1717 (s, C=O), 1614 (w, C=C). ^{1}H NMR (90 MHz, $CDCl_3$, TMS intern): δ = 6.51–5.81 (CH_2=CH-), 4.33 (t, CH_2O), 4.1–3.9 (m, CH_2N), 2.4–2.1 (m, -CH_2-). M.p. 69–71 °C.
[5] B. Corain, M. Zecca, F. O. Sam, S. Lora, G. Palma, A. C. Veronese, *Makromol. Chem., Rapid. Commun. 10* (1990) 697.
[6] L. Malatesta, F. Bonati: *Isocanide Complexes of Metals*, Wiley, New York 1969, p. 158.
[7] M. Carenza, S. Lora, G. Palma, E. Boccu, R. Largajolli, F. M. Veronese. *Radiat. Phys. Chem. 31* (1988) 657.
[8] U. Casellato, B. Corain, M. Zecca, R. A. Michelin, M. Mozzon, R. Graziani, *Inorg. Chim. Acta. 156* (1989) 165.
[9] B. Corain, M. Zecca, S. Rancan, G. Palma, S. Lora, *J. Mol. Catal 55* (1990) 209.
[10] B. Corain, M. Zecca, R. A. Michelin, M. Mozzon in U. Schubert (Ed.): *Advances in Metal—Carbene Chemistry*, Kluwer, Dordrecht 1989, p. 75
[11] E. Singleton, H. Oosthuizen, *Adv. Organomet. Chem. 22* (1984) 209.

Grahamine, an Unusual Tropane Alkaloid from *Schizanthus grahamii***

By *Rudolf Hartmann, Aurelio San-Martin, Orlando Muñoz,* and *Eberhard Breitmaier**

Alkaloids with cyclobutane partial structure are rare. A CAS on-line search resulted in bis(2-methoxycarbonyltropyl) α-truxillate from leaves of the coca plant, *Erythroxylum coca*,[1] and santiaguine, the diamide formed from truxillic acid and 1,2,3,4-tetrahydro-5-(2-piperidyl)pyridine.[2] In *Schizanthus grahamii*, we have now found a further tropane alkaloid containing a 2-methyl-4-phenylcyclobutane-1,2,3-tricarboxylic triester as central partial structure.

Schizanthus grahamii (Gill) belongs to the *Solanaceae* or nightshade family and to the Salpiglossideae branch native to Chile. The plant grows up to 60 cm high and possesses doubly pinnatifid leaves and large, butterfly-like, purple-pink blossoms.[3] Several tropane alkaloids have been isolated from the plant, including hygrolinhydroxytropane esters and schizanthine, in which two 3α-(6β-hydroxytropane) esters of angelic acid are linked as a mesaconic diester.[4, 5]

Using previously described methods,[5] we isolated an extract from the dried and pulverized aboveground parts of the plant and subjected it to countercurrent distribution (dichloromethane and McIlvaine buffer, pH = 5.4). Column chromatography of the first nine fractions (alumina 60/E, petroleum ether (40–60 °C): ethyl acetate = 4:5) gave, besides the known schizanthine, the new compound grahamine as an oily, but pure, fairly stable substance $[[\alpha]_{586}^{20} = +6.21°$ (c = 0.0016 M in $CHCl_3$), R_f = 0.1125 (thin layer chromatography, neutral alumina, $CHCl_3$)].

Fast atom bombardment (FAB) mass spectrometry gave a molecular mass of 871 for grahamine. The best-resolved NMR spectrum in the proton region was obtained in hexadeuteriobenzene as solvent.[6] The ^{1}H-broadband-decoupled ^{13}C-NMR spectrum contains 46 signals, two of which, displaying double intensity, belong to a monosubstituted benzene ring, so that 48 C atoms may be assumed. The DEPT subspectra reveal seven methyl (C_7H_{21}), nine aliphatic methylene (C_9H_{18}), twenty-two methine ($C_{22}H_{22}$), and ten quaternary C atoms (C_{10}). The sum of these CH_n fragments, $C_{48}H_{61}$, corresponds to a molecular mass of 637, a difference of 234 from the actual molecular mass of 871. The typical shifts (δ = 40.5, 41.1, 41.2), splittings (quartets), and CH coupling constants (^1J = 134–140 Hz) of *N*-methyl groups indicate the presence of three nitrogen atoms. If their molecular mass of 42 is subtracted from the above difference, the resulting mass (192) corresponds exactly to twelve oxygen atoms. The empirical formula thereby obtained, $C_{48}H_{61}N_3O_{12}$, respresents twenty double-bond equivalents.

Further structure elucidation was accomplished by one- and two-dimensional NMR methods (400- and 600- MHz ^{1}H NMR; 100- and 150-MHz ^{13}C NMR; Scheme 1). All 38

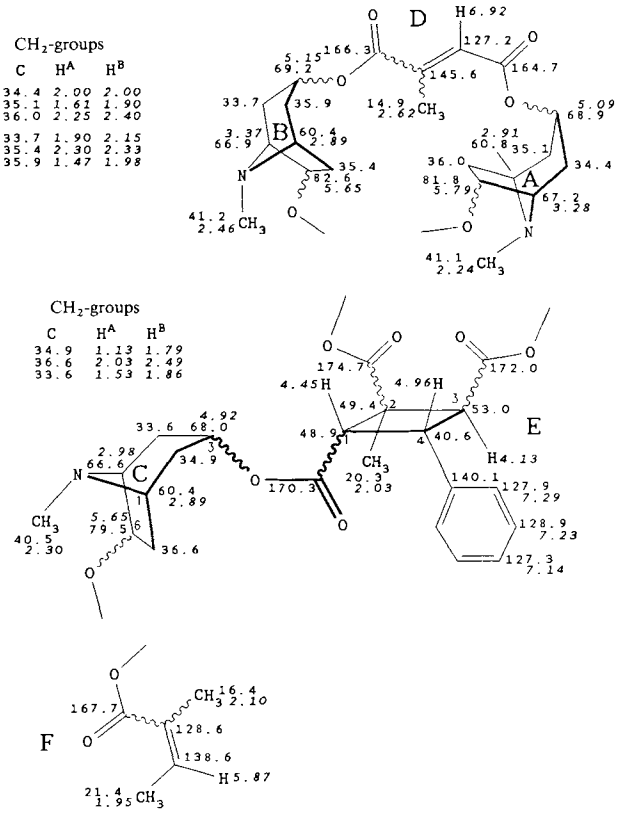

Scheme 1. Partial structures **A**–**F** of grahamine (**1**). ^{13}C- and ^{1}H-NMR chemical shifts, the latter in italics.

CH_n fragments of the molecule can be assigned in the C,H COSY contour diagram. All 61 H atoms of the molecule are bonded to carbons, so that no OH or NH groups are present. The cross signals of an H,H COSY diagram reveal three 3,6-dihydroxytropane rings, **A**, **B**, and **C**, as well as a methyl-

[*] Prof. Dr. E. Breitmaier, Dr. R. Hartmann
Institut für Organische Chemie der Universität
Gerhard-Domagk-Strasse 1., D-5300 Bonn (FRG)
Prof. Dr. A. San-Martin, Dr. O. Muñoz
Faculty of Science, Department of Chemistry
University of Chile, Santiago (Chile)

[**] This work was supported by the Ministerium für Wissenschaft und Forschung des Landes Nordrhein-Westfalen. We thank Dr. *G. J. Wolff* and *M. Mörtter* (Bruker, Rheinstetten) for allowing us to use a 600-MHz NMR spectrometer.

cyclobutane partial structure, which was identified from the typical CH coupling constants (^1J = 140–145 Hz) in the coupled ^{13}C-NMR spectrum. In the C,H COLOC diagram, the connectivity of all six carboxyl C atoms (δ = 164.7–174.7) is clearly revealed by the two- and three-bond coupling constants $^2J_{CH}$ and $^3J_{CH}$, respectively. Accordingly, tropane rings **A** and **B** are linked as mesaconic diester **D**. Further cross signals in the C,H COLOC diagram show that a 2-methyl-4-phenylcyclobutane-1,2,3-tricarboxylic ester **E** is present, whereby the carboxylic acid function on C1 forms an ester linkage with the third 3,6-dihydroxytropane **C** at its 3-hydroxyl group. Furthermore, the C,H COLOC diagram reveals an angelic ester partial structure **F**, which is linked to tropane ring **C** through the 6-hydroxyl group. Combination of all partial structures gives the constitution of grahamine (**1**), which accounts for the twenty double-bond equivalents.

The relative configuration of the *O*-acyl groups on the tropane rings may be derived from the HH coupling constants. All signals of protons in a 3-position are split into a doublet of doublets ($^3J_{HH}$ = 4–5 Hz) owing to coupling with the pseudo-axial protons 2-H and 4-H (interplanar angle ca. 60°). Signal broadening occurs as a result of unresolved HH coupling to the pseudo-equatorial protons in 2- and 4-positions (interplanar angle ca. 90°). Accordingly, the 3-H protons are pseudo-equatorial and the 3-*O*-acyl groups pseudo-axial. The signals of the 6-H protons are each a doublet of doublets with $^3J_{HH}$ = 7.8–8.8 Hz to 7-H_{endo} and 3.5–3.8 Hz to 7-H_{exo}. Further couplings with 5-H are again unresolved (interplanar angle nearly 90°); examination of the interplanar angle between the protons 5-H and 6-H in a Dreiding model reveals that only 6-H in *endo* position allows an interplanar angle to 5-H of about 90°. Thus, the 6-*O*-acyl groups are *exo*.

The CH coupling constants of the carboxyl C atoms at δ = 166.3 (**D**) and 167.7 (**F**) reflect the relative configuration of the two C–C double bonds. A $^3J_{CH}$ coupling of 15 Hz between the carboxy signal at δ = 167.7 and the proton signal at δ = 5.87 is characteristic of the *trans* configuration of the methyl group of angelic ester **F**. A correspondingly large coupling with the proton signal at δ = 6.92 is absent for the carboxyl signal at δ = 166.3, which confirms the **E** configuration of the mesaconic diester partial structure **D**.

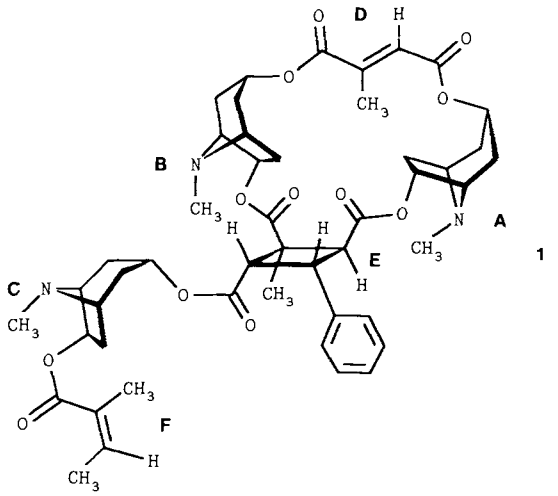

Since the $^3J_{HH}$ couplings of the *cis* and *trans* protons in cyclobutane derivatives differ only slightly,[7] the relative configuration of this ring was determined by H,H NOE difference spectroscopy. Pronounced nuclear Overhauser effects corresponding to a *cis* relationship are found between the protons at δ = 4.45 and 4.96 as well as 4.13 and 2.03 (methyl). Saturation of the resonance at δ = 2.03 also leads to an NOE at the *N*-methyl proton of tropane ring **B** (δ = 2.46). Accordingly, the partial structures may be joined as shown by **1**.

Presumably, the plants, which grow at sunny sites, form the cyclobutane ring from mesaconic diester (left half in **1**) and cinnamic ester (right half) by [2+2] cycloaddition.

Received: November 30, 1989 [Z 3660 IE]
German version: *Angew. Chem. 102* (1990) 441

CAS Registry number:
grahamine, 24583-56-0.

[1] C. Liebermann, *Ber. Dtsch. Chem. Ges. 21* (1888) 2342; *ibid. 22* (1889) 672; W. C. Evans, *J. Ethnopharmacol. 3* (1981) 265.
[2] I. Ribas, E. Riviera, *An. R. Soc. Esp. Fis. Quim. Ser. B49* (1953) 707.
[3] E. Petersen: *Praktisches Gartenlexikon*, 3rd ed. Nymphenburger Verlagshandlung, München 1982.
[4] H. Ripperger, *Phytochemistry 18* (1979) 717; A. San-Martin, J. Rovirose, V. Gambaro, M. Castillo, *ibid. 19* (1980) 1007.
[5] A. San-Martin, C. Labbe, M. Castillo, *Phytochemistry 22* (1983) 1838; *ibid. 26* (1987) 819.
[6] R. Hartmann, *Dissertation*, Universität Bonn 1989 (detailed description of the interpretation and documentation of the spectra).
[7] D. J. Pasto, S. H. Yang, *J. Am. Chem. Soc. 106* (1984) 152.

Enzyme-Catalyzed Synthesis of (*S*)-Cyanohydrins**

By *Uwe Niedermeyer* and *Maria-Regina Kula**

The enzyme-catalyzed addition of hydrogen cyanide to aldehydes leads to optically active cyanohydrins.[1] These compounds open up a simple route to chiral β-amino alcohols,[2] α-hydroxy acids, and pyrethroid insecticides.[3] However, obtaining cyanohydrins with high optical purity is fundamentally difficult, since the optical yield of the enzyme-catalyzed asymmetric synthesis is decreased by the concomitant nonselective chemical addition of hydrogen cyanide. This reaction cannot be completely suppressed in most solvent systems.[4] The importance of optically active cyanohydrins, on the one hand, and the lack of methods for asymmetric synthesis of cyanohydrins, on the other, prompted us to investigate in more detail the potential of enzyme-catalyzed cyanohydrin formation.

The synthesis of (*R*)-cyanohydrins is documented by numerous examples. One of the most effective catalysts is an oxynitrilase (4.1.2.10) from *Prunus amygdalus* (bitter almond).[1, 5, 6] By contrast, the enzymatic synthesis of (*S*)-cyanohydrins has not yet been studied.[***] We have now found that an oxynitrilase from *Sorghum bicolor* (4.1.2.11), which was described mainly from a botanical viewpoint in the 1960s,[7a, b] allows the preparative synthesis of (*S*)-cyanohydrins with high optical purity.[8]

[*] Prof. Dr. M.-R. Kula, Dr. U. Niedermeyer
Institut für Enzymtechnologie der Universität Düsseldorf
in der KFA Jülich
Postfach 2050, D-5170 Jülich (FRG)

[**] This work was supported by the Deutsche Forschungsgemeinschaft and the Fonds der Chemischen Industrie.

[***] Editorial note (March 16, 1990): A communication concerning the enzyme-catalyzed synthesis of (*S*)-cyanohydrins has been published in issue No. 9/1990 of *Tetrahedron Lett.*: F. Effenberger, B. Hörsch, S. Förster, T. Ziegler, *Tetrahedron Lett. 31* (1990) 1249 (Received: December 22, 1989).

By detailed investigations of the reaction kinetics of enzymatic and nonenzymatic cyanohydrin formation, we were able to show that the enantiomeric excess of the product could be controlled, especially through the pH value. Figure 1 shows, for example, the pH dependence of the enzymatic reaction of 4-hydroxybenzaldehyde. Under otherwise identical conditions, lower pH values clearly result in higher optical rotations, that is, higher enantiomeric purity, but lead to a decrease in reaction rate.

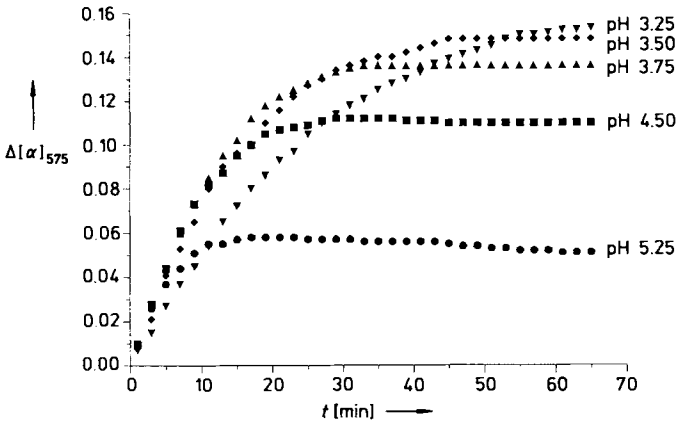

Fig. 1. Effect of the pH value on the asymmetric cyanohydrin synthesis at 25 °C (determined from the change in optical rotation $\Delta[\alpha]_{575}$). Starting concentrations: 27.5 mM 4-hydroxybenzaldehyde, 500.0 mM HCN, 1.7 U mL^{-1} (*S*)-oxynitrilase.

Carbonyl compounds react with hydrogen cyanide at different rates in the nonenzymatic reaction.[9] This differing reactivity of the starting materials in the spontaneous formation of cyanohydrins, as well as the affinity of the enzyme for the substrates, governs the conditions under which almost exclusive enzyme-catalyzed cyanohydrin formation occurs.

Although the rate of the reaction catalyzed by the (*S*)-oxynitrilase decreases with decreasing pH value, reactions can be carried out down to a pH value of 3.0. Thus, a relatively broad pH range is available for optimizing the reaction. The results obtained in batch runs with a number of aldehydes under optimized conditions are summarized in Table 1. In contrast to the (*R*)-oxynitrilase from *Prunus amygdalus*, the (*S*)-oxynitrilase from *Sorghum bicolor* is apparently unable to catalyze the reaction of aliphatic aldehydes. The procedure presented here affords homocyclic aromatic (*S*)-cyanohydrins with very high optical purity.

Table 1. Enzymatic synthesis of (*S*)-cyanohydrins in sodium citrate buffer at 20 °C. The starting material (0.5 mmol) was treated with excess hydrogen cyanide and the (*S*)-cyanohydrin was isolated after the reaction times indicated (batch runs).

Carbonyl compound	*t* [min]	pH	Yield [%]	*ee* value [%]
Benzaldehyde	45	3.25	80	96
3-Hydroxybenzaldehyde	40	3.20	90	98
4-Hydroxybenzaldehyde	25	3.75	87	99
3-Methylbenzaldehyde	90	3.25	80	96
Furfural	60	4.00	no conversion	
Acetaldehyde	60	3.25	no conversion	
(*R*/*S*)-3-Methylcyclohexanone	60	4.50	no conversion	

In a continuous run the (*S*)-oxynitrilase, immobilized on Eupergit C,[10] was employed in a stirred tank reactor (10 mL); 4-hydroxybenzaldehyde (21 mM) was converted under identical conditions as described above into the corresponding (*S*)-cyanohydrin (*ee* value 98%). For a residence time of 66 min and a conversion of 85%, a space–time yield of 58 g L^{-1} d^{-1} was obtained. The productivity, as well as the enantiomeric excess, can be further improved by using higher concentrations of catalyst.[11]

To determine the *ee* values, the cyanohydrins were reduced to the corresponding aminoethanols.[12] These compounds were perfluoropropionylated and then analyzed directly by gas chromatography on a chiral column.[13]

Experimental Procedure

The enzyme preparation was obtained from five-day-old shoots of *Sorghum bicolor* by standard biochemical methods of protein isolation. The (*S*)-oxynitrilase stock solution had an activity of 83 U mL^{-1} (53 U mg^{-1}), whereby 1 U catalyzes the formation of one micromole of 4-hydroxymandelonitrile per minute at 20 °C at pH 3.75.

Example: 4-Hydroxybenzaldehyde (61 mg, 0.5 mmol) was dissolved in 9.4 mL of 50 mM sodium citrate buffer (pH 3.75) and incubated at 20 °C. After addition of 500 μL of oxynitrilase solution and 800 μL of 4.2 M aqueous HCN solution, the reaction was monitored polarimetrically. The reaction is complete after 15–30 min (constant optical rotation). The reaction mixture was extracted with 4 × 10 mL of diethyl ether and the combined organic phases were dried over Na_2SO_4. The solvent was then removed with a rotary evaporator, the residue washed with 3 × 10 mL of pentane, and the product dried in vacuo. Yield: 64.8 mg (83%).

To determine the optical purity, 1–2 mg of the cyanohydrin was reduced by treatment with 250 μL of a 1 M solution of diborane (Aldrich Chemie, Steinheim) in tetrahydrofuran at room temperature for 30 min. After hydrolysis of the excess diborane with a few drops of ethanol and removal of the solvent, the resulting amino alcohol was acylated directly by treatment with 20 μL of pentafluoropropionic anhydride at room temperature in dichloromethane. The excess anhydride was removed in a rotary evaporator and the residue was dissolved in dichloromethane and then analyzed by gas chromatography (FS-Chirasil-Val, Macherey-Nagel, Düren).

Received: November 15, 1989 [Z 3635 IE]
German version: *Angew. Chem. 102* (1990) 423

CAS Registry numbers:
benzaldehyde, 100-52-7; 3-hydroxybenzaldehyde, 100-83-4; 4-hydroxybenzaldehyde, 123-08-0; 3-methylbenzaldehyde, 620-23-5; furfural, 98-01-1; acetaldehyde, 75-07-0; (*R*/*S*)-3-methylcyclohexanone, 625-96-7; (*S*)-benzaldehydecyanohydrin, 28549-12-4; (*S*)-3-hydroxybenzaldehydecyanohydrin, 125781-60-4; (*S*)-4-hydroxybenzaldehydecyanohydrin, 71807-09-5; (*S*)-3-methylbenzaldehydecyanohydrin, 105367-21-3; (*S*)-oxynitrilase, 9024-43-5.

[1] W. Becker, U. Benthin, E. Eschenhof, E. Pfeil, *Biochem. Z. 337* (1963) 156.
[2] W. Becker, H. Freund, E. Pfeil, *Angew. Chem. 77* (1965) 1139; *Angew. Chem. Int. Ed. Engl. 4* (1965) 1079.
[3] T. Matsuo, T. Nishioka, M. Hirano, Y. Suzuki, K. Tsushima, N. Itaya, H. Yoshioka, *Pestic. Sci. 1980*, 202.
[4] H.-H. Hustedt, E. Pfeil, *Justus Liebigs Ann. Chem. 640* (1961) 15.
[5] F. Effenberger, T. Ziegler, S. Förster, *Angew. Chem. 99* (1987) 491; *Angew. Chem. Int. Ed. Engl. 26* (1987) 458.
[6] J. Brussee, E. C. Roos, A. van der Gen, *Tetrahedron Lett. 29* (1988) 4485.
[7] a) C. Bové, E. E. Conn, *J. Biol. Chem. 236* (1961) 207; b) M. K. Seely, R. S. Criddle, E. E. Conn, *ibid. 241* (1966) 4457.
[8] U. Niedermeyer, M.-R., Kula, Patentanmeldung P 3823866 (July 14, 1988).
[9] J. W. Baker, W. L. Bright, *J. Am. Chem. Soc. 71* (1949) 1089.
[10] Röhm Pharma: Produktinformation und Dotenblätter zu Eupergit C and Eupergit C 250 L, Darmstadt 1987.
[11] U. Kragl, U. Niedermeyer, C. Wandrey, M.-R. Kula, *Enzyme Eng. 10*, in press.
[12] M.-L. Anhoury, P. Crooy, R. De Neys, J. Eliars, *J. Chem. Soc. Chem. Commun. 1974*, 1015.
[13] W. König, I. Benecke, S. Sievers, *J. Chromatogr. 238* (1982) 427.

Continuous Generation of NADH from NAD$^{\oplus}$ and Formate Using a Homogeneous Catalyst with Enhanced Molecular Weight in a Membrane Reactor**

By *Eberhard Steckhan,** *Sabine Herrmann, Romain Ruppert, Jörg Thömmes*, and *Christian Wandrey*

Homogeneous catalysts, which are often highly efficient and selective even at low reaction temperatures, have usually been restricted to use in batch processes. On the other hand, heterogeneous catalysts, though well suited for continuous processes, often exhibit low selectivity. Only moderate success has been achieved so far in attempts to exploit the potential advantages of homogeneous catalysts by binding them to polymers in order to make them heterogeneous. Many problems remain to be solved; these include the nonuniform and partly unknown structures of the heterogeneous catalysts thereby obtained, hindered diffusion due to extensive crosslinking of the polymer matrix, low catalytic activity, loss of metal, and self-poisoning of the active centers.[1] Recently, we reported that the Rh^{III} complex **1** is an effective homogeneous catalyst for regeneration of the enzyme cosubstrates nicotinamide adenine dinucleotide (NADH) and nicotinamide adenine dinucleotide phosphate (NADPH) either with formate as hydride donor[2] or electrochemically. The rhodium catalyst reacts with NAD(P)$^{\oplus}$ much faster than with carbonyl compounds, thereby allowing selective reduction of the cofactors, provided that suitable concentration ratios are chosen.[3] After 100 catalytic cycles involving **1**, no formation of 1,6-NADH could be detected enzymatically.

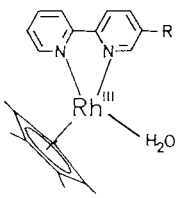

1, R = H
2, R = CH_2OPEG
3, R = CH_2OEt

An effective system for in situ regeneration of these expensive cosubstrates in enzymatic reactions is a prerequisite for the use of oxidoreductases as extraordinarily active catalysts in stereospecific organic synthesis. The usual enzymatic regeneration is not unproblematic.[4] A system employing formate dehydrogenase (FDH) as regeneration enzyme and formate as hydride donor has been brought to technical perfection.[5] Continuous production of enantiomerically pure amino acids is achieved by retaining the amino acid dehydrogenases, FDH, and polymer-bound high-molecular-weight NADH (PEG-NADH)[6] in an enzyme membrane reactor (EMR) behind an ultrafiltration membrane.

In principle, **1** could serve the same function as FDH.[2] Compared with the FDH system, this nonenzymatic generation of NADH has the following important advantages: (1) The reaction is zero order in NAD$^{\oplus}$ and, in contrast to FDH, **1** exhibits no product inhibition. (2) NADPH can be generated under the same conditions. (3) Complex **1** is more stable than an enzyme and not oxygen-sensitive.

By binding **1** to polyethyleneglycol (PEG, MW 20000), we have obtained, for the first time, a homogeneous catalyst (**2**) that can be retained by an ultrafiltration membrane, but which does not give rise to the problems associated with a heterogeneous catalyst, since it remains water soluble. The properties of **1** are therefore largely maintained. We were thus able to replace the FDH in the ultrafiltration flow reactor and generate NADH continuously in a homogeneous catalytic reaction. Because of the improved solubility of the PEG-bound complex, the stationary concentrations of catalyst can be larger than those possible with FDH. In addition, the reaction parameters can be widely varied.

In order to demonstrate that the catalytic properties of the rhodium complex **2**,[7] with enhanced molecular weight, are maintained in the ultrafiltration flow reactor, the kinetic parameters for the reduction of NAD$^{\oplus}$, NADP$^{\oplus}$, and PEG-NAD$^{\oplus}$[6] with formate catalyzed by **2** must be determined and compared with the values obtained for the analogous low-molecular-weight complex **3**.[8] The turnover frequencies[9] for the reduction of (PEG-)NAD(P)$^{\oplus}$ are only lowered by a factor of 0.56–0.66 by the increased molecular (MW 20000) weight of the rhodium complex (Table 1). The

Table 1. Turnover frequencies [h^{-1}] for complexes **2** and **3** in the catalysis of the reduction of NAD$^{\oplus}$, NADP$^{\oplus}$, and PEG-NAD$^{\oplus}$ (0.5 M HCOONa, 3.8×10^{-4} M cosubstrate, 2.5×10^{-5} M **2** or **3** in degassed, thermostated 0.1 M sodium phosphate buffer at pH 7.0; UV absorption at 340 nm monitored as a function of time).

	NAD$^{\oplus}$		NADP$^{\oplus}$		PEG–NAD$^{\oplus}$	
T [°C]	**3**	**2**	**3**	**2**	**3**	**2**
25	20.3	13.3	20.7	12.3	16.6	9.9
38	67.5	43.3	67.5	39.5	56.4	31.8

increase in molecular weight has no effect, however, on the activation energies of the reactions determined from the Arrhenius equation.[10] The reaction catalyzed by **2** is also zero order in NAD$^{\oplus}$. This can be determined by simple variation of the initial concentration of NAD$^{\oplus}$.[11] The reaction mechanism may be formulated as follows:

$$[Cp^*Rh(bpy\text{-}5\text{-}CH_2OPEG)(H_2O)]^{2\oplus} + HCOO^{\ominus} \rightleftharpoons [Cp^*Rh(bpy\text{-}5\text{-}CH_2OPEG)(HCOO)]^{\oplus} + H_2O$$

$$[Cp^*Rh(bpy\text{-}5\text{-}CH_2OPEG)(HCOO)]^{\oplus} \rightleftharpoons [Cp^*Rh(bpy\text{-}5\text{-}CH_2OPEG)H]^{\oplus} + CO_2$$

$$[Cp^*Rh(bpy\text{-}5\text{-}CH_2OPEG)H]^{\oplus} + NAD^{\oplus} + H_2O \rightleftharpoons [Cp^*Rh(bpy\text{-}5\text{-}CH_2OPEG)(H_2O)]^{2\oplus} + NADH$$

The retention of the catalytic properties of **2**, even in the reduction of PEG-NAD$^{\oplus}$, is of great importance, because this allows **2** to be used in a membrane reactor as shown in Figure 1. NADH generation was used to check the suitability of the polymer-bound high-molecular-weight complex **2** for use in a flow reactor. For this purpose, a novel, pressure-stable (to 3 bar) glass flow reactor equipped with an overhead stirrer was employed (Fig. 2). Unlike the reaction in the EMR, the reaction chamber is situated above the ultrafiltration membrane. This reactor has several basic advantages: Since it is made of glass, the reaction can be followed visual-

[*] Prof. Dr. E. Steckhan, Dr. S. Herrmann, Dr. R. Ruppert [+]
Institut für Organische Chemie und Biochemie der Universität
Gerhard-Domagk-Strasse 1, D-5300 Bonn 1 (FRG)
Dipl.-Chem. J. Thömmes, Prof. Dr. C. Wandrey
Kernforschungsanlage Jülich, Institut für Biotechnologie
D-5170 Jülich (FRG)

[+] Present address:
ENSCL, Laboratoire de Chemie Organique Appliquée,
U.A. C.N.R.S 402, Cité Scientifique
F-59652 Villeneuve d'Ascq (France)

[**] This work was supported by the Fonds der Chemischen Industrie and by BASF AG. We thank Prof. Dr. *M. R. Kula* for PEG-NADH.

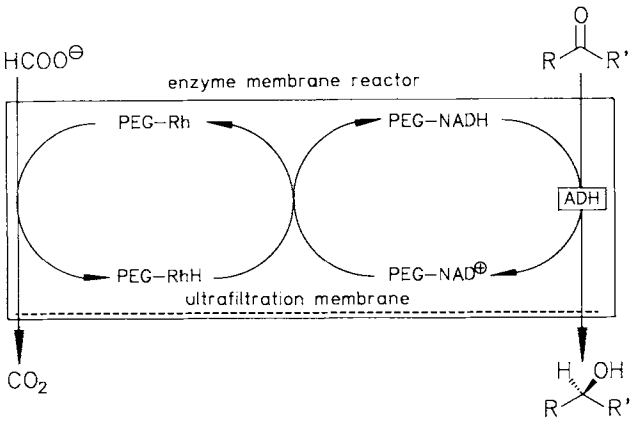

Fig. 1. Concept for the use of **2** in an enzyme membrane reactor (ADH: alcohol dehydrogenase).

ly. In addition, the reactor material should have no effect on the reaction. Moreover, the reactor can be employed for a wide variety of purposes; for example, a continuous electrochemical generation of NADH could be easily achieved by

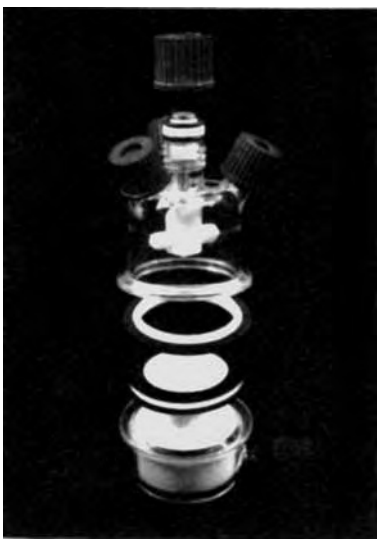

Fig. 2. Flow-through membrane reactor for continuous generation of NADH.

introducing electrodes. Reactions involving gaseous species also pose no problems. A schematic drawing of the experimental setup for continuous generation of NADH is shown in Figure 3.

With the aim of easily isolating the NADH formed, we used an unbuffered ammonium formate/$NAD^{\oplus}$ substrate solution (pH 5.6) in the initial continuous run. After addition of **2**, the conversion of $NAD^{\oplus}$ rapidly climbs to 70%, whereby **2** affords a turnover frequency of 26.3 h^{-1} (Fig. 4A). Although the subsequent decrease in conversion can be slowed by a longer residence time (Fig. 4B), only after replacement of ammonium formate by sodium formate after 30 h of continuous operation (Fig. 4C) does the conversion increase from 30 to 45%. A stationary state is then reached. The large decrease in conversion in the presence of ammonium formate could be due to the incorporation of NH_3 into the ligand sphere of the Rh atom. This ligand exchanges more slowly than H_2O and $Cl^{\ominus}$ with formate. Accordingly, the use of strongly coordinating ligands in the reaction medium should be avoided. In a second experiment with an $NAD^{\oplus}$/sodium formate substrate solution (4.1 mM/0.5 M) buffered to pH 8 with phosphate (0.1 M), the conversion increases at 25 °C in the presence of a doubled concentration of

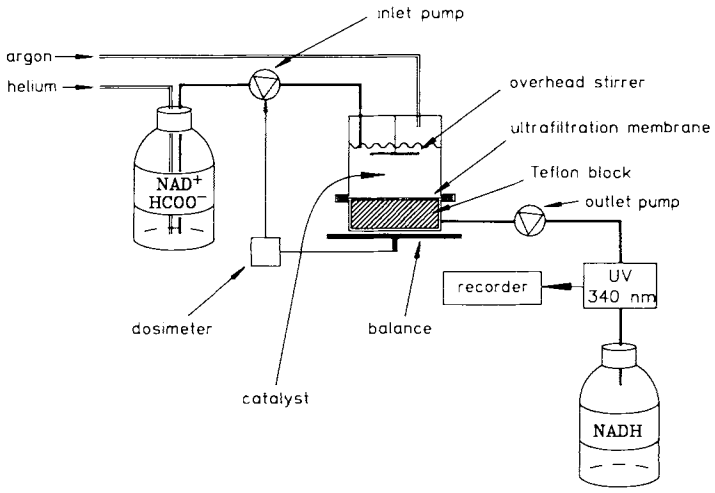

Fig. 3. Experimental setup for continuous generation of NADH.

2 to 70% and then decreases, though more slowly than in the first experiment, over twenty residence times to a stationary conversion of 50%. Before the stationary state was reached, the residence time was doubled by doubling the reaction volume. Conversions of up to 80% were sometimes

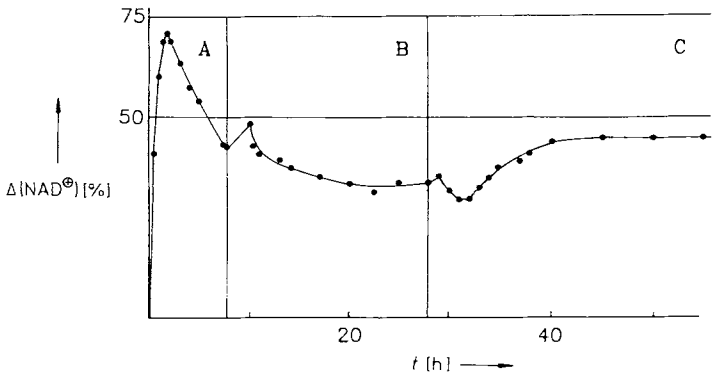

Fig. 4. Dependence of $NAD^{\oplus}$ conversion $\Delta(NAD^{\oplus})$ on time t for continuous generation of NADH (5 mM $NAD^{\oplus}$, 0.13 mM **2**; A,B, 0.5 M $HCOONH_4$; C, 0.5 M HCOONa; residence time A,C, 1 h; B, 2 h; membrane precoated with 300 mg PEG 35000).

achieved. The quantification of $NAD^{\oplus}$ in the substrate and product solution shows that material balance is maintained over the entire period of the experiment. The cause of the decrease in conversion has not yet been determined. However, loss of complex end groups due to hydrolysis, as well as washing out of **2**, can be excluded.[12] The increase in the conversion caused by temporarily doubling the reaction volume in the second experiment shows that an irreversible deactivation of **2** cannot be a reason for the decrease in conversion.

The experiments show that the increased-molecular-weight redox catalyst **2** exhibits the same properties as the low-molecular-weight model. In the flow reactor, a continu-

ous conversion of 45–50% can be maintained after the stationary state has been reached. The redox catalyst thereby displays a turnover frequency of 16.9 h^{-1}. The entire period of the experiment involved more than 1000 reaction cycles. The space–time yield is 44.4 mmol L^{-1} d^{-1}. Taking into consideration the kinetic reaction data, complete conversion can be expected for analogous runs at the stationary state when a 2.2-fold concentration of **2** is employed. This would correspond to a space–time yield of 98.4 mmol L^{-1} d^{-1}. Thus, the rhodium catalyst **2**, with enhanced molecular weight, is very well suited for the continuous regeneration of NADH and NADPH, as well as of their polymer-bound high-molecular-weight forms in coupled enzymatic reactions. The procedure described here offers a widely variable alternative for the enzymatic regeneration of NAD(P)H.

Received: November 8, 1989 [Z 3626 IE]
German version: *Angew. Chem. 102* (1990) 445

CAS Registry numbers:
1, 125568-56-1; **2**, 125591-72-2; **3**, 125591-71-1; PEG, 25322-68-3; $NAD^{\oplus}$, 53-84-9; $NADP^{\oplus}$, 53-59-8; PEG-$NAD^{\oplus}$, 53-84-9; NADH, 58-68-4; NADPH, 53-57-6; NaHCOO, 141-53-7; PEG-2,2′-bipyridyl-5-methyl deriv., 125591-70-0; 5-ethoxymethyl-2,2′-bipyridine, 125568-55-0; 5-brommethyl-2,2′-bipyridine, 98007-15-9.

[1] G. Braca, *Catalisi 1988*, 23; F. A. Cotton, G. Wilkinson: *Advanced Inorganic Chemistry*, 5th ed., Wiley-Interscience, New York 1988, p. 1271.
[2] R. Ruppert, S. Herrmann, E. Steckhan, *J. Chem. Soc. Chem. Commun. 1988*, 1150.
[3] R. Ruppert, S. Herrmann, E. Steckhan, *Tetrahedron Lett. 28* (1987) 6583.
[4] J. B. Jones, J. F. Beck in J. B. Jones, C. J. Sih, D. Perlman (Eds.): *Applications of Biochemical Systems in Organic Chemistry, Part 1*, Wiley-Interscience, New York 1976, pp. 370–376; J. B. Jones in R. Porter, S. Clark (Eds.): *Enzymes in Organic Synthesis*, Pitman, London 1985, p. 3; G. M. Whitesides, *ibid.* p. 76; H. Simon, *GIT Fachz. Lab. 32* (1988) 458.
[5] C. Wandrey, R. Wichmann, A. F. Bückmann, M. R. Kula, *Umschau 84* (1984) 88; C. Wandrey, R. Wichmann, W. Berke, M. Morr, M. R. Kula, *Prepr. Eur. Congr. Biotechnol. 3rd 1984*, 239; C. Wandrey, R. Wichmann in A. I. Laskin (Ed.): *Enzymes and Immobilized Cells in Biotechnology*, Benjamin/Cummings, Menlo Park, CA, 1985, p. 177; M. R. Kula, C. Wandrey in K. Mosbach (Ed.): *Methods Enzymol. 136* (1986) p. 9.
[6] Polyethyleneglycol-(20000)-N^6-(2-aminoethyl)-NADH and -$NAD^{\oplus}$: A. F. Bückmann, M. R. Kula, R. Wichmann, C. Wandrey, *J. Appl. Biochem. 3* (1981) 301.
[7] Experimental procedure for **2**: Freshly sublimed potassium *tert*-butyl alkoxide (115 mg, 1 mmol) was added under argon atmosphere to a solution of PEG (MW 20000; 5 g, 0.25 mmol) in 1 L of dry THF. After refluxing for 20 h, the reaction solution was treated with 5-bromomethyl-2,2′-bipyridine (500 mg, 2 mmol) and then refluxed for an additional 28 h. It was then allowed to cool, 200 mL of water was added, and the THF was removed in vacuo. After dialysis and freeze-drying, 4.7 g of colorless, cotton-wool-like product was obtained. UV: λ_{max} [nm] = 242, 303. Part of the product (4.3 g) was dissolved in 1 L of dry methanol and the resulting solution was treated with di-μ-chloro(dichloro)bis(pentamethylcyclopentadienyl)dirhodium(III) (400 mg, 0.65 mmol) (synthesis: B. L. Booth, R. N. Hazeldine, M. Hill, *J. Chem. Soc. A. 1969*, 1299) and stirred for 1 h. Water (1 L) was then added and the organic solvent was removed in vacuo. After dialysis and freeze-drying, 4.1 g of a pale orange product was obtained. UV (H_2O, pH 7.5, 25 °C): λ_{max} [nm] (ε[L mol^{-1} cm^{-1}]) = 233 (12700), 308 (6150), 318 (6300).
[8] Physical data for 5-ethoxymethyl-2,2′-bipyridine and for **3**: Synthesis of 5-ethoxymethyl-2,2′-bipyridine from 5-bromomethyl-2,2′-bipyridine (synthesis: J. G. Eaves, H. S. Munro, D. Parker, *Inorg. Chem. 26* (1987) 644) by reaction with $EtO^{\ominus}$. ^1H NMR (60 MHz, $CDCl_3$, TMS int.): δ = 1.26 (t, 3H, ^3J = 7 Hz), 3.57 (q, 2H, ^3J = 7 Hz), 4.53 (s, 2H), 7.07–8.73 (m, 7H). MS (70 eV, 300 μA): *m/z* 214 ($M^{\oplus}$, 42%), 185 ($M^{\oplus}$ – Et, 28), 169 ($M^{\oplus}$ – OEt, 100), 157 (bpy + H, 55), 141(22), 115(5), 78 (py, 13), 51(8). UV (H_2O; pH 3.0; 25 °C): λ_{max} [nm] (ε[L mol^{-1} cm^{-1}]) = 242 (8900), 304 (1680). Preparation of the rhodium complex was carried out in analogy to U. Kölle, M. Grätzel, *Angew. Chem. Int. Ed. Engl. 26* (1987) 567; ^1H NMR (60 MHz, D_2O): δ = 1.23 (t, 3H, ^3J = 7 Hz), 1.58 (s, 15H), 3.63 (q, 2H, ^3J = 7 Hz), 7.57–8.97 (m, 7H). UV (H_2O; pH 7.5; 25 °C): λ_{max} [nm] (ε[L mol^{-1} cm^{-1}]): 233 (31600), 308 (15300), 318 (15700). Correct elemental analysis (C, H, N).
[9] Turnover frequency = (PEG-)NAD(P)H concentration/(catalyst concentration × time).
[10] The activation energies for the reaction of $NAD^{\oplus}$ and (PEG-)$NAD^{\oplus}$ (3.8×10^{-4} M each) in sodium formate (0.5 M) in the presence of **2** and **3**, respectively (2.6×10^{-5} M each) were determined at 17.3, 25.7, 32.1, and 40.0 °C in sodium phosphate buffer at pH 7.0. For the reduction of $NAD^{\oplus}$, E_a is 64.0 and 68.2 kJ mol^{-1} for **2** and **3**, respectively; for the reduction of (PEG-)$NAD^{\oplus}$, E_a is 70.3 and 68.6 kJ mol^{-1} for **2** and **3**, respectively.
[11] The reaction order of zero in $NAD^{\oplus}$ was confirmed by applying a differential method of determining the reaction order to two NADH concentration–time curves.
[12] Complex **2** is stable upon dialysis (six times against 9 L of bidistilled H_2O) and under flow-through conditions in H_2O (six residence times) in an Amicon ultrafiltration unit.

$Se_{10}^{2\ominus}$, a Bicyclic Polyselenide

By *Dieter Fenske, Gertrud Kräuter*, and *Kurt Dehnicke**

With the exception of the undecaselenide **1**, whose anion has a spirocyclic structure,[1] and the recently described hexadecaselenide 2, whose anion consists of Se_6 rings and two $Se_5^{2\ominus}$ chains,[2] all other structurally investigated polyselenides are acyclic. Known compounds are the diselenide **3**,[3] the tetraselenides **4**–**8**,[4–7] the pentaselenides **9**–**12**,[7–10] and the hexaselenides **13** and **14**.[11,12]

$(PPh_4)_2Se_{11}$ **1** Cs_4Se_{16} **2** Na_2Se_2 **3** [Ba(222-Crypt)]Se_4 **4** $[Ba(en)_4]Se_4$ **5**

$(NC_4H_8O)_2Se_4$ **6** $(NC_5H_{10})_2Se_4$ **7** $[Ph_3PNPPh_3]_2Se_4 \cdot 4CH_3CN$ **8**

Rb_2Se_5 **9** Cs_2Se_5 **10** $[Cs([18]crown-6)]_2Se_5 \cdot CH_3CN$ **11** $(PPh_4)_2Se_5$ **12**

$(NBu_4)_2Se_6$ **13** $[(CH_3)_3N(CH_2)_{13}CH_3]_2Se_6$ **14**

Although the conditions leading to formation of polyselenides are not understood in detail, important factors include reaction conditions such as solvent and temperature in addition to the size, charge, and shape of the counterion. For instance, the tetraselenide **8** is formed from Cs_3TaSe_4 in acetonitrile in the presence of $[Ph_3PNPPh_3]Cl$ at room temperature,[7] whereas, as we report here, heating of a polyselenide solution in dimethylformamide (DMF) at 100 °C in the presence of $[Ph_3PNPPh_3]Cl$, followed by cooling of the solution, affords the previously unknown bicyclic decaselenide $[Ph_3PNPPh_3]_2Se_{10} \cdot DMF$ as black crystals in very good yield.

The crystal structure analysis[13] showed that, per formula unit, the compound contains one molecule of DMF disordered over two mutually orthogonal positions. The $Se_{10}^{2\ominus}$ ion is located on a crystallographic twofold axis; its symmetry corresponds to point group C_2. The two selenium six-membered rings have chair conformation (Fig. 1). Compared to the decalin molecule, the decaselenide ion contains four additional valence electrons if a selenium atom is regarded as isolobal to a CH_2 group. This has several consequences for the central Se–Se unit: The selenium atoms are coordinated in a distorted pseudo-trigonal-bipyramidal fashion, whereby the selenium atoms Se3 und Se3′ are linked equatorially. The two lone pairs on these selenium atoms can

[*] Prof. Dr. K. Dehnicke, G. Kräuter
Fachbereich Chemie der Universität
Hans Meerwein-Strasse, D-3550 Marburg (FRG)
Prof. Dr. D. Fenske
Institut für Anorganische Chemie der Universität Karlsruhe (FRG)

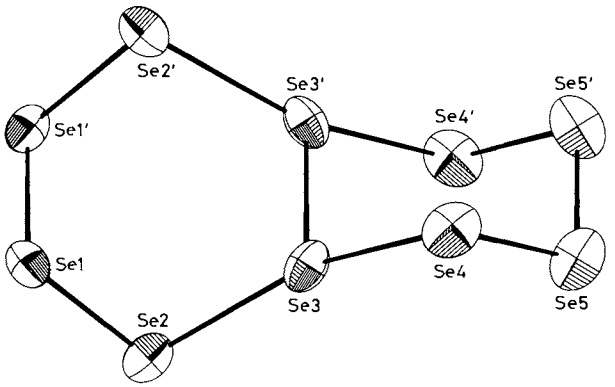

Fig. 1. Molecular structure of the $Se_{10}^{2\ominus}$ ion (ORTEP plot, 50% probability level at −70 °C).

occupy equatorial positions as well, in accordance with the Gillespie–Nyholm rules[14] (Scheme 1).

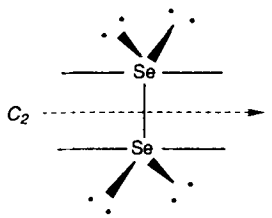

Scheme 1. Idealized formulation of the central Se3–Se3′ unit of the $Se_{10}^{2\ominus}$ ion with equatorial-equatorial linking of the two selenium atoms having trigonal-bipyramidal bonding geometry.

This arrangement allows a relatively short Se3–Se3′ bond (246 pm), whereas the Se–Se distances to the axially arranged Se atoms are 257 and 276 pm. These distances permit the $Se_{10}^{2\ominus}$ ion to be regarded also as consisting of a central $^{\oplus}\dot{\dot{S}}\dot{\dot{e}}$-$\dot{\dot{S}}\dot{\dot{e}}^{\oplus}$ fragment and two $Se_4^{2\ominus}$ ions, insofar as the Se–Se distances of these fragments are in good agreement with those in tetraselenide ions.[4–7]

Table 1. Bond lengths [pm] and angles [°] in the $Se_{10}^{2\ominus}$ ion.

Se1-Se2	232.0(2)	Se2-Se1-Se1′	105.62(6)
Se1-Se1′	232.6(2)	Se1-Se2-Se3	100.65(7)
Se2-Se3	275.9(3)	Se2-Se3-Se4	159.85(8)
Se3-Se3′	246.0(2)	Se2-Se3-Se3′	101.61(8)
Se3-Se4	257.2(3)	Se4-Se3-Se3′	98.32(9)
Se4-Se5	231.8(3)	Se3-Se4-Se5	101.94(8)
Se5-Se5′	234.2(3)	Se4-Se5-Se5′	102.76(6)

Dichalcogen units are also found in the inclusion compound $(Te_2)_2I_2$,[15] in which the Te_2 "dumb-bells" have a Te–Te distance of 271 pm and are arranged to form double layers through longer Te–Te bonds (332 pm). The structure reveals electronic and topological relationships to compounds from β-SnS to black phosphorus.[16] The formulation of partially oxidized units, $^{2}_{\infty}[Te_2^{\delta\oplus}]$, which are indicated by extended Hückel calculations, is reflected in the lengthening of the I–I distances in the intercalated iodine molecules.[17]

Experimental Procedure

Gray selenium (0.96 g, 12.16 mmol) and a trace of iodine as catalyst for polyselenide formation were added to a mixture of Li and Se in a molar ratio of 1:1 (0.26 g = 1.52 mmol) and $[Ph_3PNPPh_3]Cl$ (1.75 g, 3.04 mmol). The resulting mixture was heated for 3 h in 30 mL of DMF at 100 °C. After cooling, the reaction mixture was filtered to remove LiCl and unreacted selenium, 20 mL of ether was added, and the solution was allowed to stand for 2 d. The resulting black single crystals were filtered, washed with EtOH, and dried briefly in vacuo. Yield 2.1 g (72%, based on $[Ph_3PNPPh_3]Cl$).

Received: December 1, 1989 [Z 3663 IE]
German version: *Angew. Chem. 102* (1990) 420

[1] B. Krebs, cited in [16]; see also M. G. Kanatzidis, S.-P. Huang, *Inorg. Chem. 28* (1989) 4667.
[2] W. S. Sheldrick, H. G. Braunbach, *Z. Naturforsch. B44* (1989) 1397.
[3] H. Föppl, E. Busmann, F.-K. Frorath, *Z. Anorg. Allg. Chem. 314* (1962) 12.
[4] T. König, B. Eisenmann, H. Schäfer, *Z. Anorg. Allg. Chem. 498* (1983) 99.
[5] T. König, B. Eisenmann, H. Schäfer, *Z. Naturforsch. B37* (1982) 1245.
[6] O. Foss, V. Janicks, *J. Chem. Soc. Dalton Trans. 1980*, 620.
[7] N. E. Brese, C. R. Randall, J. A. Ibers, *Inorg. Chem. 27* (1988) 940.
[8] P. Böttcher, *Z. Kristallogr. 150* (1979) 65.
[9] U. Kretschmann, P. Böttcher, *Z. Naturforsch. B40* (1985) 895.
[10] G. Kräuter, K. Dehnicke, D. Fenske, *Chem.-Ztg. 114* (1990) 7.
[11] R. G. Teller, L. J. Krause, R. C. Haushalter, *Inorg. Chem. 22* (1983) 1809.
[12] F. Weller, J. Adel, K. Dehnicke, *Z. Anorg. Allg. Chem. 548* (1987) 125.
[13] Crystal data (−70 °C): space group $C2$, $a = 2691.4(9)$, $b = 1252.5(5)$, $c = 1106.8(5)$ pm, $\beta = 90.21(2)°$, $Z = 2$; Stoe-Stadi-IV four-circle diffractometer, $Mo_{K\alpha}$ radiation, graphite monochromator, ω scans, $\theta = 3–54°$, 3162 observed unique reflections, isotropic refinement for the H atoms, $R = 0.046$, $R_w = 0.029$. Further details of the crystal structure investigation may be obtained from the Fachinformationszentrum Karlsruhe, Gesellschaft für wissenschaftlich-technische Information mbH, D-7514 Eggenstein-Leopoldshafen 2 (FRG), on quoting the depository number CSD-54323, the names of the authors, and the journal citation.
[14] R. J. Gillespie: *Molekülgeometrie*, Verlag Chemie, Weinheim 1975; *Molecular Geometry*, van Nostrand-Reinhold Comp., London 1972.
[15] R. Kniep, H.-J. Beister, *Angew. Chem. 97* (1985) 399; *Angew. Chem. Int. Ed. Engl. 24* (1985) 393.
[16] P. Böttcher, *Angew. Chem. 100* (1988) 781; *Angew. Chem. Int. Ed. Engl. 27* (1988) 759.
[17] W. Tremel, R. Hoffmann, *Inorg. Chem. 26* (1987) 118.

Water-Soluble Metal Complexes of the Sulfonated Triphenylphosphane TPPTS: Preparation of the Pure Compounds and their Use in Catalysis**

By *Wolfgang A. Herrmann,** *Jürgen A. Kulpe, Jürgen Kellner, Herbert Riepl, Helmut Bahrmann,* and *Werner Konkol*

Dedicated to Professor Günther Wilke on the occasion of his 65th birthday

The large-scale industrial use of water-soluble rhodium complexes of the sulfonated triphenylphosphane $P(C_6H_4\text{-}m\text{-}SO_3^{\ominus}Na^{\oplus})_3$ (TPPTS) in the Ruhrchemie/Rhône-Poulenc process can be regarded as a methodological advance in homogeneous catalysis by means of organometallic complexes.[1,2] The use of water as the solvent for the catalyst in a two-phase system makes possible its ready separation from the hydrophobic products. In addition, the hydroformyla-

[*] Prof. Dr. W. A. Herrmann, Dr. J. A. Kulpe, Dr. J. Kellner, H. Riepl
Anorganisch-chemisches Institut der Technischen Universität München,
Lichtenbergstrasse 4, D-8046 Garching (FRG)
Dr. H. Bahrmann, Dr. W. Konkol
Hoechst Aktiengesellschaft, Werk Ruhrchemie
Postfach 13 01 60, D-4200 Oberhausen 11 (FRG)

[**] Water-soluble Metal Complexes and Catalysts, Part 1.—TPPTS = sodium salt of 3,3′,3″-phosphanetriyltribenzenesulfonic acid

tion of propene in this process occurs with increased regioselectivity;[3] the scale of butyraldehyde production lies presently at about 300 000 tons per year. Catalysts whose water-solubility is based on the presence of COOH, NH_2, and SO_3H groups in the ligand appear also to be slowly gaining in importance in other processes[4] and in the stabilization of metal colloids.[5]

Of particular importance is the TPPTS ligand introduced by *Kuntz*, since it is inexpensive and can easily be prepared in large quantities.[6] It is also expected to form complexes with most transition metals, just as does triphenylphosphane (TPP). However, the analytical characterization of the TPPTS–metal complexes described previously in the literature has been either incomplete or inaccurate.[1, 7] This is mainly due to the extreme water-solubility of TPPTS (ca. 1.1 kg L^{-1} [1b]), which poses extreme limits to the choice of solvents and purification methods which can be used.

By means of adaption and optimization of the *gel permeation chromatography* technique we have now established the prerequisites for a wide-ranging development of the water-soluble TPPTS complexes: about 40 analytically pure complexes of the general type $[L_xM_y(TPPTS)_z \cdot (H_2O)_{3z}]$ have been synthesized.[8] The syntheses are carried out either by replacing other ligands such as CO, THF, or TPP by TPPTS or by reacting TPPTS with metal salts, if necessary in the presence of additional reagents which act as ligands or reducing agents. Product mixtures are separated in aqueous solution using hydrophilic gels with eluents which are suited for the particular separation problem in hand. The best carrier materials within the temperature range 0–40 °C have been found to be Sephadex G-15/G-25 and Fractogel TSK HW-40. Decomposition occurs very seldom, and the chromatographic separation is followed via either UV/VIS or refractive index detectors. Such a procedure makes it possible to separate amounts of substance up to 10 g on a laboratory scale in one step.[2e] In contrast to previous work,[6] it is also possible to obtain the free ligand TPPTS rapidly and without losses in a pure state using Sephadex G-15; phosphane oxide impurities ($\delta(P) = 34.8$) that cannot be removed by other means can be reduced to below 0.1 % (according to HPLC measurements).

The TPPTS complexes contain *one water molecule per sodium ion* after drying in vacuo (oil pump) at room temperature. The following information may be useful for practical applications of this procedure:

1. TPPTS forms soluble complexes with transition-metal salts in water, though these are not necessarily stable in an aqueous medium. The solvent water can lead to the formation of hydroxo complexes, which are seldom encountered in the chemistry of TPP: examples are the isolable rhodium complexes **2** and **4** (Scheme 1). The former rather than the expected hydrido complex is formed rapidly in attempts to carry out a Cl/H exchange starting from the nonahydrate of **1**, and more slowly directly from $RhCl_3 \cdot 3H_2O$ and TPPTS. If a solution of the hydroformylation catalyst **3** in water is heated at reflux, the hydroxo complex **4** is formed; however, the latter is reconverted quantitatively into **3** under process conditions (CO/H_2) and therefore does not interfere with the hydroformylation reaction. In spite of the importance of TPPTS-containing rhodium complexes for hydrogenation and hydroformylation, this aspect has previously not been taken into account. Both types of complex (hydrido and hydroxo complexes) are formed in TPPTS/water, even when no other hydride source is present (Scheme 1). This is probably due to the catalytic shift of the water gas equilibrium according to Equation (a), which leads to the formation of hydride.

$$CO + H_2O \rightleftharpoons CO_2 + H_2 \qquad (a)$$

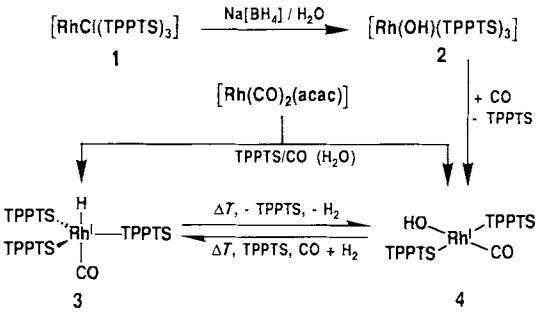

Scheme 1. Solvate water molecules are not shown; acac = acetylacetonate.

2. TPP and TPPTS complexes of analogous composition have almost identical ^{31}P NMR data, and the spectroscopic data for other ligands (e.g., NO, CO, H) are also similar; thus, the ligand TPPTS does not exhibit stereoelectronic peculiarities.

3. TPPTS complexes generally have lower coordination numbers (CN) than homoleptic TPP analogues. Thus, while the complex $Ni(TPP)_4$ is known, the nickel complex described incorrectly in the literature as $Ni(TPPTS)_4$[1] in fact has the formula $Ni(TPPTS)_3$ (as nonahydrate; Pd shows the same behavior[8b]). The TPPTS analogue of $[HRh(TPP)_4]$ is also nonexistent; attempts to prepare such a complex via ligand exchange led to the new binuclear hydroxo complex $[(TPPTS)_2Rh(\mu\text{-}OH)]_2$. We believe this tendency for the formation of phosphane-poorer complexes to be due to the high charge accumulation within the ligand sphere (three electrons per TPPTS!).

4. A sodium-poorer form of complexed TPPTS is possible if the excess of negative charge is compensated by the complexed metal ion. A typical example is provided by the silver complex **5** (CN = 3) with eight rather than nine sodium ions[9] (Scheme 2). The corresponding TPP complex has the formula $[Ag(TPP)_4]^{\oplus}$ (CN = 4). This example indicates the larger diversity of complexation to be expected from sulfonated phosphane ligands.

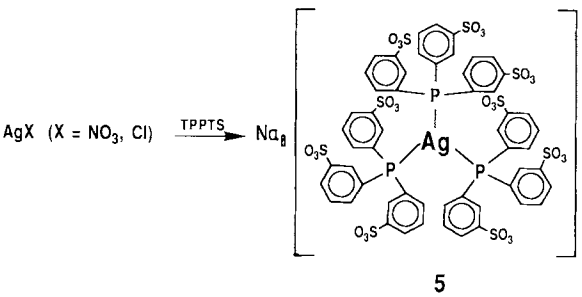

Scheme 2.

5. The specific advantage of the new TPPTS complexes lies in their ready separability in catalytic reactions. This property has, for example, been taken advantage of in the 1,4-addition of diethylamine to isoprene using the new catalyst *cis*-$[PtCl_2(TPPTS)_2 \cdot 6H_2O]$ according to Equation (b). At an amine/catalyst ratio of 1000/1 (temperature 80 °C) the amine consumption after 48 h is 99 % and the 1,4-selectivity 91 %. The aqueous catalyst solution can be reused after phase separation.

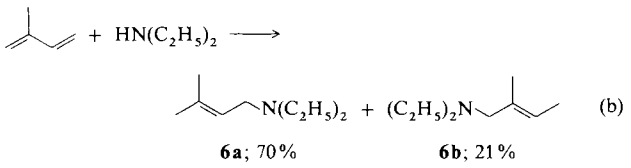

6a; 70% **6b**; 21% (b)

Gel-chromatographic purification has thus made possible the systematic preparation of analytically pure, water-soluble TPPTS complexes, so that their lack of volatility and the unwillingness of such compounds to crystallize is no longer a problem. The availability of pure samples of these complexes now also makes it much easier to probe the mechanisms by which such compounds act as catalysts.

Experimental Procedure

a) Purification of TPPTS: A solution of crude TPPTS in water, obtained from the sulfonation of TPP with subsequent amine extraction[6] contains ca. 30% (w/w) TPPTS. Purification was carried out by introducing 50 mL of such a solution onto a Sephadex G-15 column ($l = 95$, $d = 4$ cm). At a flow rate of 54 mL cm^{-2} h^{-1}, five fractions were obtained (UV detection at $\lambda = 330$ nm and refractive index detection) after 85, 123, 159, 201, and 268 min. The fourth fraction contained pure TPPTS (as the trihydrate after drying under oil-pump vacuum at room temperature). ^{31}P NMR (D_2O, 5 °C). $\delta = -5.3$ ppm. Correct elemental analysis (C, H, O, P).

b) **2**: To a solution of $RhCl_3 \cdot 3H_2O$ (260 mg, 1 mmol) in 20 mL of H_2O was added TPPTS (10 mmol) in 10 mL of H_2O; the mixture was stirred for ca. 40 h at room temperature. The solution, which contained **1**, **2**, TPPTS-oxide (phosphane oxide), and $[Rh(\mu\text{-}OH)(TPPTS)_2]_2$, was chromatographed over Sephadex G-15; chloride-free **2** (nonahydrate) was obtained in 92% yield as a red glass. Correct elemental analysis (C, H, O, P, Rh, S). ^{31}P NMR (109.3 MHz, D_2O, 21 °C): $\delta = 35.2$ [dd; $^1J(Rh, P_A) = 144$ Hz], 53.5 [dt; $^1J(Rh, P_B) = 195$, $^2J(P, P) = 41$ Hz]. IR (KBr): $\tilde{\nu}$ [cm^{-1}] = 1220 (sh,vs), 1196 (vs), 1038 (vs), 787 (m), 624 (m), 527 (s).

c) Hydroamination of isoprene: a solution of *cis*-$[PtCl_2(TPPTS)_2 \cdot 6H_2O]$ (120 mg, 0.08 mmol)[8b] in 6 mL of H_2O, isoprene (8.16 g, 0.12 mmol), and diethylamine (5.86 g, 80 mmol) were introduced into a 100-mL laboratory autoclave. The mixture was warmed for 2 d to 80 °C. After cooling and phase separation, the following components were obtained from the organic phase: 70% **6a**, 21% **6b**, and 8% *N,N*-diethylaminodimethyloctadiene (characterization by means of GC/MS, GC/IR, and ^1H NMR after product isolation); amine consumption 99%.

Received October 10, 1989;
revised November 27, 1989 [Z3589 IE]
German version: *Angew. Chem. 102* (1990) 408

[1] a) E. G. Kuntz, Fr. Pat. 2314910 (June 20, 1975), Rhône-Poulenc; b) *Chemtech 1987*,570; DBP 2 700 904 C2 (October 20, 1983), Rhône-Poulenc.

[2] Further publications: a) C. Larpent, R. Dabard, H. Patin, *Inorg. Chem. 26* (1987) 2922; b) C. Larpent, H. Patin, *J. Appl. Organomet. Chem. 1* (1987) 529; c) P. Kalck, P. Escaffre, F. Serein-Spirau, A. Thorez, B. Beson, V. Colleuille, R. Perron, *New J. Chem. 12* (1988) 687; d) H. Bahrmann, H. Bach, *Phosphorus Sulfur 30* (1987) 611; e) W. A. Herrmann, P 3921295.5 (June 29, 1989), DE 3822036 (June 23, 1989), Hoechst AG; f) I. T. Horváth, R. V. Katsrup, A. A. Oswald, E. J. Mozeleski, *Catal. Lett. 2* (1989) 85.

[3] K. Weissermel, H.-J. Arpe: *Industrielle Organische Chemie*, 3rd edit., VCH Verlagsgesellschaft, Weinheim 1988, p. 142.

[4] Water-soluble sulfonated chiral phosphanes have recently been introduced as ligands in enantioselective catalysis: a) F. Alario, Y. Amrani, Y. Colleuille, T. P. Dang, J. Jenck, B. Morell, D. Sinou, *J. Chem. Soc. Chem. Commun. 1986*, 202; b) Y. Amrani, L. Lecomte, B. Sinou, J. Bakus, I. Toth, B. Heil, *Organometallics 8* (1989) 542; *J. Organomet. Chem. 370* (1989) 277.

[5] a) C. Larpent, H. Patin, *J. Mol. Catal. 44* (1988) 191; b) G. Schmid, A. Lehnert, *Angew. Chem. 101* (1989) 773; *Angew. Chem. Int. Ed. Engl. 28* (1989) 780.

[6] B. Cornils, EP 0107006 (May 2, 1984), Ruhrchemie AG.

[7] C. Larpent, R. Dabard, H. Patin, *New J. Chem. 12* (1988) 907. The problems of separating other reaction products obtained in the preparation of TPPTS metal complexes have already been referred to in the literature: [2c] and B. Fontal, J. Orlewski, C. C. Santini, J. M. Basset, *Inorg. Chem. 25* (1986) 4322.

[8] a) W. A. Herrmann, J. A. Kulpe, H. Bahrmann, W. Konkol, *J. Organomet. Chem.*, in press; b) H. Kellner, *Dissertation*, Technische Universität München 1989.

[9] Chromatography on Sephadex G-15; colorless, slightly light-sensitive powder, yield 90%. ^{31}P NMR (D_2O/C_2H_5OH, −30 °C): $\delta = 8.9$ [dd; $^1J(^{107}Ag, ^{31}P) = 314$, $^1J(^{109}Ag, ^{31}P) = 358$ Hz]. Correct elemental analysis (C, H, Ag, Na, O, P, S).

Novel Planar π-Systems

By *Henning Hopf** and *Martin Kreutzer*

Tetracyanoethylene **1**, discovered in 1957,[2] is the most frequently used cyanocarbon compound in organic synthesis.[1] In the eyes of the hydrocarbon chemist, **1** may be regarded as a tetraaza derivative of the hitherto unknown tetraethynylethene **3**, R = H, presumably also a very reactive and preparatively valuable cross-conjugated π-system. We have set ourselves the target of preparing both **3**[3] as well as the cyano(ethynyl)ethenes **2a–d**, which are formally formed from **1** by successive replacement of its cyano functions by $Me_3Si-C\equiv C-$ groups. In addition we are interested in the lower substituted cyano(ethynyl)ethenes **2e–j** for comparison. What some of the intermediary members **2**, which are listed in Table 1 without taking into account diastereomers, lack in symmetry, they might—because of the polarization of their π-electrons—gain in reactivity. Herein we describe the synthesis of **2b** and **2g** and a modified route to **2e**,[4] and report on the first reactions of these novel, electron-rich π-systems.

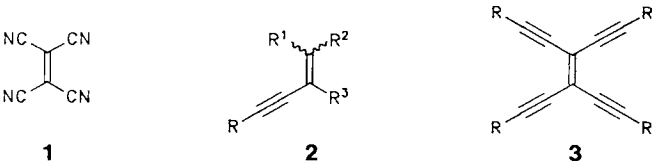

1 **2** **3**

Table 1. Structures of the cyano(ethynyl)ethenes **2** presented in this communication. 2-[3-trimethylsilyl-1-(trimethylsilylethynyl)-2-propynylide]malononitrile **2b** and 5-trimethylsilyl-3-(trimethyl-silylethynyl)pent-2-en-4-yne nitrile **2g** were synthesized for the first time; in the case of **2e** [4] a modified route was developed. R in **2** is always $SiMe_3$.

	R^1	R^2	R^3		R^1	R^2	R^3
2a	CN	CN	CN	**2f**	CN	H	CN
2b	CN	CN	C≡CR	**2g**	CN	H	C≡CR
2c	C≡CR	CN	CN	**2h**	C≡CR	CN	H
2d	CN	C≡CR	C≡CR	**2i**	CN	H	H
2e	CN	CN	H	**2j**	H	H	CN

As starting material for the two novel dialkynes we used 1,5-bis(trimethylsilyl)-1,4-pentadiyn-3-one **4**,[5] which can be condensed in a Wittig reaction with diethylphosphonoacetonitrile to give **2g**[6] and with malononitrile to give **2b**, and the yields are good in each case.[6] The reaction **4** → **2b**, instead of being carried out under the conditions quoted in Scheme 1, can also be carried out under typical Knoevenagel conditions (β-alanine; ethanol/acetic acid; 72%); this type of reaction has hitherto rarely been described for conjugated acetylenic ketones or aldehydes.[4] The aluminum oxide-catalyzed reaction[7] proved to be better than the procedure described in the literature,[4] even for the coupling of trimethylsilylpropynal **5**[8] with malononitrile to give **2e**.

Since the derivatives **2** are formally enynes, and these have been employed as diene components in Diels-Alder additions,[9] attempts were first made to react **2b** and **2e** with maleic anhydride and tetracyanoethylene **1**; however, no reaction took place, even after prolonged reaction times (2 weeks, room temperature). As expected the three model dienes 2,3-dimethyl-1,3-butadiene **8**, cyclopentadiene **11**, and

[*] Prof. Dr. H. Hopf, Dipl.-Chem. M. Kreutzer
Institut für Organische Chemie der Universität
Hagenring 30, D-3300 Braunschweig (FRG)

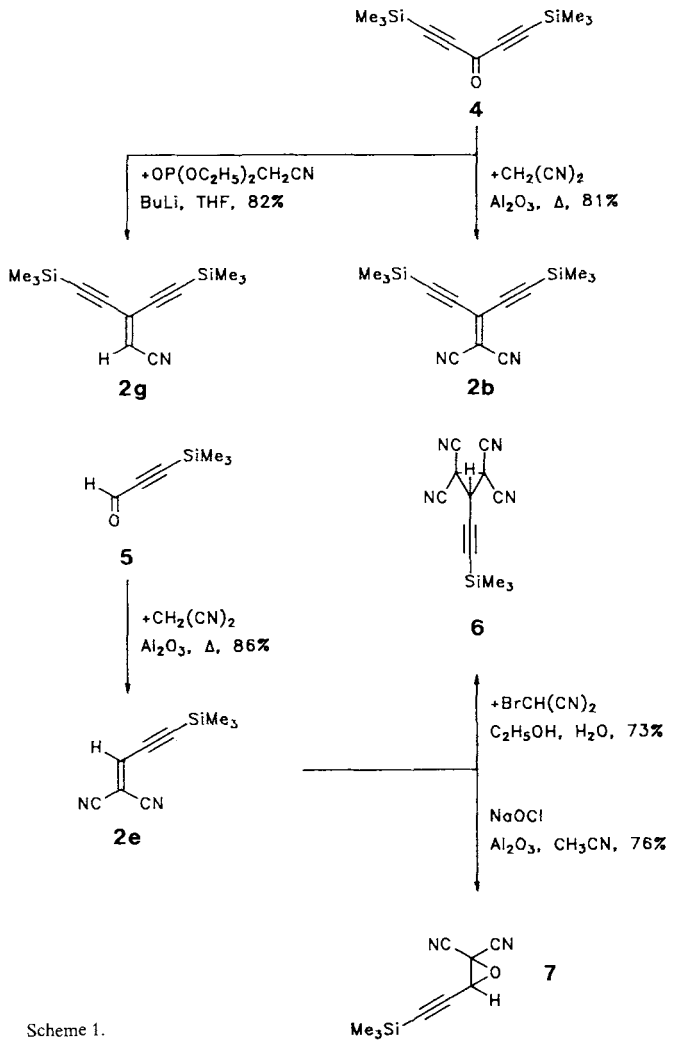

Scheme 1.

9,10-dimethylanthracene **14** underwent smooth [2+4]-cycloadditions, which, however, were markedly different in their positional selectivity.[10] Their reactions with **2e** led to formation of the expected adducts **10**, **13** and **15**[6] (the electron attracting effect of the cyano substituent manifests itself directly at the neighboring double bond), whereas **2b** reacts with **8** and **11** in the sense of a vinylogous dienophile whose double bond remains intact. To what extent this drastic difference in reactivity also occurs in other dienes or whether a change in the reaction mechanism is involved, will have to be established by further investigations. The relative reactivity of double and triple bonds in addition reactions is often difficult to predict; it strongly depends on the type of reaction and can also be influenced by comparatively simple changes in structure.[11, 12] **2b**, which is less reactive than **2e**, does not react with **14**; neither **2b** nor **2e** participate in Diels-Alder additions with inverse electron demand (no addition to tetracyclone and 1,2,3,4-tetrachloro-5,5-dimethoxycyclopentadiene). The greater reactivity of **2e** also manifests itself in a cyclopropanation reaction[13] with bromomalononitrile and in the epoxidation with sodium hypochlorite,[14] which lead in good yields to the ethnylcyclopropane **6**[6] and to the oxirane **7**, respectively.[6] Under the conditions quoted in Scheme 1, **2b** does not undergo these reactions. The above condensation reactions can also be extended to aryl-substituted acetylenic ketones and aldehydes[15] and thus open up a general route to substituted cyano(ethynyl)ethenes **2**.

Received: November 15, 1989 [Z 3636 IE]
German version: *Angew. Chem. 102* (1990) 425

CAS Registry numbers:
1, 670-54-2; **2b**, 125781-52-4; **2e**, 69656-67-3; **2g**, 125781-51-3; **4**, 60836-10-4; **5**, 2975-46-4; **6**, 125781-58-0; **7**, 125781-59-1; **8**, 513-81-5; **9**, 125781-53-5; **10**, 125781-56-8; **11**, 542-92-7; **12**, 125781-54-6; **13**, 125781-55-7; **14**, 781-43-1; **15**, 125781-57-9; $(O)P(OC_2H_5)_2CH_2CN$, 2537-48-6; $CH_2(CN)_2$, 109-77-3; $BrCH(CN)_2$, 1885-22-9; maleic anhydride, 108-31-6; tetracyclone, 479-33-4; 1,2,3,4-tetrachloro-5,5-dimethoxy-1,3-cyclopentadiene, 2207-27-4.

[1] A. J. Fatiadi, *Synthesis 1986*, 249, and references cited therein.
[2] T. L. Cairns, R. A. Carboni, D. D. Coffman, V. A. Engelhardt, R. E. Heckert, E. L. Little, E. G. McGeer, B. C. McKusick, W. J. Middleton, *J. Am. Chem. Soc. 79* (1957) 2340.
[3] Derivatives of **3** with R = CMe_3, CH_3 and $SiMe_3$ have been prepared by Hauptmann: H. Hauptmann, *Angew. Chem. 87* (1975) 490; *Angew. Chem. Int. Ed. Engl. 14* (1975) 498. The tetraphenyl compound **3**, R = C_6H_5, has been described as the very first tetraethynylethene derivative: Y. Hori, K. Noda, S. Kobayashi, H. Taniguchi, *Tetrahedron Lett. 1969*, 3563.

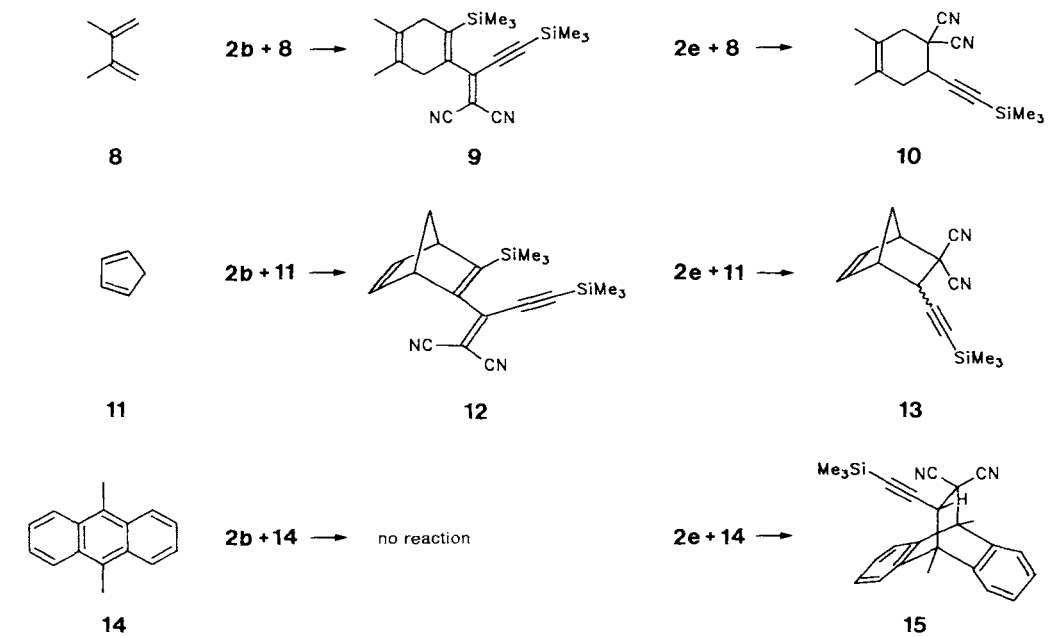

[4] A. Borisova, N. S. Vyazankin, A. S. Medvedeva, I. D. Kalikhman, *Zh. Obshch. Khim. 48* (1978) 2800; *J. Gen. Chem. USSR 48* (1978) 1307. Complex ynamines containing **2e** as subsystem have been described by G. Himbert, W. Brunn, *Liebigs Ann. Chem. 1985*, 2206. Reaction of **5** with diethylphosphonoacetonitrile leads to **2i**: N. I. Nesterov, E. V. Komissarova, N. N. Belyaev, M. D. Stadnichuk, A. A. Petrov, *Zh. Obshch. Khim. 47* (1977) 1425; *J. Gen. Chem. USSR 47* (1977) 1307.
[5] H. Hauptmann, *Tetrahedron 32* (1976) 1293.
[6] All the new compounds were characterized by the usual analytical and spectroscopic data.
[7] F. Texier-Boullet, A. Foucaud, *Tetrahedron Lett. 23* (1982) 4927.
[8] L. Brandsma: *Preparative Acetylenic Chemistry*, 2nd Edit., Elsevier, Amsterdam 1988, p. 102.
[9] Review: A. S. Onishchenko: *Diene Synthesis*, Israel Program Sci. Transl., Jerusalem 1964, p. 635ff; cf. H. Neunhoeffer, W. K. Franke in Houben-Weyl-Müller (Ed.): *Methoden der Organischen Chemie*, Bd. V/1d, Thieme, Stuttgart 1972, p. 690ff.
[10] For definition see I. Fleming: *Grenzorbitale und Reaktionen organischer Verbindungen*, VCH Verlagsgesellschaft, Weinheim 1988, p. 193ff.
[11] See Ref. [10], p. 181ff., and G. H. Schmid, K. Yates, T. W. Regulski, D. G. Garrat, H.-W. Leung, R. McDonald, *J. Am. Chem. Soc. 95* (1973) 160.
[12] G. H. Schmid in S. Patai (Ed.): *The Chemistry of the Carbon-Carbon Triple Bond, Vol. I*, Wiley, New York 1978, p. 275ff.
[13] H. Hart, Y. C. Kim, *J. Org. Chem. 31* (1966) 2784.
[14] A. Foucaud, M. Bakouetila, *Synthesis 1987*, 854.
[15] M. Kreutzer, unpublished.

$[Ni_3(\mu_3\text{-}CNMe)(\mu_3\text{-}I)(CNMe)_2(Ph_2PCH_2PPh_2)_2]I$, a *triangulo* Nickel Cluster with an Unprecedented Symmetric Linear μ_3-η^1 Isocyanide Ligand**

By *Kevin S. Ratliff, Gregory K. Broeker, Phillip E. Fanwick,* and *Clifford P. Kubiak**

There continues to be much interest in the interactions between small unsaturated molecules and metal clusters. While much work has been devoted to the reactivity of carbon monoxide with metal clusters and surfaces, the isoelectronic isocyanides, CNR, have received little attention. Isocyanides can bind to trinuclear clusters by adopting any of the five limiting structures **I**–**V**. *Muetterties* found that

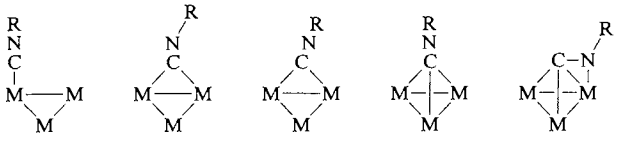

methyl isocyanide is bound to nickel surfaces in an η^2 fashion (**V**) with a considerable interaction between the nitrogen atom of the isocyanide and the metal surface.[1]

Molecular examples of the type-**V** interaction have been observed in only a few cases. The complexes $[Pt_7(2,6\text{-}Me_2C_6H_3NC)_{12}]$,[2] $[Os_6(CO)_{18}(4\text{-}MeC_6H_4NC)_2]$,[3] and $[Fe_3(CO)_9(CNtBu)]$[4] all possess μ_3-η^2 isocyanides. The complex $[Ru_5(CO)_{14}(CNtBu)_2]$ contains an isocyanide which is bound to all five ruthenium atoms in a μ_5-η^2 fashion and acts as a six-electron donor.[5] The striking feature common to all of these isocyanide clusters is that the bridging isocyanides prefer η^2 coordination with considerable interaction between the isocyanide nitrogen and the metal atoms. *Fortune* et al. have described the crystal structure of $[Co_3(C_5H_5)_3(\mu_3\text{-}CNC_6H_{11})(\mu_3\text{-}S)]$, which was refined only to $R = 0.092$ and $R' = 0.120$ and which showed no significant interaction between the nitrogen atom and the three cobalt atoms.[6] The isocyanide C–N–C bond angles of 141° and 129° for the two independently refined isomers of the cobalt cluster, however, was unexpected and puzzling. If a capping isocyanide is truly symmetrically bound to a *triangulo* cluster, the π^* orbitals of the μ_3-CNR ligand are degenerate and thus no isocyanide bending should occur.

We report here the first example of a symmetric, linear, μ_3-η^1, type-**IV** isocyanide. Several symmetric μ_3-η^1 CO clusters are known. These include $[Pt_3(\mu_3\text{-}CO)(dppm)_3]^{2\oplus}$ (dppm = $Ph_2PCH_2PPh_2$),[7] $[Pd_3(\mu_3\text{-}CO)(dppm)_3]^{2\oplus}$,[8] and $[(C_5H_5)_3Ni_3(\mu_3\text{-}CO)_2]$,[9] which has two CO ligands capping each face of the Ni_3 triangle. A unique example of a coordinatively unsaturated μ_3-η^1 CO nickel cluster, $[Ni_3(\mu_3\text{-}CO)(Me_2PCH_2PMe_2)_4][Na(NCBH_3)_3]_2$, was recently prepared by *Puddephatt* et al.[10] This recent result, together with our work described here, strongly suggests that diphosphino ligands can be used to stabilize *triangulo* Ni_3 clusters with unusual properties.

$[Ni_2(\mu_2\text{-}CNMe)(CNMe)_2(dppm)_2]$ **1**

The binuclear Ni^0 complex **1** reacts with electrophiles and other metal ions by both μ-CNMe ligand-centered[11,17] and metal-centered[12,13] pathways. Reaction of **1** with CH_2I_2 in toluene at 50 °C gives the *triangulo* cluster **2** in high yield.[14]

$[Ni_3(\mu_3\text{-}CNMe)(\mu_3\text{-}I)(CNMe)_2(dppm)_2]I$ **2**

IR spectroscopy reveals a strong terminal methyl isocyanide band at 2170 cm^{-1}. The single μ_3-CNMe ligand $\tilde{\nu}$(CN) band occurs at unusually high energy ($\tilde{\nu}$(N) = 1943 cm^{-1}),[15] as compared to $\tilde{\nu}$(CN) = 1550 cm^{-1} for $[Co_3(C_5H_5)(\mu_3\text{-}CNC_6H_{11})(\mu_3\text{-}S)]$.[6] Replacement of the μ_3-CNMe ligand with $^{13}CNMe$ resulted in $\tilde{\nu}(^{13}CN)$ = 1910 cm^{-1}. The ^1H NMR spectrum of **2** shows two inequivalent methyl isocyanides in a 2:1 ratio at $\delta = 3.17$ and 3.70, respectively, in CD_3CN. The ^{31}P NMR spectrum of **2** is an AA'BB' spin system centered at $\delta = 0.5$, characteristic of an asymmetrically coordinated dppm complex. X-ray-quality crystals were obtained by slow diffusion of Et_2O into an acetone solution of **2**. An ORTEP drawing of **2** is shown in Figure 1.[16]

The most striking feature of the cluster is the symmetrically triply bridging methyl isocyanide. The capping isocyanide

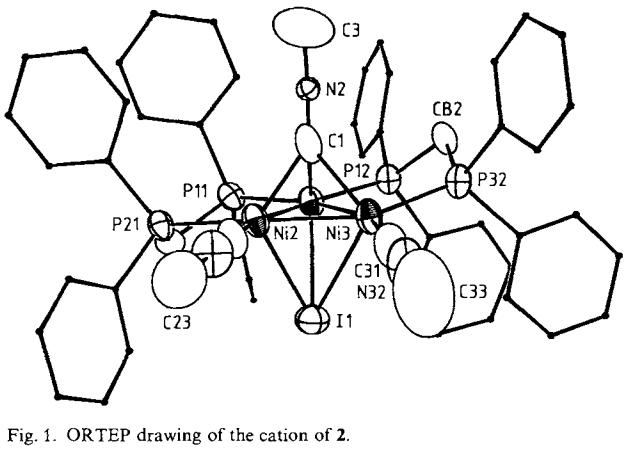

Fig. 1. ORTEP drawing of the cation of **2**.

[*] Prof. C. P. Kubiak [+], K. S. Ratliff, G. K. Broeker, P. E. Fanwick
Department of Chemistry, Purdue University
West Lafayette, IN 47907 (USA)
[+] Research Fellow of the Alfred P. Sloan Foundation, 1987–1991
[**] This work was supported by the National Science Foundation (CHE-8707963).

is essentially linear with a C–N–C angle of 170(1)°. The remainder of the cluster consists of a trinuclear nickel core with similar nickel–nickel distances (d_{Ni-Ni} (average) = 2.38(1) Å), consistent with a strongly bonded $Ni_3^{2\oplus}$ core. Ni1 is bridged to Ni2 and Ni3 by two dppm ligands. Both Ni2 and Ni3 have two terminally bound isocyanides, thus completing a nearly planar $[Ni_3L_6]^{2\oplus}$ core. The three nickels are capped by a μ_3-iodide (d_{Ni-I} (average) = 2.75(3) Å). A triply bridging isocyanide occupies the other capping position (d_{Ni-C} (average) = 2.04(4) Å). A skeletal view of the cluster core with bond distances is given in Figure 2.

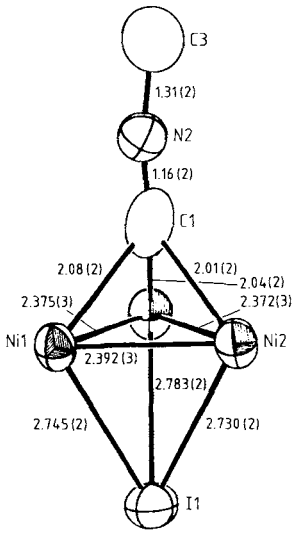

Fig. 2. Skeletal view of **2** with bond distances. Selected bond angles [°]: Ni1-Ni2-Ni3 59.79(8), Ni2-Ni1-Ni3 59.68(8), Ni2-Ni3-Ni1 60.53(8), Ni1-C1-Ni2 71.5(6), Ni2-C1-Ni3 71.6(6), Ni3-C1-Ni1 70.4(6), Ni-I-Ni 51.2(5) (average), C1-N1-C3 170(1).

Preliminary reactivity studies indicate that the capping iodide is essential to the stability of the cluster. For example, reaction of **1** with CH_2Br_2 in toluene results in precipitation of an intermediate which decomposes in all solvents. Similarly, removal of $I^{\ominus}$ by treatment of **2** with two equivalents of CF_3SO_3Ag leads to cluster degradation to $[Ni_2(CNMe)_3(dppm)_2]^{2\oplus}$ [17] and an unidentified nickel species. The capping iodide also poses an intriguing question concerning the electron count of the cluster. If the capping $I^{\ominus}$ is counted as a two-electron donor, then the resulting cluster electron count would be 44, suggesting coordinative unsaturation. The triply bridging iodide, however, could act as a four- or even six-electron donor. All previous examples of nickel clusters are coordinatively saturated with 48 or more electrons.[10] If $I^{\ominus}$ is viewed as a six-electron donor, then cluster **2** can achieve coordinative saturation without the usual μ_3-η^2 (type **V**) isocyanide bonding. MO calculations may clarify the nature of the donor/acceptor relationship between the capping iodide and the unprecedented μ_3-η^1 isocyanide.

Received: May 31, 1989;
revised: January 9, 1990 [Z 3367 IE]
German version: *Angew. Chem. 102* (1990) 405

[1] E. L. Muetterties: *New Horizons in Catalysis: Proc. 7th Int. Congr. Catal.*, Tokyo, June 30–July 4, 1980, p. 36.
[2] Y. Yamamoto, K. Aoki, H. Yamazake, *Organometallics 2* (1983) 1377.
[3] C. R. Eady, P. D. Gavens, B. F. G. Johnson, J. Lewis, M. C. Malatesta, M. J. Mays, A. G. Orpen, A. V. Rivera, G. M. Scheldrick, M. B. Hursthouse, *J. Organomet. Chem. 149* (1978) C43.
[4] M. I. Bruce, T. W. Hambley, B. K. Nicholson, *J. Chem. Soc. Chem. Commun. 1982*, 353.
[5] M. I. Bruce, J. G. Matisons, J. R. Rodgers, R. C. Wallis, *J. Chem. Soc. Chem. Commun. 1981*, 1070.
[6] J. Fortune, A. R. Manning, F. S. Stephens, *J. Chem. Soc. Chem. Commun. 1983*, 1071.
[7] G. Ferguson, B. R. Lloyd, R. J. Puddephatt, *Organometallics 5* (1986) 344.
[8] L. Manojlovic-Muir, K. W. Muir, B. R. Lloyd, R. J. Puddephatt, *J. Chem. Soc. Chem. Commun. 1983*, 1336.
[9] E. O. Fischer, C. Palm, *Chem. Ber. 91* (1958) 1725.
[10] G. Ferguson, M. C. Jennings, H. A. Mirza, R. J. Puddephatt, private communication.
[11] D. L. DeLaet, P. E. Fanwick, C. P. Kubiak, *Organometallics 5* (1986) 1807.
[12] J. Ni, P. E. Fanwick, C. P. Kubiak, *Inorg. Chem. 27* (1988) 2017.
[13] H. P. Kim, P. E. Fanwick, C. P. Kubiak, *J. Organomet. Chem. 346* (1988) C39.
[14] Complex **2** can be prepared in 80% yield by the direct reaction of **1** with anhydrous NiI_2.
[15] This assignment has been confirmed by the recent preparation and X-ray crystallographic characterization of $[Ni_3(\mu_3\text{-}CNMe)(\mu_3\text{-}I)(PPh_2CH_2PPh_2)_3]$ I, in which there is only a single μ_3-η^1 CNMe ligand with $\tilde{\nu}$(CN) = 1922 cm^{-1}: K. S. Ratliff, P. E. Fanwick, C. P. Kubiak, *Polyhedron*, in press.
[16] Crystal data for **2**: $C_{56}H_{53}Ni_3I_2N_3P_4$, M = 1321.90, monoclinic, space group $P2_1/c$, a = 19.730(4), b = 24.659(4), c = 12.536(3) Å, V = 6054(4) $Å^3$, Z = 4, ϱ_{calcd} = 1.450 $g\,cm^{-3}$. Crystal dimensions: 0.56 × 0.22 × 0.08 mm^3. The structure was solved by MULTAN least-squares Fourier methods and was refined to R and R_w values of 0.061 and 0.080, respectively, for 608 variables and 3873 observed reflections with $I > 3.0\,\sigma(I)$, $Mo_{K\alpha}$ radiation. Data were corrected for absorption empirically, μ = 20.76 cm^{-1}. Further details of the crystal structure investigation may be obtained from the Fachinformationszentrum Karlsruhe, Gesellschaft für wissenschaftlich-technische Information mbH, D-7514 Eggenstein-Leopoldshafen 2 (FRG), on quoting the depository number CSD-54157, the names of the authors, and the journal citation.
[17] D. L. DeLaet, R. Del Rosario, P. E. Fanwick, C. P. Kubiak, *J. Am. Chem. Soc. 109* (1987) 754.

$[\{Ni_2(\mu\text{-}CNMe)(CNMe)_4(Ph_2PCH_2PPh_2)\}_2Hg][NiCl_4]$, a Spirocyclic Ni_4Hg Cluster with an Hg^{II}-Center**

By *Jinkang Gong, Jean Huang, Phillip E. Fanwick,* and *Clifford P. Kubiak**

Metal–metal bonds between two or more different metals are of fundamental interest. The chemical and physical consequences of combining different metals on a molecular level may include (1) cooperative reactivity, (2) charge-separated excited states, and (3) unusual magnetic properties. The N-atom Lewis basicity of the μ-isocyanide ligand of complex **1** is quite well established.[1] Metalations of **1** afford a surprising variety of structures. For example, metalation of **1** with $[Pd(CNMe)_4]^{2\oplus}$, $(PPh_3)AuCl$, or NiI_2 produces linear trinuclear Ni-Pd-Ni,[2a] linear binuclear Ni-Au,[2b] and *triangulo*-Ni_3 frameworks, respectively.[2c,d] Complex **1** may react by either μ-ligand-[1] or metal-centered[2,3] pathways. We now report the reaction of **1** with $HgCl_2$, which gives an extraordinary metalation product.

$[Ni_2(\mu\text{-}CNMe)(CNMe)_2(PPh_2CH_2PPh_2)_2]$

1

$[\{Ni_2(\mu\text{-}CNMe)(CNMe)_4(Ph_2PCH_2PPh_2)\}_2Hg][NiCl_4]$

2

[*] Prof. C. P. Kubiak, J. Gong, J. Huang, P. E. Fanwick
Department of Chemistry, Purdue University
West Lafayette, IN 47907 (USA)

[**] This work was supported by the National Science Foundation (CHE-870963) and NASA (NAG-3-977). *J.H.* gratefully acknowledges a fellowship from Upjohn Corporation.

The reaction of **1** with $HgCl_2$ (molar ratio 1:1) in THF at 25 °C for 12 h produces the Ni_4Hg cluster **2** in 25% yield. Complex **2** has also been prepared quantitatively by the direct reaction of $Ni(CNMe)_4$, $Ph_2PCH_2PPh_2$, and $HgCl_2$ (molar ratio 5:2:2) in THF. IR spectroscopy (KBr) reveals the presence of both terminal ($\tilde{\nu}$(CN) = 2151 vs) and bridging ($\tilde{\nu}$(CN) = 1737, 1718 cm^{-1}) isocyanides. The $^{31}P\{^1H\}$ NMR spectrum consists of a singlet (δ = 44.2) with weak ^{199}Hg satellites ($J_{P\text{-}Hg}$ = 603 Hz). The values of $^1J_{P\text{-}Hg}$ for complexes with direct P–Hg bonds typically range from about 4300 to 5700 Hz.[4, 5] The $^{31}P\{^1H\}$ data are therefore clearly not consistent with direct P–Hg bonding. The ^1H NMR data indicate the presence of $Ph_2PCH_2PPh_2$ (δ = 7.22–7.61 (m, 40H, Ph_2P), 2.77 (m, 4H, CH_2) as well as terminal (δ = 3.10 (s, 24H, $CNCH_3$)) and bridging (δ = 2.19 (s, 6H, μ-$CNCH_3$) isocyanides. X-ray-quality crystals were obtained by slow diffusion.[6] An ORTEP drawing of the cation of **2** is shown in Figure 1.

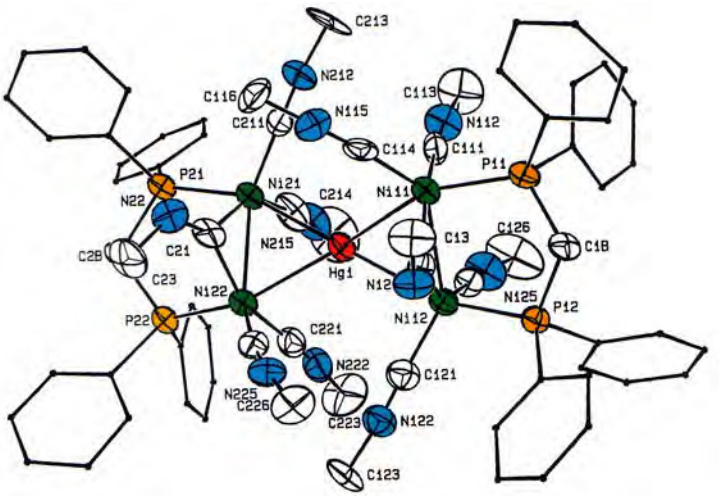

Fig. 1. ORTEP drawing of the molecular cation of **2**: Hg (red), Ni (green) P (orange) N (blue) C (black). Selected bond distances [Å] and angles [°]: N22-C21 1.23(2), N222-C221 1.18(2), N225-C224 1.17(2), Ni12-C121 1.86(2); Ni11-C11-N12 82.1(6), Ni21-C21-Ni22 82.6(7), Hg1-Ni11-Ni12 62.40(6), Hg1-Ni12-Ni11 62.48(6), Hg1-Ni21-Ni11 62.15(6), Hg1-Ni22-Ni21 62.75(6).

The cation of **2** consists of a central mercury(II) ion coordinated only by four nickel atoms ($d_{Ni\text{-}Hg}$ (average) = 2.65(3) Å). The four nickel atoms exhibit two close pairwise Ni–Ni interactions ($d_{Ni\text{-}Ni}$ (average) = 2.542(2) Å). Each Ni_2 pair is bridged by one $Ph_2PCH_2PPh_2$ and one CNMe ligand. Each nickel atom is additionally coordinated by two terminal CNMe ligands. The overall structure can be viewed as a central $Hg^{2\oplus}$ ion coordinated by two neutral $[Ni_2(\mu\text{-CNMe})(CNMe)_4Ph_2PCH_2PPh_2)]$ fragments. The μ-CNMe ligands are *cis* with respect to one another. A skeletal view of the $[HgNi_4(Ph_2PCH_2PPh_2)_2]$ core is presented in Figure 2.

The $[HgNi_4]^{2\oplus}$ core is slightly nonplanar with a torsion angle of 34.6(1)°. The Ni–Hg bond lengths vary from 2.617(2) to 2.682(2) Å and are somewhat longer than the value of 2.462(3) Å reported for the only other structurally characterized example of a Ni–Hg bond, $[(Ph_3Ge)Hg\text{–}Ni(GePh_3)(C_5H_5)]_x$.[7] We note that the overall interaction between the two $[Ni_2(\mu\text{-CNMe})(CNMe)_4(Ph_2PCH_2PPh_2)]$ fragments and $Hg^{2\oplus}$ may be viewed similarly to that of a linear (π donor)$_2$Hg complex. The midpoints of the Ni11–Ni12 and Ni21–Ni22 bonds are separated from the central $Hg^{2\oplus}$ ion by 2.002(2) Å and 1.963(2) Å, respectively. The angle (Ni11-Ni12)-Hg-(Ni21-Ni22) is 170.3°. Extended

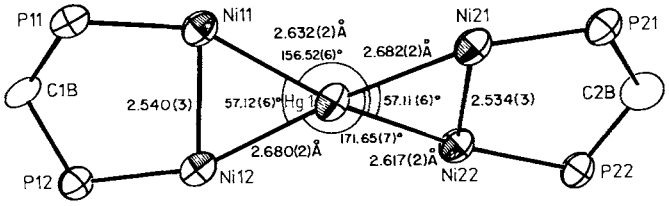

Fig. 2. ORTEP drawing of the $[HgNi_4(Ph_2PCH_2PPh_2)_2]$ core (phenyl rings omitted for clarity), with selected bond distances and angles.

Hückel calculations indicate that the HOMO of **1** possesses $Ni_2(d_{\pi^*})$ character.[1d, 8] The stability of **2** therefore appears to result in part from an $Ni_2(d_{\pi^*}) \rightarrow Hg^{2\oplus}(p_\pi)$ interaction. Complex **2** is unprecedented. *Shaw* et al. have prepared several Ni–Hg mixed-metal binuclear complexes, but they apparently do not contain direct Ni–Hg bonds.[4] Perhaps the closest analogues to **2** are $[\mu_4\text{-}Hg\{(\mu_3\text{-}C_2tBu)(CO)_9Ru_3\}_2]$ prepared by *Rosenberg*[9] and the linear "sandwich" cluster $[\{Hg(Pt_3(2,6\text{-}Me_2C_6H_3NC)_6\}_2]$ prepared by *Yamamoto* et al.[10]

Received: July 14, 1989;
revised: January 9, 1990 [Z 3442 IE]
German version: *Angew. Chem. 102* (1990) 407

[1] a) D. L. DeLaet, P. E. Fanwick, C. P. Kubiak, *Organometallics 5* (1986) 1807; b) D. L. DeLaet, R. Del Rosario, P. E. Fanwick, C. P. Kubiak, *J. Am. Chem. Soc. 109* (1987) 754; c) D. L. DeLaet, P. E. Fanwick, C. P. Kubiak, *J. Chem. Soc. Chem. Commun. 1987*, 1412; d) F. R. Lemke, D. L. DeLaet, J. Gao, C. P. Kubiak, *J. Am. Chem. Soc. 110* (1988) 6904.

[2] a) J. Ni, P. E. Fanwick, C. P. Kubiak, *Inorg. Chem. 27* (1988) 2017; b) H. P. Kim, P. E. Fanwick, C. P. Kubiak, *J. Organomet. Chem. 346* (1988) C39; c) K. S. Ratliff, G. K. Broeker, P. E. Fanwick, C. P. Kubiak, *Angew. Chem. 102* (1990) 405; *Angew. Chem. Int. Ed. Engl. 29* (1990) 395; d) K. S. Ratliff, P. E. Fanwick, C. P. Kubiak, *Polyhedron*, in press.

[3] J. Gong, C. P. Kubiak, *Inorg. Chim. Acta 162* (1989) 19.

[4] X. L. R. Fontaine, S. J. Higgins, C. R. Langrick, B. L. Shaw, *J. Chem. Soc. Dalton Trans. 1987*, 777.

[5] A. L. Balch, U. M. Olmsted, S. P. Rowley, *Inorg. Chem. 27* (1988) 227 S.

[6] Crystals of the complex were obtained as $2 \cdot MeCN \cdot MeOH \cdot H_2O$ by slow diffusion of Et_2O into an acetonitrile solution of **2**. The unexpected presence of MeOH and H_2O in the crystals cannot be readily explained, but their presence was confirmed in the ^1H-NMR spectrum of crystalline material dissolved in CD_3CN. Crystal data for $2 \cdot MeCN \cdot MeOH \cdot H_2O$: $HgNi_5Cl_4P_4O_2N_{11}C_{73}H_{83}$, M = 1906.40, triclinic, space group $P\bar{1}$, a = 16.511(6), b = 16.694(4), c = 17.927(8) Å, α = 66.48(3)°, β = 65.76(3)°, γ = 74.93(2)°, V = 4103(2) Å^3, Z = 2, ϱ_{calcd} = 1.543 g cm^{-3}. Crystal dimensions: 0.47 × 0.26 × 0.17 mm^3. The structure was solved by SHELX-86. The remaining atoms were located using DIRDIF and successive least-squares/difference Fourier syntheses. The structure was refined to R and R_w values of 0.056 and 0.061, respectively, for 5273 observed reflections with $I > 3\,\sigma(I)$ with $Mo_{K\alpha}$ radiation. Data were corrected for absorption empirically, μ = 32.5 cm^{-1}. Further details of the crystal structure investigation may be obtained from the Fachinformationszentrum Karlsruhe, Gesellschaft für wissenschaftlich-technische Information mbH, D-7514 Eggenstein-Leopoldshafen 2 (FRG), on quoting the depository number CSD-54156, the names of the authors, and the journal citation.

[7] L. N. Zakharov, Y. T. Struchkov, *Cryst. Struct. Commun. 9* (1980) 549.

[8] K. S. Ratliff, D. L. DeLaet, J. Gao, C. P. Kubiak, *J. Am. Chem. Soc. 112* (1990) in press.

[9] a) S. Hajela, B. M. Novak, E. Rosenberg, *Organometallics 8* (1989) 468; b) E. Rosenberg, K. King, R. Fahmy, A. Tiripicchio, *J. Am. Chem. Soc. 102* (1980) 3626; c) E. Rosenberg, K. Hardcastle, S. Ermer, K. King, A. Tiripicchio, *Inorg. Chem. 22* (1983) 1339; d) E. Rosenberg, J. Wang, R. G. Gellert, *Organometallics 7* (1988) 1093.

[10] Y. Yamamoto, H. Yamazaki, T. Sakurai, *J. Am. Chem. Soc. 104* (1982) 2329.

 © VCH Verlagsgesellschaft mbH, D-6940 Weinheim, 1990 0570-0833/90/0404-0397 $ 02.50/0

Structure of a Non-classically Bridged Methyleneborane in the Crystal**

By *Christine Wieczorek, Jürgen Allwohn, Günter Schmidt-Lukasch, Ralf Hunold, Werner Massa,* and *Armin Berndt**

Dedicated to Professor Paul von Ragué Schleyer on the occasion of his 60th birthday

Three-membered ring systems with boron as ring member are effective σ-components for strong σ-π interactions. We have recently described the geometric consequences of such interactions in **1** with tricoordinated boron as π-component.[1] Dicoordinated boron atoms with formally empty p-orbital on boron are effective π-components for σ-π interactions, which give rise to significant changes in bond

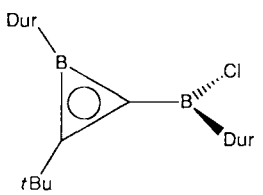

1

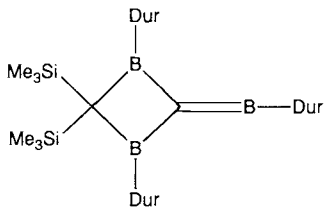

2

lengths[4] in **2**[2] and similar methyleneboranes.[3] The combination of a boracyclopropane unit with a dicoordinated boron atom in **3** (**3a**[6]) would lead one to expect a particularly strong σ-π interaction. According to calculations[7, 8] this results in the bridged structure[9] **4** with a B–C–B angle not less than 65° smaller than in **3** (Scheme 1). In the present communication we report experimental confirmation of this prediction.

The crystalline methyleneboranes **4b, c** are accessible from **5b, c**[11] and Bogdanović magnesium[12] in diethyl ether (3

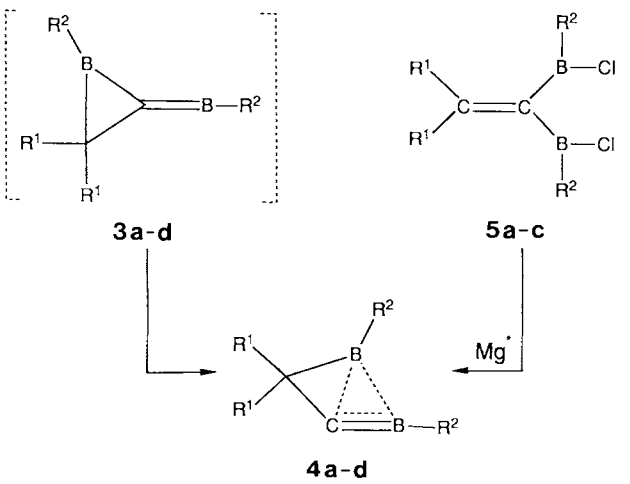

Scheme 1. **a**: $R^1 = SiMe_3$, $R^2 = t$Bu; **b**: $R^1 = SiMe_3$, R^2 = dur(=2,3,5,6-tetramethylphenyl); **c**: $R^1 = GeMe_3$, R^2 = dur; **d**: $R^1 = R^2 = H$.

[*] Prof. Dr. A. Berndt, Dr. G. Schmidt-Lukasch, C. Wieczorek, J. Allwohn, Dr. R. Hunold, Prof. Dr. W. Massa
Fachbereich Chemie der Universität
Hans-Meerwein-Strasse, D-3550 Marburg (FRG)

[**] This work was supported by the Deutsche Forschungsgemeinschaft and the Fonds der Chemischen Industrie.

days' stirring). Only **4c** can be isolated in the form of single crystals (from hexane, toluene) which are suitable for an X-ray structure investigation; **4b** forms fine fibrous needles. Figure 1 shows the structure of **4c** in the crystal;[13] important bond lengths and angles of **4c** are listed in Table 1, together with those calculated for the unsubstituted **4d**.[7, 8] The good agreement between experimental and calculated data illustrates the reliability of the results of high-level ab-

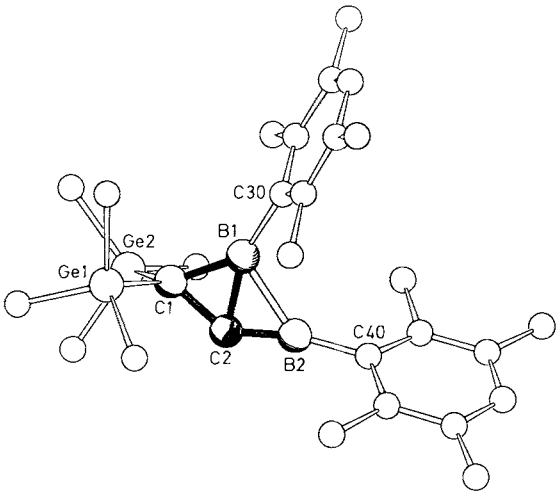

Fig. 1. Schakal drawing of the structure of **4c** in the crystal.

Table 1. Experimental and calculated structural data of **4c** and **4d** (distances in pm, angles in degrees).

	4c	4d	
		6-31G* [7]	DZ + P [8]
C2-B2	135.1(9)	133.9	134.6
C2-B1	154.5(9)	152.7	153.9
C2-C1	147.5(8)	145.4	145.6
C1-B1	161.7(8)	158.1	159.0
B1-B2	183.9(9)	182.5	182.4
B1-C2-B2	78.5(4)	78.8	78.1
C2-B2-C40 [a]	168.8(6)	172.3	170.4
C2-B1-C30 [b]	162.4(5)	160.6	–
C1-B1-C30 [b]	140.3(5)	–	142.5

[a] In the case of **4d**: H instead of C40. [b] In the case of **4d**: H instead of C30.

initio calculations. Apparently, the substituents used by us have no great influence on the structure of the skeletal framework of **4**. Even the chemical shifts of the skeletal atoms[15] remain essentially unchanged upon varying the substituents, as shown in Table 2.

The boron atoms of the B–C double bond[16] of the bridged methyleneboranes **4** are more strongly shielded than

Table 2. NMR data of the skeletal atoms of the methyleneboranes **4a–c** and **2**.

		4a	4b	4c	2 [2]
$\delta(^{11}B)$	B2 (C=*B*)	18	19	20	71
	B1	52	51	48	62
$\delta(^{13}C)$	C2 (*C*=B)	115.2	121.2	126.0	115.5
	C1	25.0	26.0	30.5	56.5

 © VCH Verlagsgesellschaft mbH, D-6940 Weinheim, 1990 0570-0833/90/0404-0398 $ 02.50/0

the corresponding boron atom in the unbridged species **2** (see Table 2). This is consistent with the finding that cationic C atoms in non-classical carbocations such as the symmetrically bridged species **6**[17] and the unsymmetrically bridged species **7**[18] are much more strongly shielded than in classical cations such as **8**.

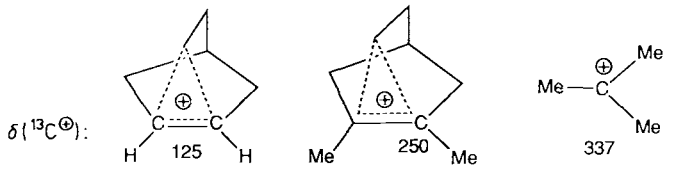

6 **7** **8**

Structural deformation and NMR spectroscopically detectable shielding of the π-centers, as depicted in Scheme 2, are general consequences of appreciable σ-π interaction.

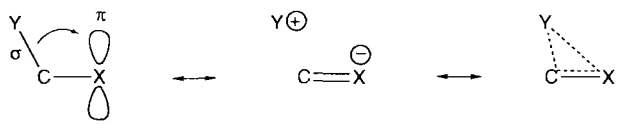

Scheme 2. Consequences of a σ-π interaction for the structure and electron density distribution.

This is also demonstrated by recent calculations for the isopropyl and other carbocations.[19]

Received: October 9, 1989 [Z 3587 IE]
German version: *Angew. Chem. 102* (1990) 435

[1] A. Höfner, B. Ziegler, W. Massa, A. Berndt, *Angew. Chem. 101* (1989) 188; *Angew. Chem. Int. Ed. Engl. 28* (1989) 186.
[2] R. Hunold, M. Pilz, J. Allwohn, M. Stadler, W. Massa, P. von R. Schleyer, A. Berndt, *Angew. Chem. 101* (1989) 759; *Angew. Chem. Int. Ed. Engl. 28* (1989) 781.
[3] M. Stadler, R. Hunold, J. Allwohn, W. Massa, A. Berndt, *Angew. Chem. 101* (1989) 761; *Angew. Chem. Int. Ed. Engl. 28* (1989) 784.
[4] Also the finding that the B–C double bond in $(Me_3Si)_2C=B$–*t*Bu [5] with formal empty p-orbital on the boron is markedly shorter than in $(Me_2Si)_2C=B=NiPr_2$ with p-orbital on boron filled by π-π delocalization can be readily explained by σ-π interaction (C–Si hyperconjugation).
[5] R. Boese, P. Paetzold, A. Tapper, R. Ziembinski, *Chem. Ber. 120* (1989) 1057, and references cited therein.
[6] H. Klusik, A. Berndt, *Angew. Chem. 95* (1983) 895; *Angew. Chem. Int. Ed. Engl. 22* (1983) 877.
[7] P. H. M. Budzelaar, P. von R. Schleyer, K. Krogh-Jespersen, *Angew. Chem. 96* (1984) 809; *Angew. Chem. Int. Ed. Engl. 23* (1984) 825; P. H. M. Budzelaar, K. Krogh Jespersen, T. Clark, P. von R. Schleyer, *J. Am. Chem. Soc. 107* (1985) 2773.
[8] G. Frenking, H. F. Schaefer III, *Chem. Phys. Lett. 109* (1984) 521.
[9] Accordingly, very strong σ-π interaction in the cyclopropylidenemethyl cation **I** leads to the bridged structure **II** [10].

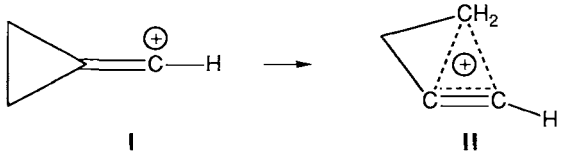

I **II**

[10] H. Fischer, K. Hummel, M. Hanack, *Tetrahedron Lett. 1969*, 2169; Y. Apeloig, J. B. Collins, D. Cremer, T. Bally, E. Haselbach, J. A. Pople, J. Chandrasekhar, P. von R. Schleyer, *J. Org. Chem. 45* (1980) 3496.
[11] **5b** and **5c** are accessible from 1,2-dichloro-1,2-diduryldiborane(4) [1] and bis(trimethylsilyl)- or bis(trimethylgermyl)acetylene, respectively, in pentane.
[12] B. Bogdanović, S.-T. Liao, K. Schlichte, U. Westeppe in R. B. King, J. J. Eisch (Eds.): *Organometallic Synthesis, Vol. IV*, Elsevier, Amsterdam 1988, p. 410.
[13] X-ray structure analyses: $C_{28}H_{44}B_2Ge_2$, space group $P2_1/n$, $Z = 4$, $a = 894.0(4)$, $b = 1305.3(2)$, $c = 2482.7(12)$, $\beta = 90.09(3)°$; 2987 independent reflections with $F_0 > 3\sigma$ measured on a four-circle diffractometer (CAD4 Enraf-Nonius) with $Cu_{K\alpha}$ radiation at −80 °C; columnar crystal ($\mu = 24.37\ cm^{-1}$), loss of crystal after the measurement by decomposition, absorption correction by "DIFABS" [14]; hydrogen atoms at calculated positions with isotropic factors incorporated groupwise in the calculation. Anisotropic temperature factors used for the remaining atoms. Refinement by full matrix methods. 323 parameters. $R = 0.044$, $wR = 0.035$ (weighting $w = 1/\sigma^2(F_0)$). Further details of the crystal structure investigation are available on request from the Fachinformationszentrum Karlsruhe, Gesellschaft für wissenschaftlich-technische Information mbH, D-7514 Eggenstein-Leopoldshafen 2 (FRG), on quoting the depository number CSD-320071, the names of the authors and the journal citation.
[14] N. Walker, D. Stuart, *Acta Crystallogr. Sect. A 39* (1983) 158.
[15] The following chemical shifts δ have been calculated (IGLO, MP2/6-31G*//): B2: 9.1, B1: 44.9, C2: 141.2, C1: 19.9; P. von R. Schleyer (Erlangen), private communication.
[16] We thank Prof. *B. Wrackmeyer* (Bayreuth) for NMR double resonance investigations, which confirm the assignment of $\delta^{11}B = 18$ in **4a** to the boron atom of the B–C double bond.
[17] G. A. Olah, G. K. S. Prakash, M. Arvanghi, F. A. L. Anet, *J. Am. Chem. Soc. 104* (1982) 7105; recent review: D. Lenoir, *Nachr. Chem. Tech. Lab. 36* (1988) 1210, and references cited therein.
[18] P. C. Myhre, K. L. McLaren, C. S. Yannoni, *J. Am. Chem. Soc. 107* (1985) 5294; T. Laube, *Angew. Chem. 99* (1987) 580; *Angew. Chem. Int. Ed. Engl. 26* (1987) 560, zit. Lit.
[19] P. von R. Schleyer, W. Koch, B. Liu, U. Fleischer, *J. Chem. Soc. Chem. Commun. 1989*, 1098, and references cited therein.

A Mesityl-bridged Methyleneborane**

By *Monika Pilz, Jürgen Allwohn, Werner Massa*, and *Armin Berndt**

Dedicated to Professor Paul von Ragué Schleyer on the occasion of his 60th birthday

The bridging of electron-deficient sites by aryl groups is well known in dimeric arylaluminum compounds **1**.[1] With **2**, we now present a molecule in which two boron atoms are bridged by an aryl group.

Opening of the aryl bridge in **1** can already be accomplished with the weak Lewis base diethyl ether (Scheme 1), whereas in the case of **2** the stronger Lewis base 4-*tert*-butylpyridine is required. The formation of the adduct **3** compares with the formation of **5**[2] from the bridged methyleneborane **4**.[3] We therefore regard **2** as a mesityl-bridged methyleneborane. **2** differs appreciably from **6**,[4] whose strong B–H–B bridge is inert towards 4-*tert*-butylpyridine and even towards *tert*-butyllithium.

2 is formed upon oxidation of the dilithium compound **7**[5] with $SnCl_2$ (yield 86%). Intermediates of this reaction, in which a mesityl residue migrates from boron to carbon, may well be the electrophilic diborylcarbene **8** and the methyleneborane **9**. The mesomerism characteristic for *C*-borylmethyleneboranes[6] creates, corresponding to resonance formula **9B**, a marked deficiency of electrons at the dicoordinated boron atom, which is compensated by bridging with the mesityl group at the other boron atom.

[*] Prof. Dr. A. Berndt, M. Pilz, J. Allwohn, Prof. Dr. W. Massa
Fachbereich Chemie der Universität
Hans-Meerwein-Strasse, D-3550 Marburg (FRG)

[**] This work was supported by the Deutsche Forschungsgemeinschaft and the Fonds der Chemischen Industrie.

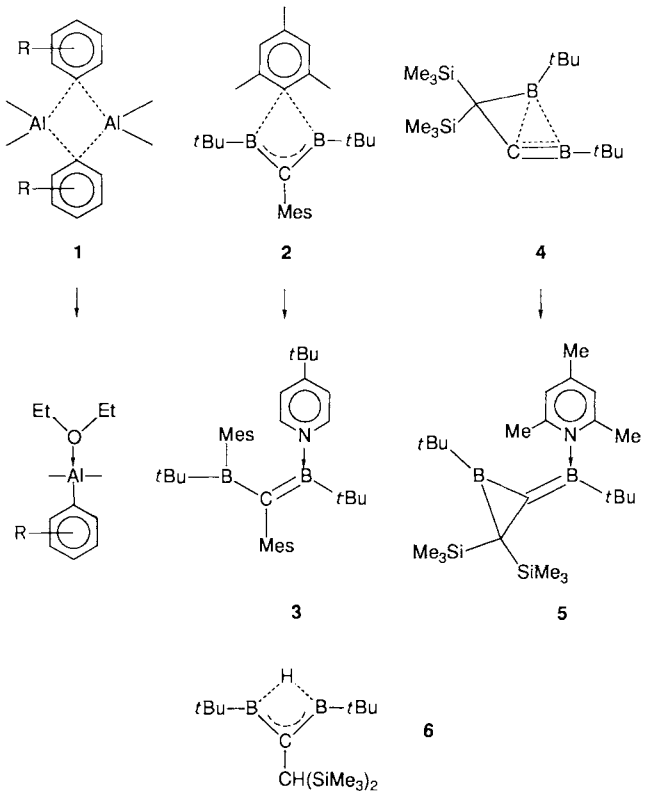

Scheme 1. Mes = 2,4,6-trimethylphenyl.

Figure 1 shows the crystal structure of **2**.[7] The bridging bonds from the boron atoms to the mesityl ring (174.8(9) and 176.9(8) pm, respectively) are comparable in length with the corresponding Al–C bridging bonds in **1** (R = *o*-CH_3: 213 pm[1a]), if one takes into account the 38 pm greater covalent radius of aluminum. The bridging aryl ring in **1** is perpendicular (91.0°) to the least-square plane through C–Al–C–Al, while that in **2** is perpendicular (89.1°) to the least-square plane through B1–C2–B3–C4. The mesityl ring bound to C2 forms an angle of 85.9° with this plane.

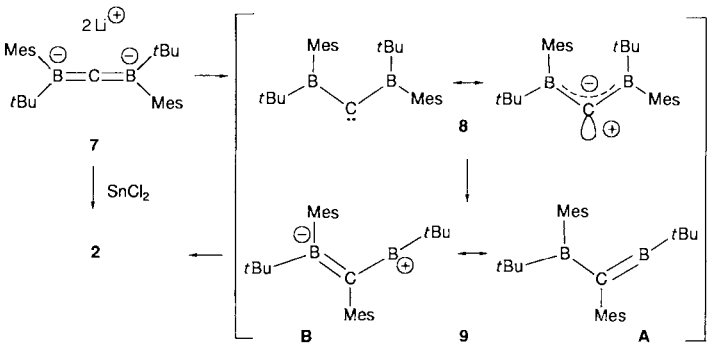

The NMR data (Table 1) indicate that the bridged structure **2** is also present in solution. A rapid topomerization of **9** with migration of the mesityl group from the tricoordinated to the dicoordinated boron atom (Scheme 2) should have no influence on the chemical shifts of the mesityl groups bound to the boron.

The *ortho* and *para* C atoms of this mesityl group are, however, noticeably deshielded (Table 1, δ = 160.8 and

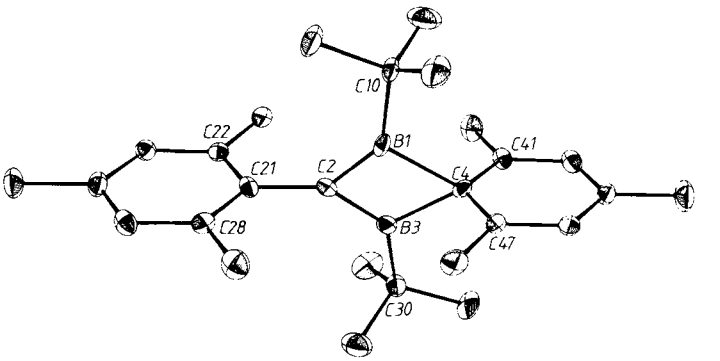

Fig. 1. ORTEP plot of the crystal structure of **2**. The vibration ellipsoids are drawn at the 50% probability level. Projection almost onto the B1, C2, B3 plane. Important bond lengths [pm] and angles [°]: B1-C2 144.8(8), B3-C2 146.2(8), B1-C4 176.9(8), B3-C4 174.8(9), C2-C21 146.5(5), B1-C10 161.0(7), B3-C30 158.9(7), C4-C41 142(1), C4-C47 142.6(8); B1-C2-B3 80.7(4), B1-C4-B3 64.8(4), C2-B1-C4 106.7(4), C2-B3-C4 107.2(4), C41-C4-C47 117.7(5); B1-C2-C21-C22 80.8(7), B3-C2-C21-C28 91.8(6), C2-B1-C4-C47 114.8(6), C2-B3-C4-C-41 102.2(5).

Table 1. Some physical data of the compounds **2** and **3**. Spectra in $CDCl_3$, TMS as standard for ^{1}H- and ^{13}C-NMR spectra, $BF_3 \cdot OEt_2$ for ^{11}B-NMR spectra.

2: yellow crystals, m.p. = 207 °C, yield 86%.—^{1}H NMR (300 MHz, 25 °C): δ = 0.55 (s, 18H, $C(CH_3)_3$), 2.23, 2.47 (each s, each 6H, *o*-CH_3), 2.26, 2.33 (each s, each 3H, *p*-CH_3), 6.83, 7.08 (each s, each 2H, *m*-H); ^{13}C NMR (100 MHz, −40 °C): δ = 21.0, 22.0 (each q, each 1C, *p*-CH_3), 22.6, 25.0 (each q, each 2C, *o*-CH_3), 28.3 (br. s, 2C, $C(CH_3)_3$), 28.6 (q, 6C, $C(CH_3)_3$), 113.4 (s, 1C, B-*i*-C), 127.1, 129.3 (each d, each 2C, *m*-C), 130.3 (br. s, 1C, CB_2), 130.8, 146.1 (each s, each 1C, *p*-C), 130.9, 160.4 (each s, each 2C, *o*-C), 140.3 (s, 1C, C-*i*-C); ^{11}B NMR (96 MHz, 25 °C): δ = 42 ($\nu_{1/2}$ = 595 Hz)

3: yellow crystals, m.p. = 142 °C, yield: NMR spectroscopically quantitative.—^{1}H NMR (300 MHz, 25 °C): δ = 0.37, 0.51, 1.27 (each s, each 9H, $C(CH_3)_3$), 2.06, 2.27 (each s, each 3H, *p*-CH_3), 2.17, 2.47 (each s, each 6H, *o*-CH_3), 6.26, 6.83 (each s, each 2H, *m*-H), 7.00, 7.92 (each d, each 2H, *m*-, *o*-H_{pyr}); ^{13}C NMR (75 MHz, 25° C): δ = 21.3, 24.3, 24.4 (each q, each 2C, *o*- und *p*-CH_3), 25.2, 27.1 (each s, each 1C, $BC(CH_3)_3$), 29.9, 30.3, 31.2 (each q, each 3C, $C(CH_3)_3$), 35.5 (s, 1C, $C(CH_3)_3$), 117.6 (br. s, 1C, CB_2), 120.2 (d, 2C, *m*-C_{pyr}), 126.8, 127.4 (each d, each 2C, *m*-C), 131.4, 131.7 (each s, each 1C, *p*-C), 135.6, 137.6 (each s, each 2C, *o*-C), 142.6 (d, 2C, *o*-C_{pyr}), 149.8 (s, 1C, C-*i*-C), 153.9 (s, 1C, B-*i*-C), 164.8 (s, 1C, *p*-C_{pyr}); ^{11}B NMR (96 MHz, 25 °C): δ = 48, 65 ($\nu_{1/2}$ = 1088, 1769 Hz).

146.3, resp.) relative to the corresponding atoms in **3** (δ = 135.6 or 137.6 and 131.4 or 131.7, resp.), whereas the *ipso* C atom is, in contrast, strongly shielded (δ = 113.4) as compared to **3** (δ = 153.9). Similar consequences of bridging were observed in the case of **1**[8] (R = *p*-CH_3; δ: *o*-C 155, *p*-C 150, *i*-C 118). The chemical shifts of the tri- and dicoordinated B atoms would be averaged in a rapid equilibrium (Scheme 2). On the basis of the classical methyleneborane

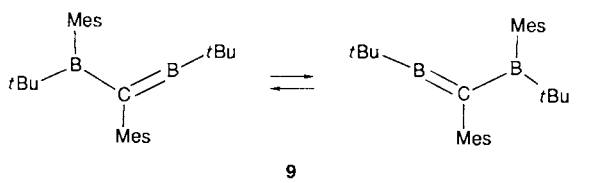

Scheme 2.

10[3] the unaveraged shifts for **9** can be predicted to be $\delta = 65 \pm 5$ and 70 ± 5. The average value $\delta = 65 \pm 5$ differs very markedly from that measured for **2** (δ (^{11}B) = 42).

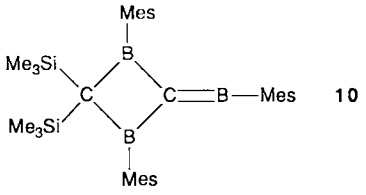

10

Aryl bridging is, after π-π[9] and σ-π conjugation,[3, 6] a third route to the stabilization of methyleneboranes by intramolecular filling of the empty p-orbital on the boron atom.

Received: November 27, 1989 [Z 3655 IE]
German version: *Angew. Chem. 102* (1990) 436

CAS Registry numbers:
2, 125734-71-6; **3**, 125715-36-8; **7**, 125715-35-7; 4-*tert*-butylpyridine, 3978-81-2.

[1] a) M. Barber, D. Liptak, J. P. Oliver, *Organometallics 1* (1982) 1307, and references cited therein; b) D. J. Brauer, C. Krüger, *Z. Naturforsch. B34* (1979) 1293.

[2] H. Lukasch, G. Schmidt-Lukasch, U. Lippold, A. Berndt, *Angew. Chem. 100* (1988) 959; *Angew. Chem. Int. Ed. Engl. 27* (1988) 960.

[3] C. Wieczorek, J. Allwohn, G. Schmidt-Lukasch, R. Hunold, W. Massa, A. Berndt, *Angew. Chem. 102* (1990) 435; *Angew. Chem. Int. Ed. Engl. 29* (1990), 398.

[4] R. Wehrmann, H. Meyer, A. Berndt, *Angew. Chem. 97* (1985) 779; *Angew. Chem. Int. Ed. Engl. 24* (1985) 788.

[5] M. Pilz, J. Allwohn, R. Hunold, W. Massa, A. Berndt, *Angew. Chem. 100* (1988) 1421; *Angew. Chem. Int. Ed. Engl. 27* (1988) 1370.

[6] R. Hunold, M. Pilz, J. Allwohn, M. Stadler, W. Massa, P. von R. Schleyer, *Angew. Chem. 101* (1989) 759; *Angew. Chem. Int. Ed. Engl. 28* (1989) 781; J. Allwohn, R. Hunold, M. Pilz, R.-G. Müller, W. Massa, A. Berndt, *Z. Naturforsch 45b* (1990), in press.

[7] X-ray structure analysis: $C_{27}H_{40}B_2$, space group $P2_1$, $Z = 2$, $a = 943.2(3)$, $b = 1359.7(1)$, $c = 947.8(3)$ pm), $\beta = 99.28(2)°$; 14771 independent reflections with $F_o > 3\sigma$ measured on a four-circle diffractometer (CAD4 Enraf-Nonius) with $Cu_{K\alpha}$ radiation at $-80\,°C$; no absorption correction ($\mu = 3.62\,cm^{-1}$), methyl groups refined as rigid groups, whereby isotropic temperature factors were used groupwise for the H atoms. Anisotropic temperature factors were used for all the remaining atoms. At the end of the refinement the *tert*-butyl groups and the mesityl groups bound to C were fixed as rigid groups because of the poor reflection/parameter ratio. Refinement by full matrix method. 235 parameters, $R = 0.053$, $wR = 0.048$ (weighting $w = 1/\sigma^2(F_o)$). Further details of the crystal structure investigation are available on request from the Fachinformationszentrum Karlsruhe, Gesellschaft für wissenschaftlich-technische Information mbH, D-7514 Eggenstein-Leopoldshafen 2 (FRG), on quoting the depository number CSD-320070, the names of the authors, and the journal citation.

[8] G. A. Olah, G. K. S. Prakash, G. Liange, K. L. Henold, G. B. Haigh, *Proc. Natl. Acad. Sci. USA 74* (1977) 5217.

[9] B. Glaser, E. Hanecker, H. Nöth, H. Wagner, *Chem. Ber. 120* (1987) 659, and references cited therein; R. Boese, P. Paetzold, A. Tapper, *ibid. 120* (1987) 1069.

portant role as β-Si effect[5] in organic chemistry. However, such cations have proven to be too unstable for NMR spectroscopic investigations.[6] Recently,[7] we were able to show that hyperconjugation and stronger σ-π interactions in methyleneboranes have similar consequences as in carbocations. We now demonstrate NMR spectroscopically the consequences of strong C–Sn hyperconjugation in the methyleneborane **1**.

The bis(*C*-stannyl)methyleneborane **1** postulated as a product of the thermolysis of the 1,3-diboretane **3** (Scheme 1) can

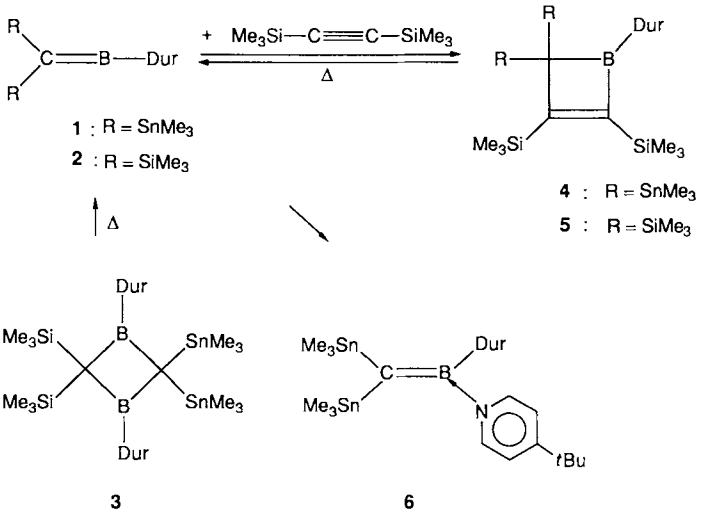

Scheme 1. Dur = 2,3,5,6-tetramethylphenyl.

be detected NMR spectroscopically along with **2**[8] after rapid removal from the reaction mixture by condensation and trapping in cooled solvents. The separation of **2** is accomplished via the cycloadduct **4**, which is formed from **1** and bis(trimethylsilyl)acetylene at room temperature; **2** reacts only at 135 °C to give **5**. **4** can be separated from the mixture of **4** and **2** by crystallization at −30 °C (pentane).

The thermal cycloreversion of **4**, the first reported for a 1,2-dihydroborete, already takes place at 120 °C. Destillation into CD_2Cl_2 cooled to −80 °C afforded a solution of **1** and bis(trimethylsilyl)acetylene, which was investigated ^{13}C- and ^{11}B-NMR spectroscopically (Table 1). Treatment of this solution at −78 °C with 4-*tert*-butylpyridine yielded the adduct **6**, whose $^1J(^{119}Sn,^{13}C)$ value is required for comparison purposes (see below). NMR data of **1**, **2**, **7**, and **8** relevant for the following discussion are collected in Scheme 2.

Strong C–Sn Hyperconjugation in a Distannylmethyleneborane**

By *Monika Pilz, Holger Michel,* and *Armin Berndt**

Dedicated to Professor Paul von Ragué Schleyer on the occasion of his 60th birthday

Kinetic measurements show that carbocations are more strongly stabilized by C–Sn hyperconjugation[1–4] than by C–Si hyperconjugation, an interaction which plays an im-

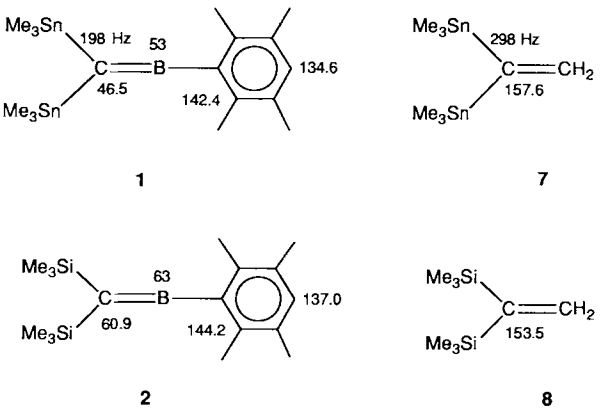

Scheme 2.

[*] Prof. Dr. A. Berndt, M. Pilz, H. Michel
Fachbereich Chemie der Universität
Hans-Meerwein-Strasse, D-3550 Marburg (FRG)

[**] This work was supported by the Deutsche Forschungsgemeinschaft and the Fonds der Chemischen Industrie.

Table 1. Some physical data of the compounds **1**, **4** and **6**. Standard for ^{1}H- and ^{13}C-NMR spectra TMS, for ^{11}B-NMR spectra $BF_3 \cdot OEt_2$.

1: yield, NMR spectroscopically ca. 95% – ^{1}H NMR (300 MHz, $CDCl_3$, 25 °C): $\delta = 0.27$ (s, 18H, $Sn(CH_3)_3$), 2.23, 2.59 (each s, each 6H, *o*- and *m*-CH_3), 7.09 (s, 1H, p-H); ^{13}C NMR (100 MHz, CD_2Cl_2, −80 °C): $\delta = -5.2$ (q, 6C, $Sn(CH_3)_3$, $^1J(^{119}Sn, ^{13}C) = 355.7$), 19.7, 21.3 (each q, each 2C, *o*- and *m*-CH_3), 46.5 (br. s, 1C, CB, $^1J(^{119}Sn,^{13}C) = 198$ Hz), 126.5 (br. s, 1C, *i*-C), 133.6, 142.4 (each s, each 2C, *m*- and *o*-C), 134.6 (d, 1C, *p*-C); ^{11}B NMR (96 MHz, CD_2Cl_2, 20 °C): $\delta = 53$ ($\nu_{1/2} = 680$ Hz)

4: pale yellow, m.p. = 106 °C, yield 12%. – ^{1}H NMR (300 MHz, $CDCl_3$, 25 °C): $\delta = 0.00$ (s, 18H, $Sn(CH_3)_3$), 0.09, 0.32 (each s, each 9H, $Si(CH_3)_3$), 2.07, 2.16 (each s, each 6H, *o*- and *m*-CH_3), 6.82 (s, 1H, *p*-H); ^{13}C NMR (100 MHz, $CDCl_3$, −40 °C): $\delta = -6.9$ (q, 6C, $Sn(CH_3)_3$, $^1J(^{119}Sn,^{13}C) = 313.6$ Hz), 0.0, 0.6 (each q, each 3C, $Si(CH_3)_3$), 19.9 (q, 4C, *o*- and *m*-CH_3), 54.3 (br. s, 1C, Sn_2CB, $^1J(^{119}Sn,^{13}C) = 277.7$ Hz), 129.7 (d, 1C, *p*-C), 132.5, 133.6 (each s, each 2C, *o*- and *m*-C), 138.4 (br. s, 1C, *i*-C), 171.8 (s, 1C, SiCC, $^2J(^{119}Sn,^{13}C) = 37$ Hz), 197.1 (br. s, 1C, SiCB, $^3J(^{119}Sn,^{13}C) = 101$ Hz); ^{11}B NMR (96 MHz, $CDCl_3$, 25 °C): $\delta = 39$ ($\nu_{1/2} = 764$ Hz)

6: yield NMR spectroscopically quantitative.—^{1}H NMR (300 MHz, CD_2Cl_2, 25 °C): $\delta = -0.41$, −0.30 (each s, each 9H, $Sn(CH_3)_3$), 1.26 (s, 9H, $C(CH_3)_3$), 2.05, 2.21 (each s, each 6H, *o*- and *m*-CH_3), 6.72 (s, 1H, *p*-H), 7.19, 8.39 (each br. s, each 2H, *o*- and *m*-H_{pyr}); ^{13}C NMR (100 MHz, CD_2Cl_2, −80 °C): $\delta = -6.8$, −6.2 (each q, each 6C, $Sn(CH_3)_3$, $^1J(^{119}Sn,^{13}C) = 294.2$, 299.7 Hz), 20.2, 20.7 (each q, each 2C, *o*- and *m*-CH_3), 29.6 (q, 3C, $C(CH_3)_3$), 34.3 (s, 1C, $C(CH_3)_3$), 80.1 (br. s, 1C, CB, $^1J(^{119}Sn\text{-}^{13}C) = 325$ Hz), 122.7 (d, 2C, *m*-C_{pyr}), 129.3 (d, 1C, *p*-C_{dur}), 132.4, 135.6 (each s, each 2C, *o*- and *m*-C_{dur}), 142.7 (d, 2C, *o*-C_{pyr}), 165.1 (s, 1C, *p*-C_{pyr}), *i*-C could not be located; ^{11}B NMR (96 MHz, CD_2Cl_2, 25 °C): $\delta = 41$ ($\nu_{1/2} = 1445$ Hz).

The C atom of the B–C bond in **1** is $\Delta\delta = 14.4$ more strongly *shielded* than in **2**, whereas the correspondingly substituted C atom in **7**[9] is *deshielded* by $\Delta\delta = 4.1$ relative to that in **8**.[10] Apparently the B–C double bond is more strongly polarized in corresponding to resonance formula **B** in **1** than in **2**.[11] The *ortho* and *para* C atoms in **1** are less deshielded than in **2**. The thus indicated smaller delocalization of π electrons of the duryl ring to the boron atom and the stronger polarization of the B–C double bond according to **B** point to a smaller π-electron density at the boron atom of **1** than of **2**. This should lead to a small *deshielding* of the boron atom in **1** relative to that in **2**. Experimentally, however, we find a *shielding* of $\Delta\delta = 10$, which we attribute to C–Sn hyperconjugation corresponding to resonance formula **C**. In methyleneboranes with extremely strong σ-π interaction (bridging),[7] $\delta(^{11}B)$ is 18–20, $\Delta\delta \approx 45$.

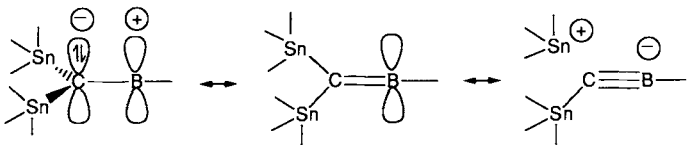

B **A** **C**

The weakening of the C_{sp^2}–Sn bonds to be expected in accord with the corresponding resonance formula **C** is experimentally confirmed[13] by the small coupling constant $^1J(^{119}Sn, ^{13}C)$ of **1**, which is only 198 Hz.[12] In the adduct **6**, in which C–Sn hyperconjugation plays no role because of the filling of the p-orbital on the boron atom by 4-*tert*-butylpyridine, the corresponding coupling (325 Hz) lies in the range characteristic for C_{sp^2}–Sn bonds in geminal trimethylstannyl groups (cf. 298 Hz in **7**[9]).

Received: November 27, 1989 [Z 3656 IE]
German version: *Angew. Chem. 102* (1990) 438

CAS Registry numbers:
1, 125685-57-6; **2**, 120638-21-3; **3**, 120638-19-9; **4**, 125685-58-7; **5**, 125685-59-8; **6**, 125685-60-1; bis(trimethylsilyl)acetylene, 14630-40-1; 4-*tert*-butylpyridine, 3978-81-2.

[1] C. Eaborn, K. C. Pande, *J. Chem. Soc. 1960*, 1566; C. Eaborn, *J. Chem. Soc. Chem. Commun. 1972*, 1255, and references cited therein.
[2] T. G. Traylor, H. J. Berwin, J. Jerkunica, M. L. Hall, *Pure Appl. Chem. 30* (1972) 599, and references cited therein.
[3] J. B. Lambert, G. Wang, D. H. Teramura, *J. Org. Chem. 53* (1988) 5422, and references cited therein.
[4] The σ^+ values of CH_2–$SnMe_3$ (−0.92) and CH_2–$SiMe_3$ (−0.62) enable a quantitative comparison: W. Hanstein, H. J. Berwin, T. G. Traylor, *J. Am. Chem. Soc. 92* (1970) 829.
[5] X. Li, J. A. Stone, *J. Am. Chem. Soc. 111* (1989) 5586, and references cited therein.
[6] G. A. Olah, A. L. Berrier, L. D. Field, G. K. S. Prakash, *J. Am. Chem. Soc. 104* (1982) 1349.
[7] C. Wieczorek, J. Allwohn, G. Schmidt-Lukasch, R. Hunold, W. Massa, A. Berndt, *Angew. Chem. 102* (1990) 435; *Angew. Chem. Int. Ed. Engl. 29* (1990) 398.
[8] M. Pilz, M. Stadler, R. Hunold, J. Allwohn, W. Massa, A. Berndt, *Angew. Chem. 101* (1989) 761; *Angew. Chem. Int. Ed. Engl. 28* (1989) 784.
[9] T. N. Mitchel, A. Amamria, B. Fabisch, H. G. Kuivila, T. J. Karol, K. Swami, *J. Organomet. Chem. 259* (1983) 157.
[10] G. Fritz, W. Himmel, *Z. Anorg. Allg. Chem. 448* (1979) 55.
[11] The part of the shielding of the C atoms of the B–C double bond of **1** and **2**, which is due to anisotropy by proximity to the dicoordinated boron atom, might be equally as large as the shielding of the *ipso* C atoms in **1** and **2** relative to those in **4** and **5**, respectively, which are bound to tricoordinated boron atoms ($\Delta\delta \approx 12$). The remaining shielding of 99 in **1** (81 in **2**) indicates polarization corresponding to resonance formula **B**.
[12] For an overview of $J(^{119}Sn,^{13}C)$ see: B. Wrackmeyer, *Annu. Rep. NMR Spectrosc. 16* (1985) 73.
[13] That the $^1J(^{119}Sn,^{13}C)$ coupling within the $SnMe_3$ groups in **1** is 56 and 61.5 Hz *greater* than in **6** can also be regarded as an indication of the participation of resonance formula **C**.

Transition-Metal-Induced Generation of C_2H_4 from 1,7-Octadiene: Regiospecific Activation of Internal C–C Bonds instead of Metathesis-like Coupling of Terminal CH_2 Groups**

By *Norbert Steinrück, Oliver Dange, Detlef Stöckigt*, and *Helmut Schwarz**

The metathesis reaction of 1,7-octadiene (**1**) has been more extensively studied than that of almost any other olefin.[1] *Grubbs* et al.[2] were able to show that ethylene is generated from **1** and metal carbene complexes **2** in a chain reaction; metallacyclobutanes **3** are involved as intermediates, and carbene complexes **4** are presumed to be the second product [Eq. (a)]. Metathesis reactions have also been observed repeatedly in bimolecular and unimolecular reactions of transition-metal ions in the gas phase.[3, 4]

Here we report on a reaction of "naked" transition-metal ions $M^{\oplus}$ (M = Fe, Ni, Cr) with **1** which cannot be explained

[*] Prof. Dr. H. Schwarz, Dipl.-Chem. N. Steinrück, Dipl.-Chem. O. Dange, D. Stöckigt
Institut für Organische Chemie der Technischen Universität
Strasse des 17. Juni 135, D-1000 Berlin 12

[**] This work was supported by the Deutsche Forschungsgemeinschaft, the Volkswagen-Stiftung, the Fonds der Chemischen Industrie, and the Gesellschaft von Freunden der Technischen Universität Berlin. We thank Prof. *H. Lehmkuhl*, Max-Planck-Institut Mülheim, and Dr. *K. Weiss*, Universität Bayreuth, for stimulating discussions.

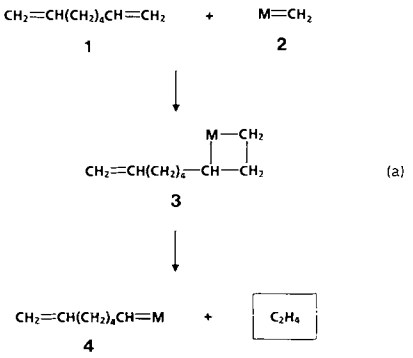

in terms of the type of metathesis reaction predominating in solution. Instead, the reaction for $M^{\oplus} = Fe^{\oplus}$ is presumably a rare example of *directed* activation of C–C bonds *without* prior C–H bond activation.[5]

Electron-impact ionization (100 eV) of a 10:1 mixture of **1** and a suitable substrate for the generation of $M^{\oplus}$ (such as $Fe(CO)_5$, $Ni(acac)_2$, or $Cr(acac)_3$) in the ion source of a modified ZAB-HF-3F mass spectrometer with BEBE configuration (B, magnetic sector; E, electric sector) affords ionic complexes of the type **1**-$M^{\oplus}$. The ions, accelerated to 8 keV, are mass-selected with sectors B(1)E(1), and their unimolecular decompositions[6] are monitored by scanning B(2). All three metal ions, $Fe^{\oplus}$, $Ni^{\oplus}$, and $Cr^{\oplus}$, induced loss of C_2H_4 from **1** (8, 7, and 10% of the total ion current, respectively).

Investigations using partially deuterated (and ^{13}C-labeled) isotopomers of **1** and naked metal ions (Table 1) allow the following conclusions to be drawn:

1. The fact that C_2D_4 ($\Delta m = 32$) was formed from none of the complexes [1,1,8,8-$^2H_4$] **1**-$M^{\oplus}$ compellingly rules out a metathesis reaction involving coupling of the terminal methylene groups, for example, isomerization to a bicyclo[4.2.0]octane derivative and metal insertion to give **5**, which could react to give **6** and ethylene [Eq. (b)].

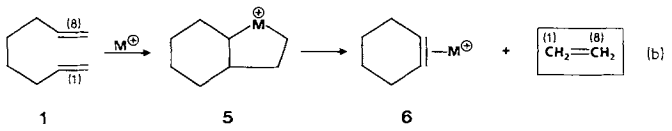

2. The relative intensity for $\Delta m = 28$ requires that, for the complexes with $Fe^{\oplus}$, more than 90% of the total ethylene formed originate from the *internal* CH_2 groups, C(4) and C(5) [Eq. (c)]. Although these experiments still do not distinguish among the many possible mechanistic variants[7] for the highly selective generation of C_2H_4 from

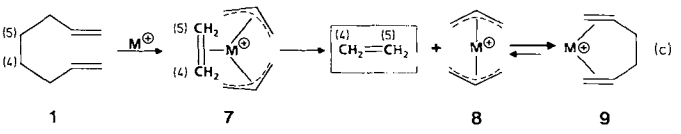

1-$Fe^{\oplus}$, we favor the reaction via **7** shown in Equation (c), which provides a further example of an activation of C–C bonds without prior activation of C–H bonds.[5] For **1**-$Cr^{\oplus}$, we estimate that this mechanism accounts for ca. 20% of the reaction;[8] for **1**-$Ni^{\oplus}$, not even a semiquantitative estimate is possible owing to substantial exchange processes. However, the internal positions are also unquestionably involved in C_2H_4 generation from **1**-$Ni^{\oplus}$.

3. The data in Table 1 indicate that, for the generation of ethylene from **1**-$Cr^{\oplus}$, two further, independent processes presumably take place. The first is the generation of C_2H_4 from C(3) and C(4); we estimate that this process accounts for ca. 30% of the reaction. The second process, accounting for ca. 50% of the reaction, involves coupling of one of the two vinyl groups in a transannular fashion with a hydrogen atom of the allylically activated CH_2 group to give C_2H_4. The mechanistic details of this reaction pathway have not yet been explored.
4. Decomposition of the iron complex of **1** proceeds extremely selectively and three reaction pathways could be characterized for **1**-$Cr^{\oplus}$. However, the nickel complex **1**-$Ni^{\oplus}$ defies clear analysis, since ethylene loss is preceded by extensive exchange processes.[9]

The high selectivity with which C_2H_4 is formed from **1**-$Fe^{\oplus}$ encouraged us to carry out an experiment to determine whether the resulting ions have the structure **8** or **9**. Mass selection of the corresponding ion in a tandem experiment,[10] followed by collisional activation (CA[11]), affords a CA spectrum that is identical with the CA spectrum of $Fe(C_3H_5)_2^{\oplus}$ generated independently by reaction of $Fe^{\oplus}$ with $CH_2=CHCH_2Cl$.[12] This result does not mean, however, that the loss of C_2H_4 from **1**-$Fe^{\oplus}$ necessarily leads to **8**, since the CA spectrum of an authentic (1,5-hexadiene)$Fe^{\oplus}$ complex is also indistinguishable from the spectrum given in Ref. [12]. A coupling of the two allyl fragments also presumably occurs during C_2H_4 loss from **1**-$Fe^{\oplus}$ (i.e., **8** rearranges to **9**), as indicated by the following observation: in the CA spectrum of the ion obtained after C_2H_4 loss from [1,1,3,3-$^2H_4$] **1**-$Fe^{\oplus}$, for example, the entire signal group of the base peak ($\Delta m = 42$, loss of propene) is distributed over five m/z values ($\Delta m = 42-46$). This is best explained by a C–C coupling of the two ligands followed by H rearrangements.[13]

Received: November 15, 1989;
revised: January 15, 1990 [Z 3637 IE]
German version: *Angew. Chem. 102* (1990) 429

CAS Registry numbers:
1, 3710-30-3; Cr, 14067-03-9; Fe, 14067-02-8; Ni, 14903-34-5.

Table. 1. Metal-induced loss of ethylene from 1,7-octadiene isotopomers in the mass spectrometer. $\Delta m = m/z$ (molecular ion) – m/z (fragment ion). The relative intensities are give in % and normalized so that their sum is 100%. $\Delta m = 32$ *not* observed in any system.

Δm	[1,1,8,8-$^2H_4$]-**1**			[1,1,3,3-$^2H_4$]-**1**			[1,1,2,3,3-$^2H_5$]-**1**			[3,3-$^2H_2$]-**1**			[1-^{13}C,3,3-$^2H_2$]-**1** [a]			[1-^{13}C,5,5-$^2H_2$]-**1** [a]			[4,4-$^2H_2$]-**1**		
	$Fe^{\oplus}$	$Ni^{\oplus}$	$Cr^{\oplus}$	$Fe^{\oplus}$	$Ni^{\oplus}$	$Cr^{\oplus}$	$Fe^{\oplus}$	$Ni^{\oplus}$	$Cr^{\oplus}$	$Fe^{\oplus}$	$Ni^{\oplus}$	$Cr^{\oplus}$	$Fe^{\oplus}$	$Ni^{\oplus}$	$Cr^{\oplus}$	$Fe^{\oplus}$	$Ni^{\oplus}$	$Cr^{\oplus}$	$Fe^{\oplus}$	$Ni^{\oplus}$	$Cr^{\oplus}$
28	92	43	48	93	50	43	91	41	33	95	66	68	93	60	41	4	50	37	8	60	62
29	4	29		5	25	23	3	24	22	2	23	15	4	30	43	5	25	27	2	15	
30	4	28	52	2	25	34	2	20	27	3	11	17	3	10	16	91	25	36	90	25	38
31							4	15	18												

[a] $\Delta m = 29$ presumably corresponds to a doublet $C_2H_3D/^{13}CCH_4$; analogously, $\Delta m = 30$ may have been formed from a doublet $C_2H_2D_2/^{13}CCH_3D$. The resolution attainable in a MIKES experiment (MIKE = mass-analyzed ion kinetic energy spectrometry) was not sufficient to achieve separation.

[1] For a review, see K. J. Irvin: *Olefin Metathesis*, Academic Press, New York 1983.
[2] R. H. Grubbs, D. D. Carr, C. Hoppin, P. L. Burk, *J. Am. Chem. Soc. 98* (1976) 3478.
[3] A. E. Stevens, J. L. Beauchamp, *J. Am. Chem. Soc. 101* (1979) 6449; L. F. Halle, P. B. Armentrout, J. L. Beauchamp, *Organometallics 2* (1983) 1829; D. B. Jacobson, B. S. Freiser, *J. Am. Chem. Soc. 107* (1985) 2605; H. Kang, J. L. Beauchamp *ibid. 108* (1986) 5663; S. W. Buckner, J. R. Gord, B. S. Freiser *ibid. 110* (1988) 6606; S. W. Buckner, B. S. Freiser, *Polyhedron 7* (1988) 1583; S. Karrass, K. Eller, C. Schulze, H. Schwarz, *Angew. Chem. 101* (1989) 634; *Angew. Chem. Int. Ed. Engl. 28* (1989) 607; S. Karrass, T. Prüsse, K. Eller, H. Schwarz, *J. Am. Chem. Soc. 111* (1989) 9018.
[4] For recent reviews on the activation of C–H and C–C bonds by naked transition-metal ions, see H. Schwarz, *Acc. Chem. Res. 22* (1989) 282; P. B. Armentrout, J. L. Beauchamp, *ibid. 22* (1989) 315; D. H. Russell (Ed.): *Gas Phase Inorganic Chemistry*, Plenum, New York 1989; K. Eller, H. Schwarz, *Chimia 43* (1989) 371.
[5] This topic is currently a focus of much controversy (see [4]). For recent examples, see S. Karrass, H. Schwarz, *Helv. Chim. Acta 72* (1989) 633; *Organometallics*, in press; S. Karrass, K. Eller, H. Schwarz, *Chem. Ber.*, in press.
[6] Besides loss of C_2H_4 ($\Delta m = 28$), further unimolecular reactions have been observed: **1**-$Fe^{\oplus}$: $\Delta m = 2$ (7%), 4 (9), 16 (13), 18 (4), 28 (8), 42 (50), 44 (1), 56 (8). **1**-$Ni^{\oplus}$: $\Delta m = 2$ (8), 4 (< 1), 16 (2), 18 (< 1), 28 (7), 42 (69), 54 (< 1), 56 (12). **1**-$Cr^{\oplus}$: $\Delta m = 2$ (38), 28 (10), 42 (15), 54 (13), 56 (24). For a discussion, see O. Dange, *Diplomarbeit*, Technische Universität Berlin 1989.
[7] We thank Dr. *Karin Weiss* for pointing out an alternative mechanism, according to which **1** first undergoes $Fe^{\oplus}$-induced isomerization to 2,6-octadiene and then loses the originally internal C(4) and C(5) methylene groups via Cope rearrangement and metathesis reaction.
[8] Primary and secondary isotope effects of unknown magnitude prevent a precise description of the process involved in C_2H_4 generation from **1**-$Cr^{\oplus}$. The values given in the text are therefore only rough estimates.
[9] Diverse isomerizations of olefins catalyzed by M(CO), (M = Fe, Ni), although they cannot explain the results reported here, have been described in J. E. Arnet, R. Pettit, *J. Am. Chem. Soc. 83* (1961) 2954; P. A. Pinke, R. D. Stauffer, R. G. Miller, *ibid. 96* (1974) 4229.
[10] F. W. McLafferty (Ed.): *Tandem Mass Spectrometry*, Wiley, New York 1983; K. L. Busch, G. L. Glish, S. A. McLuckey: *Mass Spectrometry/Mass Spectrometry: Techniques and Applications of Tandem Mass Spectrometry*, VCH Publishers, New York 1988.
[11] K. Levsen, H. Schwarz, *Mass Spectrom. Res. 2* (1983) 77.
[12] In CA spectra (collision gas, helium; 80% transmission) of $Fe(C_3H_5)_2^{\oplus}$, the following signals are observed: $\Delta m = 2$ (14%), 16 (3), 28 (15), 56 (5), 67 (4), and $Fe^{\oplus}$ (13).
[13] The most recent results of other research groups indicate that $M(C_3H_5)_2^{\oplus}$ complexes are also formed in the reaction of $Fe(CO)_x^{\oplus}$ with C_3H_5Cl or of $Co(C_3H_6)^{\oplus}$ with 1-propene; these complexes are best described as **9**. (H. Mestdagh, C. Rolando, *J. Am. Chem. Soc. 111* (1989) 3476; R. L. Hettich, B. S. Freiser, *Organometallics 8* (1989) 2447). Our attempts to achieve a differentiation between **8** and **9** by selective ligand exchange and use of Fourier transform ion cyclotron resonance (FTICR) have so far failed.

Ionic Isomer Distinction by Neutralization-Reionization Mass Spectrometry (NRMS): Carbonic Acid Radical Cations, $(HO)_2CO^{\cdot\oplus}$ versus $(H_2O/CO_2)^{\cdot\oplus}$ Clusters **

By *Johan K. Terlouw, Detlev Sülzle*, and *Helmut Schwarz* *

Dedicated to Professor Paul von Ragué Schleyer on the occasion of his 60th birthday

The interaction of carbon dioxide with water is a topic of central importance in biological, atmospheric, and industrial processes.[1] Whereas earlier studies[2] suggested the occurrence of free carbonic acid, $(HO)_2CO$ (**1**), in the gas-phase reactions of H_2O with CO_2, both theoretical[1h, 3] and experimental studies[4] later provided evidence that a weakly bound van der Waals complex was generated. From the detailed spectroscopic analyses it was further concluded that a planar structure **2** (C_{2v}) rather than a hydrogen-bridged isomer **3** (C_s) was formed. The long-sought free carbonic acid **1** is, however, readily accessible by thermolysis of NH_4HCO_3.[5] Mass-spectrometric studies further demonstrate[5] that both **1** and its radical cation $\mathbf{1}^{\cdot\oplus}$ are perfectly stable species in the gas phase, since they are prevented by significant barriers (> 40 kcal mol^{-1})[1g, h, 5, 6] from undergoing spontaneous isomerization and dissociation reactions. In addition, by using neutralization-reionization mass spectrometry (NRMS),[7] it was possible to reduce $\mathbf{1}^{\cdot\oplus}$ to its neutral counterpart.[5]

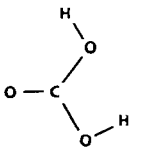

1 s/a (C_s)

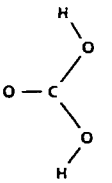

1 s/s (C_{2v})

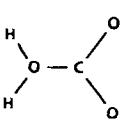

2 (C_{2v})

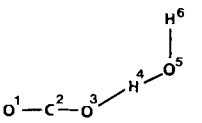

3 (C_s)

Here we describe experiments on the electron-impact ionization (70 eV) of an H_2O/CO_2 mixture (90% CO_2/10% H_2O, total ion source pressure ca. 2×10^{-4} torr). We shall demonstrate that the charged cluster $(H_2O/CO_2)^{\cdot\oplus}$ formed under these conditions by ion/molecule reactions does not have the structure of the radical ions $\mathbf{1}^{\cdot\oplus}$ or $\mathbf{2}^{\cdot\oplus}$ but rather is the proton-bridged radical ion $\mathbf{3}^{\cdot\oplus}$.[8] In addition, the data presented clearly support the view[9] that NRMS can also be used to characterize *isomeric ions*. The experimental findings are supported by ab initio MO calculations (HF/6-31G** + ZPVE)[10] (Table 1).

Table 1. Total energies, zero-point vibrational energies (ZPVE), relative energies, and $<S^2>$ values (6-31G**//6-31G**).

	E_{total} [Hartree]	ZPVE [Hartree]	E_{rel} [kcal mol^{-1}]	$<S^2>$
1 s/a	−263.657029	0.043412	0	
1 s/s	−263.660912	0.043736	−2.3	
2	−263.662995	0.037283	−7.2	
3	−263.660514	0.043898	−1.9	
1 $s/a^{+\cdot}$	−263.312272	0.041832	0	0.76
1 $s/s^{+\cdot}$	−263.312136	0.041822	0.1	0.76
$\mathbf{2}^{+\cdot}$ [a]	−263.147185	0.038805	101.8	0.78
$\mathbf{3}^{+\cdot}$	−263.292329	0.034851	8.6	0.76

[a] Corresponds to a transition structure.

[*] Prof. Dr. H. Schwarz, Dipl.-Chem. D. Sülzle
Institut für Organische Chemie der Technischen Universität
Strasse des 17. Juni 135, D-1000 Berlin 12
Prof. Dr. J. K. Terlouw
Department of Chemistry, McMaster University
1280 Main Street West
West Hamilton, Ontario L8S 4M1 (Canada)

[**] This work was supported by the Deutsche Forschungsgemeinschaft, the Fonds der Chemischen Industrie, the Graduiertenkolleg Chemie zu Berlin, and the Gesellschaft von Freunden der Technischen Universität Berlin

Electron-impact ionization of a mixture of H_2O and CO_2 gives rise to, among others, a signal at m/z 62, which, according to exact mass measurements, corresponds to the elemental composition CH_2O_3. Mass selection of this ion in an MS/MS experiment,[11] followed by collisional activation (CA),[12] yields the CA mass spectrum shown in Figure 1b. The ion is characterized by three major dissociation processes yielding $HOCO^{\oplus}$ (m/z 45) + $OH^{\bullet}$, $CO_2^{\bullet\oplus}$ (m/z 44) + H_2O, and $H_2O^{\bullet\oplus}$ (m/z 18) + CO_2 with enthalpies of formation, derived from known thermochemical data,[13] of 150, 165, and 139 kcal mol^{-1}, respectively. These results are fully compatible with a radical cation having the connectivity **3**, which should undergo three competing bond cleavages to afford the radical cations $HOCO^{\bullet\oplus}$, $CO_2^{\bullet\oplus}$, and $H_2O^{\bullet\oplus}$. For the isomers $\mathbf{1}^{\bullet\oplus}$ and $\mathbf{2}^{\bullet\oplus}$, on the other hand, rearrangement prior to dissociation has to be invoked to account for the formation of fragments with m/z 44 (loss of H_2O) and m/z 18 (loss of CO_2) from $\mathbf{1}^{\bullet\oplus}$ and m/z 45 (loss of $OH^{\bullet}$) from $\mathbf{2}^{\bullet\oplus}$. This is at odds with the result obtained for the $[H_2{}^{18}O/CO_2]^{\bullet\oplus}$ system (Fig. 1a); the CA mass spectrum clearly demonstrates the nonoccurrence of oxygen exchange or hydrogen migration. In addition, a comparison of Figure 1b with the CA spectrum of authentic $\mathbf{1}^{\bullet\oplus}$ [5] (in particular the loss of $OH^{\bullet}$ versus H_2O) rules out the generation of $\mathbf{1}^{\bullet\oplus}$ in the reaction of $H_2O^{\bullet\oplus}$ with CO_2. The ab initio MO calculations also support our conclusion: $\mathbf{2}^{\bullet\oplus}$ does not correspond to a minimum but rather to a transition structure (one negative eigenvalue), which is 93.2 kcal mol^{-1} higher in energy than $\mathbf{3}^{\bullet\oplus}$. The latter ion is 8.6 kcal mol^{-1} less stable than the two conformers of $\mathbf{1}^{\bullet\oplus}$ (which are practically isoenergetic, with $\mathbf{1s/a}^{\bullet\oplus}$ 0.1 kcal mol^{-1} more stable than $\mathbf{1s/s}^{\bullet\oplus}$).

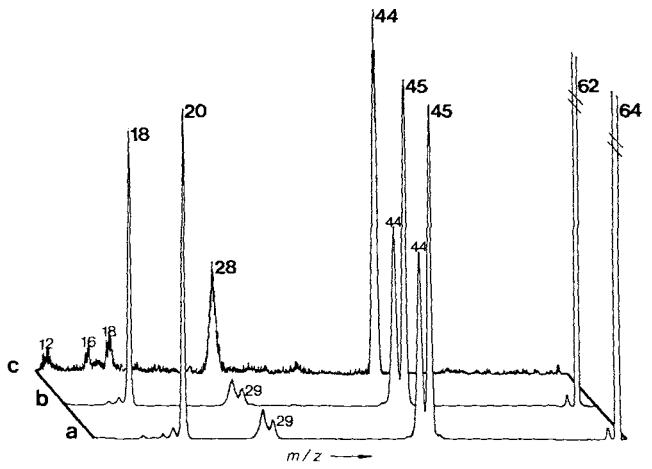

Fig. 1. a) CA mass spectrum (collision gas: helium) of $(H_2{}^{18}O/CO_2)^{\bullet\oplus}$. b) CA mass spectrum of $(H_2O/CO_2)^{\bullet\oplus}$ obtained under the same conditions. c) NR mass spectrum of $(H_2O/CO_2)^{\bullet\oplus}$ (xenon for neutralization, oxygen for reionization).

Obviously, under the prevailing reaction conditions, the Lewis acid-base type interaction so characteristic for the generation of many *neutral* van der Waals complexes (including **2**) cannot compete with the formation of a proton-bound radical cation complex $\mathbf{3}^{\bullet\oplus}$. The fact that $\mathbf{3}^{\bullet\oplus}$ is not capable of surmounting the high barrier leading to the most stable isomer $\mathbf{1}^{\bullet\oplus}$ is quite likely a result of collisional stabilization of the encounter complex formed under high-pressure conditions.

What happens if $\mathbf{3}^{\bullet\oplus}$ is subjected to an NRMS experiment? Is the unknown *neutral* van der Waals complex **3** formed? Or does $\mathbf{3}^{\bullet\oplus}$ undergo rearrangement/dissociation processes? The prospects of generating a stable, neutral, hydrogen-bridged complex **3** are not very promising. In view of the fact that the electron transfer operative in NRMS is a vertical process, large structural differences between the ionic and neutral counterparts will strongly diminish the Franck–Condon factors; to put the situation in a different perspective, a vibrationally "hot" species will be formed having a lifetime too short for detecting a recovery signal.[14] A comparison of the calculated data for $\mathbf{3}^{\bullet\oplus}$ and **3** (Table 2)

Table 2. Molecular data of **3** and $\mathbf{3}^{\bullet\oplus}$ calculated at the 6-31G** level [a] and charge distributions of $\mathbf{3}^{\bullet\oplus}$.

Bond length [Å]	**3**	$\mathbf{3}^{\bullet\oplus}$	Charge distribution of $\mathbf{3}^{\bullet\oplus}$	
O1-C2	1.141	1.122	O1	−0.31
C2-O3	1.146	1.164	C2	0.98
O3-H4	2.317	1.477	O3	−0.60
H4-O5	0.944	1.028	H4	0.56
O5-H6	0.943	0.975	O5	−0.11
			H6	0.48
Bond angle [°]	**3**	$\mathbf{3}^{\bullet\oplus}$		
O1-C2-O3	179.8	179.3		
C2-O3-H4	139.5	201.0		
O3-H4-O5	171.0	177.5		
H4-O5-H6	105.9	113.2		

[a] Molecular data of the remaining molecules discussed in the text: *H. Schwarz* et al., unpublished.

leaves little doubt that the chances of generating stable **3** by vertical reduction of $\mathbf{3}^{\bullet\oplus}$ are quite remote indeed. Whereas, for example, the O3–H4 bond length of $\mathbf{3}^{\bullet\oplus}$ (1.477 Å) is quite normal for this kind of proton-bridged structure,[15] the corresponding bond of the neutral analogue **3** is elongated to 2.317 Å. Another significant geometry change concerns the decrease of the H4–H5 bond length from 1.028 Å in $\mathbf{3}^{\bullet\oplus}$ to 0.944 Å in **3**. In fact, the NR mass spectrum of $\mathbf{3}^{\bullet\oplus}$ (Fig. 1c) shows not even a trace of a recovery signal. The spectrum is dominated by a signal at m/z 44, due to collisionally ionized CO_2 generated by dissociative neutralization ($\mathbf{3}^{\bullet\oplus} + e^{\ominus} \rightarrow CO_2 + H_2O$). The much lower intensity of the complementary $H_2O^{\bullet\oplus}$ signal (m/z 18) may reflect a lower collisional ionization cross-section of H_2O versus CO_2, due in part to a translational energy effect.[7g] We note that the absence of a recovery signal at m/z 62 in Figure 1c provides further evidence that the $CH_2O_3^{\bullet\oplus}$ species (m/z 62) formed from $H_2O^{\bullet\oplus}$ and CO_2 does *not* correspond to the radical cation of carbonic acid ($\mathbf{1}^{\bullet\oplus}$): authentic $\mathbf{1}^{\bullet\oplus}$, generated upon electron-impact ionization of **1**,[5] gives rise to an intense recovery signal and a strong peak at m/z 45 ($CO_2H^{\oplus}$).

In conclusion, the ion/molecule reactions occurring in the $(H_2O/CO_2)^{\bullet\oplus}$ system generate exclusively the proton-bridged radical cation $\mathbf{3}^{\bullet\oplus}$. The ionic form of the van der Waals complex **2** (which is formed in *neutral* mixtures of H_2O and CO_2[3,4]) is not generated nor is the radical cation of carbonic acid, $\mathbf{1}^{\bullet\oplus}$.[16]

Received: December 11, 1989 [Z 3679 IE]
German version: *Angew. Chem. 102* (1990) 431

CAS Registry numbers:
CO_2, 124-38-9; H_2O, 7732-18-5.

[1] a) D. M. Kern, *J. Chem. Educ. 37* (1960) 14; b) M. Eigen, G. G. Hammes, *Adv. Enzymol. Relat. Subj. Biochem. 25* (1964) 1; c) E. Magid, B. O. Turbeck, *Biochim. Biophys. Acta 165* (1968) 515; d) I. Zelitch, *Annu. Rev.*

Biochem. 44 (1975) 923; e) B. Jönsson, G. Karlström, H. Wennerström, B. Roos, *Chem. Phys. Lett. 41* (1976) 317; f) Y. Pocker, D. W. Bjorkquist, *J. Am. Chem. Soc. 99* (1977) 6537; g) K. M. Merz, Jr., R. Hofmann, M. J. S. Dewar, *ibid. 111* (1989) 5636; h) J. R. Damewood, Jr., R. A. Kumpf, W. C. F. Mühlbauer, *J. Phys. Chem. 93* (1989) 7640.

[2] C. R. Coon, A. D. King, Jr., *J. Am. Chem. Soc. 93* (1971) 1857.

[3] B. Jönsson, G. Karlström, H. Wennerström, *Chem. Phys. Lett. 30* (1975) 58.

[4] a) L. Fredin, B. Nelander, G. Ribbegard, *Chem. Scr. 7* (1975) 11; b) K. I. Peterson, W. Klemperer, *J. Chem. Phys. 80* (1984) 2439.

[5] J. K. Terlouw, C. B. Lebrilla, H. Schwarz, *Angew. Chem. 99* (1987) 352; *Angew. Chem. Int. Ed. Engl. 26* (1987) 354.

[6] a) B. Jönsson, G. Karlström, H. Wennerström, S. Forsén, B. Roos, J. Almlöf, *J. Am. Chem. Soc. 99* (1977) 4628; b) J. O. Williams, C. von Alsenoy, L. Schäfer, *J. Mol. Struct. (THEOCHEM) 76* (1981) 109; c) Y. Jean, F. Volatron, *Chem. Phys. 65* (1982) 107; d) C. McMichel Rohlfing, L. C. Allan, *J. Chem. Phys. 79* (1983) 4958; e) M. T. Nguyen, T.-K. Ha, *J. Am. Chem. Soc. 106* (1984) 599.

[7] Reviews a) J. K. Terlouw, P. C. Burgers, B. L. M. van Baar, T. Weiske, H. Schwarz, *Chimia 40* (1986) 357; b) C. Wesdemiotis, F. W. McLafferty, *Chem. Rev. 87* (1987) 485; c) J. K. Terlouw, H. Schwarz, *Angew. Chem. 99* (1987) 829; *Angew. Chem. Int. Ed. Engl. 26* (1987) 805; d) H. Schwarz, *Pure Appl. Chem. 61* (1989) 685; e) J. L. Holmes, *Adv. Mass Spectrom. 11* (1989) 53; f) J. K. Terlouw, *ibid. 11* (1989) 984; g) J. L. Holmes, *Mass Spectrom. Rev. 8* (1989) 513; h) F. W. McLafferty, *Science (Washington, DC)*, in press.

[8] On thermochemical grounds it is most likely that the reactants in the formation of $(H_2O/CO_2)^{\cdot\oplus}$ are $H_2O^{\cdot\oplus}$ and neutral CO_2 and *not* H_2O and $CO_2^{\cdot\oplus}$. This is based on the different ionization energies of H_2O (12.62 eV) and CO_2 (13.78 eV): K. Kimura, S. Katsumata, Y. Achiba, T. Yamazaki, S. Iwata: *Handbook of HeI Photoelectron Spectra of Fundamental Organic Molecules*, Japan Scientific Press, Tokyo 1981.

[9] For an extensive discussion of this *analytical* aspect of NRMS, see F. W. McLafferty, C. Wesdemiotis, *Org. Mass Spectrom. 24* (1989) 663.

[10] The MO calculations were performed using the CRAY-XMP version of *Pople*'s GAUSSIAN 82 and 86 series of programs. Stationary points (minima and transition structures) were characterized by analyzing the force constant matrix. Uncorrected zero-point vibrational energies (ZPVE) were included in the calculations of relative energies. The degree of spin contamination for the radical cations was estimated by calculating the $<S^2>$ values. For the species of interest the values were very close (< 10%) to the "pure" value $<S^2> = 0.75$.

[11] Reviews: a) F. W. McLafferty (Ed.): *Tandem Mass Spectrometry*, Wiley Interscience, New York 1983; b) K. L. Busch, G. L. Glish, S. A. McLuckey: *Mass Spectrometry/Mass Spectrometry: Techniques and Applications of Tandem Mass Spectrometry*, VCH Verlagsgesellschaft, Weinheim 1988.

[12] Review: K. Levsen, H. Schwarz, *Mass Spectrom. Rev. 2* (1983) 77.

[13] S. G. Lias, J. E. Bartmess, J. F. Liebman, J. L. Holmes, R. D. Levin, W. G. Mallard, *J. Phys. Chem. Ref. Data 17* (1988) Suppl. 1.

[14] Typical cases in which neutralization of an ion does *not* give rise to a detectable recovery signal of the otherwise stable neutral molecules are discussed in a) C. Wesdemiotis, R. Feng, E. R. Williams, F. W. McLafferty, *Org. Mass Spectrom. 21* (1986) 689; b) T. Drewello, *Dissertation* (D83), Technische Universität Berlin, 1989; c) H. Egsgaard, L. Carlsen, H. Florencio, T. Drewello, H. Schwarz, *Ber. Bunsen-Ges. Phys. Chem. 93* (1989) 76; d) M. C. Blanchette, J. L. Holmes, F. P. Lossing, *Org. Mass Spectrom. 22* (1987) 701.

[15] For many leading references, see N. Heinrich, H. Schwarz in J.-P. Maier (Ed.): *Ion and Cluster Spectroscopy and Structure*, Elsevier, Amsterdam 1989.

[16] For the formation of *structurally uncharacterized* $(H_2O/CO_2)^{\cdot\oplus}$ clusters in the reaction of $(CO_2)_x^{\cdot\oplus}$ clusters with H_2O, see G. Romanowski, K. P. Wanczek, *Int. J. Mass Spectrom. Ion Processes 95* (1989) 223.

Vanadium Tetrafluoride**

By *Stephan Becker* and *Bernd G. Müller**

The tetrafluorides of numerous transition metals have long been known, but little information is available on their structure and actual composition (e.g. $OH^{\ominus}$ or $O^{2\ominus}$ instead of $F^{\ominus}$).

In some cases (e.g., PdF_4[1]), neutron diffraction studies of powders have led to structural proposals. However, structure determinations of single crystals have been carried out for only a few compounds (e.g., ZrF_4[2] and NbF_4[3]). Whereas several tetrafluorides MF_4 could be assigned to known structure types on the basis of powder data (e.g., the tetrafluorides of M = Pt, Rh, Ir are isotypes of the PdF_4 structure and those of M = Hf, Ce, Th of the ZrF_4 structure), such information is completely lacking for the corresponding compounds of the 3d metals (with the exception of MnF_4[4]). It was expected that these compounds—like MnF_4—might form unique structures, as already indicated by the literature data on the unit cell of VF_4 (according to Ref. [5], hexagonal with $a = 5.38$, $c = 5.16$ Å, according to Ref. [6], orthorhombic with $a = 5.33$, $b = 5.16$, $c = 9.35$ Å, no further structural details).

Preparative difficulties—for example, the tendency to disproportionate (e.g., with M = V, Cr, Ru, Re) or the ready thermal decomposition to lower-valent compounds and elemental fluorine (e.g., with M = Pd, Rh, Ni)—have been the primary factors preventing the growth of suitable single crystals.

Preparation of VF_4, however, is achieved relatively "simply" by reaction of vanadium powder (99.99%, under argon) with elemental fluorine in a Monel autoclave. Use of a slight excess of F_2 ($V:F \approx 1:4.1$) should influence the disproportionation equilibrium ($2\,VF_4 \rightleftarrows VF_3 + VF_5$) by leading to formation of small amounts of volatile VF_5; in addition, formation of VOF_3 should result in removal of traces of oxygen).

In this way, bright, light-green, coarse, relatively moisture-sensitive crystals were obtained after a reaction time (annealing in a temperature gradient: $T_1 = 280 \rightarrow T_2 = 180\,^{\circ}C$) of about ten weeks. Under dry argon or perfluoroalkanes, the crystals may be handled without decomposition.

Careful analysis of long-exposure films (Weissenberg and precession photographs) unequivocally confirmed monoclinic symmetry. To calculate the interatomic distances listed in Table 1, the lattice constants derived from Guinier–de Wolff photographs were used. In addition, the motives of mutual adjunction[8] and the coordination number are given; all F–V–F angles within an octahedron lie very close to 90 or 180°.

Table 1. Motives of mutual adjunction, distances [pm], and coordination numbers (C.N.).

	F1	F2	C.N.
V	2/1 169.6	2 + 2/2 191.8 + 192.3	6
C.N.	1	2	

In order to show clearly the relationship with the SnF_4 structure,[8, 9] a monoclinic unit cell for VF_4 in the arrangement $P2_1/n$ of space group No. 14 (with $a = 5.381$, $b = 5.170$, $c = 5.340$ Å, $\beta = 59.74°$) is drawn instead of one in the usual $P2_1/c$ arrangement in the tetragonal unit cell of SnF_4 in Figure 1. The relationship between the two arrangements is given by the following transformation matrix:

$$P2_1/c \rightarrow P2_1/n: \quad \begin{pmatrix} 1 & 0 & 0 \\ 0 & 1 & 0 \\ 1 & 0 & 1 \end{pmatrix}$$

[*] Dr. B. G. Müller, Dipl.-Chem. S. Becker
Institut für Anorganische und Analytische Chemie I
Heinrich-Buff-Ring 58, D-6300 Giessen (FRG)

[**] This work was supported by the Deutsche Forschungsgemeinschaft. We thank Prof. Dr. *Rudolf Hoppe* for his personal and material support.

The relationship of the two structures is thereby directly shown. Both structures contain layers of corner-sharing $[VF_6]$ octahedra in accordance with $^2_\infty[VF_{4/2}F_{2/1}]$ with two *trans* $F^\ominus$ ions; the layers are also stacked in the same way. The crucial difference between the two structure types is that the $[VF_6]$ octahedra within a layer are tilted toward one another; the bond angle of the fluorine bridge V-F2-V is 150.7° (SnF_4: 180°).

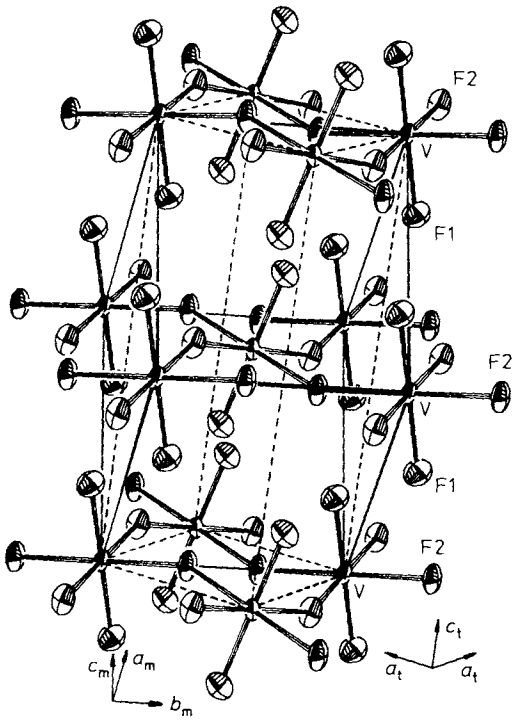

Fig. 1. Unit cell of SnF_4 (dashed line) and VF_4 (solid line) [7].

Comparison of the interatomic distances of the three isotype or structurally related compounds MF_4 (M = Sn, Nb, V) reveals that, for VF_4, the difference between the distances d(M-terminal $F^\ominus$) and d(M-bridging $F^\ominus$) is more pronounced than for SnF_4 or NbF_4[9] (Table 2).

Table 2. Comparison of the interatomic distances in four compounds of the type MF_4.

M	V	Nb	Sn	Mn
d_1 (M-F)$_{\text{term.}}$	1.696	1.859	1.861	1.697
d_2 (M-F)$_{\text{bridging}}$	1.918	2.042	2.024	1.948
d_1/d_2	0.884	0.919	0.910	0.871

The reason for this is unclear, since, even for MnF_4—albeit with *cis*-oriented terminal $F^\ominus$ and $d = 0.871$—a comparable quotient is found.

Susceptibility measurements on several samples of VF_4 crystals between 4.2 and 251 K (μ_{eff}(251 K) = 1.43 B.M.) provided evidence for the absence of oxygen (VOF_3 is diamagnetic) and confirmed the complicated collective magnetic interactions;[5] the determination of the magnetic structure by neutron diffraction is in progress.

Experimental Procedure

Vanadium powder (500 mg, Ventron) was placed in a Monel autoclave under inert gas (Braun glovebox). At −196 °C, 0.8 mL of F_2 was condensed into the autoclave, which was then placed in an oven preheated to 280 °C and kept for about ten weeks at this temperature. After stepwise cooling (25 °C per day), the autoclave was opened under inert gas (Ar, glovebox) and the VF_4 thus obtained was transferred to glass ampoules for further analysis.

Received: December 4, 1989;
supplemented: January 29, 1990 [Z 3665 IE]
German version: *Angew. Chem. 102* (1990) 426

CAS Registry numbers:
V, 7440-62-2; F, 7782-41-4; VF_4, 10049-16-8.

[1] A. F. Wright, B. E. F. Fender, N. Bartlett, K. Leorg, *Inorg. Chem. 17* (1978) 748.
[2] R. D. Burbank, F. N. Bensey, *USA E.C. Rep.* (1956) K-1280.
[3] H. Schäfer, H. G. von Schnering, K. J. Niehues, H. G. Nieder-Vahrenholz, *J. Less-Common Met. 9* (1965) 95.
[4] B. G. Müller, M. Serafin, *Z. Naturforsch. B42* (1987) 1102.
[5] R. G. Cavell, H. C. Clark, *J. Chem. Soc. 1962*, 2692.
[6] A. J. Edwards, P. Taylor, *Chem. Commun. 1970*, 1474.
[7] $P2_1/c$; $a = 5.340(3)$, $b = 5.170(2)$, $c = 5.381(3)$ Å, $\beta = 119.89(0)$, $Z = 2$; Phillips PW 1100 AgK_α four-circle diffractometer; 528 symmetry-independent reflections, $R = 0.060$, $R_w = 0.045$. Further details of the crystal structure investigation may be obtained from the Fachinformationszentrum Karlsruhe, Gesellschaft für wissenschaftlich-technische Information mbH, D-7514 Eggenstein-Leopoldshafen 2 (FRG), on quoting the depository number CSD-54336, the names of the authors, and the journal citation.
[8] R. Hoppe, *Z. Kristallogr. 150* (1979) 23.
[9] H. G. von Schnering, *Festkörperkolloquium Kiel*, März 1987; personal communication.

Intramolecular Interconversion of *syn*- and *anti*-Tricarbonyl(1-ethoxy-1,2-dihydrocyclobutabenzene)chromium. Trapping of the *ortho*-Quinodimethane Intermediate**

By *Ernst Peter Kündig,* Gérald Bernardinelli, James Leresche,* and *Patrick Romanens*

1,2-Dihydrocyclobutabenzenes are convenient and widely used precursors of the highly reactive *ortho*-quinodimethanes, which are synthetically important dienes in Diels-Alder reactions.[1, 2] Although syntheses of π-cyclobutabenzene-transition metal complexes have been reported and reactions of the complexed cyclobutabenzene (nucleophilic addition, lithiation) have been the subject of several studies,[3 – 5] the effect of coordination on the transformation cyclobutabenzene/*ortho*-quinodimethane has thus far remained unexplored. We report here on the thermal ring opening of complexed 1-ethoxy-1,2-dihydrocyclobutabenzene **1**, and on a [4 + 2]-cycloaddition of the postulated intermediary *ortho*-quinodimethane complex.

We chose **1** in this study for the following reasons: firstly, reversible electrocyclic ring-opening of 1-alkoxy-substituted 1,2-dihydrocyclobutabenzenes occurs at moderate temperatures (80–110 °C)[6] and, secondly, the $Cr(CO)_3$ complexes of **1** are readily accessible by exchange of the arene ligand of tricarbonyl(naphthalene)chromium; the 2:3 mixture of diastereomers (*syn*-**2** and *anti*-**2**) that is formed[7] can be readily separated by flash chromatography. The benzyl protons in benzocycloalkene complexes readily undergo stereoselective

[*] Prof. Dr. E. P. Kündig, J. Leresche, P. Romanens
Department de Chimie Organique, Université de Genève
30 Quai Ernest Ansermet, CH-1211 Genève-4 (Switzerland)

Dr. G. Bernardinelli
Laboratoire de Crystallographie Université de Genève
24 Quai Ernest Ansermet, CH-1211 Genevé-4 (Switzerland)

[**] This work was supported by the Swiss National Science Foundation.

base-catalyzed hydrogen/deuterium exchange;[8] this enables assignment of the structures of *syn*-**2** and *anti*-**2**. Upon addition of a catalytic amount of *t*BuOK to *syn*-**2** or to *anti*-**2** in [D_6]DMSO, the ^{1}H-NMR signal of one of the two methylene protons disappeared, and monodeuteriated complexes were formed. These signals were assigned to the *anti*-H atoms. The tertiary benzylic C–H bond remained unaffected in both diastereomers. The vicinal coupling constant of the remaining benzyl protons is 4 Hz in *anti*-**2** (J_{cis}) and 1.5 Hz in *syn*-**2** (J_{trans}), in accord with data on uncomplexed 1-substituted 1,2-dihydrocyclobutabenes.[9] This assignment was confirmed by an X-ray analysis of *syn*-**2** (Fig. 1).

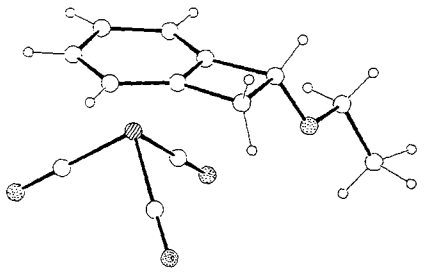

Fig. 1. Structure of *syn*-tricarbonyl(1-ethoxy-1,2-dihydrocyclobutabenzene)-chromium *syn*-**2** in the crystal; ◎ = Cr, ◎ = O [10].

On heating in benzene, *syn*-**2** and *anti*-**2** interconvert. The reaction can be conveniently followed by ^{1}H NMR in a sealed tube. Clean first-order kinetics are observed for the reversible reaction in the temperature range of 130–180 °C (Fig. 2).

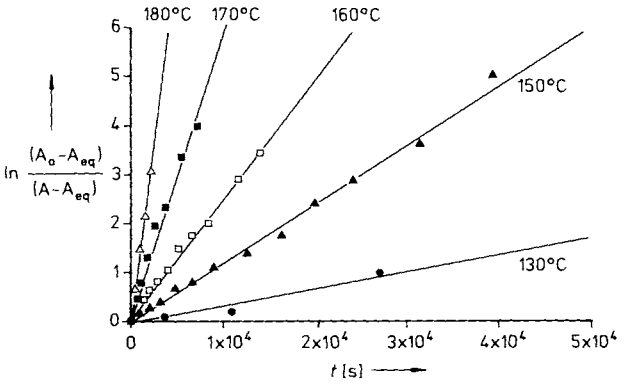

Fig. 2. First order kinetic plots for the interconversion of *syn*-**2** and *anti*-**2**, as measured by growth and decay of the 1H-NMR signals of the methyl protons.

Attempts to detect an intermediate failed. The ^{1}H-NMR spectrum at 150 °C merely showed the resonances of *syn*-**2** and *anti*-**2**. The activation parameters calculated from the data listed in Table 1 are: $\Delta H^{\neq} = 29.9 \pm 1.0$ kcal mol^{-1} and $\Delta S^{\neq} = -8.5 \pm 3$ cal mol^{-1} K^{-1}.[11] For comparison, the values calculated from the data obtained by *Sammes* et al. for the racemization of 1-methoxy-1,2-dihydrocyclobutabenzene are $\Delta H^{\neq} = 30.7$ kcal mol^{-1} and $\Delta S^{\neq} = 3.0$ cal mol^{-1} K^{-1}.[6]

At 130 °C, the reaction of **2** is about 100 times slower than that of non-complexed 1-methoxy-1,2-dihydrocyclobutabenzene ($k = 1.14 \times 10^{-3}$ s^{-1}).[6] Comparison of the activation parameters show the activation entropy rather than the

Table 1. Rate constants for the reaction *syn*-**2** ⇌ *anti*-**2**. A first order reversible reaction was assumed by using the equation $\ln (A_o\text{-}A_{eq})/(A\text{–}A_{eq}) = (k_1 + k_2)\,t$. The correlation was in the range 0.992 to 0.999 for all plots.

T [°C]	k_2 [s]	$t_{1/2}$ [h]	k_1 [s]	$t_{1/2}$ [h]
130	0.78×10^{-5}	25	1.0×10^{-5}	19
140	2.1×10^{-5}	13	2.8×10^{-5}	7
150	5.2×10^{-5}	4	6.8×10^{-5}	2.8
160	10.0×10^{-5}	2	13.3×10^{-5}	1.43
170	23.0×10^{-5}	0.8	30.3×10^{-5}	0.63
180	56.0×10^{-5}	0.33	74.4×10^{-5}	0.26

enthalpy to be the source of this rate difference. If we assume an *o*-quinodimethane-$Cr(CO)_3$ complex as intermediate, the activation entropy difference may indicate a more ordered transition state.[12] An 18-electron configuration of Cr^0 would be achieved if the metal coordinates to the cyclic diene as well as to one of the exocyclic double bonds of the *o*-quinodimethane. This presumably would increase the barrier of rotation around the metal ligand bond and could be the cause of the entropy difference (loss of a degree of freedom). An intramolecular process for the interconversion of *syn*-**2** and *anti*-**2** also concurs with the observation that no arene exchange with the solvent (C_6D_6) takes place in the temperature range investigated. This would have been expected if the $Cr(CO)_3$ group were coordinated only to the diene portion of the *o*-quinodimethane or if the mechanism of interchange involved metal-arene bond dissociation. Similar bonding situations are known in an *o*-quinodimethane complex[13] and a methylene/cyclohexadiene complex[14] with tricarbonylchromium as well as in η^6-fulvene and η^6-azulene complexes.[15]

Experimental evidence for the proposed *o*-quinodimethane intermediate was obtained via a [4 + 2]-cycloaddition reaction. Slow addition of several olefin dienophiles to the equilibrating mixture of *syn*- and *anti*-**2** resulted in decomposition of the complex, possibly due to a CO/olefin exchange. We therefore turned to *trans*-1,2-bis(trimethylsilyl)ethene,[16] which we considered to be too bulky to interact readily with the metal. Thermolysis of *syn*-**2** in this dienophile (solvent and reactant) at 160 °C for 6 h resulted in a 56% conversion of **2** into a 17:1 mixture of complexes **4** and **5**.

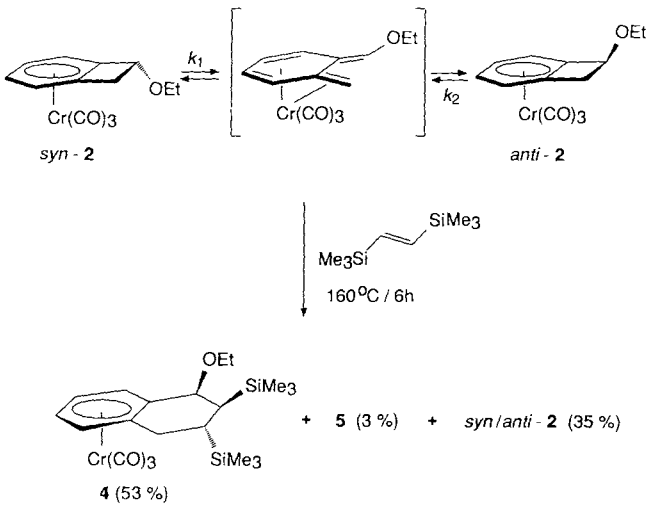

35% of **2** was recovered from the reaction as a *syn*/*anti* mixture.[17] Structural assignment of complex **4** was based

on NMR spectral analysis and an X-ray diffraction study (Fig. 3). The X-ray structure of complex **4** reveals a boat conformation of the saturated ring of the tetralin complex with a *cis* arrangement of the C(1) ethoxy and the C(2) trimethylsilyl groups. The structure of **5**, a stereoisomer of **4**, has not yet been assigned unequivocally.

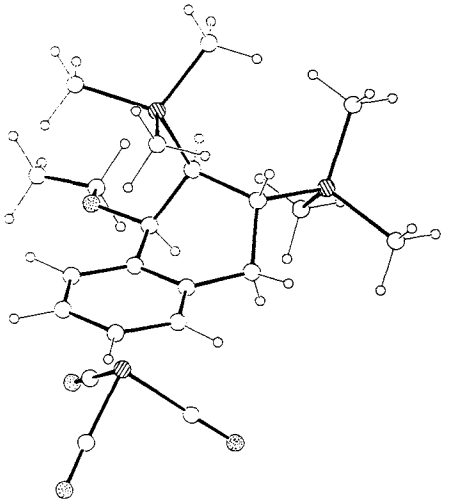

Fig.3. Structure of the adduct **4** in the crystal; ⊗ = Si [10].

This first study of a transition metal bound 1.2-dihydrocyclobutabenzene/*o*-quinodimethane reaction has focused on mechanistic aspects. We are presently extending these studies to more synthetically oriented projects. As the metal completely shields one face of the *o*-quinodimethane intermediate, high stereoselectivity can be expected in Diels-Alder reactions and this will be of particular import in reactions with chiral complexes. The present, severe limitation of useful dienophiles may be overcome by judicious choice of benzocyclobutene complexes with other organometallic fragments, by using milder ring opening reactions and/or different routes to π-complexed *ortho*-quinodimethane complexes.

Experimental

The mixture of diastereomers *syn*-**2** and *anti*-**2** obtained in 70% yield from the arene exchange in tricarbonyl(naphthalene)chromium was separated by flash chromatography using hexane/ether 4/1 (*syn*-**2**: $R_f = 0.13$; *anti*-**2**: $R_f = 0.19$).

syn-**2**: M.p.(hexane): 59–60 °C. IR (hexane, ν(CO)): $\tilde{\nu}$ [cm^{-1}]): 1984 (s), 1918 (s). ^{1}H NMR (360 MHz, C_6D_6): $\delta = 1.18$ (t, 3H, $J = 7$ Hz; $-CH_3$), 2.60 (dd, 1H, $J = 5.5$, 14 Hz; H_{anti}-C(2)), 2.80 (dd, 1H, $J = 1.5$, 14 Hz; H_{syn}-C(2)), 3.18–3.46 (m, 2H; OCH_2CH_3) 4.12 (t, 1H, $J = 6$ Hz; $H_{arom.}$), 4.20 (dd, 1H, $J = 2$, 5.5 Hz; *H*-C(1), 4.46 (t, 1H, $J = 6$ Hz; $H_{arom.}$), 4.52 (d, 1H, $J = 6$ Hz; $H_{arom.}$), 4.83 (d, 1H, $J = 6$ Hz; $H_{arom.}$). Correct elemental analysis.

anti-**2**: M.p.(hexane): 71.5–72.5 °C. IR (hexane, ν(CO) [cm^{-1}]): 1984 (s), 1918 (s). ^{1}H NMR (360 MHz, C_6D_6): $\delta = 1.02$ (t, 3H, $J = 7$ Hz; CH_3), 2.59 (dd, 1H, $J = 1.7$, 14 Hz; H_{anti}-C(2)), 2.98 (dd, 1H, $J = 4$, 14 Hz; H_{syn}-C(2)), 3.08–3.24 (m, 2H; OCH_2CH_3), 4.16 (t, 1H, $J = 6$ Hz; $H_{arom.}$), 4.33 (t, 1H, $J = 6$ Hz, $H_{arom.}$), 4.60 (d, 1H, $J = 6$ Hz; $H_{arom.}$), 4.69 (dd, 1H, $J = 1.7$, 4 Hz; H-C(1)), 5.02 (d, 1H, $J = 6$ Hz; $H_{arom.}$). Correct elemental analysis.

4: A degassed solution of complex *syn*-**2** (0.200 g, 0.70 mmol) in *trans*-bis(trimethylsilyl)ethene was stirred at 160 °C for 6 h in a closed tube. After cooling to 20 °C, the excess olefin was recovered by short path distillation, the residue was taken up in ether, filtered, and evaporated to dryness. Flash chromatography on silica (hexane/ether = 4/1) furnished **4** (170 mg, 53%, $R_f = 0.48$) followed by **5** (10 mg, 3%, $R_f = 0.35$) and *syn*/*anti*-**2** (70 mg, 35%).

M.p.(EtOH/H_2O): 78–80 °C. IR (hexane, ν((CO):$\tilde{\nu}$ [cm^{-1}]): 1970 (s), 1900(s). ^{1}H NMR (200 MHz, C_6D_6): $\delta = -0.20$ (s, 9H, $Si(CH_3)_3$), 0.00 (s, 9H, $Si(CH_3)_3$), 0.80–0.94 (m, 1H, H–C(3)), 1.10 (t, 3H, $J = 6.9$ Hz; CH_3CH_2O), 1.55 (dd, 1H, $J = 4$, 6.7 Hz, H–C(2)), 2.00 (dd, 1H, $J = 7.5$, 15.6 Hz; H_{anti}-C(4)), 2.55 (dd, 1H, $J = 13$, 15.6 Hz; H_{syn}–C(4)), 3.42–3.58 (m, 2H, OCH_2CH_3), 4.44 (d, 1H, $J = 6.7$ Hz; H–C(1)), 4.49–4.58 (m, 2H, H–C(6,7)), 4.70 (d, 1H, $J = 5.5$ Hz; H–C(5)), 5.55 (d, 1H, $J = 5.7$ Hz; H–C(8)). ^{13}C NMR (50 MHz, C_6D_6): $\delta = 234.20$, 112.74, 110.14, 93.23, 92.29, 90.75, 90.56, 77.71, 66.47, 28.16, 27.71, 18.65, 15.58. Correct elemental analysis.

Received: December 11, 1989 [Z 3677 IE]
German version: *Angew. Chem. 102* (1990) 421

CAS Registry numbers:
1, 125685-98-5; *anti*-**2**, 99571-34-3; *syn*-**2**, 99537-80-1; **4**, 125685-99-6; **5**, 125761-44-6; tricarbonyl(napthalene)chromium, 12110-37-1; *trans*-bis(trimethylsilyl)ethene, 18178-59-1.

[1] J. L. Charlton, M. J. Alauddin, *Tetrahedron 40* (1987) 2873.
[2] W. Oppolzer, *Synthesis 1978*, 793.
[3] E. P. Kündig, *Pure Appl. Chem. 57* (1985) 1855.
[4] C. Elschenbroich, J. Koch, S. Schneider, B. Sprangenberg, P. Schiess, *J. Organomet. Chem. 317* (1986) 41.
[5] H. G. Wey, H. Butenschön, *J. Organomet. Chem. 350* (1988) C8.
[6] B. J. Arnold, P. G. Sammes, T. W. Wallace, *J. Chem. Soc. Perkin Trans 1 1974*, 409.
[7] E. P. Kündig, C. Perret. S. Spichiger, G. Bernardinelli, *J. Organomet. Chem. 286* (1985) 183. All reactions in this study were carried out with racemic **1**. The arene exchange reaction yields two diastereomeric pairs of complexes. For the sake of brevity, only one *syn*- and one *anti*-enantiomer are schown in the equation and in the figures.
[8] W. S. Trahanovsky, R. J. Card, *J. Am. Chem. Soc. 94* (1972) 2897.
[9] W. A. Bubb, S. Sternhell, *Aust. J. Chem. 29* (1976) 1685.
[10] Crystal data for *syn*-**2**: A suitable crystal of average dimensions $0.25 \times 0.25 \times 0.30$ mm was sealed in a Lindemann capillary under Ar. The lattice parameters and intensities were measured at room temperature on a Philips PW 1100 diffractometer with a graphite monochromated $Mo_{K\alpha}$ radiation. Orthorhombic, space group $P2_12_12_1$. $a = 9.938(2)$, $b = 10.296(3)$, $c = 12.330(2)$ Å. $V = 1261.6(5)$ Å^3. $Z = 4$, $F_{calcd} = 1.496$ g cm^{-3}, $\mu(Mo_{K\alpha}) = 0.886$ mm^{-1} $I \approx 295$ K. $F(OOO) = 584$. 1584 Friedel pairs were recorded (ω-2θ scan) of which 2002 had $|F_o| > 3\sigma(F_o)$ and $|F_o| > 4$, The structure was solved by direct methods (Multan 80) and refined by full matrix least squares methods (XRAY 76). The refinement of the absolute structure parameter (x = 0.51(4))[18] clearly indicates that the sample is an inversion twin with 50% of each enantiomer. The final *R* factor, based on 2002 observed reflexions, was 0.032. $R_w = 0.035$. – Crystal data for **4**: A suitable crystal of average dimensions $0.05 \times 0.20 \times 0.35$ mm was sealed in a Lindemann capillary under Ar. The lattice parameters and intensities were measured at room temperature on a Philips PW 1100 diffractometer with a graphite monochromated $Mo_{K\alpha}$ radiation. Triclinic, space group $P\bar{1}$. $a = 8.494(1)$, $b = 11.331(1)$, $c = 14.513(2)$ Å, $\alpha = 78.57(2)$, $\beta = 74.40(2)$, $\gamma = 68.26(3)°$. $V = 1233.7(4)$ Å^3. $Z = 2$, $F_{calcd} = 1.23$ g cm^{-3}, $\mu(Mo_{K\alpha}) = 0.568$ mm^{-1}. $F(000) = 484.3014$ independent reflections were recorded (ω-2θ scan), of which 1864 had $|F_o| > 4\sigma(F_o)$. The structure was solved by direct methods (Multan 87) and refined by full matrix least squares methods (XTAL 2.4). The final *R* factor, based on 1864 observed reflexions, was 0.072. $R_w = 0.044$. Further details of the crystal structure investigations are available on request from the Director of the Cambridge Crystallographic Data Center, University Chemical Laboratory, Lensfield Road, Cambridge CB2 1EW (UK).
[11] The error limits for the activation parameters represent 90% confidence limits in the rate constants.
[12] While an *o*-quinodimethane intermediate is a plausible proposal in view of the structural analogy of isolated complexes [13–15], other intermediates, e.g. an η^6-arene diradical complex, cannot be excluded as yet. Likewise, the entropy effect could result from a transition state with more (zwitter)-ionic character.
[13] M. Yalpani, R. Benn, R. Goddard, G. Wilke, *J. Organomet. Chem. 240* (1982) 49.
[14] J. Blagg, S. G. Davies, G. L. Goodfellow, K. H. Sutton, *J. Chem. Soc. Chem. Commun. 1986*, 1283.
[15] a) F. Edelmann, S. Töfke, U. Behrens, *J. Organomet. Chem. 309* (1986) 87; b) S. Töfke, U. Behrens, *Angew. Chem. 99* (1987) 134; *Angew. Chem. Int. Ed. Engl. 26* (1987) 147; c) J. Bandy, V. S. B. Mtetwa, K. Prout, J. C. Green, C. E. Davies, M. L. H. Green, M. J. Hazel, A. Izquierdo, J. J. Martin-Polo, *J. Chem. Soc. Dalton Trans 1985* 2037.
[16] J. Dunoguès, R. Calas, N. Ardoin, C. Biran, P. Ladouyade, *J. Organomet. Chem. 32* (1971) C31.
[17] Although no kinetic study has been carried out, samples removed in the course of the trapping reaction, and analyzed by HPLC, indicate the rate of formation of **4** to be considerably slower than the interchange of *syn*- and *anti*-**2**. The rate of the latter appears to be roughly the same in the ethene **7** medium as in benzene.
[18] G. Bernardinelli, H. D. Flack, *Acta Crystallogr. Sect. A 41* (1985) 500.

[PhLiNCH$_2$CH$_2$NLiPh] · 3HMPA, a Monomeric Dilithiumethylenediamide Complex with N_2Li_2 Double Bridging: Synthesis, Crystal Structure, and Model MO Calculations**

By *David R. Armstrong, Donald Barr, Alan T. Brooker, William Clegg, Karina Gregory, Susan M. Hodgson, Ronald Snaith,** and *Dominic S. Wright*

Dedicated to Professor Paul von Ragué Schleyer on the occasion of his 60th birthday

We have recently begun to investigate the lithiation of amines having heteroatom groups (e.g., Me_2N,[1a] MeO,[1b] >C=S[1c]) nearby (α,β,γ) their NH centers. The aim has been to probe the inter- and intra-molecular involvements that these heteroatoms may have with the *N*-attached Li in the resulting lithium amide structure.[2] For example, in the structure of [{PhCH(CH$_2$OMe)}$_2$NLi]$_2$ the MeO-side arms merely add to the coordination sphere of the Li centers in their (NLi)$_2$ ring.[1b] In contrast, in the dilithiated thiourea [PhNLiC(=NPh)SLi·2HMPA]$_2$ the >C=S moiety becomes much more crucially involved: the monomeric units contain both N(μ_2-Li)N and S–Li bonds, these monomers then associating through N → Li coordinations.[1c] As part of this study, it was of interest to dilithiate a diamine, i.e. a precursor whose heteroatom group is a further N(H). In particular, it seemed likely that the two $N^{\delta\ominus}$ centers generated after dilithiation would become mutually involved with the two $Li^{\delta\oplus}$ centers. This would be the di-heteroatom equivalent of the double bridged C_2Li_2 "ion-triplet" structures shown, through the many studies (theoretical and experimental) of *Schleyer* et al.[2a, 3–5] and *Streitwieser* et al.,[6] to be frequently adopted by dilithiated hydrocarbons.

Here we describe the results of dilithiating *N,N'*-diphenylethylenediamine, PhHNCH$_2$CH$_2$NHPh, in the presence of hexamethylphosphoric acid triamide [HMPA, O=P(NMe$_2$)$_3$], which leads to the dilithium diamide **1**. The crystal structure of the product, **1**, reveals a monomeric binuclear complex containing the anticipated N_2Li_2 double bridging and, in addition, a Li(μ_2-O)Li bridge provided by one of the HMPA ligands.

[PhLiNCH$_2$CH$_2$NLiPh] · 3HMPA **1**

Prior to the experimental work, ab initio MO calculations (at the 6-31G basis set level) were performed on the model species ethylenediamine as well as on the *N*-mono and *N,N'*-dilithiated derivatives. The minimum energy optimized structures (confirmed by frequency analysis using the complete harmonic force constants) are shown in Figure 1; these structures were freely optimized, without symmetry constraints. The amine itself adopts a *gauche*-like structure, with the –NH$_2$ and –CH$_2$ groups being slightly twisted relative to each other (Fig. 1a). In the mono-lithium derivative, this orientation persists, but the key finding is that the Li involves itself with *both* N centers (Fig. 1b). Such involvement is asymmetric, with a short (H)$N^{\delta\ominus}$–$Li^{\delta\oplus}$ distance of 1.784 Å and a much longer (H$_2$)N–$Li^{\delta\oplus}$ one of 2.032 Å. The optimized structure of HLiNCH$_2$CH$_2$NLiH (Fig. 1c) confirms the anticipated N_2Li_2 double bridge arrangement. The two

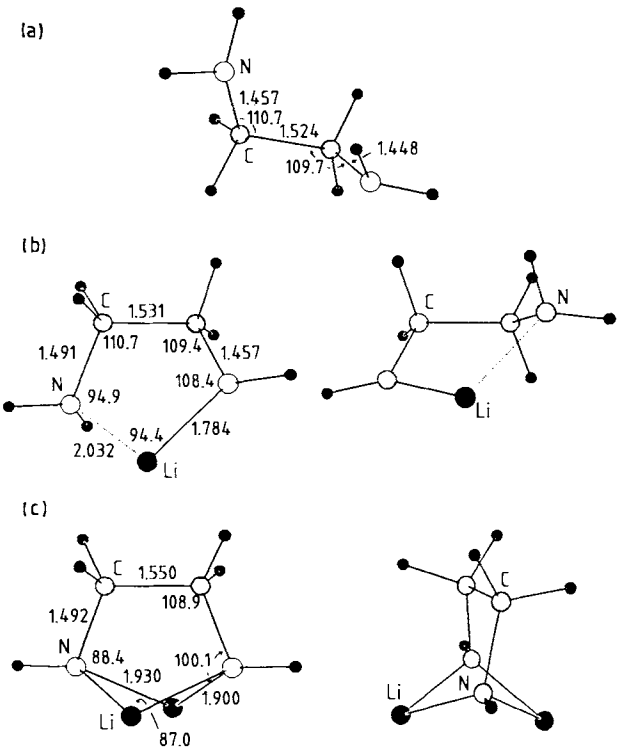

Fig. 1. Bond distances [Å] and angles [°] of the ab initio (6-31G) optimized structures of a) H$_2$NCH$_2$CH$_2$NH$_2$, b) HNLiCH$_2$CH$_2$NH$_2$, and c) HNLiCH$_2$CH$_2$NHLi.

$Li^{\oplus}$ centers sit on either side of the HNCH$_2$CH$_2$NH framework, so forming an Li_2N_2 "butterfly". However, this situation is again asymmetric, with each $Li^{\oplus}$ having distances to two N centers of 1.900 and 1.930 Å. The asymmetry seems to be caused by the continued slight twist of the CH$_2$ groups relative to each other: when C_{2v} symmetry is imposed, making the CH$_2$ groups equivalent (i.e., eclipsed), the resulting structure, with all N–Li distances equal (1.906 Å), is slightly less stable (by 1.2 kcal mol^{-1}).

In the experimental study, PhHNCH$_2$CH$_2$NHPh in hexane/toluene was allowed to react with two equivalents of *n*-butyllithium in the presence of just two equivalents of HMPA. In fact, the tris-complexed dilithium diamide, **1**, was isolated (see *Experimental*). The molecular structure of **1**, determined by X-ray diffraction,[7] is shown in Figure 2. As predicted by theory, the two $Li^{\oplus}$ ions are positioned on opposite sides of the NCH$_2$CH$_2$N dianion framework. The four N–Li distances fall into two sets, each Li having a short and a long bond to two N centers [Li(1)–N(1) 2.055(8), Li(1)–N(2) 2.137(7) Å; Li(2)–N(1) 2.146(9), Li(2)–N(2) 2.088(8) Å]. Two HMPA ligands are attached terminally to the Li atoms [Li(1)–O(2) 1.888(6), Li(2)–O(3) 1.868(7) Å]. The third HMPA ligand bridges these metal atoms so that

[*] Dr. R. Snaith, Dr. D. Barr, Dr. D. S. Wright, A. T. Brooker
University Chemical Laboratory
Lensfield Road,
Cambridge, CB2 1EW (UK)
Dr. D. R. Armstrong
Department of Pure and Applied Chemistry
University of Strathclyde
Glasgow, G1 1XL (UK)
Dr. W. Clegg, S. M. Hodgson
Department of Chemistry, The University,
Newcastle upon Tyne, NE1 7RU (UK)
K. Gregory
Institut für Organische Chemie der Universität Erlangen-Nürnberg
D-8520 Erlangen (FRG)

[**] This work was supported by the UK Science and Engineering Research Council, by Gonville and Caius College, Cambridge (Research Fellowship for *D. S. W.*) and by Ciba-Geigy (Award for Collaboration in Europe scheme).

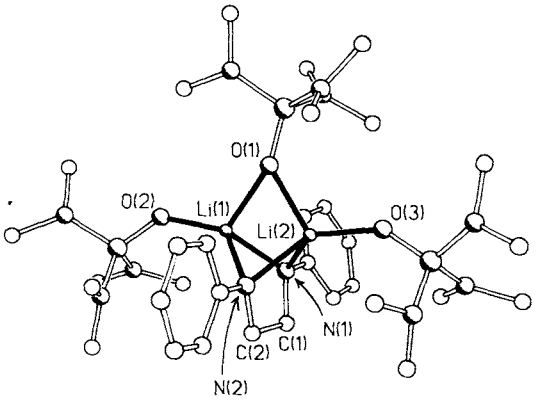

Fig. 2. Molecular structure of **1** [7].

the core of the molecule can be viewed as three co-fused "butterflies" (one NLi_2N, two OLi_2N frameworks). The bridging O–Li distances are also unequal, the shorter one involving Li(2) [Li(1)–O(1) 2.068(9), Li(2)–O(1) 1.994(7) Å]; perhaps significantly, the summed or mean N–Li distances are rather longer for Li(2) than for Li(1).

The structure of **1** (to our knowledge, the first dilithiated diamide to be so characterized) fits clearly into the pattern established earlier for dilithiated hydrocarbons. In particular, numerous studies have shown a marked preference for double bridged C_2Li_2 arrangements, e.g., by theory for species such as dilithiopropene[3, 5, 6] and by crystallography for species such as *o,o'*-dilithiobiphenyl.[2a, 4, 5] The explanation[6] of such a preference is based on simple electrostatics: a doubly bridged $Li^{\oplus}(C^{\ominus}\cdots C^{\ominus})Li^{\oplus}$ "ion triplet", having four attractive $Li^{\oplus}\cdots C^{\ominus}$ terms and only two repulsive terms ($Li^{\oplus}\cdots Li^{\oplus}$, $C^{\ominus}\cdots C^{\ominus}$), will have electrostatic stability except when one set of charges is quite far from the other (specifically, when $R_{--}/R_{++} < 0.14$ or > 6.9, R being the charge-charge distance). In **1**, the core can be considered as a collection of three ion-triplets, one $Li^{\oplus}(N^{\ominus}\cdots N^{\ominus})Li^{\oplus}$ and two $Li^{\oplus}(N^{\ominus}\cdots O^{\delta\ominus})Li^{\oplus}$. The Li(1)–Li(2) distance (2.286(8) Å) is one of the shortest known; the closest analogy is with the O_2Li_2 ring dimer $[Me_2PCH_2CtBu_2OLi]_2$ ($Li\cdots Li$, 2.30 Å),[8] though even shorter contacts (ca. 2.20 Å) occur in the complicated Li_8 core of $(o\text{-}LiC_6H_4CH_2NLiCH_2CH_2NMe_2)_4$.[1a] However, such a short distance does not reflect metal $\cdots$ metal bonding (the interaction is a repulsive one). It is rather, as described above, the balanced and optimized separation when taken in conjunction with the $N\cdots N$ distance [2.68(1) Å], the two $N\cdots O$ distances (mean, 3.14(1) Å), and the four N–Li and two O–Li ones.

The other significant feature of **1** is the incorporation of a third HMPA ligand; **1** is obtained whether two (one per Li), three, or four equivalents of HMPA are provided experimentally. Its presence, as an intramolecular bridging ligand, allows each Li to attain four-coordination. Several other examples of lithium structures (with both organic and inorganic anions) containing μ_2-HMPA ligands have been reported,[2a] e.g., the O_2Li_2 isomer of [Ph(2-py)NLi·HMPA]$_2$ (mean Li–O length 1.924 Å)[9a] and the cation of $[Li(H_2O)_2.HMPA]_2Cl_2$ (mean Li–O length 1.976 Å).[9b] However, in all of these examples the μ_2-HMPA operates intermolecularly, usually causing dimerization.

Experimental

1: *n*BuLi (2.5 mL of a 1.60 M solution in hexane, 4 mmol) was added under nitrogen to a chilled solution (−50 °C) of *N,N'*-diphenylethylenediamine (0.42 g, 2 mmol) in hexane/toluene (5 mL/5 mL) containing HMPA (0.72 g, 4 mmol). At room temperature a cloudy yellow solution was obtained. After filtration, the filtrate was stored in dry-ice, producing an oil from which small crystalline blocks formed. These were filtered, washed with hexane, and identified as **1**, [yield 0.70 g (69% based on 4 mmol HMPA), m.p. 141–143 °C; correct elemental analysis. ^{1}H NMR (C_6D_6, 250 MHz, 20 °C) δ = 7.39 (t, 4H), 6.80 (d, 4H), 6.52 (t, 2H), 3.70 (s, 4H, $(CH_2)_2$), 2.35 (d, 54H, 3HMPA). Single crystals suitable for X-ray crystallography were sealed under N_2 in Lindemann capillary tubes prior to data collection.

The ab initio optimized geometries described were obtained from the computer program GAMESS [10] using the 6-31G basis set [11]. The total energies (in a.u.) calculated for the optimized structures of $H_2NCH_2CH_2NH_2$, $HNLiCH_2CH_2NH_2$, and $HNLiCH_2CH_2NHLi$ are −189.19058, −196.08025, and −202.98654 respectively.

Received: November 30, 1989 [Z 3662 IE]
German version: *Angew. Chem. 102* (1990) 443

[1] a) D. Barr, W. Clegg, S. M. Hodgson, R. E. Mulvey, D. Reed, R. Snaith, D. S. Wright, *J. Chem. Soc. Chem. Commun. 1988*, 367; b) D. Barr, D. J. Berrisford, R. V. H. Jones, A. M. Z. Slawin, R. Snaith, J. F. Stoddart, D. J. Williams, *Angew. Chem. 101* (1989) 1048; *Angew. Chem. Int. Ed. Engl. 28* (1989) 1044; c) D. R. Armstrong, R. E. Mulvey, D. Barr, R. Snaith, D. S. Wright, W. Clegg, S. M. Hodgson, *J. Organomet. Chem. 362* (1989) C1.

[2] a) For a review of the crystal structures of organolithium compounds (including ones with Li–N bonds), see W. N. Setzer, P. von R. Schleyer, *Adv. Organomet. Chem. 24* (1985) 353; b) For a review of heteroatom (O,N) involvement in lithium-containing structures, see G. W. Klumpp, *Recl. Trav. Chim. Pays-Bas 105* (1986) 1.

[3] a) E. D. Jemmis, J. Chandrasekhar, P. von R. Schleyer, *J. Am. Chem. Soc. 101* (1979) 2848; b) P. von R. Schleyer, A. J. Kos, *J. Chem. Soc. Chem. Commun. 1982*, 448.

[4] U. Schubert, W. Neugebauer, P. von R. Schleyer, *J. Chem. Soc. Chem. Commun. 1982*, 1184.

[5] P. von R. Schleyer, *Pure Appl. Chem. 55* (1983) 355; *56* (1984) 151, and references therein.

[6] A. Streitwieser, *Acc. Chem. Res. 17* (1984) 353, and references therein.

[7] **1**: $C_{32}H_{68}Li_2N_{11}O_3P_3$, M_r = 761.8, monoclinic, space group $P2_1/n$, a = 18.427(1), b = 14.036(1), c = 19.130(1) Å, β = 115.683(4)°, V = 4459.1 Å^3, Z = 4, ϱ_{calcd} = 1.135 g cm^{-3}, $F(000)$ = 1648, CuK_α radiation, λ = 1.54184 Å, μ = 1.56 mm^{-1}. The structure was determined by direct methods and refined from 3639 unique observed reflections measured at room temperature with a Stoe-Siemens diffractometer ($2\theta_{max}$ 110°), with anisotropic thermal parameters, and with isotropic H atoms in calculated positions; R = 0.063, R_w = 0.049, S = 1.18 for 461 parameters. Further details of the crystal structure investigation can be obtained from the Director of the Cambridge Crystallographic Data Centre, University Chemical Laboratory, Lensfield Road, Cambridge, CB2 1EW (UK). Any request should be accompanied by the full literature citation for this communication.

[8] L. M. Engelhardt, J. MacB. Harrowfield, M. F. Lappert, I. A. MacKinnon, B. H. Newton, C. L. Raston, B. W. Skelton, A. H. White, *J. Chem. Soc. Chem. Commun. 1986*, 846.

[9] a) D. Barr, W. Clegg, R. E. Mulvey, R. Snaith, *J. Chem. Soc. Chem. Commun. 1984*, 700; b) *ibid. 1984*, 974.

[10] a) M. Dupuis, D. Spangler, J. J. Wendoloski, *GAMESS, N.R.C.C. Software Catalogue*, Program No. 2 GOI, 1980, Vol. 1; b) M. F. Guest, J. Kendrick, S. A. Pope. *GAMESS Documentation*, Daresbury Laboratory, 1983.

[11] a) W. J. Hehre, R. Ditchfield, J. A. Pople, *J. Chem. Phys. 56* (1972) 2257; b) P. C. Hariharan, J. A. Pople, *Theor. Chim. Acta 28* (1973) 213; c) J. D. Dill, J. A. Pople, *J. Chem. Phys. 62* (1975) 2921.

Reversible Photoisomerization of Ketene to Ethynol**

By *Remo Hochstrasser* and *Jakob Wirz**

Ethynol and substituted hydroxyacetylenes have been characterized in recent years by tandem mass spectrome-

[*] Prof. Dr. J. Wirz, Dr. R. Hochstrasser
Institut für Physikalische Chemie der Universität Basel
Klingelbergstrasse 80, CH-4056 Basel (Switzerland)

[**] This work is part of project No. 2000-5.515 of the Swiss National Science Foundation. Support by Ciba-Geigy SA, Sandoz SA, F. Hoffmann–LaRoche & Cie. SA, the Ciba-Stiftung, and the Stipendienfonds der Schweizerischen Chemischen Industrie is gratefully acknowledged.

try,[1] matrix IR spectroscopy,[2] and flash photolysis in aqueous solution.[3] They were generated by cycloreversion reactions induced by electron impact[1] and thermal[2a] or photochemical[2b, 3] activation of suitable precursors. We now report that prolonged irradiation of matrix-isolated ketene with 308-nm pulses from a XeCl excimer laser cleanly yields ethynol which is free from the perturbing effects of eliminated fragments such as CO in the matrix cage. The reverse photoisomerization of ethynol to ketene takes place upon deep-UV irradiation (248, 222, or 185 nm), as reported previously (Scheme 1).[2b]

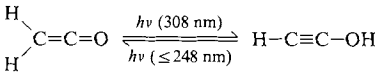

Scheme 1.

Ketene was generated by pyrolysis of acetic anhydride,[4] mixed with 200 to 500 parts of argon, and matrix-isolated on a CsI target window which was held at 23 K in order to allow annealing of the matrix during the deposition. The sample was then cooled to 12 K and its FTIR spectrum recorded in the range of 3630 to 630 cm^{-1} at a resolution of 0.2 cm^{-1} using a mercury-cadmium-telluride (MCT) narrow-band detector cooled with liquid nitrogen. Six different isotopomeric mixtures of acetic anhydride were prepared by allowing sodium acetate to react with $POCl_3$ in order to identify the six $^1H/^2H$ and $^{16}O/^{18}O$ isotopomers of ketene.[5] The fundamental bands are listed in Table 1; the band positions of the three $^1H/^2H$ ketenes agree within a few cm^{-1} with those reported by *Moore* and *Pimentel*.[6]

Table 1. Fundamental modes $\tilde{\nu}$[cm^{-1}] of ketene and its ^2H and ^{18}O isotopomers.

Mode	$^1H_2CC^{16}O/^{18}O$		$^1H^2HCC^{16}O/^{18}O$		$^2H_2CC^{16}O/^{18}O$	
$\nu_1(A_1, \nu_s(CH))$	3063.0	3062.9	3108.8	3109.0	2259.8	2255.9
$\nu_2(A_1, \nu(C=O))$	2142.2	2115.4	2131.9	2102.3	2112.7	2087.9
$\nu_2(A_1, \nu(^{13}C=O))$	2085.6	2058.0				
$\nu_3(A_1, \delta(CH_2))$	1380.4	1376.6	1287.5	1278.3	1225.0	1213.5
$\nu_4(A_1, \nu(C=C))$	1111.4	1108.0			920.2	915.2
$\nu_5(B_1, \nu_{as}(CH))$	3154.8	3154.6	2311.1	2307.9	2374.2	2373.8
$\nu_6(B_1, \varrho(CH_2))$	973.2	972.2	860.9	858.9	848.9	847.4
$\nu_7(B_1, \gamma(C=C=O))$	438	434	398	395	371	368
$\nu_8(B_2, \omega(CH_2))$	590	587	555	550	542	537
$\nu_9(B_2; \delta(C=C=O))$	524	524	492	492	433	433

Ketene exhibits a weak absorption band in the near UV; $\lambda_{max} = 310$ nm ($\varepsilon = 10\ M^{-1}\ cm^{-1}$),[7] where ethynol is expected to be transparent. Therefore, the samples were irradiated with a XeCl excimer laser (308 nm, 20 ns, 50 mJ per pulse) and the reaction progress was monitored by IR spectroscopy; irradiation for 5 d at pulse repetition rates of 20 Hz was necessary to convert about 90% of the starting material. Most of the new bands were readily attributed to the ν_1 to ν_5 bands of ethynol and its isotopomers (Table 2) by comparison with our earlier results.[2b] All of these bands gained in intensity with increasing irradiation dose and were free from site splittings; moreover, their intensity ratios remained constant throughout the experiment. Three new bands were identified as belonging to carbon monoxide (2138 cm^{-1} for $C^{16}O$ and 2087 cm^{-1} for $C^{18}O$) and to ethene (1439 and 952 cm^{-1}); some weak bands between 2110 and 1900 cm^{-1} could not be assigned. The OH group proved

Table 2. Fundamental modes $\tilde{\nu}$[cm^{-1}] above 630 cm^{-1} (relative intensity in parentheses) of isolated ethynol and its ^2H and ^{18}O isotopomers formed by photoisomerization of ketene.

Mode	ν_1 (A′, ν(OH))	ν_2 (A′, ν(CH))	ν_3 (A′, ν(C≡C))	ν_4 (A′, ν(CO))	ν_5 (A′, δ(COH))
$^1HCC^{16}O^1H$	3588.2(70)	3345.2(75)	2202.1(80)	1054.6(15) [a]	1231.3(100)
$^1HCC^{16}O^2H$	2650.2(35)	3345.1(30)	2199.4(100)	1043.6(25)	944.4(15)
$^2HCC^{16}O^1H$	3588.2(30)	2624.6(100)	2099.1(10)	1045.8(20)	1230.1(30)
$^2HCC^{16}O^2H$	2650.6(20)	2624.4(100)	2094.5(20)	1040.9(60)	943.0(15)
$^1HCC^{18}O^1H$	3577.0(50)	3344.2(90)	2194.2(100)	1019.0(50)	1226.3(70)
$^1HCC^{18}O^2H$	2634.0(30)	3344.2(40)	2192.4(100)	1009.6(30)	937.2(30)
$^2HCC^{18}O^1H$	3577.0(40)	2623.3(100)	2068.7(30)	1018.1(60)	1224.8(40)
$^2HCC^{18}O^2H$	2635.2(10)	2623.3(100)	2066.0(50)	1009.6(20)	936.2(30)

[a] Broad (ca. 5-cm^{-1} width at half height). Based on the sum rule, this band is expected to lie at ca. 1049 cm^{-1}.

to be most sensitive to changes in the matrix environment: the O^1H stretching vibrations of the CO-complexed sites[2b] were red shifted by 90–130 cm^{-1} relative to that of isolated ethynol.

A DTGS detector (DTGS = deuterated triglycine sulfate) was used to monitor the region from 630 to 220 cm^{-1}; here the resolution had to be kept at 1 cm^{-1} in order to avoid interference caused by vibrations of the closed-cycle He-refrigerator. The spectral changes arising from the photolysis of ketene were, however, too small to allow an unambiguous identification of the ethynol bending modes ν_6 to ν_9. Higher concentrations of ethynol could be built up by irradiation of hydroxycyclobutenedione,[2b] but this reaction gave rise to site splittings which could not always be cleanly resolved. Ranges for the position of the bending vibrations ν_6 to ν_9 are listed in Table 3. Some of these assignments remain questionable and it must be recalled that these values are perturbed by interaction of the ethynol molecules with the CO fragments in the matrix.

Table 3. Ranges of fundamental modes [cm^{-1}] below 630 cm^{-1} (including all sites; intensity designated as medium, weak, or very weak) of ethynol and its ^2H isotopomers formed by photolysis of hydroxycyclobutenedione.

	ν_6 (A′, δ(CCH))	ν_7 (A′, δ(CCO))	ν_8 (A″, γ(CCH))	ν_9 (A″, γ(CCO))
$^1HCCO^1H$	590–605(w)	380–390(vw)	520–535(m)	330–350(w)
$^1HCCO^2H$	590–605(w) [a]	290–300(vw)	520–535(m)	260–270(w)
$^2HCCO^1H$	450–460(w)	380–390(vw) [b]	370–380(m) [b]	330–350(w)
$^2HCCO^2H$	450–460(w) [a]	290–300(vw)	370–380(m)	260–270(w)

[a] Not unambiguously identifiable due to overlap with the ν_6 band of the O^1H isotopomers present in the mixture. [b] Ranges of sites may be overlapping.

Two theoretical force fields for ethynol have been reported (3-31G[8a] and MP2/6-31G**[8b]). The observed band positions of the fundamental vibrations ν_1 to ν_5 of all isotopomers agreed within 2% with those calculated[9] from the purely ab initio (unscaled) harmonic force field obtained by the second calculation.[8b] The five highest diagonal elements of the computed force field were then adjusted to fit the experimental data of Table 1. The resulting semiempirical force constants[10] gave satisfactory agreement (40 data pairs, 15-cm^{-1} standard deviation). Further adjustment of cross terms did not significantly improve the quality of the fit. Relatively large deviations were found for the O^1H/O^2H ratio of the stretching mode ν_1 (found 1.35, calculated 1.40; presumably due to anharmonicity effects) and for the C≡C

stretching modes ν_3 of $^2HCC^xO^yH$. The latter deviations may be attributed to Fermi coupling of $2\nu_4$ with ν_3, which is negligible when the acetylenic hydrogen is not labeled. This is also borne out by significant deviations from the sum rule in the ν_3 bands and by the fact that these are red shifted by ca. 60 cm^{-1} upon complexation with CO[2b] for $^2HCC^xO^yH$, whereas the corresponding bands for the $^1HCC^xO^yH$ isotopomers are shifted by only 7 cm^{-1}.

By combining the vibrational data obtained in this work with the theoretical rotational constants,[8b] a reliable estimate for the absolute entropy, $S_m^\ominus$ (298 K) = 250 J $K^{-1}mol^{-1}$, and the thermal heat content, $H_m^\ominus$ (298 K) − $H_m^\ominus$ (0 K) = 12.8 kJ mol^{-1}, of gaseous ethynol can be made using standard statistical mechanics. The entropy change for the conversion of ketene[6b] to ethynol is calculated to be $\Delta_r S_m^\ominus$ (298 K) = 8 J K^{-1} mol^{-1}.

Our experiments establish that ethynol is formed by photolysis of ketene in an argon matrix. The following observations suggest that this reaction takes place via decarbonylation of ketene, followed by insertion of CO into the C–H bond of methylene. 1) The quantum yield of ketene photoenolization in the matrix is quite low, $\phi \approx 10^{-3}$.[11] Decarbonylation of ketene is known to occur with high quantum yield upon 308-nm photolysis in the gas phase.[12] Presumably, the in-cage recombination of the primary fragments CH_2 and CO yields predominantly ketene rather than ethynol. 2) Irradiation of matrix-isolated methylketene yields CO and ethene exclusively, as expected if methylcarbene is the primary photoproduct formed by decarbonylation. 3) The reaction of parent ketene is clean at sufficiently high dilution. At lower host/guest ratios, dimerization of two methylene fragments to ethene becomes increasingly important.

Oxirene, oxiranylidene, and formylmethylene have been considered as possible intermediates in isomerization reactions of ketene and ethynol.[13] The same species may play a role in the Wolff rearrangement.[14] We find no evidence for the occurrence of such intermediates in the reversible photoisomerization of ketene to ethynol in an argon matrix at 12 K.

Received: December 27, 1989 [Z 3707 IE]
German version: *Angew. Chem. 102* (1990) 454

[1] a) B. van Baar, T. Weiske, J. K. Terlouw, H. Schwarz, *Angew. Chem. 98* (1986) 275; *Angew. Chem. Int. Ed. Engl. 25* (1986) 282; b) J. K. Terlouw, P. C. Burgers, B. L. M. van Baar, T. Weiske, H. Schwarz, *Chimia 40* (1986) 357; c) J. K. Terlouw, H. Schwarz, *Angew. Chem. 99* (1987) 829; *Angew. Chem. Int. Ed. Engl. 26* (1987) 805.

[2] a) C. Wentrup, P. Lorenčak, *J. Am. Chem. Soc. 110* (1988) 1880; b) R. Hochstrasser, J. Wirz, *Angew. Chem. 101* (1989) 183; *Angew. Chem. Int. Ed. Engl. 28* (1989) 181.

[3] Y. Chiang, A. J. Kresge, R. Hochstrasser, J. Wirz, *J. Am. Chem. Soc. 111* (1989) 2355.

[4] G. J. Fisher, A. F. MacLean, A. W. Schnizer, *J. Org. Chem. 18* (1953) 1055.

[5] Partly deuterated acetic acid was obtained by partial exchange of malonic acid and subsequent decarboxylation; ^{18}O was introduced by basic hydrolysis of acetonitrile in ^{18}O-enriched (75%) heavy water. The following H- and O-isotopic compositions (approximate % contents) of ketene were obtained: $^1H_2{}^{16}O$(99); $^2H_2{}^{16}O$(97); $^1H_2{}^{16}O$(50) + $^1H^2H^{16}O$(40) + $^2H_2{}^{16}O$(10); $^2H_2{}^{16}O$(64) + $^2H_2{}^{18}O$(35); $^2H_2{}^{18}O$(64) + $^2H_2{}^{16}O$(32) + $^1H^2H^{18}O$(3) + $^1H^2H^{16}O$(1); $^2H_2{}^{18}O$(36) + $^1H^2H^{18}O$(24) + $^2H_2{}^{16}O$(20) + $^1H^2H^{16}O$(12) + $^1H_2{}^{18}O$(4) + $^1H_2{}^{16}O$(2).

[6] a) C. B. Moore, G. C. Pimentel, *J. Phys. Chem. 38* (1963) 2816; b) P. D. Mallinson, L. Nemes, *J. Mol. Spectrosc. 59* (1976) 470.

[7] C. Reid, *Chem. Rev. 71* (1971) 73.

[8] a) D. J. DeFrees, A. D. McLean, *J. Phys. Chem. 86* (1982) 2835; b) J. Dommen, M. Rodler, T.-K. Ha, *Chem. Phys. 117* (1987) 65.

[9] D. F. MacIntosh, M. R. Peterson, *QCPE-program No. 342.*

[10] S(OH) = 7.25; S(CO) = 8.07; S(CC) = 15.55, S(CH) = 5.94 mdyn $Å^{-1}$; S(COH) = 0.73 mdyn Å rad^{-2}. The other force constants are given in Table 2 in [8 b]. The empirical scaling factors suggested in that paper were ignored.

[11] This estimate is based on the amount of ketene deposited on the 5-cm^2 target (ca. 0.05 mmol), the extinction coefficient of ketene (ca. 10 M^{-1} cm^{-1} at 308 nm),[7] and the amount of light (ca. 0.2 mol) needed to photoenolize half of the ketene.

[12] a) R. K. Lengel, R. N. Zare, *J. Am. Chem. Soc. 100* (1978) 7495; b) C. C. Hayden, D. M. Neumark, K. Shobatake, R. L. Sparks, Y. T. Lee, *J. Chem. Phys. 76* (1982) 3607; c) H. Petek, D. J. Nesbitt, P. R. Ogilby, C. B. Moore, *J. Phys. Chem. 87* (1983) 5367; d) H. M. Frey, R. Walsh, *ibid. 89* (1985) 2445.

[13] a) K. Tanaka, M. Yoshimine, *J. Am. Chem. Soc. 102* (1980) 7655; b) W. J. Bouma, R. H. Nobes, L. Radom, C. E. Woodward, *J. Org. Chem. 47* (1982) 1869; c) S. Schröder, W. Thiel, *J. Am. Chem. Soc. 108* (1986) 7985; d) M. Yoshimine, *J. Chem. Phys. 90* (1989) 378.

[14] a) G. Maier, H. P. Reisenauer, T. Sayraç, *Chem. Ber. 115* (1982) 2192; b) E. G. Lewars, *Chem. Rev. 83* (1983) 519.

The Bicyclo[1.1.1]pentane Framework—an Excellent Relay for π/σ Conjugation**

By *Rolf Gleiter,* Karl-Heinz Pfeifer, Günter Szeimies,** and *Uwe Bunz*

Dedicated to Professor Franz Effenberger on the occasion of his 60th birthday

A convenient measure for the interaction of two π moieties, such as two vinylene units, is the energy difference between their occupied π MOs. This interaction can be a direct one (through space)[1] or it can be mediated via a σ skeleton (through bond)[1, 2]. By means of He(I) photoelectron (PE) spectroscopy, such an interaction can be measured. If the validity of Koopmans' approximation is assumed,[3] the above effects can be directly observed in the PE spectra. Examples of conjugation, homoconjugation, and through-bond interaction are shown in Scheme 1, together with the corresponding splitting, ΔI_π, of the ionization energies assigned to the π MOs.[4]

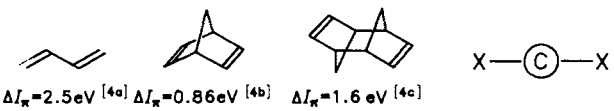

1 2 3 4

Scheme 1.

Instead of a σ bond connecting two π systems, one can also use a rigid σ skeleton of a bicyclic system as shown in **4**. Recent experiments with cubane,[5a] bicyclo[2.2.1]heptane,[5b] and bicyclo[2.2.2]octane[5c] as central unit, with two bromine atoms or two ethynyl moieties as X, showed only a very small splitting.[5]

Here we report that the splitting is large when the bicyclo[1.1.1]pentane framework is used as a relay. To demonstrate this, we show in Figure 1 the PE spectra of bicyclo[1.1.1]pentane[6a] (**5**), 1,3-diethynylbicyclo[1.1.1]pentane[6b] (**6**), and 1,3-dibromobicyclo[1.1.1]pentane[6c] (**7**). For comparison we also list in Table 1 the PE data of 1-ethynyl-

[*] Prof. Dr. R. Gleiter, Dipl.-Chem. K.-H. Pfeifer
Organisch-chemisches Institut der Universität
Im Neuenheimer Feld 270, D-6900 Heidelberg (FRG)
Prof. Dr. G. Szeimies, Dipl.-Chem. U. Bunz
Institut für Organische Chemie der Universität
Karlstrasse 23, D-8000 München (FRG)

[**] This work was supported by the Deutsche Forschungsgemeinschaft and the Fonds der Chemischen Industrie. We thank *A. Flatow* for recording the PE spectra.

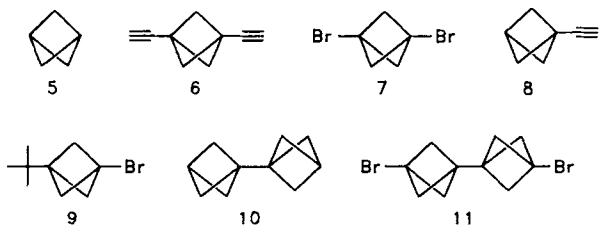

bicyclo[1.1.1]pentane[8a] (**8**) and 1-bromo-3-*tert*-butylbicyclo[1.1.1]pentane[6d] (**9**).

A comparison between the calculated results[9] (Table 1) and the PE data suggests that the first two peaks (bands ①, ②, and ③, ④) in the PE spectrum of **6** can be assigned to the ionizations from the π MOs 2e″ and 4e′. The small splitting of the peaks (Jahn–Teller effect) confirms this assignment. The same assignment is given for the first four bands in the PE spectrum of **7**. Here the ^{2}2E″ and the ^{2}4E′ states are split by 0.2–0.3 eV owing to the spin–orbit coupling usually observed for bromine compounds.[12] Both **6** and **7** show an energy splitting between ^{2}2E″ and ^{2}4E′ of about 0.7 eV, which indicates a considerable interaction between the π units.

Table 1. Comparison between the vertical ionization energies $I_{v,j}$ for **5**–**11** and the calculated orbital energies ε_j. All values in eV.

Compound	Band	$I_{v,j}$	Assignment	$-\varepsilon_j$(STO-3G)	$-\varepsilon_j$(4-31G)	$-\varepsilon_j$(AM1)
5	1	10.60	$2a_2''$	10.88	11.93	11.05
	2	11.10	3e′	11.00	12.03	11.40
	3	11.50	1e″	11.35	12.36	12.09
	4	12.50	$1a_2'$	12.69	13.48	12.17
6	1	9.55	2e″(π)	8.86	10.15	10.47
	2	9.80				
	3	10.31	4e′(π)	9.38	10.77	10.80
	4	10.40				
	5	11.73	3e′(σ)	11.90	12.96	12.39
7	1	9.84	2e″(π)	8.35		10.69
	2	10.15				
	3	10.61	4e′(π)	8.83		11.12
	4	10.83				
	5	11.16, 11.31, 11.43	$3a_2''$(σ)	9.98		11.84
	6	12.10	3e′(σ)	12.29		12.54
8	1	9.90	5e(π)	8.95	10.27	10.53
	2	11.00	4e(σ)	11.31	12.33	11.67
	3	11.55	$7a_1$(σ)	11.45	12.76	11.73
9	1	9.60	6e [a]	8.17 [a]		10.57 [a]
	2	9.97				
	3	10.80	$7a_1$	9.97		11.51
10	1	9.50	$5a_{1g}$	9.64	10.90	10.59
	2	10.00	$4e_g$	10.06	11.15	10.75
	3	11.00	$3e_g$	11.04	12.02	11.59
	4	11.40	$4e_u$	11.09	12.13	11.52
11	1	9.70	$5e_g$	8.27		10.63
	2	9.90				
	3	10.10	$5e_u$	8.38		10.77
	4	10.40				
	5	11.60	$6a_{1g}$	9.45		11.17

[a] The assignment and the calculated orbital energies refer to 1-bromo-3-methylbicyclo[1.1.1]pentane.

This splitting is due to a difference in the interaction between the valence MOs of **5** with the π MOs of the substituents. The assignment of the PE spectrum of **5** yields five close-lying MOs (2a″, 3e′, 1e″) with high 2p character (see Table 1, Fig. 2). For reasons of symmetry only 1e″ and 3e′

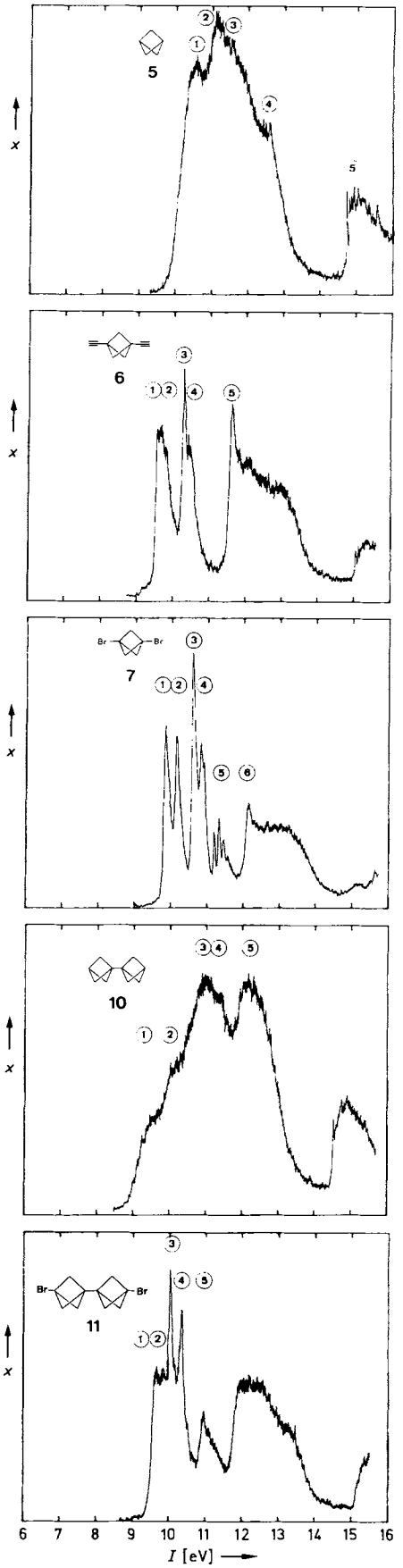

Fig. 1. He(I) PE spectra of **5**–**7**, **10**, and **11**. x = count rate.

interact with the π MOs of the substituents in **6** and **7**. Owing to the localization of e″ at the carbon skeleton only, the interaction between e″ (π) and e″ (σ) is stronger than the interaction between the two e′ linear combinations.

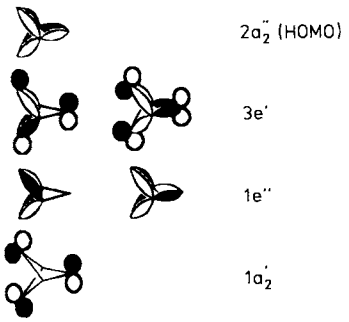

Fig. 2. Schematic drawing of the highest occupied MOs of **5**.

In view of efforts to use the bicyclo[1.1.1]pentyl moiety as a building block for oligomers,[13] it was also of interest to study the PE spectra of 1,1′-bi(bicyclo[1.1.1]pentane)[8b] (**10**) and 3,3′-dibromo-1,1′-bi(bicyclo[1.1.1]pentane)[6c] (**11**) (Fig. 1, Table 1). Our investigations of **10** reveal a region between 9 and 13 eV with strongly overlapping bands. The MO calculations carried out on **10** show that the valence MOs of **10** corresponding to these bands[3] can be described as linear combinations of those of **5** (Table 1). For **11** we notice a broad band on top of which are two small peaks (① and ② in Fig. 1, bottom) followed by two sharp peaks (③ and ④). The first broad peak is assigned to $5e_g$. The corresponding wave function is predicted to be a mixture between 4p orbitals at the bromine centers and large coefficients at the carbon skeleton (Fig. 3). This explains why the spin–orbit coupling is difficult to detect. The two sharp peaks are due to a spin–orbit splitting of the $5e_u$ band. The wave function of the latter is mainly centered at the bromine atoms (Fig. 3). Based on this interpretation, the splitting between $5e_g$ and $5e_u$ is 0.4 eV, indicating also good relay properties for the bi(bicyclo[1.1.1]pentane) unit. This effect is also important in view of energy-transfer processes via a σ skeleton.[14]

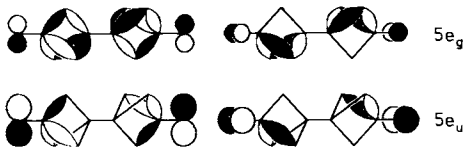

Fig. 3. Schematic drawing of the highest occupied MOs of **11**.

Received: November 29, 1989 [Z 3659 IE]
German version: *Angew. Chem. 102* (1990) 418

[1] R. Hoffmann, *Acc. Chem. Res. 4* (1971) 1; H.-D. Martin, B. Mayer, *Angew. Chem. 95* (1983) 281; *Angew. Chem. Int. Ed. Engl. 22* (1983) 283.
[2] R. Gleiter, *Angew. Chem. 86* (1974) 770; *Angew. Chem. Int. Ed. Engl. 13* (1974) 696; M. N. Paddon-Row, *Acc. Chem. Res. 15* (1982) 245.
[3] T. Koopmans, *Physica 1* (1934) 104.
[4] a) D. W. Turner, C. Baker, A. D. Baker, C. R. Brundle: *Molecular Photoelectron Spectroscopy*, Wiley-Interscience, London 1970; K. Kimura, S. Katsumata, Y. Achiba, T. Yamazaki, S. Iwata: *Handbook of He(1) Photoelectron Spectra of Fundamental Organic Molecules*, Japan Scientific Societies Press, Tokio 1981; b) P. Bischof, J. A. Hashmall, E. Heilbronner, V. Hornung, *Helv. Chim. Acta 52* (1969) 1745; c) W. Grimme, L. Schumachers, R. Gleiter, K. Gubernator, *Angew. Chem. 93* (1981) 98; *Angew. Chem. Int. Ed. Engl. 20* (1981) 113.
[5] a) E. Honegger, E. Heilbronner, T. Urbanek, H.-D. Martin, *Helv. Chim. Acta 68* (1985) 23; b) E. Honegger, E. Heilbronner, N. Hess, H.-D. Martin, *Chem. Ber. 118* (1985) 2927; c) *ibid. 120* (1987) 187.
[6] a) Compound **5** was prepared in 30% yield by reduction of bicyclo[1.1.1]-pent-1-yl phenyl thioether [7a] with lithium sand (containing 2% sodium) in triglyme and 1,6-diaminohexane. b) Compound **6** was obtained in 70% yield from 1,3-di(1-chlorovinyl)bicyclo[1.1.1]pentane by elimination with sodium amide in liquid ammonia. 1,3-Di(1-chlorovinyl)bicyclo[1.1.1]-pentane was synthesized in 80% yield by treatment of 1,3-di(acetyl)bicyclo[1.1.1]pentane [7b] with PPh_3/dibromotetrachloroethane in benzene. c) Compound **7** was prepared in 31% yield by irradiation of [1.1.1]propellane [7a] in PPh_3/dibromotetrachloroethane. As second product we isolated 3,3′-dibromo-1,1′-bi(bicyclo[1.1.1]pentane) (**11**) in 21% yield. d) Compound **9** was synthesized in 30% yield by irradiation of [1.1.1]propellane in *tert*-butylbromide [7c].
[7] a) K. Semmler, G. Szeimies, J. Belzner, *J. Am. Chem. Soc. 107* (1985) 6410; b) P. Kaszynski, J. Michl, *J. Org. Chem. 53* (1988) 4593; c) J. Belzner, G. Szeimies, *Tetrahedron Lett. 28* (1987) 3099.
[8] a) U. Bunz, G. Szeimies, *Tetrahedron Lett. 30* (1989) 2087; b) U. Bunz, K. Polborn, H.-U. Wagner, G. Szeimies, *Chem. Ber. 121* (1988) 1785.
[9] The MO calculations for **5**–**11** were carried out with the HF-SCF method using a STO-3G basis [10] as well as the AM1 procedure [11]. For the smaller molecules a 4-31G basis could also be employed [10]. The geometrical parameters for **5**–**8** and **10** were calculated with the STO-3G basis and the AM1 method. For the ab initio calculations on **11** we adopted the X-ray parameters reported in the literature for the bisthioether of **10** [8b]. For **9** we adopted the geometrical parameters for the bicyclo[1.1.1]pentane skeleton of **5**; the *tert*-butyl group was replaced by a methyl group.
[10] W. J. Hehre, L. Radom, P. von R. Schleyer, J. A. Pople: *Ab Initio Molecular Orbital Theory*, Wiley, New York 1986.
[11] M. J. S. Dewar, S. Olivella, J. J. P. Steward, *J. Am. Chem. Soc. 108* (1986) 5771.
[12] J. A. Hashmall, E. Heilbronner, *Angew. Chem. 82* (1970) 320; *Angew. Chem. Int. Ed. Engl. 9* (1970) 305.
[13] G. Szeimies in A. de Meijere, S. Blechert (Eds.): *Strain and its Implications in Organic Chemistry*, NATO ASI-Series, Kluwer, Dordrecht 1988, p. 361ff; J. Michl, P. Kaszynski, A. C. Friedli, G. S. Murthy, H.-C. Yang, R. E. Robinson, *ibid.*, p. 463; G. S. Murthy, K. Hassenrück, V. M. Lynch, J. Michl, *J. Am. Chem. Soc. 111* (1989) 7262; A.-D. Schlüter, *Angew. Chem. 100* (1988) 283, *Angew. Chem. Int. Ed. Engl. 27* (1988) 296.
[14] M. N. Paddon-Row, K. D. Jordan in J. F. Liebmann, A. Greenberg (Eds.): *Modern Models of Bonding and Delocalization*, VCH, Weinheim/New York 1988, p. 115ff and references cited therein.

A Stable Triradical Compound and its Unusual Magnetic Properties**

By *Lothar Dulog** and *Jeong Soo Kim*

Organic ferromagnetism is a subject of current controversy, and several theoretical models for it have been proposed.[1] The spin polarization model of *McConnell* and the spin multiplicity of the ground state have been used to explain organic ferromagnetism.[2] A spin multiplicity different from 1 is much more difficult to obtain for organic compounds than for inorganic compounds, since the former usually possess low symmetry and orbital orthogonality. Here we report on the synthesis and unusual magnetic properties of compound **4**, which contains three stable $^{\ominus}O\text{–}\overset{\oplus}{N}R = CR'\text{–}NR'' \dot{-} O$ units ("nitronyl nitroxide" radicals) in a single molecule.

[*] Prof. Dr. L. Dulog, J. S. Kim, M. Sc.
2. Institut für Technische Chemie der Universität,
Pfaffenwaldring 55, D-7000 Stuttgart 80 (FRG)
and
Forschungsinstitut für Pigmente und Lacke e. V.
Allmandring 37, D-7000 Stuttgart 80 (FRG)

[**] We thank Prof. Dr. *A. Simon* and Dr. *R. Kremer*, Max-Planck-Institut für Festkörperforschung, for the measurements of magnetic susceptibility.

To generate the triradical compound **4**, we used the known condensation reaction between an aldehyde (**1**) and a hydroxylamine (**2**), followed by oxidation (**3** → **4**) with lead dioxide.[3]

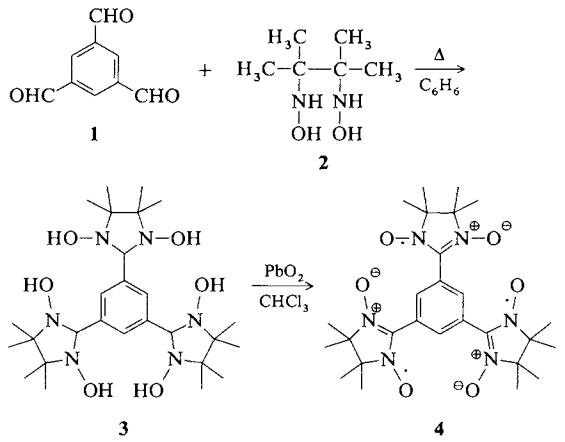

The product, **4**, is a blue powder, which is readily soluble in chloroform and dichloromethane. We have not found further solvents for **4** and have been unsuccessful in growing crystals of **4**.

The ESR spectrum of a dilute solution of **4** displays a broad maximum, which indicates strong intramolecular spin–spin interaction (Fig. 1).

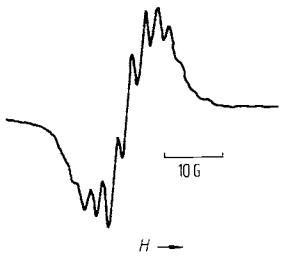

Fig. 1. ESR spectrum of triradical **4** in chloroform ($c = 3.38 \times 10^{-5}$ mol L^{-1}).

The magnetic susceptibility of **4** is very unusual. It shows strong deviations from the Curie law and surprisingly high values at high temperatures (Fig. 2). The findings can be explained neither by ferromagnetism nor by antiferromagnetism. Such properties are unknown for organic compounds and rarely observed for transition-metal complexes.

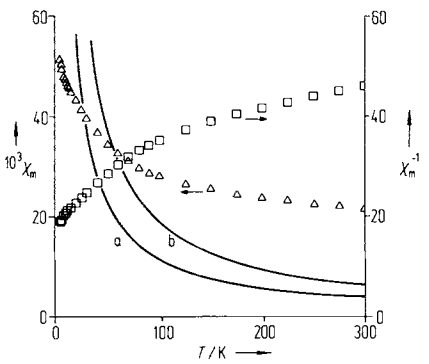

Fig. 2. Molar susceptibility (left axis, △) and reciprocal molar susceptibility (right axis, □) of **4** at a field strength of 10 000 Gauss. a) Theoretical curve for χ_m according to the Curie law with three radical centers per molecule. b) Theoretical curve for χ_m according to the Curie law for an $S = 3/2$ ground state. Unit of χ_m: 10^{-6} m^3 mol^{-1} = emu mol^{-1}.

The effective spin per molecule is larger than the theoretical value of 3.87 (without spin–orbit coupling) for $S = 3/2$ metal atoms (Fig. 3). Because of the weak spin–orbit coupling between the spin and the p orbital, we presume that this coupling can be nearly neglected for **4**. The molar susceptibility of triradical **4** shows field-strength dependence, which is not characteristic of usual paramagnetism (Fig. 4).

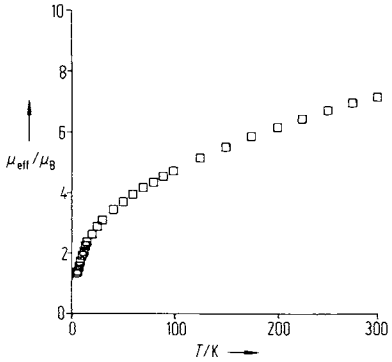

Fig. 3. Effective spin per molecule of **4** at a field strength of 10 000 Gauss.

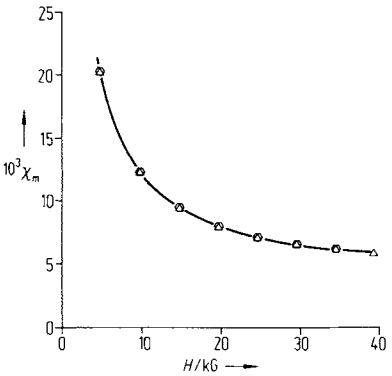

Fig. 4. Field-strength dependence of the molar susceptibility of **4** at 270 K. Susceptibility determined for increasing field strength (△) and for decreasing field strength (○).

In order to interpret the high molar susceptibility as a property of **4**, it is necessary to rule out the presence of ferromagnetic impurities introduced by the oxidizing agent, lead dioxide. Reaction of **4** with HCl gas results in an equilibrium between **4** and its "hydrochloride", which only contains nitroxyl radicals.[3] After reaction for three hours, 71% of the initial molar susceptibility is still found, as observed earlier for other $^{\ominus}O-\overset{\oplus}{N}R = CR'-NR'' \doteq O$ radicals.[3] By contrast, ferromagnetic particles in lead dioxide are rapidly reduced by HCl vapor and show no noticeable susceptibility after three hours. The susceptibility remaining after treatment of **4** with HCl indicates that the high susceptibility is indeed a property of **4**.

Elemental analysis of **4** left no ash. The molecular mass determined by vapor-pressure osmometry was 559.02 g mol^{-1} (calcd 543.64 g mol^{-1}). A molecular mass of 543.2921 g mol^{-1} was obtained from the mass spectrum. The hydroxylamine **3** can also be oxidized with diamagnetic sodium periodate; the resulting triradical **4** also exhibits high susceptibility, greater than the value calculated for a paramagnetic substance.

The magnetic properties of **4** appear to be similar to those of some low-symmetry or noncrystalline inorganic compounds, such as FeF_3. The unusual properties of these inorganic compounds have been explained in terms of the antiferromagnetic interaction in the lattice and the ferromagnetic interaction between the lattices.[4] Extension of this explanation to **4** would mean that, in **4**, an intramolecular antiferromagnetic and an intermolecular ferromagnetic interaction are present.

A quantitative explanation of the molar susceptibility of **4** might be possible in terms of the intermolecular ferromagnetic spin polarization perpendicular to the benzene plane and a weak intramolecular antiferromagnetic interaction. Further investigations are in progress.

The magnetic susceptibility of **4** at room temperature varies from 16 to 57×10^{-3} emu mol^{-1} depending on the pretreatment, whereas the calculated value is 3.75×10^{-3} emu mol^{-1}. This may support the explanation proposed above.

Experimental Procedure

1: 1,3,5-Benzenetricarboxylic acid was converted into 1,3,5-benzenetricarbonyl chloride, which was then hydrogenated with $Pd/BaSO_4$ as catalyst to give **1**; see [5].

2: 2-Nitropropane was coupled to give 2,3-dimethyl-2,3-dinitrobutane, which was then reduced with Zn/NH_4Cl to **2**; see [6].

Compounds **1** (0.50 g, 3.08 mmol) and **2** (1.40 g, 9.44 mmol) were placed in 150 mL of benzene. The vigorously stirred reaction mixture was then heated while N_2 was admitted. The water thereby formed was removed. Slow cooling of the solution resulted in precipitation of **3**. The crude product was collected by filtration and, after drying, could be used in subsequent reaction. Yield: 0.75 g (44%). IR(KBR): $\tilde{\nu} = 3440$, 2980, 1450, 1370, 1160 cm^{-1}. ^1H NMR(60 MHz, CD_3OD): $\delta = 1.37$ (s, 12 CH_3), 3.40 (br., 3 CH), 5.00 (s, 6 OH), 8.83 (s, C_6H_3).

4: The crude product **3** (0.1 mg) was suspended in 10 mL of chloroform and 1.5 g of lead dioxide was added. The reaction mixture was then vigorously stirred at room temperature and the lead dioxide subsequently separated. After removal of chloroform in vacuo, **4** was isolated as a dark blue powder. The oxidation was quantitative. Purification of **4** was accomplished by redissolving it in chloroform and adding benzene dropwise to the gently stirred solution. The blue powder reprecipitated. IR(KBr): $\tilde{\nu} = 3100$, 2980, 2930, 1450, 1265, 1210, 1170, 1130, 860, 670 cm^{-1}. MS(70eV): *m/z* (%) 543 (2.2; $M^{\oplus}$), 527 (1.8; $M^{\oplus} - O$), 511 (2.0; $M^{\oplus} - O_2$), 480 (3.8; $M^{\oplus} + 1\text{–}2O_2$), 465 (4.4; $M^{\oplus}\text{–}NO_2\text{–}O_2$), 450 (31.1; $M^{\oplus}\text{–}1\text{–}2\ NO_2$), 433 (15.6; $M^{\oplus}\text{–}NO_2\text{–}2O_2$). Elemental analysis: found C 59.45, H 7.25, N 15.02; calcd C 59.65, H 7.23, N 15.46.

Received: June 12, 1989;
supplemented: December 21, 1989 [Z 3390 IE]
German version: *Angew. Chem. 102* (1990) 403

CAS Registry numbers:
1, 3163-76-6; **2**, 14384-45-3; **3**, 125520-16-3; **4**, 125520-11-4.

[1] a) J. S. Miller, A. J. Epstein, W. M. Reiff, *Chem. Rev. 88* (1988) 201; b) Z. Yoshida, T. Sugimoto, *Angew. Chem. 100* (1988) 1633; *Angew. Chem. Int. Ed. Engl. 27* (1988) 1573.

[2] a) H. M. McConnell, *J. Chem. Phys. 39* (1963) 1910; b) A. A. Ovchinnikov, *Theoret. Chim. Acta 47* (1978) 297.

[3] E. F. Ullman, J. H. Osiecki, D. G. B. Boocock, R. Darcy, *J. Am. Chem. Soc. 94* (1972) 7049.

[4] a) A. Barnshaw, B. N. Figgs, J. Lewis, *J. Chem. Soc. A 1966*, 1656; b) B. N. Figgs, J. Lewis, *Prog. Inorg. Chem. 6* (1964) 91.

[5] W. Ried, F. J. Königstein, *Chem. Ber. 92* (1959) 2532.

[6] a) L. W. Seigle, H. B. Hass, *J. Org. Chem. 5* (1940) 100; b) R. Sayre, *J. Am. Chem. Soc. 77* (1955) 6689.

Isolation of an L-Stereospecific *N*-Acyl-L-proline-Acylase and its Use as Catalyst in Organic Synthesis**

By *Ulrich Groeger,** *Karlheinz Drauz*, and *Herbert Klenk*

Dedicated to Professor Franz Effenberger on the occasion of his 60th birthday

The importance of the amino acid L-proline has increased tremendously in the past few years. Aside from the now already classical use of L-proline and its derivatives in asymmetric synthesis,[1] L-proline is a constituent of the three most important ACE (angiotensin converting enzyme) inhibitors captopril **1**, enalapril **2a**, and lisinopril **2b**, which count among the world's most successful antihypertensive agents. The demand for L-proline is currently satisfied by fermentation methods[3] as well as by the hydrolysis of gelatins and extractive recovery of the proline with ion-exchangers.[2]

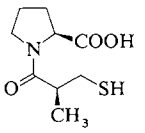

1

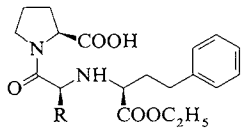

2a: R = CH_3
2b: R = $(CH_2)_4\text{–}NH_2$

Although some good syntheses are known for D,L-proline,[2, 4a] the usual route of racemate resolution (either via separation of diastereomeric pairs of salts or via an enzymatic cleavage of suitable precursors[5]) used in the case of many amino acids could thus far not be realized in the case of L-proline. Even transformations of other chiral amino acids into L-proline have not, as yet, acquired any importance as preparative methods.[6] Our interest therefore focused on an enzyme system with which L-proline should be obtainable from an *N*-acyl-D,L-proline precursor.

Enrichment cultures of a sewage clarifier sample led to selection of the microorganism *Comamonas testosteroni* DSM 5416. Upon growth in the presence of *N*-acetyl-L-proline, this bacterium produces an enzyme which hydrolyzes *N*-acetyl-L-proline. This *N*-acyl-L-proline-acylase was enriched 53-fold with a yield of 50% from the cell-free extract by heat treatment, membrane filtration, and ion-exchange chromatography. The enzyme, with a molecular weight of 380 000 ± 40 000 Da is made up of eight identical subunits (molecular weight 45,000 ± 5,000 Da). The enzyme does not only exhibit a good pH-stability (four weeks at room temperature in the pH range 5–10) but also a remarkable temperature stability (30 min at 70 °C and pH 7.5). A pH of 6.8 ± 0.5, a temperature of 65 °C and a K_M value of 5 mM [0.1 M 2-amino-2-(hydroxymethyl)propane-1,3-diol(tris)-HCl, pH 7.0; 30 °C] were found to be optimal for the resolution of *N*-acetyl-L-proline. Figure 1 shows plots of the hydrolysis versus time of *N*-acetyl-L-proline, *N*-acetyl-D,L-proline and *N*-acetyl-D-proline.

The enzyme hydrolyzes *N*-acetyl-L-proline stereospecifically. After 2 hours the conversion of *N*-acetyl-L-proline was quantitative, that of *N*-acetyl-D,L-proline 48% (theoretically 50%). *N*-acetyl-D-proline was not hydrolyzed. This permits

[*] Dr. U. Groeger, Dr. K. Drauz, Dr. H. Klenk
Degussa AG, Fachbereich Forschung Chemie Organisch
Postfach 13 45, D-6450 Hanau 1 (FRG)

[**] Amino Acid Transformation, Part 4.—Part 3: H.-P. Krimmer, K. Drauz, A. Kleemann, *Chem.-Ztg. 111* (1987) 357.

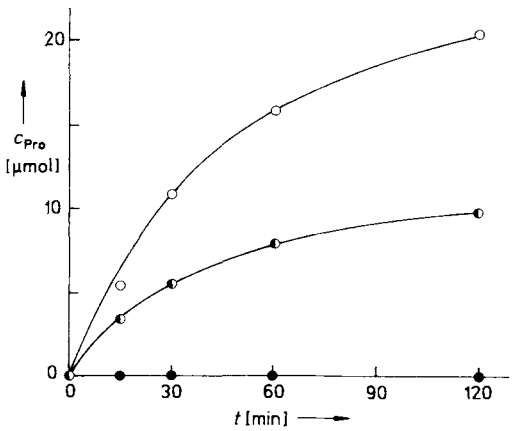

Fig. 1. Reaction kinetics of the hydrolysis of *N*-acetyl-L-proline (○), *N*-acetyl-D,L-proline (◐), and *N*-acetyl-D-proline (●). The reaction mixture (2 mL) contained 0.2 mmol of tris-HCl pH 7.0, 20 μmol of substrate, and 0.4 U of purified *N*-acyl-L-proline-acylase from *Comamonas testosteroni* DSM 5416. The specific activity of the purified enzyme was 85.2 U mg^{-1} at 30 °C and pH 7.0 with *N*-acetyl-L-proline as substrate. One unit (U) of the enzyme activity corresponds to the amount of enzyme which catalyzes formation of 1 μmol of proline per minute. The reaction mixture was incubated at 30 °C and treated for the quoted times with one aliquot of 10% (w/v) trichloroacetic acid. The precipitated protein was centrifuged off (10 min, 11 000 pm), the supernate diluted 1:5 or 1:50 with a 0.1 M citrate buffer, 0.1% (v/v) phenol, 0.5% (v/v) thiodiethanol, pH 2.2, and the resulting proline quantified with a Biotronic LC 5001 amino acid analyzer. The enzyme activity was determined in the usual way by ninhydrin detection of the reaction product L-proline according to the method of *Yaron* and *Mlynar* [7].

an enzyme-catalyzed racemate resolution of D,L-proline via *N*-acetyl-D,L-proline, a technique analogous to that already used for the industrial production of L-amino acids employing an aminoacylase from *Aspergillus oryzae*;[8] However, this technique could not be used for the recovery of L-proline, since the aminoacylases known so far do not hydrolyze *N*-acyl-L-proline because of their substrate specificity.[9]

The following *N*-acetyl- and *N*-chloroacetyl-amino acids are converted by the *N*-acyl-L-proline-acylase: *N*-acetyl-L-proline (relative activity ≡100) *N*-acetyl-L-alanine (9) *N*-chloroacetyl-L-proline (362), *N*-chloroacetyl-L-thiazolidine-4-carboxylic acid (462), *N*-chloroacetyl-L-methionine (17), *N*-chloroacetyl-L-valine (14), *N*-chloroacetyl-L-leucine (2), *N*-chloroacetyl-L-phenylalanine (1), *N*-chloroacetyl-L-tyrosine (1). In the case of the following *N*-acetyl- and *N*-chloroacetylamino acids the relative activities are less than 1: *N*-acetyl-L-valine, *N*-acetyl-D,L-serine, *N*-acetyl-L-cysteine, *N*-acetyl-L-tyrosine and *N*-chloroacetyl-L-isoleucine.

These findings illustrate the high substrate specificity of the enzyme for acylated *L*-proline and its derivatives. Aside from the acyl-*D*,*L*-proline compounds, the *N*-acylthiazolidine-4-carboxylic acid readily accessible from cysteine and formaldehyde is also cleaved. This concomitantly opens up a novel entry to *L*-cysteine and *L*-cysteine derivatives by enzymatic racemate resolution.

The chloroacetyl compounds of *L*-proline and of *L*-thiazolidine-4-carboxylic acid are hydrolyzed respectively 3.6 times and 4.6 times more rapidly than *N*-acetyl-L-proline. This is consistent with findings for other aminoacylases, and is due to the electronegativity of the chloroacetyl group.[9] Table 1 shows further data for the substrate- and stereospecifity of the enzyme.

The derivatization of the carboxyl group of *N*-acetyl-L-proline results in a complete loss of the enzymatic activity, from which it can be presumed that this group is essential for the binding of the substrate to the enzyme. On introducing an OH group into the 4-position of the proline the activity decreases by a factor of 10. *N*-Protecting groups of the urethane type are not hydrolyzed. The enzyme has no amidase activity, and only minimal peptidase activity.

Table 1. Substrate- and stereo-specificity of *N*-acyl-L-proline-acylase towards some proline compounds. The reactions were carried out under the conditions described in the caption to Figure 1. *N*-Ac-L-Pro-OH: relative activity ≡100.

Substrate	Relative activity
N-Ac-L-Pro-OH	100
N-Ac-D-Pro-OH	0
N-Ac-L-Pro-NH_2	0
N-Ac-L-Pro-OMe	0
N-Ac-L-Pro(4-OH)-OH	10
N-ClAc-L-Pro-OH	362
N-ClAc-L-thiazolidine-4-carboxylic acid	462
N-Z-L-Pro-OH	0
N-Z-D-Pro-OH	0
N-Z-L-Pro-NH_2	0
N-Boc-L-Pro-OH	0
H-L-Pro-NH_2	0
N-Ac-L-Ala-L-Pro-OH	0
N-Z-L-Pro-L-Ala-OH	0
N-Z-Gly-L-Pro-OH	11
H-L-Ala-L-Pro-OH	0
H-Gly-L-Pro-OH	4
H-L-Pro-Gly-OH	0

The enzyme is inhibited, in particular, by phosphate, 1,10-phenanthroline, 2-mercaptoethanol, 4-(chloromercurio)-benzoate, 4-(hydroxymercurio)-benzoate, $Hg^{2\oplus}$, $Cu^{2\oplus}$, $Fe^{2\oplus}$, $Fe^{3\oplus}$, $Sn^{2\oplus}$, and $Zn^{2\oplus}$ ions. An activation of the native enzyme by divalent metal ions was not observed, but the enzyme inactivated by 1,10-phenanthroline could be reactivated to 80% and 54% of the starting activity by addition of $Co^{2\oplus}$ and $Zn^{2\oplus}$ ions, respectively. This indicates that the *N*-acyl-L-proline-acylase from *Comanomas testosteroni* DSM 5416 is a cobalt- or zinc-dependent amidohydrolase, which according to the EC classification is assigned to the subgroup EC 3.5.1.[10]

The novel, thermostable *N*-acyl-L-proline-acylase from *Comamonas testosteroni* DSM 5416 is a highly specific and robust enzyme by which L-proline can be recovered from acyl-D,L-precursors. A similar enzyme from *Pseudomonas spec.* has been described by *Kikuchi* et al.[11]

This enzyme, however, is much more temperature-labile (rapid inactivation at 50 °C) and considerably larger (597,000–623,000 Da, ten to twelve identical subunits of 55,000 Da), and it has a noticeably higher peptidase activity (*N*-Z-Gly-L-Pro-OH is hydrolyzed 2.7 times and H-Gly-L-Pro-OH 1.2 times more rapidly than *N*-Ac-L-Pro-OH).

Received: December 20, 1989 [Z 3693 IE]
German version: *Angew. Chem. 102* (1990) 428

[1] K. Drauz, A. Kleemann, J. Martens, *Angew. Chem. 94* (1982) 590; *Angew. Chem. Int. Ed. Engl. 21* (1982) 584; J. Martens, *Top. Curr. Chem. 125* (1984) 165, and references cited therein; E. J. Corey, R. K. Bakshi, S. Shibata, *J. Am. Chem. Soc. 109* (1987) 5551.

[2] a) J. P. Greenstein, M. Winitz: *Chemistry of the Amino Acids, Vol. 3*, R. E. Krieger Publishing Company 1961; b) [2a], Chap. 35, p. 2178.

[3] Kyowa Hakko Kogyo Co. Ltd., EPS 98 122 dated 5.31. 1989, and references cited therein.

[4] a) For examples of syntheses which, in our opinion, could also be carried out on an industrial scale see: K Hasse, A. Wieland, *Chem. Ber. 93* (1960) 1686; U. Schmidt, H. Poisel, *Angew. Chem. 89* (1977) 824; *Angew. Chem. Int. Ed. Engl. 16* (1977) 7; K. Drauz, A. Kleemann, M. Samson, *Chem. Ztg. 108* (1984) 391; b) T. Shiraiwa, K. Shinjo, H. Kurokawa, *Chem. Lett.*

1989, 1413; C. Hongo, M. Sibazaki, S. Yamada, I. Chibata, *J. Agric. Food Chem. 24* (1976) 903; S. Yamada, C. Hongo, I. Chibata, *Agric. Biol. Chem. 41* (1977) 2413.
[5] J. Peisach, H. J. Strecker, *J. Biol. Chem. 237* (1962) 2255; [2a], Chap. 35, p. 2195, and references cited therein.
[6] K. Drauz, A. Kleemann, J. Martens, P. Scherberich, F. Effenberger, *J. Org. Chem. 51* (1986) 3494, and references cited therein; S. Lafquih Tizonani, J.-P. Lavergue, P. Viallefont, R. Jaquier, *Tetrahedron 36* (1980) 2961.
[7] A. Yaron, D. Mlynar, *Biochem. Biophys. Res. Commun. 32* (1968) 658.
[8] W. Leuchtenberger, U. Plöcker, *Chem. Ing. Tech. 60* (1988) 16.
[9] S. Kang, Y. Minematsu, Y. Shimohigashi, M. Waki, N. Izumiya, *Mem. Fac. Sci. Kyushu Univ. Ser. C 16* (1987) 61.
[10] Nomenclature Committee of the International Union of Biochemistry: *Enzyme Nomenclature*, Academic Press, New York 1984, p. 366.
[11] M. Kikuchi, I. Koshiyama, D. Fukushima, *Biochim. Biophys. Acta 744* (1983) 180.

Facile Synthesis of 3-(ω-Haloalkyl)thiophenes as Key Building Blocks for Functionalized Thiophenes and Polythiophenes**

By *Peter Bäuerle,* Frank Würthner,* and *Stephan Heid*

Dedicated to Professor Franz Effenberger on the occasion of his 60th birthday

3-Alkylthiophenes containing a terminal leaving group in the alkyl chain are central intermediates for the synthesis of functionalized 3-alkylthiophenes and poly(3-alkylthienylenes), which are currently under intensive investigation.[1] The coupling of monomeric thiophenes to form conjugated polymers occurs at the 2- and 5-positions,[2] thereby allowing covalent attachment of functional groups via alkyl chains in the 3-position (or 4-position). Functionalized 3-alkylthiophenes were previously only accessible starting from 3-methylthiophene[3] or 3-(2-hydroxyethyl)thiophene[4] by a tedious sequence of chain-lengthening steps. Moreover, those with shorter alkyl chains are difficult to polymerize.[4a]

We have now developed a facile synthesis of 3-alkylthiophenes containing a terminal halogen substituent on an alkyl chain of length $n \geq 4$. These compounds may be used as key building blocks for the preparation of functionalized 3-alkylthiophenes and poly(3-alkylthienylenes).[5]

Since the use of 3-lithiothiophene in alkylation reactions is restricted,[6] the synthesis of 3-alkylthiophenes was approached via nickel-catalyzed Grignard couplings[7] of alkylmagnesium bromides with 3-bromothiophene, which is readily accessible by a new procedure.[8] The direct extension of this reaction to α,ω-dihaloalkanes, however, does not lead to the necessary mono-Grignard compounds.[9] On the other hand, the ω-(*p*-methoxyphenoxy)alkyl bromides **1**, easily prepared from α,ω-dihaloalkanes and hydroquinone monomethyl ether (HCM),[10] react readily with magnesium to give the corresponding Grignard compounds **2** [Eq. (a)]. Compounds **1a–e** (n = 4–6, 8, 10) undergo nearly quantitative Grignard reaction to afford **2a–e** (GC monitoring), whereas 3-(*p*-methoxyphenoxy)propyl bromide (**1**, n = 3),[10d] like 1,3-dihalopropanes, undergoes elimination on reaction with magnesium to yield cyclopropanes.[11]

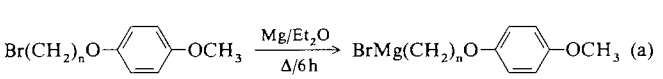

(a)

1 **2**

The nickel-catalyzed Grignard coupling of 3-bromothiophene (**3**) and the alkylmagnesium bromides **2a–e** in the presence of 0.1–1 mol% $NiDPPPCl_2$[12] as catalyst in refluxing ether [Eq. (b)] leads to the previously unknown,

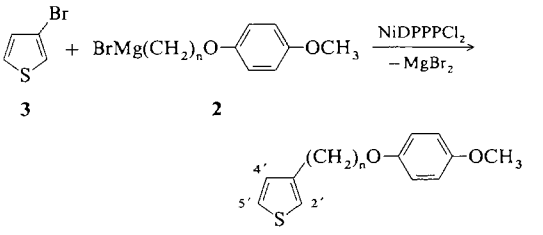

3 **2** **4**

(b)

terminally protected 3-[ω-(*p*-methoxy-phenoxy)alkyl]thiophenes **4**, which may be obtained, after a single recrystallization, in 63–81% yield as a colorless, analytically pure solid[13] (Table 1).

Table 1. Results of the nickel-catalyzed Grignard coupling of **3** with the alkylmagnesium bromides **2a–e** to give the terminally HCM-protected thiophenes **4** and their ether cleavage with hydrogen halides to give the 3-(ω-bromoalkyl)-thiophenes **5** or the 3-(ω-iodoalkyl)thiophenes **6**.

	n	**4**		**5**		**6**	
		Yield [%]	M.p. [°C]	Yield [%]	B.p. at 10^{-3} torr [°C]	Yield [%]	B.p. at 10^{-3} torr [°C]
a	4	76 [a, b]	34–35	51[c]	60–65	60	70
b	5	81 [b]	52	75	80	64	80
c	6	79	41	76	90	68	100
d	8	63	30–31	70	105	59	115
e	10	70	48–49	73 [d]	120	70 [e]	135

[a] Three isomeric butenes identified as byproducts by GC/MS(EI): *m/z* 56 ($M^{\oplus}$). [b] 1.5% of 1,(2n)-bis(*p*-methoxyphenoxy)alkane isolated as byproduct. [c] 10% 4,5,6,7-tetrahydrobenzo[*b*]-thiophene isolated as byproduct. [d] Addition of 5 mol% hexadecyltrimethylphosphonium bromide. [e] Addition of 5 mol% methyltriphenylphosphonium iodide.

Of the numerous ether cleavage methods,[14] that with hydrogen halide/acetic anhydride[10, 14] proved best suited for the cleavage of the HCM protecting group in **4**. Thiophenes **4** were thus converted directly and—with the exception of **4a**—free of byproducts into the 3-(ω-bromoalkyl)-thiophenes **5** and the 3-(ω-iodoalkyl)thiophenes **6** [Eq. (c)].

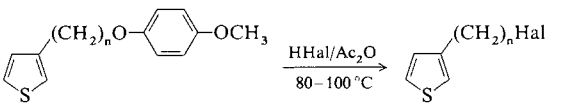

4 **5**, Hal = Br; **6**, Hal = I

(c)

The best yields were obtained using HBr/Ac_2O at 100 °C/20–25 h for **5** and HI/Ac_2O at 80 °C/15–25 h for **6**. Addition of phase-transfer catalysts helps keep within the given limits the time required for ether cleavage of the longer-chain homologues, which become increasingly insoluble. After separation of the simultaneously formed hydroquinone followed

[*] Dr. P. Bäuerle, F. Würthner, S. Heid
Institut für Organische Chemie, Biochemie und Isotopenforschung der Universität
Pfaffenwaldring 55, D-7000 Stuttgart 80 (FRG)

[**] Thiophenes, Part 1. This work was supported by the Volkswagen-Stiftung (AZ I/61584), the Deutsche Forschungsgemeinschaft, and Hoechst AG (donation of 3-bromothiophene). We thank Dr. *A. Bandi* (Universität Stuttgart) for the GC/MS(EI) analyses.

by chromatographic and distillative workup, halides **5** and **6** were obtained as analytically pure compounds in 51–76% yield[15] (Table 1). The 3-(ω-iodoalkyl)thiophenes **6** are also accessible by Finkelstein reaction[10] from bromides **5**, as was shown for the conversion of bromide **5b** to iodide **6b** (85% yield).

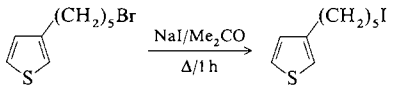

(d)

5b **6b**

The methods described here allow a two-step synthesis—with the exception of **6a**[4b]—of the previously unknown terminal bromine- and iodine-substituted 3-alkylthiophenes **5** and **6**, respectively, with chain lengths $n \geq 4$, starting from 3-bromothiophene (**3**).

General Experimental Procedure

4: Compound **1** (0.125 mol) in 40 mL of anhydrous ether was added under inert atmosphere to magnesium turnings (3.16 g, 0.13 mol) in 10 mL of ether. The reaction mixture was then refluxed for 5–6 h. The Grignard solution of **2** was subsequently transferred via cannula to a second apparatus and added dropwise at 0 °C to $NiDPPPCl_2$ (70 mg, 0.1 mol%) and **3** (17.2 g, 0.106 mol) over 1 h. The reaction mixture was refluxed for 12–15 h and afterwards hydrolyzed with 40 mL of 1 N HCl and 150 mL of ice water followed by extraction with several portions of ether. Washing to neutrality and drying of the combined organic phases and removal of the solvent in vacuo afforded a yellowish-white solid, which was recrystallized from *n*-hexane or methanol to give analytically pure **4**.

5: A mixture of HBr (48%; 20.2 g, 0.12 mol) and acetic anhydride (20.2 g, 0.198 mol) was added under inert atmosphere to **4** (0.02 mol) and the reaction mixture was heated at 100 °C for 20–25 h. After dilution with water, the mixture was extracted several times with ether and the combined organic phases were washed to neutrality with saturated $NaHCO_3$ solution. Drying of the organic phase and removal of the solvent afforded a yellow-brown oil, from which hydroquinone was precipitated by addition of an *n*-hexane/ether mixture. The solution was then filtered, transferred to a short silica gel column, and eluted with hexane. Removal of the solvent gave **5**, mostly analytically pure, as a colorless oil, which may be further purified by kugelrohr distillation.

6: A mixture of freshly distilled HI (57%; 26.9 g, 0.12 mol) and acetic anhydride (20.2 g, 0.198 mol) was added under inert atmosphere to **4** (0.02 mol) and the reaction mixture was heated at 80 °C for 15–25 h. After dilution with water, the mixture was extracted several times with ether and the combined organic phases were decolorized by treatment with a thiosulfate solution. Further workup was carried out as described for **5**.

Received: October 25, 1989 [Z 3609 E]
German version: *Angew. Chem. 102* (1990) 414
Publication delayed at authors' request

CAS Registry numbers:
1a, 2033-83-2; **1b**, 125878-81-1; **1c**, 20744-11-0; **1d**, 125878-82-2; **1e**, 125878-83-3; **3**, 872-31-1; **4a**, 125878-84-4; **4b**, 125878-85-5; **4c**, 125878-86-6; **4d**, 125878-87-7; **4e**, 125878-88-8; **5a**, 125878-89-9; **5b**, 125878-90-2; **5c**, 125878-91-3; **5d**, 125878-92-4; **5e**, 125878-93-5; **6a**, 114896-68-3; **6b**, 125878-94-6; **6c**, 125878-95-7; **6d**, 125878-96-8; **6e**, 125878-97-9; 4,5,6,7-tetrahydrobenzo[b]thiophene, 13129-17-4.

[1] F. Garnier, *Angew. Chem. Adv. Mater. 101* (1989) 529; *Angew. Chem. Int. Ed. Engl. Adv. Mater. 28* (1989) 513; *Adv. Mater. 1989*, 117.
[2] G. Tourillon in T. Skotheim (Ed.): *Handbook of Conducting Polymers, Vol. 1*, Marcel Dekker, New York 1986, p. 293 ff.
[3] a) P. Cagniant, G. Merle, D. Cagniant, *Bull. Soc. Chim. Fr. 1970*, 308; b) C. F. Shu, M. S. Wrighton, *ACS Symp. Ser. 378* (1988) 408.
[4] a) P. Audebert, G. Bidan, M. Lapkowski, D. Limousin in M. Kuzmany, M. Mehring, S. Roth (Eds.): *Electronic Properties of Conjugated Polymers, (Springer Ser. Solid State Sci. 76*, (1987) 366); b) Y. Ikenoue, N. Uotani, A. O. Patil, F. Wudl, A. J. Heeger, *Synth. Met. 30* (1989) 305.
[5] P. Bäuerle, K.-U. Gaudl, *Adv. Mater. 2* (1990) 185.
[6] For example, a) W. Baarschers, *Can. J. Chem. 54* (1976) 3056; b) S. Gronowitz, T. Frejd, O. Karlsson, K. Lawitz, P. Pedaja, K. Petterson, *Chem. Scr. 18* (1981) 192; c) J. A. Elvidge, S. P. Jones, T. L. Peppard, *J. Chem. Soc. Perkins Trans. 1 1982*, 1089.
[7] a) K. Tamao, S. Kodama, I. Nakajima, M. Kumada, A. Minato, K. Suzuki, *Tetrahedron 28* (1982) 3347; b) C. Van Pham, H. B. Mark, Jr., H. Zimmer, *Synth. Commun. 16* (1986) 689.
[8] a) U. Dettmaier, K. Eichler, K. Kühlein, E. I. Leupold, H. Litterer, *Angew. Chem. 99* (1987) 470; *Angew. Chem. Int. Ed. Engl. 26* (1987) 468; b) S. Kato, M. Ishizaki, Jpn. Kokai Tokkyo Koho JP 62148480 (1987), Tokuyama Soda Co., Ltd.; *Chem. Abstr. 108* (1988) 150299s.
[9] J. von Braun, W. Sobecki, *Chem. Ber. 44* (1911) 1918.
[10] a) K. Ziegler, H. Weber, *Chem. Ber. 70* (1937) 1275; b) K. Ziegler, H. Weber, H. G. Gellert, *ibid. 75* (1942) 1715; c) A. W. Nineham, *J. Chem. Soc. 1953*, 2601; d) J. N. Ashley, R. F. Collins, M. Davis, N. E. Sirett, *ibid. 1958*, 3303.
[11] The collected gas was characterized by GC/MS(EI): *m/z* 42 ($M^{\oplus}$); see also N. Zelinsky, J. Gutt, *Chem. Ber. 40* (1907) 3049.
[12] $NiDPPPCl_2$ = [1,3-bis(diphenylphosphino)propanedichloronickel(II)]: G. R. van Hecke, W. de W. Horrocks, Jr., *Inorg. Chem. 5* (1966) 1968.
[13] All thiophenes **4** gave satisfactory C, H, S analyses and ^{1}H NMR spectra (300 MHz, $CDCl_3$, TMS as standard): e.g., **4c,d**: $\delta_H = 7.213$ (dd, $^3J(5',4') = 4.96$, $^4J(5',2') = 2.91$ Hz, 1H; H-5'), 6.918 (dd, $^3J(4',5') = 5.00$, $^4J(4',2') = 1.31$ Hz, 1H; H-4'), 6.900 (dd, $^4J(2',5') = 2.98$, $^4J(2',4') = 1.27$ Hz, 1H; H-2'), 6.815 (s, 4H; H_{Ph}), 3.879 (t, $^3J(1,2) = 6.49$ Hz, 2H; H-1), 3.714 (s, 3H; OCH_3), 2.629 (t, $^3J(6,5) = 7.48$ Hz, 2H; H-6), 1.745 (m, 2H; H-2), 1.610 (m, 2H; H-5), 1.53–1.35 (m, 4H; H-3,4).
[14] a) R. L. Burwell, *Chem. Rev. 54* (1954) 615; b) H. Meerwein in: *Houben-Weyl-Müller, Methoden der Organischen Chemie, 4. Aufl., Bd. 6/3*, Thieme, Stuttgart 1965, p. 143 ff.; c) M. V. Bhatt, S. U. Kulkarni, *Synthesis 1983*, 249.
[15] All thiophenes **5** and **6** gave satisfactory C, H, halogen, S analyses and ^{1}H NMR spectra (300 MHz, $CDCl_3$, TMS as standard), e.g., **5d**: $\delta_H = 7.147$ (dd, $^3J(5',4') = 4.86$, $^4J(5',2') = 2.95$ Hz, 1H; H-5'), 6.843 (dd, $^3J(4',5') = 4.86$, $^4J(4',2') = 1.21$ Hz, 1H; H-4'), 6.828 (dd, $^4J(2',5') = 2.86$, $^4J(2',4') = 1.28$ Hz, 1H; H-2'), 3.310 (t, $^3J(1,2) = 6.82$ Hz, 2H; H-1), 2.548 (t, $^3J(6,5) = 7.62$ Hz, 2H; H-6), 1.770 (m, 2H; H-2), 1.555 (m, 2H; H-5), 1.43–1.21 (m, 4H; H-3,4). **6c**: $\delta_H = 7.220$ (dd, $^3J(5',4') = 4.86$, $^4J(5',2') = 2.99$ Hz, 1H; H-5'), 6.917 (dd, $^3J(4',5') = 4.85$, $^4J(4',2') = 1.20$ Hz, 1H; H-4'), ca. 6.90 (dd, $^4J(2',4') = 1.22$ Hz, $^4J(2',5')$ not determinable, 1H; H-2'), 3.161 (t, $^3J(1,2) = 7.01$ Hz, 2H; H-1), 2.619 (t, $^3J(6,5) = 7.61$ Hz, 2H; H-6), 1.82 (m, 2H; H-2), 1.65 (m, 2H; H-5) 1.48–1.27 (m, 4H; H-3,4).

CH Activation of Acetonitrile by Alkyl Compounds of the Early Lanthanoids: Dimeric Cyanomethyl-Lanthanoid Complexes with CH_2CN Bridges**

By *Hero J. Heeres, Auke Meetsma*, and *Jan H. Teuben**

Considerable progress has been made in the exciting field of CH bond activation of saturated and unsaturated hydrocarbons by highly electrophilic $d^0(f^n)$ organolanthanoids, actinoids and early transition metal compounds.[1] An outstanding example is the activation of the normally inert CH bonds of methane by complexes of the type Cp^*_2MMe ($Cp^* = \eta^5$-pentamethylcyclopentadienyl; M = Lu, Sc and Y).[2] Recently, we have shown that $Cp^*_2LnCH(SiMe_3)_2$ compounds (Ln = La and Ce) are efficient catalysts for the cyclodimerization of alkynes $MeC{\equiv}CR$ (R = Me, Et, *n*Pr) to substituted 3-alkylidenecyclobutenes.[3] The first step in the reaction sequence is a propargylic metalation of one of the relatively acidic methyl protons of $MeC{\equiv}CR$. This prompted us to study the interactions between Cp^*_2Ln-alkyl compounds and other substrates containing active C–H bonds. Initially, we focused our attention on nitriles containing at least one α-C–H bond. Metalated nitriles, well-known for group 1 elements,[4] are highly reactive species which are very useful intermediates in organic synthesis.[5] In this communication the novel and facile metalation of acetonitrile by pen-

[*] Prof. Dr. J. H. Teuben, Drs. H. J. Heeres, Drs. A. Meetsma
Groningen Centre for Catalysis and Synthesis, Department of Chemistry
University of Groningen
Nijenborgh 16, 9747 NL-AG Groningen (The Netherlands)

[**] This work was supported by Shell Research BV.

tamethylcyclopentadienyl-stabilized alkyl compounds **1a** and **1b** of the early lanthanoids lanthanum and cerium is reported.

Treatment of benzene solutions of the monomeric compounds **1** with 1 mmol acetonitrile/mmol Ln results in the quantitative formation of **3** (NMR) and cyanomethyllanthanoid species **2**.

$$Cp^*_2LnCH(SiMe_3)_2 + CH_3C{\equiv}N \longrightarrow 1/n[Cp^*_2LnCH_2C{\equiv}N]_n + CH_2(SiMe_3)_2$$

1a, Ln = La — **2a**, Ln = La, n = 2 — **3**

1b, Ln = Ce — **2b**, Ln = Ce, n = 2

2a and **2b** were isolated as beautiful crystals (whitish and pink, respectively) in good yields (65–70%). Both compounds are only sparingly soluble in all the solvents investigated (THF, toluene, benzene, pentane). The compounds show almost identical IR spectra with cyanomethyl absorptions at 2140, 2120 and 2050 cm^{-1} (**2a**) implicating a somewhat reduced C≡N bond order.[6] The NMR spectrum of the diamagnetic compound **2a** ([D_8]toluene, 70 °C) shows two singlets at $\delta = 2.03$ and 0.55 for the Cp* and CH_2 protons respectively.

Interactions of nitriles with group 3, lanthanoid and actinoid alkyls and hydrides normally lead to insertion of the C≡N bond into the M–C or M–H σ-bond and the formation of monomeric or dimeric azomethine complexes.[7] Metalation of nitriles by these elements has hitherto not been observed. The compounds **2a** and **2b** represent the first examples of cyanomethyl compounds of the said elements.

To determine the bonding mode of the CH_2CN fragment, an X-ray diffraction study was conducted on the lanthanum species **2a** (Fig. 1).[8] **2a** crystallizes in dimeric units. Each

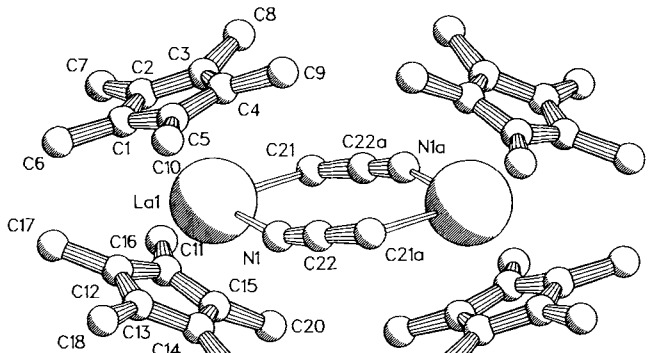

Fig. 1. Molecular Structure of $[Cp^*_2LaCH_2CN]_2$ **2a** (hydrogen atoms omitted for clarity). Selected bond lengths [Å] and angles [°]: La(1)-La(1A) = 5.8479(8), La(1)-C(21) = 2.748(4), La(1)-C(1) = 2.817(4), La(1)-C(2) = 2.808(4), La(1)-C(3) = 2.790(5), La(1)-C(4) = 2.802(5), La(1)-C(5) = 2.807(4), La(1)-N(1) = 2.537(4), N(1)-C(22) = 1.162(6), C(22)-C(21a) = 1.393(6) Å, N(1)-La(1)-C(21) = 95.7(1), N(1)-C(22)-C(21a) = 175.6(5), La(1)-C(21)-C(22a) = 105.6(3) La(1)-N(1)-C(22) = 157.5(4)°.

molecule consists of two Cp^*_2La units connected by two almost linear CCN fragments which form an eight-membered $La(CH_2CN)_2La$ ring in a chair conformation. Particularly interesting is the bonding situation of the bridging CH_2CN groups. The La–C(21) bond length (2.748(4) Å) is significantly longer than a pure La–C σ-bond (2.52–2.65 Å),[9] whereas the La–N(1) distance (2.537(4) Å) is much shorter than an La–N dative bond (ca. 2.77 Å).[10] Furthermore, the CCN units are almost linear (N(1)–C(22)–C(21a) = 175.6(5)°) with a short C(22)–C(21A) bond length of 1.393(6) Å. Hence, the bonding of the CCN unit is best described as intermediate between a *C*-metalated structure **A** and an *N*-metalated ketenimine **B**. Structures of type **B**, but

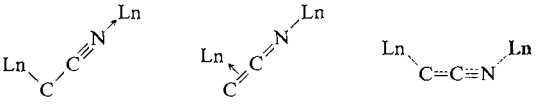

with both metal atoms coordinated to nitrogen, have already been detected in a number of dimeric lithiated nitriles,[11] whereas structures of type **A** are present in various square-planar late transition metal complexes.[12] To our knowledge, compound **2a** is the first structurally characterized example with a CCN coordination of type **C**. Interestingly, MNDO calculations by *Schleyer* et al. for unsolvated lithiated acetonitrile have predicted that an eight-membered $M(CH_2CN)_2M$ ring dimer, similar to what we actually observe for **2a**, is the most favorable structure.[13]

This study provides evidence that metalation of heteroatomic substrates containing active C–H bonds by alkyl(organo)lanthanoid compounds is well possible. In this regard, monomeric Cp^*_2Ln-alkyl compounds strongly resemble organic compounds of group 1 elements[5, 11] and indicate that the Ln–C σ-bonds in these compounds are very polar.

Experimental

2a: Acetonitrile (75 µL, 1.34 mmol) was added to a solution of 762 mg (1.34 mmol) of **1a** in benzene (15 mL). Upon standing at room temperature without stirring, colorless crystals of **2a** deposited. 397 mg (0.44 mmol, 66%) of **2a** could be isolated as beautiful, whitish crystals. IR (KBr/Nujol): $\tilde{\nu}$ [cm^{-1}] = 2710(w), 2140(s), 2120(sh), 2050(m), 1030(m), 1020(m), 800(w), 750(s), 670(w), 540(w), 440(m); ^1H NMR (300 MHz, [D_8]toluene, 70 °C): $\delta = 2.03$ (s, 30H; C_5Me_5), 0.55 (s, 2H; $LaCH_2$); ^{13}C NMR (75 MHz, [D_8]toluene, 50 °C): $\delta = 119.6$ (s; C_5Me_5), 11.2 (q, $^1J(C,H) = 124$ Hz; C_5Me_5), unequivocal assignment of the cyanomethyl carbon resonances was not possible.—Correct elemental analysis.

2b was prepared by a similar procedure and isolated as pink crystals in 72% yield. IR (KBr/Nujol): $\tilde{\nu}$ [cm^{-1}] = 2710(w), 2150(s), 2120(sh), 2060(m), 1030(m), 1020(w), 800(w), 750(s), 550(w), 460(m); ^1H NMR (300 MHz, [D_6]benzene, 30 °C): $\delta = 3.12$ (s, 30H, lw = 23 Hz; C_5Me_5), −45 (s, 2H, lw = 80 Hz; $CeCH_2$).—Correct elemental analysis.

Received: November 24, 1989 [Z 3653 IE]
German version: *Angew. Chem. 102* (1990) 449

CAS Registry numbers:
1a, 98720-36-6; **1b**, 106333-13-5; **2a**, 125803-84-1; **2b**, 125827-93-2; **3**, 2117-28-4; $CH_3C{\equiv}N$, 75-05-8.

[1] a) P. L. Watson, *J. Chem. Soc. Chem. Commun. 1983*, 276; b) M. E. Thompson, S. M. Baxter, A. R. Bulls, B. J. Burger, M. C. Nolan, B. D. Santarsiero, W. P. Schaefer, J. E. Bercaw, *J. Am. Chem. Soc. 109* (1987) 203; c) K. H. den Haan, Y. Wielstra, J. H. Teuben, *Organometallics 6* (1987) 2053; d) J. W. Bruno, G. M. Smith, T. J. Marks, C. K. Fair, A. J. Schultz, J. M. Williams, *J. Am. Chem. Soc. 108* (1986) 40; e) I. P. Rothwell, *Acc. Chem. Res. 21* (1988) 153; f) H. Rabaâ, J. Y. Saillard, R. Hoffman, *J. Am. Chem. Soc. 108* (1986) 4327.

[2] a) P. L. Watson, *J. Am. Chem. Soc. 105* (1983) 6491; b) M. E. Thompson, J. E. Bercaw, *Pure Appl. Chem. 56* (1984) 1.

[3] H. J. Heeres, A. Heeres, J. H. Teuben, *Organometallics*, in press.

[4] a) C. Krüger, *J. Organomet. Chem. 9* (1967) 125; b) R. Das, C. A. Wilkie, *J. Am. Chem. Soc. 94* (1972) 4555; c) I. N. Juchnovski, J. S. Dimitrova, I. G. Binev, J. Kaneti, *Tetrahedron 34* (1978) 779.

[5] S. Arseniyadis, K. S. Kyler, D. S. Watt, *Org. React.* (N.Y.) 31 (1984) 1.

[6] a) IR spectra for free $CH_3C{\equiv}N$ (Nujol mull) show C≡N absorptions at 2293 and 2257 cm^{-1}, see: M. R. M. Bruce, D. R. Tyler, *Organometallics 4* (1985) 528; b) the C≡N stretching frequencies for α-cyanomethyl complexes of Fe, Pt and Cu are reported to lie between 2210 and 2165 cm^{-1}, see: S. D. Ittel, C. A. Tolman, A. D. English, J. P. Jesson, *J. Am. Chem. Soc. 100* (1978) 7577.

[7] a) J. E. Bercaw, D. L. Davies, P. T. Wolczanski, *Organometallics 5* (1986) 443; b) W. J. Evans, J. H. Meadows, W. E. Hunter, J. L. Atwood, *J. Am. Chem. Soc. 106* (1984) 1291; c) R. E. Cramer, K. Panchanatheswaran, J. W. Gilje, *ibid. 106* (1984) 1853.

[8] **2a**: $(C_{22}H_{32}LaN)_2$, $M_r = 898.81$, monoclinic, space group $P2_1/n$, $a = 8.448(1)$, $b = 26.262(2)$, $c = 10.148(1)$ Å, $\beta = 113.78(1)°$, $V = 2060.3(4)$ Å^3, $Z = 2$, $\varrho_{calcd} = 1.449$ g cm^{-3}, $\lambda(Mo_{K\alpha}) = 0.71073$ Å, $\mu = 20.8$ cm^{-1}, $F(000) = 912$, $T = 130$ K. The structure was solved by Patterson methods and subsequent partial structure expansion (SHELXS86). Refinement on F with anisotropic thermal parameters for the non-hydrogen atoms and isotropic thermal parameters for the hydrogen atoms converged at $R_F = 0.035$ ($wR = 0.048$) for 3895 unique reflections with $F \geq 4.0\,\sigma(F)$ and 346 parameters. Further details of the crystal structure investigation can be obtained from the Director of the Cambridge Crystallographic Data Centre, University Chemical Laboratory, Lensfield Road, Cambridge, CB2 1EW (UK). Any request should be accompanied by a full literature citation for this communication.

[9] a) J. L. Atwood, M. F. Lappert, R. G. Smith, H. Zhang, *J. Chem. Soc. Chem. Commun. 1988*, 1308; b) H. van der Heijden, C. J. Schaverien, A. G. Orpen, *Organometallics 8* (1989) 255.

[10] M. R. Spirlet, J. Rebizant, C. Apostolidis, B. Kanellakopulos, *Acta Crystallogr. C43* (1987) 2322, and references cited herein.

[11] G. Boche, *Angew. Chem. 101* (1989) 286; *Angew. Chem. Int. Ed. Engl. 28* (1989) 277, and references cited herein.

[12] a) H. H. Murray, J. P. Fackler, A. M. Mazany, L. C. Porter, J. Shain, L. R. Falvello, *Inorg. Chim. Acta 114* (1986) 171; b) N. Bresciani-Pahor, L. Randaccio, M. Summers, P. J. Toscano, *ibid. 68* (1983) 69; c) P. S. Pregosin, R. Favez, R. Roulet, T. Boschi, R. A. Michelin, R. Ros, *ibid. 45* (1980) L7.

[13] J. Kaneti, P. von R. Schleyer, T. Clark, A. J. Kos, G. W. Spitznagel, J. G. Andrade, J. B. Moffat, *J. Am. Chem. Soc. 108* (1986) 1481.

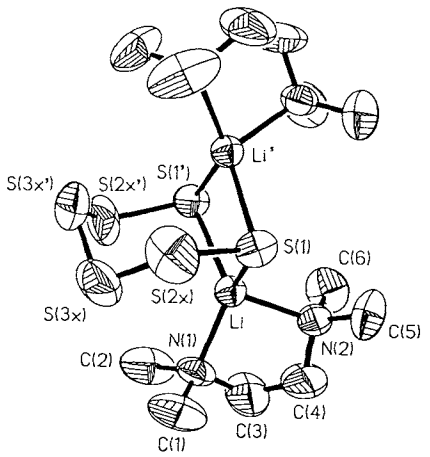

Fig. 1. Perspective drawing of $[Li(tmeda)_2][S_6]$ **1** showing the atom-labeling scheme. Of the disordered inner sulfurs, those of 59% occupancy are shown (x series). Thermal ellipsoids represent the 50% probability surfaces. Selected bond distances [Å] and angles [°]: Li-S(1) 2.497(7), Li-S(1') 2.489(7), Li-N(1) 2.138(8), Li-N(2) 2.136(8), Li-Li' 3.25(1), S(1)-S(2x) 2.044(9), S(2x)-S(3x) 2.05(1), S(3x)-S(3x') 2.079(7), Li-S(1)-Li' 81.3(3), S(1)-Li-S(1') 98.3(2), S(1)-Li-N(1) 132.2(3), S(1)-Li-N(2) 102.1(3), S(1')-Li-N(1) 119.4(3), S(1')-Li-N(2) 117.3(3), Li-S(1)-S(2x) 108.2(3), S(1)-S(2x)-S(3x) 108.2(4).—For the "inner" sulfur atoms with 41% occupancy (y series) the following metric data apply: S1-S2y 1.97(2), S2y-S3y 1.96(2), S3y-S3y' 2.04(1); Li-S1-S2y 95.9(4), S1-S2y-S3y 114.1(6)

Synthesis and Structure Determination of Bicyclic $[Li(tmeda)]_2[S_6]$***

By *Kazuyuki Tatsumi,* Yoshihisa Inoue, Akira Nakamura,* Roger E. Cramer,* William VanDoorne*, and *John W. Gilje*

Despite the recognized potential of the lithium–sulfur battery as a high-energy density power source,[1] there are so far no well characterized examples of lithium sulfides. In the binary lithium–sulfur system, only Li_2S and Li_2S_2 have been considered stable, although higher polysulfides may exist as in the analogous sodium–sulfur system.[2, 3] On the other hand, the crystal structures of some heavier alkali- and alkaline earth-polysulfides are known.[4, 5] These all contain ionic zigzag chains of $S_x^{2\ominus}$ (x = 3–6) which are well separated from the counterions. Here, we report that addition of *N,N,N',N'*-tetramethylethylenediamine (tmeda) to Li_2S_x (x = 2–6) in toluene induces formation of orange crystals of **1**,*** the X-ray analysis of which reveals a bicyclic Li_2S_6 molecular frame.[6]

$[Li(tmeda)_2][S_6]$ **1**

[*] Dr. K. Tatsumi, Prof. Dr. A. Nakamura, Y. Inoue
Department of Macromolecular Science, Faculty of Science
Osaka University
Toyonaka, Osaka 560 (Japan)
Prof. Dr. R. E. Cramer, Prof. Dr. W. VanDoorne [+],
Prof. Dr. J. W. Gilje
Department of Chemistry, University of Hawaii
Honolulu, HI 96822 (USA)

[+] Present address: Department of Chemistry, Calvin College
Grand Rapids, MI 49506 (USA)

[**] This work was supported by the National Science Foundation (Grant CHE 85-19289 for *R. E. C.* and *J. W. G.*) and by the donors of the Petroleum Research Fund administered by the American Chemical Society.

[***] Editorial note (March 16, 1990): Another synthesis of **1** and its structural characterization are described in a communication which appeared after this manuscript had been accepted: A. J. Banister, D. Barr, A. T. Brooker, W. Clegg, M. J. Cunnington, M. J. Doyle, S. R. Drake, W. R. Gill, K. Manning, P. R. Raithby, R. Snaith, K. Wade, D. S. Wright, *J. Chem. Soc. Chem. Commun. 1990*, 105.

The crystal structure of **1** is not an ionic lattice, but consists of discrete molecular units, in each of which two lithiums coordinate to one $S_6^{2\ominus}$ anion. A perspective drawing is shown in Figure 1, along with the salient intramolecular metric parameters. The most important aspect of the structure of **1** is that two lithium ions bridge the terminal sulfurs of $S_6^{2\ominus}$, one from above the $S_6^{2\ominus}$ unit and the other from below, thus making an unusual bicyclic Li_2S_6 geometry. This type of coordination is unique among the alkali- and alkaline earth-sulfides and also differs from the known structures of transition metal polysulfides.[7] For BaS_3, BaS_4, K_2S_5, and Cs_2S_6, the polysulfides have ionic acyclic geometries, and the cations do not bind specific sulfur atoms. In contrast, lithium in **1** is not an innocent counter cation. Instead its coordination to sulfur atoms is sufficiently strong to hold together the two ends of the semicircular S_6 chain, and is indicative of some degree of covalency in the Li–S bonds.

A crystallographic twofold axis passes through the midpoint of a line connecting the two terminal sulfur atoms and that of the two central sulfurs. The four "inner" sulfur atoms, of which two, S(2x) and S(3x), are related to the other two by the twofold axis of symmetry, are disordered with an occupancy factor of 0.591(9). Their complements, which are 0.409(9) occupancy, are labeled as S(2y) and S(3y). The two sets of S_6^{2-} ligands are located so that S(1) and S(1'), as well as Li and Li', are at the same position for both sets. In each the $S_6^{2\ominus}$ adopts a 'crown' conformation. In Figure 1, only the $S_6^{2\ominus}$ unit of 59% occupancy is shown for clarity.

The mean value of the S–S bond distances at 2.018 Å is normal.[8] The LiS(1)Li'S(1') quadrilateral is puckered with the dihedral angle between the two LiS_2 triangular faces being 10.6°. The Li–S distances (av. 2.493 Å) compare favorably with those in the compounds **2** (2.4 Å),[9a] **3** (2.52 Å),[9b] **4** (av. 2.42 Å),[9c] and **5** (av. 2.48 Å),[9d] and are shorter than

$[CH_3SLi]_n$ **2**

$[Li(tmeda)]_2[SCH_2CH_2CH_2SC(CH_3)]_2$ **3**

$[Li(dme)]_4[U(SCH_2CH_2S)_4]$ **4**

$[Li(dme)_2]_2(S_2CSCH_2CH_2SCS_2)$ **6**

the Li–S bonds in **6** (av. 2.747 Å).[9c] Further chelation by tmeda completes each lithium's pseudo-tetrahedral LiS_2N_2 coordination sphere. In order to ease steric congestion between the tmeda methyl groups and the $S_6^{2\ominus}$ ligand, the tmeda swings away from the polysulfide, as reflected by the notably larger S(1,1')–Li–N(1) angles relative to the S(1,1')–Li–N(2) angles.

The Raman spectrum of **1** (crystals) shown by the solid curve in Figure 2 is of interest. Alkali- and alkaline earth-polysulfides characterized thus far exhibit Raman bands in

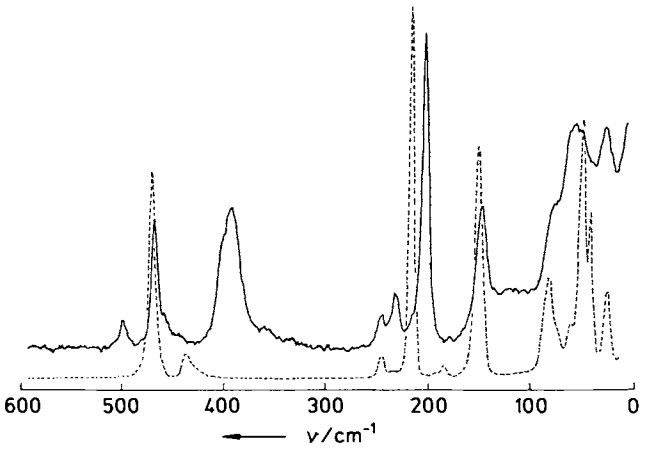

Fig. 2. Comparison of the Raman spectra of crystalline $[Li(tmeda)_2][S_6]$ **1** (——) and S_8 powder (– – –). The spectra were measured with a JASCO R-800 spectrometer equipped with an He–Ne laser. The samples were mounted in glass capillaries.

the 350–500 cm^{-1} region arising from S–S stretching vibrations.[10] Likewise for **1** the S–S stretches probably give rise to the bands at 395 cm^{-1} (broad) and 471 cm^{-1}. No other intense bands usually appear in the spectra of other polysulfides, while rather weak low-frequency bands have been assigned to lattice or bending modes. In this respect, the presence of strong lines at 205 cm^{-1} and 148 cm^{-1} for **1** deserves comment. These low-frequency Raman lines are not due to tmeda, and seem to be associated with the cyclic arrangement of Li_2S_6. As a matter of fact, the spectrum of **1** closely resembles that of elemental sulfur, S_8 (powder), which also shows intense lines at 218 cm^{-1} and 152 cm^{-1} (Figure 2, dashed curve). The two low-frequency S_8 bands were interpreted as e_1 and e_2 bending modes characteristic of the cyclic S_8 geometry,[11] and we think the corresponding bands for **1** are of a similar origin.

The complex **1** is the only lithium sulfide we could isolate from the tmeda/Li_2S_x (x = 2–6) system.[12] At present it is not entirely clear how the sulfur composition of **1** is controlled. In most transition metal polysulfides, a specific polysulfide ring size is thermodynamically stable. In other words, the ring size varies depending on the choice of the transition metal moiety.[13] Therefore, it would be interesting to examine whether a change in the 'auxiliary' ligand at Li affects the size of the $S_x^{2\ominus}$ fragment; and further studies in this direction are currently underway.

Experimental

An excess of tmeda (6 ml, 40 mmol) was added to a toluene slurry (60 mL) of a yellow powder obtained from the brown-red THF washings (4 × 30 mL) of Li_2S_2 [14] (2.6 g, 34 mmol), to give a homogeneous orange-red solution. Orange crystals (1.6 g, 3.7 mmol, 11% isolated yield based on Li) of **1** formed after the solution was concentrated and stored overnight at −20 °C [15]. The highly hygroscopic product is soluble in benzene, toluene, and THF, assuming a yellow color, but is not soluble in hexane. On the other hand, a DMF solution of **1** assumes a blue color (absorption maximum at 615 nm), which may be attributed to generation of the $S_3^{\ominus}$ radical anion in solution [16].

Received: November 10, 1989;
supplemented: January 3, 1990 [Z 3628 IE]
German version: *Angew. Chem. 102* (1990) 455

[1] J. R. Birk, R. K. Steunenberg *Adv. Chem. Ser. 140* (1975) 186, and references therein.

[2] According to phase diagram studies Li_2S_3 or Li_2S_4 may be a stable species above 360 °C: a) P. T. Cunningham, S. A. Johnson, E. J. Cairns, *J. Electrochem. Soc. 119* (1972) 1448; b) R. A. Sharma, *ibid. 119* (1972) 1439.

[3] a) D.-G. Oei, *Inorg. Chem. 12* (1973) 435, 438; b) L. S. Marcoux, E. T. Seo *Adv. Chem. Ser. 140* (1975) 216.

[4] a) R. Tegman, *Acta Crystallogr. Sec. B: Struct. Crystallogr. Cryst. Chem. 29* (1973) 1463; b) B. Kelly, P. Woodward, *J. Chem. Soc. Dalton Trans.* 1976, 1314; c) S. C. Abrahams, J. L. Bernstein, *Acta Crystallogr. Sec. B: Struct. Crystallogr. Cryst. Chem. 25* (1969) 2365; d) S. C. Abrahams, E. Grison, *Acta Crystallogr. 6* (1953) 206; e) A. Hordvik, E. Stetten, *Acta Chem. Scand. 22* (1968) 3029.

[5] $(Ph_4P)_2S_7$ and Tl_2S_5 contain ionic acyclic polysulfides as well. Cf. a) M. G. Kanatzidis, N. C. Baenziger, D. Coucouvanis, *Inorg. Chem. 22* (1983) 290; b) B. Leclerc, T. S. Kabré, *Acta Crystallogr. Sec. B: Struct. Crystallogr. Cryst. Chem. 31* (1975) 1675.

[6] A single crystal of **1** was mounted in a glass capillary and sealed under argon. Crystal size 0.7 × 0.5 × 0.2 mm, monoclinic, space group *C2/c*, $a = 22.808(4)$, $b = 9.194(1)$, $c = 15.038(2)$ Å, $\beta = 129.80(1)°$, $\varrho_{calcd} = 1.48$ g cm^{-3}, $Z = 4$, $\mu(Mo_{K\alpha}) = 5.13$ cm^{-1}. X-ray data were collected on a Nicolet *P3* diffractometer in the $\theta/2\theta$ mode using graphite-monochromated $Mo_{K\alpha}$ radiation. The data were corrected for Lorentz and polarization effects, and an empirical absorption correction was applied. The 931 observed reflections with $F_o^2 > 3.0\,\sigma(F_o^2)$ from 1255 measured reflections were used for the structure determination. The structure was solved by direct methods and the subsequent full-matrix least squares refinements gave final R values of $R = 0.0463$ and $R_G = 0.0444$. The inner four sulfur atoms of the S_6 unit, of which two are related to the other two by a crystallographically imposed C_2 axis, were found to be disordered with 0.591(9)/0.409(9) occupancy factors (x/y series). GOF = 1.81, $\Delta/\sigma = 0.49$, $(\varrho)_{max} = 0.20$ e $Å^{-3}$, $N_o/N_v = 8.8$. All computations with a Nicolet SHELXTL PLUS package with micro VAX II. Further details of the crystal structure analysis can be obtained from the Fachinformationszentrum Karlsruhe, Gesellschaft für wissenschaftlich-technische Information mbH, D-7514 Eggenstein-Leopoldshafen 2 (FRG), by quoting the depository number CSD-54331, the names of the authors, and the journal citation.

[7] M. Draganjac, T. B. Rauchfuss, *Angew. Chem. 97* (1985) 745; *Angew. Chem. Int. Ed. Engl. 24* (1985) 742, and references therein.

[8] D. Coucouvanis, P. R. Patil, M. G. Kanatzidis, B. Detering, N. C. Baenziger, *Inorg. Chem. 24* (1985) 24.

[9] a) E. Weiss, U. Joergens, *Chem. Ber. 105* (1972) 481; b) R. Amstutz, D. Seebach, P. Seiler, B. Achweizer, J. Dunitz, *Angew. Chem. 92* (1980) 59; *Angew. Chem. Int. Ed. Engl. 19* (1980) 53; c) K. Tatsumi, I. Matsubara, Y. Inoue, A. Nakamura, R. E. Cramer, G. J. Tagoshi, J. A. Golen, J. W. Gilje, unpublished; d) K. Tatsumi, Y. Inoue, A. Nakamura, R. E. Cramer, W. VanDoorne, J. W. Gilje, *J. Am. Chem. Soc. 111* (1989) 782.

[10] a) H. H. Eysel, G. Wieghardt, H. Kleinschmager, G. Weddingen, *Z. Naturforsch. B 31* (1976) 415; b) F. P. Daly, C. W. Brown, *J. Phys. Chem. 79* (1975) 350; c) G. J. Janz, E. Roduner, J. W. Coutts, J. R. Downey, Jr., *Inorg. Chem. 15* (1976) 1751; d) G. J. Janz, J. W. Coutts, J. R. Downey, Jr., E. Roduner, *ibid. 15* (1976) 1755; e) G. J. Janz, J. R. Downey, Jr., G. J. Wasilczyk, J. W. Coutts, A. Eluard, *ibid. 15* (1976) 1759; f) H. Ziemann, W. Bues, *Z. Anorg. Allg. Chem. 455* (1979) 69.

[11] a) D. W. Scott, J. P. McCullough, *J. Mol. Spectrosc. 13* (1964) 313; b) R. Steudel, H.-J. Mäusle, *Z. Naturforsch. A 33* (1978) 951, and references therein.

[12] Lithium polysulfides in liquid ammonia have recently been characterized by Raman and UV/VIS spectroscopy; suggest existence of Li_2S_2, Li_2S_4, Li_2S_5, and Li_2S_6, in addition to $S_3^{\ominus}$ and probably Li_2S. Interestingly, the least reduced polysulfide in the solution was claimed to be $S_6^{2\ominus}$: P. Dubois, J. P. Lelieur, G. Lepoutre, *Inorg. Chem. 27* (1988) 73.

[13] For example, the size of the polysulfide ring in the $(C_5H_5)_2MS_x$ and $(C_5Me_5)_2MS_x$ systems seems to depend on the organometal fragment; x = 5 for $(C_5H_5)_2M$ (M = Ti, Zr, Hf, V) and $(C_5Me_5)_2Th$, x = 4 for $(C_5H_5)_2Mo$ and $(C_5H_5)_2W$, x = 3 for $(C_5Me_5)_2Ti$: E. Samuel, *Bull. Soc. Chim. Fr. 1966*, 2548; M. Schmidt, B. Block, H. D. Block, H. Köpf, E. Wilhelm, *Angew. Chem. 80* (1968) 660; *Angew. Chem. Int. Ed. Engl. 7* (1968) 632; E. F. Epstein, I. Bernal, H. Köpf, *J. Organomet. Chem. 26* (1971) 229; E. G. Müller, J. L. Petersen, L. F. Dahl, *ibid. 111* (1976) 91; J. M. McCall, A. Shaver, *ibid. 193* (1980) C 37; H. Köpf, *Angew. Chem. 81* (1969) 332; *Angew. Chem. Int. Ed. Engl. 8* (1969) 375; B. R. Davis, I. Bernal, H. Köpf, *ibid. 83* (1971) 1018 and *10* (1971) 921; P. H. Bird, J. M.

McCall, A. Shaver, U. Siriwardane, *ibid. 94* (1982) 375 and *21* (1982) 384; D. A. Wrobleski, D. T. Cramer, J. V. Ortiz, T. B. Rauchfuss, R. R. Ryan, A. P. Sattelberger, *J. Am. Chem. Soc. 108* (1986) 174.

[14] "Li_2S_2" was prepared as a light yellow powder by reaction of lithium metal and elemental sulfur (1:1) in liquid ammonia. According to the Raman spectra, this material is nearly identical with that prepared from $LiEt_3BH$ ("superhydride") and 1/8 S_8, and presumably contains small quantities of other lithium sulfides, e.g., Li_2S, Li_2S_3, Li_2S_4 as well as S_8. Disproportionation might occur in THF, and in view of the dark color, the sulfur content in the THF washings is probably higher than the original Li_2S_2 stoichiometry. The other polysulfides Li_2S_x (x = 3–6) were also prepared in liquid ammonia.

[15] a) All manipulations were carried out under argon using dry solvents. b) Addition of tmeda directly to a slurry of "Li_2S_2" in toluene followed by standard work-up furnished crystals of **1** in a higher yield, but this method occasionally gave a small amount of S_8 crystals as a side product. As was to be expected, **1** was obtained from Li_2S_x (x = 3–6) + tmeda systems as well. ^{1}H NMR of **1** (100 MHz, C_6D_6, room temperature) $\delta = 2.00$ (s, 4H, CH_2), 2.18 (s, 12H, CH_3). c) The ^{1}H-NMR spectrum of free tmeda (neat) shows two singlets at $\delta = 2.39$ (CH_2) and 2.26 (CH_3).

[16] a) R. Bonnaterre, G. Cauquis, *J. Chem. Soc. Chem. Commun. 1972*, 293; b) D. M. Gruen, R. L. McBeth, A. J. Zielen, *J. Am. Chem. Soc. 93* (1971) 6691.

A Monocyclic Selenepine: Synthesis and Characterization of Diethyl 2,7-Di-*tert*-butyl-4,5-selenepinedicarboxylate**

By *Hideaki Hori, Shoko Yamazaki, Kagetoshi Yamamoto,** and *Ichiro Murata**

Although much interest has recently been focused on selenium heterocycles,[1] the field of selenepines still remains unexplored.[2] Preparation and characterization of selenepines have been confined to only a few dibenzo[*b*,*f*]-selenepine derivatives owing to facile loss of selenium.[3] The characteristic features of bond length, bond angle, and bond dissociation energy associated with the C–Se bond predict that selenepines should have a different geometry from that of other "heteropines" and should be thermally less stable than thiepines.

The synthesis of monocyclic selenepines, like that of monocyclic thiepines, must take into account their expected thermal instability. The findings on monocyclic thiepines[4, 5] and 1,4-thiazepine[6] indicate that an isolable selenepine has to posses at least one bulky group at both C-2 and C-7 positions. Here we report the first synthesis and characterization of diethyl 2,7-di-*tert*-butyl-4,5-selenepinedicarboxylate (**1c**).

The synthesis of the three selenepines **1a**–**1c** was carried out via the key intermediate cation salts **4a**–**4c**, prepared in the usual manner. Reaction of **2**[7] with lithium aluminum hydride and with methyllithium in ether gave the alcohols **3a** and **3b**, respectively, which were not isolated owing to their susceptibility to air oxidation. Treatment of **3a** and **3b** with aqueous 42% HBF_4 gave **4a** (66%) and **4b** (86%), respectively. The cation **4a** was reduced with $LiAlH_4$ to the selenapyran **7**. Treatment of **7** with lithium diisopropylamide at −78 °C in THF–HMPA gave the corresponding anion, which was quenched with dry CO_2 to afford the carboxylic acid **8a**. Compound **8a** was converted into the ester **8b** (68%) with diazoethane. On treatment with Ph_3CBF_4 in dichloromethane at room temperature for 20 h, **8b** was transformed into the cation **4c** (58% from **4a**).

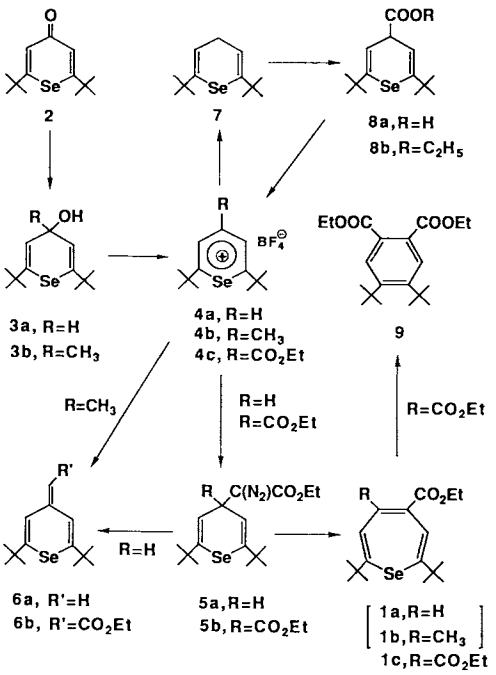

Reaction of **4a** and **4c** with ethyl lithiodiazoacetate, generated in THF–ether at −110 °C from ethyl diazoacetate, gave **5a** (16%) and **5b** (21%), respectively. The 4-position of the diazoester group is clearly shown by the symmetrical signal patterns in the ^{1}H-NMR spectra. Unfortunately, reaction of **4b** with ethyl lithiodiazoacetate led to exclusive formation of a deprotonation product **6a** under the usual conditions as well as under a variety of modified conditions.

The final conversion of **5a** to **1a** met with obstacles. Treatment of **5a** with a catalytic amount of di-μ-chlorobis(π-allyl)palladium(II) gave **6b** instead of **1a**. No identifiable product could be isolated from **5a** under acidic conditions. However, the ring expansion of **5b** proceeds smoothly in the presence of $[Pd(C_3H_5)_2Cl_2]$ at −20 °C and can be monitored by ^{1}H-NMR spectroscopy in $CDCl_3$. The signals due to **5b**

Table 1. Some physical data for compounds **1c**, **4a**, **4b**, **4c**, and **8b**.

1c: ^{1}H NMR (90 MHz, $CDCl_3$): $\delta = 1.17$ (s, 18H; $C(CH_3)_3$), 1.24 (t, $J = 7.0$ Hz, 6H; OCH_2CH_3), 4.25 (q, $J = 7.0$ Hz, 4H; OCH_2CH_3), 6.58 (s, 2H; H-3)

4a: colorless crystals, m.p. 183–183.5 °C (from EtOH/hexane, (1:1)); ^{1}H NMR (100 MHz, CD_2Cl_2): $\delta = 1.66$ (s, 18H; $C(CH_3)_3$), 8.56 (AB_2, $J = 6.7$ Hz, 2H; H-3, H-5), 8.95 (AB_2, $J = 6.7$ Hz, 1H; H-4); IR (KBr): $\tilde{\nu} = 1083$ cm^{-1} ($BF_4^{\ominus}$)

4b: colorless needles, m.p. 153–154.5 °C (from EtOH/hexane, (1:1)); ^{1}H NMR (60 MHz, $CDCl_3$): $\delta = 1.64$ (s, 18H; $C(CH_3)_3$), 2.78 (s, 3H; CH_3), 8.24 (s, 2H; H-3, H-5); IR (KBr): $\tilde{\nu} = 1055$ cm^{-1}

8b: colorless oil. ^{1}H NMR (60 MHz, $CDCl_3$): $\delta = 1.16$ (s, 18H; $C(CH_3)_3$), 1.30 (t, $J = 7$ Hz, 3H; OCH_2CH_3), 4.20 (q, $J = 7$ Hz, 2H; OCH_2CH_3), 3.03 (t, $J = 4$ Hz, 1H; H-4), 5.96 (d, $J = 4$ Hz, 2H; H-3, H-5). IR (neat): $\tilde{\nu} = 1730$ cm^{-1}

4c: colorless crystals, m.p. 161.5–162.5 °C (from THF). ^{1}H NMR (90 MHz, $CDCl_3$): $\delta = 1.70$ (s, 18H; $C(CH_3)_3$), 1.49 (t, $J = 7.0$ Hz, 3H; OCH_2CH_3), 4.56 (q, $J = 7.0$ Hz, 2H; OCH_2CH_3), 8.86 (s, 2H; H-3, H-5). IR (KBr): $\tilde{\nu} = 1720$, 1050 cm^{-1}

[*] Prof. Dr. I. Murata, Prof. Dr. K. Yamamoto, Dipl.-Chem. H. Hori
Department of Chemistry, Faculty of Science, Osaka University
Toyonaka, Osaka 560 (Japan)
Prof. Dr. S. Yamazaki
Nara University of Education
Takabatake-cho, Nara 630 (Japan)

[**] This work was supported by a Grant-in-Aid for Scientific Research on Priority Areas (No. 01 648 003) from the Ministry of Education, Science and Culture (Japan).

[11] J. Friedrich, S. Davies, R. Freeman, *J. Magn. Reson. 75* (1987) 390; S. Davies, J. Friedrich, R. Freeman, *ibid. 75* (1987) 540; H. Kessler, H. Oschkinat, C. Griesinger, *ibid. 70* (1986) 106; R. Freeman, J. Friedrich, S. Davies, *Magn. Reson. Chem. 26* (1988) 903.
[12] R. Brüschweiler, J. C. Madsen, C. Griesinger, O. W. Sørensen, R. R. Ernst, *J. Magn. Reson. 73* (1987) 380; J. Cavanagh, J. P. Waltho, J. Keeler, *ibid. 74* (1987) 386.
[13] P. Pfändler, G. Bodenhausen, B. U. Meier, R. R. Ernst, *Anal. Chem. 57* (1985) 2510.
[14] B. U. Meier, Z. L. Mádi, R. R. Ernst, *J. Magn. Reson. 74* (1987) 565; M. Nović, G. Bodenhausen, *Anal. Chem. 60* (1988) 582.
[15] P. Pfändler, G. Bodenhausen, *Magn. Reson. Chem. 26* (1988) 888.
[16] H. Oschkinat, W. Bermel, *J. Magn. Reson. 81* (1989) 220.
[17] L. Emsley, G. Bodenhausen, *J. Magn. Reson. 82* (1989) 211.
[18] L. Emsley, G. Bodenhausen, *Magn. Reson. Med. 10* (1989) 273; *J. Magn. Reson. 87* (1990), in press.
[19] L. Emsley, G. Bodenhausen, *Chem. Phys. Lett. 165* (1990) 469.

Synthesis of (±)-Phyllanthocin via a Metal-Catalyzed Cycloreduction**

By *Barry M. Trost** and *Eric D. Edstrom*

The novel molecular architecture and promising biological activity of phyllanthoside[1] has made its aglycone, phyllanthocin (**1**),[2] an attractive synthetic target.[3] The development of a cycloisomerization[4] and of a reductive cyclization[5] of enynes under very mild conditions suggested a convenient convergent strategy from two relatively simple building blocks of about equal size (cf. Scheme 1). The failure of many transition-metal-catalyzed reactions with more elaborate structures led us to test the feasibility of such processes for the construction of oxygen heterocycles in general[6] and to assess the feasibility of its applicability for complex molecule construction by undertaking a synthesis of (±)-phyllanthocin (**1**).

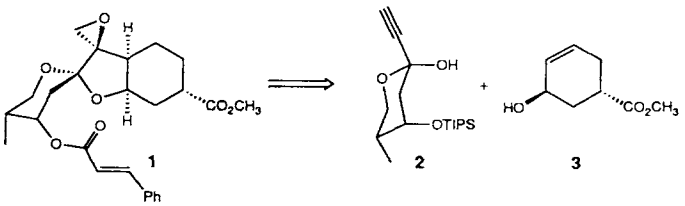

Scheme 1.

The known cyclohexenol **3**[7] is conveniently available from the *cis*-diastereomer[8] in 85% yield by application of the Mitsunobu reaction (Scheme 2).[9]

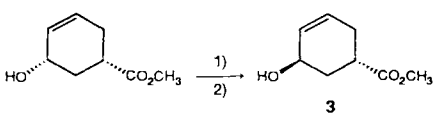

Scheme 2. Synthesis of the cyclohexenol component **3**. 1) PPh_3, DEADCAT ($C_2H_5O_2CN{=}NCO_2C_2H_5$), HCO_2H, THF; 2) $KHCO_3$, CH_3OH.

[*] Professor B. M. Trost, Dr. E. D. Edstrom
Department of Chemistry, Stanford University
Stanford, CA 94305-5080 (USA)

[**] This work was supported by the National Institutes of Health (NIH), Institute of General Medical Sciences. Mass spectra were provided by the Mass Spectrometry Facility, University of California-San Francisco, supported by the NIH Division of Research Resources.

The lactol **2** is available in four steps from the known (2*R**,3*S**)-2-methyl-1-(phenylmethoxy)hex-5-en-3-ol (**4**)[10] (Scheme 3). The choice of protecting group proved crucial owing to the ease of β-elimination during nucleophilic additions to lactone **7**. The triisopropylsilyl protecting group (TIPS) proved efficacious both in terms of its introduction and removal, as well as in terms of its chemical stability in subsequent transformations.[11] Oxidative olefin cleavage proceeded efficiently with buffered potassium permanganate under phase transfer conditions[12] or, for this particular substrate, using the *Lemieux* and *von Rudloff* protocol.[13] Hydrogenolysis of the benzyl ether **6** followed by acidification produces the lactone **7**.[14] Maintaining the acetylide addition at −78 °C followed by quenching with methanol:acetic acid (10:1) prevents the undesired β-elimination. In this way, the lactol **2**[14] is available in 68% overall yield from olefin **4**.

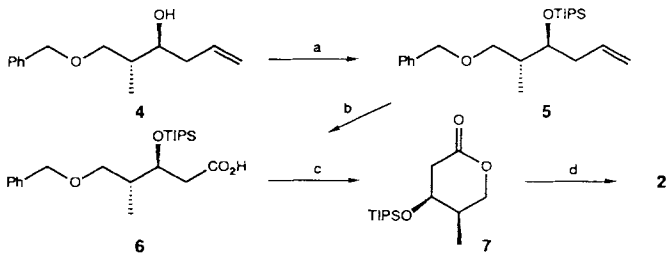

Scheme 3. Synthesis of the lactol component **2**. a) TIPS-OSO_2-CF_3, 2,6-lutidine, CH_2Cl_2, 99%. b) $NaIO_4$, $KMnO_4$ (cat.), *tert*-C_4H_9OH, H_2O, RT, pH 7. c) H_2, 10% Pd/C, C_2H_5OH, directly thereafter pyridinium *p*-toluenesulfonate, 5 Å molecular sieve, benzene, 74% overall yield referred to **5**. d) $(CH_3)_3SiC{\equiv}CLi$, THF, −78 °C, 93%. TIPS = $[(CH_3)_2CH]_3Si$.

The glycosidic coupling event entails treating a solution of the lactol **2** with 2 equivalents of hydroxy ester **3** in benzene (0.3 M) containing K 10 montmorillonite clay[15] and powdered 5 Å molecular sieves at room temperature (75% yield). Due to the fact that our starting materials are racemic, a mixture of **8a**[14] and **9a** is produced which cleanly separates after desilylation to **8b**[14] and **9b**[14] (K_2CO_3, CH_3OH, 0 °C) (Scheme 4). The production of such a mixture does not

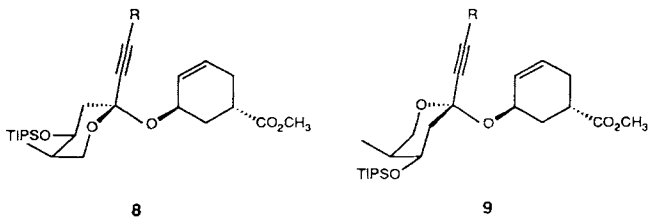

Scheme 4. Products of the reaction of **2** with **3**. **a**, R = $(CH_3)_3Si$; **b**, R = H.

constitute a shortcoming of the synthesis since it can be totally avoided simply by using enantiomerically pure building blocks **2** and **3**.[16] For our purposes, exploring the cyclization of both isomers (**8b** and **9b**) is desirable. Using carefully defined catalytic conditions with proper choice of silane effects (Scheme 5) excellent yields (86% and 78% of **10a**[14] and **11a**,[14] respectively) of the requisite polyhydrobenzofurans. For characterization, **10a** and **11a** were

subjected to ozonolysis and hydrolysis; the ketols **10b**[14] and **11b**[14, 17] were formed in 89% and 88% yields, respectively. For subsequent comparison purposes, the cyclized product **11a** was also transformed into the *epi*-compound **12**.

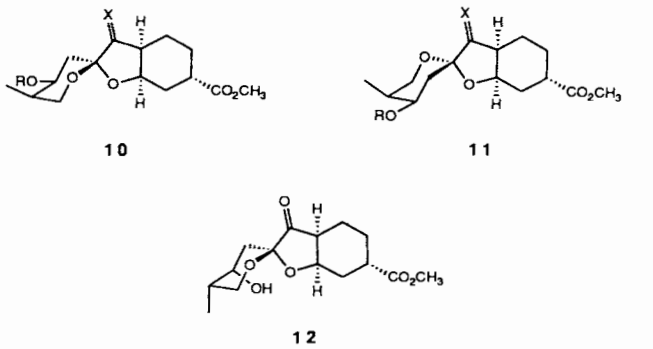

Scheme 5. Products derived from **8b** and **9b**. **a**, R = TIPS, X = CH_2; **b**, R = H, X = O. Reactions **8b** → **10a** and **9b** → **11a**: polymethylsilanol, $[(dba)_3Pd_2CHCl_3]$ (dba = dibenzylideneacetone), *N*,*N*′-dibenzylideneethylenediamine, CH_3COOH, CH_2Cl-CH_2Cl, RT. Reactions **10a** → **10b** and **11a** → **11b**: 1) O_3, CH_3OH, CH_2Cl_2, −78 °C; 2) $ZnBr_2$, CH_2Cl_2, RT; 3) O_3, CH_3OH, CH_2Cl_2, −78 °C.

In pursuing our objective of phyllanthocin, its entire carbon skeleton with the correct stereochemistry (see **13**[14]) arises by desilylation of **10a** as readily discerned by the appearance of the protons at C-6′ [3.76 (t, J = 11.8 Hz) and 3.48 (dd, J = 11.8, 4.9 Hz)] (cf. Scheme 6). Ozonolysis provides the ketone **14**[14]—a common intermediate in many of the previous syntheses of phyllanthocin. Following the literature sequence of epoxidation with dimethylsulfonium methylide (96%) and cinnamoylation (68%)[3] completes the formation of synthetic phyllanthocin, spectroscopically identical to the natural product.

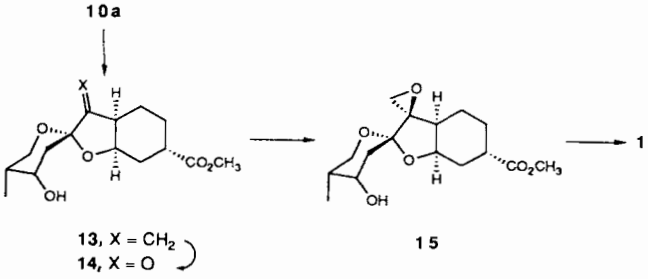

Scheme 6. Last step of the synthesis of **1**. Reaction **10a** → **13**: aqueous HF (30%), CH_3CN, RT, 82%. Reaction **13** → **14**: O_3, CH_3OH, CH_2Cl_2, −78 °C, 95%.

Three aspects of this synthesis are noteworthy. The successful glycosylation catalyzed by K 10 montmorillonite clay efficiently joins the two halves and should prove more generally useful (**2** + **3** → **8** + **9**). The excellent yields in the reductive cyclization (**8b** → **10a**) are particularly gratifying, especially since attempts to close the ring by thermal Alder ene reactions completely fail. The availablity of this new reaction for the synthesis of oxygen heterocycles creates a very simple strategy to phyllanthocin which proceeds in only five steps (38% unoptimized overall yield) from the two halves which, themselves, require few steps (two and four, respectively) from simple known starting materials. The introduction of this palladium-catalyzed cycloreduction appears to be a powerful complement to Alder ene chemistry in not only effecting reactions that otherwise fail but also providing novel variation of the types of products available.

Table 1. Selected spectroscopic data for key intermediates. IR (neat); 400-MHz ^1H NMR ($CDCl_3$); ^{13}C NMR ($CDCl_3$). J in Hz. Correct elemental analyses (C,H).

7: IR: $\tilde{\nu}$ = 1730, 1460 cm^{-1}. ^1H NMR: δ = 4.30 (t, J = 10.3, 1H), 4.23 (m, 1H), 4.16 (dd, J = 10.8, 4.4, 1H), 2.68 (t, J = 4.0, 2H), 2.12 (m, 1H), 1.07 (b, 21H), 1.02 (d, J = 6.8, 3H). ^{13}C NMR (75 MHz): δ = 170.1 (C), 70.3 (CH), 67.8 (CH_2), 39.4 (CH), 33.7 (CH_2), 17.8 (CH_3), 12.2 (CH_3), 11.8 (CH)

8a: IR ($CHCl_3$): $\tilde{\nu}$ = 2170, 1735, 1460 cm^{-1}. ^1H NMR: δ = 5.86 (m, 1H), 5.78 (m, 1H), 4.51 (m, 1H), 4.19 (dt, J = 10.3, 5.4, 1H), 3.84 (dd, J = 11.4, 2.3, 1H), 3.70 (s, 3H), 3.47 (dd, J = 11.4, 1.4, 1H), 2.76 (m, 1H), 2.35 (m, 2H), 2.14 (m, 1H), 1.98 (bs., 1H), 1.96 (d, J = 4.8, 1H), 1.85 (m, 1H), 1.69 (m, 1H), 1.05 (d, J = 7, 3H), 1.04 (b, 21H), 0.18 (s, 9H). ^{13}C NMR (75 MHz): δ = 176.6 (C), 129.3 (CH), 127.7 (CH), 103.2 (C), 95.7 (C), 88.5 (C), 66.0 (CH), 65.7 (CH), 65.5 (CH_2), 51.6 (CH_3), 40.2 (CH_2), 35.2 (CH), 34.7 (CH), 32.1 (CH_2), 27.6 (CH_2), 17.8 (CH_3), 12.0 (CH_3), 9.2 (CH), −0.6 (CH_3)

8b: IR: $\tilde{\nu}$ = 3320, 2120, 1740 cm^{-1}. ^1H NMR: δ = 5.87 (ddd, J = 9.8, 4.4, 2.0, 1H), 5.79 (m, 1H), 4.53 (m, 1H), 4.20 (m, 1H), 3.85 (dd, J = 11.6, 2.4, 1H), 3.70 (s, 3H), 3.47 (dd, J = 11.6, 2.0, 1H), 2.77 (dddd, J = 12.4, 10.8, 5.6, 3.2, 1H), 2.56 (s, 1H), 2.35 (dt, J = 18.0, 5.0, 1H), 2.28 (br.d, J = 13.6, 1H), 2.15 (dddd, J = 16.4, 10.8, 3.6, 1.8, 1H), 2.02 (br. s, 1H), 2.00 (br.d, J = 4.8, 1H), 1.84 (m, 1H), 1.72 (ddd, J = 13.2, 12.8, 4.0, 1H), 1.05 (br., 24H). ^{13}C NMR (100 MHz): δ = 176.2 (C), 129.3 (CH), 127.3 (CH), 95.7 (C), 81.8 (C), 72.1 (C), 66.0 (CH), 65.9 (CH), 65.6 (CH_2), 51.7 (CH_3), 40.7 (CH_2), 35.3 (CH), 34.8 (CH), 32.2 (CH_2), 27.7 (CH_2), 18.0 (CH_3), 12.2 (CH_3), 9.4 (CH)

10a: IR: $\tilde{\nu}$ = 1735, 1460, 880 cm^{-1}. ^1H NMR: δ = 5.18 (d, J = 1.5, 1H), 5.07 (d, J = 1.5, 1H), 4.29 (dt, J = 11.3, 4.9, 1H), 4.12 (m, 1H), 4.04 (dd, J = 11.5, 2.4, 1H), 3.67 (s, 3H), 3.55 (dd, J = 11.4, 1.3, 1H), 2.64 (m, 1H), 2.55 (m, 1H), 2.13 (dt, J = 14.4, 4.3, 1H), 1.86 (m, 4H), 1.74 (m, 1H), 1.67 (dd, J = 13.1, 4.3, 1H), 1.47 (m, 1H), 1.10 (d, J = 7.0, 3H), 1.05 (br., 21H). ^{13}C NMR (75 MHz): δ = 176.5 (C), 155.7 (C), 107.7 (CH_2), 106.2 (C), 74.5 (CH), 67.3 (CH), 66.5 (CH_2), 51.5 (CH_3), 41.6 (CH), 38.0 (CH_2), 37.5 (CH), 35.3 (CH), 30.1 (CH_2), 25.4 (CH_2), 25.3 (CH_2), 17.8 (CH_3), 12.0 (CH_3), 9.0 (CH)

13: IR: $\tilde{\nu}$ = 3530, 1730 cm^{-1}. ^1H NMR: δ = 5.10 (d, J = 1.8, 1H), 5.08 (d, J = 1.8, 1H), 4.31 (m, 1H), 3.85 (dq, J = 10.3, 5.2, 2.5, 1H), 3.76 (t, J = 11.8, 1H), 3.68 (s, 3H), 3.48 (dd, J = 11.3, 4.9, 1H), 3.33 (d, J = 10.4, 1H), 2.55 (m, 2H), 2.30 (dddd, J = 15.0, 4.1, 2.1, 2.0, 1H), 2.06 (dd, J = 14.0, 3.0, 1H), 1.95 (dd, J = 14.0, 3.0, 1H), 1.90 (m, 2H), 1.77 (m, 2H), 1.22–1.59 (m, 2H), 0.91 (d, J = 7.0, 3H). ^{13}C NMR (75 MHz): δ = 176.4 (C), 156.8 (C), 108.1 (CH_2), 104.3 (C), 74.6 (CH), 68.6 (CH), 62.5 (CH_2), 51.6 (CH_3), 41.2 (CH), 40.3 (CH_2), 37.0 (CH), 34.3 (CH), 29.3 (CH_2), 28.5 (CH_2), 26.7 (CH_2), 12.8 (CH_3)

14, **15**, **1**: Spectral data identical to authentic sample [3].

Received: January 8, 1990 [Z 3726 IE]
German version: *Angew. Chem. 102* (1990) 541

CAS Registry numbers:
1, 62948-37-2; **2**, 126544-28-3; **3**, 126640-65-1; **4**, 94233-74-6; **5**, 126544-29-4; **6**, 126544-30-7; **7**, 126544-31-8; **8a**, 126544-32-9; **8b**, 126544-33-0; **9a**, 126640-66-2; **9b**, 126640-67-3; **10a**, 126544-34-1; **10b**, 126544-36-3; **11a**, 126544-35-2; **11b**, 89690-43-7; **12**, 119719-67-4; **13**, 126544-37-4; **14**, 126640-68-4.

[1] G. R. Pettit, G. M. Cragg, D. Gust, P. Brown, *Can. J. Chem. 60* (1982) 544; G. R. Pettit, G. M. Cragg, D. Gust, P. Brown, J. M. Schmidt, *Can. J. Chem. 60* (1982) 939; G. R. Pettit, G. M. Cragg, M. L. Niven, L. R. Nassimbeni, *ibid. 61* (1983) 2630; G. R. Pettit, G. M. Cragg, M. I. Suffness, D. Gust, F. E. Boettner, M. Williams, J. A. Saenz-Renauld, P. Brown, J. M. Schmidt, P. D. Ellis, *J. Org. Chem. 49* (1984) 4258; G. R. Pettit, G. M. Cragg, M. Suffness, *ibid. 50* (1985) 5060.

[2] S. M. Kupchan, E. J. LaVoie, A. R. Braufman, B. Y. Fei, W. M. Bright, R. F. Bryan, *J. Am. Chem. Soc. 99* (1977) 3199.

[3] a) P. R. McGuirk, D. B. Collum, *J. Am. Chem. Soc. 104* (1982) 4496; b) D. R. Williams, S.-Y. Sit, *ibid. 106* (1984) 2949; c) P. R. McGuirk, D. B. Collum, *J. Org. Chem. 49* (1984) 843; d) S. D. Burke, J. E. Cobb, K. Takeuchi, *ibid. 50* (1985) 3420; e) A. B. Smith III, M. Fukui, *J. Am. Chem. Soc. 109* (1987) 1269; f) S. F. Martin, M. S. Dappen, B. Dupré, C. J. Murphy, *J. Org. Chem. 52* (1987) 3706; g) S. F. Martin, M. S. Dappen, B. Dupré, C. J. Murphy, J. A. Colapret, *ibid. 54* (1989) 2209.

[4] B. M. Trost, M. Lautens, *J. Am. Chem. Soc. 107* (1985) 1781.

[5] B. M. Trost, F. Rise, *J. Am. Chem. Soc. 109* (1987) 3161.

[6] B. M. Trost, E. Edstrom, M. B. Carter-Petillo, *J. Org. Chem. 54* (1989) 4489.
[7] B. M. Trost, T. R. Verhoeven, *J. Am. Chem. Soc. 102* (1989) 4730.
[8] a) M. Kato, M. Kogeyama, R. Tanaka, K. Kumahara, A. Yoshikoshi, *J. Org. Chem. 40* (1975) 1932; b) B. M. Trost, J. Timko, J. Stanton, *J. Chem. Soc. Chem. Commun. 1989*, 436.
[9] O. Mitsunobu, M. Eguchi, *Bull. Chem. Soc. Jpn. 44* (1971) 3427; G. Grynkiewicz, H. Burzynska, *Tetrahedron 32* (1976) 2109.
[10] C. H. Heathcock, S. Kiyooka, T. A. Blumenkopf, *J. Org. Chem. 49* (1984) 4214.
[11] E. J. Corey, H. Cho, C. Rücker, D. H. Hua, *Tetrahedron Lett. 22* (1981) 3455; R. F. Cunico, L. Bedell, *J. Org. Chem. 45* (1980) 4797.
[12] D. G. Lee, V. S. Chang, *J. Org. Chem. 43* (1978) 1532.
[13] R. V. Lemieux, E. von Rudloff, *Can. J. Chem. 33* (1955) 1701; J. W. ApSimon, A. S. Y. Chau, W. G. Craig, *ibid. 45* (1967) 1439.
[14] A complete spectroscopic analysis has been carried out and the elemental composition has been established by combustion analysis and/or high resolution mass spectroscopy.
[15] For brief reviews on the use of clays in synthesis, see A. M. McKillop, O. W. Young, *Synthesis 1975*, 481; P. Laszlo, *Science 210* (1987) 1473.
[16] The enantiomerically pure precursor of **2** is known [3 f, g, 8 b] as is also that for **3**, see H. C. Brown, K. S. Bhat, R. S. Randad, *J. Org. Chem. 54* (1989) 1570; A. I. Meyers, K. A. Babiak, A. L. Campbell, D. L. Comins, M. P. Fleming, R. Henning, M. Heuschmann, J. P. Hudspeth, J. M. Kane, P. J. Reider, D. M. Roland, K. Shimizu, K. Tomioka, R. D. Walkup, *J. Am. Chem. Soc. 103* (1983) 5015.
[17] *Martin* et al. [3 g] report a tentative assignment of structure **10 b** for a minor product of his spiroketalization. However, our data for **11 b** corresponds to the compound described by *Martin* et al.

Bis(*N,N*-diisopropylamino)trimethylsiloxyphosphane: A Novel Flexible Phosphitylating Reagent in Nucleoside Chemistry and Its Application in the Synthesis of *P*-Modified Nucleotides **

By *Wojciech Dąbkowski, Jan Michalski,** and *Wang Qing*

Dedicated to Professor Günther Wilke on the occasion of his 65th birthday

In 1976, *Letsinger* et al.[1] developed a method for the linking of nucleosides via phosphite groups with phosphorochloridites which was more convenient than earlier routes. This method was further improved by the phosphoroamidite approach of *Caruthers* et al.[2] Since then a variety of modified Letsinger reagents have been proposed.[3] However, only those containing simple alkoxy groups attached to the tricoordinate phosphorus are suitable for constructing intermediates for the synthesis of *P*-modified nucleotides via the Michaelis-Arbuzov reaction.[4] Prior to our present studies phosphitylating reagents containing siloxy groups were almost unknown.[5]

Bis(*N,N*-diethylamino)trimethylsiloxyphosphane had already been characterized by *Alfonsov* et al. in 1976 and was used for the silylation of ethyl alcohol.[6]

$$(Et_2N)_2POSiMe_3 + EtOH \rightarrow (Et_2N)_2P(O)H + EtOSiMe_3$$

In contrast we were able to demonstrate that bis(*N,N*-diisopropylamino)trimethylsiloxyphosphane (**1**) as well as other *N,N*-dialkylamino analogues exhibit phosphitylating properties in the presence of 1*H*-tetrazole. Due to its ready availability, stability, and relatively high phosphitylating power, the phosphane **1** seems to be the current reagent of choice.

The title phosphane **1** was prepared from readily available chlorobis(*N,N*-diisopropylamino)phosphane[7] in almost quantitative yield (Scheme 1). This new phosphitylating reagent, which can be distilled without decomposition in vacuo, solidifies to a low-melting solid. It can be stored at room temperature and used in phosphitylating procedures without special precautions.

$$(iPr_2N)_2PCl \xrightarrow{H_2O} (iPr_2N)_2POH \xrightarrow{Me_3SiCl} (iPr_2N)_2POSiMe_3$$

1

Scheme 1. One-pot synthesis of **1**. H_2O/Et_3N (1/1) in ether, 2 h, 20 °C; Me_3SiCl/Et_3N (1/1), 2 h, 20 °C; yield 90%. **1**, b.p. 100–102 °C/0.01 torr; ^1H NMR ($CDCl_3$, TMS int.): δ = 0.3 (s, 9H), 0.9 (d, 24H), 3.0–3.7 (m, 4H); ^{31}P NMR ($CDCl_3$, 85% H_3PO_4 ext.): δ = 108.23. DMTr = 4,4′-dimethoxytrityl.

The most important property of the siloxyphosphane **1** is its ability to undergo highly selective nucleophilic substitution at the tricoordinate phosphorus atom without affecting the silicon center under conditions which are commonly used in the phosphite triester approach. In the phosphitylation of alcohols the reactivity of the phosphane **1** is similar to that of the corresponding alkoxy derivatives. A number of 3′,5′-dinucleoside trimethylsilylphosphites **3** have been prepared in this way in very high yield without isolation of the intermediate **2** (Scheme 2).

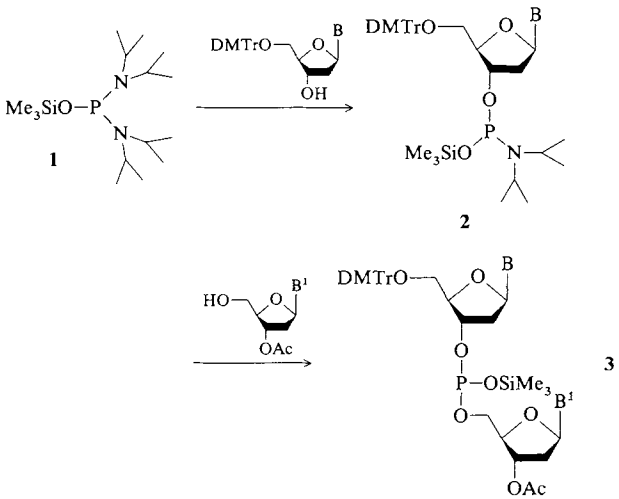

3a, B = B¹ = Thy[8a]; 3b, B = B¹ = Ade(bz); **3c**, B = Thy, B¹ = Ade(bz); **3d**, B = Ade(bz), B¹ = Thy

Scheme 2. One-pot synthesis of **3** (via **2**). Nucleoside with a free 3′-hydroxy-group/diisopropylammoniumtetrazolide (1/1), 15 min, 20 °C, CH_3CN; nucleoside with a free 5′-hydroxy group/diisopropylammonium tetrazolide, 5 min, 20 °C, CH_3CN. Yield (determined by ^{31}PNMR spectroscopy) 95–97%. ^{31}P NMR ($CDCl_3$, 85% H_3PO_4 ext.): δ = 117.6, 116.8 (**3a**); 117.6, 116.0 (**3b**); 118.1, 117.5 (**3c**); 118.5, 118.0 (**3d**). The mononucleoside **2** can be isolated quantitatively.

The trimethylsilylphosphites of type **3** can also be obtained by silylation[8] of phosphonates with P–H bonding.[9]

The esters **3** exhibit remarkable chemical properties characteristic of trimethylsilylphosphites.[10] The value of the esters **3** in nucleotide chemistry is clearly evident from their selective and efficient participation in Michaelis-Arbuzov-

[*] Prof. Dr. J. Michalski, Dr. W. Dąbkowski, Wang Qing [+]
Centre of Molecular and Macromolecular Studies,
Polish Academy of Sciences
Sienkiewicza 112, 90-363 Łódź (Poland) and
Max-Planck Institut für experimentelle Medizin Abteilung Chemie
Hermann-Rein-Strasse 3, D-3400 Göttingen (FRG)
[+] Permanent address: Chemical Research Institute, Beijing (Peoples Republic of China)

[**] The authors thank Prof. *Friedrich Cramer*, the Polish Academy of Sciences and the Max-Planck-Gesellschaft for support of this work. We are grateful to Dr. *Dieter Gauss* for help in preparing the manuscript.

type reactions and from reactions which are unique for this reagent, for example the one-pot synthesis of the biologically interesting methylphosphonates of type **4**[11] (Scheme 3) and phosphorofluoridates.[12] The chemical and enzymatic properties of **4** compare with those of other dinucleoside methylphosphonates.[4, 5]

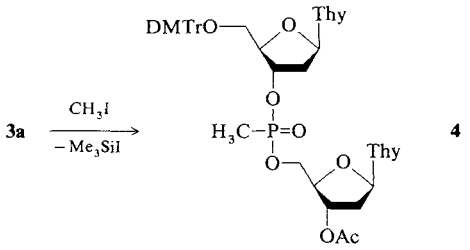

Scheme 3. Synthesis of **4** (2 h, 20 °C) [8b]. ^{31}P-NMR ($CDCl_3$, 85% H_3PO_4 ext.): δ = 32.7, 32.5.

Unique for reagents of type **3** is the reaction with oxalylazolides and anilides to form in excellent yields the dinucleotide azolides **5a, b** and anilides **5c** (Scheme 4).

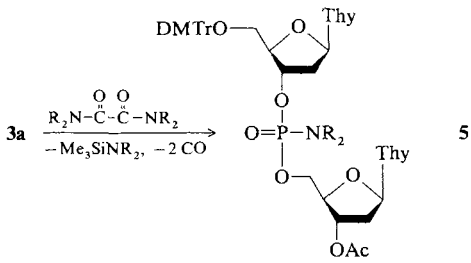

5a, R_2NH = imidazole; **5b**, R_2NH = triazole; **5c**, R_2NH = aniline

Scheme 4. Synthesis of **5** from **3a** and $(R_2N-CO)_2$ (1/1); 3 h, 20 °C. Yield. (determined by ^{31}P NMR spectroscopy) 90–94%. ^{31}P NMR ($CDCl_3$, 85% H_3PO_4 ext.): δ = −12.0, −11.5 (**5a**); −10.6, −10.3 (**5b**); +2.0, +1.6 (**5c**).

In this way the anilides of type **5c** have become readily accessible for the first time. Nucleotide anilides are of importance for the stereospecific synthesis of nucleoside phosphorothioates.[13]

The reaction of **5a** leading to the anhydrides **6a** and **6b** further illustrates the potential of this approach (Scheme 5).

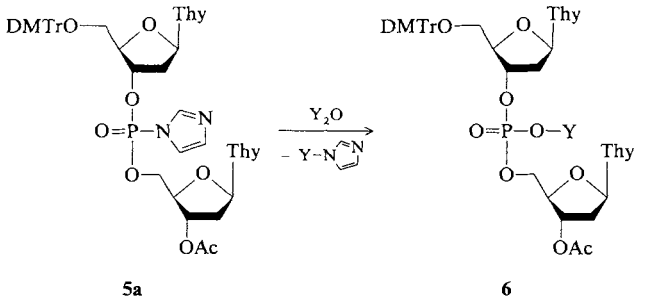

6a, Y = CH_3SO_2; **6b**, Y = CF_3CO

Scheme 5. Synthesis of **6** (15 min, 20 °C, CH_3CN). Yield (determined by ^{31}P NMR spectroscopy) 95–97%. ^{31}P NMR ($CDCl_3$, 85% H_3PO_4 ext.): δ = −15.6, −15.3 (**6a**); −9.8, −9.5 (**6b**).

All compounds **3**–**6** are mixtures of diastereoisomers. Phosphonates with P–H bonding, which are versatile intermediates in nucleotide chemistry, can be readily obtained by hydrolysis from **2** and **3** in a one-pot procedure.

Received: December 13, 1989;
revised: February 12, 1990 [Z 3684 IE]
German version: *Angew. Chem. 102* (1990) 565

CAS Registry numbers:
1, 114071-78-2; **2a**, 126256-30-2; **2b**, 126256-31-3; **3a** p_R isomer, 126256-32-4; **3a** P_S isomer, 126373-38-4; **3b** P_R isomer, 126451-68-1; **3b** p_S isomer, 126256-40-4; **3c** P_R isomer, 126256-35-7; **3c** P_S isomer, 126373-40-8; **3d** P_R isomer, 126256-36-8; **3d** P_S isomer, 126373-41-9; **4a** P_R isomer, 90865-75-1; **4a** P_S isomer, 90865-76-2; **5a** P_R isomer, 126256-33-5; **5a** P_S isomer, 126373-45-3; **5b** P_R isomer, 126256-37-9; **5b** P_S isomer, 126373-42-0; **5c** P_R isomer, 126256-39-1; **5c** P_S isomer, 126373-44-2; **6a** P_R isomer, 126256-34-6; **6a** P_S isomer, 126373-39-5; **6b** P_R isomer, 126256-38-0; **6b** P_S isomer, 126373-43-1; $[(iPr)_2N]_2PCl$, 56183-63-2; 3′-*o*-Ac-thymidine, 21090-30-2; 5′-*o*-DMT-thymidine, 40615-39-2; 3′-*o*-Ac-N^6-benzoyl-2′-deoxyadenosine, 25152-95-8; 5′-*o*-DMT-N^6-benzoyl-2′-deoxyadenosine, 64325-78-6.

[1] R. L. Letsinger, W. B. Lunsford, *J. Am. Chem. Soc. 98* (1976) 3655–3661.
[2] L. J. McBride, M. H. Caruthers, *Tetrahedron Lett. 24* (1983) 245–248.
[3] S. A. Narang (Ed.): *Synthesis and Applications of DNA and RNA*, Academic Press, Orlando, FL 1987.
[4] a) M. J. Nemer, K. K. Ogilvie, *Tetrahedron Lett. 21* (1980) 4149–4252; b) S. A. Noble, E. F. Fisher, M. H. Caruthers, *Nucleic Acids Res. 12* (1984) 3387–3404; c) W. J. Stec, G. Zon, W. Egan, R. A. Byrd, L. R. Philips, K. A. Gallo, *J. Org. Chem. 50* (1985) 3908–3913; d) A. Wilk, W. J. Stec, *Nucleic Acids Res. Symp. Ser. 18* (1987) 289–292.
[5] a) K. Imai, T. Ito, S. Kondo, T. Takaku, *Nucleosides & Nucleotides 4* (1985) 669–679; b) W. Dąbkowski, F. Cramer, J. Michalski, *Tetrahedron Lett. 28* (1987) 3559–3560.
[6] E. S. Batyeva, V. A. Alfonsov, A. N. Pudovik, *Izv. Akad. Nauk SSSR, Ser. Khim. 1976*, 463–466.
[7] a) R. B. King, P. M. Sundaram, *J. Org. Chem. 49* (1984) 1784–1789; b) S. Hamamoto, H. Takaku, *Chem. Lett. 1986*, 1401–1404.
[8] a) A. Kume, M. Fujii, M. Sekine, T. Hata, *J. Org. Chem. 49* (1984) 2139–2143; b) E. de Vroom, M. L. Spierenburg, C. E. Dreef, G. A. van der Marel, J. H. van Boom, *Recl. Trav. Chim. Pays-Bas 106* (1987) 65–66.
[9] a) R. H. Hall, A. Todd, R. F. Webb, *J. Chem. Soc. 1957*, 3291–3296; b) P. J. Garegg, T. Regberg, J. Stawinski, R. Strömberg, *Chem. Scr. 25* (1985) 280–282; c) B. C. Froehler, M. D. Matteucci, *Tetrahedron Lett. 27* (1986) 469–472; d) J. E. Marugg, M. Tromp, E. Kuyl-Yeheskiely, G. A. van der Marel, J. H. van Boom, *ibid. 27* (1986) 2661–2664; e) M. Fujii, K. Ozaki, M. Sekine, T. Hata, *Tetrahedron 43* (1987) 3395–3407, and references cited therein.
[10] a) A. Łopusiński, J. Michalski, M. Potrzebowski, *Phosphorus Sulfur 28* (1986) 299–305; b) W. Dąbkowski, J. Michalski, *J. Chem. Soc. Chem. Commun. 1987*, 755–756; c) W. Dąbkowski, F. Cramer, J. Michalski, *Tetrahedron Lett. 28* (1987) 3559–3560; d) A. Skowrońska, R. Dembiński, R. Kamiński, J. Michalski, *J. Chem. Soc., Perkin Trans. 1 1988*, 2197–2201.
[11] P. S. Miller, P. O. P. Ts'o, *Annu. Rep. Med. Chem. 23* (1988) 295–304, and references cited therein.
[12] W. Dąbkowski, F. Cramer, J. Michalski, *Tetrahedron Lett. 29* (1988) 3301–3302.
[13] Z. J. Lésnikowski, W. Niewiarowski, W. S. Zieliński, W. J. Stec, *Tetrahedren 40* (1984) 15–32.

Catalytic Hydration of Acrylonitrile to Acrylamide under Mild Conditions**

By *Jik Chin** and *J. H. Kim*

Numerous articles have been written on the development of catalysts that hydrolyze amides, esters and nitriles. Due to the stability of these substrates, most studies have been focused on model systems involving activated substrates[1] or intramolecular catalysis.[2] Perhaps it is now time to exploit

[*] Prof. J. Chin, J. H. Kim
Department of Chemistry, McGill University
801 Sherbrooke Street West, Montreal, Quebec H3A 2K6 (Canada)

[**] Support by the National Science and Engineering Research Council of Canada is gratefully acknowledged.

the knowledge gained from extensive model studies to the development of true catalysts that hydrolyze unactivated substrates.[3] We recently showed[4] that **1** is highly efficient at catalyzing the hydrolysis of unactivated esters such as methyl acetate. The hydrolysis of amides and nitriles poses an even greater challenge than the hydrolysis of esters, since amides and nitriles are thousands of times more stable than esters. For example, the second-order rate constants for hydroxide-catalyzed hydrolysis of methyl acetate,[5] acetonitrile[6] and acetamide[7] are 1.5×10^{-1} M s^{-1}, 1.6×10^{-6} M s^{-1}, and 7.4×10^{-5} M s^{-1}, respectively. Herein we report on the hydrolysis of acetonitrile under mild conditions using **1**, **2** and **3** as catalysts.

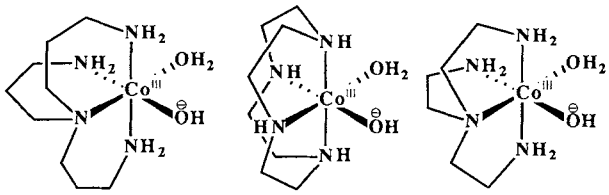

1 2 3

In a typical kinetically controlled experiment, acetonitrile (0.1–0.5 M) was added to a D_2O solution of **2** (0.01 M, perchlorate salt) at pD 7.0 and 40 °C. Figure 1 shows that, as the reaction proceeds, the ^{1}H-NMR signal of acetonitrile

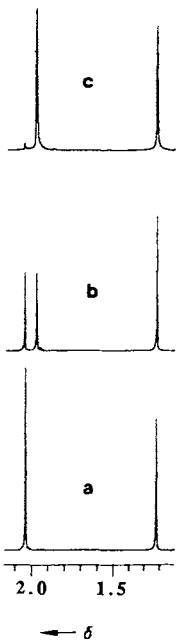

Fig. 1. ^{1}H-NMR chemical shift of the α proton of acetonitrile (0.1 M) after addition of **2** (0.01 M) at pD 7.0 and 40 °C. *tert*-Butyl alcohol as standard ($\delta = 1.22$). Measurements after a) 0 h, b) 5.5 h, c) 23 h.

($\delta = 2.04$) decreases while that of acetamide ($\delta = 1.96$) increases. The reaction is zero order with respect to acetonitrile concentration and first order with respect to the catalyst concentration. Under the above conditions, the rate of the hydrolysis is 3.2×10^{-6} M s^{-1}. **3** is about 20 times less reactive than **2**. **1** is active but deligates to give free tris(3-aminopropyl)amine after initial production of acetamide.

$Cu^{2\oplus}$, $Ni^{2\oplus}$ and $Zn^{2\oplus}$ have all been shown to catalyze the hydration of nitriles when the nitrile function is covalently linked to metal-coordinating functional groups.[8, 9] For example, 2-cyanopyridine and 2-cyano-1,10-phenanthroline are rapidly hydrated to the corresponding amides when $Cu^{2\oplus}$ is added to the aqueous reaction mixture under mild conditions. It has been shown that, under reflux conditions, $Pt^{2\oplus}$-complexes catalyze the hydrolysis of simple nitriles that do not contain any additional metal-coordinating functionalities.[10] Simple nitriles directly coordinated to Co^{III}-,[6] Rh^{III}-,[11] Ru^{III}-[12] and Ir^{III}[11]-complexes can be easily hydrolyzed to the corresponding amido complexes at ambient temperature. However, there is no catalytic turnover with the substitutionally inert Co^{III}-, Rh^{III}-, Ru^{III}- and Ir^{III}-complexes. Interestingly, ten turnovers can be easily detected for the hydrolysis of acetonitrile by **2** in neutral water (pH 7) at 40 °C (Fig. 1). The turnover time is approximately 3×10^3 s. This represents the first example of turnover for a Co^{III}-complex-catalyzed hydrolysis of a nitrile. Although Co^{III}-complexes are generally substitutionally inert the coordinated water molecules in **2** can be rapidly displaced under mild conditions.[13]

There are three possible mechanisms for the hydrolysis of acetonitrile when catalyzed by **2**. The first mechanism involves intermolecular attack of the metal hydroxide on acetonitrile (**A**). The second involves coordination of acetonitrile followed by intermolecular hydroxide-attack (**B**).[6] The third involves coordination of acetonitrile followed by intramolecular attack of the metal hydroxide (**C**). Mechanism

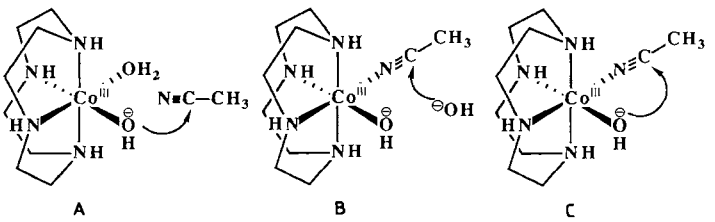

A B C

A can be ruled out on the basis that **3** is much less reactive than **2**. If mechanism **A** were correct, **2** and **3** would be expected to have comparable reactivities, since the basicities of the metal hydroxides are about the same.[16] Mechanism **B** can also be ruled out. The pseudo-first-order rate constant for the hydrolysis of $[(NH_3)_5Co(NCCH_3)]^{3\oplus}$ in water to give the acetamide-bound cobalt complex is 3.4×10^{-7} s^{-1} at pH 7.0 and 25 °C.[6] Hence, if mechanism **B** is correct, the expected maximum rate constant for hydrolysis of acetonitrile (0.5 M) catalyzed by **2** (0.01 M) would be 3.4×10^{-9} M s^{-1}. This is too slow to account for the observed rate of hydrolysis (3.2×10^{-6} M s^{-1}). Furthermore, hydroxide-catalyzed hydrolysis of $[(NH_3)_5Co(NCCH_3)]$ is accompanied by a proton exchange for the methyl group.[6] In sharp contrast, the hydrolysis of acetonitrile catalyzed by **2** does not show any proton exchange for the methyl group. Mechanism **C** is consistent with the observed rate-enhancement as well as the lack of any proton exchange for the methyl group. Related mechanisms involving intramolecular metal-hydroxide attack on metal-coordinated substrates have been proposed for the Co^{III} complex-promoted hydrolysis of phosphate esters and carboxylate esters.[14]

There has been considerable industrial interest in developing catalysts for the hydrolysis of acrylonitrile to acrylamide without hydrolyzing the carbon–carbon double bond. Intramolecular metal-hydroxide attack on coordinated acrylo-

nitrile according to mechanism **C** should result in clean hydrolysis of the cyano group with retention of the C–C double bond. Indeed acrylonitrile is quantitatively converted into acrylamide by **2** (Fig. 2).

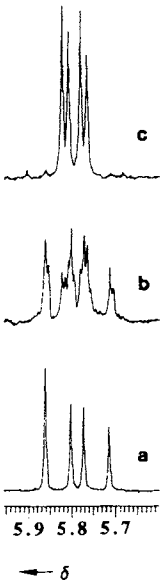

Fig. 2. ^{1}H-NMR chemical shift of the α proton of acrylonitrile (0.1 M) after addition of **2** (0.01 M) at pD 6.3 and 40 °C. Measurements after a) 0 h, b) 3.5 h, c) 20 h.

We have shown that **2** forms four-membered ring intermediates much more readily than does **3**.[14] Since mechanism **C** involves the formation of a four-membered ring intermediate, it is not surprising that **2** is so much more reactive than **3** in hydrolyzing acetonitrile. Although **1** also catalyzes the hydrolysis of acetonitrile, it starts to decompose after initial reaction due to acetamide-promoted deligation of the tetraamine ligand. Amide-promoted deligation of Co^{III}-amine complexes is a known phenomenon.[11] Deligation does not take place with **2**, apparently because the cyclic tetraamine ligand binds very tightly to the cobalt atom.

The three most important criteria in developing a "perfect" catalyst are reactivity, selectivity, and turnover number. Unlike enzymes, simple catalysts are far from being perfect. Nevertheless, **2** is an excellent catalyst for the hydrolysis of nitriles. The catalytic mechanism involving intramolecular metal-hydroxide-attack on the Co^{III}-complex-coordinated nitrile allows for unprecedented reactivity and selectivity. Furthermore, rapid dissociation of the product from the metal complex allows for catalytic turnover to take place for the first time using a Co^{III}-complex.

Received: November 24, 1989 [Z 3644 IE]
German version: *Angew. Chem. 102* (1990) 580

[1] a) R. Breslow, G. Trainor, A. Ueno, *J. Am. Chem. Soc. 105* (1983) 2739; b) D. J. Cram, P. Y. Lam, S. P. Ho, *ibid. 108* (1986) 839; c) J. M. Lehn, C. Sirlin, *J. Chem. Soc. Chem. Commun. 1978*, 949; d) J. Chin, X. Zou, *J. Am. Chem. Soc. 106* (1984) 3687.

[2] a) H. Kroll, *J. Am. Chem. Soc. 74* (1952) 2036; b) M. L. Bender, B. W. Turnquist, *ibid. 79* (1957) 1889; c) P. A. Sutton, D. A. Buckingham, *Acc. Chem. Res. 20* (1987) 357, and references cited therein; d) P. Nanjappan, T. Czarnik, *J. Am. Chem. Soc. 109* (1987) 1826; e) A. J. Kirby, P. W. Lancaster, *J. Chem. Soc. Perkin Trans. 2 1972*, 1206; f) R. Kluger, J. Chin, *J. Am. Chem. Soc. 104* (1982) 2891.

[3] a) D. Kahn, W. C. Still, *J. Am. Chem. Soc. 110* (1988) 7529; b) F. M. Menger, M. Ladika, *ibid. 109* (1987) 3145.

[4] J. Chin, M. Banaszczyk, *J. Am. Chem. Soc. 111* (1989) 2724.

[5] J. P. Guthrie, P. A. Cullimore, *Can. J. Chem. 58* (1980) 1281.

[6] D. A. Buckingham, F. R. Keene, A. M. Sargeson, *J. Am. Chem. Soc. 95* (1973) 5649.

[7] T. Yamana, Y. Mizukami, A. Tsuji, Y. Yasuda, K. Masuda, *Chem. Pharm. Bull. 20* (1972) 881–891.

[8] P. F. B. Barnard, *J. Chem. Soc. A 1969*, 2140.

[9] R. Breslow, R. Fairweather, J. Keana, *J. Am. Chem. Soc. 89* (1969) 2135.

[10] a) M. A. Bennett, G. B. Robertson, P. O. Whimp, T. Yoshida, *J. Am. Chem. Soc. 95* (1973) 5649; b) C. M. Jensen, W. C. Trogler, *ibid. 108* (1986) 723.

[11] N. J. Curtis, A. M. Sargeson, *J. Am. Chem. Soc. 106* (1984) 625.

[12] a) A. W. Zanella, P. C. Ford, *J. Chem. Soc. Chem. Commun. 1974*, 795; b) A. W. Zanella, P. C. Ford, *Inorg. Chem. 14* (1975) 42.

[13] J. Chin, M. Banaszczyk, V. Jubian, X. Zou, *J. Am. Chem. Soc. 111* (1989) 186.

[14] a) J. Chin, M. Banaszczyk, *J. Am. Chem. Soc. 111* (1989) 4103; b) J. Chin, V. Jubian, *J. Chem. Soc. Chem. Commun. 1989*, 839.

Oligorylene as a Model for "Poly(perinaphthalene)" **

By *Angelika Bohnen, Karl-Heinz Koch, Wolfgang Lüttke*, and *Klaus Müllen**

Dedicated to Professor Wolfgang Roth on the occasion of his 60th birthday

The annelated arenes derived formally by connecting all the *peri*-positions of naphthalene have been designated by *Clar* as "rylenes".[1] Although chemical and physical properties of the first member of this series of naphthalene oligomers, perylene **2a**, have been thoroughly investigated,[2–4] the higher homologues terrylene **3a** and quaterrylene **4a** have resisted all attempts at characterization even though they are known compounds. This is primarily due to the fact that they are difficult to synthesize and extremely insoluble in organic solvents.[5]

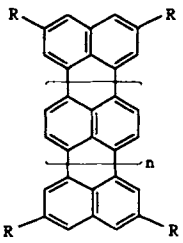

1: R = H
2a: R = H, n = 0
3a: R = H, n = 1
4a: R = H, n = 2
2b: R = *t*Bu, n = 0
3b: R = *t*Bu, n = 1
4b: R = *t*Bu, n = 2

Theoretical studies suggest that these higher rylenes should be of considerable interest, however. Thus, a low-lying energy gap has been predicted for poly(*peri*-naphthalene) **1**, which might give rise to intrinsic conductivity.[6, 7]

As part of an attempt to extrapolate from existing experimental data to the properties of **1**, we have succeeded

[*] Prof. Dr. K. Müllen, Dipl.-Chem. A. Bohnen, Dipl.-Chem. K.-H. Koch
Max-Planck-Institut für Polymerforschung
Ackermannweg 10, D-6500 Mainz 1 (FRG)
Prof. Dr. W. Lüttke
Institut für Organische Chemie der Universität Göttingen

[**] Polyarylenes and Polyarylenevinylenes, Part 2. This work was supported by the Volkswagen Stiftung and the Bundesministerium für Forschung und Technologie. Part 1: [10].

in developing a straightforward approach to structural analogues of terrylene **3a** and quaterrylene **4a**. The method is based on alkali metal-induced cyclization of oligonaphthalene precursors, and it leads directly to the compounds **3b** and **4b**, which thanks to their alkyl substituents are soluble. The resulting homologous series of soluble rylenes (**2b**–**4b**) now makes it possible to study rylene physical properties as a function of molecular size. We present here various pieces of spectroscopic information together with evidence of significant redox activity and, in the case of doped derivatives, electrical conductivity.

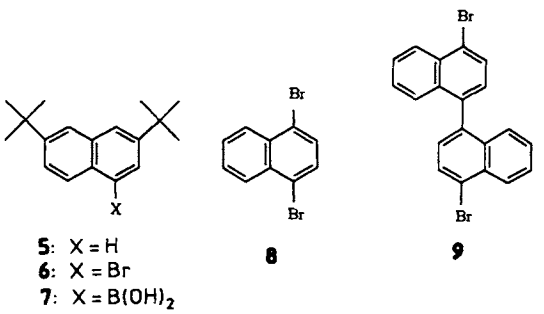

5: X = H
6: X = Br
7: X = $B(OH)_2$

8 **9**

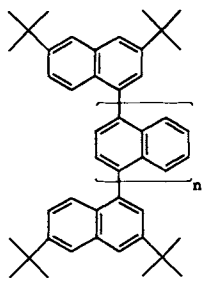

10: n = 0
11: n = 1
12: n = 2

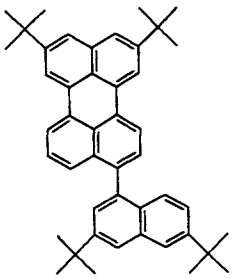

13

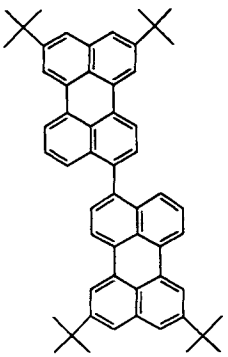

14

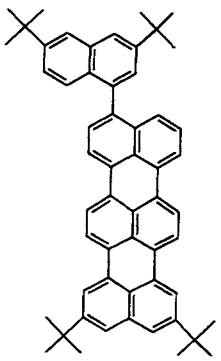

15

The starting point for the syntheses is 2,7-di-*tert*-butylnaphthalene **5**, which is readily prepared by Friedel-Crafts alkylation of naphthalene. This compound can be separated via its thiourea inclusion complex from the 2,6-isomer that forms concurrently.[8] **5** is subsequently converted into the monobromo derivative **6**[9] (86%) by a method we have described previously,[10] after which it is transformed into the monoboronic acid **7** (76%). Palladium-catalyzed coupling of **7** with **6** (molar ratio 1:1), with 1,4-dibromonaphthalene **8** (2:1), or with 4,4'-dibromo-1,1'-binaphthyl **9** (2:1) leads to the 1,4-coupled oligonaphthalenes **10** (74%), **11** (83%), and **12** (75%).[11]

In preparing the rylenes themselves we took advantage of the fact that 1,1'-binaphthyl cyclizes spontaneously to perylene upon reduction with alkali metals.[12] The corresponding cyclization of the oligonaphthalenes **10**–**12** was accomplished by treatment with potassium (vacuum, 1,2-dimethoxyethane, room temperature, 3d), followed by oxidation with anhydrous cadmium chloride and column chromatographic purification over aluminum oxide. The perylene **2b** is obtained in a yield of 40%. Ternaphthyl **11** leads to two cyclization products: the naphthylperylene **13** (42%) and the terrylene **3b** (24%). Cyclization apparently occurs only at the *peri*-positions of the naphthalene. The course of the cyclization evidently depends upon the extent of the redox activity of the π system, since the quaternaphthyl derivative **12** leads to the biperylenyl **14** (48%) rather than to the desired quaterrylene **4b**. Byproducts include the nonseparable naphthylperylenes (10%), as well as the naphthylterrylene derivative **15** which could be isolated (5%). Cyclization to **4b** can nevertheless be accomplished by treatment of **14** with copper(II) chloride and aluminum chloride in carbon disulfide (Kovacic conditions[13]). Chromatographic purification of the crude product (aluminum oxide, cyclohexane) results in elution only of the byproducts (perylene chromophores). The target compound **4b** was recovered from the column packing (dried under nitrogen) by multiple extraction with refluxing chloroform (48%). In an analogous fashion, **13** can be cyclized to the terrylene **3b** (42%).[11]

The parent compounds **3a** and **4a** can be prepared by dealkylation of **3b** and **4b**, respectively (aluminum trichloride/sodium chloride melt, 5:1, 130°C, 15 min).

As can be seen from Table 1, the series of soluble rylenes **2b**, **3b**, and **4b** exhibits an intense bathochromic shift for the longest wavelength ^1L_a band, which is in each case characterized by a similar vibrational structure. The observed peak positions are in good agreement with calculated values (PPP-SCF[14]). As with perylene, the fluorescence spectra of the homologues show only very small Stokes shifts. Whereas both perylene **2b** and terrylene **3b** demonstrate very intense fluorescence (fluorescence quantum yields Φ_F of 0.94 and 0.70, respectively[15a]), the fluorescence intensity of **4b** is surprisingly weak ($\Phi_F \approx 0.05$[15]).

Table 1. Selected spectroscopic data for the compounds **2b**, **3b**, and **4b**.

Cpd.	Color	Absorption [nm]			Fluorescence [nm] [c]	
		λ_{max}	(ε) [a]	$\lambda_{PPP}(f)$ [b]	λ_{max}	Φ_F [d]
2b	yellow	439	(28000)	446 (1.02)	446	0.94
3b	red	560	(65000)	566 (1.80)	573	0.70
4b	blue	660	(138000)	672 (2.54)	678	≈0.05 [15b]

[a] Absorption spectra at room temperature in 1,4-dioxane. [b] Calculated absorption positions [14], f = oscillator strength. [c] Fluorescence spectra in degassed 1,4-dioxane at room temperature. [d] Reference material for fluorescence measurements: [15a] **2b**: perylene; **3b**: rhodamine 101; **4b**: 3-diethylamino-7-diethyliminophenoxazonium perchlorate (oxazine 1).

Electrochemical oxidation and reduction under cyclovoltammetric control reveals the oligorylenes to be very effective electrophores (Table 2). **2b** is transformed reversibly into a radical cation and a dication as well as a radical anion and a dianion. In the case of **3b** a radical trication is also formed, and with **4b** it is even possible to demonstrate a reversible redox sequence covering seven successive steps

Table 2. Cyclovoltammetrically determined redox potentials for the oligorylenes **2b**, **3b**, and **4b**. [a]

	E° (Oxidation)				E° (Reduction)		
	−4e	−3e	−2e	−1e	+1e	+2e	+3e
2b			1.45	0.78	−1.99	−2.55	
3b		2.43 [b]	0.94	0.43	−1.57	−1.98	
4b	2.23 [c]	1.90 [b]	0.66	0.23	−1.42	−1.72	−2.97 [b]

[a] Oxidation in CH_2Cl_2; reduction in tetrahydrofuran; redox potentials of reversible pairs in V vs. SCE (ferrocene calibration 310 mV); nBu$_4$N$^\oplus$PF$_6^\ominus$ as supporting electrolyte; scan rate 100 mV s^{-1}; temperature 0 °C. [b] Temperature −25 °C. [c] Temperature −50 °C.

from a tetracation to a radical trianion. Not surprisingly, electron transfer is also possible by chemical means. Thus, reduction of **2b** and **3b** with potassium, for example, leads to the dianionic salts **2b**$^{2\ominus}$/2K$^\oplus$ (violet) and **3b**$^{2\ominus}$/2K$^\oplus$ (blue), as shown by the corresponding ^{1}H-NMR spectra.[16]

The energy gap in polymer **1** is a quantity of considerable significance from the standpoint of electrical conductivity. In the case of the discrete molecules **2b**–**4b** this corresponds to the HOMO/LUMO energy difference ΔE(Table 3). One of

Table 3. HOMO-LUMO energy differences ΔE [eV] as a function of degree of annelation [18] (cf. Tables 1 and 2).

	ΔE_{elec} [a]	ΔE_{opt} [b]	ΔE_{theor} [c]
2b	2.77	2.67	2.78
3b	2.00	2.14	2.19
4b	1.64	1.80	1.84

[a] Difference between the electrochemically determined redox potentials for the radical cation and radical anion. [b] Based on the energy of the longest wavelength optical transition, determined at 1/10 of the maximum absorption. [17] [c] Corresponds to the energy determined by the PPP–SCF method [14] for the transition $S_0 \rightarrow S_1$.

the ways of characterizing it experimentally is to measure the potential difference for the first stage of reduction or oxidation. Alternatively, one can determine the energy of the longest wavelength optical transition[17, 18] (Tables 1 and 2). A graphic treatment of the observed ΔE values as a function of the number of naphthalene units present fails to display convergence, but it does reveal a considerable decrease with increasing molecular size. The observed ΔE for the discrete species **4b** (ca. 1.6 eV) is significantly less than that for polymers of either the polyphenylene (ca. 3.4 eV)[19] or poly-*p*-phenylenevinylene type (ca. 2.5 eV),[20] and is comparable to that determined for polyacetylene.[20]

p-Doping with iodine in saturated dichloromethane solution converts **3b** and **4b** into slightly soluble charge-transfer complexes, whereas the complex from **2b** remains in solution. The powder conductivity was found to be 10^{-2} S cm^{-1} for **3b** and, interestingly, 5 S cm^{-1} in the case of **4b**.

Received: December 27, 1989;
supplemented: March 2, 1990 [Z 3700]
German version: *Angew. Chem. 102* (1990) 548

[1] E. Clar, *Chem. Ber. 81* (1948) 52.
[2] E. Clar: *Polycyclic Hydrocarbons, Vol. II*, Springer, Berlin 1964, p. 25.
[3] J. B. Birks: *Organic Molecular Photophysics, Vol. I and II*, Wiley, London 1986.
[4] H. J. Keller, D. Nöthe, H. Pritzkow, D. Wehe, M. Werner, *Mol. Cryst. Liq. Cryst. 62* (1980) 181.
[5] E. Clar, W. Kelly, R. M. Laird, *Monatsh. Chem. 80* (1956) 391.
[6] J. L. Brédas, R. H. Baughman, *J. Chem. Phys. 83* (1985) 1316.
[7] A. K. Bakhshi, J. Ladik, *Synth. Met. 30* (1989) 115.
[8] H. van Bekkum, T. J. Niewstad, J. van Barneveld, P. Klapwijk, B. M. Wepster, *Recl. Trav. Chim. Pays-Bas 88* (1969) 1028.
[9] L. Erichomovitch, M. Ménard, F. L. Chubb, Y. Pépin, J. C. Richer, *Can. J. Chem. 44* (1966) 2305.
[10] U. Fahnenstich, K. H. Koch, K. Müllen, *Makromol. Chem. Rapid Commun. 10* (1989) 563.
[11] The structures of all new compounds were established on the basis of spectroscopic data and elemental analysis. For example: 2,5,10,13-tetra-*tert*-butylterrylene **3b**: mp = 369–370 °C; ^{1}H-NMR (200 MHz, $CDCl_3$): δ = 1.49 (s, CH_3), 7.65 (d, 3-H), 8.27 (d, 1-H), 8.30 (s, 7-H); $J_{1,3}$ = 3 Hz.—2,5,12,15-tetra-*tert*-butylquaterrylene **4b**: mp = 520–528 °C; ^{1}H NMR (200 MHz, $CDCl_3$): δ = 1.45 (s, CH_3), 7.58 (br. s, 3-H), 8.18 (m, 1-, 6-, 7-H).
[12] S. P. Solodovnikov, Y. B. Zaks, S. T. Ioffe, M. I. Kabachnik, *Isv. Akad. Nauk. SSSR Ser. Khim. 1968*, 442.
[13] P. Kovacic, M. B. Jones, *Chem. Rev. 87* (1987) 357.
[14] PPP-SCF-CI calculations taking into account a maximum of 100 simple excited configurations and a maximum of 25 SCF iterations.
[15] a) We wish to thank *M. Strauch*, Universität Göttingen, for fluorescence measurements on **2b**, as well as Priv.-Doz. *A. R. Holzwarth*, MPI für Strahlenchemie, Mülheim a. d. Ruhr (FRG), for fluorescence investigations on **3b** and **4b**; b) the unusually weak fluorescence of **4b** is the subject of further study.
[16] ^{1}H NMR (200 MHz, [D]$_8$THF, −20 °C): **2b**$^{2\ominus}$/2K$^\oplus$: δ = 5.8 (s, 1H), 4.97 (s, 1H), 1.11 (s, 9H); **3b**$^{2\ominus}$/2K$^\oplus$: δ = 6.58 (s, 1H), 6.19 (s, 1H), 5.97 (s, 1H), 1.23 (s, 9H).
[17] H. H. Hörhold, M. Helbig, *Makromol. Chem. Macromol. Symp. 12* (1987) 229.
[18] In view of the differing experimental conditions, the relatively good agreement between the optically and electrochemically determined ΔE values must be regarded as coincidental.
[19] L. W. Shacklette, H. Eckhardt, R. R. Chance, G. C. Miller, D. M. Ivory, R. H. Baughman, *J. Chem. Phys. 73* (1980) 4098.
[20] R. R. Chance, D. S. Boudreaux, H. Eckhardt, R. L. Elsenbauner, J. E. Frommer, J. L. Brédas, R. Silbey in J. Ladik, J. M. André, M. Seel (Eds.): *Quantum Chemistry of Polymers: Solid State Aspects*, Reidel, Dordrecht 1984, p. 235.

Synthesis of Enantiomerically Pure Heterosteroids by Intramolecular Hetero-Diels-Alder Reaction**

By *Lutz F. Tietze*,* *Uwe Beifuss, Magdolna Lökös, Matthias Rischer, Axel Göhrt*, and *George M. Scheldrick*

Heterocyclic steroids[1] are of considerable interest because of their pharmalogical properties, which frequently deviate from those of the carbocyclic compounds.[2] Although the synthesis of carbocyclic steroids by intramolecular Diels-Alder reaction of *o*-quinodimethanes according to the synthetic scheme AD → ABCD has been the subject of numerous studies for about ten years,[3] heterosteroids have so far never been synthesized in this way. As the first example of a novel, general, convergent and enantioselective entry to heterosteroids we describe here the synthesis of enantiomerically pure 6-oxa-2,4-diazasteroids and related compounds. The synthetic strategy employed is based on the tandem Knoevenagel-hetero-Diels-Alder reaction, which has already proven to be a valuable method for the stereoselective synthesis of annulated dihydropyrans.[4]

[*] Prof. Dr. L. F. Tietze, Dr. U. Beifuss, Dr. M. Lökös, Dipl.-Chem. M. Rischer
Institut für Organische Chemie der Universität
Tammannstrasse 2, D-3400 Göttingen (FRG)
Dipl.-Chem. A. Göhrt, Prof. Dr. G. M. Sheldrick
Institut für Anorganische Chemie der Universität
Tammannstrasse 4, D-3400 Göttingen (FRG)

[**] Inter- and Intramolecular Hetero-Diels-Alder Reactions, Part 29. This work was supported by the Deutsche Forschungsgemeinschaft and the Fonds der Chemischen Industrie.—Part 28: [4c].

Knoevenagel condensation of the enantiomerically pure cyclopentane derivative **2** with cyclic 1,3-dioxo compounds **1** in the presence of catalytic amounts of ethylenediammonium diacetate (EDDA) affords the alkylidene compounds **3**, which react in situ to give the cycloadducts **4**. Thus, reaction

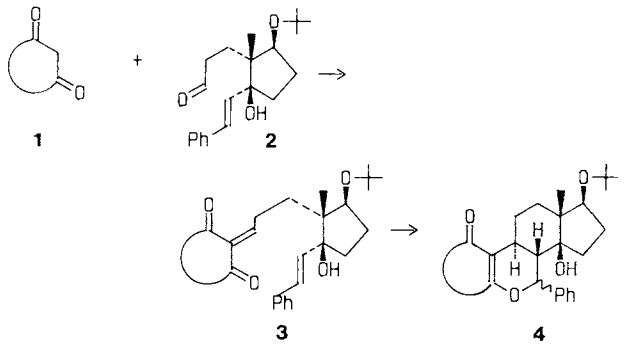

of **2** with *N,N'*-dimethylbarbituric acid in boiling acetonitrile ultimately furnishes the *trans*-annulated hetero-Diels-Alder products **5a** and **5b**, which differ only in the configuration at C-7, in 55 and 24% yield, respectively. The constitution and configuration of the two epimers were determined by analysis of the ^{1}H- and ^{13}C-NMR spectra,[5] and, in the case of **5a**, also by X-ray structure analysis.[6] For both isomers, the *trans*-fusion of the rings B and C follows from the coupling constants $^3J_{8-H,9-H} = 11$ Hz. In the reaction of **2** with Meldrum's acid in boiling toluene the cycloaddition is followed by cleavage of acetone and CO from the initially formed cycloadducts **6**, so that in this case the lactones **7a** (57%) and **7b** (18%) were the only products isolated. Similar results, i.e. exclusive formation of products with *trans*-annulated rings B and C, are found for the cyclization reactions of **2** with indane-1,3-dione and 3-methyl-1-phenylpyrazolin-5-one. In non-optimized reactions the cycloadducts **8** and **9** were obtained in 58 and 45% yield,

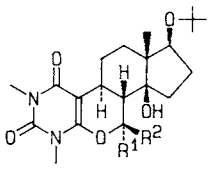

5a: R^1 = H, R^2 = Ph
5b: R^1 = Ph, R^2 = H

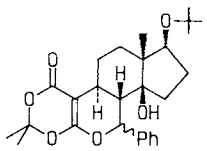

6

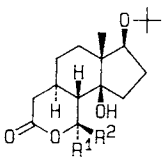

7a: R^1 = H, R^2 = Ph
7b: R^1 = Ph, R^2 = H

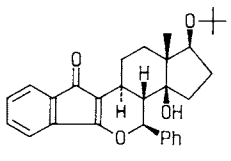

8

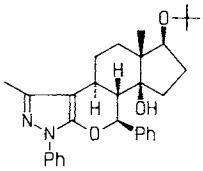

9

respectively. The remarkably high diastereoselectivity in the formation of the *trans*-annulated products can best be explained by assuming an *exo-E-anti*-transition state as depicted in **10**. The poor stereochemical control in the formation of the stereogenic center C-7 in **5a/b** is attributed to a carbocationic intermediate in the cycloaddition. On the basis of isomerization experiments with **5a, b** a thermodynamically controlled epimerization at C-7 after the cycloaddition should also be taken into consideration.[7]

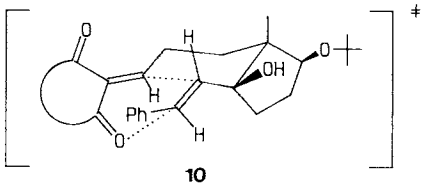

10

The synthesis of the aldehyde **2** required for the intramolecular cycloadditions was accomplished by using the readily accessible tetrahydroindanedione **11**[8] as starting material, which was converted into the *tert*-butyl ether **12a**.[9] Oxidative cleavage of the C–C double bond in **12a** with ozone[10] and subsequent esterification of the initially formed oxocarboxylic acid **13a** with methyl iodide and 1,8-diazabicyclo[5.4.0]undec-7-ene (DBU) in acetonitrile[11] afforded the methyloxocarboxylate **13b** (86%).

Aside from the *tert*-butyl ether **12a**, the ethers **12a–f** were prepared and converted into the enantiomerically pure oxocarboxylates **13c–g** in 67–83% yield.[12] The *tert*-butoxide **13h** was accessible by ozonolysis of **12h** and subsequent treatment with *tert*-butyl alcohol in the presence of dicyclohexylcarbodiimide and 4-(dimethylamino)pyridine (Table 1).[13] Due to their availability in both enantiomeric forms,

Table 1. Preparation of enantiomerically pure cyclopentanones **13** by ozonolysis of the tetrahydroindanedione derivatives **12**.

Educt R		Product	R^1	R^2	Yield [%]
12a	*t*Bu	**13a**	*t*Bu	H	–
12a	*t*Bu	**13b**	*t*Bu	Me	86
12b	$SiMe_2tBu$	**13c**	$SiMe_2tBu$	Me	69
12c	$SiPh_2tBu$	**13d**	$SiPh_2tBu$	Me	83
12d	SEM [a]	**13e**	SEM [a]	Me	74
12e	Ac	**13f**	Ac	Me	67
12f	Bzl	**13g**	Bzl	Me	83
12a	*t*Bu	**13b**	*t*Bu	*t*Bu	59 [13]

[a] SEM = Me_3Si-C_2H_4-O-CH_2.

their ready accessibility, and their different functional groups, oxocarboxylates **13b–h** could be of general interest for the synthesis of cyclopentanoid natural products and related compounds.

The addition of lithiophenylacetylene[14] in THF at 0 °C to the methyl ester **13b** does not proceed chemoselectively. Besides 34% of the expected product **15** also 14% of the trisadduct **16** is formed. To avoid addition of the nucleophile to the carboxylate group, the bulky *tert*-butoxide **13h** was employed; thus, exclusively **17** (77%) is obtained in a completely chemo- and diastereoselective reaction. The stereoselective addition of the nucleophile to the keto group in **13h** probably succeeds as a result of the shielding of the Re-side by the *tert*-butyl ether group. Since the configuration of the

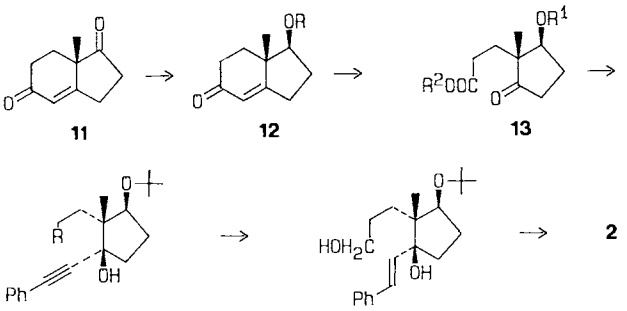

15: R = CO_2Me
16: R = $C(OH)(C{\equiv}C\text{-}Ph)_2$
17: R = CO_2tBu

products **15** and **17** could not be unequivocally determined by NMR spectroscopy, an X-ray structure analysis was carried out on **15**.[6] Reaction of **17** with $LiAlH_4$ led, with reduction of the ester to the alcohol and reduction of the triple bond to the *E*-double bond, to **14** (91%). Swern oxidation[15] of the light- and acid-sensitive alcohol **14** finally gave the aldehyde **2** (68%) required for the tandem-Knoevenagel-hetero-Diels-Alder reaction.

By variation of the diene, of the dieneophile, and of the connecting chain, the synthetic strategy presented here enables the synthesis of a variety of other heterocyclic steroid derivatives.

Received: December 27, 1989 [Z 3702 IE]
German version: *Angew. Chem. 102* (1990) 545

[1] a) H. O. Huisman, *Angew. Chem. 83* (1971) 511; *Angew. Chem. Int. Ed. Engl. 10* (1971) 450; b) S. R. Ramadas, J. Radhakrishnan, *J. Sci. Ind. Res. 31* (1972) 145; c) S. R. Ramadas, A. P. Chundhuri, *ibid. 34* (1975) 563; d) H. O. Huisman, W. N. Speckamp, *Int. Rev. Sci. Org. Chem. Ser. Two 8* (1976) 207; e) S. R. Ramadas, S. Padmanabhan, N. S. Chandrakumar, *J. Sci. Ind. Res. 39* (1980) 275; f) S. R. Ramadas, P. C. Chenchaiah, N. S. C. Kumar, M. V. Krishna, P. S. Srimivasan, V. V. S. K. Sastry, J. A. Rao, *Heterocycles 19* (1982) 861; g) A. A. Frimer, J. Hameiri-Buch, S. Ripshtos, P. Gilinsky-Sharon, *Tetrahedron 42* (1986) 5693; h) C. R. Engel, D. Mukherjee, M. N. R. Chowdhury, V. S. Salvi, *Steroids 47* (1986) 381; i) S. R. Ramadas, D. V. Ramana, R. Bakthavatchalam, *Phosphorus Sulfur 31* (1987) 141; j) H. Suginome, S. Yamada, *Bull. Chem. Soc. Jpn. 60* (1987) 2453; k) M. S. Ahmad, Z. Alam, *Ind. J. Chem. B 27* (1988) 336; l) M. Husain, R. Habib, S. Fazal, A. Fazal, M. Husain, *ibid. B 27* (1988) 435; m) T. G. Back, K. Brunner, *J. Org. Chem. 54* (1989) 1904.

[2] a) G. H. Rasmusson, G. F. Reynolds, N. G. Steinberg, E. Walton, G. F. Patel, T. Liang, M. A. Cascieri, A. H. Cheung, J. R. Brooks, C. Berman, *J. Med. Chem. 29* (1986) 2298; b) Yu. A. Sokolov, *Vestsi Akad. Navuk BSSR Ser. Khim. Navuk 1988*, 69; c) B. B. Kuz'mitskii, I. G. Dad'kov, Yu. L. Zhuravkov, N. A. Konoplya, G. S. Lyubin, A. E. Mashkovich, V. M. Nasek, O. V. Gulyakevich, V. N. Pshenichnyi, V. A. Khripach, *ibid. 1989*, 64; d) A. Vermeulen, V. A. Giagulli, P. De Schepper, A. Buntinx, E. Stoner, *Prostate (N.Y.) 14* (1989), 45.

[3] a) R. L. Funk, K. P. C. Vollhardt, *Chem. Soc. Rev. 9* (1980) 41; b) T. Kametani, H. Nemoto, *Tetrahedron 37* (1981) 3; c) G. Quinkert, H. Stark, *Angew. Chem. 95* (1983) 651; *Angew. Chem. Int. Ed. Engl. 22* (1983) 637; d) M. B. Groen, F. J. Zeelen, *Recl. Trav. Chim. Pays-Bas 105* (1986) 465.

[4] a) W. Bartmann, B. M. Trost (Hrsg.): *Selectivity—A Goal for Synthetic Efficiency*, VCH, Weinheim 1984; b) L. F. Tietze in [4a], p. 299; c) L. F. Tietze, H. Meier, H. Nutt, *Liebigs Ann. Chem., 1990*, 253, and references cited therein; d) L. F. Tietze, J. Fennen, E. Anders, *Angew. Chem. 101* (1989) 1420; *Angew. Chem. Int. Ed. Engl. 28* (1989) 1371.

[5] **5a**: m.p. 195–197 °C; $[\alpha]_D^{20} = +92.0°$ ($c = 1.0$ in $CHCl_3$); ^1H NMR (500 MHz, $CDCl_3$): $\delta = 0.99$ (s, 3H; 18-CH_3), 1.08 (s, 9H; *tert*-butyl-H), 1.14–2.28 (m, 7H; 11-H_{ax}, 12-H_2, 15-H_2, 16-H_2), 2.2 (dd, $J = 10$, 11 Hz, 1H; 8-H), 2.68 (dt, $J = 3$,11 Hz, 1H; 9-H), 2.81 (s, 1H; 14-OH), 3.1 (mc, 1H; 11-H_{eq}), 3.27 and 3.36 (2s, 2 × 3H; 2 × N–CH_3), 3.53 (d, $J = 5$ Hz, 1H; 17-H), 4.92 (d, $J = 10$ Hz, 1H; 7-H) 7.36–7.46 (m, 5H; phenyl-H); ^{13}C NMR 50 MHz, $CDCl_3$): $\delta = 15.50$ (13-CH_3), 24.13 (C-11), 27.76 (N–CH_3), 28.18 [C(CH_3)$_3$], 28.65 (N–CH_3), 31.21, 32.28 and 34.77 (C-12, C-15 and C-16), 35.93 (C-9), 47.66 (C-8), 50.51 (C-13), 74.02 [$C(CH_3)_3$], 80.83 (C-17), 82.21 (C-14), 85.84 (C-7), 89.68 (C-10), 127.8, 127.9, 128.0 and 128.2 (C-Ph), 139.3 (*ipso*-C-Ph), 150.9 (C-3), 156.3 (C-5), 162.6 (C-1).

5b: $[\alpha]_D^{20} = -96.0°$ ($c = 1.0$ in $CHCl_3$); ^1H NMR (500 MHz, $CDCl_3$): $\delta = 0.68$–1.87 (m, 7H; 11-H_{ax}12-H_2, 15-H_2, 16-H_2), 0.85 (s, 3H; 18-CH_3), 1.1 (s, 9H; *tert*-butyl-H), 1.58 (s br, 1H; 14-OH), 1.79 (dd, $J = 9.5$, 11 Hz; 8-H), 3.02 (mc, 1H; 11-H_{eq}), 3.03 (ddd, $J = 3.5$, 11, 11.5 Hz; 1H, 9-H), 3.32 and 3.37 (2s, 2 × 3H; 2 × N–CH_3), 3.56 (t, $J = 8$ Hz, 1H; 17-H), 5.07 (d, $J = 9.5$ Hz, 1H; 7-H), 5.13–5.2 (m, 5H; phenyl-H); ^{13}C-NMR (126 MHz, $CDCl_3$): $\delta = 16.94$ (13-CH_3), 24.70 (C-11), 26.92 (N–CH_3), 27.92 (N–CH_3), 28.70[C(CH_3)$_3$], 29.46, 30.35 and 33.71 (C-12, C-15, C-16), 33.52 (C-9), 48.51 (C-13), 72.35 (C-17), 72.86 [$C(CH_3)_3$], 79.87 (C-14), 85.20 (C-7), 91.18 (C-10), 127.9, 127.9, 128.6 and 129.0 (C-Ph), 139.3 (*ipso*-C-Ph), 151.2 (C-3), 156.4 (C-5), 162.8 (C-1).

[6] Further details of the crystal structure investigation are available on request from the Fachinformationszentrum Karlsruhe, Gesellschaft für wissenschaftlich-technische Information mbH, D-7514 Eggenstein-Leopoldshafen 2 (FRG), on quoting the depository number CSD-54461, the names of the authors, and the journal citation.

[7] Conversion of **5a** under the reaction conditions for the tandem Knoevenagel hetero Diels-Alder reaction (acetonitrile, reflux, EDDA) afforded after 52 h, **5a** and **5b** in the ratio 1:2.2 ± 0.1; the analogous reaction of **5b** leads to **5a** and **5b** in the ratio 1:2.2 ± 0.1 after 24 h.

[8] a) U. Eder, G. Sauer, R. Wiechert, *Angew. Chem. 83* (1971) 492; *Angew. Chem. Int. Ed. Engl. 10* (1971) 496; b) Z. G. Hajos, D. R. Parrish, *J. Org. Chem. 39* (1974) 1615.

[9] a) Z. G. Hajos, R. A. Micheli, D. R. Parrish, E. P. Oliveto, *J. Org. Chem. 32* (1967) 3008; b) R. A. Micheli, Z. G. Hajos, N. Cohen, D. R. Parrish, L. A. Portland, W. Sciamanna, M. A. Scott, P. A. Wehrli, *ibid. 40* (1975) 675.

[10] a) R. B. Turner, *J. Am. Chem. Soc. 72* (1950) 579; b) W. G. Dauben, H. G. Wight, G. A. Boswell, *J. Org. Chem. 23* (1958) 1787; c) E. Winterfeldt in [4a], S. 349; d) S. Takano, S. Sato, E. Goto, K. Ogasawara, *J. Chem. Soc. Chem. Commun. 1986*, 156.

[11] C. G. Rao, *Org. Prep. Proced. Int. 12* (1980) 225.

[12] **13b**: A solution of **12a** (15 mmol) in CH_3CO_2Et (135 mL), CH_3COOH (135 mL) and water (80 mL) was ozonized at −15 °C with 2.5 equivalents of O_3. The reaction solution was treated with 100 mL of toluene, evaporated in vacuo (repeated to constant weight), and dried under high vacuum. A solution of the resulting carboxylic acid **13a** in 15 mL of anhydrous CH_3CN was treated at room temperature under N_2 and with vigorous stirring with 15 mmol of DBU and 17 mmol of CH_3I. After 1 h, the mixture was treated with 15 mL of H_2O and extracted with 3 × 50 mL of Et_2O. The combined ethereal phases were washed with H_2O, dried over $MgSO_4$, and evaporated in vacuo. Flash chromatography of the crude product (ethyl acetate/*n*-hexane 1:4) affords the analytically pure oxocarboxylate **13b**.

[13] a) Varying yields, best result given; b)B. Neises, W. Steglich, *Angew. Chem. 90* (1978) 556; *Angew. Chem. Int. Ed. Engl. 17* (1978) 522; c) A. Hassner, V. Alexanian, *Tetrahedron Lett.* 1978, 4475.

[14] J. E. Baldwin, R. C. Thomas, L. I. Kruse, L. Silberman, *J. Org. Chem. 42* (1977) 2846.

[15] A. J. Mancuso, D. Swern, *Synthesis 1981*, 165.

Synthesis of the First Silaamidide **

By *Gail E. Underiner* and *Robert West**

Amidines and their conjugate bases (amidides) have been extensively studied in carbon chemistry,[1] and while their silicon analogues $R_2N-Si(R)=NR$ are unknown,[2] a 1,3-diphospha-2-silaallyl anion has recently been reported.[3] We now report the isolation and characterization of the first silaamidide anion, as the salt lithium *N,N'*- bis(2,4,6-tri-*tert*-butylphenyl)phenylsilaamidide (**3**) and its ether complexes **2** and **4**.

Reaction of *n*BuLi with 2,4,6-tri-*tert*-butylaniline followed by addition of one-half equivalent of $PhSiCl_3$ affords silanediamine **1** (Table 1). Treatment of **1** with two equivalents of *t*BuLi in diethyl ether yields lithium silaamidide **2**,

[*] Prof. R. West, Dr. G. E. Underiner
Department of Chemistry
The University of Wisconsin
Madison, WI 53706 (USA)

[**] This work was supported by the Air Force Office of Scientific Research, Air Force Systems Command, USAF under Contract No. F49620-86-C-0010 and the National Science Foundation, Grant No. CHE-8318810-02.

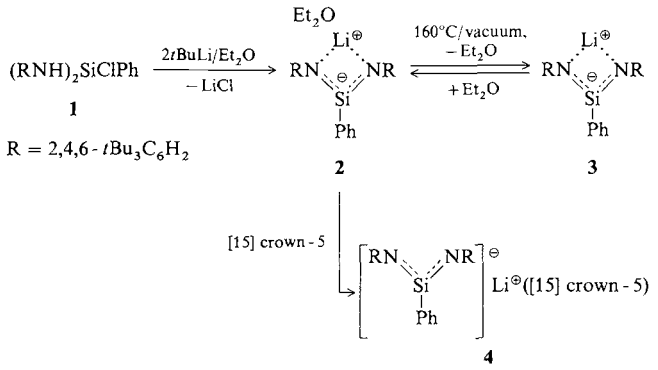

in which the lithium cation is coordinated to two N atoms of silaamide and to one molecule of diethyl ether. Ether may be reversibly removed from **2** by heating at 160 °C for several hours under vacuum to give the ether-free silaamidide salt **3**. Addition of [15]crown-5 to a benzene solution of **2** yields the salt **4** in the form of large yellow benzene-containing crystals. The lithium cation is no longer coordinated to the two N atoms, and the crystals lose benzene on exposure to X-rays and become a powder that cannot be fully characterized. The silaamidide salts are thermally stable but decompose rapidly upon exposure to atmospheric moisture or oxygen.

Table 1. Melting points and ^{29}Si NMR Data for **1**–**7**.

Compound	M.p. [°C]	^{29}Si NMR [δ values]
1 [a, b]	156–157	−28.8
2 [a]	212 (dec.)	3.2
3 [a]	140 (dec.)	7.0
4		−37.5
5 [b]	160–163	
6 [b]	226–227	−54.6
7 [a, b]	220–228	

[a] Satisfactory elemental analysis obtained for C, H, and N. [b] Correct high-resolution mass spectrum.

The ether-free silaamidide salt **3** exhibits a ^{29}Si NMR resonance at $\delta = 7$, shifted strongly downfield from the resonance for **1** ($\delta = -29$). **2** and **4** have ^{29}Si NMR chemical shifts of $\delta = 3$ and $\delta = -37.5$, respectively. This trend is reasonable, since the Si atom becomes more shielded by the greater negative charge in the allylic system as the lithium cation is more effectively solvated. Silaamidide salts **2**, **3**, and **4** show only one set of resonances for the tBu$_3$C$_6$H$_2$ groups in the ^{1}H and ^{13}C NMR spectra. This suggests that these anions, like amidides in organic chemistry,[5] are symmetrical. Rapid equilibration between unsymmetrical species cannot, however, be excluded. We attribute an intense band in the IR spectra (Nujol mull) of **2** at 1304 cm^{-1} to $\tilde{\nu}_{as}$ of [NSiN]. As expected, this frequency is lower than the previously reported value of $\nu_{Si=N}$ for tBu$_2$NSitBu$_3$ (1326 cm^{-1}).[4]

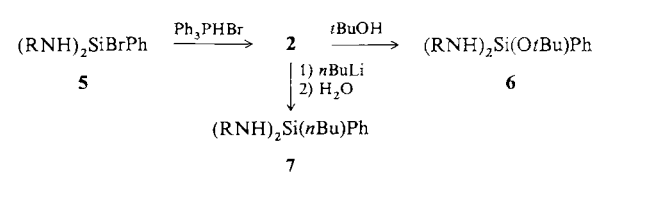

The silaamidide anion of **2** reacts rapidly with HBr and tBuOH. Since silylamines are prone to cleavage by strong acids, Ph$_3$PHBr was utilized as a gentle source of HBr.[6] It reacts with **2** in solution over several hours at room temperature, protonating one nitrogen atom and adding across the double bond of the silaamidine to afford **5**. Chlorosilane **1** does not react under these conditions. Compound **2** reacts with tBuOH to yield **6**. Addition of nBuLi to **2** followed by quenching with water gives **7**, presumably by addition of nBuLi across an Si···N bond to form the dianion, which is then protonated.

Experimental Procedure

1: 2,4,6-Tri-*tert*-butylaniline (6.0 g, 23 mmol) in 120 mL of hexane was treated with n-BuLi (9.2 mL of a 2.5 M solution in hexane, 23 mmol). After stirring the resulting white suspension for 1 h followed by 40 min of reflux, the reaction mixture was cooled to room temperature and PhSiCl$_3$ (2.4 g, 12 mmol) was added by syringe. After refluxing for 48 h, the solution was filtered and the salts washed several times with hexane. Solvent was removed from the filtrate under vacuum to give a sticky solid. Recrystallization in hexane yielded 5.30 g (67%) of colorless **1**.

2: A solution of **1** (2.00 g), 3.16 mmol) in 10 mL of ether and 50 mL of hexane was treated at −78 °C with tBuLi (3.72 mL of a 1.7 M solution in hexane, 6.32 mmol). After several hours the reaction mixture was warmed to room temperature and stirred for 24 h. Salts were removed by filtration under nitrogen and the filtrate was evaporated to dryness, giving a colorless solid. Recrystallization in hexane furnished 1.24 g (56%) of colorless **2**.

Received: November 14, 1989 [Z 3633 IE]
German version: *Angew. Chem. 102* (1990) 579

CAS Registry numbers:
1, 126256-41-5; **2**, 126256-46-0; **3**, 126256-42-6; **4**, 126256-48-2; **5**, 126256-43-7; **6**, 126256-44-8; **7**, 126256-45-9; Ph$_3$PHBr, 6399-81-1; PhSiCl$_3$, 98-13-5; 2,4,6-tri-*tert*-butylamine, 961-38-6.

[1] For a review of amidines see S. Patai (Ed.): *The Chemistry of Amidines and Imidates*, Wiley, London 1975.
[2] Within recent years, several examples of silaimines (Si=N) have been reported. a) U. Klingebiel, A. Meller, *Angew. Chem. 88* (1976) 304; *Angew. Chem. Int. Ed. Engl. 15* (1976) 313; b) U. Klingebiel, D. Bentmann, A. Meller, *J. Organomet. Chem. 144* (1978) 381; c) S. S. Ziegler, L. Johnson, R. West, *ibid. 341* (1988) 187; d) N. Wiberg, K. Schurz, G. Fischer, *Angew. Chem. 97* (1985) 1058; *Angew. Chem. Int. Ed. Engl. 24* (1985) 1053. e) U. Klingebiel, M. Hesse, *ibid. 98* (1986) 638; and *ibid. 25* (1986) 649.
[3] E. Niecke, E. Klein, M. Nieger, *Angew. Chem. 101* (1989) 792; *Angew. Chem. Int. Ed. Engl. 28* (1989) 751.
[4] N. Wiberg, K. Schurz, *Chem. Ber. 121* (1988) 581.
[5] J. D. Halliday, E. H. Symons, P. E. Binder, *Can. J. Chem. 56* (1978) 1470.
[6] A. Hercouret, M. LeCorre, *Synthesis 1988*, 157.

A Facile Synthesis of β-Selenolactams

By *Hideharu Ishihara, Michinari Yoshimi*, and *Shinzi Kato**

Although considerable progress has been made in the chemistry of β-lactams[1] and β-thiolactams[2] during the past forty years, very little is known about the biologically and spectroscopically interesting β-selenolactams because of the difficulties encountered in their synthesis.[3] We now wish to report a convenient method for synthesizing and characterizing β-selenolactams **3a** to **3e** (see Table 1). These β-selenolactams were obtained by reaction of lithium alkyneselenolate **1** with the alkylidenamines **2** below −20 °C. The structures were determined by ^{1}H NMR, ^{13}C NMR, ^{77}Se

[*] Prof. Dr. S. Kato, Dr. H. Ishihara, M. Yoshimi
Department of Chemistry, Faculty of Engineering
Gifu University
1-1 Yanagido, Gifu 501-11 (Japan)

Table 1. Yields and some spectral data for β-selenolactams **3a–3e**.

	R^1	R^2	Reaction conditions [a]	Yield [%]	m.p. [c] [°C]	^{13}C NMR [d] δ (C=Se)	^{77}Se NMR [e] δ	^1H NMR [f] $J(^3CH-^4CH)$ [Hz]
3a	C_6H_5	C_6H_5	B	89 (*cis*)	180–181	202.0	664.4	5.49
3b	4-$CH_3C_6H_4$	*i*-C_3H_7	A	59 (*cis*) [b]	oil	204.9	442.7	4.70
3b′				10 (*trans*) [b]	oil	206.1	–	0.70
3c	4-$CH_3C_6H_4$	4-$CH_3C_6H_4$	B	77 (*cis*)	186–188	200.9	632.5	5.50
3d	4-$CH_3C_6H_4$	$C_6H_5CH_2$	B	70 (*cis*)	115–116	206.3	432.8	4.77
3e	4-$CH_3C_6H_4$	4-ClC_6H_4	B	86 (*cis*)	184–185	203.0	679.9	5.50

[a] A: Mole ratio of **1**/**2**/AcOH = 1/1/0.5, tetrahydrofuran, −20 °C, 3 h; B: Mole ratio of **1**/**2**/AcOH = 1/1/1.2, tetrahydrofuran, −20 °C, 1 h. [b] Purified by preparative thin-layer chromatography (hexane/ether = 5/1, **3b**: R_f = 0.2, **3b′**: R_f = 0.3). [c] Satisfactorily exact mass data for **3b** and **3b′** as well as elemental analyses for **3a, 3c–e** (C ±0.33, H ±0.16%) were obtained; [d] Relative to Me_4Si in $CDCl_3$. [e] Relative to Me_2Se in $CDCl_3$ (60%). [f] In $CDCl_3$.

NMR, IR, and mass spectra as well as by elemental analysis. The configurations of R^1 and R^2 were determined to be *cis* on the basis of vicinal coupling constants J_{HH} = 4 to 6 Hz.[4] All the reactions of **2** (except for **2b**) led to the exclusive formation of the *cis* isomer of **3**. A plausible explanation for

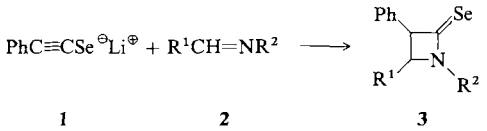

1 **2** **3**

this [2+2] cycloaddition to **3** is the participation of the canonical resonance structure **1′** in analogy to the reactions of the corresponding thio congeners.[5]

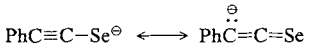

1 **1′**

The reaction pathway described here for synthesizing β-selenolactams, although until now only carried out with 1-alkynes, avoids many difficulties inherent in other methods: (1) The reaction conditions are mild, the procedures very easy. (2) The yields of **3** are high, and *cis* isomers are obtained almost exclusively. (3) The starting compounds are readily available. (4) Since it is conducted in solution, the reaction is free of the small-scale synthesis problems that are encountered in the heterogeneous reaction using phosphorus pentaselenide.[3a]

Experimental Procedure

3a: A solution of **1** (1 mmol), prepared from phenylethynyllithium (1 mmol) and selenium (powder) in tetrahydrofuran (10 mL), was treated with **2a** (181 mg, 1 mmol) for 1 h and then with acetic acid (72 mg, 1.2 mmol) at −20 °C under argon. The mixture was stirred at this temperature for 15 min. After adding ether (20 mL), the mixture was washed with water (3 × 50 mL) and the organic phase dried over anhydrous sodium sulfate. The solvents were removed by evaporation in vacuo. Recrystallization of the residue with ether/hexane (5/1) afforded (**3a**) in 89% yield: m.p. 180–181 °C. ^1H NMR ($CDCl_3$): δ = 4.59 (d, J = 5.49 Hz, 1H, ^3CH), 6.10 (d, J = 5.49 Hz, 1H, ^4CH), 7.0–7.4 (m, 13H, H_{Aryl}), 8.23 (d, 2H, H_{Aryl}). ^{13}C NMR ($CDCl_3$): δ = 63.3 (^3CH), 71.1 (^4CH), 118.2, 126.8–138.9 (C_{Aryl}), 202.0 (C=Se). Satisfactory C,H analysis.

Received: November 17, 1989 [Z 3640 IE]
German version: *Angew. Chem. 102* (1990) 572

CAS Registry numbers:
1, 78531-03-0; **2a**, 538-51-2; **2b**, 80275-06-5; **2c**, 16979-20-7; **2d**, 24431-15-0; **2e**, 29574-09-2; **3a**, 126134-17-6; **3b**, 126134-18-7; **3b′**, 126134-19-8; **3c**, 126134-20-1; **3d**, 126134-21-2; **3e**, 126134-22-3.

[1] M. S. Manhas, A. K. Bose: *Synthesis of Penicillin, Cephalosporin C and Analogs*, Dekker, New York, 1969; M. S. Manhas, A. K. Bose: *β-Lactams, Natural and Synthetic*, Part 1, Wiley-Interscience, New York, 1971; D. A. Koppel, *Chem. Heterocycl. Compd. 42* (1983) 219; J. G. Gleason, *Org. Compd. Sulphur Selenium Tellurium 3* (1975) 190; R. Mecke, Jr., R. Mecke, *Chem. Ber. 89* (1956) 343.

[2] The CAS online search (1968 to October 1989) of β-thiolactams provided 220 β-lactams and 52 literature citations for the preparation of thiolactams.

[3] Only two β-selenolactams have been reported; either the yield was not mentioned at all or a relatively low yield was obtained. The methods used were as follows: a) the heating of β-lactam with stoichiometric amounts of red phosphorus and selenium in xylene: H. E. Hallam, C. M. Jones, *J. Chem. Soc. A 1969* 1033; b) the cycloaddition of a selenoketene with 3,4-dihydroisoquinoline: E. Schaumann, F. F. Grabley: *Tetrahedron Lett. 21* (1980) 4251.

[4] The coupling constants J(H,H) of *cis*- and *trans*-β-lactams are 4–6 Hz and 2–3 Hz, respectively: H. B. Kagan, J. J. Bassetier, J. L. Luche, *Tetrahedron Lett.* (1964), 941; K. D. Barrow, T. M. Spotswood, *ibid. 1965*, 3325; R. H. Cox, S. L. Smith, *J. Phys. Chem. 71* (1967) 1809. The *cis* and *trans* β-thiolactams show similar coupling constants: A. Vigerani, G. G. Gallo, *J. Heterocycl. Chem. 4* (1967) 583.

[5] N. Miyaura, T. Yanagi, A. Suzuki, *Chem. Lett. 1979*, 535.

$Zn^{II}Fe^{III}$ and $Fe^{II}Fe^{III}$ Complexes Containing a Novel (μ-Phenoxo)bis(μ-diphenylphosphato)-dimetal(II,III) Core as Model Complexes for Active Sites of Purple Phosphatases**

By *Klaus Schepers, Bernd Bremer, Bernt Krebs,* Gerald Henkel, Erika Althaus, Bernd Mosel,* and *Werner Müller-Warmuth*

Purple, acid phosphatases are important iron-containing non-heme proteins which catalyze the hydrolysis of activated phosphoric acid esters.[1] The active site of uteroferrin (PP 1[1b]) and of phosphatase from bovine spleen[1d,e,f] consists of an $Fe^{II}Fe^{III}$ moiety in its inactive purple form in which

[*] Prof. Dr. B. Krebs, Dipl.-Chem. K. Schepers, Dipl.-Chem. B. Bremer
Anorganisch-chemisches Institut der Universität
Wilhelm-Klemm-Strasse 8, D-4400 Münster (FRG)
Prof. Dr. G. Henkel
Fachgebiet Anorganische Chemie/Festkörperchemie der Universität
Lotharstrasse 1, D-4100 Duisburg (FRG)
Prof. Dr. W. Müller-Warmuth, Dipl.-Chem. E. Althaus, Dr. B. Mosel
Institut für Physikalische Chemie der Universität
Schlossplatz 7, D-4400 Münster (FRG)

[**] This work was supported by the Deutsche Forschungsgemeinschaft, the Bundesminister für Forschung und Technologie and the Fonds der Chemischen Industrie. We thank Prof. Dr. *W. Haase*, Dipl.-Ing. *H.-P. Fleischhauer* and Dipl.-Ing. *S. Gehring* for carrying out and evaluating the magnetic measurements. We also thank Prof. Dr. Dr. *H. Witzel* for stimulating discussions.

the iron ions have a high-spin configuration and are coupled strongly antiferromagnetically ($-J > 150\ cm^{-1}$[1d]). The enzymatically active pink form of PP1 contains a mixed valence $Fe^{II}Fe^{III}$ center with a more weakly antiferromagnetic coupling of the high-spin ions ($J = -19.8(5)\ cm^{-1}$[2]). A tightly bound phosphate group was detected in the oxidized form of PP1; however, it is so far controversial as to whether this phosphate group is bridging or terminally coordinated.[3] A purple, mixed valence uteroferrin(red)-phosphate complex which shows a pH-dependent absorption maximum between 530 and 561 nm has been characterized both spectroscopically and kinetically.[4] The antiferromagnetic spin interactions are only weak ($J = -6.0(5)\ cm^{-1}$[2]).

In contrast, a phosphatase (PP2) isolated from kidney beans contains a heterobinuclear $Zn^{II}Fe^{III}$ center, whose structure is presumably very similar to that of the $Fe^{II}Fe^{III}$ unit in the reduced form of PP1.[5] PP2 shows an absorption band at $\lambda_{max} = 560$ nm which can be assigned to a charge transfer transition from a tyrosine ligand to the Fe^{III}. A further enzymatically active $Fe^{II}Fe^{III}$ derivative of PP2 has the same ESR spectrum as the mixed valence form of PP1.[6]

Diiron(III) model complexes with (μ-oxo)bis(μ-phosphato), (μ-oxo)bis(μ-phenylphosphato), tris(μ-phosphato) or tris(μ-phenylphosphato) groups could be obtained with the ligand 1,4,7-trimethyl-1,4,7-triazacyclononane; a bridging coordination of diphenylphosphate is present in the dinuclear Fe^{III} complex $[Fe_2O\{O_2P(OC_6H_5)_2\}_2L_2]$ (L = hydrotris(1-pyrazolyl)borate).[7]

Attempts to synthesize and characterize mixed valence phosphate-bridged model compounds for the active form of the purple phosphatases have hitherto failed. We report here on the first model complexes for the active centers of PP1 and PP2, in which phosphoric acid esters are coordinated to the dinuclear $Fe^{II}Fe^{III}$ and $Zn^{II}Fe^{III}$ units. 2,6-Bis[bis(2-pyridylmethyl)aminomethyl]-4-methylphenol (Hbpmp), which has proven to be suitable for the synthesis of dinuclear mixed valence iron complexes,[8] was used as ligand.

Reaction of equimolar amounts of $Fe(ClO_4)_3 \cdot 9H_2O$ and $ZnBr_2$ in methanol with Hbpmp leads, after addition of diphenyl phosphate, to bluish-black crystals of **1**. The analogous reaction with two equivalents of $Fe(ClO_4)_3 \cdot 9H_2O$ yielded dark green crystals of **2**.

$[Zn^{II}Fe^{III}(bpmp)(O_2P(OPh)_2)_2](ClO_4)_2 \cdot 1.5\,CH_3OH \cdot H_2O$ **1**

$[Fe^{II}Fe^{III}(bpmp)(O_2P(OPh)_2)_2](ClO_4)_2 \cdot CH_3OH \cdot H_2O$ **2**

The structure of **1** is shown in Figure 1.[9] The molecule contains a μ-phenoxo-bridged $Zn^{II}Fe^{III}$ unit in which the metal centers are additionally linked by two μ-diphenylphosphato bridges. The nitrogen donors of the ligand $bpmp^{\ominus}$ complete an octahedral environment of the two metal centers by facial coordination. The Zn···Fe distance of 3.695 Å in **1** (and the similar Fe···Fe distance in **2**[10]) is significantly larger than in the carboxylate-bridged $Zn^{II}Fe^{III}$- and $Fe^{II}Fe^{III}$-analogues (3.438 and 3.365 Å, respectively[8d]), presumably as a result of the larger bite distance of the phosphate. This indicates a remarkable structural flexibility of the hydroxo-(alkoxo)-bridged dimetal(II,III) center (possibly important for the catalytic activity). On the other hand, d(Zn···Fe) compares with the value of 3.65 Å determined from EXAFS measurements on the native kidney bean phosphatase in the presence of phosphate.[11]

1 has a magnetic moment of 6.15 μ_B at room temperature. The magnetic susceptibilities (Faraday method) for crystalline **2** between 4.2 and 289.5 K can be fitted based on an isotropic Heisenberg model, $H' = -2J \cdot S_1 \cdot S_2$ ($S_1 = 2$, $S_2 = 5/2$) and $g = 2.06(4)$. Weak antiferromagnetic behavior was established; the coupling constant ($J = -6.2(5)\ cm^{-1}$) is in good agreement with the value determined for the reduced uteroferrin-phosphate complex.

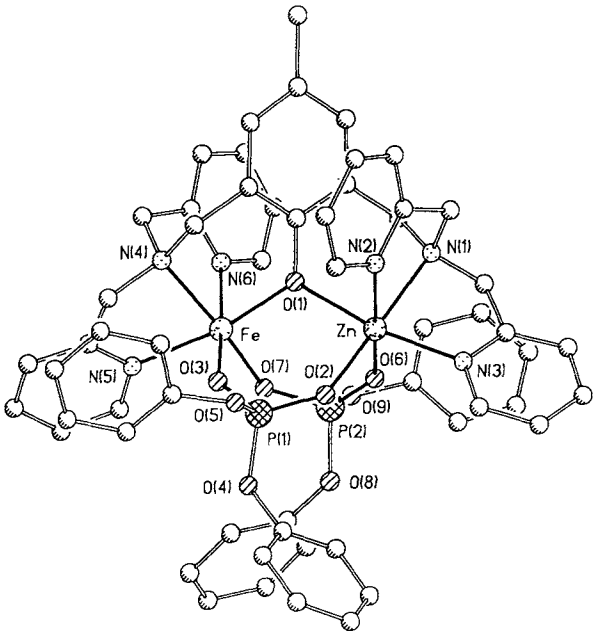

Fig. 1. Structure of the cation $[Zn^{II}Fe^{III}bpmp(O_2P(OPh)_2)_2]^{2\oplus}$ in the crystal of **1**. Important bond lengths [Å] and angles [°]: Fe···Zn 3.695(1), Fe···P1 3.281(1), Zn···P1 3.212(1), Fe···P2 3.183(1), Zn···P2 3.325(1), Fe–O1 2.031(2), Zn–O1 2.176(2), Fe–O3 1.984(3), Zn–O6 2.065(3), Fe–O7 1.966(2), Zn–O2 2.026(3), Fe–N4 2.177(3), Zn–N1 2.180(3), Fe–N5 2.104(3), Zn–N3 2.119(3), Fe–N6 2.125(3), Zn–N2 2.127(3), P1–O2 1.490(3), P1–O3 1.492(3), P2–O6 1.475(3), P2–O7 1.505(2); Fe–O1–Zn 122.8(1).

Electrochemical investigations on **1** show a reversible one-electron charge transfer at a potential of +143 mV. The transfer observed at +765 mV with only a very small peak current can be attributed to slight contamination of **1** with Fe^{II}. In the case of **2** two reversible one-electron transfers are observed at potentials of $E_1 = +135$ mV and

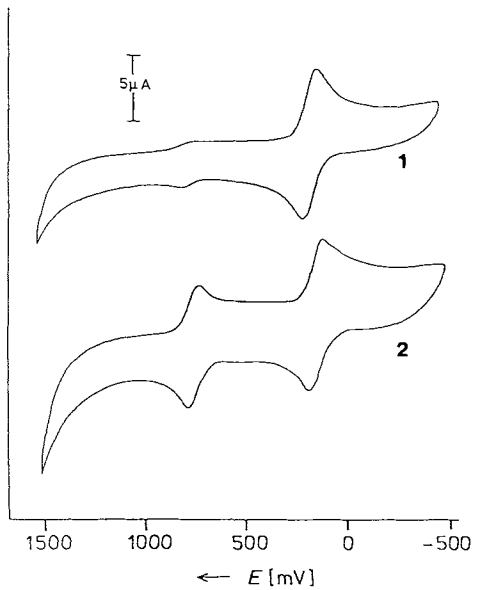

Fig. 2. Cyclovoltammograms of **1** and **2** (vs. SCE). 0.1 M $(n\text{Bu})_4NClO_4$ in MeCN under argon. Measuring rate: 100 mV s^{-1}.

$E_2 = +755$ mV, which are assigned to the redox pairs $Fe^{II}Fe^{II}/Fe^{II}Fe^{III}$ and $Fe^{II}Fe^{III}/Fe^{III}Fe^{III}$. The cyclovoltammograms of **1** and **2** are shown in Figure 2.

Using the relationship $E_2 - E_1 = R \cdot T \cdot F^{-1} \cdot \ln K$, the thermodynamic stability constant of the mixed valence complex **2** can be estimated to be $K = 3.2 \times 10^{10}$ for the comproportionation equilibrium. The Mössbauer spectrum of **1** at

$$(Fe^{II}Fe^{II}) + (Fe^{III}Fe^{III}) \rightleftarrows 2(Fe^{II}Fe^{III})\,.$$

298 K shows, in addition to the Fe^{III} doublet, broad signals that can be assigned to Fe^{II}. At 4.2 K additional splittings are observed which can be ascribed to magnetic hyperfine interactions. The Mössbauer spectra of **2** could be fitted for the temperatures 300, 100 and 50 K (Fig. 3). The values of the

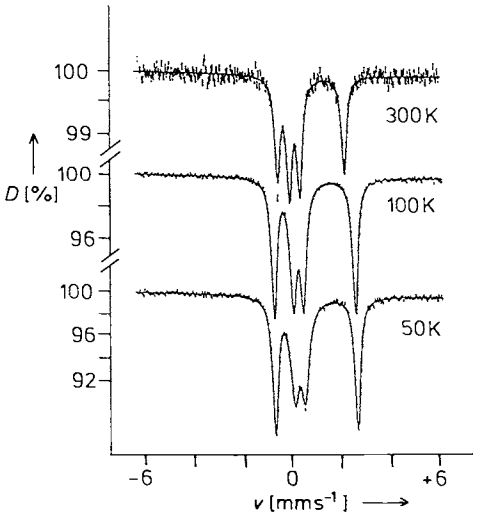

Fig. 3. ^{57}Fe-Mössbauer spectra of a polycrystalline sample of **2**. *v*: rate, *D*: transmission.

isomeric shifts δ (referred to metallic iron at 298 K) and the quadrupole splittings ΔE_Q are listed in Table 1. All the spectra of **2** show two separate quadrupole doublets of equal intensity, indicating localized high-spin-Fe^{II}- and high-spin-Fe^{III}-valence states. The corresponding values for the uteroferrin(red)-phosphate complex at 119 K are $\delta = 1.23$ and 0.54 mm s^{-1} ($\Delta E_Q = 2.76$ and 0.78 mm s^{-1}) respectively, for uteroferrin(red) without phosphate[4] $\delta = 1.22$ and 0.53 mm s^{-1} ($\Delta E_Q = 2.63$ and 1.78 mm s^{-1}), respectively, and for bovine spleen phosphatase(red) at 77 K[1f] $\delta = 1.17$ and 0.67 mm s^{-1} ($\Delta E_Q = 2.65$ and 1.27 mm s^{-1}), respectively. Similar Mössbauer data as for **2** have been obtained for the carboxylate-bridged complex $[Fe_2(bpmp)(OPr)_2](BPh_4)_2$ ($\delta = 1.13$ and 0.48 mm s^{-1}, respectively, $\Delta E_Q = 2.69$ and 0.50 mm s^{-1}, respectively, at 55 K).[8c] A valence fluctuation more rapid than 10^{-7} s is not observed in the room-temperature spectrum of **2**. The spectra at 25, 10 and 4.2 K indicate

Table 1. Mössbauer parameters of **2** ($\delta \pm 0.01$ mm s^{-1}; $\Delta E_Q \pm 0.02$ mm s^{-1}).

	Fe^{II}		Fe^{III}	
T [K]	δ_1 [mm s^{-1}]	ΔE_{Q1} [mm s^{-1}]	δ_2 [mm s^{-1}]	ΔE_{Q2} [mm s^{-1}]
300	1.05	2.75	0.37	0.43
100	1.16	3.35	0.48	0.41
50	1.17	3.39	0.49	0.43

magnetic hyperfine interactions which so far, however, could not be fitted.

The electron spectrum of **1** in methanol shows only one absorption maximum at $\lambda_{max} = 569$ nm ($\varepsilon \approx 800$ cm^{-1} mol^{-1}), which is assigned to a charge transfer transition from phenolate to the Fe^{III} ion. The UV/VIS spectrum of **2** in methanol shows the corresponding transition at $\lambda_{max} = 610$ nm ($\varepsilon \approx 950$ cm^{-1} mol^{-1}). In addition, a shoulder is observed at $\lambda = 365$ nm ($\varepsilon \approx 3480$ cm^{-1} mol^{-1}), which can be assigned to a charge-transfer transition from the Fe^{II} to pyridine.[8d]

Experimental Procedure

1: A solution of 0.44 g of Hbpmp (0.8 mmol) in 30 mL of methanol was treated with a solution of 0.41 g of $Fe(ClO_4)_3 \cdot 9H_2O$ (0.8 mmol) in 10 mL of methanol and a solution of 0.18 g of $ZnBr_2$ (0.8 mmol) in 10 mL of methanol. After addition of 0.4 g of diphenyl phosphate (1.6 mmol) in 10 mL of methanol, bluish-black crystals of **1** separated out. Small amounts of oxidizing agents (H_2O_2, $S_2O_8^{2\ominus}$) did not prevent the slight contamination with Fe^{II}.

2: The synthesis was accomplished by an analogous reaction of 0.82 g of $Fe(ClO_4)_3 \cdot 9H_2O$ (1.6 mmol) with 0.44 g Hbpmp (0.8 mmol) and 0.4 g of diphenyl phosphate (1.6 mmol).

Received: January 8, 1990 [Z 3730 IE]
German version: *Angew. Chem. 102* (1990) 582

[1] a) B. C. Antanaitis, P. Aisen, *Adv. Inorg. Biochem. 5* (1983) 111; b) R. B. Lauffer, B. C. Antanaitis, P. Aisen, L. Que, Jr., *J. Biol. Chem. 258* (1983) 14212; c) J. T. Sage, Y.-M. Xia, P. G. Debrunner, D. T. Keough, J. de Jersey, B. Zerner, *J. Am. Chem. Soc. 111* (1989) 7239, and references cited therein; d) B. A. Averill, J. C. Davis, S. Burman, T. Zirino, J. Sanders-Loehr, T. M. Loehr, J. T. Sage, P. G. Debrunner, *ibid. 109* (1987) 3760; e) D. Münstermann, M. Dietrich, H. Suerbaum, H. Witzel, *Eur. J. Biochem.*, in press; f) K. Cichutek, H. Witzel, F. Parak, *Hyperfine Interact. 42* (1988) 885.

[2] E. P. Day, S. S. David, J. Peterson, W. R. Dunham, J. J. Bonvoisin, R. H. Sands, L. Que, Jr., *J. Biol. Chem. 263* (1988) 15561.

[3] D. T. Keough, J. L. Beck, J. de Jersey, B. Zerner, *Biochem. Biophys. Res. Commun. 108* (1982) 1643.

[4] J. W. Pyrz, J. T. Sage, P. G. Debrunner, L. Que, Jr., *J. Biol. Chem. 261* (1986) 11015.

[5] J. L. Beck, L. A. McConachie, A. C. Summors, W. N. Arnold, J. de Jersey, B. Zerner, *Biochim. Biophys. Acta 869* (1986) 61.

[6] J. L. Beck, J. de Jersey, B. Zerner, M. P. Hendrich, P. G. Debrunner, *J. Am. Chem. Soc. 110* (1988) 3317.

[7] a) S. Drüeke, K. Wieghardt, B. Nuber, J. Weiss, H. P. Fleischhauer, S. Gehring, W. Haase, *J. Am. Chem. Soc. 111* (1989) 8622; b) W. H. Armstrong, S. J. Lippard, *ibid. 107* (1985) 3730.

[8] a) M. Suzuki, H. Kanatomi, I. Murase, *Chem. Lett. 1981*, 1745; b) M. Suzuki, A. Uehara, H. Oshio, K. Endo, M. Yanaga, S. Kida, K. Saito, *Bull. Chem. Soc. Jpn. 60* (1987) 3547; *ibid. 61* (1988) 3907; c) A. S. Borovik, L. Que, Jr., *J. Am. Chem. Soc. 110* (1988) 2345; A. S. Borovik, L. Que, Jr., V. Papaefthymiou, E. Münck, L. F. Taylor, O. P. Anderson, *ibid. 110* (1988) 1986; d) A. S. Borovik, V. Papaefthymiou, L. F. Taylor, O. P. Anderson, L. Que, Jr., *ibid. 111* (1989) 6183.

[9] Crystal structure data of **1**: triclinic, $P\bar{1}$, $a = 10.179(3)$, $b = 13.312(5)$, $c = 23.950(7)$ Å, $\alpha = 100.47(3)$, $\beta = 93.32(2)$, $\gamma = 98.49(3)°$, $Z = 2$, $V = 3144.2$ Å^3, measuring temperature 150 K, $Mo_{K\alpha}$ radiation ($\lambda = 0.71069$ Å), 11623 symmetry independent reflections, 7624 with $I > 1.96\sigma(I)$, $R = 0.0495$, $R_w = 0.0448$, structure solution by direct methods; both metal atom positions were considered as occupied by (Zn + Fe) and were refined with coupled occupation factors (sum 1). The result of this refinement (with 100% Fe at position 1 and 90% Zn + 10% Fe at position 2) can be interpreted, in agreement with the thermal parameters, with structural chemical considerations (bond lengths) and with spectroscopic data, as ordered occupation of the position 1 with Fe^{II} and of position 2 with $Zn^{II}(+Fe^{II})$. Further details of the crystal structure investigation are available on request from the Fachinformationszentrum Karlsruhe, Gesellschaft für wissenschaftlich-technische Information mbH, D-7514 Eggenstein-Leopoldshafen 2 (FRG), on quoting the depository number CSD-54476, the names of the authors, and the journal citation.

[10] K. Schepers, B. Bremer, G. Henkel, B. Krebs, unpublished.

[11] a) B. Krebs, G. Henkel, S. Priggemeyer, P. Eggers-Borkenstein, H. Witzel, M. Körner, D. Münstermann, H.-F. Nolting, C. Hermes, *J. Inorg. Biochem. 36* (1989) 263; b) P. Eggers-Borkenstein, S. Priggemeyer, B. Krebs, G. Henkel, H. Witzel, M. Körner, H.-F. Nolting, C. Hermes, unpublished.

A New Route to 1,3-Diphospholide Ions. Synthesis and X-Ray Structure Analysis of a 1,3-Diphosphaferrocene

By *Nicole Maigrot, Louis Ricard, Claude Charrier,* and *François Mathey**

Presently, only one 1,3-diphospholide ion is known. This 2,4,5-tri-*tert*-butyl derivative is formed as a by-product in the synthesis of the 3,5-di-*tert*-butyl-1,2,4-triphospholide ion from *tert*-butylphosphaacetylene.[1-3] The development of the chemistry of this very interesting species is thus hampered by the lack of a convenient and specific access to derivatives of the 1,3-diphospholide ion. We have now found a way of filling this gap starting from the readily accessible 1,2-dihydro-1,2-diphosphete ring.[4]

The P–P bond of the 1,2,3,4-tetraphenyl-substituted four-membered ring compound **1** was first cleaved by reaction with lithium in THF.[5] Treatment of the resulting dianion with carbon disulfide followed by alkylation with methyl iodide then afforded the five-membered 2,3-dihydro-1,3-diphospholes **2a, b** in 80% yield (Scheme 1).

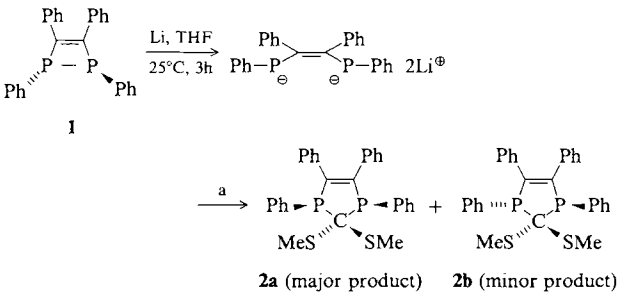

Scheme 1. a: 1) CS_2, −80 °C, 15 min, 2) 2 equiv. MeI, −80 to 25 °C.

Both isomers were obtained in the pure state by chromatography. The ^1H and ^{13}C NMR spectra of the *cis* isomer **2a** obtained as major product (Table 1) display two nonequivalent MeS groups, whereas the spectra of the *trans* isomer obtained in smaller amounts contain only one MeS signal.

Table 1. Most important spectroscopic data of **2a, 2b, 5** [a].

2a: ^{31}P NMR: $\delta = 60.3$; ^1H NMR: $\delta = 1.62$ (s, 3H, SMe), 2.44 (t, ^4J(H–P) = 1.36 Hz, 3H; SMe); ^{13}C NMR: $\delta = 13.97$ (s, SMe), 14.99 (t, ^3J(C–P) = 21.3 Hz, SMe), 57.90 (t, ^1J(C–P) = 41.5 Hz, P–*C*–P), 147.50 (dd, ^1J(C–P) = 12.5 Hz, ^2J(C–P) = 5.7 Hz, Ph–*C*=); MS = *m/z* 500 ($M^\oplus$, 34%), 453 ($M^\oplus$ − SMe, 100%), 406 ($M^\oplus$ − 2SMe, 27%)

2b: ^{31}P NMR (CH_2Cl_2): $\delta = 74.2$; ^1H NMR: $\delta = 1.98$ (s, 6H, SMe); ^{13}C NMR (C_6D_6): $\delta = 13.27$ (t, ^3J(C–P) ≈ 9 Hz, SMe), 52.79 (t, ^1J(C–P) = 37.9 Hz, P–*C*–P), 147.52 (s, Ph*C*=)

5: ^{31}P NMR: $\delta = 5.1$; ^1H NMR: $\delta = 3.67$ (t, ^2J(H–P) = 32.5 Hz, 1H, P–C*H*–P), 4.54 (s, 5H, Cp), 7.13 (s, 10H, Ph); ^{13}C NMR: $\delta = 74.95$ (s, Cp), 81.59 (t, ^1J(C–P) = 71.6 Hz, P–*C*–P), 110.79 (m, Ph–*C*=); MS: *m/z* 374 ($M^\oplus$, 100%).

[a] NMR spectra in CD_2Cl_2 and 70-eV EI mass spectra unless noted otherwise. ^1H NMR, 200.1 MHz; ^{13}C NMR, 50.3 MHz; ^{31}P NMR 32.4 MHz.

[*] Prof. F. Mathey, Dr. N. Maigrot, Dr. L. Ricard, Dr. C. Charrier
Laboratoire de Chimie du Phosphore et des Métaux de Transition
DCPH Ecole Polytechnique
F-91128 Palaiseau Cedex (France)

The mixture **2a, 2b** was treated with six equivalents of lithium in THF at room temperature. The initial ^{31}P NMR signals of **2a** and **2b** slowly disappeared and were replaced by a larger signal at $\delta = 229$ (**3**) and a smaller signal at $\delta = 193$ (**4**). Addition of *tert*-butyl chloride (or, alternatively, of dry powdered NH_4Cl) led to transformation of **3** into **4** (Scheme 2). Apparently, **4** is formed by protonation of **3**. Indeed, the phosphorus atoms of **3** show no sizable PH coupling, whereas the phosphorus atoms of **4** are strongly coupled with one proton: $J(^{31}P^1H) = 36.6$ Hz. The position of the P signal of **4** in the ^{31}P NMR spectrum is similar to that recorded for the 2,4,5-tris-*tert*-butyl-1,3-diphospholide ion ($\delta^{31}P = 187.6$ in THF[2]) and the PH coupling is similar to those found in phospholide anions.[6] Compound **4** was unequivocally identified as the 4,5-diphenyl-1,3-diphospholide ion via its reaction with (η^5-cyclopentadienyl)(η^6-*p*-xylene)iron hexafluorophosphate,[7] which afforded the expected 1,3-diphosphaferrocene **5** (Scheme 2).

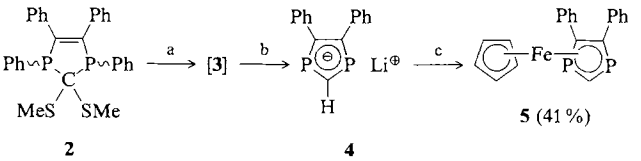

Scheme 2. a: 6 equiv. Li, THF, 25 °C, 24 h; b: *t*BuCl, 25 °C, 24 h or NH_4Cl, 25 °C, 5 min; c: $[(\eta^5\text{-}C_5H_5)(\eta^6\text{-}1,4\text{-}Me_2C_6H_4)Fe]^\oplus PF_6^\ominus$, 25 °C, 4 h.

Only one 1,3-diphosphaferrocene had been previously described in the literature.[8] It was obtained as a mixture with the corresponding 1,2,4-triphosphaferrocene and was only characterized by ^1H and ^{31}P NMR spectroscopy. Therefore, we decided to carry out the X-ray structure analysis of **5** (Fig. 1). The 1,3-diphospholide ring is almost planar. The two rings are eclipsed and parallel. The iron atom is closer to the phospholide plane [1.6224(7) Å] than to the cyclopentadienyl plane [−1.6694(7) Å]. The two most striking differences between the structure of **5** and 3,4-dimethyl-1-phosphaferrocene[10] are the parallelism of the two planes in **5** (in 3,4-dimethyl-1-phosphaferrocene the dihedral angle is

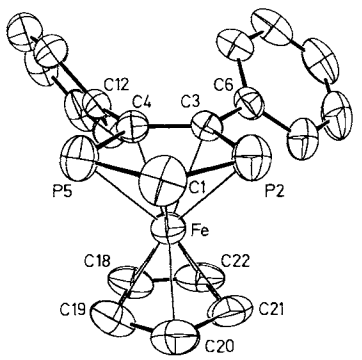

Fig. 1. Structure of **5** in the crystal [9]. Ellipsoids are scaled to enclose 50% of the electronic density. Hydrogen atoms are omitted for clarity. Important bond distances [Å] and angles [°]: Fe–P2 2.285(1), Fe–P5 2.277(1), Fe–C1 2.094(5), Fe–C3 2.094(4), Fe–C4 2.084(4), Fe–(C18–C22) 2.045 to 2.065(5), P2–C1 1.745(5), P2–C3 1.779(4), P5–C1 1.760(6), P5–C4 1.785(4), C3–C4 1.418(6), C–C (C_6H_5) 1.394(8) to 1.422(8); P2–C1–P5 119.7(3), C1–P2–C3 93.5(2), C1–P5–C4 92.9(2), P2–C3–C4 116.7(3), P5–C4–C3 117.1(3).

 © VCH Verlagsgesellschaft mbH, D-6940 Weinheim, 1990 0570-0833/90/0505-0534 $ 02.50/0

3.18° [10]) and the widening of the intracyclic angle at C_1. Open-chain η^3-1,3-diphosphaallyl complexes show smaller P–C–P angles.[11]

The quantitative conversion of **2** into **4** (^{31}P NMR) opens up several new perspectives: (1) the easy variation of the substitution pattern of **4** via the choice of the starting 1,2-diphosphete;[4] (2) the optional η^1-coordination of the two phosphorus atoms of these unhindered 1,3-diphospholide species (such a coordination appears to be difficult in the case of the strongly hindered 2,4,5-tris-*tert*-butyl derivative[8]); (3) the 2-H atom the 1,3-diphospholide ligand in η^5-complexes such as **5** could be substituted. We are currently investigating these possibilities.

Experimental Procedure

Synthesis of **2a, 2b**: The P–P bond of **1** (3.94 g, 10 mmoles) was cleaved under an argon atmosphere by stirring with lithium (140 mg, 20 mmol) in 20 mL of THF for 3 h. The solution was then cooled to −80 °C and one equivalent of CS_2 (600 μL, 10 mmol) was added. After fifteen minutes, two equivalents of methyl iodide (1.24 mL, 20 mmol) were added dropwise. After stirring for an additional fifteen minutes at −80 °C, the reaction mixture was slowly warmed to room temperature. After evaporation of THF, the mixture was chromatographed over silica gel 60 with hexane/toluene (50/50) to remove any unconsumed **1**, and then with toluene. About 10% unconsumed **1** was thus recovered and 80% pale yellow crystals of a mixture of the two isomers **2a** and **2b**.

Synthesis of **5**: A solution of **2** (2 g, 4 mmoles) in 20 mL of THF was stirred with 170 mg (24 mmol) of lithium wire (1% Na) under an argon atmosphere for 24 h at room temperature. The product **3** was treated with 1 mL (12 mmol) of *t*BuCl and the reaction mixture left to stand for an additional 24 h, thus yielding **4**. Finally, **4** was allowed to react with 1.5 g (4 mmol) of $[CpFe(C_8H_{10})]^{\oplus}PF_6^{\ominus}$ at room temperature for 4 h to yield **5**. The reaction mixture was quickly chromatographed on a short silica gel column (20 g, l = 8 cm, ∅ = 26 mm) and eluted with CH_2Cl_2. After evaporation of the solvent, the residue was chromatographed a second time over silica gel (100 g, l = 21 cm, ∅ = 36 mm) and eluted with a mixture of hexane and CH_2Cl_2 (70/30). The expected product **5** is obtained with the bright red head fraction, yield 41%. **5** can be purified by heating under vacuum (0.1 torr) in a sublimer at 120 °C to remove an oily residue that cannot be removed by chromatography. **5** can be recrystallized from a mixture of toluene and methanol (5/95).

Received: November 30, 1989 [Z 3661 IE]
German version: *Angew. Chem. 102* (1990) 575

CAS Registry numbers:
1, 96693-28-6; **2a**, 126134-65-4; **2b**, 126134-66-5; **4**, 126134-67-6; **5**, 126134-68-7; $[CpFe(C_8H_{10})]^{\oplus}PF_6^{\ominus}$, 34978-37-5.

[1] R. Bartsch, P. B. Hitchcock, J. F. Nixon, *J. Chem. Soc. Chem. Commun. 1987*, 1146.
[2] A. H. Cowley, S. W. Hall, *Polyhedron 8* (1989) 849.
[3] R. Bartsch, J. F. Nixon, *Polyhedron 8* (1989) 2407.
[4] L. Ricard, N. Maigrot, C. Charrier, F. Mathey, *Angew. Chem. 99* (1987) 590; *Angew. Chem. Int. Ed. Engl. 26* (1987) 548.
[5] C. Charrier, J. Guilhem, F. Mathey, *J. Org. Chem. 46* (1981) 3; C. Charrier, N. Maigrot, F. Mathey, F. Robert, Y. Jeannin, *Organometallics 5* (1986) 623.
[6] C. Charrier, F. Mathey *Tetrahedron Lett. 28* (1987) 5025.
[7] The reaction of cationic (η^5-cyclopentadienyl)(η^6-arene)iron complexes with phospholide anions yields the corresponding monophosphaferrocenes: R. M. G. Roberts, A. S. Wells, *Inorg. Chim. Acta 112* (1986) 171.
[8] R. Bartsch, P. B. Hitchcock, J. F. Nixon, *J. Organomet. Chem. 340* (1988) C37.
[9] Crystals of **5**, $C_{20}H_{16}FeP_2$ were grown at −18 °C from a methanol-toluene solution of the compound. Data were collected at 18° ± 1° on an Enraf Nonius CAD4 diffractometer. The crystal structure was solved and refined using an Enraf Nonius CAD4 diffractometer. The compound crystallizes in the space group $P2_1/n$, a = 10.194(1) Å, b = 9.841(1) Å, c = 16.818(1) Å, β = 95.05(1)°; V = 1680.71() Å^3; Z = 4; ϱ_{calcd} = 1.487 g/cm^3; $Cu_{K\alpha}$ radiation (λ = 1.54184 Å) graphite monochromator; μ = 90.6 cm^{-1}; $F(000)$ = 768. A total of 3683 unique reflexions were recorded in the range $2° \le 2q \le 150.0°$, of which 1683 were considered as unobserved ($F^2 < 3.0\sigma(F^2)$), leaving 2000 for solution and refinement. The structure was solved by direct methods, yielding a solution for 12 of the 23 heavy atoms. The hydrogen atoms positional parameters were refined in the final stages of a least-squares refinement with fixed thermal parameters equal to 1.3 times that of the attached carbon atom while using anisotropic temperature factors for all other atoms. A non-Poisson weighting scheme was applied with a p factor equal to 0.08. The final R factors were R = 0.047, Rw = 0.064, G.O.F. = 1.27. Further details of the crystal structure investigation are available on request from the Fachinformationszentrum Karlsruhe, Gesellschaft für wissenschaftlich-technische Information mbH, D-7514 Eggenstein-Leopoldshafen 2(FRG), on quoting the depository number CSD-54551, the names of the authors, and the journal citation.
[10] F. Mathey, A. Mitschler, R. Weiss, *J. Am. Chem. Soc. 99* (1977) 3537.
[11] R. Appel, W. Schuhn, F. Knoch, *Angew. Chem. 97* (1985) 421; *Angew. Chem. Int. Ed. Engl. 24* (1985) 420.

Clays Direct Aromatic Nitration**

By *Christine Collet, Alfred Delville*, and *Pierre Laszlo**

Dedicated to Professor Paul von Ragué Schleyer on the occasion of his 60th birthday

Modified clays can act as efficient catalysts of organic reactions.[1–3] Among clays, kaolinites have seldom been used for such purposes,[2] although they do intercalate molecules as polar as water,[4] formamide,[5] *N*-methylformamide,[5] dimethyl sulfoxide,[6,7] and dimethyl selenoxide[7] within their layers. Therefore, we set about exploring the catalytic potential of kaolinites for reactions proceeding through highly polar transition states. Discrimination between transition states differing in polarity and in steric bulk was our goal. We chose to study the nitration of *p*-anisaldehyde (**1**).

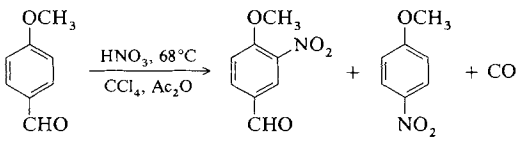

1 **2** **3**

The methoxy substituent directs nitration to the *ortho* and *para* positions.[8] In the former case, the resulting Wheland intermediate has only to lose a proton for product **2** to be formed. In the latter case, that of nitration *ipso* to the 4-formyl-substituted position, expulsion of protonated carbon monoxide is a prerequisite for the appearance of product **3**. Accordingly, under *homogeneous* reaction conditions, only minuscule quantities of the minor **3** form (Table 1). The two Wheland intermediates[9,11] leading to products **2** and **3** are highly polar, with calculated dipole moments (MINDO-3[15]) of 4.49 and 5.57 D, respectively. Accordingly, the expectation that the high acidity (Hammett acidity function $H_0 = -6$ to -8)[16] and perhaps also the intense electric field at the interface of a montmorillonite clay[17,18] would favor the **1** → **3** pathway was borne out (Table 1): in the presence of montmorillonite K10[1–3] the proportion of **3** in the product mixture **2** + **3** goes up by more than one order of magnitude, and increases as the Brønsted acidity at

[*] Prof. Dr. P. Laszlo, C. Collet, Dr. A. Delville
Laboratoire de chimie fine aux interfaces
Université de Liège
Sart Tilman par B-4000 Liège (Belgium)
and Ecole Polytechnique,
F-91128 Palaiseau (France)

[**] We thank Professor *Jacques Thorez* and Mr. *Diano Antenucci*, University of Liège, for the X-ray diffractograms.

Table 1. Proportion of *p*-nitroanisole formed (±1.2%) as a function of the solid present (0.15 g per mmol of **1**)[a].

Solid support	**3** (%)
(none)	1.1
Silica	2.3
Kieselguhr	1.6
$Cu(NO_3)_2 \cdot 3H_2O$ on kieselguhr	2.2
$Cu(NO_3)_2 \cdot 3H_2O$ on acidic alumina	2.1
$Cu(NO_3)_2 \cdot 3H_2O$	1.3
K10	9.6
Claycop	10
K10-$Cu^{2\oplus}$	13
K10-$Al^{3\oplus}$	15
K10-$Ti^{4\oplus}$	16
K10-$Zr^{4\oplus}$	21
Kaolinite	27 [b]

[a] 1.5 g of the solid + 10 mmol **1** + 3.1 ml Ac_2O i.e. an excess relative to HNO_3 plus the residual water in the clay [12] are introduced in that order in CCl_4 (25 ml) and refluxed for 15 min while 0.5 mL of fuming HNO_3 (Merck, p.a., 99.5% min.) is added dropwise. [b] 73% of **2**. Claycop is clay-supported cupric nitrate [3].

the surface is enhanced by the Lewis-acidic interstitial cations.[1-2] Likewise, in a still more pronounced manner, a kaolinite, also a clay with a strongly acidic surface ($H_0 = -3$ to -6),[16] favors *ipso* nitration: the yield of **3** rises to 27%, boosted by a factor of 25 compared to homogeneous conditions!

The percentage of **3** varies with the amount of kaolinite present (Fig. 1): such a plot, with a strong resemblance to a Langmuir isotherm, is consistent with a single type of catalytic site. In the most conservative estimate, the catalytic turnover is at least 300.[20] The enhanced production of **3** is observed only with phyllosilicates, such as the K10 montmorillonite and kaolinites. Conversion is quantitative when the amount of the nitrating reagent has been well-adjusted to equal that of the aldehyde substrate, taking into account (minor) losses as vapors of nitrogen oxides. Conversion does not occur significantly (Table 1) on the surface of microporous solids such as alumina or silica.

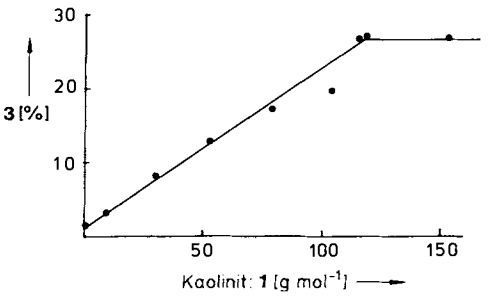

Fig. 1. Percentage of **3** formed as a function of the ratio (g mol^{-1}) of the mass of kaolinite (g) to the amount of **1** (mol).

These effects do not seem to require intercalation.[21] Protonation of the incipient carbon monoxide leaving group,[11] in the adsorbed state, is the probable cause for the considerable increases in the amount of *ipso* nitration in the *para* position, by a factor 10 with the montmorillonite, and by a factor 25 with the kaolinite.

Received: November 13, 1989 [Z 3630 IE]
German version: Angew. Chem. 102 (1990) 563

CAS Registry numbers:
1, 123-11-5; **2**, 31680-08-7; **3**, 100-17-4; Kaolinite, 1318-74-7.

[1] P. Laszlo *Science 235* (Washington D. C.) (1987) 1473–1477.
[2] P. Laszlo in P. Laszlo (Ed.): *Preparative Chemistry Using Supported Reagents*, Academic Press, San Diego 1987, p. 3
[3] A. Cornélis, P. Laszlo *Aldrichimica Acta 21* (1988) 97–103.
[4] a) P. Costanzo, R. F. Giese, M. Lipsicas *Clays Clay Miner. 32* (1984) 419–428; b) M. Lipsicas, C. Straley, P. Costanzo, R. F. Giese, *J. Colloid Interface Sci. 107* (1985) 221–230.
[5] M. Lipsicas, R. Raythatha, R. F. Giese, P. Costanzo, *Clays Clay Miner. 34* (1986) 635–644.
[6] J. G. Thompson, C. Cuff *Clays Clay Miner. 33* (1985) 490–500.
[7] M. Raupach, P. F. Barron, J. G. Thompson *Clays Clay Miner. 35* (1987) 208–219.
[8] K. Schofield: *Aromatic Nitration*, Cambridge University Press, Cambridge 1980.
[9] Aromatic nitration of an activated substrate such as **1** has a late transition state resembling the Wheland intermediate [8], a statement not overturned by recently proposed SET mechanisms [10].
[10] a) C. L. Perrin *J. Am. Chem. Soc. 99* (1977) 5516–5518; b) L. Eberson, F. Radner *Acc. Chem. Res. 20* (1987) 53–59; c) M. J. Thompson *Tetrahedron 45* (1989) 191–202; d) J. F. Johnston, J. H. Ridd, J. P. B. Sandall *J. Chem. Soc. Chem. Commun. 1989*, 244–246.
[11] The proportion of **3** formed is identical when the reaction is run either under dinitrogen or carbon monoxide pressure (20 bar); which rules out carbon monoxide loss in the rate-determining step.
[12] Acetic anhydride plays a role in dehydrating both the clay and the nitrating agent. Under such conditions [13], acetyl nitrate is the likely nitrating species [14]. Furthermore, acetic acid could serve as the base and pull off a highly acidic proton, the pK_a of its conjugate acid being 0.58 in H_2SO_4.
[13] J. B. Menke *Recl. Trav. Chim. Pays-Bas 44* (1925) 141–149.
[14] M. A. Paul *J. Am. Chem. Soc. 80* (1958) 5332–5333; A. Cornélis, L. Delaude, A. Gerstmans, P. Laszlo *Tetrahedron Lett. 29* (1988) 5657–5660.
[15] R. C. Bingham, M. J. S. Dewar, D. H. Lo. *J. Am. Chem. Soc. 97* (1975) 1294–1301.
[16] H. A. Benesi *J. Am. Chem. Soc. 78* (1956) 5490–5494.
[17] The magnitude of the electric field was calculated from Gauss's law, at a distance of 6 Å from a clay sheet with a charge density, appropriate for a smectite (the Upton bentonite) of 6.8 me $Å^{-2}$. The electric field at the interface has limiting values of 1.6×10^8 V m^{-1} for a dielectric constant of 78.5 (water), and of 1.2×10^{10} V m^{-1} for a dielectric constant of unity. The energy gain for the more polar of two transition states differing by 1 D in their dipole moments is 5.5 kJ mol^{-1} for a local dielectric constant of 5.
[18] The *Bertrán* group has shown recently that strong electric fields of ca. 10^{10} V m^{-1} can remove an activation energy barrier. They showed, using the example of the $F^{\ominus} + CH_3F$ Walden inversion, that increasing the strength of the electric field gradually deletes the barrier [19]. The heuristic interpretation is that electrons donated by the nucleophile follow the field which pumps the system from its initial to its final state.
[19] J. L. Andrés, A. Lledós, M. Duran, J. Bertrán *Chem. Phys. Lett. 153* (1988), 82–86.
[20] Source Clay Minerals Repository, Department of Geology, University of Missouri Columbia, Missouri 65201 (USA). BET specific surface = 8.8 $m^2 \cdot g^{-1}$.
[21] X-ray diffractograms of the kaolinite are identical before and after the reaction.

Formation of an Aminoreductone from Glucose

By *Sabine Estendorfer, Franz Ledl,** and *Theodor Severin**

In many heated foodstuffs, reducing sugars react with amino acids or proteins to give, inter alia, brown products and characteristic aromas of roasting (non-enzymatic browning, Maillard reaction). Such reactions have for some time attracted interest among physicians and biochemists, since one presumes that morbid alterations in diabetic per-

[*] Prof. Dr. T. Severin, S. Estendorfer
Institut für Pharmazie und Lebensmittelchemie der Universität
Sophienstr. 10, 8000 München 2 (FRG)
Prof. Dr. F. Ledl
Institut für Lebensmittelchemie der Universität
Pfaffenwaldring 55, 7000 Stuttgart 80 (FRG)

sons, clouding of the eye lenses, cross-linking of proteins, and possibly ageing processes can be attributed to reactions of sugars with proteins.[1]

Only the first steps of the Maillard reaction have so far been elucidated in detail. Glucose reacts with amino acids or other primary or secondary amines, leading firstly to glycosylamines, which readily transform by Amadori rearrangement into the corresponding *N*-substituted 1-amino-1-deoxyfructoses.[2] In proteins, the lysine side chain is preferentially attacked. Secondary reactions lead to the formation of an extraordinarily complex mixture containing many still unidentified compounds. Substances with reductone character, which can protect foodstuffs against oxidative damage and thus contribute to storage stability, are also formed.

We have isolated an open-chain C_6-aminoreductone as transformation product of an Amadori compound. Thus far, only a C_4-aminoreductone which can be formed in very small amounts in heated sugar–amine mixtures has been reported in the literature.[3] The "piperidinohexose reductone" containing a C_5 ring, which was isolated by *Hodge* et al., is formed only with secondary amines[4] and therefore is of no great importance in foodstuffs.[5]

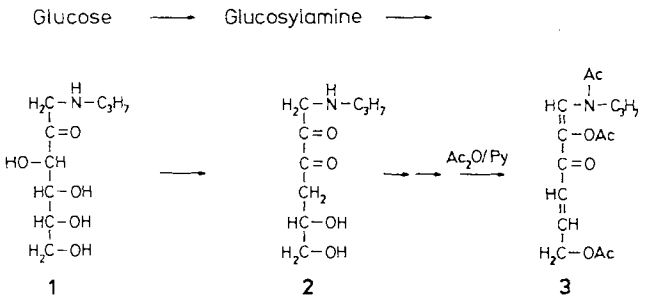

When the Amadori compound **1** obtainable from glucose and propylamine is heated in buffered, neutral, aqueous solution for several days at 37 °C or briefly at elevated temperatures (e.g. 5 h at 60 °C) it decomposes with formation of novel reducing compounds which can be separated by chromatography on silica gel. After acetylation and thin-layer chromatographic separation the aminoreductone **3** could be isolated in pure form. The structure of **3** was derived from its spectral data. The coupling constants of the protons on C-4 and C-5 show that the compound is present in the *trans* form. We were recently able to trap the dicarbonyl compound **2**, formulated as intermediate, with *o*-phenylenediamine.[6] Experiments carried out so far indicate that the Amadori compound **1** releases the amine more readily at elevated temperatures and is thereby transformed, inter alia, into 1-deoxy-2,3-hexodiulose and 3-deoxy-1,2-hexosulose, as well as secondary products.

In reactions of glucose with protein, reductones of type **3** in lysine side chains should be easily detectable by their redox behavior.

Experimental

A solution of the oxalate of 1-propylamino-1-deoxyfructose **1** (4.8 g, 18 mmol) in 20 mL of water was adjusted to pH 7 with ca. 2 g of $NaHCO_3$ and allowed to stand for ca. 70 h at 37 °C (or, e.g., 5 h at 60 °C). The solution was then filtered, evaporated under vacuum and chromatographed on a silica gel column with ethyl acetate/methanol (2/1). The fraction containing reductone colored an alkaline solution of triphenyltetrazolium chloride (TTC). The eluate was evaporated down and acetylated for ca. 12 h at room temperature with Ac_2O/Py. The resulting mixture was taken up in ice-water/dichloromethane and separated on thin-layer plates (silica gel, 0.5 mm) with hexane/ethyl acetate/triethylamine (50/48/2). The fluorescence quenching zone at $R_f = 0.4$ was eluted with warm ethyl acetate. The yield of **3** was 0.1%.

3: ^{1}H NMR (400 MHz, $CDCl_3$, TMS int.): $\delta = 0.92$ (t, $J = 7$ Hz, 3H; CH_2-CH_3), 1.62 (sext., $J = 7$ Hz, 2H; CH_2-CH_3), 2.11 (s, 3H; N-CO-CH_3), 2.28, 2.31 (s, each 3H; O-CO-CH_3), 3.68 (t, $J = 7$ Hz, 2H; N-CH_2), 4.76 (dd, $J = 4.4$, 1.5 Hz, 2H; =CH-CH_2-O), 6.63 (br. d, $J = 15$ Hz, 1H; =CH-C=O), 6.88 (dt, $J = 15$, 4.4 Hz, 1H; =CH-CH_2), 7.77 (br.s, 1H; CH-N).—^{13}C NMR (100 MHz, $CDCl_3$, TMS int.): $\delta = 11.11$ (CH_2-CH_3), 20.49, 20.65, 22.05 (CO-CH_3), 22.38 (CH_2-CH_3), 47.40 (N-CH_2), 63.01 (CH_2-O), 124.04 (=CH-C=O), 127.71 (HC-N), 130.80 (CO-C=), 140.31 (=CH-CH_2), 168.43, 170.28, 170.46 (CH_3-C=O), 183.21 (=HC-C=O).—MS (70 eV): m/z [%]: 311 (4.4, $M^{\oplus}$), 269 (4.1), 251 (13.9), 238 (5.0), 227 (7.5), 209 (40.4), 196 (13.3), 167 (70.7), 150 (14.6), 138 (27.4), 110 (8.3), 96 (11.5), 84 (6.6), 68 (8.1), 43 (100).—IR (KBr): $\tilde{\nu}$ [cm^{-1}] = 2995(m), 1780(s), 1620(s), 800(m).—UV(ethanol: λ_{max} [nm] (log ε) = 300 (4.24).—Correct analysis.

Received: December 4, 1989 [Z 3666 IE]
German version: *Angew. Chem. 102* (1990) 547

CAS Registry numbers:
1 oxalate, 71231-91-9; **3**, 126134-91-6.

[1] J. W. Baynes, V. M. Monnier: "*The Maillard Reaction in Aging, Diabetes and Nutrition*," *Prog. Clin. Biol. Res. 304* (1989) 1.
[2] H. Paulsen, K. W. Pflughaupt in W. Pigman, D. Horton (Eds.): *The Carbohydrates: Chemistry and Biochemistry, Vol. IB*, Academic Press, New York 1980, p. 881.
[3] F. Ledl, T. Severin, *Z. Lebensm.-Unters. Forsch. 169* (1979) 173.
[4] F. Weygand, H. Simon, W. Bitterlich, J. E. Hodge, B. E. Fischer, *Tetrahedron 6* (1958) 123.
[5] F. Ledl, G. Fritsch, J. Hiebl, O. Pachmayr, T. Severin in M. Fujimaki, M. Namiki, H. Kato (Eds): "*Amino-Carbonyl Reaction in Food and Biological Systems*"—Proceedings of the 3rd International Symposium on the Maillard Reaction, Kodansha Ltd., Tokyo 1986, p. 173.
[6] J. Beck, F. Ledl, T. Severin, *Z. Lebensm.-Unters. Forsch. 188* (1989) 118; B. Huber, F. Ledl, *Carbohydr. Res.*, in press.

Atomic Structure and Superstructure of α-$RuCl_3$ by Scanning Tunneling Microscopy**

By *Hans-Joachim Cantow**, *Harald Hillebrecht*, *Sergej N. Magonov*, *Heinz Wilhelm Rotter*, *Markus Drechsler*, and *Gerhard Thiele*

Dedicated to Professor Christoph Rüchardt on the occasion of his 60th birthday

Scanning tunneling microscopy (STM) enables the study of conductive and semiconductive surfaces at the atomic level.[1] The tunneling of electrons in such systems is determined by the local density of states (LDOS) at the Fermi level. In many cases the LDOS is strongly modulated by the arrangement of the surface atoms. In the following communication we report on the STM characterization of α-$RuCl_3$.

Figures 1–3 show atomic scale top-view images of the surface of α-$RuCl_3$. Figures 1 and 2 represent the best qual-

[*] Prof. Dr. H.-J. Cantow, Dr. S. N. Magonov[+]
Institut für Makromolekulare Chemie der Universität
Stefan-Meier-Strasse 31, D-7800 Freiburg (FRG)
Dipl.-Chem. H. Hillebrecht, Dr. H. W. Rotter, Prof. Dr. G. Thiele
Institut für Anorganische und Analytische Chemie
der Universität Freiburg (FRG)
Dipl.-Phys. M. Drechsler
Institut für Biophysik und Strahlenbiologie der Universität Freiburg (FRG)
[+] Permanent address: Institute of Physical Chemistry
USSR Academy of Science
SU-117977 Moscow (USSR)

[**] This work was supported by the Deutsche Forschungsgemeinschaft (grant for *S.N.M.*).

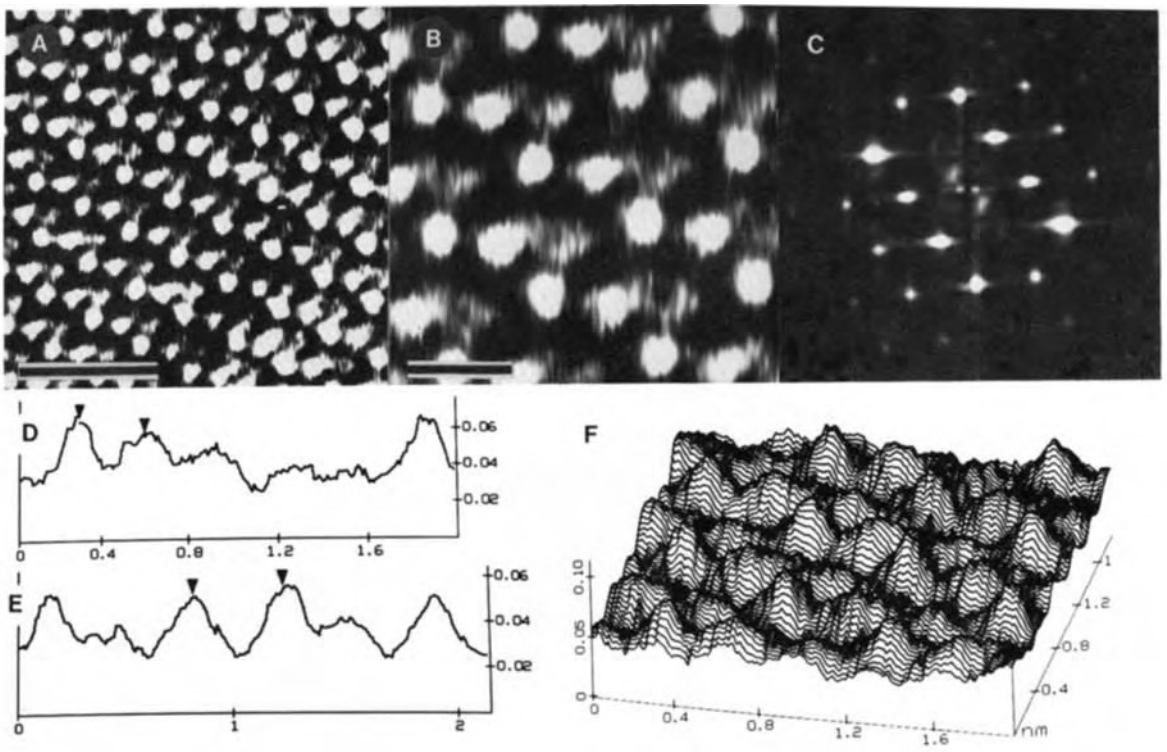

Fig. 1. STM images of α-$RuCl_3$ in air at 300 K. $I = 2.6$ nA, $U = -241$ mV. A) Top view, bar = 10 nm, B) zoomed top view, bar = 5 nm, C) two-dimensional Fourier transform, D), E) cross-section contours (units for obscissa and ordinate in nm, F) three-dimensional line plot of image B.

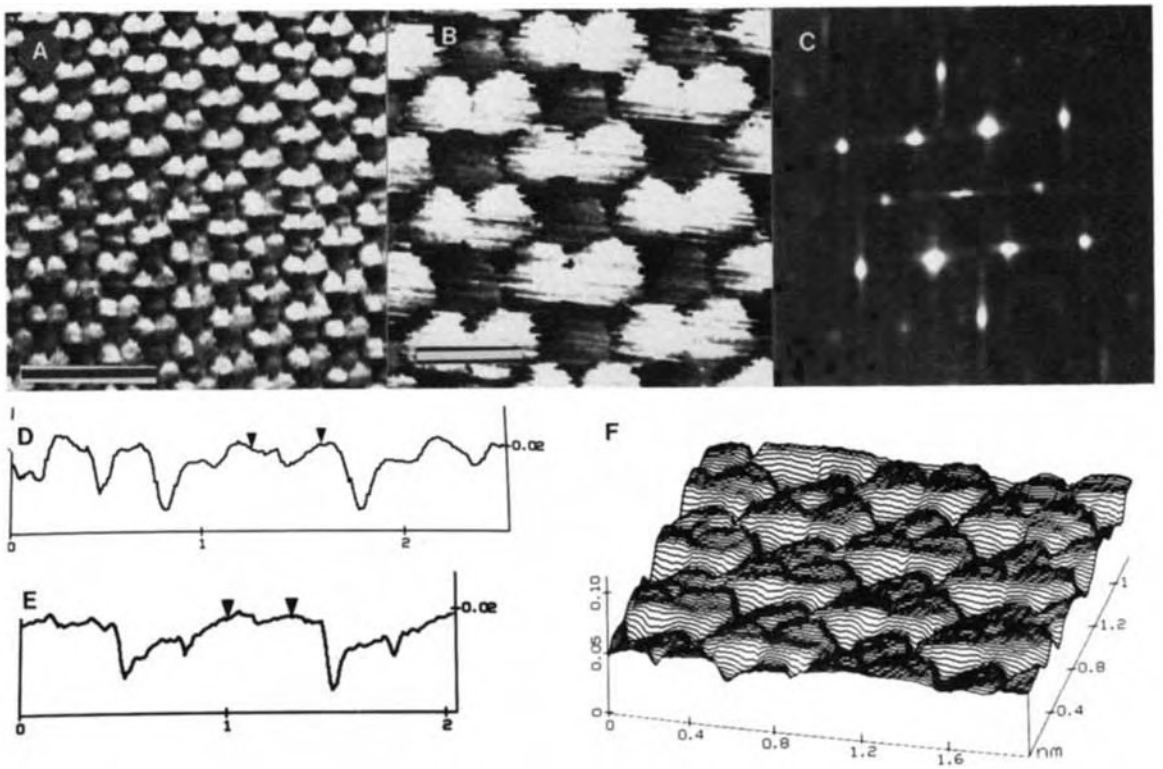

Fig. 2. STM images of α-$RuCl_3$ in silicone oil at 300 K. $I = 27.3$ nA, $U = -785$ mV. A) Top view, bar = 10 nm, B) zoomed top view image, bar 5 nm, C) two-dimensional Fourier transform, D), E) cross-section contours (units for the abscissa and ordinate in nm), F) three-dimensional line plot of image B.

ity images obtained in air ($I = 2.6$ nA, $U = -241$ mV) and under silicone oil ($I = 27.3$ nA, $U = 785$ mV). The images depicted in Figure 3 were obtained by variation of the tunneling current. On increasing the tunneling current from 2.6 (Fig. 3, top) to 5.7 nA (Fig. 3, middle) the features of the images change from diffuse to well separated. At still higher tunneling current (44 nA; Fig. 3, bottom) a higher contrast image is observed. The same trend in the quality of the imag-

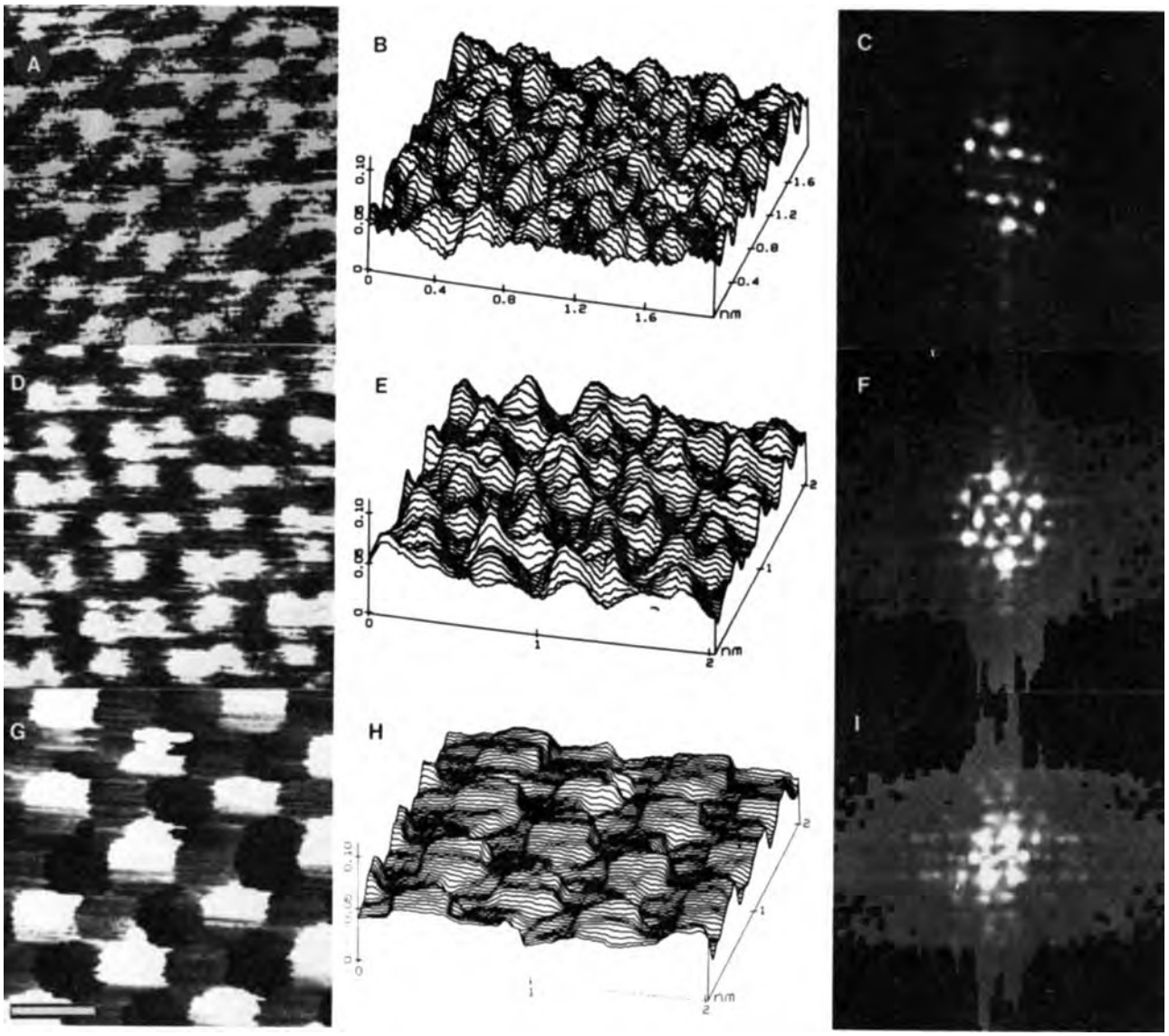

Fig. 3. STM images of α-$RuCl_3$ in air at 300 K. Constant voltage of $U = 300$ mV. Top: $I = 2.6$ nA; middle: $I = 5.7$ nA; bottom: $I = 44$ nA. A, D, G) Top views, bar 5 nm, B, E, H) three-dimensional line plots, C, F, I) two-dimensional Fourier transforms.

ing is achieved even when the polarity of the bias voltage is changed (− 300 mV). The best quality images were observed at higher tunneling currents. The bright areas correspond to increases in the local surface charge density in the z-direction perpendicular to the surface. Increasing the tunnel current induces a flattening of the "hills" of electron density. An increase of current at constant potential generally signifies an increase in the distance between measuring tip and sample surface and thus a stronger influence of the tip on the electronic structure of the sample. In the optimum-quality and high-contrast images of α-$RuCl_3$ these effects are manifested as changes in the size of the round shape patterns and the shape of the corrugation (superstructures).

On using silicone oil between measuring tip and sample surface more stable images are obtained at high tunneling currents. We have found that the best quality images of an α-$RuCl_3$ surface are obtained at a definite tunneling gap resistance. For one of the α-$RuCl_3$ samples the best quality images were obtained at bias voltages of $U = (400 + n \times 50)$ mV and corresponding tunneling currents of $I = (7 + n \times 1)$ nA ($n = 0.1 - 20$). The resistance of the tunneling gap in these cases is 57 MΩ. It varies up to 20% from sample to sample, but the aforementioned dependence remains the same. Attempts to increase the tunneling current under optimum conditions for best quality images without changing the bias voltage led to a disappearance of the image, presumably because of multiple point contacting of the measuring tip with the sample surface. Nevertheless, the tips are not damaged by such possible point contacts, as increasing the voltage or decreasing the current renders this effect reversible.

The two-dimensional Fourier transformed images (Figs. 1C, 2C, 3C, F, I) afford information about the symmetry of the electronic surface features—the "hills" of charge density. They show hexagonally arranged reflections which change in intensity under different experimental conditions. The outer hexagon delineates the "hills" with distances ranging from 2.8 to 4.1 Å, the inner hexagon those with distances ranging from 5.8 to 6.5 Å. Intensity measurements along a line (section images, Figs. 1D, E, 2D, E) yield more accurate information: The difference in the z values between the "hill peaks" for various values of U and I lie in the range 0.2 to 0.5 Å. The difference in the z values between the highest point of a hill and the lowest point of the adjoin-

 © VCH Verlagsgesellschaft mbH, D-6940 Weinheim, 1990 0570-0833/90/0505-0539 $ 02.50/0

ing hollow varies between 0.3 and 2.3 Å. A strong dependence of the size of this difference (i.e. the corrugation) on the experimental conditions has been observed in the case of graphite[1] and TaS_2.[4]

Figure 4 shows graphical representations of α-$RuCl_3$ based on X-ray data. The space group $C2/m$ (monoclinic, $AlCl_3$-type) was assumed for the crystal structure of α-

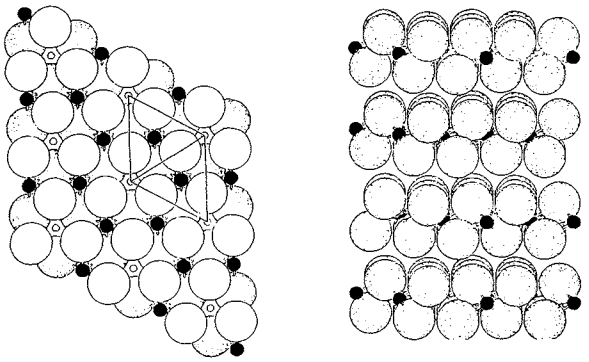

Fig. 4. Layered structure of α-$RuCl_3$ from X-ray data. Left: computer-simulated top view; right: side view of the α-$RuCl_3$ lattice. ●: Ru.

$RuCl_3$.[2] Each layer of the crystal consists of two outer layers of chlorine atoms with an inner layer of ruthenium atoms (octahedral bonding between ruthenium and chlorine atoms). The chlorine atoms lie thereby in an almost undistorted close-packed arrangement, the in-plane distances between the chlorine atoms being 3.265 Å (averaged X-ray data). The ruthenium atoms occupy 2/3 of the vacant positions in the octahedron and are thereby packed hexagonally in a graphite-like manner. The X-ray data yield distances of 3.46 Å between the ruthenium atoms, which leads one to assume that the STM images represent the surface charge density distribution modulated by the chlorine atom positions in the surface layer. If the surface electron density were modulated by ruthenium atoms one would expect a non-centered hexagonal structure in the STM images, which however is not observed. A more detailed assignment of the STM images of α-$RuCl_3$ is presented in Figure 5 (top).

Scanning tunneling microscopy is an attractive technique for the structure analysis of the crystal surfaces of compounds whose surface electron distribution is modulated by the arrangement of the atoms, as is apparently the case with α-$RuCl_3$. STM data for the distances between neighboring chlorine atoms under different experimental conditions are listed in Table 1. The discrepancies between these data and those obtained from X-ray data are of a fundamental nature, since X-ray structure analyses afford average values. With the STM technique, the distorted hexagonal packing of the surface chlorine atoms is detectable. The distortion is mainly due to the lower position of the central atom in the hexagon (0.2 to 0.5 Å). Significant niveau differences of ca. 0.1 Å are detectable however, even between the chlorine atoms of the hexagon. These effects could be caused by weak Ru–Ru pairing interactions. This type of metal-metal bonding with retention of the hexagonal arrangement has also been found for other transition metal halides.[3] The specific distorted structure of α-$RuCl_3$ leads to the formation of a hexagonal superlattice with $R = a\sqrt{3}$ (a = 3.3 Å, averaged lattice constant). The angle between the main axes of the unit cell and the superlattice is 30°. With the STM technique different superstructures were observed in the case of TiS_2, TaS_2, $TaSe_2$[5,6] and VS_2. A comparison of electron diffraction and conductivity data with STM results for TaS_2 and some other layered materials[6] shows that the influences of charge density waves are detected by scanning tunneling microscopy. A correlation of STM results for α-$RuCl_3$ with those obtained by other techniques has not yet been reported.

Figure 5 (bottom) shows the distorted Cl unit cell derived from averaged STM data. The height and width of the hexagon are in good agreement with the X-ray data. In Figure 5 (top) the corresponding subunit is marked. In our

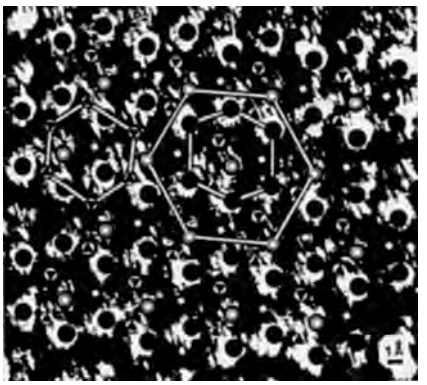

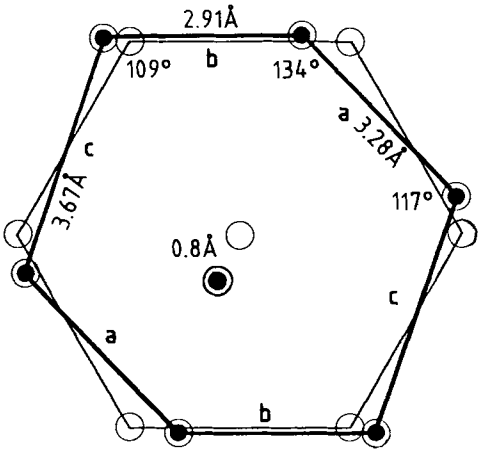

Fig. 5. Detailed images of α-$RuCl_3$. Top: top view of α-$RuCl_3$ with indicated atomic positions. Upper Cl atoms: filled circle; central lower Cl atoms: circle in circle; possible positions of the Ru atoms: triangle in circle; unoccupied sites of the Ru-lattice: square. Bottom: distortion of the hexagonal Cl-unit cell in α-$RuCl_3$. Regular hexagonal cells: thin line; distorted hexagonal cells: thick line; positions of the Cl atoms: circles; distances and angles are given for the distorted hexagonal unit cell with sides *a*, *b*, *c*.

opinion the changes in the STM images on increasing the tunneling current are due to a decrease in the gap between measuring tip and sample surface. This is supported by the similarity of the STM images recorded at different tunneling currents but at the same gap resistance. The variation of the images reflects the profiles of LDOS at different distances from the surface. The more diffuse image of Figure 3a (I = 2 nA, U = 300 mV) may indicate that those orbitals of the chlorine atoms which accept electrons, although localized near atomic positions, are spatially more diffuse. This is not the case with electron-donating orbitals which are more concentrated near atoms. They reflect the smaller z values (z-damping) of one of the chlorine atoms of the unit cell

($I = 2.6$ nA, $U = -241$ mV, Fig. 1A. Orbitals which can accept electrons are actually less sensitive to vertical (z-) deflections of the atoms, as shown by the image measured at $I = 5.7$ nA, $U = 300$ mV (Fig. 3D). The approach of the measuring tip to the sample surface leads to images with well separated patterns of electron density triplets which emphasize the surface distortion of the unit cells. A closer approach of the tip to the surface gives rise to high-quality images with circular patterns and flattened electron density hills. It has been shown that at extremely close tip-to-surface distances, or even at point contact, the resistance no longer decreases exponentially with decreasing distance, but reaches a constant value (plateau).[7] In this case the tip has scarcely any vertical sensitivity and thus causes "flattening". Perhaps attractive intermolecular forces are thereby involved in image formation.[8]

Table 1. Distances r_a, r_b and r_c between neighboring chlorine atoms in the distorted lattice of α-$RuCl_3$ at various bias voltages U and tunneling currents I[a] (cf. Fig. 5, bottom).

U [mV]	I [nA]	r_a [Å]	r_b [Å]	r_c [Å]
−241	2.6	3.4	3.1	4.1
−299	17.8	3.0	2.7	3.5
−300	2.0	3.3	2.9	3.6
−300	5.2	3.3	2.7	3.5
−785	27.3	3.2	3.0	3.5
150	27.1	3.4	3.0	3.9
300	2.0	3.2	2.8	3.6
300	5.7	3.4	2.9	3.7
300	46.2	3.3	3.1	3.6
–	–	3.28[b]	2.91[b]	3.67[b]

[a] Average over all distances 3.29 Å (STM), 3.265 Å (X-ray diffraction). [b] Mean value.

Scanning tunneling microscopy has proven very useful for investigations of the structure of α-$RuCl_3$. It was immediately clear that the hexagonal structure is three-dimensionally distorted. In addition, quantitative evaluations could be carried out. A superlattice exists at room temperature.

Experimental

The α-$RuCl_3$ crystals were prepared by sublimation at 800 to 500 °C; thin-layer samples were cleaved from the crystals with the aid of self-adhesive tape and fixed on metallic supports with conductive silver glue. The measuring tips for the STM investigations (Nanoscope II, Digital Instruments) were mechanically cut from PT(70)/Ir(30) wire, tested on highly oriented pyrolytic graphite, and calibrated in the x and y directions (accuracy ± 0.1 Å). The z values are reproducible within ≤0.1 Å, but variations of up to 30% are possible. The imaging current was plotted against x and y sensitivity at constant tunneling current. All measurements were carried out at room temperature in air or under silicone oil. Oxygen effects could be ruled out.

Bias voltages and tunneling currents of $U = \pm 11$ to ± 1500 mV and $I = 0.01$ to 46 nA, respectively were chosen for the investigations. The scanning frequencies for the y direction were 26 and 39 Hz. Data arrays of 400 × 400 points of top-view images were collected and subjected to 2DFFT or represented as three-dimensional line plots. The images presented here were obtained without applying any filtering routines.

Received: August 14, 1989;
revised: February 21, 1990 [Z 3497 IE]
German version: *Angew. Chem. 102* (1990) 551

CAS Registry number:
α-$RuCl_3$, 10049-08-8.

[1] G. Binnig, H. Rohrer, *Angew. Chem. 99* (1987) 622; *Angew. Chem. Int. Ed. Engl. 26* (1987) 606, and references cited therein.
[2] K. Brodersen, G. Thiele, H. Ohnsorge, I. Recke, F. Moers, *J. Less-Common Met. 15* (1968) 347.
[3] K. Brodersen, H. K. Breitbach, G. Thiele, *Z. Anorg. Allg. Chem. 357* (1968) 162.
[4] M. Weimer, J. Kramer, C. Bai, J. D. Baldeschwieler, *Phys. Rev. B37* (1988) 4292.
[5] R. E. Thomson, U. Walter, E. Glanz, J. Clarke, A. Zettl, P. Rauch, F. J. DiSalvo, *Phys. Rev. B38* (1988) 10734.
[6] R. V. Coleman, P. Drake, P. K. Hansma, G. Slough, *Phys. Rev. Lett. 55* (1985) 394.
[7] J. K. Gimzewski, R. Möller, *Phys. Rev. B36* (1987) 1284.
[8] J. M. Soler, A. M. Baro, N. Garsia, H. Rohrer, *Phys. Rev. Lett. 57* (1986) 444.

Stability and Cyclization of Enol Radical Cations: A Mechanistic Study of One-Electron Oxidation of β,β-Dimesityl Enols**

By *Michael Schmittel** and *Ulrich Baumann*

The thermodynamic reversal of the keto/enol equilibrium on going from neutral molecules to radical cations has been consistently supported by thermochemical investigations[1] in the gas phase and MO studies.[2] Enol radical cations in the gas phase are always considerably more stable than the tautomeric keto radical cations (e.g., the propen-2-ol radical cation is about 14 kcal mol^{-1} more stable than the acetone radical cation[1]). By contrast, the chemistry of enol radical cations in solution[3] has hardly been investigated, since only a few simple enols[4] are available as stable starting materials.

Two enols of type **1**, investigated initially by *Fuson* et al.[5] and, more recently, by *Rappoport* and co-workers,[6, 7] were chosen as model compounds for the first direct study of the stability and reactivity of enol radical cations in solution. Enols **1** and their tautomeric ketones/aldehydes **2** can be prepared in tautomerically pure form and thus allow the direct determination of their oxidation potentials in solution.

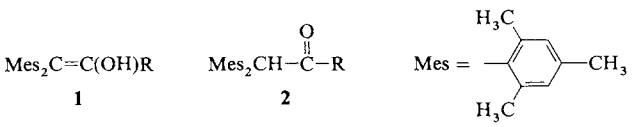

1 **2**

a, R = *t*Bu; **b**, R = H

Cyclovoltammetric measurements in acetonitrile and in dichloromethane at room temperature and −40 °C, however, showed only irreversible oxidation waves,[8] which indicates that the radical cations undergo rapid reaction at the electrodes. Moreover, several attempts to obtain stable radical cations by oxidation of the enols with dioxygen(1+) hexafluoroarsenate at low temperatures[9] failed. Even at −100 °C, no paramagnetic products could be detected by ESR spectroscopy.

In agreement with known ionization potentials,[7] the anodic peak potentials of enols **1** in acetonitrile are considerably lower than those of the tautomeric carbonyl compounds **2**. The peak potentials[8] and the equilibrium constants of

[*] Dr. M. Schmittel, Dipl.-Chem. U. Baumann
Institut für Organische Chemie und Biochemie der Universität
Albertstrasse 21, D-7800 Freiburg (FRG)

[**] Enol Radical Cations in Solution, Part 1. This work was supported by the Fonds der Chemischen Industrie, the Land Baden-Württemberg, and the Wissenschaftliche Gesellschaft Freiburg. We thank *D. Morat* for her skillful assistance as well as Prof. *J. Heinze* and Dipl.-Chem. *M. Diedrich* for help with the electroanalytical investigations.

the keto/enol equilibrium determined by *Rappoport* and coworkers[6] allow an estimate of the relative stabilities of the tautomeric radical cations $\mathbf{1}^{\bullet\oplus}$ and $\mathbf{2}^{\bullet\oplus}$ in acetonitrile, although the ΔG^0 values for $\mathbf{1} \rightarrow \mathbf{2}$ determined originally in hexane[10] need to be corrected by -1 kcal mol^{-1} in order to account for the greater stabilization of the enols by hydrogen bonding in acetonitrile. However, thermochemical data cannot be derived directly from the kinetically controlled peak potentials E_p. Nonetheless, it is generally true that, for aromatic compounds, heterogeneous electron transfer is rapid and reversible. Accordingly, the standard potentials differ only slightly from the peak potentials.[11] The free energies ΔG^0 ($\mathbf{1}^{\bullet\oplus} \rightarrow \mathbf{2}^{\bullet\oplus}$) are therefore estimated via a thermochemical cycle involving the peak potentials. A marked thermodynamic preference for enol radical cations is also found in condensed phase (Table 1).

Table 1. Peak potentials E_p[8] of **1** and **2** as well as reaction free energies ΔG°.

R	E_p (**1**) [V]	E_p (**2**) [V]	ΔG^0 ($\mathbf{1} \rightarrow \mathbf{2}$) [kcal mol^{-1}]	ΔG^0 ($\mathbf{1}^{\bullet\oplus} \rightarrow \mathbf{2}^{\bullet\oplus}$) [kcal mol^{-1}]
a *t*Bu	0.97	1.85	2.6	−17.7
b H	1.00	1.98	−3.1	−25.7

What reactions do the short-lived enol radical cations undergo? The cyclovoltammogram of **1a** in acetonitrile (Fig. 1) provides an indication of the subsequent reactions of the enol radical cation. It shows, in addition to the irreversible oxidation wave of **1a**, a reversible wave ($E_{1/2} = 1.25$ V, $\Delta E_p = 60$ mV) shifted by 300 mV toward anodic potential. Analogously, a second, though irreversible, oxidation wave at $E_p = 1.39$ V is observed for **1b**.

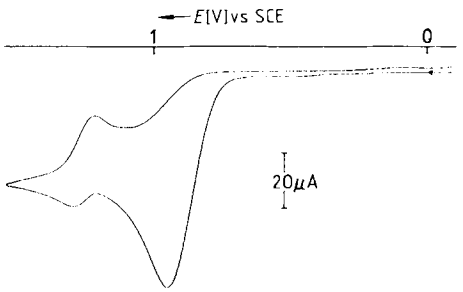

Fig. 1. Cyclovoltammogram of **1a** in acetonitrile [8].

To elucidate the reactions occurring at the electrode, enols **1a,b** were allowed to react in acetonitrile with tris(*p*-bromophenyl)ammoniumyl hexachloroantimonate (**3**) as a one-electron oxidizing agent.[12] Complete conversion was attained with 200 mol% of **3**, which indicates the occurrence of a formal two-electron oxidation. For short reaction times (ca. 20 s), benzofurans **4**[13, 14] were formed in good yields (**4a**, 82%; **4b**, 85%). Tris(*o*-phenanthroline)iron (III) hexafluorophosphate (**5**), known as an "outer-sphere" oxidizing agent,[15] also allows the synthesis of **4** in good yields (**4a**, 91%; **4b**, 81%).

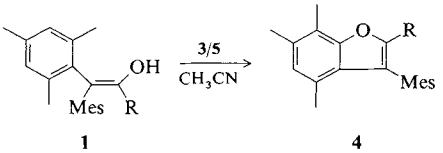

After isolation of benzofurans **4**, it was possible to show by cyclic voltammetry that the second oxidation wave in the enol oxidation (Fig. 1) is due to the benzofurans formed at the electrode.[16] This is sufficient evidence that $\mathbf{1a,b}^{\bullet\oplus}$ are involved as reactive intermediates in formation of the benzofurans.

Two reaction mechanisms are conceivable for the formation of benzofurans **4**; they differ essentially in the primary reaction of $\mathbf{1}^{\bullet\oplus}$ (Scheme 1). According to mechanism 1, the enol radical cation is rapidly deprotonated[17] and then immediately oxidized further, whereas, according to mechanism 2, the enol radical cation first cyclizes and is then deprotonated.

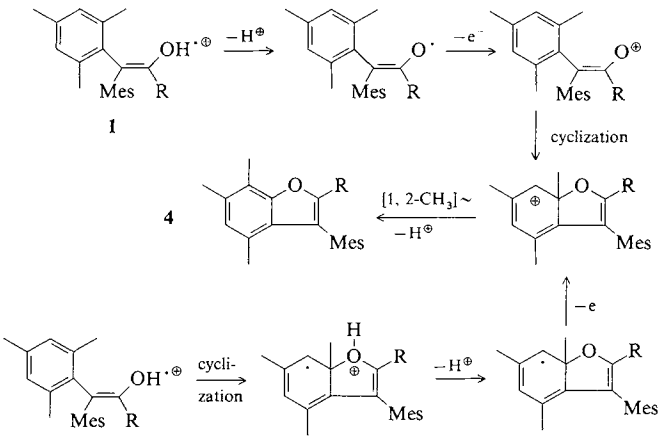

Scheme 1. Possible mechanisms for the formation of **4**. Top: Mechanism 1. Bottom: Mechanism 2.

The thermodynamic reversal of the keto/enol equilibrium by one-electron oxidation in solution opens up interesting synthetic possibilities. By suitable choice of the oxidizing agent, it should be possible, starting from a ketone, to oxidize selectively the enol form alone. Since the enol is continuously formed from the ketone, carbonyl compounds could thus react via enol radical cation intermediates. Corresponding studies have already proved successful.

Received: October 13, 1989 [Z 3590 IE]
German version: *Angew. Chem. 102* (1990) 571

CAS registry numbers:
1a, 89959-16-0; $\mathbf{1a}^{\bullet\oplus}$, 126188-87-2; **1b**, 54288-04-9; $\mathbf{1b}^{\bullet\oplus}$, 126135-11-3; **2a**, 96040-95-8; **2b**, 94203-58-4; **3**, 24964-91-8; **4a**, 126135-09-9; **4b**, 126135-10-2; **5**, 28277-57-8.

[1] J. L. Holmes, F. P. Lossing, *J. Am. Chem. Soc. 102* (1980) 1591; *ibid. 104* (1982) 2648.
[2] N. Heinrich, W. Koch, G. Frenking, H. Schwarz, *J. Am. Chem. Soc. 108* (1986) 593; W. J. Bouma, J. K. MacLeod, L. Radom, *ibid. 101* (1979) 5540.
[3] J. Yoshida, K. Sakaguchi, S. Isoe, *J. Org. Chem. 53* (1988) 2525.
[4] H. Hart, *Chem. Rev. 79* (1979) 515.
[5] R. C. Fuson, S. P. Rowland, *J. Am. Chem. Soc. 65* (1943) 992.
[6] D. A. Nugiel, Z. Rappoport, *J. Am. Chem. Soc. 107* (1985) 3669; Z. Rappoport, S. E. Biali, *Acc. Chem. Res. 21* (1988) 442.
[7] J. Lecoultre, E. Heilbronner, S. E. Biali, Z. Rappoport, *Helv. Chim. Acta 69* (1986) 2108; I. Rabin, S. E. Biali, Z. Rappoport, C. Lifshitz, *Int. J. Mass Spectrom. Ion Processes 70* (1986) 301.
[8] The oxidation potentials (versus SCE) were determined in acetonitrile (100 mV s^{-1}): 3–4 mM substrate, 0.1 M tetra-*n*-butylammonium hexafluorophosphate, ferrocene as reference. Compound **1b** was also oxidized irreversibly at 50 V s^{-1}.

[9] J. P. Dinnocenzo, T. E. Banach, *J. Am. Chem. Soc. 108* (1986) 6063.
[10] E. M. Arnett, E. J. Mitchell, T. S. S. R. Murty, *J. Am. Chem. Soc. 96* (1974) 3875.
[11] Using $10 < k < 10^{10}\ s^{-1}$ for the rate constant of the subsequent chemical reaction, one obtains the following value for the standard oxidation potential E^0: $E_p + 0.01\ V < E^0 \approx E_{1/2} < E_p + 0.26\ V$; cf. R. S. Nicholson, I. Shain, *Anal. Chem. 36* (1964) 706.
[12] W. Schmidt, E. Steckhan, *Chem. Ber 113* (1980) 577.
[13] The spectroscopic data are in agreement with the proposed structures. The substitution pattern of benzofurans **4** was made plausible by increment calculations of the ^{13}C NMR chemical shifts: G. Y. Kuo, S. T. Ross, *J. Heterocycl. Chem. 15* (1978) 1489; N. Platzer, J.-J. Basselier, P. Demerseman, *Bull. Soc. Chim. Fr. 1974* 905.
[14] ^1H NMR (250 MHz): **4a** (C_6D_6): δ = 1.29 (s, 9H, *t*Bu), 1.88 (s, 3H, CH_3), 2.05 (s, 6H, 2 CH_3), 2.14 (s, 3H, CH_3), 2.16 (s, 3H, CH_3), 2.33 (s, 3H, CH_3), 6.67 (s, 1H, benzofuran H), 6.78 (s, 2H, Mes-H); **4b** (C_6D_6): δ = 1.99 (s, 3H, CH_3), 2.02 (s, 6H, 2 CH_3), 2.13 (s, 3H, CH_3), 2.14 (s, 3H, CH_3), 2.34 (s, 3H, CH_3), 6.69 (s, 1H, 5-H), 6.80 (s, 2H, Mes-H), 6.99 (s, 1H, 2-H). ^{13}C NMR (100 MHz): **4a** ($CDCl_3$): δ = 11.44 (7-CH_3), 17.18 (4-CH_3), 19.01 (6-CH_3), 20.96 (2 *o*-CH_3), 21.26 (*p*-CH_3), 29.12 (C(CH_3)$_3$), 34.55 (*C*(CH_3)$_3$), 112.80, 116.70, 124.92, 125.57, 127.64, 128.06, 131.46, 131.94, 136.72, 137.71, 153.18, 157.61; **4b** ($CDCl_3$): δ = 11.45 (7-CH_3), 17.27 (4-CH_3), 19.06 (6-CH_3), 20.78 (2 *o*-CH_3), 21.20 (*p*-CH_3), 117.52, 120.24, 123.61, 126.03, 127.87, 128.46, 129.32, 132.56, 137.31, 138.10, 140.63, 155.10. High-resolution MS (70 eV): **4a**: *m/z* 334.2288 (calcd 334.2297); **4b**: *m/z* 278.1671 (calcd 278.1671).
[15] J. K. Kochi, *Angew. Chem. 100* (1988) 1331; *Angew. Chem. Int. Ed. Engl. 27* (1988) 1227.
[16] In agreement with the observations on the oxidation of enols **1a,b**, compound **4a** is oxidized reversibly ($E_{1/2}$ = 1.23 V) and **4b** irreversibly (E_p = 1.38 V) at the given potentials.
[17] This mechanism was originally postulated by *Bailey* et al., when they observed the formation of the corresponding benzofuran in 3% yield during ozonolysis of trimesitylethenol: P. S. Bailey, F. E. Potts III, J. W. Ward, *J. Am. Chem. Soc. 92* (1970) 230.

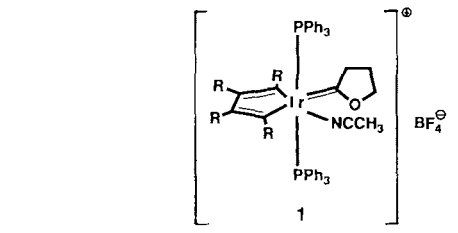

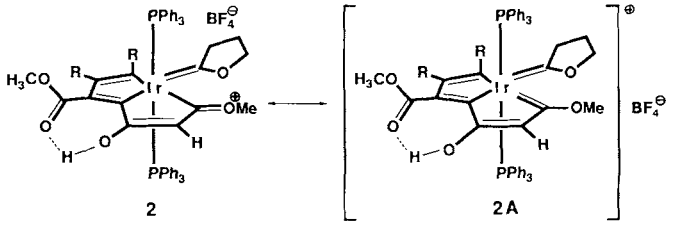

vinylidene ligand was not present, since the only downfield signal detected was at δ = 286 (t, J_{CP} = 7.6 Hz). However, a signal indicative of an acyl carbon was observed at δ = 229.5 (t, J = 7.5 Hz). Elemental and mass spectral analysis indicated a loss of CO_2 and the incorporation of a C_2H_2 fragment from propiolic acid into the original iridium complex.

We resorted to an X-ray crystal structure determination in order to characterize **2** (Fig. 1, Table 1).[6] From the X-ray

Synthesis and Structure of Annelated Carbon Rings Containing a Bridgehead Transition Metal**

By *Joseph M. O'Connor,* Lin Pu*, and *Raj Chadha*

The structure and bonding of metallacycle complexes continues to come under extensive investigation due to the diverse array of catalytic and stoichiometric reactions exhibited by this class of compounds.[1] Herein we report the serendipitous preparation and structural characterization of metallabicyclooctatriene complexes in which a metal occupies the bridgehead site. We recently discovered a new coupling reaction of the carbene ligands in metallacycle-bis(carbene) complexes,[2] and sought to extend this chemistry to the vinylidene ligand. In an attempt to prepare a carbene-vinylidene complex, we examined the reaction of propiolic acid[3] and the cationic metallacycle-carbene complex **1**.[4]

Heating **1** and propiolic acid in $CDCl_3$ at 50 °C leads to the quantitative formation of the new complex **2** as indicated by ^1H NMR spectroscopy. The ^1H NMR spectrum of **2** shows signals at δ = 13.22 (s, 1H) and 5.98 (br, 1H); four singlets at 3.34, 3.48, 3.60, and 3.67 (OCH_3); and the expected resonances attributed to the hydrogen atoms of the triphenylphosphane ligand and the carbene ligand.[5] From the $^{13}C\{^1H\}$ NMR spectrum of **2** it was clear that the desired

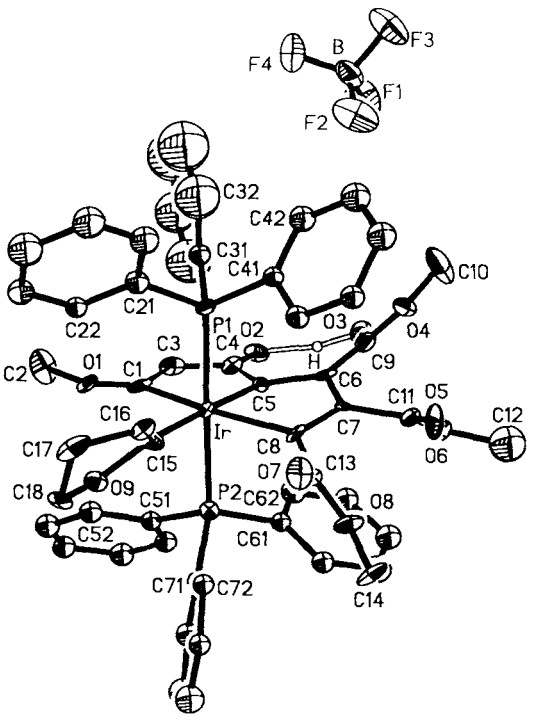

Figure 1. Molecular structure and partial numbering scheme for **2**.

structure it is clear that a new metallacycle unit has formed across one of the original bonds of the metallacycle. The carbon atoms C1 and C3 presumably originate from propi-

[*] Professor J. M. O'Connor, L. Pu
Department of Chemistry D-006
University of California at San Diego
La Jolla, CA 92093 (USA)
Dr. Raj Chadha
UCSD Crystallographic Laboratory

[**] This work was funded by the U.S. National Science Foundation (CHE-8721344). We also thank Johnson-Matthey for a generous loan of precious metals.

Table 1. Selected bond distances [Å] and angles [°] for **2** and **3**.

Bond Distances			Bond Angles		
	2	**3**		**2**	**3**
Ir–C1	2.019(25)	2.084(14)	C1-Ir-C5	83.2(9)	77.2(5)
Ir–C5	2.034(19)	2.053(13)	C1-Ir-C8	166.6(9)	154.6(5)
Ir–C8	2.178(22)	2.100(13)	C5-Ir-C8	83.5(8)	77.8(5)
Ir–C15	1.982(27)	2.029(14)	C1-Ir-C15	97.4(10)	102.6(5)
O1–C1	1.157(31)	1.354(16)	C5-Ir-C15	177.3(14)	178.6(7)
O1–C2	1.520(33)	1.384(18)	C8-Ir-C15	95.8(10)	102.3(5)
O2–C4	1.270(22)	1.206(17)	Ir-C1-C3	105.8(17)	116.5(10)
O3–C9	1.225(31)	1.202(28)	Ir-C1-O1	131.9(18)	121.0(10)
O4–C9	1.389(36)	1.333(29)	O2-C4-C5	127.0(18)	123.4(13)
O4–C10	1.379(38)	1.404(24)			
C1–C3	1.520(32)	1.356(21)			
C3–C4	1.374(31)	1.421(21)			
C4–C5	1.412(26)	1.497(19)			
C5–C6	1.499(29)	1.364(18)			
C6–C7	1.459(28)	1.477(18)			
C6–C9	1.406(31)	1.487(18)			
C7–C8	1.453(27)	1.389(19)			

olic acid. Unexpectedly, the methoxy unit from one of the methyl carboxylate ring substituents is now bonded to C1 of the new metallacycle.

The most unusual aspect of the structure of **2** is the presence of iridium at the bridgehead position of a [3.3.0] fused ring system. This bonding feature results in pronounced distortion from ideal octahedral geometry about iridium. The C1-Ir-C8 angle is 166.6(9), the C8-Ir-C15 angle is 95.8(10), and the C1-Ir-C15 angle is 97.4(10)°. The ca. 83° C-Ir-C angle in both metallacycle rings of **2** is opened up by ca. 6° compared to the corresponding angle in related iridacyclopentadiene structures.[1, 7]

A second surprising structural feature of **2** is the presence of a methylated acyl oxygen, indicated by distances of 1.520(33) Å for O1–C2 and 1.157(31) Å for C1–O1. The alternative metallapentalene resonance form, **2A**, is not unreasonable for an Ir–C1 distance of 2.019(25) Å; however, the chemical shift of C1 ($\delta = 230$) is more typical of an acyl carbon than a carbene carbon. The Ir–C5 distance of 2.034(19) Å is unusually short and may indicate some carbenoid character in that bond as well. The C–C bond lengths for C5–C8 indicate a high degree of electron delocalization over these atoms.

The final unusual feature of **2** is the presence of an enol unit (C3, C4, O2, H) within the new metallacycle. The H atom was located by X-ray analysis, and its position is consistent with the observed C–C and C–O bond lengths. We attribute the preference for the enol tautomer in **2** to both hydrogen bonding to O3 and a greater degree of conjugation in the enol form than in the keto form.

In order to further clarify these unusual bonding features, complex **2** was deprotonated with methylamine to give the neutral metallabicyclooctatrienone complex **3**,[8] whose structure was also determined by X-ray crystallography (Fig. 2, Table 1).[9]

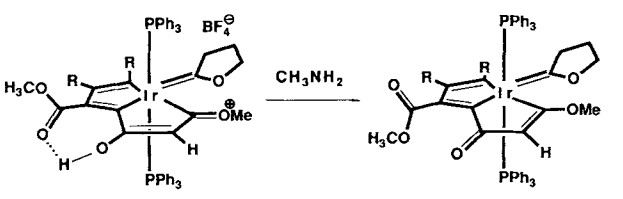

2 **3**

With a C1-Ir-C8 angle of 154.6°, complex **3** is even more dramatically distorted from ideal octahedral geometry than **2**. The C4–O2 distance in **3** has shortened to 1.206(17) Å and the methyl carboxylate group bonded to C6 has rotated out of the plane of the metallacycle, an indication that the proton which bridged O2 and O3 is no longer present. In addition, the C–C double bond has shifted from C3–C4 to C1–C3, and the C1–O1 distance has lengthened to 1.354(16) Å. This lat-

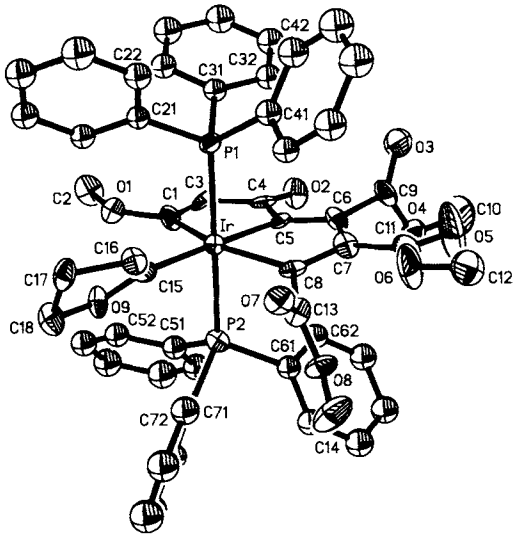

Figure 2. Molecular structure (ORTEP) and partial numbering scheme for **3**.

ter observation is consistent with the existence of a methylated acyl oxygen in **2**. In both **2** and **3** the ring containing Ir and C5–C8 deviates significantly from planarity; the angle between the C5, Ir, C8 plane and the C5–C8 mean plane is 16.9° for **2** and 12.6° for **3**. Efforts are currently underway to determine the mechanism of the formation of **2** from **1** and propiolic acid.

Received: December 27, 1989 [Z 3701 IE]
German version: *Angew. Chem. 102* (1990) 586

CAS Registry numbers:
1, 126256-50-6; **2**, 126256-52-8; **3**, 126256-53-9; **3**·$2C_6H_6$, 126256-54-0; propiolic acid, 471-25-0.

[1] N. E. Schore, *Chem. Rev. 88* (1988) 1081; J. P. Collman, L. S. Hegedus, J. R. Norton, R. G. Finke: *Principles and Applications of Organotransition Metal Chemistry*, University Science Books, Mill Valley, CA, USA 1987, Chap. 9; E. Lindner, *Adv. Heterocycl. Chem. 39* (1986) 237; K. P. C. Vollhardt, *Angew. Chem. 96* (1984) 525; *Angew. Chem. Int. Ed. Engl. 23* (1984) 539; S. D. Chappell, D. J. Cole-Hamilton, *Polyhedron 1* (1982) 739.

[2] J. M. O'Connor, L. Pu, A. L. Rheingold, *J. Am. Chem. Soc. 111* (1989) 4129.

[3] Alkynes with terminal C≡C groups are well-precedented vinylidene-ligand precursors in iridium systems: A. Höhn, H. Otto, M. Dziallas, H. Werner, *J. Chem. Soc. Chem. Commun. 1987*, 852; F. J. Garcia Alonso, A. Höhn, J. Wolf, H. Otto, H. Werner, *Angew. Chem. 97* (1985) 401; *Angew. Chem. Int. Ed. Engl. 24* (1985) 406; H. Werner, J. Wolf, G. Müller, C. Krüger, *ibid. 96* (1984) 421 and *23* (1984) 431; *J. Organomet. Chem. 342* (1988) 381; M. D. Fryzuk, N. T. McManus, S. J. Rettig, G. S. White, *Angew. Chem. 102* (1990) 67; *Angew. Chem. Int. Ed. Engl. 29* (1990) 73.

[4] Complex **1** was prepared by halide ligand abstraction from [Ir(CR=CRCR=CR)$(PPh_3)_2${=$C(CH_2)_3O$}Cl]: J. M. O'Connor, L. Pu, A. L. Rheingold, *J. Am. Chem. Soc. 109* (1987) 7578; *ibid.*, in print.

[5] **2**: ^{1}H NMR (300 MHz, $CDCl_3$): δ = 13.22 (s, 1H, OH), 7.1–7.4 (m, 30H, 6 C_6H_5), 5.98 (br, 1H, =C(H)-), 4.69 (t, J = 8.0 Hz, 2H, -CH_2O-), 3.67 (s, 3H, OCH_3), 3.60 (s, 3H, OCH_3), 3.48 (s, 3H, OCH_3), 3.34 (s, 3H, OCH_3), 3.24 (t, J = 7.8 Hz, 2H, =CCH_2-), 1.76 (quintet, J = 7.8 Hz, 2H, -$CH_2CH_2CH_2$-). $^{13}C\{^1H\}$ NMR (75 MHz, $CDCl_3$): δ = 286.4 (t, J = 7.6 Hz), 229.5 (t, J = 7.5 Hz), 189.4, 182.0 (t, J = 5.4 Hz), 176.0, 168.7,

168.1, 161.1 (t, J = 8.0 Hz), 157.7(br), 147.1, 134.3(br), 130.9(br), 128.0(br, superimposed on a triplet, J = 51.3 Hz), 87.8, 61.0, 60.3, 52.8, 51.2, 51.1, 21.6. IR (CH_2Cl_2): $\tilde{\nu}$ = 1690, 1720 cm^{-1}. MS(FAB): m/z 1097 ($M^{\oplus} - BF_4$). Correct C,H analyses.

[6] **2** (296 K): $C_{54}H_{50}BO_9F_4P_2Ir$, monoclinic, Cc, a = 14.757(7), b = 20.652(5), c = 17.054(4) Å, β = 105.36(3)°, V = 5012(3) Å^3, Z = 4, $\varrho_{calcd.}$ = 1.569 g cm^{-3}, μ = 27.84 cm^{-1}. Yellow acicular crystal (0.10 × 0.11 × 0.20 mm); 4678 data were collected (Nicolet R3m/V, $Mo_{K\alpha}$, 3.5 < 2Θ < 50°): 4540 were unique (R_{int} = 0.0688), and 3230 reflexes were observed ($F_0 > 6\sigma(F_0)$) and corrected for absorption (T_{max}/T_{min} = 1.10), R = 0.0538, R_w = 0.0743. Further details of the crystal structure analysis may be obtained from the Fachinformationszentrum Karlsruhe, Gesellschaft für wissenschaftlich-technische Information mbH, D-7514 Eggenstein-Leopoldshafen 2 (FRG), by quoting the depository number CSD-54398, the names of the authors, and the journal citation.

[7] For structural characterization of iridacyclopentadiene complexes see ref. [2, 4], and J. M. O'Connor, L. Pu, A. L. Rheingold *Organometallics* 7 (1988) 2060.

[8] **3**: ^1H NMR (300 MHz, $CDCl_3$): δ = 7.3–7.4 (m, 30H, $6C_6H_5$), 4.88 (br. 1H, =C(H)-), 4.10 (t, J = 8.0 Hz, 2H, -CH_2O-), 3.87 (s, 3H, OCH_3), 3.37 (s, 3H, OCH_3), 3.33 (s, 3H, OCH_3), 3.12 (s, 3H, OCH_3), 2.98 (t, J = 8.0 Hz, 2H, =CCH_2-), 1.37 (quintet, J = 8.0 Hz, 2H, -$CH_2CH_2CH_2$-). $^{13}C\{^1H\}$ NMR (75 MHz, $CDCl_3$) δ = 293.0 (t, J = 8.8 Hz), 200.7, 196.2 (t, J = 10.2 Hz), 178.2, 172.9 (t, J = 7.7 Hz), 171.9, 166.0 (t, J = 9.2 Hz), 164.2, 150.4, 147.7, 134.5(br), 130.0 (t, J = 50.2 Hz), 129.7(br), 127.4(br), 123.0(br), 85.4, 59.9, 57.2, 51.3, 50.5, 50.0, 21.3. IR (CH_2Cl_2): $\tilde{\nu}$ = 1700(br, s), 1580(m), 1540(w) cm^{-1}. MS(FAB), m/z 1095.2520. (calcd for $C_{54}H_{49}O_9P_2Ir$ + H: 1095.2536).

[9] **3**·2C_6H_5 (T = 298 K): $C_{54}H_{49}O_9P_2Ir \cdot 2C_6H_6$ orthorhombic, $P_{na}2_1$, a = 19.226(4), b = 17.120(3), c = 17.240(2) Å, V = 5675(2) Å^3, Z = 4, $\varrho_{calcd.}$ = 1.466 g cm^{-3}, μ = 54.7 cm^{-1}. Pale yellow crystal (0.13 × 0.14 × 0.15 mm); 3985 data were collected (Nicolet R3m/V, $Cu_{K\alpha}$, 3 ≤ 2Θ < 110°): 3700 were unique (R_{int} = 0.00), and 3059 were observed ($F_0 > 6\sigma(F_0)$) and corrected for absorption (T_{max}/T_{min} = 1.37). R = 0.0463, R_w = 0.0723. For further details see [6].

A Borate Propeller Compound as Chiral Catalyst for an Asymmetrically Induced Diels-Alder Reaction

By *Dieter Kaufmann** and *Roland Boese*

We have already reported success in achieving asymmetrically induced Diels-Alder reactions[1] with the aid of catalytic amounts of haloorganoboranes such as **1**, compounds that are derived from naturally occurring terpenes.[2] We subsequently described a seven-step preparation of the axially chiral boron catalyst **2a**, which incorporates a 1,1'-binaphthyl fragment.[3]

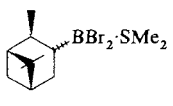

1

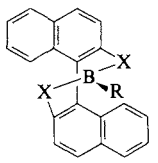

2a, X = CH_2, R = Cl
2b, X = O, R = Br
2c, X = O, R = OAryl

An attempted synthesis of the dioxaborepine **2b** by treatment of (*S*)-(−)-1,1'-bi-2-naphthol[4] [(−)-**3**, a substance available in a single step] with monobromoborane dimethylsulfide[5] **4** led to an unexpected result, in that the sole product that actually resulted proved to be a crystalline material with a mass of 874. This can only be explained by assuming reaction of **3** with **4** in a 3:2 molar ratio, together with elimination of both molecular hydrogen and hydrogen bromide. Though lacking spectroscopic proof, *Kelly* et al.[6] have postulated the intermediacy of a *B*-aryloxy substituted dioxaborepine of the structural type **2c** in the reaction of juglone with borane-tetrahydrofuran and (*S*)-3,3'-diphenyl-1,1'-bi-2-naphthol (1:1:1).

To our surprise, X-ray structural analysis[7] of crystals obtained upon treatment of (*R*,*S*)-**3** with **4** revealed exclusive formation of a C_3-symmetric tetradecacyclic diborate **5** (Fig. 1), and no **2b** whatsoever. The unit cell was shown to contain both enantiomers of the compound. To the best of our knowledge, formation of a propeller compound with axially chiral 1,1'-binaphthyl groups as "blades" is heretofore without precedent.

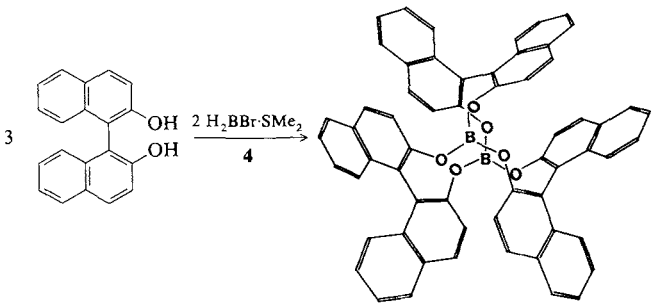

3 **5**

Since both an acyloxyborane catalyst[8] and a borate-activated dienophile[6] had already been successfully employed in asymmetrically induced Diels-Alder reactions, we next examined the applicability of (+)- and (−)-**5** to the reaction of cyclopentadiene **6** with methacrolein **7** at −78 °C. Whereas the uncatalyzed cycloaddition provided only a 15% yield (*exo*-**8**/*endo*-**8** 86/14) after 42 h even at 20 °C, conducting the

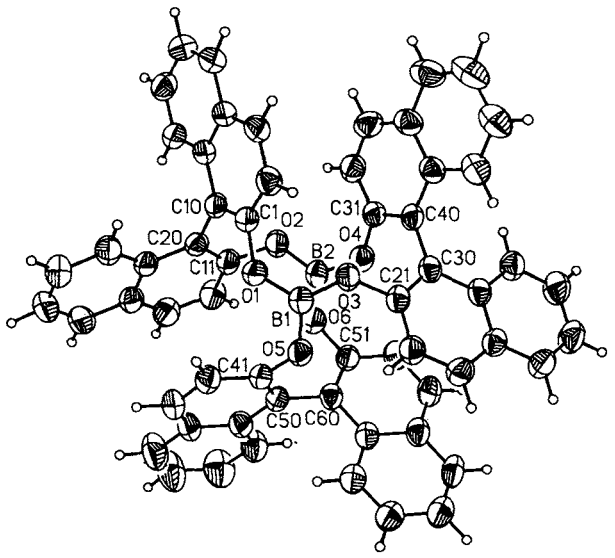

Fig. 1. Structure of crystalline **5**. [7] Average values for important distances [Å] and angles [°] (maximum standard deviations for B-O and B-C bonds 0.004 Å, for C-C bonds 0.006 Å): B-O 1.358, O-C 1.392, C-C bonding of the naphthyl groups (e.g., C10-C20) 1.495, C(O)-C(bonded) (e.g., C1-C10) 1.367; C(O)-C(nonbonded) 1.406, C-C (central bond of the naphthyl groups) 1.419, B···B 3.397; O-B-O 120.0, B-O-C 124.9, O-C-C(bonded) (e.g., O1-C1-C10) 116.8, torsional angle (C(O)-C(bonded)-C(bonded)-C(O) (e.g., C1-C10-C20-C11) 80°.

[*] Priv.-Doz. Dr. D. Kaufmann
Bayer AG, Zentrale Forschung und Entwicklung
D-5090 Leverkusen (FRG)
Dr. R. Boese
Institut für Anorganische Chemie
der Universität-Gesamthochschule Essen
Universitätsstrasse 3–5, D-4300 *Essen* 1 (FRG)

reaction in dichloromethane at −78 °C in the presence of 3 mol-% (−)-**5** led to the isolation of an 85% yield of the cycloadduct (+)-**8**. The *exo*-selectivity[9] (97.4%) of the reaction is outstanding, as is the observed enantioselectivity (90% *ee*). Use of (+)-**5** leads in analogous fashion to the (−)-*exo*-aldehyde **8**.

6 **7** **8**

Since this new catalyst is available from two commercial[10] reagents in a single step, asymetrically induced cycloaddition becomes an exceptionally simple synthetic operation. In the event that the catalyst is not to be re-used it can be cleaved at room temperature with sodium hydrogen carbonate solution; optically active **3** can be recovered nearly quantitatively, and there is no racemization.

At the present time we can only speculate about the mechanism of the catalysis. The first step is probably complexation of the carbonyl group of methacrolein with a boron atom, which might lead to a distortion of the propeller molecule. Subsequent cycloaddition could then occur within the sphere of influence of the binaphthyl moiety.

Experimental

(−)-**5**: To a solution of 286.3 mg (1.0 mmol) of (*S*)-(−)-**3** in 25 mL of anhydrous dichloromethane was added with a syringe at −20 °C under nitrogen 154.9 mg (1.0 mmol) of **4**. The mixture was allowed to warm slowly to room temperature, after which volatile components were removed in vacuo and the residue was dried at 50 °C/0.01 torr. Yield 282.8 mg (97%) (−)-**5**, mp > 350 °C.—^{1}H-NMR (400 MHz, $CDCl_3$, *J* in Hz): δ = 6.64 and 6.68 (AB system, ^3J = 8.8, 4H), 7.06 (d, ^3J = 8.3, 2H), 7.22 (ddd, ^3J = 8.3, 6.7, ^4J = 1.3, 2H), 7.47 (ddd, ^3J = 8.1, 6.7, ^4J = 1.1, 2H), 7.74 (d, ^3J = 8.1, 2H) (numbers of hydrogens are based on a single binaphthyl unit).

(+)-*exo*-**8**: To a cooled (−78 °C) solution of 282.6 mg (0.32 mmol) of (−)-**5** in 25 mL of anhydrous dichloromethane was added dropwise under nitrogen (through a syringe) 736 mg (10.5 mmol) of methacrolein. This was followed after 15 min by 661 mg (10.0 mmol) of cyclopentadiene. The reaction mixture was kept at −78 °C for 2 d. It was then warmed slowly to 0 °C and washed with two 10 mL portions of saturated aqueous sodium hydrogen carbonate solution. Volatile components were removed at room temperature with a gentle vacuum, after which the product was distilled at 50 °C/0.01 Torr. Yield 1.16 g (85%) of a mixture consisting of 97.4% (+)-*exo*- and 2.6% *endo*-**8** (GC, ^{1}H-NMR). The enantiomeric excess of the *exo* product was determined to be 90% by ^{1}H NMR after addition of the shift reagent Eu(hfc)$_3$ and integration of the aldehyde proton signals.

Received: December 23, 1988 [Z 3103]
German version: *Angew. Chem. 102* (1990) 568
Publication delayed at authors' request.

[1] K. Krohn, *Nachr. Chem. Tech. Lab. 35* (1987) 836.
[2] G. Bir, D. Kaufmann, *Tetrahedron Lett. 28* (1987) 777.
[3] U.-M. Gross, M. Bartels, D. Kaufmann, *J. Organomet. Chem. 344* (1988) 277.
[4] F. Toda, K. Tanaka, L. Nassimbeni, M. Niven, *Chem. Lett. 1988*, 1371.
[5] H. C. Brown, N. Ravindran, *Inorg. Chem. 16* (1977) 2938.
[6] T. R. Kelly, A. Whiting, N. S. Chandrakumar, *J. Am. Chem. Soc. 108* (1986) 3510.
[7] X-ray structure analysis of **5** at room temperature, crystal growth at 0 °C from pentane/dichloromethane (2/1); the unit cell contained one molecule of dichloromethane: $P\bar{1}$. a = 9.3537(10), b = 14.4558(13), c = 19.1677(19) Å, α = 111.931(7), β = 91.371(8), γ = 100.487(8)°, V = 2352.2(4) Å^3, Z = 2. ϱ_{calc} = 1.335 g cm^{-3}; $Mo_{K\alpha}$ radiation (graphite monochromator); scan range 3° ≤ 2Θ ≤ 50°; total number of reflections: 8272, observed reflections: 5749 ($F_0 \geq 4\sigma(F)$), R = 0.0526, R_w = 0.0612. Nicolet-R3m/V four-circle X-ray diffractometer, data calculated with SHELXTL-PLUS on a MicroVAX II.—Further details of the crystal structure investigation are available on request from the Fachinformationszentrum Karlsruhe, Gesellschaft für wissenschaftlich-technische Information mbH, D-7514 Eggenstein-Leopoldshafen 2 (FRG) on quoting the depository number CDS-320095, the names of the authors, and the journal citation.
[8] K. Furuta, S. Shimizu, Y. Miwa, H. Yamamoto, *J. Org. Chem. 54* (1989) 1483.
[9] Y. Kobuke, T. Fueno, J. Furukawa, *J. Am. Chem. Soc. 92* (1970) 6548.
[10] Aldrich Chemical Company, Inc.

Fast Heteronuclear 3D NMR Spectroscopy **

By *Peter Schmieder, Horst Kessler,* and *Hartmut Oschkinat**

Three-dimensional NMR spectroscopy plays an important role in the structure determination of complex compounds.[1, 2] Since isotopically labeled proteins readily became accessible by gene-technology techniques, it has been possible to use the chemical shifts of heteronuclei to resolve complicated two-dimensional proton NMR spectra of large proteins by dispersing them into a third dimension. The application of 3D techniques to smaller molecules such as peptides shorter than 20 amino acids seems to be an overkill, since the acquisition time needed to obtain a spectrum with sufficient resolution is prohibitively long. On the other hand, there is a potential demand for 3D NMR spectra when peptides containing many amino acids with long aliphatic side chains such as arginine, lysine, and proline are being investigated. Herein, we wish to show that the time necessary to record a heteronuclear 3D NMR spectrum useful enough for the assignment of side-chain protons of these amino acids is in fact rather short: the net acquisition time needed to record the spectrum of a cyclic hexapeptide without isotopic labeling presented here was 8.2 h. The resolution is comparable to that of a normal 2D spectrum.

Several examples of the use of heteronuclear 3D NMR spectroscopy have already been described.[3, 4] In most cases ^{15}N is used as heteronucleus since its signals appear in a limited range; hence a good resolution can be obtained within a reasonable measurement time. It is more difficult to record a 3D NMR spectrum with ^{13}C as heteronucleus, since the spectral ranges of the carbons and the protons directly attached to them are much larger.

The measurement time needed to record a 3D NMR spectrum with sufficient resolution may then be reduced by restricting the chemical shift ranges in one or both of the two virtual dimensions on the basis of semiselective excitation.[5–8] Using this approach may not always allow an appropriate selection of the chemical shift ranges and may have experimental disadvantages.

Another way to select a certain chemical shift range in the carbon dimension is to excite only certain types of carbon signals by a DEPT-type pulse sequence,[9] which should be extremely useful in assigning side-chain protons of amino

[*] Prof. Dr. H. Kessler, Dipl.-Chem. P. Schmieder
Organisch-Chemisches Institut der Technische Universität München
Lichtenbergstrasse 4, D-8046 Garching (FRG)
Dr. H. Oschkinat
Max-Planck-Institut für Biochemie,
Am Klopferspitz, D-8033 Martinsried (FRG)

[**] This work was supported by the Deutsche Forschungsgemeinschaft and the Fonds der Chemischen Industrie. We thank Dipl. Chem. *M. Kurz* for providing a sample of the cyclic hexapeptide. *P.S.* thanks the Fonds der Chemischen Industrie for a fellowship grant.

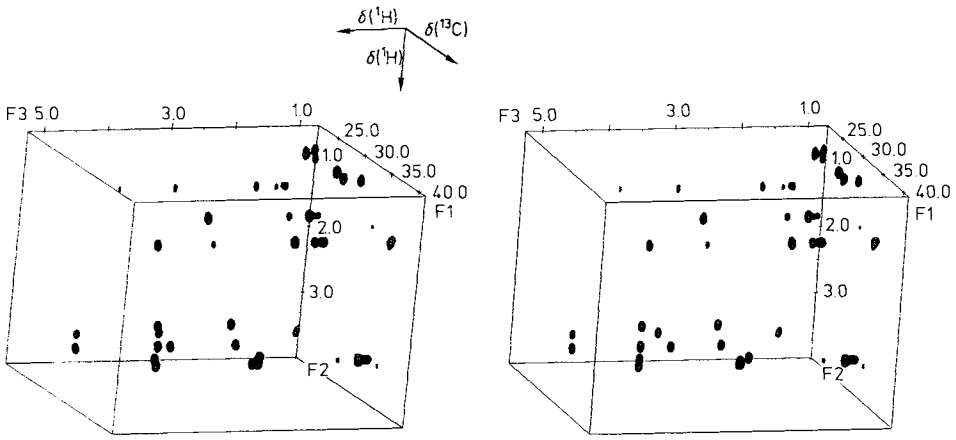

Fig. 1. Stereo picture of the 3D DEPT-TOCSY spectrum of *cyclo*(-D-Ala-Phe-Trp-Lys(Z)-Val-Phe-). 64 experiments were recorded in t_1, 96 experiments in t_2. The delay Δ was set to 3.57 ms, the mixing time to 35 ms. The spectrum was recorded on a Bruker AM 500 spectrometer and processed on a CONVEX with our own software [8]. Residual signal bands at the frequency $\omega_1 = 0$ (^{13}C axial peaks) were removed with a "whitewash" procedure to improve the display.

acids. However, the creation of heteronuclear double quantum coherence by an "inverse" DEPT sequence depends in a different manner on the flip angle of the editing pulse.[10] If, for example, a 90°-pulse is chosen, only CH_2 groups are selected. The particular advantage of this type of selective excitation is its virtually rectangular excitation profile—all CH_2 groups are excited with their full intensity, but other groups are not—which is hardly achievable with soft pulses. This should reduce the spectral width dramatically if the suppression is good enough to prevent distortions from remaining signals, which are then folded into the spectrum.

We have used this approach in combination with a BIRD pulse[11] for saturating protons bound to nonmagnetic carbons to obtain a carbon-resolved TOCSY spectrum of 25 mg of the cyclic hexapeptide *cyclo*(-D-Ala-Phe-Trp-Lys(Z)-Val-Phe-) in 0.5 mL of DMSO (Fig. 1). The application of the BIRD pulse for the inversion of nonsatellite protons prior to the execution of the pulse sequence is not recommendable in all cases, since in molecules with a strong negative NOE a severe attenuation of the signals may occur. However, in the case of small- or medium-sized peptides with positive or weakly negative NOE it provides a powerful method for shortening the measuring time. In our application, a BIRD pulse was inserted into the relaxation delay, splitting it into two delays of length 193 and 255 ms. This, together with an acquisition time of 92 ms, led to a good and simultaneous suppression of nearly all ^1H signals from protons bound to ^{12}C.[12] Since t_1 is usually short in the case of a small peptide, rapid pulsing with two scans per second is possible.

Figure 2 shows the pulse sequence of the 3D DEPT-TOCSY without the BIRD sequence, which can easily be added to any kind of heteronuclear technique. It can be seen from Figure 2 that only CH_2 groups have been excited sufficiently enough to show TOCSY cross peaks. Signals due to the excitation of C_α carbons do not appear at this contour level. The assignment of the signals and the chemical shifts may be taken from the 2D CH_2-selected inverse DEPT-HMQC spectrum shown in Figure 3. To test the quality of the suppression, a similar 3D spectrum with a larger spectral width was recorded, proving that the suppression is better than 90%. In principle, the same editing effect could be achieved by the application of a heteronuclear triple quantum filter,[13] since CH groups cannot form heteronuclear triple quantum coherences. CH_3 groups are suppressed as well, since they form heteronuclear quadruple quantum coherences very effectively and cannot pass the filter.

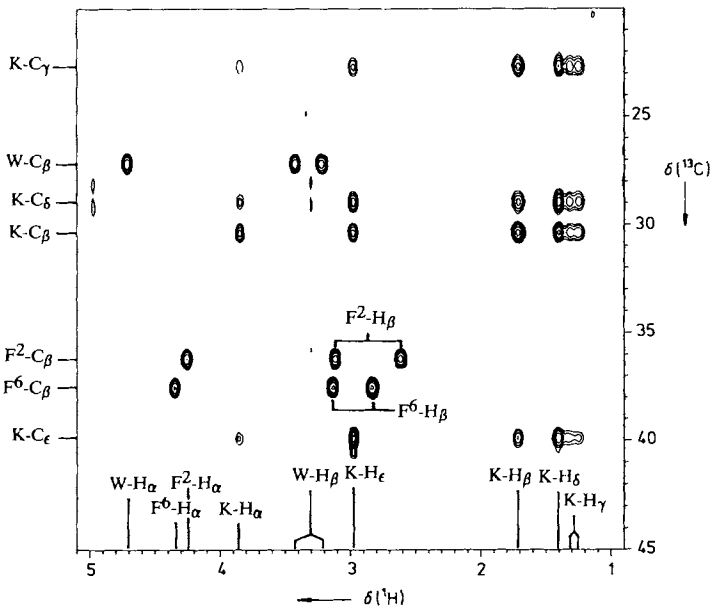

Fig. 3. Region of the 2D DEPT-HMQC spectrum with TOCSY transfer of *cyclo*(-D-Ala-Phe-Trp-Lys(Z)-Val-Phe-) showing the assignment of the resonances that are also visible in Figure 2. This spectrum corresponds to a projection of all signals of the spectrum to the top of the cube shown in Figure 1 (F_1/F_3).

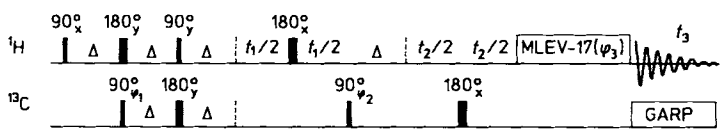

Fig. 2. Pulse sequence of the 3D DEPT-TOCSY, which is a combination of the 2D DEPT-HMQC [10] and the TOCSY experiment. The delays Δ are set to $(2^1J_{CH})^{-1}$, the heteronuclear decoupling during acquisition by the GARP sequence [14] is optional. The MLEV-17 sequence [15] was used during the spin-lock period. The phase cycle is: φ_1 = x, −x, x, −x; φ_2 = x, x, −x, −x; φ_3 = x, x, x, x, −x, −x, −x, −x; rec = x, −x, −x, x. Quadrature detection in t_1 was achieved by applying TPPI (time proportional phase increment) to phase φ_1 and the phase of the following carbon π pulse, in t_2 by applying TPPI to the phase of the first seven pulses of the sequence.

The net acquisition time to record the spectrum with 64 experiments in t_1 and 96 experiments in t_2 was 8.2 h using 8 scans/experiment. On our Bruker AM 500 spectrometer two dummy scans were necessary, since no "buffered acquisi-

tion" is available yet, giving the still acceptable measuring time of 10.2 h. The mixing time was set to 35 ms, the delays Δ were optimized for $^1J_{CH} = 140$ Hz (3.57 ms). The spectral width was 2500 Hz in F_1 and F_2 resulting in a limiting resolution of 0.38 ppm (46.9 Hz) in F_1 and 0.063 ppm (31.3 Hz) in F_2. In comparison the limiting resolution in the 2D NMR spectrum shown in Figure 3 is 0.3 ppm (36.6 Hz) in F_1, which is sufficient in medium-sized compounds.

We have shown that the application of DEPT-type pulse sequences to restrict the spectral width in a 3D spectrum can lead to a well-resolved spectrum in an acceptable measuring time. In the case of small peptides, the described experiment utilizing a BIRD pulse may be completed overnight.

Received: December 15, 1989 [Z 3690 IE]
German version: *Angew. Chem. 102* (1990) 588

[1] C. Griesinger, O. W. Sørensen, R. R. Ernst, *J. Am. Chem. Soc. 109* (1987) 7227–7228.
[2] H. Oschkinat, C. Griesinger, P. J. Kraulis, O. W. Sørensen, R. R. Ernst, A. M. Gronenborn, G. M. Clore, *Nature (London) 332* (1988) 374–376.
[3] S. W. Fesik, E. R. Zuiderweg, *J. Magn. Reson. 78* (1988) 588–593.
[4] D. Marion, L. E. Kay, S. W. Sparks, D. A. Torchia, A. Bax, *J. Am. Chem. Soc. 111* (1989) 1515–1517.
[5] C. Bauer, R. Freeman, T. Frenkiel, J. Keeler, A. K. Shaka, *J. Magn. Reson. 58* (1984) 442–457.
[6] J. Cavanagh, J. P. Waltho, J. Keeler, *J. Magn. Reson. 74* (1987) 386–393.
[7] H. Kessler, U. Anders, G. Gemmecker, S. Steuernagel, *J. Magn. Reson. 85* (1989) 1–14.
[8] H. Oschkinat, C. Cieslar, T. A. Holak, G. M. Clore, A. M. Gronenborn, *J. Magn. Reson. 83* (1989) 450–472.
[9] D. M. Doddrell, D. T. Pegg, M. R. Bendell, *J. Magn. Reson. 48* (1982) 323–327.
[10] H. Kessler, P. Schmieder, M. Kurz, *J. Magn. Reson. 85* (1989) 400–405.
[11] J. R. Garbow, D. P. Weitekamp, A. Pines, *Chem. Phys. Lett. 93* (1982) 504; cf. also H. Kessler, M. Gehrke, C. Griesinger, *Angew. Chem. 100* (1988) 507–554; *Angew. Chem. Int. Ed. Engl. 27* (1988) 490–536.
[12] A. Bax, S. Subramanian, *J. Magn. Reson. 67* (1986) 565–569.
[13] J. M. Schmidt, H. Rüterjans, *J. Am. Chem. Soc. 112* (1990) 1279–1280.
[14] A. J. Shaka, P. B. Barker, R. Freeman, *J. Magn. Reson. 64* (1985) 547–552.
[15] A. Bax, D. G. Davis, *J. Magn. Reson. 65* (1985) 355–360.

Synthesis and 2D-(^{1}H,^{103}Rh)-NMR Study of the First "Non-Classical" Polyhydrido Complex Stabilized by a Nitrogen Donor Ligand**

By *Urs E. Bucher, Thomas Lengweiler, Daniel Nanz, Wolfgang von Philipsborn*, and *Luigi M. Venanzi**

The so-called "non-classical" transition-metal hydrido-complexes, i.e., those containing coordinated molecular hydrogen, have aroused great interest in recent years.[1–3] Most of the complexes of this type described hitherto have also contained tertiary phosphanes or arsanes as co-ligands.

We report here the synthesis and 2D-(^{1}H,^{103}Rh)-NMR characterization of a new "non-classical" rhodium hydride with the structure $[\{HB(3,5\text{-}Me_2pz)_3\}Rh(H_2)H_2]$, **1**, containing the terdentate anionic tris-(3,5-dimethylpyrazolyl) borate as co-ligand.

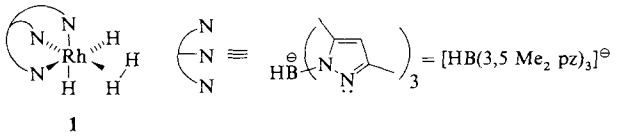

1

This off-white solid was obtained from **3**,[4] as shown in Scheme 1. The complex appears to be indefinitely stable in the solid state at room temperature but decomposes slowly in solution with formation of metallic rhodium.

$[HB(3,5\text{-}Me_2pz)_3RhCl_2(MeOH)]$ **3**

↓ $PPh_4Cl / CHCl_3$

$[PPh_4][HB(3,5\text{-}Me_2pz)_3RhCl_3]$ **2**

↓ $NaBH_4 / EtOH$

$[HB(3,5\text{-}Me_2pz)_3Rh(H_2)H_2]$ **1**

Scheme 1.

The ^{1}H-NMR spectrum of **1** (CD_2Cl_2, 253 K) in the hydride region consists of a doublet centered at $\delta = -12.76$ with an apparent $J(^{103}Rh,^1H)$ value of 18.1 Hz. The corresponding longitudinal relaxation time T_1 is extremely short with a minimum value of 42 ms at 166 K (400.13 MHz, $CD_2Cl_2/CDCl_3$ 2/1). On the basis of known relaxation criteria[15] this strongly indicates the presence of coordinated molecular hydrogen.

The presence of four coordinated hydrogen atoms was first inferred from careful integration of this signal relative to those of the organic ligand and was unambiguously confirmed by ^{1}H-detected 2D-(^{1}H,^{103}Rh)-NMR spectroscopy. Although experiments of this type were first reported in 1979[6] only few applications involving the central metal atom of an organometallic complex have been published, e.g. those by *Cabeza* et al.[7] and by *Benn* and *Rufińska*.[8] The technique features a twofold coherence transfer allowing for both initial excitation as well as detection at the higher frequency. In the "classical" pulse sequence (Fig. 1)[9] heteronuclear (H,M) two-spin coherences are generated during the preparation period.

Omission of the refocussing π-pulse leads to an additional modulation of the signal during t_1 due to the coupling of the remaining n – 1 protons of the MH_n fragment with these coherences. The splitting of the signal in $F1$ corresponds to the (M-^{1}H)-coupling, since scalar interactions between the four dynamically equivalent protons do not influence the

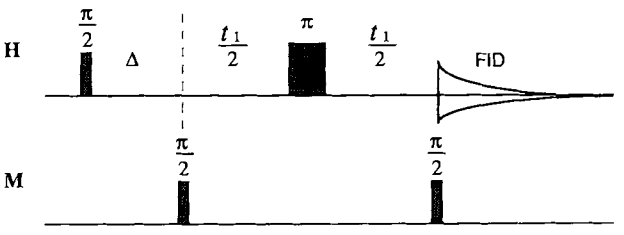

Fig. 1. Standard pulse sequence for indirect 2D-(^{1}H,M)-NMR spectroscopy [9].

[*] Prof. Dr. L. M. Venanzi, Dipl.-Chem. U. E. Bucher, Dipl.-Chem. T. Lengweiler
Laboratorium für Anorganische Chemie der Eidgenössischen Technischen Hochschule, ETH-Zentrum
Universitätstrasse 6, CH-8092 Zürich (Switzerland)
Prof. Dr. W. von Philipsborn, Dipl.-Chem. D. Nanz,
Organisch-chemisches Institut der Universität Zürich
Winterthurerstrasse 190, CH-8057 Zürich (Switzerland)

[**] *U. E. B., T. L.* and *L. M. V.* gratefully acknowledge the support of the Swiss National Science Foundation

spectra. The number of lines in the resulting multiplet is equal to n, in contrast to n + 1 in fully coupled M-NMR spectra. The metal chemical shift and the number of hydrido ligands can be read directly from the spectrum (Fig. 2) if the ^{1}H-transmitter frequency is on resonance with the hydride signal.

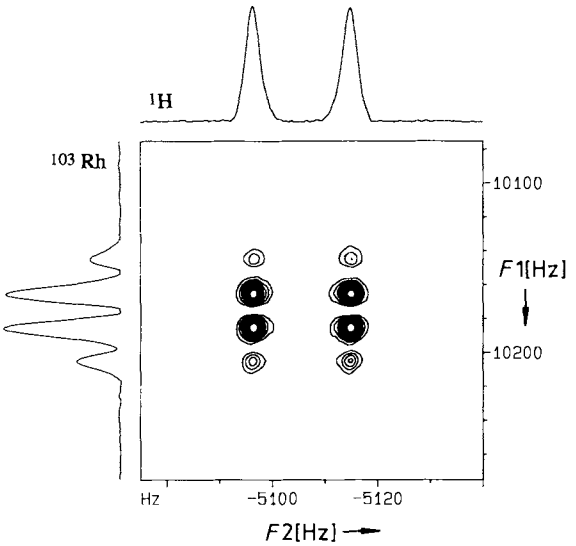

Fig. 2. Contour plot of a two-dimensional (^{1}H,^{103}Rh)-correlated spectrum of **1** in CD_2Cl_2 at 253 K (10 mg in 0.6 mL solvent, measuring time 8 min, Bruker AM-400-WB). Four FIDs were collected for each of the 48 traces in t_1. Prior to Fourier Transformation the data in t_2 and t_1 were weighted with sine and sine squared functions, respectively.

We consider the technique described above to be the method of choice for the determination of the number of protons coupled to a magnetically insensitive spin ½ metal center.

Hamilton et al.[10] have reported the preparation of two rhenium polyhydride complexes containing polypyrazolyl ligands, i.e., $[\{HB(pz)_3\}ReH_6]$ and $[\{CH_2(pz)_2\}ReH_7]$ (pz = pyrazolyl). These, however, contain only "classical" hydride ligands. Furthermore, *Tanke* and *Crabtree*[11] have recently described some iridium hydrido complexes with pyrazolylborate ligands where, however, there are other donors in addition to hydrogen and nitrogen and the Ir–H bonds are of the classical type. To our knowledge **1** is the first example of a platinum metal polyhydrido complex containing only nitrogen donors as co-ligands and also the first example of a complex containing coordinated molecular hydrogen, stabilized only by nitrogen donors.

Thus it appears that, as found in the phosphane-containing polyhydrido complexes, "non-clasical" behavior is more common in compounds of the second than those of the third transition series even when nitrogen donors are present as co-ligands.

Experimental

2: 372.8 mg (1 mmol) of PPh_4Cl was added to a suspension of 500 mg (1 mmol) of compound **3** in 10 mL of $CHCl_3$ and the mixture was refluxed for 3 h. The resulting solution was evaporated to dryness under reduced pressure and the residue was recrystallized from CH_2Cl_2/THF. Yield: 798 mg (95%). Satisfactory C,H,N,Cl analyses. IR (RbI): $\tilde{\nu}$(B–H) = 2532(s), $\tilde{\nu}$(Rh–Cl) = 330 and 316 cm^{-1}(m); ^{1}H NMR (CD_2Cl_2, 200 MHz, 298 K): δ = 7.9–7.6 (m, 20H, phenyl), 5.7 (s, 3H, CH), 2.7 (s, 9H, CH_3), 2.4 (s, 9H, CH_3).

1: 1 g (1.18 mmol) of **2** was suspended in 10 mL of ethanol under argon. A solution of 179 mg (4.7 mmol) of $NaBH_4$, in 5 mL ethanol was then gradually added. After a short time gas-evolution occurred and an off-white solid was formed. This was filtered off, washed with ethanol and methanol successively and dried under high vacuum. Yield: 339.5 mg (71%). Satisfactory C,H,N analyses. IR (RbI): $\tilde{\nu}$(B–H) = 2532 cm^{-1}(s), $\tilde{\nu}$(Rh–H) = 2035 cm^{-1}(vs), ^{1}H NMR (CD_2Cl_2, 250 MHz, 273 K): δ = 5.82 (s, 3H, CH), 2.36 (s, 9H, CH_3), 2.13 (s, 9H, CH_3), −12.76 (d, 4H, Rh–H), ^1J(Rh,H) = 18.1 Hz. ^{11}B NMR (80.2 MHz, CD_2Cl_2, 298 K): δ = − 27.7 (vs. $B(OMe)_3$) ^1J(B,H) = 105 Hz; ^{103}Rh NMR (CD_2Cl_2, 12.6 MHz, 253 K): δ = 805 (Ξ = 3.16 MHz). The compound **1** can also be prepared starting from **3** using the above method. However, it is obtained in lower yield (ca. 20%) and is less pure.

Received: December 27, 1989 [Z 3704 IE]
German version: *Angew. Chem. 102* (1990) 573

[1] G. J. Kubas, R. R. Ryan, B. I. Swanson, P. J. Vergamini, H. J. Wasserman, *J. Am. Chem. Soc. 106* (1984) 451.
[2] R. H. Morris, J. F. Sawyer, M. Shiralian, J. D. Zubowski, *J. Am. Chem. Soc. 107* (1985) 5581.
[3] R. H. Crabtree, M. Lavin, L. Bonneviot, *J. Am. Chem. Soc. 108* (1986) 4032.
[4] S. May, P. Reinsalu, J. Powell, *Inorg. Chem. 19* (1980) 1582.
[5] D. G. Hamilton, R. H. Crabtree, *J. Am. Chem. Soc. 110* (1988) 4126; C. Ammann, F. Isaia, P. S. Pregosin, *Magn. Reson. Chem. 26* (1988) 236; F. A. Cotton, R. L. Luck, *Inorg. Chem. 28* (1989) 8.
[6] L. Müller, *J. Am. Chem. Soc. 101* (1979) 4481.
[7] J. A. Cabeza, B. E. Mann, C. Brevard, P. M. Maitlis, *J. Chem. Soc. Chem. Commun.* 1985, 65.
[8] R. Benn, A. Rufińska, *Magn. Reson. Chem. 26* (1988) 895.
[9] M. R. Bendall, D. T. Pegg, D. M. Doddrell, *J. Magn. Reson. 52* (1983) 81; A. Bax, R. H. Griffey, B. L. Hawkins, *ibid. 55* (1983) 301.
[10] D. G. Hamilton, X. Luo, R. H. Crabtree, *Inorg. Chem. 28* (1989) 3198.
[11] R. S. Tanke, R. H. Crabtree, *Inorg. Chem. 28* (1989) 3444.

On the Way to Ligating Oligocyclopentadienyls: Synthesis and Preliminary Reactions of the Two Isomeric Tercyclopentadienyls and Their Transition Metal Complexes**

By *Roland Boese, Randy L. Myrabo, David A. Newman,* and *K. Peter C. Vollhardt**

While the synthesis and chemistry of homo- and heterobimetallic organometallic compounds,[1–3] often bridged by ligands[1,2] intended[3] to anchor the metals in close proximity, is well-explored, much less is known about the acyclic higher metal homologues.[2,4] Linked pairs of η^5-cyclopentadienyl (Cp) moieties,[5] as in fulvalene,[5,6] have played a significant role in these developments because of their exceptional binding ability.[7] We report a rational (and potentially generalizable) synthesis of the first "cyclopentadienologs" of fulvalene, namely the two isomers of tercyclopentadienyl,[8] their sequence-specific metal-complexation, the structure determination of two of these trimetallic products, and some preliminary ligand transfer chemistry. The intramolecular nature of the latter bodes well for catalytic applications of systems of this type.

[*] Prof. Dr. K. P. C. Vollhardt, R. L. Myrabo, Dr. D. A. Newman
Department of Chemistry, University of California, Berkeley,
and the Materials and Chemical Sciences Division
Lawrence Berkeley Laboratory
Berkeley, CA 94720 (USA)
Dr. R. Boese
Institut Für Anorganische Chemie der Universität-Gesamthochschule
Universitätsstrasse 5–7, Postfach 103764, D-4300 Essen 1 (FRG)

[**] This work was supported by the Director, Office of Energy Research, Office of Basic Energy Sciences, Materials Sciences Division of the U.S. Department of Energy under Contract DE-AC03-76SF00098. We thank Dr. *F. J. Hollander* for solving the crystal structure of **8a**.

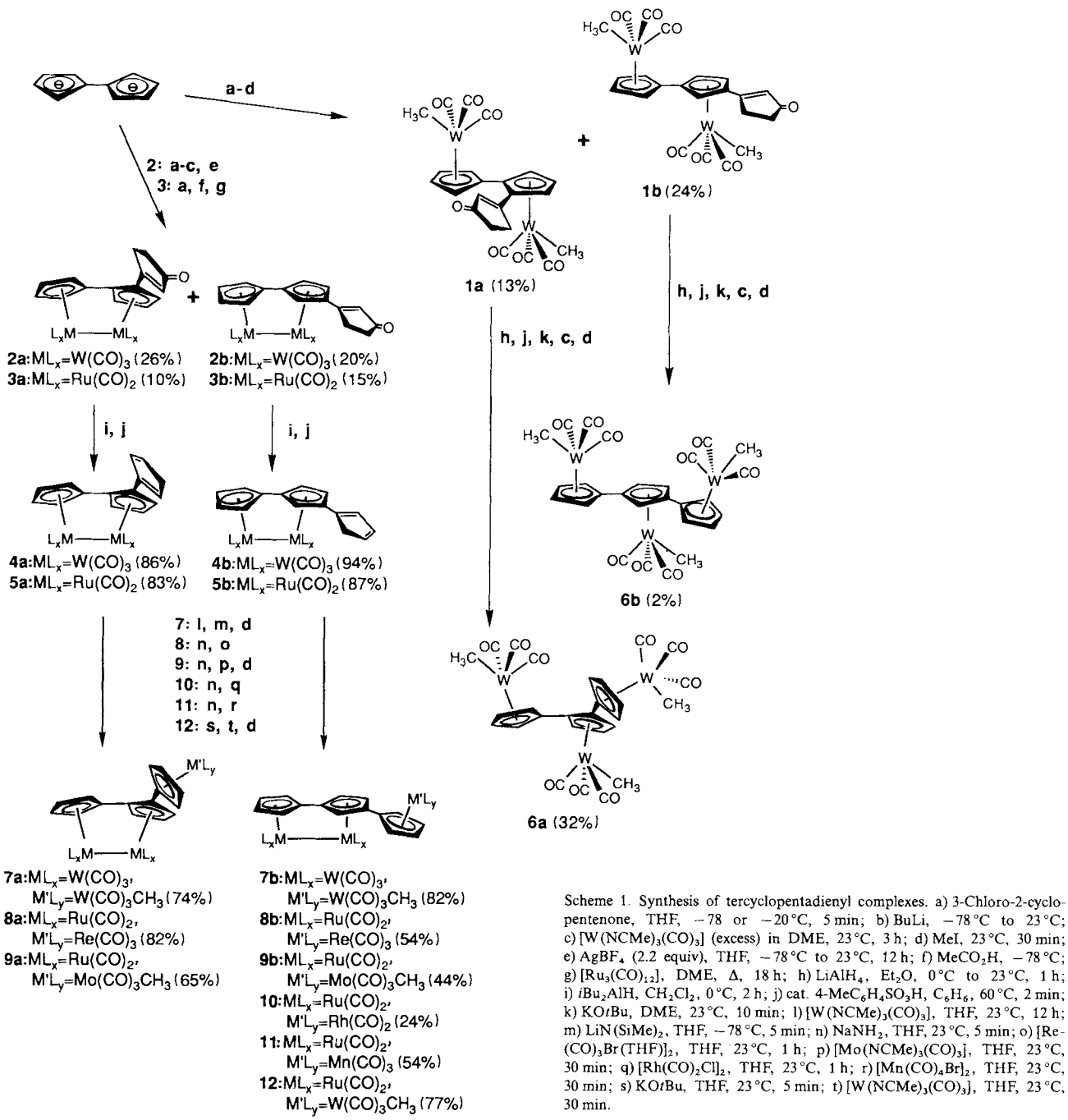

Scheme 1. Synthesis of tercyclopentadienyl complexes. a) 3-Chloro-2-cyclopentenone, THF, −78 or −20 °C, 5 min; b) BuLi, −78 °C to 23 °C; c) $[W(NCMe)_3(CO)_3]$ (excess) in DME, 23 °C, 3 h; d) MeI, 23 °C, 30 min; e) $AgBF_4$ (2.2 equiv), THF, −78 °C to 23 °C, 12 h; f) $MeCO_2H$, −78 °C; g) $[Ru_3(CO)_{12}]$, DME, Δ, 18 h; h) $LiAlH_4$, Et_2O, 0 °C to 23 °C, 1 h; i) iBu_2AlH, CH_2Cl_2, 0 °C, 2 h; j) cat. 4-$MeC_6H_4SO_3H$, C_6H_6, 60 °C, 2 min; k) KO*t*Bu, DME, 23 °C, 10 min; l) $[W(NCMe)_3(CO)_3]$, THF, 23 °C, 12 h; m) $LiN(SiMe_2)$, THF, −78 °C, 5 min; n) $NaNH_2$, THF, 23 °C, 5 min; o) $[Re(CO)_3Br(THF)]_2$, THF, 23 °C, 1 h; p) $[Mo(NCMe)_3(CO)_3]$, THF, 23 °C, 30 min; q) $[Rh(CO)_2Cl]_2$, THF, 23 °C, 1 h; r) $[Mn(CO)_4Br]_2$, THF, 23 °C, 30 min; s) KO*t*Bu, THF, 23 °C, 5 min; t) $[W(NCMe)_3(CO)_3]$, THF, 23 °C, 30 min.

The cornerstone of our synthetic strategy is the discovery that Cp-anions undergo efficient conjugate addition-elimination reactions[9] to 2-cyclopentenones bearing leaving groups at C3. Scheme 1 depicts the synthesis of the title compounds, starting with fulvalene dianion.[10] The respective regioisomeric components, **a** and **b**, of the intermediates **1**–**3**[11] were separated by chromatography and then converted independently into the desired target compounds **6**–**12**.

A 1,1′:3′,1″- and a 1,1′:2′,1″-tercyclopentadienyl compound (**7b** and **8a**, respectively) have been characterized crystallographically (Figs. 1 and 2).[11] Comparison of **7b** and **8a** reveals steric inhibition of coplanarity for only the 1,1′:2′,1″-tercyclopentadienyl ligand.

An iterative synthetic alternative to that shown in Scheme 1 allows complete control of the metal sequence to be associated with the evolving oligocyclopentadienyl chain, as exemplified in Scheme 2 for the heterotrinuclear complexes **15** and **16**, starting from **13**.[6]

A prerequisite for potentially synergistic chemical behavior toward organic substrates of these systems is intramolecular metal-to-metal ligand transfer. Attempts to uncover such rearrangements has led to some remarkable observations. Thus, treatment of the cyclopentadiene intermediates **4a** and **4b** with basic D_2O [CD_3COCD_3, Et_3N, 23 °C, 2 h] resulted in regiospecific deuterium incorporation (95%) into the uncomplexed ring, a process uncomplicated by potential metal transfer along the chain.[14] Surprisingly, *complete* label scrambling between the two terminal rings occurred on conversion of [D_5]**4b** into [D_4]**7b**, whereas [D_4]**7a** was formed from [D_5]**4a** bearing deuterium only on the η^5-$(C_5D_4)W(CO)_3CH_3$ substituent to the fulvalene unit! A

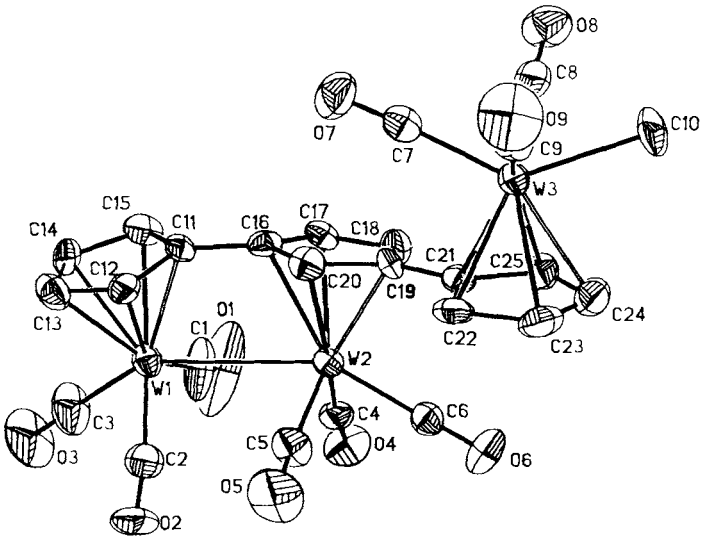

Fig. 1. Molecular structure of **7b** in the crystal (SHELXTL). Selected distances [Å] and angles [°]: W1-W2 3.266(1), W-CO (average) 1.96, W3-C10 2.324(11), W1-Cp1 (ring centroid) 1.975, W2-Cp2 1.994, W3-Cp3 2.017, C23-C24 1.375(18), C22-C23 1.459(16), C11-C16 1.453(13), C19-C21 1.468(14); C21-C22-C23 106.2(9), C22-C23-C24 109.2(10), C12-C11-C16 124.1(9), Cp2-Cp3 9.6, C15-C11-C16-C20 −179.9(1.1), C12-C11-C16-C17 153.7(1.0).

possible rationale for this divergent behavior is that the metal-anion precursor before methylation is responsible for the scrambling in [D_4] **7b** by reversible nucleophilic displacement of the metal-bound tungsten at the other terminus.[15]

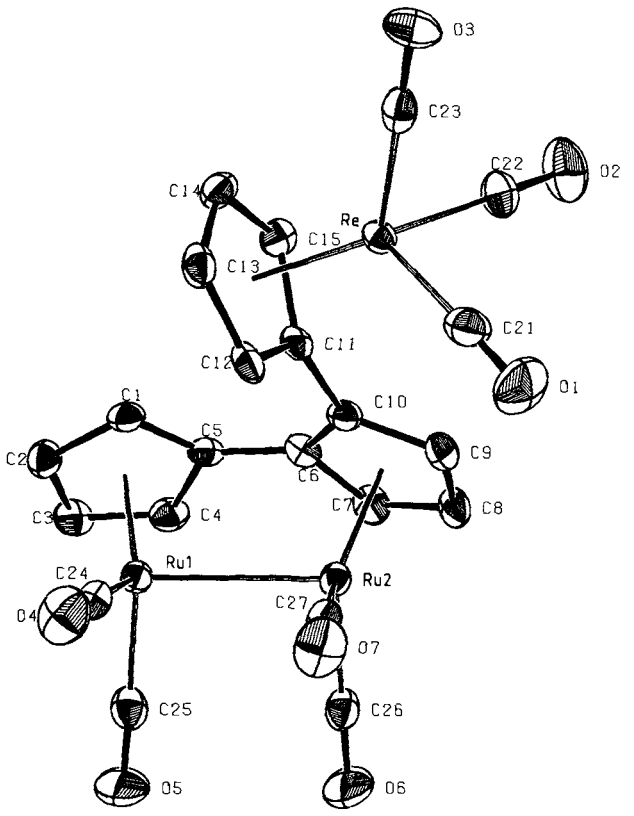

Fig. 2. Molecular structure of **8a** in the crystal (ORTEP). Selected distances [Å] and angles [°]: Ru1-Ru2 2.8190(4), Ru-CO (average) 1.86, Re-CO (average) 1.91, Ru1-Cp1 1.8981(3), Ru2-Cp2 1.8993(3), Re-Cp3 1.9531(2), C14-C15 1.397(6), C6-C10 1.457(6), C5-C6 1.436(6), C10-C11 1.491(5); C1-C5-C4 106.1(4), C8-C9-C10 109.3(4), C4-C5-C6 123.8(4), Cp2-Cp3 104.7(2), C1-C5-C6-C7 162.6(6), C4-C5-C6-C10 −154.1(6).

In contrast, in the analogous intermediate on route to [D_4]-**7a**, steric constraints prevent coplanarity (or a favorable angle) of attack of the cyclopentadienyl ring of the attached non-metal-bound anionic tungsten. In support of this mechanism, following the course of the reaction of [D_5]**4b** with [$W(NCMe)_3(CO)_3$] (23 °C, 2 h, 40% conversion) by ^{1}H-NMR spectroscopy revealed the generation of [η^5-(C_5D_4)W(D)(CO)$_3$]{η^5:η^5-(C_5H_3-C_5H_4)}$W_2(CO)_6$], [D_5]-**17b**, "exchange" of label taking place only with time (23 °C,

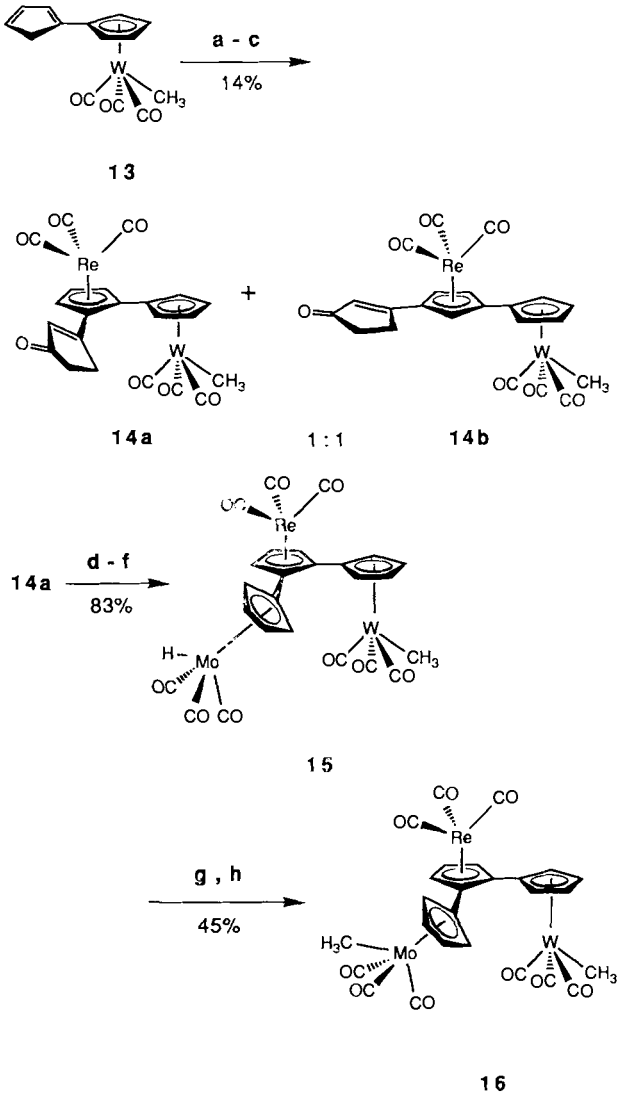

Scheme 2. Synthesis of **15** and **16**. a) NaH (3 equiv), THF, 0 °C, 20 min; b) 3-chloro-2-cyclopentenone, 0 °C, 1.5 h, then 23 °C, 30 min; c) [$Re(CO)_3(THF)_2Br$] [13], THF, Δ, 4.5 h; d) *i*Bu_2AlH, CH_2Cl_2, 0 °C, 2 h; e) 4-$MeC_6H_4SO_3H$, C_6H_6, 60 °C, 2 min; f) [$Mo(NCEt)_3(CO)_3$], THF, 23 °C, 19 h; g) KO*t*Bu, THF, 23 °C, 40 *min*; h) MeI, 23 °C, 2.5 *h*.

19 h), presumably by dedeuteration at tungsten, since scrambling was suppressed in the presence of added CH_3COOD.[16] Conversely, metalation of [D_4]**4b**$^{\ominus}$ at 23 °C led to instant label redistribution in the resulting anion between two outer Cp units. This process was sufficiently slow at −78 °C to allow access to regiochemically deuterated [D_4]**7b** by methylation, the stability of the latter ruling out methyl transfer[14] as another pathway for exchange. This

species is also stable in this regard on irradiation,[17] significantly, considering that chlorination[18] of $[D_5]$**17a** and $[D_5]$**17b** (CCl_4, THF, 23 °C, 10 min) to tetradeuteriated $[\eta^5\text{-}(C_5H_4)W(CO)_3(Cl)\{\eta^5\text{:}\eta^5\text{-}(C_5H_3\text{-}C_5H_4)\}W_2(CO)_6]$ provided results that completely paralleled those obtained in the generation of $[D_4]$ **7a** and $[D_4]$ **7b** with respect to the integrity of the position of the label.

Methyl migration could, however, be induced by reduction of the W–W bond in **7b** (1% Na–Hg, THF, 23 °C, 1 h) to furnish $[\eta^5\text{:}\eta^5\text{:}\eta^5\text{-}(C_{15}H_{11})W_3(CO)_9(CH_3)]^{2\ominus}$ in the form of two isomers bearing the methyl group at both the terminal and internal positions in a ratio of 1:2.7, respectively, changing to 1:6 on prolonged standing. Treatment with CD_3I furnished $[D_6]$**6b**, the unlabeled methyl remaining mainly (2.2:0.9) bound to the central tungsten. Isomer **7a** behaved similarly, being converted into to the corresponding dianions (1.5:1) and, ultimately, $[D_6]$**6a** (1.2:1.8). The uniquely intramolecular nature of these processes could be established by cross-over experiments involving **7a** and **7b**, respectively, admixed with their $[(\eta^5\text{-}C_5D_4)W(CO)_3(CD_3)]$-substituted counterparts. It appears that in reduced **7a** the terminal Cp-metal fragments are sufficiently mobile to allow for methyl transfer, although other details of this transformation have yet to be established.[14, 15, 19]

Experimental

2a, b: To fulvalenedilithium (1.00 mmol) in THF (15 mL) at −20 °C under nitrogen was added 3-chloro-2-cyclopentenone (116.5 mg, 1.00 mmol). The resulting dark brown mixture was cooled to −78 °C and treated with BuLi/hexane (0.59 mL, 1.70 M, 1.00 mmol). After warming to room temperature, a DME (10 mL) slurry of $[W(NCMe)_3(CO)_3]$ (821 mg, 2.10 mmol) was added. After three hours' stirring, the solution was cooled to −78 °C and allowed to react with a suspension of $AgBF_4$ (428 mg, 2.20 mmol) in THF (5 mL). Once the mixture had been allowed to slowly warm to room temperature, it was preadsorbed on silica gel. Chromatography with acetone/CH_2Cl_2 as eluent [gradient 1:19 to 1:4] afforded two major purple bands, **2a** (198 mg, 25.6%), followed closely by **2b** (154 mg, 19.9%).

4b: To a cooled (0 °C) CH_2Cl_2 (2.5 mL) slurry of **2b** (19.9 mg, 0.0269 mmol) was added a 1 M solution of diisobutylaluminum hydride (0.0403 mmol) in CH_2Cl_2. The resulting purple mixture was stirred for 2 h at 0 °C and then quenched with 10% aq. NH_4Cl (1 mL). The organic phase was filtered through alumina, the alumina washed with acetone, and the solvents removed to yield the cyclopentenol as a mixture of diastereomers (19.1 mg, 95%). A solution of this mixture (72 mg, 0.097 mmol) in benzene (20 mL) was added to a warm (60 °C) benzene solution (70 mL) of *p*-toluenesulfonic acid monohydrate (2.3 mg, 0.012 mmol). After stirring for 3 minutes, the acid was neutralized with saturated $NaHCO_3$ (2 × 35 mL). Filtration through alumina and removal of solvents yielded **4b** (70 mg, 99%) as a mixture of diene isomers.

7b: A solution of **4b** (64 mg, 0.088 mmol) and $W(NCMe)_3(CO)_3$ (69 mg, 0.176 mmol) in THF (12 mL) was stirred for 12 h under nitrogen. The mixture was cooled (−78 °C), treated with 0.1 M $LiN[SiMe_3]_2$ (0.118 mmol) in THF, and then with methyl iodide (30.2 mg, 0.214 mmol). The product was purified by chromatography (silica, acetone/hexane 1:3) to yield crystalline **7b** (73 mg, 82%).

Received: December 27, 1989 [Z 3706 IE]
German version: *Angew. Chem. 102* (1990) 589

CAS-Registry Numbers:
1a, 126541-40-0; **1b**, 126541-41-1; **2a**, 126541-38-6; **2b**, 126504-20-9; **2b** (precursor alcohol) (isomer 1), 126504-21-0; **2b** (precursor alcohol) (isomer 2), 126638-17-3; **3a**, 126504-25-4; **3b**, 126504-26-5; **4a** (isomer 1), 126504-27-6; **4a** (isomer 2), 126504-43-6; **4b** (isomer 1), 126504-22-1; **4b** (isomer 2), 126504-42-5; **5a** (isomer 1), 126504-28-7; **5a** (isomer 2), 126504-44-7; **5b** (isomer 1), 126504-29-8; **5b** (isomer 2), 126504-45-8; **6a**, 126504-37-8; **6b**, 126504-36-7; **7a**, 126541-39-7; **7b**, 126504-23-2.

[1] a) H. A. Jenkins, S. J. Loeb, D. W. Stephan, *Inorg. Chem. 28* (1989) 1998; b) L. B. Kool, M. Ogasa, M. D. Rausch, R. D. Rogers, *Organometallics 8* (1989) 1785; c) R. H. Fong, W. H. Hersh, *J. Am. Chem. Soc. 109* (1987) 2843; d) P. Johnston, G. J. Hutchings, L. Denner, J. C. A. Boeyens, N. J. Coville, *Organometallics 6* (1987) 1292; e) A. Vogler, A. H. Osman, H. Kunkely, *Inorg. Chem. 26* (1987) 2337.

[2] R. J. Puddephatt, *Chem. Soc. Rev. 12* (1983) 99.

[3] Examples of the failure of this concept are provided by the bridging phosphido group, see a) S.-G. Shyu, M. Calligaris, G. Nardin, A. Wojcicki, *J. Am. Chem. Soc. 109* (1987) 3617; b) N. M. Doherty, G. Hogarth, S. A. R. Knox, K. A. Macpherson, F. Melchior, A. G. Orpen, *J. Chem. Soc. Chem. Commun. 1986*, 540.

[4] a) S. J. Davies, J. A. K. Howard, R. J. Musgrove, F. G. A. Stone, *Angew. Chem. 101* (1989) 613; *Angew. Chem. Int. Ed. Engl. 28* (1989) 624; b) M. A. Ciriano, S. Sebastian, L. A. Oro, A. Tiripicchio, M. Tiripicchio Camellini, F. J. Lahoz, *ibid. 100* (1988) 406 and *27* (1988) 402; c) A. L. Balch, L. A. Fossett, M. M. Olmstead, P. E. Reedy, Jr., *Organometallics 7* (1988) 430; d) P. Braunstein, C. de Meric de Bellefon, M. Ries, *ibid. 7* (1988) 332.

[5] a) P. Härter, G. Bogoth, E. Herdtweck, J. Riede, *Angew. Chem. 101* (1989) 1058; *Angew. Chem. Int. Ed. Engl. 28* (1989) 1008; b) T. J. Lynch, M. C. Helvenston, A. L. Rheingold, D. L. Staley, *Organometallics 8* (1989) 1959; c) M.-H. Desbois, D. Astruc, J. Guillin, F. Varret, A. X. Trautwein, G. Villeneuve, *J. Am. Chem. Soc. 111* (1989) 5800; d) W. L. Bell, C. J. Curtis, A. Miedaner, C. W. Eigenbrot, Jr., R. C. Haltiwanger, C. G. Pierpont, J. C. Smart, *Organometallics 7* (1988) 691; e) U. T. Mueller-Westerhoff, *Angew. Chem. 98* (1986) 700; *Angew. Chem. Int. Ed. Engl. 25* (1986) 702; f) C. Riekar, G. Ingram, P. Jaltner, H. Schottenberger, K. E. Schwarzhans, *J. Organomet. Chem. 381* (1990) 127.

[6] M. A. Huffman, D. A. Newman, M. Tilset, W. B. Tolman, K. P. C. Vollhardt, *Organometallics 5* (1986) 1926, and references therein.

[7] a) D. B. Jacobsen, B. S. Freiser, *J. Am. Chem. Soc. 107* (1985) 7399; b) H. A. Skinner, J. A. Connor, *Pure Appl. Chem. 57* (1985) 79; c) C. D. Hoff, *J. Organomet. Chem. 282* (1985) 201.

[8] The only precedence for these ligands is found in ferrocene oligomers a) E. W. Neuse in C. E. Carraher, Jr., J. E. Sheats, C. U. Pittman, Jr. (Eds.): *Advances in Organometallic and Inorganic Polymer Science*, Marcel Dekker, New York 1982, p. 3; b) M. D. Rausch, *Pure Appl. Chem. 30* (1972) 523.

[9] E. Breitmaier, F.-W. Ullrich, B. Potthoff, R. Böhme, H. Bastian, *Synthesis 1987*, 1.

[10] J. C. Smart, C. J. Curtis, *Inorg. Chem. 16* (1977) 1788.

[11] All new compounds were fully characterized. For example; **7b**: purple crystals, m.p. 240 °C (dec); ^1H NMR (300 MHz, CD_3COCD_3): δ = 6.22 (ddd, J = 1.8, 1.8, 2.9 Hz, 1H), 6.09 (dd, J = 1.8, 3.0 Hz, 1H), 5.75 (ddd, J = 1.8, 1.9, 2.8 Hz, 1H), 5.6–5.7 (m, 5H), 5.08 (m, 2H), 5.00 (ddd, J = 1.7, 1.7, 2.9 Hz, 1H), 0.42 [s, $J(^{183}W\text{-}^1H)$ = 3.7 Hz, 3H); IR (CH_2Cl_2): $\tilde{\nu}$ = 2011, 1967, 1927, 1882 cm^{-1}; MS: *m/z* 1010 ($M^{\oplus}$, 35), 868(70), 840(94), 782(100). Correct elemental analysis. Monoclinic space group: $P2_1/n$, a = 13.432(3), b = 7.036(2), c = 25.968(11) Å, β = 90.97(3)°, V = 2453(1) Å^3, Z = 4, μ = 148.8 cm^{-1}, empirical absorption correction; $Mo_{K\alpha}$ radiation (graphite monochromator); scan range $3° \le 2\Theta \le 50°$; 4042 reflections collected; 3304 treated as observed [$F_o \ge 3.5\sigma(F)$], R = 0.0348, R_w = 0.0310.—**8a**: Triclinic space group: $P\bar{1}$, a = 7.4479(18), b = 11.8063(23), c = 12.6793(20) Å, α = 110.618(14), β = 90.532(16), γ = 93.966(18)°, V = 1040.3(7) Å^3, Z = 2, μ = 73.3 cm^{-1}, empirical absorption correction; $Mo_{K\alpha}$ radiation (graphite monochromator); scan range $3° \le 2\Theta \le 45°$; 2709 reflections collected; 2534 treated as observed [$F_o \ge 3\sigma(F)$], R = 0.0212, R_w = 0.0258. Further details of the crystal structure investigations may be obtained from the Fachinformationszentrum, Karlsruhe, Gesellschaft für wissenschaftlich-technische Information mbH, D-7514 Eggenstein-Leopoldshafen 2 (FRG), on quoting the depository number CSD-54505, the names of the authors, and the journal citation.—**16**: yellow crystals, m.p. 142–145 °C; ^1H NMR (300 MHz, CD_3COCD_3) δ = 5.85 (dd, J = 2.0, 2.7 Hz, 1H), 5.82 (dd, J = 2.0, 2.9 Hz, 1H), 5.72 (m, 4H), 5.67 (dd, J = 2.9, 2.9 Hz, 1H), 5.62 (m, 2H), 5.50 (m, 1H), 5.43 (m, 1H), 0.48 [s, $J(^{183}W\text{-}^1H)$ = 3.5 Hz, 3H], 0.44 (s, 3H); IR (Et_2O): $\tilde{\nu}$ = 2027, 2016, 1937 cm^{-1}; MS: *m/z* 940 ($M^{\oplus}$, 6), 896(28), 884(48), 868(53), 854(56), 840(72), 826(61), 812(72), 798(75), 770(44), 754(68), 728(63), 698(55), 670(80), 658(88), 57(100). For the pairs of regioisomers **1a, b**, **2a, b**, **3a, b**, and their respective derivatives, the connectivity of the three rings (1,1′:3′,1″ versus 1,1′:2′,1″) could be determined from their ^1H-NMR spectra. [6] The signals due to hydrogens located on the disubstituted ring appeared as doublets of doublets, whose coupling constants ($^3J \approx$ 2.9 Hz and $^4J \approx$ 1.9 Hz) allowed the connectivity to be determined. [12] In several cases these results were confirmed by NOE studies.

[12] P. Johnston, M. S. Loonat, W. L. Ingham, L. Carlton, N. J. Coville, *Organometallics 6* (1987) 2121.

[13] D. Vitali, F. Calderazzo, *Gazz. Chim. Ital. 102* (1972) 587.

[14] a) P. E. Garrou, *Adv. Organomet. Chem. 23* (1984) 95; b) H. Werner, *ibid. 19* (1981) 155.

[15] C. P. Casey, C. R. Cyr, R. L. Anderson, D. F. Marten, *J. Am. Chem. Soc. 97* (1975) 3053.

[16] E. J. Moore, J. M. Sullivan, J. R. Norton, *J. Am. Chem. Soc. 108* (1986) 2257.

[17] D. B. Pourreau, G. L. Geoffroy, *Adv. Organomet. Chem. 24* (1985) 249.

[18] a) M. P. Castellani, D. R. Tyler, *Organometallics 8* (1989) 2113; b) N. W. Hoffman, *Inorg. Chim. Acta. 88* (1984) 59.

[19] W. E. Geiger, N. G. Connelly, *Adv. Organomet. Chem. 24* (1985) 87.

Solid-State NMR Studies of the Structure and Reactivity of Metakaolinite**

By *João Rocha* and *Jacek Klinowski**

Although the kaolinite-mullite reaction series, one of the most important in the entire field of ceramic technology, has been studied for more than 100 years,[1] many questions are still unanswered. The most important are the structure of metakaolinite and the relationship between the various high-temperature phases, whose solution would help to explain the remarkable reactivity of metakaolinite, the starting material for the synthesis of important solids such as zeolites, ultramarine, chinaware, cements and ceramics. We have studied this reaction series using high-resolution ^{27}Al and ^{29}Si solid-state NMR with magic-angle spinning (MAS). Several similar studies have been published,[2-6] but since they fail to provide details of the important NMR parameters used for the acquisition of spectra, it is impossible to evaluate their usefulness.

Samples of kaolinite with different degrees of crystallinity: Cornish (sample 1) and Brazilian (sample 2), with Hinckley Indices[7] of 1.24 (highly crystalline) and 0.42 (poorly crystalline) were calcined in air for 1 h at temperatures in the range 400–1000 °C at 50 °C intervals (bed depths of 6–7 mm). In another experiment a sample of kaolinite was calcined for 24 h at 600 °C and then treated with 1 M KOH at 80 °C for 2 hours.

Kaolinite exhibits one ^{29}Si resonance at $\delta = -91.5$, assigned to a Q^3 Si environment,[1,6] and one ^{27}Al resonance at ca. $\delta = 0$, assigned to hexacoordinate Al (see Fig. 1a). NMR shows the presence of short-range order in metakaolinite and some differences in the dehydroxylation process of kaolinites with different degree of crystallinity. We have been able to resolve clearly, for the first time, three ^{29}Si MAS NMR signals, centered at $\delta = -91.5$, -96.7 and -100.5 in samples of poorly and highly crystalline kaolinite heated at 480 °C and 500 °C, respectively (Fig. 2). These spectra and the spectra of kaolinite treated at 550–900 °C can be simulated in terms of a minimum of five resonances centered at $\delta = -91.5$, -96.7, -100.5, -103.4 and -107.7 (Fig. 2). The presence of fine structure in the ^{29}Si NMR spectra of metakaolinite has been claimed,[5-6] but we are not satisfied that their presence has been convincingly demonstrated; in one case the argument relied on resolution enhancement. Our saturation recovery experiments show that the ^{29}Si spin-lattice relaxation time is about 17 s. However, most published results were obtained using recycle times of 2–5 s, and it is likely that some of the component signals in the spectrum of metakaolinite are saturated under these conditions.

In the temperature range of 480 to 920 °C metakaolinite shows three resolved ^{27}Al resonances at ca. $\delta = 0$, 28 and 57 assigned to hexa-, penta-[8,9] and tetracoordinate Al, respectively. The treatment of metakaolinite with KOH produces dramatic changes in the intensities of the signals due to penta- and hexacoordinate Al. The hexa-:penta-:tetracoordinate Al intensity ratios in untreated and treated metakaolinite are 0.6:1:1 and 0.1:0.4:1, respectively, showing that the treatment converts some penta- and hexacoordinate Al into tetracoordinate. Atomic absorption measurements reveal

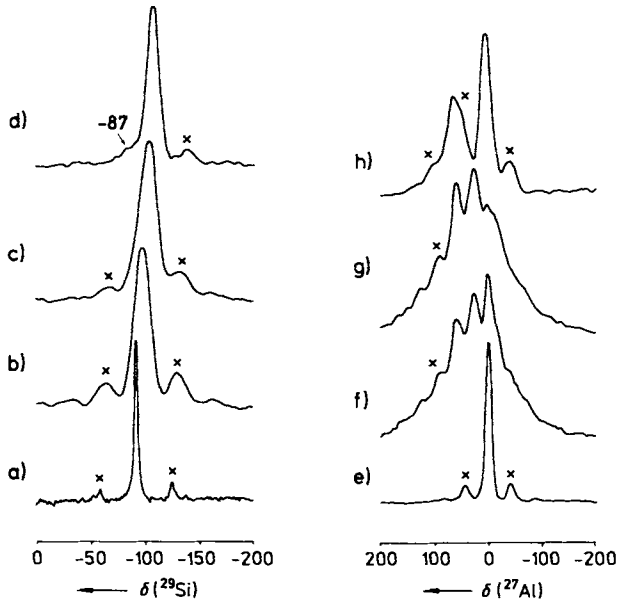

Fig. 1. ^{29}Si (left) and ^{27}Al MAS NMR (right) spectra of sample 1 (a) and e), $T = 20$ °C] and samples prepared from it by thermal treatment at $T = 550$ [(b) and (f)], 800 [(c) and (g)] and 1000 °C [(d) and (h)]. Spectra (a)–(c), and (e), (g) and (h) are characteristic of both kaolinites; spectra (d) and (f) are for the highly crystalline sample 1. ^{29}Si spectra (79.5 MHz) were measured with a Bruker MSL-400 multinuclear spectrometer. An Andrew-Beams probehead was used with rotors spinning at 3 kHz with air as the driving gas. 50°radiofrequency pulses were applied with a 30 s recycle delay. ^{29}Si chemical shifts δ relative to external tetramethylsilane (TMS). ^{27}Al MAS NMR spectra were measured at 104.2 MHz with very short and powerful (0.6 μs, equivalent to 9° pulse angle) rf pulses and a 0.2 s recycle delay. Rotors were spun in air at 5 kHz. Chemical shifts δ relative to external $Al(H_2O)_6^{3\oplus}$. × denotes spinning sidebands.

that only 2.6 mol-% of the Al is dissolved during treatment, which indicates that spectral changes are due to the change of coordination of the aluminum and not to its removal from the solid. It is striking that the ^{29}Si MAS NMR spectra of treated and untreated samples are very similar, which suggests that some regions of the sample contain Al–O–Al and

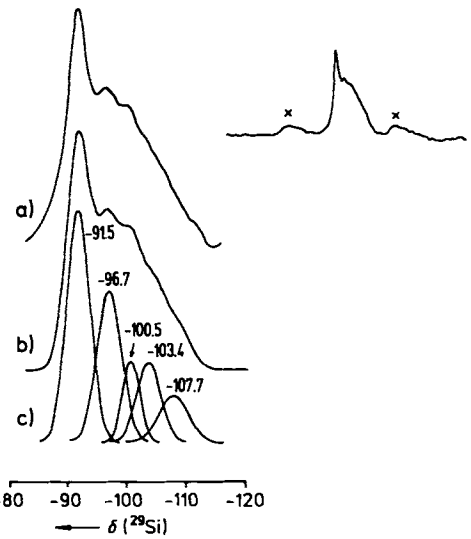

Fig. 2. (a) ^{29}Si MAS NMR spectrum characteristic of both kaolinites after thermal treatment at 480–500 °C; (b) simulated spectrum using (c) a number of Gaussian signals with chemical shifts as indicated. The spectrum on the right is from a highly crystalline kaolinite treated at 500 °C.

[*] Dr. J. Klinowski, J. Rocha
Department of Chemistry
University of Cambridge
Lensfield Road, Cambridge CB2 1EW (UK)

[**] We are grateful to E.C.C. International Limited for support and for providing kaolinite samples, to the University of Aveiro for support and to Dr. *G. Engelhardt*, Dr. *J. M. Adams* and Dr. *M. W. Anderson* for discussions.

Al–OH–Al bonds, but not Si–O–Al bonds. We also note that at temperatures as low as 480–500 °C the Q^4 Si environment is already present (at $\delta = -107.7$). These facts are consistent with the incipient separation of Al and Si.

The assignment of all ^{29}Si resonances is still an open question. The possibilities are: a) simultaneous presence of several distinct Si–O–Si bond angles; b) different Q^3 (mAl) and/or Q^4 (nAl) sites[16] with $0 < n,m < 4$ especially[10] Q^3 (1 Al) (at $\delta = -100.5$) and Q^4 (1 Al) and/or Q^4 (2 Al) (at $\delta = -96.7$); c) Si sites with associated residual OH groups.[6]

At 950–1000 °C the ^{29}Si spectra of both kaolinites exhibit an NMR signal centered at ca. $\delta = -110$ with a FWHM (full-width-at-half-maximum) of $\Delta\delta = 13.5$, narrower than the similar signal given by samples heated at lower temperatures (FWHM of $\Delta\delta = 17-20$). This suggests that cristobalite germs are likely to be present in the amorphous matrix in samples heated to high temperatures. The spectrum of sample 1, heated at 1000 °C, clearly shows the presence of an additional faint resonance from mullite at ca. $\delta = -87$. The XRD data reveal the presence in samples 1 and 2 (heated at 950–1000 °C) of mullite and γ-alumina, probes derived from sample 1 being richer in mullite.

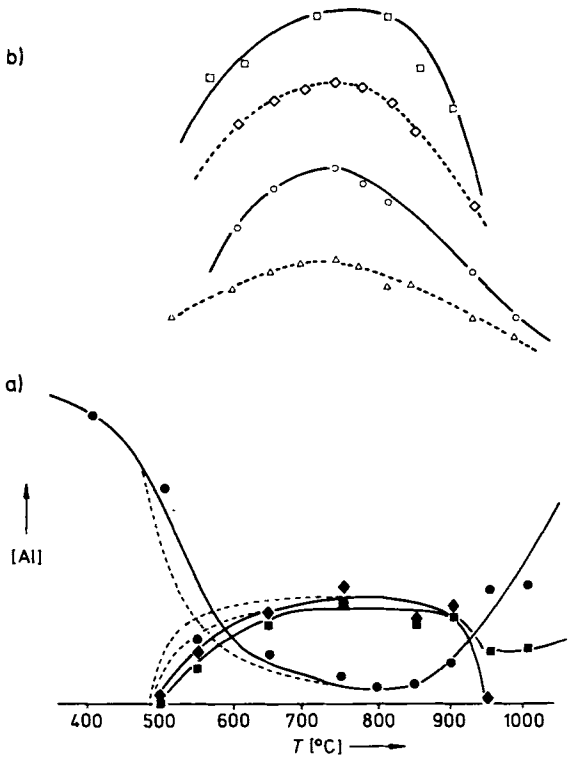

Fig. 3. (a) The change of tetra-(■), penta-(◆) and hexacoordinate (●) Al populations versus the temperature of treatment of kaolinite samples. Dotted lines show the differences between sample 2 (which follows these lines) and sample 1. Deconvolution of the spectra is described elsewhere. [13] (b) Dependence of several properties of metakaolinite on the calcining temperature. △: Variation of the compressive strength of the geomaterials obtained by hydraulic binding of metakaolinite with $Ca(OH)_2$ as chemical activator; ○: IR disorder index of the 460–470 cm^{-1} band; ◇: dissolution enthalpy of kaolinite in HF [14] and □: of the yield of zeolite X synthesis as a function of temperature [15] (in the last case the temperature of firing of the kaolinite precursor).

We suggest that metakaolinite contains: a) segregated amorphous silica regions in which Q^4 units predominate; b) a "main framework" with Q^4 (nAl) units (containing one or two tetracoordinate Al atoms) probably with a small number of associated residual (5–10% as measured by TGA at 650 °C) OH groups; c) traces of the parent kaolinite with Q^3 silicon environments and hexacoordinate Al, probably with a relatively significant amount of associated residual OH groups; d) regions of segregated amorphous alumina in which Al–O–Al (or Al–OH–Al) bonds are present but no Si–O–Al bonds; e) regions where silicon atoms *may* be associated with some residual OH groups; f) penta-coordinate sites, acting as structural defects, randomly and widely distributed in all regions, with a significant number of associated residual OH groups.

Figure 3a shows the variation in the three ^{27}Al populations, monitored by NMR as a function of temperature (a plot of Al occupancy as a function of the degree of dehydroxylation gives a similar plot, Figure 3b) which is compared with the temperature dependence of several known properties of metakaolinite. All the curves go through a maximum at 750–800 °C. Similar curves are obtained for the temperature dependence of the electrical conductivity of solutions of metakaolinite in HF extrapolated to zero time, of the specific initial dissolution rate of metakaolinite in HF,[11] and of the point of zero charge of $H^{\oplus}$-kaolinite/metakaolinite.[12]

It is interesting to consider the changes in the three Al populations in the light of published data. The reactivity of metakaolinite is at a maximum at 750–800 °C when the population of hexacoordinate Al is at a minimum and tetra- and pentacoordinate populations at a maximum. As pentacoordinate Al is a transition state characteristic of the temperature domain in which metakaolinite is metastable, one is tempted to choose this coordination as the best measure of the remarkable chemical reactivity of metakaolinite. On the other hand, the reactivity can only be fully understood in terms of the coexistence of several kinds of regions. It is thus essential that many early literature experiments be repeated and the results discussed in terms of the concepts described above. This work is now in progress.

Received: December 4, 1989 [Z 3667 IE]
German version: *Angew. Chem. 102* (1990) 539

[1] H. Le Chatelier, *Bull. soc. franç. minéral., 10* (1887) 208.
[2] S. Kormaneni, C. A. Fyfe, G. J. Kennedy, *Clay Minerals, 20* (1985) 327.
[3] T. Watanabe, H. Shimizu, K. Nagasawa, A. Masuda and H. Saito, *Clay Miner. 22* (1987) 37.
[4] J. Sanz, A. Madani, J. M. Serratosa, J. S. Moya, S. Aza, *J. Am. Ceram. Soc. 71* (1988) C418.
[5] J. F. Lambert, W. S. Millman, J. J. Fripiat, *J. Am. Chem. Soc. 111* (1989) 3517.
[6] R. H. Meinhold, K. J. D. Mackenzie, I. W. M. Brown, *J. Mat. Sci. Lett., 4* (1985) 163.
[7] D. N. Hinckley, *Clays and Clay Miner. Proc. Conf. 11* (1963) 229.
[8] E. Lippmaa, A. Samoson, M. Mägi, *J. Am. Chem. Soc. 108* (1986) 1730.
[9] J. P. Gilson, C. Edwards, A. Peters, R. Koppuswamy, R. F. Wormsbecher, T. G. Roberie, M. P. J. Shatlock, *J. Chem. Soc. Chem. Commun. 1987*, 91.
[10] G. Engelhardt, D. Michel, *High-Resolution Solid-State NMR of Silicates and Zeolites*, Wiley, New York 1987.
[11] M. Murat, M. Driouche, *Clay Miner. 23* (1988) 55.
[12] M. Tschapek, L. Tcheichvili, C. Wasowski, *Clay Miner. 10* (1974) 219.
[13] J. Rocha, J. Klinowski, *Phys. Chem. Miner.*, in press.
[14] A. Bachiorrini, M. Murat, *C.R. Acad. Sc. Paris, Ser. 2 303* (1986) 1783.
[15] Br. Pat. 980 891 (1965), Union Carbide Corp.
[16] The $Q^{(n)}$ nomenclature defines the number of Si-O-Si bridges that an SiO_4 unit takes part in. For example see H. Eckert, *Angew. Chem. Int. Ed. Engl. Adv. Mater. 28* (1989) 1723; *Angew. Chem. Adv. Mater. 101* (1989) 1763; *Adv. Mater. 1989*, 423. Q^a (b Al) signifies an SiO_4 group which is bound via O atoms to b Al atoms and (a–b) other Si atoms.

New Chiral Auxiliaries for Enolate Alkylations**

By *Kyu-Sung Jeong, Kevin Parris, Pablo Ballester,* and *Julius Rebek, Jr.**

Asymmetric transformations are the concern of modern synthetic chemistry, and chiral auxiliaries are one means by which high stereoselection can be achieved.[1] We recently introduced a system which shows exceptional selectivity in cycloaddition reactions;[2] here we demonstrate its applicability in alkylation reactions.

The molecular skeleton of the new auxiliaries derives from the commercially available Kemp triacid **1**.[3] Its imide acid chloride **2a**[4] readily acylates amines or alcohols. For example, the amide **2b** (m.p. 113–115 °C) was obtained from **2a** and (*S*)-1-phenylethylamine, and the ester **2d** (m.p. 160–162 °C) from **2a** and (*S*)-1-naphthylethanol, each in high yield (87 and 70%, respectively).[5] The esters **2c** and **2e** have been described in detail elsewhere[4] (Scheme 1).

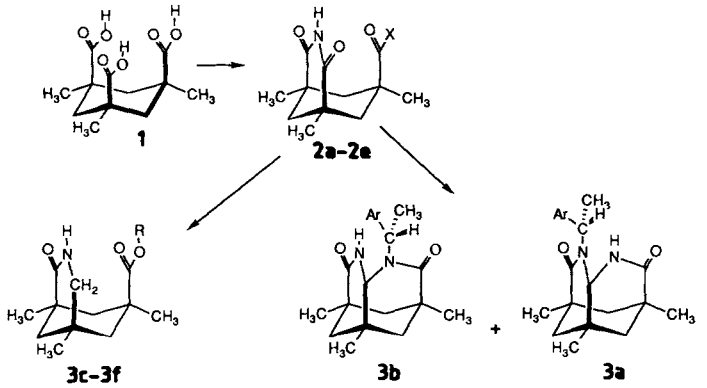

Scheme 1. **2a**, X = Cl; **2b**, X = (*S*)-NH-CH(CH$_3$)C$_6$H$_5$; **2c**, X = OMe; **2d**, X = (*S*)-O-CH(CH$_3$)-2-naphthyl; **2e**, X = O-CH$_2$CH$_2$-2-naphthyl; **3c**, R = H; **3d**, R = Me; **3e**, R = 2-naphthyl; **3f**, R = CH$_2$-CH$_2$-2-naphthyl. Ar = phenyl.

Reduction of **2b** (NaBH$_4$/EtOH, 0 °C) followed by acid treatment (*p*-TsOH/CH$_2$Cl$_2$) gave the tricyclics **3a** and **3b** as an easily separable mixture of diastereomers [flash chromatography; **3a** (55%, m.p. 107–109 °C), **3b** (34%, m.p. 187–189 °C)]. The structure of **3b**, established by X-ray crystallography,[6] features the N–H bond near the asymmetric microenvironment. The methyl ester **2c** was reduced, firstly with NaBH$_4$/EtOH and then with Et$_3$SiH/CF$_3$CO$_2$H, to give the bicyclic lactam **3d** (m.p. 141–143 °C). Saponification, activation (SOCl$_2$), then coupling with β-naphthol gave **3f** (m.p. 82–84 °C). A parallel sequence of reductions afforded **3f** from **2e**, and the *optically active* **3c** was obtained from **2d**.

The tricyclic compound **3b** proved to be a most effective auxiliary for asymmetric alkylation reactions. Acylation of **3b** (NaH/RCH$_2$COCl/THF) furnished the propionyl and the 3-phenylpropionyl derivatives **4a** and **4b**, respectively. Deprotonation (LDA/THF, −78 °C) and alkylation of **4a** with benzyl bromide (−78 °C, 10 min → 0 °C, 3–5 h) *gave a single diastereomer* (**5**) (Scheme 2). Parallel alkylation of **4b** with MeI *gave only the other diastereomer* (**6**). With 500-MHz NMR and HPLC as assays, the diastereoselectivity was judged to be at least 200:1. Regeneration of the alkylation products as optically active carboxylic acids[7] with simultaneous recovery of the auxiliaries can be easily achieved using Evans' procedure[8] (LiOH/H$_2$O$_2$).

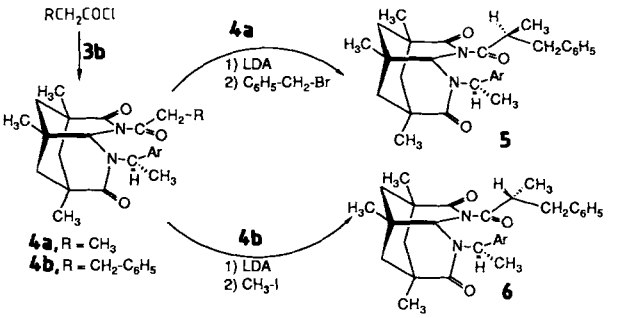

Scheme 2. Ar = phenyl; LDA = lithium diisopropylamide.
5 → (*S*)-C$_6$H$_5$-CH$_2$-CH(CH$_3$)-COOH + **3b** (CH$_3$ = R)
6 → (*R*)-C$_6$H$_5$-CH$_2$-CH(CH$_3$)-COOH + **3b** (CH$_2$-C$_6$H$_5$ = R)

The alkylation results are summarized in Table 1. A comparison of the reactions of the diastereomers **3a** and **3b**, clearly reveals that both the asymmetry of the cyclohexyl moiety as well as that of the α-phenylethyl moiety contributes to the selectivity. An X-ray crystallographic study[6] of the alkylation product of **4b** (No. 5) established its structure as shown in **6**. The product of entry No. 3 was also obtained in suitable form for crystallographic analysis and the structure was established as **7**.

Table 1. Alkylation of enolate derivatives (cf. **8**) from which the acyl derivatives were obtained by lithiation. E = electrophile. The products still contain the auxiliary compound.
R-CH$_2$-COCl → R-CHE-COOH, R = Me, E = PhCH$_2$ or R = PhCH$_2$, R = Me

No.	R	Auxil. cpd.	Acyl deriv.	EX	Product	Diast. ratio	Yield [%]
1	Me	**3a**		PhCH$_2$Br		63:37	76
2	Me	**3b**	**4a**	PhCH$_2$Br	**5**	>99:1	63
3	Me	**3e**		PhCH$_2$Br	**7**	>99:1	56
4	PhCH$_2$	**3a**		MeI		>99:1	84
5	PhCH$_2$	**3b**	**4b**	MeI	**6**	>99:1	64
6	PhCH$_2$	**3e**		MeI		98:2	73

The efficacy of the new systems is demonstrated by their control of electrophile approach to the enolate system. The extended aromatic nucleus in these structures, shown in the

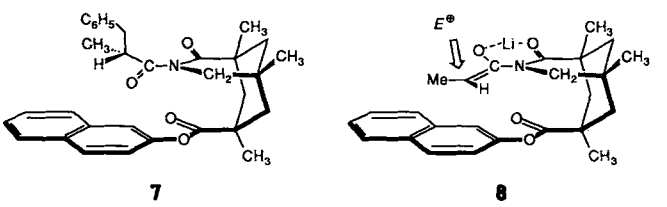

enolate **8**, provides an effective barrier to external reagents, while Li$^{\oplus}$-chelation fixes the configuration of the enolate.

[*] Prof. Dr. J. Rebek, Jr., K.-S. Jeong, K. Parris, P. Ballester
Department of Chemistry, University of Pittsburgh,
Pittsburgh, PA 15260 (USA)
and
Department of Chemistry, Massachusetts Institute of Technology,
Cambridge, MA 02139 (USA)

[**] Research supported by the Hoechst Celanese Co., Inc.

The configuration of the alkylation products (e.g., **6** and **7**) are fully in accord with this analysis.

In summary, chiral auxiliary compounds (**3**) of a new shape have been described, and their action can be related to the stereoelectronics of enolate alkylations. The asymmetric environment of the auxiliary compounds is so well defined in structures such as **3b** that such materials show efficiency as asymmetric protonation agents.

Received: December 13, 1989;
revised: February 16, 1990 [Z 3686 IE]
German version: *Angew. Chem. 102* (1990) 550

CAS Registry numbers:
2a, 109216-50-4; **2b**, 126295-07-6; **2c**, 126451-72-7; **2d**, 126295-08-7; **2e**, 126451-73-8; **3a**, 124223-11-6; **3b**, 124154-23-0; **3c**, 126295-09-8; **3d**, 126295-10-1; **3e**, 126451-74-9; **3f**, 126295-11-2; **4a**, 126295-12-3; **4b**, 126295-13-4; **5**, 126295-14-5; **6**, 126451-75-0; **7**, 126295-15-6; $MeCH_2COCl$, 79-03-8; $PhCH_2CH_2COCl$, 645-45-4; (*S*)-1-phenylethylamine, 2627-86-3; (*S*)-1-(2-naphthyl)ethanol, 27544-18-9; B-naphthol, 135-19-3.

[1] a) J. K. Whitesell, *Acc. Chem. Res. 18* (1985) 280; b) W. Oppolzer, *Tetrahedron 43* (1987) 1969; c) K. A. Lutomski, A. I. Meyers, in J. E. Morrison (Ed.): *Asymmetric Synthesis*, Academic Press, New York 1984, Vol. 3, Chap. 1; d) S. G. Davies, *Chem. Brit. 25* (1989) 268; e) H. Kuntz, D. Schanzenbach, *Angew. Chem. 101* (1989) 1042; *Angew. Chem. Int. Ed. Engl. 28* (1989) 1068; f) D. A. Evans, M. D. Ennis, D. J. Mathre, *J. Am. Chem. Soc. 109* (1982) 1737; g) M. Ihara, M. Takahashi, H. Niitsuma, N. Taniguchi, K. Yasui, K. Fukumoto, *J. Org. Chem. 59* (1989) 5413; h) R. Schmierer, G. Grotemeier, G. Helmchen, A. Selim, *Angew. Chem. 93* (1981) 209; *Angew. Chem. Int. Ed. Engl. 20* (1981) 207.

[2] D. P. Curran, K.-S. Jeong, T. A. Heffner, J. Rebek, Jr., *J. Am. Chem. Soc. 111* (1989) 9238.

[3] D. S. Kemp, K. S. Petrakis, *J. Org. Chem. 46* (1981) 5140. **1** is available from the Aldrich Chemical Company. For a convenient synthesis, see J. Rebek, Jr., B. Askew, M. Killoran, D. Nemeth, F.-T. Lin, *J. Am. Chem. Soc. 109* (1987) 2426.

[4] B. Askew, P. Ballester, C. Buhr, K.-S. Jeong, S. Jones, K. Parris, K. Williams, J. Rebek, Jr., *J. Am. Chem. Soc. 111* (1989) 1082.

[5] All new compounds were characterized by a full complement of high-resolution spectra (^{1}H-NMR, FT-IR, MS).

[6] Complete details of the crystallographic studies of **3b**, **6** and **7** will be published elsewhere.

[7] The (*S*)- and (*R*)-2-methyl-3-phenylpropionic acids released from **5** and **6**, respectively, were coupled to optically active 1-phenylethylamine; NMR analysis showed >99:1 enantiomeric purity.

[8] D. A. Evans, J. A. Ellman, T. C. Britton, *Tetrahedron Lett. 28* (1987) 6141.

1-Amino- and 1,3-Diaminoimidazolium Salts**

By *Helmut Link*,* *Wilhelm Klötzer*, *Eva Maria Karpitschka*, *Marc Montavon*, *Renate Müssner*, and *Nicolas Singewald*

Stepwise amination of imidazoles to give the previously unknown 1,3-diaminoimidazolium salts **3** may be accomplished with *O*-(diphenylphosphinoyl)hydroxylamine (DPH).[1,2] Some derivatives of these quaternary salts have interesting chemical and biological properties. For example, the 1,3-bis[(*p*-aminobenzylidene)amino]imidazolium salts **7** are surprisingly stable in aqueous media. In screening experiments using the animal models *Litomosoides carinii*/cotton rat and *Onchocerca gibsoni*/cattle, these salts show a high activity against filaria.[3] The latter model is best suited for the evaluation of potential drugs against the human parasite *Onchocerca volvulus*, which causes river blindness (onchocerciasis). Here we report on the synthesis of *N*-aminated imidazolium salts.

The amination of imidazole (**1a**) with sodium hydroxylamine *O*-sulfonate in water leads to a mixture of the 1-amino- and 1,3-diaminoimidazolium salts **2a** · HX and **3a**, respectively, which can be separated as their benzylidenamino derivatives **4a** and **7a**, R′ = R″ = H (Scheme 1). This amination method is also suitable for water-soluble 2-, 4-, and 5-substituted imidazoles such as 2-methyl-, 2-ethyl-, and 2-methyl-4-hydroxymethylimidazole. 2-Isopropylimidazole, 2-phenylimidazole, and 2-methylbenzimidazole can only be diaminated in very small yield by this method. We have now found that DPH is a suitable reagent for the amination of water-insoluble imidazoles. For example, the sodium salt of 2-phenylimidazole (**1b**) reacts in *N*-methylpyrrolidone with 1 molar equivalent of DPH to give 1-amino-2-phenylimidazole (**2b**; 50–70% yield after chromatography). Further amination with DPH in dichloromethane to give 1,3-diamino-2-phenylimidazolium salt **3b** proceeds in high yield (88% after conversion to the chloride with Amberlite). We also obtained product **3b**, X = Cl, in 40–50% yield by treatment of **1b** with *O*-(mesitylenesulfonyl)hydroxylamine (MSH) in tetrahydrofuran in the presence of sodium hydrogen carbonate followed by anion exchange (Amberlite).

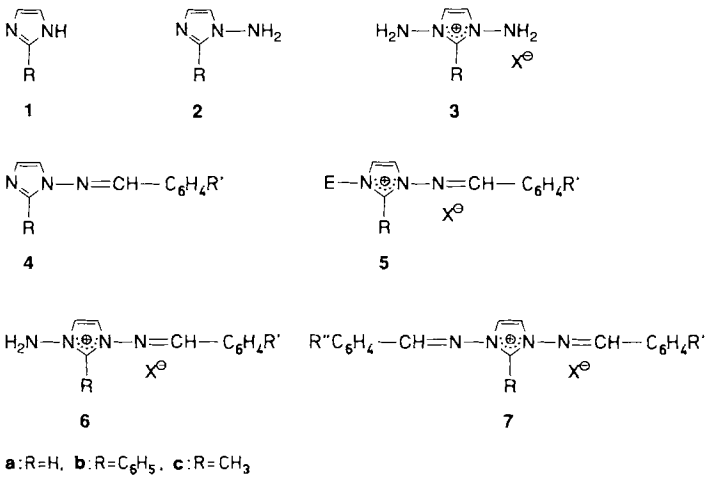

Scheme 1.

1-Amino- and 1,3-diaminoimidazolium salts may be stored at room temperature without noticeable decomposition. 1-Aminoimidazole (**2**, R = H, alkyl, phenyl) undergoes condensation with aldehydes such as *p*-dimethylaminobenzaldehyde in glacial acetic acid to give **4**, which reacts, in turn, with electrophilic reagents such as α-halo esters or benzyl halides to give **5**. Treatment of **4** with DPH results in amination to give **6**, which can be converted into **7** by reaction with aldehydes. The 1,3-bis(benzylidenamino)imidazolium salts with identical substituents R′,R″ may also be obtained directly from **3**. The stepwise condensation of **3** with two different aldehydes to give **7** (R′ ≠ R″) is also possible, but requires careful purification of the first condensation product **6**.

[*] Dr. H. Link, Dr. M. Montavon
Pharmazeutische Forschungsabteilung, F. Hoffmann-LaRoche AG
CH-4002 Basel (Switzerland)
Prof. Dr. W. Klötzer†, Dr. E. M. Karpitschka, Dr. R. Müssner, Dr. N. Singewald
Institut für Organische und Pharmazeutische Chemie der Universität
A-6020 Innsbruck (Austria)

[**] We thank Dr. *W. Arnold* (NMR), Dr. *W. Vetter* and *W. Meister* (MS), Dr. *M. Grosjean* (IR), and Dr. *A. Dirscherl* (microanalysis) for spectroscopic and analytical investigations as well as *B. Schaffner*, *U. Brombacher*, *R. Villard*, *D. Wechsler*, and *R. Schlagbauer* for synthetic work.

The C-methyl group of 2-methylimidazolium chloride (**7c**, $R' = R'' = p\text{-}NMe_2$, X = Cl) can be condensed with aldehydes and amino acetals. For example, refluxing this compound for 20 h with *p*-dimethylaminobenzaldehyde and piperidine (in molar equivalent amounts) in ethanol affords **8** in 89% yield (Scheme 2). Reaction of **7c** with *N,N*-dimethyl-

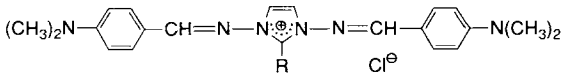

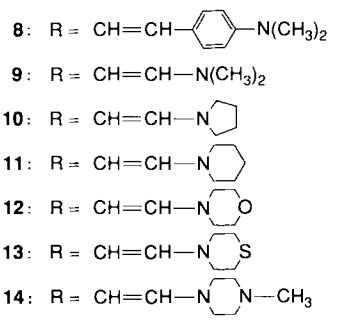

Scheme 2.

formamide diethyl acetal to give **9** requires 4 d in DMF at 50 °C; as expected, the reaction is faster with *N,N*-dimethylformamide di-*tert*-butyl acetal (1 d at room temperature). In both cases, the yield is 84–87%. Compounds **10**–**14** were obtained similarly.

In the following discussion, we wish to report on the synthesis of 2-amino derivatives of **7** (Scheme 3). 1,3-Bis(benzylidenamino)imidazolium chloride (**7a**, R′ = R″ = H, X = Cl) adds sulfur in the presence of triethylamine and pyridine. The resulting compound **15** can be methylated to give 2-(methylthio)imidazolium tetrafluoroborate (**16**) by

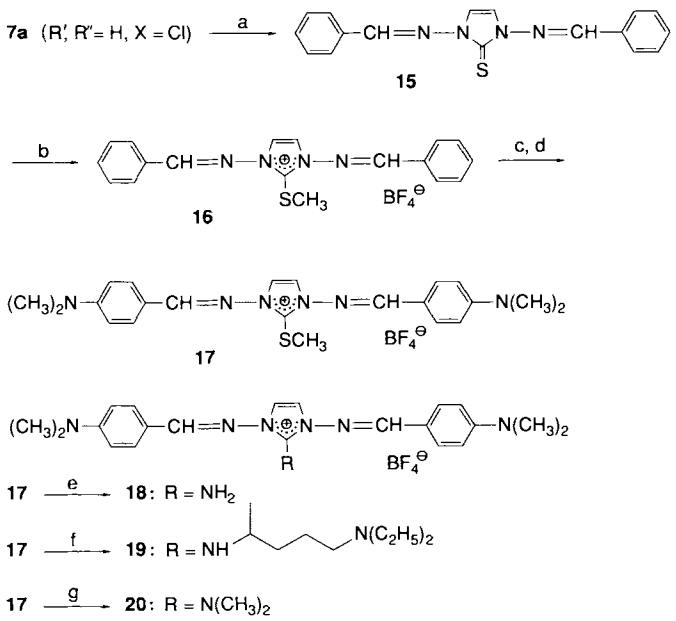

Scheme 3. a: 1.0 molar equiv. S, 1.0 molar equiv. NEt_3, Pyridine, 15 min room temperature (RT), 30 min reflux, 85% yield; b: 1.0 molar equiv. $Me_3O^{\oplus}BF_4^{\ominus}$, CH_2Cl_2, 3 h RT, 95%; c: HBF_4, steam distillation; d: 2 molar equiv. *p*-dimethylaminobenzaldehyde, 3 h RT, 75%; e: NH_3, anhydrous DMF, 71%; f: ca. 10 molar equiv. 2-amino-5-(diethylamino)pentane, CH_3CN, 24 h, RT, 50%; g: $NH(CH_3)_2$, anhydrous DMF, 70%.

treatment with Meerwein salt. At this stage in the synthesis, the substituent at position 2 can be replaced by amino groups. Subsequently, the benzylidenamino groups can be replaced by *p*-(dimethylamino)benzylidenamino groups. However, it is also possible (see Scheme 3) to eliminate benzaldehyde by steam distillation in acid medium. The resulting 1,3-diamino-2-(methylthio)imidazolium tetrafluoroborate may then be converted into **17** by treatment with *p*-(dimethylamino)benzaldehyde. Substitution of the methylthio group by ammonia or amines then leads to the desired compounds **18**–**20** (Table 1).

Table 1. Physical data for compounds **7b**, **8**, **9**, and **17**–**20**. The NMR spectra were recorded at 25 °C with TMS as standard on a 250-MHz instrument.

7b: ($R' = R'' = p\text{-}NMe_2$, X = Cl). m.p. 241 °C (dec.) (from EtOH/Et_2O). ^1H NMR ($CDCl_3$): δ = 9.23 (s, 2H), 8.94 (s, 2H), 7.79 (d, J = 9 Hz, 4H), 7.76–7.85 (m, 2H), 7.56–7.68 (m, 3H), 6.69 (d, J = 9 Hz, 4H), 3.08 (s, 12H)
7b: ($R' = R'' = p\text{-}NMe_2$, X = CH_3COO): m.p. 162–164 °C (from MeOH/Et_2O). ^1H NMR ([D$_6$]DMSO): δ = 9.02 (s, 2H), 8.80 (s, 2H), 7.8–7.9 (m, 2H), 7.6–7.7 (m, 7H), 6.82 (d, J = 9 Hz, 4H), 3.04 (s, 12H), 1.55 (s, 3H)
8: m.p. 238–240 °C (dec.) (from CH_2Cl_2/Et_2O). ^1H NMR ([D$_6$]DMSO): δ = 8.96 (s, 2H), 7.17–7.97 and 6.51–6.98 (m, 14H), 3.03 (s, 3H)
9: m.p. 246–248 °C (dec.) (from EtOH). ^1H NMR ([D$_6$]DMSO): δ = 8.79 (s, 2H), 8.34 (d, J = 13 Hz, 1H), 8.30 (s, 2H), 7.73 (d, J = 9 Hz, 4H), 6.84 (d, J = 9 Hz, 4H), 5.46 (d, J = 13 Hz, 1H), 2.9–3.4 (6H), 3.05 (s, 12H)
17: m.p. 250–253 °C (dec.) (from CH_3CN/Et_2O). ^1H NMR ([D$_6$]DMSO): σ = 8.75 (s, 2H), 8.52 (s, 2H), 7.59–7.84 (m, 4H), 6.69–6.92 (m, 4H), 3.06 (s, 12H), 2.82 (s, 3H)
18: m.p. 260 °C (dec.) (from DMF/Et_2O). ^1H NMR ([D$_6$]DMSO): δ = 8.48 (s, 2H), 7.50–7.80 (m, 6H), 6.50–6.88 (m, 4H), 2.98 (s, 12H)
19: m.p. 187–191 °C (dec.) (from MeOH/Et_2O). ^1H NMR ([D$_6$]DMSO): δ = 8.28 (s, 2H), 7.45–7.80 (m, 6H), 6.40–6.76 (m, 4H), 4.5 (br.s, 1H), 2.97 (s, 12H), 2.25–2.60 (m, 6H), 1.22–1.86 (m, 7H), 0.95 (t, 6H)
20: m.p. 248–252 °C (dec.) (from DMF/Et_2O). ^1H NMR ([D$_6$]DMSO): δ = 8.53 (s, 2H), 8.02 (s, 2H), 7.45–7.74 (m, 4H), 6.58–6.95 (m, 4H), 3.26 (s, 6H), 3.00 (s, 12H)

A large number of the 1,3-bis[(*p*-aminobenzylidene)-amino]imidazolium chorides and bromides (**7**) we prepared were only sparingly soluble in water. More soluble salts were desired for biological evaluation. Our observation that hydrogen carbonates are even less soluble prompted us to convert the chlorides and bromides via hydrogen carbonates to more soluble salts such as acetates. This salt interconversion method proved successful and avoided the necessity of interconverting the salts at the stage of the water-soluble salts **3** and **6**.

Received: December 4, 1989 [Z 3668/3669 IE]
German version: *Angew. Chem. 102* (1990) 559

CAS Registry numbers:
1b, 7164-98-9; **2b**, 26286-54-4; **3b**, 115053-15-1; **3c**, 111132-20-8; **7a**, 115053-24-2; **7b** (R′ = R″ = NMe_2, X = Cl), 111132-51-5; **7b** (R′ = R″ = NMe_2, X = CH_3COO), 111132-24-2; **8**, 126135-24-8; **9**, 115052-79-4; **10**, 126135-25-9; **11**, 115052-80-7; **12**, 115052-81-8; **13**, 115053-11-7; **14**, 126135-26-0; **15**, 118968-97-1; **16**, 115053-26-4; **17**, 115052-91-0; **18**, 126135-28-2; **19**, 115052-97-6; **20**, 115052-93-2; *p*-dimethylaminobenzaldehyde, 100-10-7; *N,N*-dimethylformamide diethyl acetal, 1188-33-6; 1-pyrrolidine carboxaldehyde, 3760-54-1; 1-piperidine carboxaldehyde, 2591-86-8; 4-morpholine carboxaldehyde, 4394-85-8; 4-thiomorpholine carboxaldehyde, 61907-20-8; 4-methyl-1-piperazine carboxaldehyde, 7556-55-0; 2-amino-5-(diethylamino)pentane, 140-80-7.

[1] E. W. Colvin, G. W. Kirby, A. C. Wilson, *Tetrahedron Lett. 23* (1982) 3835.
[2] *N*-Amination with DPH: W. Klötzer, H. Baldinger, E. M. Karpitschka, J. Knoflach, *Synthesis 1982*, 592; W. Klötzer, R. Widmann, S. Ayoub, *Sci. Pharm. 52* (1984) 46; W. Klötzer, J. Stadlwieser, J. Raneburger, *Org. Synth. 64* (1986) 96; W. Hanefeld, H.-J. Staude, *Arch. Pharm. Weinheim Ger. 320* (1987) 67; G. Laus, W. Klötzer, *Synthesis 1989*, 269.
[3] E. M. Karpitschka, W. Klötzer, H. Link, M. Montavon, R. Müssner, Swiss Patent Application 1778/85 (1985); W. Klötzer, H. Link, R. Müssner, W. Schiestl, N. Singewald, Swiss Pat. Appl. 1940/86 (1986); H. Link, Swiss Pat. Appl. 3955/86 (1986); F. Hoffmann-LaRoche AG.

Novel Diphosphinoiridium Catalysts for the Enantioselective Hydrogenation of *N*-Arylketimines

By *Felix Spindler*,* *Benoit Pugin*, and *Hans-Ulrich Blaser*

Homogeneous enantioselective hydrogenation is an important method for the synthesis of optically active compounds;[1] however, most applications are limited to Rh or Ru catalysts and to functionalized olefins or ketones.[2] And despite the reduction of imines to the corresponding amines being preparatively important,[3] only few enantioselective hydrogenations with attractive optical yields have so far been described.[4, 5] The diphosphinorhodium complexes used in these hydrogenations generally show rather low activities, even at high hydrogen pressures (>70 bar). In the present communication we describe novel diphosphinoiridium catalysts for the enantioselective hydrogenation of *N*-arylketimines, which are important intermediates in the synthesis of herbicides.[6, 7]

In the presence of a catalyst prepared in situ from bis[(1,5-cyclooctadiene)iridium chloride] $[Ir(cod)Cl]_2$ and a chiral diphosphino compound $\widehat{PP}$, imines of type **1** react with molecular hydrogen in high yields to give the corresponding anilines. Both the structure of the diphosphino compound as well as the anion strongly influence the catalyst's properties (halogen effect).

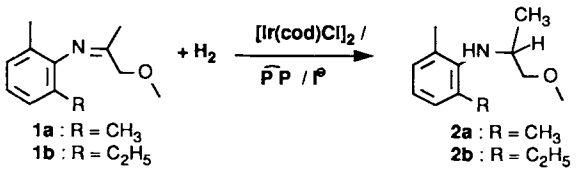

1a : R = CH_3
1b : R = C_2H_5

2a : R = CH_3
2b : R = C_2H_5

Good activities and enantioselectivities are obtained with chiral ligands which can form a conformationally flexible six- or seven-membered metallacycle (BDPP,[4a] DIOP[8] or BPPM[9]). 1,2-Diphosphino compounds (e.g. CHIRAPHOS,[10] NORPHOS[11]) give catalysts with low

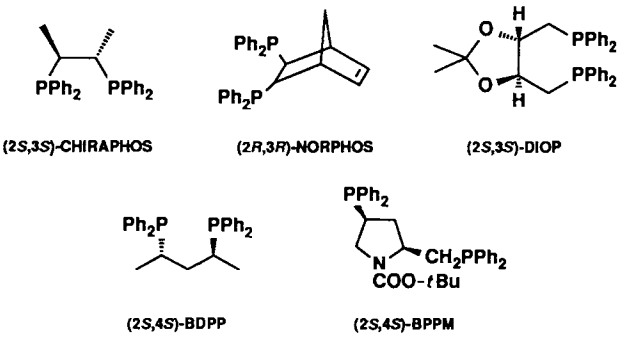

activity. A strong halogen effect is observed: the halogen-free catalytic system $[Ir(cod)_2]BF_4$/(2*S*, 3*S*)-DIOP yields the (*R*)-enantiomer of **2a** with only 4% *ee*, whereas addition of 1 equivalent of iodide leads to a considerably more active catalyst producing the (*S*)-enantiomer of **2a** with 68% *ee* (Table 1). Whether this effect is also observed with other imines was not investigated. In the in-situ preparation of the catalyst from $[Ir(cod)Cl]_2$ and DIOP the addition of $I^{\ominus}$ (less strongly $Cl^{\ominus}$, $Br^{\ominus}$) also has a positive influence on the activity and selectivity: The addition of 2 equivalents of $I^{\ominus}$ leads to an increase in the initial reaction rate from 0.2 min^{-1} to 1.8 min^{-1} (for imine **1a**), and the enantiomeric excess increases from 58% *ee* to 70% *ee* (Table 1). A significant catalyst deactivation is observed, with the iodide-containing catalyst being the less rapidly deactivated. There are indications that inactive dinuclear iridium complexes are formed, as proposed for the hydrogenation of alkenes.[12, 13]

Table 1. Enantioselective hydrogenation of imines **1** with $[Ir(cod)Cl]_2/\widehat{PP}$ to **2**[a].

Ligand $\widehat{PP}$	Imine	$I^{\ominus}$/Ir	*T* [°C]	*t* [h]	Conversion [%]	*ee*[b] [%]
(2*S*, 3*S*)-CHIRAPHOS[10]	**1a**	–	50	24	54	37 (*R*)
(2*R*, 3*R*)-NORPHOS[11]	**1a**	–	50	66	60	27 (*R*)
(2*S*, 3*S*)-DIOP[8] [c]	**1a**	–	50	48	30	4 (*R*)
(2*S*, 3*S*)-DIOP[c]	**1a**	1	18	21	91	68 (*S*)
(2*S*, 3*S*)-DIOP	**1a**	–	18	21	87	58 (*S*)
(2*S*, 3*S*)-DIOP	**1a**	2	18	21	95	70 (*S*)
(2*S*, 3*S*)-DIOP	**1b**	2	18	24	77	56 (*S*)
(2*S*, 3*S*)-DIOP[d]	**1b**	60	25	50	100	62 (*S*)
(2*S*, 4*S*)-BPPM[9]	**1a**	–	18	22	99	73 (*S*)
(2*S*, 4*S*)-BDPP[4a]	**1a**	2	18	45	49	72 (*S*)
(2*S*, 4*S*)-BDPP	**1a**	2	0	16	98	84 (*S*)

[a] Reaction conditions: 40 mmol imine, imine/catalyst 100:1, $[Ir(cod)Cl]_2$/PP 1:1.1, solvent 10 mL MeOH/10 mL benzene, $p(H_2)$ = 20 bar, $I^{\ominus}$ from tetrabutylammonium iodide. [b] *ee* determined polarimetrically [14] and ^{1}H-NMR spectroscopically [15]. [c] $Ir(cod)_2BF_4$ instead of $[Ir(cod)Cl]_2$. [d] 0.5 mol imine, imine/catalyst 10000:1, $p(H_2)$ = 100 bar; remaining reaction conditions as in [a].

The reaction conditions influence both the optical yields as well as the productivity. Lower temperatures favor higher enantiomeric excesses (72% *ee* at 18 °C, 84% *ee* at 0 °C; imine **1a** and BDPP). At normal pressure no reaction takes place. At pressures of H > 10 bar, productivities increase with pressure even though the enantioselectivities are not affected. The average turnover number at 20 bar lies in the range 100–500, under optimized reaction conditions around 10000. For the analogous rhodium complexes the average value is 100 at 70 bar H_2 and in the best case 700.

The imines **3**–**7** are further examples of substrates that can be hydrogenated with the catalyst $[Ir(cod)Cl]_2$/DIOP/2$I^{\ominus}$. Under standard conditions (cf. Table 1) the following *ee* values [%][15] are obtained: 66(**3**), 52(**4**), 16(**5**), 22(**6**), 58(**7**).

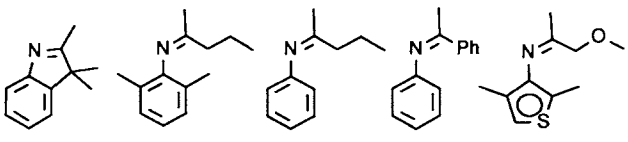

3 **4** **5** **6** **7**

Our results indicate that the conformational freedom of motion of the imino group has to be restricted (hindered rotation about the *N*-aryl bond), in order to obtain good enantioselectivities.

[*] Dr. F. Spindler, Dr. B. Pugin, Dr. H.-U. Blaser
Zentrale Forschungslaboratorien Ciba-Geigy AG
Postfach, CH-4002 Basel (Switzerland)

All the imines used (aside from **3**) consist of a mixture of *syn*- and *anti*-isomers; in the case of the imine **1a** the *anti*/*syn* ratio is 5:1 (^{1}H-NMR measurements). Since both the equilibrium *syn*-isomer $\rightleftarrows$ *anti*-isomer as well as the equilibrium imine $\rightleftarrows$ enamine proceed more rapidly than the hydrogenation (^{1}H-NMR measurements, H/D exchange with [D_4]-methanol) we conclude that the *anti*/*syn* ratio is not selectivity-determining. More detailed investigations on the elucidation of the reaction mechanism are currently under way.

Experimental

All operations were carried out under argon. A solution of $[Ir(cod)Cl]_2$ (134.4 mg, 0.2 mmol) in 10 mL of a 1:1 solvent mixture of benzene and methanol was treated with 219.7 mg (0.44 mmol) of (2*S*, 3*S*)-DIOP and, after 15 min, with 295.8 mg (0.8 mmol) of tetrabutylammonium iodide; the mixture was then stirred for a further 15 min. A separate solution of the imine **1a** (7.65 g, 40 mmol) in methanol (5 mL)/benzene (5 mL) was now prepared. The imine solution and catalyst solution were successively transferred via a steel capillary into a 50 mL steel autoclave under an inert atmosphere. The inert gas was replaced in the autoclave by hydrogen in three cycles (20 bar/normal pressure). Finally 20 bar of hydrogen were compressed into the autoclave. After completion of reaction the conversion was determined gas chromatographically and the product distilled under high vacuum. After flash chromatographic purification of the crude product **2a** (silica gel, hexane/ethyl acetate 1:1), the optical yield was determined by polarimetry[14] and ^{1}H-NMR spectroscopy[15].

Received: October 14, 1989;
revised: February 14, 1990 [Z 3581 IE]
German version: *Angew. Chem. 102* (1990) 561

CAS Registry numbers:
1a, 85385-06-4; **1b**, 118604-68-5; (*R*)-**2a**, 118604-66-3; (*S*)-**2a**, 118604-67-4; (*S*)-**2b**, 118604-70-9; $[Ir(COD)Cl]_2$, 12112-67-3; $[Ir(COD)_2]BF_4$, 35138-23-9; (2*S*, 3*S*)-chiraphos, 64896-28-2; (2*R*, 3*R*)-norphos, 71042-54-1; (2*S*, 3*S*)-diop, 37002-48-5; (*S*, 4*S*)-bppm, 61478-28-2; (2*S*, 4*S*)-bdpp, 77876-39-2.

[1] Review article: a) R. Noyori, M. Kitamura in R. Scheffold (Ed.): *Modern Synthetic Methods, Vol. 5*, Springer, Berlin 1989, pp. 115–198; b) K. Koenig in J. Morrison (Ed.): *Asymmetric Synthesis, Vol. 5*, Academic Press, New York 1985, pp. 71–101; c) L. H. Pignolet (Ed.): *Homogeneous Catalysis with Metal Phosphine Complexes*, Plenum Press, New York 1983; d) J. M. Brown, P. A. Chaloner in [1c], pp. 137–165; e) B. Heil, L. Markó, S. Törös in [1c], pp. 317–341.

[2] a) M. Kitamura, T. Ohkuma, S. Inoue, N. Sayo, H. Kumobayashi, S. Akutagawa, T. Ohta, H. Takaya, R. Noyori, *J. Am. Chem. Soc. 110* (1988) 629–631; b) T. Hayashi, N. Kawamura, Y. Ito, *Tetrahedron Lett. 29* (1988) 5969–5972; c) A. Chan, C. Landis, *J. Mol. Catal. 49* (1989) 165–173.

[3] a) K. Harada in S. Patai (Ed.): *The Chemistry of the Carbon-Nitrogen Double Bond*, Intersience, London 1970, pp. 276–293; b) P. Rylander: *Catalytic Hydrogenation over Platinum Metals*, Academic Press, New York 1967, pp. 123–138; c) K. Yamada, M. Takeda, T. Iwakuma, *Tetrahedron Lett. 22* (1981) 3869–3872.

[4] a) J. Bakos, I. Tóth, B. Heil, L. Markó, *J. Organometal. Chem. 279* (1985) 23–29; b) S. Vastag, J. Bakos, S. Törös, N. E. Takach, R. B. King, B. Heil, L. Markó, *J. Mol. Catal. 22* (1983) 283–287; c) S. Vastag, B. Heil, S. Törös, L. Markó, *Transition Met. Chem. (Weinheim, Ger.) 2* (1977) 58–59; d) J. Bakos, I. Tóth, B. Heil, G. Szalaontai, L. Párkányi, V. Fülöp, *J. Organometal. Chem. 370* (1989) 263–76.

[5] G. Kang, W. R. Cullen, M. D. Fryzuk, B. R. James, J. P. Kutney, *J. Chem. Soc. Chem. Commun. 1988*, 1466–1467.

[6] H. Moser, G. Rihs, H. Sauter, *Z. Naturforsch. B 37* (1982) 451–462.

[7] F. Spindler, B. Pugin, EP-A-0256982 (1988), Ciba-Geigy AG.

[8] 2,2-Dimethyl-4,5-bis(diphenylphosphinomethyl)-1,3-dioxolane: H. B. Kagan, T. Dang, *J. Am. Chem. Soc. 94* (1972) 6429–6433.

[9] (2*S*, 4*S*)-*N*-(*tert*-Butyloxycarbonyl)-4-(diphenylphosphino)-2-(diphenylphosphinomethyl)pyrrolidine: K. Achiwa, *J. Am. Chem. Soc. 98* (1976) 8265–8266.

[10] (2*S*, 3*S*)-Bis(diphenylphosphino)butane: M. D. Fryzuk, B. Bosnich, *J. Am. Chem. Soc. 99* (1977) 6262–6267.

[11] H. Brunner, W. Pieronczyk, *Angew. Chem. 91* (1979) 656–656; *Angew. Chem. Int. Ed. Engl. 18* (1979) 620.

[12] H. Wang, L. H. Pignolet, *Inorg. Chem. 19* (1980) 1470–1480.

[13] D. Chadosh, R. Crabtree, H. Felkin, S. Morehouse, G. Morris, *Inorg. Chem. 21* (1982) 1307-1311.

[14] Prof. *K. Bernauer*, Universität Neuchatel (Switzerland) kindly supplied us with an enantiomerically pure sample of **2a** $[[d]_{365}^{20}: -130.5°$ ($c \approx 3$, hexane) for (*S*)-**2a**]. **2b** was converted with chloroacetyl chloride into the corresponding chloracetamide. The optical rotation of the diastereomeric mixture of the atropisomers (1′*S*, *RS*) is known $[[\alpha]_D^{20}: -9°$ ($c = 2.073$, hexane)][6].

[15] ^{1}H-NMR spectroscopic determination of the enantiomeric purity with the chiral shift reagent (*S*)-(+)-2,2,2-trifluoro-1-(9-anthryl)ethanol.

BOOK REVIEWS

Book Reviews are written by invitation from the editor. Suggestions for books to be reviewed and for book reviewers are welcome. Publishers should send brochures or (better) books to the following address: Redaktion Angewandte Chemie, Postfach 101161, D-6940 Weinheim, Federal Republic of Germany. The editor reserves the right of selecting which books will be reviewed. Uninvited books not chosen for review will not be returned.

Anthracycline- and Anthracenedione-Based Anticancer Agents. Edited by *J. W. Lown*. Elsevier, Amsterdam 1988. 738 pp., hard cover, HFl 440.00.—ISBN 0-444-87275-2

"Anthracyclines represent one of the most useful and widely prescribed classes of anticancer agents" writes *J. W. Lown*, the editor of this book in the series with the general title "Bioactive Molecules". In accordance with the great clinical importance of this class of compounds, a wealth of new original papers has appeared since the last interdisciplinary multi-author volumes were published in the years 1980 to 1982. This has brought added urgency to the task of editing an up-to-date review of the field of anthracyclines, including all aspects from synthesis to clinical application.

It must be acknowledged that the editor, who has himself contributed to the field through synthetic and biophysical studies on anthracyclines, has made an excellent choice of topics to be covered. The total of 20 articles are divided into three sections as follows: Section 1: Isolation, Synthesis and Properties; Section 2: Biophysical and Biochemical Studies Related to Mechanisms of Action; Section 3: Pharmacology, Toxicity and Clinical Aspects.

Only two articles are actually devoted to synthesis, that by *F. Arcamone* and *S. Penco* on doxorubicin analogues, and that by *E. M. Acton* et al. on the very promising new class of compounds, the morpholinyl-anthracyclines. This limited choice of topics is justified, since recent comprehensive review articles on anthracycline syntheses already exist. Next comes a contribution by *T. Oki* on anthracyclines of microbial origin, including very recent results on the biogenesis of these compounds. The last three reports in Section 1 deal with topics that have scarcely been reviewed before, namely anthracycline-metal complexes (*A. Garnier-Suillerot*), and the pharmacological aspects of mitoxanthrones and ametanthrones (*F. E. Durr*), and of anthrapyrazoles (*H. D. Hollis Showalter* et al.).

Section 2 on biophysical and biochemical studies is the longest in the book, with eight articles. The interaction with DNA, which is important in relation to the effectiveness of the compounds, is treated first, in articles dealing with quantitative aspects (*E. Stutter* et al.), X-ray diffraction studies (*G. Ughetto*), computer modeling (*J. R. Brown* and *S. Neidle*), and sequence selectivity (*B. Pullman*). However, there is still no consensus among experts on the basic mechanism of action, as is shown by the general articles on anthracyclines by *C. E. Myers* et al. and on anthracenediones by *K. Reszka*. Thus, in addition to the interaction with DNA, there are discussions of the effects on DNA-topoisomerase II (*M. Potmesil*) and on lipid oxidation and prostaglandin formation (*R. F. Novak* et al.).

However, it is in clinical application that biochemical models undergo their ultimate test. This aspect, together with pharmacology and toxicity, is treated in Section 3. The introductory article by *M. Grandi* et al. on screening methods, which is fairly basic in content, is followed by newer aspects of anthracycline resistance (*D. H. Kessel*), of the pharmacology of Menogaril, which has been developed from nogalamycin (*J. P. McGovern* et al.), and that of anthracenedione (*M. D. Green* et al.), together with tumor cell differentiation by anthracyclines (*A. M. Casazza*). The short closing contribution by the editor again emphasizes the fact that, despite the wealth of experimental results, a firm understanding of antitumor activity is still a long way off. However, he urges continued research "... in order to understand the mode of action of these valuable agents and to improve their performance".

This volume is extremely useful for everyone working on synthetic, pharmacological or clinical aspects of anthracyclines or on antitumor therapy in general. Nowadays it is hardly possible for an individual to read every original paper which has an interdisciplinary connection with this topic. This collective volume makes it easier to see beyond the confines of one's own special field. Thus, it enables the synthetic chemist and the natural products chemist, for example, to learn which compounds have progressed from promising animal trials to clinical trials or use. However, sentences such as "Aclacinomycine A is therefore essentially ineffective in the major solid tumors" (p. 672), or "The side effects were in general similar to those seen with doxorubicin" have a sobering effect.

As in the parallel series "Studies in Natural Products Chemistry", also published by Elsevier, the authors' contributions are reproduced in "camera ready" form. Consequently the visual appearance is that of a wide variation in type styles and in the presentation of formulas. The incidence of typographical errors varies considerably from author to author, and in this respect the standard falls far short of that usually found in books that are typeset. These superficial shortcomings would, of course, be acceptable if they were offset by the contributions being more up-to-date and by an advantage in price. Unfortunately, however, in most of the articles the references extend only up to the end of 1986, or occasionally to the beginning of 1987. Even with this method of production it appears that at least a year has elapsed between the submission of the manuscripts and the publication of the book, a delay which this reviewer has also experienced as an author in the parallel series. The subject index consists of 8 1/2 pages. There is no index of cited authors; in the computer age it should have been easily possible to provide such an index, which would have been very useful.

Despite the fact that much of the work of publication has been off-loaded onto the authors, the price of the book is very high. Nevertheless, this should not deter libraries and scientists working in the field from buying it, as this is offset by the wealth of information that is compressed into it.

Karsten Krohn [NB 1031 IE]
Institut für Organische Chemie
der Technischen Universität Braunschweig (FRG)

Die Technik der organischen Trennungsanalyse. Eine Einführung. By *H. Laatsch*. Thieme, Stuttgart 1988. xii, 223 pp., paperback, DM 36.00. – ISBN 3-12-722801-8

Owing to the considerable advances that have occurred in chromatography (thin layer chromatography, column chromatography and gas chromatography), and the relatively little new progress that has been made in the classical organic techniques of separation and analysis ("wet chemical methods"), many chemists will take the view that it was not really necessary to add another survey to the already large number of review articles on the latter topic. However, the author of this book intends it to be used by students of experimental chemistry, who would find a readable and lucid introduction to the subject very helpful. In meeting this aim he has been very successful. However, the book should also serve as a useful introduction for advanced and post-graduate students engaged in isolating and analyzing natural products, a line of research which unfortunately tends to be neglected in the organic chemistry departments of German universities in comparison with preparative studies.

The first part of the book includes (in Section C, pp. 9–25) a very detailed description of the "ether separation process", which is successful for the majority of analytical problems. If the sample contains substances which tend to decompose easily, it is recommended that the separation should be carried out using derivatives, or by column chromatography. Attention is also drawn to the possibilities offered by the color changes exhibited by certain substances at different pH-values, which make it easier to recognize their presence. Section D (pp. 26–40) deals with methods for purifying the crude products of separation and measuring their physical constants. It is commendable that this section even includes a detailed account of the purification of solids by crystallization. Crystallization experiments are nowadays often neglected because of the availability of chromatographic separation methods, but they are in fact indispensable for isolating new natural products. The author emphasizes that one cannot claim to have a pure substance until crystals with a well-defined melting point have been obtained. A mixture of two compounds with identical or similar R_F-values can sometimes be mistaken for a pure compound.

The second part of the book (pp. 53–104) describes the reactions that can be used to demonstrate the presence of particular functional groups. Although not all such reactions are included, the most important ones undoubtedly are, and attention is drawn to compounds which can interfere with the analysis. The author describes how the substances isolated are first assigned to particular compound classes, followed by the preparation of the derivatives that are needed to arrive at an identification. Here again, only the most important derivatives, preferably those which crystallize well, are described. The preparation of crystalline derivatives from oily or amorphous compounds is of considerable interest in natural products chemistry, since in many cases the structures of complex natural products can only be determined by X-ray crystallography. The specimen analytical reports (Section H, pp. 174–195) are probably unnecessary,

 © VCH Verlagsgesellschaft mbH, D-6940 Weinheim, 1990 0570-0833/90/0505-0560 $ 02.50/0

as all students should have already learned in their preparative work how to write reports. In any case, it is not possible to lay down a report structure which can be applied universally. On the other hand, a useful feature are the exercises which the student can work through to test his or her knowledge of the methods for detecting functional groups and of the most important derivatizations for particular classes of compounds. However, the learning content of the exercises could have been further increased by including references to the IR, ^{1}H NMR and ^{13}C NMR spectra of the compounds.

Despite the fact that at some universities wet analytical methods are no longer taught, due to the shortening of studies and to the introduction of essential courses on topics such as spectroscopy and separation techniques, every student should work through this book. The experimental exercises and the practical hints are extremely valuable. It is especially worth mentioning that only a very few errors could be detected. The book has the usual high standard of production of the Thieme publishing house, and its price is reasonable, even for students.

Klaus Weinges [NB 1008 IE]
Organisch-Chemisches Institut
der Universität Heidelberg (FRG)

Dictionary of Alkaloids. Edited by *I. W. Southon* and *J. Buckingham*. Chapman and Hall, London 1989. 1161 pp./index 620 pp., hardcover, £ 675.00. – ISBN 0-412-24910-3

The alkaloids, with over 300 structural types and biosynthetic branches, form a group of secondary metabolites whose variety of structures is unrivalled by any other class of substances in nature. Since in many cases they show high toxicity or have other striking physiological effects, they have long attracted the interest of chemists; their structures continue to present challenges to analytical, synthetic and biosynthetic chemists, as befits their great importance in medicine and research, as toxins, and in chemotaxonomy and the classification of plants.

As the number of known natural products has grown, the definition of the term "alkaloid" has become widened to include not only basic plant substances but also non-basic nitrogen compounds. The editors of the present book now take this a step further by including almost all naturally occurring nitrogen-containing secondary metabolites of plant, microbial and animal origin; thus the definition is no longer based on physiological effects, nor on basicity.

In view of this wide definition of alkaloids, it is understandable that the present book contains an enormous number of compounds – about 10000. Thus the extent of this compilation is greater than in any other similar work. The only nitrogen-containing natural products that are omitted or not treated in full are a few simple lower amines, the nucleobases and nucleosides, and the pterins. Besides true peptides, the amino acids are also not covered (with only a few exceptions), but the amines such as tryptamine that are derived from these by decarboxylation are included. However, the peptide alkaloids are covered thoroughly.

In contrast to other well-known compilations, the alkaloids are not arranged according to the types of organisms that produce them, nor on the basis of (bio)chemical criteria, but are instead listed in alphabetical order. In adopting this method the editors define their aim as that of collecting together accurate and critical data on *all* known alkaloids, or at least on those whose structures are known. This necessitates summarizing the information in a concise form; each entry begins with the name, giving the most usual one where several alternatives exist, followed by the systematic name. This is followed by the stereochemical formula according to the current state of knowledge (showing the absolute configuration where this is known); the stereochemical diagrams are well-drawn and essentially free from errors. However, the representation of the sempervirin structure as an N,N-zwitterion seems rather unconventional, in contrast to the more usual representation as given, for example, for the related alkaloid melinonin E. Following the molecular formula, molecular mass and origin, the entry lists the main physical properties (melting and boiling points, specific rotation, refractive index) for the parent compound, and often also for derivatives, together with information on biological activity. For some alkaloids, however, the last item could have been more complete; for example, the toxicities of the various curare alkaloids have been very precisely determined by *Wieland*, whereas this compilation only gives these data for the main alkaloids, and even here instead of LD 50 values in most cases there is only a general statement such as "highly toxic".

For the many alkaloids whose structures are still unknown, this compilation of data is especially useful, since all the information contained in the secondary literature has been extracted from the different sources, critically evaluated, and reduced to a consensus! It would, of course, have been useful to have spectroscopic data too, but this would scarcely have been practicable within the predetermined size of the book. For these the reader is referred to the HEILBRON data bank, from which the present dictionary of alkaloids, like the dictionary of antibiotics from the same publisher, is an extract in book form. This accounts for the contents of the book being very up-to-date, a fact which is especially obvious in the literature citations.

Under each entry there is a bibliography, which includes publications up to the beginning of 1988, and is indexed under various headings such as isolation, structure determination, spectroscopic data and synthesis. Another very useful item included is the Chemical Abstracts Registry Number, which facilitates making a more extensive literature search if needed.

Preceding the alphabetically listed information on individual alkaloids there is a 32-page description of the main types of alkaloids, of which there are about 35. Here nomenclature and biosynthetic relationships are discussed in a condensed but very lucid form, with many examples. A list of review literature is provided with each section.

One can well believe the claim that all alkaloids known up to the beginning of 1988 are listed: the reviewer can hardly be expected to check this, of course, and a few tests will have to suffice. In the main part of the dictionary the simplest alkaloids, such as benzylamine, are, of course, readily found, but one can also find those with highly complex structures, such as leurosin and virotoxin. However, not all of these are listed under the expected names: whereas dimethyltryptamine and bufotenin are included under these names, serotonin appears at first glance to be absent, but is then found under 5-hydroxytryptamine. The isomeric psilocin (and also psilocybin), on the other hand, appear under their systematic names. Yet other alkaloids are not listed separately, but appear under the corresponding parent compounds. As a result one finds, for example, that only the nitrogen-free compound 12-oxooctadecanoic acid appears as a structural formula, whereas the alkaloid derived from it, lycaonic acid piperidide, does not.

In these cases, therefore, one needs to use the separately bound names index, which contains all the systematic names and common trivial names that are listed in the main work. Here it is worth noting that many of the names from the older literature have been altered to conform with modern rules of nomenclature. The index volume also contains a molecular formulas index, a list of CAS Registry Numbers, and an index of compound types. In this each alkaloid is assigned to one or more of 296 groups arranged mainly according to structural types, which enables one to easily obtain a complete survey of alkaloids of a particular type, e.g. mold alkaloids, alkaloid-*N*-oxides, tropane alkaloids, or compounds related to morphine.

The species index, containing nearly 20000 references, is without doubt an especially useful feature, even though it has a few gaps—for example, under the anhalonium types the important alkaloid mescalin is not listed. Under the botanical name *Cortinarius orellanus* one finds, as expected, a reference to orellanin. However, the peptide structure for cortinarin, which although it seems unlikely has not yet been disproved, is not mentioned here—could this be a result of critical selection?

With such an all-embracing definition of alkaloids it is inevitable that the boundaries are somewhat fluid, and this unavoidably leads to some inconsistencies. For example, although indirubin is included, the better-known indigo isomer is absent; also not mentioned are indoxyl and isatin. However, one hardly expects to find these compounds in a book on alkaloids in any case; their omission is therefore a trivial matter in this extremely up-to-date survey of the literature on alkaloids, which is the most complete printed compilation available anywhere on the subject. Of course, it goes without saying that a mammoth work of this nature, which is comprehensive and up-to-date to a degree otherwise only achieved in computerized data banks, is priced accordingly. To read this book is aesthetically pleasurable, in addition to the information that it yields; it should be in every library which is concerned with natural products.

Hartmut Laatsch [NB 1004 IE]
Institut für Organische Chemie
der Universität Göttingen (FRG)

Preparative Polar Organometallic Chemistry. Vol. 1. By *L. Brandsma* and *H. D. Verkruijsse*. Springer, Berlin 1987. 240 pp., paperback, DM 78.00. – ISBN 3-540-16916-4

When one compares the increase in the library budget (at any rate, that in Marburg) with the increase in the cost of journals and books, the effect in recent years has been to cut resources, making it necessary to exercise special care over the purchase of new books. Can we or can we not afford a certain book? In this case the answer must be an unqualified "yes", if only because, pursuing this economic theme, the book by *Brandsma* and *Verkruijsse* enables one to save money. The authors have produced an extremely practical book, a "laboratory manual", as they call it, for chemistry students and for chemists in industrial and university laboratories. Nothing has been left to chance; all the laboratory recipes have been tested several times by the authors themselves, who have a great deal of experience in the field of polar organometallic compounds. Everyone who has ever worked with a recipe which is not reproducible (or which does not work at all!) will appreciate what it means to use one that has been tested and optimized.

The book deals with polar organometallic compounds (intermediates) obtained from sp^2 compounds. Chapter 1 gives an introductory general survey entitled "Organometallic Reagents, Solvents and Laboratory Equipment". This includes useful hints on the safe handling of such compounds, and also on their disposal. The following chapters are: Chapter 2 "Reactivity of Polar Organometallic Intermediates", Chapter 3 "Metallated Olefinic and Allenic Hydrocarbons", Chapter 4 "Metallation of Hetero-Substituted Unsaturated Systems", Chapter 5 "Metallated Hetero-Aromatic Compounds", and Chapter 6 "Metallated Aromatic Compounds". There is a very useful appendix consisting of tables from which the reader can find suitable methods for preparing any particular polar organometallic compound, and for reacting it with an electrophilic species. Another table lists typical reaction conditions with a wide variety of electrophiles.

In summary, anyone who wishes to save money and avoid irritation in preparing and carrying out reactions with polar organometallic compounds should buy this book by *Brandsma* and *Verkruijsse*. The money will be well spent.

Gernot Boche [NB 1010 IE]
Fachbereich Chemie
der Universität Marburg (FRG)

Spectrometric Titrations. Analysis of Chemical Equilibria. By *J. Polster* and *H. Lachmann*. VCH Verlagsgesellschaft, Weinheim 1989. 433 pp., hardcover, DM 196.00. – ISBN 3-527-26436-1

The meaning primarily attached to the word "titration" is the method introduced by *Gay-Lussac* for the quantitative determination of dissolved substances. The end-point of such a titration is usually determined using an indicator which undergoes a color change. However, it was soon recognized that this method can be used to investigate a wide variety of other equilibrium systems. The changes in the physical condition of the system are observed in either a stepwise or a continuous fashion by means of suitable instruments which detect changes in variables such as pH, electrical conductivity, optical density, fluorescence or optical rotation. From the resulting titration curves it is then usually possible to calculate the equilibrium constants, which play a fundamental role not only in chemistry and physics, but also in biochemistry and medicine, pharmacy and toxicology, and other areas.

Part I of this book deals with the basic theory and methodology of spectrometric titration. The topics covered are the classification of the various methods, the graphical treatment of the experimental data, multiple wavelength spectrometry, and thermodynamic and electrochemical principles.

Part II discusses in detail the formal treatment of titration systems and the calculation of results. Acid-base equilibria involving one, two, three and still more stages are considered, and methods of treating the data by iterative curve fitting and statistical analysis are described. For non-overlapping multi-stage titration systems it is necessary to add an external standard proteolyte whose pK-value is known very accurately; from the simultaneous titrations one can then determine a relative pK-value for the equilibrium being investigated. Branched acid-base equilibria, metal complex equilibria, association equilibria and redox equilibria are also considered.

 © VCH Verlagsgesellschaft mbH, D-6940 Weinheim, 1990 0570-0833/90/0505-0562 $ 02.50/0

Part III of the monograph describes the apparatus needed for spectrometric titrations and the electrochemical and spectrometric techniques involved.

The appendix contains the EDIA program which the authors recommend for use with a personal computer to evaluate relative pK-values (ΔpK), together with the TIFIT program for iterative curve fitting and statistical analysis of data.

The authors have set out to critically evaluate the published work on spectrometric titrations which is widely scattered throughout the literature, and to present this in a clear and easily assimilated form, amplified by results from their own research in this area.

Perhaps it would be possible in a subsequent edition to include more detail on methods for determining points of inflection and stationary points, and measuring the true positions of shoulders in titration curves by repeated differentiation.

The care which has gone into the preparation of the figures, which are excellent from both a visual and a didactic standpoint, deserves special mention, as also does the overall quality of production and presentation. This monograph can be warmly recommended to everyone involved in studying equilibria and seeking a review of the current state of knowledge in this area. The literature references listed at the end of each chapter provide a very useful aid to further, more detailed, reading. Although it is pleasing to note that the publishers, notwithstanding the excellent quality of printing and production, have managed to keep the price down to DM 0.45 per page, one regrets that not all the students of chemistry, physics, biochemistry etc. with an interest in the topic will be able to afford the book. However, it deserves a place in all university libraries and relevant research laboratories.

Gerhard Talsky [NB 1005 IE]
Institut für Technische Chemie
der Technischen Universität München, Garching (FRG)

Methods for the Oxidation of Organic Compounds – Alcohols, Alcohol Derivatives, Alkyl Halides, Nitroalkanes, Alkyl Azides, Carbonyl Compounds, Hydroxyarenes and Aminoarenes. (Series: Best Synthetic Methods, Vol. 8). By *A. H. Haines*. Academic Press, London 1988. xx, 467 pp., hardcover, £ 69.50. – ISBN 0-12-315502-9

Series such as "Organic Synthesis", "Organic Reactions", or "Reagents for Organic Synthesis", or more recently computerized data banks of information on reactions, provide the synthetic chemist with information about preparative methods which he needs for solving problems of synthesis. Nevertheless, difficulties often arise from the fact that it is not always easy to find the required information on chemical reactions, or to decide on the best method of carrying out the search. The series "Best Synthetic Methods", of which the present book has been published as Volume 8, is intended for both advanced students and experienced chemists. It aims to provide them with overviews and critical evaluations, practical advice, and representative examples of important preparative methods, together with guidance on choosing the best one for the purpose. The author, who has already contributed the second volume of the series on methods for oxidation of hydrocarbons, has succeeded in meeting the aims of the series, with the result that this volume too does justice to the general title "Best Synthetic Methods".

A major reason for the success of the volume is the orderly and consistent arrangement of the material according to the degree of oxidation of the educts. Each of the seven chapters is further subdivided according to the reagents used. Since many of the methods described are not restricted to a single class of compounds, cross-references are provided to other chapters in which the same reagents are mentioned, thus providing the reader with additional guidance. The longest chapter is that on the oxidation of alcohols to carbonyl compounds and carboxylic acids, in accordance with the importance of these classes of compounds. Each of the methods described in this chapter is prefaced by a general introduction on "Scope and Limitations". Advantages and disadvantages compared with other reagents are pointed out, and the numerous variants of one basic method which exist in many cases are compared. Discussions of reaction mechanisms, including questions of reactivity, selectivity and stereochemistry provide the reader with additional information to help in deciding whether a method is suitable in a particular case.

Each sub-section contains examples of detailed preparative recipes in which the theory is applied to optimizing the practical results. Most of these are carefully worked out methods which have proved themselves in the exacting area of natural products syntheses.

The clarity and thoroughness of the experimental details contribute to the relative ease with which even those with limited experience can repeat the preparations. Each sub-section is completed by a comprehensive list of references which includes both review articles and important original papers. However, the policy of describing only fully proven methods reduces the topicality of the coverage. The later chapters of the book deal with oxidation reactions which are of less importance from the organic chemistry standpoint. However, the author's balanced and careful treatment of this material succeeds in also providing the user of the book with a useful account of these classes of compounds and the methods of oxidizing them.

Tables at the end of the book provide a summary of all the topics covered. These list in a clear form the educts, reaction conditions, products, yields and key literature references, enabling the reader to quickly see the main features at a glance.

Franz-Peter Montforts [NB 998 IE]
Institut für Organische Chemie
der Universität Bremen (FRG)

Colloid Chemistry of Polymers. By *Y. S. Lipatov*. Elsevier, Amsterdam 1988. ix, 460 pp., hard cover, $ 155.25.— ISBN 0-444-43006-7

This book by *Y. S. Lipatov* is the seventh volume in an ongoing series with the title "Polymer Science Library", which is published by Elsevier with *A. D. Jenkins* as consulting editor. The main topics of this volume are the microheterogeneity of polymer melts, the morphology of phase-separated systems, the colloidal aspects of polymeric systems, and the importance of interfacial properties in such systems. The main emphasis is on the thermodynamic treatment of the colloid chemistry of polymer systems.

The volume consists of 13 chapters, the first of which is a general introduction to colloid chemistry, especially as applied to dispersed colloidal polymer systems; the aims and methods of investigations of such systems are also described. Chapter 2 is concerned with the microheterogeneous structure of polymeric one- and multicomponent systems, with

the main emphasis on amorphous polymers. Chapter 3 discusses the formation of structures in dispersed polymer systems, including the thermodynamics of phase formation, the theory of spinodal breakdown of dispersed systems, phase separation, and dissipative processes resulting from microheterogeneity in polymeric systems. Chapter 4 deals with the interfacial potential in dispersed systems, including polymer solutions and melts as well as solid polymers. Chapter 5 continues this theme by treating surface active phenomena in polymers and the effects of surface active agents on the properties of polymer solutions; special attention is given to the use of surface active agents for modifying the mechanical properties of polymers. Chapter 6 is devoted to the adsorption of polymers on solid surfaces. Topics dealt with under this heading include the thermodynamic and kinetic principles of the adsorption of polymers from dilute solutions, the role of adsorbed layers in stabilizing dispersed systems, and the adsorption of polymer blends. Chapter 7 describes the theory of polymer adhesion and the thermodynamic aspects; adhesives and their mode of action are also discussed. The structure and properties of polymer boundary layers at surfaces and interfaces are described in Chapter 8; the main aspects discussed are boundary layers of polymers on solid surfaces and in polymer mixtures, structural changes in the neighborhood of interfaces in such mixtures, microheterogeneities in boundary layers, and polymer monolayers. Chapter 9 deals with filled polymers, more particularly with structures formed in the presence of dispersed fillers, the mechanical and rheological properties of filled polymers, the effect of the filler on the properties of the interface, and the use of colloidal metals as fillers. Chapter 10 discusses polymer mixtures, especially the theory of the miscibility and compatibility of different polymers, and experimental methods for measuring compatibility. This chapter also deals with typical features found in the phase diagrams of binary polymer mixtures and in the rheological behavior of polymer mixtures. Polymer-polymer systems, the thermodynamics of their formation and their colloidal and chemical structures are described in Chapter 11. Chapter 12 is devoted to gel formation in polymer solutions and to polymeric gels; aspects treated are the classification of gels, the conditions for and mechanism of gel formation, and the structure and properties of gels. Lastly Chapter 13 deals with emulsions, dispersions and foams containing polymers; topics treated are polymerization in emulsions, suspensions and dispersions, polycondensation in emulsions and at interfaces, and the properties of polymer dispersions and foams.

In all these topics the book treats the most important thermodynamic principles involved. A comprehensive bibliography is appended at the end of each chapter. A disadvantage of the book is that in translating the original 1984 Russion edition into English no more recent work has been included, and the bibliography is therefore no longer completely up-to-date. Work by Russian scientists is, as expected, especially well represented in the literature references, but there is nevertheless adequate citation of papers from the West. Regrettably, experimental results have only rarely been included as a way of elucidating results derived from theory. Despite this, the book provides many stimulating ideas, and it gives a reasonably comprehensive treatment of the field of polymer colloid science. The presentation is clear and readily comprehensible, and is supported by numerous figures and examples.

However, a real disadvantage of the book is the quality of production; it has evidently been made by direct photographic reproduction from a typescript. The Greek characters in the equations and diagram and other embellishments have been inserted by hand. Considering the high price of the book, the text certainly ought to have been properly processed and typeset.

Apart from this lack of visual appeal, the book is of a high scientific quality. The subject matter is equally suitable for chemists, physicists and engineers; however, the clarity of presentation should also enable an interested non-specialist to learn about the latest methods and developments in the colloid chemistry of polymers. For these reasons the book can be recommended.

Heinz Hoffmann [NB 1020 IE]
Institut für Physikalische Chemie
der Universität Bayreuth (FRG)

Registered names, trademarks, etc. used in this journal, even when not marked as such, are not to be considered unprotected by law.

© VCH Verlagsgesellschaft mbH, D-6940 Weinheim, 1990. – Printed in the Federal Republic of Germany by Konrad Triltsch Druck- und Verlagsanstalt Würzburg.

All rights reserved (including those of translation into foreign languages). No part of this issue may be reproduced in any form — by photoprint, microfilm, or any other means — nor transmitted or translated into a machine language without written permission from the publishers. Only single copies of contributions, or parts thereof, may be made for personal use. This journal was carefully produced in all its parts. Nevertheless, authors, editors and publisher do not warrant the information contained therein to be free of errors. Readers are advised to keep in mind that statements, data, illustrations, procedural details or other items may inadvertently be inaccurate.

Valid for users in the USA: The appearance of the code at the bottom of the first page of an article (serial) indicates the copyright owner's consent that copies of the article may be made for personal or internal use, or for the personal or internal use of specific clients. This consent is given on the condition, however, that the copier pay stated per-copy fee through the Copyright Clearance Center, Inc. (CCC), for copying beyond that permitted by Sections 107 or 108 of the U.S. Copyright Law. This consent does not extend to other kinds of copying, such as copying, for general distribution, for advertising or promotional purposes, for creating new collective works, or for resale. For copying from back volumes of this journal see 'Permissions to Photo-Copy: Publisher's Fee List' of the CCC.

Editorial office: Postfach 10 11 61, D-6490 Weinheim, Federal Republic of Germany, Telephone (06201) 60 22 55, Telex 465 516 vchwh d, Telefax (06201) 602 328.

Editor: *Peter Gölitz*

Associate editors: *D. I. Loewus, A. Stimson.* **Editorial assistant:** *E. Schweikart*

Publishers: VCH Verlagsgesellschaft mbH. (Managing Director: *Hans Dirk Köhler*), Pappelallee 3, D-6940 Weinheim, Federal Republic of Germany.

Advertising office (Advertising Manager *R. J. Roth*): Postfach 10 11 61, D-6940 Weinheim, Federal Republic of Germany, Telephone (0 62 01) 60 61 30, Telex 4 67 155, Telefax (0 62 01) 606 156.

ANGEWANDTE CHEMIE
International Edition in English
Volume 29 · Number 6
June 1990
Pages 565–706

New Aspects of the Maillard Reaction in Foods and in the Human Body

By Franz Ledl* and Erwin Schleicher*

Translated by Harry E. Nursten

Dedicated to Professor Otto H. Wieland on the occasion of his 70th birthday and to Professor Theodor Severin on the occasion of his 60th birthday

The reactions that occur during the cooking, baking, and preservation of foods of all kinds are of great importance for the production of aroma, taste, and color. However, more recently it has been shown that these reactions may be accompanied by a reduction in nutritive value and the formation of toxic compounds. For these reasons, the very complex reactions between reducing sugars and the free amino groups of amino acids or proteins, known as non-enzymatic browning or the Maillard reaction, have again caught the interest of chemists. The Maillard reaction came to be seen in a new light as it was realized that it actually occurred in the human body. As a general rule, the longer the half-life of a protein, the larger the amount of its Maillard products found, i.e., important factors are the 'age' or persistence of the protein in the body and the glucose concentration, particularly in diabetics. Many of the symptoms developed by diabetics resemble those of premature aging, which leads to the possibility that glucose, because of its reactivity towards proteins, is fundamentally involved in the normally slow progress of aging.

1. Introduction

The first substantial investigation of the reaction of reducing sugars with amino acids was carried out about 75 years ago by *Maillard*.[1] Subsequently, *Amadori*[2] reported the formation of two reaction products, which he described as the stable and the unstable isomer. *Kuhn* and *Weygand* showed later that a glycosylamine (the labile isomer) is formed first and that it then rearranges to the aminoketose (the stable isomer).[3] The elucidation of the mechanism of the reaction intrigued *Simon* and *Kraus*.[4] *Heyns* et al.[5] reported on the corresponding reactions of ketoses with amino acids that result in the formation of aminoaldoses. Further contributions to an understanding of the 'early' stage of the Maillard reaction, both with regard to the reactions occurring and to their products, came amongst others from the schools of *Hodge, Anet, Heyns, Micheel,* and *Kato*.[6] In the following sections, the significance of the Maillard reaction for foods and for the human organism will be outlined on the basis of the more recently achieved results.[7]

[*] Prof. Dr. F. Ledl
Institut für Lebensmittelchemie und Analytische Chemie der Universität Pfaffenwaldring 55, D-7000 Stuttgart 80 (FRG)
Dr. rer. nat. habil. E. Schleicher
Institut für Klinische Chemie und Institut für Diabetesforschung am Städtischen Krankenhaus München-Schwabing
Kölner Platz 1, D-8000 München 40 (FRG)

 © VCH Verlagsgesellschaft mbH, D-6940 Weinheim, 1990 0570-0833/90/0606-0565 $ 03.50+.25/0

2. Reaction Paths

2.1. Preamble

The Maillard reaction, or non-enzymatic browning, embraces not only one reaction but a whole network of different reactions. Accordingly, when sugars react with amines, one obtains an extraordinarily complex mixture of compounds, which are present in very different amounts. Besides substances which may be formed in relatively high yields (up to 30%) under certain conditions, other compounds are formed whose concentrations lie in the ppb range or even lower. Contrary to preparative chemistry, here the significance of a reaction and of a product is determined not so much by the yield but by its effect (e.g., aroma, taste). A few μg of a product may well be sufficient to characterize the aroma of a heated food. The product pattern is subject to large variations, depending on the reaction conditions. In particular, the reaction time, the temperature, the concentrations of the reactants, and the pH play a decisive role. These factors are responsible for the differences in aroma, taste, and appearance of boiled meat and roasted meat.

Although more than 75 years have passed since the first research on the Maillard reaction and although many results have been gathered in the meantime, it is still not possible to present a complete reaction scheme. To date, only a few of the reaction products have been isolated and identified. The products that have been characterized are preponderantly those that are stable and have not undergone further change to any large extent either in the reaction mixture or during isolation or purification. Such compounds can serve as indicator substances for certain reaction paths in the Maillard reaction. Difficulties are encountered in the isolation of reactive intermediates, since they are present only in very low concentrations in the reaction mixture and they usually react further during isolation. Yet it is precisely these compounds that are of the greatest significance for the Maillard reaction, since they play an important role in the formation of browning products, aroma compounds, high molecular weight substances, and so on.

In the following, an attempt will be made to describe the reaction sequence of the Maillard reaction without going into details that can often be unnecessarily confusing. Consequently the results of some studies are not or only partly taken into account, without any intention of detracting from their importance.

2.2. Initial Reactants

In foods, it is essentially the monosaccharides, glucose and fructose, and the disaccharides, maltose and lactose, as well as in some cases (e.g., meat) reducing pentoses, that react with amino acids and/or proteins. Sugar linked glycosidically in glycoproteins, glycolipids, flavonoid compounds, or in disaccharides, such as sucrose, participate in the Maillard reaction only after cleavage of the glycosidic bond. Hexuronic acids, insofar as they occur in the free form at all, behave like pentoses, i.e., in the course of the Maillard reaction decarboxylation takes place. In certain cases (e.g., cheese), biogenic amines can react as the amino component. Ammonia constitutes a special case; it can be formed in small amounts from amino acids during the Maillard reaction (cf. Section 2.7.1) and it is used in large amounts in the production of one type of caramel coloring.

In the human body, the reaction between glucose and the free amino groups of proteins as the amino component has been the primary subject of investigation. More recent results have indicated that fructose and pentoses also play a role as sugar components (cf. Sections 4.2 and 4.5). In general, for the Maillard reaction, primary amines are more im-

Franz Ledl was born in Starnberg, Germany in 1946. He studied food chemistry at the University of Munich where he received his Dr. rer. nat in 1973 under the supervision of Th. Severin and habilitated in 1987. At present he is Professor of Food Chemistry and Analytical Chemistry at Stuttgart University. His research interests include several areas of the Maillard reaction in foods and in vivo.

Erwin Schleicher was born in Bamberg in 1946. He studied chemistry in Munich at the Technical University from 1968–1972. After graduation he remained in Munich studying under the supervision of H. Simon and receiving his doctorate in 1974. He spent the following years (1975–1976) carrying out postdoctoral research with H. G. Floss at Purdue University (Indiana, USA). After returning to Munich he investigated the mechanism of redox enzymes. Since 1977 he has been working as a clinical chemist at the institutes for clinical chemistry and diabetes research group at the academic hospital Munich-Schwabing with O. H. Wieland. In 1986 he habilitated at TU Munich. His interests revolve around the theme of structural-functional relationship of glycoproteins, especially extracellular proteins, and the mechanism of signal transmission through cell membranes.

portant than secondary amines. Thus, in proteins, it is the primary amino groups of the lysine side-chains that react predominantly and, insofar as they occur in foods in the free form, primary amino acids take precedence. However, in cereals and in cereal products (malt, beer), considerable amounts of the secondary amino acid proline occur; since cereals are staple items of the diet, attention will also be paid to the behavior of secondary amines in the Maillard reaction.

2.3. Model Reactions

Investigations of the Maillard reaction in foods and also in vivo have been carried out predominantly with the help of model systems. The main reason for this is to be sought in the wide range of reactants and other substances present in even the simplest of natural systems. Not only do they make the situation that much more complex, but they make the separation, isolation, and purification of Maillard products extremely difficult. Fortunately, it has become evident that the relationships and conditions in foods and in the human organism can be simulated with model systems and that the results obtained can be extrapolated. The knowledge presented in Sections 2.4 to 2.8 on the reaction pathways has been largely obtained from such model systems.

2.3.1. Types of Model Systems

In general, in order to simulate conditions in foods and in vivo, aqueous solutions of the sugar and the amino component have been investigated. To study the processes occurring during roasting, fusion of the reactants has been found appropriate. Bearing in mind that the sugars and also the amines occur in foods in widely different amounts, the number of possible model systems is clearly vast. Yet care must be taken, since several preparative operations involve concentration and it is known that, for example, in drying foods, a range of concentrations has to be traversed that is optimal for the Maillard reaction to occur.

Of central significance for product formation are time and temperature (increases of up to sixfold have been recorded). As a rule of thumb, the rate at least doubles when the temperature is increased by 10 °C. If browning is used to measure the progress of the Maillard reaction, then four weeks at 20 °C, three hours at 100 °C, or five minutes at 150 °C give approximately the same result.

In the main, model systems are buffered to a pH between 4 and 7.5.

To simulate the conditions in the human or other animal organism, the sugar component, glucose, is incubated with the amine component, e.g., protein, 140 mM sodium chloride, and 5 mM potassium chloride at pH 7.4 and 37 °C (physiological conditions) and the mixture is subsequently analyzed. The progress of the Maillard reaction occurring on proteins under such conditions can be followed fluorometrically.

2.3.2. Studies on Model Systems

For the analysis, the aqueous reaction solution or the reaction melt dissolved in water is repeatedly extracted with an organic solvent. The non-polar products that are extracted into the organic phase can be analyzed gas chromatographically, provided they are sufficiently volatile, and characterized mass spectrometrically. In recent years, this has been the method by which most Maillard products have been identified. After derivatization (silylation, acylation), some of the polar products can also be identified gas chromatographically. The remaining mixture, however, presents great difficulties for the analyst, yet it constitutes the major part of the reaction products. By conventional chromatographic methods (exclusion, ion exchange, adsorption, partition), fractions are first obtained, which may yield pure substances, but usually only after several separation steps. High-performance liquid chromatography (HPLC) has provided reproducible fractionation and has facilitated the recognition of substances and of class of substance through the use of different types of detector (UV, fluorescence, electrochemical, etc.). To answer more detailed questions regarding a particular reaction mechanism or the elucidation of a new reaction path, starting substances labeled with radioactive and/or stable isotopes have been used. In the following sections, the analyses of some Maillard products are detailed and examples are given of derivatization and trapping reagents. Some problems in the investigation of protein-sugar reaction mixtures are outlined in Section 4.3.

2.4. Initial Phase

The schemes shown are based on glucose as example for the degradation of hexoses; deviations exhibited by pentoses or disaccharides will be indicated. For simplification, open-chain structures will mostly be used. In fact, the sugars and many of their products exist mainly in their cyclic half-acetal form. To start with, the structures of some reactants and primary products are illustrated (Scheme 1).

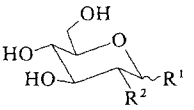

$R^1 = R^2 = OH$: D-Glucose
$R^1 = NHR$, $R^2 = OH$: D-Glucosylamine **1** (always in β-form)
$R^1 = OH$, $R^2 = NHR$: 2-Amino-2-deoxy-D-glucose **2** (Heyns-product)

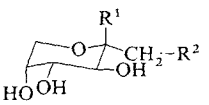

$R^1 = R^2 = OH$: β-D-Fructopyranose (also α-form and furanose)
$R^1 = NHR$, $R^2 = OH$: β-D-Fructosylamine (not isolable with aliphatic amines)
$R^1 = OH$, $R^2 = NHR$: 1-Amino-1-deoxy-β-D-fructose **3** (Amadori product; also α-form and furanose)

Scheme 1.

2.4.1. Amines Reacting as Nucleophiles

The reaction of amines as nucleophiles leads, after addition to the carbonyl group of the sugar, to the formation of

glycosylamines. Relatively stable glycosylamines of type **1** are obtained from aromatic and heterocyclic amines, e.g., purines. A biologically very widely occurring substance of this kind of structure is adenosine triphosphate. Glycosylamines of amino acids or aliphatic amines are usually only detectable in very small amounts in sugar-amine reaction mixtures. They quickly undergo further reactions and rearrange via the aminoenol **5** into the aminoketose **3** and other products.

Aminoketoses (or Amadori compounds) have been shown to be present, alongside other products, in heated and in stored foods,[8] in dried fruit, in vegetable and milk products,[9] as well as in soy sauce.[10] They also occur in infusion solutions containing glucose and amino acids, intended for parenteral nutrition (whether heat sterilized or mixed under sterile conditions).[11] They are also present in the human body, in higher amounts in diabetics (cf. Section 4.4). The biosynthesis of histidine proceeds via an aminoketose, which is formed by rearrangement of an imine.

Deoxydiketoses and deoxyaldoketoses are formed as degradation products of the aminoketoses in the pH range 4–7. 1-Deoxy-2,3-hexodiulose **6**, 1-amino-1,4-dideoxy-2,3-hexodiulose **7**, and 3-deoxy-2-hexosulose **8** are formed via the

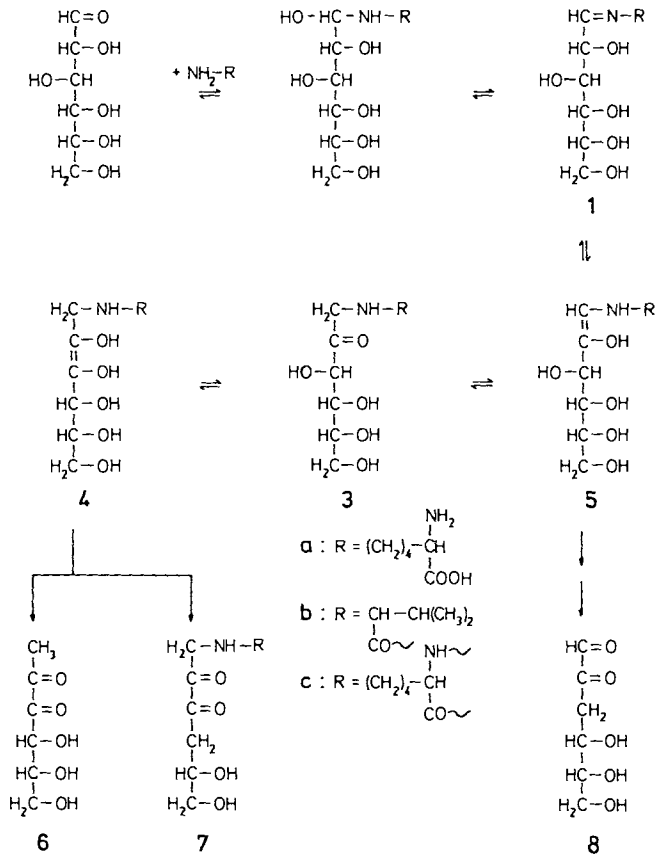

enediol **4** or the aminoenol **5**. To demonstrate the conversion of **3** into these products, trapping with *o*-phenylenediamine is useful, the corresponding quinoxalines **9**, **10**, and **11** being formed.[12] (The Group R′ in the formulas for the quinoxalines **9** and **11** is intended to indicate that, when Amadori compounds derived from disaccharides react further, the glycosidic bond in the corresponding deoxyosones is not severed and therefore the quinoxalines bear an α-glucosyl or β-galactosyl residue, depending on whether they are derived from maltose or lactose.)

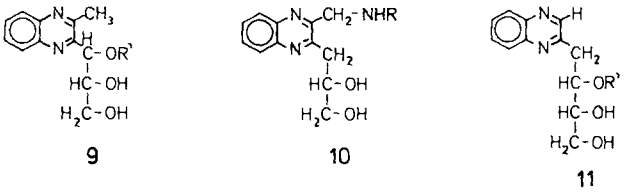

Besides the aminoketoses **3**, compounds of the type **12**[13] and **13**[14] are also obtained. The latter type of compound is also known as an intermediate in the formation of osazones.

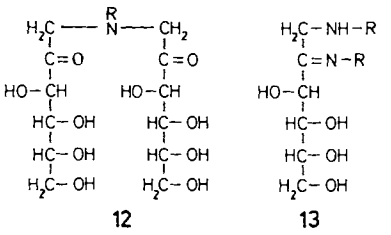

Ketoses react with amines via imines as intermediates to form aminoaldoses such as **2**, the so-called Heyns compounds.[15] In Nature, part of the biosynthesis of *N*-acetylglucosamine and *N*-acetylgalactosamine follows the same principle: fructose reacts with ammonia and rearranges to the activated glucosamine or galactosamine via the Schiff's base. Compounds of type **2** are not very stable; they readily

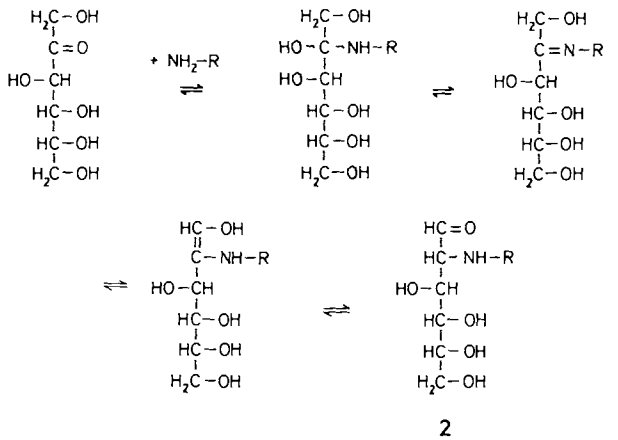

react further, forming products such as the Amadori compounds.[16] Recent work suggests that aminoaldoses are also formed in the human body. One can assume that Amadori and Heyns compounds decompose in a parallel manner. In presence of *o*-phenylenediamine, aminoaldoses yield predominantly the quinoxaline **11** via **8** as intermediate.[17] In view of the in vivo formation of Heyns compounds, further studies of their properties are called for (cf. Section 4.2).

2.4.2. *Amines as Bases or Acids*

As bases or acids (depending on the prevailing pH), the amines act as catalysts, for example, for the migration of the carbonyl group of the sugar, i.e., aldoses are converted into ketoses (fructose) and vice versa or an imine becomes an aminoketose or aminoaldose (cf. Section 2.4.1) (corresponding to the Lobry de Bruyn-Alberda van Ekenstein rearrangement). Through loss of water, the enediols **14** and **15** give the 3-deoxy-2-hexosulose **8**, and the 1-deoxy-2,3-hexodiulose **6** and the 4-deoxy-2,3-hexodiulose **16**, respectively. On heating

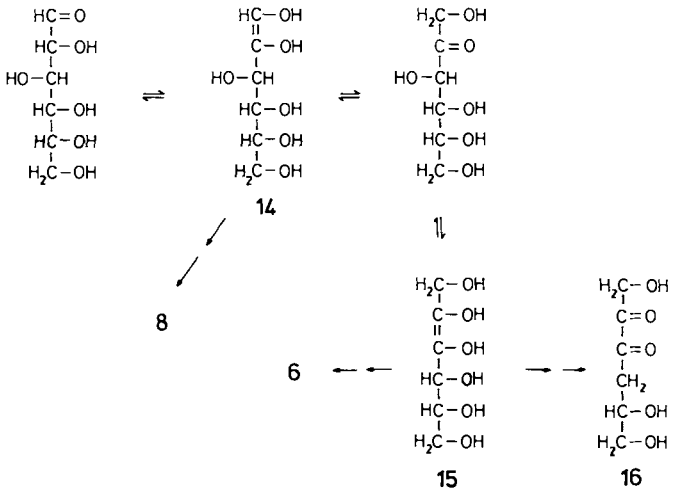

the sugar in the absence of amines, these reactions occur at pH values below 3[18] or above 8[19] or on caramelization, i.e., at temperatures above 130 °C. Thus, the significance of amines in the formation of the deoxyosones **6**–**8** and **16** lies in their ability to catalyze these sugar rearrangements under pH conditions normally encountered in foods and living organisms (pH 4–7).

2.5. Deoxyaldoketoses and Deoxydiketoses

As far as is known at present, many important reactions of sugars during the Maillard reaction take place via deoxyaldoketoses or deoxydiketoses. These compounds can be described as intramolecular disproportionation products of sugars which undergo further reactions markedly more rapidly than the original reactants; enolization, cyclization, and loss of water thereby play major roles. The presence of amines leads in addition to the formation of nitrogen-containing compounds. Products that are formed by cleavage of the original sugar's carbon chain will be considered in a separate section.

2.5.1. *Reactions of 3-Deoxyaldoketoses*

3-Deoxyhexosuloses were first shown to be present amongst the reaction products of sugars and amines about 30 years ago.[20] In solution, one would expect an equilibrium between the cyclic forms **8a** to **8d**. The best known product derived from these compounds is 5-hydroxymethyl-2-furfural **18**.[21] In the presence of amines, the formation of **18** may be limited in favor of nitrogen-containing compounds. The formation of metasaccharinic acid lactone **19** is noteworthy. Under alkaline conditions, the formation of metasaccharinic acid from **8** takes place by hydride migration.[19] In the Maillard reaction at pH 4–7, it is likely that the lactone **19** is formed from the cyclic precursor **8a** through isomerization of the keto group.[23] Formation of the furanone **20** from **8a** is conceivable after enolization involving C3, followed by elimination of the hydroxy group from the

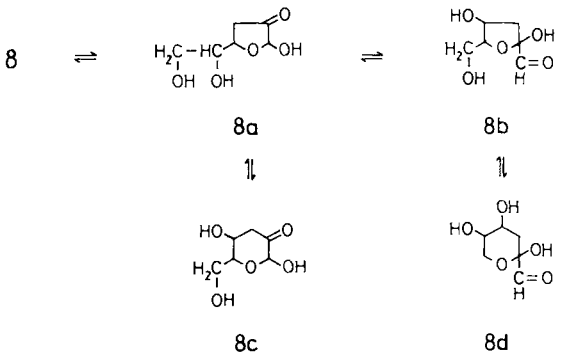

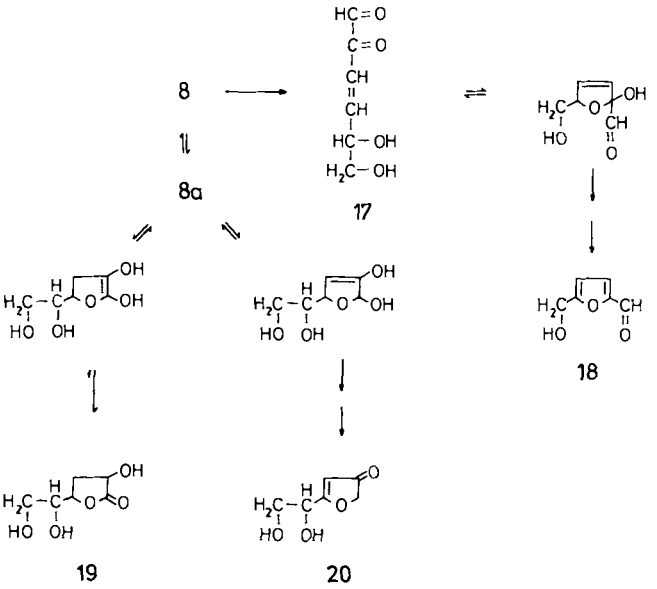

half-acetal function, but this has not yet been demonstrated. It is known that 5,6-dimethoxyglucose **21** rearranges into the corresponding compound **22**.[24] The structurally equivalent aminofuran **24** is obtained as the main product when

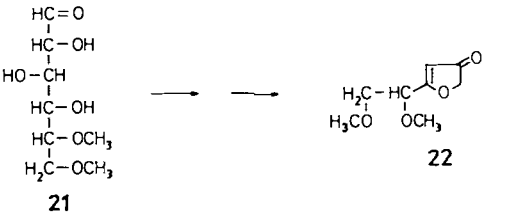

N-acetylglucosamine **23** is heated in the presence of amines. Compound **24** has been known for some time and serves as indicator for *N*-acetylglucosamine or *N*-acetylgalactosamine.[25] In Nature, these aminosugars occur almost exclusively bound glycosidically to protein and so are not available as reactants for the Maillard reaction.

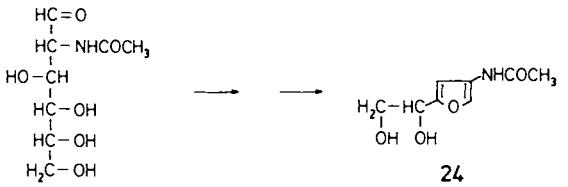

23 **24**

In the Maillard reaction of the deoxyhexosuloses **8** in the presence of larger amounts of primary amines, the formation of hydroxymethylfurfural **18** can be largely suppressed. In its place, are found pyrrolealdehydes of structure **25**,[26] as well as pyridiniumbetaines of type **26**.[27] The fact, that **25** and **26** are obtained only in very poor yield from hydroxymethylfurfural and amines, indicates that the incorporation of amine takes place in a precursor of **18**. Further nitrogen-containing products from compound **8** are the bispyrroles **27** and **28**.[28] The structures allow one to assume a dimerization of the

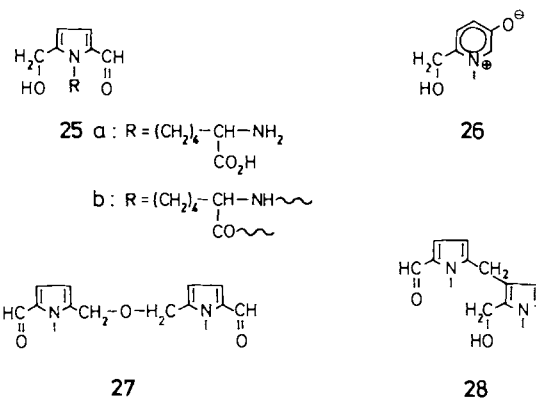

25 a: R = $(CH_2)_4$–CH(CO$_2$H)–NH$_2$; b: R = $(CH_2)_4$–CH(CO~)–NH~ **26** **27** **28**

pyrrolealdehyde **25**, whose hydroxymethyl OH group is subject to ready nucleophilic substitution (cf. Section 4.5). In the presence of amino acids, additional compounds are found: lactones of the type **29**[29] and lactams of structure **30**.[22] For the formation of these bicyclic compounds, the hydroxy

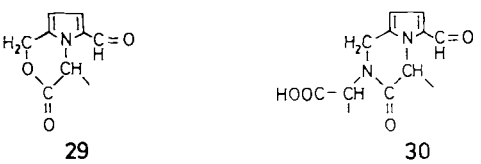

29 **30**

group of the pyrrolealdehyde **25** is again replaced by other nucleophiles. In proteins, nitrogen-containing products are mainly linked to the peptide chain through the ε-amino groups of lysine. To detect pyrrolealdehyde **25b**, an enzyme-linked immuno sorbent assay (ELISA) has been developed.[30] Lysylpyrrolealdehyde **25a** can be determined by reverse-phase HPLC after alkaline or enzymatic hydrolysis.[31]

The monosaccharide derivatives **25** and **26** are also obtained by reaction of maltose and lactose with primary amines. This can be understood as a consequence of **17** being an intermediate; for its formation, loss of the oxygen atom attached to C4 is required, regardless of whether a glucosyl or galactosyl residue is attached to it, as in maltose and lactose, respectively. Pentoses also react via the 3-deoxyaldoketoses to give the corresponding pyrroles **25**[32] and pyridiniumbetaines **26**[27] (here, the hydroxymethyl group in structures **25** and **26** needs to be replaced by hydrogen).

When reducing sugars react with secondary amines, hydroxymethylfurfural **18** is usually not formed or, if so, only in small amounts. When the secondary amino acid proline is heated with compound **8**, the so-called maltoxazine **31** can

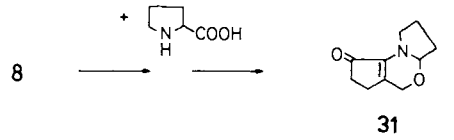

8 **31**

be isolated as the main product. Maltoxazine is a volatile component of malt and of beer and its formation will be discussed in Section 2.8.2.[33] The reaction of secondary amines and pentoses leads to the formation of the orange-colored condensation product **35**, which can be extracted with organic solvents as the main colored compound.[34] The formation of the hydroxyfuranone **34** will be considered later. Compound **35** is obtained in presence of **34** and secondary amines from the 3-deoxy-2-pentosulose **32** in good yields and from the cyclopentenedione **33** in very good yields. Compounds **31** and **35** are examples of carbocyclic

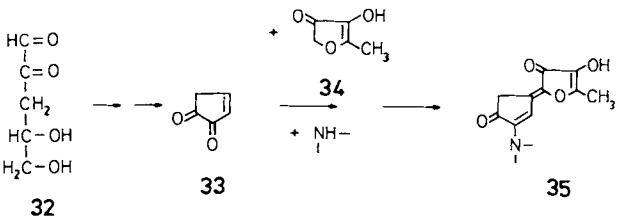

32 **33** **34** **35**

products obtained from 3-deoxyaldoketoses with secondary amines. They illustrate a general principle, found repeatedly; namely, that sugars in the presence of secondary amines are transformed into carbocyclic compounds, sometimes in substantial amounts.

3-Deoxyaldoketoses participate in the formation of yet other pyrrolealdehydes. Thus, the compounds **37** and **38** are formed upon reaction of **8** with the aminoketose **3**. In both cases, **36** functions as intermediate. The electron-attraction by the formyl group in the intermediate **36** leads to retroaldol cleavage and thus to formation of compound **37**.[35] In a competing reaction, the enamine function induces forma-

tion of the pyrrole **38**.[36] The formulas refer to products from hexoses, but the condensation proceeds analogously for pentoses.[37] As in the pyrrolealdehydes of type **25**, the hydroxy groups in the neighborhood of the pyrrole ring in **37** and **38** are readily substituted. Examples of this are the in-

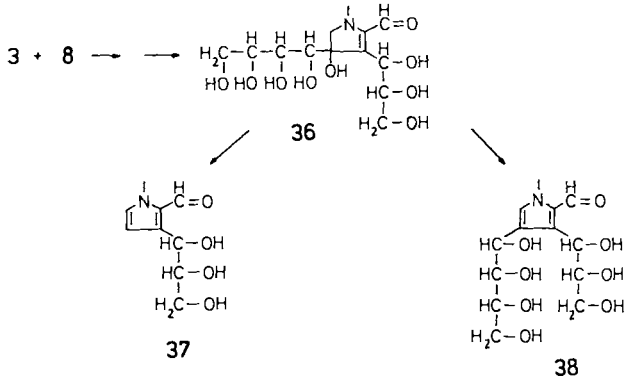

tramolecular ether formation in **39** and the partial replacement of the hydroxy group by a methoxy group during chromatographic purification (methanol/ethyl acetate as eluent) of such compounds, leading to formation of, e.g., **40**.[37b]

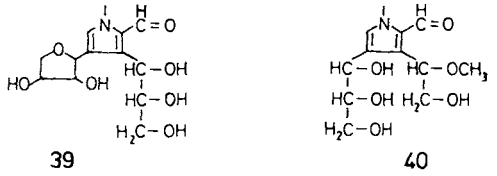

In addition to 3-deoxyaldoketoses, other α-dicarbonyl compounds can also interact with aminoketoses. Thus, the structure of the pyrrole **42** implies that 1,4-dideoxydiketose **41** participates in its formation[37b] (cf. Section 3.4). Further evidence of similar condensation reactions comes from the

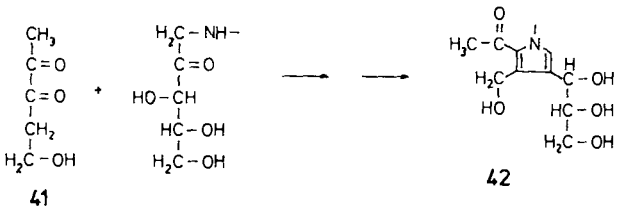

structures of the pyrrolealdehydes, which are obtained from the polar fractions from reaction mixtures of glucose and pentoses with alkylamines after addition of sodium periodate. Apart from the pyrroledialdehydes and pyrroletrialdehydes **43** and **44**, their isomers **45** and **46**, respectively, are also obtained, amongst other products, from **37** and **38**.[37b,c]

The isolation and identification of the pyrroles **37**, **38**, and **42** proves that the aminoketoses are sufficiently reactive to undergo condensation reactions. Evidence for the participa-

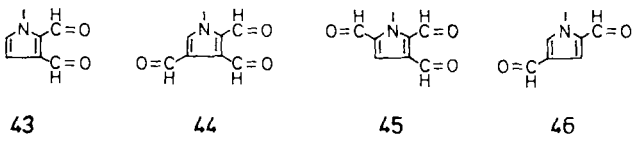

tion of other primary products of the Maillard reaction, such as the aminoaldoses, is provided by the structure of the pyrrolealdehydes obtained on periodate oxidation. This is of particular interest in relation to the Maillard reaction in vivo, since here reactions following formation of pyrroles, such as substitution of the α-hydroxy group, can lead to cross-linking and other changes in protein structure (cf. Sections 4.5 and 5).

2.5.2. Degradation of 1-Deoxydiketoses

1-Deoxydiketoses were shown only recently to be secondary products of aminoketoses.[12a,b] They are converted into compounds with the general reductone structure **47** (cf. Section 3.4). At present, nothing is known about whether the open-chain reductone **6a** is present in the reaction mixture. One would expect an equilibrium mixture between the cyclic forms **6b** to **6d** in solution.

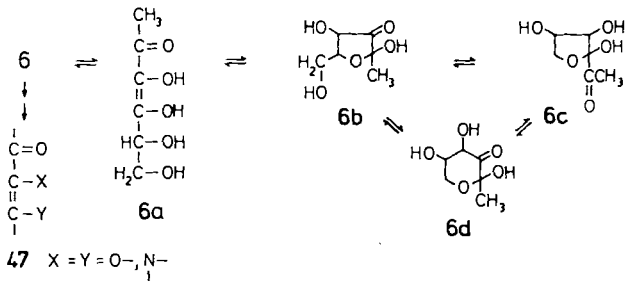

Enolization and loss of water from the hemiketal form **6b** of the 1-deoxydiketose leads to the furanone **48**,[38] which can be detected gas chromatographically after derivatization (e.g., silylation). It is worth noting that furanone **48** isomerizes to compound **49** (R = H) only to an insignificant extent

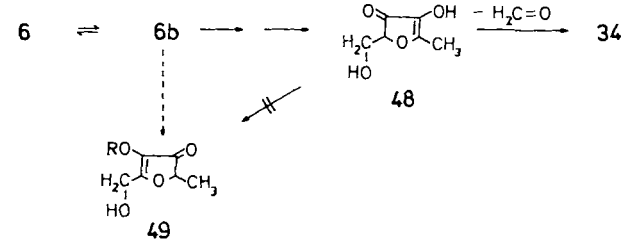

under the conditions of the Maillard reaction. Instead, formaldehyde is split off with formation of the pentose derivative **34** in considerable amounts. In this connection, the structure of the colored main product **50** from the reaction mixtures of hexoses and secondary amines is of interest, since it contains

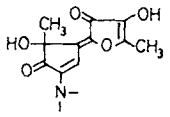

50

the furanone **34** as a building block (cf. Section 3.3).[34] Furanone **48** can only be formed from disaccharides if the glycosidic bond is broken. If one assumes that the glycosidic bond is still present in the intermediate **6b**, then the glycosylfuranones **49** (R = α-glu, β-gal) should be formed. Evidence for such compounds is, however, still lacking.

From pentoses and 6-deoxyhexoses, such as rhamnose, the corresponding furanones **34**[39] and **51**[40] are formed via

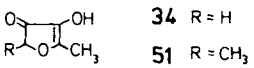

34 R = H
51 R = CH_3

the 1-deoxydiketoses. Compound **34** plays a crucial role in the browning of pentoses (see Section 3.3). In the presence of sulfur-containing compounds (e.g., cysteine), from which hydrogen sulfide is liberated on heating, **34** also exerts a considerable effect on aroma production. Substances are formed that possess interesting aroma notes (mainly resembling heated meat;[41] compounds **52** to **57** are given as exam-

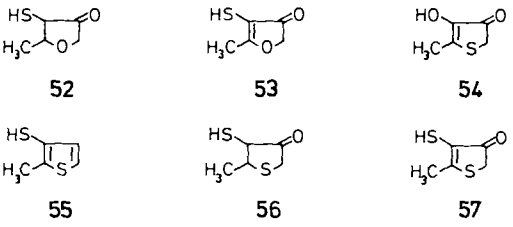

52 **53** **54**

55 **56** **57**

ples). The corresponding S-containing products with an additional methyl group are obtained from furanone **51** on heating with hydrogen sulfide. Compound **51** has a very low odor threshold and an aroma note (fruity-roast-caramel-like) that is perceived as pleasant. It is now manufactured on a relatively large scale and is added to many products.[42] It is interesting that **51** is formed also in plants.[43]

Further products are obtained from 1-deoxydiketoses via the cyclic hemiacetal form **6d**. The pyranone **59** is formed by enolization and loss of the hydroxy group from C2.[44] This compound can be used as the universal indicator substance for the occurrence of the Maillard reaction, since hexoses occur in virtually all foodstuffs. Compound **59** is formed in ppm amounts upon heating foodstuffs and is readily detectable by gas chromatography after extraction with an organic solvent.[45] If the hemiacetal **6d** loses the hydroxy group from C5, the unstable β-pyranone **58** is formed, and this rearranges in part into the lactic acid ester **60**[23] (cf. Section 2.6.1). Tautomerization of **6d** leads to a β-diketone, which is shown in its cyclic hemiacetal form **61**. This compound has not yet been shown to be an intermediate, but one can assume that it would readily undergo β-diketo scission, producing, for example, C_4-aminoreductones[46] (cf. Section 2.6.1). Acetylformoin **62**, which is formed from ketone **61** by elimination of the β-hydroxy group attached to C6 of the original sugar,[26,40] readily undergoes further reactions and is therefore only found, if at all, in low concentration in model systems or foodstuffs.

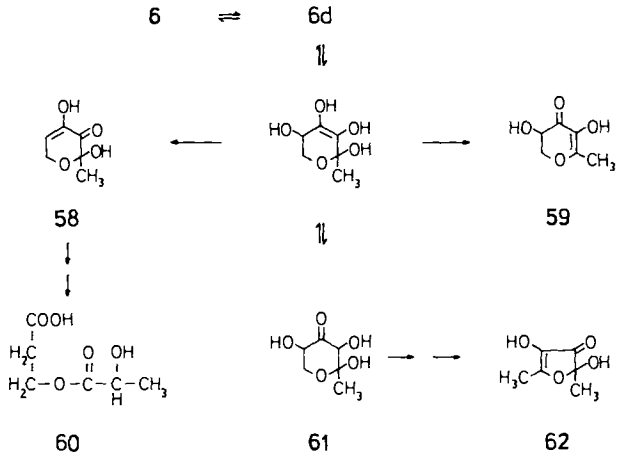

58 **59** **60** **61** **62**

The reactions of 1-deoxydiketones derived from disaccharides differ in some respects from those of monosaccharide derivatives. This is understandable, if one starts with the cyclic form **64**. After enolization without splitting the glycosidic bond, only elimination of the hydroxy group on C5 is possible, with formation of the β-pyranone **63**. The γ-pyranone **59** is therefore a product typical of monosaccharides, which can only be formed via a free hydroxy group at C4. The presence of small amounts of pyranone **59** among disaccharide reaction products can be explained by some degree of hydrolysis of the glycosidic link during the Maillard reaction (cf. Section 2.5.1), the monosaccharide formed giving rise to **59**. The β-pyranone **63**, which has so far been found in heated milk (R = β-gal)[47] and in steamed ginseng root (red ginseng, R = α-glu),[48] is a key intermediate in disaccharide degradation. Its fate depends on the nature of the glycosidically bound sugar. A β-galactosyl residue allows formation both of five- and of six-membered rings. β-Galactosylisomaltol **66** (R = β-gal), a Maillard product characteristic for lactose,[49] is formed preponderantly. The corre-

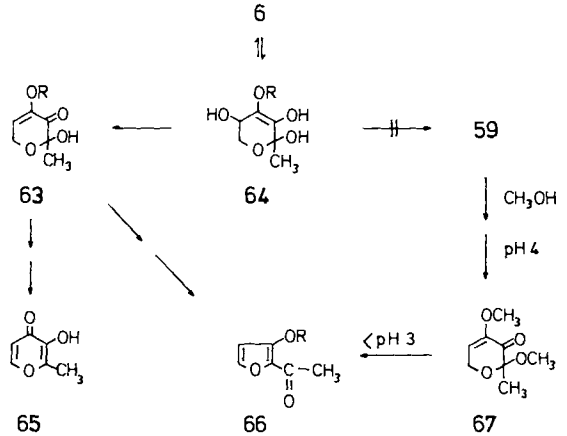

63 **64** **59** **65** **66** **67**

sponding reaction sequence can be observed with monosaccharides, when they are heated in alcoholic solution (in methanol in the scheme). The γ-pyranone **59** is converted at pH 4 into the β-pyranone **67**, which, on further lowering of the pH to split the ketal, rearranges into the isomaltol methyl ether **66** (R = methyl).[47] If these reactions are carried out in aqueous solution, isomaltol **66** (R = H) is formed only in insignificant amounts,[50] even though it corresponds to the above methyl ether. Maltose leads to a higher proportion of maltol **65**,[51] α-glucosylisomaltol **66** (R = α-glu) being formed only in trace amounts.[52] It follows that α-glucosyl-β-pyranone **63** (R = α-glu) must be subject to splitting of its glycosidic bond to a considerable extent. This can be attributed to the greater steric hindrance to flexibility of the ring of the maltose intermediate, which is not relieved by ring-contraction and formation of **66** (R = α-glu).

As already indicated, compound **62** is very reactive. The so-called aminohexosereductones **68a** are considerably more stable. They are formed from **62** in presence of secondary amines.[53] Under optimal conditions, aminohexosereductones can be obtained in yields of 30%, based on the amount of sugar employed. Indirectly, this shows the importance of **62** as an intermediate in the Maillard reaction.

The pyrrolinones **69a** have been found in reactions between hexoses and primary amines. These compounds, which can be obtained from **62** in very good yields,[54] fluoresce strongly and, like the aminohexosereductones, possess antioxidant properties (cf. Section 3.4).

Reactions of disaccharides with primary or secondary amines also lead to aminoreductones. The galactosyl and glucosyl residues remain glycosidically linked in compounds **68b** and **69b**, respectively, and the basic pyrrolinone and cyclopentenone systems are identical with those of the monosaccharide products.[55]

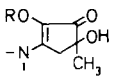

68 a : R = H
68 b : R = α-Glu,β-Gal

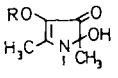

69 a : R = H
69 b : R = α-Glu, β-Gal

The main product, extractable with organic solvents from reaction mixtures of disaccharides and primary aliphatic amines, is the pyridone **71**.[56] Most likely **63** is first converted into the pyridiniumbetaines **70** (R = α-glu, β-gal), which

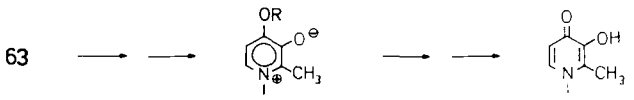

63 **70** **71**

have recently been isolated in crystalline form from mixtures of disaccharides and primary amines.[57] Pyridiniumbetaines are predominantly converted into the pyridones **71** on cleavage of the glycosidic bond. Pyridones with this type of structure are known to bind metals such as iron[58] and aluminum tightly;[59] a study of their effect on the absorption and elimination of trace elements is currently being carried out. The pyrrole derivative **72**, corresponding to galactosylisomaltol **66** (R = β-gal), has been isolated as a byproduct from reactions involving lactose.[47] Upon heating **66** together with primary and secondary amines one obtains, inter alia, the furan derivatives **73** and **74**.[60] Compounds **75**[61] and **76**

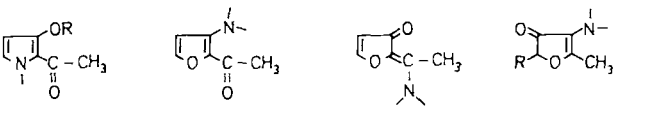

72 **73** **74** **75** R=H, CH_3

are nitrogen-containing derivatives from 1-deoxydiketoses of pentoses and 6-deoxyhexoses, respectively. So far, the pyrrolinone **76** has only been obtained from reaction mixtures of condensation products of the type **77** and primary amines. With secondary amines, compounds **77** rearranges into compounds **78**, the structures of which parallel those of aminohexosereductones **68a**.[62]

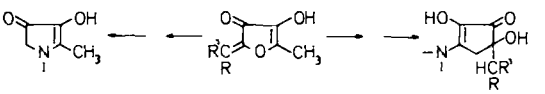

76 **77** **78**

2.5.3. *Reaction of 4-Deoxydiketoses*

The formation of 4-deoxydiketoses **16** in Maillard reaction mixtures has so far not been confirmed. However, since compounds have been isolated whose formation from sugars is best explained in terms of 4-deoxydiketoses as intermediates, one may assume that such α-dicarbonyl compounds are indeed formed.

Supporting evidence for their formation comes from the structures of compounds **79**–**81**. In the presence of larger amounts of primary amines, the formation of the hydroxyacetylfuran **79** can be largely suppressed in favor of the two nitrogenous heterocycles **80** and **81**.[26, 27, 63]

16 **79** X = O **81**
80 X = N–

As shown in Section 2.4.2, 4-deoxydiketoses are not formed from aminoketoses of type **3**. The compounds **79**–**81** are therefore indicator substances showing that the reactions have not proceeded exclusively via aminoketoses.[12b]

2.5.4. *Reactions of 1-Amino-1,4-dideoxydiketoses*

Proof that 1-amino-1,4-dideoxydiketoses **7** are reaction products of the aminoketoses has only been obtained recent-

ly.[12b,c] Cyclization and loss of water leads to the aminoacetylfuran **82**. As long as 30 years ago, the furan **82a** was obtained by heating Amadori compounds in the presence of strong acids[64] (cf. Section 4.3). In the meantime, it has been shown that **82** is also formed at pH 4 to 7. It should be noted that **82** is present as a stable salt under acid conditions, but that above pH 5 it rapidly undergoes further reactions.

Among the rearrangement and condensation products derived from **82** are the compounds **83** to **87**.[12c] From the structures of furoic acid **83**, of its amide **84**, and of furoylcarboxamide **85** it is immediately apparent that the aminoketone **82** is readily oxidized. The condensation to the aminopyrrole **87** is noteworthy (compounds **86** and **87** were isolated and identified as monoacetyl derivatives after acetylation of the total reaction mixture; the extent to which the compounds exist in the free form as pyrroles has not yet been ascertained). If such cyclizations are attributed to proteins, then aminopyrrole formation by two ε-amino groups of peptide-bound lysine residues constitutes a cross-link. The significance of cross-linking reactions in biological materials will be dealt with in Section 5.1.

In presence of ammonia aminoacetylfurans of type **82** give good yields of the imidazole **88** or its alkyl derivatives **89** respectively.[65] Compound **88** has been described recently as indicator substance for protein cross-linking (see Section 4.5). **88** was assumed to be derived from a cross-link. However, it became evident[65] that the formation of **88** takes place from furosine **82a** and ammonia during and subsequently to the acid hydrolysis of proteins. **82a** is itself formed in the process, as already mentioned, from the lysine Amadori compound **3a** or **3c**, and ammonia is liberated from asparagine and glutamine.

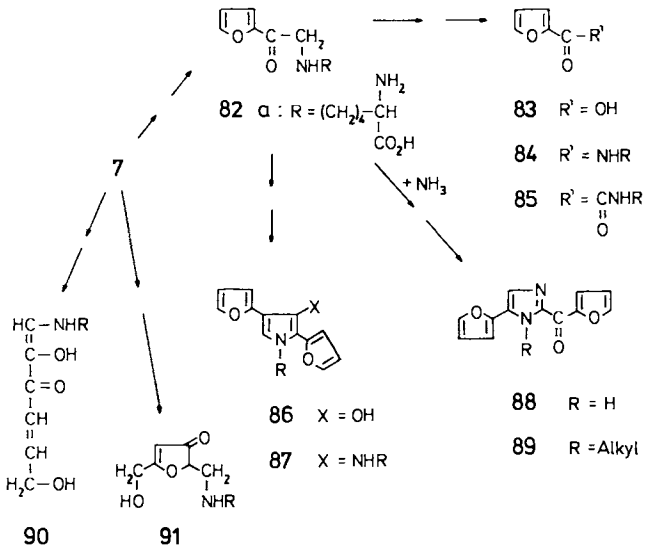

Recently, the isolation of aminoreductone **90** from a glucose-propylamine reaction mixture was achieved.[37d] It can be assumed that a 1-propylamino-1,4-dideoxydiketose of the general type **7** is formed as intermediate. This shows for the first time that an open-chain C_6-aminoreductone is present in a Maillard reaction mixture. The formation of the furanone **91** can also be derived from **7**, but so far structure **91** has been allocated only on the basis of the mass spectrum of a peak in the gas chromatogram of a silylated sugar-amine reaction mixture.[66]

2.6. Cleavage Reactions

It has already been mentioned several times that, during the reactions undergone by sugars, cleavage of the carbon chain can occur. As will be shown, some cleavage products are very reactive and can substantially accelerate the Maillard reaction.[67] Sugar fragmentation products play a considerable role in aroma formation (cf. Section 3.1).

2.6.1. Retroaldolization

Sugars and many of their derivatives can undergo retroaldol-type reactions. The structures of compounds **92** to **102**[46a,68] permit one to assume that they have been formed

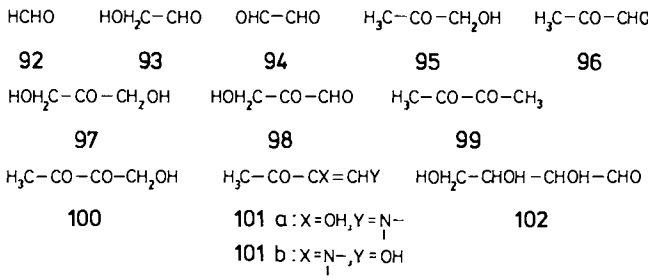

by a retroaldol cleavage. In some cases, oxidation and/or dehydration follows. Some of the cleavage products are very reactive, readily undergoing condensation reactions. The available partners consist of other retroaldol compounds, as well as of sugar derivatives with carbon chains still intact. The condensation products **103** to **111** illustrate the type of structures formed.[69,37c] Further research has shown that the progress of the degradation of the sugar is paralleled by the formation of the cleavage products. In the early phase,

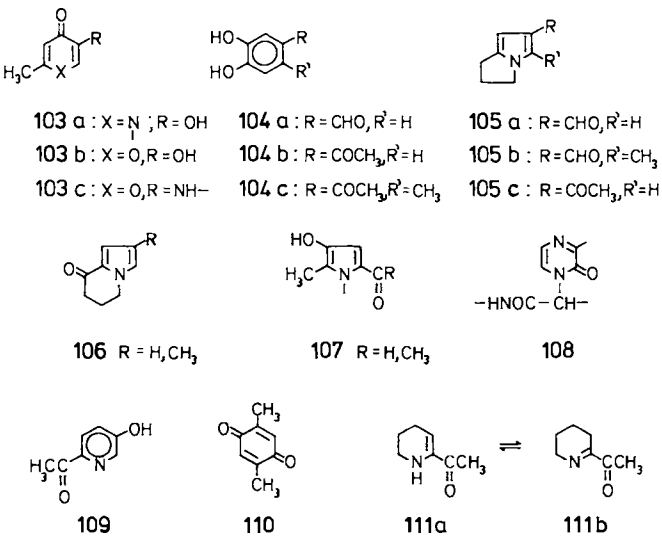

C_2 fragments preponderate, which have been formed from the sugar or the imine **1** provided that an aldose had been the starting point. Electron spin resonance spectra have provided evidence for the partial conversion of the imine cleavage product **112** into the pyridinium radical **113**, from which oxidation produces glyoxal or the corresponding nitrogenous analogs that immediately react further.[70]

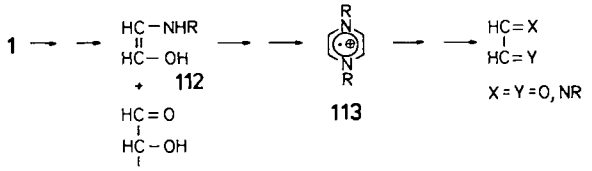

Somewhat later, C_3 compounds appear, but by then ketoses or Amadori products are already present. The amounts of the cleavage products found depends on the pH of the reaction medium, including the foodstuff. At pHs below 7, retroaldol products are likely to play only a subordinate role,[67, 71] but one must remember that even very small amounts of aroma compounds formed in this way may have great impact, if their odor threshold is very low.

If one assumes that the rate of browning depends on the amounts of the C_2 and C_3 products formed, it would follow that solutions of disaccharides become colored more slowly. Certainly, the C_3 products can be formed by retroaldolization only after hydrolysis of the glycosidic bond.[72] Possibly the configuration of the hydroxy group at C4 of glucose and galactose also affects the rates of cleavage and of browning.[73]

Labeling experiments have shown that C_4 aminoreductones **101** are formed via the β-diketone **61**. Neither C1 nor C6 of the sugar gives rise to the methyl group of the C_4 product **101**.[46] After cleavage of **61** to the tetrose (shown here in the enolized form **114**), the deoxy form **100** incorporates amine to give the product **101**. Retroaldolization is also involved in the formation of the acids **116** and **117**: the unstable β-pyranone **58** is in equilibrium with the furanone **115**, which on β-cleavage gives the ester **60**. Depending on the conditions, this, in turn, is split more or less rapidly into β-hydroxypropionic acid **116** and lactic acid **117**.[23]

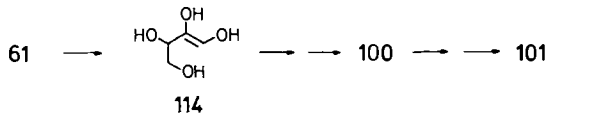

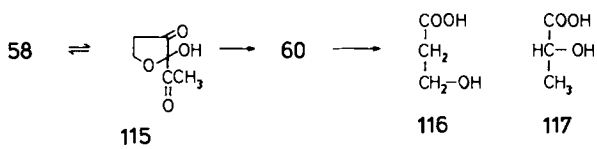

2.6.2. *Cleavage of α-Diketones*

If the 3-deoxyaldoketose **8** is heated under Maillard conditions (i.e., in neutral aqueous solution in the presence of amines), but with exclusion of oxygen, extraction with organic solvents yields amongst other products the lactone **118**, formic acid **119**, and furfuryl alcohol **120**.[74] Model experiments with glyoxal and methylglyoxal had previously already led to the identification of the acid amides **121a** and **121b**.[75] The formation of **118**–**121** requires cleavage of the α-diketo group. Such cleavages are known, even though there are hardly any proposals as to how they occur.

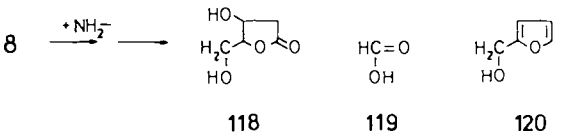

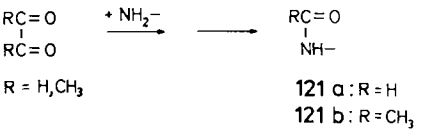

For the decarboxylation of the α-ammoniumcarboxylic acid **122**, an immoniumbetaine of the type **123** has been indicated as an intermediate,[76] which has some resemblance to the thiazoliumbetaine **124** derived from thiamine. If one assumes that, in the fission of the deoxyosone **8**, imine **125** is formed first, then it is to be expected that alongside **118** C_1-immoniumbetaines will be formed. However, so far proof or identification of such derivatives has not been unequivocally achieved. Alternatively, the intermediate **126** could lead to formic acid **119** and the C_5 fragment **127**, the latter reacting further to give furfuryl alcohol **120**. Lactone **118** and formic acid are formed in considerably greater amounts in the presence of oxygen, whereas the amount of furfuryl alcohol **120** decreases. It would seem therefore that

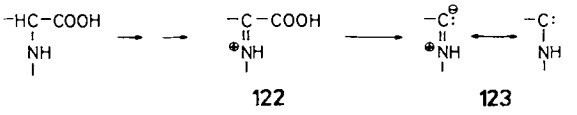

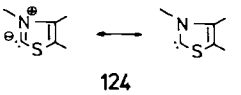

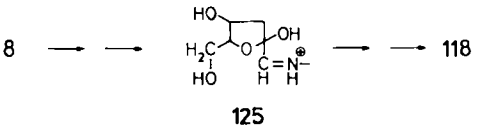

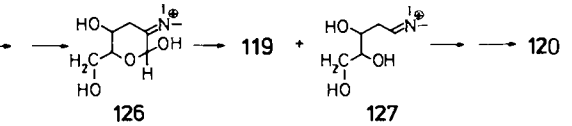

118 and **119** are formed in the reaction mixture predominantly by oxidative degradation of **8**.

Recently,[77] it proved possible to identify carboxymethyllysine **128** in the protein hydrolyzate of biological material (cf. Section 4.5). From the experimental results ob-

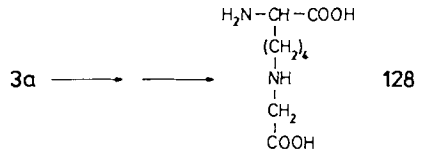

tained to date, it follows that the formation of **128** is due to oxidative cleavage of the corresponding aminoketose **3a**.[78]

2.7. The Strecker Degradation

2.7.1. Strecker Degradation of Amino Acids

The decarboxylation of amino acids on heating with sugars has been known for many years. The decarboxylation is actually brought about by reaction of the amino acids with α-dicarbonyl compounds.[79] The azavinylogous β-keto acid **129** is formed first and then loses carbon dioxide. The significance of the Strecker degradation lies in the fact that the amino acids furnish ammonia and the reactive aldehydes of type **131**, compounds that can undergo, inter alia, condensa-

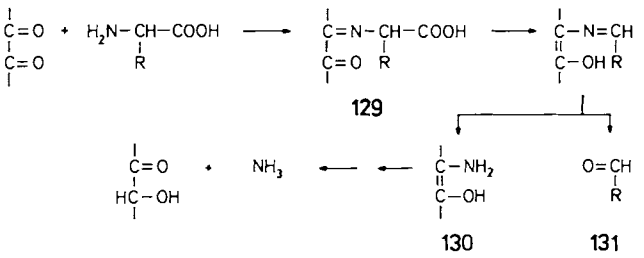

tion reactions. Thus, in reaction mixtures including lysine and phenylalanine as well as hexoses, furans **132**[80] and **133**[81] have been found, whose structures comprise the corresponding Strecker aldehyde. Ammonia in the free form or as the aminoenol **130** participates in the formation of pyridine, pyrazine, imidazole, and other derivatives.[82]

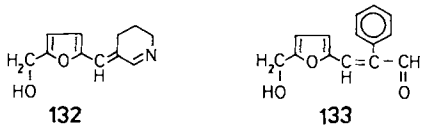

The Strecker degradation of amino acids brings about the reduction of the deoxyaldoketoses and diketoses. Cyclization and loss of water converts **8** into the furan **134** and, with the participation of ammonia, into the pyrrole **135** and the

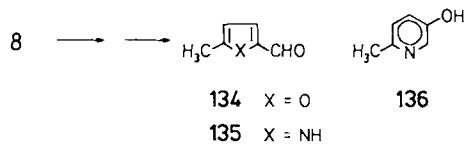

pyridine **136**.[83] Compounds such as, inter alia, **137**, **138**, and **139** are derivable from 1-deoxydiketoses of type **6**. However, there is evidence that in these compounds the methyl group is not derived from C1 of the hexose. Therefore, a degradation via the imine **1a** has been proposed as a route to the formation of **138** and **139**:[84] loss of water from **1a** leads

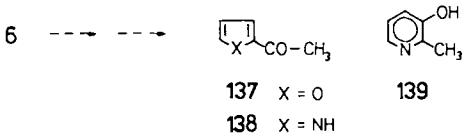

first to the 2-deoxyhexose **140**, which, after hydrolysis of the imine function, reacts further to yield the pyrrole **138** or the pyridine **139**. The Strecker degradation of proline and hydroxyproline will be considered in detail in Section 2.8.2. Another reaction sequence, that also leads to the reduction of α-dicarbonyl compounds, will be dealt with in Section 3.4.

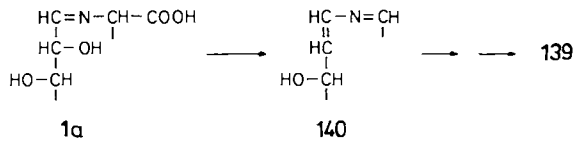

2.7.2. Strecker Degradation of Amines?

In many foodstuffs and especially in vivo, the lysine side chain is the most important amine for the Maillard reaction. This raises the question of whether, in the presence of α-dicarbonyl compounds, the formyl derivative **141** is produced. For proteins it would seem likely that reactions would follow that would be comparable to those that take place during the synthesis of collagen and that lead to cross-link-

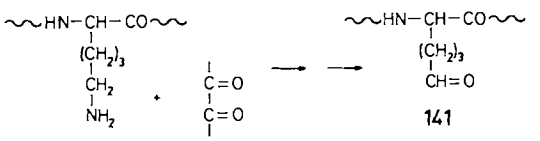

ing. It is known that primary aliphatic amines in presence of vicinal triketones such as ninhydrin and dehydroascorbic acid are converted into the corresponding aldehydes.[85] In the Maillard reaction, triketones, such as the β-pyranone **58** and oxidized reductones, are indeed formed, but the α-diketo compounds are of far greater significance. The experimental results available at present do not yet provide unequivocal proof that α-diketo compounds can lead to the splitting of

primary aliphatic amines into ammonia and aldehydes under the conditions of the Maillard reaction.

2.8. The Influence of Particular Amino Acids and Amines on the Course of the Reaction

This section is devoted to some special reactions that, due to the specific nature of the amino components, lead to unusual products.

2.8.1. *Tryptophan*

An important finding, particularly with regard to the Maillard reaction in vivo, is that protein-bound tryptophan reacts with reducing sugars only to a limited extent.[86] Thus, this essential amino acid is, in contrast to the essential lysine, hardly damaged in protein-sugar reactions. In foodstuffs, tryptophan can also occur in the free state (e.g., in soy sauce). Then, even under mild conditions, reaction with carbonyl compounds and ring-closure with formation of β-carbolines become possible. The tetrahydro derivatives **142** and **143** have been shown to be present in soy sauce[87] (cf. Section 3.5).

Under drastic reaction conditions, further β-carbolines are formed, some of which have also been found in foodstuffs.[88] It is apparent from structures **144**–**148** that, alongside cyclization, decarboxylations and dehydrogenations take place. It is likely that 3-deoxyaldoketoses participate in the formation of compounds **144** to **148**, which have been isolated from pentose-tryptophan reaction mixtures. If

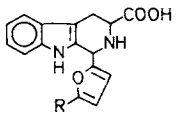

142 R = H
143 R = CH_2OH

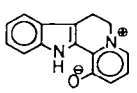

144

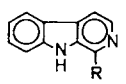

145 R = H
146 R = CH_3
147 R = $COCH_3$
148 R =

the amino group is blocked, formation of glycosyl derivatives **149** (R = β-Glu, β-Xyl) has been observed. Evidence of their further reaction, e.g., to aminoketoses via Amadori rearrangement, has not been obtained so far.[89] To what extent products of the type **149** are formed in the Maillard reaction has not been investigated. More attention has been devoted to the tryptophan derivatives **150** and **151**, because of their strong mutagenic and carcinogenic activity.[90] These substances, which were first detected in pyrolyzates of tryptophan and of tryptophan-containing proteins, have

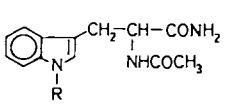

149 R = ß-Glu,ß-Xyl

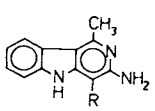

150 R = H
151 R = CH_3

since been found in foodstuffs that have been particularly severely exposed to heat.[91]

2.8.2. *Proline and Hydroxyproline*

Proline occurs in relatively large amounts in cereals and their products, such as malt. The participation of this imino acid in the formation of volatile compounds contributing to the aroma of malt has been particularly thoroughly researched. It is assumed that the dihydropyrrylium compound **152** plays a central role in the process. **152** is an intermediate of the reaction of proline with α-dicarbonyl compounds. The cation **152**, which is obtained by decarboxylation, leads to a series of nitrogen-containing hetero-

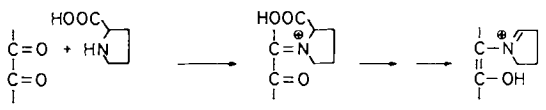

152

cycles by a variety of reactions. From the structures of compounds **31** and **153**–**162**, it can be deduced that the stabilization of the intermediate **152** is achieved by electron uptake (**153**), loss of protons (**154**), addition of heteroatoms (**31**), or

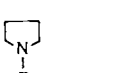

153

R = CH_2COCH_3
R =
R = H_2C

154

R = $CHCOCH_3$
R = H_2C CH_2OH

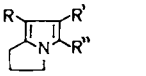

155

R = CHO, R' = H, R'' = CH_3
R = $COCH_3$, R' = H, R'' = CH_3
R = R'' = H, R' = $COCH_2CH_2COCH_3$
R = H, R' = $COCH_2CH_2COCH_3$, R'' = CH_3
R = R' = H, R'' =

addition of other nucleophiles (**155**).[92] Opening of the dihydropyrrylium ring, followed by intra- or intermolecular condensation, leads to renewed ring closure, for example, with formation of pyridine derivatives **156**–**159**,[93] as well as of

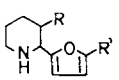

156

R' = H, CH_3
R = H, OH

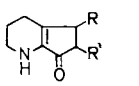

157

R = R' = H
R = H, R' = CH_3
R = CH_3, R' = H
R = , R' = H

158

R = CH_3, C_2H_5

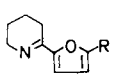

159

R = H, CH_3

the dihydroindolizine **160**, and the partially hydrogenated cyclopentazepinones **161**–**162**.[94] For the formation of maltoxazine **31**, a pathway starting from **8** via **152a** has been proposed.

Hydroxyproline occurs almost exclusively in connective tissue protein (collagen) and therefore is of no great signifi-

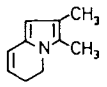

160

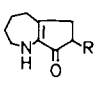

161 R = H, CH_3

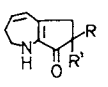

162 R = R' = H
R = H, R' = CH_3
R = OH, R' = CH_3

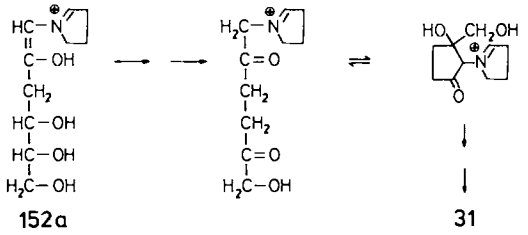

152a 31

cance for the Maillard reaction in vivo or in foodstuffs. From model systems, it appears that, as with the degradation of proline, the dihydropyrrylium compound **163** leads to volatile products. In the process, stabilization occurs preponderantly by loss of water and formation of a pyrrole ring (compounds of the type **164**), which may be built into a bicyclic system (compound **165**).[95] Hydroxyproline has a

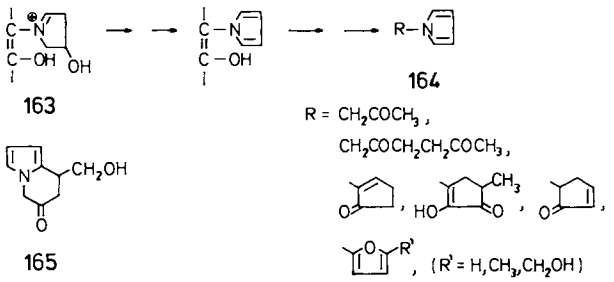

163 164

R = CH_2COCH_3, $CH_2COCH_2CH_2COCH_3$,

165

(R' = H, CH_3, CH_2OH)

certain significance, as does proline, as a starting material for the formation of volatile components of tobacco smoke.

2.8.3. Cysteine and Cystine

Cysteine and cystine do not occur free to any large extent in foodstuffs. The great significance of these amino acids for aroma formation is mainly due to the fact that, on heating, hydrogen sulfide is released. Hydrogen sulfide reacts with Maillard products to give a multitude of sulfur-containing compounds. Their important influence on the aroma is in part due to their extremely low odor thresholds. It follows that even small amounts of cysteine or cystine can affect the aroma perceived. If the extensive patent literature and the results of model experiments are taken as a guide, cysteine and cystine play an important role in the formation of the aroma of meat.[96] From model systems of cysteine with pentoses and hexoses, a broad spectrum of sulfur-containing volatile compounds has been isolated and some of these have very intense odors.[97] Mono-, di-, and trisubstituted thiazoles of the general structure **166** predominate. Thiazoles are

166

found, inter alia, in the volatile fraction of roasted coffee beans[98] and of cooked meat.[7j, 99]

Some important sulfur-containing aroma compounds are dealt with in Section 3.1. Cysteine has a retarding effect on the Maillard reaction, and this will be discussed in Section 3.7.

2.8.4. Arginine

In reports on the damage suffered by amino acids when proteins are heated in the presence of sugars, reference is frequently made to the fact that arginine, as well as lysine, undergoes extensive modification during the Maillard reaction.[100] Changes to lysine are often tantamount to loss of this amino acid and are therefore important for the nutritional value of the food, since lysine is an essential amino acid (cf. Section 3.6). During the in vivo Maillard reaction, lysine participates in cross-linking. Recently, it was discovered that arginine can also undergo such cross-linking reactions. From the structure of the product **167** it follows that arginine and lysine are linked via a imidazopyridinium bridge[101] (cf. Sections 4.5 and 5.1).

It is worth noting that the Maillard reaction is not initiated by the guanidino group.[102] Heating glucose with N^{α}-acetylarginine causes no browning of the solution and the hexose remains largely unchanged. The guanidino group of arginine bound in a protein therefore needs reactive Maillard products in order to be converted into, e.g., **167**. Heating aqueous solutions of methylguanidine (as models for arginine) with α- and β-dicarbonyl compounds at pH 7 to 8 led to the isolation of, e.g., imidazolones and pyrimidines of the general type **168** and **169**, respectively (the formation of the imidazolones re-

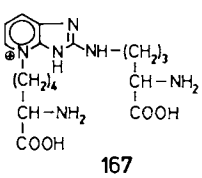

167

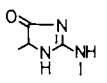

168

169

quires at least one aldehyde function).[103] Further research is required in order to ascertain which Maillard products with this function react preferentially with the guanidino group.

2.8.5. Creatine

Creatine **170a** and creatine phosphate **170b** occur in relatively large amounts (0.5%) in muscle. Heating causes mainly cyclization to creatinine **171**. For some years now, atten-

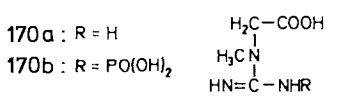

170a : R = H
170b : R = $PO(OH)_2$

171

tion has focused on these meat constituents, since they participate in the formation of the carcinogenic and strongly

mutagenic compounds **172** and **173**. Both compounds have been shown to be present in high-temperature roasted mixtures of amino acids and creatine with[104] and without hexoses[105] and later also in meat and fish products.[106]

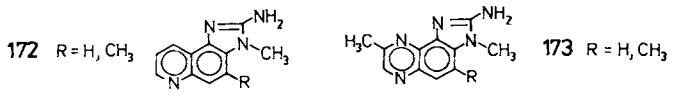

It can be assumed that creatinine, possessing a reactive methylene group, is able to condense with aldehydes (e.g., formed by Strecker degradation of amino acids) and that further reactions with sugar degradation products and ammonia follow. Certainly the concentration of **172** and **173** fell when Strecker aldehydes were trapped with tryptophan.[107] However, such a method cannot readily be adopted for foodstuffs, since tryptophan can form mutagenic and carcinogenic compounds with sugars and aldehydes (cf. Section 2.8.1).

Meanwhile, it has become apparent that the amount of carcinogens formed is largely determined by the conditions under which the foodstuff has been treated and that mild processing can to a great extent avoid their production. For example, if the food is heated to above 130 °C, the concentrations of **172** and **173** formed lie in the lower ppb range, but cooking at the boil leaves them below the limits of detection.

2.8.6. Ammonia

Unless foods have been allowed to spoil, they normally contain ammonia only in very low concentrations. To manufacture caramel as a coloring matter for foodstuffs (e.g., cola beverages), ammonia in large amounts is brought into reaction with sugars. With ammonia, the formation of pyridines,[108] pyrazines,[109] and imidazoles[110] is possible without requiring the cleavage of a C–N bond. As a consequence, these heterocycles occur in relatively large amounts in sugar-ammonia reaction mixtures. Compounds **174**–**177** are given

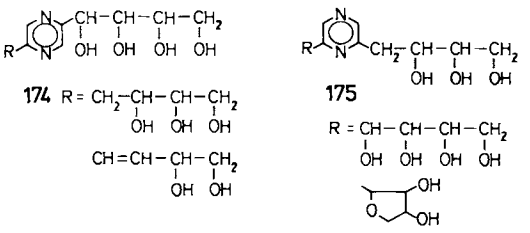

as examples. They can serve as evidence of the addition of ammonia caramel.[8a,111] This can be important for beer, bread, and other foods, where dark color can simulate the use of certain raw materials.[112]

Compound **176b** is known to reduce reversibly the number of lymphocytes in rats[110a] when fed a diet low in vitamin B_6. The methylimidazole **178** has toxic properties.[113] For both substances, upper concentration limits have been laid down for ammonia caramel.[114] Polyhydroxyalkylpyrazines are formed also from, for example, amino sugars[115] (e.g., 2-aminoglucose), but the occurrence of the

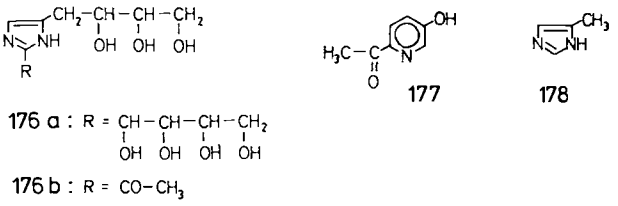

latter in foodstuffs is not significant, as already mentioned in Section 2.5.1.

2.9. High Molecular Weight Compounds (Melanoidins)

If the reaction mixtures of sugars and amines are submitted to exclusion chromatography, fractions can be obtained with molecular weights of about 7000 Da and even greater. So far it has not yet proved possible to isolate homogeneous high molecular weight Maillard products.[116] Very little is known about the structure of the high molecular weight substances, the so-called melanoidins. Knowledge has however been gained from the interpretation of spectral data, although some of the ^{1}H- and ^{13}C-NMR spectra of the melanoidins isolated by different research groups have differed substantially. Melanoidins with groups of signals that largely resemble those of Amadori compounds[117] contrast with those that exhibit signals in the olefin, aromatic, and carbonyl regions.[118] Experiments with ^{13}C- and ^{15}N-labeled sugars or amino acids have shown that the carboxy group of the amino acid survives in part in the melanoidin and that the signal of the α-carbon largely remains in the position in the melanoidin spectrum where it appears in the amino acid spectrum. Somewhat divergent from this, the ^{15}N-NMR spectrum also exhibits signals in the pyrrole, indole, and amide regions.[118] Signals for the C1 atom of the sugar can be found in all parts of the spectrum, consistent with the formation of different deoxyaldoketoses and diketoses and their derivatives. Results, obtained so far by the degradation of melanoidins with ozone and hydrogen peroxide,[119] have not led to any illuminating conclusions as regards the monomers involved in the condensation to melanoidins. Combined pyrolysis-gas chromatography of melanoidins, even when combined with mass-spectrometry, has not so far given unequivocal results either.[120] Differently produced caramel colors have been differentiated by means of Curie Point pyrolysis.[121] Electron spin resonance has also been applied to melanoidins, but so far no deductions have been drawn as regards the structure of the radicals.[122] The absorption of melanoidins in the ultraviolet and visible regions shows that condensation reactions have participated only to a limited extent in the linking of the monomers.[123] It is possible that substitution reactions play a role, as has been discussed in relation to the cross-linking of proteins.

3. Significance of the Maillard Reaction for Foods

When fire was introduced as an aid in the preparation of foods several hundred thousand years ago, the Maillard re-

action became intimately linked to food chemistry. As evident from the recipes in cookery books down the ages, the Maillard reaction serves in particular to enhance the sensory qualities of many dishes. Who does not recognize the typical aroma of warm, crusty bread, of roasted meat, or of freshly ground roast coffee? The brown shades of color of different beers, as well as of many foods that have been exposed to heat, are equally the result of the Maillard reaction. However, for some years now, it has been known that the Maillard reaction is also involved in the formation of mutagenic and carcinogenic substances and can cause a reduction in the nutritional value of foods.

3.1. Aroma

The great interest shown by the food industry in the Maillard reaction largely stems from a desire to produce and control the characteristic aromas obtained on cooking, baking, roasting, and grilling. Once the analytical technique of combined gas chromatography–mass spectrometry had been developed for the separation and identification of relatively readily volatile substances, the search for compounds with specific odors became greatly intensified. The results have been summarized in a series of review articles.[7j, 124] Herein, therefore, we shall deal only with certain aspects.

Almost invariably, it has proved possible to isolate and identify from each foodstuff (boiled, baked, roasted, etc.) hundreds of volatile compounds. The structures of compounds **166** and **179–185** are intended to give an idea of the

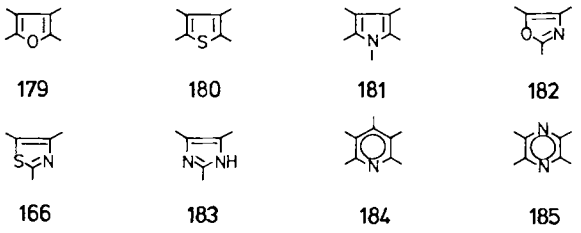

179 **180** **181** **182**

166 **183** **184** **185**

multiplicity of the heterocyclic systems encountered. To these must be added the many components based on proline and mentioned in Section 2.5.2, as well as other volatile Maillard products, such as esters, acids, ketones, aldehydes, alcohols, alkenes, alkanes, aromatic derivatives, amines, and mercaptans, that contribute to the aroma positively or negatively to a greater or lesser extent.

So far, all hopes have not been fulfilled; in particular, the aromas of boiled or grilled meat, of roasted coffee, of chocolate, and of bread cannot yet be satisfactorily reproduced by means of a single substance and one now suspects that this will never be the case. In general, reproduction of such aromas requires several components, which need to be present in the correct proportions. The so-called aromagrams allow one to estimate the contributions of the individual components to the final aroma. Aromagrams are produced by assessing with the nose, at the exit of a gas chromatograph, the volatiles separated from a complex mixture. Decisive for detection of each compound is whether its concentration in the mixture is sufficient for it to exceed the threshold at the odor port. By diluting the mixture in a stepwise manner before injection (usually by doubling the amount of solvent at each step), progressively fewer substances remain to be detected by the nose. The substances left in the later stages of the process usually carry most of the aroma of the mixture. For example, aromagrams have shown that it is not so much the trithiolane **186** and the dithiazine **187**, as previously thought,[125] that are important for the aroma of boiled meat, but the thiofuran **188** and its oxidation product **189**.[126] The acetylpyrroline **190** is one of the important contributors to the aroma of white bread,[127] whereas the typical odor of roasted nuts is in part determined by the pyrazines **191** and **192**.[128] Recently, it was shown that the concentration of the acetylpyrroline **190** is substantially dependent on the amount of C_3 products in the bread. Particularly in white bread, yeast, as well as the Maillard reaction, is an important source of these compounds (e.g., dihydroxyacetone monophosphate).[129]

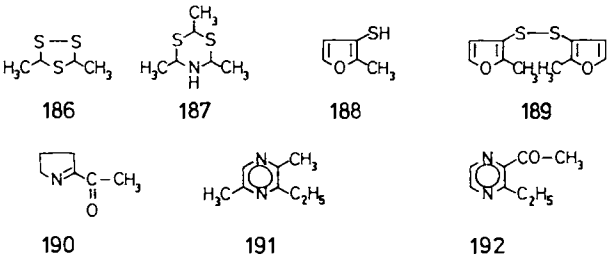

186 **187** **188** **189**

190 **191** **192**

Depending on the detailed processing conditions used and bearing in mind the variability of biological raw materials, it is not surprising that the concentrations of the intensely odorous components in foods differ greatly from sample to sample. This makes for difficulties in regulation, surveillance, and specification. Proof of the addition of aroma compounds that could have been formed by the Maillard reaction is therefore hardly possible.

3.2. Taste

When bread or meat is overheated on its surface during baking or roasting, respectively, the crust usually tastes bitter. The same effect is noted when wort boiling takes place at higher temperatures. Also model mixtures of sugars and amino acids taste bitter when they have been heated under grilling conditions. The most strongly bitter note in such experiments has been achieved with proline.[130] From reaction mixtures of this imino acid and hexoses, bitter substances **193–195** were successfully isolated.[94c, 131] It is noteworthy, that the taste threshold of the bispyrrolidine **193** lies higher by a factor of only 5 than that of quinine, i.e., **193** is already recognized as being bitter at concentrations of a few ppm. Investigations have yet to be carried out on the part played by compounds **193–195** in the bitter taste of highly heated proline-containing cereal products. A bitter taste is also exhibited by the proline-specific cyclopentazepinones **161** and **162**[94b] (cf. Section 2.8.2), as well as by the pyrroles **196** and **197**, which are formed on heating serine and threonine with hexoses.[132] However, with some

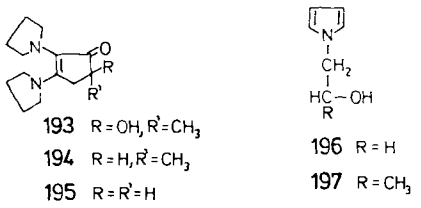

193 R = OH, R' = CH_3
194 R = H, R' = CH_3
195 R = R' = H

196 R = H
197 R = CH_3

of these compounds, the taste thresholds, so far as they have been investigated, exceed the concentrations in which they are formed.

3.3. Color

From the fact that "we also eat with our eyes", the significance of colored compounds in food chemistry can be deduced. However, the Maillard reaction contributes not only to desirable formation of color, but also to discoloration of foods, which is synonymous with a lowering of quality. The determination of the degree of browning (usually through absorbance at 420 nm) is often used analytically to assess the extent to which the Maillard reaction has taken place. Since the concentrations of the sugar and amino components in foodstuffs are very variable, measurement of the color intensity does not readily yield comparable results.

The isolation and identification of colored Maillard products has so far been achieved only with model systems. The structures of substances, in which the carbon chain of the sugar has remained intact, show that the deoxyaldoketoses and diketoses are important intermediates. Thus, the yellow compound **198** is formed by condensation of hydroxymethylfurfural **18** with the pyranone **17a**.[133] Both of these compounds are derived from the 3-deoxyaldoketose **8**. The analogous product **199** is present in reaction mixtures con-

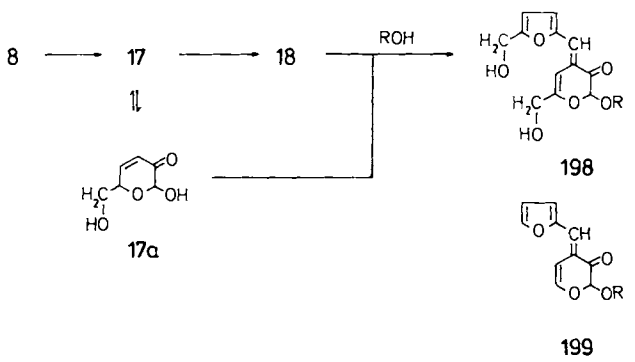

taining pentoses. These compounds may be stabilized as acetals in systems containing little water. Such systems include, for example, bread crust, from which even a short time in the baking oven removes most of the water. Reaction conditions are then favorable for acetal or ketal formation with alcohols (e.g., carbohydrates). In aqueous solution, the hemiacetal **198** (R = H) is not stable; the furanone **201** becomes the main colored product when a carbonyl compound (e.g., furfural) is added to the solution. It can be assumed that rearrangement occurs first and that subsequent condensation leads to the furanone **201**.[133] It is noteworthy that the red pyrrolinone **200** is obtained on heating furfural in the presence of a primary amine and that its structure is very like that of the furanone **201**.[134] One can deduce from this the great potential for condensation which is inherent in the 3-deoxyaldoketoses, the precursors of these colored compounds. In foodstuffs, the condensation could occur with a whole range of carbonyl compounds, so that a multitude of browning products could result by means of this type of condensation alone, quite apart from whether **200** or **201** themselves are stable end products. Indeed, this makes it understandable why the attempted isolation of colored Maillard products from heated foods has not yet been successful.

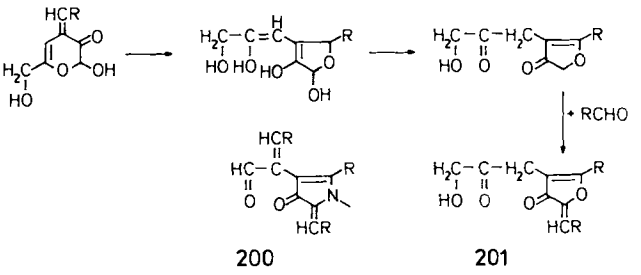

1-Deoxydiketoses can also lead to colored substances. Interaction of Amadori compounds with carbonyl compounds leads, inter alia, to the yellow compounds **202** and **203**,[135]

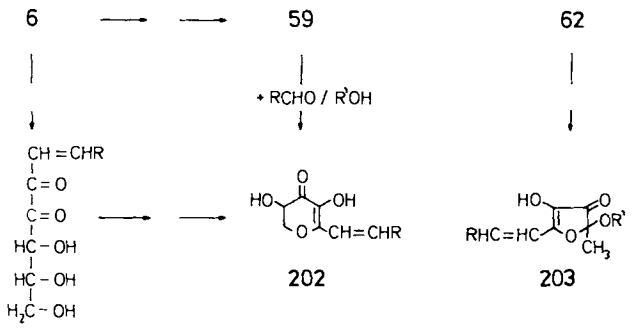

parts of which are clearly derived from 1-deoxydiketoses via **59** and **62**, respectively. The furanone **203** becomes stabilized as the ketal in media poor in water; its hemiacetal quickly reacts further.

Compound **50** (cf. Section 2.5.2) becomes the main colored product, when, to simulate media poor in water, heating is carried out in alcoholic solution. The mechanism shown is only hypothetical. As already mentioned, the furanone **48** readily loses formaldehyde with formation of the hydroxyfuranone **34**. 1-Deoxydiketose reacts in alcoholic solution to some extent as the reductone ether, which rearranges by loss of water and incorporation of the secondary amine to the cyclopentenone derivative **204**. This is subject to

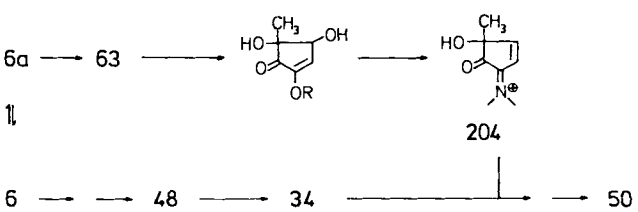

nucleophilic attack by the furanone **34** and oxidation then yields the colored product **50**.

Research on model systems has produced much data on the browning of pentoses. The structures of the yellow main products **77a** and **77b**, which are formed on heating pentoses with primary amines,[136] suggest condensation of the hydroxyfuranone **34** with furfural and pyrrolealdehyde, respectively. The formation of the colored product **35** from pentoses and secondary amines has already been mentioned in Section 2.5.1. **77a**, **77b**, and **35** also contain the hydroxyfura-

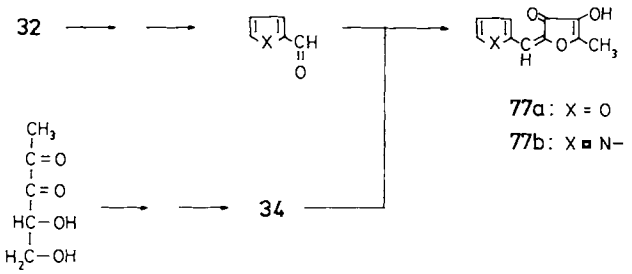

none **34** as part of their molecule. **34** is able to condense under mild conditions even with less reactive aldehydes and ketones to give colored compounds of type **77**, and, with reactive carbonyl compounds, it will even react further to give products of structure **205**.[62] Bearing in mind that, un-

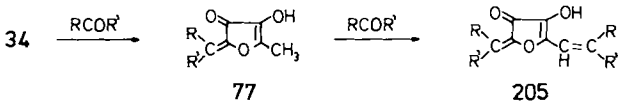

der favorable conditions, **34** may be formed in yields of 5% based on the consumed pentose, it becomes clear that this compound plays a central role in color formation. The pyranone **206** is a further colored product derived from pentoses.[134] Both 3- and 1-deoxydicarbonyl compounds can be formulated as precursors of **206**.

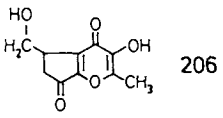

Cleavage products not only participate in the formation of volatile Maillard products, but are also found in the structures of colored compounds. The yellow pyrroles **207** and **208** were isolated from reaction mixtures of primary amines with dihydroxyacetone, pentoses, and hexoses.[34] As expected, the concentration of such pyrroles increases in these sugar reaction mixtures when the pH is raised above 7. Dihydroxyacetone and methylglyoxal, formed on loss of water, occur in smoke, so that browning products, such as **207** and

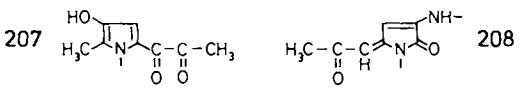

208, must be expected to be found on the surface of smoked meat and fish products.

There are further possibilities for color production during the Maillard reaction. Thus, Maillard products which possess a carbonyl function next to an enol grouping often give colored complexes with metal ions. Aqueous solutions of ferric salts turn red, violet, or blue on addition to solutions of compounds **34**, **48**, **50**, **51**, **59**, **62**, **65**, **68** (R = H), **69** (R = H), **71**, **90**, **101**, and **209**.[137] (Substance **209** is obtained from aminoketoses in the presence of oxidizing agents.) The significance of such colored complexes in the browning of heated or stored foodstuffs remains to be assessed.

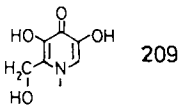

A further possibility for the formation of colored products lies in the reaction of α,β-triketones and α-dicarbonyl compounds with amino acids and peptides. As shown in Section 2.7, the Strecker degradation produces aminoenols of type **130**, which can react with further α-diketones or α,β-triketones to form colored condensation products of the general structure **210**.[138] Peptides give compounds of type **211**.[139]

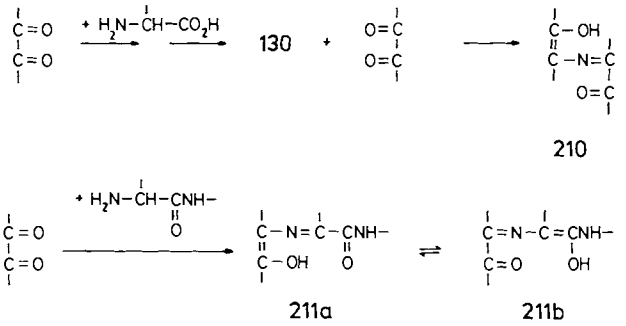

3.4. Shelf Life

It has been known for some time, that beer is stabilized against oxidative changes through substances formed by Maillard reactions occurring during the kilning of germinated barley. Without at first knowing their structure, these compounds were called reductones. The triosereductone **212** and reductic acid **213** can be prepared from sugars, but the

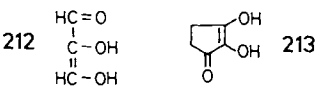

conditions required (heating in alkaline or acid solution) have no relevance to foodstuffs. It is now known that it is reductone ethers of type **34**, **48**, **51**, **59**, and **62** and aminoreductones **68**, **69**, **90**, and **101**, structurally comparable with vitamin C, that act as stabilizers. The formation of reductones in the Maillard reaction has already been dealt with (cf.

Section 2.5.2). The compounds which are preferentially reduced by reductones are only just being identified. If ascorbic acid or acetylformoin **62** reacts with diacetyl, some 3-hydroxybutan-2-one is formed, i.e., diacetyl is reduced.[140] By analogy, 1-deoxydiketoses should lead to the reduced substances **51**, **214**,[61] **215**,[141] **216**,[140] **217**,[142] and **218**,[143] as well as to the oxidized substances **219**[141] and **220**.[144]

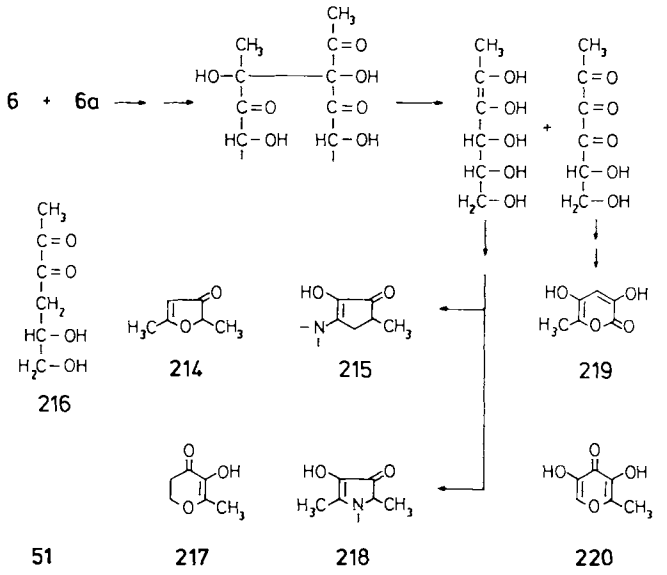

Following the same principle, one would expect the pyrrolinone **218** to be formed directly from the aminoreductone **69a**. Loss of water and addition of a second molecule allows disproportionation to **218** to take place. This mechanism at least affords an explanation for the formation of **218** upon storage of **69a**.[143]

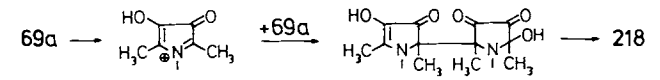

The aminohexosereductones **69a** in acid solution give good yields of the so-called methylenereductinic acid **222**.[145] Evidence for **222** in sugar–amine reaction mixtures and in foodstuffs has not yet been obtained; however, rapid condensation with carbonyl compounds to give cyclopentenediones of type **223**, as well as ready dimerization to **221**[146] provide grounds for thinking that the methylenereductic acid is too reactive to be readily detected in reaction mixtures.

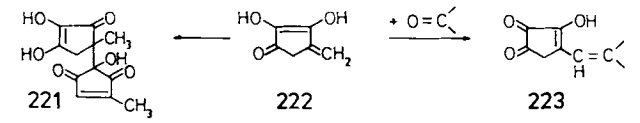

On warming the hydroxyfuranone **51**, some dimer **224** is formed, presumably via radical intermediates.[23] Longer

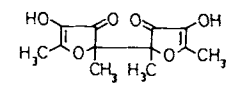

storage of the pyranone **59** leads to larger amounts of the oxidation product **220**,[144] a compound that has also been detected in heated or stored foodstuffs. The mechanism of this oxidation has not yet been ascertained, but the disproportionation of a dimeric intermediate does not seem unreasonable. Oxidation of **59** with iodine or cupric salts gives predominantly glyceric acid and lactic acid.[23]

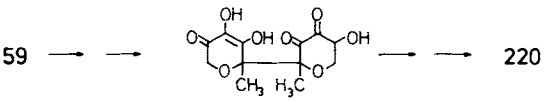

In comparative tests for antioxidant activity, aminohexosereductones **68a** perform particularly well, though their relatively high toxicity does not commend them for use in foodstuffs.[147] For detection of reductones in reaction mixtures, two methods are available: selective electrochemical determination after separation by column chromatography[148] or condensation with hydrazine to hydroxypyrazoles of type **225**, which can be determined gas chromatographically after derivatization.[149] Carbocyclic reductones cannot be con-

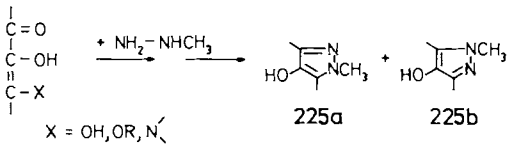

verted into hydroxypyrazoles. On treatment with methanol/toluenesulfonic acid, volatile methoxy derivatives are obtained.[141] Although it has been shown that certain melanoidins possess antioxidative properties,[150] there is no experimental evidence for the assumption that reductone groups are responsible.

3.5. Mutagenic Substances

Since the introduction of the Ames test for mutagenicity, a series of reaction mixtures, fractions, and Maillard products has been subjected to such a test. The results of experiments with foodstuffs,[151] aroma concentrates,[152] model systems,[153] and fractions derived from them are usually not comparable and are in part contradictory. At present, attention is focused on the Maillard products **172** and **173**, the carcinogenicity of which has meanwhile been thoroughly substantiated.[154] Rapid and definite detection of these compounds, which occur in some foodstuffs in ppb and less, still presents certain problems. It has been indicated already in Section 2.8.5, that steps have been taken to greatly reduce their formation. The mutagenic and carcinogenic tryptophan derivatives **150** and **151** also have a certain significance for foods.[91] Mixtures of these compounds with melanoidins isolated from reaction mixtures of glucose and glycine definitely exhibit reduced rates of mutation in the Ames test.[155] The practical implications of such results cannot yet be assessed.

The mutagenic and in part strongly carcinogenic effect of nitrosamines has been known for some time. Secondary amines present in foodstuffs can react with added nitrite during manufacture or preparation and with nitrite from saliva as they pass through the stomach. Secondary amines, such as Amadori compounds, are formed during the Maillard reaction. After addition of nitrite, except for the tryptophan derivative,[156a] no mutagenic activity is found with Amadori and Heyns compounds,[156b] but the tetrahydro-β-carbolines of postulated structure **226**[157] and nitrosothiazolidines of structure **227** exhibit unequivocal mutagenicity.[158] However, the conditions of reaction, including the

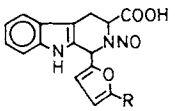

226 R = H, CH_2OH

227

concentrations of the reagents, need to be considered. For example, the incubation of soy sauce with an amount of nitrite corresponding to the maximum amount to be expected in saliva, under conditions equivalent to those in the stomach, does not lead to an enhanced rate of mutation in the Ames test, even though compounds **142** and **143** are present in this food in relatively high amounts (50 and 10 ppm, respectively).[159]

Recently, the anticarcinogenic activity of Maillard products has been reported.[160] It is postulated that reactions take place with oxygen radicals, which are trapped and thus converted into less aggressive compounds.

As well as other compounds, the Maillard products **18**, **25a**, and methylglyoxal have been shown to be mutagenic in the Ames test, while **145** and **146** have been shown to be comutagenic.[161] If, for example, one wishes to avoid the formation of compound **18** in foods, one would have to be prepared to substantially forego cooking.

3.6. Reduction in Nutritive Value

The growth of animals, which have been fed with proteins that have been heated in the presence of sugars, may be retarded. Many such studies have been carried out with milk proteins. From these, it became apparent that reaction of the sugar with the ε-amino groups of the lysine side-chains partly leads to products which the animal can no longer utilize. This is equivalent to reducing the nutritive value, since lysine is an essential amino acid. It has been shown unequivocally that the formation of the Amadori compound **3c** leads, after proteolysis of the protein in the alimentary canal, to the lysine derivative **3a**, which is worthless to the organism.[162] One of the consequences of these results has been that, in the production of milk powders and other products preferred in infant nutrition, particular attention must be paid to keeping damage to lysine to the minimum.

Amadori compounds possess good complexing properties, which lead, for example, to increased zinc excretion via urine after parenteral[11a] or oral[163] administration of such compounds. Experiments with oral intake of reaction mixtures showed that products subsequent to the aminoketoses exhibit similar effects (cf. Substance **71**).[164]

The resorption rates of higher molecular weight Maillard products from reaction mixtures of pentoses and hexoses with amino acids is very low in rats;[165] browning mixtures from proteins and sugar are somewhat better absorbed, the enzymatic hydrolysis of protein in the alimentary canal being hindered by the Maillard reaction, but not blocked.[166]

3.7. Control of the Maillard Reaction

When sterile solutions of glucose and amino acids are mixed in the cold in the preparation of infusions for parenteral nutrition and stored with refrigeration at 2 °C, evidence of the formation of aminoketoses of type **3** can be obtained in two to three weeks, and, after two months, a light yellow coloration becomes apparent.[11] A parallel situation occurs in many foodstuffs. If the Maillard reaction is to be suppressed, this can be achieved, for example, by adding sulfites[167] or, under certain circumstances, by reducing the water content/activity.[168] However, such methods are not appropriate for all foodstuffs.

It has long been known that sulfurous acid hinders the Maillard reaction. One can assume that addition of sulfite to the carbonyl group occurs,[169a] which thus becomes blocked and is no longer available for further reactions. These reactions are not always reversible, since part of the sulfite remains bound, for example, in the higher molecular weight reaction products.[169b] One of the few products isolated and identified to date has the structure **228**.[169a] It

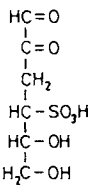

228

seems reasonable to assume that the intermediate **17** undergoes reaction with sulfite. The Maillard reaction is also hindered by the addition of divalent sulfur derivatives, such as thioglycollic acid or cysteine.[170] Since addition of sulfur-containing compounds is expected to lead to large alterations in aroma in foods, their practical application is hardly likely.

Control of the Maillard reaction in vivo by means of aminoguanidine will be discussed in Section 6.2.

4. Formation of Amadori Compounds under Physiological Conditions

4.1. Reactions of Glucose with Proteins

That the Maillard reaction also occurs in vivo only became clear when the heterogeneity of hemoglobin was discovered. Thus, it was found[171] that, when human hemoglobin is chromatographed on weakly acid ion ex-

changers, three hemoglobin fractions (HbA_{1a}, HbA_{1b}, and HbA_{1c}) elute in front of the main fraction, HbA_0 (see Fig. 1). These fast hemoglobins (designated HbA_1 as a group), which normally constitute a few per cent (5–8%) of the total hemoglobin, possess the same amino acid sequence as HbA_0. They differ only through the presence of additional, covalently bound, low molecular weight substances. The elucidation of the structure of HbA_{1c} aroused particular interest, as higher amounts of it were found by chance in the blood of diabetics.[173] With the aid of periodate oxidation, it could be shown that the hexose found in HbA_{1c} is bound at the N-terminal valine of the β-chain in the form of 1-amino-1-deoxyfructose **3b**. Since HbA_{1c} can also be obtained by in vitro incubation of HbA_0 with glucose,[175] it is clear that the formation of HbA_{1c} proceeds via the addition of glucose to the N-terminal amino group of hemoglobin, forming the Schiff's base **1**, and subsequent Amadori rearrangement to **3**. The reaction has been termed the non-enzymatic glycosylation of proteins, since, in contrast to the multitude of enzymatically formed glycoproteins, glucose is here bound to protein without mediation by enzymes. In the American literature the synonymous term 'glycation' also appears.

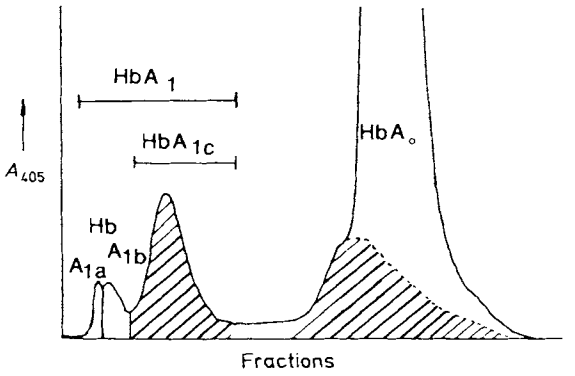

Fig. 1. Elution profile of human hemoglobin after chromatography on a weakly acid ion exchanger. Hemoglobin fraction HbA_{1c}, in which glucose is bound as structure **3b**, elutes before the main fraction HbA_0. Recently, it was shown that fraction HbA_0 also contains fructosylated hemoglobin, in which, however, glucose is bound as structure **3a** [172a]. The composition of the hemoglobin fractions HbA_{1a} and HbA_{1b} remains in part unknown. The shaded portions indicate increases with increased blood glucose concentration (diabetics). A_{405} = absorption at 405 nm.

In medical circles, 'fructosamine' is used as a synonym for **3**. Here, since the Amadori compound **3** formed is always a 1-amino-2-deoxyfructose, the term 'fructosylation' will always be employed. With hemoglobin, the preferred point of fructosylation is the amino terminal of the β-chain. The amino terminal of the α-chain is fructosylated 8–10 times less frequently in comparison.[172] Of the 22 primary amino groups of the α- and β-chains, only 3 are preferentially fructosylated. It is noteworthy, that the non-enzymatic fructosylation shows such an unexpected specificity, in which the pK_a value of the amino groups apparently plays a subordinate role. Limited steric access for glucose to the less reactive amino groups has been discussed as a possible reason for the specificity, but, meanwhile, indications have been obtained that the specificity could also be explained through acid-base catalysis by adjacent proton donor/acceptor groups.[172] As represented in a general way in Equation 1, glucose (G) reacts with the free amino groups of a protein (P), forming a Schiff's base **1**. After rearrangement to the relatively stable aminofructose **3c**, the fructosylated protein persists in the body until it is degraded.[176] The amount of fructosylated protein present in the body at a particular time represents the steady-state concentration $[\mathbf{3c}]_{SS}$.

$$G + P \underset{k_{-1}}{\overset{k_1}{\rightleftharpoons}} \mathbf{1} \underset{k_{-2}}{\overset{k_2}{\rightleftharpoons}} \mathbf{3c} \xrightarrow{k_3} \text{degradation products} \qquad (1)$$

Under steady-state conditions, when $k_{-2} \ll k_2$,[165] Equation (2) applies.[176]

$$\frac{[\mathbf{3c}]_{SS}}{[P]} = \frac{k_2'}{k_3}[G] \qquad (2)$$

The rate constant for the forward reaction is given by Equation (3),

$$k_2' = \frac{k_1 k_2}{k_{-1} + k_2} \qquad (3)$$

and that for degradation is k_3. The protein half-life can be calculated by means of the expression, $t_{1/2} = \ln 2/k_3$. The concentration of fructosylated protein (degree of fructosylation) in the steady state is therefore proportional to the glucose concentration and the ratio of the formation and decomposition constants. Since the degree of fructosylation in the steady state and the rate constant k_2' can be determined for each protein, one can calculate the decomposition constant and hence the protein half-life, provided the glucose concentration is known and constant (about 4.4 mM in the human body). On the other hand, if the rate of decomposition is known, the degree of fructosylation of a protein becomes a measure of the glucose concentration to which it has been exposed during its 'life'. In addition, the following conditions must also hold: 1. The protein must be freely accessible to the glucose in vivo (which is so for the blood proteins and the proteins of insulin-insensitive cells, where inward transport of glucose is greater than its consumption). 2. The in vivo and in vitro kinetics must correspond. Fructosylation can thus be regarded as an endogenous, non-radioactive way of marking proteins, which can be used for the estimation of the half-life of proteins.

If one determines the steady-state degree of fructosylation of human proteins that have been separated from the serum of normal subjects, and measures the corresponding in vitro rate constants k_2', the protein half-lives can be calculated.[176] Some results are presented in Table 1. The values given in the literature[177] show good agreement with the values obtained by in vitro kinetics for serum proteins. The low value obtained by the latter method for hemoglobin is associated with the fact that hemoglobin is present in red blood corpuscles not in solution, but as a concentrate (330 mg/mL).

Under conditions of increased or decreased protein turnover, as, for example, with thyroid hyper- or hypo-activity, respectively, a decreased or increased degree of fructosylation was indeed found for the human serum lipoprotein, 'low-density lipoprotein' (LDL), which is engaged in choles-

Table 1. Comparison of the half-lives $t_{1/2}$ of proteins with data from the literature. The values for the rate constant k'_2 and the degree of fructosylation in the steady state were determined in vitro.

	Mean degree of fructosylation		k'_2 [mM^{-1} d^{-1} mg^{-1}]	$t_{1/2}$	
	nmol lys-fru [a] per mg protein	mol lys-fru per mol protein		Calcd. [b]	Ref. [177]
Albumin	3.6	0.25	0.04	14.04	12–20
γ-Globulin	1.6	0.25	0.017	14.6	15–26
Fibrin peptide	0.86	0.2	0.048	3.0	4–5.5
LDL [c]	1.2	0.5	0.04	4.68	3.1–3.4
HDL [d]	1.8	0.1	0.05	5.62	4.2–4.8
Hemoglobin	2.0	0.13	0.023	13.6	70

[a] Lysines reacted at ε-amino groups; structure **3c**. [b] From $t_{1/2} = \ln 2/k_3$. [c] Low density lipoprotein (cholesterol-transporting protein). [d] High density protein (cholesterol-removing protein).

terol transport.[176b] Particularly interesting was the observation that the degree of fructosylation of LDL of normal subjects was correlated with the LDL-cholesterol level: a doubling of the level is reflected in a doubling of the degree of fructosylation of the LDL[176b] (cf. Section 5.2). In Figure 2, an experiment is presented in which a model reaction simulates the in vivo protein turnover.[176b] An albumin so-

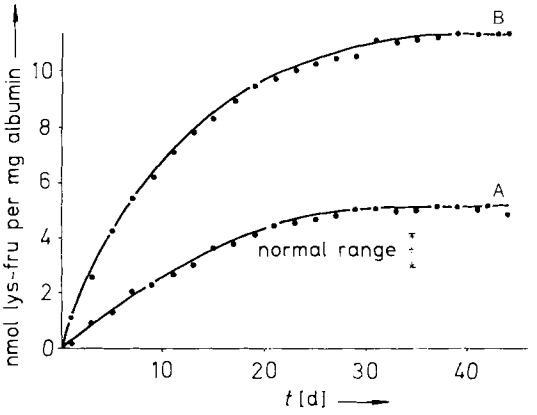

Fig. 2. Simulation of human protein-turnover in vitro. Human serum albumin incubated with 7.2 (A) and 14.4 (B) mM D-glucose, respectively. Each day, a twentieth part of the total was removed and replaced by the same amount of further original medium. Additional details appear in the text.

lution was incubated with two different concentrations of glucose and daily a twentieth of the solution was replaced by starting solution. This daily 'elimination' of 5% corresponds to a half-life of 13.8 days in a first-order degradation reaction. The border concentration between normal and raised blood-sugar level was taken to be 7.2 mM and the concentration for diabetics 14.4 mM glucose. After 40 days, equilibrium is more or less achieved. The steady-state value for 7.2 mM glucose was 5.1 nmol lys-fru per mg albumin, whereas, with the doubled glucose concentration, roughly double the degree of fructosylation was obtained (lys-fru indicates structure **3c**). From these values one can estimate that the in vitro steady-state fructosylation of 3.6 nmol albumin required a glucose concentration of about 5 mM. This concentration of glucose agrees well with the mean glucose concentration of normal subjects (4.4 mM), i.e., the in vitro reaction conditions appear to reflect those in the body relatively well.

4.2. Comparison of the Structure of Enzymatically Glycosylated and Non-enzymatically Fructosylated Proteins

In many glycoproteins, different sugars (e.g., galactose) are bound *O*-glycosidically to serine or threonine present in the peptide chain (cf. structure **229**). For a long time, only one type of *N*-glycoside had been characterized, namely, *N*-acetylglucosamine[178] bound *N*-glycosidically to the amide nitrogen of asparagine (cf. structure **230**).

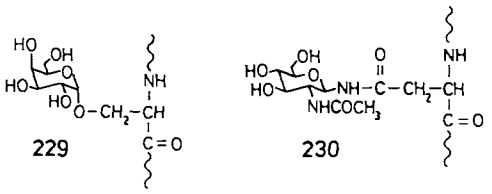

In contrast, the fructosylation of proteins takes place mainly on the free amino groups of the lysine residues[179] (cf. structure **3c** and Section 4.1). The conformation of fructosylated proteins in aqueous solution has been examined by ^{13}C-NMR spectroscopy.[180] RNase A from bovine pancreas was used as the model protein. The results showed that the protein-bound hexoses are almost exclusively present in cyclic form, as would be expected by analogy with the free hexoses. The glucosylamine **1**, as well as the ketosamine, prefers the β-pyranose form (see structural formulas in Section 2.4). Since the reference compounds, *N*-α-formyl-ε-fructoselysine and fructosylated poly-L-lysine, exhibit resonances corresponding to those of the fructosylated enzyme (RNase), it seems that the protein matrix has relatively little influence on the conformation of the hexose.

4.3. Methods for the Quantitative Determination of Non-enzymatically Fructosylated Proteins

Since many of the methods used in food chemistry to detect and determine in vivo fructosylated proteins are not specific and sensitive enough, a series of alternative methods has been developed. Most of the methods of detection depicted in Figure 3 do not proceed stoichiometrically; they constitute therefore not absolute, but only relative methods of determination. Theoretically, it should be possible to quantify **3**, bound in a protein, after hydrolysis of the protein. However, **3** is not stable under the strongly acid conditions of hydrolysis; one obtains about 50% free lysine and about 30% **82a** (cf. Section 2.5.4). It could be shown[64] that **82a**, determined by means of an amino acid analyzer, can be used to measure the degree of heat damage suffered by foodstuffs, especially milk products, through non-enzymatic browning. Considerably smaller amounts of **82a** can be determined by HPLC.[181] Use of this method allowed 50 pmol **3c** in 5–25 μg protein to be determined specifically and precisely. A further advantage of the method is that it

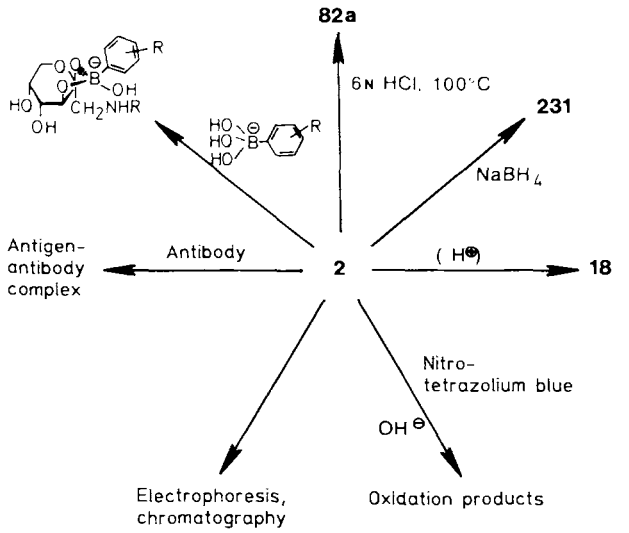

Fig. 3. Reactions providing evidence of the presence of fructosylated proteins. The reactions on the right occur with modification of structure **3**, those on the left without such modification.

permits insoluble tissues (e.g., collagenous ones) to be investigated.

Fructosylated proteins can also be determined in the amino acid analyzer after sodium borohydride reduction to **231** and subsequent hydrolysis, in which **231** dehydrates to a

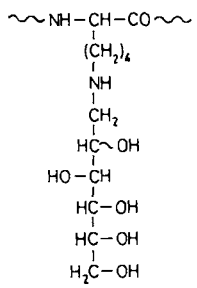

231

considerable extent. Usually the sensitivity needs to be improved, for which purpose tritiated sodium borohydride is employed. The determination of **18**, which is frequently used in food chemistry because it is readily formed from **3** on mild acid hydrolysis (cf. Section 2.5.2), can only be applied here under special circumstances.[182, 183]

The characteristic behavior of Amadori compounds on reduction was employed for their detection relatively early on.[3a, 6] In alkaline solution, **3** enolizes to the strongly reducing enaminol **5**, which can be determined and quantified by means of various redox indicators, such as dichlorophenolindophenol. Since the reductone formed also possesses reducing properties, the reaction without, firstly, unequivocal stoichiometry and, secondly, a clearly defined endpoint. To overcome these problems, it was suggested that the reaction be determined kinetically with Nitrotetrazolium Blue as the reducing agent.[184] It became evident that at pH 10.3 neither glucosylamine nor free glucose participated in the reaction to any marked extent. By appropriate choice of time window, the specificity could be improved, because other reducing substances, present in human serum, have substantially completed their reactions within the first ten minutes. The alteration in the pK_a of hemoglobin fructosylated at valine **3b**, which had led to the discovery of the fructosylated hemoglobins, was used at first by all researchers to separate and quantify **3b** by means of ion-exchange chromatography, electrophoresis, or isoelectric focusing.[185] Since, as already mentioned, most proteins are mainly fructosylated at the ε-amino groups of lysine residues (cf. structure **3a**), which exhibit substantially less change in pK_a these methods are not universally applicable (cf. Fig. 1). Attempts to detect **3** with phenylhydrazine as a carbonyl reagent failed, because of insufficient reactivity and sensitivity.[186]

Although some protein-bound sugar structures exhibit extraordinary antigenicity, early trials showed already that structure **3** becomes antigenic only after reduction to **231**. However, the binding of the antibody to **231** is not quantitative for all fructosylated proteins, probably because of steric hindrance, so that the method is not universally applicable.[187]

Fructosylated amino acids and peptides bind specifically to matrix-bound boric acid, with formation of a boric ester (see Fig. 3), and can be quantified after elution with acid or sorbitol.[188] However, this procedure also is not quantitative for many proteins and therefore not appropriate, probably again because of steric hindrance. Our own investigations have shown that boric ester formation can also take place with substituted phenylboric acids in homogeneous aqueous solution.[189] Since the absorption maximum of **232** moves to shorter wavelengths on esterification, **3** can be quantified photometrically.

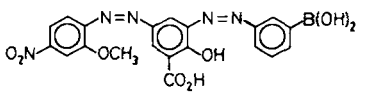

232

It can be seen that, in spite of the number of methods described, there is no generally applicable technique for determining precisely and specifically proteins that have been fructosylated in the human body. For each particular protein, the most appropriate method has to be selected from those available.

4.4. Detection of Fructosylated Proteins in Human Blood and Tissues

Only in this decade was it realized that many human proteins, not just hemoglobins, are fructosylated. About ten years ago, it was shown[190] that human serum albumin is also fructosylated. As with hemoglobin, the position of fructosylation is relatively specific. Only nine of 55 ε-amino groups are measurably fructosylated, LYS-525 being most strongly attacked (50% of the total fructosylation). The degree of fructosylation of some blood proteins is listed in Table 1. Since diabetics have higher blood-sugar values (about 2–5 fold), some proteins from diabetics may bind more than 1 mol fructose per mol protein. Other plasma

proteins, such as α_1-antitrypsin, fibronectin, plasminogen, antithrombin-III, ApoE, and ApoC II, can of course be determined, but, mainly because of their short half-life (hours, 1–3 days), they are hardly fructosylated.[191] Not only soluble proteins, but also membrane-bound proteins are subject to fructosylation, as has been demonstrated with erythrocytes.[192] With human tissue proteins, the degree of fructosylation depends, amongst other factors, on whether glucose has ready access to the proteins (as with extracellular proteins such as connective tissue) or whether (as with intracellular proteins) the glucose concentration in the cell is very low. This is particularly relevant for insulin-sensitive tissue, i.e., tissue in which glucose uptake is regulated by insulin. As a consequence, fructosylation could not be detected in the proteins of the muscles of the heart or skeleton.[193]

In contrast, in insulin-insensitive tissue, such as nerve-tissue, **3c** could be detected.[193] Tissue containing collagen has been particularly thoroughly investigated. Figure 4 shows values for the content of **3c** in tendon, aorta-wall,

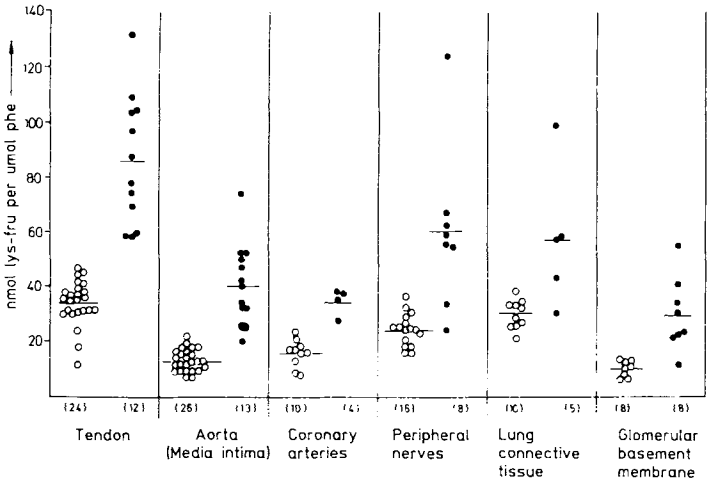

Fig. 4. Non-enzymatic fructosylation of several tissues from diabetic (●) and normal (○) patients. The horizontal lines indicate the arithmetic means. The number of cases is given in brackets for each type of tissue. Fructosylation is expressed in nmol lys-fru per μmol phenylalanine, which serves as an arbitrary measure of the amount of protein. The glomerular basement membrane is the collagenous dialysis membrane of the kidney.

nerve tissue, lung connective tissue, and glomerular basement membrane. **3c** has also been detected in hair and in finger nails (cf. Section 6.1). The mean values for the different tissues of normal subjects correspond roughly to a fructosylation of 1–3% of all the lysine residues. The mean values for individual diabetics are more variable than those for non-diabetics, corresponding to greater differences in metabolism. The degrees of fructosylation of the different tissues correlate well with each other: patients with high fructosylation of tendons also exhibit high fructosylation in other tissues. Mean blood sugar levels also correlate surprisingly well with the degree of fructosylation of tissues.

Of particular interest is the question whether the degree of fructosylation of proteins, especially that of connective tissue, increases during life. Although one paper[194] describes a doubling of the degree of fructosylation of human tendon collagen during a lifetime, other researches, using more specific methods, showed a smaller increase (about 50%) in the fructosylation of tendon and aorta tissue.[176b] However, a very clear relationship between degree of fructosylation and age has been established for lens tissue of the eye.[195]

Since, according to present knowledge, fructosylated amino acids cannot be metabolized in the mammalian organism (cf. Section 3.6) and since they have good solubility in water, they should be eliminated largely in the urine. In fact, normal subjects do excrete significant amounts of fructosylated amino acids, about 0.1–0.3 mmol per day.[188, 196] As some foodstuffs contain substantial amounts of free or bound fructoselysine, **3a** and **3c**, respectively, the question arises whether the excreted fructosylated amino acids are not in part of exogenous origin. Evidence that this is not so comes from the fact that fasting for 24 hours leaves the excretion rate unchanged, fasting for 10 days even increasing it. This increase is due to heightened protein degradation (catabolism). With animal experiments it has been shown that exogenous fructosylated amino acids and proteins are degraded by microorganisms in the gut. Mammals cannot make use of fructosylated amino acids. Diabetics excrete increased amounts of fructoselysine in their urine, corresponding to their metabolic state.[188, 196]

4.5. Do Subsequent Reactions also Occur in vivo? Formation of 'Advanced Glucosylation End Products' (AGE)

Whether the Amadori product **3**, in a way corresponding to the browning reaction of food chemistry, also reacts further in vivo and so provides a possible mechanism of aging is an interesting problem. The first support came from finding that the fluorescence specific for browning pigments increased for tendon collagen in a linear manner with age.[197] Samples obtained from diabetics did not give readings falling into the normal range, but exhibited greater fluorescence. Since **3** does not fluoresce, derivatives must have been formed. In model reaction mixtures of bovine serum albumin and glucose, a corresponding fluorescence was clearly present after 30 days.[198] From the solution obtained from the protein after acid hydrolysis, the fluorescent product **88** was isolated. As already outlined in Section 2.5.4, it is probably an artefact. Meanwhile, the pyrrolealdehyde **25b** has been shown to be present in a number of native proteins by means of a specific antibody, thus proving the presence of derivatives of **3** in vivo.[30] The mechanism of formation has already been described in Section 2.5.1.

A further derivative, carboxymethyllysine **128**, also formed in vivo, has been detected in the meantime (cf. Section 2.6.2). This therefore explains the excretion of **128** in urine, which had been known for some time.[199] **128** has also been found in the eye lens, where its concentration increases linearly with age.[199] The interesting observation has been made that in vitro **3a** leads to more browning pigments in the absence of oxygen than in its presence, but without formation of **128**.[77] It was therefore proposed that the excretion of **128** can be used as a general indicator of the age of extracellular protein and the ratio of excreted **3a**/**128** as a general indicator of oxidative stress in the human body.[199] Meanwhile, in a model reaction, a further pyrrolealdehyde,[200] **39**,

has been found, the mechanism of formation of which has already been postulated (cf. Section 2.5.1). In the presence of sodium sulfite, compound **39** accumulates, while, in the absence of sulfite, it very quickly forms cross-links with the free amino groups of proteins. One can assume that compounds of type **233** are formed.

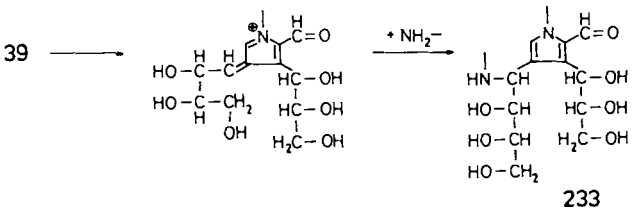

Meanwhile, the Maillard product **167** has also been isolated from human tendon.[101] The structure of this cross-link implies participation of lysine, arginine, and a pentose. Since, so far, nothing is known of the role of arginine and of pentoses in the Maillard reaction in vivo, the significance of **167** for the cross-linking of proteins cannot yet be evaluated.

Recently, it was demonstrated that the Maillard reaction is involved not only with proteins, but also with nucleic acids.[201] Incubation of DNA with reducing sugars leads to the formation of brown fluorescent substances, the spectroscopic properties of which resemble those of AGE-proteins. Such modified DNA (AGE-DNA) on transcription exhibits specific mutations, caused by insertions or deletions. Cross-linking between proteins and DNA was also evident. Whether such protein-AGE-DNA cross-linking also takes place in human cells has not yet been demonstrated, but, on the basis of the above findings, seems not unlikely.

5. Does the Maillard Reaction Lead to Modification of the Structure and Function of Proteins?

5.1. Effects on the Structure of Proteins

Fructosylation of bovine lens protein leads to a dulling of crystallin.[202] Since this opaqueness does not appear in the presence of reducing agents, it is assumed that fructosylation gives rise to a subsequent change in conformation, exposing sulfhydryl groups and thus allowing dimerization of the protein. In cataracts (lens dulling) from diabetic and galactosemic rats, evidence was obtained for aggregates of crystallin, linked by disulfide bonds.[203] As, according to other studies, crystallin is fructosylated in a time- and concentration-dependent manner, one is led to assume that the Maillard reaction plays a role in the development of cataracts with age or diabetes.

Since cross-linking of the free lysine sidechains of the long-persisting connective tissue proteins, collagen and elastin, is of essential significance, the relationship between the fructosylation of collagen and its properties has been extensively investigated. During physiological cross-linking of collagen, a lysyl oxidase oxidizes a few lysyl and hydroxylysyl residues to the corresponding aldehydes, which subsequently cross-link with the ε-amino groups of neighboring collagen molecules. The attack of glucose on a lysyl or hydroxylysyl residue should inhibit the reaction and thus lead to reduced cross-linking of collagen. In actual fact, the opposite was found. To explain these experimental results, one must therefore draw on other mechanisms. As already described (cf. Section 4.5), fructosylated lysyl groups can themselves form cross-links via derivatives such as **39** and **167**. Such non-physiological cross-links are formed in collagen fibers between collagen molecules lying alongside one another, thus increasing the mechanical stability, but lowering the solubilization by acids or enzymes. In model experiments, it has in fact been shown that tendon has greater mechanical strength after incubation with glucose. Incubating tendon with glucose simulates the increase in tensile strength which takes place with age.[204] Using RNase as an example, it has been shown that this enzyme, on fructosylation in vitro, undergoes di- and trimerization in a time-dependent manner.[205] This cross-linking continues even after removal of the glucose and can be almost completely inhibited by simultaneous incubation with L-lysine. The reaction mechanism was considered to involve condensation of an amino group of the protein with **3a** of another protein, thus producing cross-links (structure **13**). Meanwhile, it has been shown that such cross-linking can also take place between different proteins.[200, 206] When serum albumin or immunoglobulin G is added to collagen, previously incubated for a longer period with glucose, they become covalently bound. In fact, with diabetic animals, five times more immunoglobulin G is bound to collagen than with non-diabetic ones. Particularly interesting is the discovery that the cholesterol-transporting serum lipoprotein LDL can be bound covalently in this manner to fructosylated collagen (e.g., in the arterial wall).

5.2. Effects of Fructosylation on the Function of Proteins

Fructosylation occurs primarily on the free ε-amino groups of lysine bound in proteins. These amino groups of lysine are of essential significance in the active centers of numerous proteins with functions in catalysis, transport, binding, and structure. They also play an important role in interactions, such as those between hormone and hormone receptor, antigen and antibody, and enzyme and enzyme inhibitor. Hence, it is an attractive hypothesis to postulate that fructosylation of lysyl residues, occupying strategically important positions, is detrimental to the functionality of the protein affected. However, when transaminases were fructosylated in vitro, no reduction in enzyme activity was found.[189] Evidently, the lysine at the active center, which forms a Schiff's base with the cofactor, pyridoxal phosphate, must be protected from fructosylation. In contrast, on incubation with glucose, ribonuclease A loses 50% of its original activity in 24 hours, whereas cathepsin B and papain lose about 70% in 2 weeks.[207] With these enzymes, it appears that fructosylation of the lysine, which lies close to the active center, is responsible for the reduction in activity.

Changes in conformation are also possible factors, as has been shown with the β-*N*-acetyl-D-glucosaminidase from bovine kidney as example.[208] The activity was already reduced to a half after seven days' incubation with 44 mM D-glucose. Studies with the separated isoenzymes A and B

demonstrated that isoenzyme A is completely inactivated, whereas B remains fully active. The changes in functionality are accompanied by alterations in structure. Thus fructosylation changes the electrophoretic mobility. The molecular mass increases from 130 to 205 kDa. To what extent these reductions in activity and changes in structure play a role also in vivo is so far not known. A series of experiments indicates that fructosylated proteins are less readily split on proteolysis. Thus, it appears that the cross-linking of protein chains, which occurs during the course of the non-enzymatic browning reaction between reducing sugars and proteins, also affects their ease of hydrolysis (cf. Sections 3.6 and 5.1). The proteolytic cascade involved in blood clotting has been the subject of research by many groups. The inhibitory effect of antithrombin III is considerably reduced on incubation for 3 days with 100 mM glucose; 400 mM glucose reduces it to half. Such reduced functionality of antithrombin III leads to higher thrombin activity and to increased formation of fibrin peptide. The greater the degree of fructosylation of the fibrin peptide, the more slowly is it cleaved by plasmin.[209] Hormone activity can also be affected by fructosylation, as can be seen, for example, with insulin. The diminished activity of insulin can be demonstrated on fat cells through reduced glucose oxidation, increased de novo fatty acid synthesis, and reduced antilipolytic properties.[210] Since these effects only appear with very high degrees of fructosylation, it is likely that these results are not relevant to the situation in vivo. The cholesterol-transporting LDL of human blood normally contains about 0.5 mol lys-fru per mol.[191b] Detailed research in vitro showed that modification of the ε-amino groups of LDL led to a reduction in binding to the LDL-receptors, which are attached to the cell membrane.[211] The reduction in binding, uptake, and metabolism of LDL by different human cells could be demonstrated, also for fructosylated LDL, to be dependent on the amount of glucose bound. It is noteworthy that fructosylated LDL in human macrophages can stimulate cholesterol ester synthesis. It seems possible, therefore, that fructosylation of LDL and the corresponding derivatives (AGE products) favor the formation of foam cells (macrophages are taken to be precursors of the foam cells of the atherosclerotic plaques). The relevance, in this connection, of the interesting observation that raised LDL-cholesterol levels are accompanied by increased degrees of fructosylation (cf. Section 4.1), is so far not known.

5.3. Immunogenicity of Fructosylated Proteins and their Reaction Products

Several attempts to detect unequivocally antibodies against structure **3** in human blood have thus far not succeeded. This corresponds to the results of animal experiments, which indicate that fructosylated proteins possess little antigenicity (cf. Section 4.3). Since the amount of AGE products, which has been found in the different long-life body proteins, is much less than had been expected on the basis of in vitro studies, the possibility was investigated of the existence of a mechanism in the living organism that is capable of selectively removing AGE proteins. It was indeed shown that, in immunocompetent cells (macrophages), there is a high-affinity receptor, able to bind AGE proteins, to take them into the cell, and to degrade them.[212] This receptor for AGE proteins has already been extracted from the macrophage membrane and concentrated. However, this degradation system for AGE proteins does not seem to be totally efficient, since the aging products accumulate over the life span of the individual as a function of time and of the blood glucose level.

6. Medical Aspects of the Maillard Reaction

6.1. The Maillard Reaction as Diagnostic of the Metabolic State of Diabetics

The degree of fructosylation of proteins in the human body, under steady state conditions, is proportional to the half-life of the protein and to the glucose concentration (cf. Section 4.1). Thus, provided the protein half-life remains constant, the mean concentration of glucose to which that protein has been exposed during its life time in the body can be calculated. The degree of fructosylation can therefore be used to calculate the blood glucose level retrospectively. The fructosylated proteins represent a sort of blood sugar memory. Depending on the time frame one wishes to investigate, so one selects a protein with an appropriate half-life. Thus, for example, hemoglobin is suitable for checking on the blood sugar level over the last 2–3 months, whilst the determination of the fructosylated serum proteins mirrors the mean blood glucose concentration over the last 2–3 weeks. By means of the furosine method (cf. Section 4.3), raised glucose levels can even be determined from the degree of fructosylation of finger nail or hair proteins.[213] The determination of the fructosylated blood proteins thus leads to the objective assessment of the state of metabolism, which is clinically helpful both for the physician and the patient. The patient is given a straight motivating indicator and the physician can take into account the mean blood sugar values over a considerable time, without the effort of having to determine the individual values.

Since the late complications of diabetes appear, in particular, in the insulin-insensitive tissues, the fructosylation of the proteins of these tissues was compared with the severity of the late complications.[193] Diabetics with severe late complications in several organs exhibited a high degree of fructosylation of tendon or aorta tissue. These results point to a connection between poor metabolic control and the development of diabetic late complications. In accordance with this, it could be shown recently that diabetics with high amounts of AGE proteins suffer from increased damage to eyes and kidneys.[214]

6.2. Intervention in the Maillard Reaction in vivo

Once the Maillard reaction had been recognized as the cause of undesirable, glucose-dependent cross-linking of proteins in the human body, ways of suppressing the reaction were sought. For many years, food chemists have employed sulfite as an additive to inhibit the formation of Maillard products in foods (cf. Section 3.7). For administration

with **3** or other rearrangement products. It could be shown that aminoguanidine **234** inhibits the formation of AGE substances and the cross-linking of proteins in vivo as well as in vitro.[215] After administration of aminoguanidine, no accumulation was observed of immunoglobulins in the collagen network of the blood vessels of diabetic rats. Further research showed lowered cross-linking of the collagen and less deposition of the cholesterol-transporting lipoproteins on the arterial walls. Studies of toxicity in different mammals and in healthy humans provided evidence that **234** is relatively well tolerated. It is planned to test **234** as a drug to hinder the cross-linking caused by the Maillard reaction and thus to reduce late complications in diabetes and the damaging effects of aging.

It is assumed that aminoguanidine reacts preferentially with **3** to form hydrazones of type **235**. In in vitro experiments, the triazine **236** is formed to some extent. A probable mechanism for its formation is the retroaldolization of **3** to methylglyoxal **96**, which then condenses with amino-

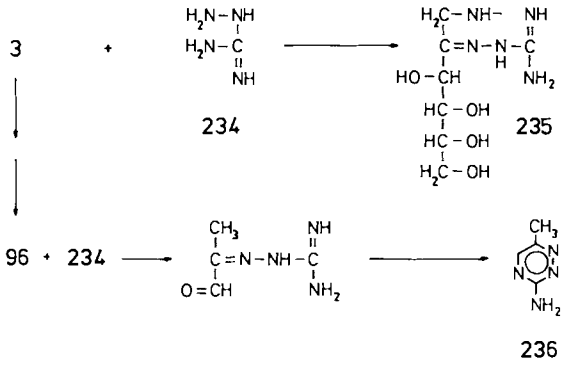

guanidine. Reaction of the hydroxyfuranone **62** with aminoguanidine at pH 7–8 leads to formation of the hydroxytriazine **237**.[216] It can be assumed that **62** is cleaved to give pyruvic acid, which then cyclizes with aminoguanidine

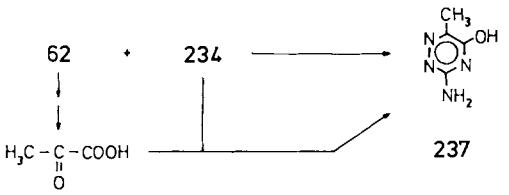

to give **237**. The extent to which the formation of triazines also occurs in vivo still needs to be ascertained.

7. Summary and Outlook

Even 78 years after its discovery, the Maillard reaction with its multitude of reaction pathways and products is still only known in outline. In food chemistry, the objectives are to have the Maillard reaction proceed in such a way that the formation of toxic substances and the reduction in nutritional value are suppressed, whilst, simultaneously, desirable components are formed in optimal amount. Although it was first realized only relatively recently that the Maillard reaction also occurs in the human body, evidence has already been provided for a series of structural and functional changes in fructosylated proteins. However, in the foreseeable future, it will continue to prove difficult to show that, from the confusing multiplicity of Maillard products, specific, defined substances are responsible for the complex processes of aging. Current efforts aim particularly to hinder the undesirable Maillard reaction in the human organism and thus the "Verzuckerung" of man and its consequences during his or her life time.

We are greatly indebted to Prof. Dr. K. D. Gerbitz, Dr. B. Olgemöller, and Dipl.-Chem. S. Prytulla for critically reading the manuscript and to Prof. Dr. Th. Severin for many helpful comments.

Received: June 21, 1989;
revised: November 27, 1989 [A 762 IE]
German version: *Angew. Chem. 102* (1990) 597
Translated by *Professor H. E. Nursten*, Reading (UK)

[1] L. C. Maillard, *C. R. Acad. Sci. Ser. 2, 154* (1912) 66; *ibid. 155* (1912) 1554.
[2] M. Amadori, *Atti R. Acad. Naz. Lincei Mem. Cl. Sci. Fis. Mat. Nat. 13* (1931) 72.
[3] a) R. Kuhn, F. Weygand, *Ber. Dtsch. Chem. Ges. B 70* (1937) 769; b) F. Weygand, *ibid. 73* (1940) 1259.
[4] H. Simon, A. Kraus, *Fortschr. Chem. Forsch.* 14 (1970) 389.
[5] K. Heyns, H. Paulsen, R. Eichstedt, M. Rolle, *Chem. Ber. 90* (1957) 2039.
[6] H. Paulsen, K. W. Pflughaupt in W. Pigman, D. Horton (Eds.): *The Carbohydrates: Chemistry and Biochemistry, Vol. IB*, Academic Press, New York 1980, p. 881.
[7] Übersichtsartikel: a) T. M. Reynolds, *Adv. Food Res. 12* (1963) 1; *ibid. 14* (1965) 167; b) M. Angrick, D. Rewicki, *Chem. Unserer Zeit 14* (1980) 149; c) C. Eriksson (Ed.): *The Maillard Reaction in Foods, Prog. Food Nutr. Sci. 5*, Pergamon Press, Oxford 1981; d) G. Waller, M. S. Feather (Eds.): *Maillard Reactions in Food and Nutrition, ACS Symp. Ser. 215*, American Chemical Society, Washington D.C. 1983; e) G. Westphal, L. Kroh, *Nahrung 29* (1985) 757, 765; f) W. Baltes, *Lebensmittelchem. Gerichtl. Chem. 40* (1986) 49; g) M. Fujimaki, M. Namiki, H. Kato (Eds.): *Amino-carbonyl Reactions in Food and Biological Systems, Dev. Food Sci. 13*, Elsevier, Amsterdam 1986; h) M. Namiki, *Adv. Food Res. 38* (1989) 115; i) J. W. Baynes, V. M. Monnier (Eds.): *The Maillard Reaction in Aging, Diabetes and Nutrition, Prog. Clin. Biol. Res. 304*, A. R. Liss Inc., New York 1989; j) T. H. Parliment, R. J. McGorrin, C.-T. Ho (Eds.): *Thermal Generation of Aromas. ACS Symp. Ser. 409*, American Chemical Society, Washington D.C. 1989; k) P. A. Finot, H. U. Aeschbacher, R. F. Hurrel, R. Liardon (Eds.): *The Maillard Reaction in Food Processing, Human Nutrition and Physiology*, Birkhäuser Verlag Basle, Brussels, Berlin 1990.
[8] a) R. Wittmann, K. Eichner, *Z. Lebensm. Unters. Forsch. 188* (1989) 212; b) H. Hashiba, *Agric. Biol. Chem. 42* (1978) 1727; c) J. Steinig, A. Montag, *Z. Lebensm. Unters. Forsch. 174* (1982) 453; d) K. Heyns, H. Paulsen, *Justus Liebigs Ann. Chem. 622* (1959) 160.
[9] a) H. Sulser, W. Büchi, *Lebensm. Wiss. Technol. 2* (1969) 105; b) M. Ciner-Doruk, K. Eichner, *Z. Lebensm. Unters. Forsch. 168* (1979) 9, 360; c) A. B. Möller, A. T. Andrews, G. C. Cheeseman, *J. Dairy Res. 44* (1977) 267; d) H. Erbersdobler, *Milchwissenschaft 25* (1970) 280.
[10] H. Hashiba, *Agric. Biol. Chem. 42* (1978) 763.
[11] a) L. D. Stegink, J. A. Shepherd, L. K. Fry, L. J. Filer, *Pediatr. Res. 8* (1974) 396; b) B. Huber, H. Krämer, F. Ledl, L. Vogel, *Krankenhauspharmazie 10* (1989) 168.
[12] a) J. Beck, F. Ledl, T. Severin, *Carbohydr. Res. 177* (1988) 240; b) *Z. Lebensm. Unters. Forsch. 188* (1989) 118; c) H. Huber, F. Ledl, *Carbohydr. Res.*, in press.
[13] E. F. L. J. Anet, *Austr. J. Chem. 10* (1957) 193.
[14] a) W. Baltes, K. Franke, *Z. Lebensm. Unters. Forsch. 167* (1978) 403; b) L. Kroh, G. Westphal, *Z. Chem. 23* (1983) 293.
[15] a) J. F. Carson, *J. Am. Chem. Soc. 77* (1955) 1881, 5957; b) K. Heyns, R. Eichstedt, K. H. Meinecke, *Chem. Ber. 88* (1955) 1551.
[16] K. Heyns, G. Müller, H. Paulsen, *Justus Liebigs Ann. Chem. 703* (1967) 202.
[17] W. Nedvidek, F. Ledl, unpublished.
[18] M. S. Feather, J. F. Harris, *Adv. Carbohydr. Chem. Biochem. 28* (1973) 161.

[19] G. Machell, G. N. Richard, *J. Chem. Soc. 1960*, 1924, 1932, 1938.
[20] a) E. F. L. J. Anet, *Austr. J. Chem. 13* (1960) 396; b) *J. Am. Chem. Soc. 82* (1960) 1502; c) H. Kato, *Bull. Agric. Chem. Soc. Jpn. 24* (1960) 1.
[21] a) E. F. L. J. Anet, *Chem. Ind. (London) 1962*, 262; b) *J. Chromatogr. 9* (1962) 291.
[22] K. Olsson, P. A. Pernemalm, O. Theander, *Acta Chem. Scand. Ser. B 32* (1978) 249.
[23] J. Beck, F. Ledl, M. Sengl, T. Severin, *Z. Lebensm. Unters. Forsch. 190* (1990) 212.
[24] a) E. F. L. J. Anet, *Tetrahedron Lett. 1966*, 1649; b) *Carbohydr. Res. 2* (1966) 448.
[25] a) R. Kuhn, G. Krüger, *Chem. Ber. 90* (1957) 264; b) J. N. BeMiller, R. L. Whistler, *J. Org. Chem. 27* (1962) 1161.
[26] G. R. Jurch, J. H. Tatum, *Carbohydr. Res. 15* (1970) 233.
[27] O. Pachmayr, F. Ledl, T. Severin, *Z. Lebensm. Unters. Forsch. 182* (1986) 294.
[28] K. Olsson, P. A. Pernemalm, T. Popoff, O. Theander, *Acta Chem. Scand. Ser. B 31* (1977) 469.
[29] H. Shigematsu, T. Kurata, H. Kato, M. Fujimaki, *Agric. Biol. Chem. 35* (1971) 2097.
[30] F. Hayase, R. H. Nagaraj, S. Miyata, F. G. Njoroge, V. M. Monnier, *J. Biol. Chem. 264* (1989) 3758.
[31] a) F. Ledl, M. Sengl, T. Severin, *J. Chromatogr. 463* (1989) 119; b) U. Schüssler, F. Ledl, *Z. Lebensm. Unters. Forsch. 189* (1989) 32.
[32] H. Kato, *Agric. Biol. Chem. 31* (1967) 1086.
[33] R. Tressl, B. Helak, D. Rewicki, *Helv. Chim. Acta 65* (1982) 483.
[34] F. Ledl, U. Krönig, T. Severin, H. Lotter, *Z. Lebensm. Unters. Forsch. 177* (1983) 267.
[35] F. G. Njoroge, A. A. Fernandes, V. M. Monnier, *J. Carbohydr. Chem. 6* (1987) 553.
[36] J. G. Farmar, P. C. Ulrich, A. Cerami, *J. Org. Chem. 53* (1988) 2346.
[37] a) T. Severin, U. Krönig, *Z. Lebensm. Unters. Forsch. 152* (1973) 42; b) S. Estendorfer, F. Ledl, T. Severin, unpublished; c) U. Krönig, *Dissertation*, Universität München 1974; d) Estendorfer, F. Ledl, T. Severin, *Angew. Chem. 102* (1990) 547; *Angew. Chem. Int. Ed. Engl. 29* (1990) 536.
[38] J. Hiebl, F. Ledl, T. Severin, *J. Agric. Food Chem. 35* (1987) 990.
[39] T. Severin, W. Seilmeier, *Z. Lebensm. Unters. Forsch. 134* (1967) 230.
[40] J. E. Hodge, B. E. Fisher, E. C. Nelson, *Proc. Am. Soc. Brew. Chem. 1963*, 84.
[41] G. A. M. van den Ouweland, H. G. Peer, *J. Agric. Food Chem. 23* (1975) 501.
[42] A. O. Pittet, P. Rittersbacher, R. Muralidhara, *J. Agric. Food Chem. 18* (1970) 929.
[43] a) J. O. Rodin, C. M. Himel, R. M. Silverstein, R. W. Leeper, W. A. Gortner, *J. Food Sci. 30* (1965) 280; b) B. Willhalm, M. Stoll, A. F. Thomas, *Chem. Ind. (London) 1965*, 1629.
[44] a) T. Severin, W. Seilmeier, *Z. Lebensm. Unters. Forsch. 137* (1968) 4; b) F. D. Mills, D. Weisleder, J. E. Hodge, *Tetrahedron Lett. 1970*, 1243.
[45] a) F. Ledl, W. Schnell, T. Severin, *Z. Lebensm. Unters. Forsch. 160* (1976) 367; b) F. Ledl, *Lebensmittelchem. Gerichtl. Chem. 41* (1987) 83.
[46] a) F. D. Mills, B. G. Baker, J. E. Hodge, *Carbohydr. Res. 15* (1970) 205; b) H. Simon, G. Heubach, *Chem. Ber. 98* (1965) 3703; c) F. Ledl, T. Severin, *Z. Lebensm. Unters. Forsch. 169* (1979) 173.
[47] F. Ledl, G. Ellrich, H. Kostermeyer, *Z. Lebensm. Unters. Forsch. 182* (1986) 12.
[48] H. Matsüüra, Y. Yoshida, K. Kumihiro, T. Fuwa, R. Kasai, O. Tanaka, *Chem. Pharm. Bull. 32* (1984) 4674.
[49] J. E. Hodge, E. C. Nelson, *Cereal Chem. 38* (1961) 207.
[50] J. Rothmoser, *Dissertation*, Universität München 1981.
[51] a) J. Brand, *Ber. Dtsch. Chem. Ges. 37* (1894) 807; b) S. Patton, *J. Biol. Chem. 184* (1950) 131.
[52] J. C. Goodwin, *Carbohydr. Res. 115* (1983) 281.
[53] F. Weygand, H. Simon, W. Bitterlich, J. E. Hodge, B. E. Fisher, *Tetrahedron 6* (1958) 123.
[54] F. Ledl, G. Fritsch, *Z. Lebensm. Unters. Forsch. 178* (1984) 41.
[55] F. Ledl, *Z. Lebensm. Unters. Forsch. 179* (1984) 381.
[56] T. Severin, A. Loidl, *Z. Lebensm. Unters. Forsch. 161* (1976) 119.
[57] F. Ledl, H. Osiander, O. Pachmayr, T. Severin, *Z. Lebensm. Unters. Forsch. 188* (1989) 207.
[58] G. J. Kontoghiorghes, R. W. Evans, *FEBS Lett. 189* (1985) 141.
[59] W. O. Nelson, S. J. Rettig, C. Orvig, *J. Am. Chem. Soc. 109* (1987) 4121.
[60] H. G. Peer, G. A. M. van den Ouweland, C. N. De Groot, *Recl. Trav. Chim. Pays-Bas 87* (1968) 1011.
[61] T. Doornbos, G. A. M. van den Ouweland, S. B. Tjan in [7c], p. 57.
[62] F. Ledl, T. Severin, *Z. Lebensm. Unters. Forsch. 167* (1978) 410.
[63] R. E. Miller, S. M. Cantor, *J. Am. Chem. Soc. 74* (1952) 5236.
[64] a) K. Heyns, J. Heukeshoven, K. H. Brose, *Angew. Chem. 80* (1968) 62, *Angew. Chem. Int. Ed. Engl. 7* (1968) 628; b) P. A. Finot, J. Bricout, R. Viani, J. Mauron, *Experientia 24* (1968) 1097; c) H. Erbersdobler, H. Zucker, *Milchwissenschaft 21* (1966) 564.
[65] a) B. Huber, F. Ledl, T. Severin, A. Stangl, G. Pfleiderer, *Carbohydr. Res. 182* (1988) 301; b) F. G. Njoroge, A. A. Fernandes, V. M. Monnier, *J. Biol. Chem. 263* (1988) 10646.
[66] G. Westphal, L. Kroh, E. Sandner, *Nahrung 25* (1981) 893.
[67] T. Hayashi, M. Namiki in [7g], p. 29.
[68] a) F. Hayase, H. Kato in [7g], p. 39; b) T. Severin, J. Hiebl, H. Popp-Ginsbach, *Z. Lebensm. Unters. Forsch. 178* (1984) 284.
[69] a) G. Manninger, T. Severin, *Z. Lebensm. Unters. Forsch. 161* (1976) 45; b) K. Heyns, U. Sage, H. Paulsen, *Carbohydr. Res. 2* (1966) 328; c) M. Piloty, W. Baltes, *Z. Lebensm. Unters. Forsch. 168* (1979) 374; d) T. Severin, T. Wieland, *ibid. 153* (1973) 201; e) N. van Chuyen, T. Kurata, M. Fujimaki, *Agric. Biol. Chem. 37* (1973) 1613.
[70] a) M. Namiki, T. Hayashi in [7c], p. 81; b) in [7d], p. 21; c) T. Hayashi, S. Mase, M. Namiki, *Agric. Biol. Chem. 49* (1985) 3131.
[71] a) T. Hayashi, S. Mase, M. Namiki, *Agric. Biol. Chem. 50* (1986) 1959; b) T. Hayashi, M. Namiki in [7g], p. 29.
[72] Y. Kato, T. Matsuda, N. Kato, K. Watanabe, R. Nakamura, *J. Agric. Food Chem. 34* (1986) 351.
[73] Y. Kato, T. Matsuda, N. Kato, R. Nakamura, *J. Agric. Food Chem. 36* (1988) 806.
[74] M. Sengl, F. Ledl, T. Severin, unpublished.
[75] F. Hayase, H. Kato, *Agric. Biol. Chem. 49* (1985) 467.
[76] M. F. Aly, R. Grigg, *Tetrahedron 23* (1988) 7271.
[77] M. U. Ahmed, S. R. Thorpe, J. W. Baynes, *J. Biol. Chem. 261* (1986) 4889; J. A. Dunn, D. G. Dyer, K. J. Knecht, S. R. Thorpe, D. R. McCance, K. Bailie, G. Silvestri, T. J. Lyons, J. W. Baynes in [7k], p. 425.
[78] R. Liardon, D. de Weck-Gaudard, G. Philippossian, P. A. Finot, *J. Agric. Food Chem. 35* (1987) 427.
[79] A. Schönberg, R. Moubacher, *Chem. Rev. 50* (1952) 261.
[80] R. Miller, K. Olsson, P. A. Pernemalm, *Acta Chem. Scand. Ser. B 38* (1984) 689.
[81] A. F. Gluron, B. Quack, T. P. Mawhinney, M. S. Feather, *J. Agric. Food Chem. 36* (1988) 677; W. Baltes, L. Mevissen, *Z. Lebensm. Unters. Forsch. 187* (1988) 209.
[82] M. P. Piloty, W. Baltes, *Z. Lebensm. Unters. Forsch. 168* (1979) 368, 374.
[83] P. E. Shaw, R. E. Berry, *J. Agric. Food Chem. 25* (1977) 641.
[84] T. Nyhammar, K. Olsson, P. A. Pernemalm, *Acta Scand. Chem. Ser. B 37* (1983) 879.
[85] M. Namiki, A. Terao, S. Ueda, T. Hayashi, *Agric. Biol. Chem. 49* (1986) 3139.
[86] a) H. K. Nielsen, D. de Weck, P. A. Finot, R. Liardon, R. F. Hurrell, *Br. J. Nutr. 53* (1985) 281; b) F. Hayase, H. Kato, M. Fujimaki, *Agric. Biol. Chem. 43* (1979) 2459.
[87] S. Nakasuka, B. Feng, T. Goto, K. Kihara, *Tetrahedron Lett. 27* (1986) 3399.
[88] a) T. Severin, B. Heidenhain, *Z. Lebensm. Unters. Forsch. 132* (1966) 65; b) T. Severin, K. H. Bräutigam, *Chem. Ber. 106* (1973) 2943; c) K. H. Bräutigam, T. Severin, *Z. Lebensm. Unters. Forsch. 154* (1974) 80; d) E. Knoch, W. Baltes, *Lebensmittelchem. Gerichtl. Chem. 42* (1988) 110; e) T. R. Bosin, S. Krogh, D. Mais, *J. Agric. Food Chem. 34* (1986) 843.
[89] T. Nyhammar, P. A. Pernemalm, *Food Chem. 17* (1985) 289.
[90] a) T. Sugimura, T. Kawachi, M. Gajao, T. Gakagi, Y. Seino, T. Okamoto, K. Shodo, T. Kosuge, K. Tsuji, K. Watabayashi, Y. Iitaka, A. Itai, *Proc. Jpn. Acad. 53* (1977) 58; b) M. Nagao, S. Sato, T. Sugimura in [7d], p. 521.
[91] Z. Yamaizumi, T. Shiomi, H. Kasai, S. Nishimura, Y. Takahashi, M. Nagao, T. Sugimura, *Cancer Lett. (Shannon Irel.) 9* (1980) 75.
[92] a) H. Shigematsu, S. Shibata, T. Kurata, H. Kato, M. Fujimaki, *J. Agric. Food Chem. 23* (1975) 233; b) R. Tressl, B. Helak, H. Kamperschröer, N. Martin, D. Rewicki, *ibid. 33* (1985) 919; c) B. Helak, E. Kersten, K. Sprengler, R. Tressl, D. Rewicki, *ibid. 33* (1985) 919; c) *ibid. 37* (1989) 405.
[93] a) R. Tressl, D. Rewicki, H. Kamperschröer, B. Helak, *J. Agric. Food Chem. 33* (1985) 924; b) B. Helak, K. Sprengler, R. Tressl, D. Rewicki, *ibid. 37* (1989) 400.
[94] a) R. Tressl, B. Helak, K. Sprengler, A. Schröder, D. Rewicki, *Liebigs Ann. Chem. 1985*, 2017; b) R. Tressl, B. Helak, D. Rewicki, *J. Agric. Food Chem. 33* (1985) 1132; c) H. M. E. Pabst, F. Ledl, H.-D. Belitz, *Z. Lebensm. Unters. Forsch. 181* (1985) 386.
[95] a) R. Tressl, K. G. Grünewald, E. Kersten, D. Rewicki, *J. Agric. Food Chem. 34* (1986) 347; b) *ibid. 33* (1985) 1137.
[96] a) R. A. Wilson, I. Katz, *Flavour Ind. 1974*, 30; b) G. MacLeod in G. G. Birch, M. G. Lindley (eds.): *Developments in Food Flavours*, Elsevier Applied Science, London, New York 1986, p. 191; c) M. J. Lane, H. E. Nursten in [7d], p. 141.
[97] a) E. J. Mulders, *Z. Lebensm. Unters. Forsch. 152* (1973) 193; b) F. Ledl, T. Severin, *Chem. Mikrobiol. Technol. Lebensm. 2* (1973) 155; c) F. Ledl, T. Severin, *Z. Lebensm. Unters. Forsch. 154* (1974) 29.
[98] a) O. G. Vitzthum, P. Werkhoff, *J. Food Sci. 39* (1974) 1210; b) R. Tressl in [7j], p. 285.
[99] R. A. Wilson, C. J. Mussinan, I. Katz, A. Sanderson, *J. Agric. Food Chem. 21* (1973) 873.
[100] a) R. K. Cho, A. Okitani, H. Kato in [7g], p. 439; b) D. B. Shin, F. Hayase, H. Kato, *Agric. Biol. Chem. 52* (1988) 1451.
[101] D. R. Sell, V. M. Monnier, *J. Biol. Chem. 264* (1989) 21597.
[102] K. Heyns, H. Noack, *Chem. Ber. 95* (1962) 720.

[103] E. Klein, B. Kramhöller, F. Ledl, T. Severin, unpublished.
[104] T. Nyhammar, S. Grivas, K. Olsson, M. Jägerstad in [7g], p. 323.
[105] D. Yosida, Y. Saito, G. Mizugaki, *Agric. Biol. Chem. 48* (1984) 241.
[106] a) H. Kasai, Z. Yamaizumi, K. Wakabayashi, M. Nagao, T. Sugimura, S. Yokoyama, T. Miyazawa, S. Nishimura, *Chem. Lett. 1980*, 1391; b) H. Kasai, Z. Yamaizumi, T. Shimoi, S. Yokoyama, T. Miyazawa, K. Wakabayashi, M. Nagao, T. Sugimura, S. Nishimura, *ibid. 1981*, 485; c) K. Wakabayashi, M. Takahashi, M. Nagao, S. Sato, N. Kinae, I. Tomita, T. Sugimura in [7g], p. 363.
[107] R. C. Jones, J. H. Weisburger, *Mutat. Res. 206* (1988) 343; b) *Jpn. J. Cancer Res. (Gann) 79* (1988) 222.
[108] K. Aso, *Nippon Nogei Kagaku Kaishi 16* (1939) 249.
[109] a) H. Tsuchida, M. Komoto, K. Kato, M. Fujimaki, *Agric. Biol. Chem. 37* (1973) 2571; b) H. Tsuchida, K. Morinaka, S. Fujii, M. Komoto, S. Mizuno in [7g], p. 85; c) H. Tsuchida, S. Tachibana, M. Komoto, *Agric. Biol. Chem. 40* (1976) 1241; d) M. Komoto, H. Tsuchida, *ibid. 44* (1980) 1189.
[110] a) U. Kröplien, J. Rosdorfer, J. Van der Greef, R. C. Long, J. H. Goldstein, *J. Org. Chem. 50* (1985) 1131; b) S. Fujii, H. Tsuchida, M. Komoto, *Agric. Biol. Chem. 30* (1966) 73.
[111] H. Tsuchida, K. Kitamura, M. Komoto, *Carbohydr. Res. 67* (1978) 549.
[112] W. Seibel, J. M. Brümmer, *Dtsch. Lebensm. Rundsch. 83* (1987) 171.
[113] a) K. Nishie, A. C. Weiss, A. C. Keyl, *Toxicol. Appl. Pharmacol. 14* (1969) 301; b) I. F. Gaunt, A. G. Lloyd, P. Grasso, S. D. Gangolli, K. R. Butterworth, *Food Cosmet. Toxicol. 15* (1977) 509.
[114] a) J. F. Lawrence, C. F. Charbonneau, *J. Chromatogr. 407* (1987) 405; b) U. Kröplien, *ibid. 362* (1986) 286.
[115] a) R. Kuhn, G. Krüger, H. J. Haas, A. Seliger, *Justus Liebigs Ann. Chem. 644* (1961) 122; b) G. Candiano, G. M. Ghiggeri, R. Gusmano, L. Zetta, E. Benfenati, G. Icardi, *Carbohydr. Res. 184* (1988) 67.
[116] a) H. Motai, S. Inone, *Agric. Biol. Chem. 38* (1974) 233; b) S. Homma, T. Tomura, M. Fujimaki, *ibid. 46* (1982) 1791.
[117] K. Olsson, P. A. Pernemalm, O. Theander in [7c], p. 47.
[118] a) H. Kato, S. B. Kim, F. Hayase in [7g], p. 215; b) M. S. Feather, R. D.-Huang in [7g], p. 183; c) L. M. Benzing-Purdie, C. I. Ratcliffe in [7g], p. 193; d) R. D. Huang, M. S. Feather, *J. Agric. Food Chem. 36* (1988) 673.
[119] a) S. B. Kim, F. Hayase, H. Kato, *Agric. Biol. Chem. 49* (1985) 785; b) F. Hayase, S. B. Kim, H. Kato, *ibid. 48* (1984) 2711.
[120] a) F. Hayase, H. Kato, *Agric. Biol. Chem. 45* (1981) 2559; b) F. Hayase, M. Sato, H. Tsuchida, H. Kato, *ibid. 46* (1982) 2987; c) H. Tsuchida, M. Komoto, H. Kato, M. Fujimaki, *ibid. 40* (1976) 2051; d) K. Heyns, R. Hauber, *Justus Liebigs Ann. Chem. 733* (1970) 159; e) W. Baltes, K. Franke, W. Hörtig, R. Otto, U. Lessig in [7c], p. 137; f) H. Kato, H. Tsuchida in [7c], p. 147.
[121] a) R. Hardt, W. Baltes, *Z. Lebensm. Unters. Forsch. 185* (1987) 275; b) A. Dross, R. Hardt, W. Baltes, *Fresenius Z. Anal. Chem. 328* (1987) 495.
[122] C. H. Wu, G. Russell, W. D. Powrie, *J. Food Sci. 52* (1987) 813.
[123] M. Hermann, F. Ledl, unpublished.
[124] a) S. Fors in [7d], p. 185; b) G. Ohloff, I. Flament, *Heterocycles 11* (1978) 663; c) W. Baltes, *Dtsch. Lebensm. Rundsch. 75* (1979) 2; d) H. E. Nursten, *Food Chem. 6* (1981) 263; e) J. P. Danehy, *Adv. Food Res. 30* (1986) 77.
[125] H. W. Brinkman, H. Copier, J. J. M. de Leuw, S. B. Tjan, *J. Agric. Food Chem. 20* (1972) 177.
[126] U. Gasser, W. Grosch, *Z. Lebensm. Unters. Forsch. 186* (1988) 489.
[127] a) P. Schieberle, W. Grosch, *Z. Lebensm. Unters. Forsch. 177* (1983) 173; *ibid. 178* (1984) 479; *ibid. 180* (1985) 474; b) *J. Agric. Food Chem. 35* (1987) 252.
[128] a) I. Flament, B. Willhalm, M. Stoll, *Helv. Chim. Acta 50* (1967) 2233; b) R. G. Buttery, R. M. Seifert, D. G. Guadagni, L. C. Ling, *J. Agric. Food Chem. 19* (1971) 969; c) C. A. Pittet, D. Hruza, *ibid. 22* (1974) 264.
[129] P. Schieberle, in [7j], p. 350 and in [7k], p. 184.
[130] C. Wan-Chung, *Dissertation,* Technische Universität München 1979.
[131] a) H. M. E. Pabst, F. Ledl, H.-D. Belitz, *Z. Lebensm. Unters. Forsch. 178* (1984) 356; b) H. M. E. Pabst, H. Lotter, H.-D. Belitz, *ibid. 186* (1988) 311.
[132] W. Baltes, G. Bochmann, *J. Agric. Food Chem. 35* (1987) 340.
[133] F. Ledl, J. Hiebl, T. Severin, *Z. Lebensm. Unters. Forsch. 177* (1983) 353.
[134] F. Ledl, H. Lotter, unpublished.
[135] F. Ledl, T. Severin, *Z. Lebensm. Unters. Forsch. 175* (1982) 262.
[136] a) T. Severin, U. Krönig, *Chem. Mikrobiol. Technol. Lebensm. 1* (1972) 153; b) U. Krönig, T. Severin, *ibid. 2* (1973) 49; c) H. E. Nursten, R. O'Reilly in [7d], p. 103.
[137] H. Hashiba in [7g], p. 155.
[138] a) T. Kurata, M. Fujimaki, Y. Sakurai, *Agric. Biol. Chem. 37* (1973) 1471; b) T. Hayashi, Y. Hoshi, M. Namiki, *ibid. 47* (1983) 1003; *ibid. 48* (1984) 2377; c) T. Kurata, T. Imai, N. Arakawa in [7g], p. 67.
[139] H. Sakurai, K. Ishii, *Bull. Coll. Agric. Vet. Med. Nihon Univ. 45* (1988) 50, 59.
[140] B. Huber, P. Noll, F. Ledl, unpublished.
[141] H. Pehr, G. Manninger, T. Severin, *Carbohydr. Res. 64* (1978) 1.
[142] L. Mevissen, W. Baltes, *Z. Lebensm. Unters. Forsch. 176* (1983) 206.
[143] P. Noll, F. Ledl, unpublished.
[144] P. E. Shaw, J. H. Tatum, R. E. Berry, *Carbohydr. Res. 16* (1971) 207.
[145] F. Ledl, G. Fritsch, T. Severin, *Z. Lebensm. Unters. Forsch. 175* (1982) 208.
[146] F. D. Mills, J. E. Hodge, W. K. Rohwedder, L. W. Tjarks, *J. Org. Chem. 38* (1973) 2512.
[147] J. E. Hodge, C. D. Evans, US-Pat. 2 806 794 (1957).
[148] R. Schnee, K. Eichner, *Z. Lebensm. Unters. Forsch. 185* (1987) 188.
[149] F. Ledl, G. Fritsch, J. Hiebl, T. Severin, *Z. Lebensm. Unters. Forsch. 176* (1983) 294.
[150] a) H. Lingnert, C. E. Eriksson in [7d], p. 335; b) N. Yamaguchi in [7g], p. 291.
[151] B. Commoner, A. J. Vitayathil, P. Dolara, G. Nair, P. Madyastha, G. C. Cuca, *Science (Washington D.C.) 201* (1978) 913.
[152] M. Scheutwinkel-Reich, G. Reese, W. van der Hude, *Z. Lebensm. Unters. Forsch. 180* (1985) 207.
[153] a) M. Jägerstadt, A. L. Reuterswärd, R. Öste, M. Dahlquist in [7d], p. 507; b) K. Shinohara, R. T. Wu, N. Jahan, M. Tanaka, N. Moringa, H. Murakami, H. Omura, *Agric. Biol. Chem. 44* (1980) 671.
[154] a) H. Ohgaki, K. Kusama, N. Matsukura, K. Marino, H. Hasegawa, S. Sato, S. Takayama, T. Sugimura, *Carcinogenesis (London) 5* (1984) 921; b) H. Ohgaki, H. Hasegawa, T. Kato, M. Suenaga, M. Ubutaka, S. Sato, S. Takayama, T. Sugimura, *Proc. Jpn. Acad. Ser. B 61* (1985) 137; T. Sugimura, S. Takayama, H. Ohgaki, K. Wakabayashi, M. Nagao in [7k], p. 323.
[155] a) S. B. Kim, F. Hayase, H. Kato in [7g], p. 383; b) T. Kada, K. Morita, T. Inone, *Mutat. Res. 53* (1978) 351; c) R. I. M. Chan, H. F. Stich, M. P. Rosin, W. D. Powrie, *Cancer Lett. (Shannon Irel.) 15* (1982) 27.
[156] a) D. W. Gruenwedel, S. C. Lynch, G. F. Russell, *Adv. Exp. Med. Biol. 177* (1984) 269; b) K. Heyns, S. Röper, H. Röper, B. Meyer, *Angew. Chem. 91* (1979) 940; *Angew. Chem. Int. Ed. Engl. 18* (1979) 878.
[157] N. Kinae in [7g], p. 343.
[158] S. Mihara, T. Shibamoto, *J. Agric. Food Chem. 28* (1980) 62.
[159] A. Nagahara, K. Ohshita, S. Nasuno in [7g], p. 373.
[160] H. U. Aeschbacher in [7k], p. 335.
[161] a) H. Omura, N. Jahan, K. Shimohara, H. Murakami in [7d], p. 537; b) M. Nagao, T. Yahagi, M. Honda, Y. Seino, T. Matsushima, T. Sugimura, *Proc. Jpn. Acad. 53* (1977) 34.
[162] a) J. Mauron, F. Mottu, *Arch. Biochem. Biophys. 77* (1958) 312; b) P. A. Finot, J. Mauron, *Helv. Chim. Acta 52* (1969) 1488; c) J. Mauron, *Int. J. Vitam. Nutr. Res. 40* (1970) 209; d) P. A. Finot, E. Magnenat, F. Mottu, E. Bujard, *Ann. Nutr. Aliment. 32* (1978) 325; e) B. Sherr, C. M. Lee, C. Jelesciewicz, *J. Agric. Food Chem. 37* (1989) 119.
[163] D. E. Furniss, R. F. Hurrell, P. A. Finot, *Acta Pharmacol. Toxicol. 59* (1986) 188.
[164] P. A. Finot, D. E. Furniss in [7i], p. 343.
[165] M. Fujimaki, S. Homma, N. Arakawa, C. Inagaki, *Agric. Biol. Chem. 43* (1979) 497.
[166] G. J. Pintauro, T. C. Lee, C. O. Chichester in [7d], p. 467.
[167] a) H. S. Burton, D. J. McWeeny, D. O. Biltcliffe, *J. Sci. Food Agric. 14* (1963) 911; b) B. L. Wedzicha (Ed.): *Chemistry of Sulfur Dioxide in Foods,* Elsevier Applied Science, London, New York 1984.
[168] H. E. Nursten in D. MacCarthy (Eds.): *Concentration and Drying of Foods,* Elsevier Applied Science, London, New York 1986, p. 53.
[169] a) M. E. Knowles, *Chem. Ind. 1971*, 910; B. Lindberg, J. Tanaka, O. Theander, *Acta Chem. Scand. 18* (1964) 1164; E. F. L. J. Anet, D. L. Ingles, *Chem. Ind. 1964*, 1319. b) B. L. Wedzicha, M. T. Kaputo, *J. Food Sci. Technol. 22* (1987) 643.
[170] a) R. G. Arnold, *J. Dairy Sci. 52* (1969) 1857; b) L. Kroh, S. Zeise, G. Westphal, R. Macholz, *Nahrung 33* (1989) 51; c) L. Kroh, S. Zeise, R. Stösser, G. Westphal, *Z. Lebensm. Unters. Forsch. 188* (1989) 115.
[171] D. W. Allen, W. A. Schroeder, J. Balog, *J. Am. Chem. Soc. 80* (1958) 1628.
[172] a) H. F. Bunn, D. N. Haney, K. H. Gabbay, P. M. Gallop, *Biochem. Biophys. Res. Comm. 67* (1975) 103. H. F. Bunn, R. Shapiro, M. McManns, L. Garrick, M. J. McDonald, K. H. Gallop, *J. Biol. Chem. 254* (1979) 3892; b) A. L. Trivelli, H. M. Ranney, H. T. Lai, *N. Engl. J. Med. 284* (1971) 353; see also Ref. [174].
[173] S. Rahbar, O. Blumenfeld, H. M. Ranney, *Biochem. Biophys. Res. Commun. 36* (1969) 838.
[174] H. F. Bunn, D. N. Haney, K. H. Gabbay, P. M. Gallop, *Biochem. Biophys. Res. Commun. 67* (1975) 103.
[175] a) R. Flückiger, K. H. Winterhalter, *FEBS Lett. 71* (1976) 356; b) R. Dolhofer, A. Städele, O. H. Wieland, *Klin. Wochenschr. 55* (1977) 945.
[176] a) J. W. Baynes, S. R. Thorpe, M. M. Murtiashaw, *Methods Enzymol. 106* (1984) 88; b) E. Schleicher, O. H. Wieland, *Biochim. Biophys. Acta 884* (1986) 199.
[177] H. E. Schultze, J. F. Heremans (Eds.): *Molecular Biology of Human Proteins,* Elsevier, Amsterdam 1966, p. 473.
[178] A glucoprotein from *Halobacterium halobium* has been described which contains glucose bound *N*-glycosidically to the amide nitrogen of the asparagine. F. Wieland, R. Heitzer, W. Schäfer, *Proc. Natl. Acad. Sci. USA 80* (1983) 5470.

[179] Fructose also reacts to a certain extent with proteins in vivo to give 2-amino-2-deoxyglucose **2** (Heyns-product): J. D. McPherson, B. H. Shilton, D. J. Walton, *Biochemistry 27* (1988) 1901.
[180] C. I. Neglia, H. J. Cohen, A. R. Garber, P. D. Ellis, S. R. Thorpe, J. W. Baynes, *J. Biol. Chem. 258* (1983) 14279.
[181] E. Schleicher, O. H. Wieland, *J. Clin. Chem. Clin. Biochem. 19* (1981) 81.
[182] O. H. Wieland, R. Dolhofer, E. Schleicher, *Int. Congr. Ser. Excerpta Med. n 500* (1980) 721.
[183] a) R. Dolhofer, O. H. Wieland, *Diabetes 29* (1980) 417; b) *Clin. Chim. Acta 112* (1981) 197.
[184] R. N. Johnson, P. A. Metcalf, J. R. Baker, *Clin. Chim. Acta 127* (1983) 87.
[185] a) R. Flückiger, P. M. Gallop, *Methods Enzymol. 106* (1984) 77; b) K. Miedema, T. Casparie, *Ann. Clin. Biochem. 21* (1984); b) E. Schleicher, *Internist 26* (1985) 372.
[186] R. W. Fischer, K. H. Winterhalter, *FEBS Lett. 135* (1981) 145.
[187] L. K. Curtiss, J. L. Witztum, *J. Clin. Invest. 72* (1983) 1427.
[188] M. Brownlee, H. Vlassara, A. Cerami, *Diabetes 29* (1980) 1044.
[189] E. Schleicher, R. Maier, unpublished.
[190] a) J. F. Day, S. R. Thorpe, J. W. Baynes, *J. Biol. Chem. 254* (1979) 595; b) R. Dolhofer, O. H. Wieland, *FEBS Lett. 103* (1979) 282.
[191] a) M. Cohen (Ed.): *Diabetes and Protein Glycosylation*, Springer, Berlin 1986; b) E. D. Schleicher, T. Deufel, O. H. Wieland, *FEBS Lett. 129* (1981) 1; c) E. D. Schleicher, K. D. Gerbitz, R. Dolhofer, E. Reindel, O. H. Wieland, E. Edelmann, M. Haslbeck, W. Kemmler, H. Walter, H. Mehnert, *Diabetes Care 7* (1984) 548.
[192] E. Schleicher, R. Scheller, O. H. Wieland, *Biochem. Biophys. Res. Commun. 99* (1981) 1011.
[193] B. W. Vogt, E. D. Schleicher, O. H. Wieland, *Diabetes 31* (1982) 1123.
[194] S. L. Schnider, R. R. Kohn, *J. Clin. Invest. 67* (1981) 1630.
[195] R. L. Garlick, H. F. Bunn, R. Spiro, *Diabetes 37* (1988) 1144.
[196] E. Reindl, *Dissertation*, Universität München 1983.
[197] V. M. Monnier, R. R. Kohn, A. Cerami, *Proc. Natl. Acad. Sci. USA 81* (1984) 583.
[198] S. Pongor, P. C. Ulrich, F. A. Bencsath, A. Cerami, *Proc. Natl. Acad. Sci. USA 81* (1984) 2684.
[199] T. J. Lyons, G. Silvestri, J. A. Dunn, J. W. Baynes, Conference on "Glycated Proteins in Diabetes mellitus", Adelaide, Australia 1988.
[200] A. Cerami, H. Vlassara, M. Brownlee, *Diabetes Care 11 Suppl. 1* (1988) 73.
[201] R. Bucala, P. Model, A. Cerami, *Proc. Natl. Acad. Sci. USA 81* (1984) 105.
[202] V. J. Stevens, C. A. Rouzer, V. A. Monnier, A. Cerami, *Proc. Natl. Acad. Sci. USA 75* (1978) 2918.
[203] a) S. H. Chiou, L. T. Chylack, H. F. Bunn, J. H. Kinoshita, *Biochem. Biophys. Res. Commun. 95* (1980) 894; b) V. M. Monnier, A. Cerami, *Science (Washington D.C.) 211* (1981) 491.
[204] a) D. E. Harrison, J. R. Archer, *Exp. Gerontol. 13* (1978) 75; b) M. J. C. Kent, N. D. Light, A. J. Bailey, *Biochem. J. 225* (1985) 745.
[205] A. S. Eble, S. R. Thorpe, J. W. Baynes, *J. Biol. Chem. 258* (1983) 9406.
[206] M. Brownlee, H. Vlassara, A. Cerami, *Diabetes 34* (1985) 938.
[207] H. Vlassara, M. Brownlee, A. Cerami, *Clin. Chem. (Winston-Salem N.C.) 32* (1986) 37.
[208] R. Dolhofer, E. A. Siess, O. H. Wieland, *Hoppe-Seyler's Z. Physiol. Chem. 363* (1982) 1427.
[209] a) M. Brownlee, H. Vlassara, A. Cerami, *Diabetes 32* (1983) 680; b) *Diabetologia 33* (1984) 532.
[210] R. Dolhofer, O. H. Wieland, *FEBS Lett. 100* (1979) 133.
[211] a) J. L. Witztum, E. H. Mahoney, M. J. Branks, M. Fisher, R. Elam, D. Steinberg, *Diabetes 31* (1982) 283; b) E. D. Schleicher, B. Olgemöller, J. Schön, T. Dürst, O. H. Wieland, *Biochim. Biophys. Acta 846* (1985) 226.
[212] H. Vlassara, H. Brownlee, A. Cerami, *J. Exp. Med. 160* (1984) 197.
[213] a) M. Oimoni, H. Hatanaka, K. Ishikawa, S. Kubota, Y. Yoshimura, S. Baba, *Klin. Wochenschr. 62* (1984) 477; b) M. Oimoni, S. Nishimoto, T. Kitamura, S. Matsumoto, H. Hatanaka, K. Ishikawa, S. Baba, *ibid. 63* (1985) 728.
[214] V. M. Monnier, V. Vishwanath, K. F. Frank, A. E. Graig, P. Dauchot, R. R. Kohn, *N. Eng. J. Med. 314* (1986) 403.
[215] M. Brownlee, H. Vlassara, A. Kooney, P. Ulrich, A. Cerami, *Science (Washington D.C.) 232* (1986) 1629.
[216] M. Wissfeld, P. Noll, F. Ledl, unpublished.

The Chemistry of Interstellar Space

By Eric Herbst*

Within the last ten to twenty years, radioastronomers have discovered the existence of almost 100 different molecules in interstellar space. Ranging in complexity from two to thirteen atoms, these molecules are found in cold, rarefied regions called interstellar clouds, which are giant accumulations of gas and dust located in our galaxy as well as many others. Interstellar clouds are also the birthplaces of future generations of stars and are of great interest to astronomers. The observation of the large sample of gaseous molecules, detected mainly via their rotational spectral patterns, tells astronomers about the detailed physical conditions in interstellar clouds, and tells chemists about the extent of molecular synthesis possible under the seemingly harsh conditions of low temperature and density. The molecules are mainly organic in nature and comprise species known to be both stable and common in the laboratory as well as those both unstable and uncommon under terrestrial conditions, including radicals and molecular ions. Although the gas phase of interstellar clouds is well studied via spectroscopic techniques, the dust particles are much more poorly characterized via their scattering and absorption of visible radiation as well as some broad resonances in the ultraviolet and infrared regions of the spectrum. It is normally thought that these submicron-sized particles consist of cores that are composites of silicate and carbonaceous materials with mantles that contain material deposited from the gas such as ices of water, ammonia, and methane. In addition to the dust particles and gaseous molecules, there is some evidence for very large aromatic molecules (the so-called polycyclic aromatic hydrocarbons or PAH's) which occupy a nether region in between large gas-phase species and small dust particles. As our understanding of the chemical processes in interstellar clouds increases, it may be possible to speculate how large interstellar molecules can come into existence and whether or not there is a clear connection between interstellar chemistry and the start of life on earth.

1. Introduction

Although the existence of planets outside of the solar system has yet to be proven unequivocally, organic chemistry is known to be widespread in the universe. Almost 100 different molecular species, both organic and inorganic in nature and ranging in complexity up to thirteen atoms and possibly many more, have been discovered in between the stars, in regions of space called interstellar clouds. These interstellar clouds are large agglomerations of gas and dustlike particles which take up a significant portion of the volume of interstellar space. The largest interstellar clouds have linear dimensions in excess of 100 light years. Unless they are hot enough to emit in the visible region of the spectrum, like stars, interstellar clouds are not immediately apparent on glancing at the night sky. To a trained observer, however, cool interstellar matter is apparent because it scatters and absorbs the light of distant stars, rendering areas of the sky black. Although interstellar clouds are mainly gaseous in content, the approximately 1% of the matter in particulate form is responsible for extinguishing starlight since dust particles interact much more strongly with visible radiation than do gaseous atoms and molecules.

Not all interstellar clouds contain enough matter to extinguish background starlight completely; there are some in which visible radiation manages to penetrate. The gas in these clouds, labeled "diffuse", can be studied via optical and ultraviolet absorption spectroscopy, and it was this technique that was first used to study the interstellar medium. The existence of the interstellar radicals CH, $CH^{\oplus}$, and CN has been known for about fifty years due to this technique; an account of the early identifications can be found in *Herzberg*'s book on diatomic molecules.[1] The gas in diffuse clouds turns out to be mainly atomic in nature since the gas density is very low and since stellar radiation, which penetrates these regions, can photodissociate molecules rather rapidly by astronomical standards. In the years since the initial identification of interstellar molecules, only additional diatomic molecules such as H_2, CO, OH, and C_2 have been found via optical and ultraviolet spectroscopy to be in diffuse clouds.

The story is a very different one for those interstellar clouds in which there is sufficient interstellar matter that stellar radiation cannot penetrate. These clouds, which are labeled "dense", can only be studied at longer wavelengths, which are not extinguished by the tiny dust particles. Most of the studies of dense interstellar clouds performed to date have been accomplished by radioastronomers. The term "radioastronomy" is somewhat of a misnomer in that astronomers use it to refer to studies at all wavelengths longer than infrared, including microwave, millimeter and even submillimeter waves. Radioastronomy can be undertaken from the ground since the atmosphere is relatively benign in this spectral region, whereas infrared astronomy is strongly hindered by atmospheric attenuation due to water. The projected use of satellites to do high-resolution infrared spec-

[*] Prof. E. Herbst
Department of Physics, Duke University
Durham, NC 27706 (USA)

troscopy will allow infrared astronomers to study dense interstellar clouds in more detail than has previously been the case.

The temperature in most regions of dense interstellar clouds is quite low ($10 < T < 70$ K) and these regions emit only at so-called "radio" wavelengths. The emission is overwhelmingly discrete in nature and derives from the rotational spectra of gaseous molecules; a weak continuum is due both to the 3 K black-body background temperature of the universe and to the dust particles.[2] An emission spectrum of the well-studied Orion Nebula in the millimeter region of the spectrum is shown in Figure 1. Although virtually all of the high-resolution spectral lines in this figure have been identified, there is room to label only a limited number of molecules. There are continuous radio sources in our galaxy and others, and if an interstellar cloud is fortuitously located in the foreground of such a source, absorption spectroscopy can be undertaken. Although infrared radiation is not emitted from the bulk of dense interstellar clouds, these clouds are the sites of star formation since the gas and dust slowly collapse and, in localized regions, heat up sufficiently that nuclear fusion processes are initiated. Around newly formed stars and in areas in which stars are forming, hot dust particles emit a continuum in the infrared which can be used as a background source for absorption spectroscopic studies of molecules located in cooler regions in the foreground. Although this infrared technique does not yet result in spectra with a high signal-to-noise ratio from interstellar clouds, it has been used more successfully to probe selected circumstellar clouds surrounding evolved (old) stars. In the best studied of the circumstellar sources (IRC + 10216), a significant number of molecules have been discovered both in emission in the radio and absorption in the infrared.[3]

Spectra such as those shown in Figure 1 can be used to learn much about dense interstellar clouds. Molecular identification can often be made by comparing interstellar spectral transitions with those previously obtained by spectroscopists in the laboratory. However, a significant percentage of interstellar molecules are highly unusual radicals and molecular ions; these have been tentatively identified by their interstellar rotational spectra since rotational spectral frequencies are uniquely characteristic of molecular structure and, in most cases, confirmed by subsequent laboratory experiment. In addition to molecular identification, analysis of interstellar spectral lines allows a determination of the relative concentrations or "abundances" of molecules and of their temperatures.[4] Given the low gas densities, temperatures of different molecules need not all be the same, since equilibrium is not achieved. However, the derived temperatures are all quite low outside of star-forming regions. In the so-called "dark" clouds, in which star formation is not strongly evident, typical temperatures around 10 K are derived. In the so-called "giant" molecular clouds where star formation is more noticeable, of which the Orion Nebula is the best studied example, bulk temperatures of the order of 70 K are prevalent. In star-forming regions, emission from highly excited states can occur and, in addition, maser emission is far from uncommon.[5] Finally, the existence of spectral features seen in emission implies a minimum overall gas density because of the necessity that the rate of collisional excitation of excited rotational states of molecules at least equal the emission rate of the particular transitions seen. The deduced gas densities in dense interstellar clouds range from a low of 10^3 molecules cm^{-3} to a high of perhaps 10^5 cm^{-3} in regions near the centers of the clouds. In star-forming regions, much higher gas densities can be achieved. Although all of these gas densities are very low compared with the atmospheric density on the earth, the large sizes of interstellar clouds translate into huge masses, up to perhaps a million times the mass of the sun.

Although the gas phase of interstellar clouds is well characterized by spectroscopic studies, the same cannot be said of the dust particles. Based on extremely limited information, it is normally suggested that the dust particles are typically 0.1 microns in size, and composed of a refractory core (e.g., silicates) surrounded by a mantle of material deposited from the gas. The evidence derives mainly from the scattering of visible radiation, from one broad ultraviolet resonance in diffuse clouds, and from broad features in the infrared which coincide with fundamental vibrational transition frequencies.[6] Recently, a series of broad unidentified emission lines in the infrared from warm regions of the interstellar medium has been tentatively assigned to the fluorescence of large aromatic molecules which absorb ultraviolet radiation from nearby stars and reradiate it in the infrared.[7] The assignment is based on a functional group analysis and comparison with laboratory absorption spectra. The intensities and line widths are suggestive of large individual molecules contain-

Born in Brooklyn, New York, USA, on January 15, 1946, Eric Herbst received his B.A. degree in Chemistry from the University of Rochester in 1966, and his M.A. and Ph.D. degrees in Chemistry from Harvard University in 1969 and 1972, respectively. In the latter stages of his thesis work, he became interested in molecular astronomy because of the keen interest of his research supervisor, Professor William Klemperer, in this line of inquiry. After a postdoctoral research position in Professor Klemperer's laboratory, he took a second postdoctoral research position in the laboratory of Professor Carl Lineberger at the Joint Institute for Laboratory Astrophysics, University of Colorado, in the field of laser ion spectroscopy. He then accepted a faculty position in chemistry at the College of William and Mary, Williamsburg, Virginia, where he taught for six years. Since 1980, he has been in the physics department at Duke University, Durham, North Carolina, where he is currently Professor of Physics. His research interests are divided between molecular astronomy and millimeter-wave spectroscopy. During the year 1988–89, he was at the University of Cologne, FRG, as an Awardee of the Alexander von Humboldt Stiftung.

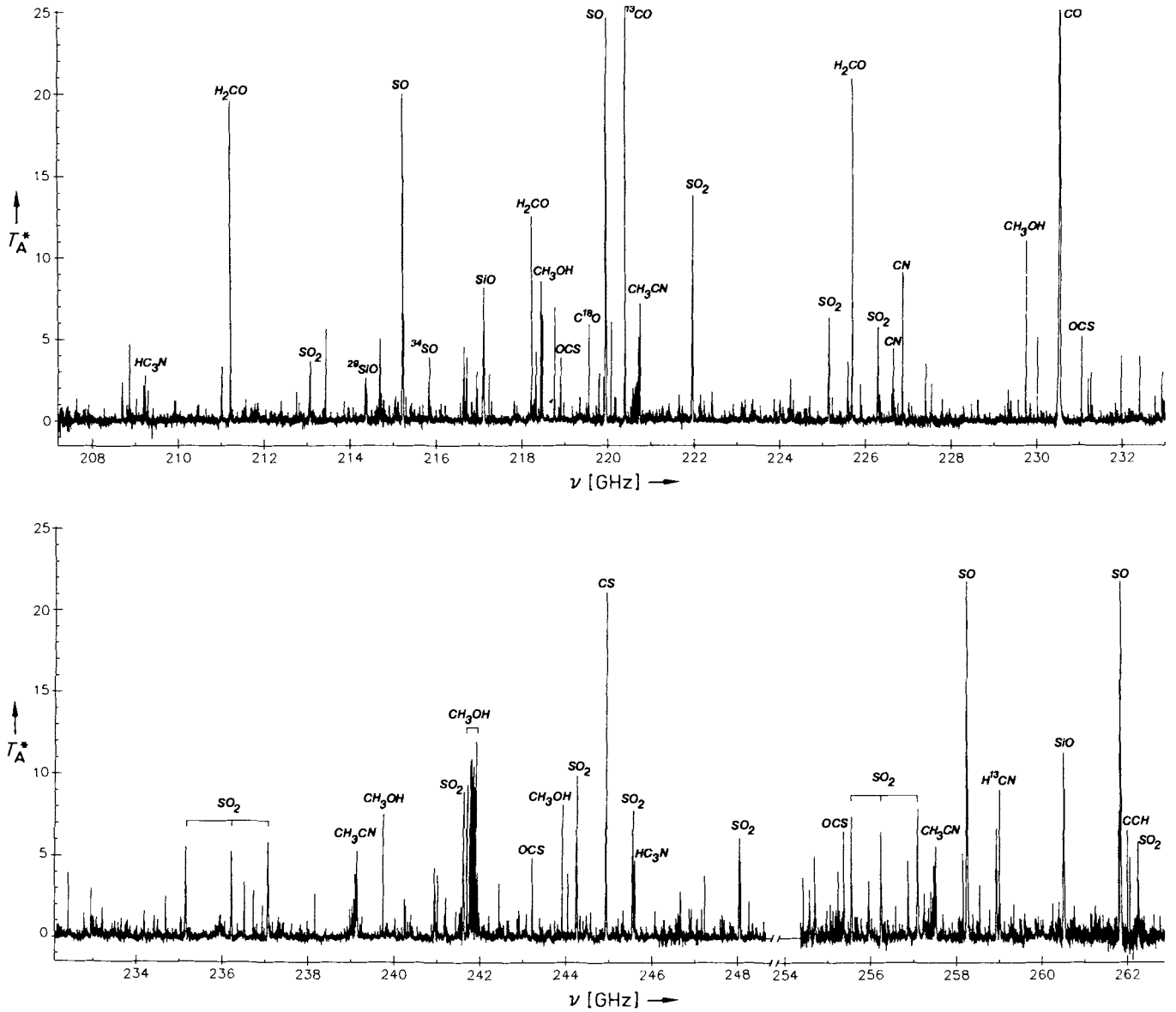

Fig. 1. The millimeter-wave spectrum of the Orion Nebula in the direction of the so-called Kleinmann-Low area. Rotational spectra from many molecules are seen. Taken from [69]. ν = frequency, T_A^* = antenna temperature, a measure of emission intensity.

ing perhaps 50 carbon atoms rather than graphitic particles and the molecules are known as polycyclic aromatic hydrocarbons (PAH's). These molecules are rather stable against ultraviolet radiation and will not be destroyed rapidly by the ultraviolet photons which it is thought lead to the infrared fluorescence which is their signature. Although the spectral assignment is reasonable, laboratory study of the efficacy of the proposed mechanism for the infrared emission of radiation is a prerequisite for further progress. PAH's have also been suggested as the source of a series of unidentified diffuse spectral features seen in absorption spectroscopy in diffuse interstellar clouds.[8]

A list of the nearly 90 interstellar molecules discovered from high-resolution spectral features is given in Table 1. In addition, many of these species have been detected in more than one isotopic variant with deuterium and ^{13}C being the most frequent isotopic atoms encountered. Most of the molecular species have been detected via radio-astronomical

Table 1. Interstellar (and circumstellar) molecules. An asterisk signifies circumstellar detection only. A question mark signifies tentative detection.

H_2	H_2O	NH_3	HCOOH	$HCOOCH_3$
CH	H_2S	H_2CO	HCCCN	CH_3CCCN
$CH^{\oplus}$	HCN	H_2CS	C_4H	
OH	HNC	C_2H_2	C_4Si*	C_2H_5OH
HCl	$HCO^{\oplus}$	$HCNH^{\oplus}$	C_5*	CH_3OCH_3
C_2	$HOC^{\oplus}$ (?)	CCCH		CH_3CCCH
CN	$H_2D^{\oplus}$ (?)	c-CCCH	C_2H_4*	CH_3CH_2CN
NO	$HN_2^{\oplus}$	HNCO	CH_3OH	HC_7N
CO	HCO	$HOCO^{\oplus}$	CH_3SH	
CS	CCH	HNCS	$HCONH_2$	CH_3COCH_3
SiO	HNO	CCCN	HC_2CHO	CH_3C_5N (?)
NS	$HCS^{\oplus}$	CCCO	CH_3CN	
SO	CCC*	CCCS	CH_3NC	HC_9N
$SO^{\oplus}$	SO_2		C_5H	
SiS	SiC_2*	CH_4*		$HC_{11}N$
SiC*	CCS	SiH_4*	CH_3NH_2	
PN	OCS	H_2CNH	CH_3CCH	
NaCl*		H_2NCN	CH_3CHO	
AlCl*		c-C_3H_2	C_2H_3CN	
KCl*		CH_2CO	C_6H	
KF (?)*		CH_2CN	HC_5N	

spectra in dense interstellar clouds although I have also included optical and ultraviolet detections in diffuse clouds as well as infrared detections in circumstellar sources. As can be seen from Table 1, many of the molecules are indeed standard organic species, of which the most complex is $H(C\equiv C)_5CN$, a linear unsaturated nitrile. A significant number of molecular ions have been discovered as well. Indeed, the initial discovery of the ion $HCO^{\oplus}$ has helped to promote a vigorous laboratory effort in both infrared and microwave spectroscopy of molecular ions. The story behind the $HCO^{\oplus}$ discovery is of some interest. The original detection of a single line at 89.190 GHz (labeled "X-ogen" by its discoverers) prompted my thesis adviser, Professor *William Klemperer* at Harvard University, to suggest $HCO^{\oplus}$ as the carrier of the line, based on estimated bond lengths (reasonably correct) and ideas concerning the chemistry (not correct).[9] The initial suggestion, derided in some quarters, was confirmed by both the later detection of the analogous line of $H^{13}CO^{\oplus}$ in the interstellar medium[10] and the laboratory detection by *Woods* et al.[11]

In addition to molecular ions, a large number of carbon-containing radicals have been discovered in interstellar space. Prominent among these are the linear C_nH radicals, which are alkynes with one hydrogen removed. Also prominent are the linear organo-sulfur radicals CCS and CCCS, and the linear organo-silicon radical CCCCSi. Unusual ring species include cyclopropenylidene (c-C_3H_2) and SiC_2, as well as a cyclic form of C_3H which is metastable, since it lies higher in energy than the linear species. Another prominent metastable species is HNC. Although these molecules seem bizarre to the terrestrial chemist, their existence in space is proven beyond any doubt and testifies to the differing physical conditions in the interstellar and terrestrial environments.

What are the relative concentrations of the molecules in dense interstellar clouds? By far the most abundant molecule is H_2; it is so much more abundant than any other species that its abundance can be equated to the total gas density. Molecular hydrogen has no dipole moment and consequently does not possess a strong rotational spectrum. However, there is enough of it so that its weak quadrupolar transitions have been identified. In addition, its ultraviolet spectrum in diffuse clouds has been seen and indicates that even in these sources, it is a significant percentage of the total gas density. The next most abundant molecule is carbon monoxide, with a relative concentration ("fractional abundance") of 1×10^{-4} compared with H_2. All more complex molecules have even lower fractional abundances, which vary somewhat depending on which source one is looking at. Fractional abundances for the well-studied source TMC-1 (Taurus Molecular Cloud I) are shown in Table 2. Although organic molecules possess low abundances in a fractional sense, the large masses of interstellar clouds tell us that the absolute amount of material in organic form is very large indeed compared with the amount of such matter on earth. The low fractional abundance of $HCO^{\oplus}$, the most abundant molecular ion yet detected, indicates that the clouds are overwhelmingly neutral in composition.

Why are interstellar clouds dominated by hydrogen? Unlike the earth, which possesses a weak gravitational field, most objects in the universe, be they stars or interstellar clouds, have gravitational fields strong enough to retain atoms independent of their mass. In such objects, a wealth of spectroscopic studies, mainly on stars, shows hydrogen to be the dominant element, with helium in second place, and heavy elements such as carbon, oxygen, nitrogen lower in abundance by factors of 10^4 or so. The distribution of matter among the elements derives from the Big Bang, in which only hydrogen and helium were produced in significant abundance, and nuclear fusion in stars, in which heavier elements are synthesized. Dying stars then release these heavier elements into the interstellar medium, either gently or explosively, and new generations of stars are produced that incorporate them. It is interesting to note that astronomers, whose training in chemistry must be minimal, refer to all elements heavier than helium as "metals".

Table 2. Selected molecular fractional abundances in TMC-1 [a].

Molecule	Fractional Abundance Observed	Theory [b]	Molecule	Fractional Abundance Observed	Theory [b]
CO	8(-5)	8(-5)	CH	2(-8)	1(-8)
OH	3(-7)	2(-8)	C_2	5(-8)	2(-8)
C_2H	8(-8)	7(-8)	C_3H	5(-10)	5(-8)
C_4H	2(-8)	1(-7)	C_5H	4(-10)	6(-9)
C_6H	1(-9)	3(-9)	c-C_3H_2	2(-8)	3(-8)
CH_3CCH	6(-9)	2(-10)	CH_3C_4H	2(-9)	4(-9)
CN	3(-8)	7(-8)	HCN	2(-8)	1(-7)
HNC	2(-8)	6(-8)	CH_3CN	1(-9)	6(-9)
C_3N	1(-9)	1(-8)	HC_3N	6(-9)	3(-8)
HC_5N	3(-9)	5(-9)	HC_7N	1(-9)	7(-10)
HC_9N	3(-10)	1(-10)	$HC_{11}N$	1(-10)	
CH_3C_3N	5(-10)	2(-10)	NH_3	2(-8)	2(-8)
H_2CO	2(-8)	2(-7)	CH_2CO	1(-10)	5(-8)
C_3O	1(-10)	3(-11)	CH_3OH	4(-9)	4(-9)
CH_3CHO	6(-10)	4(-11)	CS	1(-8)	3(-8)
CCS	8(-9)	1(-9)	CCCS	2(-9)	4(-10)
SO	5(-9)	1(-10)	H_2S	7(-10)	6(-11)
OCS	2(-9)	3(-9)	H_2CS	4(-9)	3(-9)
$HCO^{\oplus}$	8(-9)	5(-9)	$N_2H^{\oplus}$	5(-10)	4(-13)
$HCS^{\oplus}$	6(-10)	5(-10)			

[a] Fractional abundances are expressed with respect to H_2; a(-b) signifies $a\times10^{-b}$. [b] Theoretical results mainly from the calculations of [52b]. Results of sulfur-containing species from [66].

Although it is difficult to obtain the elemental distribution in the gas phase of dense interstellar clouds, since the material is dominated by molecules, it is possible to obtain such information from diffuse cloud studies. Lists of elemental abundances that pertain to normal stars as well as to the gas phase of diffuse clouds are shown in Table 3. The diffuse

Table 3. Elemental abundances in the gas phase[a].

Element	Abundance in diffuse clouds[b]	Abundance in stars
H	1.0	1.0
He	0.14	0.10
O	1.8(-4)	6.9(-4)
C	7.3(-5)	4.2(-4)
N	2.1(-5)	8.7(-5)
S	8.0(-6)	1.6(-5)
Si	8.0(-7)	4.5(-5)
Fe	3.0(-7)	3.2(-5)
Na	2.0(-7)	1.9(-6)
Mg	7.0(-7)	3.2(-5)

[a] The expression a(-b) signifies $a\times10^{-b}$. [b] The abundances are by number not mass. In dense clouds it is now normally assumed that the elements, S, Si, Fe, Na, and Mg are additionally depleted from the diffuse cloud values by two orders of magnitude.

cloud abundances are depleted in "metallic" elements, which are incorporated into the dust particles. It is often assumed that elemental abundances in the gas phase of dense clouds are similar to those in diffuse clouds with the exception of "heavy metals" such as S, Si, and actual metals, which are further depleted. Astronomers often refer to two sets of "heavy metal" abundances—"high" and "low"—which differ by two orders of magnitude.

Despite the uncertainty in our knowledge of the exact elemental abundances in the gas phase of dense clouds, the large abundance of hydrogen suggests that molecular hydrogen will be dominant and the much smaller abundances of carbon, oxygen, and nitrogen suggest that molecules with these elements will have small fractional abundances. Indeed, the fractional abundance of CO suggests that much of the elemental abundance of carbon resides in this species.

Although the relative abundances of the elements are a boundary condition on the molecular abundances, they do not tell us how the molecules are synthesized. In the next section of the article, the chemical processes that synthesize molecules are discussed.

2. The Formation of Interstellar Molecules

Before a discussion of how interstellar molecules are synthesized, it is necessary to ask where they are formed. Basically there are two possibilities: they are formed in the interstellar clouds where they are seen or they are formed elsewhere. Why should we consider their formation elsewhere? First, physical conditions in dense clouds would not appear to be conducive to chemistry. The very low gas densities mean that collisions between atoms and molecules in the gas do not occur billions of times per second, as on the earth, but instead occur once every day or even longer, depending on the cloud density. In addition, the low temperatures would appear to indicate that the vast majority of collisions will not be reactive. Secondly, conditions in stellar atmospheres, especially extended atmospheres of older stars, include higher densities and temperatures. These regions are known to be the birthplace of dust particles, which are then blown out into space.[12] In addition, polyatomic molecule formation in certain types of extended atmospheres is known to take place.[3, 13] It is therefore tempting to suggest that these molecules can also be blown out into space and eventually form the material in interstellar clouds. However, this scenario cannot be correct. Although it is certainly true that the gas and dust ejected from elder stars is the material from which interstellar clouds are formed, it is also true that ultraviolet radiation in interstellar space is sufficiently intense to photodissociate small molecular species in time periods extremely short compared with the time necessary to travel from a star to an interstellar cloud.[14] Thus, the material that forms interstellar clouds will probably consist of dust particles, which can withstand ultraviolet radiation, and atoms. It is also possible that PAH molecules are large enough to resist photodissociation by ultraviolet radiation for long periods of time. Despite the apparent difficulties, the synthesis of the smaller gas-phase molecules seen in interstellar clouds must be accomplished locally. Once produced inside dense interstellar clouds, molecules are shielded somewhat from the interstellar ultraviolet radiation field by the dust particles.

There are two types of chemical processes that can synthesize molecules from atoms in interstellar clouds—gas-phase reactions and reactions on the surfaces of dust particles. Let us consider gas-phase reactions first. Although it shall be shown in Section 2.2 that gas-phase reactions can indeed account for the abundances of almost all molecules seen outside of star-forming regions, it is difficult to account for the primary step in molecule formation—the synthesis of diatomic species from the initial atomic gas using these reactions. Under the low-density conditions of interstellar clouds, the formation of diatomic species can only occur when two atoms stick together in a binary collision; so-called "three-body" collisions, in which two bodies come together to form an intermediate "collision complex" which is then stabilized by inelastic collision with a third body, while prominent in the laboratory, do not occur.[15] Under low-density conditions, the only manner in which the collision complex can be stabilized is via the emission of radiation. This process, known as "radiative association", is inefficient for atom-atom collisions. In particular, the radiative association of two hydrogen atoms to form molecular hydrogen occurs in fewer than one in 10^{10} collisions and cannot produce enough H_2 to account for its overwhelmingly large abundance.[2] Although several other gas-phase routes to H_2 have been suggested, it is clear that interstellar H_2 must be formed via reactions on the surfaces of dust particles.[16] The mechanisms for this process and other possible reactions on dust surfaces are considered in Section 2.1. In this discussion, the possibility that the dust particles are some type of universal catalyst is ignored (although some astronomers have come perilously close to such an assertion) and the assumption that gas-phase molecules are held onto the dust particles by weak physical adsorption forces is utilized. The possibility of chemisorption for selected species cannot be ruled out.

2.1. Surface Chemistry on Interstellar Dust Particles

The process by which two hydrogen atoms form a hydrogen molecule consists of several steps. First, the two hydrogen atoms must stick to the surface of a dust particle. This is an efficient process, unlike the sticking of hydrogen atoms to each other, because the dust particles are macroscopic particles that possess large numbers of energy modes which can accept the kinetic energy of the impacting hydrogen atoms and convert it into an increase in temperature. Once the hydrogen atoms have stuck to the grain, they must recombine before desorption occurs. Migration on the dust surfaces can occur via a classical random walk mechanism. For the special case of light hydrogen atoms, a more rapid quantum-mechanical tunneling process can occur.[16] Once the hydrogen atoms are in the vicinity of one another, they can form a chemical bond by imparting energy to the dust particle, which then increases its temperature once again. The final step in the synthesis is the thermal evaporation of the newly formed hydrogen molecule. The likelihood that these processes indeed occur has been strengthened by numerous laboratory studies. Under typical dense interstellar cloud conditions, formation of H_2 takes roughly 10^5 years, which

is approximately the time scale for a collision between an individual H atom and a grain. The process accounts for the total conversion of H into H_2 since the molecule, once formed, is relatively immune from photodissociation even under diffuse cloud conditions because it is self-shielded.[17]

If H_2 is formed on grain surfaces, what about other molecules? One must remember that hydrogen atoms are somewhat unique on grain surfaces because of their lightness and consequent ability to tunnel from site to site. If H atoms can rapidly find each other on grain surfaces, then they can also find heavier, more stationary atoms of high abundance such as C, O, and N. The sticking of H atoms to these heavier species will produce the radicals CH, OH, and NH. Subsequent sticking reactions between these species and H atoms should also occur without activation energy, leading eventually to the saturated molecules CH_4, H_2O, and NH_3.[18] The formation of other molecules on dust surfaces is not well understood and a variety of ideas have been presented.[19-23] *Allen* and *Robinson*[19] have listed a large number of reactions which they feel occur on grains. These reactions are sticking processes that occur between atoms and/or radicals so that activation energy barriers are not present. *Allen* and *Robinson* consider only very small grains so that even relatively heavy species can migrate appreciably. Large molecules are synthesized via sequences of sticking reactions in which radicals are formed as well as more stable, and therefore inert isomers. *Tielens* et al.[6, 20] consider larger (standard) grains and therefore are more concerned with which species can migrate appreciably. In their models, only H, H_2, C, N, and O can undergo appreciable migration and react with other, including more stationary species. In addition, they show that certain reactions with small amounts of activation energy can occur. Complex molecules are not built up in their approach. Finally, *Greenberg* et al.[21, 22] have shown from laboratory studies that complex organic molecules can be synthesized via photochemical processes when cold surfaces containing simple species are subjected to intense photon fluxes. These authors argue for a similar chemistry in the interstellar medium despite the very different time scales and far more modest photon fluxes involved.[23]

It can be seen that there is no unanimity of opinion on the synthesis of most molecules on dust particles. In my view, if it is correct that H_2 is formed on grains, it is also most probable that simple saturated species such as water, ammonia, and methane are also formed. The formation of more complex species than these is problematical. In addition to the problem of not really knowing which species are produced on dust particle surfaces, an even more vexing problem is how these species can be desorbed from the dust particles at the low temperatures prevailing in non-star-forming regions of interstellar clouds. Since evaporation is far too slow for molecules heavier than H_2, other mechanisms must be considered. These mechanisms can be divided into two types—continual and intermittent.[24] A variety of continual mechanisms which are nonthermal in origin have been considered; these include photodesorption, grain-grain collisions, grain explosions, use of the exothermicity of chemical reactions either directly or indirectly (grain heating), sputtering by cosmic rays, etc. None of these has been shown conclusively to operate efficiently under interstellar conditions although much research remains to be undertaken. The intermittent mechanisms have to do with the process of star formation. When stars form or are forming, the rise in temperature and the existence of shock waves can drive the desorbed material off interstellar dust particles.[25, 26] In my view, the intermittent mechanisms, especially simple thermal desorption based on a higher temperature, are on a more solid footing. In the simplest scenario then, heavy molecules are not appreciably released from dust particle surfaces unless star formation occurs nearby. One should then look for any evidence of heavy molecules formed on dust grains and desorbed into the gas in the vicinity of protostars and newly formed stars. In regions distant from star-forming regions, there may be no evidence at all in the gas phase of the chemistry of heavy molecules occurring on the surfaces of grains. Since the largest number of interstellar molecules are discovered under such conditions, it is most probable that they are formed in the gas phase.

2.2. Gas-Phase Interstellar Chemistry

Once molecular hydrogen is formed on the surfaces of dust particles and evaporates into the gas phase, gas-phase chemical processes leading to complex molecules occur. These processes are restricted in non-star-forming regions by the low gas densities and temperatures to binary reactions without activation energy. Ternary reactions, in which a collision complex is stabilized via an inelastic collision with a third body, are important in the laboratory[15] but do not occur at the low densities of even the most dense interstellar clouds. In the realm of neutral-neutral chemistry, most reactions have appreciable activation energy even if exothermic. These reactions have rate coefficients k that are given by the simple Arrhenius formula [Eq. (1)].

$$k = A(T)\exp(-E_a/kT) \tag{1}$$

T is the temperature, k is the Boltzmann constant, E_a is the activation energy, and $A(T)$ is a weakly temperature-dependent factor which derives from the actual shape of the reaction potential surface as the reactants approach one another. Activation energies of 1–5 eV are normal; when these are inserted into the right-hand-side of Equation 1, at say a temperature of 10 K, it is easily seen that the rate coefficient approaches zero. As an example, consider a reaction with an activation energy of 1 eV. At a temperature of 10 K, the factor appearing in the exponential is -1160! Since collisions between species are themselves rare in interstellar clouds, it is clear that only efficient gas-phase reactions with no activation energy need be considered.

What types of reactions do not possess activation energy? Probably reactions involving atoms and neutral radicals obey this constraint. However, if these were the only reactions to be considered, it would be difficult if not impossible to produce most of the observed interstellar molecules. In addition, there is little experimental evidence concerning the rates of radical reactions at very low temperatures and current theoretical ideas are widely divergent. More important than neutral-neutral reactions are so-called ion-molecule re-

actions, in which one species possesses a charge (e.g., Equation 2, where the species are atomic or molecular). These

$$A^{\oplus} + B \rightarrow C^{\oplus} + D \quad (2)$$

reactions have been studied in the laboratory by a variety of investigators utilizing different experimental techniques.[15,27-30] A temperature range from considerably above room temperature to near 1 K has been probed and it is found that the vast majority of exothermic ion-molecule reactions do not have rate coefficients that have an exponential dependence on temperature as seen in Equation 1; rather, their rate coefficients are large and only weakly dependent on temperature. The rapidity of ion-molecule reactions can be understood in terms of very attractive long-range potential surfaces that often lead to long-lived collision complexes (potential minima) rather than transition states (potential maxima). The simplest case occurs when the neutral reactant B does not possess a permanent dipole moment. Then, if the long-range attraction is dominated by the ion-induced dipole force and if it is assumed that every strong collision leads to reaction, a simple formula for the rate coefficient is obtained which was first derived by *Langevin*[31] [Eq. (3)]. α is the polarizability of the neutral

$$k = 2\pi e(\alpha/\mu)^{1/2} \approx 10^{-9}\ \mathrm{cm^3\ molecule^{-1}\ s^{-1}} \quad (3)$$

species (in cm^3), μ is the reduced mass of the reactants (in gm), and e is the electronic charge in esu. Note that this expression shows no temperature dependence at all, in good agreement with experiment, and that the absolute value of the rate coefficient is 10–100 times the size of the standard "gas kinetic" value for neutral-neutral reactions at room temperature. Thus, exothermic ion-molecule reactions are rapid and will occur at low temperatures. From the point of view of interstellar chemistry, reactions involving neutrals with permanent dipole moments are even better in that their rate coefficients have been found to increase with decreasing temperature, typically as $T^{-1/2}$.[32-33] Unfortunately, no simple formula can be derived in this case, although much theoretical interest has centered on ion-polar neutral reactions.[34-35] Rate coefficients for these processes can reach $10^{-7}\ \mathrm{cm^3\ molecule^{-1}\ s^{-1}}$ at 10 K.

The above discussion makes it clear that ion-molecule reactions can occur rapidly under interstellar conditions. What is still unclear is (1) how ions are produced in low-temperature clouds and (2) how ion-molecule reactions can actually synthesize polyatomic species. Ions are produced mainly via cosmic ray bombardment.[36] Cosmic rays are high-energy nuclei, mainly protons, and formed in high-energy events such as supernovae; they penetrate dense interstellar clouds, unlike ultraviolet photons. These species ionize neutral atoms and molecules in their paths. The most important ionization process involves the dominant neutral H_2 [Eq. (4)], and leads to the formation of the $H_2^{\oplus}$ ion.[36] The

$$H_2 + \text{cosmic ray} \rightarrow H_2^{\oplus} + e + \text{cosmic ray} \quad (4)$$

first-order rate coefficient for cosmic-ray-induced ionization is designated ζ by astronomers and is equal to approximately $10^{-17}\ s^{-1}$; this small number means that interstellar clouds are not bombarded by large numbers of cosmic rays, which, of course, would destroy rather than enhance molecular buildup, but rather "tickled" by small numbers of these species.

After the $H_2^{\oplus}$ ion is formed, it is "immediately" destroyed by reaction with ubiquitous H_2 via the well-studied reaction shown in Equation 5 to produce the simplest polyatomic ion $H_3^{\oplus}$.

$$H_2^{\oplus} + H_2 \rightarrow H_3^{\oplus} + H \quad (5)$$

In general, if an ion can react with H_2, no other reaction need be considered because reaction with H_2 is so rapid due to the ubiquity of this neutral species. The rate for reaction with H_2 in a standard dense cloud of gas density $n = 10^4\ \mathrm{cm^{-3}}$ is $10^{-9}\ \mathrm{cm^3\ s^{-1}}$ times $10^4\ \mathrm{cm^{-3}}$ or $10^{-5}\ s^{-1}$, which leads to a time scale of $10^5\ s \approx 1$ day. This is "immediate" by interstellar standards! When $H_3^{\oplus}$ is formed, it can react with a wide variety of other neutral species present in the primeval mix. Let us first follow what happens if reaction with oxygen atoms occurs. The following sequence of reactions leading to $H_3O^{\oplus}$ is well-studied in the laboratory [Eqs. (6)–(8)], and consists of a "proton transfer" reaction followed by two "H atom" transfer reactions.

$$H_3^{\oplus} + O \rightarrow OH^{\oplus} + H_2 \quad (6)$$

$$OH^{\oplus} + H_2 \rightarrow H_2O^{\oplus} + H \quad (7)$$

$$H_2O^{\oplus} + H_2 \rightarrow H_3O^{\oplus} + H \quad (8)$$

The oxonium ion $H_3O^{\oplus}$, a saturated species, is resistant to further reaction with H_2, and reacts much more slowly with other species, including the dominant carrier of negative charge in dense clouds. This is normally assumed to be free electrons, formed primarily via cosmic ray bombardment, although the suggestion has been made that if polycyclic aromatic hydrocarbons are present and abundant in dense clouds, electrons will stick to them to form negatively charged ions more abundant than free electrons.[37] Ignoring this possibility for the moment, we must consider the reaction between $H_3O^{\oplus}$ and electrons. Recombination reactions between positive molecular ions and electrons have been studied extensively in the laboratory[38] and proceed rapidly in almost all cases with rate coefficients in the range 10^{-6}–$10^{-7}\ \mathrm{cm^3\ molecule^{-1}\ s^{-1}}$ at room temperature and with a weak inverse temperature dependence. The products of these reactions are neutral fragments rather than the parent neutral species and the reactions are termed "dissociative recombination" reactions. However, it is only recently that laboratory measurements of the neutral-product branching ratios have begun to be available and interstellar chemists previously had to estimate these branching ratios based on a variety of often conflicting simple theoretical models.[39] The simplest such model suggests that there is a 50% probability that one hydrogen atom will dissociate from the parent neutral, a 50% probability that two hydrogen atoms (or an H_2 molecule) will dissociate from the parent neutral, and that breakage of multiple heavy atom-heavy atom bonds is unlikely. This model predicts for the case of $H_3O^{\oplus}$ + e that OH and H_2O will each be produced on 50% of collisions. The reaction between oxonium ions and electrons has now been

studied via laser-induced fluorescence of product OH radicals[40] and found to produce the radical OH (+ either H_2 or 2 H) on 65 ± 10% of collisions, with water presumably being formed on ≤ 35% of collisions since three-body product channels are also exothermic. Thus, $H_3O^{\oplus}$ is a precursor to interstellar OH and (presumably) H_2O as well. Once formed, these species are depleted by gas-phase reactions. Water is a stable neutral species and can only react via ion-molecule reactions, whereas OH is depleted via neutral-neutral reactions as well and, hence, will have a lower concentration.

The ion-molecule synthesis of water is an example of how a polyatomic neutral can be produced via such reactions; first a complex ion is synthesized, then some of this complexity is lost when the ion recombines with electrons. Laboratory studies are currently underway in several places to completely determine the neutral products of a variety of dissociative recombination reactions such as that of $H_3O^{\oplus}$ and electrons via the techniques of laser-induced fluorescence and ultraviolet absorption spectroscopy. Preliminary results indicate a complex pattern in which generalizations are difficult. If the dominant carrier of negative charge in dense interstellar clouds is not electrons but rather $PAH^{\ominus}$ (negatively charged polycyclic aromatic hydrocarbons), the final neutral products of ion-molecule syntheses will form from ion-ion neutralization processes. Although the products of such reactions are not known, it appears on theoretical grounds that in general they will involve less dissociation of the parent neutral than do ion-electron reactions.[39c]

Ion-molecule chemical pathways, whether they synthesize inorganic species, hydrocarbons, or more complex organic molecules, often result in highly unusual neutrals by terrestrial standards. The principal reason for this lies in the assumption that dissociative recombination reactions produce assorted neutral products including radicals (e.g., OH) and metastable isomers (e.g., HNC) seen in Table 1. In the main, this assumption remains to be tested by experimental investigation.

Let us now consider the synthesis of organic molecules via ion-molecule reactions. One initiating reaction is that between $H_3^{\oplus}$ and neutral atomic carbon [Eq. (9)], which has not yet been studied in the laboratory due to the difficulty in producing C. However, ab initio quantum-chemical studies

$$C + H_3^{\oplus} \rightarrow CH^{\oplus} + H_2 \quad (9)$$

show that reaction (9) proceeds readily.[41] Another initiating reaction of importance starts with $C^{\oplus}$ rather than C since, because of the ease in photoionizing atomic carbon, it is probable that the initial atomic population of carbon is mainly in the form of $C^{\oplus}$ once it reaches dense interstellar clouds. Interestingly, there is no exothermic reaction between $C^{\oplus}$ and H_2 and the only possibility under low-temperature conditions is the radiative association reaction[42] [Eq. (10)] in which the $CH_2^{\oplus}$ complex is stabilized by emission of a photon.

$$C^{\oplus} + H_2 \rightarrow CH_2^{\oplus} + h\nu \quad (10)$$

Until recently, this and other radiative association reactions had been studied by theoretical methods only due to their low efficiency and the fact that low gas densities are needed in the laboratory so that three-body association does not dominate.[43] The theoretical methods show that radiative association tends to become more probable as temperature decreases ($k \propto T^{-n}$; $n \geq 2$), as the size of the collision complex increases, and as its dissociation energy increases. For the three-atom system in Equation 10, the latest calculated rate coefficient is $\approx 10^{-15}$ cm^3 molecule^{-1} s^{-1} at 10 K.[44,45] Given the standard Langevin value for the collision rate coefficient, the probability of radiative association is approximately one collision in 10^6. Although this is a low number, it is higher than in the case of two hydrogen atoms mentioned above. In addition, the large abundance of H_2 in dense interstellar clouds makes this process competitive. Very recently, the process shown in Equation 10 has been studied in the laboratory in a low-pressure ion trap and found to have a rate coefficient in reasonable agreement with the theoretical value.[46]

Once $CH^{\oplus}$ and $CH_2^{\oplus}$ are formed, $CH_3^{\oplus}$ is produced "immediately" via well-studied H-atom transfer reactions [Eqs. (11) and (12)]. The H-atom transfer reaction between

$$CH^{\oplus} + H_2 \rightarrow CH_2^{\oplus} + H \quad (11)$$

$$CH_2^{\oplus} + H_2 \rightarrow CH_3^{\oplus} + H \quad (12)$$

$CH_3^{\oplus}$ and H_2 is endothermic and does not occur under interstellar conditions. A slower radiative association process has been proposed and its rate coefficient at 10 K calculated[45] to be $\approx 10^{-13}$–10^{-14} cm^3 molecule^{-1} s^{-1} or even greater.[47] The theoretical values have been somewhat corroborated by two recent and somewhat conflicting experimental values.[48,49] Once $CH_5^{\oplus}$ is produced via radiative association, it can react with electrons to form a variety of single-carbon-atom hydrocarbons such as methane [Eq. (13)].

$$CH_5^{\oplus} + e^{\ominus} \rightarrow CH_4 + H,\ CH_3 + H_2, \text{ etc.} \quad (13)$$

In addition, methane is known to form via the ion-molecule reaction shown in Equation 14; the reactant CO is formed by a series of neutral-neutral and ion-molecule reactions.

$$CH_5^{\oplus} + CO \rightarrow CH_4 + HCO^{\oplus} \quad (14)$$

Once simple hydrocarbons are synthesized, more complex ones can be produced by several different pathways. A well-studied type of reaction in the laboratory, called "carbon insertion",[28] is important in dense interstellar clouds. In this type of reaction, $C^{\oplus}$ reacts with a simple hydrocarbon to produce a more complex hydrocarbon ion and one or more hydrogen atoms. An example is given in Equation 15.

$$C^{\oplus} + CH_4 \rightarrow C_2H_2^{\oplus} + H_2;\ C_2H_3^{\oplus} + H \quad (15)$$

Two-carbon-atom hydrocarbon ions can possibly also be synthesized via analogous insertion reactions involving neutral carbon atoms and hydrocarbon ions; however, these processes have yet to be studied in the laboratory. A third synthetic mechanism involves the so-called condensation reactions in which hydrocarbon ions and neutrals react to

form larger hydrocarbon ions as well as hydrogen atoms or molecules. Equation 16 gives an example; in general, con-

$$CH_3^{\oplus} + CH_4 \rightarrow C_2H_5^{\oplus} + H_2 \quad (16)$$

densation reactions are less efficient than the other two mechanisms under interstellar conditions. Yet a fourth possibility involves radiative association reactions between hydrocarbon ions and neutrals; there is some experimental evidence for this in low-pressure ion cyclotron resonance experiments[28] but further experimental studies are necessary to confirm theoretical determinations of rate coefficients.

After two-carbon-atom hydrocarbon ions are produced, they can react with H_2 or neutrals of lesser abundance, or dissociatively recombine with electrons to produce neutral hydrocarbons such as the radical C_2H or acetylene. In general, reactions between hydrocarbon ions with more than one carbon atom and H_2 do not occur except for very unsaturated ions,[50] presumably because they are endothermic. Thus, for two-carbon-atom ions only $C_2^{\oplus}$, $C_2H^{\oplus}$, and $C_2H_2^{\oplus}$ react with H_2; for $C_2H_2^{\oplus}$, it is currently unclear whether the reaction is predominantly a normal one (to produce $C_2H_3^{\oplus}$ + H) or an associative one. The net result of the difficulty in hydrogenating ions produced in reactions such as (15) is that unsaturated hydrocarbon ions and neutrals are predicted to be dominant despite the large abundance of H_2. This prediction is in agreement with observational results in non-star-forming regions (Table 2).

Let us continue on to three-carbon-atom hydrocarbons. The well-known ion-molecule reaction shown in Equation 17

$$C^{\oplus} + C_2H_2 \rightarrow C_3H^{\oplus} + H \quad (17)$$

produces an ion with a linear backbone which does not react rapidly with hydrogen but does associate with it under high-pressure laboratory conditions. The association, which leads 50% of the time to a cyclic form of the ion $C_3H_3^{\oplus}$, presumably occurs radiatively under low-density interstellar conditions.[51] Once the cyclic $C_3H_3^{\oplus}$ ion is produced, it can recombine dissociatively with electrons to form the widespread interstellar ring molecule c-C_3H_2 (cyclopropenylidene, [Eq. (18)].

$$c\text{-}C_3H_3^{\oplus} + e^{\ominus} \rightarrow c\text{-}C_3H_2 + H \quad (18)$$

Ion-molecule syntheses analogous to what has been described here have been written down for hydrocarbons with up to nine carbon atoms.[52] In general, as the size of the hydrocarbon increases, the amount of laboratory information decreases and it is necessary to deduce reaction pathways by analogy with other reaction studies.

Organic molecules with atoms other than carbon and hydrogen can be formed via reactions that involve hydrocarbon neutrals or ions. For example, organonitrogen species can be formed via ion-atom reactions between hydrocarbon ions and nitrogen atoms; a well-studied example is shown in Equation 19,[53] which presumably leads to cyanoacetylene (HC_3N), a well-known interstellar molecule, via the dissociative recombination channel [Eq. (20)].

$$N + C_3H_3^{\oplus} \rightarrow C_3H_2N^{\oplus} + H \quad (19)$$

$$C_3H_2N^{\oplus} + e \rightarrow HC_3N + H \quad (20)$$

Other organonitrogen species can be formed from the simple precursors HCN and NH_3, both of which are themselves formed by series of ion-molecule reactions.[54] Examples include the above radiative association reactions [Eqs. (21) and (22)], which are calculated to be sufficiently rapid at low

$$CH_3^{\oplus} + HCN \rightarrow CH_3CNH^{\oplus} + h\nu \quad (21)$$

$$CH_3^{\oplus} + NH_3 \rightarrow CH_3NH_3^{\oplus} + h\nu \quad (22)$$

interstellar temperatures, due to the large size and bond energies of the collision complexes, to lead to large amounts of methyl cyanide and methylamine after dissociative recombination.[52, 55]

Oxygenated organic molecules are also formed via a variety of ion-molecule processes. The production of interstellar methanol for example is thought to proceed via a radiative association reaction[52, 55] [Eq. (23)] followed by dissociative recombination, and interstellar ketene is thought to be synthesized via a radiative association reaction [Eq. (24)], followed by dissociative recombination.

$$CH_3^{\oplus} + H_2O \rightarrow CH_3OH_2^{\oplus} + h\nu \quad (23)$$

$$CH_3^{\oplus} + CO \rightarrow CH_3CO^{\oplus} + h\nu \quad (24)$$

All of the association reactions [Eqs. (21)–(24)] have only been studied under high-pressure three-body conditions in the laboratory. A detailed discussion of ion-molecule synthetic pathways to various types of molecular products has recently been published.[52]

2.3. Deuterium Isotopic Fractionation

Ion-molecule processes also explain to a great extent the considerable isotopic fractionation observed in interstellar clouds, especially regarding deuterium. Although the deuterium-to-hydrogen abundance ratio, which is a remnant of the Big Bang, is only of the order of 10^{-5}, the abundance ratio of singly deuterated to normal molecules in dense interstellar clouds can rise orders of magnitude above this for trace constituents of the clouds. The mechanism for such strong isotopic fractionation is the difference in zero-point energy between ordinary and deuterated species. In dense clouds, the repository of deuterium is mainly HD, and the HD to H_2 abundance ratio is approximately twice the Big Bang D/H value, or $\approx 3 \times 10^{-5}$. Consider the well-studied ion-molecule reaction between $H_3^{\oplus}$ and HD [Eq. (25)], which is exothermic by an energy equivalent to a few hundred Kelvin due to zero-point energy differences.

$$H_3^{\oplus} + HD \rightarrow H_2D^{\oplus} + H_2 \quad (25)$$

At temperatures significantly lower than this exothermicity, the back reaction will have a much slower rate than the forward reaction [Eq. (1)] and the equilibrium will lie far to

the right. Thus, it is to be expected that at low temperatures the $H_2D^{\oplus}/H_3^{\oplus}$ ratio will be much larger than 3×10^{-5}. Although this ratio has not been measured in interstellar clouds, many other abundance ratios have been. For example, in TMC-1, a cold cloud with a temperature of 10 K, the $DCO^{\oplus}/HCO^{\oplus}$ abundance ratio is 0.015. The ions $HCO^{\oplus}$ and $DCO^{\oplus}$ arise principally from the reactions of CO with $H_3^{\oplus}$ and $H_2D^{\oplus}$, respectively, so that the measured $DCO^{\oplus}/HCO^{\oplus}$ abundance ratio reflects that of $H_2D^{\oplus}/H_3^{\oplus}$. A complete study of interstellar deuterium fractionation reactions akin to Equation 25 has recently been published.[56] Fractionation can also occur on dust particle surfaces. The abundant ion $DCO^{\oplus}$ recombines with electrons to give deuterium atoms which eventually stick to the grain surfaces and combine with atoms and radicals in a manner analogous to that of H atoms.[57] Unlike the gas-phase processes, processes on dust surfaces can lead to large abundances of doubly deuterated species as well.[57]

3. Chemical Models of Interstellar Clouds

To determine whether or not ion-molecule processes are responsible for most of the interstellar molecules seen, it is necessary to include them in computer models which lead to calculated concentrations. These models consist of coupled kinetic equations. Each kinetic equation relates the time derivative of the concentration of a molecule to its formation and depletion rates. Consider as a simple example the molecule $C^{\oplus}$ formed in the reaction shown in Equation 2 and destroyed by reaction with a species E [Eq. (26)]. The kinetic

$$C^{\oplus} + E \rightarrow \text{products} \tag{26}$$

equation for species $C^{\oplus}$ is presented in Equation 27, where the symbol [ ] indicates concentration or, as the astronomers

$$d[C^{\oplus}]/dt = k_2[A^{\oplus}][B] - k_{26}[C^{\oplus}][E] \tag{27}$$

prefer, abundance. Kinetic equations for all molecules in the model can be written down. Although a few models involving the formation of heavy molecules on dust particles have appeared, most models ignore grain chemistry except for the formation of molecular hydrogen.

When interstellar modeling started in the early 1970s, computers were not as advanced as today and instead of solving large numbers of simultaneous coupled differential equations, investigators used the steady-state approximation in which the time derivatives are all set to zero and algebraic equations obtained. The first such models of diffuse clouds[58] and dense clouds[36, 59] were quite successful. Their success and the detection of interstellar ions have shown that ion-molecule processes do occur in interstellar clouds and can explain much of the chemistry. The original dense cloud model of *Herbst* and *Klemperer*[36] contained only 100 gas-phase reactions involving 35 species of up to five atoms in size.

Although the steady-state hypothesis is fine for diffuse clouds, since chemical steady state can be shown to be reached in a relatively short time due to the rapid photodissociation of molecules via external ultraviolet radiation, the approximation may not be applicable to dense clouds. The first non-steady-state solutions of the coupled kinetic equations in dense clouds showed that steady state can be reached in about 10^7 yrs from standard starting materials (either all atoms or atoms plus those diatomic molecules—especially H_2—seen in diffuse clouds).[60] This time is much longer than the time necessary for a molecule to stick on a grain surface ($\approx$ a few per 10^5 years for a cloud of gas density 10^4 molecules cm^{-3}). Therefore, if a desorption mechanism does not exist, neither can the gas phase of dense interstellar clouds exist past this amount of time. If there is no gas, there is clearly no gas-phase steady-state solution. The paradox remains to this day—workers in the field either ignore the problem, invoke some desorption mechanism, or abandon the steady-state hypothesis.

Compared with early models of dense interstellar clouds, modern models are much larger, include much larger molecules, and incorporate time dependence. The time dependence can be purely chemical, in which case physical conditions such as density and temperature do not change, or it can include physical time dependence. Time dependence of physical conditions can be treated simply (e.g., by simple isothermal free-fall collapse) or hydrodynamically. Complications, such as the effect of ultraviolet radiation on cloud edges, the effect of PAH's, and the effect of photodissociation caused by cosmic ray excitation of H_2 can also be considered.[61, 62] Models of both non-star-forming and star-forming regions have been undertaken in recent years and these are discussed separately. A hydrodynamic model in which chemistry occurs as a star begins to form will not be mentioned[63] nor will current models of diffuse clouds.[64]

3.1. Models of Non-Star-Forming Regions of Dense Clouds

Most models of cool regions of dense interstellar clouds contain only chemical time dependence. Some results from a recent model of this type for a cool dense cloud (T = 10 K, $n = 10^4$ cm^{-3}) containing almost 300 chemical species and 2600 gas-phase chemical reactions (most unmeasured in the laboratory) are depicted in Figures 2 and 3.[52] Somewhat smaller but similar models have been developed by competing groups.[65] Figure 2 shows the fractional abundance of

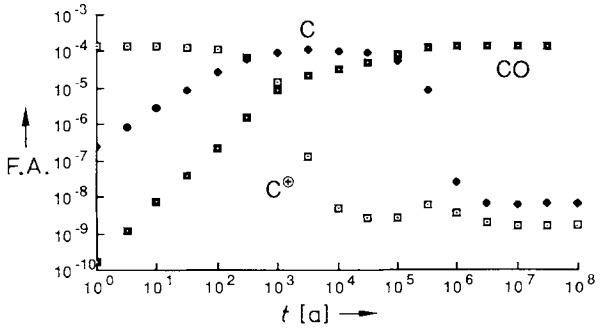

Fig. 2. The calculated abundances with respect to H_2 (F.A.) of the dominant carbon-containing species in a chemical model of cool (10 K) dense interstellar clouds plotted against time (see [52]). □ = $C^{\oplus}$, ◆ = C, ■ = CO.

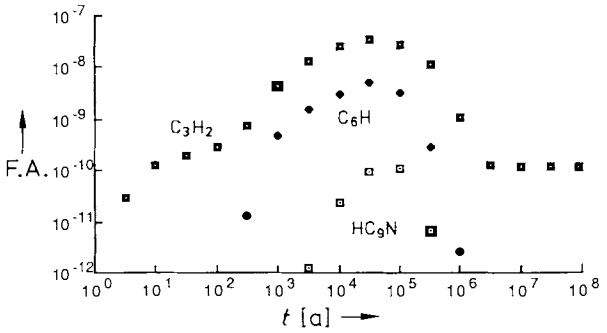

Fig. 3. The calculated abundances with respect to H_2 (F.A.) of several organic molecules in a chemical model of cool (10 K) dense interstellar clouds plotted against time (see [52]). □ = HC_9N, ◆ = C_6H, ■ = c-C_3H_2.

the dominant carbon-containing species as a function of time from initial conditions to steady state. It can be seen that the initially large abundance of $C^{\oplus}$ gradually disappears as the abundance of neutral C increases. Finally, as steady state is reached, the neutral C abundance drops dramatically and the CO fractional abundance rises to its steady-state value of 10^{-4}, in agreement with observation. If one wishes to abandon the steady-state hypothesis because of the dust adsorption problem, one can choose a time as early as $\approx 10^5$ years without a noticeable drop in the calculated CO abundance. In general, this is true for most smaller molecules in the models—choice of a time before steady state is reached such as 10^5 years does not greatly affect the calculated abundances. Use of this so-called "early time" has recently received some support from the observation of large amounts of atomic carbon in selected dense clouds; the calculated steady-state abundance of C is far too small to explain the observations, but at a time of 10^5 years the calculated abundance is indeed quite large. The idea of using "early-time" abundances for dense clouds is still a controversial one since it is clear that the overall ages of clouds are much greater than this. Thus, if one accepts the early-time chemical hypothesis, the time clock in chemical models is not really starting when the cloud is being born but at some later time, perhaps after a dissociative shock wave has ripped through the cloud or material has been processed by turbulent motions pushing it to the cloud edge where it can be photodissociated. In any event, if one wishes to maintain the steady-state hypothesis, as some astronomers do, one can argue either (1) that the atomic C comes from only the outer shells of clouds in which ultraviolet starlight penetrates and dissociates CO into C and O and/or (2) that our knowledge of elemental abundances in the gas phase of dense clouds is quite insecure and that if there is more carbon than oxygen, there will be a large abundance of C even at steady state. The usual assumption is to choose elemental abundances based on stellar and diffuse cloud observations, in which oxygen is normally (but not always) dominant (Table 3). In my view, it is pointless to maintain a steady-state hypothesis unless the problem of desorption from the grains is understood.

Figure 3 shows the calculated abundances of three representative organic molecules. Unlike most smaller species such as CO, the abundances of organic species show an extreme difference between early time and steady state. At a time of 10^5 years, the abundances show clear peaks before diminishing to their steady-state values. The reason for this dichotomy is clear enough—organic molecules are synthesized via reactions involving $C^{\oplus}$ and C. Once most of the carbon is converted into CO and the abundances of $C^{\oplus}$ and C become low, then the synthesis of organic species is inefficient. The more complex the species, the sharper the dichotomy. The calculated early-time peak abundances of organic molecules are much closer to what is observed in some well-studied clouds such as TMC-1, although they can sometimes exceed the observed values even in this remarkable source. Table 2 contains a comparison between observed and peak calculated abundances in TMC-1[52] for almost 40 species. Although it is buried in this table, there appear to be two major problems with using early-time as opposed to steady-state abundances—these concern the small molecules $HN_2^{\oplus}$ and SO, the calculated abundances of which are quite low until times somewhat larger than 10^5 years. Some authors have advocated using slighter longer times than 10^5 years to achieve still better agreement between theory and observation.[66] Still, a glance at Table 2 shows the considerable extent of the agreement. (Of course, if one ignores the dust desorption problem and one carefully chooses a C/O elemental abundance ratio of greater than unity, one can probably achieve general agreement at steady state as well.) The agreement between observation and theory for the cyanoacetylene series (sometimes referred to as the cyanopolyyne series) in TMC-1 is depicted in Figure 4 where the peak results of two

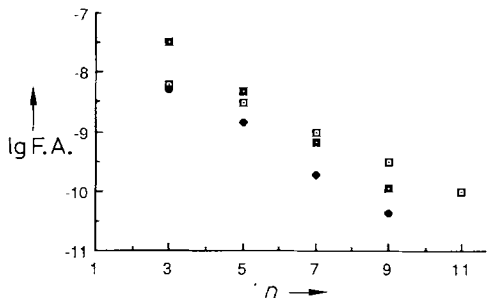

Fig. 4. The peak calculated and observed abundances of cyanopolyynes ($HC_{2n+1}N$) with respect to H_2 (F.A.) plotted against number n of carbon atoms. The observed abundances (□) are from the well-known interstellar source TMC-1. The calculated results (◆, ■) are taken from two slightly different models [52].

slightly different current models are contained.[52] Note that for this series of species, the peak abundances do not greatly exceed the observed values, indicating that if the time evolution shown in Figures 2 and 3 is correct, TMC-1 may be serendipitously at the correct age for peak abundances. Interestingly, the large cyanopolyyne abundances in TMC-1 do appear to be unique!

Within the last year, a novel idea for removing the large dichotomy between early-time and steady-state abundances has been proposed.[67] A large body of observational data shows that the gas in dense interstellar clouds is not homogeneous but is clumped; i.e., relatively dense regions exist inside a lower density medium. This is shown in Figure 5 where a telescope beam of low spatial resolution is shown failing to resolve the clumped material. The diffuse material is pervad-

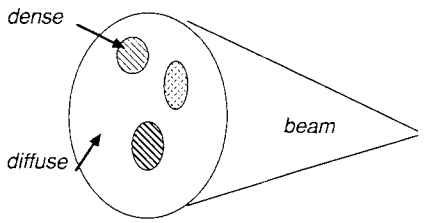

Fig. 5. If the beam of a radiotelescope is large enough, it cannot resolve dense clumps of gas existing in a much more diffuse medium. It is likely that most dense interstellar clouds have such a clumpy nature.

ed by external ultraviolet radiation and the carbon is mainly in the form of C and $C^{\oplus}$. The recent observation of $C^{\oplus}$ as well as C in dense clouds is in harmony with this picture.[68] Since C and $C^{\oplus}$ are the precursors to organic molecule development, the synthesis of organic molecules in the dense clumps would be aided at steady state if mixing between the diffuse gas and the dense gas in the clumps would occur.[67] Models to quantify this effect are currently underway; it would appear that the early-time, steady-state dichotomy can be removed if the diffuse gas is rich in C rather than $C^{\oplus}$. Even if the idea of mixing allows the abundances of complex molecules to be high at steady state, it is unclear what causes the mixing. In addition, the problem of desorption from the dust particles is not solved unless the additional radiation penetrating the dense clumps can photodesorb material.

3.2. Models of Star-Forming Regions of Dense Clouds

In the vicinity of star formation, the collapsing gas results in higher densities and temperatures. It would be surprising if the chemistry were unaffected by this process and there is ample observational evidence to show that it is indeed affected. The chemistry in star-forming regions is clearly a severe function of how distant the material is from the center of the star-formation activity. Present-day observations do not yet have the spatial resolution to peer into the chemistry in the immediate vicinity of stars and protostars although this situation will soon change. Given the spatial resolution that has been brought to bear on the problem, unusual chemistries over wider scales, perhaps 0.3 light year, in the vicinity of protostars have been examined. The best-studied region is the so-called Kleinmann-Low Nebula in the Orion Molecular Cloud, in which three chemically different areas have been observed. These are termed the "Plateau", "Hot Core", and "Compact Ridge" regions.[69] All appear to be associated with a strong infrared source called IRc2 suspected of being a protostar. The "Plateau" source shows very wide line widths in its molecular spectral features and is associated with gas heated strongly (to perhaps thousands of degrees) but temporarily by a shock wave passing outward from the protostar. The other two sources are more quiescent in nature. The "Hot Core" source has a density of 10^6-10^7 cm^{-3} and a temperature of perhaps 100 K or more. It contains high abundances of normal "saturated" species such as H_2O and NH_3, as well as saturated species such as CH_3CH_2CN not even detected in the normal interstellar medium. It does not appear to be associated directly with star formation but is perhaps a piece of material that did not fully take part in the collapse to form a protostar. Finally, the "Compact Ridge" source, although possessing physical conditions similar to the "Hot Core", has abnormally high abundances of the oxygen-containing molecules methanol, methyl formate, and dimethyl ether. Given its physical location, it is probably formed by the intersection of heated gas coming outwards from IRc2 and the quiescent material of the normal interstellar cloud. Models for each of these unusual regions have been proposed.

Much research has gone into the chemical and physical effects of interstellar shock waves.[70-71] The properties of the shocked gas depend critically on the speed of the shock front and the size of the magnetic field. In the absence of a magnetic field, even a shock of moderate velocity can heat the gas to temperatures in excess of several thousand K from which it cools rapidly. Nevertheless, while the gas is hot, numerous exothermic reactions with activation energy barriers and even some endothermic reactions can occur between abundant species, totally changing the chemical composition of the material. In the presence of even a small (μGauss) magnetic field, the shock characteristics change dramatically and the neutral gas does not jump discontinuously in temperature as the shock passes by but rises gradually in temperature. However, a net velocity between the ionic and neutral phases of the gas appears which can power endothermic ion-molecule reactions such as that in Equation 28 which is 0.39 eV endothermic. Reaction (28) is actually thought to be

$$C^{\oplus} + H_2 \rightarrow CH^{\oplus} + H \qquad (28)$$

the process that produces $CH^{\oplus}$ in regions of diffuse interstellar clouds subjected to shock waves.

In the "Plateau" source in Orion, shock models[71] have been proposed to explain the enhanced abundances of certain sulfur-bearing species such as H_2S, OCS, and SO, which cannot be accounted for by normal ion-molecule chemical models.[66, 69] These shock models have met with mixed success and have produced widely differing results.

The chemistry of the "Hot Core" source in Orion has been more successfully explained in terms of the desorption of saturated material from grain surfaces caused by the relatively high temperature ($T \geq 100$ K). Much of the saturation presumably occurs via H-atom addition on grain surfaces, as discussed in Section 2.1. In a current detailed model, it is proposed[72] that the chemistry can be divided into three phases. In the first phase, normal gas-phase chemistry occurs while the cloud undergoes free-fall isothermal collapse and gas-phase molecules stick to the dust particle surfaces. On these surfaces, reactions involving H atoms occur and produce saturated species such as H_2O, NH_3, and CH_4. After a period of time of approximately 10^6 years, the gas phase has been depleted of most of its condensible species whereas the H_2 density has reached the high value characteristic of the "Hot Core". In the second phase, star formation is assumed to occur nearby, with the result that the temperature rises sufficiently to drive adsorbed species off the grains. In the third and final phase, gas-phase chemistry once again occurs. However, at the high gas density, the ion content of the gas is so low that the ion-molecule chemistry is very slow and the chemical makeup of the gas reflects that achieved in the first

phase for a considerable length of time. Although not quantitatively successful, the model results do explain the enhanced abundances of saturated species seen in this source. Improvements will have to await a better understanding of interstellar dust particles and the chemical processes that can occur on them.

No detailed model of the chemistry of the "Compact Ridge" source has yet appeared in the literature although work on such a model is underway.[73] It has been suggested that the oxygen-rich organic molecules found at high abundance in this source are produced by a chemical pathway in which large amounts of water, mixing into the quiescent gas from the protostellar source IRc2, supply the oxygen.[69] Preliminary calculations do not support this view and, currently, it appears as if there is no gas-phase mechanism sufficiently rapid to explain the large abundances of molecules such as methyl formate, methanol, and dimethyl ether. If this tentative conclusion is correct, then dust-based chemistry is responsible.

4. Summary and Outlook

Since the first observations of polyatomic molecules in the interstellar medium about twenty years ago, the field of interstellar chemistry has progressed significantly. Approximately ninety different molecules have been discovered in the gas phase of dense interstellar clouds, ranging up to thirteen atoms in size. In addition to these unambiguous detections, based on high-resolution spectra, there are low-resolution spectra that have been interpreted in terms of large aromatic molecules ("PAH's") as well as material adsorbed on the surfaces on interstellar dust particles. The dust particles themselves have not been well characterized but are presumably mixtures of silicates and carbonaceous material.

Our understanding of the low-temperature chemistry of interstellar molecules has also grown appreciably in the last two decades. Although molecular hydrogen is synthesized on the surfaces of dust particles, it would appear that most interstellar molecules are produced via gas-phase reactions, especially in regions distant from star-forming regions. These gas-phase reactions must possess no activation energy; the major class of such reactions are ion-molecule processes. Chemical models incorporating large numbers of gas-phase reactions, many of which have been studied in the laboratory, have been quite successful in reproducing observed abundances in sources such as TMC-1. This does not mean that reactions on the surfaces of dust particles do not occur, but rather that the products of these reactions remain on these surfaces. Although the gas-phase models appear to be successful, much work remains to be accomplished in understanding the assorted chemical processes, especially dissociative recombination and radiative association. In addition, it is not at all clear that the extreme time dependence calculated in simple one-phase models is correct; work on two-phase models with mixing between the phases is just beginning.

In regions of the interstellar medium where stars are forming, the chemical situation is much more complex. Star formation heats up the surrounding material, driving off the adsorbed layers from dust particles, results in so-called "winds" of outwardly driven material to interact with the quiescent gas, and leads to shock waves which can heat the material in a transient manner to thousands of degrees. Although chemical models have been propounded which take one or more of these effects into account, they do not yet have the success of models of non-star-forming regions. As astronomers begin to use interferometric methods and look at star-forming regions with greater and greater spatial resolution, models of the chemistry in these regions will be further developed.

In addition to using higher spatial resolution, astronomers are beginning to probe the chemistry of interstellar regions in different galaxies from our own. Two particular galaxies of focus are the "Magellanic Clouds" which are seen from the southern hemisphere and are very close to our own galaxy. These galaxies appear to have less matter in the form of atoms heavier than helium than our own galaxy has, with interesting consequences for the chemistry. Chemical models of interstellar clouds in the Magellanic Clouds are already being undertaken.[74]

Another area of future research concerns the extent of the growth of interstellar molecules. Improvements in observational techniques should permit high-resolution spectral detection of larger molecules than seen previously and additional laboratory work on appropriate reactions should enable modelers to make predictions concerning these larger molecules.

Finally, an area of growing interest is the relationship between interstellar chemistry and the chemistry of the solar system. More than five billion years ago, our area of space was a cool dark interstellar cloud in which a low-mass star (our sun) managed to form via gravitational collapse of a portion of the cloud. In the immediate vicinity of the newly formed sun, certainly all traces of a previous chemistry were lost due to the extreme heat. Further away from the new sun however, interstellar molecules could have survived, especially if they had already been adsorbed on the surfaces of dust particles, which subsequently coagulated to form larger bodies such as planetesimals. There is increasing evidence from meteoritic and cometary studies that such a close relationship between interstellar chemistry and at least some of the matter in these objects exists.[75]

In summary, interstellar chemistry is a young and vibrant field in which many advances have been made, but in which much more needs to be learned.

The work carried out by my group was supported by the National Science Foundation (USA).

Received: December 14, 1989 [A 764 IE]
German version: *Angew. Chem. 102* (1990) 627

[1] G. Herzberg: *Spectra of Diatomic Molecules*, Van Nostrand, Princeton 1950.
[2] W. D. Watson, *Rev. Mod. Phys. 48* (1976) 513–552.
[3] a) A. Omont, *Rev. Mod. Astron. 1* (1988) 102; b) M. S. Vardya, S. P. Taraf-dar (Eds.): *Astrochemistry*, Reidel, Dordrecht 1987; c) A. Betz in [3b], p. 327.
[4] a) D. J. Hollenbach, H. A. Thronson, Jr. (Eds.): *Interstellar Processes* Reidel, Dordrecht 1987; b) W. M. Irvine, P. F. Goldsmith, Å. Hjalmarson in [4a], p. 561.
[5] M. Elitzur in [4a], p. 763.
[6] A. G. G. M. Tielens, L. J. Allamandola in [4a], p. 397.

[7] L. J. Allamandola, A. G. G. M. Tielens, J. R. Barker in [4a], p. 471.
[8] a) A. Léger, L. d'Hendecourt, *Astron. Astrophys. 146* (1985) 81–85; b) M. K. Crawford, A. G. G. M. Tielens, L. J. Allamandola, *Astrophys. J. Lett. 293* (1985) L45–L48.
[9] W. Klemperer, *Nature (London) 227* (1970) 1230.
[10] L. E. Snyder, J. M. Hollis, F. J. Lovas, B. L. Ulich, *Astrophys. J. 209* (1976) 67–74.
[11] R. C. Woods, T. A. Dixon, R. J. Saykally, P. G. Szanto, *Phys. Rev. Lett. 35* (1975) 1269–1272.
[12] C. G. Seab in [4a], p. 491.
[13] a) L. A. M. Nejad, T. J. Millar, *Astron. Astrophys. 183* (1987) 279–286; b) G. A. Mamon, A. E. Glassgold, A. Omont, *Astrophys. J. 323* (1987) 306–315.
[14] a) T. J. Millar, D. A. Williams (Eds.): *Rate Coefficients in Astrochemistry*, Kluwer, Dordrecht 1988; b) E. F. Van Dishoeck in [14a], p. 49.
[15] D. Smith, N. G. Adams in M. T. Bowers (Eds.): *Gas Phase Ion Chemistry*, Academic Press, New York 1979, p. 1.
[16] a) R. J. Gould, E. E. Salpeter, *Astrophys. J. 138* (1963) 393–407; b) D. Hollenbach, E. E. Salpeter, *J. Chem. Phys. 53* (1970) 79–86.
[17] A. Dalgarno, T. L. Stephens, *Astrophys. J. Lett. 160* (1970) L107–L109.
[18] W. D. Watson, E. E. Salpeter, *Astrophys. J. 174* (1972) 321–340; *175* (1972) 659–671.
[19] M. Allen, G. W. Robinson, *Astrophys. J. 212* (1977) 396–415.
[20] A. G. G. M. Tielens, W. Hagen, *Astron. Astrophys. 114* (1982) 245–260.
[21] J. M. Greenberg in [3b], p. 501.
[22] L. B. d'Hendecourt, L. J. Allamandola, F. Baas, J. M. Greenberg, *Astron. Astrophys. 109* (1982) L12–L14.
[23] L. B. d'Hendecourt, L. J. Allamandola, J. M. Greenberg, *Astron. Astrophys. 152* (1985) 130–150.
[24] A. Léger, M. Jura, A. Omont, *Astron. Astrophys. 144* (1985) 147–160.
[25] D. A. Williams, T. W. Hartquist, *Mon. Not. R. Astron. Soc. 210* (1984) 141–145.
[26] C. M. Walmsley, W. Hermsen, C. Henkel, R. Mauersberger, T. L. Wilson, *Astron. Astrophys. 172* (1987) 311–315.
[27] D. Smith, N. G. Adams, *Adv. At. Mol. Phys. 24* (1989) 1–49.
[28] V. G. Anicich, W. T. Huntress, Jr., *Astrophys. J. Suppl. Ser. 62* (1986) 553–672.
[29] a) B. R. Rowe in [14a], p. 135; b) T. L. Mazely, M. A. Smith, *Chem. Phys. Lett. 144* (1988) 563–569.
[30] F. C. Fehsenfeld, E. E. Ferguson, *J. Chem. Phys. 56* (1972) 3066–3070.
[31] a) E. Herbst in [4a], p. 611; b) R. D. Levine, R. B. Bernstein: *Molecular Reaction Dynamics*, Clarenden Press, Oxford 1974.
[32] N. G. Adams, D. Smith, D. C. Clary, *Astrophys. J. Lett. 296* (1985) L31–L34.
[33] J. B. Marquette, C. Rebrion, B. R. Rowe, *Astron. Astrophys 213* (1989) L29–L32.
[34] D. C. Clary, *Mol. Phys. 54* (1985) 605–618.
[35] D. R. Bates, *Proc. R. Soc. London A 384* (1982) 289–300.
[36] E. Herbst, W. Klemperer, *Astrophys. J. 185* (1973) 505–533.
[37] A. Omont, *Astron. Astrophys. 164* (1986) 159–178.
[38] N. G. Adams, D. Smith in [14a], p. 173.
[39] a) E. Herbst, *Astrophys. J. 222* (1978) 508–516; b) S. Green, E. Herbst, *ibid. 229* (1979) 121–131; c) D. R. Bates, E. Herbst in [14a], p. 41; d) E. Herbst in J. B. A. Mitchell, S. L. Guberman (Eds.): *Dissociative Recombination*, World Scientific, Singapore 1989, p. 303.
[40] C. R. Herd, N. G. Adams, D. Smith, *Astrophys. J. 349* (1990) 388–392.
[41] E. Herbst, D. J. DeFrees, A. D. McLean, unpublished.
[42] J. H. Black, A. Dalgarno, *Astrophys. Lett. 15* (1973) 79–82.
[43] a) D. R. Bates, E. Herbst in [14a], p. 17; b) L. M. Bass, R. D. Cates, M. F. Jarrold, N. J. Kirchner, M. T. Bowers, *J. Am. Chem. Soc. 105* (1983) 7024–7033.
[44] E. Herbst, *Astrophys. J. 252* (1982) 810–813.
[45] I. M. W. Smith, *Astrophys. J. 347* (1989) 282–288.
[46] D. Gerlich, private communication.
[47] D. R. Bates, *Astrophys. J. 312* (1987) 363–366.
[48] S. E. Barlow, G. H. Dunn, K. Schauer, *Phys. Rev. Lett. 52* (1984) 902–905; *53* (1984) 1610.
[49] D. Gerlich, G. Kaefer, *Astrophys. J. 347* (1989) 849–854.
[50] a) N. G. Adams, D. Smith, K. Giles, E. Herbst, *Astron. Astrophys. 220* (1989) 269–271; b) E. Herbst, N. G. Adams, D. Smith, *Astrophys. J. 285* (1984) 618–621.
[51] N. G. Adams, D. Smith, *Astrophys. J. Lett. 317* (1987) L25–L27.
[52] a) E. Herbst, C. M. Leung, *Astrophys. J. Suppl. Ser. 69* (1989) 271–300; b) *Astron. Astrophys.*, in press.
[53] W. Federer, H. Villinger, W. Lindinger, E. E. Ferguson, *Chem. Phys. Lett. 123* (1986) 12–16.
[54] a) E. Galloway, E. Herbst, *Astron. Astrophys. 211* (1989) 413–418; b) W. M. Irvine, F. P. Schloerb, Å. Hjalmarson, E. Herbst in D. C. Black, M. S. Matthews (Eds.): *Protostars and Planets II*, University of Arizona, Tucson, AZ 1985, p. 579.
[55] W. T. Huntress, Jr., G. F. Mitchell, *Astrophys. J. 231* (1979) 456–467.
[56] T. J. Millar, A. Bennett, E. Herbst, *Astrophys. J. 340* (1989) 906–920.
[57] P. D. Brown, T. J. Millar, *Mon. Not. R. Astron. Soc. 237* (1989) 661–671; *ibid. 240* (1989) 25P–29P.
[58] a) P. M. Solomon, W. Klemperer, *Astrophys. J. 178* (1972) 389–421; b) J. H. Black, A. Dalgarno, *Astrophys. J. Suppl. Ser. 34* (1977) 405–423.
[59] G. F. Mitchell, J. L. Ginsburg, P. J. Kuntz, *Astrophys. J. Suppl. Ser. 38* (1978) 39–68.
[60] a) S. S. Prasad, W. T. Huntress, Jr., *Astrophys. J. Suppl. Ser. 43* (1980) 1–35; b) T. E. Graedel, W. D. Langer, M. A. Frerking, *ibid. 48* (1982) 321–368.
[61] S. Lepp, A. Dalgarno, *Astrophys. J. 324* (1988) 553–556.
[62] R. Gredel, S. Lepp, A. Dalgarno, E. Herbst, *Astrophys. J. 347* (1989) 289–293.
[63] S. P. Tarafdar, S. S. Prasad, W. T. Huntress, Jr., K. R. Villere, D. C. Black, *Astrophys. J. 289* (1985) 220–237.
[64] E. F. Van Dishoeck, J. H. Black in [14a], p. 209.
[65] a) T. J. Millar, L. A. M. Nejad, *Mon. Not. R. Astron. Soc. 217* (1985) 507–522; b) T. J. Millar, C. M. Leung, E. Herbst, *Astron. Astrophys. 183* (1987) 109–117; c) W. D. Langer, T. E. Graedel, *Astrophys. J. Suppl. Ser. 69* (1989) 241–270.
[66] T. J. Millar, E. Herbst, *Astron. Astrophys.*, in press.
[67] J. P. Chieze, G. Pineau des Forets, *Astron. Astrophys. 221* (1989) 89–94.
[68] J. Stutzki, G. J. Stacey, R. Genzel, A. I. Harris, D. T. Jaffe, J. B. Lugten, *Astrophys. J. 332* (1988) 379–399.
[69] G. A. Blake, E. C. Sutton, C. R. Masson, T. G. Phillips, *Astrophys. J. 315* (1987) 621–645.
[70] a) J. M. Shull, B. T. Draine in [4a], p. 283; b) D. R. Flower, T. S. Monteiro, G. Pineau des Forets, E. Roueff in [14a], p. 271; c) G. F. Mitchell in [3b], p. 275.
[71] a) T. M. Leen, M. M. Graff, *Astrophys. J. 325* (1988) 411–416; b) T. W. Hartquist, M. Oppenheimer, A. Dalgarno, *ibid. 236* (1980) 182–188.
[72] P. D. Brown, S. B. Charnley, T. J. Millar, *Mon. Not. R. Astron. Soc. 231* (1988) 409–417.
[73] T. J. Millar, E. Herbst, S. B. Charnley, unpublished.
[74] T. J. Millar, E. Herbst, *Mon. Not. R. Astron. Soc. 242* (1990) 92–97.
[75] a) V. Vanysek in [3b], p. 461; b) U. Marvin in [3b], p. 469.

Stereocontrolled Construction of Complex Cyclic Ketones via Oxy-Cope Rearrangement

New Synthetic Methods (81)

By Leo A. Paquette*

Convergency is a highly serviceable aspect of organic synthesis, particularly when its application is accompanied by high levels of chirality transfer and regiocontrol. A reaction that is notably well suited to these objectives is the oxy-Cope rearrangement. In addition, the benefits that can accrue from suitable condensation of β,γ-unsaturated ketones with a vinyl organometallic and subsequent [3,3] sigmatropic shift are substantive enhancement in structural complexity and the ability to generate a myriad of polycyclic frameworks. Another profitable feature is the complementary regeneration of the carbonyl group in a new structural context. In view of the pivotal role played by the carbonyl functionality in synthetic transformations, reacquisition of such a reaction site translates into heightened chemical versatility. The trajectories followed by vinyl organometallics as they engage in 1,2 addition to ketones are gradually being understood. Proper diastereoselective control of this bond-making process, when coupled with full awareness of the chair or boat topography adopted during the ensuing oxy-Cope electronic reorganization, provides for exciting new strategy-level dimensions not often available in other contexts. The use of this two-step sequence as a prelude to a third chemical event clearly serves to expand the possibilities for molecular construction still more. While a considerable amount of the work to date has focused on the preparation of rather elaborate carbocyclic molecules, principally with a view to gaining access to complex natural products, the possibilities for heterocyclic synthesis are currently being accorded increased attention.

1. Introduction

The philosophy of the financial investor, namely, to buy low and sell high, is often adopted by the synthetic organic chemist at the molecular level. By making recourse to conventional bond constructions known for their high efficiency and subsequently bringing about a structural rearrangement that generates a stereochemically more intricate entity, one can gain considerable complexity relative to the level of input. Thus, the "profit margin" can be substantial.

In this connection, sigmatropic rearrangements have evolved as particularly reliable synthetic tools since a detailed understanding of these processes in terms of orbital symmetry was advanced.[1] Among these, the oxy-Cope rearrangement has been accorded rapidly increasing attention because of its exceptional flexibility and broad applicability.[2–5] As illustrated in Scheme 1, the substrate destined to

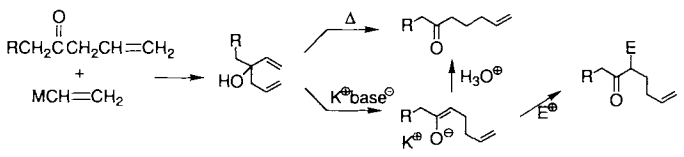

Scheme 1. Thermal and anionic oxy-Cope sequences.

undergo isomerization is often prepared by coupling a vinyl organometallic with a β,γ-unsaturated ketone. Such simple condensations can often proceed with exceptional diastereoselectivity. The important issue to emphasize is the convergency associated with this initial step and the considerable latitude this feature can bring to the overall sequence.

While oxy-Cope rearrangements can be effected thermally,[6,7] enormous rate accelerations (up to 10^{15}) can be realized by conversion to the potassium alkoxide.[8] The greatly decreased reaction temperatures made possible by this innovation are often tolerant of sensitive functional groups. The alkoxide oxygen must be linked to the bond that is about to be broken, since it is the "electron push" that induces weakening and facilitates rupture.[9,10]

The thermal and anionic oxy-Cope variants share in common an irreversibility component that distinguishes them from classical Cope reactions and extends their overall utility well beyond that customarily available to classical [3,3] sigmatropic processes. In the first case, irreversibility stems from the greater thermodynamic stability of a carbonyl group relative to a C–C double bond. In the anionic mode, the resonance energy of the enolate anion is key. Note that enolate generation is regiospecific.

Near-quantitative asymmetric transmission can arise as a direct consequence of the highly ordered cyclic transition states involved. Chairlike conformations are often preferred,[11] but boat alternatives are also energetically accessible and can be demanded by the structural features of the system. This aspect needs to be clearly appreciated in every instance, since the exceptional associated stereospecificity can allow for the ready construction of complex molecules having in excess of six stereogenic centers.

While the above features are enormously attractive, attention needs also to be drawn to the fact that Scheme 1 constitutes a fundamental two-step carbonyl regenerative process.[5] Invariably, the ketone end product is appreciably more embellished structurally than the starting material, especially when polycyclic systems are involved.[5,12] Few will discount the importance of the carbonyl functionality to syn-

[*] Prof. L. A. Paquette
Department of Chemistry
The Ohio State University
Columbus, OH 43210 (USA)

thetic design. In actuality, the oxy-Cope product carries two different sites of unsaturation, either of which can be selectively adapted to specific synthetic goals. In this review, we compile those developments in the area of oxy-Cope chemistry that have application in particular to the elaboration of cyclic and polycyclic ketones, many of which have direct relevance to the field of natural products.

2. Relevant Features of the Sigmatropic Event

As mentioned above, two limiting transition-state conformations can be realized during suprafacial-suprafacial [3,3] sigmatropy. The preference for involvement of a chairlike conformation needs to be correlated with the demands by substituents for occupying equatorial and not axial positions. A direct consequence of this energetic ordering is the formation of *E* double bonds when groups are equatorial. Axial substituents give rise to *Z* olefin geometries. In those examples where both double bonds are β-substituted, two new chiral centers are formed. Chirality transfer then becomes an issue, since the asymmetry inherent in these vinyl groups is translated predictably and specifically into an *erythro* or *threo* product. An instructive example is available from the early work of *Evans* [Eqs. (1) and (2)].[13]

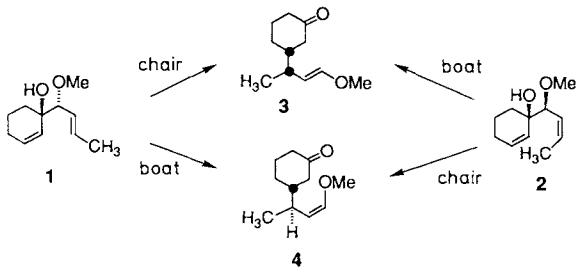

(1)

Since **1** and **2** are exclusive precursors to **3** and **4**, and **5** and **6** afford only **7** and **8**, the operation of one or more nonconcerted pathways seems highly improbable. The product ratios (**1** → **3** (96%) + **4** (4%); **2** → **4** (70%) + **3** (30%); **5** → **7** (77%) + **8** (23%); **6** → **8** (98%) + **7** (2%)) indicate further that **1** and **6** isomerize almost exclusively via the chair transition states **9a** and **9b**, respectively (Scheme 2). The diastereomers with β-methoxyl groups (**2** and **5**) experience greater destabilization during analogous bond relocation because of the presence of a pseudoaxial methoxyl group in **10a** and **10b**. Consequently, the latter two oxy-Cope processes proceed in part (23–30%) via competitive boat geometries. This study eventuated in a stereoselective total synthesis of (±)-juvabione.

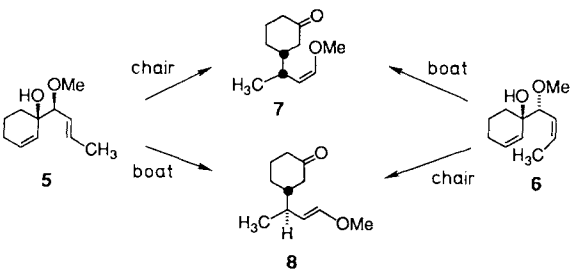

(2)

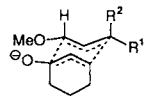

9a, $R^1 = CH_3$, $R^2 = H$
b, $R^1 = H$, $R^2 = CH_3$

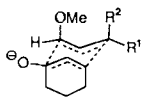

10a, $R^2 = CH_3$, $R^1 = H$
b, $R^2 = H$, $R^1 = CH_3$

Scheme 2. Chair transition states **9a**, **9b**, **10a**, and **10b** for dienols **1**, **6**, **2**, and **5**, respectively.

In addition to being serviceable for producing simple bicyclic ketones [Eq. (3)],[14] the oxy-Cope sequence has been utilized for preparing polyfunctionalized molecules of various types [Eqs. (4),[15] (5),[16] (6),[17] and (7)[18]]. These transformations have provided the basis for efficient new syntheses of pseudoionone (from a relative of **11**), (3*E*,8*E*)-suspensolide (from **12**), and gnididione (from **13**).

One of the most advantageous features of the oxy-Cope rearrangement is its ability to generate new stereogenic centers with virtually complete stereospecificity and without need for external chiral reagents and the like. Furthermore,

Leo A. Paquette (born in 1934 in Worcester, Massachusetts) obtained a B.S. in 1956 from Holy Cross College and a Ph.D. in 1959 from the Massachusetts Institute of Technology. In that same year, he joined the Upjohn Company, where he served as a Research Associate in the Discovery Research Department for four years. In 1963, he joined the Department of Chemistry at The Ohio State University as Assistant Professor, becoming Associate Professor in 1966 and Professor in 1969. In 1981, he was appointed Kimberly Professor of Chemistry and has served as University Distinguished Professor since 1987. His research interests include the preparation and properties of unusual organic molecules of theoretical interest, the synthesis of natural products, and the development of new synthetic methodology. The development of chemospecific and stereoselective chemical transformations hold particular attention, as does the possible stereocontrol of organic reactions. His extensive contributions have been recognized by a number of awards, including the Arthur C. Cope Scholar Award (1987) and the American Chemical Society Award for Creative Work in Synthetic Organic Chemistry (1984). Leo Paquette has been a Sloan, Guggenheim, and Humboldt Fellow and was elected a member of the National Academy of Sciences in 1984.

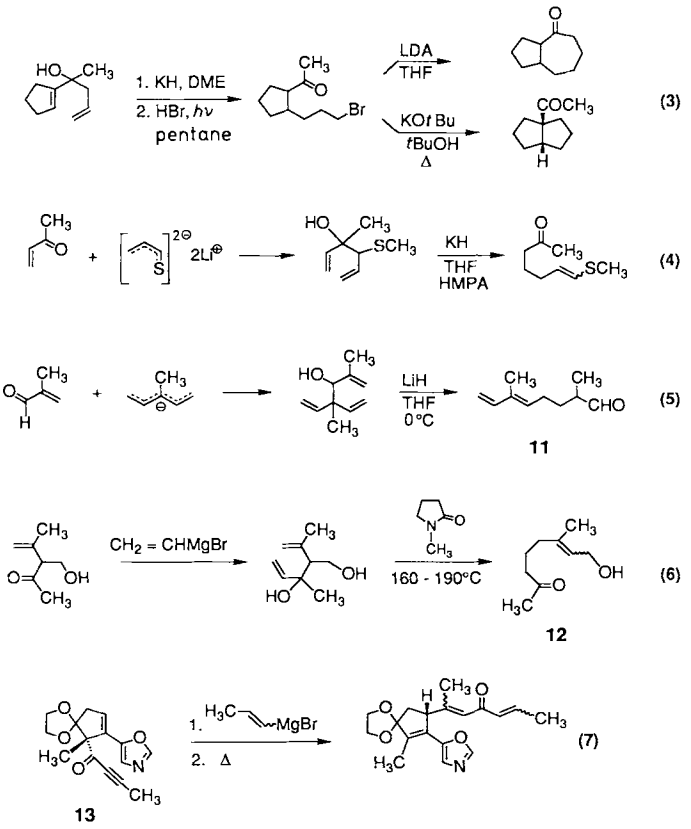

the resultant configuration can often be predicted in terms of simple cyclohexane conformational analysis. *Koreeda*'s clever application of this chemistry to set C-20 of the desmosterol side chain in the correct (*R*) configuration illustrates the point [Eq. (8)].[19] The same group has made the remarkable finding that allylmagnesium chloride adds to **14** with a >50:1 preference for axial entry. This unexpectedly high selectivity makes viable in turn the stereocontrolled conversion of **15** to the isomeric lactones **16** (31%) and **17** (26%) [Eq. (9)].[20]

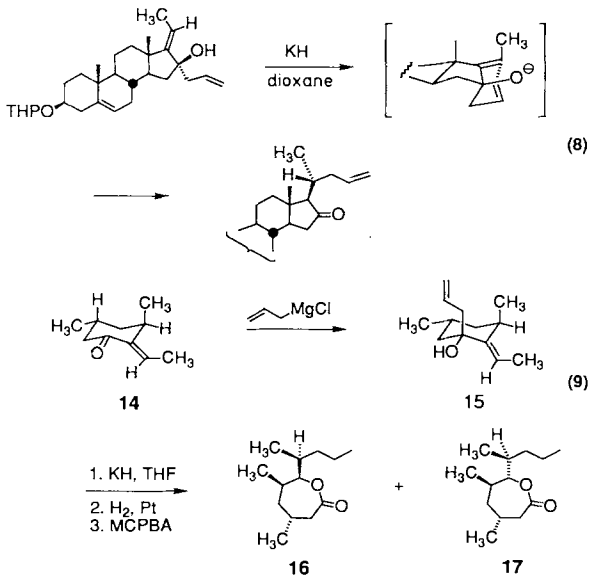

THP = tetrahydropyranyl; MCPBA = *m*-chloroperbenzoic acid

3. Oxy-Cope Ring Contractions

Use of the oxy-Cope rearrangement for effecting ring contraction has seen only limited service because of the relative unavailability of the necessary medium-ring alcohols. However, several important kinetic relationships have been made clearly apparent by these systems. For example, thermal activation of **18** results in exclusive [1,5] hydrogen migration to deliver **19** [Eq. (10)]. This pathway is totally overridden, however, by conversion of **18** to the potassium alkoxide, which is rapidly transformed into **20** at room temperature.[21] This aldehyde holds significance as a precursor to all of the primary prostaglandins[22] as well as to the algal sperm attractant multifidene.[23]

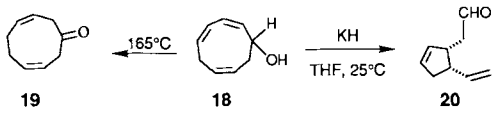

Compound **21**, the methyl analogue of **18**, is cleanly converted into **22** at −25 °C with an excess of potassium hydride in dry tetrahydrofuran containing 18-crown-6. For comparison, heating **21** with sodium hydride in tetrahydrofuran results instead in transformation predominantly (90%) into **23** [Eq. (11)].[24] These observations establish that the fraction of rearrangement of **21** which passes through the oxy-Cope manifold increases as the donor properties of the oxygen center are decreased and the rate of isomerization falls off.

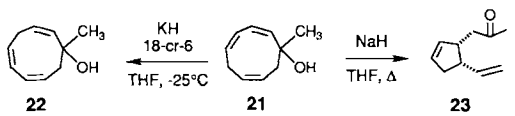

18-cr-6 = 18-crown-6

The high basicity of alkoxides in polar aprotic solvents and the corresponding stability of the enolate anion act in concert to shift the equilibrium toward the carbanion. The addition of complexing agents generally exacerbates the situation and results in rate acceleration. Besides the well-known order of dissociation (Cs > K > Na > Li), steric inhibition to ion pairing, as well as the inherent capability of the substrate for competitive isomerization along a different reaction channel, needs to be reckoned with.

Potassium bases, often in conjunction with 18-crown-6, are most frequently employed to effect anionic oxy-Cope rearrangement. They do not necessarily function identically, particularly in difficult cases. Commercial potassium hydride is quite useful, but impurities should be removed by the Macdonald procedure if the chances for reproducibility are to be maximized.[25] Potassium hexamethyldisilazanide is a conveniently available soluble reagent. However, when rearrangement is slow, silylation of the unrearranged alcohol can often become the kinetically favored process.[26] Potassium diethylamide is reliable, but somewhat tedious to prepare.[27] Finally, potassium *tert*-butoxide is found to work best, if at all, when the substrate alcohol is especially prone to anionic [3,3] sigmatropy.[26]

4. Diastereoselectivity in the Initial Coupling Reaction

Until recently, no example of the first step in the carbonyl regenerative sequence had been documented where both reaction partners are chiral. There exists good reason for this. The 1,2 addition necessarily generates yet another stereogenic center and consequently gives rise to at least eight diastereomeric products. However, the problem can be conveniently dealt with and high levels of molecular recognition attained if the following criteria are accorded proper consideration:[28]

1. Nucleophilic capture by the carbonyl should be relegated exclusively to one prochiral face by suitable steric control. If this stereoselectivity is strictly governed, only a maximum of four diastereomeric alcohols can result.
2. If respectable levels of diastereoselectivity were to operate under these circumstances, then the number of possible products would be halved again. At this point, the use of either reagent in optically pure form would result in net kinetic resolution (single product formation).

Our understanding of the extent and direction of diastereoselection attainable in such reactions is still founded on a limited number of cases. However, interesting trends and predictabilities are beginning to emerge. Bicyclic ketone (±)-**24** adds nucleophiles only from its *exo* surface. However, the conformational mobility of its vinyl group lessens the overall capacity of the molecule for steric discrimination. Consequently, the potential for diastereocontrol falls off rapidly [**25**:**26** = 1.65:1, Eq. (12)].[28] On a positive note, the cyclobutoxide character of the first-formed intermediate results in spontaneous sigmatropy above −78 °C and leads (via boat transition states) to products carrying six stereogenic centers.

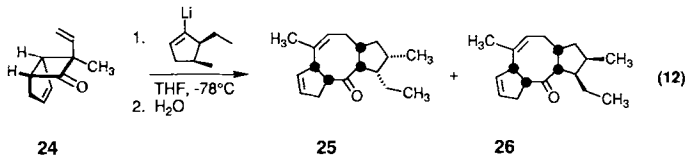

24 **25** **26**

Comparative analysis of the response of racemic ketones **27** and **28** to capture by chiral organocerates has revealed that the additional σ bond in **28** does not appreciably enhance key intermolecular interactions of steric origin (Scheme 3).[28] For the series **29**–**33**, the extent of diastereoselection reaches a maximum at **33**.[29] These data have allowed the formulation of a transition-state model consistent with the greater discriminatory power of substituents positioned in the vicinity of the four-membered ring.

The most well understood scenarios at present comprise *endo* addition to such unsaturated 7,7-disubstituted norbornanones as **34**[27] and **35**[30] on the one hand and *exo* addition to **36** and **37** on the other (Scheme 4).[30] The extent of intermolecular recognition can reach quite useful levels when *endo* attack is involved. In contrast, diastereomeric differentiation is significantly reduced when the *exo* trajectory is followed and little sensitivity is reflected toward the *exo*-3-methyl substituent in **36**. These observables can be rationalized in terms of an essentially coplanar arrangement of the reactants with appropriate stacking during the *endo* face-selective process (see **38**). In contrast, a knife-edge alignment as in **39** is presumably adopted by cyclopentenyl anions as *exo* attack on the norbornanone carbonyl group begins. Thus, we see that the trajectories of approach can indeed be widely divergent. It is precisely our awareness of these distinctions that will ultimately allow for broader, more reliable application of oxy-Cope methodology in the future.[31]

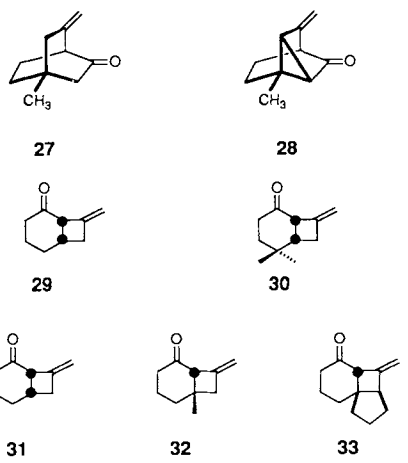

27 **28** **29** **30** **31** **32** **33**

Scheme 3. Select bicyclic β,γ-unsaturated ketones.

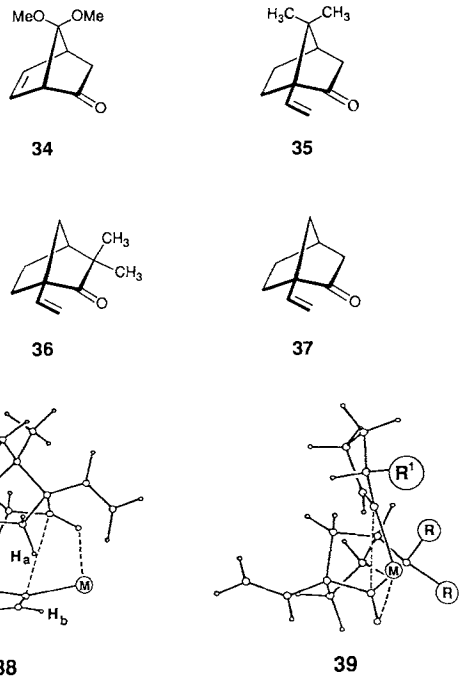

34 **35** **36** **37** **38** **39**

Scheme 4. Unsaturated norbornanones **34**–**37** and prototypical transition-state models for *endo* (**38**) and *exo* addition (**39**) of cyclopentenylmetal derivatives to **35** and **36**, respectively.

In those circumstances where chiral racemic reaction partners are brought into condensation, 1:1 stoichiometry can be used because double diastereoselection operates. The two enantiomers of both reagents are consumed with equal rapidity. However, if either reagent is optically pure, the (*R*)

and (*S*) forms of the racemic coreactant will necessarily be consumed at different rates. Studies involving (*R*)-(−)-isopiperitenone have ascertained that the maximum yields of homochiral 1,2 addends can be most efficiently and economically realized with an RLi-to-ketone ratio of 3:1.[32]

Face selection during the oxy-Cope step proper has been accorded far less attention. The only experiments designed to probe this question involve the (*RR,SS*)- and (*RS,SR*)-fluoroadamantane alcohols **40** and **41** [Eq. (13)].[33] The goal was to assess directly those electronic contributions stemming from the halogen atom. A pair of chair transition states is available to each diastereomer. While **42** has the phenyl group axial, **43** has it equatorial. Consequently, steric factors would favor reaction via **42** in both instances. In contrast,

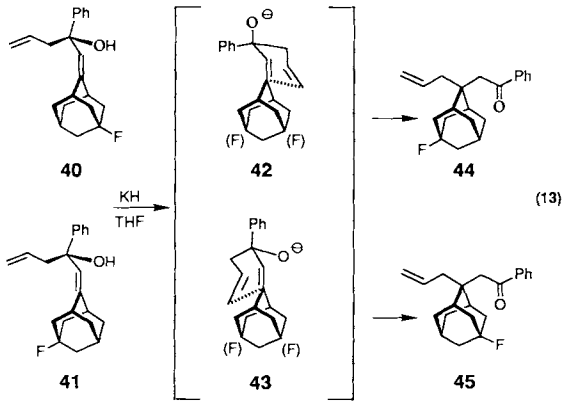

(13)

the hyperconjugative effect of the electronegative fluorine atom would prefer to induce bond formation "*syn*" to the halogen. Whereas **40** gave rise to an 81:19 ratio of diastereomeric acetophenones **44** and **45** (here the effects operate in the same direction), the product distribution from **41** was 36:64. Thus, *syn* approach is favored (by a factor of 1.4), in line with *Cieplak*'s hyperconjugation model.[34]

5. Expansion of Six-Membered Rings

5.1. Expansion of Cyclohexanones

Marvell and *Whalley* recognized twenty years ago that the thermal oxy-Cope rearrangement of *trans*-1,2-divinylcyclohexanol constitutes an excellent means for ring enlargement by four carbon atoms.[35] Moreover, the exclusive formation of *trans*-5-cyclodecen-1-one signaled that isomerization proceeded by way of the chair transition state. This pathway would require that the transient enol double bond have *Z* geometry, a stereochemical feature that was established later by others via trapping experiments conducted under anionic conditions [Eq. (14)].[25]

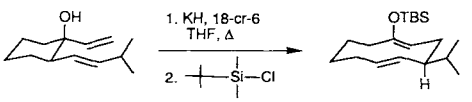

(14)

Comparable heating of *cis*-1,2-divinylcyclohexanol to 220 °C does not eventuate in an equally stereoselective process. A 60:40 mixture of *trans*- and *cis*-5-cyclodecen-1-one results.[35] This loss of stereocontrol was given further attention by *Clive* et al., who examined the fate of potassium alkoxide **46** at a considerably reduced temperature (refluxing tetrahydrofuran).[36] Only 3% of **48** is produced (via **47**), **46** finding it kinetically preferable to undergo conformational inversion to **49** prior to isomerization via **50** to **51** [97%, Eq. (15)]. It remains to establish whether **48** is disadvantaged because of its *Z* double-bond geometry or whether the equatorially disposed electron-rich substituent in **46** is responsible (in **49** the alkoxide oxygen is axial).

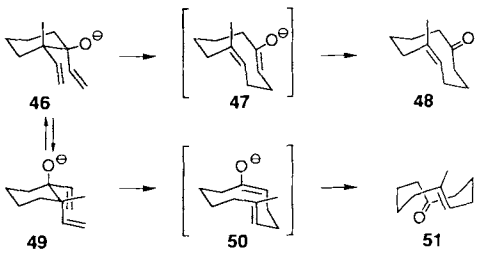

(15)

Schreiber et al. have used this effect in an approach to germacrane derivatives [Eq. (16)].[37] An advantage offered by the [2+2] photoaddition of allene to 2-cyclohexenones is its regioselectivity for generation of the β,γ-enone. Forma-

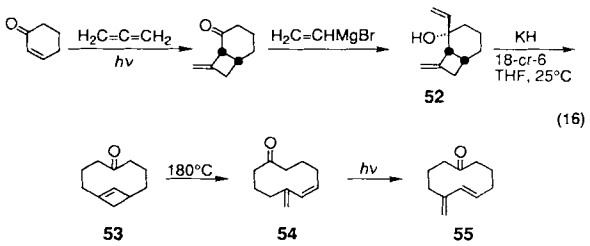

(16)

tion of **52** is followed by anionic oxy-Cope rearrangement to produce the bicyclic bridgehead olefin **53** in 71% yield. Thermolysis of **53** furnished **54** and **55** in a 5:1 ratio. When this mixture was irradiated in cyclohexane, a photostationary state favoring **55** was quickly reached (**54**:**55** = 1:10).

Compound **56**, the isopropyl analogue of **52**, was analogously transformed into **57** [Eq. (17)]. The high re-

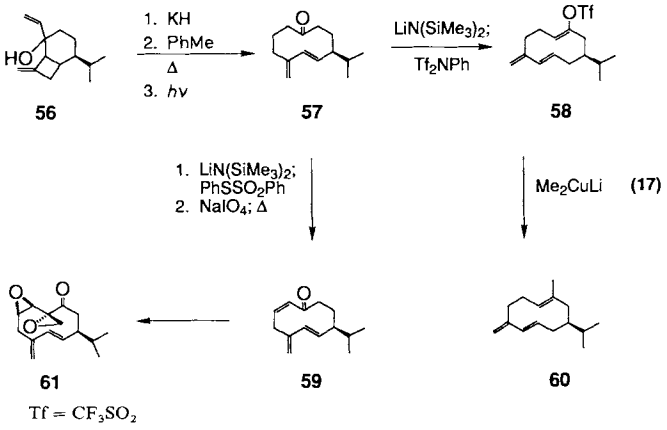

(17)

gioselectivity exhibited by **57** for enolate formation made possible the preparation of **58** and **59**, viable precursors to germacrene D (**60**)[38] and the cockroach sex pheromone periplanone B (**61**)[39].

5.2. Expansion of 2-Cyclohexenones

A more expeditious route to germacranes has been realized starting from suitably functionalized 2-cyclohexenones. *Still*'s early syntheses of acoragermacrone (**64**) and preisocalamendiol (**65**) are illustrative of the approach [Eq. (18)].[40] Addition of 2-lithio-3-methyl-1-butene to isopiperitenone (**62**) and anionic oxy-Cope rearrangement of the resultant alcohol afforded **63**. An elegant addition-elimination sequence was next utilized to isomerize the conjugated double bond and arrive directly at **64**. Alternatively, simple "deconjugation" of **63** delivered **65**.

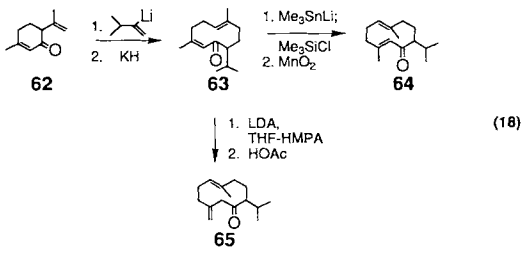

62 63 64 65 (18)

In like fashion, changing the electrophilic partner to **66** permitted arrival at **67**. Ring expansion of this intermediate by the oxy-Cope pathway, direct treatment with trimethylsilyl chloride, and workup with *m*-chloroperbenzoic acid provided **68**. This acyloin was in turn transformed into periplanone B (**61**) and to its inactive diastereomers **69** and **70** [Eq. (19)].[41]

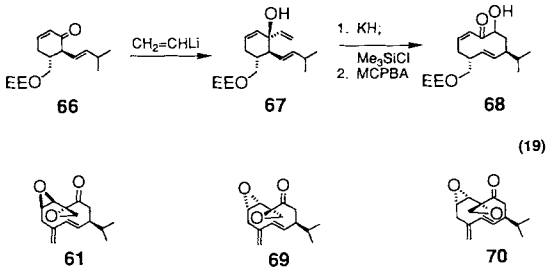

66 67 68 (19)

61 69 70

EE = ethoxyethyl

A more recent, strategically related approach to (±)-**61** has been documented by *Hauptmann* et al.,[42] and *Mori* et al. have prepared (−)-periplanone B in 18 steps from (*S*)-3-cyclohexene-1-carboxylic acid by means of a very similar oxy-Cope ring expansion.[43]

Extension of this protocol so as to permit the concise elaboration of germacranolides has been accomplished independently by *Still* et al.[44] and *Takahashi* et al.[45,46] Not only did stereochemical and regiochemical uncertainties need to be overcome, but potential elimination reactions had to be skirted and the proper direction of lactonization controlled effectively. One way to bypass these possible pitfalls involves the coupling of **71**, prepared readily from (+)-carvone, to lithiocyclobutene **72**. Oxy-Cope ring expansion of the resulting *trans* divinyl alcohol exhibits the usual strong preference for a chairlike transition state since macrocycle **73** was obtained after thermodynamic alkaline equilibration [Eq. (20)]. Hydroxy lactone **74** is obtained after further processing, thereby setting the stage for proper interchange of the direction of lactonization and adjustment of the configurations at C-7 and C-8. This was accomplished via **75** to give eucannabinolide (**76**).[44]

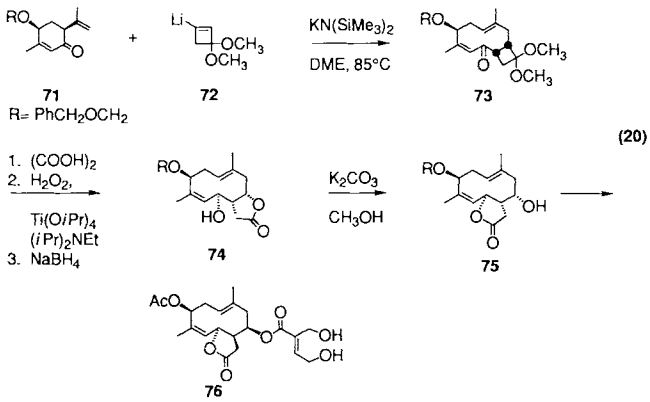

71 72 73 (20)

74 75 76

Preparation of the optically active 3-oxygenated 13-norheliangolide **79** was successfully realized by crafting of **77** from (−)-carvone, oxy-Cope rearrangement followed by alkylative introduction of the final two carbons, and closure of the lactone ring [Eq. (21)].[45]

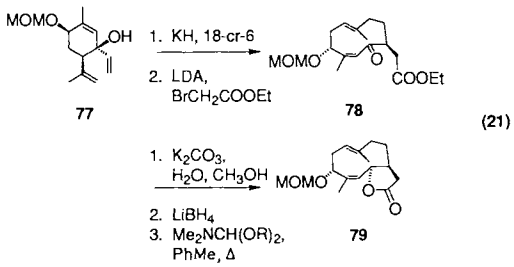

77 78 (21)

79

MOM = methoxymethyl, LDA = lithium diisopropylamide

Of significance in the present context is the tolerance of various carbonyl substituents to oxy-Cope sigmatropy. A classic example is due to *Rajagopalan* et al., who noted that addition of vinylmagnesium bromide to **80** and subsequent refluxing in tetrahydrofuran resulted in conversion to **81** [Eq. (22)].[47] The structural features of **81** were recognized to be conducive to transannular cyclization under mildly

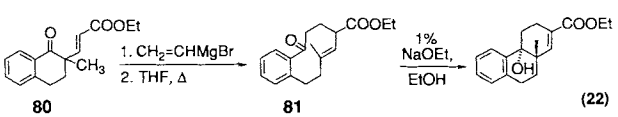

80 81 (22)

basic conditions. *Sworin* and *Lin* have also carried out interesting studies on ring expansion.[48]

The most well studied oxy-Cope system is undoubtedly the conversion of **82** to **83**. Initially rationalized by *Swaminathan* et al. as the exclusive result of a fragmentation-recombination pathway,[49] the process is currently viewed as capable of operating as well in the concerted sigmatropic mode depending on conditions. These deductions have been made possible chiefly on the strength of studies conducted more recently on optically active substrates.[50] When isomerized with potassium hydride in tetrahydrofuran, the (1*R*,8a*S*) alcohol **82** gives **83** in optically active form. The use of potassium hydroxide in methanol affords racemic product. These findings have been plausibly rationalized at the mechanistic level as outlined in Eq. (23).

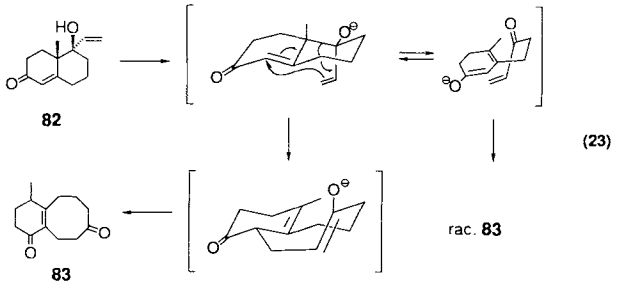

(23)

These rearrangements have proven to be general in scope, having been applied successfully, inter alia, to **84**,[51] **85**[52] and **86**[53] [Eq. 24)].

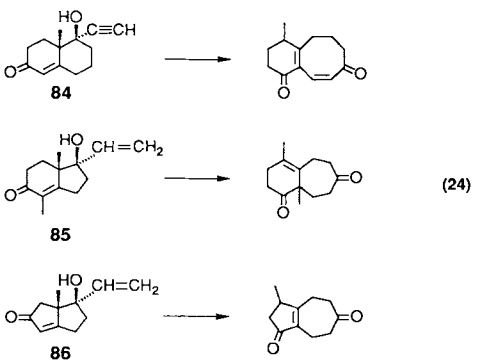

(24)

6. Expansion of 2-Vinylcyclobutanones and -cyclopentanones

Recourse to 2-vinylcyclobutanones permits extension of the oxy-Cope strategy to cyclooctenone and cyclooctadienone formation. This aspect of the methodology has attracted interest in recent years because the number of known eight-membered ring natural products has increased substantially during this period. The strain inherent in cyclobutane rings allows for the ready isomerization of alcohols such as **87** and **88** [Eq. (25)].[54]

Gadwood et al. have reported that both *cis*- and *trans*-1,2-dialkenylcyclobutanols undergo [3,3] sigmatropic ring enlargement upon treatment with potassium hydride.[55] Initial *trans–cis* isomerization was invoked to explain the ability of the latter systems to engage in oxy-Cope chemistry. More recently, *Salaun* et al. have pointed out that the reactivity of these isomers is clearly distinguished on the basis of their stereochemical features. Contrary to the earlier claim, the Orsay group has found the *trans* alcohols to be capable only of retro-ene fragmentation [Eq. (26)].[56]

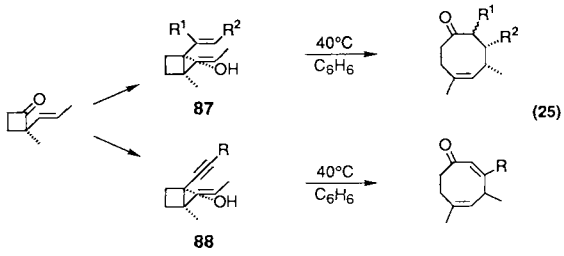

(25)

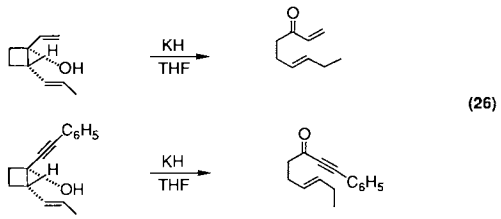

(26)

Notwithstanding, the methodology represents a powerful tool for the rapid elaboration of cyclooctanoid terpenes. For example, the sesquiterpene alcohols poitediol (**90**) and dactylol (**91**) can be formed via ring expansion of the bicyclic vinylcyclobutanone **89** [Eq. (27)].[57] Good overall yields were realized if the lithium acetylide adduct was isomerized under neutral conditions. Geminal dimethylation and carbonyl transposition then set the stage for proper oxygenation of the framework. Reduction of poitediol (**90**) with sodium in liquid ammonia provided dactylol (**91**).

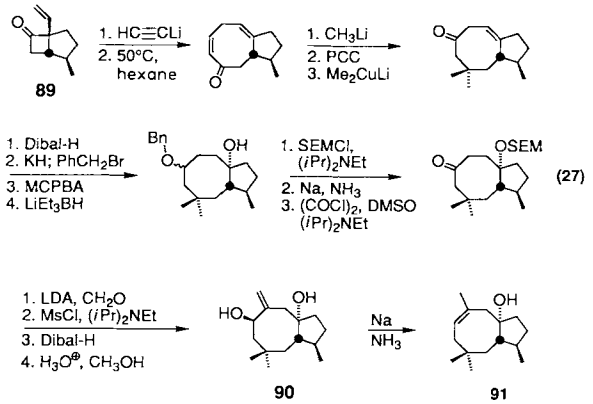

(27)

PCC = pyridinium chlorochromate, Dibal-H = diisobutylaluminum hydride, SEMCl = $Me_3Si-CH_2-CH_2-O-CH_2Cl$, MsCl = methansulfonyl chloride

The addition of cyclopentenyllithiums to **24** results in spontaneous oxyanionic Cope rearrangement. If the resultant regiospecifically positioned enolate (e.g., **92**) is trapped with methyl iodide, functionalized all-*cis*-dicyclopenta[*a*,*d*]-

cyclooctane products such as **93** result [Eq. (28)].[58] This angularly fused 5-8-5 framework, which comprises the fundamental architectural element of the ophiobolins, ceroplastols, and fusicoccins, is consequently available in only two laboratory manipulations (**24** is prepared from vinylketene and cyclopentadiene).[59]

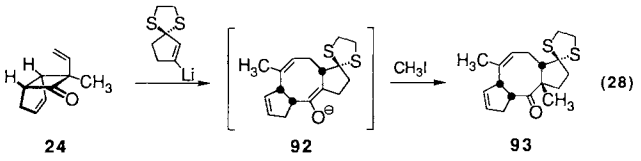

Divinylation of 2-chlorocyclopentanone provides for the formation of an 81:19 mixture of isomers **94** and **95**.[60] Thermal activation of the composite sample resulted in exclusive formation of (*E*)-5-cyclononen-1-one [**96**, Eq. (29)]. This stereochemical result conforms to expectation if chair-like transition-state geometries are involved.

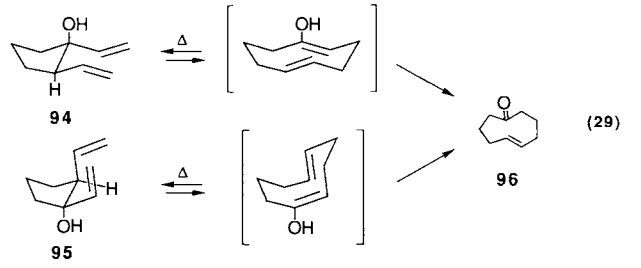

(+)-Phoracantholide I (**99**), the defensive substance of the Australian coleoptera, has been synthesized in concise fashion by taking advantage of the efficient response of **97** to being heated neat at 170 °C. The acetylenic oxy-Cope reaction that is triggered affords the nine-membered *Z,Z* dienone **98** cleanly [Eq. (30)].[61] The *trans* isomer of **97** proved unreactive at temperatures as high as 200 °C. Once **98** was in hand, the volatile oily **99** was arrived at in five additional steps.

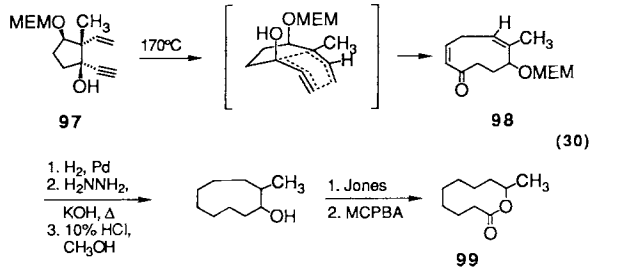

MEM = methoxymethyl

7. Expansion of Medium-Ring Systems

The *trans*- and *cis*-1,2-divinylcyclododecanols have been subjected to thermal rearrangement with interesting results. Thus, while **100** gives **104** as the single product, **101** provides a 24:76 mixture of **104** and **105** under the same conditions [Eq. (31)].[60] To the extent that concerted stereospecific reactions are involved, the *trans* isomer **100** probably passes entirely through chair transition state **102**. This behavior is identical to that followed by *trans*-1,2-divinylcyclohexanol.

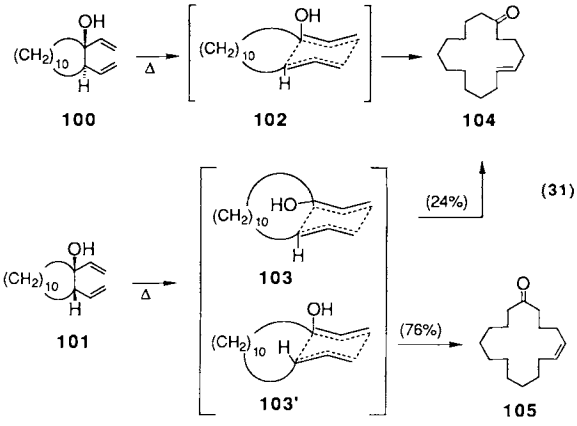

This *cis* arrangement in **101** fosters competition between the involvement of **103** and **103'**. Of these, the pathway leading to *Z* enone **105** clearly dominates, in contrast to the partitioning exhibited by the six-ring lower homologue **46**, which favors formation of the *E* isomer by a small margin. The intermediate ring sizes have not been scrutinized in comparable detail.[60]

When one of the double bonds is endocyclic, the alcohols exhibit a greatly reduced capability for oxy-Cope behavior. A pronounced tendency for undergoing [1,3] sigmatropy surfaces instead. Representative examples are compiled in Equation (32).[62] This alternative ring expansion scheme has been developed by *Thies* et al. into a short synthesis of muscone (**106**).[63]

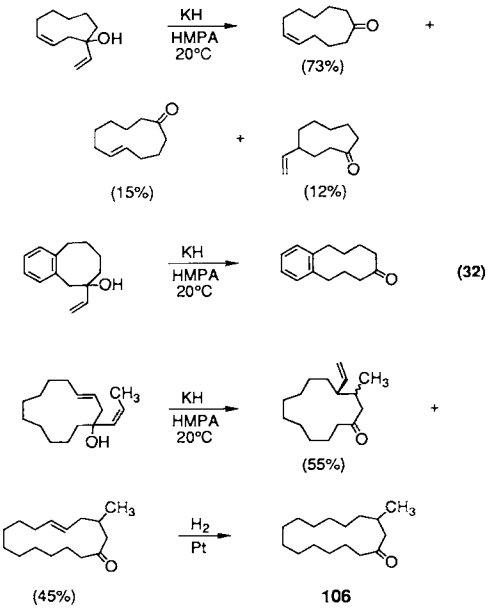

8. Expansion of Spirocyclic β,γ-Unsaturated Ketones

Spirocyclic compounds offer two alternatives as oxy-Cope templates. When the β,γ double bond occurs in the form of a methylene group as in **107** and **108**, octahydrobenzocyclooctenones result [Eq. (33)].[55] As a general rule, the allylic alcohols isomerize too rapidly to permit their isolation, the rigid s-*cis* boat orientation of the double bonds further reducing the activation energy of the rearrangement step.

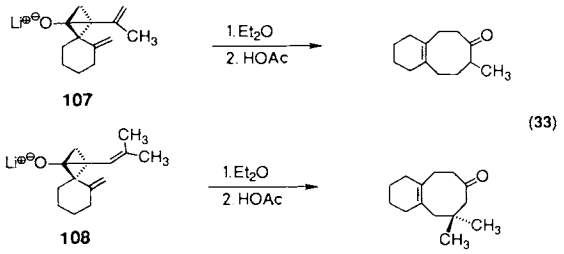

(33)

An important distinction surfaces when the double bond is situated internal to the ring. The *syn* capture of vinyl organometallics by such ketones provides vinyl alcohols, oxyanionic Cope rearrangement of which delivers bicyclic bridgehead olefins having a carbonyl group in the largest bridge [Eq. (34)].[55, 64, 65] Ring systems as small as that found in **109**, a pleuromutilin prototype, can be conveniently acquired in this manner. *Levine* et al. have transformed the homologous ketone **110** into the oxocyclododecanecarboxylic acid **111**.

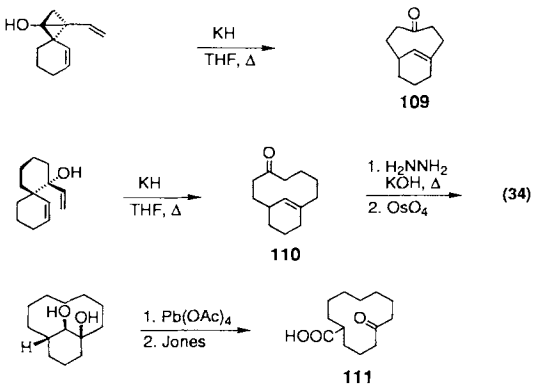

(34)

An interesting example of this particular isomerization begins with a stereocontrolled three-step synthesis of **112** from 2-(hydroxymethylene)cyclohexanone [Eq. (35)].[66]

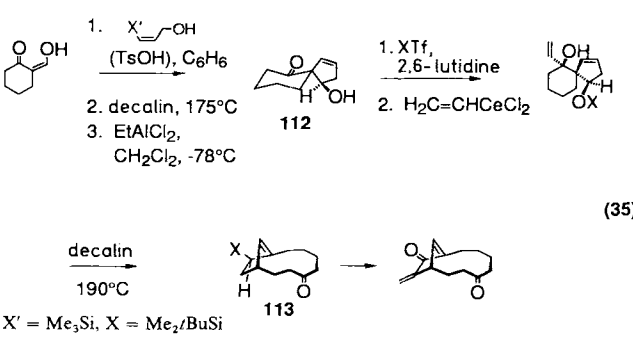

(35)

Once the hydroxyl group is silylated, vinylcerium(III) dichloride is captured selectively to provide a vinyl compound, which, upon heating in decalin, undergoes [3,3] sigmatropy with formation of **113**. A diene dione, which constitutes the bridgehead olefin core of the cytotoxic 8,9-seco-ent-kaurene diterpenes, was subsequently elaborated.

9. Reactions of Bicyclic Ketones with Internal Double Bonds

9.1. Reactions of 7-Substituted 5-Norbornen-2-ones

Jung was the first to call attention to the enormous latent potential of 7,7-dimethoxy-5-norbornen-2-one (**114**) in the oxy-Cope area.[67] A nucleophilic vinyl species, forced to approach the ketone carbonyl from the *endo* surface for obvious steric reasons, becomes ultimately positioned in adequate proximity to the strained bicyclic double bond to enable operation of the [3,3] shift. In the examples of Equation (36), richly functionalized *cis*-hydrindanones are seen to form irrespective of other possible bonding options.[67, 68]

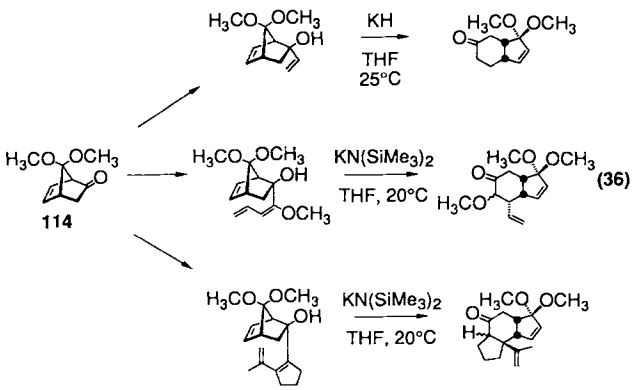

(36)

Bicyclic ketone **114** is sufficiently reactive to enter into anionic oxy-Cope rearrangement with aromatic components, a feat not otherwise easily accomplished.[62, 69] The α-naphthyl derivative **115** illustrates the power of the method for the rapid elaboration of steroidal hormone analogues [Eq. (37)].[67] The benzofuran analogue of **115** has been similarly transformed expeditiously into coronafacic acid (**116**).[68] Another ingenious variant of this concept has resulted in a route to reserpine intermediates.[70]

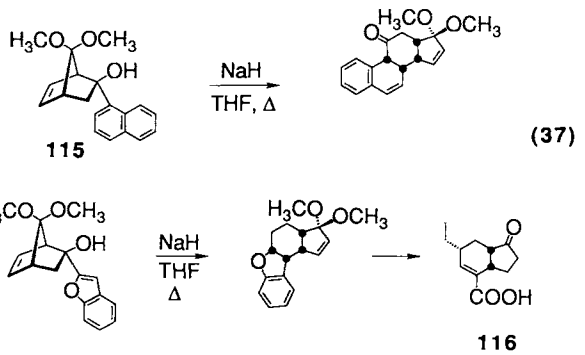

(37)

The coupling of (±)-**114** with racemic **117** exhibits a strong diastereoselectivity bias (12:1) in favor of **118**.[71] Anionic oxy-Cope rearrangement of **118** afforded the trans AB-locked keto ketal **119** efficiently [Eq. (38)]. Later arrival at **120** set the stage for kinetic resolution by the Koga method[72] and a successful total synthesis of natural (+)-ikarugamycin (**121**).[73]

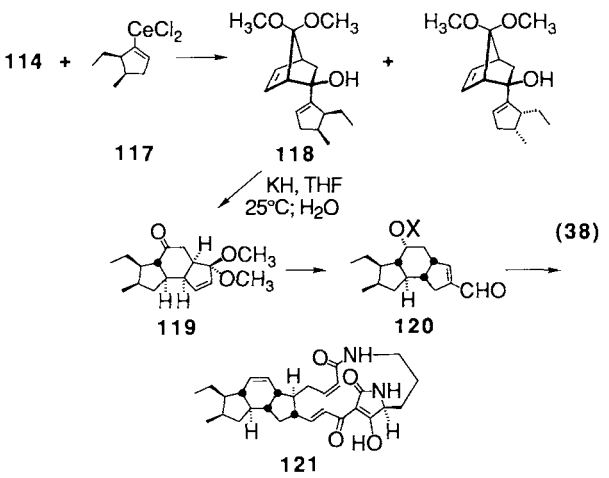

X = Me_2tBuSi

In reality, there need only be a *syn* substituent on C-7 of the norbornenone skeleton to guarantee *endo* directionality for attack by the vinyl organometallic.[74] The geminal methoxyl groups in **114** serve, of course, as a masked ketone carbonyl. This feature need not be relevant for certain specific objectives, *Chang*'s formal synthesis of (±)-9-isocyanopupukeanane (**126**) being a case in point [Eq. (39)].[75] The crucial steps in this study are the stereocontrolled isopropenylmagnesium bromide addition to **122** and anionic oxy-Cope rearrangement of diol **123**. This isomerization

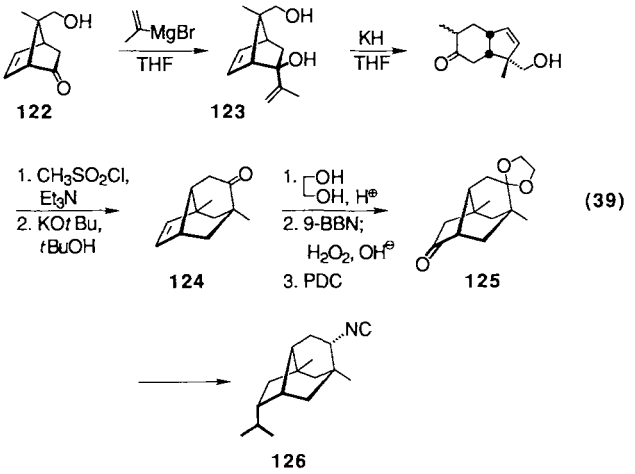

9-BBN = 9-borabicyclo[3.3.1]nonane, PDC = pyridinium dichromate

transforms one of the hydroxyl groups into a ketone carbonyl, thereby allowing for chemospecific mesylation and intramolecular cyclization to form **124**. Hydroboration-oxidation of the ketal of **124** led logically to **125**, a ketone that had been previously transformed into **126**.[76]

The rearrangement of norbornenol **127** was found to proceed stereoselectively via a boat transition state as in the earlier examples. This geometry serves admirably to provide an all-*cis* product [Eq. (40)].[77] The two rings in **128** were then cleaved sequentially to permit arrival at dimethyl secologanoside *O*-methyl ether (**129**).

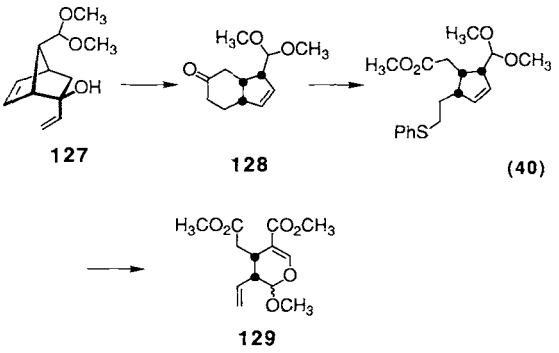

Fallis et al. have demonstrated that the presence of an additional *exo*-fused cyclohexane ring on the bicyclic nucleus, as in **130**, is inadequate to direct preferential nucleophilic attack to the *endo* surface of the carbonyl group. Only 25% of the vinylation leads to **131** [Eq. (41)].[78] The potassium salt of **131** is subject to smooth sigmatropic rearrangement in refluxing tetrahydrofuran. The tricyclic ketone **132** so formed is considered to be a prototype for the structurally unique sesterterpene gascardic acid.

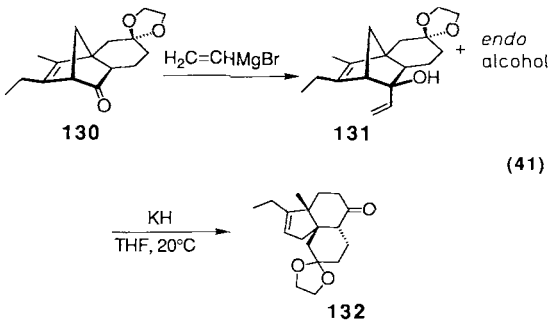

Two protocols are currently available for producing *exo*-norbornenols when the usual methods for preparing these particular isomers are not kinetically favored. The Fallis solution begins with the *endo* alcohol and inverts stereochemistry by implementing a [2,3] sulfenate–sulfoxide rearrangement cycle.[79] Whereas 2-vinylnorbornanols can undergo direct reaction with phenylsulfenyl chloride, a

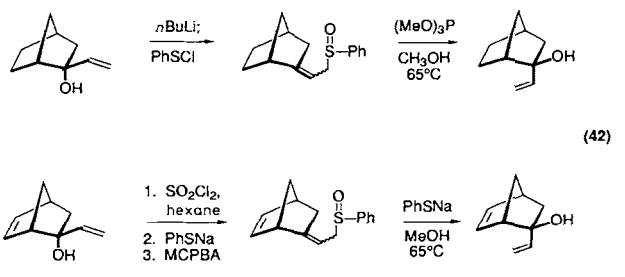

somewhat more circuitous route is necessitated in the case of **133** because of complications arising from competing electrophilic attack on the strained double bond [Eq. (42)].

In the Fleming scheme, advantage is taken of a stereospecific allylsilane epoxidation [Eq. (43)].[80] The possibility

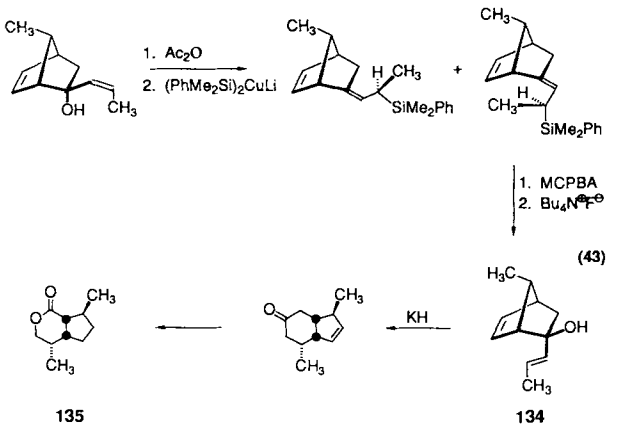

135 134 (43)

of producing **134** cleanly despite the *anti* stereochemistry of its 7-methyl substituent opened the way for an expedient total synthesis of dihydronepetalactone (**135**).

9.2. Reactions of Bicyclo[2.2.2]oct-5-en-2-ones

Established by the seminal studies on bicyclo[2.2.2]oct-5-en-2-ones was the anticipated similarity in transition-state characteristics (boatlike) to the norbornenols. As a consequence, recourse to this class of starting materials serves as an especially efficient stereoselective pathway to *cis*-fused decalins.[8] The preparation of **136** is illustrative [Eq. (44)].[81] An excellent test of the process is the stereospecific synthesis of (±)-α-amorphene (**138**) achieved by *Mirrington* et al.[82] Relevantly, the *Z* isomer of **137** failed to undergo

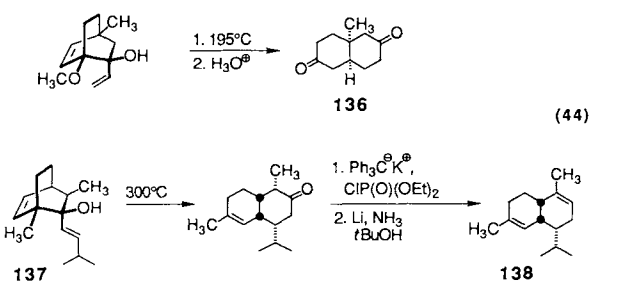

136 (44)

137 138

oxy-Cope rearrangement, presumably as a consequence of the considerable steric crowding between the isopropyl group and olefinic bridge as the side chain begins to adopt the conformation necessary for the sigmatropic event.

Variations are possible that result in structurally more complex products. *Rigby* et al. have shown that isomerization of **139** makes directly available the tricyclic ring system of the aristolane sesquiterpenes [Eq. (45)].[83] A general method of [4.4.4]propellane synthesis has also been devised.[81,84]

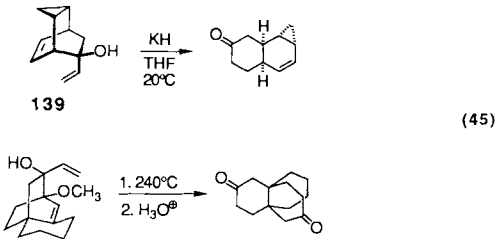

139 (45)

Two groups[85,86] have employed a related alkoxide-accelerated rearrangement to prepare the cranberry constituent cannivonine (**141**), only to find that the structure reported for this compound is incorrect [Eq. (46)]. The unusual isoquinuclidine nucleus was accessed by transannular cyclization of **140**.

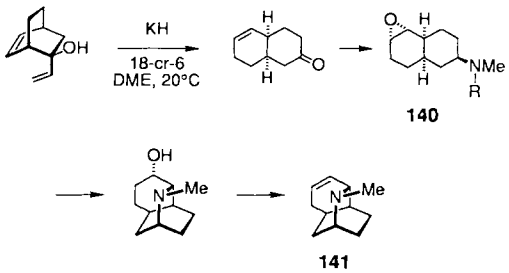

140 (46)

141

Introduction of a heteroatom within the allylic alcohol component can seemingly have an influence on the oxy-Cope reaction rate and accelerate enolate anion equilibration after the sigmatropic event. An early manifestation of the latter phenomenon was seen with **142**.[86] Oxy-Cope rearrangement of its potassium salt required heating in tetrahydrofuran. During the short reaction period, initially formed α-alkoxy enolate **143** equilibrated completely to **144**, as reflected in the efficient isolation of **145** following addition of phenylselenenyl chloride [Eq. (47)]. This example illustrates

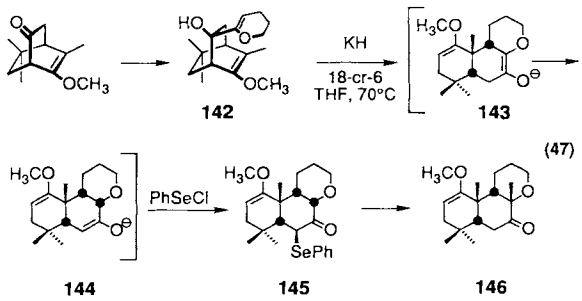

142 143 (47)

144 145 146

the feasibility of assembling the forskolin prototype **146** in only a few steps. However, compounds related to **142**, but carrying additional substituents on the dihydropyran ring, showed no tendency to undergo a comparable [3,3] shift.[87]

9.3. Reactions of Higher Homologues

Whereas bicyclo[3.2.2]non-6-en-2-ols typified by **147a** and **147b** are recognized to possess the ability to undergo the

oxyanionic Cope transposition,[88] a dependence on substituent location and type has surfaced [Eq. (48)]. For example, the phenylthio derivative **147c** is destroyed under the same conditions.[88] Furthermore, the parent alcohol **148** and bridgehead functionalized analogues such as **149** experience [1,3] sigmatropy (with inversion of configuration) instead.[89] More study is needed before those factors responsible for this dichotomy are made clear.

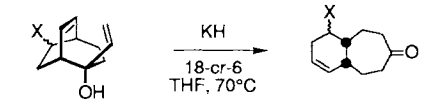

147a, X = *n*BuO
b, X = *n*BuS
c, X = PhS

(48)

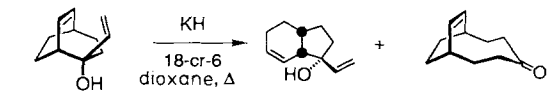

148

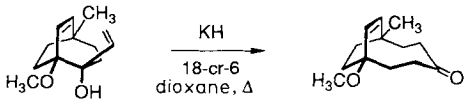

149

Although a smaller number of isomeric 8-ols have been scrutinized, this variant has proven to be spectacularly successful in providing tricyclic ketones such as **150** and **151** having well-defined all-*cis* ring-juncture stereochemistry [Eq. (49)].[90, 91] The chirality transfer exhibited during the formation of **151** is an attractive asset of this strategy.

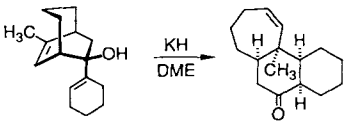

150

(49)

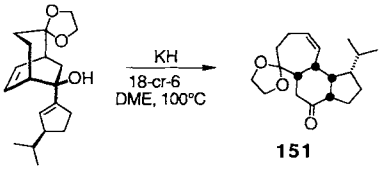

151

Placement of the homoallylic double bond at an exocyclic site as in **152** has the consequence of making available a

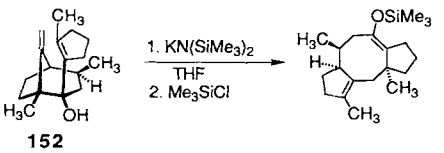

152

(50)

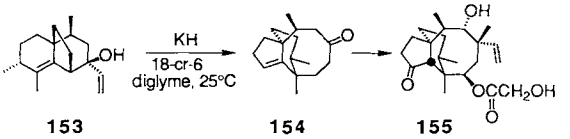

153 **154** **155**

synthetic entry to multiply fused cyclooctanones and their derivatives [Eq. (50)].[92] An elaborate application of this specific rearrangement can be found in *Boeckman*'s stereocontrolled assembly of (±)-pleuromutilin (**155**).[93] Because alcohol **153**, like **152**, possesses only one rotational degree of freedom, isomerization to **154** occurs quantitatively in the presence of potassium hydride and diglyme at 100 °C.

10. Reactions of Bicyclic Ketones Whose Double Bonds Are Exocyclic

Martin et al. have examined the conversion of **27** and structurally related ketones to alcohols of the **156** variety because anionic-accelerated rearrangement of these compounds delivers products such as **157** that possess the basic [5.3.1]bicyclic unit of the tricyclic taxane diterpenes [Eq. (51)].[94]

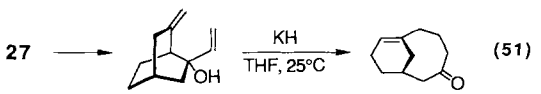

156 **157**

(51)

The tricyclic variant **28**,[95] on the other hand, has been shown to serve as a precursor to **158**, a ketone constituting the ABC core of cerorubenic acid-III [Eq. (52)].[96] The molecular architecture of **158** is unique in that a vinylcyclopropane is embedded centrally in such a manner that thermal ring expansion to a cyclopentene is precluded by the constraints of Bredt's rule.

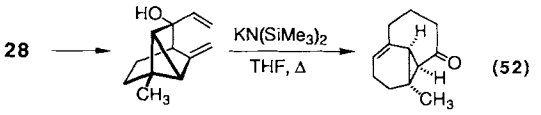

158

(52)

The exceptionally high potential of the oxy-Cope reaction for elaborating ketones carrying bridgehead double bonds has been duly recognized only in the past few years. The readiness with which such fascinating structures[97] can be formed has earlier been outlined in Equations (16), (34), (45), (51), and (52). The rather unique example **159** → **160** uncovered by *Snider* et al. should be included with this group [Eq. (53)].[98]

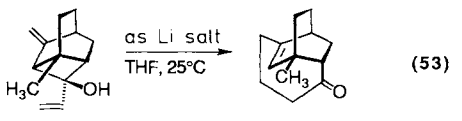

159 **160**

(53)

In all of the examples just surveyed, little conformational latitude is available to the divinyl alcohol because of the rather substantive rigidity of the bicyclic framework where a number of reaction centers are located. 1-Alkenyl-2-(1-cy-

clopentenyl)-*endo*-norbornan-2-ols and their *exo* isomers, in contrast, enjoy a great deal more latitude since neither the bridgehead double bond nor the unsaturated center linked to C-2 is formally constrained [cf. **161** and **162** in Eq. (54)].

In the *endo* series, there exist four possible geometric arrangements that bring the appropriate trigonal carbons into proximity (Scheme 5). Two are chairlike and two are of the

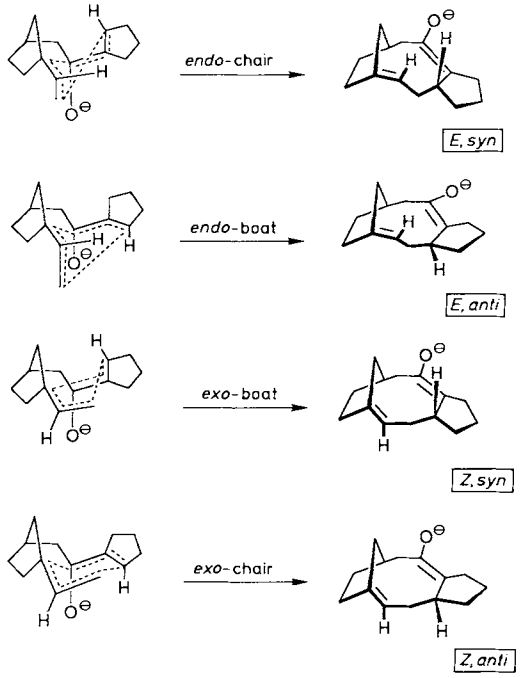

Scheme 5. Transition-state options for 1-alkenyl-2-cyclopentyl-*endo*-norbornan-2-ols (see text).

boat type. Each can be categorized uniquely by a combination of two descriptors, the first defining the specific orientation of the bridgehead vinyl group relative to the norbornyl framework and the second the spatial arrangement of the developing six-membered ring. Each orientation generates a product having a very specific and distinctive combination of stereochemical features at the double bond and ring fusion sites. *Endo* alignment of the bridgehead vinyl group serves ultimately to lock the olefinic proton into a *syn* relationship with the methano bridge in the product enolate. The alternative *exo* vinyl orientation necessarily leads to *Z* olefin geometry. The relative stereochemistry of the cyclopentyl ring fusion site that is positioned β to the enolate anion center is inextricably linked to whether chair or boat topography is adopted.

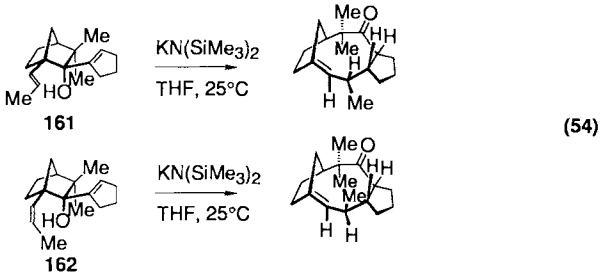

(54)

The exclusive formation from **161**, **162**, and related alcohols of the *Z,syn* product requires that each isomerize with a strong kinetic preference for the *exo*-boat transition state [Eq. (54)].[99] In the examples shown, an additional stereogenic center is seen to be unambiguously defined as a consequence of this remarkably exclusive sigmatropic pathway.

For entirely similar reasons, the stereochemistry of the products arising from the epimeric *exo* alcohols is likewise inextricably linked to the particular operational transition state (Scheme 6). Here also, rearrangement proceeds rapidly

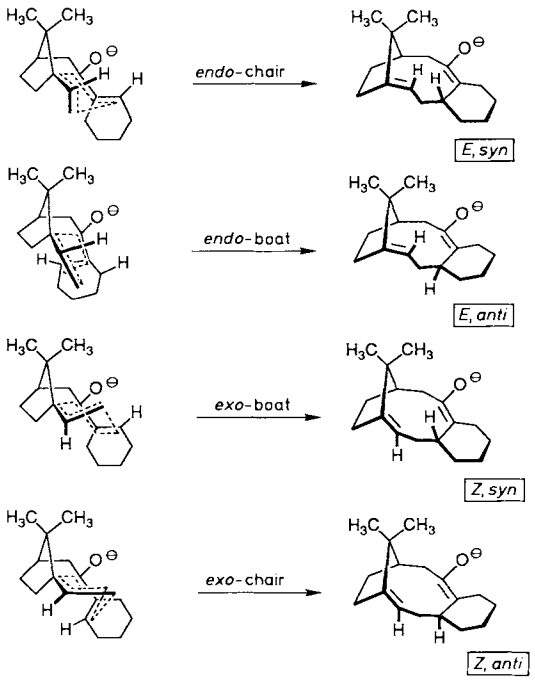

Scheme 6. Transition-state options for 1-alkenyl-2-cyclohexenyl-*exo*-norbornan-2-ols (see text).

at room temperature. Strikingly, only a single transition-state geometry, the *endo*-chair, is utilized during [3,3] sigmatropy.[100] For **163**, conversion to **164** proceeds with 100% stereoselectivity [Eq. (55)]. Since the oxyanionic Cope reac-

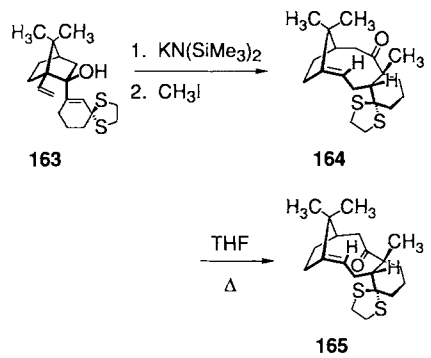

(55)

tion proceeds at 20 °C, an opportunity is offered that would permit the existence of discrete atropisomers. This is indeed the case. When refluxed in tetrahydrofuran for several days, **164** is irreversibly transformed into its conformational iso-

mer **165**. The several σ-bond rotations that must occur during this process are impeded from taking place readily because of the structural features present in **164**. Once the carbonyl oxygen becomes "tucked under" as in **165**, a lower-energy framework is attained. The conversion of **163** to a single atropisomer constitutes an example of a rare atropselective reaction, the first in an oxy-Cope setting.

11. 2-Norbornen-7-ones and Other Fragmentation-Prone Substrates

Gas-phase pyrolysis of **166** leads predominantly (88%) to **167**, in accord with the particular susceptibility of this vinylnorbornenol for fragmentation-recombination [Eq. (56)].[7] The study by *Berson* et al. of more heavily substituted examples established that this biradical-mediated [1,3] sigmatropic rearrangement proceeds with retention of configuration in the migrating group.[101]

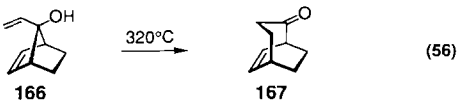

(56)

Oxyanion generation within such systems is known to foster rearrangement via antarafacial-retention [1,3] bridgehead-carbon migration. However, oxy-Cope reorganization now takes place concurrently, the product ratio being dependent on the structural characteristics of the 7-vinyl substituent.[102] Alcohol **168** responds by delivering a mixture of two ketones in the relative ratio of 3:1 [Eq. (57)]. The level of

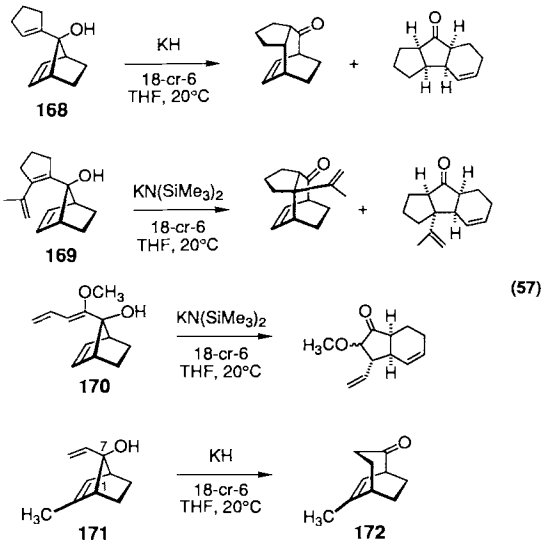

(57)

[3,3] sigmatropy is enhanced for **169** (1:20) and becomes exclusive when **170** is the substrate.[68] The pair of [1,3] shifts capable of operating within **171** are not at all competitive, the exclusive formation of **172** revealing a decided preference for C-1/C-7 bond cleavage.[102]

The propensity for two-carbon homologation persists in larger bicyclic frameworks such as found in **173** [Eq. (58)].[103] In parallel fashion, the potassium salt of benzo analogue **174** is transformed quantitatively into **175** within two minutes at 24 °C. On progressing to lower temperatures, *Mukai* et al. were able to establish that treatment of **174** with potassium hydride leads quickly to establishment of

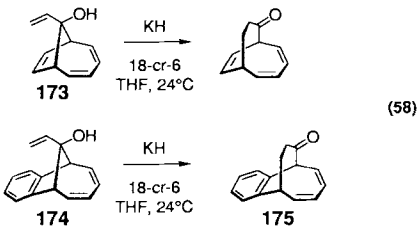

(58)

an equilibrium with the three isomeric allylic alcohols **176**–**178** (Scheme 7). With the passage of time, the proportion of **175** increases at the expense of these base-sensitive benzobicyclononatrienols.[103]

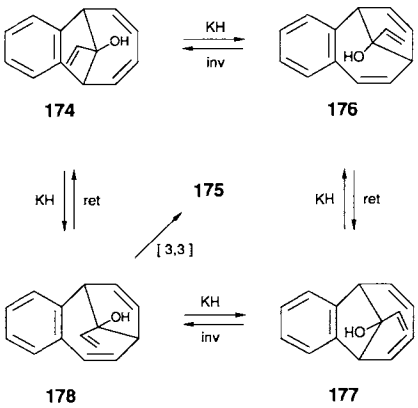

Scheme 7. Anionically accelerated circumambulatory [1,3] sigmatropic rearrangements in **174**.

Hydroxy ketone **179** is so configured that its olefinic centers cannot become proximate. Nevertheless, when exposed to base, **179** is transformed into either **183** or **184** depending on the reaction conditions [Eq. (59)].[104] The use of KOH in aqueous methanol provides **183**. With excess KH in tetrahydrofuran, **184** results. These events have been rationalized in terms of initial ring fission and reclosure to **180** or **181**. Both

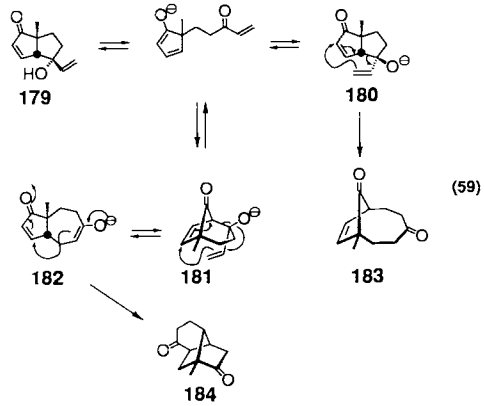

(59)

of these intermediates are structurally disposed for oxy-Cope isomerization. While **180** is the obvious immediate precursor of **183**, the enolate anion formed from **181** must undergo aldol closure prior to arriving at **184**.

12. Dianionic Oxy-Cope Processes

Dianionic oxy-Cope rearrangements have received remarkably little attention, although divinyl alcohols are well recognized to be quite susceptible to thermal [3,3] sigmatropy.[105] In the few examples that have been studied, large ring dienolates have resulted and these intermediates have undergone transannular aldolization during workup. The *trans* diol **185**, available from 9,10-phenanthraquinone, is isomerized initially to **186** when heated with KH in tetrahydrofuran. The actual isolated product is the dibenzotropone **187**, probably formed as indicated [Eq. (60)].[106] The *trans* stereochemistry is a necessary prerequisite for this rearrangement since the vinyl groups must both be equatorially disposed to be within bonding distance.

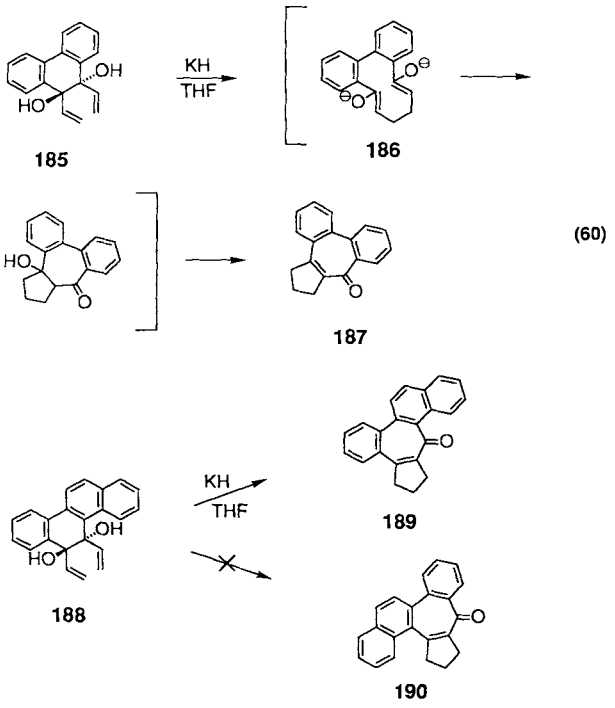

Diol **188** behaves analogously, giving rise to **189** and not to **190**.[106]

13. Tandem Pairing of the Oxy-Cope Rearrangement with a Second Chemical Event

13.1. [3,3] Sigmatropy Occurring First

The powerful capacity of the anionic oxy-Cope rearrangement for stereoselective molecular construction can be usefully expanded by direct linking of this isomerization to a sequential reaction. Described above are examples where the regiospecifically generated enolate anion is trapped at oxygen [Eqs. (14) and (17)] or alkylated at the α carbon [Eqs. (28) and (55)]. When enolate equilibration operates, advantage can often be taken of the new locus of negative charge [Eq. (47)]. An expedient means for preparing polycyclic α-hydroxy ketones has been developed by taking advantage of in situ enolate hydroxylation [Eq. (61)].[107] The locus of the newly introduced oxygen atom depends, of course, on the regiochemistry of enolate formation. Products **191** and **192** provide two contrasting examples. The acid-catalyzed closure of **192** to **193** adds yet another interesting parameter to these transformations.

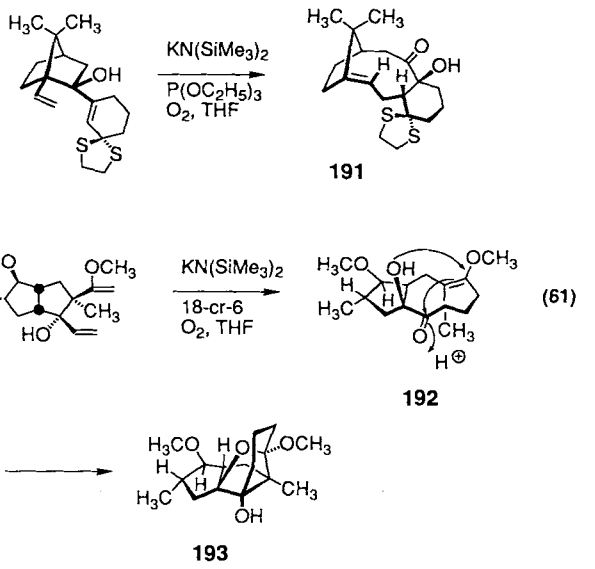

Since the oxy-Cope process is tolerant of various functional groups, it is often convenient to incorporate within the starting alcohol features that are conducive to subsequent transannular cyclization [Eqs. (33), (59), and (60)]. Four ingenious examples are collected in Equation (62). Arrival at

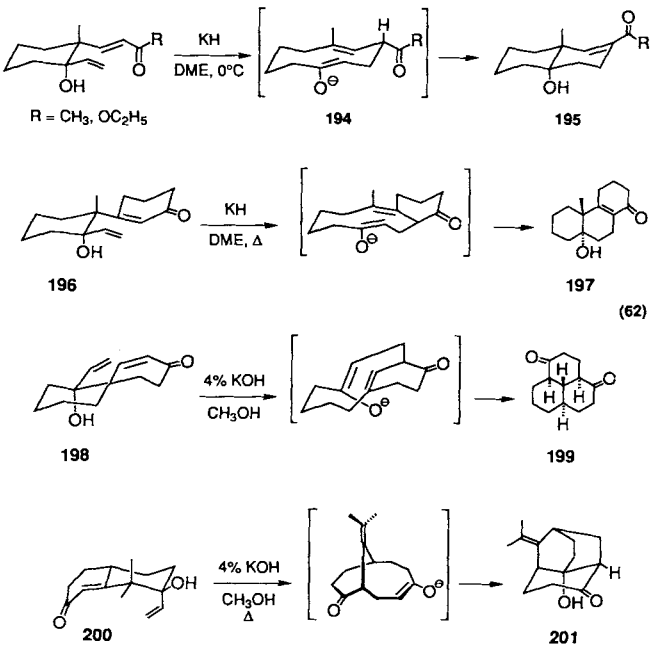

195 is seemingly dependent on proton transfer within **194** to generate a new enolate that is suitably aligned stereoelectronically for intramolecular nucleophilic capture of the nonconjugated carbonyl.[108] The conversions **196** → **197**,[109] **198** → **199**,[51] and **200** → **201**[110] are predicated on similar considerations of orbital overlap control.

The feasibility of trapping an enol in an irreversible intramolecular alkylation step has been demonstrated [Eq. (63)].[48] When a halide leaving group is involved as in **202**, the oxy-Cope rearrangement must be performed thermally. Attempts to implement charge acceleration techniques resulted instead in premature intramolecular ether formation as exemplified by **203**.

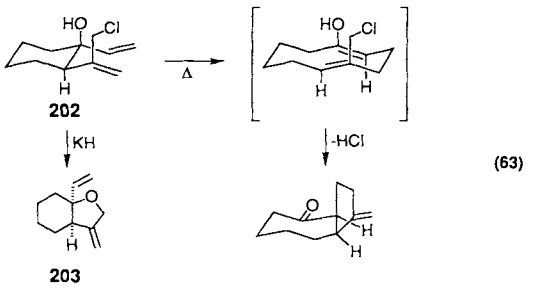

(63)

In contrast, medium-ring enolate anions generated by [3,3] sigmatropy do successfully undergo transannular cyclization concomitant with S_N' displacement of a methoxyl leaving group, provided that the C–OCH_3 bond is properly aligned with the flanking π orbital. Structurally intricate polycyclic ketones are thereby constructed with rapidity and efficiency. As an illustrative example, **204** is smoothly transformed in a single maneuver via **205** into the complex diquinane **206** at room temperature [Eq. (64)].[111] In yet another fascinating reaction, heating of the potassium alkoxide of **207** gives **208** as the first-formed intermediate. As a consequence of the enormous strain that would result from intramolecular methoxide displacement within this intermediate, there is ample time for enolate equilibration with **209** to transpire in advance of conversion to **210**.

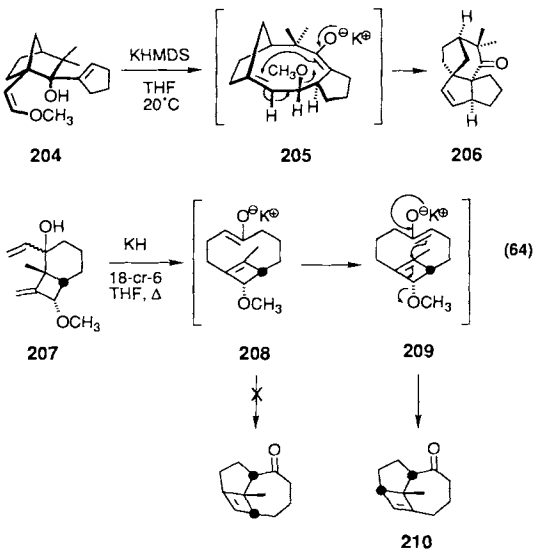

(64)

KHMDS = potassium hexamethyldisilazanide

The possibility of achieving the stereocontrolled construction of hydroazulenones by sequential anionic oxy-Cope rearrangement with S_N' allylic ether displacement has been examined with considerable success. Thus, ring expansion of **211** proceeds via **212** to give **213** as the first-formed tetracyclic product [Eq. (65)].[112] Alcohol **214** also enjoys a kinetic predisposition for generation of a *trans,trans*-cyclodecadiene (namely, **215**) and ultimately delivers **216**. Whereas the geometry present in **212** and **215** is necessary to bring the double bonds into a closely proximate arrangement, the ensuing S_N' displacement of methoxide ion is found to occur with equal facility from the frontside or backside.

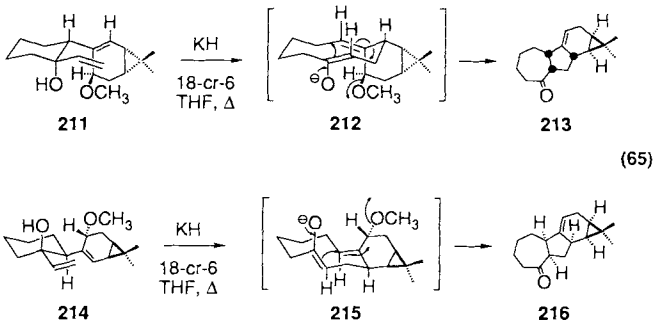

(65)

Wender et al. have found that **217** rearranges under alkaline conditions to give the 14-membered ketone **219**, which has served as a precursor to (±)-muscone[113] and to (−)-(3*Z*)-cembrene A.[114] Although the observed macroexpansion is consistent with the direct involvement of enolate anion **218** or its macrocyclic isomer [Eq. (66)],[115] later investigation has provided solid indication that the stepwise process is the more favored.[116] Since **218** does not accumulate during this fast reaction, it is necessary that the presence of the enolate in **218** accelerate the Cope rearrangement that leads to **219**. The synthetic advantages that accrue to this remarkable type of charge acceleration are beginning to receive attention.[117]

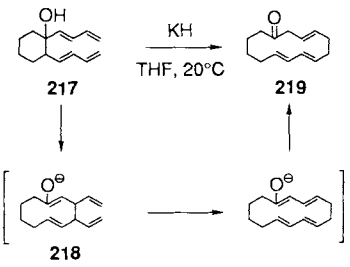

(66)

The regiochemical control assured by the geometrical constraints of the oxy-Cope reaction can be utilized further to set the stage for subsequent intramolecular cycloaddition or electrocyclization. *Jacobi* et al. have been responsible for uncovering examples of each tandem process. Heating the pure *Z* alcohol **220** at 160 °C resulted in direct conversion to ketal **222**, mild acid hydrolysis of which afforded gnididione (**223**) [Eq. (67)].[118] This elegant transformation owes its success to the capacity of intermediate **221** for intramolecular Diels–Alder addition involving the electron-deficient triple bond and isoxazole ring.

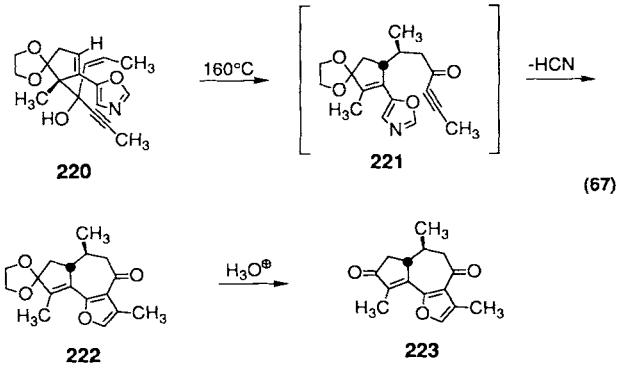

(67)

Bis-acetylenic alcohols such as **224** undergo facile oxy-Cope rearrangement to afford mixtures of *E* and *Z* enynones. Upon enolization, these latter compounds experience electrocyclic ring closure with the formation of methylenecyclopentenones (e.g., **225**) [Eq. (68)].[118]

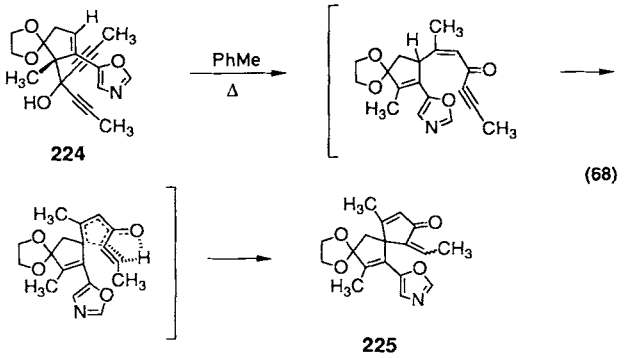

(68)

13.2. [3,3] Sigmatropy Occurring Last

While tandem rearrangements of the Claisen–Cope variety are well known,[119] there appear to be no known examples of two-step reaction sequences where the final stage is of the oxy-Cope type (excluding, of course, syntheses of the alcohols themselves).

14. Summary and Outlook

In either its neutral or anionic version, the oxy-Cope rearrangement constitutes an intrinsically sophisticated means for achieving internal chirality transfer within the context of polycyclic ketone construction. To the extent that diastereoselectivity can be controlled during formation of the divinyl alcohol, the ensuing [3,3] sigmatropic shift will lead to products having well-defined networks of stereogenic centers. Variation of the nucleophile has been very limited and clearly will expand as more complex vinyl anions become increasingly available. Access to more structurally diverse β,γ-unsaturated ketones will undoubtedly bring about new opportunities for isomerizations of this type. All existing signs suggest that growth in this area will not only be feasible but intensively pursued.

The ring systems capable of being accessed by the oxy-Cope process seem limited only by the imagination of the researcher. The convergency of the carbonyl regeneration scheme allows for combinatorial possibilities that assure the exercise of many more options in the future. Perhaps the most exciting and challenging feature of this two-step process will be suitable development of reliable transition-state models that shall ultimately allow for simultaneous kinetic resolution—an area in which studies have been made, but more needs to be done.

The oxy-Cope reaction offers great opportunities for realizing totally new dimensions in the synthesis of complex molecules. The flexibility, stereochemical reliability, brevity, and efficiency of the scheme bode especially well for extensive future application.

The theory and experiment for which we are responsible has been brought to fruition by the enthusiasm, dedication, intellectual prowess, and experimental skills of a relatively small number of students. These efforts have been made possible by the financial support of the National Institutes of Health. Fellowships from the Deutsche Forschungsgemeinschaft (FRG), NATO/SERC (UK), NSERCC (Canada), and the CNRS (France) have contributed support to my postdoctoral associates from these countries.

Received: January 25, 1990 [A 765 IE]
German version: *Angew. Chem. 102* (1990) 642

[1] R. B. Woodward, R. Hoffmann: *Die Erhaltung der Orbitalsymmetrie;* Verlag Chemie, Weinheim 1970; *The Conservation of Orbital Symmetry,* Verlag Chemie, Weinheim/Academic Press, New York 1970; *Angew. Chem. 81* (1969) 797; *Angew. Chem. Int. Ed. Engl. 8* (1969) 781.
[2] S. Swaminathan, *J. Indian Chem. Soc. 61* (1984) 99.
[3] R. K. Hill in J. D. Morrison (Ed.): *Asymmetric Synthesis, Vol. 3A,* Academic Press, London 1984, S. 503; R. K. Hill in L. A. Paquette (Ed.): *Comprehensive Organic Synthesis, Vol. 5,* Pergamon Press, Oxford 1990.
[4] S. R. Wilson, *Org. React.* (NY), in press.
[5] L. A. Paquette, *Synlett* (1990) 67.
[6] M. Urion, *Ann. Chem. (Paris)* (1934) 5.
[7] J. A. Berson, M. Jones, Jr., *J. Am. Chem. Soc. 86* (1964) 5017, 5019.
[8] D. A. Evans, A. M. Golob, *J. Am. Chem. Soc. 97* (1975) 4765.
[9] D. A. Evans, D. J. Baillargeon, *Tetrahedron Lett. 1978,* 3315, 3319; M. L. Steigerwald, W. A. Goddard III, D. A. Evans, *J. Am. Chem. Soc. 101* (1979) 1994.
[10] B. K. Carpenter, *Tetrahedron 34* (1978) 1877; G. Ahlgren, *Tetrahedron Lett. 1979,* 915; M. D. Rozeboom, J. P. Kiplinger, J. E. Bartmess, *J. Am. Chem. Soc. 106* (1984) 1025; M. J. S. Dewar, C. Xie, *ibid. 109* (1987) 5893.
[11] W. von E. Doering, W. R. Roth, *Tetrahedron 18* (1962) 67.
[12] G. Mehta, P. Azario, R. Barone, M. Chanon, *Tetrahedron 45* (1989) 1985.
[13] D. A. Evans, D. J. Baillargeon, G. V. Nelson, *J. Am. Chem. Soc. 100* (1978) 2242; D. A. Evans, J. V. Nelson, *ibid. 102* (1980) 774.
[14] H. O. House, T. S. B. Sayer, C.-C. Yau, *J. Org. Chem. 43* (1978) 2153.
[15] D. Seebach, K.-H. Geiß, M. Pohmakotr, *Angew. Chem. 88* (1976) 449; *Angew. Chem. Int. Ed. Engl. 15* (1976) 437.
[16] S. R. Wilson, D. T. Mao, K. M. Jernberg, S. T. Ezmirly, *Tetrahedron Lett. 1977,* 2559; see also T. Anishi, Y. Fujita, T. Nishida, *Synthesis 1980,* 651.
[17] M. A. Battiste, J. R. Rocca, R. L. Wydra, J. H. Tumlinson, III, T. Chuman, *Tetrahedron Lett. 29* (1988) 6565.
[18] P. A. Jacobi, H. G. Selnick, *J. Am. Chem. Soc. 106* (1984) 3041.
[19] M. Koreeda, Y. Tanaka, A. Schwartz, *J. Org. Chem. 45* (1980) 1172.
[20] M. Koreeda, Z. You, *J. Org. Chem. 54* (1989) 5195.
[21] L. A. Paquette, G. D. Crouse, A. K. Sharma, *J. Am. Chem. Soc. 104* (1982) 4411.
[22] L. A. Paquette, G. D. Crouse, A. K. Sharma, *J. Am. Chem. Soc. 102* (1980) 3972; L. A. Paquette, G. D. Crouse, *Tetrahedron 37* (1981) 281.
[23] L. A. Paquette, M. J. Coghlan, P. C. Hayes, *J. Org. Chem. 49* (1984) 4516.
[24] G. D. Crouse, L. A. Paquette, *Tetrahedron Lett. 22* (1981) 3167; see also L. A. Paquette, G. D. Crouse, *J. Am. Chem. Soc. 103* (1981) 6235.
[25] T. L. Macdonald, K. J. Natalie, Jr., G. Prasad, J. S. Sawyer, *J. Org. Chem. 51* (1986) 1124.
[26] Unpublished observations of our group.

[27] L. A. Paquette, K. S. Learn, *J. Am. Chem. Soc. 108* (1986) 7873; L. A. Paquette, K. S. Learn, J. L. Romine, H.-S. Lin, *ibid. 110* (1988) 879.
[28] L. A. Paquette, W. He, R. D. Rogers, *J. Org. Chem. 54* (1989) 2291.
[29] L. A. Paquette, D. T. DeRussy, J. C. Gallucci, *J. Org. Chem. 54* (1989) 2278.
[30] L. A. Paquette, D. T. DeRussy, T. Vandenheste, R. D. Rogers, *J. Am. Chem. Soc. 112* (1990), in press.
[31] L. A. Paquette in O. Chizhov (Ed.): *Organic Synthesis: Modern Trends*, Blackwell, Oxford 1987.
[32] L. A. Paquette, D. T. DeRussy, C. E. Cottrell, *J. Am. Chem. Soc. 110* (1988) 890.
[33] M. Lin, W. J. le Noble, *J. Org. Chem. 54* (1989) 997.
[34] A. S. Cieplak, *J. Am. Chem. Soc. 103* (1981) 4540.
[35] E. N. Marvell, W. Whalley, *Tetrahedron Lett. 1970*, 509.
[36] D. L. J. Clive, C. G. Russell, S. C. Suri, *J. Org. Chem. 47* (1982) 1632.
[37] S. L. Schreiber, C. Santini, *Tetrahedron Lett. 22* (1981) 4651.
[38] S. L. Schreiber, R. C. Hawley, *Tetrahedron Lett. 26* (1985) 5971.
[39] S. L. Schreiber, C. Santini, *J. Am. Chem. Soc. 106* (1984) 4038.
[40] W. C. Still, *J. Am. Chem. Soc. 99* (1977) 4186.
[41] W. C. Still, *J. Am. Chem. Soc. 101* (1979) 2493.
[42] H. Hauptmann, G. Mühlbauer, N. P. C. Walker, *Tetrahedron Lett. 27* (1986) 1315.
[43] S. Kuwahara, K. Mori, *Heterocycles 28* (1989) 167.
[44] W. C. Still, S. Murata, G. Revial, K. Yoshihara, *J. Am. Chem. Soc. 105* (1983) 625.
[45] C. Kuroda, H. Hirota, T. Takahashi, *Chem. Lett. 1982*, 249; C. Kuroda, T. Nakamura, H. Hirota, E. Enomoto, T. Takahashi, *Bull. Chem. Soc. Jpn. 58* (1985) 146.
[46] A. Utagawa, H. Hirota, S. Ohno, T. Takahashi, *Bull. Chem. Soc. Jpn. 61* (1988) 1207.
[47] S. P. Ganesh Raj, S. Janardhanan, K. Rajagopalan, *Synth. Commun. 19* (1989) 1341.
[48] M. Sworin, K.-C. Lin, *J. Org. Chem. 52* (1987) 5640; *J. Am. Chem. Soc. 111* (1989) 1815.
[49] J. P. John, S. Ramachandran, S. Swaminathan, *Tetrahedron Lett. 1962*, 720; J. P. John, K. G. Srinivasan, P. S. Venkataramani, S. Swaminathan, *Tetrahedron 25* (1969) 2661; S. Swaminathan, K. G. Srinivasan, P. S. Venkataramani, *ibid. 26* (1970) 1453.
[50] R. Uma, S. Swaminathan, K. Rajagopalan, *Tetrahedron Lett. 25* (1984) 5825; R. Uma, K. Rajagopalan, S. Swaminathan, *Tetrahedron 42* (1986) 2757.
[51] C. S. S. Rao, G. Kumar, K. Rajagopalan, S. Swaminathan, *Tetrahedron 38* (1982) 2195.
[52] P. V. Ramani, J. P. John, K. V. Narayanan, S. Swaminathan, *J. Chem. Soc. Perkin. Trans. 1 1972*, 1516.
[53] N. Raju, A. Geetha, K. Rajagopalan, S. Swaminathan, *Indian J. Chem. Sect. B 20* (1981) 238.
[54] S. A. Miller, R. C. Gadwood, *J. Org. Chem. 53* (1988) 2214.
[55] R. C. Gadwood, R. M. Lett, *J. Org. Chem. 47* (1982) 2268.
[56] J. P. Barnier, J. Ollivier, J. Salaun, *Tetrahedron Lett. 30* (1989) 2525.
[57] R. C. Gadwood, R. M. Lett, J. E. Wissinger, *J. Am. Chem. Soc. 106* (1984) 3869; *ibid. 108* (1986) 6343.
[58] L. A. Paquette, D. R. Andrews, J. P. Springer, *J. Org. Chem. 48* (1983) 1148; L. A. Paquette, J. A. Colapret, D. R. Andrews, *ibid. 50* (1985) 201.
[59] R. L. Danheiser, C. Martinez-Davila, H. Sard, *Tetrahedron 37* (1981) 3943; R. Huston, M. Rey, A. S. Dreiding, *Helv. Chim. Acta 65* (1982) 451.
[60] T. Kato, H. Kondo, M. Nishino, M. Tanaka, G. Hata, A. Miyoke, *Bull. Chem. Soc. Jpn. 53* (1980) 2958.
[61] T. Ohnuma, N. Hata, N. Miyachi, T. Wakamatsu, Y. Ban, *Tetrahedron Lett. 27* (1986) 219.
[62] R. W. Thies, E. P. Seitz, *J. Chem. Soc. Chem. Commun. 1976*, 846; *J. Org. Chem. 43* (1978) 1050; R. W. Thies, M. Meshgini, R. H. Chiarello, E. P. Seitz, *ibid. 45* (1980) 185.
[63] R. W. Thies, K. P. Daruwala, *J. Chem. Soc. Chem. Commun. 1985*, 1188; *J. Org. Chem. 52* (1987) 3798.
[64] M. Kahn, *Tetrahedron Lett. 21* (1980) 4547.
[65] S. G. Levine, R. L. McDaniel, Jr., *J. Org. Chem. 46* (1981) 2199.
[66] L. A. Paquette, G. Ladouceur, *J. Org. Chem. 54* (1989) 4278.
[67] M. E. Jung, J. P. Hudspeth, *J. Am. Chem. Soc. 100* (1978) 4309.
[68] L. A. Paquette, D. T. DeRussy, R. D. Rogers, *Tetrahedron 44* (1988) 3139.
[69] E. N. Marvel, S. W. Almond, *Tetrahedron Lett. 1979*, 2779.
[70] M. E. Jung, L. A. Light, *J. Am. Chem. Soc. 106* (1984) 7614.
[71] L. A. Paquette, J. L. Romine, H.-S. Lin, *Tetrahedron Lett. 28* (1987) 31.
[72] K. Tomioka, K. Koga in J. D. Morrison (Ed.): *Asymmetric Synth. Vol. 2 A*, Chapter 7, Academic Press, London 1983.
[73] L. A. Paquette, D. Macdonald, L. G. Anderson, J. Wright, *J. Am. Chem. Soc. 111* (1989) 8037.
[74] M. E. Jung, G. L. Hatfield, *Tetrahedron Lett. 24* (1983) 2931.
[75] N.-C. Chang, W.-F. Lu, C.-Y. Tseng, *J. Chem. Soc. Chem. Commun. 1988*, 182; S.-L. Hsieh, C.-T. Chiu, N.-C. Chang, *J. Org. Chem. 54* (1989) 3820.
[76] H. Yamamoto, H. L. Sham, *J. Am. Chem. Soc. 101* (1979) 1609.
[77] N.-C. Chang, H.-M. Day, W.-F. Lu, *J. Org. Chem. 54* (1989) 4083.
[78] G. Bérubé, A. G. Fallis, *Tetrahedron Lett. 30* (1989) 4045.
[79] W. L. Brown, A. G. Fallis, *Tetrahedron Lett. 26* (1985) 607; *Can. J. Chem. 65* (1987) 1828.
[80] I. Fleming, N. K. Terrett, *Tetrahedron Lett. 25* (1984) 5103.
[81] D. A. Evans, W. L. Scott, L. K. Truesdale, *Tetrahedron Lett. 1972*, 137.
[82] R. P. Gregson, R. N. Mirrington, *J. Chem. Soc. Chem. Commun. 1973*, 598.
[83] J. H. Rigby, J.-P. Denis, *Synth. Commun. 16* (1986) 1789.
[84] K. Pramod, G. S. R. Subba Rao, *Indian J. Chem. 218* (1982) 984.
[85] D. A. Evans, A. M. Golob, N. S. Mandel, G. S. Mandel, *J. Am. Chem. Soc. 100* (1978) 8170.
[86] J. A. Oplinger, L. A. Paquette, *Tetrahedron Lett. 28* (1987) 5441.
[87] L. A. Paquette, J. A. Oplinger, *Tetrahedron 45* (1989) 107.
[88] J. H. Rigby, J.-M. Sage, J. Raggon, *J. Org. Chem. 47* (1982) 4815.
[89] T. Uyehara, K. Ohmori, Y. Kabasawa, T. Kato, *Chem. Lett. 1984*, 1879.
[90] R. E. Ireland, W. J. Thompson, G. H. Srouji, R. Etter, *J. Org. Chem. 46* (1981) 4863.
[91] K. R. Dahnke, unpublished.
[92] S. Liang, unpublished.
[93] R. K. Boeckman, Jr., D. M. Springer, T. R. Alessi, *J. Am. Chem. Soc. 111* (1989) 8284.
[94] S. F. Martin, J. B. White, R. Wagner, *J. Org. Chem. 47* (1982) 3190.
[95] M.-A. Poupart, L. A. Paquette, *Tetrahedron Lett. 29* (1988) 269.
[96] L. A. Paquette, M.-A. Poupart, *Tetrahedron Lett. 29* (1988) 273.
[97] K. J. Shea, *Tetrahedron 36* (1980) 1683.
[98] B. B. Snider, R. B. Beal, *J. Org. Chem. 53* (1988) 4508.
[99] L. A. Paquette, C. A. Teleha, R. T. Taylor, G. D. Maynard, R. D. Rogers, J. C. Gallucci, J. P. Springer, *J. Am. Chem. Soc. 112* (1990) 265.
[100] L. A. Paquette, N. A. Pegg, D. Toops, G. D. Maynard, R. D. Rogers, *J. Am. Chem. Soc. 112* (1990) 277.
[101] J. A. Berson, T. Miyashi, G. Jones, II, *J. Am. Chem. Soc. 96* (1974) 3468.
[102] L. A. Paquette, F. Pierre, C. E. Cottrell, *J. Am. Chem. Soc. 109* (1987) 5731.
[103] T. Miyashi, A. Hazato, T. Mukai, *J. Am. Chem. Soc. 104* (1982) 891; *ibid. 100* (1978) 1008.
[104] C. M. Tice, C. H. Heathcock, *J. Org. Chem. 46* (1981) 9.
[105] S. J. Rhoads, N. R. Raulins, *Org. React. (NY) 22* (1975) 63.
[106] P. Geetha, C. A. M. A. Hug, K. Rajagopalan, S. Swaminathan, *Tetrahedron Lett. 23* (1982) 569.
[107] L. A. Paquette, D. T. DeRussy, N. A. Pegg, R. T. Taylor, T. M. Zydowsky, *J. Org. Chem. 54* (1989) 4576.
[108] K. Thangaraj, P. C. Srinivasan, S. Swaminathan, *Tetrahedron Lett. 23* (1982) 4983.
[109] G. Sathyamoorthi, K. Thangaraj, P. C. Srinivasan, S. Swaminathan, *Tetrahedron Lett. 30* (1989) 4427.
[110] N. Raju, K. Rajagopalan, S. Swaminathan, J. N. Schoolery, *Tetrahedron Lett. 21* (1980) 1577.
[111] L. A. Paquette, J. Reagan, S. L. Schreiber, C. A. Teleha, *J. Am. Chem. Soc. 111* (1989) 2331.
[112] L. A. Paquette, Y.-J. Shi, *J. Org. Chem. 54* (1989) 5205.
[113] P. A. Wender, D. A. Holt, S. M. Sieburth, *J. Am. Chem. Soc. 105* (1983) 3348.
[114] P. A. Wender, D. A. Holt, *J. Am. Chem. Soc. 107* (1985) 7771.
[115] P. A. Wender, S. M. Sieburth, J. J. Petraitis, S. K. Singh, *Tetrahedron 37* (1985) 3967.
[116] P. A. Wender, R. J. Ternansky, S. M. Sieburth, *Tetrahedron Lett. 26* (1985) 4319.
[117] For example: G. Majetich, K. Hull, *Tetrahedron Lett. 29* (1988) 2773.
[118] P. A. Jacobi, L. M. Armacost, J. I. Kravitz, M. J. Martinelli, H. G. Selnick, *Tetrahedron Lett. 29* (1988) 6865.
[119] F. E. Ziegler, *Chem. Rev. 88* (1988) 1423.

The Coordination Chemistry and Organometallic Chemistry of Tridentate Oxygen Ligands with π-Donor Properties

By Wolfgang Kläui*

Metal complexes are capable of accomplishing almost anything, provided they contain the proper metal/ligand combinations. A host of essential biochemical transformations—but also a great many industrially significant reactions—occur within the coordination spheres of metal ions. For instance, the particular arrangement of ligands in the zinc-containing enzyme carboanhydrase is responsible for an acceleration in the hydration of CO_2 by a factor of 10^9. It is the ligands that determine whether an iron atom will transfer molecular oxygen, as in the case of hemoglobin, or electrons, as with the cytochromes. By varying the ligands it is possible to establish in advance whether a metal ion in the presence of synthesis gas will cause an olefin to be hydrogenated or hydroformylated. Stated more generally, it is the ligands that stabilize the particular oxidation states of a metal and determine how substrate molecules will be coordinated and undergo reaction. The synthesis of new ligands that confer specific reactivity on metal ions is thus an important challenge for the coordination chemist. The following article describes organometallic compounds of the type $[CpCo\{P(O)R'R''\}_3]^{\ominus}$, which have developed from an extremely unreactive laboratory curiosity into versatile oxygen-containing ligands whose steric and electronic properties promise a series of interesting applications.

1. Introduction

Most chemistry students encounter multidentate ligands (chelating ligands) for the first time in the course of an EDTA determination of the metal content of an aqueous solution. Chelating ligands important in analytical chemistry, biochemistry, and industrial extraction processes often feature one or more nitrogen atoms as donor centers. Important oxygen chelate ligands include the β-diketonates present as components in NMR lanthanide shift reagents, such natural antibiotic ionophores as valinomycin, and the crown ethers introduced by *Pedersen*. The present contribution describes the coordination chemistry of a class of monoanionic tridentate ligands in which all three of the complexing donor atoms are oxygen. These ligands display various remarkable properties. Chemically, they are extremely robust; even though they represent organometallic compounds of the "half-sandwich" type, they nevertheless dissolve without decomposition in aqueous sulfuric acid. They are not oxidized at all by atmospheric oxygen, and only with difficulty by nitric acid. At the same time, some of the ligands offer the surprising ability of producing sodium salts that are highly soluble, not only in water but also in pentane. All the ligands have the general constitution $[(C_5R_5)M\{P(O)R'R''\}_3]^{\ominus}$, with $C_5R_5 = C_5H_5$, C_5Me_5; M = Co, Rh; and R',R'' = alkyl, aryl, or *O*-alkyl (compare **2** in Scheme 1). They will be uniformly abbreviated by $L^{\ominus}$.[1] In Scheme 2, **3** is mentioned as a rhodium analogue.

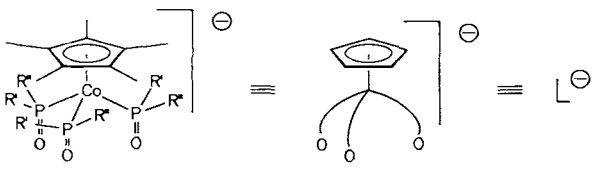

[*] Prof. Dr. W. Kläui
Institut für Anorganische Chemie der Technischen Hochschule
Templergraben 55, D-5100 Aachen (FRG)

Thus, the species in question are anionic cyclopentadienyl complexes, which because of the three P=O-functions[2] prove to be excellent tridentate oxygen ligands. In order to call attention to their C_{3v} symmetry they have been described[2] as oxygen tripod (i.e., "three-footed") ligands. This article constitutes a summary answer to the following questions: How are such tripod ligands synthesized? What is unusual about them? What can they do that other ligands cannot?

2. Synthesis of the Ligands

When cobaltocene is heated without solvent to ca. 100 °C in the presence of diesters of phosphorous acid[10] or secondary phosphane oxides,[11] one obtains directly the cobalt(II) complexes CoL_2 **1** containing oxygen tripod ligands. The free ligands $L^{\ominus}$ can be released by cleaving the compounds CoL_2 with cyanide in the presence of atmospheric oxygen.[12] The mechanism for the first step is only part explained,[13] but the second step can be regarded as a simple ligand substitution, which is followed by oxidation and further reaction of the intermediate ion $[Co(CN)_5]^{3\ominus}$ to give the stable Co^{III} complex $[Co(CN)_6]^{3\ominus}$. The synthesis can actually be carried out as a one-pot reaction and enables the introduction of almost any substituent R (Scheme 1).

If the two groups R' and R'' differ, what one obtains is a tripod ligand in which the three phosphorus atoms are stereogenic centers. This means that 16 stereoisomeric complexes CoL_2 are possible (seven pairs of enantiomers and two meso compounds), and if substituents R' and R'' are small, then all 16 are formed in comparable amounts.[15,16] On the other hand, if R' and R'' differ in size, cleavage with cyanide leads to a uniform ligand $L^{\ominus}$ consisting only of the (*R*, *R*, *R*)- and (*S*, *S*, *S*)-enantiomers[17] (Fig. 1).

These ligands can also be prepared stepwise. The CO- and iodo-ligands in $[(C_5H_5)M(CO)I_2]$, M = Co, Rh, are first re-

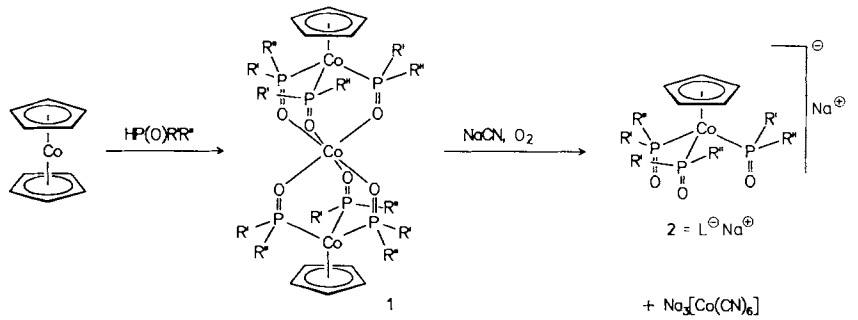

R', R'' = OCH_3, OC_2H_5, $OCH(CH_3)_2$, $OCH_2CH(CH_3)_2$, OC_4H_9, $OCH_2C(CH_3)_3$
CH_3, C_2H_5, C_4H_9, $CH_2C_6H_5$, C_6H_5, p-ClC_6H_4

Scheme 1. Synthesis of **2** = $L^{\ominus}Na^{\oplus}$ from cobaltocene via **1**.

placed by trimethylphosphite, after which the three coordinated trimethylphosphite ligands may be converted successively into dimethylphosphito ligands with the aid of the

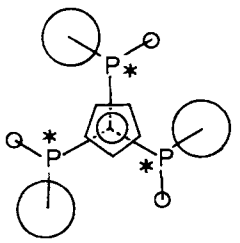

Fig. 1. Newman projection along the three-fold axis of a chiral ligand $L^{\ominus}$ with the (*R,R,R*)- or (*S,S,S*)-configuration.

Michaelis–Arbuzov reaction.[18] With this synthetic route one has, in addition to the cobaltocene route, also an entry to the analogous rhodium ligands. The synthesis of ligands of type **3** containing a C_5Me_5 (= Cp*)R fragment is possible via the route shown in Scheme 2.

Phosphorus compounds with the general composition $P(OR)_2(OMe)$ (= dialkylmethylphosphites), $PR(OR)(OMe)$ (= alkylmethylphosphonites), and $PR_2(OMe)$ (= methylphosphinites) can also be introduced in place of trimethylphosphite.

3. What Typifies the Complex Chemistry of the Ligands $L^{\ominus}$?

The two synthetic pathways described above are complementary in the sense that $L^{\ominus}$ is subject to modification at each position, permitting the preparation of an entire class of monoanionic oxygen tripod ligands with C_{3v} symmetry. Were one to attempt a characterization of this new type of ligand, the following questions would all need to be taken into account:

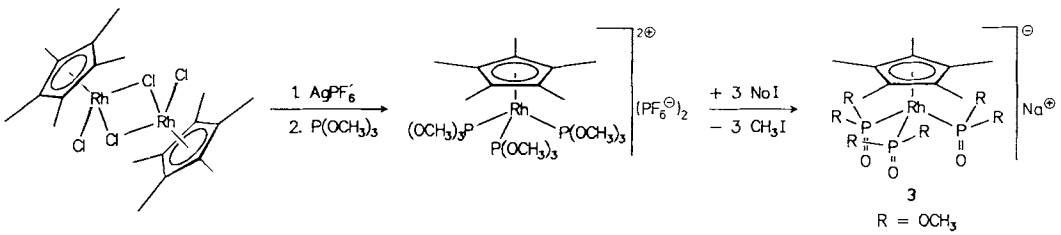

Scheme 2. Synthesis of the rhodium analogue **3** of $L^{\ominus}Na^{\oplus}$ **2** via the Michaelis-Arbuzov reaction.

Wolfgang Kläui was born in 1945 in Zürich, Switzerland. He received his Dipl.-Chem. (1971) and Dr. phil. (1973) degrees at the University of Zürich where he worked under H. Werner. In 1974 he was granted a fellowship of the Royal Society to work with Sir Jack Lewis (now Lord Lewis) in Cambridge (UK). He completed his Habilitation in 1979 at the University of Würzburg (FRG), became a "Privatdozent" there, and was appointed Professor of Inorganic Chemistry in 1982 at the Rheinisch-Westfälische Technische Hochschule in Aachen (FRG).

- With which metals and in what oxidation states do the ligands prefer to form complexes?
- How stable are the resulting complexes?
- What coordination geometries are favored?
- Are the ligands $L^{\ominus}$ strong or weak; i.e., do they induce large or small ligand field splittings Δ?
- Are they hard or soft ligands?

3.1. With which Metals does $L^{\ominus}$ form Complexes?

In the course of our first experiments with the ligand $L^{\ominus}_{OEt}$ [*] we were struck by the fact that it formed complexes with almost every metal ion examined[12, 19–23] (Fig. 2). Its behavior with respect to ions of the third main group[10, 12]

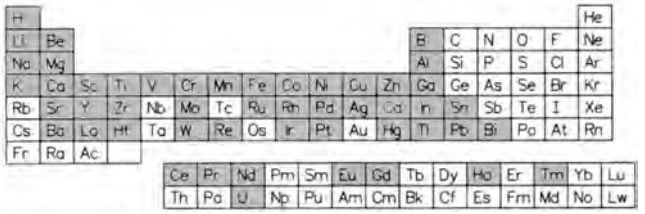

Fig. 2. All the elements shaded in gray are known to form complexes with the ligands $L^{\ominus}$.

is instructive to consider in this context. In the case of $Al^{3\oplus}$, $Ga^{3\oplus}$, $In^{3\oplus}$, and $Tl^{3\oplus}$ one obtains the expected 2:1 complexes $[ML_2]^{\oplus}$, with an octahedral arrangement of oxygen atoms. Reaction with $BF_4^{\ominus}$ or $BPh_4^{\ominus}$ produces the cations $[LBF]^{\oplus}$ and $[LBPh]^{\oplus}$, which may be regarded as 1:1 complexes of $L^{\ominus}$ with the unknown ions $BF^{2\oplus}$ and $BPh^{2\oplus}$. This is rather remarkable, since relatively few ligands are known to show such a willingness to form both metal and nonmetal derivatives. In this sense $L^{\ominus}$ resembles the fluoride ion, with which it also has much in common electronically (see Section 3.3).

The ligand $L^{\ominus}$ displays a strong tendency to undergo facial tridentate binding even with metal ions that do not favor this coordination (see, e.g., Ref. [23]). Trimetaphosphate $[P_3O_9]^{3\ominus}$ **4** or trimetaphosphimate $[P_3O_6(NH)_3]^{3\ominus}$ **5** would appear to represent simple models for $L^{\ominus}$ if they were characterized by the same coordination behavior as the latter.

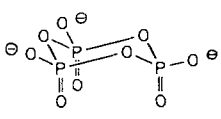

4

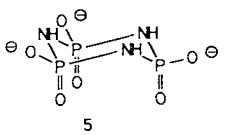

5

This hypothesis cannot actually be tested in the case of trimetaphosphate, since there are very few trimetaphosphate–metal complexes whose crystal structures have been characterized.[6, 7] By contrast, the coordination chemistry of the isoelectronic trimetaphosphimate ion with metal aqua ions has been thoroughly investigated by *Sokol, Rozanov* et al. The results indicate that this particular *O,O,O*-tripod ligand displays much weaker chelate formation than $L^{\ominus}$ due to the flexibility of its six-membered ring. For example, it acts only as a bidentate P=O ligand with respect to $Cu^{2\oplus}$ in the complex $[Cu(H_2O)_2\{P_3O_6(NH)_3\}_2]^{4\ominus}$.[24] The original chair conformation of the six-membered ring is so distorted that the third coordination site is turned away from the copper ion, leaving the axial position of the CuO_6 octahedron occupied by water. Consequently, the Cu^{II} ion acquires a coordination polyhedron that is quite elongated. On the other hand, the ligands $L^{\ominus}$ in the analogous compound $[Cu(L_{OEt})_2]$ function as tridentate P=O ligands, and the Jahn–Teller distortion of the CuO_6 octahedron is particularly small.[21] Trimetaphosphimate in the polymeric compounds $NaM^{II}\{P_3O_6(NH)_3\}\cdot 7H_2O$, M = Zn, Co, acts as a tridentate ligand bridging two zinc or cobalt ions, forming two M–O bonds to one metal ion and one bond to the other.[25] The praseodymium ion achieves the coordination number eight in the complex salt $K_{1.3}(NH_4)_{1.7}Pr\{P_3O_6(NH)_3\}_2\cdot 8H_2O$ through the fact that one trimetaphosphimate serves as a tridentate terminal ligand, while the second assumes the function of a pentadentate bridging ligand.[26]

3.2. How Stable are the Complexes?

In order to characterize the complexing ability of the ligands $L^{\ominus}$ quantitatively and to ascertain why the observed values are so high, *Anderegg* determined a series of stability constants and conducted thermochemical measurements.[27]

Close examination of the data in Table 1 reveals three striking facts:

Table 1. Complex stability constants $\log K_1$ and $\log \beta_2$ for $L^{\ominus}_{OEt}$ with mono- and divalent ions in 95% methanol/water.

$\log K_1$	$\log K_1/\log \beta_2$	$\log K_1/\log \beta_2$
H 8.8	Mg 9.2/15.9	Mn 9.4/16.6
Li 6.1	Ca 9.1/16.5	Co 9.4/15.6
Na 4.1	Sr 8.1/13.7	Ni 8.6
K 3.6	Ba 7.7/12.9	Cu 9.4/15.8
	Pb 9.2/14.6	Zn 9.1/14.6
		Cd 7.7/14.8

1) K_1 and β_2 are nearly independent of the size of the metal ions; a difference of only 1.5 logarithmic units (corresponding to a factor of 30) separates the smallest ion, $Mg^{2\oplus}$ (r = 65 pm), from the largest, $Ba^{2\oplus}$ (r = 135 pm). Apparently the "bite" of this tripod ligand is sufficiently flexible to accommodate the steric demands of the metal ion with little loss in stability.
2) The 1:1 complex with $Na^{\oplus}$ is less stable than *Lehn*'s cryptand complexes, but it is nevertheless more stable than crown ether complexes of $Na^{\oplus}$.
3) No selectivity is observed with respect to the 3d transition metal ions (Fig. 3). In the case of ethylenediamine, glycinate, malonate, and many other ligands, the complex stability constants increase along the Irving–Williams series from manganese through iron, cobalt, and nickel up to copper, decreasing again with zinc. The effect is especially

[*] In order to specify the substituent R on the phosphorus atom of $L^{\ominus}$, the abbreviation $L^{\ominus}_R$ will be used from this point on.

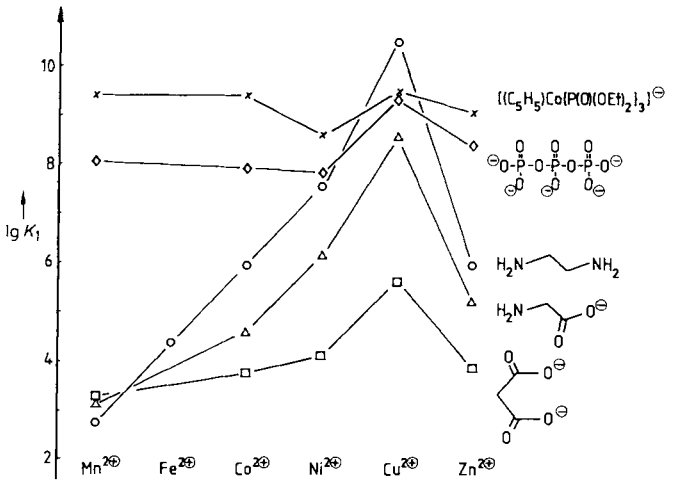

Fig. 3. Graphic representation of the complex stability constants $\log K_1$ of $L^{\ominus}_{OEt}$ and several typical chelating ligands with the metal ions $Mn^{2\oplus}$–$Zn^{2\oplus}$. K_1 is valid for the reaction $M^{2\oplus}$ + ligand $\rightleftharpoons$ M(ligand)$^{n\oplus}$.

prominent with ethylenediamine. Two ligands fail to conform to the Irving–Williams series: the oxygen tripod ligand $L^{\ominus}_{OEt}$ and tripolyphosphate. For both of these ligands, *all* the complex stability constants are high, and they are essentially independent of the nature of the metal ion. Thermochemical data explain the difference: ligands such as ethylenediamine conform to the Irving–Williams series because complex formation becomes increasingly *exothermic* from Mn to Cu, ΔH turning less strongly negative once again only with Zn. By contrast, complex formation with tripolyphosphate is significantly *endothermic*! The large K_1 values for tripolyphosphate are a consequence of an extraordinarily high entropy of complexation. The same is apparently true for the oxygen tripod ligands $L^{\ominus}$ as well.

$$Mg^{2\oplus}_{aq} + 2L^{\ominus} \overset{25\,^{\circ}C}{\rightleftharpoons} MgL_2, \quad \log\beta_2 = 16 \qquad (a)$$
$$\Delta S = 73\ \text{cal mol}^{-1}\,\text{K}^{-1}$$
$$T\Delta S = 22\ \text{kcal mol}^{-1}$$
$$\Delta H = 0\ \text{cal mol}^{-1}$$

Thermodynamic data confirm that the large formation constant in complexation according to Equation (a) (10^{16}) is a consequence solely of the entropy term. The value for ΔS (73 cal mol^{-1} K^{-1}) is many times larger than one would expect for the replacement of 6 mol of water by 2 mol of tripod ligand. An explanation is to be found in the fact that the oxygen tripod ligand $L^{\ominus}_{OEt}$ induces a considerable amount of structure in the solvent water, and this structure largely disappears upon complexation.

3.3. Oxygen Tripod Ligands $L^{\ominus}$; Weak and Hard!

Determining whether a ligand forms stable or unstable complexes with metal ions provides no insight whatsoever into the question of whether the ligand is strong or weak in terms of ligand field theory. The electronic spectra of complexes between oxygen tripod ligands and 3d transition metal ions such as $Ti^{3\oplus}$, $Co^{2\oplus}$, $Ni^{2\oplus}$, and $Cu^{2\oplus}$ present a clear picture: the spectra can be described to a close approximation as representing a summation of the (d-d)spectra for the MO_6 fragment and the ligand-internal transitions. Evaluation[18,28] of the (d-d)band positions makes it possible to arrange a set of ligands in both a spectrochemical[29] and a nephelauxetic series[29,30] (Fig. 4).

The oxygen tripod ligands are among the weakest of the oxygen ligands. They are significantly weaker than water, and fall roughly together with fluoride. They are also extremely hard ligands, with a position in the nephelauxetic series corresponding approximately to that of water or dimethylsulfoxide coordinated via oxygen. This finding may be interpreted as showing that the CpCo and Cp*Rh fragments provide no opportunity for delocalization of the d electron density of metal ions coordinated through the P=O bridges.[31] To a first approximation, the electronic properties of the tripod ligands are equivalent to those of fluoride or oxide.[32]

3.4. $[CoL_2]^{\oplus}$, the First Octahedral "Spin-Crossover" Co^{III} Complex

Co^{III} complexes are unusually numerous, and virtually all of them are hexacoordinate, kinetically inert, and diamagnetic, with d^6 low-spin electronic configurations.[33] This generalization has been a consistent feature of cobalt complex chemistry since the days of *S. M. Jörgensen* and *A. Werner*. The most prominent exception cited in textbooks is the paramagnetic d^6 high-spin ion $[CoF_6]^{3\ominus}$, first described by *Klemm* et al.[34] Since $[Co(H_2O)_6]^{3\oplus}$ displays a low-spin configuration[35] and $L^{\ominus}$ has electronic properties intermediate between those of fluoride and water, a question naturally arises about the magnetic characteristics of cobalt(III) complexes bearing the ligand $L^{\ominus}$. Are the $[CoL_2]^{\oplus}$ complexes also low-spin, or do they represent a second example of

Spectrochemical series $\Delta_o = f(\text{Ligand})$

$$\underline{Br}^{\ominus} < \underline{SCN}^{\ominus} < \underline{Cl}^{\ominus} < \underline{N_3}^{\ominus} < \underline{F}^{\ominus} \approx \boxed{L^{\ominus}} \approx \underline{DMSO} \approx \underline{OH}^{\ominus} < \underline{ox}^{2\ominus} < \underline{H_2O} < \underline{NH_3} < \underline{SO_3}^{2\ominus} < \underline{NO_2}^{\ominus} < \underline{CN}^{\ominus}$$

0.72 0.75 0.78 0.83 0.9 0.91 0.99 1.00 1.25 1.3 ~1.4 ~1.7

Nephelauxetic series

$$F^{\ominus} > H_2O > \boxed{L^{\ominus}} > DMSO > NH_3 > ox^{2\ominus} > en > \underline{SCN}^{\ominus} > \underline{Cl}^{\ominus} \approx \underline{CN}^{\ominus} > \underline{Br}^{\ominus} > \underline{N_3}^{\ominus} > \underline{I}^{\ominus}$$

Fig. 4. Positions of the ligands $L^{\ominus}$ in the spectrochemical and nephelauxetic series. Elements that are directly bound to the central atom of the complex are underlined.

octahedral cobalt(III) with a high-spin configuration, joining $[CoF_6]^{3\ominus}$?

We were able to prepare $[Co(L_{OEt})_2]PF_6$ by electrochemical oxidation of $[Co(L_{OEt})_2]$.[36, 37] The compound is dark green and paramagnetic at room temperature, but cooling causes it to become lemon-yellow and diamagnetic. The energy difference between the d^6/high-spin and d^6/low-spin electronic configurations for this compound apparently is of the same order of magnitude as kT. This situation is depicted graphically in Figure. 5. The magnetic properties of the compound are thus highly temperature-dependent. The observed thermochromism is also easily explained, because d^6/high-spin and d^6/low-spin correspond to two different chromophores.

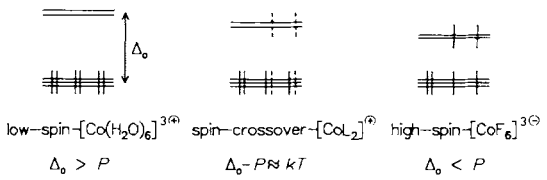

Fig. 5. d-Orbital splitting and magnetism of cobalt(III) complexes in an octahedral ligand field (one-electron approximation, Δ_0 = ligand field splitting, P = spin-pairing energy).

Altering the substituents on the phosphorus atoms of the tripod ligands makes it possible to adjust the state of the spin equilibrium in almost any way desired.[28, 38] Figure 6 illustrates this point through the temperature dependence of the chemical shift δ of the ^{31}P-NMR signal in the complexes $[Co(L_R)_2]^{\oplus}$ (**6a–6e**, R = Et, OMe, OEt, O*n*Bu, O*i*Pr). The cobalt(III) complexes **6b–e** containing O-alkyl-substituted ligands display temperature-dependent high-spin/low-spin equilibria, whereas complex **6a** with an ethyl-substituted ligand is diamagnetic throughout the examined temperature range. Apparently, replacing the electron-withdrawing O-alkyl group by the electron-releasing ethyl substituent leads to a larger ligand-field splitting, which in turn stabilizes the diamagnetic low-spin configuration.

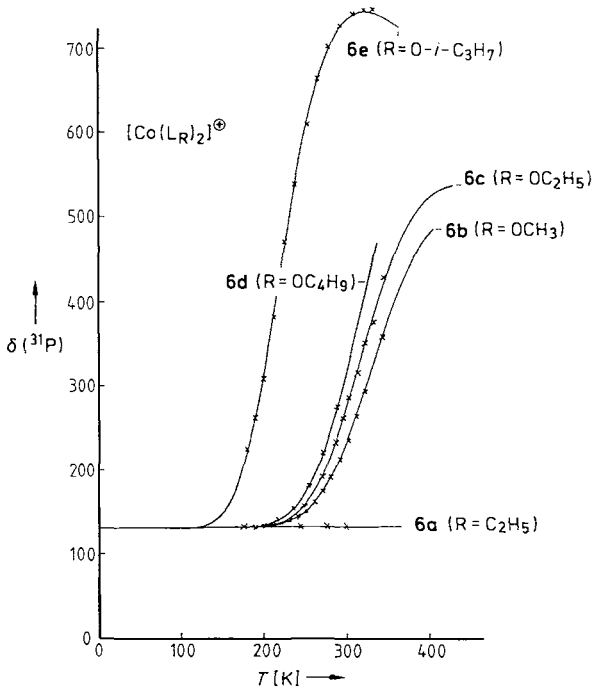

Fig. 6. Temperature dependence of ^{31}P-NMR chemical shifts of the cobalt(III) complexes $[Co(L_R)_2]^{\oplus}$ **6a–e**.

$L^{\ominus}_{OiPr}$ is the weakest ligand—but for steric, not electronic reasons. Repulsive intramolecular ligand-ligand interactions in $[Co(L_R)_2]^{\oplus}$ lead to an increased metal–ligand distance. This causes the ligand field strength to become smaller and the high-spin configuration more stable. The effect is most evident with **6e**, which at room temperature is almost 75% in the high-spin form. Spectroscopic characterizations and magnetic data provide a consistent picture of the tripod ligands: electronic or steric effects of substituents R make it possible to fine-tune the ligand field strength, but the ligands always display the characteristics of oxygen ligands that are both very weak *and* hard.

4. Organometallic Chemistry of the Oxygen Ligands $L^{\ominus}$

The placement of $L^{\ominus}$ between water and fluoride in the spectrochemical series means that these ligands can be compared in terms of their electronic characteristics with oxo ligands. Consequently, one might expect them to be quite effective at stabilizing metal ions in their middle and high oxidation states. Indeed, 2:1 complexes of $L^{\ominus}$ ligands are known for titanium (II, III, or IV) and vanadium(II, III, or IV), as are 1:1 complexes with molybdenum(V) and tungsten(VI).[39] The reduction potentials (III/II) for vanadium, chromium, and iron complexes of the type ML_2 are 950–1050 mV more negative than those of the corresponding aqua ions![37, 39] It is thus remarkable that the ligands $L^{\ominus}$ are also capable of stabilizing carbonylmetal fragments. For example, hexacarbonyltungsten reacts with NaL_{OEt} to produce the air-stable, dark red binuclear compound $[L_2W_2(CO)_4]$ **7**, which consists of two $LW(CO)_2$ fragments joined by a W≡W triple bond.[40]

Scheme 3 shows the reaction of NaL with the tropylium complexes $[(C_7H_7)M(CO)_3]^{\oplus}$ (M = Mo, W). Here, one carbon monoxide ligand is displaced, and the symmetrically η^7-coordinated C_7H_7 ring is transformed into a ring system with allylic (η^3) binding. The resulting free coordination sites are occupied by the three oxygen "teeth" of the tripod ligand. The compounds **8** may be regarded as analogous to the complexes **9**, since both $L^{\ominus}$ and $Cp^{\ominus}$ formally represent facially coordinated, monoanionic 6e ligands. Nevertheless, the CO-vibrational frequencies listed in Scheme 3 indicate that the similarity does not extend to electronic properties: the CO bands in **8** are 25–50 wave numbers lower than the CO bands in **9**.

The fluxional behavior characteristic of η^3 bound tropylium rings is present with both the $L^{\ominus}$ complexes and the isoelectronic cyclopentadienyl compounds[41] (cf. Fig. 7, upper half). Metallotropic rearrangement proceeds much more slowly with the tripod derivatives than in the case of the cyclopentadienyl compounds. This makes it possible by cooling to reduce the rate of the degenerate rearrangement of

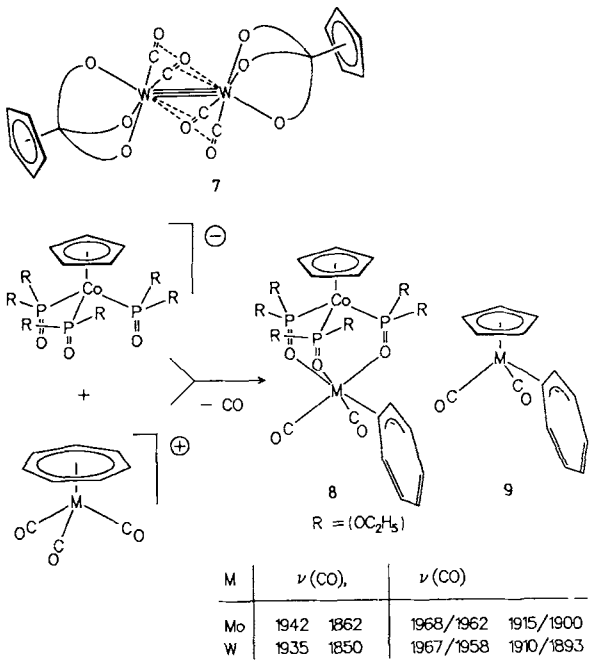

M	ν(CO),		ν(CO)	
Mo	1942	1862	1968/1962	1915/1900
W	1935	1850	1967/1958	1910/1893

Scheme 3. Synthesis and CO vibrational frequencies [cm^{-1}] of the tropylium complexes **8**. For purposes of comparison, the corresponding frequencies are also provided at the right for the Cp-analogues **9**.

the tropylium ring to such an extent that the molecules appear static on the NMR time scale (Fig. 7, lower half).

The higher stability of these compounds compared to the corresponding cyclopentadienyl derivatives is astonishing, since no oxygen ligands other than $L^{\ominus}$ are known to be capable of efficiently stabilizing the fragment $[Mo(\eta^3\text{-}C_7H_7)(CO)_2]^{\oplus}$. In contrast to $Cp^{\ominus}$, $L^{\ominus}$ is only weakly basic,[27] so many tripod complexes of carbonyl-metal fragments can be both prepared and subjected to reaction in aqueous medium. For example, the acetonitrile complexes $[(CH_3CN)_3M(CO)_3]$ (M = Cr, Mo, W) react smoothly in

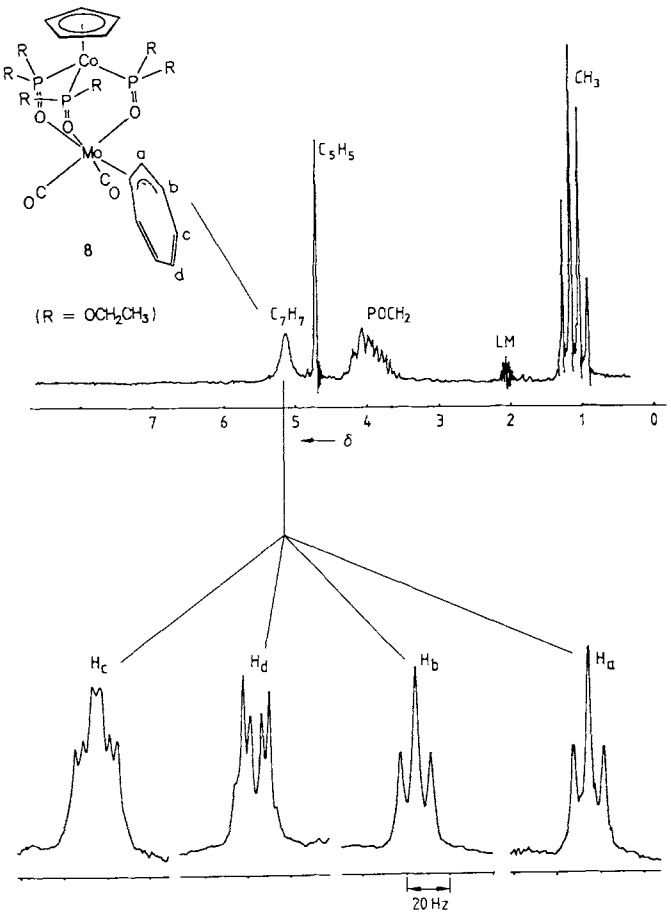

Fig. 7. ^{1}H-NMR spectrum of **8** for M = Mo. Above: entire spectrum (298 K, 60 MHz; LM = solvent [D_6]acetone). Below: region of C_7H_7 signal at 193 K (270 MHz).

water to give $[LM(CO)_3]^{\ominus}$ **10**.[42] Allyl, hydride, alkyl, and carbyne derivatives of carbonyl molybdenum and tungsten complexes can be equally effectively stabilized by $L^{\ominus}$. The

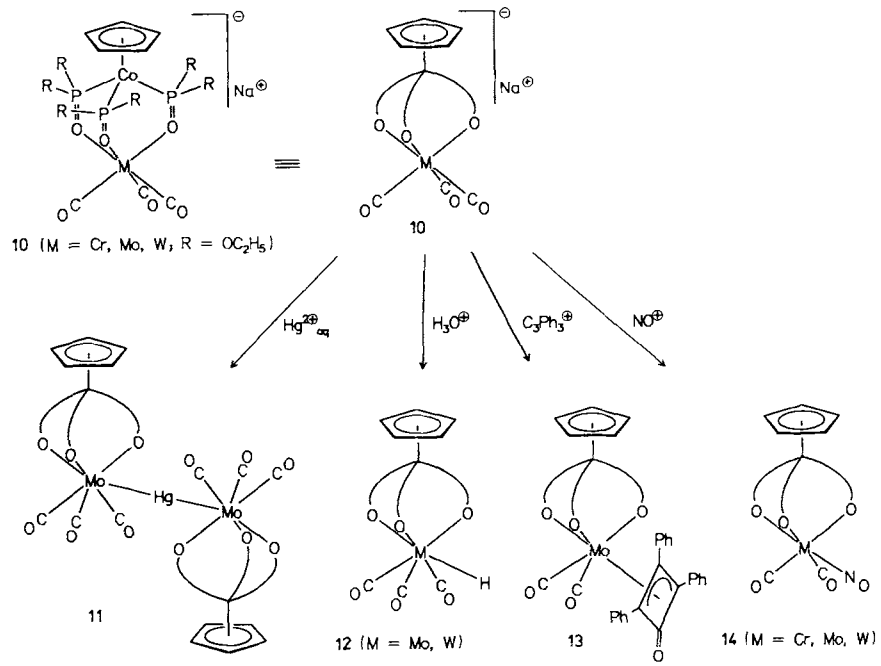

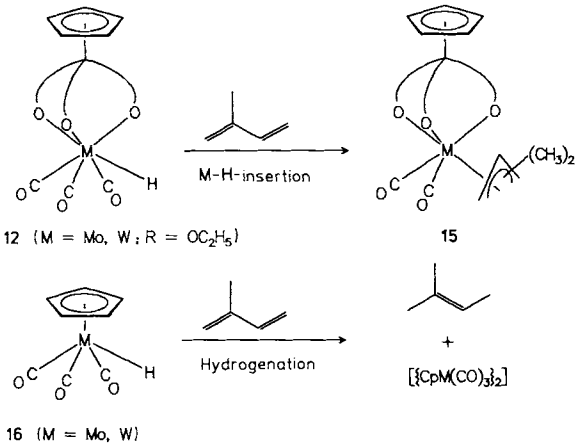

anionic tricarbonyl complexes **10** can be protonated to generate the hydrido species **12**; nevertheless, they also react with typical soft Lewis acids such as $Hg^{2\oplus}$, $C_3Ph_3^{\oplus}$, and $NO^{\oplus}$ to give **11**, **13** and **14**, respectively.[43]

In the reaction sequence $[LW(CO)_3]^{\ominus} \rightarrow [LW(CO)_3H] \rightarrow [L_2W_2O_5]$,[39] tungsten is oxidized from the oxidation state 0 to +VI. The "bite" of the tripod ligand apparently accommodates itself well to the sharply diminishing ionic radius, since the ligand is not cleaved during reaction. Isoprene can be inserted into the metal–hydrogen bond of the hydrido complex **12** (M = Mo, W, R = OC_2H_5), leading to the allylic complexes **15**,[39] while the analogous cyclopentadienyl compounds **16** react with conjugated dienes to give hydrogenation of the olefin and formation of the binuclear complexes $[\{(C_5H_5)M(CO)_3\}_2]$.[44]

The numerous examples of L/Mo and L/W combinations suggest that the oxophilicity of the early transition metals contributes to stability in these compounds. Nevertheless, most of the d elements have now been shown to form organometallic compounds with tripod ligands. Examples

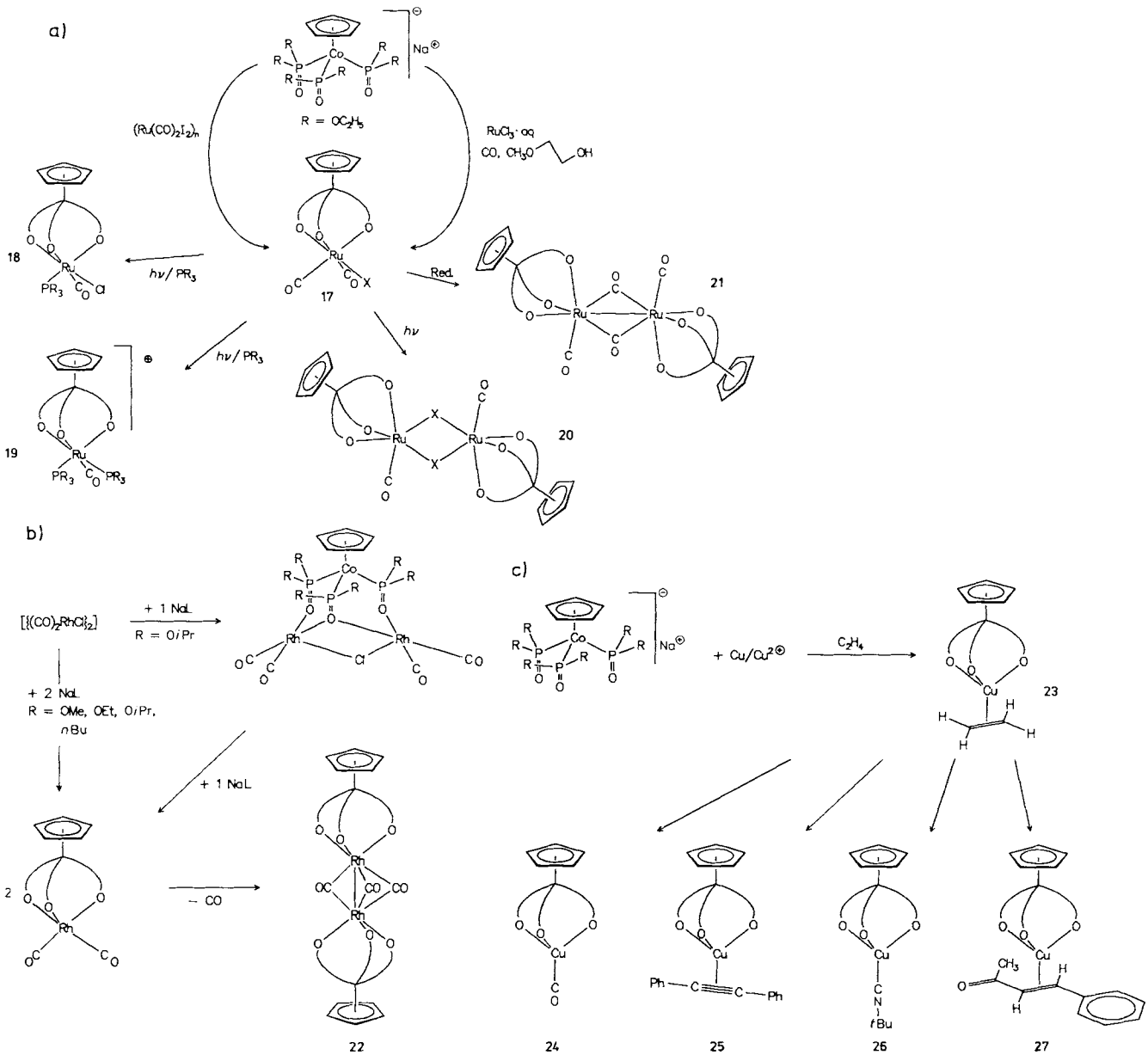

Scheme 4. Synthetic routes to a) ruthenium, b) rhodium, and c) copper(I) complexes with $L^{\ominus}$. **23**: synthesis in H_2O/pentane. ^1H NMR: $\delta = 4.0$ (C_2H_4) (Free C_2H_4: $\delta = 5.3$). **24**, R = C_2H_5: $\nu(CO) = 2040\ cm^{-1}$; cleavage of CO at 150 °C.

include $[LMn(CO)_3]$,[45] $[LRe(CO)_3]$,[45] the ruthenium complexes **17**–**21**,[43] $[LRu(C_6H_6)PF_6$,[18] Rh^I complexes of the type $[LRh(olefin)_2]$,[46] $[LRh(\mu\text{-}CO)_3RhL]$ **22**,[47,48] $[LRh(C_5Me_5)PF_6$,[18] $[LIr(CO)_2]$,[49] [LPd(dmba)] (where dmba = *o*-(*N*,*N*-dimethylaminobenzyl)-C^2,*N*-),[50] $[LPtMe_3]$,[51] and the Cu^I complexes **23**–**27**[16,52] (Scheme 4).

A characteristic feature is the clear increase in compound stability for the sequence 3d < 4d < 5d with metal ions of the sixth through eighth subgroups.

5. Oxygen Tripod Ligands $L^{\ominus}$: Good π-Donor Ligands!

Given the diversity of the organometallic compounds containing oxygen tripod ligands, a basic question arises as to why so many $LM(CO)_x$ complexes are so stable, even though the classification of the ligands $L^{\ominus}$ as "hard" suggests they should be best suited to stabilizing higher oxidation states of the metals. The key to understanding this situation lies in the apparent contradiction that, while $L^{\ominus}$ is a weak ligand according to ligand field theory, it nevertheless induces more extensive M → CO back-bonding in many carbonylmetal derivatives (i.e., a higher electron density at the metal) than is observed with other monoanionic 6e ligands. For example, the wave numbers of the CO vibrations in the molybdenum and tungsten carbyne complexes with the general composition [(6e ligand)M(≡CR)$(CO)_2$] decline by 25–50 cm^{-1} through the sequence $C_5H_5^{\ominus} > C_5Me_5^{\ominus} \approx B(pz)_4^{\ominus} \approx HB(pz)_3^{\ominus} > L_{OMe}^{\ominus} > L_{OiPr}^{\ominus}$ (pz = pyrazolyl).[53] The solution to the problem has already been disclosed in the title of this section: the oxygen tripod ligands are good π-donors. This phenomenon is further clarified in the MO-scheme in Fig. 8, which shows how σ- and π-interactions between metal and ligands affect the ligand field splitting in an octahedral complex.[54] In a), only the σ-donor capacity of the ligands is taken into account. Hence, the t_{2g} orbitals are precisely nonbonding, and the e_g orbitals are antibonding. With increasing σ-donor capacity the energy of the e_g orbitals increases, thus increasing the ligand field splitting Δ_0. The supplemental π interactions are treated separately in b) and c). A π-donor interaction causes the t_{2g} orbitals also to become antibonding, making Δ_0 smaller. On the other hand, π-acceptor interaction lowers the energy of the t_{2g} orbitals, and Δ_0 becomes larger. The experimentally observed ligand field splitting Δ_0 results from a combination of these three factors.

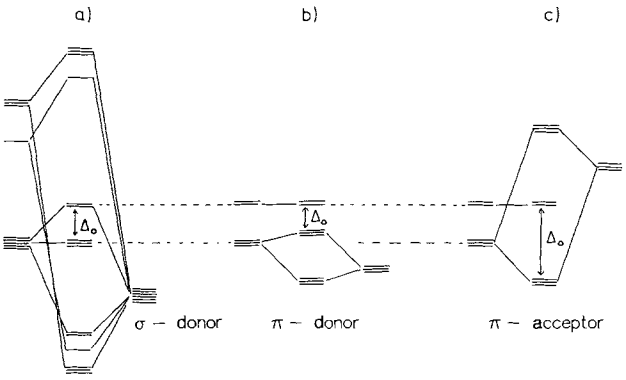

Fig. 8. The influence of σ-donor, π-donor, and π-acceptor capacity on the ligand field splitting Δ_0.

The remarkably small value of Δ_0 for complexes of the oxygen tripod ligands $L^{\ominus}$ can be explained by assuming that in comparison with most other oxygen ligands their π-donor capacity is stronger relative to their σ-donor capacity, whereas their π-acceptor capacity is negligible. The strong π-donor capacity of $L^{\ominus}$ causes an increase in energy in the t_{2g} orbitals, resulting in a smaller energy difference from the π* orbitals of coordinated CO ligands. This implies the possibility of better overlap and consequently stronger M → CO back-bonding, resulting in a lower CO-vibrational frequency. The stability of the $L^{\ominus}$-carbonylmetal derivatives containing oxygen tripod ligands is therefore a consequence of the interaction of two factors: the strong chelating effect of the ligands supports coordination at the metal center, and their extensive π-donor capability induces strong back-bonding in the existing metal-CO bonds. Interestingly, comparable effects can be observed in polyoxometallates, as has been demonstrated in the groundbreaking efforts of *Klemperer* et al.[55] and *Finke* et al.,[56] who showed that these materials can serve as models for metal oxide surfaces, and that they are capable of complexing organometallic fragments in the same way as the ligands $L^{\ominus}$. In the case of the alkoxide complexes of molybdenum and tungsten, the even higher π-donor capacity of the oxygen ligands is largely responsible for reactivity with respect to organic substrates, as demonstrated by *Chisholm* et al. in a series of experimental studies supported by Fenske–Hall MO calculations on model compounds.[57] Just as with complexes of the oxygen tripod ligands, clusters containing alkoxide ligands demonstrate especially large π-donor effects with the early heavy transition metals, an observation that can be explained by the reduction in d orbital energies within a given period as the atomic number increases.

6. Applications and Future Prospects

Several factors would indicate the potential for a broad spectrum of applications for the ligands $L^{\ominus}$, including their strong tendency to form complexes with ions of both transition and main-group metals, the fact that the phosphorus substituent R can be varied as a way of adjusting solubility over the range from exclusive water solubility to high solubility in saturated hydrocarbons, the thermal stability of the complexes, and their insensitivity with respect to acids and oxidizing agents. This review concludes with consideration of a few important new developments and certain specific applications that are already foreseeable.

Shinar and *Navon* have recently discovered the ionophoric characteristics of the ligands $L^{\ominus}$, noting that $L_{OEt}^{\ominus}$ is a very efficient transporter of alkali metal ions through phospholipid membranes. Moreover, the lithium ions in a LiCl/NaCl solution are transported through a membrane composed of phosphatidylcholine vesicles much more rapidly than sodi-

um ions. Competition experiments have shown the lithium/sodium selectivity to exceed a factor of 40.[58] The transport mechanism itself has not yet been fully clarified, but the principal cause of the selectivity may be the fact that the lithium salt LiL_{OEt} exists as the dimer **28** in lipophilic medium,[59] whereas NaL_{OEt} forms trimers with the composition $Na_3L_3(H_2O)_2$ **29**.[39]

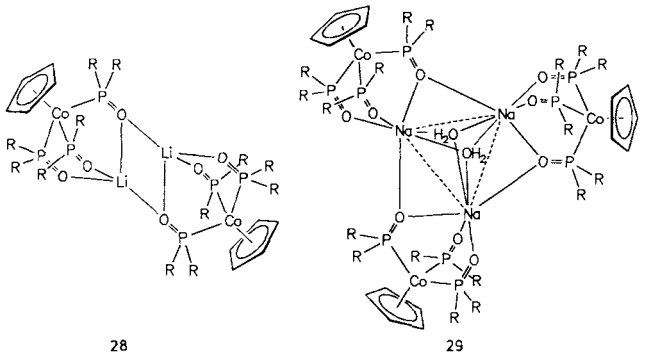

28 29

The biochemistry of such ionophores is currently under intensive investigation due to potential medical significance in the context of lithium therapy.

Other studies in which we are currently engaged relate to the use of $L^{\ominus}$ species as components in phase-transfer reactions and in catalysts for organometallic conversions. One particularly attractive feature in this regard is the fact that (see Scheme 2) it is relatively easy to synthesize chiral ligands $L^{\ominus}$ possessing C_{3v} symmetry.

In Section 5, a plausible argument was made for interpreting the stabilization of low oxidation states in transition metal complexes by oxygen tripod ligands as a consequence of synergistic effects between opposing π-donor and π-acceptor ligands. For many catalytic applications this means that either the energies of key intermediates are much too high, or else the tripod complexes formed as intermediates are too stable. On the other hand, the situation becomes considerably more promising if the metal ion coordinated to $L^{\ominus}$ remains in a high oxidation state throughout the catalytic cycle. In this case, stability is essentially a function of the chelate effect and electrostatic interaction between the tripod ligand and the metal ion, a typical situation in oxygen-transfer reactions, for example.

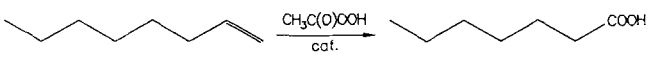

Scheme 5. The oxidation of 1-octene to heptanoic acid by peracetic acid, using $[L_{OEt}Ru(CO)_2Cl]$ as catalyst precursor. Reaction conditions: aqueous solution, 10% excess of peracetic acid, 60 → 20 °C. Yield: 75% (with catalyst 1:4000), 4% (without catalyst)

Scheme 5 illustrates an application of this type, in which a ruthenium tripod complex catalyzes the peracetic acid oxidation of 1-octene to heptanoic acid.[60] The oxoruthenium complex that presumably forms here has not yet been identified. Similarly, oxovanadium tripod complexes can play a role as catalyst precursors in other oxygen-transfer reactions.[61]

Many reactions of low-valent organometallic fragments in tripod ligand complexes might be regarded as attractive models for reactions at the surfaces of heterogeneous metal oxide catalysts, but for the reasons described above the observed catalytic activity is not particularly great. In an attempt to achieve higher reactivities we are currently pursuing two different strategies. On the one hand, we have synthesized tripod ligands such as **30** that contain long, functionalized side-chains. These supplementary donor centers are intended to behave as "dangling ligands" that could assist in the stabilization of unsaturated intermediates in catalytic cycles, adding a type of coordinative stabilization that is easily displaced. Such functionalized ligands have permitted

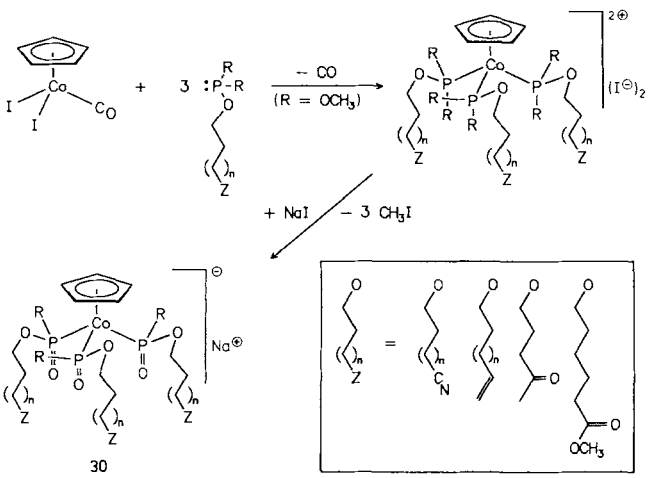

us, for example, to develop catalysts for the hydrogenation of C=C double bonds, the oligomerization of acetylenes, and hydroformylation, catalysts that are significantly more reactive than the corresponding complexes with non-functionalized ligands. Ligands of this novel type appear promising for a host of other catalytic cycles as well.[62]

As a second possibility for controlling the reactivity of tripod ligands, we have designed structures that possess only two strongly coordinating P=O centers, where a halogen, for example, serves as a weak third ligand site. Such an *O,O,X*-tripod ligand must of course be inert—a species that, apart from its function as a chelating ligand, enters into no other chemical reactions—and this imposes severe restrictions on the choice of potential candidates. Of the many systems we have investigated, the ruthenium(II) complex $\mathbf{31}^{\ominus}$ appears to be the most suitable. The protonated form of this *O,O,Cl*-ligand (**31** H) is readily accessible, and we have recently described its synthesis, together with preliminary information regarding its coordination chemistry.[63]

We were somewhat astonished by the discovery that the copper(II) complex **32** is transformed in the space of a few hours into the carbonylcopper complex **33** by room-temperature treatment with CO gas and copper metal in methanol.[63] It is remarkable how rapidly the copper dissolves and **33** forms in this reaction, especially since **32** is virtually insoluble in methanol. Another interesting reaction we have observed is the oxidative addition of the O-H bond of **31** · H to tungsten(0) and molybdenum(0) centers, leading to the hydrido-metal complexes **34**.[64] The willingness with which the

carbonylcopper complex **33** and the hydrido complex **34** arise suggests interesting potential syntheses for these ligands in the field of organometallic chemistry. One can foresee that the synthetic pathway[64] to *O,O,Cl*-ligands **31**$^{\ominus}$ might be broadened to include other *O,O,X*-ligands in which

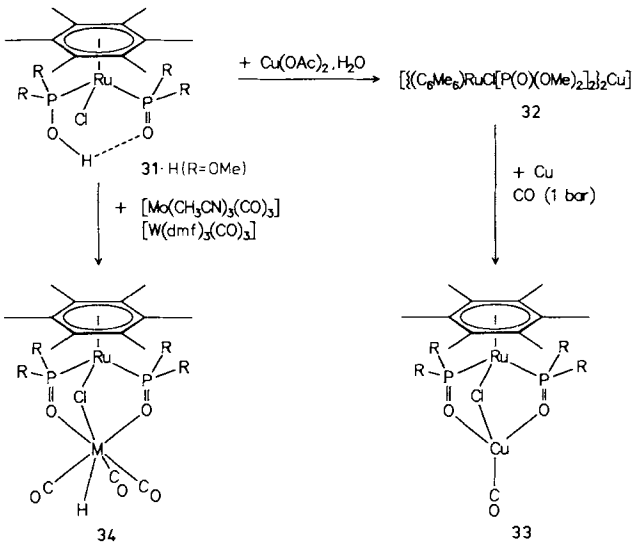

X might represent not only halogen, but also a sulfur or a nitrogen donor center. The extent to which such ligands would also be suited to conferring other new and interesting reaction possibilities on metal ions remains to be determined.

I wish to express my appreciation to all those colleagues who have been involved in this work, in particular to my co-workers H.-O. Asbahr, E. Buchholz, W. Eberspach, B. Engels, K. Evertz, H. Hamers, B. Lenders, A. Müller, H.-J. Schulte, C-E. Song, and A. Weber-Schuster. I am especially grateful to my colleague M. Scotti for his friendly collaboration, made possible by financial support from the Volkswagen-Stiftung. Thanks are due to the firms Bayer, Hoechst, BASF, Degussa, and Heraeus for gifts of chemicals. The Deutsche Forschungsgemeinschaft and the Fonds der Chemischen Industrie have regularly provided generous support for my scientific efforts.

Received: May 3, 1989 [A 763 IE]
German Version: *Angew. Chem. 102* (1990) 661
Translated by Dr. *W. E. Russey*, Huntingdon, PA (USA)

[1] The systematic names of the ligands L$^{\ominus}$ [e.g., cyclopentadienyltris(diorganylphosphito-*P*)cobaltate, also -phosphinito- or -phosphonito-] are based on the groups P(O)R'R'' bound to the cobalt(III) center. The anions P(O$^{\ominus}$)(OR)$_2$ are called phosphito ligands since they represent phosphorous acid diesters, while the anions P(O$^{\ominus}$)R$_2$ (phosphinito ligands) and P(O$^{\ominus}$)(OR)R (phosphonito ligands) are derivatives of phosphinic and phosphonic acid, respectively.

[2] Review articles dealing with the chemistry of the P=O functional group: a) E. E. Nifant'ev, *Russ. Chem. Rev. (Engl. Transl.) 47* (1978) 835; b) D. M. Roundhill, R. P. Sperline, W. B. Beaulieu, *Coord. Chem. Rev. 26* (1978) 263; c) B. Walther, *ibid. 60* (1984). 67.

[3] The complexes of the type L$^{\ominus}$ constitute the first examples of monoanionic tridentate oxygen ligands with C_{3v} symmetry. No organic ligands of this type exist. Hexaethyl-*P,P',P''*-phosphanetriyltris(phosphonate) P{P(O)(OEt)$_2$}$_3$[4] (described by *Weber* and *Fluck*[5]), the trimetaphosphate ion $[P_3O_9]^{3\ominus}$,[6, 7] and the trimetaphosphimate ion $[P_3(NH)_3O_3]^{3\ominus}$[8, 9] are also capable of acting through their P=O groups as tridentate oxygen ligands.

[4] H. W. Roesky, H. Djarrah, M. Thomas, B. Krebs, G. Henkel, *Z. Naturforsch. B38* (1983) 168.

[5] D. Weber, E. Fluck, *Z. Naturforsch. B30* (1975) 60.
[6] C. J. Besecker, W. G. Klemperer, *J. Organomet. Chem. 205* (1981) C31.
[7] C. I. Besecker, V. W. Day, W. G. Klemperer, *Organometallics 4* (1985) 564.
[8] V. L. Sokol, M. A. Porai-Koshits, V. R. Berdnikov, I. A. Rozanov, L. A. Butman, *Sov. J. Coord. Chem. (Engl. Transl.) 1* (1975) 341.
[9] L. K. Shubochkin, O. V. Popov, E. F. Shubochkina, V. I. Sokol, I. A. Rozanov, L. A. Butman, *Sov. J. Coord. Chem. (Engl. Transl.) 3* (1977) 700.
[10] W. Kläui, H. Neukomm, H. Werner, G. Huttner, *Chem. Ber. 110* (1977) 2283.
[11] W. Kläui, W. Eberspach, R. Schwarz, *J. Organomet. Chem. 252* (1983) 347.
[12] W. Kläui, *Z. Naturforsch. B34* (1979) 1403.
[13] We have recently shown that the first step of the reaction of cobaltocene with secondary phosphane oxides HP(O)R$_2$ proceeds via hydrogen elimination to thermally labile cobalt(I) complexes with the composition $[(C_5H_5)Co\{exo\text{-}1\text{-}[P(O)R_2]C_5H_5\}]$.[14] The subsequent steps have not yet been clarified.
[14] W. Kläui, C.-E. Song, *Inorg. Chem. 28* (1989) 3845.
[15] K. Evertz, *Diplomarbeit*, Technische Hochschule Aachen 1984.
[16] W. Kläui, B. Lenders, B. Hessner, K. Evertz, *Organometallics 7* (1988) 1357.
[17] *R* and *S* refer to the configurations of the three phosphorus centers in L$^{\ominus}$.
[18] W. Kläui, H. Otto, W. Eberspach, E. Buchholz, *Chem. Ber. 115* (1982) 1922.
[19] W. Kläui, *Helv. Chim. Acta 60* (1977) 1296.
[20] W. Kläui, K. Dehnicke, *Chem. Ber. 111* (1978) 451; B. Kamenar, A. Hergold-Brundić, M. Bruvo, *Z. Kristallogr. 184* (1988) 103.
[21] E. Dubler, L. Linowsky, W. Kläui, *Transition Met. Chem. (Weinheim Ger.) 4* (1979) 191.
[22] W. Kläui, *J. Organomet. Chem. 184* (1980) 49.
[23] E. M. Holt, W. Kläui, J. J. Zuckerman, *J. Organomet. Chem. 335* (1987) 29.
[24] V. I. Sokol, L. Ya. Medvedeva, L. A. Butman, I. A. Rozanov, *Sov. J. Coord. Chem. (Engl. Transl.) 2* (1976) 434.
[25] I. A. Rozanov, L. Ya. Medvedeva, E. N. Beresnev, Yu. A. Sokolov, V. I. Sokol, *Russ. J. Inorg. Chem. (Engl. Transl.) 26* (1981) 359.
[26] V. I. Sokol, M. A. Porai-Koshits, V. R. Berdnikov, I. A. Rozanov, L. A. Butman, *Sov. J. Coord. Chem. (Engl. Transl.) 5* (1979) 865.
[27] G. Anderegg, W. Kläui, *Z. Naturforsch. B36* (1981) 949.
[28] W. Kläui, W. Eberspach, P. Gütlich, *Inorg. Chem. 26* (1987) 3977.
[29] C. K. Jørgensen: *Modern Aspects of Ligand Field Theory*, North-Holland Amsterdam, 1971.
[30] C. K. Jørgensen, *Prog. Inorg. Chem. 4* (1962) 73.
[31] For this reason it is also understandable that the pentamethylcyclopentadienyl rhodium ligands are electronically almost indistinguishable from the cyclopentadienyl cobalt ligands.
[32] The ligand field strength and hardness of oxide ions can of course not be discussed without taking into consideration the influence of the host lattice. That this influence can be of decisive importance has been demonstrated by *Reinen* on the basis of ligand field spectra of Ni^{II} on oxide host lattices: D. Reinen, *Theor. Chim. Acta 5* (1966) 312.
[33] F. A. Cotton, G. Wilkinson: *Advanced Inorganic Chemistry*, 5th Ed. Wiley, New York 1988, Chapters 18 - F-4.
[34] W. Klemm, W. Brandt, R. Hoppe, *Z. Anorg. Allg. Chem. 308* (1961) 179.
[35] D. A. Johnson, A. G. Sharpe, *J. Chem. Soc. A 1966*, 798.
[36] W. Kläui, *J. Chem. Soc. Chem. Commun. 1979*, 700.
[37] N. El Murr, A. Chaloyard, W. Kläui, *Inorg. Chem. 18* (1979) 2629.
[38] W. Eberspach, N. El Murr, W. Kläui, *Angew. Chem. 94* (1982) 919; *Angew. Chem. Int. Ed. Engl. 21* (1982) 915; *Angew. Chem. Suppl. 1982*, 1943.
[39] W. Kläui, A. Müller, W. Eberspach, R. Boese, I. Goldberg, *J. Am. Chem. Soc. 109* (1987) 164.
[40] W. Kläui, A. Müller, R. Herbst, E. Egert, *Organometallics 6* (1987) 1824.
[41] W. Kläui, A. Müller, G. Hägele, unpublished.
[42] W. Kläui, A. Müller, M. Scotti, *J. Organomet. Chem. 253* (1983) 45.
[43] A. Müller, *Dissertation*, Technische Hochschule Aachen 1985.
[44] A. Miyake, H. Kondo, *Angew. Chem. 80* (1968) 663, 968; *Angew. Chem. Int. Ed. Engl. 7* (1968) 631, 880.
[45] W. Kläui, J. Okuda, M. Scotti, M. Valderrama, *J. Organomet. Chem. 280* (1985) C26.
[46] M. Scotti, M. Valderrama, S. Rojas, W. Kläui, *J. Organomet. Chem. 301* (1986) 369.
[47] W. Kläui, M. Scotti, M. Valderrama, S. Rojas, G. M. Sheldrick, P. G. Jones, T. Schroeder, *Angew. Chem. 97* (1985) 697; *Angew. Chem. Int. Ed. Engl. 24* (1985) 683.
[48] C.-E. Song, *Dissertation*, Technische Hochschule Aachen 1988.
[49] W. Kläui, H.-O. Asbahr, unpublished.
[50] W. Kläui, M. Pfeffer, unpublished.
[51] A. Nettle, M. Valderrama, R. Contreras, M. Scotti, K. Peters, H. G. von Schnering, H. Werner, *Polyhedron 7* (1988) 2095.
[52] B. Lenders, *Dissertation*, Technische Hochschule Aachen 1988; B. Lenders, W. Kläui, M. Irmler, G. Meyer, *J. Chem. Soc.*, Dalton Trans., in press; W. Kläui, B. Lenders, *Chem. Ber.*, in press.
[53] W. Kläui, H. Hamers, *J. Organomet. Chem. 345* (1988) 287 and references cited therein.

[54] See, for example, J. K. Burdett: *Molecular Shapes – Theoretical Models of Inorganic Stereochemistry*, Wiley, New York 1980, Chapters 9 and 12.
[55] C. J. Besecker, V. W. Day, W. G. Klemperer, M. R. Thompson, *Inorg. Chem. 24* (1985) 44, and references cited therein.
[56] R. G. Finke, B. Rapko, P. J. Domaille, *Organometallics 5* (1986) 175, and references cited therein.
[57] M. H. Chisholm, D. L. Clark, *Comments Inorg. Chem. 6* (1987) 23; M. H. Chisholm, B. K. Conroy, D. L. Clark, J. C. Huffman, *Polyhedron 7* (1988) 903, and references cited therein.
[58] H. Shinar, G. Navon, W. Kläui, *J. Am. Chem. Soc. 108* (1986) 5005.
[59] I. Goldberg, H. Shinar, G. Navon, W. Kläui, *J. Inclusion Phenom. 5* (1987) 181.
[60] M. Sojka, unpublished.
[61] E. Roman, F. Tapia, M.-T. Barrera, M. Garland, J.-Y. Le Marouille, C. Giannotti, *J. Organomet. Chem. 297* (1985) C 8.
[62] W. Bertleff, D. Köffer, W. Kläui, C.-E. Song, EP 89 109 979.8, 1989 (BASF AG).
[63] W. Kläui, E. Buchholz, *Angew. Chem. 100* (1988) 603; *Angew. Chem. Int. Ed. Engl. 27* (1988) 580.
[64] W. Kläui, E. Buchholz, *Inorg. Chem. 27* (1988) 3500.

Communications may be submitted in English *or* in German. Further details regarding the submission of communications can be found in the "Notice to Authors" reproduced in the January issue of the journal. Copies thereof may be obtained from the editorial office upon request.

Synthesis, Structure, and Gas-Phase Decomposition of $[Cd(EC_6H_2tBu_3)_2]_2$ (E = S, Se): First Examples of Low-Coordinate Volatile Cadmium Chalcogenolato Complexes[**]

By *Manfred Bochmann,* Kevin Webb, Mary Harman,* and *Michael B. Hursthouse*

As is well known, most thiolato and selenolato complexes of zinc, cadmium, and mercury are soluble only in coordinating polar solvents and possess polymeric nonmolecular lattice frameworks with bridging ligands.[1] For cadmium, these characteristics are exemplified by the polyadamantanoid structure of $[Cd(SPh)_2]_n$.[2] Although attempts have been made to use nonvolatile thiolato compounds such as $[M(SMe)_2]_n$ (M = Zn, Cd) as sources for metal sulfides,[3] polymeric compounds are clearly not suitable for the deposition of metal chalcogenides under more typical MOCVD[4] conditions. However, the introduction of ligands with high steric hindrance is highly effective in reducing the degree of association and thereby increasing the volatility of chalcogenide complexes. Following the demonstration of this principle for the gas-phase deposition of TiS films,[5] we now report the synthesis, structure, and gas-phase thermolysis of volatile cadmium thiolato and selenolato complexes.

The reaction of the bulky thiol **1a** with $Cd[N(SiMe_3)_2]_2$ in hexane at room temperature gives **2a** as colorless crystals [Eq. (a)]. The analogous reaction with the selenol **1b** affords

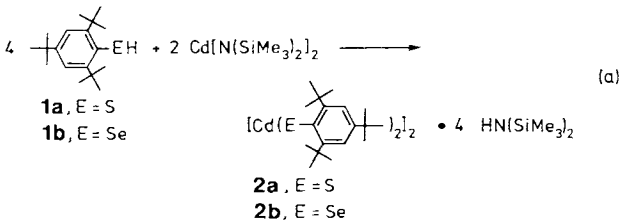

(a)

the bright yellow complex **2b**. Both complexes are moderately soluble in noncoordinating solvents such as toluene from which they are recrystallized.

The structure of **2a** (Fig. 1)[6] confirms that the complex is dimeric in the solid state with two terminal and two asymmetrically bridging thiolato ligands. Each cadmium is coordinated to three sulfur atoms in a trigonal-planar arrangement; there are no close contacts between neighboring dimer units in the crystal. To our knowledge such a coordination geometry has not been observed before for a cadmium chalcogenide complex.[8] In general, cadmium chalcogenides show a strong preference for a tetrahedral ligand environment, even in cases of significant steric crowding, as found for example in **3**.[9]

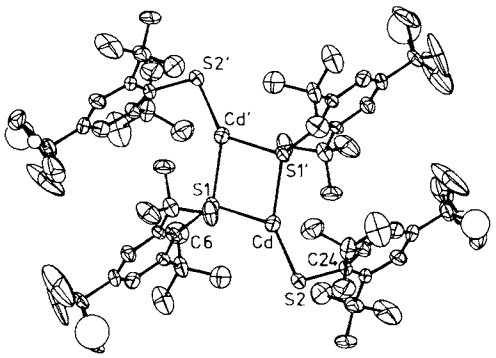

Fig. 1. Molecular structure of **2a** (ORTEP, ellipsoids correspond to 50% probability). Severe disorder in some *tert*-butyl groups required modeling with more than three carbon positions. Selected bond lengths [Å] and angles [°]: Cd-S1 2.499(6), Cd-S1' 2.583(7), Cd-S2 2.377(6), Cd-Cd' 3.798(6); S1-Cd-S1' 83.3(2), Cd-S1-Cd' 96.8(2), S1-Cd-S2 133.4(1), Cd-S1-C6 115.3(6), Cd-S2-C24 97.9(6).

$[Cd(SC_6H_2iPr_3)_2(1\text{-methylimidazole})_2]$ **3**

The Cd_2S_2 four-membered ring forms a planar parallelogram, with the two Cd–S distances differing by almost 0.1 Å [2.499(6) vs. 2.583(7) Å]. In $[Cd(SPh)_2]_n$, by comparison, intermediate Cd–S bond lengths are found (2.543 and 2.530 Å).[2] By contrast, the terminal Cd–S2 distances in **2a** are remarkably short [2.377(4) Å], even compared to Cd–S distances of terminal thiolato ligands in related complexes such as the tetrahedral monomeric complex **3** [average 2.46 Å],[9] and may suggest a degree of Cd–S multiple bonding due to interaction of the coordinatively unsaturated cadmium with a sulfur lone pair. Preliminary X-ray data confirm that **2b** has an analogous dimeric structure.[10]

The ^1H NMR spectra of **2a** and **2b** in weakly coordinating solvents (CD_2Cl_2, $CDCl_3$, $[D_8]$toluene) are surprisingly simple and show only one singlet each for the *ortho*- and *para*-*tert*-butyl groups and the aromatic *meta*-protons. The spectra are essentially temperature-independent. On cooling the solutions to −40 °C the signals for the *ortho*-*tert*-butyl groups broaden due to hindered rotation, before the compounds precipitate on further cooling. There is no evidence for ligand-exchange processes or for the appearance of two separate signal sets which would be expected for the terminal and bridging ligands on the basis of the solid-state structures. The data suggest therefore that the complexes **2a** and **2b** are monomeric in solution, with two-coordinate metal

[*] Dr. M. Bochmann, K. Webb
School of Chemical Sciences
University of Chemical Sciences
University of East Anglia
GB-Norwich NR4 7TJ (UK)
Dr. M. Harman, Prof. M. B. Hursthouse [*]
Department of Chemistry
Queen Mary and Westfield College
Mile End Road, GB-London E1 4NS (UK)

[+] X-ray crystallography

[**] This work was supported by the Science and Engineering Research Council (UK) and the Royal Signals and Radar Establishment. We thank Dr. *J. E. Hails* for valuable discussions.

centers.[11] The cadmium complexes resemble in this respect comparable sterically hindered compounds of mercury, such as $Hg(EC_6H_2R_3\text{-}2,4,6)_2$ (E = S, R = *i*Pr, *t*Bu; E = Se, R = *t*Bu).[12]

Compounds **2a** and **2b** are thermally very stable and sublime at 10^{-2} torr above 320 and 240 °C, respectively. Under mass spectrometry conditions both monomeric and dimeric species are present in the gas phase [**2a**: $Cd(SAryl)_2^{\oplus}$, *m/z* 668, 100%; $Cd_2(SAryl)_3^{\oplus}$, *m/z* 1057, 22%]. Compound **2a** decomposes thermally above ca. 400 °C, **2b** above ca. 300 °C. The volatility of **2a** and **2b** has been utilized for the deposition of metal chalcogenides from the gas phase under reduced pressure. In preliminary experiments on glass targets, **2a** produced smooth transparent golden-yellow films of CdS at 450 °C/10^{-2} torr. The main organic byproduct is $(C_6H_2tBu_3)_2S$. Under comparable conditions at 350 °C, **2b** deposits brown films of CdSe; scanning electron microscopy reveals that these are polycrystalline. The composition of the films was confirmed by energy-dispersive X-ray analysis. Deposition studies on crystalline targets such as GaAs are in progress.

Experimental Procedure

2a: All experiments were carried out under inert gas. To a solution of thiol **1a** (1.0 g, 3.6 mmol) [13] in 20 mL of light petroleum ether (b.p. 40–60 °C) at room temperature was added via syringe a solution of $Cd[N(SiMe_3)_2]_2$ (0.77 g, 1.8 mmol) [14] in 5 mL of petroleum ether. After a few seconds a white precipitate was formed. The mixture was stirred for 1 h before the residue was filtered off and washed with 2 × 20 mL of petroleum ether. The product was recrystallized from warm toluene to give **2a** as colorless needles (0.67 g, 56%). The solid complex is air-stable, but solutions are subject to slow hydrolysis with liberation of **1a**. ^1H NMR (400 MHz, CD_2Cl_2, 25 to −40 °C): δ = 1.25 (s, 9H, *p*-*t*Bu), 1.77 (s, 18H, *o*-*t*Bu), 7.2 (s, 2H).

1b: The compound has been briefly mentioned in a footnote [13]. To a solution of $(C_6H_2tBu_3Se)_2$ (0.685 g, 1.06 mmol) [15] in 40 mL of THF under nitrogen and with exclusion of light was added via syringe 2.1 mmol of $LiBEt_3H$ (1 M solution in THF, 2.1 mL) at room temperature. The pale yellow solution was stirred for 30 min and cooled to −78 °C. After the dropwise addition of $HBF_4 \cdot Et_2O$ (1.0 g, 6 mmol) over 5 min, the mixture was allowed to warm to room temperature. The solvent was removed and the residue taken up in 30 mL of 40/60 petroleum ether, filtered, and concentrated to give **1b** as a white crystalline solid (0.55 g, 1.69 mmol, 80%), m.p. 172–173 °C (lit. [13] 176.5–177.5 °C). Correct elemental analysis. ^1H NMR (60 MHz, $CDCl_3$): δ = 1.40 (s, 9H, *p*-*t*Bu), 1.66 (s, 18H, *o*-*t*Bu), 1.92 (s, 1H, Se-H), 7.35 (s, 2H). ^{77}Se NMR (17.08 MHz, $CDCl_3$, relative to neat Me_2Se): δ = 139.9 (d, ^1J(Se,H) 51.9 Hz).

2b: The complex was prepared following the procedure given for **2a** from **1b** (0.456 g, 1.4 mmol) and $Cd[N(SiMe_3)_2]_2$ (0.31 g, 0.7 mmol) as bright yellow crystals (0.42 g, 0.55 mmol, 79%). Correct elemental analysis. ^1H NMR (90 MHz, $CDCl_3$): δ = 1.28 (s, 9H), 1.56 (s, 18H), 7.24 (s, 2H).

Received: February 6, 1990 [Z 3783 IE]
German version: *Angew. Chem. 102* (1990) 703

CAS Registry numbers:
2a, 127086-57-1: **2b**, 127086-58-2; CdS, 1306-23-6; CdSe, 1306-24-7.

[1] I. G. Dance, *Polyhedron 5* (1986) 1037.
[2] D. Craig, I. G. Dance, R. Garbutt, *Angew. Chem. 98* (1986) 178; *Angew. Chem. Int. Ed. Engl. 25* (1986) 165.
[3] K. Osakada and T. Yamamoto, *J. Chem. Soc. Chem. Commun. 1987*, 1117. Polymeric cadmium thiolates of S-N ligands (e.g., cadmiumbis(pyridine-1-thiolate)) depolymerize at elevated temperatures and produce CdS: P. O'Brien, Queen Mary and Westfield College, London, personal communication.
[4] MOCVD = Metal-Organic Chemical Vapor Deposition.
[5] M. Bochmann, I. Hawkins, L. M. Wilson, *J. Chem. Soc. Chem. Commun. 1988*, 344.
[6] **2a**: Needles from toluene. A needle fragment of the dimensions 0.15 × 0.5 × 0.3 mm^3 was used. Monoclinic, space group $P2_1/n$, a = 10.068(2), b = 19.991(2), c = 17.874(2) Å, β = 91.76(1)°, V = 3595.91 $Å^3$, Z = 4, ϱ_{calcd} = 1.23 g cm^{-3}, μ = 7.364 cm^{-1} ($Mo_{K\alpha}$); $1.5 \le \theta \le 22°$, 4395 unique reflections measured, 2677 observed [$F_o > 3\sigma(F_o)$], 367 parameters in least squares, final R = 0.060 (R_w = 0.079, $w = [\sigma^2(F_o) + 0.00188\,F_o]^{-1}$). The structure was solved via the heavy-atom method following previously detailed procedures [7]. Further details on the crystal structure analysis are available from the Director of the Cambridge Crystallographic Data Centre, University Chemical Laboratory, Lensfield Road, GB-Cambridge CB2 1EW, on quoting the full journal citation.
[7] R. A. Jones, M. B. Hursthouse, K. M. A. Malik, G. Wilkinson, *J. Am. Chem. Soc. 101* (1979) 4128.
[8] Another example for a trigonal-planar coordination geometry of cadmium is $[MeCdPtBu_2]_3$: B. L. Benac, A. H. Cowley, R. A. Jones, C. M. Nunn, T. C. Wright, *J. Am. Chem. Soc. 111* (1989) 4986. Since the submission of this communication a report on the structure of $[Cd(SC_6H_2iPr_3\text{-}2,4,6)_3]^{\ominus}$ has appeared: E. S. Gruff, S. A. Koch, *J. Am. Chem. Soc. 112* (1990) 1245.
[9] D. T. Corwin, E. S. Gruff, S. A. Koch, *J. Chem. Soc. Chem. Commun. 1987*, 966.
[10] M. B. Hursthouse, M. Mazid, unpublished.
[11] The complexes **2a** and **2b** were insufficiently soluble in benzene for reliable molecular weight determinations.
[12] M. Bochmann, K. Webb, unpublished.
[13] W. Rundel, *Chem. Ber. 101* (1968) 2956.
[14] H. Bürger, W. Sawadny, U. Wannagat, *J. Organomet. Chem. 3* (1965) 113.
[15] H. Kessler, W. Rundel, *Chem. Ber. 101* (1968), 3350; L. Lange, W.-W. du Mont, *J. Organomet. Chem. 286* (1985) C1.

Structural Characterization of the Pseudoenantiomeric *cis*-Dioxo Osmium(VI) Esters of Chiral Diols with Cinchona Alkaloid Ligands**

By *Ronald M. Pearlstein, Brent K. Blackburn, William M. Davis,* and *K. Barry Sharpless**

The catalytic asymmetric dihydroxylation (ADH, Scheme 1) of olefins,[1] utilizing cinchona alkaloid derivatives as chiral ligands, was substantially improved in generality and speed by our understanding of the multiple diol-producing catalytic cycles that are accessible.[2] By maintaining a low olefin concentration via its slow addition throughout the course of the reaction, a nonenantioselective cycle can be avoided. This permits catalytic production of diols with enantiomeric excesses comparable to those obtained in the corresponding stoichiometric reaction. Further enhancements of the ADH reaction are therefore most likely to come from optimization of the chiral auxiliary for its inherent (stoichiometric) enantioselectivity.

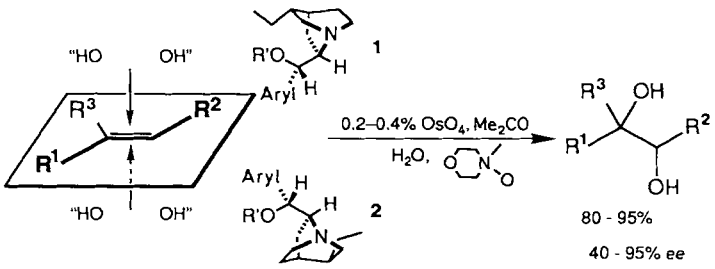

Scheme 1. Catalytic asymmetric dihydroxylation of olefins in the presence of dihydroquinidine or dihydroquinine *p*-chlorobenzoate, **1** or **2**, respectively. R' = *p*-ClC_6H_4CO, Aryl = 4-(6-methoxy)quinolyl.

Structural studies on both the free[3] and OsO_4-bound[4] chiral ligands have been reported recently. Though some alkaloid derivatives showed an interesting conformational

[*] Prof. K. B. Sharpless, Dr. R. M. Pearlstein, Dr. B. K. Blackburn, Dr. W. M. Davis
Massachusetts Institute of Technology
Cambridge, MA 02139 (USA)

[**] This work was supported by the U. S. National Science Foundation (Grant CHE-8303355).

change on metal binding,[4] the origin of face selectivity towards the olefin was unclear. We have now undertaken the structural characterization of the product osmate esters from the stoichiometric reactions of the *trans*-1,2-disubstituted olefins 2,2,5,5-tetramethylhex-3-ene ($R^1 = R^2 = t$Bu, $R^3 = H$) and 2,5-dimethylhex-3-ene ($R^1 = R^2 = i$Pr, $R^3 = H$) with **2** and **1**, respectively, as auxiliaries in order to obtain information regarding the steric interactions possible between various parts of the alkaloid and the reacting olefin. Such studies are aimed at the rational design of new alkaloid derivatives for improved enantioselectivities.

The dioxo[(3*S*,4*S*)-2,2,5,5-tetramethyl-3,4-hexanediolato]osmium(VI) complex containing **2** (**3**)[5] and the dioxo[(3*R*,4*R*)-2,5-dimethyl-3,4-hexanediolato]osmium(VI) complex containing **1** (**4**)[6] were prepared by combining equimolar amounts of OsO_4 with the alkaloid derivative followed by the corresponding olefin. Single crystals suitable for X-ray structure analysis were grown from either CH_2Cl_2/heptane (**3**)[7, 8] or from toluene alone (**4**)[7, 9].

Both structures, shown in Figure 1, show similar coordination geometry, which is approximately trigonal-bipyramidal. The equatorial plane consists of the two terminal oxo ligands and one of the diolate oxygen atoms, with the osmium atom lying <0.11 Å out of this plane. Other osmate esters possessing just one nitrogen donor have crystallized as oxo-bridged dimers,[10] thereby obscuring the five-coordinate geometry assumed[11] to be present in solution. In the complexes containing **1** and **2**, however, there are no nonbonded contacts to the Os atom within 3.6 Å; hence the complexes are monomers.

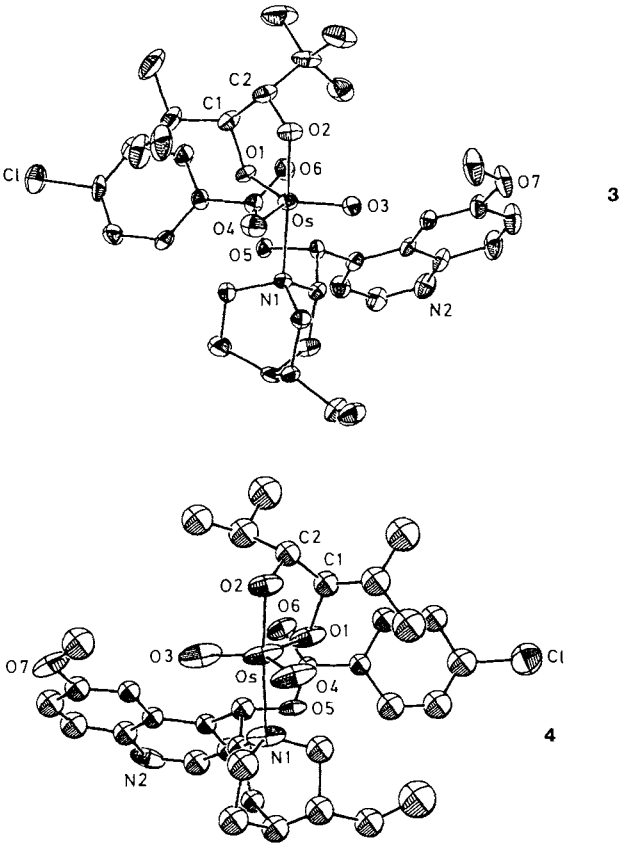

Fig. 1. ORTEP representations of **3** and **4**, showing 35% and 25% thermal probability ellipsoids, respectively. Selected bond distances [Å] and angles [°] for **3**: Os-O1 1.874(5), Os-O2 1.909(5), Os-O3 1.706(5), Os-O4 1.704(5), Os-N1 2.243(5), C1-C2 1.53(1); O1-Os-O2 83.9(2), O1-Os-O3 116.9(2), O1-Os-O4 112.9(3), O1-Os-N1 92.3(2), O2-Os-O3 96.5(2), O2-Os-O4 96.5(3), O2-Os-N1 176.1(2), O3-Os-O4 129.4(3), O3-Os-N1 84.6(2), O4-Os-N1 85.6(2). Selected bond distances [Å] and angles [°] for **4**: Os-O1 1.82(1), Os-O2 1.90(1), Os-O3 1.76(2), Os-O4 1.70(1), Os-N1 2.27(2), C1-C2 1.50(3); O1-Os-O2 85.0(6), O1-Os-O3 113.1(6), O1-Os-O4 110.3(8), O1-Os-N1 91.3(6), O2-Os-O3 97.4(6), O2-Os-O4 95.9(6), O2-Os-N1 175.8(7), O3-Os-O4 135.4(8), O3-Os-N1 85.8(7), O4-Os-N1 83.6(6).

This study therefore represents the first structural characterization of a truly[10, 11] five-coordinate Os(VI)mono-diolate complex, revealing a *cis*-dioxo coordination mode which is exceedingly rare for d^2 transition-metal complexes.[12, 13] The closest previously reported structural analogue is the tris(acetato)dioxoosmate(VI) anion,[14] which has an O=Os=O angle of 125.2(3)°. This value corresponds well with those of 129.4(3)° in **3** and 135.4(8)° in **4**; and all are close to the idealized value of 120°.

The conformation of **1** in complex **4** is virtually identical to that observed in the OsO_4 adduct of the related **1**-dimethylcarbamate.[4] In addition, the α-methylene linkages to the Os-bound quinuclidine moiety of the alkaloid remain staggered relative to the equatorial oxygen atoms. There are, however, two structural differences other than those due to the differing oxygen derivatization. The Os–N distance in **4** has shortened to 2.27(2) Å, indicative of a stronger, more covalent bond. Also, the ethyl group bound in the β-position of the quinuclidine for **4** is rotated towards the nitrogen atom, almost opposite the rotation seen in the OsO_4 adduct of **1**-dimethylcarbamate. This difference may be due to simple crystal-packing forces.

As expected, the absolute configurations of the coordinated diols correspond to those of the major enantiomers reported for the catalytic reactions with the respective chiral ligands. As pointed out in a recent structural study[15] of an asymmetric osmylation system employing a stoichiometric amount of a chiral diamine, explanation of enantioselectivity depends strongly on the basic mechanism of vicinal dihydroxylation, which has not yet been unequivocally determined. Nevertheless, features of **3** and **4** suggest possible interactions between the substituents of the diol and parts of the alkaloid derivatives. These features can be best appreciated in the stereoviews of Figure 2. In both structures, the

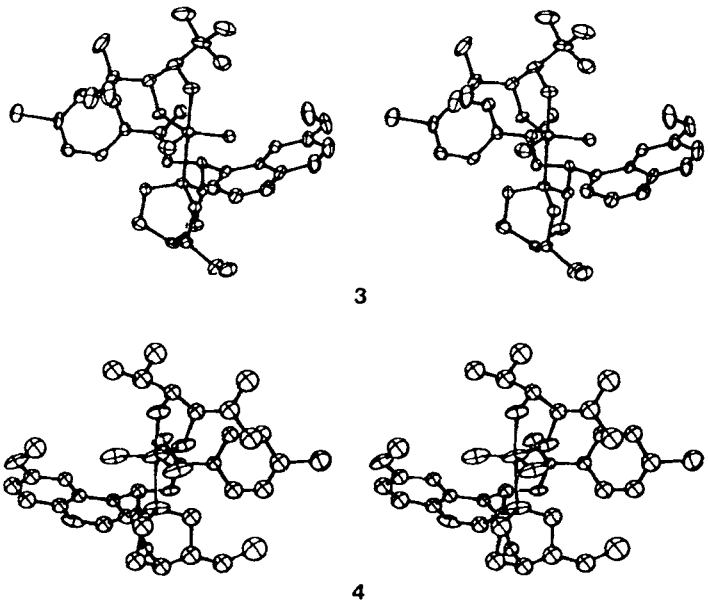

Fig. 2. ORTEP stereoview of **3** and **4**.

planar O5-C = O6 grouping of the ester approaches to within approximately 3 Å of O1, the equatorial diolate oxygen atom. The alkyl substituent of the carbon (C1) that is bound to O1 points away from this ester grouping, leading to the appropriate relative stereochemistry. In practice, it has been noted that the enantiomeric excess of the product diols is exquisitely sensitive to changes in the derivatization of the alcohol moiety of the alkaloids. Furthermore, esters and related derivatives have generally proven to give the highest enantioselectivities.

As may be noted in Figure 1, the 6-methoxy substituent of the quinoline moieties is coplanar with the fused aromatic rings, and in both cases, points towards one of the terminal oxo ligands. Although the nature of the interaction is unexplained, this structural feature is remarkably constant for the osmate esters and the OsO_4 adduct of **1**-dimethylcarbamate.

The most notable difference between the "pseudoenantiomers" **1** and **2** is the stereochemistry of the ethyl substituent on the quinuclidine system. In **4**, this ethyl group approaches the *p*-chlorobenzoyl group, seemingly directing it even closer to the coordinated diolate than in the case of **3**, in which the ethyl group points into empty space. It is tempting to correlate this effect with the rather consistently better *ee* values obtained with quinidine derivatives than with their quinine analogues.

In such a conformationally nonrigid system, it is dangerous to ascribe too much significance to any particular solid-state structural feature; nevertheless, the spectral data[16] are consistent with a similar conformation in solution. The structures of **3** and **4**, therefore, provide a starting point for the development of a structure–activity correlation for the ADH reaction.

Received: August 31, 1989;
revised: March 7, 1990 [Z 3529IE]
German version: *Angew. Chem. 102* (1990) 710

CAS Registry numbers:
3, 126979-52-0; **4**, 126979-51-9; 2,2,5,5-tetramethylhex-3-ene, 22808-06-6.

[1] E. N. Jacobsen, I. Markó, W. S. Mungall, G. Schröder, K. B. Sharpless, *J. Am. Chem. Soc. 110* (1988) 1968.

[2] J. S. M. Wai, I. Markó, J. S. Svendsen, M. G. Finn, E. N. Jacobsen, K. B. Sharpless, *J. Am. Chem. Soc. 111* (1989) 1123.

[3] G. D. H. Dijkstra, R. M. Kellogg, H. Wynberg, J. S. Svendsen, I. Markó, K. B. Sharpless, *J. Am. Chem. Soc. 111* (1989) 8069.

[4] J. S. Svendsen, I. Markó, E. N. Jacobsen, C. Pulla Rao, S. Bott, K. B. Sharpless, *J. Org. Chem. 54* (1989) 2263.

[5] **3**: m.p. 193–196 °C. ^{1}H NMR (300 MHz, $CDCl_3$): δ = 8.68(d,1), 8.06(m,4), 7.51(d,2), 7.42(dd,1), 7.28(s,1), 7.07(br.,1), 4.11(br.,2), 3.8(br.,2), 3.3(br.,2), 3.1(br.,1), 2.6(br.,1), 2.0(br.,3), 1.75(s,1), 1.7(br.,2), 1.5(br.,1), 1.25(m,3), 0.95(d,6), 0.81(m,15). ^{13}C NMR (75 MHz, $CDCl_3$): δ = 159.2, 147.6, 145.4, 143.1, 140.6, 132.3, 131.4, 129.7, 129.0, 127.1, 123.1, 118.6, 102.1, 99.6, 97.6, 75.0, 56.7, 38.1, 37.9, 28.8, 27.8, 27.2, 26.7, 25.9, 25.5, 23.9, 11.9. $[\alpha]_D^{23} = +39$ (C_6H_6, c = 0.31 g mL^{-1}). Satisfactory C,H,N,Cl analysis.

[6] **4**: m.p. 164–167 °C. ^{1}H NMR (300 MHz, $CDCl_3$): δ = 8.73(d,1), 8.14(d,2), 8.08(d,2), 7.51(d,2), 7.41(dd,1), 7.33(d,1), 7.28(s,1), 4.12(s,3), 3.5(br.,2), 3.4(br.,1), 3.2(t,2), 3.1(br.,1). 2.28(t,1), 1.9(s,1), 1.7(m,7), 1.2(br.,2), 1.00(t,3), 0.87(d,6), 0.60(br.,6). ^{13}C NMR (75 MHz, $CDCl_3$): δ = 164.2, 159.2, 147.7, 144.9, 140.3, 131.7, 131.1, 129.2, 128.7, 126.7, 123.3, 118.1, 101.6, 95.8, 74.5, 62.3, 56.4, 37.3, 31.7, 26.8, 26.2, 25.1, 22.8, 19.5, 18.3, 11.3. $[\alpha]_D^{23} = -50$ (C_6H_6, c = 0.25 g mL^{-1}).

[7] All measurements were made with an Enraf-Nonius CAD-4 diffractometer at 23 °C with graphite-monochromated $Mo_{K\alpha}$ radiation (λ = 0.71069 Å). Solution of the structures was accomplished by using the Patterson method. Structure refinement was performed with standard least-squares methods by using the TEXSAN software package, Molecular Structure Corporation (1985). In both structures, the residuals for the mirror-image structure were shown to be significantly larger, confirming the assumed configuration. Hydrogen atoms were not refined, but included in calculated positions.

[8] **3**: monoclinic, $P2_1$ (No. 4), a = 9.722(1), b = 17.687(2), c = 11.1114(8) Å, β = 102.191(7)°, V = 1867.6(6) Å^3, Z = 2, ρ_{calcd} = 1.53 g cm^{-3}. A total of 6683 reflections having $I > 3\sigma(I)$ were used in the calculations (including both Friedel mates). All non-hydrogen atoms refined anisotropically to R = 0.038, R_w = 0.036. An empirical absorption and a secondary extinction correction were applied.

[9] **4**: orthorhombic, $P2_12_12_1$ (No. 19), a = 9.7226(3), b = 10.865(6), c = 33.837(6) Å, V = 3576(4) Å^3, Z = 4, ρ_{calcd} = 1.54 g cm^{-3}. A total of 3342 reflections having $I > 3\sigma(I)$ were used in the calculations (including both Friedel mates). Carbon atoms were refined with isotropic thermal parameters, and all remaining non-hydrogen atoms were refined anisotropically to R = 0.066, R_w = 0.067. An analytical absorption correction was applied.

[10] B. A. Cartwright, W. P. Griffith, M. Schröder, A. C. Skapski, *J. Chem. Soc. Chem. Commun. 1978*, 853.

[11] M. Schröder, A. J. Nielson, W. P. Griffith, *J. Chem. Soc. Dalton Trans. 1979*, 1607.

[12] R. H. Holm, *Chem. Rev. 87* (1987) 1401.

[13] Other notable examples: a) S. Perrier, J. K. Kochi, *Inorg. Chem. 27* (1988) 4165; b) J. C. Dobson, K. J. Takeuchi, D. W. Pipes, D. A. Geselowitz, T. J. Meyer, *ibid. 25* (1986) 2357; c) G. F. Ciani, G. D'Alfonso, P. F. Romiti, A. Sironi, M. Freni, *Inorg. Chim. Acta 72* (1983) 29.

[14] T. Behling, M. V. Capparelli, A. C. Skapski, G. Wilkinson, *Polyhedron 1* (1982) 840.

[15] K. Tomioka, M. Nakajima, Y. Iitaka, K. Koga, *Tetrahedron Lett. 29* (1988) 573.

[16] For instance, the unusually low chemical shifts (δ = 0.81 in **3** and 0.60, 0.87 in **4**)[5,6] for the methyl protons of the coordinated diols are consistent with their observed position within the shielding region of the *p*-chlorophenyl rings.

Synthesis of Cyclosilanylethynes

By *Edwin Hengge,* Alfred Baumegger, Markus Eibl, Erhard Hohenester*, and *Christoph Kratky**

Silanylethynes have recently attracted much interest because of the possibility of σ–π interactions between the silicon skeleton and the CC triple bond. Electron delocalizations of this kind have already been observed in simple silanylethynes and cyclic (poly)silanylethynes.[1] We recently reported a method for synthesizing bis(silanyl)-substituted ethynes by reaction of acetylene with halosilanes and alkali metals.[2] Using the same reaction route, we have now succeeded in synthesizing cyclosilanylethynes. As starting materials for these syntheses we used mono- and difunctional cyclosilanes.[3]

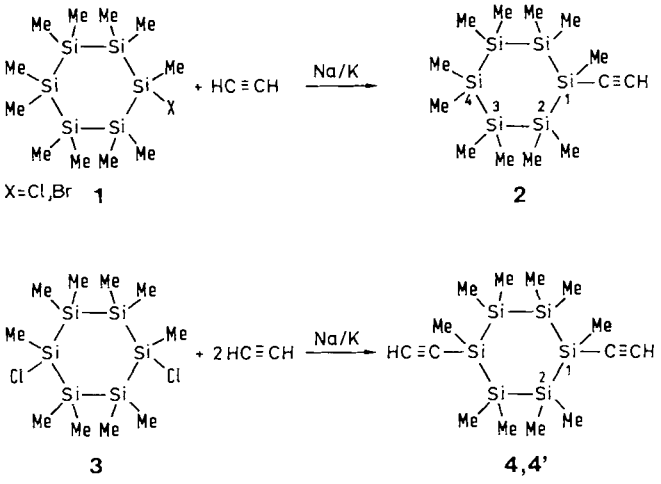

Scheme 1. Synthesis of **2** and 4 (**4'**).

[*] Prof. Dr. E. Hengge, A. Baumegger, M. Eibl
Institut für Anorganische Chemie der Technischen Universität
Stremayrgasse 16, A-8010 Graz (Austria)
Doz. Dr. C. Kratky, E. Hohenester
Institut für Physikalische Chemie der Universität
Heinrichstrasse 28, A-8010 Graz (Austria)

The reaction of the chlorocyclohexasilane derivative **1** (X = Cl) with acetylene and K/Na alloy gives the previously unknown cyclohexasilanylethyne **2**. In an analogous reaction the 1,4-dichlorocyclohexasilane **3** gives the 1,4-diethynylcyclohexasilane **4** (and its isomer **4'**, which will not be discussed separately here; Scheme 1).

Treating **2** with K/Na alloy in an ultrasonic bath gives the corresponding alkali-metal acetylide; this was not isolated, but was allowed to react directly with **1** or **3** to give, respectively, the bis(cyclohexasilanyl)ethyne **5** and the 1,4-bis[(cyclohexasilanyl)ethynyl]cyclohexasilane **6** (Scheme 2). All the

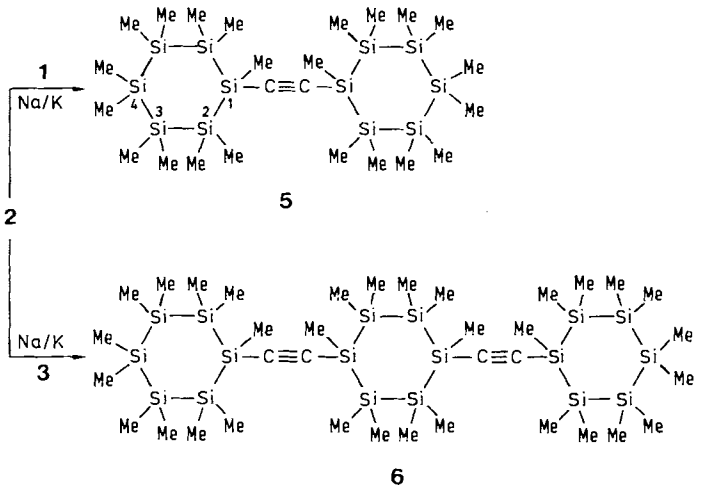

Scheme 2. Synthesis of **5** and **6**.

compounds were thoroughly characterized; they are colorless crystalline compounds that are stable in air and withstand increased temperatures.

From the frequencies of the C≡C vibrations in the Raman and IR spectra it is evident that the silicon ring does not exert an effect on the CC triple-bond system.

The signals in the ^{29}Si NMR spectra have been assigned on the basis of the ^{29}Si–^{29}Si couplings, which were determined by modified INEPT-INADEQUATE experiments.[4] Here again, no change in the bonding could be detected, since the values of $^{1}J_{Si,Si}$ and $^{2}J_{Si,Si}$ show no significant deviation from the coupling constants in other derivatives with the general formula $Si_6Me_{11}X$.[5] The value of $^{1}J_{Si,C\equiv}$ for **2** is also within the expected range.[6] Table 1 lists all the relevant physical data for the compounds **2**, **4**, **5**, and **6**.[7]

An X-ray crystallographic analysis of **5** enabled the structure to be determined very precisely[8] (Fig. 1). The two symmetrically equivalent cyclohexasilane rings are joined diaxially. The C–C distance was determined as 121 pm, which corresponds to that in a normal triple bond, and the value of 177.0° for the C1A–C1–Si1 bond angle is scarcely different

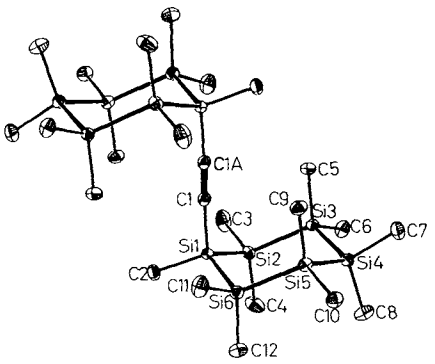

Fig. 1. Crystal structure of **5** (ORTEP, thermal ellipsoids at the 50% probability level, hydrogen atoms not shown). Selected bond lengths [pm] and angles [°]: C1-Si1 183.3(4), C1A-C1 121.2(5); C1A-C1-Si1 177.0(3).

from that expected for an sp-hybridized carbon atom. No useful crystals of **6** could be obtained, possibly owing to the occurrence of two isomeric 1,4-disubstituted cyclohexasilanes,[2] a fact which is also clearly evident from the NMR spectra.

Table 1. Physical data for compounds **2** and **4**–**6** [a].

2: ^{1}H NMR: σ = 2.424 (s, 1H), 0.560, 0.527, 0.476, 0.411, 0.367 (all m, 33H). ^{13}C NMR: σ = 98.03, 87.36, 6.85, 5.63, 5.50, 5.32. ^{29}Si NMR: σ = −58.39 (Si1), −40.96(Si2), −41.30 (Si3), −41.71 (Si4), ^{1}J(Si1,Si2) = 63.8, ^{2}J(Si1,Si3) = 11.0, ^{2}J(Si2,Si4) = 9.5, ^{1}J(Si1,C≡) = 60.9, ^{1}J(Si,CH$_3$) = 32.6 Hz. – IR (Nujol): $\tilde{\nu}$ [cm^{-1}] = 3280 (≡C-H), 2010 (-C≡C-), 1240, 830, 800, 780, 725, 685, 645, 585, 400, 340, 300. MS (70 eV): *m/z* 358 ($M^{\oplus}$). M.p. 207–210 °C. Elemental analysis in agreement with formula.

4, **4'**: ^{1}H NMR: σ = 2.249, 2.225, 0.449, 0.358, 0.328, 0.207. ^{13}C NMR: σ = 98.16, 87.36, 86.95, −5.07, −5.27, −5.37, −5.62, −5.63, −6.83. ^{29}Si NMR: σ = −58.83 (Si1), −58.31 (Si1'), −40.64 (Si2), −40.52 (Si2'), ^{1}J(Si1,Si2) = 64.3 and 64.5 Hz, ^{2}J(Si1,Si3) = 11.2 and 10.8 Hz. IR (Nujol): $\tilde{\nu}$ [cm^{-1}] = 3280 (≡C–H), 2010 (–C≡C–), 840, 805, 780, 735, 690, 660, 650, 590, 410, 330. MS (70 eV): *m/z* 368 ($M^{\oplus}$). M.p. 190 °C (decomp.). Elemental analysis in agreement with formula.

5: ^{1}H NMR: σ = 0.28, 0.29, 0.33, 0.34, 0.43, 0.47, 0.53 (all m). ^{13}C NMR: σ = 116.09, −6.34 to −4.61 (m). ^{29}Si NMR: σ = −60.29 (Si1), −41.05 (Si2), −41.26 (Si3), −41.75 (Si4), ^{1}J(Si1,Si2) = 64.3, ^{2}J(Si1,Si3) = 10.8, ^{2}J(Si2,Si4) = 9.5 Hz. IR (Nujol): $\tilde{\nu}$ [cm^{-1}] = 840, 830, 805, 785, 780, 760, 730, 685, 680, 650, 630, 480, 390. Raman: $\tilde{\nu}$ [cm^{-1}] = 2100. MS (70 eV): *m/z* 690 ($M^{\oplus}$). M.p. 154–156 °C. Elemental analysis in agreement with formula.

6: ^{1}H NMR: σ = 0.27, 0.28, 0.32, 0.34, 0.37, 0.43, 0.46, 0.54, 0.64 (all m). ^{13}C NMR: σ = 116.05, 115.48, −4.64 to −6.42(m). ^{29}Si NMR: σ = −60.13, −59.59, −41.78, −41.28, −41.06, −40.15. IR (Nujol): $\tilde{\nu}$ [cm^{-1}] = 1246, 840, 803, 783, 763, 734, 688, 675, 653, 395. Raman: $\tilde{\nu}$ [cm^{-1}] = 2100. MS (70 eV): *m/z* 1032 ($M^{\oplus}$). M.p. 210 °C (dec.).

[a] ^{1}H NMR (300.13 MHz, C_6D_6), ^{13}C NMR (75.460 MHz, C_6D_6), ^{29}Si NMR (59.627 MHz, C_6D_6); 20 °C, saturated solutions, all shift values referred to TMS.

Experimental Procedures

2: 1.32 g of K/Na alloy was prepared as a suspension in 500 mL of toluene, acetylene was introduced, and simultaneously a solution of **1** (X = Cl) (9.40 g, 25.5 mmol) in 50 mL of toluene was slowly added dropwise. After extraction with water the product was purified by sublimation at 60 °C/0.01 mbar. Yield 6.7 g (73%).

4: 0.85 g of K/Na alloy was prepared as a suspension in 100 mL of toluene, and acetylene was introduced while stirring vigorously; simultaneously a solution of **3** (X = Cl) (1.16 g, 2.98 mmol) in 20 mL of toluene was slowly added dropwise. The solvent was distilled off and the residue was purified by sublimation at 80 °C/0.01 mbar, giving 0.5 g of the product (yield 45%).

5: **2** (0.96 g, 2.7 mmol) was added to a suspension of 0.24 g of K/Na alloy in toluene and ultrasonically irradiated. A solution of **1** (0.9 g, 2.2 mmol) (X = Br) in 20 mL of toluene was then added dropwise to the resulting brown suspension. After filtering and removing the solvent the white residue was recrystallized from benzene. Yield 0.6 g (39%). **5** can be sublimed at 135 °C/0.01 mbar.

6: **2** (2.3 g, 6.4 mmol) was added to a suspension of 0.36 g of K/Na alloy in 80 mL of toluene and ultrasonically irradiated. A solution of **3** (X = Cl) (1.22 g, 3.1 mmol) in 20 mL of toluene was added dropwise to this suspension and the mixture was then stirred for about 12 h. The product was extracted in the same way as for **5**, the colorless crystals being recrystallized from benzene. Yield 0.3 g (9%).

Received: February 14, 1990 [Z 3796 IE]
German version: *Angew. Chem. 102* (1990) 722

CAS Registry numbers:
1 (Cl), 23118-87-8; **1** (Br), 110624-83-4; **2**, 127208-72-4; **3**, 99128-54-8; **4**, 127208-73-5; **4'**, 127208-77-9; **5**, 127208-74-6; **6**, 127208-75-7; **6'**, 127208-76-8; HC≡CH, 74-86-2.

[1] H. Sakurai, *Pure Appl. Chem. 59* (1987) 1637–1646; T. Iwahara, R. West, *J. Chem. Soc. Chem. Commun. 1988*, 954–955; R. Gleiter, W. Schäfer, H. Sakurai, *J. Am. Chem. Soc. 107* (1985) 3046–3050; H. Bock, *Angew. Chem. 101* (1989) 1659–1682; *Angew. Chem. Int. Ed. Engl. 28* (1989) 1627.

[2] E. Hengge, A. Baumegger, *J. Organomet. Chem. 369* (1989) C39–C42.
[3] F. K. Mitter, E. Hengge, *J. Organomet. Chem. 332* (1987) 47–52.
[4] O. W. Sorensen, R. Freeman, T. Frenkiel, T. H. Mareci, R. Schuck, *J. Magn. Reson. 46* (1982) 180.
[5] E. Hengge, M. Eibl, F. Schrank, *J. Organomet. Chem. 369* (1989) C23–C26 and unpublished results.
[6] K. Kamienska-Trela, *J. Organomet. Chem. 159* (1978) 15–21.
[7] Bruker MSL-300 spectrometer; accuracy of quoted coupling constants J [Hz] is better than ± 0.3 Hz. Values of J(Si,Si) across one and two bonds were determined using a modified INEPT-INADEQUATE pulse sequence; the development delay time for the double quantum coherence was optimized for coupling constant values of 60 Hz (^1J) or 10 Hz (^2J). ^1J(Si2,Si3) and ^1J(Si3,Si4) could not be determined owing to the smallness of the quotient $\Delta\delta/J$ (cf. A. Bax, R. Freeman, *J. Magn. Reson. 41* (1980) 507–511). ^1J(Si,C≡) and ^1J(Si,CH_3) were determined from the satellites in the ^{13}C NMR spectrum with broad-band decoupling and from those in the ^{29}Si INEPT spectrum of **2**.
[8] Crystallographic data for **5**, $Si_{12}C_{24}H_{66}$, $M = 691.82$: monoclinic, space group $P2_1/n$, $a = 10.061(6)$, $b = 12.272(9)$, $c = 17.867(13)$ Å, $\beta = 89.96(5)°$, $V = 2206.0(2.6)$ Å^3, $Z = 2$, $\varrho_{calcd} = 1.042$ g cm^{-3}, $\mu(Mo_{K\alpha}) = 3.6$ cm^{-1}, $T = 93(2)$ K, 10 604 independent reflections, 3622 with $I > 4\sigma(I)$, modified STOE diffractometer, graphite monochromator, $(\sin\theta\lambda^{-1})_{max} = 0.81$ Å^{-1}, $Mo_{K\alpha}$ radiation, $\lambda = 0.71069$ Å. Structure determined by direct methods (SHELX-86), $R = 0.0285$ (295 parameters, 3622 reflections, unit weightings, Si and C anisotropic, H isotropic, d(CH) = 1.07 Å, SHELX-76). $\Delta\varrho_{fin} = 0.33$ Å^{-3}. Further details of the crystal structure investigations can be obtained on request from the Director of the Cambridge Crystallographic Data Centre, University Chemical Laboratory, Lensfield Road, Cambridge CB2 1EW (UK), on quoting the full literature reference.

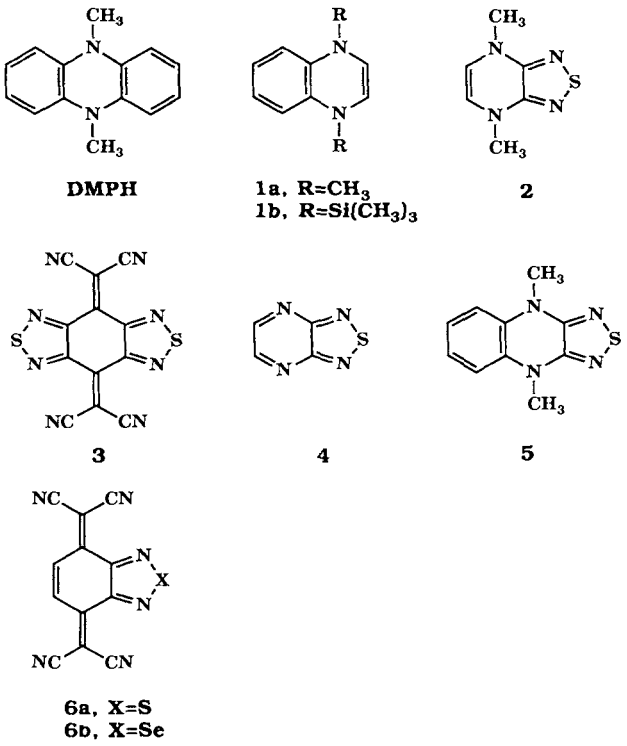

4,7-Dimethyl-4,7-dihydro[1,2,5]thiadiazolo-[3,4-*b*]pyrazine, a Novel Electron Donor with a 12π-Electron Ring System

By *Yoshiro Yamashita,* Junko Eguchi, Takanori Suzuki, Chizuko Kabuto, Tsutomu Miyashi,* and *Shoji Tanaka*

5,10-Dimethyl-5,10-dihydrophenazine (DMPH) is a strong electron donor due to the 16π-electron ring system[1] and affords conducting charge-transfer (CT) complexes with electron acceptors.[2] However, 1,4-dimethyl-1,4-dihydroquinoxaline (**1a**), containing a 12π-electron ring system, has not been isolated, probably due to its extremely electron-donating property,[3] although a derivative, **1b**, containing trimethylsilyl groups was synthesized.[4] In order to enhance the stability of **1a**, we substituted a 1,2,5-thiadiazole ring, an electron-withdrawing heterocycle, for the benzene ring to give the title compound **2**. This substitution is also expected to lead to interactions between sulfur and nitrogen atoms in the solid state, as found in thiadiazole-fused TCNQ derivatives such as **3**.[5] We report here the preparation and properties of **2**, a novel 12π-electron heterocycle.

Compound **2** was obtained as yellow crystals (m.p. 102–104 °C) in 22% yield by reduction of [1,2,5]thiadiazolo[3,4-*b*]pyrazine (**4**)[6] with potassium followed by methylation with methyl iodide. The new donor is stable in the solid state under air and absorbs at longer wavelengths[7] than the benzo derivative **5**.[8] The half-wave oxidation potentials ($E_1 = +0.15$, $E_2 = +0.95$ V (irreversible) versus the saturated calomel electrode) were measured by cyclic voltammetry.[9] Although the first oxidation potential is higher than that of **1a** due to the electron-withdrawing heterocycle, the value is still very low, indicating that **2** is a strong electron donor.

In order to investigate the molecular structure of **2** as well as the possible interheteroatom interactions, X-ray structural analysis of **2** was carried out.[10] The molecule is completely planar except for hydrogens of the methyl groups. The bond lengths given in Figure 1 show a pronounced bond

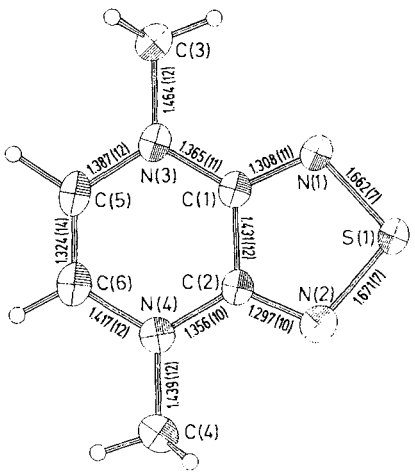

Fig. 1. Molecular structure of **2** with bond lengths [Å] (ORTEP).

alternation. Thus, the C5–C6 bond length (1.324 Å) is very close to a pure C–C double-bond distance, while the C5–N3 (1.387 Å) and C6–N4 (1.417 Å) bond lengths are close to a C–N single-bond length.[11, 12] The S–N and C–N bonds of the thiadiazole moiety are a little longer and shorter, respectively, than the corresponding bonds of 1,2,5-thiadia-

[*] Prof. Dr. Y. Yamashita, Dr. S. Tanaka
Institute for Molecular Science
Myodaiji, Okazaki 444 (Japan)
J. Eguchi, Dr. T. Suzuki, Dr. C. Kabuto, Prof. Dr. T. Miyashi
Department of Chemistry, Faculty of Science
Tohoku University
Aramaki, Sendai 980 (Japan)

zoles.[13] The increase in the double-bond character of the C–N bonds results in the longer C1–C2 bond.

The molecules of **2** are uniformly stacked along the *a* axis, the dihydropyrazine parts overlapping as shown in Figure 2. The dihedral angle between the upper and lower molecules is

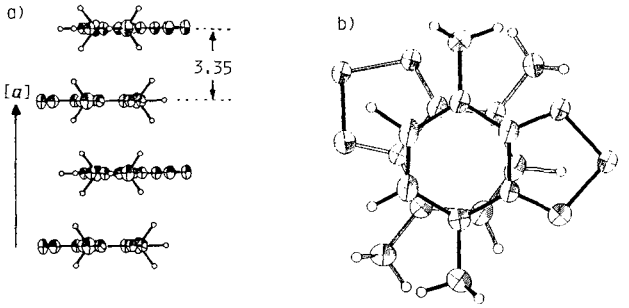

Fig. 2. Crystal structure of **2**. a) One-dimensional column along the *a* axis. b) Overlapping of **2** (projection).

0° and the distance between the molecular planes is 3.35 Å. The molecules are connected by S···N contacts to form a coplanar dyad. The contact distance of 3.05 Å is significantly shorter than the sum of the van der Waals radii (3.35 Å). The dyad is held together by hydrogen bonding (2.50 Å) between olefinic hydrogens and nitrogens of thiadiazole rings to form a coplanar sheetlike network (Fig. 3), which is stacked to give an unusual crystal structure resembling graphite.

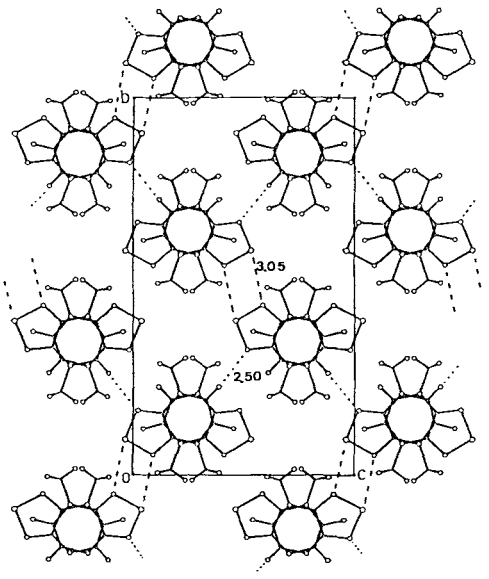

Fig. 3. Sheetlike network of **2**. Broken lines: S···N interactions and hydrogen bonding.

The strong S···N interactions can be attributed to an electrostatic effect, which is suggested from the atomic charges calculated by the MNDO method[14] (Fig. 4). The calculation also shows that, besides the enediamine part, the sulfur atom of the thiadiazole has a large coefficient in its HOMO.

The donor **2** formed no complexes with tetracyanoquinodimethane (TCNQ), chloranil, or 2,3-dichloro-5,6-dicyano-1,4-benzoquinone (DDQ). However, it gave conducting complexes with acceptors **3**, **6a**,[15] and **6b**,[16] which contain a 1,2,5-thiadiazole ring or a selenadiazole ring. This

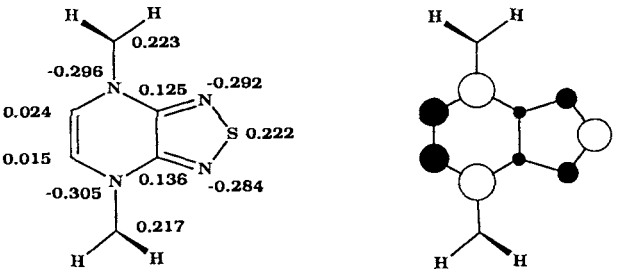

Fig. 4. The net atomic charges and HOMO of **2** calculated by the MNDO method.

Table 1. Properties of charge-transfer complexes of **2** (donor, D) with electron acceptors (A).

Acceptor	E_{red}[a] [V]	D:A ratio[b]	σ[c] [S cm^{-1}]
3	−0.02	1:1	5.6×10^{-2}
6a	+0.12	2:3	2.6×10^{-2}
6b	+0.04	2:3	1.2×10^{-1}

[a] Versus the saturated calomel electrode. [b] Based on elemental analyses. [c] Electrical conductivities measured on compressed pellets by two-probe technique at room temperature.

fact seems to suggest that interheteroatom interactions also play an important role in the complexation. The properties of the complexes are summarized in Table 1.

Received: December 20, 1989 [Z 3694IE]
German version: *Angew. Chem. 102* (1990) 709

[1] R. F. Nelson, D. W. Leedy, E. T. Seo, R. N. Adams, *Z. Anal. Chem. 224* (1967) 184–196; K. Dietz, H. J. Keller, D. Nöthe, D. Wehe, *J. Am. Chem. Soc. 104* (1982) 7581–7585.
[2] L. R. Melby, *Can. J. Chem. 43* (1965) 1448–1453.
[3] W. Kaim, *Heterocycles 23* (1985) 1363–1366.
[4] W. Kaim, *Angew. Chem. 93* (1981) 621–622; *Angew. Chem. Int. Ed. Engl. 20* (1981) 600–601.
[5] C. Kabuto, T. Suzuki, Y. Yamashita, T. Mukai, *Chem. Lett. 1986*, 1433–1436; T. Suzuki, C. Kabuto, Y. Yamashita, T. Mukai, T. Miyashi, G. Saito, *Bull. Chem. Soc. Jpn. 61* (1988) 483–493.
[6] A. P. Komin, M. Carmack, *J. Heterocycl. Chem. 13* (1976) 13–22.
[7] UV (cyclohexane): $\lambda(\log\varepsilon)$ = 354 (3.83), 368 (3.91), 387 (3.86), 410 nm (3.52).
[8] Y. Yamashita, K. Saito, T. Mukai, T. Miyashi, *Tetrahedron Lett. 30* (1989) 7071–7074.
[9] Measured at a Pt electrode in acetonitrile with 0.1 M Et_4NClO_4 as a supporting electrolyte: scan rate 100 mV s^{-1}. The irreversible second oxidation potential was calculated from the anodic peak potential $E_{pa} = -0.03$. The oxidation potentials of **5** and tetrathiafulvalene measured under the same conditions were +0.54, +1.30 V (irreversible) and +0.31, +0.68 V, respectively.
[10] X-ray structure data for **2**: orthorhombic, space group *Cmca* (No. 64), $a = 6.707(2)$, $b = 20.248(2)$, $c = 11.503(1)$ Å, $V = 1562.2(5)$ Å^3, $Z = 8$, $\varrho_{calcd} = 1.431$ g cm^{-3}. Rigaku AFC-5R, $Mo_{K\alpha}$ radiation, graphite monochromator; 981 reflections for $2\theta_{max} = 52$; solution of structure by direct methods; refinement by block-diagonal least-squares method to $R = 0.0637$ for 458 reflections with $F_0 > 3\sigma F_0$. Further details of the crystal structure investigation are available on request from the Director of the Cambridge Crystallographic Data Centre, University Chemical Laboratory, Lensfield Road, GB-Cambridge CB21EW (UK), on quoting the full journal citation.

[11] The π-bond orders calculated from the bond lengths according to established equations[12] are 1.00 for the C5–C6 bond, 0.34 for the C5–N3 bond, and 0.15 for the C6–N4 bond.
[12] G. Häfelinger, *Chem. Ber. 103* (1970) 2902–2921.
[13] A. Gieren, V. Lamm, R. C. Haddon, M. L. Kaplan, *J. Am. Chem. Soc. 101* (1979) 7277–7281.
[14] MNDO calculations [MOPAC program: J. J. P. Stewart, *Q. C. P. E. Bull. 3* (1983) 43] were performed by using the geometry determined from the X-ray analysis. These calculations were carried out at the Computer Center of the Institute for Molecular Science.
[15] T. Suzuki, Y. Yamashita, C. Kabuto, T. Miyashi, *J. Chem. Soc. Chem. Commun. 1989*, 1102–1103.
[16] Compound **6b** was recently prepared by us.

Asymmetric Heterodinuclear $[L'Ru(\mu\text{-}O)(\mu\text{-}CH_3CO_2)_2ML]^{2\oplus}$ Complexes (M = Fe, Mn, V): Electronic Structure and Magnetic Properties**

By *Rainer Hotzelmann, Karl Wieghardt,* Ulrich Flörke,* and *Hans-Jürgen Haupt*

Dedicated to Professor Wolfgang Roth on the occasion of his 60th birthday

Since it was discovered that in some iron- and manganese-containing metalloproteins the active center is a dinuclear μ-oxo-bis(μ-carboxylato)dimetal(III) unit,[1, 2] inorganic chemists have synthesized various low-molecular-weight model complexes of this kind and have determined their structures and investigated their electronic structure and magnetic properties. In this study we have in particular sought to clarify the mechanism of the spin exchange coupling between the two paramagnetic metal centers. In the series of homodinuclear complexes $[L'_2M^{III}_2(\mu\text{-}O)(\mu\text{-}CH_3CO_2)_2]^{2\oplus}$ (L' = *N,N',N''*-trimethyl-1,4,7-triazacyclononane,[3–7] antiferromagnetic or ferromagnetic coupling can occur, depending on the d-electron configuration of the metal ions (Table 1). We have started to prepare heterodinuclear complexes of this type and to study their magnetic properties, with the object of identifying the magnetic orbitals responsible for the spin exchange coupling in structures of this type.[8]

Table 1. Structural data and magnetic properties for homodinuclear complexes of the form $[L'_2M_2^{III}(\mu\text{-}O)(\mu\text{-}CH_3CO_2)_2]^{2\oplus}$ [a].

M	M-O_{oxo} [Å]	M···M [Å]	M-O-M [°]	J [cm^{-1}][b]	Ref.
Ti^{III} (d^1)	1.81(2)	3.20(1)	122.7(8)	diamagnetic	[3]
V^{III} (d^2)	1.792(4)	3.250(2)	130.2(2)	> +200	[4]
Mn^{III} (d^4, h.s.)[c]	1.810(4)	3.084(3)	120.9(1)	+9	[5]
Fe^{III} (d^5, h.s.)[c]	1.800(3)	3.120(3)	119.7(2)	−119	[6]
Ru^{III} (d^5, l.s.)[c]	1.884(2)	3.258(1)	119.7(2)	diamagnetic	[7]

[a] L' = *N,N',N''*-trimethyl-1,4,7-triazacyclononane. [b] $H = -2JS_1 \cdot S_2$. [c] h.s. = high spin; l.s. = low spin.

In dinuclear linear oxo-bridged complexes of chromium(III) (d^3) the strong antiferromagnetic coupling (ground state $S = 0$) is attributed to the overlapping of one t_{2g} orbital from each of the chromium ions with a p orbital of the oxo bridge ("magnetic superexchange", Fig. 1).[9] Since this interaction

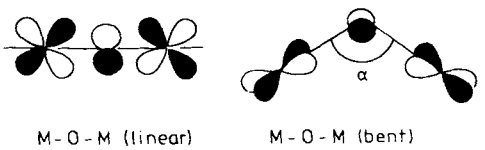

Fig. 1. Schematic representation of the orbitals involved in the magnetic superexchange mechanism.

is in principle independent of the Cr^{III}–O–Cr^{III} bond angle, the same exchange mechanism should also occur in μ-oxo-bis(μ-carboxylato)dimetal(III) complexes if the two corresponding t_{2g} orbitals are each occupied by one electron. To test this hypothesis we have synthesized the asymmetric heterodinuclear complexes **1**–**3**.

$[L'Ru(\mu\text{-}O)(\mu\text{-}CH_3CO_2)_2FeL]X_2$ **1**, X = PF_6; **1'**, X = ClO_4
$[L'Ru(\mu\text{-}O)(\mu\text{-}CH_3CO_2)_2MnL](PF_6)_2$ **2**
$[L'Ru(\mu\text{-}O)(\mu\text{-}CH_3CO_2)_2VL](PF_6)_2$ **3**
L' = *N,N',N''*-trimethyl-1,4,7-triazacyclononane;
L = 1,4,7-triazacyclononane

The hydrolysis of equimolar amounts of $L'RuCl_3$ and $LMCl_3$ (M = Fe, Mn, V) in a methanolic sodium acetate solution, followed by addition of $NaPF_6$, results in precipitation of the crystalline compounds **1**–**3**. Addition of $NaClO_4$ or $NaPF_6$ to aqueous solutions of the respective chlorides yielded single crystals of **1** and **3** suitable for structure determination by X-ray diffraction.

Figure 2 shows the structure of the dication of **1'**.[10] The atoms N3, Fe1, O1, Ru1, and N2 lie in a crystallographic mirror plane. The two metal centers are linked by a weakly asymmetric oxo bridge and two bidentate acetate groups. The Ru···Fe distance of 3.176(3) Å is not consistent with a metal–metal bond. The iron ion is coordinated to L and the ruthenium ion to L'; thus, no ligand exchange occurs during the synthesis.

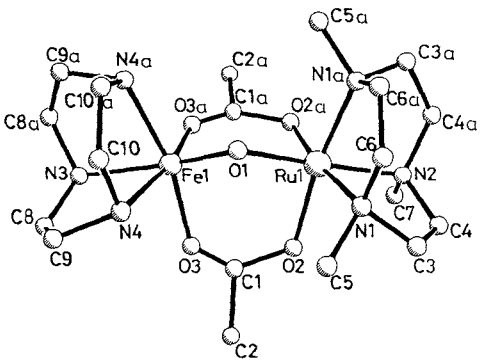

Fig. 2. Structure of the dication in crystals of **1'**, showing important bond lengths [Å] and angles [°]: Ru1···Fe1 3.176(3), Ru1-O2 2.05(2), Ru1-N2 2.10(3), Fe1-O3 2.00(2), Fe1-N4 2.12(2), Ru1-O1 1.95(1), Ru1-N1 2.04(2), Fe1-O1 1.73(2), Fe1-N3 2.26(2); Ru1-O1-Fe1 119.3(8).

[*] Prof. Dr. K. Wieghardt, Dipl.-Chem. R. Hotzelmann
Lehrstuhl für Anorganische Chemie I der Universität
Postfach 102148, D-4630 Bochum (FRG)
Dr. U. Flörke, Prof. Dr. H.-J. Haupt
Lehrstuhl für Allgemeine Anorganische und Analytische Chemie
der Universität-Gesamthochschule
D-4790 Paderborn (FRG)

[**] This work was supported by the Fonds der Chemischen Industrie. L' = *N,N',N''*-trimethyl-1,4,7-triazacyclononane; L = 1,4,7-triazacyclononane.

Figure 3 shows the structure of the dication of **3**. The Ru–O–V bridge is highly asymmetric: the Ru–O distance is quite long, 2.053(10) Å, whereas the V–O distance is very short, 1.665(8) Å. This points to the existence of a $Ru^{II}V^{IV}$ complex with a $Ru^{II}-O=V^{IV}$ bridge.

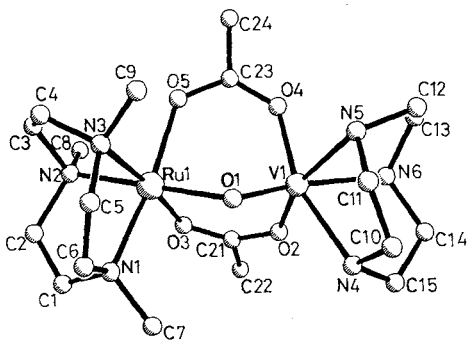

Fig. 3. Structure of the dication in crystals of **3**, showing important bond lengths [Å] and angles [°]: Ru1···V1 3.153(3), Ru1-O1 2.053(10), Ru1-O3 2.12(1), Ru1-O5 2.106(9), Ru1-N1 2.09(1), Ru1-N2 2.08(1), Ru1-N3 2.07(1), V1-O1 1.665(8), V1-O2 1.98(1), V1-O4 1.98(1), V1-N4 2.16(1), V1-N5 2.16(1), V1-N6 2.23(1); Ru1-O1-V1 115.6(5).

Measurements of the susceptibility as a function of temperature[11] on powdered samples of **1**, **2**, and **3** in the range 4.2–295 K using a Foner magnetometer gave temperature-independent magnetic moments (Curie behavior) with values of 4.7 μ_B for **1**, 3.9 μ_B for **2**, and 1.8 μ_B for **3**. These values correspond to spin states of $S = 2$, 3/2, and 1/2 for **1**, **2**, and **3**, respectively.

Assigning oxidation states to the metal ions in **1**, **2**, and **3** is not a trivial matter. Although the syntheses start from the trivalent mononuclear compounds $L'Ru^{III}Cl_3$ and $LM^{III}Cl_3$, there are no a priori grounds for ruling out intramolecular transfer in **1**, **2**, or **3**; thus, **1** could be formulated as a complex of $Ru^{II}Fe^{IV}$, **2** as one of Ru^{II} Mn^{IV}, and **3** as one of $Ru^{II}V^{IV}$, each with a diamagnetic Ru^{II} ion (d^6, low spin) and a paramagnetic M^{IV} ion. On the other hand, the metal ions in **1**–**3** could instead be in their trivalent forms ($Ru^{III}Fe^{III}$, $Ru^{III}Mn^{III}$, $Ru^{III}V^{III}$). In this case the single electron of the Ru^{III} ion (d^5, low spin) would have a very strong antiferromagnetic coupling ($-J > 300\ cm^{-1}$) to one of the unpaired electrons of a high-spin Fe^{III} (5e), Mn^{III} (4e), or V^{III} (2e) ion. Both descriptions are consistent with the observed magnetic behavior. For **1** and **2** the formulas with $Ru^{III}Fe^{III}$ and $Ru^{III}Mn^{III}$ are preferred on the grounds of the electronic spectra (Fig. 4), both of which show at least one strong

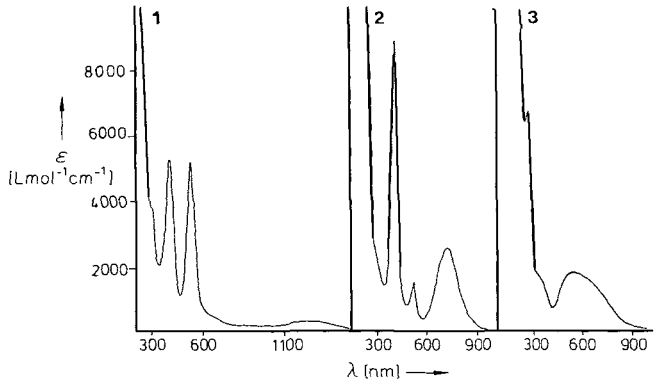

Fig. 4. Electronic spectra of **1**–**3** in acetonitrile.

$O_\mu \rightarrow M(III)$ charge transfer (CT) band in the visible region between 400 and 600 nm. Similar strong CT bands have also been observed for the analogous homonuclear complexes containing Fe^{III}, Mn^{III}, Ru^{III}, and V^{III}.[2–7, 12] In the spectrum of **3**, which resembles that of an octahedral $VO^{2\oplus}$ complex, these absorption peaks are absent. Compound **3** should therefore be described as a $Ru^{II}V^{IV}$ complex, which is also supported by the X-ray structural analysis.

The Mössbauer spectrum of **1** at 78 K with no applied magnetic field[11] shows a symmetrical doublet with an isomer shift of $\delta = 0.42(3)\ mm\ s^{-1}$ and a quadrupole splitting of $\Delta E_Q = 1.58(5)\ mm\ s^{-1}$. These values are typical for an octrahedrally coordinated high-spin Fe^{III} ion and are similar to those for the homodinuclear complex $[L'_2Fe_2(\mu\text{-}O)(\mu\text{-}CH_3CO_2)_2](PF_6)_2$.[6] Therefore, **1** is a $Ru^{III}Fe^{III}$ complex.

The assignment of oxidation states is also supported by the X-band ESR spectra of solid samples of the tetraphenylborate salts of **1**, **2**, and **3** at 10 K (Fig. 5).[13] The spectrum of **2** shows ^{99}Ru and ^{101}Ru hyperfine splittings and also a six-line signal at $g \approx 2.0$, which is assigned to the ^{55}Mn hyperfine interaction. However, the spectrum of **3** shows only one well-resolved eight-line signal at $g \approx 2.0$. Such a signal is typical for octahedral V^{IV} complexes.[14] In contrast **1** gives no ESR signal owing to its $S = 2$ ground state.

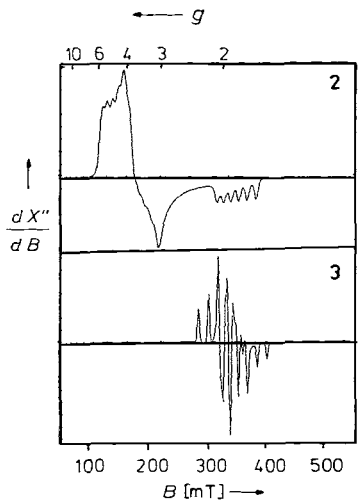

Fig. 5. ESR spectra (X-band) of solid samples of **2** and **3** as BPh_4 salts (not PF_6 salts) at 10 K. (Measurement conditions: 9.436 GHz; 20.0 μW/40 dB; modulation amplitude: 10.0 G).

Thus, the picture that emerges is the following. **1** and **2** are complexes of $Ru^{III}Fe^{III}$ and $Ru^{III}Mn^{III}$ with spin states $S = 2$ and $S = 3/2$, respectively, which are formed by strong antiferromagnetic coupling of the metal centers through a magnetic superexchange mechanism (magnetic orbital "d_{xz}"–"d_{xz}"; spin exchange coupling constant $-J > 300\ cm^{-1}$; $H = -2JS_1S_2$). On the other hand, **3** must be regarded as a complex of $Ru^{II}V^{IV}$ ($S = 1/2$) with a diamagnetic Ru^{II} ion (d^6) and a V^{IV} ion (d^1).

Experimental Procedure

To a solution of 0.5 g of sodium acetate in 40 mL of methanol under argon were added 0.15 g of $L'RuCl_3$ [7] and an equimolar amount of $LMCl_3$ (M = Fe^{III} [15], Mn^{III} [5], or V^{III} [4]), and the mixture was then heated under reflux for 1 h. $NaPF_6$ (0.8 g) was then added, and a stream of argon was passed through until the solution was reduced to half its original volume. At 0 °C crystals of **1**, **2**, or **3** precipitated out; these were then separated by filtration, washed with ethanol

and ether, and dried in air (yield 50–60%). All the complexes gave elemental analyses (C, H, N, Fe, Mn, V) in agreement with the formulas.

Received: January 11, 1990;
supplemented: March 7, 1990 [Z 3732 IE]
German version: *Angew. Chem. 102* (1990) 720

CAS Registry numbers:
1, 127132-96-1; **1'**, 127132-97-2; **2**, 127132-99-4; **3**, 127133-01-1; $L'RuCl_3$, 115140-50-6; $LFeCl_3$, 86823-88-3; $LMnCl_3$, 127133-02-2; $LVCl_3$, 127133-03-3; $[L'Ru(\mu\text{-}O)(\mu\text{-}CH_3CO_2)_2MnL](BPh_4)_2$, 127133-04-4; $[L'Ru(\mu\text{-}O)(\mu\text{-}CH_3CO_2)_2VL](BPh_4)_2$, 127133-05-5.

[1] S. J. Lippard, *Angew. Chem. 100* (1988) 353; *Angew. Chem. Int. Ed. Engl. 27* (1988) 344.
[2] K. Wieghardt, *Angew. Chem. 101* (1989) 1179; *Angew. Chem. Int. Ed. Engl. 28* (1989) 1153.
[3] A. Bodner, S. Drüeke, K. Wieghardt, B. Nuber, J. Weiss, *Angew. Chem. 102* (1990) 60; *Angew. Chem. Int. Ed. Engl. 29* (1990) 68.
[4] M. Köppen, G. Fresen, K. Wieghardt, R. M. Llusar, B. Nuber, J. Weiss, *Inorg. Chem. 27* (1988) 721.
[5] K. Wieghardt, U. Bossek, B. Nuber, J. Weiss, J. Bonvoisin, M. Corbella, S. E. Vitols, J. J. Girerd, *J. Am. Chem. Soc. 110* (1988) 7398.
[6] J. R. Hartman, R. L. Rardin, P. Chaudhuri, K. Pohl, K. Wieghardt, B. Nuber, J. Weiss, G. C. Papaefthymiou, R. B. Frankel, S. J. Lippard, *J. Am. Chem. Soc. 109* (1987) 7387.
[7] P. Neubold, K. Wieghardt, B. Nuber, J. Weiss, *Inorg. Chem. 28* (1989) 459.
[8] U. Bossek, T. Weyhermüller, K. Wieghardt, J. Bonvoisin, J. J. Girerd, *J. Chem. Soc. Chem. Commun. 1989*, 633.
[9] a) J. Glerup, *Acta Chem. Scand. 26* (1972) 3775; b) E. Pedersen, *ibid. 26* (1972) 333.
[10] Crystal structure data for **1'**: orthorhombic, space group *Pnma*, $a = 14.765(3)$, $b = 9.917(2)$, $c = 23.251(6)$ Å, $V = 3404(3)$ Å^3, $Z = 4$, $\varrho_{calcd} = 1.542$ g cm^{-3}, $R = 0.120$, $R_w = 0.119$ for 4144 observed reflections ($F \geq 4\sigma(F)$) and 132 parameters, $Mo_{K\alpha}$ radiation. The ClO_4 ions show considerable disorder; the site symmetry *m* for the dication is not compatible with the ($\lambda\lambda\lambda$) or ($\delta\delta\delta$) conformations of the M-N-C-C-N chelate rings. This disorder is responsible for the relatively poor *R* value and large standard deviations. However, the structure analysis unambiguously confirms the asymmetry of the complex and the atomic connectivities. Crystal structure data for **3**: monoclinic, space group $C2/c$, $a = 23.912(4)$, $b = 19.611(4)$, $c = 17.108(3)$ Å, $\beta = 119.35(1)°$, $V = 6992.8$ Å^3, $Z = 8$, $\varrho_{calcd} = 1.665$ g cm^{-3}. $R = 0.095$ for 4370 observed reflections ($F > 5\sigma(F)$) and 287 parameters, $Mo_{K\alpha}$ radiation. The PF_6 ions show a small disorder. Further details of the crystal structure investigations may be obtained from the Fachinformationszentrum Karlsruhe, Gesellschaft für wissenschaftlich-technische Information mbH, D-7514 Eggenstein-Leopoldshafen 2 (FRG), on quoting the depository number CSD-54378, the names of the authors, and the journal citation.
[11] We thank Dipl.-Chem. *H. Romstedt*, Dr. *J. Ensling*, and Prof. Dr. *P. Gütlich* (Universität Mainz) for the susceptibility measurements and for recording the Mössbauer spectrum of **1**.
[12] J. Sanders-Loehr, W. D. Wheeler, A. K. Shiemke, B. A. Averill, T. M. Loehr, *J. Am. Chem. Soc. 111* (1989) 8084.
[13] We thank Dr. *E. Bill* and Prof. Dr. *A. X. Trautwein* (Medizinische Universität Lübeck) for recording the ESR spectra.
[14] A similar ESR spectrum was also observed for $[(NH_3)_5Ru^{II}\text{-}O=V^{IV}(Hedta)]^{\oplus}$ in solution: F. J. Kristine, R. E. Shepherd, *Inorg. Chem. 17* (1978) 3145.
[15] K. Wieghardt, K. Pohl, W. Gebert, *Angew. Chem. 95* (1983) 739; *Angew. Chem. Int. Ed. Engl. 22* (1983) 727.

^{17}O NMR Spectroscopy of Benzoyl Compounds $Y-C_6H_4-COX$: Sensitivity to Ring Substituents as a Measure of the Electron Demand of the Carbonyl Group**

By *Hans Dahn,* Peter Péchy*, and *Vien Van Toan*

The electrophilicity of a carbonyl group diminishes when it is bound to an electron-donating group (as in $-CONH_2$); however, a numerical scale of electrophilicities seems still to be lacking. The "tool of increasing electron demand"[1] has been devised to measure the electron demand of carbocations. Its principle is that the greater the electron demand of a given center, the more sensitive its properties (reaction rates, spectral data, etc.) will respond to electron-donating or withdrawing substituents; usually the latter are fixed in the *para* position of an aromatic ring directly attached to the center. Applying the "tool" to the problem of carbonyl electrophilicities, one would vary the ring substituent Y in benzoyl compounds $Y-C_6H_4-COX$ and expect that, for a measured carbonyl property, the sensitivity to variation of Y should increase with increasing electrophilicity of the carbonyl group (e.g., aldehydes should be more sensitive than amides). In principle the effect can be measured by any suitable (e.g., spectroscopic) technique; until now, however, promising techniques like determination of IR stretching vibration[2] or bond length[3] have not been successful for this problem. In particular it should be stressed that ^{13}C NMR chemical shifts do *not* yield a measure of the electron density and π-bond order at the carbonyl carbon atom, probably due to internal compensations;[4] moreover, ^{13}C NMR of carbonyl carbon shows an inverse substituent effect; that is, electron-withdrawing substituents increase the shielding instead of diminishing it.[5] We now report results showing that ^{17}O NMR chemical shifts provide an appropriate measure for the characterization of carbonyl groups and for applying the "tool of increasing electron demand" via substituent effects.

^{17}O NMR spectroscopy is distinguished by a large spectral window (>600 ppm for oxygen bound to carbon); shift values are reproducible to ±0.5 ppm, without isotopic enrichment.[6] We have shown that the shift values of carbonyl oxygen atoms, appearing at lower field than bridging oxygen atoms, are particularly sensitive to resonance effects.[7] For instance, while a cyclopropanone (without resonance interaction) shows a shift of $\delta = 524$, a value close to a normal ketone, a cyclopropenone (strong interaction) appears at much higher field ($\delta = 233$), closer to an enolate.[8]

Substituent effects for four series of aromatic carbonyl ^{17}O chemical shifts have already been reported.[9–12] We have measured 12 series of Aryl–COX (Table 1), varying the para substituent Y of the aryl group for each type of –COX (aldehydes, amides, etc.; 6 to 13 compounds in each series).

Table 1. ^{17}O NMR chemical shifts and substituent sensitivity in the aromatic carbonyl compounds *p*- (and *m*-) $Y-C_6H_4-COX$ [a].

COX	δ [b]	ϱ^+ [c]	*R* [d]	SD [e]	n [f]
$COCF_3$	543.6	29.0(C)	0.988	3.7	10
CHO	562.1	26.3(C)	0.993	2.6	9
COCOOEt	538.2	26.2	0.999	0.71	6
COMe [g]	548.6	22.5 [g]	0.986	2.9	8
COBr	513.3	23.8	0.999	0.29	7
COCl	483.6	20.5(C)	0.998	0.75	8
COSEt	489.5	16.0	0.998	0.90	8
COOCOAr	386.4	13.2	0.991	1.5	9
COF	352.6	14.1	0.999	0.43	9
COOMe	337.3	8.5	0.991	0.78	13 [h]
$CONH_2$	326.2	7.3	0.981	1.2	10
COOH	246.1	7.3	0.979	0.87	7
COONa	265.3(W)	5.1(W)	0.979	0.85	12

[a] Chemical shifts were measured at natural abundance on a Bruker WH-360 spectrometer operating at 48.8 MHz; for spectral acquisition parameters see [8]. Standard: tap water; a positive value indicates lower shielding. [b] For Y=H; solvent acetonitrile, unless indicated: W = water depleted in ^{17}O. [c] $\varrho^+ = \delta(0)/\sigma^+$. σ^+ values [14]; solvent acetonitrile, unless indicated: C = tetrachloromethane, W = water depleted in ^{17}O. [d] Correlation coefficient. [e] Standard deviation of regression line. [f] Number of data points (in *p* position, unless indicated). [g] Values from [9]; ϱ^+ recalculated. [h] In *m* and *p* position.

[*] Prof. Dr. H. Dahn, Dr. P. Péchy, Dr. V. V. Toan
Institut de Chimie Organique, Université de Lausanne
rue de la Barre 2, CH-1005 Lausanne (Switzerland)

[**] This work was supported by the Swiss National Science Foundation.

We used aprotic solvents (MeCN, CCl_4), with the exception of water for ArCOONa.[13] The substituent sensitivity was expressed by Hammett-type correlations; as expected for carbonyl group properties, the σ^+ scale[14] gave the statistically best fits. Dual substituent parameter treatment,[15] which separates polar and resonance effects, did not improve the correlations.

As shown in Table 1, ϱ^+ diminishes from trifluoroacetophenones to benzoate anions by a factor of 6, following the diminishing electron demand of the group. The order of decreasing sensitivity corresponds to increasing resonance by electron donation from X. The classical qualitative rules of chemical electrophilicity (and acylating power) are well reflected by the ϱ^+ values ($COO^{\ominus} < CONH_2 \ll COMe$; $COF < COCl < COBr$; $COOR < COSR$; $COMe < COCF_3$). Bridging oxygen atoms show smaller sensitivity:[11] we found a Hammett-type $\varrho = 5.6$ for –O– of methyl benzoates.

Table 1 also gives the shift values δ of the unsubstituted benzoyl derivatives (measured in MeCN, except for –COONa). The shielding increases (lower δ) with increasing donor action of X, as expected for increasing importance of the polar bond structure $C(=X^{\oplus})-O^{\ominus}$. We find a general parallel between ϱ^+ and δ values, which can be expressed by a reasonably good correlation with the slope $\delta/\varrho^+ = 13.1$ ($R = 0.950$). On the other hand, purely inductive effects (as in $COCF_3$ and COCOOEt[16]) do not affect the shift values as much as does resonance.

The chemical shifts of ^{17}O are essentially determined by paramagnetic shielding, which is approximated by the Karplus–Pople equation.[7a] It contains an electronic excitation energy term and a bond-order/charge-density matrix term. The latter term is related to the π-electron density and to chemical electrophilicity. Very often, however, the relative importance of the two terms is not known; for some carbonyl groups the preponderance of the bond order term has been demonstrated, either by calculation[9] or via comparison with NQR values.[16, 17] In our results the correlation between δ and ϱ^+ (which is related to bond order) confirms the importance of the π-electron density term in the benzoyl ^{17}O chemical shifts. This means that the electronic excitation energy term of the Karplus–Pople equation does not vary in a systematic way from one type of benzoyl compound to another; indeed, there exists in this class no correlation between ^{17}O NMR and UV spectra.[18]

In conclusion it appears that ϱ^+ values give a convenient measure of electrophilicity; δ values (simpler to obtain) are more sensitive to resonance than to polar effects.

Received: January 11, 1990 [Z 3733 IE]
German version: *Angew. Chem. 102* (1990) 681

CAS Registry numbers:
$PhCOCF_3$, 434-45-7; PhCHO, 100-52-7; $PhCOCO_2Et$, 1603-79-8; PhCOBr, 618-32-6; PhCOCl, 98-88-4; PhCOSEt, 1484-17-9; $PhCO_2H \cdot Na$, 532-32-1; PhCOF, 455-32-3; $PhCO_2Me$, 93-58-3; $PhCONH_2$, 55-21-0; $PhCO_2H$, 65-85-0.

[1] P. G. Gassmann, A. F. Fentiman, *J. Am. Chem. Soc. 91* (1969) 2549; H. C. Brown, C. G. Rao, M. Ravindranathan, *ibid. 99* (1977) 7663; H. C. Brown, P. v. R. Schleyer: *The Nonclassical Ion Problem*, Plenum Press, New York 1977, p. 163.
[2] R. T. C. Brownlee, J. Di Stefano, R. D. Topsom, *Spectrochim. Acta 31 A* (1975) 1685; R. D. Topsom, *Prog. Phys. Org. Chem. 16* (1987) 193.
[3] F. H. Allen, O. Kennard, D. Watson, L. Brammer, A. G. Orpen, R. Taylor, *J. Chem. Soc. Perkin Trans. 2 1987*, S1.
[4] C. Delseth, T. Nguyen, J.-P. Kintzinger, *Helv. Chim. Acta 63* (1980) 498; H. C. Brown, E. N. Peters, *J. Am. Chem. Soc. 99* (1977) 1712.
[5] J. B. Stothers: *Carbon-13 NMR Spectroscopy*, Academic Press, New York 1972, pp. 279–310; W. F. Reynolds, *Prog. Phys. Org. Chem. 14* (1982) 165.
[6] Reviews: a) J.-P. Kintzinger in P. Diehl, E. Fluck, R. Kosfeld (Eds.): *NMR, Basic Principles and Progress, Vol. 17*, Springer, Berlin 1981, pp. 1–64; b) W. G. Klemperer, *Angew. Chem. 90* (1978) 258; *Angew. Chem. Int. Ed. Engl. 17* (1978) 246.
[7] H. A. Christ, P. Diehl, H. R. Schneider, H. Dahn, *Helv. Chim. Acta 44* (1961) 865.
[8] H. Dahn, M. N. Ung-Truong, *Helv. Chim. Acta 70* (1987) 2130.
[9] R. T. C. Brownlee, M. Sadek, D. J. Craik, *Org. Magn. Reson. 21* (1983) 616.
[10] T. E. S. Amour, M. I. Burgar, B. Valentine, D. Fiat, *J. Am. Chem. Soc. 103* (1981) 1128.
[11] P. Balakrishnan, A. L. Baumstark, D. W. Boykin, *Org. Magn. Reson. 22* (1984) 753.
[12] K.-T. Liu, T.-R. Wu, Y.-C. Lin, *J. Phys. Org. Chem. 2* (1989) 363.
[13] Solvent effects upon individual δ values can be important: H. A. Christ, P. Diehl, *Helv. Phys. Acta 36* (1969) 170. Controls of our series showed, however, only small solvent effects on ϱ^+.
[14] H. C. Brown, Y. Okamoto, *J. Am. Chem. Soc. 80* (1958) 4979; O. Exner: *Correlation Analysis of Chemical Data*, Plenum Press, New York 1988, p. 61.
[15] S. Ehrenson, R. T. C. Brownlee, R. W. Taft, *Prog. Phys. Org. Chem. 10* (1973) 1.
[16] Also –COCN, $\delta = 559$: C. P. Cheng, S. C. Lin, G.-S. Shaw, *J. Magn. Reson. 69* (1986) 58.
[17] C. P. Cheng, T. L. Brown, *J. Am. Chem. Soc. 101* (1979) 2327.
[18] K. Yates, S. L. Klemenko, I. G. Csizmadia, *Spectrochim. Acta 25 A* (1969) 765.

Lithium-Ion-Catalyzed Epoxidation by Triplet Dioxygen: An ab initio Study **

By *Heinz Hofmann* and *Timothy Clark* *

Dedicated to Paul von Ragué Schleyer on the occasion of his 60th birthday

Our recent studies on the metal-ion catalysis of radical,[1, 2] closed-shell,[3] and triplet[4] reactions have demonstrated that complexation to a metal cation or radical cation may facilitate open- or closed-shell reactions, respectively. Most significantly in the context of the present communication, complexation of triplet dioxygen, $^3O_2$, with $Li^{\oplus}$ lowers the barrier to hydrogen abstraction from C-H donors and favors the O-H product thermodynamically.[4] This result, which may have far-reaching consequences for biological systems, encouraged us to consider another important oxidation reaction, the epoxidation of olefins. Both the silver-catalyzed epoxidation of ethylene[5] and the epoxidation of aromatics by cytochrome P450[6] suggest that metals may have a large effect on the course of this reaction. Our H-abstraction work[4] has revealed the predominantly electrostatic nature of this type of catalysis, so that $Li^{\oplus}$ catalysis provides a useful model for the electrostatic component of transition-metal catalysis. We have therefore used ab initio molecular orbital theory[7] to investigate the two related reactions (a) and (b) (adduct formation is indicated by, for example, $[Li:O_2]^{\oplus}$).

$$^3O_2 + C_2H_4 \xrightarrow{(1^*)} {}^3[\underset{\mathbf{2}}{O\text{-}O\text{-}CH_2\text{-}CH_2}] \xrightarrow{(3^*)} \text{oxirane} + {}^3O \qquad \text{(a)}$$

$$^3[Li:O_2]^{\oplus} + C_2H_4 \xrightarrow{(4^*)} {}^3[\underset{\mathbf{5}}{Li:O\text{-}O\text{-}CH_2\text{-}CH_2}]^{\oplus} \xrightarrow{(6^*)} {}^3[\underset{\mathbf{7}}{\text{oxirane}:Li:O}]^{\oplus} \qquad \text{(b)}$$

Both reactions involve two distinct steps with an intermediate minimum (**2** and **5**). The first step, the addition of the

[*] Dr. T. Clark, Dipl.-Chem. H. Hofmann
Institut für Organische Chemie der Universität Erlangen-Nürnberg
Henkestrasse 42, D-8520 Erlangen (FRG)

[**] This work was supported by the Deutsche Forschungsgemeinschaft, the Fonds der Chemischen Industrie, the Volkswagen-Stiftung, and Convex Computer GmbH.

Table 1. Absolute [Hartrees] [a] and relative [kcal mol^{-1}, in parentheses] [b] energies of **1**–**7**.

Species	NIMAG [c]	HF [a]	MP2	MP3	MP4sdtq	ZPE [d]
$^3O_2 + C_2H_4$	0	−227.64963 (0.0)	−228.22566 (0.0)	−228.24518 (0.0)	−228.27600 (0.0)	37.2
1	1	−227.58736 (38.6)	−228.15111 (46.3)	−228.17521 (43.4)	−228.21057 (40.6)	36.8
2	0	−227.60923 (26.5)	−228.16717 (37.9)	−228.19326 (33.7)	−228.22305 (34.4)	38.4
3	1	−227.58936 (37.3)	−228.10892 (72.7)	−228.14640 (61.4)	−228.17702 (61.6)	36.7
^3O + oxirane	0	−227.65129 (0.8)	−228.18166 (29.5)	−228.21124 (23.1)	−228.23487 (27.7)	39.1
$^3O_2$:$Li^{\oplus}$ + C_2H_4	0	−234.90058 (0.0)	−235.47695 (0.0)	−235.49624 (0.0)	−235.52041 (0.0)	37.7
4	1	−234.87603 (15.8)	−235.45406 (14.7)	−235.47393 (14.4)	−235.50866 (7.8)	38.1
5	0	−234.90005 (2.0)	−235.46566 (8.8)	−235.48948 (5.9)	−235.52179 (0.8)	39.4
6	1	−234.88410 (10.4)	−235.41616 (38.2)	−235.45097 (28.5)	−235.48494 (22.3)	37.8
7	0	−234.96912 (−40.0)	−235.50181 (−12.6)	−235.53100 (−18.8)	−235.55593 (−19.3)	40.7
^3O:$Li^{\oplus}$ + oxirane	0	−234.90544 (−1.2)	−235.43804 (26.2)	−235.46770 (19.7)	−235.49176 (19.8)	39.5

[a] Restricted Hartree–Fock (RHF) for closed-shell systems and unrestricted Hartree–Fock (UHF) for radicals. [b] Energies include correction for zero-point vibrations. [c] Number of imaginary frequencies (1, transition state; 0, minimum). [d] Zero-point energy [kcal mol^{-1}].

dioxygen species to the olefin to give a triplet dimethyleneperoxy diradical, **2**, is calculated to be endothermic by 34.4 kcal mol^{-1} in the unperturbed reaction (a) and to have an activation energy of 40.6 kcal mol^{-1} (via transition state **1**). Although it might be expected on the basis of other UHF-based calculated activation energies[8] that the calculated activation energy should be too high because of spin contamination in the UHF wave function, we can still conclude that the barrier to addition of triplet oxygen to olefins is considerably higher than those for, say, oxygen radicals.[9] This result reflects the expected[10] kinetic inactivity of triplet oxygen, even in a reaction that stays on the triplet potential energy surface.

Complexation of the oxygen with $Li^{\oplus}$ [Eq. (b)] changes this situation considerably. The activation energy for the initial addition reaction leading to **5** via transition state **4** is only 7.8 kcal mol^{-1}. The addition reaction is essentially thermoneutral with a calculated energy of 0.8 kcal mol^{-1}. Thus, both the odd-electron bond stabilization of the transition state **4** observed previously for radical addition to olefins[11] and the thermodynamic preference for products with as many bonds as possible between oxygen and an electropositive element (hydrogen or carbon) are found in the effect of $Li^{\oplus}$ complexation on this addition reaction. Triplet oxygen addition to ethylene becomes a fast, reversible process in the presence of $Li^{\oplus}$.

The second stage of the reaction is the concurrent closing of the oxirane ring and cleavage of the O–O bond. This process is found to have a high (61.6 kcal mol^{-1}, transition state **3**) activation energy for the unperturbed reaction (a). The entire process shown in Equation (a) is found to be endothermic by 27.7 kcal mol^{-1}. The calculated activation energy for the $Li^{\oplus}$-catalyzed reaction (b) is, however, only 22.3 kcal mol^{-1} (transition state **6**) and the reaction sequence (b) as far as the complex **7** is exothermic by 19.3 kcal mol^{-1}. Schematic energy profiles for the two reactions are shown in Figure 1. There is comparatively little effect of the $Li^{\oplus}$ on this second stage of the reaction compared with the first step, but the overall effect is significant. In both transition states for the ring closure/bond cleavage (**3**, **6**), the O–O bond stretching precedes the closure of the C–C–O angle. Because these transition states (**3**, **6**) bear little resemblance to the final products, the intrinsic reaction coordinates were followed from the transition states to the products using the IRC option in Gaussian 88.[11] We also note that the orientation of triplet oxygen addition via an s-*trans* transition state is opposite to the s-*cis* orientation found for singlet oxygen addition to ethylene.[12]

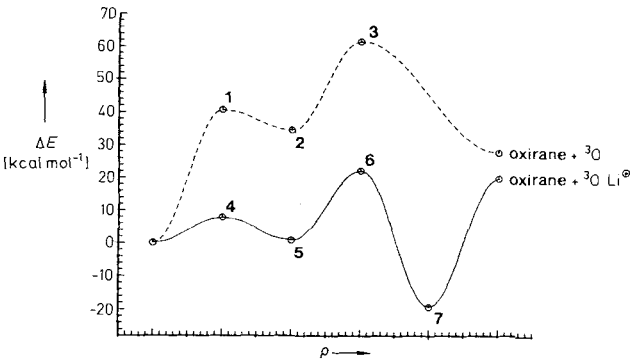

Fig. 1. Schematic energy profiles for the epoxidation of ethylene by $^3O_2$ (dashed line) and by $^3[O_2:Li]^{\oplus}$ (solid line). Energies are relative to the starting materials and the numbering of the stationary points corresponds to that used in the text and structures. ϱ = reaction coordinate.

We emphasize once more[1–4] that such results should be quite general for $^3O_2$ complexed to metal cations. Lithium, which is a computationally convenient model, is expected to show a large effect,[4, 13] but should not be unique. Although our model studies cannot be considered to relate directly to enzymatic systems, we should like to point out that $^3[O_2:Li]^{\oplus}$ can perform both hydrogen abstraction[4] and epoxidation reactions analogous to the reactivity of cytochrome P450.[6] Our calculations thus suggest indirectly that the electrostatic component of cytochrome P450 catalysis may be greater than generally thought. Furthermore, reaction (b) also produces an oxygen atom, so that two epoxidations should be possible with one oxygen molecule. Our results and the remarkable gas-phase reactivity of tran-

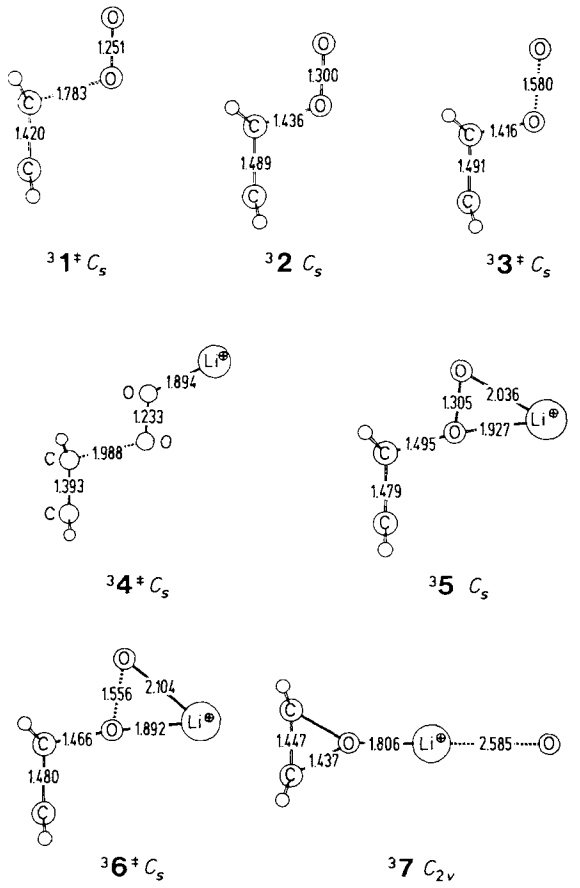

Scheme 1. Structural parameters for **1**–**7** calculated at the UHF/6-31G* level.

sition-metal ions[14] suggest that "naked ion chemistry" may be a remarkably good model for far more complex systems such as zeolites[3, 15] or enzymes.

Received: January 15, 1990 [Z 3740 IE]
German version: *Angew. Chem. 102* (1990) 697

CAS Registry numbers:
C_2H_4, 74-85-1; $Li^{\oplus}$, 17341-24-1.

[1] T. Clark, *J. Chem. Soc. Chem. Commun. 1986*, 1774–1776.
[2] A. von Onciul, T. Clark, *J. Chem. Soc. Chem. Commun. 1989*, 1082–1084.
[3] T. Clark, *J. Am. Chem. Soc. 110* (1988) 1672–1678.
[4] H. Hofmann, T. Clark, unpublished.
[5] See, for instance, K. A. Jørgensen, *Chem. Rev. 89* (1989) 431–458.
[6] V. Ullrich, *Top. Curr. Chem. 83* (1979) 67–104.
[7] All calculations used the Gaussian 88 (M. J. Frisch, M. Head-Gordon, H. B. Schlegel, K. Raghavachari, J. S. Binkley, C. Gonzalez, D. J. Defrees, D. J. Fox, R. A. Whiteside, R. Seeger, C. F. Melius, J. Baker, L. R. Kahn, J. J. P. Stewart, E. M. Fluder, S. Topiol, J. A. Pople, Gaussian, Inc., Pittsburgh PA.) or Cadpac 4.0 (R. D. Amos, J. E. Rice, CADPAC: *The Cambridge Analytic Derivatives Package*, issue 4.0, Cambridge 1987) programs on a Convex C 2 or a Cray YMP-432. The 6-31 G* basis set (P. C. Hariharan, J. A. Pople, *Theor. Chim. Acta. 28* (1973) 213.) was used throughout. The natures of the stationary points were confirmed by diagonalization of the force-constant matrices calculated at the same level. The energies discussed in the text are corrected for zero-point energies and include a fourth-order Møller-Plesset correction for electron correlation including single, double, triple, and quadrupole excitations (MP4sdtq; C. Møller, M. S. Plesset, *Phys. Rev. 46* (1934) 618; J. S. Binkley, J. A. Pople, *Int. J. Quantum Chem. 9* (1975) 229; J. A. Pople, J. S. Binkley, R. Seeger, *Int. J. Quantum Chem. Suppl. 10* (1976) 1; M. J. Frisch, R. Krishnan, J. A. Pople, *Chem. Phys. Lett. 75* (1980) 66). Because the transition state **3** occurs very early in the ring-closure reaction, the intrinsic reaction coordinate was followed downhill from the transition state to the oxirane product in order to confirm the nature of the reaction.
[8] C. Gonzalez, C. Sosa, H. B. Schlegel, *J. Phys. Chem. 93* (1989) 2435–2440, 8388.
[9] C. Sosa, H. B. Schlegel, *J. Am. Chem. Soc. 109* (1987) 4193–4198.
[10] See, for instance, G. A. Hamilton in O. Hayaishi (Ed.): *Molecular Mechanism of Oxygen Activation*, Academic Press, New York 1974, pp. 405–451.
[11] Note that possible alternative reactions, such as dioxetane formation, have not been considered in this study and that they may compete with the epoxidation considered here.
[12] G. Tonachini, H. B. Schlegel, F. Bernardi, M. A. Robb, *THEOCHEM 31* (1986) 221–227.
[13] T. Clark, *J. Am. Chem. Soc. 111* (1989) 761–763.
[14] H. Schwarz, *Acc. Chem. Res. 22* (1989) 282–287.
[15] A. K. Ghosh, L. Kevan, *J. Phys. Chem. 92* (1988) 4439–4446.

Structure Determination of $NaCD_3$ Powders at 1.5 and 300 K by Neutron and Synchrotron-Radiation Diffraction**

By Erwin Weiss, Siegfried Corbelin, Jeremy Karl Cockcroft,* and *Andrew Nicholas Fitch*

Dedicated to Professor Paul von Ragué Schleyer on the occasion of his 60th birthday

We reported earlier[1] the synthesis of methylsodium containing variable amounts of $LiCH_3$ and were able to determine the structures of these preparations from their X-ray powder data. The preparations were formed from $LiCH_3$ and sodium *tert*-butoxide by a metal–metal exchange reaction [Eq. (a)] and, depending on the composition of the di-

$$LiCH_3 + NaO\mathit{t}Bu \xrightarrow{\text{ether/hexane}} NaCH_3 + LiO\mathit{t}Bu \quad (a)$$

ethyl ether/hexane solvent system, contained $NaCH_3$ and $LiCH_3$ in a molar ratio of about 3:1 to 36:1. The amount of $LiCH_3$ was lowest in pure ether. In all these reactions, $LiCH_3$ was first prepared and dissolved $NaO\mathit{t}Bu$ then added.

X-ray investigation of the fine powder gave a cubic macrocell ($a = 2020$ pm, space group $F\bar{4}3c$) containing 24 tetrameric $(NaCH_3)_4$ aggregates. Although the structure is therefore closely related to that of methyllithium,[2] the arrangement of the $(NaCH_3)_4$ units in the lattice is considerably more complicated. They form a zeolite-like structure with large cavities, which can incorporate complete $(LiCH_3)_4$ units up to the structurally determined $NaCH_3$ ratio of 3:1 without noticeable lattice expansion.

A phase transition, involving formation of a more compact structure, is observed at about 80 °C on drying lithium-poor methylsodium preparations. We have now succeeded in directly preparing this methylsodium by dropwise addition of the $LiCH_3$ solution to a previously prepared $NaO\mathit{t}Bu$

[*] Prof. Dr. E. Weiss, Dipl.-Chem. S. Corbelin
Institut für Anorganische und Angewandte Chemie der Universität
Martin-Luther-King-Platz 6, D-2000 Hamburg 13 (FRG)
Dr. J. K. Cockcroft
Institut Laue-Langevin, 156 X
F-Grenoble 38042 Cedex (France)
Dr. A. N. Fitch
Department of Chemistry, University of Keele
GB-Staffordshire ST5 5BG (UK)

[**] Metal-Alkyl and Metal-Aryl Compounds, Part 43. This work was supported by the Deutsche Forschungsgemeinschaft and the Fonds der Chemischen Industrie. We thank ILL and SERC Daresbury for making possible the neutron and synchrotron-radiation diffraction investigations. We also are grateful to Dipl.-Chem. *H. Viebrock* for his help in analyzing the data. Part 42: N. P. Lorenzen, E. Weiss, *Angew. Chem. 102* (1990) 322; *Angew. Chem. Int. Ed. Engl. 29* (1990) 300.

solution, followed by workup at room temperature without addition of hexane. The dried preparations are stable at room temperature, but they still contain small amounts of $LiCH_3$ (ca. 20:1). As shown by the structure investigation described below, this preparation is, in fact, *true methylsodium*. The formation of the $NaCH_3$–$LiCH_3$ inclusion compounds obtained earlier was apparently due to a template effect. Addition of NaO*t*Bu to methyllithium, which is also tetrameric in diethyl ether,[3] results in precipitation of $NaCH_3$, which forms a unique host lattice around these tetramers.

X-ray structure investigations of the $NaCH_3$ powders afforded diagrams containing numerous lines, which owing to insufficient resolution, could not be indexed. This was only accomplished by neutron-diffraction studies using the high-resolution powder diffractometers of the Laue-Langevin Institut in Grenoble. These investigations required deuterated methylsodium, $NaCD_3$, which we prepared from $LiCD_3$[4] and NaO*t*Bu.[5]

Measurements were carried out at 1.5 and 300 K and revealed no phase transformations. We will report details of these measurements elsewhere[5] (cf. also Refs. [4, 2c]). Although the multilined diagram showed numerous overlaps, it could finally be indexed as orthorhombic *I*-centered.

Further structure determination was possible by synchrotron-radiation diffraction investigations, carried out at the SERC Daresbury Laboratory.[6] These studies allowed determination of the positions of the Na and C atoms by direct methods[7] and then of the total structure (space group *I*222), including the D atoms, from the neutron-diffraction data. Refinement was performed by the Rietveld method[8, 9] (Fig. 1).

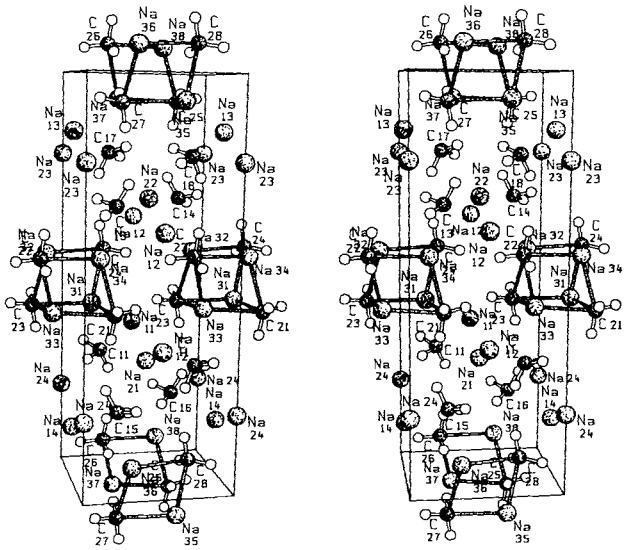

Fig. 1. Stereoscopic view [13] of the unit cell of $NaCD_3$ with atom numbering (symmetry-related atoms differ in the value of the second digit). Tetramers are highlighted by showing the heterocubane framework. $a = 676.86(1)$, $b = 1860.16(4)$, $c = 657.62(1)$ pm, $\varrho_{calcd} = 1.315$ g cm^{-3} ($NaCD_3$); refinement to R_{wp} (profile) $= \{\Sigma[w(y_o - y_c)^2]\}^{1/2}/\Sigma[w(y_o)^2] = 0.057$. Anisotropic for D, isotropic for Na and C (all values for neutron diffraction at 1.5 K). Values for 300 K as well as further details (including those of the synchrotron-radiation investigations) will be presented elsewhere [5].

The use of neutron diffraction to determine complicated structures has so far been used only in special cases. The structure elucidation described here is one of the first ab initio structure determinations combining neutron and synchrotron-radiation diffraction.[11] It gave the structure shown in Figures 1 to 3.

The methylsodium structure is a unique, relatively complicated structure type. The unit cell contains 16 formula units distributed over positions having different coordination numbers [e.g., four Na1 (in *h*), four Na2 (in *i*), and eight Na3 (in *k*)[12]]. Examination of several neighboring unit cells (Fig. 2) clearly reveals that half of the ions (eight Na3, eight

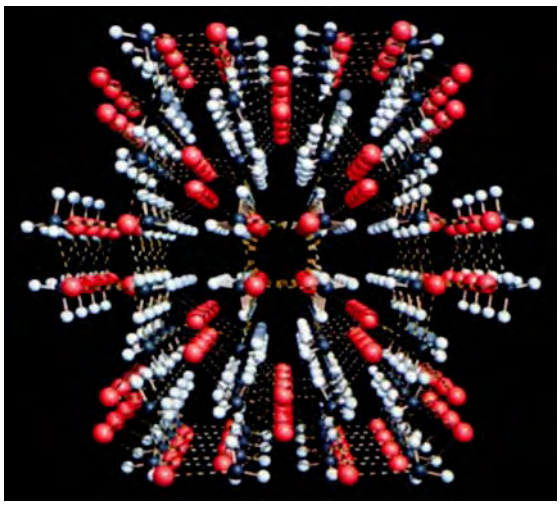

Fig. 2. Ball-and-stick model of the methylsodium lattice ($Na^{\oplus}$, red; C, gray; *x* axis horizontal, *y* axis vertical to projection plane, as in Fig. 1). In the middle of the picture and on the right and left sides are four tetramers, one behind the other (the long yellow broken lines correspond to short Na–C distances). Half tetramers lie at the top and bottom of the picture. The Na–C distances to the ions lying in between and not belonging to the tetramers are shorter (broken lines) or longer (dotted lines) depending on the orientation of the methanide ions.

C2 together with associated D atoms) are part of tetramers, $(NaCD_3)_4$, which are arranged in rows parallel to the *x* and *z* axes. The remaining eight $Na^{\oplus}$ and eight $CD_3^{\ominus}$ ions (Na1, Na2, C1 together with associated D atoms) lie between these rows and the $Na^{\oplus}$ ions form a zigzag chain parallel to the *z* axis. All ions that are not part of tetramers link them through Na–C contacts.

In the tetramers (space-filling model, Fig. 3), the central Na_4C_4 unit forms a strongly distorted cube. The $CD_3^{\ominus}$ ions together with their D atoms are directed outward and, as observed for methyllithium,[2] staggered with respect to the three neighboring $Na^{\oplus}$ atoms.

The Na–C distances to and between the eight $Na^{\oplus}$ and eight methanide ions outside the tetramers vary much more strongly than those within the tetramers (cf. also Fig. 2). They are short (252.8 and 256.9 pm) for direct contact between $Na^{\oplus}$ and the lone pair of the methanide ion and markedly longer when $Na^{\oplus}$ is located on the side opposite the lone pair (283.4 and 291.1 pm; at 1.5 K in each case).

For KCD_3 we have already discussed in detail the structure of the methanide ion.[4] The precise structure determinations of $LiCD_3$[2c] and $NaCD_3$ once again reveal the *trigonal-pyramidal structure of methanide ions* in the solid state. The methanide parameters for $NaCD_3$ (C-D 109.4 pm,

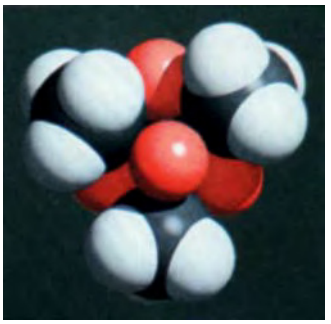

Fig. 3. Space-filling model of the $(NaCD_3)_4$ unit. The $Na^{\oplus}$ radii were arbitrarily set at 110 pm (usual ionic radius 97 pm). Owing to slight distortion, the Na–Na and Na–C distances vary somewhat (Na-Na 297–317, Na-C 257–264 pm, at 1.5 K). Each tetramer is surrounded by four methanide ions (not shown), which are arranged with their lone pairs directed toward the $Na^{\oplus}$ ions, resulting in short distances (256.9 pm).

D-C-D 106.2°; average values, 1.5 K) are in agreement with those for $LiCD_3$ and KCD_3.

This study thus closes the gap that existed for the structures of alkali-metal methanides. The structure of methylsodium is intermediate between that of methyllithium and methyl compounds of the heavy metals,[4, 14, 15] insofar as both tetrameric aggregates (as in methyllithium) and discrete ions (as in methanides of the higher alkali metals) are present. The optimal packing in the crystal causes the density of $NaCH_3$ to be appreciably larger than that of the $LiCH_3$-stabilized forms.

Received: December 15, 1989 [Z 3691 IE]
German version: *Angew. Chem. 102* (1990) 728

CAS Registry number:
$NaCD_3$, 126752-83-8.

[1] E. Weiss, G. Sauermann, G. Thirase, *Chem. Ber. 116* (1983) 74.
[2] a) E. Weiss, E. A. C. Lucken, *J. Organomet. Chem. 2* (1964) 197; b) E. Weiss, G. Hencken, *ibid. 21* (1970) 265; c) E. Weiss, T. Lambertsen, B. Schubert, J. K. Cockroft, A. Wiedenmann, *Chem. Ber. 123* (1990) 79.
[3] P. West, R. Waack, *J. Am. Chem. Soc. 89* (1967) 4395.
[4] E. Weiss, T. Lambertsen, B. Schubert, J. K. Cockcroft, *J. Organomet. Chem. 358* (1988) 1.
[5] E. Weiss, S. Corbelin, J. K. Cockcroft, A. N. Fitch, *Chem. Ber.*, in print.
[6] Synchroton Radiation Source (SRS), SERC Daresbury Laboratory, Warrington, UK. Measurements on the 9.1 diffractometer at 300 K, wavelength 109.67 pm.
[7] G. Sheldrick, *SHELXS-86: Programs for Crystal Structure Solution*, Universität Göttingen 1986.
[8] H. M. Rietveld, *J. Appl. Crystallogr. 2* (1969) 65. The refinement was carried out with a program [9] that also takes into consideration pseudo-Voigt reflection profiles, a mixture of Gaussian and Lorentzian profiles. The following scattering lengths [fm] were used: 3.630 (Na), 6.6484 (C), 6.674 (D)[10].
[9] J. K. Cockcroft: *PROFIL, a Rietveld Refinement Program with Chemical Constraints*, Institut Laue-Langevin, Grenoble, France.
[10] G. Koester, H. Rauch: *Recommended Values of Neutron Scattering Lengths (IAEA Rep. 2517/RB)*, IAEA, Vienna 1983.
[11] A. N. Christensen, D. E. Cox, M. S. Lehmann, *Acta Chem. Scand. 43* (1989) 19, and references cited therein.
[12] T. Hahn (Ed.): *International Tables for X-ray Crystallography, Vol. A*, D. Reidel, Dordrecht 1983.
[13] Structures drawn with *SCHAKAL, a FORTRAN Program for the Graphical Representation of Molecular and Crystallographic Models*: E. Keller, *J. Appl. Crystallogr. 22* (1989) 19; color graphics obtained with IBM 6150 (display screen 5081, 1000 × 1000 pixels).
[14] a) E. Weiss, G. Sauermann, *Angew. Chem. 80* (1968) 123; *Angew. Chem. Int. Ed. Engl. 7* (1968) 133; b) *Chem. Ber. 103* (1970) 265.
[15] E. Weiss, H. Köster, *Chem. Ber. 110* (1977) 717.

Optically Active Deltacyclanes and Deltacyclenes by Enantioselective Catalysis**

By *Henri Brunner,** *Manfred Muschiol*, and *Franz Prester*

Norbornadiene reacts with olefins and acetylenes in the presence of catalysts to form deltacyclanes and deltacyclenes, respectively. We report here that by carrying out such reactions using enantioselective transition-metal catalysts it is possible to obtain asymmetric inductions with remarkably high values.

Phosphane-modified nickel cyanide catalysts have been found to be effective in catalyzing the reaction of norbornadiene with acrylonitrile to give **1**.[1] 3 mL of norbornadiene is reacted with 3 mL of acrylonitrile in the presence of about 0.2 g of catalyst in an autoclave for 20 h at 120 °C. After filtering to remove the catalyst the product **1** is purified by distillation. The enantiomer analysis is carried out by first saponifying the isomeric nitriles **1** to give the corresponding carboxylic acids, which are then converted to the diastereomeric menthyl esters, and these are separated by gas chromatography in a 50-m CP-Sil-88-Fame quartz capillary column.[2] Using $(PPh_3)_2Ni(CN)_2$ as the catalyst gives **1** in 70–80% yield, with a diastereomeric ratio of 80:20. Enantioselective control was achieved by using, instead of PPh_3, the optically active phosphanes Diop[3] and Norphos.[4, 5] Whereas catalysts containing Diop gave a quantitative yield with a diastereomeric ratio of 60:40, the yield using Norphos-containing catalysts fell to about 10% (diastereomeric ratio 55:45). The asymmetric induction values obtained with catalysts based on Norphos (12 and 15% *ee*) are somewhat higher than those for catalysts based on Diop (4 and 3% *ee*).

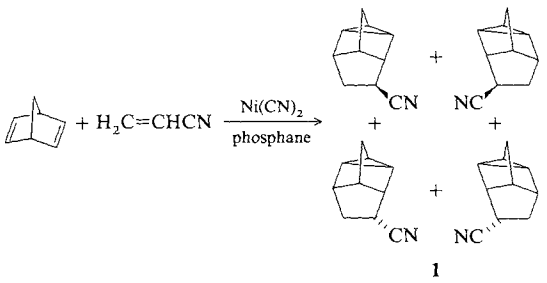

1

In contrast to the reaction with acrylonitrile, in the reaction of norbornadiene with phenylacetylene no diastereomers are possible; the deltacyclene **2** consists only of the two enantiomers. For this reaction in situ catalysts based on $Co(acac)_3$, Diphos and Et_2AlCl have been used.[6, 7] When Norphos is used instead of Diphos the reaction of approximately 1 mL of norbornadiene with 1 mL of phenylacetylene in THF at 35 °C is complete in 4 h. The yield of the phenyl-substituted deltacyclene **2** is quantitative. The enantiomeric purity was determined by gas chromatography using a perpentylated β-cyclodextrin column,[8] which gives a peak separation down to the baseline for the enantiomers of **2**. For Norphos-based catalysts the value was 98.4% *ee*, with (−)-**2** having the shorter retention time and (+)-**2** the longer.

[*] Prof. Dr. H. Brunner, M. Muschiol, Dipl.-Chem. F. Prester
Institut für Anorganische Chemie der Universität
Universitätsstrasse 31, D-8400 Regensburg (FRG)

[**] Asymmetric Catalysts, Paper 55. This work was supported by the Deutsche Forschungsgemeinschaft, the Fonds der Chemischen Industrie and BASF AG, Ludwigshafen. Paper 54: H. Brunner, M. Muschiol, T. Wischert, J. Wiehl, *Tetrahedron Asymmetry, 1* (1990) 159.

When (−)-Norphos is used the main product is (−)-**2**, no second peak for (+)-**2** being detectable in the gas chromatogram following the large (−)-**2** peak. Catalysts made from (+)-Norphos give predominantly (+)-**2**. In this case the first peak in the chromatogram is that of the minor component (−)-**2**. Under these measurement conditions it was possible to determine the isomer ratio as 0.8:99.2, corresponding to an enantiomeric purity of 98.4% *ee*. With Diop-based catalysts in THF at 35 °C no reaction occurred within 4 h. In benzene there was a reaction giving **2**, but the enantiomeric purity was only about 20% *ee*.

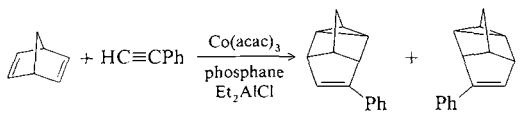

2

The reaction of norbornadiene with acrylonitrile using Ni catalysts made from Diop or Norphos, giving **1**, only occurs under harsh conditions, and gives a mixture of diastereomers with low asymmetric induction; it is not very suitable as a preparative method. The reaction of norbornadiene with phenylacetylene using Norphos-Co catalysts to give **2** proceeds under mild conditions and requires only small amounts of catalyst (0.2–0.3 mol %; norbornadiene:phenylacetylene:Norphos:cobalt = 500:500:1.5:1). The chemical yield is quantitative, with a remarkably high enantiomeric purity of 98.4% *ee*. The reaction of norbornadiene with phenylacetylene to give the deltacyclene **2** therefore ranks as one of the best enantioselective reactions catalyzed by transition-metal complexes that have so far been reported.

Experimental Procedure

4-Phenyltetracyclo[4.3.0.0^{2,9}.0^{3,7}]non-4-ene **2**: 0.95 mL (9.4 mmol) of norbornadiene and 1.00 mL (9.1 mmol) of phenylacetylene were added under nitrogen to 7.1 mg (2×10^{-2} mmol) of Co(acac)$_3$ and 14 mg (3×10^{-2} mmol) of (+)-Norphos in 1 mL of dry THF. The catalytically active Co species was then generated by adding 5 mL of a 1 M solution of diethylaluminum chloride in hexane. The reaction mixture was stirred for 4 h at 35 °C. 5 mL of isopropanol was then dripped in to decompose the Et$_2$AlCl. The volatile constituents were removed by vacuum distillation at room temperature. **2** was then isolated by vacuum distillation at 100 °C in a Kugelrohr apparatus. $[\alpha]_D^{20}$ 56.3 (c = 1, CHCl$_3$). The ^{1}H NMR spectrum and mass spectrum of **2** were identical to those of a reference sample. [6] Yield 100%, enantiomeric purity 98.4% *ee*, both determined by gas chromatography with naphthalene as standard using a 40-m-Lipodex-C column. [8] Retention times: (−)-**2** 120.7 min, (+)-**2** 123.7 min (column temperature 104 °C, carrier gas H$_2$, flow rate 4–5 mL min^{-1} at 1.7 bar, injection temperature 170 °C).

Received: February 2, 1990 [Z 3776 IE]
German version: *Angew. Chem. 102* (1990) 680

CAS Registry numbers:
(−)-**2**, 127279-29-2; (+)-**2**, 127256-90-0; Co(acac)$_3$, 21679-46-9; norbornadiene, 121-46-0; phenylacetylene, 536-74-3; (+)-Norphos, 71042-54-1; diethylaluminum chloride, 96-10-6.

[1] G. N. Schrauzer, P. Glockner, *Chem. Ber. 97* (1964) 2451.
[2] H. Brunner, M. Muschiol, *Monatsh. Chem.*, in press.
[3] H. B. Kagan, T. P. Dang, *J. Am. Chem. Soc. 94* (1972) 6429.
[4] H. Brunner, W. Pieronczyk, *Angew. Chem. 91* (1979) 655; *Angew. Chem. Int. Ed. Engl. 18* (1979) 620.
[5] H. Brunner, W. Pieronczyk, B. Schönhammer, K. Streng, I. Bernal, J. Korp, *Chem. Ber. 114* (1981) 1137.
[6] J. E. Lyons, H. K. Myers, A. Schneider, *Ann. N. Y. Acad. Sci. 333* (1980) 273.
[7] M. Lautens, C. M. Crudden, *Organometallics 8* (1989) 2733.
[8] J. Ehlers, W. A. König, S. Lutz, G. Wenz, H. tom Dieck, *Angew. Chem. 100* (1988) 1614; *Angew. Chem. Int. Ed. Engl. 27* (1988) 1556.

Reactivity in Intramolecular Radical Reactions: A Comparison of Hydrogen Transfer with Alkene Addition**

By *Corrado Berti, Lebert Grierson, Jean A.-M. Grimes, M. John Perkins,** and *Bulent Terem*

Intramolecular hydrogen-atom transfers and intramolecular radical additions have been extensively studied and have found important roles in synthesis,[1] yet the use of effective molarities (EM values)[2] as a means of relating the rates of these free-radical rearrangements to rates of suitable intermolecular models has only occasionally been mentioned.[3]

EM values for ionic reactions have been widely reported, and figures approaching, or greater than, the entropy-controlled limit[4] of ca. 10^8 M have been encountered for examples of nucleophilic attack on carbonyl carbon.[2] In contrast, when the intramolecular process involves rate-limiting proton transfer, EM values are several orders of magnitude smaller (generally less than 100 M). In this communication we examine both published and new rate data, which suggest that in radical chemistry a similar dichotomy exists between intramolecular addition and intramolecular hydrogen-atom transfer.

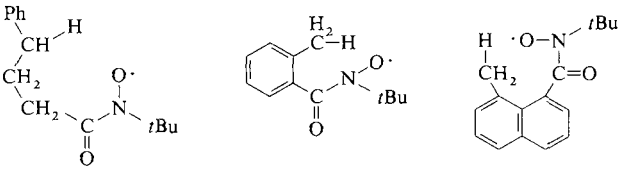

1 **2** **3**

The new results have been obtained with acyl *tert*-butylnitroxides R′CON(O·)*t*Bu. These may often be isolated,[5] yet are sufficiently reactive to oxidize a variety of organic substrates.[6] Some intramolecular reactions have also been noted;[7] comparison of the reported rate of intramolecular benzylic hydrogen-atom transfer (k_{intra}) in **1** with that of intermolecular reaction (k_{inter}) between undecanoyl *tert*-butyl nitroxide and ethylbenzene yields an EM value close to unity (Table 1).

Table 1. Some EM values for intramolecular reactions of nitroxides.

	Compound	T [K]	EM [M]
Intramolecular benzylic hydrogen abstraction	**1**	382	1.4 [a]
	2	358	12.8 [b]
	3	358	44 [b]
Alkene addition	**5**	398	$5(\pm3)\times10^5$ [b]

[a] Based on data in [7]. [b] This work; for compounds **2** and **3**, inter- and intramolecular rates were measured at the same temperatures.

[*] Prof. M. J. Perkins, C. Berti, L. Grierson, J. A.-M. Grimes, B. Terem
Department of Chemistry, Royal Holloway and Bedford New College
GB-Egham, Surrey TW20 0EX (UK)

[**] We are grateful to the Royal Society and the S. E. R. C. for financial support. *M. J. P.* is particularly indebted to Dr. *K. U. Ingold* and Dr. *D. Griller* (N. R. C. Ottawa) and Prof. *A. L. J. Beckwith* (A. N. U. Canberra) for their generous hospitality during which parts of this investigation were completed.

We have now examined more constrained species. Thus, rate measurements on intramolecular reaction in **2** (formed by oxidation[5] of the corresponding hydroxamic acid[8]) and on the intermolecular reaction between benzoyl *tert*-butyl nitroxide and toluene give an EM value of 12.8 M for **2**. Although this increase relative to **1** is consistent with an entropic factor of ca. 10 expected for freezing one internal rotation,[9] it takes no account of the small polar effect of the carbonyl substituent in **2**.[10] A somewhat higher EM value (44 M) was obtained for **3** for which any polar effect would be minimized (rate comparison with the reaction between α-methylnaphthalene and α-naphthoyl *tert*-butyl nitroxide).

Recognizing the parallel between these low EM values and those found in proton-transfer reactions, we then turned our attention to intramolecular addition. Benzoyl *tert*-butyl nitroxide affords a 2:1 adduct with *trans*-stilbene.[11] We therefore prepared the hydroxamic acid **4**,[8] which, by one-electron oxidation, was expected to give **5**, whose cyclization rate could then be compared with that of the intermolecular addition of benzoyl *tert*-butyl nitroxide to stilbene.

Compound **4** is *different in kind* from other *N*-*tert*-alkylhydroxamic acids in that it undergoes rapid, spontaneous, and essentially quantitative autoxidation to a mixture of two hydroperoxides identified as the stereoisomers **6**.[12] This

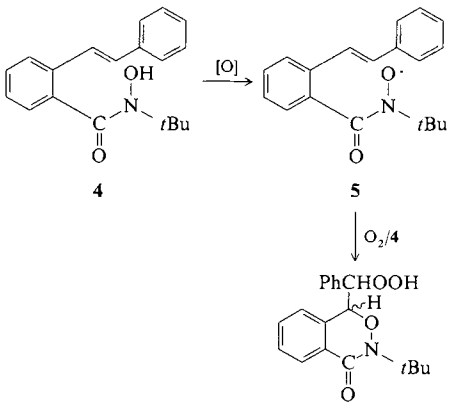

suggests that the cyclization of **5** is indeed very fast. Nitroxide **5** (a_N = 7.8 G) was therefore generated in the absence of oxygen by ultraviolet irradiation of degassed solutions of **4** in *tert*-butylbenzene containing 10% di-*tert*-butyl peroxide and its first-order decay was monitored by ESR spectroscopy over the temperature range −40 to −10 °C, giving $\log A = 9.08$ and $E_a = 12.3$ kcal mol^{-1}.

There is no detectable reaction between benzoyl *tert*-butyl nitroxide and *trans*-stilbene at room temperature, either in the presence or absence of oxygen. The rate constant for the addition of this radical to stilbene was found to be 0.0125 M^{-1} s^{-1} in O_2-free *tert*-butylbenzene at 125 °C.[13] Extrapolation of the cyclization rate data to 125 °C gives an EM value for the intramolecular reaction of $5(\pm 3) \times 10^5$ M. Any polar effect of carbonyl on the intramolecular reaction is again expected to be very small.[14]

Although EM values of ca. 1–100 M have been deduced previously[3] for hydrogen-transfer processes, a similarly low value, ca. 40 M, was also estimated for intramolecular addition (in the rearrangement of 5-hexenyl radicals[15]). However, this estimate is based on comparison with intermolecular reaction *at the unsubstituted* carbon of a terminal alkene. A more acceptable comparison may be made between cyclization of the 6-methyl-5-heptenyl radical (**7**) and alkyl addition to 2-methylbut-2-ene. Careful consideration of published

7

rate data for these reactions[16] suggests that EM values for hexenyl rearrangements may be as high as 10^5 M.

These data, taken together with the direct measurements on nitroxide reactions reported here for the first time, support the hypothesis that intramolecular hydrogen-atom transfers, like proton transfers, generally have low EM values, whereas intramolecular radical additions, like their nucleophilic counterparts, may generally have much higher ones.

For ionic reactions, more than one interpretation of this divergent behavior has been considered,[2, 17, 18] and it seems probable that several factors may contribute. The suggestion that intramolecular proton transfer has a significant enthalpic disadvantage due to the inaccessibility of a colinear (X···H···Y) transition state,[18–20] while attractive, seems to be contradicted by recent calculations by *Dorigo* and *Houk*.[21]

From the standpoint of synthesis it is clear that intramolecular atom transfer, like intramolecular addition, is often sufficiently rapid to accomplish preparatively useful transformations, although our efforts to achieve remote functionalization of a steroid by oxidation of the

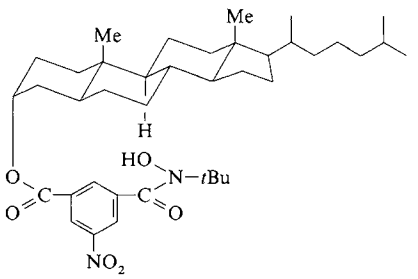

8

3α-cholestanol derivative **8** (m.p. 159–160°)[8] gave a highly persistent nitroxide showing no evidence of intramolecular reaction.

Received: November 21, 1989;
revised: March 12, 1990 [Z 3645 IE]
German version: *Angew. Chem. 102* (1990) 684

CAS Registry numbers:
1, 73312-31-9; **2**, 127063-88-1; **3**, 127063-89-2; **4**, 127085-51-2; **5**, 127063-90-5; **6**, 127063-91-6; **8**, 127085-52-3; (*E*)-(PhCH=)$_2$, 103-30-0; PhCON(O)*t*Bu, 35822-90-3.

[1] Hydrogen-atom transfers include the well-known Hofmann-Löffler-Freytag [M. E. Wolff, *Chem. Revs. 63* (1963) 55] and Barton reactions [R. H. Hesse, *Adv. Free Rad. Chem. 3* (1969) 83]. Intramolecular additions have been widely exploited recently: see, e.g., D. P. Curran, *Synthesis* 1988, 417, 489; A. L. J. Beckwith, B. P. Hay, *J. Am. Chem. Soc. 111* (1989) 2674; T. V. Rajan Babu, T. Fukunaga, G. S. Reddy, *ibid. 111* (1989) 1759; M. D. Bachi, D. Denenmark, *ibid. 111* (1989) 1886; D. L. J. Clive, T. L. B. Boivin, *J. Org. Chem. 54* (1989) 1997; H. Ishibashi, T. S. So, T. Sato, K. Kuroda, M. Ikeda, *J. Chem. Soc. Chem. Commun. 1989*, 762, and references therein.

[2] EM = k_{intra}/k_{inter}; see, e.g., A. J. Kirby, *Adv. Phys. Org. Chem. 17* (1980) 183.

[3] A. L. J. Beckwith, K. U. Ingold in P. de Mayo (Ed.), *Rearrangements in Ground and Excited States, Vol. 1*, Academic Press, New York 1980, p. 161.

[4] M. C. Page, W. P. Jencks, *Proc. Natl. Acad. Sci. USA 68* (1971) 1678.
[5] P. F. Alewood, S. A. Hussain, T. C. Jenkins, M. J. Perkins, A. H. Sharma, N. P. Y. Siew, P. Ward, *J. Chem. Soc. Perkin Trans. 1 1978*, 1066.
[6] M. J. Perkins, *Rev. Chem. Intermed. 7* (1986) 133, and references therein.
[7] C. Berti, M. J. Perkins, *J. Chem. Soc. Chem. Commun. 1979*, 1167.
[8] All new compounds had satisfactory elemental analyses and/or mass spectra, as well as IR and ^{1}H NMR spectra consistent with the proposed structures.
[9] See, for example, F. D. Lewis, R. W. Johnson, D. R. Kory, *J. Am. Chem. Soc. 96* (1974) 6188.
[10] S. A. Hussain, T. C. Jenkins, M. J. Perkins, *J. Chem. Soc. Perkin Trans. 1 1979*, 2809.
[11] S. A. Hussain, T. C. Jenkins, M. J. Perkins, N. P. Y. Siew, *J. Chem. Soc. Perkin Trans. 1 1979*, 2803.
[12] The isomers cocrystallized; only one (m.p. 138–140°) was freed from its diastereomer. The alternative structures that would have arisen from 7-*endo* cyclization were excluded by dehydration of **6** with CH_3COCl/pyridine [N. A. Porter, J. S. Wujek, *J. Org. Chem. 52* (1987) 5085] to give the ketone **A**, characterized by the presence (^{1}H NMR) of an unsubstituted benzoyl group.

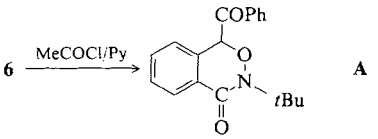

[13] [Stilbene] = 0.3 M; competing first-order self-reaction of the radical accounts for only ca. 10% reaction. Pseudo-first-order plots were linear over the radical concentration range studied (ca. 10^{-4} M); at lower concentration there was evidence that the initial radical addition to stilbene is reversible. Experimental rate constants for both this and the intramolecular reaction were halved to allow for reaction of the initial adduct with a second molecule of nitroxide.
[14] Data are not available for nitroxide additions to substituted stilbenes, but the carbonyl substituent might be expected to retard the intramolecular reaction very slightly; c.f. data for CCl_3 addition: J. I. G. Cadogan, P. W. Inward, *J. Chem. Soc. 1962*, 4170.
[15] See also B. Giese: *Radicals in Organic Synthesis*, Pergamon, Oxford 1986, pp. 141, 142.
[16] Based on data in: A. L. J. Beckwith, I. A. Blair, G. Phillipou, *Tetrahedron Lett. 1974*, 2251 and A. G. Shostenko, V. E. Myshkin, L. G. Khamidova, *High Energy Chem. Engl. Tansl. 12* (1978) 368, adjusted assuming $k(Et^{\cdot} + Et^{\cdot}) \approx 5 \times 10^9$ M^{-1} s^{-1}.
[17] F. M. Menger, *Acc. Chem. Res. 18* (1985) 128.
[18] L. Mandolini, *Adv. Phys. Org. Chem. 22* (1986) 1.
[19] *Wentrup* has discussed the low preexponential factors for intramolecular atom-transfer reactions and has also concluded that strained transition-state geometry is the most likely cause; C. Wentrup: *Reactive Molecules*, Wiley, New York 1984, p. 92.
[20] In a few cases in which very high EM values have been reported for hydrogen transfer, other factors, including steric compression, may be present in the reactant: e.g., P. J. Wagner, B. P. Giri, J. C. Scaiano, D. L. Ward, E. Gabe, F. L. Lee, *J. Am. Chem. Soc. 107* (1985) 5483; see also P. J. Wagner *Acc. Chem. Res. 22* (1989) 83.
[21] A. E. Dorigo, K. N. Houk, *J. Org. Chem. 53* (1988) 1650.

A First Step toward the Phosphorus Analogues of Polythiophenes

By *Marc-Olivier Bevierre, François Mercier, Louis Ricard,* and *François Mathey**

The electroconductivity of polythiophenes has been the subject of considerable study during the last few years.[1] More recently, it has been shown that high carrier mobility could also be achieved with well-defined thiophene oligomers such as α-sexithienyl.[2] Phospholyl anions are strictly isoelectronic with thiophenes and show a high degree of electronic delocalization according to theoretical,[3] NMR,[4] and structural studies.[5] Hence, the idea of replacing thiophene by phospholyl rings in a polythiophene chain was very attractive. Indeed, in contrast to thiophene, the phospholyl ring retains a high coordination ability towards transition metals via its heteroatom.[6] A polyphospholyl conductor or semiconductor might thus offer the opportunity of modifying, for example, the catalytic, redox, or magnetic properties of coordinated metallic centers by an electric current.

In order to investigate such possibilities, it was first necessary to devise a simple access to such still-unknown polyphospholyl chains. The classical routes used for the synthesis of polythiophene chains (e.g., the oxidative coupling of 2-lithio derivatives[7] or the reductive coupling of 2-bromo derivatives[8]) cannot be transposed to their phosphorus analogues because the necessary 2-lithio or 2-bromo derivatives are unknown[9] and because tervalent phosphorus compounds display a high sensitivity toward oxidation at the heteroatom. We now wish to report on a straightforward synthesis of a six-unit mixed chain containing four thiophene and two phospholyl rings.

Earlier[10] we showed that prolonged heating of 1-phenyl-3,4-dimethylphosphole (**1**) ultimately leads to the tetramer **2** [Eq. (a)]. Since the various H and Ph migrations involved in

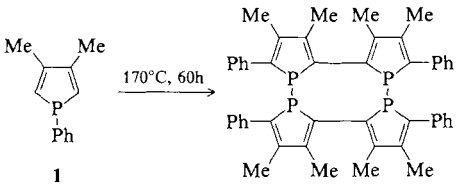

such a transformation were thought to proceed via concerted [1,5] sigmatropic shifts,[11] we reasoned that, if we replaced the phenyl at phosphorus by an α-thienyl substituent, we would retain the α substitution during the thermal conversion, thus creating the desired α-thienyl-α-phospholyl links. Accordingly, we first prepared the bithienyl-substituted phosphole **4** from readily available 1-cyano-3,4-dimethylphosphole (**3**).[12] Under prolonged heating, phosphole **4**[13] undergoes the same transformation as phosphole **1** [Eq. (b)].[14] The poorly soluble red-black tetramer **5**[15]

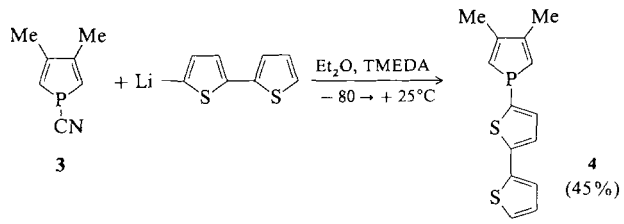

(b)

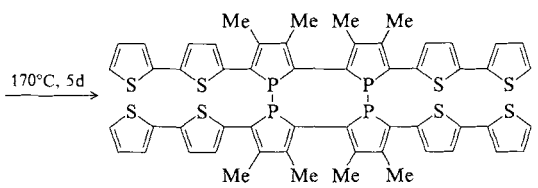

5 (ca. 30%)

could be very slowly recrystallized in 1,3,5-trichlorobenzene at 120 °C.[16]

[*] Prof. Dr. F. Mathey, Dr. M.-O. Bevierre, Dr. F. Mercier, Dr. L. Ricard
Laboratoire de Chimie du Phosphore et des Métaux de Transition
DCPH, CNRS-Ecole Polytechnique
F-91128 Palaiseau Cedex (France)

Compound **5** can serve as a convenient starting point for the synthesis of the dianion **6**, which is isoelectronic with α-sexithienyl [Eq. (c)]. The cleavage of the P–P bonds of **5**

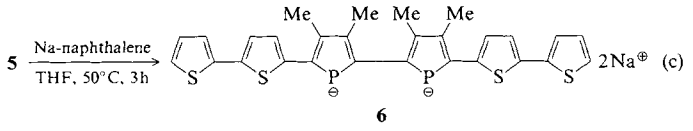

6

appears to be quantitative according to ^{31}P NMR analysis. The ^{31}P NMR resonance of **6** ($\delta = +65$) is in the normal range for a phospholyl anion.[4] Compound **6** was more fully characterized by methylation. The biphosphole **7** ($\delta(^{31}P) = +7.5$) is sensitive to oxidation and was allowed to react with sulfur to give **8** as a mixture of two diastereoisomers[17] [Eq. (d); overall yield of **8** from **5**, ca. 50%].

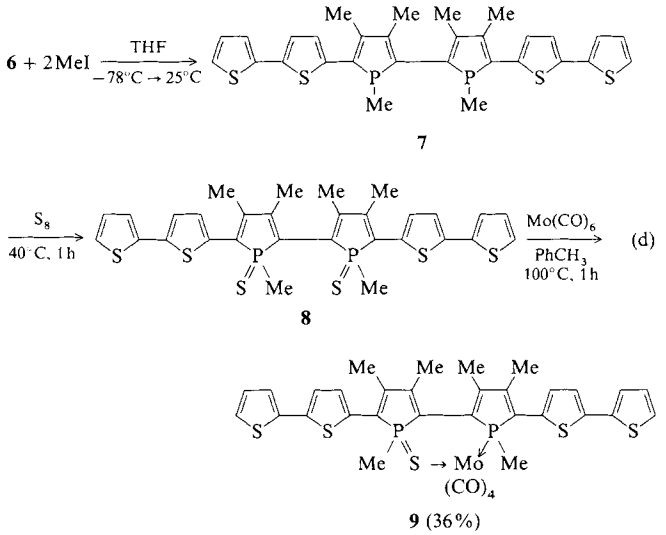

In order to characterize unambiguously the six-unit chain by X-ray diffraction, we also prepared a molybdenum complex **9** [Eq. (d)] and a tungsten complex **10** [Eq. (e)]. Both

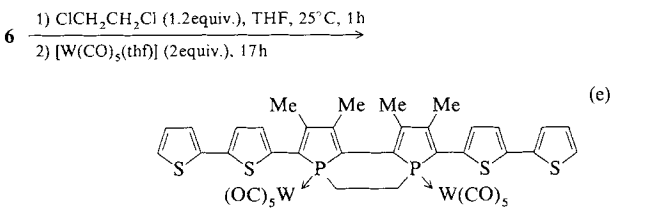

10 (ca. 30%)

complexes **9** and **10** were obtained as single isomers[18, 19] and gave good crystals for the X-ray study[20, 21] (Fig. 1). In complex **9**, the thiophene rings are planar and have normal bond lengths and angles. The phosphole ring containing P1 is also planar, whereas the phosphole ring containing P2 is puckered as expected:[9] P2 lies outside of the C13–C16 mean plane by 0.115(2) Å. The first half of the chain (S_1, S_2 and P_1 rings) is quasi-planar. The angles between the rings are 4.81 ± 3.15 and $2.57 \pm 4.72°$, respectively. The other half of the chain is more puckered (15.25 ± 1.26 and $154.75 \pm 0.71°$, respectively.). The angle between the two phosphole rings is $55.6 \pm 0.3°$. The C–C links between the rings are shorter in the first half of the chain (1.42(1) and 1.43(1) Å, respectively) than in the second half (1.46(1) and 1.47(1) Å, respectively.). All these data suggest a higher delocalization in the first than in the second half.

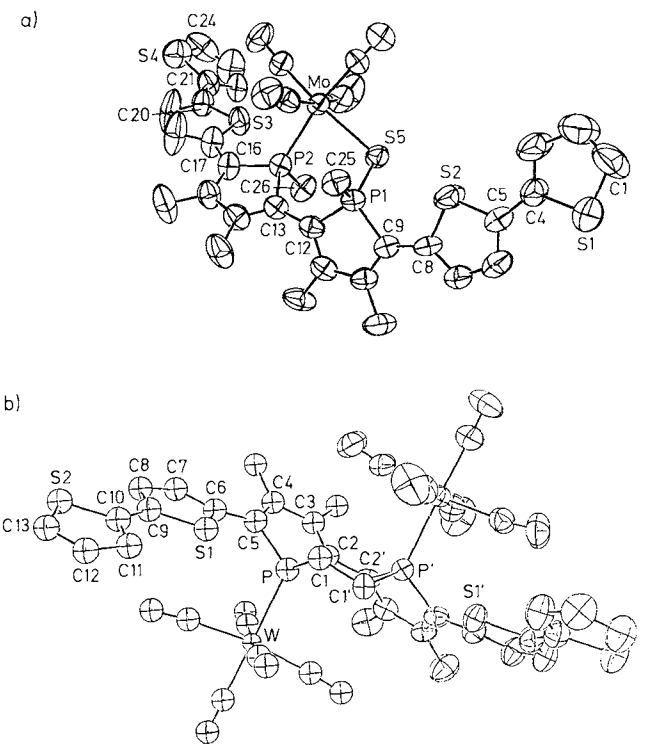

Fig. 1. Structures of **9** (a) and **10** (b) in the crystal. Ellipsoids are scaled to enclose 50% of the electronic density. Hydrogen atoms are omitted for clarity. Important bond distances [Å] and angles [°]: **9**: Mo-S5 2.632(2), Mo-P2 2.525(2), S5-P1 1.980(3), S1-C1 1.73(1), S1-C4 1.676(8), S2-C5 1.701(8), S2-C8 1.740(7), S3-C17 1.695(8), S3-C20 1.702(8), S4-C21 1.692(9), S4-C24 1.73(1), P1-C9 1.810(7), P1-C12 1.773(8), P1-C25 1.795(8), P2-C13 1.800(8), P2-C16 1.798(8), P2-C26 1.814(8), C4-C5 1.43(1), C8-C9 1.42(1), C12-C13 1.43(1), C16-C17 1.46(1), C20-C21 1.47(1); S5-Mo-P2 84.52(7), Mo-S5-P1 106.2(1), C1-S1-C4 92.3(5), S1-C4-C5 121.1(7), C4-C5-S2 121.5(7), C5-S2-C8 95.1(4), S2-C8-C9 120.6(6), C8-C9-P1 122.6(6), C9-P1-C12 95.3(4), P1-C12-C13 124.4(6), C12-C13-P2 121.7(6), C13-P2-C16 92.2(4), P2-C16-C17 123.4(7), C16-C17-S3 121.5(6), C17-S3-C20 93.9(4), S3-C20-C21 121.1(7), C20-C21-S4 120.7(7), C21-S4-C24 90.6(6). **10**: W-P 2.495(2), S1C6 1.732(8), S1-C9 1.735(7), S2-C10 1.699(7), S2-C13 1.695(9), P-C1 1.856(6), P-C2 1.798(6), P-C5 1.807(7), C1-C1' 1.529(12), C2-C2' 1.442(12), C2-C3 1.349(8), C3-C4 1.487(10), C4-C5 1.353(10), C5-C6 1.453(12), C6-C7 1.387(10), C7-C8 1.395(10), C8-C9 1.348(10), C9-C10 1.453(11), C10-C11 1.396(12), C11-C12 1.410(12), C12-C13 1.307(13); W-P-C1 118.3(2), W-P-C2 114.9(2), W-P-C5 118.2(2), C1-P-C2 101.2(2), C1-P-C5 107.8(3), C2-P-C5 92.1(3), P-C1-C1' 111.9(4), P-C2-C2' 116.9(3), P-C5-C6 121.0(5), C5-C6-S1 118.7(5), C6-S1-C9 93.6(4), S1-C9-C10 119.6(6), C9-C10-S2 120.1(6), C10-S2-C13 91.2(4).

In complex **10**, the four thiophene rings are planar, whereas the phosphorus atoms are outside of the corresponding diene mean planes by 0.15 Å. The thiophene–thiophene, thiophene–phosphole, and phosphole–phosphole interplane angles are, respectively, 6.35 ± 1.63, 24.34 ± 0.46, and $66.26 \pm 0.14°$. The C–C links between the rings are almost equal at 1.44–1.45 Å and similar to those found in α-terthienyl.[22]

The comparison between the structures of **9** and **10** underlines the flexibility of the six-unit chain and the sensitivity of the electronic delocalization within the chain to the substitution patterns of the phosphorus atoms. We are currently

studying the electrochemistry of these new types of conjugated oligomers.

Experimental Procedure

All reactions were carried out under argon.

4: Compound **3** was prepared in situ from 40 g (210 mmol) of **1** as previously described [12]. *n*-Butyllithium (95 mL, 1.6 M in hexane) was added dropwise at room temperature to 2,2'-bithienyl (25 g, 150 mmol) and anhydrous TMEDA (22.7 mL) in 150 mL of anhydrous Et_2O. The mixture was stirred for 3 h and was then added dropwise to the solution of **3** at $-80\,^{\circ}C$. The temperature was subsequently raised to 25 °C. After hydrolysis, neutralization, extraction with Et_2O, drying, and evaporation, the crude residue was chromatographed on silica gel with hexane. Overall yield 45%. The product could be recrystallized in hexane at 6 °C.

5: A sample of recrystallized phosphole **4** (6 g, 22 mmol) was sealed in a glass tube under argon. The tube was heated for 5 d at 170 °C. Compound **5** slowly precipitated as pure red-black crystals from the reaction mixture. These crystals were washed with dichloromethane. Yield ca. 30%.

6: A solution of sodium naphthalenide was first prepared from sodium (0.08 g, 3.5 mmol) and naphthalene (0.46 g, 3.5 mmol) in THF (10 mL). Compound **5** (1 g, 0.9 mmol) was then added without precaution to the dark green solution at room temperature. The reaction was complete after stirring for 3 h at 50 °C. Pure **6** could also be obtained by cleavage of **5** with sodium in diglyme at 120 °C.

8: To the solution of dianion **6** was added 0.23 mL (3.7 mmol) of methyl iodide at $-80\,^{\circ}C$. The temperature was raised to 25 °C. Then, sulfur (0.2 g, 6.2 mmol) was added to the reaction medium. After 1 h at 40 °C, the solution was filtered, the THF evaporated, and the naphthalene sublimed. The residue was chromatographed on silica gel with hexane/CH_2Cl_2 30/70 as the eluent. The product thus obtained (0.5 g, 43%) could be recrystallized in hexane/CH_2Cl_2 20/80.

9: Disulfide **8** (0.64 g, 1 mmol, major isomer) and $Mo(CO)_6$ (0.53 g, 2 mmol) were heated in toluene (20 mL) at 100 °C for 1 h. After filtration and evaporation, the organic residue was chromatographed on silica gel. Hexane/CH_2Cl_2 50/50 was first used as the eluent to remove impurities, then complex **9** was eluted with pure CH_2Cl_2 (0.3 g, 36%).

10: To the solution of dianion **6** was added dropwise 0.17 mL (2.2 mmol) of 1,2-dichloroethane with 2 mL of THF at $-80\,^{\circ}C$. The temperature was raised to 25 °C. Then, the reaction mixture was added to a solution of [$W(CO)_5$(thf)] obtained by UV irradiation of 1 g (2.8 mmol) of $W(CO)_6$ in 100 mL of THF for 1 h (125-W medium-pressure mercury lamp). After stirring for one night, the solvent was evaporated and the residue dissolved in dichloromethane. The solution was filtered and chromatographed on silica gel with hexane/CH_2Cl_2 80/20 as the eluent. The product thus obtained could be recrystallized in toluene/hexane 80/20 at room temperature.

Received: January 31, 1990;
supplemented: March 13, 1990 [Z 3770 IE]
German version: *Angew. Chem. 102* (1990) 672

[1] See, for example, F. Galluzi, M. Schwarz, *Chem. Phys. Lett. 105* (1984) 95; S. Glenis, G. Horowitz, G. Tourillon, F. Garnier, *Thin Solid Films 111* (1984) 93; M. Kaneko, M. Yamada, T. Kenmoshi, E. Tsuschida, *J. Polym. Sci. Polym. Lett. Ed. 23* (1985) 629; H. Tomozawa, D. Braun, S. Phillips, A. J. Heeger, H. Kroemer, *Synth. Met. 22* (1987) 63; J. Roncali, A. Yassar, F. Garnier, *J. Chem. Soc. Chem. Commun. 1988,* 581.

[2] F. Garnier, G. Horowitz, D. Fichou, *Synth. Met. 28* (1989) C705; D. Fichou, G. Horowitz, Y. Nishikitani, F. Garnier, *ibid. 28* (1989) C723; D. Fichou, G. Horowitz, Y. Nishikitani, J. Roncali, F. Garnier, *ibid. 28* (1989) C729; D. Fichou, G. Horowitz, Y. Nishikitani, F. Garnier, *Chemtronics 3* (1988) 176; G. Horowitz, D. Fichou, F. Garnier, *Solid State Commun. 70* (1989) 385.

[3] G. Kaufmann, F. Mathey, *Phosphorus Relat. Group V Elem. 4* (1974) 231; C. Guimon, G. Pfister-Guillouzo, F. Mathey, *Nouv. J. Chim. 3* (1979) 725; N. M. Kostic, R. F. Fenske, *Organometallics 2* (1983) 1008.

[4] L. D. Quin, W. L. Orton, *J. Chem. Soc. Chem. Commun. 1979,* 401; C. Charrier, F. Mathey, *Tetrahedron Lett. 28* (1987) 5025.

[5] T. Douglas, K. H. Theopold, *Angew. Chem. 101* (1989) 1394; *Angew. Chem. Int. Ed. Engl. 28* (1989) 1367.

[6] S. Holand, F. Mathey, J. Fischer, *Polyhedron 5* (1986) 1413.

[7] J. Kagan, S. K. Arora, *Heterocycles 20* (1983) 1937.

[8] T. Yamamoto, K. Sanechika, A. J. Yamamoto, *Polym. Sci. Polym. Lett. Ed. 18* (1980) 9; K. Tamao, S. Kodama, I. Nakajima, M. Kumada, *Tetrahedron 38* (1982) 3347.

[9] F. Mathey, *Chem. Rev. 88* (1988) 429.

[10] F. Mathey, F. Mercier, F. Nief, J. Fischer, A. Mitschler, *J. Am. Chem. Soc. 104* (1982) 2077.

[11] For a general discussion of these [1,5] sigmatropic shifts, see [9].

[12] S. Holand, F. Mathey, *Organometallics 7* (1988) 1796.

[13] **4**: m.p. 69 °C. ^{31}P NMR(C_6D_6): $\delta = -25.2$. ^1H NMR(C_6D_6): $\delta = 1.79$ (d, ^4J(H,P) = 3.3 Hz, 6H, Me), 6.37 (d, ^2J(H,P) = 38.9 Hz, 2H, =CH–P), 6.56–7.20 (m, 5H, bithienyl). ^{13}C NMR(C_6D_6; selected): $\delta = 17.45$ (d, ^3J(C,P) = 3.5 Hz, Me), 149.44 (d, ^2J(C,P) = 8.6 Hz, Me–*C*). MS (EI, 70 eV) *m/z* 276 ($M^{\oplus}$, 100%). Correct C,H elemental analysis.

[14] Besides **5**, the thermal transformation of **4** produces several compounds of lower molecular weights and higher solubilities. For the discussion of a similar transformation [see Eq. (a)] and for the structures of the postulated intermediates, see [9].

[15] **5**: m.p. > 350 °C. ^{31}P NMR ($C_2H_2Cl_4$): $\delta = -2.1$. Correct C,H elemental analysis for $C_{56}H_{44}P_4S_8$.

[16] X-ray structure determination for **5**: Because of the low solubility of the compound, crystals were grown in a 100 K temperature gradient using $C_6H_3Cl_3$ as solvent. Data were collected at 20 ± 1 °C on an Enraf-Nonius CAD4 diffractometer. The structure was solved and refined using the Enraf-Nonius-supplied SDP package. The compound crystallizes in space group *P*1; $a = 11.463(2)$, $b = 16.528(2)$, $c = 27.185(3)$ Å, $\alpha = 91.96(1)$, $\beta = 101.91(1)$, $\gamma = 89.90(1)°$; $V = 5036.64(2.3)$ Å^3; $Z = 4$; $\varrho_{calcd} = 1.447$ g cm^{-3}; $Cu_{K\alpha}$ radiation ($\lambda = 1.54184$ Å), graphite monochromator; $\mu = 47.7$ cm^{-1}; $F(000) = 2272$. A total of 12233 unique reflections were recorded in the range $2° \le 2\theta \le 130.0°$; 7319 were considered as unobserved ($F^2 < 3.0\sigma(F^2)$), leaving 4914 for solution and refinement. The crystals were of medium quality and a scan width of 1.3° had to be adopted for data collection. Moreover, since the diffraction intensity falls off quite rapidly, a scan time of two min was used to improve the signal to noise ratio. The structure was solved by direct methods, yielding a solution of 90 of the 136 independent heavy atoms. Although the general shape of the molecule can be well established from the present study, it has not yet been possible to refine the structure to a level suitable for full publication. Three factors make it difficult to refine the model: the large average thermal agitation of the molecule, the large correlation coefficients between atoms of the two molecules that result from the presence of a pseudo mirror plane at [0,0,1/2], the lack of data with *l* odd (ten percent of all observed data) that results from this special packing. A non-Poisson weighting scheme was applied with a *p* factor equal to 0.08. The present isotropic *R* factors are $R = 0.156$, $R\omega = 0.200$, GOF = 3.79.

[17] **8** (main isomer): ^{31}P NMR ($CDCl_3$): $\delta = 48.9$. ^1H NMR($CDCl_3$; selected): $\delta = 2.04$ (d, ^2J(H,P) = 15.4 Hz, 6H, Me-P), 2.06 (s, 6H, Me-C), 2.35 (s, 6H, Me-C). ^{13}C NMR($CDCl_3$; selected): $\delta = 15.86$ (d, ^3J(C,P) = 12.6 Hz, *Me*-C), 16.81 (d, ^3J(C, P) = 12.6 Hz, *Me*-C), 21.10 (d, ^1J(C,P) = 50.3 Hz, Me-P); MS (EI, 70 eV): *m/z* 642 ($M^{\oplus}$, 100%), 610 ($M^{\oplus}$–S, 87%), 565 (88%). Correct C,H analysis.

[18] **9**: ^{31}P NMR(CD_2Cl_2): $\delta = +53.1$, +47.4 (^3J(P,P) = 7.3 Hz). MS (70 eV): *m/z* 786 ($M^{\oplus}$–S, 2%), 702 ($M^{\oplus}$–S–3CO, 3%), 578 ($M^{\oplus}$–S–4CO–Mo, 100%). IR(CH_2Cl_2): $\tilde{\nu}$-(CO) = 2018 s, 1915, 1900 vs, 1860 s. Correct C,H analysis.

[19] **10**: ^{31}P NMR(C_6D_6): $\delta = +30.5$ ($^1J(^{31}P,^{183}W) = 231.9$ Hz). ^1H NMR (C_6D_6): $\delta = 1.94$ (d, ^4J(H,P) = 1.7 Hz, 6H, Me), 1.99 (s, 6H, Me), 2.34–2.73 (m, 4H, CH_2), 6.64–7.08 (m, 10H, thiophene).

[20] a) X-ray structure determination for **9**: Crystals were grown by slow evaporation of a dichloromethane solution of the compound. Data were collected at 18 ± 1 °C on an Enraf-Nonius CAD4 diffractometer. The crystal structure was solved and refined using the Enraf-Nonius-supplied SDP package. The compound crystallizes in space group *C*2/*c*; $a = 30.001(3)$, $b = 11.322(1)$, $c = 26.54(3)$ Å, $\beta = 128.01(1)°$; $V = 7104.59(3.10)$ Å^3; $Z = 8$; $\varrho_{calcd} = 1.531$ g cm^{-3}; $Mo_{K\alpha}$ radiation ($\lambda = 0.71073$ Å), graphite monochromator; $\mu = 7.7$ cm^{-1}; $F(000) = 3328$. A total of 6228 unique reflections were recorded in the range $2° \le 2\theta \le 50.0°$; 3469 were considered as unobserved ($F^2 < 3.0\sigma(F^2)$), leaving 2759 for solution and refinement. The structure was solved by direct methods, yielding a solution for the twenty atoms. The hydrogen atoms were included as fixed contribution in the final stages of least-squares refinement while using anisotropic temperature factors for all other atoms. A non-Poisson weighting scheme was applied with a *p* factor equal to 0.08. The final *R* factors were $R = 0.046$, $R_\omega = 0.063$, GOF = 1.21. b) Further details of the crystal structure investigation are available on request from the Fachinformationszentrum Karlsruhe, Gesellschaft für wissenschaftlich-technische Information mbH, D-7514 Eggenstein-Leopoldshafen 2 (FRG), on quoting the depository number CSD-54479, the names of the authors, and the journal citation.

[21] X-ray structure determination for **10**: Crystals were grown at room temperature from a toluene-pentane solution of the compound. Data were collected at 18 ± 1 °C. The compound crystallizes in space group *Pbcn*; $a = 17.547(1)$, $b = 8.404(1)$, $c = 29.125(3)$ Å; $V = 4294.87(1.2)$ Å^3; $Z = 4$; $\varrho_{calcd} = 1.877$ g cm^{-3}; $Mo_{K\alpha}$ radiation ($\lambda = 0.71073$ Å), graphite monochromator; $\mu = 57.3$ cm^{-1}; $F(000) = 2352$. A total of 6240 unique reflections were recorded in the range $2° \le 2\theta \le 60.0°$; 3336 were considered as unobserved ($F^2 < 3.0\sigma(F2)$), leaving 2904 for solution and refinement. The structure was solved by Patterson methods, yielding a solution for the tungsten and phosphorus atoms. The hydrogen atoms were included as fixed contribution in the final stages of least-squares refinement while using anisotropic temperature factors for all other atoms. A non-Poisson weighting scheme was applied with a *p* factor equal to 0.07. The final *R* factors were $R = 0.035$, $R_\omega = 0.047$, GOF = 1.07 [20b].

[22] F. Van Bolhuis, H. Wynberg, E. E. Havinga, E. W. Meijer, E. G. J. Staring *Synth. Met. 30* (1989) 381.

Solvent and Structure Effects in the Photobromination of Benzyltrimethylsilanes. A Mechanistic Changeover from Hydrogen-Atom Transfer to Electron Transfer**

By *Enrico Baciocchi** and *Manuela Crescenzi*

It has long been known that the bromine atom is very effective in abstracting benzylic hydrogens.[1] However, $Br^{\cdot}$ is also a good oxidant ($E^{\circ} = 2.0$ V vs NHE in H_2O)[2] and, with electron-rich substrates, it could behave as an electron-abstracting species as well. This mechanistic dichotomy, it is recognized nowadays, should characterize all reactions occurring between species with complementary electron-donor/electron-acceptor properties.[3]

We wish now to report on quite dramatic solvent and structure effects observed during a study of the photobromination of benzyltrimethylsilane (**1**) and (4-methoxybenzyl)trimethylsilane (**2**). We suggest that these effects provide us with the first evidence of a mechanistic dichotomy (hydrogen-atom transfer versus electron transfer) in the reactions of $Br^{\cdot}$ with aromatic compounds.

When **1** (1 mmol) is allowed to react (20 min at 60 °C) with Br_2 (1 mmol) in CCl_4 or AcOH (10 mL), under external irradiation (Pyrex filter) by a 500-W high-pressure mercury vapor lamp, only the expected product of side-chain substitution, (α-bromobenzyl)trimethylsilane (**3**), is obtained. There is little doubt, also on the basis of a recent kinetic study,[4] that this reaction occurs by a mechanism involving hydrogen-atom transfer.

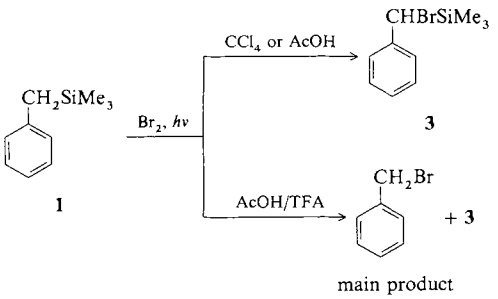

Scheme 1.

When the solvent is changed to an 1:1 AcOH:TFA mixture (TFA = trifluoroacetic acid), however, a drastic change in the product composition occurs (Scheme 1). Compound **3** is now a minor product (15%), whereas most of the reaction leads to benzyl bromide (52%).[5] Of course, we have checked that both **1** and **3** are photochemically stable in the mixed solvent and that, in the absence of light, no desilylation occurs but only ring-brominated products form.

It is difficult to rationalize this observation by simply suggesting that in AcOH-TFA an attack of $Br^{\cdot}$ at silicon is also occurring. Apart from the very scanty information on such a process,[6] there is no plausible reason why no hint of it has been found in both AcOH and CCl_4. The homolytic substitution by $Br^{\cdot}$ at hydrogen and at silicon would have to be subject to drastically different solvent effects, which is not reasonable.

On the other hand, there is overwhelming evidence that benzyltrimethylsilane radical cations undergo an extremely fast desilylation reaction to give benzyl radicals.[7] The formation of benzyl bromide observed in AcOH-TFA can be much better interpreted on the basis of a mechanism [Eqs. 1–3] involving the transfer of an electron from **1** to $Br^{\cdot}$ as the first step. The radical cation thereby formed then undergoes a nucleophile-assisted reaction (presumably by the solvent)[7a, 8] to give the benzyl radical, which propagates the chain by reaction with Br_2, leading to benzyl bromide.

$$Br^{\cdot} + ArCH_2SiMe_3 \rightarrow Br^{\ominus} + ArCH_2SiMe_3^{\cdot\oplus} \quad (1)$$

$$ArCH_2SiMe_3^{\cdot\oplus} + AcOH \rightarrow ArCH_2^{\cdot} + Me_3SiOAc + H^{\oplus} \quad (2)$$

$$ArCH_2^{\cdot} + Br_2 \rightarrow ArCH_2Br + Br^{\cdot} \quad (3)$$

There are at least two factors which can contribute to shift the mechanism from hydrogen-atom transfer to electron transfer on going from AcOH to AcOH-TFA. First, increasing the acidity of the solvent should result in a higher E° value of the $Br^{\cdot}/Br^{\ominus}$ couple, due to better solvation of $Br^{\ominus}$ via hydrogen bonds. Second, TFA is very effective in solvating aromatic radical cations,[9] thereby lowering the oxidation potential of **1** ($E_p = 2.09$ V vs. NHE in MeCN).[7b, 10] Thus, in AcOH-TFA, $Br^{\cdot}$ and **1** are a better oxidant and a better reductant, respectively, than in AcOH. We therefore suggest that the combined effect of these two factors in AcOH-TFA so much facilitates the electron-transfer step as to make this step competitive with hydrogen-atom transfer.[11]

A similar mechanistic shift can also be induced, in the same solvent, by increasing the electron availability of the substrate. Accordingly, whereas photobromination of **1** in AcOH leads exclusively to (α-bromobenzyl)trimethylsilane, in the corresponding reaction of **2**, 4-methoxybenzyl acetate,[5] which certainly derives from the acetolysis of the initially formed 4-methoxybenzyl bromide (Scheme 2), is the exclusive product of the side-chain process.[14]

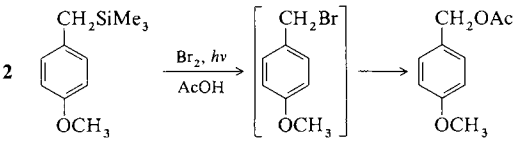

Scheme 2.

Thus, in AcOH, on going from **1** to **2** the nature of the products changes, again suggesting a changeover from a hydrogen-transfer to an electron-transfer mechanism, this time induced by the much easier oxidizability of the latter substrate (the E_p value of **2** is ca. 0.5 V lower than that of **1**).[7a]

Clearly, these results confirm the previous view[7b] that the study of the reactions of benzyltrimethylsilanes can be an excellent tool for distinguishing hydrogen-transfer from electron-transfer mechanisms.

Received: January 17, 1990 [Z 3741 IE]
German version: *Angew. Chem. 102* (1990) 687

CAS Registry numbers:
1, 770-09-2; **2**, 17988-20-4; **3**, 17903-41-2; benzyl bromide, 100-39-0; 4-methoxybenzyl acetate, 104-21-2.

[*] Prof. Dr. E. Baciocchi, Dr. M. Crescenzi
Dipartimento di Chimica, Università "La Sapienza"
P. le A. Moro 5, 00185 Roma (Italy)
and
Centro CNR di Studio sui Meccanismi di Reazione, Rome

[**] This work was supported by the Ministero della Pubblica Istruzione and the National Council of Research (CNR).

[1] G. A. Russel in J. K. Kochi (Ed.): *Free Radicals, Vol. 1*, Wiley, New York 1973, Chapter 7.
[2] L. Eberson, *Adv. Phys. Org. Chem. 18* (1982) 1ff.
[3] L. Eberson: *Electron Transfer Reactions in Organic Chemistry*, Springer, Berlin 1987.
[4] J. S. Swenton, M. Platz, L. D. Venham, *J. Org. Chem. 53* (1988) 2764.
[5] In this case photobromination was carried out in the presence of small amounts of AcONa to neutralize HBr developed during the reaction, because, *under irradiation*, HBr promoted a fast protodesilylation of the starting benzyltrimethylsilane. Addition of AcONa had no effect on the product composition of the photobromination of **1** in AcOH.
[6] P. J. Barker in F. R. Hartley, S. Patai (Eds.): *The Chemistry of the Metal Carbon-Bonds, Vol. 2*, Wiley, New York 1985, 3; H. Sakurai in J. K. Kochi: *Free Radicals, Vol. II*, Wiley, New York 1973, p. 774; A. G. Davis, B. P. Roberts, *ibid. Vol. I*, p. 583.
[7] a) J. P. Dinnocenzo, S. Farid, J. L. Goodman, I. R. Gould, W. P. Todd, S. L. Mattes, *J. Am. Chem. Soc. 111* (1989) 8973; b) E. Baciocchi, T. Del Giacco, C. Rol, G. V. Sebastiani, *Tetrahedron Lett. 30* (1989) 3753; c) K. Mizuno, M. Ikeda, Y. Otsuji, *ibid. 26* (1985) 461; J. Yoshida, T. Murata, S. Isoe, *ibid. 27* (1986) 3373; R. M. Borg, R. O. Heuckeroth, A. J. Y. Lan, S. L. Quillen, P. S. Mariano, *J. Am. Chem. Soc. 109* (1987) 2728.
[8] When benzyldimethyloctylsilane was photobrominated in place of **1**, the reaction product contains dimethyloctylsilyl acetate as the main silicon-containing compound together with small amounts of dimethyloctylsiloxane. No other side products were detected.
[9] J. O. Howell, J. M. Goncalves, C. Amatore, L. Klasinc, R. M. Wightman, J. K. Kochi, *J. Am. Chem. Soc. 106* (1984) 3968. For general papers concerning medium effects on ET reactions see: D. Rehm, A. Weller, *Z. Phys. Chem. (Wiesbaden) 69* (1970) 183; J. Mattay, *Angew. Chem. 99* (1987) 849, *Angew. Chem. Int. Ed. Engl. 26* (1987) 825; M. A. Fox, M. Chanon (Eds.): *Photoinduced Electron Transfer*, Elsevier, Amsterdam 1988, Section 3 in Part B.
[10] A higher value is, however, reported in [7a].
[11] It is also conceivable that benzyltrimethylsilane radical cation is formed by irradiation of the charge-transfer complex between **1** and Br_2 [12]: $(PhCH_2SiMe_3,\ Br_2) \xrightarrow{h\nu} (PhCH_2SiMe_3,\ Br_2)^* \longrightarrow PhCH_2SiMe_3^{\bullet\oplus}Br_2^{\ominus}$ However, the excitation of the charge-transfer complex is unlikely since its λ_{max} is around 300 nm in CCl_4 and lower values are expected in AcOH-TFA [13].
[12] J. K. Kochi, *Angew. Chem. 100* (1988) 1331; *Angew. Chem. Int. Ed. Engl. 27* (1988) 1227.
[13] S. Fukuzumi, J. K. Kochi, *J. Org. Chem. 46* (1981) 4116.
[14] Small amounts of ring-brominated products also form. It was confirmed that these are the exclusive reaction products of the bromination of **2** in the dark.

Direct Evidence for a Nitrile Imine–Imidoylnitrene Rearrangement: X-Ray Crystal Structure of an Unusual Nitrene Complex

By *Michel Granier, Antoine Baceiredo, Hansjörg Grützmacher, Hans Pritzkow*, and *Guy Bertrand**

Dedicated to Professor Rolf Huisgen on the occasion of his 70th birthday

Diazomethane is unique among small molecules with regard to the number of its potentially accessible isomers.[1] Usually, six of them are considered: cyanamide, diazirine, carbodiimide, isocyanamide, nitrile imine, and isodiazirine. According to theoretical calculations,[2] cyanamide is the most stable isomer; the less stable ones, namely, nitrile imine[3] and isodiazirine are higher in energy by 84.8 and 99.0 kcal mol^{-1}, respectively. Most of these isomers are interconvertible. The rearrangement of nitrile imine to carbodiimide has been detected only at very high temperature (> 500 °C)[4a] or photochemically in a matrix.[4b] It is of particular interest since it is isoelectronic with the nitrile oxide–isocyanate rearrangement,[5] and it is strongly related to the Wolff-type rearrangement starting from imidoyl azide (or acyl azide).[6] If the nitrile imine is regarded as a carbene, this process is also analogous to the rearrangement of acyl carbenes to ketenes.[7] One of the remaining questions is to know whether these rearrangements are concerted or involve isodiazirine (or oxazirene) **A** and imidoylnitrene (or acylnitrene) **B** as intermediates.

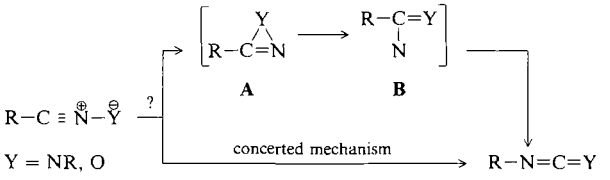

According to theoretical calculations, the rearrangement of RCNO to RNCO is predicted to pass through structures which may be termed oxazirine and (singlet) acylnitrene, but they are not true intermediates and should not be observable compounds.[8] *Wentrup* et al. reported evidence for nitrile imine–imidoylnitrene rearrangement through an isodiazirine intermediate, based on the nature of the products obtained in the pyrolysis at 500 to 960 °C of different nitrile imine precursors.[4a] Here we wish to report definitive proof for the nitrile imine–imidoylnitrene rearrangement including the X-ray crystal structure of a nitrogen-substituted oxonium compound.

We have shown that *C*-[thiophosphoranyl]-*N*-phosphanyl nitrile imine **1a** is stable at room temperature (m.p. 100 °C) and rearranges to the isomeric diazo derivative **2a** only on heating in solution at 55 °C for six hours. The *C,N*-diphosphanyl nitrile imine **1b**, on the other hand, is not stable enough to be spectroscopically observed even at −78 °C.[9]

From these results, it is clear that the hybridization state of the phosphorus atom is of primary importance to the stability of the nitrile imine. *o*-Quinones are well-known to react with phosphanes to give the corresponding pentacoordinated, pentavalent phosphoranes. Thus, we chose to study the reaction of tetrachloro-*o*-benzoquinone (TCBQ) with nitrile imine **1a**. A very clean reaction occurred leading, after workup, to product **3** as colorless crystals. A doublet of quintets at $\delta = -24.1$ ($J_{PP} = 2.6$, $J_{PH} = 16.0$ Hz) in the ^{31}P NMR spectrum was in the range expected for a $\sigma^5\lambda^5$-phosphorus atom bearing two diisopropylamino groups and the quinone residue; its counterpart at $\delta = 56.5$ (d quint., $J_{PP} = 2.6$, $J_{PH} = 21.9$ Hz) was in good agreement with the

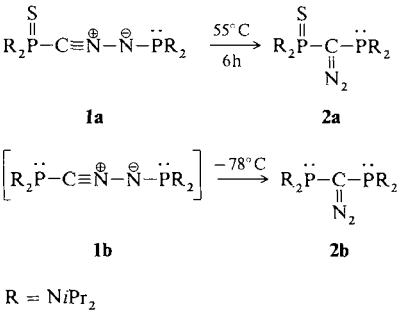

[*] Dr. G. Bertrand, M. Granier, Dr. A. Baceiredo,
Laboratoire de Chimie de Coordination du CNRS
205, Route de Narbonne, F-31077 Toulouse Cédex (France)
Dr. H. Grützmacher, Dr. H. Pritzkow
Anorganisch-chemisches Institut der Universität
Im Neuenheimer Feld 270, D-6900 Heidelberg (FRG)

presence of a bis(diisopropylamino)thiophosphoranyl group. The absence of IR absorptions above 2000 cm^{-1} allowed us to rule out nitrile imine **4** or carbodiimide **5** as possible structures, but the mass spectrum (EI *m/z* 778) demonstrated that no nitrogen elimination had occurred, indicating that **3** was a structural isomer of **4** and **5**. These spectroscopic data as a whole and the presence of a signal at $\delta = 154.3$ (dd, $J_{PC} = 183.3$, 6.1 Hz) in the ^{13}C NMR spectrum[10] left only the isodiazirine derivative **6** as a possible candidate from the usual R_2CN_2 isomers.

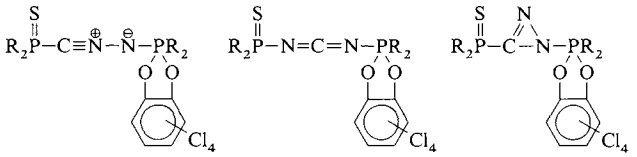

4 **5** **6**

R = N*i*Pr$_2$

The surprising thermal stability (m.p. > 300 °C without decomposition) and lack of chemical reactivity (no reaction in boiling methanol) made it necessary to carry out an X-ray diffraction study of **3** for unambiguous structural characterization (Fig. 1).[11] The most surprising feature is the presence of a planar tricoordinate oxygen bonded to the aryl ring (O2-C7 1.378(5) Å), to P1 (O2-P1 1.729(3) Å), and also to N2 (O2-N2 1.394(4) Å). C1 is also planar and the C1–N1 and C1–N2 distances (1.332(4) and 1.290(5) Å) are between those of a single and a double bond. P1 is at the center of a slightly distorted trigonal bipyramid with expected P–O and P–N bond lengths. The P1-O1-C2-C7-O2 and P1-O2-N2-C1-N1 fragments are almost planar (maximum deviation ± 0.055 and 0.043 Å, respectively). Thus, this compound is best represented as **3a** but can also be regarded as an imidoylnitrene **3b** stabilized by a donor–acceptor interaction with an oxygen atom. Note that the stabilization of nitrenes by coordination at nitrogen is well known,[12] but has only previously been postulated for oxygen.[13]

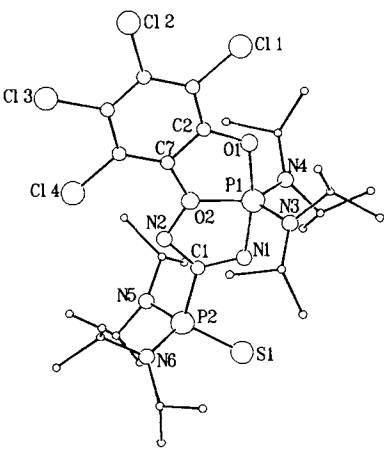

Fig. 1. Molecular structure of **3**. Important bond lengths [Å] and angles [°]: P1-N1 1.743(3), P1-O1 1.741(3), P1-O2 1.729(3), P1-N3 1.657(3), P1-N4 1.658(3), C1-N1 1.332(4), C1-N2 1.290(5), C1-P2 1.854(4), N2-O2 1.394(4), O1-C2 1.349(4), O2-C7 1.378(5), C2-C7 1.387(6); O1-P1-N1 167.7(1), O2-P1-N1 82.9(1), O2-P1-O1 85.0(1), N3-P1-N1 92.8(1), N3-P1-O1 95.3(1), N2-P1-O2 123.3(1), N4-P1-N1 94.9(1), N4-P1-O1 90.8(1), N4-P1-O2 125.8(1), N4-P1-N3 110.9(1), N2-C1-N1 118.3(3), P2-C1-N1 119.2(2), P2-C1-N2 122.4(2), C1-N1-P1 114.0(2), O2-N2-C1 105.4(2), C2-O1-P1 115.2(2), N2-O2-P1 118.9(2), C7-O2-P1 117.8(2), C7-O2-N2 123.3(2).

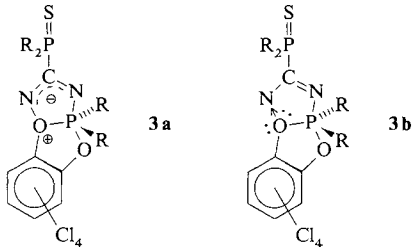

3a **3b**

When the reaction of nitrile imine **1a** with TCBQ was monitored by NMR spectroscopy at − 50 °C, an intermediate could be detected which rearranged to **3** at − 45 °C. The ^{31}P NMR spectrum ($\delta = 58.5$ and 2.6, $J_{PP} = 13.0$ Hz) was in agreement with a $\sigma^4\lambda^5$ and a $\sigma^5\lambda^5$ phosphorus, and the presence of a signal at $\delta = 151.1$ (dd, $J_{PC} = 191.6$, 24.4 Hz) in the ^{13}C NMR spectrum[10] could be in agreement with the isodiazirine structure **6**.[14] Attempts to confirm this structure are under investigation.

In summary, the reaction of nitrile imine **1a** with TCBQ probably affords a transient new nitrile imine **4**, which rearranges into imidoylnitrene **3**, possibly via a spectroscopically observable isodiazirine **6**.

Experimental Procedure

All operations were performed under dried atmosphere. A chloroform solution (1.5 mL) of tetrachloro-*o*-benzoquinone (0.15 g, 0.61 mmol) was added at − 78 °C to a chloroform solution (1.5 mL) of nitrile imine **1a** (0.30 g, 0.56 mmol). The reaction mixture was then allowed to warm to room temperature and **3** (0.37 g, 84% yield) crystallized slowly from the solution.

Received: February 9, 1990 [Z 3788 IE]
German version: *Angew. Chem. 102* (1990) 671

CAS Registry numbers:
1a, 113533-22-5; **3**, 127104-08-9; **3** · $CHCl_3$, 127104-09-0; *o*-TCBQ, 2435-53-2.

[1] a) J. B. Moffat in S. Patai (Ed.): *The Chemistry of the Diazonium and the Diazo groups*, Wiley, London, 1977; b) B. T. Hart, *Aust. J. Chem. 26* (1973) 461.
[2] J. B. Moffat, *J. Mol. Struct. 52* (1979) 275.
[3] Reviews on nitrile imines: a) R. Huisgen, *Angew. Chem. 75* (1963) 604, 742; *Angew. Chem. Int. Ed. Engl. 2* (1963) 565, 742; b) P. Caramella, P. Grünanger in A. Padwa (Ed.): *1,3 Dipolar Cycloaddition Chemistry*, Wiley, Interscience, New York 1984.
[4] a) S. Fischer, C. Wentrup, *J. Chem. Soc. Chem. Commun. 1980*, 502; b) N. H. Toubro, A. Holm, *J. Am. Chem. Soc. 102* (1980) 2093.
[5] C. Wentrup, *Adv. Heterocycl. Chem. 28* (1981) 231.
[6] a) W. Lwowski in S. Patai (Ed.): *The Chemistry of the Azido Group*, Wiley, London 1971; b) T. L. Gilchrist, C. J. Moody, C. W. Rees, *J. Chem. Soc. Perkin Trans. 1 1979*, 1871.
[7] M. Regitz, G. Maas: *Diazo Compounds, Properties and Synthesis*, Academic Press, London 1986.
[8] a) D. Poppinger, L. Radom, J. A. Pople, *J. Am. Chem. Soc. 99* (1977) 7806; b) D. Poppinger, L. Radom, *ibid. 100* (1978) 3674.
[9] a) G. Sicard, A. Baceiredo, G. Bertrand, *J. Am. Chem. Soc. 110* (1988) 2663; b) M. Granier, A. Baceiredo, G. Bertrand, *Angew. Chem. 100* (1988) 1397; *Angew. Chem. Int. Ed. Engl. 27* (1988) 1350.
[10] Selected spectroscopic data: **3**: ^1H NMR ($CDCl_3$): $\delta = 1.12$ (d, J(HH) = 6.7 Hz, 24H; CH_3), 1.32 (d, J(HH) = 6.8 Hz, 12H; CH_3), 1.37 (d, J(HH) = 6.8 Hz, 12H; CH_3), 3.68 (sept. d, J(HH) = 6.8, J(PH) = 21.9 Hz, 4H; CH), 4.00 (sept d, J(HH) = 6.7, J(PH) = 16.0 Hz, 4H; CH). ^{13}C NMR ($CDCl_3$): δ = 22.60, 22.64, 22.85, 22.87, 23.67, 23.72, 23.79, CH), 113.79 (d, J(PC) = 5.4 Hz; OCC), 113.96 (s; OCC), 123.23 (s; OCCC), 123.92 (s; OCCC), 126.07 (d, J(PC) = 32.79 Hz; OC), 140.36 (s; OC), 154.30 (dd, J(PC) = 183.3, 6.1 Hz; C=N). – **7**: ^{13}C NMR ($CDCl_3$,

218 K): δ = 23.61 (m; CH_3), 47.37 (m; CH), 125.22 (d, J(PC) = 6.0 Hz; OCC), 126.48, 126.97, 128.13 (s; OCC, OCCC), 138.07 (d, J(PC) = 5.1 Hz; OC), 147.49 (d, J(PC) = 3.4 Hz; OC), 151.06 (dd, J(PC) = 191.6, 24.4 Hz; C=N).

[11] Crystal data for **3**: $C_{31}H_{56}Cl_4N_6O_2P_2S \cdot CHCl_3$, monoclinic, a = 13.376(11), b = 13.811(12), c = 24.179(18) Å, β = 98.88(6)°, V = 4413.5 Å^3, space group $P2_1/n$, Z = 4. Intensity data were collected on a Stoe-Siemens four-circle diffractometer ($Mo_{K\alpha}$ radiation, graphite monochromator) in the range $3° \leq 2\theta \leq 50°$ using the ω-scan technique; 8130 unique reflections were collected with 4282 observed ($I > 2\sigma I$). An empirical absorption correction was applied ($0.875 < T < 0.999$). The structure was solved by direct methods (SHELXS 86). All non-hydrogen atoms were refined anisotropically; the $CHCl_3$ was strongly disordered and was refined as two rigid CCl_3 groups. Hydrogen atoms were placed in calculated positions (not refined) or as rigid CH_3 groups having one common isotropic temperature factor. At final convergence, R = 0.060; Rw = 0.074 ($w = 1.2/(\sigma^2 F + 0.0004 F^2)$). Further details of the crystal structure investigation are available on request from the Fachinformationszentrum Karlsruhe, Gesellschaft für wissenschaftlich-technische Information mbH, D-7514 Eggenstein-Leopoldshafen 2 (FRG), on quoting the depository number CSD-54569, the names of the authors, and the journal citation.

[12] P. A. S. Smith in E. F. V. Scriven (Ed.): *Azides and Nitrenes*, Academic Press, London 1984.

[13] L. Horner, A. Christmann, A. Gross, *Chem. Ber. 96* (1963) 399.

[14] The synthesis and structure of a phosphorus isologue of an isodiazirine has recently been reported: E. Niecke, R. Streubel, M. Nieger, D. Stalke, *Angew. Chem. 101* (1989) 1708; *Angew. Chem. Int. Ed. Engl. 28* (1989) 1673.

Intramolecular Insertion of Arylcarbenes into C–Si Bonds

By *Wolfgang Kirmse** and *Wolfgang Konrad*

Dedicated to Professor Wolfgang R. Roth on the occasion of his 60th birthday

Recently, we reported on arylcarbenes that contain an ether function in an *ortho* side chain.[1] *Electrophilic* attack of the carbenes **1** at the oxygen produces oxonium ylides **2**, which are trapped by protic solvents or rearranged to **3** and **4**. The observed migration tendencies (allyl,benzyl > alkyl > methyl, phenyl) are consistent with the radical-pair mechanism of the Stevens rearrangement.[2]

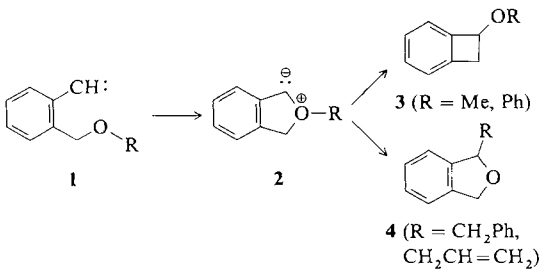

1 2

With the intention of reversing the polarities, we have now examined the analogous silicon compounds. We obtained the necessary starting compounds by double metalation and silylation[3] of 2-methylbenzyl alcohol **5** (Scheme 1), followed by hydrolysis of the silyl ethers **6** to **7** and oxidation to the aldehydes **8**. On treatment with 50% NaOH/dioxane, at 80–90 °C,[4] the tosylhydrazones **9** furnish the diazo compounds **10**; with D_2O/DONa, H/D exchange leads to formation of the deuteriated diazo compounds ArylCDN_2. We generated the carbenes **11** by thermolysis of the tosylhydrazone sodium salts **9**-Na or the diazo compounds **10** at 280–300 °C.

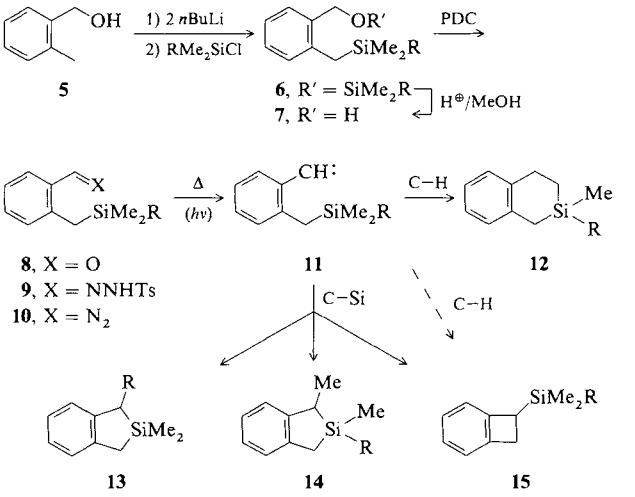

Scheme 1. **a**, R = CH_3; **b**, R = Ph; **c**, R = CH_2Ph. PDC = pyridinium dichromate.

Insertion of the carbenes **11** into the C–H bonds of the methyl groups leads to the silacyclohexanes **12**, insertion into Si–R and Si–Me bonds to the silacyclopentanes **13** and **14**, respectively. The benzocyclobutenes **15** can be formed by insertion into the benzyl–Si bond and by insertion into the benzylic C–H bonds. These two reaction routes can be differentiated with the help of the deuteriated carbenes [^{2}H]-**11**.

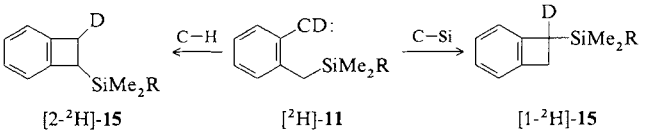

[2-^{2}H]-**15** [^{2}H]-**11** [1-^{2}H]-**15**

As revealed by the NMR data of [^{2}H]-**15**, C–Si insertion is the preferred, but not exclusive bonding mode of **15** (see Table 1).

Table 1. Reaction products of the carbenes **11** (amounts in mol-% from thermolyses of **10** at 280–300 °C).

	C-H			C-Si			Addition	
R	**12**	**15**	**19**	**13**	**14**	**15**	**17**	**18**
CH_3	55	5		7		33		
Ph	21	4		22	5	16	32	
$PhCH_2$	25	7	32	1	2	29		4

Aside from the previously discussed reactions, intramolecular addition is observed with **11b** and **11c**. In **11b** the C-1′–C-2′ bond of the Si-phenyl moiety is reactive; the cycloheptatriene **17** and its double bond isomers are formed via **16** (by 1,5 H-shift). In contrast, **11c** adds to the C-2′–C-3′ bond of the Si-benzyl residue to give the stable norcaradiene **18** (opening of the three-membered ring would yield a bridgehead alkene). We attribute the regioselectivity to substituent effects of Me_3Si and Me_3SiCH_2 respectively: electrophiles preferentially attack the *ipso*-position of Me_3SiPh, but the

[*] Prof. Dr. W. Kirmse, Dr. W. Konrad
Fakultät für Chemie der Ruhr-Universität
Universitätsstrasse 150, D-4630 Bochum 1 (FRG)

o,p-position of Me_3SiCH_2Ph.[5] Apart from **12c–14c** and **18**, **11c** affords still another C–H insertion product, namely **19**.

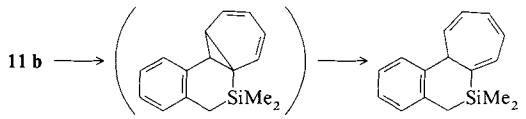

16 **17** (+ isomers)

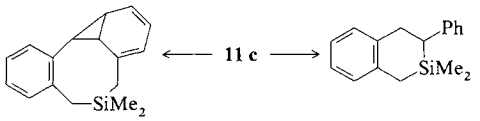

18 **19**

In the arylcarbenes **11**, the intramolecular insertion into C–Si bonds (30–40%, Table 1) may effectively compete with the insertion into C–H bonds and the addition to arenes. In contrast, intermolecular C–Si insertions have previously only been detected in reactions of the strained siletanes **20** and **21** with dichlorocarbene[6] and methylene.[7] We likewise found no insertion into Si–phenyl and Si–benzyl bonds, respectively, during thermolyses or photolyses of phenyldiazomethane in trimethylphenylsilane and benzyltrimethylsilane. Further experiments will have to show what causes the high intermolecular reactivity of these bonds and

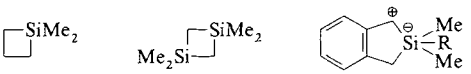

20 **21** **22**

whether "inverse ylides" **22** are involved with pentacoordinated silicon.[8] The "migration tendency" in C–Si insertions (Ph > alkyl, benzyl) is reminiscent of cationic rearrangements[9] and differs strongly from the behavior of the oxonium ylides **2**. Intermediates of type **22** would be compatible with these observations.

Received: February 8, 1990 [Z 3786 IE]
German version: *Angew. Chem. 102* (1990) 682

[1] W. Kirmse, K. Kund, *J. Am. Chem. Soc. 111* (1989) 1465.
[2] a) U. Schöllkopf, U. Ludwig, *Chem. Ber. 101* (1968) 2224; b) U. Schöllkopf, J. Schossig, G. Ostermann, *Liebigs Ann. Chem. 737* (1970) 158; c) J. E. Baldwin, W. F. Erickson, R. E. Hackler, R. M. Scott, *Chem. Commun. 1970*, 576; d) H. Iwamura, M. Iwamura, T. Nishida, M. Yoshida, J. Nakayama, *Tetrahedron Lett. 1971*, 63; e) W. D. Ollis, M. Rey, I. O. Sutherland, G. L. Closs, *J. Chem. Soc. Chem. Commun. 1975*, 543; f) U. H. Dolling, G. L. Closs, A. H. Cohen, W. D. Ollis, *ibid. 1975*, 545; g) H. Iwamura, Y. Imahashi, K. Kushida, K. Aoki, S. Satoh, *Bull. Chem. Soc. Jpn. 49* (1976) 1690; h) W. Kirmse, P. V. Chiem, *Tetrahedron Lett. 26* (1985) 197.
[3] Y. Ito, M. Nakatsuka, T. Saegusa, *J. Am. Chem. Soc. 104* (1982) 7609.
[4] a) A. Jonczyk, J. Wlostowa, *Synth. Commun. 8* (1978) 569; b) X. Creary, *Org. Synth. 64* (1986) 207.
[5] A. R. Bassindale, P. G. Taylor in S. Patai, Z. Rappoport (Eds.): *The Chemistry of Organic Silicon Compounds, Part 2*, Wiley, Chichester 1989, p. 893.
[6] D. Seyferth, R. Damrauer, S. B. Andrews, S. S. Washburne, *J. Am. Chem. Soc. 93* (1971) 3709.
[7] H. M. Frey, R. Walsh, I. M. Watts, *J. Chem. Soc. Chem. Commun. 1989*, 284.
[8] R. J. P. Corriu, J. C. Young in S. Patai, Z. Rappoport (Eds.): *The Chemistry of Organic Silicon Compounds, Part 2*, Wiley, Chichester 1989, p. 1241.
[9] P. Vogel: *Carbocation Chemistry*, Elsevier, Amsterdam 1985.

Isolation of Conformational Isomers of α- and β-Ionones by Inclusion Complex Formation

By *Fumio Toda*,* *Koichi Tanaka*, and *Takaji Fujiwara*

Conformational study of β-ionone (**1**) has long been interesting because **1** is closely related to the retinal chromophore, whose binding within rhodopsin is known to be conformationally dependent.[1] However, no conformational isomer of **1** has yet been isolated in pure state. NMR studies of the solution conformation of β-ionone[2] have shown it to exist mainly in the s-*cis* form (**1a**).

We now report the isolation of the s-*trans* conformer **1a** and the s-*cis* conformer **1b** of β-ionone (**1**) as inclusion complexes with the host compounds **3**[3] and **4**,[4] respectively. We also report the isolation of the axial quasi-chair form **2a** of α-ionone (**2**) as an inclusion compound with 9,9′-bianthryl (**5**).[5]

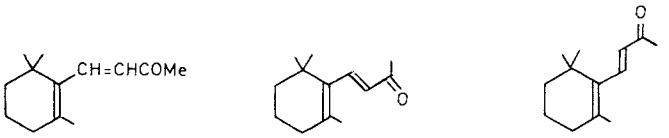

1 **1b** **1a**

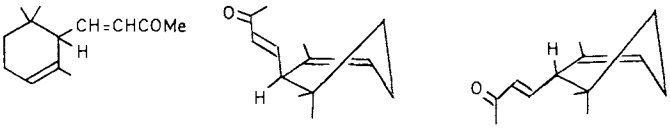

2 **2a** **2b**

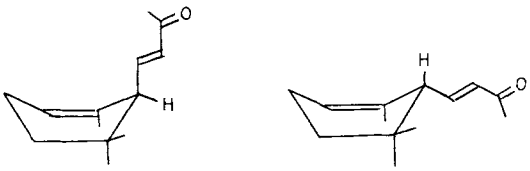

2c **2d**

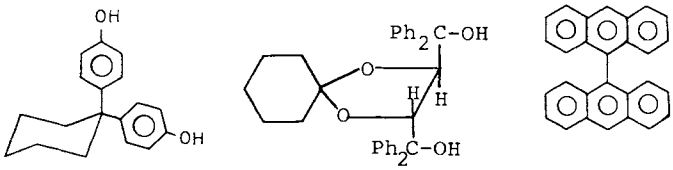

3 **4** **5**

β-Ionone (**1**) and **3** form a 2:1 inclusion compound, **6**, in which, according to X-ray crystal structure analysis, **1** is accommodated in an almost planar s-*trans* form (**1a**) be-

[*] Prof. F. Toda, Dr. K. Tanaka
Department of Industrial Chemistry, Faculty of Engineering
Ehime University, Matsuyama, Ehime 790 (Japan)
Prof. Dr. Takaji Fujiwara
Department of Chemistry, Faculty of Science
Shimane University, Matsue, Shimane 690 (Japan)

tween two molecules of the host **3** (Fig. 1).[6] It is energetically easier for **3** to form a cavity which accommodates **1a** through van der Waals and hydrogen-bonding interactions.

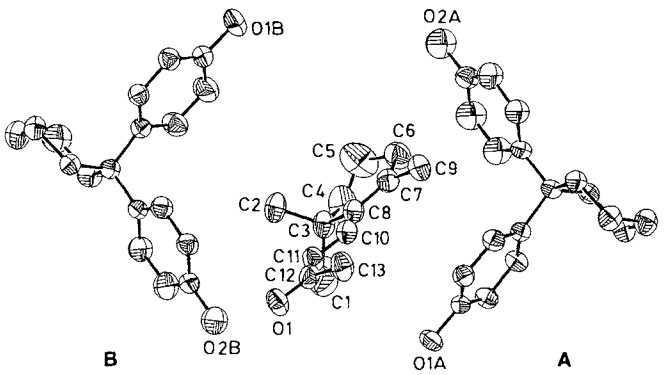

Fig. 1. Molecular structure of **6**. $M_r = 729.01$, triclinic, space group $P\bar{1}$, $Z = 2$, $a = 17.598(6)$, $b = 12.484(3)$, $c = 10.955(4)$ Å, $\alpha = 113.59(2)$, $\beta = 110.90(3)$, $\gamma = 76.70(3)°$, $V = 2050(1)$ Å^3, $\varrho_{exp} = 1.188(2)$, $\varrho_{calcd} = 1.181$ Mg m^{-3}, $\mu = 5.92$ cm^{-1}, $R = 0.056$ for 5360 reflections with $F_0 > 3\sigma(F_0)$. The C4, C5, and C10 atoms are displaced by 0.300(8), − 0.370(8), and − 0.049(7) Å, respectively, out of the best plane through the C3, C6, C7, and C8 atoms (maximum deviation = 0.014 Å). The C10 atom deviates slightly from the plane. The hosts **A** are connected by the hydrogen bond of O2A-H···O1A [$(x, y, 1+z) = 2.778(3)$ Å], and the hosts **B** by the O1B-H···O2B [$(x, y, 1+z) = 2.731(3)$ Å] hydrogen bond. The host and guest are linked by the hydrogen bonds O2B-H···O1 [2.686(3) Å] and O1···H-O1A [$(1-x, -y, -z) = 2.682(3)$ Å], where O1 connects both chains of hosts **A** and **B**. The structural unit of the zigzag chain formed by hosts **A**, the guest molecules, and the zigzag chain formed by hosts **B** repeats along the c axis [6].

On the other hand, **1** and **4** form a 1:1 inclusion compound, **7**, in which **1** exhibits the s-*cis* form (**1b**). Although an X-ray crystal structure analysis of **7** could not be carried out because of difficulty in obtaining a good crystal, the s-*cis* conformation of **1** in **7** was determined by spectroscopic methods. In the IR spectrum, the C=O band ($\tilde{\nu} = 1675$ cm^{-1}) of **1b** in **7** was at higher frequencies than the C=O band ($\tilde{\nu} = 1590$ cm^{-1}) of **1a** in **6**. It has been well established that s-*cis* enones show the C=O absorption at higher frequencies than do the s-*trans* isomers.[7] In the UV spectrum in the solid state, **1b** in **7** showed λ_{max} at shorter wavelengths than did **1a** in **6** (Fig. 2). It has also been established that s-*cis* enones absorb in the UV at shorter wavelengths than do s-*trans* enones.[8]

In the relatively small cavity of the 1:1 complex **7**, the less bulky s-*cis* isomer **1b** should be accommodated favorably. By contrast, the more bulky s-*trans* isomer **1a** should be accommodated favorably in the relatively large cavity of the 2:1 complex **6**. α-Ionone **2** also forms inclusion compounds, but not with **3**. Thus, by exploiting this selective inclusion, **1** and **2** can be separated efficiently.

Interestingly, α-ionone (**2**) and **5** form a 1:1 inclusion compound, **8**, in which the quasi-chair form with an axial enone group, **2a**, is present. X-ray crystal structure analysis of **8** shows that the molecules of **5** are arranged so as to form a channel-type complex with **2a**. In a channel, two molecules of **2a** of the same chirality face each other and display contacts through their acyl groups (Fig. 2). The structure of the axial quasi-chair form **2a** is shown in Figure 3. The cavity formed by **5** is fitted to accommodate **2a** but not the equatorial quasi-chair form **2b**, the axial quasi-boat form **2c**, or the equatorial quasi-boat form **2d**. Hydrocarbon hosts such as **5**,[5] 1,1,2,2-tetraphenylethane,[9] and 1,2,4,5-hexatetraene derivatives[10] are known to form inclusion compounds with a wide variety of guests including hydrocarbons.

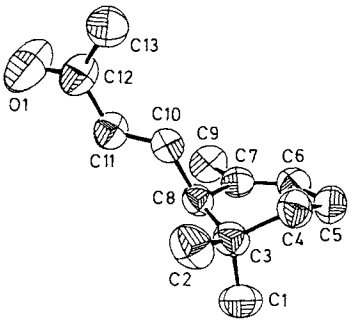

Fig. 3. Conformation of **2a** in the inclusion compound **8**.

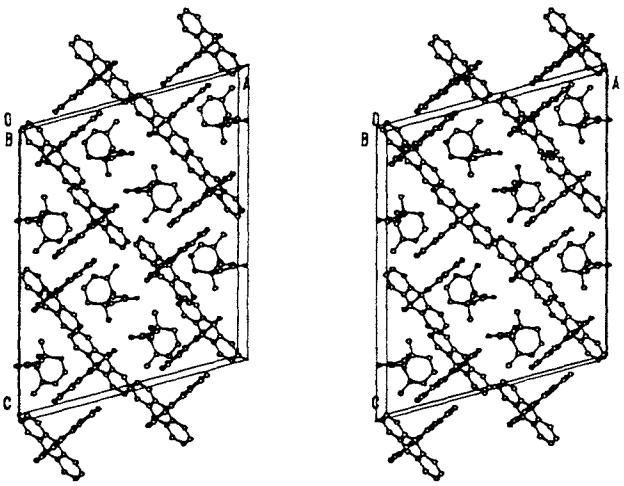

Fig. 2. Packing diagram of **8**. $M_r = 546.8$, monoclinic, space group $C2/c$, $Z = 8$, $a = 21.293(2)$, $b = 11.244(1)$, $c = 27.199(1)$ Å, $\beta = 105.98(1)°$, $V = 6260(1)$ Å^3, $\varrho_{exp} = 1.160$ Mg m^{-3}, $\mu = 6.23$ cm^{-3}, $R/wR = 0.045/0.056$ for reflections with $F_0 > 3\sigma(F_0)$ [6].

The above results suggest that the inclusion complexation method is applicable to the isolation of unstable conformers of various organic compounds.

Experimental Procedure

6: When a solution of **3** (1 g) in **1** (5 g) was kept at room temperature for 12 h, the 2:1 inclusion complex **6** was obtained as pale yellow prisms (1.2 g); m.p. 132–134 °C, $\tilde{\nu}$(C=O) (Nujol mull) = 1590 cm^{-1}.

7: When a solution of **4** (1 g) in **1** (5 g) was treated as above, the 1:1 inclusion complex **7** was obtained as colorless plates (0.9 g); m.p. 68–70 °C, $\tilde{\nu}$(C=O) (Nujol mull) = 1675 cm^{-1}.

8: When a solution of **5** (0.5 g) in *rac*-**2** (5 g) was treated as above, the 1:1 inclusion complex **8** was obtained as colorless prisms (0.35 g); m.p. not clear, $\tilde{\nu}$(C=O) (Nujol mull) = 1675 cm^{-1}. Separation of **1** and **2** by complexation with **3**: When a solution of **3** (1 g) and a 1:1 mixture of **1** and **2** (1.43 g) in EtOAc (2 mL) was kept at room temperature for 2 h, **6** was formed (0.85 g). Upon distillation in vacuo, **6** gave **1** of 95.3% purity (by gas chromatography) (0.35 g, 46% yield).

Received: December 27, 1989 [Z 3703]
German version: *Angew. Chem. 102* (1990) 688

CAS Registry numbers:
1, 79-77-6; **2**, 127-41-3; **6**, 127063-79-0; **7**, 127128-06-7; **8**, 127063-80-3.

[1] H. Matsumoto, R. S. H. Liu, C. J. Simmons, K. Seff, *J. Am. Chem. Soc. 102* (1980) 4259; R. S. H. Liu, A. E. Asato, M. Denny, D. Mead, *ibid. 106* (1984) 8298.
[2] B. Honig, B. Hudson, B. D. Sykes, M. Karplus, *Proc. Natl. Acad. Sci. USA 68* (1971) 1289; K. Müllen, H. Schmickler, B. Frei, H. R. Wolf, *Tetrahedron Lett. 27* (1986) 477.
[3] I. Goldberg, Z. Stein, A. Kai, F. Toda, *Chem. Lett. 1987*, 1617.
[4] F. Toda, A. Satō, K. Tanaka, T. C. W. Mak, *Chem. Lett. 1989*, 873.
[5] F. Toda, *Top. Curr. Chem. 140* (1987) 43.
[6] Further details of the crystal structure investigations are available on request from the Director of the Cambridge Crystallographic Data Centre, University Chemical Laboratory, Lensfield Road, Cambridge CB2 1EW (UK), on quoting the full journal citation.
[7] R. L. Erskine, E. S. Waight, *J. Chem. Soc. 1960*, 3425.
[8] E. S. Waight, R. L. Erskine in G. W. Gray (Ed): *Steric Effects in Conjugated Systems*, Butterworths, London 1958, Chapter 7.
[9] F. Toda, K. Tanaka, Y. Wang, G.-H. Lee, *Chem. Lett. 1986*, 109.
[10] F. Toda, K. Tanaka, H. Tsukada, H. Shimanouchi, Y. Sasada, *Chem. Lett. 1979*, 1381.

Synthesis, Structure, and Reactivity of Aryloxo(imido)titanium Complexes**

By *John E. Hill, Robert D. Profilet, Phillip E. Fanwick*, and *Ian P. Rothwell**

The chemistry of transition-metal terminal oxo (M=O)[1-3] and related alkylimido (M=NR)[1,4-7] functional groups has received considerable research attention over the past few years. In particular, the work of *Bergman* et al.[6] and *Wolczanski* et al.[7] has shown that terminal alkylimido compounds of zirconium can exhibit interesting reactivity including the activation of hydrocarbon C–H bonds. During our study of the chemistry of titanium supported by ancillary, aryloxide ligation we have isolated various terminal alkylimido derivatives of this metal. Here we report on the various synthetic strategies possible for the isolation of these compounds as well as on their structure and reactivity.[8]

Previous work by our group has shown that the η^2-imine complex **1** (py′ = pyridine or 4-substituted pyridine) is a very useful intermediate for the formation of both high- and low-valent compounds of titanium.[9,10] Reaction of this η^2-imine complex with azobenzene in the presence of 4-pyrrolidinopyridine (py′) leads to the formation of the highly colored η^2-azobenzene complex **2** in high yield (Scheme 1).[11] The pyridine analogue of **2** has been structurally characterized previously.[9b] In hydrocarbon solvents, compound **2** is thermally unstable. At 100 °C over days the formation of a new titanium complex **3**[12] along with free azobenzene is observed. The identity of **3** as a terminal phenylimido complex was confirmed by a single-crystal X-ray diffraction analysis (Fig. 1).[13]

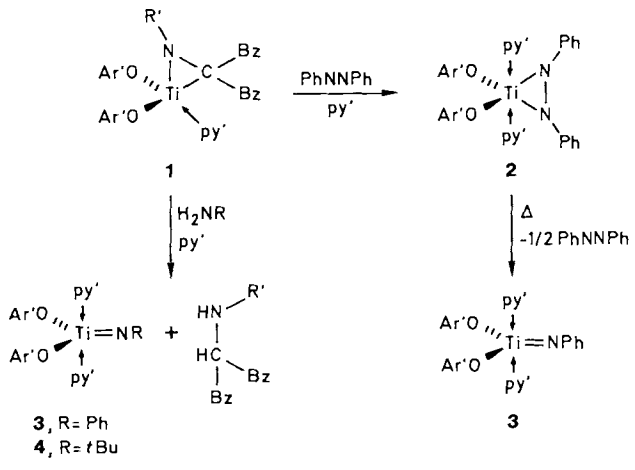

Scheme 1. Synthesis of **3** and **4**. Bz = CH_2Ph; py′ = 4-pyrrolidinopyridine; Ar′O = 2,6-$iPr_2C_6H_3O$; R′ = *t*Bu.

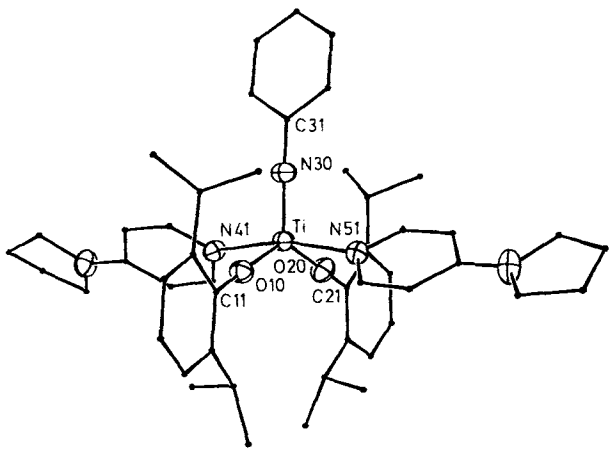

Fig. 1. ORTEP view of the phenylimido compound **3**. Selected distances [pm] and angles [°]: Ti-N30 171.9(3), Ti-N41 220.6(3), Ti-N51 222.3(3), Ti-O10 188.0(3), Ti-O20 186.7(3); Ti-N30-O31 173.1(3), N41-Ti-N51 165.8(1), O10-Ti-O20 133.2(1), Ti-O10-O11 172.0(2), Ti-O20-O23 173.8(3).

The coordination environment about the metal center in **3** is best described as distorted trigonal-bipyramidal with *trans*, axial pyridine ligands [py′-Ti-py′ = 165.8(1)°]. The remaining two aryloxide ligands and terminal phenylimido group occupy the three equatorial sites. Compound **3** represents the first structurally characterized terminal alkylimido derivative of titanium.[1,8,13] The Ti–N distance of 171.9(3) pm is considerably shorter than the distances found to terminal amido ligands (compare the Ti–NHPh distances of 188.1(3) and 189.(3) pm in **5**).[14] An interesting structural comparison can also be made between **3** and the related terminal oxo compound $[(2,6\text{-}iPr_2C_6H_3O)_2Ti(=O)(py')_2]$,[10] where an essentially identical coordination environment is present with a Ti–O distance of 165.7(6) pm.

Besides the cleavage of azobenzene, an alternative method for the formation of **3** involves direct reaction of the η^2-imine complex **1** with aniline in the presence of pyrrolidinopyridine (Scheme 1). This latter reaction also allows the formation of the *tert*-butylimido complex **4**.[15]

In a directly related study, the reactivity of the dialkyl compounds $[(2,6\text{-}Ph_2C_6H_3O)_2TiR_2]$ ($R = CH_2SiMe_3$, C_6H_5)[16] with aniline has also been investigated. Although reaction of the trimethylsilylmethyl derivative is slow, treatment of the diphenyl compound with two equivalents of $PhNH_2$ in benzene solution at room temperature was found to lead to the deep-red bis(phenylamido) complex **5** in high yield (Scheme 2).[17] A single-crystal X-ray diffraction analysis of **5** was carried out and confirmed the stoichiometry.[18] Treatment of **5** with 4-pyrrolidinopyridine (py′) rapidly leads to the elimination of one equivalent of aniline and formation of the phenylimido complex **6**.

[*] Prof. I. P. Rothwell, J. E. Hill, R. D. Profilet, Dr. P. E. Fanwick
Department of Chemistry, Purdue University
West Lafayette, IN 47907 (USA)

[**] This work was supported by the National Science Foundation.

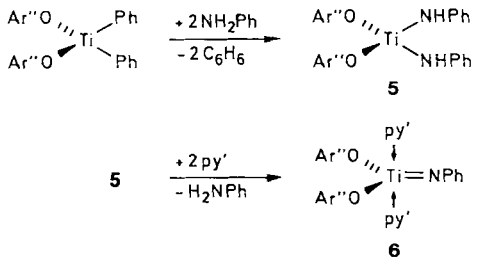

Scheme 2. Synthesis of **5** and **6**. Ar″O = 2,6-$Ph_2C_6H_3O$.

The new terminal aryl- and alkylimido compounds **3**, **4**, and **6** are surprisingly unreactive. Neither significant decomposition nor evidence for reaction with 3-hexyne is observed upon thermolysis at 110 °C for days in [D_6]benzene. Furthermore, given the fact that the previously reported zirconium imido compounds undergo reaction with a range of carbon–hydrogen bonds,[6b, 7] it is of note that compound **6** does not undergo cyclometalation of the 2,6-diphenylphenoxide ligands.[19] Moreover, although the phenylimido complex **6** does not react with 3-hexyne, the bis(phenylamido) complex **5** will catalyze the reaction of aniline with 3-hexyne to produce the *N*-phenylimine of 3-hexanone.[6b] Whether this reaction proceeds via an unsolvated, and hence more reactive, phenylimido intermediate is presently being investigated.

Received: January 30, 1990 [Z 3766 IE]
German version: *Angew. Chem. 102* (1990) 713

[1] W. A. Nugent, J. M. Mayer: *Metal–Ligand Multiple Bonds*, Wiley, New York 1988.

[2] a) W. A. Hermann, *Angew. Chem. 100* (1988) 1269; *Angew. Chem. Int. Ed. Engl. 27* (1988) 1297; b) W. A. Hermann, *J. Mol. Catal. 41* (1987) 109; c) S. Cai, D. M. Hoffman, D. A. Wierda, *J. Chem. Soc. Chem. Commun. 1988*, 1489; d) G. Parkin, J. E. Bercaw, *J. Am. Chem. Soc. 111* (1989) 559; e) G. Parkin, J. E. Bercaw, *Polyhedron 7* (1988) 2053; f) J. W. Faller, M. Jinong, *Organometallics 7* (1988) 559; g) P. Legzdins, E. C. Phillips, S. J. Rettig, L. Sanchez, J. Trotter, V. C. Yee, *ibid. 7* (1988) 1877.

[3] a) R. H. Holm, *Chem. Rev. 87* (1987) 1401; b) F. Bottomley, N. Sutin, *Adv. Organomet. Chem. 28* (1988) 339.

[4] a) M. H. Chisholm, I. P. Rothwell in G. Wilkinson, R. Gillard, J. A. McCleverty (Eds.): *Comprehensive Coordination Chemistry Vol. 2*, Pergamon Press, Oxford 1987, Chapter 13.4, b) W. A. Nugent, B. L. Haymore, *Coord. Chem. Rev. 31* (1980) 123.

[5] E. W. Harlan, R. H. Holm, *J. Am. Chem. Soc. 112* (1990) 186, and references therein.

[6] a) M. J. Carney, P. J. Walsh, F. J. Hollander, R. G. Bergman, *J. Am. Chem. Soc. 111* (1989) 8751; b) P. J. Walsh, F. J. Hollander, R. G. Bergman, *ibid. 110* (1988) 8729.

[7] C. C. Cummins, S. M. Baxter, P. T. Wolczanski, *J. Am. Chem. Soc. 110* (1988) 8731.

[8] After submission of this manuscript we learned of the characterization of an imidotitanium complex by *Roesky* et al. also described in this issue: W. W. Roesky, H. Voelker, M. Witt, M. Noltemeyer, *Angew. Chem. 102* (1990) 712; *Angew. Chem. Int. Ed. Engl. 29* (1990) 669.

[9] a) L. D. Durfee, P. E. Fanwick, I. P. Rothwell, K. Folting, J. C. Huffman, *J. Am. Chem. Soc. 109* (1987) 4710; b) L. D. Durfee, J. E. Hill, P. E. Fanwick, I. P. Rothwell, *Organometallics 9* (1990) 75; c) L. D. Durfee, J. E. Hill, J. L. Kerschner, P. E. Fanwick, I. P. Rothwell, *Inorg. Chem. 28* (1989) 3095.

[10] J. E. Hill, P. E. Fanwick, I. P. Rothwell, *Inorg. Chem. 28* (1989) 3602.

[11] Correct C, H, N elemental analysis

[12] Correct C, H, N elemental analysis ^{1}H NMR (200 MHz, C_6D_6, 30 °C): δ = 4.57 (sept., $CHMe_2$), 1.49 (d, $CHMe_2$), 8.79 (d, *ortho* protons on py), 5.67 (d, *meta* protons on py), 2.13(m), 1.13(m, pyrrolidine protons), 6.6–7.4 (m, orther aromatic protons). Selected ^{13}C NMR data (C_6D_6, 30 °C): δ = 161.7(Ti=N-*C*), 26.4 ($CHMe_2$), 24.1 ($CHMe_2$), 24.5 and 46.2 (pyrrolidine ring carbons).

[13] Crystal data at −100 °C for **3**: space group $P2_1/n$, a = 14.234(4), b = 13.818(3), c = 23.087(6) Å, β = 95.99(1)°, Z = 4, ρ_{calcd} = 1.162 g cm^{-3}; 6196 unique data with $I > 3\sigma(I)$ yielded R = 0.054, R_w = 0.065.

[14] The previously structurally characterized mononuclear zirconium alkylimido complex [$Cp_2Zr(NtBu)(thf)$] has a Zr–N distance of 182.6(4) pm [6b].

[15] Selected spectroscopic data for **4**: ^{1}H NMR (C_6D_6, 30 °C): δ = 1.39 (s, $NCMe_3$), 4.60 (sept., $CHMe_2$), 1.48 (d, $CHMe_2$), 8.77 (d, *ortho* protons on py), 5.73 (d, *meta* protons on py), 1.34 (m), 2.33 (m, pyrrolidine protons). ^{13}C NMR (C_6D_6, 30 °C): δ = 68.0 ($NCMe_3$), 32.3 ($NCMe_3$), 25.7 ($CHMe_2$), 24.4 ($CHMe_2$).

[16] R. W. Chesnut, L. D. Durfee, P. E. Fanwick, I. P. Rothwell, K. Folting, J. C. Huffman, *Polyhedron 6* (1987) 2019.

[17] Selected spectroscopic data for **5**: IR (Nujol mull), $\tilde{\nu}$ (NH) = 3,301 cm^{-1}. ^{1}H NMR (C_6D_6, 30 °C): δ = 8.22 (s, Ti-N*H*Ph), 6.4–7.4 (m, aromatic protons). ^{13}C NMR (C_6D_6, 30 °C): δ = 161.4 (Ti-N-*C*), 161.3 (Ti-O-*C*), 151.9 (*para* carbon on py), 118.7–142.5 (aromatic carbons), 46.8, 25.3 (pyrrolidine carbons).

[18] Crystal data at 20 °C for **5**: space group $P2_1/n$, a = 11.427(3), b = 18.722(3), c = 18.811(5) Å, β = 105.25(1)°, Z = 4, ρ_{calcd} = 1.236 g cm^{-3}; 2919 unique data with $I > 3\sigma(I)$ yielded R = 0.041, R_w = 0.048. Further details of the crystal structure investigations are available on request from the Fachinformationszentrum Karlsruhe, Gesellschaft für Wissenschaftlich-technische Information mbH, D-7514 Eggenstein-Leopoldshafen 2 (FRG), on quoting the depository number CSD-54481, the names of the authors, and the journal citation.

[19] The lack of cyclometalation of 2,6-diphenylphenoxide ligands by organoimido groups bound to Nb, Ta, and W has also been reported: see a) R. W. Chesnut, P. E. Fanwick, I. P. Rothwell, *Inorg. Chem. 27* (1988) 752; b) J. L. Kerschner, Y. S. Yu, P. E. Fanwick, I. P. Rothwell, J. C. Huffman, *Organometallics 8* (1989) 1414.

Intramolecular Hetero-Diels–Alder Reactions of Oxadienes: Influence of Substituents of the Tether on the Diastereoselectivity**

By *Lutz F. Tietze,* Siegbert Brand, Thomas Brumby*, and *Jens Fennen*

Intramolecular cyclization reactions such as the intramolecular Diels–Alder and ene reactions are widely used for synthesizing carbo- and heterocycles.[1] There is considerable interest in the extent to which substituents on the tether influence such reactions in the formation of new stereogenic centers. The stereoselectivity of reactions of this type depends crucially on the energy differences between the conformational transition states which lead to the diastereomeric products. Whereas the influence of substituents on the conformations of molecules in the ground state has been very thoroughly studied, especially for cyclohexane,[2] there have so far been scarcely any similar energetic studies on transition states, despite the fact that many examples of intramolecular cyclizations of substrates having substituents on the tether are already known.[3] The aim of our study is to use accurate analyses of the product mixtures from intramolecular pericyclic, free radical, and ionic cyclizations to deduce the geometry of the transition states, and hence to determine quantitatively, as accurately as possible, the effects of tether substituents.

In this communication we investigate how the stereochemistry of the intramolecular Diels–Alder reaction of oxadienes[4] is influenced by a methyl group at different positions on a C_4 tether. We chose as a model the alkylidene-α,α′-

[*] Prof. Dr. L. F. Tietze, S. Brand, T. Brumby, J. Fennen
Institut für Organische Chemie der Universität
Tammanstrasse 2, D-3400 Göttingen (FRG)

[**] Inter- and Intramolecular Hetero-Diels–Alder Reactions, Part 30. This research was supported by the Deutsche Forschungsgemeinschaft and the Fonds der Chemischen Industrie. Part 29: L. F. Tietze, U. Beifuss, M. Lökös, M. Rischer, A. Göhrt, G. M. Sheldrick, *Angew. Chem. 102* (1990) 545; *Angew. Chem. Int. Ed. Engl. 29* (1990) 527.

dioxo compound **3**, which can be prepared by condensation of 7-methyl-6-octenal (**1**) with *N*,*N*-dimethylbarbituric acid (**2**) in the presence of catalytic amounts of ethylenediammonium diacetate. The intramolecular cycloaddition of **3**, formed in situ, gives, within 2 h at 20 °C, a 98.8:1.20 mixture of the diastereomeric cycloadducts *rac*-**5a** and *rac*-**5c**.[5] This is assumed to be a concerted reaction,[6] in which the *trans*-annelated product is formed via an *exo-E-anti* transition state and the *cis*-annelated product via an *endo-E-syn* and/or an *exo-Z-syn* transition state.[7] In addition, 17% of the ene reaction product *rac*-**4** is obtained; this can be cyclized to give *rac*-**5a** by reaction with $BF_3 \cdot OEt_2$.

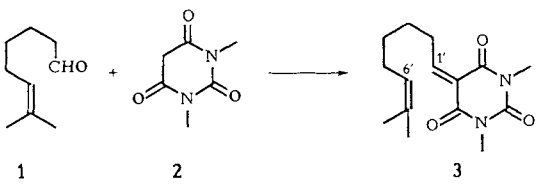

1 **2** **3**

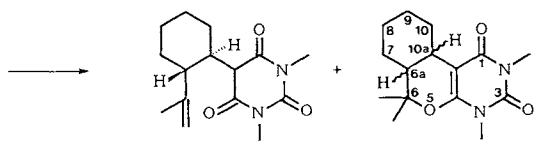

4 (17%) **5** (58%)

rac-**5a** : *rac*-**5c** = 98.8 : 1.2 (±0.1)

5, 7, 9, 11, 13	6a-H	10a-H
a	α	β (*trans*)
b	β	α (*trans*)
c	α	α (*cis*)
d	β	β (*cis*)

The tandem Knoevenagel–hetero-Diels–Alder reaction of the aldehyde **6**[8] with **2** affords, in addition to ene products, only one *trans* and one *cis* cycloadduct, **7a** and **7d**, respectively, which have been isolated and identified by NMR spectroscopy.[5] The induced diastereoselectivity[9] for the formation of **7a** is found to be greater than 99.5:0.5, whereas the noninduced diastereoselectivity,[9] with a value of 97.9:2.10, is slightly lower than that for the synthesis of the unsubstituted system **5**.[10] In the transition state leading to **7a** the methyl group on the tether adopts an equatorial position; here, it should be noted that force-field calculations[11] indicate that **7a** is about 12.5 kJ mol^{-1} less stable than **7b** with the methyl group in the axial position; **7b** is not found in this reaction. The lower thermodynamic stability of **7a** is probably caused by a strong interaction between the methyl group and one of the C=O groups.

The reaction of the aldehyde **8** with **2** yields all four possible diastereomers **9a–d**, with **9b** as the main product (Table 1). In this case, too, all the diastereomers were isolated by preparative HPLC and identified by NMR spectroscopy.[5] Surprisingly, it was found that there is a high induced diastereoselectivity for the formation of the *trans* cycloadducts **9a** and **9b** and almost no selectivity for that of the *cis* compounds **9c** and **9d**. The noninduced diastereoselectivity is the same as for the cycloaddition of **3**. A similar result is also found for the reaction of the aldehyde **10** with **2**. In this case, however, only the *trans* products **11a** and **11b** could be identified by NMR spectroscopy.[5] An additional HPLC peak with a retention time similar to that of **9c** was observed and assigned to the *cis* products **11c** and/or **11d** (Table 1).

Table 1. Selectivities [%]/$\Delta\Delta G^{\neq}$ values [kJ mol^{-1}] in the intramolecular hetero-Diels–Alder reaction of alkylidenebarbiturates.

Product	a	b	c	d
7	97.9/0.0	<0.5/–	<0.5/–	2.10/9.12
9	3.60/8.12	95.2/0.0	0.5/13.0	0.7/12.1
11	94.1/0.0	4.7/7.37	1.2/10.8	
13	<0.5/–	98.3/0.0	0.9/11.7 ⟷	0.8/12.1

The aldehyde **12** yields, with high induced diastereoselectivity (>99.5:0.5), the *trans* cycloadduct **13b** as the main product.[5] Two additional peaks were observed in the HPLC chromatogram and assigned to the *cis* products **13c** and **13d** (Table 1).

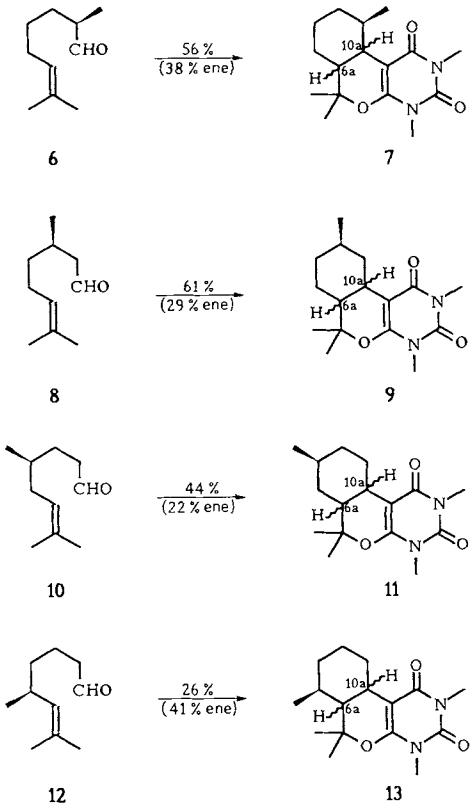

6 **7** **8** **9** **10** **11** **12** **13**

The high noninduced diastereoselectivity of the hetero-Diels–Alder reactions of **3** and its methyl-substituted analogues is surprising, since the intramolecular Diels–Alder reaction of the related hydrocarbon 1,3,9-decatriene yields an approximately 1:1 mixture of the two cycloadducts. *Houk* et al. assumed that this reaction occurs via a nearly symmetrical transition state, and their experimental results were in good agreement with calculations on that basis.[12] Thus, we explain the observed high *trans* selectivity of the reactions of **3**, **6**, **8**, **10**, and **12** by the existence of nonsymmetric transition states.[13]

The observed diastereofacial differentiation in the cycloaddition is basically due to two contributions, which can either act in the same sense or oppose each other: (1) steric

interactions of the substituents with the diene or dienophile moiety ("steric effect") and (2) 1,3-diaxial interactions between the substituents on the tether ("conformational effect"). Thus, the high induced diastereoselectivity in the reactions of the aldehydes **6** and **12** (with a methyl group at the α position relative to the diene or dienophile moiety) can be attributed to steric interactions between the methyl group and the diene or dieneophile moiety of the molecule, whereas in the aldehydes **8** and **10** (methyl group at the β position relative to the diene or dienophile moiety) conformational effects are dominant. The geminal substitution of the acceptor alkene unit confers high conformational rigidity on the transition states due to the "partial" 1,3-allyl strain (sp^2 geminal effect[15]).[14] It can be assumed that the formation of the *trans* products **9b**, **9a**, **11a**, and **11b** occurs via a chairlike transition state, with the methyl group in either the equatorial (**9b**, **11a**) or axial (**9a**, **11b**) position. The calculated ΔG value for the transition states leading to **9b** and **9a** is 8.12 kJ mol^{-1} and for the transition states leading to **11a** and **11b**, 7.37 kJ mol^{-1}. These values are greater than the experimentally measured energy difference between the methylcyclohexane conformers with the methyl group in the equatorial and axial positions.[2] It must be assumed, therefore, that in the transition states leading to **9a** and **11b** there is a stronger 1,3-diaxial interaction due to close approach of the axial methyl group to the "inwardly" directed hydrogen atom on C-1′ and C-6′, respectively (with the carbon atoms numbered as in **3**).

Received: December 29, 1989 [Z 3710 IE]
German version: *Angew. Chem. 102* (1990) 675

[1] J. Sauer, R. Sustmann, *Angew. Chem. 92* (1980) 773; *Angew. Chem. Int. Ed. Engl. 19* (1980) 779–807; D. L. Boger, S. M. Weinreb: *Hetero-Diels-Alder Methodology in Organic Synthesis*, Academic Press, San Diego, CA, USA 1987; D. F. Taber: *Intramolecular Diels-Alder and Alder Ene Reactions*, Springer, Berlin 1984; A. G. Fallis, *Can. J. Chem. 62* (1984) 183; E. Ciganek, *Org. React. (N.Y.) 32* (1984) 1; W. Oppolzer, *Angew. Chem. 96* (1984) 840; *Angew. Chem. Int. Ed. Engl. 23* (1984) 876.

[2] J. A. Hirsch, *Top. Stereochem. 1* (1967) 199; D. H. R. Barton, O. Hassel, *ibid. 6* (1971) 1; W. Klyne, *Prog. Stereochem. 1* (1954) 36.

[3] D. Craig, *Chem. Soc. Rev. 16* (1987) 187.

[4] Reviews: L. F. Tietze, *J. Heterocyclic Chem. 27* (1990) 47; L. F. Tietze in W. Bartmann, B. M. Trost (Eds.): *Selectivity—A Goal for Synthethic Efficiency*, Verlag Chemie, Weinheim 1984, p. 299; L. F. Tietze, G. von Kiedrowski, K. Harms, W. Clegg, G. Sheldrick, *Angew. Chem. 92* (1980) 130 131; *Angew. Chem. Int. Ed. Engl. 19* (1980) 134; L. F. Tietze, T. Brumby, M. Pretor, G. Remberg, *J. Org. Chem. 53* (1988) 810; L. F. Tietze, S. Brand, T. Pfeiffer, J. Antel, K. Harms, G. Sheldrick, *J. Am. Chem. Soc. 109* (1987) 921.

[5] The products were isolated as pure substances by column chromatography, preparative HPLC, or fractional crystallization; they were identified by X-ray crystallography and/or NMR spectroscopy. **5a**: ^{1}H NMR (200 MHz, $CDCl_3$): $\delta = 0.82$ (qm, $J = 12$ Hz, 1H, 10-H_{ax}), 1.0–1.5 (m, 4H, 6a-H, 7-H_{ax}, 8-H_{ax}, 9-H_{ax}), 1.15 (s, 3H, 6-$CH_{3,ax}$), 1.42 (s, 3H, 6-$CH_{3,eq}$), 1.65–1.9 (m, 3H, 7-H_{eq}, 8-H_{eq}, 9-H_{eq}), 2.19 (ddd, $J = 11$, 11, 3 Hz, 1H, 10a-H), 3.14 (dm, $J = 13$ Hz, 1H, 10-H_{eq}), 3.30 (s, 3H, N-CH_3), 3.31 (s, 3H, N-CH_3). **7a**: ^{1}H NMR (200 MHz, $CDCl_3$): $\delta = 1.08$ (d, $J = 6$ Hz, 3H, 10-CH_3), 1.10 (s, 3H, 6-$CH_{3,ax}$), 1.04–1.19 (m, 1H), 1.30–1.49 (m, 2H), 1.44 (s, 3H, 6-$CH_{3,eq}$), 1.49–1.65 (m, 2H, 6a-H, 10-H), 1.71–1.94 (m, 3H), 2.18 (dd, $J = 10.3$, 9.0 Hz, 1H, 10a-H), 3.31 (s, 6H, N-CH_3). **9b**: ^{1}H NMR (80 MHz, $CDCl_3$): $\delta = 0.4$–2.0 (m, 7H, 6a-H, 7-H 8-H, 9-H, 10-H_{ax}), 0.95 (d, $J = 6$ Hz, 3H, 9-CH_3), 1.19 (s, 3H, 6-CH_3), 1.47 (s, 3H, 6-CH_3), 2.30 (dt, $J = 3$, 10 Hz, 1H, 10a-H), 3.18 (dq, $J = 2$-3, 12 Hz, 1H, 10-H_{eq}), 3.30 (s, 6H, N-CH_3). **11a**: ^{1}H NMR (200 MHz, $CDCl_3$): $\delta = 0.66$–0.90 (m, 1H, 10-H_{ax}), 0.96 (d, $J = 6.5$ Hz, 3H, 8-CH_3), 0.90–1.30 (m, 2H, 7-H_{ax}, 9-H_{ax}), 1.17 (s, 3H, 6-$CH_{3,ax}$), 1.46 (s, 3H 6-$CH_{3,eq}$), 1.34–1.60 (m, 2H, 6a-H, 8-H), 1.70–1.90 (m, 2H, 9-H_{eq}, 7-H_{eq}), 2.18 (td, $J = 11.0$, 3.0 Hz, 1H, 10a-H), 3.10–3.24 (m, 1H, 10-H_{eq}), 3.34 (s, 6H, N-CH_3). **13b**: ^{1}H NMR (200 MHz, $CDCl_3$): $\delta = 0.85$ (tdd, $J = 13.0$, 11.0, 4.0 Hz, 1H, 10-H_{ax}), 1.05 (d, $J = 6.5$ Hz, 3H, 7-CH_3), 1.18–1.35 (m, 2H), 1.21 (s, 3H, 6-$CH_{3,ax}$), 1.36–1.57 (m, 2H), 1.60 (s, 3H, 6-$CH_{3,eq}$), 1.71–1.87 (m, 2H), 2.28 (ddd, $J = 11.0$, 10.0, 3.0 Hz, 1H, 10a-H), 3.11 (br. d, $J = 13$ Hz, 1H, 10-H_{eq}), 3.31 (s, 6H, N-CH_3).

[6] L. F. Tietze, M. Bratz, R. Machinek, G. v. Kiedrowski, *J. Org. Chem. 52* (1987) 1638.

[7] The conventions used in describing the structures of the transition states are as follows: (1) *Endo/exo* refer to the position of the tether relative to the diene moiety of the molecule. If the chain is below the diene moiety, the transition state has an *endo* structure. (2) *E/Z* refer to the configuration of the C–C double bond of the oxadiene, with the higher priority given to the reacting C=O group. (3) *Syn/anti* refer to the relative positions of the hydrogens which appear at the linking positions of the newly formed ring in the product. In *ortho* additions, *syn* and *anti* transition states give, respectively, *cis*- and *trans*-annelated products.

[8] The aldehydes **6**, **8**, **10**, and **12** were used as racemic mixtures, and consequently the corresponding products **7**, **9**, **11**, and **13** were also obtained as racemic mixtures. The syntheses of the aldehydes **6**, **10**, and **12** will be described elsewhere.

[9] L. F. Tietze, U. Beifuss, *Angew. Chem. 97* (1985) 1067; *Angew. Chem. Int. Ed. Engl. 24* (1985) 1042.

[10] The ratios of the diastereomers were determined by HPLC. For this purpose three reactions were carried out under identical conditions in each case, followed by three HPLC measurements on the mixtures. The standard deviation was less than 0.5%.

[11] L. F. Tietze, J. Fennen, unpublished results.

[12] K. N. Houk, M. N. Paddon-Row, N. G. Rondan, Y.-D. Wu, F. K. Brown, D. C. Spellmayer, J. T. Metz, Y. Li, R. J. Loncharich, *Science (Washington) 231* (1986) 1108.

[13] L. F. Tietze, T. Brumby, S. Brand, M. Bratz, *Chem. Ber. 121* (1988) 499; L. F. Tietze, J. Fennen, E. Anders, *Angew. Chem. 101* (1989) 1420; *Angew. Chem. Int. Ed. Engl. 28* (1989) 1371.

[14] R. W. Hoffmann, *Chem. Rev. 89* (1989) 1841.

[15] L. F. Tietze, U. Beifuss, M. Ruther, A. Rühlmann, J. Antel, G. M. Sheldrick, *Angew. Chem. 100* (1988) 1200; *Angew. Chem. Int. Ed. Engl. 27* (1988) 1186.

Reductive Scission of a Cyclopropane σ-Bond During the Action of Elemental Lithium on Cyclopropylacetylenes – A *cis*-1,2-Dilithioalkene as Intermediate**

By *Adalbert Maercker** and *Ulrich Girreser*

Dedicated to Professor Paul von Ragué Schleyer on the occasion of his 60th birthday

The first observation of the scission of a cyclopropane σ-bond was in the reaction of 2-cyclopropyl-1,1-diphenylethylene **1** with lithium metal (giving **3**),[1] but the existence of the postulated primary adduct **2** could not be proven experimentally.

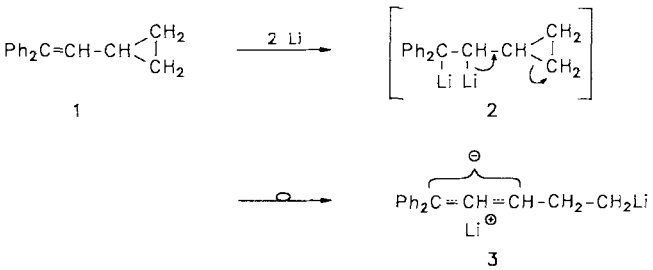

1 2 3

However, such proof has now been obtained for the analogous reaction of cyclopropylphenylacetylene **4** with

[*] Prof. Dr. A. Maercker, Dipl.-Chem. U. Girreser
Institut für Organische Chemie der Universität
Adolf-Reichwein-Strasse, D-5900 Siegen (FRG)

[**] Polylithiumorganic Compounds, Part 12. This research was supported by the Ministerium für Wissenschaft und Forschung, Nordrhein-Westfalen, and by the Fonds der Chemischen Industrie.—Part 11: A. Maercker, F. Brauers, W. Brieden, B. Engelen, *J. Organomet. Chem. 377* (1989) C45.

elemental lithium at $-30\,^{\circ}C$ in diethylether, by the observation of the vicinal dilithioalkene **5**, in which the lithium atoms, which are thought to be in a bridging configuration,[2] are in any case exclusively in the *cis* configuration. This was shown by derivatization with CH_3OD, dimethyl sulfate and CO_2 in turn, which gave the products **10** (77%),[3] **11** (83%)[4] and **12** (22%) respectively, not even trace amounts of the corresponding *trans* derivatives being detected in each case (Table 1).

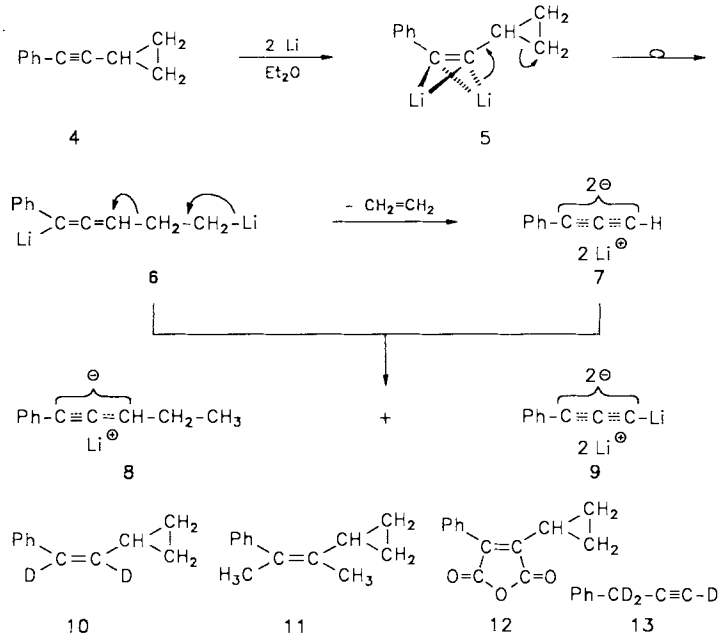

Previously the *cis* addition of lithium has only been observed for cyclooctyne[5] and, under certain conditions, for diphenylacetylene;[6] aliphatic alkynes react much more slowly and undergo exclusively *trans* addition.

Above $-30\,^{\circ}C$ the cyclopropylmethyl part of **5** undergoes a ring–chain rearrangement, but the open-chain dilithium compound **6**, like **3**, is unstable. In contrast to **3** in diethyl ether,[1] **6** converts to a more stable form, not by loss of lithium hydride, but by loss of ethylene to give **7**, a "sesquiacetylene",[7] which then undergoes deprotonation to give the already known trilithium compound **9**.[8] Following deuterolysis (1 h at room temperature) the compound **13**[8] was finally isolated with a yield of 18%. Also formed in this reaction were the isomeric hydrocarbons phenylallene (4%) and 1-phenyl-1-propyne (2%), both of which were also triply deuterated to a level of more than 80%. The fragmentation of **6** is reminiscent of the loss of ethylene from 3,3-diphenylpropyllithium forming diphenylmethyllithium.[9]

If the phenyl group in **4** is replaced by a second cyclopropyl group (**14**), it is found that the compound no longer undergoes reaction with lithium metal. Even several hours' heating in diethyl ether or THF under reflux and with ultrasonic activation produced no result. In contrast, **14** reacts readily with lithium-4,4'-di-*tert*-butylbiphenyl[10] in THF even at $-30\,^{\circ}C$, requiring only catalytic amounts of 4,4'-di-*tert*-butylbiphenyl. However, the expected primary product, the 1,2-dilithioethylene derivative, is not observed. The first

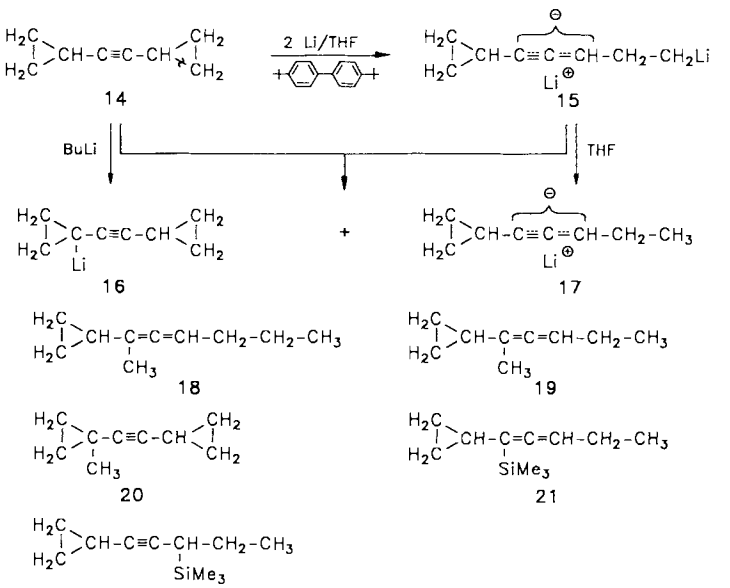

Table 1. Relevant physical data for the compounds **10**–**13** and **18**–**22**[a].

10: ^1H NMR: $\delta = 7.55-7.10$ (m; C_6H_5), 2.20–1.60 (m; cyclopropyl-CH), 1.00–0.35 (m; 2 cyclopropyl-CH_2). – ^{13}C NMR: $\delta = 137.9, 128.6, 128.1, 126.3$ (C_6H_5), 136.2, 126.9 (= CD), 10.9, 8.0 (cyclopropyl). – IR (CCl_4): $\tilde{\nu} = 3045$ (m), 2250 (m) cm^{-1}. – MS: *m/z* 146 ($M^{\oplus}$, 59%), 145(31), 131(100), 130(77), 129(45), 117(22), 116(17). – B.p. 40–45 °C/0.3 torr. – cf. [3].

11: ^1H NMR: $\delta = 7.40-7.10$ (m; C_6H_5), 1.99 (m; CH_3), 1.45 (m; CH_3), 1.60–1.10 (m; cyclopropyl-CH), 0.60–0.30 (m; 2 cyclopropyl-CH_2). – ^{13}C NMR: $\delta = 145.2$, 128.8, 127.9, 125.7 (C_6H_5), 130.5, 103.4 (= C), 21.5, 12.6 (CH_3), 15.0, 4.6 (cyclopropyl). – MS: *m/z* 172 ($M^{\oplus}$, 21%), 157(100), 143(31), 142(50), 129(61), 128(26), 115(30). – B.p. 55–60 °C/0.002 torr. – cf. [4].

12: ^1H NMR: $\delta = 7.80-7.40$ (m; C_6H_5), 2.10–1.90 (m; cyclopropyl-CH), 1.70–1.00 (m; 2 cyclopropyl-CH_2). – ^{13}C NMR (20.1 MHz): $\delta = 164.3$, 163.8, (C=O), 144.8, 139.4 (= C), 130.4, 129.4, 128.8, 127.4 (C_6H_5), 10.5, 10.2 (cyclopropyl). – IR (KBr): $\tilde{\nu} = 3060$ (w), 1820 (s), 1755 (s) cm^{-1}. – MS: *m/z* 214 ($M^{\oplus}$, 24%), 142(44), 141(100), 115(67), 63(33), 43(33), 39(25). – M.p. 58–60 °C (from ethanol/water).

13: ^1H NMR: $\delta =$ 7.35 (s, br; C_6H_5). – ^2H NMR (61.4 MHz, $CDCl_3$): $\delta = 3.60$ (s; CD_2), 2.20 (s; ≡CD). – ^{13}C NMR (20.1 MHz): $\delta = 136.0$, 128.5, 127.9, 126.7 (C_6H_5), 81.5, 70.2 (≡C), 24.3 (CD_2). – MS: *m/z* 119 ($M^{\oplus}$, 89%), 118(100), 117(50), 91(12), 64(12), 58(11), 51(12). – cf. [8].

18: ^1H NMR: $\delta = 5.10$ (m; =CH), 2.10–1.80 (m; $=CCH_2$), 1.71 (d, $^5J = 3.2$ Hz; $=CCH_3$), 1.80–0.95 (m; CH_2Me and cyclopropyl-CH), 0.92 (t, $^3J = 6.7$ Hz; CH_2Me), 0.90–0.25 (m; 2 cyclopropyl-CH_2). – ^{13}C NMR: $\delta =$ 200.3 (= C=), 101.9 (= CMe), 91.9 (= CH), 31.6, 22.5, (CH_2), 18.4, 13.7 (CH_3), 13.7, 6.1, 5.8 (cyclopropyl). – IR ($CDCl_3$): $\tilde{\nu} = 3050$ (m), 1955 (w) cm^{-1}. – MS: *m/z* 136 ($M^{\oplus}$, 4%), 108(57), 107(46), 93(43), 91(68), 79(100), 77(46).

19: ^1H NMR: $\delta = 5.30-4.95$ (m; =CH), 2.20–1.70 (dq, $^3J = 7.3$, 7.6 Hz; CH_2), 1.72 (d, $^5J = 3.1$ Hz; $=CCH_3$), 1.30–0.90 (m; cyclopropyl-CH), 0.95 (t, $^3J = 7.6$ Hz; CCH_3), 0.80–0.25 (m; 2 cyclopropyl-CH_2). – ^{13}C NMR (20.1 MHz): $\delta = 200.1$ (= C=), 102.8 (= CMe), 93.5 (= CH), 22.5 (CH_2), 18.5, 13.8 (CH_3), 13.5, 6.2, 5.7 (cyclopropyl). – IR (film): $\tilde{\nu} = 3080$ (m), 1955 (w) cm^{-1}. – MS: *m/z* 122 ($M^{\oplus}$, 31%), 107(62), 93(42), 91(92), 79(100), 77(65), 39(38). Elemental analysis in agreement with formula.

20: ^1H NMR: $\delta = 1.18$ (s; CH_3), 1.30–0.90 (m; cyclopropyl-CH), 0.90–0.40 (m; 4 cyclopropyl-CH_2). – ^{13}C NMR (20.1 MHz): $\delta = 81.9$, 79.1 (≡C), 16.4 (CH_3), 24.8, 8.2, 7.2, 0.1 (cyclopropyl). – IR (film): $\tilde{\nu} = 3090$ (s), 2980 (vs), 2240 (vw) cm^{-1}. – MS: *m/z* 120 ($M^{\oplus}$, 5%), 116(76), 91(100), 79(49), 78(46), 77(43), 51(41). B.p. 46–48 °C/10 torr. Elemental analysis in agreement with formula.

21: ^1H NMR: $\delta = 4.96$ (td, $^3J = 6.2$, $^5J = 2.0$ Hz; =CH), 1.93 (qd, $^3J = 6.2$, 7.0 Hz; CH_2), 1.20–0.90 (m; cyclopropyl-CH), 0.94 (t, $^3J = 7.0$ Hz; CH_3), 0.80–0.20 (2 m; 2 cyclopropyl-CH_2), 0.13 (s; $Si(CH_3)_3$). – ^{13}C NMR: $\delta = 203.1$ (= C=), 101.4, 89.4 (= C), 21.5 (CH_2), 13.9 (CH_3) 9.5, 7.8, 6.9 (cyclopropyl), – 1.4 ($Si(CH_3)_3$). – IR ($CDCl_3$): $\tilde{\nu} = 3090$ (m), 1925 (s), 1240 (s) cm^{-1}. – MS: *m/z* 180 ($M^{\oplus}$, 10%), 123(8), 106(12), 74(13), 73(100), 59(15), 45(14).

22: ^1H NMR: $\delta = 1.60-1.20$ (m; $CHCH_2$), 1.20–0.90 (m; cyclopropyl-CH and CH_3), 0.80–0.50 (m; 2 cyclopropyl-CH_2), 0.05 (s; $Si(CH_3)_3$) – ^{13}C NMR (C_6D_6): $\delta = 84.1$, 77.1 (≡C), 22.8 (CH_2), 14.4 (CH_3), 22.0, 8.4 (cyclopropyl), – 0.1 (SiCH), – 3.1 ($Si(CH_3)_3$). – IR ($CDCl_3$): $\tilde{\nu} = 3100$ (m), 2200 (vw), 1250 (s) cm^{-1}. – MS: *m/z* 180 ($M^{\oplus}$, 9%), 123(13), 106(18), 74(13), 73(100), 59(21), 45(13).

[a] 80 MHz ^1H- and 100.6 MHz ^{13}C-NMR spectra in $CDCl_3$ unless stated otherwise; mass spectra at 70 eV.

detectable dilithium compound is **15**; derivatizing this with dimethyl sulfate gave the allene **18** in 40% yield, together with 1% of the isomeric 1-substituted 1-hexyne derivative. Unlike **6**, **15** does not undergo fragmentation with loss of ethylene, but instead, like **3** in THF,[1] it gradually becomes protonated, forming **17**. In this reaction the educt **14** also serves to some extent as a source of protons, as is shown by the formation of a small amount of **20** (6%) in addition to the main product **19** (65%) in the derivatization with dimethyl sulfate (12 h, 0 °C, Table 1). The lithium compound **16** could also be obtained in a yield of 80% by deprotonation of **14** with *n*-butyllithium.[11] In this case too, the main product of methylation is the allene **19**; the isomeric 1-cyclopropyl-3-methyl-1-pentyne is formed in only trace amounts (3%). A different situation is found when **17** is derivatized using chlorotrimethylsilane, which in addition to the allene **21** (30%) gives the alkyne **22** (15%) (Table 1). It is interesting that the second cyclopropane ring is not opened under the conditions used.

Experimental

5: A suspension of 0.7 g (100 mmol) of lithium powder (2% sodium)[12] in 130 mL of dry diethyl ether was prepared, and into this at 0 °C under argon was first dropped about 5% of a solution of 2.0 g (14 mmol) of **4**[13] in 20 mL of diethyl ether. When the reaction had got under way (as shown by a yellow coloration of the reaction mixture), the rest of the solution was added at − 30 °C. To obtain a good yield it was extremely important to carry this out very slowly over a period of 6 h, preferably using a syringe metering system (such as that made by INFORS AG, Bottmingen, Switzerland). The mixture was then stirred for a further 1 h at − 30 °C and the deep-red solution was then filtered under inert gas to remove excess lithium. The derivatization was carried out at − 70 °C. Yield: 77–83%.

15: 0.5 g (2 mmol) of 4,4'-di-*tert*-butylbiphenyl and 0.5 g (70 mmol) of lithium powder (2% sodium)[12] were mixed together in 80 mL of dry THF and stirred for 2 h at 0 °C. To the resulting deep-green solution at − 30 °C under argon was slowly added over a period of 6 h, using a syringe metering system, a solution of 1.05 g (10 mmol) of **14**[11] in 20 mL of THF, and the mixture was then stirred for a further 1 h at − 30 °C. After filtering to remove excess lithium, the derivatization was carried out at − 80 °C under inert gas. Yield: 41% of **15**, together with 16% of the educt **14**, 15% of **17** and 7% of **16**. If instead the reaction is carried out at − 45 °C, one obtains only 7% of **17** and 2% of **16** together with 31% of **15**, but in this case 41% of the educt **14** is left behind (the rest presumably consists of polymers).

Received: January 9, 1990 [Z 3727 IE]
German version: *Angew. Chem. 102* (1990) 718

CAS Registry numbers:
4, 21777-85-5; **5**, 127063-70-1; **10**, 127063-71-2; **11**, 52692-56-5; **12**, 127063-72-3; **13**, 10147-10-1; **14**, 27998-49-8; **15**, 127063-73-4; **16**, 39225-18-8; **17**, 127063-78-9; **18**, 127063-74-5; **19**, 127063-75-6; **20**, 67538-98-1; **21**, 127063-76-7; **22**, 127063-77-8; Li, 7439-93-2.

[1] A. Maercker, *Justus Liebigs Ann. Chem. 732* (1970) 151.
[2] Cf. ab initio calculations on unsubstituted *cis*-1,2-dilithioethylene: P. von R. Schleyer, E. Kaufmann, A. J. Kos, T. Clark, J. A. Pople, *Angew. Chem. 98* (1986) 164; *Angew. Chem. Int. Ed. Engl. 25* (1986) 169.
[3] For the non-deuterated compound see G. M. Underwood, A. K. Chan, T. Green, C. T. Watts, C. A. Kingsbury, *J. Org. Chem. 38* (1973) 2735.
[4] For the corresponding *E*/*Z* mixture see G. A. Olah, P. W. Westerman, J. Nishimura, *J. Am. Chem. Soc. 96* (1974) 3548.
[5] A. Maercker, T. Graule, U. Girreser, *Angew. Chem. 98* (1986) 174; *Angew. Chem. Int. Ed. Engl. 25* (1986) 167.
[6] G. Levin, J. Jagur-Grodzinski, M. Szwarc, *J. Am. Chem. Soc. 92* (1970) 2268.
[7] J. Klein, S. Brenner, *J. Am. Chem. Soc. 91* (1969) 3094; J. Klein, J. Y. Becker, *J. Chem. Soc. Chem. Commun. 1973*, 576.
[8] J. E. Mulvaney, T. L. Folk, D. J. Newton, *J. Org. Chem. 32* (1967) 1674.
[9] A. Maercker, M. Passlack, *Chem. Ber. 116* (1983) 710.
[10] P. K. Freeman, L. L. Hutchinson, *J. Org. Chem. 45* (1980) 1924; *ibid. 48* (1983) 4705.
[11] G. Köbrich, D. Merkel, *Justus Liebigs Ann. Chem. 761* (1972) 50.
[12] A. Maercker, M. Theis, *Organomet. Synth. 3* (1986) 378.
[13] M. Hanack, E. Weber, *Chem. Ber. 116* (1983) 777.

Synthesis and Structure of $Ph_2P(S)N=TiCl_2 \cdot 3C_5H_5N$, the First Imidotitanium Complex**

By *Herbert W. Roesky,** *Heike Voelker, Michael Witt,* and *Mathias Noltemeyer*

Compounds containing M=N bonds are well known for the elements of subgroups 5 to 8.[1] In contrast, for titanium and its homologues up to now only imidozirconocenes have been isolated and characterized.[2] *Wolczanski* et al. have also reported the occurrence of $(t\mathrm{Bu_3SiNH})_2\mathrm{Zr}=\mathrm{NSi}t\mathrm{Bu_3}$ as a reactive intermediate.[3] No corresponding titanium compounds have yet been reported, despite the fact that they would be of great interest as catalysts for the activation of C–H bonds or for polymerizations.[4]

In the course of our studies on metal-nitrogen bonds,[5, 6] *N*,*N*-bis(trimethylsilyl)diphenylthiophosphinamide **1**, prepared from *N*,*N*-bis(trimethylsilyl)aminodiphenylphosphane[7] and elemental sulfur, was allowed to react with titanium tetrachloride. In this reaction chlorotrimethylsilane is eliminated with the formation of a yellow amorphous solid whose ^{31}P-NMR spectrum consists of three singlets (δ = 47.3, 49.0, 51.5). This intermediate is then treated with pyridine to form the title compound **2**. In contrast, reaction of the oxygen analogue of **1** with $TiCl_4$ leads to an eight-membered ring compound.[8] Similar cyclic structures can be assumed for the intermediate involved in the formation of **2**.

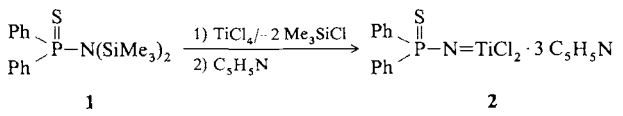

1 **2**

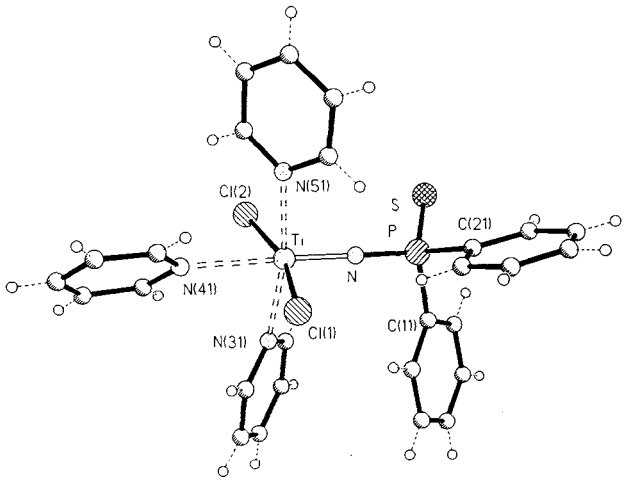

Fig. 1. Crystal structure of **2**. Selected bond lengths [pm] and angles [°]: Ti-Cl1 238.4(1), Ti-Cl2 234.9(1), Ti-N 172.0(2), Ti-N31 222.9(2), Ti-N41 243.9(2), Ti-N51 222.4(3), N-P 164.7(2), P-S 195.4(1); Cl1-Ti-Cl2 163.5(1), Cl1-Ti-N 97.4(1), Cl2-Ti-N 99.1(1), Cl1-Ti-N31 90.8(1), Cl2-Ti-N31 87.8(1), N-Ti-N31 94.0(1), Cl1-Ti-N41 81.1(1), Cl2-Ti-N41 82.4(1), N-Ti-N41 177.9(1), N31-Ti-N41 84.4(1), Cl1-Ti-N51 89.7(1), Cl2-Ti-N51 88.9(1), N-Ti-N51 95.9(1), N31-Ti-N51 169.9(1).

[*] Prof. Dr. H. W. Roesky, H. Voelker, Dr. M. Witt, Dr. M. Noltemeyer
Institut für Anorganische Chemie der Universität
Tammannstraße 4, D-3400 Göttingen (FRG)

[**] This work was supported by the Deutsche Forschungsgemeinschaft, the Volkswagen Foundation and the Fonds der Chemischen Industrie.

2 is an orange-red crystalline solid whose ^{31}P-NMR spectrum exhibits a singlet ($\delta = 42.0$). Crystallization of **2** from pyridine/*n*-hexane (2/1) yields single crystals suitable for determining the structure by X-ray diffraction[9] (Fig. 1). The titanium atom has a distorted octahedral coordination, the corners of the octahedron being formed by three pyridine molecules (N31, N41, N51), two chlorine atoms (Cl1, Cl2) and the nitrogen atoms of the imido ligand. The Ti–N bond length (172.0(2) pm) is similar to that in the Ti–N unit of the eight-membered P-O-N-Ti heterocycle $[Ph_2PONTiCl_2 \cdot 2MeCN]_2$ (173.9 pm).[8] The coordination of the imido ligand to the titanium atom is almost linear (Ti–N–P 172.5(2)°), showing that the ligand acts as a four-electron donor. The pyridine molecule *trans* to the imido ligand is much more loosely bound (Ti–N41 243.9(2) pm) than the other two pyridine molecules (average Ti–N 222.7 pm).

Evidently, therefore, the imidotitanium compounds that have so long been sought can be stabilized by coordination with electron pair donors on the titanium atom. The first results on the chemistry of these compounds are reported by *Rothwell* et al. in another communication.[4]

Experimental

1: 10 g (29.0 mmol) of *N*,*N*-bis(trimethylsilyl)aminodiphenylphosphane was dissolved in 150 mL of benzene, mixed with 0.93 g of sulfur (3.625 mmol, referred to S_8), and heated for 3 h at 50–60 °C. After evaporating off the solvent under vacuum the colorless residue was recrystallized from MeCN. Yield 9.7 g (89%); m.p. 116 °C. ^{31}P NMR (101.26 MHz, 85% H_3PO_4, C_6H_6, $CDCl_3$): $\delta = 61.0$ (s); ^{29}Si NMR (49.69 MHz, TMS, C_6H_6, $CDCl_3$): $\delta = 10.7$ (d, $^2J(^{29}Si,^{31}P) = 1.2$ Hz); MS (EI): *m/z* 377 ($M^{\oplus}$, 16%), 362 ($M^{\oplus}$ – Me, 100%).

2: Into a solution of 1.5 g (4.0 mmol) of **1** in 50 mL CH_2Cl_2 at –15 °C was slowly added a solution of 0.76 g (4.0 mmol) of $TiCl_4$ in 25 mL of CH_2Cl_2. The mixture was then allowed to slowly warm up to room temperature and was stirred for a further 20 h. After evaporating off the solvent under vacuum the yellow residue was recrystallized from pyridine/*n*-hexane (2/1). This yielded a mixture of a yellow powdery solid and orange-red crystals of **2**. The solvent and the powdery solid were decanted off from the crystals, which were then sorted to find a crystal suitable for the X-ray structure determination. Yield of **2** 0.63 g (27%). M.p. 125 °C (decomp.). IR (Nujol/KBr): $\nu = 1605$(st), 1377(st), 1110(st), 1070(st), 1012(st), 698(st), 520(st) cm^{-1}.

Received: January 10, 1990 [Z 3731 IE]
German version: *Angew. Chem. 102* (1990) 712

[1] W. A. Nugent, J. M. Mayer: *Metal Ligand Multiple Bonds*, Wiley, New York 1988.
[2] P. J. Walsh, F. J. Hollander, R. G. Bergman, *J. Am. Chem. Soc. 110* (1988) 8729.
[3] C. C. Cummins, S. M. Baxter, P. T. Wolczanski, *J. Am. Chem. Soc. 110* (1988) 8731.
[4] Another imidotitanium complex is described in this issue by *Rothwell* et al.: J. E. Hill, R. D. Profilet, P. E. Fanwick, I. P. Rothwell, *Angew. Chem. Int. Ed. Engl. 29* (1990) 664; *Angew. Chem. 102* (1990) 713.
[5] M. Witt, H. W. Roesky, D. Stalke, F. Pauer, T. Henkel, G. M. Sheldrick, *J. Chem. Soc. Dalton Trans. 1989*, 2173.
[6] H. W. Roesky, Y. Bai, M. Noltemeyer, *Angew. Chem. 101* (1989) 788; *Angew. Chem. Int. Ed. Engl. 28* (1989) 754.
[7] H. Nöth, L. Meinel, *Z. Anorg. Allg. Chem. 349* (1967) 225.
[8] M. Witt, H. W. Roesky, D. Stalke, T. Henkel, G. M. Sheldrick, *J. Chem. Soc. Dalton Trans.*, in press.
[9] $C_{27}H_{25}Cl_2N_4PSTi$, $M_r = 587.3$, monoclinic, $P2_1/c$, $a = 969.2(1)$, $b = 1392.2(2)$, $c = 2103.3(5)$ pm, $\beta = 91.74(1)°$, $V = 2.8368(8)$ nm^3, $Z = 4$, $\varrho_{calc.} = 1.375$ g cm^{-3}, $\mu(Mo_{K\alpha}) = 0.636$ mm^{-1}, crystal dimensions: $0.6 \times 0.4 \times 0.3$ mm^3, Siemens-Stoe-AED2 four-circle diffractometer, 7950 reflections with 2θ from 7.0° to 45°, of which 3690 are symmetry-independent and 3099 with $F_o > 3\sigma(F_o)$ were used in the structure refinement (SHELXTL Plus): $R = 0.0335$, $R_w = 0.0345$, $w^{-1} = \sigma^2(F_o) + 0.0001(F_o^2)$, GOF 1.58. Further details of the crystal structure determination are available on request from the Fachinformationszentrum Karlsruhe, Gesellschaft für wissenschaftlich-technische Information mbH, D-7514 Eggenstein-Leopoldshafen 2 (FRG), on quoting the depository number CSD-54478, the names of the authors, and the journal citation.

Electron Transfer between Covalently Linked Porphyrin and Quinone Units: Synthesis, Magnetic Resonance and Picosecond Fluorescence Spectroscopy**

By *Jörg von Gersdorff, Martina Huber, Heike Schubert, Dominique Niethammer, Burkhard Kirste, Martin Plato, Klaus Möbius,* Harry Kurreck,* Rainer Eichberger, Reinhard Kietzmann*, and *Frank Willig**

Quinones covalently linked with porphyrin are suitable as biomimetic models for the study of light-induced charge separations in the primary process of photosynthesis with the help of spectroscopic methods and electron transfer (ET) theories.[1]

We have synthesized the porphyrin-quinones **1a** and **2a**, linked via flexible bridges, as well as the essentially rigid porphyrin derivative **3** and its fragments **5** and **6**.

The functionalized porphyrins **1c** and **2d** were obtained by condensation of pyrrole, benzaldehyde, and *p*-nitrobenzaldehyde or 4(e)-(hydroxymethyl)cyclohexane-(e)-aldehyde in boiling propionic acid and subsequent chromatographic work-up (**6** was synthesized analogously with cyclohexanealdehyde). The 4-(hydroxymethyl)cyclohexanealdehyde was accessible by single tosylation[2] of 1(e),4(e)-bis(hydroxymethyl)cyclohexane and subsequent oxidation of the tosylate with DMSO.[3] For the synthesis of **1b**, the compound **1c**, after reduction of the nitro group with $SnCl_2$/HCl, was allowed to react with acetylated gentisic acid in the presence of ethyl 2-ethoxy-1,2-dihydroquinoline-1-carboxylate (EEDQ).[4] **1b** is formed after removal of the protecting groups with methanolic HCl. Compound **2b** was obtained by esterification of **2d** with acetylated gentisic chloride and subsequent removal of the protecting groups (see above). Oxidation to the porphyrin-quinones **1a** and **2a** was achieved with activated PbO_2 immediately before the measurement.[5]

For the synthesis of **5**, methyl 1,4-cyclohexanedicarboxylate was linked with *p*-benzoquinone in an oxidative-decarboxylating reaction using $(NH_4)_2S_2O_8/AgNO_3$.[6] After conversion of **5** into the corresponding hydroquinone with sodium dithionite, the aldehyde **4** was accessible by reduction of the ester group with diisobutylaluminum hydride (DIBAH).[7] Condensation of **4** with pyrrole and benzaldehyde in boiling propionic acid in the presence of atmospheric oxygen yielded directly, after chromatographic work-up, the porphyrin-quinone **3**. The porphyrin derivatives (final yields 2–4%) were metalated with zinc acetate in methanol/chloroform.

Since the ET rates are essentially determined by the geometric arrangement of donor, bridge and quinone, we have ascertained the preferred conformations by NMR measure-

[*] Prof. Dr. K. Möbius, Dr. M. Plato
Freie Universität, Institut für Molekülphysik
Arnimallee 14, D-1000 Berlin 33
Prof. Dr. H. Kurreck, Dipl.-Chem. J. von Gersdorff, Dr. M. Huber [+], Dipl.-Chem. H. Schubert, Dipl.-Chem. D. Niethammer, Priv.-Doz. Dr. B. Kirste
Freie Universität, Institut für Organische Chemie
Takustrasse 3, D-1000 Berlin 33
Prof. Dr. F. Willig, Dr. R. Eichberger, Dr. R. Kietzmann
Fritz-Haber-Institut der Max-Planck-Gesellschaft
Faradayweg 4–6, D-1000 Berlin 33
[+] Present address:
University of California San Diego, Department of Physics B-019
La Jolla CA 92093 (USA)

[**] This work was supported by the Deutsche Forschungsgemeinschaft (SFB 337 and Normalverfahren) and the Fonds der Chemischen Industrie.

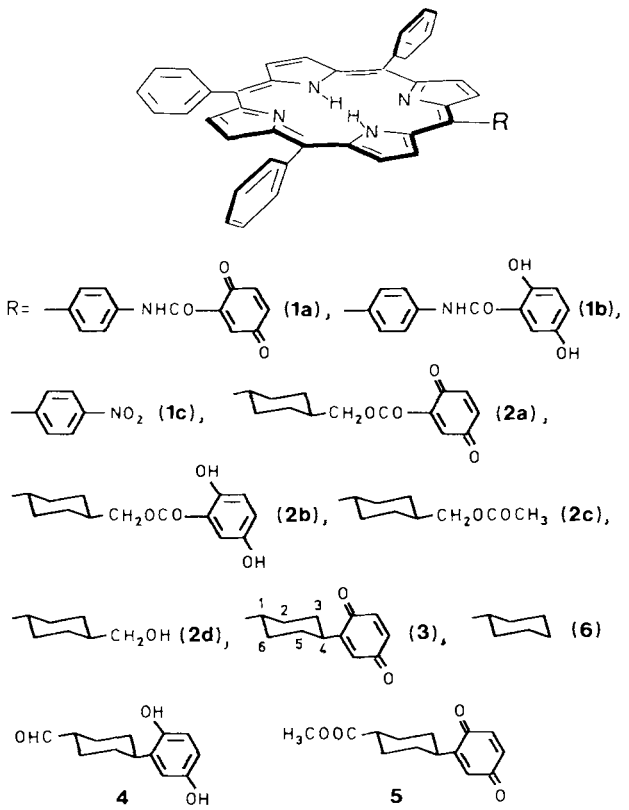

ments (NOE) on the fragments Zn-**6** and cyclohexylbenzoquinone and by electron nuclear double resonance (ENDOR) measurements[8] on the corresponding radical ions. In the case of Zn-**6**, strong nuclear Overhauser effects (9–16%) between the cyclohexyl proton in position 1 and the axial protons in positions 2 and 6 and the neighboring pyrrole protons (at $\delta = 9.83$) were observed. From this a perpendicular arrangement of the two ring planes is deduced, which also follows from the hyperfine coupling constants (HFC; all < 2 MHz) of the radical cation of Zn-**6** ($AgClO_4$/iodine oxidation, CH_2Cl_2[9]) on applying the Heller-McConnell relationship.[10] In the case of 2-cyclohexyl-1,4-benzoquinone a considerable NOE (10%) between the axial protons in positions 2 and 6 and the neighboring quinone proton was observed, thus indicating a preferred conformation with the proton in position 1 in the neighborhood of the oxygen atom. From the HFC (3.2 MHz) of the corresponding proton of the cyclohexyl substituent in the radical anion of **5** (benzoin reduction, trimethylbenzylammonium hydroxide, isopropanol) there follows, by comparison with the methyl HFC of the corresponding methylsemiquinone radical anion (5.6 MHz), a (mean) dihedral angle of ca. 60°.[10] RHF-INDO/SP calculations[11] gave an energy minimum for the radical cation of Mg-**6**[12] with approximately perpendicular arrangement of porphyrin and cyclohexane planes. In contrast, several flat local energy minima of comparable depth were obtained for the radical ion of the cyclohexylquinone; the best agreement with the measured HFC was found for a dihedral angle of ca. 70°.

The electron transfer rates k_{ET} were estimated for the compound **3**, which is characterized by a relatively rigid conformation.[13] The quotient of the k_{ET} values for the charge separation (CS) and charge recombination (CR) is a measure of the efficiency of the separation process and thus also a measure of the suitability of donor (D)–acceptor(A) complexes as model systems for the primary processes of photosynthesis. For non-adiabatic electron transfer, Equation (1) applies,[14]

$$k_{ET} = \frac{2\pi}{\hbar} |V_{DA}|^2 \cdot F \qquad (1)$$

where $\hbar = h/2\pi$ is Planck's constant, V_{DA} the electronic interaction matrix element between D and A and F the thermally averaged Franck-Condon factor. The explicit calculation of V_{DA}[15] enables the influence of the distance and orientation of D and A as well as the influence of the MO coefficients in the frontier orbitals of D and A on k_{ET} to be investigated.[16] V_{DA} was calculated for a perpendicular arrangement of the mean cyclohexane plane and porphyrin plane for several orientations of the quinone.[13]

The ratios $V_{DA}(CS)/V_{DA}(CR)$ for the two arrangements of the quinone perpendicular to the mean cyclohexane plane are 0.82 and 1.06, respectively (dihedral angle $\pm 90°$); for non-orthogonal orientations the quotient is $\ll 1$. This unfavorable ratio for a biomimetic model compound [in analogy to the photosynthetic primary processes, $k_{ET}(CS) \gg k_{ET}(CR)$ would be desired, which, e.g., would be realizable by $V_{DA}(CS) \gg V_{DA}(CR)$] is mainly attributed to the large MO coefficients of the HOMOs at the site of linkage of the porphyrin with the cyclohexane, whereby $k_{ET}(CR)$ is increased.[13]

The efficiency of the charge separation is determined by the product of $V_{DA}(CS)/V_{DA}(CR)$ and the ratio of the Franck-Condon factors, $F(CS)/F(CR)$. An estimation according to the classical method of *Marcus* et al.[17] shows that $F(CS)/F(CR)$ can compensate an unfavorable ratio $V_{DA}(CS)/V_{DA}(CR)$ for biomimetic models. The experimental checking of this prediction will only be possible by measurement of $k_{ET}(CR)$ in combination with the measurements of $k_{ET}(CS)$ described below.

The rate constants for the charge separation were determined by picosecond fluorescence spectroscopy. Fluorescence decay curves were recorded[20] by time-resolved single-photon counting[18] or with a Streak synchroscan camera.[19] In the case of Zn-**1b**, **2b**, Zn-**2b**, Zn-**2c**, and Zn-**6** the fluorescence intensity decreases monoexponentially over more than five lifetimes. Variation of the substituents in the *meso* position has no measurable influence on the decay curve. The incorporation of zinc into the metal-free compounds, on the other hand, effects a drastic shortening of the lifetime, since the intersystem crossing then becomes the dominating decay channel.[21] Both results agree with stationary measurements of the fluorescence yield.[22]

For the excited singlet state of the porphyrin-quinones, $^1P^*$, a further decay channel is opened up if an electron (with k_{ET}) can be transferred to the quinone fragment. The rate constant for the decay of $^1P^*$ is then $k = \tau^{-1} + k_{ET}$, where τ is the lifetime of the analogous compound with hydroquinone instead of quinone residue. The decay curve of Zn-**2a** differs from those of the compounds with hydroquinone moiety (Zn-**2b**) and without quinone moiety (Zn-**2c**, Zn-**6**), respectively.

As expected, the k_{ET} values (Table 1) become smaller with increasing length of the bridge between porphyrin and quinone. They are also in good agreement with the data quoted in the literature for other similar porphyrin-quinone complexes.[23] A comparison of measured ET rate constants and calculated $k_{ET}(CS)$ values with structural information obtained from the ENDOR data is possible in the case of the relatively rigid Zn-**3**. The values of $V_{DA}(CS)$ calculated for

Table 1. Measured fluorescence lifetimes k^{-1} and electron transfer rates k_{ET} (room temperature).

Cpd.	k^{-1}	k_{ET} [s^{-1}]
Zn-**1a**	253 ps	3.4×10^9
Zn-**1b**	1.7 ns	–
2a	500 ps	1.9×10^9
2b	7.3 ns	–
Zn-**2a**	275 ps	3.0×10^9
Zn-**2b**	1.8 ns	–
Zn-**2c**	1.8 ns	–
3	107 ps	9.2×10^9
Zn-**3**	25 ps	40.0×10^9
Zn-**6**	1.8 ns	–

different conformations (dihedral angle) of comparable energy vary between 0.2×10^{-3} and 3.9×10^{-3} eV. A value of $V_{DA}(CS) = 2.4 \times 10^{-3}$ eV is obtained for the conformation with a dihedral angle of 70° (see above). With this value and the parameters ΔG° and λ[17] one obtains for $T = 293$ K according to Equations (1) and (2)[17] $k_{ET}(CS) = 5.7 \times 10^{10}$ and 9.9×10^{10} s^{-1} for $\lambda = 0.62$ and 0.9 eV, respectively, in satisfactory agreement with the experimentally determined ET rate constant of 4×10^{10} s^{-1} (Table 1).

Summary: For an efficient charge separation in quinones coupled covalently with porphyrin, the MO coefficient in the HOMO of the porphyrin at the site of coupling should be as small as possible and the orientation of the quinone to the cyclohexane bridge as orthogonal as possible.

Received: January 19, 1990 [Z 3748 IE]
German version: *Angew. Chem. 102* (1990) 690.

[1] See, for example, S. Boxer, *Biochim. Biophys. Acta 726* (1983) 265; T. A. Moore, D. Gust, P. Mathis, J.-C. Mialocq, C. Chachaty, R. V. Bensasson, E. J. Land, D. Doizi, P. A. Liddell, W. R. Lehmann, G. A. Nemeth, A. L. Moore, *Nature (London) 307* (1984) 630; A. R. Joran, B. A. Leland, G. G. Geller, J. J. Hopfield, P. B. Dervan, *J. Am. Chem. Soc. 106* (1984) 6090; J. L. Sessler, M. R. Johnson, *Angew. Chem. 99* (1987) 679; *Angew. Chem. Int. Ed. Engl. 26* (1987) 678; M. R. Wasielewski in M. A. Fox, M. Chanon (Eds.): *Photoinduced Electron Transfer, Part A*, Elsevier, Amsterdam 1988, p. 161; D. Gust, T. A. Moore, *Science (Washington D.C.) 244* (1989) 35.
[2] G. A. Haggis, L. N. Owen, *J. Chem. Soc. 1953*, 404.
[3] N. Kornblum, W. J. Jones, G. J. Anderson, *J. Am. Chem. Soc. 81* (1959) 4113.
[4] B. Belleau, G. Malek, *J. Am. Chem. Soc. 90* (1968) 1651.
[5] R. Kuhn, I. Hammer, *Chem. Ber. 83*(1950) 413.
[6] N. Jacobsen, K. Torssell, *Justus Liebigs Ann. Chem. 763* (1972) 135.
[7] L. I. Zakharkin, L. P. Sorokina, *J. Gen. Chem. USSR Engl. Transl. 37* (1967) 525; *Zh. Obshch. Khim. 37* (1967) 561.
[8] ENDOR method, see K. Möbius, M. Plato, W. Lubitz, *Phys. Rep. 87* (1982) 171; H. Kurreck, B. Kirste, W. Lubitz, *Angew. Chem. 96* (1984) 171; *Angew. Chem. Int. Ed. Engl. 23* (1984) 173; *Electron Nuclear Double Resonance Spectroscopy of Radicals in Solution*, VCH, Weinheim 1988.
[9] H. J. Shine, A. G. Padilla, S.-M. Wu, *J. Org. Chem. 44* (1979) 4069.
[10] C. Heller, H. M. McConnell, *J. Chem. Phys. 32* (1960) 1535.
[11] M. Plato, E. Tränkle, W. Lubitz, F. Lendzian, K. Möbius, *Chem. Phys. 107* (1986) 185; M. Plato, W. Lubitz, F. Lendzian, K. Möbius, *Isr. J. Chem. 28* (1988) 109.
[12] In order to avoid complications in the INDO parametrization, Mg was used instead of Zn in the MO calculations [13].
[13] M. Huber, *Dissertation*, Freie Universität Berlin 1989.
[14] R. A. Marcus, N. Sutin, *Biochim. Biophys. Acta 811* (1985) 265.
[15] See, for example, P. Siders, R. J. Cave, R. A. Marcus, *J. Chem. Phys. 81* (1984) 5613; H. Heitele, M. E. Michel-Beyerle, *J. Am. Chem. Soc. 107* (1985) 8068; B. A. Leland, A. R. Joran, P. M. Felker, J. J. Hopfield, A. H. Zewail, P. B. Dervan, *J. Phys. Chem. 89* (1985) 5571; G. L. Closs, L. T. Calcaterra, N. J. Green, K. W. Penfield, J. R. Miller, *ibid. 90* (1986) 3673; L. Otha, G. L. Closs, K. Morokuma, N. J. Green, *J. Am. Chem. Soc. 108* (1986) 1319; M. R. Wasielewski, M. P. Niemczyk in M. Gouterman, P. M. Rentzepis, K. D. Straub (Eds.): *Porphyrins—Excited States and Dynamics*, Am. Chem. Soc., Washington, D.C., 1986, p. 154; R. J. Cave, P. Siders, R. A. Marcus, *J. Phys. Chem. 90* (1986) 1436; H. Heitele, M. E. Michel-Beyerle, P. Finckh, *Chem. Phys. Lett. 134* (1987) 273; A. M. Oliver, D. C. Craig, M. N. Paddon-Row, J. Kroon, J. W. Verhoeven, *ibid. 150* (1988) 366.
[16] In the case of **3**, V_{DA} was calculated by the MO method RHF-INDO [11] in analogy to a concept with which V_{DA} was recently determined for the primary ET step in bacterial photosynthesis from the atomic coordinates of the participating pigments [cf. H. Michel, O. Epp, J. Deisenhofer, *EMBO J. 5* (1986) 2445]: M. Plato, K. Möbius, M. E. Michel-Beyerle, M. Bixon, J. Jortner, *J. Am. Chem. Soc. 110* (1988) 7279. Unlike the pigments of the photosynthesis, D and A in Zn-**3** are linked covalently via the cyclohexanediyl bridge. The influence of the bridge on the electronic structure of D and A was taken into account in the MO calculations.
[17] According to *Marcus* et al. [14] Equation (2) holds true,

$$F = (4\pi\lambda k_B T)^{-1/2} \exp\left[-(\lambda + \Delta G^0)^2/(4\lambda k_B T)\right] \quad (2)$$

where λ is the total reorganization energy, ΔG^0 the free standard reaction enthalpy, k_B the Boltzmann constant, and T the absolute temperature. ΔG^0 values for the charge separation and charge recombination were estimated from the cyclovoltammetrically determined redox potentials of Zn-**6** and **5** and the energy of the first singlet excitation state E_{00} of zinc tetraphenylporphyrin [$E_{00} = 2.1$ eV, cf. M. R. Wasielewski, M. P. Niemczyk, *J. Am. Chem. Soc. 106* (1984) 5043] to be $\Delta G^0(CS) = -0.84$, $\Delta G^0(CR) = -1.26$ eV. In the estimation of $\lambda = \lambda_i + \lambda_0$ [λ_i is the internal reorganization energy arising from changes in geometry of the reacting porphyrins (P) and quinones (Q) and λ_0 is the external reorganization energy by changes in the surrounding medium], λ_i was neglected, since the changes in geometry between the $^1P^*Q$ and $P^{\oplus}Q^{\ominus}$ states caused by photoinduced charge separation can be regarded as small [13, 23]; cf. also M. R. Wasielewski, M. P. Niemczyk, W. A. Svec, E. B. Pewitt, *J. Am. Chem. Soc. 107*, (1985) 1080. λ_0 was estimated according to the method of *Marcus* [R. A. Marcus, *J. Chem. Phys. 24* (1956) 966] using geometric data ($r_P = 6$, $r_Q = 4$, $r_{P,Q} = 10.6$ Å) and dielectric data of the solvent CH_2Cl_2 ($n_D = 1.42$, $\varepsilon = 9.08$) to be $\lambda_0 = 0.62$ eV [13]. With these ΔG^0 and λ values, Equation (2) gives $F(CS)/F(CR) = 320$. This value is regarded as the upper limit, since the decrease in F in the inverted region ($-\Delta G^0 > \lambda$) is, according to investigations on comparable systems [cf. J. Ulstrup, J. Jortner, *J. Chem. Phys. 63* (1975) 4358] significantly smaller than is predicted according to Equation (2). For comparison with the value of λ calculated here, an experimentally determined value of $\lambda = 0.9$ eV can be resorted to which was obtained by M. R. Wasielewski et al. (see above) from measurements of the transient absorption for porphyrin-quinones with comparably large center-to-center separation $r_{P,Q}$ as in the case of Zn-**3**. With this value of λ, $F(CS)/F(CR) = 4$.
[18] T. Murao, I. Yamazaki, K. Yoshihara, *Appl. Opt. 21* (1982) 2297.
[19] R. Eichberger, F. Willig, W. Storck, *Mol. Cryst. Liq. Cryst. 175* (1989) 19.
[20] Excitation was repetitive with laser pulses (6 ps halfwidth, $< 10^{10}$ photons per pulse) at 590 nm and a repetition frequency of 800 kHz upon time-resolved photon counting and 4 MHz upon measurement with the synchroscan camera. The first method of measurement with 40 ps apparent laser pulse width was used if the time constants of the decay curves were greater than 150 ps. If the smallest time constant of the decay curves was less than 150 ps then the second method of measurement was used with 15–25 ps apparent laser pulse width, depending on the integration time.
[21] J. A. Schmidt, A. R. McIntosh, A. C. Weedon, J. R. Bolton, J. S. Connolly, J. K. Hurley, M. R. Wasielewski, *J. Am. Chem. Soc. 110* (1988) 1733.
[22] P. G. Seybold, M. Goutermann, *J. Mol. Spectrosc. 31* (1969) 1.
[23] M. D. Archer, V. P. Y. Gadzekpo, J. R. Bolton, J. A. Schmidt, A. Weedon, *J. Chem. Soc. Faraday Trans. 2 82* (1986) 2305; J. A. Schmidt, A. Siemiarczuk, A. C. Weedon, J. R. Bolton, *J. Am. Chem. Soc. 107* (1985) 6112; J. A. Schmidt, J. Y. Lin, J. R. Bolton, M. D. Archer, V. P. Y. Gadzekpo, *J. Chem. Soc. Faraday Trans. 1 85* (1989) 1027.

Concanavalin A Binds Pyranosides and Their Tetraacetates Stereoselectively**

By *Jürgen-Hinrich Fuhrhop** and *Michael Arlt*

The protein concanavalin A (= Con A) stereoselectively binds carbohydrate head groups that appear as neighboring hexose units on the surfaces of glycoproteins[1] or vesicles.[2]

[*] Prof. Dr. J.-H. Fuhrhop and Dipl.-Chem. M. Arlt
Institut für Organische Chemie der Freien Universität
Takustrasse 3, D-1000 Berlin 33

[**] This work was supported by the Deutsche Forschungsgemeinschaft (SFB 312 "Vectorial Membrane Processes"), the Förderungskommission für Forschung und wissenschaftlichen Nachwuchs der Freien Universität, and the Fonds der chemischen Industrie.

D-Glucopyranose and D-mannopyranose units are agglutinated, whereas D-galactopyranose units are not. Clefts,[3] shallow pockets,[4] as well as nonspecific[5] or substrate-dependent[6] binding sites have been characterized by X-ray crystal structure analyses of monosaccharide complexes. None of the resulting binding models agree with the experimental results described in this paper.

Agglutination experiments with 10^{-4} M aqueous suspensions of the glycolipids **1a–1d**[7] and 1 mg of Con A per mL[8] yielded expected results: D-glucose and D-mannose

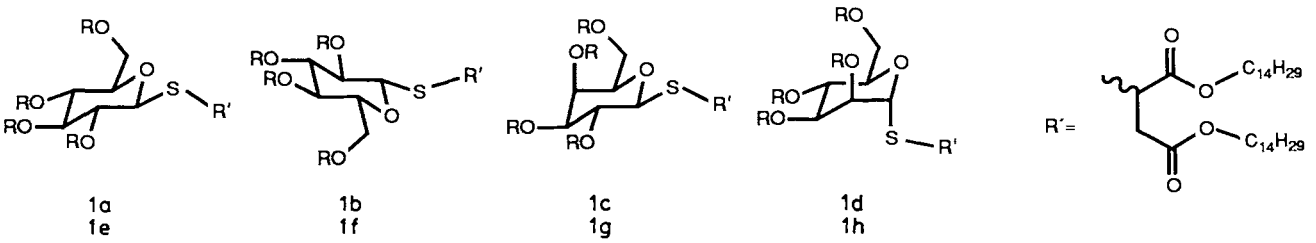

were bound, D-galactose and L-glucose were not. Con A therefore differentiates not only between diastereomers but also between enantiomers. Furthermore, we found that on sonication the tetraacetates **1e–1h** formed spherical aggregates similar to those obtained from lipids **1a–1d**. Electron micrographs of negatively stained specimens (pH 7; phosphotungstate) showed vesicles (diameter approx. 400 ± 100 Å) and were identical for both the glucose derivatives **1a** and **1e**. Light scattering measurements after gel chromatography (Sephadex G100) gave identical results in the dead volume for **1a** and its tetraacetate **1e**. Entrapment experiments with the water-soluble fluorescence dye pyranine, however, were only successful with **1a**. In the case of the tetraacetate aggregates, the dye dispersed equally between the dead volume and the fractions that followed. We assume that the mechanical stability of the "hydrophobic" tetraacetate membrane does not suffice for remaining impermeable during gel chromatography. Surface monolayers of **1a** on water were also more stable (collapse pressure: $\pi_c = 50 \pm 5\ mN\ m^{-1}$; molecular area: 39 ± 3 Å^2) than in the case of the tetraacetate **1e** (34 ± 3 mN m^{-1}; 54 ± 3 Å^2 per molecule).

Agglutination experiments with Con A showed that the vesicles made of the tetraacetates **1e–1h** (≥99.8% purity) were precipitated with the same binding constants and velocities as the free carbohydrates **1a–1d** (Fig. 1). This means that four acetate groups on the vesicle surfaces are bound stereoselectively by Con A in the same way as four hydroxy groups. Minute traces of non-acetylated carbohydrate head groups (≪ 0.1%) cannot possibly cause the observed precipitation, since a tenfold diluted vesicular solution shows no precipitate whatsoever under the given reaction conditions. Electron micrographs of Con A-agglutinated vesicles show a flattening of the membranes at the contact areas. We therefore assume that the Con A-covered membranes make direct contact, without a protein link between vesicle surfaces. Micrographs of unbound vesicles show exclusively monomeric spheres in the presence of Con A. At tenfold higher concentrations of Con A all stereoisomeric vesicles are precipitated.

None of the binding models of Con A given in the literature accomodate four or eight acetyl groups (assuming the binding of two carbohydrate head groups) in place of protons. We therefore propose a binding site without a "cleft" or "pocket" but consisting of planar or slightly convex β-pleated sheets, which constitute 60% of the Con A surface. Such a binding site would offer a much better explanation for the observed stereoselective binding of smooth vesicle surfaces, since there is no obvious driving force for drawing a carbohydrate pair out of the vesicle surface and into a cleft on the Con A surface. Furthermore, the low solubility of hydrophobic oligomethylene chains in the region of hydrophilic head groups would strongly oppose such movement, and in polymerized vesicles, which are also stereoselectively recognized by Con A,[2] such movement would be almost impossible.

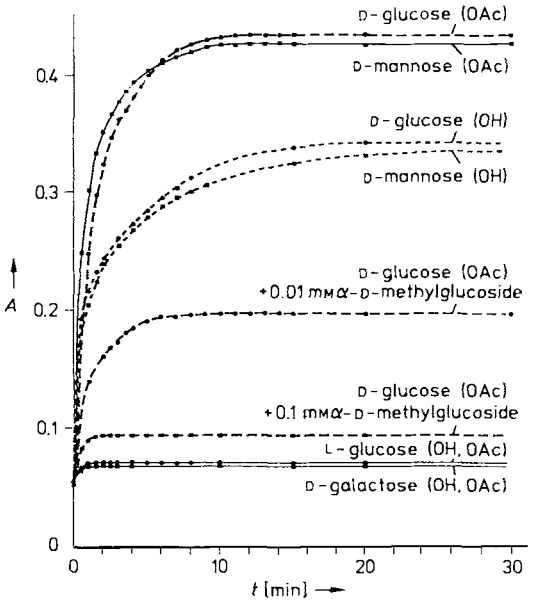

Fig. 1. Time-dependent absorption A at $\lambda = 360$ nm for the four diastereomeric and enantiomeric glycolipids **1a–1d** ("OH") and their tetraacetates ("OAc") in aqueous suspensions after addition of 10^{-4} M Con A.

We therefore propose an essentially planar binding site, whose stereospecifity is presumably caused by the arrangement of six dipoles.

The binding energy between Con A and a glycoprotein is known to be 23 kJ mol^{-1}.[9] This energy can be attributed to the dipole-dipole interactions of these six dipole pairs at an average distance of 0.45 nm.[10] Such a distance leaves ample room for the proposed acetyl groups (Fig. 2). There is even

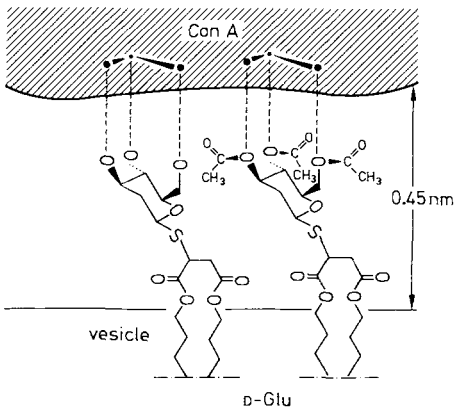

Fig. 2. Model of the stereoselective binding of D-glucose with and without acetyl groups at a smooth surface of Con A with a planar binding site distribution (hatched surface is tilted through 90°).

enough space for an additional hydration sphere between both surfaces, which would explain the observed similarities of binding constants and rates. The carbonyl dipoles of the acetyl groups obviously do not play an important role in the binding process. Formal attempts to bind the wrong enantiomers or diastereomers in the model yield at least two distances which are 20% larger. This is in agreement with the observed decrease of binding energies and equilibrium constants.

Received: November 24, 1989 [Z 3650 IE]
German version: *Angew. Chem. 102* (1990) 699

CAS Registry numbers:
1a, 101009-69-2; **1b**, 127062-38-8; **1c**, 127062-39-9; **1d**, 127062-40-2; **1e**, 101009-70-5; **1f**, 126979-69-9; **1g**, 126979-70-2; **1h**, 126979-71-3; Con A, 11028-71-0.

[1] L. Bhattacharyya, C. F. Brewer, *Biochem. Biophys. Res. Commun. 137* (1986) 670–674.
[2] H. Bader, K. Dorn, B. Hupfer, H. Ringsdorf, *Adv. Polym. Sci. 64* (1985) 1.
[3] J. P. Carver, A. E. Mackenzie, K. D. Hardman, *Biopolymers 24* (1985) 49–63.
[4] J. W. Becker, G. N. Reeke, B. A. Cunningham, G. M. Edelman, *Nature (London) 259* (1976) 406–409.
[5] I. J. Goldstein, C. E. Hayers, *Adv. Carbohydr. Chem. 35* (1978) 128–316.
[6] Z. Derewenda, J. Yariv, J. R. Helliwell, A. J. Kalb, E. J. Dodson, M. Z. Papiz, T. Wan, J. Campbell, *EMBO J. 8* (1989) 2189–2193.
[7] J. H. Fuhrhop, H. H. David, J. Mathieu, U. Liman, H. J. Winter, E. Boekema, *J. Am. Chem. Soc. 108* (1986) 1785–1791.
[8] Con A, Grade IV, Sigma, salt free; exact conditions are given in R. D. Brown III, C. F. Brewer, S. H. Koenig, *Biochemistry 16* (1977) 3883–3896. 1 mg of Con A per mL gave total stereoselectivity; with 25 mg Con A per mL nonselective precipitations of all vesicles were observed.
[9] T. G. I. Ling, B. Mattiason in T. C. Bøg-Hansen, E. van Driessche (Eds): *Lectins, Vol. 2*, de Gruyter, Berlin 1982, p. 563–571.
[10] Derived from the point dipole model:

$$E_{dipole} = \frac{1}{4\pi\varepsilon_0} \times \frac{2\mu_{OH}^2}{r^3} N_A \times 6$$

Synergic Destabilization by Geminal Ester Groups**

By *Sergej Verevkin, Barbara Dogan, Hans-Dieter Beckhaus* and *Christoph Rüchardt**

Dedicated to Professor Rolf Huisgen on the occasion of his 70th birthday

Stabilization by synergic interaction of geminal donor substituents on a saturated carbon atom, e.g. alkoxy groups in acetals, and its consequences, have long been known qualitatively as the "anomeric effect".[1] This anomeric stabilization and its dependence on structure was recently determined quantitatively by us.[2] In contrast, geminal nitro groups on a saturated C atom lead to destabilization.[3a] Results of ab-initio calculations and other theoretical studies,[3b–e] point to analogous effects in the case of other acceptor groups. We have now examined the synthetically important malonates **1a–c** and the methanetricarboxylates **2** in order to establish whether geminal ester groups are also synergically destabilizing.

Despite the universal use of malonates, to our knowledge no measurements of their standard enthalpies of formation have thus far been reported.[4] In the case of **1a–c**, **2**, and the reference compounds ethyl 2-methylbutyrate **3** and ethyl pivalate **4** they were now obtained from their combustion enthalpies $\Delta H_c^0(1)$ and vaporization enthalpies ΔH_v[3a] (Table 1.).

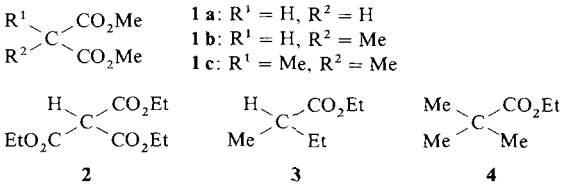

Table 1. Combustion enthalpies $\Delta H_c^0(1)$, vaporization enthalpies ΔH_v, and standard enthalpies of formation ΔH_f^0 of **1a–c** and **2–4** [kcal mol^{-1}] [a].

	$\Delta H_c^0(l)$	ΔH_v	$\Delta H_f^0(l)$	$\Delta H_f^0(g)$
1a	−552.38 ± 0.15	14.78 ± 0.19	−191.13 ± 0.15	−176.35 ± 0.24
1b	−708.38 ± 0.13	13.81 ± 0.17	−197.50 ± 0.13	−183-69 ± 0.21
1c	−863.08 ± 0.10	13.31 ± 0.19	−205.17 ± 0.10	−191.86 ± 0.19
2	−1187.73 ± 0.20	18.93 ± 0.17	−299.30 ± 0.20	−280.37 ± 0.26
3	−1002.62 ± 0.33	10.59 ± 0.07	−133.94 ± 0.33	−123.35 ± 0.34 [b]
4	−1001.08 ± 0.25	9.86 ± 0.03 [4]	−135.48 ± 0.25	−125.62 ± 0.26 [c]

[a] Standard deviation of the mean value from 5–8 measurements in each case. [b] Literature value [4]: −124.86 ± 2.02. [c] Literature value [4]: −128.10 ± 2.00.

For the determination of the extra stabilization or destabilization the method based on group increments, as developed for anomerically stabilized acetals,[2] was used, and not that

[*] Prof. Dr. C. Rüchardt, Dr. B. Dogan, Dr. H.-D. Beckhaus
Institut für Organische Chemie und Biochemie der Universität
Albertstrasse 21, D-7800 Freiburg (FRG)
Dr. S. Verevkin
Kuibyshew Politechnisches Institut, Kuibyshew (UdSSR)

[**] Geminal Substitution Effects, Part 3. This work was supported by the Deutsche Forschungsgemeinschaft and the Fonds der Chemischen Industrie, *S. V.* thanks Prof. *Alexandr M. Roznov* (Kuibyschew) for special support and the DAAD (Deutscher Akademischer Austauschdienst) for an exchange grant.–Part 2: [2].

of the isodesmic reactions which is otherwise frequently used. A possible influence of different alkyl branching on the central C atom can be tested, on the basis of the variously substituted malonic diesters **1a–c**.

Increments for the carboxy group, ΔH_f^0(g) CO_2[2C], and the O-bound carbon, ΔH_f^0(g) $CH_3^0[CO_2]$, $CH_2^0[CO_2,C]$, as well as for the ester-bearing alkyl groups, ΔH_{ester} $CH_3[CO_2]$, $CH_2[CO_2,C]$, $CH[CO_2,2C]$, $C[CO_2,3C]$ could be calculated from the known ΔH_f^0(g) values of monocarboxylates[6] with the help of already known increments for alkanes, ΔH_{alkyl}[5] (Table 2). The increments for alkyl groups with two ester groups as neighbors, $\Delta H_{diester}$, were determined from the new thermochemical data for the malonic diesters **1a–c** (see Table 1), while the increments for CH with three ester groups as neighbors, $\Delta H_{triester}$ were determined from the data for **2** (Table 2). On introducing an ester substituent instead of an alkyl group the increments hardly change; the destabilization energy ΔH_{ester}-ΔH_{alkyl} lies between 0.2 and 0.7 kcal mol^{-1} (Table 3). A second ester group, however, gives rise to a significant destabilization: the destabilization energy $\Delta H_{diester}$-ΔH_{ester} is 2.6 to 3.2 kcal mol^{-1}. The corresponding destabilization by the third ester group ($\Delta H_{triester}$-$\Delta H_{diester}$), with a value of 6.6 kcal mol^{-1}, is substantial. The extra destabilization $\Delta\Delta H_{gem} = \Delta H_{diester} - 2\Delta H_{ester} + \Delta H_{alkyl}$ and $\Delta\Delta H_{gem,gem} = \Delta H_{triester} - 2\Delta H_{diester} + \Delta H_{ester}$, i.e. the energy in excess of the additive destabilization energy is 1.9 to 2.8 kcal mol^{-1} in the case of malonic diesters and 3.5 kcal mol^{-1} in the case of tricarboxylates.

Table 2. Increments in enthalpy of formation [kcal mol^{-1}] for pure alkyl groups (ΔH_{alkyl}) and alkyl groups substituted by one (ΔH_{ester}), two ($\Delta H_{diester}$), or three ($\Delta H_{triester}$) [a] ester groups.

ΔH_{alkyl} [5]	ΔH_{ester} [b]	$\Delta H_{diester}$ [c]	$\Delta H_{triester}$ [d]	
CH_3 [C] − 10.05	$[CO_2]\equiv$ − 10.05	–	–	
CH_2 [2C] − 5.13	$[CO_2,C]$ − 4.74	$[2CO_2]$ − 1.57	–	
CH [3C] − 2.16	$[CO_2,2C]$ − 1.92	$[2CO_2,C]$ + 1.14	$[3CO_2]$	+ 7.74
C [4C] − 0.30	$[CO_2,3C]$ + 0.40	$[2CO_2, 2C]$ + 3.02	$[3CO_2,C]$	–

[a] Neighboring atoms in square brackets. [b] From monocarboxylates [6] with CO_2[2C] −77.34, $CH_3^0[CO_2]$ −10.05 and $CH_2^0[CO_2,C]$ −8.80. [c] From the malonic diesters **1a–c** (Table 1). [d] From tricarboxylates **2** (Table 1).

Table 3. Destabilization of geminal di- and tricarboxylates from the difference in group increments in Table 2 [kcal mol^{-1}]

	ΔH_{ester} [a] − ΔH_{alkyl} [d]	$\Delta H_{diester}$ [b] − ΔH_{ester} [a]	$\Delta H_{triester}$ [c] − $\Delta H_{diester}$ [b]	$\Delta\Delta H_{gem}$ [e]	$\Delta\Delta H_{gem,gem}$ [f]
$CH_2[xCO_2,(2-x)C]$	+ 0.39	+ 3.17	–	+ 2.78	–
$CH[xCO_2,(3-x)C]$	+ 0.24	+ 3.06	+ 6.60	+ 2.82	+ 3.54
$C[xCO_2,(4-x)C]$	+ 0.70	+ 2.62	–	+ 1.92	–

[a] x = 1. [b] x = 2. [c] x = 3. [d] x = 0. [e] $(\Delta H_{diester} - \Delta H_{ester}) - (\Delta H_{ester} - \Delta H_{alkyl})$. [f] $(\Delta H_{triester} - \Delta H_{diester}) - (\Delta H_{diester} - \Delta H_{ester})$.

The classical anomeric effect is enhanced by alkyl groups on the central carbon atom.[2] The analogous dependence of the "inverse anomeric effect" on the degree of substitution is only slight in the case of the malonates.

The confirmation of the presumed inverse anomeric destabilization in the case of **1** and **2** indicates that the concept under discussion is a generally valid one. We shall next determine the extent of geminal effects and their dependence on the structure of some other substituents.

When discussing the CH-acidity of malonic esters and other geminally substituted compounds one must not only consider the stabilization of the anion but also the destabilization of the ground state as contributing to the acidity.

Received: January 18, 1990 [Z 3745 IE]
German version: *Angew. Chem. 102* (1990) 693

CAS Registry numbers:
1a, 108-59-8; **1b**, 609-02-9; **1c**, 6065-54-9; **2**, 6279-86-3; **3**, 7452-79-1; **4**, 3938-95-2.

[1] A. J. Kirby: *The Anomeric Effect and Related Stereoelectronic Effects at Oxygen*, Springer, Berlin 1983, and references cited therein.
[2] H.-D. Beckhaus, B. Dogan, S. Verevkin, J. Hädrich, C. Rüchardt, *Angew. Chem. 102* (1990) 313; *Angew. Chem. Int. Ed. Engl. 29* (1990) 320.
[3] a) K. Fritzsche, B. Dogan, H.-D. Beckhaus, C. Rüchardt, *Thermochim. Acta*, in press; b) W. J. Hehre, L. Radom, P. von R. Schleyer, J. A. Pople: *Ab initio molecular orbital theory*, Wiley, New York 1986, p. 356; c) G. Leroy, *Adv. Quantum Chem. 17* (1985) 6393; d) N. S. Zefirov, N. M. Sergeev, D. I. Makhon'kov, L. Ya. D'yachkova, *J. Org. Chem. USSR (Engl. Transl.) 13* (1977) 1; e) N. D. Epiotis, *New J. Chem. 12* (1988) 231.
[4] a) J. B. Pedley, R. D. Naylor, S. P. Kirby: *Thermochemical Data of Organic Compounds*, Chapman and Hall, London 1986; b) J. D. Cox, G. Pilcher: *Thermochemistry of Organic and Organometallic Compounds*, Academic Press, London 1970.
[5] P. von R. Schleyer, J. E. Williams, K. P. Blanchard, *J. Am. Chem. Soc. 92* (1970) 2377.
[6] The ΔH_f^0(g) values of the following monocarboxylates were used in the calculation of the group increments ΔH_{ester} (Table 2): methyl acetate, ethyl acetate, butyl acetate, ethyl propionate, methyl *n*-pentenoate, ethyl *n*-pentenoate, propyl *n*-pentenoate, ethyl α-methylbutyrate (Table 1), methyl pivalate, ethyl pivalate (Table 1), methyl hexanoate, methyl heptanoate, methyl octanoate, methyl nonanoate, methyl decanoate ([**4a**] and own measurements).

Some Valenes of Benzannelated Five-Membered Heteroarenes – Synthesis and NMR Spectra**

By *Manfred Christl,* Stefan Krimm* and *Arno Kraft*

Dedicated to Professor Rolf Huisgen on the occasion of his 70th birthday

The chemical shifts of the C-atoms common to both three-membered rings of *endo,endo'*-bridged bicyclobutanes stretch over the unusually large range of $\Delta\delta \approx 90$ (δ = − 13.4 to 75.5).[1] In the valenes of naphthalene, 1,4-disubstituted phthalazines,[1a] and quinoxaline-2,3-dicarbonitrile[2] recently investigated by us the corresponding δ-values lie between 42.4 and 48.6. We now present the first valenes of benzannelated five-membered heteroarenes and their NMR spectra.

The majority of the conventional methods for the synthesis of five-membered heteroarenes are unsuitable in the case of benzvalene-annelated derivatives. Thus, we were unable to dehydrogenate the benzvalene adducts of benzonitrile oxide and diphenyl nitrile imine.[3, 4a] We therefore carried out 1,3-dipolar cycloadditions[5] with benzvalenyl phenyl sulfone **1**.[6] This reacts with even more 1,3-dipolar compounds than does benzvalene.[3, 4] Moreover, the phenylsulfonyl

[*] Prof. Dr. M. Christl, Dipl.-Chem. S. Krimm, Dr. A. Kraft
Institut für Organische Chemie der Universität
Am Hubland, D-8700 Würzburg (FRG)

[**] This work was supported by the Fonds der Chemischen Industrie and by the Deutsche Forschungsgemeinschaft.

function introduced with **1** serves as leaving group in the elimination required en route to the target molecules.

Two nitrile oxides, diphenyl nitrile imine, (4-nitrophenyl)-phenyl nitrile ylide, two azides and two diazoalkanes afforded the dihydroheteroarenes **2** and **3**. Benzonitrile oxide,[5b] diphenyl nitrile imine[5b] and 4-nitrophenyl phenyl nitrile

1 2 3

ylide[5c] were slowly generated in situ from their hydrogen chloride adducts with triethylamine, while the other 1,3-dipolar compounds were used as such. Data on the reaction conditions, yields and isomeric ratios are listed in Table 1. The regioselectivity compares with that of known 1,3-dipolar cycloadditions of vinyl sulfones.

Since the phenylsulfonyl function is only a moderately good leaving group the elimination of phenylsulfinic acid[8] from **2** and **3** did not succeed in all cases. With potassium *tert*-butoxide in tetrahydrofuran at 20 °C we obtained the isoxazole **4** (5 h, 77% yield) from **2b**, and the pyazoles **5** (5 h, 23%), **6a** (1 h, 29%) and **6b** (25 h, 68%), respectively, from **2c**, **3g** and **2h**.[7] There is no doubt about the structure of **5**, whereas in the case of **6a**, **b** tautomeric forms also have to be taken into consideration; however, on the basis of the ^{13}C-NMR spectra we prefer the structures **6**.

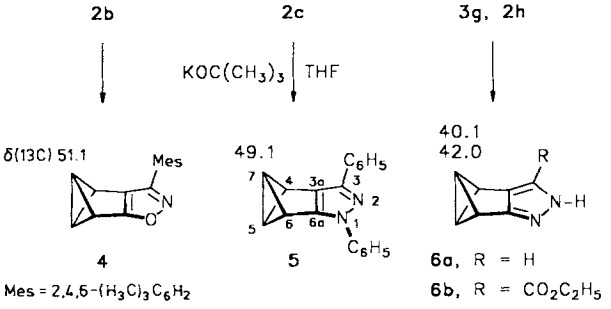

The success of these aromatizations seems to be dependent, inter alia, on the acidity of the protons that have to be split off. Thus, on using the mixture **2c**, **3c**, the reaction of **2c** proceeded smoothly, while **3c** remained unchanged and could then be readily isolated in isomerically pure form. In the case of **3e** the elimination reaction leading to the valene of phenylbenztriazole was not complete, and attempted separation of product and unconsumed starting material met without success.

3-Methyl-2,4-diphenyloxazolium-5-olate *N*-methyldiphenyl munchnone underwent reaction with **1** in dichloromethane, but the expected product was not obtained. In contrast, in the presence of ethyldiisopropylamine the desired pyrrole **7**[7] was immediately formed in 41% yield. Presumably, after cycloaddition and elimination of CO_2, the phenylsulfinate ion splits off at the stage of the transient azomethine ylide.[5d] The cationic precursor of **7** then transfers a proton even to the weak base ethyldiisopropylamine.

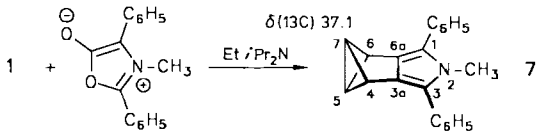

1 7

Starting from *cis*-3,4-dibenzoyltricyclo[3.1.0.0^{2,6}]hexane[1a] **8** and tricyclo[3.1.0.0^{2,6}]hexanedione **9**[2] there are several conceivable possibilities for the synthesis of the desired type of compound. However, only two reactions have thus far met with success: those to the thiophenes **10** (20% yield) and **11** (9%)[7] from **8** and Lawesson's reagent (toluene, triethylamine, 22 °C, 7 d) and from **9** and bisphenacylthioether (KOH in methanol, 20 °C, 18 h), respectively. The latter reaction provided the glycol product first, which was dehydrated with thionyl chloride in pyridine (0 °C, 1.5 h). 3,4-Diaminothiophene converted **9**, in analogy to known reactions,[2] into **12** (27%),[7] the valene of thieno[3,4-*b*]quinoxaline.

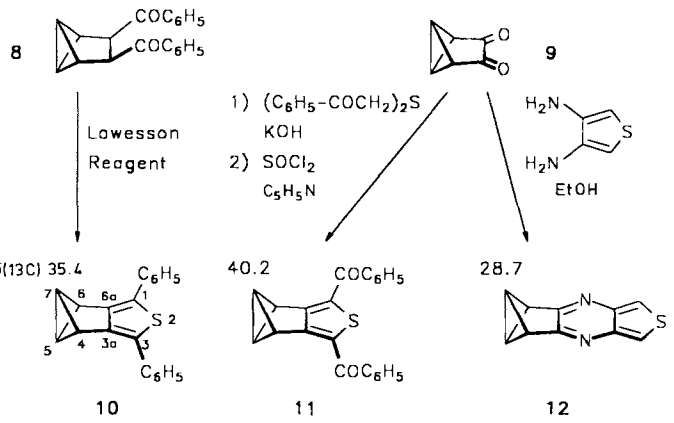

Table 1. Reactions of **1** with two nitrile oxides, diphenyl nitrile imine, 4-nitrophenyl phenyl nitrile ylide, two azides, and two diazoalkanes leading to the isomers **2** and **3**.

2, 3	1,3-Dipole XNY	Solvent	Time	X	Y	Yield [%]	Ratio **2:3**
a	C_6H_5-CNO	CH_2Cl_2	6 h	C-C_6H_5	O	76	>95: 5
b	Mes-CNO	$CHCl_3$	16 h	C-Mes	O	78	>95: 5
c	C_6H_5-CNN-C_6H_5	C_6H_6	32 h	C-C_6H_5	N-C_6H_5	97	66:34
d	C_6H_5-CNCH-C_6H_4-4-NO_2	CH_2Cl_2	26 h	C-C_6H_5	CH-C_6H_4-4-NO_2	27	>95: 5
e	C_6H_5-N_3	CH_2Cl_2	7 d	N	N-C_6H_5	25	< 5:95
f	4-$NO_2C_6H_4$-N_3	CH_2Cl_2	5 d	N	N-C_6H_4-4-NO_2	25	< 5:95
g	CH_2N_2	$(C_2H_5)_2O$	[a]	N	CH_2	96	15:85[b]
h	$C_2H_5O_2C$-CHN_2	CH_2Cl_2	2 d	C-$CO_2C_2H_5$	NH	46	>95:5

[a] First 4 h at 0 °C then 2 d at 20 °C. [b] **2g** was not isolated but only characterized NMR spectroscopically.

The ^{13}C-NMR chemical shifts of the bicyclobutane bridgehead atoms of the valenes are quoted alongside the formulas. They generally lie at considerably lower field than the values of the dihydro derivatives **2** and **3**. Especially noteworthy are the differences between the heteroarenes which are formally benzvalene derivatives, and those which can be derived from bismethylenetricyclo[3.1.0.0^{2,6}]hexane.[9] Thus, **4** and **5**, with $\delta = 51.1$ and 49.1, respectively, show the furthest downfield shifts of all tricyclo [3.1.0.0^{2,6}]hexane derivatives, whereas the corresponding signals of **7**, **10** and **11** with $\delta = 37.1$, 35.4 and 40.2 lie at considerably higher field. A comparison of the δ values of the pyrazoles **6** ($\delta = 40.1$, 42.0) and **5** accordingly supports the proposed structure **6**. The expansion of the aromatic system in **12** leads to a further upfield shift to $\delta = 28.7$. In comparison to the corresponding absorption of the valene in which the thiophene moiety of **12** is replaced by a benzene ring,[2] a shielding of $\Delta\delta = 6.2$ is observed in **12** which is possibly due to stronger double bond localization.

The majority of the valenes synthesized underwent isomerization under more or less energetic conditions to the benzannelated heteroarenes. In the case of **6b** and **7** this took place at 100–150 °C in C_6D_6, in the case of **10** and **11** during attempts at chromatographic purification. The isoxazole **4**, on the other hand, was converted into the acylazirine **13** (67% yield) upon heating.[7] Reactions of this type have already been reported, but thermally initiated ones generally do not terminate at the stage of the acylazirine.[10]

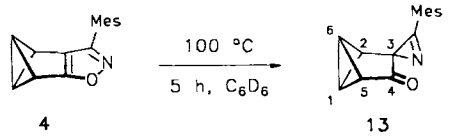

4 13

Received: September 28, 1989;
revised: December 12, 1989 [Z 3566 IE]
German version: *Angew. Chem. 102* (1990) 704
Publication delayed at authors' request

CAS Registry numbers:
1, 51991-05-0; **2a**, 126664-51-5; **2b**, 126664-52-6; **2c**, 126664-53-7; **2d**, 126664-54-8; **2e**, 126664-55-9; **2f**, 126664-56-0; **2g**, 126664-57-1; **2h**, 126664-58-2; **3a**, 126664-59-3; **3b**, 126664-60-6; **3c**, 126664-61-7; **3d**, 126664-62-8; **3e**, 126664-63-9; **3f**, 126664-64-0; **3g**, 126664-65-1; **3h**, 126664-66-2; **4**, 126664-67-3; **5**, 126664-68-4; **6a**, 126664-69-5; **6b**, 126664-70-8; **7**, 126664-71-9; **8**, 96598-12-8; **9**, 85358-63-0; **10**, 126664-72-0; **11**, 126664-73-1; **12**, 126664-74-2; **13**, 126664-75-3; bisphenylacylthioether, 2461-80-5; 2,4,6-triphenyl benzonitrile *N*-oxide, 2904-57-6; diphenyl nitrile imine, 15409-32-2; 4-nitrophenyl phenyl nitrile ylide, 10494-67-4; 5-hydroxy-3-methyl-2,4-diphenyl oxazolium hydroxide, inner salt, 13712-75-9; benzonitrile oxide, 873-67-6; phenyl azide, 622-37-7; *p*-nitrophenyl azide, 1516-60-5; diazomethane, 334-88-3; ethyl diazoacetate, 623-73-4; 3,4-diaminothiophone, 78637-85-1.

Table 2. Selected physical data of **2**–**7** and **10**–**13**: 200- and 400-MHz ^{1}H-NMR and 50- and 100-MHz ^{13}C-NMR spectra in $CDCl_3$ (δ values, coupling constants in Hz), IR (KBr, cm^{-1}).

2a: m.p. 137–139 °C – **2b**: m.p. 173–176 °C

2c: ^{1}H NMR: $\delta = 2.19$ (dq, $J_{5,7} = 8.2$, $J_{3a,7} = J_{4,7} = J_{6,7} = 1.7$; 7-H), 2.66 (dq, $J_{4,6} = 5.0$, $J_{3a,4} = J_{4,5} = 1.7$;4-H), 2.83 (m; 5-H), 3.21 (dt, $J_{5,6} = 1.7$; 6-H), 4.43 (br.s; 3a-H), 6.97–7.95 (several m; 3 C_6H_5). – ^{13}C NMR: $\delta = 3.6$ (d, C-7), 10.7 (d; C-5), 38.6, 39.2 (each d; C-4, -6), 64.3 (d; C-3a), 100.8 (s; C-6a), 117.8, 121.8, 125.7, 128.1, 128.4–129.2, 133.8 (each d, each 3 *o*-, *m*-, p-C); 131.1, 137.2, 143.5, 149.2 (each s; 3 *ipso*-C, C-3)

3c: m.p. 167–170 °C. – ^{1}H NMR: $\delta = 2.34$ (dq, $J_{5,7} = 7.9$, $J_{4,7} = J_{6,7} = J_{6a,7} = 1.7$; 7-H), 2.82 (m; 6-H), 2.84 (m; 5-H), 3.39 (dt, $J_{4,6} = 4.9$, $J_{4,5} = 1.7$; 4-H), 5.18 (br.s; 6a-H), 6.86 (tt; 1 *p*-H), 7.03 (m; 2 *o*-H), 7.18–7.52 (m; 10H), 7.81 (m; 2 *o*-H). – ^{13}C NMR: $\delta = 3.4$ (d; C-7), 8.9 (d; C-5), 38.9, 40.3 (each d; C-4, -6), 74.9 (d; C-6a), 90.8 (s; C-3a), 112.8, 126.8, 128.3, 128.6, 129.0, 129.2 (each d; *m*-, *o*-C), 120.0, 128.5, 133.9 (each d; *p*-C), 131.4, 137.9, 141.2, 142.7 (each s; 3 *ipso*-C, C-3)

2d: m.p. 216–219 °C – **3e**: m.p. = 142–145 °C – **3f**: m.p. = 215–217 °C

3g: m.p. 121–124 °C (still contains a few % **2g**)

2h: m.p. 170 °C (decomp.). – IR: $\tilde{\nu} = 3350$ (n-H), 1685 (C=O)

4: m.p. 104–107 °C

5: m.p. 136–139 °C. – ^{1}H NMR: $\delta = 2.73$, 2.84 (each dt, $J_{4,6} = 4.6$, $J_{4,5} = J_{5,6} = 1.5$; 4-, 6-H), 4.51 (t; 5.7-H), 7.22 (tt; *p*-H), 7.26 (tt; *p*-H), 7.37 (m; 2 *m*-H), 7.41 (m; 2 *m*-H), 7.67 (m; 2 *o*-H), 7.80 (m; 2 *o*-H). – ^{13}C NMR: $\delta = 31.7$, 33.4 (each ddt, $J_{C,H} = 175$, 11, 3; C-4, -6), 49.1 (dd, $J_{C,H} = 211$, 4; C-5,7), 119.0 (dt; *o*-C), 125.8 (dt; *p*-C), 126.0 (dt; *o*-C), 127.4 (dt; *p*-C), 128.4 (dd; *m*-C), 129.2 (dd; *m*-C), 133.4 (particularly high intensity), 140.0, 144.2, 160.0 (each s; C-3, -3a, -6a, 2 *ipso*-C)

6a: m.p. 80–83 °C – IR: $\tilde{\nu} = 3180$ (breit; N-H)
6b: m.p. 88–90 °C – IR: $\tilde{\nu} = 3140$ (breit; N-H), 1710 (C=O)

7: m.p. 150–151 °C – ^{1}H NMR: $\delta = 2.68$ (t, $J_{4,5} = 1.5$; 4-H), 3.39 (s; CH_3), 3.87 (t; 5-H), 7.24 (tt; *p*-H), 7.41 (m; *m*-H), 7.45 (m, *o*-H). – ^{13}C NMR: $\delta = 32.4$ (ddt, $J_{C,H} = 172$, 11, 4; C-4), 34.7 (q, $J_{C,H} = 138$; CH_3), 37.1 (dd, $J_{C,H} = 212$, 5; C-5), 126.1 (dt; *p*-C), 128.1 (dt; *o*-C), 128.5 (dd; *m*-C), 130.1, 133.2, 135.6 (each s; C-1, -3a, *ipso*-C)

10: m.p. 148–151 °C. – ^{1}H NMR: $\delta = 2.91$ (t, $J_{4,5} = 1.7$; 4-H), 4.03 (t; 5-H), 7.23 (tt; *p*-H), 7.36 (m; *m*-H), 7.53 (m; *o*-H). – ^{13}C NMR: $\delta = 34.1$ (ddt, $J_{C,H} = 173$, 11, 3; C-4), 35.4 (dd, $J_{C,H} = 217$, 5; C-5), 128.2 (s; C-1), 150.4 (s; C-3a), 126.2 (dt; *o*-C), 126.8 (dt; *p*-C), 128.8 (dd; *m*-C), 134.4 (s; *ipso*-C)

11: m.p. 120–122 °C. – IR: $\tilde{\nu} = 1640$, 1625 (C=O)

12: m.p. 140–143 °C.

13: m.p. 131–132 °C. – IR: $\tilde{\nu} = 1735$ (C=O, C=N). – ^{1}H NMR: $\delta = 2.03$, 2.61 (each dt; $J_{2,5} = 4.9$, $J_{1,2} = J_{1,5} = J_{2,6} = J_{5,6} = 1.9$; 2-, 5-H), 3.27, 3.42 (each dt, $J_{1,6} = 7.2$; 1-, 6-H), 2.34 (s; *p*-CH_3), 2.53 (s; 2 *o*-CH_3), 6.97 (br.s; 2 *m*-H). – ^{13}C NMR: $\delta = 9.4$, 11.9 (each d; C-1, -6), 33.2, 42.8 (each d; C-2, -5), 43.1 (s; C-3), 159.4 (s; C=N), 212.9 (s; C-4), 20.3 (q; 2 *o*-CH_3), 21.6 (q; *p*-CH_3), 117.8 (s; *ipso*-C), 129.5 (d; 2 *m*-C), 141.9 (s; 2 *o*-C), 144.1 (s; *p*-C)

[1] a) M. Christl, S. Freund, *Chem. Ber. 118* (1985) 979, and references cited therein; b) other compounds with extreme δ values: Y. Sugihara, S. Wakabayashi, N. Saito, I. Murata, *J. Am. Chem. Soc. 108* (1986) 2773, and references cited therein; M. Christl, C. Herzog, *Tetrahedron Lett. 28* (1987) 187.
[2] M. Christl, A. Kraft, *Angew. Chem. 100* (1988) 1427; *Angew. Chem. Int. Ed. Engl. 27* (1988) 1369.
[3] M. Christl, B. Mattauch, H. Irngartinger, A. Goldmann, *Chem. Ber. 119* (1986) 950.
[4] a) M. Christl, *Angew. Chem. 85* (1973) 666; *Angew. Chem. Int. Ed. Engl. 12* (1973) 660; b) M. Christl, H. Leininger, *Tetrahedron Lett. 1979*, 1553; c) M. Christl, E. Brunn, W. R. Roth, H.-W. Lennartz, *Tetrahedron 45* (1989) 2905.
[5] a) A. Padwa (Ed.): *1,3-Dipolar Cycloaddition Chemistry*, Wiley, New York 1984; b) P. Caramella, P. Grünanger in [5a], *Vol. 1*, p. 291; c) H.-J. Hansen, H. Heimgartner in [5a], *ibid.*, *Vol. 1*, p. 177; d) K. T. Potts in [5a], *Vol. 2*, p. 1.
[6] T. J. Katz, K. C. Nicolaou, *J. Am. Chem. Soc. 96* (1974) 1948.
[7] Elemental analyses and IR, NMR and mass spectra support the proposed structures. Selected physical data are collected in Table 2.
[8] T. Durst in D. H. R. Barton, W. D. Ollis (Eds.): *Comprehensive Organic Chemistry, Vol. 3*, Pergamon, Oxford 1979, p. 171.
[9] F. Lanzendörfer, M. Christl, *Angew. Chem. 95* (1983) 896; *Angew. Chem. Int. Ed. Engl. 22* (1983) 871.
[10] S. A. Lang, Jr., Y.-i Lin in A. R. Katritzky, C. W. Rees (Eds.): *Comprehensive Heterocyclic Chemistry, Vol. 6*, Pergamon, Oxford 1984, p. 1.

Nitrogen Triiodide**

By *Inis Tornieporth-Oetting* and *Thomas Klapötke**

In addition to the stable NF_3,[1] only the binary nitrogen trihalides NCl_3, which is explosive, and NBr_3,[2] which was

[*] Dr. T. Klapötke, Dipl.-Chem. I. Tornieporth-Oetting
Institut für Anorganische und Analytische Chemie
der Technischen Universität
Strasse des 17. Juni 135, D-1000 Berlin 12

[**] This research was supported by the Deutsche Forschungsgemeinschaft, the Fonds der Chemischen Industrie and the Bundesministerium für Bildung und Wissenschaft within the framework of the graduate seminars "Synthesis and Structure Determination of Small Molecular Compounds" (Lecturer: *I. T.-O.*).

first isolated in 1975, have as yet been described. Nitrogen triiodide NI_3,[3] the longest-known nitrogen-halogen compound could hitherto only be prepared in the form of a donor-acceptor complex with one or three molecules of coordinated ammonia;[4] the X-ray crystal structure analysis reveals that $[NI_3 \cdot NH_3]_n$ consists of chains in which N is surrounded approximately tetrahedrally by I.[5] We recently reported the formation of $[NI_3 \cdot NH_3]_n$ from $I_3^{\oplus}AsF_6^{\ominus}$ and NH_3.[6] The aim of the present study was the synthesis of adduct-free nitrogen triiodide as the last missing member in the series of nitrogen trihalides.

The synthesis of free NI_3 can only be performed in the absence of ammonia, since $[NI_3 \cdot NH_3]_n$ cannot be transformed into NI_3 by the removal of ammonia,[4] and according to thermochemical considerations the adduct $NI_3 \cdot NH_3$ should be ca. 30 kJ mol^{-1} more stable than NH_3 and NI_3.[7] As boron nitride reacts readily with hydrogen fluoride to form ammonium tetrafluoroborate [Eq. (a)],[8] we were interested in the behavior of boron nitride towards iodine monofluoride.

$$BN + 4\,HF \longrightarrow NH_4^{\oplus}BF_4^{\ominus} \qquad (a)$$

Boron nitride reacts with IF in $CFCl_3$ according to Equation (b) to form NI_3, a red-black, highly volatile solid, very unstable at room temperature (**danger of explosion** [9]) and soluble in $CFCl_3$ giving a deep red color[10].

$$BN + 3\,IF \xrightarrow{CFCl_3} NI_3 + BF_3 \qquad (b)$$

In solution NI_3 decomposes rapidly at 0 °C and within several hours at − 60 °C. This explains the relatively small (30%) yield (see *Experimental*). In the solid state NI_3 is stable at − 196 °C, decomposes slowly at −78 °C and spontaneously at 0 °C. The driving force for the formation of the endothermic species NI_3[7] may certainly be ascribed to the large tendency for formation of BF_3 to take place.[11] After evaporation of the solvent at − 50 °C, NI_3 may be sublimed directly into a glass tube cooled to − 196 °C. In the process a small amount of decomposition takes place (iodine residue). NI_3 was characterized by Raman spectroscopy.[12]

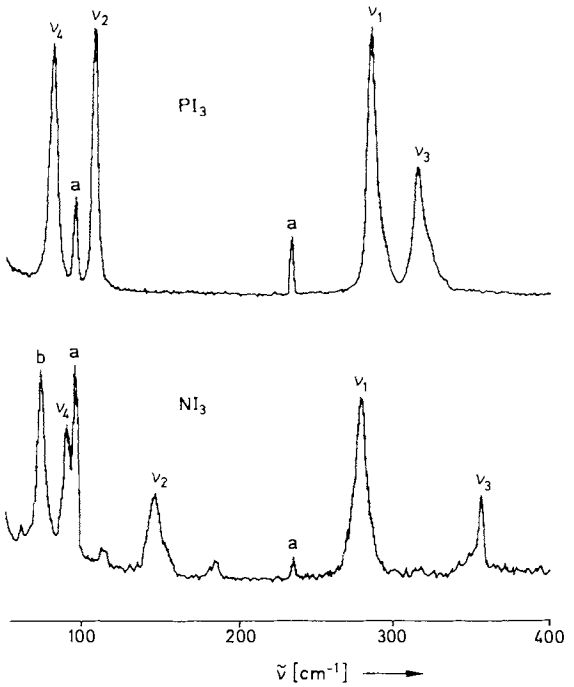

Fig. 1. Raman spectrum of NI_3[12] and PI_3 (see Table 1). ν_1–ν_4: NI_3; a: Laser lines; b: Lattice vibrations.

Table 1. Wave numbers [cm^{-1}] and relative intensities (in brackets) of the Raman active fundamental vibrations ν_1–ν_4 of the nitrogen trihalides NCl_3 and NI_3, and of PI_3.

	ν_1	ν_2	ν_3	ν_4
NCl_3[a]	535 (s)	347 (s)	637 (w)	254 (m)
NI_3[b]	279 (10)	146 (5)	354 (3)	90 (5)
PI_3[c]	285 (10)	107 (6)	315 (5)	81 (7)

[a] In CCl_4 solution, room temperature [15]. [b] Solid, − 100 °C. [c] Solid, room temperature.

The four most intense lines in the low-temperature Raman spectrum of NI_3 (Fig. 1) can be assigned to the NI_3 species with C_{3v} symmetry.[12] In Table 1 the Raman data of NI_3, of the Cl-analog NCl_3, and of PI_3 are compared. From the trend in the intensities as well as in the position of the frequencies, the four bands can be unambiguously assigned to the Raman active fundamental vibrations ν_1 to ν_4. For comparison, Figure 1 also shows the Raman spectrum of solid PI_3. The IR spectrum of $[NI_3 \cdot NH_3]_n$ contains a weak band at $\tilde{\nu} = 176\ cm^{-1}$ and a strong one at $\tilde{\nu} = 488\ cm^{-1}$, which can be assigned to the symmetric N-I stretching vibration.[13] However, as a result of the polymeric structure this assignment and the comparison with the Raman spectrum of NI_3 is problematic. On the other hand, the location of the observed N-I stretching vibration for iodine azide at 338 cm^{-1}[14] agrees well with the observed N-I stretching frequency for NI_3[12] (cf. ClN_3: $\tilde{\nu}_{N-Cl} = 719\ cm^{-1}$[14]).

When NI_3 is allowed to evaporate into the unheated ion source of a mass spectrometer (EI, 70 eV, 30 °C), it decomposes completely: the spectrum consists only of peaks of $I^{\oplus}$ (100%) and $I_2^{\oplus}$ (20%).

Freshly sublimed, deep red NI_3 reacts spontaneously with anhydrous NH_3 at − 45 °C, accompanied by a color change to green and the formation of $[NI_3 \cdot 3\,NH_3]_n$.[16] With methyl iodide, solid NI_3 reacts already below − 30 °C, losing I_2 and forming tetramethylammonium iodide,[17] as shown in Equation (c).

$$NI_3 + 4\,MeI \rightarrow NMe_4^{\oplus}I^{-} + 3\,I_2 \qquad (c)$$

Although NI_3 exists only at low temperature, the compound is more stable than one expects from the decrease in stability within the series NF_3, NCl_3, NBr_3.[4] This effect is certainly partially explained by the similar trend in the bond energies of the N–I and N-Cl bonds (E (N–Cl) = 190 kJ mol^{-1},[18] E (N–I) = 169 kJ mol^{-1}[7], which reflect the fact that I is considerably more electropositive than Cl and Br (Allred-Rochow electronegativities: Cl 2.83, Br 2.74, I 2.21).

Experimental

NI_3: All apparatus were deactivated with F_2. 20 mL of $CFCl_3$ (dried over P_4O_{10}) was condensed into a 50-mL quartz ampoule fitted with a stainless steel valve and containing a mixture of 1.00 g (3.94 mmol) of iodine and 0.065 g (2.63 mmol) of boron nitride (Aldrich). 0.157 g (4.14 mmol, i.e. 5% excess) of fluorine (Union Carbide; HF absorption by NaF) was thereafter condensed into the ampoule at − 196 °C; the reaction mixture was warmed to − 30 °C over 2 h with constant agitation. After a further 8 h at − 30 °C the mixture was irradiated for 5 minutes in an ultrasonic bath (**danger of explosion** [9]), then slowly warmed to − 10 °C, the $CFCl_3$ pumped off at − 50 °C and the NI_3 isolated as a deep-red solid from the black residue by sublimation (− 20 °C, receiving vessel − 196 °C; yield ca. 0.3 g, 30%). NI_3 already decomposes below 0 °C to iodine and nitrogen (proof via gas discharge). 0.08 g of NI_3 sets free 0.075 g I_2, corresponding to 94% I_2 (calc. 96%).

Received: January 17, 1990 [Z 3742 IE]
German version: *Angew. Chem. 102* (1990) 726

[1] N. N. Greenwood, A. Earnshaw: *Chemistry of the Elements*, Pergamon, Oxford 1984; *Chemie der Elemente*, VCH Verlagsgesellschaft, Weinheim 1988.
[2] J. Jander, J. Knackmuss, K.-U. Thiedemann, *Z. Naturforsch. B30* (1975) 464.
[3] J. Jander, U. Engelhardt in C. B. Colburn (Ed.): *Developments in Inorganic Nitrogen Chemistry, Vol. 2: Nitrogen Compounds of Chlorine, Bromine, and Iodine*, Elsevier, Amsterdam 1973, p. 184.
[4] The names nitrogen triiodide, nitrogen bromide and nitrogen chloride conform to IUPAC nomenclature, although the actual polarization would be better described as trihalide nitride.
[5] a) H. Hartl, H. Bärnighausen, J. Jander, *Z. Anorg. Allg. Chem. 375* (1968) 225; b) J. Jander, L. Bayersdorfer, K. Höhne, *ibid. 357* (1968) 215.
[6] I. Tornieporth-Oetting, T. Klapötke, J. Passmore, *Z. Anorg. Allg. Chem.*, in press.
[7] R. H. Davies, A. Finch, P. N. Gates, *J. Chem. Soc. Chem. Commun. 1989*, 1461.
[8] O. Glemser, H. Haeseler, *Z. Anorg. Allg. Chem. 279* (1955) 141.
[9] **Warning**: Although pure NI_3 is stable at low temperatures in $CFCl_3$, the synthesis and isolation presents particular problems. On occasion the reaction of BN with IF does not start immediately. One of our samples cooled to $-18\,^{\circ}C$ and covered with a 10-cm thick layer of ice exploded and flying splinters caused considerable damage, for example to the full visor face protection of the experimenter.
[10] In the reaction of BN with four equivalents of IF, analogous to Equation (a), NI_3 is also formed. Byproducts: I_3BF_4 and an, as yet, not unambiguously identified yellow solid, possibly $IF_2^{\oplus}BF_4^{\ominus}$: $2\,BN + 8\,IF \rightarrow 2\,NI_3 + 2\,BF_3 + 2\,IF \rightarrow 2\,NI_3 + BF_3 + I_2F^{\oplus}BF_4^{\ominus}$; $2\,I_2F^{\oplus}BF_4^{\ominus} \rightarrow I_3^{\oplus}BF_4^{\ominus} + IF_2^{\oplus}BF_4^{\ominus}$. Up till now no indication of the existence of $NI_4^{\oplus}BF_4^{\ominus}$ could be found.
[11] A rough estimate of the enthalpy of reaction for Equation (b), neglecting the correct aggregation states, yields ΔH°_{298} (c) $= -312$ kJ mol^{-1} (ΔH°_f: BN(soln.) -254[19], IF(g) -95[18], BF_3(g) -1137[18], NI_3(g) $+287$ kJ mol^{-1} [7].
[12] Excitation wavelength: 647.09 nm, Laser energy: 15 mW, $T: -100\,^{\circ}C$. $\tilde{\nu}$ [cm^{-1}] = 72(m), 91(m), 113(vw), 146(m), 179(vw), 279(s), 354(w); Note added in proof: In the meantime it has also been possible to record a ^{15}N-NMR spectrum of NI_3 (98% ^{15}N) in $CFCl_3$ [20]. The appearance of only one singlet [$\delta = +183$ ppm, rel. to $MeNO_2$, 50.653 MHz (^{15}N), $-30\,^{\circ}C$] in the expected range points to the presence of only one species in solution. We shall report on the measurement conditions and the synthesis of $^{15}NI_3$ in a further communication..
[13] a) K. Knuth, J. Jander, U. Engelhardt, *Z. Naturforsch. B 24* (1969) 1473; b) *Z. Anorg. Allg. Chem. 392* (1972) 279; c) J. Jander, Adv. Inorg. Chem. Radiochem. 19 (1976) 1.
[14] K. Dehnicke, *Angew. Chem. 88* (1976) 612; *Angew. Chem. Int. Ed. Engl. 15* (1976) 240.
[15] P. J. Hendra, J. R. Mackenzie, *Chem. Commun. 1968*, 760.
[16] Depending on the temperature a residue which is either brown $[NI_3 \cdot NH_3]_n$ (room temperature, excess NH_3 in the gas phase), green $[NI_3 \cdot 3\,NH_3]_n$ ($-33 > T > -75\,^{\circ}C$) or red $[NI_3 \cdot 5\,NH_3]_n$ ($T < -75\,^{\circ}C$) remains [4], but NI_3 cannot be recovered by removal of NH_3 in vacuo.
[17] ^1H NMR ($CDCl_3$): $\delta(Me_4N^{\oplus}I^{\ominus}) = 3.02$; cf. $\delta(MeI) = 2.17$.
[18] D. A. Johnson: *Some Thermodynamic Aspects of Inorganic Chemistry*, Cambridge University Press, Cambridge 1982.
[19] I. Barin: *Thermochemical Data of Pure Substances, Part I*, VCH Verlagsgesellschaft, Weinheim 1989.
[20] We thank Dr. *Klein*, BASF AG, for recording the ^{15}N-NMR spectrum.

Doubly Stereodifferentiating Hiyama Addition with Mismatched Reactants; Enantio- and Diastereocontrolled Synthesis of Dihydrocanadensolide**

By *Johann Mulzer** and *Lars Kattner*

Dedicated to Professor Rolf Huisgen on the occasion of his 70th birthday

Owing to its four chirality centers and the bicyclic paraconic acid lactone structure, dihydrocanadensolide **1**, a metabolite of *Penicillium canadense*,[1] is an attractive synthetic target molecule. The configuration first proposed for **1** was later revised[2,3] but is still not unequivocally elucidated.

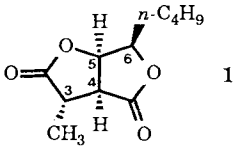

1

The physiological properties of the compound are unknown. We report here on the total synthesis of natural **1** and its enantiomer (Scheme 1).

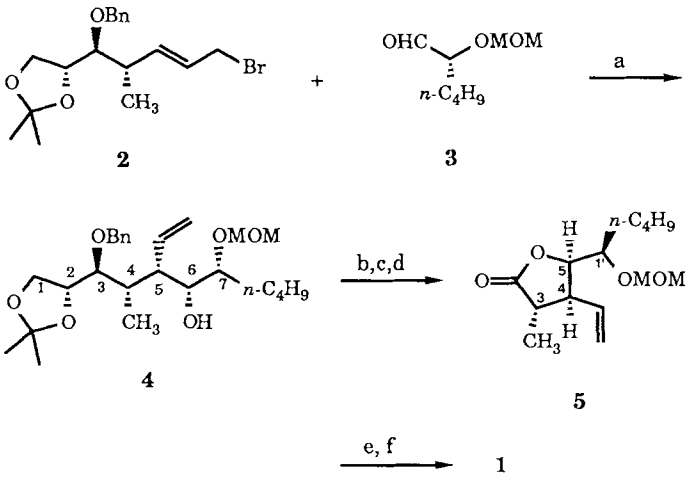

Scheme 1. a) $CrCl_3/LiAlH_4$, THF, 0 °C, 36 h, 63%; b) Na/NH_3, THF, $-40\,^{\circ}C$, 20 min, 86%; c) pyridinium *p*-tosylate (PPTS), MeOH, 22 °C, 24 h, 64%; d) H_5IO_6, Et_2O/THF, 22 °C, 10 min; pyridinium chlorochromate (PCC), CH_2Cl_2, 22 °C, 2 h, 85%; e) HCl/MeOH/THF, 60 °C, 1 h, 98%; f) O_3/PPh_3, CH_2Cl_2, $-78\,^{\circ}C$; PCC, CH_2Cl_2, 22 °C, 2 h, 67%.

The key step is the Hiyama addition[4] of the allyl bromide derivative **2** to the aldehyde **3** (MOM = methoxymethyl). Both components are accessible in pure form in a few steps from (*R*)-2,3-isopropylideneglycerinaldehyde[5] and react highly stereoselectively (> 97% according to ^1H- and ^{13}C-NMR analysis) to give the adduct **4** (Table 1). This is the first Hiyama reaction of a chirally substituted acyclic allyl bromide derivative.[6] The configuration at the new chirality center C-6 was confirmed by conversion of **4** into the diacetal **6**, in which the *trans* position of 6-H and 7-H could be detect-

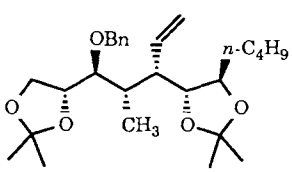

6

ed by NOE difference spectroscopy. The relative configuration at C-5/6 follows from the successful conversion of the monolactone **5** into the bislactone **1**, which is possible only in the case of *cis*-annelation[2] (Scheme 1).

[*] Prof. Dr. J. Mulzer, Dipl.-Chem. L. Kattner
Institut für Organische Chemie der Freien Universität
Takustrasse 3, D-1000 Berlin 33

[**] This work was supported by the Graduiertenkolleg "Synthese and Strukturaufklärung niedermolekularer Verbindungen".

Table 1. Analytical data of some key compounds (correct combustion analyses were obtained for all compounds; ^{1}H-(^{13}C-)NMR at 270 (62.5) MHz in $CDCl_3$ with internal TMS).

1: ^{1}H NMR: δ = 0.94 (t, 3H, J = 7.5 Hz, *n*Bu-CH_3), 1.35–1.58 (m, 4H, *n*Bu-CH_2), 1.44(d, 3H, J = 7.5 Hz, 3-CH_3), 1.85 (mc, 2H, *n*Bu-CH_2), 3.07 (dq, 1H, J = 7.5, 1 Hz, 3-H), 3.13 (dd, 1H, J = 6, 1 Hz, 4-H), 4.54 (ddd, 1H, J = 8, 7, 4 Hz, 6-H), 5.08 (dd, 1H, J = 6, 4 Hz, 5-H). ^{13}C NMR: δ = 13.78, 17.08, 22.37, 27.45, 28.49, 38.33, 48.98, 78.27, 82.37, 174.62, 176.70. $[\alpha]_D^{20}$ = −31 (c = 0.26, MeOH), m.p. = 94.5 °C

4: ^{1}H NMR: δ = 0.89 (t, 3H, J = 7 Hz, 11-H), 0.96 (d, 3H, J = 7 Hz, 4-CH_3), 1.12–1.64 (m, 6H, 8-H, 9-H, 10-H), 1.34, 1.39 (each s, each 3H, isopropylidene-CH_3), 2.15 (m, 1H, 4-H), 2.36 (ddd, 1H, J = 10, 7, 3 Hz, 5-H), 3.24 (s, 1H, OH), 3.35 (m, 1H, 7-H), 3.41 (s, 3H, MOM-CH_3), 3.66 (m, 1H, J = 8, 3 Hz, 6-H), 3.76 (dd, 1H, J = 7, 6 Hz, 3-H), 3.79 (dd, 1H, J = 8.8 Hz, 1-H), 4.05 (dd, 1H, J = 8, 6 Hz, 1-H), 4.20 (m, 1H, J = 8, 7, 6 Hz, 2-H), 4.52–4.76 (m, 4H, MOM-CH_2,Ph-CH_2), 4.96 (dd, 1H, J = 17, 2 Hz, vinyl-CH_2), 5.14 (dd, 1H, J = 10, 2 Hz, vinyl-CH_2), 5.80 (ddd, 1H, J = 17, 10, 10 Hz, vinyl-CH), 7.28 (mc, 5H, Aryl-H). ^{13}C NMR: δ = 12.73, 13.88, 22.70, 25.33, 26.44, 27.61, 30.23, 35.33, 47.33, 55.78, 67.08, 72.36, 72.60, 75.56, 79.51, 84.39, 98.00, 108.64, 117.64, 127.32, 127.66, 128.13, 136.57, 138.79. $[\alpha]_D^{20}$ = +26 (c = 1.08, $CHCl_3$)

5: ^{1}H NMR: δ = 0.90 (t, 3H, J = 7 Hz, 5'-CH_3), 1.19 (d, 3H, J = 7 Hz, 3-CH_3), 1.30 (mc, 4H, 3'-CH_2, 4'-CH_2), 1.72 (mc, 2H, 2'-CH_2), 2.88 (mc, 2H, 3-H, 4-H), 3.38 (s, 3H, MOM-CH_3), 3.64 (ddd, 1H, J = 8, 6, 2 Hz, 1'-H), 4.47 (dd, 1H, J = 8, 2 Hz, 5-H), AB system: δ_A = 4.64, δ_B = 4.70 (2H, J_{AB} = 7 Hz, MOM-CH_2), 5.22 (dd, 1H, J = 16.5, 1.5 Hz, vinyl-CH_2), 5.24 (dd, 1H, J = 10, 1.5 Hz, vinyl-CH_2), 5.88 (ddd, 1H, J = 16.5, 10, 10 Hz, vinyl-CH), ^{13}C NMR: δ = 13.94, 14.20, 22.77, 27.67, 30.04, 39.44, 51.40, 56.26, 77.14, 80.26, 95.75, 119.66, 133.93, 179.51. $[\alpha]_D^{20}$ = −73 (c = 0.65, $CHCl_3$)

9: ^{1}H NMR (numbering as for **4**): δ = 0.86 (t, 3H, J = 7 Hz, 11-H), 0.99 (d, 3H, J = 7 Hz, 4-CH_3) 1.16–1.66 (m, 6H, 8-H, 9-H, 10-H), 1.40, 1.44 (each s, each 3H, isopropylidene-CH_3), 2.06 (m, 1H, 4-H), 2.42 (ddd, 1H, J = 10, 6.5, 4 Hz 5-H), 3.07 (s, 1H, OH), 3.40 (mc, 5H, 6-H, 7-H, MOM-CH_3), 3.62 (dd, 1H, J = 7, 4 Hz, 3-H), 3.75 (dd, 1H, J = 8.8 Hz, 1-H), 4.07 (dd, 1H, J = 8, 7 Hz, 1-H), 4.36 (ddd, 1H, J = 8, 7, 7 Hz, 2-H), AB system: δ_A = 4.59, δ_B = 4.70 (2H, J_{AB} = 7 Hz, MOM-CH_2), AB system: δ_A = 4.63, δ_B = 4.78 (2H, J_{AB} = 12 Hz, Ph-CH_2), 5.00 (dd, 1H, J = 17.5, 2 Hz, vinyl-CH_2), 5.18 (dd, 1H, J = 10, 2 Hz, vinyl-CH_2), 5.86 (ddd, 1H, J = 17.5, 10, 10 Hz, vinyl-CH), 7.33 (mc, 5H, aryl-H). ^{13}C-NMR: δ = 13.83, 15.23, 22.82, 25.64, 26.61, 27.14, 30.60, 37.12, 47.04, 55.85, 66.65, 73.70, 73.74, 78.24, 82.77, 82.84, 97.74, 108.94, 117.85, 127.32, 127.70, 128.17, 136.73, 139.24. $[\alpha]_D^{20}$ = +26 (c = 1.66, $CHCl_3$)

The all-*syn* arrangement[7] at the chirality centers C-4 to C-6 in **4** can be explained as follows. The relative configuration at C-4/5 is the result of the diastereofacial control exercised by the chirality centers of **2** which can be interpreted in terms of a Felkin-Anh-analogous transition state **7**.[8] The

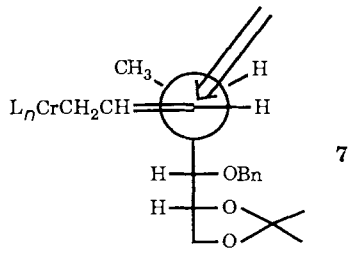

7

relative configuration at C-5/6 corresponds to the normal "simple diastereoselection" of the Hiyama reaction.[9] Since C-7 is introduced into the reaction with a given configuration, the *syn*-arrangement at C-6/7 follows automatically, which is contrary to the stereochemical course of the Hiyama addition of *achiral* allyl bromides to α-alkoxyaldehydes.[10] The formation of **4** is therefore a case of double stereodifferentiation with mismatched reactants.[11] The influence of the allyl bromide surpasses by far that of the aldehyde. After debenzylation and hydrolysis of the acetal moiety the triol unit of **4** is oxidatively degraded and the compound two C-atoms shorter is converted into the lactol, which can be oxidized quantitatively to the lactone **5** (Table 1). The second

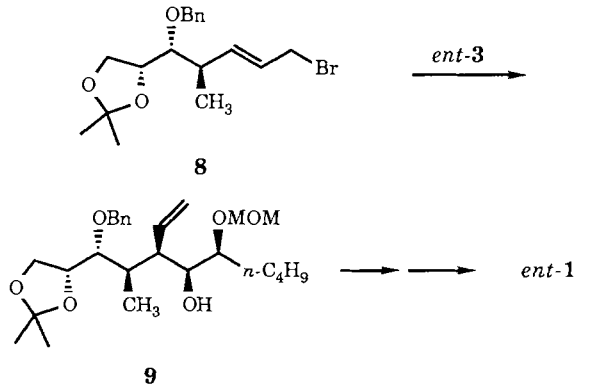

lactone ring is obtained by oxidative cleavage of the vinyl group. According to its melting point, rotation, and ^{1}H-/^{13}C-NMR data (Table 1) the product thus obtained is identical with the natural product,[12] whose structure was thus confirmed for the first time. Access to the enantiomer was accomplished by Hiyama addition of the allyl bromide derivative **8** to *ent*-**3**,[5] which affords the adduct **9** in >97% diastereomeric purity (Table 1). **9** is converted into *ent*-**1** analogously to the conversion of **4** into **1**.

Received: February 13, 1990 [Z 3795 IE]
German version: *Angew. Chem. 102* (1990) 717

[1] N. J. McCorkindale, J. L. C. Wright, P. W. Brian, S. M. Clarke, S. A. Hutchinson, *Tetrahedron Lett. 1968*, 727.
[2] M. Kato, M. Kageyama, R. Tanaka, K. Kuwahara, A. Yoshikoshi, *J. Org. Chem. 40* (1975) 1932.
[3] R. C. Anderson, B. Fraser-Reid, *Tetrahedron Lett. 1978*, 3233.
[4] a) Y. Okude, S. Hirano, T. Hiyama, H. Nozaki, *J. Am. Chem. Soc. 99* (1977) 3179; b) T. Hiyama, K. Kimura, H. Nozaki, *Tetrahedron Lett. 22* (1981) 1037; c) T. Hiyama, Y. Okude, K. Kimura, H. Nozaki, *Bull. Chem. Soc. Jpn. 55* (1982) 561.
[5] We shall report elsewhere on the syntheses of **2**, **3**, *ent*-**3**, and **8** from (*R*)-isopropylideneglycerinaldehyde, which largely involve routine steps.
[6] For a cyclic-chiral Hiyama reagent see S. Hatakeyama, H. Numata, K. Osanai, S. Takano, *J. Org. Chem. 54* (1989) 3515.
[7] We use the Masamune nomenclature: S. Masamune, S. A. Ali, D. L. Snitman, D. S. Garvey, *Angew. Chem. 92* (1980) 573; *Angew. Chem. Int. Ed. Engl. 19* (1980) 557.
[8] For a discussion of the Felkin-Anh-Model see J. Mulzer, *Nachr. Chem. Tech. Lab. 32* (1984) 16.
[9] C. T. Buse, C. H. Heathcock, *Tetrahedron Lett. 1978*, 1685.
[10] J. Mulzer, T. Schulze, A. Strecker, W. Denzer, *J. Org. Chem. 53* (1988) 4098.
[11] S. Masamune, W. Choy, J. S. Petersen, L. R. Sita, *Angew. Chem. 97* (1985) 1; *Angew. Chem. Int. Ed. Engl. 24* (1985) 1.
[12] In [1]: m.p. 94–94.5 °C, $[\alpha]_D^{20}$ = −31 (CH_3OH). We thank Dr. *McCorkindale*, University of Glasgow, for an authentic sample.

Synthesis of Enantiomerically Pure (−)-Hypnophilin**

By *Klaus Weinges,* Uwe Dietz, Thomas Oeser,* and *Hermann Irngartinger*

In 1981 *Steglich* et al.[1] described the isolation, structure determination, and biological properties of (−)-hypnophilin

[*] Prof. Dr. K. Weinges, Dipl.-Chem. U. Dietz, Dipl.-Chem. T. Oeser[+], Prof. Dr. H. Irngartinger[+]
Organisch-Chemisches Institut der Universität
Im Neuenheimer Feld 270, D-6900 Heidelberg 1 (FRG)
[+] X-ray structure analysis.

[**] Chemistry and Stereochemistry of the Iridoids, Part 12. This work was supported by the Deutsche Forschungsgemeinschaft – Part 11: [3].

10, a sesquiterpene with triquinane structure. Two recent communications[2] concerning the synthesis of racemic **10** have motivated us to report the synthesis of enantiomerically pure **10** from catalpol **1**.

Catalpol **1** can be converted by simple reactions into all-(*R*)-**2** (Scheme 1), whose constitution and absolute configuration have been confirmed by an X-ray structure analysis.[3]

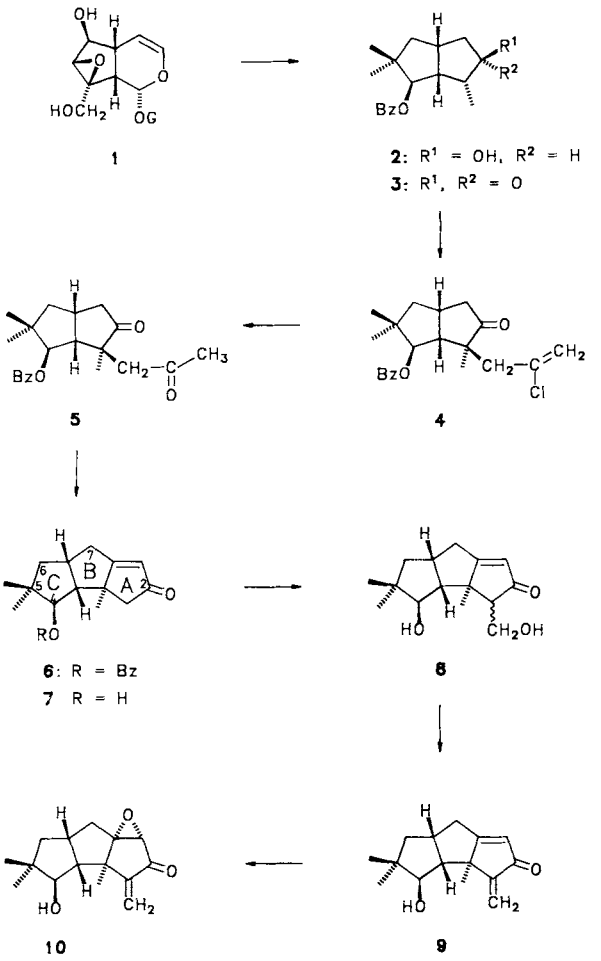

Scheme 1. **1** → **2**: [3]; **2** → **3**: pyridinium chlorochromate (PCC), $NaOCOCH_3$, CH_2Cl_2, room temperature (RT), 4 h, 85%; **3** → **4**: 2,3-dichloropropene, *t*BuOK, *t*BuOH, C_6H_6, 80 °C, 2.5 h, 60%; **4** → **5**: $Hg(CF_3CO_2)_2$, CH_2Cl_2, RT, 45 min, 80%; **5** → **6**: *t*BuOK, *t*BuOH, 35 °C, 15 min, 85%; **6** → **7**: NaOH, MeOH, 80 °C, 12 h, 78%; **7** → **8**: lithium diisopropylamide (LDA), THF, CH_2O, −78 °C bis −30 °C, 10 min, 73%; **8** → **9**: *p*-toluenesulfonchloride, pyridine, CH_2Cl_2, RT, 4 d, 1,8-diazabicyclo[5.4.0]undec-7-ene (DBU), RT, 2 h, 75%; **9** → **10**: H_2O_2, K_2CO_3, CH_2Cl_2, RT, 2 d, 51%. Bz = benzoyl, G = glucosyl.

Oxidation of **2** with pyridinium chlorochromate in dichloromethane affords the crystalline ketone **3**. Alkylation of **3** with 2,3-dichloropropene leads to **4**, which is hydrolyzed with mercury(II) trifluoroacetate in dichloromethane within 45 min to the diketone **5**. This reaction has already been carried out on several α-(chlorobutenyl)cycloalkanones by *Matsumoto* et al.,[4] and proceeds in high yields. Aldol condensation of **5** affords the triquinane derivative **6**. The ester group is subsequently hydrolyzed with sodium hydroxide at 80 °C. Condensation and hydrolysis can also be carried out in one reaction step; however, the yield of **7** is then lowered. Hydroxymethylation, removal of water and epoxidation lead via **8** and **9** to enantiomerically pure (−)-hypnophilin **10**. The physical data (specific rotation, CD, and IR, ^{1}H-NMR, ^{13}C-NMR and mass spectra) of **10** are identical with those of the natural product.[1b] Hypnophilin is a colorless oil and decomposes after a few days (monitored chromatographically (TLC)). For this reason we have prepared the intermediate **9**, which is crystalline and stable, in larger amounts and epoxidized it to **10** when required.

The cyclopenta[*a*]pentalene derivative **7** (correct elemental analysis) is crystalline (m.p. 102 °C) and has a specific rotation of + 34 (c = 1 in $CHCl_3$). The IR and ^{1}H-NMR spectra are in good agreement with those for racemic **7**.[2a] The ^{13}C-NMR signals[5] are consistent with the constitution quoted for **7**. Compound **7** has already been described as intermediate in the total synthesis of enantiomerically pure (−)-coriolin; in this case, however, a specific rotation of − 115.4 (c = 0.2 in $CHCl_3$) was quoted.[6] The large difference in the values of rotation made an X-ray structure analysis necessary. Since the absolute configuration of **2** was confirmed by X-ray diffraction,[3] the absolute configurations at C3b and C6a of **7** must also be confirmed because no reaction was carried out at these C atoms. Relative to these, an *S*-configuration was found for C3a and an *R*-configuration for C4. The rings A and C are attached *anti* to each other, corresponding to the sterically most favorable conformation (Fig. 1). Ring C assumes an almost flat envelope conformation with a folding angle of 36.6° between the planes C4/C3b/C6a/C6 and C4/C5/C6. Due to the enone structure, ring A is planar within a maximum deviation of 0.08 Å, and the central ring has a slightly twisted envelope shape. The bond angles and bond lengths are, within the limits of error, as would be expected.[7]

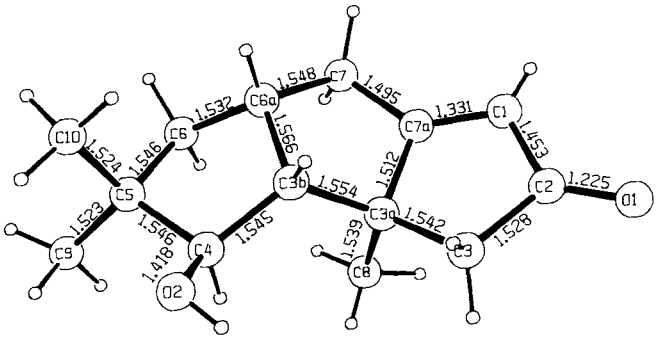

Fig. 1. Crystal structure of **7** with bond lengths [A°] (standard deviation 0.003-0.004 Å) [8].

Received: February 14, 1990 [Z 3797 IE]
German version: *Angew. Chem. 102* (1990) 685

CAS Registry numbers:
1, 2415-24-9; **2**, 119433-11-3; **3**, 127060-82-6; **4**, 127060-83-7; **5**, 127060-84-8; **6**, 127001-14-3; **7**, 102628-62-6; **8**, 127000-11-7; **9**, 127000-12-8; **10**, 80677-96-9.

[1] a) J. Kupka, T. Anke, B.-M. Giannetti, W. Steglich, *Arch. Microbiol. 130* (1981) 223; b) B.-M. Giannetti, B. Steffan, W. Steglich, J. Kupka, T. Anke, *Tetrahedron 42* (1986) 3587; c) W. Steglich, *Pure Appl. Chem. 53* (1981) 1233.

[2] a) L. Van Hijfte, R. D. Little, J. L. Petersen, K. D. Moeller, *J. Org. Chem. 52* (1987) 4647; b) T. L. Fevig, R. L. Elliott, D. P. Curran, *J. Am. Chem. Soc. 110* (1988) 5064.

[3] K. Weinges, H. Iatridou, H.-G. Stammler, J. Weiss, *Angew. Chem. 101* (1989) 485; *Angew. Chem. Int. Ed. Engl. 28* (1989) 447.

[4] H. Yoshioka, K. Takasaki, M. Kobayashi, T. Matsumoto, *Tetrahedron Lett. 1979*, 3489.

[5] ^{13}C-NMR spectrum (75.46 MHz, $CDCl_3$) of **7**: δ = 19.86, 24.88, 26.54 (3q;3 CH_3), 33.30 (t; C-6), 40.17 (d; C-6a), 45.45 (s; C-5), 46.54 (t;C-7), 48.13 (s; C-3a), 53.39 (t; C-3), 56.87 (d; C-3b), 80.94 (d; C-4), 122.33 (d; C-1), 194.09 (s; C-7a), 210.61 (s; C-2).

[6] M. Demuth, P. Ritterskamp, E. Weigt, K. Schaffner, *J. Am. Chem. Soc. 108* (1986) 4149. In this work formula **18** is identical with that quoted by us for formula **7**. Unfortunately, in the Experimental Section the *R/S* nomenclature for **18** has been used incorrectly.

[7] F. H. Allen, O. Kennard, D. G. Watson, L. Brammer, A. G. Orpen, R. Taylor, *J. Chem. Soc. Perkin Trans. 2, 1987*, S1.

[8] X-ray structure analysis of **7**: crystal dimensions 0.3 × 0.3 × 0.5 mm. Space group $P2_12_12_1$, Z = 4, a = 7.200(1), b = 12.855(3), c = 13.440(3) Å, V = 1244.0(7) Å^3, ϱ_{calcd} = 1.176 Mgm^{-3}. CAD4 diffractometer (Enraf-Nonius), graphite monochromator, $Mo_{K\alpha}$ radiation, $\omega - 2\theta$ scan in the range to $\sin\theta/\lambda^{-1}$ = 0.661 Å^{-1}. The structure was solved with the program MULTAN 11/82 [P. Main, S. J. Fiske, S. E. Hull, L. Lessinger, G. Germain, J.-P. Declereq, M. M. Woolfson, York (England)] and refined in a full matrix method (C and O anisotropically, hydrogen atom positions localized by difference Fourier syntheses and subsequently refined isotropically). Lorentz and polarization corrections were carried out. R = 0.043 (R_w = 0.053). All calculations were carried out with the SDP Program packet [B A. Frenz and Ass., Inc., College Station Texas (USA) and Enraf-Nonius, Delft (Holland) 1982]. Further details of the crystal structure investigation are available on request from the Fachinformationszentrum Karlsruhe, Gesellschaft für wissenschaftlich-technische Information mbH, D-7514 Eggenstein-Leopoldshafen 2 (FRG), on quoting the depository number CSD-54515, the names of the authors, and the journal citation.

scavenging reagents, except for a more recent result where the reaction of *tert*-butyllithium with tmpB(Cl)PHAryl led to the boranylphosphanide [tmp(*t*Bu)BPAryl]Li (tmp = 2,2,6,6-tetramethylpiperidino; Aryl = 2,4,6-tBu$_3$C$_6$H$_2$).[9]

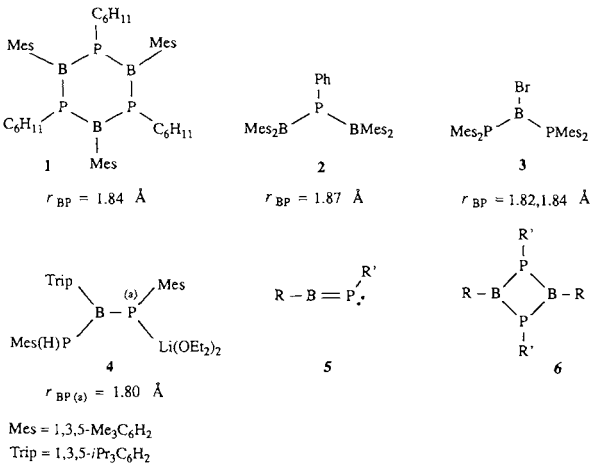

An Allene-analogous Boranylidenephosphane with B=P Double Bond: 1,1-Diethylpropyl(2,2,6,6-tetramethylpiperidino)-boranylidenephosphane-*P*-pentacarbonylchromium

By *Gerald Linti, Heinrich Nöth*, Kurt Polborn*, and *R. T. Paine*

Compounds of boron with coordination number 2 are stabilized electronically by multiple bonds. However, in most cases additional sterically bulky substituents are necessary to suppress oligomerization. Examples are provided by boroxanes R–B≡O featuring a B≡O triple bond,[1] imino- and aminoiminoboranes RB≡NR'[2] and R_2N–B≡NR'[3] respectively, characterized by B≡N triple bonds, and alkylidene boranes containing a B=C double bond.[4] That elements of the third row of the periodic table such as phosphorus are also capable of forming multiple bonds to boron can be seen in formulas **1**–**4**.[5–8]

The planar triphosphatriborinane ring **1** with planar tricoordinated phosphorus atoms and relatively short B–P bonds (average: 1.84 Å) provides convincing evidence of this type of bonding. Planar coordinated phosphorus atoms are also present in the diborylphosphane **2** and in the borylated lithium phosphide **4**, while the phosphorus atoms in **3** exhibit a slightly pyramidal coordination. A common feature of these four compounds is the presence of tricoordinated boron atoms.

In spite of the introduction of very bulky substituents R and R', the preparation of boranylidene phosphanes **5** was still not possible. Their attempted synthesis led to the 1,3,2,4-diphosphadiboretane dimers **6**.[5] Also, the fleeting existence of **5** as an intermediate could not be clearly identified with

Apparently, the substituents selected up to now have been insufficient for a kinetic stabilization of a boranylidenephosphane **5**. Therefore, we tried to enhance steric shielding at the phosphorus atom in **5** by introducing an additional bulky ligand. For this purpose compounds of type **6** were treated with [(CO)$_5$Cr(thf)] at ambient temperature.[10] With **7**[11] as an example, ring cleavage results in the formation of the yellow 1,1-diethylpropyl-(2,2,6,6-tetramethylpiperidino)boranylidenephosphane **8**, complexed at P, in high yields [Eq. (a)].

In contrast, the sterically less hindered diphosphadiboretane **9**[12] reacts with $Cr(CO)_6$ under photolytic conditions to give only complex **10** [Eq. (b)]. This difference in the course of two comparable reactions is reflected in the mass spectra of **7** and **9**. The radical cation $(tmpB{=}PCEt_3)^{\oplus}$ is the base peak in **7**; i.e., the diphosphadiboretane has dissociated to a boranylidene phosphane, while no monomeric $(Me_2NB{=}PCMe_3)^{\cdot\oplus}$ is observed during the fragmentation of **9**.[12]

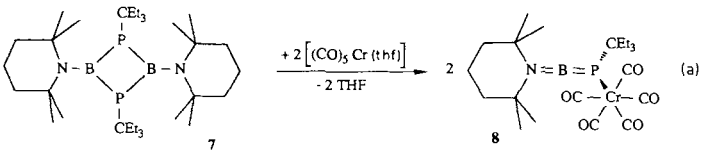

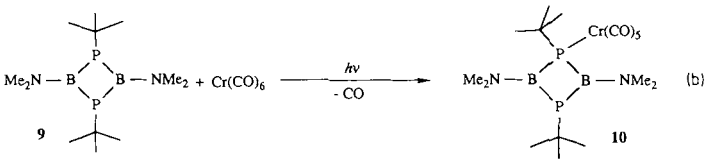

Compared with **7** there is little change in the shielding of the boron atom in **8** ($\Delta\delta^{11}$B = 3). δ^{31}P exhibits a more pronounced upfield shift ($\Delta\delta$ = 25). ^{1}H-NMR and ^{13}C-NMR spectra suggest that the molecule **8** is fairly symmetrical. However, a convincing prediction for the structure of **8** can-

[*] Prof. Dr. H. Nöth, Dr. G. Linti, Dr. K. Polborn
Institut für Anorganische Chemie der Universität
Meiserstrasse 1, D-8000 München 2 (FRG)
Prof. Dr. R. T. Paine
Department of Chemistry, University of Albuquerque
New Mexico (USA)

not be put forward solely on the basis of NMR data. If there is a true p(π)–p(π) bond between boron and phosphorus in **8**, then one must expect an allene type structure for $(tmp)=B=P(CEt_3)Cr(CO)_5$ as is found in the N-analogue $(tmp)=B=N(CMe_3)Cr(CO)_5$.[13] The X-ray structure analysis,[14] depicted in Figure 1, shows an almost linear arrangement for the NBP unit (176.1(3)°) and a nearly orthogonal arrangement for C1NC5 and CrPC10 (angle between the normals to the planes: 96.0°) (Fig. 1). The very short B–N

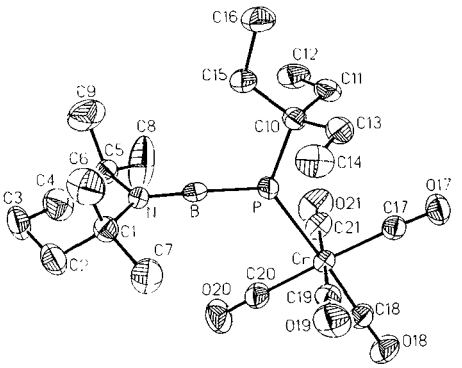

Fig. 1. Crystal structure of **8** (in ORTEP, thermal ellipsoides represent a 30% probability, hydrogen atoms are not shown). Selected bond lengths [Å] and angles [ ]: B-P 1.743(5), B–N 1.339(5), P–C10 1.885(4), P–Cr 2.420(1); N-B-P 176.1(3), B-P-C10 109.0(2), B-P-Cr 123.1(2), C10-P-Cr 127.6(1), B-N-C1 119.8(3). B-N-C5 120.0(3).

bond (1.339(5) Å) is consistent with the presence of a B=N double bond. The B–P bond length (1.743(5) Å) is 0.06 Å shorter than the shortest B–P bond length with double bond character reported for **4** (for a more recent value see Ref. [15]), and 0.18 Å shorter than the B–P bond length in **7**;[11] this corresponds with a change from a single to a double bond. Consistent with the presence of a B=P double bond, the sum of the bond angles at the phosphorus atom is, within experimental error, 360°, suggesting sp^2 hybridization. However, due to the significantly different steric requirements of the substituents at the phosphorus atom, the BPC6 bond angle deviates strongly (109.0°) from the ideal 120° expected for sp^2 hybridization. It follows that the $Cr(CO)_5$ group adds to the steric shielding of the boron atom by pushing the 1,1-diethylpropyl group toward the N=B=P system. A comparable situation to **8** exists in the isoelectronic phosphaallene complex $Ph_2C=C=P(Aryl)Ni(CO)_3$;[16] its allene skeleton remains almost unchanged compared to the free phosphaallene ligand.[17]

MNDO calculations predict for the dimerization of boranylidenephosphanes **5** (R = R′ = H, CH_3) to 1,3,2,4-diphosphadiboretanes **6** an energy barrier of only 21 kJ mol^{-1}. This barrier is more than 80 kJ mol^{-1} lower than for the dimerization of iminoboranes RN≡BR′.[18] One of the reasons for this energy difference is that the bent structure of boranylidenephosphanes in the ground state differs markedly from the linear structure of iminoboranes.[10] Nevertheless, boranylidenephosphanes carrying less bulky groups should be able to be generated in the gas phase[10] because gaseous boranylidenesulfanes of type X–B=S (X = H, F, Cl, CH_3)[19] are already well characterized. The existence of these sulfur compounds as intermediates in solution is ascertained by scavenging reactions.[20] A kinetic stabilization of boranylidenesulfanes by bulky substituents, in analogy with boranylidenephosphanes **5**, will be much more difficult. However, the present results are a promising sign that boranylidenesilanes $RB=SiR'_2$ will become accessible.[21]

Experimental

8: A solution of 1.52 g (6.9 mmol) of $Cr(CO)_6$ in 50 mL of THF was irradiated with a mercury lamp (Hanovia S 200 W). After evolution of gas ceased, a solution containing 0.67 g (1.19 mmol) of **7** in 20 mL of hexane was added. The course of the reaction was monitored by ^{31}P NMR. Five days were required for completion of the reaction. All volatile components were then removed *in vacuo* from the red-orange solution. Extraction of the residue with 50 mL of pentane furnished a yellow solution from which 0.97 g (86%) of **8** crystallized out at 20 °C as intensely yellow prisms; m.p. 95–98 °C. NMR data (C_6D_6, 25 °C, Bruker AC 200): $\delta^{11}B = 62.9$ ($h_{1/2} = 540$ Hz); $\delta^{31}P = -45.3$ ($h_{1/2} = 340$ Hz); $\delta^{13}C = 218.3$ (d, $^2J(P,C) = 14$ Hz, *cis*-CO), 211.5 (*trans*-CO), 55.9 (*d*, $^3J(P,C) = 8$ Hz, C-1,5), 37.9 (C-2,4), 33.4 (d, $^4J(P,C\text{-}6) = 3$ Hz), 32.4 (d, $^4J(P,C\text{-}9) = 2$ Hz, 16.5 (C-4), 46.6 (d, $^1J(P,C\text{-}10) = 5$ Hz, 30.3 (d, $^2J(P,C\text{-}11) = 4$ Hz, 9.3 (d, $^3J(P,C\text{-}12) = 5$ Hz); $\delta^1H = 1.32$, 1.16 (6H each, $NCCH_3$) 1.06 (6H, $NCCH_3$), 1.53 (m, 6H, $PCCH_2$ H-11), 0.89 (t, 9H, $^3J(H,H) = 7$ Hz $PCCH_2CH_3$).

10: An ice cooled suspension of 0.31 g (1.1 mmol) of **9** and 0.58 g (2.7 mmol) of $Cr(CO)_6$ in 30 mL of hexane was irradiated with a mercury lamp (Hanovia S 200 W) for one hour. CO evolution ceased after this time and 1.2 mmol of CO were collected. Addition of 5 mL of THF to the solution and additional irradiation set free another 0.8 mmol of CO. After removal of all volatiles *in vacuo* the residue was extracted with 20 mL of hexane. On cooling the extract to −78 °C the product precipitated as a sand-colored powder. Yield: 0.36 g, 70%; m.p. 120 °C (dec.). NMR data (C_6D_6, 25 °C, Bruker AC 200): $\delta^{11}B = 45.9$ ($h_{1/2} = 300$ Hz); $\delta^{31}P = -34.5$, −42.0 ($h_{1/2}$ 300 Hz each); $\delta^{13}C = 45.6$ (t, $^3J(P,C) = 8$ Hz, NMe_2), 45.3 (dd, $^3J(P_a,C) = 6$, $^3J(P_b,C) = 8$ Hz, NMe_2), 35.9 (d, $^2J(P,C) = 7$ Hz, CMe_3), 32.9 (d, $^2J(P_a,C) = 5$ Hz, CMe_3), quarternary C-atoms not observed since the DEPT sequence was used; $\delta^1H = 2.82$ (d, $^4J(P,H) = 1.5$ Hz, NMe_2), 2.68 (s, NMe_2), 1.30, 1.15 (each a dd, $^3J(P,H) = 9.5$, $^5J(P,H) = 0.5$ Hz, CMe_3).

Received: December 29, 1989 [Z 3715 IE]
German version: *Angew. Chem. 102* (1990) 715

CAS Registry numbers:
7, 102651-91-2; **8**, 126821-93-0; **9**, 112438-33-2; **10**, 126821-94-1; $Cr(CO)_5THF$, 15038-41-2; $Cr(CO)_6$, 13007-92-6.

[1] M. Groteklaes, P. Paetzold, *Chem. Ber. 121* (1988) 809; K. Kawaguchi, Y. Endo, E. Hirota, *J. Mol. Spectrosc. 93* (1982) 38; D. C. Frost, C. Kirby, W. M. Lau, A. McDowell, W. P. C. Westwood, *J. Mol. Struct. 100* (1983) 87.
[2] P. Paetzold, *Adv. Inorg. Chem. 31* (1987) 123.
[3] H. Nöth, *Angew. Chem. 100* (1988) 1664; *Angew. Chem. Int. Ed. Engl. 27* (1988) 1603.
[4] H. Klusik, A. Berndt, *Angew. Chem. 95* (1983) 895; *Angew. Chem. Int. Ed. Engl. 22* (1983) 877; G. Maier, J. Henkelmann, H. P. Reisenauer, *Angew. Chem. 97* (1985) 1061, *Angew. Chem. Int. Ed. Engl. 24* (1985) 1065; B. Glaser, H. Nöth, *Angew. Chem. 97* (1985) 424; *Angew. Chem. Int. Ed. Engl. 24* (1985) 416; B. Glaser, E. Hanecker, H. Nöth, B. Wagner, *Chem. Ber. 100* (1987) 659; R. Boese, P. Paetzold, A. Tapper, *Chem. Ber. 120* (1987) 1069.
[5] H. V. R. Dias, P. P. Power, *J. Am. Chem. Soc. 111* (1989) 114; *Angew. Chem. 99* (1987) 1320; *Angew. Chem. Int. Ed. Engl. 26* (1987) 1270; R. A. Bartlett, H. V. R. Dias, X. Feng, P. P. Power, *J. Am. Chem. Soc. 111* (1989) 1306.
[6] R. A. Bartlett, H. V. R. Dias, P. P. Power, *Inorg. Chem. 27* (1988) 3919.
[7] H. Karsch, G. Hanika, B. Huber, K, Meindl, S. König, C. Krüger, G. Müller, *J. Chem. Soc. Chem. Commun. 1989*, 373.
[8] R. A. Bartlett, X. Feng, P. P. Power, *J. Am. Chem. Soc. 108* (1986) 6817.
[9] C. Courét, J. Escudie, B. Garrigues, M. Lazraq, J. Satgé, *Can. J. Chem. 65* (1987) 1230.
[10] A. H. Cowley, *Phosphorus Sulfur 30* (1987) 129; A. M. Arif, J. E. Boggs, A. H. Cowley, J. G. Lee, M. Pakulski, J. M. Power, *J. Am. Chem. Soc. 108* (1986) 6083; in this work $tmpBPC_6H_2tBu_3$ is identified as a thermolysis product by mass spectrometry, and a reaction between $(tmp\ BPC_6H_2tBu_3)_2$ and $Fe_2(CO)_9$ is mentioned; however, the products were not characterized.
[11] P. Kölle, H. Nöth, R. T. Paine, *Chem. Ber. 199* (1986) 2681.
[12] P. Kölle, G. Linti, H. Nöth, G. L. Wood, C. K. Narula, R. T. Paine, *Chem. Ber. 121* (1988) 871.
[13] U. Wietelmann, Dissertation, Universität München 1986.
[14] Data for the X-ray structure determination of **8**: Single crystals were mounted in glass capillaries under argon. An Enraf-Nonius CAD4-diffractometer was used with graphite monochromatated $Mo_{K\alpha}$-radiation (λ = 0.71069 Å). A DEC-VAX II computer and the SHELXTL PLUS software package were used for all calculations. $C_{21}H_{33}BCrNO_5P$, M = 473.3, size of single crystal: 0.2 × 0.45 × 0.35 mm, temperature 20 °C, monoclinic,

space group $P2_1/n$, $a = 11.015(2)$, $b = 14.851(2)$, $c = 15.752(2)$ Å, $\beta = 91.22(2)°$, $V = 2576.3(5)$ Å^3, $\varrho = 1.22$ g cm^{-3}, $Z = 4$, $\mu = 5.21$ cm^{-1}. ω-scan, range: $2\theta = 4-46°$ in $\pm hkl$, scan width: $0.8 + 0.35 \tan\theta$, variable scan speed: 90 s max., 3802 reflections collected, internal consistency: 0.019, 3317 unique reflections, 2891 reflections considered observed with $F \geq 4\sigma(F)$. Structure solution with direct methods, anisotropic decription of non-hydrogen atoms, isotropic description of H-atoms. $R = 0.052$, $R_w = 0.055$ with $w^{-1} = \sigma^2(F) + .000235\,F^2$, highest $\Delta/\sigma = 0.048$, highest residual electron density: 0.68 e/Å^3.—Further details of the crystal structure determination are available from the Fachinformationszentrum Karlsruhe, Gesellschaft für wissenschaftlich-technische Information mbH, D-7514 Eggenstein-Leopoldshafen 2 (FRG), on quoting the depository number CSD-54482, the names of the authors, and the journal citation.

[15] K_3BP_2 contains a linear P = B = P anion, related to **8**, its B–P bond length being 1.767 Å, which is somewhat longer than in **8**: H. G. von Schnering, M. Somer, M. Hartweg, K. Peters, *Angew. Chem. 102* (1990) 63; *Angew. Chem. Int. Ed. Engl. 29* (1990) 65.

[16] R. Appel, F. Knoch, V. Winkhaus, *J. Organomet. Chem. 307* (1986) 93.

[17] R. Appel, P. Fölling, B. Josten, M. Siray, V. Winkhaus, F. Knoch, *Angew. Chem. 96* (1984) 620; *Angew. Chem. Int. Ed. Engl. 23* (1984) 619.

[18] P. Kölle, *Dissertation*, Universität München 1987.

[19] R. W. Kirk, P. L. Timms, *J. Chem. Soc. Chem. Commun. 1967*, 18; E. F. Pearson, R. V. McCormick, *J. Chem. Phys. 58* (1973) 1619; E. F. Pearson, C. L. Norris, W. H. Flygare, *ibid. 60* (1974) 1761; H. W. Kroto, R. J. Suffolk, N. P. C. Westwood, *Chem.-Phys. Lett. 22* (1973) 495; C. Kirby, H. W. Kroto, M. J. Taylor, *J. Chem. Soc. Chem. Commun. 1978*, 19; C. Kirby, H. W. Kroto, *J. Mol. Spectrosc. 83* (1980) 1.

[20] W. Rattay, *Dissertation*, Universität München 1985.

[21] V. Hyna, *Dissertation*, Universität München 1989.

Measuring the Optical Activity of Chiral Imprints in Insoluble Highly Cross-linked Polymers**

By *Günter Wulff** and *Günter Kirstein*

In recent years there has been increasing interest in the technique of using template molecules to produce imprints in cross-linked polymers, then applying these for molecular recognition purposes.[1, 2] To prepare these, polymerizable monomer molecules possessing suitable binding groups are first attached to template molecules. The "template monomer" is then converted into a macroporous polymer by polymerizing in the presence of a large excess of a cross-linking agent. The template can then be removed, leaving microvoids in the polymer; the shape of the voids and the configuration of the binding groups are determined by the template molecule. For example, the template monomer **1** (consisting of phenyl-α-D-mannopyranoside **2** as a template and two 4-vinylphenylboronic acid residues attached by esterification

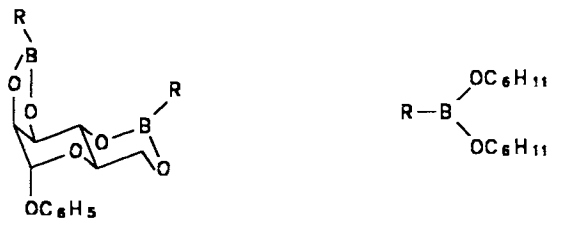

1 **3**

[*] Prof. Dr. G. Wulff, Dr. G. Kirstein
Institut für Organische Chemie und Makromolekulare Chemie der Universität
Universitätsstrasse 1, D-4000 Düsseldorf (FRG)

[**] Polymers with Enzyme-Analogous Structures, Paper 28. This work was supported by the Deutsche Forschungsgemeinschaft and the Fonds der Chemischen Industrie. Paper 27: [1c].

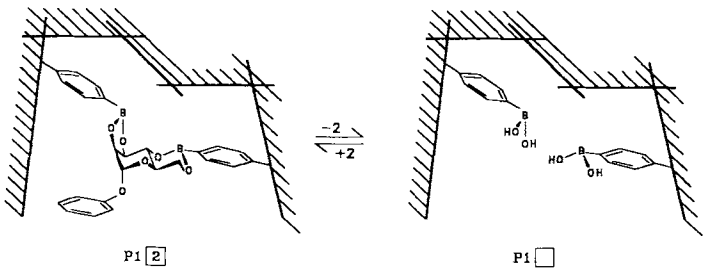

Scheme 1.

as binding groups) can be converted into the polymer **P-1-2**. After detaching the template **2** the polymer **P-1-□**, whose voids each contain two projecting free boronic acid groups, is obtained (see Scheme 1). This polymer can be used to achieve highly selective chiral separations of both the racemate of the template **2**[3] and D,L-mannose.[1c]

As these polymers are completely insoluble the chiral voids cannot be characterized by direct methods, and the usual method of investigating the racemate separation behavior only gives indirect information. If chiroptical measurements could be made on such polymers this would certainly make possible major advances. *Vogl, Pino* et al.[4] have recently described a method for measuring the optical rotation of helical atropisomeric polymers in the solid phase. We have investigated the possibility of applying this method to macroporous polymers with chiral voids, and of using it, for example, to determine the contribution of the chiral imprints to the specific rotation for the polymers **P-1-2** and **P-1-□**.

To measure the specific rotation of a solid it must be examined as a suspension in a medium whose refractive index is as close as possible to that of the substance being investigated. Where measurements are made in media with different refractive indices (Fig. 1), different values are obtained for the

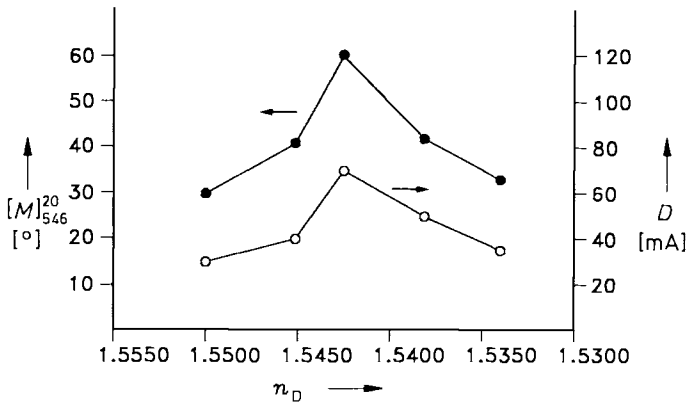

Fig. 1. Molar optical rotation $[M]^{20}_{546}$ and optical transmission D (measured in *mA* obtained from a photomultiplier) for suspensions of **P-1-2** in media with different refractive indices [5]. $c = 2.0$.

optical transmission D and the specific rotation. Only in the optimum range with 80–95% transmission does one obtain the maximum, and correct, value for the specific rotation of the substance.[4] To test the reliability of such measurements, the refractive index of the medium was adjusted to the optimum value and the molar optical rotation was measured as a function of the concentration (Fig. 2). It is also important that the density of the medium should be as similar as possible to that of the solid, so as to avoid sedimentation.[4, 5] Since birefringence effects can be mistaken for optical rota-

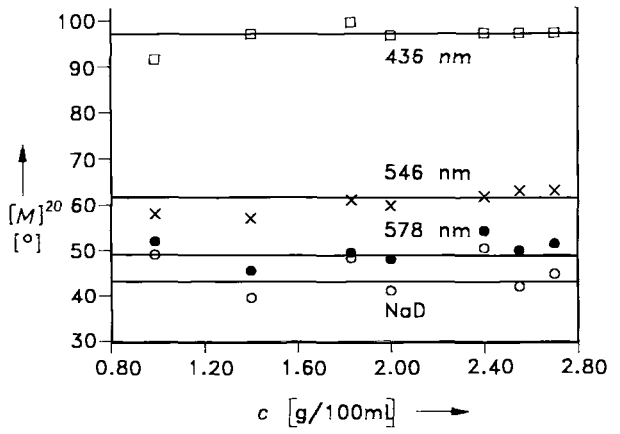

Fig. 2. Molar optical rotation of **P-1-[2]** as a function of suspension concentration c in a medium with a refractive index $n_D^{20} = 1.5424$. The average molar rotation values $\bar{x}$ and the standard deviations σ for the measurements at each wavelength are as follows: 436 nm: $\bar{x} = 97.1°$, $\sigma = 2.4°$; 546 nm: $\bar{x} = 61.7°$, $\sigma = 3.1°$; 578 nm: $\bar{x} = 48.7°$, $\sigma = 3.0°$; Na D-line: $\bar{x} = 43.3°$, $\sigma = 3.9°$.

tions,[4] an achiral macroporous polymer, which was otherwise similar to the polymers **P-1-[2]** and **P-1-□** was first prepared from the monomer **3**. From this polymer **P-3-[4]** the cyclohexanol moiety **4** was then detached to give the polymer **P-3-□**. Neither polymer showed any optical rotation under optimal measurement conditions.[5] The achiral polymer **P-3-□**, with free boronic acid groups, was then esterified by reacting in turn with an excess of (*S*)- or of (*R*)-1-phenyl-1,2-ethanediol, [(*S*)-**5** and (*R*)-**5** respectively], achieving esterification of about 96% of the boronic acid groups. Optical rotation measurements were then made on this polymer also (see Table 1). The observed molar rotation values $[M]_{546}^{20}$ for the polymers containing the (*S*) and (*R*) enantiomers were + 357° and − 366° respectively, thus giving absolute values which are identical within the limits of error, and are also of the same order of magnitude as the molar rotation value for the corresponding monomeric phenyl ester **6**. From these results one may proceed on the assumption that optical rotation values can be determined with reasonable accuracy on highly cross-linked macroporous polymers. It appears that the achiral matrix has only a small effect on the contribution of optically active side-groups to the observed rotation values.

Table 1. Optical rotation values for achiral polymers after reacting with optically active diols, and for reference samples [a].

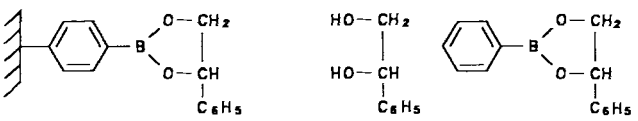

		P-3-[5]	5	6
$[\alpha]_{546}^{20}$	(*S*)	+ 23.4 ± 1°	+ 72.0° (95.0% *ee*)	+ 159.0°
	(*R*)	− 24.0 ± 1°	− 72.6° (95.8% *ee*)	-
$[M]_{546}^{20}$	(*S*)	+ 357 ± 15°	+ 99.5°	+ 356.3°
	(*R*)	− 366 ± 15°	− 100.3°	-

[a] Macroporous polymer **P-3-[5]** prepared by removing the cyclohexanol residues from **P-3-[4]** then loading with (*S*)- or (*R*)-1-phenyl-1,2-ethandiol **5** to a level of 96.3% occupancy. Suspension medium: 6.60 g of 1,2-dichlorobenzene plus 1.00 g of a mixture of 9.00 g of dichloroethane with 2.00 g of tetrachloroethylene. $n_D^{20} = 1.5386$. Polymer concentrations: 2.748 g in 100 mL for the polymer containing (*S*)-phenylethandiol and 1.758 g in 100 mL for that with the (*R*) enantiomer. Measured rotations: + 0.643° and − 0.422° respectively.

To investigate the effects of the template and of the void structure on the optical rotation, the polymer **P-1-[2]** made from the template monomer **1** was studied in greater detail.[6] As can be seen from Figure 1 and Table 2, this gave a molar rotation value $[M]_{546}^{20}$ of − 60.6°. The measurements over a range of concentrations (Fig. 2) showed good agreement between the values, with an average $[M]_{546}^{20}$ value of − 61.7° and a mean error for the average of $m = 1.2°$. Taking into account possible systematic errors, the overall limit of error is estimated as ± 5–10%.

Table 2. Optical rotation values for various polymers with voids. The measurements were made on suspensions in a mixture of 1,2-dichlorobenzene, dichloroethane and tetrachloroethylene.[5]

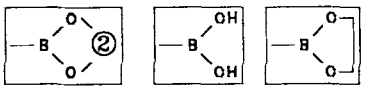

	Template monomer **1**	Template **2**	P-1-[2] [a]	P-1-□ [b]	P-1-[7] [c]
α_{546}^{20}	-	-	− 0.040°	− 0.067°	+ 0.040°
$[\alpha]_{546}^{20}$	− 93.5°	+ 142.6°	− 2.0°	− 2.7°	+ 3.1°
$[M]_{546}^{20}$	− 448.9°	+ 365.3°	− 60.6°	− 76.4°	+ 110.0°
			[$\bar{x}$ = − 61.7°] [d]		

[a] $n_D^{20} = 1.5424$, $c = 2.00$, $D = 80\%$. [b] $n_D^{20} = 1.5424$, $c = 2.58$, $D = 80\%$. [c] $n_D^{20} = 1.5401$, $c = 1.28$, $D = 95\%$. [d] $\bar{x}$ was calculated from the measurements at different concentrations (see Fig. 2). D is the optical transmission of the suspension expressed as a percentage of that for the pure solvent.

If we compare the value of − 61.7° given in Table 2 for the molar rotation $[M]_{546}^{20}$ of the polymer **P-1-[2]** with the value − 448.9° for the template monomer **1**, it becomes apparent that, in contrast to the situation in **P-3-[(*R*)-5]**, the molar rotation value has decreased considerably as a result of the polymerization. It must be assumed that this has been caused by the polymer matrix. Its effect can be determined by splitting off the optically active template **2**. Since optically active boronic acid groups usually have rotation values greatly different from those of their esters,[7] it is necessary to convert **P-1-□** with ethylene glycol **7** into the ester **P-1-[7]** in order to allow a meaningful comparison. The polymer **P-1-[7]** gives a positive molar rotation $[M]_{546}^{20} = + 110.0°$. This shows that in **P-1-[7]** the imprints generated in the polymer make a positive contribution to the rotation value, and this is responsible for the low molar rotation value found for **P-1-[2]**. In this case the optical rotation is not caused by individual chiral centers, as is usual, but by the imprint as a whole. Evidently, therefore, the contribution of chiral voids to the rotation values in highly cross-linked polymers can be measured satisfactorily.

Measuring the optical rotation in the solid phase allows one to directly determine the properties of a chiral void in the polymer. For example, it is possible to recognize different binding situations of the template in the cavity. If the polymer **P-1-□** with empty voids is recharged with the template **2**, the resulting polymer, in contrast to **P-1-[2]**, has a very large positive rotation value of $[M]_{546}^{20} = + 323°$. If this loaded polymer is heated in acetonitrile in the presence of a 3 Å molecular sieve, the molar rotation $[M]_{546}^{20}$ changes to − 68°, i.e. about the same as for the original polymer **P-1-[2]**. Evidently most of the template molecules are at first bonded only by a single point of attachment (formed by esterification of only one boronic acid group in the cavity), and this

then changes to a double attachment. Results from calorimetric studies lend support to this assumption.[8]

Further interesting results can be expected from studies of the optical rotation, and of the circular dichroism where appropriate, for polymers under different swelling conditions and at different temperatures. This method could also become very important as a means of characterizing chiral stationary phases for use in separating racemates. In cases where a cross-linked polymer has been prepared with optically active side-groups there is often speculation about effects caused by an asymmetric matrix,[9] and it should now be possible to measure this directly.

Received: January 29, 1990 [Z 3764 IE]
German version: *Angew. Chem. 102* (1990) 706

[1] a) G. Wulff, A. Sarhan, *Angew. Chem. 84* (1972) 364; *Angew. Chem. Int. Ed. Engl. 11* (1972) 341; b) G. Wulff, A. Sarhan, K. Zabrocki, *Tetrahedron Lett. 1973*, 4329; c) G. Wulff, S. Schauhoff, *J. Org. Chem.*, in press; d) K. J. Shea, E. A. Thompson, S. D. Pandey, P. D. Beauchamp, *J. Am. Chem. Soc. 102* (1980) 3149; e) J. Damen, D. C. Neckers, *ibid. 102* (1980) 3265; f) B. Sellergren, M. Lepistö, K. Mosbach, *ibid. 110* (1988) 5853; g) Review: G. Wulff in W. T. Ford (Ed.): *Polymeric Reagents and Catalysts, ACS Symp. Ser. 308* (1986) 186.

[2] G. Wulff, B. Heide, G. Helfmeier, *J. Am. Chem. Soc. 108* (1986) 1089; K. J. Shea, T. K. Dougherty, *ibid. 108* (1986) 1091; K. J. Shea, D. Y. Sasaki, *ibid. 111* (1989) 3442.

[3] G. Wulff, J. Vietmeier, H.-G. Poll, *Makromol. Chem. 188* (1987) 731.

[4] P. Pino, J. Bartus, O. Vogl, *Polym. Prepr. Am. Chem. Soc. Div. Polym. Chem. 29/1* (1988) 254; J. Bartus, L. S. Corley, G. D. Jaycox, O. Vogl, *Polym. Prepr. Jpn. [Engl. Ed.] 36* (1987) Nr. 5–10, E23; for earlier studies see also: P. Pino, *Fortschr. Hochpolym. Forsch. 4* (1965) 417.

[5] The measurements by *Vogl, Pino* et al. [4] were made using polymers with a particle diameter <45 μm suspended in a medium with the same refractive index contained in a 10 mm UV cuvette. The suspension was stirred to avoid sedimentation. For our measurements, in order to obtain larger rotations, we used an ordinary thermostatically controlled polarimeter cuvette with an optical path length of 100 mm. Sedimentation was prevented by aerating with a peristaltic pump or by shaking occasionally. Suspension media with different refractive indices were prepared by mixing two components, namely 1,2-dichlorobenzene ($n_D^{20} = 1.5513$) and a mixture of 1,2-dichloroethane and tetrachloroethylene (9:2 w/w, $n_D^{20} = 1.4528$). See also Figure 1.

[6] The polymer **P-1-2** used here was prepared by the usual method. [3] 24.43 g of ethylene glycol dimethacrylate, 4.60 g of **1** and 0.18 g of azo-bis-(isobutyronitrile) were polymerized in 18 g of tetrahydrofuran for 9 h at 65 °C. The polymer contained 0.33 mmol g^{-1} of the template monomer **1**. It was found possible to remove 88% of the template. In calculating the molar rotation values for **P-1-□** and **P-1-7** given in Table 2, the rotation caused by the residual 12% of the template monomer was subtracted. The molar rotation values relate to the fraction for which the given structure applies.

[7] G. Wulff, H. Stellbrink, *Recl. Trav. Chim. Pays-Bas 109* (1990) 216.

[8] G. Wulff, G. Kirstein, H.-G. Poll, unpublished.

[9] G. Blaschke, *Angew. Chem. 92* (1980) 14; *Angew. Chem. Int. Ed. Engl. 19* (1980) 13.

Dicobalt Complexes with *syn*- and *anti*-Coordinated μ-Cycloheptatriene Bridges**

By *Hubert Wadepohl,** *Wolfgang Galm*, and *Hans Pritzkow*

Dedicated to Professor Günter Wilke on the occasion of his 65th birthday

In binuclear complexes cycloheptatriene, as a six-electron ligand, can bind in different ways to the metal atoms. Apart from the symmetrical *syn*-coordination **A** ($\eta^3:\eta^3$; examples: $[\{(CO)_3M\}_2(\mu\text{-}C_7H_8)]$, M = Fe **1**,[1] M = Ru **2**,[2] an unsymmetrical *syn*-binding **B** of cycloheptatriene to the $(L_nM)_2$ unit is known ($\sigma^1, \eta^2:\eta^3$; example: $[(CpRh)_2(\mu\text{-}C_7H_8)]$ **3**[3]).

Here we report on the synthesis, structure and dynamic behavior of *syn*-$[(CpCo)_2(\mu\text{-}C_7H_8)]$ **6a** and *anti*-$[(Cp^*Co)_2(\mu\text{-}C_7H_8)]$ **6b** (Cp = η-cyclopentadienyl, Cp* = η-pentamethylcyclopentadienyl). In **6b** an *anti*-bound cycloheptatriene bridge **C** ($\eta^4:\eta^4$) has been realized for the first time.

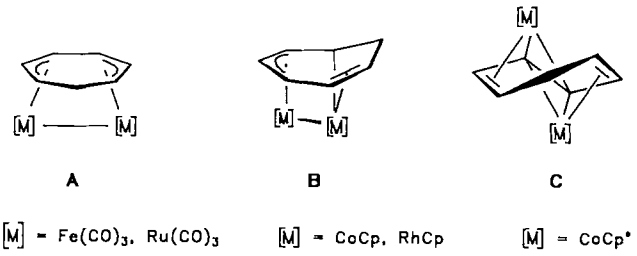

A **B** **C**

[M] = Fe(CO)$_3$, Ru(CO)$_3$ [M] = CoCp, RhCp [M] = CoCp*

Reaction of $[CpCo(1\text{-}4\text{-}\eta\text{-}C_7H_8]$ **4a**[4] with $[CpCo(C_2H_4)_2]$ **5a**[5] affords the *syn*-binuclear complex **6a** in good yields. From $[Cp^*Co(1\text{-}4\text{-}\eta\text{-}C_7H_8)]$ **4b** and $[Cp^*Co(C_2H_4)_2]$ **5b**[6] the *anti*-binuclear complex **6b** is exclusively formed. The ethene complexes **5** probably attack at the uncomplexed CC double bond of the η^4-bound cycloheptatriene ligand of **4**. The two bulky Cp*Co groups prevent the formation of a Co–Co bond, which would lead to the *syn*-binuclear complex, and force the *anti*-coordination. The high stability of **4b** prevents the formation of a "mixed" Cp*/Cp derivative of **6**. Hence, **4b** reacts neither with **5a** nor $[CpCo(C_6Me_6)]$,[5] both of which are sources of the CpCo fragment. Reaction of **4a** or $[CpRh(\eta^4\text{-}C_7H_8)]$[3, 7] with **5b** yields **4b** only, via ligand exchange.

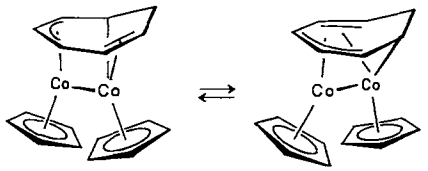

6a

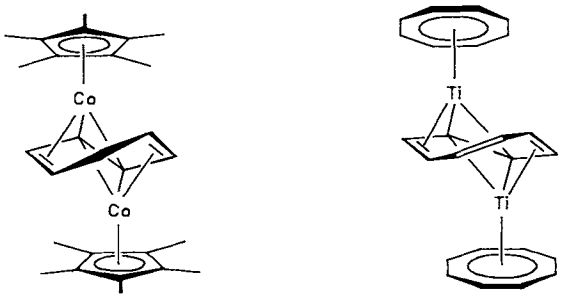

6b **7**

The *syn*-orientation of the CpCo groups in **6a** causes the bridging ligand to appear as five ^{1}H-NMR signals in the intensity ratio 2:2:1:2:1. Like **3**, **6a** is also non-ridgid in

[*] Priv.-Doz. Dr. H. Wadepohl, W. Galm, Dr. H. Pritzkow
Anorganisch-Chemisches Institut der Universität
Im Neuenheimer Feld 270, D-6900 Heidelberg (FRG)

[**] This work was supported by the Deutsche Forschungsgemeinschaft (Sonderforschungsbereich 247 der Universität Heidelberg).

solution. The temperature-dependent NMR spectra[8] indicate two dynamic processes with different activation energies.[9] At low temperatures the data are in accordance with a dynamic structure in which the two valence tautomers with a μ-1-σ,5-6-η:2-4-η-cycloheptatrienebridge are rapidly interconverting. The Co–C σ-bond is verified by the high field shift of the averaged ^{13}C-NMR signal of C-1 and C-6 ($\delta = 2.6$). The coalescence of the Cp proton resonances at 313 K ($\Delta G^{\neq}(313\ K) = 67.5\ kJ\ mol^{-1}$) can be explained either by a symmetrical $\eta^3:\eta^3$-binding of the cycloheptatriene to the $(CpCo)_2$ unit, or by an unhindered rotation of the cycloheptatriene ligand.

A quite different bonding situation, however, exists in the case of **6b**. The symmetrically *anti*-coordinated cycloheptatriene bridge gives rise to four multiplets (intensity ratio 2:2:2:2) in the temperature-independent ^{1}H-NMR spectrum.[10] **6b** also has C_2 molecular symmetry in the crystal (Fig. 1).[11] Each Cp*Co fragment is bound to four carbon atoms of the twisted cycloheptatriene; C1 and C1′ each have a longer and a shorter bond to both cobalt atoms. The C1–C1′ bond, which is coordinated to both metal atoms, has been elongated to 1.516(6) Å.[12]

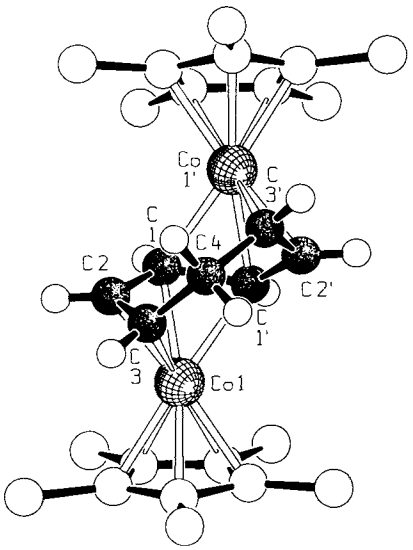

Fig. 1. Molecular structure of **6b** in the crystal (SCHAKAL [20]). Important bond lengths [Å] and angles [°] with standard deviations in parentheses: C1-C1′ 1.516(6), C1-C2 1.418(5), C2-C3 1.394(5), C3-C4 1.497(4), Co-C1 2.039(3), Co-C1′ 2.103(3), Co-C2 1.920(3), Co-C3 2.012(4), Co-C(Cp*) 1.987(8)...2.172(4), C1′-C1-C2 121.5(5), C1-C2-C3 117.3(3), C2-C3-C4 123.3(3), C3-C4-C3′ 116.7(4); torsion angles C2C1C1′C2′ −64.6°, C1′C1C2C3 15.9°.

In **6a** the bridging ligand is formally a three-electron donor to each CpCo fragment. The valence electron (VE) count of 18 per cobalt atom is attained through a metal–metal bond. In **6b** the cycloheptatriene is also a six-electron ligand. Here the large Co–Co distance (3.707 Å) precludes any direct metal-metal interaction. However, similarly to the triple-decker sandwich complexes,[13] the two metal atoms are electronically coupled via the bridging ligand, so that a closed 34 VE shell is obtained.

Among the binuclear complexes of cyclooctatetraene (cot) there are structures which are analogous to the complexes of type **B** and **C**. Here the CH_2 group of the seven-membered ring in **6** has been formally replaced by a HC=CH group which is not coordinated to the metal. However, of the 34-VE complexes $[\{(CO)_3Ru\}_2(\mu\text{-cot})]$,[14] *syn*-$[(CpRh)_2(\mu\text{-cot})]$,[15] $[(CpRh)_2(\mu\text{-cot})]^{2\oplus}$,[16] and $[(CpFe)_2(\mu\text{-cot})]$,[17] all of which are isoelectronic with **6**, only the first two have a *syn*-(μ-σ^1, $\eta^2:\eta^3$) coordination of the cot bridge (corresponding to **B**). In the latter two complexes an *anti*-(μ-$\eta^5:\eta^5$) structure is adopted. In the dititanium complex $[\{(\eta\text{-cot})\text{-Ti}\}_2(\mu\text{-cot})]$ **7**[18] (30 VE, paramagnetic[19]) the *anti*-(μ-$\eta^4:\eta^4$)cot bridge is bound similarly to **C**. However, the C–C bond lengths in the metal coordinated part of the bridging ligand exhibit a different pattern from those in **6b**.[18b]

Experimental

4b: A mixture of 0.70 g (2.8 mmol) of **5b** and 0.48 g (5.2 mmol) of cycloheptatriene in ca. 15 mL of petroleum ether (boiling range 30–60 °C) was heated under reflux for 2.5 h. After removal *in vacuo* of all volatile components at room temperature (until the mass was constant) the crude product could be used directly. For purification, the product was chromatographed on silanized silica gel (Merck RP60, ca. 3 × 2.5 cm) with petroleum ether. After reduction of the volume by evaporation, red **4b** (0.20 g, 25%) crystallized from the eluate at −80 °C. m.p. 68 °C. ^{1}H NMR (200 MHz, C_6D_6): $\delta = 5.8$ (m, 1H, H-6), 5.2 (m, 1H, H-5), 4.3 (m, 1H, H-3), 4.1 (m, 1H, H-2), 2.5 (m, 1H, H-1), 2.3 (m, 1H, H-4), 2.0 (m, 1H, CH_2), 1.69 (s, 15H, Cp*), 0.9 (m, 1H, CH_2). ^{13}C{^{1}H} NMR (50 MHz, C_6D_6): $\delta = 130.0$ (CH, C-5 or C-6), 123.6 (CH, C-6 or C-5), 89.4 (C, C_5Me_5), 88.7 (CH, C-2 od. C-3), 82.4 (CH, C-3 or C-2), 54.6 (CH, C-1 or C-4), 51.1 (CH, C-4 or C-1), 30.9 (CH_2), 9.9 (C_5Me_5). MS (EI, 70 eV): *m/z* 286 ($M^{\oplus}$, 100%), 271 ($[M-CH_3]^{\oplus}$, 54), 206 (46), 194 ($[Cp^*Co]^{\oplus}$, 48), 133 ($[Cp^*-2H]^{\oplus}$, 56), 119 (65), 91 ($[C_7H_7]^{\oplus}$, 50), 59 ($Co^{\oplus}$, 17). Correct C,H analysis.

6a: A mixture of 1 g (4.6 mmol) of **4a** and 0.9 g (5.0 mmol) of **5a** in 100 mL petroleum ether was heated at 50–60 °C for 1 h. A dark precipitate was formed. After removal of solvent *in vacuo* the residue was recrystallized from toluene. At −20 °C 0.73 g (46%) of **6a** (dark brown microcrystalline solid, sublimation at 180 °C) was obtained. MS (EI, 70 eV): *m/z* 340 ($M^{\oplus}$, 77%), 274 ($[M-C_5H_6]^{\oplus}$, 100), 216 ($[M-CpCo]^{\oplus}$, 13), 196(9), 189 ($[Cp_2Co]^{\oplus}$, 85), 124 ($[CpCo]^{\oplus}$, 22), 91 ($[C_7H_7]^{\oplus}$, 9), 59 ($Co^{\oplus}$, 9). Correct C,H analysis.

6b: A mixture of 0.81 g (2.8 mmol) of **4b** and 0.71 g (2.8 mmol) of **5b** in ca. 20 mL toluene was heated under reflux for 2.5 h. After removal of solvent *in vacuo* the residue was redissolved in ca. 10 mL petroleum ether. At −20 °C 0.76 g of (56%) **6b** was obtained as dark brown crystals (decomp. 170 °C). ^{13}C{^{1}H} NMR (50 MHz, C_6D_6): $\delta = 88.6$ (C_5Me_5), 75.5 (CH), 44.3 (CH), 38.6 (CH), 29.7 (CH_2), 9.9 (C_5Me_5). MS (EI, 70 eV): *m/z* 480 ($M^{\oplus}$, 5%), 286 ($[Cp^*Co(C_7H_8)]^{\oplus}$, 100), 271 ($[Cp^*Co(C_7H_8)-CH_3]^{\oplus}$, 54), 206 (44), 192 ($[Cp^*Co-2H]^{\oplus}$, 48), 133 ($[Cp^*-2H]^{\oplus}$, 54), 91 ($[C_7H_7]^{\oplus}$, 37), 59 ($Co^{\oplus}$, 18). Correct C,H analysis.

Received: January 22, 1990 [Z 3750 IE]
German version: *Angew. Chem. 102* (1990) 701

CAS Registry numbers:
4a, 78318-94-2; **4b**, 127255-85-0; **5a**, 69393-67-5; **5b**, 80848-36-8; **6a**, 127255-86-1; **6b**, 127255-87-2; C_7H_8, 544-25-2; $CpRh(C_2H_4)_2$, 12211-95-9; $CpRh(C_7H_8)$, 82512-24-1.

[1] G. F. Emerson, J. E. Mahler, R. Pettit, R. Collins, *J. Am. Chem. Soc. 86* (1964) 3590; F. A. Cotton, B. G. DeBoer, T. J. Marks, *ibid. 93* (1971) 5069.
[2] R. Bau, J. C. Burt, S. A. R. Knox, R. M. Laine, R. P. Phillips, F. G. A. Stone, *J. Chem. Soc. Chem. Commun. 1973*, 726; J. C. Burt, S. A. R. Knox, F. G. A. Stone, *J. Chem. Soc. Dalton Trans. 1975*, 731.
[3] J. Evans, B. F. G. Johnson, J. Lewis, R. Watt, *J. Chem. Soc. Dalton Trans. 1974*, 2368.
[4] A. Salzer, P. Bigler, *Inorg. Chim. Acta 48* (1981) 199.
[5] K. Jonas, E. Deffense, D. Habermann, *Angew. Chem. 95* (1983) 729; *Angew. Chem. Int. Ed. Engl. 22* (1983) 716; *Angew. Chem. Suppl. 1983*, 1005.
[6] a) U. Kölle, F. Khouzami, B. Fuss, *Angew. Chem. 94* (1982) 132; *Angew. Chem. Int. Ed. Engl. 21* (1982) 131; *Angew. Chem. Suppl. 1982*, 230. b) S. A. Frith, J. L. Spencer, *Inorg. Synth. 23* (1985) 15.
[7] Contrary to a previous report [P. Caddy, M. Green, E. O'Brien, L. E. Smart, P. Woodward, *Angew. Chem. 89* (1977) 671; *Angew. Chem. Int. Ed. Engl. 16* (1977) 648] $[CpRh(C_7H_8)]$ can be prepared from $[CpRh(C_2H_4)_2]$ by refluxing for 3 h in cycloheptatriene (40% yield).
[8] **6a**: ^{1}H NMR (200 MHz, C_6D_6, $T = 283$ K): $\delta = 4.77$ (s, 5H, Cp), 4.69 (s, 5H, Cp), 4.2 (m, 2H, H-3, H-4), 3.6 (m, 2H, H-2, H-5), 2.4 (m, 1H, CH_2), 1.9 (m, 2H, H-1, H-6), 1.2 (m, 1H, CH_2); ^{1}H NMR (200 MHz, [D_8]toluene, $T = 333$ K): $\delta = 4.75$ (s, 10H, Cp), 4.3 (m, 2H, H-3, H-4), 3.6 (m, 2H, H-2, H-5), 2.3 (m, 1H, CH_2), 1.9 (m, 2H, H-1, H-6), 1.2 (m, 1H, CH_2). ^{13}C{^{1}H} NMR (50 MHz, C_6D_6, 283 K): $\delta = 84.0$ (Cp), 80.4 (Cp), 60.0 (CH), 55.3 (CH), 35.1 (CH_2), 2.6 (CH, C-1, C-6); ^{1}H- and ^{13}C-NMR spectra are temperature-invariant between 190 and 280 K.

[9] The energy barriers for **6a** are lower than for the dirhodium complex **3** where structure **B** can be frozen out below 200 K [3].
[10] **6b**: ^{1}H NMR (200 MHz, C_6D_6): δ = 4.6 (m, 2H, C_7H_8), 1.9 (m, 2H, C_7H_8), 1.67 (s, 30H, Cp*), 1.1 (m, 2H, C_7H_8), 1.0 (m, 2H, C_7H_8).
[11] Monoclinic, space group $C2/c$, a = 20.914(16), b = 8.369(7), c = 14.532(12) Å, β = 106.71(6)°, V = 2436 Å^3, Z = 4, Stoe-Siemens four-circle diffractometer ($Mo_{K\alpha}$-radiation, ω-scan, empirical absorption correction) 1930 unique reflections with $I \geq 2\sigma(I)$, all non-hydrogen atoms anisotropic, Cp*-rings disordered (refined as two five membered rings with site occupation 0.5), all hydrogen atoms of the cycloheptatriene localized in difference Fourier syntheses and refined isotropically, R = 0.036; R_w = 0.034, $w = 1/\sigma^2(F)$ (SHELX-76 [G. M. Sheldrick, University of Cambridge 1976]). Further details of the crystal structure investigation may be obtained from the Fachinformationszentrum Karlsruhe, Gesellschaft für wissenschaftlich-technische Information mbH, D-7514 Eggenstein-Leopoldshafen 2 (FRG), on quoting the depository number CSD-54480, the names of the authors, and the journal citation.
[12] This can be explained by the strong bonding interaction of the LUMO of the bridging ligand (π-antibonding with respect to C1-C1') with the half-filled e_1-orbitals of the Cp*Co-fragments.
[13] J. W. Lauher, M. Elian, R. H. Summerville, R. Hoffmann, *J. Am. Chem. Soc. 98* (1976) 3219.
[14] F. A. Cotton, W. T. Edwards, *J. Am. Chem. Soc. 90* (1968) 5412.
[15] J. H. Bieri, T. Egolf, W. von Philipsborn, U. Piantini, R. Prewo, U. Ruppli, A. Salzer, *Organometallics 5* (1986) 2413.
[16] J. Edwin, W. E. Geiger, A. L. Rheingold, *J. Am. Chem. Soc. 106* (1984) 3052.
[17] C. Böhle, W. Siebert (Universität Heidelberg), personal communication 1980; X-ray crystal structure analysis: C. Krüger, Mülheim a.d. Ruhr.
[18] a) H. Breil, G. Wilke, *Angew. Chem. 78* (1966) 942; *Angew. Chem. Int. Ed. Engl. 5* (1966) 898; b) H. Dietrich, H. Dierks, *ibid. 78* (1966) 943 resp. *5* (1966) 899; *Acta Crystallogr. B24* (1968) 58.
[19] S. P. Kolesnikov, J. E. Dobson, P. S. Skell, *J. Am. Chem. Soc. 100* (1978) 999.
[20] E. Keller: *SCHAKAL 88, A FORTRAN Program for the Graphical Representation of Molecular and Crystallographic Models*, Universität Freiburg 1988.

The Monofluorooxonium(0) Hexafluorometalate(VI)s $H_2OF^{\oplus}MF_6^{\ominus}$ (M = As,Sb)**

By *Rolf Minkwitz** and *Gabriele Nowicki*

The protonated hypofluorous acid $H_2OF^{\oplus}$ is isoelectronic with the recently prepared monofluoramine H_2NF.[1] According to ab initio calculations the cation $H_2OF^{\oplus}$ has C_s symmetry with the parameters d(OF) = 144, d(OH) = 96 pm, $\sphericalangle$(HOH) = 108, $\sphericalangle$(FOH) = 120°.[2] These values are, with exception of the FOH angle, in satisfactory agreement with the values determined by microwave spectroscopy for the corresponding parameters of H_2NF ($\sphericalangle$ FNH = 101°).[3]

An attempt to synthesize monofluorooxonium(0) salts $H_2OF^{\oplus}MF_6^{\ominus}$ in analogy to those of the hydronium salts[4] according to Equation (a) by protonation of HOF in

$$H_2O + HF + MF_5 \longrightarrow H_3O^{\oplus}MF_6^{\ominus} \quad (M = As,Sb) \qquad (a)$$

aqueous acidic media met without success.[5] On the contrary, because of the polarity $HO^{\delta\oplus}F^{\delta\ominus}$ the proton attacked at the fluorine, resulting in a decomposition into H_2O_2 and HF.[5] Also in the direct fluorination of H_2O to HOF and HF there were no indications of an $H_2OF^{\oplus}$ ion being formed.[5] The same holds true for the reaction of H_2O with XeF_2 leading to O_2, HF and Xe.[6]

$XeF^{\oplus}MF_6^{\ominus}$ salts have a high oxidation potential. Nevertheless, they are very selective fluorinating agents,[7-10] since reactions with them in anhydrous HF still proceed extremely smoothly at 195 K, and even temperature-sensitive products can thus be prepared.

Fluorination of H_2O with $XeF^{\oplus}MF_6^{\ominus}$ [Eq. (b)] leads almost quantitatively to the pale reddish salts **1**.

$$XeF^{\oplus}MF_6^{\ominus} + H_2O \xrightarrow[213\ K]{(HF)} \underset{\mathbf{1}}{H_2OF^{\oplus}MF_6^{\ominus}} + Xe \quad (M = As,Sb) \qquad (b)$$

Both salts can be stored without decomposition for a few weeks in sealed vessels at 233 K, and for up to 2 h at room temperature. In a high vacuum apparatus, however, HOF (ν(OH): 3540s; δ (HOF): 1361; ν (OF): 890 ms cm^{-1}) and HF can already be isolated in an inert gas matrix at 223 K[11] [Eq. (c)]. SbF_5 remains in the reaction vessel at this temperature.

$$\underset{\mathbf{1}}{H_2OF^{\oplus}MF_6^{\ominus}} \xrightarrow{\Delta} HOF + HF + MF_5 \qquad (c)$$

Consistent with this finding the following fragments are observed mass spectrometrically (EI, 30 eV): m/z (%) 36(2.8) $HOF^{\oplus}$, 32(32.8) $O_2^{\oplus}$, 20(10) $HF^{\oplus}$, 19(3.6) $F^{\oplus}$, 18(100) $H_2O^{\oplus}$, 17(14.3) $OH^{\oplus}$. These fragments and their intensities are characteristic for HOF.[12]

Table 1. IR vibration frequencies [cm^{-1}] of $X_2{}^{16}OF^{\oplus}MF_6^{\ominus}$, $X_2{}^{18}O^{\oplus}MF_6^{\ominus}$, and X_2NF (X = H,D; M = As,Sb) at 153 K.

$H_2{}^{16}OF^{\oplus}$		$H_2{}^{18}OF^{\oplus}$		$D_2{}^{16}OF^{\oplus}$		$D_2{}^{18}OF^{\oplus}$		H_2NF	D_2NF	Assignment
$AsF_6^{\ominus}$	$SbF_6^{\ominus}$	$AsF_6^{\ominus}$	$SbF_6^{\ominus}$	$AsF_6^{\ominus}$	$SbF_6^{\ominus}$	$AsF_6^{\ominus}$	$SbF_6^{\ominus}$	[1]	[1]	[a]
3386s	3385s			2340s	2339s			3234	2250	$\nu_1(a')\nu_sEX_2$
		3172vbr,s	3180vbr,s			2249vbr,s	2247vbr,s			
3225vs	3226vs			2270vs	2280vs			3346	2500	$\nu_5(a'')\nu_{as}EX_2$
1630m	1630m	1587m	1583m	1100m	1097m	1082m	1080m	1564	1145	$\nu_2(a')\delta EX_2$
1261m	1261m	1215m	1218m	939mw	950mw	930mw	932mw	1241	965	$\nu_6(a'')\delta XEF$
1067w	1070w	1011w	1014w	[b]	[b]	[b]	[b]	1233	970	$\nu_3(a')\omega EX_2$
865s	863s	831s	830s	860s	858s	840s	843s	891	882	$\nu_4(a')\nu EF$
712s	665s	703s	666s	700s	666s	702s	668s			$\nu_3MF_6^{\ominus}$
397	287	397	285	395	287	395	286			$\nu_4MF_6^{\ominus}$

[a] E = O,N. [b] Masked by $\nu_4(a')$.

For both salts, the NMR spectroscopic characterization of **1** in HF at 213 K yields: δ (^{1}H)(300 MHz, CH_4 as external standard) = 8.06 (as shoulder alongside the solvent signal at δ = 7.47); δ(^{19}F)(282 MHz, F_2 as external standard) = −490.9 (broad, no splitting of signal).[13] The ^{19}F-NMR

[*] Prof. Dr. R. Minkwitz, Dipl.-Chem. G. Nowicki
Fachbereich Chemie der Universität
Postfach 50 05 00, D-4600 Dortmund 50 (FRG)

[**] This work was supported by the Minister für Wissenschaft und Forschung des Landes Nordrhein-Westfalen.

signals of the anions are observed at $\delta = -480.7$ ($AsF_6^\ominus$) and -534.9 ($SbF_6^\ominus$).

Assignment of the vibrations in the $H_2OF^\oplus$ cation in accord with Table 1 followed unambiguously by comparison with the assignment of the vibrations in the case of H_2NF, which is confirmed by calculations.[1] Only the situation $\nu_s(OH) > \nu_{as}(OH)$ is open to doubt. It is merely based on the difference in the intensities of the bands in the IR spectrum. However, because of the large half-widths of the vibration bands (Fig. 1), one can assume strong hydrogen bonding

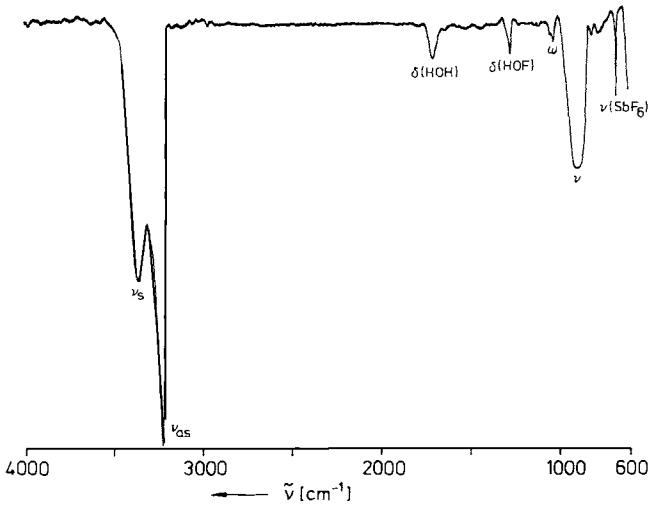

Fig. 1. IR spectrum of solid $H_2OF^\oplus SbF_6^\ominus$ at 153 K (without mull) between NaCl or polyethylene plates in an IR low-temperature cuvette.

between the ions to influence the intensities. These interactions also preclude a force field calculation, although adequate isotopic data have been measured. All frequency shifts of the isotopomers lie in the range to be expected according to the product rule.[14]

For further characterization of **1** the reactions (d)–(h) have been carried out; these afforded known compounds. They show that the cation **1** is bifunctional: depending upon

$$\mathbf{1} + SCl_2 \xrightarrow[213\ K]{} OSF_2 + 2HCl + MF_5 \quad (d)$$

$$\mathbf{1} + SF_4 \xrightarrow[213\ K]{(HF)} OSF_3^\oplus MF_6^\ominus\,[15] + 2HF \quad (e)$$

$$\mathbf{1} + ClF_3 \xrightarrow[195\ K]{(HF)} OClF_2^\oplus MF_6^\ominus\,[16] + 2HF \quad (f)$$

$$\mathbf{1} + H_2O \xrightarrow[213\ K]{(HF)} H_2OOH^\oplus MF_6^\ominus\,[17] + HF \quad (g)$$

$$\mathbf{1} + CH_3OH \xrightarrow[233\ K]{} \text{explosion} \quad (h)$$

the reaction partners it is formally either an $OF^\oplus$ or an $OH_2^\oplus$ moiety. Owing to its instability the hypofluorous acid cannot be used preparatively, whereas its protonated salts could be valuable synthetic building blocks because of the ease with which they can be handled.

Experimental

A solution of 1 mmol of $XeF^\oplus MF_6^\ominus$ (M = As,Sb) in 5 mL of XF(X = H,D) was prepared in a 30 mL KEL-F reactor fitted with a valve of the same material. An equimolar amount of $X_2^{16}O$ or $X_2^{18}O$ was then pipetted into the solution under an inert gas (N_2). After 12 hours' stirring at 213 K, Xe and the solvent XF were removed from the mixture in a high vacuum at the same temperature. The remaining pale reddish solid is only sparingly soluble in HF and immediately deliquesces on exposure to air. Contamination by iron fluorides can be ruled out as being responsible for the color. It is possibly attributable to charge-transfer transitions in the solid state.

Received: December 27, 1989 [Z 3699 IE]
German version: *Angew. Chem. 102* (1990) 692

CAS Registry numbers:
1 (M = As), 126876-05-9; **1** (M = Sb), 126898-38-2; $XeF^\oplus AsF_6^\ominus$, 26024-71-5; $XeF^\oplus SbF_6^\ominus$, 36539-18-1; H_2O, 7732-18-5; SF_4, 7783-60-0; ClF_3, 7790-91-2; CH_3OH, 67-56-1; OSF_2, 7783-42-8; HCl, 7647-01-0; AsF_5, 7784-36-3; SbF_5, 7783-70-2; $OSF_3^\oplus AsF_6^\ominus$, 51320-88-8; HF, 7664-39-3; $OClF_2^\oplus AsF_6^\ominus$, 36544-27-1; $H_2OOH^\oplus AsF_6^\ominus$, 70850-29-2; SCl_2, 10545-99-0; $OSF_3^\oplus SbF_6^\ominus$, 126876-06-0; $OClF_2^\oplus SbF_6^\ominus$, 38199-85-8; $H_2OOH^\oplus SbF_6^\ominus$, 70850-28-1.

[1] R. Minkwitz, R. Nass, *Z. Naturforsch. B43* (1988) 1478.
[2] A. Johansson, P. A. Kollman, J. F. Liebman, S. Rothenberg, *J. Am. Chem. Soc. 96* (1974) 3750.
[3] D. Christen, R. Minkwitz, R. Nass, *J. Am. Chem. Soc. 109* (1987) 7020.
[4] K. O. Christe, C. J. Schack, R. D. Wilson, *Inorg. Chem. 14* (1975) 2224.
[5] E. H. Appelman, *Acc. Chem. Res. 6* (1973) 113.
[6] J. H. Holloway, *J. Fluorine Chem. 33* (1986) 149.
[7] R. Minkwitz, A. Werner, *Z. Naturforsch. B43* (1988) 403.
[8] R. Minkwitz, A. Werner, *J. Fluorine Chem. 39* (1988) 141.
[9] R. Minkwitz, G. Nowicki, H. Preut, *Z. Anorg. Allg. Chem. 573* (1989) 185.
[10] R. Minkwitz, G. Nowicki, *Z. Naturforsch B44* (1989) 1343.
[11] J. A. Goleb, H. H. Claassen, M. H. Studier, E. H. Appelman, *Spectrochim. Acta Part A 28* (1972) 65.
[12] M. H. Studier, E. H. Appelman, *J. Am. Chem. Soc. 93* (1971) 2349.
[13] NMR data of pure HOF: $\delta(^{19}F) = 402$ (F_2 as external standard); $\delta(^1H) = -16$ (CH_4 as external standard); positive signs correspond to an upfield shift: J. C. Hindman, A. Svirmichas, E. H. Appelman, *J. Chem. Phys. 57* (1972) 4542.
[14] H. Siebert: *Anwendungen in der Schwingungsspektroskopie*, Springer, Berlin 1966, p. 21.
[15] M. Brownstein, P. A. W. Dean, R. J. Gillespie, *J. Chem. Soc. Chem. Commun. 1970*, 9.
[16] K. O. Christe, C. J. Schack, *Inorg. Chem. 11* (1972) 2212.
[17] K. O. Christe, W. W. Wilson, E. C. Curtis, *Inorg. Chem. 18* (1979) 2578.

Ring Closure and Ring Expansion Reactions in Bridged Triarylphosphanes and Triarylarsanes with *o*-Isopropenyl Substituents. Novel Candidates for Turnstile Geometry**

By *Dieter Hellwinkel,* Andreas Wiel, Gerhard Sattler,* and *Bernd Nuber*

Despite optimum prerequisites – combination of a C_3-symmetric tridentate ligand with a C_2 symmetric bidentate ligand system – the phosphorane **1** does not have the ideal turnstile geometry **TS**[1] but a distorted trigonal-bipyramidal structure **TS'** ≙ **TBP**.[2] Similar deviations from the ideal type **TS** structure are also known for phosphoranes of analogous composition, with adamantane skeletal frameworks such as **2**.[3]

In the hope of perhaps still being able to realize the undistorted turnstile-type **TS** structure with the aid of an extremely rigid tridentate ligand we have now synthesized triphenylphosphane **5a**,[4] triply bridged by isopropylidene groups, starting from 5-phenyl-10,10-dimethyl-5,10-dihydroacrido-

[*] Prof. Dr. D. Hellwinkel, Dipl.-Chem. A. Wiel, Dr. G. Sattler, Dr. B. Nuber
Institut für Organische Chemie der Universität
Im Neuenheimer Feld 270, D-6900 Heidelberg (FRG)

[**] This work was supported by the Fonds der Chemischen Industrie and by BASF AG (FRG)

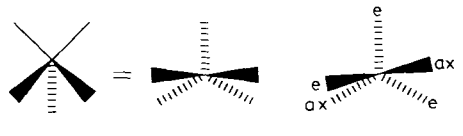

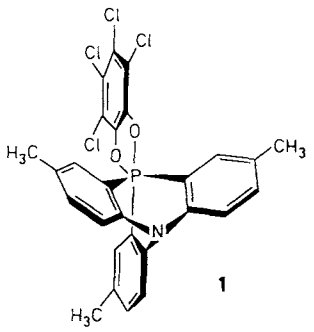

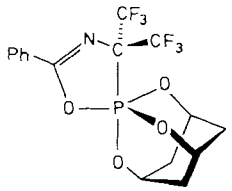

phosphane **3a**, which was obtained by cyclization of (2-isopropenyl)diphenylphosphane. Removal of the phenyl group in **3a** with Li in THF and reaction of the secondary phosphane **4** isolable after hydrolysis with phosgene affords the chlorophosphane **7a**, which reacts with 2,6-bis(isopropenyl)phenyllithium to give the tertiary phosphane **8a**. This can be converted in good yields into **5a** by acid-catalyzed cyclization.

The analogous arsane **5b** is accessible via essentially the same route except that the lithium arsenide obtained by Li-cleavage is converted oxidatively into the cyclic arsinic acid **6**, which is then reduced with PCl_3 to chloroarsane **7b**.[5] The doubly bridged derivatives **10a,b** can also be synthesized in a similar way. However, of the compounds **11a,b** prepared by reaction of diphenylchloroarsane and diphenylchlorophosphane, respectively, with 2,6-bis(isopropenyl)phenyllithium, only **11a** can be cyclized acid-catalytically to give **10a**.[6] **10b**, on the other hand, is obtainable by cyclization of the singly bridged arsane **9**, which in turn is accessible from 2-isopropenylphenyllithium and **7b**. The structurally relevant NMR data and melting points of the new compounds are listed in Table 1.

Table 1. Melting points, ^{31}P- and methyl-^1H-NMR signals ($CDCl_3$, δ values rel. 85% H_3PO_4 and TMS) of the compounds **3**–**10** and **12**.

	M.p. [°C][a]	^{31}P	Me_{eq}	Me_{ax}	$^5J_{P,H}$[b]
3a	134	−22.9	2.02	1.45	2.20 Hz
3b	140	–	2.07	1.49	–
4	[c]	−70.7	1.42	1.12	2.65 Hz
5a	287	−76.7	2.05	1.81	2.65 Hz
5b	311	–	2.05	1.89	–
6	286	–	1.30		–
7a	[d]	+63.4	1.70	1.45	[e]
7b	102	–	2.01	1.37	–
8a	133	−36.5	1.79	1.27	1.80 Hz
8b	125	–	2.00	1.29	–
9	141	–	2.07	1.48	–
10a	173	−54.6	2.05	1.61	2.60 Hz
10b	180	–	2.06	1.66	–
12	260	−63.3	2.08	1.78	–

[a] All the new compounds gave correct elemental analyses: ± 0.3%. [b] Coupling is observed only for the axial methyl groups [7]. [c] B.p 140–150 °C/0.1 torr. [d] B.p. 154 °C/0.1 torr. [e] Signals very broad, no ^5J(P, H) coupling.

The single-crystal X-ray structure analyses of **5a,b** showed only slight deviations from the C_{3v} structure type for the bond lengths and angles (Table 2). The element–aryl bonds are somewhat shorter than those in triphenylphosphane (182.8 pm)[8] and triphenylarsane (195.7 pm),[9] while the CPC and CAsC angles are markedly smaller than those in triphenylphosphane (103°) and triphenylarsane (100.1°), respectively, which leads to a stronger pyramidalization of the central atoms. Figure 1 shows the structure of **5b**,[10] which is virtually identical with that of **5a**.[10]

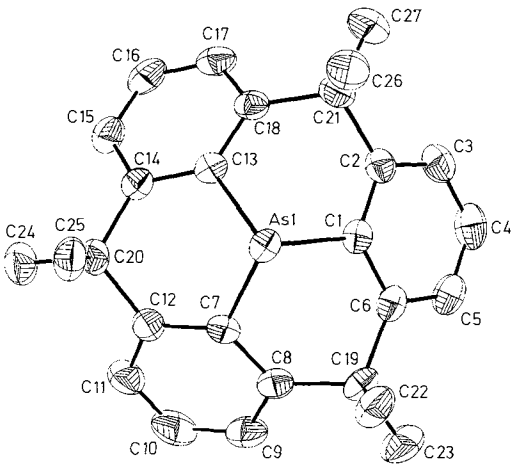

Fig. 1. Crystal structure of **5b** (without H atoms).

Reaction of **5a** with *o*-chloranil in boiling benzene leads, with concomitant decoloration of the solution, to formation of the pentacoordinated phosporane **12**, whose ^1H-NMR spectrum shows only two methyl signals of equal intensity, even at −60 °C (Table 1), which suggest a flexible structure in solution, but do not afford any further useful information. We have therefore carried out a single-crystal X-ray structure analysis of **12** too,[10] the most important informative

Table 2. Selected bond lengths [pm] and angles [°] (standard deviations in brackets) of the new compounds **5a**, **5b**, and **12**.

	5a (X = P)	**5b** (X = As)	**12** (X = P)
X1-C1	181.0(2)	194.2(3)	180.3(3)
X1-C7	181.2(3)	194.2(3)	178.6(3)
X1-C13	181.5(2)	194.7(3)	175.4(4)
X1-O1	–	–	168.4(2)
X1-O2	–	–	192.1(2)
C1-X1-C7	98.0(1)	93.5(1)	97.8(1)
C1-X1-C13	98.2(1)	92.9(1)	100.2(1)
C7-X1-C13	97.5(1)	92.7(1)	105.5(2)
C7-X1-O1	–	–	136.6(1)
C13-X1-O1	–	–	116.5(1)
C1-X1-O1	–	–	86.0(1)
O1-X1-O2	–	–	83.3(1)
C1-X1-O2	–	–	167.2(1)
C7-X1-O2	–	–	85.2(1)
C13-X1-O2	–	–	90.8(1)

data of which can be gleaned from Table 2 and Figure 2. Here again, the trigonal-bipyramidal structural principle has largely prevailed – albeit in a strongly distorted form – which manifests itself in a very long axial bond (192.1 pm) along with a normal length equatorial P–O bond (168.4 pm) in the symmetrical bidentate 1,2-phenylenedioxy ligand. Despite its rigidity and inherent C_3 symmetry, the tridentate ligand system also shows a clear tendency to formation of one longer axial (180.3 pm) and two shorter equatorial (175.4 and 178.6 pm, resp.) P–C bonds as well as a larger eq-eq (105.5°) and two smaller eq-ax (100.2 and 97.8°, resp.) C-P-C bond angles.

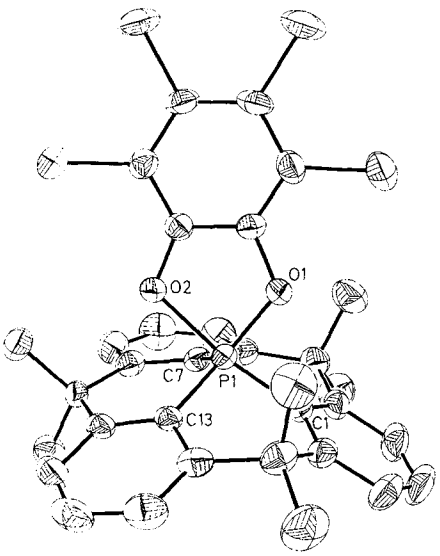

Fig. 2. Structure of **12** in the crystal (without H atoms).

On attempting to gain access, analogously to the cyclization of **8b** to **5b**, to comparable arsacycles with a zero- or one-oxygen bridge, we discovered a completely different reaction type. Reaction of **14**, which is obtainable from 5-chlorodibenzarsole **13**[11] and 2,6-bis(isopropenyl)phenyllithium, with methanesulfonic acid in glacial acetic acid affords a product whose ^{1}H-NMR spectrum shows three methyl signals and one olefinic proton signal. These data (Table 3) are only compatible with a completely unsymmetrical molecule in which, in addition, one methyl group must have been modified to an olefin function.

Table 3. Melting points and structurally relevant ^{1}H- and (in brackets) ^{13}C-NMR data (δ values rel. TMS) of the new arsacycles **16**, **18**, **19**, and **21**.

	M.p. [°C][a]	Me_a	Me_b	Me_c	$H_{olef.}$
16	180	0.79	1.96	2.31	6.77
		(36.59)	(33.10)	(18.73)	
18	171	1.82	1.87	–	–
		(33.98)	(32.11)	–	–
19	>330	1.85[b]		–	–
		(31.94)		–	–
21	135	1.72	2.03	2.17	6.68
	(decomp.)	(34.53)	(30.87)	(18.79)	–

[a] All the new compounds gave correct elemental analyses ± 0.3%. [b] Accidental isochronism!

An unsymmetrical product is formed if the initial attack of the protonated isopropenyl group in **14H**$^\oplus$ does not take place, as usual, at the *ortho*- but at the *ipso*-position of the dibenzarsole unit. The resulting arsanylium center, incorporated in an eight-membered ring system **15**, can then attack the terminal C-atom of the second isopropenyl group, the reaction sequence finally ending in formation of the novel heterocycle **16**.

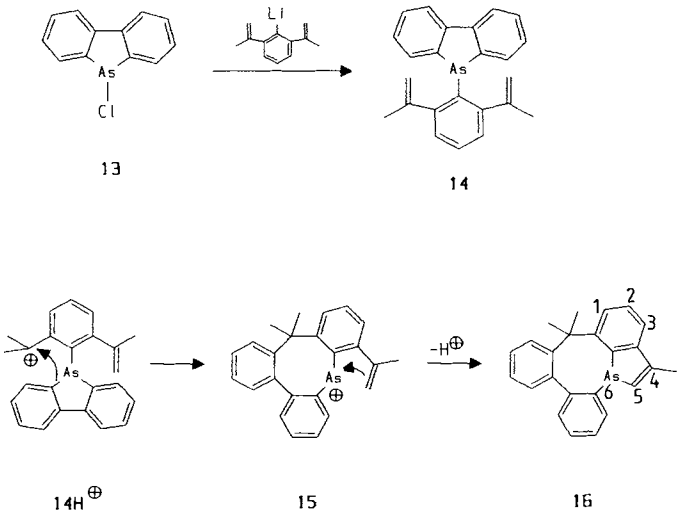

Definite proof of this is provided by the single-crystal X-ray structure analysis,[10] which basically reveals an almost planar arsindole moiety and a central eight-membered ring system with a highly distorted boat conformation (Fig. 3). The bond lengths and angles compare very well with those expected for a strainless molecule.[12]

An analogous *ipso*-attack of an activated isopropenyl group in the reaction of 10-(2-isopropenylphenyl)-10*H*-phenoxarsine **17** with $TiCl_4$ in cyclohexane leads to the expanded heterocycle **18**. This is also formed upon PCl_3-reduction[5] of the oxide **19**, which is obtained upon formic acid-catalyzed ring expansion of **17** (and subsequent oxidative work-up). Finally, also on treating 10-[2,6-bis(isopropenyl)-phenyl]-10*H*-phenoxarsine **20**, obtainable from 10-chloro-10*H*-phenoxarsine[13] and 2,6-bis(isopropenyl)phenyllithium, with formic acid, an isomer can be isolated whose spectroscopic data are consistent with the structure **21** (Table 3) and whose formation can be envisaged in the same

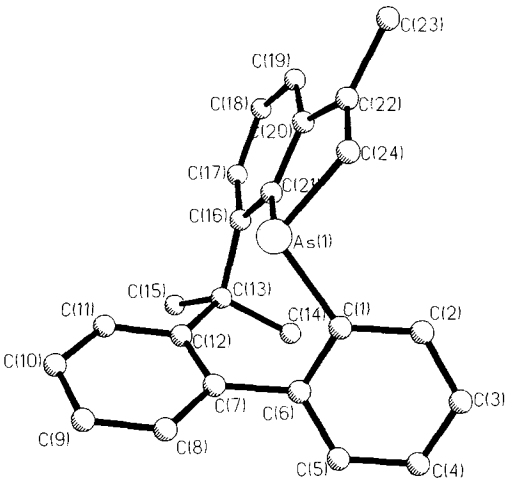

Fig. 3. Structure of **16** in the crystal (without H atoms). Selected bond lengths [pm] and angles [°] (standard deviations in brackets): As1-C1 195.2(2), As1-C21 194.6(2), As1-C24 191.8(4); C1-As1-C21 101.3(1), C1-As1-C24 105.1(1), C21-As1-C24 86.0(1).

way as that of **16** as a result of a tandem ring expansion/cyclization.

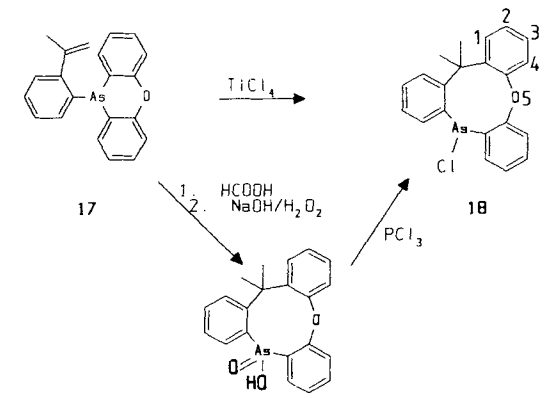

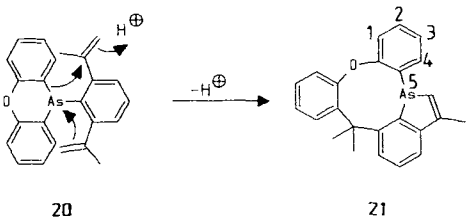

We are presently investigating whether this novel ring expansion in the form of a 1,2-phenylenemethylene moiety can also be extended to analogous derivatives of other main group elements (in particular N, P, Sb, Si, C).

Received: January 31, 1990 [Z 3771/3772 IE]
German version: *Angew. Chem. 102* (1990) 677

CAS Registry numbers:
3a, 127445-64-1; **3b**, 127445-65-2; **4**, 127445-66-3; **5a**, 127445-61-8; **5b**, 127445-62-9; **6**, 127445-67-4; **7a**, 127445-68-5; **7b**, 127445-69-6; **8a**, 127445-70-9; **8b**, 127445-71-0; **9**, 127445-72-1; **10a**, 96897-82-4; **10b**, 127445-73-2; **11a**, 127445-79-8; **11b**, 127445-80-1; **12**, 127472-31-5; **13**, 2866-58-2; **16**, 127445-63-0; **17**, 127445-77-6; **18**, 127445-74-3; **19**, 127445-75-4; **20**, 127445-78-7; **21**, 127445-76-5; *o*-chloranil, 2435-53-2; 10-chloro-10*H*-phenoxarsine, 2865-20-5.

[1] a) P. Gillespie, P. Hoffmann, H. Klusacek, D. Marquarding, S. Pfohl, F. Ramirez, E. A. Tsolis, I. Ugi, *Angew. Chem. 83* (1971) 691; *Angew. Chem. Int. Ed. Engl. 10* (1971) 687; b) W. S. Sheldrick, *Top. Curr. Chem. 73* (1978) 1; c) D. Hellwinkel, *ibid. 109* (1979) 1; d) P. Lemmen, R. Baumgartner, I. Ugi, F. Ramirez, *Chem. Scr. 28* (1988) 451.
[2] D. Hellwinkel, W. Blaicher, W. Krapp, W. S. Sheldrick, *Chem. Ber. 113* (1980) 1406.
[3] H. L. Carell, H. M. Bermann, J. S. Ricci, W. S. Hamilton, F. Ramirez, J. F. Marecek, L. Kramer, I. Ugi, *J. Am. Chem. Soc. 97* (1975) 38.
[4] For analogous systems with nitrogen and carbon centers see: D. Hellwinkel, G. Aulmich, M. Melan, *Chem. Ber. 114* (1981) 86; D. Hellwinkel, M. Melan, *ibid. 107* (1974) 616.
[5] S. Samann in *Houben-Weyl-Müller: Methoden der organischen Chemie, Bd. XIII/8*, Thieme, Stuttgart 1978, p. 250.
[6] **10a** has already been prepared by *Chen* et. al. via a completely different, less effective route: C. H. Chen, J. J. Doney, J. L. Fox, H. R. Russ, *J. Org. Chem. 50* (1985) 2914.
[7] The same effects were also observed by *Chen* et. al.: see [6] and literature cited therein.
[8] J. J. Daly, *J. Chem. Soc. 1964*, 3799.
[9] A. N. Sobolev, V. K. Belsky, N. Yu. Chernikova, F. Yu. Akhamadulina, *J. Organomet. Chem. 244* (1983) 129.
[10] Crystallographic data: **5a**: monoclinic, space group $P2_1/n$, $a = 12.498(3)$, $b = 9.961(2)$, $c = 21.027(5)$ Å, $\beta = 102.83(2)°$, $Z = 4$, $R = 0.052$, $R_w = 0.045$ for 3240 unique reflections. **5b**: monoclinic space group $P2_1/a$, $a = 11.838(3)$, $b = 11.557(2)$, $c = 14.798(3)$ Å, $\beta = 90.13(2)°$, $Z = 4$, $R = 0.04$, $R_w = 0.032$ for 3556 unique reflections. **12**: monoclinic, space group $P2_1/c$, $a = 10.918(7)$, $b = 28.32(1)$, $c = 11.036(5)$ Å, $\beta = 110.73(4)°$ $Z = 4$, $R = 0.043$, $R_w = 0.037$ for 3561 unique reflections. **16**: triclinic, space group $P\bar{1}$, $a = 8.339(4)$, $b = 8.595(7)$, $c = 13.865(9)$, $\alpha = 99.90(6)$, $\beta = 99.80(5)$, $\gamma = 105.39(5)°$, $Z = 2$, $R = 0.045$, $R_w = 0.04$ for 3937 unique reflections. Further details of the crystal structure investigations are available on request from the Fachinformationszentrum Karlsruhe, Gesellschaft für wissenschaftlich-technische Information mbH, D-7514 Eggenstein-Leopoldshafen 2 (FRG), on quoting the depository number CSD-54475, the names of the authors, and the journal citation.
[11] J. A. Aeschlimann, N. D. Lees, N. P. McCleland, G. N. Nicklin, *J. Chem. Soc. 127* (1925) 66.
[12] Cf. A. Tzschach, J. Heinicke: *Arsenheterocyclen*, VEB Deutscher Verlag für Grundstoffindustrie, Leipzig 1978.
[13] V. I. Gavrilov, V. N. Khlebnikov, A. A. Komleva, B. D. Chernokal'skii, *Zh. Obshch. Khim. 44* (1974) 2506; *Chem. Abstr. 82* (1975) 140 268m.

Electrochemical Solid-State Studies on Oligomeric *p*-Phenylenes as Model Compounds for Conductive Polymers**

By *Klaus Meerholz* and *Jürgen Heinze**

The characteristic current plateau in the cyclovoltammograms of conductive polymers has been the subject of intensive discussion for some time. On the one hand, capacitive charges in the sense of a molecular condenser are assumed as the reason for such plateaus,[1-3] while on the other there are increasing indications that capacitance effects play only a subordinate role and that the plateau current can largely be attributed to faradaic redox processes.[4-7]

Our voltammetric investigation of soluble oligomers of defined structure from the *p*-phenylenevinylene and *p*-phenylene series[8,9] has shown that the number of possible redox states increases with increasing chain length, and that the energy gap strongly increases between the lowest and highest redox states.

We have now investigated for the first time voltammetrically the redox behavior of defined oligomers of the *p*-phenylene series in the solid state. For comparison, Figure 1 a shows a typical cyclic voltammogram for the reduction of

[*] Prof. Dr. J. Heinze, Dipl.-Chem. K. Meerholz
Institut für Physikalische Chemie der Universität
Alberstrasse 21, D-7800 Freiburg (FRG)

[**] This work was supported by the Deutsche Forschungsgemeinschaft, the Fonds der Chemischen Industrie, and Bayer AG (gifts of chemicals).

p-quaterphenyl in solution.[9] The system is apparently reversibly reduced to the dianion in two separate redox steps at − 2.28 and − 2.45 V. Surprisingly, in the solid-state experiment (Fig. 1 b), irrespective of the chosen scan rate only one

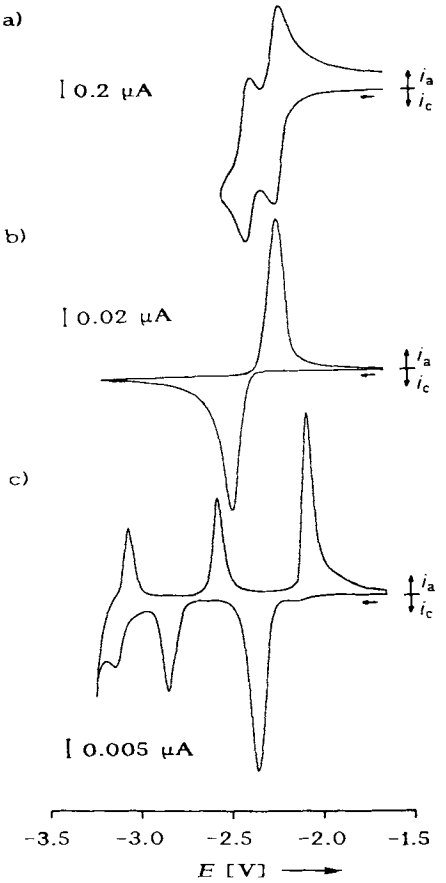

Fig. 1. Cyclovoltammograms in Me_2NH/0.1 M Bu_4NBr of a) *p*-quaterphenyl (saturated solution; $T = 10\,^{\circ}C$, $v = 100\,mV\,s^{-1}$), b) *p*-quaterphenyl (thin layer on Pt; $T = -75\,^{\circ}C$, $v = 10\,mV\,s^{-1}$), and c) *p*-sexiphenyl (thin layer on Pt; $T = -75\,^{\circ}C$, $v = 10\,mV\,s^{-1}$); potentials calibrated with $Cp_2Co^{\oplus}/Cp_2Co$ vs Ag/AgCl.

cathodic and one anodic wave are observed (at − 2.54 and − 2.25 V, resp.), both of which correspond to the transfer of two electrons per quaterphenyl molecule (see *Experimental*).

In our opinion the different redox transitions in the two voltammograms (Fig. 1 a, 1 b) are closely coupled with the structural properties of quaterphenyl in solution and in the solid state. In solution the phenyl rings can rotate freely about the linked bonds and thus also assume the conformation with the conjugation between the phenylene subunits that is optimum for the redox process. In the solid state, on the other hand, this free rotation is strongly hindered by intermolecular interactions. The molecules are present in a twisted conformation with a lesser degree of conjugation than is actually possible. Therefore, the first reduction in the solid state takes place at a more negative potential than in solution. In the monoionic state the molecules stabilize through a change in geometry from the twisted benzoid structure into a partially planar quinoid-like structure with better conjugation between the rings. Similar structural changes have been observed with substituted 5,6-dihydrobenzo[*c*]cinnolines in solution[10] and with tetrathiafulvalene in a Nafion matrix.[11, 12] As a consequence of this change in structure at the stage of the monoanion the redox potential for dianion formation shifts to more positive potentials and results in a formal two-electron transfer. At the dianion stage a further stabilizing change of structure takes place. During the reoxidation, which, because of the stabilization, takes place at more positive potentials than the reduction, a formal two-electron transfer is again observed, which is now attributable to the relaxation of the system into the initially twisted structure.

In a further solid state experiment we have investigated the electrochemical reduction of *p*-sexiphenyl voltammetrically (Fig. 1 c). In both scan directions three waves are observed, between which the current drops to almost zero. Coulometric measurements indicate transfer of two electrons for the first wave, of one electron for the second and up to one for the third (Tables 1 b–d). *p*-Sexiphenyl can accordingly be reversibly charged to the tetraanion. This finding is consistent with the rule that the number of possible redox states increases with increasing chain length of the oligomer. Particularly striking is the fact that the reoxidation waves lie at very much more positive potentials than the corresponding reduction waves.

In our opinion these effects clearly show that *p*-sexiphenyl molecules also stabilize through the transition from a benzoid into a quinoid-like structure upon uptake of electrons. This geometric stabilization still continues even after formation of the dianion. However, the extent of the additional stabilization is significantly less after the fourth electron transfer.

Table 1. Coulometric data for the reduction and oxidation of *p*-quaterphenyl and *p*-sexiphenyl. n = number of charging and discharging cycles, f = average binding number of a monomer unit, $Q_{a,c}$ = anodic and cathodic charge, respectively.

Exp.[a]	Educt	n	E_λ [V]	Q_a[b,d] [μC]	$-Q_c$[b,d] [μC]	ΔQ[b] [μC]	f
a	*p*-Quaterphenyl	1	−3.22		2.16 (2.00)	0	1.50
b	*p*-Sexiphenyl	1	−2.55		0.50 (2.00)	0	1.66
c		1	−2.95		0.75 (3.00)	0	1.66
d		1	−3.25		0.94 (3.76)[e]	0	1.66
e	*p*-Sexiphenyl	1	1.65	6.44 (2.00)		0	1.66
f		20[c]	1.76	140.20 (43.8)	137.00 (42.8)	3.20 (0.99)	-
g		1	1.76	6.85 (2.14)		0	1.83
h		4[c]	2.10	54.00 (16.88)	45.28 (14.15)	8.72 (2.73)	-
i		1	2.10	11.32 (3.54)		0	2.29
j		1	1.76	7.26 (2.27)		0	2.29

[a] The experiments b–d and e–j were carried out successively on the same sample. [b] Charges after subtraction of background currents. The charge equivalents transferred per mole of educt are quoted in brackets (see Experimental). [c] Solid-state polymerization. [d] $Q_a = -Q_c$ except in the case of f and h. [e] It was not possible to measure the last reduction wave entirely because the reduction of the electrolyte system starts at − 3.25 V.

In principle, similar results are obtained in the anodic oxidation of a *p*-sexiphenyl film as in the reduction. In a low-temperature experiment, reversible generation of the trication is possible. Upon further anodic charging the tetracation is formed, which, however, is not indefinitely stable and undergoes a coupled solid state reaction. The reactivity of the system increases when the temperature is raised, so that the *p*-sexiphenyl trication already reacts at room temperature.

If formation of the trication is completely excluded ($E_\lambda = 1.65$ V), *p*-sexiphenyl can be reversibly converted into the dication more than 500 times without loss of activity (Fig. 2a, Table 1e). Particularly striking are the extremely narrow waves and the large potential difference between the anodic and the cathodic peak potential of $\Delta E_p = 410$ mV, which indicates a strong energetic stabilization of the charged system.

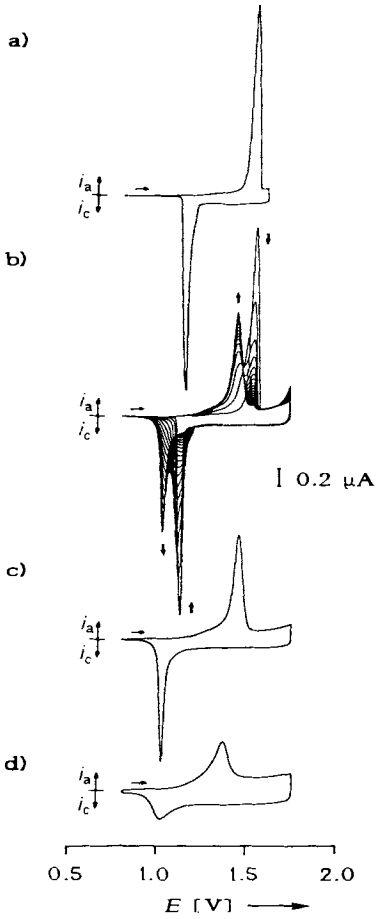

Fig. 2. Cyclovoltammograms in CH_2Cl_2/0.1 M Bu_4NPF_6 of a) *p*-sexiphenyl (thin layer on Pt), b) *p*-sexiphenyl in the multisweep experiment with $E_\lambda = 1.75$ V, c) the dodecaphenyl isomer, d) polyphenylene; potentials calibrated with $Cp_2Fe/Cp_2Fe^{\oplus}$ vs Ag/AgCl, $T = 10\,^{\circ}C$, $v = 20\ mV\,s^{-1}$.

If the switching potential in the multisweep experiment is set in the ascent of the anodic trication wave ($E_\lambda = 1.76$ V), two new, gradually increasing waves appear, whilst the original signals decrease (Fig. 2b). The resulting isopotential point confirms that *p*-sexiphenyl reacts to give a new electroactive species without side reactions. This reaction is quantitative. In addition, at high scan rates, broad waves as are typical for the reduction of protons are observed at low potentials in the cathodic reverse scan. The coulometric analysis of the voltammograms shows that one charge is lost per molecule (by proton cleavage) in the condensation reaction (Table 1f). The material formed is, in contrast to *p*-sexiphenyl, completely insoluble in all conventional solvents, and its voltammetric peak potentials lie negative to those of *p*-sexiphenyl. Furthermore, the halfwidths of the waves are still very small (Fig. 2c), and the peak-potential difference ($\Delta E_p = 430$ mV) resembles that of *p*-sexiphenyl. These are clear indications that a material of definite composition is formed. From all these observations we conclude that *p*-sexiphenyl dimerizes quantitatively in this solid state reaction to give a dodecaphenyl isomer whose redox steps each correspond to the transfer of four electrons per molecule.

If still higher electrode potentials (e.g. $E_\lambda = 2.1$ V) are applied in the multisweep experiment, further polymerization steps are induced. Depending upon the oxidation potential, 2–4 charge equivalents are thereby lost by cleavage of protons (Table 1h). The waves are once again shifted to more negative potentials, but are now also significantly broader, and the difference in peak potential decreases ($\Delta E_p = 350$ mV). An isopotential point is once again observed. The voltammogram, with its characteristic current plateau, is now typical for conductive polymers (Fig. 2d).

The amount of charge consumed in a pure charging and discharging cycle remains almost constant for all the materials investigated (Fig. 2a, c, d; Table 1e, g, j); on average, every third phenyl unit becomes charged. (The slight difference in charge of 8% between the experiments g and j can be attributed to the fact that the redox potentials in experiment j are shifted negative relative to those in g.) We can deduce from this that no material is lost or decomposed during the experiment. This is additionally supported by the appearance of isopotential points during the polymerization. The characteristic plateau region can thus be attributed unequivocally to faradaic redox processes.

Since the amount of charge that is additionally consumed for the solid-state polymerization is greater than that which is theoretically required for the complete linkage of all chains, the average binding number f of a monomeric unit must be greater than the limiting value $f = 2$ for chains of indefinite length (see Table 1i, j). A value of $f > 2$, however, signifies that coupling reactions leading to a network take place in addition to chain-lengthening steps. The chains are coupled via the *ortho* and *meta* positions of the phenyl units. Such a formation of defects has already been detected by FTIR-ATR measurements on polythiophene.[13]

The network formed exclusively by solid-state polymerization is apparently made up of numerous different structural segments. As a consequence the individual charge transitions, other than in ideal, linear chains, no longer take place in distinctly separate potential steps but are distributed over a large number of closely adjacent redox states. The typical voltammogram of conductive polymers corresponds to the superposition of all redox waves. Due to formation of the network, the mobility of the subunits formed in the polymer matrix is reduced. This might explain why a smaller peak-potential difference is observed for the polymer than for the oligomers.

Our investigations show that polyphenylene not only contains long, linear, *p*-coupled chains, as was previously assumed, but a polymer network. Since polypyrrole and polythiophene exhibit similar voltammograms, we presume that a network is partially formed also in those cases.

Experimental

For the solid state investigations, the oligomer to be investigated was deposited onto a Pt-disk electrode (∅ = 1 mm) by sublimation or by dipcoating the respective oligomer in dichloromethane. In this way, fully chargeable ($i \sim v$) homogenous layers of differing thickness could be prepared.

The amount of material employed was determined from the integral under the redox waves (= charge). In the reduction of *p*-sexiphenyl the charge numbers of the redox steps could be derived unambiguously from the observed charge ratio of 2:1 for the first two redox steps (Table 1 b,c). In the case of quaterphenyl an experiment was carried out with a large electrode and a weighable amount of material; this gave a value of 2 for the charge number. A similar experiment with sexiphenyl confirmed the above described direct method for the quantitative measurement.

By reduction and oxidation of one and the same sample of *p*-sexiphenyl it was confirmed that the integral under the first reduction wave is identical with that under the first oxidation wave ($E_\lambda = 1.65$ V), i.e., two electrons per molecule are transferred in both cases.

Received: January 24, 1990;
supplemented: April 2, 1990 [Z 3755 IE]
German version: *Angew. Chem. 102* (1990) 695

[1] S. W. Feldberg, *J. Am. Chem. Soc. 106* (1984) 4671.
[2] a) J. Tanguy, N. Mermilliod, M. Hoclet, *J. Electrochem. Soc. 134* (1987) 795; b) J. Tanguy, N. Mermilliod, *Synth. Met. 21* (1987) 129.
[3] R. C. M. Jakobs, L. J. J. Janssen, E. Barendrecht, *Recl. Trav. Chim. Pays-Bas 103* (1984) 275.
[4] a) J. Heinze, M. Dietrich, J. Mortensen, *Makromol. Chem. Makromol. Symp. 8* (1987) 73; b) J. Heinze, R. Bilger, K. Meerholz, *Ber. Bunsenges. Phys. Chem. 92* (1988) 1266; c) J. Heinze, *Top. Curr. Chem. 152* (1990) 1.
[5] S. Bruckenstein, J. W. Sharkey, *J. Electroanal. Chem. 241* (1988) 211.
[6] R. S. Hutton, M. Kalaji, L. M. Peter, *J. Electroanal. Chem. 270* (1989) 429.
[7] J. Heinze, M. Störzbach, J. Mortensen, *Ber. Bunsenges. Phys. Chem. 91* (1987) 960.
[8] J. Heinze, J. Mortensen, K. Müllen, R. Schenk, *J. Chem. Soc. Chem. Commun. 1987*, 701.
[9] K. Meerholz, J. Heinze, *J. Am. Chem. Soc. 111* (1989) 2325.
[10] M. Dietrich, J. Heinze, H. Fischer, F. A. Neugebauer, *Angew. Chem. 98* (1986) 999; *Angew. Chem. Int. Ed. Engl. 25* (1986) 1021.
[11] T. P. Henning, A. J. Bard, *J. Electrochem. Soc. 130* (1983) 613.
[12] M. D. Ward, *J.Electroanal. Chem. 273* (1989) 79.
[13] H. Neugebauer, A. Neckel, N. Brinda-Konopik in H. Kuzmany, M. Mehring, S. Roth (Eds.): *Electronic Properties of Polymers and Related Compounds*, Springer, Berlin 1985, p. 227.

Zwitterions as Intermediates of the 1,3-Dipolar Cycloaddition of Electrophilic Azides to 5-Alkylidenedihydrotetrazoles – the Other Non-Concerted Limiting Case **

By *Helmut Quast,* Dieter Regnat, Eva-Maria Peters, Karl Peters* and *Hans Georg von Schnering*

Dedicated to Professor Rolf Huisgen on the occasion of his 70th birthday

The perturbational treatment of 1,3-dipolar cycloadditions[1] predicts for extreme HOMO-LUMO energy differences two limiting cases of a non-concerted two-step mechanism in which zwitterions occur as intermediates. *Huisgen* et al. realized one of the non-concerted limiting cases by reaction of strongly nucleophilic thiocarbonyl ylides with particularly electrophilic alkenes.[2] We report here on the first example for the other non-concerted limiting case which is to be expected in the cycloaddition of strongly electrophilic 1,3-dipoles to particularly nucleophilic alkenes. In a comparable Diels-Alder reaction with inverse electron demand a zwitterion was recently isolated and identified as intermediate.[3]

1,3-Dipolar cycloaddition of alkyl and aryl azides RN_3 to 5-alkylidenedihydrotetrazoles **2** leads to spirocycles of type **4**.[4] On the other hand, in reactions with the strongly *electrophilic* azides **1a–c** in toluene the zwitterions **3** or the 5-iminotetra-hydro-1,2,3,4-tetrazines **5** – together with molecular nitrogen – are obtained. The latter are formed from the corresponding spirocycles **4**, which, however, are not observed directly. The ring expansion of the tetrazole to the tetrahydro-1,2,3,4-tetrazine ring is an example of the rare 1,2-shift of a nitrogen atom.[5]

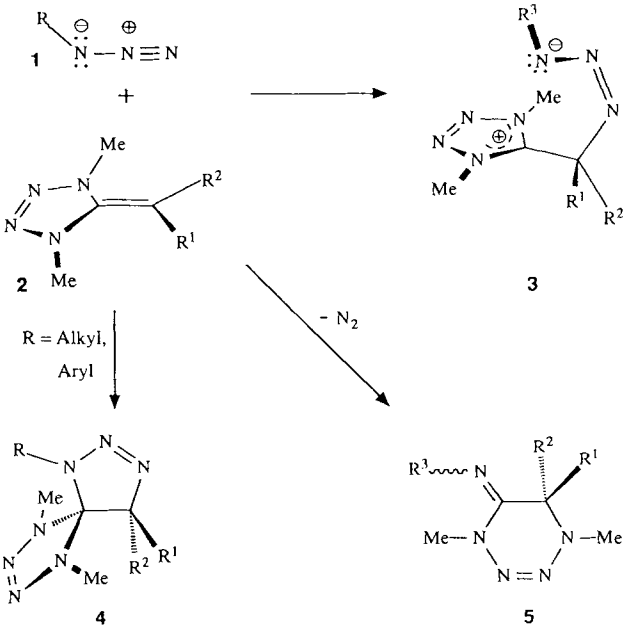

1a: R = 2,4,6-$(NO_2)_3$-C_6H_2; **1b**: R = 4-Me-C_6H_4-SO_2; **1c**: R = Me-SO_2

2a: $R^1 = R^2$ = Me; **2b**: R^1 = H, R^2 = *t*Bu

Table 1. Substituents, yields and melting points of the zwitterions **3** and of the 5-iminotetrahydro-1,2,3,4-tetrazines **5**.

Cpd.	R^1	R^2	R^3	Yield [%]	M.p. [°C]
3a	Me	Me	2,4,6-$(NO_2)_3$-C_6H_2	90	125–126
3b	H	*t*Bu	2,4,6-$(NO_2)_3$-C_6H_2	37	115
3c	Me	Me	4-Me-C_6H_4-SO_2	quant.	
5c	Me	Me	4-Me-C_6H_4-SO_2	73	172–173
3d	H	*t*Bu	4-Me-C_6H_4-SO_2	quant.	139–140
5d	H	*t*Bu	4-Me-C_6H_4-SO_2	68	107–108
3e	H	*t*Bu	Me-SO_2	52	111–112
5f	Me	Me	Me-SO_2	86	106–107

The zwitterions **3a, d, e** (Table 1) can be recrystallized from boiling 2-propanol. The structure of the zwitterion **3e** (Fig. 1) was confirmed by X-ray diffraction analysis.[6] It shows some remarkable features in the crystal which may

[*] Prof. Dr. H. Quast, Dipl.-Chem. D. Regnat
Institut für Organische Chemie der Universität
Am Hubland, D-8700 Würzburg (FRG)
E.-M. Peters, Dr. K. Peters, Prof. Dr. H. G. von Schnering
Max-Planck-Institut für Festkörperforschung
Heisenbergstraße 1, D-7000 Stuttgart 80 (FRG)

[**] This work was supported by the Fonds der Chemischen Industrie. *D. R.* thanks the Fonds der Chemischen Industrie for a postgraduate grant.

essentially remain unaltered in solution. The N–N distances in the triazenide moiety resemble those in uncharged triazenes[7] and suggest a considerable localization of the negative charge on N10. Particularly striking is the short distance of 258.5 pm between the centers of the opposite charges, C5 and N10. The resulting coulomb attraction is balanced by the steric repulsion between the methyl group on N4 and the *tert*-butyl group on C6, which is oriented almost orthogonally to the plane of the tetrazole ring. Thus, ring closure to the cycloadduct **4e** is sterically hindered, and the particular stability of the zwitterions of the *tert*-butyl series (**3b, d, e**) compared to the dimethyl compound **3c** apparently has steric origins.

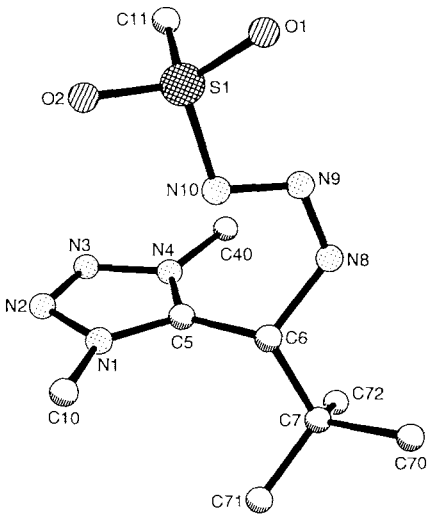

Fig. 1. Structure of the zwitterion **3e** in the crystal. Selected bond lengths [pm] and angles [°]: N1–N2 135.7(4), N1–C5 132.6(3), N2–N3 127.1(4), N3–N4 136.1(3), N4–C5 132.4(4), C5–C6 151.5(4), C6–C7 154.8(4), C6–N8 149.7(4), N8–N9 127.1(4), N9–N10 134.8(3), N10–S1 162.9(3), S1–O1 143.3(2), S1–O2 142.9(3), S1–C11 177.0(4); C5–C6–C7 115.5(2), C5–C6–N8 109.5(2), C7–C6–N8 110.5(2), C6–N8–N9 115.6(2), N8–N9–N10 116.5(2), N9–N10–S1 111.0(2).

Whereas the zwitterion **3c** quantitatively affords tetrazine **5c** and iminotetrazole **6** (97:3) at temperatures as low as −10 to 0 °C (in $CDCl_3$), **3d** reacts very slowly in CD_3CN at 20–25 °C (38% conversion in 850 h) and completely only in 5 h at 80 °C. Tetrazine **5d** and iminodihydrotetrazole **6** are formed in the ratio 4:1. Numerous analogies are known for the decomposition of the intermediate cycloadducts **4c, d** into **6** and **7**.[8] The NMR spectroscopic data of some zwitterions **3** and tetrazines **5** are collected in Table 2.

Are the zwitterions **3** intermediates of a two-step 1,3-dipolar cycloaddition or do they only participate in a dead-end equilibrium alongside a concerted cycloaddition? The following observations help towards answering this question.

1. Only the zwitterions **3c, d** are formed from **2** and tosyl azide **1b** at −78 °C in CD_2Cl_2. Neither the cycloadducts **4c, d** nor the tetrazines **5c, d** could be detected by ^{1}H-NMR spectroscopy (200 MHz) at −60 °C.

2. The deuterated zwitterion [D_7] **3c** formed from deuterated tosyl azide [D_7]**1b** and **2a** at −30 °C in [D_8]toluene reacts at −10 to 0 °C in $CDCl_3$ in the presence of 20 equivalents of **1b** to give the isotopomeric tetrazines [D_7]**5c** and **5c** in the ratio (93 ± 1):(7 ∓ 1). That is, the cleavage of the zwitterion **3c** plays only a minor role compared to its cyclization.

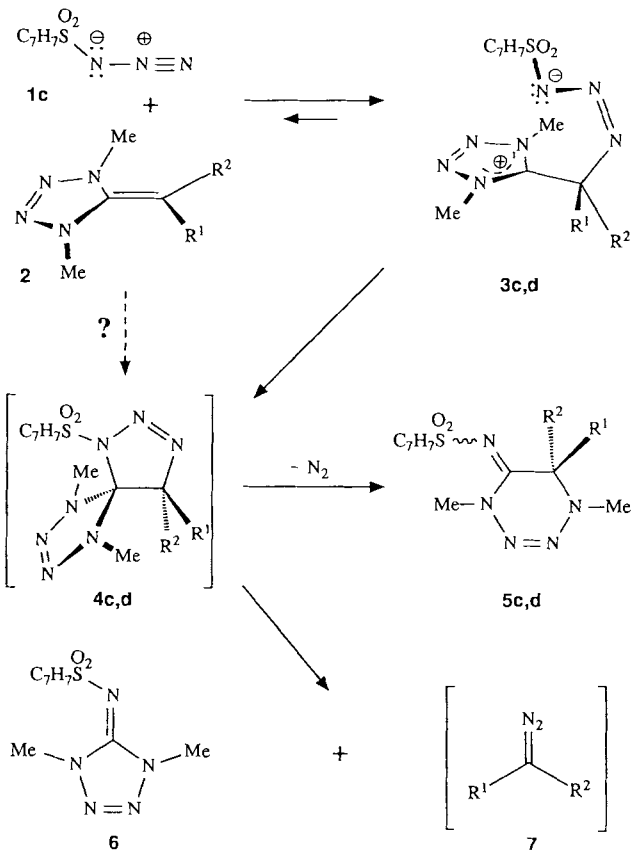

3. Within 3 h in CD_3CN solution at 80 °C in the presence of 20 equivalents of **1b**, the zwitterion [D_7]**3d** yields 20% of the iminotetrazoles [D_7]**6**, **6** and 80% of the tetrazines [D_7]**5d**, **5d** with an isotopomeric ratio of (65 ± 3):(35 ∓ 3). Under the same conditions, **3d** in the presence of 20 equivalents of [D_7]**1b** affords ca. 35% of non-deuterated tosyl azide **1b** as well as 20% of iminotetrazoles **6**, [D_7]**6** and 80% of tetrazines **5d**, [D_7]**5d** in the ratio (65 ± 3):(35 ∓ 3). That is, the zwitterion **3d** partially decomposes into its components **1b** and **2b** at 80 °C.

Since the zwitterions **3c, d** are formed much more rapidly from tosyl azide **1b** and the alkylidene tetrazoles **2** than are the tetrazines **5c, d**, and since the zwitterions **3c, d** cyclize more rapidly to the intermediate cycloadducts **4c, d** than

Table 2. ^{1}H-NMR (200 or 250 MHz) and ^{13}C-NMR (50 or 62.5 MHz) data of the zwitterions **3a, c, d** and tetrazines **5c, d**.

3a: ^{1}H NMR (CD_3CN): δ = 1.79 (2 Me), 4.28 (2 NMe), 8.24 (2 *m*/H). ^{13}C NMR ([D_6]DMSO): δ = 25.4 (2 Me), 40.0 (2 NMe), 63.7 (*C*Me$_2$), 122.1 (*m*-C), 130.9, 139.5, 147.6 (*ipso*-, *o*-, *p*-C), 156.2 (C=N)

3c: ^{1}H NMR ($CDCl_3$, −20 °C): δ = 1.81 (2 Me), 2.46 (*p*-Me), 3.89 (2 NMe), 7.35, 7.60 (AA'XX', 4H, *o*-, *m*-H). ^{13}C NMR ($CDCl_3$, −20 °C): δ = 20.6 (*p*-Me), 22.4 (2 Me), 37.9 (2 NMe), 56.1 (*C*Me$_2$), 141.1 (*ipso*-C), 125.8 (*o*-C), 128.4 (*m*-C), 139.0 (*p*-C), 155.5 (C=N)

3d: ^{1}H NMR ($CDCl_3$): δ = 1.16 (*t*Bu), 2.37 (*p*-Me), 3.60 (NMe), 4.33 (NMe), 4.58 (1H), 7.19, 7.58 (AA'XX', 4H, *o*-, *m*-H). ^{13}C NMR ($CDCl_3$): δ = 21.4 (*p*-Me), 27.2 (*CMe*$_3$), 37.0 (*C*Me$_3$), 37.7 (NMe), 38.8 (NMe), 62.4 (*CH*$_2$*t*Bu), 141.6 (*ipso*-C), 127.1 (*o*-C), 129.0 (*m*-C), 139.9 (*p*-C), 154.0 (C=N)

5c: ^{1}H NMR ($CDCl_3$): δ = 1.35 (2 Me), 2.39 (*p*-Me), 3.24 (NMe), 3.82 (NMe), 7.25, 7.83 (AA'XX', 4H, *o*-, *m*-H). ^{13}C NMR (C_6D_6): δ = 21.1 (*p*-Me), 19.2 (2 Me), 37.0 (NMe), 41.5 (NMe) 54.9 (*C*Me$_2$), 142.7 (*ipso*-C), 126.7 (*o*-C), 129.3 (*m*-C), 142.0 (*p*-C), 150.5 (C=N)

5d: ^{1}H NMR ($CDCl_3$): δ = 1.08 (*t*Bu), 2.41 (*p*-Me), 3.44 (NMe), 3.50 (NMe), 5.29 (1H), 7.83, 7.28 (AA'XX', 4H, *o*-, *m*-H). ^{13}C NMR ($CDCl_3$): δ = 21.5 (*p*-Me), 28.1 (*CMe*$_3$), 39.9 (*C*Me$_3$), 37.4 (NMe), 44.3 (NMe), 60.4 (*CH*$_2$*t*Bu), 142.7 (*ipso*-C), 126.4 (*o*-C), 129.3 (*m*-C), 140.5 (*p*-C), 145.5 (C=N)

they decompose into their components, *the zwitterions* **3c, d** *are intermediates of a two-step 1,3-dipolar cycloaddition. A concerted cycloaddition of* **1b** *and* **2** *cannot be detected at low temperatures*. It seems unlikely that it begins to play a role at 80 °C in the case of **1b** and **2b**, since the rate-determining step of the two-step cycloaddition, i.e. the cyclization of the zwitterion **3d** probably has a less negative activation entropy than the hypothetical concerted cycloaddition.[9]

The first step of the two-step 1,3-dipolar cycloaddition described here is influenced by the HOMO (dipolarophile)–LUMO (1,3-dipole) separation, the second step by the electronic stabilization of the zwitterion and by steric effects on its cyclization. In the case of the 1,3-dipolar cycloaddition of phenyl azide to *N*-(1-cyclohexenyl)pyrrolidine, which is regarded as concerted, the HOMO(dipolarophile)–LUMO(1,3-dipole)separation is ca. 7.3 eV.[9] The HOMO of isopropylidenedihydrotetrazole **2a** lies at −6.95 eV[10] and the LUMO of the sulfonyl azides **1b** and **1c**, according to MNDO calculations, lie at −0.14 and −0.19 eV, respectively.[11] That is, with a separation of 6.8 eV between HOMO (dipolarophile) and LUMO (1,3-dipole), a 1,3-dipolar cycloaddition can proceed in two steps. 2-Alkylidenedihydrobenzimidazoles and 2-alkylidenetetrahydroimidazoles behave like the 5-alkylidenedihydrotetrazoles **2** towards electrophilic azides. Whether this also holds true in the case of other electrophilic 1,3-dipoles remains an open question.

Received December 13, 1989 [Z 3683 IE]
German version: *Angew. Chem. 102* (1990) 724
Publication delayed at authors' request.

CAS Registry numbers:
1a, 1600-31-3; **1b**, 941-55-9; **1b** (D_7), 126822-18-2; **1c**, 624-90-8; **2a**, 54986-15-1; **2b**, 54986-16-2; **3a**, 126822-10-4; **3b**, 126822-11-5; **3c**, 126822-12-6; **3c** (D_7), 126822-19-3; **3d**, 126822-14-8; **3d** (D_7), 126822-21-7; **3e**, 126822-16-0; **5c**, 126822-13-7; **5c** (D_7), 126822-20-6; **5d**, 126822-15-9; **5d** (D_7), 126822-23-9; **5f**, 126822-17-1; **6**, 6456-14-0; **6** (D_7), 126822-22-8.

[1] R. Sustmann, *Pure Appl. Chem. 40* (1974) 569–593.
[2] R. Huisgen, G. Mloston, E. Langhals, *J. Am. Chem. Soc. 108* (1986) 6401–6402; *J. Org. Chem. 51* (1986) 4085–4087; R. Huisgen, E. Langhals, H. Nöth, *Tetrahedron Lett. 27* (1986) 5475–5478; G. Mloston, E. Langhals, R. Huisgen, *ibid. 30* (1989) 5373–5376; R. Huisgen in D. P. Curran (Ed.): *Advances in Cycloaddition, Vol. 1*, JAI Press, London 1988, p. 1–31.
[3] K.-P. Hartmann, M. Heuschmann, *Angew. Chem. 101* (1989) 1288–1290; *Angew. Chem. Int. Ed. Engl. 28* (1989) 1267.
[4] H. Quast, L. Bieber, G. Meichsner, D. Regnat, *Chem. Ber. 121* (1988) 1285–1290.
[5] R. Ohme, H. Preuschhof, *Justus Liebigs Ann. Chem. 721* (1969) 25–33; A. Heesing, G. Imsieke, G. Maleck, R. Peppmöller, H. Schulze, *Chem. Ber. 103* (1970) 539–552; A. S. Bailey, R. Scattergood, W. A. Warr, *J. Chem. Soc. C 1971*, 3769–3778; M. Regitz, G. Weise, B. Lenz, U. Förster, K. Urgast, G. Maas, *Bull. Soc. Chim. Belg. 94* (1985) 499–520; *Chem. Abstr. 105* (1986) 24225q.
[6] Crystals of **3e** (0.6 × 0.85 × 0.4 mm, from 2-propanol) are ortho-rhombic, space group *Fdd2*, $a = 2179(1)$, $b = 2881(5)$, $c = 953.5(7)$ pm, $V = 5987(7) \times 10^6$ pm^3, $Z = 16$, $\varrho_{calc} = 1.284$ g cm^{-3}, $\mu(Mo_{K\alpha}) = 2.2$ cm^{-1}. Nicolet R3m/V diffractometer. Of 1934 measured reflections ($1.75 < \theta < 27.5°$) 1836 were unique. The 1749 reflections with $F > 3\sigma(F)$ were used for the refinement with the program system SHELXTL PLUS. $R = 0.037$, $R_w = 0.036$. Further details of the crystal structure investigation are available on request from the Fachinformationszentrum Karlsruhe, Gesellschaft für wissenschaftlich-technische Information mbH, D-7514 Eggenstein-Leopoldshafen 2 (FRG), on quoting the depository number CSD-54282, the names of the authors, and the journal citation.
[7] A. J. Randall, C. H. Schwalbe, *J. Chem. Soc. Perkin Trans. 2 1984*, 251–253.
[8] M. Regitz, G. Maas: *Diazo Compounds*, Academic Press, New York 1986, p. 386–389.
[9] R. Huisgen in A. Padwa (Ed.): *1,3-Dipolar Cycloaddition Chemistry, Vol. 1*, Wiley, New York 1984, p. 1–176.
[10] P. Rademacher (Universität Essen) private communication.
[11] E. Huda, *Dissertation*, Universität Düsseldorf 1989. We thank Professor Dr. *H.-D. Martin* for these data.

BOOK REVIEWS

Book Reviews are written by invitation from the editor. Suggestions for books to be reviewed and for book reviewers are welcome. Publishers should send brochures or (better) books to the following address: Redaktion Angewandte Chemie, Postfach 101161, D-6940 Weinheim, Federal Republic of Germany. The editor reserves the right of selecting which books will be reviewed. Uninvited books not chosen for review will not be returned.

Schrödinger—Life and Thought. By *W. Moore*. Cambridge University Press, Cambridge/UK 1989. xi, 513 pp., hardcover, $ 39.50.—ISBN 0-521-35434-X

The success and recognition gained by a scientist are usually measured by the frequency with which his or her publications are cited. Only a few reach a status which transcends such criteria, and these become the subjects of biographies. As a result, suddenly it is not only their already well known scientific achievements that are of interest, but also their childhood, upbringing and private lives. The theoretical physicist *Erwin Schrödinger* was virtually predestined to be the subject of a biography, being an individualist and a scientific loner whose life and achievements therefore stood out unusually clearly from those of his contemporaries. The Emeritus Professor of Physical Chemistry *Walter Moore* has meticulously gathered together information on *Schrödinger*'s private and scientific life, some of it practically unknown up to now, and assembled this into an imposing work. Even the list of names of the people in many different countries whom he has consulted in writing the book fills a whole page. As a result this biography of *Schrödinger* far exceeds all previous ones in size and comprehensiveness.

The accounts of *Schrödinger*'s youth in Vienna, of his student days, and of his early years as a professor of theoretical physics, first in Jena, then in Stuttgart and Breslau, occupy the initial third of the biography. The development of the ideas that led to *Schrödinger* taking his place in the history of physics and related disciplines begins in 1924 with *Louis de Broglie*'s prediction of the existence of particle-waves. At that time *Schrödinger* held a professorship in Zürich, and was fortunate in having the mathematician *Hermann Weyl* nearby. *Moore* has succeeded admirably in describing the development of wave mechanics with a minimum of mathe-

matical formulas. This is especially valuable, since the six lengthy original papers published by *Schrödinger* would be very laborious for the reader to tackle himself. The supreme moment in *Schrödinger*'s life was essentially the few days of the Christmas holiday of 1925. Compared with this the meetings of the Nobel committee to evaluate *Schrödinger*'s work, extending up to 1933, seem very long. It was not at first clear whether wave mechanics should be regarded as merely an extension of *de Broglie*'s particle-waves hypothesis or whether it contained ideas that were fundamentally new. The most absorbing section of the book is concerned not so much with the birth of wave mechanics as with how the theory stood up to objections by *Planck, Einstein, Born, Heisenberg, Lorentz* and others. The manner in which the Schrödinger equation was proved correct against these criticisms was a matter of surprise rather than of logic. At this point the reader is given the impression that the only problem actually solved by *Schrödinger* was that of the hydrogen atom, and in the final analysis this is true. Some of his contemporaries, such as *Paul Dirac* and *Friedrich Hund*, recognized immediately that *Schrödinger*'s equation had also laid the foundation stone for what was to become the most successful branch of theoretical chemistry, but this insight was denied to *Schrödinger* himself during his lifetime. In fact, he could not accept the interpretation of the wave function in terms of *Born*'s model. The dispute on this aspect, which *Schrödinger* pursued in a vindictive and emotional way against *Born*, is only briefly mentioned in this biography. *Schrödinger*'s later positions, such as those in Berlin (1927–1933), Graz (1936–1938) and Dublin (1939–1956), to mention only a few, appear to the reader interested in wave mechanics as no more than an epilogue.

The occasional comments of a political nature about *Schrödinger* are, as one might expect, questionable and contradictory. Nevertheless, here for the first time a biographer has ventured to reproduce *Schrödinger*'s emotional "declaration of allegiance to the Führer" of 31 March 1938 (which is the correct date), even though it is not accompanied by the no less revealing comments on this by the then rector of Graz University. I found only a few names of people and places in this biography that need to be corrected.

Schrödinger had a personality with inner conflicts. Frequent affairs at a personal level made it difficult for him to carry out his normal duties to the full. As a result of this, and the frequent changes of location which were partly connected with it, *Schrödinger*, unlike some of his other well-known colleagues, never founded institutes or produced eminent students. However, the author puts a different interpretation on the *Schrödinger* phenomenon, recognizing an essential inner connection between the rapid succession of affairs and the striving towards scientific versatility.

This biography, which is also very attractively presented and contains excellent illustrations and source references, can be recommended to every scientist.

Rudolf Janoschek [NB 1047 IE]
Institut für Theoretische Chemie
der Universität Graz (Austria)

The Conformational Analysis of Cyclohexenes, Cyclohexadienes and Related Hydroaromatic Compounds. Edited by *P. W. Rabideau*. VCH Verlagsgesellschaft, Weinheim/VCH Publishers, New York 1989. ix, 323 pp., hardcover, DM 154.00.—ISBN 3-527-26860-X/0-89573-702-7

This monograph belongs to the series "Methods in Stereochemical Analysis" (series editor: *A. P. Marchand*), and consists of eight chapters, an appendix and a brief subject index. The authors and short titles of the individual contributions, together with some statistical data (numbers of pages and details of literature citations) are listed in Table 1.

Table 1.

Author(s)	Short title	Number of pages	References		
			Total number	Number (and %) for 1984 onward	Number (and %) of self-citations
F. A. L. Anet	Cyclohexenes	42	137	19 (14)	4 (3)
J. B. Lambert	6-Membered rings with exocyclic double bonds	14	41	4 (10)	13 (32)
P. W. Rabideau, A. Sygula	1,3-Cyclohexadienes	21	75	3 (4)	3 (4)
P. W. Rabideau	1,4-Cyclohexadienes	35	84	17 (20)	19 (23)
F. G. Morin, D. M. Grant	^{13}C NMR Spectroscopy	38	43	6 (14)	10 (23)
S. A. Evans	Hetero-6-ring-olefins (thioxanthenes)	40	119	19 (16)	5 (4)
K. B. Lipkowitz	Applications of force field calculations	53	47	6 (13)	3 (6)
R. G. Harvey	Metabolites of carcinogenic hydrocarbons	29	97	25 (26)	44 (45)
K. B. Lipkowitz	Methodology of force field calculations (Appendix)	19	32	8 (25)	1 (3)
	Subject index	3			
Totals		294	675	107 (16)	102 (15)

The first contribution attests that virtually everything is known about the conformational behavior of cyclohexene, and that on this firm basis many of the properties of cyclohexene derivatives can be understood. The short second chapter does not really fit into the book's context, unless a rather artificial one is constructed by, for example, emphasizing the enol form of cyclohexanone as a cyclohexene derivative. The following two chapters on 1,3- and 1,4-cyclohexadienes (and their benzo derivatives) bring us back to the primary topic; these chapters include a neat analysis of the factors governing the geometry of the six-membered ring (planar or non-planar?) and of the preferred positions occupied by substituents. Chapter 5 is concerned with applications of ^{13}C NMR spectroscopy to the conformational analysis of partially hydrogenated naphthalenes, anthracenes and phenanthrenes, and includes a six-page table listing chemical shifts. The title of Chapter 6 announces an account of conformational studies on hetero-six-membered ring olefins in general, but the chapter is almost exclusively devoted to thioxanthenes of pharmacological importance. At this point one would have been pleased to find a discussion on nicotinamide adenine dinucleotide (NAD), which is so important biochemically, and whose reduced form (NADH) is of course a derivative of aza-1,4-cyclohexadiene. In contrast, Chapter 7 contains for the most part what the title promises, i.e. force field calculations on hydrocarbons with cyclohexene and cyclohexadiene units. However, 1,3-cyclohexadienes

are not included here, as they are less amenable to force field calculations, having conjugated double bonds. Apart from this omission, a remarkably wide variety of interesting strained hydrocarbons is covered, all of which indeed fit into the subject. This may help to allay doubts about the justification to publish this book as a whole, originating from its rather narrow scope. Chapter 7 is supplemented by an appendix, which gives a brief outline of force field methods. In fact, this appendix appears more or less superfluous. The material is presented very loosely and seems to stem from a casual seminar talk rather than rigorous planning; literature citations in the text are almost nil. The eighth and last chapter is on a topic that one would not expect in this book. As it concerns structure-bioactivity relationships of hydroaromatic metabolites of carcinogenic hydrocarbons, its topicality is obvious and reflected by many very recent literature citations (Table 1). A prominent feature is the discussion of NMR spectroscopic results, including many from the author's own laboratory.

As already mentioned, the book as a whole raises the question of whether the narrowly defined subject matter really justifies a monograph to itself. Further doubt is nourished by the notion that a "nugget" of the book (Chapter 8) might more appropriately have been published elsewhere. Clearly, specialization is inevitable in view of the ever increasing tide of new scientific knowledge, but is it really necessary to take this as far as has been done here? The book can be recommended to a limited number of experts; it is unlikely to reach a large readership, also in view of the frustrations ensuing from its high price.

Otto Ermer [NB 1024 IE]
Institut für Organische Chemie
der Universität Köln (FRG)

Comprehensive Polymer Science: The Synthesis, Characterization, Reactions and Applications of Polymers. 7 volumes. Edited by *G. Allen* and *J. C. Bevington*. Pergamon Press, Oxford 1989. 5367 pp., hardcover, $ 1995.00.—ISBN 0-08-032516-5

Volume 1 of this work contains a comprehensive review of "Polymer Characterization", and Volume 2 deals with "Polymer Properties". In the latter volume a somewhat more detailed treatment of high temperature polymers and liquid crystal polymers would have been desirable. Polymer synthesis is treated in volumes 3 to 5, under "Chain Polymerization" (Volumes 3 and 4) and "Step Polymerization" (Volume 5). The contributions vary from very detailed and comprehensive to very brief, and cover all aspects, usually with the main emphasis on scientific problems.

Volume 6 is concerned with reactions involving macromolecules. The chapter on "Thermal Degradation" neglects to cover aromatic polymers. Volume 7, "Specialty Polymers and Polymer Processing", is by the nature of the subject heterogeneous. The chapter on "Polymer Blends" is very good as regards the theoretical part, but a section on methods of production and on polymer blends of technological importance would have been a welcome addition. The least satisfactory part is that on "Polymer Processing" (230 pp.).

The editors and the authors (of whom there are 250 from 20 different countries!) have set out to produce "a milestone in the literature of polymer science", covering the fields of synthesis, characterization, reactions and applications. Have they succeeded in fulfilling this ambitious self-proclaimed promise? In the opinion of the reviewers, they have only been partly successful. However, it is doubtful whether it is actually possible to cover these four aspects of such an extensive area of knowledge equally well in a single work, even in a multi-volume compendium such as this.

"Comprehensive Polymer Science" should be regarded as a valuable addition to the already existing encyclopedias and handbooks in the polymer field, and it also succeeds as a comprehensive textbook presenting the latest state of knowledge. It is recommended for readers wishing to familiarize themselves with specific areas of polymer research, including especially synthesis, characterization and reactions. In many of the chapters this objective is particularly helped by the manner of presentation, with numerous tables summarizing the information and thus making the reader's task easier. Also the bibliographies, extending partly up to 1988, give comprehensive access to the original literature.

Some defects need to be remedied in a future edition of the work. The contributions vary greatly in the amount of detail covered, and some of them only deal with selected aspects; in a few cases the format is merely that of an expanded synopsis. Also the balance between scientific and practically orientated information varies greatly. It would also be highly desirable to have a consistent nomenclature and terminology. Lastly, cross-references within the individual contributions and between them would be very useful.

Ludwig Böhm, Harald Cherdron, Manfred Fleissner, Willi Kreuder, Arnold Schneller [NB 1019 IE]
Hoechst AG
Frankfurt/Main (FRG)

Spectroelectrochemistry. Edited by *R. J. Gale*. Plenum, New York 1988. 450 pp., hardcover, $ 85.00.—ISBN 0-306-42855-5

Spectroelectrochemistry—the application of spectroscopic methods to solving electrochemical problems—is currently the fastest growing branch of electrochemistry. The numerous results that it has produced have in many cases lent further support to conclusions reached from classical electrochemical studies, and in a few cases have refuted them. Often spectroscopic methods have for the first time opened up the way to obtaining a detailed picture, on a microscopic scale, of the mechanism of an electrochemical reaction and of the structure of the electrochemical double layer. Therefore, despite the fact that in journals and monographs there are review articles covering nearly all the different methods of spectroelectrochemistry with varying degrees of depth and completeness, the idea of publishing a book which gives a comprehensive and coherent description of all the *in situ* methods is to be welcomed. The deliberate restriction to *in situ* methods, thereby avoiding the potential sources of error involved in transferring electrodes from the electrochemical sampling cell to the analytical instrument, is also sensible. However, the exclusion (which is presumably intentional) of methods whose main strength lies in identifying and quantifying species in solution as opposed to those on the electrode surfaces is incomprehensible and disappointing.

A short introductory chapter by the editor is followed by seven chapters on methods that are *in situ* in nature and essentially surface specific (although there is some doubt as to whether the second of these criteria applies to electrochemical ESR spectroscopy). The seven chapters deal with: X-ray spectroscopy, photoemission measurements, UV-VIS reflection spectroscopy, IR reflection spectroscopy, surface-

enhanced Raman spectroscopy, electron spin resonance spectroscopy and Mössbauer spectroscopy.

All the chapters are written by recognized experts, although they vary in the quality of detailed coverage, and in some cases the choice of examples and literature citations is unduly selective. Unfortunately, as in many multi-author works of this kind, it appears that each author has been unaware of what the others planned to include, and there is therefore no coordination between the contents of the chapters, especially with regard to the examples of experimental studies and results. This is all the more annoying in view of the fact that the rational use of several spectroelectrochemical methods in combination can lead to results that are considerably more accurate, reliable and complete. Examples that could have been included are studies of conducting polymers, of chemically modified electrodes, or of compounds adsorbed on electrodes. These would have provided striking illustrations of the enormous potential of using different methods in combination.

Also disappointing is the lack of completeness in the book; several methods (e.g. electrochemical mass spectrometry and the generation of surface optical waves) are missing, or are mentioned only in passing, and with outdated references. On the other hand, the treatments of Mössbauer spectroscopy and electrochemical ESR spectroscopy seem disproportionately lengthy, in view of the fact that these techniques have been relatively little used and have a limited application potential. It is true that the popularity of a technique cannot always be equated with its scientific importance, but the reader could have been helped by providing a fuller and more comprehensive introductory survey of the methods, and some justification of the choice of methods for detailed treatment.

Except for some minor errors and inaccuracies (e.g. on Raman fluorescence (p. 2), and the description of electrochemical impedance measurements as a form of absorption spectroscopy (p. 2)) the chapters seem to be clearly written and factually correct. The index is brief, and the opportunity of using it to open up the field is scarcely used.

After reading the book one is left with an overall impression that it fails to meet the expectation, from the title and publisher's blurb, that it will give the reader a comprehensive overview of the field of spectroelectrochemistry. Instead it offers a collection of competently written individual review articles that are uncoordinated with each other. In some cases (e.g. the article on IR spectroscopy) these reviews have already appeared before in a form which differs only slightly; it was therefore hardly necessary to publish them again in this book, and they were apparently included only for completeness. The book certainly contains some valuable chapters which are useful for the electrochemist seeking specific information about special techniques. However, the reader interested in finding a sound, coordinated and comprehensive review of the subject will soon put the book down in disappointment.

Rudolf Holze [NB 1011 IE]
Fachbereich Chemie
der Universität Oldenburg (FRG)

The Elements. By *J. Emsley*. Clarendon Press, Oxford 1989. 256 pp., paperback, £ 9.95.—ISBN 0-19-855237-8

Important data and properties of the chemical elements have in the past been widely scattered throughout textbooks, tabulated works of reference and other specialist literature. Attempts to provide information of this kind in a compact form for those interested in finding it have usually been limited to footnotes in tables showing the Periodic Classification of the elements. Thus *John Emsley*'s idea of preparing a convenient work of reference in book form, giving the most important properties of all the elements up to nobelium, is very much to be welcomed.

The elements are arranged alphabetically, and each is given exactly two pages. These all follow the same pattern as follows: historical information (discovery, naming), chemical and physical properties, and data on the structures and properties of the nucleus and the electron shells. Lastly there is information on natural occurrence and biological importance. The "chemical" properties given for each element include its appearance, occurrence, reactivity, uses, ionic radii, electronegativity, effective nuclear charge, standard reduction potentials and oxidation states. The information listed under physical properties includes melting and boiling points, thermodynamic data, thermal and electrical conductivities, crystal structure(s) and X-ray absorption coefficient. The nuclear properties listed include information on the main isotopes (including artificial nuclides) and NMR data. Finally, under "electronic properties", ionization energies and data on atomic spectra are given.

Owing to the way in which the work has been planned, some vagueness creeps in for elements that occur in several different modifications (e.g. B, S). Some random tests confirmed the reliability of the data. A wealth of information on sources is provided for those wishing to undertake extensive searches.

The advantage offered by this miniature encyclopedia is that it gives comprehensive and reliable information at a glance. For chemists the question arises as to whether there is a need for more information, especially with regard to history, occurrence and biological importance, matters that are given only marginal coverage here; however, the book is likely to prove an important aid, mainly for those in chemistry-related disciplines.

Joachim Wachter [NB 1015 IE]
Institut für Anorganische Chemie
der Universität Regensburg (FRG)

Activation and Functionalization of Alkanes. Edited by *C. L. Hill*. Wiley, Chichester 1989. x, 372 pp., hardcover, £ 39.30.—ISBN 0-471-60016-4

Alkanes are the most abundant naturally occurring organic compounds, and are therefore a rich source of chemical feedstocks. However, their low reactivity and the problems of achieving regioselectivity in reactions limit their usefulness for manufacturing higher value products. Consequently there is growing interest among chemists in various methods for the functionalization of CH bonds. Whereas only a few papers on this topic had been published up to 1980, their number now runs into thousands. This book concentrates on studies by eminent organometallic, organic, bioorganic and inorganic chemists that are aimed at developing stable catalysts for selective functionalization of CH bonds with high yields. In each case the articles describe the principles, mechanisms and preparative potential of the reactions discussed.

In Chapter 1 (Historical Evolution of Homogeneous Alkane Activation Systems, 24 pp., 66 refs.) *A. E. Shilov* describes the oxidation of methane using platinum complexes, and the development and properties of iron porphyrins as models for monooxygenases that depend on cytochrome P-450.

Chapter 2 (Electrophilic Chemistry of Alkanes, 51 pp., 114 refs.) by *G. A. Olah, O. Farooq* and *G. K. S. Prakasch* is devoted to the oxidation of secondary and tertiary CH bonds in magic acid to carbocations and their subsequent reaction products. In this medium H_2O_2 and ozone react as electrophiles with alkanes, to give ketones; chlorine and bromine in the presence of acidic catalysts give chlorides and bromides respectively.

Chapters 3–5 deal with the activation of alkanes by three organometallic systems. Chapter 3 (Some Recent Advances in Alkane Functionalization: Metal Phosphine Catalysts and Mercury Photosensitization, 30 pp., 33 refs.) by *R. Crabtree* describes thermal or photochemical oxidative additions of CH bonds with complexes of iridium, rhodium or rhenium; this is an interesting reaction, although the catalysts are of poor stability. On the other hand, the photosensitized dehydrodimerization of alkanes, discovered more or less accidentally, uses as a catalyst elemental mercury, which is efficient, simple to use and robust, leading to interesting preparative applications.

Chapter 4 (Alkane Activation Processes by Cyclopentadienyl Complexes of Rhodium, Iridium and Related Species, 38 pp., 61 refs.) by *W. D. Jones* shows that although these complexes all react in a similar way with alkanes, the reaction rates differ widely. After photochemical activation they undergo oxidative addition at CH bonds, in some cases at temperatures as low as −20 °C. The reaction mechanisms are thoroughly discussed.

In Chapter 5 (Homogeneous Activation of Carbon-Hydrogen Bonds by High Valent Early d-Block Lanthanide and Actinide Metal Systems, 43 pp., 128 refs.) *I. P. Rothwell* discusses reactions whereby α-, β- and γ-hydrogen atoms are abstracted from alkyl, amino, mercapto and alkoxy ligands of the d°-transition metals specified in the title.

Chapters 6 and 7 and parts of Chapter 10 deal with the functionalization of alkanes by metal porphyrins. In Chapter 6 (Alkane Functionalization by Cytochrome P-450 and by Model Systems Using O_2 or H_2O_2, 20 pp., 74 refs.) by *D. Mansuy* and *P. Battioni*, the mechanism of the cytochrome P-450 hydroxylation reaction is discussed. Starting from Fe^{II} porphyrin, reactio with oxygen and reduction gives an $Fe^{IV}=O$ porphyrin radical cation, which inserts itself into the CH bond. This appears to be followed by further free radical reactions, since epimerizations and rearrangements are observed. Other iron porphyrin systems are described which are activated by H_2O_2, hydroperoxides, iodoso compounds or, in less favorable yields, by oxygen and reducing agents; in these catalysts the porphyrin ring has chlorophenyl substituents which give at least partial protection from oxidative autodecomposition. These reagents can be used for epoxidation of olefins and for hydroxylation of alkanes such as adamantane or cyclohexane.

In Chapter 7 (Shape Selective Oxidation of Hydrocarbons, 20 pp., 71 refs.) *K. Suslick* describes how the stability of porphyrins can be increased by steric shielding. The regioselectivity is improved too, as rates of oxidation for methylene groups at the outermost positions in hydrocarbons are 2–3 times greater than those for internal methylene groups. Although hydroxylations can be carried out in microheterogeneous systems (e.g. vesicles) or microporous systems (e.g. zeolites) with selectivities that are in some cases better, the isolation of the products is more difficult with these methods, and the catalyst only remains active for a small number of cycles.

In Chapter 8 (Catalytic Oxygenation of Unactivated CH-Bonds: Superior Oxo Transfer Catalysts and the Inorganic Metalloporphyrins, 30 pp., 118 refs.) *C. L. Hill* reviews this topic and shows that catalysts based on the polyoxometallate structure combine the selectivity and controllability of homogeneous catalysts with the stability of metal oxides. The transition metal substituted polyoxometallates such as $[MPW_{11}O_{39}]^{5\ominus}$ with $M = Co^{II}$ or Mn^{II} are several orders of magnitude more stable than sterically protected metalloporphyrins.

Chapter 9 (Selective Functionalization of Saturated Hydrocarbons by the "Gif" and "Gif-Orsay" Systems, 18 pp., 36 refs.) by *D. H. R. Barton* and *N. Ozbalik* gives an impressive account of the development of the Gif system, e.g. Gif IV consists of pyridine, glacial acetic acid, iron(II/III), zinc and O_2, and oxidizes adamantane preferentially at the methylene groups, with a life of up to 2000 cycles, or breaks down the side chain of cholestenone to give progesterone. The Gif-Orsay system, in which zinc is replaced by the cathode and a mediator, is superior to the Gif system, and oxidizes cyclohexane with a current efficiency of 49%. From a mechanistic standpoint the CH_2 selectivity can be explained in terms of intermediate metal carbene complexes which undergo oxidative scission.

The final chapter (Alkane Oxidation Studies in Du Pont's Central Research Department, 55 pp., 54 refs.) by *C. A. Tolman, J. D. Druliner, M. J. Nappa* and *N. Herron* describes research to elucidate the reaction steps in the industrial cyclohexane oxidation process giving cyclohexanol and cyclohexanone. By carrying out microreactor experiments and computer simulations of more than 150 reaction sequences the process conditions have been optimized. By using metalloporphyrins in zeolites it is possible to preferentially oxidize smaller hydrocarbon molecules compared with larger ones, although the catalyst life is only a small number of cycles. The iron/palladium/zeolite system which is a completely inorganic model for P-450 gives selective oxidation of octane by oxygen in the presence of cyclohexane.

The book fully achieves its aim of reporting on this rapidly developing interdisciplinary field in a concise form limited to the essential facts. Its usefulness is enhanced by the orderly arrangement of the text, the clear tables and structural formulas, and a comprehensive subject index. It can be strongly recommended to everyone working on reactions at non-activated CH bonds, or planning to do so.

Hans J. Schäfer [NB 1048 IE]
Organisch-chemisches Institut
der Universität Münster (FRG)

The Language of Biotechnology. A Dictionary of Terms. By *J. M. Walker* and *M. Cox*. American Chemical Society, Washington, D.C. (USA) 1988. viii, 225 pp., paperback, $ 47.95 (USA & Canada: $ 39.95).—ISBN 0-8412-1490-5; hardcover, $ 59.95 (USA & Canada: $ 49.95).— ISBN 0-8412-1489-1

This little 250-page ABC of biotechnology, a work of reference which includes terms from *Abomasum* to *Zygomycotina*, gives clear and concise definitions. It should help biotechnologists to better understand the language used by colleagues in specialist fields other than their own, which is an essential prerequisite for effective team work.

The multitude of terms used in biotechnology would be enough to fill a dictionary of several volumes. The value of this little book lies in the fact that it covers a broad range of selected words and expressions used in the different specialist areas of biotechnology. To compile such a selection in an interdisciplinary field of study is no easy task. The essential

feature of the dictionary is the explanations of terms from such widely different specialist fields as microbiology, genetics, molecular biology, plant and animal cell culture, enzyme technology, fermentation technology, process control and biochemical engineering. Explanations of the more complex technological aspects are supported by diagrams and formulas.

The authors have succeeded in putting together a very useful small dictionary of biotechnology. It will help to make this wide field of research a little more comprehensible.

Gunnar Pommerening [NB 993 IE]
Institut für Enzymtechnologie
der Universität Düsseldorf
in der Kernforschungsanlage Jülich (FRG)

Crystal Chemistry and Refractivity. By *H. W. Jaffe*. Cambridge University Press, Cambridge (UK) 1988. x, 335 pp., hardcover, £ 55.00.—ISBN 0-521-25505-8

Introduction to Crystal Chemistry. Student Edition. By *H. W. Jaffe*. Cambridge University Press, Cambridge (UK) 1988. 161 pp., paperback, £ 15.00.—ISBN 0-521-36985-1

In the last few decades chemistry has made considerable advances in the area of theory, and also in synthesis and analysis. The same also applies to crystallography, where the progress achieved includes remarkable improvements in the methods for determining crystal structures by X-ray and neutron diffraction. As a result of this a very large number of precisely determined crystal structures, including even those of very complex inorganic and organic compounds, are now known. These advances have been incorporated into a number of excellent new textbooks dealing with both chemistry and crystallography.

However, if *crystal chemistry* is understood to include not only the geometrical description of crystal structures, but also the study of the relationships between chemical composition, temperature and pressure on the one hand and, on the other hand, the structure and the factors which alter it, such as thermal expansion, compression, phase transformations and solid state reactions, then it must be said that there is a lack of good new textbooks on crystal chemistry. The textbooks by *H. Krebs* ("Anorganische Kristallchemie" (1968)) and by *R. C. Evans* ("Crystal Chemistry" (1964)) cannot be said to reflect the present state of knowledge, and the book by *A. F. Wells* ("Structural Inorganic Chemistry", 5th Edition (1984)), although an excellent work of reference, is not a student textbook. Several publishers have promised textbooks on crystal chemistry which have not yet appeared. The arrival of the book "Crystal Chemistry and Refractivity", by *H. W. Jaffe*, will therefore be greeted with much interest and curiosity.

The work consists of two parts. Part I, on the fundamentals of crystal chemistry and the refraction of light (146 pp.), contains a concise and accurate description of general principles such as atomic structure, types of chemical bonding, Pauling's rules, crystal field theory, polymorphism, diadochy and isotypes. Two separate sections are devoted to the packing density of atoms and the relationship between crystal structure and optical properties.

Although Part II (178 pp.) is entitled "Descriptive Crystal Chemistry", it is by no means restricted to the geometrical description of crystal structures. It includes a discussion, illustrated by examples, of the effects of chemical composition and temperature, and also in some cases of pressure, on the structures of crystals and the transformations which they undergo. Thus *Jaffe*'s book fulfills its claim to be a modern textbook of crystal chemistry in the sense of the definition given above, to an extent not achieved in any other book known to this reviewer. It can certainly be recommended to everyone whose work is concerned with inorganic solids.

Regrettably, it seems likely that this book by *Jaffe* will not reach as wide a readership as it deserves to, owing to the fact that, in accordance with the author's special interests, the structural examples chosen are nearly all from the minerals field. Despite this, the wide chemical and structural variety of minerals, and the fact that in a great many mineral systems the approach to thermodynamic equilibrium occurs so slowly that the progress of the reactions can be studied at leisure, means that minerals offer particularly suitable examples of crystal chemical phenomena. The book can therefore be recommended just as warmly to chemists and materials scientists as to geoscientists.

The paperback "Introduction to Crystal Chemistry" by *H. W. Jaffe*, published simultaneously with the above book, is almost completely identical to Part I of that book, and it is no doubt intended as a short textbook on crystal chemistry that students can afford. Regrettably, however, there must be some doubt as to whether the abridged version can fulfill this aim, when measured against the high standard of the total work. The fact that the description of the fundamentals in this part is so concise means that the student's appreciation of the significance and implications of these principles will probably be severely limited, if he or she is unable to draw on the carefully chosen structural examples and related discussion that are contained in Part II of the full work. The six-page appendix which is offered as a substitute, containing a few structural diagrams without the associated discussion, does not really give much help in this respect. Moreover, as the treatment of the effects of temperature and pressure on the structures of the minerals is nearly all contained in Part II of the complete work, the paperback version is lacking in some important aspects of crystal chemistry.

It appears that in deciding to publish the "Student Edition", the desire on the part of the publishers for a quick source of extra profit has taken precedence over their duty to the readers. One hopes very much that there will soon be a new paperback edition of the excellent full work, printed on cheaper paper if necessary, but at a reduced price.

Friedrich Liebau [NB 1007 IE]
Mineralogisch-Petrographisches Institut
der Universität Kiel (FRG)

Organisch-chemischer Denksport. Ein Seminar für Fortgeschrittene. By *R. Brückner*. Vieweg, Braunschweig/Wiesbaden 1989. xvii, 270 pp., paperback, DM 39.80.—ISBN 3-528-06329-7

Working through exercise problems is a necessary activity; one tests whether one has mastered the material that has been learnt and can apply it. Often, however, this task is only undertaken reluctantly, in particular by using the exercises in textbooks. In most cases one is here concerned with mature knowledge which, although of fundamental importance, is often already covered with the dust of the years. The atmosphere in the book of exercises reviewed here is quite different. There is a strong emphasis on topics taken from the most recent literature. At the outset the word "Denksport" in the title avoids creating the distance that conventionally exists between the teacher setting the exercises and the person doing them, and instead emphasizes challenge and competition.

The author also uses apt and racy quotations to break down any atmosphere of authority other than that based on facts (although for some tastes these may contain too many Americanisms). In this way the previously tiresome duty of doing exercises is transformed into a welcome activity.

In his 70 exercises, many of which are very tough nuts to crack, the author covers a remarkably wide range of topics in organic chemistry. In the answers he analyzes the basic essentials of problems that are concerned with stereochemistry, mechanisms, spectroscopy, and especially synthesis. By including many references he encourages the reader to follow up each exercise by looking into the problem in more detail with the help of the original literature, and to form his or her own opinion on the basis of the experimental facts. This is definitely to be recommended, since the author also interprets observations for which the original papers offer no explanation. In the interests of topicality he even exposes himself to the risk of being overtaken by events. This is the case, for example, in Exercise 7, which concerns an unsuccessful attempt to synthesize compound **246**. This compound has since been successfully prepared (*J. Am. Chem. Soc. 109* (1987) 2857), and the author's speculations concerning the thermal decomposition of **246** (p. 105) can now be compared with the actual behavior of **246**.

It is not unreasonable to recognize in the exercises the author's favorite hobby-horses, and also the school of chemistry from which he comes. There one often works with numerical values, in order to at least arrive at a qualitative understanding, if a quantitative treatment is not possible. This philosophy has prompted the author to include an appendix in which are tabulated bond enthalpies, stabilization energies, strain energies, the dependence of equilibrium ratios and product ratios on the difference in free enthalpies and free activation enthalpies respectively, and other quantities, all of which one often needs but never has to hand. The widespread use of kinetics, which is generally too little used in organic chemistry, and which the author therefore actively promotes, is again a feature carried over from his training. However, in accordance with his present research interests the majority of the exercises are concerned with problems of synthesis, especially natural products syntheses involving tricky stereochemical requirements. Several of these relate to natural products that have only recently been isolated, and thus the synthetic routes suggested in the answers are still awaiting experimental verification.

However, into this wine one must now pour a little water. There are a considerable number of errors, including some which alter the meaning, and some of the interpretations can be countered by alternatives that are at least equally valid. Here are some samples to illustrate these points: In Answer 3 (p. 90) formulas **3** and **205** do not match up with the problem (p. 5). In Answer 6 (p. 102) the word "Tautomerie" in the 5th line should read "Mesomerie". The suggestion for converting **248** into **12a** and **12b** (Answer 7, p. 106) seems very unlikely. In Problem 22 (p. 23) only the initiated are likely to realize that P(cyclo-C_6H_{11}) actually means HP(cyclo-C_6H_{11})$_2$. The explanations for the formation of the dibromide **75** from **403** (Answer 33, p. 165) and of the lactones **183** and **184** (Answer 7, pp. 247, 248) violate the principle of Occam's Razor. A carbon atom is missing from the precursor of **114** (Answer 44, p. 188). On p. 60 (Problem 55) reference is made to Perylen, but in the answer (p. 210) we instead find "Piperylen". In the preparation of **177** (Answer 66, p. 245) the final step requires 3,4-dihydro-2*H*-pyran, not cyclohexene. In Answer 69 (pp. 254 f.) the configurations in formulas **615**–**617** are incorrect, causing confusion. Since the book is intended primarily for advanced readers (final year undergraduates and graduate students), any compromise in the care of presentation detracts from the aims of the book as a learning aid. In the preface the author playfully lays the blame for any remaining errors onto his friend who has read the proofs. With a wink, one should compare this with the principle followed by the author's teacher, that in publications no part of the task should be left to chance, least of all to a friend. Lastly, a word of criticism to the publishers: the inadequate standard of production of the book means that the frequent leafing to and fro between the problem and answer sections soon leads to loose pages.

However, only he who never attempts anything makes no mistakes. With this motto in mind, the book's shortcomings need to be set against the gain in knowledge and pleasure afforded by this "Denksport". The result of this is a balance well on the positive side, and therefore every advanced student of organic chemistry is warmly recommended to carefully work through the book. Moreover, the price does not present a serious obstacle to buying one's personal copy.

Manfred Christl [NB 1013 IE]
Institut für Organische Chemie
der Universität Würzburg (FRG)

Introduction to Inductively Coupled Plasma Atomic Emission Spectroscopy. (Series: Analytical Spectroscopy Library, Vol. 3.). By *G. L. Moore*. Elsevier, Amsterdam 1989. 340 pp., hardcover, DFl 190.00.—ISBN 0-444-43029-6

This book of 15 chapters deals with the basic principles and analytical capabilities of optical emission spectroscopy using an inductively coupled radiofrequency plasma (ICP-OES). It is practically orientated, and provides the analyst in a straightforward way with the knowledge needed for optimizing the variables, recognizing sources of systematic errors, and performing analyses. The book is therefore intended mainly for technicians in analytical laboratories. The author has successfully translated his experience in emission spectroscopy into a lively and readily understandable, but nevertheless accurate, account of the subject.

The first chapter treats atomic spectra and classical spectroscopic analysis, with special emphasis on the capabilities of all the different types of excitation sources that are now available for emission spectroscopy (electric arcs, spark discharges, glow discharges, lasers, microwave plasmas). The account of the development of the ICP source and of the excitation mechanisms is limited to that needed for optimizing the adjustment of the ICP and performing ICP analyses. The following chapter is concerned mainly with the design of optical spectrometers for both sequential and simultaneous analysis, and with their performance data. Generators for ICP spectroscopy are treated only briefly, whereas the various alternative spectrometer arrangements in commercial instruments are clearly described in detail.

In the chapter on the analytical performance characteristics of ICP-OES, the method is compared with atomic absorption spectroscopy, X-ray fluorescence spectroscopy and DCP-OES (DCP = direct current plasma). The capabilities of ICP sources with low gas throughput and working with organic solutions are also discussed. The chapter on nebulization techniques describes the use of pneumatic and ultrasonic nebulizers for producing aerosols, and techniques for working with microsamples. The reader is referred to relevant literature, including recently published work.

The chapters that follow are concerned more with matters of practical detail. The chapter on sample preparation tech-

niques is concerned with digestion and extraction methods for multielement analyses, the decomposition of organic matrices, and conventional methods such as acid digestion at both atmospheric and high pressures; also discussed are sintering techniques, fusion with fluxes and microwave digestion. Special attention is given to digestion methods for geological samples.

The chapter on alternative techniques for sample introduction describes the capabilities of the hydride method and of electrothermal vaporization, of the direct introduction of powders in a gas jet, of techniques using suspensions, of direct sample insertion and of spark ablation. In the chapter on quantitative analysis by emission spectroscopy, methods of calibration using synthetic standards, certified reference materials, and standard addition are described. The meanings of the terms detection limit, determination limit and precision are explained. In describing the various analytical applications of ICP-OES, environmental analysis receives relatively little attention, but this is compensated by the detailed discussions of development trends in on-line analysis, automation of sample handling, etc.

The discussion of random and systematic errors is clear and straightforward. The usual statistical test procedures are described, as also is the importance of the spectral background and the methods used to measure it. The use of an internal standard is not so necessary in ICP-OES as in arc and spark emission spectroscopy, with which the author is equally familiar, but nevertheless it can be useful in ICP-OES for correcting fluctuations in the rate of sample introduction, especially for high concentrations.

In the chapter on optimization of the operating variables, the several different versions of the simplex procedures are described. Here the author makes full use of the experience gained from his own work, and presents this in a clearly understandable form. A simple computer program for simplex optimization is also given.

The most complex problem encountered in the analysis of real samples is that of interferences and the choice of suitable emission lines. Nebulization interferences and matrix effects arising from the plasma are briefly described. The relationship between interferences and optimization of variables is discussed with regard to source power and height of observation. The analytical errors caused by background and interfering lines depend critically on the spectrometer resolution achieved in practice. This dependence on resolution, although understood, is often complicated, and instead of treating it in detail the reader is referred to relevant literature.

The chapter on combined techniques, in which ICP-OES is coupled to various other analytical methods, describes in particular the coupling to electrothermal vaporization and the ICP-mass spectometry technique. The power of detection, the effects of other elements on the observed signals and the spectral interferences which occur in ICP-MS for the lighter elements are critically discussed.

The book is especially suitable as an introduction and learning aid for practical ICP spectroscopy in the laboratory, and it contains an adequate number of relevant literature references for this purpose. For practical work it would perhaps also have been useful to include data on emission lines commonly used in ICP-OES. The spectroscopic fundamentals can be found in the standard works by *Boumans* and *Montaser*. This book by *Moore* is likely to be of special interest to technicians and geology students, since it contains more of relevance for these groups than for environmental analysts or users in the ultra-pure chemicals or biological fields, a fact which is not surprising in view of the author's own field of work. Thus, for example, there are no chapters on the problems of trace analysis in relation to reagent purity and purification, on working in dust-free environments, nor on blanks and their relationship to ambient concentrations. The book makes easy reading and has a pleasing format. It will undoubtedly find a lot of use in the laboratory and in the vicinity of the ICP spectrometer. For many newcomers to ICP-OES as a modern multielement analytical technique it will ease their introduction to the subject.

Jose A. C. Broekaert [NB 1036 IE]
Institut für Spektrochemie
Dortmund (FRG)

Photoinduced Electron Transfer. Parts A–D. Edited by *M. A. Fox* and *M. Chanon*. Elsevier, Amsterdam 1988. Part A: Conceptual Basis. xviii, 640 pp., DFl 360.00.—ISBN 0-444-87122-5; Part B: Experimental Techniques and Medium Effects. xviii, 748 pp., DFl 410.00.—ISBN 0-444-87123-3; Part C: Photoinduced Electron Transfer Reactions—Organic Substrates. xviii, 754 pp., DFl 410.00.—ISBN 0-444-87124-1; Part D: Photoinduced Electron Transfer Reactions—Inorganic Substrates and Applications. xviii, 790 pp., DFl 425.00.—ISBN 0-444-87125-X, hardcover, set: DFl 1350.00.—ISBN 0-444-87121-7

The type of elementary reaction described as photoinduced electron transfer (PIET) has been studied both theoretically and, to a now increasing extent, experimentally. One factor that has contributed to this considerable growth of interest is the rapid progress achieved in the area of ultrafast techniques such as picosecond laser spectroscopy, which provides remarkably short time resolution in studying the dynamics of molecules and thereby of fast chemical processes. For the synthetic chemist the main significance of PIET studies lies in the enticing prospect of gaining a better understanding of such reactions so as to be able to develop more efficient catalytic and energy conversion processes; this is the reason for the current attraction of this area of research.

M. A. Fox and *M. Chanon*, as editors of this very comprehensive work, have tried to bring together in four volumes as many different aspects of this interdisciplinary field as possible. The 2600-page work consists of individual chapters in the form of photographically reproduced manuscripts by 46 authors or author groups. Starting from an essentially theoretical conceptual basis (Vol. A), Vol. B deals with the experimental techniques and with medium effects, then Volumes C and D describe actual examples in organic and inorganic chemistry respectively, and some particular areas of application such as solar energy conversion and information storage.

In the excellent introductory chapter of Volume A *M. Chanon, M. D. Hawley* and *M. A. Fox* give a general overview of PIET processes and a clear account of the relevant physical quantities. This is followed by a very technically orientated chapter by *J. P. Schermann, J. P. Astruc, C. Desfrançois* and *R. Barbe* describing electron transfer between excited atoms and molecules. Some theoretical aspects based on the Marcus equation are explained and discussed in two articles by *K. F. Purcell* and *B. Blaive*, and by *M. R. Wasielewski* and *F. Wilkinson*. The clear presentation by *D. C. Mauzerall* of the problem of reverse electron transfer deserves special mention. Another well-organized chapter is that by *G. Jones II* on the photochemistry and photophysics of organic charge transfer complexes. Next come articles on

exciplexes (*Y. Haas* and *O. Anner*), on the origin of solvent effects (*D. F. Calef*), and on the photochemistry of organic free radicals, cations and anions (*J. Eriksen*). Finally, *M. Chanon* and *L. Eberson* discuss in detail the fascinating phenomenon of photoinduced chain reactions; a highlight of this is a very useful compilation of frequently used components and sensitized electron transfer reactions.

Part B begins with a status report by *J. A. Delaire* and *J. Fauré* on laser spectroscopic methods; the development of nanosecond, picosecond and even femtosecond pulsed lasers for studying transient species is described. Two articles on the application of pulse radiolysis to inorganic reactions to generate short-lived species, by *W. L. Waltz* and by *P. Neta* and *A. Harriman*, are followed by a discussion of organic systems, arranged according to classes of organic compounds, with special emphasis on porphyrins and redox catalysts. These chapters illustrate the complex character of photolysis and radiolysis as applied to understanding intra- and intermolecular electron transfer processes. *S. G. Boxer, R. A. Goldstein* and *S. Franzen* describe how reaction dynamics can be influenced by applying magnetic and electric fields. Here the reader is first introduced to the theory of CIDNP and its application to the photosynthetic reaction center and to other organic donor-acceptor systems. A comparison between photoconductivity and the processes occurring in the photosynthetic reaction center serves to illustrate the effects of electric fields on PIET reactions. Next comes a lengthy article in which *M. Julliard* surveys the various classical methods and experiments for detecting PIET reactions. A large number of studies on donor-acceptor systems are cited and tabulated according to the criteria used in the investigations. Using various experimental data as examples, the reader is made aware not only of the methods and criteria for proving the occurrence of a PIET, but also of the difficulties and possible sources of error. *L. Brus* describes studies of electron transfer reactions based on measuring inelastic scattering of photons by transient species (time-resolved resonance Raman spectroscopy). In particular, applications to studying homogeneous reactions in liquids and heterogeneous electron transfer at semiconductor–electrolyte interfaces are discussed. *L. Kevan* describes the use of conventional ESR spectroscopy as well as modern double resonance (ENDOR) and electron spin-echo modulation (ESEM) techniques for the identification of paramagnetic intermediates. The advantages of the ESEM method for characterizing heterogeneous structures (semiconductors, micelles, vesicles) are clearly pointed out. Next *J. E. Baggott, C. H. Langford* and *C. Moralejo*, and in a separate article *A. D. Kirk*, describe temperature, wavelength and pressure effects in PIET reactions from a mechanistic point of view. It appears that there are still uncertainties about some aspects, in particular the interpretation of activation volumes, where the theory is not yet well developed.

In Part 2 of Volume B, *J. Santamaria* begins with a lucid treatment of solvent and salt effects on energetics and kinetics. *S. Baral* and *J. H. Fendler* provide a link from this to PIET reactions in "organized" media, which range from mimetic vesicles and lipid bilayer membranes to biological systems. After an introduction to the preparation of organizates of this kind, they give an interesting account of some recent PIET experiments. The article also discusses the stabilization of semiconducting colloids in organizates and their potential application in redox catalysis.

S. Nakabayashi and *T. Kawai* extend this connection further to electron transfer processes at semiconductor interfaces, which are important in relation to photoelectrodes, photocatalysis and sensitization. The theory of PIET through boundary layers is described, as well as spectroscopic analysis, electron transfer dynamics and the design of such materials. *J. Rabani* provides a lucid account of how PIET processes can be influenced by polyelectrolytes. Carefully controlled tailoring of polymers by incorporating donors, acceptors or sensitizers can result in a slowing down of the reverse electron transfer process which presents a serious problem in photochemical systems for energy conversion and storage. This article is very topical, and the presentation is clear and comprehensible.

In Part C (PIET in organic and biochemical substrates), *F. D. Lewis* begins by reporting on electron transfer reactions in compounds with multiple CC bonds. He succeeds in classifying the many different ways in which olefinic radical cations and anions can react. *P. G. Gassman* gives an excellent introduction and review of PIET reactions of strained hydrocarbons. The clear presentation and logical structure give the reader an insight into what the author describes at the end of the article as a "fascinating area of photochemistry". *A. Albini* and *A. Sulpizio* classify the PIET reactions of arenes according to their reaction mechanisms, i.e. the subsequent reactions of the radical species produced. Unfortunately, the authors give hardly any information about the *photoinduced* $S_{RN}1$ reactions of arenes, justifying this by the fact that review articles already exist (although these were published in 1983 or earlier). An update on this topic would have been appropriate. Next *A. Lablache-Combier*, in a contribution of nearly 180 pages, extends the $S_{RN}1$ concept to the synthesis of heteroarenes and to their subsequent reactions. Numerous physical-chemical relationships are introduced, so that the combination of synthetic aspects with photochemical data provides the reader with a clear idea of the advantages and difficulties of such reactions. The following article, by *M. Hoshino* and *H. Shizuka*, gives a very explicit account, supported by a few examples, of the photophysics and photochemistry of aromatic carbonyl compounds. Also clearly written is the chapter by *P. S. Mariano* on photochemical reactions of iminium ions. The reader interested in synthetic aspects will certainly profit from the application of such reactions to complex systems such as alkaloids and condensed heterocycles. *N. J. Pienta* gives a general survey of the photochemistry of amines, thiols and thioethers (with 300 references). The article includes informative comparisons with other chemical and electrochemical methods for generating reactive radical cations. Well arranged tables are provided which also cover biochemical, inorganic, organometallic and polymeric systems. The chapter by *W. R. Bowman* is devoted entirely to photoinduced nucleophilic substitutions at sp^3 carbon atoms. Numerous examples, arranged according to substrates, leaving groups, nucleophiles and mechanisms, give the reader an idea of the applicability of these reactions and their limitations. *X. Ci* and *D. G. Whitten* adopt a mechanistic viewpoint in discussing photoreductions using tertiary amines as donors, and photoinduced redox fragmentations of aminoalcohols. Part C ends with two chapters by *S. Fukuzumi* and *T. Tanaka* which deal in a clear, precise and comprehensive way with the (photoinduced) redox chemistry of biological systems, which are covered rather too scantily in the work as a whole; the examples described here are the 1,4-dihydropyridines NAD(P)H and the flavines. The reader is given an excellent and informative introduction to the redox properties of these compounds in the ground and excited states, followed by a detailed discussion of their PIET reactions. In making it easier to understand complicated photocatalytic cycles in systems analogous to that of photosynthesis, this article offers much more than a mere introductory survey.

Volume D begins with a concise summary by *M. A. Fox* of O_2 activation by PIET, which again is of biological importance. The following chapter by *H. R. Mäcke* and *A. F. Williams* on transition metal complexes of O_2 is unfortunately too brief and conventional in content. In somewhat greater detail *N. Serpone* describes PIET reactions of classical hexacoordinated complexes, in particular those containing polypyridyl ligands. PIET reactions occur, often unexpectedly, in weakly interacting systems such as ion pair complexes or "supramolecular" complexes; these highly topical reactions are described by *V. Balzini* and *F. Scandola*. This is followed by a short chapter in which *A. Vogler* describes the intramolecular electron transfer between weakly coupled redox centers, e.g. in multinuclear complexes. The chapter by *C. Giannotti, S. Gaspard* and *P. Krausz* on PIET in organometallic transition metal compounds is disappointing, not just because of the poor visual impression given by the typescript, but due to the fact that essentially all that it contains is a compilation of results on cyano complexes together with a few metallocenes and carbonyl complexes. Readers interested in this topic are better served by the recent monographs by *Kochi* or by *Hennig* and *Rehorek*.

The final chapter of Volume D contains articles on the actual and potential applications of PIET. On the basis of well documented examples, *R. Pichat* and *M. A. Fox* describe photochemical "catalysis" at semiconductor surfaces. Semiconductors are also at the center of the article by *M. Grätzel* on solar energy applications. Also related to this theme, *J. S. Connolly* and *J. R. Bolton* have put together a comprehensive "historical" account of the attempts at producing artificial photosynthesis, but it is not easy reading except for insiders. The following articles, on the importance of PIET in polymerization initiation reactions (*Y. Shirota*), in the processing and storage of information (*M. V. Alfimov* and *V. A. Sazhnikov*), in modern photoresist technology, (*F. Schue, L. Giral, C. Montiginoul* and *B. Serre*), and in phototoxicity, either involving or not involving O_2 (*N. Paillous* and *M. Comtat*), each give only a brief insight into areas of application where the PIET concept has already proved its usefulness.

At the end of Volume D, in addition to a large subject index, there is a very long and comprehensive author index (137 pp.) for the collected literature citations in all the articles. It would have been equally useful to have included, along with these pages reminiscent of the Science Citation Index, a list of the most important commonly used acronyms; the lack of such a list means that many of the articles make difficult reading if one is unprepared. With such a large number of authors and a field of a very interdisciplinary nature, it is probably unavoidable that some basic concepts, some frequently used experimental techniques and some particularly relevant chemical systems are described several times. In some respects this is an advantage from the reader's standpoint, since there are inevitably variations in the quality and comprehensiveness of the articles with such a heterogeneous team of authors. Nevertheless, we must notice that, despite the claim regarding comprehensive coverage, two important topics receive rather too little attention, namely PIET processes in organometallic chemistry and in biochemistry.

And now to what is undoubtedly a negative aspect of the work: the price of the four volumes! For a work in this price range the photographic reproduction of 47 typescripts in different formats, with the poor visual impression that this gives, is quite unacceptable. Consequently one can predict, regretfully, that although this is on the whole a very useful collection of articles on a subject of high topicality, the wide readership which is desirable will not be realized in practice.

Peter Bäuerle [NB 1012 IE]
Institut für Organische Chemie
der Universität Stuttgart
Wolfgang Kaim
Institut für Anorganische Chemie
der Universität Stuttgart (FRG)

Registered names, trademarks, etc. used in this journal, even when not marked as such, are not to be considered unprotected by law.

© VCH Verlagsgesellschaft mbH, D-6940 Weinheim, 1990. – Printed in the Federal Republic of Germany by Konrad Triltsch Druck- und Verlagsanstalt Würzburg.

All rights reserved (including those of translation into foreign languages). No part of this issue may be reproduced in any form — by photoprint, microfilm, or any other means — nor transmitted or translated into a machine language without written permission from the publishers. Only single copies of contributions, or parts thereof, may be made for personal use. This journal was carefully produced in all its parts. Nevertheless, authors, editors and publisher do not warrant the information contained therein to be free of errors. Readers are advised to keep in mind that statements, data, illustrations, procedural details or other items may inadvertently be inaccurate.

Valid for users in the USA: The appearance of the code at the bottom of the first page of an article (serial) indicates the copyright owner's consent that copies of the article may be made for personal or internal use, or for the personal or internal use of specific clients. This consent is given on the condition, however, that the copier pay stated per-copy fee through the Copyright Clearance Center, Inc. (CCC), for copying beyond that permitted by Sections 107 or 108 of the U.S. Copyright Law. This consent does not extend to other kinds of copying, such as copying, for general distribution, for advertising or promotional purposes, for creating new collective works, or for resale. For copying from back volumes of this journal see 'Permissions to Photo-Copy: Publisher's Fee List' of the CCC.

Editorial office: Postfach 10 11 61, D-6490 Weinheim, Federal Republic of Germany, Telephone (06201) 60 22 55, Telex 465 516 vchwh d, Telefax (06201) 602 328.

Editor: *Peter Gölitz*

Associate editors: *D. I. Loewus, A. Stimson.* **Editorial assistant:** *E. Schweikart*

Publishers: VCH Verlagsgesellschaft mbH. (Managing Director: *Hans Dirk Köhler*), Pappelallee 3, D-6940 Weinheim, Federal Republic of Germany.

Advertising office (Advertising Manager *R. J. Roth*): Postfach 10 11 61, D-6940 Weinheim, Federal Republic of Germany, Telephone (0 62 01) 60 61 30, Telex 4 67 155, Telefax (0 62 01) 606 156.

ANGEWANDTE CHEMIE
International Edition in English
Volume 29 · Number 7
July 1990
Pages 707–822

Retroviruses and Oncogenes I (Nobel Lecture)**

By Harold E. Varmus*

Introduction

The story that *Mike Bishop*[***] and I will tell in these two lectures is one in which retroviruses, oncogenes, our personal histories, and the history of tumor virology are closely interwoven. It begins with some simple questions about the origin and behavior of viral genes and takes us to a vantage point from which we can survey many aspects of retroviruses and animal cells, including some of the aberrations that lead to cancer. We now know that retroviruses capture normal cellular genes and convert them into cancer-causing genes, called oncogenes; such transductions are rare, but depend upon the normal events of an intricate virus life cycle. Retroviruses have introduced us to more than forty cellular genes with the potential to become oncogenes, some discovered as components of viral genomes, others as genetic targets for viral insertion mutations. It has been our privilege to participate in a generous share of the experiments that established these principles. But we have required the help of many talented people in our laboratories at the University of California, San Francisco (UCSF), as well as the collaboration and friendly competition of others elsewhere. (I mention as many names as the narrative can bear, but inevitably I must apologize to valued colleagues who remain anonymous here.) Several viruses also figure in our tale, but Rous sarcoma virus (RSV) again has the leading role, yet another of many tributes to the pioneering work of *Peyton Rous* and to the principle of delayed gratification in science. The product of his diligence in pursuing a single chicken tumor nearly eighty years ago,[1] *Rous*' virus remains the only retrovirus that could have satisfied the genetic and biochemical criteria for the work we accomplished in the era that preceded molecular cloning.

[*] Prof. H. E. Varmus
Department of Microbiology and Immunology
and Department of Biochemistry and Biophysics
University of California, San Francisco
San Francisco, California 94143 (USA)

[**] Copyright © The Nobel Foundation, 1990. We thank The Nobel Foundation, Stockholm, for permission to print this lecture.

[***] J. M. Bishop, *Angew. Chem. 102* (1990) 765; *Angew. Chem. Int. Ed. Engl. 29* (1990) 716.

First Taste of Molecular Biology: Hybridizations with the *lac* Operon

My commitment to experimental science occurred, by today's standards, dangerously late in a prolonged adolescence. As an undergraduate at Amherst College, I was devoted to Dickensian novels and anti-Establishment journalism, while marginally fulfilling premedical requirements. I then indulged myself with a year of Anglo-Saxon and metaphysical poetry at Harvard graduate school, before beginning medical studies at Columbia University, with a primary interest in psychiatry. But my ambitions soon turned towards an academic career in internal medicine. So just after graduation in 1966, like many of my contemporaries, I applied for research training at the National Institutes of Health. Perhaps because his wife was a poet, *Ira Pastan* agreed to take me into his laboratory, despite my lack of scientific credentials.

At the time, *Ira* was studying the biochemical effects of thyroid stimulating hormone (TSH) on tissue slices, a subject close enough to clinical endocrinology not to be intimidating. But one day, while still an intern at Columbia-Presbyterian Hospital, I received a telephone call from *Ira*, telling me

that a lecture by *Earl Sutherland* had inspired him to begin work on the effects of cyclic AMP on regulation of the *lac* operon in *E. coli*. Late that night, alone in the house staff library, I peered for the first time into the *Journal of Molecular Biology*—it is no small tribute to Columbia that this journal was there—and attempted to read the seminal papers on the *lac* operon by *Jacob* and *Monod*.[2] I knew then that, one way or another, my life was about to change.

Science is largely the making of measurements, and I soon learned from *Ira* how much more important a new measurement could be than an old theory. He and *Bob Perlman* had just discovered that cyclic AMP reversed catabolite repression of the *lac* operon.[3] They suggested that I use the relatively new technique of molecular hybridization to ask whether regulation by cyclic AMP occurs at the transcriptional level. Apart from the pleasures of just getting results (as *Gunther Stent* has said, results are wonderful because they give us something to talk about[4]), these measurements had enormous intellectual appeal, because they very simply resolved the ambiguity of hypothesis, demonstrating unequivocal changes in synthesis of *lac* messenger RNA.[5] Furthermore, they were carried out with technical subtleties that ultimately shaped the way I later thought about the problems of detecting single genes in more complex, eukaryotic cells. We annealed radiolabeled *E. coli* RNA to filter-bound DNA from a pair of bacteriophages that differed only by the presence or absence of the *lac* operon; and we minimized irrelevant hybridization by including, as competitor, unlabeled RNA from an *E. coli* mutant from which the *lac* operon was deleted. An aesthetic merger of genetics with molecular biology, itself as pleasing as the results!

Introduction to the Provirus and the Virogene–Oncogene Hypotheses

A major feature of life at the NIH in the late 1960s was the extraordinary offering of evening courses for physicians attempting to become scientists as they neared thirty. Two classes had direct and specific effects on my subsequent work because they introduced me to important problems I believed approachable with the methods I had acquired in my brief apprenticeship.

Like many of my peers, I was excited by the prospect of applying reductionist methods to eukaryotic organisms, particularly in a way that might be informative about human disease. From some dilatory reading in the early 1960s, I knew enough about viruses and their association with tumors in animals to understand that they might provide a relatively simple entry into a problem as complex as cancer. In fact, for anyone interested in the genetic basis of cancer, viruses seemed to be the only game in town. What surprised and beckoned me were two rather simple but heretical hypotheses that described curious ways the genes of RNA tumor viruses might mingle with the chromosomes of host cells.

The more daring of these two hypotheses was the provirus hypothesis, first enunciated by *Howard Temin*.[6] (*John Bader*, one of our NIH lecturers, was among the few others to espouse it in public.[7]) The provirus hypothesis stated that the genes of RNA tumor viruses were copied into DNA, which became stably associated with the host cell; the proviral DNA then provided the information for production of new virus particles. With its existence supported principally—some said feebly—by studies with inhibitors of DNA and RNA synthesis, and its plausibility doubted in the absence of any precedent for information transfer from RNA to DNA, the provirus seemed to be a provocative target for a definitive decision with molecular hybridization.

The other hypothesis, the virogene–oncogene hypothesis, was more complex.[8] *George Todaro* and *Robert Huebner* proposed that normal cells must contain genes related to those found in RNA tumor viruses, since viral proteins could often be found in cells of apparently uninfected animals, especially chickens and mice. Such genes, known as virogenes, were believed to be transmitted vertically as components of chromosomes, expressed in response to a variety of agents, and acquired by infection of germ cells at some time in the past. Since some RNA tumor viruses were known to be highly oncogenic, it was also proposed that tumor-inducing genes of such viruses (viral oncogenes) might also be transmitted through the germ line as a consequence of ancient infection. Activation of these endogenous viral oncogenes by substances we recognize as carcinogens—chemicals, radiation, other viruses—could serve to initiate a neoplastic process.

Transition to RNA Tumor Virology in Revolutionary Times

During the summer of 1969, I combined a backpacking vacation in California with a search for a suitable place to study tumor viruses. Acting on a tip from *Harry Rubin* in Berkeley, I sought out a small group, composed of *Mike Bishop, Leon Levintow*, and *Warren Levinson*, that was beginning to work with Rous sarcoma virus at the University of California, San Francisco. (*Rubin*, it should be said, was more eager for me to meet *Peter Duesberg*, but *Duesberg* was out of town.) A brief conversation with *Mike* was sufficient to convince me of our intellectual compatibility (happily, one of the few convictions to have survived twenty years in this field), and I made plans to join the UCSF group as a postdoctoral fellow the following summer.

Before the intervening year had passed, however, two major discoveries changed the landscape of tumor virology. *Satoshi Mizutani* and *Temin*[9] and *David Baltimore*[10] found the predicted enzyme, reverse transcriptase, in virus particles, thereby erasing most of the skepticism about the provirus hypothesis by providing a means to synthesize the heretical DNA copy of an RNA genome. And *Steve Martin* isolated a crucial mutant of Rous sarcoma virus,[11] one that lost its ability to transform cells at elevated temperature and regained it when the temperature was reduced. *Martin*'s mutant offered the first clear definition of the gene we later called *src*, and it showed that the gene—and, by implication, a protein the gene encoded—was required to instigate and sustain the transformed state. Since the mutant virus grew normally at the temperature that blocked transformation, oncogenic and replicative functions could be dissociated, a facet of the story that will soon resurface.

First Forays with RSV: Seeking Proviral DNA

Reverse transcriptase was properly greeted as strong evidence for the provirus hypothesis, and defused the urgency of challenging it. Yet it still seemed important to detect the provirus directly, most obviously by molecular hybridization, and to follow the pathway of its synthesis, especially in infected cells, not just in vitro. Reverse transcriptase obligingly offered a means to simplify the job, through the synthesis of potentially powerful probes, radioactive virus-specific DNA copied from a template of viral RNA.

Some of my initial efforts to proceed with these problems look, in retrospect, frustrating, if not quixotic—though the results were published in prominent journals. We chose at first to use double-stranded products of the RSV reverse transcriptase as hybridization probes, in order to measure gene copies through the accelerating effects of cellular DNA on reassociation kinetics.[12] However, the RNA template was unevenly copied by reverse transcriptase in vitro,[13] so that the products had complicated reannealing kinetics and did not uniformly represent the viral genome (whose genetic composition was in any case still unknown). When I attempted to measure RSV-related DNA in the most obvious settings—uninfected and RSV-infected chicken cells—I found multiple copies of virus-related DNA in the normal cells, in apparent confirmation of at least some aspects of the virogene–oncogene hypothesis.[14] But I was unable to detect the anticipated increment of RSV DNA in infected chicken cells, until I switched to the use of single-stranded DNA as probes.[15] But by then *Paul Neiman* had already measured the increment by hybridization with radiolabeled RNA from virions.[16] And, in the meantime, *Hill* and *Hillova* had provided more dramatic support for the provirus hypothesis in an entirely different way, by DNA transfection: addition of DNA from RSV-infected cells to new cells allowed the recovery of the original virus.[17] So the entire viral genome must have been present in the DNA of infected cells.

Our approach to the provirus was eased when I abandoned chicken cells, the traditional hosts for RSV in culture, in favor of cells from other birds—ducks and quail—and from mammals.[18] Because we could detect little virus-related DNA in these cells prior to infection, it was relatively simple to measure new copies of RSV DNA following infection, to follow the time course of DNA synthesis, to show that reverse transcription occurred in the cytoplasm, and to define linear, circular, and integrated forms of viral DNA.[19]

Making a Probe to Test the Virogene–Oncogene Hypothesis

The varied abilities of normal avian DNAs to anneal to RSV-derived probes helped to focus our attention upon the sorts of virus-related sequences we could detect in chicken DNA. Did these sequences constitute genes for viral structural proteins? More importantly, did they include the viral transforming gene, as predicted by the oncogene–virogene hypothesis? To approach these questions, it was imperative to have more rigorously defined probes. This was not a trivial challenge in the early 1970s, before restriction mapping and molecular cloning were available to us.

But one potent reagent was available. In 1971, *Peter Vogt* reported the isolation of transformation-defective, replication-competent mutants of RSV.[20] The genomic RNA subunits of these "td" mutants were shown by *Duesberg* and his colleagues to be about 15 percent shorter than the subunits of wild-type virus.[21] The provisional interpretation was that the missing sequences (initially called "x" and later

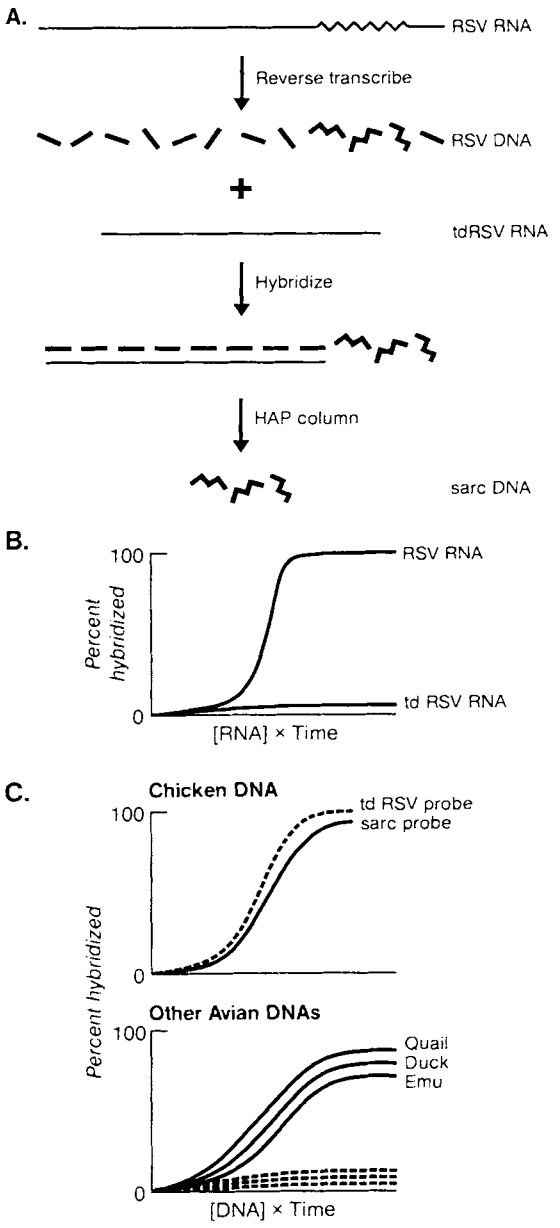

Fig. 1. Schematic summary of initial experiments with the sarc probe (see [22, 23] for primary data and further details). Panel A: Radiolabeled sarc-specific DNA was prepared by subtractive hybridization of the products of reverse transcription of RSV RNA to RNA from a transformation-defective deletion mutant of RSV (td RSV). The basis for the strategy is described in the text. Thin lines represent RNA, thick lines represent DNA, jagged portions represent sarc sequences (i.e., those present in RSV but not in td-RSV genomes). HAP, hydroxyapatite. Panel B: sarc DNA is specific for sequences that differentiate RSV and td RSV. The probe was hybridized to RSV RNA and td-RSV RNA and results monitored by HAP chromatography. Panel C: sarc probe (solid curves) anneals to DNA from many species of birds, whereas probe for other components of the RSV genome (td-RSV probe, dashed curves) anneals poorly to DNA from species other than chicken. The extent of annealing (normalized values shown here) was determined by HAP chromatography.

"sarc") included some or all of the viral transforming gene (v-*src*) earlier defined by temperature-sensitive (ts) mutants. Like *Martin*'s ts mutants, the deletion mutants retained the functions required for replication, despite the extensive loss of sequence, so it was tempting to presume that the deletion was coextensive, or nearly coextensive, with the transforming gene.

Mike and I were intimately acquainted with these conjectures through a collaborative consortium of Californian laboratories, directed by *Vogt, Duesberg*, and us, which met every six weeks or so, in Los Angeles or the Bay Area. Through these discussions, we recognized that if we could prepare radioactive DNA specific for the sequences deleted in the td-RSV mutants, we would have a reagent that would approximate a specific probe for the transforming gene of RSV.

The strategy for doing this was straightforward in principle, but difficult in practice (Fig. 1A). In essence, single-stranded, radiolabeled DNA fragments were synthesized from a template of wild-type RSV RNA, then hybridized to td-RSV RNA to remove unwanted components by hydroxyapatite chromatography, leaving the sarc-specific DNA. *Ramareddy Guntaka* first put this protocol into motion with some encouraging results. But it was ultimately the ministrations of *Dominique Stehelin* that produced a sarc probe that met rigorous standards: nearly complete annealing to RSV RNA, no significant annealing to td-RSV RNA (Fig. 1B), and representation of over 10 percent of the RSV genome, most of the sarc region, in the probe.[22]

Sarc Probe Detects Conserved Sequences in Avian DNA

When *Stehelin* incubated the sarc probe with normal chicken DNA, it annealed extensively (as, of course, did probe made from td-RSV RNA) (Fig. 1C). The results, unambiguously exciting, were still fully consistent with the original oncogene–virogene hypothesis. So we were yet more excited when the next results seemed to violate it: although the "virogene" probe from td-RSV annealed poorly to DNAs from several other avian species, the sarc probe annealed extensively, even to DNA from the Australian emu—a ratite (we learned, from our Berkeley colleague, *Allan Wilson*) at a great evolutionary distance from chickens.[23] The extent and fidelity of the hybrids formed with the sarc probe indicated that its homologues in normal cells had diverged during avian evolution at a rate similar to that of cellular genes used in the few earlier forays into molecular evolution, suggesting that the sequences had been conserved for at least 100 million years.

From these findings, we drew conclusions that seem even bolder in retrospect, knowing they are correct, than they did at the time.[23] We said that the RSV transforming gene is indeed represented in normal cellular DNA, but not in the form proposed by the virogene–oncogene hypothesis. Instead, we argued, the cellular homologue is a normal cellular gene, which was introduced into a retroviral genome in slightly altered form during the genesis of RSV. Far from being a noxious element lying in wait for a carcinogenic signal, the progenitor of the viral oncogene appeared to have a function valued by organisms, as implied by its conservation during evolution. Since the viral *src* gene allows RSV to induce tumors, we speculated that its cellular homologue normally influenced those processes gone awry in tumorigenesis, control of cell growth or development.

Firming Up the Result: Sarc Represents the c-*src* Proto-oncogene

Despite the broad claims, the first round of experiments with the sarc probe left many worrisome questions unanswered.

The most pressing question, and one foremost in the minds of our critics, seems now both essential and mundane: Was the sarc probe actually detecting a functional, protein-encoding homologue of the viral transforming gene (v-*src*)? Or were the still ill-defined genetic and physical maps of the RSV genome leading us astray? Some support came from geneticists who mapped a large number of the existing transformation mutations of RSV within the region of the viral genome lost during formation of td-RSV deletion mutants.[24] More exciting and stronger support came from protein biochemists: *Joan Brugge* and *Ray Erikson* discovered that the long-sought product of v-*src* was a protein of about 60 000 daltons,[25] one that would require about 1600 nucleotides of coding sequence and could account for most of what was missing from td-RSV. *Hermann Oppermann* and others[26] then detected a protein in normal cells that seemed virtually indistinguishable from v-*src* protein, confirming the idea that the sarc probe was measuring a gene (now called c-*src*) that resembled v-*src*. Ultimately, the molecular cloning and nucleotide sequencing of the RSV genome revealed how fortunate we had been in the design of our probe:[27] most td-RSV mutants lack all of v-*src* and little else.

The second question was more subtle: Did the conservation of c-*src* during avian speciation accurately imply that it was a cellular gene? Or might it still represent an inherited viral gene more conserved than other viral elements? Answers came from several quarters, all confirming the arguments based on evolution. Using chicken chromosomes fractioned according to size by *Elton Stubblefield* in Texas, we found that c-*src* and virogenes are unlinked; the viral genes we could detect were on one or more large chromosomes, but c-*src* was on a small chromosome.[28] *Steve Hughes* then used restriction enzymes to gauge the diversity of sequences in and around viral genes and c-*src* in many individual chickens;[29] the pattern generated with the sarc probe was monotonous, as would be expected for a conserved cellular gene (and shown to be the case for genes such as globin, ovalbumin, and others). The pattern produced with a probe for viral structural genes, however, suggested variety in number and context, as though they had been introduced into the chicken genome by recent, independent germ-line infections. When we examined the transcripts emanating from c-*src* and from virus-related genes, individual chicken embryos contained various amounts and types of viral RNAs but similar quantities of a single, differently sized species of c-*src* RNA.[30]

The most powerful evidence for the cellular nature of c-*src* required molecular cloning. For then it was possible to show that the coding sequences of c-*src* were interrupted in many places by introns,[31] in the manner recently discovered to be characteristic of cellular genes. In contrast, as described in greater detail below, endogenous virogenes have the insignia of proviruses, being composed of continuous coding domains, flanked by repeated sequences.

The third question was most informative about the mechanism by which v-*src* causes cancer: What accounted for the proposed physiological differences between a beneficial proto-oncogene and a pathogenic viral oncogene derived from it? From the first measurements of *src* gene expression, it was apparent that the viral gene, controlled by a potent viral transcriptional promoter, was expressed much more vigorously than its cellular counterpart.[32] But the levels of v-*src* protein required for transformation proved to be lower than nononcogenic amounts of c-*src* protein,[33] implying qualitative differences as well. *Mark Collett* in *Erikson*'s laboratory[34] and *Art Levinson* in ours[35] had discovered that *src* proteins are protein kinases, which *Tony Hunter* and *Bart Sefton* later showed to be specific for tyrosine residues.[36] *Hidesaburo Hanafusa*'s laboratory then defined the subtle structural and physiological differences between the viral and cellular versions of the gene:[37] at least three of several amino acid differences between $p60^{v\text{-}src}$ and $p60^{c\text{-}src}$ enhance the protein-tyrosine kinase activity of the transforming protein. Thus, quantitative and qualitative factors conspire to produce the *src* oncogene.

Finally, how well conserved is the cellular *src* gene? Early on, *Deborah Spector* showed that, under conditions of reduced stringency, most or all of the sarc probe could anneal to the genomes of all vertebrates, not just birds.[38] Since the implicated mammals included man, these findings helped to create a larger audience for our work, and they raised the possibility that retroviral proto-oncogenes might have a role in human cancer. New technologies ultimately extended the list of organisms that carry c-*src* to include virtually all metazoans—insects,[39] worms,[40] sponges,[41] and hydras[42]—reminders of our evolutionary origins that are at once exhilarating and sobering.

The *src* story remains unfinished. We cannot tell you how c-*src* benefits normal organisms or cells, although recent work implicates c-*src* both in development, especially in the central nervous system,[43] and in growth control during mitosis.[44] We do not know the physiological targets for the *src* kinase, although numerous phosphotyrosine-containing proteins have been identified.[45] And we do not know how the enzymatic activity of p60 is regulated, although phosphorylation is important.[46] Nevertheless, the *src* paradigm has stimulated our field to move in several directions: to identify many new viral oncogenes and their cellular progenitors,[47] to characterize a stunning variety of oncogenic proteins,[48] to make unexpected connections with elements of growth regulatory networks,[49] and to describe mutant proto-oncogenes in human tumors.[50] These developments are recounted in the accompanying lecture by *Mike Bishop*. It is my mission to stay with the virus—and especially the provirus.

Deciphering Proviral Structure

By the early 1970s the provirus was a well-accepted idea, but the organization of viral DNA and its position within chromosomes were still matters of conjecture. Several peculiarities of viral RNA and the viral life cycle hinted that proviral DNA must have special attributes.[19] First, the priming site for the first strand of viral DNA was near the 5′ rather than at the 3′ end of viral RNA,[51] implying that synthesis must be a complex process and that the provirus must not be a simple copy of viral RNA. Next, a short sequence (R) was found at both ends of viral RNA, and hence present in two copies, but appeared to be copied only once during synthesis of viral DNA;[52] how was the second copy of R regenerated? Finally, it was difficult to account for the efficient synthesis of viral RNA without the prospect of a strong transcriptional promoter upstream of the start site; how was that promoter provided?

These problems were solved by the unexpectedly elegant configuration of viral DNA, as worked out mainly by *Peter Shank, Steve Hughes*, and *Hsing-Jien Kung* in our group[53] and independently by *John Taylor*'s laboratory in Philadelphia.[54] Once again, RSV was the instrument of discovery, and again the results depended upon hybridization with specific probes, this time for terminal regions of the viral genome. In essence, viral genes were found to be flanked in the provirus by long terminal repeats (LTRs) derived from sequences present at both ends of viral RNA (Fig. 2). (The

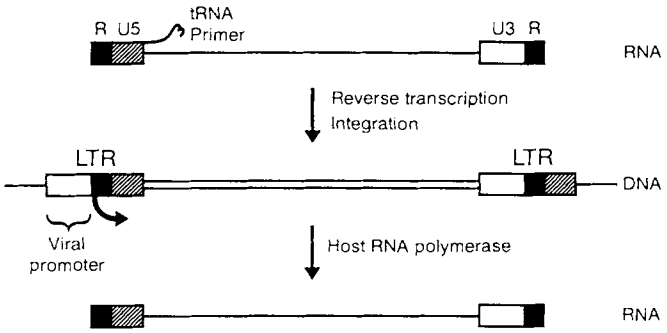

Fig. 2. The organization of proviral DNA in comparison to retroviral RNA. The top line shows one subunit of a viral dimeric genome, with host tRNA positioned near the 5′ end where it serves to prime synthesis of the first strand of viral DNA. R, short sequence present at both ends of viral RNA; U5 and U3 are sequences unique to the 5′ and 3′ regions of the RNA that are duplicated during DNA synthesis to form the long terminal repeats (LTRs). The middle line shows a provirus integrated into host-cell DNA (single line). The viral coding sequences reside between the LTRs (double line). The region encompassing the viral promoter in U3 of the upstream LTR is bracketed; the curved arrow denotes the start site and direction of transcription of the provirus by host RNA polymerase. The bottom line shows the composition of the primary viral transcript after 3′ processing; the poly(A) tract at the 3′ end is not illustrated.

ends of the LTRs correspond to the priming sites for the two DNA strands and thereby helped unravel a strategy of DNA synthesis too convoluted to review here.[19]) Because the R sequence is present once in each LTR, it can be reconstituted by transcribing parts of both LTRs. And viral sequences that contain strong transcriptional signals reside upstream of the RNA start site. Mapping of integration sites showed that many regions of the host genome could accommodate a pro-

virus; thus, transcriptional self-sufficiency of the provirus allowed it to function in varied chromosomal contexts.

Proviruses as Mobile Elements that Cause Insertion Mutations

But the structure of the provirus did more than solve some perplexities of the retrovirus life cycle. In general form and even in selected short sequences, proviruses resemble an abundant type of mobile DNA element, described by now in plants, bacteria, yeast, insects, and many other organisms (Fig. 3),[55] another arresting example of conservation throughout evolution. Their connection with retroviruses has been strengthened in recent years by discoveries that several such elements are duplicated and relocated by using reverse transcriptases to make new DNA copies from RNA transcripts,[56] although they never produce extracellular viruses. These properties also apply to endogenous proviruses, cloned from the germ lines of many vertebrates,[57] reemphasizing the profound differences between inherited virogenes and cellular proto-oncogenes.

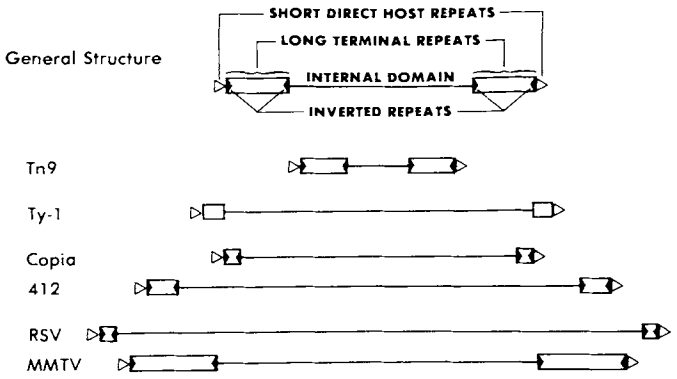

Fig. 3. Many mobile DNAs are organized like proviruses. The figure demonstrates some common features of many transposable elements, including LTRs (rectangular boxes), inverted repeats within the LTRs (closed triangles), and short duplications in host DNA generated during insertion (open triangles). The illustrated mobile elements include retroviral proviruses (RSV and mouse mammary tumor virus (MMTV)), retrotransposons of *Drosophila* (copia and 412) and budding yeast (Ty1), and a conventional transposon of *E. coli* (Tn9). (Taken from [55]).

One practical consequence of the startling similarities between retroviral proviruses and mobile elements was to consider the possibility that proviruses, like mobile DNA, might cause insertion mutations. In 1978, while on sabbatical in *Mike Fried*'s laboratory at the Imperial Cancer Research Fund, I designed an experiment to test this idea. *John Wyke* provided me with a rat cell line transformed by a single RSV provirus, which could serve as a target for insertion mutation by proviruses introduced by superinfection with mouse leukemia virus (MLV). By sifting through many clones of cells that had lost their transformed properties after infection with MLV, *Suzanne Ortiz* and I found two that contained an MLV provirus inserted at different sites within the pre-existing RSV provirus, interfering with the expression of v-*src*.[58]

This experiment established the principle that retroviruses could serve as insertional mutagens to inactivate genes. It also had the heuristic benefit of stimulating us to think about insertion mutations that acted in a dominant fashion by activating gene expression. *Greg Payne* was then attempting to explain how avian leukosis virus (ALV), a virus virtually indistinguishable from td-RSV and lacking any evidence of a viral oncogene, could nevertheless induce tumors (most commonly B-cell lymphomas) within several weeks after infection of susceptible chickens.[59] Might ALV proviruses occasionally integrate adjacent to a cellular proto-oncogene and augment expression through a viral LTR? *Greg*'s evidence for this idea,[60] however provocative, was nearly drowned out by the commotion caused by *Hayward, Neel,* and *Astrin*'s discovery[61] that ALV DNA in B-cell lymphomas was adjacent to c-*myc*—a known progenitor of a retroviral oncogene[62]—and that the viral LTR was driving c-*myc* expression.

ALV-induced tumors taught us several new principles: Retroviruses can induce neoplasia by insertionally activating proto-oncogenes;[63] proviruses and their target genes can be variously arranged with similar effects on transcription;[64] and proto-oncogenes need not be transduced to participate in oncogenesis. The last was an especially important point that presaged the later outpouring of mutant proto-oncogenes in human tumors unassociated with any virus.[50]

Using Proviruses as Transposon Tags for Novel Proto-oncogenes: The *int*-1 Story

However important, ALV has failed to introduce us to any proto-oncogenes not already known as forefathers of retroviral oncogenes. For this, we made use of another retrovirus without a viral oncogene, the mouse mammary tumor virus (MMTV). Like RSV, MMTV has a venerable history.[65] Found in the milk of inbred mice with a high incidence of mammary cancer over fifty years ago in Holland[66] and at the Jackson Laboratories in Maine,[67] MMTV was the first mammalian retrovirus to be discovered; it remains the only efficient viral agent of mammary carcinoma and thus a model for one of the most common of human cancers.

MMTV-induced mammary tumors are quasi-clonal growths of virus infected cells.[68] To ask whether the tumor cells result from insertion of viral DNA near a heretofore unknown proto-oncogene, *Roel Nusse* examined many tumors to find one with only a single new provirus; he then cloned that provirus and its flanking cellular DNA in *E. coli*. An unfamiliar gene, which we called *int*-1, was nearby, and it was expressed in that tumor and several others with nearby insertions, but not in normal mammary glands.[69]

But this was not sufficient to implicate *int*-1 as an oncogene. First, there was the circumstantial force of repetition: over three-quarters of mammary tumors in the C3H mouse strain harbor insertion mutations in the *int*-1 locus. Then, *Tony Brown* did what nature had not done, by placing the *int*-1 gene within a retroviral genome; the resulting virus alters the growth and morphology of cultured mammary cells.[70] Finally, *Ann Tsukamoto* followed a strategy pioneered by *Ralph Brinster* and *Richard Palmiter* and by *Philip*

Leder[71] and introduced the *int*-1 gene, linked to an MMTV LTR, into the mouse germ line.[72] All the transgenic mice, male or female, experience dramatic hyperplasia of the mammary epithelium, and most of the females develop mammary carcinoma within six months. This is about as close as we can come to fulfilling *Koch*'s postulates for a genetic disease: by placing the virally mutated form of the gene into the germ line--ironically, much as envisioned to occur naturally in the virogene–oncogene hypothesis—we have recreated the disease.

I cannot leave our transgenic mice without making a more general point. In California and many other places, misguided efforts to abolish the use of laboratory animals seriously threaten medical science. If *Peyton Rous* had been denied his chickens, our field would have no past; if all of us are now denied mice and other animals, it will have little future.

A Tentative Scheme for Transduction of Proto-oncogenes

The *int*-1 gene is but the first entry on a now substantial list of proto-oncogenes discovered as loci repeatedly activated by proviruses in tumors.[63] Thus, retroviruses usher in the genetic cast in the drama of cancer in two ways: by transduction and insertion mutation. Not surprisingly, the two phenomena appear to be mechanistically related: insertion mutation is probably the first step in the sequence of events that occasionally spawns a viral oncogene as its end product. What we can predict, but not yet fully substantiate by direct observation, is that two recombination events are required for transduction (Fig. 4).[73] The first occurs during proviral integration, placing viral DNA upstream from the activated cellular gene that will be acquired. The second occurs during virus replication in the tumor that results from the insertion mutation; the second step joins viral sequences to cellular sequences derived from the downstream region of the gene. We suppose that more or less in this fashion a close relative of ALV acquired a slightly mutated version of a chicken's *src* gene nearly a century ago, and set us on a path we are still traveling.

The Prospects for Retrovirology

The story thus far confirms *David Baltimore*'s statement of thanksgiving:[74] "A virologist is among the luckiest of biologists because he can see into his chosen pet down to the details of all its molecules." Because retroviruses, our chosen pets, are such remarkable agents, it has been enough to train our sights on two brief questions—how do retroviruses grow? and how do retroviruses cause cancer?—to have extended our concerns outward to the cellular host, as well as to have focused them inward upon the viruses themselves.[75] As a result, we have entered into some of the liveliest arenas in modern biology: the genetic basis of cancer, the transposition of DNA through RNA intermediates, the control of gene expression in eukaryotes, and the molecular evidence for evolution.

At this point, the study of oncogenes and proto-oncogenes

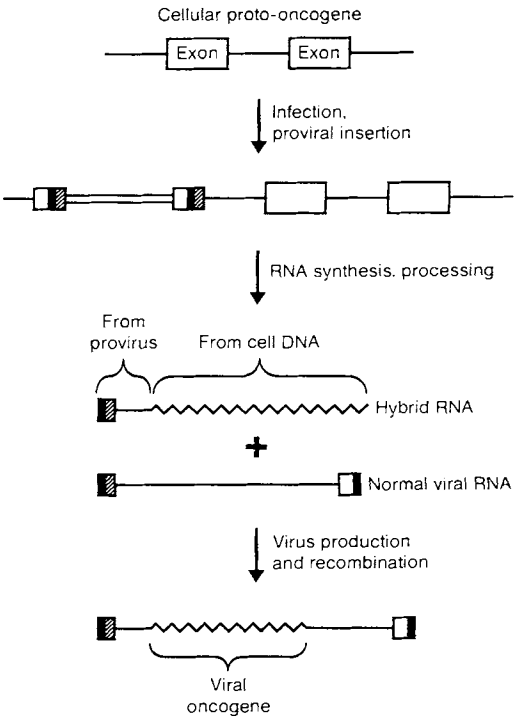

Fig. 4. Model for transduction of cellular proto-oncogenes to form retroviral oncogenes. Exons of a proto-oncogene are located downstream of a retroviral provirus recently introduced by infection and denoted as in Fig. 2. Virus-host chimeric RNA, a product of the proviral insertion mutation, recombines with normal viral RNA during virus replication to join viral sequences downstream of the cellular sequences. For further details, see [73].

has attained a degree of maturity that allows it to be conducted with astonishing little virology. Yet retroviruses remain vital tools for the isolation of important new oncogenes; witness in the past few years the discoveries of the *jun* and *crk* genes.[76] Likewise, since the discovery of reverse transcriptase nearly two decades ago, seemingly exhaustive attention has been given to the life cycle of retroviruses,[19] yet many central features are just now coming into view.[75] Cell surface receptors for viral attachment and entry have been recently identified and show a remarkable range of biochemical properties;[77] the proviral integration reaction has been recapitulated in vitro with nucleoprotein complexes,[78] allowing a description of integrative precursors and intermediates;[79] retroviruses have been recognized as pliable genetic vectors[80] that may one day be used clinically to correct gene deficiencies, in the manner used in nature to transport host-derived oncogenes; many unexpected aspects of viral gene expression have been discovered, including translational frame-shifting during the synthesis of reverse transcriptase[81] and complex viral regulatory genes that govern the behavior of two classes of human retroviruses;[82] and the principles of virus assembly are emerging through physical and genetic assaults on viral structural proteins and proteases.[83] These inherently fascinating problems have now taken on a special urgency, because we are all threatened by the worldwide dissemination of a lethal human retrovirus, the human immunodeficiency virus.[84] Thus, retroviruses continue to challenge our intellects in ways that may help us grapple with major diseases, cancer, and now AIDS, while also revealing fundamental features of the lives of our cells.

My indebtedness is large: to the many co-workers and colleagues mentioned here, and to many more unnamed, for communal labor, ideas, and criticism; to several institutions (especially the National Institutes of Health, the American Cancer Society, and the University of California, San Francisco) for nurturing my career with financial support and other resources; and to my family, for affectionate tolerance. My approach to science has been most profoundly influenced by Ira Pastan, who showed me that laboratory life was preferable to the clinic; by Peter Vogt, who taught me viral genetics when I needed it; and by Mike Bishop, who has been a generous and challenging colleague for nearly two decades. My gratitude would be incomplete if I did not especially mention the friendship and assistance of Suzanne Ortiz, Nancy Quintrell, Jean Jackson, Leon Levintow, Warren Levinson, and Don Ganem.

Received: January 26, 1990 [A 770 IE]
German version: *Angew. Chem. 102* (1990) 756

[1] P. Rous, *J. Exp. Med. 132* (1911) 397; *Science (Washington, D.C.) 157* (1967) 24.
[2] F. Jacob, J. Monod, *J. Mol. Biol. 3* (1961) 318; F. Jacob, A. Ullmann, J. Monod, *ibid. 13* (1965) 704.
[3] R. L. Perlman, B. DeCrombrugghe, I. Pastan, *Nature (London) 223* (1969) 810; R. Perlman, B. Chen, B. DeCrombrugghe, M. Emmer, M. Gottesman, H. Varmus, I. Pastan, *Cold Spring Harbor Symp. Quant. Biol. 35* (1970) 419–423.
[4] G. Stent in L. Wolpert, A. Richards (Eds.): *A Passion for Science*, Oxford University Press, Oxford 1988, pp. 109–119.
[5] H. E. Varmus, R. L. Perlman, I. Pastan, *J. Biol. Chem. 245* (1970) 2259, 6366.
[6] H. M. Temin, *Natl. Cancer Inst. Monogr. 17* (1964) 557; H. M. Temin, *Science (Washington, D.C.) 192* (1976) 1075.
[7] J. P. Bader, *Virology 26* (1965) 253.
[8] R. J. Huebner, G. J. Todaro, *Proc. Natl. Acad. Sci. (USA) 64* (1969) 1087.
[9] H. M. Temin, S. Mizutani, *Nature (London) 226* (1970) 1211.
[10] D. Baltimore, *Nature (London) 226* (1970) 1209.
[11] G. S. Martin, *Nature (London) 227* (1970) 1021.
[12] L. Gelb, D. Kohne, M. Martin, *J. Mol. Biol. 57* (1971) 129.
[13] H. E. Varmus, W. E. Levinson, J. M. Bishop, *Nature New Biol. 233* (1971) 19.
[14] H. E. Varmus, R. A. Weiss, R. Friis, W. E. Levinson, J. M. Bishop, *Proc. Natl. Acad. Sci. USA 69* (1972) 20.
[15] H. E. Varmus, S. Heasley, J. M. Bishop, *J. Virol 14* (1974) 895.
[16] P. E. Neiman, *Science (Washington, D.C.) 178* (1972) 750.
[17] M. Hill, J. Hillova, *Nature New Biol. 237* (1972) 35; *Virology 49* (1972) 309.
[18] H. E. Varmus, P. K. Vogt, J. M. Bishop, *J. Mol. Biol. 74* (1973) 613; *Proc. Natl. Acad. Sci. USA 70* (1973) 3067.
[19] a) R. Weiss, N. Teich, H. Varmus, J. Coffin (Eds.): *RNA Tumor Viruses*, Cold Spring Harbor Laboratory, Cold Spring Harbor; b) H. Varmus, R. Swanstrom in [19a], Chapter 5 (1982), pp. 369–512; c) H. Varmus, R. Swanstrom in [19a], Chapter 5S (1985) pp. 75–134.
[20] P. K. Vogt, *Virology 46* (1971) 939.
[21] G. S. Martin, P. H. Duesberg, *Virology 47* (1972) 494; L.-H. Wang, P. Duesberg, K. Beemon, P. K. Vogt, *J. Virol. 16* (1975) 1051.
[22] D. Stehelin, R. V. Guntaka, H. E. Varmus, J. M. Bishop, *J. Mol. Biol. 101* (1976) 349.
[23] D. Stehelin, H. E. Varmus, J. M. Bishop, P. K. Vogt, *Nature (London) 260* (1976) 170.
[24] A. Bernstein, R. MacCormick, G. S. Martin, *Virology 70* (1976) 206.
[25] J. S. Brugge, R. L. Erikson, *Nature (London) 269* (1977) 346.
[26] M. S. Collett, J. S. Brugge, R. L. Erikson, *Cell 15* (1978) 1363; H. Oppermann, A. D. Levinson, H. E. Varmus, L. Levintow, J. M. Bishop, *Proc. Natl. Acad. Sci. USA 76* (1979) 1804; L. R. Rohrschneider, R. N. Eisenman, C. R. Leitch, *ibid. 76* (1979) 4479.
[27] A. P. Czernilofsky, A. D. Levinson, H. E. Varmus, J. M. Bishop, E. Tischer, H. M. Goodman, *Nature (London) 287* (1980) 198; T. Takeya, H. Hanafusa, *J. Virol. 44* (1982) 12.
[28] T. Padgett, E. Stubblefield, H. E. Varmus, *Cell 10* (1977) 649; S. H. Hughes, E. Stubblefield, F. Payvar, J. D. Engel, J. B. Dodgson, D. Spector, B. Cordell, R. T. Schimke, H. E. Varmus, *Proc. Natl. Acad. Sci. USA 76* (1979) 1348.
[29] S. H. Hughes, F. Payvar, D. Spector, R. T. Schimke, H. L. Robinson, J. M. Bishop, H. E. Varmus, *Cell 18* (1979) 347.
[30] D. Spector, B. Baker, H. E. Varmus, J. M. Bishop, *Cell 3* (1978) 381; D. Spector, K. Smith, T. Padgett, P. McCombe, D. Roulland-Dussoix, C. Moscovici, H. E. Varmus, J. M. Bishop, *ibid. 3* (1978) 371.
[31] R. C. Parker, H. E. Varmus, J. M. Bishop, *Proc. Natl. Acad. Sci. USA 78* (1981) 5842; T. Takeya, H. Hanafusa, R. P. Junghans, G. Ju, A. M. Skalka, *Mol. Cell. Biol. 1* (1981) 1024; D. Shalloway, A. D. Zelenetz, G. M. Cooper, *Cell 24* (1981) 531.
[32] J. M. Bishop, H. Varmus in [19a], Chapter 9 (1982), pp. 999–1108.
[33] R. P. Parker, H. E. Varmus, J. M. Bishop, *Cell 37* (1984) 131; E. B. Jakobovits, J. E. Majors, H. E. Varmus, *ibid. 38* (1984) 757.
[34] M. S. Collett, R. L. Erikson, *Proc. Natl. Acad. Sci. USA 75* (1978) 2021; T. W. Hsu, J. L. Sabran, G. E. Mark, R. V. Guntaka, J. M. Taylor, *J. Virol. 28* (1978) 810.
[35] A. Levinson, H. Oppermann, L. Levintow, H. E. Varmus, J. M. Bishop, *Cell 15* (1978) 561.
[36] T. Hunter, B. M. Sefton, *Proc. Natl. Acad. Sci. USA 77* (1980) 1311.
[37] T. Takeya, H. Hanafusa, *Cell 32* (1983) 881.
[38] D. H. Spector, H. E. Varmus, J. M. Bishop, *Proc. Natl. Acad. Sci. USA 75* (1978) 4102.
[39] B.-Z. Shilo, R. A. Weinberg, *Proc. Natl. Acad. Sci. USA 78* (1981) 6789; M. A. Simon, B. Drees, T. Kornberg, J. M. Bishop, *Cell 42* (1985) 831.
[40] A. Kamb, M. Weir, B. Rudy, H. E. Varmus, C. Kenyon, *Nature (London) 337* (1989) 364.
[41] A. Barnekow, M. Schartl, *Mol. Cell. Biol. 4* (1984) 1179.
[42] T. C. Bosch, T. F. Unger, D. A. Fisher, R. E. Steele, *Mol. Cell. Biol. 9* (1989) 4141.
[43] J. S. Brugge, P. C. Cotton, A. E. Queral, J. N. Barrett, D. Nonner, R. W. Kenne, *Nature (London) 316* (1985) 554; P. F. Maness, M. Aubry, C. G. Shores, L. Frame, K. H. Pfenninger, *Proc. Natl. Acad. Sci. USA 85* (1988) 5001; R. Martinez, B. Mathey-Provot, A. Bernards, D. Baltimore, *Science (Washington, D.C.) 237* (1987) 411.
[44] D. O. Morgan, J. M. Kaplan, M. J. Bishop, H. E. Varmus, *Cell 57* (1989) 775; S. Shenoy, J.-K. Choi, S. Bagrodia, T. D. Copeland, J. L. Maller, D. Shalloway, *ibid. 57* (1989) 763.
[45] T. Hunter, J. A. Cooper, *Annu. Rev. Biochem. 54* (1984) 897.
[46] T. Hunter, *Cell 49* (1987) 1.
[47] J. M. Bishop, H. Varmus in [19a], Chapter 9S (1985), pp. 249–356.
[48] H. E. Varmus, J. M. Bishop (Eds.): *Cancer Surveys—Proteins Encoded by Oncogenes, Vol. 5*, Number 2, Oxford University Press, Oxford 1986.
[49] H. E. Varmus in G. Stamatoyannopoulos, A. W. Nienhuis, P. Leder, P. W. Majerus (Eds.): *Molecular Basis of Blood Diseases*, Chapter 9, W. B. Saunders, London 1987, pp. 271–346.
[50] H. E. Varmus, *Annu. Rev. Genet. 18* (1984) 553; J. M. Bishop, *Science (Washington, D.C.) 235* (1987) 305.
[51] J. M. Taylor, R. Illmensee, *J. Virol. 16* (1975) 553.
[52] J. M. Coffin, W. A. Haseltine, *Proc. Natl. Acad. Sci. USA 74* (1977) 1908; M. S. Collett, P. Dierks, J. F. Cahill, A. J. Faras, J. T. Parsons, *ibid. 74* (1977) 2389; W. A. Haseltine, J. M. Coffin, T. C. Hageman, *J. Virol. 30* (1979) 375; R. P. Junghans, S. Hu, C. A. Knight, N. Davidson, *Proc. Natl. Acad. Sci. USA 74* (1977) 477; E. Stoll, M. A. Billeter, A. Palmenberg, C. Weissmann, *Cell 12* (1977) 57.
[53] S. Hughes, P. K. Vogt, P. R. Shank, D. Spector, H.-J. Kung, M. L. Breitman, J. M. Bishop, H. E. Varmus, *Cell 15* (1978) 1397; P. R. Shank, S. Hughes, H.-J. Kung, J. Majors, N. Quintrell, R. V. Guntaka, J. M. Bishop, H. E. Varmus, *ibid. 15* (1978) 1383; H. E. Varmus, P. R. Shank, S. Hughes, H.-J. Kung, S. Heasley, J. Majors, P. K. Vogt, J. M. Bishop, *Cold Spring Harbor Symp. Quant. Biol. 43* (1979) 851.
[54] T. W. Hsu, J. L. Sabran, G. E. Mark, R. V. Guntaka, J. M. Taylor, *J. Virol. 28* (1978) 810; J. L. Sabran, T. W. Hsu, C. Yeater, A. Kaji, W. S. Mason, J. M. Taylor, *ibid. 29* (1979) 170.
[55] H. E. Varmus, in J. Shapiro (Ed.): *Transposable Elements*, Chapter 10, Academic Press, New York 1983, pp. 411–503; H. E. Varmus, P. O. Brown in M. Howe, D. Berg (Eds.): *Mobile DNA*, ASM Publications, New York 1989, pp. 35–56.
[56] D. Baltimore, *Cell 40* (1985) 481; H. E. Varmus, *Nature (London) 314* (1985) 583.
[57] J. Stoye, J. Coffin, in [19a], Chapter 10 (1985), pp. 357–404.
[58] H. E. Varmus, N. Quintrell, S. Ortiz, *Cell 25* (1981) 23.
[59] N. Teich, J. Wyke, T. Mak, A. Bernstein, W. Hardy in [19a], Chapter 8 (1982), pp. 785–998.
[60] G. S. Payne, S. A. Courtneidge, L. B. Crittenden, A. M. Fadly, J. M. Bishop, H. E. Varmus, *Cell 23* (1981) 311.
[61] W. S. Hayward, B. G. Neel, S. M. Astrin, *Nature (London) 290* (1981) 475; B. G. Neel, W. S. Hayward, H. L. Robinson, J. Fang, S. M. Astrin, *Cell 23* (1981) 323.
[62] D. Sheiness, J. M. Bishop, *J. Virol. 31* (1979) 514; M. Roussel, S. Saule, C. Lagrou, C. Rommens, H. Beug, T. Graf, D. Stehelin, *Nature (London) 281* (1979) 452.
[63] H. E. Varmus: *Cancer Surveys, Vol. 2*, Oxford University Press, Oxford 1982, p. 301; R. Nusse, A. Berns in G. Klein (Ed.): *Cellular Oncogene Activation*, Chapter 3, Marcel Dekker, New York 1988.
[64] G. S. Payne, J. M. Bishop, H. E. Varmus, *Nature (London) 295* (1982) 209.
[65] J. Hilgers, P. Bentvelzen, *Adv. Cancer Res. 26* (1978) 143.

[66] R. Korteweg, *Genetics 18* (1936) 350.
[67] J. J. Bittner, *Science (Washington, D.C.) 84* (1936) 162.
[68] J. C. Cohen, P. R. Shank, V. Morris, R. Cardiff, H. E. Varmus, *Cell 16* (1979) 333.
[69] R. Nusse, H. E. Varmus, *Cell 31* (1982) 99; R. Nusse, A. van Ooyen, D. Cox, Y. K. T. Fung, H. Varmus, *Nature (London) 307* (1984) 131.
[70] A. M. C. Brown, R. S. Wildin, T. J. Prendergast, H. E. Varmus, *Cell 46* (1986) 1001.
[71] T. A. Stewart, P. K. Pattengale, P. Leder, *Cell 38* (1984) 627; R. D. Palmiter, R. L. Brinster, *Annu. Rev. Genet. 20* (1986) 465; S. Cory, J. M. Adams, *Annu. Rev. Immunol. 6* (1988) 25; D. Hanahan, *Science (Washington, D.C.) 246* (1989) 1265.
[72] A. S. Tsukamoto, R. Grosschedl, R. C. Guzman, T. Parslow, H. E. Varmus, *Cell 55* (1988) 619.
[73] H. E. Varmus, *Science (Washington, D.C.) 216* (1982) 812; J. M. Bishop, *Annu. Rev. Biochem. 52* (1983) 301; R. Swanstrom, R. C. Parker, H. E. Varmus, J. M. Bishop, *Proc. Natl. Acad. Sci. USA 80* (1983) 2519.
[74] D. Baltimore, *Science (Washington, D.C.) 192* (1976) 632.
[75] H. E. Varmus, *Science (Washington, D.C.) 240* (1988) 1427.
[76] Y. Maki, T. J. Bos, C. Davis, M. Starbuck, P. K. Vogt, *Proc. Natl. Acad. Sci. USA 84* (1987) 2848; P. K. Vogt, T. J. Box, R. F. Doolittle, *ibid. 84* (1987) 3316; B. J. Mayer, M. Hamaguchi, H. Hanafusa, *Nature (London) 332* (1988) 272.
[77] P. J. Maddon, A. G. Dalgleish, J. S. McDougal, P. R. Clapham, R. A. Weiss, R. Axel, *Cell 47* (1986) 333; J. S. McDougal, M. S. Kennedy, J. M. Sligh, S. P. Cort, A. Mawle, J. K. A. Nicholson, *Science (Washington, D.C.) 231* (1986) 382; L. M. Albritton, L. Tseng, D. Scadden, J. M. Cunningham, *Cell 57* (1989) 659.
[78] P. O. Brown, B. Bowerman, H. E. Varmus, J. M. Bishop, *Cell 49* (1987) 347.
[79] T. Fujiwara, K. Mizuuchi, *Cell 55* (1988) 497; P. O. Brown, B. Bowerman, H. E. Varmus, J. M. Bishop, *Proc. Natl. Acad. Sci. USA 86* (1989) 2525.
[80] J. Coffin in [19a], Chapter 4 (1985), pp. 17–74; E. Gilboa, *BioEssays 5*, (1987) 252.
[81] T. Jacks, H. D. Madhani, F. R. Masiarz, H. E. Varmus, *Cell 55* (1988) 447; T. Jacks, M. D. Power, F. R. Masiarz, P. A. Luciw, P. J. Barr, H. E. Varmus, *Nature (London) 331* (1988) 280.
[82] H. Varmus, *Genes Dev. 2* (1988) 1055; B. R. Franza, B. R. Cullen, F. Wong-Staal (Eds.): *The Control of Human Retrovirus Gene Expression*, Cold Spring Harbor Laboratory, Cold Spring Harbor 1988.
[83] C. Dickson, R. Eisenman, H. Fan in [19a], Chapter 6 (1985), pp. 135–146; A. M. Skalka, *Cell 56* (1989) 911.
[84] *The Science of AIDS: Readings from Scientific American Magazine*, W. H. Freeman, New York 1988.

Retroviruses and Oncogenes II (Nobel Lecture)**

By J. Michael Bishop *

I am grateful to the family in whose embrace I formed my aspirations; the institutions modest and grand that helped me nurture those aspirations; the many colleagues with whom I have shared the pursuit of nature's secrets; the Nobel Foundation and the Karolinska Institute for glorious hospitality; and Swedish Medicine, which restored my larynx to some semblance of function.

The English critic *Cyril Connolly* once remarked that "The true index of a man's character is the health of his wife." My life in science has been rich and rewarding. I have sacrificed very little. But my partner in that life has sacrificed a great deal: *Kathryn*, my wife of thirty years. I take this moment to speak my gratitude for her forbearance, and to acknowledge that matters are not likely to improve.

If I were asked to choose a biographical theme for today, it would have to be procrastination, *Peyton Rous* withdrew from medical school for a year to spend time on a ranch in Texas, ostensibly to recover from tuberculosis.[1] Once back in medicine, he found himself "unfit to be a real doctor" (in his own words) and turned to pathology for an entry into research. *Harold Varmus* dallied with English literature before entering medical school, as you have heard.[2] And I came close to abandoning medicine entirely at an early age.

I entered Harvard Medical School knowing nothing of research. But during my first two years there, I was awakened to research by new-found friends among my classmates, particularly *John Menninger* (now at the University of Iowa) and *Howard Berg* (now at Harvard University). I sought summer work in a neurobiology laboratory at Harvard but was rebuffed because of my inexperience. My interest in practicing medicine declined. I becamed ambivalent about continuing in medical school, yet at a loss for an alternative.

Like *Peyton Rous*, I was rescued by pathologists. *Benjamin Castleman* offered me a year of independent study in his department at the Massachusetts General Hospital, and *Edgar Taft* of that department took me into his research laboratory. There was little hope that I could do any investigation of substance during that year, and I did not. But I was riotously free to read and think, which lead me to a new passion: molecular biology. I began my efforts to consummate that passion with two novitiates.

Novitiates

I served the first novitiate with *Elmer Pfefferkorn* and Sindbis virus. I had no credentials, other than my desire. Yet *Elmer* took me into his laboratory, and Harvard Medical School excused me from all but one of my fourth-year courses so that I could try research unencumbered. Both were enlightened acts, for which I remain grateful beyond measure.

I sought out *Elmer* and Sindbis virus because I had perceived that the inner sanctum of molecular biology was closed to me, that I would have to find an outer chamber in which to pursue my passion. Through *Elmer*, I found animal viruses, ripe for study with the tools of molecular biology, yet still accessible to the innocent.

I was innocent, but I was brash. I resolved to test the ability of the Sindbis RNA genome to serve as mRNA in vitro and to trace the fate of the genome following its entry into the host cell. These were novel ventures in their time (1961). They were also technically foolish. But they sired an abiding interest in how the genomes of RNA viruses commandeer the molecular machinery of the host cell, an interest that led me eventually to retroviruses.

My work with *Elmer* was sheer joy, teaching me the inebriation of research, the practice of rigor and the art of disappointment. But it produced nothing of substance. Twenty-five years later, on the occasion of my fiftieth birthday, *Elmer* recalled my first novitiate in science with a quote from *T. H. Huxley*: "There is great practical benefit in making a few failures early in life."

After two years of clinical training at the Massachusetts General Hospital, I began my second novitiate by entering the Research Associates Program at the National Institutes of Health in Bethesda, Maryland, where my mentor was *Leon Levintow*. My subject was the replication of poliovirus, which had become a test case for the view that the study of animal viruses could tease out the secrets of the vertebrate cell. In my first publishable research, I obtained evidence that the replication of polioviral RNA engendered a multistranded intermediate, although my description of that intermediate proved flawed in its details.[3]

Midway through my postdoctoral training, *Levintow* departed for the faculty at the University of California, San Francisco. In his stead came *Gebhard Koch*, who soon lured me to his home base in Hamburg, Germany, for a year. Together *Gebhard* and I explored the basis for the infectivity of multistranded RNAs.[4] I continued this work for several years to come, eventually showing that the double-stranded form of polioviral RNA is infectious because the positive strand of the duplex can be expressed in mammalian cells, as if the duplex RNA might be unraveling within the cell.[5] This finding perplexed us and seemed abstruse, but it appears to have been a harbinger of unanticipated enzymatic activities whose existence and functions are coming into view only now.[6]

Retroviruses

As my year in Germany drew to a close, I chose to join *Levintow* as a member of the faculty at the University of California, San Francisco. The decision proved providential

[*] Prof. J. M. Bishop
Department of Microbiology and Immunology,
Department of Biochemistry and Biophysics, and
The G. W. Hooper Research Foundation
University of California, San Francisco
San Francisco, CA 94143 (USA)

[**] Copyright © The Nobel Foundation, 1990. We thank The Nobel Foundation, Stockholm, for permission to print this lecture.

beyond all measure. In San Francisco, I found *Warren Levinson*, who had set up a program to study Rous sarcoma virus, an archetype for what we now call retroviruses. At the time, the replication of retroviruses was one of the great puzzles of animal virology. *Levinson, Levintow*, and I joined forces in the hope of solving that puzzle. We had hardly begun before *David Baltimore* and *Howard Temin* announced that they had solved the puzzle with the discovery of reverse transcriptase,[7, 8] work that brought them Nobel Prizes a scant five years later.

The discovery of reverse transcriptase was sobering: a momentous secret of nature, mine for the taking, had eluded me (and others, of course). But I was also exhilarated because the DNA synthesized by reverse transcriptase in vitro represented an exquisite probe for viral nucleic acids, a reagent that would give us unprecedented access to the life cycle of retroviruses. To paraphrase a memorable simile from *Arthur Kornberg*,[9] we now had a wedge with which to pry open the infected cell, and the hammer to drive that wedge would be molecular hybridization.

I had become enamored of molecular hybridization while working on poliovirus, because of the exceptional sensitivity and specificity the technique offered in the pursuit of viral nucleic acids. It was a tool made to order for the study of retroviral replication, which proceeds in concert with and is obscured by the normal metabolism of the host cell.

Improvising assays as we went, my colleagues and I soon had our first glimpse of viral RNA in cells infected with

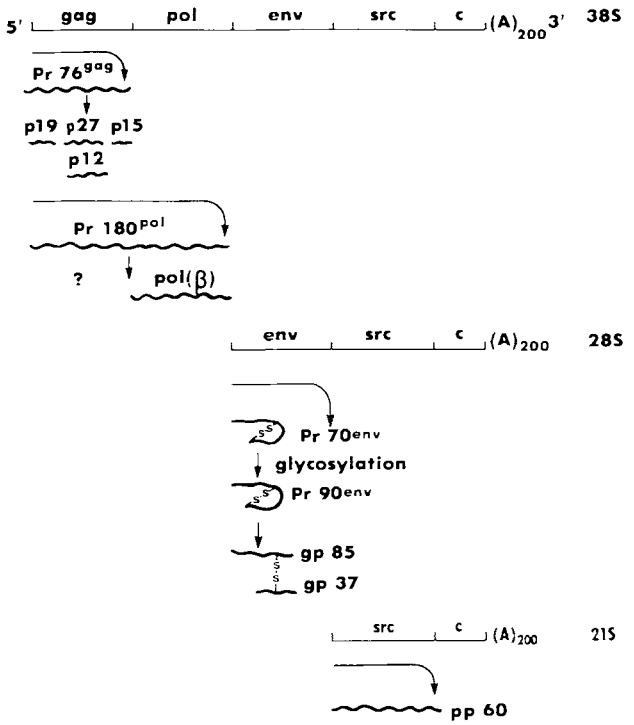

Fig. 1. Expression of the Rous sarcoma virus genes. The diagram was prepared in 1980 to portray how splicing and the processing of proteins facilitate expression of the Rous sarcoma virus genome. In the interim, we have learned that frame-shifting during translation is also required to produce the *gag-pol* polyprotein [13]. Individual genes are designated by conventional nomenclature, according to the proteins they encode: *gag*, structural proteins of the capsid and nucleocapsid; *pol*, reverse transcriptase; *env*, the glycoproteins of the viral envelope; and *src*, the oncogene of the virus. Other viral functions not illustrated include the protease that mediates maturation of several viral proteins and integrase, the enzyme that catalyzes integration of viral DNA.

retroviruses.[10] We were to pursue the character and genesis of those RNAs for years to come, laying out the manner of viral gene expression in considerable detail (Fig. 1). The work helped uncover an early example of RNA splicing[11, 12] and set the stage for the much later discovery of frame-shifting in the translation of retroviral mRNAs.[13] But our exercises with viral RNA had a larger resonance, as well, because we had constructed the technical stage on which the discovery of retroviral transduction would eventually play out.

I also picked up the study of reverse transcriptase itself, perhaps to exorcise my sense of failure at not discovering the enzyme in the first place. We began by working in vitro to explore the details of DNA synthesis by the enzyme.[14] The most notable outcome was the demonstration that the reverse transcriptase of Rous sarcoma virus uses the cellular tRNA for tryptophan as a primer to initiate transcription from the retroviral genome (Fig. 2).[14, 15] The point was soon generalized to other retroviruses and is now a feature that serves as a signature of retrotransposons at large.[16]

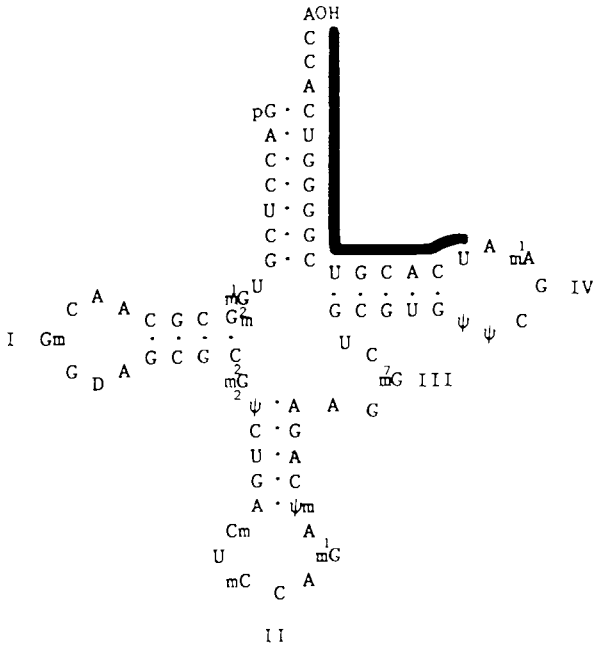

Fig. 2. The tRNA primer for reverse transcription in Rous sarcoma virus. The avian tRNA for tryptophan serves as primer for reverse transcription from the genome of Rous sarcoma virus. The RNA is displayed here in a conventional representation of secondary structure. The first sixteen nucleotides at the 3′ end of the tRNA are paired with the genome by hydrogen-bonded complementarity, as highlighted here.

But what I wanted most to know was the course of events in the infected cell. Could we find the proviral DNA first imagined by *Howard Temin* and then foretold in substance by the discovery of reverse transcriptase? Where in the cell was this DNA synthesized following infection? What form did it take before and after integration into chromosomal DNA? *Harold Varmus* arrived to provide the answers[2] and to alter my life and career irrevocably. Within the year, his name became consubstantial with expertise on the synthesis and integration of retroviral DNA. In the process, I had lost a postdoctoral fellow and gained a coequal.

Oncogenes

To this point, we had thought little of cancer. But as the virus of *Peyton Rous* first lured me away from poliovirus, now it lured us to the study of neoplastic transformation. *Peyton Rous* received his Nobel Prize two years before my initial encounter with his virus. The award dramatized the great mystery of how Rous sarcoma virus might cause cancer. It was a mystery whose solution lay in genetics.

Soon after arrival in San Francisco, a graduate student and I had conducted a search for temperature-sensitive conditional mutants of poliovirus and Rous sarcoma virus, without a particle of success. But where we had failed, others succeeded, and the study of viral tumorigenesis was transformed.[17-19] The data showed with luminous clarity that a gene within Rous sarcoma virus is responsible for cancerous growth of infected cells, that continuous action of the gene is required to sustain cancerous growth, and that the gene probably works by directing the synthesis of a protein. The oncogene *src* had been sighted.

The genetic identification of *src* was reported in the same year as the biochemical discovery of reverse transcriptase. The two became themes that intertwined and nourished one another in the daily life of our laboratory. Much as our deployment of molecular hybridization in the study of viral replication set the stage for the discovery of cellular *src*, so our ensuing success in isolating viral proteins from infected cells[20] emboldened us to seek the protein encoded by *src*.

We were in the midst of efforts to prepare antisera that would recognize the *src* protein when news of success came from Denver.[21] *Erikson* and his colleagues had obtained persuasive evidence that the oncogene encodes a 60-kilodalton protein. Once the product of *src* was a physical reality, the puzzle of its action loomed larger than ever. How could this single protein elicit the pleiotropic change in cellular phenotype that we call neoplastic transformation?

The answer came quickly. The *src* gene encodes a protein kinase,[22,23] whose amino acid substrate later proved unexpectedly to be tyrosine.[24] By phosphorylating numerous cellular proteins, the enzyme could rapidly change myriad aspects of cellular structure and function; by being the first exemplar of protein-tyrosine kinases, it gave notice of a previously unappreciated regulatory device that we now realize is second to none in the signaling pathways of the cell.[25]

The ways in which these answers emerged are illuminating. In Denver, insight came from an inspired guess, based on the pleiotropism of *src*:[22] protein phosphorylation ranks among the most versatile agents of change known to biochemists. In our laboratory, enzymological reasoning led the way:[23] Phosphorylation of the *src* protein in cellular extracts displayed properties suggestive of a unimolecular reaction, as if the protein were phosphorylating itself—which indeed it was.[26] And at the Salk Institute, the use of an erroneous buffer led to the fortuitous separation of phosphotyrosine from phosphothreonine for the first time in recorded history, the only example of productive laziness that I have ever seen acknowledged with both candor and gratitude in the biomedical literature.[25]

The sighting and subsequent characterization of *src* opened the way to a biological cornucopia. We now know of more than twenty retroviral oncogenes, whose diverse specificities in tumorigenesis provide experimental models for most forms of cancer that afflict human kind (Table 1). Each of these genes encodes a protein whose biochemical action provides distinctive purchase on the mechanisms of neoplastic growth.[27,28]

Table 1. The oncogenes of retroviruses (1989).

Oncogene	Pathogenicity	Oncogene	Pathogenicity
abl	B-cell-tumors and fibrosarcomas	*kit*	sarcomas
		mil/raf	sarcomas and supplemental
akt	thymomas	*mos*	sarcomas
cbl	B-cell- and myeloid tumors	*myb*	myeloblastosis
		myc	carcinomas; myelocytomatosis; sarcomas
crk	sarcomas		
erb-A	supplemental	*ras*	sarcomas; erythroleukemia
erb-B	erythroleukemia and fibrosarcomas	*rel*	B-cell tumors
		ros	sarcomas
ets	supplemental	*sea*	sarcomas; leukemias
fes/fps	sarcomas	*sis*	sarcomas
fgr	sarcomas	*ski*	carcinomas
fms	sarcomas	*src*	sarcomas
fos	osteosarcomas	*yes*	sarcomas
jun	sarcomas		

The products of oncogenes are deployed to various reaches of the cell, including the nucleus, the cytoplasm, the plasma membrane, even the exterior beyond the cell.[27,28] And they act in different ways, which for the moment are subsumed by three genre: (1) the phosphorylation of proteins, with either serine and threonine, or tyrosine as substrates—the immediate role of the oncogene product may be induction of the phosphorylation (as in the case of growth factors) or catalysis itself (as with the receptors for growth factors);[25] (2) the transmission of signals by GTP-binding proteins, as exemplified by the products of *ras* genes—whose exact position in signaling pathways remains unresolved;[29] (3) the control of transcription from DNA.[30]

Diversification of this list in the future seems likely, since the functions of many oncogenes have yet to be elucidated. But the list displays an economy of style that may survive because it reflects the need for pleiotropism: nature may have only a limited number of ways to achieve the manifold changes that create the neoplastic phenotype.

Retroviral Transduction

At first it seemed that the lessons to be learned from retroviral oncogenes might apply only to the cancers induced by viruses in animals, that the oncogenes of retroviruses might be alley cats of evolution with little importance to human kind. The discovery of cellular *src* and the inference that it gave rise to the oncogene of Rous sarcoma virus inspired hope that this narrow view might be wrong.[31] If cells contain genes capable of becoming oncogenes by transduction into retroviruses, perhaps the same genes might also become oncogenes within the cell, without ever encountering a virus. By means of accidental molecular piracy, retroviruses may have brought to view the genetic keyboard on which many different causes of cancer can play, a final common pathway to the neoplastic phenotype (Fig. 3).

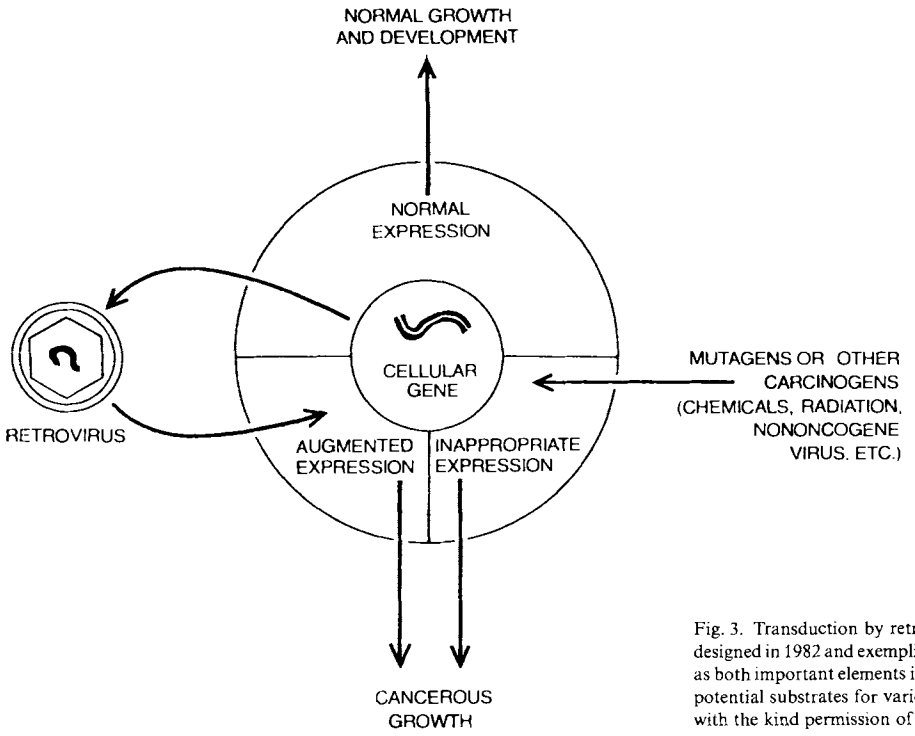

Fig. 3. Transduction by retroviruses uncovers cancer genes. The cartoon was designed in 1982 and exemplifies the now conventional view of proto-oncogenes as both important elements in the governance of normal cellular phenotype and potential substrates for various causes of cancer. (The figure is reprinted here with the kind permission of *Scientific American 246* (1982), No. 3, pp. 68–79.

The hope had its detractors.[32] Even transduction itself was challenged. But for us in San Francisco, the reality of transduction seemed inescapable. The cellular homologue of *src* had been conserved through eons of evolution, whereas the other genes of Rous sarcoma virus could be found only in chickens and a few close kin.[2] The ineluctable conclusion was that the two sorts of genes, an oncogene on the one hand and genes devoted to viral replication on the other, had separate origins.

We would eventually muster more sophisticated arguments, all of which pointed to the same conclusion: the progenitor of *src* was a conserved (and hence vital) cellular gene that found its way into Rous sarcoma virus by recombination.[2] The images of cellular and viral *src* gained eventually from molecular cloning sustained our argument in a gratifying manner,[33] but for me, they were anticlimactic.

Arguing for the cellular origins of *src* provided my first experience with the heuristic force of evolution. "Nothing in biology makes sense except in the light of evolution", to recall a famous aphorism from *Dobzhansky*.[34] The aphorism embodies a truth that has been dishonored in the United States, where religious zealots continue their efforts to hound the teaching of evolution from public schools, and men of little learning assail the truth of evolution under the fraudulent rubric of "creation science".

The genesis of retroviral oncogenes by recombination with cellular genes had been postulated by several observers. Although it may sound self-serving, I confess my ignorance of those speculations when we began our work on cellular *src*. I was motivated by a desire to test the virogene–oncogene hypothesis of *Huebner* and *Todaro*,[35] not by an interest in the origins of oncogenes. But in due course, *Howard Temin* provided a useful inspiration with his suggestion that all retroviruses arose by the cobbling together of disparate genetic elements in the cell, with intermediates that he called proto-viruses.[36] The inspiration was for taxonomy, not experiment.

As transduction by retroviruses came into common discourse, the need arose for a generic term to describe the cellular progenitors of *src* and other retroviral oncogenes. The first to find general usage was "cellular oncogene". Although I was a nominal member of the responsible committee on nomenclature, I was uncomfortable with this term because of its unwarranted implication that the native cellular genes carried intrinsic tumorigenic potential, that they need not be changed to cause trouble. So in playful homage to *Howard Temin*, I began to use the term "protosarc".[37] The generic "proto-oncogene" followed in short order.

In the interim, proto-oncogene has come into general use, as the colloquial counterpoise to oncogene. It has also become an embarrassment, because the precise connotation of the word is that of prototype rather than progenitor, not far removed from the offensive connotation of cellular oncogene. But the intent of the taxonomic invention was clear: numerous investigators (ourselves included) have spent the past decade exploring the sorts of genetic damage that can convert a harmless proto-oncogene into a pathogenic oncogene.[38]

The manuscript that announced our discovery of cellular *src* concluded with the speculation that the gene might be involved in "the normal regulation of cell growth and development or in the transformation of cell behavior by physical, chemical or viral agents".[39] These words were pure bravado, particularly because we then had no assurance that cellular *src* was in fact a full-fledged gene. The assurance accrued over the ensuing two years, first in the form of evidence that cellular *src* was transcribed in normal cells,[40,41] and then with the identification of the protein encoded by the gene.[42,43]

Expanding the Repertoire

As our confidence in the reality of cellular *src* grew, a new challenge took shape. Could we generalize the principle of transduction? Had the oncogenes of other retroviruses also originated from cellular genes? In order to pursue the generality of transduction, we turned first to a retrovirus known as MC29,[44] which attracted our attention because it offers a model for the induction of carcinomas, the most prevalent of human cancers.

During the search for an oncogene in MC29, the impatience of molecular biologists held sway, the rigor of formal genetics was cast aside. Some investigators (ourselves included) used molecular hybridization to detect nucleotide sequences unique to the genome of MC29,[45, 46] others used chemical procedures to identify the same sequences and to map their position on the viral genome.[47] Both strategies took liberties that we had not allowed ourselves with *src*. Lacking a deletion mutant that might define the oncogene, we and others made the assumption that the genomes of MC29 and its necessary helper virus were congenic except for the presence or absence of the oncogene (Fig. 4).

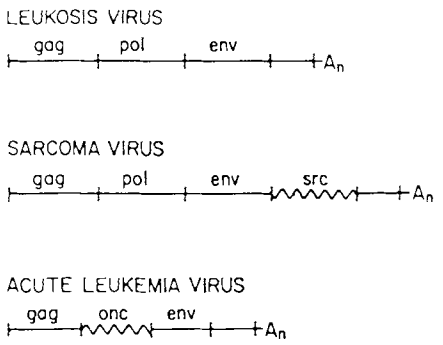

Fig. 4. The genomes of Rous sarcoma virus and related avian retroviruses. The genomes of Rous sarcoma virus, avian leukosis viruses, and acute avian leukemia viruses appear to have a common origin and, thus, are congenic with the exception of oncogenes, inserted into the genomes by transduction from host cells. The leukosis viruses have no oncogenes and induce malignancy by insertional mutagenesis [2, 38]. The viral genes are designated as in Fig. 1, except for the use of *onc*, the generic term for retroviral oncogenes.

The same assumption had been applied previously in an effort to define the oncogene of a murine sarcoma virus and had led to a molecular quagmire.[48] But now the lessons from *src* told us more precisely what we might be seeking. So we forged ahead and soon had a molecular probe that represented nucleotide sequences found in MC29 and other retroviruses with similar tumorigenicities, but not in the related helper viruses.[45]

The newly found locus was taken to be the oncogene of MC29 and eventually designated *myc*, in deference to the form of leukemogenesis (myelocytomatosis) from which the virus acquired its name. Over the next several years, the authenticity of *myc* would be ascertained by molecular cloning,[49] nucleotide sequencing,[50] and gene transfer.[51] To this day, the gene has never been defined by the strategies of classical genetics, and there is now no need to do so. The new biology is upon us.

The lessons of *src* were powerful. We and others were able to argue that the molecular probes for the oncogene of MC29 were legitimate because they also detected nucleotide sequences in the DNA of normal vertebrates,[46, 52] sequences that were transcribed into RNA in normal cells[52, 53] and that diverged among species in rough accord with phylogenetic distance.[46, 52, 53] No other portion of the MC29 genome displayed these properties. Similar findings were described in parallel for the avian retroviral oncogenes *erb* (in reality, two oncogenes) and *myb*.[46] The example of cellular *src* was not an exotic anomaly; it was an archetype.

In the years that followed, *myc* proved to be a great provider, a vehicle for several seminal discoveries that included the activation of cellular genes by insertional mutagenesis,[54] the involvement of proto-oncogenes in chromosomal translocations,[55, 56] and the amplification of proto-oncogenes in human tumors.[57] These discoveries had exceptional logical force because they involved a gene whose tumorigenic potential was already known from the study of retroviruses.

No sooner had the bounty of transduction become evident than other routes to proto-oncogenes took shape, some serendipitous, others designed:[58] the ability of retroviruses to mutate cellular genes, creating oncogenes at their place of residence within the cell; the dissection of chromosomal abnormalities in cancer cells, such as translocations and amplifications; the use of gene transfer to detect mutant proto-oncogenes by means of their biological activity; and the pursuit of phylogenetic kinships. The definition of proto-oncogene had now become more expansive, subsuming any gene with the potential for conversion to an oncogene—by the hand of nature in the cell or by the hand of the experimentalist in the test tube.

The Normal Functions of Proto-oncogenes

The tally of proto-oncogenes has now reached sixty or more. Most are genes never glimpsed before by any other means. What are these genes in their normal guise? What purposes preserved them through one billion years of evolution? Why do they harbor the potential to wreak cellular mayhem?

We formed our hypotheses from the lessons of transduction. The properties of retroviral oncogenes must echo the functions of proto-oncogenes. Three properties seemed especially telling: the stimulation of cellular proliferation; the specificity of tumorigenesis, as if each gene were designed to work in only certain cells; and the ability of many oncogenes to interrupt or sometimes reverse cellular differentiation.[59] Like father, like son: it seemed possible that the actions of viral oncogenes are merely caricatures of what proto-oncogenes are normally intended to do. Retroviruses may have revealed to us not only touchstones of tumorigenesis, but clues to the nerve center that governs the normal cell cycle and the differentiation of cellular function.

Eager to explore these thoughts in a living organism, we turned to the fruit fly, *Drosophila melanogaster*. Why the fruit fly? First, because the full collection of genes in this creature is within our scope. Second, because we have in

hand a rich catalogue of normal and mutant genes from the fruit fly, the products of more than half a century of labor. Third, because the fruit fly is for the moment the only metazoan organism in which we can manipulate genes with reasonable facility, although a soil worm on the one hand and the laboratory mouse on the other are now making strong bids for our favor. Fourth, because when reduced to essentials, the fruit fly and *Homo sapiens* are not very different. And fifth, because the fruit fly has a large complement of proto-oncogenes with counterparts in mammals.[60]

What we have learned of proto-oncogenes from *Drosophila* vindicates at least some of the bravado in our first publication on cellular *src*. Mutant alleles have been identified for the counterparts of six proto-oncogenes in the fruit fly (Table 2). In two instances, the *abl* and *myb* proto-oncogenes, the

Table 2. Mutant alleles of proto-oncogenes in *Drosophila melanogaster*.

Proto-oncogene	*Drosophila* counterpart	Biochemical function	Mutant phenotype
abl	*abl*	tyr kinase	embryonic lethal/defects in late development
int-1	*wingless*	? growth factor	segment polarity
raf	*pole hole*	ser/thr kinase	defective cellular proliferation
rel	*dorsal*	?	dorsal-ventral polarity
erbb-1	*flb/top*	tyr kinase	embryonic lethal/dorsoventral patterning
myb	*myb*	transcription factor	embryonic and pupal lethality

search for mutations was deliberate; in the remainder, mutations recognized first by their phenotypes later proved to be in *Drosophila* counterparts of mammalian proto-oncogenes. All of the mutations elicit profound disturbances of development. The work from our own hands has revealed a requirement for activity of the proto-oncogene *myb* during two distinct stages of development, embryogenesis and pupation (unpublished data of *A. Katzen* and *J. M. B.*). More precisely, a deficiency in *myb* appears to reduce the number of cell divisions that can occur in certain developmental lineages.

The actions of proto-oncogenes in development have their underpinnings in the elaborate circuitry that governs the behavior of vertebrate cells (Fig. 5). The junction boxes in this circuitry include polypeptide hormones that act on the surface of the cell, receptors for these hormones, proteins that convey signals from the receptors to the deeper recesses of the cell, and nuclear functions that orchestrate the genetic response to afferent commands (typically, by regulating transcription). Diverse lines of inquiry have brought these junction boxes to view, but the study of proto-oncogenes has been among the richest sources. Time and again, the several lines of inquiry have converged on the same junction box. We may have most of the circuitry in view. The cell is not infinitely complex; the cell can be understood.

Seeds of Cancer

But what of cancer? Are proto-oncogenes the seeds of this disease in all our cells? Are they a common keyboard for many different players in tumorigenesis? As a physician, I found these questions attractive. As a scientist, I found them intimidating. Exploration of the cancer cell is akin to archaeology: we must infer the past from its remnants in the present, and the remnants are often cryptic.

But the first remnants to emerge from the proto-oncogenes of human cancer cells told a vivid story. Molecular dissections revealed that chromosomal translocations in human and murine tumors often affect proto-oncogenes already familiar from the study of retroviruses, with the great provider *myc* prominent among them.[55,61] Emboldened by these findings, my colleagues and I mounted a belated excavation for the genetic shards of tumorigenesis. But we chose a neglected terrain in which to dig: amplified DNA.

Focal amplification of domains within chromosomes is a scheduled and purposeful event during the life cycles of diverse organisms.[62] In mammals, however, gene amplification is an unscheduled aberration that gives rise to karyotypic abnormalities known as double-minute chromosomes and homogeneously staining regions. When my colleagues and I

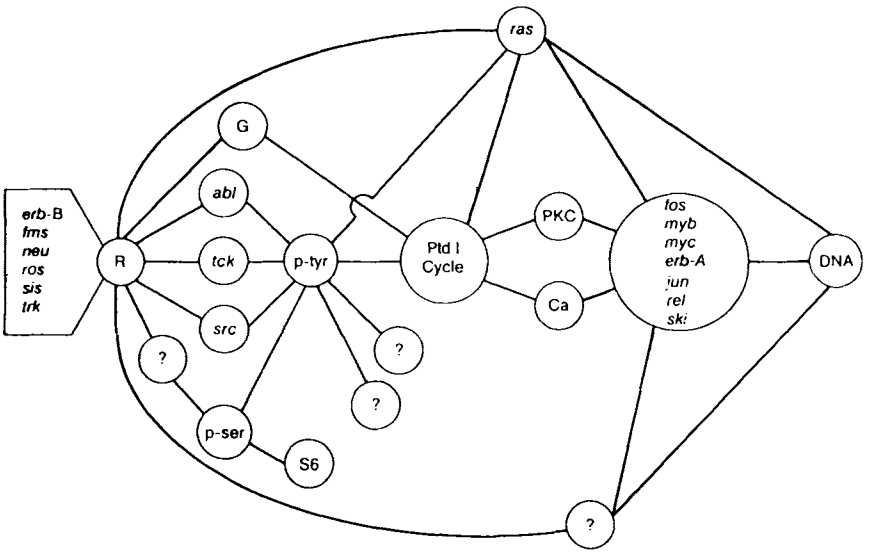

Fig. 5. The biochemical circuitry that mediates cellular phenotype. The diagram illustrates how some of the functions encoded by proto-oncogenes fit into the circuitry that regulates the phenotype of vertebrate cells. The scheme is in part hypothetical and is not intended to be comprehensive. Functions encoded by proto-oncogenes have been designated by the conventional terminology for the genes themselves. Other abbreviations include: G, GTP-binding proteins that transduce signals from cell-surface receptors; R, generic receptor; p-Ser, phosphorylation of serine in proteins; p-Tyr, phosphorylation of tyrosine in proteins; PtdI, phosphatidylinositol; S6, a ribosomal protein that is phosphorylated in response to diverse mitogenic signals; PKC, protein kinase C. (Reprinted here with the kind permission of *Science (Washington, D. C.) 235* (1987) 305–311.

began our excavations, gene amplification in cancer cells was known principally as a consequence of selection by chemotherapeutic agents. But the literature also contained occasional examples of double-minute chromosomes and homogeneously staining regions in untreated cancers. When a limited sampling of these were examined by ourselves and others, they proved to involve previously identified proto-oncogenes (yet again, *myc* was prevalent).[57] In due course, it became apparent that gene amplification is relatively common in untreated tumors and that it affects proto-oncogenes.

Intent on a more systematic study, we chose human neuroblastomas, in which gene amplification seemed exceptionally common. We resolved to ask whether the amplified DNA in neuroblastoma cells contained any of the proto-oncogenes then known. When we got to *myc*, we struck rich ore of an unexpected sort: a gene related to *myc*, sighted for the first time in the parallel work on neuroblastoma by ourselves and others, and eventually designated N-*myc*.[63-65] In due course, it became apparent that N-*myc* is an authentic proto-oncogene, a close kin of *myc* itself that apparently evolved to serve a separate purpose in the normal organism.[66-68]

As the survey of neuroblastomas broadened, a fertile correlation became apparent. Amplification of N-*myc* was found only in the more aggressive variants of the tumor, in perhaps one-quarter of all the specimens examined.[69, 70] Moreover, within single tumors, N-*myc* was expressed abundantly only in neuroblasts, the least differentiated (and presumably most malignant) cells of the tumor.[64] These correlations had two implications: first, that amplification of N-*myc* might embody a step in tumor progression, one of several events that exacerbate the malignancy of neuroblastomas; second, that we had brought to hand a prognostic tool, a device with which to supplement the conventional staging of the disease.

The passage of time has dealt kindly with these hopes. The *New England Journal of Medicine* has now provided its imprimatur by arguing that "in neuroblastoma, amplification of the N-*myc* gene is of greater prognostic value than the clinical stage of the disease".[71] Thirty years after deserting the bedside, I have found clinical relevance in my research.

The excavation that unearthed N-*myc* was a pedestrian exercise in both concept and execution. Yet in one fell swoop, it served up an important proto-oncogene without the assistance of a retrovirus, hinted at a major role for gene amplification in tumorigenesis, foreshadowed the molecular dissection of tumor progression, and gave first notice that the emerging knowledge of oncogenes would eventually prove useful at the bedside.

These themes have since found wider resonance. First, we can point to a variety of human malignancies in which damage to one or another proto-oncogene has been found with some consistency (Table 3). The damage takes diverse forms, including translocations, amplifications, and point mutations, all of which appear to have dominant effects on gene function. The list of malignancies containing these lesions is impressive: because of the diversity of tumors involved; because of their identities—several can be counted among the principal nemeses of humankind; and because the list has been assembled after only a few years of pursuit, with imperfect tools—there is doubtless more to come. Beyond this list, there lies the burgeoning repertoire of recessive lesions in human cancers, whose nature, prevalence, and unquestionable importance are just now coming into focus.[72]

Table 3. Proto-oncogenes and human tumors; some consistent incriminations.

Proto-oncogene	Neoplasm	Lesion
abl	chronic myelogenous leukemia	translocation
erbb-1	squamous cell carcinoma glioblastoma	amplification
erbb-2 (neu)	adenocarcinoma of breast and ovary	amplification
myc	Burkitt's lymphoma	translocation
	small cell carcinoma of lung	amplification
	carcinoma of the breast	
	carcinoma of the cervix	
l-myc	small cell carcinoma of lung	amplification
n-myc	neuroblastoma	amplification
	small cell carcinoma of the lung	
k-ras	carcinomas of colon, lung, and pancreas	point mutation
n-ras	acute myelogenous and acute lymphoblastic leukemia; carcinoma of thyroid	point mutation
h-ras	carcinomas of genitourinary tract and thyroid	point mutation

Second, catalogues of genetic damage within individual tumors are taking shape, showing us how the malfunction of several different genes might combine to produce the malignant phenotype:[58] for example, carcinomas of the colon contain no less than five different yet prevalent lesions—some genetically dominant, others recessive; carcinoma of the breast, at least five lesions; carcinoma of the lung, at least four; and neuroblastoma, at least three. Moreover, detection of the lesions is likely to provide information for prognosis, perhaps even for therapeutic management. Examples include neuroblastoma,[69-71] carcinoma of the breast[73, 74] and ovary,[74] and preleukemias.[75-77]

For those of us who first studied cancer more than thirty years ago in medical school, then returned to the disease decades later to find it little less a mystery, the contemporary image of the cancer cell is both thrilling and an unexcelled vindication for fundamental research. The image was forged from the vantage point of molecular genetics and with the tools of that discipline. The lines of discovery trace back to minuscule columns of hydroxyapatite from which the molecular probe for *src* first flowed; to *src* itself, which even now has not been persuasively implicated in the genesis of human cancer; and to the chickens in which *Peyton Rous* first found his tumor. From these humble roots, a great tree of knowledge has grown. And a great truth has been reiterated: we cannot prejudge the utility of scholarship, we can only ask that it be sound.

Prospects for Therapy

What of treatment? Will we acquire new antidotes for cancer from our study of oncogenes? There is little likelihood that we will be able to repair or replace damaged proto-oncogenes in the foreseeable future, particularly in the individual already burdened with countless tumor cells. There is talk of restoring functional copies of recessive oncogenes to tumors in which they are defective.[78] But realization of this objective in human subjects presently seems many years distant.

If we focus on the protein handmaidens of genes, however, we can see more cause for hope. Given sufficient information about how these proteins act, the pharmaceutical chemist or the immunotherapist may be able to invent ways to interdict their action, even to exploit the specificity of genetic damage and thus to reverse the effects of oncogenes. We are not close to implementing this strategy, but it is a reasonable hope.

I am eager not to appear naive. No single therapy against an oncogene product is likely to become a panacea. We must deal with a large variety of oncogenes, whose products are deployed to the many reaches of the cell and whose actions present great chemical and enzymological diversity; and we must be prepared to cope with evolving genetic damage within cancer cells that can bring a variety of oncogenes into play sequentially. Nevertheless, the search for genetic damage in cancer cells and the explication of how that damage affects the biochemical functions of genes have become our best hope to understand and thus to thwart the ravages of cancer.

Conclusion

At the beginning of this century, the Austrian engineer and novelist *Robert Musil* offered a description of progress in science that foreshadowed modern views of epistemology and that now exemplifies the course of contemporary cancer research.

> ... every few years, ... something that up to then was held to be error suddenly revolutionizes all views, ... an unobtrusive, despised idea becomes the ruler over a new realm. ...[79]

Harold Varmus, I, and our numerous colleagues have been privileged to assist as a despised idea became the ruler over a new realm. The notion that genetic changes are important in the genesis of cancer has met strenuous resistance over the years. But now that notion has gained ascendancy. In the event, I have learned that there is no single path to creativity: we are constrained not by the necessary discipline of rigor, but by the limits to our imaginations and our intellectual courage. In the words of an American sage: "Dare to be wrong, or you may never be right."[80]

Discovery takes two forms. The first is mundane, but nevertheless legitimate: we grope our way to reality and then recognize it for what it is. The second is legitimate, but also sublime: we imagine reality as it ought to be and then find the proof for our imaginings. I have been fortunate to know the first form of discovery and am thankful for the privilege. I have miscarried opportunities to know the second and am diminished by the failure. Redemption lies in more imaginings.

"The real truths are those that can be invented."[81]

I owe a lifelong debt to Harold Varmus, with whom I shared most of the events described here. The whole has been greater than the sum of the two parts, or so I believe. Numerous students and postdoctoral fellows have participated in the discovery and pursuit of proto-oncogenes with Harold and myself. Without their dedicated and talented efforts, I would have no story to tell. Since I could not name them all in the text, I have named none. Many of their contributions are documented in the bibliography to this manuscript. I recall the memory of Richard Parker, for his special impact. I am also grateful to colleagues in the scientific community who have helped me at crucial times in my career, including David Baltimore, Howard Berg, Peter Duesberg, Howard Goodman, Robert Huebner, Malcolm Martin, John Menninger, Aaron Shatkin, Howard Temin, and Peter Vogt. I acknowledge my many colleagues at the University of California, San Francisco, whose friendship and support have been vital, particularly Bruce Alberts, Mitzi Best, Herbert Boyer, Lois Fanshier, Julius Krevans, Jean Jackson, Marc Kirschner, Tom Kornberg, Suzanne Ortiz, Nancy Quintrell, Rudi Schmid, Lois Serxner, Holly Smith, and Karen Smith. I thank my wife and family for a gift of forbearance that cannot be repaid. My work has been supported by both the National and California Divisions of the American Cancer Society and by the National Institutes of Health. The support of biomedical research in the United States is an act of public altruism unexcelled in history. I dedicate this manuscript to the countless individuals who sustain that support, by voluntary contributions and by the payment of state and federal taxes.

Received: January 26, 1990 [A 771 IE]
German version: *Angew. Chem. 102* (1990) 765

[1] R. Dulbecco (Nat. Acad. Sci. USA) *48* (1976) 275–306.
[2] H. E. Varmus, *Angew. Chem. 102* (1990) 756; *Angew. Chem. Int. Ed. Engl. 29* (1990) 707.
[3] J. M. Bishop, D. F. Summers, L. Levintow, *Proc. Natl. Acad. Sci. USA, 54* (1965) 1273–1281.
[4] J. M. Bishop, G. Koch, B. Evans, M. Merriman, *J. Mol. Biol. 46* (1969) 235–249.
[5] M. Best, B. Evans, J. M. Bishop, *Virology 47* (1972) 592–603.
[6] B. L. Bass, H. Weintraub, R. Cattaneo, M. A. Billeter, *Cell 56* (1989) 331.
[7] D. Baltimore, *Nature* (London) *226* (1970) 1209–1211.
[8] H. M. Temin, S. Mizutani, *Nature* (London) *226* (1970) 1211–1213.
[9] A. Kornberg, *Science* (Washington, D.C.) *131* (1960) 1503–1508.
[10] J. Leong, et al., *J. Virol. 9* (1972) 891–902.
[11] S. R. Weiss, H. E. Varmus, J. M. Bishop, *Cell 12* (1977) 983–992.
[12] B. Cordell, S. R. Weiss, H. E. Varmus, J. M. Bishop, *Cell 15* (1978) 79–92.
[13] T. Jacks, H. E. Varmus, *Science* (Washington, D.C.) *230* (1985) 1237–1246.
[14] A. J. Faras, J. M. Taylor, W. Levinson, J. Goodman, J. M. Bishop, *J. Mol. Biol. 79* (1973) 163–183.
[15] J. E. Dahlberg et al., *J. Virol. 13* (1974) 1126–1133.
[16] H. E. Varmus, *Sci. Am. 257* (1987) No. 9, pp. 56–66.
[17] G. S. Martin, *Nature* (London) *227* (1970) 1021–1023.
[18] S. Kawai, H. Hanafusa, *Virology 46* (1971) 470–479.
[19] P. K. Vogt in H. Fraenkel-Conrat, R. R. Wagner (Eds.): *Comprehensive Virology, Vol. 9*, Plenum Press, New York 1977, pp. 341–455.
[20] H. Opperman, J. M. Bishop, H. E. Varmus, L. Levintow, *Cell 12* (1977) 993–1005.
[21] J. S. Brugge, R. L. Erikson, *Nature* (London) *269* (1977) 346–347.
[22] M. S. Collett, R. L. Erikson, *Proc. Natl. Acad. Sci. USA 75* (1978) 2021–2024.
[23] A. Levinson, H. Oppermann, L. Levintow, H. E. Varmus, J. M. Bishop, *Cell 15* (1978) 561–572.
[24] T. Hunter, B. M. Sefton, *Proc. Natl. Acad. Sci. USA 77* (1980) 1311–1315.
[25] T. Hunter, J. A. Cooper, *Annu. Rev. Biochem. 54* (1985) 897–931.
[26] A. D. Levinson, H. Oppermann, H. E. Varmus, J. M. Bishop, *J. Biol. Chem. 255* (1980) 11973–11980.
[27] J. M. Bishop, *Cell 42* (1985) 23–38.
[28] T. Hunter, *Sci. Am. 251* (1984) Nr. 8, S. 70–80.
[29] M. Barbacid, *Annu. Rev. Biochem. 56* (1987) 779–827.
[30] P. K. Vogt, R. Tjian, *Oncogene 3* (1988) 3–9.
[31] J. M. Bishop, *Cell 23* (1981) 5–6.
[32] P. H. Duesberg, *Science (Washington, D.C.) 228* (1985) 669.
[33] R. Jove, H. Hanafusa, *Annu. Rev. Cell Biol. 3* (1987) 31–57.
[34] T. Dobzhansky, cited in D. J. Futuyama: *Science on Trial: The Case for Evolution*, Pantheon Books, New York 1983, p. 114.
[35] R. J. Huebner, G. J. Todaro, *Proc. Natl. Acad. Sci. USA 64* (1969) 1087–1094.
[36] H. Temin in: *Nobel Lectures in Molecular Biology 1933–1975*, Elsevier-North Holland, New York 1977, pp. 509–529.

[37] J. M. Bishop et al. in P. O. P. Ts'o (Ed.): *The Molecular Biology of the Mammalian Genetic Apparatus, Vol. 2*, North-Holland, Amsterdam 1977, pp. 277–287.
[38] H. E. Varmus, *Annu. Rev. Genet. 18* (1984) 553–612.
[39] D. Stehelin, H. E. Varmus, J. M. Bishop, P. K. Vogt, *Nature* (London) *260* (1976) 170–173.
[40] D. Spector et al., *Cell 3* (1978) 371–379.
[41] D. Spector, B. Baker, H. E. Varmus, J. M. Bishop, *Cell 3* (1978) 381–386.
[42] M. S. Collett, E. Erikson, A. F. Purchio, J. S. Brugge, R. L. Erikson, *Proc. Natl. Acad. Sci. USA 76* (1979) 3159–3163.
[43] H. Oppermann, A. D. Levinson, H. E. Varmus, L. Levintow, J. M. Bishop, *Proc. Natl. Acad. Sci. USA 76* (1979) 1804–1808.
[44] A. J. Langlois, S. Sankaran, P. H.-L. Hsuing, J. W. Beard, *J. Virol. 1* (1967) 1082–1084.
[45] D. Sheiness, K. Bister, L. Fanshier, C. Moscovici, J. M. Bishop, *J. Virol. 33* (1980) 963–968.
[46] M. Roussel et al., *Nature* (London) *281* (1979) 452–455.
[47] P. Mellon, A. Pawson, K. Bister, G. S. Martin, P. H. Duesberg, *Proc. Natl. Acad. Sci. USA 75* (1978) 5874–5878.
[48] R. W. Ellis et al., *J. Virol. 36* (1980) 408–420.
[49] B. Vennstrom, D. Sheiness, J. Zabielski, J. M. Bishop, *J. Virol. 42* (1982) 773–779.
[50] K. Alitalo et al., *Proc. Natl. Acad. Sci. USA 80* (1983) 100–104.
[51] B. Vennstrom et al., *EMBO J. 3* (1984) 3223–3231.
[52] D. Sheiness, J. M. Bishop, *J. Virol. 31* (1979) 514–521.
[53] D. K. Sheiness, S. H. Hughes, H. E. Varmus, E. Stubblefield, J. M. Bishop, *Virology 105* (1980) 415–424.
[54] W. S. Hayward, B. G. Neel, S. M. Astrin, *Nature* (London) *290* (1981) 475–480.
[55] G. Klein, *Cell 32* (1983) 311–315.
[56] M. D. Cole, *Annu. Rev. Genet. 20* (1986) 361–378.
[57] K. Alitalo, M. Schwab, *Adv. Cancer Res. 47* (1986) 235–282.
[58] J. M. Bishop, *Science* (Washington, D. C.) *235* (1987) 305–311.
[59] H. Beug, M. J. Hayman, T. Graf in M. F. Greaves (Ed.): *Cancer Surveys, Vol. 1*, Oxford University Press, Oxford 1982, pp. 205–230.
[60] B.-Z. Shilo, *Trends Genet. 1987*, 69–73.
[61] F. G. Haluska, Y. Tsujimoto, C. M. Croce, *Annu. Rev. Genet. 21* (1987) 321–347.
[62] G. R. Stark, M. Debatisse, E. Giulotto, G. M. Wahl, *Cell. 57* (1989) 901–908.
[63] M. Schwab et al., *Nature* (London) *305* (1983) 245–248.
[64] M. Schwab et al., *Proc. Natl. Acad. Sci. USA 81* (1984) 4940–4944.
[65] N. E. Kohl et al., *Cell 35* (1983) 359–367.
[66] L. W. Stanton, M. Schwab, J. M. Bishop, *Mol. Cell. Biol. 83* (1986) 1772–1776.
[67] N. E. Kohl et al., *Nature* (London) *319* (1986) 73–77.
[68] K. M. Downs, G. R. Martin, J. M. Bishop, *Genes Dev. 3* (1989) 860–869.
[69] G. M. Brodeur et al., *Science* (Washington, D.C) *224* (1984) 1121–1124.
[70] R. C. Seeger et al., *New Engl. J. Med. 313* (1985) 1111–1116.
[71] D. J. Slamon, *New Engl. J. Med. 317* (1987)955–957.
[72] G. Klein, *Science* (Washington, D.C.) *238* (1987) 1539–1545.
[73] D. J. Slamon et al., *Science* (Washington, D.C.) *235* (1987) 177–182.
[74] D. J. Slamon et al., *Science* (Washington, D.C.) *244* (1989) 707–712.
[75] E. Liu, B. Hjelle, R. Morgan, F. Hecht, J. M. Bishop, *Nature* (London) *330* (1987) 186–189.
[76] H. Y. Hirai et al., *Nature* (London) *327* (1987) 430–432.
[77] R. A. Padua, *Leukemia 2* (1988) 503–510.
[78] H.-J. S. Huang et al., *Science* (Washington, D.C.) *242* (1988) 1563–1566.
[79] R. Musil (A. Frisé, Ed.): *Der Mann ohne Eigenschaften*. Rowohlt, Reinbek 1978, p. 40; *The Man Without Qualities—I*, (E. Wilkins, E. Kaiser, Trans.), Pan Books, London 1979, p. 41.
[80] Attributed to *Fats Waller*, on constructing musical chords.
[81] K. Kraus, *Die Fackel* 360–362 (1912) 6; *Half-Truths & One-and-a-Half Truths* (H. Zohn, Ed. and Trans.), Carcanet Press, Manchester, 1986, p. 61.

Experiments with Separated Oscillatory Fields and Hydrogen Masers (Nobel Lecture)**

By Norman F. Ramsey*

I am honored to receive the Nobel Prize, which I feel is also an honor to the physicists and engineers in many countries who have done beautiful experiments using the methods I shall be discussing. In addition, I am grateful to my great teacher *I. I. Rabi*, to my friends and colleagues, to my eighty-four Ph.D. students who were close friends and collaborators and especially to *Daniel Kleppner* and *Daniel Larson*, who contributed so much to the success of our laboratory.

The Method of Successive Oscillatory Fields

In the summer of 1937, following two years at Cambridge University, I went to Columbia University to work with *I. I. Rabi*. After I had been there only a few months, *Rabi* invented[1-4] the molecular beam magnetic resonance method so I had the great good fortune to be the only graduate student to work with *Rabi* and his colleagues[1-2] on one of the first two experiments to develop and utilize magnetic resonance spectroscopy, for which *Rabi* received the 1944 Nobel Prize in Physics.

By 1949, I had moved to Harvard University and was looking for a way to make more accurate measurements than were possible with the Rabi method and in so doing I invented the method of separated oscillatory fields.[3-6] In this method the single oscillatory magnetic field in the center of the Rabi device is replaced by two oscillatory fields, one at the entrance and one at the exit of the space in which the properties of the atoms or molecules are studied. As I shall point out, the separated oscillatory fields method had many advantages over the single oscillatory field method, and in the following years it was extended to many experiments beyond those of molecular beam magnetic resonance. The device shown in Figure 1 is a molecular beam apparatus embodying successive oscillatory fields that has been used at Harvard for an extensive series of experiments.

Fig. 1. Molecular beam apparatus with separated oscillatory fields. The beam of molecules emerges from a small source aperture in the left third of the apparatus, is focussed there and passes through the middle third in an approximately parallel beam. It is focussed gain in the right third to a small detector aperture. The separated oscillatory electric fields at the beginning and end of the middle third of the apparatus produce resonance transitions that reduce the focussing and therefore weaken the detected beam intensity.

Let me now review the successive oscillatory field method, particularly in its original and easiest-to-explain application—the measurement of nuclear magnetic moments. The extension to more general cases is then straightforward.

The method was initially an improvement on *Rabi*'s resonance method for measuring nuclear magnetic moments, whose principles are illustrated schematically in Figure 2.

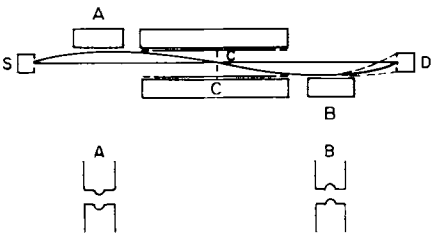

Fig. 2. Schematic diagram of a molecular beam magnetic resonance apparatus. A typical molecule which can be detected emerges from the source S, is deflected by the inhomogeneous magnetic field A, passes through the collimator C and is deflected to the detector D by the inhomogeneous magnetic field B. If, however, the oscillatory field in the C region induces a change in the molecular state, the B magnet will provide a different deflection and the beam will follow the dashed lines with a corresponding reduction in detected intensity. In the Rabi method, the oscillatory field is applied uniformly throughout the C region as indicated by the long rf lines inside the C-magnet, whereas in the separated oscillatory field method the rf is applied only in the short regions at the beginning and end of the C-magnet.

Consider a classical nucleus with spin angular momentum $\hbar \boldsymbol{J}$ and magnetic moment $\boldsymbol{\mu} = (\mu/J)\boldsymbol{J}$. Then in a static magnetic field $\boldsymbol{H}_0 = H_0 \boldsymbol{k}$, the nucleus, due to the torque on the nuclear angular momentum, will precess like a top about $\boldsymbol{H}_0$ with the Larmor frequency ν_0 and angular frequency ω_0 given by (1),

$$\omega_0 = 2\pi\nu_0 = \frac{\mu H_0}{\hbar I} \tag{1}$$

as shown in Figure 3. Consider an additional magnetic field $\boldsymbol{H}_1$ perpendicular to $\boldsymbol{H}_0$ and rotating about it with angular frequency ω. Then, if at any time $\boldsymbol{H}_1$ is perpendicular to the plane of $\boldsymbol{H}_0$ and $\boldsymbol{J}$, it will remain perpendicular to it provided $\omega = \omega_0$. In that case, in a coordinate system rotating with $\boldsymbol{H}_1$, $\boldsymbol{J}$ will precess about $\boldsymbol{H}_1$ and the angle φ will continuously change in a fashion analogous to the motion of a "sleeping top"; the change of orientation can be detected by allowing the molecular beam containing the magnetic moments to pass through inhomogeneous fields as in Figure 2. If ω is not

[*] Prof. N. F. Ramsey
Physics Department, Harvard University
Cambridge, MA 02138 (USA)

[**] Copyright © The Nobel Foundation 1990.—We thank the Nobel Foundation, Stockholm, for permission to print this lecture.

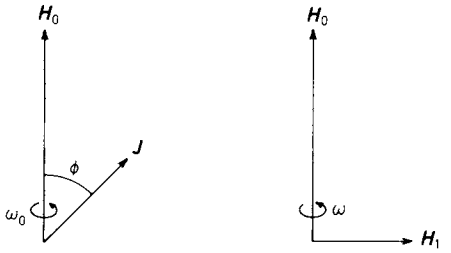

Fig. 3. Precession of the nuclear angular momentum $\boldsymbol{J}$ (left) and the rotating magnetic field $\boldsymbol{H}_1$ (right) in the Rabi method.

equal to ω_0, $\boldsymbol{H}_1$ will not remain perpendicular to $\boldsymbol{J}$; so φ will increase for a short while and then decrease, leading to no net change. In this fashion the Larmor precession frequency ω_0 can be detected by measuring the oscillator frequency ω at which there is maximum reorientation of the angular momentum and hence a maximum change in beam intensity for an apparatus as in Figure 2. This procedure is the basis of the *Rabi* molecular beam resonance method.

The separated oscillatory field method in this application is much the same except that the rotating field $\boldsymbol{H}_1$ seen by the nucleus is applied initially for a short time τ, the amplitude of $\boldsymbol{H}_1$ is then reduced to zero for a relatively long time t and then increased to $\boldsymbol{H}_1$ for a time τ, with phase coherency being preserved for the oscillating fields as shown in Figure 4. This

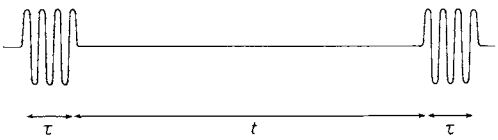

Fig. 4. Two separated oscillatory fields, each acting for a time τ, with zero amplitude oscillating field acting for time t. Phase coherency is preserved between the two oscillatory fields so it is as if the oscillation continued, but with zero amplitude for time t.

can be done, for example, in the molecular-beam apparatus of Figure 2 in which the molecules first pass through a rotating field region, then a region with no rotating field and finally a region with a second rotating field driven phase coherently by the same oscillator.

If the nuclear spin angular momentum is initially parallel to the fixed field (so that φ is equal to zero initially) it is possible to select the magnitude of the rotating field so that φ is 90° or $\pi/2$ radians at the end of the first oscillating region. While in the region with no oscillating field, the magnetic moment simply precesses with the Larmor frequency appropriate to the magnetic field in that region. When the magnetic moment enters the second oscillating field region there is again a torque acting to change φ. If the frequency of the rotating field is exactly the same as the mean Larmor frequency in the intermediate region there is no relative phase shift between the angular momentum and the rotating field.

Consequently, if the magnitude of the second rotating field and the length of time of its application are equal to those of the first region, the second rotating field has just the same effect as the first one—that is, it increases φ by another $\pi/2$, making $\varphi = \pi$, corresponding to a complete reversal of the direction of the angular momentum. On the other hand, if the field and the Larmor frequencies are slightly different, so that the relative phase angle between the rotating field vector and the precessing angular momentum is changed by π while the system is passing through the intermediate region, the second oscillating field has just the opposite effect to the first one; the result is that φ is returned to zero. If the Larmor frequency and the rotating field frequency differ by an amount such that the relative phase shift in the intermediate region is exactly an integral multiple of 2π, φ will again be left at π just as at exact resonance.

In other words: if all molecules had the same velocity, the transition probability would be periodic as in Figure 5. However, in a molecular beam resonance experiment one can easily distinguish between exact resonance and the other cases. In the case of exact resonance, the condition for no change in the relative phase of the rotating field and of the precessing angular momentum is independent of the molecular velocity. In the other cases, however, the condition for an integral multiple of 2π relative phase shift is velocity dependent, because a slower molecule is in the intermediate region longer and so experiences a greater shift than a faster molecule. Consequently, for the non-resonance peaks the reorientations of most molecules are incomplete, so the magnitudes of the non-resonance peaks are smaller than at exact reso-

Norman F. Ramsey, who was born in 1915 in Washington D.C., completed his formal studies at the Columbia University and the University of Cambridge. In 1940, under the supervision of I. Rabi, he received a PhD from Columbia University for molecular beam studies of the rotational magnetic moments of molecules. He was awarded an Sc. D. by Cambridge University in 1954 and by Oxford University in 1973, as well as honorary degrees from numerous universities. He was Executive Secretary of the group of scientists who established Brookhaven National Laboratory and was the first Chairman of its Physics Department. Since 1947 he has been at Harvard University, where he is Higgins Professor of Physics. To mention only a small selection of his various other activities, Norman Ramsey was in 1973/74 the George Eastman Professor at Oxford University, from 1966–1981 President of the Universities Research Association, and from 1980–1986 the Chairman of the Board of Governors of the American Institute of Physics. Books authored by him include "Experimental Nuclear Physics", "Nuclear Moments", "Molecular Beams", and "Quick Calculus". Of the many awards he had already received before the Nobel Prize only those of the last five years might be mentioned: Monie Ferst Award, Rabi Prize and Rumford Premium, Compton Medal and Oersted Medal, IEEE Centennial Medal, and National Medal of Science.

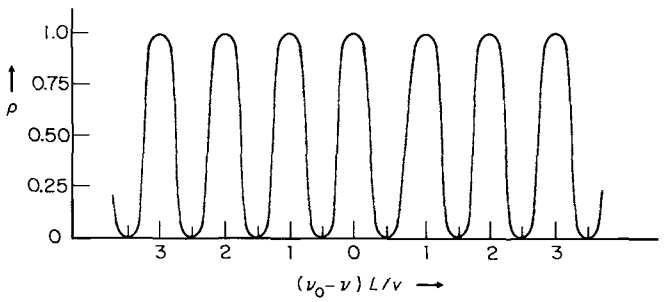

Fig. 5. Transition probability ϱ as a function of the frequency $\nu = \omega/2\pi$ that would be observed in a separated oscillatory field experiment if all the molecules in the beam had a single velocity v. L is the distance between the two separated oscillatory field regions.

nance, and one expects a resonance curve similar to that shown in Figure 6 in which the transition probability for a particle of spin 1/2 is plotted as a function of frequency.

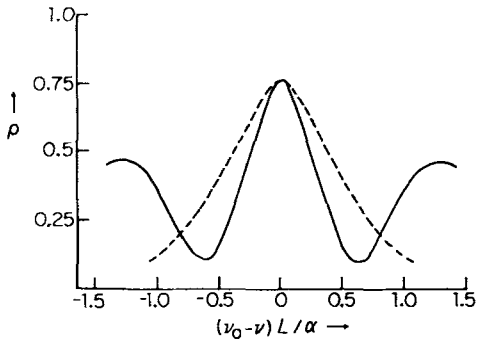

Fig. 6. When the molecules have a Maxwellian velocity distribution, the transition probability is as shown by the full line for optimum rotating field amplitude. (L is the distance between oscillating field regions, α is the most probable molecular velocity and ν is the oscillatory frequency $= \omega/2\pi$.) The dashed line represents the transition probability with the single oscillating field method when the total duration is the same as the time between separated oscillatory field pulses (Fig. 4).

Although the above description of the method is primarily in terms of classical spins and magnetic moments, the method applies to any quantum mechanical system for which a transition can be induced between two energy states W_i and W_f which are differently focussed. The resonance frequency ω_0 is then given by Equation (2) and one expects a resonance curve similar to that shown in Figure 6.

$$\omega_o = (W_i - W_f)/\hbar \qquad (2)$$

From a quantum-mechanical point of view, the oscillating character of the transition probability in Figures 5 and 6 is the result of the cross term in the calculation of the transition probability from probability amplitudes. Let C_{iif} be the probability amplitude for the nucleus to pass through the first oscillatory field region with the initial state i unchanged and for there to be a transition to state f in the final field, and let C_{iff} be the amplitude for the alternative path with the transition to the final state f being in the first field with no change in the second. Then the cross term $C_{iif}C^*_{iff}$ produces an interference pattern and gives the narrow oscillatory pattern of the transition probability shown in the curves of Figures 5 and 6. Alternatively, the pattern can in part be interpreted as resulting from the Fourier spectrum of an oscillating field which is on for a time τ, off for t and on again for τ (Fig. 4). This interpretation is however not fully valid since with finite rotations of $\boldsymbol{J}$ the problem is a non-linear one. Furthermore, the Fourier interpretation obscures some of the key advantages of the separated oscillatory field method. I have calculated the quantum mechanical transition probabilities[3, 5, 7, 8] and these calculations provide the basis for Figure 6.

The separated oscillatory field method has a number of advantages including the following:

(1) The resonance peaks are only 0.6 as broad as the corresponding ones with the single oscillatory field method. The narrowing is somewhat analogous to the peaks in a two slit optical interference pattern being narrower than the central diffraction peak of a single wide slit whose width is equal to the separation of the two slits.

(2) The sharpness of the resonance is not reduced by nonuniformities of the constant field since both from the qualitative description and from the theoretical quantum analysis, it is only the space average value of the energies along the path that enter Equation (2) and are important.

(3) The method is more effective and often essential at very high frequencies where the wavelength of the radiation used may be comparable to or smaller than the length of the region in which the energy levels are studied.

(4) Provided there is no unintended phase shift between the two oscillatory fields, first order Doppler shifts and widths are eliminated.

(5) The method can be applied to study energy levels in a region into which an oscillating field cannot be introduced; for example, the Larmor precession frequency of neutrons can be measured while they are inside a magnetized iron block.

(6) The lines can be narrowed by reducing the amplitude of the rotating field below the optimum. The narrowing is the result of the low amplitude favoring slower than average molecules.

(7) If the atomic state being studied decays spontaneously, the separated oscillatory field method permits the observation of narrower resonances than those anticipated from the lifetime and the Heisenberg uncertainty principle provided the two separated oscillatory fields are sufficiently far apart; only states that survive sufficiently long to reach the second oscillatory field can contribute to the resonance. This method, for example, has been used by *Lundeen* et al.[9] in precise studies of the Lamb shift.

The advantages of the separated oscillatory field method have led to its extensive use in molecular and atomic beam spectroscopy. One of the best known is in atomic cesium standards of frequency and time which will be discussed later.

Although in most respects, the separated oscillatory field method offers advantages over a single oscillatory field, there are sometimes disadvantages. In studying complicated overlapping spectra the subsidiary maxima (Fig. 6) can cause confusion. Furthermore, it is sometimes difficult at the required frequency to obtain sufficient oscillatory field strengths with two short oscillatory fields, whereas adequate

field strength may be achieved with a weaker, longer oscillatory field. Therefore, for most molecular beam resonance experiments it is best to have both separated oscillatory fields and a single long oscillatory field available; one can then use the most suitable method under the circumstances.

As in any high precision experiment, care must be exercised with the separated oscillatory field method to avoid obtaining misleading results. Ordinarily these potential distortions are more easily understood and eliminated with the separated oscillatory field method than are their counterparts in most other high-precision spectroscopy. I have discussed the various effects in detail elsewhere[3, 7, 8, 10] but I will briefly summarize them here.

Variations in the amplitudes of the oscillating fields from their optimum values may markedly change the shape of the resonance, including the replacement of a maximum transition probability by a minimum. However, symmetry about the exact resonance frequency is preserved, so no measurement error need be introduced by such amplitude variations.[7, 8]

Variations of the magnitude of the fixed field between, but not in, the oscillatory field regions do not ordinarily distort a molecular beam resonance provided the average transition frequency (Bohr frequency) between the two fields equals the values of the transition frequencies in each of the two oscillatory field regions alone. If this condition is not met, there can be some shift in the resonance frequency.[7, 8]

If, in addition to the two energy levels between which transitions are studied, there are other energy levels partially excited by the oscillatory field, there will be a pulling of the resonance frequency as in any spectroscopic study and as analyzed in detail in the literature.[3, 7, 8]

Even in the case when only two energy levels are involved, the application of additional rotating magnetic fields at frequencies other than the resonance frequency will produce a net shift in the observed resonance frequency.[3, 7, 8] A particularly important special case is the effect identified by *Bloch* and *Siegert*[11] which occurs when oscillatory rather than rotating magnetic fields are used. Since an oscillatory field can be decomposed into two oppositely rotating fields, the counter-rotating field component automatically acts as such an extraneous rotating field. Another example of an extraneously introduced rotating field is that which results from the motion of an atom through a field $\boldsymbol{H}_0$ whose direction varies in the region traversed. The theory of the effects of additional rotating fields at arbitrary frequencies has been developed by myself,[7, 8, 10, 12] *Winter*,[10] *Shirley*,[13] *Code*,[12] and *Greene*.[14]

Unintended relative phase shifts between the two oscillatory field regions will produce a shift in the observed resonance frequency.[13–15] This is the most common source of possible error, and care must be taken to avoid it either by eliminating such a phase shift or by determining the shift—say by measurements with the molecular beam passing through the apparatus first in one direction and then in the opposite direction.

A number of extensions to the separated oscillatory field method have been made since its original introduction:

(1) It is often convenient to introduce phase shifts deliberately to modify the resonance shape.[15] As discussed above, unintended phase shifts can cause distortions of the observed resonance, but some distortions are useful. Thus, if the change in transition probability is observed when the relative phase is shifted from $+\pi/2$ to $-\pi/2$ one sees a dispersion curve[15] (Fig. 7). A resonance of this shape provides maximum sensitivity for detecting small shifts in the resonance frequency.

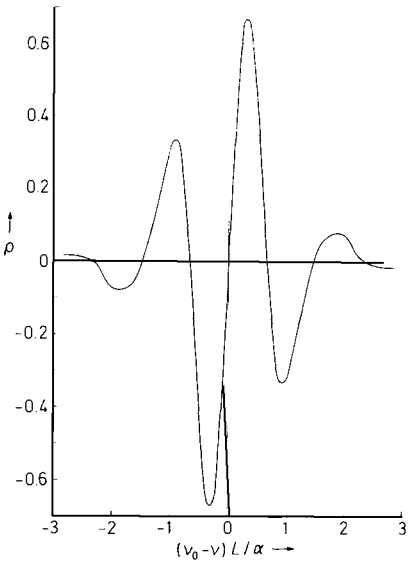

Fig. 7. Theoretical change in transition probability on reversing a $\pi/2$ phase shift. At the resonance frequency there is no change in transition probability, but the curve at resonance has the steepest slope.

(2) For most purposes the highest precision can be obtained with just two oscillatory fields separated by the maximum time, but in some cases it is better to use more than two separated oscillatory fields.[4] The theoretical resonance shapes[7] with two, three, four and infinitely many oscillatory fields are shown in Figure 8. The infinitely many oscillatory field case, of course, by definition becomes the same as the single long oscillatory field if the total length of the transition region is kept the same and the infinitely many oscillatory fields fill in the transition region continuously as we assumed

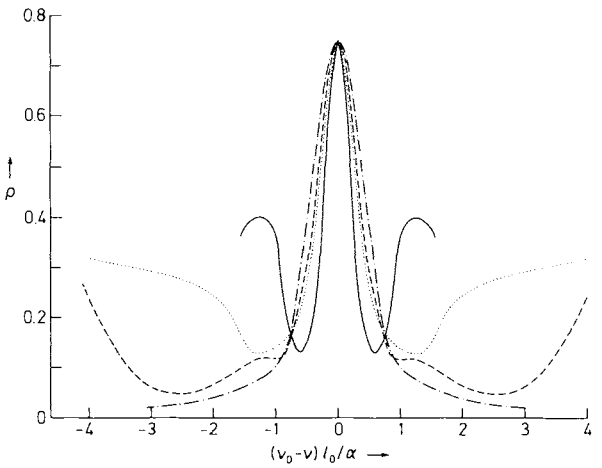

Fig. 8. Multiple oscillatory fields. The curves show molecular beam resonances with two (——), three (···), four (---) and infinitely many (–·–) successive oscillating fields. The case with an infinite number of oscillating fields is essentially the same as Rabi's single oscillatory field method (l = L).

in Figure 8. For many purposes this is the best way to think of the single oscillatory field method, and this point of view makes it apparent that the single oscillatory field method is subjected to complicated versions of all the distortions discussed in the previous section. It is noteworthy that, as the number of oscillatory field regions is increased for the same total length of apparatus, the resonance width is broadened; the narrowest resonance is obtained with just two oscillatory fields separated the maximum distance apart. Despite this advantage, there are valid circumstances for using more than two oscillatory fields. With three oscillatory fields the first and largest side lobe is suppressed, which may help in resolving two nearby resonances; for a larger number of oscillatory fields additional side lobes are suppressed, and in the limiting case of a single oscillatory field there are no side lobes. Another reason for using a large number of successive pulses can be the impossibility of obtaining sufficient power in a single pulse to induce adequate transition probability with a small number of pulses.

(3) The earlier use of the separated oscillatory field method involved two oscillatory fields separated in space, but it was soon realized that the method with modest modifications could be generalized to a method of successive oscillatory fields with the separation being in time, say by the use of coherent pulses.[16]

(4) If more than two successive oscillatory fields are utilized it is not necessary for the success of the method that they be equally spaced in time;[4] the only requirement is that the oscillating fields be coherent—as is the case if they are all derived from a single continuously running oscillator. In particular, the separation of the pulses can even be random,[16] as in the case of the large-box hydrogen maser[17] discussed later. The atoms being stimulated to emit move randomly into and out of the cavities with oscillatory fields and spend the intermediate time in the large container with no such fields.

(5) The full generalization of the successive oscillatory field method is excitation by one or more oscillatory fields that vary arbitrarily with time in both amplitude and phase.[7, 8]

(6) *V. F. Ezhov* et al.[6, 18] carried out a neutron-beam experiment, using an inhomogeneous static field in the region of each oscillatory field such that initially when the oscillatory field is applied conditions are far from resonance. Then, when the resonance condition is slowly approached, the magnetic moment that was originally aligned parallel to $\boldsymbol{H}_0$ will adiabatically follow the effective magnetic field on a coordinate system rotating with $\boldsymbol{H}_1$ until at the end of the first oscillatory field region the moment is parallel to $\boldsymbol{H}_1$. This arrangement has the theoretical advantage that the maximum transition probability can be unity even with a velocity distribution, but the method may be less well adapted to the study of complicated spectra.

(7) I emphasized earlier that one of the principal sources of error in the separated oscillatory field method is that which arises from uncertainty in the exact value of the relative phase shift in the two oscillatory fields. *Jarvis*, et al.[19] have pointed out that this problem can be overcome with a slight loss in resolution by driving the two cavities at slightly different frequencies so that there is a continual change in the relative phase. In this case the observed resonance pattern will change continuously from absorption to dispersion shape. The envelope of these patterns, however, can be observed and the position of the maximum of the envelope is unaffected by relative phase shifts. Since the envelope is about twice the width of a specific resonance there is some loss of resolution in this method, but in certain cases this loss may be outweighed by the freedom from phase-shift errors.

(8) The method has been extended to electric as well as magnetic transitions and to optical laser frequencies as well as radio- and microwave-frequencies. The application of the separated oscillatory field method to optical frequencies requires considerable modifications because of the short wavelengths, as pointed out by *Blaklanov, Dubetsky*, and *Chebotsev*.[20] Successful applications of the separated oscillatory field method to lasers have been made by *Bergquist*,[21] *Lee*,[21] *Hall*,[21] *Salour*,[22] *Cohen-Tannoudji*,[22] *Bordé*,[23] *Hänsch*,[24] *Chebotayev*[25] and many others.[25]

(9) The method has been extended to neutron beams and to neutrons stored for long times in totally reflecting bottles.

(10) In a recent beautiful experiment, *S. Chu* et al.[26] have successfully used the principle of separated oscillatory fields with a fountain of atoms that rises up slowly, passes through an oscillating field region, falls under gravity and passes again through the same oscillatory field region. This fountain experiment was attempted many years ago by *J. R. Zacharias* et al.,[3] but it was unsuccessful because of the inadequate number of very slow atoms. *Chu* et al. used laser cooling[27, 28, 29] to slow the atoms to a low velocity and obtained through the separated oscillatory fields a beautifully narrow resonance pattern.

The Atomic Hydrogen Maser

The atomic hydrogen maser grew out of my attempts to obtain even greater stability in atomic beam experiments. By the Heisenberg uncertainty principle (or by the Fourier transform), the width of a resonance in a molecular beam experiment cannot be less than approximately the reciprocal of the time the atom is in the resonance region of the apparatus. For atoms moving through a 1 m long resonance region at 100 m/s this means that the resonance width is approximately 100 Hz. To decrease this width and hence increase the precision of the measurements required an increase in this time. To increase the time by drastically lengthening the apparatus or selecting slower molecules would decrease the already marginal beam intensity or greatly increase the cost of the apparatus. I therefore decided to plan an atomic beam in which the atoms, after passing through the first oscillatory field would enter a storage box with suitably coated walls where they would bounce around for a period of time and then emerge to pass through the second oscillatory field. My Ph.D. student, *Daniel Kleppner*,[30] undertook the construction of this device as his thesis project. The original configuration required only a few wall collisions and was called a broken atomic beam resonance experiment. Initially the beam was cesium and the wall coating was teflon. The experiment[30] was a partial success in that a separated oscillatory field pattern for an atomic hyperfine transition was obtained, but it was weak and disappeared after a few wall

collisions. The results improved markedly when paraffin was used for the wall coating and a hyperfine resonance was eventually obtained after 190 collisions giving a resonance width of 100 Hz, but with the resonance frequency shifted by 150 Hz.

To do much better than this, we decided we would have to use an atom with a lower mass and a lower electric polarizability to reduce the wall interactions. Atomic hydrogen appeared ideal for this purpose, but atomic hydrogen is notoriously difficult to detect. We, therefore, calculated the possibility of detecting the transitions through their effects on the electromagnetic radiations. *Townes* et al.[31] had a few years earlier made the first successful maser (acronym for *M*icrowave *A*mplifier by *S*timulated *E*mission of *R*adiation) but no one had previously made a maser based on a magnetic dipole moment or at a frequency as low as that of an atomic hyperfine transition. We concluded, however, that if the resonance could be made narrow enough by multiple wall collisions, we should be able to obtain maser oscillations. The apparatus was designed and constructed by *Goldenberg*, *Kleppner* and myself[32] and after a few failures we obtained maser oscillations at the atomic hydrogen hyperfine frequency. Both the proton and the electron have spin angular momenta $\boldsymbol{I}$ and $\boldsymbol{J}$ as well as magnetic moments. The atomic hyperfine transitions are those for which there is a change of the relative orientation of these two magnetic moments between the initial and final states in Equation (2). We studied H atoms in the $1^2S_{1/2}$ ground electronic state and mostly observed the transitions $F = 1,\ m = 0 \rightarrow F = 0,\ m = 0$, where F is the quantum number of the total angular momentum $\boldsymbol{F} = \boldsymbol{I} + \boldsymbol{J}$ and m is the associated magnetic quantum number.

The principles of an atomic hydrogen maser are shown schematically in Figure 9. An intense electrical discharge in

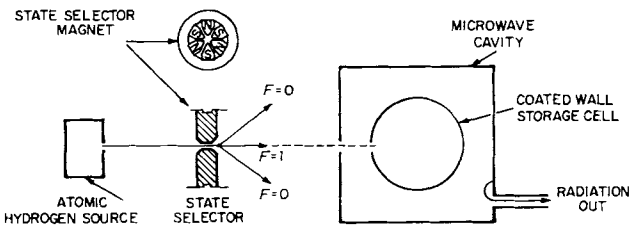

Fig. 9. Schematic diagram of atomic hydrogen maser. Only the paths of the $m = 0$ atoms are shown since the $m = 1$ atoms are not involved in the $\Delta m = 0$ transitions studied.

the source converts commercially available molecular hydrogen (H_2) into atomic hydrogen (H). The atoms emerge from the source into a region that is evacuated to 10^{-6} torr and enter a state selecting magnet which has three north poles alternating in a circle with three south poles. By symmetry, the magnetic field is zero on the axis and increases in magnitude away from the axis. Since the energy of a hydrogen atom in the $F = 1$ $m = 0$ state increases with magnetic field and since mechanical systems are accelerated toward lower potential energy, an atom in the $F = 1$ state that is slightly off axis will be accelerated toward the axis, i.e. the $F = 1$ state will be focussed onto the small aperture of the 15-cm-diameter storage cell, whereas the lower energy $F = 0$ state is defocussed. As a result, if the atomic beam flows steadily, the storage bottle in equilibrium will contain more high energy $F = 1$ atoms than low energy $F = 0$ atoms. If these atoms are exposed to microwave radiation at the hyperfine frequency, more atoms are stimulated to go from the higher energy state to the lower one than in the opposite direction. Energy is then released from the atoms and makes the microwave radiation stronger. Thus the device is an amplifier or maser. If the storage cell is placed inside a tuned cavity, an oscillation at the resonance frequency will increase in magnitude until an equilibrium value is reached. At this level the oscillation will continue indefinitely, with the energy to maintain the oscillation coming from the continuing supply of hydrogen atoms in the high energy hyperfine state. The device then becomes a free running maser oscillator at the atomic hyperfine splitting frequency.

The atomic hydrogen maser oscillator has unprecedented high stability due to a combination of favorable features. The atoms typically reside in the storage cell for 10 seconds, which is much longer than in an atomic beam resonance apparatus, so the resonance line is much narrower. The atoms are stored at low pressure, so they are relatively free and unperturbed while radiating. The first order Doppler shift is removed, since the atoms are exposed to a standing wave and since the average velocity is extremely low for atoms stored for 10 seconds. Masers have very low noise levels, especially when the amplifying elements are isolated atoms. Over periods of several hours the hydrogen maser stability is better than 1×10^{-15}.

The major disadvantage of the hydrogen maser is that the atoms collide with the walls at intervals, changing slightly the hyperfine frequency and giving rise to wall shifts of 1×10^{-11}. However, the wall shifts can be experimentally determined by measurements utilizing storage bottles of two different diameters or with a deformable bulb whose surface to volume ratio can be altered. As in all precision measurements, care must be taken in adjusting and tuning the hydrogen maser to avoid misleading results. These limitations and precautions are discussed in a series of publications by various authors.[32-34] The designs of hydrogen masers have been modified in many ways either for special purposes or for increased stability and reliability. For example, different hyperfine transitions have been used and masers have been operated in relatively strong magnetic fields. A hydrogen maser has also been operated[17] with a storage bottle that is much larger than the wavelength of the stimulating radiation by confining the microwave power to two small cavities so that it functions as a separated oscillatory field device. As shown in Figure 10 the atoms that are stimulated to emit radiation move randomly into and out of the two oscillatory field cavities and spend the intermediate time in the large container where there is no oscillatory field. Due to the larger size of the storage box the storage times are longer and wall collisions are less frequent, so the resonances are narrower and the wall shifts are smaller than for a normal hydrogen maser.

Now that I have discussed extensively the principles of the separated oscillatory field method and of the atomic maser, I shall give some illustrations as to their value. One major category of applications is to precision spectroscopy, espe-

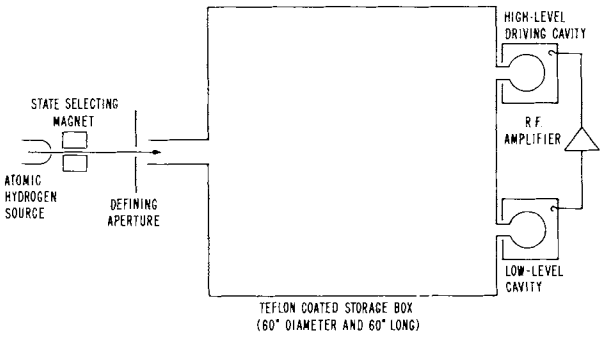

Fig. 10. Schematic diagram of a large box hydrogen maser. The two cavities on the right act as two separated oscillating fields with that of the high level cavity being obtained by amplification from the low level cavity.

cially at radio and microwave frequencies. Another category of applications is to atomic clocks and frequency standards.

Precision Spectroscopy

It is difficult to summarize the spectroscopic applications since there are so many of them. Beautiful experiments have been done by a large number of scientists in different countries. I shall, therefore use just a few illustrations from experiments in which I have been personally involved.

My graduate students have made precision measurements of the radiofrequency spectra of different molecules in various rotational states. For each of these states more than seven different molecular properties can be inferred and thus the variations of the properties with changes in the rotational and vibrational quantum numbers can be determined. These properties include nuclear and rotational magnetic moments, nuclear quadrupole interactions, nuclear spin-spin magnetic interactions, spin rotational interactions, etc. I shall illustrate the accuracy and significance of the measurements with a single example. With both D_2 and LiD we have accurately measured[35, 36] the deuteron quadrupole interaction eqQ where e is the proton electric charge, q is the gradient of the molecular electric field at the deuteron and Q is the deuteron quadrupole moment which measures the shape of the deuteron and in particular its departure from spherical symmetry. These measurements were made with the high-resolution molecular beam apparatus based on the method of separated oscillatory fields that is shown in Figure 1. We found for eqQ the value $+225\,044 \pm 20$ Hz in D_2 and $+34\,213 \pm 33$ Hz in LiD. Since q has been calculated[37, 38] for each of these quite different molecules, two independent values of Q can be calculated. The results agree to within 1.5%, which confirms the validity of the difficult calculation of q; with it we find $Q = 2.9 \times 10^{-27}$ cm^2.

In an experiment with collaborators[39] at the Institut Laue-Langevin at Grenoble, France, we have used the separated oscillatory field method with a beam of slow neutrons to make an accurate measurement of the neutron magnetic moment and found[37, 40] it to be $-1.91304275 \pm 0.00000045$ nuclear magnetons. In a somewhat different experiment with neutrons moving so slowly that they can be bottled for more than 80 s in a suitable storage vessel, we have used the method of successive oscillatory fields with the two coherent radiofrequency pulses being separated in time rather than space. In this manner and as a fundamental test of time reversal symmetry, we have recently set a very low upper limit for the neutron electric dipole moment by finding[41] its value to be $(-3 \pm 5) \times 10^{-26}$ e cm.

The atomic hydrogen maser gives very accurate data on the microwave spectrum of the ground electronic state of the hydrogen atom. The hyperfine frequency $\Delta\nu$ for atomic hydrogen has been measured in our laboratory and in a number of other laboratories. The best value[42, 43] is $\Delta\nu_H = 1\,420\,405\,751.7667 \pm 0.0009$ Hz.

This value agrees with present quantum electromagnetic theory[44] to within the accuracy of the theoretical calculation and can be used to obtain information on the proton structure. Similarly accurate values have been found for atomic deuterium and tritium and the dependence[45] of these results on the strengths of externally applied electric fields has been measured. With a modified form of the hydrogen maser designed to operate at high magnetic fields, the ratio of the magnetic moment of the electron to that of the proton is found[40, 46] to be -658.210688 ± 0.000006. Incidentally, when this result is combined with the beautiful electron measurements from Professor *Dehmelt*'s laboratory[40, 47, 48] one obtains the best values for the free proton magnetic moment in both Bohr μ_B and nuclear magnetons (μ_N).

Atomic Clocks

In the past 50 years there has been a major revolution in time keeping, with the accuracy and reproducibility of the best clocks at the end of that period being approximately a million times those at the beginning. This revolution in timekeeping and frequency control is due to atomic clocks.

Any clock or frequency standard depends on some regular periodic motion such as the pendulum of the grandfather's clock. In the case of atomic clocks the periodic motion is internal to the atoms and is usually that associated with an atomic hyperfine structure as discussed in the section on the atomic hydrogen maser.

In the most widely used atomic clocks, the atom whose internal frequency provides the periodicity is cesium and the usual method of observing it is with a separated oscillatory field magnetic resonance apparatus as in Figure 2. The first commercial cesium beam clock was developed in 1955 by a group led by *J. R. Zacharias*[4] and in the same year *L. Essen* and *V. L. Parry*[4] constructed and operated the first cesium beam apparatus that was extensively used as an actual frequency standard. Subsequently, many scientists and engineers throughout the world contributed to the development of atomic clocks, as discussed in greater detail elsewhere.[4]

Cesium atomic clocks now have an accuracy and stability of about 10^{-13} which was so far superior to all previous clocks that in 1967 the internationally adopted definition of the second was changed from one based on motion of the earth around the sun to 9 192 631 770 periods of the cesium atom.

For many purposes even greater stability is required over shorter time intervals. When such stability is needed the hy-

drogen maser is frequently used with a stability of 10^{-15} over periods of several hours.

Atomic clocks based on the above principles have for a number of years provided the greatest stability and accuracy and these are sufficiently great that further improvements might seem to be neither desirable nor feasible. But as we shall see in our final section, there are applications that already push atomic clocks to their limits and there are many current developments with great promise for the future. These include improvements to the existing devices, use of higher frequency, use of lasers, electromagnetic traps for storing both ions and atoms, laser cooling, etc.

Applications for Accurate Clocks

Accurate atomic clocks are used for so many different purposes that a list of them all is tediously long so I shall here just briefly mention a few that push clock technology to its limit.

In radio astronomy one looks with a parabolic reflector at the radio waves coming from a star just as in optical astronomy one looks with an optical telescope at the light waves coming from a star. Unfortunately, in radio astronomy the wavelength of the radiation is about a million times longer than the wavelength of light. The resolution of the normal radio telescope is therefore about a million times worse since the resolution of a telescope depends on the ratio of the wavelength to the telescope aperture. However, if there are two radio telescopes on opposite sides of the earth looking at the same star and if the radio waves entering each are matched in time, it is equivalent to a single telescope whose aperture is the distance between the two telescopes and the resolution of such a combination exceeds that of even the largest single optical telescope. However, to do such precise matching in time each of the two radio telescopes needs a highly stable clock, usually an atomic hydrogen maser.

One of the exciting discoveries in radio astronomy has been the discovery of pulsars, that emit their radiation in short periodic pulses. Precision clocks have been needed to measure the pulsar periods and the changes in the periods with time; these changes sometimes occur smoothly and sometimes abruptly. Of particular interest from the point of view of time measurements, are the millisecond pulsars which have remarkable constancy of period, rivaling the stability of the best atomic clocks.[49] Another millisecond pulsar is part of a rapidly rotating binary star that is slowly changing its period of rotation.[49] This slow change in rotation can be attributed to the loss of energy by the radiation of gravity waves—the first experimental evidence for the existence of gravity waves.

Time and frequency can now be measured so accurately that wherever possible other fundamental measurements are reduced to time or frequency measurements. Thus, the unit of length by international agreement has recently been defined as the distance light will travel in a specified time, and voltage may soon be represented in terms of frequency measurements.

Accurate clocks have provided important tests of both the special and general theories of relativity. In one experiment,[50] a hydrogen maser was shot in a rocket to a 6000 mile altitude and its periodic rate changed with speed and altitude just as expected by the special and general theories of relativity. In other experiments, observers have measured the delays predicted by relativity for radio waves passing near the sun.

Precision clocks make possible an entirely new and more accurate navigational system, the global positioning system or GPS. A number of satellites containing accurate atomic clocks transmit signals at specific times so any observer receiving and analyzing the signals from four such satellites can determine his position to within ten yards and the correct time within one hundredth of a millionth of a second (10^{-8} s).

A particularly fascinating navigational feat dependent on accurate clocks was the recent and highly successful tour of the Voyager spacecraft to Neptune. The success of this mission depended upon the ground controllers having accurate knowledge of the position of the Voyager. This was accomplished by having three large radio telescopes at different locations on the earth, each of which transmitted a coded signal to Voyager which in turn transmitted the signals back to the telescopes. The distances from each telescope to Voyager could be determined from the elapsed times and thus Voyager could be located. To achieve the required timing accuracy, two hydrogen masers were located at each telescope. Due to the rotation of the earth in the eight hours required for the electromagnetic wave to travel from the earth to Voyager and back again at the speed of light, the telescope transmitting the signal in some cases had to be different from the one receiving it; this placed an additional stringent requirement on the clocks. Thus, the spectacular success of the Voyager mission depended on the availability of highly stable clocks.

Received: January 30, 1990 [A 769 IE]
German version: *Angew. Chem. 102* (1990) 790

[1] I. I. Rabi, J. R. Zacharias, S. Millman, P. Kusch, *Phys. Rev. 53* (1938) 318; *ibid. 55* (1939) 526.
[2] J. M. B. Kellogg, I. I. Rabi, N. F. Ramsey, J. R. Zacharias, *Phys. Rev. 55* (1939) 729; *ibid. 56* (1939) 728; *ibid. 57* (1940) 677.
[3] N. F. Ramsey: *Molecular Beams*, Oxford Press 1956 and 1985.
[4] N. F. Ramsey, *Natl. Bur. Stand. (US) 88* (1983) 301, and references cited therein.
[5] N. F. Ramsey, *Phys. Rev. 76* (1949) 996; *ibid. 78* (1950) 695.
[6] N. F. Ramsey, *Phys. Today 33* (1980), No. 7, p. 25.
[7] N. F. Ramsey, *Phys. Rev. 109* (1958) 822.
[8] N. F. Ramsey, *J. Phys. Radium 19* (1958) 809.
[9] S. R. Lundeen, P. E. Jessop, F. M. Pipkin, *Phys. Rev. Lett. 34* (1975) 377, 1368.
[10] N. F. Ramsey, *Phys. Rev. 100* (1955) 1191.
[11] F. Bloch, A. Siegert, *Phys. Rev. 57* (1940) 522.
[12] R. F. Code, N. F. Ramsey, *Phys. Rev. A 4* (1971) 1945.
[13] J. H. Shirley, *J. Appl. Phys. 34* (1963) 783.
[14] G. Greene, *Phys. Rev. A 17* (1978) 1057.
[15] N. F. Ramsey, H. B. Silsbee, *Phys. Rev. 84* (1951) 506.
[16] N. F. Ramsey, *Rev. Sci. Inst. 28* (1957) 57.
[17] E. Uzgiris, N. F. Ramsey, *Phys. Rev. A 1* (1970) 429.
[18] V. F. Ezhov, S. N. Ivanov, I. M. Lobashov, V. A. Nazarenko, G. D. Porsev, A. P. Serebrov, R. R. Toldaev, *Sov. Phys. JETP (Engl. Transl.) 24* (1976) 39.
[19] S. Jarvis, D. J. Wineland, H. Hellwig, *J. Appl. Phys. 48* (1977) 5336.
[20] Y. V. Blaklanov, B. V. Dubetsky, V. B. Chebotsev, *Appl. Phys. 9* (1976) 171.
[21] J. C. Bergquist, S. A. Lee, J. L. Hall, *Phys. Rev. Lett. 38* (1977) 159; *Proc. Third. Int. Conf. Laser Spectrosc.* (1978) 142.

[22] M. M. Salour, C. Cohen-Tannoudji, *Phys. Rev. Lett. 38* (1977) 757; *Proc. Third. Int. Conf. Laser Spectrosc.* (1978) 149; *Appl. Phys. 15* (1978) 119; *Phys. Rev. A 17* (1978) 614.
[23] C. J. Bordé, *C.R. Seances Acad. Sci. Ser. B 284* (1977) 101.
[24] T. W. Hänsch, *Proc. Third. Int. Conf. Laser Spectrosc.* (1978) 149.
[25] V. P. Chebotayev, A. V. Shishayev, B. Y. Yurshin, L. S. Vasilenko, N. M. Dyuba, M. I. Skortsov, *Appl. Phys. 15* (1978) 43, 219, 319.
[26] M. Kasevich, E. Riis, S. Chu, R. S. DeVoe, *Phys. Rev. Lett. 63* (1989) 612.
[27] D. Wineland, H. Dehmelt, *Bull. Am. Phys. Soc. 18* (1973) 1521; *ibid. 20* (1975) 60, 61, 637.
[28] T. W. Hänsch, A. L. Schawlow, *Opt. Commun. 13* (1975) 68; reviewed by U. S. Letokhow, *Comments At. Mol. Phys. 6* (1977) 119.
[29] D. Wineland, W. M. Itano, *Phys. Today 40* (1987) No. 6, p. 34.
[30] D. Kleppner, N. F. Ramsey, P. Fjelstadt, *Phys. Rev. Lett. 1* (1958) 232.
[31] J. P. Gordon, H. Z. Geiger, C. H. Townes, *Phys. Rev. 95* (1954) 282; *ibid. 99* (1955) 1264.
[32] H. M. Goldenberg, D. Kleppner, N. F. Ramsey, *Phys. Rev. Lett. 5* (1960) 361; *Phys. Rev. 126* (1962) 603.
[33] D. Kleppner, H. C. Berg, S. B. Crampton, N. F. Ramsey, R. F. C. Vessot, H. E. Peters, J. Vanier, *Phys. Rev. 138* (1965) A 972.
[34] J. M. V. A. Koelman, S. B. Crampton, H. T. C. Luiten, B. J. Verhaar, *Phys. Rev. A 38* (1988) 3535. This paper contains an extended series of references to other papers on hydrogen maser limitations, principles, and practices.
[35] See [12].
[36] R. R. Freeman, A. R. Jacobson, D. W. Johnson, N. F. Ramsey, *J. Chem. Phys. 63* (1975) 2597.
[37] R. V. Reid, M. L. Vaida, *Phys. Rev. A 7* (1973) 1841.
[38] K. K. Docken, R. R. Freeman, *J. Chem. Phys. 61* (1974) 4217.
[39] G. L. Green, N. F. Ramsey, W. Mampe, J. M. Pendlebury, K. Smith, W. B. Dress, P. D. Miller, P. Perrin, *Phys. Rev. D 20* (1979) 2139.
[40] E. R. Cohen, B. Taylor, *Rev. Mod. Phys. 59* (1987) 1121.
[41] K. F. Smith, N. Crampin, J. M. Pendlebury, D. J. Richardson, D. Shiers, K. Green, A. I. Kilvington, J. Moir, H. B. Prosper, D. Thompson, N. F. Ramsey, B. R. Heckel, S. K. Lamoreaux, P. Ageron, W. Mampe, A. Steyerl, *Phys. Lett. B 136* (1984) 327; *Phys. Lett. B 234* (1990) 191.
[42] H. Hellwig, R. F. Vessot, M. Levine, P. W. Zitzewitz, D. W. Allan, D. T. Glaze, *IEEE Trans. Instrum. Meas. IM-19* (1970) 200.
[43] L. Essen, M. J. Donaldson, M. J. Bangham, E. G. Hope, *Nature (London) 229* (1971) 110.
[44] G. L. Baldwin, D. R. Yennie, *Phys. Rev. D 37* (1988) 498.
[45] P. C. Gibbons, N. F. Ramsey, *Phys. Rev. A 5* (1972) 73.
[46] P. F. Winkler, D. Kleppner, T. Myint, F. G. Walther, *Phys. Rev. A 5* (1972) 83; E. Cohen, B. Taylor, *Phys. Lett. B 204* (1988) 1.
[47] R. S. van Dyck, P. B. Schwinberg, H. Dehmelt, *At. Phys. 9* (1984) 53.
[48] R. S. van Dyck, F. L. Moore, D. L. Farnum, P. B. Schwinberg, *Bull. Am. Phys. Soc. 31* (1986) 244; *At. Phys. 9* (1984) 75.
[49] J. H. Taylor, L. A. Fowler, P. M. McCulloch, *Nature (London) 277* (1979) 437; M. M. Davis, J. H. Taylor, J. M. Weisberg, D. C. Backer, *ibid. 315* (1985) 547.
[50] R. F. C. Vessot, M. W. Levine, E. M. Mattison, E. L. Blomberg, T. E. Hoffman, G. U. Nystrom, B. F. Farrel, R. Decher, P. B. Eby, C. R. Baugher, J. W. Watts, D. L. Teuber, F. D. Wills, *Phys. Rev. Lett. 45* (1980) 2081.

Experiments with an Isolated Subatomic Particle at Rest (Nobel Lecture)**

By Hans Dehmelt*

"You know, it would be sufficient to really understand the electron."

Albert Einstein

The 5th century B. C. philosopher *Democritus*' smallest conceivable in-divisible entity, the "a-tomon" (the un-cuttable), is a most powerful but not an immutable concept. By 1930 it had already metamorphosed twice: from something similar to a molecule, say a slippery atomon of water, to *Mendeleyev*'s chemist's atom and later to electron and to proton, both particles originally assumed to be of small but finite size. With the development of *Dirac*'s theory of the electron in the late twenties their size shrunk to mathematically zero. Everybody "knew" then that electron and proton were indivisible Dirac point particles with radius $R = 0$ and gyromagnetic ratio $g = 2.00$. The first hint of cuttability or at least compositeness of the proton came from *Otto Stern*'s 1933 measurement of proton magnetism in a Stern-Gerlach molecular beam apparatus. However, this was not realized at the time. He found for its normalized dimensionless gyromagnetic ratio not $g = 2$ but $g \approx 5$ [Eq. (1)],

$$g = (\mu/A)(2M/q) \approx 5, \tag{1}$$

where μ, A, M, q are respectively magnetic moment, angular momentum, mass and charge of the particle. For comparison the obviously composite $^4He^{\oplus}$ ion, also with spin 1/2, has according to the above formula the $|g|$ value 14 700, much larger than the Dirac value 2. Also, along with this large $|g|$ value went a very finite radius of this atomic ion of 3×10^{-11} m. And indeed, with *Hofstadter*'s high-energy electron scattering experiments in the fifties the proton radius grew again to $R = 0.86 \times 10^{-15}$ m, roughly in proportion to the excess in g of 3. Similar later work at still higher energies led to the discovery of three quarks inside the "indivisible" proton. Today, everybody "knows" that the *electron* is an indivisible atomon, a Dirac point particle with radius $R = 0$ and $g = 2.00$. ... But is it? Like the proton, it could be a composite object. History may well repeat itself once more. This puts a high premium on precise measurements of the g factor of the electron.

Geonium Spectroscopy

The metastable pseudo-atom geonium[1,2] has been expressly synthesized for studies of the electron g factor under optimal conditions. It consists of an individual electron permanently confined in an ultrahigh vacuum Penning trap at 4 K. The trap employs a homogeneous magnetic field $B_0 = 5$T and a weak electric quadrupole field. The latter is produced by hyperbolic electrodes, a positive ring and two negative caps spaced $2Z_0 = 8$ mm apart (see Fig. 1). The

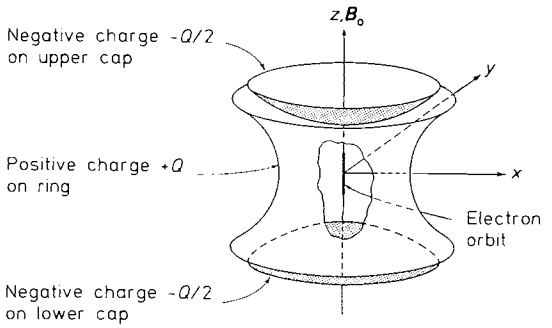

Fig. 1. Penning trap. The simplest motion of an electron in the trap is along its symmetry axis, along a magnetic field line. Each time it comes too close to one of the negatively charged caps it turns around. The resulting harmonic oscillation took place at about 60 MHz in our trap. (After [12].)

potential $\varphi(xyz)$, with A a constant, is given by Equation (2). The axial potential well depth D is 5 eV [Eq. (3)].

$$\varphi(xyz) = A(x^2 + y^2 - 2z^2) \tag{2}$$

$$D = e[\varphi(000) - \varphi(00Z_0)] = 2eAZ_0^2 = 5\,\text{eV} \tag{3}$$

The trapping of the electron is mostly magnetic. The large magnetic field dominates the motion in the geonium atom.

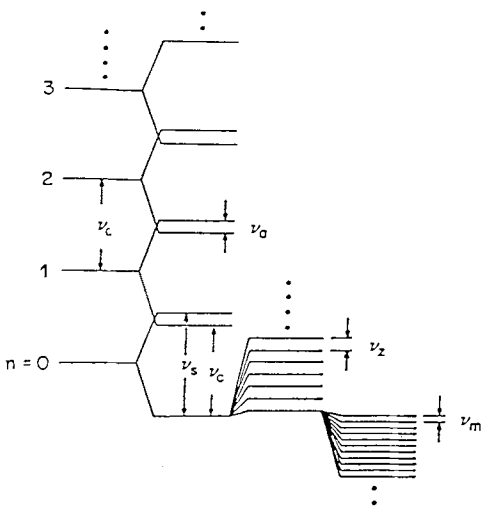

Fig. 2. Energy levels of geonium. Each of the cyclotron levels labeled n is split first by the spin–magnetic field interaction. The resulting sublevels are further split into the oscillator levels, and finally into the manifold of magnetron levels. (After [1].)

[*] Prof. Dr. H. Dehmelt
Department of Physics, University of Washington
Seattle, WA 98195 (USA)

[**] Copyright © The Nobel Foundation 1990.—We thank the Nobel Foundation, Stockholm, for permission to print this lecture.

The energy levels of this atom shown in Figure 2 reflect the cyclotron motion at frequency $\nu_c = eB_0/2\pi m = 141$ GHz, the spin precession at $\nu_s \approx \nu_c$, the anomaly or $g-2$ frequency $\nu_a = \nu_s - \nu_c = 164$ MHz, the axial oscillation at $\nu_z = 60$ MHz, and the magnetron or drift motion at a frequency $\nu_m = 13$ kHz. The electron is continuously monitored by exciting the ν_z-oscillation and detecting via radio the 10^8-fold enhanced spontaneous 60 MHz emission. A corresponding signal is seen in Figure 3. Doppler side band cooling has

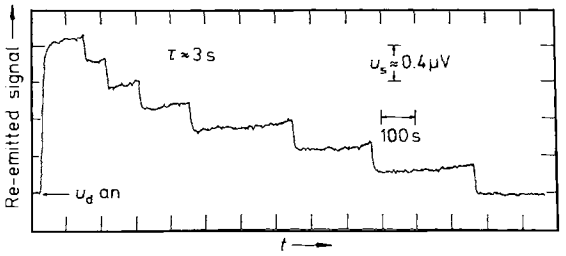

Fig. 3. Rf signal produced by trapped electron. When the electron is driven by an axial rf field, it emits a 60-MHz signal, which was picked up by a radio receiver. The signal shown was for a very strong drive and an initially injected bunch of seven electrons. One electron after the other was randomly "boiled" out of the trap until finally only a single electron was left. By reducing the drive power somewhat, this last electron could be observed indefinitely. (After [13].)

made continuous confinement of an electron in the trap center for 10 months possible.[3] This process makes the electron absorb rf photons deficient in energy and supply the balance from energy stored in the electron motion to be cooled.

The corresponding shrinking of the radius of the magnetron motion is displayed in Figure 4. Extended into the optical region, the cooling scheme is most convincingly demonstrated in Figure 5. The transitions of primary interest at ν_c, ν_a, ν_m are much more difficult to detect than the ν_z oscillation. Nevertheless, the task may be accomplished by means of the continuous Stern-Gerlach effect,[4] whereby the geonium atom itself is made to work as a 10^8-fold amplifier. In the scheme a single ν_a-photon of only about 1 μeV energy gates the absorption of approximately 100 eV of rf power at ν_z. The continuous effect uses an inhomogeneous magnetic field in a similar way as the classic one. However, the field now takes the form of a very weak Lawrence cyclotron trap or magnetic "bottle" (cf. Fig. 6a). The "bottle" adds only a minute monitoring well D_m to the axial potential well of large electrostatic depth $D = 5$ eV [Eq. (4)], where m and n respec-

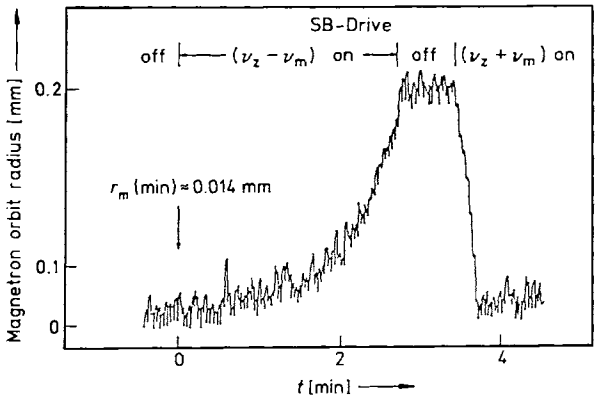

Fig. 4. Side-band "cooling" of the magnetron motion at ν_m. By driving the axial motion not on resonance at ν_z but on the lower Doppler side-band at $\nu_z - \nu_m$, it is possible to force the metastable magnetron motion to provide the energy balance $h\nu_m$, and thereby expand the magnetron orbit radius. Conversely, an axial drive at $\nu_z + \nu_m$ shrinks the radius. The roles of upper and lower side bands are reversed here from the case of a particle in a well, where the energy increases with amplitude because the magnetron motion is metastable and the total energy of this motion *decreases* with radius. (After [1].)

$$D_m = (m + n + 1/2)\,0.1\ \mu\text{eV} \tag{4}$$

tively denote the spin and cyclotron quantum numbers. Thus, jumps in m or n show up as jumps in ν_z [Eq. (5)].

$$\nu_z = \nu_{z0} + (m + n + 1/2)\,\delta \tag{5}$$

In our experiments $\delta = 1.2$ Hz, and ν_{z0} corresponds to the axial frequency of a hypothetical electron without magnetic moment. Random jumps in m and n occur when spin or cyclotron resonances are excited. Figure 6b shows an early example of a series of such jumps in m (spin flips). For the spin, spontaneous transitions are totally negligible. Standard text books discuss transitions between two sharp levels induced by a broad electromagnetic spectrum $\varrho(\nu)$: The transition rate from either level is the same and is proportional to the spectral power density $\varrho(\nu_s)$ of the radiation field at the transition frequency ν_s. Ergo, the average dwell times in either level are the same, (cf. Fig. 6a). In the geonium experiments the frequency of the weak rf field is sharp, but the spin resonance is broadened and has a shape $G_s(\nu)$. One may convince oneself that moving the sharp frequency of the rf field upwards over the broad spin resonance should produce the same results as moving a broad rf field of spectral shape $\varrho(\nu) \propto G_s(\nu)$ downwards over a sharp spin resonance: The

Hans Georg Dehmelt was born on September 9, 1922 in Görlitz (GDR). He studied physics at the Universities of Breslau and Göttingen. As a student of H. Kopfermann he also met up with Wolfgang Paul in Göttingen, where he was awarded his Dr. rer. nat. in 1950 for his Studies on Nuclear Quadrupole Resonance (title of his Dissertation) under the supervision of H. Krüger. His studies on and co-discovery of nuclear quadrupole resonance were of great importance for the study of chemical bonding. In 1952 he joined Walther Gordy's laboratory at Duke University in Durham, NC, USA, as a postdoctoral associate. Since 1955 he has been a faculty member of the University of Washington in Seattle, USA. He has been a naturalized American citizen for more than 30 years.

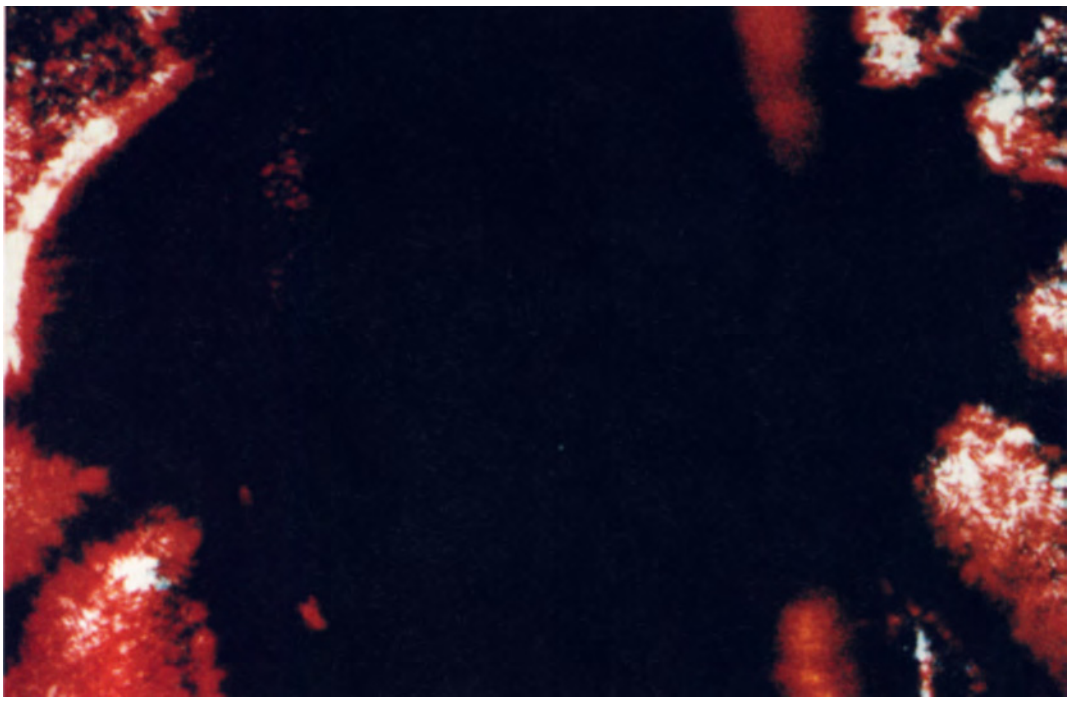

Fig. 5. Visible blue (charged) barium atom "Astrid" at rest in the center of a Paul trap photographed in natural color. The photograph strikingly demonstrates the close localization ($\ll 1$ μm) attainable with geonium cooling techniques. Stray light from the lasers focussed on the ion also illuminates the ring electrode of the tiny rf trap of about 1 mm internal diameter. (After [4].)

rate of all spin flips or jumps in m in either direction counted in the experiment is proportional to $G_s(\nu)$. To obtain the plot of $G_s(\nu)$ in Figure 7 the frequency of the rf field was increased in small steps, and at each step spin flips were counted for a fixed period of about half an hour. From our ν_s, ν_c data for electron and positron[5] we have determined the value shown

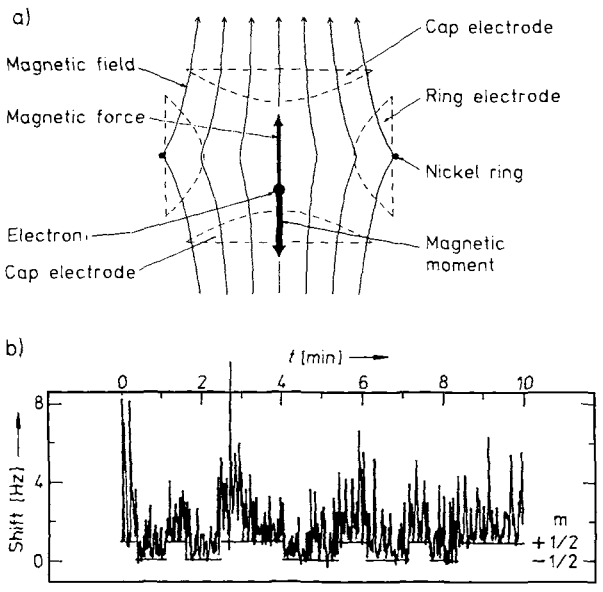

Fig. 6. a) Weak magnetic bottle for continuous Stern-Gerlach effect. When in the lowest cyclotron and magnetron level the electron forms a 1-μm long wave packet, 30 nm in diameter, which may oscillate undistorted in the axial electric potential well. The inhomogeneous field of the auxiliary magnetic bottle produces a minute spin-dependent restoring force that causes the axial frequency ν_z for spin ↑ and ↓ to differ by a small but detectable value. (After [14].) b) Spin flips recorded by means of the continuous Stern-Gerlach effect. The random jumps in the base line indicate jumps in m at a rate of about 1 per minute when the spin resonance is excited. The upwards spikes or "cyclotron grass" are explained by expected rapid random thermal excitation and spontaneous decay of cyclotron levels with an average value $\langle n \rangle \approx 1.2$. (After [15].)

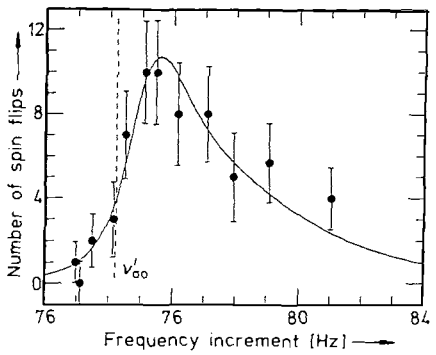

Fig. 7. Plot of electron spin resonance in a geonium atom near 141 GHz. A magnetic radiofrequency field causes random jumps in the spin quantum number. As the frequency of the exciting field is stepped through the resonance in small increments, the number of spin flips occurring in a fixed observation period of about 1/2 hour are counted and then plotted vs frequency. (Actually the 141 GHz field flipping the spin is produced by the cyclotron motion of the electron through an inhomogeneous magnetic rf field at $\nu_s - \nu_c = 164$ MHz.) (After [5].)

in (6), both for the particle and for the anti-particle. The

$$\tfrac{1}{2} g^{exp} = \nu_s/\nu_c = 1.001\ 159\ 652\ 188(4) \qquad (6)$$

error in the difference of their g factors is only half as large. Heroic quantum electrodynamical calculations by *Kinoshita*[6] have yielded for the shift of the g factor of a point

electron associated with turning on the interaction with the electromagnetic radiation field the expression (7).

$$\tfrac{1}{2}(g^{\text{point}} - 2) = \tfrac{1}{2}\Delta g^{\text{Kinoshita}} = 0.001\ 159\ 652\ 133(29) \quad (7)$$

In the calculations $\Delta g^{\text{Kinoshita}}$ is expressed as a power series in α/π. *Kinoshita* has critically evaluated the experimental α input data on which he must rely. He warns that the error in his result, which is dominated by the error in α, may be underestimated. Muonic, hadronic and other small contributions to g amount to less than about 4×10^{-12} and have been included in the shift. *Kinoshita*'s result may be used to correct the experimental g value, and leads to (8).

$$g = g^{\text{exp}} - \Delta g^{\text{Kinoshita}} = 2 + 11(6) \times 10^{-11} \quad (8)$$

Electron Radius R?

Extrapolation from known to unknown phenomena is a time-honored approach in all the sciences. Thus, from known g and R values of other "near-Dirac particles" and our *measured* g value of the electron I attempt to extrapolate a value for its radius. Stimulated by the theoretical works of *Brodsky* and *Drell* in the year 1980,[7] I have plotted $g - 2$ vs $R/\lambda\!\!\!^{-}_{C}$ in Figure 8 for the helium-3 nucleus, triton, proton, and electron.[8] Here, $\lambda\!\!\!^{-}_{C}$ is the Compton wavelength of the respective particle. The plausible relation [Eq. (9), (10)], given by *Brodsky* and *Drell* for the simplest composite theoretical model of the electron,[7] fits the admittedly sparse data surprisingly well. Even for such a very different spin ½ structure as the atomic ion $^4He^{\oplus}$ composed of an α-particle and an electron the data point does not fall too far off the full line. Intersection in Figure 8 of this line with the line

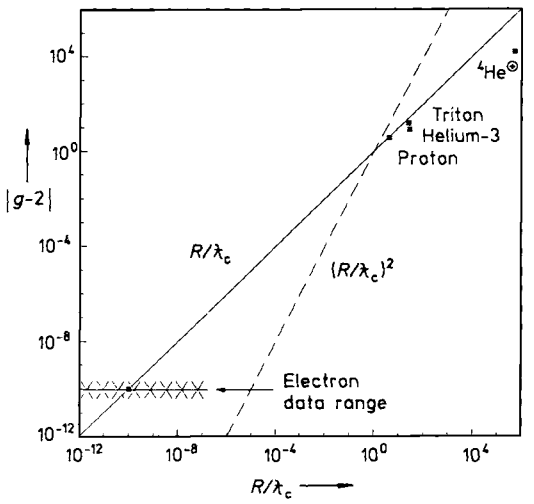

Fig. 8. Plot of $|g - 2|$ values, with radiative shifts removed, vs reduced rms radius $R/\lambda\!\!\!^{-}_{C}$ for near-Dirac particles. The full line $|g - 2| = R/\lambda\!\!\!^{-}_{C}$ predicted by the simplest theoretical model provides a surprisingly good fit to the data points for proton, triton and helium-3 nucleus. It may be used to obtain a new radius value for the *physical* electron from its intersection with the line $|g - 2| = 1.1 \times 10^{-10}$ representing the Seattle electron g data. The data are much less well fitted by the relation $|g - 2| = (R/\lambda\!\!\!^{-}_{C})^2$, which is shown for comparison in the dashed line. The atomic ion $^4He^{\oplus}$ is definitely *not* a near-Dirac particle, but even its data point does not fall too far off the full line.

$g - 2 = 1.1 \times 10^{-10}$ for our g value yields for the electron the extrapolated point shown and gives with $\lambda\!\!\!^{-}_{C} = 0.39 \times 10^{-10}$ cm an electron radius of $R \approx 10^{-20}$ cm.

$$|g - 2| = R/\lambda\!\!\!^{-}_{C} \quad (9)$$

$$|g - g_{\text{Dirac}}| = (R - R_{\text{Dirac}})/\lambda\!\!\!^{-}_{C} \quad (10)$$

The row of X's in Figure 8 reflects the data range defined by the uncertainty in our g data and the upper limit $R < 10^{-17}$ cm determined in high energy collision experiments. It appears that this combination of current data is not in harmony with electron structure models assuming special symmetries that predict the quadratic relation $|g - 2| \approx (R/\lambda\!\!\!^{-}_{C})^2$ (shown by the dashed line in Fig. 8). This favors the linear relation used in the above extrapolation of R for the electron. Thus, the electron may have *size* and *structure*!

If one feels that the excess g value $11(6) \times 10^{-11}$ measured is not significant because of its large relative error, then the value $R \approx 10^{-20}$ cm given here still constitutes an important new upper limit. Changing the point of view the close agreement of g^{point} with g^{exp} provides the most stringent experimental test of the fundamental theory of quantum electrodynamics in which $R = 0$ is assumed. Furthermore, the near-identity of the g values measured by us for electron and positron constitutes the most severe test of the CPT theorem (CPT = *C*harge-*P*arity-*T*ime reversal theory) or mirror symmetry of a *charged* particle-antiparticle pair.

Lemaître's "L'Atome Primitif" Revisited—A Speculation

From 1974 on *Salam* and others have proposed composite electron and quark models.[9] On the strength of these proposals and with an eye on Figure 8, I view the electron as the third approximation of a Dirac particle, d_3 particle for short, and as composed of three fourth-approximation Dirac or d_4 particles. The situation is taken to be quite similar to that previously encountered in the triton and proton subatomic particles, respectively assumed to be of type d_1 and d_2. In more detail, three d_4 subquarks of huge mass $m' \approx 10^{10}\, m_e$ in a deep square well make up the electron in this working hypothesis. However, their mass $3m_4$ is almost completely compensated by strong binding to yield a total relativistic mass equal to the observed mass m_e of the electron. Figure 8 may even suggest a more speculative extrapolation: The constituents of the electron in the infinite regression $N \rightarrow \infty$ proposed in Figure 9 have ever more massive, ever smaller sub-sub-..... constituents d_N. However, these higher order subquarks are realized only up to the "cosmon" with $N = C$, the most massive particle ever to appear in this universe. At the beginning of the universe, a lone bound cosmon-anticosmon pair or lifetime-broadened cosmonium atomic state of near-zero total relativistic mass/energy was created from *Vilenkin*'s metastable "nothing" state of zero relativistic energy[10] in a spontaneous quantum jump of cosmic rarity. Similar, though much more frequent, quantum jumps that have recently been observed in a trapped $Ba^{\oplus}$ ion are shown in Figure 10. In this case the system also jumps spontaneous-

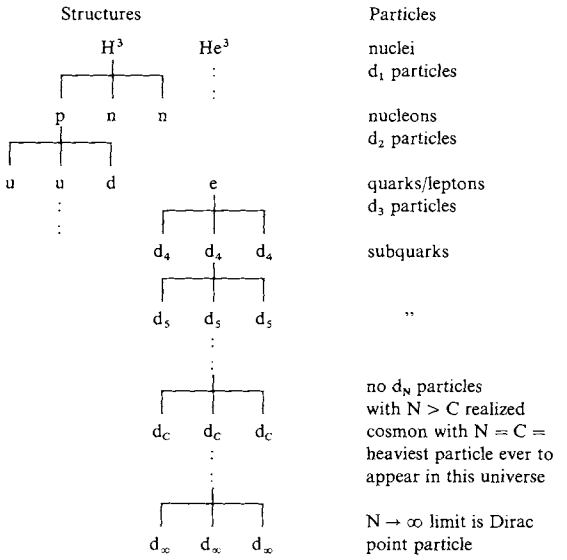

Fig. 9. Triton model of "near-Dirac particles". (After [17].)

ly from one state (ion in metastable $D_{5/2}$ level plus no photon) to a new state (ion in $S_{1/2}$ ground level plus photon) of the same total energy. The "cosmonium atom" introduced here is merely a modernized version[19] of Lemaître's "l'atome primitif"[11] or world-atom whose explosive radioactive decay created the universe. At the beginning of the world the short-lived cosmonium atom decayed into an early gravitation-dominated standard big bang state that eventually developed into a state, in which again rest mass energy, kinetic, and Newtonian gravitational potential energy add up to zero (see formula 8 in Ref. [20]). The electron is a much more complex particle than the cosmon. It is composed of 3^{C-3} cosmon-like d_C particles, but only two particles of this type formed the cosmonium world-atom from which sprang the universe. In closing, I should like to cite a line from *William Blake*: *"To see a world in a grain of sand ---"*, and allude to a conceivable parallel: to see worlds in an electron —.

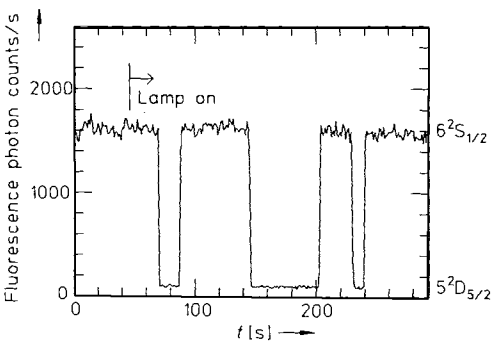

Fig. 10. Spontaneous decay of $Ba^{\oplus}$ ion in metastable $D_{5/2}$-level. Illuminating the ion with a laser tuned close to its resonance line produces strong resonance fluorescence and an easily detectable photon count of 1600 photons per second. Later, when an auxiliary, weak $Ba^{\oplus}$ spectral lamp is turned on, the ion is randomly transported into the metastable $D_{5/2}$ level of 30 s lifetime and becomes invisible. After dwelling in this shelving level for 30 s on the average, it drops down to the $S_{1/2}$ ground state *spontaneously* and becomes visible again. This cycle then repeats. (After [18].)

Received: January 30, 1990 [A 766 IE]
German version: *Angew. Chem. 102* (1990) 774

[1] R. S. Van Dyck, Jr., P. B. Schwinberg, H. G. Dehmelt, *Electron Magnetic Moment from Geonium Spectra*, in B. Kursunoglu, A. Perlmutter, L. Scott (Eds.): *New Frontiers in High Energy Physics*, Plenum, New York 1978.
[2] R. S. Van Dyck, Jr., P. B. Schwinberg, H. G. Dehmelt, Electron Magnetic Moment from Geonium Spectra: *Early Experiments and Background Concepts, Phys. Rev. D 34* (1986) 722.
[3] G. Gabrielse, H. Dehmelt, W. Kells, *Observation of a Relativistic, Bistable Hysteresis in the Cyclotron Motion of a Single electron, Phys. Rev. Lett. 54* (1985) 537.
[4] H. Dehmelt, *Single Atomic Particle Forever Floating at Rest in Free Space: New Value for Electron Radius, Phys. Scr. T22* (1988) 102.
[5] R. S. Van Dyck, Jr., P. B. Schwinberg, H. G. Dehmelt, *New High Precision Comparison of Electron/Positron g-Factors, Phys. Rev. Lett. 59* (1987) 26.
[6] T. Kinoshita, *Fine-Structure Constant Derived from Quantum Electrodynamics, Metrologia 25* (1988) 233.
[7] S. J. Brodsky, S. D. Drell, *Anomalous Magnetic Moment and Limits on Fermion Substructure, Phys. Rev. D 22* (1980) 2236.
[8] H. Dehmelt: *Geonium Spectra - Electron Radius - Cosmon, AIP Conf. Proc. 187* (1989) 319.
[9] L. Lyons, *An Introduction to the Possible Substructure of Quarks and Leptons, Prog. Part. Nucl. Phys. 10* (1983) 227, and references cited therein.
[10] A. Vilenkin, *Quantum Creation of Universe, Phys. Rev. D 30* (1984) 509–515.
[11] G. Lemaître: *The Primeval Atom*, Van Nostrand, New York 1950, p. 77.
[12] H. Dehmelt, *Stored Ion Spectroscopy*, in F. T. Arecchi, F. Strumia, H. Walther (Eds.): *Advances in Laser Spectroscopy*, Plenum, New York 1983.
[13] D. Wineland, P. Ekstrom, H. Dehmelt, *Monoelectron Oscillator, Phys. Rev. Lett. 31* (1973) 1297.
[14] H. Dehmelt, *New Continuous Stern-Gerlach Effect and a Hint of "the" Elementary Particle, Z. Phys. D: At. Mol. Clusters 10* (1988) 127–134.
[15] R. S. Van Dyck, Jr., P. Ekstrom, H. Dehmelt, *Precise Measurement of Axial, Magnetron, and Spin-Cyclotron Beat Frequencies on an Isolated 1-meV Electron, Phys. Rev. Lett. 38* (1977) 310.
[16] H. Dehmelt, *Less is more: Experiments with an Individual Atomic Particle at Rest in Free Space, Am. J. Phys. 58* (1990) 17.
[17] H. Dehmelt, *Triton, ... electron, ... cosmon ...: An infinite regression?, Proc. Natl. Acad. Sci. USA 86* (1989) 8618–8619.
[18] W. Nagourney, J. Sandberg, H. Dehmelt, *Shelved optical electron amplifier: Observation of quantum jumps, Phys. Rev. Lett. 56* (1986) 2797.
[19] This is by no means the first modernization attempt. *M. Goldhaber* has kindly brought it to my attention that he had introduced a different "cosmon" already in 1956 in his paper *Speculations on Cosmogony, Science (Washington) 124* (1956) 218.
[20] P. Jordan, *Die physikalischen Weltkonstanten, Naturwissenschaften 25* (1937) 513.

Electromagnetic Traps for Charged and Neutral Particles (Nobel Lecture)**

By Wolfgang Paul*

Introduction

Experimental physics is the art of observing the structure of matter and of detecting the dynamic processes within it. But in order to understand the extremely complicated behavior of natural processes as an interplay of a few constituents governed by as few as possible fundamental forces and laws, one has to measure the properties of the relevant constituents and their interaction as precisely as possible. And as all processes in nature are interwoven one must separate and study them individually. It is the skill of the experimentalist to carry out clear experiments in order to get answers to his questions undisturbed by undesired effects and it is his ingenuity to improve the art of measuring to ever higher precision. There are many examples in physics showing that higher precision revealed new phenomena, inspired new ideas, or confirmed or dethroned well established theories. On the other hand, new experimental techniques conceived to answer special questions in one field of physics became very fruitful in other fields too, be it in chemistry, biology, or engineering. In awarding the Nobel prize to my colleagues *Norman Ramsey, Hans Dehmelt* and me for new experimental methods the Swedish Academy indicates its appreciation for the aphorism the Göttingen physicist *Georg Christoph Lichtenberg* wrote two hundred years ago in his notebook "one has to do something new in order to see something new". On the same page *Lichtenberg* said: "I think it is a sad situation in all our chemistry that we are unable to suspend the constituents of matter free".

Today, the subject of my lecture will be the suspension of such constituents of matter or in other words, traps for free charged and neutral particles without material walls. Such traps permit the observation of isolated particles, even of a single one, over a long period of time and therefore according to Heisenberg's uncertainty principle enable us to measure their properties with extremely high accuracy.

In particular, the possibility to observe individual trapped particles opens up a new dimension in atomic measurements. Until a few years ago all measurements were performed on an ensemble of particles. Therefore, the measured value—for example, the transition probability between two eigenstates of an atom—is a value averaged over many particles. Tacitly one assumes that all atoms show exactly the same statistical behavior if one attributes the result to the single atom. On a trapped single atom, however, one can observe its interaction with a radiation field and its own statistical behavior alone.

The idea of building traps grew out of the molecular beam physics, mass spectrometry and particle accelerator physics I was involved in during the first decade of my career as a physicist more than 30 years ago. In these years (1950–55) we had learned that plane electric and magnetic multipole fields are able to focus particles with a magnetic or electric dipole moment in two dimensions. Lenses for atomic and molecular beams[1, 2, 3] were conceived and realized, improving considerably the molecular beam method for spectroscopy or for state selection. These lenses facilitated the development of both the ammonia as well as the hydrogen maser.[4]

The question "What happens if one injects charged particles, ions or electrons, into such multipole fields" led to the development of the linear quadrupole mass spectrometer. It employs not only the focusing and defocusing forces of a high-frequency electric quadrupole field acting on ions but also exploits the stability properties of their equations of motion in analogy to the principle of "strong focusing" for accelerators which had just been conceived in the same year.

If one extends the rules of two-dimensional focusing to three dimensions one possesses all ingredients for particle traps.

As already mentioned the physics or the particle dynamics in such focusing devices is very closely related to that in accelerators or storage rings for nuclear or particle physics. In fact, multipole fields were used in molecular beam physics first. But the two areas have complementary goals: the storage of particles, even of a single one, of extremely low energy down to the micro electron volt region on the one side, and of as many particles as possible of extremely high energy on the other. Today we will limit ourselves to the low energy region.

At first I will deal with the physics of dynamic stabilization of ions in two- and three-dimensional radio frequency quadrupole fields, the quadrupole mass spectrometer, and the ion trap. I shall then report on the trapping of neutral particles with emphasis on an experiment with magnetically stored neutrons.

As in most cases in physics, especially in experimental physics, the achievements are not the achievements of a single person, even if he contributed in posing the problems and some basic ideas in solving them. All the experiments I am awarded for were done together with research students or young colleagues in mutual inspiration. In particular, I have to mention in the very early days *H. Friedburg* and *H. G. Bennewitz, C. H. Schlier* and *P. Toschek* in the field of molecular beam physics, and in conceiving and realizing the linear quadrupole spectrometer and the r.f. ion trap *H. Steinwedel, O. Osberghaus* and especially the late *Erhard Fischer*. Later *H. P. Reinhard, U. v. Zahn* and *F. v. Busch* played an important role in developing this field.

Focusing and Trapping of Particles

What are the principles of focusing and trapping particles? Particles are elastically bound to an axis or a coordinate in

[*] Prof. Dr. W. Paul
Physikalisches Institut der Universität
Nussallee 12, D-5300 Bonn (FRG)

[**] Copyright © The Nobel Foundation 1990. – We thank the Nobel Foundation, Stockholm, for permission to print this lecture.

space if a binding force acts on them which increases linearly with their distance r [Eq. (1)],

$$F = -cr \tag{1}$$

in other words if they move in a parabolic potential (2).

$$\Phi \sim (\alpha x^2 + \beta y^2 + \gamma z^2) \tag{2}$$

The tools appropriate for generating such fields of force to bind charged or neutral particles with a dipole moment are electric or magnetic multipole fields. In such configurations the field strength and the potential increases according to a power law and shows the desired symmetry. Generally, if m is the number of "poles" or the order of symmetry the potential is given by

$$\Phi \sim r^{m/2} \cos(m/2\,\varphi) \tag{3}$$

For a quadrupole $m = 4$ it gives $\Phi \sim r^2 \cos 2\varphi$, and for a sextupole $m = 6$ one gets $\Phi \sim r^3 \cos 3\varphi$ corresponding to a field strength increasing with r and r^2 respectively.

Trapping of Charged Particles in Two- and Three-Dimensional Quadrupole Fields

In the electric quadrupole field the potential is quadratic in the cartesian coordinates.

$$\Phi = \frac{\Phi_0}{2r_0^2}(\alpha x^2 + \beta y^2 + \gamma z^2) \tag{4}$$

The Laplace equation $\Delta\Phi = 0$ imposes the condition $\alpha + \beta + \gamma = 0$. There are two simple ways to satisfy this condition.

a) $\alpha = 1 = -\gamma$, $\beta = 0$ results in the two-dimensional field

$$\Phi = \frac{\Phi_0}{2r_0^2}(x^2 - z^2) \tag{5}$$

b) $\alpha = \beta = 1$, $\gamma = -2$ generates the three-dimensional configuration, in cylindrical coordinates

$$\Phi = \frac{\Phi^0(r^2 - 2z^2)}{r_0^2 + 2z_0^2} \quad \text{with} \quad 2z_0^2 = r_0^2. \tag{6}$$

The Two-Dimensional Quadrupole or the Mass Filter [5, 6]

The configuration a) is generated by four hyperbolically shaped electrodes linearly extended in the y-direction as shown in Figure 1. The potential on the electrodes is $\pm\Phi_0/2$

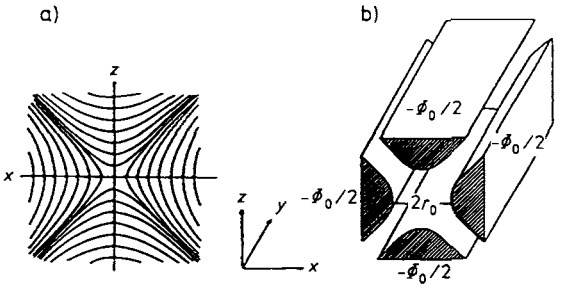

Fig. 1. a) Equipotential lines for a plane quadrupole field. b) the electrodes structure for the mass filter.

if one applies the voltage Φ_0 between the electrode pairs. The field strength is given by (7).

$$E_x = -\Phi_0 x/r_0^2, \quad E_z = \Phi_0 z/r_0^2, \quad E_y = 0 \tag{7}$$

If one injects ions in the y-direction it is obvious that for a constant voltage Φ_0 the ions will perform harmonic oscillations in the x–y plane but due to the opposite sign in the field E_z their amplitude in the z-direction will increase exponentially. The particles are defocused and will be lost by hitting the electrodes.

This behavior can be avoided if the applied voltage is periodic. Due to the periodic change of the sign of the electric force one gets focusing and defocusing in both the x- and z-directions alternating in time. If the applied voltage is given by a dc voltage U plus an r.f. voltage V with the driving frequency ω [Eq. (8)] the equations of motion are as given in (9) and (10).

$$\Phi_0 = U + V\cos\omega t \tag{8}$$

$$\ddot{x} + \frac{e}{mr_0^2}(U + V\cos\omega t)\,x = 0 \tag{9}$$

$$\ddot{z} - \frac{e}{mr_0^2}(U + V\cos\omega t)\,z = 0 \tag{10}$$

Wolfgang Paul, one of the most outstanding physicists of our time was born in 1913. He obtained his doctorate at the Technische Hochschule Berlin in 1939 and his habilitation at the University of Göttingen in 1944. Since 1952 he has been Professor for Experimental Physics at the University of Bonn. In the years 1958 and 1959 he was visiting professor at CERN in Geneva. 1960–1962 he was director of the KFA Jülich, 1964–1967 of the physics department at CERN, and from 1970–1973 of DESY in Hamburg. In 1970 he was Loeb Lecturer at Harvard University and in 1977 he was awarded an honorary doctorate by the University of Uppsala and by the Technische Hochschule Aachen. He is a member of the Akademie der Wissenschaften zu Düsseldorf und Leopoldina zu Halle. Since 1979 he has been the President of the Alexander-von-Humbold Stiftung. In 1989 he was awarded the Robert-Wichard-Pohl prize of the German Physical Society. Of his numerous discoveries and inventions, the Quadrupole Mass Spectrometer is of outstanding importance to the chemist.

At first sight one expects that the time-dependent term of the force cancels out in the time average. But this would be true only in a homogenous field. In a periodic inhomogenous field, like the quadrupole field there is a small average force left, which is always in the direction of the lower field, in our case toward the center. Therefore, certain conditions exists that enable the ions to traverse the quadrupole field without hitting the electrodes, i.e. their motion around the y-axis is stable with limited amplitudes in the x- and z-directions. We have learned these rules from the theory of the Mathieu equations, as this type of differential equation is called.

In dimensionless parameters these equations are written as in (11) and (12). By comparison with equations (9, 10) one obtains (13).

$$\frac{d^2x}{d\tau^2} + (a_x + 2q_x \cos 2\tau)\, x = 0 \tag{11}$$

$$\frac{d^2z}{d\tau^2} + (a_z + 2q_z \cos 2\tau)\, z = 0 \tag{12}$$

$$a_x = -a_z = \frac{4eU}{mr_0^2\omega^2}, \quad q_x = -q_z = \frac{2eV}{mr_0^2\omega^2}, \quad \tau = \frac{\omega t}{2} \tag{13}$$

The Mathieu equation has two types of solution:

1. Stable motion: the particles oscillate in the x–z-plane with limited amplitudes. They pass the quadrupole field in the y-direction without hitting the electrodes.

2. Unstable motion: the amplitudes grow exponentially in the x or z direction, or in both directions. The particles will be lost.

Whether stability exists depends only on the parameters a and q and not on the initial parameters of the ion motion, e.g. their velocity. Therefore, in an a,q-map there are regions of stability and instability (Fig. 2). Only the overlapping region for x and z stability is of interest for our problem. The most relevant region $0 < a,q < 1$ is plotted in Figure 3. The motion is stable in the x and z directions only within the triangle.

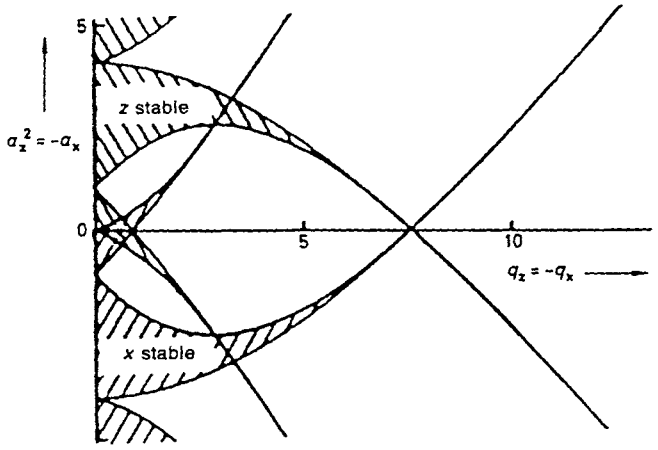

Fig. 2. The overall stability diagram for the two-dimensional quadrupole field.

For fixed values r_0, ω, U and V all ions with the same m/e have the same operating point in the stability diagram. Since

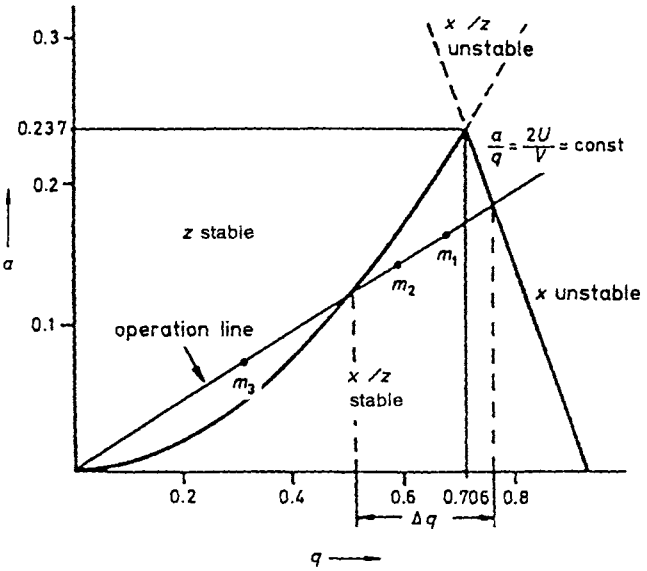

Fig. 3. The lowest region for simultaneous stability in x- and z-direction. All ion masses lie on the operation line. $m_2 > m_1$.

a/q is equal to $2U/V$ and does not depend on m, all masses lie along the operating line a/q = const. On the q axis ($a = 0$, no d.c. voltage) one has stability for $0 < q < q_{max} = 0.92$ with the consequence that all masses between $\infty > m > m_{min}$ have stable orbits. In this case the quadrupole field works as a high-pass mass filter. The mass range Δm becomes narrower with increasing dc voltage U, i.e. with a steeper operating line, and approaches $\Delta m = 0$ if the line goes through the tip of the stability region. The bandwidth in this case is given only by the fluctuation of the field parameters. If one changes U and V simultaneously and proportionally in such a way that a/q remains constant, one brings the ions of the various masses successively into the stability region, thus scanning through the whole mass spectrum in this way. That is the quadrupole acts as a mass spectrometer. A schematic representation of a quadrupole mass spectrometer is given in Figure 4.

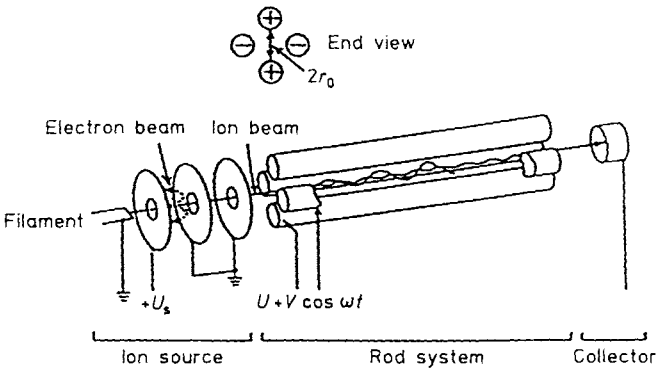

Fig. 4. Schematic view of the quadrupole mass spectrometer or mass filter.

Figures 5a and 5b show the first mass spectra obtained in 1954.[6] One can clearly see the influence of the d.c. voltage U on the resolving power.

The performance and application of such instruments were the subject of a number of theses at Bonn Universi-

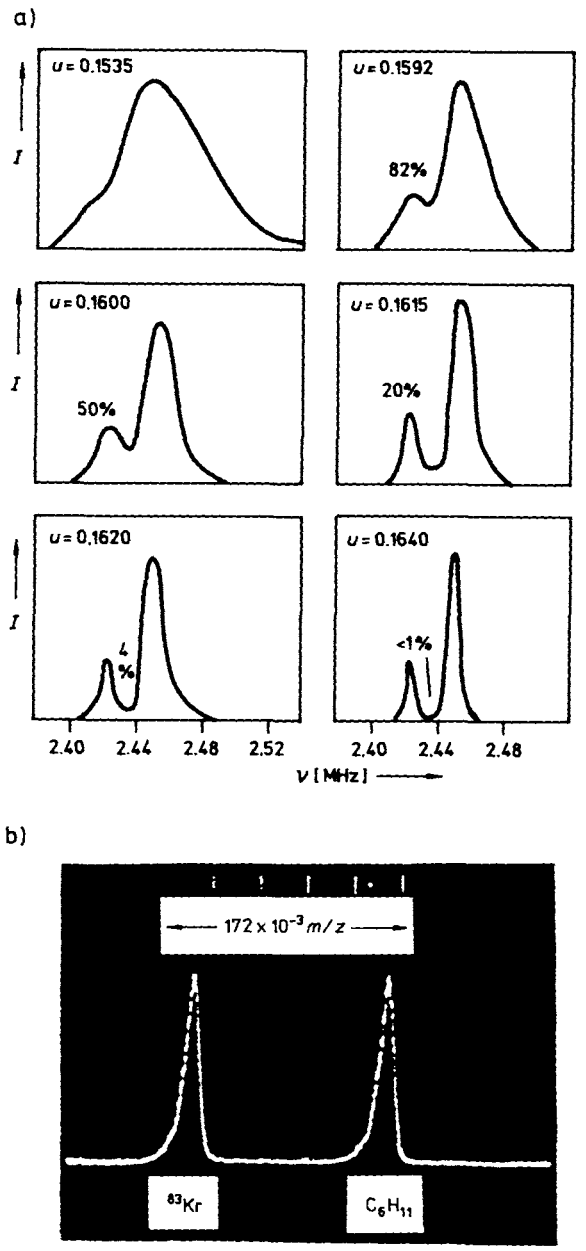

Fig. 5. a) First mass spectrum of rubidium. Mass scanning was achieved by periodic variation of the driving frequency ν. Parameter: $u = U/V$, at $u = 0.164$ ^{85}Rb and ^{87}Rb are fully resolved. I = ion current. b) Mass doublet ^{83}Kr—C_6H_{11}. Resolving power $m/\Delta m = 6500$ [9].

ty.[7–9] Thus, we studied the influence of geometrical and electrical imperfections giving rise to higher multipole terms in the field. A very long instrument ($l = 6$ m) for high precision mass measurements was built achieving an accuracy of 2×10^{-7} in determining mass ratios at a resolving power of $m/\Delta m = 16\,000$. On the other hand, very small instruments have been used in rockets to measure atomic abundances in the upper atmosphere. In another experiment we succeeded in separating isotopes in amounts of milligrams using a resonance method to shake single masses out of an intense ion beam guided into the quadrupole.

In the past years the r.f. quadrupole, whether as mass spectrometer or beam guide, has, owing to its versatility and technical simplicity, found broad applications in many fields of science and technology. It became a kind of standard instrument and its properties have been reported extensively in the literature.[10]

The Ion Trap

Already at the very beginning of our thinking about the dynamic stabilization of ions we were aware of the possibility of using it for trapping ions in a three-dimensional field. We called such a device an "Ionenkäfig" (ion cage).[11–13] Nowadays the word "ion trap" is preferred.

The potential configuration in the ion trap is given by Equation (6). This configuration is generated by an hyperbolically shaped ring and two hyperbolic rotationally symmetric caps as is shown schematically in Figure 6a. Figure 6b shows a section through the first realized trap in 1955.

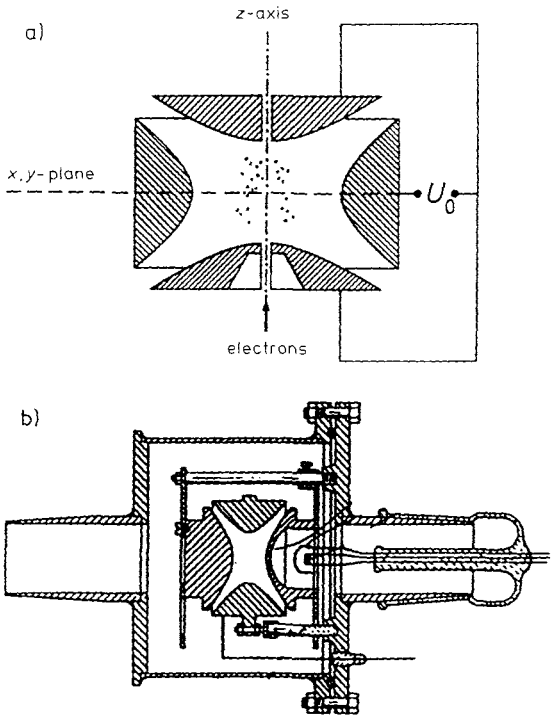

Fig. 6. a) Schematic view of the ion trap. b) Cross section of the first trap (1955).

If one brings ions into the trap, which is easily achieved by ionizing a low-pressure gas inside by electrons passing through the volume, they perform the same forced motions as in the two-dimensional case. The only difference is that the field in the z-direction is stronger by a factor 2. Again a periodic field is needed for the stabilization of the orbits. If the voltage $\Phi_0 = U + V \cos \omega t$ is applied between the caps and the ring electrode the equations of motion are represented by the same Mathieu functions [Eq. (11), (12)]. The relevant parameters for the r motion correspond to those in the x-direction in the two-dimensional case. Only the z parameters are changed by a factor 2.

Accordingly, the region of stability in the a, q-map for the trap (Fig. 7) has a different shape. Again the mass range of

the storable ions (i.e. ions in the stable region) can be chosen by the slope of the operation line $a/q = 2U/V$. Starting with operating parameters in the tip of the stable region one can trap ions of a single mass number. By lowering the d.c. voltage one brings the ions near the q-axis where their motions are much more stable.

For many applications it is necessary to know the frequency spectrum of the oscillating ions. From mathematics we learn that the motion of the ions can be described as a slow (secular) oscillation with the fundamental frequencies $\omega_{r,z} = \beta_{r,z}\omega/2$ modulated by a micromotion, a much faster oscillation of the driving frequency ω if one neglects higher harmonics. The frequency determining factor β is a function only of the Mathieu parameters a and q and therefore mass dependent. its value varies between 0 and 1; lines of equal β are drawn in Figure 7.

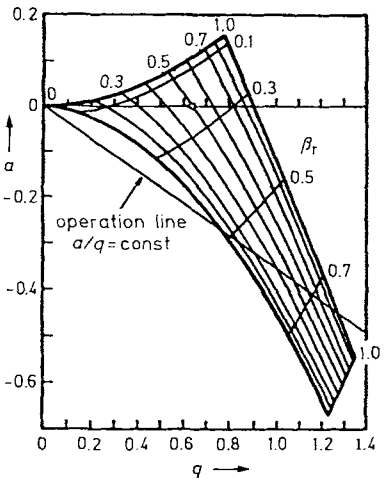

Fig. 7. The lowest region for stability in the ion trap. On the lines inside the stability region β_z and β_r respectively are constant.

Due to the stronger field, the frequency ω_z of the secular motion becomes twice ω_r. The ratio ω/ω_z is a criterion for the stability. Ratios of 10:1 are easily achieved and therefore the displacement by the micromotion averages out over a period of the secular motion.

The dynamic stabilization in the trap can easily be demonstrated in a mechanical analogue device. In the trap the equipotential lines form a saddle surface as is shown in Figure 8. We have machined such a surface on a round disc. If one puts a small steel ball on it, then it will roll down: its position is unstable. But if one let the disk rotate with the right frequency appropriate to the potential parameters and the mass of the ball (in our case a few turns/s) the ball becomes stable, makes small oscillations and can be kept in position over a long time. Even if one adds a second or a third ball they stay near the center of the disk. The only condition is that the related Mathieu parameter q be in the permitted range.[*]

This behavior gives us a hint of the physics of dynamic stabilization. The ions oscillating in the r- and z-directions

[*] I brought the device with me. It is made out of plexiglass, permitting the demonstration of the particle motions with the overhead projector.

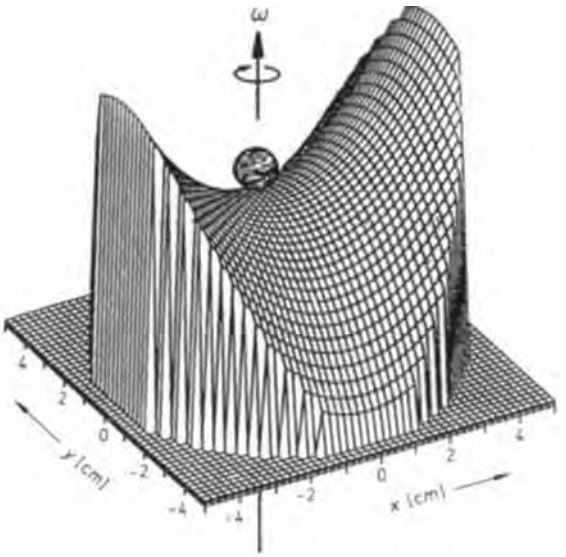

Fig. 8. Mechanical analogue model for the ion trap with steelball as "particle".

behave, to a first approximation, harmonically, as if they are moving in a pseudo potential well which increases quadratically in all coordinates. From their frequencies ω_r and ω_z we can calculate the depth of this well for both directions. It is related to the amplitude V of the driving voltage and to the parameters a and q. Without any d.c. voltage the depth is given by $D_z = (q/8)V$; in the r-direction it is half of this value. As in practice, V amounts to a few hundred volts, the potential depth is of the order of 10 volts. The width of the well is given by the geometric dimensions. The resulting configuration of the pseudo potential[14] is therefore given by Equation (14).

$$\Phi = D\frac{(r^2 + 4z^2)}{r_0^2 + 2z_0^2} \tag{14}$$

Cooling Process

As already mentioned, the depth of the relevant pseudo potential in the trap is of the order of a few volts. Accordingly the permitted kinetic energy of the stored ions is of the same magnitude and the amplitude of the oscillations can reach the geometrical dimensions of the trap. But for many applications one needs particles of much lower energy and well concentrated in the center of the trap. For precise spectroscopic measurements, in particular, it is desirable to have extremely low velocities to get rid of the Doppler effect and an eventual Stark effect, caused by the electric field. It becomes necessary to cool the ions. Relatively crude methods of cooling are the use of a cold buffer gas, or the damping of the oscillations by an external electric circuit. The most effective method is the laser-induced side-band fluorescence developed by *Wineland* and *Dehmelt*.[5]

In 1959 *Wuerker* et al.[16] performed an experiment trapping small charged aluminum particles ($\Phi \sim \mu$m) in the quadrupole trap. The necessary driving frequency was around 100 Hz. They studied all the eigenfrequencies and took photographs of the particle orbits (Figs. 9a, b). After

they had damped the motion with a buffer gas they observed that the randomly moving particles arranged themselves in a regular pattern. They formed a crystal.

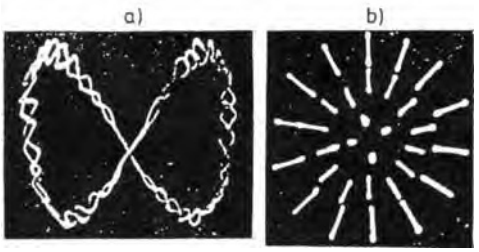

Fig. 9. a) Photomicrograph of a Lissajous orbit in the r–z-plane of a single charged particle of aluminum. The micro motion is visible. b) Pattern of "condensed" Al particles [16].

In recent years one has succeeded in observing optically single trapped ions by laser resonance fluorescence.[17] Using a high resolution image intensifier *Walther* et al. observed the pseudo crystallization of ions in the trap after cooling them with laser light. The ions move to such positions where the repulsive Coulomb force is compensated by the focusing forces in the trap and the energy of the ensemble has a minimum. Figures 10a, b show such a pattern with seven ions.

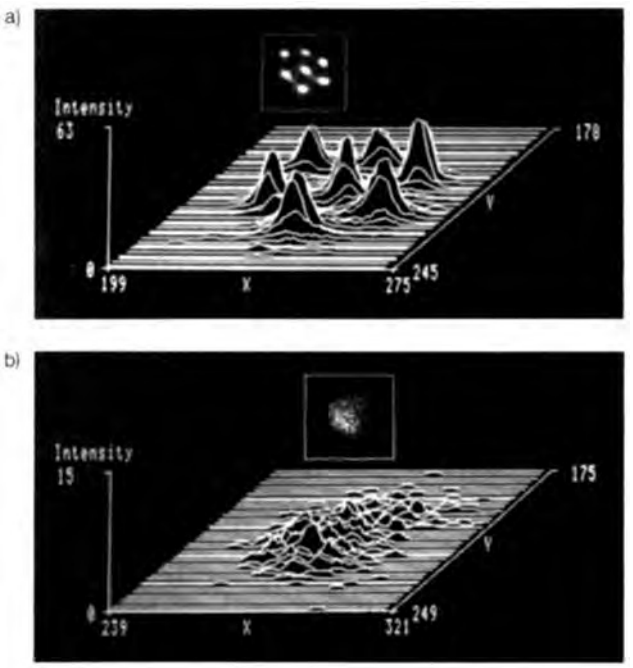

Fig. 10. a) Pseudo crystal of seven magnesium ions. Particle distance 23 μm. b) The same trapped particles at "higher temperature"; The crystal has melted [18].

Their separation distance is of the order of a few micrometers. These observations opened a new field of research.[18]

The Ion Trap as Mass Spectrometer

As mentioned earlier the ions perform oscillations in the trap with frequencies ω_r and ω_z which at fixed field parameters are determined by the mass of the ion. This enables a mass selective detection of the stored ions. If one connects the cap electrodes with an active r.f. circuit of eigenfrequency Ω, in the case of resonance $\Omega = \omega_z$ the amplitude of the oscillations increases linearly with time. The ions hit the cap or leave the field through a borehole and can easily be detected by an electron multiplier device. By modulating the voltage V determining the ion frequency in a sawtooth mode one brings the ions of the various masses one after the other into resonance, thus scanning the mass spectrum. Figure 11

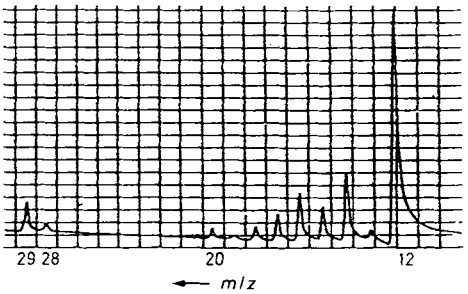

Fig. 11. First mass spectrum achieved with the ion trap. Gas: air at 2×10^{-9} torr [19].

shows the first spectrum of this kind achieved by *Rettinghaus*[19].

The same effect with a faster increase of the amplitude is achieved if one inserts a small band of instability into the stability diagram. It can be generated by superimposing on the driving voltage $V \cos \omega t$ a small additional rf voltage, e.g., with frequency $\omega/2$, or by adding a higher multipole term to the potential configuration.[5b, 20]

In summary the ion trap works as ion source and mass spectrometer at the same time. It became the most sensitive mass analyzer available, as only a few ions are necessary for detection. The underlying theoretical principles and applications are reviewed in detail in a monograph by *R. E. March* and *R. J. Hughes*.[21]

The Penning Trap

If one applies to the quadrupole trap only a d.c. voltage in such a polarity that the ions perform stable oscillations in the z-direction with the frequency $\omega_z^2 = \dfrac{2eU}{mr_0^2}$ the ions are unstable in the x–y-plane, since the field is directed outwards. Applying a magnetic field in the axial direction, the z-motion remains unchanged but the ions perform a cyclotron motion ω in the x–y-plane. It is generated by the Lorentz force F_L directed towards the center. This force is partially compensated by the radial electric force $F_r = eUr/r_0^2$. As long as the magnetic force is much larger than the electric force, we also have stability in the radial direction. No r.f. field is needed. The resulting rotational frequency is given by Equation (15).

$$\omega = \omega_c - \frac{\omega_z^2}{2\omega} \tag{15}$$

It is slightly smaller than the undisturbed cyclotron frequency $\omega_c = eB/m$. The difference is due to the magnetron frequency ω_m [Eq. (16)], which is independent of the particle mass.

$$\omega_M = \frac{\omega_z^2}{2\omega} \tag{16}$$

The Penning trap,[22] as this device is called, is of advantage if the magnetic properties of particles have to be measured, as for example Zeeman transitions in spectroscopic experiments, or cyclotron frequencies for a very precise comparison of masses, as have been performed, e.g., by *G. Werth*. The most spectacular application the trap has found is in the experiments of *G. Gräff*[23] and *H. Dehmelt* for measuring the anomalous magnetic moment of the electron. This method was brought by *H. Dehmelt*[24] to an admirable precision by observing only a single electron stored for many months.

Traps for Neutral Particles

In the last examination I had to pass as a young man I was asked if it would be possible to confine neutrons in a bottle in order to prove if they are radioactive. This question, at that time only to be answered with "no", pursued me for many years until I could have had replied: Yes, by means of a magnetic bottle. It took 30 years until by the development of superconducting magnets its realization became feasible.

Using the example of such a bottle I would like to demonstrate the principle of confining neutral particles. Once again this goes back to our early work on focusing neutral atoms and molecules having a dipole moment by means of multipole fields, making use of their Zeeman or Stark effect to first and second order.[1-3] Both effects can be used for trapping. Until now only magnetic traps have been realized for atoms and neutrons. In particular, *B. Martin, U. Trinks* and *K. J. Kügler* contributed to their development with great enthusiasm.

The Principle of Magnetic Bottles

The potential energy U of a particle with a permanent magnetic moment $\boldsymbol{\mu}$ in a magnetic field is given by $U = -\mu B$. If the field is inhomogenous it corresponds to a force $F = \text{grad}(\boldsymbol{\mu B})$. In the case of the neutron, with its spin $\hbar/2$, only two spin directions relative to the field are permitted. Therefore, its magnetic moment can be oriented only parallel or antiparallel to $\boldsymbol{B}$. In the parallel position the particles are drawn into the field and in the opposite orientation they are repelled. This permits their confinement to a volume with magnetic walls.

The appropriate field configuration to bind the particles harmonically is in this case a magnetic sextupole field. As I have pointed out such a field $\boldsymbol{B}$ increases with r^2, $\boldsymbol{B} = \boldsymbol{B}_0\, r^2/r_0^2$ and the gradient $\partial B/\partial r$ with r, respectively.

In such a field, neutrons with orientation $\mu \uparrow\uparrow \boldsymbol{B}$ satisfy the confining condition, as their potential energy $U = +\mu B \sim r^2$ and the restoring force $\mu \,\text{grad}\, \boldsymbol{B} = -cr$ is always oriented towards the center. They oscillate in the field with the frequency $\omega^2 = \frac{2\mu B_0}{m r_0^2}$. Particles with $\mu \uparrow\downarrow \boldsymbol{B}$ are defocused and leave the field. This is valid only as long as the spin orientation is conserved. In the sextupole, of course, the direction of the magnetic field changes with the azimuth, but as long as the particle motion is not too fast the spin follows the field direction adiabatically, conserving the magnetic quantum state. This behavior permits the use of a magnetic field constant in time, in contrast to the charged particle in an ion trap.

An ideal linear sextupole in the x–z-plane is generated by six hyperbolically shaped magnetic poles of alternating polarity extended in the y-direction (Fig. 12a). It might be approximated by six straight current leads with alternating current directions arranged in a hexagon (Fig. 12b). Such a configuration works as a lens for particles moving along the y-axis.

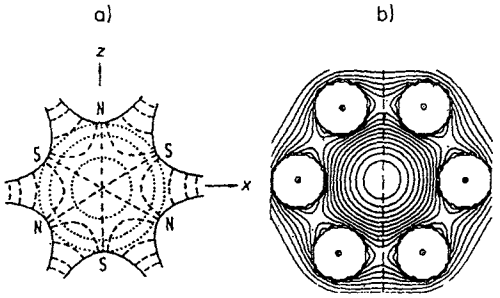

Fig. 12. a) Ideal sextupole field. Dashed: magnetic field lines, dotted: lines of equal magnetic potential (B = const.). b) Linear sextupole made of six straight current leads with alternating current direction.

There are two possible ways of achieving a *closed storage volume:* a sextupole sphere and a sextupole torus. We have realized and studied both. In particular *B. Martin, U. Trinks* and *K. J. Kügler* have participated enthusiastically in this development.

The spherically symmetric field is generated by three ring-currents in an arrangement shown in Figure 13. The field B

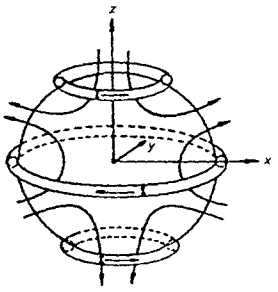

Fig. 13. Sextupole sphere.

increases in all directions with r^2 and has its maximum value B_0 at the radius r_0 of the sphere. Using superconducting current leads we achieved $B_0 = 3$T in a sphere with a radius of 5 cm. But due to the low magnetic moment of the neutron

$\mu = 6 \times 10^{-8}$ eV/T the potential depth μB_0 is only 1.8×10^{-7} eV, and hence the highest velocity of storable neutrons is only 6m/s. Due to their stronger moment, in the case of Na atoms these values are 2.2×10^{-4} eV and 37 m/s, respectively.

The main problem with such a closed configuration is the filling process, especially the cooling inside in order to avoid that the particles injected from outside are again leaving the storage volume. However, in 1975 in a test experiment we succeeded in observing a storage time of three seconds for sodium atoms evaporated inside a bottle with helium cooled walls.[25] But the break through in confining atoms was achieved by *W. D. Phillip* and *H. J. Metcalf* using the modern technique of laser cooling.[26]

The problem of storing neutrons becomes easier if one uses a linear sextupole field bent to a closed torus with a radius R (Fig. 14). The magnetic field in the torus volume is

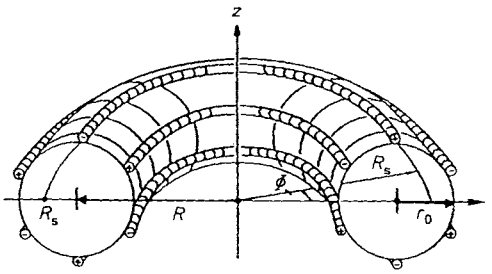

Fig. 14. Sextupole torus. R_s orbit of circulating neutrons.

unchanged $\boldsymbol{B} = \mathbf{B}_0\, r^2/r_0^2$ and has no component in the azimuthal direction. The neutrons move in a circular orbit with Radius R_s if the centrifugal force is compensated by the magnetic force [Eq. (17)].

$$F_c = \frac{m v_\varphi^2}{R_s} = \mu \left.\frac{\partial B}{\partial r}\right|_{R_s} \tag{17}$$

In such a ring the permitted neutron energy is limited by

$$E_{max} = \mu B_0 \left(\frac{R}{r_0} + 1\right) \tag{18}$$

It is increased by a factor $(R/r_0 + 1)$ compared to the case of the sextupole sphere. As the neutrons have not only an azimuthal velocity but also components in the r and z directions they are oscillating around the circular orbit.

But this toroidal configuration has not only the advantage of accepting higher neutron velocities, it also permits an easy injection of the neutrons in the ring from the inside. The neutrons are not only moving in the magnetic potential well but they also experience the centrifugal barrier. Accordingly, one can lower the magnetic wall on the inside by omitting the two inward current leads. The resulting superposition of the magnetic and the centrifugal potential still provides a potential well with its minimum at the beam orbit. But there is no barrier for the inflected neutrons.

It is obvious, that the toroidal trap in principle works analogous to the storage rings for high energy charged particles. In many respects the same problems of instabilities of the particle orbits by resonance phenomena exist, causing loss of the particles. But also new problems arise like, e.g., undesired spin flips or the influence of the gravitational force.

In accelerator physics one has learned to overcome such problems by shaping the magnetic field by employing the proper multipole components.

This technique is also appropriate in the case of the neutron storage ring. The use of the magnetic force $\mu \cdot \mathrm{grad}\boldsymbol{B}$ instead of the Lorentz force, which is proportional to B, just requires multipole terms of one order higher. Quadrupoles for focusing have to be replaced by sextupoles and, e.g., octupoles for stabilization of the orbits by decapoles.

In the seventies we designed and constructed such a magnetic storage ring with orbits of a diameter of 1 m. The achieved usable field of 3.5 T permits the confinement of neutrons in the velocity range of 5–20 ms^{-1}, corresponding to a kinetic energy up to 2×10^{-6} eV. The neutrons are injected tangentially into the ring by a neutron guide with totally reflecting walls. The inflector can be moved mechanically into the storage volume and shortly afterwards be withdrawn.

The experimental set up is shown in Figure 15. A detailed description of the storage ring and the underlying theoretical principles is given in Ref. [27].

In 1978 in a first experiment we tested the instrument at the Grenoble high flux reactor. We could observe neutrons stored up to 20 min after injection by moving a neutron counter through the confined beam after a preset time. As in the detection process the neutrons are lost, one has to refill the ring, starting a new measurement. But due to the relative-

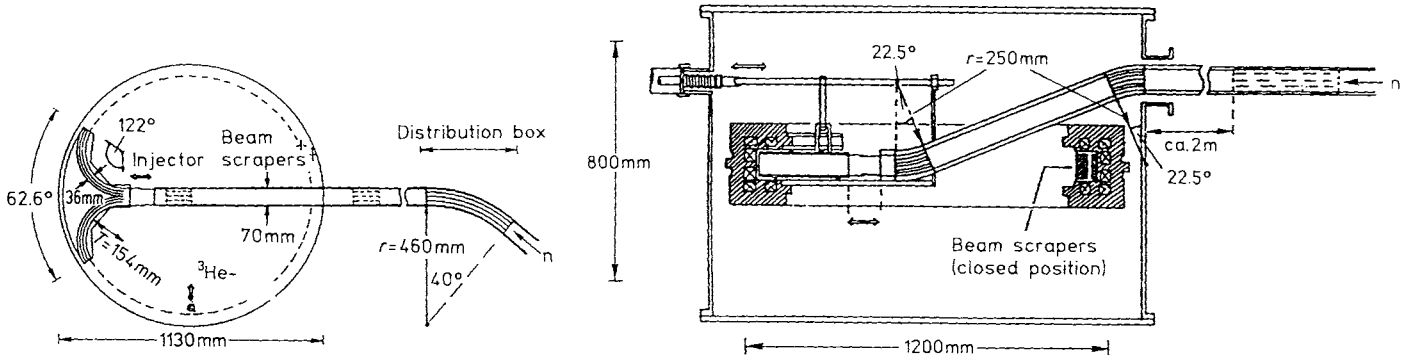

Fig. 15. Schematic top view and side view of the neutron storage ring experiment.

ly low flux of neutrons in the acceptable velocity range, their number was too low to make relevant measurements.

In a more recent experiment,[28] using a new neutron beam with a flux improved by a factor 40 we could observe neutrons up to 90 min, i.e. roughly six times the radioactive decay time of the neutron. Figure 16 shows the measured

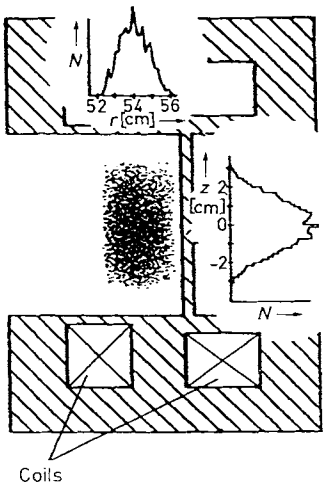

Fig. 16. Beam profile of the stored neutrons inside the magnet gap 400 s after injection.

profile of the neutron beam circulating inside the magnetic gap. Measuring carefully the number of stored neutrons as a function of time we could determine the lifetime as $\tau = 877 \pm 10$ s (Fig. 17).

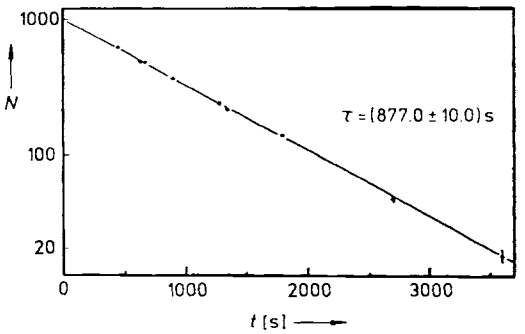

Fig. 17. Logarithmic decrease of the number of stored neutrons with time (τ = half-time).

The analysis of our measurements let us conclude that the intrinsic storage time of the ring for neutrons is at least about one day. It shows that we had understood the relevant problems in its design.

The Storage Ring as a Balance

This very reproducible performance permitted another interesting experiment. As I have already explained, neutrons are elastically bound to the symmetry plane of the magnetic field. Due to their low magnetic moment the restoring force is of the order of the gravitational force. Hence it follows that the weight of the neutron stretches the magnetic spring that the particle is hanging on; the equilibrium center of the oscillating neutrons is shifted downwards.

The shift z_0 is given by the balance $mg = \mu \operatorname{grad} \boldsymbol{B}$. One needs a gradient $\partial B/\partial z = 173\ \mathrm{Gcm}^{-1}$ for compensating the weight. As the gradient in the ring increases with z and is proportional to the magnetic current I one can calculate the shift z_0 according to Equation (19).

$$z_0 = \text{const.}\ mg/I. \tag{19}$$

It amounts in our case to $z_0 = 1.2$ mm at the highest magnet current $I = 200$ A and 4.8 mm at 50 A accordingly.

By moving a thin neutron counter through the storage volume we could measure the profile of the circulating neutron beam and its position in the magnet. Driving the counter alternately downwards and upwards in many measuring runs we determined z_0 as a function of the magnetic current.

The result is shown in Figure 18. The measured data taken with different experimental parameters follow the predicted line. A detailed analysis gives for the gravitational mass of the neutron the value $m_g = (1.63 \pm 0.06) \times 10^{-24}$ g. It agrees within 4% with the well known inertial mass.

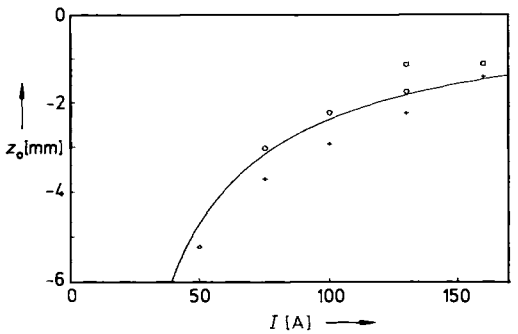

Fig. 18. Downward shift of the equilibrium center of the neutron orbits due to the weight of the neutron as function of the magnetic current I. Size of injection aperture: ±35.3(+), ±21.3(○), ±18.8 mm. (◇), ±14.5 mm □. The curve gives the theoretical shift.

Thus the magnetic storage ring represents a balance with a sensitivity of 10^{-25} g. It is only achieved because the much higher electric forces play no role at all.

I am convinced that the magnetic bottles developed in our laboratory and described here are potentially very useful instruments for many other experiments in the future, as the ion trap has already proven in the past.

Received: February 20, 1990 [A 768 IE]
German version: *Angew. Chem. 102* (1990) 780

[1] H. Friedburg, W. Paul, *Naturwissenschaften 38* (1951) 159.
[2] H. G. Bennewitz, W. Paul, *Z. Phys. 139* (1954) 489.
[3] H. G. Bennewitz, W. Paul, *Z. Phys. 141* (1955) 6.
[4] C. H. Townes, *Proc. Natl. Acad. Sci. USA 80* (1983) 7679.

[5] a) W. Paul, H. Steinwedel, *Z. Naturforsch. A8* (1953) 448; b) DBP Nr. 944900, US-Pat. 2939958.
[6] W. Paul, M. Raether, *Z. Phys. 140* (1955) 262.
[7] W. Paul, H. P. Reinhardt, U. von Zahn, *Z. Phys. 152* (1958) 143.
[8] F. von Busch, W. Paul, *Z. Phys. 164* (1961) 581.
[9] U. von Zahn, *Z. Phys. 168* (1962) 129.
[10] P. H. Dawson: *Quadrupole Mass Spectrometry and its Application*, Elsevier, Amsterdam 1976.
[11] W. Paul, O. Osberghaus, E. Fischer, *Forschungsber. Wirtsch. Verkehrsminist. Nordrhein-Westfalen 415* (1958).
[12] K. Berkling, *Dissertation*, Universität Bonn 1956.
[13] E. Fischer, *Z. Phys. 156* (1959) 1.
[14] H. Dehmelt, *Adv. At. Mol. Phys. 3* (1967).
[15] D. J. Wineland, H. Dehmelt, *Bull. Am. Phys. Soc. 20* (1975) 637.
[16] R. F. Wuerker, R. V. Langmuir, *Appl. Phys. 30* (1959) 342.
[17] W. Neuhauser, M. Hohenstett, P. Toschek, H. Dehmelt, *Phys. Rev. A22* (1980) 1137.
[18] F. Dietrich, E. Chen, J. W. Quint, H. Walther, *Phys. Rev. Lett. 59* (1987) 2931.
[19] G. Rettinghaus, *Z. Angew. Phys. 22* (1967) 321.
[20] F. von Busch, W. Paul, *Z. Phys. 164* (1961) 580.
[21] R. E. March, R. J. Hughes: *Quadrupole Storage Mass Spectrometry*, Wiley, New York 1989.
[22] F. M. Penning, *Physica (Amsterdam) 3* (1936) 873.
[23] G. Gräff, E. Klempt, G. Werth, *Z. Phys. 222* (1969) 201.
[24] R. S. van Dyck, P. B. Schwinberg, H. G. Dehmelt, *Phys. Lett. 38* (1977) 310.
[25] B. Martin, *Disertation*, Universität Bonn 1975.
[26] A. L. Migdal, J. Prodan, W. D. Phillips, T. H. Bergmann, H. J. Metcalf, *Phys. Rev. Lett. 54* (1985) 2596.
[27] K. J. Kügler, W. Paul, U. Trinks, *Nucl. Instrum, Methods Phys. Res. Sect. A 228* (1985) 240.
[28] W. Paul, F. Anton, L. Paul, S. Paul, W. Mampe, *Z. Phys. C45* (1989) 25.

Enzymatic Cleavage of RNA by RNA (Nobel Lecture)**

By Sidney Altman*

Introduction

The transfer of genetic information from nucleic acid to protein inside cells can be represented as shown in Scheme 1. This simple scheme reflects accurately the fact that the information contained in the linear arrangement of the nucleotides in DNA is copied accurately into the linear arrangement of nucleotides in RNA, which, in turn, is translated by machinery inside the cell into proteins, the macromolecules responsible for governing many of the important biochemical processes in vivo. The straightforward transfer of information from DNA to protein is carried out by a class of molecules called messenger RNAs (mRNAs). The diagram shown does not elaborate on the properties of other RNA molecules that are transcribed from DNA, namely, transfer RNA (tRNA) and ribosomal RNA (rRNA) and many other minor species of RNA found in vivo that had no identifiable function prior to 1976, nor does it indicate that the information in DNA and RNA can be replicated as daughter DNA and RNA molecules, respectively.[1]

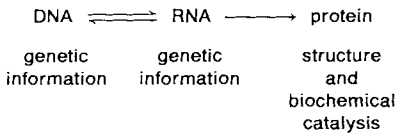

Scheme 1. A representation of the flow of information inside cells from DNA to protein. This diagram is not a complete representation of the central dogma (see [1]).

Ribosomes are complexes which, in *Escherichia coli*, are made of about 50 proteins and three RNA molecules. It is on these particles that mRNA directs the synthesis of protein from free amino acids. tRNA molecules (Fig. 1) perform an adaptor function in the sense that they match particular amino acids to groups of three specific nucleotides on the mRNA to be translated and ensure that the growing polypeptide (protein) chain contains the right linear sequence of amino acid subunits. Thus, rRNA and tRNA participate in the process of information transfer inside cells, but they clearly do so in a comparatively complex manner.

My work on RNA began as a study of certain mutants that disrupt the ability of tRNA molecules to function normally during translation.[2] This research, in turn, led to the identification of another RNA molecule that had, unexpectedly, all the properties of an enzyme.[3] Aside from its intrinsic interest to students of catalysis and enzymology, our finding of an enzymatic activity associated with RNA has stimulated reconsideration of the role of RNA in biochemical systems today (Scheme 1; see *Cech*[4] and *Altman*[5] for reviews) and of the nature of complex biochemical systems eons ago.[6-11]

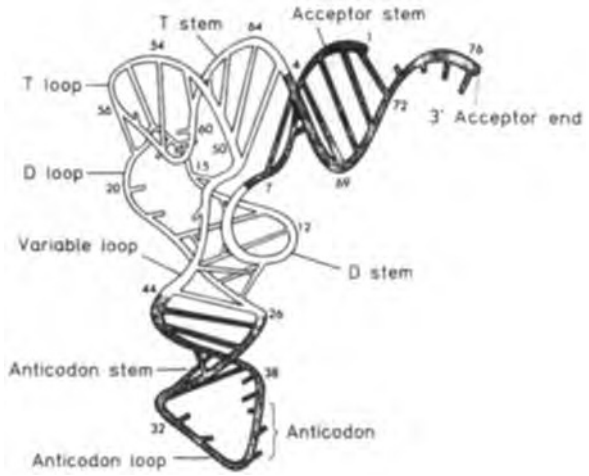

Fig. 1. A diagram illustrating the folding of the yeast $tRNA^{Phe}$ molecule. The ribose–phosphate backbone is drawn as a continuous ribbon and internal hydrogen bonding is indicated by crossbars. Positions of single bases are indicated by bars that are intentionally shortened. The anticodon and acceptor arms are shaded. (Reprinted with permission from [63].)

As was first pointed out over twenty years ago by *Woese*,[12] *Crick*,[13] and Orgel,[14] if RNA can act as a catalyst then the origin of the genetic code plays a much less critical role in the early stages of the evolution of the first biochemical systems that were capable of replicating themselves. The variety of biochemical reactions now known to be governed by RNA (Table 1)[5] allows one to consider the possibility that a large number of different enzymatic reactions might indeed occur in the absence of protein. To add further substance to these ideas about life on our planet over a billion years ago, it is important to expand our understanding of how modern catalytic RNAs work and of the roles they play in vivo today. This discussion deals primarily with the discovery and characterization of the catalytic RNA subunit of the enzyme ribonuclease P from *Escherichia coli*.

Table 1. Some properties of catalytic RNAs.

RNA	End groups [a]	Cofactor	Mechanism
1. Group I introns	5'-P, 3'-OH	Yes	Transesterification
2. Group II introns	5'-P, 3'-OH	No	Transesterification
3. M1 RNA	5'-P, 3'-OH	No	Hydrolysis
4. Viroid/satellite	5'-OH, 2',3'-cyclic phosphate	No	Transesterification
5. Lead ion/tRNA	5'-OH, 2',3'-cyclic phosphate	No	Similar to RNase A

[a] The end groups are those produced during the initial cleavage step of self-splicing reactions or during the usual cleavage reactions of other RNA species.

[*] Prof. S. Altman
Department of Biology, Yale University
New Haven, CT 06520 (USA)

[**] Copyright © The Nobel Foundation 1990. We thank The Nobel Foundation, Stockholm, for permission to print this lecture.

A Brief Account of Studies of Ribonuclease P

Finding the Substrate

In October 1969, I arrived at the Medical Research Council Laboratory of Molecular Biology in Cambridge, England, ostensibly to study the three-dimensional structure of tRNA through the use of physical-chemical methods. On my arrival, *Sydney Brenner* and *Francis Crick* informed me that the crystal structure of yeast $tRNA^{Phe}$ had just been solved,[15,16] and that there was no need to engage in the studies originally outlined for me. I was further instructed to get settled, to think about a new problem for a week or two, and then to return for another discussion. Although some of my colleagues remember me as being disappointed after that conversation with *Brenner* and *Crick*, the feeling must have passed quickly because I only recall being presented with a marvelous opportunity to follow my own ideas.

I proposed to make acridine-induced mutants of $tRNA^{Tyr}$ from *E. coli* to determine whether altering spatial relationships in tRNA, by deleting or adding a nucleotide to its sequence, would drastically alter the function of the molecule. Since *Brenner* and *John D. Smith* and their colleagues[17–19] had just completed a classic series of studies of base-substitution mutants of $tRNA^{Tyr}$, they were not overly excited by the prospect of someone simply producing more mutants. Nevertheless, *Brenner* and *Crick* did not prevent me from pushing ahead and *John Smith*, in time, provided valuable advice about the genetics of the system in use in the laboratory.

The mutants I made lacked the usual function of suppressor tRNAs and made no mature tRNA in vivo, but they reverted at a very high rate (about 1%) to wild type. These properties indicated that there might be an unstable duplication or partial duplication of the gene for tRNA in the DNA that contained the information for the tRNA. Furthermore, it seemed likely that RNA would be transcribed from this mutant gene. I reasoned that if I could isolate the RNA transcript, which had to be unstable since no mature tRNA was made, I might be able to understand the nature of the duplication event.

The simple expedient of quickly pouring an equal volume of phenol into a growing culture of *E. coli* labeled with $^{32}PO_4^{3\ominus}$ enabled me to isolate and characterize not only the transcript of the gene for $tRNA^{Tyr}$ mutated by acridines, but also transcripts of the gene for $tRNA^{Tyr}$ (Fig. 2),[2] which had been previously mutated by other means by *Brenner*, *Smith*, and their colleagues. These gene transcripts contained sequences in addition to the mature tRNA sequences at both ends of the molecules (Fig. 3)[20a] and were, therefore, tRNA precursor molecules. The ability to isolate the precursors depended on the rapid phenol extraction technique and the fact that the mutated molecules, by virtue of having altered conformations in comparison to the wild type, were less susceptible to attack by intracellular ribonucleases than the transcripts of the wild-type gene. The "extra" sequences, themselves, though of interest because such segments of gene transcripts had not been characterized at that time, proved not to be particularly revealing.

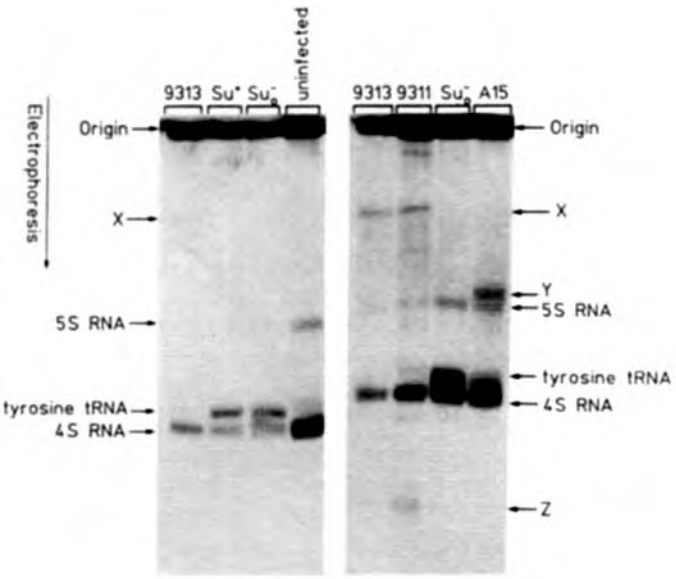

Fig. 2. Separation by electrophoresis of labeled RNA from *E. coli* infected with derivatives of bacteriophage $\phi 80$ that carried various genes for $tRNA^{Tyr}$. The figure shows an autoradiogram of polyacrylamide gels. Experimental details are given in and the figure is taken from [2]. Each column in the gel patterns is titled according to the $tRNA^{Tyr}$ gene carried by the infecting phage. 9313 and 9311 are acridine-induced mutants of the suppressor $tRNA^{Tyr}su_3^+$. A15 is a mutant derivative carrying the G15–A15 mutation and su_0^- is the wild-type $tRNA^{Tyr}$ gene. (Reprinted with permission from [2].)

Although the earlier work of *Darnell*[21a] and *Burdon*[21b,c] and their co-workers had shown that tRNAs were probably made from precursor molecules in eukaryotic cells, further characterization of the enzymes involved in the biosynthesis of tRNA, or tRNA-processing events, could not proceed without a radiochemically pure, homogeneous substrate of the kind that I had isolated.

Sidney Altman, born in 1939 in Montreal, received his undergraduate education in physics at the Massachusetts Institute of Technology. He began graduate studies in physics at Columbia University, but switched to biophysics at the University of Colorado Medical Center (with Leonard Lerman) and then molecular biology at Harvard University (with Mathew Meselson). His work with Sydney Brenner and Francis Crick at the Medical Research Council Laboratory of Molecular Biology in Cambridge, England, led to the discovery of RNase P and the enzymatic properties of the RNA subunit of that enzyme. In 1971 he began work as an assistant professor at Yale University and became a professor in 1980. In 1989 he received, together with Thomas R. Cech, the Nobel Prize in chemistry.

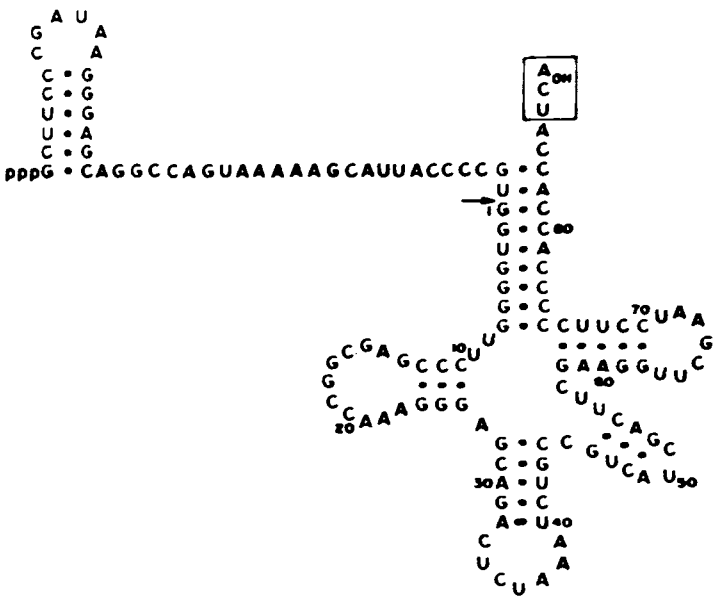

Fig. 3. Nucleotide sequence of the precursor to $tRNA^{Tyr}su_3^+$. The arrow pointing toward the sequence indicates the site of cleavage by RNase P on the 5′ side of nucleotide 1 of the mature tRNA sequence. The boxed nucleotides are extra nucleotides at the 3′ terminus (after [20a]).

When the precursor to one of the mutant $tRNA^{Tyr}$ molecules was mixed with an extract of *E. coli*, it was immediately apparent that enzymatic activities were present in the cell extract that could remove the "extra" nucleotides from both the 5′ and 3′ ends of the mature tRNA sequence (Fig. 4).[20a,b] The activity that processed the 5′ end of the tRNA precursor, which we named Ribonuclease P, did so by a single endonucleolytic cleavage event, in contrast to what appeared to be nonspecific exonucleolytic degradation at the 3′ end of the molecule. In fact, no ribonucleases with such high specificity with respect to site of cleavage as that exhibited by RNase P were known at that time, so the novelty of this reaction assured our continuing interest. Some characterization of the reaction was immediately carried out in collaboration with *Hugh Robertson* and *John Smith*.[20b]

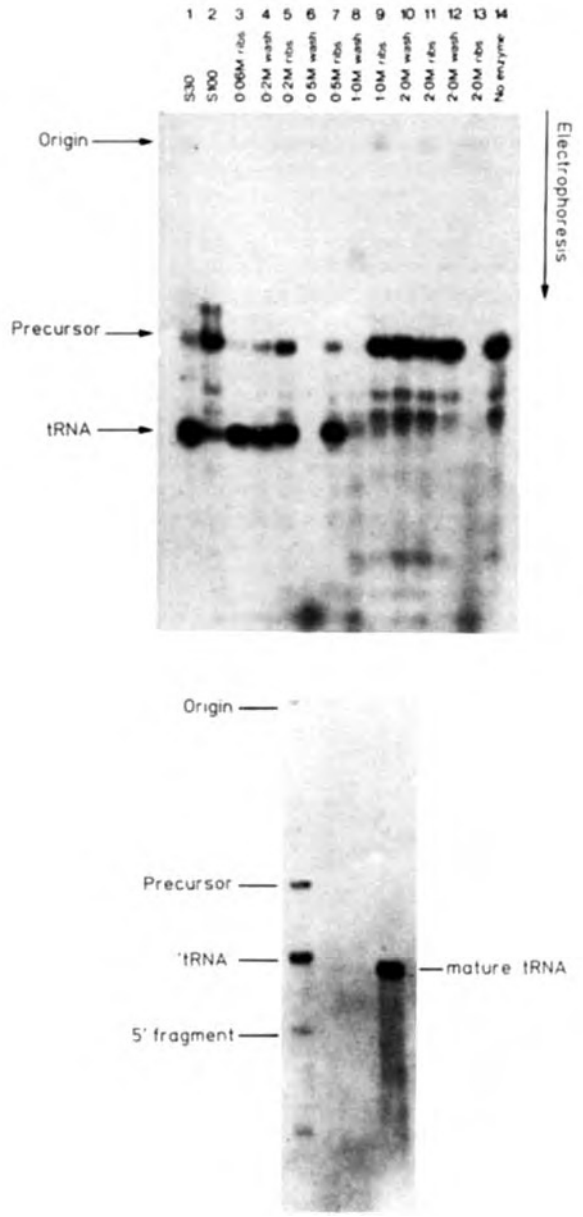

Fig. 4. Top: RNase P activity in extracts of *E. coli*. Extracts of *E. coli*, partial purification of RNase P, and cleavage reactions were carried out as generally described in [20b]. The substrate used was the precursor to *E. coli* $tRNA^{Tyr}$. The column titles in the figure refer to fractions from crude cell extracts of *E. coli* and washes, with buffers that contained increasing concentrations of NH_4Cl, of ribosomes prepared by centrifugation of the S100 fraction. About 100 μg of protein was added to the reaction in lane 1 and lesser amounts to each of the other reactions. There are spontaneous breakdown products of the substrate visible between the "precursor" and "tRNA" bands in the gels. Bottom: Separation by gel electrophoresis of the products of cleavage in vitro of the precursor to $tRNA^{Tyr}A25$ by a partially purified preparation (DEAE-Sephadex fraction) of RNase P. The 3′ end fragment ("tRNA") includes the additional nucleotides of the precursor. (Reprinted with permission from [20b].)

Characterization of Ribonuclease P from *Escherichia coli*

At the MRC laboratory, we showed that RNase P produced 5′-phosphate and 3′-hydroxyl groups at its site of cleavage,[20b] unlike most nonspecific nucleases which produce 5′-hydroxyl and 3′-phosphate groups. This observation fitted with the fact that mature tRNAs have a 5′ phosphate at their 5′ termini. While some progress was made in terms of chromatographic purification of the enzyme, in retrospect the most striking observation made in the early studies was that "it is possible that the active form of RNase P, which must have a strong negative charge, could be associated with some nucleic acid." The next important step was taken a few years later by *Benjamin Stark*, a graduate student in my laboratory at Yale, who showed that an RNA of high molecular weight copurified with the enzymatic activity and, in a classic experiment, demonstrated that this RNA molecule was essential for enzymatic activity.[22] The RNA was named M1 RNA and had a fingerprint that was similar to that of a stable RNA species (band IX) of unknown function that had been described by *Ikemura* and *Dahlberg*[23] as one of a series of minor RNA species found in *E. coli*; the protein subunit of RNase P from *E. coli* was named C5 protein.

The essential role of the RNA component was established by first treating RNase P with micrococcal nuclease, an enzyme that destroys RNA, and subsequently assaying the treated enzyme for RNase P activity: there was none after

treatment with micrococcal nuclease (Fig. 5) or, for that matter, after treatment with various proteinases. Thus, under the conditions we were then using (that is, buffers that contained 5 mM $MgCl_2$), both protein and RNA components were shown to be essential for enzymatic activity. Concurrently we showed that the enzyme had a buoyant density in CsCl of 1.72 g mL^{-1},[22] characteristic of an RNA–protein complex that consists predominantly of RNA. Velocity sedimentation experiments had previously determined the sedimentation coefficient to be about 11.5 S.[20b]

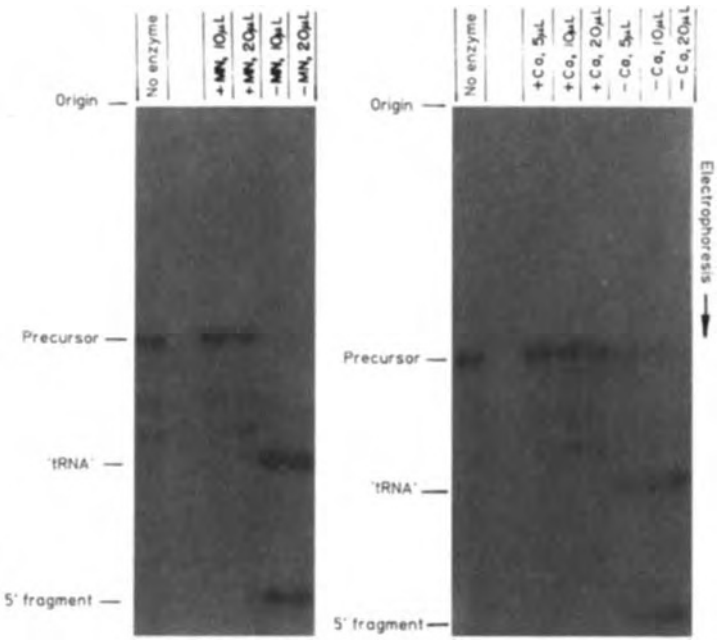

Fig. 5. Inactivation of RNase P by pretreatment with ribonuclease. Control reactions were performed without micrococcal nuclease (MN) in the pretreatment mixture (left) or without $CaCl_2$ (right). RNase P pretreated with MN had less than 5% of the activity of the control reaction RNase P. The extent of inactivation can be varied by changing the reaction conditions as shown. (Reprinted with permission from [22].)

While the biochemical purification was proceeding, studies of temperature-sensitive mutants of *E. coli* made by *Schedl* and *Primakoff* et al.[24,25] and *Shimura, Ozeki,* and their co-workers[26,27] showed that RNase P is essential in *E. coli* for the biosynthesis of all tRNAs and that both RNA and protein subunits are required in vivo. Furthermore, work from the laboratories of *William McClain*[28,65] and *John Carbon*[29] added to the evidence that RNase P is responsible for the processing of many different tRNA precursor molecules. Although appropriate genetic analyses could not be performed, we also showed that RNase P-like activities exist in the extracts of cells from many other organisms, including humans.[30,31] These early studies showed that RNase P was capable of cleaving many different tRNA precursor molecules and that there was no identifiable similarity in terms of nucleotide sequence around the sites of cleavage. The manner in which the enzyme recognized its sites of cleavage in different substrates with such selectivity seemed worthy of study, and recognition of some feature of the structure in solution, common to all tRNA precursor molecules, was suspected.

When *Stark*'s experiments were published we did not have the temerity to suggest, nor did we suspect, that the RNA component alone of RNase P could be responsible for its catalytic activity. The fact that a simple enzyme had an essential RNA subunit, in itself, seemed heretical enough. Shortly thereafter, however, when *Ryszard Kole* demonstrated that the enzyme consisted of an RNA (M1 RNA) and a protein subunit (C5 protein; $M_r \approx 14000$), which were not covalently linked and which could be separated into inactive subunits and then reconstituted to form an active enzyme,[32] the similarities in chemical composition and properties of assembly of this system to those of the ribosome were sufficiently striking that we could not escape thinking about the possibility that the RNA, at the very least, participated in the formation of the active site of the enzyme. Indeed, making the comparison with ribosomes proved to be important in overcoming some resistance to the idea that an enzyme could have an RNA subunit.[33] From a purely chemical point of view, there was no reason why RNA could not participate in formation of the active site or even in catalysis itself.

The advent of recombinant-DNA technology and powerful systems for the transcription in vitro of isolated pieces of DNA enabled us to characterize in some detail the RNA subunit of RNase P (377 nucleotides in length)[34] and to prepare large quantities for biochemical experiments. Concurrent progress in our purification of the protein subunit prepared us for a series of experiments, conducted in collaboration with *Norman Pace*'s group at Indiana University, in which we made hybrid enzymes with subunits from *E. coli* (prepared in our laboratory) and from *B. subtilis* (prepared in *Pace*'s laboratory). As an offshoot of these experiments, *Cecilia Guerrier-Takada* in my laboratory assayed reconstituted RNase P from *E. coli* under ionic conditions optimal for the activity of the holoenzyme from *B. subtilis* and different from the ones we had previously employed. She found, in control experiments in which she tested the RNA and protein subunits separately, that the RNA subunit from *E. coli,* exhibited catalytic activity of its own in buffers that contained 60 mM $MgCl_2$. (An example of such reactions is shown in Figure 6.) In fact, the catalytic activity of M1 RNA is evident when the concentration of $Mg^{2\oplus}$ is greater than 20 mM.[3] The protein subunit of the enzyme increased the k_{cat} by a factor of 10–20 but had little effect on the K_m. We quickly determined that M1 RNA had all the properties of a true enzyme as defined in biochemistry textbooks:[35] it was unchanged (in size) during the course of the reaction; it had a true turnover number as measured by Michaelis–Menten analysis of the kinetics (Fig. 7) and, therefore, it was a catalyst; it was needed in only small amounts and it was stable. These observations were possible because of the purity of our preparations of M1 RNA and the use of a natural substrate, the precursor to $tRNA^{Tyr}$ from *E. coli*.

We soon proposed a model of the secondary structure of M1 RNA based on its susceptibility to nucleases in solution and some simple notions of the stability of RNA structures. We also outlined the general ionic requirements of the reaction (Table 2).[36] The curve of the dependence of the rate of the reaction on the pH is flat between 5 and 9 and is suggestive of the involvement of more than one group with a pK_a not characteristic of those found on nucleotides alone in solution. It is reasonable to expect, therefore, that the active

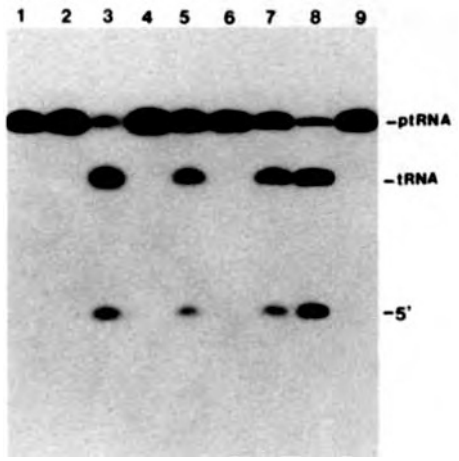

Fig. 6. Dependence of the catalytic activity of M1 RNA on the concentration of $Mg^{2\oplus}$. The precursor to $tRNA^{Tyr}$, abbreviated as pTyr, is the substrate. Reactions and reconstitution of RNase P were carried out as described in [3]. Lane 1: No enzyme added; 10 mM $MgCl_2$. Lane 2: M1 RNA (2×10^{-8} M); 10 mM $MgCl_2$. Lane 3: M1 RNA (0.1×10^{-8} M) plus C5 protein (2×10^{-8} M); 10 mM $MgCl_2$. Lane 4: No enzyme added; 100 mM $MgCl_2$. Lane 5: M1 RNA (2×10^{-8} M); 100 mM $MgCl_2$. Lane 6: M1 RNA (0.1×10^{-8} M) plus C5 protein (2×10^{-8} M); 100 mM $MgCl_2$. Lane 7: M1 RNA (2×10^{-8} M); 100 mM $MgCl_2$ and 4% polyethylene glycol. Lane 8: M1 RNA (2×10^{-8} M) plus C5 protein (4×10^{-7} M); 100 mM $MgCl_2$. Lane 9: C5 protein (4×10^{-7} M); 10 mM $MgCl_2$.

site of M1 RNA is embedded in a folded structure and that the local environment of the active site is not precisely identical to that of the aqueous buffer in which the whole molecule is dissolved.

Table 2. Catalytic activity of M1 RNA.

M1 RNA active [a]:	
	≥ 20 mM $MgCl_2$
	10 mM $MgCl_2$ plus C5 protein
	10 mM $MgCl_2$ plus 5 mM polyamine
M1 RNA not active:	
	10 mM $MgCl_2$

[a] The table summarizes data of *Guerrier-Takada* et al. [3]. The complete composition of reaction mixtures is given in the reference.

These findings complemented those of *Thomas Cech*'s group[37,38] on self-splicing RNA and started intense speculation about the role RNA may have played in the origin of life. However, our immediate interest was in determining precisely how the enzyme works, what its role is in vivo, and how it manages to recognize 60 or so different substrates in *E. coli* that have no apparent sequence similarity around their sites of cleavage.

Recent Work

Structure

The original model[64] of the secondary structure of M1 RNA has been extensively refined by phylogenetic analysis (Fig. 8) carried out primarily by *Pace* et al.[39] This analysis has not yet yielded a satisfactory correlation between the phenotypes of mutants[40] and features of the secondary structure of M1 RNA or its analogues from other bacteria (see below). However, it does provide the basis for hypotheses about the regions of M1 RNA that are essential for function,[41] as indicated by evolutionary conservation, and it highlights the necessity of determining the three-dimensional features of the structure. To this end, both additional phylogenetic comparisons, utilizing data concerning the homologue of M1 RNA from several eukaryotic species,[42-45] and crystallographic studies are in progress. One observation of continuing interest from these studies is that the evolutionary clock for both the RNA and protein subunits of RNase P seems to be very fast in comparison with that for rRNAs.[46,47] Although the function of RNase P, as judged by the antigenic properties of the protein[48a,b] and its ability to cleave various substrates and to reconstitute active enzyme with subunits from different organisms[3,46,49] has been highly conserved, the nucleotide sequences of the genes for the subunits of the enzyme have drifted extremely rapidly.[45,47]

Mechanism

The detailed mechanism of the reaction catalyzed by RNase P is not known, but two proposals have been made. In one case,[36] a variation of the S_N2 in-line displacement mechanism has been suggested in which a complex between one magnesium ion and six water molecules facilitates the nucleophilic action of a water molecule in solution (Fig. 9).

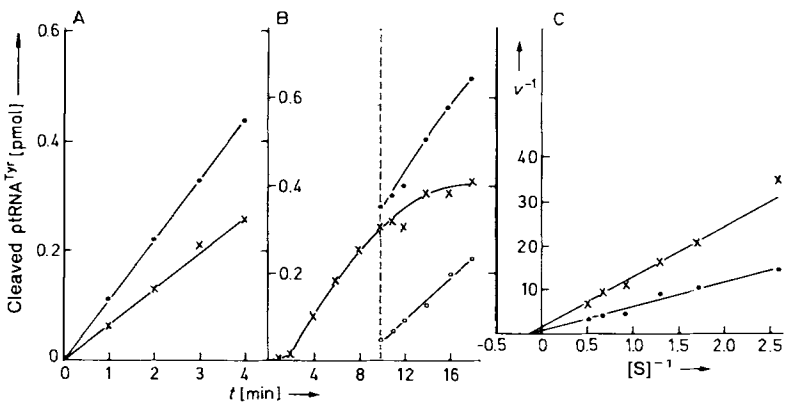

Fig. 7. Kinetic analysis of the reactions of M1 RNA and RNase P with the precursor to $tRNA^{Tyr}$ (pTyr) as substrate. A) Comparison of the kinetics of reconstituted (by dialysis) *E.coli* RNase P in buffer that contained 5 mM $MgCl_2$ with those of M1 RNA in buffer that contained 60 mM $MgCl_2$ that had been treated in the same way. •, RNase P activity; x, M1 RNA activity. B) Kinetics of the reaction catalyzed by M1 RNA in buffer that contained 60 mM $MgCl_2$. M1 RNA was incubated with a fivefold excess of pTyr. Ten minutes after the start of incubation a further threefold excess of pTyr, or buffer alone, was added to the reaction mixture. •, pTyr added after 10 min; x, buffer alone added after 10 min; o, net added pTyr cleaved after 10 min (all in pmol). C) Determination of K_m and V_{max} for the reactions shown in A. A Lineweaver–Burk double-reciprocal plot was constructed from the appropriate kinetic data. •, RNase P in buffer that contained 5 mM $MgCl_2$; x, M1 RNA in buffer that contained 60 mM $MgCl_2$. Units: $[S]^{-1}$ (pmol $\times 5 \times 10^{-4})^{-1}$; v^{-1} [(pmol substrate cleaved per min)$^{-1}$]. (Reprinted with permission from [3].)

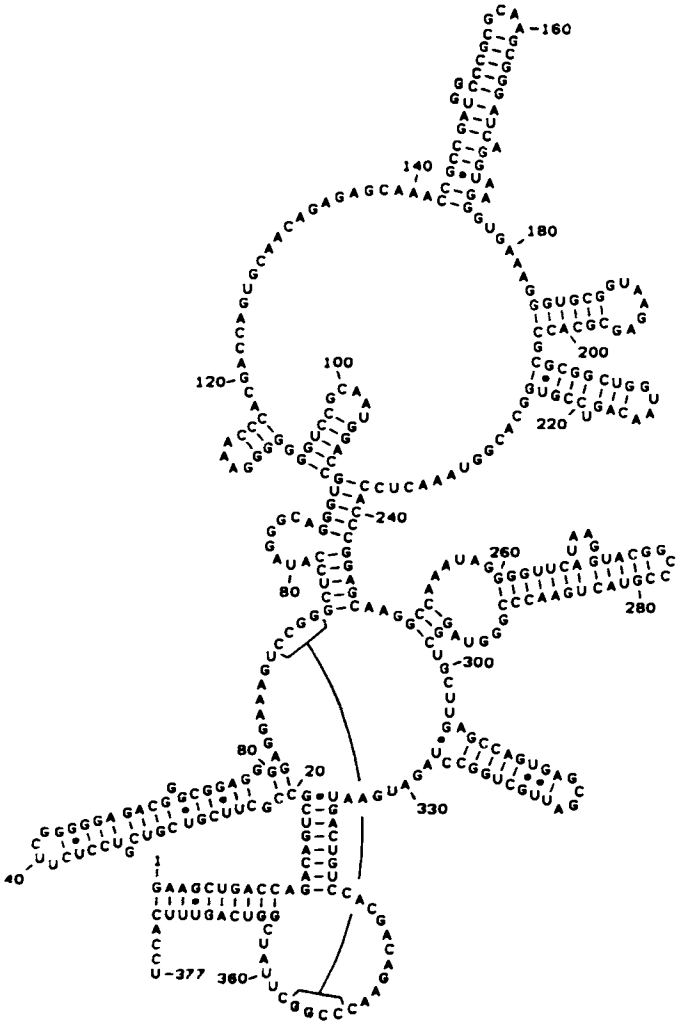

Fig. 8. A model for the secondary structure of M1 RNA based on extensive phylogenetic analysis of the nucleotide sequence of the RNA subunit of RNase P from several eubacteria. (Reprinted with permission from [39].)

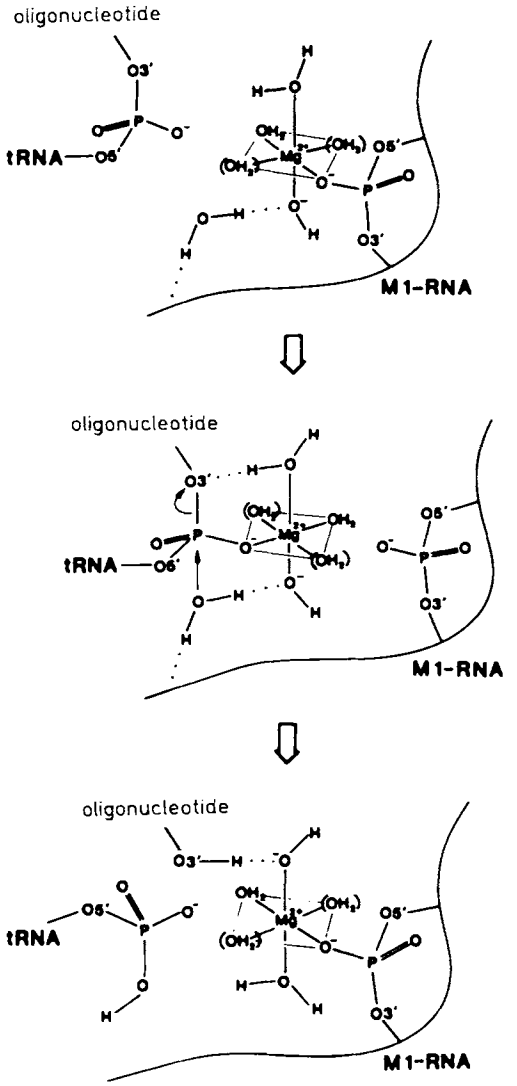

Fig. 9. Hypothetical electronic mechanism of tRNA precursor hydrolysis by M1 RNA of RNase P. The reaction is catalyzed by an Mg–H_2O complex that is initially bound to a phosphate of M1 RNA. $Mg^{2\oplus}$ is formally shown as hexacoordinated, but it may well be tetracoordinated as indicated by the parentheses around the two equatorial water ligands. Top: A water molecule form the solvent that will participate in hydrolysis is positioned by a hydrogen bond to an O or N atom in M1 RNA. Middle and bottom: The tRNA precursor substrate is bound by the water molecule attached to M1 RNA and passes through a transition state prior to cleavage of the "extra" oligonucleotide and prior to the addition of OH to its O5′ terminal phosphate. After the reaction steps shown here, a solvent water chain between the axial ligands of $Mg^{2\oplus}$ recocks the enzyme for the next cycle. (Reprinted with permission from [36].)

Investigations of the rRNA self-splicing reaction in *Tetrahymena* in *Thomas Cech*'s laboratory indicate that the S_N2 mechanism proposed for the RNase P reaction may also be relevant in the self-splicing reaction.[4, 50] In the other proposal for the mechanism of the RNase P reaction,[51] the nucleophile is derived from groups on the surface of the enzyme and the role of the magnesium ion is not as clearly specified. Attempts are underway in our laboratory to test the first model, by the insertion of a phosphothioate bond at the cleavage site and analysis of the stereochemistry of the cleaved product.

While many aspects of the RNase P reaction may be revealed if the crystal structure of the enzyme becomes available, the determination of a crystal structure may prove to be elusive. We have, therefore, embarked on an attempt to identify regions of M1 RNA that are critical for the reaction by cross-linking the substrate to the enzyme by irradiation with ultraviolet light. Such experiments have revealed that a cross-link is formed between a nucleotide close to the site of cleavage in the substrate (C-3; see Fig. 3) and residue C92 in M1 RNA.[52] If C92 is deleted from M1 RNA, the kinetics of the enzymatic reaction and the site of cleavage of particular substrates are significantly altered. Furthermore, the region of secondary structure around C92 in M1 RNA resembles that of the tRNA E site in 23 S rRNA (Fig. 10). Additional studies have shown that this site is important in the binding of the aminoacyl stem of a tRNA precursor to the enzyme and that, as in the binding of tRNA to the E site of 23 S rRNA,[53] the 3′-terminal CCA sequence plays a critical role in the interaction of the enzyme with the substrate. These results, in addition to allowing the identification of domains with similar structural and functional properties in RNA molecules with very different cellular functions, delineate a region of importance for function in M1 RNA and suggest further experiments aimed at a more

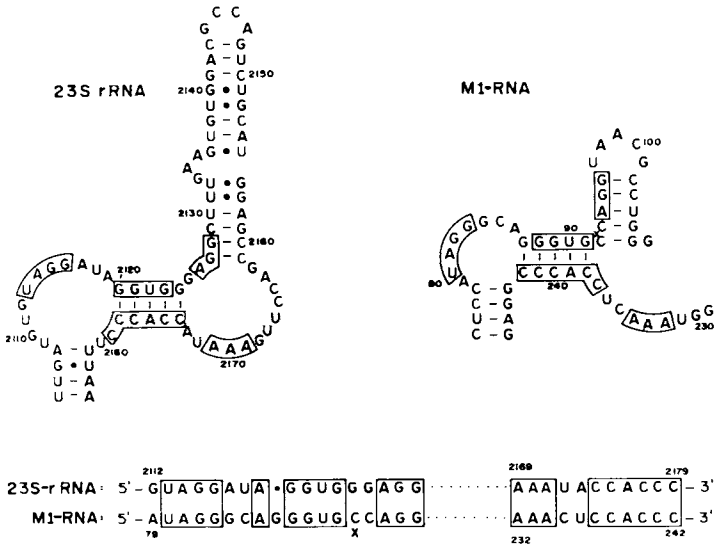

Fig. 10. Comparison of part of the E site of 23 S rRNA with a region in M1 RNA that surrounds the cross-link with the substrate. The secondary structures are taken from [53] and [39]. The "x" marks C92, the nucleotide in M1 RNA that is cross-linked to the substrate. Nucleotides shown in boxes are found in approximately the same relative positions in the structures shown (see [52].)

detailed definition of the interactions between enzyme and substrate and of the particular steps in the enzymatic reaction that involve this region.

Recognition of the Substrate

Early notions of the features important for the recognition by RNase P of its substrate focused either on the possibility of Watson–Crick pairing of nucleotide sequences common to all tRNAs (e.g., CCA and GUUCG) with sequences in M1 RNA[54] or some other, incompletely specified, measuring mechanism that recognizes the three-dimensional structure of the tRNA moiety of the precursor.[55] Results of several experiments indicated that extensive base-pairing between enzyme and substrate was not essential for the enzymatic reaction[54, 56] and attention was focused on the conformation of the substrate in solution. It had been demonstrated early on that RNase P from any one source can cleave tRNA precursors from any other source. Thus, when an unusual tRNA that lacked the D stem and loop was found, namely, $tRNA^{Ser}$ from bovine mitochondria,[57] we examined whether M1 RNA could cleave an analogue of a precursor to that tRNA.

In collaboration with *William McClain*,[58] we showed not only that the D stem and loop were not essential for recognition, but also that the anticodon stem and loop were dispensable, too (Fig. 11). A substrate that consisted merely of a single-stranded region at the 5′ end of a mini-tRNA, containing only the T stem and loop stacked on the aminoacyl acceptor stem, was cleaved almost as efficiently as the parent tRNA precursor from which it was derived. This minimal substrate contains an RNA helix that is analogous to the part of the intact three-dimensional structure of a normal tRNA that contains the T stem stacked on the acceptor stem (Fig. 1). Recently, we have also shown that cleavage by M1 RNA requires neither the loop segment of the structure nor more than six base pairs in the helical region and (in separate experiments) that no more than one "extra" nucleotide at the 5′ terminus is required. While substrates with these features are not cleaved as efficiently as either a normal precursor tRNA or pAT1 (the substrate shown in Fig. 11 that resembles a hairpin), they must, nevertheless, contain sufficient recognition elements to allow the reaction to proceed. All these model substrates have the 3′-terminal CCA sequence and none are cleaved efficiently when the CCA sequence is altered. Therefore, it appears that the CCA sequence, as we had recognized earlier with normal tRNA precursors,[59]

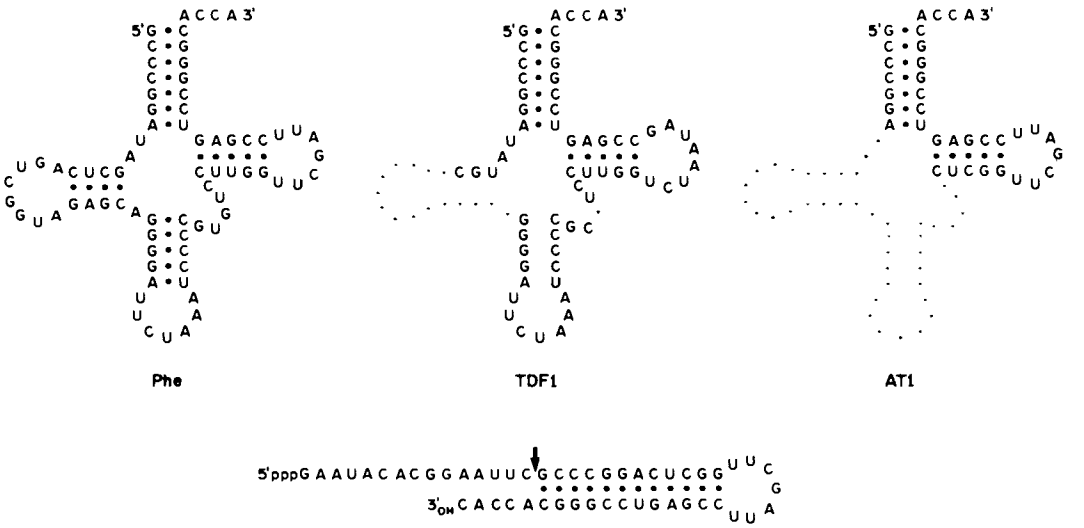

Fig. 11. Structure of mature $tRNA^{Phe}$ and derivatives of it, encoded by synthetic genes. Top: The sequences are shown without the modified nucleotides characteristic of mature $tRNA^{Phe}$ because they are not present in the transcripts made in vitro. The transcripts contain "extra" nucleotides at both ends of the molecules (after [58]). Bottom: Structure of the AT-1 precursor drawn in a stem and loop structure similar to the corresponding region in $tRNA^{Phe}$. The arrows mark the site of cleavage by RNase P or M1 RNA. The sequence of mature AT-1 is shown in the upper part of the figure. (Reprinted with permission from [58].)

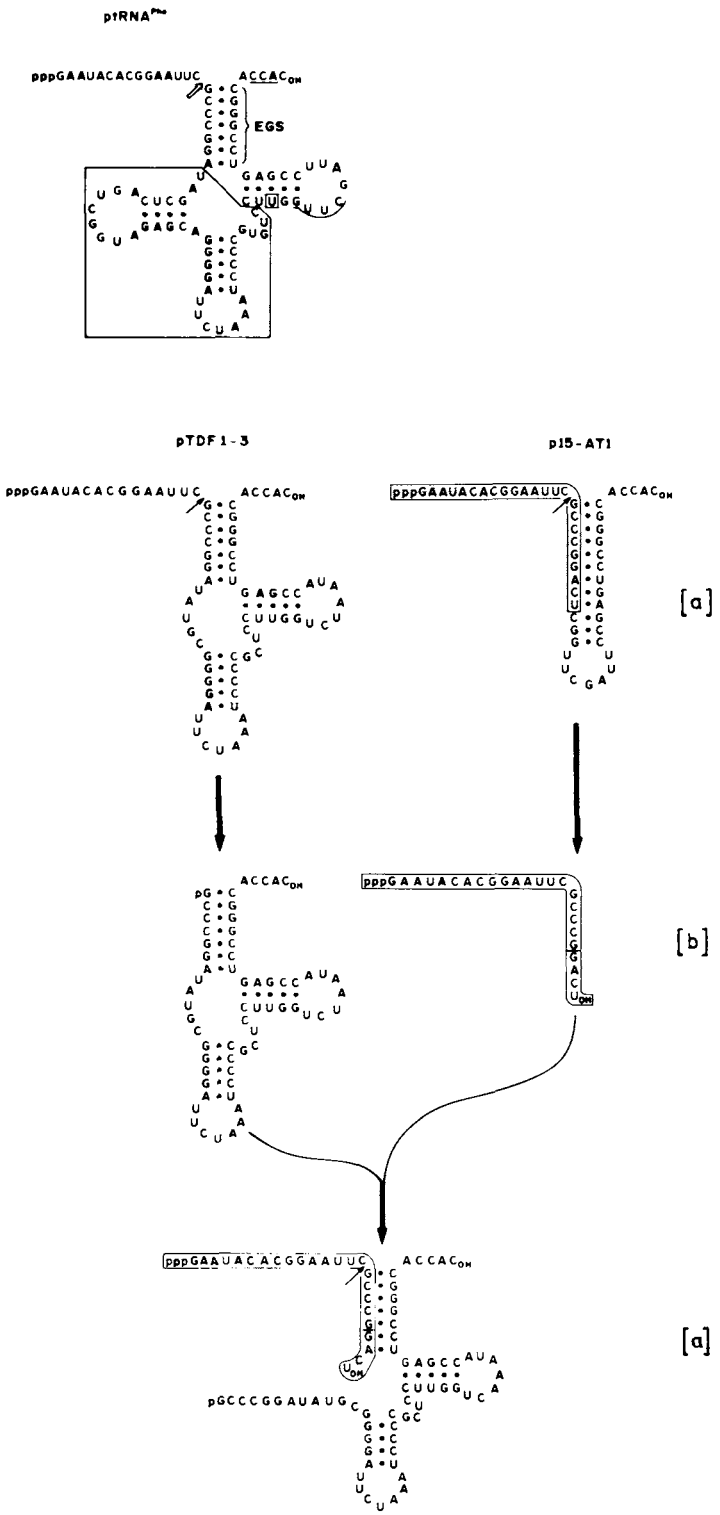

Fig. 12. Scheme for the formation of substrates for RNase P by hybridization of two oligoribonucleotides. TDF-1 (see Fig. 11) was prepared by cleavage by RNase P in vitro of its precursor molecule that had been transcribed in vitro [58]. A portion (boxed sequence) of the precursor to AT-1 (Fig. 11) was prepared by transcription in vitro of a restriction fragment of the DNA that encoded the AT-1 synthetic gene (A.C. Forster and S. Altman, *Science (Washington, D.C.)* (1990), in press). [a], cleaved; [b] uncleaved.

and at least one half turn of a RNA helix play an essential role in recognition of small substrates.

Conclusions from experiments with model substrates have to be tempered by the knowledge that some recognition elements, which appear to play a prominent role in these examples, may not play as important a role and/or may be supplemented by other elements in the normal tRNA precursors found in cells. It is certainly the case that a change in the D stem or anticodon stem of a normal tRNA precursor can have a dramatic effect on the rate of cleavage by RNase P even though these regions of the substrate are entirely absent from the model substrates.

Through the hybridization of two oligoribonucleotides, as shown in Figure 12, we can create and manipulate novel substrates. An "external guide sequence" which can guide RNase P to its target, can be hybridized in theory to any other RNA of known sequence and will form the 3′ or downstream part of the substrate. RNase P should then cleave the hybrid target at the junction between the single- and double-stranded region at the 5′ side of the double-stranded region. This new method presents opportunities to investigate more precisely the details of the recognition mechanism and it also provides, in principle, a means to inactivate any RNA of known sequence in vivo (Fig. 13). Aside from the problem

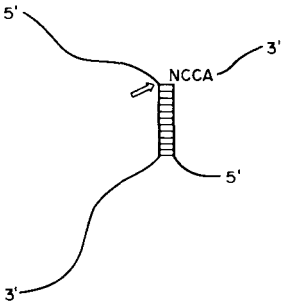

Fig. 13. Targeting of RNA for cleavage by RNase P. An external guide sequence (EGS) is shown by the shorter line ending in NCCA. N is most frequently found to be A in tRNA molecules. The region of the EGS shown as hydrogen-bonded is designed to be complementary to a region of known sequence in the RNA to be targeted.

of the expression of the external guide sequence in vivo, the method does have the advantage that RNase P is already present in cells of all types. Providing that the hybrid can be designed to be compatible with the cleavage-site specificity of the enzyme in the particular host organism of choice, the target RNA should be inactivated.

In this example of the use of one oligoribonucleotide to target another RNA that is to be cleaved by RNase P, substrate recognition by the enzyme resembles, in a formal sense, selection of the site of cleavage by some of the other known RNA catalysts. Group I introns and the satellite and similar RNAs use guide sequences[4,5] in the selection of cleavage sites or to form structures in which a cleavage site becomes defined. In virtually all other respects, these reactions are quite distinct from that carried out by RNase P.

The Past, Present, and Future of RNase P

The discovery of RNA catalysis has led to new hypotheses about the origin of the earliest self-replicating biochemical systems. Models of these early systems rely entirely on RNA

as the genetic material and as the source of catalytic activity (Scheme 2).[6, 7, 10, 11] All this speculation clearly presupposes that what we see in present-day systems reflects, in some manner, the properties of RNA over a billion years ago. Should that indeed be the case, the richness of biochemical mechanisms exhibited by RNA (see Table 1) is impressive and can allow for the development of rather complex systems in the absence of protein and DNA. In this context, we shall allow ourselves to consider very briefly some aspects of the reactions governed by RNase P in vitro.

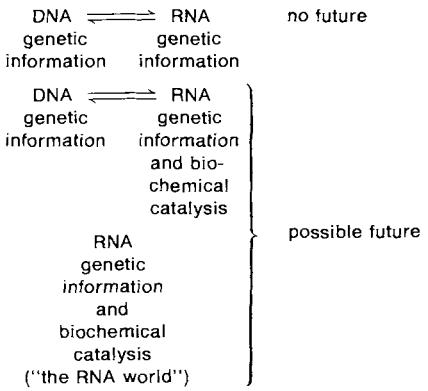

Scheme 2. A representation of three possible schemes of information transfer before proteins were part of the scheme. The mechanisms, nonenzymatic or enzymatic, of information transfer between DNA and RNA are unspecified. The phrase "the RNA world" was coined by *Gilbert* [7].

Although M1 RNA can cleave very simple substrates, it is apparent that these particular cleavage reactions cannot occur in vivo today because such cleavages would occur too frequently in the population of RNA in any cell: that is, the entire population of RNA molecules would be too susceptible to degradation by RNase P. However, one can imagine that in an RNA world, there was considerable advantage to having an RNA molecule that could identify many sites in very long molecules generated by enzymatic or nonenzymatic mechanisms. The proliferation of many smaller molecules from larger ones would give rise to the possibility of a great variety of conformations of RNA in solution, some of which may have endowed RNA with catalytic activity or other useful functions that very long transcripts did not have.

Setting aside for the moment the details of the origin of the genetic code and the appearance of proteins, one can ask why a protein subunit became associated with M1 RNA? We recently showed that the protein subunit of RNase P can alter the site of cleavage and affect the rate of the reaction in a manner sensitive to the nature of the particular substrate being used.[52, 60] Thus, it is possible that proteins may have fine-tuned the site specificity of RNA enzymes by enhancing the rates of reaction at particular sites and with particular substrates. What we see today as the "normal" cleavage sites of RNA enzymes may have been selected for over the eons, in conjunction with the appearance of protein cofactors, as physiological conditions changed during evolutionary time. The "unselected" reactions—for example, those with very small hairpin substrates—became in consequence second- or lower-order reactions and are no longer relevant to events in vivo.

Finally, why do RNA enzymes only cleave phosphodiester bonds? Three answers come readily to mind. First and most trivially, RNA enzymes may cleave or form other classes of bonds and we just have not yet made the critical observations or found the right reaction conditions (the last part of the answer is a generic response to questions about the lack of success in performing any reaction in vitro). Second, it is possible that, in the RNA world, RNA molecules could only cleave or form phosphodiester bonds: it was a primitive world and no other reactions were governed by enzymes. Once proteins appeared on the scene there was no further need to diversify RNA enzymes. Lastly, and most important, the chemistry of RNA enzymes and enzymes with RNA subunits,[61,62] when sufficiently well-understood, may indicate to us that there is a compelling reason why RNA molecules cleave only phosphodiester bonds. The validity, or lack of it, of this last answer can be tested by direct experimentation, and therein lies the work of the next several years.

My indebtedness to so many people makes it impractical to list them all here. Nevertheless, I wish to express my gratitude to my parents, my family, my teachers (especially Leonard Lerman, Mathew Meselson, Sydney Brenner, John D. Smith, and Lee Grodzins), my professional colleagues and collaborators (especially Hugh Robertson and William H. McClain) and my students and co-workers (especially Cecilia Guerrier-Takada) in my laboratory. The taxpayers of the United States, through the agencies of the National Institutes of Health and the National Science Foundation, have generously supported my work.

Received: January 30, 1990 [A 772 IE]
German version: *Angew. Chem. 102* (1990) 735

[1] F. Crick, *Nature (London) 277* (1970) 561–563.
[2] S. Altman, *Nature (London) New Biol. 229* (1971) 19–21.
[3] C. Guerrier-Takada, K. Gardiner, T. Marsh, N. Pace, S. Altman, *Cell (Cambridge Mass.) 35* (1983) 849–857.
[4] T. R. Cech, *Science (Washington, D.C.) 236* (1987) 1532–1539.
[5] S. Altman, *Adv. Enzymol. Relat. Areas Mol. Biol. 62* (1989) 1–36.
[6] J. E. Darnell, W. F. Doolittle, *Proc. Natl. Acad. Sci. USA 83* (1986) 1271–1275.
[7] W. Gilbert, *Nature (London) 319* (1986) 618.
[8] H. D. Robertson, *Nature (London) 322* (1986) 16–17.
[9] F. H. Westheimer, *Nature (London) 319* (1986) 534–535.
[10] A. M. Weiner, N. Maizels, *Proc. Natl. Acad. Sci. USA 84* (1987) 7383–7387.
[11] G. F. Joyce, *Nature (London) 338* (1989) 217–223.
[12] C. R. Woese: *The Origins of the Genetic Code*, Harper and Row, New York 1967.
[13] F. Crick, *J. Mol. Biol. 38* (1968) 367–379.
[14] L. Orgel, *J. Mol. Biol. 38* (1968) 381–393.
[15] S. H. Kim, F. L. Suddath, G. J. Quigley, A. McPherson, J. L. Sussman, A. H. J. Wang, N. C. Seeman, A. Rich, *Science (Washington D.C.) 185* (1974) 435–440.
[16] J. D. Robertus, J. E. Ladner, J. T. Finch, D. Rhodes, R. S. Brown, B. F. C. Clark, A. Klug, *Nature (London) 250*, (1974) 546–551.
[17] J. N. Abelson, M. L. Gefter, L. Barnett, A. Landy, R. L. Russell, *J. Mol. Biol. 47* (1970) 15–28.
[18] R. L. Russell, J. N. Abelson, A. Landy, M. L. Gefter, S. Brenner, J. D. Smith, *J. Mol. Biol. 47* (1970) 1–13.
[19] J. D. Smith, L. Barnett, S. Brenner, R. L. Russell, *J. Mol. Biol. 54* (1971) 1–14.
[20] a) S. Altman, J. D. Smith, *Nature (London) New Biol. 233* (1971) 35–39; b) H. D. Robertson, S. Altman, J. D. Smith, *J. Biol. Chem. 247* (1972) 5243–5251.
[21] a) D. Bernhardt, J. E. Darnell, *J. Mol. Biol. 42* (1967) 43–56; b) R. H. Burdon, *Prog. Nucleic Acids Res. Mol. Biol. 11* (1971) 33–79; c) R. H. Burdon, *Brookhaven Symp. Biol. 26* (1974) 138–153.

[22] B. C. Stark, R. Kole, E. J. Bowman, S. Altman, *Proc. Natl. Acad. Sci. USA 75* (1978) 3717–3721.
[23] T. Ikemura, J. E. Dahlberg, *J. Biol. Chem. 248* (1973) 5024–5032.
[24] P. Schedl, P. Primakoff, *Proc. Natl. Acad. Sci. USA 70* (1973) 2091–2095.
[25] P. Schedl, P. Primakoff, J. Roberts, *Brookhaven Symp. Biol. 26* (1974) 53–76.
[26] H. Ozeki, H. Sakano, S. Yamada, T. Ikemura, Y. Shimura, *Brookhaven Symp. Biol. 26* (1974) 89–105.
[27] H. Sakano, S. Yamada, T. Ikemura, Y. Shimura, H. Ozeki, *Nucleic Acids Res. 1* (1974) 355–371.
[28] W. H. McClain, *Acc. Chem. Res. 10* (1977) 418–425.
[29] J. Carbon, S. Chang, L. L. Kirk, *Brookhaven Symp. Biol. 26* (1974) 26–36.
[30] S. Altman, H. D. Robertson, *Mol. Cell. Biochem. 1* (1973) 83–93.
[31] R. L. Garber, M. A. Q. Siddiqui, S. Altman, *Proc. Natl. Acad. Sci. USA 75* (1978) 635–639.
[32] R. Kole, S. Altman, *Proc. Natl. Acad. Sci. USA 76* (1979) 3795–3799.
[33] R. Kole, S. Altman, *Biochemistry 20* (1981) 1902–1906.
[34] R. Reed, M. Baer, C. Guerrier-Takada, H. Donis-Keller, S. Altman, *Cell (Cambridge Mass.) 30* (1982) 627–636.
[35] J. Fruton, S. Simmonds: *General Biochemistry*, 2nd ed., Wiley, New York 1958, p. 211.
[36] C. Guerrier-Takada, K. Haydock, L. Allen, S. Altman, *Biochemistry 25* (1986) 1509–1515.
[37] T. R. Cech, A. J. Zaug, P. J. Grabowski, *Cell (Cambridge Mass.) 27* (1981) 487–496.
[38] T. R. Cech, B. L. Bass, *Annu. Rev. Biochem. 55* (1986) 599–629.
[39] B. James, G. J. Olsen, J. Lin, N. Pace, *Cell (Cambridge Mass.) 52* (1988) 19–26.
[40] N. Lumelsky, S. Altman, *J. Mol. Biol. 202* (1988) 443–454.
[41] D. S. Waugh, C. J. Green, N. R. Pace, *Science (Washington D.C.) 244* (1989) 1569–1571.
[42] D. L. Müller, N. C. Martin, *Cell (Cambridge Mass.) 34* (1983) 911–917.
[43] G. Krupp, B. Cherayil, D. Frendeway, S. Nishikawa, D. Soll, *EMBO J. 5* (1986) 1697–1703.
[44] J.-Y. Lee, D. R. Engelke, *Mol. Cell. Biol. 9* (1989) 2536–2543.
[45] M. Bartkiewicz, H. Gold, S. Altman, *Genes Dev. 3* (1989) 488–499.
[46] N. P. Lawrence, A. Richman, R. Amini, S. Altman, *Proc. Natl. Acad. Sci. USA 84* (1987) 6825–6829.
[47] H. A. Gold, *Ph. D. Thesis*, Yale University, New Haven, CT USA 1988.
[48] a) H. A. Gold, J. Craft, J. A. Hardin, M. Bartkiewicz, S. Altman, *Proc. Natl. Acad. Sci. USA 85* (1988) 5483–5487; b) M. J. Mamula, M. Baer, J. Craft, S. Altman, *Proc. Natl. Acad. Sci. USA 86* (1990) 8717–8721.
[49] H. A. Gold, S. Altman, *Cell (Cambridge Mass.) 44* (1986) 243–249.
[50] J. A. McSwiggen, T. R. Cech, *Science (Washington D.C) 244* (1989) 679–683.
[51] C. I. Reich, G. J. Olsen, B. Pace, N. R. Pace, *Science (Washington D.C.) 239* (1988) 178–181.
[52] C. Guerrier-Takada, N. Lumelsky, S. Altman, *Science (Washington D.C.) 246* (1989) 1578–1584.
[53] D. Moazed, H. F. Noller, *Cell (Cambridge Mass.) 57* (1989) 585–597.
[54] C. Guerrier-Takada, S. Altman, *Cell (Cambridge Mass.) 45* (1986) 177–183.
[55] A. L. M. Bothwell, B. C. Stark, S. Altman, *Proc. Natl. Acad. Sci. USA 73* (1976) 1912–1916.
[56] M. F. Baer, R. M. Reilly, G. M. McCorkle, T.-Y. Hai, S. Altman, U. L. RajBhandary, *J. Biol. Chem. 263* (1988) 2344–2351.
[57] M. H. L. de Bruijn, A. Klug, *EMBO J. 2* (1983) 1309–1321.
[58] W. H. McClain, C. Guerrier-Takada, S. Altman, *Science (Washington D.C.) 238* (1987) 527–530.
[59] C. Guerrier-Takada, W. H. McClain, S. Altman, *Cell (Cambridge Mass.) 38* (1984) 219–224.
[60] C. Guerrier-Takada, A. van Belkum, C. W. A. Pleij, S. Altman, *Cell (Cambridge Mass.) 53* (1988) 267–272.
[61] D. D. Chang, D. A. Clayton, *Science (Washington D.C.) 235* (1987) 1178–1184.
[62] C. W. Greider, E. H. Blackburn, *Cell (Cambridge Mass.) 51* (1987) 887–898.
[63] J. D. Watson, N. H. Hopkins, J. W. Roberts, J. A. Steitz, A. M. Weiner: *Molecular Biology of the Gene*, 4th ed., Benjamin/Cummings, Menlo Park, CA, 1987, p. 388.
[64] C. Guerrier-Takada, S. Altman, *Biochemistry 23* (1984) 6327–6334.
[65] C. Guthrie, J. G. Seidman, S. Altman, B. G. Barrell, J. D. Smith, W. H. McClain, *Nature (London) New Biol. 246* (1973) 6–11.

Self-splicing and Enzymatic Activity of an Intervening Sequence RNA from *Tetrahymena* (Nobel Lecture)**

By Thomas R. Cech*

Introduction

A living cell requires thousands of different chemical reactions to utilize energy, move, grow, respond to external stimuli, and reproduce itself. While these reactions take place spontaneously, they rarely proceed at a rate fast enough for life. Enzymes, biological catalysts found in all cells, greatly accelerate the rates of these chemical reactions and impart to them extraordinary specificity. In 1926, *James B. Sumner* crystallized the enzyme urease and found that it was a protein. Skeptics argued that the enzymatic activity might reside in a trace component of the preparation rather than in the protein,[1] and it took another decade for the generality of *Sumner*'s finding to be established. As more and more examples of protein enzymes were found, it began to appear that biological catalysis would be exclusively the realm of proteins. In 1981 and 1982, my research group and I found a case in which RNA, a form of genetic material, was able to cleave and rejoin its own nucleotide linkages. This self-splicing RNA provided the first example of a catalytic active site formed of ribonucleic acid. This lecture gives a personal view of the events that led to our realization of RNA self-splicing and the catalytic potential of RNA. It provides yet another illustration of the circuitous path by which scientific inquiry often proceeds. The decision to expend so many words describing the early experiments means that much of our current knowledge about the system will not be mentioned. For a more comprehensive view of the mechanism and structure of the *Tetrahymena* self-splicing RNA and RNA catalysis in general, the reader is directed to a number of recent reviews.[2-7] Possible medical and pharmaceutical implications of RNA catalysis have also been described recently.[8]

Why *Tetrahymena*?

In the pre-recombinant DNA era of the early 1970s, much of the research on the structure and function of eukaryotic chromosomes utilized entire genomes as experimental systems. My own research with *John Hearst* in Berkeley and with *Mary Lou Pardue* at the Massachusetts Institute of Technology (MIT) concerned the organization of DNA sequences and chromosomal proteins in the mouse genome. During my stay at MIT, I began to be dissatisfied with this global approach and became interested in the prospect of being able to dissect the structure and expression of some particular gene. Thus, when I set up my own laboratory in Boulder in 1978, I turned my attention entirely to the rDNA (gene for the large ribosomal RNAs) of the ciliated protozoan *Tetrahymena* (Fig. 1).

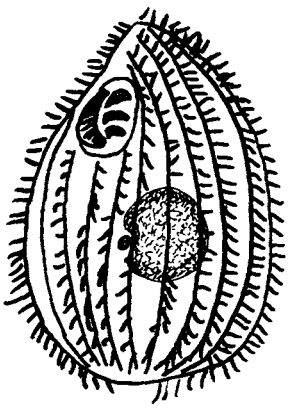

Fig. 1. *Tetrahymena thermophila*, showing the transcriptionally active macronucleus and the germ-line micronucleus.

Unlike most nuclear genes, which are embedded in giant chromosomes, the genes for rRNA in *Tetrahymena* are located on small DNA molecules in the nucleoli; they are extrachromosomal.[9, 10] Furthermore, in the transcriptionally active macronucleus the gene is amplified to a level of approximately 10000 copies.[11] These properties made it possible to purify a significant amount of the rDNA. The ability to purify the gene was not in itself a major attraction, because by this time the availability of recombinant DNA techniques ensured that no gene would long escape isolation and sequence analysis. Rather, the attractive feature was the prospect of being able to isolate the gene complete with its associated structural proteins and proteins that regulated transcription (the synthesis of an RNA copy by RNA polymerase).

One feature of the *Tetrahymena* rDNA that was of only peripheral interest to me at that time was the presence of an intervening sequence (IVS) or intron, which interrupted the rRNA-coding sequences of the rDNA of some strains of *Tetrahymena pigmentosa*.[12] In the course of mapping the RNA-coding regions of the rDNA of *Tetrahymena thermophila, Don Rio* and I found that this species also harbored an IVS in its rDNA (Fig. 2;[13] independently described by *Din* et al.[14]). Although intervening sequences had been discovered only two years before by *Phil Sharp*'s lab at MIT and a group from Cold Spring Harbor Laboratory, there were already a large number of examples. Thus, the finding of another IVS was hardly cause for us to be distracted from our plan to investigate the proteins that regulated rDNA transcription.

[*] Prof. T. R. Cech
Howard Hughes Medical Institute
Department of Chemistry and Biochemistry
University of Colorado
Boulder, CO 80309-0215 (USA)

[**] Copyright © The Nobel Foundation, 1990. We thank the Nobel Foundation, Stockholm, for permission to print this lecture.

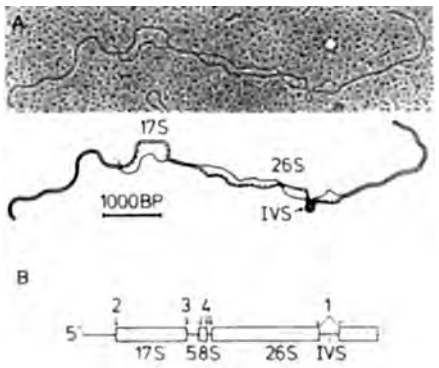

Fig. 2. A) Visualization of the RNA-coding portions of the *T. thermophila* rDNA by electron microscopy. The mature, processed rRNA was hybridized to the DNA under R-loop conditions. In the interpretation, each solid line indicates a single strand of DNA and each dashed line a strand of RNA. (Reproduced from [13].) BP = base pair. B) The pre-rRNA, thin lines representing portions that are removed during processing and open boxes representing the mature rRNA sequences. Numbered arrows indicate the usual order of RNA processing events: 1, splicing; 2–4, endonucleolytic cleavages.

RNA Splicing in Vitro

The first step towards biochemical dissection of the transcriptional process was to see if rRNA synthesis would proceed in a crude cell-free system. We isolated nuclei from *T. thermophila* (the nuclei provided both the RNA polymerase and the ribosomal chromatin templates) and incubated them with the nucleoside triphosphates and salts necessary for transcription. We also included α-amanitin, a mushroom toxin known to inhibit the polymerases that transcribe mRNA, tRNA, and other small RNAs, which enabled us to focus on synthesis of the large rRNA.

When the products of these in vitro transcription reactions were separated by gel electrophoresis, they were found to consist of a somewhat heterogeneous distribution of high-molecular-weight RNA (≥ 26 S), the size expected for full-length pre-rRNA (Fig. 3). In addition, there was a discrete low-molecular-weight product (ca. 9 S). The small RNA accumulated post-transcriptionally.[15] Thus, it seemed likely to be one of several short regions of the pre-rRNA that was cut out and ultimately discarded during the maturation process. These candidate regions included an external transcribed spacer at the 5′ end, the internal transcribed spacers flanking the 5.8 S rRNA, and the IVS (cf. Fig. 2B).

Driven more by curiosity than by any conviction that the results would be of central importance to our research goals, I encouraged *Art Zaug* to identify the sequences encoding the small RNA. He confirmed that the small RNA was encoded by the rRNA gene, and then mapped it to the intervening sequence.[15, 16]

Fig. 3. Transcription and splicing of pre-rRNA in vitro in isolated *T. thermophila* nuclei. Lanes 1–4: RNA produced by incubation of nuclei at 30 °C for times ranging from 5 to 60 min. The 0.4-kilobase species is the excised IVS RNA. Lanes 5 and 6: Purified *Tetrahymena* 26 S and 17 S rRNAs, serving as molecular weight standards. RNA was analyzed by polyacrylamide gel electrophoresis. (Reproduced from [15].)

This was a finding of considerable excitement: the intervening sequence, synthesized as part of the pre-rRNA in our in vitro transcription reactions, was also being cleanly excised from the pre-rRNA in vitro. Despite a great deal of interest in the mechanism of RNA splicing,[17–20] in only one other case—pre-tRNA in yeast—had RNA splicing been confirmed to occur in vitro.[21, 22] It seemed reasonable that rRNA splicing in *Tetrahymena* might follow a quite different path than tRNA splicing in yeast, so that detailed study of both systems would be justified.

Furthermore, in each *Tetrahymena* cell there were 10 000 identical genes, each pumping out unspliced pre-rRNA at the rate of one copy per gene per second. I reasoned that the nuclei might contain an unusually high concentration of the splicing enzyme to accomplish so much reaction, which could facilitate isolation of the first splicing enzyme. Little did we guess that the splicing "enzyme" would not exist in the traditional sense, but that something much more interesting lay in wait for us.

Thomas R. Cech, born on December 8, 1947, studied chemistry at Grinnell College, Iowa (B. A., 1970) and at the University of California, Berkeley (Ph. D., 1975). Following postdoctoral research in the Department of Biology at MIT, he joined the faculty of the University of Colorado, Boulder, in 1978. His finding of self-splicing RNA and subsequent analysis of the mechanisms of RNA catalysis have led to many national and international awards and prizes, culminating in the Nobel Prize in Chemistry in 1989. In 1987, Dr. Cech was elected to the National Academy of Sciences (USA). He remains at the University of Colorado, where he is American Cancer Society Professor and Investigator, Howard Hughes Medical Institute.

Self-splicing Unrecognized

Our strategy for purifying the splicing enzyme was conventional. We would find conditions in which pre-rRNA transcription occurred but splicing was inhibited, and purify the accumulated pre-rRNA to use as a substrate. We would then treat the pre-rRNA with extracts of *Tetrahymena* nuclei, which we already knew contained splicing activity, and would use gel electrophoresis to monitor the splicing reaction. Finally, we would obtain ever-purer subfractions of the nuclear extract that retained activity, eventually isolating the splicing enzyme.

Isolation of unspliced pre-rRNA substrate proved to be straightforward.[23] *Art Zaug* purified this RNA by standard SDS-phenol (SDS = sodium dodecyl sulfate) extraction and used it in a series of RNA splicing reactions. One set of test tubes contained substrate RNA and nuclear extract dissolved in the same solution of simple salts and nucleotides that had been conducive to RNA transcription and splicing in our earlier experiments with intact nuclei. Another tube, containing the same components except with the nuclear extract omitted, was to serve as the "splicing minus" control.

The very first attempt was successful. The RNA in the tubes containing the nuclear extract gave rise to the small band of RNA characteristic of the IVS. Surprisingly, however, the control RNA incubated only in salts and nucleotides produced the same amount of IVS. "Well, Art, this looks very encouraging, except you must have made some mistake making up the control sample." Yet several careful repetitions of the experiment gave the same result: release of the IVS occurred independently of the addition of nuclear extract and therefore apparently independently of any enzyme. I became concerned that we weren't observing RNA splicing at all; perhaps the RNA we had been calling "precursor" had already been spliced in vivo, and what we were observing in vitro was some disaggregation or release of the IVS from already-spliced RNA. Clearly, the reaction would be worthy of further pursuit only if we could show that a chemical transformation was occurring in vitro, and that it was the same cutting and rejoining that occurred in the living cell. We would have to teach ourselves some RNA chemistry.

The Mystery of the Extra G

To verify the accuracy of RNA splicing in nuclei, we decided to determine the nucleotide sequence of the IVS RNA product. (It was not obvious that this would be particularly illuminating, since we had already shown that the IVS product came from the IVS region of the rDNA and that, within the error limits of our measurements, it was the correct size to account for the entire IVS.) When *Art Zaug* labeled the RNA on its 5′ end with ^{32}P and subjected it to sequencing reactions, he determined a sequence 5′-GAAAUAGNAA ... (where N represents an unidentified nucleotide). The DNA sequence across the exon–IVS junction had been reported earlier for *T. pigmentosa* by *Wild* and *Sommer*[24] and was being determined for *T. thermophila* by *Nancy Kan* in *Joe Gall*'s laboratory. The *T. thermophila* DNA sequence predicted that the IVS RNA would begin with 5′-AAAUAGCAA ...

Thus, our RNA sequence was a perfect match to the DNA sequence except for the extra G residue on its 5′ end. *Art Zaug* meticulously checked and rechecked the identity of this terminal nucleotide using a variety of enzyme treatments and chromatography systems until there was no doubt: the IVS RNA began with an ordinary guanosine residue, linked to the next nucleotide by a standard 3′–5′ phosphodiester bond such as that produced by RNA polymerase. Clearly the *Gall* lab, known for the high quality of their science, must have made an error. We telephoned them, advising them that they had determined most of the sequence correctly but had apparently missed one G right at the 5′ end of the IVS. Much to our surprise, they defended every nucleotide of their sequence: no ambiguity in the DNA sequence, at least in that region, and no chance of a G at the 5′ splice site.

At about the same time, I was working to define the minimum components necessary for the release of the IVS from pre-rRNA. The original experiments had been done in a "transcription cocktail" that included the four nucleoside triphosphates, building blocks for RNA synthesis. I found that removal of three of the NTPs had no effect on the reaction, but the fourth, GTP, was required in micromolar concentration. In addition, IVS release required $MgCl_2$ and was stimulated by certain salts such as $(NH_4)_2SO_4$.

Was it a coincidence that GTP, the nucleotide required for IVS release in our simple in vitro system, was also the nucleotide that was found unexpectedly at the 5′ end of the excised IVS? Or might there be a causal relationship between the two observations? The obvious hypothesis was that GTP was required so that it could be added to the 5′ end of the IVS during splicing. The test was simple: mix ^{32}P-labeled GTP with unlabeled pre-rRNA, and look for labeling of the IVS RNA concomitant with its excision. The experiment was the strangest I had ever performed. On the one hand, its success was a straightforward prediction from our existing knowledge of the system. On the other hand, it seemed incredibly naive and unrealistic to expect that simple mixing of a nucleotide with phenol-extracted, proteinase-treated RNA could possibly result in formation of a covalent bond. I certainly didn't want to be embarrassed in front of my graduate students and colleagues by the failure of such an experiment, so I did it very quietly.

The next day I ran the gel, exposed it for autoradiography, and developed the X-ray film. In the sample containing ^{32}P-GTP plus $MgCl_2$ there was a bright signal of radioactivity at the position of the IVS RNA. In a sample containing ^{32}P-GTP but no $MgCl_2$, and in a sample in which ^{32}P-ATP had been substituted for the ^{32}P-GTP, there was no labeled IVS.

Over the next weeks, we confirmed several major features of the reaction. GTP addition was stoichiometric, one GTP per IVS RNA. The GTP was added precisely to the 5′ end of the IVS by a normal 3′–5′ phosphodiester bond. Finally, the triphosphate was unnecessary; GMP and even guanosine were active. The last of these observations eliminated one otherwise very reasonable hypothesis, that the GTP was providing an energy source for ligation much as ATP is used by phage T4 RNA ligase. Had that been the case, forms such as guanosine and GMP, which are missing the phosphoanhydride moiety, would have been inactive.

It took only a few moments of thought to devise a simple splicing pathway that integrated our new information about

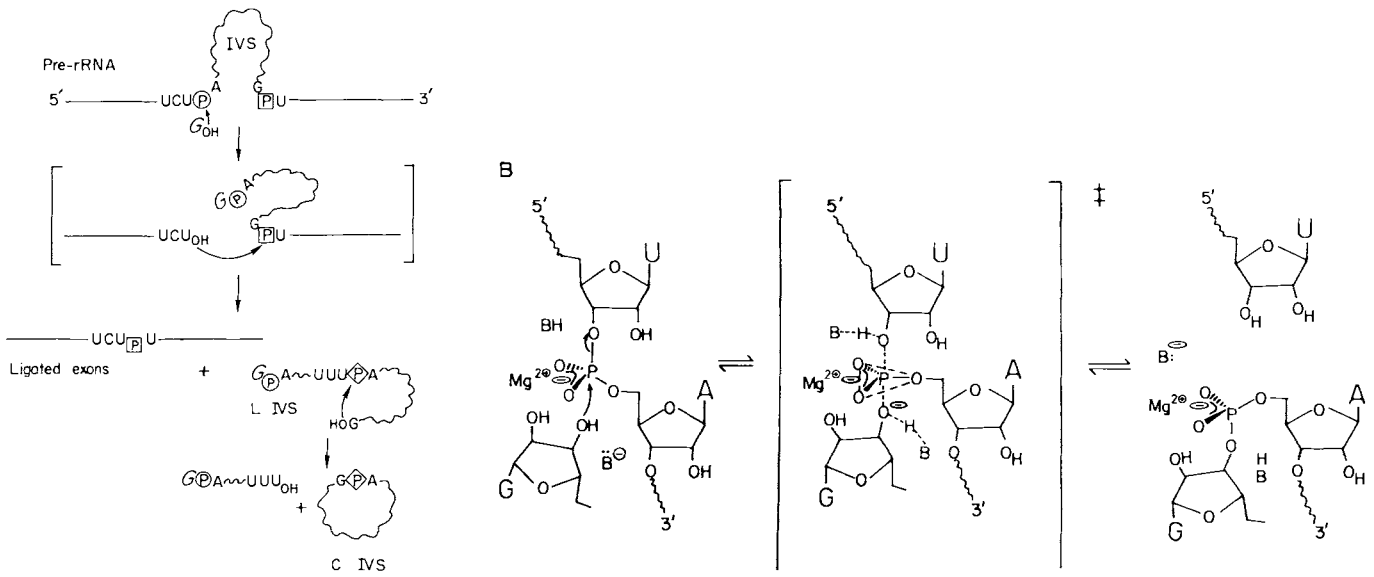

Fig. 4. A) Self-splicing of the *Tetrahymena* pre-rRNA by consecutive transesterification reactions. Straight lines, exons (mature rRNA sequences); wavy line, IVS; circle, 5′ splice-site phosphate; square, 3′ splice-site phosphate; diamond, cyclization site phosphate. B) Model for the initial step involving nucleophilic attack by the 3′-hydroxyl group of guanosine on the phosphorus atom at the 5′ splice site. The hypothesis of an in-line, S_N2 (P) reaction with inversion of configuration around phosphorus was subsequently confirmed [31]. The hypotheses of acid-base catalysis and coordination of $Mg^{2\oplus}$ to the phosphate, enhancing the electrophilicity of the phosphorus atom and stabilizing the trigonal-bipyramid transition state, are untested. (Reproduced from [3].)

the reaction. Addition of guanosine to the phosphorus atom at the 5′ splice site must be occurring by a transfer of phosphate esters, or transesterification reaction (Fig. 4A). Such a reaction would free the 5′ exon, leaving a new 3′-hydroxyl group at its 3′ end. The simplest way to proceed from such proposed intermediates to the final observed products was to invoke a second transesterification reaction: attack of the 3′ hydroxyl of the 5′ exon at the 3′ splice site. Thus, a single active site capable of promoting transesterification could be responsible for the entire splicing reaction.

The model shown in Figure 4A has undergone little change since we first described it in 1981 and drew a more explicit version in 1982.[23, 25] It has been a good predictor of a great many other IVS-catalyzed reactions since then.[26, 27] Furthermore, the model has been strongly bolstered by the isolation and characterization of the proposed intermediates,[28] by the demonstration of the reversibility of the reactions,[29, 30] and by determination of the stereochemical course.[31, 32] An atomic-level model of transesterification occurring by an S_N2 (P) mechanism is presented in Figure 4B.

Self-splicing Recognized

The guanosine-addition reaction provided us with the proof we needed: specific RNA bond breakage and formation were occurring in our simple in vitro splicing reaction. Such a chemically difficult reaction between very unreactive molecules certainly had to be catalyzed. But what was the catalyst?

Our first hypothesis was that the splicing activity was a protein tightly bound (perhaps even covalently bonded) to the pre-rRNA isolated from *Tetrahymena* nuclei. This would have to be a very unusual protein–RNA complex to survive the multiple forms of abuse to which we had subjected it: boiling in the presence of the detergent SDS, SDS-phenol extraction at temperatures as high as 65 °C, and extensive treatment with several nonspecific proteases (Fig. 5). That we took this hypothesis seriously provides an indication of how deeply we were steeped in the prevailing wisdom that only proteins were capable of highly efficient and specific biological catalysis.

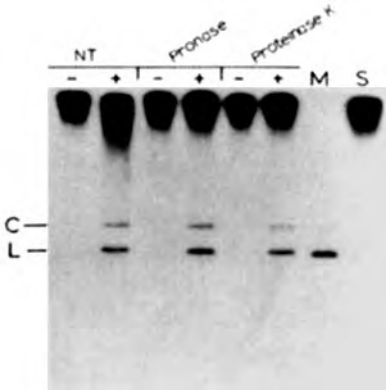

Fig. 5. IVS RNA excision and cyclization activities are resistant to protease treatment. Lane S: Pre-rRNA, purified by SDS-phenol extraction. This RNA was then treated exhaustively with proteases or not treated (NT). Incubation with GTP was performed, in the absence of $MgCl_2$ (lanes −) or with 10 mM $MgCl_2$ (lanes +). Excision of the IVS RNA as a linear molecule (L) and subsequent conversion to a circular form (C) were undiminished by protease treatment. Lane M: Isolated linear and circular IVS RNAs. (Reproduced from [96].)

In the same paper, we described an alternative hypothesis:[23]

The resistance of the splicing activity to phenol extraction, SDS and proteases can also be interpreted in a

more straightforward manner. The rRNA precursor might be able to undergo splicing without the participation of a protein enzyme. A portion of the RNA chain could be folded in such a way that it formed an active site or sites that bound the guanosine cofactor and catalyzed the various bond-cleavage and ligation events. If one of the RNA molecules produced in the reaction (for example, the free IVS) retained its activity and catalyzed additional splicing events, then it would be an example of an RNA enzyme.

As we accumulated negative result upon negative result trying to identify a protein stuck to the pre-rRNA, the alternative "RNA only" hypothesis began to appear more and more attractive. But how could we obtain a positive result to prove it?

The best strategy we could devise was to synthesize the RNA in as artificial a manner as possible, so that it was never in contact with the *Tetrahymena* cells that up to now had been our sole source of the RNA. Complete chemical synthesis of an RNA the size of the pre-rRNA (or even the size of the IVS) was and still is beyond the scope of available technology. The next best approach was to synthesize RNA from a recombinant DNA template using purified RNA polymerase.

A bacterial plasmid (Fig. 6) encoding the IVS and a portion of the flanking rRNA sequences, situated so as to allow

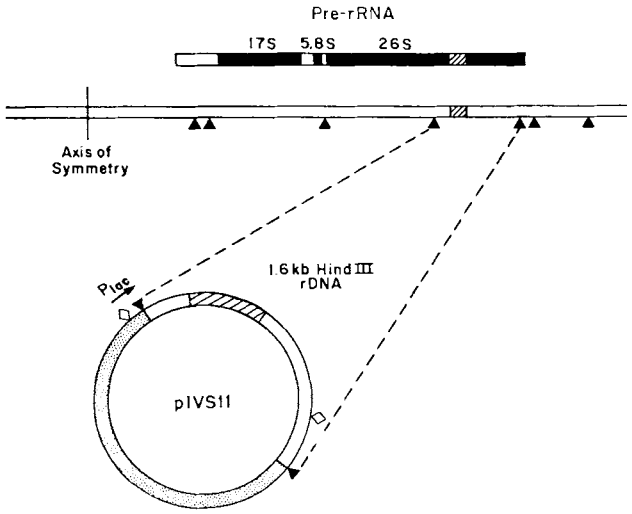

Fig. 6. Plasmid constructed to enable synthesis of an artificial, shortened version of the pre-rRNA. Top: Diagram of the natural pre-rRNA, with transcribed spacers shown as open boxes, mature rRNA sequences as solid boxes, and the IVS as a hatched box. Middle: The *T. thermophila* rDNA. One half of a palindromic rDNA molecule is shown. Bottom: Plasmid pIVS11 containing the 1.6-kilobase Hind III fragment of the rDNA inserted adjacent to P_{lac}, a promotor for transcription by *E. coli* RNA polymerase. Restriction endonuclease sites are Hind III (▲) and *Eco* RI (◇). (Adapted from [34].)

transcription by *Escherichia coli* RNA polymerase, was already being constructed in the lab by *Kelly Kruger*. The original purpose was to facilitate synthesis of large quantities of pre-rRNA substrate for isolation of the splicing enzyme. The cloning took longer than any of us had anticipated, such that by the time it was accomplished early in 1982 we were desperate to have the plasmid for a different purpose: to produce synthetic pre-rRNA for the self-splicing test.

The plasmid was grown up in *E. coli*, carefully deproteinized, and incubated with purified *E. coli* RNA polymerase under conditions that we already knew were inhibitory for splicing. The polymerase was then destroyed and the RNA purified by gel electrophoresis under denaturing conditions. Upon addition of GTP, $MgCl_2$, and salt, the IVS RNA was released from this artificial, shortened pre-rRNA. The site at which GTP broke the RNA chain was exactly the position that served as the 5′ splice site in vivo, providing some confidence that self-splicing was relevant to splicing as it occurred in the living cell.

We held a relatively subdued celebration in the lab. Between sips of champagne we compiled a list of possible general names for RNA molecules able to lower the activation energy for specific biochemical reactions. It was then that we coined the term "ribozyme" for a ribonucleic acid with enzymelike properties.

RNA in Circles

Concurrent with our studies of pre-rRNA splicing in isolated nuclei, we were pursuing a post-splicing phenomenon: the conversion of the excised intervening-sequence RNA into a circular RNA molecule in isolated *Tetrahymena* nuclei.[33] The circular form survived treatment with protease and various denaturants, which suggested that it was a covalently closed circle of RNA. As *Paula Grabowski*, then a graduate student in the laboratory, characterized the cyclization reaction, she found that it occurred with extensively deproteinized RNA in a simple buffered $MgCl_2$ solution. I dismissed her original observation of protein-free cyclization as being an artifact of incomplete denaturation of the linear RNA. Yet, as the experiments proved reproducible, I began to derive some solace in the knowledge that two researchers, *Zaug* and *Grabowski*, studying two different reactions, splicing and cyclization, were both finding activity in the absence of added protein. Having two strange results somehow made me more comfortable than having just a single strange result. The two sets of observations came together when we found that the plasmid transcripts that underwent self-splicing produced IVS RNA that underwent self-cyclization.[34]

The circular IVS RNA was not formed by end-to-end joining of the linear form. Instead, the 3′ end of the linear IVS attacked an internal phosphorus atom near the 5′ end of the molecule, clipping off a short oligonucleotide in the process (Fig. 4A). Thus cyclization, like RNA splicing, occurred by transesterification.[26]

How Does the RNA Do It?

At first glance, RNA seemed ill-suited to be a catalyst. With its four rather similar bases, RNA would appear greatly limited in its ability to form a specific substrate-binding pocket. In contrast, the 20 amino acids found in proteins explore a wide range of sizes and shapes, hydrophilicity and hydrophobicity. In terms of promoting chemistry, RNA has a dearth of functional groups that are ionizable near neutral

pH, whereas proteins have histidine and cysteine (pK_a's in the range of 6–8). How, then, was the *Tetrahymena* IVS able to catalyze transesterification?

The first glimpse of the catalytic mechanism came from detailed studies of the guanosine requirement. *Brenda Bass* tested every available guanosine analogue and found great variation in their activity.[35, 36] Derivatives carrying bulky substituents on the 7 or 8 position of the guanine base or on the 5′ position of the ribose sugar were as active as guanosine, indicating that these positions did not interact with the IVS RNA. Other derivatives were fully active but only at high concentration, or were inactive as substrates but acted as competitive inhibitors of the reaction of guanosine. Using the K_m or K_i of these guanosine analogues, we could assign free energy contributions to individual functional groups of guanosine. All the data pointed to the IVS containing a well-behaved binding site for guanosine. The site has recently been located within the IVS in elegant work by *Michel* et al.[37]

The existence of a G-binding site explained the high specificity for guanosine. In addition, by orienting the nucleophile with respect to the 5′-splice-site phosphate, the G site would contribute substantially to rate acceleration. RNA catalysis was suddenly in a familiar context; the loss of entropy and orientation of reacting groups achieved by formation of a specific enzyme–substrate complex is central to catalysis by protein enzymes.[38, 39]

The other reactant in the first transesterification step, the phosphorus atom at the 5′ splice site, is also held in place by a binding interaction. As first proposed by *Davies* et al.[40] and also apparent in models of *Michel* et al.,[41] a 5′ exon-binding site within the IVS base-pairs to the last few nucleotides of the 5′ exon. This pairing interaction specifies the site of guanosine addition and also holds the 5′ exon in place for the second step of splicing, exon ligation.[42–45]

The IVS does much more than simply hold the reacting groups in place. In the absence of guanosine, hydrolysis occurs specifically at the splice-site phosphodiester bonds, producing 5′-phosphate/3′-hydroxyl termini.[28, 46] A 3′ hydroxyl is the same as the product of self-splicing but opposite to the product of random alkaline hydrolysis of RNA. This site-specific hydrolysis reaction reflects the ability of the catalytic center of the IVS to activate the splice-site phosphates (or perhaps activate the nucleophile, in which case it must be able to activate $OH^{\ominus}$ as well as the hydroxyl of guanosine). While the structural basis of this activation is unknown, reasonable hypotheses include stabilization of the pentacoordinate transition-state structure of the phosphate and specific coordination of a $Mg^{2\oplus}$ ion.[3, 46–49] Once again, in a general sense the RNA catalyst is recapitulating a major catalytic strategy of protein enzymes, or vice versa.

Tetrahymena Is Not Alone

While we were intently characterizing splicing of the *Tetrahymena* IVS, we were also wondering when (and perhaps if) related intervening sequences would be found in other organisms. The differences in nucleotide sequences near the splice sites made it seem unlikely that *Tetrahymena* rRNA splicing would be related to nuclear tRNA or mRNA splicing. The related intervening sequences came from an unexpected direction: yeast mitochondria. This was unanticipated because mitochondria, thought to have arisen from symbiotic prokaryotes, do not usually have genes or modes of gene expression similar to those of eukaryotes. Furthermore, yeast is evolutionarily extremely distant from *Tetrahymena*.

In 1982, several groups identified short sequence elements that were conserved among a group of fungal mitochondrial intervening sequences.[40, 41, 50] Furthermore, both the Michel group[41] and the Davies group[40] had proposed that the conserved sequence blocks interacted to form a common set of short base-paired regions, serving to fold the intervening sequences into the same fundamental secondary structure (Fig. 7, top). *Michel* called these the group I in-

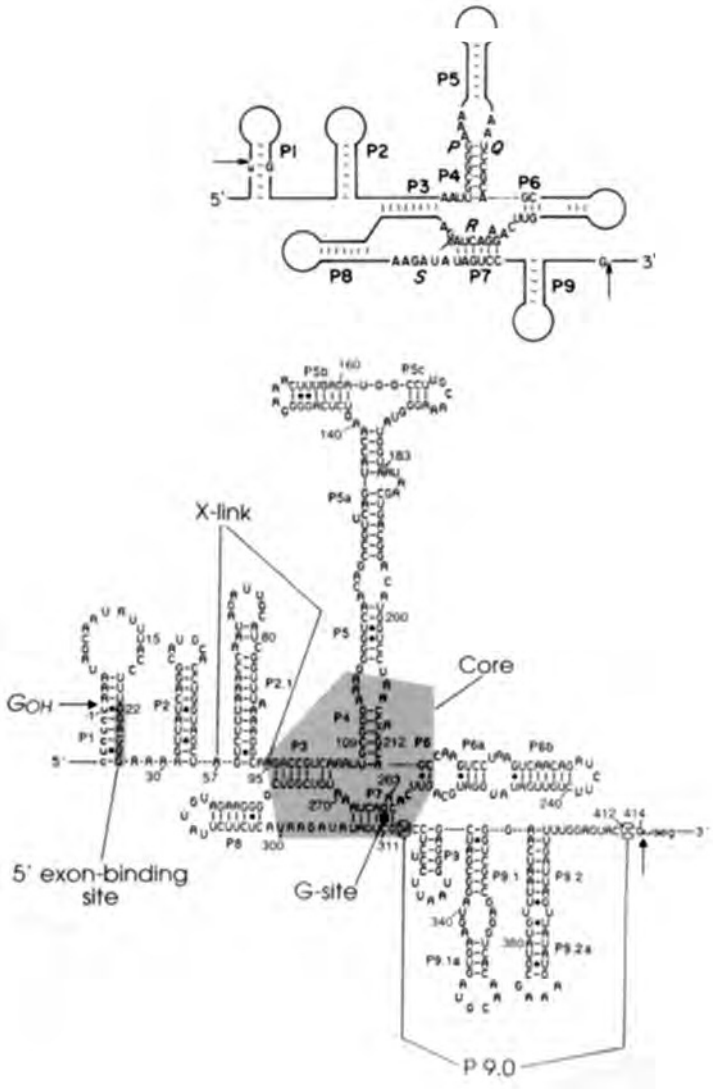

Fig. 7. Secondary structure of group I intervening sequences determined by *Michel* et al. [41] and Davies et al. [49] by the method of comparative sequence analysis [97, 98]. A) Generalized structure indicating conserved base-paired elements P1–P9. Conserved sequence elements, P, Q, R, and S are represented by their most common nucleotide sequences. Filled arrows, 5′ and 3′ splice sites. Open arrow, site of insertion of extra stem loop(s) in group IA structures. B) Secondary structure of the *T. thermophila* rRNA IVS, with the 5′ exon-binding site and the core structure most conserved in group I IVSs shaded. Guanosine-binding site (G site) was located by *Michel* et al. [37]. UV-induced cross-link (X-link) identifies a tertiary structure interaction [99]. Lowercase letters, exons; uppercase letters, IVS. (Adapted from [4].)

trons, to distinguish them from a second group of mitochondrial introns that shared a different structure.[51]

The *Tetrahymena* rRNA IVS contained the conserved sequence elements and secondary structures characteristic of the mitochondrial group I.[51,52] Furthermore, a very similar structure model of the *Tetrahymena* IVS was independently derived by another method, free-energy minimization as constrained by experimentally determined sites of cleavage of the folded RNA by various nucleases.[53] A current version of the secondary structure is shown in Figure 7, bottom.

This convergence of two previously noninteracting sets of ideas was important in several respects. In terms of splicing mechanisms, it was now unlikely that the *Tetrahymena* intron would be unique; we could extend our knowledge of its mechanism by comparing and contrasting splicing of different members of the group. Second, a believable model of the secondary structure of the *Tetrahymena* IVS was now in hand, and one could begin to formulate structure–function relationships. Finally, the similarity between the *Tetrahymena* rRNA and fungal mitochondrial introns might be revealing their origin; perhaps they were transposable elements able to enter both nuclear and mitochondrial compartments.[53]

Waiting for Number Two

If RNA catalysis were of any general significance to biology, there would be additional examples. Throughout 1982 and most of 1983, none came forth. Yet there seemed to be some reasonable candidates. In the fall of 1983, we wrote an article in which we speculated:[35]

> Several enzymes, such as RNase P, 1,4-α-glucan branching enzyme and potato *o*-diphenol oxidase, have RNA components essential for their catalytic activities. The peptidyl transferase activity of ribosomes also requires an RNA-protein complex. It remains to be seen whether the RNA is directly involved in the active site of any of these ribonucleoprotein enzymes.

The speculation about RNase P was already outdated when our paper was published in 1984, because by that time *Guerrier-Takada* et al.[54] had announced that the RNA component was the catalytic subunit of that ribonucleoprotein enzyme. This was followed by the report early in 1984 that a synthetic *E. coli* RNase P RNA, transcribed in vitro from a recombinant DNA template, also had intrinsic catalytic activity; the possibility that catalysis was due to protein contamination was thereby eliminated.[55] Similarly, the RNA subunit of *Bacillus subtilis* RNase P acted as an enzyme in vitro.[54,56] The RNase P discovery was very exciting to us. Not only did it provide a second example of an RNA molecule that lowered the activation energy for a specific biochemical reaction, but it was the first proven case of an RNA molecule that catalyzed a reaction without itself undergoing any net change. RNA catalysis was not restricted to the realm of intramolecular catalysis.

Within the next year, self-splicing of additional group I intervening sequences was reported. *Garriga* and *Lambowitz*[57] found that the first IVS of the cytochrome *b* pre-mRNA from *Neurospora* mitochondria underwent self-splicing in vitro. Several self-splicing group I RNAs from yeast mitochondria were characterized by *van der Horst* and *Tabak*.[58] Most unexpectedly, self-splicing group I IVSs were found in three bacteriophage T4 mRNAs;[59–61] RNA splicing took place in a prokaryote. In all cases, splicing occurred by the same G-addition pathway as splicing of the *Tetrahymena* nuclear rRNA IVS.

The mitochondrial group II intervening sequences have conserved sequences and secondary structures distinct from those of group I.[51] *Peebles* et al.[62] and *Van der Veen* et al.[63] discovered that pre-mRNA containing a group II intervening sequence was self-splicing in vitro. The reaction did not require guanosine and occurred by formation of a branched "lariat" RNA. The proposed mechanism is shown in Figure 8.

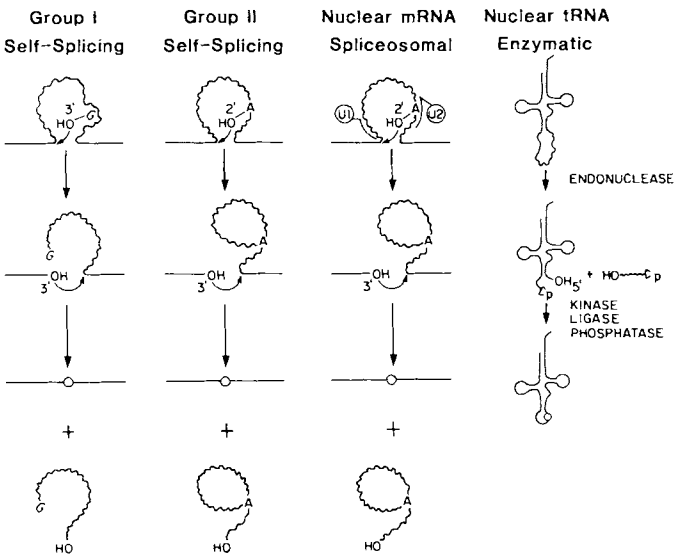

Fig. 8. Mechanism of splicing of the four major groups of precursor RNAs. Wavy lines indicate IVSs, smooth lines indicate flanking exons. For nuclear mRNA splicing, many components assemble with the pre-mRNA to form the spliceosome; only the U1 and U2 small nuclear ribonucleoproteins are shown here. (Adapted from [102].)

The fundamental chemistry of group II RNA splicing appears to be the same as that of nuclear pre-mRNAs, which do not self-splice. Instead, nuclear mRNA splicing requires assembly of the substrate with a large complex of proteins and small nuclear ribonucleoproteins to form the spliceosome.[64–67] The mechanistic similarities have led to the speculation that nuclear mRNA splicing may also be RNA catalyzed, with much of the catalysis being provided in the form of the small nuclear RNAs.[34,67]

Enzymologists Outraged

Although our description of RNA self-splicing was shocking to many, it was quickly accepted by the scientific community. In contrast, our use of the words "catalysis" and

"enzymelike" to describe the phenomenon provoked some much more heated reactions.

Our reasons for emphasizing the relationship between RNA self-splicing and biological catalysis might be better appreciated in the context of the definition given in Table 1. First, biological catalysts achieve rate accelerations of the order of 10^6 to 10^{13}, bringing the reactions into a time scale that is useful for living systems. Self-splicing clearly meets

Table 1. Defining characteristics of biological catalysis (from [95]).

Characteristic	Self-splicing	L – 19 IVS RNA
1. Rate acceleration	+	+
2. Specificity	+	+
3. Catalyst regenerated	[a]	+

[a] No, although the active site is preserved through the reactions.

this criterion; although the quantitation of rate acceleration can be done only for the site-specific hydrolysis reaction promoted by the RNA active site, even the rate of this relatively slow side-reaction is 10^{10}-fold higher than the estimated uncatalyzed rate (Fig. 9). Second, the extraordinary

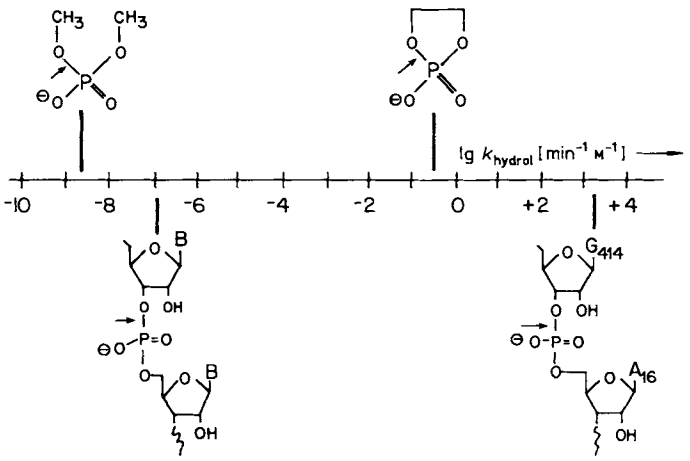

Fig. 9. The IVS RNA has an extremely efficient catalytic center. Second-order rate constants (42 °C) for the alkaline hydrolysis of phosphate diesters are displayed on a logarithmic scale. Arrows designate the P–O bond that undergoes cleavage. Above line: Data for dimethyl phosphate and ethylene phosphate from *Kumamoto* et al. [100] and *Haake* and *Westheimer* [101]. Below line: Hydrolysis of RNA uncatalyzed (left) and catalyzed (right) by the catalytic center of the *Tetrahymena* IVS. (Reproduced from [3].)

specificity of biological catalysts is evident in the self-splicing reaction; the molecule selects GTP as the attacking group for the first step of the reaction and is able to choose 2 of the 6000 nucleotides in the pre-rRNA as splice sites. On the other hand, the IVS RNA is clearly not regenerated in exactly the same form as it entered the reaction; after all, the purpose of self-splicing is to convert pre-rRNA into ligated exons plus excised IVS. Nevertheless, enzymologists do speak of intramolecular catalysis,[38, 39, 68] and we thought that such a descriptor was particularly appropriate for self-splicing.

The enzymologists who reviewed our article (*Bass* and *Cech*[35]) were far from convinced. All three referees wrote thoughtful reviews, expressing considerable interest in the data but chastising us for our naivete about enzymes. For example:

> Enzymes are true catalysts: they speed the rate of a reaction, but are themselves unchanged by the reaction. In the present instance, the ribozyme acts in a "one-shot" reaction and is permanently changed so that it can no longer cycle as does a true catalyst. The authors are well aware of this, but appear to ignore this key feature in making their comparisons.

How fundamental was this distinction between self-splicing and catalysis? Opinions would probably vary as much today as they did six years ago. Instead of engaging in a protracted argument, we decided to test experimentally whether the self-splicing RNA could be converted into a multiple-turnover catalyst. *Arthur Zaug* made a slight alteration of the self-splicing IVS, removing its first 19 nucleotides. The resulting L – 19 IVS RNA met all three criteria of a biological catalyst[69] (Table 1).

Shortened forms of the *Tetrahymena* IVS have multiple enzymatic activities. Depending on the substrates with which they are presented, these RNA enzymes can catalyze nucleotidyl-transfer, phosphotransfer, and hydrolysis reactions; nucleotidyl transfer can result in either endonucleolytic cleavage or polymerization of RNA.[43, 69–74]

As an example, consider the reaction diagramed in Figure 10. A form of the IVS RNA missing both its splice sites catalyzes the cleavage of other RNA molecules after sequences resembling that of the normal 5′ exon, CUCU. The reaction is an intermolecular version of the first step of RNA self-splicing, in which RNA cleavage is accompanied by covalent joining of guanosine to the 5′ end of the 3′ cleavage product. Because the IVS RNA is unaltered by the reaction, it can sequentially bind and process a large number of substrate RNA molecules. The k_{cat}/K_m for cleavage of an oligoribonucleotide substrate containing a CCCUCU recognition sequence is 10^8 M^{-1} min^{-1},[75] well within the range of protein enzymes.

Site-directed mutagenesis of the 5′ exon-binding site of the IVS redirects substrate specificity as predicted by the rules of Watson–Crick base-pairing.[71, 76] Thus, it has been possible to create a whole set of "RNA restriction endonucleases" that may be of use for the sequence-specific cleavage of RNA.

Converting a self-processing RNA into an RNA enzyme by physically separating its internal substrate from its catalytic center has been generally successful. The "hammerhead" and "hairpin" ribozymes, both found in plant infectious agents (viroids or viral satellite RNAs), undergo self-cleavage leaving 2′,3′-cyclic phosphate termini.[77, 78] Both have been converted into RNA enzymes.[79–81] A group II IVS can cleave RNA containing a 5′ splice site or ligated exon RNA in an intermolecular reaction,[82, 83] although in these cases multiple turnover was not demonstrated. Even the intramolecular lead-cleavage reaction of tRNA can be converted into an enzymatic system.[84] The ability of pieces of a structured RNA molecule to self-assemble, recreating an active unit, therefore appears to be a general property of the RNA biopolymer. In addition, if the fragment that undergoes reaction is secured to the rest of the molecule by a

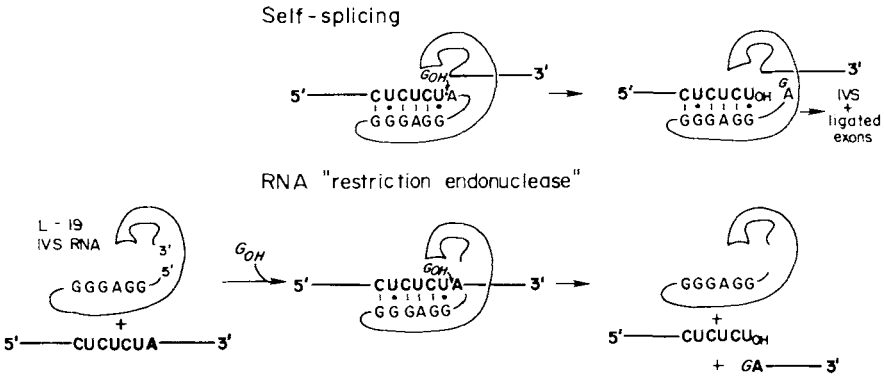

Fig. 10. A shortened version of the *Tetrahymena* IVS RNA has enzymatic activity as an endonuclease. The mechanism is an intermolecular version of the first step of pre-rRNA self-splicing. Thin letters and lines, IVS sequences; bold letters and thick lines, exon sequences (top) or substrate RNA sequences (bottom); G in italics, free guanosine or GTP. (Reproduced from [71].)

relatively weak interaction such as a few base pairs, it will dissociate quickly enough to permit multiple turnovers.

Origin of Life Fantasies

The discoveries of RNA self-splicing and the enzymatic activity of RNase P RNA rekindled earlier speculation concerning the possible role of RNA in the origin of life.[85-87] Contemporary cells depend on a complex interplay of nucleic acids and proteins, the former serving as informational molecules and the latter as the catalysts that replicate and express the information. Certainly the first self-reproducing biochemical system also had an absolute need for both informational and catalytic molecules. The dilemma was therefore, *Which came first, the nucleic acid or the protein, the information or the function?* One solution would be the coevolution of nucleic acids and proteins.[88] The finding that RNA can be a catalyst as well as an information carrier lent plausibility to an alternative scenario: the first self-reproducing system could have consisted of RNA alone.[87, 89, 90]

Perhaps coincidentally or perhaps because of its ancestry, one of the reactions catalyzed by the *Tetrahymena* IVS RNA enzyme is a nucleotidyl-transfer reaction with fundamental similarity to the reaction catalyzed by RNA replicases.[69, 73] A specific model for RNA self-replication based on the properties of the catalytic center of the *Tetrahymena* IVS RNA is given in Figure 11. The RNA enzyme (ribozyme*) differs from the L-19 IVS RNA in that it utilizes an external rather than an internal template.[91] Separation of the template region from the rest of the catalytic center of the RNA with retention of activity has recently been achieved by *Doudna* and *Szostak*.[74]

Now that we have examples of catalytic RNAs, it has been entertaining to look back at earlier speculations about the catalytic potential of RNA. As a representative example, consider the following:[92]

> ... in the evolutionary scheme, folded nucleic acid structures were abandoned by nature in favour of proteins. Although nucleic acids may have performed many enzymatic tasks in primitive cells, this is much more efficiently done by proteins....With nucleic acids the four bases are all of one structural type, though the existence of many modified bases points to an evolutionary proliferation giving much greater possibilities in forming structures. Nevertheless, the use of bases cannot match the enormous flexibility provided by having twenty amino acids which fall into three or four different structural types.

One implication is that nucleic acids, if they could have any such activity, would by nature be inferior catalysts. At one time I had a similar bias, but it was gradually dispelled as we quantitated the rate acceleration and specificity inherent to the catalytic center of the *Tetrahymena* ribozyme. The

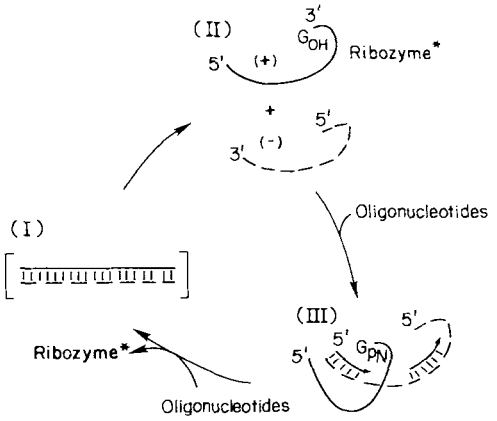

Fig. 11. Hypothetical model for RNA self-replication involving an RNA catalyst (ribozyme*). Double-stranded RNA (I) undergoes strand separation to give ribozyme* ((+) strand) and the complementary (-) strand (II). The ribozyme* catalyzes synthesis of a new (+) strand, using the (-) strand as a template (III). The detailed mechanism is described in [91]. Completion of synthesis re-forms the double-stranded RNA (I). A second cycle is needed to achieve replication of the starting material.

second conclusion, regarding the limited versatility of RNA catalysts, still strikes me as being correct. In all well-established examples, the substrate for an RNA catalyst or ribonucleoprotein enzyme is RNA or DNA or, in the case of protein synthesis on ribosomes, the closely related aminoacyl-tRNA. To its credit, RNA can form a specific binding site for at least one amino acid,[93] and there is evidence that covalent linkage of the terminal protein to poliovirus RNA is at least in part RNA-catalyzed.[94] Nevertheless, it seems unlikely that RNA can match the enormous variety of binding sites that can be formed from amino-acid side chains. The list of RNA catalysts is still growing quite rapidly. Yet it seems likely that if an entire list of biological catalysts is ever complete, it will include more proteins than RNA molecules.

I dedicate this lecture to my wife Carol and to my parents, Robert and Annette. I am indebted to my co-workers over the past decade, who performed the experiments and contributed many of the ideas about RNA catalysis described here. In addition to those whose work I have described, there are many who made important contributions that have gone unmentioned here but not at all unappreciated. Funding for our research has been provided principally by the National Institutes of Health and the American Cancer Society, and more recently by the Howard Hughes Medical Institute; I thank them for their uninterrupted and enthusiastic support. Finally, I have enjoyed the comradeship and helpful criticism of the RNA research community, both in Boulder and worldwide.

Received: January 30, 1990 [A 767 IE]
German version: *Angew. Chem. 102* (1990) 745

[1] J. B. S. Haldane: *Enzymes*, Longmans, Green & Co., UK 1930, M. I. T. Press, Cambridge, MA, 1965.
[2] T. R. Cech, B. L. Bass, *Annu. Rev. Biochem. 55* (1986) 599–629.
[3] T. R. Cech, *Science (Washington D.C.) 236* (1987) 1532–1539.
[4] T. R. Cech, *Gene 73* (1988) 259–271.
[5] T. R. Cech, *Annu. Rev. Biochem. 59* (1990), in press.
[6] J. M. Burke, *Gene 73* (1988) 273–294.
[7] S. Altman, *Adv. Enzymol. Relat. Areas Mol. Biol. 62* (1989) 1–36.
[8] T. R. Cech, *J. Am. Med. Assoc. 260* (1988) 3030–3034.
[9] J. Engberg, J. R. Nilsson, R. E. Pearlman, V. Leick, *Proc. Natl. Acad. Sci. USA 71* (1974) 894–898.
[10] J. G. Gall, *Proc. Natl. Acad. Sci. USA 71* (1974) 3078–3081.
[11] M.-C. Yao, A. R. Kimmel, M. A. Gorovsky, *Proc. Natl. Acad. Sci. USA 71* (1974) 3082–3086.
[12] M. A. Wild, J. G. Gall, *Cell 16* (1979) 565–573.
[13] T. R. Cech, D. C. Rio, *Proc. Natl. Acad. Sci. USA 76* (1979) 5051–5055.
[14] N. Din, J. Engberg, W. Kaffenberger, W. Eckert, *Cell 18* (1979) 525–532.
[15] A. J. Zaug, T. R. Cech, *Cell 19* (1980) 331–338.
[16] See also M. Carin, B. F. Jensen, K. D. Jentsch, J. C. Leer, O. F. Nielson, O. Westergaard, *Nucleic Acids Res. 8* (1980) 5551–5566.
[17] J. E. Darnell, Jr., *Science (Washington D.C.) 202* (1978) 1257–1260.
[18] J. Abelson, *Annu Rev. Biochem. 48* (1979) 1035–1069.
[19] F. H. C. Crick, *Science (Washington D.C.) 204* (1979) 264–271.
[20] M. R. Lerner, J. A. Boyle, S. M. Mount, S. L. Wolin, J. A. Steitz, *Nature (London) 283* (1980) 220–224.
[21] G. Knapp, R. C. Ogden, C. L. Peebles, J. Abelson, *Cell 18* (1979) 37–45.
[22] C. L. Peebles, R. C. Ogden, G. Knapp, J. Abelson, *Cell 18* (1979) 27–35.
[23] T. R. Cech, A. J. Zaug, P. J. Grabowski, *Cell 27* (1981) 487–496.
[24] M. A. Wild, R. Sommer, *Nature (London) 283* (1980) 693–694.
[25] A. J. Zaug, T. R. Cech, *Nucleic Acids Res. 10* (1982) 2823–2838.
[26] A. J. Zaug, P. J. Grabowski, T. R. Cech, *Nature (London) 301* (1983) 578–583.
[27] H. F. Tabak, G. Van der Horst, A. M. J. E. Kamps, A. C. Arnberg, *Cell 48* (1987) 101–110.
[28] T. Inoue, F. X. Sullivan, T. R. Cech, *J. Mol. Biol. 189* (1989) 143–165.
[29] F. X. Sullivan, T. R. Cech, *Cell 42* (1985) 639–648.
[30] S. A. Woodson, T. R. Cech, *Cell 57* (1989) 335–345.
[31] J. A. McSwiggen, T. R. Cech, *Science (Washington D.C.) 244* (1989) 679–683.
[32] J. Rajagopal, J. A. Doudna, J. W. Szostak, *Science (Washington D.C.) 244* (1989) 692–694.
[33] P. J. Grabowski, A. J. Zaug, T. R. Cech, *Cell 23* (1981) 467–476.
[34] K. Kruger, P. J. Grabowski, A. J. Zaug, J. Sands, D. E. Gottschling, T. R. Cech, *Cell 31* (1982) 147–157.
[35] B. L. Bass, T. R. Cech, *Nature (London) 308* (1984) 820–826.
[36] B. L. Bass, T. R. Cech, *Biochemistry 25* (1986) 4473–4477.
[37] F. Michel, M. Hanna, R. Green, D. P. Bartel, J. W. Szostak, *Nature (London) 342* (1989) 391–395.
[38] W. P. Jencks: *Catalysis in Chemistry and Enzymology*, McGraw-Hill, New York 1969.
[39] A. Fersht: *Enzyme Structure and Mechanism*, 2nd ed., Freeman, New York 1985.
[40] R. W. Davies, R. B. Waring, J. A. Ray, T. A. Brown, C. Scazzocchio, *Nature (London) 300* (1982) 719–724.
[41] F. Michel, A. Jacquier, B. Dujon, *Biochimie 64* (1982) 867–881.
[42] R. B. Waring, P. Towner, S. J. Minter, R. W. Davies, *Nature (London) 321* (1986) 133–139.
[43] M. D. Been, T. R. Cech, *Cell 47* (1986) 207–216.
[44] J. V. Price, J. Engberg, T. R. Cech, *J. Mol. Biol. 196* (1987) 49–60.
[45] E. T. Barfod, T. R. Cech, *Mol. Cell. Biol. 9* (1989) 3657–3666.
[46] A. J. Zaug, J. R. Kent, T. R. Cech, *Science (Washington D.C.) 224* (1984) 574–578.
[47] C. Guerrier-Takada, K. Haydock, L. Allen, S. Altman, *Biochemistry 25* (1986) 1509–1515.
[48] C. A. Grosshans, T. R. Cech, *Biochemistry 28* (1989) 6888–6894.
[49] N. Sugimoto, M. Tomka, R. Kierzek, P. C. Bevilacqua, D. H. Turner, *Nucleic Acids Res. 17* (1989) 355–371.
[50] J. M. Burke, U. L. RajBhandary, *Cell 31* (1982) 509–520.
[51] F. Michel, B. Dujon, *EMBO J.* 2 (1983) 33–38.
[52] R. B. Waring, C. Scazzocchio, T. A. Brown, R. W. Davies, *J. Mol. Biol. 167* (1983) 595–605.
[53] T. R. Cech, N. K. Tanner, I. Tinoco, Jr., B. R. Weir, M. Zuker, P. S. Perlman, *Proc. Natl. Acad. Sci. USA 80* (1983) 3903–3907.
[54] C. Guerrier-Takada, K. Gardiner, T. Marsh, N. Pace, S. Altman, *Cell 35* (1983) 849–857.
[55] C. Guerrier-Takada, S. Altman, *Science (Washington D.C.) 223* (1984) 285–286.
[56] T. L Marsh, N. R. Pace, *Science (Washington D.C.) 229* (1985) 79–81.
[57] G. Garriga, A. M. Lambowitz, *Cell 39* (1984) 631–641.
[58] G. Van der Horst, H. F. Tabak, *Cell 40* (1985) 759–766.
[59] M. Belfort, J. Pedersen-Lane, D. West, K. Ehrenman, G. Maley, F. Chu, F. Maley, *Cell 41* (1985) 375–382.
[60] K. Ehrenman, J. Pedersen-Lane, D. West, R. Herman, F. Maley, M. Belfort, *Proc. Natl. Acad. Sci. USA 83* (1986) 5875–5879.
[61] J. M. Gott, D. A. Shub, M. Belfort, *Cell 47* (1986) 81–87.
[62] C. L. Peebles, P. S. Perlman, K. L. Mecklenburg, M. L. Petrillo, J. H. Tabor, K. A. Jarrell, H.-L. Cheng, *Cell 44* (1986) 213–223.
[63] R. Van der Veen, A. C. Arnberg, G. Van der Horst, L. Bonen, H. F. Tabak, L. A. Grivell *Cell 44* (1986) 225–234.
[64] E. Brody, J. Abelson, *Science (Washington D.C.) 228* (1985) 963–966.
[65] D. Frendewey, W. Keller, *Cell 42* (1985) 355–367.
[66] P. J. Grabowski, S. R. Seiler, P. A. Sharp, *Cell 42* (1985) 345–353.
[67] T. Maniatis, R. Reed, *Nature (London) 325* (1987) 673–678.
[68] M. L. Bender, R. J. Bergeron, M. Komiyama, *The Bioorganic Chemistry of Enzymatic Catalysis*, Wiley, New York 1984.
[69] A. J. Zaug, T. R. Cech, *Science (Washington D.C.) 231* (1986) 470–475.
[70] A. J. Zaug, T. R. Cech, *Biochemistry 25* (1986) 4478–4482.
[71] A. J. Zaug, M. D. Been, T. R. Cech, *Nature (London) 324* (1986) 429–433.
[72] P. S. Kay, T. Inoue, *Nature (London) 327* (1987) 343–346.
[73] M. D. Been, T. R. Cech, *Science (Washington D.C.) 239* (1988) 1412–1416.
[74] J. A. Doudna, J. W. Szostak, *Nature (London) 339* (1989) 519–522.
[75] D. Herschlag, T. R. Cech, unpublished.
[76] F. Murphy, T. R. Cech, *Proc. Natl. Acad. Sci. USA 86* (1989) 9218–9222.
[77] G. A. Prody, J. T. Bakos, J. M. Buzayan, I. R. Schneider, G. Bruening, *Science (Washington D.C.) 231* (1986) 1577–1580.
[78] A. C. Forster, R. H. Symons, *Cell 49* (1987) 211–220.
[79] O. C. Uhlenbeck, *Nature (London) 328* (1987) 596–600.
[80] J. Haseloff, W. L. Gerlach, *Nature (London) 334* (1988) 585–591.
[81] A. Hampel, R. Tritz, *Biochemistry 28* (1989) 4929–4933.
[82] A. Jacquier, M. Rosbash, *Science (Washington D.C.), 234* (1986) 1099–1104.
[83] K. A. Jarrell, C. L. Peebles, R. C. Dietrich, S. L. Romiti, P. S. Perlman, *J. Biol. Chem. 263* (1988) 3432–3439.
[84] J. R. Sampson, F. X. Sullivan, L. S. Behlen, A. B. DiRenzo, O. C. Uhlenbeck, *Cold Spring Harbor Symp. Quant. Biol. 52* (1987) 267–277.
[85] C. Woese: *The Genetic Code: The Molecular Basis for Genetic Expression*, Harper and Row, New York 1967, p. 186.
[86] F. H. C. Crick, *J. Mol. Biol. 38* (1968) 372.
[87] L. E. Orgel, *J. Theor. Biol. 123* (1986) 127–149.
[88] M. Eigen, *Naturwissenschaften 58* (1971) 465–523.
[89] P. A. Sharp, *Cell 42* (1985) 397–400.
[90] N. R. Pace, T. L. Marsh, *Origins Life 16* (1985) 97–116.
[91] T. R. Cech, *Proc. Natl. Acad. Sci. USA 83* (1986) 4360–4363.
[92] A. Klug, J. Ladner, J. D. Robertus, *J. Mol. Biol. 89* (1974) 511–516.
[93] M. Yarus, *Science (Washington D.C.) 240* (1988) 1751–1758.
[94] G. J. Tobin, D. C. Young, J. B. Flanegan, *Cell 59* (1989) 511–519.
[95] T. R. Cech, *Harvey Lect. 82* (1988) 123–144.
[96] P. J. Grabowski, S. L. Brehm, A. J. Zaug, K. Kruger, T. R. Cech in D. H. Hamer, M. J. Rosenberg (Eds.): *Gene Expression, Vol. 8*, Alan R. Liss, New York 1983, pp. 327–342.
[97] G. Fox, C. R. Woese, *Nature 256* (1975) 505–507.
[98] H. F. Noller, C. R. Woese, *Science (Washington D.C.) 212* (1981) 403–410.
[99] W. D. Downs, T. R. Cech, *Biochemistry 29* (1990), in press.
[100] J. Kumamoto, J. R. Cox, Jr., F. H. Westheimer, *J. Am. Chem. Soc. 78* (1956) 4858–4860.
[101] P. C. Haake, F. H. Westheimer, *J. Am. Chem. Soc. 83* (1961) 1102–1109.
[102] T. R. Cech, *Cell 44* (1986) 207–210.

Communications may be submitted in English *or* in German. Further details regarding the submission of communications can be found in the "Notice to Authors" reproduced in the January issue of the journal. Copies thereof may be obtained from the editorial office upon request.

A Spacious Cyclophane Host for Inclusion Complexation of Steroids and [m.n]Paracyclophanes**

By *Daniel R. Carcanague* and *François Diederich**

Over the past years, we have investigated the binding properties of tetraoxa[n.1.n.1]paracyclophanes such as **1**.[1, 2] The two diphenylmethane units in these water-soluble hosts shape cavities with pronounced apolar character suitably sized for inclusion of flat aromatic and, to some extent, also alicyclic guests.[1-4] Here we describe the synthesis and complexation properties of the new host **2**. Contrary to **1**, compound **2** possesses a wider apolar binding site for the inclusion of larger, more spherical guests.[5, 6] In **1**, the distance between the two oxygens of one diphenylmethane unit, which defines the cavity width, is 8.41 Å (X-ray analysis).[2] At about 10.6–11.2 Å, depending on the host conformers (MMX force-field calculations),[7] the O···O distance at the naphthylphenylmethane units in **2** is considerably larger.

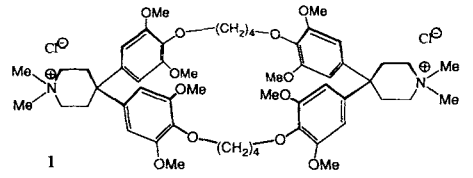

1

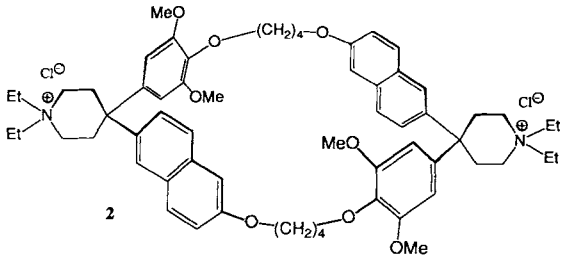

2

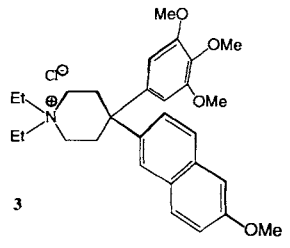

3

The selective complexation of cholesterol from aqueous solution and the complexation-induced dissolution of solid cholesterol deposits represent worthwhile targets in molecular recognition. Therefore, exploring the binding of steroids was of interest in our first studies with **2**.[5, 6, 8] Furthermore, by forming inclusion complexes of [m.n]paracyclophanes, we intended to show unambiguously that the dimensions of the binding site of **2** are suitable for incorporation of two π systems in a sandwich-type orientation. Such a demonstration would be followed by investigations of the supramolecular catalysis of reactions between two included guests (e.g., the Diels–Alder reaction).[9, 10]

The synthesis of cyclophane **2** is shown in Scheme 1.[11] Steroid complexation by **2** was investigated by ^{1}H NMR spectroscopy in D_2O/CD_3OD (1:1 v/v) at 293 K. Table 1 shows the results of binding titrations, performed at concentration ranges below the critical aggregation concentration of the host (cac ≈ 5 mM). The complexation-induced shifts of the isolated signals of the steroid methyl groups were best monitored and evaluated in these titrations. Cholic acid derivatives, corticoids, and androgenic steroids form stable complexes with **2**. According to CPK model examinations, the steroids are included in an axial geometry as depicted in Figure 1. Axial rotation is maintained in the complex. This geometry allows the highly solvated polar functional groups of the steroids at C-3 in ring A and at ring D to orient into the solution. In agreement with an axial inclusion geometry, the ^{1}H NMR resonances of the steroid methyl groups show characteristic upfield complexation shifts.

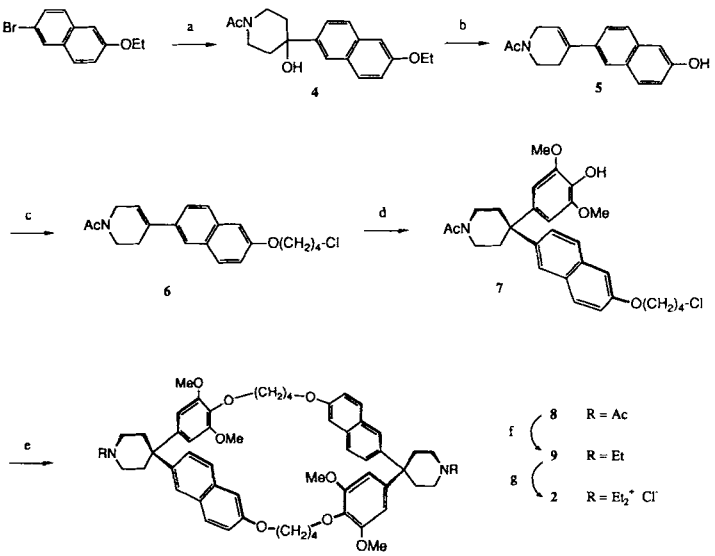

Scheme 1. a) Mg, THF, 1-acetyl-4-piperidone; 50–60% yield; **4**, m.p. 169–171 °C. b) 3.5 equiv. BBr_3, CH_2Cl_2, 40 °C, 3 h; **5**, m.p. 193 °C (dec.). c) NaH, DMF, 10 equiv. 1,4-dichlorobutane; 65% yield (from **4**); **6**, m.p. 89 °C. d) 7 equiv. $BF_3 \cdot Et_2O$, CH_2Cl_2, 6 equiv. 2,6-dimethoxyphenol, 20 °C, 6 d; 80% yield; **7**, m.p. 139–141 °C. e) 3 equiv. Cs_2CO_3, DMF, 80 °C, 2 d; 25% yield; **8** m.p. 308 °C (dec.). f) $BH_3 \cdot$ THF, reflux; 24 h; 60% yield; **9**, m.p. 248–250 °C (dec.). g) EtI, $CHCl_3$, followed by ion exchange ($Cl^\ominus$); 93% yield; **2** · $2H_2O$, m.p. 258–260 °C (dec.).

[*] Prof. F. Diederich, D. R. Carcanague
Department of Chemistry and Biochemistry
University of California
Los Angeles, CA 90024-1569 (USA)

[**] This work was supported by Merck Sharp & Dohme, the National Science Foundation, and a Chlorox Research Fellowship (*D. R. C.*)

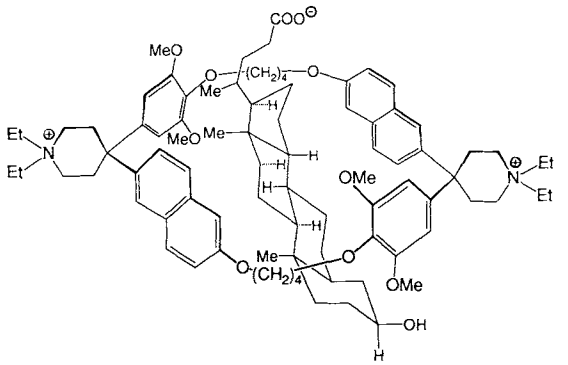

Fig. 1. Schematic representation of the axial inclusion of lithocholic acid (**10e**).

High binding selectivity is observed in the series of structurally related bile acid derivatives **10a–e**. The complex formed by deoxycholic acid (**10b**) (K_a = 250 L mol^{-1}) is approximately 2 kcal mol^{-1} less stable than the complex of lithocholic acid (**10e**) (K_a = 7075 L mol^{-1}) due to the presence in **10b** of only one additional hydroxyl group at C-12α. In the complex of lithocholic acid (**10e**), the apolar surfaces of rings B, C, and D interact favorably with the cavity walls of complementary polarity. In contrast, complexes of the other cholic acid derivatives **10a–d** are destabilized by unfavorable interactions between the strongly solvated hydroxyl groups at their rings B and C and the apolar cavity walls. Similarly, in the series **11a–c**, testosterone (**11c**) forms a more stable complex than the two corticoids **11a**, **b** having polar functional groups at ring C.

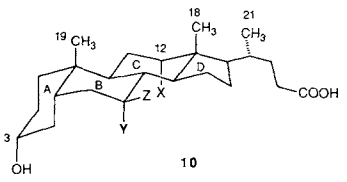

10

Steroid	X	Y	Z
a cholic acid	OH	OH	H
b deoxycholic acid	OH	H	H
c chenodeoxycholic acid	H	OH	H
d ursodeoxycholic acid	H	H	OH
e lithocholic acid	H	H	H

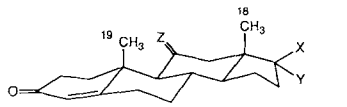

11

a hydrocortisone	$COCH_2OH$	OH	αH, βOH
b cortisone	$COCH_2OH$	OH	O
c testosterone	OH	H	H_2

The presence of polar, highly solvated groups at the central rings B and C of the steroid skeleton also affects the geometry of the complexes. Characteristic upfield shifts of the steroid methyl resonances in the ^{1}H NMR spectra indicate that ring B of **10a** and **10b** is preferentially encapsulated (Table 1). The derivatives **10c–e** are preferentially included at rings C and D, whereas the corticoids **11a**, **b** and testosterone (**11c**) are incorporated at rings A and B.

Cyclophane **2** shows high selectivity for apolar steroids. Other alicyclic systems, such as the sodium salt of 1-adamantylacetic acid (K_a = 115 L mol^{-1}, ΔG° = − 2.77 kcal mol^{-1}) or camphor (K_a = 145 L mol^{-1}, ΔG° = − 2.90 kcal mol^{-1}) are more weakly bound. These guests[12] are unable to fill the large cavity of **2**. The nonmacrocyclic comparison compound **3** and cyclophane **1** do not undergo complexation with steroids under the above-mentioned conditions.

Table 1. Association constants K_a and free binding energies $-\Delta G^0$ for the steroid complexes of cyclophane **2** [a] and upfield complexation shifts $\Delta\delta$, calculated for saturation binding, of the ^{1}H NMR resonances of the steroid methyl groups in positions 18, 19, and 21 in the complexes of **2**; D_2O/CD_3OD (1:1 v/v), T = 293 K.

Steroid	K_a [L mol^{-1}]	$-\Delta G^0$ [kcal mol^{-1}]	$\Delta\delta$ CH_3 (19)	CH_3 (18)	CH_3 (21)
10a[b]	145	2.90	0.73	0.56	0.25
10b[b]	250	3.21	0.76	0.66	0.39
10c[b]	810	3.91	0.47	1.40	0.89
10d[b]	1750	4.35	0.30	1.49	1.23
10e[b]	7075	5.18	0.55	1.49	0.90
11a	1095	4.08	1.44	0.22	
11b	1510	4.26	1.48	0.30	
11c	3545	4.76	1.48	0.43	

[a] All values obtained by nonlinear least-squares curve fitting of 500-MHz ^{1}H NMR binding titrations. Concentration ranges during titrations were chosen to provide approximately 20–90% complexation of the steroid present at constant total concentration. Accuracy of the K_a values: ± 10%. [b] Solutions contain 0.01 M Na_2CO_3.

The formation of structurally defined inclusion complexes by [m.n.]paracyclophanes as guests[13] was observed for the first time with cyclophane **2** as the host (Table 2). Cavity inclusion of compounds **12–18** is supported by strong upfield shifts of the aromatic guest resonances and characteristic up- and downfield shifts of the host resonances in ^{1}H NMR spectra of solutions of their complexes. For example, the upfield shifts of the aromatic guest resonances at saturation binding of **12** are $\Delta\delta$ = 0.86 and 0.63 (1-H and 5-H, respectively) and $\Delta\delta$ = 1.82 and 2.03 (2-H and 4-H, respectively). In the ^{1}H NMR spectrum of a solution of **2** (1 mM) and **12** (4 mM), the signals of the bridges in the host are shifted upfield ($\Delta\delta$ = 0.04 to 0.15) and those of the phenyl protons weakly downfield ($\Delta\delta$ = − 0.04). For the naphthyl resonances of the host, characteristic downfield complexation shifts are observed [$\Delta\delta$ = − 0.14 (1-H), − 0.21 (3-H), − 0.18 (4-H), − 0.13 (5-H), − 0.14 (7−H), − 0.15 (8-H)]. These shifts indicate a preference for an inclusion geometry in which the four benzene rings of host and guest are aligned in a fourfold π–π stacking array (Fig. 2).[14]

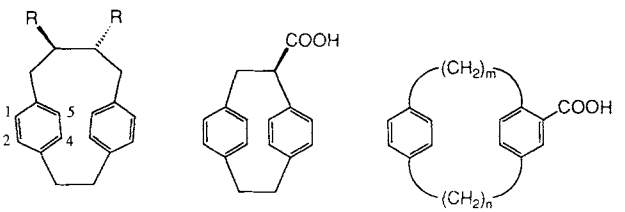

12 R = COOH
13 R = OH

14

15 m = n = 2
16 m = n = 3
17 m = 3, n = 4
18 m = n = 4

The binding strength is strongly dependent on the site of attachment of carboxylate residues to the paracyclophane skeleton. The complexes of **12** and **14** with carboxyl residues attached to the paracyclophane bridges are the most stable. In contrast, a [4.4]paracyclophanedicarboxylic acid bearing one carboxyl function at each benzene ring no longer forms a complex with **2**. Upon inclusion, the two carboxylates of this guest would be positioned deeply inside the apolar cavity. Apparently, the costs for desolvation of two carboxyl residues are too large for such a process to take place.

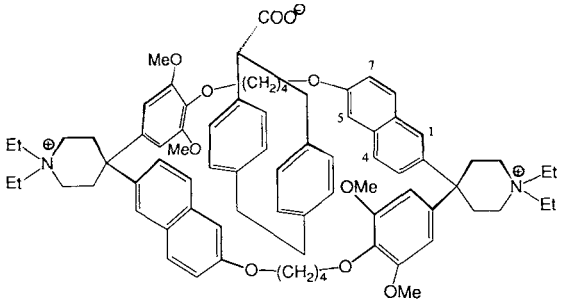

Fig. 2. Schematic representation of the geometry of the [m.n]paracyclophane complexes which, according to ^{1}H NMR analysis, is favored in solution.

Apolar interactions and desolvation rather than ion pairing provide the major driving force for efficient steroid or cyclophane complexation by **2**. This is demonstrated by the favorable binding of the neutral guests **11a–c** and **13**. The stability of all complexes formed in the solvent mixture D_2O/CD_3OD (1:1 v/v) is remarkably high. Based on previous experience, association constants for the complexes in pure water should be about two magnitudes higher than those shown in Tables 1 and 2 for the binary mixture.[15]

Table 2. Association constants K_a and free binding energies $-\Delta G^0$ for the complexes formed between [m.n]paracyclophanes **12–18** and host **2** in D_2O/CD_3OD (1:1 v/v) containing 0.01 M Na_2CO_3, $T = 293$ K [a].

[m.n]Paracyclophane	K_a[L mol^{-1}]	$-\Delta G^0$[kcal mol^{-1}]
12	840	3.92
13[b]	460	3.57
14	530	3.64
15	200	3.07
16	375	3.43
17	440	3.54
18	425	3.54

[a] For the method, see Table 1. [b] No Na_2CO_3 added.

With compound **2**, we have prepared a host which widens considerably the spectrum of guests to be complexed. The cholesterol complex of **2** is insoluble, and its stability could not be determined. The development of modified derivatives of **2** which form water-soluble cholesterol complexes and investigations of supramolecular reactivity in 1:2 host–guest complexes of **2** are currently being pursued in our laboratory.

Received: March 14, 1990 [Z 3856 IE]
German version: *Angew. Chem. 102* (1990) 836

[1] F. Diederich, *Angew. Chem. 100* (1988) 372; *Angew. Chem. Int. Ed. Engl. 27* (1988) 362.
[2] S. B. Ferguson, E. M. Seward, F. Diederich, E. M. Sanford, A. Chou, P. Inocencio-Szweda, C. B. Knobler, *J. Org. Chem. 53* (1988) 5593.
[3] K. Odashima, K. Koga in P. M. Keehn, S. M. Rosenfeld (Eds.): *Cyclophanes, Vol. 2*, Academic Press, New York 1983, p. 629.
[4] H.-J. Schneider, W. Müller, D. Güttes, *Angew. Chem. 96* (1984) 909; *Angew. Chem. Int. Ed. Engl. 23* (1984) 910.
[5] S. Kumar, H.-J. Schneider, *J. Chem. Soc. Perkin Trans. 2 1989*, 245.
[6] H. Kawakami, O. Yoshino, K. Odashima, K. Koga, *Chem. Pharm. Bull. 33* (1985) 5610.
[7] PCMODEL-MMX, Version 2.0, Serena Software, P.O. Box 3076, Bloomington, IN 47402-3076, USA.
[8] Cyclodextrin–steroid interactions: a) J. Szejtli: *Cyclodextrin Technology*, Kluwer, Dordrecht 1988; b) K. Shimada, Y. Komine, T. Oe, *J. Liq. Chromatogr. 12* (1989) 491.
[9] D. Rideout, R. Breslow, *J. Am. Chem. Soc. 102* (1980) 7816.
[10] H.-J. Schneider, N. K. Sangwan, *Angew. Chem. 99* (1987) 924; *Angew. Chem. Int. Ed. Engl. 26* (1987) 896.
[11] Spectroscopic data (IR, ^{1}H NMR, EI-MS, or FAB-MS) and elemental analyses support the structures proposed for new compounds.
[12] For the complexation of alicyclic guests, see: a) J. Franke, F. Vögtle, *Angew. Chem. 97* (1985) 224; *Angew. Chem. Int. Ed. Engl. 24* (1985) 219; b) M. A. Petti, T. J. Shepodd, R. E. Barrans, Jr., D. A. Dougherty, *J. Am. Chem. Soc. 110* (1988) 6825; c) K. Odashima, H. Kawakami, A. Miwa, I. Sasaki, K. Koga, *Chem. Pharm. Bull. 37* (1989) 257.
[13] We are grateful to Professor *Donald J. Cram* for providing us with samples of all the [m.n]paracyclophanes used in this study. Remarkably, all samples, prepared in the fifties and sixties, had maintained their analytical purity.
[14] Multiple stacks in complexes of cyclophane hosts: J.-Y. Ortholand, A. M. Z. Slawin, N. Spencer, J. F. Stoddart, D. J. Williams, *Angew. Chem. 101* (1989) 1402; *Angew. Chem. Int. Ed. Engl. 28* (1989) 1394.
[15] F. Diederich, M. R. Hester, M. A. Uyeki, *Angew. Chem. 100* (1988) 1775; *Angew. Chem. Int. Ed. Engl. 27* (1988) 1705.

The Synthesis and Structure of Stibaindoles**

By *Stephen L. Buchwald,* Richard A. Fisher,* and *Bruce M. Foxman*

Heterocyclic compounds are ubiquitous in organic chemistry and have, consequently, been a popular synthetic target. The vast majority of these efforts have focused on naturally occurring heterocyclic skeletons containing second- and third-row elements with significantly less attention directed to their heavier main-group analogues.[1] As a consequence, an impressive array of useful reactions is available to the chemist wishing to construct heterocycles of N, O, P, and S, while methods for the synthesis of their heavier analogues are limited.[2] Here we report the synthesis and characterization of a series of new metalloid heterocycles, benzo[*b*]stiboles.[3]

In the course of developing new zirconocene-based methodology for organic synthesis, we,[4i–k] and others,[4a–h] have established that sequential treatment of zirconocene(methyl) chloride with an aryllithium and an alkyne, followed by heating, affords the metallacycle **A**.

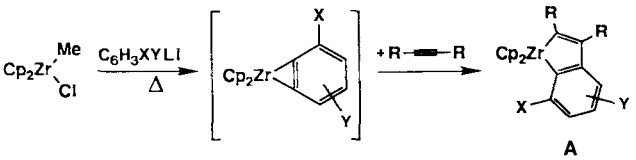

The generality of this reductive coupling reaction is documented elsewhere.[4] Treatment of benzene solutions of the zirconacycles **1–3** with one equivalent of $XSbCl_2$ (**a**, X = Cl; **b**, X = Ph) produces the benzo[*b*]stiboles **4–6**.[5] The only byproduct of the reaction, Cp_2ZrCl_2, is removed by flash chromatography on alumina III (**4b–6b**) or anhydrous $MgSO_4$ (**4a–6a**).

[*] Prof. S. L. Buchwald, R. A. Fisher
Department of Chemistry
Massachusetts Institute of Technology
Cambridge, MA 02139 (USA)
Prof. B. M. Foxman
Department of Chemistry, Brandeis University
Waltham, MA 02254 (USA)

[**] This work was supported, in part, by the Office of Naval Research and by Union Carbide,whom we gratefully acknowledge.

The antimony metallacycles **4**–**6** are moderately air stable, crystalline solids. The 1-chloro derivatives slowly decompose, when stored for prolonged periods in air, to give as yet uncharacterized species. They may be stored indefinitely in a dry nitrogen atmosphere. The 1-phenyl derivatives are substantially more robust and may be stored in the laboratory atmosphere without detectable decomposition. Complexes **4**–**6** are all considerably more prone to decomposition in

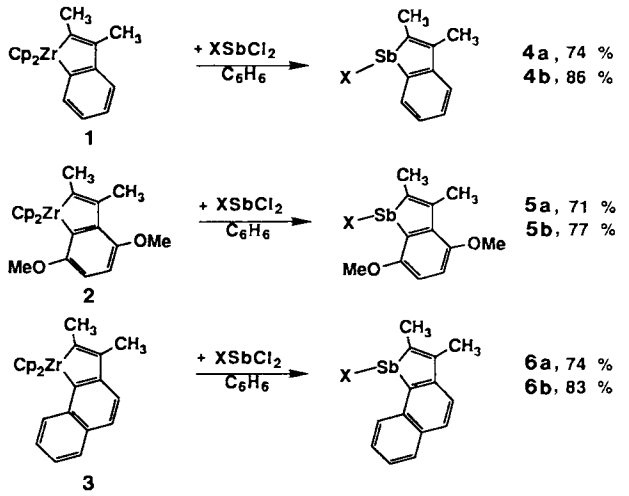

solution than in the solid state. All the compounds were characterized by ^{1}H NMR, ^{13}C NMR, IR, and combustion analysis or high-resolution mass spectrometry. Solution molecular-weight determinations indicate that the stibaindoles are monomeric in benzene solution.[6]

An X-ray crystal structure determination was carried out on compound **5b**,[7] and the structure is shown in Figure 1.

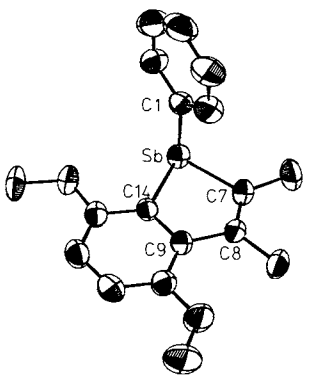

Fig. 1. Molecular structure of **5b**. Bond distances [Å] and angles [°]: Sb-C1 2.164(4), Sb-C7 2.131(3), Sb-C14 2.119(3), C7-C8 1.334(4), C8-C9 1.504(3), C9-C14 1.387(4); C1-Sb-C7 96.5(1), C1-Sb-C14 95.5(1), C7-Sb-C14 79.9(1).

The stibaindole ring is planar, as anticipated (no deviations greater than 0.03 Å), and orthogonal to the plane of the phenyl ring. The shortest intermolecular Sb–Sb distance is 4.75 Å. The highly pyramidalized geometry about the antimony atom, the bond distances, and bond angles are all in good agreement with other structurally characterized stibole derivatives.[7]

Continued interest in heterocyclic compounds coupled with recent applications of main-group organometallics in materials science provides a powerful incentive for the development of new and more selective synthetic routes to main-group metallacycles. Results from this laboratory, and elsewhere, indicate that early-transition-metal complexes may play an important role in the discovery of new and valuable classes of main-group compounds.

Experimental Procedure

General procedure for the preparation of stibaindoles: The zirconacycle (1.00 mmol) was dissolved in 20 mL of benzene in a nitrogen-filled dry box. Either antimony trichloride (0.228 g, 1.00 mmol) or phenylantimony dichloride (0.270 g, 1.00 mmol), was added, all at once, as a solid. After 5 min, the flask was sealed with a septum, brought out of the dry box, and the solvent removed, in vacuo, on a Schlenk line. Zirconocene dichloride and the desired stibaindoles were the only species detectable in the crude reaction mixture as determined by ^{1}H NMR. The zirconocene dichloride was separated from the product by extraction with 10/1 hexanes/ether followed by rapid chromatography on either anhydrous $MgSO_4$ (**4a**, **5a**, **6a**) or alumina II (**4b**, **5b**, **6b**).

Received: December, 22, 1989 [Z 3697 IE]
German version: *Angew. Chem. 102* (1990) 820

CAS Registry numbers:
1, 127399-46-6; **2**, 127399-47-7; **3**, 127399-48-8; **4a**, 127399-41-1; **4b**, 127399-42-2; **5a**, 127399-43-3; **5b**, 127421-13-0; **6a**, 127399-44-4; **6b**, 127399-45-5; $SbCl_3$, 10025-91-9; $PhSbCl_2$, 5035-52-9.

[1] B. J. Aylett: *Organometallic Compounds, Fourth Edition, Part Two*, Wiley, New York 1979; b) G. O. Doak, L. D. Freedman: *Organometallic Compounds of Arsenic, Antimony, and Bismuth*, Wiley, New York 1970.

[2] a) O. Meth-Cohn (Ed.): *Comprehensive Heterocyclic Chemistry, Vol. 1*, Pergamon, Oxford 1984; b) R. E. Atkinson in [2a], pp. 539–560; c) D. A. Armitage in [2a], pp. 614–617; d) G. Märkl, H. Hauptmann, A. Merz, *J. Organomet. Chem. 249* (1983) 335.

[3] To our knowledge, no previous reports of monobenzostiboles, stibaindoles, have appeared. Bisbenzostiboles, stibafluorenes, are well known [3a, b] and are readily synthesized using 2,2'-dilithiobiphenyl reagents [3c–e]: a) R. E. Atkinson in [2a], p. 548; b) [1a], p. 454; c) H. A. Meinema, H. F. Martens, J. G. Noltes, N. Bertazzi, R. Barbieri, *J. Organomet. Chem. 136* (1977) 173; d) H. A. Meinema, J. G. Noltes, *ibid. 160* (1978) 435; e) D. Hellwinkel, M. Bach, *ibid. 17* (1969) 389; see also: f) I. G. M. Campbell, *J. Chem. Soc. 1950*, 3109; g) *ibid. 1952*, 4448; h) *ibid. 1955*, 1662, and references therein.

[4] a) G. Erker, P. Czisch, R. Schlund, K. Angermund, C. Krüger, *Angew. Chem. 98* (1986) 356; *Angew. Chem. Int. Ed. Engl. 25* (1986) 364; b) G. Erker, U. Dorf, P. Czisch, J. L. Peterson, *Organometallics 5* (1986) 668; c) K. Kropp, V. Skibbe, G. Erker, C. Krüger, *J. Am. Chem. Soc. 105* (1983) 3353; d) V. Skibbe, G. Erker, *J. Organomet. Chem. 241* (1983) 15; e) G. Erker, K. Kropp, *Chem. Ber. 115* (1982) 2437; f) G. Erker, K. Kropp, C. Krüger, A. P. Chiang, *ibid. 115* (1982) 2447; g) G. Erker, F. Rosenfeldt, *J. Organomet. Chem. 224* (1982) 29; h) F. Rosenfeldt, G. Erker, *Tetrahedron Lett. 21* (1980) 1637; i) S. L. Buchwald, B. T. Watson, J. C. Huffman, *J. Am. Chem. Soc. 108* (1986) 7411; j) S. L. Buchwald, B. T. Watson, R. T. Lum, W. A. Nugent, *ibid. 109* (1987) 7137.

[5] a) P. J. Fagan, W. A. Nugent, *J. Am. Chem. Soc. 110* (1988) 2310; b) P. J. Fagan, E. G. Burns, J. C. Calabrese, *ibid. 110* (1988) 2979; c) S. L. Buchwald, R. A. Fisher, W. M. Davis, *Organometallics 8* (1989) 2082.

[6] a) Solution molecular-weight determinations were performed for compounds **4a** and **5b** as described in [6b] and the results were taken to be representative [4c]; b) J. E. Bercaw, B. J. Burger in A. L. Wayda, M. Y. Darensbourg (Eds.): *Experimental Organometallic Chemistry: A Practicum in Synthesis and Characterization (ACS Symp. Ser. 357* (1987) 79–102).

[7] Crystals of **5b** are triclinic, space group $P\bar{1}$; $a = 10.458(3)$, $b = 10.458(3)$, $c = 8.298(2)$ Å; $\alpha = 109.86(3)$, $\beta = 94.47(3)$, $\gamma = 80.49(3)°$; $Z = 2$; $\varrho_{calcd} = 1.574\ g\,cm^{-3}$. Using a Syntex $P2_1$ diffractometer, 3809 reflections were measured using graphite-monochromated $Mo_{K\alpha}$ radiation. The structure was refined, using 3198 data for which $I > 1.96\sigma(I)$, to convergence with $R = 0.0285$ and $R_w = 0.0316$. Anisotropic thermal parameters were assigned to Sb, C, and O atoms, while H atoms were included as fixed contributions to the structure factors. Further details of the crystal structure investigation are available on request from the Director of the Cambridge Crystallographic Data Centre, University Chemical Laboratory, Lensfield Road, GB-Cambridge CB2 1EW (UK), on quoting the full journal citation.

[8] a) A. J. Ashe III, W. Butler, T. R. Diephouse, *J. Am. Chem. Soc. 103* (1981) 207; b) A. J. Ashe III, C. M. Kausch, O. Eisenstein, *Organometallics 6* (1987) 1185; c) V. K. Bel'skii, *Zh. Strukt. Khim. 25* (1984) 138.

Cp*Ru(acac)—A Coordinatively Unsaturated, Stable 16-Valence-Electron Complex**

By *Ulrich Kölle,** *Janusz Kossakowski*, and *Gerhard Raabe*

According to extended Hückel MO calculations of *P. Hofmann*,[1] the MLL plane in d^6 complexes of the $CpML_2$ type should be tilted with respect to the MCp normal (C_s symmetry). This prediction is of importance for the retention of configuration on substitution at the central atom of "chiral metal" complexes CpMLL'L''. In many cases, such substitutions proceed stereospecifically with retention.[2] For example, the "pyramidal" cation $[CpRe(NO)PPh_3]^{\oplus}$ [3] generated from optically active $[CpRe(NO)PPh_3Me]$ not only undergoes stereospecific substitution reactions,[4] but also adds olefins enantioselectively.[5] Furthermore, the inversion of the pyramidal cation $[CpCo(PR_3)Et]^{\oplus}$ results in equilibration of the protons of the ethyl group.[6]

In $[Cp^*RuP(cyclo\text{-}C_6H_{11})_3Cl]$[7] the coordination gap at Ru is filled by the bulky phosphane ligand; accordingly, the P-Ru-Cl plane is orthogonal to the Cp* plane. The title compound represents the first structurally characterized, coordinatively unsaturated, fivefold coordinated d^6 complex with a pyramidal structure in the ground state.

The discovery of the alkoxo complex ["Cp"RuOR]$_2$ (**1**, "Cp" = η^5-C_5Me_5 (Cp*), η^5-C_5Me_4Et),[8] which is formed surprisingly readily [Eq. (a)] and, for **1a** (R = Me, "Cp" = Cp*), practically quantitatively from the halides ["Cp"$RuCl_2]_2$, provided an entry to a series of valuable starting materials, which allowed the preparative chemistry of the "Cp"Ru fragment to be extensively explored.[9, 10]

$$[\text{"Cp"}Ru^{III}Cl_2]_2 + 2ROH \xrightarrow[-2KCl,\ -R'CHO]{K_2CO_3} \underset{\mathbf{1}}{[\text{"Cp"}Ru^{II}OR]_2} \qquad (a)$$

Reaction of **1a** with acetylacetone in a molar ratio of 1:2 at room temperature in ether [Eq. (b)] affords, within a few minutes, the acac derivative **2**.[11] Compound **2**, like complexes **1**, is air-sensitive and displays a similar intense red color (λ_{max} = 520 nm); it crystallizes from pentane as red needles.

$$\underset{\mathbf{1a}}{1/2[Cp^*RuOMe]_2} + acacH \xrightarrow{-MeOH} \underset{\mathbf{2}}{Cp^*Ru(acac)} \qquad (b)$$

In accordance with its coordinatively unsaturated character, **2** (like **1**) readily adds two-electron ligands to give compounds **3**[12] [Eq. (c)].

$$\underset{\mathbf{2}}{Cp^*Ru(acac)} + L \xrightarrow[\text{pentane}]{} \underset{\mathbf{3}}{Cp^*Ru(acac)L} \qquad (c)$$

L	CO	PMe_3	$P(OMe)_3$	PPh_3
3	**a**	**b**	**c**	**d**

The carbonyl compound **3a**, like **1a**,[10a] is not very stable; on the other hand, more stable complexes are formed with phosphane and phosphite ligands. Reaction (c) is a rare example of simple addition to a coordinatively unsaturated system and therefore proceeds very fast.[13]

Of preparative interest is the reaction of **2** with hard Lewis acids such as $Zn^{2\oplus}$ or $Mg^{2\oplus}$, which, similar to the reaction of **1** with protonic acids,[9a, 10a] results in degradation to the cationic $Cp'Ru^{\oplus}$ fragment. This fragment is thus accessible without the use of protonic or strong Lewis acids and can therefore be widely used in complexation reactions such as (d).[14, 15]

$$\underset{\mathbf{2}}{Cp^*Ru(acac)} + 1/2\ Zn(BF_4)_2 \begin{cases} \xrightarrow[MeOH]{C_4H_4S} \underset{\mathbf{4}}{[Cp^*Ru(\eta^5\text{-}C_4H_4S)]BF_4} \\ \xrightarrow[MeOH]{C_7H_8} \underset{\mathbf{5}}{[Cp^*Ru(\eta^6\text{-}C_7H_8)]BF_4} \end{cases} \qquad (d)$$

The crystal structure of complex **2**[17] (Fig. 1) exhibits two independent molecules in the asymmetric unit and does not show the intermolecular metal–acac interactions[18] often observed for acac complexes (shortest intermolecular distance, Ru···C13, > 5 Å). Unlike the ligand in most other acac complexes, the ligand here is not coplanar with the metal–O–O plane, but rather tilted along the O1–O2 vector by the angle α (Fig. 3), "inward" by 9° in **2** and "outward" by 16° in **3c**. The average Ru–O distances (2.114(4) Å) are short, but longer than in **1a** (Table 1). The most striking feature in **2** is the tilting of the Ru–O1–O2 plane with respect

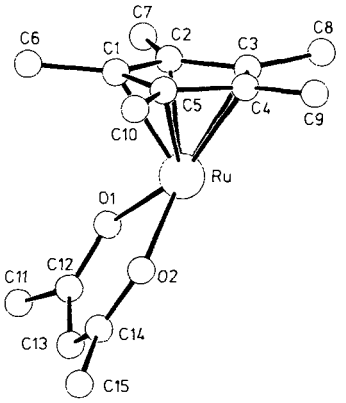

Fig. 1. Molecular structure of **2**.

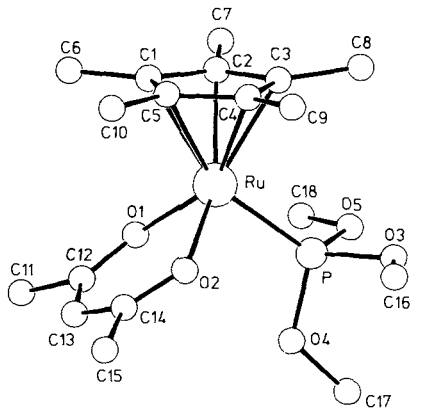

Fig. 2. Molecular structure of **3c**.

[*] Prof. Dr. U. Kölle, Dr. J. Kossakowski
Institut für Anorganische Chemie der Technischen Hochschule Templergraben 55, D-5100 Aachen (FRG)
Dr. G. Raabe
Institut für Organische Chemie der Technischen Hochschule Aachen

[**] This work was supported by the Deutsche Forschungsgemeinschaft, the Fonds der Chemischen Industrie, and Johnson-Matthey (donation of $RuCl_{3aq}$). We thank Prof. Dr. *C. Krüger*, Max-Planck-Institut für Kohlenforschung, Mülheim a. d. Ruhr, for the opportunity to carry out the structure determination in his laboratory and Prof. Dr. *P. Hofmann*, Technische Universität München, for valuable suggestions.

to the Ru–Cp* normal by $\beta = 37.5°$; that is, the Ru atom has a free, easily accessible coordination site.

On addition of $P(OMe)_3$ to **3c**[19] this tilting increases by only 3° and the Ru–O distances are increased by about 0.02 Å; that is, the structure changes only slightly (Figs. 2 and 3).

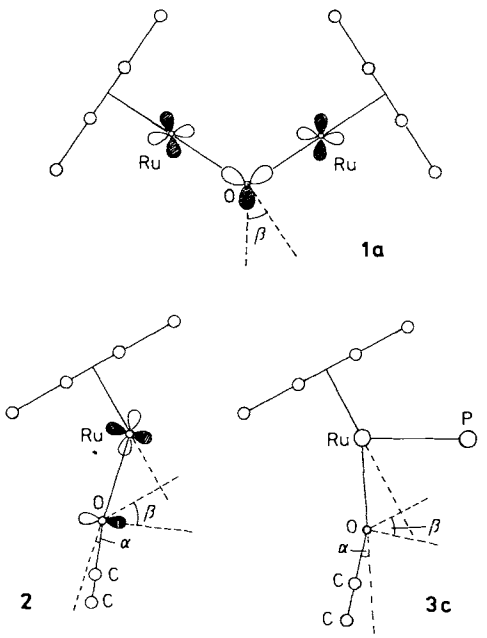

Fig. 3. Schematic drawing of the bonding in **1a**, **2**, and **3c**. The angle β is the angle between the O pz (hybrid) orbitals and the Ru–Cp* normals.

In the methoxo complex **1a**,[10, 16] the Ru–Cp* normals deviate by only 2° from the respective Ru–O–O planes; however, since the two Ru–O–O planes form an angle of 115°, the oxygen p orbitals, as in **2**, are tilted with respect to the RuCp* normals (ca. 34°). Thus, the Cp*–Ru–O orbital arrangement is similar for **1**, resulting here in an opening of the Ru-O-Ru-O rectangle against the van der Waals repulsion of the Cp* methyl groups.

The structural features of **1a**, **2**, and the phosphite complex **3c** are summarized in Table 1.

Table 1. Characteristic bonding parameters in $[Cp^*RuOMe]_2$ (**1a**), Cp*Ru(acac) (**2**), and [Cp*Ru(acac) $(P(OMe)_3]$ (**3c**). Bond lengths in Å, angles in °; see also Fig. 3.

	1a	**2**	**3c**
Ru-O	2.055 (5)	2.114 (4)	2.131 (3)
Ru-C(Cp*)	2.125 (8)	2.132 (6)	2.167 (5)
O-Ru-O	70.9 (2)	85.3 (2)	86.8 (2)
α	-	9.0	16.3
β	33.8	37.5	40.5

Preliminary EHT (EHT = extended Hückel type) calculations indicate that, in comparison to isolobal 16-electron complexes containing acceptor ligands (e.g., $CpMn(CO)_2$[11]), the increased stability of **2** is due, at least in part, to a larger HOMO–LUMO separation.

Received: January 24, 1990 [Z 3756 IE]
German version: *Angew. Chem. 102* (1990) 839

CAS Registry numbers:
1a, 120883-04-7; **2**, 127473-50-1; **3a**, 127473-51-2; **3b**, 127473-53-4; **3c**, 127473-54-5; **3d**, 126368-59-0; **4**, 127473-52-3; **5**, 121162-85-4.

[1] P. Hofmann, *Angew. Chem. 89* (1977) 551; *Angew. Chem. Int. Ed. Engl. 16* (1977) 536.
[2] H. Brunner, *Top. Curr. Chem. 56* (1975) 67.
[3] C. H. Winter, A. M. Arif, J. A. Gladysz, *J. Am. Chem. Soc. 109* (1987) 7560.
[4] J. M. Fernández, J. A. Gladysz, *Inorg. Chem. 25* (1986) 2672.
[5] G. S. Bodner, J. M. Fernández, A. M. Arif, J. A. Gladysz, *J. Am. Chem. Soc. 110* (1988) 4082.
[6] a) R. B. Cracknell, A. G. Orpen, J. L. Spencer, *J. Chem. Soc. Chem. Commun. 1986*, 1005; b) M. Brookhart, D. M. Lincoln, A. F. Volpe, Jr., G. F. Schmidt, *Organometallics 8* (1989) 1212.
[7] B. K. Campion, R. H. Heyn, T. Don Tilley, *J. Chem. Soc. Chem. Commun. 1988*, 278.
[8] a) U. Kölle, J. Kossakowski, *J. Chem. Soc. Chem. Commun. 1988*, 549; b) *J. Organomet. Chem. 362* (1989) 383.
[9] a) U. Kölle, M. H. Wang, *Organometallics 9* (1990) 195; b) U. Kölle, B.-S. Kang, G. Raabe, C. Krüger, *J. Organomet. Chem. 386* (1990) 261; c) U. Kölle, B.-S. Kang, U. Thewalt, *ibid. 386* (1990) 267.
[10] a) U. Kölle, J. Kossakowski, R. Boese, *J. Organomet. Chem. 378* (1989) 449; b) U. Kölle, *Abstr. XXVI. Conf. Organomet. Chem.*, Turin 1988.
[11] **2**: ^{1}H NMR (80 MHz, C_6D_6): $\delta = 1.64$ (15H; Cp*), 1.95 (6H; CH_3), 5.11 (1H; CH). Correct C, H elemental analysis. MS (70 eV): *m/z* 366 ($M^{\oplus} + CH_2O$, 37%), 336 ($M^{\oplus}$, 100) 293 ($M - CH_3CO^{\oplus}$, 58), 251 (63), 236 ($Cp^*RuCH_3^{\oplus}$, 63), 236 ($Cp^*Ru^{\oplus}$, 84).
[12] **3a**: IR(KBR): $\tilde{\nu}$[cm^{-1}] = 1915 (CO). ^{1}H NMR: **3a** ($CDCl_3$): $\delta = 1.58$ (Cp*), 1.88, 5.15 (acac). **3b** (C_6D_6): $\delta = 1.60$ (Cp*), 1.80, 5.10 (acac), 1.11 (d, J(P, H) = 8 Hz, PMe_3). **3c** (C_6D_6): $\delta = 1.60$ (d, J (P, H) = 2 Hz, Cp*), 1.78, 5.11 (acac), 3.50 (d, J (P, H) = 2 Hz, POMe). **3d** (C_6D_6): $\delta = 1.41$ (d, J (P, H) = 2 Hz, Cp*), 1.66, 4.86 (acac), ca. 7.50 (m, PPh).
[13] In the synthesis of **3d**, only roughly the last 10% of the reaction could be followed with a simple stopped-flow apparatus. A lower limit for the rate constant, $k_2 = 2 \times 10^3$ M^{-1}s^{-1}, was thereby measured. Conditions: Hi-Tech SFA-11, mixing time 50 ms, Zeiss spectrophotometer PM6, solvent ether, 0 °C, $\lambda_{obs.} = 520$ nm, [**2**] = 4.0 10^{-2} M, [PPh_3] = 2.0 10^{-1} M.
[14] **4**: ^{1}H NMR ($CDCl_3$): $\delta = 2.04$ (Cp*), 5.97 (pseudo s, 4H, thiophene). Correct C, H elemental analysis. Cf. $[CpRu(C_4H_4S)]BF_4$: M. Draganjac, C. J. Ruffing, T. B. Rauchfuss, *Organometallics 4* (1985) 1909; G. H. Spies, R. J. Angelici, *J. Am. Chem. Soc. 107* (1985) 5569; $[Cp^*Ru(3\text{-}MeC_4H_3S)]PF_6$: B. Chaudret, F. A. Jalon, *J. Chem. Soc. Chem. Commun. 1988*, 711.
[15] **5**: ^{1}H NMR ($CDCl_3$): $\delta = 1.94$ (Cp*), 1.82 (d, $2J = 10$ Hz, H (7)), 3.21 (m, H (1, 6)), 5.09 (m, H (2,5)), 6.39 (m, J (4, 5) = 4.5 Hz, H (3, 4)). Correct C, H elemental analysis. Cf. $[CpRu(C_7H_8)]PF_6$: M. O. Albers, D. J. Robinson, A. Shaver, E. Singleton, *Organometallics 5* (1986) 2199.
[16] S. D. Loren, B. K. Campion, R. H. Heyn, T. Don Tilley, B. E. Bursten, K. W. Luth, *J. Am. Chem. Soc. 111* (1989) 4712.
[17] Crystals suitable for X-ray structure analysis were obtained at − 20 °C from pentane. Space group $P\bar{1}$, $a = 8.872$ (2), $b = 11.483$ (2), $c = 15.260$ (1) Å, $\alpha = 88.99$ (1), $\beta = 88.85$ (1), $\gamma = 74.10$ (1)°, $V = 1495.8$ Å^3, $M_{calcd} = 335.4$, $Z = 4$, F(OOO) = 688, $\varrho_{calcd} = 1.49$ g cm^{-3}, $\mu = 10.21$ cm^{-1}. Enraf-Nonius four-circle diffractometer, 20 °C, $Mo_{K\alpha}$ radiation ($\lambda = 0.71069$ Å, graphite monochromator). 5409 unique and 4359 observed ($I > 2\sigma(I)$, R = 0.06) reflections ($\pm h \pm k + l$), $\sin\theta/\lambda_{max} = 0.60$. The solution of the structure was accomplished by the heavy-atom method using the XTAL 2.6 program package [20]; hydrogen atoms calculated. 325 refined parameters, $R = 0.041$ ($R_w = 0.048$), residual electron density $\varrho = 1.3$ e Å^{-3}
[18] See A. Siedle in G. Wilkinson (Ed.): *Comprehensive Coordination Chemistry Vol. 2*, Pergamon, Oxford 1987, p. 370 ff.
[19] Crystals suitable for X-ray structure analysis were obtained at − 30 °C from pentane. Space group $P1$, $a = 8.575$ (1), $b = 9.882$ (1), $c = 13.459$ (1) Å, $\alpha = 79.42$ (1), $\beta = 77.32$ (1), $\gamma = 74.01$ (1)°, $V = 1060.3$ Å^3, $M_{calcd} = 459.5$, $Z = 2$, F(OOO) = 476, $\varrho_{calcd} = 1.44$ g cm^{-3}, $\mu = 8.20$ cm^{-1}. Enraf-Nonius four-circle diffractometer, 20 °C, $Mo_{K\alpha}$ radiation ($\lambda = 0.71069$ Å, graphite monochromator). 3837 unique and 3423 observed ($I > 2\sigma(I)$, $R = 0.02$) reflections ($\pm h \pm k + l$), $\sin\theta/\lambda_{max} = 0.60$. The solution of the structure was accomplished by the heavy-atom method using the XTAL 2.6 program package [20]; hydrogen atoms calculated. 227 refined parameters, $R = 0.037$ ($R_w = 0.045$), residual electron density $\varrho = 0.8$ e Å^{-3}. The relatively large temperature factors of the methyl C atoms of the Cp* ligands are due to torsional vibration of this group. Further details of the crystal structure investigation may be obtained from the Fachinformationszentrum Karlsruhe, Gesellschaft für wissenschaftlich-technische Information mbH, D.7514 Eggenstein-Leopoldshafen 2 (FRG), on quoting the depository number CSD-54380, the names of the authors, and the journal citation.
[20] S. R. Hall, J. M. Stewart (Eds.): *XTAL 2.6 Users Manual*, Universities of Western Australia and Maryland 1989.

A Paramagnetic μ-Methylene Complex with a Short Cr^{III}–Cr^{III} Bond**

By *Seok Kyun Noh, Robert A. Heintz, Christoph Janiak, Shawn C. Sendlinger*, and *Klaus H. Theopold**

Despite the intensive study of μ-methylene complexes,[1] representatives of this class of organometallic compounds with unpaired electrons are rare,[2] and μ-CH_2 complexes of chromium are unknown. Our ongoing study of the reactivity of paramagnetic chromium(III) alkyls[3] has now produced an unusual molecule with one bridging methylene group and two bridging methyl ligands spanning a Cr–Cr bond. From an inorganic viewpoint this complex represents an unprecedented example of metal–metal bonding between two Cr^{III} ions of a face-sharing bioctahedron.[4]

We have recently reported the synthesis of the methyl-bridged dimer $[Cp^*(CH_3)Cr(\mu\text{-}CH_3)]_2$ (**1**) (Cp^* = pentamethylcyclopentadienyl).[3g] In solution this electron-deficient compound decomposed with a half-life of ca. 4.5 hours at room temperature. Toepler pump experiments and gas-chromatographic analysis showed that 0.92 equivalents of methane were produced in this reaction. In the ^1H NMR spectrum the Cp^* resonance of **1** ($\delta = 0.56$ in C_6D_6) was cleanly replaced with a new signal at $\delta = 3.0$. Recrystallization of the organometallic product from hexanes at $-30\,^\circ C$ yielded analytically pure $[\{Cp^*Cr(\mu\text{-}CH_3)\}_2(\mu\text{-}CH_2)]$ (**2**) in 45% yield (Scheme 1).[5] The mechanism of this intramolecular C–H activation may involve either a concerted "σ-bond metathesis" (transition structure **A**) or an oxidative addition yielding the *cis*-(alkyl)hydride **B** as an intermediate. While the former reaction pathway is well precedented only for d^0 alkyls,[6] the intermediacy of **B** is made plausible by the existence of alkyls and hydrides of Cr^{IV}.[7]

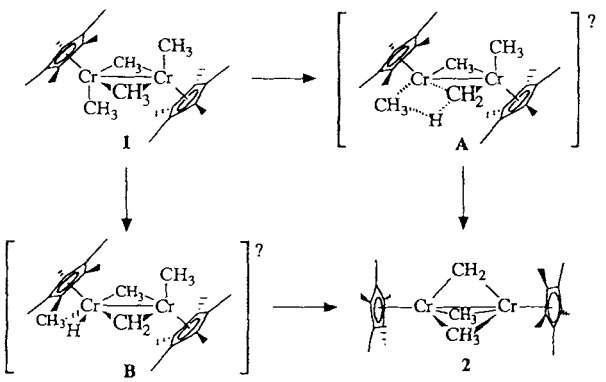

Scheme 1.

The crystal structure of **2** was determined by X-ray diffraction at $-65\,^\circ C$ (Fig. 1).[8] Complex **2** is a binuclear chromium complex and possesses no crystallographic symmetry.

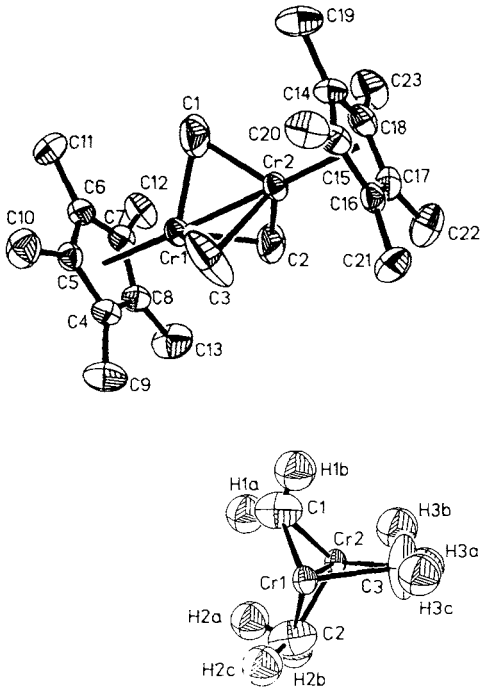

Fig. 1. The molecular structure of $[\{Cp^*Cr(\mu\text{-}CH_3)\}_2(\mu\text{-}CH_2)]$ (**2**). Selected bond distances [Å] and angles [°]: Cr1-Cr2 2.394(1), Cr1-C1 2.033(7), Cr2-C1 2.050(8), Cr1-C2 2.119(8), Cr2-C2 2.103(6), Cr1-C3 2.177(6), Cr2-C3 2.197(7), C1-H1a 0.905, C1-H1b 0.981, C2-H2a 1.064, C2-H2b 0.936, C2-H2c 1.086, C3-H3a 1.007, C3-H3b 0.868, C3-H3c 0.826; Cr1-C1-Cr2 71.8(3), Cr1-C2-Cr2 69.1(2), Cr1-C3-Cr2 66.3(2), C1-Cr1-C2 90.4(3), C1-Cr1-C3 92.0(3), C2-Cr1-C3 91.2(3), C1-Cr2-C2 90.4(3), C1-Cr2-C3 91.0(3), C2-Cr2-C3 91.1(3).

Each chromium is bonded to an η^5-Cp^* ligand, one bridging methylene group, and two bridging methyl ligands, thus placing the metal atom in the pseudooctahedral coordination environment of a three-legged piano stool. The two individual octahedra are joined via a trigonal face, resulting in a very close interaction between the two chromium atoms. Indeed, the Cr–Cr distance of 2.394(1) Å falls squarely within the range found in binuclear Cr^{II} carboxylates (2.28–2.54 Å), which are generally assigned quadruple bonds.[9] Thus **2**, which exhibits the shortest Cr^{III}–Cr^{III} distance found to date, certainly contains a metal–metal bond (see below). All hydrogen atoms of the bridging ligands were located in a difference map, and their positions were refined. Considering the limitations of an X-ray diffraction experiment, the C–H distances and H–C–H angles are reasonable, adding some credibility to the structural results overall. The Cr–C bonds to the methylene group (2.033(7) and 2.050(8) Å) are somewhat shorter than comparable σ bonds to terminal alkyl groups (ca. 2.09 Å).[3] Unexpectedly, the two methyl groups exhibit significantly different Cr–C bond lengths. While the bonds to C3 (2.177(6) and 2.197(7) Å) are similar to those found in **1** (2.170(5) and 2.206(4) Å), C2 features much shorter Cr–C distances (2.103(6) and 2.119(8) Å).

The extremely short Cr–Cr distance of **2** might be expected to lead to pairing of the d electrons in bonding molecular orbitals and thus we were surprised to find that the effective magnetic moment of **2** at room temperature substantially exceeds that of **1** (2.1 μ_B at room temperature), which exhibits a longer Cr–Cr distance (2.606(4) Å). The magnetic susceptibility of solid **2** in the temperature interval 60–280 K was measured with a Faraday balance; μ_{eff} increased with temperature and reached a value of 3.3 μ_B at room temperature. This behavior is consistent with merely antiferromagnetic coupling[10] of the two chromium centers (note that

[*] Prof. K. H. Theopold [+], Dr. S. K. Noh, R. A. Heintz, Dr. C. Janiak, Dr. S. C. Sendlinger
Department of Chemistry, Baker Laboratory
Cornell University, Ithaca, NY 14853 (USA)

[+] New address:
Department of Chemistry and Biochemistry
University of Delaware
Newark, DE 19716 (USA)

[**] This research was supported by the National Science Foundation (CHE-8820354) and by the Deutscher Akademischer Austauschdienst (NATO postdoctoral fellowship to *C. J.*).

$[Cp^*Cr(\mu\text{-}Cl)CH_3]_2$ has no Cr–Cr bond (d_{Cr-Cr}: 3.278 Å)[11] and $\mu_{eff} = 3.5\ \mu_B$ at 280 K[3e]).

To address the extent of metal–metal bonding in **2** and to reconcile the structural data with the magnetic measurements, we have performed an EHMO calculation on the model compound $[\{\eta^5\text{-}Cp)Cr(\mu\text{-}CH_3)\}_2(\mu\text{-}CH_2)]$ (**2a**).[12] It is important to realize that one does not have to invoke metal–metal bonding to explain the short metal–metal contact found in **2**. A simple geometric calculation—assuming average $Cr\text{–}C_{bridge}$ bond distances of 2.11 Å and ideal octahedral geometry (all C–Cr–C angles 90°)—yields a Cr–Cr distance of 2.44 Å for a confacial bioctahedral structure. Thus, a strong metal–metal interaction may be a consequence rather than the cause of the observed structure. Figure 2 shows a partial interaction diagram of the fragment orbitals of two CpCr moieties and the hybrid orbitals of the bridging

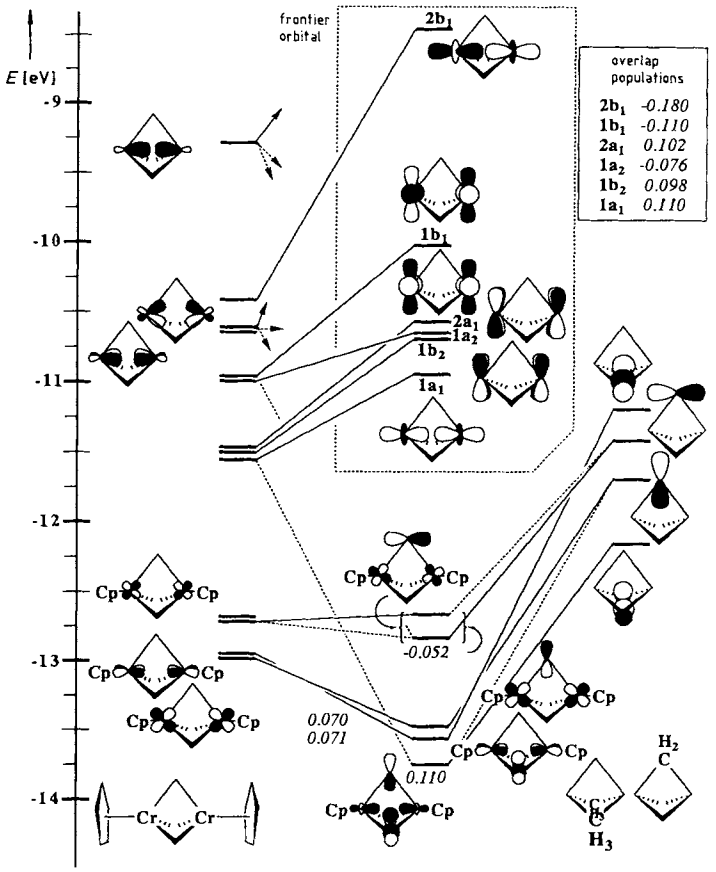

Fig. 2. Partial interaction diagram for $[\{CpCr(\mu\text{-}CH_3)\}_2(\mu\text{-}CH_2)]$ (**2a**). Numbers in italics are overlap populations; symmetry labels were assigned assuming C_{2v} symmetry. The overlap populations for the frontier d orbitals (inner box) were calculated for doubly occupied levels. Cp denotes substantial charge density on the cyclopentadienyl ligand.

ligands. As in the theoretical analysis of **1**,[3g] we find that the two three-center two-electron methyl bridges provide for substantial M–M overlap population (0.206) due to core orbitals. The three-center four-electron methylene bridge, on the other hand, makes only a minor contribution, as its filled Cr–C bonding combinations also give rise to metal–metal antibonding core levels.

Concerning the frontier d orbitals, Figure 2 shows the lower six levels (the two "t_{2g} sets" of the local octahedra) of the general 4-over-6 pattern expected for a confacial bioctahedron.[13] In idealized D_{3h} symmetry these are split into a_1' (σ), e′ (δ), e″ (δ^*), and a_2'' (σ^*) levels, the details of the pattern and energy gaps depending strongly on the metal and the M–X–M bridge angles. In the present case the σ^* level ($2b_1$ in C_{2v} symmetry) is too high in energy (1.5 eV above $1b_1$) to be populated in the electronic ground state. The remaining five levels lie within 1.0 eV and are available for filling with a total of six electrons. The extended Hückel method[14] does not take into account electron–electron interactions and thus cannot reliably predict the ground state of **2a**. However, the calculations are entirely consistent with a spin equilibrium between singlet, triplet, and pentet configurations. Herein lies the explanation for the higher magnetic moment of **2** when compared with **1**. Complex **1** features both σ and π bonding between the metals; both σ^* and π^* levels are thus destabilized beyond possible occupation, leaving only four MOs for six electrons (possible spin multiplicities $S = 0,1$). However, **2** exhibits σ and δ overlap and only the σ^* orbital is destabilized sufficiently to prevent occupation by electrons, thus leaving five MOs to be filled with six electrons (possible spin multiplicities $S = 0, 1, 2$).

We believe **2** is best described as having a chromium–chromium single bond. One aim of further experiments in our laboratory is the preparation of molecules with even shorter Cr^{III}–Cr^{III} distances. The "supershort" Cr^{II}–Cr^{II} quadrupole bonds (down to 1.828(2) Å)[9] provide a challenge, and the discovery of further examples of metal–metal bonding involving trivalent chromium is anticipated.

Received: February 6, 1990 [Z 3784 IE]
German version: *Angew. Chem. 102* (1990) 805

CAS Registry numbers:
1, 124242-59-7; **2**, 127446-27-9; **2a**, 127446-28-0.

[1] a) W. A. Herrmann, *Adv. Organomet. Chem. 20* (1982) 159; b) J. Holton, M. F. Lappert, R. Pearce, P. I. W. Yarrow, *Chem. Rev. 83* (1983) 135; c) J. E. Hahn, *Prog. Inorg. Chem. 31* (1984) 205; d) R. J. Puddephatt, *Polyhedron 7* (1988) 767.

[2] a) P. J. Krusic, F. N. Tebbe, *Inorg. Chem. 21* (1982) 2900; b) K. I. Goldberg, R. G. Bergmann, *J. Am. Chem. Soc. 110* (1988) 4853.

[3] a) D. S. Richeson, S.-W. Hsu, N. H. Fredd, G. Van Duyne, K. H. Theopold, *J. Am. Chem. Soc. 108* (1986) 8273; b) D. S. Richeson, J. F. Mitchell, K. H. Theopold, *ibid. 109* (1987) 5868; c) B. J. Thomas, J. F. Mitchell, K. H. Theopold, *J. Organomet. Chem. 348* (1988) 333; d) B. J. Thomas, K. H. Theopold, *J. Am. Chem. Soc. 110* (1988) 5902; e) D. S. Richeson, J. F. Mitchell, K. H. Theopold, *Organometallics 8* (1989) 2570; f) S. K. Noh, R. A. Heintz, K. H. Theopold, *ibid. 8* (1989) 2071; g) S. K. Noh, S. C. Sendlinger, C. Janiak, K. H. Theopold, *J. Am. Chem. Soc. 111* (1989) 9127.

[4] a) F. A. Cotton, D. A. Ucko, *Inorg. Chim. Acta 6* (1972) 161; b) D. B. Morse, T. B. Rauchfuss, S. R. Wilson, *J. Am. Chem. Soc. 112* (1990) 1860; in contrast to these authors we do not believe that the Cr–Cr distance of 3.00(1) Å in $[Cp_2^*Cr_2(\mu\text{-}I)_3]^{\oplus}$ indicates significant metal–metal bonding between two Cr^{III} ions.

[5] **2**: ^1H NMR (C_6D_6): $\delta = 3.0$ (br, Cp*), 85.7 (v br, CH_3 and CH_2?). IR (KBr): $\tilde{\nu} = 2908$(s), 2852(m), 1437(m), 1375(s), 1161(w), 1109(w), 1024(m), 912(w), 565(w), 498(w) cm^{-1}. Correct elemental analysis.

[6] M. E. Thompson, S. E. Baxter, A. R. Bulls, B. J. Burger, M. C. Nolan, B. D. Santarsiero, W. P. Schaefer, J. E. Bercaw, *J. Am. Chem. Soc. 109* (1987) 203.

[7] F. A. Cotton, G. Wilkinson: *Advanced Inorganic Chemistry*, 5th ed, New York 1988, p. 691.

[8] Purple crystals from hexanes; monoclinic $P2_1/c$; $a = 10.166(2)$, $b = 14.260(4)$, $c = 16.328(3)$ Å, $\beta = 106.26(2)°$; $Z = 4$; $R = 0.060$. Further details of the crystal structure determination are available on request from the Fachinformationszentrum Karlsruhe, Gesellschaft für wissenschaftlich-technische Information mbH, D-7514 Eggenstein-Leopoldshafen 2 (FRG), on quoting the depository number CSD-54477, the names of the authors, and the journal citation.

[9] a) F. A. Cotton, R. A. Walton, *Multiple Bonds Between Metal Atoms*, Wiley, New York 1982, p. 150, b) *Struct. Bonding (Berlin) 62* (1985) 1.

[10] a) R. L. Martin in E. A. V. Ebsworth, A. G. Maddock, A. G. Sharp (Eds.): *New Pathways in Inorganic Chemistry*, Cambridge University Press, Cambridge 1968, Chapter 9; b) R. L. Carlin: *Magnetochemistry*, Springer Verlag, Berlin, 1986, Chapter 5; c) C. J. Cairns, D. H. Busch, *Coord. Chem. Rev. 69* (1986) 1.
[11] W. A. Herrmann, W. R. Thiel, E. Herdtweck, *J. Organomet. Chem. 353* (1988) 323.
[12] The computations were performed within the extended Hückel formalism with weighted H_{ij}'s [14]. The atomic and geometric parameters were (H_{ii}, ζ): Cr4s, − 8.66 eV, 1.70; 4p, − 5.24 eV, 1.70; 3d, − 11.22 eV, 4.95, 1.60 (coefficients for double ζ expansion: 0.4876, 0.7205) [15]; C 2s, − 21.4 eV, 1.625; 2p, − 11.4 eV, 1.625; H 1s, − 13.6 eV, 1.3 [14]. Cr-Cr 2.40 Å, Cr-CH_2 2.04 Å, Cr-CH_3 2.15 Å, C-H 0.96 Å, Cr-Cp(center) 1.906 Å, C-C (Cp) 1.41 Å; idealized C_{2v} symmetry.
[13] R. H. Summerville, R. Hoffmann, *J. Am. Chem. Soc. 101* (1979) 3821.
[14] a) R. Hoffmann, *J. Chem. Phys. 39* (1963) 1397; b) R. Hoffmann, W. N. Lipscomb, *ibid. 36* (1962) 2179, *37* (1962) 2872; c) J. H. Ammeter, H. B. Bürgi, J. C. Thibeault, R. Hoffmann, *J. Am. Chem. Soc. 100* (1978) 3686.
[15] T. A. Albright, P. Hofmann, R. Hoffmann, C. P. Lillya, P. A. Dobosk, *J. Am. Chem. Soc. 105* (1983) 3396.

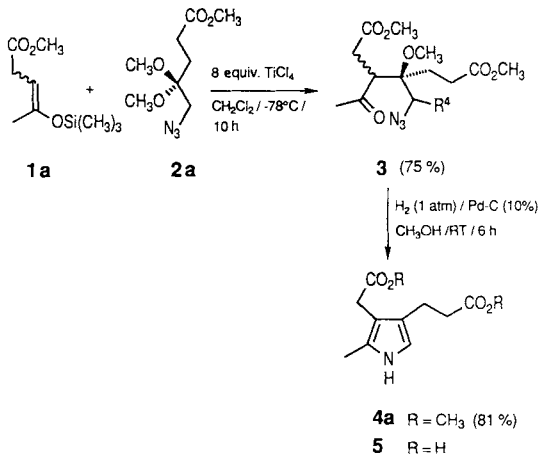

Scheme 1. Synthesis of the pyrrole **4a** via crossed aldol reaction (RT = room temperature).

A Novel Pyrrole Synthesis**

By *Hugo Bertschy, Anne Meunier*, and *Reinhard Neier**

The importance of pyrroles as natural products can be traced to the many functions which are fulfilled by tetrapyrrolic ligands.[1] The most important example of a natural alkyl-substituted pyrrole is porphobilinogen, the precursor for all tetrapyrrolic ligands. Biosynthetically, porphobilinogen is formed with the help of δ-aminolevulinic acid dehydratase (EC 4.2.1.24) in a condensation reaction starting from two molecules of δ-aminolevulinic acid.[2] Formally, this transformation corresponds to a Knorr pyrrole synthesis. Up to now, however, this synthetic path could not be imitated in vitro.

Two mechanisms have been postulated for the enzyme-catalyzed synthesis of porphobilinogen, but no unequivocal proof for either of them has been put forward.[3] The mechanism proposed by *Shemin* is especially attractive for chemists, because the reaction sequence starts with the key step, the formation of the C–C bond. The problem of regioselectivity is solved right at the beginning and all the successive steps follow from the natural reactivity of the intermediates. This is in contrast to the proposed mechanism for the Knorr pyrrole synthesis,[4] where the C–N bond is formed first. In the Knorr synthesis the C–C bond formation occurs regioselectively only if the intermediate enamine is stabilized by conjugation. It is therefore difficult to synthesize alkyl-substituted pyrroles using a Knorr reaction.

We report here the regioselective synthesis of alkyl-substituted pyrroles, which follows *Shemin*'s proposal for the biosynthesis of porphobilinogen. Regioselectively formed silyl enol ethers are used in a crossed aldol reaction[5] (Scheme 1). The aldol products are transformed into mono-, di-, tri-, and tetraalkyl-substituted pyrroles (Table 1). Annelated and aryl-substituted pyrroles can also be synthesized via this sequence. The substitution pattern is determined by the aldol reaction. This sequence allows the synthesis of pyrroles starting with aldol products under very mild conditions.

[*] Priv.-Doz. Dr. R. Neier, Dipl.-Chem. H. Bertschy, Dr. A. Meunier
Organisch-chemisches Institut der Universität
Pérolles, CH-1700 Fribourg (Switzerland)

[**] This work was supported by the Swiss National Science Foundation and CIBA Geigy AG. We thank *E. Bard, F. Nydegger, F. Fehr*, and Dr. *T. A. Jenny* for the spectra.

In order to use *Mukaiyama*'s crossed aldol reaction for the synthesis of pyrroles, adequate derivatives of α-amino ketones had to used. The azido group has been used successfully as a synthetic equivalent for amino groups. The acetal of α-azido ketones can be easily synthesized in two steps starting from α-halo ketones.[6] The synthesis of the second component, the silyl enol ethers, has been described already.[7]

Table 1. Synthesis of alkylpyrroles using the regioselective aldol reaction followed by cyclization.

No.	Silyl enol ether [a]	Acetal [b]	Reaction conditions [c]	Product (yield [%]) [d]
1	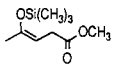 **1a**	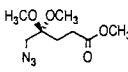 **2a**	1. A, 75 % 2. B, 81 %	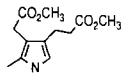 **4a** (61 %)
2	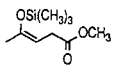 **1a**	**2b**	1. A, 84 % 2. B, 52 %	**4b** (44 %)
3	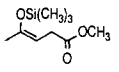 **1a**	**2c**	1. A, 80 % 2. B, 63 %	**4c** (50 %)
4	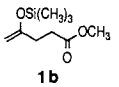 **1b**	**2c**	1. A, 98 % 2. B, 26 %	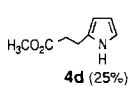 **4d** (25%)
5	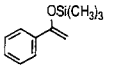 **6**	**2b**	1. A, 85 % 2. C, 89 %	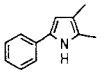 **4e** (76%)

[a] Acetal:silyl enol ether = 1:1.1. [b] Acetals **2a** and **2b** were synthesized starting from the azido ketones [6]. Compound **2c** was synthesized starting from commercially available 2-bromo-1,1-dimethoxyethane (1.5 equiv. NaN_3/DMSO/KI (cat.)/90 °C/5 d). [c] A: 6 equiv. $TiCl_4/CH_2Cl_2/-78$ °C/6–8 h (trial 1:8 equiv. $TiCl_4$), yield calculated starting from the acetal; B: H_2/Pd-C 10%/CH_3OH/room temperature 6 h–2 d; C: PBu_3/C_6H_6/room temperature/5 d. yield relative to the unpurified aldol product; after crystallization (trial 1), after flash chromatography (hexane/EtOAc) (trials 4, 5), after kugelrohr distillation (80–120 °C/10^{-3} Torr) (trials 2, 3). [d] Total yield.

However, only the synthesis of the mixture of the two regioisomers **1a** and **1b** has been reported. We succeeded in synthesizing **1a** and **1b** regioselectively starting from the corresponding bromides (Scheme 2). The α-bromo ketones could be transformed reductively with zinc and trimethylchlorosilane into the pure silyl enol ethers **1a** and **1b** (69% and 76% yield, respectively). The addition of tetramethylethylenediamine after the reduction but before workup is crucial for the success of the reductive silylation.[8]

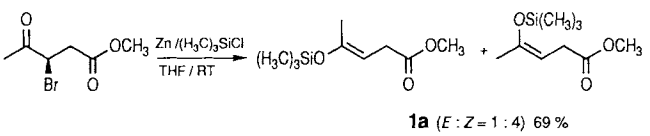

1a ($E:Z = 1:4$) 69%

Scheme 2. Regioselective synthesis of the silyl enol ether **1a** under reductive conditions (RT = room temperature).

The key step of our synthetic plan, the aldol reaction between a silyl enol ether and an α-azido acetal generally gave product in good yield (75%–98%, compare Table 1). A great excess of $TiCl_4$ was used to accelerate the aldol reaction. The separation of the mixture of diastereoisomers formed in the aldol reaction was not necessary for the synthesis of pyrroles. The aldol product could be directly treated with phosphanes in a Staudinger reaction or reduced with hydrogen[9] to give pyrroles in good yields (26%–89%, compare Table 1). Only the corresponding pyrrole could be isolated. The purification of the sensitive alkyl-substituted pyrroles was the most difficult task in this reaction sequence. The products are very unstable in the presence of tiny amounts of acids. Therefore, the workup for each product had to be optimized. The catalytic reduction has been successful in most cases. Removal of the catalyst by filtration followed by evaporation of the solvent often furnished a product of good spectroscopic purity.

This novel pyrrole synthesis allows the formation of unstablized alkylpyrroles in a regioselective manner. The synthetic strategy follows the proposal of *Shemin* for the biosynthesis of porphobilinogen. The enzymatic synthesis of the pyrrole **5** starting from one molecule of levulinic acid and one molecule of δ-aminolevulinic acid has been described.[10] Therefore, the synthesis of the pyrrole **4a** mimics formally the biosynthetic process by which the pyrrole **5** is formed.

Typical Experimental Procedure

Aldol product **3**: To a solution of azido acetal **2a** (2.17 g, 0.01 mol) in 50 mL of CH_2Cl_2, 8.8 mL (0.08 mol) of $TiCl_4$ was added in two portions at −78 °C under nitrogen atmosphere. Silyl enol ether **1a** (2.43 g, 0.012 mol) in 50 mL of CH_2Cl_2 was slowly added in such a manner that the temperature did not rise above −70 °C. The red-brown suspension was stirred for 10 h at −78 °C. The reaction was then quenched by adding 100 mL of ice water. After the separation of the two phases, the water phase was extracted with 3 × 50 mL of CH_2Cl_2. The organic phases were washed with 2 × 50 mL of saturated NaCl and dried with $MgSO_4$ and the solvent was removed. Removing methyl levulinate by distillation (40 °C, 10^{-3} Torr) gave 2.58 g of a raw material with the following composition: aldol product **3** as a mixture of diastereoisomers (71%); two products of elimination (4%); methyl 5-azidolevulinate (9%, yields are calculated relative to **2a**).

Received: February 26, 1990 [Z 3819 IE]
German version: *Angew. Chem. 102* (1990) 828

[1] R. B. Frydman, B. Frydman, A. Valasinas in D. Dolphin (Ed.): *The Porphyrins, Vol. VI*, Academic Press, New York 1979, pp. 1–123.
[2] F. F. Leeper, *Nat. Prod. Rep. 6* (1989) 171–203.
[3] a) G. F. Barnard, R. Itoh, L. Hohberger, D. Shemin, *J. Biol. Chem. 252* (1977) 8965–8974; b) P. M. Jordan, J. S. Seehra, *J. Chem. Soc. Chem. Commun. 1980*, 240.
[4] R. J. Sundberg in C. W. Bird, G. W. H. Cheeseman (Eds.): *Comprehensive Heterocyclic Chemistry, Vol. 4*, Pergamon Press, Oxford 1984, p. 331.
[5] T. Mukaiyama, *Angew. Chem. 89* (1977) 858–866; *Angew. Chem. Int. Ed. Engl. 16* (1977) 817–825.
[6] a) S. G. Wilkinson in J. F. Stoddard (Ed.): *Comprehensive Organic Chemistry, Vol. 1*, Pergamon Press, Oxford 1979, p. 624; b) M. O. Forster, H. E. Fierz, *J. Chem. Soc. 93* (1908) 669–678.
[7] R. D. Miller, D. R. McKean, *Synthesis 1979*, 730–732.
[8] a) G. M. Rubottom, R. C. Mott, D. S. Krueger, *Synth. Commun. 7* (1977) 327–332; b) A. Itoh, K. Oshima, H. Yamamoto, H. Nozaki, *Bull. Chem. Soc. Jpn. 53* (1980) 2050–2054.
[9] E. F. V. Scriven, K. Turnbull, *Chem. Rev. 88* (1988) 298–368.
[10] D. L. Nandi, D. Shemin, *J. Biol. Chem. 243* (1968) 1236–1242.

Heptasila[7]paracyclophane

By *Wataru Ando,* Takeshi Tsumuraya*, and *Yoshio Kabe*

In recent years [n]paracyclophanes having a short bridge have attracted considerable interest because of the unique properties resulting from bending of the benzene ring.[1–4] The smallest [n]paracyclophane so far isolated is the [6] isomer, first prepared by *Jones* et al. in 1974.[2] Recently, *Bickelhaupt* succeeded in spectroscopic characterization of [5]paracyclophane, which is stable at low temperature in solution, but not isolable,[3] and, more recently, a [4]paracyclophane system has been proposed as a reactive intermediate.[4] In contrast to rather extensive studies of [n]paracyclophane bridged by methylenes, there is no report of preparation of [n]paracyclophanes bridged by heteroatom chains. We report here successful synthesis of the first type of these compounds, heptasila[7]paracyclophane **1**, including the crystal structure of **1**.

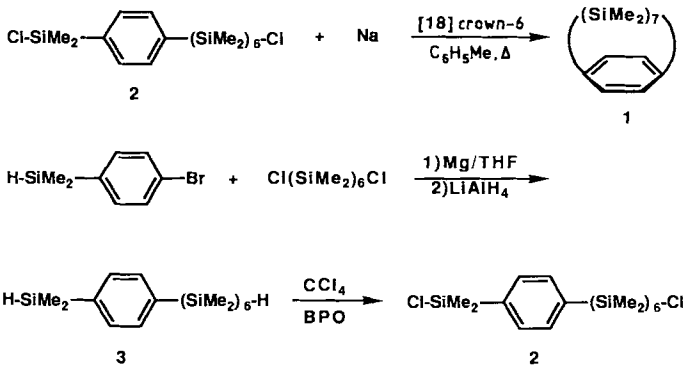

Reductive coupling of 1-chloro-6-[4-(chlorodimethylsilyl)-phenyl]-1,1,2,2,3,3,4,4,5,5,6,6-dodecamethylhexasilane (**2**)[5] by treatment with sodium in refluxing toluene in the presence of [18]crown-6 produced heptasila[7]paracyclophane **1** in 1.2% yield.

Compound **1**, obtained as colorless crystals [UV(hexane): $\lambda_{max} = 248$ nm ($\log\varepsilon = 4.63$)], is stable toward atmospheric oxygen and moisture and does not decompose even when heated to its melting point of 88–88.5 °C. The presence

[*] Prof. W. Ando, Dr. T. Tsumuraya, Dr. Y. Kabe
Department of Chemistry, The University of Tsukuba
Tsukuba, Ibaraki 305 (Japan)

of [18]crown-6 is essential for the formation of **1**; only polymeric substances were obtained in the absence of [18]crown-6.[6] The spectral data are consistent with the proposed structure. The high-resolution mass spectrum and the isotopic ratios of the molecular ion [*m/z* (relative intensity in %) 482 (100), 483 (57), 484 (38), 485 (16), 486 (6), 487 (2)] show that the molecule has composition $C_{20}H_{46}Si_7$. The ^1H, ^{13}C, and ^{29}Si NMR spectra show the presence of a twofold symmetry axis in the molecule [^1H NMR (500 MHz, $CDCl_3$): $\delta = -0.16$ (s, 6H), 0.02 (s, 12H), 0.13 (s, 12H), 0.41 (s, 12H), 7.45 (s, 4H). ^{13}C NMR (125 MHz, $CDCl_3$): $\delta = -5.13$(q), -4.42(q), -3.31(q), -1.80(q), 133.10(d), 140.18(s); ^{29}Si NMR (18 MHz, $CDCl_3$): $\delta = -39.2$, -38.7, -37.1, -18.0.

X-ray structural determination established unequivocally the molecular structure of **1** as shown in Figure 1.[7] Owing to

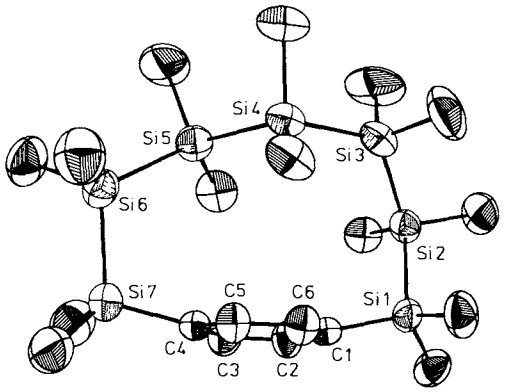

Fig. 1. Molecular structure of **1** (ORTEP) Selected bond lengths [Å] and angles [°]: Si1-Si2 2.376(4), Si2-Si3 2.350(5), Si3-Si4 2.336(5), Si4-Si5 2.350(5), Si5-Si6 2.371(4), Si6-Si7 2.338(5), C1-C2 1.40(1), C1-C6 1.41(1), C2-C3 1.41(1), C3-C4 1.39(1), C4-C5 1.40(1), C5-C6 1.40(1); C2-C1-C6 119.4(9), C1-C2-C3 119.7(9), C2-C3-C4 120.8(9), C3-C4-C5 118.8(9), C4-C5-C6 120.8(9), C1-C6-C5 119.9(9); for further data see text.

the unsymmetrical orientation of the central Si atom (Si4), the molecule has no crystallographic symmetry. Although the Si–Si bond lengths are normal and range between 2.336(5) and 2.371(4) Å, there is interestingly an alternation in the bond angles around the polysilane chain; the bond angles of C1-Si1-Si2 (105.5(3)°) and C4-Si7-Si6 (107.4(3)°) are contracted while those of Si1-Si2-Si3 (117.7(2)°), Si2-Si3-Si4 (126.5(2)°), Si3-Si4-Si5 (116.2(2)°), Si4-Si5-Si6 (115.6(2)°), and Si5-Si6-Si7 (113.7(2)°) are considerably expanded from the normal bond angles.

The most interesting feature in the structure of **1** is the deformation of the benzene ring from planarity, which is represented by the deviation angles θ_1 and θ_2. The deformation angles θ_1 of compound **1** are 6.6 and 4.5° and θ_2 are 6.5 and 9.0°, which are comparable with those observed in octamethyltetrasila[2,2]paracyclophane (**4**) ($\theta_1 = 4.3°$, $\theta_2 = 15.0°$)[8] and its chromium complex **5** ($\theta_1 = 2.5$, 2.2°, $\theta_2 = 10.1$, 10.9°).[9] These θ values are smaller than those of the [7]paracyclophane derivative **6** ($\theta_1 = 17°$, $\theta_2 = 24°$)[10a] and those of the [8]paracyclophane derivative **7** ($\theta_1 = 9°$, $\theta_2 = 15°$).[10b] The deformation in the benzene ring is less in **1** than in the analogue **6**, but an increase in the deformation in the polysilane chain of **1** is definitely noticeable. These observations are best explained by high flexibility of the conformation in the polysilane chain compared to the methylene chain, involving expansion of the Si–Si–Si angles.

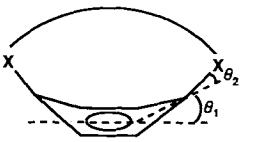

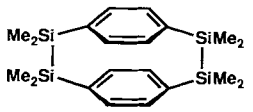

4

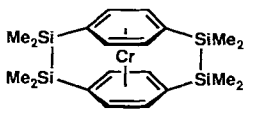

5

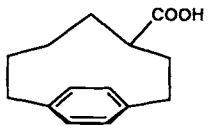

6

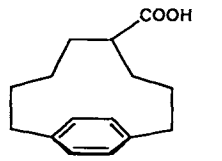

7

The structure of **1** reveals two new aspects of paracyclophane chemistry: (1) polysilane chains could stabilize [n]paracyclophanes and (2) thermal or photochemical silylene extrusion might give lower homologous [n]paracyclophanes.

Experimental Procedure

To a mixture of molten sodium (101 mg, 4.4 mmol) and [18]crown-6 (618 mg, 2.3 mmol) in refluxing toluene (20 mL) was added dropwise a toluene (20 mL) solution of **2** (1.11 g, 2.0 mmol) under dry argon. The mixture was chromatographed on a silica gel with hexane; subsequent separation by preparative HPLC (Japan Analytical Ind. Co., Ltd. LC-08 with JAIGEL-1H column) gave **1** in 1.2% yield as colorless crystals.

Received: January 16, 1990 [Z 3739 IE]
German version: *Angew. Chem. 102* (1990) 813

CAS Registry numbers:
1, 127472-87-1; **2**, 127472-88-2; **3**, 127472-89-3; $Cl(SiMe_2)_6Cl$, 812-54-4; $4\text{-}BrC_6H_4SiHMe_2$, 1637-65-6.

[1] Recent reviews: P. M. Rosenfeld, K. A. Choe in P. M. Keehn, S. M. Rosenfeld (Eds.) *Cyclophanes, Vol. I,* Academic Press, New York 1983, Chapter 5.

[2] a) V. V. Kane, A. D. Wolf, M. Jones, Jr., *J. Am. Chem. Soc. 96* (1974) 2643; b) S. L. Kammula, L. D. Iroff, M. Jones, Jr., J. W. von Straten, W. H. de Wolf, F. Bickelhaupt, *J. Am. Chem. Soc. 99* (1977) 5815; c) H. Günther, P. Schmitt, H. Fischer, W. Tochtermann, J. Liebe, C. Wolff, *Helv. Chim. Acta 68* (1985) 801; d) J. Liebe, C. Wolff, C. Krieger, J. Weiss, W. Tochtermann, *Chem. Ber. 118* (1985) 4144, and references cited therein; e) Y. Tobe, K. Ueda, K. Kakiuchi, Y. Odaira, Y. Kai, N. Kasai, *Tetrahedron 42* (1986) 1851; f) Y. Tobe, A. Nakayama, K. Kakiuchi, Y. Odaira, Y. Kai, N. Kasai, *J. Org. Chem. 52* (1987) 2639; g) Y. Tobe, K. Ueda, T. Kaneda, K. Kakiuchi, Y. Odaira, Y. Kai, N. Kasai, *J. Am. Chem. Soc. 109* (1987) 1136.

[3] a) L. W. Jenneskens, F. J. J. de Kanter, P. A. Kraakman, L. A. M. Turkenburg, W. E. Koolhaas, W. H. de Wolf, F. Bickelhaupt, *J. Am. Chem. Soc. 107* (1985) 3716; b) Y. Tobe, T. Kaneda, K. Kakiuchi, Y. Odaira, *Chem. Lett. 1985*, 1301; c) G. B. M. Kostermans, W. H. de Wolf, F. Bickelhaupt, *Tetrahedron Lett. 27* (1986) 1095; d) *Tetrahedron 43* (1987) 2955.

[4] a) T. Tsuji, S. Nishida, *J. Chem. Soc. Chem. Commun. 1987*, 1189; b) *J. Am. Chem. Soc. 110* (1988) 2157; c) G. B. M. Kostermans, P. van Dansik, W. H. de Wolf, F. Bickelhaupt, *J. Org. Chem. 53* (1988) 4531; d) G. B. M. Kostermans, M. Bobeldijk, W. H. de Wolf, F. Bickelhaupt, *J. Am. Chem. Soc. 109* (1987) 2471; e) T. Tsuji, S. Nishida, *ibid. 111* (1989) 368.

[5] **2**: ^1H NMR (60 MHz, CCl_4): δ 0.12 (s, 6H), 0.14 (s, 6H), 0.20 (s, 6H), 0.22 (s, 6H), 0.40 (s, 6H), 0.50 (s, 6H), 0.68 (s, 6H), 7.40 (AB, $J_{AB} = 6.0$ H_z, $\Delta\nu_{AB} = 6.7$ Hz, 4H). MS: *m/z* (%) 517 (0.6, $M^{\oplus}$-Cl), 383 (2, $Si_6Me_{12}Cl$), 325 (13, $Si_5Me_{10}Cl$), 267 (100, Si_4Me_8Cl), 209 (13, Si_3Me_6Cl). **3**: ^1H NMR (60 MHz, CCl_4): $\delta = 0-0.5$ (m, 4H), 3.70 (sept, $J = 4$ Hz, 1H), 4.40 (sept, $J = 4$ Hz, 1H), 7.35 (s, 4H). ^{13}C NMR (125 MHz, $CDCl_3$): $\delta = -5.63$(q), -5.34(q), -5.07(q), -4.51(q), -4.24(q), -3.61(q),

– 2.72(q), 133.41(d), 133.45(d), 137.54(s), 141.29(s). MS: *m/z* (%). 484 (4, $M^{\oplus}$), 367 (5, $M^{\oplus}-2\ Me_2Si-H$), 309 (10, $M^{\oplus}-3\ Me_2Si-H$), 291 (41, $M^{\oplus}-2\ Me_2Si-C_6H_4$), 233 (100, $M^{\oplus}-3\ Me_2Si-C_6H_4-H$).

[6] Addition of crown ether has been reported to increase the reactivity of the silyl anion by forming a crown ether–sodium ion complex; A. Sekiguchi, T. Yatabe, C. Kabuto, H. Sakurai, *Angew. Chem. 101* (1989) 778; *Angew. Chem. Int. Ed. Engl. 28* (1989) 757; M. Fujino, H. Isaka, *J. Chem. Soc., Chem. Commun. 1989*, 466.

[7] A single crystal with dimensions of $0.5\times0.2\times0.2$ mm, obtained from ethanol was used for the X-ray analysis. Lattice constants were determined by the least-squares method with an angular setting of 25 reflections within the range $11<\theta<13°$. Intensity data were obtained on a Enraf-Nonius CAD4 diffractometer equipped with graphite monochromatized $Mo_{K\alpha}$ radiation and using the $\omega-2\theta$ scan technique ($2\theta<50°$). During data collection three standards, measured every 120 min, indicated a total loss in intensity of 18.4%. A linear decay correction was applied. Of 3158 independent reflections measured, only 2298 were considered as observed on the basis of the criterion $I>3.0\ \sigma(I)$. All intensities were corrected for Lorentz and polarization effects but not for absorption. Crystal data for **1**: $M_r=483.19$; orthorhombic; P_{na21}; $a=15.037(3)$, $b=9.029(3)$, $c=23.231(5)$ Å; $V=3154.3$ Å^3; $Z=4$; $\varrho_{calcd}=1.02$ g cm^{-3}; μ ($Mo_{K\alpha}$) = 3.0 cm^{-1}. The structure of **1** was solved by direct methods and refined by full-matrix least-squares methods. The final refinements with anisotropic temperature factors for the non-hydrogen atoms lowered R and R_w values to 0.059 and 0.072, respectively.

[8] H. Sakurai, S. Hoshi, A. Kamiya, A. Hosomi, C. Kabuto, *Chem. Lett. 1986*, 1781.

[9] C. Elschenbroich, J. Hurley, W. Mass, B. Baum. *Angew. Chem. 100* (1988) 727; *Angew. Chem. Int. Ed. Engl. 27* (1988) 684.

[10] a) N. L. Allinger, T. J. Walter, M. G. Newton, *J. Am. Chem. Soc. 96* (1974) 4588; b) M. G. Newton, T. J. Walter, N. L. Allinger, *ibid. 95* (1973) 5652.

Base-Free Cationic 14-Electron Titanium and Zirconium Alkyls: In situ Generation, Solution Structures, and Olefin Polymerization Activity**

By *Manfred Bochmann,* Andrew J. Jaggar,* and *Julian C.Nicholls*

Various lines of evidence suggest that cationic group IV metal alkyl complexes of the type $[Cp_2M-R]^{\oplus}$ (M = Ti, Zr, Hf) are the catalytically active species in homogeneous metallocene-based Ziegler–Natta polymerization systems.[1] We have earlier reported the synthesis of a number of ligand-stabilized cationic titanium complexes[2] and, with the aid of model compounds, have demonstrated the mechanistic pathway which is available to unsaturated substrates capable of insertion into the Ti–C σ bond.[3] In independent work it was shown that cationic alkyl complexes that contain weakly coordinating ligands such as THF[4] and base-free zwitterionic compounds such as $[Cp_2^*Zr\text{-}C_6H_4BPh_3]$[5] polymerize ethylene in the absence of aluminum alkyl activators, sometimes requiring elevated temperatures and pressures.[5] While these findings are highly suggestive of the catalytic role played by cationic metal alkyls, no information has as yet been available about the structure of such species under the conditions of polymerization catalysis. We now report the generation in solution of some cationic titanium and zirconium alkyls and the observation of multiple ethylene insertion into the $Ti-CH_3$ bond.

Treatment of a dichloromethane solution of bis(indenyl)dimethyltitanium (**1a**) with one equivalent of dimethylanilinium tetraphenylborate (**2a**) gives methane and the deep brown cation of **3a**, $[Ind_2TiMe]^{\oplus}$ (Scheme 1). The reaction can be conveniently followed by high-field NMR spectroscopy (see *Experimental Procedure*). The methyl signal of the starting material **1a** ($\delta=-0.94$) is replaced by a singlet at $\delta=-0.15$; the ^{13}C NMR signal for the methyl group of **3a** at $\delta=70.8$ lies within the range expected for cationic titanium alkyl complexes.[2b]

$$[R_2MMe_2] + [R'_3NH]BPh_4 \xrightarrow[CH_2Cl_2]{-CH_4/-NR'_3} [R_2M-Me]BPh_4$$

1a, R = Ind, M = Ti; **1b**, R = Cp, M = Ti; **1c**, R = Cp, M = Zr

2a, R'_3N = $PhNMe_2$; **2b**, R'_3N = nBu_3N

3a/3a', R = Ind, M = Ti; **3b**, R = Cp, M = Ti; **3c/3c'**, R = Cp, M = Zr

$$\left[Ind_2Ti\begin{matrix}Me\\OEt_2\end{matrix}\right]BPh_4 \quad (\mathbf{4}) \xleftarrow{Et_2O} \mathbf{3a} \xrightarrow{C_2H_4} [Ind_2Ti(CH_2CH_2)_nMe]^{\oplus}$$

Scheme 1. Ind = indenyl, Cp = cyclopentadienyl.

By an analogous procedure, deep orange $[Cp_2TiMe]BPh_4$ (**3b**) and pale yellow $[Cp_2ZrMe]BPh_4$ (**3c**) are synthesized in dichloromethane solution by allowing **1b** and **1c**, respectively, to react with $[PhNMe_2H]BPh_4$ (**2a**). The reaction of **1a**, or **1c** with $[nBu_3NH]BPh_4$ (**2b**) proceeds equally facilely to give **3a** and **3c**, respectively. The addition of diethyl ether to solutions of **3a** results in the formation of $[Ind_2TiMe(Et_2O)]BPh_4$ (**4**) as poorly soluble black microcrystals, while the addition of acetonitrile to **3b** produces the known[2b] adduct $[Cp_2TiMe(NCMe)]BPh_4$.

Various structural possibilities (**A**–**E**; Scheme 2) can be envisaged for the complex cations. A trigonal-planar geometry (**A**) is ruled out by the observed inequivalence of H-1 and H-3 of the indenyl five-membered ring in **3a**; the signal pattern resembles that of isolated pseudo-tetrahedral complexes of the type $[Ind_2TiMe(L)]^{\oplus}$.[2b] Although not necessarily conclusive, a comparison of the C-H coupling constants of the methyl groups of **3a** ($J=128.7$ Hz) and of the nonagostic $[Ind_2TiMe_2]$ ($J=125.2$ hz) makes an agostic structure (**B**) appear unlikely; neutral scandium complexes isoelectronic to **3b** have also failed to provide conclusive evidence for an agostic methyl ligand.[6]

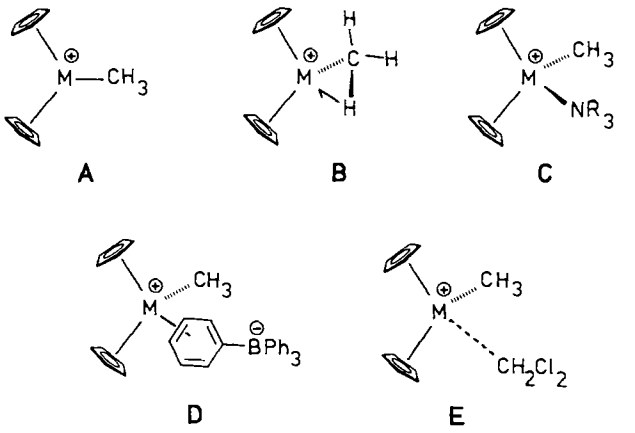

Scheme 2.

[*] Dr. M. Bochmann, A. J. Jaggar, Dr. J. C. Nicholls
School of Chemical Sciences
University of East Anglia
Norwich NR4 7TJ (UK)

[**] This work was supported by the Science and Engineering Research Council (UK). We thank Dr. *J. A. Daniels* (ICI Wilton) for gel permeation chromatography measurements.

It could be expected that Lewis-acidic cationic metal centers such as those present in **3a–3c** would have a tendency to interact with $BPh_4^{\ominus}$. Solutions of **3a–3c**, prepared using $[PhNMe_2H]BPh_4$ (**2a**), show a complex ^1H NMR pattern in the aromatic region. In $[PhNMe_2H]BPh_4$ (**2a**) the chemical shifts of the phenyl groups of the anion are strongly influenced by the presence of the anilinium cation, presumably due to ion pairing, while solvent-separated $BPh_4^{\ominus}$ ions as in $[nBu_3NH]BPh_4$ (**2b**) gives rise to three well-separated ^1H NMR signals for the *para, meta,* and *ortho* protons.[7] Solutions of **3a–3c** at $-40\,^{\circ}C$ show the presence of both ion-paired and solvated $BPh_4^{\ominus}$ ions in ratios varying from 3:1 to 3:2. In addition, the signals of free dimethylaniline are identified; an adduct of type **C** is not found. There is also no evidence that one phenyl ring of a $BPh_4^{\ominus}$ ion is coordinated to a metal center or subject to an environment different from the other three (cf. structure **D**), even at low temperature. This finding contrasts with our recent isolation of an η^6-$BPh_4^{\ominus}$ complex of a trialkylzirconium cation, $[Zr(CH_2Ph)_3(\eta^6\text{-}C_6H_5BPh_3)]$.[8] The observations suggest that base-free bis(cyclopentadienyl)metal alkyl cations have a pseudo-tetrahedral solvated structure of type **E**.[9]

By contrast, titanium and zirconium cations prepared from $[nBu_3NH]BPh_4$ (**2b**) and **1** show only solvated $BPh_4^{\ominus}$; there is no indication of an association between anions and cations. Because of the basicity of nBu_3N, the formation of labile amine complexes as indicated in **C** is likely in these cases. In agreement with this assumption, the ethylene polymerization activity of **3a′** and **3c′**, prepared with **2b**, is reduced to ca. 20% of the activity of **3a** and **3c**.

Exposure of a solution of **3a** in CD_2Cl_2 at $-40\,^{\circ}C$ to ca. 5 equivalents of ethylene leads to a reduction in intensity of the Ti-CH_3 signal at $\delta = -0.15$ and the appearance of new signals in the alkyl region at $\delta = 0.7$, 0.9, and 1,2, indicating the insertion of ethylene into the titanium–carbon bond. These signals grow further on prolonged exposure to an excess of ethylene, until the precipitation of polyethylene is seen.[12] The Ti-Me signal does not disappear completely during the initial stages of the chain-growth reaction; this observation suggests that subsequent C_2H_4 insertions proceed more readily than the first.[13]

Solutions of **3a** polymerize ethylene at 1 bar over a temperature interval of $+10$ to $-60\,^{\circ}C$; the activity shows a maximum at ca. $-20\,^{\circ}C$ and decreases rapidly above ca. $+15\,^{\circ}C$. The polymerization rate is fast for the first 10 to 15 minutes before it decays to a more steady lower level. The polydispersity of the resulting polyethylene decreases with the polymerization temperature from $\bar{M}_w/\bar{M}_n = 2.5$ at $+10\,^{\circ}C$ to 2.0 at $-40\,^{\circ}C$; such a narrow distribution is typical of chemically homogeneous active sites. The IR spectra of hot-pressed films showed the absence of pendent-methylene and terminal unsaturation.[14] The catalytic activities of **3b** and **3c** under identical conditions are lower than that of **3a**. Of the three catalysts, the zirconium complex is the thermally most stable and, although operating at a lower initial activity than **3a**, appears less susceptible to catalyst deactivation. Propylene is polymerized by **3a** at $0\,^{\circ}C$ at a slower rate. In agreement with earlier observations on non-stereorigid catalysts operating at comparable temperatures,[15] the resulting polypropylene is atactic.

Experimental Procedure

All reactions were performed under purified argon. Reactions with $[PhNMe_2H]BPh_4$ (**2a**): For NMR experiments, **2a** (37 mg, 0.084 mmol) was suspended in 0.3 mL of CD_2Cl_2 and cooled to $-80\,^{\circ}C$. A solution of $[Ind_2TiMe_2]$ (**1a**) (26.5 mg, 0.086 mmol) in 0.3 mL of CD_2Cl_2 was injected, the tube was sealed, and the sample allowed to warm to $0\,^{\circ}C$. The solution began to darken at $-60\,^{\circ}C$, and the reaction was complete after 10–15 min at $0\,^{\circ}C$ to give **3a**. Samples of **3b** and **3c** were prepared on a similar way. In all cases the formation of methane was observed ($\delta = 0.22$).

3a: ^1H NMR (400 MHz, CD_2Cl_2, $-40\,^{\circ}C$): $\delta = -0.15$ (s, 3 H, Ti-Me), 5.98 (dd, poorly resolved, 1 H, indenyl H-1), 5.78 (t, 1 H, indenyl H-2, $J = 3.3$ Hz), 6.21 (dd, poorly resolved, 1 H, indenyl H-3), 7.2–7.8 (indenyl H-4 to H-7), unresolved); associated $BPh_4^{\ominus}$: 7.63 ("d", *ortho*-H), 7.51 ("t", *meta*-H), 7.56 ("t", *para*-H); solvent-separated $BPh_4^{\ominus}$: 7.21 (unresolved, *ortho*-H), 7.07 ("t", *meta*-H), 6.93 ("t", *para*-H); free dimethylaniline: 2.92 (s, N-Me), 6.71 ("d", *ortho*-H), 7.22 ("t", *meta*-H), 6.68 ("t", *para*-H). ^{13}C NMR: $\delta = 70.8$ (Ti-Me, J(C-H) 128.7 Hz). In some samples, a second, as yet unidentified titanium species is also formed, characterized by ^1H NMR signals at $\delta = -0.19$ (Ti-Me), 5.94, 6.01, and 6.35 (indenyl); this species does not participate in polymerization reactions. **3b**: ^1H NMR (400 MHz, CD_2Cl_2, $-40\,^{\circ}C$): $\delta = 1.26$ (s, 3 H, Ti-Me), 6.28 (s, 10 H, Cp). **3c**: ^1H NMR (400 MHz, CD_2Cl_2, $-40\,^{\circ}C$): $\delta = 0.27$ (s, 3 H, Zr-Me), 6.25 (s, 10 H, Cp). The values for solvent-separated and associated $BPh_4^{\ominus}$ and for dimethylaniline present in solutions of **3b** and **3c** closely correspond to those given for **3a**. **4**: A solution of $[Ind_2TiMe_2]$ (**1a**) (0.37 g, 1.2 mmol) in 5 mL of toluene was added to a suspension of 0.441 g of $[PhNMe_2H]BPh_4$ **2a** in 20 mL of dichloromethane–diethyl ether 1:1 at $-70\,^{\circ}C$. On warming to room temperature, black microcrystalline **4** separated and was filtered off, washed with CH_2Cl_2–Et_2O, and dried (0.2 g, 0.29 mmol, 29%). Satisfactory elemental analysis. ^1H NMR (60 MHz, C_5D_5N): $\delta = 0.23$ (s, 3 H, Ti-Me), 1.09 (t, 6H, OCH_2CH_3), 3.36 (q, 4 H, OCH_2CH_3), 6.38 (m, 2 H, indenyl), 6.51 (m, 4H, indenyl), 7.2 (m, 20 H, indenyl, $BPh_4^{\ominus}$, 8.08 (m, broad, 8 H, $BPh_4^{\ominus}$).

Reactions with $[nBu_3NH]BPh_4$ (**2b**): Procedure as described for $[PhNMe_2H]BPh_4$ (**2a**). **3a′** ^1H NMR (400 MHz, CD_2Cl_2, $-40\,^{\circ}C$): $\delta = -0.15$ (Ti-Me), 5.99 (dd, poorly resolved, 1 H, indenyl H-1), 5.79 (t, 1 H, indenyl H-2, $J = 3.3$ Hz), 6.22 (dd, poorly resolved, 1 H, indenyl H-3), 7.3–7.7 (m, indenyl H-4 to H-7); $BPh_4^{\ominus}$: 7.41 (unresolved, *ortho*-H), 7.08 ("t", *meta*-H), 6.93 ("t", *para*-H); nBu_3N: $\delta = 0.89$, 0.94, 1.18, 2.11, 2.43. **3c′**: ^1H NMR (400 MHz, CD_2Cl_2, $-40\,^{\circ}C$): $\delta = 0.27$ (s, 3 H, Zr-Me), 6.24 (s, 10 H, Cp); the values for $BPh_4^{\ominus}$ and nBu_3N closely correspond to those given for **3a′**.

General procedure for polymerization reactions: $[PhNMe_2H]BPh_4$ (**2a**) (0.240 g, 0.544 mmol) was suspended in 30 mL of dichloromethane and cooled to $-40\,^{\circ}C$. 3.05 mL of a 0.18 M solution of $[Ind_2TiMe_2]$ (**1a**) in toluene (0.549 mmol) was injected with rapid stirring and purified ethylene was admitted. After two hours the reaction was quenched by the injection of 10 mL of methanol and polyethylene (3.25 g) was isolated ($\bar{M}_w$ relative to NBS1475 standard: 16000; $\bar{M}_w/\bar{M}_n = 2.0$).

Received: March 5, 1990 [Z 3824 IE]
German version: *Angew. Chem. 102* (1990) 830

CAS Registry numbers:
1a, 49596-02-3; **1b**, 1271-66-5; **1c**, 12636-72-5; **2a**, 118573-45-8; **2b**, 64167-39-1; **3a**, 127686-08-2; **3b**, 127686-09-3; **3c**, 127686-10-6; **4**, 127686-12-8; $[Cp_2TiMe(NCMe)]BPh_4$, 109630-95-7; C_2H_4, 74-85-1.

[1] a) F. S. Dyachkowski, A. K. Shilova, A. E. Shilov, *J. Polym. Sci. Part C 16* (1967) 2333; b) J. J. Eisch, A. M. Piotrowski, S. K. Brownstein, E. J. Gabe, F. L. Lee, *J. Am. Chem. Soc. 107* (1985) 7219; c) P. G. Gassman, M. R. Callstrom, *ibid. 109* (1987) 7875; d) C. A. Jolly, D. S. Marynick, *ibid. 111* (1989) 7968.

[2] a) M. Bochmann, L. M. Wilson, *J. Chem. Soc. Chem. Commun. 1986*, 1610; M. Bochmann, L. M. Wilson, M. B. Hursthouse, R. L. Short, *Organometallics 6* (1987) 2556; M. Bochmann, A. J. Jaggar, L. M. Wilson, M. B. Hursthouse, M. Motevalli, *Polyhedron 8* (1989) 1838.

[3] M. Bochmann, L. M. Wilson, M. B. Hursthouse, M. Motevalli, *Organometallics 7* (1988) 1148.

[4] a) R. F. Jordan, C. S. Bajgur, R. Willet, B. Scott, *J. Am. Chem. Soc. 108* (1986) 7410; b) R. F. Jordan, R. E. LaPointe, C. S. Bajgur, S. F. Echols, R. Willet, *ibid. 109* (1987) 4111; c) R. Taube, L. Krukowka, *J. Organomet. Chem. 347* (1988) C9.

[5] G. G. Hlatky, H. W. Turner, R. R. Eckman, *J. Am. Chem. Soc. 111* (1989) 2728.

[6] M. E. Thompson, S. M. Baxter, A. R. Bulls, B. J. Burger, M. C. Nolan, B. D. Santarsiero, W. P. Schaefer, J. E. Bercaw, *J. Am. Chem. Soc. 109* (1987) 203.

[7] $[PhNMe_2H]BPh_4$ (**2a**): ^1H NMR (400 MHz, CD_2Cl_2, 25 °C); cation: $\delta = 2.92$ (N-Me), 6.87 ("d", *ortho*-H, $J \approx 8$ Hz), 7.26 ("t", *meta*-H), 6.83 ("t", *para*-H), anion: 7.61 ("d", *ortho*-H, $J \approx 8$ Hz), 7.46 ("t", *meta*-H), 7.55 ("t", *para*-H). $[nBuNH]BPh_4$ (**2b**): $\delta = 0.89$, 1.10, 1.17, 2.13 (N-Bu), 7.44 (unresolved, *ortho*-H), 7.09 ("t", *meta*-H), 6.95 ("t", *para*-H, $J \approx 7.3$ Hz).

[8] M. Bochmann, G. Karger, A. J. Jaggar, *J. Chem. Soc. Chem. Commun.*, in press.

[9] The coordination of CH_2Cl_2 to Lewis-acidic metal centers has precedence, for example, in $[CpM(CO)_3(CH_2Cl_2)]PF_6$ [10] and $[Pd(\mu\text{-}OTeF_5)_4][Ag(\eta^2\text{-}CH_2Cl_2)_2]_2$ [11].

[10] W. Beck, K. Schloter, *Z. Naturforsch. 33B* (1978) 1214.

[11] T. D. Newbound, M. R. Colsman, M. M. Miller, G. P. Wulfsberg, O. P. Anderson, S. H. Strauss, *J. Am. Chem. Soc. 111* (1989) 3762.

[12] No species containing ethylene coordinated prior to insertion into the Ti–C σ bond (**I**→**II**) was detected. In the absence of d electrons, group IV metal centers are unable to stabilize π complexes through back-donation, and species of type **I** are unlikely to have significant lifetimes. For a theoretical treatment of the ethylene insertion step, see [1d]. Occupancy of d orbitals in early transition metals leads to energetically highly favorable back-bonding as a barrier against insertion: O. Eisenstein, R. Hoffmann, *J. Am. Chem. Soc. 102* (1980) 6148; *ibid. 103* (1981) 4308.

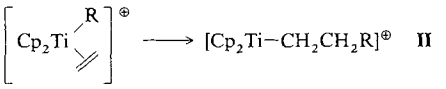

[13] This observation is in agreement with earlier results on a $Cp_2TiMeCl/AlMeCl_2$ catalytic system where only a fraction of the available Ti–Me bonds were shown to participate in chain-growth reactions: G. Fink, W. Fenzl, R. Mynott, *Z. Naturforsch. 40B* (1985) 158.

[14] J. Haslam, H. A. Willis, D. C. M. Squirrel: *Identification and Analysis of Plastics*, 2nd ed., Heyden, London 1980.

[15] W. Kaminsky, *Angew. Makromol. Chem. 145/146* (1986) 149. By contrast, the thermally unstable Cp_2TiPh_2/methylalumoxane system at temperatures below −45 °C gives isotactic polypropylene: J. A. Ewen, *J. Am. Chem. Soc. 106* (1984) 6355.

Development of Tailor-Made Cytostatics Activable by Acid-Catalyzed Hydrolysis for Selective Tumor Therapy**

By *Lutz F. Tietze,* Matthias Beller, Roland Fischer, Michael Lögers, Eckhard Jähde, Karl-Heinz Glüsenkamp,* and *Manfred F. Rajewsky*

The chemotherapy of malignant tumors is extremely problematic because of the narrow therapeutic range of the cytostatics currently available and the resulting side effects.[1] The goal of our work[2] is to exploit phenotypic differences between malignant and normal cells for the development of tumor-selective cytostatic drugs. Several groups have independently shown that, owing to an increase in the blood-sugar level of a tumor-bearing host, the rate of glycolysis in malignant cells is increased relative to that in the normal cell population.[3] The resulting increase in the amount of lactic acid results in a lowering of the pH value in the tumor tissue to 6.2 on the average, whereas the pH value of normal tissue remains nearly constant (pH 7.2). We use this pH difference to release selectively within the tumor tissue a cytostatic drug generated from a nontoxic precursor by acid-catalyzed hydrolysis. A crucial problem here is the development of functional groups that, on the one hand, guarantee the detoxification of the cytocidal component and, on the other, ensure sufficient acid lability that, at pH 6.2, the active species is released fast enough. To this end, we have developed the acetal glycosides[4] of general formula **1**, which can release a cytotoxic aldehyde or ketone, **3**, together with an alcohol, **4** and a sugar, **2**. Although the compounds

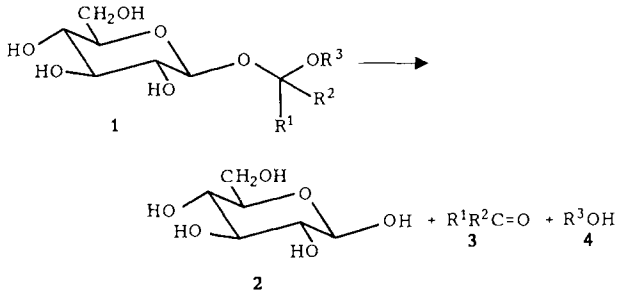

we have so far synthesized exhibited increased selectivity in vitro, their rate of hydrolysis was too low.[5] Here we describe the preparation of the glucoside **10c**, which satisfies the above requirements very well.

Reaction of trimethylsilyl-2,3,4,6-tetra-*O*-acetyl-β-D-glucopyranoside (**5**) with three equivalents of 4-(*tert*-butyldiphenylsiloxy)butan-2-one (**6**) and one equivalent of the corresponding acetal **7** in the presence of a catalytic amount of trimethylsilyl trifluoromethanesulfonate (TMSOTf) in dichloromethane at −70 °C gave exclusively the acetal-β-glucoside **8a** (β:α >99:1) in 39% yield. Owing to the minimal difference between the substituents at the carbonyl group, however, a nearly 1:1 mixture of C-2′ epimers was obtained. The lower yield, compared with the formation of acetal glucosides from aldehydes, is due to the lower reactivity of ketones.[4] Trehaloses were formed as side products in the reaction. Cleavage of the trialkylsilyl group with tetrabutylammonium fluoride (TBAF) led to a 94% yield of an epimeric mixture of alcohols **8b**, which, upon treatment with [(bis(2-chloroethyl)amido]phosphoric acid dichloride (**9**)[6] in the presence of triethylamine (CH_2Cl_2, 36 h, 20 °C) followed by reaction with NH_3 (CH_2Cl_2, 1.5 h, 20 °C), afforded the diamidophosphate **10b** in 74% yield via **10a**. Cleavage of the acetyl groups to give **10c** was accomplished by solvolysis

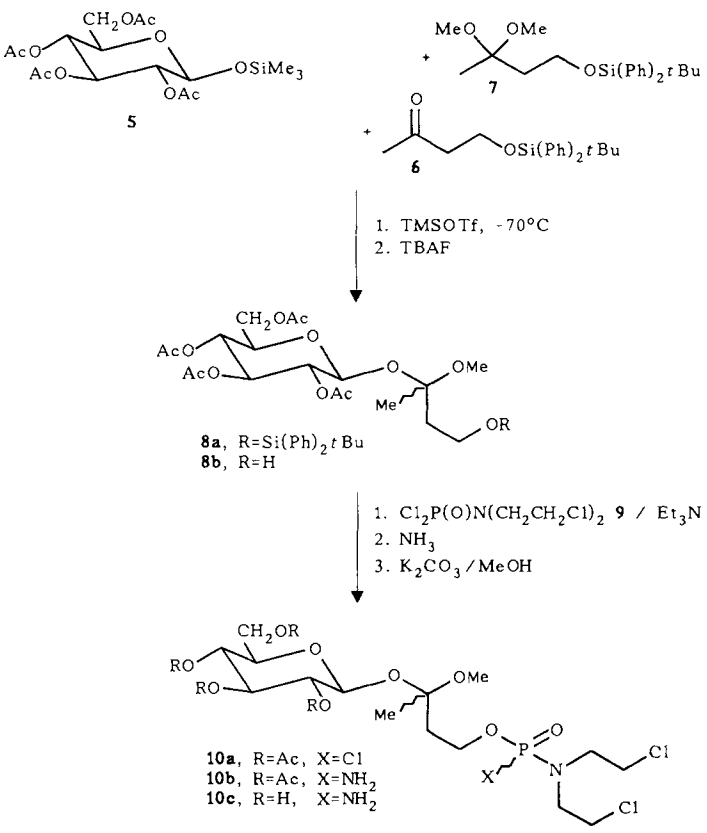

[*] Prof. Dr. L. F. Tietze, Dr. M. Beller, Dr. R. Fischer, Dipl.-Chem. M. Lögers
Institut für Organische Chemie der Universität
Tammannstrasse 2, D-3400 Göttingen (FRG)
Prof. Dr. M. F. Rajewsky, Dr. E. Jähde, Dr. K.-H. Glüsenkamp
Institut für Zellbiologie (Tumorforschung) der Universität
Hufelandstrasse 55, D-4300 Essen (FRG)

[**] Glycosidation, Part 16; Anticancer Drugs, Part 12. This work was supported by the Bundesminister für Forschung und Technologie (Förderkennzeichen 03189-52A9) and the Fonds der Chemischen Industrie. Glycosidation, Part 15, and Anticancer Drugs, Part 11: L. F. Tietze, M. Beller, *Liebigs Ann. Chem.* (1990), in press.

with potassium carbonate in methanol. Compound **10c**[7] was obtained as a mixture of four stereoisomers, since the phosphorus atom is also a stereogenic center and the phosphorylation with **9** proceeded, as expected, in a nonstereoselective fashion. All the compounds reported here are very acid labile, so that chromatography is only possible in the presence of triethylamine.

The stereochemistry of **10c** at the anomeric center is revealed by the doublet for 1-H at $\delta = 4.53$ ($J = 8$ Hz) in the ^{1}H NMR spectrum.[8] The configuration at C-2′ is assigned on the basis of the ^{13}C NMR signals for C-1′ and C-3′. We assume that, by analogy to the NMR data[4] for the acetal glycosides of aldehydes, the signals in the spectrum of the (2′*R*) epimer lie at lower field for C-1′ and higher field for C-3′, compared to the corresponding signals of the (2′*S*) isomer.

The kinetics of the acid-catalyzed hydrolysis[9] of **10c** was determined using NMR spectroscopy. The first-order rate constant for deuterolysis at pD = 6.10 in phosphate buffer at 35 °C (0.10 M, $I = 0.5$ M) is $k = 2.45 \times 10^{-5}$ s^{-1}. Assuming a $k_{D^\oplus}/k_{H^\oplus}$ value of 1.5,[10] **10c** has a half-time for hydrolysis of 15 h at pH = 6.2 and 35 °C. This value roughly corresponds to the desired value. Cleavage of **10c** yields besides glucose and methanol, the diamidophosphate **11** (ketophosphamide),[11] which, via either elimination or hydrolysis, is converted into the cytotoxic phosphoramide mustard **12** in the cell. This compound is also the active metabolite of the clinically used cytostatic drug cyclophosphamide.[12]

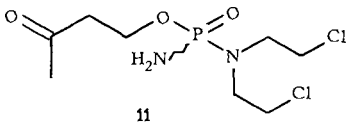

11

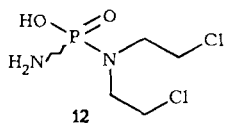

12

The dependence of the cytostatic activity of **10c** on pH was determined in vitro by treating mammary carcinoma cells (M1R) of Marshall rats for 24 h. At physiological extracellular pH ($pH_e = 7.4$) and a concentration of 10 μg mL^{-1}, nearly no toxicity was observed; at $pH_e = 6.2$, however, under otherwise indentical conditions, the survival rate of the cancer cells decreased by a factor of 5×10^4. We are currently using transplanted tumors to investigate whether this surprisingly high selectivity is also exhibited in vivo.

Received: February 20, 1990 [Z 3808 IE]
German version: *Angew. Chem. 102* (1990) 812

CAS Registry numbers:
5, 19126-95-5; **6**, 97250-25-4; **7**, 127619-80-1; **8a** (isomer 1), 127619-78-7; **8a** (isomer 2), 127619-83-4; **8b** (isomer 1), 127619-79-8; **8b** (isomer 2), 127619-84-5; **9**, 127-88-8; **10a** (isomer 1), 127619-81-2; **10a** (isomer 2), 127708-55-8; **10a** (isomer 3), 127707-74-8; **10a** (isomer 4), 127619-85-6; **10b** (isomer 1), 127645-49-2; **10b** (isomer 2), 127708-56-9; **10b** (isomer 3), 127708-57-0; **10b** (isomer 4), 127708-58-1; **10c** (isomer 1), 127619-82-3; **10c** (isomer 2), 127707-75-9; **10c** (isomer 3), 127707-76-0; **10c** (isomer 4), 127707-77-1; **11**, 100993-83-7; **12**, 10159-53-2.

[1] W. E. G. Müller: *Chemotherapie von Tumoren, Biochemische Grundlagen*, Verlag Chemie, Weinheim 1975; D. Schmähl (Ed.): *Maligne Tumoren*, Edition Cantor, Aulendorf 1981; W. Forth, D. Henschler, W. Rummel: *Allgemeine und spezielle Pharmakologie und Toxikologie*, 5th ed. BI Wissenschaftsverlag, Mannheim 1987; E. Frei III, *Cancer Res. 47* (1987) 3907.

[2] L. F. Tietze in E. Borowski, D. Shugar (Eds.): *Molecular Aspects of Chemotherapy*, Pergamon Press, Oxford 1990; L. F. Tietze, *Nachr. Chem. Tech. Lab. 36* (1988) 728.

[3] E. Jähde, M. F. Rajewsky, *Cancer Res. 42* (1982) 1505; O. Warburg: *Über den Stoffwechsel der Tumoren*, Springer, Berlin 1926; *The Metabolism of Tumours*, Constable, London 1930; A. C. Aisenberg: *The Glycolysis and Respiration of Tumors*, Academic Press, New York 1961; F. Schneider, *Naturwissenschaften 68* (1981) 20; I. F. Tannock, D. Rotin, *Cancer Res. 49* (1989) 4373; S. Osinsky, L. Bubnovskaja, T. Sergienko, *Anticancer Res. 7* (1987) 199; M. von Ardenne, P. G. Reitnauer, *Acta Biol. Med. Ger. 25* (1970) 483; J. A. Dickson, S. K. Calderwood, *JNCI, J. Natl. Cancer Inst. 63* (1979) 1371.

[4] [a] L. F. Tietze, R. Fischer, *Angew. Chem. 93* (1981) 1002; *Angew. Chem. Int. Ed. Engl. 20* (1981) 969; [b] L. F. Tietze, R. Fischer, H.-J. Guder, *Synthesis 1982*, 946; [c] L. F. Tietze, R. Fischer, H.-J. Guder, M. Neumann, *Liebigs Ann. Chem. 1987*, 847.

[5] L. F. Tietze, M. Neumann, R. Fischer, T. Möllers, K.-H. Glüsenkamp, M. F. Rajewsky, E. Jähde, *Cancer Res. 49* (1989) 4179.

[6] O. M. Friedman, A. M. Seligman, *J. Am. Chem. Soc. 76* (1954) 655.

[7] **10c**: $R_f = 0.30$ (dichloromethane/petroleum ether/ethanol 3:1:1). ^{1}H NMR ([D$_6$]acetone/D$_2$O): $\delta = 1.30$, 1.32 (2s, 3H; CH$_3$), 1.95–2.08 (m, 2H; 3′-H$_2$), 3.06–3.44 (*m*, 10H; 2CH$_2$N, 2-H, 3-H, 4-H, 5-H, 6-H$_2$), 3.19 (s, 3H; CH$_3$O), 3.56 (t, $J = 7$ Hz, 4H; 2CH$_2$Cl), 3.83–4.04 (m, 2H; CH$_2$OP), 4.55 (d, $J = 8$ Hz, 1H; 1-H). ^{13}C NMR ([D$_6$]acetone/D$_2$O): $\delta = 21.78$, 21.82 (CH$_3$, [2′*S*]), 23.47, 23.52 (CH$_3$, [2′*R*]), 37.40 (d, $^3J_{POCC} = 7.1$ Hz; C-3′ [2′*R*]), 39.27 (d, $^3J_{POCC} = 7.9$ Hz; C-3′, [2′*S*]), 42.41 (2CH$_2$Cl), 48.20, 48.24 (2d, $^2J_{PNC} = 4.2$, 4.7 Hz; 2CH$_2$N), 49.51 (CH$_3$O), 60.99, 61.06 (C-6), 62.15, 62.25, 62.48, 62.58, 62.99, 63.10 (CH$_2$OP), 69.91, 70.06, 73.46, 76.15 (C-2, C-3, C-4, C-5), 95.30 (C-1, [2′*S*]), 95.41 (C-1, [2′*R*]), 103.3 (C-2′, *R*), 103.5 (C-2′, *S*). All new compounds were identified spectroscopically; in addition, correct elemental analyses were obtained.

[8] In the NMR spectrum, C-1 refers to the anomeric center of the pyranose and C-1′ to the carbon atom of the methyl group of the exocyclic acetal.

[9] E. H. Cordes, H. G. Bull, *Chem. Rev. 74* (1974) 582; M. M. Kreevoy, R. W. Taft, Jr., *J. Am. Chem. Soc. 77* (1955) 5590.

[10] The kinetic solvent isotope effect $k_{D^\oplus}/k_{H^\oplus}$ was determined for 1-methoxy-1-methylethyl-β-D-glucopyranoside by UV spectroscopy: L. F. Tietze, M. Lögers, unpublished results.

[11] M. Thomson, M. Colvin, *Cancer Res. 34* (1974) 981; P. J. Cox, P. B. Farmer, M. Jarman, *Biochem. Pharmacol. 24* (1975) 599; J. A. Montgomery, R. F. Struck, *Cancer Treat. Rep. 60* (1976) 381.

[12] N. E. Sladek, *Pharmacol. Ther. 37* (1988) 301.

Heteronuclear Complexes Containing $CuCo(CO)_4$ Structural Units and Nitrogen Ligands**

By *Matthias Achternbosch, Heinrich Braun, Ralf Fuchs, Peter Klüfers,* Alexandra Selle*, and *Ulf Wilhelm*

Dedicated to Professor Hans-Uwe Schuster on the occasion of his 60th birthday

Bonds between different metal atoms can form according to Equation (a) if M′L′$_m$ is a Lewis acidic metal complex fragment containing ligands capable of being substituted

$$M'L'_m + ML_n \rightarrow L'_iM'\text{-}ML_n + (m-1)\,L' \qquad (a)$$

(e.g., $[CuCl_2]^\ominus$) and ML$_n$ is a nucleophilic metalate ion such as $[Co(CO)_4]^\ominus$, $[(C_5H_5)Mo(CO)_3]^\ominus$, or $[Fe(CO)_4]^{2\ominus}$.[1, 2] Heteronuclear clusters (M′M)$_x$ are formed when the metalate ion bridges M′L′ fragments with displacement of several ligands L′.

The compounds $[\{CuCo(CO)_4\}_4]$ (**1a**) and $[\{CuCo(CO)_4\}_\infty]$ (**1b**), made up of Cu atoms and μ_2-bridging $Co(CO)_4$ fragments, are formed upon reaction of chlorocuprate(I) and tetracarbonylcobaltate(−I) in such a cluster-forming reaction.[1a, b] μ_3-ML$_n$ groups are present in the anions $[Cu_5Fe_4(CO)_{16}]^{3\ominus}$ and $[Cu_6Fe_4(CO)_{16}]^{2\ominus}$, in which the $Fe(CO)_4$ fragments are each coordinated to three copper atoms of the cluster.[2] Here we report new compounds con-

[*] Prof. Dr. P. Klüfers, Dipl.-Chem. M. Achternbosch, Dr. H. Braun, Dipl.-Chem. R. Fuchs, Dipl.-Chem. A. Selle, Dipl.-Chem. U. Wilhelm
Institut für Anorganische Chemie der Universität
Engesserstrasse, Gebäude 30.45, D-7500 Karlsruhe (FRG)

[**] Heteronuclear Complexes with Metal–Metal Bonds, Part 4. This work was supported by the Deutsche Forschungsgemeinschaft and the Fonds der Chemischen Industrie. Part 3: [1a].

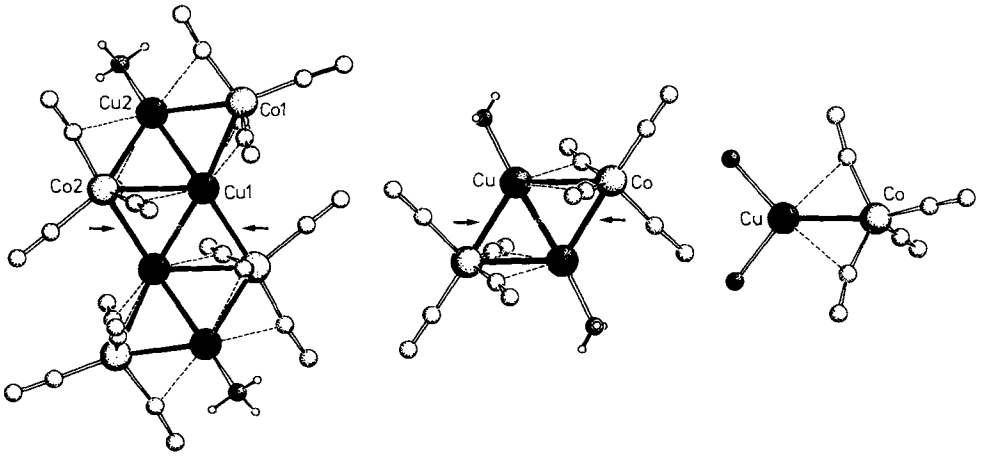

Fig. 1. Left: Structure of **2a** in the crystal. Selected distances [pm]: Cu1-Co1 253.0(1), Cu1-Co2 268.2(2), Cu1-Co2^z 258.2(1), Cu-Co1 252.3(1), Cu2-Co2 257.1(1); Cu1-Cu2 253.1(1), Cu1-Cu1^z 254.8(1). Atoms marked with a superscript z are generated by the symmetry center shown. Maximal deviation of the metal atoms from the best plane: 45 pm. The Cu–Co bond is formally cleaved by NH_3 at the positions marked with an arrow (→**2b**). Broken lines: Semibridging CO groups. Middle: Structure of **2b** in the crystal. Selected distances [pm]: Cu-Co 258.9(1), Cu-Co^z 255.6(1), Cu-Cu^z 249.4(1). Arrows: Formal bond cleavage converting **2b** into **2c**. Right: Structure of **2c** in the crystal. The Cu–Co distance is 242.9(2) pm.

taining $CuCo(CO)_4$ structural units, in which stronger ligands L′ compete with the metalate for the Lewis acidic copper(I) and thus oppose cluster formation. The more donor atoms are bonded to copper, the fewer $Co(CO)_4$ bridges are formed. Eventually, after formation of a heteronuclear binuclear complex, the M′–M bond is cleaved.

$CuCo(CO)_4$–NH_3 adducts are formed in the reaction of CuCl in aqueous ammonia with $Na[Co(CO)_4]$. Recrystallization from dichloromethane or toluene affords, depending on the experimental conditions, the crystalline compounds $(NH_3)_x CuCo(CO)_4$ (**2**) with x = 0.5 (**2a**), 1 (**2b**), and 2 (**2c**). As the concentration of NH_3 is increased, the tendency of the $Co(CO)_4$ groups to bridge the copper atoms and thus the degree of oligomerization of the $CuCo(CO)_4$ units decreases. In the crystal, **2a** is present as a tetramer, $[(NH_3)_2\{CuCo(CO)_4\}_4]$ (Fig. 1, left). Two μ_3-$Co(CO)_4$ and two μ_2-$Co(CO)_4$ groups together with four copper atoms form a nearly planar Cu_4Co_4 cluster. Since the Cu–Co and Cu–Cu distances differ only slightly, the arrangement of the metal atoms corresponds to a section of a closest-packed layer of spheres. Crystals of **2b** consist of the dimer $[\{(NH_3)CuCo(CO)_4\}_2]$ (Fig. 1, middle). The two additional ammine ligands (based on one molecule of **2a**) each formally cleave one of the Cu–Co bonds to the μ_3-$Co(CO)_4$ moieties of **2a**, so that, in **2b**, only μ_2-$Co(CO)_4$ groups are present. Finally, in **2c**, a further ammine ligand per copper displaces the $Co(CO)_4$ fragment from a bridging to a terminal position. Complex **2c** is therefore monomeric in accordance with the formula $[(NH_3)_2CuCo(CO)_4]$ (Fig. 1, right). The Cu–Co distance in **2c** (242.9 pm) is somewhat longer than those in **1a** and **1b** (236.5 and 237.4 pm, respectively); the values for the Cu–Co bond order based on the isolobal relationship between $Co(CO)_4$ and CH_3 (1 for **2c** and 0.5 for **1**) thus do not show the expected pattern based on the simple model. In **2a** and **2b**, the distances between copper and μ_2-$Co(CO)_4$ are increased by almost 20 pm compared to that of **1** for *steric* reasons. The Cu_2 units in **1** are each bridged by only one $Co(CO)_4$ group, whereas in **2a** and **2b** two such opposite-lying groups are present; any further approach to the Cu_2 unit is opposed, however, by the mutual repulsion of the carbonyl groups (estimated by use of the van der Waals shape of a CO group in $[Co(CO)_4]^{\ominus}$ [4]).

No evidence has so far been found for a homologous compound containing *three* ammine ligands per $CuCo(CO)_4$ unit. High NH_3 concentrations seem instead to lead directly to a compound with x = 4. Pale yellow **2c** dissolves in liquid ammonia with formation of a colorless solution, the conductivity of which indicates that the Cu–Co bond is cleaved with formation of $[Cu(NH_3)_4]^{\oplus}$ and $[Co(CO)_4]^{\ominus}$ ions.[5] Coordination of three nitrogen donor centers is achieved, however, when **2c** is allowed to react with the tridentate chelate ligand diethylenetriamine (dien), which results in loss of NH_3 and formation of $[(dien)CuCo(CO)_4]$ (**3**). Reaction of **2c** with other amines also results in loss of NH_3 and formation of further adducts with $CuCo(CO)_4$. Thus, reaction of **2c** with equimolar amounts of the chelate ligands ethylenediamine (en) and 1,10-phenanthroline (phen) leads to $[(en)CuCo(CO)_4]$ (**4a**) and $[(phen)CuCo(CO)_4]$ (**4b**); reaction with twice the molar amount of morpholine results in $[(C_4H_9ON)_2CuCo(CO)_4]$ (**5**). In the crystal,[3] all these amine adducts, like **2c**, are monomeric; morpholine is present in chair conformation and is coordinated only through nitrogen. The Cu–N distances become somewhat larger in the series N_2-chelate < 2 N < N_3-chelate (average values [pm]: 204.9 (**4a**) ≈ 205.3 (**4b**) < 208.2 (**2c** and **5**) < 212.7(3)). Independent of the number of nitrogen donor atoms, all complexes in the crystal contain semibridging CO ligands in which the C atoms of the Co-C-O unit concerned are directed toward a copper atom (e.g., **4b**, $(Cu\text{-}C)_{min}$ = 212.9(4) pm for Co-C = 176.2(3) pm and Co-C-O = 164.4(3)°). According to the classification of *Crabtree* and *Lavin*,[6] the semi-μ-CO groups found here belong to the common class of bent semibridging carbonyls. For the present class of substances, a limiting Cu–C distance of 260 pm is found, below which the semibridging bonding mode begins. All carbonyl ligands that, according to this rule, are semibridging are indicated in Figure 1. For higher-nuclear compounds, semi-μ_2-CO but not semi-μ_3-CO ligands are found.

Experimental Procedure

2c: NaOH (5 g, 125 mmol) and $Co_2(CO)_8$ (10.2 g, 30 mmol) were allowed to react in 100 mL of THF to give $Na[Co(CO)_4]$. The filtered solution was evaporated almost to dryness, the residue redissolved in water, the resulting solution evaporated once again, and the resulting residue diluted with water and added to a stirred solution of CuCl (4 g, 40 mmol) in 100 mL of concentrated NH_3. Cooling of the reaction mixture to −5 °C resulted in formation of a bright precipitate of **2**, which, after filtration under N_2, was dissolved in CH_2Cl_2. The resulting solution, after drying over Na_2SO_4, was saturated with NH_3 gas and, after addition of pentane until the onset of turbidity, cooled to −40 °C. Compound **2c** was obtained as pale yellow, needle-shaped crystals. Yield 65% (based on $Co_2(CO)_8$), m.p. 64 °C. IR (KBr): $\tilde{\nu}$(CO) = 2050(m), 2025(s), 1985(m), 1965(s), 1930(vs), 1895(vs) cm^{-1}. ^1H NMR (300 MHz, TMS, CH_2Cl_2): δ = 2.10 (s, NH_3).

2b: N_2 was bubbled through a solution of **2c** (1 g) in 30 mL of CH_2Cl_2 at −5 °C. After 6 h, any precipitate formed was redissolved by addition of a small amount of CH_2Cl_2 and a layer of pentane was added. Yellow crystals formed after about one week at −2 °C. Yield 80%, m.p. 77 °C. IR (KBr): $\tilde{\nu}$(CO) = 2088(w), 2045(sh), 2025(m), 1926(s; half-width, 71 cm^{-1}) cm^{-1}. ^1H NMR (CH_2Cl_2, −70 °C): δ = 2.43 (s, NH_3).

2a: Red crystals of **2a** formed upon an (unsuccessful) attempt to convert **2c** into **1** by reaction with a strongly acidic ion exchanger ($H^{\oplus}$ form) in CH_2Cl_2 solution. An efficient synthesis has not yet been developed; m.p. 79–80 °C. Replacement of NH_3 by an amine: A solution of **2c** in CH_2Cl_2 or toluene was treated with the calculated amount of dien or morpholine; NH_3 was removed by brief application of a vacuum. After addition of pentane, **3**, **4a**, or **5** were obtained as bright yellow crystals. Addition of phen to a solution of **2c** resulted in immediate formation of an orange precipitate; after recrystallization from hot acetone, **4b** was obtained as orange crystalline needles. **4a**: IR (CH_2Cl_2): $\tilde{\nu}$ (CO) = 2010(m), 1940(s), 1900(m), 1850(m) cm^{-1}. **4b**: IR (KBr): $\tilde{\nu}$ (CO) = 2017(st), 1938(st), 1900(st), 1840(s) cm^{-1}. **5**: IR (CH_2Cl_2): $\tilde{\nu}$ (CO) = 2010(s), 1900(s) cm^{-1}.

Received: January 26, 1990 [Z 3761 IE]
German version: *Angew. Chem. 102* (1990) 825

[1] a) P. Klüfers, *Angew. Chem. 97* (1985) 59; *Angew. Chem. Int. Ed. Engl. 24* (1985) 70; b) *ibid. 96* (1984) 288; and *23* (1984) 307; c) *Z. Kristallogr. 166* (1984) 143; d) G. Doyle, K. A. Eriksen, D. van Engen, *Organometallics 4* (1985) 877; e) *ibid.* 2201.

[2] G. Doyle, K. A. Eriksen, D. van Engen, *J. Am. Chem. Soc. 107* (1985) 7914; *ibid. 109* (1986) 445.

[3] **2a**: $C_{16}H_6Co_4Cu_4N_2O_{16}$, $M = 972.144$; $P\bar{1}$, $a = 859.8(4)$, $b = 892.5(5)$, $c = 1037.3(5)$ pm, $\alpha = 95.55(2)$, $\beta = 98.50(2)$, $\gamma = 117.42(2)°$; $Z = 1$, $V/Z = 686.4(6) \times 10^6$ pm^3, $\varrho_{calcd} = 2.352(2)$ g cm^{-3}; 2955 unique reflections (*hkl*); anisotropic temperature factors (T. F.), H with common isotropic T. F., 195 variables, $R = 0.026$, $R_w = 0.020$. **2b**: $C_8H_6Co_2Cu_2N_2O_8$, $M = 503.102$; $P2_1/n$, $a = 811.2(7)$, $b = 1126.3(6)$, $c = 852.8(11)$ pm, $\beta = 99.0(1)°$; $Z = 2$, $V/Z = 384.8(6) \times 10^6$ pm^3, $\varrho_{calcd} = 2.171(3)$ g cm^{-3}; 1362 *hkl*; anisotropic T. F., H with common isotropic T. F., 111 variables, $R = 0.055$, $R_w = 0.021$. **2c**: $C_4H_6CoCuN_2O_4$, $M = 268.582$; $P2_1/c$, $a = 868.2(8)$, $b = 1335(2)$, $c = 818.4(6)$ pm, $\beta = 113.84(6)°$; $Z = 4$, $V/Z = 216.9(4) \times 10^6$ pm^3, $\varrho_{calcd} = 2.056(4)$ g cm^{-3}; 1352 *hkl*; anisotropic T. F., no H positions, 110 variables, $R = 0.049$, $R_w = 0.039$. **3**: $C_8H_{13}CoCuN_3O_4$, $M = 337.688$; $P2_1/n$, $a = 791.9(4)$, $b = 1639(5)$, $c = 994(1)$ pm; $\beta = 95.72(8)°$; $Z = 4$, $V/Z = 321(1) \times 10^6$ pm^3, $\varrho_{calcd} = 1.747(5)$ g cm^{-3}; 1990 *hkl*; anisotropic T. F., H in calculated positions with common isotropic T. F., 168 variables, $R = 0.059$, $R_w = 0.024$; Cu-Co = 242.6(1) pm. **4a**: $C_6H_8CoCuN_2O_4$, $M = 294.619$; $P2_1/n$, $a = 1246.7(4)$, $b = 609.0(4)$, $c = 1401.6(5)$ pm; $\beta = 98.21(3)$; $Z = 4$, $V/Z = 263.3(2) \times 10^6$ pm^3, $\varrho_{calcd} = 1.858(2)$ g cm^{-3}; 1849 *hkl*; anisotropic T. F., H in calculated positions with common isotropic T. F., 141 variables, $R = 0.040$, $R_w = 0.031$; Cu-Co = 236.9(1) pm. **4b**: $C_{16}H_8CoCuN_2O_4$, $M = 414.729$; $P\bar{1}$, $a = 726.4(3)$, $b = 1053.1(4)$, $c = 1067.6(4)$ pm, $\alpha = 69.58(3)$, $\beta = 84.75(3)$, $\gamma = 80.63(3)°$; $Z = 2$, $V/Z = 377.3(3) \times 10^6$ pm^3, $\varrho_{calcd} = 1.825(2)$ g cm^{-3}; 3316 *hkl*; anisotropic T. F., H with individual isotropic T. F., absorption correction (ψ scans), 250 variables, $R = 0.042$, $R_w = 0.023$; Cu-Co = 239.4(1) pm. **5**: $C_8H_{18}CoCuN_2O_6$, $M = 408.76$; $P2_1/n$; $a = 963.0(4)$, $b = 1307(1)$, $c = 1399(1)$ pm, $\beta = 97.20(5)°$; $Z = 4$, $V/Z = 436.7(5) \times 10^6$ pm^3, $\varrho_{calcd} = 1.554(2)$ g cm^{-3}; 2606 *hkl*; anisotropic T. F., methylene H (calculated positions) and amine H each with common isotropic T. F., 232 variables, R = 0.051, $R_w = 0.032$; Cu-Co = 241.6(1) pm. Enraf–Nonius CAD4 and Siemens Stoe AED diffractometer, $Mo_{K\alpha}$, 295 K, structure solution and refinement with SHELXS-86 and SHELX-76, distances and angles with PLATON, drawings with ORTEP and SCHAKAL. Further details of the crystal structure investigation may be obtained from the Fachinformationszentrum Karlsruhe, Gesellschaft für wissenschaftlich-technische Information mbH, D-7514 Eggenstein-Leopoldshafen 2 (FRG), on quoting the depository number CSD-54567, the names of the authors, and the journal citation.

[4] P. Klüfers, *Z. Kristallogr. 167* (1984) 275.

[5] *D. Nichols* reports values roughly twice as high for the equivalent conductivity of typical 1:1 electrolytes in NH_3 (infinite dilution) as that determined for a 0.09 M solution of **2c** (≈ 150 cm^2 Ω^{-1} mol^{-1} at −30 °C): D. Nichols: *Inorganic Chemistry in Liquid Ammonia*, Elsevier, Amsterdam 1979.

[6] H. Crabtree, M. Lavin, *Inorg. Chem. 25* (1986) 805.

A New Way to SiC Ceramic Precursors by Catalytic Preparation of Preceramic Polymers**

By *Bruno Boury, Leslie Carpenter,* and *Robert J. P. Corriu**

The preparation of ceramic materials by organometallic processes has opened a new chapter in chemical research. In order to show the importance of the nature of the starting organometallic polymer, we have prepared a new ceramic precursor of the polycarbosilane type containing bifunctional silicon atoms. After characterization of the nature and the structure of the units along the chains, we obtained SiC ceramic via direct pyrolysis.

The discoveries of *Yajima* et al.[1] and *Verbeek*[2] opened very interesting perspectives for the chemist, since it was the first time that a ceramic material was prepared in a very useful form as fibers by a set of chemical transformations starting from organosilicon monomers.

Yajima obtained SiC fibers by a process which starts from dichlorodimethylsilane and involves first the synthesis of a polysilane and then, via Kumada rearrangement,[3] a polycarbosilane (Scheme 1). However, in spite of the great novelty of this discovery, the process has some disadvantages:

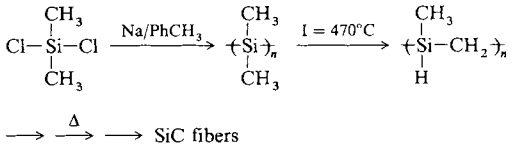

Scheme 1. Preparation of SiC fibers by the Yajima procedure.

1. It does not provide a general route to preceramic polymers, since it is limited to the preparation of polysilanes. This preparation requires a stoichiometric amount of sodium and it is only possible to modify the nature of the substituents at silicon.

2. The preceramic polymer formed in the thermolysis at 470 °C has a structure which is not well-defined, since it is the result of thermal rearrangement of the original polysilane polymer. It was demonstrated by *Dunoguès* et al.[4] and *Interrante* et al.[5] that the linear structure $-(SiHMe-CH_2)_n-$ without further reticulation does not give a high yield of ceramic.

In fact, the structure of *Yajima*'s preceramic polymer has been shown to be more complex as a result of some cross-linking.[6] This feature renders it difficult to study pyrolysis processes and mechanisms, since the chemical structure of the preceramic polymer is not precisely known.

Our approach to this problem is to try to achieve the following targets:

1. The preparation of preceramic polymer by a direct route avoiding polysilane synthesis.

2. The elaboration of the polymer by a catalytic process able to provide well-defined structures.

3. The development of a process as general as possible.

The hydrosilylation reaction is a very promising one for these purposes since it is a catalytic and very flexible reaction.[7] In this process we can choose both the nature of the substituents at silicon and the nature of the group between two silicon atoms. We can thus obtain well-defined polymers allowing studies of the pyrolysis process.

As starting monomer, we chose vinyldichlorosilane (**1**), produced by redistribution. The polymerization was performed using platinum on charcoal (Pt/C). The resulting chlorine-containing oligomer **2** was reduced by $LiAlH_4$ to **3**, an oligomer containing SiH_2 groups (Scheme 2).

[*] Prof. R. J. P. Corriu, B. Boury, L. Carpenter
Unité Mixte CNRS/RP/USTL
Université de Montpellier II – case 007
Place Eugène Bataillon, F-34095 Montpellier Cédex 5 (France)

[**] This work was supported by CNRS and Rhône-Poulenc Company.

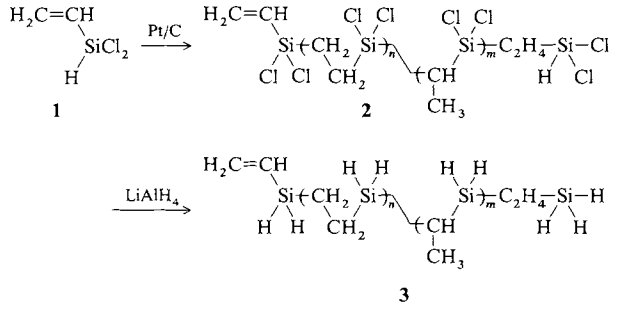

Scheme 2. Synthesis of oligomers containing SiC_x units from dichlorovinylsilane (**1**).

The ^1H, ^{13}C and ^{29}Si NMR spectra of **3** (Table 1) showed that hydrosilylation occurred mainly at the β carbon giving SiH_2-CH_2-CH_2 linear units rather than, as expected, at the α carbon, which would have produced SiH_2-CHMe units. Thus, the ^{29}Si NMR spectrum shows two main signals in the ratio 4/1 and a strong proton signal of the methylene group is observed in the ^1H NMR spectrum. The number-average molecular weight, M_n, was determined by both gel permeation chromatography and vapor-phase osmometry. From this we can determine that the oligomer **3** exhibits a DP_n value in the range of 15 to 20 units. In all polymerization experiments the formation of dimeric and trimeric species as an isomeric mixture of six- and five-membered rings was observed. The end groups of **3** are (vinyl)H_2Si and -H_3Si units.

Table 1. NMR assignments for oligomers of type **3** (200-MHz ^{29}Si NMR and 250-MHz ^1H NMR spectra).

Oligomer	δ(^{29}Si)[a]	δ(^{1}H)
$H_2C{=}CH{-}\overset{2}{Si}H_2{-}(CH_2{-}CH_2{-}\overset{1}{Si}H_2{-}CH_2{-}CH_2)_p{-}\overset{3}{Si}H_3$	Si1 −21.9	Ha 3.9
a b c	Si2 −31.8	Hb 3.75
	Si3 −55.0	Hc 3.5
$H_2C{=}CH{-}\overset{2}{Si}H_2{-}(CH_2{-}CH_2{-}\overset{1}{Si}H_2{-}\underset{CH_3}{\overset{e}{CH}})_q{-}\overset{3}{Si}H_3$	Si1 −19.8	Hd 0.75 / 0.77
	Si2 −28.9	
d f	Si3 −51.9	He 0.35
		Hf 1.25

[a] The assignments have been confirmed by spin echo experiments and comparison with the spectra of oligomers **4** and **5**

In the same way we have prepared oligomers **4** and **5** having the same groups at each end by polymerization in the presence of terminating agents (Scheme 3). These oligomers allow confirmation of the assignments for the end groups of **3**.

Thermogravimetric analysis (TGA) was performed by constant heating (5 K per min) up to 1300 °C. A very large loss of weight occurred in the case of **4** and only 12% of ceramic residue was obtained instead of the 69% expected from the theoretical conversion $SiC_2H_6 \rightarrow SiC$. Interestingly, **4** does not exhibit at 180 °C any exothermicity as observed in the differential thermal analysis (DTA) curves for the other two oligomers **3** and **5** (Fig. 1). Furthermore, the TGA curve of **4** corresponds to a regular loss of weight. Apparently the ceramization process follows a different course for **4** than in the cases of **3** and **5**. This observation can be related to the

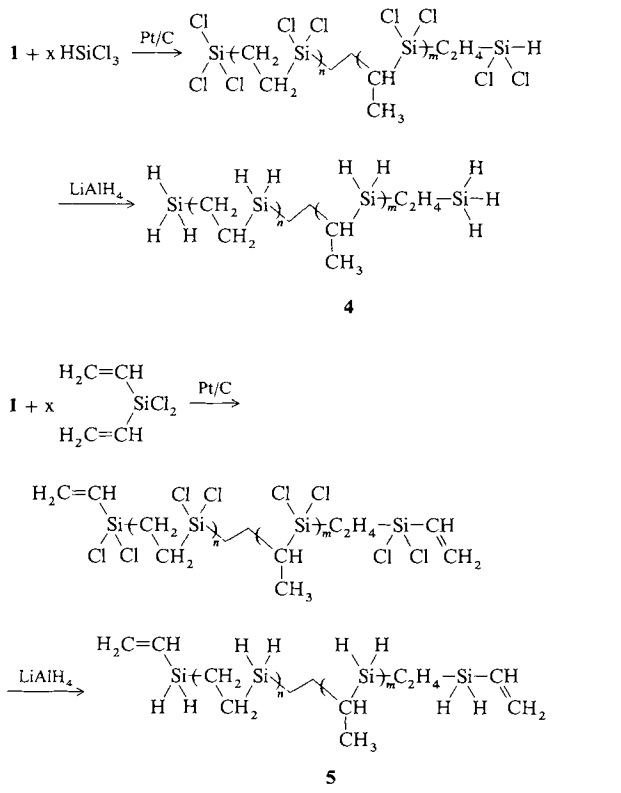

Scheme 3. Synthesis of oligomers having the same groups at each end. x = 0.1, 0.2.

presence of vinyl groups: **5** exibits a high ceramic yield (52%), much better than the 32% observed for **3**, which contains only one vinyl group.

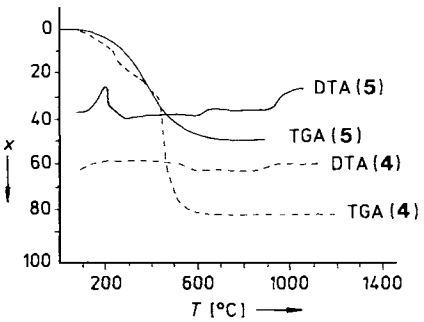

Fig. 1. DTA and TGA curves for the oligomers **4** (---) and **5** (—). x = weight loss in %.

The simplest explanation is that hydrosilylation is occurring between the vinyl groups and the Si-H functions. This hydrosilylation corresponds to the exothermic reaction observed in the DTA curves and gives a more reticulated polymer. It avoids the elimination of volatile compounds (by distillation). The efficiency of the cross-linking for increasing the yield of ceramic residues has been well demonstrated in the case of silicon nitride[8] and silicon carbide.[9]

The SiC obtained from **3** and **5** remained amorphous up to 1000–1100 °C. Crystallization occurred above 1100 °C: β-SiC was identified by X-ray diffraction. The microanalysis of

a sample prepared at 950 °C corresponds precisely to the stoichiometry Si/C = 1. The oxygen content (0.3 to 3%) is highly dependent on the experimental conditions both in the preparation of the oligomer and during ceramization. Careful control of the experimental conditions minimizes the oxygen content. The residue obtained appears as a compact solid with a density 2.1 $g\,cm^{-3}$ lower than that of β-SiC (3.12) and a specific surface between 0.5 and 2 m^2g^{-1} depending on the thermal treatment.

In agreement with the initial aims, we have demonstrated a catalytic procedure leading to the direct synthesis of preceramic oligomers which are precursors of SiC ceramics. This route may hopefully open possibilities for the preparation of new precursors of SiC given the wide chemical variation possible in the hydrosilylation reaction. In fact, as our results show, it is not necessary to use high-molecular-weight polymers since we obtained a good ceramic yield of SiC from oligomeric carbosilanes. The key point is the cross-linking of chains by chemical means (hydrosilylation in our case).

Finally, a comparison of the behavior during the direct pyrolysis of our oligomer containing SiH_2-CH_2-CH_2 units with that of the isomeric polymer having SiHMe-CH_2 units, which contains the alternating Si-C-Si-C arrangement of SiC, shows that the latter is not necessary for a high ceramic yield.[4,5] The good ceramic yields we have obtained can perhaps be explained by the bifunctionality of H_2Si groups.

The β elimination reaction,[10] which could lead to complete depolymerization, does not significantly compete with the mineralization process in the case of cross-linked polymers. Since our linear system does not undergo depolymerization either, we assume that the linear chain can undergo appropriate rearrangements during ceramization.

Experimental Procedure

Preparation of **3**: **1** (4.48 g, 35 mmol), 1,2-dichloroethane (4 mL), and Pt(5%)/C (0.2 g) were heated at reflux for 10 h. A white precipitate formed and was separated by filtration. This solid (5.25 g), as a suspension in Et_2O (150 mL), was reduced by $LiAlH_4$ (1.8 g, 47.3 mmol) in Et_2O (50 mL) at 0 °C. The mixture is allowed to warm to room temperature and then refluxed for 2 h. After acid hydrolysis, evaporation of solvent yielded 1.74 g (72.8%) of a clear, colorless oil (elemental analysis: calcd, C 41.4, H 10.3, Si 48.3; found, C 39.4, H 9.6, Si 43.2; Cl 0.04%).

Received: February 5, 1990 [Z 3777 IE]
German version: *Angew. Chem. 102* (1990) 818

CAS Registry numbers:
1, 18076-99-8; $HSiCl_3$, 10025-78-2; $Cl_2Si(CH=CH_2)_2$, 1745-72-8; $Cl(CH_2)_2Cl$, 107-06-2; Pt, 7440-06-4; $LiAlH_4$, 16853-85-3; SiC, 409-21-2.

[1] a) S. Yajima, J. Hayashi, M. Omori, *Chem. Lett. 1975*, 931; b) S. Yajima, K. Okamura, J. Hayashi, *ibid. 1975*, 1209.
[2] W. Verbeek, US-Pat. 2853567 (1974).
[3] a) M. Kumada, *J. Org. Chem. 23* (1958) 139; b) H. Sakurai, K. Ryongsu, A. Hosomi, M. Kumada, *Bull. Chem. Soc. Jpn. 39* (1966) 2050.
[4] J. Dunoguès, M. Birot, J. P. Pillot, E. Bacqué, *Macromolecules 21* (1988) 30, 34.
[5] H. J. Wu, L. V. Interrante, *Chem. Mater. 1* (1989) 564.
[6] Y. Hasegawa, K. Okamura, *J. Mater. Sci. 21* (1986) 321.
[7] E. Lukevics, Z. V. Belyakova, M. G. Pomenratseva, M. G. Voronkov, *J. Organomet. Chem. Libr. 5* (1977).
[8] a) D. Seyferth, G. H. Wiseman in L. L. Hench, D. R. Ulrich (Eds.): *Ultrastructure Processing of Ceramics, Glasses and Composites 2*, Wiley, New York 1986, Chapter 38; b) Y. D. Blum, K. B. Schwartz, R. M. Laine, *J. Mater. Sci. 24* (1989) 1707.
[9] D. Seyferth in M. Zeldin, K. Wynne, H. R. Allock (Eds.): *Inorganic and Organometallic Polymers (ACS Symp. Ser. 360* (1988), Chapter 3).
[10] L. H. Sommer, D. L. Bailey, F. C. Whitmore, *J. Am. Chem. Soc. 70* (1948) 2869; L. H. Sommer, L. J. Tyler, F. C. Whitmore, *ibid. 70* (1948) 2872; L. H. Sommer, G. L. Baughman, *ibid. 83* (1961) 3346.

The Re–Re Bond in Binuclear Di-μ-oxorhenium Complexes Containing the 1,4,7-Triazacyclononane Ligand**

By *Georg Böhm, Karl Wieghardt,* Bernhard Nuber,* and *Johannes Weiss*

Dedicated to Professor Wolfgang Kirmse on the occasion of his 60th birthday

Rhenium compounds have played a central role in the development of our understanding of metal–metal multiple bonds in binuclear complexes.[1] Thus, the $[Re_2Cl_8]^{2\ominus}$ ion provides the classic example of a nonbridged M–M quadruple bond (Re-Re 2.24 Å).[2] In binuclear complexes containing bridging ligands, however, the identification of an M–M bond is problematical—particularly if the formal bond order is small. M–M double bonds have been characterized for only a small number of molecules.[1] Rhenium(v) possesses a d^2 electron configuration and is therefore ideally suited for the formation of M–M double bonds. In recent years, *Herrmann* and his co-workers have synthesized and structurally characterized a series of binuclear Re^V compounds.[3] They have observed an unusually wide range of Re–Re distances in complexes containing the $[Re_2(\mu\text{-}O)_2]^{6\oplus}$ structural element: **1**[3a] has a planar Re_2O_2 framework and *no* Re–Re bond, whereas **2**, **3**, and **4** exhibit a puckered Re_2O_2 framework with a Re–Re double bond[3] (Scheme 1). The crystal

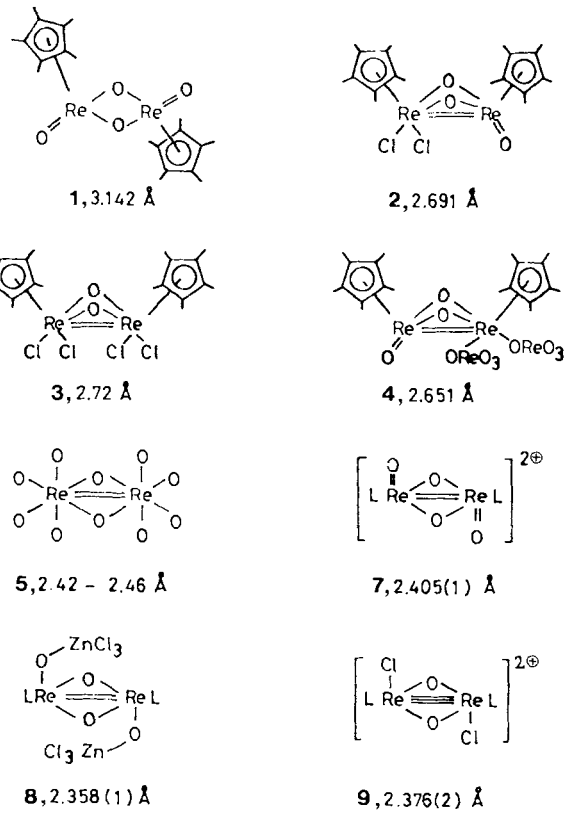

Scheme 1. Structural formulas of compounds **1**–**5** and **7**–**9** along with Re–Re distances.

[*] Prof. Dr. K. Wieghardt, Dipl.-Chem. G. Böhm
Lehrstuhl für Anorganische Chemie I der Universität
Postfach 102148, D-4630 Bochum (FRG)
Dr. B. Nuber, Prof. Dr. J. Weiss
Anorganisch-chemisches Institut der Universität
Im Neuenheimer Feld 270, D-6900 Heidelberg (FRG)

[**] This work was supported by the Fonds der Chemischen Industrie.

structures of $Nd_4Re_2O_{11}$[4a] and $La_6Re_4O_{18}$[4b] display edge-sharing dimeric units, **5**, having a $Re^{V}_2O_2$ framework, and show the shortest Re^{V}–Re^{V} distances so far found (2.42 and 2.46 Å, respectively). Binuclear coordination compounds of the Werner type, **5**, were previously unknown.

In recent years, we have repeatedly pointed out the structural and chemical relationship of the organometallic fragments CpM and Cp*M ($Cp = C_5H_5^{\ominus}$; $Cp^* = C_5Me_5^{\ominus}$) to the classic, isoelectronic fragment LM, where L is the cyclic triamine 1,4,7-triazacyclononane (or its *N*-trimethylated derivative). For example, the cation $[LReO_3]^{\oplus}$[5] can be prepared by oxidative decarbonylation of the corresponding carbonyl complex (here, $[LRe(CO)_3]^{\oplus}$[6]) with H_2O_2, in full analogy to the preparation of $[Cp^*ReO_3]$[7]. We have now synthesized two binuclear analogues of *Herrmann*'s compounds **1**–**4** and characterized them by X-ray analysis.

Reaction of ethylene glycol, L, and $[ReOCl_3(PPh_3)_2]$[8] in THF leads to formation of a pale violet precipitate, **6**Cl,

$[LReO(C_2H_4O_2)]Cl$ **6**Cl

which can be transformed in aqueous solution into the violet bromide or iodide by addition of NaBr or NaI, respectively. Compound **6** is analogous to $[Cp^*ReO(C_2H_4O_2)]$[9] and, like that compound, **6**I loses ethylene quantitatively upon heating, resulting in formation of colorless $[LRe^{VII}O_3]I$ [Eq. (a)]. Differential thermal analysis of $\mathbf{6}I \cdot H_2O$ gives a

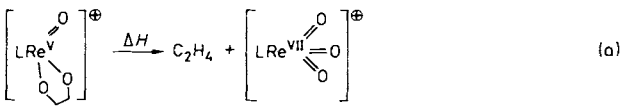

(a)

6

peak at 144 °C (loss of C_2H_4 and H_2O). Figure 1 shows the structure of the cation[10] in crystals of $\mathbf{6}Br \cdot H_2O$; the $[ReO(C_2H_4O_2)]^{\oplus}$ fragment is very similar to that in $[Cp^*ReO(C_2H_4O_2)]$.[9]

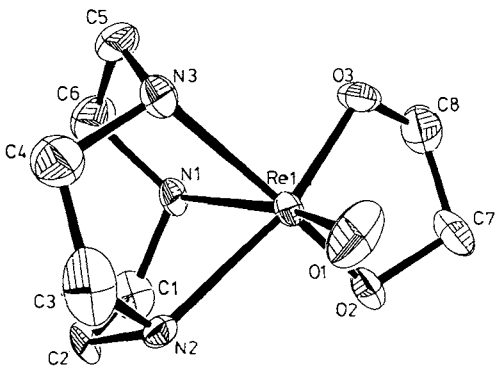

Fig. 1. Structure of the cation in $\mathbf{6}Br \cdot H_2O$. Important distances [Å]: Re1-N1 2.27(1), Re1-N2 2.175(11), Re1-N3 2.18(1), Re1-O1 1.702(15), Re1-O2 1.93(1), Re1-O3 1.939(9), C7-C8 1.51(2), C8-O3 1.42(2), C7-O2 1.45(2).

Reduction of $\mathbf{6}I \cdot H_2O$ with zinc amalgam in aqueous solution under argon at 40 °C results in formation of a green-brown solution, which, after separation of Zn/Hg, air oxidation, and addition of NaI, affords violet crystals of **7**. When an aqueous solution of $ZnCl_2$ and NaCl (1:2) is treated with CH_3SO_3H until the solution is no longer turbid and then **7** is added, dark brown crystals of **8** crystallize from the clear, green-brown solution within 2 d.

$[L_2Re_2(OZnCl_3)_2(\mu\text{-}O)_2]$ **8**

Figure 2 shows the structure of the dication in **7** and Figure 3 that of the neutral complex **8**.[10] In **7**, two Re^{V} ions are joined through two oxo bridges; the Re_2O_2 ring is planar.

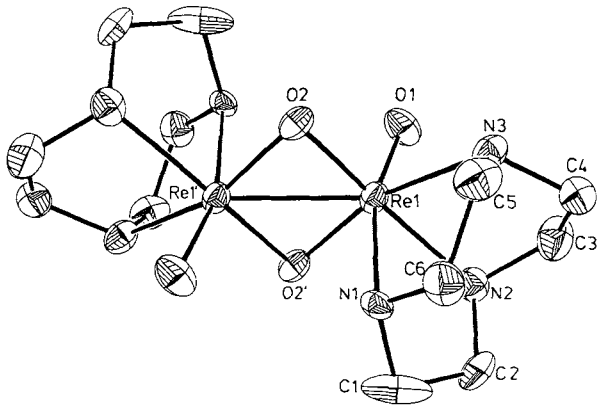

Fig. 2. Structure of the dication in **7**. Important distances [Å] and angles [°]: Re1-Re1' 2.405(1), Re1-O1 1.779(8), Re1-O2 1.933(10), Re1-N1 2.215(9), Re1-N2 2.16(1), Re1-N3 2.17(1), Re1-O2' 1.96(1), O2···O2' 3.07(1); Re1-O2-Re1' 76.2(4), O2-Re1-O2' 103.8(4).

Each Re^{V} ion possesses a terminal oxo group and a tridentate, facially coordinated amine ligand. The Re–Re distance (2.405(1) Å) is very short. Interestingly, the structure of **8** is very similar. However, the presence of a $ZnCl_3^{\ominus}$ fragment on each of the two terminal oxo ligands leads to a dramatic increase in the terminal Re=O distance in **8** and to a decrease in the Re–Re distance to 2.358(1) Å.

The cause is presumably the lower π-donor ability of the Cl_3Zn-substituted O atom. The occupied p orbitals of the oxo ligand can overlap with the unoccupied σ* and π* or-

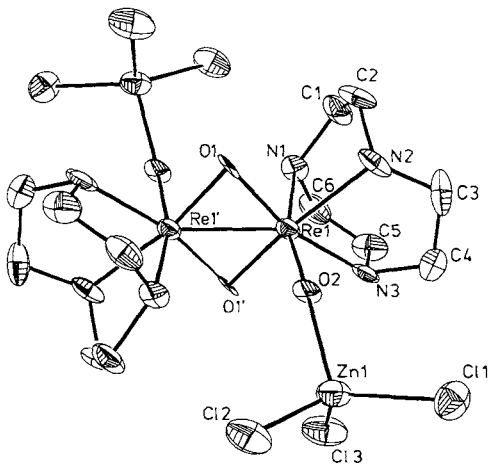

Fig. 3. Structure of the neutral complex **8**. Important distances [Å] and angles [°]: Re1-Re1' 2.358(1), Re1-O1 1.910(9), Re1-O1' 1.926(9), Re1-O2 2.075(8), Re1-N1 2.14(1), Re1-N2 2.19(1), Re1-N3 2.14(1), Zn1-Cl1 2.270(4), Zn1-Cl2 2.257(5), Zn1-Cl3 2.219(5), Zn1-O2 1.994(8); Re1-O1-Re1' 75.9(3), O1-Re1-O1' 104.1(3), Re1-O2-Zn1 137.1(5).

bitals of the Re–Re bond more strongly in **7** than in **8**.[11] The Re_2O_2 ring in **8** is also planar; the Re–μ-O distances of 1.933(10) Å in **7** and 1.910(9) Å in **8** are identical within experimental error. The corresponding distances in **1–5** are in the same range.

Refluxing of a solution of **6I** · H_2O in 0.5 M HCl for 3 h followed by cooling and treatment with NaI results in the formation of black crystals of **9** within 2 d, together with colorless $[LReO_3]I$.

$[L_2Re_2Cl_2(\mu\text{-}O)_2]I_2 \cdot 2H_2O$ **9**

Compound **9** is a dimeric Re^{IV} (d^3) compound. Figure 4 shows the structure of the cation in **9**;[10] a planar Re_2O_2 framework is again observed; each Re^{IV} ion is bonded to a

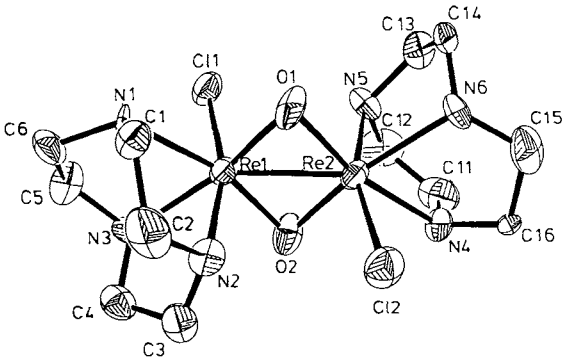

Fig. 4. Structure of the dication in **9**. Important distances [Å] and angles [°]: Re1-Re2 2.376(2), Re1-Cl1 2.385(7), Re1-O1 1.94(2), Re1-O2 2.00(2), Re1-N1 2.24(2), Re1-N2 2.12(2), Re1-N3 2.21(2), Re2-Cl2 2.391(8), Re2-O1 1.99(2), Re2-O2 1.95(2), Re2-N4 2.22(2), Re2-N5 2.13(2), Re2-N6 2.22(2); Re1-O1-Re2 74.2(6), Re1-O2-Re2 73.9(7), O1-Re1-O2 105.9(7), O1-Re2-O2 106.0(7).

terminal $Cl^{\ominus}$ ligand. The Re^{IV}–Re^{IV} distance (2.376(2) Å) is nearly as short as that in the anion of **10** (2.362(1) Å).[12] In

$K_4[Re_2^{IV}(\mu\text{-}O)_2(C_2O_4)_4] \cdot 3H_2O$ **10**

octahedral, edge-sharing complexes, a σ, a π, and a δ metal–metal bond can form between the metal ions.[11, 13] A formal Re–Re double bond ($\sigma^2\pi^2$) results for **7** and **8** and a triple bond ($\sigma^2\pi^2\delta^2$) for **9**.[18] We described earlier the complexes *anti*-$[L_2MO_2(\mu\text{-}O)_2]^{2\oplus}$ (M = Mo^V,[14a] W^V[14b]), which have an M–M single bond (2.56 Å) and a *planar* $M_2(\mu\text{-}O)_2$ ring; in the *syn* isomers, with a *puckered* M_2O_2 ring, the M–M distance is just as large. $[L_2Mo_2^{III}(\mu\text{-}OH)_2Cl_2]^{2\oplus}$[15] is isoelectronic to **9**; the Mo–Mo distance is 2.501(3) Å and corresponds to a triple bond. In the electron-rich organometallic complexes **2–4**, the Re–Re distance is up to approximately 2.7 Å long, though still in the range of Re–Re double bonds.

The reason for the absence of a Re–Re bond in **1** is therefore still unclear. The fact that the oxo bridges are involved in strong hydrogen bonding to H_2O molecules cannot explain the enormous increase in the Re–Re distance, since even $M_2(\mu\text{-}OH)_2$ complexes can exhibit strong M–M bonds. The theoretical analysis of *Bursten* et al.[16] on the relative stability of planar versus puckered M_2O_2 rings in $[Cp_2^*M_2O_4]$ complexes is not relevant to complexes **7–9**, since a *short* Mo–Mo single bond is observed in the classical compound *syn*-$[L_2Mo_2^VO_2(\mu\text{-}O)_2]^{2\oplus}$ *and* in its organometallic counterpart *syn*-$[Cp_2^*Mo_2^VO_2(\mu\text{-}O)_2]$[17] (Mo-Mo 2.555(1) and 2.587(1) Å, respectively). Both complexes have a puckered M_2O_2 ring. Furthermore, the M–M distance is just as large in the complex *anti*-$[L_2M_2O_2(\mu\text{-}O)_2]^{2\oplus}$ (M = Mo^V, W^V), which has a planar M_2O_2 ring.

Experimental Procedure

6X · H_2O (X = Br, I): $[ReOCl_3(PPh_3)_2]$[8] (1.57 g, 1.88 mmol) was added under argon to a solution (60 mL) of dry THF, L (0.52 g, 4.02 mmol), and ethylene glycol (0.19 g, 3.06 mmol), which had been dried over molecular sieves. After stirring for 3 h at 20 °C, the solution was filtered to collect the pale violet precipitate of **6**Cl. Compound **6** was then crystallized from water as the bromide or iodide by addition of NaBr or NaI (yield ca. 75%). IR (KBr): $\tilde{\nu}$ = 961 (Re=O), 654 and 615 cm^{-1} (Re-OC). UV/VIS (H_2O): λ_{max} [nm] (ε[L mol^{-1} cm^{-1}]) = 546(29).

7: **6I** · H_2O (0.27 g, 0.55 mmol) was dissolved in 25 mL of water and the resulting solution was stirred under argon over Zn/Hg at 40 °C for 3 h. The green-brown solution was then separated from Zn/Hg and stirred under air at 20 °C for 24 h, whereby the solution turned intense violet. Addition of 5 mL of a saturated aqueous NaI solution resulted in formation of a violet, microcrystalline precipitate of **7**. Single crystals suitable for X-ray structure analysis were grown by slow cooling of an aqueous solution, saturated at 50 °C (yield 60%). IR (KBr): $\tilde{\nu}$ = 818 and 794 (Re=O), 729 cm^{-1} (Re_2O_2). UV/VIS (H_2O): λ_{max} [nm] (ε[L mol^{-1} cm^{-1} per binuclear unit]) = 556 (1560), 730 (300).

8: 0.1 M CH_3SO_3H was added to 20 mL of an aqueous solution of $ZnCl_2$ (0.82 g, 6.01 mmol) and NaCl (0.70 g, 11.98 mmol) until a clear solution resulted. After addition of **7** (0.47 g, 0.50 mmol), the solution was stirred for 3 h at 30 °C. Dark brown crystals of **8** crystallized from the clear green-brown solution within 2 d (yield 0.21 g, 40%). IR (KBr): $\tilde{\nu}$ = 712 (Re_2O_2), 555, 535 cm^{-1} (Zn-O or Re-OZn).

9: A solution of **6I** · H_2O (0.27 g, 0.55 mmol) in 20 mL of 0.5 M HCl was refluxed for 3 h and then cooled to 20 °C. Addition of NaI (1.5 g, 10.01 mmol) resulted in the crystallization within 2 d of black crystals of **9** together with colorless crystals of $[LReO_3]I$. The black crystals were sorted manually and recrystallized from a small amount of 0.5 M HCl (yield 0.15 g, 30%). IR (KBr): $\tilde{\nu}$ = 694 cm^{-1} (Re_2O_2). UV/VIS (1 M NaCl): λ_{max} [nm] (ε[L mol^{-1} cm^{-1}]) = 461 (4500), 520 (sh), 621 (272), 757 (217).

Compounds **7**, **8**, and **9** are diamagnetic (Faraday method). All compounds gave correct elemental analyses (C, H, N, halogen).

Received: January 23, 1990 [Z 3754 IE]
German version: *Angew. Chem. 102* (1990) 832

[1] a) F. A. Cotton, R. A. Walton: *Multiple Bonds between Metal Atoms*, Wiley, New York 1981; b) A. Perrin, M. Sergent, *New J. Chem. 12* (1988) 337.
[2] F. A. Cotton, N. F. Curtis, C. B. Harris, B. F. G. Johnson, S. J. Lippard, J. T. Magne, W. R. Robinson, J. S. Wood, *Science (Washington) 145* (1964) 1305.
[3] a) W. A. Herrmann, M. Flöel, J. Kulpe, J. K. Felixberger, E. Herdtweck, *J. Organomet. Chem. 355* (1988) 297; b) W. A. Herrmann, R. Serrano, U. Küsthardt, M. L. Ziegler, E. Guggolz, T. Zahn, *Angew. Chem. 96* (1984) 498; *Angew. Chem. Int. Ed. Engl. 23* (1984) 515.
[4] a) K. A. Wilhelmi, E. Lagervall, O. Müller, *Acta Chem. Scand. 24* (1970) 3406; J.-P. Besse, G. Baud, R. Chevalier, M. Gasparin, *Acta Crystallogr. Sect. B 34* (1978) 3532.
[5] K. Wieghardt, C. Pomp, B. Nuber, J. Weiss, *Inorg. Chem. 25* (1986) 1659.
[6] C. Pomp, S. Drüeke, H.-J. Küppers, K. Wieghardt, C. Krüger, B. Nuber, J. Weiss, *Z. Naturforsch. B 43* (1988) 299.
[7] a) W. A. Herrmann, R. Serrano, H. Bock, *Angew. Chem. 96* (1984) 364; *Angew. Chem. Int. Ed. Engl. 23* (1984) 383; b) W. A. Herrmann, R. Serrano, A. Schäfer, U. Küsthard, *J. Organomet. Chem. 272* (1984) 55.
[8] N. P. Johnson, C. J. Lock, G. Wilkinson, *J. Chem. Soc. 1964*, 1054.
[9] W. A. Herrmann, D. Marz, E. Herdtweck, A. Schäfer, W. Wagner, H.-J. Kneuper, *Angew. Chem. 99* (1987) 462; *Angew. Chem. Int. Ed. Engl. 26* (1987) 462.
[10] Crystal structure analyses: **6**Br · H_2O: monoclinic space group $P2_1$ (C_2^2; No. 4), a = 7.248(5), b = 13.562(6), c = 7.349(9) Å, β = 113.97(5)°, V = 660.09 Å^3, Z = 2, ϱ_{calcd} = 2.37 g cm^{-3}; $Mo_{K\alpha}$ radiation; R = 0.048; R_w = 0.042 for 2584 unique reflections with $I > 2.5\sigma(I)$. **7**: monoclinic space group $P2_1/c$ (C_{2h}^5)) a = 6.815(4), b = 11.362(9), c = 14.721(9) Å, β = 90.43(5)°, V = 1139.8 Å^3, Z = 2, ϱ_{calcd} = 2.76 g cm^{-3}; $Mo_{K\alpha}$ radiation; R = 0.050; R_w = 0.046 for 2648 unique reflections with $I > 2.5\sigma(I)$. **8**: monoclinic space group $P2_1/n$ (C_{2h}^5), a = 8.101(5), b = 18.27(1), c = 9.463(4) Å, β = 100.53(4)°, V = 1377 Å^3, Z = 2, ϱ_{calcd} = 2.50 g cm^{-3}; $Mo_{K\alpha}$ radiation; R = 0.055; R_w = 0.048 for 2704 unique reflections with $I > 2.5\sigma(I)$. **9**: orthorhombic space group $Pbca$ (D_{2h}^{15}; No. 61), a = 11.617(8), b = 15.782(8), c = 28.40(1) Å, V = 5206. 8 Å^3, Z = 8, ϱ_{calcd} = 2.61 g cm^{-3}; $Mo_{K\alpha}$ radiation; R = 0.052; R_w = 0.046 for 2297 unique reflections with $I > 2.5\sigma(I)$. Further details of the crystal structure investigations may be obtained from the Fachinformationszentrum Karlsruhe, Gesellschaft für wissenschaftlich-technische Information mbH, D-7514 Eggenstein-Leopoldshafen 2 (FRG), on quoting the depository number CSD 54513, the names of the authors, and the journal citation.

[11] F. A. Cotton, *Polyhedron 6* (1987) 667.
[12] T. Lis, *Acta Crystallogr. Sect. B31* (1975) 1594.
[13] S. Shaik, R. Hoffmann, C. R. Fisel, R. H. Summerville, *J. Am. Chem. Soc. 102* (1980) 4555.
[14] a) K. Wieghardt, M. Hahn, J. Weiss, W. Swiridoff, *Angew. Chem. 95* (1983) 499; *Angew. Chem. Int. Ed. Engl. 22* (1983) 491; b) P. Schreiber, K. Wieghardt, U. Flörke, H.-J. Haupt, *Inorg. Chem. 27* (1988) 2111.
[15] K. Wieghardt, M. Hahn, W. Swiridoff, J. Weiss, *Inorg. Chem. 23* (1984) 94.
[16] B. E. Bursten, R. H. Clayton, *Inorg. Chem. 28* (1989) 2846.
[17] H. Arzoumanian, A. Baldy, M. Pierrot, J.-F. Petrignani, *J. Organomet. Chem. 294* (1985) 327.
[18] A $\sigma^2\pi^2\delta^{*2}$ electron configuration, as proposed for $[(H_2edta)Tc^{IV}(\mu\text{-}O)_2Tc^{IV}(H_2edta)]\cdot 5H_2O$ with a Tc–Tc distance of 2.33 Å (H. B. Bürgi, G. Anderegg, P. Bläuenstein, *Inorg. Chem. 20* (1981) 3829) is equally conceivable for **9**.

The Tautomeric Equilibrium between Cyclopentadienyl-1-carboxylic Acid and Fulvene-6,6-diol in Aqueous Solution**

By *Bernhard Urwyler* and *Jakob Wirz**

The light-induced decomposition of diazoketones has been studied since the origins of organic photochemistry.[1] Quinone diazides find commercial application as positive photoresists in microlithography.[2] *Süs* first described the mechanism of the photochemical ring contraction of *o*-quinone diazides and identified cyclopentadienyl carboxylic acids as the final products of photolysis in aqueous solution.[3] Recent kinetic studies of this photoreaction have, however, led to contradictory interpretations.[4]

The primary photoproduct of the parent compound 1,2-benzoquinone diazide (**1**) in a nitrogen matrix has been identified as 6-fulvenone **2** by IR spectroscopy.[5] We generated the ketene **2** by laser flash photolysis of **1**[6] as well as of 2-bromophenol (**3**)[7] and report here its reaction kinetics in aqueous solution (Scheme 1). The hydrolysis of **2** proceeds via the metastable intermediate 6,6-fulvenediol (**4**) to give 1,3-cyclopentadienyl-1-carboxylic acid (**5**). Combination of the two dissociation constants of the OH- and CH-acid **5** with the kinetic data of the decay of **4** provides the first complete characterization of the equilibrium and kinetics of the enolization of a carboxylic acid.[8]

The quantum yield of photohydrolysis of 2-bromophenol (**3**) drops to almost zero[7] in acidic solutions [pH < pK_a (**3**) = 8.45].[9] On the other hand, 1,2-benzoquinone diazide (**1**) is unstable in basic aqueous solutions. Therefore, we used the diazide **1** in acidic solutions and the phenol **3** in basic solutions (both ca. 0.5×10^{-4} M, 24 ± 2 °C) as precursors to the ketene **2** in the flash photolysis experiments (excimer laser, 248 or 308 nm, ca. 100 mJ per pulse, pulse width ca. 25 ns). Control experiments with weakly basic aqueous solutions confirmed that both **1** and **3** give the same transient intermediates upon photolysis. In the proton concentration range from 10^{-1} to 10^{-13} M all solutions were adjusted to an ionic strength of $I = 0.1$ M by the addition of NaCl. The reaction was not affected by oxygen except for the oxidation of $\mathbf{4}^{2\ominus}$ in strongly basic solutions (vide infra). Thus, in most cases air saturated solutions were used. Experiments with basic buffers such as tris(hydroxymethyl)methylamine, phosphate, and borax showed that the ketene **2** reacted with the basic buffer components, whereby the formation of **4** was suppressed. Therefore, only dilute NaOH could be used to prepare weakly basic solutions. These solutions were prepared under argon and controlled by a glass electrode.

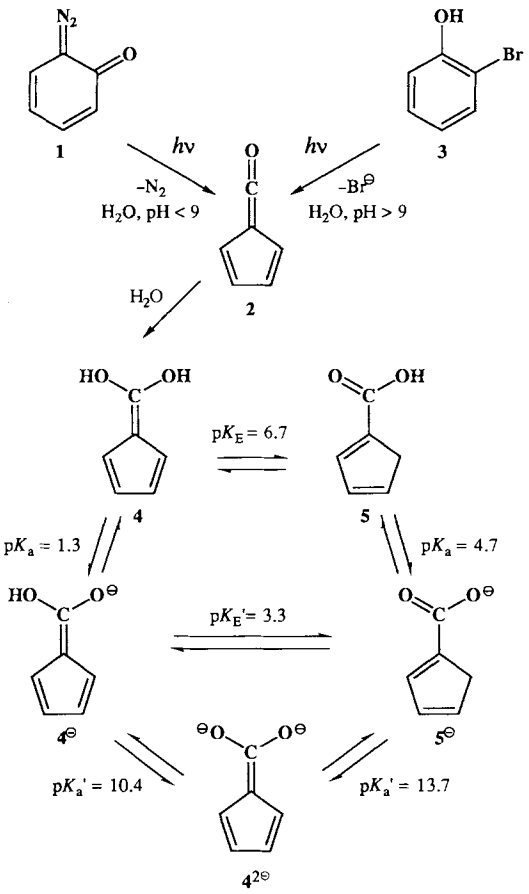

Scheme 1. All equilibrium constants are concentration quotients in aqueous solution (I = 0.1 M, 24 ± 2 °C).

A mixture of dimers of **5** is readily accessible by reaction of the cyclopentadienyl anion with CO_2.[10] The monomeric acid **5**[11] was isolated by fractional vacuum sublimation of the dimers (3×10^{-2} torr, 180 °C). The acid may be stored at −70 °C in crystalline form and is stable for hours in dilute aqueous solution at ambient temperature. Twofold deprotonation in aqueous base gave the conjugate dianion $\mathbf{4}^{2\ominus}$ reversibly, which, however, was stable only when air was strictly excluded. The oxygen and carbon dissociation constants (concentration quotients at I = 0.1 M) of **5** were measured by spectrophotometric titration,[12] pK_a = 4.71 ± 0.02, pK_a' = 13.71 ± 0.04. The second titration required NaOH concentrations of up to 1.2 M. The H_{2-} acidity function defined by *Yagil*[13] was used to calculate the concentration quotient for I = 0.1 M. A possible systematic error arising from this procedure should be less than ±0.1 pK units.

Upon flash excitation of basic solutions of **3** we observed the formation and subsequent decay of a transient intermediate absorbing in the range 280 to 320 nm (see insert in Fig. 1). Both reactions obeyed a first-order rate law (τ_1 = 1 μs, τ_2 = 7 μs at pH ≈ 10). Below 280 nm, the first reaction appeared as a decay of transient absorbance. The

[*] Prof. Dr. J. Wirz, Dipl.-Chem. B. Urwyler
Institut für Physikalische Chemie der Universität Basel
Klingelbergstrasse 80, CH-4056 Basel (Switzerland).

[**] This work is part of project No. 2000-5.515 of the Swiss National Science Foundation. It was supported by Ciba-Geigy SA, Sandoz SA, F. Hoffmann-LaRoche & Cie. SA and by the Ciba-Stiftung.

absorption maximum of the ketene **2** is at 260 nm.[5] The first reaction is thus attributed to hydrolysis of the ketene **2** yielding the enediol **4**. This assumption is fully corroborated by the following observations.

The rate of hydrolysis of **2** remained constant in aqueous solution from pH = 2 to 11, $k_0 = (9.0 \pm 0.4) \times 10^5\ s^{-1}$. In basic solutions (pH > 11) it increased with the concentration of hydroxyl ions. Linear regression of the rates measured in the range $[OH^\ominus] = 10^{-3}$ to 10^{-1} M gave the intercept $k_0 = (9.5 \pm 0.1) \times 10^5\ s^{-1}$ and the slope $k_{OH^\ominus} = (4.8 \pm 0.1) \times 10^7\ M^{-1}\ s^{-1}$. Similar rate profiles were reported by *Tidwell, Kresge* et al. for the hydrolysis of alkyl and aryl ketenes.[14]

Upon addition of KCN to a solution of **3** in aqueous NaOH (3×10^{-4} M), the decay rate of **2** increased linearly with the concentration of cyanide, $k_{KCN} = (1.6 \pm 0.2) \times 10^8\ M^{-1}\ s^{-1}$, and the intensity of the subsequent decay of **4** was reduced accordingly. The formation of a new photoproduct ($\lambda_{max} = 340$ nm) in the presence of KCN was confirmed by 400-MHz ^{1}H-NMR spectroscopy: irradiation ($\lambda > 300$ nm) of $\mathbf{3}^\ominus$ (10 mg) in 10 ml D_2O/KCN (1 M) gave rise to new signals of equal intensity at $\delta(J[Hz]) = 6.81$(d, 4), 6.79(d, 4), 6.57 (dd, 4 and 2) and 6.46 (dd, 4 and 2) which we attribute to 6-cyanofulven-6-olate ($\mathbf{6}^\ominus$). Attempts to isolate the enol **6** failed. Presumably, **6** tautomerizes to the cyclopentadiene **7**, which in turn yields a complex product mixture.

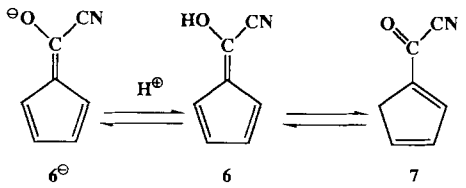

$\mathbf{6}^\ominus$ **6** **7**

The ketonization of the enediol **4** to the carboxylic acid **5** was monitored at 315 nm. The V-shaped rate profile approaches maximum values of ca. $10^6\ s^{-1}$ at both the acidic and the basic ends of the scale (Fig. 1, curve b). This is clear evidence that two acid-base equilibria are established prior to the decay of **4**: In the pH range from 2 to 10, the predominant species is $\mathbf{4}^\ominus$. Its rate profile has the same shape as that of simple enols.[15] The maximum lifetime of $\mathbf{4}^\ominus$ is about 20 ms at pH 6. Due to preequilibration with the more reactive dianion $\mathbf{4}^{2\ominus}$, the reaction rate increases with increasing concentration of $OH^\ominus$ and approaches its maximum value when the equilibrium shifts to the dianion. With increasing $H^\oplus$ concentration, the rate increases again due to protonation of $\mathbf{4}^\ominus$ at carbon; the plateau is reached in strong acid as the equilibrium shifts to the less reactive, neutral enediol **4**. Since, as usual,[15] the protonation of the enediol and its anions at carbon is rate determining, the rate law[16] for the ketonization reaction of the enol **4** is given by Equation (a).

$$\log(k_{obs}) = \log\left\{k + \frac{k' K_a}{[H^\oplus]} + \frac{k'' K_a K'_a}{[H^\oplus]^2}\right\} - \log\left\{1 + \frac{K_a}{[H^\oplus]} + \frac{K_a K'_a}{[H^\oplus]^2}\right\} \quad (a)$$

Least squares fitting of Equation (a) to the measured rate constants k_{obs} gave the first-order rate constant of the ketonization of the enediol **4**, $k = (1.08 \pm 0.08) \times 10^6\ s^{-1}$, and of the dianion $\mathbf{4}^{2\ominus}$, $k'' = (9.6 \pm 0.9) \times 10^5\ s^{-1}$, as well as the two dissociation constants of the enediol **4**, $pK_a = 1.31 \pm 0.05$ and $pK'_a = 10.4 \pm 0.1$. Due to poor buffering of the solutions at the second inflection we need to consider an additional systematic error of at most ± 0.1 pK units. As expected, the "uncatalyzed" reaction of the anion $\mathbf{4}^\ominus$ did not contribute significantly to the observed rate ($k' < 40\ s^{-1}$).

Flash photolysis ($\lambda = 308$ nm) of 2-bromophenol (**3**) in 1 M NaOH gave the dianion $\mathbf{4}^{2\ominus}$ within 100 ns after excitation. Its oxidation in air-saturated solution could thus be monitored directly; it occurs at a nearly diffusion-controlled rate, $k_{O_2} = (4.70 \pm 0.05) \times 10^9\ M^{-1}\ s^{-1}$. Indeed, the oxidation potentials of -0.62 V and -0.67 V (vs. SCE),[17] measured for the dilithium salts of phenyl- and diphenylacetic acid in THF/HMPA, are close to the first reduction potential of oxygen in aqueous solution (1 M NaOH, -0.563 V).[18]

The equilibrium constant for the enolization of the carboxylic acid **5** may be calculated through the thermodynamic cycle of Scheme 1: $pK_E = pK_a(\mathbf{5}) + pK'_a(\mathbf{5}) - pK_a(\mathbf{4}) - pK'_a(\mathbf{4}) = 6.71 \pm 0.2$. The quoted error range includes, by the law of error propagation, the conservative estimates given above for possible systematic errors in $pK'_a(\mathbf{5})$ and $pK'_a(\mathbf{4})$. The enolization constant of the carboxylic acid anion $\mathbf{5}^\ominus$ is obtained similarly as $pK'_E = pK'_a(\mathbf{5}) - pK'_a(\mathbf{4}) = 3.3 \pm 0.2$. The enol content of the carboxylic acid **5** is thus nearly nine orders of magnitude higher than that of mandelic acid.[8] It is also interesting to compare the pK_a values of **4** with those of the structurally related carbonic acid, $CO(OH)_2$: $pK_a = 3.9$ and $pK'_a = 10.3$.[19] The high enol content of **5** and the high acidity of the enediol **4** reflect the stabilization of the electron-rich dioxy function by charge transfer to the five-membered ring.

Figure 1 summarizes the rate profiles for the hydrolysis of the ketene **2**, the ketonization of the enediol **4**, and the enolization of **4**, calculated from the latter via the equilibrium constants. Note that the enolization reaction is catalyzed by base, but hardly by acid. The readily accessible dianion $\mathbf{4}^{2\ominus}$ might be useful as a reactive, electron-rich diene component for synthetic purposes.

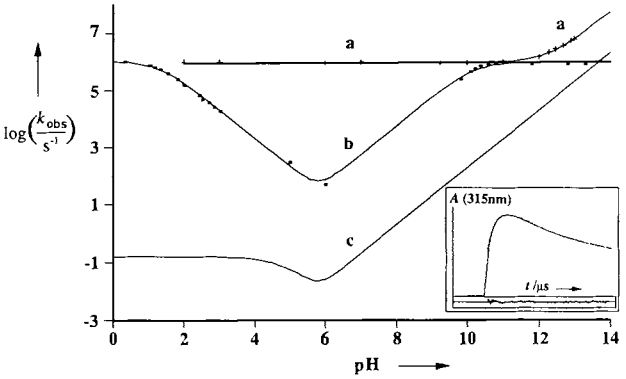

Fig. 1. Rate profiles for a) the hydrolysis of **2**, b) the ketonization of **4**, and c) the enolization of **5**. All pH values reported in this work refer to proton *concentrations* rather than activities. They were adjusted by HCl in the range pH = 1 to 3, by dilution series with acetic acid buffer at 5 and 6 and with NaOH above 9.8; $I = 0.1$ M. The inset shows the formation and subsequent decay of the transient intermediate **4** at pH = 10.

Received: March 15, 1990 [Z 3859 IE]
German version: *Angew. Chem. 102* (1990) 807

CAS Registry numbers:
1, 4024-72-0; **2**, 4727-22-4; **3**, 95-56-7; **4**, 78559-02-1; $\mathbf{4}^\ominus$, 127571-03-3; $\mathbf{4}^{2\ominus}$, 127571-05-5; **5**, 85004-15-5; $\mathbf{5}^\ominus$, 127571-04-4; **6**, 127571-01-1; **7**, 127571-02-2.

[1] H. D. Roth, *Angew. Chem. 101* (1989) 1220; *Angew. Chem. Int. Ed. Engl. 28* (1989) 1193.

[2] a) F. A. Vollenbroek, W. P. M. Nijssen, C. M. J. Mutsaers, M. J. H. J. Geomini, M. E. Reuhman, R. J. Visser, *Polym. Eng. Sci. 29* (1989) 928; b) W. S. Deforest, *Photoresist: Materials and Processes*, McGraw-Hill, New York 1975, p. 132.

[3] O. Süs, *Justus Liebigs Ann. Chem. 556* (1944) 65, 85.

[4] a) K. Nakamura, S. Udagawa, K. Honda, *Chem. Lett. 1972*, 763; b) K. Tanigaki, T. W. Ebbesen, *J. Am. Chem. Soc. 109* (1987) 5883; *J. Phys. Chem. 93* (1989) 4531; c) J. A. Delaire, J. Faure, F. Hassine-Renou, M. Soreau, *New J. Chem. 11* (1987) 15; d) M. Tsuda, S. Oikawa, K. Nagayama, *Chem. Pharm. Bull. 35* (1987) 1; e) T. Shibata, K. Koseki, T. Yamaoka, M. Yoshizawa, H. Uchiki, T. Kobayashi, *J. Phys. Chem. 92* (1988) 6269.

[5] M. S. Baird, I. R. Dunkin, N. Hacker, M. Poliakoff, J. J. Turner, *J. Am. Chem. Soc. 103* (1981) 5190.

[6] a) M. Yagihara, Y. Kitahara, T. Asao, *Chem. Lett. 1974*, 1015; b) R. Clinging, F. M. Dean, G. H. Mitchell, *Tetrahedron 30* (1974) 4065.

[7] C. Guyon, P. Boule, J. Lemaire, *Tetrahedron Lett. 23* (1982) 1581; *New J. Chem. 11* (1987) 685.

[8] See also the accompanying paper on the enol of mandelic acid: Y. Chiang, A. J. Kresge, P. Pruszynski, N. P. Schepp, J. Wirz, *Angew. Chem. 102* (1990) 810; *Angew. Chem. Int. Ed. Engl. 29* (1990) 792.

[9] P. D. Bolton, F. M. Hall, I. H. Reece, *J. Chem. Soc. B 1966*, 717.

[10] D. Peters, *J. Chem. Soc. 1961*, 1042.

[11] M.p. 70 °C (dec., presumably dimerization); UV [λ_{max} [nm] (log ε)] in H_2O: 277 nm (3.9); in NaOH, 0.1 M: 272 (3.8); ^{1}H-NMR (CD_3CN/CD_3ONa): δ = 7.38(m); 6.72 (dd, J = 6, 2 Hz); 6.62(m); 3.25(m). In D_2O/NaOD (1 M) the signals of all protons disappear due to exchange with the solvent.

[12] H. Gampp, M. Maeder, C. J. Meyer, A. D. Zuberbühler, *Talanta 32* (1985) 95.

[13] G. Yagil, *J. Phys. Chem. 71* (1967) 1034.

[14] A. D. Allen, T. T. Tidwell, *J. Am. Chem. Soc. 109* (1987) 2774; A. D. Allen, A. J. Kresge, N. P. Schepp, T. T. Tidwell, *Can. J. Chem. 65* (1987) 1719.

[15] Y. Chiang, M. Hojatti, J. R. Keefe, A. J. Kresge, N. P. Schepp, J. Wirz, *J. Am. Chem. Soc. 109* (1987) 4000. Y. Chiang, A. J. Kresge, J. A. Santabella, J. Wirz, *ibid. 110* (1988) 5506.

[16] A detailed analysis of the reaction kinetics of **4** and its benzo derivative will be given in a full paper.

[17] P. Renaud, M. A. Fox, *J. Am. Chem. Soc. 110* (1988) 5705.

[18] G. Milazzo, S. Caroli: *Tables of Standard Electrode Potentials*, Wiley-Interscience, New York 1978.

[19] R. P. Bell *The Proton in Chemistry*, 2nd. edit., Chapman and Hall, London 1973, p. 93.

The Enol of Mandelic Acid, Detection, Acidity in Aqueous Solution, and Estimation of the Keto-Enol Equilibrium Constant and Carbon Acidity of Mandelic Acid**

By *Y. Chiang, Alexander J. Kresge,* P. Pruszynski, N. P. Schepp,** and *Jakob Wirz*.

The current renaissance of interest in the chemistry of enols is providing a wealth of new information about enol isomers of simple aldehydes and ketones.[1] Little, however, is as yet known about enols of other carbonyl compounds, such as carboxylic acids and esters: we are aware of only two previous observations of carboxylic acid enols in solution.[2] One of these[2a] was of the enol of bis(pentamethylphenyl)-acetic acid **1** (Ar = Me_5C_6), whose bulky aryl groups give it remarkable stability, reminiscent of the unusually stable hindered enols of aldehydes and ketones prepared by *Fuson* some 40 years ago[3] and currently being reinvestigated by *Rappoport* et al.[1b] We wish to report that we have now generated an unhindered and very much more reactive carboxylic acid enol **2**, namely the enol of mandelic acid in aqueous solution, and have begun investigating its chemistry in this medium.

1 **2**

We prepared this enol by two different flash photolytic methods: Norrish type II photoelimination of methyl or isobutyl benzoylformate **3** [Eq. (a), R = H, *i*Pr], and photo-Wolff reaction of diazophenylacetate **6** [Eq. (b)].

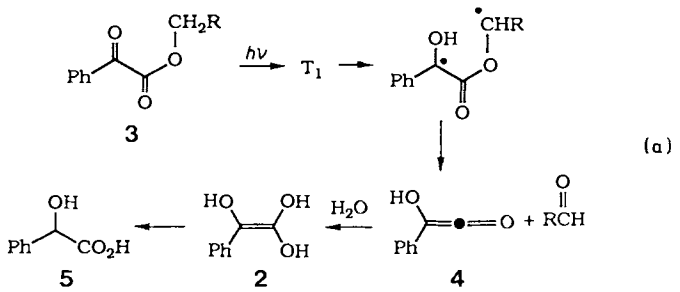

(a)

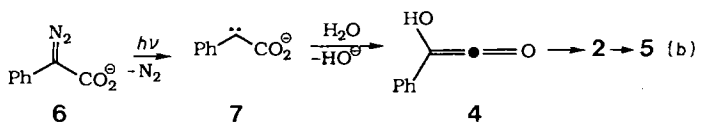

(b)

Reports in the literature[4] suggest that the first of these processes involves generation of a triplet excited state of **3** (T_1), followed by diradical formation and cleavage to hydroxyphenylketene **4**, which may then combine with water to give mandelic acid **5** via its enol **2**. Consistent with this we find that flash photolysis of methyl or isobutyl benzoylformate gives rise to triphasic UV spectral changes (Fig. 1),

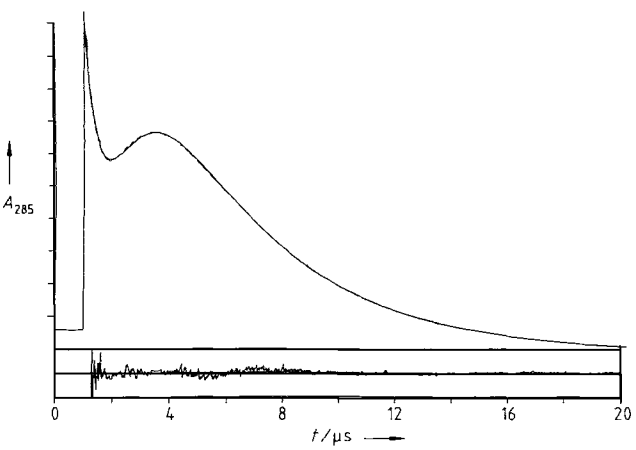

Fig. 1. Absorbance changes at λ = 285 nm upon flash photolysis of methyl benzoylformate in aqueous biphosphate buffer solution ($[H_2PO_4^{\ominus}]$ = 0.002 M, $[HOP_4^{2\ominus}]$ = 0.006 M, I = 0.10 M) at 25 ° using an excitation pulse from a KrF eximer laser. λ_{exc} = 248 nm, 20 ns pulse width, 200 mJ per pulse; the bottom trace shows residuals from a least squares fit of the data to a triple exponential expression.

[*] Prof. Dr. A. J. Kresge, Y. Chiang, Dr. P. Pruszynski
Department of Chemistry, University of Toronto
Toronto, Ontario M5S 1A1 (Canada)
Dr. N. P. Schepp, Prof. Dr. J. Wirz
Institut für Physikalische Chemie
Universität Basel, CH-4056 Basel (Switzerland)

[**] This work was supported by the Natural Sciences and Engineering Research Council of Canada, the Donors of the Petroleum Research Fund, administered by the American Chemical Society, and the Swiss National Science Foundation (Project No. 200-5. 515).

implying the production of three successively formed transient species. Flash photolysis of **6** also gives the second and third of these transients, as expected from rearrangement of a carbene intermediate to **4** followed by hydration of the ketene to mandelic acid enol **2**. Both reactions also produce mandelic acid **5** as a major product.

Decay of the shortest-lived transient formed by flash photolysis of **3** is not catalyzed by acids or bases over the pH range investigated (2–8), and the lifetime of the transient, $\tau \approx 300$ ns, is similar to that reported for the triplet excited states of benzoylformate esters in water ($\tau = 300$ ns)[5] and other solvents ($\tau = 400$–700 ns).[4] This, plus the fact that its lifetime increases to $\tau = 450$ ns in degassed aqueous solution, as well as its broad UV spectrum extending from $\lambda = 300$ to 500 nm, serves to identify this species as the triplet.

Decay of the transient attributed to **4** is also not catalyzed by $H^{\oplus}$ or $HO^{\ominus}$ over the pH range investigated (2–8), and only weakly if at all by phosphate or tris(hydroxymethyl)-methylamine (TRIS) buffers. Its rate of reaction with water is $6.7 \times 10^5\ s^{-1}$ and it exhibits a solvent isotope effect $k_{H_2O}/k_{D_2O} = 1.3$. This is the behavior expected for hydration of a phenyl-substituted ketene; for example, hydration of phenylketene itself shows no acid catalysis and catalysis by hydroxide ion becomes significant only above pH = 12, and the reaction exhibits a solvent isotope effect $k_{H_2O}/k_{D_2O} = 1.4$.[6]

Since **4** also contains an enol functional group, it could, at least in principle, undergo a formally uncatalyzed ketonization reaction [Eq. (c)] by ionization of the enol followed by

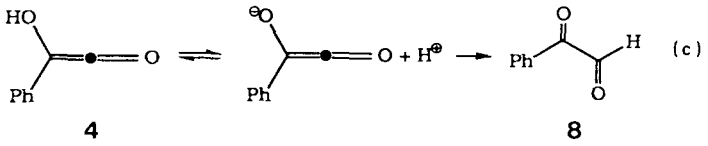

4 8 (c)

rate-determining protonation of the enolate ion on carbon. This process, however, would by expected to give a solvent isotope effect much greater than the $k_{H_2O}/k_{D_2O} = 1.3$ observed: the acid ionization step of Equation (c) would contribute a factor of $K_{H_2O}/K_{D_2O} = 3$–4, and the rate-determining step another factor of $k_H^{\oplus}/k_D^{\oplus} = 2$–$3$, for an overall prediction of $k_{H_2O}/k_{D_2O} = 6$–12. This reaction, moreover, produces benzoylformaldehyde **8**, but no **8** was found in the reaction product. Reaction by this route would also give rise to one transient less than the number observed.

The absorbance of the transient attributed to mandelic acid enol shifts to longer wavelength in basic solution, as expected for conversion of an enol into its enolate ion.[7] The decay of **2** is catalyzed by both $H^{\oplus}$ and $HO^{\ominus}$, and it also shows strong catalysis by phosphate and TRIS buffers. This is characteristic of the ketonization of enols. Decay of this transient also gives a rate profile (Fig. 2) which is typical of such a process.[1c] In particular, the apparent hydroxide ion catalysis that becomes saturated above pH = 7 can be attributed to ionization of the enol [Eq. (d)], followed by rate-determining protonation of the much more reactive enolate ion on carbon by water [Eq. (e)]. Standard treatment of rate data

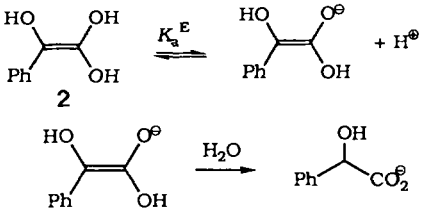

(d)

(e)

obtained in the region of transition from catalysis to saturation gives the equilibrium constant for the ionization step, which is the acidity constant of the enol. The present data produce the result, $pK_a^E = 6.62 \pm 0.07$.[8,10]

We also attempted to measure the rate of enolization of mandelic acid **5** in order to provide an estimate of the keto-enol equilibrium constant as the ratio of enolization to ketonization rate constants, $K_E = k_E/k_K$. Since **5** contains an asymmetric carbon atom which will lose its chirality upon enolization [Eq. (f)], we chose to do this by monitoring the

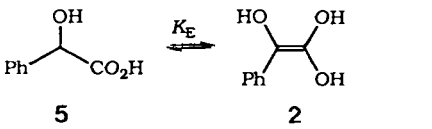

(f)

racemization of optically active mandelic acid by polarimetry. The rates of racemization proved to be very slow, and we were forced to make measurements at elevated temperatures (138–155 °C) in concentrated acid solutions (1.1–4.5 M HCl). Acid-catalyzed enolization is a classic example of a reaction whose rate is proportional to acid concentration rather than some steeper acidity function,[11] and we found this to be the case for the present racemization in the range [HCl] = 1–2 M. Above this region, however, rates increased more rapidly than in direct proportion to acid concentration, suggesting that some process in addition to enolization – perhaps nucleophilic substitution – was intervening. We plan to investigate this matter, but in the meantime, working on the assumption that the component of the racemization reaction whose rate is proportional to acid concentration is in

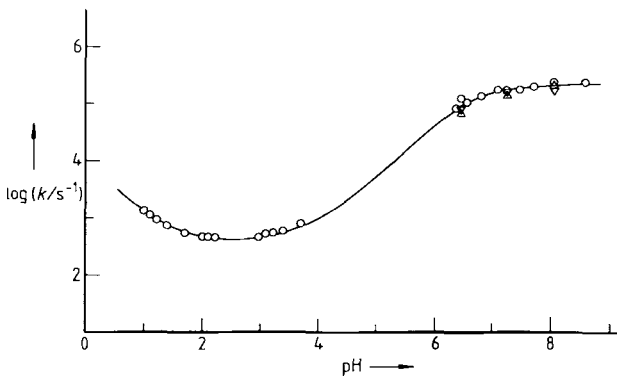

Fig. 2. Rate profile for the ketonization of **2** in aqueous solution at 25 °C; ○: enol generated from **3**, R = H; △: enol generated from **3**, R = *i*Pr; ▽: enol generated from **6**. The data for the pH range ≈6–9 were obtained from measurements in $H_2PO_4^{\ominus}$ and TRIS buffers extrapolated to zero buffer concentration. All pH data in this work refer to proton *concentrations* and not to proton activities.

fact enolization, we can estimate a hydronium-ion catalytic coefficient of $k^{E}_{H\oplus} = 4 \times 10^{-12}\ M^{-1}\ s^{-1}$ for the enolization reaction at 25 °C. Combination of this with the hydronium-ion catalytic coefficient for ketonization measured at 25 °C, $k^{E}_{H\oplus} = 9.3 \times 10^{3}\ M^{-1}\ s^{-1}$,[12] then leads to the keto-enol equilibrium constant $pK_E = 15.4$.

This keto-enol equilibrium [Eq. (f)] and the acid ionization of the enol, [Eq. (d)] form two branches of a thermodynamic cycle whose third member is the deprotonation of mandelic acid **5** as a carbon acid [Eq. (g)]. The equilibrium constant for this reaction may therefore be calculated from the other two: $pK^{K}_{a} = pK_E + pK^{E}_{a} = 22.0$.

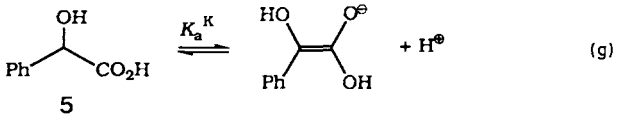

(g)

These three equilibrium constants, pK_E, pK^{E}_{a}, and pK^{K}_{a}, are the first ever measured for a simple carboxylic acid keto-enol system in aqueous solution.[13] They show the enol content to be very low—orders of magnitude less than of simple aldehydes and ketones—as expected from stabilization of the keto tautomer of the carboxylic acid system through conjugative interaction of its carbonyl and hydroxyl groups. The carboxylic acid enol, on the other hand, is more acidic than those of simple aldehydes and ketones, and that makes the carbon acidity of this carboxylic acid greater than it would otherwise be.

Received: March 27, 1990 [Z 3881 IE]
German version: *Angew. Chem. 102* (1990) 810

CAS Registry numbers:
2, 127645-81-2; **5**, 90-64-2.

[1] For reviews see: a) B. Capon, B.-Z. Guo, F. C. Kowk, A. K. Siddhanta, C. Zucco *Acc. Chem. Res. 21* (1988) 135; b) Z. Rappoport, S. E. Biali, *ibid. 21* (1988) 442; c) A. J. Kresge *ibid. 23* (1990) 43.
[2] a) P. O'Neill, A. F. Hegarty, *J. Chem. Soc. Chem. Comm. 1987*, 744; b) T. Shibata, K. Koseki, T. Yamaoka, M. Yoshizawa, H. Uchiki, T. Kobayashi, *J. Phys. Chem. 92* (1988) 6269.
[3] For a brief review of *Fuson*'s work, see H. Hart, *Chem. Rev. 79*, (1979) 515.
[4] See, e.g., M. V. Encinas, E. A. Lissi, A. Zanocco, L. C. Stewart, J. C. Scaiano, *Can. J. Chem. 62* (1984) 386.
[5] H. J. Kuhn, H. Görner, *J. Phys. Chem. 92* (1988) 6208.
[6] A. D. Allen, A. J. Kresge, N. P. Schepp, T. T. Tidwell, *Can. J. Chem. 65* (1987) 1719.
[7] P. Haspra, A. Sutter, J. Wirz, *Angew. Chem. 91* (1979) 652; *Angew. Chem. Int. Ed. Engl. 18* (1979) 617.
[8] This pK_a probably refers to ionization of the hydroxy group *trans* to phenyl [Eq. (d)] rather than the *cis* hydroxyl, inasmuch as the *trans* enol of phenylacetaldehyde has been found to be a stronger acid than its *cis* isomer [9]. Ionization of the hydroxy group geminal to phenyl can be ruled out because this would produce phenylglyoxal, which is not found in the reaction product.
[9] Y. Chiang, A. J. Kresge, P. A. Walsh, Y. Yin, *J. Chem. Soc. Chem. Comm. 1989*, 869.
[10] This is a concentration ionization constant for $I = 0.10$ M.
[11] L. P. Hammett: *Physical Organic Chemistry*, McGraw Hill, New York 1940, pp. 273–277; F. A. Long, M. A. Paul *Chem. Rev. 57* (1957) 935.
[12] $I = 0.10$ M.
[13] See, however, the accompanying paper by *Urwyler* and *Wirz* [14] for similar data on a somewhat more unusual carboxylic acid enol.
[14] B. Urwyler, J. Wirz, *Angew. Chem. 102* (1990) 807; *Angew. Chem. Int. Ed. Engl. 29* (1990) 790.

A Bicyclo[1.1.1]pentasilane Derivative. Synthesis, Molecular Structure, and Comments on Structural Homology**

By *Yoshio Kabe, Takeshi Kawase, Joji Okada, Osamu Yamashita, Midori Goto*, and *Satoru Masamune**

In recent years we have witnessed a surge of activities in constructing strained polycyclic systems with the Group 14 elements, Si, Ge, and Sn. Those systems whose members have yielded to synthesis and are now adequately characterized include bicyclo[1.1.0]tetrasilane,[1a] bicyclo[2.2.0]-hexasilane,[1b] octasilacubane,[1c] hexagermaprismane,[1d] bicyclo[2.2.0]hexastannane,[1e] pentastanna[1.1.1]propellane,[1f] tricyclo[2.2.0.$0^{2,5}$]hexasilane,[1g] and tetracyclo-[3.3.0.$0^{2,7}$.$0^{3,6}$]octasilane,[1g] and octagermane.[1h,i] We wish to add to this list the bicyclo[1.1.1]pentasilane system **1**, which has been an object of recent theoretical investigation.[2a,b]. Comparison of the molecular structure of 1,3-bis(4-*tert*-butyl-2,6-diisopropylphenyl)-2,2,4,4-tetraisopropylbicyclo[1.1.1]pentasilane (**1a**), with the corresponding carbon analog **2** (Scheme 2) reveals a high degree of structural homology. This *approximate* homology applies also to other Si ring systems and can provide useful information on the unique Si,Si non-bonding distance in unknown compounds.

Treatment of the trichlorodisilane **3** with five equivalents of naphthalenelithium in THF at −78 °C led to the formation of the dianion **4**[3] (Scheme 1) which was quenched with

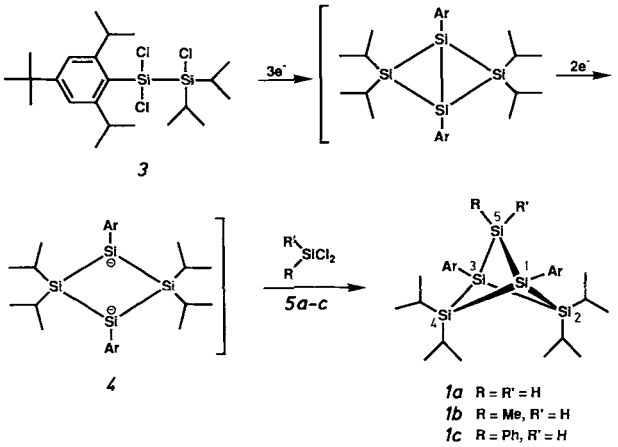

Scheme 1. Synthesis of **1a–c** (Ar = aryl).

excess dichlorosilane (**5a–c**) to provide **1a** in 31%, **1b** in 12%, and **1c** in 15% yield, respectively. The spectral data of these compounds (Table 1) are consistent with the proposed structures. Particularly revealing are the ^{29}Si-NMR spectra,

[*] Prof. Dr. S. Masamune, Dr. T. Kawase
Department of Chemistry, Massachusetts Institute of Technology
Cambridge, MA 02139 (USA)
Dr. Y. Kabe, J. Okada, Dr. O. Yamashita
Institute for Fundamental Research and
Tochigi Research Laboratory, Kao Corporation
Ichikai-machi Haga-gun, Tochigi 321-34 (Japan)
Dr. M. Goto
National Chemical Laboratory for Industry
Tsukuba, Ibaraki 305 (Japan)

[**] The work at M. I. T. was supported by a grant from the National Science Foundation, USA (Grant CHE-8706760).

Table 1. Some spectroscopic data of **1a–c**. ^{1}H NMR (270 MHz, C_6D_6), ^{13}C NMR (67.9 MHz, C_6D_6), ^{29}Si NMR (53.7 MHz, C_6D_6), mass spectra (EI, 20 eV).

1a: m.p. 200.4–202.8 °C; ^{1}H NMR: δ = 1.27 (s; 18H), 1.33 (d; 7.6 Hz; 12H), 1.40 (d; 7.6 Hz; 12H), 1.45 (d; 7 Hz; 24H), 1.85 (sept; 7.6 Hz; 2H), 2.05 (sept; 7.6 Hz; 2H), 4.13 (sept; 7 Hz; 4H), 4.32 (s; 2H), 7.37 (s; 4H); ^{13}C NMR: δ = 16.74 (d), 20.16 (d), 22.98 (q), 23.43 (q), 25.75 (q), 31.34 (s), 34.83 (d), 36.76 (s), 120.84 (d), 126.61 (s), 151.92 (s); 155.92 (s) ^{29}Si NMR: δ = −96.48 [Si(1), Si(3)], −76.64 [Si(5)], 6.26 [Si(2), Si(4)]; MS: calcd. *m/z* for $C_{44}H_{80}Si_5$: 748.5106, found 748.5062 IR: ν = 2116 cm^{-1}

1b: m.p. 179.9–182.6 °C; ^{1}H NMR: δ = 0.81 (d; 4 Hz; 3H), 1.28 (s; 18H), 1.33 (d; 7.5 Hz; 12H), 1.38 (d; 7.5 Hz; 6H), 1.40 (d: 7.5 Hz; 6H), 1.44 (d; 6.5 Hz; 12H), 1.45 (d; 6.5 Hz; 12H), 1.83 (m; 7,5 Hz; 3H), 2.18 (sept; 7.5 Hz; 1H), 4.08 (sept; 6.5 Hz; 4H), 4.62 (q; 4 Hz; 1H), 7.38 (s; 4H); ^{13}C NMR: δ = 3.60 (q), 15.84 (d), 20.04 (d), 20.69 (d), 21.03 (d), 23.01 (q), 23.37 (q), 23.65 (q), 23.70 (q) 25.73 (q), 26.04 (q), 31.36 (q), 34.81 (s), 36.72 (d), 120.82 (d), 151.56 (s), 155.96 (s); ^{29}Si NMR: δ = 91.86 [Si(1), Si(3)], −50.91 [Si(5)], −2.79, 9.37 [Si(2), Si(4)]; MS: *m/z* calcd for $C_{45}H_{82}Si_5$ 762.5263, found 762.5256; IR: ν = 2086 cm^{-1}

1c: m.p. 174.6–177.4 °C; ^{1}H NMR: δ = 1.24 (s; 18H), 1.3–1.5 (m; 48H), 1.8–2.0 (m; 3H), 2.40 (sept; 7.4 Hz; 1H), 4.13 (sept; 7 Hz; 4H), 5.34 (s; 1H), 7.00 (m; 2H), 7.36 (s; 4H), 7.84 (m; 3H); ^{13}C NMR: δ = 15.98 (d), 19.88 (d), 21.00 (d), 21.76 (d), 23.45 (q), 23.73 (q), 23.78 (q), 25.96 (q), 26.10 (q), 31.30 (q), 34.76 (s), 36.76 (d), 120.94 (d), 127.05 (d), 128.85 (d), 136.52 (s), 137.93 (d), 151.66 (s), 156.12 (s); ^{29}Si NMR: δ = 89.86 [Si(1), Si(3)], −41.14 [Si(5)], −6.24, 9.97 [Si(2), Si(4)]; MS: calcd for $C_{47}H_{77}Si_5$ ($M^{\oplus}-i$Pr) 781.4872 found 781.4955; IR: ν = 2092 cm^{-1}

whose analysis, based on the molecular symmetry of **1a–c**, readily permits signal assignments without recourse to 2D ^{29}Si NMR.[4] The assignments are indicated in Table 1.

An X-ray analysis of **1a** discloses several interesting structural features (Fig. 1).[5] As expected, the three cyclotetrasilane rings making up **1a** are highly puckered with an average dihedral angle of 60°, which contrasts with the 0–37° angles normally found in the monocyclic system. The Si–Si–Si bond angles at the bridge head atoms Si(1) and Si(3) approximate to 84° and those at the bridging silicon atoms Si(2), Si(4), and Si(5) are 78°. These values are in accord with the X-ray[6a] and electron diffraction[6b,c] (gas phase) data recorded for the carbon analogues, bicyclo[1.1.1]pentanes (**2**) showing that **1a** and **2** are homologous.

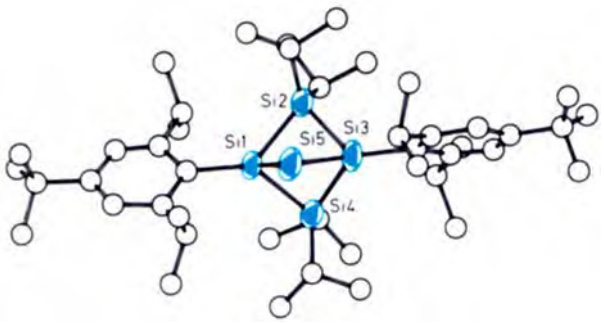

Fig. 1. Molecular structure of **1a**. Since two independent molecules in the asymmetric unit contain almost the same geometry, bond lengths [Å] and angles [°] of only one molecule are given below: Si1–Si2 2.38(1), Si1–Si4 2.34(1), Si1–Si5 2.32(1), Si2–Si3 2.34(1), Si3–Si4 2.36(1), Si3–Si5 2.35(1); Si2–Si1–Si4 87.4(3), Si2–Si1–Si5 82.6(4), Si4–Si1–Si5 83.2(4), Si1–Si2–Si3 78.0(4), Si2–Si3–Si4 87.6(5), Si2–Si3–Si5 82.2(4), Si4–Si3–Si5 82.1(4), Si1–Si4–Si3 78.5(3), Si1–Si5–Si3 79.1(5).

In **1a** the ratio of the "non-bonding distance" (NBD, Si1···Si3 2.98 Å) to the averaged length of the single bond (BL, Si–Si 2.35 Å) is 1.26 and, as a result of the homology discussed above, this ratio should be and indeed is close to that (1.22) calculated for NBD (1.89 Å)/BL (1.54) in **2**. Two other examples having the same ring framework as **1a** and **2** are the known tricyclo[2.2.0.0^{2,5}]hexasilane derivative **6**[1g] and the unknown trioxo analog **7**[2b,c] whose geometry was computed recently. Remarkably, both **6** and **7** exhibit an NBD/BL ratio of 1.21 and the latter has an Si···Si NBD of 2.06 Å, a distance well below the normal Si–Si BL. Even this unusual, predicated NBD conforms with the *approximate* homology rule.

The validity of the rule is not confined to the compounds of the above series I (Scheme 2) but also applies to those of three other series. Thus, a nearly constant NBD/BL ratio obtains for each of series II (cyclobutane[8a,9–13]), III (bicyclo[2.2.1]heptane[8b,14,15]), and IV (bicyclo[3.3.1]nonane.[8c,16] Of particular interest is **12** in series II. The finding that the Si···Si distance in this compound falls within the

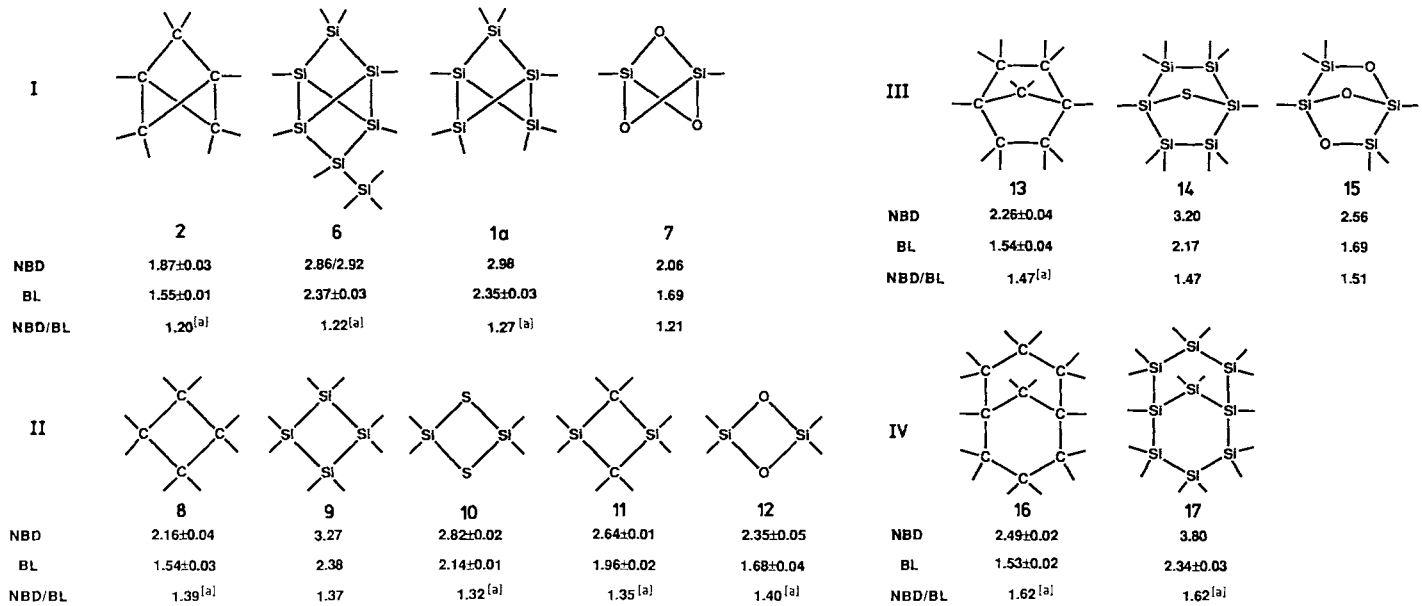

Scheme 2. The ratio NBD/BL (NBD: distance between non-bonding Si atoms; BL: bond lengths Si–X) in bi- and monocycles, data in [Å]. The analogous carbacyclic systems are also shown for comparison. [a] NBD/BL from averaged distances.

normal Si–Si bond length has aroused much discussion as to the nature of the bonding between those Si atoms.[7, 9] The remarkable consistency observed for series II implies that: 1) the shortening of the Si···Si distance in **12** is due mainly to the short Si–O (1.66 Å) BL compared to other BD's in other compounds of this series and 2) the "effective" van der Waals radius of the Si atom along the direction toward the other Si atom is smaller than that normally estimated for this atom. This inference is admittedly simplistic, but the *approximate* homology rule appears to provide an instant, good estimate on the NBD of unknown silicon compounds.

Received: March 5, 1990 [Z 3829 IE]
German version: *Angew. Chem. 102* (1990) 823

[1] a) S. Masamune, Y. Kabe, S. Collins, D. J. Williams, R. Jones, *J. Am. Chem. Soc. 107* (1985) 5552; R. Jones, D. J. Williams, Y. Kabe, S. Masamune, *Angew. Chem. 98* (1986) 173; *Angew. Chem. Int. Ed. Engl. 25* (1986) 173; b) H. Matsumoto, H. Miyamoto, N. Kojima, Y. Nagai, M. Gato, *Chem. Lett. 1988*, 629; c) H. Matsumoto, K. Higuchi, Y. Hoshino, H. Koike, Y. Naoi, Y. Nagai, *J. Chem. Soc. Chem. Commun. 1988*, 1083; d) A. Sekiguichi, C. Kabuto, H. Sakurai, *Angew. Chem. 101* (1989) 97; *Angew. Chem. Int. Ed. Engl. 28* (1989) 55; e) L. R. Sita, R. D. Bickerstaff, *ibid. 111* (1989) 3769; f) L. R. Sita, R. D. Bickerstaff, *J. Am. Chem. Soc. 111* (1989) 6454; g) Y. Kabe, M. Kuroda, Y. Honda, O. Yamashita, T. Kawase, S. Masamune, *Angew. Chem. 100* (1989) 1793; *Angew. Chem. Int. Ed. Engl. 27* (1988) 1725; h) M. Weidenbruch, F.-T. Grimm, S. Pohl, W. Saak, *ibid. 101* (1989) 201 and *28* (1989) 198; i) A. Sekiguchi, H. Naito, H. Nameki, K. Ebata, C. Kabuto, H. Sakurai, *J. Organomet. Chem. 368* (1989) C1.

[2] a) P. von R. Schleyer, R. Janoscheck, *Angew. Chem. 99* (1987) 1312; *Angew. Chem. Int. Ed. Engl. 26* (1987) 1267; b) S. Nagase, T. Kudo, T. Kurakake, *J. Chem. Soc. Chem. Commun. 1988*, 1063; c) A. Streitwieser *ibid. 1989*, 1261.

[3] T. Kawase, S. A. Batcheller, S. Masamune, *Chem. Lett. 1987*, 227.

[4] a) M. Kuroda, Y. Kabe, M. Hashimoto, S. Masamune, *Angew. Chem. 100* (1988) 1795; *Angew. Chem. Int. Ed. Engl. 27* (1988) 1727; b) J. Maxka, B. R. Adams, R. West, *J. Am. Chem. Soc. 111* (1989) 3447; c) E. Hengge, F. Schrank, *J. Organomet. Chem. 362* (1989) 11.

[5] Crystals suitable for X-ray crystallography were obtained by recrystallization from EtOH. Monoclinic, $a = 32.228(13)$, $b = 16.373(6)$, $c = 20.689(5)$, $\beta = 114.49(2)$, $V = 9934$ Å^3, space group Cc, $Z = 8$, $\varrho_{calcd} = 1.00$ g/cm^3. The 5722 independent observed reflections [$2\theta \leq 126°$; $|F_o| > 3\sigma|F_o|$] were measured on a Rigaku four-circle diffractometer using $Cu_{K\alpha}$ radiation and ω-2θ scan. The structure was solved by direct methods and all non-hydrogen atoms were refined anisotropically to $R = 0.071$ ($w = 1.0$). Further details of the crystal structure investigation are available on request from the Director of the Cambrigde Crystallographic Data Centre, University Chemical Laboratory, Lensfied Road, Cambridge CB2 1EW (UK), on quoting the full journal citation.

[6] a) A. Padwa, E. Shefter, E. Alexander, *J. Am. Chem. Soc. 90* (1968) 3717; b) J.-F. Chiang, S. H. Bauer, *ibid. 92* (1970) 1614; c) A. Almenningen, B. Andersen, B. A. Nyhus, *Acta. Chem. Scand. 25* (1971) 1217.

[7] a) T. Kudo, S. Nagase, *J. Am. Chem. Soc. 107* (1985) 2589; b) S. M. Bachrach, A. Streitwieser, *ibid. 107* (1985) 1186; c) E. D. Jemmis, P. N. P. Pavan Kumar, N. R. Sreenivas Kumar, *J. Chem. Soc. Dalton Trans. 1987*, 271.

[8] a) 56 cyclobutane derivatives of the 504 available form the Cambridge data base were used to calulate the averaged NBD and BL; b) 56 norbornane derivatives of the 304 available; c) 9 bicyclo[3.3.1]nonane derivatives of the 36 available.

[9] C. J. Hurt, J. C. Calabrese, R. West, *J. Organomet. Chem. 91* (1975) 273.

[10] W. E. Schklower, Yu, T. Strutschkow, L. E. Guselnikov, W. W. Wolkowa, W. G. Awakyan, *Z. Anog. Allg. Chem. 501* (1983) 153; W. Wojnowski, K. Peters, D. Weber, H. G. von Schnering, *ibid. 519* (1984) 134.

[11] K. M. Baines, A. G. Brook, P. D. Lickiss, J. F. Sawyer, *Organometallics 8* (1989) 709.

[12] (a) M. J. Fink, K. J. Haller, R. West, J. Michl, *J. Am. Chem. Soc. 106* (1984) 822; (b) M. J. Michalczyk, M. J. Fink, K. J. Haller, R. West, J. Michl, *Organometallics 5* (1986) 531; (c) H. B. Yokelson, A. J. Millevolte, B. R. Adams, R. West, *J. Am. Chem. Soc. 109* (1987) 4116.

[13] Compounds **8** and **9** are puckered, while compounds **10**–**12** are planar or almost planar. Despite this discrepancy the NBD/BL values remain surprisingly constant.

[14] W. Wojnowski, B. Dreczewski, H. Herman, K. Peters, E.-M. Peters, H. G. von Schnering, *Angew. Chem. 97* (1985) 978; *Angew. Chem. Int. Ed. Engl. 24* (1985) 992.

[15] R. Jones, D. J. Williams, H. Tobita, S. Collins, S. Masumune, unpublished.

[16] W. Stallings, J. Donohue, *Inorg. Chem. 15* (1976) 524.

Synthesis and Structure of Novel Cu-Clusters: $[Cu_{30-x}Se_{15}(PiPr_3)_{12}]$ (x = 0,1) and $[Cu_{36}Se_{18}(PtBu_3)_{12}]$**

By *Dieter Fenske,* Harald Krautscheid,* and *Silke Balter*

Silyl derivatives of the elements P,As,S,Se and Te react with complexes of transition metal halides containing cyclopentadienyl, allyl or phosphane ligands to form cluster complexes. In our investigations to date we have found a large number of examples justifying this synthetic principle both in the case of electron-deficient (Ti,V) as well as in the case of electron-rich (Ni,Pd) transition metals.[1] We have also checked whether phosphane complexes of the elements Cu, Ag and Au react with $E(SiMe_3)_2$ (E = S,Se) to give metal-rich complexes.

When, for example, $[AgCl(PPh_3)_3]$ is allowed to react with $E(SiMe_3)_2$ in organic solvents, one observes the formation of binary sulfides and selenides of Ag. In contrast, in the analogous reaction of $[CuCl(PPh_3)]_4$, $[Cu_2Cl_2(PPh_3)_3]$, and $[CuCl(PPh_3)_3]$ with $Se(SiMe_3)_2$ in THF, deep-colored solutions are formed, from which black crystals precipitate; they are, however, X-ray amorphous. According to elemental analyses, the amorphous products are metal-rich compounds.

When carried out with ether as solvent, the reaction with CuCl, $PiPr_3$ and $Se(SiMe_3)_2$ now led to rapid formation of a dark colored solution, from which a mixture of **1** and **2** crystallized out within a few hours, whereas under the same conditions reaction of CuCl, $PtBu_3$ and $Se(SiMe_3)_2$ led to formation of **3**.[2]

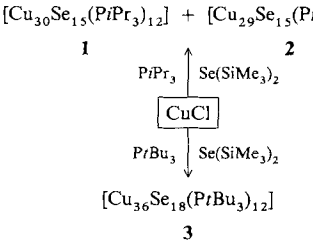

Normally, microcrystalline products which are sparingly soluble in organic solvents are formed in these reactions. However, crystals suitable for a structure analysis are obtained if the reaction temperature is allowed to increase from -30 °C to room temperature over the course of several days. **1** and **2** form black (in thin layers brown) crystals, whereas crystals of **3** are brown. As expected, **1** and **3** are diamagnetic, whereas **2** is paramagnetic.

The IR spectra are not very informative, since they only contain characteristic vibrations for the $PiPr_3$ and $PtBu_3$ ligands. X-ray structure analyses were carried out, in order to clarify the molecular structures of **1**, **2**, and **3**.[3] It was found that the structures of **1** and **2** are almost identical. In contrast to **2**, **1** contains a further Cu atom in the center of the molecule. An exact determination of the structure, however, is rendered difficult by a disordering of the *i*Pr groups.

Like **1**, in the crystalline state **2** contains (Fig. 1) five parallel layers of Cu atoms and μ_4- to μ_7-bridging Se ligands;

[*] Prof. Dr. D. Fenske, Dipl.-Chem. H. Krautscheid und S. Balter
Institut für Anorganische Chemie der Universität
Engesserstrasse, Geb.-Nr. 30.45, D-7500 Karlsruhe (FRG)

[**] This work was supported by the Deutsche Forschungsgemeinschaft, the Fonds der Chemischen Industrie, and Degussa AG.

consequently the Cu–Se bonds are of various lengths. In the case of the μ_4-Se ligands, Se4–Se6 and Se10–Se12, which bridge the Cu atoms of the 2nd and 3rd and 3rd and 4th layers, respectively, one finds in each case two short (**1**: 236–241(1); **2**: 236.3–238.8.8(6) pm and two longer Cu–Se bonds (**1**: 243–252(1); **2**: 244.4–249.8(6) pm).

The μ_5-Se ligands Se1–Se3 and Se13–Se15 bridge the Cu atoms of the 1st and 2nd and 4th and 5th layers, respectively. In each case there are three long bonds to the outer layers (**1**: 250–256(1); **2**: 247.7–256.1(6) pm) and two short bonds to the Cu atoms of the 2nd and 4th layers, respectively (**1**: 235–241(1); **2**: 238.7–241.0(6) pm).

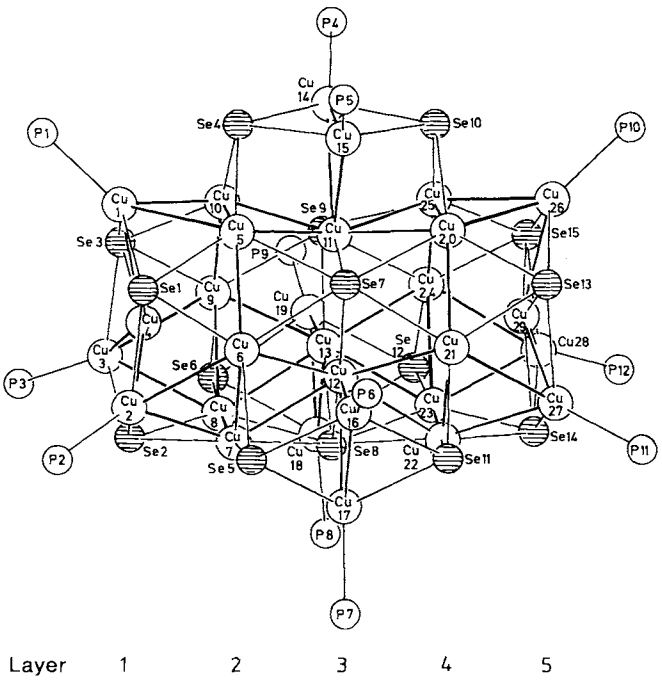

Fig. 1. Structure of **2** in the crystal (*i*Pr groups omitted, Cu–Cu distances up to 290 pm are shown). Important bond lengths [pm] and angles [°] (error ± 0.6 pm and ± 0.2°): 1st layer: Cu1-Cu4 260.6 Cu2-Se2 252.0 Se1-Cu4 247.7–252.3 Cu1-Se1-Cu2 122.1 Se1-Cu4-Se2 119.2 Se1-Cu4-Cu2 60.1. 2nd layer: Cu9-Cu10 255.5 Cu8-Cu9 267.1 Cu9-Se6 236.5 Cu5-Cu6-Cu7 120.0 Se5-Cu6-Cu5 175.4 Cu6-Se5-Cu7 68.4 3rd layer: Cu12-Se8 238.1 Cu12-Cu16 283.2 Cu16-Cu17 271.8. Se7-Cu12-Se8 161.1 Cu11-Se7-Cu12 82.2 Cu16-Cu12-Cu17 57.0 Cu12-Cu16-P6 153.7. Cu-P 223(1) pm. Cu-Cu (between layers): Cu1-Cu5 263.8 Cu2-Cu6 264.1 Cu3-Cu8 266.7 Cu5-Cu11 261.9 Cu9-Cu13 259.7.

The μ_6-Se ligands in **2** and μ_7-Se ligands in **1** (Se7–Se9) function as bridges between the inner layers, in each case with two short (**1**: 242–252(1); **2**: 235.5–240.0(7) pm) and four long Cu–Se distances (**1**: 252–261(1); **2**: 255.7–261.0(6) pm). Differently coordinated chalcogen ligands also occur in other compounds;[1, 4] overall, the Cu–Se bond lengths in **1** and **2** are comparable with those in binary copper selenides and in the few copper complexes with Se-ligands which have already been structurally characterized such as $[Cu_3Cl_4MoOSe_3]^{3\ominus}$, $[Cu_3ClMoSe_4(PPh_3)_3]$, and $[Cu_4(Se_4)_{2.4}(Se_5)_{0.6}]^{2\ominus}$.[5, 6]

The structures of the layers in **1** and **2** are shown in Figure 2. The 3rd layer is approximately a mirror plane, i.e. the 1st and 5th and 2nd and 4th layers are almost identical. **2** can accordingly be described as a sequence of Cu_3Se_3 six-membered rings (Fig. 2a), Cu_6Se_3 planes and Cu_9Se_3 planes (Fig. 2b, 2c). The deviations from the best fitting planes are never greater than 13 pm. In contrast the deviation of Cu4

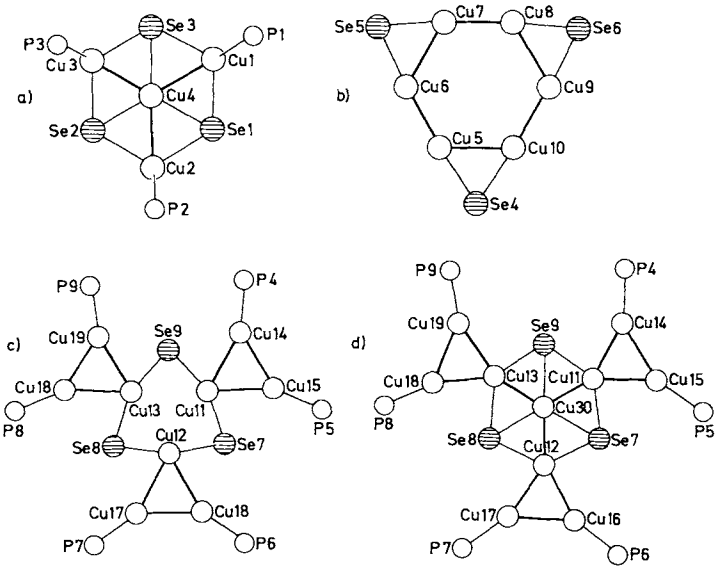

Fig. 2. Structures of the Cu,Se,P layers in **1** and **2**. a) 1st and 5th layers; respectively b) 2nd and 4 layers respectively; c) 3rd layer in **2**, d) 3rd layer in **1**.

and Cu29 from the plane of the Cu_3Se_3 rings is 41 pm in **2** and 50 pm in **1**. Of the 29 Cu atoms in **2** and 30 Cu atoms in **1**, 12 Cu atoms of the cluster periphery are in each case bound to $PiPr_3$ groups.

Unlike **2**, **1** contains a further Cu atom (Cu30) in the cluster center (Fig. 2d), and as a result the Cu-Cu contacts in the central Cu_3Se_3 ring (Cu11–C13, Se7–Se9) are noticeably expanded. In **2** they are 310–322 (0.6) pm and in **1** 402–414(1) pm,[7] while the distances between Cu30 and Cu11–Cu13 (238–244(1) pm) are remarkably short. Although Se and Cu are not clearly distinguishable by means of X-ray diffraction, we are certain that the atom in the cluster center of **1** is a Cu atom, as indicated by elemental analysis and diamagnetic behavior. The structures of **1** and **2** consist of a cluster core of 24 and 23 Cu atoms, respectively. In addition, Cu pairs (Cu14, Cu15; Cu16, Cu17; Cu18, Cu19) are bound via Se bridges to this core. The distances of these Cu pairs from the core are 252–260(1) pm (**1**) and 271.4–284.4(5) pm (**2**). All other Cu–Cu contacts lie in the range of distances that has already been found in metallic copper (256 pm) and in copper selenides.[5]

Figure 3 shows the crystal structure of **3**. The complex **3** contains a twofold axis and consists of a cluster of 36 Cu atoms having no structural relationship with **1** or **2**.

As in **1** and **2**, μ_3- (Se7), μ_4- (Se1,Se9), μ_5- (Se2–Se6,Se8) and a μ_6-Se ligands (Se10) are also found in **3**. The Cu–Se distances lie in a similar range to those in **1** and **2** (Cu–(μ_3-Se): 237.5(6); Cu–(μ_4-Se): 235.8–245.3(6); Cu–(μ_5-Se): 240.0–261.3(6) pm). The μ_3-, μ_4- and μ_5-Se ligands cover the surface of the Cu cluster. In contrast, Se10 resides in the cluster center and is surrounded by six Cu atoms and is trigonal-prismatically coordinated (Cu–Se: 243.2(6) pm). Alternatively, the central unit of the cluster can be described as two Cu_6Se_2 cubes bridged by Se10 (Fig. 4).

As shown in Figure 3 this structural unit (Cu atoms dotted) is bound by twelve Cu atoms (striped: Cu5–Cu8, Cu5′–Cu8′, Cu14, C15, C14′, C15′) which are coupled via the μ_5-Se ligands with three Cu_4 units (checkered: Cu1–Cu4, Cu1–Cu4′, Cu16, Cu17, Cu16′, Cu17′). The twelve phosphane ligands are bound to Cu atoms of the cluster periphery and effect complete shielding of the $C_{36}Se_{18}$ cluster. The Cu atoms bound to P (Cu1, Cu4, Cu6, Cu7, Cu15, Cu16) are all

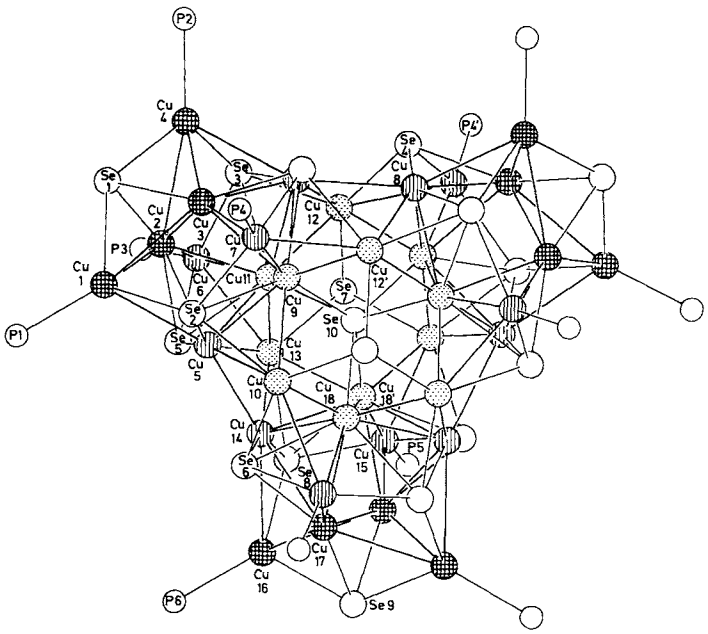

Fig. 3. Structure of **3** in the crystal (*t*Bu groups omitted, Cu–Cu distances up to 290 pm shown). Important bond lengths [pm] and angles [°] (error ± 0.5 pm and ± 0.2°): Cu1-Cu2 266.4 Cu1-Cu3 288.9 Cu1-Cu5 282.9 Cu2-Cu3 269.1 Cu2-Cu4 286.7 Cu2-Cu5 280.2 Cu2-Cu6 273.3 Cu6-Cu11 264.1 Cu6-Cu13 271.6 Cu9-Cu10 262.2 Cu9-Cu11 281.5 Cu9-Cu12 250.3 Cu9-Cu3 257.5 Cu9-Cu5 252.3 Cu9-Cu7 264.5 Cu9-Cu8 275.6 Cu10-Cu15 271.8 Cu10-Cu18 250.8 Cu10-Cu9 262.2 Cu9-Cu5 266.4 Cu-P 226–230(1) Cu9-Cu10 244.5 Cu11-Se10 243.0 Cu18-Se10 242.4 Cu-Se7-Cu 99.4-100.8 Cu-(μ_4-Se)-Cu 67.1–73.8, 130.9–131.6 Cu-(μ_5-Se)-Cu 57.3–69.8, 82.1–89.3, 106.1–137.7 Cu18-Se10-Cu9' 142.5 Cu18-Se10-Cu9 91.2 Cu11-Se10-Cu9 91.1 Cu18-Se10-Cu11 90.8.

bound to two Se atoms and three Cu atoms (Cu–Cu: 264–287(1) pm).

In contrast, higher coordination numbers are found for other Cu atoms (Cu2, Cu3, Cu5, Cu8: 2 Se and 6 Cu, Cu–Cu: 252.3–288.9(5) pm; Cu9, Cu11, Cu18: 3 Se and 7 Cu, Cu–Cu: 250.2–281.5(5) pm; Cu10, Cu12, Cu13: 3 Se and 4 Cu, Cu–Cu: 250.2–278.1(6) pm).

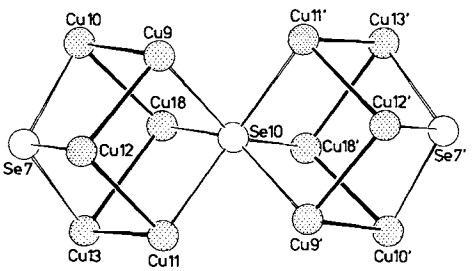

Fig. 4. Central $Cu_{12}Se_3$ unit in **3**.

The shortest Cu–Cu distances are observed in the central $Cu_{12}Se_3$ skeleton. They are comparable with those that have been found in other multinuclear Cu-complexes, for example in [Cu(tolyl)NNNNN(toly)]$_3$ (235 pm), [CuMes]$_5$ (245 pm), [Me_3SiCH_2Cu]$_4$ (242 pm), $[Cu_3I_7]^{2\ominus}$ (258 pm), $[Cu_6(S_4)_3S_5]^{2\ominus}$ (270 pm), $[Cu_{12}S_8]^{4\ominus}$ (277–295 pm), $[Cu_4(SPh)_6]^{2\ominus}$ (275 pm), [$Cu(SC_6H_4SiMe_3)$]$_{12}$ (274–317 pm).[8]

If one assumes that $Se^{2\ominus}$ ligands are present, then the clusters in **1**, **2** and **3** have the formal charge $Cu_{30}^{30\oplus}$, $Cu_{29}^{30\oplus}$ and $Cu_{36}^{36\oplus}$.[7] Accordingly, the clusters in **1** and **3** should contain copper in the formal oxidation state + 1 (d^{10} configuration). Although the contribution of d^{10}–d^{10} interactions to the metal–metal bonding is controversial, examples are known which show that this can be significant.[9] The Cu–Cu distances found in **1**, **2**, and **3**, however, clearly indicate only weak interactions.

The formation of these large clusters is surprising; however, so far we have not found any evidence of the formation of smaller multinuclear complexes. Examples of metal clusters of similar size are known for other transition elements. Examples include compounds such as: $[Au_{18}Ag_{19}Br_{11}(P\text{-}p\text{-}Tol_3)_{12}]^{2\oplus}$, $[Ni_{38}Pt_6(CO)_{48}H_{6-n}]^{n\ominus}$, $[Pd_{38}(CO)_{28}(PEt_3)_{12}]$, and $[Au_{55}(PPh_3)_{12}Cl_6]$.[10]

Steigerwald et al. recently reported on the reaction of [$(COD)_2$Ni] with Et_3PTe.[11] Depending on the reaction conditions $[Ni_9Te_6(PEt_3)_8]$ and $[Ni_{20}Te_{18}(PEt_3)_{12}]$ or $NiTe_x$ is formed. Consistent with this observation we find that **1**–**3** are formed in good yields (60%) at temperatures below 20 °C. In contrast, a binary copper selenide of unknown structure is formed at temperatures above 100 °C.

Received: March 15, 1990 [Z 3858 IE]
German version: *Angew. Chem. 102* (1990) 799

[1] D. Fenske, J. Ohmer, J. Hachgenei, K. Merzweiler, *Angew. Chem. 100* (1988) 1300; *Angew. Chem. Int. Ed. Engl. 27* (1988) 1277; D. Fenske, H. Fleischer, C. Persau, *ibid. 101* (1989) 1740 and *28* (1989) 1665; D. Fenske, A. Hollnagel, *ibid. 101* (1989) 1412 and *28* (1989) 1392; P. G. Maué, D. Fenske, *Z. Naturforsch. B43* (1988) 1213; D. Fenske, P. G. Maué, *Z. Naturforsch. B44* (1989) 531.

[2] Procedures: **1** and **2**: 0.4 g (4 mmol) of CuCl was suspended in 50 mL of ether. On addition of 1.5 mL (8 mmol) of P*i*Pr$_3$ the CuCl dissolved. Upon subsequent treatment with 0.5 mL (2 mmol) of Se(SiMe$_3$)$_2$ the solution turned dark brown, and within 2 d a mixture of **1** and **2** precipitated in the form of black crystals. These could be separated from each other by virtue of their different habits (yield 60%).
3: A suspension of CuCl (0.4 g, 4 mmol) in THF (50 mL) was treated with 1 mL (4 mmol) of P*t*Bu$_3$. After addition of 0.5 mL (2 mmol) of Se(SiMe$_3$)$_2$ at − 30 °C, the mixture was allowed to warm to room temperature over the course of several days. Brown crystals of **3** precipitated from the brown solution (yield 30%).

[3] X-ray structure analyses: Stoe Stadi IV, $Mo_{K\alpha}$, empirical absorption correction; data collection and refinement: ω scan; Cu, Se, P anisotropic, C isotropic. **1** (from diethyl ether): lattice constants (200 K): a = 1998.6(8), b = 1898.2(7), c = 2367.7(10) pm, α = 89.80(3), β = 93.86(4), γ = 92.05(4)°, $V = 8956 \times 10^6$ pm^3; space group, $P\bar{1}$, Z = 2, $\mu(Mo_{K\alpha})$ = 64.9 cm^{-1}. Profile analysis, $2\theta_{max}$ = 45°, 25400 reflections, 10895 with $I > 2\sigma(I)$, 854 parameters, R_1 = 0.12; R_2 = 0.10. The poor R value arises as the result of a disorder of the *i*Pr groups. **2** (from diethyl ether): lattice constants (190 K): a = 2396.6(13), b = 2624.9(12), c = 2831.4(12), β = 91.80(4), $V = 17804 \times 10^6$ pm^3. Space group $P2_1/c$, Z = 4, $\mu(Mo_{K\alpha})$ = 65.2 cm^{-1}. Profile analysis, $2\theta_{max}$ = 45°, 23251 reflections, 11875 with $I > 2\sigma(I)$, 937 parameters, R_1 = 0.081, R_2 = 0.073. **3** (from THF): **3** crystallizes with six molecules THF/formula unit. Lattice constants (200 K): a = 2117.4(12), b = 3593.2(13), c = 3059.2(6) pm, β = 89.22(2)°, $V = 23273 \times 10^6$ pm^3. Space group $C2/c$, Z = 4, $\mu(Mo_{K\alpha})$ = 59.7 cm^{-1}. Profile analysis, $2\theta_{max}$ = 48°, 19243 reflections, 11430 with $I > 2\sigma(I)$, 631 parameters, R_1 = 0.063, R_2 = 0.060. Further details of the crystal structure investigations are available on request from the Fachinformationszentrum Karlsruhe, Gesellschaft für wissenschaftlich-technische Information mbH, Eggenstein-Leopoldshafen 2 (FRG), on quoting the depository number CSD-54560, the names of the authors, and the journal citation.

[4] W. A. Herrmann, *Angew. Chem. 98* (1986) 57; *Angew. Chem. Int. Ed. Engl. 25* (1986) 56; D. Fenske, J. Ohmer, K. Merzweiler, *Z. Naturforsch. B42* (1987) 803.

[5] R. D. Heyding, R. McLaren Murray, *Can. J. Chem. 54* (1976) 841.

[6] A. Müller, U. Wienböker, M. Penk, *Chimia 43* (1989) 50; J. Cusick, M. L. Scudder, D. C. Craig, I. G. Dance, *Polyhedron 8* (1989) 1139.

[7] The refinement of the structure of **2** yielded a residual electron density of 6–8 electrons in the cluster center. We cannot as yet make any statements about the nature of the atom that has been encapsulated.

[8] J. Beck, J. Strähle, *Angew. Chem. 97* (1985) 419; *Angew. Chem. Int. Ed. Engl. 24* (1985) 409; S. Gambarotta, C. Floriani, A. Chiesi-Villa, C. Guastini, *J. Chem. Soc. Chem. Commun. 1983*, 1156; J. A. J. Jarvis, B. T. Kilbourn, R. Pearce, M. F. Lappert, *J. Chem. Soc. Chem. Commun. 1973*, 475; H. Hartl, F. Mahdjour-Hassan-Abadi, *Angew. Chem. 96* (1984) 359;

Angew. Chem. Int. Ed. Engl. 23 (1984) 378; G. Henkel, P. Betz, B. Krebs, *J. Chem. Soc. Chem. Commun. 1984*, 314; P. Betz, B. Krebs, G. Henkel, *Angew. Chem. 96* (1984) 293; *Angew. Chem. Int. Ed. Engl. 23* (1984) 311; I. G. Dance, J. C. Calabrese, *Inorg. Chim. Acta 1976*, L41; D. Coucouvanis, C. N. Murphy, S. K. Kanodia, *Inorg. Chem. 19* (1980) 2993; E. Block, M. Gernon, H. Kang, S. Liu, J. Zubieta, *J. Chem. Soc. Chem. Commun. 1988*, 1031.

[9] F. A. Cotton, X. Feng, M. Matusz, R. Poli, *J. Am. Chem. Soc. 110* (1988) 7077; R. Mason, D. M. P. Mingos, *J. Organomet. Chem. 50* (1973) 53; P. K. Mehrotra, R. Hoffmann, *Inorg. Chem. 17* (1978) 2187; C. Kölmel, R. Ahlrichs, *J. Phys. Chem.*, in press; K. M. Merz, R. Hoffmann, *Inorg. Chem. 27* (1988) 2120.

[10] B. K. Teo, M. C. Hong, H. Zhang, D. B. Huang, *Angew. Chem. 99* (1987) 943; *Angew. Chem. Int. Ed. Engl. 26* (1987) 897; A. Ceriotti, F. Demartin, G. Longoni, M. Manassero, M. Marchionna, G. Piva, M. Sansoni, *Angew. Chem. 97* (1985) 708; *Angew. Chem. Int. Ed. Engl. 24* (1985) 697; E. G. Mednikov, N. K. Eremenko, Y. L. Slovokhotov, Y. T. Struchkov, *J. Chem. Soc. Chem. Commun. 1987*, 218; G. Schmid, R. Pfeil, R. Boese, F. Bandermann, S. Meyer, G. H. M. Calis, J. W. A. van der Velden, *Chem. Ber. 114* (1981) 3634; J. P. Fackler, C. J. McNeal, R. E. P. Winpenny, *J. Am. Chem. Soc. 111* (1989) 6434.

[11] J. G. Brennan, T. Siegrist, S. M. Stuczynski, M. L. Steigerwald, *J. Am. Chem. Soc. 111* (1989) 9240.

Synthesis and Structure of a $1\lambda^5,4\lambda^5$-Diphosphapentalene

By *Jürgen Silberzahn, Hans Pritzkow*, and *Hans Peter Latscha**

Molecules containing activated C-C multiple bonds react with trivalent phosphorus compounds with formation of P-C double bonds to give phosphoranes. Thus, alkynes such as dimethyl acetylenedicarboxylate **1** react with tertiary phosphanes **2** in the molecular ratio 1:2 to give stable 1,2-bis(triorganophosphoranylidene)alkanes such as **3**. Reaction with diphosphanoalkanes **4** leads to cyclic diphosphoranes **5**.[1]

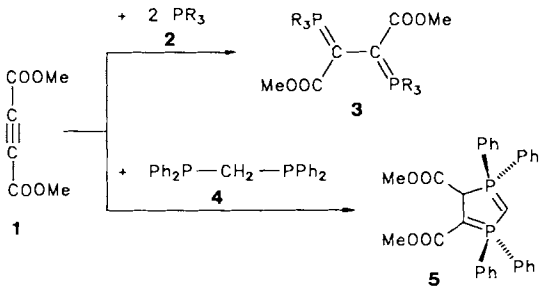

We now wish to report the isolation of brilliant orange-red crystals of $1\lambda^5,4\lambda^5$-diphosphapentalene **7** upon reaction of **1** with acetylenebis(phosphonousbis(dimethylamide)) **6** in the ratio 2:1.[2]

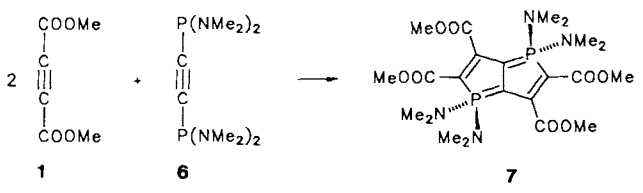

[*] Prof. Dr. H. P. Latscha, Dipl.-Chem. J. Silberzahn, Dr. H. Pritzkow
Anorganisch-chemisches Institut der Universität
Im Neuenheimer Feld 270, D-6900 Heidelberg (FRG)

Compound **7**, the first analogue of pentalene with a phosphorus atom in each ring, has a high melting point (194 °C) and is stable towards air and hydrolysis. Its extraordinary stability compared to that of carbocyclic pentalenes[3] leads to the molecular peak (*m/z* 546) in the mass spectrum being simultaneously the base peak. The stability is apparently due to the formation of ylidic structures. Figure 1 shows the crystal structure[4] of the planar ring system with a symmetry center on the C1–C1′ axis.

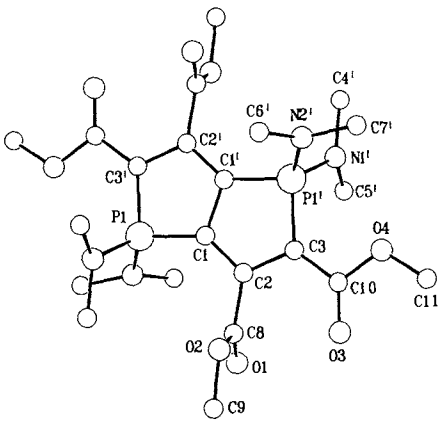

Fig. 1. Structure of **7** in the crystal. Important bond lengths [Å] and angles [°]: C1-C2 1.379(2), C2-C3 1.423(2), C3-P1′ 1.759(1), P1′-C1′ 1.758(1), C1′-C1 1.466; C1-C2-C3 115.1(1), C2-C3-P1′ 109.4(1), C3-P1′-C1′ 93.5(1), P1-C1-C1′ 108.7(1), C1′-C1-C2 111.8(1).

Cyclovoltammetric measurements indicate that the 8π-electron system of **7** can be both oxidized to the 6π-electron system as well as reduced to the 10π-electron system, in each case in two reversible steps.

Experimental

A solution of **1** (5.8 g, 41 mmol) in benzene (25 mL) was treated dropwise at 10 °C with a solution of **6** (5.3 g, 20.3 mmol) in benzene (25 mL). The resulting dark orange-brown reaction mixture was then heated under reflux for 1h. The reaction product **7**, which precipitated upon cooling the mixture, was filtered off and recrystallized from benzene or ethyl acetate (brilliant orange-red crystals). Yield: 7.9 g (71 %); Fp = 194 °C; ^{1}H NMR (200 MHz, $CDCl_3$): δ = 2.52, 3.48, 3.71; ^{13}C NMR (50 MHz, $CDCl_3$): δ = 36.7, 49.9, 51.9, 74.6, 96.2, 144.6, 164.8, 168.3; ^{31}P NMR (80 MHz, $CDCl_3$): δ = 51.7; MS: *m/z* 546 ($M^{\oplus}$); correct elemental analysis (C,H,N,P).

Received: February 19, 1990 [Z 3803 IE]
German version: *Angew. Chem. 102* (1990) 815

CAS Registry numbers:
1, 762-42-5; **6**, 29936-20-7; **7**, 127445-55-0.

[1] M. A. Shaw, J. C. Tebby, R. S. Ward, D. H. Williams, *J. Chem. Soc. C 1967*, 2442–2446; *ibid. 1970*, 504–507.

[2] W. Kuchen, K. Koch, *Z. Anorg. Allg. Chem. 394* (1972) 74–92.

[3] K. Hafner, *Nachr. Chem. Tech. Lab. 28* (1980) 222–226.

[4] **7**: $P2_1/n$, a = 8.352(4), b = 16.533(6), c = 10.316(4) Å, β = 102.12(3)°, V = 1393 Å^3, Z = 2. Four-circle diffractometer ($Mo_{K\alpha}$ radiation), ω scan, θ_{max} = 30°), 3000 observed reflections ($I > 2\sigma_I$), non-hydrogen atoms anisotropic (235 parameters), R = 0.042, R_w = 0.051. Further details of the crystal structure investigation are available on request from the Fachinformationszentrum Karlsruhe, Gesellschaft für wissenschaftlich-technische Information mbH, D-7514 Eggenstein-Leopoldshafen 2 (FRG), on quoting the depository number CSD-54517, the names of the authors and the journal citation.

$Na_{10}\{Li_2[MnO_4]_4\}$, a Compound in Which LiO_4 and MnO_4 Tetrahedra Form Chains Consisting of Six- and Eight-Membered Rings**

By *Dieter Fischer* and *Rudolf Hoppe**

Little is known about the structure of oxides of the type $A_3[MO_4]$ with A = K, Rb, Cs and M = P^V, As^V, V^V, Cr^V, Mn^V. In all single crystals so far obtained, the $[MO_4]$ structural unit exhibits disorder. This situation abruptly changes when derivatives such as $K_2\{Li[VO_4]\}$[1] and $Cs_2\{Li[VO_4]\}$[2] are synthesized. In these "lithovanadates", the linkage of $[MO_4]$ and $[LiO_4]$ groups ensures an ordered structure. An especially important example of this kind is $K_{11}\{Li[OMnO_3]_4\}$,[3] which contains an anion not found so far for pentaphosphates, for example. Upon attempting to prepare $Na_2\{Li[MnO_4]\}$,[4] we surprisingly obtained $Na_{10}\{Li_2[MnO_4]_4\}$, which has an unexpected structure.

The structure determination[5] afforded the motifs of mutual adjunction[7] and distances given in Table 1. Included are the "naive" coordination numbers (C. N.) and the effective coordination numbers (ECoN).[7-9]

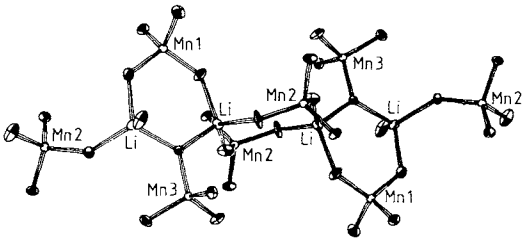

Fig. 1. Section of the Li-Mn-O chains along [010] in $Na_{10}\{Li_2[MnO_4]_4\}$; the oxygen atoms are drawn as thermal ellipsoids (ORTEP at 50% probability).

consist of alternating six- and eight-membered rings. The eight-membered rings, $\{Li[O_{1/2}Mn(O_{2/1})O_{1/2}]_2Li\}$, lie roughly parallel to (001). The six-membered rings, $\{Li[O_{1/2}Mn(O_{2/1})O_{1/2}][O_{1/2}(MnO_{3/1})]Li\}$, are oriented parallel to (100). The chains are linked through Na^+ ions.

The structure of the chainlike anion $\{Li_2[MnO_4]_4\}^{10-}$, formed from two kinds of rings, is even more bizarre than

Table 1. $Na_{10}\{Li_2[MnO_4]_4\}$: motifs of mutual adjunction, distances [pm], naive coordination numbers (C. N.), and effective coordination numbers (ECoN).

Atom	1 O1	2 O2	2 O3	1 O4	2 O5	2 O6	2 O7	1 O8	2 O9	1 O10	C. N.	ECoN [a, c]
2 Li				1/2 191.4	1/1 191.0		1/1 195.6		1/1 193.2		4	4.0
1 Mn1							2/1 169.4	1/1 170.9		1/1 168.9	4	4.0
2 Mn2		1/1 170.2	1/1 168.4		1/1 170.1				1/1 170.5		4	4.0
1 Mn3	1/1 170.4			1/1 172.2		2/1 170.0					4	4.0
2 Na1		1/1 234.8	1/1 241.3		1/1 305.7	1/1 259.7	1/1 246.0		1/1 248.9		6 5 + 1	5.0
2 Na2		1/1 1/1 241.7 270.3	1/1 247.4			1/1 230.2		1/2 264.4		1/2 289.6	6	5.0
2 Na3	1/2 236.4	1/1 252.8	1/1 255.7		1/1 242.2	1/1 234.7			1/1 237.6		6	5.8
1 Na4	1/1 247.4			1/1 275.3	2/1 247.4	2/1 267.5		1/1 231.5			7	6.2
2 Na5		1/1 247.4	1/1 229.0		1/1 291.6		1/1 1/1 262.5 286.5	1/2 244.4		1/2 244.4	7	5.5
1 Na6	1/1 236.7			1/1 236.2					2/1 283.1	1/1 230.3	5 3 + 2	3.7
C. N.	6	6	5	5	6	5	5	6	5	6		
ECoN [b, c]	5.0	5.6	4.7	4.7	4.6	4.5	4.7	5.5	4.4	4.8		

[a] Cations/ΣO. [b] O/Σ cations. [c] Starting values for the ionic radii: ionic radii with $r(O^{2\ominus})$ = 140 pm were derived from the averaged distances weighted according to the ECoN concept.

Primary structure: Lithium and manganese are surrounded in a tetrahedral fashion by O (distances: Li-O, 191.0–195.6 pm; Mn-O, 168.4–172.2 pm). The coordination spheres of the Na^+ ions are irregular; the naive coordination numbers are 5–7.

Secondary and tertiary structure: The structure is characterized by unusual chains along [010] (Fig. 1). The chains

those of the many other intriguing anions we have so far obtained during the synthesis of new oxides of alkali metals.

We have found mono- and multinuclear anions such as those in $K_2[O\text{-}Ni\text{-}O]$[10] (analogous to XeF_2[11]), in $K_4[ZnO_3]$,[12] and in $Na_4[FeO_3]$,[13] with structural units analogous to $CO_3^{2\ominus}$. Furthermore, we have found compounds containing two-tetrahedra units, for example, $K_6[O_2FeO_2FeO_2]$,[14] three-octahedra units, for example, $K_2Li_{14}[M_3O_{14}]$ with M = Pb,[15] Zr,[16] Tb,[17] and four-triangle units ($Na_{10}[Co_4O_9]$).[18] Ring-shaped anions are present in oxides such as $K_4[Cu_4O_4]$, $Na_4[Ag_4O_4]$,[19] and $Cs_4[Au_4O_4]$,[20] zigzag chains in $Cs[CuO_{2/2}]$,[21] "Zweier-Einfach-Tetraederketten", for example in $K_2Na_4[(FeO_3)_2]$,[22] "Vierer-Einfachketten" of this kind in

[*] Prof. Dr. R. Hoppe, Dipl.-Chem. D. Fischer
Institut für Anorganische und Analytische Chemie I der Universität Heinrich-Buff-Ring 58, D-6300 Giessen (FRG)

[**] Taken from the Dissertation of *D. Fischer*, Universität Giessen. This work was supported by the Deutsche Forschungsgemeinschaft and the Fonds der Chemischen Industrie.

$Cs_2Na_{10}[(GaO_3)_4]$,[23] and mixed chains consisting of tetrahedra and squares in $Rb_5[O_{2/2}SiO_2LiO_2SiO_2NiO_{2/2}]$.[24] A unique kind of chain is present in $K_4Be_3O_5$, in which planar triple coordination and tetrahedral coordination alternate according to the formula $^1_\infty[O_{4/2}Be^{[3]}OBe^{[3]}O_{4/2}Be^{[3]}]$;[25] that is, the "butterfly motif" of oxides such as $K_2Na_4[O_2MOMO_2]$ with M = Be,[26] Co,[27] and Fe[28] (in $Cs_2K_4[Fe_2O_5]$) is combined with BeO_4 tetrahedra. In addition, there are layer structures ($Na_4[Fe_2O_5]$[29]) and framework structures such as $KGaO_2$.[23]

However, chains consisting of rings are rare for such oxides. So far, we have found only one other example, $Na_{14}[Fe_6O_{16}]$, in which twelve- and eight-membered rings made up of Fe and O alternate.[30] $\{Li_2[MnO_4]_4\}^{10-}$, consisting of alternating cyclohexane- and cyclooctane-like rings, is much more complicated, since $[MnO_4]^{3-}$ groups are involved in the structure.

The Madelung Part of Lattice Energy (MAPLE)[31] was calculated and a value of MAPLE(Mn_2O_5) = 9694 kcal mol^{-1} was obtained. This value is in good agreement (−0.2%) with the MAPLE values for Mn_2O_5 from the $K_{11}\{Li[OMnO_3]_4\}$ structure determination[3] and for V_2O_5 from the orthovanadates(v) (A_2LiVO_4 with A = K, Rb, Cs[1,2] and $Rb_4V_2O_7$[32]).

Received: January 26, 1990 [Z 3762 IE]
German version: *Angew. Chem. 102* (1990) 835

[1] J. Kissel, R. Hoppe, *Z. Anorg. Allg. Chem. 750* (1989) 109–118.
[2] J. Kissel, R. Hoppe, *Z. Anorg. Allg. Chem. 751* (1989) 113–126.
[3] D. Fischer, R. Hoppe, *Z. Anorg. Allg. Chem.*, in press.
[4] The preparation was carried out by annealing thoroughly mixed amounts of Na_2O_2 and $LiMnO_4$ (Na:Mn = 2.8:1) in Ag bombs (580 °C, 30 d). Both the starting materials and the product were handled under dry argon.
[5] Crystal data: $Na_{10}\{Li_2[MnO_4]_4\}$ crystallizes orthorhombically, space group *Pnma* (No. 62) with $a = 1048.1(7)$, $b = 1518.4(9)$, $c = 1044.4(6)$ pm (diffractometer data), $Z = 16$, $\mu(Mo_{K\alpha}) = 31.4\ cm^{-1}$. 2469 unique reflections ($3° \le \Theta \le 30°$) were measured (Siemens AED 2 four-circle diffractometer with $Mo_{K\alpha}$ radiation, graphite monochromator); absorption correction. The structure was solved by the use of direct methods in conjunction with difference Fourier syntheses (SHELX-76 and -86)[6]. The subsequent refinement of the parameters, carried out with "anisotropic" temperature factors (least-squares method), gave $R = 8.6\%$, $R_w = 3.6\%$ ($w = 0.5451\ \sigma^{-2}(F_o)$ for 2450 reflections; goodness of fit = $[\Sigma w(F_o - F_c)^2/(N_{observns} - N_{parameters})]^{1/2} = 1.138$. Further details of the crystal structure investigation may be obtained from the Fachinformationszentrum Karlsruhe, Gesellschaft für wissenschaftlich-technische Information mbH, D-7514 Eggenstein-Leopoldshafen 2 (FRG), on quoting the depository number CSD-54425, the names of the authors, and the journal citation.
[6] G. Sheldrick, *SHELX-76 and SHELXS-86 Programmsystem*, Cambridge University, England, and Universität Göttingen, FRG.
[7] R. Hoppe, *Angew. Chem. 92* (1980) 106; *Angew. Chem. Int. Ed. Engl. 19* (1980) 110.
[8] G. Meyer, R. Hoppe, *Z. Anorg. Allg. Chem. 420* (1976) 40.
[9] R. Hoppe, *Z. Kristallogr. 150* (1979) 23.
[10] H. Rieck, R. Hoppe, *Z. Anorg. Allg. Chem. 400* (1973) 311.
[11] R. Hoppe, *Angew. Chem. 76* (1964) 455; *Angew. Chem. Int. Ed. Engl. 3* (1964) 532.
[12] R. Baier, R. Hoppe, *Z. Anorg. Allg. Chem. 546* (1987) 122.
[13] H. Rieck, R. Hoppe, *Naturwissenschaften 61* (1974) 126.
[14] H. Rieck, R. Hoppe, *Angew. Chem. 85* (1973) 589; *Angew. Chem. Int. Ed. Engl. 12* (1973) 673.
[15] B. Brazel, R. Hoppe, *Z. Anorg. Allg. Chem. 493* (1982) 93.
[16] R. Werthmann, R. Hoppe, *Z. Anorg. Allg. Chem.* in press.
[17] R. Wolf, R. Hoppe, *Z. Anorg. Allg. Chem. 539* (1985) 39.
[18] B. Burow, R. Hoppe, *Z. Anorg. Allg. Chem. 467* (1980) 158.
[19] W. Losert, R. Hoppe, *Z. Anorg. Allg. Chem. 524* (1985) 7.
[20] H. D. Wasel-Nielen, R. Hoppe, *Z. Anorg. Allg. Chem. 359* (1968) 36.
[21] H. Klassen, R. Hoppe, *Z. Anorg. Allg. Chem. 497* (1983) 70.
[22] K. Mader, *Diplomarbeit*, Universität Giessen 1990.
[23] H.-P. Müller, *Dissertation*, Universität Giessen 1990.
[24] R. Hofmann, R. Hoppe, *Z. Anorg. Allg. Chem. 569* (1989) 31.
[25] D. Schuld, R. Hoppe, *Z. Anorg. Allg. Chem.*, in press.
[26] D. Schuld, R. Hoppe, *Z. Anorg. Allg. Chem.*, in press.
[27] R. Hoppe, J. Birx, *Z. Anorg. Allg. Chem. 557* (1988) 171.
[28] H.-P. Müller, R. Hoppe, *Z. Anorg. Allg. Chem. 569* (1989) 16.
[29] G. Brachtel, R. Hoppe, *Naturwissenschaften 64* (1977) 271.
[30] G. Brachtel, R. Hoppe, *Angew. Chem. 89* (1977) 45; *Angew. Chem. Int. Ed. Engl. 16* (1977) 43.
[31] R. Hoppe, *Angew. Chem. 78* (1966) 52; *Angew. Chem. Int. Ed. Engl. 5* (1966) 95; *ibid. 82* (1970) 7 and 9 (1970) 25.
[32] J. Kissel, R. Hoppe, *Z. Anorg. Allg. Chem.*, in press.

Highly Selective Synthesis of (*E*)-Alkene Isosteric Dipeptides With High Optical Purity via $RCu(CN)Li \cdot BF_3$ Mediated Reaction**

By *Toshiro Ibuka,* Hiromu Habashita, Susumu Funakoshi, Nobutaka Fujii,* Yusaku Oguchi, Tadao Uyehara,* and *Yoshinori Yamamoto**

The concept of replacing the scissile C-N unit of a peptide bond in enzyme substrates by suitable isosteric units that could provide potential protease inhibitors has drawn a lot of attention in recent years.[1] Thus, it has been suggested that replacement of the amide bond (-CO-NH-) of a peptide **1** by an (*E*)-double bond might provide "(*E*)-CH=CH isosteres" **2** possessing high lipophilicity as well as enhanced resistance to biodegradation.[2]

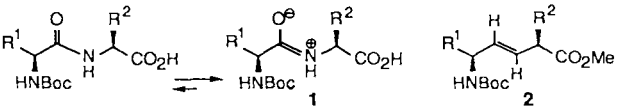

The (*E*)-CH=CH- bonding in **2** closely resembles the three-dimensional shape (rigidity, bond angle, and bond length) of the parent amide **1**.[3] Except in a few cases,[4] however, published synthetic routes to such peptide mimics give unsatisfactory results with regard to double bond geometry and/or stereochemistry at the α-position.[5] For example, the reaction of α,β-unsaturated esters with lithium diisopropylamide (LDA) followed by alkyl halides gave, as one might expect, both α-alkylation isomers and a dialkylated by-product.[6] Clearly, development of an efficient synthetic route to compounds of type **2** would be extremely valuable.

We now report another solution, based on the 1,3-chirality transfer reaction of γ-mesyloxy-α,β-enoates, to the problem of controlling the double bond geometry at the β,γ-position and the stereochemistry of the chiral carbon center at the α-position. The requisite γ-mesyloxy-(*E*)-α,β-enoates (**3**, **5**,

[*] Associate Prof. Dr. T. Ibuka, Prof. Dr. N. Fujii, H. Habashita, Associate Prof. Dr. S. Funakoshi
Faculty of Pharmaceutical Sciences, Kyoto University
Kyoto 606 (Japan)
Prof. Dr. Y. Yamamoto, Y. Oguchi, Associate Prof. Dr. T. Uyehara
Department of Chemistry, Faculty of Science, Tohoku University,
Sendai 980 (Japan)

[**] We thank Dr. G. J. Hanson, Department of Medicinal Chemistry, G. D. Searle & Co., Skokie, Ill, USA., for sending us the ^{1}H-NMR spectra of authentic *tert*-butyl *N*-[(1*S*, 2*S*)-1-benzyl-2-hydroxy-3-butenylcarbonate and its (1*S*, 2*R*)-isomer. We also thank Dr. *P. Herold*, Ciba-Geigy AG, Zentrale Forschungslaboratorien, Basel, Switzerland, for providing us with the ^{1}H-NMR spectra of authentic *tert*-butyl (4*S*, 1′*S*)-4-(1-hydroxy-2-propenyl-2,2-dimethyl-1,3-oxazolidine-3-carboxylate and its isomer. This work was supported by the Sound Technology Promotion Foundation.

16, and **18**), (**4** and **6**), (**15**), and (**17** and **19**) for the present isosteric dipeptide synthesis were readily prepared in acceptable yields from (*S*)-serine, (*S*)-threonine, (*S*)-alanine, and (*S*)-phenylalanine, respectively, according to the usual method.[7] Reaction of the mesylate (**3**) with $MeCu(CN)Li \cdot BF_3$ (LiBr) in THF/Et_2O (ca. 15/1), iso-$BuCu(CN)Li \cdot BF_3$ in THF, and $PhCH_2Cu(CN)Li \cdot BF_3$ in THF/cyclohexane (ca. 5/1) at −78 °C for 30 min gave the regio-, (*E*)-stereo-, and diastereoselective 1,3-chirality transfer products **7** (98% yield), **8** (97% yield), and **9** (97% yield), respectively, after flash chromatography over silica gel (Table 1, entries 1, 2, and 3). In a similar manner, other substrates **4**–**6** and **15**–**19**) gave the desired products in acceptable chemical and optical yields by treatment with organocyanocopper as shown in

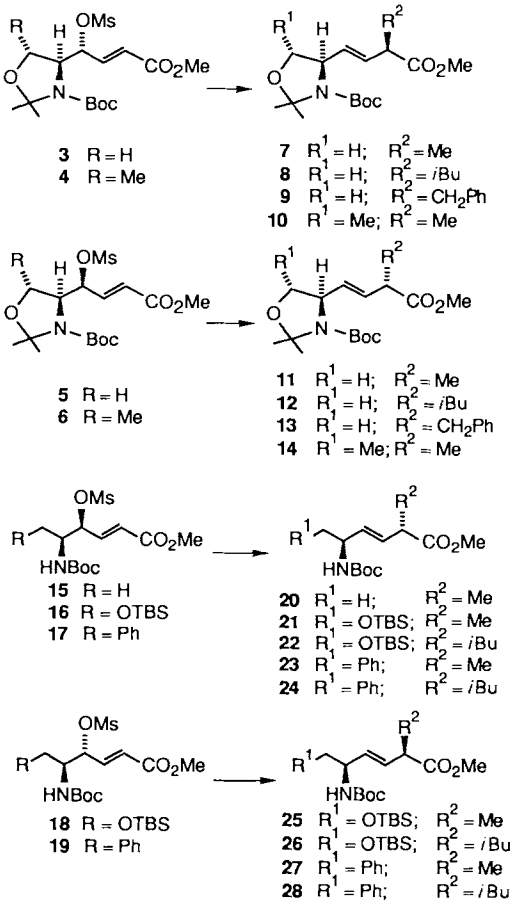

Scheme 1. Abbreviations: OMs = methanesulfonyloxy; OTBS = *tert*-butyldimethylsilyloxy; Boc = *tert*-butoxycarbonyl.

Scheme 1 and Table 1. The diastereoselectivities shown in Table 1 were determined by ^1H NMR in $CDCl_3$ for isolated compounds; >99:1 indicates that the other diastereomer was not detectable. Additionally, in some cases (Table 1, entries 1, 4, 11, 14), diastereoselectivities were determined by capillary gas-chromatography (50 m × 0.2 mm).

To achieve very high chemical and optical yields, it should be noted that a γ-mesyloxy group in the substrate, organocyanocopper · BF_3 reagent, and THF or a mixed solvent involving THF are essential.[8] Addition of $BF_3 \cdot Et_2O$ is essential for the clean 1,3-chirality transfer.[8] The reactions with organocyanocopper · BF_3 reagents in a solvent involving THF were very fast at −78 °C and went to completion within a few minutes, although the reaction mixture was stirred for 30 min. Furthermore, the geometry of the β,γ-double bond of the products (**7**–**14** and **20**–**28**) is exclusively the desired geometry (*E*) and the diastereoselectivity is in the range of 97:3 to >99:1—except in the case of entries 4, 7, and 8. The presence of an HNBoc group at the δ-position in the substrates (**15**–**19**) does not exert any influence on the course of the *anti*-S_N2' reaction.

Table 1. Synthesis of protected (*E*)-CH = CH isosteres by reaction of δ-*N*-Boc-amino-γ-mesyloxy-(*E*)-α,β-enoates with organocyanocopper-boron trifluoride reagents.[a]

Entry	Substrate	Reagent[b]	Product	Isolated yield [%] (Diastereoselectivity at C-2)[c]
1	**3**	$MeCu(CN)Li \cdot BF_3(LiBr)$	**7**	98% (>99:1)
2	**3**	iso-$BuCu(CN)Li \cdot BF_3$	**8**	97% (>99:1)
3	**3**	$PhCH_2Cu(CN)Li \cdot BF_3$	**9**	97% (>99:1)
4	**4**	$MeCu(CN)Li \cdot BF_3(LiBr)$	**10**	79% (>95:5)
5	**5**	$MeCu(CN)Li \cdot BF_3(LiBr)$	**11**	94% (>97:3)
6	**5**	iso-$BuCu(CN)Li \cdot BF_3$	**12**	97% (>97:3)
7	**5**	$PhCH_2Cu(CN)Li \cdot BF_3$	**13**	73% (>85:15)
8	**6**	$MeCu(CN)Li \cdot BF_3(LiBr)$	**14**	80% (>94:6)
9	**15**	$MeCu(CN)Li \cdot BF_3(LiBr)$	**20**	93% (>99:1)
10	**16**	$MeCu(CN)Li \cdot BF_3(LiBr)$	**21**	92% (>99:1)
11	**16**	iso-$BuCu(CN)Li \cdot BF_3$	**22**	93% (>99:1)
12	**17**	$MeCu(CN)Li \cdot BF_3(LiBr)$	**23**	96% (>99:1)
13	**17**	iso-$BuCu(CN)Li \cdot BF_3$	**24**	97% (>99:1)
14	**18**	$MeCu(CN)Li \cdot BF_3(LiBr)$	**25**	91% (>97:3)
15	**18**	iso-$BuCu(CN)Li \cdot BF_3$	**26**	94% (>97:3)
16	**19**	$MeCu(CN)Li \cdot BF_3(LiBr)$	**27**	98% (>99:1)
17	**19**	iso-$BuCu(CN)Li \cdot BF_3$	**28**	96% (>99:1)

[a] All reactions were carried out at −78 °C for 30 min with 3–4 molar equiv. of reagents. [b] The notation $MeCu(CN)Li \cdot BF_3(LiBr)$ is intended to indicate that the reagent has been prepared from ethereal MeLi as the LiBr complex (see, Ref. [8c] and [8d]). Substrates **4** and **6** gave comparable results on treatment with $MeCu(CN)Li \cdot BF_3(LiI)$ as for the entries 4 and 8. [c] All the new compounds have been fully characterized spectrally [IR($CHCl_3$), ^1H-NMR ($CDCl_3$) and CD (isooctane)] and their elemental compositions have been determined by high-resolution mass spectroscopy and/or combustion analysis. Diastereoselectivities were determined by ^1H NMR (200, 270, 300, and/or 400 MHz).

The absolute configuration of the alkyl-bearing carbon center, although apparent from the reaction course of the *anti*-S_N2' attack of the organocopper reagents[8–10, 11a, b] and from the *E*-geometry of the β,γ-double bond of the products, could be established by chemical degradation. For example, ozonolysis of benzyl ether **29** and **31**, derived from **7** and **20** by a two-step reaction (1. diisobutylaluminum hydride, room temperature (DIBAL) in CH_2Cl_2, −78 °C; 2. NaH/BnBr in DMF, 0 °C ~ room temperature), followed by reduction with DIBAL, gave the known alcohols **30**,

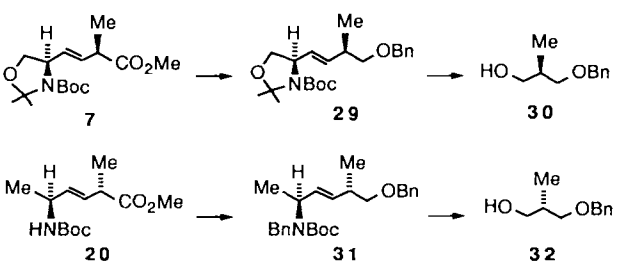

$[\alpha]_D^{22} = +17.2$ ($CHCl_3$), and **32**, $[\alpha]_D^{20} = -17.2°$ ($CHCl_3$). The optical rotations of **30** and **32** exactly match the reported values.[8d, 8e, 11]

Although all of the controlling factors in the present organocyanocopper·BF_3-mediated reaction of δ-*tert*-butoxycarbonylamino-γ-mesyloxy-α,β-enoates are not clear, the following explanation concerning the *anti*-S_N2' reaction could be drawn. Conformer **15A**, which would lead to the (*Z*)-olefin, would be destabilized in comparison with **15B** owing to unfavorable interaction between the bulky R group and the hydrogen. Consequently, elimination of the leaving group (OMs group) will take place only when the attacking copper reagent and the leaving group are in a mutual antiperiplanar disposition.

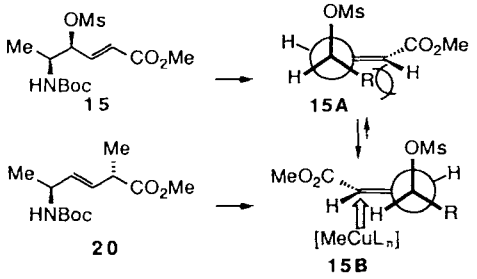

It is apparent from these preliminary data that by judicious selection of organocopper-Lewis acid reagents, the described method offers facile entry to stereochemically pure isosteric dipeptides.

Experimental

Synthesis of (*E*)-CH=CH isosteric dipeptides, for example **23**: To a stirred slurry of CuCN (72 mg, 0.8 mmol) in 5 mL of dry THF at −78 °C was added by syringe 0.533 mL (0.8 mmol) of 1.5 M MeLi/LiBr in Et_2O; the mixture was allowed to warm to −20 °C and was stirred at this temperature for 10 min. $BF_3 \cdot Et_2O$ (0.1 mL, 0.8 mmol) was added to the above mixture at −78 °C and the mixture was stirred for 5 min. A solution of γ-mesyloxy-α,β-enoate (**17**)(85 mg, 0.2 mmol) in dry THF (4 mL) was added dropwise to the above reagent at −78 °C with stirring, and stirring was continued for 30 min followed by quenching with 3 mL of a 2:1 saturated NH_4Cl–28% NH_4OH solution. The mixture was then extracted with Et_2O and the extract was washed successively with 5% citric acid, 5% $NaHCO_3$, and water, and dried over $MgSO_4$. Concentration under reduced pressure gave a crystalline residue, which was purified by flash chromatography over silica gel (*n*-hexane/EtOAc (4/1)) followed by recrystallization from *n*-hexane/Et_2O (4/1) gave the title compound **23** (66 mg, 96% yield) as colorless crystals.—m.p. 74 °C; $[\alpha]_D^{20} = +36.36$ ($c = 0.902$, $CHCl_3$); IR ($CHCl_3$) cm^{-1} = 3460, 3010, 2960, 1727 (shoulder), 1713, 1498, 1459, 1440, 1372, 1174, 974; ^{1}H-NMR (300 MHz, $CDCl_3$): $\delta = 1.19$ (d, $J = 7.08$ Hz, 3H), 1.40 (s, 9H), 1.63 (broad s, 1H), 2.75–2.89 (m, 2H), 3.11 (m, 1H), 3.66 (s, 3H), 4.30–4.50 (m, 2H), 5.49 (dd, $J = 15.22$, 4.42 Hz, 1H), 5.57 (dd, $J = 15.22$, 6.83 Hz, 1H), 7.14–7.30 (m, 5H); ^{13}C NMR (75 MHz, $CDCl_3$): $\delta = 17.21$, 28.35, 41.76, 42.45, 51.85, 126.46, 128.28, 129.55, 129.66, 131.43, 137.34, 155.11, 174.89. Satisfactory elemental analysis (C, H, N).

Received: March 8, 1990 [Z 3842 IE]
German version: *Angew. Chem. 102* (1990) 816

[1] a) A. Spatola in B. Weinstein (Ed.): *Chemistry and Biochemistry of Amino Acids, Peptides and Proteins. Vol. 7*, Marcel Dekker, New York 1983, p. 267; b) R. L. Johnson, *J. Med. Chem. 27* (1984) 1351; c) Nomenclature, see: IUPAC-IUB Joint Commission on Biochemical Nomenclature, *Eur. J. Biochem. 138* (1984) 9; c) For syntheses of non-proteinogenic amino acids, see: M. T. Reetz, D. Röhrig, *Angew. Chem. 101* (1989) 1732; *Angew. Chem. Int. Ed. Engl. 28* (1989) 1706, and references cited therein.

[2] Incorporation of CH=CH isosteres into peptides, see: a) M. T. Cox, J. J. Gormley, C. F. Hayward, N. N. Petter, *J. Chem. Soc. Chem. Commun. 1980*, 800; b) G. Precigoux, E. Ouvrard, S. Geoffre, in C. M. Deber, V. J. Hruby, K. D. Kopple (Ed.): *Peptides: Structure and Function*, Pierce, Rockford, IL, USA, 1985, p. 763; c) J. S. Kaltenbronn, J. P. Hudspeth, E. A. Lunney, B. M. Michinewicz, E. D. Nicolaides, J. T. Repine, W. H. Roark, M. A. Stier, F. J. Tinney, P. K. W. Woo, A. D. Essenburg, *J. Med. Chem. 33* (1990) 838.

[3] M. M. Hann, P. G. Sammes, P. D. Kennewell, J. B. Taylor, *J. Chem. Soc. Chem. Commun. 1980*, 234.

[4] a) A. Spaltenstein, P. A. Carpino, F. Miyake, P. B. Hopkins, *J. Org. Chem. 52* (1987) 3759; b) L. S. Lehman de Gaeta, M. Czarniecki, A. Spaltenstein, *ibid. 54* (1989) 4004.

[5] Y.-K. Shue, G. M. Carrera, A. M. Nadzan, *Tetrahedron Lett. 28* (1987) 3225.

[6] N. J. Miles, P. G. Sammes, P. D. Kennewell, R. Westwood, *J. Chem. Soc. Perkin Trans. 1* 1985, 2299.

[7] The syntheses of the homochiral substrates will be reported in the near future. **17** and **19** were synthesized by the method of *Hanson*: G. J. Hanson, T. Lindberg, *J. Org. Chem. 50* (1985) 5399.

[8] a) T. Ibuka, T. Nakao, S. Nishii, Y. Yamamoto, *J. Am. Chem. Soc. 108* (1986) 7420; b) T. Ibuka, M. Tanaka, S. Nishii, Y. Yamamoto, *J. Chem. Soc. Chem. Commun. 1987*, 1596; c) T. Ibuka, N. Akimoto, M. Tanaka, S. Nishii, Y. Yamamoto, *J. Org. Chem. 54* (1989) 4055; d) T. Ibuka M. Tanaka, S. Nishii, Y. Yamamoto, *J. Am. Chem. Soc. 111* (1989) 4864; e) T. Ibuka, M. Tanaka, Y. Yamamoto, *J. Chem. Soc. Chem. Commun. 1989*, 967; f) Y. Yamamoto, *Angew. Chem. 98* (1986) 945, *Angew. Chem. Int. Ed. Engl. 25* (1986) 947; g) C. Girard, I. Romain, M. Ahmar, R. Bloch, *Tetrahedron Lett. 30* (1989) 7399.

[9] Nearly all known organocopper reactions with allylic halides, acetates, and their congeners proceed via *anti*-S_N2' displacement. For excellent reviews on S_N2' reactions, see: J. A. Marshall, *Chem. Rev. 89* (1989) 1503; R. M. Magid, *Tetrahedron 36* (1980) 1901; for *anti*-S_N2' reactions, see: B. M. Trost, T. P. Klun, *J. Org. Chem. 45* (1980) 4256; E. J. Corey, N. W. Boaz, *Tetrahedron Lett. 25* (1984) 3063; I. Fleming, D. Higgins, *ibid. 30* (1989) 5779, and references cited therein.

[10] For *syn*-S_N2' reactions with organocopper reagents, see: J. A. Marshall, V. H. Audia, *J. Org. Chem. 52* (1987) 1106; see also, J. P. Marino, R. Fernandez de la Pradilla, E. Laborde, *ibid. 52* (1987) 4898.

[11] a) J. A. Marshall, J. D. Trometer, D. J. Cleary, *Tetrahedron 45* (1989) 391 and references cited therein; b) J. A. Marshall, B. E. Blough, *J. Org. Chem. 55* (1990) 1540; c) H. Nagaoka, Y. Kishi, *Tetrahedron 37* (1981) 3873.

Gas-Phase Thermolysis of 6-Cyclopropyl- and 6-Oxiranylpentafulvenes: Novel Routes to Dihydroindenes and Vinylcyclopentadienes**

By *Axel G. Griesbeck,* Karl Peters, Eva-Maria Peters,* and *Hans Georg von Schnering*

The electrocyclic ring closure of 6-vinylpentafulvenes **1**[1] via gas-phase thermolysis is an efficient and flexible route to 1,5-dihydropentalenes **2**.[2] We have now investigated the $[\pi^6 + \sigma^2]$ variant, which should open up a route to the homologous dihydroindenes and oxa analogues thereof.

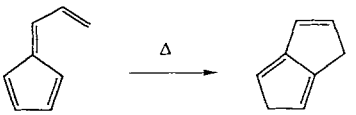

1 2

Both series of compounds are of importance for the synthesis of terpenoid natural products.[3] The employment of 6-oxiranylfulvenes in the synthesis of natural products has already been reported: *Fallis* et al.[4] were able to prepare a

[*] Dr. A. G. Griesbeck
Institut für Organische Chemie
Am Hubland, D-8700 Würzburg (FRG)
Dr. K. Peters, E.-M. Peters, Prof. Dr. H. G. von Schnering
Max-Planck-Institut für Festkörperforschung
Heisenbergstrasse 1, D-7000 Stuttgart 80 (FRG)

[**] *A. G. G.* thanks the Fonds der Chemischen Industrie for a Liebig-Stipendium

series of spiroannelated cyclopentadienes by reaction of these compounds with alkyllithium. Gas-phase thermolysis with 6-oxiranyl- and 6-cyclopropylpentafulvenes, on the other hand, were not investigated.

6-Cyclopropyl-6-methylpentafulvene **3**[5] is accessible in good yields by a standard method.[6] Upon gas-phase thermolysis (580–620 °C/0.08 torr, unpacked quartz tube, 30-cm thermolysis zone) a mixture of three isomeric dihydroindenes is formed in a total yield of 90–94%. **6** is formed as main component (62%) together with the isomers **7** (ca. 20%) and **5** (ca. 10%).[7]

It cannot be ruled out that this reaction proceeds via a corresponding spiro [4.4]nonatriene[8] as a primary product (as a result of a vinylcyclopropane-cyclopentene rearrangement). However, no intermediate product was observed even at significantly lower thermolysis temperatures (520–550 °C, ca. 20% conversion), i.e. the opening of the cyclopropane ring could lead directly to the indene derivative **4**, which then spontaneously undergoes 1,5-hydrogen shifts with formation of **5**–**7**. When this mixture of isomers was allowed to react with dienophiles such as tetracyanoethylene (TCNE), 4-methyl-1,2,4-triazole-3,5(4*H*)-dione (MTAD) and benzoquinone (BQ) only a 2:1 adduct of the dienophile and isomer **6** could be isolated in each case. The crystal structure analysis[9] of the MTAD adduct **9**[10] confirmed the *anti* arrangement of the two triazolidine rings (Fig. 1).

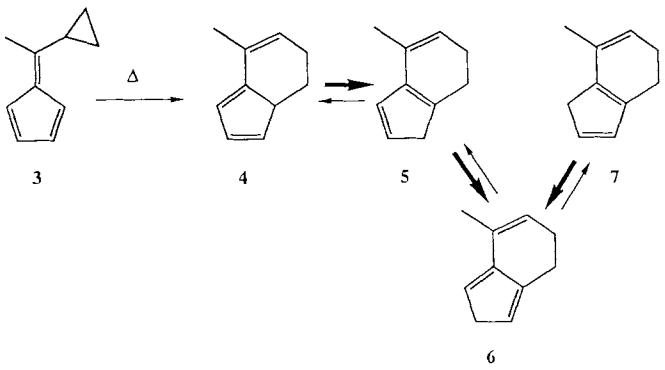

This high stereoselectivity upon attack of the second dienophile can doubtles be attributed to the shielding effect of the first triazolidine ring[11] and shows that the primary adduct of **6** and the first MTAD molecule has to be regarded as a norbornene derivative (which are usually attacked *exo*-selectively[12]) rather than as an isodicyclopentadiene derivative (which exhibit opposite activity[12]). The NMR data of the compound **9** are analogous to those of the adducts **8** and **10**, thus suggesting the same stereochemistry for these derivatives. In the adduct **10** the benzoquinone rings can be arranged *exo* as well as *endo* to the norbornane skeleton. The attack of the first benzoquinone molecule results in formation of the *endo* primary adduct, which in a subsequent step adds a second dienophile *anti* and *exo* to the newly formed diene system. No photocycloaddition (which is to be expected in the case of the *endo,endo* isomer) could be observed upon irradiation of **10**.

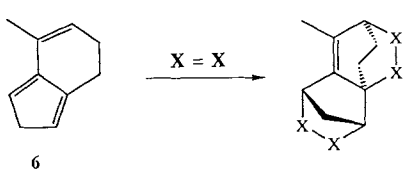

X=X :
TCNE **8** (52%)
MTAD **9** (58%)
BQ **10** (62%)

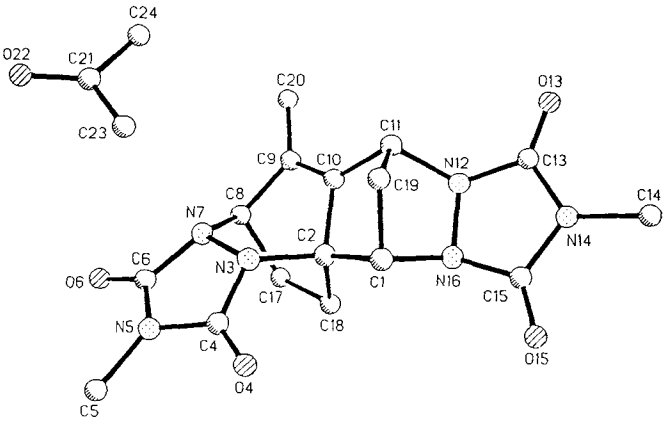

Fig. 1. Crystal structure of **9**.

The formation of the isomers **5**–**7** in a ratio which cannot be significantly altered even by distillation or prolonged heating of the thermolyzate, corresponds with the results of the dihydropentalene formation in the thermolysis of vinylpentafulvene **1**[1,2] or cyclooctatetraene.[13] The results of the MNDO calculation[14] on five different dihydroindene species are listed together with those on the dihydropentalenes[16] in Table 1. A striking result is that the annelation of a six-membered ring to cyclopentadiene strongly reduces the energy difference between the isomers **A**, **B**, and **C** unsaturated at the bridgeheads. The triene **A**, $n = 2$, remains as in the dihydropentalene series, the stabilomer.[17,18]

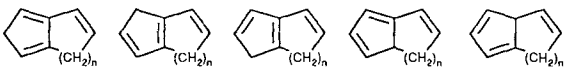

Table 1. Heats of formation ΔH_f [kcal mol^{-1}] of the isomers **A**–**E** (n = 1,2) according to MNDO.

	A	B	C	D	E
n = 1 [16]	50.7	54.9	55.4	59.0	60.0
n = 2 [14]	32.2	32.5	33.0	39.0	40.0

The epoxy compound **11** analogous to **3**[4] yielded no ring-annelation products upon gas-phase thermolysis. When the thermolysis was carried out at temperatures above 600 °C (0.08 torr), the two vinylcyclopentadienes **13a** and **13b**[19] could be isolated quantitatively. Under milder conditions (460–580 °C/0.01 torr) the aldehyde **12** could be detected to an extent of 10–15% in the thermolyzate. 6,6-Dimethylpentafulvene **14** is not formed as intermediate (formally via 1,2-H-migration) upon cleavage of carbon monoxide from **12**.

We were able to show that **14** undergoes isomerization to **13a**, **b** only to a small extent under the aforementioned conditions, as had already been established by *Zimmermann* et

al.[20] The isomeric ratio **13a**:**13b** was identical with the equilibrium ratio (64:36 ± 4%) in all experiments. In particular, in none of the cases could the 5-alkylated cyclopentadiene isomer be detected, so it must be assumed that the dienes **13** already completely equilibrate under the thermolysis conditions.

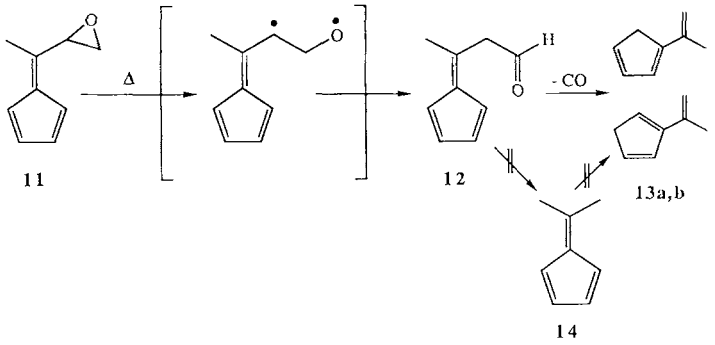

Thus, whereas an electrocyclic $[\pi^6 + \sigma^2]$-reaction had to be noted with the cyclopropylfulvene **3**, the rapid formation of the carbonyl group hinders a corresponding reaction in the case of the oxiranylfulvene **11**. We are presently trying to force a ring closure reaction also in the thermolysis of 6-oxiranylpentafulvenes by blocking the oxirane positions, and thus to facilitate an entry to iridoid compounds (oxa-analogous dihydroindenes).

Received: January 26, 1990 [Z 3759 IE]
German version: *Angew. Chem. 102* (1990) 801

CAS Registry numbers:
3, 61010-59-1; **5**, 127382-14-3; **6**, 127382-15-4; **7**, 127382-16-5; **8**, 127382-17-6; **9**, 127382-18-7; **10**, 127399-02-4; **11**, 92119-15-8; **12**, 127382-19-8; **13a**, 26385-00-2; **13b**, 26385-01-3.

[1] J. J. Gajewski, C. J. Gavender, *Tetrahedron Lett. 1971*, 1057.
[2] A. G. Griesbeck, *J. Org. Chem. 54* (1989) 4981; *Synthesis 1990*, 144.
[3] T.-L. Ho, *Carbocycle Construction in Terpene Synthesis*, VCH, Weinheim 1988.
[4] K. Antczak, J. F. Kingston, A. G. Fallis, *Tetrahedron Lett. 25* (1984) 2077; *Can. J. Chem. 62* (1984) 2451.
[5] G. A. Olah, G. K. Surya Prakash, G. Liang, *J. Org. Chem. 42* (1977) 661. The ^{1}H-NMR spectrum quoted therein is incorrect. The signals of the fulvene ring protons appear at 6.40 (mc, 3H) and 6.55 (mc, 1H) (200 MHz, $CDCl_3$).
[6] K. J. Stone, R. D. Little, *J. Org. Chem. 49* (1984) 1849.
[7] Isomeric ratios from ^{1}H- und ^{13}C-NMR integration; NMR data of **6**: ^{1}H NMR (200 MHz, $CDCl_3$): $\delta = 1.92$ (d, 3H, $J = 0.8$ Hz), 2.20 (m, 2H), 2.53 (m, 2H), 2.98 (br. s, 2H), 5.8 (m, 1H), 5.95–6.05 (m, 2H).—^{13}C NMR (50 MHz, $CDCl_3$): $\delta = 18.9$(q), 23.4(t), 24.7(t), 40.2(t), 122.1(d), 123.5(d), 125.6(d), 137.2(s), 143.1(s), 143.6(s).
[8] M. F. Semmelhack, H. N. Weller, J. S. Foos, *J. Am. Chem. Soc. 99* (1977) 292.
[9] Crystal structure analysis of **9**: colorless platelets with one molecule of acetone per molecule of **9**, crystallized from acetone. Triclinic, space group $P\bar{1}$, 3323 measured reflections, 2939 reflections with $F > 3\sigma(F)$ used for the full-matrix least squares refinement. Lattice constants: $a = 1004.9(6)$, $b = 1291.3(7)$, $c = 797.7(4)$ pm, $\alpha = 101.25(5)$, $\beta = 96.31(5)°$, $\gamma = 95.37(5)°$, $Z = 2$; $R = 0.071$, $R_w = 0.076$. Further details of the crystal structure investigation are available on request from the Fachinformationszentrum Karlsruhe, Gesellschaft für wissenschaftlich-technische Information mbH, D-7514 Eggenstein-Leopoldshafen 2 (FRG), on quoting the depository number CSD-54327, the names of the authors, and the journal citation.
[10] M.p. 253–256 °C (decomp.): ^{1}H NMR (200 MHz, [D$_6$]DMSO): $\delta = 1.81$ (d, 1H, $J = 8.0$ Hz), 2.02 (d, 1H, $J = 8.0$ Hz), 2.07 (s, 3H), 2.25 (mc, 2H), 2.93 (m,2H), 3.00 (s, 3H), 3.04 (s, 3H), 4.71 (s, 1H), 5.30 (s, 1H), 5.42 (s, 1H). ^{13}C NMR (50 MHz, [D$_6$]DMSO): $\delta = 15.9$(q), 23.2(t), 24.8(t), 25.4(q), 25.9(q), 39.6(t), 54.9(d), 58.7(d), 62.7(d), 65.8(s), 131.4(s), 135.5(s), 154.4(s), 154.6(s), 158.2(s), 158.8(s).
[11] This pronounced stereoselectivity could also be established in the corresponding reaction with a furo[3, 4-*b*]furan: W. Eberbach, H. Fritz, N. Laber, *Angew. Chem. 100* (1988) 599; *Angew. Chem. Int. Ed. Engl. 27* (1988) 568.
[12] F. K. Brown, K. N. Houk, *J. Am. Chem. Soc. 107* (1985) 1971.
[13] H. Meier, A. Pauli, P. Kochhan, *Synthesis 1987*, 573.
[14] We thank Dr. *Markus Dörr* (Sandoz AG, Basle) for carrying out the MNDO calculations. [15].
[15] M. J. S. Dewar, W. Thiel, *J. Am. Chem. Soc. 99* (1977) 4907.
[16] H. Meier, A. Pauli, H. Kolshorn, P. Kochhan, *Chem. Ber. 120* (1987) 1607.
[17] Defined as the isomer with the lowest heat of formation at 25 °C in the gas-phase, after S. A. Godleski, P. von R. Schleyer, E. Osawa, W. T. Wipke, *Prog. Phys. Org. Chem. 13* (1981) 63.
[18] The corresponding dihydroindene with fulvene structure ($\Delta H_f = 36.8$ kcal mol^{-1}) has a considerably higher heat of formation than the isomers **A**, **B**, and **C**.
[19] H. M. R. Hoffmann, O. Koch, *J. Org. Chem. 51* (1986) 2939.
[20] G. Zimmermann, M. Remmler, B. Ondruschka, F. D. Kopinke, B. Olk, *Chem. Ber. 121* (1988) 1855.

A Surface Organometallic Approach for Controlling the Pore Opening Size of Zeolites: the Case of Mordenite Modified via Grafting of Dineopentylmagnesium **

By *Albert Théolier, Emmanuel Custodero, Agnès Choplin, Jean-Marie Basset** and *Francis Raatz*

Shape selectivity is one of the most important properties of zeolites in their application in the field of adsorption and catalysis.[1] For a given zeolite, this property is related, inter-alia, to the pore size and/or to the size of the pore openings. For a number of applications in the fields of adsorption and the synthesis of fine chemicals, a certain cut-off pore diameter is often desired; this cannot be achieved, however, via direct synthesis. One way to circumvent this problem is to modify, post synthesis, the pore opening of a given zeolite. This has recently been attempted by way of the chemical vapor deposition (CVD) of alkoxysilanes.[2–9] Subsequent calcination then led to a coating of silica on the external surface of the zeolite. However, although a layer by layer build up of such a coating seems to be achieved, the deposit is sometimes heterogeneous, some pores being fully blocked whereas others are not modified.[10, 11]

Another way of adjusting the shape selectivity could be to chemically graft a bulky organometallic complex at the external surface of a given zeolite and more specifically and efficiently at the pore entrance. The steric hindrance of the organometallic fragment could then be easily modulated via the bulkiness of the organic moiety. We wish to report here, to our knowledge, the first example illustrating the feasibility of such an approach; we have modified the adsorptive properties of a mordenite via the reaction of dineopentylmagnesium [$MgNp_2$] with its external OH groups.[12]

Two methods have been used for this surface reaction: a sublimation method (method A)[13] and a liquid phase method (method B).[14] In order to characterize the surface reaction between $MgNp_2$ and mordenite, preliminary experiments were carried out on a silica ($SiO_{2(400)}$) previously

[*] Dr. J. M. Basset, A. Théolier, E. Custodero, Dr. A. Choplin
Institut de Recherches sur la Catalyse
2 Avenue Albert Einstein, F-69626 Villeurbanne Cedex (France)
Dr. F. Raatz
Institut Français du Pétrole
1-4 Avenue de Bois-Préau, F-92506 Rueil-Malmaison (France)

[**] The Ministère de la Recherche et de l'Enseignement Superieur is acknowledged for financial support (contract n° 86B0777)

treated under vacuum at 400 °C. It has been possible to prove the occurrence of the surface reaction (1) on the basis of IR

$$\equiv\text{Si-OH} + \text{MgNp}_2 \longrightarrow \equiv\text{Si-O-Mg-Np} + \text{NpH} \quad (1)$$

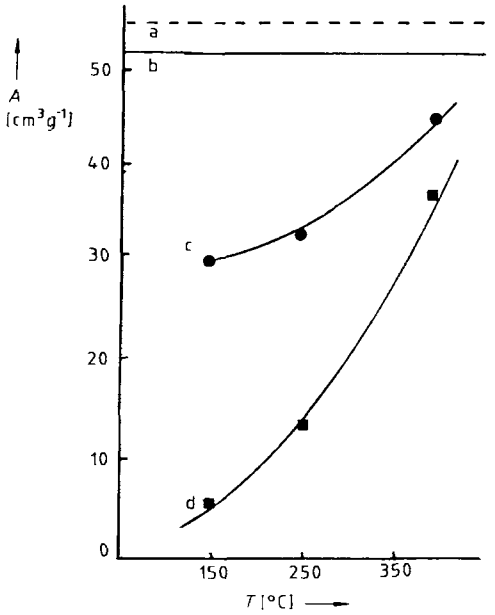

Fig. 1. Adsorption capacity A of H–mordenite (a, b) and MgNp–H-mordenite (c, d) as a function of the temperature T of treatment in the case of hexane (a, c) and isooctane (b, d).

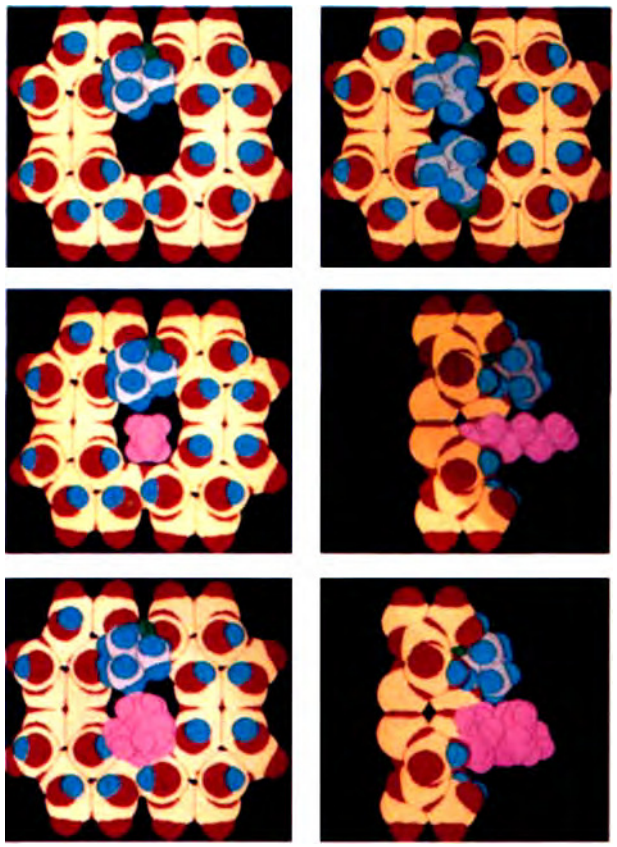

Fig. 2. Computer generated representation of (from top to bottom): one possible site of grafting –MgNp at the pore entrance of mordenite (left) and the steric crowding at pore entrance if two –MgNp moieties are grafted (right); the free passage of *n*-hexane if one –MgNp moiety is grafted (front view and side view); the steric barrier for isooctane (front view and side view). Red: oxygen; yellow: silica; green: magnesium; gray: carbon; blue: hydrogen. Host molecule: pink. The Van der Waals radii of the atoms are shown.

data,[15] volumetric measurements,[16] elemental analysis,[17] and ^{13}C-MAS-NMR data. The neopentyl group exhibits two distinct ^{13}C-NMR signals at $\delta = 31.82$ (CH_3) and 28.51 (CH_2), respectively. This surface species is thermally[18] stable, as is to be expected for compounds of the type Mg(R)(OR).[19] Total disappearance of the ν(CH) bands occurs only above 300 °C.

The reaction of $MgNp_2$ with the mordenite has been followed by in situ IR spectroscopy. Sublimation of $MgNp_2$ on a mordenite causes the disappearance of the band at 3745 cm^{-1}, characteristic of surface silanol groups and the appearance of weak bands at 2955 and 2869 cm^{-1}, typical of $\nu(CH_3)$ vibrations. This behavior is similar to that observed under comparable conditions with silica. The amount of magnesium which can be grafted by both methods (A or B) never exceeds 0.2 wt.-%. As in the case of silica, the grafted organometallic fragment is stable up to ca. 200 °C, a temperature above which it starts to decompose into neopentane and an unidentified magnesium species.

Although we have no direct evidence that dineopentylmagnesium is grafted exclusively on the external surface of the mordenite, a number of observations support this hypothesis. The amount of grafted magnesium never exceeds 0.2 wt-%, in good agreement with the number of available external surface OH groups.[20] The Van der Waals radius of solvated $MgNp_2$ ($MgNp_2 \cdot 2Et_2O$) is greater than that of the pore entrance of the mordenite (6.7 × 7.0 Å). Consequently, the method of impregnation in solution (Method B) should not allow easy access of the complex into the pore system. For the unsolvated gas phase $MgNp_2$, the Van der Waals radius is close to that of the pore entrance. Nevertheless, the fact that both methods lead to similar results (e.g. Mg content and adsorption data) suggests that the solvated $MgNp_2$ mainly reacts with the external surface of the zeolite.

The adsorptive properties of these MgNp-modified mordenites have been measured by a pulse-chromatographic method.[21] The adsorption capacities thus determined for *n*-hexane (kinetic diameter $\sigma = 4.2$ Å) and isooctane ($\sigma = 6.3$ Å) are shown in Figure 1 as a function of the temperature of treatment of the Mg-mordenite. Two points should be emphasized: (i) the grafting of the organometallic moiety -Mg-Np reduces the adsorption capacity of the mordenite for *n*-hexane by a factor of 2 and nearly suppresses the adsorption of isooctane; (ii) as the temperature of treatment of the modified mordenite increases, this selectivity toward *n*-hexane is reduced and finally suppressed above 400 °C. This phenomenon is correlated to the thermal stability of the grafted organometallic fragment.

The above results indicate that the grafting of an organometallic species on the external surface of mordenite is indeed a way of controlling the shape selectivity of zeolites.

Computer modeling[22] of the interaction of $MgNp_2$ with the silanol groups available on the external surface of mordenite indicates that on the (001) face, two types of sites are available: the first type allows grafting of an MgNp moiety via one surface O atom [giving (≡Si–O-)MgNp]; the second type would allow the grafting via two O atoms: a 1e-donor (≡Si–O) and a 2e-donor (adjacent ≡Si–OH, able to coordinate to the Mg atom) [giving (≡Si–O)(≡Si–OH)MgNp] (Fig. 2). On the (010) and (100) faces, only 1e-donor O atoms are available, leading to (≡Si–O)MgNp. Once a MgNp fragment is grafted, the reaction of a second molecule of $MgNp_2$ in the close vincinity may be difficult for steric reasons. In any case, no more than 2 MgNp moieties can be grafted in the vicinity of a pore aperture. (Fig. 2) Computer modeling also suggests that only a minor fraction of the surface-grafted MgNp fragments efficiently controls the pore entrance

aperture and thus the selectivity of the adsorptive properties. When one MgNp is grafted per pore aperture, the discrimination capacity between *n*-hexane and isooctane by MgNp-modified mordenite can be easily visualized (Fig. 2): numerous short contact distances seem to exist between the organic molecule and the organometallic fragment in the case of isooctane, but none or very few in the case of *n*-hexane. When two MgNp fragments are grafted per pore aperture no hydrocarbon can enter the pore system (Fig. 2), as is consistent with the lowering of the *n*-hexane adsorption capacity.

This preliminary study indicates that it should be possible to design a shape selective system for a given application, starting from a readily available zeolite, modified by an organometallic complex, whose steric bulk can be accurately tuned. Studies are now in progress to fully characterize these new solids (precise localization of the organometallic entity) and to extend this new method to different couples of zeolites and complexes. The solid obtained by this approach suggests applications in the field of adsorption or catalysis at low temperature. One can nevertheless imagine that successive reactions (such as hydrolysis, complex grafting ...) should lead to the build-up in a layer by layer fashion of an oxide coating on the zeolite. Such solids may find more applications in catalytic reactions occurring at higher temperatures.

Received: February 15, 1990 [Z 3799 IE]
German version: *Angew. Chem. 102* (1990) 803

[1] N. Y. Chen, W. E. Garwood, *Catal. Rev. Sci. Eng. 28* (1986) 185.
[2] H. Olson, P. G. Rodewald, US-Pat. 4 379 761 (1983), Mobil Oil Co.
[3] P. G. Rodewald, US-Pat. 4 465 886 and 4 477 583 (1984) Mobil Oil Co.
[4] P. T. Allen, B. M. Drinkard, E. H. Hunger, US-Pat. 3 724 170 (1973) Mobil Oil Co.
[5] I. A. Cody, US-Pat. 4 451 572 (1983), EXXON Research.
[6] M. Niwa, H. Ito, S. Kato, T. Hattori, Y. Murakami, *J. Chem. Soc. Chem. Commun. 1983*, 819; *Proc. 8th Int. Congr. Catal*, (1984) 701.
[7] M. Niwa, S. Kato, T. Hattori, Y. Murakami, *J. Chem. Soc. Faraday Trans. 1 80* (1984) 3135.
[8] Y. Murakami, A. Furuta, H. Ito, S. Okada, JP-Pat. 60 187 317, 60 187 318, 60 187 319 (1985).
[9] M. Niwa, K. Yamazaki, Y. Murakami, *Chem. Lett. 1989*, 441.
[10] M. Niwa, C. V. Hidalgo, T. Hattori, Y. Murakami, *Proc. 7th Int. Zeolite Conf. 1986*, 297.
[11] M. Niwa, Y. Kawashima, T. Hibino, Y. Murakami, *J. Chem. Soc. Faraday Trans. 1 84* (1988) 4327.
[12] $MgNp_2$ was synthesized from NpBr and Mg following published procedures (R. R. Schrock, G. D. Feldmann, *J. Am. Chem. Soc. 100* (1978) 3360. The mordenites (large pore, from Norton, Si/Al = 6.5 and Toyosoda Si/Al = 10.2) were used in their Na or H forms; they were pretreated under vacuum (400 °C, 16 h) to remove any trace amount of water. Diethyl ether was distilled prior to use. All experiments were performed with strict exclusion of air and water by standard Schlenk tubes or break and seal techniques.
[13] Method A. $MgNp_2$ was sublimed (150 °C, 10^{-4} mm Hg) on the zeolite at 150 °C; excess of complex, physisorbed on the surface of the zeolite, was removed by evacuation at the same temperature for 4 h.
[14] Method B. The zeolite (1 g) was placed in contact with a solution of the complex (50 mg) in ether (10 mL), at room temperature. After ca. ½ h, the solution was removed via a syringe and the solid was washed two times with 10 mL aliquots of ether, then evacuated at room temperature for 6 hours.
[15] Reaction of $MgNp_2$ with a silica dehydroxylated at 400 °C led to total consumption of the silanol groups (disappearance of the band at 3745 cm^{-1}) and to the appearance of ν(C–H) bands at $\tilde{\nu}$ = 2955 and 2869 cm^{-1} corresponding to the grafted neopentyl moiety.
[16] Reaction of $MgNp_2$ with a $silica_{(400)}$ led to the evolution of 1 mole of NpH per mole of Mg.
[17] The Mg/C ratio after grafting was equal to 1/5, as expected for surface MgNp.
[18] The grafted organometallic began to decompose above 200 °C to give mostly neopentane and traces of methane.
[19] E. C. Ashby, G. F. Willard, A. B. Goel, *J. Org. Chem. 44* (1979) 1221.
[20] The number of surface $\equiv$Si–OH groups available for MgNp grafting on the [100] and [010] faces is approximately 2 per unit cell per plane. These two planes are those which contribute the most to the external surface, which is 27 m^2/g. A maximum amount of ca. 0.15 wt-% Mg is thus suggested.
[21] The modified zeolite was synthesized in situ or transferred in a chromatographic type column. Its adsorption capacity for a given hydrocarbon was related to the number of pulses which have to be injected on the column in order to obtain a constant signal at the outlet. Under our conditions, the pressure of the hydrocarbon, controlled by a stream of argon bubbling through it, was such that $p/p_s \approx 1$.
[22] Computer modeling has been performed using ALCHEMY (TRIPOS Assoc.). The crystallographic parameters of mordenite are those determined by Meier (*Zeit. Fur Krist. 115* (1961) 439). The bond distances and angles of the MgNp moiety are those from the electron diffraction study of $MgNp_2$ (E. C. Ashby, L. Fernholt, A. Haaland, R. Seip, R. S. Smith, *Acta Chem. Scand. A 34* (1980) 213). The chosen Mg–O distance was 1.98 Å (an average value).

^{13}C-MAS-NMR Spectra of Technical Calcium Carbide and Barium Carbide — Are the $C_2^{2\ominus}$ Ions in Ionic Carbides Surrounded Symmetrically?**

By *Bernd Wrackmeyer,* Klaus Horchler, Angelika Sebald, Lawrence H. Merwin*, and *Charles Ross II*

The $C_2^{2\ominus}$ ion is a central link in the 14-electron family of diatomic molecules[1] and a building block of fascinating structures with C_2 units.[2] The salt-like carbides MC_2 (M = Ca,Sr,Ba) provide an opportunity of obtaining ^{13}C-NMR parameters of $C_2^{2\ominus}$ ions in the solid state. In all textbooks one finds that these carbides are said to have a tetragonal structure[3] in which each metal atom is surrounded by six $C_2^{2\ominus}$ ions. Each $C_2^{2\ominus}$ ion has six metal atoms as neighbors, namely two terminal and four side-on (space group *I4/mm*): an exactly axially-symmetric environment results for the carbon atoms. In the case of CaC_2[4] at least four phases are discussed, of which three could be stable or metastable at room temperature. The preparation of single crystals for an X-ray structure analysis has so far met with little success, so that the available crystallographic data is inadequate. Tetragonal symmetry was assumed in the determination of $r_{C\equiv C}$ = 120 pm by neutron diffraction measurements on technical CaC_2.[5]

In order to help towards the structural elucidation and to investigate the question of the ionic character of the alkaline earth metal carbides we have now recorded ^{13}C-MAS-NMR spectra of technical CaC_2 and BaC_2 (Fig. 1)[6] and analyzed them concerning the tensor components σ_{11}, σ_{22} and σ_{33} (Table 1).[7] ^{13}C-NMR spectra of static samples of CaC_2[8, 9] as well as of SrC_2 and BaC_2[9] are already available; however, these are either completely uninformative[8] or their quality is not satisfactory enough for an exact analysis with regard to the uniformity of the samples, the isotropic δ^{13}C values, and the tensor components of the ^{13}C shielding constants.[9]

[*] Prof. Dr. B. Wrackmeyer, Dipl.-Chem. K. Horchler
Laboratorium für Anorganische Chemie der Universität
Postfach 101251, D-8580 Bayreuth (FRG)
Dr. A. Sebald, Dr. L. H. Merwin, Dr. C. Ross II
Bayerisches Geoinstitut
Postfach 101251, D-8580 Bayreuth (FRG)

[**] This work was supported by the Deutsche Forschungsgemeinschaft and the Fonds der Chemischen Industrie.

Table 1. Isotropic $\delta^{13}C$ values [a] and tensor components of the ^{13}C shielding constants $\sigma^i(^{13}C)$ [b] for CaC_2 (cf. Fig. 1) and BaC_2.

	$\delta^{13}C$	σ_{11}	σ_{22}	σ_{33}	$\Delta\sigma$	η
CaC_2	206.2 [c]	−350	−283	14	331	0.31 ± 0.1
BaC_2	232.1	−354	−288	−55	265	0.38 ± 0.1

[a] Relative to external Me_4Si for one of the ^{13}C resonances ($\delta^{13}C = 38.5$) of solid adamantane. [b] σ-values are likewise referred to Me_4Si but have opposite signs to the δ values; the convention is: $\sigma^i = 1/3\ (\sigma_{11} + \sigma_{22} + \sigma_{33})$ and $|\sigma_{33} - \sigma^i| \geq |\sigma_{11} - \sigma^i| \geq |\sigma_{22} - \sigma^i|$; the anisotropy of the chemical shift $\Delta\sigma = \sigma_{33} - 1/2\ (\sigma_{11} + \sigma_{22})$; the asymmetry parameter $\eta = 3/2\ (\sigma_{22} - \sigma_{11})\ (\Delta\sigma)$. [c] $\delta^{13}C$ of the second species (ca. 5–10%): 200.3 (as far as the spinning side bands are recognizable, their relative intensities compare with those of the main component.

The simulation of the ^{13}C-MAS-NMR spectra[7] shows, that in the case of CaC_2 and BaC_2, the deviation from axial symmetry for the carbon atoms is so marked that a highly symmetric structure of MC_2 is out of the question. One way in which to reconcile the widely differing information provided by the powder X-ray diffraction data and the ^{13}C-MAS-NMR spectra is to assume that the C≡C axis only statistically coincides with the *c* axis of the lattice, i.e. the orientation of the individual C_2 units deviates from this axis.[10] Numerous phases with orientational disorder are characterized by molecular units with high external symmetry and strong internal bonding which are coordinated via many weak bonds to other large atoms.[11]

Consistent with the data provided by powder X-ray diffraction diagrams[6] one finds, in the case of CaC_2 (Fig. 1),

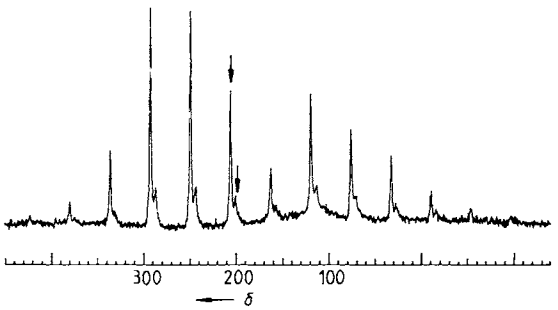

Fig. 1. 75.5 MHz ^{13}C-MAS-NMR spectrum (Bruker MSL 300) of technical calcium carbide; the isotropic $\delta^{13}C$ values are indicated with arrows and were identified by measurements at different rates of rotation. Measuring conditions: 25 °C, rotation rate 3272 Hz, pulse angle ca. 72° (4.0 μs), 800 scans, relaxation delay 300 s.

that a second modification is present to the extent of ca. 5–10%, with almost the same $\delta^{13}C$ value as the main component. In the case of the smaller component of the mixture it is impossible to glean any information about the symmetry of the environment of the $C_2^{2\ominus}$ units, since the signal-to-noise ratio is not large enough for a spectral simulation.

The $\delta^{13}C$ values depend markedly on the cation,[9] whereby the deshielding of the ^{13}C nucleus increases with increasing size of the cation. This dependence indicates that there are covalent interactions between the $C_2^{2\ominus}$ ions and the $M^{2\oplus}$ ions.[12] So far, there are scarcely any NMR data available about ionic species in solution and in the solid state. In the case of $NH_4^{\oplus}$ $NCS^{\ominus}$, however, good agreement was found between the $\delta^{15}N$ and $\delta^{13}C$ values in both states of aggregation,[13] so that this compound is the example resorted to for largely ionic bonding. The correlations with the ionization energy of M or the terminal M–C distance based on less exact $\delta^{13}C$ values for MC_2[9] are questionable and—on using our more accurate data—do not under any circumstances permit extrapolations to H–C≡C–H.

The $\delta^{13}C$ values are unusual for alkyne carbon atoms.[14] A correlation between $\delta^{13}C$ and $\delta^{15}N$ of isoelectronic and isostructural linear compounds[15] [Eq. (a)] predicts a $\delta^{13}C$ of ca. 140 for a "free" $C_2^{2\ominus}$ ion on using the $\delta^{15}N$ value for the cyanide ion ($\delta^{15}N = -106.1$).[15b]

$$\delta^{13}C = 0.536\ \delta^{15}N_{(MeNO_2 \equiv 0)} + 196.5 \qquad (a)$$

The following considerations support this $\delta^{13}C$ value for a "free" $C_2^{2\ominus}$ ion: In analogous structures the δ values should behave like the anisotropy of the chemical shift $\Delta\sigma_{(^{13}C)}$ and $\Delta\sigma_{(^{15}N)}$. With $\delta^{13}C = 140$ for the $C_2^{2\ominus}$ ion, $\Delta\sigma_{(^{13}C)} = \sigma_{\parallel} - \sigma_{\perp} = 345$, when $\sigma_{\parallel(^{13}C)} = 90$ (as reference value for linear undisturbed systems[16]). Experimentally, $\Delta\sigma_{(^{15}N)} = 654$ was determined for the N_2 molecule corresponding to the $C_2^{2\ominus}$ ion;[17] the quotient of the two $\Delta\sigma$ values is almost identical with the slope of the straight line plotted according to Equation (a).

Together with the finding that the environment of the carbon atoms in MC_2 is not axially symmetric, the large difference between the $\delta^{13}C$ value (ca. 140) expected according to Equation (a) and the experimental values (206.1 ppm for CaC_2 and 232.1 ppm for BaC_2) merely allows the conclusion that the $C_2^{2\ominus}$ unit in "ionic" carbides and the C≡C triple bond in alkynes are not comparable.

Received: January 5, 1990;
revised: March 19, 1990 [Z 3724 IE]
German version: *Angew. Chem. 102* (1990) 821

[1] a) N. L. Summers, J. Tyrell, *J. Am. Chem. Soc. 99* (1977) 3960; b) P. Pyykkö, *J. Mol. Phys. 67* (1989) 871.
[2] See examples given by R. Hoffmann, *Angew. Chem. 100* (1988) 1653; *Angew. Chem. Int. Ed. Engl. 27* (1988) 1593.
[3] M. von Stackelberg, *Z. Phys. Chem. Abt. B 9* (1930) 437.
[4] a) H. H. Franck, M. A. Bredig, G. Hoffmann, *Z. Anorg. Allg. Chem. 232* (1937) 61; b) N.-G. Vannerberg, *Acta Chem. Scand. 15* (1961) 769; c) *ibid. 16* (1962) 1212; c) W. Borchert, M. Röder, *Z. Anorg. Allg. Chem. 302* (1959) 253.
[5] M. Atoji, R. C. Medrud, *J. Chem. Phys. 31* (1959) 332.
[6] According to our powder X-ray diffraction diagrams CaC_2 (Baker) consists of two phases and contains in addition ca. 5–10% CaO; BaC_2 (Alfa Products, 99%) is a pure phase and contains little BaO.
[7] a) Simulation programs for the iterative spinning side-band analysis written by L. H. Merwin after [7b]; b) M. M. Maricq, J. S. Waugh, *J. Chem. Phys. 70* (1979) 3300; c) a graphical analysis [7d] furnishes the same results, but is very time consuming in the case of MAS-NMR spectra with many side bands; for cases with axial or almost axial symmetry both methods [7b, d] are problematic [7e]; d) J. Herzfeld, A. E. Berger, *J. Chem. Phys. 73* (1980) 6021, e) N. J. Clayden, C. M. Dobson, L.-Y. Lian, D. J. Smith, *J. Magn. Reson. 69* (1986) 476.
[8] D. T. Haworth, C. A. Wilkie, *J. Inorg. Nucl. Chem. 40* (1978) 1689.
[9] T. M. Duncan, *Inorg. Chem. 28* (1989) 2663.
[10] a) Room temperature powder X-ray diffraction data ($20° \leq 2\theta \leq 100°$, $Cu_{K\alpha}$ radiation) of BaC_2 (space group *I4/mmm*; $a = 4.3991(5)$ Å, $c = 7.1024(10)$ Å) were collected out by us in order to find evidence of orientationally-disordered C_2 units. The data were refined [10b] using different models for the distribution of the carbon atoms. For the assumption of a perfect structure these converged after absorption corrections to $R_p = 3.98$, $R_{wp} = 4.56$ and $R_{Bragg} = 23.9$. The last value (R_{Bragg}) and the extremely large isotropic thermal parameter for the carbon atoms [10.0(1) Å^2 compared with 4.1(2) Å^2 for Ba] indicate that this model does not fit (even on applying anisotropic temperature factors), obviously as a result of the orientationally-disordered C_2 units. Unfortunately, no reliable value can be quoted for $d_{C\equiv C}$ (span from 1.1 to 1.5 Å) so we can only solve this problem with the help of a neutron diffraction experiment. b) D. B. Wiles, R. A. Young, *J. Appl. Crystallogr. 14* (1981) 149.
[11] a) For a review cf. [11b], and for cyanides as example cf. [11c–e]; b) N. G. Parsonage, L. A. K. Stavely: *Disorder in Crystals*, Clarendon Press, Oxford 1978, S. 926; c) D. L. Price, J. M. Rowe, J. J. Rush, E. Prince, D. G. Hinks, S. Susman, *J. Chem. Phys. 56* (1972) 3697; d) J. M. Rowe, D. G.

Hinks, D. L. Price, S. Susman, J. J. Rush, *ibid. 58* (1973) 2039; e) K.-D. Ehrhardt, W. Press, G. Heger, *Acta Crystallogr. Sect. B39* (1983) 171.
[12] a) The influence of the cation of the C–C bond of the $C_2^{2\ominus}$ ion is also manifested in the different vibration frequencies of the C≡C stretching vibration (from Raman spectra): $\tilde{\nu} = 1847\,cm^{-1}$ (SrC_2 [12b]) and $1831\,cm^{-1}$ (BaC_2 [1b]); b) P. Pykkö (Helsinki), private communication.
[13] R. M. Dickson, M. S. McKinnon, J. F. Britten, R. E. Wasylishen, *Can. J. Chem. 65* (1987) 941.
[14] a) H.-O. Kalinowski, S. Berger, S. Braun: *^{13}C-NMR-Spektroskopie*, Thieme, Stuttgart 1984; b) B. Wrackmeyer, K. Horchler, *Prog. Nucl. Mag. Reson. Spectrosc.*, in press.
[15] a) Examples for bonding pairs in this $\delta^{13}C/\delta^{15}N$ correlation: $C\equiv N^{\ominus}$/$N\equiv N$; Bu-$C\equiv C^{\ominus}$/Bu-$C\equiv N$; H-$C\equiv C$-H/H-$C\equiv N$-$H^{\oplus}$; Me-$C\equiv C$-H/Me-$C\equiv N$-$H^{\oplus}$; $C\equiv O/NO^{\oplus}$; $CO_2NO_2^{\oplus}$; $N=C=O^{\ominus}/N=N=O$; Ph-$C\equiv N$/Ph-$N\equiv N^{\oplus}$; Ph-N$\equiv C$/Ph-N$\equiv N^{\oplus}$. $\delta^{13}C$ values from Ref. [14a, 15b, c], and references cited therein; $\delta^{15}N$ values from Ref. [15d, e, 17]; b) $\delta^{13}C$, $\delta^{15}N$ for $C\equiv N^{\ominus}$: R. E. Wasylishen, *Can. J. Chem. 60* (1982) 2194; c) $\delta^{13}C$ for Bu-$C\equiv C^{\ominus}$: D. Seebach, R. Hässig, J. Gabriel, *Helv. Chim. Acta 66* (1983) 308; d) M. Witanowski, L. Stefaniak, G. A. Webb, *Annu. Rep. NMR Spectrosc. 18* (1986) 1; e) G. J. Martin, M. L. Martin, J. P. Gouesnard, *NMR Basic Princ. Prog. 18* (1981) 1.
[16] A. J. Beeler, A. M. Orendt, D. M. Grant, P. W. Cutts, J. Michl, K. W. Zilm, J. W. Downing, J. C. Facelli, M. S. Schindler, W. Kutzelnigg, *J. Am. Chem. Soc. 106* (1984) 7672.
[17] J. Mason in J. Mason (Ed.): *Multinuclear NMR*, Plenum, London 1987, S. 338.

Semisynthetic Rhodomycins: Novel Glycosylation Methods for the Synthesis of Anthracycline Oligosaccharides

By *Cenek Kolar** and *Günther Kneissl*

β-Rhodomycinone A **1**[1] as well as other microbial anthracyclines of the aclacinomycin-type contain one or two oligosaccharide chains consisting of α(1 → 4)-linked oligodeoxy sugars.[1,2] The most frequently occurring partial sequences are 2-deoxy-α-L-fucosyl-(1 → 4)-L-rhodosamine, contained in **1**, and α-L-rhodosaminyl-(1 → 4)-L-rhodosamine.

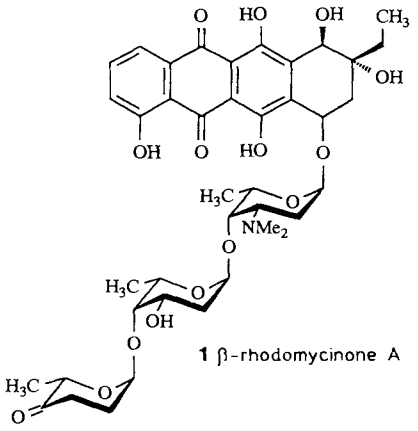

1 β-rhodomycinone A

The synthesis of these disaccharides is difficult, since only a poorly reactive axial 4-hydroxy group of a daunosamine moiety must be glycosylated.[3,4] The established procedures such as the Koenigs-Knorr method[5] or the *N*-iodosuccinimide (NIS) glycosylation technique[6] have proven unsuitable for this purpose. The recently introduced $(Bu_3Sn)_2O$/NIS method indeed affords α(1 → 4)-disaccharides in good yields (74–82%), but the iodine on C-2′ of the product must then be removed in a reductive step.[7]

We have now found that the 1-*O*-*t*$BuMe_2Si$-2,6-dideoxy-β-*lyxo*-hexopyranoses[8a] **4** and **12** as well as the 3-trifluoroacetylamino-*lyxo*- and 3-trifluoroacetylamino-*arabino*-glycals **14** and **15**, respectively, are suitable as glycosyl donors for the preparation of anthracycline oligosaccharides. In the case of the glycosyloxysilanes, so far only the 1-*O*-trimethylsilylated derivatives have been used [9–11] in combination with trimethylsilyl triflate (TMSOTf) or other catalysts, in particular for the synthesis of acetal-glycosides.[8b] In the case of the glycals **14** and **15**, reactions with anthracyclinones in the presence of *p*-toluenesulfonic acid as promoter have thus far been described.[12,13]

For the preparation of the 2-deoxy-L-fucosyl donor **4**, fucal **2**[14] was converted by hydrolysis[14] (30% CF_3COOH) into the diacetate **3**, which, in turn can be converted selectively with *t*$BuMe_2SiCl$/imidazole in 1,2-dichloromethane into the β-L-anomer **4** ($[\alpha]_D^{24} = 17.2°$ ($c = 1.02$, $CHCl_3$): 200-MHz ^{1}H-NMR (C_6D_6, TMS): $\delta = 5.08$ (4-H), 4.74 (3-H), 4.41 (1-H). Under standard conditions (DMF as medium)[15] the silylation furnishes a mixture of both α- and β-anomers (α:β = 1:4).

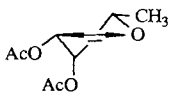

2

3

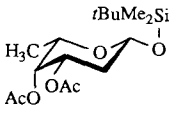

4

The 3-azido-*arabino*-hexopyranose **5**,[16] which is readily accessible from L-rhamnal and must be epimerized in the 4-position,[17] was chosen as starting compound for the synthesis of the daunosaminyl donor **12**. For the regioselective silylation, **5**, like **3**, was allowed to react with *t*$BuMe_2SiCl$/imidazole in CH_2Cl_2. The β-anomer **6** ($[\alpha]_D^{24} = +2°$ ($c = 1.0$, $CHCl_3$)) obtained in 92% yield was deacetylated under Zemplén conditions to **7**, which was converted under previously tested conditions[17] (trifluoromethanesulfonic anhydride, pyridine/dichloromethane at −30 °C) into the triflate **8**. Epimerization[18] of the *arabino*-compound **8** with a mixture of cesium and sodium acetates adjusted to pH 8 afforded the *lyxo*-acetate **9** in 72% yield ($[\alpha]_D^{24} = +5.6°$ ($c = 1.0$, $CHCl_3$)). After deacetylation of **9** to **10**, the azido group in **10** was reduced (10% Pd/C, ammonia/ethanol, pH 9), and the resulting amino group converted into a trifluoroacetamido group. Introduction of the acetyl group into **11** finally furnished the glycosyl donor **12**[19] ($[\alpha]_D^{24} = -24.4°$ ($c = 1.0$, $CHCl_3$); 200-MHz ^{1}H-NMR ($CDCl_3$ TMS): $\delta = 6.44$ (NH), 5.02 (4-H), 4.84 (1-H).

To check the linkability of the glycosyl donors **4** and **12** we chose the benzyldaunosaminide **13**[4] as glycosyl acceptor

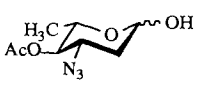

5

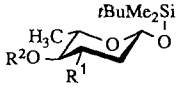

6 R^1=N_3 R^2=Ac
7 R^1=N_3 R^2=H
8 R^1=N_3 R^2=SO_2CF_3

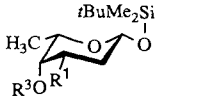

9 R^1=N_3 R^3=Ac
10 R^1=N_3 R^3=H
11 R^1=$NHCOCF_3$ R^3=H
12 R^1=$NHCOCF_3$ R^3=Ac

[*] Dr. C. Kolar, G. Kneissl
Behringwerke AG
Postfach 1140, D-3550 Marburg (FRG)

and TMSOTf as promotor,[20, 21] and employed equimolar amounts of the glycosylation components.[22] In the presence of 0.3 equivalents of TMSOTf and 4 Å molecular sieve (CH_2Cl_2), **4** reacts at $-50\,^{\circ}C$ with **13** to give the disaccharide **16**[4] ($[\alpha]_D^{24} = -170^{\circ}$ ($c = 1.0$, $CHCl_3$); 400-MHz ^{1}H-NMR ($CDCl_3$, TMS): $\delta = 7.99$ (N-H), 5.26 (3′-H), 5.14 (4′-H), 4.91 (1-H, 1′-H)) in 73% yield. With an excess of the promoter (0.6 equiv) the terminal glycoside bond in **16** is attacked, leading to formation of the benzylglycoside **18** (ca. 8%)[23a] and the trisaccharide **20** (ca. 5%).[24a] **12** reacts in the same way (0.4 equiv. TMSOTf) with 13 to give the disaccharide **17** in 75% yield ($[\alpha_D^{24} = 127.9^{\circ}$ ($c = 0.99$, $CHCl_3$); 200-MHz ^{1}H-NMR ($CDCl_3$, TMS): $\delta = 8.02$ (3-NH), 6.58 (3′-NH), 5.15 (4′-H), 5.05 (1-H, 1′H), 3.55 (4-H); with an excess of the promoter, the mono- and the trisaccharide **19**[23b] and **21**,[24b] respectively, are then formed besides **17**.

The 3-trifluoroacetylamino-*lyxo*- and 3-trifluoroacetylamino-*arabino*-glycals **14**[12] and **15**[13] were also used for the glycosylation of **13** (pNO_2Bz = *para*-nitrobenzoyl), but TMSOTf was used instead of *p*-toluenesulfonic acid as promoter. In the presence of TMSOTf and 4 Å molecular sieve (CH_2Cl_2) **13** reacts with **14** or **15** at $-40\,^{\circ}C$ to give the disaccharides **22**[25a] and **23**,[25b] respectively, in 60–70% yield, and, as in the reaction of **12** with **13**, the benzylglycosides **24**[23c, 26] and **25**[23d] and the trisaccharides **26**[24c]

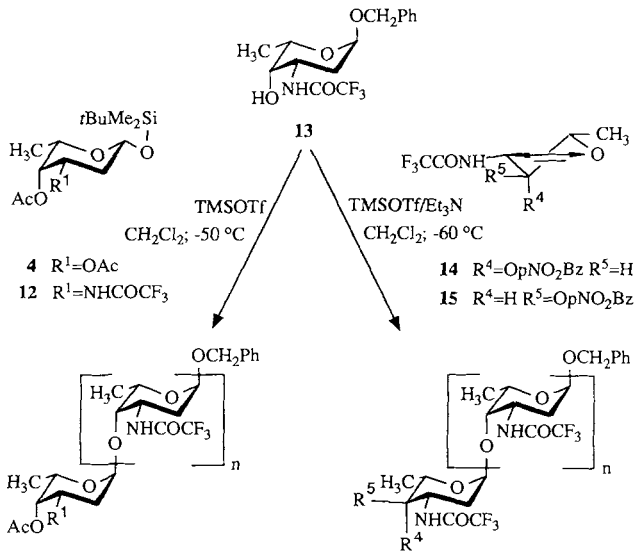

and **27**,[24d] respectively, are also formed. When, however, the glycoside syntheses are carried out in the presence of TMSOTf/triethylamine (5:1) at $-60\,^{\circ}C$ the glycals are activated by the triethylammonium triflate formed in situ, and the disaccharides **22** and **23**, respectively, are formed in over 90% yield.[27] The mono- and trisaccharides are formed in only trace amounts.

The route via the disaccharide **28**, which is obtained after cleavage (0.1M, NaOH) of the acyl groups in **17** or **22**, is more suitable for the preparation of the trisaccharides, even though transglycosylations also occur. The glycosylation of **28** with **4**, **12**, **14** or **15** under the above-mentioned conditions affords the trisaccharides **20**, **21**, **26** and **27**, respectively, in 40–65% yield.

As these glycoside syntheses demonstrate, the β-glycosyloxysilanes as well as the 3-trifluoroacetylaminoglycals are very reactive readily linkable glycosyl donors. Since α-*O*-glycosidally-linked 2-deoxy sugars are present as building blocks in natural products of microbial and plant origin these glycosylation techniques can contribute immensely to their preparation. The β-glycosyloxysilanes could find wide application in glycoside syntheses.

Received: February 26, 1990 [Z 3816 IE]
German version: *Angew. Chem. 102* (1990) 827

[1] T. Oki in H. S. El Khadem (Ed.): *Anthracycline Antibiotics*, Academic Press, New York 1982, S. 75.
[2] F. Arcamone: *Doxorubicin*, Academic Press, New York 1981, p. 243.
[3] H. S. El Khadem, D. Matsuura, *Carbohydr. Res. 88* (1981) 332.
[4] H. S. El Khadem, D. Matsuura, *Carbohydr. Res. 101* (1982) C1–C4; for **16** $[\alpha]_D = -209^{\circ}$ ($CHCl_3$) has been quoted, ^{1}H-NMR data are lacking.
[5] A. Martin, M. Pais, C. Monneret, *J. Chem. Soc. Chem. Commun. 1983*, 306; *Tetrahedron Lett. 27* (1986) 575.
[6] J. Thiem, H. Karl, J. Schwentner, *Synthesis 1978*, 696.
[7] J. Thiem, W. Klaffke, *J. Org. Chem. 54* (1989) 2006.
[8] With regard to the glycosylation, the *tert*-butyldimethylsiloxy group in these glycosyloxysilanes is a leaving group. b) L. F. Tietze, R. Fischer, H. J. Guder, A. Goerlich, M. Neumann, T. Krach, *Carbohydr. Res. 164* (1987) 177. As reported therein, a carbenium ion attacks the anomeric oxygen of the glycosyloxytrimethylsilane, leading to cleavage of the bond between the oxygen and trimethylsilyl group upon reaction with triflate.
[9] A. Klemer, E. Buhe, *Tetrahedron. Lett. 1969*, 1689; A. Klemer, E. Buhe, R. Kutz, S. Chahin, L. Kleefeld, *Justus Liebigs Ann. Chem. 739* (1970) 185.
[10] L.-F. Tietze, R. Fischer, *Tetrahedron Lett. 22* (1981) 3239; L.-F. Tietze, R. Fischer, H.-J. Guder, *ibid. 23* (1982) 4661; L.-F. Tietze, A. Goerlach, M. Beller, *Liebigs Ann. Chem. 1988*, 565.
[11] J. Yoshimura, K. Hara, T. Sato, H. Hashimoto, *Chem. Lett. 1983*, 319.
[12] H. Umezawa, Y. Takahashi, M. Kinoshita, H. Naganawa, K. Tatsuta, T. Takeuchi, *J. Antibiot. 33* (1980) 1581.
[13] J. Boivin, M. Pais, C. Monneret, *Carbohydr. Res. 79* (1980) 193.
[14] B. Iserlin, T. Reichstein, *Helv. Chim. Acta 27* (1944) 1200.
[15] B. Kraska, A. Klemer, H. Hagedorn, *Carbohydr. Res. 36* (1974) 389.
[16] J.-C. Florent, C. Monneret, *J. Chem. Soc. Chem. Commun. 1987*, 1171.
[17] a) J. P. Marsch, C. W. Moser, E. M. Acton, L. Goodman, *Chem. Commun. 1967*, 973; b) R. W. Binkley: *Modern Carbohydrate Chemistry*, Marcel Dekker, New York 1988, p. 181.
[18] J. Thiem, D. Springer, *Carbohydr. Res. 136* (1985) 325.
[19] The 4-epimeric *arabino*-donor can be prepared from **5** in the same way as **12** from **9**; C. Kolar, unpublished.
[20] a) H. Vorbrüggen, K. Krolikiewicz, B. Blunuf, *Chem. Ber. 114* (1981) 1234; b) Y. Kimura, M. Suzuki, T. Matsumoto, R. Abe, S. Terashima, *Chem. Lett. 1984*, 501.
[21] C. Kolar, K. Dehmel, U. Knödler, M. Paal, P. Hermentin, M. Gerken, *J. Carbohydr. Chem. 8* (1989) 295.
[22] General procedure: A mixture of **13** (0.75 g, 2.25 mmol), glycosyloxysilane (2.25 mmol), 3.5 g of molecular sieve 4 Å and 100 mL of CH_2Cl_2 was treated at $-50\,^{\circ}C$ under N_2 with 0.3 equiv. TMSOTf. After seven hours' stirring at $-50\,^{\circ}C$ a further 0.1 equiv TMSOTf was added if necessary, and the mixture was stirred for a further 6 h, then treated at $-50\,^{\circ}C$ with 0.75 mL of Et_3N and 100 mL of CH_2Cl_2, and finally filtered. The filtrate was washed with 0.1M citrate buffer (adjusted to pH 5 with NaOH) and then with water, dried (Na_2SO_4), and evaporated to dryness in vacuo. Column chromatographic separation of the residue (200 g silica gel; eluent: petroleum ether/CH_2Cl_2/acetone 8:5:1) furnished an α(1 → 4)-linked disaccharide. The course of the glycoside syntheses can be controlled by the addition of a polar solvent (acetone, THF). The reactions conducted in CH_2Cl_2/acetone (20:1) proceed slower, but require increased concentration of the promotor.
[23] Benzyl glycosides: a) **18** syrup; $[\alpha]_D^{24}$ -123° ($c = 1.05$, $CHCl_3$); b) **19**: m.p. 152°C, $[\alpha]_D^{24} = -147.1^{\circ}$ ($c = 1.0$, $CHCl_3$)), Ref. [4]: $[\alpha]_D = -179^{\circ}$ ($CHCl_3$); c) **24**: m.p. 80–82°C, $[\alpha]_D^{24} = -142^{\circ}$ ($c = 1.0$, $CHCl_3$), Ref. [22]: $[\alpha]_D = -137^{\circ}$ ($c = 0.6$, $CHCl_3$); d) **25**: m.p. 145–146°C, $[\alpha]_D^{24} = -89^{\circ}$ ($c = 1.01$, $CHCl_3$).

[24] Trisaccharides: a) **20** $[\alpha]_D^{24} = -181°$ ($c = 0.28$, $CHCl_3$); b) **21**: $[\alpha]_D^{24} = -190°$ ($c = 0.1$, $CHCl_3$); c) **26**: $[\alpha]_D^{24} = -149.2°$ ($c = 1.02$, $CHCl_3$), FAB-MS: m/z 939 ($M + Li^{\oplus}$), 825 ($M - OCH_2Ph$), 600 [$M - (N$-TFAc-Dau-$OCH_2Ph)$], 375 [$M - \{(N$-TFAc-Dau$)_2$-$OCH_2Ph\}$], (N-TFAc-Dau = N-trifluoroacetyl-L-daunosaminyl); 400-MHz ^1H NMR ($CDCl_3$, TMS): $\delta = 5.52$ (4″-H), 5.15 (1-H), 4.98 (1′-H, 1″); d) **27**: $[\alpha]_D^{24} = -143°$ ($c = 0.1$, $CHCl_3$).

[25] a) **22**: $[\alpha]_D^{24} = -157°$ ($c = 1.03$, $CHCl_3$), 400-MHz ^1H NMR ($CDCl_3$, TMS): $\delta = 7.85$ (3-NH), 6.67 (3′-NH), 5.41 (4′-H), 5.05 (1′-H), 4.95 (1-H); b) **23**: $[\alpha]_D^{24} = -130°$ ($c = 0.96$, $CHCl_3$), 400-MHz ^1H NMR ($CDCl_3$, TMS): $\delta = 7.71$ (3-NH), 6.68 (3′-NH), 4.98 (1′-H), 4.93 (1-H), 4.84 (4′-H).

[26] H. S. El Khadem, A. Liav, *Carbohydr. Res. 74* (1979) 345.

[27] General procedure: A mixture of **13** (0.75 g, 2.25 mmol), glycal (2.25 mmol), 3.5 g of molecular sieve 4 Å and 100 mL CH_2Cl_2 was treated at -60 °C under N_2, firstly with triethylamine (0.18 mmol, 0.024 mL) and then with TMSOTf (0.67 mmol, 0.12 mL). After 1.5 hours' stirring at -60 °C the mixture was treated with 0.75 mL of Et_3N and 100 mL of CH_2Cl_2 and worked up as described above.

μ-Hydroxobis(μ-formato)hexaaquadichromium(III), an Intermediate in the Formation of Basic Chromium Carboxylates**

By *Petra N. Turowski, Avi Bino*, and *Stephen J. Lippard**

A century ago, violet compounds, variously formulated as $[Cr_3(O_2CR)_5(OH)_2](OH)_2 \cdot 2H_2O$ and $[Cr_2(OH)_3(O_2CR)_3]$, were obtained during formation of the now classical dark green basic chromium carboxylates, $[Cr_3O(O_2CR)_6L_3]^{\oplus}$ **1**. We here report the identification of this elusive violet species, isolated and structurally characterized as the formate derivative [μ-hydroxobis(μ-formato)hexaaquadichromium(III)], **1**. Its preparation and reaction to form basic chromium for-

$$Cr_2(OH)(O_2CH)_2(H_2O)_6]^{3\oplus} \quad \mathbf{1}$$

mate closely parallel results obtained for the violet complexes observed by *Weinland* and others.[1d, e]

1 was isolated, after reduction of chromium(VI) oxide in formic acid or reaction of Cr^{III} salts in aqueous formic acid at 50 °C, in the form of the salt **1**, $[p\text{-}CH_3C_6H_4SO_3]_3 \cdot 2H_2O$.[2] The complex consists of two octahedrally coordinated chromium atoms bridged by an hydroxo ligand and two bidentate formato ligands (Fig. 1). The remaining, terminal coordination sites are occupied solely by aqua ligands, a unique feature in complexes of this class. The structural parameters of the bridging unit of **1** are compared with those of selected hydroxo-bridged species in Table 1. Note that the Cr–OH distances in **1** (1.920 Å) are rather short. The core geometry is very similar to that of an analogous diiron(III) complex, $[Fe_2(OH)(O_2CCH_3)_2(HBpz_3)_2](ClO_4)$,[3] and it is intermediate between the structures of more nearly linear $\{Cr_2(OH)\}^{5\oplus}$ complexes and those of di- and trihydroxo-bridged dichromium(III) species.[4] The complex is extensively hydrogen-bonded in the crystal, mostly to the *p*-toluenesulfonate ions. The bridging ligands provide a pathway for antiferromagnetic

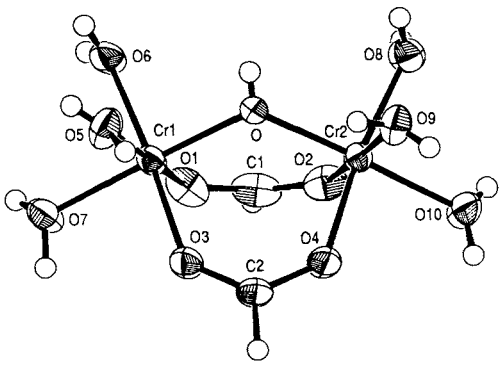

Fig. 1. Structure of **1** in the crystal (ORTEP, showing 50% probability thermal ellipsoids and atom labeling schemes for non-hydrogen atoms of the cation. Hydrogen atoms are included as arbitrary isotropic spheres). Selected interatomic distances [Å] and angles [°]: Cr1-O, 1.923(3); Cr1-O1, 1.957(4); Cr1-O3, 1.956(3); Cr1-O5, 1.983(4); Cr1-O6, 1.965(4); Cr1-O7, 2.008(4); Cr2-O, 1.916(4); Cr2-O2, 1.963(3); Cr2-O4, 1.958(3); Cr2-O8, 1.983(4); Cr2-O9, 1.974(4); Cr2-O10, 1.983(5); Cr1···Cr2, 3.381(1); Cr1-O-Cr2, 123.4(2); O-Cr1-O1, 91.6(2); O-Cr1-O3, 91.9(1); O1-Cr1-O3, 94.1(2); O-Cr2-O2, 92.4(2); O-Cr2-O4, 92.4(1); O2-Cr2-O4, 93.8(2).

exchange coupling between the Cr^{III} centers in **1** ($J = -11.2(2)$ cm^{-1}).[5] The metal atoms in the other complexes listed in Table 1 are also antiferromagnetically coupled to one another, as indicated.[3, 4]

Table 1. Comparison of structural and magnetic features of hydroxo-bridged dichromium(III) and diiron(III) complexes.

Compound	M-OH [Å]	M···M [Å]	M-OH-M [°]	$-J$ [cm^{-1}]
1 $[p\text{-}CH_3C_6H_4SO_3]_3 \cdot 2H_2O$	1.920(4)	3.381(1)	123.4(2)	11.2(2)
$[Fe_2(OH)(O_2CCH_3)_2(HBpz_3)_2](ClO_4)$ [3]	1.956(4)	3.439(1)	123.1(2)	17(1)
$[Cr_2(OH)(NH_3)_{10}]Cl_5 \cdot H_2O$ [4]	1.97	3.852(9)	165.6(9)	16
Δ,Λ-$[Cr_2(OH)(en)_2(OH)_2](ClO_4)_3$ [4]	1.99	3.677(2)	135.4(2)	–
$[Cr_2(OH)_2(NH_3)_8](S_2O_6)_2$ [4]	1.97	3.045(1)	101.5	14
$\Delta,\Delta/\Lambda,\Lambda$-$[Cr_2(OH)_2(phen)_4]I_4$ [4]	1.92	2.986(4)	102.1(3)	6.5
$[Cr_2(OH)_3(metacn)_2]I_3$ [4a, c]	1.97	2.642(2)	84.1(3)	64

We noticed in the preparation of **1** that, if the temperature of the exothermic reaction exceeds 50 °C, a green material gradually forms. The product was characterized by visible spectroscopy as the basic chromium formate, $[Cr_3O(O_2CH)_6(H_2O)_3]^{\oplus}$. This result suggested that **1** and its analogues might be intermediates in the formation of basic chromium carboxylates. This hypothesis was confirmed by heating a solution of pale green "$CrCl_3 \cdot 6H_2O$" in formic acid and water to 70 °C and monitoring its visible spectrum. Formation of the blue dichromium(III) complex **1** was observed in the first 20 min, after which the characteristic dark green color of basic chromium formate appeared over a period of 5 h. The spectral changes observed after 30 min were identical to those of **1** in aqueous formic acid at 70 °C. A similar series of reactions was observed upon heating chromium (III) chloride in aqueous acetic acid. The conversion of the dinuclear into the trinuclear complex could be reversed by adding water and driving off carboxylic acid from the basic chromium carboxylate.

These studies have thus provided structural characterization of a new kind of dichromium(III) complex which contains one hydroxide and two formate bridging ligands. Previously, structures of oxo- or hydroxo-bridged compounds

[*] Prof. Dr. S. J. Lippard, P. N. Turowski, Prof. Dr. A. Bino[+]
Department of Chemistry, Massachusetts Institute of Technology
Cambridge, MA 02139 (USA)

[+] Permanent address: Department of Inorganic and Analytical Chemistry
The Hebrew University of Jerusalem

[**] This work was supported by Grants from the National Institute of General Medical Sciences and the National Science Foundation. *A. B.* was on sabbatical leave from the Hebrew University of Jerusalem. *P. N. T.* was supported under Training Grant CA-09112 from the National Cancer Institute.

containing two additional carboxylate bridges were obtained for transition metal systems such as Fe_2^{III}, Fe_2^{II}, Mn_2^{III}, Mn_2^{II}, V_2^{III}, Os_2^{IV}, and Ru_2^{III},[3, 6] but not for Cr_2^{III}, although many other types of dichromium(III) complexes are known.[4] Such carboxylate-bridged units with iron and with manganese are important in biology, in proteins such as hemerythrin and manganese catalases.[6a, b, 7] Recently, *Wieghardt* et al. reported the synthesis of the red complex, $[Cr_2(OH)(O_2CCH_3)_2(metacn)_2](ClO_4)_3$,[4c] which, although not structurally characterized, most likely has the same μ-hydroxobis(μ-acetato)dichromium(III) core as **1**.[8] Significantly, we have demonstrated that **1** is an intermediate in reactions leading to the well-known basic chromium formate. It is possible that similar complexes of other transition metals are also intermediates in the formation of their trinuclear basic carboxylates. Mechanistic studies are in progress.

Received: January 25, 1990 [Z 3758 IE]
German version: *Angew. Chem. 102* (1990) 841

[1] a) M. P. Schützenberger, *Bull. Soc. Chim. Fr. 4* (1965) 86; b) C. Haeussermann, *J. Prakt. Chem. 50* (1984) 383; c) A. Werner, *Ber. Dtsch. Chem. Ges. 41* (1908) 3447; d) R. F. Weinland, K. Höhn, *Z. Anorg. Allg. Chem. 69* (1910) 158; e) E. Gussmann, *ibid. 69* (1910) 217; f) B. N. Figgis, G. B. Robertson, *Nature (London) 205* (1965) 694; g) R. D. Cannon, R. P. White, *Prog. Inorg. Chem. 36* (1988) 195.

[2] Experimental procedure for **1**: A solution of 0.60 g (10.0 mmol) of chromium(VI) oxide in 5 mL of water was added dropwise to 50 mL of formic acid (88%). The resulting blue solution was diluted with 50 mL of water and adsorbed on a 1.5 × 7 cm column of Dowex 50X2-200 cation exchange resin. After washing the column with water, the blue ion was removed with 0.5 M aqueous *p*-toluenesulfonic acid solution. Upon slow evaporation, violet crystals of **1** $[p\text{-}CH_3C_6H_4SO_3]_3 \cdot 2H_2O$ were obtained, which were separated from solid *p*-toluenesulfonic acid by extensively washing with acetone. These crystals (0.53 g, 20%) were suitable for X-ray diffraction studies. Correct elemental analysis (C,H,S). ^1H NMR (300 MHz, CD_3OD): $\delta = 7.7$ (br, 6H), 7.24 (s, 6H), 4.88 (s, 17H + HOD), 2.36 (s, 6H); FT-IR (KBr): $\tilde{\nu}[cm^{-1}] = 3337, 3141, 2471, 1604, 1497, 1457, 1409, 1390, 1376, 1214, 1203, 1155, 1127, 1036, 1011, 813, 761, 729, 718, 686, 619, 565$; UV/VIS ($H_2O$): $\lambda[nm] = 254(\varepsilon = 1180\ mol^{-1}\ cm^{-1}/Cr)$, 410(44), 572(46), 632(sh); magnetic susceptibility: $\mu_{eff}/Cr = 3.54$ (290 K, solid state), 3.5 μ_B (293 K, CD_3OD solution); crystal data at 295 K: monoclinic, space group $C2/c$ (No. 15), $a = 15.920(3)$ Å, $b = 17.381(3)$ Å, $c = 26.517(4)$ Å, $\beta = 91.77(1)°$, $V = 7334(4)$ Å^3, $M_r = 868.73\ g\ mol^{-1}$, $\varrho_{obsd} = 1.57(1)\ g\ cm^{-3}$, $\varrho_{calcd} = 1.573\ g\ cm^{-3}$, $Z = 8$. For 4552 unique, observed reflections with $F^2 > 3\sigma(F^2)$ and 526 variable parameters, the current discrepancy indices are $R = 0.051$ and $R_w = 0.067$. Further details of the crystal structure determination may be obtained from the Fachinformationszentrum Karlsruhe Gesellschaft für Wissenschaftlich-technische Information mbH, D 7514 Eggenstein-Leopoldshafen 2 (FRG), by quoting the depository number CSD-54568, the names of the authors, and the journal citation.

[3] W. H. Armstrong, S. J. Lippard, *J. Am. Chem. Soc. 106* (1984) 4632; pz = pyrazolyl.

[4] a) J. Springborg, *Adv. Inorg. Chem. Radiochem. 32* (1988) 55; b) D. J. Hodgson, *Prog. Inorg. Chem. 19* (1975) 173; c) en = 1,2-diaminoethane, phen = 1,10-phenanthroline, metacn = 1,4,7-trimethyl-1,4,7-triazacyclononane.

[5] Determined by fit of solid-state SQUID susceptometry from 6-300 K to the theoretical expression for $\boldsymbol{H} = -2JS_1 \cdot S_2$ with $S_1 = S_2 = 3/2$, $g = 1.978(1)$, $p = 1.03(1)\%$; see a) C. J. O'Connor, *Prog. Inorg. Chem. 29* (1982) 203; b) J. R. Hartman, R. L. Rardin, P. Chaudhuri, K. Pohl, K. Wieghardt, B. Nuber, J. Weiss, G. C. Papaefthymiou, R. B. Frankel, S. J. Lippard, *J. Am. Chem. Soc. 109* (1987) 7387.

[6] a) L. Que, Jr., R. C. Scarrow, *A.C.S. Symp. Ser. 372.* (1988) *152*; b) K. Wieghardt, *Angew. Chem. 101* (1989) 1179; *Angew. Chem. Int. Ed. Engl. 28* (1989) 1153; c) K. Wieghardt, M. Köppen, B. Nuber, J. Weiss, *J. Chem. Soc. Chem. Commun. 1986*, 1530; d) J. E. Armstrong, W. R. Robinson, R. A. Walton, *Inorg. Chem. 22* (1983) 1301; e) Y. Sasaki, M. Suzuki, A. Tokiwa, M. Ebihara, T. Yamaguchi, C. Kabuto, T. Ito, *J. Am. Chem. Soc. 110* (1988) 6251.

[7] a) S. J. Lippard, *Angew. Chem. 100* (1988) 353; *Angew. Chem. Int. Ed. Engl. 27* (1988) 344; b) J. Sanders-Loehr in T. M. Loehr (Ed.): *Iron Carriers and Iron Proteins*, VCH Publishers, New York 1989, p. 373.

[8] P. Chaudhuri, M. Winter, H.-J. Küppers, K. Wieghardt, B. Nuber, J. Weiss, *Inorg. Chem. 26* (1987) 3302.

Synthesis and Characterization of the Linear Trinuclear Complexes $[M_3^{II}(O_2CCH_3)_6(biphme)_2]$, M = Mn, Fe**

By *R. Lynn Rardin, Avi Bino, Peter Poganiuch, William B. Tolman, Shuncheng Liu,* and *Stephen J. Lippard**

Recent interest in polynuclear complexes of iron and manganese with oxygen donor and nitrogen donor ligands has been motivated by the occurrence of a growing class of metalloproteins known or believed to contain such polymetallic units as their functional cores.[1-3] The hydrolytic polymerization of iron or manganese in the presence of carboxylate and varying amounts of nitrogen donor ligands has led to the formation of dinuclear, trinuclear and higher nuclearity complexes.[1, 2, 4] Some of these species accurately mimic the spectroscopic and physical properties of the metal centers in hemerythrin, ribonucleotide reductases[1, 2] or the oxygen evolving complex of Photosystem II.[2, 4b] Our recent studies in this area have focused on complexes of first row transition metals with biomimetic carboxylate and imidazole containing ligands.[5-7] Here we report the synthesis and characterization of the divalent linear, trinuclear complexes

$[M_3^{II}(O_2CCH_3)_6(biphme)_2]$ **1**: M = Mn; **2**: M = Fe

biphme = 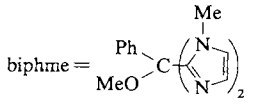

1 and **2**, the central structural unit of which is a striking departure from the triangular $\{M_3O(O_2CR)_6\}$ core that has dominated the chemistry of trivalent manganese and iron carboxylates for decades.[8]

Compounds **1** and **2** were synthesized by reaction of $M(O_2CCH_3)_2 \cdot x\ H_2O$ (M = Mn, x = 4 for **1**; M = Fe, x = 0 for **2**) with biphme in methanol.[9-11] Two geometric isomers of **1** have been structurally characterized, which we designate as *syn*-**1** and *anti*-**1**[9, 10] depending on the disposition of biphme imidazole groups with respect to the best plane passing through the three metal atoms and two monodentate oxygen atom bridges (Fig. 1). Only the *anti* isomer of **2** has been structurally characterized to date.[11]

Complexes **1** and **2** are comprised of a linear array of three M^{II} ions in which a central, hexacoordinate metal, that resides on a crystallographic inversion center in the *anti* isomers, is flanked by two metal ions that are essentially pentacoordinate. The metals are bridged by four bidentate and two relatively rare monodentate μ-acetato ligands.[12-14] Bidentate biphme ligands cap the $\{M_3(O_2CCH_3)_6\}$ core. The

[*] Prof. Dr. S. J. Lippard, Prof. Dr. A. Bino,[+] R. L. Rardin, Dr. P. Poganiuch, Dr. W. B. Tolman, Dr. S. Liu
Department of Chemistry, Massachusetts Institute of Technology
Cambridge, MA 02139 (USA).

[+] Permanent Address: Department of Inorganic and Analytical Chemistry The Hebrew University of Jerusalem.

[**] This work was supported by grants from the U. S. National Institute of General Medical Sciences and the National Science Foundation (NSF). *R. L. R.* is grateful to the NIH for support under Training Grant CA-09112, *P. P.* to the Deutscher Akademischer Austauschdienst for a NATO Science Fellowship and *W. B. T.* to the American Cancer Society for a postdoctoral fellowship. *A. B.* was on sabbatical leave from the Hebrew University of Jerusalem, Israel. We thank Dr. *G. C. Papaefthymiou* for assistance in obtaining Mössbauer data at the Francis Bitter National Magnet Laboratory, which is supported by the NSF. biphme = methoxybis(1-methylimidazol-2-yl)phenylmethane.

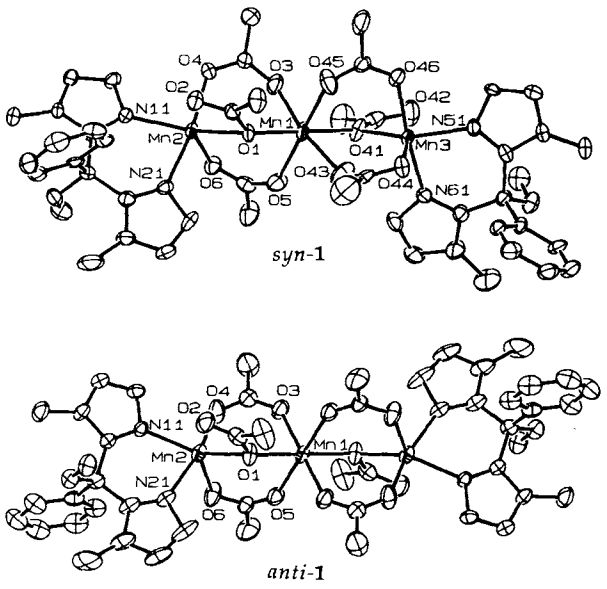

Fig. 1. Structure of *syn*-**1** (top) and *anti*-**1** (bottom) in the crystal. ORTEP drawings showing 50% probability thermal ellipsoids. Selected interatomic distances [Å] and angles [°]: *syn*-**1**: Mn1-O1, 2.181 (6); Mn1-O3, 2.151 (7); Mn1-O5, 2.144 (6); Mn1-O41, 2.200 (6); Mn1-O43, 2.183 (7); Mn1-O45, 2.143 (7); Mn2-O1, 2.242 (6); Mn2-O4, 2.141 (6); Mn2-O6, 2.120 (6); Mn2-N11, 2.210 (7); Mn2-N21, 2.208 (7); Mn2···O2, 2.370 (6); Mn3-O41, 2.138 (6); Mn3-O46, 2.127 (6); Mn3-O44, 2.228 (7); Mn3-N51, 2.155 (7); Mn3-N61, 2.202 (7); Mn3···O42, 2.790 (7); Mn1···Mn2, 3.560 (3); Mn1···Mn3, 3.370 (3); Mn1-O1-Mn2, 107.2 (2); Mn1-O41-Mn3, 101.9 (3); O1-Mn1-O3, 91.9 (2); O1-Mn1-O5, 88.5 (2); O41-Mn1-O43, 80.9 (3); O41-Mn1-O45, 90.2 (2); O1-Mn2-O4, 92.8 (2); O1-Mn2-N11, 149.3 (2); O4-Mn2-N21, 171.5 (2); O41-Mn3-O46, 91.8 (2); O41-Mn3-N51, 133.8 (3); O46-Mn3-N61, 173.1 (3); Mn2-Mn1-Mn3, 176.63 (5). *anti*-**1**: Mn1-O1, 2.205 (5); Mn1-=O3, 2.168 (6); Mn1-O5, 2.164 (6); Mn2-O1, 2.172 (5); Mn2-O4, 2.104 (6); Mn2-O6, 2.141 (6); Mn2-N11, 2.198 (6); Mn2-N21, 2.214 (7); Mn2···O2, 2.488 (7); Mn1···Mn2, 3.635 (1); Mn1-O1-Mn2, 112.3 (2); O1-Mn1-O3, 91.6 (2); O1-Mn1-O5, 87.4 (2); O1-Mn2-O4, 97.2 (2); O1-Mn2-N11, 142.5 (2); O4-Mn2-N21, 164.0 (2). *anti*-**2** (same labelling scheme as for *anti*-**1**): Fe1-O1, 2.151 (3); Fe1-O3, 2.063 (4); Fe1-O5, 2.208 (3); Fe2-O1, 2.027 (3); Fe2-O4, 2.093 (4); Fe2-O6, 2.082 (3); Fe2-N11, 2.095 (4); Fe2-N21, 2.127 (4); Fe2···O2, 3.005 (4); Fe1···Fe2, 3.3251 (9); Fe1-O1-Fe2, 105.4 (1); O1-Fe1-O3, 90.6 (1); O1-Fe1-O5, 87.3 (1); O1-Fe2-O4, 94.0 (1); O1-Fe2-N11, 124.6 (1); O4-Fe2-N21, 171.4 (1).

geometry of the terminal metal ions is trigonal bipyramidal with the pseudo-C_3 axes defined by N21-Mn2-O4 and N61-Mn3-O46 for *syn*-**1** and N21-M2-O4 for *anti*-**1**/**2**. Distortions arise from weak interactions of the terminal metal with the dangling oxygen from the monodentate μ-acetate ligand. In particular, the O-M-N angle in the trigonal plane, where O refers to the bridging oxygen atom from the monodentate carboxylate, e.g. O1, is correlated with the degree of interaction between the metal and the dangling oxygen atom. Thus, e.g., the angle O1-Mn2-N11 is widened by about 29° compared to the expected angle of 120°. This M···O interaction inhibits ligation at the potential sixth coordination site on the terminal metal ions, possibly limiting the formation of higher order oligomers.

The Mössbauer spectrum of **2**[11] consists of two quadrupole doublets arising from Fe^{II}, judging by the isomer shifts, with an intensity ratio of 2:1. The large quadrupole splitting for the more intense of the two doublets is consistent with the more distorted trigonal bipyramidal environment of the terminal Fe^{II} ions. Moreover, the relative quadrupole splitting of the pentacoordinate Fe^{II} ions in **2** and the recently reported $[Fe_2(O_2CH)_4(biphme)_2]$, **3**,[5] correlates nicely with the extent of the distortion of the coordination from trigonal bipyramidal geometry discussed above, varying from $\Delta E_Q = 3.30$ mm s^{-1} for Fe2 in **3**[5] to 3.60 mm s^{-1} for Fe2 in **2**.

A noteworthy feature of the two structures of **1** is the variation in the intramolecular Mn···Mn distances, from 3.370 (3) Å to 3.635 (1) Å. Although the observed values fall within the range reported for doubly and triply bridged dinuclear Mn^{II} complexes,[2a, 15] a difference of 0.27 Å in M···M distance within a single structural motif is extraordinary. This variability in Mn···Mn distances observed for **1** underscores the need for caution in interpreting EXAFS data for metalloproteins, in which details of the metal core geometry, especially M···M distances, are frequently used in postulating a specific structural model.[16]

The linear M^{II}_3-core geometry in **1** and **2** is unique among carboxylato-bridged trimanganese und triiron complexes, most of which have basic metal carboxylate[2c, 8] or other triangular structural motifs.[17] Aspects of the core geometries of **1** and **2** are known in related compounds, however. The $\{M_2(O_2CCH_3)_3(biphme)\}^{\oplus}$ unit comprising half the trinuclear complexes **1** and **2** is similar in structure to that reported for **3**.[5] The $\{M_3(O_2CCH_3)_6\}$ structure also appears in polymeric $Mn(O_2CCH_3)_2 \cdot 4\ H_2O$.[18] Here, however, all Mn^{II} ions are hexacoordinate and, instead of interacting weakly with terminal Mn^{II} ions as in the $\{M_3(O_2CCH_3)_6\}$ unit of **1** and **2**, the second oxygen atom from the monodentate bridging acetate binds to a Mn^{II} center that is part of another $\{Mn_3(O_2CCH_3)_6\}$ unit. A complex that appears to be very similar to **1**, $[Mn_3(O_2CPh)_6(bipy)_2]$ (bpy = 2,2'-bipyridine), has been mentioned recently, but detailed structural information is not yet available.[2c] Several linear homo- and heterotrinuclear complexes have been reported[14, 19] that contain a $\{M_2M'(O_2CR)_6\}$ core (M = M' = Co, Zn; M = Zn, M' = Mg, Ca, Sr, Co, Ni, Mn, Cd) similar to that found for **1** and **2**. Finally, a linear trinuclear complex, $[Mn_3(O_2CCH_3)_4(Saladhp)_2(CH_3OH)_2]$ [Saladhp = 2-methyl-2-(salicylideneamino)-propane-1,3-diol], was recently synthesized.[20] No linear carboxylatotriiron complexes are known.

Analysis of the structural parameters of the monodentate bridging carboxylate ligands in the present and a few related complexes[5, 21] reveals an interesting trend. In particular, a linear relationship exists between the bridging (B) and dangling (D) metal-to-oxygen distances as the carboxylate ligand moves from monodentate bridging toward bidentate bridging (Scheme 1). This movement, which we term the

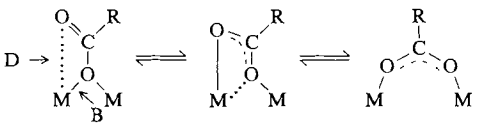

Scheme 1. Transition from monodentate to bidentate μ-carboxylato ligand ("carboxylate shift").

"carboxylate shift", may be of general importance in the active site structures of metalloproteins. In particular, concanavalin A is known to contain a monodentate bridging carboxylate[22] and a similar unit may well occur in the reduced form(s) of ribonucleotide reductase.[23]

Received: February 26, 1990 [Z 3821 IE]
German version: *Angew. Chem.* *102* (1990) 842

[1] a) S. J. Lippard, *Angew. Chem. 100* (1988) 353–371; *Angew. Chem. Int. Ed. Engl. 27* (1988) 344–361; b) L. Que, Jr., R. C. Scarrow in L. Que, Jr. (Ed.): *Metal Clusters in Proteins (ACS Symp. Ser. 372* (1988) 152–178) c) P. C. Wilkins, R. G. Wilkins, *Coord. Chem. Rev. 79* (1987) 195–214.

[2] a) K. Wieghardt, *Angew. Chem. 101* (1989) 1179–1198; *Angew. Chem. Int. Ed. Engl. 28* (1989) 1153–1172; b) J. B. Vincent, G. Christou, *Adv. Inorg. Chem. Radiochem. 33* (1989) 197–257; c) G. C. Christou, *Acc. Chem. Res. 22* (1989) 328–335; d) G. W. Brudvig, R. H. Crabtree, *Prog. Inorg. Chem. 37* (1989) 99–142; e) G. W. Brudvig, W. F. Beck, J. C. de Paula, *Annu. Rev. Biophys. Biophys Chem. 18* (1989) 25–46; f) G. C. Christou, J. B. Vincent in L. Que, Jr. (Ed.): *Metal Clusters in Proteins (ACS Symp. Ser. 372* (1988) 238–255); g) G. W. Brudvig, *ibid.* 221–237; h) G. Renger, *Angew. Chem. 99* (1987) 660–678; *Angew. Chem. Int. Ed. Engl. 26* (1987) 643–660.

[3] R. Cammack, A. Chapman, W.-P. Lu, A. Karagouni, D. P. Kelly, *FEBS Lett. 253* (1989) 239–243.

[4] a) W. Micklitz, S. J. Lippard, *Inorg. Chem. 27* (1988) 3067–3069; b) W. Micklitz, S. G. Bott, J. G. Bentsen, S. J. Lippard, *J. Am. Chem. Soc. 111* (1989) 372–374; c) W. Micklitz, S. J. Lippard, *ibid. 111* (1989) 6856–6858.

[5] W. B. Tolman, A. Bino, S. J. Lippard, *J. Am. Chem. Soc. 111* (1989) 8522–8523.

[6] R. H. Beer, W. B. Tolman, S. G. Bott, S. J. Lippard, *Inorg. Chem. 28* (1989) 4557–4559.

[7] W. B. Tolman, R. L. Rardin, S. J. Lippard, *J. Am. Chem. Soc. 111* (1989) 4532–4533.

[8] R. D. Cannon, R. P. White, *Prog. Inorg. Chem. 36* (1988) 195–298.

[9] a) Experimental procedure for *syn*-**1**: A slurry of $Mn(O_2CCH_3)_2 \cdot 4\,H_2O$ (0.13 g, 0.53 mmol) and biphme (0.10 g, 0.35 mmol) in methanol (2 mL) was allowed to stir in air for 15 min, affording a clear, nearly colorless solution. Complex **1** was precipitated as a beige solid (0.154 g, 81% yield) by addition of diethyl ether. Correct elemental analysis (C, H, N). FT-IR (KBr): ν [cm^{-1}] = 3130, 3047, 3030, 3004, 2962, 2930, 2831, 1597 (ν_{asym} CO_2), 1497, 1448, 1416 (ν_{sym} CO_2), 1338, 1281, 1174, 1155, 1138, 1089, 1068, 1018, 988, 895, 757, 721, 704, 672, 646. X-ray quality crystals of *syn*-**1** were obtained by vapor diffusion of diethyl ether into a methylene chloride solution of **1** in air. Crystal data for *syn*-**1** $\cdot$ 3 CH_2Cl_2 at $-75\,^{\circ}C$: monoclinic, space group $P2_1/c$ (No. 14), $a = 12.672(11)$ Å, $b = 21.422(16)$ Å, $c = 22.279(21)$ Å, $\beta = 100.36(4)^{\circ}$, $V = 5949(9)$ Å^3, $Z = 4$, $M_r = 1338.57$ g mol^{-1}, $\varrho_{calcd} = 1.494$ g cm^{-3}. For 4771 unique, observed reflections with $F^2 > 3\sigma(F^2)$ and 703 variable parameters, the current discrepancy indices are $R = 0.058$ and $R_w = 0.080$. b) Further details of the crystal structure investigation are available on request from the Fachinformationszentrum Karlsruhe, Gesellschaft für wissenschaftlich-technische Information mbH, D-7514 Eggenstein-Leopoldshafen 2 (FRG), on quoting the depository number CSD-54570, the names of the authors, and the journal citation.

[10] Experimental procedure for *anti*-**1**: the preparation, analytical data and FTIR spectrum of **1** are reported in Ref. [9a]. X-ray quality crystals of *anti*-**1** were obtained by slow evaporation of a methylene chloride solution in air. Crystal data for *anti*-**1** $\cdot$ 2 CH_2Cl_2 at $-45\,^{\circ}C$: monoclinic, space group $P2_1/c$ (No. 14), $a = 10.754(2)$ Å, $b = 19.466(2)$ Å, $c = 13.724(2)$ Å, $\beta = 100.74(1)^{\circ}$, $V = 2823(1)$ Å^3, $Z = 2$, $M_r = 1253.64$ g mol^{-1}, $\varrho_{calcd} = 1.475$ g cm^{-3}. For 2501 unique, observed reflections with $F^2 > 3\sigma(F^2)$ and 358 variable parameters, the current discrepancy indices are $R = 0.064$ and $R_w = 0.076$; for further details see Ref. [9b].

[11] Experimental procedure for *anti*-**2**: A slurry of $Fe(O_2CCH_3)_2$ (1.85 g, 10.64 mmol) and biphme (2.00 g, 7.08 mmol) in methanol (22 mL) was allowed to stir under argon at 50 °C for 1 hr, affording a clear, pale green solution. The volume of the solution was reduced by 50% *in vacuo*, then tetrahydrofuran was vapor-diffused into the solution, affording X-ray quality crystals of **2** $\cdot$ 2 THF (2.77 g, 71% yield) in 1 week. Correct elemental analysis (C, H, N). FT-IR (KBr): ν [cm^{-1}] = 3126, 3107, 2974, 2967, 2871, 1597 (ν_{asym} CO_2), 1500, 1448, 1417 (ν_{sym} CO_2), 1372, 1306, 1285, 1142, 1068, 989, 895, 798, 762, 723, 704, 656, 645. Mössbauer (zero field, 4.2 K) δ_1 [mm s^{-1}, versus iron metal] = 1.36, ΔE_{Q1} [mm s^{-1}] = 2.64, intensity = 34%; $\delta_2 = 1.14$, $\Delta E_{Q2} = 3.60$, intensity = 66%. Crystal data for **2** $\cdot$ 2 THF at $-75\,^{\circ}C$: monoclinic, space group $P2_1/c$ (No. 14), $a = 10.3105(8)$ Å, $b = 19.924(3)$ Å, $c = 14.009(1)$ Å, $\beta = 102.563(6)^{\circ}$, $V = 2809(1)$ Å^3, $Z = 2$, $M_r = 1230.71$ g mol^{-1}, $\varrho_{calcd} = 1.455$ g cm^{-3}. For 2590 unique, observed reflections with $F^2 > 3\sigma(F^2)$ and 358 variable parameters, the current discrepancy indices are $R = 0.043$ and $R_w = 0.056$; for further details see Ref. [9b].

[12] R. C. Mehrotra, R. Bohra: *Metal Carboxylates*, Academic, New York 1983.

[13] a) R. Alcalá, J. Fernández García, *Rev. Acad. Cienc. Exactas Fis. Quim. Nat. Zaragoza 28* (1973) 303–325; b) F. A. Cotton, M. P. Diebold, M. Matusz, W. J. Roth, *Inorg. Chim. Acta 112* (1986) 147–152; c) T. C. W. Mak, W.-H. Yip, E. J. O'Reilly, G. Smith, C. H. Kennard, *ibid. 100* (1985) 267–273; d) T. Lis, *Acta Crystallogr. Sect. B33* (1977) 2964–2966; e) M. L. Post, J. Trotter, *J. Chem. Soc. Dalton Trans. 1974*, 674–678; f) W. Clegg, I. R. Little, B. P. Straughan, *Acta Crystallogr. Sect. C42* (1986) 1319–1322; g) H. Puff, R. Sievers, G. Elsner, *Z. Anorg. Allg. Chem. 413* (1975) 37–44; h) H. C. Freeman, F. Huq, G. N. Stevens, *J. Chem. Soc. Chem. Commun. 1976*, 90–91; i) C. K. Prout, J. R. Carruthers, F. J. C. Rossotti, *J. Chem. Soc. A 1971*, 3350–3354.

[14] a) J. Catterick, P. Thornton, *J. Chem. Soc. Dalton Trans. 1976*, 1634–1640; b) W. Clegg, I. R. Little, B. P. Straughan, *ibid. 1986*, 1283–1288; c) *J. Chem. Soc. Chem. Commun. 1985*, 73–74; d) *Inorg. Chem. 27* (1988) 1916–1923.

[15] A. Caneschi, F. Ferraro, D. Gatteschi, M. C. Melandri, P. Rey, R. Sessoli, *Angew. Chem. 101* (1989) 1408–1409; *Angew. Chem. Int. Ed. Engl. 28* (1989) 1365–1367.

[16] a) G. N. George, R. C. Prince, S. P. Cramer, *Science (Washington) 243* (1989) 789–791; b) V. K. Yachandra, R. D. Guiles, A. E. McDermott, J. L. Cole, R. D. Britt, S. L. Dexheimer, K. Sauer, M. P. Klein, *Biochemistry 26* (1987) 5974–5981; c) J. A. Kirby, A. S. Robertson, J. P. Smith, A. C. Thompson, S. R. Cooper, M. P. Klein, *J. Am. Chem. Soc. 103* (1981) 5529–5537.

[17] a) S. M. Gorun, S. J. Lippard, *J. Am. Chem. Soc. 107* (1985) 4568–4570; b) N. Auger, J.-J. Girerd, M. Corbella, A. Gleizes, J.-L. Zimmerman, *ibid. 112* (1990) 448–450; c) R. Bhula, G. J. Gainsford, D. C. Weatherburn, *ibid. 110* (1988) 7550–7552.

[18] E. F. Bertaut, D. Tran Qui, P. Burlet, M. Thomas, J. M. Moreau, *Acta Crystallogr. Sect. B30* (1974) 2234–2236.

[19] a) J. Catterick, M. B. Hursthouse, D. B. New, P. Thornton, *J. Chem. Soc. Chem. Commun. 1974*, 843–844; b) W. Clegg, P. A. Hunt, B. P. Straughan, M. A. Mendiola, *J. Chem. Soc. Dalton Trans. 1989*, 1127–1131.

[20] X. Li, D. P. Kessissoglou, M. L. Kirk, C. J. Bender, V. L. Pecoraro, *Inorg. Chem. 27* (1988) 1–3.

[21] R. L. Rardin, A. Bino, P. Poganiuch, W. B. Tolman, S. Liu, D. P. Goldberg, S. J. Lippard, unpublished.

[22] K. D. Hardman, R. C. Agarwal, M. J. Freiser, *J. Mol. Biol. 157* (1982) 69–86.

[23] a) J. Stubbe, *J. Biol. Chem. 265* (1990) 5329–5332; b) J. B. Lynch, C. Juarez-Garcia, E. Münck, L. Que, Jr., *J. Biol. Chem. 264* (1989) 8091–8096.

Book Reviews are written by invitation from the editor. Suggestions for books to be reviewed and for book reviewers are welcome. Publishers should send brochures or (better) books to the following address: Redaktion Angewandte Chemie, Postfach 101161, D-6940 Weinheim, Federal Republic of Germany. The editor reserves the right of selecting which books will be reviewed. Uninvited books not chosen for review will not be returned.

Conformational Analysis of Medium-Sized Heterocycles. Edited by *R. S. Glass*. VCH Verlagsgesellschaft, Weinheim/VCH Publishers, New York 1988. 274 pp., DM 126.00.—ISBN 3-527-26789-1/0-89573-283-1

Is there a justification for a book which, in the form of a collection of review articles, treats heterocycles with seven to twelve atoms in the ring?

In a total of six chapters some well-known authors have here attempted to give as complete as possible an overview of this topic. Chapters 2–5 deal with heterocycles having O, N, S and P atoms in the ring, and in addition there is a chapter on small cyclopeptides. The main emphases within the chapters reflect the interests of their authors, but it is apparent throughout that an effort has been made to give as complete a survey as possible, at least through the literature references.

Medium-sized aliphatic cyclic hydrocarbons can adopt many different stable conformations, and consequently several conformers are present in equilibrium in solution or in the gas phase. Nevertheless, the book makes it clear that in heterocycles, and especially in partially unsaturated compounds, there are conformational restrictions which greatly reduce the number of stable conformations.

In Chapter 1, *D. A. Case* gives a concise review (30 pages) of computational methods for determining conformations. Quantum mechanical methods are still seldom applied to medium-sized rings, partly due to the long computing times involved (for *ab initio* calculations), and partly because of the uncertainty of the results obtained (for semiempirical methods). More space is given to force field calculations, where *D. A. Case* describes, in summary at least, the most important force field computer programs, and tests their effectiveness using cyclooctane as an example. The data given on the force fields in peptides are useful; however, the treatment of Ramachandran diagrams as applied to alanine model dipeptides seems rather too detailed (even though it was of considerable interest to this reviewer), in view of the fact that on other topics the reader is only given a few references to the original papers (e.g. in the case of the "anomeric effect"). In contrast the sections on the problem of multiple energy minima are well furnished with references, although here molecular dynamics calculations are treated rather too briefly.

In Chapter 2 *F. A. L. Anet* first sets out definitions and the conformational nomenclature for medium-sized rings, then discusses cyclic hydrocarbons, followed by the additional geometrical restrictions that are imposed on the rings by oxygen atoms, sometimes combined with (partial) double bonds. He then gives a survey of O-heterocycles, arranged according to ring size, which is as complete as existing knowledge allows. The general part of the chapter is systematically set out and makes easy reading; it provides a useful introduction, not only to this chapter but also to the other parts of the book.

In Chapter 3 *R. W. Alder* and *J. M. White* deal with N-heterocycles, using a similar sequence. Especially noteworthy are the sections on transannular interactions and bicyclic N-heterocycles, which are the author's special fields of interest. The conformations of sulfur-containing cyclic compounds, including studies using photoelectron spectroscopy, are discussed by *W. N. Setzer* and *R. S. Glass* in Chapter 4. In general, however, spectroscopic methods are mentioned only briefly in the rest of the chapters, without any detailed discussion (Chapter 6 is an exception). Medium-sized rings containing phosphorus (Chapter 5 by *L. D. Quin*) are found less frequently, and could offer a large field of research in the future. In particular few medium-sized rings containing CPC units have so far been synthesized.

In Chapter 6 *V. J. Hruby* and *P. S. Hill* present a survey of cyclic tri- and tetrapeptides, peptide antibiotics and disulfide peptides. The chapter begins with a section on analytical methods (NMR, CD, IR), describing the basic features of these techniques as applied to the conformational analysis of peptides. The exclusion of larger cyclopeptides seems rather arbitrary, since these show the same conformational features, apart from the more frequent occurrence of *cis*-amide bonds and cyclol formation in the small rings.

Thus the publishers are offering here a book which brings together a heterogeneous area of knowledge from the viewpoint of ring size; this is done in such a way that, despite having different authors, a consistent picture of conformations in medium-sized rings emerges. The book draws together, from many different areas of chemistry, a wealth of information which it would not be easy to find by searching the literature directly. It is recommended for use as a work of reference by every chemist who seeks to control conformations in reactions, complexations or rearrangements, and therefore needs to be concerned with medium-sized rings.

Martin Feigel [NB 1017 IE]
Institut für Organische Chemie
der Universität Erlangen-Nürnberg (FRG)

Bioorganic Chemistry. A Chemical Approach to Enzyme Action. 2nd Edition. By *H. Dugas*. Springer, Berlin 1989. xv, 651 pp., hard cover, DM 98.00.—ISBN 3-540-96795-8

Bioorganic chemistry reached a high point in the fifties and sixties, mainly through the use of isotopes for elucidating biosynthetic pathways and enzyme mechanisms, but also through chemical synthetic work mimicking biogenesis; in the last few years it has been undergoing a powerful renaissance. The reason for this is a shift in research objectives, with a greater emphasis now on investigating the factors which influence biological processes, instead of merely aiming to describe the sequence of events, e.g. in terms of an enzymic mechanism. Recently, there have been efforts to gain a better understanding of the non-covalent interactions which play the key role in all biological processes. A whole new area of bioorganic chemistry that reaches far beyond the original concept of enzyme chemistry has been opened up by the magic phrase "molecular recognition". During the last

few years various monographs, some of them quite excellent, have appeared dealing with different aspects of this topic from a variety of viewpoints. With the publication of this second edition of "Bioorganic Chemistry" we now have a work which aims to treat the whole area in textbook style.

The same division of the material into seven chapters, as in the first edition, has been retained. However, this is a very coarse structure for the wide range of topics now covered, and leads to some unexpected classifications, such as the inclusion of the "suicide" deactivators in the chapter on coenzymes.

Chapter 1 provides a good introduction outlining some basic principles, although it includes the misleading comment that bioorganic chemistry began only in the 1950s with the work of *F. H. Westheimer* (on this side of the Atlantic the biomimetic syntheses carried out by *Clemens Schöpf* and *Sir Robert Robinson* in the twenties are still well remembered). However, this discussion has been kept very short (22 pp.) and consequently it is unavoidably superficial. The following chapters on amino acids and peptides (86 pp.) and on phosphate esters and polynucleotides (60 pp.) not only treat these topics comprehensively, from the basic features of peptide and phosphate ester chemistry through to the biosynthesis of the corresponding polymers, but also include interesting sections on newer and very recent developments such as catalytic antibodies, semisynthetic enzymes and DNA-intercalating compounds. Chapter 4 (enzyme chemistry, 91 pp.) and Chapter 5 (enzyme models, 136 pp.) form the core of the book. In Chapter 4 the author first defines and explains the use in this context of terms such as "catalysis" (although even in this latest textbook we find the frequently used expression "intramolecular catalysis", which is incompatible with the definition of catalysis given earlier), "prochirality" and "specificity". Examples of actual enzyme reactions are then discussed, followed by short sections on enzyme technology (including immobilization) and the increasingly important use of enzymes in organic synthesis.

The sections that are also included here on enzyme-analog-built polymers and on the construction of non-macrocyclic molecular clefts could more appropriately have been added to the next chapter on enzyme models. These describe all the important strategies and design approaches whose common denominator is the mimicking of biological host-guest relationships. As well as recent developments based on the now already classic cyclodextrin and crown ether parent structures, the discussion also includes systems without a precisely defined structure (functionalized polymers and micelle-forming species). Also noteworthy is the treatment in this chapter of biomimetic reactions which, although they are models for biological specificity, do not need a molecular host; these include polyene cyclizations and functionalizations at non-activated steroid sites.

Chapter 6 is concerned with models that mimic the role of metal ions in biological processes. The ions of the transition metals Zn, Fe, Cu and Co are treated in turn; for these artificial systems, some of which seem very contrived, the ions are mainly introduced using porphyrin ligands. The simulation, using cobalt complexes, of enzymic reactions that depend on vitamin B_{12} links up with Chapter 7, which is devoted to the chemistry of coenzymes. This classic field of bioorganic chemistry is here subdivided according to the functions and structures of the coenzymes (redox enzymes: NAD, flavine etc.), and the most recent findings concerning reaction mechanisms and model reactions are described by means of well chosen examples. However, no reference is made to the wide variety of new coenzymes obtained from methanogenic bacteria (methanofuran, methoxatin, factor F_{430} etc.), for which details of the reaction mechanisms as well as some model reactions are already known.

These omissions are not very serious when one considers the wealth of information that is here very well presented, in both textual and diagrammatic form. Nevertheless, it is clear that the limitation of bioorganic chemistry to the chemistry of enzymes, and therefore also the book's subtitle, is obsolete and does not adequately describe the subject.

"Bioorganic Chemistry" is certainly not a textbook in the popular sense, as the emphasis is less on general principles and "proven" knowledge than on illustration by examples. This is no doubt intentional, and as a result the book makes stimulating reading. However, one would have preferred the author of such a textbook—especially one on an interdisciplinary topic like this—to be bolder in critically evaluating the material and expressing his opinions. This applies especially to situations where there is controversy between alternative approaches, which are here simply not mentioned. The reductionistic approximation for bioorganic systems, although it is currently by far the most successful approach to understanding the action of enzymes, is by no means the only one, or even the only useful one.

Despite this criticism, *H. Dugas* has succeeded in producing a book which clearly describes the beauty and subtlety of both living and abiotic molecular architecture. As well as the readership for whom the book is mainly intended (i.e. advanced students), I can warmly recommend it to everyone who seeks a comprehensive account, at a moderate price, of current front-line developments in this highly topical field of research.

Franz P. Schmidtchen [NB 1026 IE]
Lehrstuhl für Organische Chemie und Biochemie
der Technischen Universität München, Garching (FRG)

Fundamentals of Molecular Spectroscopy. By *W. S. Struve*. Wiley, Chichester 1989. 379 pp., hard cover, £ 31.95.—ISBN 0-471-85424-7

A good training in the fundamentals of molecular spectroscopy is important for all chemists and for many physicists and biologists. Several generations of young scientists have grown up with *Herzberg*'s three-volume classic work "Molecular Spectra and Molecular Structure", Volume 1 of which was originally published in German in 1939 (*Molekülspektren und Molekülstruktur*, Steinkopff Verlag). *Herzberg*'s books are still unsurpassed in scientific thoroughness and depth of treatment. Moreover, it is pedagogic masterpiece because of the many well chosen examples and the clear, usually simple, manner of presentation. However, the third and last volume was published as long ago as 1966, and since then the books have not been revised (except for the publication of a supplementary volume of tables, K. P. Huber and G. Herzberg: *Constants of Diatomic Molecules*, van Nostrand, 1979). Since 1966 great developments have taken place in molecular spectroscopy. On the experimental side Fourier transform spectroscopy and laser spectroscopy have become well established, while on the theoretical side quantitative quantum chemical calculations have become possible, developments which one could at best only have guessed at in 1966. Thus, there has for some time been an urgent need for up-to-date textbooks on molecular spectroscopy. This has now been partly covered, e.g. by the textbooks of Kroto: *Molecular Rotation Spectra*, Wiley, 1975, and Hollas: *High Resolution Spectroscopy*, Butterworth, 1982, both of which can be recommended in this context.

The book by *W. S. Struve* is based on lectures to American graduate students between 1974 and 1987; in Germany this level corresponds approximately to the final semesters of the diploma course and to special lecture courses for Doktoranden (post-graduate students), although the latter courses are now often neglected, unfortunately. Radiative transitions are treated first in an elementary way, followed by atomic spectra (40 pp.), diatomic molecules (90 pp.), polyatomic molecules (100 pp.) and, in the concluding chapters, line shapes and intensities, lasers, two-photon processes and non-linear optics. The treatment is generally competent and appropriate for teaching purposes. The book as a whole is comparable with the corresponding chapters of typical physical chemistry textbooks, but goes a little further. However, it is disappointing to find some quite outdated material, and the coverage of recent developments is very incomplete. Thus, there are examples of IR spectra of HCl from around 1960, and the information that the student will gain from this book concerning the development of techniques such as FT-IR spectroscopy is hardly adequate. Furthermore, in discussing the theory of molecular spectra there is no mention of such an important aspect as the development of the concept of molecular symmetry groups by *Longuet-Higgins, Hougen* and *Watson*, which was already mentioned as a new development in 1966 in Volume 3 of "Herzberg", and about which a textbook (by *P. R. Bunker*) has been in existence for ten years. Also some other developments belonging to the "post-*Herzberg*" era, such as *Watson*'s theory of the spectra of asymmetric rotor molecules and many other topics, are only mentioned in passing. On the other hand, some new special techniques (CARS and others) are treated in Chapter 11.

In summary one may say that this book by *W. Struve* is suitable for the bookshelves of a university teacher preparing a lecture course on this subject, and it should also be available as a rule in departmental libraries.

Martin Quack [NB 1054 IE]
Laboratorium für Physikalische Chemie
der Eidgenössischen Technischen Hochschule,
Zürich (Switzerland)

Electrochemical Reactors, Their Science and Technology. Part A: Fundamentals, Electrolysers, Batteries and Fuel Cells. Edited by *M. I. Ismail*. Elsevier, Amsterdam 1989. xviii, 548 pp., hard cover, HFl 265.00.—ISBN 0-444-87139-X

This book is the first of three volumes with the general title "Electrochemical Reactors". As the series editor explains in the preface, Volume A deals with the basic principles of electrochemical reactors and with batteries and fuel cells, Volume B will deal with special types of reactors, and Volume C with production techniques for commercial reactors and mathematical modeling of the processes occurring in electrochemical reactors. The series is intended for both specialists and students.

The first volume contains a short general introduction to the field, followed by 14 longer articles in which recognized experts report on the current state of knowledge in individual areas. These deal with fundamental aspects (thermodynamics, electrode kinetics, transport of heat and matter, flow mechanics), with more general considerations (concepts used in describing electrochemical processes, general technical problems, regulating systems) and with special aspects (electrodes, electrolytes, diaphragms, materials of construction, process control systems). Batteries and fuel cells are treated in separate articles.

The quality of the individual contributions strikes the reviewer as being just as heterogeneous as the impression given by the overall visual appearance of the book. They range from very good review articles (e.g. those on thermodynamics and electrode kinetics) to tabulated compilations of equations with virtually no discussion (as in the article on transport of heat and matter). Also the SI system is not employed universally.

The articles on fundamentals can be recommended as an introduction for newcomers to the extensive field of electrochemical processes, and experts will value the comprehensive bibliography provided. The book will be hindered from reaching a wider readership by the weaknesses mentioned above, and more especially by its high price, which the poor visual appearance (with typography and figures which are sometimes difficult to read) does nothing to counteract.

Thomas Hahn [NB 1044 IE]
Institut für chemische Verfahrenstechnik
der Universität Karlsruhe (FRG)

The Chemistry of Soils. By *G. Sposito*. Oxford University Press, Oxford 1989. 277 pp., hardcover, £ 25.00.—ISBN 0-19-504615-3

The declared aim of this book is to develop soil chemistry from the level of purely qualitative description into an exact science which makes use of all available techniques, ranging from spectrometers to computer modeling. This means that it should not only meet the needs of modern agriculture, but should also provide a basis for understanding and solving many environmental problems. The reader who already has the necessary basic knowledge of soil science, mineralogy and chemistry will find here an interesting textbook, which deals in the first few chapters with the chemical composition of soils, then goes on to describe soil chemical processes, and finally discusses questions of acidity, salt excess and fertility.

Starting from the elemental composition of soils, the mineral constituents and trace elements are discussed. The three-phase system consisting of soil solids, soil air and soil water leads on to the stages in weathering. In discussing the inorganic constituents those which mainly feature are, of course, ionic solids, primary silicates and clay minerals, oxides and hydroxides, carbonates and sulfates. Coming to the organic soil constituents, the account of humus-related problems is concise but very instructive. However, the interactions with organic trace impurities are not treated in sufficient detail; for example, pesticide-related problems are an important topic which could usefully have been included. The topic of soil solvation begins with a brief discussion of sampling methods, then continues with the most important equilibria and calculations on these. Solubility calculations are given for several minerals, and the corresponding activity-partition diagrams are developed. Under electrochemical properties the pE concept (including pE–pH diagrams), redox reactions, relevant measurement techniques and conditions in water-saturated soils are included. The characteristics of the particle surface are discussed in terms of the functional groups present, the adsorption equilibria, surface charges, the points of zero charge and the adsorbed water. The treatment of the effects of adsorbed cations, anions and molecules is extended to include descriptions of batch and column experiments, together with thermodynamic and kinetic modeling of the processes. The range of functionalities that occur

in soils is completed by discussions of ion exchange mechanisms and their quantitative treatment, together with colloid chemistry aspects and models related thereto. The chapters concerned with applications include the acidification of soils, with the main emphasis here on proton cycles, dissolved aluminum compounds, redox effects and methods for neutralizing soils. Next salt excess is discussed, including definitions, ion exchange processes, boron chemistry and irrigation problems, followed by soil fertility, including investigations on both essential and toxic elements, with sections on bioavailability, the kinetics of nutrient uptake by plants, and the effects of the pH and pE values.

The value of this comprehensive work from a learning standpoint lies in the clear diagrams and formula schemes, the comprehensive literature references (up to 1987), and the numerous exercises included in the individual chapters. The emphasis placed on calculations and modeling throughout the range of topics covered is extremely valuable. However, in cases where insufficient basic data are available for this purpose, the reader is unfortunately not helped to determine these by experiment.

A useful appendix lists units and physical constants used in soil chemistry. Regrettably there is no list of the numerous symbols and abbreviations that appear in the text. The provision of a comprehensive index and seven blank pages for notes reinforce the impression of a typical American style student textbook. The book can be recommended for everyone with an interest in soil science. For university teachers it will provide valuable additional class material, and it will enable students to rapidly become familiar with modern methods of treating problems in soil science. The style and presentation of the book are exemplary.

Fritz H. Frimmel [NB 1038 IE]
Lehrstuhl für Wasserchemie
der Universität Karlsruhe (FRG)

The Chemistry of Antitumor Antibiotics. Vol. 2. By *W. A. Remers*. Wiley, New York 1988. 290 pp., hard cover, £ 31.95.—ISBN 0-471-08180-9

This series, which was begun in 1979 by the same author, is now continued with the publication of Volume 2. It consists of seven chapters, each dealing with a further antitumor antibiotic isolated from microorganisms. This volume does not contain any extension or updating of the material covered in Volume 1, which reported on actinomycins, anthracyclines, the aureolic acid group of antibiotics, bleomycins and phleomycins, together with mitomycins and porphyromycins. This is not a serious omission, since there are enough up-to-date review articles and proceedings of symposia.

The antibiotics covered in this second volume are: streptozocin; pyrrolo-1,4-benzodiazepines; saframycins, renieramycins and safracins; naphthyridomycins, cyanocyclins and quinocarcin, CC-1065, nogalamycin and related compounds, and lastly streptonigrin and lavendomycin.

Each chapter is divided into six sections: discovery, isolation and characterization, structure determination and chemical transformations, mechanism of action, synthesis, biosynthesis, and structure-activity relationships. The efforts involved in the development of cytostatic agents, often extending over long periods, and all the problems associated with indications in view of the narrow dividing line that exists between high antitumor activity and unacceptable toxicity, are vividly described.

The author notes critically that biological data from different laboratories are often not comparable. He also emphasizes that difficulties often arise in transfering results from animal tests into the clinical situation, owing to the highly species-specific nature of tumor diseases. Regrettably, though, there is no explicit mention of the changes that have been introduced into preclinical testing methods in the last decade, mainly in the pharmaceutical industry, and recently also at the US National Cancer Institute (NCI); these involve using human tumors at a very early stage instead of animal tumors, both in cell cultures and as implants in experimental animals.

Current ideas regarding molecular activity mechanisms and structure-activity relationships in antitumor antibiotics are thoroughly discussed, and experimental models and results are clearly described. The only exception is Figure 5.2 (p. 155), showing a stereopair for a CC-1065-DNA adduct, which can only be understood with difficulty. The chemical synthetic work is illustrated by reaction schemes which are very clear and well drawn. In addition, the history of the discovery of each antibiotic, the problems arising in fermentation, the process of isolating it and the determination of the structure (including many figures showing spectra), the question of side effects, and last but not least, analytical aspects, are very well described.

The index is comprehensive and clear; a particularly good feature is the ability to search using group and generic names. Unfortunately, though, adriamycin, which is widely used as a standard compound and mentioned as such in the text, is not in the index. One does not expect to find an exhaustive list of all the many names that are used in the literature for a given antibiotic, due to the fact that in many cases it was independently discovered and named in several different places; however, for such an important compound as CC-1065 the alternative name "Rachelmycin" which occurs in the literature ought to have been mentioned. The text makes easy reading, and the incidence of printing errors, most of which do not alter the meaning, is in accordance with modern standards.

The treatment of the various topics is balanced, and the information given is sufficiently comprehensive to benefit even specialist readers. The coverage of the original literature which the book provides is considerable, the most recent references being to work published in 1988. If it appears that the bibliography is predominantly weighted towards American and Japanese research groups, this is, regrettably, a true reflection of the present distribution of research activity on the chemotherapy of tumor diseases. Some random checks indicated that the author has carefully surveyed and evaluated the literature.

Readers with a chemical background will probably find the accounts of synthetic research of most interest; such work has in many cases led to wide departures from the natural product originally discovered, as is convincingly demonstrated by the example of CC-1065. As the quantities of material that need to be produced, even for clinical applications of antitumor agents, are usually only in the region of a few kilogrammes, it is quite appropriate to use relatively expensive modern synthetic methods; the quantities needed for preclinical testing and for characterization are often surprisingly small.

Although the likely source of the next generation of clinically usable antitumor agents is still an open question, it seems highly probable that natural products will play an important role. Books such as that reviewed here can exert a beneficial influence on progress in this respect. Unfortunately, the reviewer has no information on how wide a readership

has been achieved by the first volume in this series; however, by reason of their content and presentation both volumes deserve to be widely read, especially as the price seems reasonable. As the present book treats all aspects of the subject equally thoroughly, it can be recommended both as an introduction and as more advanced reading for those engaged in the research areas covered.

Hans Gerd Berscheid [NB 1023 IE]
Frankfurt/Main (FRG)

Flow Injection Atomic Spectroscopy. (Series: Practical Spectroscopy, Vol. 7). Edited by *J. L. Burguera*. Marcel Dekker, New York 1989. 353 pp., hard cover, $125.00.— ISBN 0-8247-8059-0

In this book, the 7th volume in the "Practical Spectroscopy" series, the editor and the authors have succeeded in producing a concise, comprehensive work on the principles and applications of flow injection analysis (FIA) in atomic spectroscopy. The experimental aspects and practical hints occupy more space in the book than the theory, an emphasis which is opportune and appropriate at this time, but nevertheless the theory is not neglected.

The quality of printing and presentation is excellent, and the many clear figures and tables make for easy understanding of the main text. Although there are considerable variations in the style of the contributions by different authors, a consistently high quality is maintained throughout.

Chapters 1–3 deal with general and theoretical aspects of the method (including the introduction of the physical quantities used to describe the technique) and instrumental considerations, whereas Chapters 4 and 5 are devoted to the main areas of application of FIA in atomic spectroscopy. Chapters 6 and 7 provide those using the technique in the special fields of environmental and clinical analysis with advice on many aspects and methods for solving practical problems. Lastly Chapter 8 offers a critical appraisal of FIA, together with many stimulating ideas for the further development of instruments and techniques.

However, at this point one must mention the one drawback of this otherwise commendable book. Chapter 1, "General Introduction", fails to do full justice to its subject. The author, instead of aiming his article at beginners in the FIA technique, has chosen to discuss at some length the everyday problems encountered in using the FIA method. Only readers already familiar with FIA are likely to understand this chapter; the spectroscopist who wishes to begin using the method and needs an introduction to it is badly served by the article.

The rest of the articles are all good, and I especially recommend those interested to read Chapter 3, "Basic Components and Automation" by *J. F. van Staden*, Chapter 4, "Analytical Methods and Techniques" by *Z. Fang*, and Chapter 5, "Separation Techniques" by *M. Valcarel* and *M. Gallego*. The book is worth buying for these three fundamental chapters alone, which are recommended not only for advanced readers but also for beginners in the FIA-AS method. They enable one to quickly become familiar with the many different valve systems, instrumental arrangements, sample preparation methods and other options which make the FIA method so useful to the spectroscopist.

Chapters 6 and 7 offer the experienced FIA user much advice regarding the special problems encountered in environmental and clinical analysis, and these two chapters alone contain over 140 literature references. Despite its apparent brevity, the character of the book is in fact more that of a work of reference than of a collection of review articles, as the treatment of the subject is so masterly and concise. It contains altogether more than 700 literature references, covering publications up to 1987 in all but a few cases.

Because of its clear structure and the high quality of the individual articles, the book will be an excellent aid to becoming familiar with the subject and for work planning, both for newcomers to this interesting area of application of flow injection analysis and for those already experienced in the method. One can therefore do no more than advise potential readers not to be deterred from buying this very interesting and informative book by the rather high price of $ 125.00 ($ 150.00 in Europe). It is definitely worth it!

Frank Winter [NB 1034 IE]
Lehrstuhl für Analytische Chemie
der Universität Münster (FRG)

Modern Synthetic Methods. Volume 5. Edited by *R. Scheffold*. Springer, Berlin 1989. 304 pp., paperback, DM 78.00.— ISBN 3-540-51060-5

Following the established sequence of triennial meetings, the 5th International Seminar on Modern Synthetic Methods took place in Interlaken on 27–28 April 1989. It was held under the auspices of the Schweizerischer Chemiker-Verband, and was organized by Prof. *R. Scheffold*. This seminar-type conference can always be relied on to turn out successfully. The form is based on presentations of topical themes by a few leading researchers, each reporting comprehensively on his or her special subject, including the most recent developments, from as practical a standpoint as possible.

To enable others as well as the participants to benefit from the seminar, the papers presented are here collected together, as for the previous meetings, in a book with the ambitious title "Modern Synthetic Methods"; this is the fifth such publication since 1976. The general theme of this meeting was catalysis; a wide range of topics was covered under this heading, as is evident from the titles of the contributions: "Biotransformations in Organic Synthesis" by *D. H. G. Crout* and *M. Christen*; "Enantioselective Catalysis with Metal Complexes: An Overview" by *R. Noyori* and *M. Kitamura*; "Enantioselective Catalysis with Chiral Cobalt and Copper Complexes" by *A. Pfaltz*; "Clays, Zeolites and Other Microporous Solids for Organic Synthesis" by *J. M. Thomas* and *C. R. Theocharis*. All the papers include typical laboratory recipes and detailed lists of literature references. It can be seen that the range of topics extends from tailored inorganic catalysts through organometallic compounds to biocatalysts.

Within the broad field of biotransformations the authors have confined their discussion to well established methods with general applicability. Reactions that can be carried out using esterases, lipases and proteases are described in detail, as are those using redox enzymes, especially baker's yeast. Particular enzyme-catalyzed syntheses that are described are those of amino acids, amides, peptides, glycosides and oligosaccharides. Important applications of enzymes for the formation or scission of C-C bonds are also discussed.

Coming now to the contributions on enantioselective catalysis with metal complexes, *Noyori* and *Kitamura* give an excellent review of this rapidly growing field and the recent fascinating developments that have occurred, while *Pfaltz*, taking as an example his highly promising semicorrin com-

plexes with C_2 symmetry, offers an interesting detailed insight into the development work needed to achieve spectacular successes of this kind.

The last contribution in the book describes the structures of zeolites and ways of modifying them for specific purposes, then indicates how they can be used for organic syntheses; up to now these have been used mainly on an industrial scale for producing basic chemicals.

Altogether the book is a very useful guide to the subject of catalysts in organic synthesis, which has a promising future; in particular it offers beginners a straightforward introduction to this field. All the articles are competently written and thorough, and are therefore likely to be frequently cited. It would be difficult at present to find other reviews presenting the current state of knowledge in such a concentrated form. One can only hope that the price, which has increased further to DM 78.00—too much for a paperback in my view—will not prevent this interesting book from reaching a wide readership that will include students.

Hans-J. Altenbach [NB 1051 IE]
Institut für Organische Chemie
der Universität-Gesamthochschule Paderborn (FRG)

Nucleotide Analogues as Antiviral Agents. (ACS Symposium Series, Vol. 401). Edited by *J. C. Martin*. American Chemical Society, Washington, DC (USA) 1989. viii, 190 pp., hard cover, $ 53.95.—ISBN 0-8412-1659-2

This book is a collection of papers presented at a symposium held on the occasion of the 196th meeting of the American Chemical Society in September 1988. As the editor notes in his introduction, efforts to develop antiviral nucleoside and nucleotide analogues as an answer to the AIDS epidemic have been greatly increased in the last few years. The majority of the nucleoside analogues used up to now, of which 3′-azidothymidine and 9-(hydroxyethoxymethyl)guanine (Acyclovir) are the two most important, are effective in the form of 5′-triphosphates. The phosphorylation proceeds via three steps, one of which is often a bottleneck—for example, in the case of azidothymidine this is the phosphorylation of the 5′-monophosphate to the diphosphate. Thus it already became apparent some time ago that, instead of nucleoside analogues, one might try to introduce nucleotide analogues with potential antiviral activity into the cells. Since one of the obstacles to the uptake of nucleotides is that they can be broken down by enzymes in the plasma membrane, phosphate analogues that cannot be broken down in this way seem to offer especially good chances for successful uptake. Consequently several chapters of the book are mainly concerned with results obtained using the stable phosphonate derivatives. In addition, however, there are separate chapters dealing with other derivatives, e.g. with nucleoside-5′-amines and -acetamides (Chapter 7), nucleoside-5′-sulfamates (Chapter 9), nucleotide dimers (Chapter 11) and oligonucleotides (Chapter 12).

As the book is a collection of articles by different authors, the quality of the contributions varies. For example, some contain unnecessarily extensive tables (pp. 10, 57, 60, 61 and 67) which make it difficult for the reader to distinguish essentials from non-essentials. Also very often the absence of compound names under their structural formulas—where these are given—is confusing, as it makes it difficult to quickly relate them to the text. The book is evidently intended for experts, for whom the meanings of the many abbreviations are obvious, and who will know, for example, that DHPG, which incidentally does not appear in the index, is identical to Ganciclovir. As is often the case in symposium proceedings, every article stands alone and no account is taken of other articles with which there is an overlap of subject matter or an amplification of a topic, as, for example, in contributions 4 and 5 which deal with the compounds 9-(2-phosphonylmethoxy)ethyladenine (PMEA) and 9-(2-phosphonylmethoxy)ethylguanine (PMEG). No doubt in order to produce this symposium volume as cheaply as possible, the text is very closely printed throughout, and this has not exactly made the book user-friendly. Also it seems a little strange that in the index entries referring to azidothymidine are found not only under this abbreviated name but also under "3′-azido-2′,3′-dideoxythymidine".

In addition to the more general discussions the book contains a few items of information which I found especially interesting, not least because they could provide a stimulus for future experiments. For example, it is remarked on pages 80 and 85 that phosphonate derivatives often show higher *in vivo* than *in vitro* activity. Unfortunately no further commentary on this is given. Another interesting result reported but not explained further is that some phosphonate alkyl esters also show antiviral activity (p. 32).

This book is the first of its kind on antiviral nucleotide analogues. Although none of the compounds discussed here has yet been cleared for clinical use, it becomes evident from reading the book that this is a class of compounds with great potential, and that further systematic research on these is justified. Despite the shortcomings mentioned, the book provides a good basis of material for the specialist.

Fritz Eckstein [NB 1053 IE]
Max-Planck-Institut für Experimentelle Medizin,
Göttingen (FRG)

Nitration. Methods and Mechanisms (Organic Nitro Chemistry Series). By *G. A. Olah, R. Malhotra*, and *S. C. Narang*. VCH Verlagsgesellschaft, Weinheim, VCH Publishers, New York 1989. xii, 330 pp., hard cover, DM 145.00.—ISBN 3-527-26698-4/0-89573-144-4

The third volume to appear in the Organic Nitro Chemistry Series, this book deals exclusively with aspects of nitration in organic chemistry. In keeping with the preceding two volumes (*Nitrazoles* and *Nitrile Oxides, Nitrones and Nitronates in Organic Synthesis*), it provides a broad survey of the subject, encompassing in four chapters many of the methods and mechanisms for the nitration of aromatic and aliphatic compounds.

After a brief introduction in Chapter 1 (8 pages, 21 literature citations), the authors go on in Chapter 2 (108 pages, 264 literature citations) to describe preparative methods for aromatic nitration. Numerous examples of the great many reagents used for nitrating arenes appear mainly in tabular form, accompanied in the text by the corresponding methods.

The authors have devoted a great deal of space in one section of Chapter 2 to nitration with nitronium ions; unfortunately, the examples in this section are not as complete as those from the section on nitration with nitric-sulfuric acid (isomer-distribution data). Although this format does not allow for comparison of aromatic nitration methods by way of example, it gives the reader a good, comprehensive overview. Some neglect is also apparent in the cursory treatment of homolytic (i.e., free-radical) and, more importantly, nucleophilic nitration, considering the significance of these

topics. One other disturbing feature of this chapter is the citation of patents in the reference section with no reference to the appropriate Chem. Abstr. Citation.

Chapter 3 (101 pages, 160 literature citations) is divided into three sections, covering mechanisms for electrophilic, free radical, and nucleophilic nitration of arenes. These fully detailed sections provide insight into the current level of understanding of nitration mechanisms. As in Chapter 2, however, the discussion of nucleophilic nitration is somewhat short (2 pages) compared to the coverage of electrophilic nitration.

In Chapter 4 (92 pages, 269 literature citations) the nitration of aliphatic compounds is surveyed. Here again, well-arranged examples accompany the text. The book ends with author and subject indexes that leave no stone unturned.

At this high price, one would have expected better-quality structural formulas. Nevertheless, this third volume of the series on nitro compounds, like its predecessors, merits recommendation.

Thomas Ziegler [NB 1060 IE]
Institut für Organische Chemie
Biochemie und Isotopenforschung
der Universität Stuttgart (FRG)

Symmetrien der Natur. Ein Handbuch der Natur- und Wissenschaftsphilosophie. By *K. Mainzer*. De Gruyter, Berlin 1988. 739 pp., hard cover, DM 365.00.—ISBN 3-11-011507-7

Most important are those areas of pure science in which there is no longer a mention of practical applications, but where pure thought investigates the hidden harmonies of the universe. This inner circle, where one can hardly distinguish between science and art, is perhaps the only place where humanity today is confronted with pure truth, that is no longer veiled by human ideology and desires.

W. Heisenberg

Among his contemporaries in the development of the "new physics" during the early decades of this century, it was particularly *W. Heisenberg* who pointed out the fundamental importance to physics of abstract symmetry (i.e. symmetry in a general sense, not only geometrical). This importance is now universally accepted, and is part of the common knowledge of every young physicist and chemist. Furthermore, we now regard symmetry as providing a fascinating link between very different fields of human thought and knowledge. There have thus been many minor and major attempts to treat this subject in book form.

This book by *Klaus Mainzer* occupies a special position in view of its comprehensiveness, exemplary depth, and thoroughness. In the words of the subtitle, it is in fact a "handbook on natural philosophy and science". In over 700 pages it treats, or at least touches on, almost every aspect of this theme. Its five chapters are arranged as follows: 1. The early history of symmetry; 2. Symmetry properties in modern mathematics; 3. Symmetry properties in classical physics and natural philosophy; 4. Symmetry properties in modern physics and science; 5. Symmetry and philosophy (also art and architecture). The book also includes a comprehensive bibliography and index, which serve as an encyclopedic guide to specific topics, specific facts, people, and historical aspects. It would be useful to enlarge the index in future editions so as to increase still further the value of the book as an "encyclopedia of symmetry".

It would not be appropriate in this short review to try to summarize the contents of this comprehensive work. The book combines many functions, being at the same time an encyclopedia, a textbook and an intellectually stimulating entertainment. There is scarcely a single aspect of the subject on which one fails to find a chapter, or at least a brief comment with literature references. Whole chapters of the book can be used by the student who needs an "introduction to symmetry for chemists" (or for physicists, mathematicians etc.). Perhaps the most remarkable comment I can offer is that, in avoiding the effort of "textbook-reading" I have read many of the book's 700 pages for pleasure and relaxation and was never bored. This is literary writing for scientists in the best possible sense.

Let us cite two sentences from the introduction to *Mainzer*'s book: "In the end, therefore, there remains the need to achieve an understanding of nature which will enable Man to act in harmony with nature, even more so because of his scientific knowledge and technological capabilities. For this reason the traditional approach of the philosophy of nature, which views research as part of human history and nature, is becoming again an important component of a scientific education".

"Symmetrien der Natur" could and should be used as a textbook of general scientific education by all science students, and is also basically suitable for students of the philosophically orientated humanities. Regrettably, the very high price, which is only partly justified by the excellent quality of production and presentation, is likely to prove an obstacle to this readership. One can therefore only hope that "Symmetrien der Natur" will achieve enough sales to persuade the publishers soon to bring out a second edition at a lower price. Meanwhile, I recommend to all who can afford it to buy the book. They will not regret it.

Martin Quack [NB 1055 IE]
Laboratorium für Physikalische Chemie
der Eidgenössischen Technischen Hochschule,
Zürich (Switzerland)

Patai's Guide to the Chemistry of Functional Groups. By *S. Patai*. Wiley, Chichester 1989. 455 pp., hard cover, £ 24.95.—ISBN 0-471-91256-2

In the well-known series "The Chemistry of Functional Groups", 40 titles were published up to the end of 1988, comprising 59 volumes with over 700 chapters and more than 43 000 closely printed pages. In the book reviewed here the series editor *S. Patai* has set out to provide an overall picture of this impressive amount of material, to accompany the immense stack of volumes that he has edited. So as to make the information contained in this monumental series more readily accessible, *Patai* has taken up a suggestion by *H. C. Brown*, providing a 455-page summary of the entire work with a detailed description of what the volumes contain.

The contents of the individual chapters are here described, including important information such as the number of pages, number of literature citations and the period that they cover, and the nature of the tables, formula schemes etc. that are included. This goes far beyond a mere summary of the list of contents for each volume; *Patai* also summarizes the most important chemical results, supported by many formulas. As well as the author and subject indexes he also includes two very useful sorts of cross-references: "complementary" cross-references, which refer to descriptions of *the same*

functional group in other volumes, and "relevant", referring to similar types of reactions for *other* functional groups.

The need for such a summary arises from the structure of "Patai": some overlapping of the material is unavoidable in view of the self-contained and monographic character of the chapters. This book is an effective guide to the series.

Karsten Krohn [NB 1061 IE]
Institut für Organische Chemie
der Technischen Universität Braunschweig (FRG)

The Elements—Their Origin, Abundance and Distribution. By *P. A. Cox*. Oxford University Press, Oxford 1989. viii, 207 pp., paperback, £ 9.95.—ISBN 0-19-855298-X

The reader interested in buying this book should not allow him- or herself to be irritated by the symbols used for the elements and compounds, which seem reminiscent of alchemy. Notwithstanding the historical references in the book, *P. A. Cox*, a senior lecturer in inorganic chemistry, is concerned here not with the history of chemistry, but instead gives an interdisciplinary account of the origin, abundance and distribution of the elements and of their physical and chemical properties. The special feature of this book of six chapters is the interdisciplinary treatment of the various topics, which range from the chemistry of the sun and the universe (Chapter 4) and geochemistry (Chapter 5) to isotopic distributions (Chapter 6) and the chemical and physical properties of nuclei and atoms (Chapter 2).

Chapter 3 deals with the origin of the elements, beginning with a description of the universe in early times and the formation of the stars. This is followed by detailed accounts of the fusion of hydrogen and of helium. Excellent summaries and references to more advanced literature (with brief descriptions indicating what these books contain) are given at the end of each chapter. Chapter 1 contains a short introduction to the Periodic System, and to the elements of the earth, solar system and universe, and discusses the factors that determine the occurence and distribution of the elements.

The book is intended for first and second year students and for those teaching these groups. In the preface *P. A. Cox* states that the main aim in this book is to trace the history of the elements from their origin in the cosmos to their occurrence as minerals. In the course of this he also brings in knowledge from nuclear physics, astronomy and geology. The introductory character of the book, which is based on the author's lecture courses, is maintained by the easily comprehensible style and by a suitable form of presentation, which includes an orderly arrangement of topics and appropriate historical aspects (e.g. the historic experiment of *Geiger* and *Marsden* as described on p. 27), theories, figures and tables, with important terms emphasized by bold type.

The student is familiarized with the relationships and terminology that are important for a basic course, without going into excessive detail. Nevertheless, the topics are not treated too briefly, as can be seen by comparing the chapter on "The Origin of the Elements. Isotopes and Atomic Masses" in "Greenwood and Earnshaw", which consists of 25 pages of text, with the 36 pages devoted to the same topic in "Cox", even though the latter has about 20% fewer characters per page. The appendix contains tables giving isotope distributions and data on the occurrence of the elements (in the earth, sun, meteorites, earth's crust, the oceans and the human body), information which could otherwise only be obtained by searching through several other books. In summary this book seems to me well worth reading and recommending to students, especially when one considers that it is written in easily comprehensible English and has an interdisciplinary character which is becoming increasingly important.

Georg Schwedt [NB 1056 IE]
Institut für Anorganische und Analytische Chemie
der Technischen Universität Clausthal (FRG)

Registered names, trademarks, etc. used in this journal, even when not marked as such, are not to be considered unprotected by law.

© VCH Verlagsgesellschaft mbH, D-6940 Weinheim, 1990. – Printed in the Federal Republic of Germany by Konrad Triltsch Druck- und Verlagsanstalt Würzburg.

All rights reserved (including those of translation into foreign languages). No part of this issue may be reproduced in any form — by photoprint, microfilm, or any other means — nor transmitted or translated into a machine language without written permission from the publishers. Only single copies of contributions, or parts thereof, may be made for personal use. This journal was carefully produced in all its parts. Nevertheless, authors, editors and publisher do not warrant the information contained therein to be free of errors. Readers are advised to keep in mind that statements, data, illustrations, procedural details or other items may inadvertently be inaccurate.

Valid for users in the USA: The appearance of the code at the bottom of the first page of an article (serial) indicates the copyright owner's consent that copies of the article may be made for personal or internal use, or for the personal or internal use of specific clients. This consent is given on the condition, however, that the copier pay stated per-copy fee through the Copyright Clearance Center, Inc. (CCC), for copying beyond that permitted by Sections 107 or 108 of the U.S. Copyright Law. This consent does not extend to other kinds of copying, such as copying, for general distribution, for advertising or promotional purposes, for creating new collective works, or for resale. For copying from back volumes of this journal see 'Permissions to Photo-Copy: Publisher's Fee List' of the CCC.

Editorial office: Postfach 10 11 61, D-6490 Weinheim, Federal Republic of Germany, Telephone (06201) 60 22 55, Telex 465 516 vchwh d, Telefax (06201) 602 328.

Editor: *Peter Gölitz*

Associate editors: *D. I. Loewus, A. Stimson.* **Editorial assistant:** *E. Schweikart*

Publishers: VCH Verlagsgesellschaft mbH. (Managing Director: *Hans Dirk Köhler*), Pappelallee 3, D-6940 Weinheim, Federal Republic of Germany.

Advertising office (Advertising Manager *R. J. Roth*): Postfach 10 11 61, D-6940 Weinheim, Federal Republic of Germany, Telephone (0 62 01) 60 61 30, Telex 4 67 155, Telefax (0 62 01) 606 156.

ANGEWANDTE CHEMIE
International Edition in English
Volume 29 · Number 8
August 1990
Pages 823–938

Syntheses, Conformations and X-Ray Structure Analyses of the Saccharide Chains from the Core Regions of Glycoproteins

By Hans Paulsen*

The covalently bound carbohydrate moiety in glycoproteins can stabilize the protein molecule intramolecularly, or it may have an intermolecular function as receptor in biological recognition. The discovery of these biological phenomena has led to a renaissance of the chemistry and biochemistry of carbohydrates. Both *N*-glycoproteins as well as *O*-glycoproteins contain special, invariant oligosaccharide chains in the protein-binding region, which occur again in all glycoproteins, and are described as the "core regions." This review describes the various methods of oligosaccharide synthesis that may be used to arrive at the basic core structures by chemical means. Methods of oligosaccharide synthesis have improved so much that it is possible to synthesize complex lactosamine-type structures, and "bisected"-type structures up to nona- and undecasaccharides respectively. Oligosaccharide chains are considerably less flexible than peptide chains. Using modern methods of NMR spectroscopy, their preferred solution conformation can readily be determined. In the case of one branched octasaccharide, a comparison of the conformations in solution and in the crystal is possible. Oligosaccharides may be linked to the amide group of an asparagine, or to the hydroxyl groups of serine or threonine. By using suitable protecting groups, the glycosyl amino acids obtained can be extended with further amino acids at the *N*- or *C*-terminus, thus arriving at the desired glycopeptide sequences. In the linkage region, glycopeptides prefer certain conformations. Future research into glycoprotein functions may involve the synthesis and biochemical study of modified glycoprotein segments.

1. Introduction

The enormous growth in interest in glycoproteins over the past decade is not without reason. Glycoproteins contain highly variable amounts of saccharide (up to $> 85\%$).[1, 2] Thanks to improved analytical techniques, carbohydrate residues have now also been found in compounds which were earlier considered to be pure proteins. Carbohydrate residues can influence the stability, conformation, protease lability, thermal properties, and solubility of proteins. Glycoproteins are found in soluble form in blood and in numerous secretions, and in a fixed state in the bilayer of the membrane,[3, 4] where the carbohydrate residue is extracellularly directed. In both cases the carbohydrate moiety performs important functions. This is especially true for the specific receptor interaction with functional proteins. Glycoproteins are active in the binding and transport of enzymes, hormones and antibodies, and in cell-cell interactions.[7, 8] The carbohydrate moiety can bind hormones, enzymes, antibodies and lectins, but also toxins, viruses, and bacteria. In this connection the reader is referred to the relevant review articles.[1–8]

The most important chemical forms of the linkage between the protein and oligo- or polysaccharide chains are of two types,[1] which also differ in their biosynthesis. In *N*-glycoproteins, one finds a β-*N*-glycosidic linkage between 2-acetamido-2-deoxy-D-glucose (GlcNAc) and the amide group of an asparagine side chain. Because of its amide na-

[*] Prof. Dr. H. Paulsen
Institut für Organische Chemie der Universität
Martin-Luther-King-Platz 6, D-2000 Hamburg 13 (FRG)

 © VCH Verlagsgesellschaft mbH, D-6940 Weinheim, 1990 0570-0833/90/0808-0823 $ 3.50+.25/0

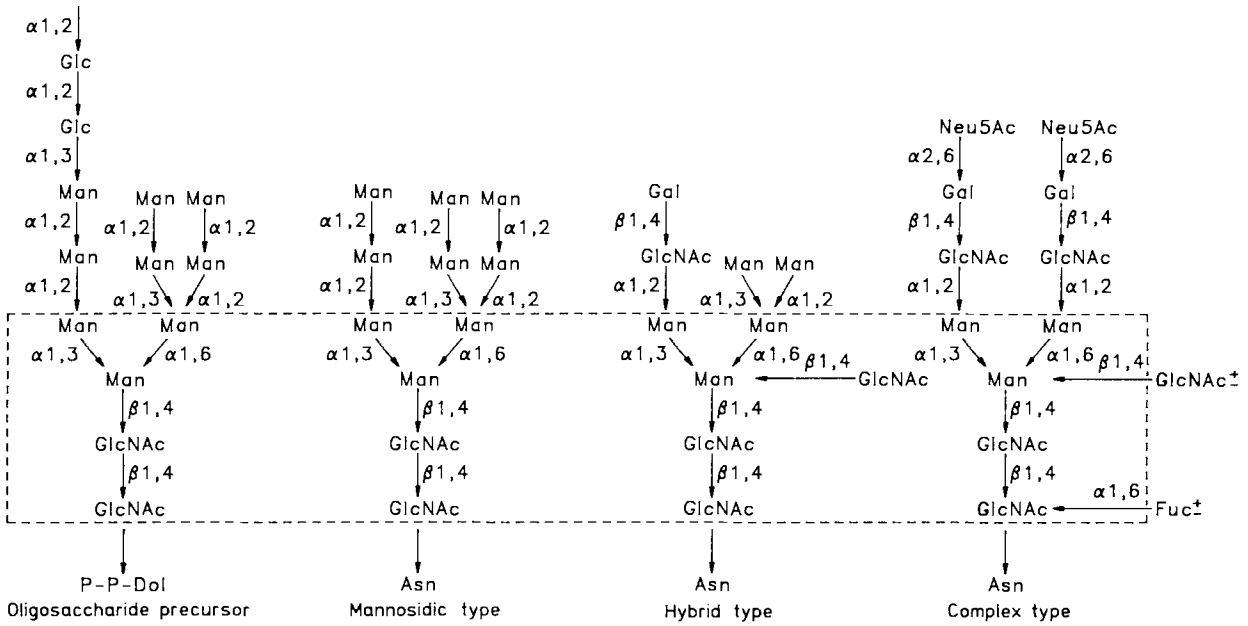

Fig. 1. Basic structures of *N*-glycoproteins. Glc = glucose, Man = mannose, P-P-Dol = dolicholpyrophosphate, Asn = asparagine, Neu5Ac = *N*-acetylneuraminic acid, Fuc = fucose.

ture, the basicity of the nitrogen atom is so reduced that the otherwise labile glycosylamine group is well stabilized. In the second type, the *O*-glycoproteins, there is either an α-*O*-glycosidic linkage of 2-acetamido-2-deoxy-D-galactose (GalNAc) or a β-*O*-glycosidic linkage of D-xylose (Xyl) to a serine or threonine hydroxy group. It is interesting that, despite the great variety of glycoproteins, the saccharide in the binding region retains a very similar, indeed partially identical sequence. This constant sequence, bound directly to the protein, is described as the "core structure."[1, 2] The appearance of a core structure characteristic for either *N*- or *O*-glycoproteins is determined by the biosynthesis of the respective glycoproteins.[9, 10]

The chemical synthesis of segments of this binding region is of interest for structure determination, for studies of glycoprotein function, and for determination of the specificity of biosynthetic addition and removal of sugar residues. Oligosaccharide segments bound to larger molecules via a spacer act as suitable antigens for the production of monoclonal antibodies. After binding oligosaccharides to a solid phase column, the column may be used for affinity chromatography of enzymes and antibodies. This review describes the chemical synthesis and molecular arrangement of such binding regions of glycoproteins.

2. *N*-Glycoproteins: Asparagine-bound Oligosaccharides

2.1. Basic Structures and Biosynthesis

The most important types of *N*-glycoprotein basic structures are summarized in Figure 1.[1, 10] Apart from the oligosaccharide precursor, they include the mannosidic structure, the hybrid structure, and the complex structure, of which the last is the most common. As can be seen, all these structural types contain a similar core pattern, consisting of two GlcNAc residues and a branching element of three mannose units (Man). This pentasaccharide structure occurs in all the formulas (circled structure). Variations in the structure of glycoproteins arise outside this core structure by fur-

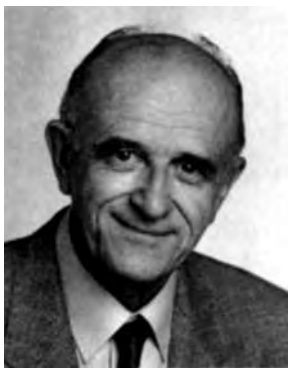

Hans Paulsen was born in 1922 in Hamburg, where he gained his PhD in 1955 in the research group headed by Professor Kurt Heyns. In 1962 he received his habilitation from the Faculty of Mathematics and Natural Sciences of the University of Hamburg, and, in 1972 he accepted a newly founded position as Professor for the Chemistry of Natural Products at the same University. His studies embraced the whole field of saccharide chemistry; however, in the last fifteen years his interests have centered on oligosaccharide syntheses. In addition he has concerned himself with biologically active compounds such as blood-group substances, glycolipids and glycoproteins, whose great importance is becoming more and more evident. His activities have found international recognition; all the honors carbohydrate chemistry has to offer have been bestowed on him. In 1980 the German Chemical Society awarded him the Emil Fischer Medal, in 1983 the Royal Society of Chemistry honored him with the Haworth Memorial Medal, and in 1985 the American Chemical Society presented him with the Claude S. Hudson award. In 1989 he received the J. Heyrovsky Medal from the Czechoslovakian academy of Sciences.

ther extension and branchings of the chains at the top of the diagram.

In order to understand the uniformity of the core structures in all *N*-glycoproteins, the principle of their biosynthesis should be explained.[10] The oligosaccharide precursor (Fig. 1) is synthesized from dolichol phosphate by specific glycosyl transferases in the rough endoplasmic reticulum. Within the dolichol phosphate cycle, the entire oligosaccharide of fourteen saccharide units is transferred to the asparagine of a polypeptide chain, wherever the signal sequence of Asn-X-Ser/Thr is found. Here, X can be any amino acid, but the presence of the adjacent hydroxy amino acid serine or threonine is essential for the transfer process.

The *N*-glycoprotein now passes through the cisternae of the Golgi apparatus, where the trimming process begins.[10] The desired structure is obtained by the action of glycosidases and glycosyl transferases removing and adding residues, respectively. However, the core pentasaccharide structure on the asparagine is not touched in this process, and it therefore appears unchanged in all products. In the mannosidic structure one sees merely degradation of one of the chains. In the hybrid type, lactosamine is coupled to one chain. This type of structure usually contains an additional GlcNAc unit, linked to the branch-point mannose. The complex type contains several lactosamine units and can be greatly branched and extended at the chain ends. An additional fucose (Fuc) is sometimes also bound to the GlcNAc linked to the asparagine. In addition, both the complex and hybrid types of structure may have an additional GlcNAc unit bound to the branch residue. This gives rise to the so-called "bisected" type, which is of great importance in biosynthesis and will be dealt with separately later.

2.2. Chemical Synthesis

2.2.1. *Reliable Glycoside Coupling Methods*

In constructing large oligosaccharides, three methods have proved themselves in glycosidic linkage: the halogenide, imidate and thioglycoside methods. The fluorides, chlorides or bromides **1** may be used as halogenide donors, while mercury or silver salts are good catalysts.[11] The imidate procedure uses donor **3** with addition of Lewis acid catalysts.[12] In the thioglycoside method, activation of the sulfur in donor **5** is necessary; by conversion into a sulfonium form it becomes a good leaving group. $Me_2SS^{\oplus}Me$ triflate and a series of other reagents have been used as catalysts.[13a]

In all three methods, neighboring group interactions lead stereoselectively to the *trans*-glycosidation product, which means that in the D-*gluco* and the D-*galacto* series only the β-glycoside of **2**, **4**, or **6** can be formed. In the absence of neighboring group participation, all three procedures yield preferentially the α-glycoside, but varying amounts of the anomeric β-glycosides are produced simultaneously. The proportion of α-glycoside is strongly dependent on conditions such as solvent, catalyst, and structure of the reaction partners. Optimization of the process is always required here. It is not simple to carry out an S_N2-type reaction on a normally labile β-anomeric donor to obtain an α-glycoside. Experience so far suggests that the most suitable donor here is a β-glycosyl chloride. With β-glycosyl fluorides a preferred α-glycosidation was observed in the presence of the catalyst $Cp_2ZrCl_2 \cdot AgClO_4$.[13b]

With D-mannose, the situation is somewhat different, since the configuration at C2 is reversed. The methods all yield the α-glycoside **8**, with Lewis acid catalysis with or without neighboring group participation. The β-glycoside **9**

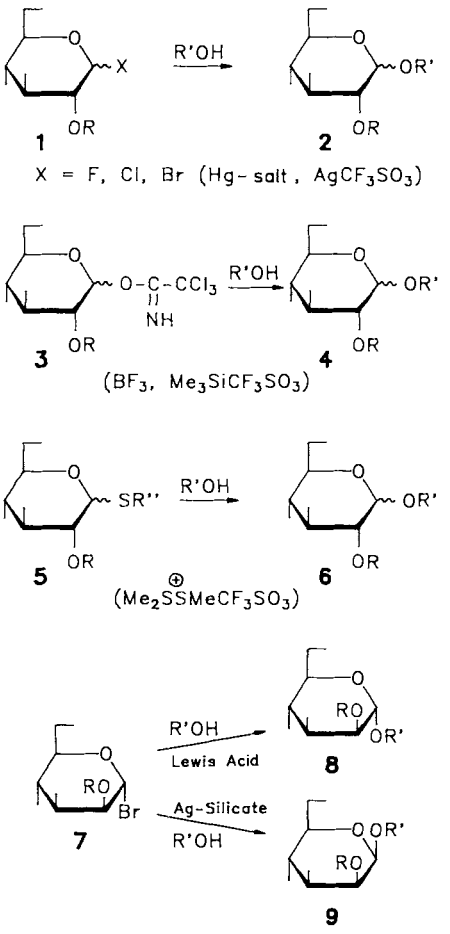

is not obtainable by these routes. Its synthesis can only be achieved by the method we have developed, which uses a heterogeneous catalyst such as silver silicate.[14] By this means donor **7** may be converted into the β-glycoside **9** in the absence of Lewis acid.

2.2.2. *Synthesis of the Basic Core Structure*

Early studies of the synthesis of the basic core structure (cf. Fig. 1) were carried out by *Jeanloz* et al.[15] The main difficulty to be encountered was the formation of the (1 → 4)-β-glycosidic linkage between the branch-point mannose and the adjacent GlcNAc unit. This bond could not be formed at the time. For that reason, a suitably protected β-D-Glc-(1 → 4)-D-GlcNAc disaccharide was first synthesized, since the β-glycosidic linkage to glucose is much easier to produce with neighboring group participation. The 2-OH group of the Glc unit then had to be selectively deprotected and oxidized to a keto group. Finally, selective reduction converted

this unit into the *manno* configuration, yielding the key disaccharide β-D-Man-(1 → 4)-D-GlcNAc.[15] This route requires several steps, and was also used for the synthesis of the tetrasaccharide β-D-Man-(1 → 4)-β-D-GlcNAc-(1 → 4)-D-GlcNAc.[16]

A new variation of this method has recently been reported by *Kunz*.[17] The starting material is the same disaccharide β-D-Glc-(1 → 4)-D-GlcNAc. With neighboring group participation from a vicinal phenylurethane residue, intramolecular nucleophilic substitution led to inversion of a 2-*O*-triflate group on the Glc unit. The same key disaccharide is hence obtained, without an oxidation reaction.

Direct synthesis of the desired β-mannosidic linkage is only possible by heterogeneous catalysis with silver silicate.[18] A reactive donor and acceptor are needed here. Donor **10** is activated at the anomeric center by the presence of ether substituents,[11] while in acceptor **11**, the 4-OH group is made more reactive by conversion of the *gluco* configuration into the 1,6-anhydro form, since it is now in the axial position. Reaction of **10** and **11** in the presence of silver silicate affords the desired β-linked disaccharide **12** in about 70% yield.[19]

After cleavage of the allyl groups in **12** to give **13**, reaction with mannose donor **14** is possible, with neighboring group participation, leading stereoselectively to the α-glycosidic bond. This reaction is considerably simpler than that described previously. Two moles of **14** can react smoothly with **13** to give the branched tetrasaccharide in 82% yield. By deprotection of **15**, the important branched sequence of the basic core structure **16** can thus be obtained.[19]

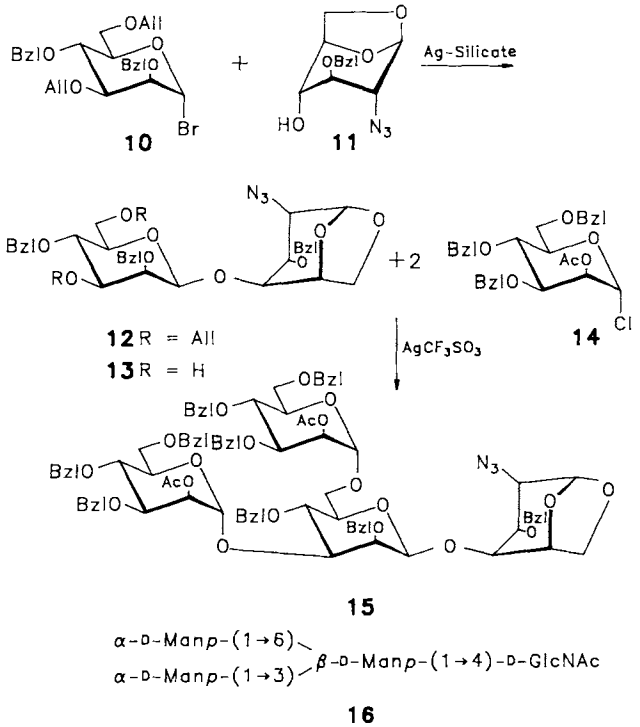

16

The tetrasaccharide **16** was also extended by a further GlcNAc unit at the reducing end to give the complete core structure. In addition, disaccharide **12** was converted into the glycosyl donor **17** and treated with **18**, yielding stereoselectively the β-linked trisaccharide **19**. After cleavage of the allyl groups to give **20**, this again reacts smoothly with two moles of the mannose derivative **14**, to give pentasaccharide

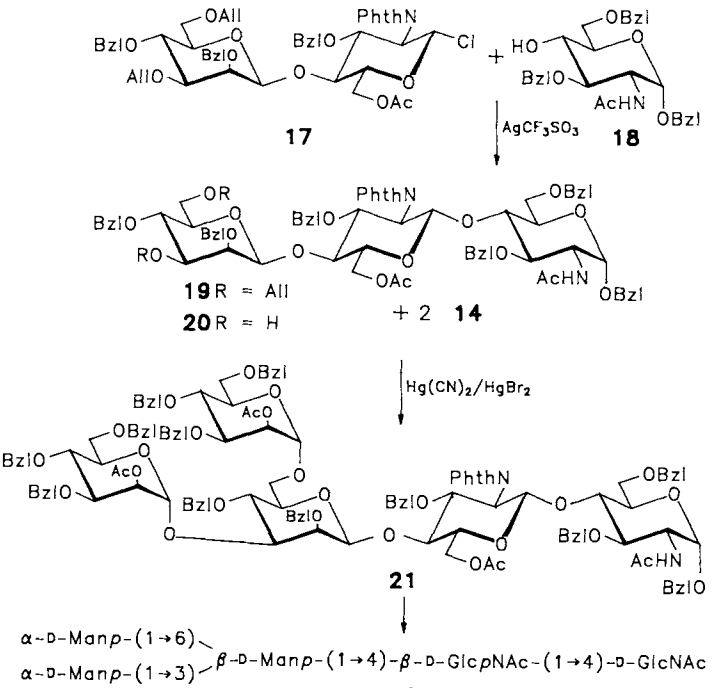

22

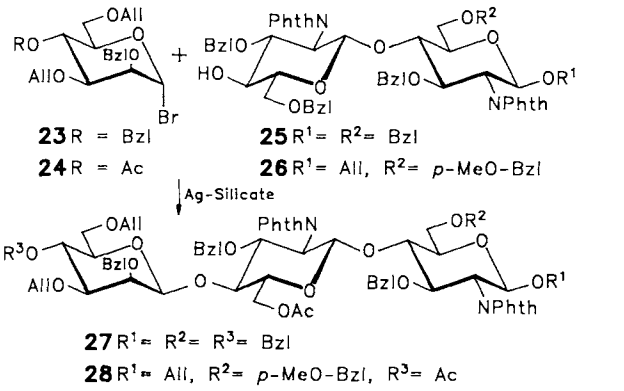

21 in one step.[20] Deprotection then leads to the complete branched core pentasaccharide **22**, which is directly bound to asparagine.

Ogawa et al.[21] followed a different route to arrive at the trisaccharide chain corresponding to **19**. On reaction of mannose donor **23** with disaccharide **25** by the silver silicate method, they isolated the β-linked trisaccharide **27** in 40% yield, as well as significant amounts of the α-linked product. This is remarkable, since the 4'-OH group in **25** is only very poorly reactive. The trisaccharide **27** was used as an intermediate for further reactions.

Van Boeckel et al.[22] have carried out systematic studies on β-mannoside synthesis by the silver silicate procedure, and conclude that the substitution pattern in the glycosyl donor is crucial. C3 and C6 should, if possible, carry electron-donating substituents, while C4 should have an electron-withdrawing group to promote β-glycosidation. Donor **24**, with its 4-OAc group, is therefore optimally substituted.

Reaction of **24** with **26** by the silver silicate method indeed yields the desired β-linked trisaccharide **28** in an increased yield of 48%, while only 19% of the α-glycoside is produced.[23] The trisaccharide **28** thus synthesized was also used for further reactions.

2.2.3. *Synthesis of Lactosamine-type Structures (Complex Type)*

The most important of the structures shown in Figure 1 is the complex type, and it is the commonest found in glycoproteins. Here, lactosamine residues, also called lactosamine antennae, are linked to the inner core structure. Depending on the number of lactosamine residues bound, these compounds are described as di-, tri- or tetra-antennary structures. The external residues may show further variations, such as additional residues or branchings.[1, 2] 5-*N*-Acetylneuraminic acid (Neu5Ac) and L-fucose (Fuc) occur frequently as the terminal residues. Most of the syntheses that have been carried out have been of compounds of this important lactosamine type, or of the so-called "bisected" type (also a complex type in Fig. 1). This review will therefore consider these syntheses closely.

Selective deprotection of the simple tetrasaccharide **15** at the 2-OH group of the terminal mannose residues leads to acceptor **29**. Disaccharide **30** is available as an excellent lactosamine donor,[24] and in one step two residues of **30** may be stereoselectively linked by β-glycosidic bonds to afford octasaccharide **31** in over 70% yield. A series of deprotection steps then leads to **32**. This route enabled us to synthesize a "bi-antennary" lactosamine type structure for the first time.[25, 26]

Ogawa et al.[27, 28] have synthesized a structure in which an additional GlcNAc unit is present at the reducing end. In the *N*-glycoprotein this is bound directly to the asparagine. They used trisaccharide **33** as acceptor, which is available by a few modifications from **27**. The glycosyl donor **34** is a most interesting trisaccharide of lactosamine and mannose. Reaction of **33** with two equivalents of bromide **34** in the presence of silver triflate leads to nonasaccharide **35** in 59% yield.[27] This reaction is remarkable in that it is a reaction of an α-D-mannosyl bromide without neighboring group participation. In the presence of the Lewis-acid-type catalyst silver triflate, the reaction leads stereoselectively to the product with α-linked mannose residues. This peculiarity of mannose has already been remarked upon in Section 2.2.1. Stepwise deprotection of **35** yields **36**, which contains the complete core structure with two lactosamine residues.[27]

Since 5-*N*-acetylneuraminic acid is very often bound to lactosamine in a terminal position, experiments have also been carried out to construct intermediates containing Neu5Ac that could then couple to other residues as such. There are two fundamental difficulties in glycoside synthesis with 5-*N*-acetylneuraminic acid.[29] One observes a competing β-elimination reaction, brought about by the adjacent

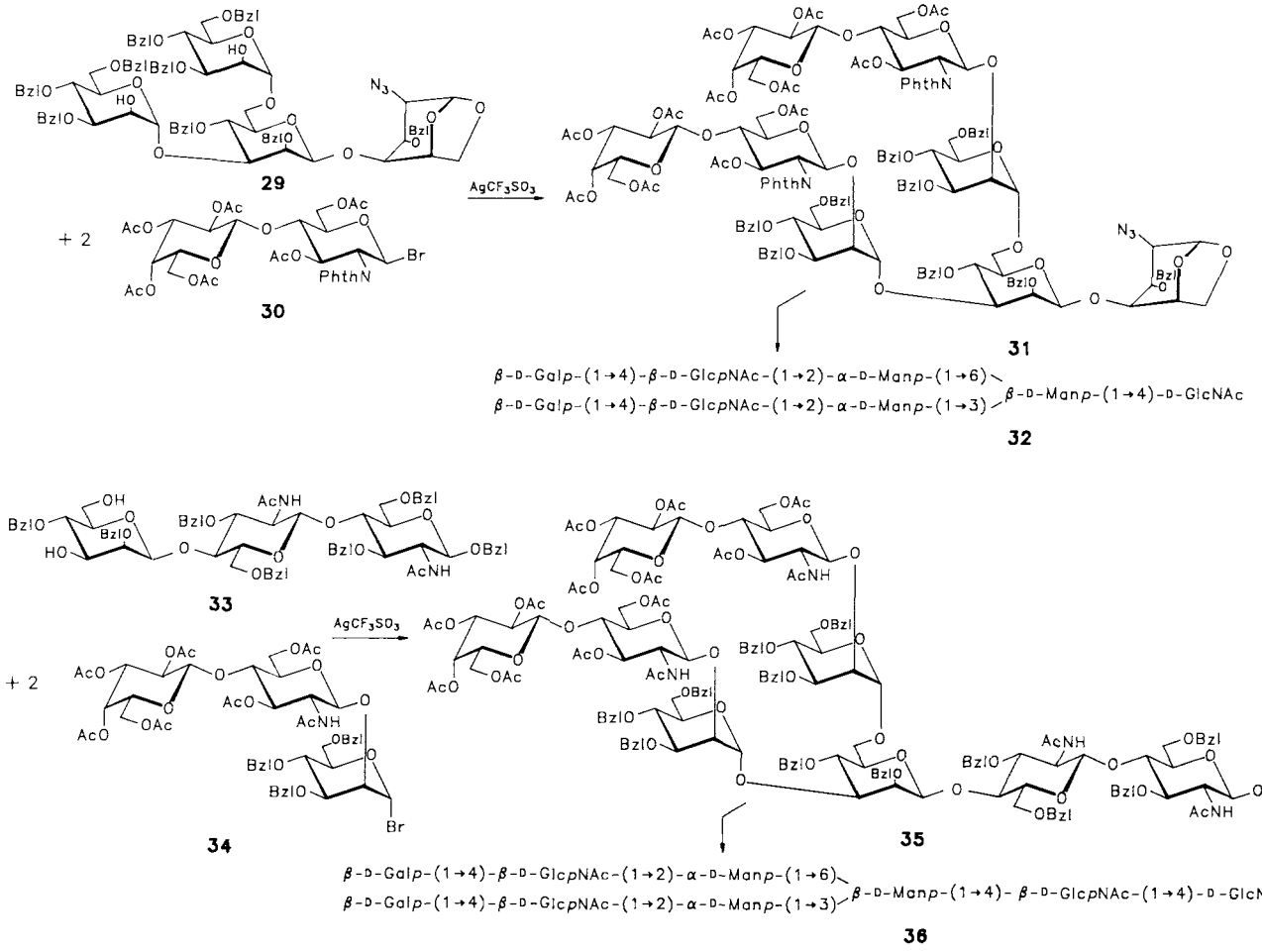

carboxylate group, which gives rise to a 2,3-unsaturated derivative that cannot take part in glycoside synthesis. Furthermore, glycoside synthesis with 5-*N*-acetylneuraminic acid proceeds non-stereoselectively, and α and β products are obtained in varying amounts depending on the reaction conditions. A purification step is required to remove the undesired anomers. Despite these serious obstacles to glycoside synthesis, a number of interesting synthetic intermediates have been synthesized.

Reaction of neuraminic acid donor **38** with lactosamine acceptor **39** gives trisaccharide **43** in 25% yield. If **43** is then converted into the acetate **44**, one has a very useful neuraminic acid-containing glycosyl donor. An example of this is the glycosidation of the mannose derivative **45**. In this case, trimethylsilyl triflate is used as a catalyst, and the 1-*O*-acetyl group acts as a leaving group, with neighboring group participation. The product, obtained in 47% yield, is the β-linked tetrasaccharide **46**. Deprotection leads to the free tetrasaccharide chain **47**.[30]

A different synthetic block was synthesized by *Ogawa* et al.[31] They chose trisaccharide **37** as the glycosyl acceptor for the neuraminic acid donor **38**. In all cases, the most favorable catalyst for the reaction was $HgBr_2/Hg(CN)_2$. After optimization of the reaction conditions, the reaction of **37** with **38** gave the tetrasaccharide **40** in 48% yield.[31] This product **40** could be stabilized by conversion into the fully acetylated **41**. After selective hydrolysis of the 1-*O*-acetyl group the imidate **42** was obtained, which proved to be a useful synthetic intermediate.

The trisaccharide acceptor **33** mentioned above can undergo a double reaction with **42** in the presence of boron trifluoride, though the reaction must be carried out in two steps. First, the chain of **42** is coupled to the reactive 6″-OH group of the mannose. This yields the monoglycosylated product in 48% yield, which must be purified for the second step. The 3″-OH group of the mannose is then glycosylated with **42**, and one obtains oligosaccharide **48** in 56% yield.[32] Stepwise deprotection of this product then yields the free un-

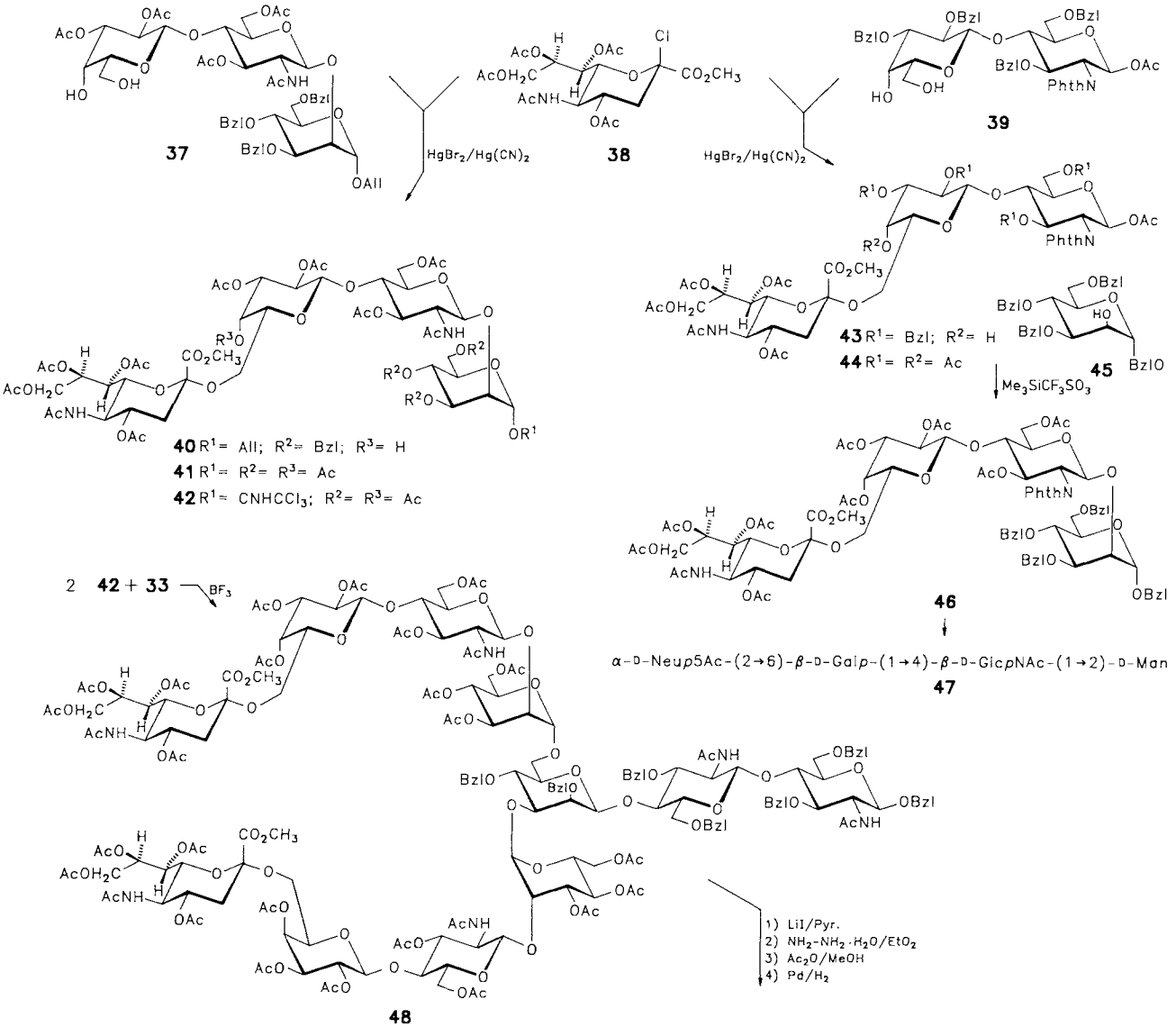

decasaccharide **49**. This synthesis can be said to mark the limits of chemical oligosaccharide synthesis at this time.

It should be mentioned that numerous attempts have been made to improve glycoside synthesis with neuraminic acid. Halogen,[33] sulfur, or selenium[34] groups can be introduced at C3, to avoid the competing elimination reaction. The deoxy form is then regenerated in the end product by reduction at C3. However, these routes require a number of additional steps, and one needs to calculate the yield over the entire pathway in order to assess which route is more favorable. Selectivity in the direction of the α-glycoside has been improved by use of the thioglycosidation method[35] (see Section 2.2.1.). This is also true for the glycosidation of secondary hydroxy groups, which are by nature even more difficult to glycosylate with neuraminic acid donors. In a more recent investigation a larger proportion of α-product was obtained in the presence of a heterogeneous catalyst.[35a]

2.2.4. *Synthesis of "Bisected" Structures*

The so-called "bisected" structures of the complex type in Figure 1 are also interesting, and are important in the biosynthetic pathway as well.[9] In the "bisected" structure, the mannose which forms the branch point bears an additional GlcNAc unit on its 4-OH group. This gives rise to an extremely branched structure, whose construction poses some interesting chemical problems.

We have constructed the trisaccharide acceptor **50**, in which the central mannose unit is intended to form the branch point. The reaction of glycosyl donor **14** with **50** is much more sluggish than that of **14** with **13**. However, by using a large excess of **14** under controlled conditions, **50** can also be coupled to two mannose residues to give **51** in 68% yield.[36] Stepwise deprotection of **51** then yields the extremely branched pentasaccharide **52**.

A number of attempts have been made to deprotect the 2-OH groups on both side-mannose residues in **51** and to link lactosamine chains to them to obtain larger units (as in the lactosamine-type synthesis).[37] However, the reaction with lactosamine donor **30**, which is so successful in the conversion of **29** into **31**, is impossible with derivatives of **51**. Pentasaccharides such as **51** have proved completely resistant to all methods of chain extension.[37] A different strategy therefore had to be adopted.

To construct the required intermediate, it was planned to couple two moles of a trisaccharide donor of lactosamine and mannose, such as **53**, with the trisaccharide diol **50**. Of the various possibilities for activating the trisaccharide donor, only imidate **53** proved sufficiently reactive. It was expected to yield the α-glycoside selectively (cf. Section 2.2.1), in a non-neighboring group active reaction. However, reaction of **50** with **53** led only to the monosubstituted product **54**, in 53% yield. Only the reactive primary hydroxy group of **50** reacts. Even with an excess of **53**, the less reactive secondary 3′-OH group of **54** could not be induced to react.[37]

A detour proved successful, however. If the reactive 6′-OH group in **50** is first protected by a chloroacetyl group

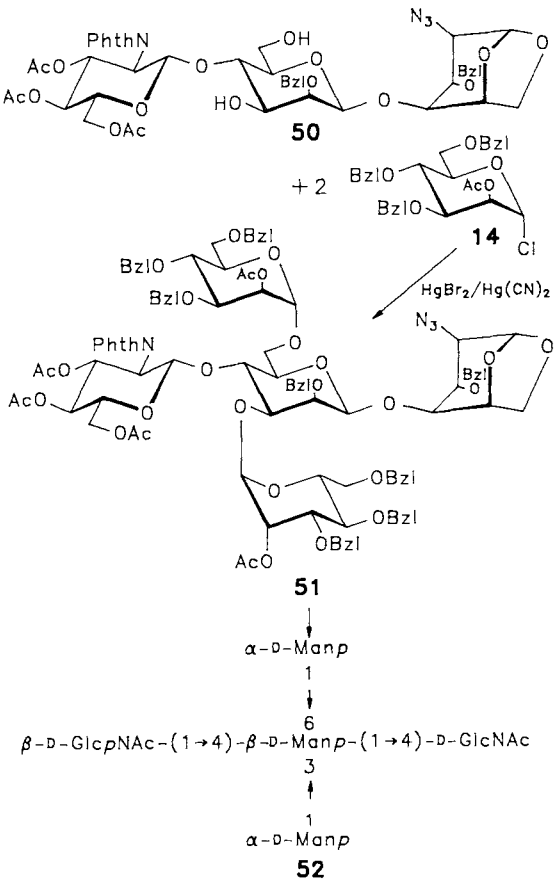

(**50** → **55**), then the reaction of **55** with **53** can be carried out. Use of excess **53** gives a 19% yield of the reversed-substituted hexasaccharide **56**. After selective cleavage of the chloroacetyl group to give **57**, the second side chain can be introduced with **53**, in 58% yield, leading to the desired nonasaccharide **58**.[37] The free "bisected" unit **59** can then be obtained by a series of deprotection steps. This series of reactions makes up an oligosaccharide synthesis of the greatest complexity.

Ogawa et al.[38] have synthesized another "bisected" structure, in which the chain is extended at the reducing end by a GlcNAc unit. As starting material they used the tetrasaccharide diol **60**, which can be obtained from a compound analogous to **33**. Like **50**, this diol can now react with a large excess of mannose donor **14** in the presence of silver triflate in a neighboring group-assisted manner. One obtains the hexasaccharide **61** in 37% yield, along with 34% of the monosubstituted product in which only the reactive, primary 6″-OH group of **60** has undergone reaction. The monoproduct can also be transformed into **61**, in 36% yield.

The 6-OH group of the reducing GlcNAc unit in **61** contains a *p*-methoxybenzyl ether residue which can be selectively cleaved with $[(NH_4)_2Ce(NO_3)_6]$ to give **62**. **62** can then react further with the thioglycoside donor of fucose **63**, in a thioglycosidation reaction in the presence of $CuBr_2 \cdot n Bu_4NBr$. Selective formation of an α-glycosidic linkage to fucose then leads to heptasaccharide **64**. From **64** one can obtain the deprotected compound **65**, which represents a complete core structure of the "bisected" type.[38]

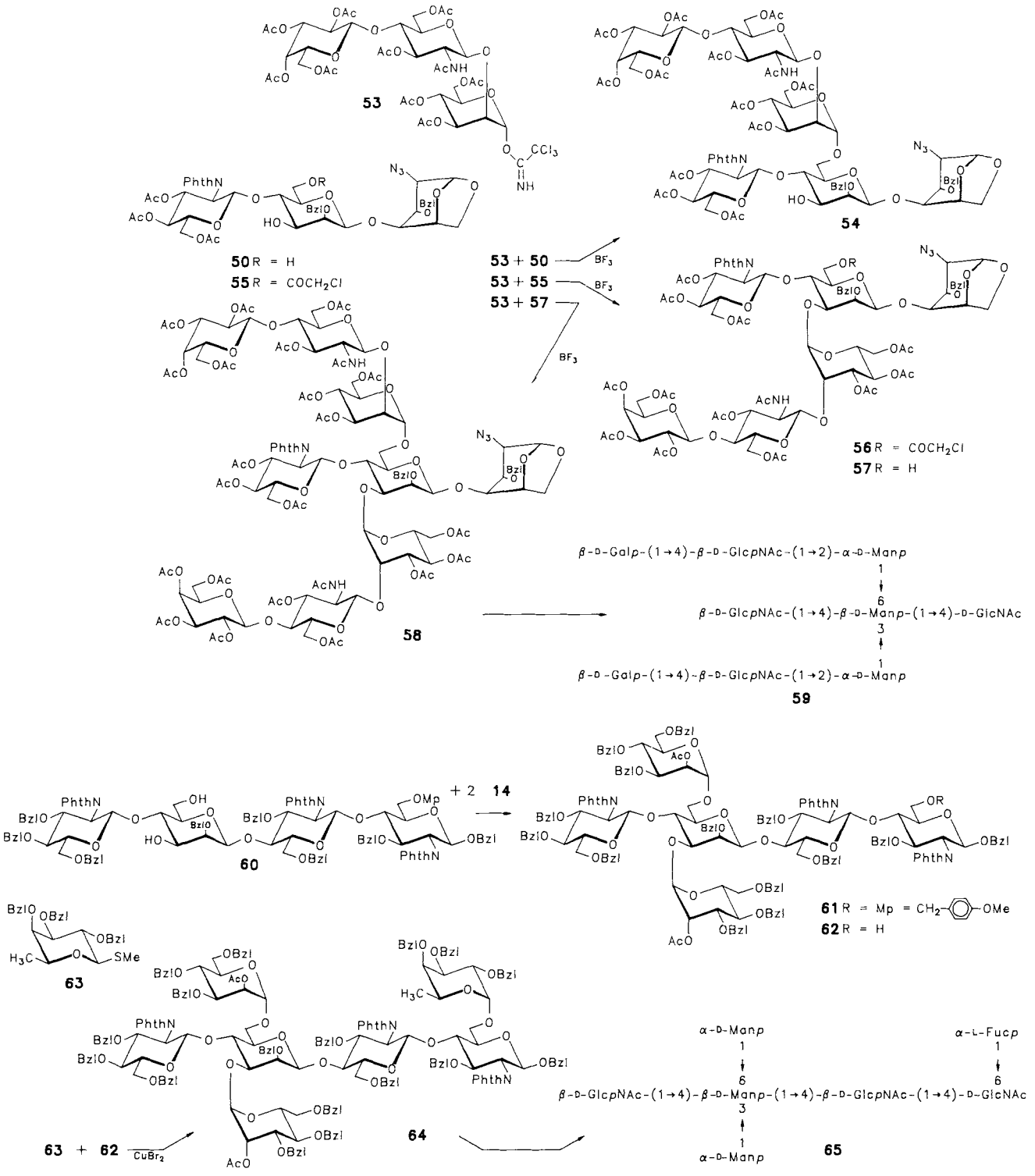

2.2.5. *Synthesis of Other Core Structures*

Of the other basic structures in Figure 1, such large structures as for the complex type have not yet been synthesized, though studies have been made on the synthesis of their side-chains. Thus, *Ogawa* et al.[39] have synthesized hexasaccharide **66** with three glucose units. This makes up one chain of the oligosaccharide precursor that is transferred to the peptide in the dolichol phosphate cycle. The chain is broken down again during the trimming process. The synthesis of these α-linked glucose residues generally gives variable amounts of the β-anomer as a side product.

In addition, *Ogawa* et al.[40] have synthesized derivatives of the branched hexasaccharide **67**, which contains only mannose residues. This chain represents one arm of the mannosidic type. The structure shortened by one mannose unit at each reducing end was also synthesized.[40] This tetrasaccharide is found in both the mannosidic and hybrid types (see Fig. 1).

α-D-Glcp-(1→2)-α-D-Glcp-(1→3)-α-D-Glcp-(1→3)-
α-D-Manp-(1→2)-α-D-Manp-(1→2)-D-Man

66

α-D-Manp-(1→2)-α-D-Manp-(1→6)
α-D-Manp-(1→2)-α-D-Manp-(1→3) α-D-Manp-(1→6)-D-Man

67

2.2.6. *Synthesis of N-Glycopeptides*

Syntheses of *N*-glycopeptides have been carried out from quite an early date, especially by *Jeanloz* et al.[41] GlcNAc[42] and chitobiose[43] were coupled *N*-glycosidically to the amide group of asparagine, which was then extended with further amino acids. The coupling reaction of the saccharide residues with the amino acid was performed by first making the β-glycosyl azide of the amino sugar. This was reduced to the β-glycosylamine, which was then reacted directly with the carboxyl group of the side chain of aspartic acid, using peptide coupling reagents (DDC, EEDQ).[41] This reaction is a critical one, since glycosylamines are relatively labile and tend to dimerize.

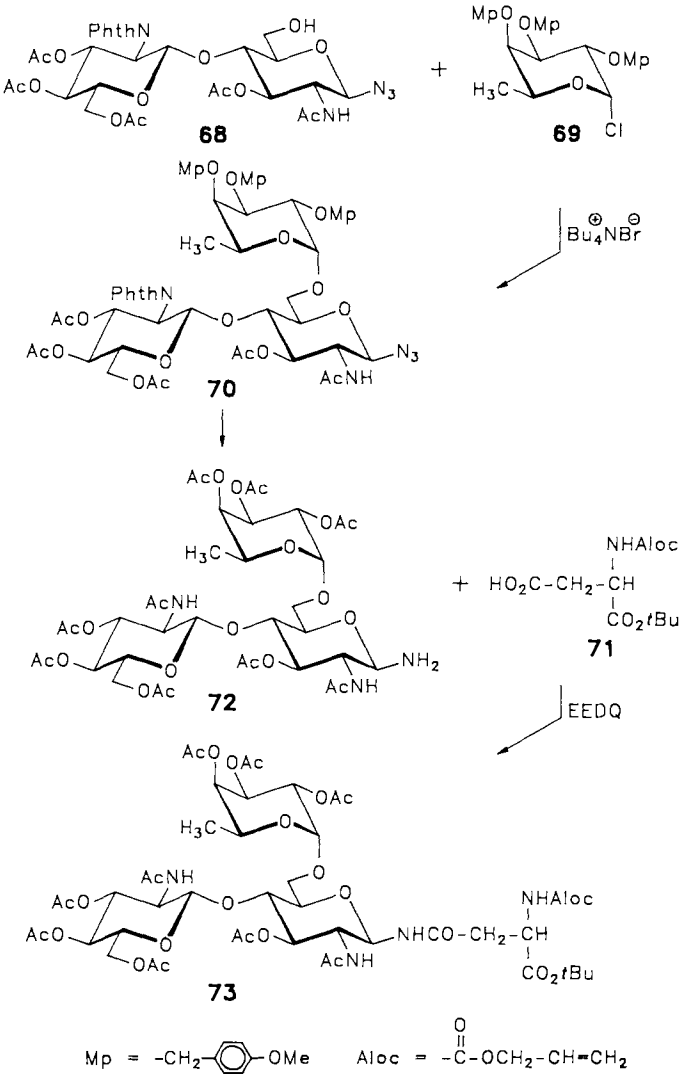

This reaction has been taken up and improved upon by *Kunz*.[44] He was able to couple the key trisaccharide of chitobiose and fucose with asparagine.[45] First the β-glycosylazide **68** was coupled with the fucose donor **69**. Under "in situ" anomerization conditions,[11] one obtains the α-linked trisaccharide **70** selectively. "In situ" anomerization reactions always proceed especially smoothly with fucose derivatives without neighboring group participation.

The *p*-methoxybenzyl substituents in **69** were chosen in order to be able to selectively remove the *O*-*p*-methoxybenzyl groups in the fucose moiety of **70** oxidatively and replace them with *O*-acetyl groups. In the fucose protected with benzyl ether groups, the glycosidic bond is so labile that it cannot tolerate the trifluoroacetic acid required later for release of the *C*-terminus of the amino acid moiety. In contrast, the acetate-protected fucose has a much stabler glycosidic bond, as would be expected. After reduction of the azide group to give glycosylamine **72**, coupling with the aspartate derivative **71** affords *N*-glycosyl amino acid **73**. The amino acid moiety contains the differentiable protecting groups Aloc/*t*Bu, allowing release of either the *C*- or the *N*-terminus. This permits chain extension with any desired amino acids, using peptide coupling methodology.[45] Details may be found in the appropriate review papers.[41,44]

2.3. Conformation of *N*-Glycoprotein Oligosaccharides

2.3.1. *Conformation of the Core Structure and of the "Bisected" Form*

Conformational analysis of the oligosaccharide chains is of great interest, since biological function is frequently correlated to the conformation. In the case of oligosaccharide chains, the number of possible conformations is severely restricted. If, as here, the residues are of *manno*, *gluco* or *galacto* configuration, then the pyranose rings adopt the $^4C_1$-chair conformation almost exclusively (e.g. C4 is above and C1 below the plane of the ring). The size of the glycosidic bond angle τ does not, therefore, vary much at all. Variations in conformation can hence only occur by twisting of the torsion angles ϕ and ψ between the glycosidic bonds (see Fig. 2). The dihedral angle ψ is severely restricted by the

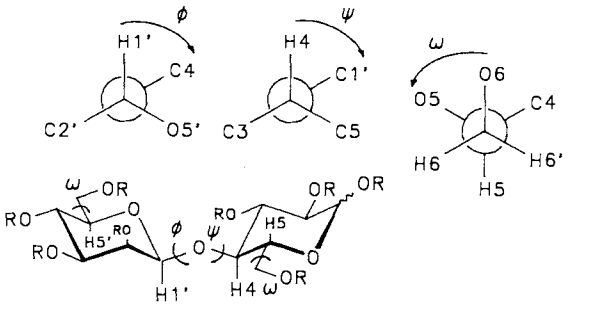

Fig. 2. Definition of the dihedral angles ϕ, ψ and ω in saccharides.

exo-anomeric effect, which predicts a preference for the *gauche* configuration of the ring oxygen with respect to the O–R bond of the aglycone. Model studies and energy calculations show that with two saccharide units that are linked by

a secondary hydroxyl group, the minimum energy form occurs when both protons in the anomeric bond (e.g. H1′- and H4 in Fig. 2) are pointing in approximately the same direction. Conformations in which one ring is reversed possess such a high energy, due to steric interactions, that they virtually do not occur. If there is a bond to a primary 6-OH group, then rotation around the C5–C6 bond constitutes a further variable, described by torsion angle ω. Where branching occurs at the 6-OH group, some variation in conformation is therefore to be expected. A new review of the conformation analysis of oligosaccharides is given by *B. Meyer*.[45a]

Conformational analysis in solution is performed by NMR spectroscopy. To do this, the chemical shift of as many protons as possible needs to be determined. Since the ring protons of the various pyranose rings show very similar chemical shifts, a great deal of overlap is observed, and it is necessary to make intensive use of modern, two-dimensional methods with various correlations.[46] NOE, NOESY or ROESY experiments afford information about NOE-effects within the molecule. ROESY experiments are needed especially when unfavorable molecule correlation times lead to a disappearance of the cross-correlation rate and the NOE-effect passes through zero. With molecules of the size described, this occurs quite often. Interglycosidic NOE-effects are currently of interest. Thus, as shown in Figure 2, one always observes strong NOE-effects over the glycosidic bond when the linkage is to a secondary hydroxyl group, e.g. between protons H1′ and H4. This gives valuable information about the conformation at the glycosidic bonds. Some quantitative evaluation of the NOE-effects is also possible.

The NMR measurements can be complemented by energy calculations using detailed semi-empirical programs such as PCILO[47] or force-field programs such as modified MM2,[48] AMBER,[49] or CHARMM.[50] A simple procedure that has been specially developed for carbohydrate sequences is the force-field program GESA.[45a, 51] This operates by the HSEA method, and is an empirical procedure in which the molecule is calculated iteratively using parametrized potential functions. The energy terms taken into consideration are van-der-Waals interactions in the form of the Kitaigorodsky expression[52] and the *exo*-anomeric effect. Pyranose rings are treated as rigid units whose coordinates are derived from X-ray structures and neutron diffraction studies. When their positions in the crystal structure are not well defined, the protons on the skeleton are not usually adopted, but are generated subsequently by a subprogram. Hydrogen atoms on the OH-groups are not considered. For suitable initial conformations, the ϕ, ψ and ω dihedral angles are optimized simultaneously, using the Fletscher-Powell algorithm.[53] Careful comparative studies by *Carver* et al.[54] have shown that the less complex GESA or HESA procedure gives very similar or identical results to the force-field programs named above. However, in assessing the variable 6-OH side-chain bond it is important to take the population distribution of the conformations into account.[55, 56]

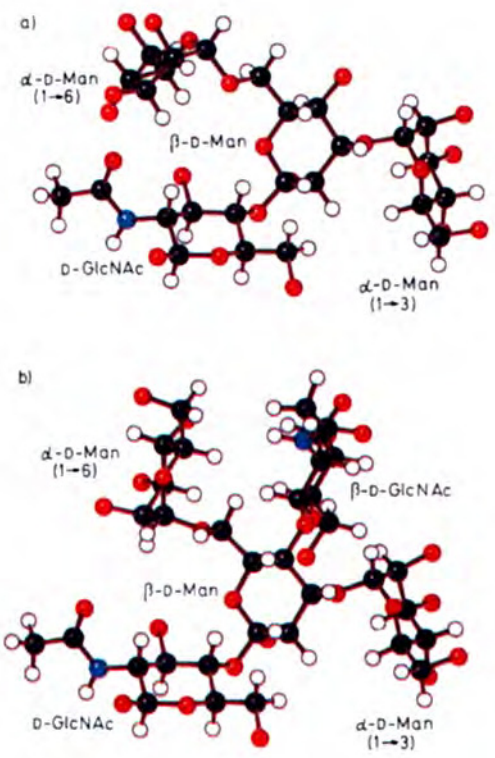

Fig. 3. Conformational minima from NMR data and GESA calculations for: a) tetrasaccharide **16**; b) "bisected" pentasaccharide **52**.

The results of one conformational analysis are given in Figure 3, where the minimum conformations of the branched, central tetrasaccharide **16**[57] and the "bisected" structure **52**[58] are presented. It is important that in both structures the part of the molecule with bonds from secondary hydroxyl groups to the (1 → 3)-arm of the mannose adopts the expected favored conformation. This agrees very well with the NMR data.[57] The flexible (1 → 6)-arm of the mannose in **16** is inclined towards the GlcNAc residue. It is interesting to compare **16** with the "bisected" form **52**. The lower part, with the (1 → 3)-arm, is virtually unchanged. The variable (1 → 6)-arm, however, now prefers a different conformation. This is supported by interglycosidic NOE-effects between the (1 → 6)-Man unit and the "bisected" (1 → 4)-GlcNAc unit.[58] As far as the (1 → 6)-arm is concerned, Figure 3 shows the forms with the highest proportions of the population distribution.

Table 1 presents the torsion angles ϕ and ψ for the individual glycosidic bonds of **16** and **52**. If one compares **16** and **52** it is clear that the values for the lower trisaccharide chain of the (1 → 3)-arm are virtually identical. The variation in the (1 → 6)-arm of the mannose, which prefers a different position in **52**, stands out clearly. The lower trisaccharide α-D-Man-(1 → 3)-β-D-Man-(1 → 4)-D-GlcNAc is the only oligosaccharide for which the X-ray structure is known.[59] For this part of both **16** and **52**, the ϕ and ψ values from the crystal structure are also included in Table 1. These values

Table 1. Torsion angles [°] of the preferred configurations of **16** and **52** determined by NMR measurements and GESA calculations, and in the crystal structure.

	β(1 → 4)		α(1 → 3)		α(1 → 6)		β-D-Man
	ϕ	ψ	ϕ	ψ	ϕ	ψ	ω
16	57	7	−48	−13	−58	179	48
52	59	−2	−48	−15	−59	152	−66
Crystal [a]	48.1	0.6	−57.6	−19.4	–	–	–

[a] X-ray structure of α-D-Man*p*-(1 → 3)-β-D-Man*p*-(1 → 4)-D-GlcNAc.

also do not differ greatly from those calculated for **16** and **52**, showing that the (1 → 3)-arm adopts very similar conformations in solution and in the crystal.

2.3.2. *Reaction of Modified Core Oligosaccharides with GlcNAc Transferase I*

Compounds **16** and **52**, whose conformations have been discussed here, are of great interest because of the difference in their behavior with GlcNAc transferase I. GlcNAc transferase I is the first enzyme to begin construction of new chains on the invariant core structure **22** during the trimming process.[9] It selectively adds the initial GlcNAc unit onto the (1 → 3)-arm of the mannose. Structure **74** (Fig. 4) corresponds to the substrate of this process, and reacts most actively (100%) with the enzyme. The two additional mannose residues on the (1 → 6)-arm in **74** are removed later by mannosidases.[9]

Tetrasaccharide **16** is also a very active substrate for this enzyme (65%). The "bisected" structure **52**, however, is not glycosylated;[60] the "bisected" arrangement is hence a stop signal for GlcNAc transferase I. It seemed reasonable to suggest that this inactivity is due to the great difference in conformation between **16** and **52** observed above, and brought about by the additional GlcNAc group on the 4′-OH in **52**.

In order to test this assumption, the modified tetrasaccharide **75** was synthesized, bearing a 4′-deoxy functionality at the branch unit.[61] **75** is not a substrate for GlcNAc transferase I either.[62] Further, **75** was also found to prefer the same conformation as **16**,[63] showing that the change in conformation in **52** is not important for the enzyme reaction. For activity, GlcNAc transferase I requires the 4′-OH group of the central mannose. Interestingly, the modified tetrasaccharide **76**,[61] which contains D-talose at the branch point, is not a substrate either.[63] If one methylates the 4′-OH group in **16** to the 4′-*O*-methyl ether, the resulting compound also does not react with GlcNAc transferase I.

From these findings, one may conclude that GlcNAc transferase I has an absolute requirement in substrate binding for an equatorial 4′-OH group (key polar group). Possibly the enzyme forms a hydrogen bond here, since the corresponding 4′-*O*-methyl ether does not react. This example shows most impressively how the synthesis of modified oligosaccharide substrates can lead to very subtle information about an enzyme binding site. However, it also shows how careful one must be in interpreting the significance of conformational changes.

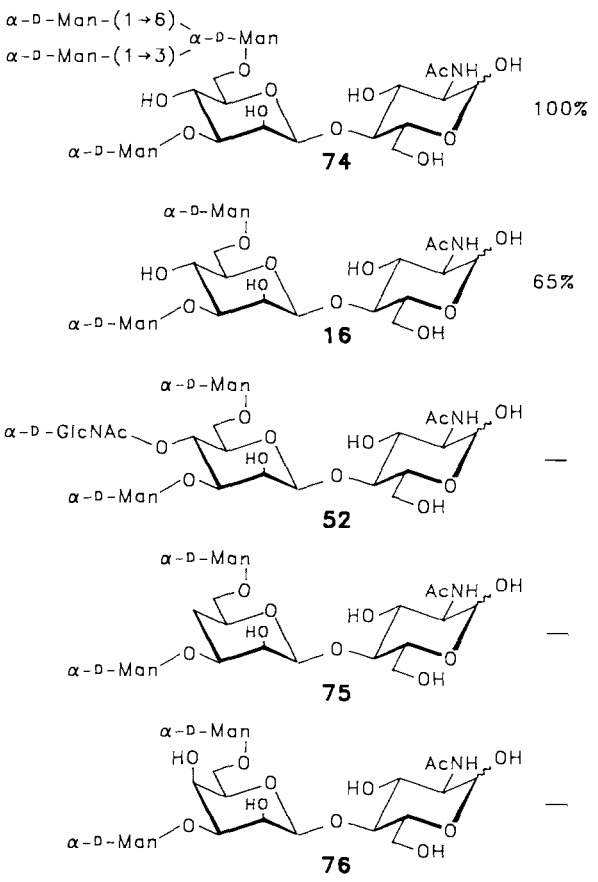

Fig. 4. GlcNAc transferase I activity with natural and modified oligosaccharide substrates.

2.3.3. *Conformation of the Lactosamine-type Structure and Comparison with the X-Ray Structure of the Saccharide Chain in Immunoglobulin*

Conformational analysis by the NMR and GESA methods described above was also carried out on the available octasaccharide **32**.[64, 65] The result is presented in Figure 6a.[64] The pentasaccharide chain with linkages to the secondary hydroxy groups of the (1 → 3)-arm shows the expected preferred conformation. The side chain of the (1 → 6)-arm is also inclined towards the reducing GlcNAc unit, as in **16**. Selective deshielding of the protons in the reducing GlcNAc unit confirm that this form indeed makes up a distinct proportion of the population.

With **32** it is now possible to make a comparison with a corresponding crystalline structure. **32** naturally does not crystallize. However, this octasaccharide is contained in an immunoglobulin which has been crystallized by *Huber*[66] and *Deisenhofer*,[67] and of which the X-ray structure has been determined. Figure 5 shows a schematic diagram of the IgG_1 immunoglobulin molecule. The upper portion contains the light chains, the lower F_c portion consists of the heavy

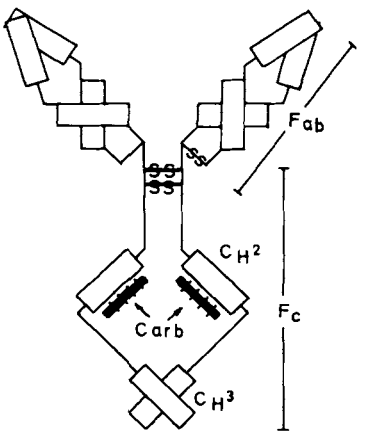

Fig. 5. Schematic model of IgG_1. Carb = oligosaccharide chain.

chains, and includes two identical carbohydrate chains facing each other in the interior of the molecule. These two chains are *N*-glycosidically linked to Asn297 and Asn597, and possess a complex lactosamine-type structure. They therefore also contain the base structure of **32**, and occur twice in the F_c-fragment.

Huber and *Deisenhofer* were able to crystallize the separated F_c-fragment, determine the protein chain structure, and also resolve the carbohydrate chain to 2.8 Å.[66–68] This resolution is remarkable. They were assisted in this by the fact that the carbohydrate chain inside the molecule is largely fixed. In other glycoprotein crystal structures, the carbohydrate moiety is usually flexible and can only be localized with difficulty. The sample studied by *Huber* and *Deisenhofer* contained no 5-*N*-acetylneuraminic acid and no "bisected" unit. The GlcNAc group bound to asparagine carried fucose at its 6-OH as a branch unit. All saccharide units were localized, except the terminal galactose on the (1 → 3)-arm. This unit has been added for completeness in Figures 6 and 7. It should be mentioned that the carbohydrate moiety in different types of immunoglobulin can vary, and deviations from the structure described here may be found.[69]

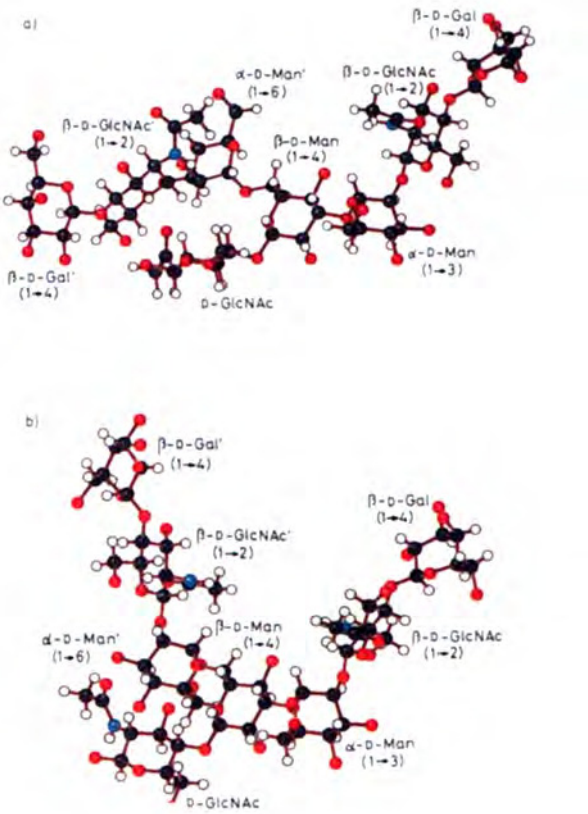

Fig. 6. Conformation of octasaccharide **32**: a) from NMR data and GESA calculations; b) in the crystal of the F_c fragment of IgG_1 immunoglobulin molecule.

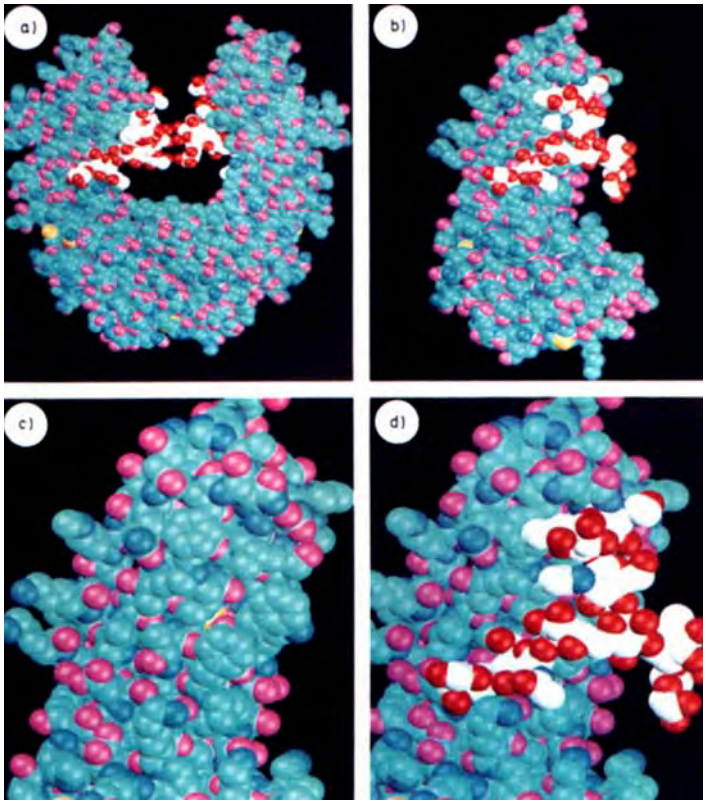

Fig. 7. a) X-ray crystal structure of the IgG_1 molecule F_c-fragment. b) One half of the F_c-fragment. c) Enlarged section of the region of the protein chain where the carbohydrate moiety is bound. The carbohydrate moiety has been omitted. d) The same section as in 7(c), with the carbohydrate chain replaced. Carbohydrate chain: C white, O red, N dark blue; protein chain: C light blue, O pink, N dark blue, S yellow.

The conformation of octasaccharide **32** in the crystal is reproduced in Figure 6b. It can be seen that the pentasaccharide chain with linkages through secondary hydroxy groups in the (1 → 3)-arm is very similar in solution and in the crystal. The flexible (1 → 6)-arm, however, is completely changed, and in the crystal points upwards. Table 2 compares the torsion angles ϕ and ψ for the two conformations. The crucial difference appears in the ψ-value for the (1 → 6)-bond (171 ° in the crystal, 79 ° in solution). The other values for bonds through secondary hydroxy groups are remarkably similar. In these portions of the molecule, quite similar conformations must be preferred both in solution and in the crystal. The deviation at the reducing GlcNAc unit is understandable, since in the crystal this is linked to a further GlcNAc residue. The variation in the (1 → 6)-arm occurs largely because this chain of the molecule lies on a protein

Table 2. Torsion angles [°] of the preferred configuration of **32** (NMR data, GESA calculations) and conformation of **32** in the crystal of the F_c-fragment of IgG_1.

	(1 → 6)-Lactosamine arm							(1 → 3)-Lactosamine arm					
	β(1 → 4)		β(1 → 2)		α(1 → 6)		C5-C6	β(1 → 4)		α(1 → 3)		β(1 → 2)		β(1 → 4)	
	ϕ	ψ	ϕ	ψ	ϕ	ψ	ω	ϕ	ψ	ϕ	ψ	ϕ	ψ	ϕ	ψ
NMR/GESA	55	2	47	0	−54	79	38	57	−5	−47	−14	52	23	52	2
X-ray structure	75	−4	51	27	−55	171	68	29	−32	−49	−4	72	28	[a]	

[a] Not fixed, due to insufficient electron density.

structure. This prompted us to examine the conformation of the entire F_c-fragment more closely.

Figure 7a shows the entire F_c-fragment in the structure derived from the X-ray analysis.[45a, 68] The two carbohydrate chains can clearly be discerned in the center, surrounded by the heavy protein chains. In the left half of the molecule one part of the carbohydrate chain is directed forward. In the right-hand portion of the molecule, the corresponding carbohydrate strand points backwards.

In order to make the structure clearer, Figure 7b shows only one half of the molecule. The coupling of the carbohydrate chain to the asparagine occurs quite high up in the molecule, where the attached fucose residue can also be identified. The mannose that functions as the crucial branching unit lies in the center of the star-like carbohydrate chain. It is most interesting that the two lactosamine arms which arise from the branching point display quite different arrangements. The flexible (1 → 6)-arm lies to the left, directly on a protein chain. The less flexible (1 → 3)-arm, in contrast, is oriented to the right and points exactly into the center of the entire molecule. This arm is not in contact with any part of the protein chain.

For clarity, Figures 7c and 7d show the carbohydrate binding region in Figure 7b, further enlarged. Figure 7c shows the regions of the protein without the carbohydrate, in the upper part of the molecule where the carbohydrate chain is eventually inserted. Phenyl rings can be clearly identified in this region, assignable to phenylalanine and tyrosine. In this section lie Phe 241, Phe 243, Val 262, Val 264 and, in the upper part, Tyr 296. The flexible (1 → 6)-arm therefore lies on a hydrophobic region of the protein chain.

This becomes particularly clear in Figure 7d: The flexible (1 → 6)-arm, at the lower left, lies on a hydrophobic section of the protein chain, and possibly acquires more hydrophobic characteristics. The (1 → 3)-arm at the lower right is unaffected, and points into the center of the molecule. It can presumably be assigned more hydrophilic properties. It should be pointed out that this arm has no contact with the other (1 → 3)-arm which is directed towards the inside from the other half of the molecule. In the upper part lies the chitobiose and the fucose that adjoins it. The arrangement is therefore an interesting one, in which lactosamine arms clearly have different functions. It can be assumed that this arrangement contributes to the special stabilization of the F_c-fragment that is required for reactions of the immunoglobulin as an antibody.

3. *O*-Glycoproteins

3.1. Basic Structures

In the *O*-glycoproteins, too, constantly recurring sequences are found as the basic core structures. The most important of these sequences are brought together in **77**–**81**. In types **77** to **80**, the key element is a galactosamine unit bound α-glycosidically to the hydroxy group of a serine or a threonine, to which galactose or glucosamine groups are then linked. Types **77** to **80** are denoted Core-I to Core-IV. The most important is the Core-I structure **77**, which is extraordinarily widespread and occurs in the most diverse glycoproteins. The Core-II, Core-III and Core-IV structures are found particularly in mucins and in a number of slimy secretions. In structure **81**, by contrast, a xylose residue is bound

β-D-Gal-(1→3)-α-D-GalNAc-L-Ser/Thr **77**
Core I

β-D-GlcNAc-(1→6)
β-D-Gal-(1→3) → α-D-GalNAc-L-Ser/Thr **78**
Core II

β-D-GlcNAc-(1→3)-α-D-GalNAc-L-Ser/Thr **79**
Core III

β-D-GlcNAc-(1→6)
β-D-GlcNAc-(1→3) → α-D-GalNAc-L-Ser/Thr **80**
Core IV

β-D-Gal-(1→3)-β-D-Gal-(1→4)-β-D-Xyl-L-Ser **81**

to the hydroxy group of the serine, with galactose residues then linked to the xylose. Sequence **81** occurs primarily as a linker element between the carbohydrate and protein chains in proteoglycans and hyaluronic acids.

The biosynthesis of the *O*-glycoproteins is, however, fundamentally different from that of the *N*-glycoproteins described above.[9] In *O*-glycoproteins, the primary step involves the transfer of an activated GalNAc residue onto the hydroxy group of serine or threonine by a specific GalNAc transferase. It is not yet known how this process is controlled, and whether there are signal sequences for it. Presumably a proline unit plays a role in the transfer. The other carbohydrate residues are then added stepwise to the GalNAc unit by the corresponding specific glycosyl transferases. Here, then, unlike in the *N*-glycoproteins, large oligosaccharide residues are not transferred onto the peptide chain, but the synthesis proceeds stepwise at the peptide chain.

3.2. Synthesis of *O*-Glycopeptides

Many studies have been made of the synthesis, in particular, of glycopeptides of the most important Core-I structural type.[44, 70] The problem is that an α-glycosidic linkage to the hydroxy amino acid has to be synthesized, without neighboring group participation. With derivatives of galactosamine, this is not possible. Halogenides of 2-azido-2-deoxy-D-galactose are excellent glycosyl donors in this reaction.[72–75]

Thus, donor **82**[71] reacts with the amino acid derivative **83** with good stereoselectivity and in good yield to afford the glycosyl amino acid **84**.[76, 77] Reduction of the azide group and subsequent acetylation then leads to the desired product **85**. Similarly, disaccharide **86**[72] can be converted into **87** with the amino acid **83**, and from **87** the synthetic intermediate **88** can then be obtained.[76, 77]

In the amino acid moiety of the compounds, protecting groups must be chosen which allow selective deprotection. Of the numerous protection possibilities that have been studied,[44, 70] the Fmoc/*t*Bu and Aloc/*t*Bu combinations have proven the most successful. Both pairs allow the selective deprotection of either the *N*-terminal or the *C*-terminal position. Using normal peptide coupling methods, further amino acids or glycosyl amino acids may then be added to either the *C*- or *N*-termini. Intermediates **85** and **88** can hence be insert-

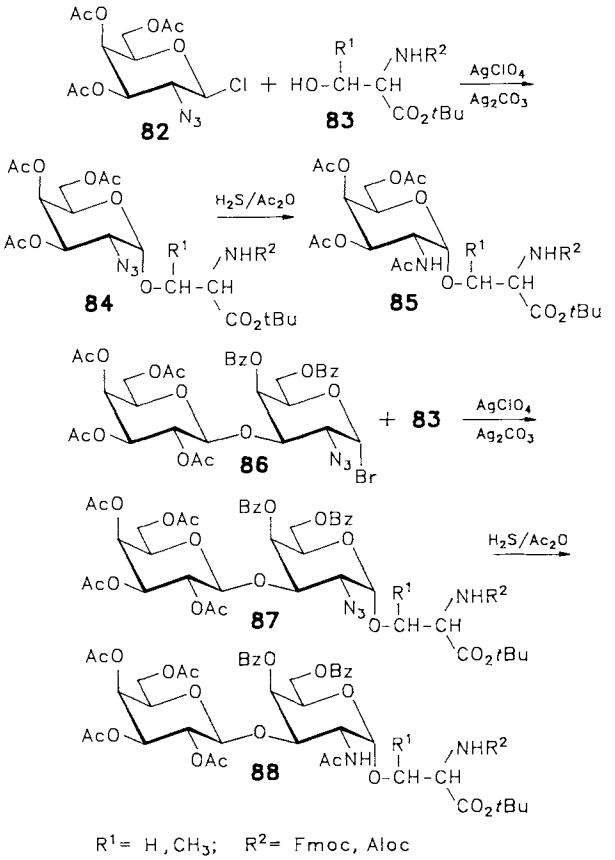

ed at any desired position in a peptide chain, wherever a glycosylated serine or threonine is required. After removal of the peptide protecting group, the acyl groups of the sugar moiety are then cleaved under carefully controlled conditions, such that β-elimination or racemization of the peptide does not occur.

O-Glycopeptide synthesis can also be carried out as a solid-phase process.[78, 79] Amongst others, Wang resin is suitable for this.[79] Wang resin contains the anchoring group shown in **89**. The initial amino acid coupled to the resin is the TDO ester **90**, to give **91**.[80] After release of the amino group as **92**,

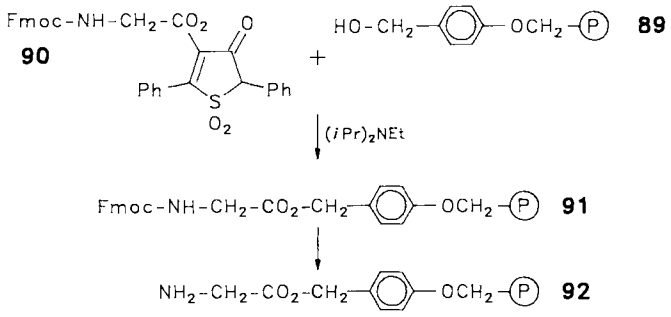

the partially deprotected amino acid building blocks of **85** or **88** can be added, as can any other amino acid required to build up the peptide chain. An example of such an *O*-glycopeptide synthesis is shown in the reaction scheme of Figure 8.[81] The completed glycopeptide can be cleaved from the solid support with trifluoroacetic acid to give **93**, without endangering the carbohydrate moiety. Deprotection of the peptide and of the sugar moiety then yields the free glycopeptide **94**. This example illustrates that even glycopeptides with complex amino acids such as arginine can be synthesized on a solid support.

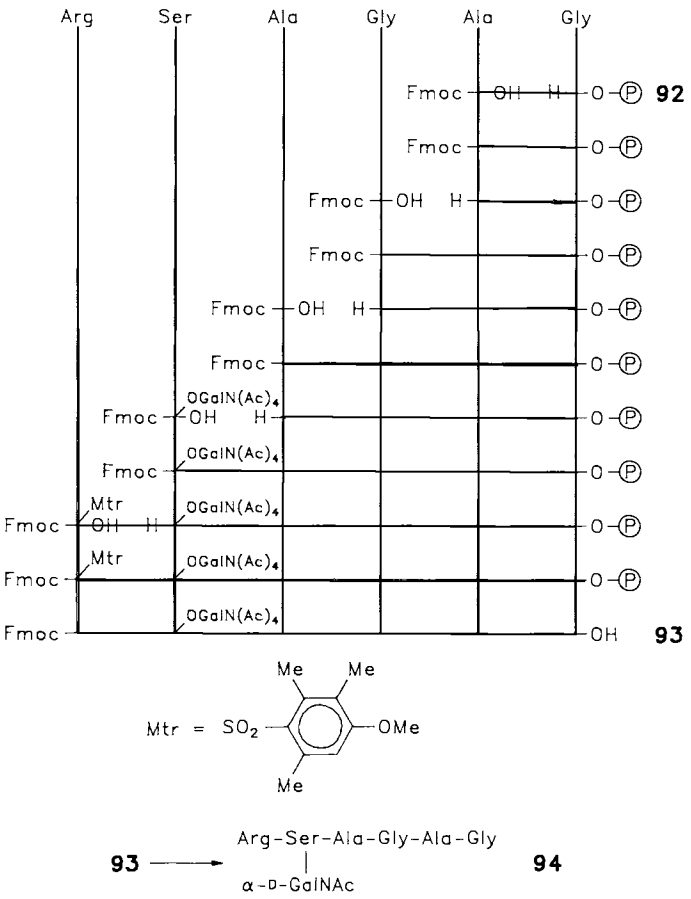

Fig. 8. Example of a solid-phase glycoprotein synthesis (Wang resin). Synthesis of Arg-Ser[α-D-GalNAc]-Ala-Gly-Ala-Gly **94**.

As well as a series of *O*-glycoproteins of the Core-I type, compound **78**, of the Core-II type, has also been synthesized.[82, 83] The xylose-containing compound **81** has been synthesized as the fragment β-D-Gal-(1 → 4)-β-D-Xyl-L-Ser[84] and also as the entire chain of **81**,[85] (for review articles see Refs.[44, 70]).

3.3. Conformational Analysis of *O*-Glycopeptides

Studies of the conformation of *O*-glycopeptides have concentrated especially on the molecular arrangement in the coupling region of the carbohydrate residue with the peptide chain. Though the peptide chain is always extremely flexible, in the carbohydrate-binding region preferred conformations are nonetheless to be expected. The question also arises of whether the peptide chain is significantly affected by the linked carbohydrate molecule.

The series of glycopeptides **95** to **98** have been studied particularly intensively.[86] These compounds make up seg-

ments of the *N*-terminus of interleukin-2. In interleukin-2, Ala is located at the *N*-terminus. Thr3 carries a carbohydrate chain of the Core-I type, which contains additional 5-*N*-acetylneuraminic acid residues. The entire molecule consists of 133 amino acids. The *N*-terminal structures **95** to **98** were synthesized by the above methods, with the peptide being extended by one or more units successively at the *C*-terminus.[76] This was done to examine whether extension of the peptide chain influenced the conformation of the sugar moiety at the link.

Ala-Pro-Thr-Ser
α-D-GalNAc **95**

Ala-Pro-Thr-Ser-Ser
α-D-GalNAc **96**

Ala-Pro-Thr-Ser-Ser-Ser
α-D-GalNAc **97**

Ala-Pro-Thr-$(Ser)_3$-Thr-$(Lys)_2$-Thr
α-D-GalNAc **98**

Ala-Ser-Gly-Ile
β-D-Xyl **99**

Conformational analysis was carried out by means of modern NMR spectroscopy, as described above. After assignment of all the protons with the aid of various correlation methods, coupling constants and NOE effects were determined using NOE, NOESY and ROESY experiments.[46] Hydrogen bonding was measured by the temperature dependence of the chemical shifts. Relaxation times afforded information about the mobility of the atoms. Evaluation of all the data yields a consistent picture which shows that there are significant amounts of preferred conformation around the coupling site.[86]

In addition, energy calculations for the molecules were carried out using the program AMBER,[49] after this had been tested for its applicability. It turned out that AMBER is suitable for calculations on peptide chains with one saccharide unit. Calculations for compound **95** led to the minimum conformation depicted in Figure 9a. This conformation turned out to be in very good agreement with the NMR data, especially with the coupling constants and NOE-effects observed. The protons between which NOE-effects were found are indicated with arrows in Figure 9a. The numbers given are the distances in Å derived from the AMBER calculation. At the distances given, it can be seen that NOE-effects are to be expected.

The arrangement between GalNAc and threonine is largely determined by the *exo*-anomeric effect of the glycosidic bond. The relationship between the peptide chain and the sugar residue, however, is probably dictated by steric influences. The conformation can be demonstrated by coupling constants and NOE-effects, e.g. between the methyl acetyl group of GalNAc and the serine. Here, one finds clearly preferred arrangements of the peptide chain and the sugar residue. It is interesting, now, to compare this with compounds **96**, **97** and **98**. It turns out that the basic arrangement for **95** given in Figure 9a appears almost completely unchanged on chain extension to **96**, **97** and **98**. Extension of the peptide chain at the *C*-terminus therefore has no significant influence on the preferred conformation around the linkage between saccharide residue and peptide chain.[86]

It should be mentioned that *Bush* et al.[87] have carried out a conformational analysis of the antifreeze-protein that is present as an anti-freezing agent in the blood of antarctic deep sea fish. The antifreeze-protein is a homopolymer of the peptide unit (L-Ala-L-Thr-L-Ala)$_n$, in which a hydroxy group of each threonine is glycosylated with a disaccharide of the Core-I structure. The preferred conformation determined by *Bush* et al. agrees well with that found for **95**. So far, there is only one X-ray analysis of a glycosyl amino acid, the rare structure α-D-Man(1 → *O*)-L-Thr, which occurs in bacteria.[88] The configuration in this X-ray structure is also in good agreement with the conformational minimum of **95** (Fig. 9a) calculated with AMBER.[86]

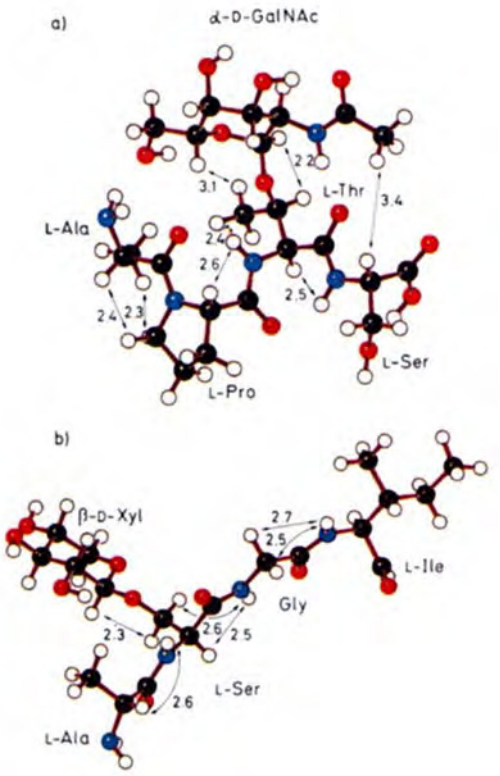

Fig. 9. Preferred conformation of *O*-glycopeptides, from NMR data and AMBER calculations. The arrows show the protons where NOE-effects were found which are important in determining the conformation. The numbers are distances in Å, from the calculations. a) Preferred conformation of Ala-Pro-Thr[α-D-GalNAc]-Ser **95**. b) Preferred conformation of Ala-Ser[β-D-Xyl]-Gly-Ile **99**.

Conformational analyses have also been carried out on *O*-glycopeptides with xylose and serine as the link.[89] This arrangement is more flexible, as shown by the NMR data of the simple compound β-D-Xyl(1 → *O*)-L-Ser. An example is the tetra-*O*-peptide **99**, which represents a sequence from proteodermatan sulfate in bovine skin. This was synthesized by direct glycosylation of the end-group-protected tetrapeptide with β-D-xylose tetraacetate, using the trimethylsilyl triflate procedure.[90] A conformational analysis was performed as for **95**, by evaluation of all available NMR data, and with an energy calculation using the program AMBER.

The result is presented in Figure 9b.[89] Here again, the arrows indicate the protons between which NOE-effects

were found, and the numbers are the distances in Å. The *exo*-anomeric effect is decisive here, too. Further, steric interactions are probably also important. The NMR measurements and energy calculations clearly show that there are also preferred conformations with structures like **99**, in which, as is shown in Figure 9b, the peptide chain adopts a particular arrangement with respect to the saccharide residue.

This review contains primarily the results of our research group. I am indebted to a large number of capable co-workers for their tireless commitment and stamina. The synthetic work was performed largely by K. Adermann, M. Heume, R. Lebuhn, G. Merz, H. Nürnberger, T. Peters, M. Raatz, H. Tietz. The conformational analyses of the N-protein structures were all carried out by Dr. T. Peters and Dr. V. Sinnwell, those of the O-protein structures by Dr. A. Pollex-Krüger. My special thanks are due to Dr. B. Meyer (Athens) for the GESA program, and for further calculations. I am also grateful to him for the diagrams of the F_c-fragment crystal structure, which were made at the University of Georgia (Complex Carbohydrate Research Center, Prof. P. Albersheim). I thank Professor R. Huber (Munich) for the data for the F_c-fragment crystal structure. Professor J. Deisenhofer (Dallas) kindly provided the corrected and refined data for the carbohydrate part of the crystal structure, which he had determined together with Dr. B. Meyer. For the programs MACROMODEL and AMBER, I thank Professor C. W. Still (New York) and Professor P. Kollman (San Francisco). The Deutsche Forschungsgemeinschaft has generously supported our work over many years.

Received: February 12, 1990 [A 775 IE]
German version: *Angew. Chem. 102* (1990) 851
Translated by Dr. *M. A. Kertesz*, Zürich (Switzerland)

[1] J. Montreuil, *Adv. Carbohydr. Chem. Biochem. 37* (1980) 157.
[2] A. Kobata in V. Ginsburg (Ed.): *Biology of Carbohydrates*, Wiley, New York 1984.
[3] A. Gottschalk (Ed.): *Glycoproteins*, Elesevier, Amsterdam 1972.
[4] M. J. Horowitz, W. Pigman (Ed.): *The Glycoconjugates, Vol. I–IV*, Academic Press, New York 1977–1982.
[5] N. Sharon, H. Lis, *Chem. Eng. News 58* (1981) 21.
[6] T. W. Rademacher, R. B. Parekh, R. A. Dwek, *Annu. Rev. Biochem. 57* (1988) 785.
[7] E. J. Goldstein (Ed.): *Carbohydrate Protein Interaction, ACS Symp. Ser. 88* (1979).
[8] T. Feizi, *Nature (London) 314* (1985) 53; *Biochem. J. 245* (1987) 1.
[9] H. Schachter, *Can. J. Biochem. Cell Biol. 64* (1986) 163.
[10] R. Kornfeld, S. Kornfeld, *Annu. Rev. Biochem. 54* (1985) 631.
[11] H. Paulsen, *Angew. Chem. 94* (1982) 184; *Angew. Chem. Int. Ed. Engl. 21* (1982) 155.
[12] R. R. Schmidt, *Angew. Chem. 98* (1986) 213; *Angew. Chem. Int. Ed. Engl. 25* (1986) 212.
[13] a) P. Füged, P. J. Garegg, H. Lönn, T. Norberg, *Glycoconjugate J. 4* (1987) 97; F. Dasgupta, P. J. Garegg, *Carbohydr. Res. 177* (1988) C 13; b) C. Muraka, T. Ogawa, *Tetrahedron Lett. 31* (1990) 2439.
[14] H. Paulsen, O. Lockhoff, *Chem. Ber. 114* (1981) 3102.
[15] M. A. E. Shaban, R. W. Jeanloz, *Carbohydr. Res. 52* (1976) 115.
[16] C. D. Warren, C. Augé, M. L. Laver, S. Suzuki, D. Power, R. W. Jeanloz, *Carbohydr. Res. 82* (1980) 71; C. Augé, C. D. Warren, R. W. Jeanloz, M. Kiso, J. Anderson, *ibid. 82* (1980) 85.
[17] H. Kunz, W. Günther, *Angew. Chem. 100* (1988) 1118; *Angew. Chem. Int. Ed. Engl. 27* (1988) 1086.
[18] H. Paulsen, R. Lebuhn, O. Lockhoff, *Carbohydr. Res. 103* (1982) C7.
[19] H. Paulsen, R. Lebuhn, *Liebigs Ann. Chem.* 1983, 1047.
[20] H. Paulsen, R. Lebuhn, *Carbohydr. Res. 130* (1984) 85.
[21] T. Ogawa, T. Kitajma, T. Nukada, *Carbohydr. Res. 123* (1983) C5.
[22] C. A. A. van Boeckel, T. Beetz, S. F. van Aelst, *Tetrahedron 40* (1984) 4097; C. A. A. van Boeckel, T. Beetz, *Recl. Trav. Chim. Pays-Bas 104* (1985) 171, 174.
[23] F. Yamazaki, T. Kukuda, Y. Ito, S. Sato, T. Ogawa, *Tetrahedron Lett. 30* (1989) 4417.
[24] J. Arnarp, J. Lönngren, *J. Chem. Soc. Chem. Commun.* 1980, 1000; *J. Chem. Soc. Perkin Trans. 1* 1981, 2070.
[25] H. Paulsen, R. Lebuhn, *Angew. Chem. 94* (1982) 933; *Angew. Chem. Int. Ed. Engl. 21* (1982) 926.
[26] H. Paulsen, R. Lebuhn, *Carbohydr. Res. 125* (1984) 21.
[27] T. Ogawa, T. Kitajma, T. Nukada *Carbohydr. Res. 123* (1983) C5, C7.
[28] T. Ogawa, H. Yamamoto, T. Nukada, T. Kitajma, M. Mamoro, *Pure Appl. Chem. 56* (1984) 779.
[29] H. Paulsen, H. Tietz, *Angew. Chem. 97* (1985) 118; *Angew. Chem. Int. Ed. Engl. 24* (1985) 128; *Carbohydr. Res. 125* (1984) 47.
[30] H. Paulsen, H. Tietz, *Angew. Chem. 94* (1982) 934; *Angew. Chem. Int. Ed. Engl. 21* (1982) 927; *Carbohydr. Res. 144* (1985) 205.
[31] T. Kitajma, M. Sugimoto, T. Nukada, T. Ogawa, *Carbohydr. Res. 127* (1984) C1.
[32] T. Ogawa, M. Sugimoto, T. Kitajma, K. K. Sadozai, T. Nukada, *Tetrahedron Lett. 27* (1986) 5739.
[33] K. Okamoto, T. Kondo, T. Goto, *Tetrahedron Lett. 27* (1986) 5229, 5233.
[34] Y. Itoh, T. Ogawa, *Tetrahedron Lett. 28* (1987) 6221.
[35] a) T. Murase, H. Ishida, M. Kiso, A. Hasegawa, *Carbohydr. Res. 184* (1988) C1; b) R. L. Thomas, A. K. Sarkar, K. Kohata, S. A. Abbas, K. L. Matta, *Tetrahedron Lett. 31* (1990) 2825.
[36] H. Paulsen, M. Heume, Z. Györgydeak, R. Lebuhn, *Carbohydr. Res. 144* (1985) 57.
[37] H. Paulsen, M. Heume, H. Nürnberger, *Carbohydr. Res. 200* (1990) 127.
[38] F. Yamazaki, T. Nukada, Y. Itoh, S. Sato, T. Ogawa, *Tetrahedron Lett. 30* (1989) 4417.
[39] T. Ogawa, T. Nukada, T. Kitajma, *Carbohydr. Res. 123* (1983) C12.
[40] T. Ogawa, T. Nukada, *Carbyhydr. Res. 136* (1985) 135.
[41] H. G. Garg, R. W. Jeanloz, *Adv. Carbohydr. Chem. Biochem. 43* (1985) 135.
[42] H. G. Garg, R. W. Jeanloz, *J. Org. Chem. 41* (1976) 2480; *Carbohydr. Res. 70* (1979) 47; *ibid. 76* (1979) 85; *ibid. 86* (1980) 68.
[43] M. Spinola, R. W. Jeanloz, *J. Biol. Chem. 245* (1970) 4158.
[44] H. Kunz, *Angew. Chem. 99* (1987) 297; *Angew. Chem. Int. Ed. Engl. 26* (1987) 294.
[45] a) H. Kunz, C. Unverzagt, *Angew. Chem. 100* (1988) 1763; *Angew. Chem. Int. Ed. Engl. 27* (1988) 1697; b) B. Meyer in J. Thiem (Ed.): *Topics in Current Chemistry 154, Carbohydrate Chemistry*, Springer, Berlin 1990.
[46] H. Kessler, M. Gehrke, C. Griesinger, *Angew. Chem. 100* (1988) 507; *Angew. Chem. Int. Ed. Engl. 27* (1988) 490.
[47] J. S. Yadav, P. Luger, *Carbohydr. Res. 119* (1983) 57.
[48] G. A. Jeffrey, R. Tailor, *J. Compt. Chem. 1* (1980) 99; K. Rasmussen, *Acta Chem. Scand. A36* (1982) 323.
[49] S. J. Weiner, P. Kollman, D. A. Case, U. S. Singh, C. Yhio, G. Alagona, S. Profeta, P. Weiner, *J. Am. Chem. Soc. 106* (1984) 765.
[50] S. N. Ha, A. Giammona, M. Field, J. W. Brady, *Carbohydr. Res. 180* (1988) 207.
[51] H. Thøgersen, R. U. Lemieux, K. Bock, B. Meyer, *Can. J. Chem. 60* (1982) 44.
[52] A. J. Kitaigorodsky, *Chem. Soc. Rev. 7* (1978) 133.
[53] R. Fletcher, M. J. D. Powell, *Comput. J. 6* (1963) 163.
[54] D. A. Cummings, J. Carver, *Biochemistry 26* (1987) 6664.
[55] D. A. Cummings, J. Carver, *Biochemistry 26* (1987) 6676.
[56] S. W. Homans, R. A. Dwek, J. Boyd, M. Mahmoudian, W. G. Richards, T. W. Rademacher, *Biochemistry 25* (1986) 6342.
[57] H. Paulsen, T. Peters, V. Sinnwell, R. Lebuhn, B. Meyer, *Liebigs Ann. Chem.* 1984, 951.
[58] H. Paulsen, T. Peters, V. Sinnwell, M. Heume, B. Meyer, *Carbohydr. Res. 156* (1986) 87.
[59] V. Varin, F. Baert, F. Fouret, G. Strecker, G. Spik, B. Fournet, J. Montreuil, *Carbohydr. Res. 76* (1979) 11.
[60] G. J. Veller, H. Paulsen, H. Schachter, *Can. J. Biochem. Cell. Biol. 62* (1984) 409.
[61] H. Paulsen, T. Peters, *Carbohydr. Res. 165* (1987) 229.
[62] Y. Nishikawa, W. Pegg, H. Paulsen, H. Schachter, *J. Biol. Chem. 263* (1988) 8270.
[63] H. Paulsen, T. Peters, V. Sinnwell, B. Meyer, *Carbohydr. Res. 165* (1987) 251.
[64] H. Paulsen, T. Peters, V. Sinnwell, R. Lebuhn, B. Meyer, *Liebigs Ann. Chem.* 1985, 489.
[65] S. W. Homans, S. W. Dwek, R. A. Rademacher, *Biochemistry 26* (1987) 6571.
[66] R. Huber, *Klin. Wochenschr. 58* (1980) 1217.
[67] J. Deisenhofer, *Biochemistry 20* (1981) 2361.
[68] B. Meyer, J. Deisenhofer, R. Huber, H. Paulsen, T. Peters, *Biochemistry*, in press.
[69] D. Burton, *Mol. Immunol. 22* (1985) 161.
[70] H. Paulsen, K. Adermann, G. Merz, M. Schultz, U. Weichert, *Starch/Staerke 40* (1988) 465.
[71] H. Paulsen, J. P. Hölck, *Carbohydr. Res. 109* (1982) 89.
[72] H. Paulsen, M. Paal, *Carbohydr. Res. 135* (1984) 71.

[73] P. Schultheiss-Reimann, H. Kunz, *Angew. Chem. 95* (1983) 64:, *Angew. Chem. Int. Ed. Engl. 22* (1983) 62.
[74] B. Ferrari, A. A. Pavia, *Tetrahedron 41* (1985) 1939.
[75] H. Paulsen, M. Schultz, *Liebigs Ann. Chem.* 1986, 1435.
[76] H. Paulsen, K. Adermann, *Liebigs Ann. Chem-* 1989, 751.
[77] H. Paulsen, G. Merz, I. Brockhausen, *Liebigs Ann. Chem.*, in press.
[78] H. Kunz, W. Günther, *Angew. Chem. 100* (1988) 1118; *Angew. Chem. Int. Ed. Engl. 27* (1988) 1086.
[79] H. Paulsen, G. Merz, U. Weichert, *Angew. Chem. 100* (1988) 1425; *Angew. Chem. Int. Ed. Engl. 27* (1988) 1365.
[80] R. Kirstgen, A. Olbrich, H. Rehwinkel, W. Steglich, *Liebigs Ann. Chem. 1988*, 437.
[81] H. Paulsen, U. Weichert, G. Merz, S. Peters, *Liebigs Ann. Chem.*, in press.
[82] H. Paulsen, W. Rauwald, U. Weichert, *Liebigs.Ann. Chem.* 1988, 75.
[83] W. Kinzy, R. R. Schmidt, *Carbohydr.Res. 166* (1987) 265.
[84] B. Erbing, B. Lindberg, T. Norberg, *Acta Chem. Scand. Ser. B 32* (1978) 308.
[85] P. J. Garegg, B. Lindberg, T. Norberg, *Acta Chem. Scand. Ser. B.33* (1979) 449.
[86] A. Pollex-Krüger, *Dissertation*, Universität Hamburg 1989.
[87] C. A. Bush, R. E. Feeney, *Int. J. Protein Res. 26* (1986) 386; B. N. N. Rao, C. A. Bush, *Biopolymers 26* (1987) 1227.
[88] N. Darbon, Y. Oddon, J. M. Lacombe, A. A. Pavia, *Carbohydr. Res. 130* (1984) 55.
[89] H. Paulsen, R. Busch, A. Pollex-Krüger, V. Sinnwell, unpublished.
[90] H. Paulsen, M. Brenken, *Liebigs Ann. Chem.* 1988, 649.

Nonmolecular Metal Chalcogenide/Halide Solids and Their Molecular Cluster Analogues

By Sonny C. Lee and Richard H. Holm*

A variety of transition-metal cluster structures are found within the extended arrays of solid-state materials. Although molecular analogues of some of these clusters have been synthesized—either by the self-assembly of smaller components in solution or by the excision of intact cluster units directly from the solid-state phase—molecular chemists are often unaware of the rich structural variety expressed in solid-state clusters. This article presents these diverse structural types as potential targets for synthetic molecular chemistry by describing fundamental solid-state cluster topologies in transition-metal chalcogenide/halide phases and detailing cases where molecular counterparts have been prepared. Particular emphasis is placed on cluster excision as a method of molecular cluster synthesis.

1. Introduction

In a broad structural sense, crystalline nonmolecular compounds of the transition elements are of three types: (I) infinite polymers with no localized organizations of metal atoms recognizable as clusters, (II) extended arrays containing recognizable but condensed clusters that are polymeric by means of apex-, edge-, or face-sharing between repeating cluster motifs, and (III) extended arrays containing discrete, recognizable clusters, independent except for the bridging interactions between them. All three types are extensively represented.

Examples of noncluster solids (type I) include binary metal sulfides with the nickel arsenide (TiS, FeS, CoS), pyrite (FeS_2), and zinc-blende structures (BeS, ZnS).[1] While coordination units such as tetrahedral ZnS_4 and octahedral FeS_6 are readily apparent in such structures, no subset of metal and sulfur atoms is locally integrated into a cluster. Polymeric condensed cluster solids (type II) have been reviewed, with many examples, by *Simon*.[2] One prominent case is $M^I_2Mo_6Se_6$,[3] in which uncapped faces of the Mo_6 octahedron within the $[Mo_6Se_6]^{2\ominus}$ repeat unit are linked by metal–metal bonds to afford infinite chains. Nonmolecular solids with discrete clusters (type III) include Re_3Cl_9,[4] NbSeBr,[5] and $PbMo_6S_8$,[6] which contain discrete triangular $[Re_3(\mu_2\text{-}Cl)_3]$, cubane-type $[Nb_4(\mu_3\text{-}Se)_4]$, and face-capped octahedral $[Mo_6(\mu_3\text{-}S)_8]$ clusters, respectively, that are connected by metal–halide or metal–chalcogenide bridges. Also included in this category are finite condensed clusters such as the $[Mo_{12}Se_{14}]$ unit in $Cs_2Mo_{12}Se_{14}$,[7] which is composed of face-sharing Mo_6 octahedra and bridging selenide ligands. Pertinent to the considerations that follow is that the $[Re_3Cl_3]$ unit has been obtained in a variety of soluble molecular forms (e.g., $[Re_3Cl_{12}]^{3\ominus}$[8]) and $[Mo_6S_8]$ has been synthesized as $Mo_6S_8(PEt_3)_6$.[9] In these cases, the cluster structure in the solid state is retained in the molecule but with small dimensional changes.

Our interest in type III solids arose most recently while examining the reactions of the cage complex $[Co_4(SPh)_{10}]^{2\ominus}$ with NaSH. We synthesized the clusters $[Co_8S_6(SPh)_6]^{4\ominus/5\ominus}$[10] and came to recognize that their nearly cubic $[Co_8(\mu_4\text{-}S)_6]$ core topology is identical with that of the rigorously cubic clusters in cobalt pentlandite (Co_9S_8).[11] The availability of these clusters provided the initial opportunity to examine the structural, electronic, and reactivity properties of *molecular* Co_8S_6 species, albeit not at the same oxidation level as the pentlandite cluster. At about the same time, *Pohl* and *Saak*[12] prepared and structurally characterized $[Fe_8S_6I_8]^{3\ominus}$, a cluster topologically equivalent to the cobalt clusters and closely related to cluster structures in certain iron–sulfur minerals and synthetic phases.[13,14]

These observations raise the intriguing question of the accessibility of molecular analogues to the impressively wide array of clusters in type III solids synthesized in the laboratory by high-temperature methods or found naturally in minerals. Such analogues are available by only two approaches. One is the synthesis of soluble molecular solids, usually by low-temperature methods. This is the usual pursuit of the cluster chemist, and it remains a largely empirical approach. The second is the removal of an intact cluster from an extended array by reactions that rupture bridge bonds and stabilize and solubilize emergent clusters by substitution of appropriate ligands at metal sites.

While the recognition of clusters in solids is quite apparent in solid-state chemistry,[2,15–19] it is not always evident that this is the case for the molecular chemist working with clusters, particularly with respect to the wide range of cluster topologies found in type III solids. We anticipate that cognizance of clusters in solids will contribute to the development of reaction chemistry directed toward their isolation in molecular form. In this way, small fragments of solids—ideally, their structural motifs—will become available for study. A conspicuous step in this direction is the preparation, by a fragment coupling reaction, of $Mo_6S_8(PEt_3)_6$,[9] whose $[Mo_6S_8]$ core is the building block of the Chevrel phases.[6]

The compounds of primary interest are nonmolecular solids with discrete clusters containing chalcogenide and/or halide ligands. Coverage of these materials and the reactions by which clusters can be removed from certain of them is extensive, and deals with many representative cluster structures, but it is not exhaustive. Metal oxides are beyond the purview of this treatment, but an analogous structural classification applies to them.

[*] Prof. R. H. Holm, S. C. Lee
Department of Chemistry, Harvard University
Cambridge, MA 02138 (USA)

 © VCH Verlagsgesellschaft mbH, D-6940 Weinheim, 1990 0570-0833/90/0808-0840 $ 3.50+.25/0

2. Noncluster Solids and Molecular Fragments

While type I solids are of only subordinate interest here, we note that fragments of their structures have been obtained in molecular form. In this and subsequent sections, the term "fragment" does not necessarily imply a strict isoelectronic or a metrically equivalent relationship with the bulk solid, but does mean core compositional identity and a structural similarity sufficient to justify a relationship to the solid. Three examples are considered. In them and others that follow, distances [Å] and angles [°] are mean values where appropriate.

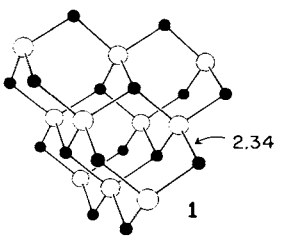

1

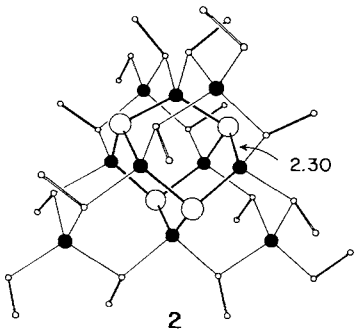

2

The mineral sphalerite (α-ZnS)[20] (**1**) exhibits one of the fundamental cubic lattices of solid-state chemistry. The molecular complex $[Zn_{10}S_4(SPh)_{16}]^{4\ominus}$[21] (**2**) can be viewed as a molecular fragment of the sphalerite lattice (the relevant Zn_6S_4 fragment is emphasized in the formula, with only the first carbon of each ligand included). The adamantanoid Zn_6S_4 center is only slightly distorted from the strict T_d symmetry found in the mineral, and Zn–S distances are comparable. A similar congruence can be observed in the case of $RbFeS_2$[22] (**3**) and the trinuclear Fe^{III} complex $[Fe_3S_4(SPh)_4]^{3\ominus}$[23] (**4**), both of which contain edge-sharing FeS_4 tetrahedra. Their Fe–S, Fe–Fe, and S···S distances are only slightly different, and both fragment **4** and polymer **3**

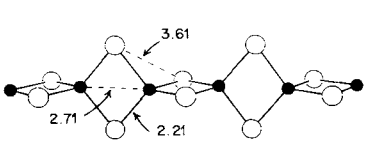

3

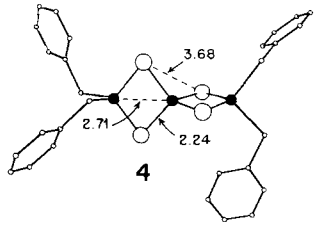

4

are antiferromagnetic. The structure **5** of the mineral patronite[24] (VS_2) consists of V^{IV} atoms bridged by η^2,η^2,μ_2-disulfide ligands with alternating short and long V–V distances. On the basis of the bond distances of its $[V_2S_4]$ core, $V_2(S_2)_2(S_2CN\mathit{i}Bu_2)_4$[25] (**6**) is a very close, solubilized version of the tight $V_2(S_2)_2$ fragment in the polymeric chain of the mineral. Note that clusters **2**, **4**, and **6** were not prepared by fragmentation of the corresponding solids.

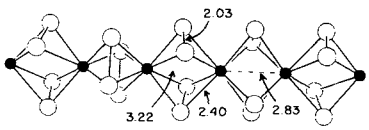

5

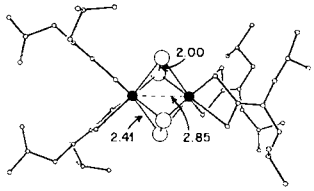

6

Patronite is included here to illustrate a compound on the edge of type I and III solids. It is an infinite polymer with $V(S_2)_2$ repeat units. However, these units are not identical owing to the large (0.39 Å) difference in alternate V–V distances. We view the $V_2(S_2)_2$ chain fragment with the shorter

Richard H. Holm was born in Boston, Massachusetts, USA, and is a graduate of the University of Massachusetts (B.S., 1955) and the Massachusetts Institute of Technology (Ph. D., 1959). He has served on the faculties of the University of Wisconsin, M.I.T., and Stanford University. Since 1980 he has been at Harvard University, where he has been department chairman and is currently Higgins Professor of Chemistry. His research interests are in the area of inorganic and bioinorganic chemistry, with particular reference to synthesis, reactions, and structures pertinent to cluster chemistry and to biological processes.

Sonny C. Lee was born in 1966 in Ping-Tung, Taiwan. He attended the California Institute of Technology as an undergraduate (B.S., 1987), where he performed research under the direction of Professor Terrence J. Collins. Currently, he is a National Science Foundation Predoctoral Fellow and Ph.D. candidate at Harvard University, where he is investigating metal–chalcogenide chemistry with Professor Holm.

V–V distance as a discrete cluster bridged to another by two disulfides. Further, the distance of 2.83 Å is short enough for there to be direct orbital interactions between the two metal atoms. Consequently, patronite and other compounds with alternating long and short distances between pairs of metal atoms are classified as type III solids. In general, the requirement for cluster designation is an organized collection of atoms with metal sites close enough for metal–metal interaction. Such interactions generally lead to spin-pairing and, in the limit, to strong metal–metal bonds.

3. Nonmolecular Solids with Discrete Clusters

3.1. Nomenclature[*]

In the tabulations of compounds that follow, X is halide, Q a chalcogenide, and Z an atom interstitial to a cluster. When for a given compound type X = Cl, Br, or I and Q = S, Se, or Te, X and Q are not further specified in the formula. Metal (M), X, Q, Z, and terminal ligand atoms are symbolized as in **7**. In describing solid-state structures, the i/a notation of *Schäfer* and *von Schnering*[15] is employed and is illustrated with the diagrams **8** adapted from *Perrin* et

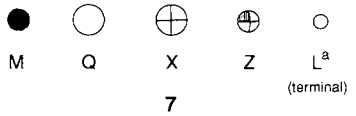

7

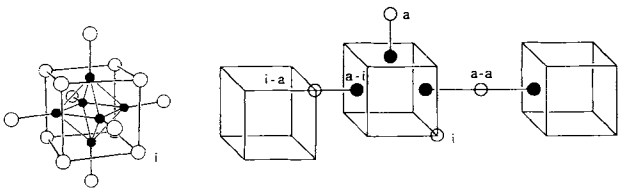

8

al.[18] The cubes represent an M_6L_8 core such as occurs in Mo_6Cl_{12}. Ligand L^i (inner) bridges metal atoms in the core of a cluster, while ligand L^a (apical) is a terminal or bridging ligand, always external to the core. These atoms can function in bridging modes L^{a-a}, L^{i-a}, and L^{a-i} between clusters, which in turn generate the connectivity of the extended solid-state array. Several examples are considered. The cluster connectivity of $Li_4Re_6S_{11}$[26] is $[Re_6S_i^i]S_{6/2}^{a-a}$; that is, the cluster contains a $[Re_6S_8]$ core (a Re_6 octahedron concentric with a S_8 cube) and a terminal sulfide at each Re site that forms a Re–S–Re bridge to another cluster. In Ta_6I_{14},[27] a more complicated connectivity pattern, $[Ta_6I_{10}^iI_{2/2}^{i-a}]I_{2/2}^{a-i}I_{4/2}^{a-a}$, is encountered. Ten iodine atoms of the $[Ta_6I_{12}]$ core (an edge-bridged Ta_6 octahedron) are unshared and two serve as apical ligands in other clusters. Two of the apical iodine atoms are part of the cores of, and four participate in Ta–I–Ta bridges to, other clusters. Illustrations of connectivity patterns appear in the following sections. Ligands involved in L^{i-i} interactions are found exclusively in type II solids. These solids are not further considered.

3.2. Clusters

Some seventeen cluster structural types have been identified in type III solids, all of which were prepared by high-temperature methods. These are collected in Tables 1–5, which are arranged in order of increasing cluster nuclearity. The great majority of these materials contain second- and third-row early transition elements in their lower oxidation states, familiar cases for the formation of metal–metal bonds. In this and subsequent sections, the emphasis is on structural patterns, synthesis, and reactivity of clusters. Electronic structural aspects of the clusters, many of which have been treated in the literature, are not included. Here, cluster structural types are briefly described.

Included in Table 1 are the bi-, tri-, and tetranuclear clusters **9**–**18**. Binuclear clusters **9** (excluding $MoCl_3$) and **11**–**13** contain metal–metal d^1–d^1 single bonds. While their connectivities are quite different, $NbCl_4$ and α-NbI_4 (**9**), NbS_3 (**11**), and VS_2 (**13**) share the characteristic of being linear polymers with alternating long and short metal–metal separations. In the other cases, the binuclear cluster units are well separated by halide bridges. In $Nb_3Se_5X_7$ (**13**), the additional niobium atom occurs in the $[Nb^{V}SeX_4]^{\ominus}$ ion, which interacts with $Nb_2^{IV}Cl_3$ bridges between clusters; this ion is not included in the connectivity description. The two d^3–d^3 cases, $MoCl_3$ (**9**) and β-$ReCl_4$ (**10**), form clusters by octahedral edge- and face-sharing, respectively. These clusters contain metal–metal triple bonds of length 2.76 Å in $MoCl_3$ and 2.73 Å in β-$ReCl_4$. Trinuclear clusters are of three structural types. The triangular planar clusters **14** are found only with the Re^{III} halides. Clusters **15** and **16** are related to **14** in possessing bonded M_3 triangles. The central triply bridging atom is displaced from the M_3 plane. Cluster **15** has the appearance of a cubane-type cluster but with one metal site vacant. In the case of **16**, the displacement of the central bridge atom is on the side of the plane opposite to that occupied by the exterior sulfur atoms of the disulfide ligands. Tetranuclear cluster **17** can be considered a derivative of **15** in which two M_3 triangles are edge-fused to form a centrosymmetric unit with a planar M_4 rhomb. The other tetranuclear cluster is the cubane-type **18**, which incorporates chalcogenides in the core. Each metal site has three halide or remaining chalcogenide terminal ligands that bridge to other clusters.

Hexanuclear clusters contain metal–metal-bonded octahedra with eight ligands capping triangular faces (**19**, **20**) or twelve ligands bridging edges (**21**, **22**). These structures are illustrated in Table 2. Structure **19** is most frequently encountered with Mo^{II} and W^{II} halides, but is also found with two Nb–I compounds. Its occurrence here is due to the size of the iodide ion, inasmuch as other Nb halides, which are also more oxidized, adopt structure **21**. At temperatures above 300 °C, Nb_6I_{11} absorbs dihydrogen at atmospheric pressure to form Nb_6HI_{11} (**20**). The interstitial atom has been located

[*] Abbreviations: acac, 2,4-pentanedionate; Cp, η^5-cyclopentadienyl; Cys, cysteinate (dianion); DMF, *N,N*-dimethylformamide; dmpe, bis(dimethylphosphino)ethane; edta, ethylenediamine-*N,N,N',N'*-tetraacetate; HMPA, hexamethylphosphoric triamide; L, ligand (generalized); PPN, bis(triphenylphosphoranylidene)ammonium; py, pyridine; thf = tetrahydrofuran; tht, tetrahydrothiophene.

Table 1. Nonmolecular solids with discrete bi-, tri-, and tetranuclear clusters.

Compound	Connectivity	Ref.
	binuclear	
	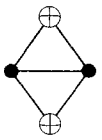 **9**	
	$M_2(\mu_2\text{-}X)_2$	
$NbCl_4$, α-NbI_4	$[Nb_2X_2^i]X_4^aX_{4/2}^{a-a}$	[28, 29]
$MoCl_3$	$[Mo_2Cl_2^i]Cl_{8/2}^{a-a}$	[30]
	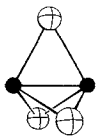 **10**	
	$M_2(\mu_2\text{-}X)_3$	
β-$ReCl_4$	$[Re_2Cl_3^i]Cl_4^aCl_{2/2}^a$	[31]
	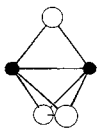 **11**	
	$M_2(\eta^4\text{-}\mu_2\text{-}Q_2)(\mu_2\text{-}X)_2$	
NbS_3	$[Nb_2(S_2)^iS_{1/3}^{i-a}](S_2)_{2/2}^{a-a}S_{2/3}^{a-i}S_{3/3}^{a-a}$	[32]
	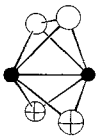 **12**	
	$M_2(\eta^4\text{-}\mu_2\text{-}Q_2)(\mu_2\text{-}X)_2$	
$Nb_2Q_2X_6$ (Q = Se, Te; X = Br, I)	$[Nb_2(Q_2)^iX_2^i]X_2^aX_{4/2}^{a-a}$	[33]
	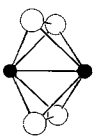 **13**	
	$M_2(\eta^4\text{-}\mu_2\text{-}Q_2)_2$	
VS_2	$[V_2(S_2)_{2/2}^i](S_2)_{2/2}^{a-a}$	[24]
$Nb_2Q_4X_4$ (Q = S, Se)	$[Nb_2(Q_2)_{\frac{1}{2}}^i]X_{8/4}^{a-a}$	[34, 35]
$Nb_3Se_5X_7$ (X = Cl, Br)	$[Nb_2(Se_2)_2^i]X_{6/2}^{a-a}$	[36]
$Mo_2S_4Cl_6$	$[Mo_2(S_2)_2^i]Cl_4^aCl_{4/2}^{a-a}$	[37]
	trinuclear	
	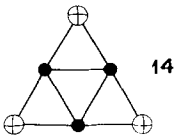 **14**	
	$M_3(\mu_2\text{-}X)_3$	
Re_3Cl_9	$[Re_3Cl_3^i]Cl_3^aCl_{6/2}^{a-a}$	[4]
Re_3I_9	$[Re_3I_3^i]I_3^aI_{4/2}^{a-a}$	[38]
	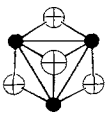 **15**	
	$M_3(\mu_2\text{-}X)_3(\mu_3\text{-}X)$	
Nb_3X_8	$[Nb_3X_4^i]X_{6/2}^{a-a}X_{3/3}^{a-a}$	[39, 40]

Table 1. (continued)

Compound	Connectivity	Ref.
	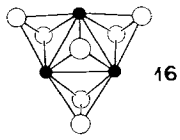 **16**	
	$M_3(\eta^4\text{-}\mu_2\text{-}S_2)_3(\mu_3\text{-}S)$	
$Mo_3S_7X_4$ (X = Cl, Br)	$[Mo_3(S_2)_{\frac{1}{2}}^iS^i]Cl_2^iCl_{4/2}^{a-a}$	[37]
$W_3S_7Br_4$	$[W_3(S_2)_{\frac{1}{2}}^iS^i]Br_2^aBr_{4/2}^{a-a}$	[41]
	tetranuclear	
	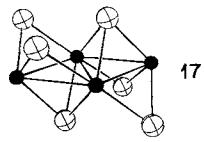 **17**	
	$M_4(\mu_2\text{-}X)_4(\mu_3\text{-}X)_2$	
$M^INb_4X_{11}$ (X = Cl, Br)	$[Nb_4X_6^i]X_{4/2}^{a-a}X_{6/2}^{a-a}$	[42]
	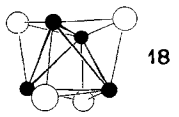 **18**	
	$M_4(\mu_3\text{-}Q)_4$	
NbQX (Q = S, Se; X = Br, I)	$[Nb_4Q_4^i]X_{12/3}^{a-a}$	[5]
MoSX	$[Mo_4S_4^i]X_{12/3}^{a-a}$	[43]
$M^{III}Mo_4Q_8$ (Q = S, Se)	$[Mo_4Q_4^i]Q_{12/3}^{a-a}$	[44, 45]
$MMo_2Re_2S_8$	$[Mo_2Re_2S_4^i]S_{12/3}^{a-a}$	[46]

by a neutron diffraction investigation of Nb_6DI_{11}.[55] Similarly, $CsNb_6I_{11}$ reacts with dihydrogen at 400 °C to afford an analogous cluster in which the interstitial atom causes small changes in cell parameters.[49] Under similar conditions, dihydrogen does not react with Ta_6Cl_{15} (**21**) and Mo_6Cl_{12} (**19**).[49]

A remarkable array of interstitial clusters **22**, principally containing Zr and with at least four connectivities, has recently been prepared by *Corbett* and co-workers.[19] All previously reported Zr_6X_{12}-type compounds are now recognized to contain interstitially substituted clusters. Size restrictions on the included atoms are not yet apparent; interstitial atoms currently range from H to first-row transition elements. Other types of interstitial cluster materials are summarized elsewhere.[2]

Hexanuclear chalcogenide and mixed chalcogenide/halide clusters are set out in Table 3. All have the face-capped octahedral motif **23**. The first two entries in the table are Chevrel phases, an extensive series of molybdenum-containing materials that also include clusters of nuclearities exceeding 6 (see below). Over 40 metals have been incorporated in the $M_xMo_6Q_8$ series. These atoms are not part of the clusters, but reside in channels in the crystal structures where they can sometimes be introduced by intercalation or removed by chemical or electrochemical reactions. Chevrel phases have been described at length.[6, 67, 68] The remaining compounds contain primarily the cubic $Re_6Q_{8-n}X_n$ units (n = 0–3). In the cases of mixed ligands, chalcogenide is always maximally incorporated within a cluster. Summaries of structural properties and further examples of these clus-

Table 2. Nonmolecular solids with discrete hexanuclear halide clusters.

Compound	Connectivity	Ref.
	face-capped	
	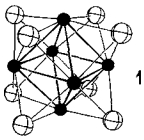 19	
	$M_6(\mu_3\text{-}X)_8$	
Nb_6I_{11}, $CsNb_6I_{11}$	$[Nb_6I_8^i]I_{6/2}^{a-a}$	[48–51]
M_6X_{12} (M = Mo, W)	$[M_6X_8^i]X_{2/2}^aX_{4/2}^{a-a}$	[30, 52]
$M^IMo_6Cl_{13}$	$[Mo_6Cl_8^i]Cl_{2/2}^aCl_{2/2}^{a-a}$	[53]
W_6Br_{16}	$[W_6Br_8^i]Br_4^a(Br_4)_{2/2}^{a-a}$	[54]
W_6Br_{18}	$[W_6Br_8^i]Br_2^a(Br_4)_{4/2}^{a-a}$	[52]
	face-capped interstitial	
	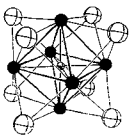 20	
	$M_6(\mu_3\text{-}X)_8Z$	
Nb_6HI_{11}, $CsNb_6HI_{11}$	$[Nb_6(H)I_8^i]I_{6/2}^{a-a}$	[48, 49, 55]
	edge-bridged	
	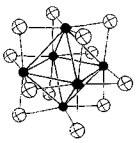 21	
	$M_6(\mu_2\text{-}X)_{12}$	
Nb_6F_{15}	$[Nb_6F_{12}^i]F_{6/2}^{a-a}$	[47]
Nb_6Cl_{14}	$[Nb_6Cl_{10}^iCl_{2/2}^a]Cl_{2/2}^{a-i}Cl_{4/2}^{a-a}$	[56]
Ta_6I_{14}	$[Ta_6I_{10}^iI_{2/2}^{i-a}]I_{2/2}^{a-i}I_{4/2}^{a-a}$	[27]
Ta_6X_{15} (X = Cl, Br)	$[Ta_6X_{12}^i]X_{6/2}^{a-a}$	[57]
	edge-bridged interstitial	
	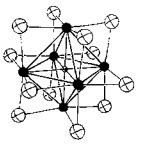 22	
	$M_6(Z)(\mu_2\text{-}X)_{12}$	
Sc_7ZX_{12} (Z = B, C, N)		[58, 59]
M_7ZI_{12} (M = Sc, Y, Pr, Gd) (Z = Mn, Fe, Co, Ni)	$[M_6(Z)X_6^iX_{6/2}^{i-a}]X_{6/2}^{a-i}$	[60]
Zr_6ZCl_{12} (Z = H, Be, B, Cr, Mn)		[60, 61]
Zr_6Cl_{12}		[62]
Zr_6ZCl_{14} (Z = B, C, P, Si, Ge)	$[M_6(Z)X_{10}^iX_{2/2}^{i-a}]X_{2/2}^{a-i}X_{4/2}^{a-a}$	[62, 63]
Zr_6ZI_{14} (Z = Fe, Co)		[60]
$M^IZr_6CX_{14}$ (X = Cl, Br)		[62]
$CsZr_6MnCl_{14}$		[60]
Zr_6NCl_{15}	$[M_6(Z)X_{12}^i]X_{6/2}^{a-a}$	[64]
$M^IZr_6ZCl_{15}$ (Z = C, N)		[64, 65]
$M_2^IZr_6BCl_{15}$		[64, 65]
$M_3^IZr_6BeCl_{15}$		[66]
$Cs_3Zr_6ZCl_{16}$ (Z = B, C)	$[M_6(Z)X_{12}^i]\ X_{4/2}^{a-a}$	[66]
$Na_4Zr_6BeCl_{16}$		[66]

Table 3. Nonmolecular solids with discrete hexanuclear chalcogenide and chalcogenide/halide clusters.

Compound	Connectivity	Ref.
	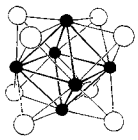 23	
	$M_6(\mu_3\text{-}Q)_8$	
$M_xMo_6Q_8$ [Q = S, Se; ca. 40 M, vacancies (x = 0)]	$[Mo_6Q_2^iQ_{6/2}^{i-a}]Q_{6/2}^{a-i}$	[6, 67–70]
$Mo_6S_6X_2$	$[Mo_6X_2^iS_{6/2}^i]S_{6/2}^{a-i}$	[71]
$Mo_4Re_2Te_8$	$[Mo_4Re_2Te_2^iTe_{6/2}^{i-a}]Te_{6/2}^{a-i}$	[68]
Mo_6QX_{10} (X = Cl, Br; X = I, Q = S, Se)	$[Mo_6Q^iX_7^i]Cl_{4/2}^{i-a}Cl_{2/2}^{a-a}$	[72, 73]
$Li_4Re_6S_{11}$, $M_2^IRe_6S_{11}$	$[Re_6S_8^i]S_{6/2}^{a-a}$	[26, 74, 75]
$M_4^IRe_6Q_{12}$ (Q = S, Se)	$[Re_6Q_8^i]Q_{4/2}^{a-a}(Q_2)_{2/2}^{a-a}$	[76–78]
$Cs_4Re_6S_{13}$	$[Re_6S_8^i]S^aS_{2/2}^{a-a}(S_2)_{3/2}^{a-a}$	[79]
$M_4^IRe_6Q_{13}$ (Q = S, Se)	$[Re_6Q_8^i]Q_{2/2}^{a-a}(Q_2)_{4/2}^{a-a}$	[77]
$Re_6Se_8Cl_2$	$[Re_6Se_4^iSe_{4/2}^{i-a}]Se_{4/2}^{a-i}Cl_2^a$	[80, 81]
$Tl_4Re_6Se_{12}$	$[Re_6Se_8^i]Se_{4/2}^{a-a}(Se_2)_{2/2}^{a-a}$	[80]
$Mo_2Re_4Se_8$	$[Mo_2Re_4Se_2^iSe_{6/2}^{i-a}]Se_{6/2}^{a-i}$	[80]
$Re_6Se_5Cl_8$	$[Re_6Se_3^iCl_3^i]Cl_{2/2}^aCl_{2/2}^{a-a}$	[80]
$Re_6Se_6Cl_6$	$[Re_6Se_6^iCl_2^i]Cl_{2/2}^aCl_{4/2}^{a-a}$	[80]
$Re_6Q_7Br_4$ (Q = S, Se)	$[Re_6Q_7^iBr^i]Br_{6/2}^{a-a}$	[80]
Re_6Te_{15}	$[Re_6Te_8^i](Te_7)_{6/6}^{a-a}$	[82, 83]

Table 4. Nonmolecular solids with discrete octanuclear clusters.

Compound	Connectivity	Ref.
	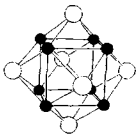 24	
	$M_8(\mu_4\text{-}S)_6$	
$K_6LiFe_{24}S_{26}Cl$	$[Fe_8S_6^i]S_{8/3}^{a-a}$	[14]
$K_6Fe_{21}S_{26}(S, Cl)$ (bartonite)	$[Fe_8S_6^i]S_{8/3}^{a-a}$	[13]
$(Fe,Ni)_9S_8$ (pentlandite)	$[M_8S_6^i]S_{8/4}^{a-a}$	[86, 87]
Co_9S_8	$[Co_8S_6^i]S_{8/4}^{a-a}$	[11]

ters and of Mo chalcogenide/halide compounds are available.[16, 18, 80, 84, 85]

The few compounds containing the discrete octanuclear clusters **24** are listed in Table 4. The cluster consists of a cube of metal atoms concentric with an octahedron of sulfur atoms. It has been found naturally in three minerals, bartonite, djerfisherite, and pentlandite. The first compound listed, while synthetic in origin, is closely related to the mineral djerfisherite. Pentlandites usually contain mixed-metal Fe/Ni clusters, with traces of Co; however, several pentlandites have been identified in which Co is the principal metal.[87] The compound Co_9S_8 is synthetic in origin but has the pentlandite crystal structure. The additional Co atom, and a corresponding Fe, Co, or Ni atom in other compounds, is located in an S_6^i octahedral site and is not included in the connectivity formula.

Lastly, clusters of nuclearity higher than six occur in the various Chevrel phases that are listed in Table 5. Cluster **25** consists of two Mo_6S_7 units bridged by four sulfur atoms, one of which is of the rare μ_6 type. Clusters **26** and **27** are composed of linear arrays of face-sharing Mo_6 octahedra indicated by the brackets. The repeat unit is $Mo_6S_6^i$. In this manner, large condensed clusters of nuclearities as high as 30 have been achieved. Compounds of this sort terminate with $M_2^IMo_6Q_6$, which are pseudo-one-dimensional solids containing $^1_\infty[Mo_3Q_3]$ chains.

Table 5. Nonmolecular solids with discrete clusters of nuclearity > 8.

Compound	Connectivity	Ref.
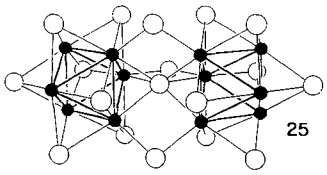	$Mo_{12}(\mu_2\text{-}S)_3(\mu_3\text{-}S)_{14}(\mu_6\text{-}S)$	
$Ba_2Mo_6S_9$	$[Mo_{12}S^{i}_{12}S^{i-a}_{6/2}]S^{a-i}_{6/2}$	[86]
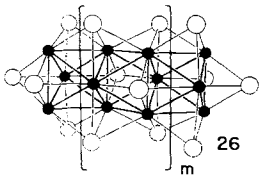	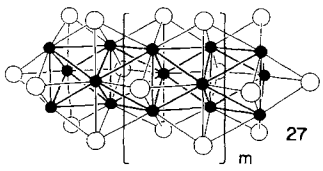	
m = 0-4	m = 0,1	
$M^{I}_{n-2}Mo_{3n}Q_{3n+2}$ (Q = S, Se; n = 4–6, 8, 10)	$[Mo_{3n}Q^{i}_{3n-4}Q^{i-a}_{6/2}]Q^{a-i}_{6/2}$	[7, 70, 88–91]
$M_xMo_{15}Q_{19}$ (Q = S, Se)	$[Mo_{3n}Q^{i}_{3n-4}Q^{i-a}_{6/2}]Q^{a-i}_{6/2}$ (n = 2, 3)	[92–96]
Mo_9Se_{11}, $Ag_{3.6}Mo_9Se_{11}$	$[Mo_{3n}Q^{i}_{3n-4}Q^{i-a}_{6/2}]Q^{a-i}_{6/2}$ (n = 3)	[97, 98]
$M^{I}_2Mo_9Q_{11}$ (Q = S, Se)	$[Mo_{3n}Q^{i}_{3n-4}Q^{i-a}_{6/2}]Q^{a-i}_{6/2}$ (n = 2, 4)	[99]

4. Synthetic Clusters Related to Those in Nonmolecular Solids

Many of the clusters present in type III solids have been prepared in molecular form by either low-temperature solution methods or removal from these solids by chemical reactions. In Table 6, clusters of crystallographically established structures whose cores are topologically (but not necessarily isoelectronically) related to those in nonmolecular solids are collected. The L^i notation is retained to designate ligands in the cluster cores. Preparations and structures of selected clusters are summarized.

4.1. Binuclear Clusters

Among the five types of binuclear clusters **9**–**13** in solids (Table 1), solubilized versions of all but **12** have been prepared. Cluster **11** has been produced in the form of $Nb_2S_3X_4(tht)_4$ (**28**) in the complex redox reaction (1) involving the reductive abstraction of sulfur from tetrahydrothiophene or solvent and the reduction of Nb^{V}.[144] The core portion of molecule **28** and cluster **11** in an extended lattice present the not uncommon situation of isoelectronic, topologically similar but metrically dissimilar structures. The latter feature is most evident in the Nb–Nb distances, which are 2.83–2.84 Å in **28** (X = Cl, Br), significantly shorter than the closest Nb–Nb separation of 3.04 Å in the NbS_3 linear polymer. Evidently, there are constraints specific to the extended structure that are relaxed upon passing to a molecular species. In this case a shorter, stronger metal–metal single bond occurs in the molecule.

$$NbSBr_3 + 5tht \xrightarrow[CS_2]{} \quad (1)$$

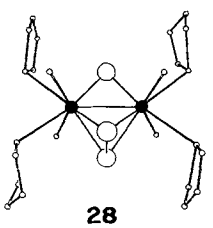

28

A molecular form of **13** as complex **6** is prepared from a mononuclear precursor in redox reaction (2).[125] Here sulfide functions as a reductant for V^{V} and the thiuram disulfide,

$$[VS_4]^{3\ominus} + 2(i\mathrm{Bu}_2\mathrm{NCSS})_2 \xrightarrow[\text{toluene}]{} V_2S_4(i\mathrm{Bu}_2\mathrm{NCS}_2)_4 + S_x^{2\ominus} \quad (2)$$

and appears as disulfide in the cluster product. The reaction of $[MoO_4]^{2\ominus}$ in aqueous polysulfide affords $[Mo_2S_{12}]^{2\ominus}$, al-

Table 6. Clusters related to those in nonmolecular solids with discrete clusters.

Cluster	Solid	Ref.
binuclear		
$V_2(S_2)^{i}_2(S_2CN\mathit{i}Bu_2)_4$ **6**	VS_2 (**13**)	[25]
$Nb_2(S_2)^{i}S^{i}X_4(tht)_4$ (X = Cl, Br) **28**	NbS_3 (**11**)	[144]
$Mo_2Cl^{i}_2Cl_4(EtSCH_2CH_2SEt)_2$	$MoCl_3$ (**9**)	[100]
$[Mo_2(S_2)^{i}_2X_8]^{2\ominus}$ (X = Cl, Br) **29**	$Mo_2S_4Cl_6$ (**13**)	[101]
$[Mo_2(S_2)^{i}_2(S_2)_4]^{2\ominus}$		[102]
$[Re_2Cl^{i}_3Cl_6]^{\ominus}$	β-$ReCl_4$ (**10**)	[103]
trinuclear		
$Nb_3Cl^{i}_4Cl_3(PMe_2Ph)_6$ **30**	Nb_3Cl_8 (**15**)	[104]
$[Nb_3Cl^{i}_4Cl_6(PEt_3)_3]^{\ominus}$		[104]
$[Mo_3(S_2)^{i}_3S^{i}(S_2)_3]^{2\ominus}$ **31**	$Mo_3S_7Cl_4$ (**16**)	[105]
$[Mo_3(S_2)^{i}_3S^{i}Cl_7]^{3\ominus}$		[143]
$[Mo_3(S_2)^{i}_3S^{i}(S_2PEt_2)_3]^{\oplus}$		[106]
$Re_3Cl^{i}_3(CH_2SiMe_3)_6$	Re_3Cl_9 (**14**)	[107]
$Re_3Cl^{i}_3Cl_6(PEt_2Ph)_3$		[108]
$[Re_3X^{i}_3X_8]^{2\ominus}$ (X = Cl, Br)		[109, 110]
$[Re_3X^{i}_3X_9]^{3\ominus}$ (X = Cl, Br)		[8, 111]
tetranuclear		
$[Mo_4S^{i}_4(NH_3)_{12}]^{4\oplus}$	MoSX, $M^{III}Mo_4S_8$ (**18**)	[112]
$[Mo_4S^{i}_4(edta)_2]^{4\ominus/3\ominus/2\ominus}$ **32**		[113, 145]
$[Mo_4S^{i}_4(NCS)_{12}]^{6\ominus}$		[114]
$[Mo_4S^{i}_4(CN)_{12}]^{8\ominus}$		[115]
$Mo_4S^{i}_4L_6$ (L = $Et_2NCS^{\ominus}_2$, $Et_2PS^{\ominus}_2$)		[116, 117]
$[Mo_4S^{i}_4(\mathit{i}PrCp)_4]^{0/\oplus/2\oplus}$		[118]
hexanuclear halide		
$Zr_6Cl^{i}_{12}(PMe_2Ph)_6$	Zr_6ZCl_{12} (**22**)	[119]
$[Zr_6BCl^{i}_{12}Cl_6]^{5\ominus}$	$Cs_3Zr_6ZCl_{16}$ (**22**)	[120]
$Nb_6I^{i}_8(MeNH_2)_6$ **42**	Nb_6I_{11}, $CsNb_6I_{11}$ (**19**)	[121]
$[Nb_6Cl^{i}_{12}Cl_6]^{2\ominus/3\ominus/4\ominus}$	Nb_6Cl_{14} (**21**)	[122–125]
$[Ta_6Cl^{i}_{12}(OH_2)_6]^{3\oplus}$	Ta_6Cl_{15} (**21**)	[126]
$Ta_6Cl^{i}_{12}Cl_2(OH_2)_4$		[127]
$[Ta_6Cl^{i}_{12}Cl_6]^{2\ominus}$		[128]
$[Mo_6Cl^{i}_8Cl_4Br_2]^{2\ominus}$ (*trans*)	Mo_6Cl_{12}, $M^{I}Mo_6Cl_{13}$ (**19**)	[129]
$[M_6Cl^{i}_8X_6]^{2\ominus}$ (M = Mo, W)		[130, 131]
$[Mo_6Cl^{i}_8(OMe)_6]^{2\ominus}$		[132]
$Mo_6Br^{i}_8Br_4(OH_2)_2$	Mo_6Br_{12} (**19**)	[133]
$M_6Cl^{i}_8Cl_4(PR_3)_2$ (M = Mo, W)	M_6Cl_{12} (**19**)	[134, 135]
$[W_6X^{i}_8X_6]^{2\ominus}$	W_6X_{12} (**19**)	[136]
$W_6Cl^{i}_{12}Cl_6$	–	[137]
$[W_6Br^{i}_8Br_6]^{\ominus}$	W_6Br_{12} (**19**)	[138]
hexanuclear halide/chalcogenide		
$[Mo_6S^{i}Cl^{i}_6Cl_6]^{3\ominus}$	Mo_6Cl_{12}, $M^{I}Mo_6Cl_{13}$ (**19**)	[139]
$Mo_6S^{i}_8(PEt_3)_6$ **34**	Chevrel phases (**23**)	[9]
$Re_6Q^{i}_4X^{i}_4X_6$ (Q = S, Se; X = Cl, Br)		[140, 141]
$[Re_6Se^{i}_5Cl^{i}_3Cl_6]^{\ominus}$	$Re_6Se_5Cl_8$ (**23**)	[80, 142]
$[Re_6Se^{i}_5Cl^{i}(OH)^{i}_2Cl_6]^{\ominus}$		[18]
$[Re_6Se^{i}_6Cl^{i}_2Cl_6]^{2\ominus}$	$Re_6Se_6Cl_6$ (**23**)	[80]
octanuclear		
$[Fe_8S^{i}_6I_8]^{3\ominus}$ **38**	$K_6LiFe_{24}S_{26}Cl$, bartonite (**24**)	[12]
$[Co_8S^{i}_6(SPh)_8]^{4\ominus/5\ominus}$ **37**	Co_9S_8 (**24**)	[10]

so containing **13**, and $[Mo_3S_{13}]^{2\ominus}$ as well, which apparently exists in equilibrium under the preparative conditions.[146]

In contrast to the foregoing processes, in which small clusters are assembled from soluble mononuclear species, heterogeneous reaction (3) in dichloromethane affords $[Mo_2S_4Cl_8]^{2\ominus}$ (**29**) in high yield.[101] This species contains

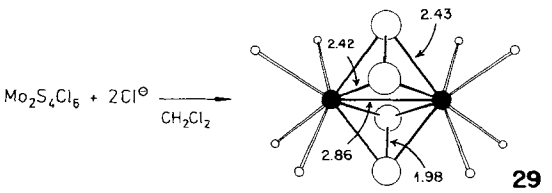

(3)

cluster unit **13** with bond distances that are within 0.03 Å of those in $Mo_2S_4Cl_6$; that is, the molecular cluster and that in the solid state are nearly identical. The reaction ostensibly removes the $Mo_2(S_2)_2$ cluster from the solid state by cleavage of the four chloride bridges linking clusters (Table 1). The reactant chloride is incorporated into the molecular product. We will hereafter term such a process a *cluster excision* reaction. We acknowledge that in no case has it been shown that a cluster remains intact in passing from the solid to the solution state; given the general structural stability of clusters with multiple bridging and metal–metal bonding, however, it is probable that most or all excision reactions result in the solubilization of intact cluster units. Reaction (3), while seemingly simple, exemplifies a large body of reactions that liberate clusters from solids in suitably ligated forms. Such reactions, which are not always recognized or described as ones of cluster excision, are considered more fully in Section 5. A second example of the apparent excision of a binuclear cluster is the isolation of $[Re_2Cl_9]^{2\ominus}$, containing **10**, by treatment of β-$ReCl_4$ with 12 N HCl followed by precipitation of the $Ph_4As^{\oplus}$ salt.[147] This species is oxidizable to the Re^{IV} complex $[Re_2Cl_9]^{\ominus}$, of known confacial bioctahedral structure.

4.2. Trinuclear Clusters

Clusters **14**–**16** (Table 1) are known in molecular form. Species containing the triangular unit **14** are generally derived from Re^{III} halides by excision reactions. The cuboidal unit **15** has been established in two Nb clusters, both prepared by the sodium amalgam reduction of $NbCl_4(thf)_2$ in toluene in the presence of a tertiary phosphane.[104] These clusters bracket by one electron the oxidation state of Nb_3Cl_8, whose Nb–Nb distance in **15** is 2.81 Å. The more reduced of these, $Nb_3Cl_7(PMe_2Ph)_6$ (**30**) with a metal–metal distance of 2.83 Å, bears the stronger resemblance to Nb_3Cl_8; the equivalent distance in the more oxidized cluster is 2.98 Å. In many respects, $[Mo_3S_{13}]^{2\ominus}$ (**31**), which we have already noted to be formed from molybdate and polysulfide, is prototypic of soluble forms of **16**. It is virtually isostructural with the cluster in $Mo_3S_7Cl_4$. Other clusters contain combinations of bidentate chelate ligands, tertiary phosphanes, and solvate ligands in place of the terminal disulfides. In addition, the pyridinium salt of $[Mo_3S_7Cl_7]^{3\ominus}$ carries six terminal chloride ligands and a seventh chloride which approaches the terminal sulfur atoms of the disulfide along a threefold axis at a distance of 2.97 Å.

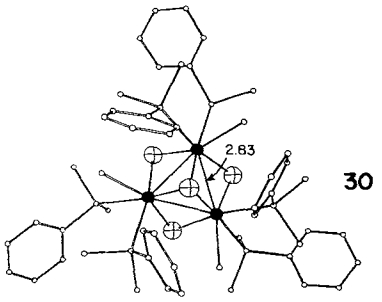

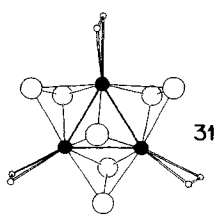

4.3. Tetranuclear Clusters

Cluster **17** (Table 1) is unknown in any molecular form. However, the cubane-type unit **18**, composed of concentric Q_4 and metal–metal-bonded M_4 tetrahedra, is a familiar structural entity in molecular clusters. No such clusters containing the Nb_4Q_4, Mo_4Se_4, or $Mo_2Re_2S_4$ cores have been prepared. However, within the last eight years, a set of Mo_4S_4 clusters in several different oxidation states has been obtained. The first of these, $[Mo_4S_4(CN)_{12}]^{8\ominus}$, was isolated as its potassium salt from the reaction of MoS_3 and aqueous cyanide.[115] Subsequently, other methods of preparation have been developed, including the reaction of $Mo(CO)_6$ and Na_2S in acetic anhydride followed by hydrolysis and workup by ion exchange[114] and by chemical[113] and electrochemical[148,149] reduction of Mo^V. The latter method is illustrated in reaction scheme (4).

Reductive electrolysis of the μ-oxo Mo^V cysteinate complex at a mercury-pool electrode followed by ion-exchange separation affords a trinuclear and a tretranuclear aquo ion [Eq. (4)]. The latter is readily converted into the edta derivative, whose oxidation and reduction affords $Mo^{IV,III}$ di- and

$$Na_2[Mo_2O_2S_2(Cys)_2] \xrightarrow[2)\ \text{cation exchange}]{1)\ \text{electrolysis}} [Mo_4S_4(OH_2)_{12}]^{5\oplus} + [Mo_3S_4(OH_2)_9]^{4\oplus} \quad (4)$$

leaf-green; dark green

$[Mo_3S_4(OH_2)_9]^{4\oplus}$ $\xrightarrow{NCS^{\ominus}}$ $[Mo_3S_4(NCS)_9]^{5\ominus}$

$[Mo_4S_4(OH_2)_{12}]^{5\oplus}$ $\xrightarrow{Na_2(edta)}$ $[Mo_4S_4(edta)_2]^{3\ominus}$

$$[Mo_4S_4(edta)_2]^{2\ominus} \xleftarrow{Br_2} [Mo_4S_4(edta)_2]^{3\ominus} \xrightarrow{NaBH_4} [Mo_4S_4(edta)_2]^{4\ominus} \quad (5)$$

tetraanions [Eq. (5)]. This series and related redox series of other Mo_4S_4 clusters can also be traversed electrochemically. The cubane core is apparent in the structure of $[Mo_4S_4(edta)_2]^{3\ominus}$ (**32**). Successive oxidation increases the

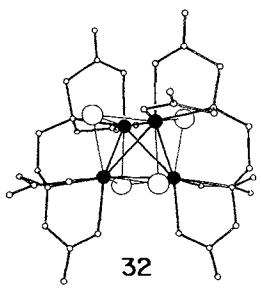

volumes of the Mo_4 tetrahedron and Mo_4S_4 core,[145] indicating that removal of electrons from electron-precise $[Mo_4S_4(edta)_2]^{4\ominus}$ (12 electrons) depopulates the six bonding Mo_4 orbitals ($a_1 + e + t_2$) in T_d symmetry. Consequently, the mean Mo–Mo distances increase by ca. 0.05 Å across the series, while the Mo–S distances are indistinguishable. The tri- and tetraanions are isoelectronic with the clusters **18** in $M^{III}Mo_4S_8$ and MoSX, respectively. Further, the molecular and solid-state clusters[43,44] are congruent in structure, inasmuch as Mo–Mo and Mo–S distances are the same to within ca. 0.02 Å. The other product of reaction (4), $[Mo_3S_4(OH_2)_9]^{4\oplus}$,[148,150] is conveniently isolated as its thiocyanate derivative. In this form and all others,[151] the $[Mo_3S_4]^{4\oplus}$ core has the cuboidal topology of **15**. However, no M_3Q_4 core has yet been detected in a type III solid.

4.4. Hexanuclear Clusters

With the exception of **20**, the solid-state halide clusters **19**–**22** (Table 2) have been isolated in molecular forms. A number of these, including the familiar ions $[M_6X_{14}]^{2\ominus}$ (M = Mo, W) and $[M_6X_{18}]^{2\ominus}$ (M = Nb, Ta), readily visualized by addition of a terminal halide at each metal site in **19** and **21**, respectively, are usually obtained by excision from solids. These reactions are illustrated in Section 5. Certain molecular clusters are also obtainable by high-temperature solid-state reactions. Examples include $LuNb_6Cl_{18}$ and $M^ILuNb_6Cl_{18}$, whose structures contain isolated $[Nb_6Cl_{18}]^{3\ominus/4\ominus}$ clusters.[152,153] The solubility properties of these solids have not been reported. Among halide clusters, a special case is W_6Cl_{18}, obtained by the reaction of W_6Cl_{12} with liquid chlorine.[137] This compound contains the core **21**. It is the only hexanuclear Mo or W cluster that is *not* based on the core **19** and thus has no solid-state analogue. Clusters of types **19** and **21** undergo terminal halide substitution, affording entry to a large group of substituted species. Examples include the reaction of $[Mo_6Cl_4]^{2\ominus}$ with NaOMe in methanol to give $[Mo_6Cl_8(OMe)_6]^{2\ominus}$[154] and the formation of the alkyl-substituted clusters $Mo_6Cl_8Cl_2R'_2(PR_3)_2$ from $Mo_6Cl_8Cl_4(PR_3)_2$ and R'_3Al in toluene.[134]

Heating a solution of $Zr_2Cl_6(PMe_2Ph)_4$ under undefined conditions gave $Zr_6Cl_{12}(PMe_2Ph)_6$ in unspecified yield.[119] This cluster is based on **21**, but it is not known if the actual core is **22** with a conceivable interstitial hydrogen atom. An "empty" cluster would be quite surprising in view of the experience of *Corbett* and co-workers with solid-state structures.[19] In those cases, an interstitial atom Z appears to be obligatory in order to achieve a cluster-based electron count at (or near) 14, which from MO arguments affords stability. A clear example of an isolated interstitially substituted cluster **22** is found in the solid phase $Rb_5Zr_6BCl_{18}$, prepared from elemental Zr and B, RbCl, and $ZrCl_4$ in a sealed Ta container at 850 °C.[120] The crystal structure consists of independent $[Zr_6BCl_{18}]^{5\ominus}$ clusters immersed in an environment of rubidium cations. Whether or not this compound is a *soluble* source of its cluster remains to be seen.

There is a much smaller set of molecular chalcogenide/halide clusters **23** (Table 3). A major advance in this area was achieved by *Saito* et al.[9] in the form of reaction (6). In this attractive conception, fragment condensation of two cuboidal Mo_3S_4 clusters **33** is employed to generate the product cluster **34**, obtained in 30% yield as dark purple crystals. The W analogue **36** has been synthesized by the related reaction (7) and isolated in 10% yield as light brown crystals.[155] In this case, the fragments are the clusters **35** present in $W_3S_7Cl_4$. Clusters **34** and **36** are mixed-valence species with 20 core electrons and essentially identical structures; **36** is the first example of a W_6Q_8 cluster in either a molecular or solid-state condition. The structures are consistent with electronically delocalized descriptions. For reasons presently unclear, the Mo–Mo distance of 2.66 Å in **34** is closer to that of Chevrel phase clusters with 24 rather than 20 electrons.[9] Both clusters can be oxidized and reduced to $[M_6S_8(PEt_3)_6]^{\oplus/\ominus}$ at potentials that, as expected, are more

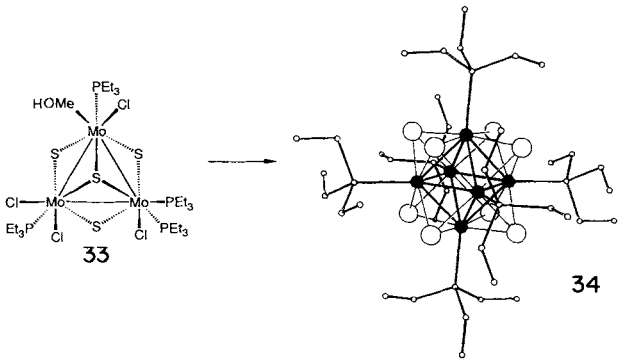

33 34

$$2[Mo_3S_4Cl_4(PEt_3)_4(MeOH)] + 2Mg \xrightarrow[THF]{} Mo_6S_8(PEt_3)_6 + 2MgCl_2 + 2Et_3PCl_2 + 2MeOH \quad (6)$$

$$2[W_3S_7Cl_4] + 10PEt_3 \xrightarrow[toluene]{} W_6S_8(PEt_3)_6 + 6Et_3PS + 4Et_3PCl_2 \quad (7)$$

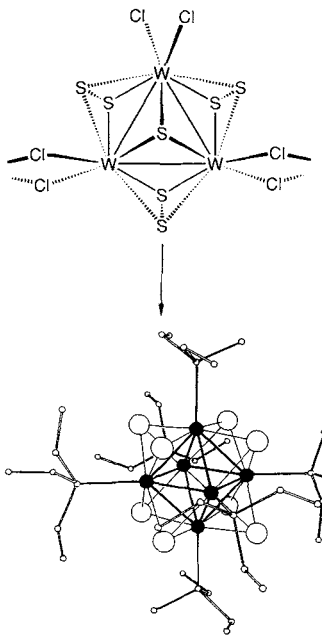

35 36

negative for **36** than for **34**. Our proposed reaction stoichiometries are consistent with the required eight-electron reductions in passing from fragments to cluster, but are not

experimentally established. If they are correct, an interesting feature is the use of Et_3P as a reducing agent for M^{IV} in both reactions and for disulfide in reaction (7) in addition to serving as a stabilizing terminal ligand in the product clusters. Most important, however, is the outcome of reaction (6), which provides the first access to a Chevrel phase cluster in *molecular* form. Prior to this work, one sulfur atom had been introduced to form the $[Mo_6SCl_7]^{3\oplus}$ core of $[Mo_6SCl_{13}]^{3\ominus}$ by the reaction of Mo_6Cl_{12} and NaSH in refluxing pyridine followed by treatment with HCl.[139] The cluster was isolated as a soluble pyridinium salt; X-ray diffraction could not distinguish sulfide from chloride in the core.

A series of compounds (see Table 6) with the $[Re_6Q_nX_{8-n}]$ core **23** have been prepared by high-temperature methods. These solids contain isolated clusters, and several are sources of solubilized clusters. The compounds $Re_6Q_4X_{10}$ (Q = Se, Te; X = Cl, Br) are claimed to be insoluble in organic solvents but dissolve upon heating in Me_2SO solution in the presence of N-donor ligands L, including Et_3N.[158] If the initial compounds all contain **23**, as is the case for $Re_6Se_4Cl_{10}$ (Table 6), the corresponding product formulations are $Re_6Q_4X_{10} \cdot 2L \cdot 2Me_2SO$; there is no structural characterization of these species. $KRe_6Se_5Cl_9$ is described as slightly soluble in ethanol, and recrystallization from aqueous ethanol gives $K[Re_6Se_5Cl(OH)_2Cl_6]$, where hydroxide has displaced chloride form the core.[19] Further, metathesis of the former compound with Bu_4NCl in absolute ethanol affords $(Bu_4N)[Re_6Se_5Cl_9]$,[142] which is soluble in organic solvents. The synthesis and properties of octahedral Re_6 clusters have been summarized.[19, 85] The availability of serveral soluble species provides an entry to the molecular chemistry of these clusters.

4.5. Octanuclear Clusters

The face-capped cubic cluster **24** has been achieved in two synthetic species. Reaction (8) affords the product cluster **37** as a black solid, which is isolated in 50% yield as the $Pr_4N^{\oplus}$ salt.[10] The cluster can be reduced to the pentaanion, in

$$2[Co_4(SPh)_{10}]^{2\ominus} + 6HS^{\ominus} \xrightarrow[Me_2CO]{} \underset{\mathbf{37}}{[Co_8S_6(SPh)_8]^{4\ominus}} + 6PhS^{\ominus} + 6PhSH \quad (8)$$

which the $[Co_8S_6]^{3\oplus}$ core is one electron more oxidized than **24** in cobalt pentlandite. The cluster in Co_9S_8 is topologically similar to **37** but is substantially smaller, with Co–Co and S^i–S^i distances that are 0.15 and 0.23 Å shorter, respectively. The black cluster $[Fe_8S_6I_8]^{3\ominus}$ (**38**) was mechanically separated in 40% yield as its $Et_4N^{\oplus}$ salt from a complicated reaction mixture initially containing Fe metal, iodine, iodide, and the prismane cluster $[Fe_6S_6I_6]^{2\ominus}$.[112] The only property of the compound that has been determined is its crystal structure. The cluster contains a nearly perfect Fe_8 cube whose range of Fe–Fe distances (2.70–2.73 Å) includes the corresponding distances in bartonite (2.73 Å) and synthetic djerfisherite (2.72 Å). Thus, in this case, the molecular cluster is topologically and dimensionally equivalent to the solid-state compounds. Investigation of the chemistry of this unique Fe–S cluster awaits the development of an efficient synthesis.

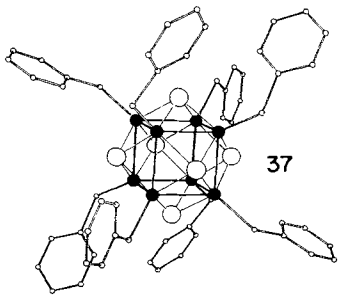

37

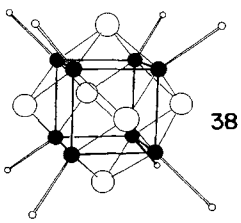

38

5. Clusters from Solids: Excision Reactions

Solubilization of discrete clusters in type III solids has been introduced by reaction (3), in which a binuclear cluster is removed from the solid phase in the form of its chloride derivative. Cluster excision is a reaction that can be recognized to occur in a range of solids where clusters are bridged by halide in a variety of connectivity patterns. Inasmuch as there are few clearcut cases of binuclear cluster excision, and such clusters are usually obtainable by low-temperature solution synthesis, we concentrate on the excision of higher nuclearity clusters. Those which have been removed from solids are of the trinuclear and hexanuclear types, and the conditions of excision are summarized in Tables 7 and 8, respectively. In recognizing these reactions, we assume that the cluster $[M_nL^i_m]$ remains intact upon its liberation from the solid phase in the form of the molecular cluster $[M_nL^i_m]L^a_x$, or if not, converts into a structurally related cluster of equal nuclearity. In nearly all cases, x is the same as the total of L^a, L^{a-a}, and L^{a-i} ligands in the solid phase. When describing the connectivities specified in Tables 1 and 2, we quote mean metal–ligand bond distances.

5.1. Trinuclear Clusters

Two types of intact clusters have been excised by the reactions in Table 7, $[Mo_3(S_2)_3S]$ (**16**) in $Mo_3S_7X_4$ and triangular Re_3X_3 (**14**) in Re_3X_9. Considering first the Mo clusters, the connectivity **39** of $Mo_3S_7X_4$ shows that the clusters are

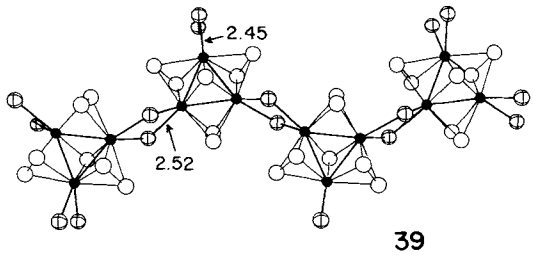

39

arranged in a zigzag chain through four chloride bridges per cluster.[37] The terminal Mo–Cl bond distance is 2.45 Å and the bridging distances range from 2.47 to 2.56 Å and average to 2.52 Å. In 1980, *Müller* et al.[183] reported the conversion of $Mo_3S_7Cl_4$ to $[Mo_3S_{13}]^{2\ominus}$ (**31**) with aqueous polysulfide (but without supporting detail). Later, this reaction was car-

Table 7. Excision of clusters from nonmolecular solids with discrete trinuclear clusters.

Compound	Conditions	Product	Ref.
$Mo_3S_7Cl_4$ **39**	Et_3P; THF, MeOH	$Mo_3S_4^iCl_4(PEt_3)_4(MeOH)$ **33** $Mo_3S_4^iCl_4(PEt_3)_3(MeOH)_2$	[156]
	Ph_3P; THF	$Mo_3S_4^iCl_4(PPh_3)_3(OH_2)_2$	[41]
	dmpe; THF	$[Mo_3S_4^iCl_3(dmpe)_3]^{\oplus}$	[41]
	Ph_3P	$Mo_3S_4^iCl_4(PPh_3)_2$	[16]
$Mo_3S_7Br_4$	Na_2S_x; H_2O (Δ)	$[Mo_3(S_2)_6^iS^i]^{2\ominus}$ **31**	[157]
$Mo_3S_7X_4$ (X = Cl, Br)	Ph_3P; MeCN (Δ)	$Mo_3S_7^iX_4(PPh_3)_2$	[16, 158]
Re_3Cl_9 **40**	solvent = Me_2CO, R_2SO, RCN, DMF, HMPA	$Re_3Cl_3^iCl_6(solv)_3$	[4, 159–161]
	L = py, RNH_2; Me_2CO, THF	$Re_3Cl_3^iCl_6L_3$	[159, 162]
	L = Ph_3E, Ph_3EO (E = P, As); Me_2CO	$Re_3Cl_3^iCl_6L_3$	[4, 162–164]
	L = $N_3^{\ominus}$, $NCS^{\ominus}$, $CN^{\ominus}$; Me_2CO, Me_2SO	$[Re_3Cl_3^iCl_nL_{9-n}]^{3\ominus}$, n = 0, 3,6	[160]
	Hacac; EtOH (Δ)	$Re_3Cl_3^iCl_3(acac)_3$	[164]
	$Na(S_2CNR_2)$ (R = Me, Et); Me_2CO	$Re_3Cl_3^iCl_6(S_2CNR_2)_3$	[162, 164]
Re_3X_9 (X = Cl, Br)	HX, $X^{\ominus}$; H_2O, EtOH	$[Re_3X_3^iX_9]^{3\ominus}$, $[Re_3X_3^iX_8]^{2\ominus}$, $[Re_3Br_3^iBr_7]^{2\ominus}$	[4, 8, 164]
Re_3Cl_9 ("aged")	RMgX; THF, Et_2O	$Re_3Cl_3^iR_6$ (R = Me, CH_2Ph, CH_2CMe_3, CH_2SiMe_3)	[165, 166, 182]

ried out in boiling aqueous polysulfide to give the same product. Reaction with Ph_3P in refluxing acetonitrile affords $Mo_3S_7X_4(PPh_3)_2$. Identification of the latter compounds, obtained in 40–48% yield, was claimed on the basis of mass spectrometry and partial elemental analysis; their structures have not been proven by X-ray analysis. The lack of firm characterization and the forcing conditions of both reactions perhaps render these two cases among the least certain of intact cluster excision.

When allowed to react with excess tertiary phosphane at room temperature over periods of hours to days, cluster **16** of $Mo_3S_7Cl_4$ was partially desulfurized to the cuboidal Mo_3S_4 core, which was solubilized as a chloro-phosphane cluster. Illustrative reaction (9) accounts for the formation of

$$Mo_3S_7Cl_4 + 6\,Et_3P \xrightarrow[MeOH]{} Mo_3S_4Cl_3(PEt_3)_3(MeOH)_2 + 3\,Et_3PS \quad (9)$$

one of the two clusters obtained in the reaction with Et_3P. It and the related transformations in Table 7 are further examples of the reduction of coordinated disulfide to sulfide with nucleophiles.[184] A related example is the conversion of $[Mo_3S_{13}]^{2\ominus}$ to $[Mo_3S_4(CN)_9]^{5\ominus}$ with cyanide.[185] Reaction of $Mo_3S_7Cl_4$ with five equivalents of Ph_3P in hot acetonitrile is reported to give three equivalents of Ph_3PS and $Mo_3S_4Cl_4(PPh_3)_2$. The terminal ligand formulation of the cluster product is subject to reexamination in view of the compositions of the four Mo_3S_4 clusters in Table 7, whose structures have been crystallographically established.[41,156] These are the only evident reactions in which clusters are removed from the solid state with modification in the bridge modality at constant nuclearity.

The Re^{III} halides are readily solubilized by a variety of means, a behavior that is readily understandable in terms of the connectivity pattern **40** of Re_3Cl_9.[5] The triangular clusters **14** are bridged to each other through one of the two Cl atoms at each Re site that are out of the Re_3 plane. The result

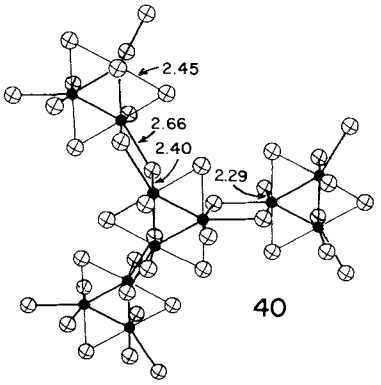

is a layer structure with four Re–Cl distances: Re–Cl^a, Re–Cl^i, and two types of Re–Cl^{a-a} distances involving Cl atoms in and out of the Re_3 plane. The three bridging interactions in the plane are ca. 0.2 Å longer than any other bond length in the crystal structure, which approaches the limit of a molecular solid. The structure of Re_3Br_9 has not been determined. That of Re_3I_9 has a different connectivity (Table 1), in which two Re atoms in a given cluster are linked through iodide bridges to adjacent clusters, leading to chains of cluster units rather than a lamellar network. Again, the longest bonds (also by ca. 0.2 Å) are the bridge bonds in the Re_3 plane. It would appear that facile cleavage of these bonds by even weak nucleophiles permits the ready excision of Re_3X_9 units from the solid. Many of these reactions are listed in Table 7.

Rhenium^{III} chloride is soluble in solvents such as acetone, acetonitrile, and DMF to afford the species $Re_3Cl_9(solv)_3$, which are readily susceptible to substitution reactions. Various observations support the lability order Cl^a (in plane) > Cl^a (out of plane) > Cl^i.[147] Because it is not known that solubilization of Re_3X_9 in the presence of added ligands occurs exclusively by solvation, reactions in the presence of such ligands are taken to fall under the excision description and are included in Table 7. In such systems, a large variety of derivatives of Re_3X_9 have been obtained including the classic ions $[Re_3X_{12}]^{3\ominus}$. These are among the simpler solubilized forms of **14** and support an extensive substitution chemistry. Substituted derivatives may be obtained directly under excision conditions, and then further modified. For example, Re_3Cl_9 has been excised as $[Re_3Cl_9(N_3)_3]^{3\ominus}$ by reaction with azide in acetone at $-10\,^{\circ}C$, and converted into $[Re_3Cl_6(N_3)_6]^{3\ominus}$ and $[Re_3Cl_3(N_3)_9]^{3\ominus}$ in subsequent reactions.[160] The substitution reactions of clusters with core **14** are beyond the scope of this review, but have been described by *Cotton* and *Walton*.[147]

5.2. Hexanuclear Clusters

Clusters of types **19**, **21**, and **22** have been excised from solids by the reactions in Table 8. A particularly interesting example of the solubilization of a face-capped cluster **19** occurs with Nb_6I_{11}, which has the connectivity pattern **41**. Each Nb atom of a given cluster is bridged by a single iodide to another Nb atom, each of these belonging to a different cluster. (In the interest of clarity, we retain only the metal

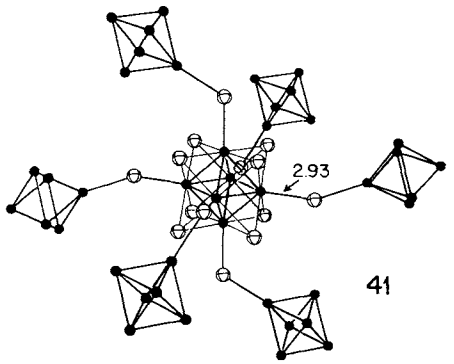

41

atoms of some clusters in this and several subsequent depictions of connectivity.) Treatment of Nb_6I_{11} with methylamine [Eq. (10)], or with *n*-propylamine under similar conditions, results in the slow dissolution of the solid-state cluster phase to afford $Nb_6I_8(RNH_2)_6$. The structure of the diamagnetic cluster **42** reveals that the I^{a-a} atoms in the solid state have been replaced by methylamine in the molecular cluster. Certain spectroscopic features of these clusters have been examined.[121,186] However, their reactivity properties have not been investigated.

$$Nb_6I_{11} \xrightarrow[\text{in EtOH}]{20\%\ MeNH_2} \quad (10)$$

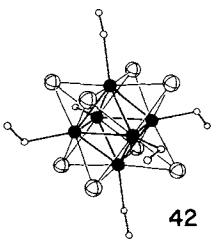

42

Replacement of two X^{a-a} atoms in a structure such as **41** by two X^a atoms produces the composition M_6X_{12} of the Mo^{II} and W^{II} halides. These compounds show the connectivity pattern **43**. The X^a atoms are *trans*, resulting in a layer

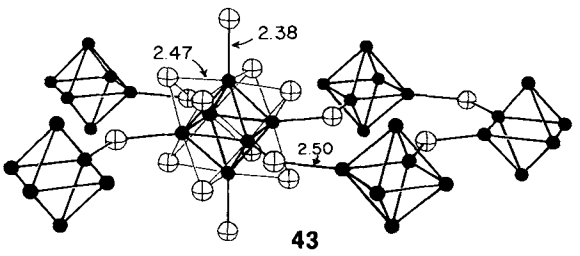

43

structure; the terminal and bridging distances given are for Mo_6Cl_{12}.[30] Bridge bonds are cleaved in the presence of polar solvents to give $Mo_6Cl_{12}(solv)_2$. Addition of other ligands to the excision system provides a simple route to clusters with a variety of terminal ligands. Depending on conditions, up to four halides may be substituted. The situation is similar to that of Re_3Cl_9, where a two-dimensional bridging network is interrupted by reaction with solvent and/or added nucleophiles.

With edge-bridged clusters **21**, four bridging interactions in the same plane result in the composition M_6X_{14} and the connectivity scheme **44**. A typical example is Nb_6Cl_{14}, whose clusters are arranged in a layer structure and connected by Nb–Cl^{a-a} bonds of 2.58 Å. The layers weakly interact through long Nb–$Cl^{i-a/a-i}$ bridge bonds of 3.01 Å. If all

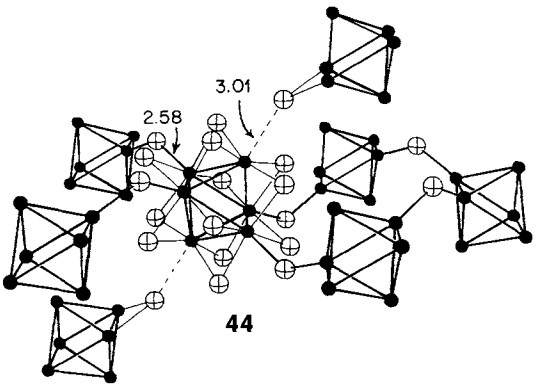

44

bridging interactions are of the M–X^{a-a} type, the composition is M_6X_{15}, as with Ta_6Cl_{15}, and the compound assumes a three-dimensional network structure similar to **41**. When anhydrous, these compounds dissolve with some difficulty in certain polar solvents in the absence of halide, but appear to be more readily soluble in the presence of halide (Table 8).

Table 8. Excision of clusters from nonmolecular solids with discrete hexanuclear clusters.

Compound	Conditions	Product	Ref.
Nb_6I_{11} (**41**)	RNH_2; EtOH	$Nb_6I_8^i(RNH_2)_6$ (R = Me **42**, Pr)	[121]
Nb_6Cl_{14}	LiCl (800 °C, 2 d)	$[Nb_6Cl_{12}^iCl_6]^{4\ominus}$	[177]
Mo_6Cl_{12} (**43**)	solvent = Me_2CO, EtOH, DMF, Me_2SO, THF, RCN	$Mo_6Cl_8^iCl_4(solv)_2$	[167–169]
	L = py, pyO, Et_3N,	$Mo_6Cl_8^iCl_4L_2$	[134, 170, 171]
	Ph_3EO (E = P, As), R_3P; EtOH, THF, CH_2Cl_2		[167–169, 172]
	R_3P; THF (Δ)	$[Mo_6Cl_8^iCl_3(PR_3)_3]^{\oplus}$	[169, 172]
	$AgClO_4$; solvent = DMF, Me_2SO	$[Mo_6Cl_8^i(solv)_6]^{4\oplus}$	[167]
	AgO_3SMe; solvent = DMF, Me_2SO	$Mo_6Cl_8^i(solv)_2(O_3SMe)_4$	[167]
	HX; EtOH	$[Mo_6Cl_8^iX_6]^{2\ominus}$	[171, 173, 174]
	M^IF; MeOH	$[Mo_6Cl_8^iF_6]^{2\ominus}$	[175]
	NaOR; ROH	$[Mo_6Cl_8^i(OR)_6]^{2\ominus}$ (R = Me, Et, Ph, C_6F_5)	[152, 175]
	$NaSC_6F_5$, HMPA; CH_2Cl_2	$Mo_6Cl_8^i(SC_6F_5)_4(HMPA)_2$	[175]
W_6Cl_{12} (**43**)	MeCN	$W_6Cl_8^iCl_4(MeCN)_2$	[176]
W_6I_{12} (**43**)	EtOH	$W_6I_8^iI_4(EtOH)_2$	[176]
W_6X_{12} (**43**)	aqueous HL; EtOH (L = Cl, Br, I)	$[W_6X_8^iL_6]^{2\ominus}$	[173, 176]
M_6X_{14} (**44**) (M = Nb, Ta; X = Cl, Br)	H_2O; aqueous HCl; MeOH; EtOH	"$[M_6X_{12}^i]^{2\oplus}$"	[177–180]
Ta_6X_{14} (**44**) (X = Cl, Br)	HX, X_2; MeOH (Δ)	$[Ta_6X_{12}^iX_6]^{2\ominus}$	[177]
Ta_6Cl_{15}	H_2O	"$[Ta_6X_{12}^i]^{2\oplus}$"	[180]
KZr_6CCl_{15}	18-crown-6, Et_4NBr; MeCN	$[Zr_6CCl_{12}^iCl_6]^{4\ominus}$	[181]
KZr_6FeCl_{15}	[2.2.2]cryptand, Et_4NBr; MeCN	$[Zr_6FeCl_{12}^iCl_3Br_3]^{4\ominus}$	[181]
$Na_4Zr_6BeCl_{16}$	[2.2.2]cryptand (PPN)Cl, MeCN	$[Zr_6BeCl_{12}^iCl_6]^{4\ominus}$	[181]

The species produced range from $[M_6X_{12}(solv)_6]^{2\oplus}$ to $[M_6X_{18}]^{2\ominus}$ or their redox products, depending on reagents used. Species written as "$[M_6X_{12}]^{2\oplus}$" are possible mixtures of solvated and solvated/halide species. Dissolution of hydrated compounds such as $M_6X_{14} \cdot nH_2O$ (M = Nb, Ta; X = Cl, Br)[178, 179, 187] is unlikely to be a reaction of cluster excision inasmuch as $Ta_6Cl_{14} \cdot 7H_2O$ contains the unbridged cluster $Ta_6Cl_{14}(OH_2)_4$ (Table 6). Lastly, we observe that, in work currently at an early stage, at least three edge-bridged interstitial clusters **22** have been excised; all possess connectivities through halide bridges. Molecular clusters have been obtained by the addition of halide and crown ether or cryptand to solubilize $Na^{\oplus}$ or $K^{\oplus}$ in the acetonitrile reaction solvent. It remains to be seen if other types of halide-bridged interstitial clusters,[188] such as Y_6RuI_{10} and those of the type M^{III} (M_6ZI_{12}), containing a six-coordinate non-cluster metal ion, can be solubilized. Their structures present $Y\text{–}I^{i-i}$ and $Y\text{–}I^{i-a}$ interactions on the one hand and $M\text{–}I^{i-i}$ and $I\text{–}M^{III}\text{-}I$ bridges on the other.

6. New Molecular Clusters from Old Solids: Some Prospects

Of cluster structural *types* having nuclearities of three or higher (**14**–**27**), clusters **14**–**16**, **18**, **19**, possibly **21** or **22**, **23**, and **24** have been prepared by low-temperature solution methods. The accessibility of **21** or **22** currently rests with $Zr_6Cl_{12}(PMe_2Ph)_6$, whose cavity occupancy is unclear as is the method of preparation and the yield. For **23**, there are just two examples, $Mo_6S_8(PEt_3)_6$ (**34**) and $W_6S_6(PEt_3)_6$ (**36**). However, a number of specific examples of these structural types have been prepared only at high temperature. Although such clusters, as well as those (**17**, **20**, **25**–**27**) thus far accessible only by high-temperature reactions, might well be assembled at low temperature, some of them may first be obtained in molecular form by excision from the solid state. A case in point is the Nb_6I_8 core **19**, acquired in the amine-derivatized form **42** by excision reaction (*10*). The starting material Nb_6I_{11} can be obtained by thermal decomposition or reduction of Nb_3I_8 with Nb at temperatures of 800 °C or higher.[51] No Nb_6I_8 species has been prepared by a low-temperature reaction. We call attention to several possibilities for cluster solubilization.

6.1. Halide-Bridged Clusters

Given that all successful reactions of cluster excision have been performed with type III solids having only *halide* bridges (Tables 7 and 8), we note several clusters that may be solubilized on this basis. Thus, the W_3S_7 core **16**, unknown in molecular form, is potentially accessible from $W_3S_7X_4$ (X = Cl, Br; Table 1). Further, from an appropriate molecular form of **16** the unknown cuboidal W_3S_4 core should be attainable by reduction of disulfide with cyanide or tertiary phosphanes in a process analogous to reaction (9).

A particularly intriguing problem is posed by the compounds containing cubane-type cluster **18** (Table 1). The compounds NbQX are prepared from the elements at ca. 700–900 °C.[5] Their crystal structure is cubic and isomorphous with MoSX. These structures have the connectivity pattern **45**. Each metal atom forms three $M\text{–}X^{a-a}$ bonds to different clusters, as part of its octahedral MQ_3X_3 coordination sphere. Consequently, the bridges are of the type

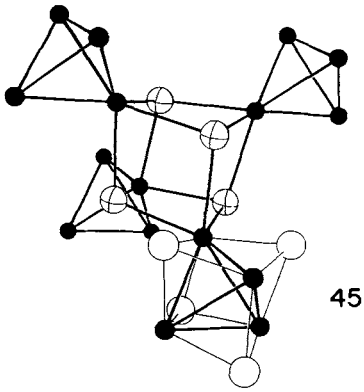

45

$M(\mu_2\text{-}Cl)_3M$. In NbSeI the Nb–I distance of 3.02 Å is longer than the bridge bond in Nb_6I_{11} (2.93 Å), which was broken in cluster excision. The phases MoSX potentially could yield the $[Mo_4S_4]^{4\oplus}$ core, although it is obtained more conveniently by low-temperature processes such as reactions (4) and (5). However, the Nb_4Q_4 core in any oxidation state has never been achieved in molecular form, or indeed in any solid phase other than NbQX. Consequently, its electronic and reactivity properties are completely unknown. Excision systems with halide to afford $[Nb_4Q_4X_{12}]^{8\ominus}$, or, better, with a halide/tertiary phosphane mixture to afford the species $[Nb_4Q_4X_{12-n}(PR_3)_n]^{(8-n)\ominus}$, appear to be reasonable possibilities. Examination of Tables 1–3 reveals other halide-bridged clusters potentially subject to solubilization. Reactions involving halide and/or phosphane might be employed to solubilize the $[Nb_4X_6]^{4\oplus}$ core **17** of $M^{I}Nb_4X_{11}$. Similarly, certain $[ReQ_nX_{8-n}]$ clusters **23** (n = 5–7) are potentially obtainable by excision. However, as already noted, the n = 4–6 species have been prepared in molecular form in high-temperature reactions (Table 6). The synthesis of interstitial clusters **22** with Z larger than a hydrogen atom by other than high-temperature methods is difficult to conceive. While several such clusters have been prepared in molecular form by high-temperature processes, the great majority of compounds containing **22** are halide-bridged in several different connectivities. Excision reactions are a promising route to these fascinating molecules, as borne out by the experiments of *Corbett* and co-workers (Table 8).

6.2. Chalcogenide-Bridged Clusters

The characteristic structural motif of Mo and Re binary and ternary chalcogenides is the face-capped octahedral cluster **23**; it has not been found in other metal chalcogenide phases. In molecular form the Mo_6Q_8 core is known only in sulfide cluster **34**. No molecular species containing any Re_6Q_8 core has been prepared; consequently, the chemistry of clusters with the core is completely unexplored. Hence, considerable interest attends solid phases containing these two units, many of which are listed in Table 3. This tabula-

tion does not include Mo_6Q_8 cluster phases with Q^{i-i} interactions (type II solids), which presumably could not be broken without substantial or complete cluster degradation. The most promising cases for cluster excision are materials in which chalcogenide bridges are of the Q^{a-a} type only. In this event all bridges are external to the cluster, a situation in common with all metal halide clusters that have been solubilized.

The connectivities of four Re–S phases are illustrated in $Li_4Re_6S_{11}$ (**46**), $K_2Re_3S_6$ (**47**), $Cs_4Re_6S_{13}$ (**48**), and $Rb_4Re_6S_{13}$ (**49**). These compounds are prepared from Re metal, the appropriate metal carbonate, and H_2S at temperatures in the 800–1350 °C range.[26, 74–79] Cluster **46** has sulfide bridges at each Re site, whereas **47**–**49** exhibit mixed sulfide/disulfide bridges. Cluster **48** presents an uncommon case of a terminal sulfide ligand. Although there is no existing measure, Re–S–Re and Re–S–S–Re bridges are expected to be more stable than metal–halide bridges. However, the bridge units, with their electrophilic and nucleophilic sites, may be subject to cleavage with retention of cluster structure. Because there is no precedent for cluster excision that does not involve cleavage of a M–X–M bridge, excision reactions of metal–chalcogenide phases necessitate development of appropriate reactions. Possibilities include the reaction of a Re–S–Re bridge with $R_3PH^{\oplus}/R_3P$ to afford terminal Re-PR_3 and $HS^{\ominus}$, and of a Re–S–S–Re bridge with R_3P/R_3PX_2 to give terminal Re-X and R_3PS. Additionally, the latter bridge might be reducible to the Re-S terminal group, which upon immediate alkylation with RX should produce terminal Re-SR and $X^{\ominus}$. These simply conceived reactions would potentially yield products such as $[Re_6S_8(PR_3)_6]^{2\oplus/3\oplus}$, $[Re_6S_8X_6]^{4\ominus/3\ominus}$, and/or mixed-ligand species. Cluster excision may be significantly assisted by the presence of a crown ether or cryptand to complex alkali-metal cations on reaction surfaces. The selection of these reagents can be guided by their kinetic and thermodynamic properties for complexation of the cation in question.[189] Other matters such as solvent, temperature, and particle size for these heterogeneous reactions must await experimentation.

Certain Re_6Se_8 cluster phases have connectivities that are analogous to those of the sulfides (Table 3) and may yield to the same reagents. A unique connectivity is found with Re_2Te_5 (**50**), which is the only proven Re–Te binary phase. It has been prepared by high-temperature reaction of the elements or by an iodine transport reaction.[82,83] Cluster **50** contains a unique planar Te_7 unit, of which each atom except the central atom acts as a Te^a ligand to a Re atom in a different Re_6Te_6 cluster. No two Re atoms in the same cluster are bonded to the same ring.

Other compounds with chalcogenide bridges solely of the Q^{a-a} type are those containing M_8S_6 clusters **24** in Table 4. However, the bridging multiplicity of the Q^a atom exceeds that in the foregoing cases. Synthetic djerfisherite has been

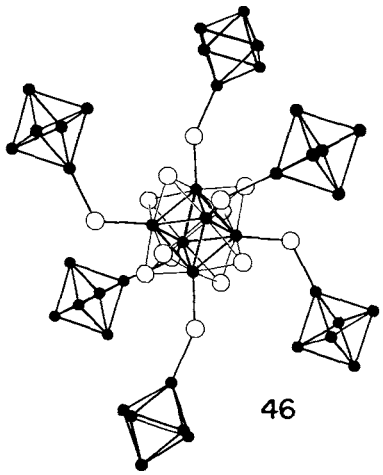

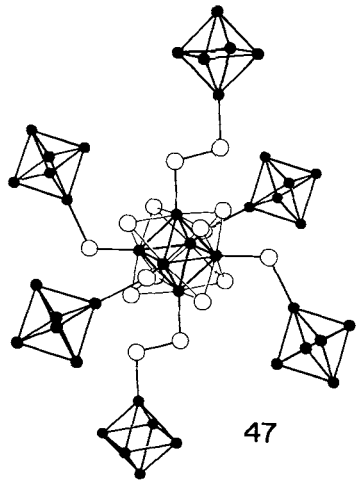

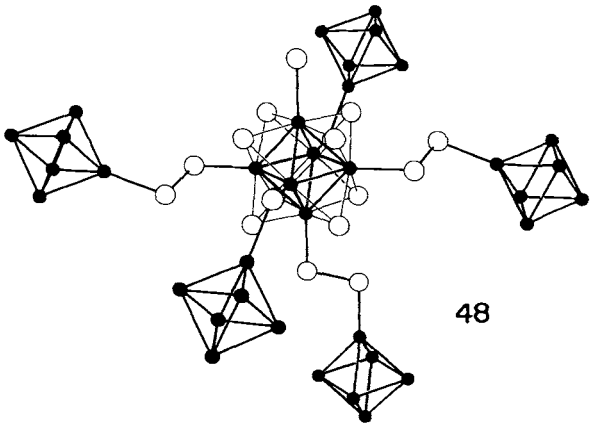

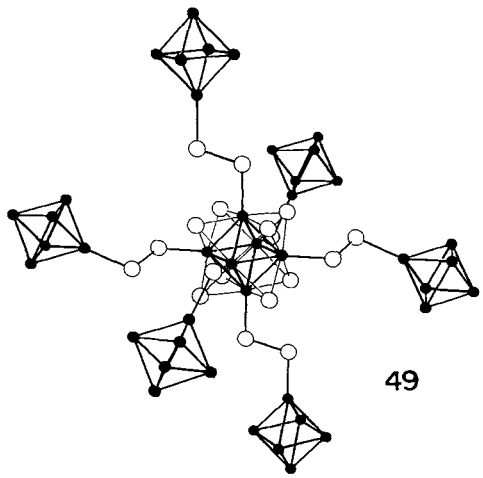

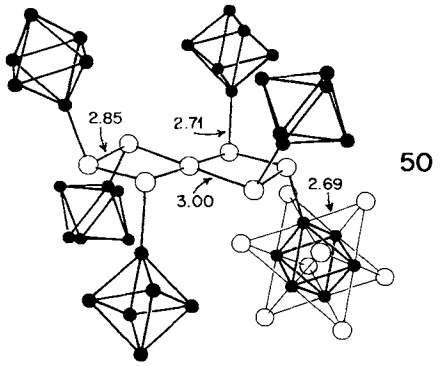

50

prepared by an electrochemical method and also from Fe metal and Li_2FeS_2 in a molten LiCl–KCl eutectic mixture at 400–450 °C.[114] The connectivity pattern **51** (exclusive of

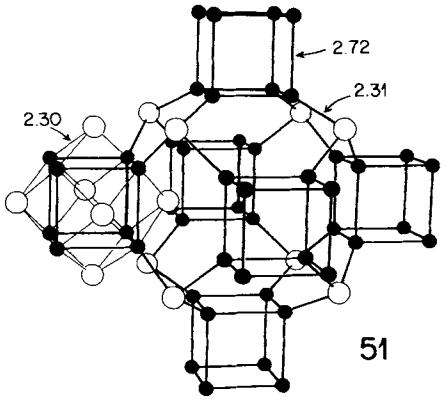

51

$K^{\oplus}$, $Li^{\oplus}$, and $Cl^{\ominus}$) is such that each Fe atom in a given cluster carries an apical sulfide ligand. It bridges to two other clusters and thus has a μ_3-S function. If the formulation is exact, the mean metal oxidation state is $Fe^{1.92\oplus}$ and the clusters are on average more reduced than **38**, the only molecular example of a Fe_8S_6 cluster. In natural and synthetic pentlandites, the clusters are linked by means of octahedral MS_6^i coordination units (**52a**) and by μ_4-S bridges between clusters (**52b**). Both djerfisherite and pentlandite

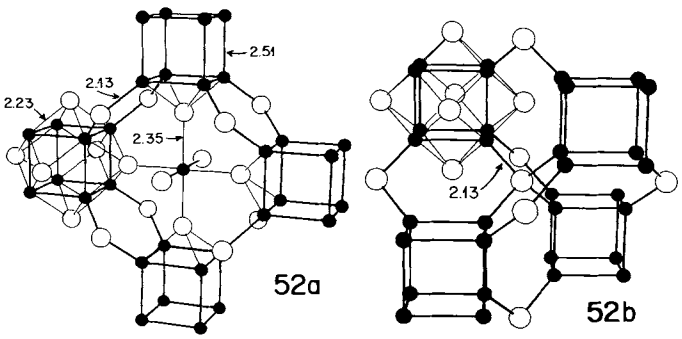

52a 52b

form tightly connected structures. Excision of clusters from these structures, especially the pentlandites in which the μ_4-S atoms have no nucleophilic character, should prove extremely difficult.

Lastly, we observe that the clusters **23** in Chevrel phases, typified by $M_xMo_6Q_8$ (Table 3), are held together tightly by twelve $Q^{i-a/a-i}$ bridges in connectivity pattern **53**. These

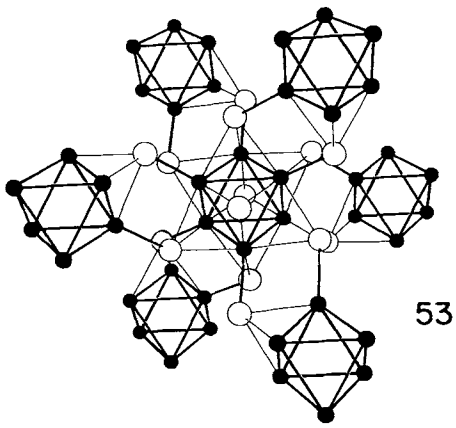

53

bonds should prove very difficult to cleave with retention of cluster structure. Unsuccessful attempts to solubilize ternary Mo chalcogenides have been noted.[190] Fortunately, with the advent of **34**, the properties of a least one individual Mo_6S_8 cluster can be examined. With the face-shared condensed clusters **26** and **27**, prospects of solubilization improve with increasing number n of repeat units $M_3Q_3^i$. Whatever the value of n, only six bridge bonds, involving the three Mo atoms at the ends of the cluster, need be cleaved. At the limit of no bridge bonds are the materials Mo_6Q_6 and $M_2^IMo_6Q_6$,[191,192] which contain the chains $^1_\infty[M_3Q_3]$ separated by the ternary element (if present). Interchain separations in these compounds are about 6.4 Å compared to intercluster Mo–Mo distances of 3.1–3.6 Å in $M_xMo_6Q_8$ and related compounds. As a consequence, the compounds $M_2^IMo_6Q_6$ (M^I = Li, Na) are soluble in highly polar solvents such as Me_2SO and *N*-methylformamide. The chain structure has been shown to be retained; these are the first soluble metal–chalcogenide polymers. In the sense of this review, the process of dissolution is not one of cluster excision inasmuch as the solid lacks intercluster bridge bonds. It remains to be seen if the larger condensed clusters **26** and **27** (n = 9–30) can be solubilized.

7. Concluding Remarks

To the molecular chemist, the existence of broad families of cluster structures in the solid state might be at first sight surprising. The dominance of thermodynamics in high-temperature synthesis would seem to preclude the formation of complex, often highly symmetric, local organizations in the lattice. That the clusters do form under these conditions is a testament to the extraordinary stability of the structural types. This stability in turn implies that, first, all structures listed in this account should be stable in molecular form (with appropriate ligation) and, second, they are probably accessible by solution syntheses. Both anecdotal and axiomatic in cluster research is the statement that all clusters are thermodynamically downhill from some combination of

starting materials; as a corollary, the units presented in Tables 1–5 must indeed lie at the bottom of the slope!

Given the vagaries of finding an auspicious starting point that leads to a given cluster, it must be said that cluster self-assembly in solution is much like a designed synthesis in the solid state: a hit-or-miss affair, with only limited rational planning. As our work on Fe–S clusters has shown,[193] the results can usually be rationalized after the fact; beforehand, however, the outcome is unpredictable. Notable advances in the rational solution syntheses of clusters have come of late with the concept of fragment condensation. Although self-assembly is arguably a process of fragment condensation (using very small fragments), the successes in truly rational syntheses have come about by employing larger, more organized starting blocks, themselves clusters, with one clearly defined condensation step. This concept is well exemplified by the fusion of two $[Mo_3S_4]$ clusters to form the $[Mo_6S_8]$ cluster **34** in reaction (6). However, this method, too, is subject to limitations, particularly in regard to accessible starting fragments.[194]

Thus, we are left with another thought unexpected to the molecular chemist: cluster excision as a rational method for accessing solid-state structures in molecular form. The clusters are clearly present in the solid state; the only question is one of a method for their excision, a question whose answer, if it exists, can be determined by rational lines of inquiry. It must also be emphasized that molecular analogues of the higher nuclearity clusters (such as **21** and **23**) have, in large part, been achieved via excision and not self-assembly. In light of the size and high symmetry of the desired products, rational synthetic routes to such clusters have proven quite difficult to formulate.

By whatever the means, the preparation of molecular analogues to the varied structural types in solid-state materials presents a worthy challenge for the molecular inorganic chemist and others interested in the synthesis of new organized assemblies.

Research on clusters in the authors' laboratory is supported by the U.S. National Institutes of Health and the National Science Foundation. S.C.L. is a recipient of a National Science Foundation Predoctoral Fellowship. We thank Professor J. D. Corbett for a preprint of reference [181] *and for helpful discussion, and C. K. Ryder for preparation of figures.*

Received: February 19, 1990 [A 773 IE]
German version: *Angew. Chem. 102* (1990) 868

[1] A. F. Wells: *Structural Inorganic Chemistry*, Clarendon, Oxford 1984, Chapter 17.
[2] A. Simon, *Angew. Chem. 93* (1981) 23; *Angew. Chem. Int. Ed. Engl. 20* (1981)1; *J. Solid State Chem. 57* (1985) 2; *Angew. Chem. 100* (1988) 163; *Angew. Chem. Int. Ed. Engl. 27* (1988) 153.
[3] M. Potel, R. Chevrel, M. Sergent, *Acta Crystallogr. Sect. B 36* (1980) 1545.
[4] F. A. Cotton, J. T. Mague, *Inorg. Chem. 3* (1964) 1402.
[5] V. E. Federov, V. K. Evstaf'ev, S. D. Kirik, A. V. Mishchenko, *Russ. J. Inorg. Chem. (Engl. Transl.) 26* (1981) 1447.
[6] R. Chevrel in S. Foner, B. B. Schwartz (Eds.): *Superconductor Materials Science: Metallurgy, Fabrication, and Applications*, Plenum, New York 1981, Chapter 10.
[7] P. Gougeon, M. Potel, J. Padiou, M. Sergent, *Mater. Res. Bull. 22* (1987) 1087; *ibid. 23* (1988) 453.
[8] J. A. Bertrand, F. A. Cotton, W. A. Dollase, *Inorg. Chem. 2* (1963) 1166.
[9] T. Saito, N. Yamamoto, T. Yamagata, H. Imoto, *J. Am. Chem. Soc. 110* (1988) 1646.
[10] G. Christou, K. S. Hagen, J. K. Bashkin, R. H. Holm, *Inorg. Chem. 24* (1985) 1010.
[11] V. Rajamani, C. T. Prewitt, *Can. Mineral. 13* (1975) 75.
[12] S. Pohl, W. Saak, *Angew. Chem. 96* (1984) 886; *Angew. Chem. Int. Ed. Engl. 23* (1984) 907.
[13] H. T. Evans, Jr., J. R. Clark, *Am. Mineral. 66* (1981) 376.
[14] B. S. Tani, *Am. Mineral. 62* (1977) 819.
[15] H. Schäfer, H. G. von Schnering, *Angew. Chem. 76* (1964) 833.
[16] V. E. Fedorov, A. V. Mishchenko, V. P. Fedin, *Russ. Chem. Rev. (Engl. Transl.) 54* (1985) 408.
[17] W. Bronger, *Pure Appl. Chem. 57* (1985) 1363.
[18] A. Perrin, C. Perrin, M. Sergent, *J. Less-Common Met. 137* (1988) 241.
[19] R. P. Ziebarth, J. D. Corbett, *Acc. Chem. Res. 22* (1989) 256.
[20] I. Kostov, J. Minčeva-Stefanova: *Sulphide Minerals: Crystal Chemistry, Parageneses, and Systematics*, E. Schweizerbart'sche Verlagsbuchhandlung, Stuttgart 1982, pp. 29–30.
[21] I. G. Dance, A. Choy, M. L. Scudder, *J. Am. Chem. Soc. 106* (1984) 6285.
[22] W. Bronger, *Z. Anorg. Allg. Chem. 359* (1968) 225.
[23] K. S. Hagen, A. D. Watson, R. H. Holm, *J. Am. Chem. Soc. 105* (1983) 3905.
[24] R. Allman, I. Baumann, A. Kutoglu, H. Rosch, E. Hellner, *Naturwissenschaften 51* (1964) 263.
[25] T. R. Halbert, L. L. Hutchings, R. Rhodes, E. I. Stiefel, *J. Am. Chem. Soc. 108* (1986) 6437.
[26] W. Bronger, H.-J. Miessen, P. Müller, R. Neugröschel, *J. Less-Common Met. 105* (1985) 303.
[27] D. Bauer, H. G. von Schnering, H. Schäfer, *J. Less-Common Met. 8* (1965) 388.
[28] L. F. Dahl, D. L. Wampler, *Acta Crystallogr. 15* (1962) 903.
[29] D. R. Taylor, J. C. Calabrese, E. M. Larsen, *Inorg. Chem. 16* (1977) 721.
[30] H. Schäfer, H. G. von Schnering, J. Tillack, F. Kuhnen, H. Wöhrle, H. Baumann, *Z. Anorg. Allg. Chem. 353* (1967) 281.
[31] M. J. Bennett, F. A. Cotton, B. M. Foxman, P. F. Stokely, *J. Am. Chem. Soc. 89* (1967) 2759.
[32] J. Rijnsdorp, F. Jellinek, *J. Solid State Chem. 25* (1978) 325.
[33] H. F. Franzen, W. Hönle, H. G. von Schnering, *Z. Anorg. Allg. Chem. 497* (1983) 13.
[34] H. G. von Schnering, W. Beckman, *Z. Anorg. Allg. Chem. 347* (1966) 231.
[35] J. Rijnsdorp, G. J. de Lange, G. A. Wiegers, *J. Solid State Chem. 30* (1979) 365.
[36] J. Rijnsdorp, F. Jellinek, *J. Solid State Chem. 28* (1979) 149.
[37] J. Marcoll, A. Rabenau, D. Mootz, H. Wunderlich, *Rev. Chim. Miner. 11* (1974) 607.
[38] M. J. Bennett, F. A. Cotton, B. M. Foxman, *Inorg. Chem. 7* (1968) 1563.
[39] H. G. von Schnering, H. Wöhrle, H. Schäfer, *Naturwissenschaften 48* (1961) 159.
[40] A. Simon, H. G. von Schnering, *J. Less-Common Met. 11* (1966) 31.
[41] F. A. Cotton, P. A. Kibala, M. Matusz, C. S. McCaleb, R. B. W. Sandor, *Inorg. Chem. 28* (1989) 2623.
[42] A. Broll, A. Simon, H. G. von Schnering, H. Schäfer, *Z. Anorg. Allg. Chem. 367* (1969) 1.
[43] C. Perrin, R. Chevrel, M. Sergent, *C.R. Seances Acad. Sci. Ser. C. 280* (1975) 23.
[44] C. Perrin, R. Chevrel, M. Sergent, *C.R. Seances Acad. Sci. Ser. C. 280* (1975) 949.
[45] H. Ben Yaich, J. G. Jegaden, M. Potel, R. Chevrel, M. Sergent, A. Berton, J. Chaussy, A. K. Rastogi, R. Tournier, *J. Solid State Chem. 51* (1984) 212.
[46] C. Perrin, R. Chevrel, M. Sergent, *J. Solid State Chem. 19* (1976) 305.
[47] H. Schäfer, H. G. von Schnering, K. J. Niehues, H. G. Nieder-Vahrenholz, *J. Less-Common Met. 9* (1965) 95.
[48] H. Imoto, A. Simon, *Inorg. Chem. 21* (1982) 308.
[49] H. Imoto, J. D. Corbett, *Inorg. Chem. 19* (1980) 1241.
[50] L. R. Bateman, J. F. Blount, L. F. Dahl, *J. Am. Chem. Soc. 88* (1966) 1082.
[51] A. Simon, H. G. von Schnering, H. Schäfer, *Z. Anorg. Allg. Chem. 355* (1967) 295.
[52] H. Schäfer, R. Siepmann, *Z. Anorg. Allg. Chem. 357* (1968) 273.
[53] M. Potel, C. Perrin, A. Perrin, M. Sergent, *Mater. Res. Bull. 21* (1986) 1239.
[54] R. Siepmann, H. G. von Schnering, *Z. Anorg. Allg. Chem. 357* (1968) 289.
[55] A. Simon, *Z. Anorg. Allg. Chem. 355* (1965) 311.
[56] A. Simon, H. G. Schnering, H. Wöhrle, H. Schäfer, *Z. Anorg. Allg. Chem. 339* (1965) 155.
[57] D. Bauer, H. G. von Schnering, *Z. Anorg. Allg. Chem. 361* (1968) 259.
[58] D. S. Dudis, J. D. Corbett, S.-J. Hwu, *Inorg. Chem. 25* (1986) 3434.
[59] S.-J. Hwu, J. D. Corbett, *J. Solid State Chem. 64* (1986) 331.
[60] T. Hughbanks, G. Rosenthal, J. D. Corbett, *J. Am. Chem. Soc. 110* (1988) 1511.
[61] R. P. Ziebarth, J. D. Corbett, *J. Solid State Chem. 80* (1989) 56.
[62] J. D. Smith, J. D. Corbett, *J. Am. Chem. Soc. 107* (1985) 5704; *ibid. 108* (1986) 1927.
[63] G. Rosenthal, J. D. Corbett, *Inorg. Chem. 27* (1988) 53.

[64] R. P. Ziebarth, J. D. Corbett, *J. Less-Common Met. 137* (1988) 21.
[65] R. P. Ziebarth, J. D. Corbett, *J. Am. Chem. Soc. 109* (1987) 4844; *ibid. 110* (1988) 1132.
[66] R. P. Ziebarth, J. D. Corbett, *Inorg. Chem. 28* (1989) 626.
[67] R. Chevrel, M. Hirrien, M. Sergent, *Polyhedron 5* (1986) 87.
[68] O. Fischer, *Appl. Phys. 16* (1978) 1.
[69] M. Potel, P. Gougeon, R. Chevrel, M. Sergent, *Rev. Chim. Mineral. 21* (1984) 509.
[70] R. Chevrel, P. Gougeon, M. Potel, M. Sergent, *J. Solid State Chem. 57* (1985) 25.
[71] C. Perrin, R. Chevrel, M. Sergent, O. Fischer, *Mater. Res. Bull. 14* (1979) 1505.
[72] C. Perrin, M. Sergent, F. Le Traon, A. Le Traon, *J. Solid State Chem. 25* (1978) 197.
[73] C. Perrin, M. Sergent, J. Prigent, *C.R. Acad. Seances Acad. Sci. Ser. C 277* (1973) 46.
[74] W. Bronger, H.-J. Miessen, D. Schmitz, *J. Less-Common Met. 95* (1983) 275.
[75] W. Bronger, H.-J. Miessen, *J. Less-Common Met. 83* (1982) 29.
[76] W. Bronger, M. Spangenberg, *J. Less-Common. Met. 76* (1980) 73.
[77] W. Bronger, H.-J. Miessen, R. Neugröschel, D. Schmitz, M. Spangenberg, *Z. Anorg. Allg. Chem. 525* (1985) 41.
[78] S. Chen. W. R. Robinson, *J. Chem. Soc. Chem. Commun. 1978,* 879.
[79] M. Spangenberg, W. Bronger, *Angew. Chem. 90* (1978) 382; *Angew. Chem. Int. Ed. Engl. 17* (1978) 368.
[80] L. Leduc, A. Perrin, M. Sergent, *C.R. Acad. Sci. Ser. 2 296* (1983) 961.
[81] L. Leduc, A. Perrin, M. Sergent, *Acta Crystallogr. Sect. C 39* (1983) 1503.
[82] V. E. Federov, N. V. Podberezskaya, A. V. Mishchenko, G. F. Khudorozko, I. P. Asanov, *Mater. Res. Bull. 21* (1986) 1335.
[83] F. Klaiber, W. Petter, F. Hulliger, *J. Solid State Chem. 46* (1983) 112.
[84] A. Perrin, M. Sergent, *New. J. Chem. 12* (1988) 337.
[85] C. Perrin, M. Sergent, *J. Less-Common Met. 123* (1986) 117.
[86] S. R. Hall, J. M. Stewart, *Can. Mineral. 12* (1973) 169.
[87] V. Rajamani, C. T. Prewitt, *Can. Mineral. 12* (1973) 178; *Amer. Mineral. 60* (1975) 39.
[88] P. Gougeon, J. Padiou, M. Potel, M. Sergent, M. Couach, *Ann. Chim (Paris) 9* (1984) 1083.
[89] P. Gougeon, M. Potel, M. Sergent, P. Monceau, *Physica B + C (Amsterdam) 135* (1985) 386.
[90] P. Gougeon, O. Peña, M. Potel, M. Sergent, R. Brusetti, *Ann. Chim. (Paris) 9* (1984) 1079.
[91] P. Gougeon, M. Potel, M. Sergent, *Acta Crystallogr. Sect. C45* (1989) 182.
[92] R. Chevrel, M. Potel, M. Sergent, M. Decroux, O. Fischer, *Mater. Res. Bull. 15* (1980) 867.
[93] A. Grüttner, K. Yvon, R. Chevrel, M. Potel, M. Sergent, B. Seeber, *Acta. Crystallogr. Sect. B35* (1979) 285.
[94] P. Gougeon, M. Potel, M. Sergent, *Acta Crystallogr. Sect. C45* (1989) 1285.
[95] M. Potel, R. Chevrel, M. Sergent, *Acta Crystallogr. Sect. B37* (1981) 1007.
[96] J. M. Tarascon, G. W. Hull, *Mater. Res. Bull. 21* (1986) 859.
[97] P. Gougeon, J. Padiou, J. Y. Le Marouille, M. Potel, M. Sergent, *J. Solid State Chem. 54* (1984) 218.
[98] P. Gougeon, M. Potel, J. Padiou, M. Sergent, C. Boulanger, J. M. Lecuire, *J. Solid State Chem. 71* (1987) 543.
[99] R. Chevrel, M. Potel, M. Sergent, M. Decroux, O. Fischer, *J. Solid State Chem. 34* (1980) 247.
[100] F. A. Cotton, P. E. Fanwick, J. W. Fitch, III, *Inorg. Chem. 17* (1978) 3254.
[101] D. Fenske, B. Czeska, C. Schumaker, R. E. Schmidt, K. Dehnicke, *Z. Anorg. Allg. Chem. 520* (1985) 7.
[102] A. Müller, W. O. Nolte, B. Krebs, *Inorg. Chem. 19* (1980) 2835.
[103] F. A. Cotton, D. A. Ucko, *Inorg. Chim. Acta 6* (1971) 161.
[104] F. A. Cotton, M. P. Diebold, X. Feng, W. J. Roth, *Inorg. Chem. 27* (1988) 3413.
[105] A. Müller, S. Pohl, M. Dartmann, J. P. Cohen, J. M. Bennett, R. M. Kirschner, *Z. Naturforsch. B34* (1979) 434.
[106] H. Keck, W. Kuchen, J. Mathow, B. Meyer, D. Mootz, H. Wunderlich, *Angew. Chem. 93* (1981) 1019; *Angew. Chem. Int. Ed. Engl. 20* (1981) 975.
[107] M. B. Hursthouse, K. M. Abdul Malik, *J. Chem. Soc. Dalton Trans. 1978,* 1334.
[108] F. A. Cotton, J. T. Mague, *Inorg. Chem. 3* (1964) 1094.
[109] M. Elder, B. R. Penfold, *Inorg. Chem. 5* (1966) 1763.
[110] J. E. Fergusson, B. R. Penfold, W. T. Robinson, *Nature (London) 201* (1964) 181.
[111] M. Elder, G. J. Gainsford, M. D. Papps, B. R. Penfold, *Chem. Commun. 1969,* 731.
[112] T. Shibahara, E. Kawano, M. Okano, M. Nishi, H. Kuroya, *Chem. Lett. 1986,* 827.
[113] T. Shibahara, H. Kuroya, K. Matsumoto, S. Ooi, *J. Am. Chem. Soc. 106* (1984) 789.
[114] F. A. Cotton, M. P. Diebold, Z. Dori, R. Llusar, W. Schwotzer, *J. Am. Chem. Soc. 107* (1985) 6735.
[115] A. Müller, W. Eltzner, H. Bögge, R. Jostes, *Angew. Chem. 94* (1982) 783; *Angew. Chem. Int. Ed. Engl. 21* (1982) 795.
[116] T. C. W. Mak, K. S. Jasim, C. Chieh, *Inorg. Chem. 24* (1985) 1587.
[117] H. Keck, A. Kruse, W. Kuchen, J. Mathow, H. Wunderlich, *Z. Naturforsch. B42* (1987) 1373.
[118] J. A. Bandy, C. E. Davies, J. C. Green, M. L. H. Green, K. Prout, D. P. S. Rogers, *J. Chem. Soc. Chem. Commun. 1983,* 1395.
[119] F. A. Cotton, P. A. Kibala, W. J. Roth, *J. Am. Chem. Soc. 110* (1988) 298.
[120] R. P. Ziebarth, J. D. Corbett, *J. Am. Chem. Soc. 111* (1989) 3272.
[121] F. Stollmaier, A. Simon, *Inorg. Chem. 24* (1985) 168.
[122] R. A. Field, D. L. Kepert, B. W. Robinson, A. H. White, *J. Chem. Soc. Dalton Trans. 1973,* 1858.
[123] F. W. Koknat, R. E. McCarley, *Inorg. Chem. 13* (1974) 295.
[124] C. Perrin, S.Ihmaine, M. Sergent, *New. J. Chem. 12* (1988) 321.
[125] A. Simon, H.-G. von Schnering, H. Schäfer, *Z. Anorg. Allg. Chem. 361* (1968) 235.
[126] N. Bričević, Ž. Ružić-Toroš, B. Kojić-Prodić, *J. Chem. Soc. Dalton Trans. 1985,* 455.
[127] R. D. Burbank, *Inorg. Chem. 5* (1966) 1491.
[128] C. B. Thaxton, R. A. Jacobson, *Inorg. Chem. 10* (1971).
[129] H. Schäfer, C. Brendel, G. Henkel, B. Krebs, *Z. Anorg. Allg. Chem. 491* (1982) 275.
[130] P. C. Healy, D. L. Kepert, D. Taylor, A. H. White, *J. Chem. Soc. Dalton Trans. 1973,* 646.
[131] L. Ouahab, P. Batail, C. Perrin, C. Garrigou-Lagrange, *Mater. Res. Bull. 21* (1986) 1223.
[132] M. H. Chisholm, J. A. Heppert, J. C. Huffman, *Polyhedron 3* (1984) 475.
[133] L. J. Guggenberger, A. W. Sleight, *Inorg. Chem. 8* (1969) 2041.
[134] T. Saito, M. Nishida, T. Yamagata, Y. Yamagata, Y. Yamaguchi, *Inorg. Chem. 25* (1986) 1111.
[135] T. Saito, H. Manabe, T. Yamagata, H. Imoto, *Inorg. Chem. 26* (1987) 1362.
[136] T. C. Zietlow, W. P. Schaefer, B. Sadeghi, N. Hua, H. B. Gray, *Inorg. Chem. 25* (1986) 2195.
[137] R. Siepmann, H. G. von Schnering, H. Schäfer, *Angew. Chem. 79* (1967) 650; *Angew. Chem. Int. Ed. Engl. 6* (1967) 637.
[138] T. C. Zietlow, W. P. Schaefer, B. Sadeghi, D. C. Nocera, H. B. Gray, *Inorg. Chem. 25* (1986) 2198.
[139] J. B. Michel, R. E. McCarley, *Inorg. Chem. 21* (1982) 1864.
[140] V. E. Federov, A. V. Mishchenko, B. A. Kolesov, S. P. Gubin, Yu. L. Slovokhotov, Yu. T. Struchkov, *Sov. J. Coord. Chem. (Engl. Transl.) 11* (1985) 980.
[141] L. Leduc, A. Perrin, M. Sergent, F. Le Traon, J. C. Pilet, A. Le Traon, *Mater. Lett. 3* (1985) 209.
[142] P. Batail, L. Ouahab, A. Penicaud, C. Lenoir, A. Perrin, *C.R. Acad. Sci. Ser. 2 304* (1987) 1111.
[143] S. Lu, M. Shang, J. Huang, *Jiegou Huaxue 3* (1984) 9.
[144] M. G. B. Drew, D. A. Rice, D. M. Williams, *J. Chem. Soc. Dalton Trans. 1983,* 2251.
[145] T. Shibahara, H. Kuroya, K. Matsumoto, S. Ooi, *Inorg. Chim. Acta 116* (1986) L 25.
[146] A. Müller, R. G. Bhattacharyya, B. Pfefferkorn, *Chem. Ber. 112* (1979) 778.
[147] F. A. Cotton, R. A. Walton: *Multiple Bonds Between Metal Atoms,* Wiley-Interscience, New York 1982, Chapters 5 and 6.
[148] M. Martinez, B.-L. Ooi, A. G. Sykes, *J. Am. Chem. Soc. 109* (1987) 4615.
[149] P. Kathirgamanathan, M. Martinez, A. G. Sykes, *J. Chem. Soc. Chem. Commun. 1985,* 953, 1437.
[150] F. A. Cotton, Z. Dori, R. Llusar, W. Schwotzer, *J. Am. Chem. Soc. 107* (1985) 6734.
[151] T. Shibahara, H. Akashi, S. Nagahata, H. Hattori, H. Kuroya, *Inorg. Chem. 28* (1989) 362.
[152] S. Ihmaine, C. Perrin, O. Peña, M. Sergent, *J. Less-Common Met. 137* (1988) 323.
[153] S. Ihmaine, C. Perrin, M. Sergent, *Acta Crystallogr. Sect. C45* (1989) 705.
[154] P. Nannelli, B. P. Block, *Inorg. Chem. 7* (1968) 2423.
[155] T. Saito, A. Yoshikawa, T. Yamagata, H. Imoto, K. Unoura, *Inorg. Chem. 28* (1989) 3588.
[156] T. Saito, N. Yamamoto, T. Yamagata, H. Imoto, *Chem. Lett. 1987,* 2025.
[157] V. P. Fedin, B. A. Kolesov, Yu. V. Mironov, V. Ye. Federov, *Polyhedron 8* (1989) 2419.
[158] V. P. Fedin, S. P. Gubin, A. V. Mishchenko, V. E. Federov, *Sov. J. Coord. Chem. (Engl. Transl.) 10* (1984) 501.
[159] F. A. Cotton, R. A. Walton, *Inorg. Chem. 5* (1966) 1802.
[160] V. Gutmann, G. Paulsen, *Monatsh. Chem. 100* (1969) 358.
[161] D. G. Tisley, R. A. Walton, *Inorg. Chem. 12* (1973) 373.
[162] R. Colton, R. Levitus, G. Wilkinson, *J. Chem. Soc. 1960,* 4121, 5275.
[163] N. P. Johnson, C. J. L. Lock, G. Wilkinson, *J. Chem. Soc. 1964,* 1054.
[164] B. H. Robinson, J. E. Fergusson, *J. Chem. Soc. 1964,* 5683.
[165] A. F. Masters, K. Mertis, J. F. Gibson, G. Wilkinson, *Nouv. J. Chim 1* (1977) 389.
[166] K. Mertis, A. F. Masters, G. Wilkinson, *J. Chem. Soc. Chem. Commun. 1976,* 858.

[167] F. A. Cotton, N. F. Curtis, *Inorg. Chem. 2* (1965) 241.
[168] W. M. Carmichael, D. A. Edwards, *J. Inorg. Nucl. Chem. 29* (1967) 1535.
[169] J. E. Fergusson, B. H. Robinson, C. J. Wilkins, *J. Chem. Soc. A 1967*, 486.
[170] R. A. Field, D. L. Kepert, D. Taylor, *Inorg. Chim. Acta 4* (1970) 113.
[171] J. C. Sheldon, *J. Chem. Soc. 1960*, 1007; *ibid. 1961*, 750, 1460.
[172] A. D. Hamer, T. J. Smith, R. A. Walton, *Inorg. Chem. 15* (1976) 1014.
[173] F. A. Cotton, R. M. Wing, R. A. Zimmerman, *Inorg. Chem. 6* (1967) 11.
[174] W. L. Jolly, *The Synthesis and Characterization of Inorganic Compounds*, Prentice-Hall, Englewood Cliffs, NJ, USA 1970, pp. 456–459.
[175] H. Schäfer, H. Plautz, H.-J. Abel, D. Lademann, *Z. Anorg. Allg. Chem. 526* (1985) 168.
[176] R. D. Hogue, R. E. McCarley, *Inorg. Chem. 9* (1970) 1354.
[177] B. G. Hughes, J. L. Meyer, P. B. Fleming, R. E. McCarley, *Inorg. Chem. 9* (1970) 1343.
[178] P. B. Fleming, L. A. Mueller, R. E. McCarley, *Inorg. Chem. 6* (1967) 1.
[179] H. S. Harned, C. Pauling, R. B. Corey, *J. Am. Chem. Soc. 82* (1960) 4815.
[180] P. J. Kuhn, R. E. McCarley, *Inorg. Chem. 4* (1965) 1482.
[181] F. Rogel, J. Zhang, M. W. Payne, J. D. Corbett, *Adv. Chem. Ser. 226* (1990) 369.
[182] P. Edwards, K. Mertis, G. Wilkinson, M. B. Hursthouse, K. M. Abdul Malik, *J. Chem. Soc. Dalton Trans. 1980*, 334.
[183] A. Müller, R. Jostes, F. A. Cotton, *Angew. Chem. 92* (1980) 921; *Angew. Chem. Int. Ed. Engl. 19* (1980) 875.
[184] A. Müller, W. Jaegermann, J. H. Enemark, *Coord. Chem. Rev. 46* (1982) 245.
[185] A. Müller, U. Reinsch, *Angew. Chem. 92* (1980) 69; *Angew. Chem. Int. Ed. Engl. 19* (1980) 72.
[186] J. Geyer-Lippmann, A. Simon, F. Stollmaier, *Z. Anorg. Allg. Chem. 516* (1984) 55.
[187] R. A. Mackay, R. F. Schneider, *Inorg. Chem. 7* (1968) 455.
[188] T. Hughbanks, J. D. Corbett, *Inorg. Chem. 27* (1988) 2022; *ibid. 28* (1989) 631.
[189] R. M. Izatt, J. S. Bradshaw, S. A. Nielson, J. D. Lamb, J. J. Christensen, D. Sen, *Chem. Rev. 85* (1985) 271.
[190] J. M. Tarascon, F. J. DiSalvo, C. H. Chen, P. J. Carroll, M. Walsh, L. Rupp, *J. Solid State Chem. 58* (1985) 290.
[191] J. M. Tarascon, G. W. Hull, F. J. DiSalvo, *Mater. Res. Bull. 19* (1984) 915.
[192] M. Potel, P. Gougeon, R. Chevrel, M. Sergent, *Rev. Chim. Miner. 21* (1984) 509.
[193] J.-F. You, B. S. Snyder, G. C. Papaefthymiou, R. H. Holm, *J. Am. Chem. Soc. 112* (1990) 1067.
[194] A procedure analogous to reaction (7) for the preparation of $Mo_6Q_8(PEt_3)_6$ has recently been reported: T. Saito, N. Yamamoto, T. Nagase, T. Tsuboi, K. Kobayashi, T. Yamagata, H. Imoto, K. Unaura, *Inorg. Chem. 29* (1990) 764. Direct reaction of $Mo_3Q_7Cl_4$ with excess PEt_3 in toluene afforded the Q = S (32%) and Se (21%) clusters in the indicated yields. In the event that a trinuclear species such as that in reaction (6) is first generated, as seems probable on the basis of reaction (9), the process involves cluster excision, partial desulfurization, and fragment reductive condensation.

Interfaces between Molecular and Polymeric "Metals": Electrically Conductive, Structure-Enforced Assemblies of Metallomacrocycles

By Tobin J. Marks*

The design, synthesis, characterization, and understanding of new molecular and macromolecular substances with "metal-like" electrical properties represents an active research area at the interface of chemistry, physics, and materials science. An important, long-range goal in this field of "materials by design" is to construct supermolecular assemblies which exhibit preordained collective phenomena by virtue of "engineered" interactions between molecular building blocks. In this review, such a class of designed materials is discussed which, in addition, bridges the gap between molecular and polymeric conductors: assemblies of electrically conductive metallomacrocycles. It is seen that efforts to rationally construct stacked metal-like molecular arrays lead logically to structure-enforced macromolecular assemblies of covalently linked molecular subunits. Typical building blocks are robust, chemically versatile metallophthalocyanines. The electrical, optical, and magnetic properties of these metallomacrocyclic assemblies and the fragments thereof, provide fundamental information on the connections between local atomic-scale architecture, electronic structure, and the macroscopic collective properties of the bulk solid.

1. Introduction

Until only a few years ago, the idea that an organic or metal-organic solid could exhibit the electrical, magnetic, and optical characteristics normally associated with bulk metals would have seemed far-fetched indeed. Among other factors, simple band-theoretical concepts tell us that such substances inherently lack the partially occupied, spatially delocalized manifolds of electronic energy levels (bands) characteristic of metals.[1] In molecular and polymeric solids, such bands are built up of contributing, molecular-level atomic and molecular orbitals, and, as in metals, only the energetically close proximity of filled and empty levels can give rise to electronic (charge) mobility and metallic character. However, typical electron-occupancy patterns found in organic and metal-organic solids lead to wide gaps between filled and unoccupied bands. Such traditional materials, as exemplified by solid benzene, polyethylene, and poly(tetrafluoroethylene), are electrical insulators. These concepts are illustrated schematically in Figure 1.

The past several years have seen a dramatic reassessment of the aforementioned historical picture. As a result of both serendipity and rational chemical synthesis, whole new classes of molecular and polymeric materials have emerged with macroscopic characteristics that are in many ways reminiscent of metals.[2] These include molecular solids which become superconducting at low temperatures[2c, 3] and flexible polymers with electrical conductivities approaching that of copper metal.[4] However, while many macroscopic properties may be similar to metals, the building blocks which compose these new substances and the synthetic chemistry necessary to prepare them are radically different. Indeed, the new "synthetic metals", "molecular metals", and "organic metals" are infinitely richer in their architectural diversity and tailorability. Furthermore, a host of fundamentally new concepts such as "soliton conductor", "bipolaron conductor", and "Mott–Hubbard insulator" have emerged to challenge and enrich our understanding of the condensed state. Equally important has been the close collaboration between chemists, physicists, materials scientists, and engineers that this new interdisciplinary area has spawned. Intellectual bridges have been built which never before existed and which allow condensed matter problems of unparalleled complexity to be attacked.

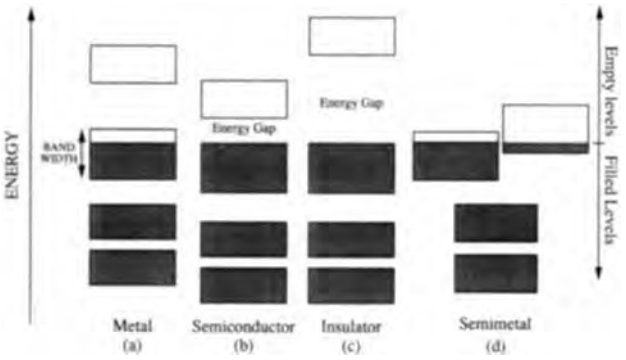

Fig. 1. Schematic depiction of electron occupancy of allowed energy bands for a classical metal, a semiconductor, an insulator, and a semimetal. The energy of the highest occupied level is called the Fermi energy. The unoccupied energy levels are white, the occupied energy levels gray.

In addition to importance in fundamental solid-state chemical and physical research, it is also apparent today that conductive, processable, functionalizable, and light-weight organic materials offer the possibility of new technologies.[2a, 4a] Applications as diverse as energy storage devices,[5] sensors,[6] switching devices,[7, 8] chemoselective electrodes,[8, 9] static charge-dissipating materials and electromagnetic shielding materials,[10] nonlinear optical materials,[11] transparent microphones,[12] "smart" windows,[12] solar energy devices,[7] and electrochromic devices[13, 14] have been proposed. Many of these concepts are in various

[*] Prof. T. J. Marks
Department of Chemistry,
Department of Materials Science and Engineering, and
the Materials Research Center
Northwestern University
Evanston, IL 60208 (USA)

stages of development and, in some cases, commercialization.

Despite the major advances that have been achieved in the areas of electrically conductive molecular and polymeric substances, we must also concede that our current level of synthetic chemical control over, ability to effectively process, and physical understanding of such materials is at a very rudimentary level. Chemically, it is apparent that while the art of synthesizing individual molecules is at a very sophisticated level, the technology for constructing lattices of molecules with precise control over molecular packing and intermolecular interactions is embarrassingly primitive. This problem of course transcends the subject of molecular metals and is fundamental to many areas of condensed matter molecular chemistry (e.g., nonlinear optics, molecular ferromagnets). Likewise, the methodology for turning the latest generations of conductive organic substances into useful films, fibers, monoliths, etc., is only now beginning to develop. For conductive polymers, it is apparent that presently achievable mechanical and electrical properties are far below the theoretical maxima that optimum processing may afford. Finally, our fundamental understanding of how macroscopic physical properties connect with microscopic details of molecular structure, crystal packing, counterion interactions, degree of band filling, disorder, interchain communication, defects, etc., is far from the level where the ab initio design of new substances can be confidently pursued.

The purpose of this review is to summarize and to analyze recent results in a research area that in many respects is at the crossroads of molecular metals and conductive polymers: electrically conductive assemblies of metallomacrocycles. The long-range goal of this effort has been to develop rational and versatile synthetic approaches to low-dimensional molecule-based conductors and, via closely connected physical and theoretical investigations, to better understand their properties. The strategies to be discussed here have progressed logically from simple systems composed of aggregates of single molecules to more elaborate, structure-enforced polymeric assemblies of linked molecular constituents. It will be seen that the design, synthesis, and properties of these assemblies impinge upon issues common to both molecular and macromolecular conductors and provide new insights of relevance to both. Due to space limitations, it is only through these regions of common overlap that it will be possible to mention the excellent work of numerous other groups now studying molecular and macromolecular conductors.

2. Design Considerations for Molecular Metals

In Figure 2 are shown some of the common building blocks of molecular conductors. It is generally recognized that two overriding features are essential for converting an unorganized collection of organic or metal-organic molecules into an electrically conductive, multimolecular array.

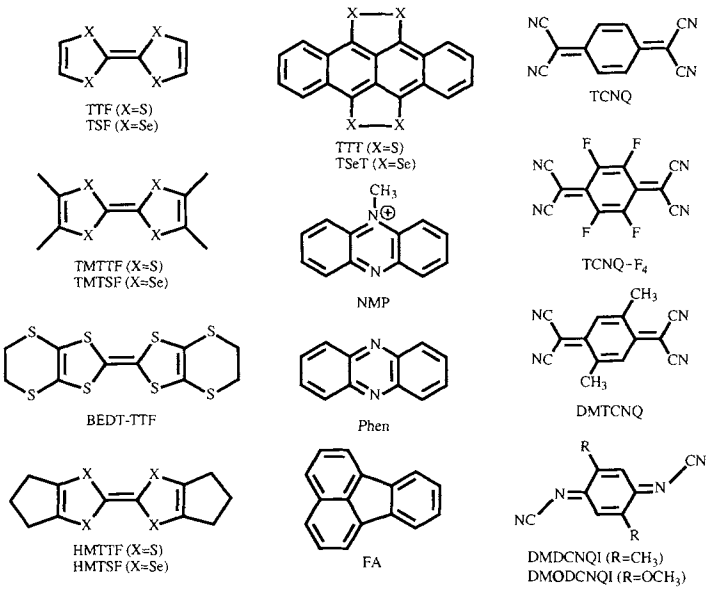

Fig. 2. Common building blocks for nonmetallomacrocylic molecular conductors. The two leftmost columns contain electron donors while the rightmost contains electron acceptors. TTF = tetrathiafulvalene, TSF = tetraselenafulvalene, TMTTF = tetramethyltetrathiafulvalene, TMTSF = tetramethyltetraselenafulvalene, BEDT-TTF = bisethylenedithiotetrathiafulvalene, HMTTF = hexamethylenetetrathiafulvalene, HMTSF = hexamethylenetetraselenafulvalene, TTT = tetrathiatetracene, TSeT = tetraselenatetracene, NMP = *N*-methylphenazinium, Phen = phenazine, FA = fluoranthene, TCNQ = tetracyanoquinodimethane, TCNQ-F_4 = tetrafluorotetracyanoquinodimethane, DMTCNQ = dimethyltetracyanoquinodimethane, DMDCNQI = dimethyl-*N*,*N*'-dicyanoquinodiimine, DMODCNQI = dimethoxydicyanoquinodiimine

First, the molecules must be located in close spatial proximity and in similar crystallographic and electronic/Coulombic environments so that an energetically uniform (i.e., devoid of

Tobin J. Marks was born in Washington, D.C., in 1944. He received a B.S. degree from the University of Maryland in 1966 and a Ph.D. from M.I.T. in 1970, working under F. A. Cotton. He moved to Northwestern University as an assistant professor in 1970. Tobin Marks is currently Charles E. and Emma H. Morrison Professor of Chemistry and Professor of Materials Science and Engineering at Northwestern. He serves on a number of editorial boards and advisory panels, has won several awards, including the American Chemical Society Award in Organometallic Chemistry, and is currently Associate Editor of Organometallics. His present research interests include polymer and solid-state chemistry, f-element organometallic chemistry, homogeneous and heterogeneous catalysis, nonlinear optical materials, metal-organic chemical vapor deposition, and carcinostatic metal complexes.

carrier-trapping hills and valleys), extended pathway exists for electronic charge diffusion. This is equivalent to saying that a band structure having sizeable bandwidths ($\gtrsim 0.5$ eV) must exist. Such a situation is commonly realized when flat, conjugated molecules crystallize in various types of stacking motifs which allow extensive overlap of the π-electron systems (e.g., **1** or **2**). The way in which a band structure is built

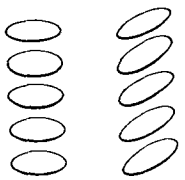

1 **2**

up from highest occupied molecular orbitals (HOMOs) as increasing numbers of molecules are added to a cofacial molecular stack is illustrated in Figure 3. In an simplistic

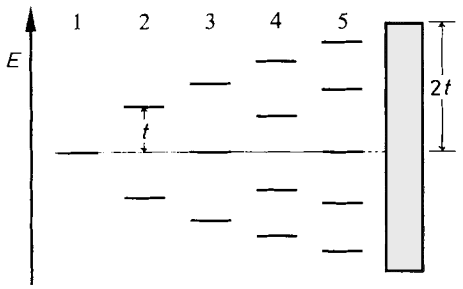

Fig. 3. Schematic illustration of how a band structure is built up by arraying increasing numbers of molecular subunit HOMOs in a molecular stack. The parameter t is the tight-binding transfer integral, analogous to the Hückel β integral. The tight-binding bandwidth is $4t$.

Hückel-like tight-binding band-structure description,[1a, b] the measure of how strongly neighboring HOMOs interact is given by the transfer integral t, which is directly analogous to the Hückel resonance integral, β. In an extended stack consisting of a very large number of molecular constituents, the bandwidth is given by $4t$ (4β). This important condensed state parameter is directly connectable to molecular properties and as such is an important quantity to accurately measure and understand.

The second key requirement for metallic characteristics in a molecular stack is that the highest energy band be incompletely filled. This characteristic has already been discussed in reference to Figure 1 for classical metals; for molecular systems, however, several important caveats must be added. In all of the molecular metals prepared to date, the substances are actually salts and the molecular subunits are in formal *fractional* oxidation states ("partial oxidation" (or reduction), "incomplete charge transfer", "mixed valence"). That is, the molecules have valence shells which, formally, are fractionally occupied as in $(TMTSF^{0.5\oplus})_2X^{\ominus}$, $TTF^{0.59\oplus}$-$TCNQ^{0.59\ominus}$, and $[H_2(Pc)^{0.33\oplus}](I_3^{\ominus})_{0.33}$; the symbol ϱ is normally used to designate the subunit oxidation state. Since each of the simple bands of the type shown in Figures 1 and 3 can accommodate two electrons per constituent molecular subunit (the occupancy of the HOMO), the quantities $(2-\varrho)/2$ and $|\varrho|/2$ give the band occupancy (e.g., 2/3-filled, 1/3-filled) for $\varrho > 0$ and $\varrho < 0$, respectively. Equally important is the observation that materials with $\varrho = 1$ (half-filled bands for classical metals) are never found to be molecular metals and are usually insulators.

The above complexities are due to a number of factors. As was first noted for certain transition-metal oxides by *Mott*, situations may occur in which the Coulombic repulsion (denoted by the parameter U) of having two charge carriers on a single site [Eq. (1)] is comparable to or exceeds the band-

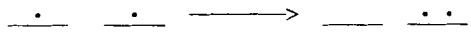

(1)

width. In the extreme case where $U \gg 4t$, a material with a half-filled band can actually be a magnetic insulator.[1, 2] That is, all carriers are confined to their individual molecules. A valence-bond picture of how mixed valency affects charge mobility in molecular conductors is shown schematically in Figure 4. Currently, the degree to which U can be

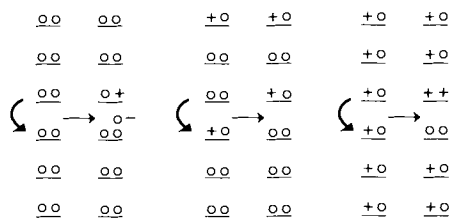

Fig. 4. Schematic depiction of how the degree of oxidation affects charge mobility in a typical molecular stack. Left: no oxidation. Middle: partial oxidation. Right: complete oxidation (one electron per subunit).

manipulated by alterations in molecular architecture, crystal packing, neighboring counterions, and level of band filling has been the subject of much speculation. Such relationships are presently obscure, large U effects may be entangled with other structural features, and accurate measurements of U are not without ambiguity. It is generally agreed that enhanced mangnetic susceptibilities are, in most molecular conductors, an indication of large U effects ("Coulomb enhancement"), as are certain types of band-filling-dependent structural distortions ($4k_F$ instabilities, where k_F refers to the electronic wave vector at the Fermi level).[1b, 15]

In addition to Coulombic effects, the properties of a molecular metal can be exceedingly sensitive to the coupling of the electronic system to certain phonons (lattice vibrations). Such an instability is analogous to a Jahn–Teller distortion and is predicted theoretically for a low-dimensional metal. The net consequence can be a periodic structural distortion and charge buildup in the stack (a charge density wave, Peierls distortion, or $2k_F$ instability), the periodicity of which reflects the filling of the highest occupied band.[1a–c, 15] In the extreme case (especially for half-filled bands or at low temperatures) the distortion "locks in" and an opening of a gap in the conduction band can induce a metal-to-insulator transition. Since other structural effects such as interactions with counterions in the crystal lattice can also induce periodic structural distortions in the stacking

geometry, identification of the origin of charge-density-wave phenomena is not always unambiguous. Qalitatively, such phenomena become less important as the molecular chain deviates strongly from unidimensionality (i.e., interchain interactions become very large). Electron–phonon interactions are also believed to play a crucial role in a variety of charge-transport mechanisms, including organic superconductivity[2c, 3, 16] and the $\sigma \sim T^{-2}$ behavior frequently observed in molecular metals.[17]

From a synthetic chemical perspective, the most obvious way to clarify many of the above phenomena would be to prepare and study molecular conductors in which there was sequential variation of one crucial parameter (e.g., molecule–molecule interplanar spacing, off-axis counterion, band filling) while all other parameters were held fixed. Unfortunately, current routes to molecular metals are not subject to such high degrees of control. Thus, conventional syntheses usually rely on crystallization combined with a chemical or electrochemical oxidation or reduction process as in Equation (2). The success of such a self-assembly process in forming segregated stacks of closely arrayed radical cations (or anions) and evenly distributed, complementary arrays of off-axis counterions is by no means guaranteed. The structural outcome hinges upon a complex and largely uncontrollable collection of Madelung, exchange, polarization, bandwidth, van der Waals, core repulsion, crystal-growth kinetic, and ionization potential/electron affinity factors, which determine, in poorly understood ways, the level of partial oxidation (ϱ) and the crystallization architecture. Thus, charge transfer may not occur, and if it does, numerous other packing modes are possible (e.g., **3**–**5**).

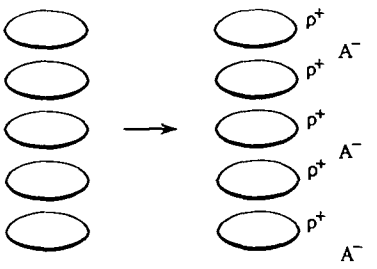

(2)

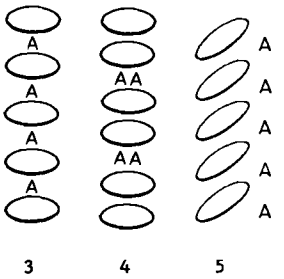

3 4 5

Most embodiments of motifs **3** and **4** lack an obvious conduction band structure and, to date, such materials have been found to be insulators.[2, 3] In addition, simple changes in the molecular building block or off-axis counterion in these syntheses typically induce major changes in stacking architecture, hence in a myriad of correlated physical properties. It is therefore apparent that any rational synthetic strategy for disentangling the numerous molecular-metal architectural/electronic structural variables must possess a means of rigorously controlling the subunit stacking rather than relying upon capricious packing forces. The principal focus of the present article, then, is upon the chemical and physical consequences of effecting, via the introduction of strong, covalent intrastack bonds, the connectivity modification shown in Equation (3).[18]

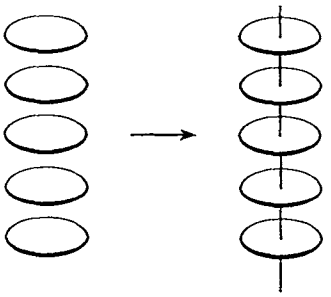

(3)

6

It should also be appreciated that structure **6** is a macromolecule. The field of electrically conductive polymers has developed in parallel to that of molecular metals, and representative structures are illustrated in Figure 5.[4] In common with stacked molecular systems, oxidation or reduction (commonly called "doping" as for conventional inorganic semiconductors) is necessary to mobilize charge carriers. However, the bandwidths of most highly conductive polymers are greater, and charge-transport mechanisms may be different. Furthermore, structural regularity is not as great as in molecular conductors, and a number of classes of conductive polymers are poorly crystalline or amorphous. This factor and the accompanying structural uncertainties severely complicate the interpretation of chemical and physical data.

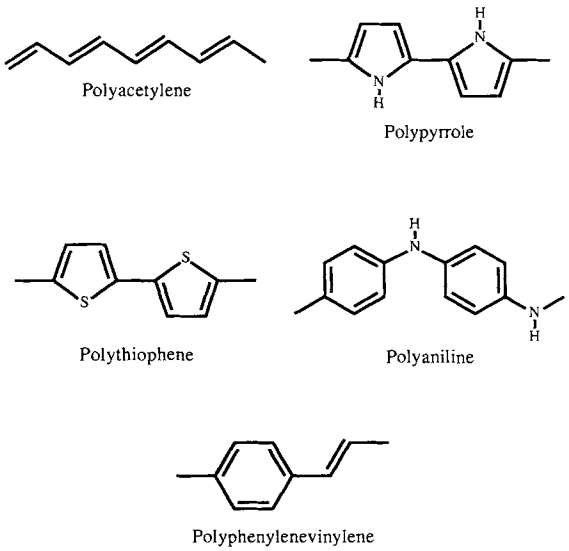

Fig. 5. Precursors of common electrically conductive polymers.

3. Building Blocks and Model Materials

Reference to target structure **6** indicates that a suitable molecular subunit must have chemical functionality perpendicular to the molecular plane. An ideal synthon for such a strategy is a metallomacrocycle in which the central metal atom has the possibility of bond formation perpendicular to the square coordination plane. Early work in this laboratory established that partial oxidation of glyoximates (**7**, **8**),[19] dibenzotetraazaannulenes (**9**),[20] hemiporphyrazines (**10**),[21] and phthalocyanines (**11**)[22] with halogens afforded new

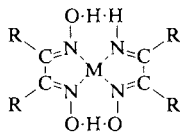

7

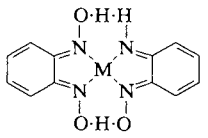

8

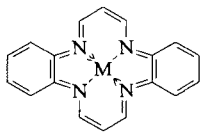

9

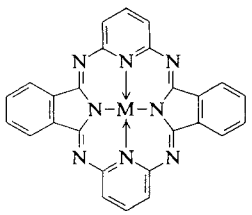

10

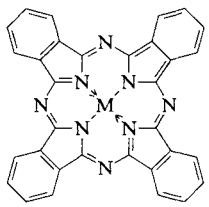

11

families of low-dimensional molecular conductors. In all cases, spectroscopic analysis of the form of the halogen present in the crystal structure showed unambiguously that the metallomacrocyclic subunits were in formal fractional oxidation states.[18b, 23]

Metallophthalocyanines, M(Pc), are robust, highly functionalizable commodity chemicals that are widely used as pigments and oxidation catalysts.[24] More importantly for the present purposes, they form the basis for a class of molecular metals in those cases where the tactic of Equation (2) is successful. A particularly informative example is $H_2(Pc)(I_3)_{0.33}$[25] (**11**, where M = two H atoms), which exhibits many of the physical properties typical of a molecular metal. As can be seen in Figure 6, the tetragonal crystal structure consists of $H_2(Pc)^{0.33\oplus}$ cations, arrayed at 3.251(2)-Å intervals and staggered by 40.0° with respect to neighboring subunits. Chains of disordered $I_3^{\ominus}$ counterions extend parallel to the stacking direction. This particular structural pattern will be seen to be ubiquitous for phthalocyanine metals. The electrical conductivity of these exceedingly thin crystals (0.07 × 0.07 × 0.65 mm) in the stacking direction ($\sigma_{\parallel}$) is ca. 700 $\Omega^{-1}cm^{-1}$ at room temperature. When normalized for the large $H_2(Pc)$ cross-sectional area, this room temperature conductivity is one of the highest yet reported for a molecular metal. The high unidimensionality of the charge transport is demonstrated by the result $\sigma_{\parallel}/\sigma_{\perp} \gtrsim 500$. As the temperature of $H_2(Pc)(I_3)_{0.33}$ crystals is slowly lowered, the stacking-axis conductivity becomes metal-like (Fig. 7, top, $d\sigma/dT < 0$), reaches a maximum at ca. 15 K, and exceeds 3500 $\Omega^{-1}cm^{-1}$ even at 1.5 K. Also shown in Figure 7, top, is the thermoelectric power (TEP) of

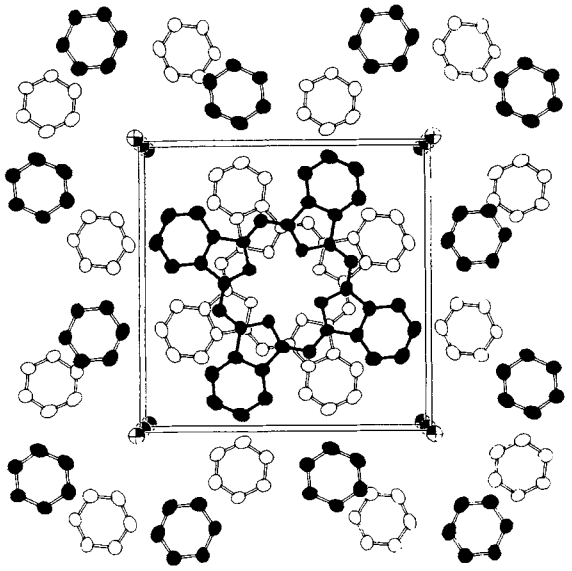

Fig. 6. The crystal structure of the macrocyclic molecular metal $H_2(Pc)(I_3)_{0.33}$ viewed parallel to the molecular stacking direction (crystallographic c axis).

an $H_2(Pc)(I_3)_{0.33}$ crystal measured in the stacking direction. The positive sign of the Seebeck coefficient (S) indicates that this material is a radical-cation conductor (the major conduction pathway is through the $[H_2(Pc)^{0.33\oplus}]_{\infty}$ chain), while the relatively small magnitude and linear dependence on temperature are classic signatures of metallic behavior.[26–28] Note the change in the thermoelectric power toward semiconducting behavior at the temperature (ca. 15 K) where $\sigma_{\parallel}(T)$ passes through a maximum. In a one-dimensional tight-binding picture, the temperature dependence of S can be related to the bandwidth ($4t$, Fig. 3) via Equation (4).[26–28, 29] Here, k_B is the Boltzmann constant. Analysis

$$S = \frac{2\pi^2 k_B^2 T \cos(\pi\varrho/2)}{3e(4t)\sin^2(\pi\varrho/2)} \tag{4}$$

of the $S(T)$ data for $H_2(Pc)(I_3)_{0.33}$ yields a tight-binding bandwidth of 1.0(1) eV. In agreement with this ligand radical-cation-based picture of charge transport, fully assigned solid-state ^{13}C CPMAS NMR data[30] evidence large, locally resolved Knight shifts (due to nuclear-conduction electron interactions) consistent with a phthalocyanine radical cation. ESR spectra are characterized by nearly free-electron g values and narrow line widths. These are signatures of a radical-cation conductor with the narrow line width indicating a high degree of unidimensional character (in accord with charge transport and optical data) and only minor interaction of the carrier spins with the $I_3^{\ominus}$ counterions (i.e., only small contributions to electron-spin relaxation by phonon-modulated spin–orbit interactions).[31, 32]

The optical and magnetic properties of $H_2(Pc)(I_3)_{0.33}$ crystals also provide classic signatures of metal-like character. In Figure 7, middle, is shown the reflectance spectrum of an $H_2(Pc)(I_3)_{0.33}$ crystal polarized parallel to and perpendicular to the macrocycle stacking direction. The small size of the crystals necessitated the development of specialized microspectrophotometry techniques.[25] The most striking feature of the spectrum is the parallel-polarized edge[33, 34] observed at ca. 3100 cm^{-1} ($\lg \nu \approx 3.49$). This feature is analogous to

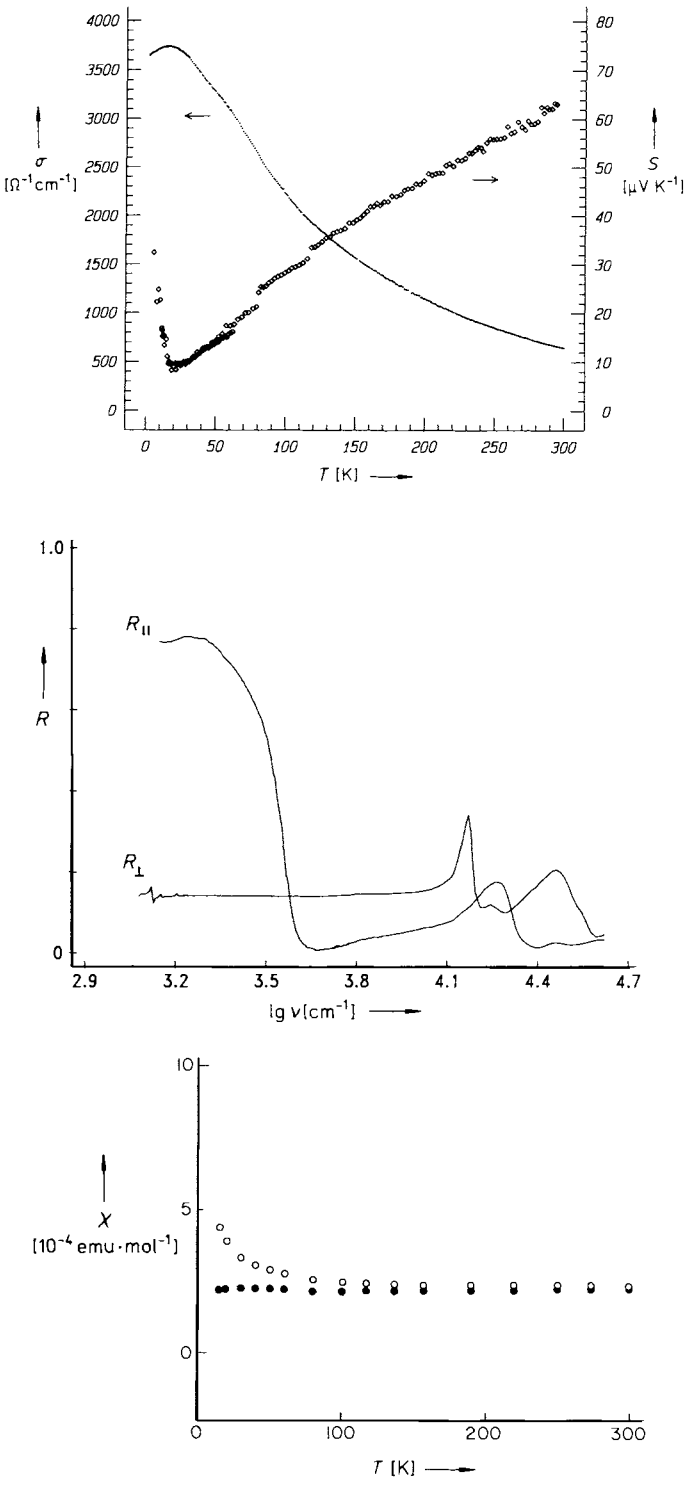

Fig. 7. Physical properties of the macrocyclic molecular metal $H_2(Pc)(I_3)_{0.33}$. Top: Variable-temperature electrical conductivity and thermoelectric power measured parallel to the molecular stacking direction. Middle: Reflectance spectrum of an $H_2(Pc)(I_3)_{0.33}$ single crystal; $R_\parallel$ and $R_\perp$ denote reflectance parallel to and perpendicular to the molecular stacking direction. The perpendicularly polarized features at 14 800 (lg $\nu = 4.17$) and 29 000 cm^{-1} (lg $\nu = 4.46$) are assigned to Pc-centered π–π^* transitions, while the parallel-polarized feature at 18 200 cm^{-1} (lg $\nu = 4.26$) is assigned to an $I_3^{\ominus}$-centered excitation. Bottom: Variable-temperature magnetic susceptibility (χ) data for a polycrystalline $H_2(Pc)(I_3)_{0.33}$ sample. The filled circles denote the Pauli-like component, the open circles the paramagnetic Curie-like component.

the plasma edge observed in the reflectivity of metals[1e] and can be associated with carrier excitation in the partially filled conduction band. The marked polarization indicates that $H_2(Pc)(I_3)_{0.33}$ is only metallic (there is a significant bandwidth) in the stacking direction. Analysis of the optical data yields the carrier relaxation time and mass, the plasma frequency (ω_p), and, via the tight-binding expression of Equation (5),[33,34] the bandwidth. Here, N_c is the carrier density. Analysis of the $H_2(Pc)(I_3)_{0.33}$ reflectivity data yields

$$4t = \frac{\varrho(\hbar\omega_p)^2}{4N_c e^2 c^2 \sin(\pi\rho/2)} \tag{5}$$

$4t = 1.3(1)$ eV, in excellent agreement with the thermopower data. Static magnetic susceptibility data for $H_2(Pc)(I_3)_{0.33}$ crystals are shown in Figure 7, bottom. When a small Curie-like component of the type normally associated with defects and impurities[35,36] is subtracted, the remaining susceptibility is only weakly paramagnetic and virtually independent of temperature. This behavior is reminiscent of the Pauli susceptibility of bulk metals,[1d,e] which is a consequence of the partially filled character of the conduction band. Assuming a one-dimensional tight-binding band and noninteracting electrons ($U = 0$), a tight-binding bandwidth can be derived from Equation (6).[37] The result for $H_2(Pc)(I_3)_{0.33}$ is that $4t = 0.37(3)$ eV, in clear disagreement with the afore-

$$\chi_{Pauli} = \frac{N\mu_B^2}{t\pi \sin(\pi\varrho/2)} \tag{6}$$

mentioned TEP and optical data. The implication of this finding is that the magnetic susceptibility is "enhanced", that is, that U and therefore Coulombic repulsions are not insignificant.[38,39] In summary, $H_2(Pc)(I_3)_{0.33}$ exhibits many of the classic features of a molecular metal, to which we will make reference in later discussion: (1) metal-like conductivity in the stacking direction; (2) thermoelectric power which is small in magnitude and the absolute value of which is linearly proportional to temperature; (3) a plasma-like edge in the reflectivity; (4) Pauli-like paramagnetism. These results also clearly demonstrate that a metal-ion substituent is not required in the core of the macrocycle for metal-like character. How reliable the formalisms are that allow extraction of $4t$ from condensed-phase TEP and optical data is an important, unanswered question which will be taken up in Section 5.

Although the molecular self-assembly tactic of Equation (2) was a useful first-generation approach, subsequent studies have shown it to have limited scope. Several additional salts have recently been prepared by high-temperature electrocrystallization procedures developed in this laboratory, such as $Ni(Pc)(BF_4)_y$[40] and $Ni(Pc)(ClO_4)_y$.[41] The crystal structure of the latter material ($y \approx 0.42$) is shown in Figure 8 and is similar to that of $H_2(Pc)(I_3)_{0.33}$, as are those of $Ni(Pc)(I_3)_{0.33}$[22c] and $Ni(Pc)(BF_4)_{0.33}$.[40]

Electrical, optical, and magnetic studies of these materials indicate metallic character in the macrocycle stacking direction and further show that the presence of the Ni ion has a relatively minor influence on the charge-transport characteristics.[40–42] Comparative charge-transport data are presented in Figure 9. $Ni(Pc)(ClO_4)_y$ also displays the interesting characteristic that y values for different crystals can vary slightly (0.39–0.47) as a function of electrocrystallization conditions,[41] presumably reflecting different occupancy levels of the anion channels. Such modest variations in

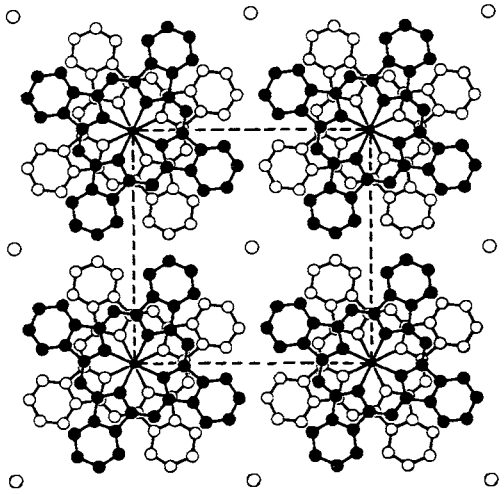

Fig. 8. The crystal structure of $Ni(Pc)(ClO_4)_{0.42}$ viewed parallel to the macrocycle stacking direction. The $ClO_4^{\ominus}$ ions are drawn as open circles for clarity.

molecular-metal band-filling/stoichiometry level are unusual but not completely unprecedented[43] and, in this case, are evident in TEP and optical measurements (cf. the ϱ dependence in Eqs. (4) and (5)). Perhaps more interestingly, the $ClO_4^{\ominus}$ ions are rotationally disordered (and likely tumbling) at room temperature in these crystals, but lock into ordered positions at lower temperatures.[44] The effects of this counterion ordering on the collective properties of $Ni(Pc)(ClO_4)_y$ are rather small compared to the effects on $(TMTSF)_2ClO_4$, where cooling-rate-dependent anion-ordering phenomena have a dramatic effect on superconducting behavior.[4, 45]

Beyond the above small anions, attempts via self-assembly to probe phthalocyanine band-structure–counterion interactions are frustrated in that electrocrystallization experiments with larger anions (e.g., $AsF_6^{\ominus}$, $SbF_6^{\ominus}$) lead to materials with different packing arrangements and ϱ values.[42f] Likewise, the use of organic oxidants such as high-potential quinones (e.g., TCNQ) fails to produce molecular metals, yielding instead insulators which are presumed to have integrated stacking as in **3** or **4**.[46] Clearly, the forces retaining the stacking architecture in these ligand-based conductors are rather delicate and unreliable. Comparative physical data on phthalocyanine molecular conductors are compiled in Tables 1 and 2.

4. Cofacial Condensation Assembly as an Approach to Enforced Molecular Stacking

A particularly attractive approach to target structure **6** employs the solid-state condensation polymerization of dihydroxy group 4 phthalocyaninato complexes (Fig. 10).[18, 47–49] These robust, highly crystalline rigid-rod polymers have been characterized by various end-group analyses (radiochemical, FT-IR),[47a] solid-state NMR spectroscopy,[30] electron microscopy,[50] and powder X-ray diffraction[47a] (aided by computer simulation techniques and single-crystal diffraction studies of model oligomers[51]), and solution diffraction techniques (for more soluble, ring-functionalized derivatives).[52] Together, these data provide a detailed picture of $[M(Pc)O]_n$ architecture and crystal

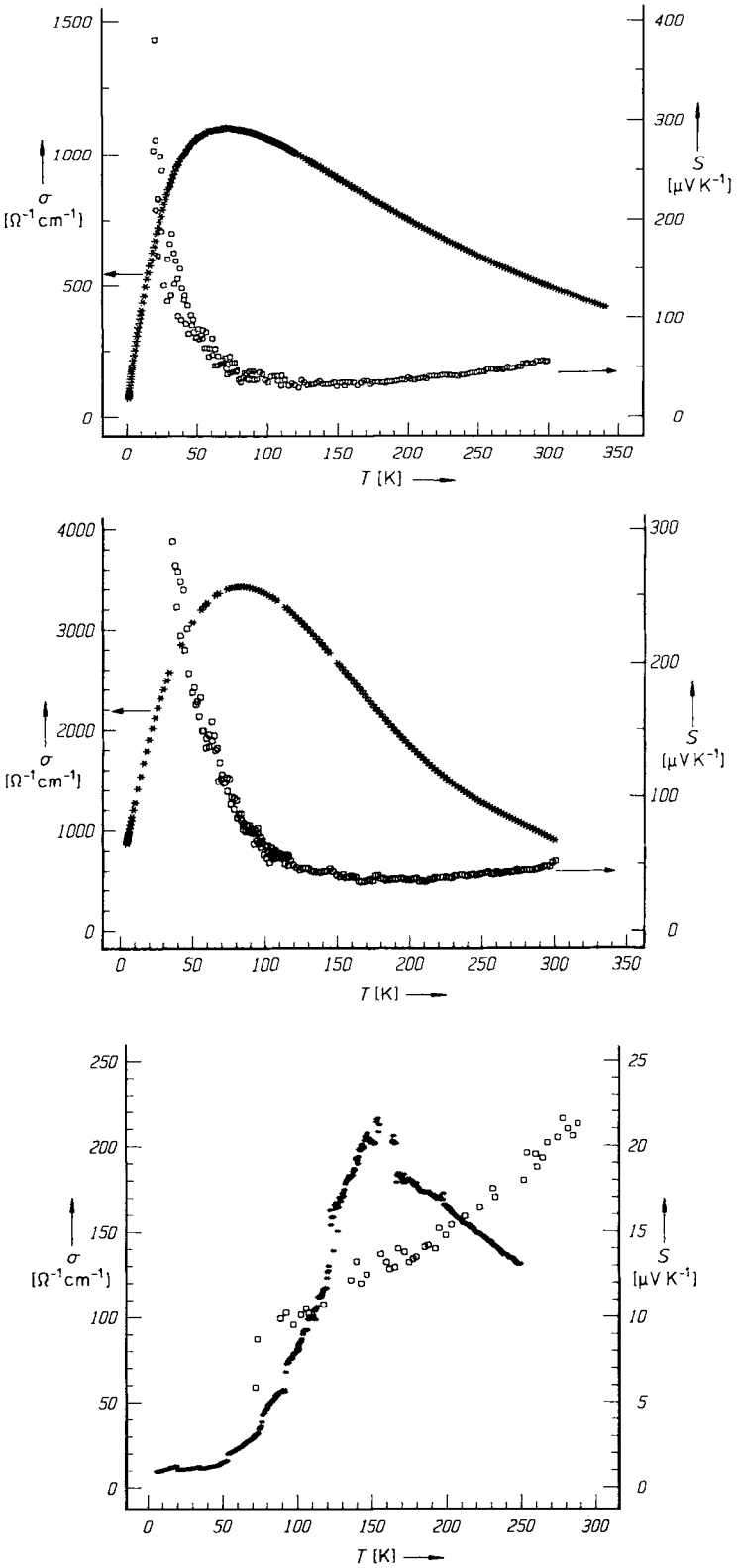

Fig. 9. Variable-temperature macrocycle stacking axis conductivity (σ) and thermoelectric power (S) data for representative crystals of $Ni(Pc)(I_3)_{0.33}$ (top), $Ni(Pc)(BF_4)_{0.33}$ (middle), and $Ni(Pc)(ClO_4)_y$, $y \approx 0.40$ (bottom). Measurements on these exceedingly fragile crystals were performed with cooling rates as low as 1 K h^{-1}.

structure. For example, n is typically 50–200, depending upon the polymerization conditions ($n \geq 100$ is used for most physical experiments), and Pc–Pc interplanar spacings expand with M ionic radius in the following order: 3.32(2)Å,

Table 1. Structural, degree of charge transfer, transport, magnetic, and optical parameters for electrically conductive phthalocyanine polymers and model compounds [a].

Compound	Tetragonal lattice [b] [Å]	ϱ	σ_{300K} [Ω^{-1} cm^{-1}]	S_{300K} [μV K^{-1}]	χ [10^{-4} emu mol^{-1}]	ω_p [cm^{-1}]
$\{[Si(Pc)O](I_3)_{0.35}\}_n$	$a = 13.97(5)$ $c = 6.60(4)$	0.35	0.60		2.35(10)	4540
$\{[Si(Pc)O](BF_4)_{0.35}\}_n$	$a = 13.70(7)$ $c = 6.58(4)$	0.35	0.10		2.22(6)	4700
$\{[Si(Pc)O](BF_4)_{0.50}\}_n$	$a = 13.96(7)$ $c = 6.66(4)$	0.50	0.13	+0.3	2.32(6)	5390
$\{[Si(Pc)O](PF_6)_{0.35}\}_n$	$a = 13.98(6)$ $c = 6.58(4)$	0.35	0.10		2.49(6)	4600
$\{[Si(Pc)O](PF_6)_{0.47}\}_n$	$a = 14.08(7)$ $c = 6.63(4)$	0.47	0.10			
$\{[Si(Pc)O](SbF_6)_{0.35}\}_n$	$a = 14.31(4)$ $c = 6.58(4)$	0.35	0.10		2.22(3)	4550
$\{[Si(Pc)O](SbF_6)_{0.41}\}_n$	$a = 14.19(7)$ $c = 6.61(4)$	0.41	0.10			
$\{[Si(Pc)O](Tos)_{0.67}\}_n$	$a = 14.39(7)$ $c = 6.64(4)$	0.67	0.04	+26	3.13(6)	5000
$\{[Si(Pc)O](SO_4)_{0.095}\}_n$	$a = 13.86(7)$ $c = 6.67(4)$	0.19	0.09	+49	1.93(14)	4870
$\{[Ge(Pc)O](I_3)_{0.35}\}_n$	$a = 13.96(5)$ $c = 6.96(4)$	0.35	0.10		2.70(10)	4210
$H_2(Pc)(I_3)_{0.33}$ [c]	$a = 13.928(5)$ $c = 6.502(3)$	0.33	ca. 700 8.0 [d]	+62	2.21(5)	6360
$Ni(Pc)(I_3)_{0.33}$ [c]	$a = 13.936(6)$ $c = 6.488(3)$	0.33	ca. 500 7.5 [d]	+59	1.90(10)	5630
$Ni(Pc)(BF_4)_{0.33}$ [c]	$a = 13.97(2)$ $c = 6.48(1)$	0.33	ca. 1000 6.0 [d]	+50	1.30(4)	6020
$Ni(Pc)(ClO_4)_{0.42}$ [c]	$a = 13.957(3)$ $c = 6.4672(9)$	0.42	100–1500	+25	2.62(8)	7700–9000

[a] All data for polycrystalline samples except where indicated. [b] Pc–Pc interplanar spacing = $c/2$. [c] Single-crystal specimen. Conductivity and thermopower measured in the Pc stacking direction. [d] Comparative polycrystalline measurement.

Table 2. Representative bandwidth information for phthalocyanine conductors.

Compound	Interplanar separation [Å]	Bandwidth [a] Optical [eV]	Bandwidth [b] TEP [eV]	Bandwidth [c] PES [eV]	Bandwidth [d] Magnetic [eV]	Bandwidth [e] Theoretical [eV]
$H_2(Pc)(I_3)_{0.33}$	3.251(2)	1.2(1)	1.0(1)	–	0.37(3)	0.85
$Ni(Pc)(I_3)_{0.33}$	3.244(2)	1.00(9)	1.0(1)	–	0.43(3)	0.85
$\{[Si(Pc)O](I_3)_{0.35}\}_n$	3.30(2)	0.60(6)		0.58(6)	0.32(3)	0.76
$\{[Si(Pc)O](BF_4)_{0.35}\}_n$	3.29(2)	0.64(6)		0.58(6)	0.37(3)	0.76
$\{[Si(Pc)O](BF_4)_{0.50}\}_n$	3.33(2)	0.63(6)	0.70(7)	0.58(6)	0.26(1)	0.76
$\{[Ge(Pc)O](I_3)_{0.35}\}_n$	3.48(2)	0.48(5)		0.38(6)	0.28(2)	0.50

[a] From optical reflectivity data analyzed via Eq. (5). [b] From thermoelectric power data analyzed via Eq. (4). [c] From gas-phase photoelectron spectrum of ROM(Pc)OM(Pc)OR dimer. [d] From magnetic susceptibility analyzed via Eq. (6). [e] From DV-Xα calculation on a cofacial dimer.

M = Si; 3.53(2)Å, M = Ge; 3.82(2)Å, M = Sn. Combined with the data base of model molecular conductors discussed above, these stacking-enforced arrays of ligand-based conductive building blocks offer a unique opportunity to probe many of the poorly understood features of molecular metals as well as conductive polymers. We begin with a discussion of chemical and electrochemical redox phenomenology and the physical properties of the resulting materials.

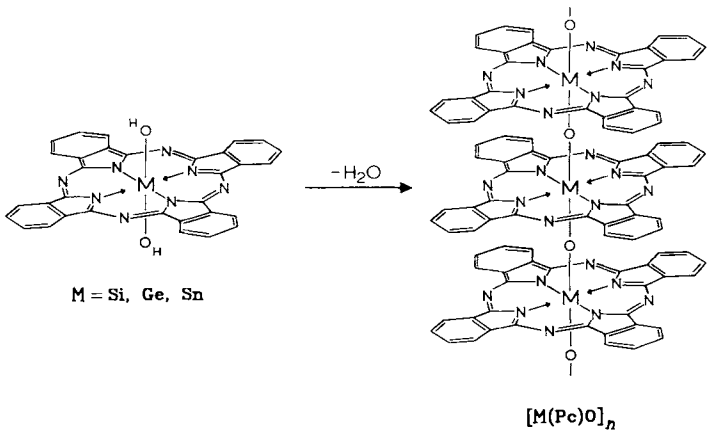

Fig. 10. Strategy for the cofacial assembly of structure-enforced group 4 metallophthalocyanine assemblies.

4.1. Chemical Doping of $[M(Pc)O]_n$ Materials: Interplanar Spacing and Counterion Effects on Collective Properties

Partial oxidation of the $[M(Pc)O]_n$ polymers with halogen[53] and nitrosyl salts[54] proceeds as shown in Equations (7) and (8). X-ray diffraction studies reveal that the doping

$$[M(Pc)O]_n + 0.53n\ X_2 \longrightarrow \{[M(Pc)O](X_3)_y\}_n \quad (7)$$
M = Si, Ge; X = Br, I; $y \approx 0.35$

$$[M(Pc)O]_n + 0.35n\ NO^{\oplus}Z^{\ominus} \longrightarrow \{[M(Pc)O]Z_{0.35}\}_n + 0.35n\ NO \quad (8)$$
M = Si; $Z^{\ominus} = BF_4^{\ominus}, PF_6^{\ominus}, SbF_6^{\ominus}$

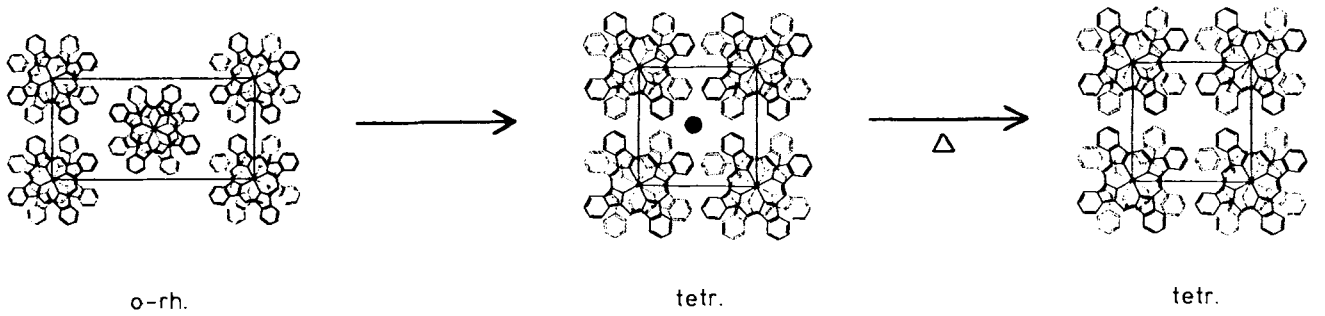

Fig. 11. Structural model of the changes accompanying chemical doping of as-polymerized $[Si(Pc)O]_n$ with I_2, followed by thermal undoping. The view is parallel to the phthalocyanine stacking direction. o-rh = orthorhombic, tetr. = tetragonal.

processes are largely inhomogeneous. That is, incremental addition of oxidant produces progressively larger amounts of the fully doped phase, having a discrete stoichiometry (fixed ϱ) and a different crystal structure. This process is illustrated schematically for $[Si(Pc)O]_n$ in Figure 11. Until full uptake of oxidant is achieved, the material is a heterogeneous mixture of starting material and product. This inhomogeneity has been verified by transmission electron microscopy.[50] X-ray diffraction studies also indicate that the tetragonal doped phases are essentially isostructural with the molecular phthalocyanine analogues (cf. $H_2(Pc)(I_3)_{0.33}$ in Fig. 6 and $Ni(Pc)(ClO_4)_{0.42}$ in Fig. 8), differing principally in interplanar spacing. Relevant structural data are compiled in Table 1. It can also be seen in Equations (7) and (8) that the ultimate degree of partial oxidation (band depletion, ϱ) is ca. $+0.35$ for all oxidants. Born–Haber cycles using proper $\Delta H_{subl.}$ and ionization potential data for molecular phthalocyanines show that this is not an unexpected result.[54] Drastic modifications in ϱ and off-axis counterions are best achieved using electrochemical techniques (see Section 4.2). Interestingly, the products of Equation (7) can be "undoped" by heating under vacuum to yield a new $[Si(Pc)O]_n$ phase which is best modeled by a tetragonal crystal structure (Fig. 11).

The series $Ni(Pc)(I_3)_{0.33}$ (**I**); $\{[Si(Pc)O](I_3)_{0.35}\}_n$ (**II**), and $\{[Ge(Pc)O](I_3)_{0.35}\}_n$ (**III**) provides an extremely informative picture of how an expansion in interplanar spacing from 3.24 to 3.30 to 3.48 Å modifies the properties of a molecular metal. Comparative variable-temperature electrical conductivity data are shown in Figure 12. In viewing these data, it should be noted that measurements on polycrystalline samples (high-quality single crystals of the doped polymers are not available) are influenced by the isotropy of the macroscopic specimen and interparticle contact effects.[55, 56] Hence, while full "metal-like" character is partially masked (cf. the $Ni(Pc)(I_3)_{0.33}$ data), an empirical rule of thumb[55, 57] suggests that polycrystalline conductivity values can be multiplied by a factor of ca. 500 to estimate single-crystal conductivity in the stacking direction ($\sigma_{\parallel}$). This approximate relationship has been verified for a number of molecular conductors and, in the present case, allows meaningful, although not strictly quantitative, comparisons to be drawn. Most importantly, the data evidence a dramatic diminution in the efficiency of charge transport as overlap decreases between the adjacent macrocycle π systems. In accord with the inhomogeneous character of the doping processes, the doping-level dependence of the conductivity is not monotonic, but exhibits an abrupt discontinuity which can be associated with a percolation threshold, as found in many composite materials.[58] Such discontinuous behavior is observed in mixtures of conductive and nonconductive particles when the volume fraction of the former reaches a certain critical threshold beyond which there is a continuous network of contacting conductive particles. At this point—the percolation threshold—the material becomes highly conductive. The temperature dependence of $\{[Si(Pc)O]X_y\}_n$ conductivity can best be fit to a fluctuation-induced carrier tunneling model[59] in which relatively large conductive regions are separated by insulating barriers having a parabolic potential. At low temperatures, transport is dominated by temperature-independent elastic tunneling, while it is thermally activated at higher temperatures. Importantly, the $\sigma(T)$ data cannot be convincingly fit to conventional carrier hopping models which apply to many conductive polymers.[4]

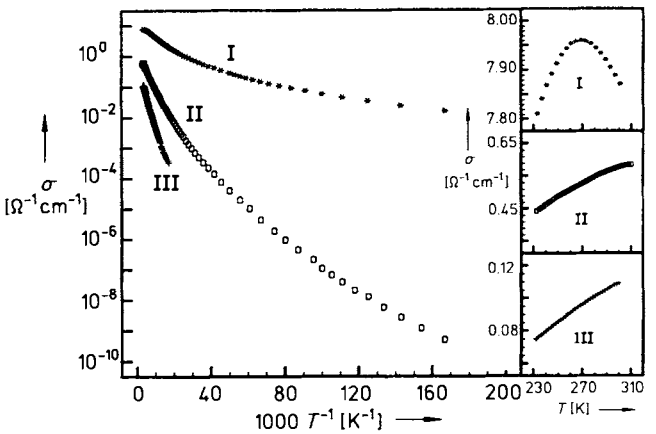

Fig. 12. Variable-temperature electrical conductivity data for compressed polycrystalline samples of $Ni(Pc)(I_3)_{0.33}$ (**I**), $\{[Si(Pc)O](I_3)_{0.35}\}_n$ (**II**), and $\{[Ge(Pc)O](I_3)_{0.35}\}_n$ (**III**). Note that metal-like behavior observed in $Ni(Pc)(I_3)_{0.33}$ single crystals (Fig. 9, top) is modified by the polycrystalline nature of the samples.

The sensitivity of band-structure-related properties to Pc–Pc interplanar separation is also evident in comparative optical reflectivity data, where a progressive shift of the plasma edge to lower energy is observed with increasing interplanar spacing (Fig. 13). This behavior is in excellent agreement with the simple tight-binding band-theoretical picture [Eq. (5)]. Finally, while the magnetic susceptibilities of **I**–**III** are all essentially Pauli-like (cf. Fig. 7), the susceptibility increases incrementally with increasing interplanar spacing, again in accord with simple theoretical notions [Eq. (6)].

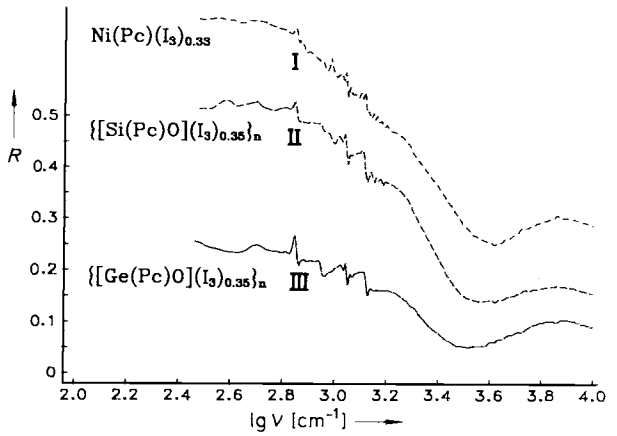

Fig. 13. Optical reflectance spectra of compressed polycrystalline samples of $Ni(Pc)(I_3)_{0.33}$ (I), $\{[Si(Pc)O](I_3)_{0.35}\}_n$ (II), and $\{[Ge(Pc)O](I_3)_{0.35}\}_n$ (III). Spectra are offset vertically by 0.2 reflectance units for ease of viewing.

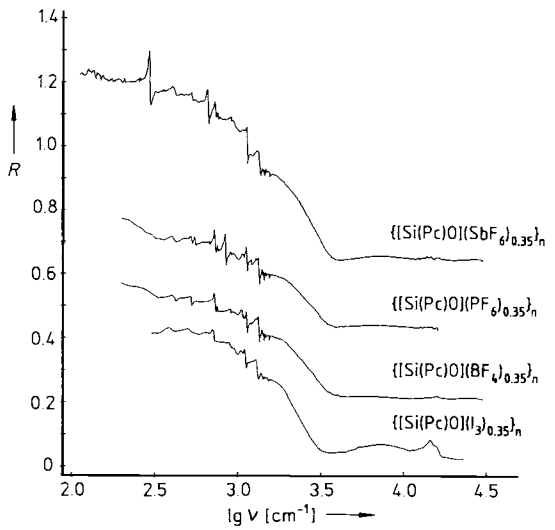

Fig. 14. Optical reflectance spectra of compressed polycrystalline samples of $\{[Si(Pc)O(SbF_6)_{0.35}\}_n$, $\{[Si(Pc)O](PF_6)_{0.35}\}_n$, $\{[Si(Pc)O](BF_4)_{0.35}\}_n$ and $\{[Si(Pc)O](I_3)_{0.35}\}_n$. Spectra are offset vertically by 0.2 reflectance units for ease of viewing.

Relevant physical data and derived $4t$ values are set out in Tables 1 and 2. It can be seen that reflectivity-derived (and susceptibility-derived) $4t$ values fall with increasing interplanar spacing. All of the susceptibility-derived bandwidths evidence some degree of Coulombic enhancement. At this stage, a completely independent measure of $4t$, for example, not tied to the many approximations inherent in the condensed-state derivation, would be highly desirable. This subject will be taken up in Section 5.

The intriguing question next arises as to the nature and magnitude of band-structure–counterion interactions. If the $[Si(Pc)^{\varrho\oplus})O]_n$ stacking is essentially frozen in these materials, to what degree are the charge carriers influenced by whether off-axis anions are large and highly polarizable (e.g., $I_3^{\ominus}$) or small and hard (e.g., $BF_4^{\ominus}$)? This question was addressed via magnetic, optical, charge-transport, and ESR measurements. Magnetic susceptibility data are one means to probe the electronic structure and population of the highest occupied band, and the result is that all of the $[Si(Pc)^{0.35\oplus}O]_n$ materials that have been studied exhibit Pauli-like paramagnetism that is virtually identical in magnitude and temperature dependence (Table 1). Any effects of the counterion on the Coulombic enhancement ("screening" effects of this type have frequently been invoked for other molecular conductors) are undetectable by this technique. Optical reflectivity studies of these materials reveal essentially identical, plasma-like edges (Fig. 14), with derived ω_p and $4t$ parameters virtually independent of counterion (Tables 1 and 2). Likewise, variable-temperature conductivity data for the partially oxidized $[Si(Pc)^{0.35\oplus}O]_n$ series evidence only slight differences of the type that can be associated with slightly different interparticle resistances and different chain-packing densities in the respective crystal structures. Data are set out in Table 1. Studies of ESR data for polycrystalline $\{[Si(Pc)^{0.35\oplus}O]X_y\}_n$ reveal nearly isotropic free-electron g values, which are consistent with ligand-based oxidation, and relatively narrow line widths that increase in the progression $BF_4^{\ominus} < PF_6^{\ominus} < SbF_6^{\ominus} < I_3^{\ominus}$ (0.36 to 2.9 G at 300 K). As noted in Section 3 for the molecular phthalocyanine conductors, narrow line widths can in general be associated with the absence of heavy atoms in extensive communication with the carriers as well as with the highly unidimensional crystal and electronic structure ($t_\perp$ is small, in agreement with the other physical measurements). The anion-dependent line width effects likely reflect minor interactions with the off-axis anions and resulting electronic relaxation via phonon-modulated spin–orbit interactions.[31]

The present results stand in sharp contrast to those for most organo-chalcogen-based molecular conductors and superconductors.[2, 3, 45] In these cases, small changes in counterion effect significant changes in crystal packing, hence major changes in charge-transport, optical, and magnetic properties; differences in resulting properties are sometimes as large as those expected for a superconductor rather than an insulator. For the present $[Si(Pc)^{0.35\oplus}O]_n$ materials, the insensitivity appears to arise from two major factors. The first and probably most important factor is the essentially frozen character of the stacking architecture, so that band-structure–counterion interactions must be Coulombic or involve subtle static or dynamic modifications in Pc–Pc staggering angles. The second factor is likely connected with the unique M(Pc) π electronic structure and will be discussed in Section 5.

4.2. Electrochemical Doping of $[M(Pc)O]_n$ Materials: Structure, Counterion, and Band-Filling Effects—Tunable ϱ

Electrochemical techniques have been employed extensively to effect the "doping" of electrically conductive polymers.[4] In general, those structural changes which accompany oxidation and reduction cycles are not well-understood. For the $[M(Pc)O]_n$ polymers, electrochemical studies offer an opportunity to address these issues as well as to vary anions and modify ϱ to an extent not readily possible with chemical reagents.

Electrochemical studies of $[Si(Pc)O]_n$ oxidative (reductive) doping have been carried out under rigorously anhydrous and anaerobic conditions in several experimental configurations in which the polymer solid is in direct contact with a

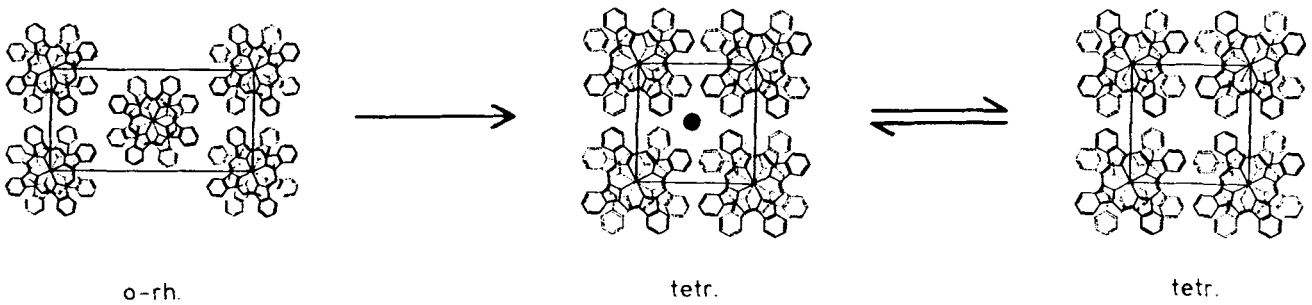

Fig. 15. Structural model of the changes accompanying initial electrochemical oxidation of as-polymerized $[Si(Pc)O]_n$. Initial "break-in" is accompanied by a transformation to a more open structure which allows more facile redox cycling. The view is parallel to the phthalocyanine stacking direction.

liquid electrolyte containing the anion (cation) of interest.[60, 61] Most studies involve an automated electrochemical potential spectroscopy (ECPS) experiment in which the applied potential is changed in steps, and at each step Coulombs of charge passed in the doping/undoping process are measured. The result is a map of applied potential versus doping stoichiometry, with the precise shape of the curve indicating where transformations between phases occur. Preparative-scale experiments are used to provide macroscopic samples for elemental analysis and diffractometric, magnetic, optical, and charge-transport characterization.

Perhaps the most interesting feature in the oxidative electrochemistry of "as-polymerized" $[Si(Pc)O]_n$ (orthorhombic; cf. Fig. 11) in common electrolytes such as $n\mathrm{Bu_4N^{\oplus}BF_4^{\ominus}}$/acetonitrile is the observation of a large overpotential/kinetic barrier upon initial oxidation.[60] The oxidation product is a tetragonal $\{[Si(Pc)O](BF_4)_y\}_n$ material, structurally similar to that prepared with $NO^{\oplus}BF_4^{\ominus}$ [Eq. (8)] except that $y \approx 0.50$ rather than 0.35. Importantly, subsequent electrochemical undoping and doping cycles for this material no longer exhibit the large overpotential, and the shape of the ECPS curve indicates that $\varrho(y)$ can be tuned smoothly between 0.00 and 0.50. The reason for the initially difficult oxidation (commonly referred to as "break-in" behavior[4, 62] but poorly understood) followed by facile cyclability can be directly correlated with the structural information. The break-in doping involves an orthorhombic to tetragonal phase transformation (Fig. 15) in which considerable reorganization of the $[Si(Pc)O]_n$ chains and expansion of the crystal lattice is required. In contrast, subsequent cycling involves interconversions between structurally similar doped and undoped tetragonal phases, requiring only anion migration through "tunnels" parallel to the stacking direction and minimal reorganization of the $[Si(Pc)O]_n$ chains (Fig. 15). The undoped phase produced in the electrochemical cycling is spectroscopically, electrochemically, and diffractometrically indistinguishable from that afforded by thermally undoping $\{[Si(Pc)O](I_3)_{0.35}\}_n$ (Fig. 11). This electrochemical behavior is unaffected by the degree to which the solid polymer sample has been finely ground, the number of redox cycles performed, or the addition of electrochemical mediators such as $[Os(bpy)]^{2\oplus}$. Further confirmation that the doping level in $\{[Si(Pc)O]BF_4)_y\}_n$ can be homogeneously tuned is provided by the observation that the tetragonal a lattice parameter varies monotonically with doping level (Fig. 16). This is the first example where the band-filling level in a molecular metal could be homogeneously tuned over a broad range

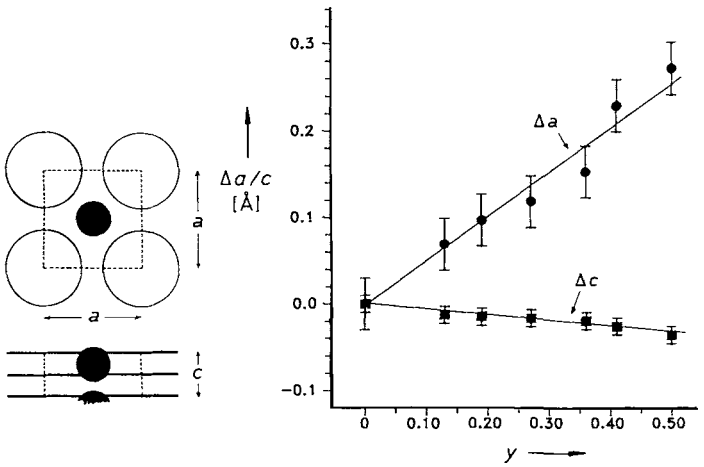

Fig. 16. Change in unit-cell parameters a and c as a function of degree of partial oxidation for $\{[Si(Pc)O](BF_4)_y\}_n$.

without a major change in crystal structure. In the closest previous example, ϱ in the system of "alloys" $(NMP)_x(Phen)_{1-x}(TCNQ)$ (NMP = *N*-methylphenazinium; Phen = phenazine) has been tuned from ca. -0.50 to -0.66 in the TCNQ band.[63, 64]

Detailed studies of $[Si(Pc)O]_n$ electrochemistry have been carried out with a wide variety of anions of differing size, shape, polarizability, and charge.[60] Representative ECPS plots are shown in Figures 17 and 18. Excepting cases where the electrochemical window of the electrolyte is exceeded, the general pattern governing the maximum stoichiometry of doping, hence the degree of band depletion that can be achieved, appears to be largely determined by the anion size. Simple packing calculations employing anion van der Waals radii show that in most cases there is good agreement between maximum possible occupancy of the anion tunnels and the doping level achieved. In the case of $n\mathrm{Bu_4N^{\oplus}BF_4^{\ominus}}$, no further oxidation of $\{[Si(Pc)O](BF_4)_{0.50}\}_n$ is observed at potentials as high as $+3.5$ V vs. the saturated calomel electrode with NaCl instead of KCl (SSCE) in liquid SO_2 at $-30\,^{\circ}C$.[65] At this point, irreversible oxidation of the polymer begins. It can also be seen in Figure 17 that the present electrochemical/synthetic results include the first case in which the charge-compensating counterion in a molecular conductor is a dianion ($SO_4^{2\ominus}$).

In the case of anions having very large dimensions, the behavior upon doping is somewhat different. For $n\mathrm{Bu_4N^{\oplus}}$ pyrenesulfonate in acetonitrile (Fig. 17), the threshold po-

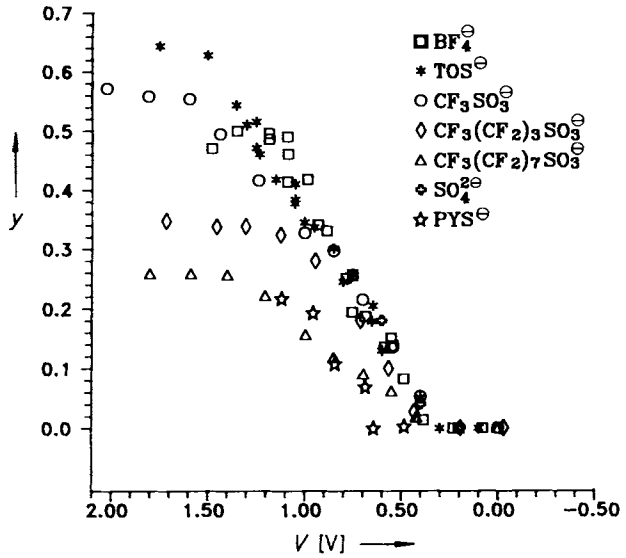

Fig. 17. Electrochemical potential spectroscopy plots for electrochemical oxidation of tetragonal $[Si(Pc)O]_n$ slurries in electrolytes composed of $nR_4N^{\oplus}$ salts (R = alkyl group) of various counterions in acetonitrile. Legend identifies the counterions. TOS = *p*-toluenesulfonate; PYS = 1-pyrenesulfonate. Potential is given vs. SSCE.

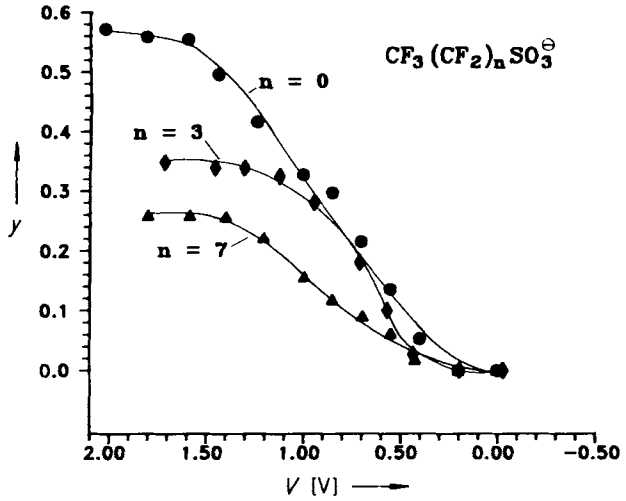

Fig. 18. Electrochemical potential spectroscopy curves for electrochemical oxidation of tetragonal $[Si(Pc)O]_n$ slurries in $nR_4N^{\oplus}CF_3(CF_2)nSO_3^{\ominus}$ (n = 0, 3, 7)/acetonitrile (R = alkyl group). Potential is given vs. SSCE.

tential for oxidative doping of tetragonal $[Si(Pc)O]_n$ is higher than for other anions studied and the ultimate doping level is rather low. In the case of $[nBu_4N^{\oplus}]_4[Mo_8O_{26}]^{4\ominus}$ in acetonitrile, an even higher threshold is observed (ca. + 0.9 V vs. SSCE) and an even lower ultimate doping level, $y \approx 0.06$, is achieved.[65] These results demonstrate the marked structure sensitivity of the $[Si(Pc)O]_n$ electrochemical doping process.

In addition to the present $[Si(Pc)O]_n$ materials, electrochemical/structural relationships have been extensively investigated for *trans*-polyacetylene.[6, 66, 67] Considerably more information is presently available for reductive doping (alkali-metal insertion) than for oxidative doping. In both cases, however, the picture is quite different than for $[Si(Pc)O]_n$ oxidative doping. Initial doping of polyacetylene is invariably found to be inhomogeneous, with the coexistence of undoped (or lightly doped) and doped $(CHX_y)_n$, $y \approx 0.06$) phases. Then, depending on the counterion, transformations are observed upon further doping to different polymer-chain/counterion packing arrangements and/or there is a modest tunability in band filling for a given crystal structure. However, in no case is the overall limiting degree of charge storage per monomer subunit as great as in the phthalocyanine polymer, nor is comparable tunability in the band filling possible. These differences no doubt reflect the far larger dimensions of the delocalized phthalocyanine π system and the attendant demonstrated capacity to store positive or negative charge, as well as the spatially closer polyacetylene-counterion interactions. The latter is understandable in terms of the higher concentration of charge per polyacetylene subunit and a polymer structure which is more favorable for close π-system–counterion interactions. The magnitudes of these interactions doubtless favor different polyacetylene packing arrangements for different stoichiometries and/or counterions, while we have shown that direct π-system–counterion interactions are small for structure-enforced phthalocyanine conductors. The factors mentioned above also suggest that doped polyacetylene crystal structures will collapse upon undoping and that well-ordered broken-in crystal structures, which are more amenable to facile doping/undoping cycles, will not be as accessible. Presently available polyacetylene data appear to confirm this.[66]

How important is the structure-enforced character of the $[Si(Pc)O]_n$ chains in the aforementioned electrochemistry? This intriguing question can be addressed via solid-state electrochemical investigations of Ni(Pc), which lacks covalent Pc–Pc structural connectivity.[60] As-sublimed Ni(Pc) has a monoclinic, slipped-stack ("β" phase) packing arrangement as shown in Figure 19. Not surprisingly, initial electrochemical oxidation is accompanied by a substantial overpotential, and the product is the tetragonal doped phase (Fig. 19). At this point, however, the behavior diverges from that of $[Si(Pc)O]_n$ in that subsequent undoping also occurs with a large overpotential, and the product is *not* an undoped tetragonal phase, but rather a second (known) monoclinic Ni(Pc) ("γ" phase). It is evident that an undoped tetragonal Ni(Pc) phase must be unstable with respect to a slipped-stack structure and that further electrochemical cycling is necessarily accompanied by $D_n \rightleftarrows$ slipped-stack structural reorganiza-

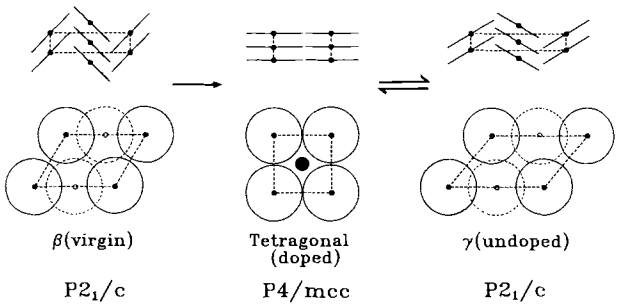

Fig. 19. Crystal structure relationships in the electrochemical oxidation of Ni(Pc) (left) to $Ni(Pc)(BF_4)_y$ where y = 0.00–0.48 (middle), followed by reduction ("undoping") (right).

tions and accompanying overpotentials. Tunability of y in the tetragonal $Ni(Pc)(BF_4)_y$ phase is rather modest.[60a]

Electrochemical experiments also answer the question of whether reductive doping of the $[Si(Pc)O]_n$ framework is possible. Partial occupancy of a band constructed from the lowest unoccupied molecular orbitals (LUMOs) of $[Si(Pc)O]_n$ might also yield a metal-like substance according to theoretical calculations.[51,68] Figure 20 shows an electrochemical

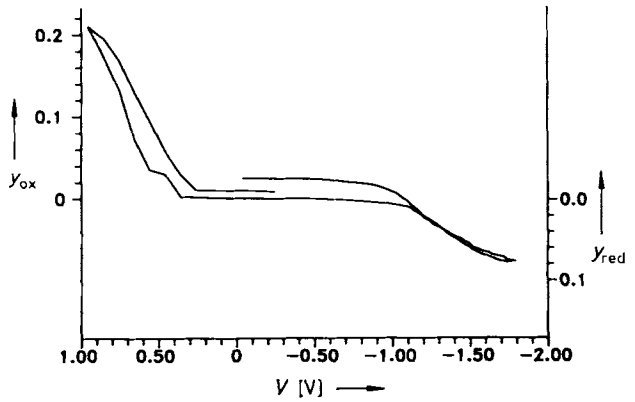

Fig. 20. ECPS data for a tetragonal $[Si(Pc)O]_n$ microcompaction in $n Bu_4N^{\oplus}BF_4^{\ominus}$/THF showing reversible reductive and oxidative doping. The anodic process is limited by the oxidation potential of THF. Potential is given vs. SSCE.

cycling experiment with solid tetragonal $[Si(Pc)O]_n$ in $Bu_4N^{\oplus}BF_4^{\ominus}$/THF. It can be seen that the polymer can be reversibly reduced with a limiting reduction stoichiometry of $y \approx 0.09$, that is, to form $\{(nBu_4N)_{0.09}[Si(Pc)O]\}_n$. Furthermore, the polymer can be cycled a number of times between the oxidized and reduced states with minor, if any, decomposition. The difference in threshold potentials measured for tetragonal $[Si(Pc)O]_n$ oxidation and reduction is ca. 1.5 V, which compares favorably with the HOMO–LUMO band gap estimated from optical spectroscopy: 1.65 eV (750 nm).[47a] Initial measurements indicate that the reductively doped $[Si(Pc)O]_n$ polymers are electrically conductive.[69]

As noted above, the electrochemically doped $\{[Si(Pc)O]X_y\}_n$ macromolecules not only incorporate a great diversity of off-axis anions (and a dianion), but also represent the first class of molecular metals in which band filling is widely tunable. Detailed charge-transport, optical, and magnetic measurements have been carried out as a function of anion and y.[60,70] Intriguing questions include whether the additional Coulombic perturbation of an off-axis dianion might cause "pinning" of the carriers and whether metal-like characteristics are tunable over the entire range of mixed valency, as suggested by simple band-theoretical considerations (Fig. 1), or whether there is a certain threshold doping level beyond which they "switch on".

In Figure 21 are shown room-temperature conductivity data for a series of polycrystalline $\{[Si(Pc)O](BF_4)_y\}_n$, $\{[Si(Pc)O](tosylate)_y\}_n$, and $\{[Si(Pc)O](SO_4)_y\}_n$ samples as a function of y. It can be seen that the $\sigma(y)$ behavior is rather insensitive to the identity of the anion and that an abrupt increase in conductivity at low doping levels is followed by a leveling off at $y \approx 0.20-0.30$. Beyond this point, the conduc-

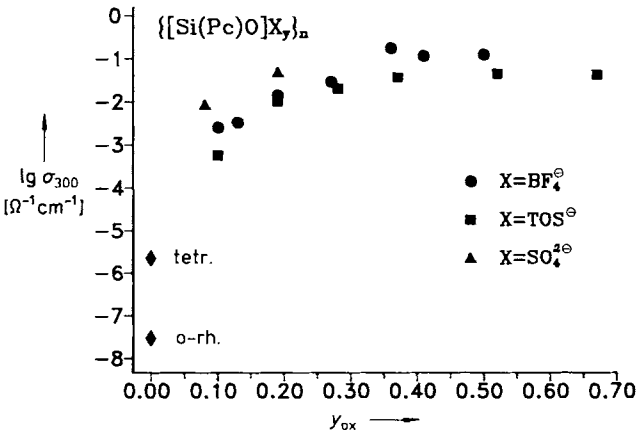

Fig. 21. Electrical conductivity (lg σ) at room temperature for polycrystalline $\{[Si(Pc)O]X_y\}_n$ samples as a function of the degree of oxidation per Si(Pc) unit (y_{ox}). The y values for $\{[Si(Pc)O](SO_4)_y\}_n$ have been multiplied by 2.0 to correct for the dinegative charge of $SO_4^{2\ominus}$.

tivity is virtually independent of y as far as $y \approx 0.67$. Variable-temperature studies indicate that, for $y \lesssim 0.20$, the $\sigma(T)$ data can be best fit to a model appropriate for a highly disordered material or one in which there is carrier hopping between localized states.[4,71-74] For $y \gtrsim 0.20$, the best fit is to the previously mentioned fluctuation-induced tunneling model.

Because the thermoelectric power measurement is a zero-current experiment and because temperature drops at grain boundaries are expected to be less important than voltage drops, this technique should be far less susceptible to polycrystalline sample effects than dc conductivity measurements.[26-28] Indeed, we find that, in contrast to conductivity measurements (cf. Figs. 9, top, and 12), variable-temperature TEP data for single crystal and polycrystalline samples of the same molecular metal are rather similar.[55] Figure 22 shows room-temperature TEP data for polycrystalline $\{[Si(Pc)O](BF_4)_y\}_n$, $\{[Si(Pc)O](tosylate)_y\}_n$, and $\{[Si(Pc)O](SO_4)_y\}_n$ samples as a function of y. With increasing y, the Seebeck coefficient (S) drops steeply from large, positive values characteristic of p-type semiconductors to small, positive values typical of p-type molecular metals (Fig. 22) and then levels off at $y \gtrsim 0.35$. Variable-temperature studies as a

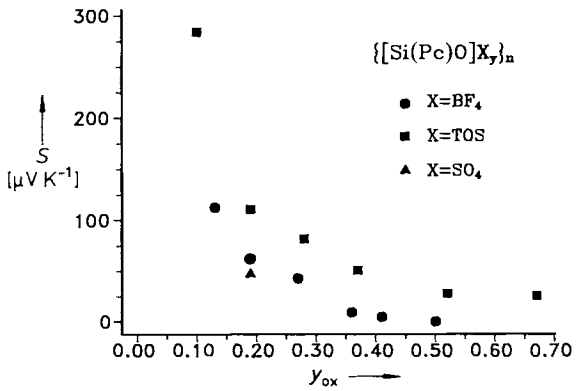

Fig. 22. Room-temperature thermoelectric power (S) data as a function of doping level for polycrystalline $\{[Si(Pc)O](BF_4)_y\}_n$, $\{[Si(Pc)O](tosylate)_y\}_n$, and $\{[Si(Pc)O](SO_4)_{0.095}\}_n$ conductive polymer samples. The y value shown for $\{[Si(Pc)O](SO_4)_{0.095}\}_n$ has been corrected for the dinegative charge of $SO_4^{2\ominus}$.

function of y have also been carried out. Although the data for the above three classes of doped polymers differ in small details, all evidence a smooth, continuous transition from behavior characteristic of a p-type semiconductor (large, positive S with $S \sim 1/T$) to a radical-cation molecular metal (small, positive S with $S \sim T$). An example is shown in Figure 23. Importantly, the transition from a semiconductor to

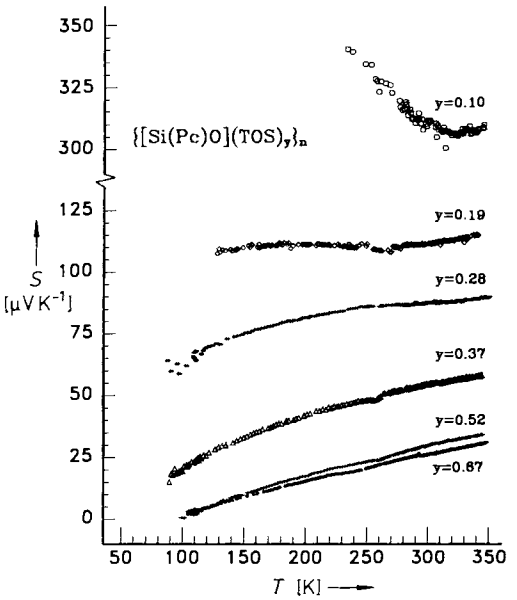

Fig. 23. Variable-temperature thermoelectric power (S) data for polycrystalline {[Si(Pc)O](tosylate)$_y$}$_n$ samples.

a metal occurs for all three series in the region $y \approx 0.20$. How do these experimental $S(y,T)$ results compare with the predictions of simple tight-binding band theory? Using Equation (4) and assuming U is negligible and $4t \approx 0.60$ eV (cf. Table 2), the curves in Figure 24 are generated. While the agreement between experiment and theory for $S(y)$ at fixed T appears reasonable (Fig. 24, top), the theory predicts continuous metallic behavior ($S \sim T$) for all doping levels (Fig. 24, bottom). In contrast, the experimental TEP data evidence a "switching on" of metallic character in the neighborhood of $y \approx 0.20$. That the thermopower of the present {[Si(Pc)O]X$_y$}$_n$ materials with $y = 0.50$ does not exhibit temperature-independent $|S| \approx 60\ \mu V\ K^{-1}$ behavior stands in marked contrast to the great majority of low-dimensional $|\varrho| = 0.50$ systems having very large $U/4t$ ratios.[26, 27]

Detailed reflectivity, magnetic susceptibility, and ESR studies have also been carried out for the {[Si(Pc)O](BF$_4$)$_y$}$_n$, {[Si(Pc)O](tosylate)$_y$}$_n$, and {[Si(Pc)O](SO$_4$)$_y$}$_n$ materials as a function of y.[70] We have shown elsewhere that single-crystal and polycrystalline optical reflectivity data for low-dimensional conductors are readily interconvertible.[33c, 53, 54] As exemplified by the optical data for the series of $BF_4^{\ominus}$ salts (Fig. 25), initial doping yields reflectance spectra characteristic of a molecular semiconductor. A well-defined plasma edge is not evident until $y \gtrsim 0.20$, beyond which doping level the energy of the edge shifts monotonically to higher energy. Indeed, for y values within the metallic regime, the adherence to Equation (5), derived for tight-binding, is quite good (Fig. 26).

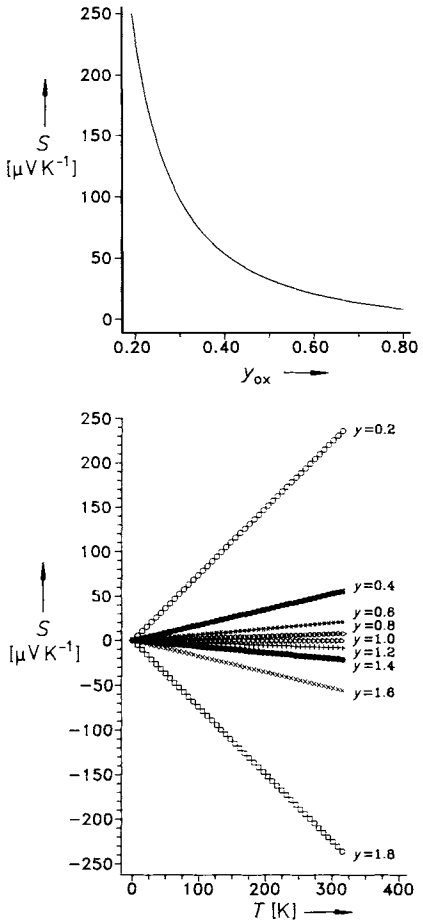

Fig. 24. Top: Band-filling dependence of thermoelectric power for a simple low-dimensional tight-binding band structure with energy-independent scattering, negligible U, $T = 300$ K, and $4t = 0.60$ eV calculated with Eq. (4). Bottom: Temperature dependence of thermoelectric power as a function of degree of oxidation ϱ calculated using Eq. (4) for a simple tight-binding band structure with energy-independent scattering, negligible U, and $4t = 0.60$ eV.

Magnetic susceptibility studies of the {[Si(Pc)O](BF$_4$)$_y$}$_n$ materials as a function of increasing y reveal a large Curie component typical of localized radical-cation states for low values of y (Fig. 27). This component of the susceptibility peaks at $y \approx 0.20$ and then falls abruptly with increasing y. Over this same y range, a Pauli component grows in and remains essentially constant beyond $y \gtrsim 0.25$. As also shown in Figure 27, this $\chi(y)$ behavior is distinctly different from that found for the chemically (inhomogeneously) doped {[Si(Pc)O](I$_3$)$_y$}$_n$ materials.[53] Because the chemical doping process is largely inhomogeneous, the Pauli contribution is linearly dependent upon the doping level (because the fraction of doped phase is linearly dependent upon the doping level). The $\chi(y)$ dependence of the homogeneously doped {[Si(Pc)O](BF$_4$)$_y$}$_n$ polymers can now be compared with the predictions of simple tight-binding band theory [Eq. (6)] in Figure 28. As for the thermopower and reflectivity data, the agreement with theory is poorest at low doping levels where, in the magnetic data, the $BF_4^{\ominus}$ salt exhibits the large, y-dependent Curie component. However, some aspects of the predicted flattening-out in $\chi(y)$ are observed at higher doping levels. Magnetic susceptibility measurements on {[Si(Pc)O](tosylate)$_{0.67}$}$_n$ and {[Si(Pc)O](SO$_4$)$_{0.095}$}$_n$ (in or near the metallic regime) also reveal large Pauli-like compo-

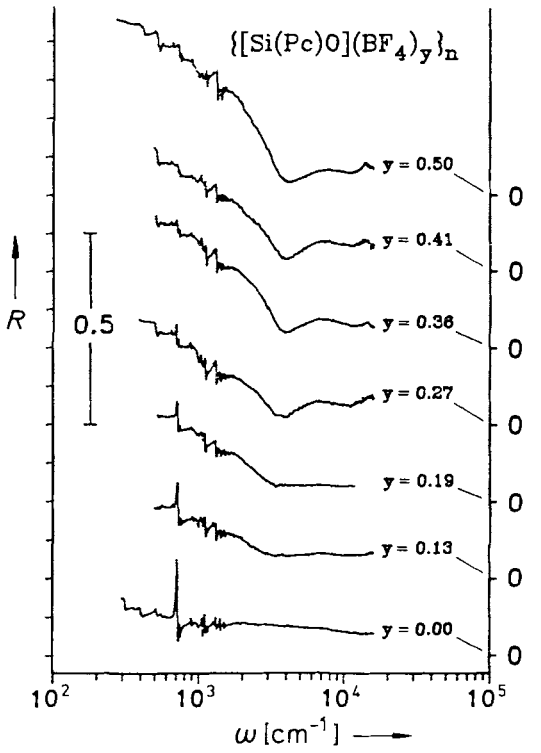

Fig. 25. Optical reflectance spectra of compressed polycrystalline $\{[Si(Pc)O](BF_4)_y\}_n$ samples as a function of y. Spectra are offset vertically for ease of viewing.

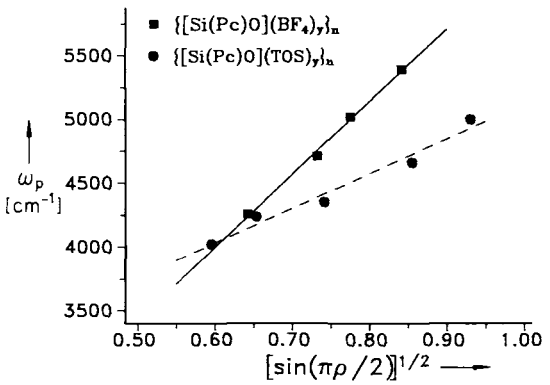

Fig. 26. Plot of $\{[Si(Pc)O](BF_4)_y\}_n$ and $\{[Si(Pc)O](tosylate)_y\}_n$ plasma frequencies ω_p (from reflectance data) as a function of degree of partial oxidation $\varrho(y)$ according to the tight-binding band theoretical expression of Eq. (5).

nents and, in the case of the latter material, no evidence of carrier localization by the dinegative counterion. Magnetic data are compiled in Table 1 and magnetically derived bandwidths in Table 2. It is found that susceptibilities are again enhanced, but also that the degree of enhancement depends upon ϱ.[70a] This is the first experimental verification of the important theoretical prediction[38a,d] that U can be ϱ (band filling) dependent.

ESR data for the above polycrystalline $\{[Si(Pc)O]X_y\}_n$ materials as a function of y are in substantial agreement with the aforementioned characterization results.[70,75] Incremental doping is accompanied by an invariance in the essentially free-electron g value (indicative of ligand-centered carriers) and by a general decrease in line width. The magnitudes and

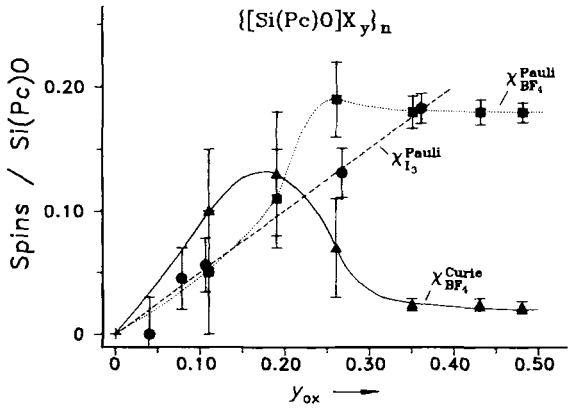

Fig. 27. Stoichiometry (y) dependence of the Pauli-like (■) and Curie-like (▲) spin susceptibilities of electrochemically (homogeneously) doped $\{[Si(Pc)O](BF_4)_y\}_n$ polymers. The dashed line indicates the Pauli-like term (●) for the chemically (inhomogeneously with I_2) doped polymer.

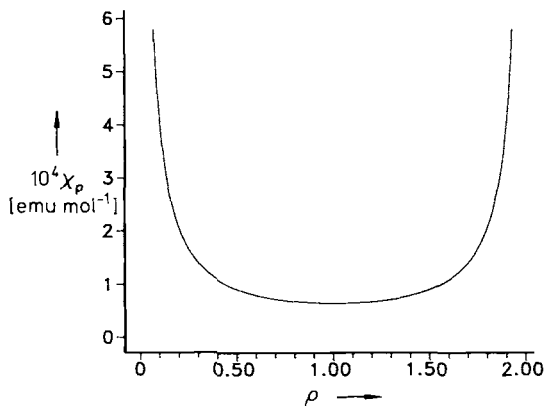

Fig. 28. Band filling dependence of the Pauli magnetic susceptibility (χ_p) calculated according to the one-dimensional tight-binding model of Eq. (6) for $4t = 0.60$ eV and $U = 0$.

y dependence of the line widths are in general accord with increasingly mobile (delocalized) conduction electrons upon doping and with a relatively unidimensional band structure (small interstack interactions). The only surprise in these data is the observation that the ESR line widths of $\{[Si(Pc)O](SO_4)_y\}_n$ are slightly larger than those of the $BF_4^{\ominus}$ and tosylate salts (ca. 1.5 G vs. 0.5–1.0 G). It is not clear at this point whether the enhanced broadening reflects decreased carrier mobility and/or greater two-dimensionality for Coulombic reasons, or whether greater carrier density on the $SO_4^{2\ominus}$ counterion induces more efficient electronic relaxation via phonon-modulated spin–orbit interactions as in the $I_3^{\ominus}$ and $SbF_6^{\ominus}$ salts discussed in Section 4.1.

4.3. Origin of the $\{[Si(Pc)O]X_y\}_n$ Insulator/Semiconductor Metal Transition

The dramatic changes in $\{[Si(Pc)O]X_y\}_n$ properties that occur in the vicinity of $y \approx 0.20$ indicate that a major change in electronic structure and carrier mobility occurs. The diffraction and electrochemical data give no indication of equally drastic structural changes, but rather evidence a fairly smooth evolution in structure as a function of y. As will be discussed below, the nature of the $y \approx 0.20$ transition is from a localized-carrier, insulating or semiconducting material to

a delocalized, metal-like material, the properties of which continue to evolve in an instructive manner as y approaches the maximum doping stoichiometry. The electronic structural model that best fits these y-dependent changes focuses on the effects of disorder and defects on the properties of a quasi-one-dimensional band structure. To do so, we make use of another band-structural concept which indicates the number of energy levels per unit energy in the band: the density of states.[1] In a classical description, many of the properties of metal-like substances (e.g., conductivity, magnetic susceptibility) are extremely sensitive to the density of states near the highest occupied band level (the Fermi level). Figure 29 A illustrates a density of states versus energy diagram for a classical, one-dimensional tight-binding band.[1] This is the idealized model from which the thermoelectric power, optical spectroscopic, and magnetic models of Equations (5) (Fig. 24), (6), and (7) (Fig. 28), respectively, are derived. The effects on this picture of disorder and defects will be to alter the density of states as shown schematically in Figure 29 B and to introduce a mobility edge (E_C) between

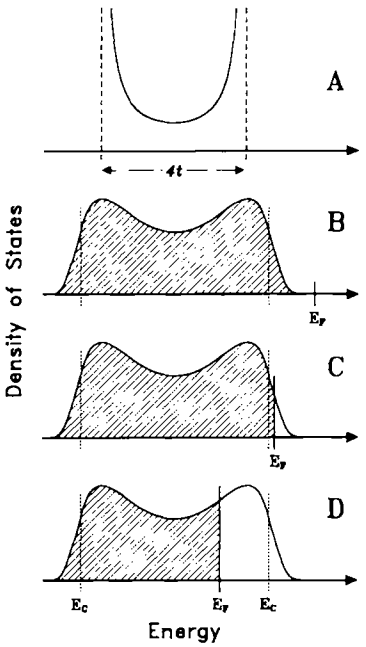

Fig. 29. Schematic density of states model of the electronic structural consequences of incrementally oxidizing $[Si(Pc)O]_n$. A: Undoped. Classical quasi-one-dimensional tight-binding description. B: Part A in the presence of disorder and defects. C: Lightly doped. D: Heavily doped. E_F represents the Fermi energy and E_C the energy of a mobility edge.

localized states at the tails of the band and the more central, delocalized (metal-like) states.[76, 77] A transition of the Fermi level (E_F) across such an edge as a function of composition or some other property is classically known as an Anderson transition.[76] In the commonly accepted description, the localized Anderson state possesses a "Fermi glass" electronic structure having a relatively continuous density of localized states.[76, 77] Whether such a situation has been truly realized in the present materials is currently under further investigation.

At low oxidation levels of $\{[Si(Pc)O]X_y\}_n$, it is reasonable that the doped polymer is significantly disordered, presumably as a consequence of varying $[Si(Pc)O]_n$ chain lengths and/or crystallographic positions as well as possibly other types of defects (including in anion locations). The effect of these perturbations will be localization of conduction band states at the tails of the band. In this regime, the carriers (holes) will therefore have low mobilities. The charge-transport data are in good accord with this model: the dc conductivity is low, exhibits high apparent activation energies, and can be fit to a transport model applicable to disordered systems or carrier hopping between localized states. At this same doping level, the magnitude and temperature dependence of the thermoelectric power is also typical of a p-type semiconductor (Figs. 22 and 23). Additional evidence for carrier localization in this regime is noted in the optical reflectivity, which is in accord with a semiconducting or insulating electronic structure (Fig. 25), and the magnetic susceptibility, which evidences a large concentration of localized Curie-like spins and little, if any, Pauli-like behavior (Fig. 27).

In the region of $y \approx 0.20$, major changes are detected. Both the magnitude and temperature dependence of the thermoelectric power evidence a transition to a metal-like substance (Figs. 22 and 23). Although interparticle contact effects are likely to obscure the sharpness of the transition, the electrical conductivity begins to level off in the vicinity of $y \approx 0.20$, while the apparent activation energies (slopes in lg σ vs. $1/T$) fall.[70a] For $y \gtrsim 0.20$, the temperature dependence of $\{[Si(Pc)O]X_y\}_n$ conductivity can be better fit to a fluctuation-induced tunneling-transport model appropriate for a more metal-like material. Also at $y \approx 0.20$, a metal-like plasma edge is first observed in the optical reflectivity, while magnetic measurements indicate that the concentration of Curie-like spins drops precipitously and the concentration of Pauli-like spins rises sharply. ESR line widths exhibit a decrease to values characteristic of more mobile spins. In terms of the model shown in Figure 29, the $y \approx 0.20$ doping region represents the region at which the Fermi level is crossing the mobility edge. This picture stands in contrast to the classical model (Fig. 29), which would predict a "turn-on" of metallic characteristics at the lowest doping levels. To our knowledge, such a doping level-dependent turn-on has not previously been observed in a molecular metal.

Depleting the band structure beyond $y \approx 0.25$ evokes a number of interesting responses. The room-temperature electrical conductivity remains remarkably constant over a very broad range, while the decrease in apparent activation energy is smaller than in the $y \approx 0.20$ region. Beyond $y \approx 0.35$, the Pauli-like component of the magnetic susceptibility remains nearly constant while the Curie-like component declines to a low, constant level. Meanwhile, the ESR line widths fall to levels typical of unidimensional phthalocyanine molecular metals not having heavy-atom counterions. For y increasing beyond ca. 0.25, the optical plasma edge shifts continuously to higher energy, in good accord with simple tight-binding band theory (Fig. 26). These observations generally agree with the picture of Figure 29 D in which the Fermi level is in the metallic portion of the conduction band and in which the density of states varies only modestly as a function of y. The latter contention is supported by the weak sensitivity of the conductivity and Pauli-like susceptibility to y. As noted elsewhere, agreement between

experimental parameters, such as bandwidths derived from a tight-binding analysis of optical reflectivity and thermopower data and those measured by other methods, is always poor at low doping levels, but more satisfactory at higher doping levels.[51, 68] Comparison of Figure 29A to Figures 29B–26D shows that one reason derives mainly from how the density of states responds to disorder and defects. The deviation of the density of states from the idealized formalism (Fig. 29A), upon which Equations (5)–(7) are based, is greatest near the tails of the band, that is, at very low and very high doping levels.

4.4. Tunable Approach to a Mott–Hubbard Insulator: Quinone Doping of $[Si(Pc)O]_n$

The maximum $\{[Si(Pc)O]X_y\}_n$ doping levels achieved via electrochemical techniques are on the order of + 0.70, corresponding to a 65%-filled classical band. With reference to Figure 4 and earlier discussion, the fascinating question next arises as to whether it is possible to incrementally tune y to even higher levels, perhaps to the half-filled band (integral oxidation state) level. Will the products be metals, semiconductors, or insulators? Doping of $[Si(Pc)O]_n$ with the strongly oxidizing reagents 2,3-dichloro-5,6-dicyano-*p*-benzoquinone (DDQ) or 2,3,5,6-tetrafluoro-7,7,8,8-tetracyanoquinodimethane ($TCNQF_4$) proceeds as shown in Equation (9).[42b, 46a, b, 78] Heating the doped polymers under vacuum

$$[Si(Pc)O]_n + yn\,Q \rightleftharpoons \{[Si(Pc)O]Q_y\}_n \qquad (9)$$

Q =

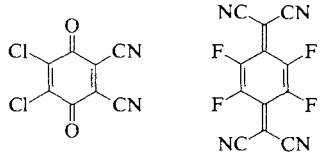

DDQ

$TCNQ\text{-}F_4$

removes the quinones and regenerates undoped $[Si(Pc)O]_n$. IR, Raman, and optical spectral data indicate that most, if not all, of the quinone molecules are present as radical anions ($Q^{\bullet\ominus}$). Hence, oxidation of the phthalocyanine subunits has occurred. X-ray diffraction data indicate that the quinone doping process is at least partially inhomogeneous and that the doped polymer crystal structures are significantly disordered/poorly crystalline.

The electrical and optical properties of the $\{[Si(Pc)O]Q_y\}_n$ materials are markedly different from those of quinone-doped *molecular* phthalocyanines. While the latter materials were found to be insulators, in agreement with the proposed integrated stacking crystal structures (**3**, **4**), the quinone-doped stacking-enforced polymers exhibit electrical and optical properties reminiscent of the halogen- and nitrosyl-doped $[Si(Pc)O]_n$ materials discussed in Section 4.1.[53, 54] Thus, a steep rise in conductivity is observed upon initial oxidation (Fig. 30) along with a drop in the thermoelectric power from that characteristic of a semiconductor to that of a π-radical-cation-based $[Si(Pc)^{e\oplus})O]_n$ molecular metal (Fig. 31). The optical reflectivity at $y \approx 0.40$ exhibits a characteristic molecular-metal plasma edge virtually identical to

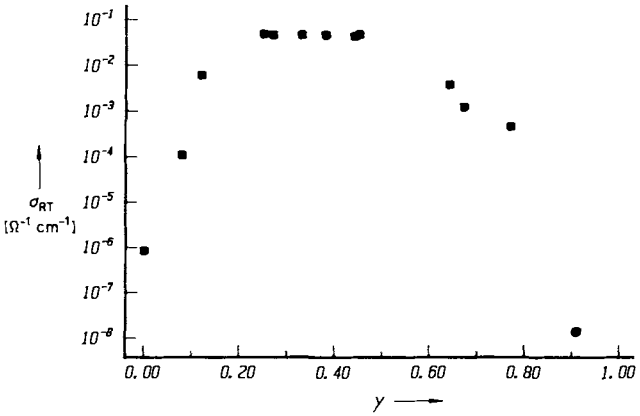

Fig. 30. Room-temperature electrical conductivity (σ_{RT}) data of compressed polycrystalline $\{[Si(Pc)O](DDQ)_Y\}_n$ samples as a function of y.

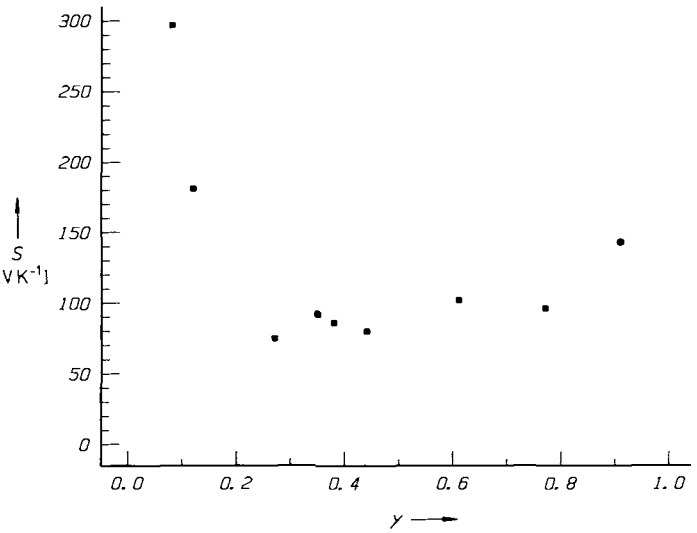

Fig. 31. Room-temperature thermoelectric power (S) data for compressed polycrystalline $\{[Si(Pc)O](DDQ)_y\}_n$ samples as a function of y.

that of the corresponding $I_3^{\ominus}$, $BF_4^{\ominus}$, and $PF_6^{\ominus}$ salts (Fig. 14).[53, 54, 78] As the $\{[Si(Pc)O]DDQ_y\}_n$ doping level is increased beyond $y \approx 0.20$, the room-temperature conductivity and thermoelectric power remain nearly constant, as observed for other $\{[Si(Pc)O]X_y\}_n$ materials (Figs. 21 and 22). In addition, the $\sigma(T)$ data can be fit to the aforementioned fluctuation-induced carrier tunneling model, while the $S(T)$ data are reminiscent of the $X^{\ominus} = BF_4^{\ominus}$ and tosylate analogues (Fig. 23).

As y is increased beyond ca. 0.50–0.60, dramatic changes occur in the $\{[Si(Pc)O]DDQ_y\}_n$ physical properties. The electrical conductivity begins to fall and, by $y \approx 0.90$, the material has become an insulator with a ca. 10^7 decrease in electrical conductivity versus that at $y \approx 0.40$ (Fig. 30). Indeed, the conductivity at $y \approx 0.90$ is lower than for $y \approx 0.00$. In this high-doping-level regime, a plasma edge is no longer discernible in the $\{[Si(Pc)O]DDQ_y\}_n$ optical reflectivity, and the strong carrier absorption commonly observed in the transmission infrared spectra of phthalocyanine molecular metals[53] is no longer apparent. As y increases beyond ca. 0.50, the room-temperature thermoelectric power of

$\{[Si(Pc)O]DDQ_y\}_n$ rises and becomes semiconducting by $y \approx 0.90$ (Fig. 31). Interpretation of magnetic susceptibility data is presently complicated by unknown and potentially varying contributions of the paramagnetic $Q^{\bullet\ominus}$ counterions.

It is evident from the above discussion that $\{[Si(Pc)O]DDQ_y\}_n$ undergoes a dramatic metal to insulator transition as y is tuned toward ca. + 1.0 (a half-filled classical band). As noted above, the admittedly simplistic model of Figure 4 implies that, all other factors being equal, electron–electron Coulombic interactions will adversely affect carrier mobility most at the integral oxidation levels of $\varrho = 0$ and 1. The latter situation would correspond to a molecular/macromolecular Mott–Hubbard insulator, and the result is effectively a gap at the center of the highest filled band. Several isolated examples are known where such a regime is believed to obtain;[2, 38a, d, 79] however, data interpretation is complicated by the crystal-structure and building-block alterations needed to produce the $\varrho = 1$ material. The present $\{[Si(Pc)O]DDQ_y\}_n$ system is the first example where the Mott–Hubbard insulator state can be incrementally tuned into a low-dimensional material. That the onset of insulating character is somewhat in advance of the $\varrho = 1.0$ oxidation level supports the not unexpected presence of localized states at the low-energy tail of the conduction band (cf. Fig. 29). If the admittedly simplistic model of Figure 4 is correct, oxidation beyond $y \approx 1.0$ should give rise to a second regime of metal-like characteristics. Preliminary results with the more strongly oxidizing dopant $TCNQF_4$ support this picture.[78] Thus, while the sharpness of the effect is likely convoluted to some degree with artifacts arising from doping inhomogeneity and disorder, it is evident that an oxidative increase of y in $\{[Si(Pc)O](TCNQF_4)_y\}_n$ materials leads (Fig. 32) initially to a

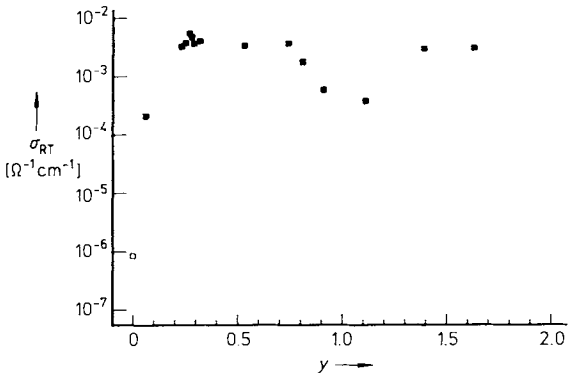

Fig. 32. Room-temperature conductivity data for compressed polycrystalline $\{[Si(Pc)O](TCNQF_4)_y\}_n$ samples as a function of y.

steep rise in conductivity followed by a leveling off by $y \approx 0.20$ as seen for DDQ (Fig. 30). At this point, a plasma edge is evident in the reflectance spectrum. As in the case of $\{[Si(Pc)O]DDQ_y\}_n$, the conductivity begins to decline by $y \approx 0.50$ and reaches a minimum near $y \approx 1.0$. However, it is possible to dope $\{[Si(Pc)O](TCNQF_4)_y\}_n$ beyond the integral oxidation state, and this chemistry effects a return in conductivity to the levels observed in the metal-like, $0.20 \lesssim 0.70$ stoichiometry region! This remarkable result suggests that oxidation beyond the $y \approx 1.0$ state involves electronic depletion of the lower Mott–Hubbard band. In terms of Figure 4, charge mobility is again increased by the creation of additional site vacancies.

5. Electronic Structure Considerations: Connections between the Microscopic and the Macroscopic

The dicussion to this point has focused upon how deliberate, chemically induced changes in metallomacrocycle stacking architecture, counterion environment, and band filling influence band structure, hence macroscopic electrical, optical, and magnetic properties. We now consider these observations in light of what is known about the composition and nature of the band structure. We also inquire as to the validity of the tight-binding formalism[1] employed here and elsewhere to extract band structure information from macroscopic, condensed-phase thermopower and optical reflectivity measurements. In particular, we ask whether small-molecule theoretical and experimental means exist to calibrate this formalism.

As depicted in Figure 3, the $[Si(Pc)O]_n$ band structure is built up by suitable combinations of Si(Pc) molecular orbitals. The highest-energy filled band, the depletion of which gives rise to metallic character, will be composed of Si(Pc) HOMOs, while the lowest-energy unfilled band, which is populated upon reductive doping, is composed of Si(Pc) LUMOs. Electronic structure calculations have been carried out at the first-principles discrete-variational local exchange (DV-Xα) level[80] on the molecules $Si(Pc)(OH)_2$ (**12**; M = Si, R = H) and the cofacial dimer HOSi(Pc)OSi(Pc)OH (**13**; M = Si, R = H).[51, 68] Species **13** is a prototype for known molecules of the type $Me_2(tBu)SiOSi(Pc)OSi(Pc)OSi(tBu)Me_2$, which have been characterized by single-crystal diffractometry[51] (structural results are in good agreement with those deduced for $[Si(Pc)O]_n$[47a]). It will be seen that the availability of cofacial dimers that model the simplest aspect of the macrocycle π–π band-forming interaction is a particularly important dividend of the $[Si(Pc)O]_n$ architectural connectivity.

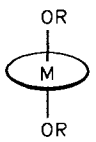

12

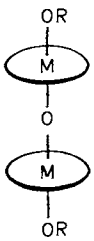

13

The DV-Xα calculations on **12** and **13** give results in excellent agreement with experimental optical and orbital ionization energy data.[51] In Figure 33 are shown graphic representations of the HOMO and LUMO of $Si(Pc)(OH)_2$. The most significant conclusion about the HOMO is that the greatest orbital amplitudes are near the core of the macrocycle with a lesser contribution from the fused benzo ring orbitals and almost negligible contribution (forbidden by symmetry) from the orbitals of the $(Si\text{-}O)_n$ chain. These ob-

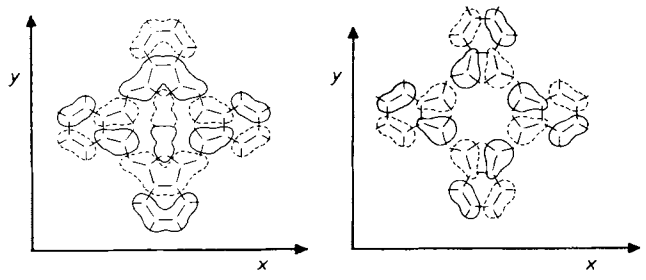

Fig. 33. Graphic representations of DV-Xα-derived molecular orbitals of $Si(Pc)(OH)_2$ viewed perpendicular to the macrocyclic plane. Left: $7e_g$(LUMO). Right: $2a_{1u}$(HOMO).

servations help to understand the largely ring-centered, π-radical-cation character of the conduction process. Furthermore, the spatial remoteness of the band-structure-forming orbitals from off-axis counterions (cf. also Figs. 6 and 8) helps to explain the observed insensitivity of the collective properties of $\{[Si(Pc)O]X_y\}_n$ to the identity of X. The DV-Xα results for the $Si(Pc)(OH)_2$ LUMO (Fig. 33) indicate that the band structure populated upon reductive doping will be of significantly different orbital composition. For example, it will have a non-negligible contribution from Si orbitals.

Calculations on dimeric structure **13** and related dimers have included an examination of how π–π interactions as expressed by 4*t* (Fig. 3) vary with interplanar eclipsing/twist angle and ring–ring interplanar spacing (Fig. 34). The DV-Xα formalism is known to be accurate in situations where relatively small π–π orbital overlap obtains.[151, 68, 81] From the upper part of Figure 34, it can be seen that the bandwidth of an infinite $[Si(Pc)O]_n$ stack is sensitive to the ring–ring eclipsing angle (with fixed interplanar spacing). It can also be seen that the experimentally observed angles on the order of 40° only approach one of two possible overlap maxima at 0° and 45°. The former may be disfavored due to nonbonded repulsions. These calculations also reveal a zero bandwidth minimum near 20°. Clearly, all synthetic strategies for a phthalocyanine molecular metal must avoid approaching this eclipsing angle. The lower part of Figure 34 shows the calculated effect on the bandwidth of varying the Pc–Pc interplanar spacing (with a fixed eclipsing angle). It can be seen that the calculated 4*t* value falls off rapidly as the stacking repeat distance increases. In Table 2, these results are compared with experimental thermopower- and reflectivity-derived tight-binding bandwidth estimates at the three experimentally accessible interplanar spacings of 3.25, 3.30, and 3.48 Å. It can be seen that the agreement between the condensed-phase measurements, interpreted within the framework of a Hückel-like formalism, and the DV-Xα theoretical calculations is quite good. However, an independent experimental calibration of the solid-state measurement would be highly desirable.

As can be appreciated from Figure 3, the electronic structure of dimers such as **13** should be directly extrapolable to the bandwidth of the corresponding polymer. That is, the HOMO–HOMO splitting of 2*t* should be one-half the tight-binding bandwidth. Molecules of structure **13** provide a

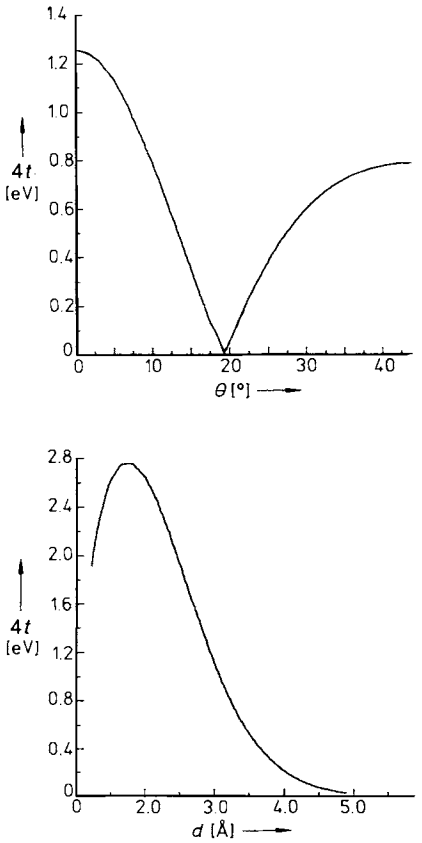

Fig. 34. Top: Calculated variation of the HOSi(Pc)OSi(Pc)OH conduction (HOMO) bandwidth as a function of Pc–Pc eclipsing (twist) angle at an interplanar separation of 3.32 Å (0° = completely eclipsed, D_{nh} Si(Pc)OSi(Pc) geometry). Bottom: Pc–Pc interplanar separation with an eclipsing angle of 37°.

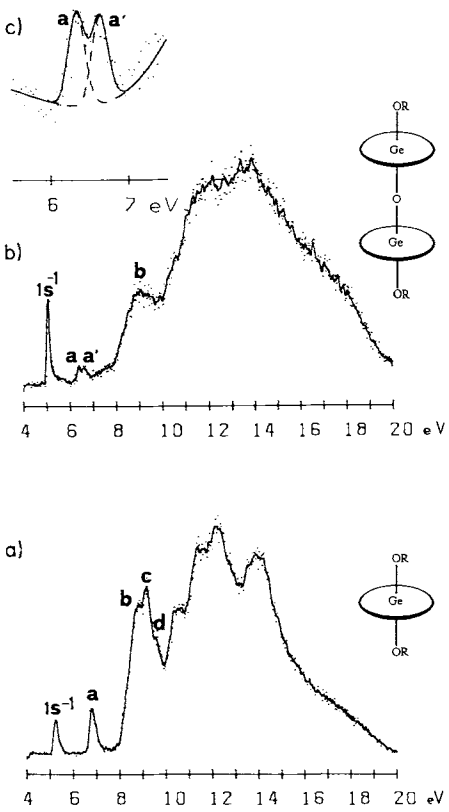

Fig. 35. Gas-phase He(I) photoelectron spectra of a) $PcGe(OSiMe_2tBu)_2$, b) $(tBu)Me_2SiOGe(Pc)OGe(Pc)OSiMe_2(tBu)$, and c) expanded-scale presentation of the aa' doublet in b.

unique ex situ measure of $4t$ since the HOMO–HOMO splitting energy can be measured in the gas phase by photoelectron spectroscopy.[51, 68d] As exemplified by Figure 35, the HOMO–HOMO interaction energy in the gaseous M = Ge compound is clearly visible in the splitting of the lowest-energy Pc π ionization (aa′ band). The measured splitting in the M = Ge dimer is 0.19(3) eV, while that in the M = Si dimer is 0.29(3) eV. Assuming molecular geometies are similar and monomer/dimer relaxation effects upon ionization are approximately constant, multiplication of these splittings by a factor of two should provide an independent measure of the tight-binding bandwidth. In Table 2 are compared $4t$ values measured in the solid state (TEP, reflectivity, magnetic), measured in the gas phase (PES), and calculated using the DV-Xα formalism. With the exception of the bandwidths derived from magnetic measurements, which are susceptible to Coulomb enhancement (see above), the agreement is quite good. Clearly, $4t$ values derived from properly analyzed condensed-phase measurements are reliable in these kinds of materials. Moreover, the era is fast approaching when first-principles quantum chemistry will play a major predictive role in guiding the design and synthesis of new electronic materials.

6. Comparison of $\{[M(Pc)O]X_y\}_n$ Materials to Other Molecular and Polymeric Conductors

The initial goal at the outset of this research was to devise a system of molecular conductors in which a number of key parameters could be perturbed while retaining control of the stacking architecture. No other system of molecular metals has allowed wide uniaxial variation of interplanar spacing or wide variation of off-axis counterions without major changes in the stacking architecture. In regard to broad excursions in the partial oxidation level, only $(NMP)_x(Phen)_{1-x}TCNQ$[63] merits comparison and contrasting. The band filling in this low-dimensional molecular conductor can be tuned from $\varrho \approx -0.50$ to -0.66 in the TCNQ stack by substitution of neutral Phen for $NMP^{\oplus}$. Electron–phonon coupling is very large, giving rise to a Peierls distortion in the stacking architecture and gap-related semiconducting charge-transport behavior even at room temperature. As x is tuned from 1.0 to 0.5, the material changes (at $x \approx 0.65$) from a two-chain conductor with a relatively small U (due to interchain screening) to a large-U single-chain (TCNQ) conductor. In the narrow region where $x \approx 0.50-0.56$, excess charge is accommodated by maintaining a commensurate (dimerized) TCNQ stacking architecture and forming pairs of charged defects (bipolarons).[63] This behavior is to be contrasted with the present phthalocyanine conductors, where the molecular $M(Pc)X_y$ systems exhibit metallic characteristics over a broad temperature range, where there is minimal to no evidence for a Peierls instability down to low temperatures, and where the lattice-stiffening of the $\{[Si(Pc)O]X_y\}_n$ backbone and the lower bandwidth are likely to further oppose electron–phonon coupling-based structural distortions. In addition to these contrasts, off-axis counterion screening effects appear to be far larger in $(NMP)_x(Phen)_{1-x}(TCNQ)$.[63]

As macromolecules, the large family of $\{[M(Pc)O]X_y\}_n$ conductors differs from the great majority of electrically conductive polymers in that the conjugation pathway does not coincide with the putative charge transport pathway and electron–phonon coupling is much smaller. Thus, initial doping of Peierls-distorted *trans*-polyacetylene results in a decrease in the magnetic susceptibility and semiconducting transport via spinless charged soliton (π free radical) defect states in the band gap.[4, 66] At the doping level of ca. $[(CH)X_{0.06}]_n$, there is an abrupt transition to a metallic state with Pauli-like magnetic susceptibility. At this point, the material has been described as having a disorder-induced metallic density of states in the band gap,[82] or as a polaron metal.[83] Polyacetylene can be prepared in highly crystalline microstructures, considerable crystal-structure-doping information is accumulating, and off-axis counterion effects are presently being explored.[4, 66, 67]

There is far less structural information on polypyrrole, polyaniline, and polyphenylenevinylene (Fig. 5). The former two materials have nondegenerate ground states and very strong electron–phonon coupling. Incremental doping of polypyrrole gives rise initially to polarons (radical-cation sites bound strongly to lattice distortions), then predominantly to spinless bipolarons in the band gap.[84] Thus, the magnetic susceptibility initially increases, goes through a broad maximum, and then drops to very low levels as partial oxidation progresses (0.0 to 0.33 holes per monomer unit). The magnitude and temperature dependence of the magnetic susceptibility is never Pauli-like. The conductivity peaks near the maximum in the susceptibility and then remains approximately constant. The temperature dependence of the conductivity at all doping levels is suggestive of carrier hopping between localized states. To our knowledge, the homogeneity and crystal-structural aspects of polypyrrole doping remain obscure. Doping (via protonation) of polyaniline[85] appears to be largely inhomogeneous using the type of $\chi(y)$ arguments presented in Section 4.2 for $\{[Si(Pc)O]I_y\}_n$ (Fig. 27). The fully doped material has been described both as a granular polaronic metal above the percolation threshold[85] and as a nonmetallic "Fermi glass".[86] A number of aspects of the undoped and doped polyaniline macromolecular structures are presently unclear.

Polyphenylenevinylene and its 1,4-dimethoxy derivative undergo chemical and electrochemical oxidation to yield conductive polymers.[87] Although doping/structural relationships are not yet fully resolved, it appears that two doped phases are present in the electrochemistry of the dimethoxy derivative. For this material, y can be brought as high as $+0.32$. Charge transport has been discussed in terms of polaron and bipolaron states in the band gap with a temperature dependence characteristic of hopping between relatively localized states.[87]

7. Conclusions

It is hoped that this review has conveyed some sense of the rich and illuminating cornucopia of solid-state chemical and physical phenomena exhibited by the $\{[M(Pc)O]X_y\}_n$ family of electrically conductive, multimolecular assemblies. Such substances clearly stand at the frontier between molecular

conductors and conductive polymers. As such, they shed new light upon each area and contribute to our better understanding of both classes of materials.

It is a sincere pleasure to acknowledge the outstanding contributions and stimulating collaboration of a host of talented colleagues. Their names can be found in the references. The author thanks the National Science Foundation through the Northwestern Materials Research Center (Grants DMR 8520280 and DMR 8821571) and the Office of Naval Research for generous financial support of this research. He thanks the Technical University of Berlin and the Free University of Berlin for a Graduiertenkolleg Lectureship, during which much of this account was written.

Received: February 12, 1990 [A 774 IE]
German version: *Angew. Chem. 102* (1990) 886

[1] For excellent introductions to relevant condensed-matter science and band-theoretical concepts, see: a) R. Hoffmann, *Angew. Chem. 99* (1987) 871; *Angew. Chem. Int. Ed. Engl. 26* (1987) 846, and references cited therein; *Solids and Surfaces. A Chemist's View of Bonding in Extended Structures*, VCH, Weinheim/New York 1988; b) M.-H. Whangbo in J. Rouxel (Ed.): *Crystal Chemistry and Properties of Materials with Quasi-One-Dimensional Structures*, Reidel, Dordrecht 1986, p. 27, and references cited therein; c) J. S. Miller, A. J. Epstein, *Prog. Inorg. Chem. 20* (1976) 1; d) H. M. Rosenberg: *The Solid State*, 3rd ed., Clarendon Press, Oxford 1986; e) C. Kittel: *Introduction to Solid State Physics*, 6th ed., Wiley, New York 1986.

[2] a) *Proc. Int. Conf. Sci. Technol. Synth. Metals, Synth. Met. 27–39* (1989); b) D. Jérome, L. G. Caron (Eds.): *Low Dimensional Conductors and Superconductors*, Plenum, New York 1987; c) J. R. Ferraro, J. M. Williams: *Introduction to Synthetic Electrical Conductors*, Academic Press, New York 1987; d) J. Y. Becker, J. Bernstein, S. Bittner (Eds.): *Isr. J. Chem. 27* (1986) No. 4; e) D. O. Cowan, F. M. Wiygul, *Chem. Eng. News 64* (1986) No. 29, p. 28; f) M. L. Cohen, *Science 234* (1986)549; g) R. L. Greene, G. B. Street, *ibid. 226* (1984) 651; h) J. S. Miller (Ed.): *Extended Linear Chain Compounds, Vol. 1–3*, Plenum, New York 1982.

[3] a) H. Inokuchi, *Angew. Chem. 100* (1988) 1817; *Angew. Chem. Int. Ed. Engl. 27* (1988) 1747, and references cited therein; b) J. M. Williams, H. H. Wang, T. J. Ernge, U. Geiser, M. A. Bens, P. C. W. Leung, K. D. Carlson, R. J. Thorn, A. J. Schultz, M.-H. Whangbo, *Prog. Inorg. Chem. 35* (1987) 51; c) D. Schweitzer, E. Gogu, I. Hennig, T. Klutz, H. J. Keller, *Ber. Bunsenges. Phys. Chem. 91* (1987) 890; d) H. Mayama, H. Yamochi, G. Saito, K. Nozaua, T. Sugano, M. Kinoshita, S. Sato, K. Oshima, A. Kawamoto, J. Tanaka, *Chem. Lett. 55* (1985); e) J. M. Williams, *Prog. Inorg. Chem. 33* (1985) 183; f) F. Wudl, *Acc. Chem. Res. 17* (1984) 227.

[4] a) J. Heinze, *Top. Curr. Chem. 152* (1990) 2; b) N. C. Billingham, P. D. Calvert, *Adv. Polym. Sci. 90* (1989) 3; c) S. Roth, H. Bleier, *Adv. Phys. 36* (1987) 385; d) T. A. Skotheim (Ed.) *Handbook of Conducting Polymers, Vol. 1, 2*, Marcel Dekker, New York 1986; e) J. E. Frommer, R. R. Chance: *Encyclopedia of Polymer Science and Engineering 5* (1986) 462; f) K. J. Wynne, G. B. Street, *Ind. Eng. Chem. Prod. Res. Dev. 21* (1982) 23; g) R. H. Baughman, J. L. Brédas, R. R. Chance, R. L. Elsenbaumer, L. W. Shacklette, *Chem. Rev. 82* (1982) 209; h) G. Wegner, *Angew. Chem. 93* (1981) 352; *Angew. Chem. Int. Ed. Engl. 20* (1981) 361.

[5] A. G. MacDiarmid, R. B. Kaner in [4d], *Vol. 1*, p. 689.

[6] a) J. J. Miasik, A. Hooper, B. C. Tofield, *J. Chem. Soc. Faraday Trans. I 82* (1985) 1117; b) F. Garnier, *Angew. Chem. Adv. Mater. 101* (1989) 529; *Angew. Chem. Int. Ed. Engl. Adv. Mater. 28* (1989) 513; *Adv. Mater. 1* (1989) 117.

[7] J. Kanicki in [4d], *Vol. 1*, p. 543.

[8] M. J. Natan, M. S. Wrighton, *Prog. Inorg. Chem. 37* (1989) 391.

[9] R. Naufi, *J. Electrochem. Soc. 130* (1983) 2126.

[10] J. R. Ellis in [4d], *Vol. 1*, p. 489.

[11] a) M. Sinclair, D. McBranch, D. Moses, A. J. Heeger in [2a], *D* 645; b) W. Wu, S. Kivelson in [2a], *D* 575.

[12] S. Miyata, *3rd Symp. Electroresponsive Molec. Polym. Systems*, Brookhaven National Laboratory, Upton, NY 1989.

[13] M. Gazard in [4d], *Vol. 1*, p. 673.

[14] K. Kaneto, H. Agawa, K. Yoshino, *J. Appl. Phys. 61* (1987) 1197.

[15] a) R. Moret, J. P. Pouget in [1b], p. 87; b) D. Jérome, H. J. Schulz, *Adv. Phys. 31* (1982) 299.

[16] S. Mazumdar, S. Ramasesha in [2a], p. *A* 105, and references cited therein.

[17] a) P. D. Hale, M. A. Ratner, *J. Chem. Phys. 83* (1985) 5277; b) E. M. Conwell, *Phys. Rev. B. 22* (1980) 1761; c) M. Weger, M. Kaveh, H. Gutfreund, *Solid State Commun. 37* (1981) 421; d) H. Gutfreund, C. Hartstein, M. Weger, *ibid. 36* (1980) 647.

[18] T. J. Marks, *Science 227* (1985) 881; b) T. J. Marks, D. W. Kalina in [2h], *Vol. 1*, p. 197.

[19] a) A. Gleizes, T. J. Marks, J. A. Ibers, *J. Am. Chem. Soc. 97* (1975) 3545; M. A. Cowie, A. Gleizes, G. W. Grynkewich, D. W. Kalina, M. S. McClure, R. P. Scaringe, R. C. Teitelbaum, S. L. Ruby, J. A. Ibers, C. R. Kannewurf, T. J. Marks, *ibid. 101* (1979) 2921, c) L. D. Brown, D. W. Kalina, M. S. McClure, S. L. Ruby, S. Schultz, J. A. Ibers, C. R. Kannewurf, T. J. Marks, *ibid. 101* (1979) 2937; d) D. W. Kalina, J. W. Lyding, M. T. Ratajack, C. R. Kannewurf, T. J. Marks, *ibid. 102* (1980) 7854.

[20] a) L.-S. Lin, M. S. McClure, J. W. Lyding, M. T. Ratajack, T.-C. Wang, C. R. Kannewurf, T. J. Marks, *J. Chem. Soc. Chem. Commun. 1980*, 954; b) L.-S. Lin, M. S. McClure, J. W. Lyding, M. T. Ratajack, T.-C. Wang, C. R. Kannewurf, T. J. Marks, unpublished.

[21] C. W. Dirk, T. J. Marks, *Inorg. Chem. 23* (1984) 4325.

[22] a) T. J. Marks, *J. Coat. Technol. 48* (1976) 53; b) J. L. Petersen, C. S. Schramm, D. R. Stojakovic, B. M. Hoffman, T. J. Marks, *J. Am. Chem. Soc. 99* (1977) 286; c) C. S. Schramm, R. P. Scaringe, D. R. Stojakovic, B. M. Hoffman, J. A. Ibers, T. J. Marks, *ibid. 102* (1980) 6702; d) D. R. Stojakovic, *Ph. D. Thesis*, Northwestern University, Evanston, IL, USA 1978.

[23] a) T. J. Marks, D. F. Webster, S. L. Ruby, S. Schultz, *J. Chem. Soc. Chem. Commun. 1976*, 444; b) T. J. Marks, *Ann. N.Y. Acad. Sci. 313* (1978) 594.

[24] F. H. Moser, A. L. Thomas: *The Phthalocyanines, Vol. I, II*, CRC Press, Boca Raton, FL, USA 1983.

[25] T. Inabe, T. J. Marks, R. L. Burton, J. W. Lyding, W. J. MacCarthy, C. R. Kannewurf, G. M. Reisner, F. H. Herbstein, *Solid State Commun. 54* (1985) 501.

[26] a) J. F. Kwak, G. Beni, P. M. Chaikin, *Phys. Rev. B 13* (1976) 641; b) J. R. Cooper, B. Alavi, L.-W. Zhou, W. P. Beyermann, G. Grüner, *ibid. 35* (1987) 8794.

[27] a) K. Mortensen, E. M. Conwell, J. M. Fabre, *Phys. Rev. B 28* (1983) 5856, and references cited therein; b) E. M. Conwell, *ibid. 18* (1978) 1818.

[28] a) D. Schweitzer, I. Hennig, K. Bender, H. Endres, H. J. Keller, *Mol. Cryst. Liq. Cryst. 120* (1985) 213; b) K. Mortensen, C. S. Jacobsen, K. Bechgaard, K. Carneiro, J. M. Williams, *ibid. 119* (1985) 401; c) A. Maaroufi, C. Coulon, S. Flandrois, P. Delhaes, K. Mortensen, K. Bechgaard, *Solid State Commun. 48* (1983) 555, and references cited therein.

[29] This expression assumes a small value of U and pragmatically neglects the energy dependence of the carrier scattering time: a) D. Ihle, T. Eifrig, *Phys. Status Solid. B 91* (1979) 135; b) P. M. Chaikin, G. Beni, *Phys. Rev. B 13* (1976) 647.

[30] a) P. J. Toscano, T. J. Marks, *J. Am. Chem. Soc. 108* (1986) 437; b) S. M. Tetrick, T. J. Marks, unpublished.

[31] a) L. Zuppiroli, in [2b], p. 307, and references cited therein; b) G. G. Maresch, M. Mehring, J. U. von Schütz, H. C. Wolf, *Chem. Phys. 85* (1984) 333, and references cited therein.

[32] a) K. Carneiro, J. C. Scott, E. M. Engler, *Solid State Commun. 50* (1984) 477, and references cited therein; b) Z. Soos, S. R. Bondeson in [2h], *Vol. 3*, p. 229; c) D. Jérome in L. Alcacer (Ed.): *The Physics and Chemistry of Low-Dimensional Solids*, D. Reidel, Dordrecht 1980, p. 123.

[33] a) C. S. Jacobsen, in [2b], p. 253; b) D. B. Tanner, in [2h], *Vol. 2*, p. 205; c) R. L. Burton, W. J. McCarthy, C. R. Kannewurf, T. Inabe, T. J. Marks, *NBS Spec. Publ. U.S. 697* (1985) 54.

[34] a) M. R. Madison, L. B. Coleman, R. B. Somoano, *Solid State Commun. 40* (1981) 979; b) B. A. Weinstein, M. L. Slade, A. J. Epstein, J. S. Miller, *ibid. 37* (1981) 643, and references cited therein; c) J. B. Torrance, B. A. Scott, B. Welber, F. B. Kaufman, P. E. Seiden, *Phys. Rev. B. 19* (1979) 730; d) P. Delhaes, C. Coulon, J. Amiell, S. Flandrois, E. Toreilles, J. M. Fabre, L. Giral, *Mol. Cryst. Liq. Cryst. 50* (1979) 43.

[35] M. Takahashi, T. Sugano, M. Kinoshita, *Bull. Chem. Soc. Jpn. 57* (1984) 26; b) P. Delhaes, C. Coulon, S. Flandrois, B. Hilti, C. W. Mayer, G. Rihs, J. Rivory, *J. Chem. Phys. 73* (1980) 1452; c) L. C. Isett, *Phys. Rev. B. 18* (1978) 439; d) J. C. Scott, A. F. Garito, A. J. Heeger, *ibid. 10* (1974) 3131.

[36] a) Z. G. Soos, S. R. Bondeson, *Mol. Cryst. Liq. Cryst. 85* (1982) 19; b) L. C. Tippie, W. G. Clark, *Phys. Rev. B. 23* (1981) 5846; c) L. J. Azevedo, W. G. Clark, *ibid. 16* (1977) 3252.

[37] a) H. Shiba, *Phys. Rev. B 6* (1972) 930; b) J. B. Torrance, Y. Tomkiewicz, B. D. Silverman, *ibid. 15* (1977) 4738.

[38] a) S. Mazumdar, S. N. Dixit, *Phys. Rev. B 34* (1986) 3683, and references cited therein; b) R. Laversanne, J. Amiell, C. Coulon, C. Garrigou-Lagrange, P. Delhaes, *Mol. Cryst. Liq. Cryst. 119* (1985) 317; c) C. S. Jacobsen, K. Bechgaard, *ibid. 120* (1985) 71; d) S. Maxumdar, A. N. Bloch, *Phys. Rev. Lett. 50* (1983) 207; e) C. Coulon, P. Delhaes, S. Flandrois, R. Lagnier, E. Bonjour, J. M. Fabre, *J. Phys. (Paris) 43* (1982) 1059.

[39] Electron–phonon coupling can also lead to susceptibility enhancement: H. Gutfreund, O. Entin-Wohlman, M. Weger, *Mol. Cryst. Liq. Cryst. 119* (1986) 457, and references cited therein.

[40] T. Inhabe, S. Nakumura, W.-B. Liang, T. J. Marks, R. L. Burton, C. R. Kannewurf, K.-I. Imaeda, *J. Am. Chem. Soc. 107* (1985) 7224.

[41] a) M. Almeida, M. G. Kanatzidis, L. M. Tonge, T. J. Marks, H. O. Marcy, W. J. McCarthy, C. R. Kannewurf, *Solid State Commun. 63* (1987) 457; b)

M. Almeida, M. G. Kanatzidis, L. M. Tonge, T. J. Marks, W. J. McCarthy, H. O. Marcy, C. R. Kannewurf, in [2a], p. *F* 37.

[42] For examples of other work on phthalocyanine molecular metals, see: a) T. Inabe, W.-B. Liang, J. F. Lomax, S. Nakamura, J. W. Lyding, W. J. McCarthy, S. H. Carr, C. R. Kannewurf, T. J. Marks, *Synth. Met. 13* (1986) 219; b) J. G. Gaudiello, H. O. Marcy, W. J. McCarthy, M. K. Moguel, C. R. Kannewurf, T. J. Marks, *ibid. 15* (1986) 115; c) M. Y. Ogawa, J. Martinsen, S. M. Palmer, J. L. Stanton, J. Tanaka, R. L. Greene, B. M. Hoffman, J. A. Ibers, *J. Am. Chem. Soc. 109* (1987) 1115; d) K. Liou, C. S. Jacobson, B. M. Hoffman, *ibid. 111* (1989) 6616; e) B. Guay, L. G. Caron, C. Bourbonnais in [2a], p. *F* 557; f) K. Yakushi, M. Sakuda, I. Hamada, H. Kuroda, A. Kawamoto, J. Tanaka, T. Sugano, M. Kinoshita, *Synth. Met. 19* (1987) 769; g) S. Hino, K. Matsumoto, H. Yamakado, K. Yakushi, H. Kuroda, *ibid. 32* (1989) 301.

[43] B. A. Scott, S. J. LaPlaca, J. B. Torrance, B. D. Silverman, B. Welber, *J. Am. Chem. Soc. 99* (1977) 6631.

[44] M. Almeida, M. G. Kanatzidis, L. M. Tonge, H. O. Marcy, W. J. McCarthy, T. J. Marks, C. R. Kannewurf, unpublished.

[45] a) T. J. Emge, H. H. Wang, M. A. Beno, J. M. Williams, M.-H. Whangbo, M. Evain, *J. Am. Chem. Soc. 108* (1986) 8215, and references cited therein; b) S. Tomic, D. Jérome, K. Bechgaard, *J. Phys. 43* (1982) L 839; c) T. Takahashi, D. Jérome, K. Bechgaard, *ibid. 43* (1982) L 565.

[46] a) T. J. Marks, C. W. Dirk, K. F. Schoch, Jr., J. W. Lyding in F. L. Carter (Ed.): *Molecular Electronic Devices*, Marcel Dekker, New York 1982, p. 195; b) T. Inabe, J. W. Lyding, M. K. Moguel, T. J. Marks, *J. Phys.* (1983) C3; c) L. J. Pace, A. Ulman, J. A. Ibers, *Inorg. Chem. 21* (1982) 199.

[47] a) T. Inabe, C. W. Dirk, K. F. Schoch, Jr., T. J. Marks, *J. Am. Chem. Soc. 105* (1983) 1539; b) C. W. Dirk, K. F. Schoch, Jr., T. J. Marks in R. B. Seymour (Ed.): *Conductive Polymers (Polymer Science and Technology Series, Vol. 15)*, Plenum, New York 1981, p. 209; c) C. W. Dirk, E. A. Mintz, K. F. Schoch, Jr., T. J. Marks, *J. Macromol. Sci.-Chem. A 16* (1981) 275; d) T. J. Marks, K. F. Schoch, Jr., B. R. Kundalkar, *Synth. Met. 1* (1980) 337; e) K. F. Schoch, Jr., B. R. Kundalkar, T. J. Marks, *J. Am. Chem. Soc. 101* (1979) 7071; f) R. D. Joyner, M. E. Kenny, *ibid. 82* (1960) 5790.

[48] For cofacial polymers with other types of metallomacrocycles or bridging groups, see: a) M. Hanack, S. Deger, A. Lange, *Coord. Chem. Rev. 83* (1988) 115; b) M. Hanack, A. Datz, R. Fay, K. Fischer, U. Keppeler, J. Koch, J. Metz, M. Mezger, O. Schneider, J. H. Schulze, in [4d], *Vol. 1*, p. 133; c) J. P. Collman, J. T. McDevitt, C. R. Leidner, G. T. Yee, J. B. Torrance, W. A. Little, *J. Am. Chem. Soc. 109* (1987) 4606; d) K. J. Wynne, *Inorg. Chem. 24* (1985) 1339, and references cited therein; e) B. N. Diel, T. Inabe, N. K. Jaggi, J. W. Lyding, O. Schneider, M. Hanack, C. R. Kannewurf, T. J. Marks, L. H. Schwartz, *J. Am. Chem. Soc. 106* (1984) 3207; f) T. J. Moyer, L. A. Schechtman, M. E. Kenney, *Polym. Prepr. 25(2)* (1984) 234; g) M. Hanack, *Chimia 37* (1983) 238; h) R. S. Nohr, P. M. Kuznesof, K. J. Wynne, M. E. Kenney, P. G. Siebenman, *J. Am. Chem. Soc. 103* (1981) 4371.

[49] K. G. Beltsios, T. J. Marks, S. H. Carr, in [2a], p. *F* 31.

[50] a) X. Zhou, T. J. Marks, S. H. Carr, *Mol. Cryst. Liq. Cryst. 118* (1985) 357; b) X. Zhou, T. J. Marks, S. H. Carr, *J. Polym. Sci. Phys. Ed. 23* (1985) 305.

[51] E. Ciliberto, K. A. Doris, W. J. Pietro, G. M. Reisner, D. E. Ellis, I. Fragalà, F. H. Herbstein, M. A. Ratner, T. J. Marks, *J. Am. Chem. Soc. 106* (1984) 7748.

[52] W. Caseri, T. Sauer, G. Wegner, *Makromol. Chem. Rapid Commun. 9* (1988) 651.

[53] B. N. Diel, T. Inabe, J. W. Lyding, K. F. Schoch, Jr., C. R. Kannewurf, T. J. Marks, *J. Am. Chem. Soc. 105* (1983) 1551.

[54] T. Inabe, J. G. Gaudiello, M. K. Moguel, J. W. Lyding, R. L. Burton, W. J. McCarthy, C. R. Kannewurf, T. J. Marks, *J. Am. Chem. Soc. 108* (1986) 7595.

[55] T. Inabe, J. C. Butler, H. O. Marcy, C. R. Kannewurf, T. J. Marks, unpublished.

[56] Single-crystal conductivity measurements are by no means immune to experimental artifacts and can be severely affected by disorder, defects, and impurities, as well as other factors related to the purity of the starting materials and the crystallization methodology [40, 56a–d]. In addition, even in cases of optimum electrical contact alignment [56e], measurement-dependent phenomena such as contact strain [41, 55] and cooling rate effects [56f] can have major and frequently unappreciated effects on the observed $\sigma(T)$. Phthalocyanine conductors are particularly treacherous in this regard. a) K. Khanna, W. W. Fuller, G. Grüner, P. M. Chaikin, *Phys. Rev. B. 24* (1981) 2958, and references cited therein; b) A. J. Heeger in J. T. Devreese, R. P. Evrard, V. E. van Doren (Eds.): *Highly Conducting One-Dimensional Solids*, Plenum Press, New York 1979, p. 105; c) I. D. Begg, K. J. Roberts, J. N. Sherwood, L. Groth-Anderson, C. S. Jacobsen, *Chem. Phys. Lett. 79* (1981) 513; d) S. S. Parkin, F. Greuzet, D. Jérome, J. M. Fabre, K. Bechgaard, *J. Phys. 44* (1983) 975; e) D. E. Schafer, F. Wudl, G. A. Thomas, J. P. Ferraris, D. O. Cowan, *Solid State Commun. 14* (1974) 347; f) S. Kagoshima, T. Yasunaga, T. Ishiguro, H. Anzai, G. Saito, *ibid. 46* (1983) 867, and references cited therein.

[57] a) C. K. Chiang, M. A. Druy, S. C. Gau, A. J. Heeger, E. J. Louis, A. G. MacDiarmid, Y. W. Park, H. Shirakawa, *J. Am. Chem. Soc. 100* (1978) 1013; b) C. K. Chaing, Y. W. Park, A. J. Heeger, H. Shirakawa, E. J. Louis, A. G. MacDiarmid, *J. Chem. Phys. 69* (1978) 5098; c) J. P. Farges, A. Brau, F. Gutmann, *J. Phys. Chem. Solids 33* (1972) 1723.

[58] a) B. Lundberg, B. Sundqvist, *J. Appl. Phys. 60* (1986) 1074, and references cited therein; b) W. Y. Hsu, J. R. Barkley, P. Meakin, *Macromolecules 13* (1980) 198; c) P. S. Clarke, J. M. Orton, A. J. Guest, *Phys. Rev. B 18* (1978) 1813; d) C. H. Seager, G. E. Pike, *ibid. 10* (1974) 1435; e) S. Kirkpatrick, *Rev. Mod. Phys. 45* (1973) 574.

[59] a) P. Sheng, *Phys. Rev. B 21* (1980) 2180; b) Y.-W. Park, A. J. Heeger, M. A. Druy, A. G. MacDiarmid, *J. Chem. Phys. 73* (1980) 946.

[60] a) J. G. Gaudiello, G. E. Kellogg, S. M. Tetrick, T. J. Marks, *J. Am. Chem. Soc. 111* (1989) 5259; b) G. E. Kellogg, J. G. Gaudiello, J. A. Schlueter, S. M. Tetrick, T. J. Marks, H. O. Marcy, W. J. McCarthy, C. R. Kannewurf, in [2a], p. *F* 15; c) M. Almeida, J. G. Gaudiello, J. C. Butler, H. O. Marcy, C. R. Kannewurf, T. J. Marks, *Synth. Met. 21* (1987) 261; d) J. G. Gaudiello, M. Almeida, T. J. Marks, W. J. McCarthy, J. C. Butler, C. R. Kannewurf, *J. Phys. Chem. 90* (1986) 4917.

[61] For an alternative approach, see: E. A. Orthmann, V. Enkelmann, G. Wegner, *Makromol. Chem. Rapid Commun. 4* (1983) 687.

[62] a) P. G. Pickup, R. A. Osteryoung, *J. Am. Chem. Soc. 106* (1984) 2294; b) F. B. Kaufman, A. H. Schroeder, E. M. Engler, S. R. Kramer, J. Q. Chambers, *ibid. 102* (1980) 483.

[63] a) J. S. Miller, A. J. Epstein, *Angew. Chem. 99* (1987) 332; *Angew. Chem. Int. Ed. Engl. 26* (1987) 287; b) H. H. S. Javadi, J. S. Miller, A. J. Epstein, *Phys. Rev. Lett. 59* (1987) 1760; c) E. M. Connell, I. A. Howard, *Phys. Rev. B. 31* (1985) 7835.

[64] Application of extreme pressures (up to 17 kbar) or cooling to liquid-helium temperatures effects more modest changes ($\lesssim 12\%$) in the ϱ of TTF-TCNQ: a) S. Kagoshima, T. Ishiguro, H. Anzai, *J. Phys. Soc. Jpn. 41* (1976) 2061; b) G. K. Khanna, J. P. Pouget, R. Conis, A. F. Garito, A. J. Heeger, *Phys. Rev. B 16* (1977) 1468; c) S. Megtert, R. Comes, C. Vettier, R. Pynn, A. F. Garito, *Solid State Commun. 37* (1981) 875.

[65] J. A. Schlueter, G. E. Kellogg, T. J. Marks, unpublished results.

[66] a) J. Chen, A. G. Heeger, *Synth. Met. 24* (1988) 311; b) M. Winokur, Y. B. Moon, A. J. Heeger, J. Barker, D. C. Bott, H. Shirakawa, *Phys. Rev. Lett. 58* (1987) 2329; c) Y. B. Moon, M. Winokur, A. J. Heeger, J. Barker, D. C. Bott, *Macromolecules 20* (1987) 2457; d) D. C. Bott, C. S. Brown, J. N. Winter, J. Barker, *Polymer 28* (1987) 601; e) L. W. Shacklette, J. E. Toth, *Phys. Rev. B 32* (1985) 5892.

[67] a) G. Wieners, R. Weizenhöfer, M. Monkenbusch, M. Stamm, G. Lieser, V. Enkelmann, G. Wegner, *Makromol. Chem. Rapid Commun. 6* (1985) 425; b) J. P. Pouget, J. C. Pouxviel, P. Robin, R. Comes, D. Begin, D. Billaud, A. Feldblum, H. W. Gibson, A. J. Epstein, *Mol. Cryst. Liq. Cryst. 117* (1985) 75; c) H. W. Hässlin, C. Riekel, K. Menke, S. Roth, *Makromol. Chem. 185* (1984) 397; d) R. H. Baughman, N. S. Murthy, G. G. Miller, *J. Chem. Phys. 79* (1983) 515; e) J. C. W. Chien, F. E. Karasz, K. Shimamura, *Macromolecules 15* (1982) 1012.

[68] a) P. D. Hale, W. J. Pietro, M. A. Ratner, D. E. Ellis, T. J. Marks, *J. Am. Chem. Soc. 109* (1987) 5943; b) K. A. Doris, E. Ciliberto, I. Fragalà, M. A. Ratner, T. J. Marks in [2d], p. 337; c) W. J. Pietro, T. J. Marks, M. A. Ratner, *J. Am. Chem. Soc. 107* (1985) 5387; d) W. J. Pietro, D. E. Ellis, T. J. Marks, M. A. Ratner, *Mol. Cryst. Liq. Cryst. 105* (1984) 273.

[69] J. A. Schlueter, T. J. Marks, unpublished results.

[70] M. Almeida, J. G. Gaudiello, G. E. Kellogg, S. M. Tetrick, H. O. Marcy, W. J. McCarthy, J. C. Butler, C. R. Kannewurf, T. J. Marks, *J. Am. Chem. Soc. 111* (1989) 5271.

[71] a) N. F. Mott, *Festkörperprobleme 21* (1979) 333; b) N. F. Mott, E. A. Davis: *Electronic Processes in Non-Crystalline Materials*, 2nd ed., Clarendon, Oxford 1979, Chapters 1, 2.

[72] a) A. J. Epstein, H. Rommelmann, R. Bigelow, H. W. Gibson, D. M. Hoffman, D. B. Tanner, *J. Phys. C3* (1983) 61; b) R. Colson, P. Nagles, *J. Non-Cryst. Solids 36* (1980) 129, and references cited therein.

[73] a) P. Sheng, B. Abeles, Y. Arie, *Phys. Rev. Lett. 31* (1973) 44; b) E. K. Sichel, J. I. Gittleman, P. Sheng, *Phys. Rev. B 18* (1978) 5712; c) E. K. Sichel, *Appl. Phys. Commun. 1* (1981) 83; d) B. Abeles, P. Sheng, M. D. Coutts, Y. Arie, *Adv. Phys. 24* (1975) 407.

[74] a) Y. Tomkiewicz, N. S. Shiren, T. D. Schultz, H. Thomann, L. R. Dalton, A. Zettl, G. Grüner, T. C. Clarke, *Mol. Cryst. Liq. Cryst. 83* (1982) 17; b) K. Mortensen, M. L. W. Thewalt, Y. Tomkiewicz, T. C. Clarke, G. B. Street, *Phys. Rev. Lett. 45* (1980) 490.

[75] S. M. Tetrick, T. J. Marks, unpublished.

[76] a) N. F. Mott: *Conduction in Non-Crystalline Materials*, Clarendon, Oxford 1987, Chapters 2, 3; b) N. F. Mott: *Metal–Insulator Transitions*, Taylor and Francis, London 1974, Chapters 1, 6; c) V. L. Berezinskii, *Sov. Phys. JETP 38* (1974) 620; d) P. W. Anderson, *Phys. Rev. 109* (1958) 1492.

[77] In a *rigorously* one-dimensional chain, disorder should lead to localization of *all* states, and conduction can only occur via phonon-assisted hopping [76b, 77a, b]. To our knowledge, such a high degree of unidimensionality has not yet been achieved, and all known molecular metals exhibit non-negligible two- or three-dimensional character. a) A. N. Bloch, R. B. Wilson, C. M. Varma, *Phys. Rev. Lett. 28* (1972) 753; b) N. F. Mott, *Adv. Phys. 16* (1967) 49.

[78] M. K. Moguel, L. M. Tonge, H. O. Marcy, W. J. McCarthy, C. R. Kannewurf, T. J. Marks, unpublished.

[79] a) J. B. Torrance, Y. Tomkiewicz, R. Bozio, C. Pecile, C. R. Wolfe, K. Bechgaard, *Phys. Rev. B 26* (1982) 2267, and references cited therein; b) J. B. Torrance, J. J. Mayerle, K. Bechgaard, B. D. Silvermann, Y. Tomkiewicz, *ibid. 22* (1980) 4960, and references cited therein; c) A. N. Bloch, S. Mazumdar, private communication.

[80] a) E. J. Baerends, D. E. Ellis, P. Ros, *Chem. Phys. 2* (1973) 41; b) Z. Berkovitch-Yellin, D. E. Ellis, M. A. Ratner, *ibid. 62* (1981) 21; c) B. Delley, D. E. Ellis, *J. Chem. Phys. 76* (1982) 1949.

[81] a) K. A. Doris, D. E. Ellis, M. A. Ratner, T. J. Marks, *J. Am. Chem. Soc. 106* (1984) 2491; b) K. A. Doris, B. Delley, M. A. Ratner, T. J. Marks, D. E. Ellis, *J. Phys. Chem. 88* (1984) 3157.

[82] a) X. Z. Yang, D. B. Tanner, M. J. Rice, H. W. Gibson, A. Feldblum, A. J. Epstein, *Solid State Commun. 61* (1987) 335; b) E. J. Mele, M. J. Rice, *Phys. Rev. B 23* (1981) 5397.

[83] J. Chen, A. J. Heeger, *Synth. Met. 24* (1988) 311; b) A. J. Heeger, in [4c], Chapter 21, and references cited therein; c) S. Kivelson, A. J. Heeger, *Phys. Rev. Lett. 55* (1985) 308.

[84] a) G. B. Street in [4c], Chapter 8; b) P. Pfluger, G. Weiser, J. C. Scott, G. B. Street in [4c], Chapter 38; c) F. Genoud, M. Guglielmi, M. Nechtschein, E. Genies, M. Salmon, *Phys. Rev. Lett. 55* (1985) 118.

[85] a) R. P. McCall, J. M. Ginder, M. G. Roe, G. E. Asturias, E. M. Scherr, A. G. MacDiarmid, A. J. Epstein, *Phys. Rev. B 39* (1989) 10174; b) F. Zuo, M. Angelopoulos, A. G. MacDiarmid, A. J. Epstein, *ibid. 36* (1987) 3475; c) J. M. Ginder, A. F. Richter, A. G. MacDiarmid, A. J. Epstein, *Solid State Commun. 63* (1987) 97.

[86] F. Wudl, R. O. Angus, Jr., F. L. Lu, P. M. Allemand, D. J. Bachon, M. Novak, Z. X. Liu, A. J. Heeger, *J. Am. Chem. Soc. 109* (1987) 3677, and references cited therein.

[87] a) J. B. Schlenoff, J. Obrzut, F. E. Karasz, *Phys. Rev. B 40* (1989) 11822; b) J. M. Madsen, B. R. Johnson, X. L. Hua, R. B. Hallock, M. A. Masse, F. E. Karasz, *ibid. 40* (1989) 11751; c) M. J. Obrzut, F. E. Karasz, *Macromolecules 22* (1989) 458; d) M. J. Obrzut, F. E. Karasz, *J. Chem. Phys. 87* (1987) 6178; e) T. Granier, E. L. Thomas, D. R. Gagnon, F. E. Karasz, R. W. Lenz, *J. Polym. Sci. Polym. Phys. Ed. 24* (1986) 2793.

Communications may be submitted in English *or* in German. Further details regarding the submission of communications can be found in the "Notice to Authors" which is reproduced in the January issue of the journal or may be obtained from the editorial office upon request.

Novel Platinum Complexes Enable Selective C-H and C-Si Activation of Tetramethylsilane at Room Temperature **

By *Peter Hofmann*,* *Helmut Heiss, Peter Neiteler, Gerhard Müller*, and *Joachim Lachmann*

Dedicated to Professor Paul von Ragué Schleyer on the occasion of his 60th birthday

The *inter*molecular activation of C–H and C–X bonds at saturated carbon [Eq. (a)] is one of the topical fields of research in organometallic chemistry.[1] Since 1982, a series of transition metal complex fragments ML_n have been reported, which can be generated in solution, and which are capable of *inter*molecular homogeneous C–H activation even at saturated (sp^3) C atoms.

Although the prerequisites for such reactions are, in principle, known, both from experiment[1] as well as from theory,[2] a directed control of reactivity patterns is still far from realizable, since the ability of ML_n to coordinate and oxidatively add even C–H bonds[3] generally implies small activation barriers, and thus low selectivities.[4] In all known systems the activation of aromatic C–H bonds is, in addition, thermodynamically[5] or kinetically favored by pre-coordination and formation of π-complexes,[6] compared to the activation of aliphatic C–H bonds. We report here an electronically and structurally unusual, two-coordinate Pt^0-intermediate, which enables the activation of C–Si bonds of tetramethylsilane (TMS) and of homologous molecules at room temperature—via prior C-H activation of a CH_3 group—but does not activate benzene.

MO model calculations showed[7] that bending of Pt^0 complexes $Pt(PR_3)_2$ **1**, which are linear in their ground states, by phosphane chelate ligands must lead to highly reactive d^{10}-ML_2 fragments (14-electron species, isolobal with CH_2).

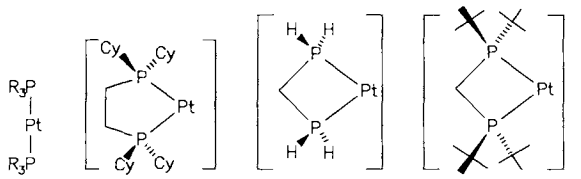

1 2 (Cy = *cyclo*-C_6H_{11}) 3 4 = [(dtbpm)Pt]

The smaller the P–Pt–P angle the higher the reactivity towards C–H and C–X bonds, since not only the total energy increases, but also the frontier orbitals change accordingly.[2c, 7] *Whitesides* et al. were able to confirm this experimentally in the case of the five-membered ring complex fragment **2**, which activates preferably aromatic, but also aliphatic, C–H bonds.[9]

On the basis of MO studies[7] of the parent system **3**, Pt^0 intermediates with four-membered ring structures, i.e. with "minimum" P–Pt–P angles were our synthetic targets. For a number of reasons,[10a] bis(di-*tert*-butylphosphino)methane (dtbpm)[11] appeared especially suitable for favoring highly strained, monomeric four-membered rings over the bridged arrangements[10b] often preferred in the case of diphosphinomethane complexes, and for suppressing side reactions.

Starting from the dichloro complex **5**[7] we were able to synthesize the *cis*-hydridoneopentyl complex **8** according to Scheme 1; complex **8**, which is stable at room temperature,

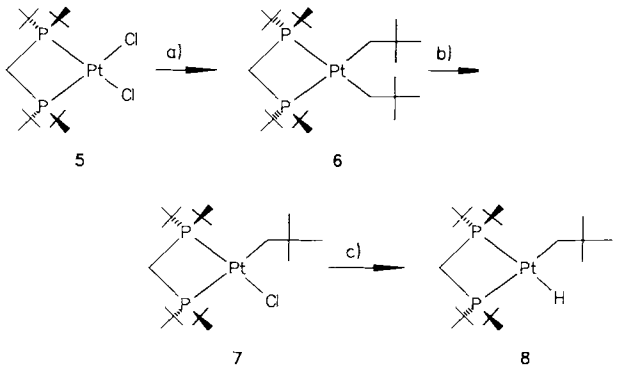

Scheme 1. Synthesis of **8**. a) $LiCH_2tBu$ in Et_2O, room temperature; b) CH_2Cl_2/CH_3OH, CH_3COCl in *n*-heptane, room temperature; c) $Na[B(OMe)_3H]$, THF, 0 °C; (synthesis of **11**, **12**: LiC_6H_5 or $LiCH_2SiMe_3$, following reaction steps as in (a).

is an ideal precursor of the 14-electron species [(dtbpm)Pt] **4**.[12] The crystal structure of **8**[13] is shown in Figure 1.[14]

The Pt atom displays planar coordination geometry (sum of angles at Pt 360.3°), the relevant P–Pt–P angle is 74.7(1)°. The Pt–P, Pt–C and Pt–H bond lengths are in the usual range. The displacement parameters of the *tert*-butyl groups, which are interlocked and sterically completely shield the four-membered ring side of complex **8**, are surprisingly small.[15]

[*] Prof. Dr. P. Hofmann, Dipl.-Chem. H. Heiss, Dipl.-Chem. P. Neiteler, Prof. Dr. G. Müller [+][++], Dipl.-Chem. J. Lachmann [+][++]
Anorganisch-chemisches Institut der Technischen Universität München
Lichtenbergstrasse 4, D-8046 Garching (FRG)

[+] X-ray structure analysis

[++] Present address: Fakultät für Chemie der Universität Konstanz
Universitätsstrasse 10, D-7750 Konstanz (FRG)

[**] This work was supported by the Deutsche Forschungsgemeinschaft, the Fonds der Chemischen Industrie, BASF AG, and DEGUSSA AG.

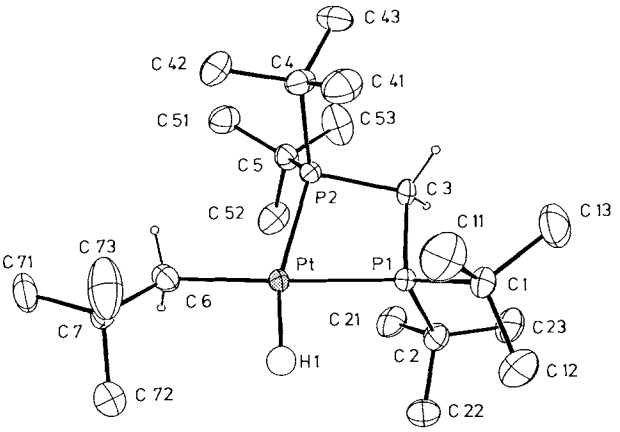

Fig. 1. Crystal structure of **8** (ORTEP, thermal ellipsoids at the 50% probability level, H atoms of the *tert*-butyl groups omitted). Selected bond lengths [Å] and angles [°]: Pt-P1 2.300(1), Pt-P2 2.338(1), Pt-H1 1.58(5), Pt-C6 2.117(5), P1-C3 1.869(5), P2-C3 1.895(5), P1-Pt-P2 74.7(1), C6-Pt-H1 96(2), P1-Pt-H1 89(2), P2-Pt-C6 100.8(1), Pt-P1-C3 93.1(2), P1-C3-P2 97.7(2).

The sought after complex fragment [(dtbpm)Pt] **4**, which, with suitable substrates L (2-butyne, 2,3-dimethyl-2-butene, acrylonitrile), can be identified as intermediate in the form of very stable alkyne or olefin complexes [(dtbpm)Pt(L)], is formed from **8** in solution already at room temperature by elimination of neopentane.

More interesting, however, are the following findings:

1) the methyltrimethylsilyl complex **9**[16a] is formed in quantitative yield from **8** in neat TMS, i.e. exclusively *C–Si activation of TMS* is observed. **9** is stable at room temperature. Reactions interrupted prior to completion show only the presence of **8** and **9**. Compound **8** also reacts smoothly with C–Si cleavage and formation of the stable products $[(dtbpm)Pt(CH_3)(SiMe_2OSiMe_3)]$[16c] and $[(dtbpm)Pt(CH_3)(SiMe_2SiMe_3)]$ analogous to **9** in pure $Me_3Si–O–SiMe_3$ and $Me_3Si–SiMe_3$ (no Si–Si cleavage as with other Pt^0 species[16b]!).

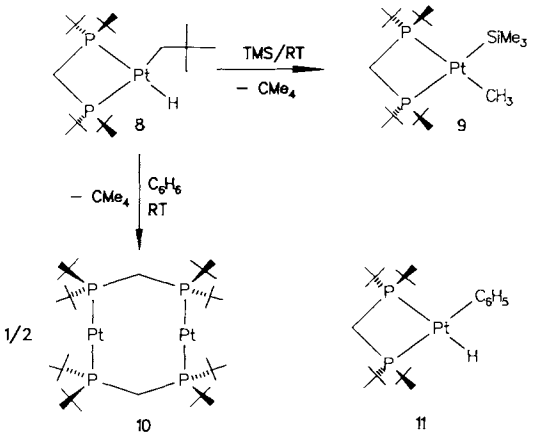

2) Decomposition of **8** at room temperature in neat benzene leads to formation of a deep-red dimer of **4**, to which we assign structure **10**, novel for Pt^0.[17] *C–H activation of benzene does not take place.*

3) Even in benzene solution with only 5 mol-% TMS, the reaction leads, with C–Si activation, to formation of **9** besides **10**; however, no hydridophenyl complex **11** is formed.

4) Complex **11**, the potential C–H activation product of benzene, synthesized according to Scheme 1, is considerably more stable than **8** and would therefore be detectable spectroscopically if it should occur in 2) and 3).

Thus, complex fragment **4** is not only capable of cleaving C–Si bonds, but of even doing so in the presence of benzene, without activating the C–H bonds of the arene. This surprising fact gains further significance in that the observed C–Si activations can only be explained consistently in terms of a prior activation of sp^3 C–H bonds. Namely, if **12**, the direct C–H activation product of TMS, is likewise prepared independently according to Scheme 1, then this alkylhydrido complex rearranges at room temperature in accordance with Scheme 2 to give the C–Si activation product **9**.

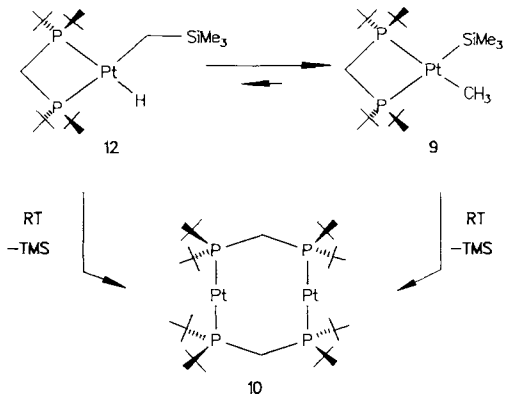

Scheme 2. RT = room temperature.

In neat TMS the rearrangement leads to **9** quantitatively, in benzene it is accompanied by the formation of dimer **10**, which according to preliminary kinetic measurements is formed by reductive elimination of TMS, both from **9** as well as from **12**. The kinetic relationships between **12**, **9** and **10** become complicated by the fact, that **9** also generates a small equilibrium concentration of **12** in benzene solution. If the, apparently, thermodynamically favored rearrangement of **12** to **9** is carried out in $[D_{12}]$TMS or in a mixture of C_6D_6/$[D_{12}]$TMS, only deuterium-free **9** is formed, thus indicating a strictly *intra*molecular reaction and ruling out intermediate reductive elimination of TMS.[18] With specifically labeled $[D_1]$**12** (Pt–D instead of Pt–H), $[D_1]$ **9** with a CH_2D group on Pt is formed, thus also clarifying the topology of this rearrangement, a topic which will be reported in more detail elsewhere (kinetics, MO model calculations, modeling studies).

Consequently, mild, quantitative C–Si activation is possible even in the case of the extremely stable and inert molecule TMS with the "hot" but readily accessible 14-electron complex fragment [(dtbpm)Pt] **4**. Not only the rearrangement of the hydrido complex **12** to **9** but also the lack of any H/D isotope effects and the purely random C–Si activation, respectively, in *inter*molecular competition experiments, where **4** is generated in TMS/$[D_{12}]$TMS, $Me_3Si–O–SiMe_3$/TMS and $Me_3Si–O–SiMe_3/Me_3Si–SiMe_3$ mixtures, suggests sp^3-C–H activation as the step prior to C–Si cleavage. A direct and selective C–Si activation by **4** seems, in contrast, much less likely, especially on steric grounds,[10a] according to the results of MO model calculations and modeling studies carried out so far. Hence, **4** would be the first ML_n fragment which activates sp^3-C–H bonds, but not the C–H bonds of benzene. Further experimental and theoretical studies are presently being carried out to gain better understanding of the anomalous reactivity of intermediate **4**, especially compared to that of **2**[19] with its essentially "more open" Pt

center and with regard to the interplay of electronic and steric effects in C–H and C–X activation processes. We also point out the importance of **9** in connection with *cis*-alkylsilyl complexes of Pt as postulated intermediates of catalytic cycles of hydrosilylation,[20] and the synthetic potential of the observed C–Si activations via subsequent insertion and elimination reactions (carbosilylation of C–C multiple bonds?).

Received: April 2, 1990
supplemented: May 15, 1990 [Z 3893 IE]
German version: *Angew. Chem. 102* (1990) 935

CAS-Registry-Numbers:
5, 113407-40-2; **6**, 128328-61-0; **7**, 128328-62-1; **8**, 128328-63-2; **9**, 128328-64-3; **10**, 128328-65-4; **11**, 128328-66-5; **12**, 128328-67-6; TMS, 75-76-3.

[1] a) J. P. Collman, L. S. Hegedus, R. J. Norton, R. G. Finke: *Principles and Applications of Organotransition Metal Chemistry*, University Science Books, Mill Valley 1987, p. 300; b) a most recent, complete list of references is given in: R. S. Shinomoto, P. J. Desrosiers, T. G. P. Harper, T. C. Flood, *J. Am. Chem. Soc. 112* (1990) 704.

[2] a) J. Y. Saillard, R. Hoffmann, *J. Am. Chem. Soc. 106* (1984) 2006; b) P. Hofmann, M. Padmanabhan, *Organometallics 2* (1983) 1273; c) P. Hofmann in A. de Meijere, H. tom Dieck (Eds.): *Organometallics in Organic Synthesis*, Springer, Berlin 1987, p. 1, and references cited therein; d) J. J. Low, W. A. Goddard, *J. Am. Chem. Soc. 108* (1986) 6115, and references cited therein.

[3] This mechanistic description concerns the "nucleophilic" C–H activation with late transition metals; other conditions prevail in the case of electron-deficient, electropositive, and strongly electrophilic metal centers. Cf. also: R. H. Crabtree, *Chem. Rev. 85* (1985) 245.

[4] a) B. H. Weiller, E. P. Wasserman, R. G. Bergman, C. B. Moore, G. C. Pimentel, *J. Am. Chem. Soc. 111* (1989) 8288; b) J. M. Buchanan, J. M. Stryker, R. G. Bergman, *J. Am. Chem. Soc. 108* (1986) 1537; c) A. H. Janowicz, R. G. Bergman, *ibid. 105* (1983) 3929; d) W. A. Kiel, R. G. Ball, W. A. G. Graham, *J. Organomet. Chem. 383* (1990) 481, and references cited therein.

[5] a) According to [4b] the Ir–phenyl bond energy is, e.g., more than 25 kcal mol^{-1} higher than that of the Ir–cyclohexyl bond; b) S. P. Nolan, C. D. Hoff, P. O. Stoutland, L. J. Newman, J. M. Buchanan, R. G. Bergman, G. K. Yang, K. S. Peters, *J. Am. Chem. Soc. 109* (1987) 3143.

[6] W. D. Jones, L. Dong, *J. Am. Chem. Soc. 111* (1989) 8722.

[7] P. Hofmann, H. Heiss, G. Müller, *Z. Naturforsch. B42* (1987) 395, and references cited therein.

[8] a) K. J. Moynihan, R. G. Goel, *Acta Crystallogr. Sect. B35* (1979) 3060; b) A. Immirzi, A. Musco, P. Zambelli, G. Carturan, *Inorg. Chim. Acta 13* (1975) L13; c) S. Otsuka, T. Yoshida, M. Matsumoto, K. Nakatsu, *J. Am. Chem. Soc. 98* (1976) 5850.

[9] a) M. Hackett, J. A. Ibers, G. M. Whitesides, *J. Am. Chem. Soc. 110* (1988) 1436; b) M. Hackett, G. M. Whitesides, *ibid. 110* (1988) 1449.

[10] a) These are: exploitation of the *gem*-dialkyl effect for the reduction of ring strain, steric shielding of the "non-reactive" side of the complex, high P-basicity, i.e. strongest possible Pt–P bonds, no aromatic P-substituents, blocking of intramolecular C–H activations, embedding of the Pt in a "hydrophobic" pocket of *rotationally invariant* space-filling *t*Bu-groups for possible control of selectivity in reactions of **4**, destabilization of dinuclear structures in the case of Pt^{II} (according to L. Manojlovic-Muir, K. W. Muir, A. A. Frew, S. S. M. Ling, M. A. Thomson, R. J. Puddephatt, *Organometallics 3* (1984) 1637); b) review of μ-diphosphinomethane complexes: R. J. Puddephatt, *Chem. Soc. Rev. 12* (1983) 99.

[11] H. H. Karsch, *Z. Naturforsch. B38* (1983) 1027.

[12] An alternative route, from $(COD)PtCl_2$ via $(COD)Pt(CH_2tBu)_2$ and $(COD)Pt(Cl)(CH_2tBu)$ to **7** (analogous to that in [9]) is possible, but less efficient.

[13] Crystal structure analysis of **8**: Syntex $P2_1$ diffractometer, $Mo_{K\alpha}$ radiation, $\lambda = 0.71069$ Å, $T = -50$ °C, crystal dimensions $0.25 \times 0.4 \times 0.5$ mm. $C_{22}H_{50}P_2Pt$, $M_r = 571.681$, monoclinic, space group $P2_1/n$, $a = 10.450(1)$, $b = 16.391(2)$, $c = 15.166(2)$ Å, $\beta = 99.92(1)°$, $V = 2558.9$ Å^3, $d_{calc} = 1.484$ g cm^{-3}, $\mu(Mo_{K\alpha}) = 56.7$ cm^{-1}, $Z = 4$, $F(000) = 1160$. 5021 unique reflections, 4531 "observed" with $F_o \leq 2\sigma^2(F_o)$ (ω scan, $\Delta\omega = 0.7°$, $(\sin\theta/\lambda)_{max} = 0.617$ Å^{-1}). $R(R_w) = 0.036\ (0.034)$, $w = 1/\sigma^2(F_o)$(anisotropic), H1 (observed) isotropic, CH_3 as rigid groups, 275 parameters, SHELX-76). Residual electron density $+2.89/-1.83$ Å^{-3}, maximum distance from Pt 0.82 Å. Further details of the crystal structure analysis are available on request from the Fachinformationszentrum Karlsruhe, Gesellschaft für wissenschaftlich-technische Information mbH, D-7514 Eggenstein-Leopoldshafen 2 (FRG), on quoting the depository number CSD-54656, the names of the authors, and the journal citation.

[14] To our knowledge **8** is only the third X-ray crystallographically characterized *cis*-hydridoalkyl complex of a transition metal besides $Cp^*Ir(PMe_3)(H)(C_6H_{11})$ [4b] and (dcpe)Pt(H)(CH_2tBu) [9a].

[15] Practically identical orientation of the *t*Bu groups is found also in the structures of **5** [7] and of $[(dtbpm)PdCl_2]$, $[(dtbpm)NiCl_2]$ and $[(dtbpm)Pt(Cl)(CH_2SiMe_3)]$: P. Hofmann, M. E. Krause, H. Heiss, G. Müller, G. Reber, J. Lachmann, unpublished. In constrast, considerable distortions on steric grounds occur in $[(dtbpm)Ni(\eta^2\text{-}trans\text{-}PhCH{=}CHPh)]$: P. Hofmann, L. A. Perez-Moya, M.-E. Krause, O. Kumberger, G. Müller, *Z. Naturforsch. B45* (1990) 897.

[16] a) Procedure for **9**: 30 mL (220 mmol) of dried TMS (over Na dust) were distilled onto 528 mg (0.923 mmol) of finely powdered **8**. After 7 days' stirring at room temperature under N_2 the white solid was filtered off and washed with 2×15 mL of TMS. After drying in high vacuum, 561 mg (0.785 mmol, 85.0%) of analytically pure, colorless **9** was obtained. When excess TMS was completely removed after completion of the reaction in a separate run formation of **9** was found to be quantitative (NMR spectroscopy). M.p. 216–217 °C (decomp.), correct elemental analysis; ^{1}H NMR (270 MHz, C_6D_6, 20 °C; C_6D_5H, int.): $\delta = 3.09$ (dd + sat, $^2J(P_A, H) = 6.4$ Hz, $^2J(P_B, H) = 7.3$, $^3J(Pt, H) = 6.8$, 2H; PCH_2P), 1.43 (dd + sat, $^3J(P_{cis}, H) = 6.8$, $^3J(P_{trans}, H) = 11.2$, $^2J(Pt, H) = 66.9$, 3H; $PtCH_3$), 1.22 (d, $^3J(P, H) = 12.2$, 18H; *t*Bu), 1.15 (d, $^3J(P, H) = 12.2$, 18H; *t*Bu), 0.73 (d + sat, $^4J(P, H) = 2.9$, $^3J(Pt, H) = 27.9$, 9H; $PtSi(CH_3)_3$); ^{13}C-NMR (67.9 MHz, C_6D_6, 20 °C; C_6D_6, int.): $\delta = 35.09$ (vt + sat, $N(P, C) = |^1J(P, C) + {}^3J(P, C)| = 13.2$ Hz, $^2J(Pt, C) = 6.4$; $P_AC(CH_3)_3$), 33.76 (dd + sat, $^3J(P, C) = 7.1$, $^1J(P, C) = 14.9$, $^2J(Pt, C)$ not resolved; $P_BC(CH_3)_3$), 33.64 (dd + sat, $^1J(P_A, C) = 4.9$; $^1J(P_B, C) = 7.3$, $^2J(Pt, C) = 31.1$; PCH_2P), 30.79 (d, $^2J(P, C) = 6.4$; $PC(CH_3)_3$), 6.91 (dd + sat, $^3J(P_{trans}, C) = 8.6$, $^3J(P_{cis}, C) = 2.7$, $^2J(Pt, C) = 82.2$, $^1J(Si, C) = 39.1$; $PtSi(CH_3)_3$), -4.59 (dd + sat, $^2J(P_{trans}, C) = 83.6$, $^2J(P_{cis}, C) = 5.9$, $^1J(Pt, C) = 594.7$; $PtCH_3$); ^{31}P-NMR (109.4 MHz, C_6D_6, 20 °C; 85% H_3PO_4, ext.): $\delta = 9.55$ (d + sat, $^2J(P_A, P_B) = 21$ Hz, $^1J(Pt, P) = 1608$; P(*trans* to CH_3)), -1.08 (d + sat, $^2J(P_A, P_B) = 21$, $^1J(Pt, P) = 656$, $^2J(Si, P) = 194$; P(*trans* to $SiMe_3$)); MS (EI, 70 eV): no $M^{\oplus}$, *m/z* 572 ($M^{\oplus} - CH_3$, 4%), 499 ($M^{\oplus} - SiMe_4$, 18), 73 ($SiMe_3^{\oplus}$, 100); IR (KBr): $\tilde{\nu}$ [cm^{-1}] = 825, 839 (C–Si), 345 (Pt–Si); b) T. Hayashi, T. Kobayashi, A. M. Kawamoto, H. Yamashita, M. Tanaka, *Organometallics 9* (1990) 280; c) an X-ray structure analysis of the C–Si activation product of hexamethyldisiloxane, $[(dtbpm)Pt(CH_3)(SiMe_2O\text{–}SiMe_3)]$ has been performed: P. Hofmann, H. Heiss, O. Kumberger, P. Bissier, unpublished.

[17] The alternative structure of a dimer of two intact, Pt^c–Pt^o bound four-membered ring fragments corresponding to the system containing 1,3-bis-(di-*tert*-butylphoshino)propane described by *Otsuka* et al. (Y. Yoshida, Y. Yamagata, T. H. Tulip, J. A. Ibers, S. Otsuka, *J. Am. Chem. Soc. 100* (1978) 2063) is ruled out on the basis of the MS, ^{1}H-, ^{13}C-, ^{31}P-, and ^{195}Pt-NMR data of **10** and a comparison of the data with the data of *Otsukas* compound and all other (dtbpm)Pt four-membered ring systems characterized by us, and also on the basis of the chemical behavior. The novel compound **10** and the corresponding palladium system (P. Hofmann, M. E. Krause, unpublished) will be reported on in a separate communication.

[18] a) A second experiment confirms the intramolecular course of the reaction: in $Me_3SiOSiMe_3$, which is itself C–Si activated by **8**, **12** also rearranges only to **9**. b) An Si–Si cleavage, which appears to be related to the rearrangement of **12** to **9** has been reported recently: L. S. Chang, M. P. Johnson, M. J. Fink, *Organometallics 8* (1989) 1639.

[19] In the meantime, the four-membered ring system $[(dcpm)Pt(H)(CH_2tBu)]$ directly corresponding to **2** has also been synthesized: P. Hofmann, J. U. Notheis, unpublished.

[20] I. Ojima in S. Patai, Zvi Rappoport (Eds.): *The Chemistry of Organic Silicon Compounds*, Wiley, New York 1989, Vol. 2, p. 1479; D. Tilley, *ibid.* p. 1415.

Heteronuclear "X-Y" Decoupling in the MAS-NMR Spectroscopy of Inorganic Solids**

By *Robert Maxwell, David Lathrop, Deanna Franke,* and *Hellmut Eckert**

It has been widely established that magic angle spinning (MAS) NMR spectroscopy can be tremendously successful in the structural elucidation of solids. Nevertheless, the spec-

[*] Prof. Dr. H. Eckert, R. Maxwell, D. Lathrop, D. Franke
Department of Chemistry
University of California, Santa Barbara
Goleta, CA 93106 (USA)

[**] Financial support by the Petroleum Research Fund (G3-20950) and the National Science Foundation (DMR-8913738) is gratefully acknowledged.

tra of many crystalline inorganic materials, ceramics and glasses are often found rather non-descript, poorly resolved, and bear little chemical information. We have found this to be the case in a variety of rare-spin resonances in crystalline and glassy metal phosphide and phosphorus chalcogenide materials, which are currently of great interest for applications in infrared optics and semiconductor technology.

In the past, much of the power of solid-state magic angle spinning (MAS)-NMR experiments has come from the ability to exploit dipolar or scalar coupling between high-γ nuclei (^{1}H or, in a few cases, ^{19}F) and lower-γ nuclei (^{13}C, ^{29}Si, ^{15}N) to facilitate detection via cross polarization or to provide spectral editing by double resonance experiments.[1] Although the application of such techniques to inorganic materials that are devoid of protons would be highly desirable, experiments of this kind are extremely scarce and have been mostly limited to spin-echo double resonance (SEDOR) experiments on non-spinning samples.[2-5]

In this communication, we wish to demonstrate that the informational content of MAS-NMR spectra can be dramatically enhanced if the standard rare-spin MAS-NMR experiment is combined with heteronuclear decoupling. Figure 1 shows the ^{113}Cd-NMR spectra of the chalcopyrite-

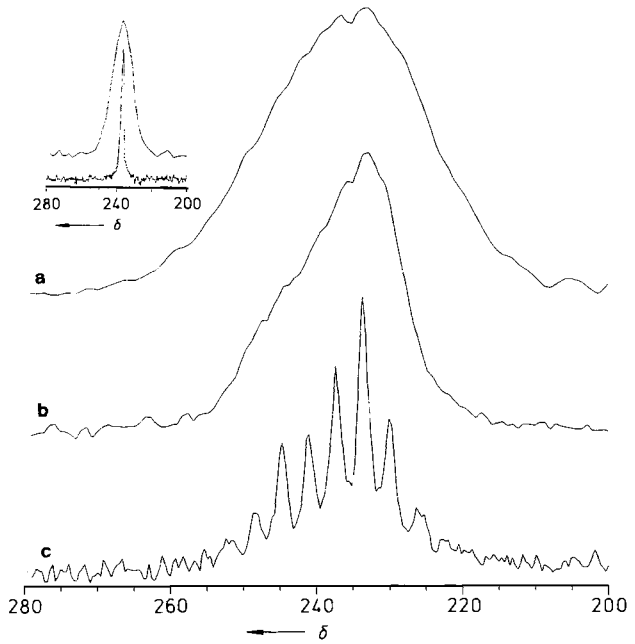

Fig. 1. 66.70-MHz ^{113}Cd-NMR spectra of crystalline $CdGeP_2$, obtained with 7-μs 90° pulses and 15-min recycle delay. a) ^{113}Cd-single-resonance MAS-NMR spectrum (rotation frequency 0.25 kHz). This spectrum is identical with the single-resonance NMR spectrum (stationary); b) {^{31}P}-^{113}Cd double-resonance NMR spectrum (stationary); c) {^{31}P}-^{113}Cd double-resonance MAS-NMR spectrum (spinning speed 0.25 kHz). The inset shows a comparison of single- and double-resonance ^{113}Cd-NMR spectra (top and bottom respectively) at a spinning speed of 5 kHz.

structured semiconductor $CdGeP_2$ with and without ^{31}P decoupling. The resolution of the single-resonance spectra is severely hampered by the sizeable dipolar coupling between ^{31}P and ^{113}Cd in this compound (Fig. 1a). As previously discussed by *Maricq* and *Waugh* for the ^{1}H-^{13}C case,[6] the ^{31}P-^{113}Cd dipolar interaction functions as a source of homogeneous line-broadening due to the magnitude of ^{31}P-^{31}P dipole couplings present in this sample. The resulting line-narrowing by MAS-NMR is only moderate even at a spinning speed of 5 kHz and non-existent at low speeds, because averaging of homonuclear interactions by MAS requires fast spinning speeds compared to the strength of the dipole coupling (in Hz). In contrast, note the superb resolution improvement obtained on combination of MAS with ^{31}P decoupling (Fig. 1c). From the distinct spinning side-band patterns observed, it is now possible to measure the chemical shift anisotropies. Using the method of *Herzfeld* and *Berger*[7] we determine $\delta_{11} = 225 \pm 2$, $\delta_{22} = 236 \pm 1$ and $\delta_{33} = 250 \pm 1$ ppm (vs. dimethylcadmium).

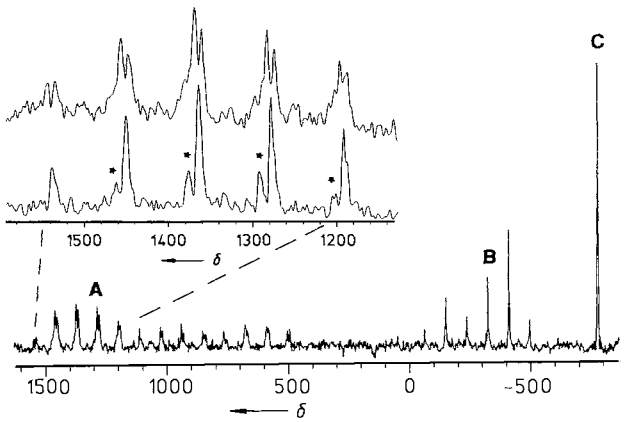

Fig. 2. 57.31-MHz ^{77}Se-NMR spectra of Ag_7PSe_6 (spinning speed 5.0 kHz). The overall spectrum shows the single-resonance case; distinct peak patterns **A**, **B**, and **C** are indicated. The inset shows the most intense part of the MAS-NMR side-band pattern with and without ^{31}P decoupling. Note the two distinct Se sites, the less intense one of which is labeled by an asterisk. Both spectra are averages of 48 scans obtained with 90°-pulses of 7-μs duration and recycle delays of 15 min.

Figure 2 shows an application to the fast ionic conductor Ag_7PSe_6. Although the X-ray powder pattern of this compound has been indexed in the cubic space group $F\bar{4}3m$ with a lattice constant of 10.768 Å,[8] its crystal structure is unknown. Differential scanning calorimetry shows that Ag_7PSe_6 undergoes a first-order phase-transition at 188 °C; presumably for this reason, we have been unable to grow single crystals of the low-temperature phase. The ^{77}Se-MAS-NMR spectrum reveals three chemically distinct species: a signal cluster **A** centered at $\delta = 1104$, a signal cluster **B** centered at $\delta = -326$, and a signal **C** at $\delta = -779$ (all shifts refered to solid CdSe at 0 ppm.[9] Signal cluster **A** and resonance **B** give rise to spinning side-band patterns due to the large ^{77}Se chemical shift anisotropy. ^{31}P decoupling leaves resonances **B** and **C** unaffected, and simplifies the spectrum of species **A** considerably: the multiplet collapses and two distinct resonances, in a ratio of approximately 3:1, become visible. Thus, the ^{77}Se{^{31}P}- double-resonance MAS-NMR experiment not only serves to differentiate between phosphorus-bound and non-phosphorus bound Se atoms, but also shows that there are two different types of phosphorus-bound Se atoms in the asymmetric unit. This result is nicely compatible with the ^{31}P-MAS-NMR spectrum of Ag_7PSe_6 shown in Figure 3. This spectrum shows a central resonance at $\delta = -51.2$ (vs 85% H_3PO_4) and two distinct pairs of ^{77}Se-^{31}P spin-spin-coupling satellites, with coupling constants of 524 ± 1.0 Hz and 430.4 ± 3.0 Hz, respectively. The intensity ratio of these satellites compares well with that observed for the respective ^{77}Se-NMR spectra of the two distinct P-bound selenium atoms. The total integrated intensity of the spin-spin-coupling pattern relative to the center band indicates, in conjunction with the natural abundance of the ^{77}Se isotope (7.0%), that P is bonded to four Se atoms.

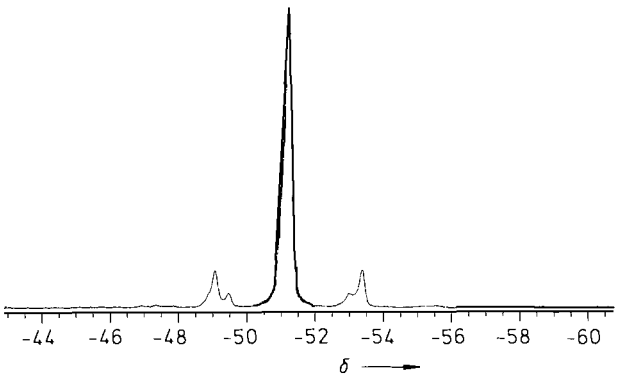

Fig. 3. 121.65-MHz ^{31}P-MAS-NMR spectrum of Ag_7PSe_6 (spinning speed 2.3 kHz), 56 scans obtained with a 45° pulse of 4-μs duration and a 1-min recycle delay.

From this NMR evidence we can conclude that the P atoms are located on sites with three-fold symmetry. Furthermore, there are two additional, nonequivalent Se atoms in the structure, which are only coordinated to Ag atoms. Thus, the ^{31}P-^{77}Se double-resonance experiment described here provides important structural insights which are crucial for our current attempt to solve the crystal structure of Ag_7PSe_6 by Rietveld X-ray analysis.

In summary, the results reported in the present communication show that heteronuclear decoupling provides an important new tool of resolution improvement and spectral editing in the MAS-NMR spectroscopy of rare nuclei in inorganic materials devoid of hydrogen. Limitations could arise if the chemical shift anisotropy of the irradiated nuclei (here ^{31}P) is very large compared to the spinning frequency. In this case only a fraction of observed nuclei would be decoupled efficiently at any given phase of the rotor cycle and hence decoupling would be incomplete. On the other hand, the sensitivity of decoupling efficiency to resonance offset effects can also be turned into an advantage for establishing connectivities by selective decoupling experiments. Other promising prospects for future applications include two-dimensional correlated spectroscopy, and measurements of heteronuclear distances by spin-echo double-resonance NMR. The development of such techniques and applications to ceramics and glasses is currently in progress.

Experimental

$CdGeP_2$ was prepared from the elements heated in stoichiometric proportions in a flame-sealed quartz container at 800 °C and 10^{-3} torr, followed by slow cooling (20 Kh^{-1}). Ag_7PSe_6 was prepared in an analogous fashion, via solid-state reaction at 500 °C. The purity of these compounds was ascertained by X-ray powder diffraction. All NMR experiments were carried out on a General Electric GN-300 NMR spectrometer using a specially designed double broadband tuned MAS-NMR probe constructed by Doty Scientific. One of the channels is tunable from 70–175 MHz (X), whereas the other one covers the frequency range 20–80 MHz (Y). The probe contains extra tuning capacitors to reject the decoupling frequency in the observe channel; additional rejection (40 dB) is provided by an external 87 MHz low-pass filter. The heteronuclear decoupling pulse is generated from the pulsed 300-MHz ^{1}H-decoupler output by mixing with a local oscillator (PTS 250) frequency, low-pass filter and two-stage amplification (up to 200 W), using Amplifier Research 50L and Henry Radio amplifiers. In all cases, the decoupling field *was applied exactly on* resonance.

Received: March 29, 1990 [Z 3884 IE]
German version: *Angew. Chem. 102* (1990) 950

[1] T. M. Duncan, C. R. Dybowski, *Surf. Sci. Rep. 1* (1981) 157.
[2] J. B. Boyce, S. E. Ready, *Phys. Rev. B38* (1988) 11 008.
[3] C. D. Mackowka, C. P. Slichter, J. H. Sinfelt, *Phys. Rev. B31* (1985) 5663.
[4] C. D. Mackowka, C. P. Slichter, J. H. Sinfelt, *Phys. Rev. Lett. 49* (1982) 379.
[5] Other heteronuclear double-resonance experiments in combination with MAS include double cross polarization (E. W. Hagaman, *J. Am. Chem. Soc. 110* (1988) 5594), Rotational Echo Double Resonance (T. Gullion, J. Schaefer, *J. Magn. Reson. 81* (1989) 196), and Rotary Resonance Recoupling (T. G. Oas, M. H. Levitt, R. G. Griffin, *J. Chem. Phys. 89* (1988) 692). All of these experiments utilize protons as an abundant-spin reservoir of magnetization.
[6] M. M. Maricq, J. S. Waugh, *J. Chem. Phys. 70* (1979) 3300.
[7] J. Herzfeld, A. E. Berger, *J. Chem. Phys. 73* (1980) 6021.
[8] F. W. Kuhs, R. Nitsche, K. Scheunemann, *Mater. Res. Bull. 14* (1979) 241.
[9] The experimental area ratio **A**/(**B** + **C**) is ca. 1.7:1; in reasonable agreement with the ratio 2:1 expected for the P-bound/non-P-bound ratio. The deviation is probably due to partial saturation of resonances **A** and **C**, which were found to have substantially longer spin-lattice relaxation times than **B**.

Hydrogenobyrinic Acid: Isolation, Biosynthesis, and Function **

By *Francis Blanche,* Denis Thibaut, Denise Frechet, Marc Vuilhorgne, Joel Crouzet, Béatrice Cameron, Kersten Hlineny, Ute Traub-Eberhard, Maureen Zboron,* and *Gerhard Müller**

Hydrogenobyrinic acid **1**, the cobalt-free analogue of the tetrapyrrolic vitamin B_{12} parent substance cobyrinic acid **2**, has been discovered for the first time in a bacterium, the B_{12}-producing *Pseudomonas denitrificans SC 510.*[1] We have now developed a biosynthetic method for its isolation, which we report herein. Surprisingly, **1** occurs a) in a non-photosynthesizing bacterium,[2] b) in both cobalt-containing as well as cobalt-free cultivation, and c) intracellularly bound to a protein *bP* specific for it. The biosynthetic entry to **1** opens up new perspectives for studies on the biosynthesis of **1** and **2** and concerning the question whether and how the biosynthetic pathways of these two compounds differ; the first relevant experiments will be reported.

The protein **1**-*bP* leading to **1** was isolated and purified.[3] **1**-*bP* is reddish-orange, in the SDS-polyacrylamide electrophoretogram the only band, corresponding to 23 kD, and the first 15 amino acids at the NH_2 terminal can be cleanly sequenced. Since **1** is set free from **1**-*bP* by heat treatment (70 °C, 10 min) there is a non-covalent protein/pigment bond present. For the isolation of **1**, **1**-*bP* or the crude extract obtained from 100 g of wet bacterium[3a] was heat-treated, centrifuged, and the **1** present in the supernate was fixed on DEAE-Sephadex A-25 (0.5 × 1 cm, 0.1 M phosphate buffer, pH 7.0). After washing with 20 mL of 0.3 M phosphate buffer, pH 7.0, **1** was eluted with 10 mL of aqueous 1 M KH_2PO_4 and transferred onto LiChroprep RP-18 (0.5 × 2 cm), washed with 10 mL of 0.25 M KH_2PO_4, and eluted with H_2O/*t*BuOH (9:1, v/v); lyophilized **1** was stored dry and protected from light at −20 °C. Yield 100 μg of **1** per 100 g of wet bacterium. For the isolation of the heptamethyl ester **1a**, **1** was treated with MeOH/H_2SO_4 (100:5, v/v) and the mixture allowed to stand for 48 h; **1a** was then isolated as described.[5]

[*] Dr. F. Blanche, D. Thibaut, D. Frechet, M. Vuilhorgne, Dr. J. Crouzet, B. Cameron
Centre de Recherche de Vitry, Rhône-Poulenc Santé
BP 14, F-94403 Vitry-sur-Seine (France)
Dr. G. Müller, Dipl.-Biol. K. Hlineny, Dipl.-Chem. U. Traub-Eberhard, Dipl.-Chem. M. Zboron
Institut für Organische Chemie,
Biochemie und Isotopenforschung der Universität
Azenbergstrasse 18, D-7000 Stuttgart (FRG)

[**] This work was supported by Rhône-Poulenc Santé (Dr. *J. Lunel*) and the Deutsche Forschungsgemeinschaft.

Identical spectra and analytical values (UV/VIS, circular dichroism, fluorescence, FAB-MS, ^1H and ^{13}C NMR, electrophoresis and thin-layer chromatography) of authentic **2** (from *P. shermanii*[4]) and of the compound obtained from **1**, after incorporation of cobalt,[5] confirm the structure of **1** (Scheme 1). The spectra of **1**[6a] match and complete the data obtained for semisynthetic **1a**.[5] Table 1 gives a complete assignment of the ^1H- and ^{13}C-NMR signals of **1**.[6b]

The in-vitro biosynthesis of **1** was achieved with the cell-free crude extracts[3a] as well as with the precursors of **2**

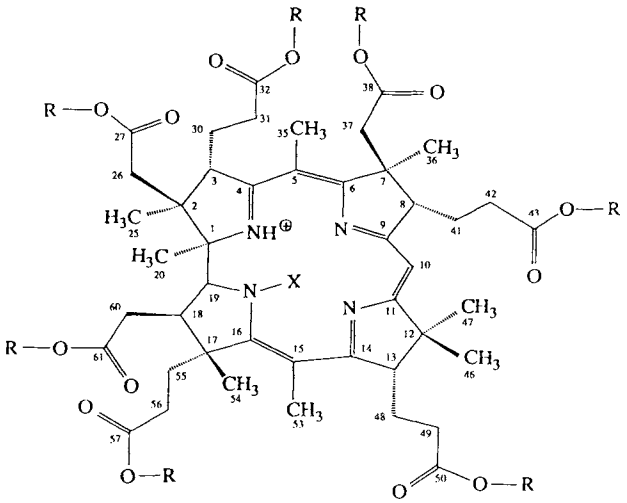

1, R = H, X = H ⟶ **2**, R = H, X = $Co^{2\oplus}(H_2O)_2$

1a, R = CH_3, X = H ⟵ **2a**, R = CH_3, X = $Co(CN)_2$

Scheme 1. a: 1 μmol of **1** or **2** in 5 mL $MeOH/H_2SO_4$ (100:5, v/v, degassed), 48 h at room temperature in the dark, then extraction and TLC as described in [4, 5]. Reaction conditions for **1** → **2** → **2a** and chromatographic purification as described in [4, 5].

Table 1. ^1H- and ^{13}C-NMR shifts (δ values) of hydrogenobyrinic acid in D_2O and assignment [a]. Position of the C atoms, cf. Scheme 1 [6b].

Position	δ(^{13}C)[b]	δ(^1H)[c]	Position	δ(^{13}C)[b]	δ(^1H)[c]
1	81.1 (s)		30	27.1 (t)	1.75, 1.85
2	47.0 (s)		31	36.0 (t)	2.08, 2.15
3	56.8 (d)	3.45	32	183.2 (s)	
4	180.5 (s)		35	15.0 (q)	1.95
5	105.7 (s)		36	20.0 (q)	1.3
6	164.4 (s)		37	47.8 (t)	2.35
7	48.2 (s)		38	179.7 (s)	
8	54.7 (d)	3.25	41	26.8 (t)	1.65, 1.85
9	173.5 (s)		42	39.0 (t)	2.05
10	90.3 (d)	5.43	43	181.0 (s)	
11	188.5 (s)		46	32.0 (q)	0.95
12	49.4 (s)		47	20.0 (q)	1.15
13	54.1 (d)	2.92	48	54.1 (t)	1.75, 1.85
14	177.4 (s)		49	27.4 (t)	1.8
15	103.7 (s)		50	183.0 (s)	
16	180.8 (s)		53	15.0 (q)	1.95
17	58.6 (s)		54	20.5 (q)	1.15
18	42.0 (d)	2.72	55	33.7 (t)	1.75, 2.05
19	68.6 (d)	4.00	56	34.3 (t)	1.75, 2.35
20	23.0 (q)	1.1	57	182.6 (s)	
25	17.2 (q)	1.2	60	37.2 (t)	2.3, 2.55
26	47.0 (t)	2.05	61	182.9 (s)	
27	180.6 (s)				

[a] The NMR spectra were recorded in D_2O with a Bruker AM-400; ^1H: 400 MHz, ^{13}C: 100.6 MHz. The HDO resonance was suppressed by gated decoupling. [b] Assignment by heteronuclear correlation experiments [10, 11], optimized for normal (130 Hz) and remote coupling (10 Hz). [c] Derived from homonuclear COSY [12] and RELAY 2D experiments [13].

known to date,[4, 7, 8] and is suitable for labeling and biosynthetic studies of **1**. The methylation process starting from uroporphyrinogen III and proceeding via the precorrins **1**–**3**[7] shows the same methylation sequence at the tetrapyrrolic ligand in the formation of **1** as in the formation of **2**: [7, 6b] C2, C7, C20, C17, C12, C1, C5/15. Figure 1A

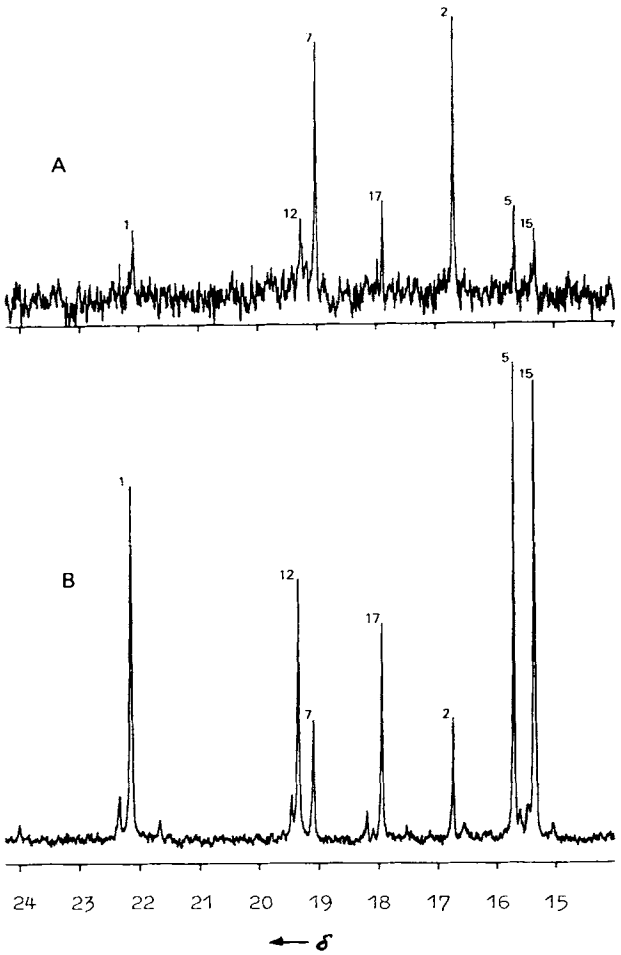

Fig. 1. ^1H broad-band decoupled 100.6-MHz ^{13}C-NMR spectra (64000 scans in [D_6]benzene) of **2a**, prepared from biosynthesized **1** [5]. *Biosynthesis:* A: crude extract from 100 g of cells [3a] + 1 μmol [C2, C7, C20-methyl-$^{13}C_3$] factor III [4c] (90 atom-% ^{13}C) + 20 μmol *S*-adenosyl-L-methionine (SAM), incubated 18 h at 30 °C. For the isolation, 3 mg of unlabeled **1** added, then heat treatment; isolation of **1** and synthesis of **2a** [5]: 2 mg. B: crude extract from 100 g of cells + 20 μmol of 5-aminolevulinic acid + 20 μmol [$^{12}CH_3$]SAM incubated 5 h at 30 °C, then 100 μmol [$^{13}CH_3$]SAM (90 atom-% ^{13}C) added, 6 h further incubation and **1** isolated; **1a**: ca. 500 μg, **2a**: 400 μg.

provides supporting evidence for the conversion of the precorrin **3** (last known precursor of **2**) into **1**: its ^{13}C-labeled didehydro-isolate and trimethylisobacteriochlorin [C2, C7, C20-methyl-$^{13}C_3$] factor III[4c, 7, 8a] was incubated with the crude extract synthesizing **1**; finally, **1** was isolated and converted by known methods[4, 5] into the dicyanoheptamethyl ester **2a** (Cobester), whose ^{13}C-NMR spectrum showed $^{13}CH_3$ signals typical for **2a** in the methyl-group region,[7] with the signals of the methyl groups C1, C12, C17, C5 and C15 corresponding to the natural ^{13}C-content of the sample. The two most intense signals arise from the $^{13}CH_3$ groups on C2 and C7 of precorrin **3**; as expected, the $^{13}CH_3$ group on C20 is not recorded and should—as in the formation of **2**—be eliminated, together with C20, as acetic acid.[8] The further methylation sequence followed—as in studies on the biosynthesis of **2**—from a ^{13}C-pulse labeling experiment.[7]

S-Adenosyl-L-[methyl-^{13}C]methionine was added to the cell extract forming **1** and preincubated for the accumulation of precursors; after further incubation **1** was isolated. Figure 1 B shows the ^{13}C-NMR of **2a**, prepared from **1**; the increase in intensity of the signals allows conclusions to be drawn about the methylation sequence.

The in-vitro transformation of radioactive **1** or **1**-*pP* into **2** could not be accomplished with *Pseudomonas dentrificans* or with *Propionibacterium shermanii*, even though the mechanism of the biosynthesis of **2** is, as far as is known, also realized in the formation of **1**. Thus, the manner and time of the cobalt incorporation leading to **2** remain unclear. The results listed in Table 2 are unequivocal and confirm conclusions drawn from experiments with unlabeled semisynthetic **1**.[5] **1** and **1**-*bP* are not utilized by the enzyme preparations synthesizing **2**, rather these are inhibitors in the formation of **2**, whereby the steps leading to the precorrin **3** are not inhibited. Additional experiments showed that the C38 mono- and C27,C38-diamide of **1** as well as the Ni^{II} analogue of **2**[9] do not inhibit formation of **2**. This finding provides a first insight into the molecular events of the inhibition, the interpretation of which is expected to provide valuable information concerning the biosynthesis of **2**. One would especially like to know whether the protein *bP* binding **1** plays a role in the formation of **2**, and if so what sort of role.

Table 2. Formation of cobyrinic acid **2** with enzyme preparations from *P. shermanii* [4, 5] and the radioactively labeled substrates hydrogenobyrinic acid **1** and protein-bound hydrogenobyrinic acid **1**-*bP* [a].

Experiment	Substrate [nmol] [f]	Cobyrinic acid **2** isolated as Cobester **2a** [nmol] [g]	[nmol] [h]
1 [i]	235 [b]		0.44
2	--	60	
3	235 [b]	10	0.17
4	450 [b]	13	0.33
5	500 [c]	5	0.10
6	700 [d]	165	102.00
7	700 [e] + 500 [c]	27	0.10

[a] In each case the same enzyme preparation from 100 g of wet bacterium per experiment [5] + 2.5 μmol $Co^{2\oplus}$ + 50 μmol *S*-adenosyl-L-methionine + substrate (specific radioactivities in brackets). [b] [Methyl-^{3}H]-**1** (762 Bq/nmol). [c] [Methyl-^{3}H]-**1**-*bP* (162 Bq/nmol, 10 mg protein). [d] [Methyl-^{3}H]-factor III [4c] (303 Bq/nmol) [e] = unlabeled [d]. [f] By in-vitro biosynthesis from 5-aminolevulinate + *S*-adenosyl-L-[methyl-$^3H_3$] methionine. [g] In all incubations **2** is formed from endogenous precursors of the enzyme preparation. [h] Based on radiochemical yields of the substrate/product conversion. [i] Incubated without enzyme, demonstrates chemical cobalt incorporation in **1**; "carried" with **2** for isolation.

Received: March 22, 1990 [Z 3868 IE]
German version: *Angew. Chem. 102* (1990) 947

[1] B. Cameron, K. Briggs, S. Pridmore, G. Brefort, J. Crouzet, *J. Bacteriol. 171* (1989) 547.

[2] The occurrence of cobalt-free corrinoids in photosynthesizing microorganisms is well known, their significance open; V. B. Koppenhagen in D. Dolphin: *Vitamin B_{12}, Vol. 2*, Wiley, New York 1983, p. 106–149.

[3] Isolation and purification of **1**-*bP* at 4 °C: a) crude extract: ultrasonic treatment of 100 g of *Pseudomonas denitrificans SC 510* bacterial wet mass in 200 mL of phosphate buffer, pH 7.4, 12 min, and centrifugation at 50 000 × g; free tetrapyrrolecarboxylic acids are fixed on DEAE-Sephadex A-25 (1 × 3 cm)[4b]. b) Ammonium sulfate fractionation, 40–60% saturation. c) Four chromatographic steps and sequences of related systems, buffer: 10 mM tris/HCl, pH 7.7: 1.) Ultrogel AcA 54 (50 × 2.5 cm). 2.) DEAE Trisacryl M, 0–0.2 M KCl. 3.) Bio-Gel HPHT, 0.15 M potassium phosphate, pH 7.7. 4.) FPLC Mono Q HR 5/5, 0–0.25 M NaCl. Yield: 2.5 mg **1**-*bP*.

[4] a) H. O. Dauner, G. Müller, *Hoppe Seyler's Z. Physiol. Chem. 356* (1975) 1353; b) R. Deeg, H. P. Kriemler, K. H. Bergmann, G. Müller, *ibid. 358* (1977) 339; c) G. Müller, K. D. Gneuss, H.-P. Kriemler, A. J. Irwin, A. I. Scott, *Tetrahedron (Suppl.) 737* (1981) 81.

[5] T. E. Podschun, G. Müller, *Angew. Chem. 97* (1985) 63; *Angew. Chem. Int. Ed. Engl. 24* (1985) 46.

[6] a) Spectroscopic data of **1**: UV/VIS (H_2O): λ_{max} = 270 nm (lg ε = 4.54), 317 (sh, 4.52), 329 (4.69), 376 (3.73), 395 (3.69), 497 (4.26), 524 (4.28); MS (FAB): *m/z* = 881 ($M^{\oplus}$ + H); b) the numbering of **1** and **2** in Scheme 1 based on NMR studies[10]. The numbering of the tetrapyrrolic ligand is conventional, but that of the peripheral substituents can lead to confusion, since C20 of uroporphyrinogen III is eliminated together with the C20 methyl group of precorrin **3** during formation of the corrin ring[7, 8]. The methyl group on C1 numbered 20 in Scheme 1 is of course introduced by *S*-adenosyl-L-methionine during the methylation process.

[7] a) H. C. Uzar, A. R. Battersby, T. A. Carpenter, F. J. Leeper, *J. Chem. Soc. Perkin Trans. 1 1987*, 1689; b) A. I. Scott, H. J. Williams, N. J. Stolowich, P. Karuso, M. D. Gonzalez, G. Müller, K. Hlineny, E. Savvidis, E. Schneider, U. Traub-Eberhard, G. Wirth, *J. Am. Chem. Soc. 111* (1989) 1897.

[8] a) C. Nussbaumer, M. Imfeld, G. Wörner, G. Müller, D. Arigoni, *Proc. Natl. Acad. Sci. USA 78* (1981) 9; b) L. Mombelli, C. Nussbaumer, H. Weber, G. Müller, D. Arigoni, *ibid. 78* (1981) 11; c) A. R. Battersby, M. J. Bushell, L. Jones, N. G. Lewis, A. Pfenniger, *ibid. 78* (1981) 13.

[9] Ni^{II}-**1a**: 1 μmol **1a** + 2.5 μmol $Ni(OAc)_2$ in CH_2Cl_2/CH_3OH (2:1, v/v) 6 h under reflux then TLC. UV/VIS (CH_2Cl_2): λ_{max} = 252 nm (rel. intensity = 0.93), 261 (sh, 0.82), 318 (sh, 0.87), 335 (1.00), 400 (sh, 0.29), 448 (0.53), 468 (sh, 0.46); MS (FAB): *m/z* 1036 ($M^{\oplus}$ + H). Ester hydrolysis with 2 M aqueous piperidine [5].

[10] A. Bax, *J. Magn. Reson. 53* (1983) 517.

[11] V. Rutar, *J. Magn. Reson. 58* (1984) 306.

[12] W. P. Aue, E. Bartholdi, R. R. Ernst, *J. Chem. Phys. 64* (1976) 2229.

[13] G. Wagner, *J. Magn. Reson. 55* (1983) 151.

Application of the Combined ab initio/IGLO/NMR Method to Resolve the B_6H_{12} Structural Question**

By *Michael Bühl* and *Paul von Ragué Schleyer**

Although B_6H_{12} was first prepared as early as 1960,[1] its accurate structure is still in doubt. On the basis of NMR spectra, a general 4212 structure (*styx* notation) was proposed.[2] As the crystals of hexaborane(12) are not suitable for X-ray structure analysis, *Beaudet* concluded in his review, "only microwave spectroscopy holds any promise for solving this structural problem".[3] Nevertheless, in the same year a gas-phase electron diffraction (GED) structure was published by *Greatrex* et al.[4] This study confirmed that the molecule possesses C_2 symmetry; the proposed structure is shown in Figure 1 a. However, the detailed dimensions differ substantially from the ones just reported by *McKee*[5] from theoretical calculations at the 3-21G and 6-31G* ab initio levels. We now decide between the two structures.

We have been employing the combined ab initio/IGLO/NMR method for the solution of structural problems.[6] In this approach, various structures derived from experiment and from ab initio geometry optimizations, are assessed by means of IGLO (individual gauge for localized orbitals)[7]

[*] Prof. Dr. P. von R. Schleyer, Dipl.-Chem. M. Bühl,
Institut für Organische Chemie der Universität Erlangen-Nürnberg,
Henkestrasse 42, D-8520 Erlangen (FRG)

[**] This work was supported by the Deutsche Forschungsgemeinschaft, Fonds der Chemischen Industrie, Volkswagenwerk and the Convex Computer Corporation. Computer time was provided by the HLRZ Jülich. A grant of the Studienstiftung des deutschen Volkes for *M. B.* is gratefully acknowledged. We thank in particular Professor *W. Kutzelnigg* and his associates, *M. Schindler* and *U. Fleischer*, for the development of the IGLO program, the preparation and release of the Convex version, and extensive discussions and advice. We thank Professor *N. N. Greenwood* and Dr. *D. W. H. Rankin* for helpful comments and criticism.

Table 1. Geometric parameters for B_6H_{12} (bond distances in Å).

Cpd.	Level of theory	B1-B2	B1-B6	B2-B3	B2-B5	B2-B6	B1-H16	B6-H16	B2-H23	B3-H23
3a[a]	3-21G	1.918	1.804	1.842	1.747	1.775	1.464	1.245	1.375	1.306
	6-31G*	1.932	1.779	1.831	1.759	1.762	1.419	1.263	1.365	1.316
3b	3-21G[b]	1.939	1.761	1.829	1.792	1.741	1.388	1.273	1.291	1.357
	6-31G*	1.941	1.747	1.825	1.798	1.738	1.376	1.283	1.291	1.357
	MP2/6-31G*	1.899	1.728	1.786	1.784	1.714	1.354	1.294	1.289	1.361
	Exp. (GED)[c]	1.778	1.913	1.699	1.821	1.777	1.416	1.200	1.308	1.308

[a] False minimum at HF-levels, see text. [b] Ref. [5]. [c] Ref. [4].

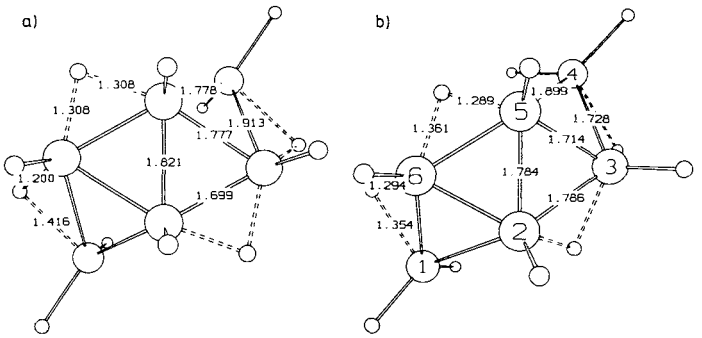

Fig. 1. Comparison of the GED (a) and MP2/6-31G* (b) structures of B_6H_{12}. Bond distances in Å, see Table 1.

NMR calculations. The chemical shifts obtained by this method for various geometries are compared with the experimental chemical shifts. Figure 2 shows the quality of the

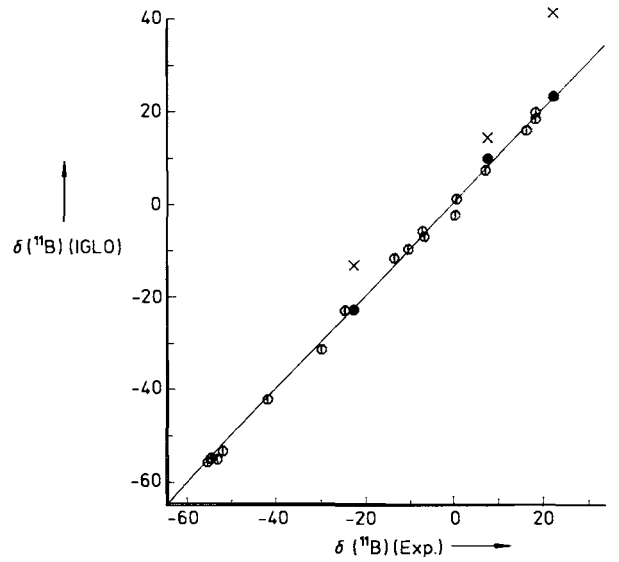

Fig. 2. Theoretical (IGLO) vs. experimental ^{11}B-NMR chemical shifts for boron hydrides. The IGLO DZ basis was used employing MP2/6-31G* optimized geometries. The ideal line with slope = 1.00 is shown. The IGLO B_6H_{12} boron chemical shifts obtained for the MP2/6–31G* structure (●) agree much better than those derived from the experimental geometry (x). Φ: B_2H_6, B_4H_{10}, B_5H_9, B_5H_{11}, B_6H_{10}, $B_2H_7^{\ominus}$, $B_3H_8^{\ominus}$, $B_4H_9^{\ominus}$ (IGLO DZ//MP2/6-31G*).

results for a collection of 9 boranes and borane anions. The geometries were calculated[8] at the MP2/6-31G* level, i.e. with a polarized basis set including electron correlation (Fig. 1b). Using these geometries, the agreement between experimental and IGLO chemical shifts is remarkably good[9] (the correlation coefficient is 0.999, the slope, 1.01, is nearly equal to the ideal value, and the standard deviation is only 1.4 ppm). In contrast, the experimental structures recommended by *Beaudet*[3] perform somewhat more poorly (correlation coefficient 0.990, slope 1.02, average deviation 4.2 ppm). We have now applied this combined ab initio/IGLO/NMR method to the B_6H_{12} structure problem.

At the time our geometry optimizations began, we were not aware of the GED structure. An assumed geometry was employed as the starting point and an optimization carried out using the small, split valence 3-21G basis set, with further refined reoptimization at the 6-31G* level (**3a**, key geometrical parameters in Table 1). As indicated by the IGLO results in Table 2, agreement of the chemical shifts using these geometries (which were shown to be minima by frequency analysis), did not give good agreement with experiment. Consequently, the structure was reoptimized at the MP2/6-31G* level. This gave somewhat different geometrical parameters (Fig. 1b, Table 1) and an excellent fit, IGLO vs. experiment (Table 2.).

Table 2. IGLO ^{11}B chemical shifts[a] (rel. $BF_3 \cdot OEt_2$) for B_6H_{12}.

Structure	Geometry	$\delta(^{11}B)$ [ppm] $B_{1,4}$		$B_{3,6}$		$B_{2,5}$	
B_6H_{12}	Exp. [b]	14.1		41.1		−13.3	
3a	3-21G	21.6		16.2		−10.9	
	6-31G*	15.5		17.2		−11.8	
3b	3-21G	14.5		22.5		−22.1	
	6-31G*	12.9		21.6		−22.4	
	MP2/6-31G*	9.6	[10.1]	22.9	[23.5]	−23.0	[−22.8]
	Exp.[c]	7.9		22.6		−22.6	

[a] In the IGLO calculations a Double Zeta (DZ) basis set was used, the values in brackets refer to calculations using a larger basis set of Triple Zeta + polarization quality, denoted as II', cf. Ref. [7]. [b] IGLO calculation carried out using the experimental geometry given in Ref. [4]. [c] Experimental chemical shifts, from I. S. Jaworiwsky, J. R. Long, L. Barton, S. G. Shore, *Inorg. Chem. 18* (1979) 56.

Puzzled by these discrepancies, we reran the 3-21G and 6-31G* optimizations using the MP2/6-31G* geometry as starting point. Indeed, new minima were obtained (**3b**) which were considerably lower in energy (ca. 27 kcal/mol^{-1}) than those obtained earlier. These lower energy minima are identical with those just reported by *McKee*.[5] The **3a** structure is a "false minimum", since it is only present at Hartree-Fock levels but disappears at a correlated level. To have two quite similar minimum energy structures (with the same symmetry), even at lower levels of theory, is unprecedented in our experience.

However, the geometrical parameters for our best theoretical structure, **3b** optimized at the MP2/6-31G* level (which was the only minimum found at that level) still differ appreciably from the GED data (Table 1). In the following, the

theoretical (MP2/6-31G*) and experimental (GED) structures are compared more critically.

The authors of the GED study pointed out an interesting structural relationship between the *arachno*-boranes B_4H_{10} **1**, B_5H_{11} **2**, and B_6H_{12} **3**.[4] The higher homologues can be thought of as arising from **1** by successive replacement of two bridging hydrogens by BH_2 groups. Figure 3 illustrates the

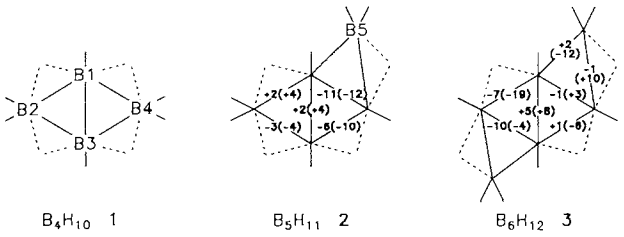

Fig. 3. The structural relationship between B_4H_{10} **1**, B_5H_{11} **2** and B_6H_{12} **3**. The changes in bond lengths (in pm) in going from **1** to **2** and from **2** to **3** are given for the MP2/6-31G* geometries (and in parentheses for the GED geometries). Notice the greater consistency of the calculated versus the experimental trends for **2** and **3**; see text.

changes in bond lengths (in pm) induced by each replacement, comparing the MP2/6-31G* and GED[4, 10] structures. Going from **1** to **2**, the replacement of one B-H-B bridge by a three-center B-B-B bond shortens the B1–B4 bond by ca. 11 pm, the adjacent B3–B4 bond by ca. 6–10 pm. Going from **2** to **3**, nearly the same "increments" are found for the corresponding bonds in the MP2 structures. In the GED structures, no analogous trend is apparent: changing the bridge between B2 and B3 in **2** from H to BH_2 mostly affects the B1–B2 distance (19 pm decrease); also, the position of the "bridging boron" B5 is considerably changed in the GED, but not in the MP2 structures. In summary, the structural relationship between **1**, **2** and **3** is more clearly visible and more consistent with the MP2 geometries.

A single point calculation at the MP2/6-31G* level on the experimental geometry shows this to be 59 kcal mol^{-1} less stable than the minimum! This enormous energetic difference strongly disfavors the GED geometry, and is in line with *McKee*'s calculations (the MP2/6-31G* energies of the GED and 3-21G structures differ by 56 kcal mol^{-1}). *McKee* also estimated the "energy loss" in the GED structure due to poor hydrogen placements to be about 37 kcal mol^{-1}.[5]

Finally, the δ values in the ^{11}B-NMR spectrum calculated for the GED structure show large deviations from the experimental chemical shifts (up to 18 ppm). For the GED structure of, e.g., B_5H_{11}, the agreement between IGLO and experiment was significantly better (maximum deviation ca. 4 ppm).[6f] The IGLO values for the false minimum **3a** also accord rather poorly with experiment (Table 2). The best agreement with the measured values, however, is found for the MP2/6-31G* geometry **3b**.

In summary, judging from structural, energetic, and NMR criteria, we conclude that the structural parameters of B_6H_{12} as derived from gas phase electron diffraction are not accurate, and that the MP2/6-31G* geometry most closely resembles the actual dimensions of B_6H_{12} both in the gas phase and in solution. Not only microwave spectroscopy, but also theoretical computations can be relied upon to provide accurate structures.

Received: April 9, 1990 [Z 3904 IE]
German version: *Angew. Chem. 102* (1990) 962

[1] a) S. G. Gibbins, I. Shapiro, *J. Am. Chem. Soc. 82* (1960) 2968; b) D. F. Gaines, R. Schaeffer, *Inorg. Chem. 3* (1964) 438.
[2] a) W. N. Lipscomb, *Inorg. Chem. 3* (1964) 1638; b) A. O. Clouse, D. C. Moody, R. R. Rietz, T. Roseberry, R. Schaeffer, *J. Am. Chem. Soc. 95* (1973) 2496.
[3] R. A. Beaudet, in J. F. Liebmann, A. Greenberg, R. E. Williams (Ed.): *Advances in Boron and the Boranes*, VCH, Weinheim 1988, p. 417, Chapter 20.
[4] R. Greatrex, N. N. Greenwood, M. B. Millikan, D. W. H. Rankin, H. E. Robertson, *J. Chem. Soc. Dalton Trans. 1988*, 2335.
[5] M. L. McKee, *J. Phys. Chem. 94* (1990) 435.
[6] For applications to carbocations see e.g. a) M. Schindler, *J. Am. Chem. Soc. 109* (1987) 1020; b) P. von R. Schleyer, J. W. de M. Carneiro, W. Koch, K. Raghavachari, *J. Am. Chem. Soc. 111* (1989) 5475; c) M. Bremer, P. von R. Schleyer, U. Fleischer, *J. Am. Chem. Soc. 111* (1989) 1147; d) M. Bremer, K. Schötz, P. von R. Schleyer, U. Fleischer, M. Schindler, W. Kutzelnigg, P. Pulay, *Angew. Chem. 101* (1989) 1063; *Angew. Chem. Int. Ed. Engl. 28* (1989) 1042; e) P. von R. Schleyer, W. Koch, B. Liu, U. Fleischer, *J. Chem. Soc. Chem. Commun. 1989*, 1098. For applications to boron compounds see f) P. von R. Schleyer, M. Bühl, U. Fleischer, W. Koch, *Inorg. Chem. 29* (1990) 153; g) P. von R. Schleyer, M. Bühl, *Angew. Chem. 102* (1990) 320; *Angew. Chem. Int. Ed. Engl. 29* (1990) 304.
[7] a) W. Kutzelnigg, *Isr. J. Chem. 19* (1980) 193; b) M. Schindler, W. Kutzelnigg, *J. Chem. Phys. 76* (1982) 1919. For a review of IGLO applications see c) W. Kutzelnigg, M. Schindler, U. Fleischer, *NMR. Basic Princip. Prog.* Springer Verlag, in press.
[8] Standard procedures and basis sets were used, cf. W. Hehre, L. Radom, P. von R. Schleyer, J. A. Pople, *Ab Initio Molecular Orbital Theory*, Wiley, New York, 1986. The MP2/6-31G* optimization was carried out using CADPAC: W. Amos, D. Rice, CADPAC: The Cambridge Analytic Derivatives Package, Issue 4.0, Cambridge, 1987.
[9] M. Bühl, P. von R. Schleyer in G. A. Olah, K. Wade, R. E. Williams (Eds.): *Electron Deficient Boron and Carbon Clusters*, Wiley, New York, in press.
[10] a) C. J. Dain, A. J. Downs, G. S. Laurenson, D. W. H. Rankin, *J. Chem. Soc. Dalton Trans. 4* (1981) 472; b) R. Greatrex, N. N. Greenwood, D. W. H. Rankin, H. E. Robertson, *Polyhedron 6* (1987) 1849.

Surprising Basicity of Low Valent Transition Metal Carbonyl Fluorides; Crystallographic Characterization of an sp^2-CH···F Hydrogen Bond**

By *Carolyn E. Osterberg, Margaret A. King, Atta M. Arif,* and *Thomas G. Richmond**

Although the chemistry of organic receptors for organic[1] and inorganic[2] guests is quite sophisticated, transition metal based reagents for molecular recognition have received little attention despite possibilities for diverse chemistry compared to wholly organic materials[3].

Hydrogen bonding is one important type of noncovalent interaction used in the design of molecular receptors. Although hydrogen bonding is frequently noted in crystallographic investigations of inorganic solids, only recently have solution equilibrium measurements demonstrated the high basicity of alkoxide ligands in low-valent transition-metal complexes.[4] In this work we report two synthetic routes to unusual carbonyl(fluoro)tungsten(II) complexes and demonstrate that the fluoro ligand rivals pyridine in its ability to hydrogen bond to phenols. A low temperature X-ray diffraction study provides evidence for an sp^2-CH···F hydrogen bond in the solid-state structure of **2**.

[*] Prof. T. G. Richmond, Dr. C. E. Osterberg, Dr. M. A. King, Dr. A. M. Arif
Department of Chemistry, University of Utah
Salt Lake City, Utah 84112 (USA)

[**] This research was supported by the National Science Foundation through a Presidential Young Investigator Award to *T.G.R.* (CHEM-895845), by the Enraf-Nonius Corporation (USA) (CHE-8811363), by the National Institutes of Health (NIH-BRSG), by the American Cancer Society (IN-178), and by the Camille & Henry Dreyfus Foundation (New Faculty Fellowship for *T.G.R.*).

As anticipated from our previous studies,[5] chelate assisted insertion of tungsten into an *ortho*-C–F bond of the unsymmetrical Schiff base ligand[6] **1** proceeds readily to afford the tungsten(II) complex **2** in 66% yield. Treatment of the chloride **3** with excess potassium fluoride affords **4** in 94%

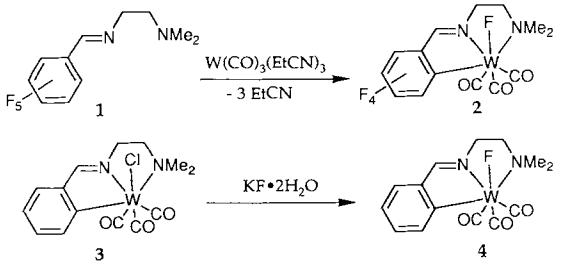

yield. The chelating monoanionic C,N,N′ ligand provides a relatively hard ligand environment for the W^{II} center.[7] This may be responsible for the high stability of these carbonyl(fluoro)metal complexes in contrast to tricarbonyl(cylopentadienyl)tungsten complexes which are unknown.[8]

Low-temperature (−140 °C) crystallographic characterization of **2** afforded a high-quality structure in which the imine hydrogen atom H1 bound to C10 was located and its position successfully refined as an isotropic contribution.[9] Examination of a unit cell of **2** (Fig. 1) revealed infinite chains by C10′–H1′···F–W interactions characterized by C10′–H = 0.98(9) Å, C10′···F = 3.099(5) Å, C10′–H1′···F = 172(7)° and H1′···F = 2.13(9) Å. This distance is significantly shorter than that defined by the H···F von der Waals[10] separation of 2.6 Å. We attribute the solid-state packing of this material to the ability of the coordinated fluoride to form an intermolecular hydrogen bond even to the weakly acidic proton on the imine carbon.[11] Of all the carbon–hydrogen bonds that have been postulated to participate in hydrogen bonding, those involving sp^2-CH groups have proved to be the most controversial.[12] However, weak interactions such as CH···X hydrogen bonds are frequently crucial in the three dimensional solid state packing of materials.[13] This result suggests that the coordinated fluoride remains a significantly basic site in this complex.[5, 6]

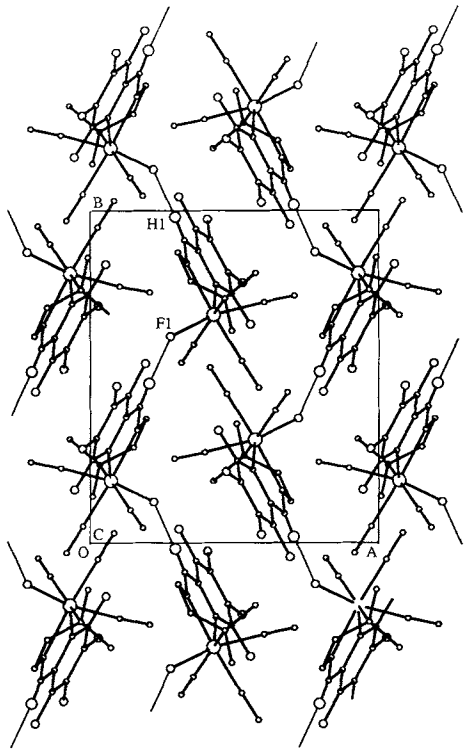

Fig. 1. PLUTO unit cell representation of **2** viewed down the *c*-axis. The intermolecular CH···F hydrogen bonds which link the molecules into chains are indicated by thin lines.

Accordingly, we have determined the equilibrium association of **2** and **4** with 4-chlorophenol in several solvents by observing the upfield shift of the ^{19}F-NMR signal assigned to the tungsten-bound fluorine as a function of phenol concentration. For the adduct **2**·4-chlorophenol in $(CD_3)_2CO$ an association constant of $K = 1\,M^{-1}$ was determined, but it increases to $K = 15\,M^{-1}$ in CH_2Cl_2, as derived from a Scatchard analysis of the titration data for 1:1 complexation.[14] Complex **4** is an even stronger base, with $K = 32\,M^{-1}$ in CH_2Cl_2 and $K = 330\,M^{-1}$ in toluene. Interaction of 4-chlorophenol with **4** is also signaled by appearance of a broad new ν_{OH} absorbance at 3177 cm^{-1} and increased terminal ν_{CO} bands for **4** in the infrared spectrum (Scheme 1).

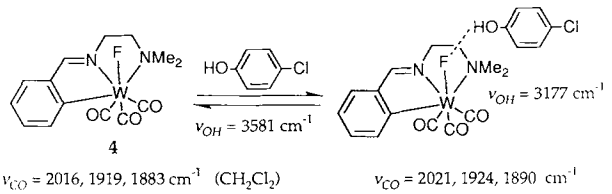

Scheme 1.

These results indicate that the tungsten(II) complexes **2** and **4** are surprisingly strong Lewis bases capable of forming strong hydrogen bonds.[15] Remarkably, the equilibrium constants reported above are in the same range as observed for pyridine/4-chlorophenol association in CCl_4.[16] We attribute the significant basicity of these low-valent metal fluorides to their electronically saturated 18-electron configuration and the lack of suitable vacant orbitals on the metal to accept π-electron density from the fluoride.[17] The propensity of the fluoride to engage in hydrogen bonding is one manifestation of the ionic character of the W^{II}–F bond. Thus, low-valent metal fluorides should be useful for the design of molecular receptors utilizing hydrogen bonding as a mode of recognition.

Experimental

2: Dissolution of 1.10 g (2.54 mmol) of $W(CO)_3(EtCN)_3$ and 0.676 g (2.54 mmol) of **1** in 25 mL of THF under a N_2 atmosphere gave a deep-red solution. After 0.5 h, the solution was evaporated to dryness to remove released EtCN and then 45 mL of THF was added. After stirring for 2 h, the solution was filtered in air and 0.896 g (1.67 mmol, 66.4%) of orange-gold crystals were obtained by addition of hexane and cooling to −10 °C. Selected characterization data: IR (THF) [cm^{-1}]: $\tilde{\nu}$ = 2020(s), 1934(vs), 1900(s); ^{19}F NMR (282 MHz) $(CD_3)_2CO$,CCl_3F): δ = −114.27 (dd,1F), −141.12 (dd, 1F), −154.12(dd, 1F), −164.46 (dd, 1F), −214.6 (br.s, 1F). C,H,N analysis.

4: A solution of **3** (3.42 g, 7.15 mmol) in 50 mL of THF was treated with excess KF · $2H_2O$ (1.35 g, 14.3 mmol). The mixture was stirred overnight, filtered in air and the filtrate concentrated by evaporation. The solid thus obtained was isolated on a glass frit and washed with 20 mL of water followed by 20 mL of Et_2O. Recrystallization from THF afforded 3.10 g (6.70 mmol) of **4** in 93.7% yield. Selected characterization data: ^{19}F NMR: δ = −229.2 (br, s). C,H,N analysis.

Received: March 8, 1990 [Z 3844 IE]
German version: *Angew. Chem. 102* (1990) 960

CAS-Registry-Numbers:
1, 126569-68-4; **2**, 128329-07-7; **3**, 126551-46-0; **4**, 126551-45-9; $W(CO)_3(EtCN)_3$, 84580-21-2; 4-chlorophenol, 106-48-9.

[1] D. J. Cram, *Angew. Chem. 98* (1986) 1041; *Angew. Chem. Int. Ed. Engl. 25* (1986) 1039; *ibid. 100* (1988) 1041 and *25* (1988) 1009; J. Rebek Jr., *ibid. 102* (1990) 261 and *29* (1990) 245.
[2] C. J. Pedersen, *Angew. Chem. 100* (1988) 1053; *Angew. Chem. Int. Ed. Engl. 27* (1988) 1021; H. M. Colquhoun, J. F. Stoddart, D. J. Williams, *ibid. 98* (1986) 483 and *25* (1986) 487.
[3] C. E. Osterberg, A. M. Arif, T. G. Richmond, *J. Am. Chem. Soc. 110* (1988) 6903; T. J. Meade, K. J. Takeuchi, D. H. Busch, *ibid. 109* (1987) 725.
[4] S. E. Kegley, C. J. Schaverien, J. J. Freudenberger, R. G. Bergman, S. P. Nolan, C. D. Hoff, *J. Am. Chem. Soc. 109* (1987) 6563; Y.-J. Kim, K. Osakada, A. Takenaka, A. Yamamoto, *ibid. 112* (1990) 1096.
[5] T. G. Richmond, C. E. Osterberg, A. M. Arif, *J. Am. Chem. Soc. 109* (1987) 8091.
[6] For Pt^{II} complexes containing the ligand **1**, see: C. M. Anderson, R. J. Puddephatt, G. Ferguson, A. J. Lough, *J. Chem. Soc. Chem. Commun. 1989*, 1297.
[7] G. Backes-Dahmann, K. Wieghardt, *Inorg. Chem. 24* (1985) 4049.
[8] W. Beck, K. Schloter, *Z. Naturforsch. B33* (1978) 1214.
[9] Crystal data for **2** at −140 °C: space group $P2_1/n$, $a = 10.903(4)$, $b = 12.387(3)$, $c = 11.374(3)$ Å, $\beta = 101.45(3)°$, $V = 1505.7$ Å^3, $Z = 4$, $\varrho_{calcd} = 2.356$ g/cm^3. Of 2751 unique reflections measured ($Cu_{K\alpha}$, $4.0 < 2\theta > 130.0$), 2527 had $I > 3\sigma(I)$ and were used in the solution and refinement with an empirical absorption correction ($\mu = 151.4$ cm^{-1}) applied. Final refinement (230 variables) gave $R = 0.0440$, $R_w = 0.0488$ and GOF = 4.03. Further details of the crystal structure investigationare available form the Director of the Cambridge Crystallographic Data Centre, University Chemical Laboratory, Lensfield Road, Cambridge CB2 1EW (UK), on quoting the full journal citation.
[10] A. Bondi, *J. Phys. Chem. 68* (1964) 441.
[11] For an intramolecular CH···F interaction see: J. A. K. Howard, S. A. R. Knox, N. J. Terrill, M. I. Yates, *J. Chem. Soc. Chem. Commun. 1989*, 640.
[12] R. D. Green: *Hydrogen Bonding by C-H Groups*, MacMillan, London 1984. W. C. Hamilton, J. A. Ibers: *Hydrogen Bonding in Solids*, Benjamin, New York 1968; R. Taylor, O. Kennard, *J. Am. Chem. Soc. 104* (1982) 5063.
[13] W. Tam, J. C. Calabrese, *Chem. Phys. Lett. 144* (1988) 79; J. A. R. P. Sarma, G. R. Desiraju, *Acc. Chem. Res. 19* (1986) 222; P. Seiler, G. R. Weisman, E. D. Glendening, F. Weinhold, V. B. Johnson, J. D. Dunitz, *Angew. Chem. 99* (1987) 1216; *Angew. Chem. Int. Ed. Engl. 26* (1987) 1175; M. C. Etter, P. W. Baures, *J. Am. Chem. Soc. 110* (1988) 639.
[14] Association constants were found to be reproducible within ± 5% in duplicate measurements. K. A. Connors, *Binding Constants*, Wiley, New York 1987.
[15] Cyclohexyl fluoride forms weak hydrogen bonds to phenol in CCl_4: R. West, D. L. Powell, L. S. Whatley, M. K. T. Lee, P. V. R. Schleyer, *J. Am. Chem. Soc. 84* (1962) 3221.
[16] J. Rubin, B. Z. Senkowski, G. S. Panson, *J. Phys. Chem. 68* (1964) 1601; J. Mullens, J. Yperman, J. P. Francois, L. C. Van Poucke, *ibid. 89* (1985) 2937.
[17] J. M. Mayer, *Comments Inorg. Chem. 8* (1988) 125.

O-Atom Insertion into Si–H Bonds by Dioxiranes: A Stereospecific and Direct Conversion of Silanes into Silanols**

By *Waldemar Adam*,* *Rossella Mello*, and *Ruggero Curci**

Dedicated to Professor Christoph Rückardt on the occasion of his 60th birthday

Dioxiranes **1** constitute a new class of reactive organic peroxides that possess great potential as oxidants.[1] Recently, we reported[2] on the efficient, highly stereoselective oxyfunctionalization of a variety of acyclic, cyclic, and polycyclic saturated hydrocarbons under extraordinary mild conditions, using solutions of methyl(trifluoromethyl)dioxirane.

Silanols serve as key intermediates in the preparation of useful "building blocks" in organosilicon chemistry.[3] Furthermore, in recent years there has been an increasing interest in optically active silanols, because they figure as useful drugs in experimental pharmacology,[4] e.g. optically active antimuscarinic agents of the sila-procyclidine type. Since the usual synthetic methodologies are encumbered by side products such as disiloxanes $R_3SiOSiR_3$,[5] there seems to be much need and interest in developing preparative methods to achieve the direct, stereoselective conversion of silanes into silanols.

For instance, by using peroxybenzoic acid, the conversion of **2c** into **3c** could be accomplished in only 49% yield;[6] ozonization of trialkylsilanes[7] afforded the corresponding silanols only as major products, by a pathway involving hydrotrioxides $R_3SiOOOH$ as intermediates.[8] We now report that silanes **2a–c**[9, 10] are quantitatively and stereospecifically converted into the corresponding silanols **3a–c**[10, 11] upon treatment with solutions of dioxirane **1a, b** at subambient temperatures [Eq. (1)]. Salient data are summarized in Table 1.

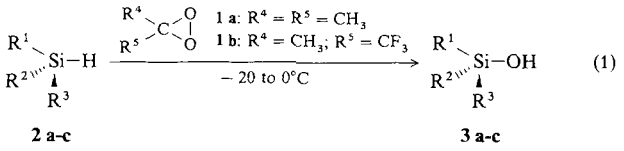

(1)

2 a-c **3 a-c**

a: $R^1 = R^2 = R^3 = Et$; **b**: $R^1 = Ph$, $R^2 = R^3 = Me$;
c: $R^1 = \alpha$-Naph, $R^2 = Ph$, $R^3 = Me$

To carry out the reaction a cold (−20 °C for **1b** and 0 °C for **1a**) standardized solution of the dioxirane **1**[2] (ca. 4 mmol) was quickly added to a cold solution of the silane **2** (ca. 4 mmol) in dry CH_2Cl_2. Capillary GC monitoring revealed ca. 100% conversion immediately on mixing of the partners (Table 1). Product isolation involved simply the removal of the volatile solvents at 10–20 °C/80–100 torr on a rotary evaporator. The IR and ^{1}H-NMR spectra[11] revealed that the isolated silanols were of high purity, obviating the necessity of further purification.

Kinetic runs (under second order reaction conditions) were performed at 0 °C by monitoring the disappearance of

Table 1. Reaction of the silanes **2a–c** with the dioxiranes **1a, b** leading to the silanols **3a–c**.

Substrate	Dioxirane	Solvent	*t* [min][a]	Yield [%][a]
Et_3SiH **2a**	**1b** [b]	CH_2Cl_2/TFP [c]	<1	≥98 **3a**
$PhMe_2SiH$ **2b**	**1b** [b]	CH_2Cl_2/TFP [c]	<1	≥98 **3b**
(+)α-Naph(Ph)(Me)SiH **2c** [e]	**1b** [b]	CH_2Cl_2/TFP [c]	<1	≥98 **3c** [d]
	1a [f]	CH_2Cl_2/acetone	18	≥98 **3c**

[a] Data refer to >98% conversion of the silane substrate (determined by GC, SE 54 capillary column, 30 m long and 0.25 mm i.d.). [b] The initial concentration of the dioxirane ranged from 0.6 to 0.7 M, the dioxirane to substrate ratio was ca. 1.0, ca. 4 mmol were used. [c] TFP = 1,1,1-trifluoropropanone, CH_2Cl_2:TFP = 4:1. [d] Viscous oil $[\alpha]_D = +20.0$ ($c = 7.0$, ether); Ref. [10]: $[\alpha]_D = +20.5$ ($c = 6.7$, ether). [e] 96.5% optical purity, $[\alpha]_D = +32.5$ ($c = 4.0$, cyclohexane), Ref. [10]: $[\alpha]_D = +33.7$ ($c = 4.0$, cyclohexane). [f] Initial dioxirane concentration was 0.03–0.04 M, dioxirane to substrate ratio ca. 1.2, ca. 4 mmol were used.

[*] Prof. Dr. W. Adam, Dr. R. Mello
Institut für Organische Chemie der Universität
Am Hubland, D-8700 Würzburg (FRG)
Prof. Dr. R. Curci
CNR Centre "Metodologie Innovative di Sintesi Organiche",
Chemistry Department, University of Bari,
Via G. Amendola 173, I-70126 Bari (Italy)

[**] This work was generously supported by the Deutsche Forschungsgemeinschaft (SFB Nr. 347 "Selektive Reaktionen Metall-aktivierter Moleküle") and the Fonds der Chemischen Industrie. *R. M.* thanks the Alexander-von-Humboldt Foundation for a postdoctoral fellowship (1989–1990).

the silane **2c** (initial concentration 0.02 to 0.04 M) via capillary GC analysis, after eliminating the dioxirane **1a,b** with PhSMe as already described.[2] Satisfactory second-order rate plots (log[(a − x)/(b − x)] versus t) were obtained, from which the rate constant ($k_2 = 0.78\ M^{-1}\ s^{-1}$) for the oxidation of **2c** with **1a** was determined. Under the same conditions, dioxirane **1b** afforded $k_2 = 450\ M^{-1}\ s^{-1}$, i.e. over 550 times more reactive than dioxirane **1a** towards **2c**.

In competition experiments,[2] the dioxirane oxidations of Et_3SiH **2a** and adamantane were investigated. It was found that **2a** was ca. 200-fold more easily hydroxylated by dioxirane **1a** than the adamantane C–H bridgehead positions, while dioxirane **1b**, a more powerful oxidant, reacted ca. 56-fold faster with **2a** than with adamantane. Since Si–H bonds are considerably weaker than C–H bonds (bond energies ca. 77. kcal mol^{-1} and 99 kcal mol^{-1}), it is understable that oxyfunctionalization by dioxiranes is remarkably easier with silanes than hydrocarbons. Employing the same competition technique, a kinetic isotope effect of $k_H/k_D = 2.6$ (at 0 °C) was determined for the oxyfunctionalization of Et_3SiH versus Et_3SiD[15] by dioxirane **1a**.

Concerning mechanistic implications, the modest size of the H/D kinetic isotope effect and the fact that oxyfunctionalization of Si–H bonds by dioxiranes occurs with complete retention of configuration suggest that free silyl radicals ($R_3Si^{\bullet}$) do not intervene in this oxygen transfer process. Although silyl radicals possess considerable configurational stability, complete retention of configuration is unlikely in radical processes;[12] for example, the photolysis of (−)-α-NaphPhMeSiOCOCH$_3$ in CCl_4 affords α-NaphPhMeSiCl in 64% optical purity[12]. On the other hand, it is known that the insertion of dichloro- or dibromocarbenes into the Si–H bond of (+)-**2c** proceeds with more than 95% retention of configuration.[13] Moreover, the isotope effect observed presently for the oxygen atom insertion into Et_3SiH by dioxirane **1a** ($k_H/k_D = 2.6$) is quite similar to that reported for the insertion of dichlorocarbene[14] into nBu$_3$SiH ($k_H/k_D = 1.23$), but quite distinct from that found in the electrophilic attack of ozone on nBu$_3$SiH ($k_H/k_D = 6.9$)[15] to give silyl hydrotrioxides. Therefore, as for the carbene insertions, an oxene mechanism is proposed for the hydroxylation of silanes by dioxiranes, which is analogous to the "butterfly" three-centered transition state **4** suggested for the oxyfunctionalization of hydrocarbons by dioxiranes.[2] The alternative five-centered transition state **4'** is consistent with all the presently acquired experimental facts on this novel oxygen insertion process, in which the attacking species is the dioxy diradical derived from peroxide bond cleavage of the dioxirane.[16] For this to apply, however, a prerequisite is that the peroxide bond homolysis is not rate determining, otherwise, the observed second-order rate law (i.e. first-order in both dioxirane and silane) would not be consistent with the proposed **4'**.

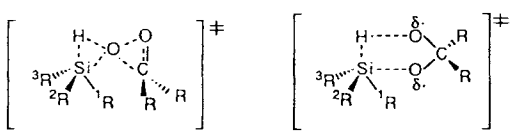

4 **4'**

We conclude that the oxene mechanism is most consistent with the present experimental facts for the oxyfunctionalization of silanes. More significant from the preparative point of view is that a convenient, efficient, and stereospecific direct conversion of silanes **2** into silanols **3** has been made available for synthetic chemistry.

Received: March 23, 1990 [Z 3871 IE]
German version: *Angew. Chem. 102* (1990) 916

CAS-Registry-Numbers:
1a, 74087-85-7; **1b**, 115464-59-0; **2a**, 617-86-7; **2b**, 776-76-1; **2c**, 1025-09-8; **3a**, 597-52-4; **3b**, 5272-18-4; **3c**, 1028-62-2.

[1] For reviews, see: a) W. Adam, R. Curci, J. O. Edwards, *Acc. Chem. Res. 22* (1989) 205; b) R. W. Murray, *Chem. Rev. 89* (1989), 1187; c) R. Curci in A. L. Baumstark (Ed): *Advances in Oxygenated Processes Vol. 2*, JAI Press, Greenwich (CT) 1990, chapter I.
[2] R. Mello, M. Fiorentino, C. Fusco, R. Curci, *J. Am. Chem. Soc. 111* (1989) 6749.
[3] R. Corriu, C. Guerin, J. Moreau, *Top. Stereochem. 15* (1984) 43.
[4] R. Tacke, H. Linoh, L. Ernst, U. Moser, E. Mutschler, S. Sarge, H. K. Cammenga, G. Lambrecht, *Chem. Ber. 120* (1987) 1229.
[5] G. L. Larson, L. del Valle, *Synth. React. Inorg. Met. Org. Chem. 11* (1981) 173.
[6] L. H. Sommer, L. A. Ulland, G. A. Parker, *J. Am. Chem. Soc. 94* (1972) 3469.
[7] P. S. Bailey in H. H. Wasserman (Ed.): *Ozonization in Organic Chemistry, Vol. 2*, Academic Press, New York 1982, p. 329.
[8] E. J. Corey, M. M. Mehrotra, A. U. Khar, *J. Am. Chem. Soc. 108* (1986) 2472.
[9] (+)-**2c** (Table 1) was obtained by $LiAlH_4$ reduction of (−)-α-naphthylphenylmethylmenthoxysilane with $LiAlH_4$ [10]; the silanes **2a, b** are commercially available.
[10] L. H. Sommer, C. L. Frye, G. A. Parker, K. W. Michael, *J. Am. Chem. Soc. 86* (1964) 3271.
[11] The isolated silanols are all known compounds and were spectrally identified.
[12] a) A. G. Brook, J. M. Duff, *J. Am. Chem. Soc. 91* (1969) 2118; b) H. Sakurai, M. Murakami, M. Kumada, *ibid. 91* (1969) 519.
[13] A. G. Brook, J. M. Duff, D. G. Anderson, *J. Am. Chem. Soc. 92* (1970) 7567.
[14] L. Spialter, W. A. Swansiger, L. Pazdernik, M. E. Freeburger, *J. Organomet. Chem. 27* (1971) C25.
[15] L. Spialter, L. Pazdernik, S. Bernstein, W. A. Swansiger, G. R. Buell, M. E. Freeburger, *Adv. Chem. Ser. 112* (1972) 65.
[16] S. A. Kafafi, R. I. Martinez, J. T. Herron in J. F. Liebman, A. Greenberg (Ed.): *Modern Models of Bonding and Delocalization*, VCH, FL-Deerfield Beach 1988.

Synthesis and Molecular Structure of *cis*-[Pd(C$_6$F$_5$)$_2$(C$_6$H$_5$CH$_2$NMe$_2$)], an Intramolecular Coordination Compound Containing an Unusual η^1-Arene Ligand

By *Larry R. Falvello, Juan Forniés,* Rafael Navarro, Violeta Sicilia,* and *Milagros Tomás*

Several arene bonding modes to transition-metal centers have been described. A wide range of η^6-arene complexes are known, and well-defined species with η^3- and η^1-arene bonding have also been prepared.[1] However, the η^3- and η^1-arene coordination types are very scarce. In fact, the platinum phenalenyl complex **A** (Scheme 1) is, as far as we know, the only example in which an η^3-arene coordination mode has been confirmed by X-ray structure determination.[2]

[*] Prof. J. Forniés, Dr. R. Navarro, Dr. V. Sicilia, Dr. M. Tomás
Departamento de Química Inorgánica
Instituto de Ciencia de Materiales de Aragón
Universidad de Zaragoza
E-50009 Zaragoza (Spain)
Dr. L. R. Falvello
Department of Chemistry and
Laboratory for Molecular Structure and Bonding
Texas A & M University, College Station TX (USA)

[**] This work was supported by the Comisión de Ciencia y Tecnología. *V.S.* thanks Ibercaja for a research grant.

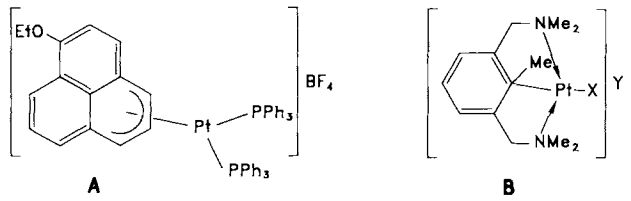

Scheme 1. **B**, X = I, Y = BF_4; X = *o*-tolyl, Y = I.

Concerning the very scarce η^1-arene coordination, two different types of structures have been reported. One contains a boat-type aryl ring which can be considered as a σ-metal-substituted arenium ion and in which a rehybridization of some of the sp^2 C centers has taken place; for example, compounds of type **B**.[3] The other contains planar aryl rings in which all the C atoms are sp^2-hydridized; for example, $AgB_{11}CH_{12} \cdot 2C_6H_6$[4] and $[Cr\{NMes(BMes_2)\}_2]$[5] (Mes = mesityl).

In the course of our research into the chemistry of *C,N*-cyclopalladated derivatives,[6] we have studied the reaction of *cis*-$[Pd(C_6F_5)_2(thf)_2]$[7] with $C_6H_5CH_2NMe_2$ (benzyldimethylamine is a typical starting material for the synthesis of the *ortho*-palladated structural unit $H_4\overline{C_6\text{-}CH_2\text{-}Me_2N}\text{-}Pd$). This process [Eq. (a)] leads to **1**, which, as established by an X-ray study, is an unprecedented palladium complex displaying η^1-arene coordination.

$$cis\text{-}[Pd(C_6F_5)_2(thf)_2] + C_6H_5CH_2NMe_2 \xrightarrow{CHCl_3} cis\text{-}[Pd(C_6F_5)_2(C_6H_5CH_2NMe_2)] + 2THF \quad (a)$$

The IR spectrum of **1** shows two bands (795, 784 cm^{-1}) assignable to the X-sensitive mode of the C_6F_5 groups,[8] which retain their *cis* positions through reaction (a). The ^{19}F NMR spectrum of **1** indicates that the two C_6F_5 groups are inequivalent.

The structure of **1**, established by a single-crystal X-ray diffraction analysis,[9] is shown in Figure 1. The palladium atom has a distorted square-planar environment formed by C1 and C1′, the *ipso*-C atoms of *cis*-C_6F_5 groups, and the N and C7 (*ipso*-C) atoms of the amine ligand. One effect of the unexpected *C,N*-chelating nature of benzyldimethylamine is to provide an acute N–Pd–C7 angle of 64.4(3)°. The Pd–C_6F_5 distances and the C1–Pd–C1′ angle are similar to those observed in *cis*-$[Pd(C_6F_5)_2\{S_2CP(C_6H_{11})_3\}]$.[10]

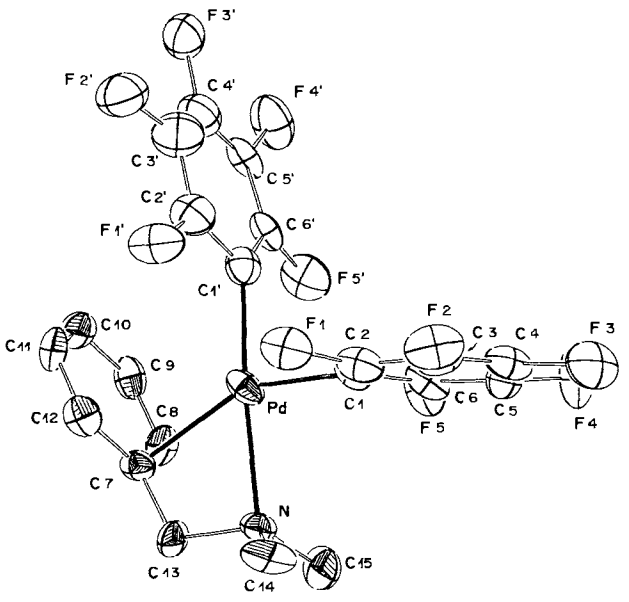

Fig. 1. Molecular structure of complex **1**. Selected bond lengths [Å] and bond angles [°]: Pd-C1 1.957(8), Pd-C1′ 2.022(11), Pd-N 2.314(6), Pd-C7 2.335(7); C1-Pd-C1′ 88.6(2), C1-Pd-N 88.0(3), C7-Pd-N 64.4(3), C13-C7-Pd 88.9(5), C12-C7-Pd 86.2(5), C8-C7-Pd 90.4(5).

The coordination mode of the phenyl ring to the palladium atom is noteworthy. The shortest Pd–C(phenyl) distance is that corresponding to Pd-C7 (2.335(7) Å). This value is higher than that corresponding to a σ Pd bond (1.9–2.1 Å) and lower than the Pd–C distances observed in the η^2-arene complex **C** (2.571(4) and 2.433(3) Å).[11] The long Pd–C8 (2.706(8) Å) and Pd–C12 (2.663(9) Å) distances exclude an η^3-coordination to the palladium center.[2] The dihedral angle between the C_6H_5 plane and the best least-squares plane through Pd-N-C1-C1′ (plane A) is 92.75(28)°. Atom C7 lies essentially on plane A, its mean position being 0.028 Å form the plane.[12]

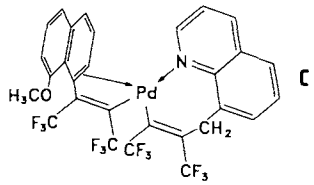

C

Moreover, the C_6H_5 ring is planar and all C–C bond lengths and C–C–C bond angles are the same within experimental error. That is an unexpected structural feature for an η^x (x ≠ 6) arene group bonded to a transition-metal center. Because of the coordination we should expect a deformation of the ring. As can be seen from the structural data, the arene ring is η^1-coordinated to the palladium atom in a similar way to that previously observed for $AgB_{11}CH_{12} \cdot 2C_6H_6$ (Ag–η^1-C distance = 2.400(7) Å)[4] and $[Cr\{NMes(BMes_2)\}_2]$ (Cr–η^1-C distances = 2.391(15) and 2.383(15) Å).[5] This structure differs significantly from the structures shown by the platinum η^1-arene complexes **B**,[3] which display a small but noticeable "boat" type puckering of the ring, and the Pt–C distances (2.183(7) and 2.293(9) Å) are shorter than the Pd–C7 distance in **1**.[13]

Concerning the bonding mode between the ring and the Pd center, several points are to be noted. (1) The values of the angles C13–C7-C12 (118.9(7)°), C8-C7-C12 (117.7(8)°), and C13-C7-C8 (123.1(8)°) indicate that the C7 atom is sp^2 hybridized. (2) C7 is basically in the plane A. (3) The Pd–C7 bond is almost perpendicular to the aryl ring plane (the deviation from the perpendicularity being only 3.72(29)°).[11] Consequently, the p(π) orbital of C7, which is perpendicular to the plane of the aryl ring, must be responsible for the interaction with the palladium center.

The study of the reactivity of **1**, including its role as a potential intermediate in an *ortho*-metalation process is in progress.

Experimental Procedure

To a solution of *cis*-$[Pd(C_6F_5)_2(thf)_2]$ (0.30 g, 0.51 mmol) in $CHCl_3$ (20 mL) at room temperature was added $C_6H_5CH_2NMe_2$ (77 μL, 0.51 mmol), and the mixture was stirred at room temperature for 30 min. After evaporation to dryness and addition of *n*-hexane (30 mL) a pale yellow solid was isolated and identified as **1**; 74% yield. Correct C, H, N elemental analysis. IR (Nujol): $\tilde{\nu}$ [cm^{-1}]: C_6F_5: 1495 vs, 1054 vs, 795 s, 784 s; $C_6H_5CH_2NMe_2$: 1374 s, 1352 s, 840 s, 746 vs, 700 s. NMR spectra in $CDCl_3$. ^1H m (200 MHz): δ = 7.79 (d, 2H, *o*-phenyl-H) 7.42 (t, 2H, *m*-phenyl-H), 7.18 (t, 1H, *p*-phenyl-H), 4.04 (s, 2H, $-CH_2-$), 2.61 (s,6H, NMe_2). ^{19}F NMR (188 MHz, standard $CFCl_3$): δ = −117.2 (*o*-F); −160.5, −161.2 (*p*-F); −163.8, −164.7 (*m*-F). Complex **1** is nonconducting in an acetone solution ($c \approx 5 \times 10^{-4}$ M).

Received: March 6, 1990 [Z 3839 IE]
German version: *Angew. Chem.* **102** (1990) 952

[1] a) F. A. Cotton, G. Wilkinson: *Advanced Inorganic Chemistry*, 5th ed., Wiley, New York 1988, p. 1177; b) E. L. Muetterties, J. R. Bleeke, E. J. Wucherer, T. A. Albright, *Chem. Rev. 82* (1982) 499.
[2] A. Keasey, P. M. Bailey, P. M. Maitlis, *J. Chem. Soc. Chem. Commun. 1978*, 142.
[3] a) G. van Koten, K. Timmer, J. G. Noltes, A. L. Spek, *J. Chem. Soc. Chem. Commun. 1978*, 250; b) D. M. Grove, G. van Koten, J. N. Louwen, J. G. Noltes, A. L. Spek, H. J. C. Ubbels, *J. Am. Chem. Soc. 104* (1982) 6609; c) J. Terheijden, G. van Koten, I. C. Vinke, A. L. Spek, *ibid. 107* (1985) 2891.
[4] K. Shelly, D. C. Finster, Y. J. Lee, W. R. Scheidt, C. A. Reed, *J. Am. Chem. Soc. 107* (1985) 5955.
[5] R. A. Barlett, H. Chen, P. P. Power, *Angew. Chem. 101* (1989) 325; *Angew. Chem. Int. Ed. Engl. 28* (1989) 316.
[6] a) J. Forniéss, R. Navarro, V. Sicilia, *Polyhedron 7* (1988) 2659; b) J. Forniés, R. Navarro, V. Sicilia, M. Tomás, *Inorg. Chim. Acta 168* (1990) 201.
[7] R. Usón, J. Forniés, M. Tomás, B. Menjón, *Organometallics 4* (1985) 1912.
[8] J. Maslowsky, Jr.: *Vibrational Spectra of Organometallic Compounds*, Wiley, New York 1977, p. 438 and references therein.
[9] Suitable crystals for X-ray study were obtained by slow diffusion at 5 °C of *n*-hexane into a solution of **1** in CH_2Cl_2. Crystal data: monoxlinix, $a = 21.0836(23)$, $b = 8.0959(10)$, $c = 13.6030(20)$ Å, $\beta = 114.690(8)°$, $V = 2109.65$ Å^3. Size: $0.25 \times 0.75 \times 0.35$ mm, $\mu(Mo_{K\alpha}) = 9.12$ cm^{-1}. Data reduction included an absorption correction (maximum and minimum transmission factors, 0.7211 and 0.5471, respectively). Siemens/STOE AED2 four-circle diffractometer. $\omega-2\theta$ scan technique at room temperature; scan range, $4 \le 2\theta \le 50°$. Total number of reflections, 4000; 2660 unique reflections with $F_o \ge 6\sigma(F_o)$ used for all calculations; $Z = 4$. Systematic absences: (*hkl*): $h + k \neq 2n$ and (*h* 0*l*): $1 \neq 2n$, consistent with either of the space groups *C*2/*c* and *Cc*. Successful refinement and detailed analysis of the structure established the space group as *Cc*. The positions of the central Pd atom and the immediately ligated atoms were found by direct methods [14] under the assumption of space group *C*2/*c*. Further development was possible only in the acentric group *Cc*. The structure has pseudosymmetry with one C_6F_5 ligand related to the other by approximate local twofold symmetry. The $C_6H_5CH_2NMe_2$ ligand, however, is clearly and unambiguously inconsistent with the presence of overall twofold symmetry. Since the bisector of the R–Pd–R angle is roughly parallel to the crystallographic *b* axis, we expected and observed a modest degree of correlation between some pairs of corresponding parameters of the two C_6F_5 groups in the final least-squares refinement of the structure. We thus applied loose observational restraints [15] on interatomic distances in the C_6F_5 groups. The correlation was not so serious as to preclude full anisotropic refinement of the structure, with 296 variables in full-matrix least-squares analysis. The final residuals for the correct enantiomorph are $R = 0.0590$. Further details of the crystal structure investigation are available form the Cambridge Crystallographic Data Centre, University Chemical Laboratory, Lensfield Road, Cambridge CB2 1EW (England), on quoting the full journal citation.
[10] R. Usón, J. Forniés, M. A. Usón, J. F. Yagüe, P. G. Jones, K. Meyer-Base, *J. Chem. Soc. Dalton Trans. 1986*, 947.
[11] H. Osser, M. Pfeffer, J. T. B. H. Jastrzebski, C. H. Stam, *Inorg. Chem. 26* (1987) 1169.
[12] M. Nardelli, *Comput. Chem. 7* (1983) 95.
[13] The covalent radii for Pt^{II} and Pd^{II} in a square-planar environment are virtually identical. F. R. Hartley: *The Chemistry of Platinum and Palladium*, Applied Science, London 1973, p. 8.
[14] G. M. Sheldrick, SHELX-86, Universität Göttingen, 1986.
[15] a) G. M. Sheldrick, SHELX-76 "Program of Crystal Structure Determination", University of Cambridge, Cambridge (England) 1976; b) J. Waser, *Acta Crystallogr. 16* (1963) 1091.

Bis(pentamethylcyclopentadienyl)silylene as Ligand in Gold(I) Chloride Complexes**

By *Peter Jutzi** and *Andreas Möhrke*

Dedicated to Professor Edwin Hengge on the occasion of his 60th birthday

After the discovery of complexes containing terminal carbene ligands,[1] there was no lack of efforts to prepare complexes in which divalent homologues of carbon were bonded as ligands to transition metals. The first germylene,[2] stannylene,[3] and plumbylene complexes[4] were followed by further representatives. Thus, these complexes now constitute a well-investigated and well-established class of compounds (type **A**).[5]

$R_2E \rightarrow ML_n$ **A**, E = C, Ge, Sn, Pb

So far, however, all attempts to prepare silylene (silanediyl) complexes analogous to carbene complexes have failed.[6] In the course of our investigations concerning the chemistry of decamethylsilicocene (**1**),[7] we have now succeeded in synthesizing the first such compound.

Reaction of **1** with carbonylgold(I) chloride in toluene at about -90 °C results in loss of CO and formation of [bis(pentamethylcyclopentadienyl)silanediyl]gold chloride (**2**) [Eq. (1)] in good yield. The silylene complex **2**, obtained as a

$$\underset{\mathbf{1}}{(\pi\text{-}Me_5C_5)_2Si} + (CO)AuCl \xrightarrow[-CO]{} \underset{\mathbf{2}}{[(\sigma\text{-}Me_5C_5)(\pi\text{-}Me_5C_5)SiAuCl]} \quad (1)$$

very dark red powder, is extremely sensitive to air and moisture and readily soluble in aprotic organic solvents such as toluene, benzene, and chloroform. The structure of **2** was established unambiguously by NMR spectroscopy, mass spectrometry and elemental analysis.

The chemical shifts in the ^{29}Si NMR spectra of **1** and **2** differ markedly. Whereas a resonance at unusually high field ($\delta = -398$) is found for **1**,[7] the ^{29}Si NMR signal for **2** lies at $\delta = +82.8$, in a region characteristic for unsaturated, low-coordinated silicon compounds (silaethenes and disilenes).[8]

Interestingly, the two pentamethylcyclopentadienyl (Cp*) ligands are differently coordinated to the silicon atom in the silylene complex **2**. This is revealed by the temperature-dependent ^{1}H NMR spectra, which indicate the presence of a σ- and a π-bonded Cp* ligand. The σ-bonded ligand gives rise to three broadened signals in a 2:2:1 ratio; at lower temperature (-60 °C) these signals clearly show fine structure. This is characteristic for σ-Cp* systems that undergo a slow sigmatropic rearrangement.[9] The π-bonded Cp* ligand gives rise, as expected, to only one signal for all methyl groups, even at low temperature. The ^{13}C NMR data for **2** are also in accord with the Cp* bonding described here (see *Experimental Procedure*). The exact hapticity of π-bonded Cp* ligands cannot generally be determined from NMR spectra. However, X-ray analysis of the structurally comparable germylene complexes $[(\pi\text{-}Me_5C_5)(Cl)GeW(CO)_5]$ and $[(\pi\text{-}Me_5C_5)\{(Me_3Si)_2CH\}GeW(CO)_5]$ has shown a dihapto coordination.[10] Examination of models supports such a mode of coordination for the π-Cp* ligand in **2** as well.

The bonding in **2** corresponds qualitatively to that in carbene complexes of the Fischer type. In the latter, the electron deficit of the carbene carbon is reduced primarily by transfer of electron density from nonbonding orbitals of heteroatoms in the α position. In the silylene complex **2**, a π ligand acts as the electron donor.

The π-bonding components in the Cp^*_2Si unit of **2** are overall significantly less than those in **1**. Presumably, the resulting electron deficit at the Si atom is at least partly compensated by electron withdrawal from the Au atom through (d–p) π back-bonding.

In the compounds of carbon homologues, the tendency for irreversible coordination of a donor molecule is very pro-

[*] Prof. Dr. P. Jutzi, Dr. A. Möhrke
Fakultät für Chemie der Universität
Universitätsstrasse, D-4800 Bielefeld (FRG)

[**] According to IUPAC rules, carbene (CH_2) homologues should have the suffix -diyl (i.e., silanediyl, stannanediyl, etc.). However, the names silylene, stannylene, etc., in analogy to methylene, are still commonly used in the chemical literature.

nounced and results in formation of donor-stabilized complexes of type **B** (ylide complexes).[5] This class of compounds now also includes examples with silicon; numerous interesting and readily accessible complexes have been reported, especially in recent years.[11]

$R_2E \rightarrow ML_n$ **B** E = C, Si, Ge, Sn, Pb
↑
donor

The silylene complex **2** can be very easily converted into the corresponding complex of type **B**. Thus, reaction of **2** with *tert*-butyl cyanide and with pyridine affords compounds **3** and **4**, respectively. These complexes can also be prepared directly from decamethylsilicocene (**1**), as shown by the reactions of **1** with (*tert*-butyl cyanide)- and pyridinegold(I) chloride [Eq. (2)].

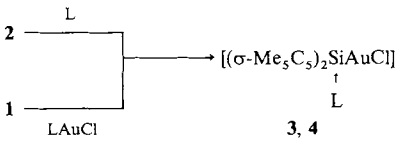

(2)

3, L = *t*-C_4H_9NC; **4**; L = C_5H_5N

The compounds, obtained as colorless (**3**) or brown (**4**) crystals, were characterized unambiguously by spectroscopy and elemental analysis. The ^1H NMR spectra reveal that, in both cases, the two Cp* ligands are σ-bonded and the fluxional process is more rapid than in **1**. The additional coordination of a σ-donor ligand apparently obviates the necessity of π coordination of Cp* ligands. In comparison to **2**, the ^{29}Si NMR signals of **3** and **4** are shifted slightly to higher field and lie in the expected range.[12] In the ^{13}C NMR spectrum of **3**, the electrophilic character of the Si atom is reflected in a significant downfield shift of the signal of the cyanide C atom.[13]

Complexes **2**, **3**, and **4**, described here for the first time, clearly exemplify that the Cp* ligand can be used as required in compounds of low-valent main-group elements by change in hapticity ($\eta^5 \rightarrow \eta^1$). In addition, the bulky σ-bonded Cp* ligand also provides for kinetic stabilization.[14]

Experimental Procedure

2: A solution of **1** (1.47 g, 4.92 mmol) in toluene (20 mL) was added to a stirred suspension of carbonylgold(I) chloride (1.28 g, 4.92 mmol) in toluene (15 mL) at − 90 °C, and the reaction mixture was stirred for 1 h. The resulting deep red solution was allowed to warm to about − 20 °C, reduced in volume to ca. 15 mL, and treated slowly with 15 mL of *n*-pentane. Compound **2**, thereby obtained as a deep red powder, was washed with *n*-pentane and dried under vaccum. Yield 2.01 g (77%), m. p. 88–90 °C (dec.). ^1H NMR (300.1 MHz, $CDCl_3$, TMS): δ = 1.25, 1.74, 1.79 (s, broad, 3H:6H:6H, σ-C_5Me_5), 1.98 (s, 15H, π-C_5Me_5). ^{13}C NMR (75.4 MHz, $CDCl_3$, TMS): δ = 11.6, 14.6, 21.1 (broad, σ-C_5Me_5), 59.2 (broad, "allyl"(σ-C_5Me_5)), 135.0, 136.5, (broad, "vinyl"(σ-C_5Me_5)) 13.7 (s, π-C_5Me_5), 127.4 (s, π-C_5Me_5). ^{29}Si NMR (59.6 MHz, $CDCl_3$, TMS): δ = + 82.8. MS (70 eV): *m/z* 530 [$M^{\oplus}$, 1%], 395 [$M^{\oplus}$ − C_5Me_5, 1], 233 [$AuCl^{\oplus}$, 7], 163 [C_5Me_5Si, 100]. Correct C, H, Cl elemental analysis.

3, **4**: a) From **2**: A stirred solution of **2** (594 mg, 1.12 mmol) in toluene (7 mL) at 0 °C was treated with an equimolar amount of *tert*-butyl cyanide or pyridine. After a few seconds (**4**) or within several hours (**3**), the deep red solution changed color. Removal of the solvent, extraction into *n*-hexane, filtration, and crystallization led to colorless **3** (80%) or brown **4** (36%). b) From **1**: A solution of (*tert*-butyl cyanide)gold(I) chloride (1.70 g, 5.4 mmol) or pyridinegold(I) chloride (1.68 g, 5.4 mmol) in toluene (10 mL) was added to a solution of **1** (1.62 g, 5.4 mmol) in toluene (10 mL) at 0 °C. After stirring for several hours, the reaction mixture was allowed to warm to room temperature, and the volatile components were removed under vacuum; the residue was then redissolved in toluene and the solution filtered. Recrystallization at about − 60 °C afforded **3** (78%) or **4** (62%). Recrystallization from *n*-hexane/toluene (4/1) led to analytically pure products. **3**: m. p. 110 °C (dec.). ^1H NMR ($CDCl_3$): δ = 1.54 (s, 9H, CMe_3), 1.68 (broad, 30H, C_5Me_5). 1H NMR ([D_8]toluene, − 60 °C): δ = 0.31 (s, 9H, CMe_3), 1.87, 1.92, 1.96, 2.32, 2.54 (s, 6H:6H:6H.6H:6H, C_5Me_5). 1H NMR ([D_8]toluene, + 60 °C): δ = 0.65 (s, 9H, CMe_3), 1.93 (s, 30H, C_5Me_5). ^{13}C NMR ($CDCl_3$):δ = 13.5 (broad, C_5Me_5), 29.7 (CMe_3), 57.8 (CMe_3), 134.5 (very broad, CMe_5), 165.0 (CN-CMe_3). ^{29}Si NMR ($CDCl_3$):δ = + 71.2. IR (CsI): $\tilde{\nu}$[cm^{-1}] = 2231, 2208 (N≡C). Correct C, H, N elemental analysis. Molecular mass (cryoscopic in benzene): 621 g mol^{-1} (calcd 614.1 g mol^{-1}) **4**: m. p. 72–74 °C ^1H NMR ($CDCl_3$): δ = 1.74 (s, broad, 30H, CMe_5), 7.56, 7.90, 8.49 (m, 2H:2H:1H, C_5H_5N). ^{13}C NMR ($CDCl_3$): δ = 13.6 (broad C_5Me_5), 65.7 (allyl-C_5Me_5), 125.9 (C_5H_5N), 135.8 (broad, vinyl-C_5Me_5), 139.2, 150.0 (C_5H_5N). ^{29}Si NMR ($CDCl_3$): δ = + 54.3. Correct C, H, N elemental analysis.

Received: January 23, 1990 [Z 3753 IE]
German version: *Angew. Chem. 102* (1990) 913

CAS Registry numbers:
1, 100189-23-9; **2**, 127762-18-9; **3**, 127762-19-0; **4**, 127762-20-3; (CO)AuCl, 50960-82-2; (*t*-C_4H_9NC)AuCl, 37131-32-1; (C_5H_5N)AuCl, 22355-16-4; *t*-C_4H_9NC, 7188-38-7; C_5H_5N, 110-86-1.

[1] E. O. Fischer, A. Maasböl, *Angew. Chem. 76* (1964) 645; *Angew. Chem. Int. Ed. Engl. 3* (1964) 580.
[2] P. Jutzi, W. Steiner, *Angew. Chem. 88* (1976) 720; *Angew. Chem. Int. Ed. Engl. 15* (1976) 684.
[3] P. J. Davidson, M. F. Lappert, *J. Chem. Soc. Chem. Commun. 1973*, 317.
[4] J. D. Cotton, P. J. Davidson, M. F. Lappert, *J. Chem. Soc. Dalton Trans. 1976*, 2275.
[5] W. Petz, Chem. Rev. 86 (1986) 1019.
[6] The existence of previously described donor-free silylene complexes appears questionable[5, 11].
[7] P. Jutzi, U. Holtmann, D. Kanne, C. Krüger, R. Blome, R. Gleiter, I. Hyla-Kryspin, *Chem. Ber. 122* (1989) 1629.
[8] T. A. Blinka, B. J. Helmer, R. West, *Adv. Organomet. Chem. 23* (1984) 195; A. G. Brook, K. M. Baines, *ibid. 25* (1986) 1.
[9] P. Jutzi, *Chem. Rev. 86* (1986) 983.
[10] An η^2 coordination of the Cp* rings can only be shown for the solid-state structures. In solution, the fluxional process is too rapid: P. Jutzi, B. Hampel, K. Stroppel, C. Krüger, K. Angermund, P. Hofmann, *Chem. Ber. 118* (1985) 2789; P. Jutzi, B. Hampel, M. B. Hursthouse, A. J. Howes, *J. Organomet. Chem. 299* (1986) 19.
[11] a) C. Zybill, *Nachr. Chem. Tech. Lab. 37* (1989) 248; b) C. Zybill, D. L. Wilkinson, C. Lewis, G. Müller, *Angew. Chem. 101* (1989) 206; *Angew. Chem. Int. Ed. Engl. 28* (1989) 203, and references cited therein.
[12] The coordination of a σ-donor molecule, accompanied by simultaneous loss of the π-(Cp*) interaction, should only slightly change the electron density at silicon.
[13] Compare with the ^{13}C NMR values in free *tert*-butyl cyanide (δ = 154.5) and in the gold(I) chloride complex (δ = 132.2).
[14] P. Jutzi, *Comments Inorg. Chem. 6* (1987) 123.

Ytterbium(II) Benzamidinates, a New Class of Highly Reactive Lanthanoid(II) Complexes**

By *Michael Wedler, Mathias Noltemeyer, Ursula Pieper, Hans-Georg Schmidt, Dietmar Stalke* and *Frank T. Edelmann**

The discovery of a simple synthesis of samarium diiodide by *Kagan* et al. marked the beginning of an impressive development of organolanthanoid(II) chemistry.[1] However, in view of the enormous increase in their importance in preparative organic chemistry,[2] the number of soluble, fully characterized divalent lanthanoid derivatives is still surprisingly small.[3, 4] The well-investigated compounds include primarily the decamethylmetallocenes $(C_5Me_5)_2M$ (M = Sm, Eu, Yb), the bis(trimethylsilyl)amides $M[N(SiMe_3)_2]_2(thf)_2$ (M = Sm, Eu, Yb), and $(C_6F_5)_2Yb(thf)_4$.[4]

[*] Dr. F. T. Edelmann, M. Wedler, Dr. M. Noltemeyer, U. Pieper, H.-G. Schmidt, Dr. D. Stalke
Institut für Anorganische Chemie der Universität
Tammannstrasse 4, D-3400 Göttingen (FRG)

[**] This work was supported by the Deutsche Forschungsgemeinschaft and the Fonds der Chemischen Industrie.

We describe here the synthesis, structure, and reactivity of silylated ytterbium(II) benzamidinates. These compounds represent a new class of soluble, highly reactive lanthanoid(II) complexes.

Ytterbium diiodide **1**[1] reacts with sodium *N,N'*-bis(trimethylsilyl)benzamidinates **2**[5, 6] in THF to give deep red solutions. The ytterbium(II)benzamidinates **3** formed in these reactions are obtained, after recrystallization from *n*-hexane, as black-red solids in high yield.

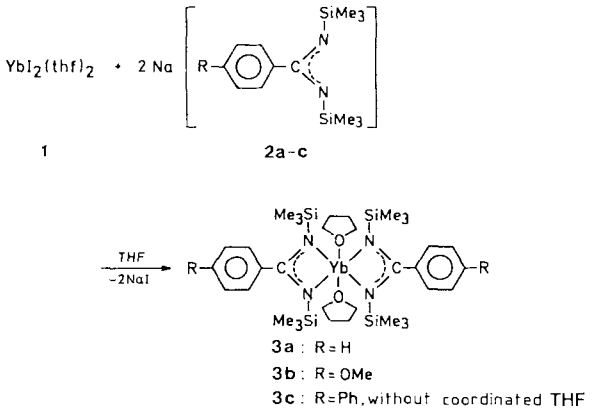

As expected, the ytterbium(II) benzamidinates **3a–c** are very sensitive to oxidation. The homoleptic ytterbium(III) benzamidinates $[RC_6H_4C(NSiMe_3)_2]_3Yb$ can be identified as oxidation products.[7] The $SiMe_3$ substituents are responsible for the excellent solubility of complexes **3** in nonpolar solvents such as toluene, cyclohexane, and *n*-hexane. In contrast, the lanthanoid(II) acetates $Sm(OAc)_2$ and $Yb(OAc)_2$ have been reported to be insoluble.[1b]

Both **3a** and **3b** are present as bis-THF adducts according to ^1H NMR spectroscopy and elemental analysis, whereas crystalline **3c** is unsolvated. Single crystals of **3a** suitable for an X-ray structure analysis (Fig. 1)[8] were obtained by cooling a saturated solution of **3a** in *n*-hexane. The ytterbium atom is coordinated in a very distorted octahedral fashion and, together with the oxygen atoms of the two *trans* THF molecules, lies on a crystallographic twofold axis. The Si-N-C-N-Si units of the benzamidinato ligands are planar. However, owing to the bulky $SiMe_3$ substituents, they are rotated by 26.3° with respect to each other. The Yb–N bond lengths (average value 248 pm) are comparable to those in $Na[Yb^{II}\{N(SiMe_3)_2\}_3]$ (Yb-N: 238, 244, 247 pm).[9] Conjugation of the π systems of the phenyl rings of the chelate ligands with the amidinato units can be ruled out by the large dihedral angle (77.3°).

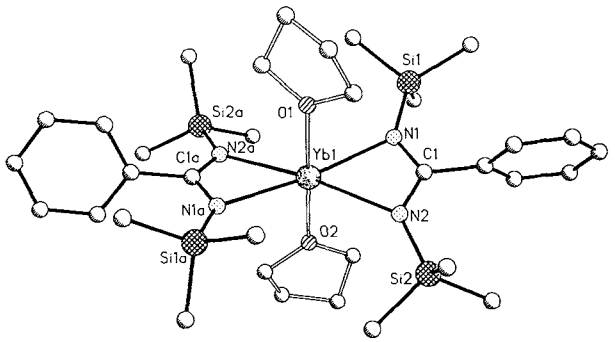

Fig. 1. Molecular structure of **3a**. Selected bond lengths [pm] and angles [°]: Yb1-N1 246.8(2), Yb1-N2 247.8(2), Yb1-O1 242.4(3), Yb1-O2 240.6(3); N1-C1-N2 120.4(2), N1-Yb1-N2 55.6(1), N1-Yb1-N1a 169.0(1), N2-Yb1-N2a 170.1(1).

Ytterbium(II) compounds are strong reducing agents ($E^\circ(Yb^{3\oplus}/Yb^{2\oplus}) = -1.15$ V).[4] The high reactivity of benzamidinates **3** can be exploited for the synthesis of novel ytterbium(III) complexes. S–S and Se–Se bonds are readily and quantitatively cleaved by **3a**. For example, the reaction of **3a** with tetramethylthiuram disulfide affords colorless **4**. Reaction with PhSeSePh yields yellow, crystalline **5** in good yield.

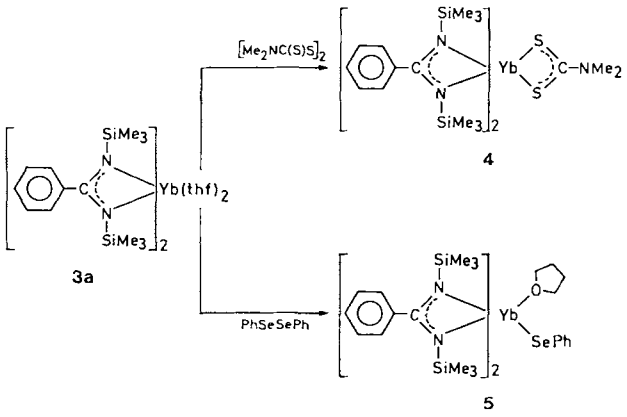

The transition from diamagnetic ytterbium(II) to paramagnetic ytterbium(III) complexes is demonstrated impressively by the strongly temperature-dependent ^1H NMR spectra of **4** and **5**. According to the X-ray structure (Figs. 2 and 3),[8] both are hexacoordinated complexes. In **4** the chelating dithiocarbamato ligand has displaced both THF molecules from the starting material. The distances and angles in the YbS_2CNMe_2 part of the molecule are largely comparable to those in $(C_5Me_5)_2Yb(S_2CNEt_2)$.[10] A monomeric ytterbium(III) selenolate with a terminal PhSe ligand is present in compound **5**. The chelating amidinate ligands, originally *trans* in **3**, are tilted with respect to each other in **4** and **5**. This feature strikingly shows the structural analogy between the Cp* complexes $(C_5Me_5)_2Yb(S_2CNEt_2)$[9] and $(C_5Me_5)_2Yb(NH_3)TePh$[10] on the one hand and the benzamidinates **4** and **5** on the other.

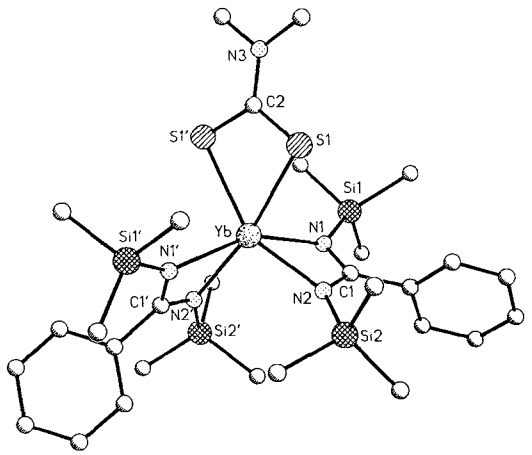

Fig. 2. Molecular structure of **4**. Selected bond lengths [pm] and angles [°]: Yb-N1 231.9(8), Yb-N2 229.8(6), Yb-N1' 230.5(8),Yb-N2' 232.3(7), Yb-S1 274.5(3), Yb-S1' 273.0(3); N1-C1-N2 119.0(8), N1-Yb-N2 59.6(2), N1'-C1'-N2' 118.2(7), N1'-Yb-N2' 59.3(3), S1-C2-S2' 120.1(5), S1-Yb-S1' 65.6(1).

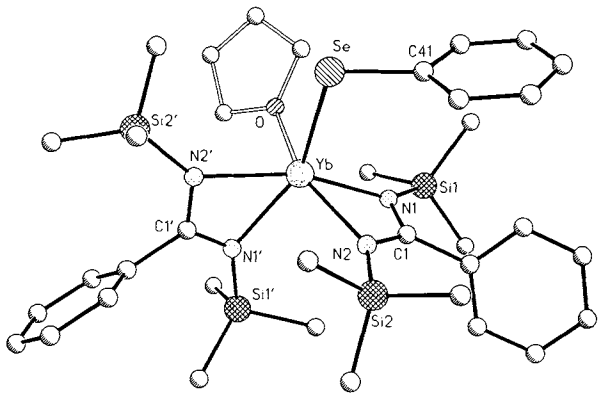

Fig. 3. Molecular structure of **5**. Selected bond lengths [pm] and angles [°]: Yb-Se 280.5(1), Yb-N1 230.5(8), Yb-N2 226.5(7), Yb-N1′ 236.6(7), Yb-N2′ 233.4(8), Yb-O 233.6(6); Yb-Se-C(41) 105.3(3), N1-C1-N2 117.8(8), N1′-C1′-N2′ 118.7(8), N1-Yb-N2 59.8(3), N1′-Yb-N2′ 58.5(3).

Experimental Procedure

All operations were performed in degassed solvents under N_2. Correct elemental analyses were obtained.

1: A solution of 1,2-diiodoethane (1.41 g, 5.00 mmol) in 150 mL of THF was added dropwise to Yb powder (1.08 g, 6.25 mmol) and the reaction mixture was stirred for 24 h at room temperature. The pale yellow solution of YbI_2 thereby obtained can be used directly in the subsequent reactions.

3a–c: Compound **2** (10 mmol), dissolved in 30 mL of THF, was added dropwise to **1** (5 mmol) in 150 mL of THF. The reaction mixture was stirred for 12 h at room temperature and the THF was then completely removed under vacuum. The residue was extracted with 150 mL of *n*-hexane (**3c**: toluene) and the resulting solution was filtered through Celite and then concentrated to ca. 30 mL. Cooling to − 25 °C afforded black-red crystals. **3a**: yield 2.30 g (55%); m.p. 150–155 °C. ^{1}H NMR (80 MHz, C_6D_6): $\delta = 7.03-7.32$ (m, 10H, Ph), 4.43 (m, 8H, THF), 2.00 (m, 8H, THF), 0.14 (s, 36H, $SiMe_3$). EI-MS (70 eV): *m/z* 844 ($M^{\oplus}$, 1%), 700 ($M^{\oplus}$ − 2 THF, 15), 263 ($PhC(NSiMe_3)_2$, 37), 146 (Si_2Me_6, 100), 73 ($SiMe_3$, 56). **3b**: Yield 1.65 g (37%); m.p. 117 °C. ^{1}H NMR (80 MHz, C_6D_6): $\delta = 7.16$ (m, 4H, C_6H_4), 6.70 (m, 4H, C_6H_4), 3.84 (m, 8H, THF), 3.26 (s, 6H, OMe), 1.57 (m, 8H, THF), 0.12 (s, 36H, $SiMe_3$). EI-MS (70 eV): *m/z* 760 ($M^{\oplus}$ − 2 THF, 5%), 133 ($MeOC_6H_4CN$, 100). **3c**: Yield 4.15 g (97%), dec. above ca. 200 °C. ^{1}H NMR (80 MHz, C_6D_6): $\delta = 7.63-7.88$ (m, 18H, PhC_6H_4), 0.22 (s, 36H, $SiMe_3$). EI-MS: *m/z* 853 ($M^{\oplus}$, 100%), 513 ($PhC_6H_4C(NSiMe_3)_2Yb$, 16).

4: $[Me_2NC(S)S]_2$ (0.29 g, 1.2 mmol) was added to a solution of **3a** (2.03 g, 2.4 mmol) in 60 mL of *n*-hexane. The reaction mixture was stirred for 12 h at room temperature and then filtered through Celite. The filtrate was concentrated to 30 mL and cooled to 0 °C. Colorless crystals formed within 2–3 days. Yield 0.64 g (33%); m.p. 147 °C. ^{1}H NMR (80 MHz, C_6D_6, 32 °C): $\delta = 7.00$ ($\nu_{1/2} = 19$ Hz, 36H, $SiMe_3$), 2.42 (s, 6H, NMe_2), − 1.94 (t, 2H, *p*-Ph), − 3.80 ($\nu_{1/2} = 16$ Hz, 4H, *m*-Ph), − 21.48 ($\nu_{1/2} = 16$ Hz, 4H, *o*-Ph). EI-MS: *m/z* 820 ($M^{\oplus}$, 24%), 700 ($M^{\oplus} - Me_2NCS_2$, 100).

5: A solution of PhSeSePh (0.26 g, 0.83 mmol) in 30 mL of *n*-hexane was added to a solution of **3a** (1.40 g, 1.66 mmol) in 70 mL of *n*-hexane. The reaction mixture was stirred for 12 h at room temperature, turning from deep red to yellow. It was then filtered through Celite and the filtrate was concentrated to 20 mL. Cooling to − 25 °C afforded 1.02 g (66%) of bright yellow crystals. M.p. 205 °C. ^{1}H NMR (80 MHz, C_6D_6, 32 °C): $\delta = 50.5$ (m, 4H, THF), 18.3 (m, 4H, THF), 13.5 ($\nu_{1/2} = 36$ Hz, 4H, SePh), 7.7 ($\nu_{1/2} = 16$ Hz, 1H, SePh), 3.5 ($\nu_{1/2} = 169$ Hz, 36H, $SiMe_3$), − 0.5 ($\nu_{1/2} = 8$ Hz, 2H, *p*-Ph), − 1.9 ($\nu_{1/2} = 17$ Hz, 4H, *m*-Ph), − 15.6 ($\nu_{1/2} = 46$ Hz, 4H, *o*-Ph). EI-MS: *m/z* 700 ($[PhC(NSiMe_3)_2]_2Yb$, 26%), 437 ($PhC(NSiMe_3)_2Yb$, 9), 73 ($SiMe_3$, 100).

Received: March 5, 1990 [Z 3832 IE]
German version: *Angew. Chem. 102* (1990) 941

[1] a) J. L. Namy, P. Girard, H. B. Kagan, *Nouv. J. Chim. 1* (1977) 5; b) J. L. Namy, P. Girard, H. B. Kagan, P. E. Caro, *ibid. 5* (1981) 479.
[2] H. B. Kagan, J. L. Namy, *Tetrahedron 42* (1986) 6573.
[3] H. Schumann, *Angew. Chem. 96* (1984) 475; *Angew. Chem. Int. Ed. Engl. 23* (1984) 474.
[4] W. J. Evans, *Polyhedron 6* (1987) 803.
[5] R. T. Boeré, R. T. Oakley, R. W. Reed, *J. Organomet. Chem. 331* (1987) 161.
[6] M. Wedler, F. Knösel, M. Noltemeyer, F. T. Edelmann, U. Behrens, *J. Organomet. Chem. 388* (1990) 21.
[7] M. Wedler, *Dissertation*, Universität Göttingen 1990.
[8] Crystal structure analyses of **3a**, **4**, and **5**: **3a** ($C_{34}H_{62}N_4O_2Si_4Yb$, $M = 844.4$ gmol^{-1}) forms orthorhombic crystals in the space group *Pbcn*, $a = 1827.5(1)$, $b = 1292.9(1)$, $c = 1789.4(1)$ pm, $V = 4.228$ nm^3, $Z = 4$, $\varrho_{calcd} = 1.33$ Mgm^{-1}, $\mu(Mo_{K\alpha}) = 2.35$ mm^{-1}. 7025 measured intensities, $2\theta_{max} = 50°$. Of 3707 unique reflections, 3027 with $F > 3\sigma(F)$ were observed. Structure solution: Patterson methods (SHELX-86[12]), 206 parameters were refined; extinction correction, refinement of the extinction coefficients to 0.00025. $R = 0.023$, $R_w = 0.024$; GOF = 1.31, residual electron density: $\pm 5.2 \times 10^2$ e nm^{-3}. **4** ($C_{30}H_{52}N_4S_2Si_4Yb$, M = 820.3 gmol^{-1}) forms monoclinic crystals in the space group $P2_1/n$, $a = 1124.8(1)$, $b = 3489.1(2)$, $c = 1166.6(1)$ pm, $\beta = 117.94(1)°$, $V = 4.045$ nm^3, $Z = 4$, $\varrho_{calcd} = 1.35$ Mgm^{-1}, $\mu(Mo_{K\alpha}) = 2.54$ mm^{-1}. 6615 measured intensities, $2\theta_{max} = 45°$. Of 5207 unique reflections, 4657 with $F > 3\sigma(F)$ were observed. Structure solution: Patterson methods (SHELX-86[12]). 370 parameters were refined. $R = 0.038$, $R_w = 0.070$, GOF = 2.27, residual electron density $\pm 6.1 \times 10^2$ e nm^{-3}. **5** ($C_{36}H_{59}N_4OSeSi_4Yb$, $M = 928.2$ gmol^{-1}) forms monoclinic crystals in the space group $P2_1/n$, $a = 1144.4(1)$, $b = 1905.6(2)$, $c = 2101.7(4)$ pm, $\beta = 105.45(4)°$. $V = 4.418$ nm^3, $Z = 4$, $\varrho_{calcd} = 1.40$ Mgm^{-1}, $\mu(Mo_{K\alpha}) = 2.99$ mm^{-1}. 6755 measured intensities, $2\theta_{max} = 45°$. Of 5728 unique reflections, 4281 with $F > 3\sigma(F)$ were observed. Structure solution: Patterson methods (SHELX-86[12]). 424 parameters were refined. $R = 0.054$, $R_w = 0.051$. GOF = 1.40, residual electron density: $\pm 1.2 \times 10^3$ e nm^{-3}. The data sets were collected on a Stoe AED with $Mo_{K\alpha}$ radiation ($\lambda = 71.073$ nm) at $T = -85$ °C (**3a**) and $T = 25$ °C (**4** and **5**). Semiempirical absorption correction (XEMP[12]) (**3a**, 216 data; **4**, 168 data; **5**, 210 data). All non-hydrogen atoms were refined anisotropically. The hydrogen atoms were placed at geometrically ideal positions and a riding model was used to include them in the refinement[11]. Further details of the crystal structure investigation may be obtained from the Fachinformationszentrum Karlsruhe, Gesellschaft für wissenschaftlich-technische Information mbH, D-7514 Eggenstein-Leopoldshafen 2 (FRG), on quoting the depository number CSD-54571, the names of the authors, and the journal citation.
[9] T. Don Tilley, R. A. Andersen, A. Zalkin, *Inorg. Chem. 23* (1984) 2271.
[10] T. Don Tilley, R. A. Andersen, A. Zalkin, D. H. Templeton, *Inorg. Chem. 21* (1982) 2644.
[11] D. J. Berg, R. A. Andersen, A. Zalkin, *Organometallics 7* (1988) 1858.
[12] G. M. Sheldrick, *SHELX-86*, Programm zur Strukturlösung und Verfeinerung, Göttingen 1986.

Oxidative Addition of Phosphorus Ylides to $Ru_3(CO)_{12}$ **

By *D. Scott Bohle, Daniel Heineke, Antonio Tiripicchio, Marisa Tiripicchio Camellini*, and *Heinrich Vahrenkamp**

The versatile reactivity of phosphorus ylides has made them important reagents in organic chemistry.[1] In inorganic chemistry their strong basicity has been the basis of a rich coordination chemistry.[2] The way has thereby been paved "for an understanding of some of the complicated reactions in the system metal/phosphane/C_1 building block".[2] This should also open a fertile area of metal-assisted organic reactions of phosphorus ylides. With this in mind we have begun to investigate the reactivity of phosphorus ylides towards organometallic cluster compounds. After observing a new type of C–C bond formation between a cluster-bound vinylidene (CCH_2) unit and the ylides $R_3P{=}CHX$,[3] we have now found a new kind of oxidative addition in which a

[*] Prof. Dr. H. Vahrenkamp, Dr. D. S. Bohle, Dipl.-Chem. D. Heineke
Institut für Anorganische und Analytische Chemie der Universität
Albertstrasse 21, D-7800 Freiburg (FRG)
Prof. A. Tiripicchio, Prof. M. Tiripicchio Camellini
Istituto di Chimica Generale ed Inorganica, Universita di Parma
Centro di Studio per la Strutturistica Diffratometrica del C. N. R.
Viale delle Scienze, I-43100 Parma (Italy)

[**] This work was supported by the European Community (grant ST 2J-0347-C), by the Volkswagen-Stiftung, and by the Fonds der Chemischen Industrie.

phosphorus ylide and $Ru_3(CO)_{12}$ react to give a phosphoniomethylidyne ligand linked to three ruthenium atoms.

Reaction of $Ru_3(CO)_{12}$ with $Ph_3P{=}CH_2$ at $-20\,^{\circ}C$ in THF results in formation of a deep red intermediate, which, after workup, affords a 23% yield of **1**.[4] Upon heating in cyclohexane, **1** is converted into **2** in 31% yield.[5] A mixture of **1** (38%) and **2** (24%) is also obtained when $Ru_3(CO)_{12}$ is

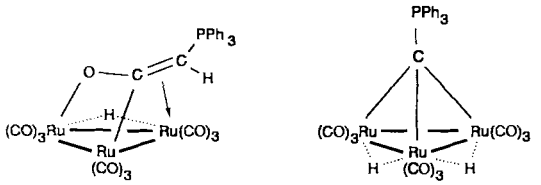

1 **2**

treated with an excess of $Ph_3P{=}CHCHO$ in refluxing cyclohexane. Our findings have coincided with those of *Deeming* et al.,[6] who isolated five products from the reaction of $[Os_3(CO)_{10}(MeCN)_2]$ with $Ph_3P{=}CHCHO$. One product is similar, but not completely analogous, to those identified here.

Both **1** and **2** are products of an oxidative addition of $Ph_3P{=}CH_2$ to $Ru_3(CO)_{12}$. Although this is immediately obvious for **2**, the formation of **1** requires an intermediate CO insertion. We believe this to occur according to Scheme 1. As observed in the reactions of $R_3P{=}CH_2$ with simple metal carbonyls[2] and based on the immediate color change, the primary product is presumably **A**, which then rearranges to **B**. Like in the reactions of electron-rich aldehydes with $Ru_3(CO)_{12}$,[7] **B** is also the product of oxidative addition of $Ph_3P{=}CHCHO$ to $Ru_3(CO)_{12}$ and has been isolated as such for the Os_3 cluster by *Deeming* et al.[6] Compound **B** has two alternatives for decarbonylation, one of which leads to **1**, the other to **C**, the initially formed, but not yet observed, intermediate in the oxidative addition of $Ph_3P{=}CH_2$ to $Ru_3(CO)_{12}$. Both **1** and **C** can further decarbonylate in the second step of oxidative addition to form the final product **2**.

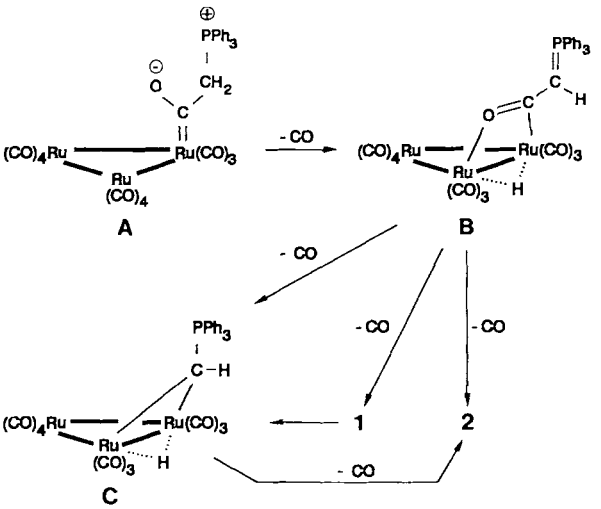

Scheme 1.

The structures of **1** and **2** have been determined by X-ray crystallography.[8] Figures 1 and 2 show that they both represent unusual bonding patterns. In **1** the ligand Ph_3PCHCO is linked via a π-bonding interaction of the C–C unit to one ruthenium atom, while the central C atom and the terminal O atom are σ-bonded to the second and third ruthenium atoms. The μ_3-bridging ligand can be called a phosphonium enolate with the P–C2 bond (181 pm) having a single-bond distance and both the C–C and the C–O bonds having between single- and double-bond distances. The C–C bond length (144 pm) is also longer than in the vinyl-bridged cluster $[HOs_3(CO)_{10}(\mu\text{-}CH{=}CH_2)]$ (140 pm).[9] Likewise, the C–O bond length (131 pm) is longer than in the acyl-bridged cluster $[HOs_3(CO)_{10}(\mu\text{-}PhCH_2C{=}O]$ (126 pm).[10] The comparatively simple structure of **2** contains a μ_3-bridging carbon atom with three normal Ru–C bond distances around 210 pm.[11] Unusual, however, is the fact that the carbon atom is ligated by the phosphane and can thus be called a cluster constituent like a metal atom. That this view is not unrealistic has been demonstrated recently by *Shriver* et al.[12a] for the substitution of CO by phosphane in the cluster $[Fe_2Co(CO)_9(\mu_3\text{-}C \cdot CO)]^{\ominus}$. *Schmidbaur*'s compound $[(Ph_3PAu)_3(\mu_3\text{-}C \cdot PMe_3]Cl$ similarly contains a phosphane-substituted μ_3-C ligand.[12b]

The formation of **2** completes the utilization of all four hydrogen atoms of methane in the sequence $CH_4 \rightarrow CH_3I \rightarrow CH_2{=}PPh_3 \rightarrow$ **2**. The resulting cluster unit should now be a useful starting point for subsequent organic reactions.[13] What this may mean has indirectly been shown by us in making the cluster compounds **3**[14] and **4**.[3] In **3** and **4** the M_3C units are isoelectronic to the one in **2**, while on top

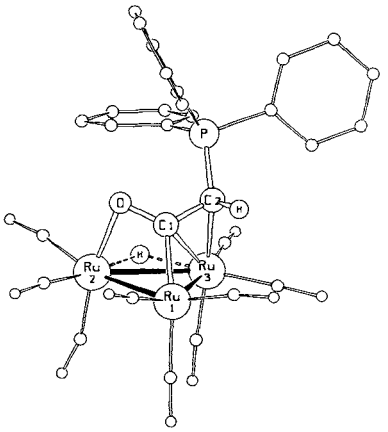

Fig. 1. Molecular structure of **1**. Important bond lengths [pm]: Ru1-Ru2 273.7(3), Ru1-Ru3 276.7(3), Ru2-Ru3 302.0(3), Ru1-C1 207(2), Ru2-O 211(2), Ru3-C1 246(2), Ru3-C2 227(2), C1-O 131(3), C1-C2 144(3), C2-P 181(2).

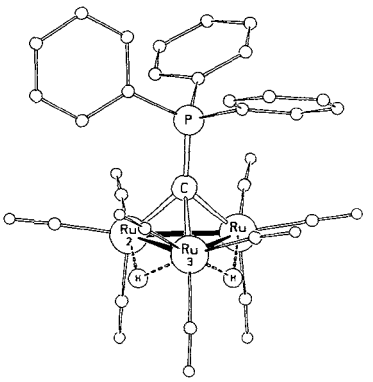

Fig. 2. Molecular structure of **2**. Important bond lengths [pm]: (two crystallographically independent molecules): Ru1-Ru2 271.7(1), 271.7(1); Ru2-Ru3 286.2(1), 287.3(1); Ru3-Ru1 283.3(1), 284.4(1); Ru1-C 209.9(4); 210.3(4); Ru2-C 210.0(4), 210.0(5); Ru3-C 212.0(4), 210.6(4); C-P 174.3(5), 174.4(4).

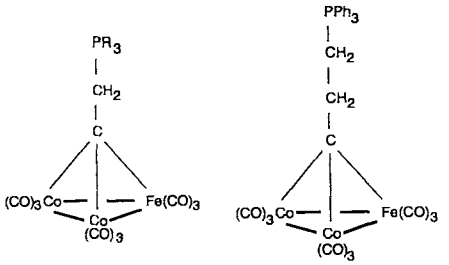

3 4

of them the C-PPh_3 unit has been homologated by the "insertion" of one and two CH_2 units, respectively.

Received: March 6, 1990 [Z 3833 IE]
German version: *Angew. Chem. 102* (1990) 938

[1] H. J. Bestmann, R. Zimmermann in: *Houben-Weyl: Methoden der Organischen Chemie, Bd. E1*, Thieme, Stuttgart 1982, p. 616.
[2] H. Schmidbaur, *Angew. Chem. 95* (1983) 980; *Angew. Chem. Int. Ed. Engl. 22* (1983) 907.
[3] D. Heineke, H. Vahrenkamp, *Organometallics 9* (1990) 1697.
[4] 0.25 mmol of $Ru_3(CO)_{12}$ and 0.5 mmol of salt-free $Ph_3P=CH_2$, 25 mL of THF, −20 °C, warmup to room temperature in 20 min, addition of 0.25 mmol of $CH_3OSO_2CF_3$ to remove anionic side products. Chromatography with hexane/CH_2Cl_2 (1:1) over silica gel: first fraction, $Ru_3(CO)_{12}$; second fraction, **1**. **1**: yellow, m.p. 125 °C (dec.). IR (CH_2Cl_2). $\tilde{\nu}$ = 2090 w, 2058 s, 2031 s, 1996 s cm^{-1}. ^1H NMR (250 MHZ $CDCl_3$): δ = 7.4–7.7 (phenyl multiplet), 2.99 (d, J = 15.9 Hz, P-C-H), −14.95 (s, Ru-H).
[5] 0.05 mmol of **1**, 20 mL of C_6H_{12}, reflux for 5 h; workup by chromatography with hexane/CH_2Cl_2 (3:1) over silica gel yielded **2** in the first fraction. **2**: yellow, m.p. 153 °C. IR (CH_2Cl_2): $\tilde{\nu}$ = 2096 m, 2062 s, 2031 vs, 1977 m, 1957 w, 1944 w cm^{-1}. ^1H NMR: δ = 7.4–7.8 (phenyl multiplet), −17.73 (s, Ru-H).
[6] A. J. Deeming, D. Nuel, N. I. Powell, C. Whittaker, *J. Chem. Soc. Chem. Commun.* 1990, 68.
[7] D. S. Bohle, H. Vahrenkamp, unpublished.
[8] Crystal data for **1**: triclinic, space group $P\bar{1}$, a = 1662.8(6), b = 1014.8(4), c = 985.2(4) pm, α = 67.69(2), β = 88.46(2), γ = 85.88(2)°, Z = 2; 2510 reflections, R = 0.090. Crystal data for **2**: triclinic, space group $P\bar{1}$, a = 1787.7(8), b = 1665.6(5), c = 1044.7(3) pm, α = 102.82(2), β = 99.15(2), γ = 93.00(2)°; Z = 4, 8389 reflections, R = 0.033. In both structures the hydride ligands could be located, but not refined. Further details of the crystal structure investigation may be obtained from the Fachinformationszentrum Karlsruhe, Gesellschaft für wissenschaftlich-technische Information mbH, D-7514 Eggenstein-Leopoldshafen 2 (FRG), on quoting the depository number CSD-54524 the names of the authors, and the journal citation.
[9] A. G. Orpen, D. Pippard, G. M. Sheldrick, K. D. Rouse, *Acta Crystallogr. B34* (1978) 2466.
[10] B. F. G. Johnson, J. Lewis, T. I. Odiaka, P. R. Raithby, *J. Organomet. Chem. 216* (1981) C56.
[11] See G. M. Sheldrick, J. P. Yesinowski, *J. Chem. Soc. Dalton Trans. 1975*, 873.
[12] a) S. Ching, M. Sabat, D. F. Shriver, *Organometallics 8* (1989) 1047; b) H. Schmidbaur, F. Scherbaum, B. Huber, G. Müller, *Angew. Chem. 100* (1988) 441; *Angew. Chem. Int. Ed. Engl. 27* (1988) 419.
[13] For the [$Fe_4(CO)_{12}(\mu_4$-C)] system, cf. J. S. Bradley, *Adv. Organomet Chem. 22* (1983) 1.
[14] T. Albiez, H. Vahrenkamp, *Angew. Chem. 99* (1987) 561; *Angew. Chem. Int. Ed. Engl. 26* (1987) 572.

Functional Tetrahedral Zinc Complexes**

By *Ralf Alsfasser, Anne K. Powell,* and *Heinrich Vahrenkamp**

In the numerous zinc-containing enzymes, the zinc ion is almost always coordinated in a tetrahedral fashion.[1] Three of the four coordination sites are occupied by peptide donor groups, while the fourth, the "functional" site, is occupied by the substrate of the enzyme (or, in the "resting state", by a water molecule). Because of the lability of zinc complexes and the diverse coordination possibilities for zinc, it is unexpectedly difficult to obtain this simple coordination pattern, L_3ZnX, in model complexes.[2] Thus, typical chelating L_3 ligands such as triazacyclononane,[3a] tris(aminomethyl)-methane,[3b] *cis*-triaminocyclohexane,[3c] and even hydrotris(pyrazolyl)borate[3d] usually also afford octahedral 1:2 complexes. Only a complicated and bulky L_3 ligand such as tris(4,5-diisopropylimidazolyl)phosphane leads to a complex, $[L_3ZnCl]^{\oplus}$, that models the structure and function of the enzyme carbonic anhydrase.[4]

To obtain novel L_3ZnX complexes **1**, we have now exploited the fact that the well-studied hydrotris(pyrazolyl)borate ligands as their 3-phenyl or 3-*tert*-butyl-substituted derivatives form stable tetrahedral complexes L_3MX, M = Co,Ni,Cu,Zn.[5] In complexes **1**, the hydrophobic pocket formed around the fourth coordination site of the zinc by the substituents of the pyrazole can accommodate a variety of groups X. The utility of this concept is demonstrated by the four compounds **1a**–**1c** and **2**, all of which have been characterized by X-ray structure analyses.[6]

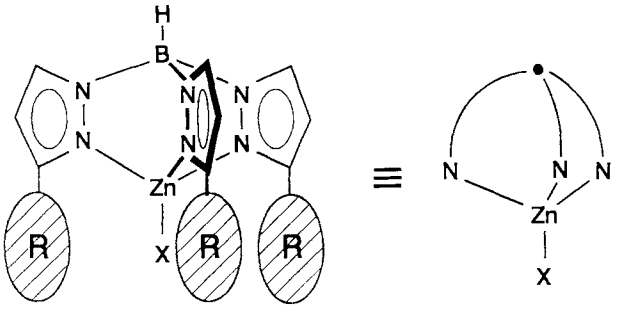

1, R = Ph, *t*Bu

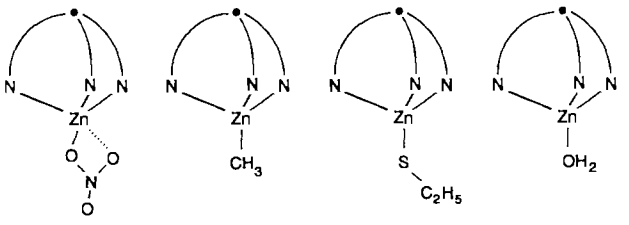

1a **1b** **1c** **1d** (?)

Hydrotris(phenylpyrazolyl)boratozinc nitrate (**1a**) precipitates when methanolic solutions of $Zn(NO_3)_2 \cdot 6H_2O$ and the potassium salt of the ligand are combined (56% yield after recrystallization from benzene). Complex **1a** is first and foremost a further example of the well-investigated class of hydrotris(pyrazolyl)boratozinc salts.[5] Its structure analysis clearly shows, however, that the coordination of the nitrato ligand, as shown in the formula, is somewhere between monodentate and bidentate (Zn-O 195 and 247 pm). Complex **1a** is thus a primitive analogue of the enzyme carbonic anhydrase in two respects: first, the pocket at zinc in L_3ZnX has room for both a monodentate X and a second, small ligand (the substrate); second, the nitrato ligand is coordinated in just the way discussed for the isoelectronic hydrogen carbonate in carbonic anhydrase.[4]

[*] Prof. Dr. H. Vahrenkamp, Dipl.-Chem. R. Alsfasser, Dr. A. K. Powell
Institut für Anorganische und Analytische Chemie der Universität
Albertstrasse 21, D-7800 Freiburg (FRG)

[**] This work was supported by the Fonds der Chemischen Industrie and the Deutsche Forschungsgemeinschaft.

Hydrotris(phenylpyrazolyl)boratozinciomethane (**1b**) is formed in 90% yield as a practically analytically pure product when methyllithium (ca. 2 M, in ether, 10% excess) is added dropwise to a solution of L_3ZnCl in benzene. After concentration of the reaction solution to dryness, the product is separated from the lithium compounds by extraction with toluene. Further such organozinc compounds are synthesized analogously. Together with the organozinc compounds of hydrotris(*tert*-butylpyrazolyl)borate recently synthesized by *Parkin* et al.,[7] they are the first monomeric representatives of the class of compounds RZnX.[8] Although their bonding alone is intriguing (the Zn–C distance in **1b** is 197 pm), their primary importance presumably lies in their reactivity toward protic reagents HX. Treatment with these reagents results in alkane elimination and formation of the corresponding Zn–X compounds. In the simplest case—for example, reaction with HCl or RCOOH—the resulting compounds may be more easily obtained by other routes (cf. also Ref. [7]). As shown for **1c** in the following discussion, however, this reaction can also lead to novel compounds, not accessible via other routes.

Hydrotris(phenylpyrazolyl)boratozinc ethanethiolate (**1c**) is obtained practically analytically pure in 85% yield when the *t*BuZn compound analogous to **1b** is allowed to react for one week in a stirred solution containing a stoichiometric amount of ethanethiol, followed by filtration of the reaction solution and concentration of the filtrate to dryness. The easy preparation and manipulation of **1c** demonstrate especially clearly the advantages of the L_3 coligand chosen here, since monomeric complexes of the type L_3ZnSR were previously unknown. Zinc thiolates are usually oligomeric,[2] and only a few monomers of the type $[Zn(SR)_4]^{2\ominus}$[9a] and $L_2Zn(SR)_2$[9b] have been described. The importance of **1c** (Zn–S distance 221 pm) lies in its structural relationship to the numerous enzymes in which zinc is surrounded in a tetrahedral fashion by histidine-imidazole and cysteine-thiolate coordination partners.[1]

[μ-Hydroxobis{tris(*tert*-butylpyrazole)zinc}] trisperchlorate (**2**) is formed within a few minutes when the potassium salt of the *tert*-butylpyrazolylborato ligand is allowed to react with $Zn(ClO_4)_2 \cdot 6H_2O$ in methanol; after recrystallization from toluene, **2** can be isolated in 42% yield. The expected product was the cationic complex **1d**. Complex **1d** may in fact be the precursor of **2** if the zinc increases the hydrolytic activity of the coordinated water molecule in **1d**, as it does in the enzymes containing the unit $L_3Zn\text{-}OH_2$ in the active site. If this zinc-catalyzed hydrolysis is directed toward the complex itself in **1d**, the BH unit can be released from the otherwise hydrolysis-stable pyrazolylborate as H_3BO_3 and a tris(pyrazole)zinc complex such as **2** can be formed. Complex **2**, more easily prepared from *tert*-butylpyrazole, KOH, and $Zn(ClO_4)_2$ in methanol, shows Zn–O distances of 190 and 192 pm and a Zn–O–Zn angle of 137°. It is the first isolable compound in which an $L_3Zn\text{-}OH$ unit is present; such a unit has been discussed for the hydrolytic function of carbonic anhydrase and carboxypeptidase.[1, 10]

Two typical hard ligands are bound to zinc in complexes **1a** and **2** and two typical soft ligands in **1b** and **1c**. The extreme cases are the coordination of an $OH^{\ominus}$ ion and a methyl group in comparable ligand environments. The fact that all four complexes are soluble in nonpolar media such as toluene supports the assumption that, even in **1a** and **2**, the very polar Zn–X units are buried within a hydrophobic ligand environment. This should result in an unusual reactivity of these Zn–X units.

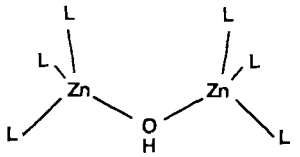

cation of **2**, L = *tert*-butylpyrazole

Received: April 11, 1990 [Z 3916 IE]
German version: *Angew. Chem. 102* (1990) 939

[1] T. G. Spiro (Ed.): *Zinc Enzymes*, Wiley, New York 1983.
[2] R. H. Prince in G. Wilkinson (Ed.): *Comprehensive Coordination Chemistry*, Pergamon, Oxford 1987, Vol. 5, pp. 926–1045.
[3] a) R. Yang, L. J. Zompa, *Inorg. Chem. 15* (1976) 1499; b) A. Sabatini, A. Vacca, *J. Chem. Soc. Dalton Trans. 1980*, 519; J. Wirbser, H. Vahrenkamp, unpublished; c) R. A. D. Wentworth, *Inorg. Chem. 7* (1968) 1030; d) S. Trofimenko, *J. Am. Chem. Soc. 89* (1967) 3170.
[4] R. S. Brown, N. J. Curtis, J. Huguet, *J. Am. Chem. Soc. 103* (1981) 6953.
[5] S. Trofimenko, J. Calabrese, J. S. Thompson, *Inorg. Chem. 26* (1987) 1507.
[6] The complete crystallographic details will be reported in a forthcoming paper. The most important compound described here, **2**, forms orthorhombic crystals, space group $P2_12_12_1$, $a = 1015.9(8)$, $b = 2275.4(5)$, $c = 2544.7(6)$ pm, $\varrho_{calcd} = 1.32$ gcm^{-3}, $Mo_{K\alpha}$ radiation, $\mu = 9.6$ cm^{-1}, 3652 reflections with $I \geq 3\sigma(I)$, $R = 0.074$.
[7] I. B. Gorrell, A. Looney, G. Parkin, *J. Chem. Soc. Chem. Commun. 1990*, 220.
[8] Cf. J. Boersma in G. Wilkinson, F. G. A. Stone, E. W. Abel (Eds.): *Comprehensive Organometallic Chemistry*, Pergamon, Oxford 1982, Vol. 2, pp. 823–851.
[9] a) P. J. Blower, J. R. Dilworth, *Coord. Chem. Rev. 76* (1987) 121; b) D. T. Corwin, S. A. Koch, *Inorg. Chem. 27* (1988) 493, and references cited therein.
[10] Cf. P. Woolley, *Nature (London) 258* (1975) 677; E. Kimura, T. Koike, K. Toriumi, *Inorg. Chem. 27* (1988) 3687.

A 1,2:2,1-Bis(2-silapropane-1,3-diyl)diborane(6): Stabilization Product of Bis(trisyl)diborane(2)?

By *Theo Mennekes, Peter Paetzold,** and *Roland Boese**

Dedicated to Professor Edwin Hengge on the occasion of his 60th birthday

In the course of our investigations of two-coordinate boron,[1] we wanted to gain 1,2-bis(trisyl)diborane(2) (**2**) by a kind of Wurtz synthesis from the known dichloro(trisyl)borane (**1**)[2] and Na/K alloy. We hoped that the bulky "trisyl" group, $(Me_3Si)_3C$, would kinetically stabilize **2**. Instead, however, the title compound **3** was obtained. Its constitution was established from the NMR, MS, and IR spectra[3] and was confirmed by an X-ray structure examination (Fig. 1).[4]

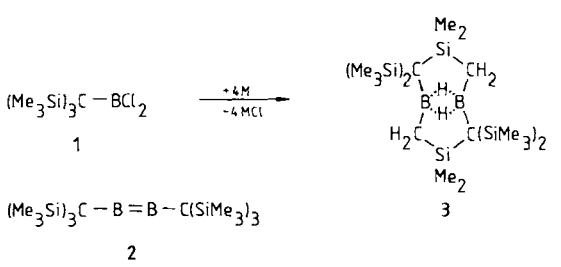

[*] Prof. Dr. P. Paetzold, T. Mennekes
Institut für Anorganische Chemie der Technischen Hochschule
Templergraben 55, D-5100 Aachen (FRG)
Dr. R. Boese
Institut für Anorganische Chemie der Universität—Gesamthochschule
Universitätsstrasse 5–7, D-4300 Essen (FRG)

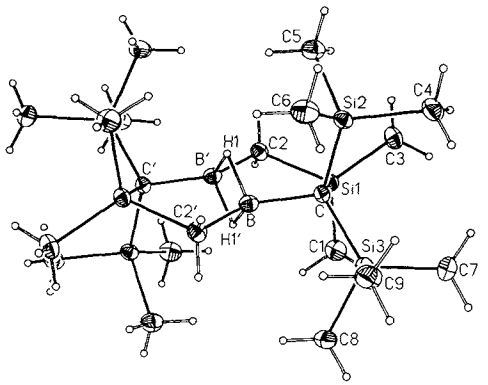

Fig. 1. Centrosymmetric molecular structure of **3**. Selected distances, angles, and torsion angles ([Å] and [°], standard deviations in parentheses): B···B' 1.856(3), B-H1 1.266(15), B'-H1 1.280(14), B-C 1.605(2), C-Si1 1.918(2), Si1-C2 1.896(2), C2-B' 1.586(3); B-H1-B' 93.6(9), H1-B-H1' 86.4(9), C-B···B 112.7(2), C-B-C2' 137.5(1), B-C-Si1 101.0(1), C-Si1-C2 104.3(1), Si1-C2-B' 103.9(1), Si1-C-Si2 110.6(1), Si1-C-Si3 113.9(1), Si2-C-Si3 112.7(1), C1-Si1-C3 106.7(1); B-C-Si1-C2 27.0, C-Si1-C2-B' −27.6, Si1-C2-B'···B 17.5, Si1-C-B···B' −17.7, C2-B'···B-C 0.4.

Compound **3** has C_i symmetry. The atoms B, B', C, C', C2, and C2' are arranged in a nearly coplanar fashion in two nonplanar five-membered rings sharing a common B–B' edge. The parallelogram B-H1-B'-H1' lies nearly perpendicular to the planes of those atoms. The distance B···B' (1.856 Å) is comparable to the B···B distance in *trans*-1,2-bis(trisyl)diborane(6), $[(Me_3Si)_3C]_2B_2H_4$[5] (1.839 Å), and markedly longer than the B···B distance in B_2H_6 (1.76 Å).[6] The 1,5-disila-3,7-diboracyclooctane structure of **3**, with a double 3,7-transannular H bridge, resembles the established structure of a likewise transannularly bridged 1,6-diboracyclodecane.[7]

Obviously, intermediates in the reaction of **1** with Na/K might be either trisylboranediyl, $(Me_3Si)_3CB$:, or dichlorobis(trisyl)diborane(4), $(Me_3Si)_3C(Cl)B\text{-}B(Cl)C(SiMe_3)_3$, which could undergo dimerization or a second dechlorination step, respectively, to give **2**. Intramolecular additions of C–H bonds to unsaturated systems, as presumed to occur in the stabilization of **2** to give the isolated product **3**, are well known. Examples in boron chemistry include the stabilization of RB≡O (R = 2,4,6-tri-*tert*-butylphenyl), $C_6F_5B{\equiv}NR$ (R = mesityl), and $R_2NB{\equiv}NNR_2$ (NR_2 = 2,6-dimethylpiperidino).[8]

Experimental Procedure

1,2:2,1-Bis[2,2-dimethyl-1,1-bis(trimethylsilyl)-2-silapropane-1,3,diyl]diborane(6), **3**: A solution of **1** (3.0 g) in 25 mL of hexane was treated at room temperature with 0.90 g of Na/K alloy (1:3). The reaction mixture was refluxed for 4 d and then filtered. The filtrate was concentrated until the crude product started to crystallize. Recrystallization once from hexane and twice from diethyl ether afforded 0.36 g of colorless **3** (15%; m.p. 250 °C). The product can be handled under air without decomposition.

Received: April 2, 1990 [Z 3891 IE]
German version: *Angew. Chem. 102* (1990) 909

CAS Registry numbers: **1**, 124408-70-4; **3**, 128054-44-4.

[1] P. Paetzold, *Adv. Inorg. Chem. 31* (1987) 123; R. Boese, P. Paetzold, A. Tapper, R. Ziembinski, *Chem. Ber. 122* (1989) 1057; H. Bock, L. S. Cederbaum, W. von Niessen, P. Paetzold, P. Rosmus, B. Solouki, *Angew. Chem. 101* (1989) 77; *Angew. Chem. Int. Ed. Engl. 28* (1989) 88.

[2] S. S. Al-Juaid, C. Eaborn, *J. Chem. Soc. Dalton Trans. 1989*, 447.

[3] **3**: NMR [$CDCl_3$, 25 °C, 80 MHz/TMS (^{1}H), 32.08 MHz/$Et_2O \cdot BF_3$ (^{11}B), 67.88 MHz/TMS (^{13}C)]: $\delta(^1H) = -0.12$–0.07 (4H, CH_2), 0.11 (s, 36H; $SiMe_3$), 0.23 (s, 12H; $SiMe_2$); $\delta(^{11}B) = 33.2$; $\delta(^{13}C) = 0.1$–6.5 (BC), 2.2, 3.2 (2q; SiMe). IR (CCl_4): $\tilde{\nu} = 1600\ cm^{-1}$ (BH_2B). MS(70 eV): *m/z* 484 ($M^{\oplus}$, 22%), 469 ($M^{\oplus} - CH_3$, 66), 411 ($M^{\oplus} - SiMe_3$, 58), 242 (1/2 $M^{\oplus}$, 57), 73 ($SiMe_3^{\oplus}$, 100).

[4] Single crystals of **3** were obtained from diethyl ether: $a = 15.950(1)$, $b = 8.938(1)$, $c = 21.417(2)$ Å, $\beta = 99.63°$, $V = 3010.2(3)$ Å^3, $Z = 4$, $\varrho_{calcd} = 1.070\ g\ cm^{-3}$, $C2/c$ (No. 15); crystal dimensions $0.50 \times 0.39 \times 0.21$ mm^3, $T = 125$ K, measuring range $3 \le 2\theta \le 45°$; 1981 unique reflections, 1891 observed with $F_o \ge 4\sigma(F)$; anisotropic temperature factors for the non-hydrogen atoms; 148 refined parameters; $R = 0.029$, $R_w = 0.036$. Further details of the crystal structure investigation may be obtained from the Fachinformationszentrum Karlsruhe, Gesellschaft für wissenschaftlich-technische Information mbH, D-7514 Eggenstein-Leopoldshafen 1 (FRG), on quoting the depository number CSD-320101, the names of the authors, and the journal citation.

[5] S. S. Al-Juaid, C. Eaborn, P. B. Hitchcock, J. D. Smith, *J. Organomet. Chem. 385* (1990) 13; P. Paetzold, L. Geret, R. Boese, *ibid. 385* (1990) 1.

[6] D. S. Jones, W. N. Lipscomb, *J. Chem. Phys. 51* (1969) 3133.

[7] M. Yalpani, R. Boese, R. Köster, *Chem. Ber. 120* (1987) 1843. Cf. also R. Köster in: *Houben-Weyl: Methoden der Organischen Chemie, Band XIII/3a*, Thieme, Stuttgart 1982, p. 328ff.

[8] M. Groteklaes, P. Paetzold, *Chem. Ber. 121* (1988) 809; P. Paetzold, A. Richter, T. Thijssen, S. Würtenberg, *ibid. 112* (1979) 3811; W. Pieper, D. Schmitz, P. Paetzold, *ibid. 114* (1981) 3801.

Boroboration of CO with Tri-*tert*-butylazadiboriridine

By *Peter Paetzold,* Burkhard Redenz-Stormanns* and *Roland Boese**

Tri-*tert*-butylazadiboriridine (**1**)[1] reacts at −78 °C with CO according to Equation (1) to form the tricyclic product **2**; NMR monitoring of the reaction indicates that it is complete. We have isolated colorless, crystalline **2** in 71% yield.

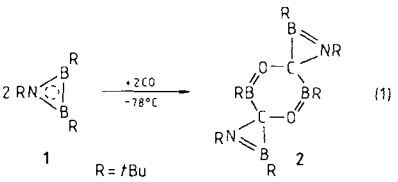

The constitution of **2** was established from the NMR and mass spectra,[2] and the unexpected structure was confirmed by X-ray structure analysis (Fig. 1).[3] In the centrosymmetric molecule **2**, two CBN three-membered rings are joined in a spirocyclic fashion to the central, planar six-membered ring, and the planes of neighboring rings are nearly perpendicular to each other. The *t*Bu groups at B3 and B3' are displaced toward the ring O atoms by the neighboring three-membered rings, as shown by the angles C1'-B3-C30 and O-B3-C30 (128 and 113°, respectively). The B–O distance of 1.36 Å supports the assumption of appreciable π contributions to the B–O bonding. Especially striking is the B–N distance of 1.33 Å, the shortest B–N double bond so far found.[4]

The surprising formation of **2** according to Equation (1) may be explained as follows: First, the carbene-like C atom of CO inserts into the B–B bond of **1** with formation of a four-membered ring; that is, the C atom is "boroborated". The four-membered ring then undergoes cyclodimerization

[*] Prof. Dr. P. Paetzold, B. Redenz-Stormanns
Institut für Anorganische Chemie der Technischen Hochschule
Templergraben 55, D-5100 Aachen (FRG)
Dr. R. Boese
Institut für Anorganische Chemie der Universität-Gesamthochschule
Universitätsstrasse 5-7, D-4300 Essen (FRG)

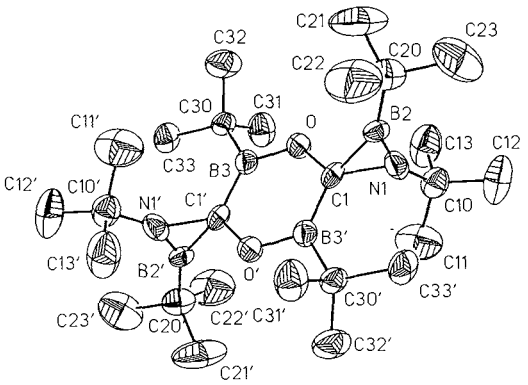

Fig. 1. Molecular structure of **2** (hydrogen atoms omitted). Selected distances and angles ([Å] and [°], standard deviations in parentheses): B3-O 1.360(5), O-C1 1.453(5), C1-B3' 1.558(6), B3-C30 1.600(6), C1-B2 1.551(6), C1-N1 1.459(5), B2-N1 1.329(9), B2-C20 1.529(9), N1-C10 1.492(8); C1'-B3-O 118.8(4), B3-O-C1 124.6(3), O-C1-B3' 116.5(3), B2-C1-N1 52.3(3), C1-B2-N1 60.3(3), C1-N1-B2 67.4(3), C1'-B3-C30 128.0(3), O-B3-C30 113.1(3).

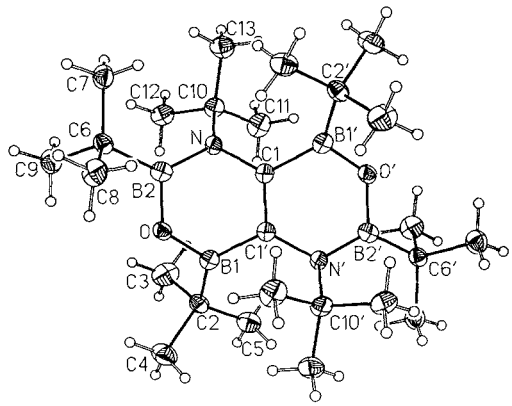

Fig. 2. Molecular structure of **3**. Selected distances, angles, and torsion angles ([Å] and [°], standard deviations in parentheses): C1-N 1.429(4), N-B2 1.449(5), B2-O 1.399(4), O-B1 1.379(4), B1-C1' 1.557(5), C1-C1' 1.390(6), B1-C2 1.581(4), B2-C6 1.594(5), N-C10 1.520(5); C1'-C1-N 120.5(3), C1-N-B2 115.3(3), N-B2-O 115.5(3), B2-O-B1 121.9(3), O-B1-C1' 112.0(2), C1'-B1-C2 130.2(3), O-B1-C2 116.2(3); C1'-C1-N-B2 30.6, C1-N-B2-O 35.1, N-B2-O-B1 0.2, B2-O-B1-C1' 36.6, B1-C1'-C1-N −6.7, C1'-C1-N-C10 −128.5, C1-C1'-B1-C2 125.0, B1-O-B2-C6 173.2, B1-C1'-C1-B1' −180.0.

along a BCO unit to form the corresponding six-membered ring. Finally, sigmatropic migration of the amino groups from the B atoms to the C atoms results in rearrangement to **2** [Eq. (2)]. This proposal is supported by the "alkyloboration" of CO with BR'_3, which occurs according to Equation (3) in a fully analogous fashion.[5]

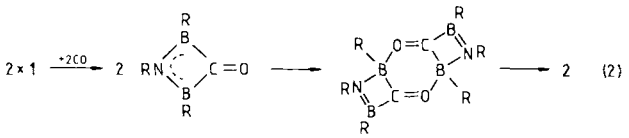

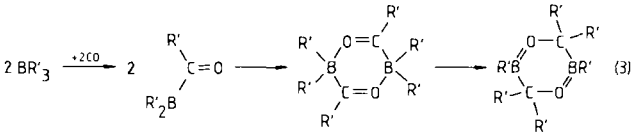

Irradiation of $Fe(CO)_5$ in the presence of **1** at −30 °C results in a product completely different from **2** but also corresponding to a 1:1 reaction of **1** and CO. The colorless, crystalline compound **3** is formed in 34% yield [Eq. (4)].

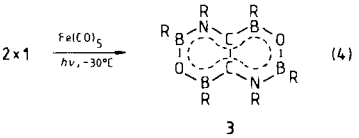

3

NMR and mass spectra[6] are in agreement with structure **3**, which was confirmed by an X-ray structure analysis (Fig. 2).[7] In the centrosymmetric molecule **3**, which is similar to naphthalene, the central ring atoms C1, C1', B1, B1', N, and N' are arranged in a planar fashion, but the trapeziform outer parts of the ring, B1-O-B2-N and B1'-O'-B2'-N', form an angle of 37.4° with the plane defined by the central ring atoms. The distances between neighboring ring atoms lie between those of typical single and double bonds involving the respective elements. This indicates a naphthalene-like cyclic delocalization of the π-electron systems despite the nonplanarity of the framework. The *t*Bu groups at B1, N and at B',N' project "below" and "above", respectively, the ring framework. The pyramidal distortion at these four ring atoms caused by the nonplanarity of the ring framework is thereby largely compensated. In the formation of **3**, the C–O triple bond is opened at −30 °C. Presumably, the Fe atom of an unknown intermediate is involved catalytically in this process.

The smooth reaction of the carbene-like molecule CO indicates that nitrenes or their precursors should react similarly. We therefore carried out the reaction of **1** with butyl azide, which resulted in loss of N_2 and formation of diazadiboretidine **4** in 65% yield [Eq. (5)]. The constitution of **4** was

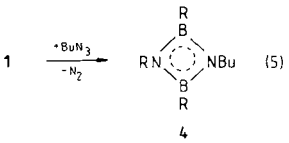

4

established unambiguously from the NMR and mass spectra.[8] The diazadiboretidines $(t\mathrm{BuBN}t\mathrm{Bu})_2$ and $(\mathrm{BuBN}t\mathrm{Bu})_2$ related to **4** have been well investigated structurally.[9] In the formation of **4**, the nitrene BuN: formally undergoes boroboration. First, one of the B atoms of **1** must attack the N1 atom of the N_3 group. The second step could involve either 1,1 boroboration or 1,3 boroboration of the N_3 group to give a six-membered ring, followed by loss of N_2. Product **4** corresponds to the hypothetical intermediate in Equation (2).

CO or BuN_3 do not react with the open-chain diborane(4) $t\mathrm{Bu}(\mathrm{Me_2N})\mathrm{B}\text{-}\mathrm{B}(\mathrm{NMe_2})t\mathrm{Bu}$, which is comparable to **1**. The boroboration tendency of **1** thus depends on its three-membered ring structure.

Experimental Procedure

1,2,5,7,8,10-Hexa-*tert*-butyl-4,9-dioxa-1,7-diaza-2,5,8,10-tetraboradispiro-[2.2.2.2]decane, **2**: CO was bubbled through a solution of **1** (0.62 g) in 50 mL of pentane at −78 °C for 30 min. Compound **2** (0.50 g, 71%) crystallized from the reaction solution.

1,3,4,5,7,8-Hexa-*tert*-butyl-2,6-dioxa-4,8-diaza-1,3,5,7-tetraboranaphthalene, **3**: A solution of **1** (1.04 g) and $Fe(CO)_5$ (0.98 g) in 60 mL of hexane was irradiated (254 nm) at −30 °C for 24 h. All volatiles were then removed under vacuum at room temperature. Compound **3** (0.40 g, 34%) was crystallized from ether.

1-Butyl-2,3,4-tri-*tert*-butyl-1,3,2,4-diazadiboretidine, **4**: Compound **1** (0.80 g) and butyl azide (0.39 g) were combined in 10 mL of pentane at 0 °C and the resulting solution was stirred for 30 min at room temperature. Distillative workup gave **4** (0.70 g, 65%) as a colorless liquid at 70 °C/0.01 Torr.

Received: April 17, 1990 [Z 3912 IE]
German version: *Angew. Chem. 102* (1990) 910

CAS Registry numbers:
1, 109976-00-3; **2**, 128270-57-5; **3**, 128270-58-6; **4**, 128270-59-7; $Fe(CO)_5$, 13463-40-6.

[1] R. Boese, B. Kröckert, P. Paetzold, *Chem. Ber. 120* (1987) 1913.
[2] **2**: NMR ($CDCl_3$; 25 °C; 60 MHz/TMS (^1H), 32.08 MHz/$Et_2O \cdot BF_3$ (^{11}B), 67.88 MHz/TMS (^{13}C)): $\delta(^1H) = 0.72, 1.12, 1.29$ (3s, 1:1:1; 3*t*Bu); $\delta(^{11}B) = 28.4, 48.1$ (2 s, 1:1); $\delta(^{13}C) = 28.7, 28.9, 30.8$ (3 q; Me of 3 *t*Bu), 53.5 (s; Cl of N*t*Bu); the two expectedly broad BC-^{13}C singlets could not be found. MS (70 eV): *m/z* 470 ($M^{\oplus}$, 68%), 413 ($M^{\oplus} - C_4H_9$, 70), 357 ($M^{\oplus} - C_4H_9 - C_4H_8$, 50), 301 ($M^{\oplus} - C_4H_9 - 2C_4H_8$, 100).
[3] Single crystals of **2** were obtained from pentane; $a = 9.3161(18)$, $b = 9.666(2)$, $c = 10.7385(17)$ Å, $\alpha = 69.941(14)$, $\beta = 80.517(13)$, $\gamma = 62.474(13)°$, $V = 805.5(2)$ Å^3, $Z = 1$, $\varrho_{calcd} = 0.969$ g cm^{-3}, $P\bar{1}$ (No. 2); crystal dimensions $0.12 \times 0.25 \times 0.13$ mm^3; $T = 155$ K; measuring range $3 \le 2\theta \le 45°$; 2113 unique reflections, 1323 observed with $F_o \ge 4.0\,\sigma(F)$; anisotropic temperature factors for the non-hydrogen atoms; 181 refined parameters $R = 0.071$, $R_w = 0.070$. Further details of the crystal structure investigation my be obtained from the Fachinformationszentrum Karlsruhe, Gesellschaft für wissenschaftlich-technische Information mbH, D-7514 Eggenstein-Leopoldshafen 2 (FRG), on quoting the depository number CSD-320105, the names of the authors, and the journal citation.
[4] P. Paetzold, *Adv. Inorg. Chem. 31* (1987) 123.
[5] A. Pelter, K. Smith, H. C. Brown: *Borane Reagents*, Academic Press, London 1988, p. 239.
[6] **3**: NMR (cf. [2]): $\delta(^1H) = 0.99, 1.06, 1.14$ (3 s, 1:1:1; 3 *t*Bu); $\delta(^{11}B) = 37.0$, 46.3 (2 s, 1:1); $\delta(^{13}C) = 28.5, 29.0, 32.3$ (3 q; Me of 3 *t*Bu), 55.3 (s; Cl of N*t*Bu), 146.5 (s; BCN); further BC-^{13}C singlets were not observed. MS (70 eV): *m/z* 470 ($M^{\oplus}$, 96%), 413 ($M^{\oplus} - C_4H_9$, 70), 357 ($M^{\oplus} - C_4H_9 - C_4H_8$, 50), 301 ($M^{\oplus} - C_4H_9 - 2C_4H_8$, 100).
[7] Single crystals of **3** were obtained from pentane; $a = 8.164(2)$, $b = 19.250(5)$, $c = 10.190(5)$ Å, $\beta = 109.39(3)°$, $V = 1510.6$ Å^3, $Z = 2$, $\varrho_{calcd} = 1.033$ g cm^{-3}, $P2_1/c$ (No. 14); crystal dimensions $0.12 \times 0.14 \times 0.21$ mm^3; $T = 103$ K; measuring range $3 \le 2\theta \le 44°$; 1861 unique reflections, 1348 observed with $F_o \le 4\sigma(F)$; anisotropic temperature factors for the non-hydrogen atoms; 190 refined parameters, $R = 0.05$, $R_w = 0.063$. For further details, see [3], CSD-320104.
[8] **4**: NMR (cf. [2]): $\delta(^1H) = 0.80 - 1.20$ (4H; C-CH_2-CH_2C of Bu), 0.89 (t, 3H; CH_3 of Bu), 1.06 (s, 18H; 2 B*t*Bu), 1.21 (s, 9H; N*t*Bu), 2.99 (t, 2H; NCH_2); $\delta(^{11}B) = 42.7$; $\delta(^{13}C) = 14.3$ (q; C4 of Bu), 20.5 (t; C3 of Bu), 29.4 (q; C2 of B*t*Bu), 34.4 (q; C2 of N*t*Bu), 37.4 (t; C2 of Bu), 42.7 (t; C1 of Bu), 48.8 (s; C1 of N*t*Bu); the BC-^{13}C singlet was not found. MS: *m/z* 278 ($M^{\oplus}$, 39%), 263 ($M^{\oplus} - CH_3$, 100), 235 ($M^{\oplus} - C_3H_7$, 71), 221 ($M^{\oplus} - C_4H_9$, 36).
[9] P. Paetzold, E. Schröder, G. Schmid, R. Boese, *Chem. Ber. 118* (1985) 3205; P. Paetzold, C. von Plotho, G. Schmid, R. Boese, B. Schrader, D. Bougeard, U. Pfeiffer, R. Gleiter, W. Schäfer, *ibid. 117* (1984) 1089.

The First Clamped and Strongly Deformed Adamantane**

By *Fritz Vögtle,* Joachim Dohm,* and *Kari Rissanen*

Can benzene rings in strained macrocycles be replaced by adamantane building blocks? If so, this would offer a general approach to varying the lipophilicity, ring strain, and cavity size and shape of cyclophanes and host compounds. Comparison of the angles in adamantane and benzene (Scheme 1) shows that the bridgehead bonds in 1,3-position, like the *m*-phenylene bonds, form an angle of ca. 120°.

Scheme 1.

The stereochemistry of the new hydrocarbon phane **1**, which we designed with this consideration in mind, was expected to be fundamentally different from that of the known [2.2]metacyclophane **2**, since *three* intraannular H_i hydrogen atoms project into the interior of the ten-membered ring.

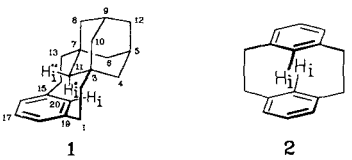

1 **2**

The synthesis of **1** (m.p. 78–79.5°) was accomplished via the dithia[3.3]cyclophane route, starting from 1,3-bis(mercaptomethyl)benzene and 1,3-bis(bromomethyl)adamantane,[1] to give dithia[3.3]phane **3** (40% yield),[2] followed by sulfone pyrolysis (50% yield)[3] (Scheme 2).

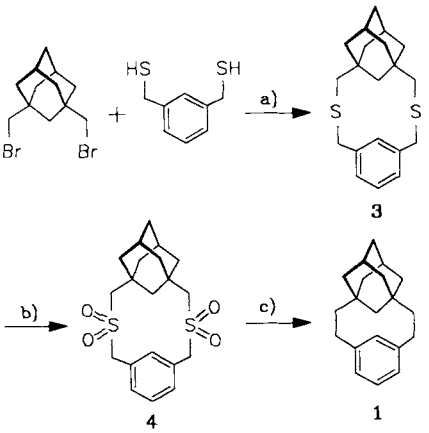

Scheme 2. a) High-dilution technique, 2 equiv. NaOH, EtOH/C_6H_6 (4:1), 78 h reflux, 12 h room temperature, 40%; b) HOAc, H_2O_2 (30%), 5 h reflux, 65%; c) 10^{-4} Torr, 550 °C, 50%.

The "[2.2](1,3)adamantanometacyclophane" **1**[4] exhibits an intense molecular peak in the mass spectrum (*m/z* 266) and characteristic ^1H and ^{13}C NMR spectra. The signals of H_i' and H_i'' are strongly shifted upfield ($\delta = -0.10$ and $+0.06$),[5] whereas H_i of the benzene ring absorbs at $\delta = 7.75$. The signals of dithiaphane **3** and disulfone **4** are even more strongly shifted upfield (up to $\delta = -2.18$; cf. Table 1).

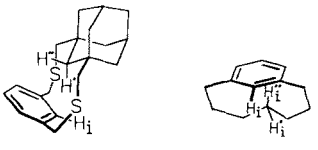

3 **5**

[*] Prof. Dr. F. Vögtle, Dipl.-Chem. J. Dohm
Institut für Organische Chemie und Biochemie der Universität
Gerhard-Domagk-Strasse 1
D-5300 Bonn 1 (FRG)
Dr. Kari Rissanen
Department of Chemistry
University of Jyväskylä
Kyllikinkatu 1–3
SF-40100 Jyväskylä (Finnland)

[**] This work was supported by the Deutsche Forschungsgemeinschaft (Sonderforschungsbereich 334: Interactions in Molecules), the Fonds der Chemischen Industrie (doctoral fellowship for *J. D.*), and Bayer AG, Leverkusen (donation of adamantane). We thank Dr. *G. Eckhardt* and *C. Schmidt* for the EI mass spectra and NMR spectra, respectively.

Table 1. ^{1}H NMR shifts of intraannular protons in **1**, **3**, and **4** as well as **5** and **2**.

Compd	δ (H_i)	δ (H'_i)	δ (H''_i)	T [°C]	Solvent
1	7.75	−0.10	0.06	25	CD_2Cl_2 [a]
		−0.18	−0.04	25	$C_2D_2Cl_4$ [b]
		−0.27	0.29	126	$C_2D_2Cl_4$ [b]
		−0.07	0.27	25	[D_8]toluene [b]
		−0.12	0.50	116	[D_8]toluene [b]
3	7.63	1.41	−2.18	25	$CDCl_3$ [a,c]
4	7.67	1.95	−1.72	25	[D_6] DMSO [a,c]
5	7.43 [d]	−0.18	−0.18	25	$CDCl_3$ [e]
		>0.50	−1.33	−73.5	$CDCl_3$ [e]
2	4.25			25	$CDCl_3$

[a] 200 MHz. [b] 90 MHz. [c] Cf. [2]. [d] 100 MHz, cf. [6]. [e] 60 MHz, cf. [6].

The ^{1}H NMR spectrum of **1** remains largely unchanged even at 116 °C (90 MHz, [D_8]toluene) and 126 °C (90 MHz, $C_2D_2Cl_4$); the AB splitting pattern of the signals of H_i' and H_i'' is merely transformed into an AM pattern, whereby the signal of the more strongly shielded H_i' is shifted to higher field, that of the less shielded H_i'' to lower field (cf. Table 1). The increase in temperature apparently affects the interaction of the solvent with the aromatic system and thus influences the ring-current effect, which causes the opposite shifts of the H_i' and H_i'' signals. From these observations we conclude that **1** is conformationally rigid and is present in the *anti* conformation.

Comparison of these findings with the ^{1}H NMR results for the corresponding [7]metacyclophane **5**,[6] for which a ring inversion has a barrier of only $\Delta G^{\ddagger} = 48$ kJ mol^{-1}, reveals that the conformational rigidity of adamantanophane **1** is remarkable. In contrast to **5**, compound **1** has a stiffened aliphatic "chain". The two aliphatic bridges in **1** and **5** therefore differ strongly in their steric demands and, in particular, in their interaction with the aromatic H_i proton.

The X-ray structure analysis reveals that, despite the "spherical" adamantane moiety, **1** adopts the *anti* conformation (Fig. 1), as observed for the [2.2]metacyclophane **2**.[7, 8]

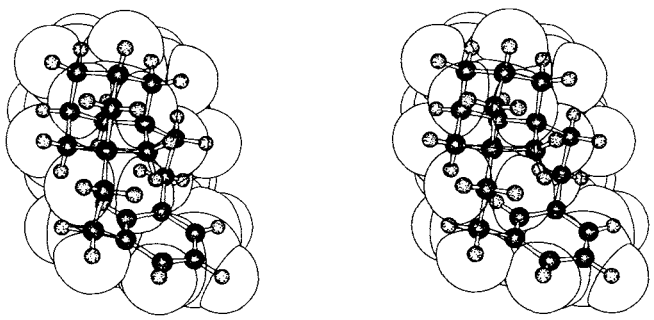

Fig. 1. Molecular structure of **1** (stereoview).

Especially striking is the strong distortion of the adamantane framework in **1**. In order to reduce the steric interactions in the interior of the macrocycle, C11 is bent away from the aromatic ring (distance C11-C20 278.6 pm, cf. Fig. 2), resulting in a flattening of the cyclohexane chair of the adamantane moiety and a decrease in the angles C10-C3-C11 and C8-C7-C11 to unusually small values (100.6° and 100.3°, respectively) for sp^3 carbon atoms (normal value: 109.5°). At the same time, the adamantane bonds C7-C8 and C3-C10 are lengthened to 154.8 and 154.5 pm, respectively, whereas the bonds C5-C6 and C4-C5 are shortened to 150.8 and 150.5, respectively. This is all the more remarkable, since known adamantane compounds encumbered sterically with substituents (e.g., biadamantane and biadamantylidene) are much less deformed.[9]

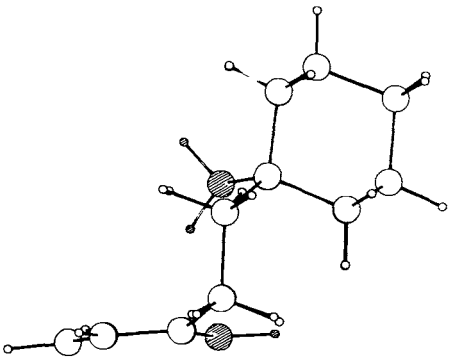

Fig. 2. Molecular structure of **1** (side view); the parts of the molecule in the "back" are exactly covered by those in the front, since this allows the intraannular atoms (hatched) and the deformations to be optimally shown.

The bond lengths and angles in the benzene ring of **1** are more strongly distorted than in the [2.2]metacyclophane **2** (values in parentheses): for example, C18-C19 141.6 pm (138.2 pm), C17-C18 136.0 pm (138.7 pm), and C18-C19-C20 116.4° (117.3°). Furthermore, the boat-shaped deformation of the benzene ring characteristic of the [2.2]metacyclophane is even more pronounced in **1**: C20 is displaced by 16.7 pm (14.3 pm) and C17 by 7.4 pm (4.2 pm) from the ring plane and the corresponding angles are 14.3° for C20 and 6.5° for C17 (11.9° and 3.5°, respectively, in **2**)! Finally, the CH_2-CH_2 bridges (157.0 and 157.8 pm) are longer in **1** than in [2.2]metacyclophane (155.9 pm).

The increased strain in **1** (compared with **2**) caused by the adamantane moiety is thus compensated by deformation of both the rigid adamantane and the benzene ring. According to MM2(85) calculations, the strain energy of **1** is nearly a factor of 2.5 higher than that of [2.2]metayclophane (**2**).[10]

The investigation shows that the rigid adamantane framework can be significantly distorted by bridging; such distortion was previously not achieved by substitution with bulky substituents. In addition, the study shows that it is possible to replace benzene rings, even in strained ring compounds, by adamantane units serving as "rigid" building blocks. These findings open up new possibilities, especially within phane chemistry, where arene units (benzene, naphthalene, pyridine, thiophene, etc.) might be replaced by adamantane and related hydrocarbons and heteropolycycles.[11, 12] Furthermore, transannular chemical reactions should be possible in these new "aliphanes"[4] and might lead—as usual for [2.2]phanes—to new polycyclic hydrocarbons hardly accessible via other routes.

Received: March 19, 1990 [Z 3862 IE]
German version: *Angew. Chem. 102* (1990) 943

CAS Registry numbers:
1, 128191-75-3; **3**, 128191-76-4; **4**, 128191-77-5; 1,3-bis(bromomethyl)adamantane, 1078-87-1; 1,3-bis(merceptomethyl)benzene, 41563-69-3.

[1] a) S. Landa, Z. Kamycek, *Collect. Czech. Chem. Commun. 24* (1959) 1320; b) an improved synthesis is described in [2].
[2] F. Vögtle, J. Dohm, M. Nieger, K. Rissanen, *Chem. Ber.*, in press.
[3] a) F. Vögtle, L. Rossa, *Angew. Chem. 91* (1979) 534; *Angew. Chem. Int. Ed. Engl. 18* (1979) 514.
[4] In a strict sense, the name "adamantanophane" is not in accord with phane nomenclature, since, according to this name, the aliphatic adamantane is treated as an "aromatic" unit. Although in violation of the rules, this name is nonetheless useful because it is short and descriptive. For comparison:

pentacyclo[9.3.3.1.1^{4,8}.1^{13,16}]eicosa-4,6,8(20)-triene (IUPAC name), pentacyclo[0.16.1^{1,5}.1^{1,7}.1^{3,7}.1^{3,7}.1^{10,14}]eicosane-10,12,14(20)-triene(nodal nomenclature[13]), [1^{3,7}.1^{3,9}.1^{5,7}][11]metacyclophane (usual phane nomenclature[14]), [2.2](1,3)adamantanometacyclophane ("araliphane" name). For this reason, corresponding names of compounds (e.g., triquinacenophane[15], cyclooctatetraenophane[16]) have already been coined in the literature. It seems reasonable to classify *arali*phatic compounds such as **1**, **3**, and **4** as "*arali*phanes" and completely *ali*phatic phane analogues as "*ali*phanes" (from *ali*phatic).

[5] Spectroscopic data for **1** (numbering shown in formula: ^{1}H NMR (200 MHz, CD_2Cl_2, TMS): $\delta = 7.75$ (s, 1H; 20-H); 7.20 (t, $^3J = 7.4$ Hz, 1H; 17-H); 6.96 (d, $^3J = 7.4$ Hz, 2H; 16,18-H); 3.14, 2.65 (AB, $^2J = 13.6$ Hz, $^3J = 12.1/3.6$ Hz, 4H; 1-H$_{ax/eq}$, 14-H$_{ax/eq}$); 2.53, 1.29 (AB, $^2J = 12.0$ Hz, 4H; 4,6-H$_{ax}$, 4,6-H$_{eq}$); 2.23 (m, 1H; 5-H); 1.98 (m, 1H;9-H); 1.65 (tt, $^3J = 3.2$ Hz, $^4J = 1.0$ Hz, 2H; 12-H); 1.41, 0.87 (AB, $^2J = 12.6$ Hz, $^3J = 12.0/3.6$ Hz, 4H; 2-H$_{ax/eq}$, 13-H$_{ax/eq}$); 1.36 (m, 4H; 8-H, 10-H); 0.06 (dt, $^2J = 16.6$ Hz, $^4J = 3.0$ Hz, 1H; 11-H$_{eq}$); -0.10 (d, $^2J = 16.6$ Hz, 1H; 11-H$_{ax}$). ^{13}C NMR (50.32 MHz, $CDCl_3$): $\delta = 145.7$ (C-15, C-19); 140.5 (C$-$20); 130.0 (C-17); 127.4 (C-18, C-16); 50.6 (C-8, C-10); 42.6 (C-2, C-13); 41.1 (C-11); 39.2 (C-12); 37.3 (C-6, C-4); 32.3 (C-1, C-14); 32.2 (C-9); 31.4 (C-3, C-7); 29.0 (C-5). The assignment was made by H,H- and C,H-COSY, spin-echo, and ^{1}H{^{1}H} NOE difference NMR spectroscopy. MS (70 eV): *m/z* 266.2027 ($M^{\oplus}$, 100%) (calcd 266.2028).

[6] S. Hirano, H. Hara, T. Hiyama, S. Fujita, H. Nozaki, *Tetrahedron 31* (1975) 2219.

[7] Crystal structure analysis of **1**: monoclinic, space group $P2_1/c$ (No. 14); $a = 1149.6(1)$, $b = 1558.7(2)$, $c = 916.7(1)$ pm, $\beta = 112.30(1)^\circ$; $V = 1519.7(3) \times 10^6$ pm^3; $Z = 4$; $\varrho_{calcd} = 1.164$ g cm^{-3}; $Mo_{K\alpha}$ ($\lambda = 0.70930$ Å); $\mu = 0.06$ mm^{-1}; $F(000) = 584$; $T = 296 \pm 1$ K; crystal dimensions, $0.20 \times 0.18 \times 0.24$ mm; CAD4 diffractometer (Enraf-Nonius); corrections: Lorentz polarization, linear 5% decrease (corrected with factors 1.000 to 1.024 on *I*); $2\theta = 4 - 50^\circ$; *hkl* range: $h = -13$–12, $k = -18$–0, $l = 0$–10; 2779 measured, unique reflections, 1417 with $I > 3.0\,\sigma I$. The structure was solved using MULTAN (least-squares Fourier method). Refinement: $R = 0.045$, $R_w = 0.055$, non-hydrogen atoms refined anisotropically, H atoms determined using the ΔF map and refined with fixed, isotropic temperature factors (SDP and PLUTO programs). Further details of the crystal structure investigations are available on request from the Director of the Cambridge Crystallographic Data Centre, University Chemical Laboratory, Lensfield Road, Cambridge CB2 1EW (UK), on quoting the full journal citation.

[8] The dithiaphane **3** was also characterized by X-ray structure analysis: cf. [2].

[9] a) S. C. Swen-Walstra, G. J. Visser, *Chem. Commun. 1971*, 82; b) R. A. Alden, J. Kraut, T. G. Traylor, *J. Am. Chem. Soc. 90* (1968) 74; c) O. Ermer, *ibid. 110* (1988) 3747; d) O. Ermer, C.-D. Bödecker, *Chem. Ber. 114* (1981) 652; e) M. A. Flamm-ter Meer, H.-D. Beckhaus, K. Peters, H.-G. von Schnering, C. Rüchardt, *ibid. 118* (1985) 4665.

[10] MM2(85)/MMP2 calculations (on an HP 9000/825S SRX) gave a σ strain energy of 217 kJ mol^{-1} for **1** and 85.5 kJ mol^{-1} for **2**; semiempirical calculations using AM1 (on a CONVEX C 220) gave an SCF standard enthalpy of formation of 50.9 kJ mol^{-1} for **1** and 182 kJ mol^{-1} for **2**. We thank Dipl.-Chem. *P. M. Windscheif* for the calculations. For strain energies of other small cyclophanes cf. F. Bickelhaupt, *Pure Appl. Chem. 62* (1990) 373.

[11] This was further substantiated by our synthesis of macrocycles of type **6**, formally obtained by replacement of two benzene rings by adamantane

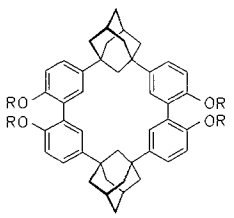

6: R = H, CH_3, CH_2COOEt

units in hexa-*m*-phenylene[17]. The poor solubility of hexa-*m*-phenylene was still exhibited even after incorporation of the adamantane framework. The following macrocycles were identified by mass spectrometry: **6** (R = H): EI-MS, *m/z* calcd 636.3228, found 636.3259 ($M^{\oplus}$); **6** (R = CH_3): EI-MS, *m/z* 692 ($M^{\oplus}$); **6** (R = $CH_2COOC_2H_5$): EI-MS, *m/z* 980 ($M^{\oplus}$).

[12] Unstrained macrocyclic polyethers containing an adamantane unit: A. A. Chaikovskaya, T. N. Kudrya, A. M. Pinchuk, *Zh. Org. Khim. 25* (1989) 2000.

[13] N. Lozac'h, A. L. Goodson, *Angew. Chem. 96* (1984) 1; *Angew. Chem. Int. Ed. Engl. 23* (1984) 1.

[14] F. Vögtle, P. Neumann, *Tetrahedron 26* (1970) 5847.

[15] W. P. Roberts, G. Shoham, *Tetrahedron Lett. 22* (1981) 4895.

[16] L. A. Paquette, M. A. Kesselmayer, *J. Am. Chem. Soc. 112* (1990) 1258.

[17] H. A. Staab, F. Binning, *Chem. Ber. 100* (1967) 293.

$CsNa_2(OH)_3 \cdot 6H_2O$: Structural Differentiation in the Hydrate of a Ternary Alkali-Metal Hydroxide**

By *Dietrich Mootz** and *Heinz Rütter*

Dedicated to Professor Dietrich Babel on the occasion of his 60th birthday

The structures of most hydrates of the lighter alkali-metal hydroxides were determined some time ago.[1, 2] More recently, structural characterizations have also been carried out for such compounds of the heavy alkali metals[3] as well as for anhydrous ternary alkali hydroxides.[4] *Hydrates*, however, of ternary alkali hydroxides, to our knowledge, have so far not been subjected to crystal structure analysis. Only one phase of this kind, to which the composition $CsOH \cdot 2\,NaOH \cdot 4H_2O$ has been assigned, can be found in the literature.[5] Our structure determination[6] unmistakably shows that the compound in question, melting congruently at 46.5 °C, is a *hexa*hydrate dominated in a characteristic way by differentiation between the cations of unequal size as well as between the H_2O molecules and the $OH^{\ominus}$ ions.[7]

In the crystal structure of $CsNa_2(OH)_3 \cdot 6H_2O$ the $Na^{\oplus}$ ions are coordinated by the six H_2O molecules to form distorted octahedra (Na–O distances between 2.275(3) and 2.688(3) Å). The octahedra are linked by common faces to form columns parallel to the crystallographic *b* axis. These are arranged according to the pattern of closest packing of cylindrical rods[8] and connected with each other by a complex system of hydrogen bonds with the H_2O molecules as twofold proton donors and the $OH^{\ominus}$ ions as fourfold proton acceptors (O···O distances between 2.633(4) and 2.798(4) Å). Thus, each $OH^{\ominus}$ ion bridges two octahedron edges in adjacent columns. Each column, together with two further ones and the associated $OH^{\ominus}$ ions, encloses in a

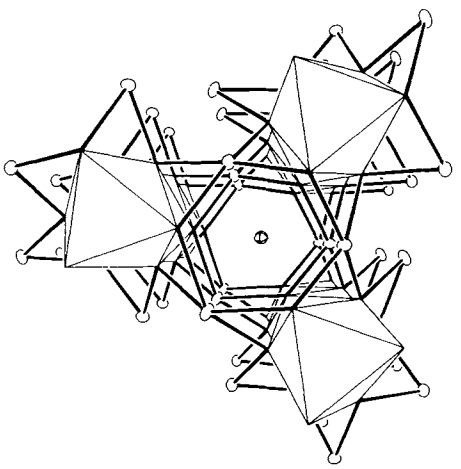

Fig. 1. Perspective drawing of the structure of $CsNa_2(OH)_3 \cdot 6H_2O$, projected down the *b* axis (atomic thermal-vibration ellipsoids at the 25% probability level, ORTEP plot[10]). Ellipsoids without equators, $OH^{\ominus}$ ions; ellipsoid with equator, $Cs^{\oplus}$ ion; bold lines, hydrogen bonds. One sees the pseudotrigonal arrangement of three columns of the face-linked $Na(H_2O)_6$ octahedra and, between them and the bridging $OH^{\ominus}$ ions, the large cavities containing the $Cs^{\oplus}$ ions. For completion of the three small cavities another column each (not shown in the figure) has to be added.

[*] Prof. Dr. D. Mootz, Dipl.-Chem. H. Rütter
Institut für Anorganische Chemie und Strukturchemie der Universität
Universitätsstrasse 1, D-4000 Düsseldorf (FRG)

[**] This work was supported by the Minister für Wissenschaft und Forschung des Landes Nordrhein-Westfalen, the Fonds der Chemischen Industrie, and the Dr. Jost Henkel-Stiftung. It is part of the doctoral dissertation in progress of *H. Rütter*, Universität Düsseldorf.

pseudotrigonal arrangement a total of three small and three large cavities, of which the latter type is highlighted in Figure 1. The H atoms of the $OH^{\ominus}$ ions probably project into the small cavities. In agreement with the generally low proton-donor strength of the $OH^{\ominus}$ion, they do *not* participarte in hydrogen bonds.[9] The large cavities enclose the $Cs^{\oplus}$ ions and may be considered as cuboctahedra consisting of nine H_2O molecules and the three $OH^{\ominus}$ groups, compressed along the pseudo-threefold axis (Fig. 2). The corresponding

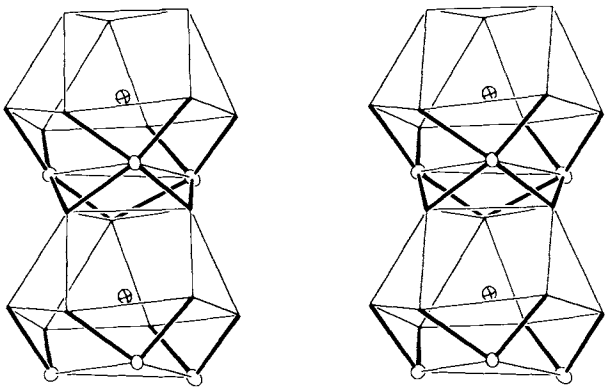

Fig. 2. Stereoscopic drawing of two cuboctahedra containing the $Cs^{\oplus}$ ions, succeeding each other along the pseudo-threefold axis, and their connection by hydrogen bonds; same way of representation as in Figure 1.

twelve Cs–O distances of 3.287(3) to 3.981(3) Å are the shortest ones; the next shortest distance, however, is already 4.113(3) Å.

In the higher hydrates of NaOH the $OH^{\ominus}$ ions are also not coordinated to the small, hard $Na^{\oplus}$ ions.[2] This generally has to do with the lowered charge density of the $OH^{\ominus}$ ions due to multiple proton-acceptor function in hydrogen bonds. Conversely, in the title compound the coordination of two of the $OH^{\ominus}$ ions to the large, softer $Cs^{\oplus}$ ion is reflected in the shortest Cs–O distances (3.287(3) and 3.296(3) Å), and also the third $OH^{\ominus}$ ion, following after five H_2O molecules, is still rather tightly bound at 3.542(3) Å.

Received: September 28, 1989;
supplemented: April 9, 1990 [Z 3567 IE]
Publication delayed at authors' request
German version: *Angew. Chem. 102* (1990) 949

CAS Registry number:
$CsNa_2(OH)_3 \cdot 6H_2O$, 128112-95-8.

[1] P. A. Agron, W. R. Busing, H. A. Levy, *Winter Meet. 1972 Crystallogr. Assoc., Albuquerque, NM, Collect. Abstr.*, p. 52; J. A. Wunderlich, *Bull. Soc. Fr. Minéral. Cristallogr. 81* (1958) 287; G. Beurskens, G. A. Jeffrey, *J. Chem. Phys. 41* (1964) 924; P. Hemily, *C. R. Hebd. Séances Acad. Sci. 236* (1953) 1579.

[2] R. Seidel, Dissertation, Universität Düsseldorf 1988.

[3] H. Jacobs, T. Tacke, J. Kockelkorn, *Z. Anorg. Allg. Chem. 516* (1984) 67; H. Jacobs, A. Schardey, *ibid. 565* (1988) 34; H. Jacobs, B. Harbrecht, P. Müller, W. Bronger, *ibid. 491* (1982) 154.

[4] H. Jacobs, A. Schardey, B. Harbrecht, *Z. Anorg. Allg. Chem. 555* (1987) 43.

[5] L. A. Sadokhina, V. V. Otdel'nov, G. V. Zimina, S. B. Stepina, *Russ. J. Inorg. Chem. (Engl. Transl.) 25* (1980) 1266.

[6] Large, colorless columns of the title compound were obtained by slow evaporation of the solvent water; space group $Pca2_1$ (No. 29), a = 13.951(3), b = 6.089(1), c = 12.508(3) Å, V = 1062.6 Å^3, Z = 4, Siemens-Stoe AED2, $Mo_{K\alpha}$ radiation, graphite monochromator, measuring range $3° < 2\theta < 70°$, 2430 measured symmetry-independent reflections, of which 2202 with $F > 4\sigma(F)$, absorption correction with ψ-scan, R = 0.026, R_w = 0.040. Due to the strongly scattering Cs atoms the H atoms could not be localized unambiguously; a neutron diffraction study is planned. Further details of the crystal structure determination can be obtained on request from the Fachinformationszentrum Karlsruhe, Gesellschaft für wissenschaftlich-technische Information mbH, D-7514 Eggenstein-Leopoldshafen 2 (FRG), on quoting the depository number CSD-54521, the names of the authors, and the journal citation.

[7] Even without definitely determined H-atom positions the assignment of H_2O and $OH^{\ominus}$ as made for the subsequent description of the structure is practically inevitable.

[8] M. O'Keeffe, S. Andersson, *Acta. Crystallogr. Sect. A 33* (1977) 914.

[9] Due to difficulties in the preparation of samples an IR spectrum of the substance suitable for a check of this result could so far not be obtained. However, apart from the O···O distances already assigned as hydrogen bonds (see text), there are no further distances with $OH^{\ominus}$ ions smaller than 3.385(5) Å in the structure.

[10] C. K. Johnson, ORTEP II, Report ORNL-5138, Oak Ridge National Laboratory, Oak Ridge, TN, 1976.

C_4O_2 (1,2,3-Butatriene-1,4-dione), the First Dioxide of Carbon with an Even Number of C Atoms

By *Günther Maier,* Hans Peter Reisenauer, Heinz Balli, Willy Brandt*, and *Rudolf Janoschek*

Dedicated to Professor Wolfgang Kirmse on the occasion of his 60th birthday

The long known dioxides of carbon, CO_2 **1** and C_3O_2 **3**, as well as that recently prepared by us, C_5O_2 **5**,[1] have an odd number of carbon atoms. Analogues with an even number of carbon atoms—C_2O_2 **2** or C_4O_2 **4**—have so far defied experimental detection.[2, 3]

O=C=O **1** O=C=C=O **2** O=C=C=C=O **3**

O=C=C=C=C=O **4** O=C=C=C=C=C=O **5**

Theoretically, the compounds **2** and **4** should—in contrast to **1**, **3** and **5**—have a triplet ground state,[4] as also indicated by simple MO considerations: the electronic situation compares with that in the O_2 molecule. The π-molecular orbitals of **1**–**5**, with a linear geometry ($D_{\infty h}$), are pairwise degenerate (x and y directions indistinguishable). This leads, with an even number of C atoms, to two electrons being available for the highest occupied pair of molecular orbitals instead of the four electrons required for a closed shell. According to *Hund*'s rule this situation should lead to a triplet ground state.

Motivated by the simple synthetic entry to **5** by photolytic or thermal decomposition of trisdiazocyclohexanetrione[1] we have prepared the structurally similar cyclic diazoketones **6**[5]–**8** by diazo-group transfer in the hope of finding an entry to **2** or **4**.

[*] Prof. Dr. G. Maier, Dr. H. P. Reisenauer
Institut für Organische Chemie der Universität
Heinrich-Buff-Ring 58, D-6300 Giessen (FRG)
Prof. Dr. H. Balli, Dipl.-Chem. W. Brandt
Institut für Farbenchemie der Universität
St. Johannsvorstadt 10, CH-4056 Basel (Switzerland)
Prof. Dr. R. Janoschek
Institut für Theoretische Chemie der Universität
Mozartgasse 14, A-8010 Graz (Austria)

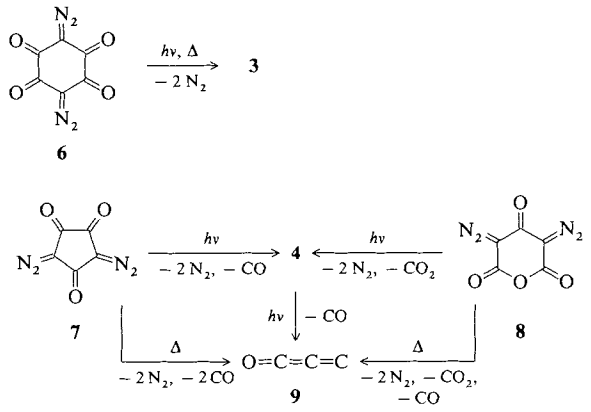

The three precursors were subjected both to a high-vacuum flash pyrolysis with subsequent isolation of the products in an argon matrix, as well as to direct irradiation in the matrix. In the thermolysis of **6** and its photolysis with a Hg low-pressure lamp (254 nm) only **3** could be detected IR spectroscopically. In contrast, the gas-phase thermolysis of the diazoketones **7** and **8** afforded the already known C_3O **9**,[6] which could be identified by its characteristic bands in the IR spectrum of the matrix-isolated products. More interesting is the photolysis of the matrix-isolated precursors **7** and **8**, which crucially depends on the wavelength of the irradiating light. With wavelengths >300 nm (Hg high-pressure lamp/long pass filter or monochromator) **9** is smoothly formed again in both cases. If, on the other hand, a Hg low-pressure lamp (254 nm) is used as light source only a small amount of **9** is formed initially. The main product is now C_4O_2 **4**, the IR spectrum of which is shown in Figure 1.

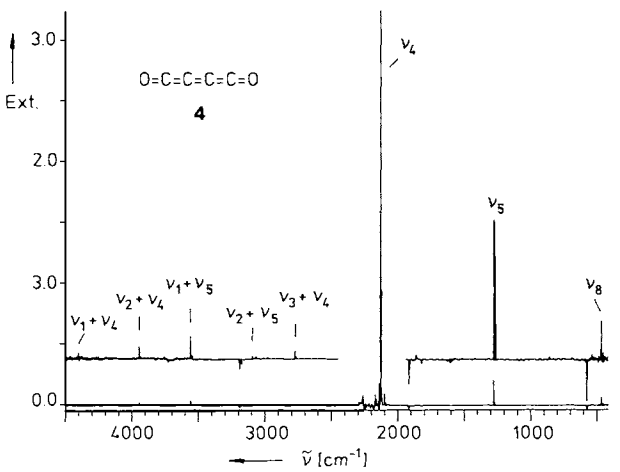

Fig. 1. Photolysis of 7 in an argon matrix: difference spectrum (5 min 254 nm – 10 min 335 nm; the bands pointing downwards belong to C_3O; numbering referred to $D_{\infty h}$ symmetry). Ext. = absorbance.

This assignment is supported by the observation that **4** rapidly dissociates into CO and **9** upon continuation of the photolysis with wavelengths > 300 nm.

To corroborate the analysis of the IR spectrum we have calculated the geometry of C_4O_2 (triplet and singlet state) by semiempirical methods (PM3 and MNDO) [optimized geometries: linear ($D_{\infty h}$) and bent (C_{2h}), resp.]. The calculated vibrational spectra are listed together with the experimental data in Table 1. The band patterns obtained for both geometries compare equally well with the experimental spectrum, so that a decision between a linear and slightly bent structure on the basis of the IR spectrum is not possible. The bands observed at 2130 and 1277 cm^{-1}, however, can be assigned to the two IR-active stretching vibrations Σ_u or B_u respectively, and the weak band at 467 cm^{-1} to the higher of the two IR-active bending vibrations Π_u or A_u respectively. The positions of the three IR-inactive stretching vibrations Σ_g and A_g can be calculated indirectly from the six observable combination bands ($\Sigma_g + \Sigma_n$ or $A_g + B_u$). They should be observable at about 2277, 1816 and 642 cm^{-1} in the Raman spectrum.

Table 1. Observed IR absorptions (argon matrix, 12 K) and calculated vibrations of **4** ($^3\Sigma_g^-$, ^1A_g) [cm^{-1}], relative IR intensities [%] in brackets.

		Calculation (PM3) $^3\Sigma_g^-$ ($D_{\infty h}$)			Calculation (PM3) ^1A_g (C_{2h})		Calculation (MNDO) $^3\Sigma_g^-$ ($D_{\infty h}$)		Experiment	
ν_1[a]	Σ_g	2515	(0.0)	A_g	2436	(0.0)	2597	(0.0)	2277[b]	–
ν_2	Σ_g	2062	(0.0)	A_g	2073	(0.0)	2144	(0.0)	1816[b]	–
ν_3	Σ_g	709	(0.0)	A_g	740	(0.0)	727	(0.0)	642[b]	–
ν_4	Σ_u	2319	(100.0)	B_u	2303	(100.0)	2481	(100.0)	2130.3	(100.0)
ν_5	Σ_u	1408	(1.1)	B_u	1374	(0.8)	1451	(0.2)	1276.9	(7.0)
ν_6	Π_g	436	(0.0)	A_g	375	(0.0)	547	(0.0)	–	–
				B_g	312	(0.0)			–	–
ν_7	Π_g	326	(0.0)	A_g	317	(0.0)	363	(0.0)	–	–
ν_8	Π_u	408	(1.3)	A_u	616	(1.2)	508	(1.5)	467.1	(2.0)
				B_u	200	(2.2)			–	–
ν_9	Π_u	107	(0.0)	A_u	115	(0.0)	127	(0.0)	–	–
				B_u	≈0[c]	(0.7)		–	–	
ν_1 (Σ_g) + ν_4 (Σ_u)									4403.0	
ν_1 (Σ_g) + ν_5 (Σ_u)									3558.6	
ν_2 (Σ_g) + ν_4 (Σ_u)									3943.4	
ν_2 (Σ_g) + ν_5 (Σ_u)									3095.8	
ν_3 (Σ_g) + ν_4 (Σ_u)									2771.3	
ν_3 (Σ_g) + ν_5 (Σ_u)									1918.9	

[a] Numbering referred to $D_{\infty h}$ symmetry. [b] Average value determined from combination bands. [c] The values for this vibration vary between 50 i and 50 cm^{-1} with very small changes in geometry. The associated differences in energy are <0.01 kcal mol^{-1}. This suggests presence of a quasilinear molecule.

The dependence of the photolysis of **7** and **8** on the wavelength of the incident light is clearly demonstrated in Figure 2. C_4O_2 absorbs at λ = 340, 334 and 212 nm; its absorption at 250 nm, on the other hand, is negligible. Consequently, the secondary cleavage into C_3O and CO proceeds decisively slower with light from a mercury low-pressure lamp (λ = 254 nm) than with light of longer wavelength. More-

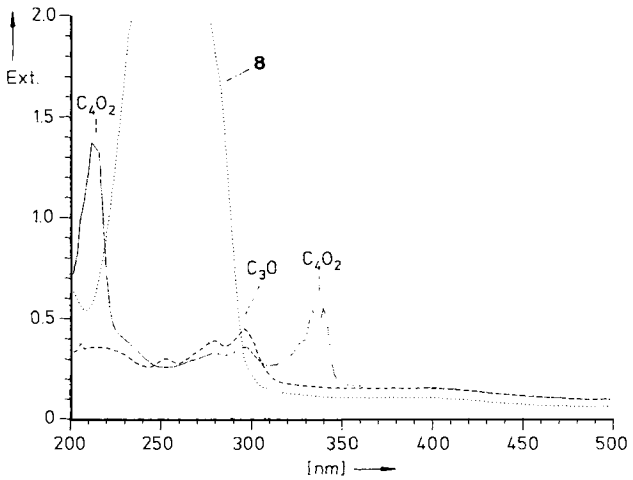

Fig. 2. Photolysis of **8** in an argon matrix: (···) unirradiated, (—) 5 min 254 nm, (---) 10 min 335 ± 10 nm.

 © VCH Verlagsgesellschaft mbH, D-6940 Weinheim, 1990 0570-0833/90/0808-0906 $ 3.50+.25/0 Angew. Chem. Int. Ed. Engl. 29 (1990) No. 8

over, C_4O_2 must also weakly absorb above 400 nm (not recognizable in the spectrum), since it also dissociates into C_3O and CO on irradiation with monochromatic light of wavelength 436 ± 10 nm.

The equilibrium structure of C_4O_2 in the triplet state was calculated both at the ab-initio UHF/3-21G(d) level as well as by the semiempirical UHF-PM3 method (Scheme 1, left). In both cases a linear structure ($D_{\infty h}$) results. The orbital situation also requires, despite *Hund*'s rule, the investigation of the lowest singlet state in order to determine the nature of the ground state of **4**, for the singlet state could, other than in the case of the O_2 molecule, be stabilized by bending and thus compete energetically with the triplet state. Both ab-initio SCF as well as PM3 calculations indicate a non-linear singlet structure with C_{2h} symmetry (Scheme 1, right).

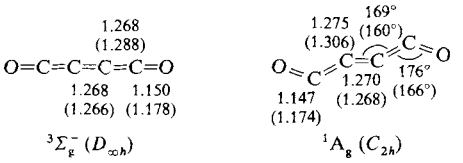

Scheme 1. Left: equilibrium structure of **4** in the lowest triplet state, calculated at the ab initio UHF/3-21G(d) level (UHF-PM3 values in brackets). The bond lengths are given in Å. Right: equilibrium structure of **4** in the lowest singlet state, calculated at the ab initio SCF/3-21G (d) level (PM3 values in brackets).

Four different sets of calculations consistently indicate a triplet ground state. The small term splittings (Table 2), however, do not permit unequivocal conclusions to be drawn about the ground state.

Table 2. Calculated relative energy [kcal mol^{-1}] of the lowest singlet and triplet states of **4** [^1A_g(C_{2h}) correlates with $^1\Delta_g$ ($D_{\infty h}$)].

	PM3-CI[7]	MCSCF[a] 3-21+G	UMP2[9] 3-21G(d)	6-31G(d)
^1A_g (C_{2h})	8.8	8.5	4.8	4.0
$^3\Sigma_g^-$ ($D_{\infty h}$)	0.0	0.0	0.0	0.0

[a] 2-Electron-4-orbital-(π_g, π_u)-MCSCF[8].

The electronically excited states and vertical excitation energies of C_4O_2 were calculated by the MCSCF method.[8] The results are listed in Table 3. There are symmetry allowed excitations at ca. 180 and 400 nm in both the triplet as well as the singlet term scheme, whereas transitions, at 330 nm are only possible from the ^1A_g state. The data for the observed absorptions of C_4O_2 (Fig. 2) are, in good agreement with the calculated singlet transitions, at 212, 334, 340 and above 400 nm. For the photolysis product C_3O we have calculated 317 and 288 nm respectively for the symmetry allowed transitions $^1\Sigma^+ \rightarrow {}^1\Pi$ and $^1\Sigma^+ \rightarrow {}^1\Sigma^+$. These values are in good agreement with measured values 295 and 280 nm.

Table 3. Calculated (2-configuration-MCSCF) vertical electronic transitions λ [nm] from $^3\Sigma_g^-$ ($D_{\infty h}$) and ^{1}Ag (C_{2h}).*: symmetry allowed transitions.

$^3\Sigma_g^-$	λ	^1A_g	λ
$^3\Delta_u$	433	$^{*1}A_u$	510
$^3\Sigma_u^+$	421	$^{*1}B_u$	435
$^{*3}\Sigma_u^-$	400	$^{*1}B_u$	412
$^3\Delta_u$	299	$^{*1}A_u$	339
$^3\Sigma_u^+$	295	$^{*1}A_u$	324
$^{*3}\Sigma_u^-$	176	$^{*1}B_u$	186

The photolysis of C_4O_2 at wavelengths of over 400 nm can be correlated with the calculated transition $^1A_g \rightarrow {}^1B_u$ at 412 nm (Fig. 3). If the photolysis starting from the C_{2h} symmetry terminates in the C_s symmetry, ^1A_g (C_4O_2 with eight π electrons) correlates with the doubly excited state $^1\Sigma^+$ (C_3O with six π electrons) + $^1\Sigma^+$ (CO with two π electrons). ^1B_u (C_4O_2 with six π electrons) correlates with the ground state $^1\Sigma^+$ C_3O with four π electrons) + $^1\Sigma^+$(CO). As a result of the avoided crossing C_4O_2 (^1B_u) can dissociate non-adiabatically to C_3O + CO in the ground states. The height of the barrier to kinetic stabilization of C_4O_2 (^1A_g) must, according to Figure 3, lie below the point of intersection of the correlation lines, i.e. below 60 kcal mol^{-1}. Literature values of 200 kcal mol^{-1} [4f] are based on unsuitable methods of calculation (SCF), which cannot describe an avoided crossing.

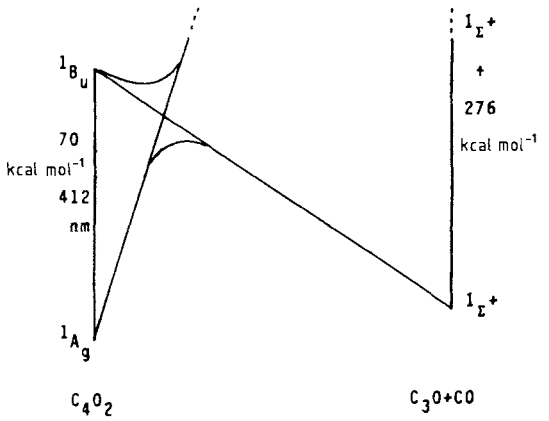

Fig. 3. State correlation diagram for the mechanism of photolysis of C_4O_2.

In the hope of obtaining direct evidence for the triplet character of C_4O_2 we have investigated the irradiated (λ = 254 nm) samples of **7** and **8** (argon matrix) ESR spectroscopically. However, up to the maximum magnetic field strength of 7000 Gauss (measuring frequency: 9.38 GHz) of the spectrometer available, no triplet signal could be recorded. On the assumption that C_4O_2 does in fact have a triplet ground state, the zero-field splitting parameter D must be greater than 1.0 cm^{-1}.[10] Such a value is not unreasonable, since very high D values have been measured for structurally similar, linear cumulenes (ground state $^3\Sigma$) such as C_nO (n even),[11] C_n (n > 2, even),[12] CNN,[13] SiCO,[14] and SiNN.[14] Hence, the negative ESR results do not in any way rule out a triplet ground state for C_4O_2.

Summarizing: C_4O_2 is a stable molecule under matrix conditions. It can be readily split photochemically into C_3O and CO. The question whether the molecule has a singlet or triplet ground state is open.

Experimental

7: A mixture of 1,2,4-cyclopentanetrione [15] (0.50 g, 4.5 mmol) and 2-azido-3-ethylbenzothiazolium tetrafluoroborate [16] (5.00 g, 17.1 mmol) in water

(200 mL) was acidified with 3 drops of 32% HCl and stirred for 15 min at 50 °C (exclusion of light). After extraction with CH_2Cl_2, the organic phase was dried (Na_2SO_4) and purified on silica gel (20 g). After removal of the solvent there remained 0.53 g (72%) of a crystalline product. For further purification the substance was recrystallized from CH_2Cl_2/Et_2O; yield 0.42 g (57%), colorless platelets. M.p. 135–137 °C (decomp.), noticeable decomposition above 120 °C. UV (CH_2Cl_2): λ_{max} (lgε) = 256 nm (4.37), 288 (4.01), 311 (3.51), 340 (3.55). IR (KBr): $\tilde{\nu}$ = 2160 cm^{-1}, 2135, 1755, 1685, 1355, 1355, 1310, 712. MS (70 eV): *m/z* (%) = 164 (9, $M^{\oplus}$), 136(7), 80(86), 68(69), 52(100). Correct elemental analysis.

8: A mixture of dihydropyran-2,4,6-trione [17] (0.60 g, 4.7 mmol) and 2-azido-3-ethylbenzothiazolium tetrafluoroborate [16] (3.00 g, 10.3 mmol) in 150 mL of 100% glacial acetic acid was stirred for 2 h at 60 °C. The crude desired product was precipitated by addition of 180 mL of Et_2O. After filtration the crystalline residue almost completely dissolved in CH_2Cl_2/CH_3CN (4:1) and was purified chromatographically on silica gel with CH_2Cl_2 as eluent. Evaporation of the liquid phase to dryness furnished a crystalline residue, which was dissolved in 60 mL of CH_2Cl_2 and 20 mL of CH_3CN. Subsequent dropwise addition of 250 mL of Et_2O and filtration afforded 0.31 g (36%) of colorless platelets. Noticeable decomposition above 150 °C. UV (CH_2Cl_2): λ_{max} (lg ε) = 244 nm (4.23, 258 (4.28), 268 (4.27), 280 (4.24). IR (KBr): $\tilde{\nu}$ = 2170 cm^{-1}, 2100, 1750, 1740, 1715, 1640, 1355, 740, 735. MS (70 eV): *m/z* (%) = 180 (30, $M^{\oplus}$), 80(10), 68(39), 52(100). Correct elemental analysis.

Received: March 5, 1990 [Z 3830 IE]
German version: *Angew. Chem. 102* (1990) 920

[1] G. Maier, H. P. Reisenauer, U. Schäfer, H. Balli, *Angew. Chem. 100* (1988) 590; *Angew. Chem. Int. Ed. Engl. 27* (1988) 566; see also: F. Holland, M. Winnewisser, G. Maier, H. P. Reisenauer, A. Ulrich, *J. Mol. Spectrosc. 130* (1988) 470.

[2] a) J. J. Bloomfield, I. R. S. Irelan, A. P. Marchand, *Tetrahedron Lett. 1968*, 5647. The bridged 1,2-diones described in this work have already been irradiated by us in an argon matrix in a previous study (unpublished experiments, 1979), and only CO was found. b) H.-D. Scharf, R. Klar, *Tetrahedron Lett. 1971*, 517; c) J. Strating, B. Zwanenburg, A. Wagenaar, A. C. Udding, *ibid. 1969*, 125; d) D. Bryce-Smith, A. Gilbert, *J. Chem. Soc. Chem. Commun. 1968*, 1319; e) D. L. Dean, H. Hart, *J. Am. Chem. Soc. 94* (1972) 687; f) M. B. Rubin, M. Weiner, H.-D. Scharf, *ibid. 98* (1976) 5699.

[3] The existence of the analogous carbon sulfides C_2S_2 and C_4S_2 has been confirmed mass spectroscopically: D. Sülzle, H. Schwarz, *Angew. Chem. 100* (1988) 1384; *Angew. Chem. Int. Ed. Engl. 27* (1988) 1591; *Chem. Ber. 122* (1989) 1803. *Note added in proof:* In the meantime we have generated C_2S_2 via an independent route, and isolated it in an argon matrix. Conversely, *H. Schwarz* and *D. Sülzle* have detected C_4O_2 by neutralization-reionization mass spectrometry (private communication, April 30, 1990).

[4] a) G. P. Raine, H. F. Schaefer III, R. C. Haddon, *J. Am. Chem. Soc. 105* (1983) 194; b) R. C. Haddon, D. Poppinger, L. Radom, *ibid. 97* (1975) 1645; c) R. C. Haddon, *Tetrahedron Lett. 1972*, 3897; d) J. Fleischhauer, M. Beckers, H.-D. Scharf, *ibid. 1973*, 4275; e) P. Lindner, Y. Öhrn, J. B. Sabin, *Int. J. Quantum Chem. Symp. 7* (1973) 261; f) R. D. Brown, E. H. N. Rice, *J. Am. Chem. Soc. 106* (1984) 6475.

[5] F. Henle, *Justus Liebigs Ann. Chem. 350* (1906) 344.

[6] a) R. L. DeKock, W. Weltner, Jr., *J. Am. Chem. Soc. 93* (1971) 7106; b) R. D. Brown, F. Eastwood, P. S. Elmer, P. D. Godfrey, *ibid. 105* (1983) 6496; c) R. D. Brown, P. D. Godfrey, P. S. Elmer, M. Rodler, L. M. Tack, *ibid. 107* (1985) 4112; d) R. D. Brown, D. E. Pullin, E. H. N. Rice, M. Rodler, *ibid. 107* (1985) 7877.

[7] J. J. P. Stewart, *J. Comput. Chem. 10* (1989) 209, 221.

[8] H. J. Werner, W. Meyer, *J. Chem. Phys. 74* (1981) 5794; H. J. Werner, E. A. Reinsch, *ibid. 76* (1982) 3144.

[9] J. S. Binkley, M. J. Frisch, D. J. DeFrees, R. Krishnan, R. A. Whiteside, H. B. Schlegel, E. M. Fluder, J. A. Pople: *GAUSSIAN 82*, Carnegie-Mellon University, Pittsburgh 1982.

[10] E. Wasserman, L. C. Snyder, W. A. Yager, *J. Chem. Phys. 41* (1964) 1763.

[11] a) R. J. Van Zee, G. R. Smith, W. Weltner, Jr., *J. Am. Chem. Soc. 110* (1988) 609; b) D. W. Ewing, *ibid. 111* (1989) 8809.

[12] R. J. Van Zee, R. F. Ferrante, K. J. Zeringue, W. Weltner, Jr., D. E. Ewing, *J. Chem. Phys. 88* (1988) 3465.

[13] a) E. Wasserman, L. Barash, W. A. Yager, *J. Am. Chem. Soc. 87* (1965) 2075; b) G. R. Smith, W. Weltner, Jr., *J. Chem. Phys. 62* (1975) 4592.

[14] R. R. Lembke, R. F. Ferrante, W. Weltner, Jr., *J. Am. Chem. Soc. 99* (1977) 416.

[15] J. H. Boothe, R. G. Wilkinson, S. Kushner, J. H. Williams, *J. Am. Chem. Soc. 75* (1953) 1732.

[16] H. Balli, F. Kersting, *Justus Liebigs Ann. Chem. 647* (1961) 1.

[17] R. Kaushal, *J. Ind. Chem. Soc. 17* (1940) 138.

Identification of Butatrienedione, Its Radical Anion, and Its Radical Cation in the Gas Phase**

By *Detlev Sülzle* and *Helmut Schwarz**

Dedicated to Professor Wolfgang Kirmse on the occasion of his 60th birthday

There are several reasons for the exceptional interest[1] in linear and quasi-linear cumulenes of the general structure XC_nY (X,Y = lone pair, H_2, O, S; n ≥ 2). The compounds, some of which have been postulated as key intermediates in the formation of interstellar species, possess unusual spectroscopic properties, and their reactivity/stability, as well as their electronic ground state (singlet versus triplet), is governed by an "even/odd alternation". Although many combinations of XC_nY have long been known for n = 3, 5, the even-numbered analogues (n = 2, 4, 6) have often eluded unambiguous experimental identification. However, this situation is not due—as originally assumed[2]—to an intrinsic instability of these cumulenes, but rather must be the result of fast bimolecular reactions. For example, the dithiocumulenes SC_nS (n = 2, 4, 6)[1, 3, 4] and also the mixed S/O cumulenes SC_2O[5] and SC_4O[6] have been identified in the gas phase by neutralization-reionization mass spectrometry (NRMS).[7]

On the other hand, all attempts so far to prepare and characterize even-numbered cumulenediones OC_nO (n = 2, 4, 6) have been unsuccessful. Although ethylenedione, OC_2O, for example, is expected to be a kinetically extremely stable triplet on the basis of ab initio calculations,[8] from the earlier attempts of *Staudinger*[9] to this day no group has succeeded in generating and identifying this compound.[10]

Here we report the generation of the radical anion, radical cation, and neutral molecule of butatrienedione, OC_4O, in the gas phase. These experiments complement the recent matrix studies of *Maier* et al.[11]

Dissociative electron attachment[12] to **1**[13] affords an intense signal at *m/z* 80, which corresponds to a compound having the elemental formula $C_4O_2^{\odot\ominus}$. Mass selection of $C_4O_2^{\odot\ominus}$ via B(1)E and subsequent collisional activation of the 8-keV ion beam (collision gas O_2; 80% transmission *T*) afford the collisional activation (CA) spectrum shown in Figure 1a. All anionic decomposition products in Figure 1a can be explained by direct bond cleavage in $\mathbf{2}^{\odot\ominus}$. The assignment of the connectivity $OCCCCO^{\odot\ominus}$ to $C_4O_2^{\odot\ominus}$ is supported by the fact that the tendency to undergo skeletal rearrangements is appreciably less for radical anions than for radical cations.[14] Accordingly, we conclude that $\mathbf{1}^{\odot\ominus}$ eliminates CO_2 and $(CH_3)_2CO$ and is transformed into $\mathbf{2}^{\odot\ominus}$ (Scheme 1). We further maintain that, except for $CO^{\odot\ominus}$ (whose electron affinity (EA) is negative), all other species (C_4O_2, C_4O, C_3O, C_2O, C_3, C_2, and C_1) must have positive EA values.

Subjection of $\mathbf{2}^{\odot\ominus}$ in a further collision experiment to a vertical charge reversal (CR)[14b, 15, 16] results in the spectrum given in Figure 1b. This spectrum contains an intense "recovery signal" for $C_4O_2^{\odot\oplus}$ and establishes that not only $C_4O_2^{\odot\ominus}$ but also $C_4O_2^{\odot\oplus}$ exists in a potential minimum. Again remarkable is that, typical for a cumulene structure $\mathbf{2}^{\odot\oplus}$, decomposition occurs via cleavage of individual bonds.

[*] Prof. Dr. H. Schwarz, Dipl.-Chem. D. Sülzle
Institut für Organische Chemie der Technischen Universität
Strasse des 17. Juni 135, D-1000 Berlin 12

[**] This work was supported by the Deutsche Forschungsgemeinschaft, the Fonds der Chemischen Industrie, and the Graduiertenkolleg Chemie Berlin.

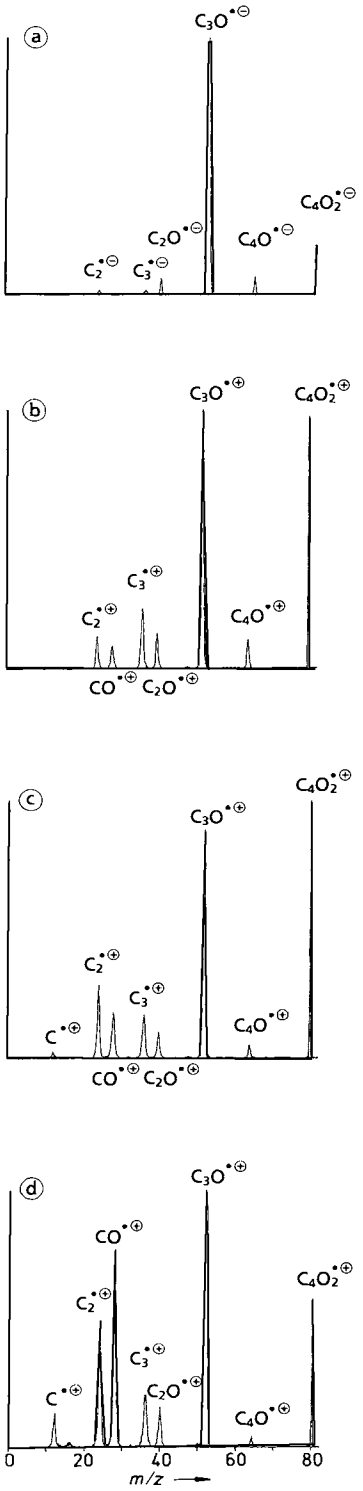

Fig. 1. a) CA spectrum of $C_4O_2^{\odot\ominus}$ (collision gas O_2, 80% T); b) CR spectrum of $C_4O_2^{\odot\ominus}$ (O_2, 80% T); c) NR spectrum of $C_4O_2^{\odot\ominus}$ (O_2, 80% T; O_2, 80% T); d) NR spectrum of $C_4O_2^{\odot\oplus}$ (Xe, 70% T; O_2, 80% T).

Is it possible to prepare neutral butatrienedione (**2**) from the radical anion $\mathbf{2}^{\odot\ominus}$ and/or radical cation $\mathbf{2}^{\odot\oplus}$ (also accessible by direct 70-eV electron-impact ionization of **1**) by electron transfer and to characterize **2** in an NRMS experiment? As revealed by Figure 1c, the answer is unequivocally yes. Oxidation of $\mathbf{2}^{\odot\ominus}$ generates **2**, which is further oxidized to $\mathbf{2}^{\odot\oplus}$ (Fig. 1c). Analogously, reduction of $\mathbf{2}^{\odot\oplus}$ yields **2**, which, upon subsequent reionization, affords the spectrum shown in Figure 1d. Noteworthy features include (1) the unusually intense recovery signal, which indicates favorable Franck–Condon transitions, and (2) the excellent agreement with the NR spectra generated under various conditions. This finding can also be viewed as evidence for comparably minor structural changes in the system $\mathbf{2}^{\odot\ominus} \rightarrow \mathbf{2} \rightleftarrows \mathbf{2}^{\odot\oplus}$.

Summary: Neutral butatrienedione, its radical anion, and its radical cation are perfectly stable molecules. If still further evidence were needed for this claim, it would be provided by an independent tandem experiment. If the reionized $C_4O_2^{\odot\oplus}$ formed via the sequence $\mathbf{2}^{\odot\oplus} \rightarrow \mathbf{2} \rightarrow \mathbf{2}^{\odot\oplus}$ is again mass-selected and subjected to collisional activation, the resulting interference-free NR spectrum is identical with the CA spectrum of $\mathbf{2}^{\odot\oplus}$ generated by direct collisional activation.

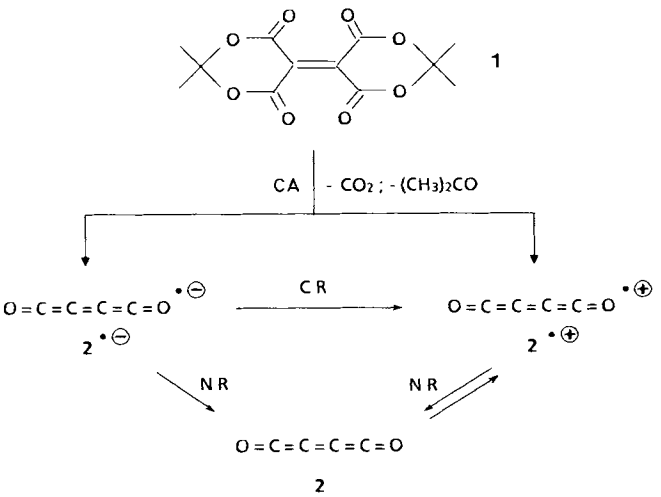

Scheme 1.

Received: May 17, 1990 [Z 3962 IE]
German version: *Angew. Chem. 102* (1990) 923

[1] Detailed report: D. Sülzle, N. Beye, E. Fanghänel, H. Schwarz, *Chem. Ber.*, in press.
[2] F. A. Cotton, G. Wilkinson: *Advanced Inorganic Chemistry*, Interscience Publisher, New York 1962, p. 226; L. D. Brown, W. N. Lipscomb, *J. Am. Chem. Soc. 99* (1977) 3968.
[3] D. Sülzle, H. Schwarz, *Angew. Chem. 100* (1988) 1384; *Angew. Chem. Int. Ed. Engl. 27* (1988) 1337.
[4] D. Sülzle, H. Schwarz, *Chem. Ber. 122* (1989) 1803.
[5] D. Sülzle, J. K. Terlouw, H. Schwarz, *J. Am. Chem. Soc. 112* (1990) 628.
[6] D. Sülzle, H. Schwarz, unpublished.
[7] Review articles: Wesdemiotis, F. W. McLafferty, *Chem. Rev. 87* (1987) 485; J. K. Terlouw, H. Schwarz, *Angew. Chem. 99* (1987) 829; *Angew. Chem. Int. Ed. Engl. 26* (1987) 805, H. Schwarz, *Pure Appl. Chem. 61* (1989) 685; J. K. Terlouw, *Adv. Mass Spectrom. 11* (1989) 984; J. L. Holmes, *Mass Spectrom. Rev. 8* (1989) 513; F. W. McLafferty, *Science (Washington D.C.) 247* (1990) 925.
[8] G. P. Raine, H. F. Schaefer III, R. C. Hadders, *J. Am. Chem. Soc. 105* (1983) 194.
[9] H. Staudinger, G. Anthes, *Ber. Dtsch. Chem. Ges. 46* (1913) 1426.
[10] For references, see [5].
[11] G. Maier, H. P. Reisenauer, H. Balli, W. Brandt, R. Janoschek, *Angew. Chem. 102* (1990) 920, *Angew. Chem. Int. Ed. Engl. 29* (1990) 905.
[12] All experiments were carried out with a four-sector mass spectrometer in the arrangement BEBE under standard conditions (B, magnetic sector; E, electric sector). NH_3 ($p \approx 10^{-5}$ torr) is used as an electron moderator.
[13] H. R. Snyder, C. W. Kruse, *J. Am. Chem. Soc. 80* (1958) 1942.
[14] a) H. Budzikiewicz, *Angew. Chem. 93* (1981) 635; *Angew. Chem. Int. Ed. Engl. 20* (1981) 624; b) J. H. Bowie, *Mass Spectrom. Rev. 3* (1984) 161.
[15] K. Levsen, H. Schwarz, *Mass Spectrom. Rev. 2* (1983) 77.
[16] J. H. Beynon, *Proc. Royal Soc. London Ser. A 378* (1981) 1.

Iron(II)-Mediated Hydride and Methanide Transfer to Carbonyl Groups**

By *Detlef Schröder* and *Helmut Schwarz**

Dedicated to Professor Dr. Günther Wilke on the occasion of his 65th birthday

The course of the metal-induced hydride transfer in the Meerwein–Ponndorf–Verley–Oppenauer (MPVO) reaction [Eq. (1)][1] still cannot be described by a single mechanism despite the claims of most textbooks. The metal M and the solvent affect the kinetics through the degree of aggregation,[2] and the substituents R govern, in addition to the reaction rate, the extent to which one-electron transfers[3] occur. There is unanimous agreement, however, that alkyl- and aryl-group transfer cannot compete with hydride migration; rearrangements with R ≠ H have not yet been described.[4]

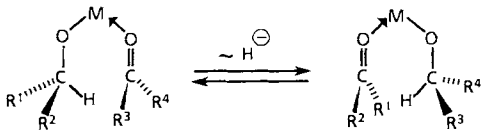

(1)

Here we report a gas-phase reaction analogous to the MPVO reaction but with the important differences that (1) the transition-metal ion $Fe^{\oplus}$ serves as metal M and (2), in addition to hydride transfer, methanide transfers have been observed for the first time. For the migration of $R = CH_3^{\ominus}$, we have found that steric manipulation on the alkoxide moiety leads to a dramatic change in the course of the reaction. Furthermore, kinetic isotope effects for the hydride transfer were determined.

We performed Fourier transform ion cyclotron resonance (FTICR) experiments, which allow the study of sequential ion/molecule reactions[5] unobscured by aggregation phenomena or the effect of counterions. In the reaction sequence (Fig. 1a–g), metal ions $M^{\oplus}$ (M = Cr, Mn, Fe, Ni) are generated by laser desorption/ionization[6] from V2A steel in the external ion source[7] of a Spectrospin CMS 47X ICR instrument[8] by use of an Nd:YAG laser (Spectron System, 1064 nm). The ions are transferred to the actual ICR cell through a system of electric potentials and lenses. The ions $M^{\oplus}$ are decelerated to nearly thermal energies and trapped in the field of a superconducting magnet (Oxford Instruments, maximum field strength 7.05 T) (Fig. 1a). Except for the ^{56}Fe isotope, all other ions present are ejected from the cell by suitable pulse sequences (Fig. 1b). The alkoxide ions $FeOR^{\oplus}$ ($R = CH_3$, C_2H_5, $i\text{-}C_3H_7$, $t\text{-}C_4H_9$, and isotopomers) required for the MPVO reaction are generated by ion/molecule reactions of $Fe^{\oplus}$ with pulsed-in[1a] neutral molecules. Nitroalkanes, alkyl nitrites, alkyl nitrates, and alkyl peroxides have proven useful for this purpose.[11] However, since ketones (necessary for the actual MPVO reaction) and argon[12] are also present in the ICR cell ($P_{ketone} \approx 10^{-8}$ mbar; $P_{Ar} \approx 10^{-7}$ mbar), numerous primary, secondary, and tertiary ions are formed in the diverse ion/molecule reactions (Fig. 1c). In the system $Fe^{\oplus}/CD_3NO_2/(CH_3)_2CO$, for example, "pure" $FeOCD_3^{\oplus}$ (1; m/z 90) can

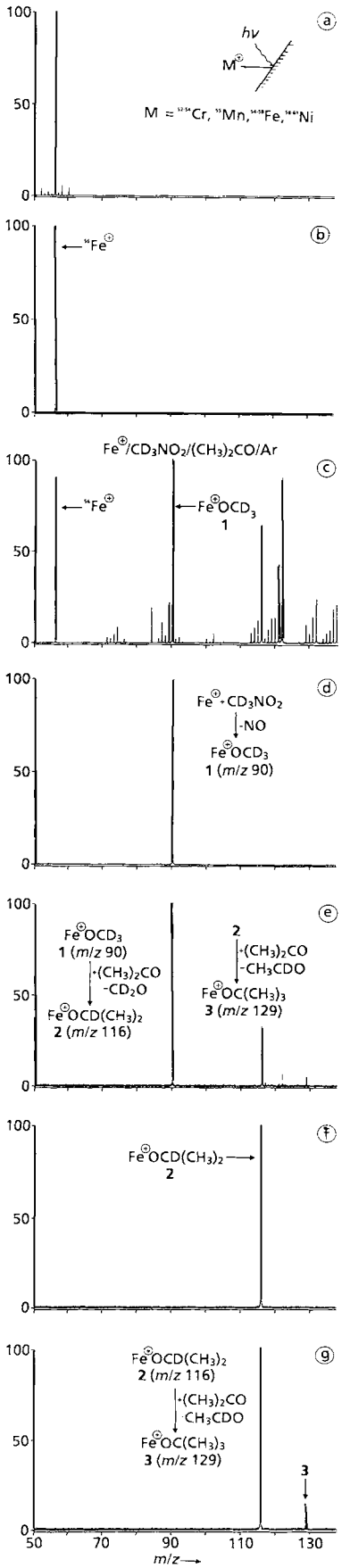

Fig. 1. a) Laser desorption/ionization of a V2A steel; b) "isolation" of $^{56}Fe^{\oplus}$; c) reaction of $^{56}Fe^{\oplus}$ with pulsed-in CD_3NO_2 and acetone (10^{-8} mbar) in the presence of Ar (10^{-7} mbar); d) "isolation" of $FeOCH_3^{\oplus}$ (m/z 90); e) reaction of $FeOCD_3^{\oplus}$ with acetone; f) "isolation" of $FeOCD(CH_3)_2^{\oplus}$ (m/z 116); g) reaction of $FeOCD(CH_3)_2^{\oplus}$ with acetone.

[*] Prof. Dr. H. Schwarz, Dipl.-Chem. D. Schröder
Institut für Organische Chemie der Technischen Universität
Strasse des 17. Juni 135, D-1000 Berlin 12

[**] This work was supported by the Deutsche Forschungsgemeinschaft, the Fonds der Chemischen Industrie, and the Gesellschaft von Freunden der Technischen Universität Berlin.

be easily isolated from the palette of products by using a suitable sequence of pulses (Fig. 1d). Reaction of **1** with $(CH_3)_2CO$ affords products **2** and **3** (*m/z* 116 and 129, respectively; Fig. 1e); the "interfering signal" appearing at *m/z* 122 is due to a reaction of **1** with residual CD_3NO_2.[13] The generation of **3** and **2** can be confirmed by "isolating" the latter (Fig. 1f) and allowing it to react selectively with acetone to give **3** (Fig. 1g). It should be noted in passing that the overall reaction sequence $M^{\oplus} \rightarrow$ **3** constitutes a fourth-order MS experiment. However, two further steps are required to characterize structurally the $FeO\textit{t}\text{-}C_4H_9^{\oplus}$ ion **3**: (1) the isolation and (2) the collision-induced decomposition of **3**.[14] Before the results of these experiments are described, we should mention briefly several other $FeOR^{\oplus}$/ketone systems in order to demonstrate that the hydride and methanide transfers implied in Figure 1 are, in fact, general.

For example, the system $Fe^{\oplus}/CH_3NO_2/(CD_3)_2CO$ affords the ions $FeOCH_3^{\oplus}$ (*m/z* 87), $FeOCH(CD_3)_2^{\oplus}$ (*m/z* 121), and $FeOC(CD_3)_3^{\oplus}$ (*m/z* 138), which are isotopomeric to **1**, **2** and **3**.[15]

That the hydride transfer occurs with a kinetic isotope effect can be shown by investigation of the pair $FeOCD_2H^{\oplus}$ (generated from $Fe^{\oplus}$ and CHD_2NO_2) and $(CH_3)_2CO$. $FeOCH(CH_3)_2^{\oplus}$ and $FeOCD(CH_3)_2^{\oplus}$ are obtained in a ratio of 0.78:1, which, after statistical correction, gives $k_H/k_D = 1.6$.

Groups R other than methyl can also serve as alkoxide ligands RO. This is exemplified by two reactions, which, in addition, reveal further aspects of the course of the reaction. The reaction of $FeOCH(CH_3)_2^{\oplus}$ (generated from $Fe^{\oplus}$ and $(CH_3)_2CHONO$) with $(CD_3)_2CO$ affords, after two seconds, the distribution of products shown in Equation (2) (given in % relative to $FeOCH(CH_3)_2^{\oplus}$). Whereas the D_6-labeled product **3c** is formed by a simple $CH_3^{\ominus}$ migration from the "nonisolated" intermediate **4** and the D_9 compound **3a** is the result of a consecutive reaction (**4** → **2b** → **3a**), the appearance of the D_3-labeled alkoxide **3b** necessitates that the lifetime of **4** be sufficiently long to allow an internal reciprocal H/CD_3 migration.

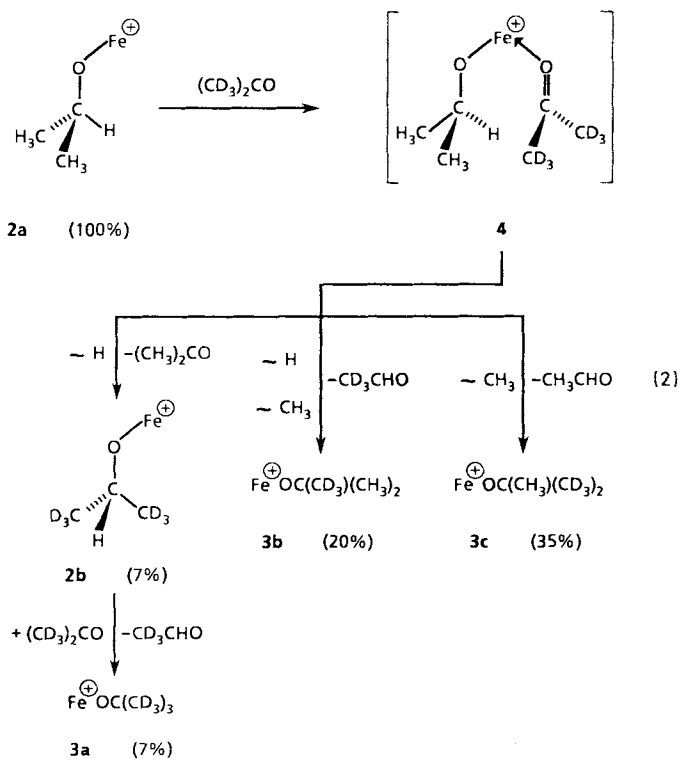

(2)

We observed a *seemingly* analogous reaction pattern for the reaction of $FeOC(CH_3)_3^{\oplus}$ (generated from $Fe^{\oplus}$ and $(CH_3)_3COOC(CH_3)_3$) with $(CD_3)_2CO$. Besides clusters, the only product is an ion that demands a transfer of $CH_3^{\ominus}$. In this case, however, an MPVO-like migration of $CH_3^{\ominus}$ to the carbonyl center of $(CD_3)_2CO$ is not involved. Otherwise, the resulting product would have contained three equivalent methyl groups [Eq. (3): **5** → **3c**]. This is not the case, as evi-

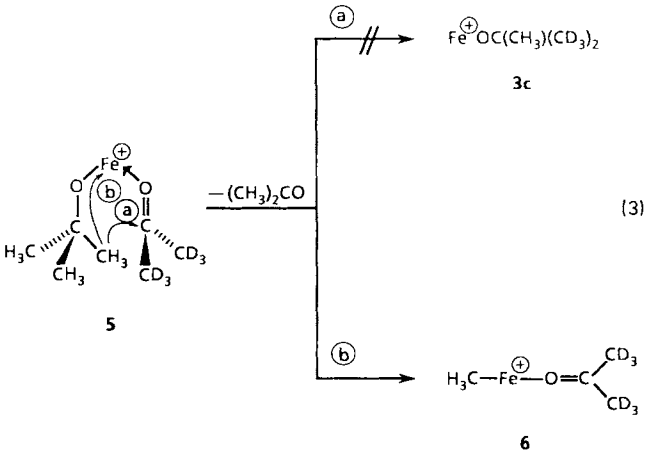

(3)

denced by the following experiment. If the product (**6**) is subjected to a CID experiment, the resulting product distribution unequivocally rules out an equivalence of CH_3/CD_3 [Eq. (4)]. Moreover, a comparison with the CID spectrum of authentic $FeOC(CH_3)_3^{\oplus}$[16] (generated directly from $Fe^{\oplus}$ and $(CH_3)_3COOC(CH_3)_3$) excludes the reaction pathway **5** → **3c**. Instead, a β-CH_3 migration to the metal center occurs.[17] The cause of this abrupt change in the reaction

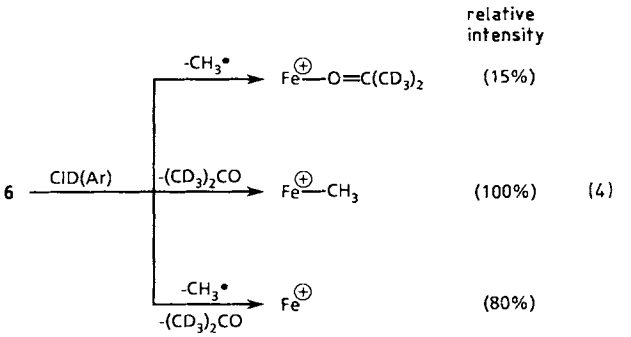

(4)

trajectory is still not clear; possibly, the steric crowding leads to a change in the geometric details at the $Fe^{\oplus}$ center (for example, an increase in the O–Fe–O angle).

It should be mentioned that the $Fe^{\oplus}$-mediated hydride/metnanide migrations of the MPVO type are not limited to acetone as acceptor. Preliminary investigations have shown that acetaldehyde, 3-pentanone, and 4-heptanone may also be reduced,[18] and the data in Table 1 for the system $FeOCHDCH_3^{\oplus}/CH_3CHO$ confirm that three kinds of reaction occur: (1) unidirectional transfer of $H^{\ominus}$, $D^{\ominus}$, or $CH_3^{\ominus}$ coupled with the loss of CH_3CDO, CH_3CHO, or CH_2O, respectively; (2) reciprocal migration of $H^{\ominus}/CH_3^{\ominus}$, followed by CH_2O loss from the original CH_3CHO moiety; (3) the formation of tertiary products of the type $FeOC(CH_3)_3^{\oplus}$.

Table 1. Reaction products of unidirectional, reciprocal, and consecutive migration of $X^{\oplus}$ (X = H, D, CH_3) in the system $FeOCHDCH_3^{\oplus}/CH_3CHO$.

		Yields of product ions [%] [a]			
t [s]	$FeOCH_2CH_3^{\oplus}$	$FeOCHDCH_3^{\oplus}$ [b]	$FeOCH(CH_3)_2^{\oplus}$	$FeOCD(CH_3)_2^{\oplus}$	$FeOC(CH_3)_3^{\oplus}$
0	–	100	–	–	–
10	14	100	39	11	2
30	11	31	100	23	28

[a] The "yields" are based on the most intense signal (100%). [b] In the present experiment, the ion generated by D transfer is identical with the precursor $FeOCHDCH_3^{\oplus}$. As a result, no H/D isotope effect is given.

Not surprisingly, the latter two reactions become increasingly important as the reaction time increases (Table 1).

Received: March 6, 1990 [Z 3861 IE]
German version: *Angew. Chem. 102* (1990) 925

CAS Registry numbers:
1 (H replaces D), 128054-63-7; **2a**, 128054-65-9; **3**, 128054-66-0; **3** (Et replaces *t*Bu), 128054-64-8; acetaldehyde, 75-07-0; 3-pentanone, 96-22-0; 4-heptanone, 123-19-3; acetone, 67-64-1; methanide, 15194-58-8; deuterium, 7782-39-0.

[1] H. Meerwein, R. Schmidt, *Justus Liebigs Ann. Chem. 444* (1925) 221; W. Ponndorf, *Z. Angew. Chem. 39* (1926) 138; A. Verley, *Bull. Soc. Chim. Fr. 37* (1925) 537; R. V. Oppenauer, *Recl. Trav. Chim. Pays-Bas 56* (1937) 137; Reviews: A. L. Wilds, *Org. React. 2* (1944) 178; C. Djerassi, *ibid. 6* (1951) 207.
[2] R. B. Woodward, N. L. Wender, F. J. Brutschy, *J. Am. Chem. Soc. 67* (1945) 1425; W. N. Moulton, R. E. van Atta, R. R. Ruch, *J. Org. Chem. 26* (1961) 290; V. J. Shiner, Jr., D. Whittacker, *J. Am. Chem. Soc. 85* (1963) 2337; B. J. Yager, C. K. Hancock, *J. Org. Chem. 30* (1965) 1174; E. W. Warnhoff, P. Reynolds-Warnhoff, M. Y. H. Wong, *J. Am. Chem. Soc. 102*(1980) 5956.
[3] E. C. Ashby, A. B. Goel, J. N. Argyropoulos, *Tetrahedron Lett. 23* (1982) 2273.
[4] Review: D. C. Bradley, R. C. Mehrota, D. P. Gaur: *Metal Alkoxides*, Academic Press, London 1978, p. 250.
[5] R. B. Cody, R. C. Burnier, C. J. Cassady, B. S. Freiser, *Anal. Chem. 54* (1982) 2225; S. W. Buckner, B. S. Freiser, *Polyhedron 7* (1988) 1583; B. S. Freiser, *Chemtracts—Anal. Phys. Chem. 1* (1989) 65.
[6] B. S. Freiser, *Talanta 32* (1985) 697; *Anal. Chim. Acta 178* (1985) 137.
[7] P. Kofel, M. Allemann, H. Kellerhans, K. P. Wanczek, *Int. J. Mass. Spectrom. Ion Processes 65* (1985) 97.
[8] For a description of the machine, see: K. Eller, H. Schwarz, *Int. J. Mass Spectrom. Ion Processes 93* (1989) 243; K. Eller, W. Zummack, H. Schwarz, *J. Am. Chem. Soc. 112* (1990) 621.
[9] R. A. Forbes, F. H. Laukien, J. Wronka, *Int. J. Mass. Spectrom. Ion Processes 83* (1988) 23.
[10] T. J. Carlin, B. S. Freiser, *Anal. Chem. 55* (1983) 571.
[11] C. J. Cassady, B. S. Freiser, *J. Am. Chem. Soc. 107* (1985) 1566; L. F. Halle, F. S. Klein, J. L. Beauchamp, *ibid. 106* (1984) 2543.
[12] Argon fulfills two functions by (1) contributing to collisional stabilization and possibly excited-state deactivation and (2) serving as a collision gas for collision-induced decompositions (CID). The latter are used for the structural characterization of the products resulting from ion/molecule reactions.
[13] This can be demonstrated, for example, by reducing the partial pressure of CD_3NO_2.
[14] According to a recently published basic text on tandem mass spectrometry, the practical limit should be $(MS)^5$ and only in extremely favorable cases should $(MS)^6$ be possible: K. L. Busch, G. L. Glish, S. A. McLuckey: *Mass Spectrometry/Mass Spectrometry. Techniques and Applications of Tandem Mass Spectrometry*, VCH Publishers, New York 1988, p. 47. A "world record" is described by *Cooks* et al., who succeeded in realizing an $(MS)^{12}$ experiment by using a modified Paul ion trap: J. N. Louris, J. S. Broadbelt-Lustig, R. G. Cook, G. L. Glish, G. J. van Berkel, S. A. McLuckey, *Int. J. Mass. Spectrom. Ion Processes 96* (1990) 117.
[15] For the system $Fe^{\oplus}/CH_3ONO/(CD_3)_2CO$, we have succeeded in structurally characterizing the encounter complex with m/z 151 in a CID(Ar) experiment. The observed fragments [intensities in % relative to m/z 151 = 100%: $HFeO(CD_3)_2^{\oplus}$ (loss of CH_2O; 44%), $CH_3OFe^{\oplus}$ (loss of $(CD_3)_2CO$; 34%), $FeCD_3^{\oplus}$ (5%), $FeH^{\oplus}$ (loss of $CH_2O/(CD_3)_2CO$; 14%), and $Fe^{\oplus}$ (elimination of $CH_3O/(CD_3)_2CO$; 10%)] are in agreement with a connectivity CH_3O-Fe-$OC(CD_3)_2^{\oplus}$.
[16] In the CID spectrum of $FeOC(CH_3)_3^{\oplus}$, we find a loss of CH_3, CH_4, $(CH_3)_2CO$ and $(CH_3)_3CO$.
[17] Detailed discussion of actual and presumed β-alkyl migrations to transition-metal ions: S. Karraß, H. Schwarz, *Organometallics* in press.
[18] D. Schröder, H. Schwarz, unpublished results.

Unsaturated C_3B_2 Rings with Neighboring Boron Atoms: Derivatives of 4-Methylene-1,2-dibora-cyclopentane, Dilithium 2,3-diboratafulvene, and 1,2-Dibora-3-cyclopentene**

By *Gerhard E. Herberich,* Christian Ganter, Lars Wesemann*, and *Roland Boese*

Unsaturated C_3B_2 rings with non-neighboring boron atoms have long been known: for example, derivatives of 1,3-dibora-4-cyclopentene (**A**)[1] and 2-methylene-1,3-dibora-4-cyclopentene (**B**).[2] Unsaturated C_3B_2 rings with *neighboring* boron atoms, by contrast, have been inaccessible so far.

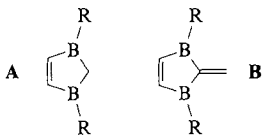

Here we describe examples of this type of compound. To form the C_3B_2 ring framework, we started from $Li_2[C(CH_2)_3]$ (**1**)[3] and used synthetic steps that have been well-tested with saturated compounds (Scheme 1). Borylation with $ClB(NR_2)_2$ (R = Et, *i*Pr) affords the diborylisobutenes **2a,b**, which react with HCl to give the chloroboryl compounds **3a,b**;[4] subsequent B–B bond formation, carried out with Na/K alloy in hexane,[5] leads to the 4-methylene-1,2-diboracyclopentanes **4a,b**. The alternative, direct formation of the C_3B_2 ring by reaction of **1** with the diborane(4) building block $Cl_2B_2(NMe_2)_2$ was unsuccessful.

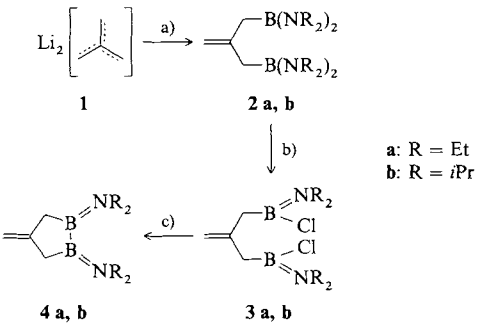

Scheme 1. a) $ClB(NR_2)_2$, THF, 0 °C; b) HCl (Et_2O), −78 °C; c) $NaK_{2.8}$, hexane, 20 °C.

The X-ray structure analysis of **4b**[6] (Fig. 1) confirms the presence of a B–B bond. Compound **4b** shows an unusual twist conformation: the dihedral angle N2-B2-B1-N1 is 56.0° and the interplanar angle between the planes C3-B2-N2 and C1-B1-N1 36.8°. The aminoborane groups are also nonplanar with dihedral angles of 14.2° between the planes C5-N1-C8 and B2-B1-C1 and of 9.4° between the planes

[*] Prof. Dr. G. E. Herberich, Dipl.-Chem. C. Ganter, Dr. L. Wesemann
Institut für Anorganische Chemie der Technischen Hochschule
Professor-Pirlet-Strasse 1, D-5100 Aachen (FRG)
Dr. R. Boese
Institut für Anorganische Chemie der Universität – Gesamthochschule
Universitätsstrasse 3–5, D-4300 Essen 1 (FRG)

[**] This work was supported by the Deutsche Forschungsgemeinschaft and the Fonds der Chemischen Industrie.

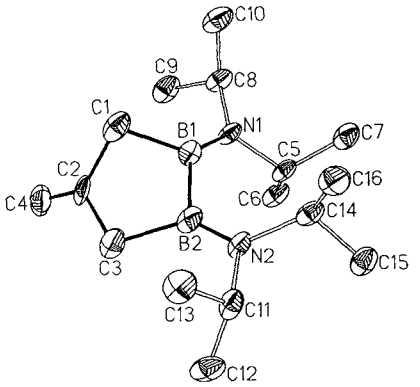

Fig. 1. Molecular structure of **4b**. Selected bond lengths [pm]: N1-B1 138.9(7), N2-B2 140.2(7), B1-B2 172.3(8), B1-C1 161.8(7), B2-C3 161.3(7), C1-C2 149.7(7), C2-C3, 151.7(7), C2-C4 130.0(8).

C11-N2-C14 and C3-B2-B1. The unusual features of the structure are due to the high steric demands of the iPr$_2$N groups. The B–C bonds (161.3(7) and 161.8(7) pm) are slightly lengthened,[7] whereas the B–N bonds (138.9(7) and 140.2(7) pm) are slightly shortened.[8]

Compound **4a** can be metalated with lithium 2,2,6,6-tetramethylpiperidide (LiTMP) in THF to give the moderately soluble, red dilithium 2,3-diboratafulvene derivative **5a**. Similarly, **4b** reacts with *tert*-butyllithium in hexane to give the orange-red bis(diisopropylamino) derivative **5b**. A singly metalated intermediate cannot be observed by NMR spectroscopy. The metalation products **5** react with tetramethylethylenediamine (TMEDA) to give the crystalline adducts **6** ($\equiv$**5** · (TMEDA)$_2$). The ^{11}B NMR signals of **6a,b** ($\delta = 43$) are slightly shifted to higher field compared with those of **4a, b** ($\delta = 52$ and 54, respectively) and lie in the same region as those of simple borataethene ions.[9]

Dianions **5** are transformed by cyclopentadiene, without any side reaction, into the 4-methyl-1,2-dibora-3-cyclopentene rings **7**, which are isomeric to the 4-methylene derivatives **4** but now contain an endoyclic double bond.

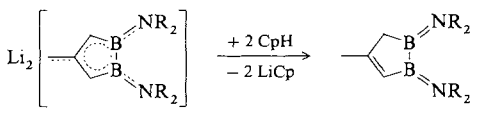

5 a, b **7 a, b**

Experimental Procedure

Standard for ^{1}H and ^{13}C NMR spectra, TMS int.; for ^{11}B NMR spectra, $BF_3 \cdot OEt_2$ ext.

2a: Distillation at 115 °C/10^{-6} bar (81%). ^{1}H NMR (80 MHz, $CDCl_3$): $\delta = 4.54$ (quint., $^4J = 1.3$ Hz, $H_2C=$), 1.63 (t, $^4J = 1.3$ Hz, 2 BCH_2), Et_2N: 2.98(q), 1.02(t). ^{11}B NMR ($CDCl_3$): $\delta = 34$.

2b: Crystallization from hexane (53%), m.p. 98–99 °C. ^{1}H NMR (80 MHz, $CDCl_3$): $\delta = 4.62$ (m, $H_2C=$), 1.71 (m, 2 BCH_2), iPr$_2$N: 3.56 (sept.), 1.15(d). ^{11}B NMR ($CDCl_3$): $\delta = 36$.

3a,b: Filtration and distillation at 85 °C/10^{-6} bar (94%) and at 150 °C/10^{-6} bar (89%).

4a: A stirred solution of **3a** (16.0 g, 0.055 mol) in hexane was allowed to react at 20 °C with $NaK_{2.8}$ (7.0 g, 0.053 mol) for 3 d. Filtration through kieselguhr, removal of the solvent, and distillation (45 °C/10^{-6} bar) gave 6.0 g (50%) of **4a**. MS: m/z 220 (100%, $M^{\oplus}$). ^{1}H NMR (80 MHz, $CDCl_3$): $\delta = 4.57$ (quint., $^4J = 1.6$ Hz, $H_2C=$), 1.89 (t, $^4J = 1.6$ Hz, 2 BCH_2); Et_2N: 3.24(q), 3.14(q), 1.11(t), 1.08(t) ^{11}B NMR ($CDCl_3$): $\delta = 52$.

4b: **3b** (3.3 g, 9.5 mmol) was allowed to react with 1.0 mL of $NaK_{2.8}$ as described for **4a** followed by refluxing for 24 h. Distillation (90 °C/10^{-6} bar) afforded 2.0 g of **4b** (76%), m.p. 47–48 °C. MS: m/z 276 (87%, $M^{\oplus}$). ^{1}H NMR (80 MHz, $CDCl_3$): $\delta = 4.58$ (quint., $^4J = 1.6$ Hz, $H_2C=$), 2.06 (t, $^4J = 1.6$ Hz, 2 BCH_2), iPr$_2$N: 3.72 (sept.), 3.34 (sept.), 1.25(d), 1.11(d). ^{11}B NMR ($CDCl_3$): $\delta = 54$.

6a: **4a** (2.0 g, 0.0091 mol) was treated in THF at −78 °C with LiTMP (2.7 g, 0.018 mol). The reaction mixture was then allowed to warm to 20 °C and the volatile components were removed under vacuum (finally, for 12 h at 10^{-6} bar). Crystallization from 10 mL of hexane and 3 mL of TMEDA (0.02 mol) at −30 °C afforded dark orange crystals. ^{1}H NMR (80 MHz, [D_8]THF): signals of 2 H6 and H1/H4 at $\delta = 1.05$ overlapped; Et_2N: 3.15(q), 1.05(t), TMEDA: 2.29(s), 2.18(s). ^{11}B NMR ([D_8]THF): $\delta = 43$. ^{13}C NMR (67.88 MHz, [D_8]THF, 203 K): $\delta = 79.4$ (t, $^1J = 150$ Hz, C6), 76.4 (d, $^1J = 130$ Hz, C1), 72.8 (d, $^1J = 128$ Hz, C4), 163.9 (s, C5), Et_2N: 47.3(t), 46.8(t), 44.6(t), 44.3(t), 16.9(q), 16.5(q), 14.9(q), 14.5(q), TMEDA: 57.4(tm), 45.9(qm); at 300 K, C1 and C4 are equivalent, as are the four Et groups.

6b: **4b** (1.0 g, 3.6 mmol) in 25 mL of pentane was treated at −78 °C with 4.5 mL of 1.7 M tBuLi (7.6 mmol, in hexane) and 1.2 mL (7.7 mol) of TMEDA. The reaction mixture was then stirred for 24 h at 20 °C. Concentration to 10 mL and crystallization at −30 °C afforded dark orange crystals. ^{1}H NMR (80 MHz, [D_{10}]Et_2O): signals of 2 H6 and H1/H4 at $\delta = 1.2$ overlapped, iPr$_2$N: 3.72 (sept.), 1.21(d), TMEDA: 2.28(s), 2.24(s), ^{11}B NMR ([D_{10}]Et_2O): $\delta = 43$. ^{13}C NMR (67.88 MHz, [D_{10}]Et_2O, 213 K): $\delta =$ 167.0 (s, C5), 77.8 (d, $^1J = 131$ Hz, C1,4), 74.4 (t, $^1J = 150$ Hz, C6), iPr$_2$N: 53.8(d), 24.3(q), 23.5(q) (at 300 K equivalent), TMEDA: 57.2(t), 46.3(q).

7a: Cyclopentadiene (3.6 g, 55 mmol) was added to **5a**, prepared from **4a** (5.45 g, 24.8 mmol) and LiTMP (7.7 g, 52.4 mmol), in THF at −78 °C. The THF was removed, the residue dissolved in hexane, and the resulting solution filtered through kieselguhr to remove the LiCp. Removal of volatile components and distillation (50 °C/10^{-6} bar) gave 4.0 g of **7a** (73%). MS: m/z 220 (68%, $M^{\oplus}$). ^{1}H NMR (270 MHz, $CDCl_3$): $\delta = 6.00$ (s, =CH), 1.97 (s, Me), 1.57 (s, BCH_2), Et N: 3.29(q), 3.26(q), 3.20(q), 3.12(q), 1.14(t), 1.12(t), 1.09(t), 1.08(t), ^{11}B NMR ($CDCl_3$): $\delta = 49$.

7b: 9.0 mL of 1.7 M tBuLi (15 mmol, in hexane) was added to **4b** (2.0 g, 7.2 mmol) in 30 mL of pentane at −78 °C and the reaction mixture was stirred for 24 h at 20 °C. The resulting precipitate was washed several times with pentane. After addition of 30 mL of pentane, cyclopentadiene (1.2 g, 18 mmol) was added at −78 °C and the reaction mixture was stirred at 20 °C until the red color had vanished (2 h). Filtration to remove LiCp, concentration, and distillation (90 °C/10^{-6} bar) gave 0.2 g of **7b** (10%), m.p. 50 °C. ^{1}H NMR (80 MHz, $CDCl_3$): $\delta = 6.23$ (s, HC=), 1.95 (s, Me), 1.72 (s br, BCH_2), iPr$_2$N: 3.74 (sept.), 3.33 (sept.), 1.24(d), 1.11(d), ^{11}B NMR ($CDCl_3$): $\delta = 51$.

Received: March 26, 1990;
revised: May 25, 1990 [Z 3879 IE]
German version: *Angew. Chem. 102* (1990) 914

CAS-Registry-Numbers:
1, 53721-69-0; **2a**, 128270-26-8; **2b**, 128270-27-9; **3a**, 128270-28-0; **3b**, 128270-29-1; **4a**, 128270-30-4; **4b**, 128270-31-5; **5a**, 128270-32-6; **5b**, 128270-33-7; **6a**, 128270-36-0; **6b**, 128270-37-1; **7a**, 128270-34-8; **7b**, 128270-35-9; $ClB(NEt_2)_2$, 868-25-7; $ClB(NiPr_2)_2$, 28049-80-1; cyclopentadiene, 542-92-7.

[1] P. Binger, *Angew. Chem. 80* (1968) 288; *Angew. Chem. Int. Ed. Engl. 7* (1968) 286; W. Siebert, U. Ender, W. Herter, *Z. Naturforsch. B 40* (1985) 326; J.-K. Uhm, H. Römich, H. Wadepohl, W. Siebert, *ibid. B 43* (1988) 306.
[2] V. Schäfer, H. Pritzkow, W. Siebert, *Chem. Ber. 122* (1989) 401.
[3] J. Klein, A. Medlik, *J. Chem. Soc. Chem. Commun. 1973*, 275.
[4] The corresponding Me_2N compound is polymeric and therefore cannot be used in the next step.
[5] R. J. Brotherton, A. L. McCloskey, L. L. Petterson, H. Steinberg, *J. Am. Chem. Soc. 82* (1960) 6242; H. Nöth, W. Meister, *Chem. Ber. 94* (1961) 509.
[6] Nicolet R3m/V, $Mo_{K\alpha}$ radiation, $T = 120$ K. **4b**: $P2_1/c$ (No. 14), $a = 627.4(8)$, $b = 1736.2(1)$, $c = 1707.3(2)$ pm, $\beta = 95.52(9)°$; $V = 1.8512(3.1)$ nm^3; $Z = 4$; $\varrho_{calcd} = 0.989$ g cm^{-3}; 2447 unique reflections, 1577 with $F_0 \geq 4\sigma(F)$. $2\theta_{max} = 45°$; non-hydrogen atoms refined anisotropically, H atoms included at calculated positions and their isotropic temperature factors refined in groups: 195 parameters, $R = 0.078$, $R_w = 0.076$ mit $w^{-1} = \sigma^2(F_0) + 0.00082\,F_0^2$. Further details of the crystal structure investigation may be obtained from the Fachinformationszentrum Karlsruhe, Gesellschaft für wissenschaftlich-technische Information mbH, D-7514 Eggenstein-Leopoldshafen 2 (FRG), on quoting the depository number CSD-320120, the names of the authors, and the journal citation.
[7] Cf. 157.8(1) pm in BMe_3: L. S. Bartell, B. L. Carroll, *J. Chem. Phys. 42* (1965) 3076; 158.0(4) pm (average) in BPh_3: F. Zettler, H. D. Hausen, H. Hess, *J. Organomet. Chem. 72* (1974) 157; 159.0(2) pm in 1,2,4,5-tetrakis-(dimethylamino)-1,2,4,5-tetraborinane: H. Fisch, H. Pritzkow, W. Siebert, *Angew. Chem. 96* (1984) 595; *Angew. Chem. Int. Ed. Engl. 23* (1984) 608.
[8] Typical for (dialkylamino)boranes are values of 141–142 pm: P. Paetzold, *Adv. Inorg. Chem. 31* (1987) 123.
[9] Typical: $\delta(^{11}B) = 41$: M. V. Garad, A. Pelter, B. Singaram, J. W. Wilson, *Tetrahedron Lett. 24* (1983) 637.

Low-Dimensional Compounds Incorporating Polychalcogenide Ligands. The Unusual Polymeric Structures of $[AuSe_5]_n^{n\ominus}$ and $[AuSe_{13}]_n^{3n\ominus}$

By *Younbong Park* and *Mercouri G. Kanatzidis**

Solid-state compounds incorporating the versatile polychalcogenide ligands $Q_x^{2\ominus}$ are rare. These ligands are thermally unstable and release chalcogen at the high temperatures commonly used in solid-state reactions. On the other hand, room-temperature synthesis of molecular polychalcogenides is a thriving field of research.[1] We believe that an enormous number of interesting polychalcogenide compounds occur at intermediate (i.e., 150–350 °C) temperatures and could be discovered, provided suitable solvents (e.g., molten salts) were available. This intermediate temperature regime has not been explored as a synthetically useful area[2] either for solid-state or molecular compounds. These temperatures do not support the conventional (non)aqueous solvents commonly used near room temperature, nor do they favor true solid-state reactions (exceedingly slow ion diffusion). This has been particularly true in chalcogenide chemistry.[3] Molten salts have been used previously at high temperatures ($T > 700$ °C) to obtain crystals of binary semiconductors.[4, 5] Alkali-metal polychalcogenide melts, in particular, show melting points as low as ca. 150 °C[6] and can serve not only as solvents but also as reagents (i.e., chalcogen and alkali-metal donors). The deliberate use of these systems for the synthesis of new materials has not been seriously pursued. Recently, the compounds $K_4Ti_3Si_{14}$,[7] $Na_2Ti_2Se_8$,[8] $K_3Nb_2Se_{11}$,[9] α- and β-$KCuS_4$,[10] $K_2Hg_3Q_4$[11] (Q = S,Se), and $K_2Hg_6S_7$[11] were reported to form in polychalcogenide melts at 210–375 °C. Here we report two remarkable ternary compounds, $KAuSe_5$ (**1**) and K_3AuSe_{13} (**2**), prepared by using a molten-salt synthetic procedure at 250 °C. The structures of **1** and **2** were established by single-crystal X-ray diffraction studies[12] and represent the first examples of solid-state gold-polyselenide compounds.

The structure of **1** is shown in Figure 1. It is made up of covalent one-dimensional $[AuSe_5]_n^{n\ominus}$ anionic chains and

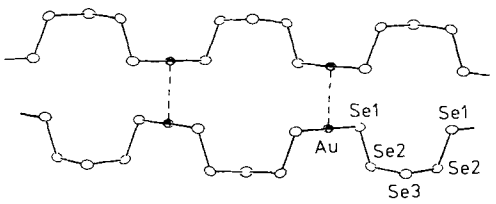

Fig. 1. ORTEP representation of the structure of the $[AuSe_5]_n^{n\ominus}$ chains with labeling scheme, showing the mode of "dimerization" via the Au···Au short contacts. Selected bond distances [Å] and angles [°]: Au-Se1 2.410(4), Se1-Se2 2.363(6), Se2-Se3 2.343(5); Se1-Se2-Se3 104.2(2), Se2-Se3-Se2 104.2(3), Au-Se1-Se2 101.4(2).

charge-compensating $K^{\oplus}$ ions. The $[AuSe_5]_n^{n\ominus}$ chains are composed of $Se_5^{2\ominus}$ ligands bridging two Au atoms via terminal Se atoms. The structure of $[AuSe_5]_n^{n\ominus}$ may be formally derived from that of $[AuSe]_n^{n\ominus}$[13] by replacing the $Se^{2\ominus}$ ions with $Se_5^{2\ominus}$ ligands. The $Au^{\oplus}$ centers show a linear coordination with a Se–Au–Se bond angle of 179.0(2)°. The $[AuSe_5]_n^{n\ominus}$ chains lack a center of symmetry, but they possess a perpendicular mirror plane passing through the Se3 atom. The chains in **1** are parallel to the crystallographic *c* axis. These chains interact with each other forming dimers through close Au···Au d^{10}–d^{10} contacts,[14] (2.950(3) Å) as depicted in Figure 1. The Au–Au contacts are considerably shorter than those observed in KAuSe[13] and in α- and β-AuSe.[15] and comparable to those in Ag_3AuSe_2.[14a] This is a beautiful example of a well-defined d^{10}–d^{10} interaction in the solid state. In general, d^{10}–d^{10} bonding contacts are not fully understood. Normally, the interaction of two filled metal orbitals results in a nonbonding situation due to the formation of a bonding and an equally antibonding state. However, recent theoretical investigations into this issue have invoked a significant admixture of s and p character (from the empty s and p orbitals) into the predominantly d metal orbitals.[16] This hybridization gives rise simultaneously to a more bonding and a less antibonding M–M interaction and therefore an overall stabilization.

The obseved Au–Se bond distances (2.410(4) Å) are similar to those found in KAuSe[13] at 2.414(1) Å. The average Se–Se bond distances in $KAuSe_5$ are normal (2.353(6) Å) and in the range found for other Se–Se bond distances in polyselenide complexes.[1] The shortest K···Se distances in $KAuSe_5$ are K1-Se1 (3.339(4) Å) and K2-Se1 (3.384(4) Å).

The structure of K_3AuSe_{13} is shown in Figure 2 and it is even more intriguing. This is a $Au^{3\oplus}$ compound, composed of centrosymmetric one-dimensional $[Au(Se_3)(Se_5)_2]_n^{3n\ominus}$ chains running parallel to the *c* axis. The makeup of the chains can be regarded as a one-dimensional assembly of square-planar $Au^{3\oplus}$ centers (situated on a center of symmetry) with two armlike *trans* $Se_5^{2\ominus}$ ligands and bridging $Se_3^{2\ominus}$ ligands. The bridging mode of the $Se_3^{2\ominus}$ ligands in **2** is similar

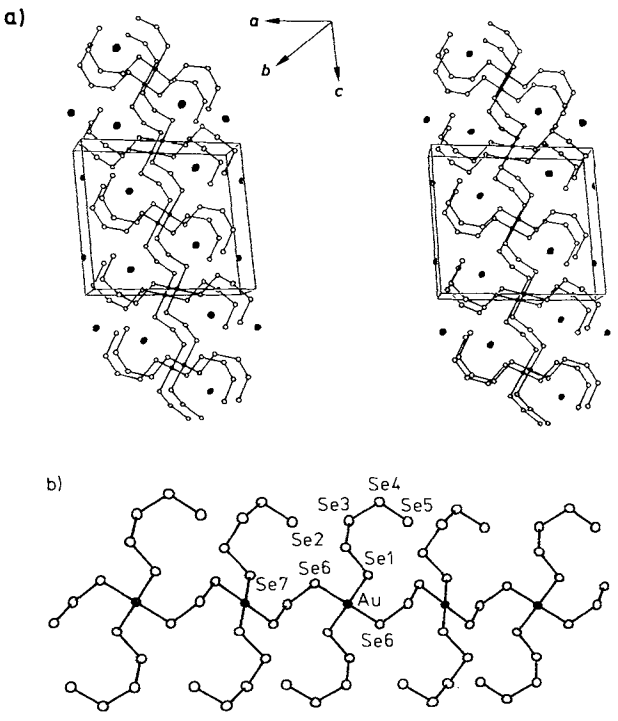

Fig. 2. ORTEP representation of the structure of the $[AuSe_{13}]_n^{3n\ominus}$ chains. a) Stereoscopic view of the unit cell. ●, K; ●, Au; ○, Se. b) A single chain with labeling scheme. Selected bond distances [Å] and angles [°]: Au-Se1 2.465(2), Au-Se6 2.485(2), Se1-Se2 2.349(3), Se2-Se3 2.368(3), Se3-Se4 2.348(3), Se4-Se5 2.343(3), Se6-Se7 2.351(3); Se1-Au-Se1 180, Se6-Au-Se6 180, Se1-Au-Se6 90.82(6); Se1-Au-Se6 89.19(6), Au-Se1-Se2 111.9(1), Au-Se6-Se7 108.92(8), Se3-Se4-Se5 109.2(1). Average Se–Se–Se angle 105.

[*] Prof. M. G. Kanatzidis, Y. Park
Department of Chemistry and
Center for Fundamental Materials Research
Michigan State University
East Lansing, MI 48824 (USA)

[**] Financial support from the National Science Foundation for a Presidential Young Investigator Award (CHE-8958451) is gratefully acknowledged.

to that of the $Se_5^{2\ominus}$ ligands in **1**. The Au···Se distances in **2** compare well with the corresponding distances in AuSe[15] (2.48 Å) and in the molecular compound $[Au_2Se_{10}]^{2\ominus}$[17] (2.45 Å). Unlike **1**, there are no close Au···Au contacts in **2**. Selected bond distances for K_3AuSe_{13} are given in the caption of Figure 2. The $K^{\oplus}$ ions reside in the cavities created by the Se atoms in the polyselenide chains. Compound **2** is the first solid-state compound to contain both $Se_3^{2\ominus}$ and $Se_5^{2\ominus}$ ligands and to our knowledge it is the most Se-rich Au compound to date. Conceptually, the $[Au(Se_3)(Se_5)_2]_n^{3n\ominus}$ chains can be viewed as the oxidative addition product of a $Se_{10}^{2\ominus}$ chain to the $Au^{\oplus}$ atoms of a hypothetical $[AuSe_3]_n^{n\ominus}$ chain, the latter being homologous to $[AuSe_5]_n^{n\ominus}$. The $[Au(Se_3)(Se_5)_2]_n^{3n\ominus}$ chain also represents the first example of a monodentate long polyselenide (i.e., $Se_5^{2\ominus}$), where one negative end is coordinated to a transition metal while the other is loose, ionically interacting with an alkali-metal ion. It should be noted that the usual binding mode of $Se_5^{2\ominus}$ is bidentate, either bridging as in **1**, $[V_2Se_{13}]^{2\ominus}$,[18] and $[In_2Se_{21}]^{4\ominus}$[19] or chelating as in $[Fe_2Se_{12}]^{2\ominus}$[20] and Cp_2TiSe_5.[21]

It is surprising that **2** forms by just changing the $K_2Se:Au:Se$ ratio from 2:1:8 (the ratio favoring formation of **1**) to 1.8:1:8. The small decrease in the K_2Se concentration results in a different K_2Se_x melt with a longer average polyselenide chain length compared to that present in the synthesis of **1**. The longer $Se_x^{2\ominus}$ chains would be more oxidizing than the corresponding short ones, which is consistent with the formation of **2**, a $Au^{3\oplus}$ compound. The slight but significant variation in the composition of the polyselenide melt (solvent) and the isolation of both $Au^{\oplus}$ and $Au^{3\oplus}$ polyselenide compounds underscores the complexity of these reaction mixtures and the delicate coordination and redox equilibria between the various $Au^{m\oplus}$ (m = 1,3) and $Se_x^{2\ominus}$ species. Such effects have been noted earlier in room-temperature solution studies on molecular Au/Se complexes.[17]

Further exploration of the effect of the polychalcogenide composition on the nature of the final K/Au/Se products is in progress.

Experimental Procedure

$KAuSe_5$, **1**: K_2Se, 0.157 g, 1.00 mmol), Au powder (0.098 g 0.5 mmol; 99.95%, Cerac), and Se powder (0.316 g, 4 mmol; 99.5%, Aldrich) were mixed in a Pyrex tube and sealed under vacuum (ca. 10^{-3} Torr). The reaction was carried out at 250 °C for 99 h before being cooled to room temperature at 2 °C h^{-1}. The reddish black needle-shaped crystals were obtained in a 74% yield by removing excess potassium polyselenides with water under inert atmosphere.

K_3AuSe_{13}, **2**: Same as for $KAuSe_5$ except that a 1.8:1:8 $K_2Se:Au:Se$ ratio was used. Black parallelpipeds were obtained. Yield 57%. The presence of K Au, and Se (semiquantitative analyses), as well as the homogeneity of the products, was established for all compounds by energy dispersive spectroscopy (EDS) in a scanning electron microscope.

Received: February 21, 1990 [Z 3812 IE]
German version: *Angew. Chem. 102* (1990) 945

[1] a) A. Müller, E. Diemann, *Adv. Inorg. Chem. Radiochem. 31* (1987) 89–122; b) M. Draganjac, T. B. Rauchfuss, *Angew. Chem. 97* (1985) 745–760; *Angew. Chem. Int. Ed. Engl. 24* (1985) 742–757; c) M. A. Ansari, J. A. Ibers, *Coord. Chem. Rev. 100* (1990) 223–266; d) M. G. Kanatzidis, *Comments Inorg. Chem. 10* (1990) 161–195.

[2] This does not include the hydrothermal synthesis technique, which also involves solvents at high pressures. However, chalcogenide synthesis under these conditions is also an unexplored area. For examples of such syntheses, see: a) W. S. Sheldrick, *Z. Anorg. Allg. Chem. 562* (1988) 23–30; b) W. S. Sheldrick, H.-J. Hauser, *ibid. 557* (1988) 98–104; c) W. S. Sheldrick, H.-J. Hauser, *ibid. 557* (1988) 105–111.

[3] a) L. E. J. Roberts: *MTP Int. Rev. Sci., Solid State Chemistry 10* (1975) p. 241; b) W. Bronger, *Angew. Chem. 93* (1981) 12–23; *Angew. Chem. Int. Ed. Engl. 20* (1981) 52–62; c) A. Meerschaut, P. Gressier, L. Guemas, J. Rouxel, *J. Solid State Chem. 51* (1984) 307–314; d) P. Böttcher, *Angew. Chem. 100* (1988) 781–794; *Angew. Chem. Int. Ed. Engl. 27* (1988) 759–772; e) B. Krebs, *ibid. 95* (1983) 113–134 and *22* (1983) 113–134.

[4] a) D. Elwell, H. J. Scheel: *Crystal Growth from High-Temperature Solutions*, Academic Press, London 1975; b) G. J. Janz (Ed.): *Molten Salts Handbook*, Academic Press, New York 1967; c) G. Mamantov: *Molten Salts*, Marcel Dekker, New York 1969.

[5] a) H. J. Scheel, *J. Cryst. Growth 24/25* (1974) 669–673; b) R. Sanjines, H. Berger, F. Levy, *Mater. Res. Bull. 23* (1988) 549–553; c) R. W. Garner, W. B. White, *J. Cryst. Growth 7* (1970) 343–347.

[6] a) W. Klemm, H. Sodomann, P. Langmesser, *Z. Anorg. Allg. Chem. 241* (1939) 281–304; b) T. G. Pearson, P. L. Robinson, *J. Chem. Soc. 1931*, 1304–1314.

[7] S. A. Sunshine, D. Kang, J. A. Ibers, *J. Am. Chem. Soc. 109* (1987) 6202–6204.

[8] D. Kang, J. A. Ibers, *Inorg. Chem. 27* (1988) 549–551.

[9] S. Schreiner, L. E. Aleandri, D. Kang, J. A. Ibers, *Inorg. Chem. 28* (1989) 392–393.

[10] M. G. Kanatzidis, Y. Park, *J. Am. Chem. Soc. 111* (1989) 3767–3769.

[11] M. G. Kanatzidis, Y. Park, *Chem. Mater. 2* (1990) 99–101.

[12] a) Crystal data for $KAuSe_5$, **1**: orthorhombic, *Ibam*, $Z = 8$, $a = 8.625(6)$, $b = 11.293(9)$, $c = 16.425(11)$ Å, $V = 1600(3)$ Å^3, 23 °C. $2\theta_{max}(Mo_{K\alpha}) = 46°$. Number of data measured 719. Number of unique data 536. Number of data having $F_0^2 > 3\sigma(F_0^2)$: 382. Number of variables 37. Number of atoms 5. $\mu = 413$ cm^{-1}. $R = 0.057$ and $R_w = 0.071$. b) Crystal data for K_3AuSe_{13}: monoclinic, $P2/c$, $Z = 2$, $a = 14.949(6)$, $b = 4.858(2)$, $c = 13.723(5)$ Å, $\beta = 93.86(3)°$, $V = 994(1)$ Å^3, 23 °C. $2\theta_{max}(Mo_{K\alpha}) = 48°$. Number of data measured 1918. Number of unique data 1570. Number of data having $F_0^2 > 3\sigma(F_0^2)$: 1167. Number of variables 81. Number of atoms 10. $\mu = 316$ cm^{-1}. $R = 0.044$ and $R_w = 0.050$. An empirical absorption correction based on ψ scans for several reflections was applied to all data sets. Further details of the crystal structure investigations may be obtained from the Fachinformationszentrum Karlsruhe, Gesellschaft für wissenschaftlich-technische Information mbH, D-7514 Eggenstein-Leopoldshafen 2 (FRG), on quoting the depository number CSD-54566, the names of the authors, and the journal citation.

[13] K. O. Klepp, W. Bronger, *J. Less-Common Met. 127* (1987) 65–71.

[14] a) M. Jansen, *Angew. Chem. 99* (1987) 1136–1149; *Angew. Chem. Int. Ed. Engl. 26* (1987) 1098–1111; b) F. Scherbaum, B. Huber, G. Müller, H. Schmitbaur, *ibid. 100* (1988) 1600–1602 and *27* (1988) 1542–1544; c) M. N. I. Kahn, C. King, D. D. Heinrich, J. P. Fackler, Jr., L. C. Porter, *Inorg. Chem. 28* (1988) 2150–2154; d) J. P. Fackler, Jr., L. C. Porter, *J. Am. Chem. Soc. 108* (1986) 2750–2751.

[15] These compounds contain both linear $Au^{\oplus}$ and square-planar $Au^{3\oplus}$ centers. Average $Au^{\oplus}$–Se and $Au^{3\oplus}$–Se distances are 2.42 Å and 2.48 Å, respectively: A. Rabenau, H. Schulz, *J. Less Common Met. 48* (1976) 89–101.

[16] a) K. M. Merz, Jr., R. Hoffmann, *Inorg. Chem. 27* (1988) 2120–2127; b) P. K. Mehrotra, R. Hoffmann, *ibid. Chem. 17* (1978) 2187–2189.

[17] M. G. Kanatzidis, S.-P. Huang, *Inorg. Chem. 28* (1989) 4667–4669.

[18] C.-N. Chau, R. W. M. Wardle, J. A. Ibers, *Inorg. Chem. 26* (1987) 2740–2741.

[19] M. G. Kanatzidis, S. Dhingra, *Inorg. Chem. 28* (1989) 2024–2026.

[20] H. Strasdeit, B. Krebs, G. Henkel, *Inorg. Chim. Acta 89* (1984) L 11–L 13.

[21] D. Fenske, J. Adel, K. Dehnicke, *Z. Naturforsch. B 42* (1987) 931–933.

Biomimetic Catalysis of an S_N2 Reaction Resulting from a Novel Form of Transition-State Stabilization**

By *David A. Stauffer, Richard E. Barrans, Jr.*, and *Dennis A. Dougherty**

Cyclophane host **1** is a general receptor for quaternary ammonium and immonium guests.[1] Complexation arises, in part, from an attractive "cation–π" interaction[1–3] between the positive charge of a guest and the polarizable, electron-rich π systems of the host. We now report that hosts such as **1** can act as biomimetic catalysts in aqueous media

[*] Prof. D. A. Dougherty, Dr. D. A. Stauffer, R. E. Barrans, Jr.
Arnold and Mabel Beckman Laboratories of Chemical Synthesis
California Institute of Technology, Mail Code: 164-30
Pasadena, CA 91125 (USA)

[**] This work (contribution No. 8010) was supported by the Office of Naval Research and the National Institutes of Health, *R.E.B.* was a Department of Education Graduate Assistance in Areas of National Need Fellow, 1989. Portions of this work were reported at the 187th National Meeting of the American Chemical Society, Dallas, TX, April 9–12, 1989.

for S_N2 reactions that develop a positive charge in their transition states.[4] In particular, the Menschutkin reaction[5] of methyl iodide with nucleophiles such as quinoline (**2**) is substantially accelerated by host **1**. We postulate that the cation–π interaction is also a major factor in the catalysis and that our findings may have implications for a broad range of biological methylation reactions.

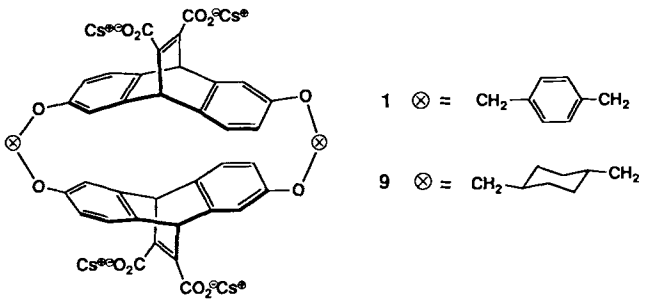

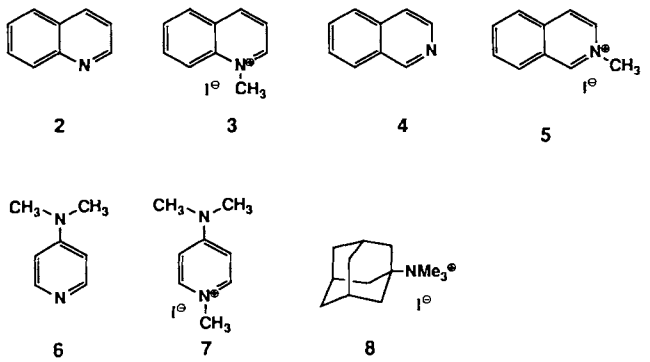

Alkylation of nucleophiles such as **2**, **4**, and **6** with CH_3I in D_2O/borate buffer[1] (pD = 9) proceeds slowly to give **3**, **5**, and **7**. Addition of host **1** greatly accelerates the reactions. When excess CH_3I is used (pseudo-first-order conditions), the results are consistent with the kinetic scheme of Figure 1.[6] This is essentially a Michaelis–Menten scheme with

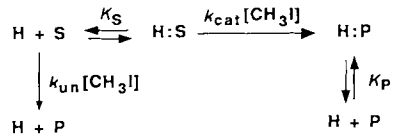

Fig. 1. Kinetic scheme applied to the alkylation reactions studied. H = host, S = substrate, P = product. k_{un} = rate constant for the uncatalyzed reaction.

some small, but important, distinctions. Since we already know[1] the binding constants for S and P (K_S and K_P), all ambiguities concerning the interpretations and interrelations[7] of the conventional Michaelis parameters (k_{cat} and K_M) are removed.[8] Another simplification is that all alkylation reactions are completely irreversible under the present conditions. Thus, the only unknown in Figure 1 is k_{cat}. A fit to the concentration vs. time data involves only one adjustable parameter, k_{cat}, so such rate constants can be obtained in a straightforward manner.

A variety of observations support the overall scheme. The reaction is first-order in CH_3I, and no rate acceleration is seen when the nonmacrocyclic analogue of **1** (dibenzyloxy derivative of 9,10-dihydro-9,10-ethenoanthrancene building block[11]) is used. In further support of the proposed kinetic scheme, the system shows competitive inhibition. Addition of adamantyltrimethylammonium iodide (**8**)[1] at a concentration that would occupy 40% of the host binding sites leads to a 40% decrease in the apparent k_{cat}. Product inhibition is also found, since the products (immonium ions) are always more tightly bound than the substrates.[1] Nevertheless, in optimal cases as many as five catalytic turnovers per host have been seen before product inhibition effectively shuts down the system. As shown in Table 1, k_{cat}/k_{un} can

Table 1. Parameters for catalyzed S_N2 reactions [a].

S	P	H	k_{cat}/k_{un} [b]	$-\Delta G^\circ_S$ [c,d]	$-\Delta G^\circ_T$ [c]	$-\Delta G^\circ_P$ [c,d]
2	**3**	**1**	100	5.4	8.1	7.6
4	**5**	**1**	10	6.3	7.8	7.2
6	**7**	**1**	5	5.8 [e]	6.7	6.5 [e]
2	**3**	**9**	20	5.9	7.7	6.6

[a] See Figs. 1 and 3 for definitions of symbols. [b] ±10% [c] kcalmol^{-1} at 300 K. [d] Ref. [1]. [e] Present work.

attain values as high as 100, indicating substantial catalysis for these simple reactions.

Figure 2 places all quantities on a free energy scale. It is a trivial matter to determine ΔG°_T, the free energy of binding of

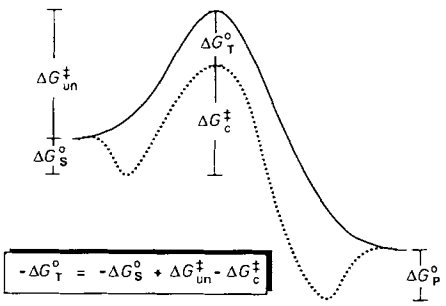

Fig. 2. Free energy diagram for catalyzed and uncatalyzed alkylations. Note that, by convention, activation energies are positive numbers, but favorable free energies of binding are negative numbers.—,uncatalyzed reaction; ····, catalyzed reaction.

the transition state (Table 1). There is no ambiguity as to the nature of ΔG°_T: it is precisely the free energy change on moving the S_N2 transition state out of water and into the receptor. Figure 3 provides a schematic of our model for the catalyzed reaction, with the receptor in the "rhomboid" conformation implicated by our previous studies[1] of the binding of flat, aromatic guests.

There are several possible interpretations of these findings. One could argue that we are simply desolvating the nucleophile by binding it, thereby enhancing its nucleophilicity. However, such reactions are generally accelerated in polar solvents,[5] and for the present systems, we have determined that the reactions of methyl iodide with both quinoline (**2**) and isoquinoline (**4**) are faster in our buffer system (without host) than in chloroform or benzene.[9] The catalysis we observe is therefore not a simple desolvation effect. Host **1** shows a substantial preference for electron-deficient guests,[1] and so it is difficult to ascribe any strong binding component to the leaving group, with its developing negative charge. The most likely origin of the catalysis, then, is the cation–π interaction. Host **9**, which is known to show a weaker cation–π effect than **1**,[1] is also a weaker catalyst (Table 1).

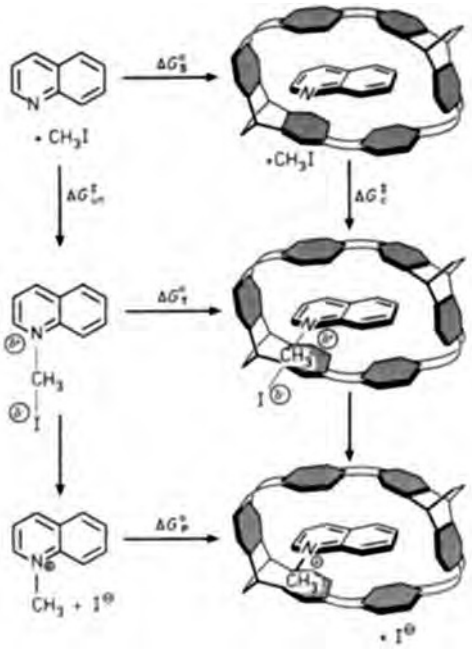

Fig. 3. Schematic of the catalyzed and uncatalyzed reactions of methyl iodide with quinoline.

Interestingly, the transition state, with only a partial positive charge, is more tightly bound than the product, with a full positive charge, in all cases. We propose that the most reasonable explanation for this observation is that transition states, because of their long, weak bonds, are inherently more polarizable than ground states.[10] Host **1** completely surrounds a guest with electron-rich π systems (Fig. 3), and we suggest that the polarization of these π components in response to a guest dominates the binding behavior of **1**. With neutral guests, electron-deficient structures such as **2** are preferred over electron-rich indoles because of π-polarization effects.[1] With a positive charge, as in **3** or **8**, even more host polarization occurs. A transition state (Fig. 3) polarizes the host, and is itself polarized, creating even more favorable interactions. Water as a surrounding medium would be much less effective in this regard. The large dielectric constant associated with water is a low-frequency dielectric constant—that is, water stabilizes charges by reorienting its molecular dipoles, a relatively slow process. However, the high-frequency dielectric constant of water is quite low (i.e., water is not at all polarizable).[11] Because transition states are very short-lived, the high-frequency component is relevant to the present case. Water is simply not capable of an instantaneous response to the changes occurring in a transition state the way π electrons are.[12]

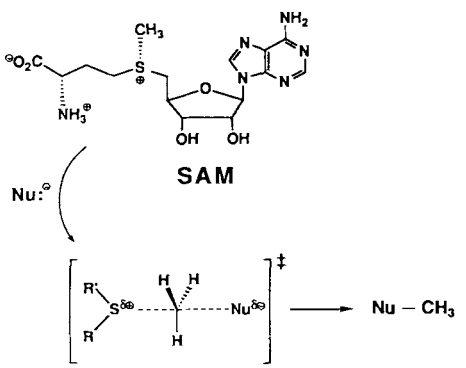

Scheme 1. Nu = DNA, tRNA, protein, sugar, olefins.

If, indeed, cation–π interactions are predominantly responsible for the transition-state binding, then the present system would represent an especially parsimonious realization of *Pauling*'s surmise[13] that enzymes preferentially bind transition states. One uses the same force—the polarization of π systems at the active site—to bind substrate, transition state, and product. The nature of the binding force, though, is such that it is most effective in binding a transition state.

Finally, we note that the overwhelming majority of biological methylation reactions are mediated by *S*-adenosylmethionine (SAM) (Scheme 1).[14] The transition states of these reactions resemble those bound by **1**, and we speculate that perhaps nature uses similar cation–π interactions to enhance these reactions. Efforts to find support for this hypothesis and to expand the scope of this type of catalysis are underway.

Received: February 26, 1990;
revised: May 3, 1990 [Z 3817 IE]
German version: *Angew. Chem. 102* (1990) 953

CAS Registry numbers:
R,R,R,R-**1**, 116300-56-2; *S,S,S,S*-**1**, 116300-55-1; **2**, 91-22-5; **4**, 119-65-3; **6**, 1122-58-3; **2**, 116265-055.

[1] a) D. A. Stauffer, D. A. Dougherty, *Tetrahedron Lett. 29* (1988) 6039–6042; b) M. A. Petti, T. J. Shepodd, R. E. Barans, Jr., D. A. Dougherty, *J. Am. Chem. Soc. 110* (1988) 6825–6840; c) T. J. Shepodd, M. A. Petti, D. A. Dougherty, *ibid. 110* (1988) 1983–1985; d) T. J. Shepodd, M. A. Petti, D. A. Dougherty, *ibid. 108* (1986) 6085–6087; e) M. A. Petti, T. J. Shepodd, D. A. Dougherty, *Tetrahedron Lett. 27* (1986) 807–810.

[2] a) In our previous work [1] we described this interaction as an "ion–dipole" effect. Although the term was intended to be descriptive only, we now believe it has an overly specific connotation. The stabilization of a positive charge by an electron-rich π system is no doubt a complex phenomenon, involving charge–dipole, charge–quadrupole, charge-induced dipole, π-polarization, and other effects. Ion–dipole implies, for example, a definite distance dependence ($1/r^2$) which may not be appropriate here. For a recent discussion of these various interactions as applied to protein chemistry, see [3a]. b) In the current system, the substrates are presumed to bind to the "rhomboid" conformation [1b] of the host. In this arrangement, face-to-face, π-stacking interactions are predominant, with both "linker" rings and two of the four aromatic rings of the ethenoanthracenes involved (see Fig. 3).

[3] a) S. K. Burley, G. A. Petsko, *Adv. Protein Che. 39* (1988) 125–189; *FEBS Lett. 203* (1986) 139–143; b) M. Meot-Ner (Mautner), C. A. Deakyne, *J. Am. Chem. Soc. 107* (1985) 469–474; C. A. Deakyne, M. Meot-Ner (Mautner), *ibid. 107* (1985) 474–479; c) H.-J. Schneider, T. Blatter, S. Simova, I. Theis, *J. Chem. Soc. Chem. Comm. 1989*, 580–581.

[4] a) Several previous examples of catalysis of S_N2 reactions have been reported, the accelerations being attributed to both "proximity" effects and electrostatic stabilization of developing charges. See, for example, F. P. Schmidtchen, *Top. Curr. Chem. 132* (1986) 101–133; H.-J. Schneider, R. Busch, *Angew. Chem. 96* (1984) 910–911; *Angew. Chem. Int. Ed. Engl. 23* (1984) 911–912; T. R. Kelly, C. Zhao, G. J. Bridger, *J. Am. Chem. Soc. 111* (1989) 3744–3745. Recent general reviews of biomimetic catalysis and related topics: b) R. Breslow, *Science 218* (1982) 532–537; I. Tabushi, *Tetrahedron 40* (1984) 269–292; J.-M. Lehn, *Angew. Chem. 100* (1988) 91–116; *Angew. Chem. Int. Ed. Engl. 27* (1988) 89–112; c) J. Rebek, Jr., *Science 235* (1987) 1478–1484; *Top. Cur. Chem. 132* (1986) 101–133; *Angew. Chem. 102* (1990) 261–272; *Angew. Chem.* Int. Ed. Engl. *29* (1990) 245–255; F. Diederich, *Angew. Chem. 100* (1988) 372–396; *Angew. Chem. Int. Ed. Engl. 27* (1988) 362–386; d) J. F. Liebman, A. Greenberg (Eds.): *Mechanistic Principles of Enzyme Activity*, VCH, New York 1988, especially Chapter 3 by A. W. Czarnik, M. I. Page, A. Williams (Eds.): *Enzyme Mechanisms*, R. Soc. Chem., London 1987, especially Chapter 1 by M. I. Page.

[5] a) A. J. Parker, *Chem. Rev. 69* (1969) 1–32; b) J. M. Cachaza, M. A. Herraez, *An. Quim. 67* (1971) 11–16.

[6] Typical conditions: host concentration, 200 μM; initial concentration of substrate, 1 mM; CH_3I in at least 40-fold excess to ensure pseudo-first-order conditions. Reactions were monitored by 400-MHz ^1H NMR in a pD = 9 cesium borate buffer [1]. The (*S,S,S,S*) isomer of **1** and the (*R,R,R,R*) isomer of **9** were used. No evidence for binding of MeI to host or host–substrate complex was found. The formation of the host–substrate complex is much more rapid than alkylation and so is not rate-limiting [1].

[7] See, for example, C. Walsh: *Enzyme Reaction Mechanisms*, Freeman, New York 1979.

[8] Our model assumes that the thermodynamic host–substrate complex is kinetically competent. If, instead, a less stable binding mode is the productive one, then the value of k_{cat} would have to increase in order to compensate for the smaller percent of substrate bound (productively), and $\Delta G_T^{\ddagger}$ would, in fact, remain unchanged.

[9] $\Delta G_{298}^{\ddagger}$ [kcalmol^{-1}] for the reaction CH_3I + **2** (solvent): 24.8 (C_6H_6) [5b]; 24.4 ($CHCl_3$) [5b]; 23.9 (present borate buffer).

[10] Theoretical studies of S_N2 reactions support this notion: a) F. Carrion, M. J. S. Dewar, *J. Am. Chem. Soc. 106* (1984) 3531–3539; b) J. Chandrasekhar, S. F. Smith, W. L. Jorgensen, *ibid. 107* (1985) 154–163; c) *ibid. 106* (1984) 3049–3050; d) C. Bunton: *Nucleophilic Substitution at a Saturated Carbon Atom*, Elsevier, New York 1963; e) E. M. Arnett, R. Reich, *J. Am. Chem. Soc. 102* (1980) 5892–5902.

[11] J. N. Israelachvili: *Intermolecular and Surface Forces*, Academic Press, London 1985, pp. 75–78.

[12] One might argue that benzene as a solvent should also be able to stabilize the transition state through cation–π interactions. However, the host enforces a perfect alignment of the π systems, whereas the fluid solvent may not have the correct orientation as the transition-state forms.

[13] L. Pauling, *Chem. Eng. News 24* (1946) 1375–1377; *Nature 161* (1948) 707–709; J. Kraut, *Science 242* (1988) 533–540.

[14] For reviews on SAM reactions G. L. Cantoni, *Annu. Rev. Biochem. 44* (1975) 435–451; S. K. Shapiro, F. Schlenk: *Transmethylation and Methionine Biosynthesis*, University of Chicago Press, Chicago 1964; H. W. Liu, C. T. Walsh in Z. Rappoport, (Ed.): *The Chemistry of the Cyclopropyl Group*, Wiley, New York 1987, pp. 959–1025; see also [7], pp. 851–863.

1,2-Dimethyl-1,2-disila-*closo*-dodecaborane(12), the First Silicon Analogue of an *ortho*-Carborane **

By *Dietmar Seyferth,* Klaus Büchner, William S. Rees, Jr.*, and *William M. Davis*

The icosahedral carboranes, especially those in which the two cluster carbon atoms are vicinal (*o*-carboranes), have received much attention since the first reports of their existence in 1963.[1] Notably absent in the many publications on this class of boron cluster compounds over the intervening 25 odd years have been examples of icosahedral clusters in which the two monosubstituted carbon atoms of an *o*-carborane have been replaced by two monosubstituted silicon, germanium, tin, or lead atoms. We report here the synthesis and structural characterization of **1**, the first such fourth-main-group analogue of an *o*-carborane: 1,2-dimethyl-1,2-disila-*closo*-dodecaborane(12) (or 1,2-dimethyl-*o*-silaborane). This compound is notable also in that it is the first example of a *formal* derivative of a disilyne, $H_3CSi \equiv SiCH_3$ in the present case, a class of unsaturated organosilicon compounds of which there are to date no known examples.

The synthesis of 1,2-dimethyl-*o*-silaborane, **1**, was the result of a deviation from the expected reaction course when a benzene solution of decaborane(14) and bis(dimethylamino)methylsilane, $CH_3(H)Si[N(CH_3)_2]_2$, **2**, was heated at reflux under nitrogen. In prior work,[2] such a reaction of $B_{10}H_{14}$ with $(CH_3)_2Si[N(CH_3)_2]_2$ in refluxing benzene had resulted in formation of a linear polymer, $[6,9\text{-}(CH_3)_2NSi(CH_3)_2N(CH_3)_2 \cdot B_{10}H_{12}]_x$, a pale yellow, resinous material from whose melt fibers could be drawn and whose pyrolysis in a stream of ammonia to 1000 °C gave boron nitride containing 2–4% Si in high yield. However, the reaction of $B_{10}H_{14}$ with **2** in refluxing benzene or toluene resulted in formation of a mixture of two white solids, **1** in 15% yield, based on $B_{10}H_{14}$, and $6,9\text{-}[(CH_3)_2NH]_2B_{10}H_{12}$, **3**, in 58% yield [Eq. (1)]. The former could be purified by sublimation at 90 °C (0.01 Torr). Its yield has not been optimized. Compound **1** may be handled without exclusion of the laboratory atmosphere since it is stable to air and moisture.

$$B_{10}H_{14} + \underset{\mathbf{2}}{CH_3(H)Si[N(CH_3)_2]_2} \xrightarrow[-2H_2,\ -2(CH_3)_2NH]{\Delta} \underset{\mathbf{3}}{6,9\text{-}[(CH_3)_2NH]_2B_{10}H_{12}} + \underset{\mathbf{1}}{\text{Si}_2\text{C}_2\text{B}_{10}\text{H}_{12}} + \cdots \quad (1)$$

Very slow crystallization of **1** from dilute benzene solution at 3 °C gave the 1:1 solvate **1** · C_6H_6 as rods whose structure was determined by single-crystal X-ray diffraction.[3] The *o*-silaborane, like the *o*-carboranes, has a slightly distorted icosahedral structure (Fig. 1). The Si–Si bond distance of

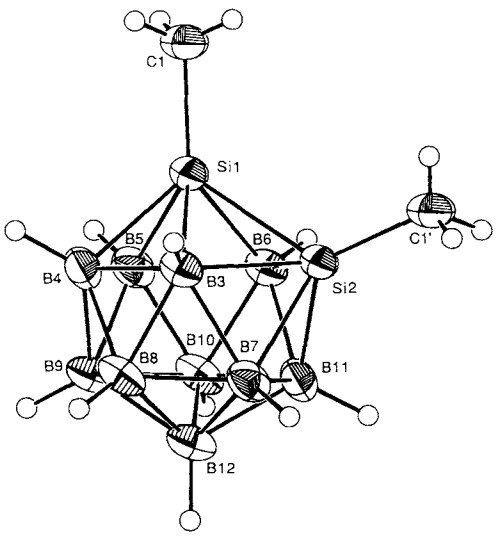

Fig. 1. ORTEP representation of **1**, drawn with 35% probability ellipsoids. Hydrogen atoms have been given arbitrary thermal parameters for clarity. Due to molecular symmetry, distances involving Si2 are equivalent to those involving Si1. Other symmetry related atoms are C1 and C2, B3 and B6, B4 and B11, B5 and B7, B8 and B10, and B9 and B12. Selected interatomic distances [Å] (standard deviations of the last digit given in parentheses): Si1-C1 1.827(3), B3-B4 1.848(5), Si1-Si2 2.308(2), B4-B5 1.859(5), Si1-B3 2.116(3), B4-B8 1.774(5), Si1-B4 2.018(3), B4-B9 1.765(5), Si1-B5 2.017(3), B5-B6 1.849(5), Si1-B6 2.113(4), B5-B9 1.769(5), B6-B10 1.771(4), B5-B10 1.765(5), B8-B12 1.782(5), B9-B12 1.775(8), B10-B12 1.784(5).

2.308(2) Å is slightly less than that of "normal" Si–Si single bonds (≈2.33–2.34 Å),[4] but significantly longer than known Si–Si double bonds.[5] In comparison, the C–C bond distances in *o*-carboranes (1.655 Å, the mean value found in X-ray and gas-phase electron diffraction studies[6]) are longer than the normal $C(sp^3)$–$C(sp^3)$ distance of 1.54 Å. This is understandable in terms of the larger size of a silicon atom (covalent radius 1.18 Å), compared with a carbon atom (covalent radius 0.77 Å). The Si–B bond distances in **1** (2.017(3), 2.018(3), 2.113(4), and 2.116(3) Å) are very close to the sum of the covalent radii of Si and B, 2.07 Å (using 0.89 Å as the average boron covalent radius in *o*-carboranes[6]). These distances may be compared to those of the

[*] Prof. D. Seyferth, Dr. K. Büchner, Dr. W. S. Rees, Jr., Dr. W. M. Davis
Department of Chemistry
Massachusetts Institute of Technology
Cambridge, MA 02139 (USA)

[**] This work was supported in part by the U.S. Office of Naval Research and by the award of a Feodor Lynen Fellowship to *K.B.* by the Alexander von Humboldt Foundation.

Si–B bonds in *commo*-3,3'-Si(3,1,2-$SiC_2B_9H_{11})_2$, which contains a single silicon atom bonded within a 12-atom boron-containing cluster: 2.05(1) and 2.14(1) Å.[7]

The ^1H, ^{13}C, ^{29}Si, and ^{11}B NMR spectra of **1** were recorded.[8] The ^{11}B NMR spectrum (160.367 MHz, [D_6]acetone, 25 °C, external $BF_3 \cdot OEt_2$) was in agreement with the 1,2-disila-*closo*-dodecaborane(12) cage structure, showing four doublets in 2:2:2:4 intensity ratio at $\delta = -11.2$ (d, $J = 147$ Hz, B9, 12), -12.6 (d, $J = 144$ Hz, B8, 10), -13.5 (d, $J = 152$ Hz, B3, 6), and -14.5 (d, $J = 147$ Hz, B4, 5, 7, 11). The assignments are based on a 2D proton-decoupled ^{11}B–^{11}B NMR spectrum. The CH_3 resonance was observed at $\delta = -0.07$ in the ^1H NMR spectrum of **1** in C_6D_6 solution. The proton-decoupled ^{29}SiNMR spectrum of **1** in C_6D_6 solution at 50 °C showed a singlet at $\delta = -37.77$, the proton-decoupled ^{13}C NMR spectrum, also in C_6D_6 at 40 °C, a singlet at $\delta = -12.80$. The upfield shifts observed in the ^{13}C and ^{29}Si spectra of **1** taken in C_6D_6 solution, as compared with TMS, are consistent with the well-documented electron-deficient nature of boron cages.

Compound **1** is less stable than the *o*-carboranes. It melts at 201–203 °C (sealed capillary) and decomposes with gas evolution above 230 °C. It remains undecomposed when heated at reflux in wet tetrahydrofuran solution for several days. It was unaffected when treated with an excess of CF_3CO_2H in THF at room temperature and remained largely undecomposed when this solution was heated at reflux for 14 hours. It was found to be stable toward $AlCl_3$ in refluxing benzene. It reacts with and is degraded by alcoholic KOH in THF at room temperature within minutes and it decolorizes a solution of bromine in carbon tetrachloride after several hours at reflux.

Now that the first member of this new class of boron cluster compounds has been isolated, it may be expected that other 1,2-$R_2Si_2B_{10}H_{10}$ compounds can be prepared. The development of their chemical reactivity at silicon and at boron will be of some interest as will a comparison of their chemistry with that of the *o*-carboranes.

Experimental Procedure

A 250-mL three-necked flask equipped with a reflux condenser, an addition funnel, and a magnetic stirring bar was flushed with argon and charged with $B_{10}H_{14}$ (6.6 g, 54.0 mmol) and dry toluene (120 mL). To the resulting solution was added dropwise at room temperature **2** (7.1 g, 53.7 mmol)[9]. The reaction mixture was stirred and heated at reflux under argon for 24 h. During this time a white solid precipitated. The reaction mixture was filtered and the filtrate evaporated at reduced pressure. The residue was extracted with two 100-mL portions of hot benzene. Filtration of the extracts and cooling to 3 °C resulted in deposition of 1.45 g of **1** as an amorphous white powder that contained a small amount of white needles. Evaporation of the remaining benzene solution gave 0.6 g of **3**, identified on the basis of its ^1H and ^{11}B NMR and mass spectra. The solid that had precipitated during the reaction was sublimed at 90 °C (0.01 Torr) to give an additional 0.15 g of **1**. The sublimation residue was 6.0 g of **3**. The total yield of the latter was 6.6 g, (58%). The total yield of **1** was 1.60 g, a yield of 15% based on $B_{10}H_{14}$. Correct C, H, Si elemental analyses; correct high-resolution mass spectrum.

Received: February 16, 1990 [Z 3801 IE]
German version: *Angew. Chem. 102* (1990) 911

CAS Registry numbers:
1, 128270-48-4; **1** · C_6H_6, 128270-49-5; **2**, 22705-33-5; **3**, 128270-50-8; $B_{10}H_{14}$, 17702-41-9.

[1] *Gmelin Handbook of Inorganic Chemistry, 8th Edition, Borverbindungen, Vols. 2* (1974), *6* (1975), *11* (1977), *12* (1977), and chapters in the first and second supplements (1980–1983), Springer, Berlin. See also: R. N. Grimes: *Carboranes*, Academic Press, New York 1970, Chapter 6 and literature cited therein.

[2] D. Seyferth, W. S. Rees, Jr., unpublished work.

[3] **1** · C_6H_6 crystallizes with crystallographic twofold symmetry. One molecule of benzene was found for every molecule of **1** in two sites of equal occupancy; each site has the same crystallographic twofold symmetry. Crystal data for **1** · C_6H_6: orthorhombic, space group *Pccn* (No. 56); $a = 10.081(1)$, $b = 10.666(8)$, $c = 16.130(5)$ Å, $V = 1734$ Å, $Z = 4$; $\varrho_{calcd} = 1.052$ g cm^{-3}, $F(000) = 592$, $\mu(Mo_{K\alpha}) = 1.78$ cm^{-1}, 2291 reflections measured, 2291 unique reflections, 1050 observed ($I > 3\sigma(I)$), 89 variables, $r = 0.044$, $R_w = 0.058$, Rigaku AFC6R diffractometer, $Mo_{K\alpha}$ ($\lambda = 0.71069$ Å). Further details of the crystal structure determination may be obtained from the Fachinformationszentrum Karlsruhe, Gesellschaft für wissenschaftlich-technische Information mbH, D-7514 Eggenstein-Leopoldshafen 2 (FRG), on quoting the deposition number CDS-54516, the names of the authors, and the journal citation.

[4] Representative Si–Si single bond distances: 2.340(9) Å in $(CH_3)_6Si_2$: B. Beagley, J. J. Monaghan, T. G. Hewis, *J. Mol. Struct. 8* (1971) 401; 2.338(4) Å in *cyclo*-$[(CH_3)_2Si]_6$: H. L. Carrell, J. Donohue, *Acta Crystallogr. Sect. B28* (1972) 1566.

[5] Si–Si double bond distances: 2.143(1) and 2.160(1) Å: M. J. Fink, M. J. Michalczyk, K. J. Haller, J. Michl, R. West, *Organometallics 3* (1984) 793; 2.140(9) Å: S. Masamune, S. Murakami, J. T. Snow, H. Tobita, D. J. Williams, *ibid. 3* (1984) 3330.

[6] V. S. Mastryukov, L. V. Vilkov, O. V. Dorofeeva, *J. Mol. Struct. 24* (1975) 217.

[7] W. S. Rees, Jr., D. M. Schubert, C. B. Knobler, M. F. Hawthorne, *J. Am. Chem. Soc. 108* (1986) 5369.

[8] NMR spectra, conditions: All measurements at 25 °C unless otherwise specified. ^{11}B, 160.37 and 96.235 MHz, $BF_3 \cdot OEt_2$; ^1H, 300 MHz, TMS; ^{29}Si, 99.34 MHz, TMS; ^{13}C, 75.43 MHz, TMS.

[9] S. S. Washburne, W. R. Peterson, Jr., *J. Organomet. Chem. 21* (1970) 59.

Helicene Dianions: Paratropicity of Twisted Phenanthrene Dianions

By *Ron Frim, Albrecht Mannschreck,* and *Mordecai Rabinovitz**

The smallest polycyclic molecule with an enforced helical structure[1] is a three-ring system, namely, phenanthrene substituted at the 4,5 positions.[2] Like the other members of the helicene series, it belongs to the C_2 point group and hence is chiral. Such systems can be resolved into stable enantiomers if the barrier to racemization is sufficiently high. The neutral hydrocarbon species do not show a severe perturbation of the diatropicity according to their ^1H NMR spectra. In the neutral system where the HOMO–LUMO gap is wide, σ_{para} has an insignificant effect on the chemical shift.[3] Therefore, variations in the helicity do not significantly modify the ^1H NMR parameters.[4, 5] This phenomenon is illustrated by the chemical shifts of the protons at positions 9 and 10 in phenanthrenes **1**–**4** (Table 1). Reduction of these hydrocarbons with alkali metals can, in principle, give paratropic dianions.

These $4n\pi$ polycyclic dianions have been studied by NMR spectroscopy[3] with respect to two major parameters: (1) the electronic structure as related to paratropicity and (2) the detailed mode of electron delocalization. The correlation between the calculated HOMO–LUMO energy gap and the paratropicity as well as the NMR line shape was studied[5] without taking into account the different paths for delocalization of the various systems.

However, no study has taken into account the effect of the potential nonplanarity of such systems on their spectroscopic parameters. Our approach is to study a series of hydrocarbons and their double negatively charged derivatives, all of which have the same sp^2 skeleton and show a known degree of deviation from planarity[2] (see above). We assume that

[*] Prof. Dr. M. Rabinovitz, Dipl.-Chem. R. Frim
Department of Organic Chemistry, The Hebrew University
Jerusalem 91904 (Israel)
Prof. Dr. A. Mannschreck
Institut für Organische Chemie der Universität
D-8400 Regensburg (FRG)

[**] Financial support from the U.S.–Israel Binational Science Foundation is gratefully acknowledged.

the gross delocalization pattern is the same as long as the sp^2 carbon skeleton is maintained, and hence the relationship between the nonplanarity of the $4n\pi$ system and the NMR spectroscopic parameters can be studied. A system of choice is the charged $4n\pi$ helicene series in general and 4,5-disubstituted phenanthrenes in particular. The effects of their deviation from planarity should be reflected by both their electronic structure and their NMR spectra. Here we report the influence of the deviations from planarity on the ^1H NMR parameters of a series of dianions of 4,5-disubstituted phenanthrenes.

We chose to concentrate on alkyl-substituted phenanthrenes for two reasons: (1) the ability to modify the twist of the phenanthrene moiety by alkylation; (2) phenanthrene dianion shows a very significant dependence of its ^1H NMR line shapes on the type of reducing metal on the one hand and temperature and solvent on the other.[5] The $4n\pi$ phenanthrene dianion displays an intermediate HOMO–LUMO energy gap.[3–5] Systems with narrower energy gaps do not show resolved NMR spectra because of the relatively high concentration of a thermally excited or even a ground-state triplet. A wider energy gap will always give well-resolved NMR spectra, since thermal excitation to the triplet state is not possible. For that very reason, we thought that any minor change in the system's geometry and therefore in its energy gap would give rise to a very significant change in the NMR spectra. Indeed, twisted dianions derived from substituted phenanthrenes show a reduced degree of paratropicity and much narrower line shapes (Fig. 1 and Table 1). Our conclusion that these ions are twisted is confirmed by DNMR studies[6] and by theoretical calculations (MNDO,[7] MMX[8a]). The theoretical calculations are in good agreement with X-ray studies.[8b]

On going from the almost planar unsubstituted phenanthrene dianion ($\mathbf{1}^{2\ominus}$) to the dianions substituted by bulky alkyl groups, the ^1H NMR line shapes become much narrower and fine structures can be observed (Table 1). Phenanthrene dianion $\mathbf{1}^{2\ominus}$ with sodium as countercation shows no ^1H NMR spectrum down to a temperature as low as $-70\,^\circ C$. When lithium is the reducing metal, broad lines emerge at $-20\,^\circ C$. The spectrum is improved in terms of line shape as the temperature is further reduced. At $-70\,^\circ C$ one observes a well-resolved, easily interpretable NMR spectrum. The NMR results for 4-*tert*-butylphenanthrene dianion are very similar to those of phenanthrene dianion itself. The reason

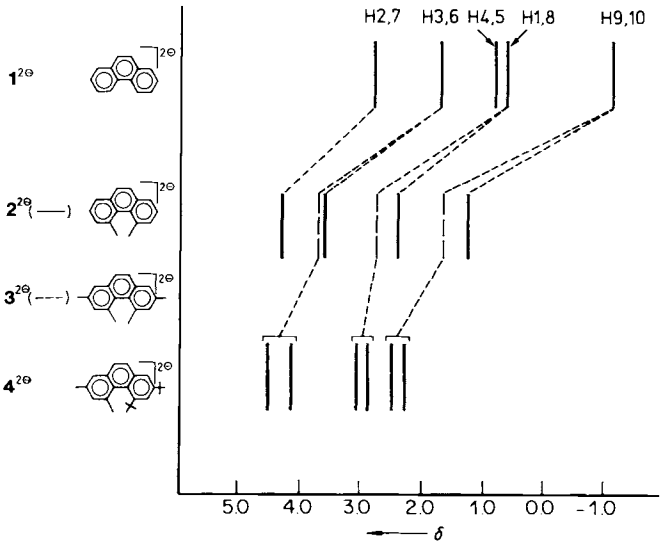

Fig. 1. ^1H NMR (200 MHz) chemical shifts of substituted phenanthrene dianions (as dilithium salts) represented by the stick diagram. The effect of helical twisting on the paratropic shift is clearly shown.

for this is the toothed-wheel effect that can take place when phenanthrene bonds become a little longer upon charging of the molecule. A greater degree of twisting can be achieved in 2,4,5,7-tetramethylphenanthrene dianion ($\mathbf{3}^{2\ominus}$), for which a significant narrowing in the line shapes is observed. When sodium was used to reduce the parent $(4n+2)\pi$ system **3**, we observed broad lines at $-20\,^\circ C$. At $-70\,^\circ C$ a spectrum with rather narrow lines (although without observable spin–spin couplings) is obtained. The lithium salt of this dianion shows a well-resolved spectrum even at room temperature. Conversion of 2,4-di-*tert*-butyl-5,7-dimethylphenanthrene (**4**) to its dianion resulted in an even more significant effect: $\mathbf{4}^{2\ominus}/2Na^{\oplus}$ shows already at $-20\,^\circ C$ a resolved spectrum, whereas, as expected, the dilithium salt shows a very well resolved spectrum at room temperature.

Dianions with additional alkyl substituents at positions other than 4 or 5 show line shapes very similar to those of the phenanthrene dianion substituted at positions 4 and 5 only

Table 1. The influence of the spatial structure of $4n\pi$ polycyclic helicenes on their ^1H NMR spectra and calculated twist angle.

	δH9,H10 [a]		Proton line shapes [b]		Calcd twist angle [°]		NMR parameters [a, c]
	Hydrocarbon	Dianion	$Na^{\oplus}$ counterion	$Li^{\oplus}$ counterion	Hydrocarbon (MMX/MNDO) [8,7]	Anion (MNDO) [7]	
1	7.83	−1.14	no spectrum	resolved −70 °C	0/2	19.87	0.62 (d,2H; H 1,8), J = 6.5 Hz; 0.80 (d,2H; H 4,5), J = 5.7 Hz; 1.69 (t,2H; H 3,6), J = 6.2 Hz; 2.75 (t,2H; H 2,7), J = 6.5 Hz
2	7.57	1.23	L.B. − 20° resolved −70 °C	resolved + 20 °C	33.02/36.86	58.82	2.40 (d,2H; H 1,8), J = 6.3 Hz; 3.62 (d,2H; H 3,6), J = 6.3 Hz; 4.32 (t,2H; H 2,7), J = 6.3 Hz
3	7.47	1.65	L.B. − 20° resolved −70 °C	resolved + 20 °C	33.15/–	–	2.74 (s,2H; H 1,8); 3.71 (s,2H; H 3,6); 0.65, 0.04 (s,6H; 6H; Me)
4	7.59 d 7.87 d J = 2 Hz	2.49 d 2.28 d J = 2 Hz	resolved − 20 °C	resolved + 20 °C	40.38/42.21	74.04	2.87, 3.07 (s,1H; 1H; H 1,8); 4.15, 4.54 (s,1H; 1H; H 3,6); 1.23, 0.73 (s,9H; 9H TtBu); 1.42, 0.84 (s,3H; 3H TMe)

[a] Lithium salts, Relative to TMS; [D_8] THF line at δ = 3.67 taken as standard. [b] Line broadening of the dianions. resolved = well-resolved spectrum; L.B. = line broadening. [c] δ values and coupling constants of the anions (except for H9, H10).

 © VCH Verlagsgesellschaft mbH, D-6940 Weinheim, 1990 0570-0833/90/0808-0920 $ 3.50+.25/0

($\mathbf{2}^{2\ominus}$, Table 1). The more twisted the helicene is, the more the paratropicity of the 4nπ system is quenched.[4]

In order to study this phenomenon, we concentrated on the proton chemical shifts at positions 9 and 10 of the substituted phenanthrenes. The same trend is observed for the protons of the other positions. The 9,10 positions have the largest charge density, as deduced from NMR spectra and ωβ-HMO calculations for a doubly charged phenanthrene ($\mathbf{1}^{2\ominus}$). Without exception, the more twisted the phenanthrene moiety is, the less the spectrum is shifted towards higher field (Table 1). For example, in the spectrum of phenanthrene dianion ($\mathbf{1}^{2\ominus}/2Li^{\oplus}$) the resonances of protons at positions 9,10 are shifted to $\delta = -1.14$, whereas the resonances of the same protons in 2,4,5,7-tetramethylphenanthrene dianion ($\mathbf{3}^{2\ominus}/2Li^{\oplus}$) are shifted to $\delta = +1.65$. Thus, a dramatic chemical shift difference of 2.79 ppm results from the different paratropicities of $\mathbf{1}^{2\ominus}$ and $\mathbf{3}^{2\ominus}$. In the spectrum of 2,4-di-*tert*-butyl-5,7-dimethylphenanthrene dianion ($\mathbf{4}^{2\ominus}/2Li^{\oplus}$) those proton resonances appear at $\delta = 2.49$ and 2.28. In all cases studied the same charge distribution pattern has been observed. Changing the countercation, solvent, and temperature did not affect the observed trend of line shape and chemical shift differences.

The paratropicity of 4nπ "antiaromatic" systems and the line shapes of their ^1H NMR signals thus correlate with the degree of twisting. Since antiaromaticity (as well as aromaticity) requires an efficient delocalization, we believe that twisting of the system quenches its antiaromatic properties. Therefore, the paratropic shift and the NMR line shapes can be applied as probes for so-called "antiaromaticity".

Received: February 19, 1990 [Z 3805 IE]
German version: *Angew. Chem. 102* (1990) ■

CAS Registry numbers:
1, 85-01-8; **1**, dianion, 67382-15-4; **1**, $2Li^{\oplus}$, 54667-02-6; **2**, 3674-69-9; **2**, dianion, 128054-52-4; **2**, $2Na^{\oplus}$, 128054-56-8; **2**, $2Li^{\oplus}$, 128054-60-4; **3**, 7396-38-5; **3**, dianion, 128054-53-5; **3**, $2Na^{\oplus}$, 128054-58-0; **3**, $2Li^{\oplus}$, 128083-45-4; **4**, 128054-51-3; **4**, dianion, 128054-54-6; **4**, $2Na^{\oplus}$, 128083-43-2; **4**, $2Li^{\oplus}$, 128054-62-6.

[1] K. P. Meurer, F. Vögtle, *Top. Curr. Chem. 127* (1985) 1.
[2] H. Scherübl, U. Fritzsche, A. Mannschreck, *Chem. Ber. 117* (1984) 336.
[3] Recent reviews a) M. Rabinovitz, *Top. Curr. Chem. 146* (1988) 99; b) M. Rabinovitz, Y. Cohen, *Tetrahedron 44* (1988) 6957; c) K. Müllen, *Chem. Rev. 84* (1984) 603.
[4] M. Karplus, J. A. Pople, *J. Chem. Phys. 38* (1963) 2803.
[5] a) A. Minsky, A. Y. Meyer, M. Rabinovitz, *Tetrahedron 41* (1985) 785; b) A. Minsky, A. Y. Meyer, R. Poupko, M. Rabinovitz, *J. Am. Chem. Soc. 105* (1983) 2164.
[6] D NMR studies of the dianions are under way. The ΔG values of neutral systems are known [2]. The ΔG value of 1,4,8-trimethyl-5-isopropylphenanthrene dianion has a lower limit of 65 kJ mol^{-1}.
[7] MNDO calculations were performed on a CDC Syber 180/855 running under NOS 2.7.1 and NOS/VE 1.4.1. Program: M. J. S. Dewar, W. Thiel, *Molecular Theory Program, Version 2.5*. Hydrogen bonding and lithium parameters included by A. Golblum, Hebrew University of Jerusalem, 1986.
[8] a) The MMX calculations were performed on an Olivetti M240 computer with a math coprocessor 18087 applying the PC Model MMX calculations Serena Software, USA. b) X-ray studies: R. Cosmo, T. W. Hambley, S. Sternhell, *J. Org. Chem. 52* 3119 (1987).
[9] The NMR spectra were recorded with a Bruker WP-200 SY pulsed-FT spectrometer operating at 200.133 MHz for ^1H NMR, equipped with a ^2H lock system and an Aspect-2000 computer (32 K).
[10] Sample preparation: Lithium or sodium wire was introduced in the upper part of an extended NMR tube containing the polycyclic compound (5–10 mg) dissolved in 0.7 mL of [D_8] THF (Aldrich). The frozen solution was degassed and sealed under vacuum. The solution was then brought into contact with the metal by turning the tube upside down.

Correlations between Magnetism and Structure in Dinuclear $Cu^{II}Fe^{III}$ Complexes with Integer Spin EPR Signals**

By *Theodore R. Holman, Kevin A. Andersen, Oren P. Anderson, Michael P. Hendrich, Carlos Juarez-Garcia, Eckard Münck,* and *Lawrence Que, Jr.**

The relationship between structure and magnetism in coupled dinuclear transition metal complexes has attracted great interest among inorganic and bioinorganic chemists, due to the unique physical properties of these complexes[1] as well as their relevance to biological systems.[1, 2] The magnetism of these systems depends on the electronic configurations of the individual metal centers, which, in turn, determine their fundamental spectroscopic properties. Recently, we have developed a systematic method for synthesizing heterobimetallic complexes of the dinucleating ligand 2,6-bis(bis-2-pyridylmethylamino)methyl)-4-methylphenol (Hbpmp),[3] affording a series of $M^{II}Fe^{III}$ compounds.[4, 5] Herein, we report the structures of two $Cu^{II}Fe^{III}$ complexes[6] of $bpmp^{\ominus}$ which exhibit integer spin EPR signals that correspond to their markedly different magnetochemistry.[7]

$[Cu^{II}Fe^{III}(bpmp)(O_2CC_2H_5)_2](PF_6)_2$ **1a**

$[Cu^{II}Fe^{III}(bpmp)(O_2CCH_3)(OCH_3)](BPh_4)_2 \cdot 0.22\ CH_3CO_2H$ **2a**

X-ray structure analyses of **1a**[8, 9] and **2a**[9, 10] revealed the following features:

In **1a** the cation consists of a discrete, dinuclear $Cu^{II}Fe^{III}$ complex (Fig. 1, top), in which the two metals are bridged by the phenolate oxygen atom of the $bpmp^{\ominus}$ ligand and by two propionate groups. The $Fe^{III}\cdots Cu^{II}$ distance is 3.401(4) Å, consistent with those of similar triply bridged dinuclear cores.[4] The $bpmp^{\ominus}$ ligand and the propionate groups provide a six-coordinate, roughly octahedral ligand array about each of the metal atoms in **1a**, but the coordination environment about the Cu^{II} atom shows the effects of Jahn-Teller elongation along the N2–Cu–O3 axis.

In **2a** (Fig. 1, bottom), one of the bridging carboxylate groups of **1a** is replaced by a terminal methoxide ligand that is coordinated only to the roughly octahedral Fe^{III} atom, leaving the Cu^{II} atom five-coordinate. One Cu-ligand bond (Cu–O1 = 2.176(4) Å) is elongated considerably relative to the other four in **2a**; this pattern suggests that the bridging phenolate oxygen atom, O1, is best regarded as the apical ligand atom of a square pyramidal coordination array about Cu^{II}. The Fe–O1 bond is also elongated due to the influence of the methoxide ligand, as the strong Fe–OCH_3 interaction affords a short (1.849(4) Å) Fe–O bond and decreases the affinity of the Fe for the phenolate bridge. The lengthening of both M–O1 bonds in **2a**, relative to those in **1a**, is the primary factor in the elongation of the Fe···Cu distance by 0.24 Å, to 3.641(1) Å.

[*] Prof. L. Que, Jr., T. R. Holman
Department of Chemistry, University of Minnesota
Minneapolis, MN 55455 (USA)
Prof. E. Münck, M. P. Hendrich, C. Juarez-Garcia
Gray Freshwater Biological Institute, University of Minnesota
Navarre, MN 55392 (USA)
Prof. O. P. Anderson, K. A. Andersen
Department of Chemistry, Colorado State University
Ft. Collins, CO 80523 (USA)

[**] This work was supported by grants from the National Institutes of Health (GM-38767(*L. Q.*) and GM-22701 (*E. M.*)), including also a predoctoral traineeship (GM-08277) for *T. R. H.*, and a postdoctoral fellowship (GM-12996) for *M. P. H.*

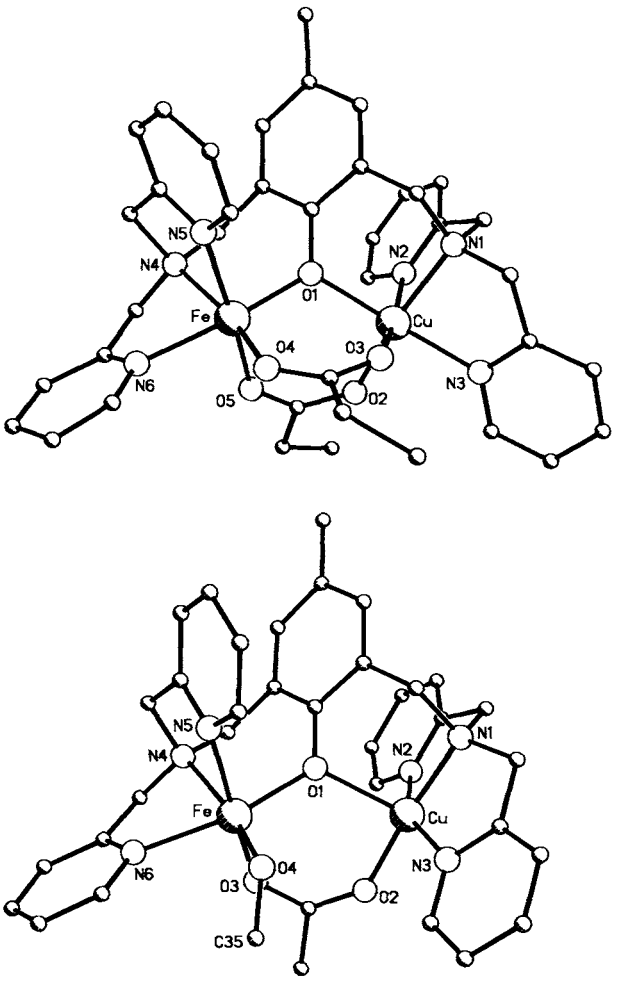

Fig. 1. Top: Structure of the dinuclear complex cation of **1a** in the crystal. Atoms are represented as spheres of arbitrary radii. Selected distances [Å] and angles [°]: Fe···Cu 3.401(4), Fe-O1 1.93(1), Fe-O4 1.90(2), Fe-O5 2.11(1), Fe-N4 2.15(1), Fe-N5 2.15(2), Fe-N6 2.12(2), Cu-O1 2.01(1), Cu-O2 1.94(1), Cu-O3 2.31(2), Cu-N1 2.09(1), Cu-N2 2.19(1), Cu-N3 2.03(1), <Fe-O1-Cu 119.3(5). Bottom: Structure of the dinuclear complex cation of **2a** in the crystal. Atoms are represented as spheres of arbitrary radii. Selected distances [Å] and angles [°]: Fe···Cu 3.641(1), Fe-O1 1.975(4), Fe-O3 2.016(4), Fe-O4 1.849(4), Fe-N4 2.255(5), Fe-N5 2.132(4), Fe-N6 2.175(5), Cu-O1 2.176(4), Cu-O2 1.945(4), Cu-N1 2.034(5), Cu-N2 2.006(4), Cu-N3 1.975(5), <Fe-O1-Cu 122.5(2).

The spectroscopic properties of the two complexes correlate well with their crystal structures. The Mössbauer parameters of **1b** ($\delta = 0.46$ mm/s; $\Delta E_Q = 0.42$ mm/s) are similar to those of other triply bridged complexes in this series.[4] In contrast, **2b** ($\delta = 0.49$ mm/s; $\Delta E_Q = 1.27$ mm/s) has the larger ΔE_Q value, most likely due to the presence of the short Fe–OMe bond. Magnetic susceptibility studies[11] indicate that the dinuclear center in **1b** is antiferromagnetically coupled ($J = 50\ cm^{-1}$ for $\mathcal{H} = JS_1 \cdot S_2$, $S_1 = 5/2$, $S_2 = 1/2$), while the center in **2b** is weakly ferromagnetically coupled ($J = -3\ cm^{-1}$) (Fig. 2). This difference in coupling

$[Cu^{II}Fe^{III}(BPMP)(O_2CCH_3)_2](BPh_4)_2$ **1b**

$[Cu^{II}Fe^{III}(BPMP)(O_2CC_2H_5)(OCH_3)](BPh_4)_2$ **2b**

interaction can be rationalized by inspection of the magnetic orbitals in the two complexes, assuming that the phenolate provides the principal coupling pathway.[1, 6c] For **1a**, the Jahn-Teller distortion on the Cu^{II} atom directs the magnetic

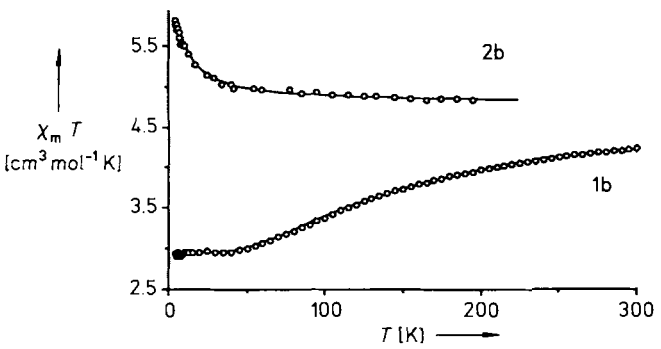

Fig. 2. Experimental (○○○) and theoretical (—) temperature dependence of $\chi_m T$ for **1b** and **2b**. Fitting parameters: **1b**, $J = 50\ cm^{-1}$, $D_{Fe} = 0.5\ cm^{-1}$, $E/D = 0.23$, $g_x = g_y = g_z = 2.0$, $D_{Cu} = 0$, $g_x = g_y = 2.08$, $g_z = 2.35$; **2b**, $J = -3\ cm^{-1}$, $D_{Fe} = 0.8\ cm^{-1}$, $E/D = 0.23$, $g_x = g_y = g_z = 2.0$, $D_{Cu} = 0$, $g_x = g_y = 2.12$, $g_z = 2.40$.

orbital along the axis of the phenolate bond and allows it to interact antiferromagnetically with the Fe^{III} magnetic orbitals. The elongation axis for the Cu^{II} atom in **2a**, however, is along the phenolate bridge; this places the magnetic orbital in the plane perpendicular to the phenolate bond and renders it orthogonal to the magnetic orbitals of the Fe^{III} atom, engendering the ferromagnetic interaction.

Interestingly, complex **1b** gives rise to a low field EPR signal at $g = 8$, while complex **2b** exhibits signals at $g = 12$ and $g = 8$ (Fig. 3). The intensity of the low field resonances

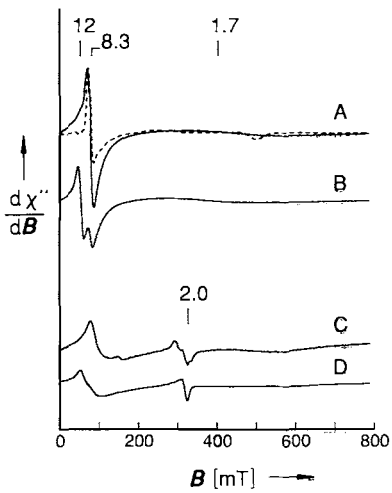

Fig. 3. EPR spectra of **1b** and **2b** in CH_3CN (4 mM) at 3 K. A) **1b**, $B_1 \| B$; B) **2b**, $B_1 \| B$; C) **1b**, $B_1 \perp B$; D) **2b**, $B_1 \perp B$. The dashed spectrum in A is a polycrystalline sample of **1b**. The signal at $g = 2.0$ is a preparation-dependent species, presumably a Cu^{II} impurity. An extremely broad signal at $g \approx 1.7$ has significant area under the absorption spectrum, but its origin is yet unclear. Instrumental parameters: 9.1 GHz at 0.02 mW, all below microwave saturation; modulation 100 kHz at 0.1 mT_{pp}; dB/dT, 3.3 $mT\,s^{-1}$. The frozen solution spectra are all properly normalized.

is approximately four times stronger when the microwave magnetic field B_1 is parallel to the static field B (parallel mode). The signal positions and enhanced parallel field intensities are indicative of transitions between levels of an integer-spin system.[12] The spectrum of polycrystalline **1b** (Fig. 3A, dashed) is similar to that of the dilute, frozen solution spectrum. This indicates that intermolecular magnetic interactions are small for the polycrystalline material and do not significantly affect the determination of J. The temperature dependence of the resonance at $g = 8$ for the complex

1b (Fig. 3A) indicates that it results from a ground-state doublet. A temperature study of complex **2b** indicates that the signals at $g = 12$ and $g = 8$ (Fig. 3B) are from ground and excited doublets, respectively. The line positions and temperature data suggest the following: for complex **1b**, the $g = 8$ resonance is from the ground state with $S = 2$ (antiferromagnetic coupling). For complex **2b**, the $g = 12$ signal is from the lowest doublet of the ground state with $S = 3$ (ferromagnetic coupling) and the $g = 8$ signal is from an excited doublet of either the $S = 2$ or $S = 3$ manifolds. The relative signs of the exchange couplings are in agreement with the magnetization results. The observation of integer spin signals from **1b** and **2b** and their correspondence to the magnetostructural data provide us with a set of complexes for further studies of integer spin systems and their spectroscopic manifestations.

Experimental

1a: A methanolic solution of Hbpmp (20 mL, 3.8 mM) was treated sequentially with 1 equiv. of $Fe(NO_3)_3$, 1 equiv. of $Cu(NO_3)_2$, and 2 equiv. of $NaO_2CC_2H_5$ to produce a purplish brown solution. After addition of 1 equiv. of NH_4PF_6, the solution was allowed to evaporate slowly to yield the crystals used for the X-ray diffraction study.

1b: A methanolic solution of Hbpmp (20 mL, 3.8 mM) was treated sequentially with 1 equiv. of $FeCl_3$, 1 equiv. $CuCl_2$, and 4 equiv. of $NaBPh_4$, resulting in a green solid (75% yield) formulated as $[Cu^{II}Fe^{III}bpmpCl_2](BPh_4)_2$. Treatment of an acetone solution of the green complex with 2.2 equiv. of AgO_2CCH_3 afforded a purplish brown solution, which was filtered to remove the AgCl solid. Vapor phase diffusion of ethyl acetate into the acetone solution furnished crystals of **1b** (50% yield). UV/VIS (CH_3COCH_3): $\lambda_{sh} = 500$ nm.

2b: A methanolic solution of Hbpmp (20 mL, 3.8 mM) was treated sequentially with 1 equiv. of $Fe(NO_3)_3$, 1 equiv. of $Cu(NO_3)_2$, and 4 equiv. of $NaO_2CC_2H_5$ to produce a red/brown solution. Metathesis with $NaBPh_4$ yielded a brown solid, which was recrystallized from acetone/methanol to yield crystals with the composition **2b** · $C_2H_5CO_2H$ (75% yield). UV/VIS(CH_3COCH_3): $\lambda_{sh} = 485$ nm.

2a: This complex was synthesized according to the procedure for **2b** with the exception that NaO_2CCH_3 was used in place of $NaO_2CC_2H_5$.

Received: April 18, 1990 [Z 3921 IE]
German version: *Angew. Chem. 102* (1990) 933

[1] a) O. Kahn, *Struct. Bonding (Berlin) 68* (1987) 89; b) O. Kahn, *Angew. Chem. 97* (1985) 837; *Angew. Chem. Int. Ed. Engl. 24* (1985) 834.

[2] a) R. C. Scarrow, L. Que, Jr., *ACS Symp. Ser. 372* (1988) 152; b) S. J. Lippard, *Angew. Chem. 100* (1988) 353; *Angew. Chem. Int. Ed. Engl. 27* (1988) 344; c) T. E. King, Y. Orii, B. Chance, K. Okunuki, (Eds.) *Cytochrome Oxidase*, Elsevier, New York 1979; d) E. Münck, V. Papaefthymiou, K. K. Surerus, J.-J. Girerd, *ACS Symp. Ser. 372* (1988) 302; e) E. I. Solomon, M. D. Allendorf, L. S. Kau, J. E. Pate, D. Spira-Solomon, D. E. Wilcox, A. G. Porras, *Life Chem. Rep. 5* (1987) 37.

[3] M. Suzuki, H. Kanatomi, I. Murase, *Chem. Lett., 1981*, 1745.

[4] A. S. Borovik, L. Que, Jr., V. Papaefthymiou, E. Münck, L. F. Taylor, O. P. Anderson, *J. Am. Chem. Soc. 110* (1988) 1986.

[5] *Suzuki* et al. have also obtained heterobimetallic complexes of bpmp: M. Suzuki, A. Uehara, H. Oshio, K. Endo, M. Yanaga, S. Kida, K. Saito, *Bull. Chem. Soc. Jpn. 60* (1987) 3547.

[6] Other CuFe complexes are reported in the following references: a) C. A. Koch, C. A. Reed, G. A. Brewer, N. P. Rath, W. R. Scheidt, G. Gupta, G. Lang, *J. Am. Chem. Soc. 111* (1989) 7645; b) G. A. Brewer, E. Sinn, *Inorg. Chem. 26* (1987) 2532; c) Y. Journaux, O. Kahn, J. Zarembowitch, J. Galy, J. Jaud, *J. Am. Chem. Soc. 105* (1983) 7585; d) C. K. Schauer, K. Akabori, C. M. Elliott, O. P. Anderson, *ibid.* (1984) 1127; e) M. J. Gunter, K. J. Berry, K. S. Murray, *ibid.* (1984) 4227.

[7] For a discussion of integer-spin state EPR signals: a) M. P. Hendrich, P. G. Debrunner, *J. Magn. Reson. 78* (1988) 133; b) *Biophys. J. 56* (1989) 489.

[8] **1a** was obtained mainly as highly efflorescent crystals which diffracted poorly. Among these crystals were a few thin, stable, plate-like crystals that belonged to the orthorhombic system, space group *Pnma* or $Pna2_1$, $Z = 4$, with $a = 20.849(6)$ Å, $b = 17.411(4)$ Å, $c = 12.587(3)$ Å, and $V = 4569$ Å^3 at 143 K. The structure was solved in $Pna2_1$ by using direct methods on 2530 unique reflections, 3371 measured. Refinement (anisotropic thermal parameters on non-hydrogen atoms, H atoms in idealized positions, 294 least squares parameters) converged at $R = 0.094$, $R_w = 0.124$, and GOF = 1.34.

[9] Details of crystallographic experiments: Nicolet R3m diffractometer, $Mo_{K\alpha}$ radiation ($\lambda = 0.7107$ Å), $\theta/2\theta$ scans, $4° < 2\theta < 45°$, $I > 1.25\sigma(I)$. Further details of the crystal structure analyses are available on request from the Director of the Cambridge Crystallographic Data Centre, University Chemical Laboratory, Lensfield Road, Cambridge CB21EW (UK), on quoting the complete journal citation.

[10] **2a** was obtained as red/green dichroic crystals in the triclinic system, space group $P\bar{1}$, $Z = 2$, with $a = 13.135(3)$ Å, $b = 13.503(3)$ Å, $c = 20.940(5)$ Å, $\alpha = 93.62(2)°$, $\beta = 93.81(2)°$, $\gamma = 92.76(2)°$, $V = 3693$ Å^3 (at 146 K). The structure was solved by using direct methods on 8886 unique reflections, 13899 measured. Refinement (anisotropic thermal parameters on non-hydrogen atoms, H atoms in idealized positions, 909 least squares parameters) converged at $R = 0.086$, $R_w = 0.082$, and GOF = 1.34 after placement of a fractional (occupancy factor = 0.22) molecule of acetic acid in the structural model.

[11] Magnetization data were collected on microcrystalline powders using a Quantum Design SQUID susceptometer over the temperature range from 1.9 to 300 K for **1b** and 1.9 to 200 K for **2b**, both at 0.31 T. We thank Dr. *E. P. Day* for his valuable help.

[12] Similar low field signals have been observed in other coupled FeCu systems [6e, 7b, 13].

[13] G. W. Brudvig, R. H. Morse, S. I. Chan, *J. Magn. Reson. 67* (1986) 189.

Torand Synthesis by Trimerization—New Receptors for Guanidinium **

By *Thomas W. Bell** and *Jia Liu*

Toroidal complexing agents having exceptionally rigid, yet accessible cavities, may be composed entirely of smaller rings fused to form the perimeter of a macrocycle.[1, 2] The first examples of such hosts, termed "torands", are **1**[2] and the parent dodecahydrohexaazakekulene.[1] Preorganization of six pyridine dipoles by the hexagonal framework of **1** leads to exceptionally stable complexes of alkali metal cations.[2] Extension of this architecture to a molecular cleft[3] afforded "hexagonal lattice receptor" **2**,[4] which tightly binds a neutral organic molecule (urea), despite the inherently weaker interactions between neutral hosts and guests. Here we describe effective syntheses of a larger torand (**3**) and its nonmacrocyclic analogue (**4**), as well as the formation of 1:1 complexes between both new hosts and guanidinium chloride.

The 1,8-naphthyridine units of both new receptors were synthesized via Friedlander condensation of heteroaromatic *o*-aminoaldehydes with annelated cyclohexanones (Scheme 1). The common intermediate in the syntheses of **1**–**4** is benzylideneketone **5**, which was prepared in five steps from cyclohexanone and pentanal by previously described methods[2, 5] (23% overall yield). Condensation of **5** with 4-aminopyrimidine-5-carboxaldehyde gave **6**, which underwent acidic hydrolysis to aminoaldehyde **7**, isolated as its HCl salt. Condensation of **7** with **5**, followed by ozonolysis afforded diketone **2**, as previously reported.[4] This urea receptor was then converted into novel guanidinium receptor **4** in one step by alkaline condensation with 2-aminonicotinaldehyde.

A key to our new torand synthesis is the discovery that the *o*-aminoaldehyde functionality of **7** survives ozonolytic cleavage of the benzylidene group. Crude ketoaminoalde-

[*] Prof. T. W. Bell, J. Liu
Department of Chemistry, State University of New York
Stony Brook, New York 11794-3400 (USA)

[**] This work was supported by the National Institutes of Health (PHS Grant GM 32937).

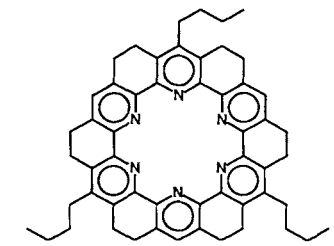

1

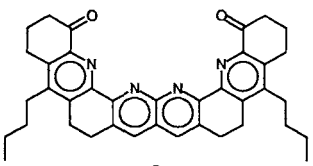

2

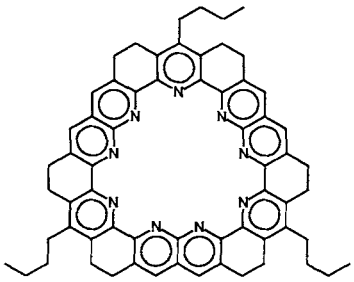

3

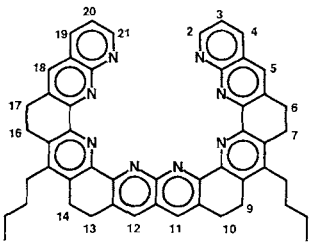

4

hyde **8** was obtained quantitatively by ozonolysis of **7** as the HCl salt. Ozonolysis of **7** as the free base did not produce isolable quantities of **8** or its free base. Intermediate **8** contains both the ketone and *o*-aminoaldehyde groups required to form **3** by cyclotrimerization. When **8** was treated with 1.1 equivalents of cesium hydroxide in ethanol, this new torand was formed in 38–49% yield according to ^{1}H-NMR analysis of the crude product with *p*-dimethoxybenzene as internal standard. It was isolated from the product mixture as a precipitate containing 1.1–1.5 equivalents of cesium per host molecule. Complexation of cesium was also demonstrated by appearance of the ion **3**·$Cs^{\oplus}$ (m/z = 1072) in the fast-atom bombardment mass spectrum (FABMS). In contrast to the high affinity of **1** toward alkali metal cations,[2] free torand **3** could be liberated simply by heating the cesium complex in boiling water. ^{1}H-NMR and ^{13}C-NMR spectra of **3** are consistent with the expected time-average symmetry (D_{3h}) and the protonated macrocycle gives rise to the base peak m/z = 940 of the FAB mass spectrum.

Torand **3** is the largest cycloarene derivative known to date.[6] Despite its larger size, **3** is available via trimerization in fewer steps and in higher overall yield than torand **2**.[2] Should this simple synthesis of a complex product be considered an example of "structure-directed" synthesis,[7] is it an example of the "cesium effect" in macrocyclization reactions,[8] or does it involve a more conventional "template effect"?[9] To address these questions we performed the cyclocondensation of **8** in the presence of potassium hydroxide, obtaining **3** in an optimum yield of 23% according to NMR spectroscopic measurements. For both CsOH and KOH, the yield of **3** was largest with 1.1 equivalents of base and dropped precipitously when more or less base was used. Whereas trimerization of intermediate **8** is in a sense preprogrammed by the geometric ideality of the product, cesium ion clearly enhances the yield of **3** relative to side products, which are probably nonmacrocyclic, higher molecular weight oligomers. Molecular modeling results suggest that although the cavity of **3** is somewhat large for cesium, this cation likely serves as a template by forming a complex with the trimeric helical intermediate, thus reducing the distance between reactive centers.[10]

Also according to molecular models, **3** and **4** are expected to bind guanidinium salts, forming 1:1 complexes **9** and **10**, respectively (Scheme 2). Results of molecular mechanics calculations (Macromodel) suggest that the lowest energy conformations of torand **3** are nearly planar, whereas those of **4** are helical, placing the terminal nitrogen nuclei approximately 7.3 Å apart. Thus, **3** should bind guanidinium to form six nearly ideal hydrogen bonds in **9** with little change in host conformation, whereas **4** must adjust to a more planar conformation in complex **10**.

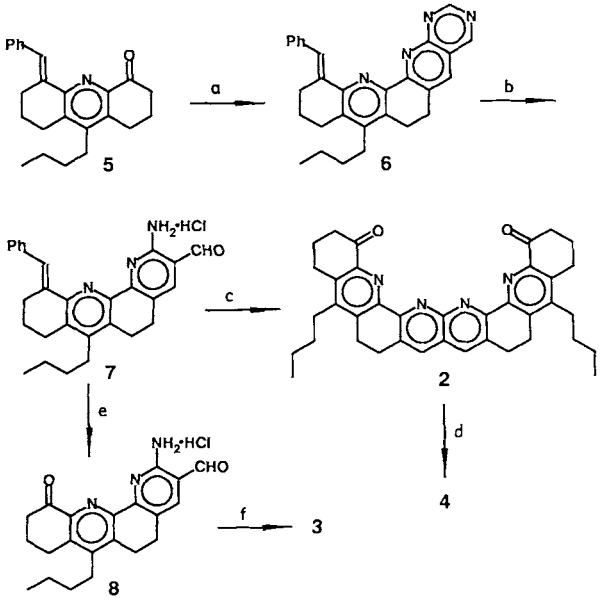

Scheme 1. a: 4-aminopyrimidine-5-carboxaldehyde, KOH, MeOH, reflux (93%). b: 2N HCl, reflux (97%). c: 1. **5**, KOH, MeOH, reflux (97%); 2. O_3, MeOH, CH_2Cl_2, −78°C; 3. Me_2S (100%, 2 steps); 4. cryst. from CH_2Cl_2, *i*PrOH (71%). d: 2-aminonicotinaldehyde, KOH, EtOH, reflux (70%). e: 1. O_3, MeOH, CH_2Cl_2, −78°C; 2. Me_2S (100%, 2 steps); f: 1. CsOH, EtOH; 2. H_2O, reflux (28%).

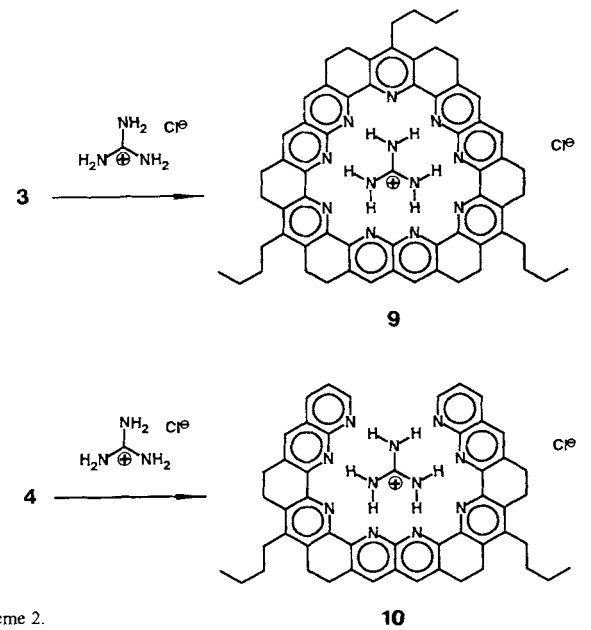

Scheme 2.

In the experiment, solid guanidinium chloride is dissolved in CD_2Cl_2 solutions of **3** and **4** to form **9** and **10** respectively, as shown by guanidinium NH resonances occurring at $\delta = 10.4-10.9$ in the ^{1}H-NMR spectra. The stoichiometries of both complexes were confirmed by microanalysis, and peaks corresponding to $\mathbf{3} \cdot CH_6N_3^{\oplus}$ and $\mathbf{4} \cdot CH_6N_3^{\oplus}$ are observed in the FABMS spectra of **9** and **10**, respectively. The

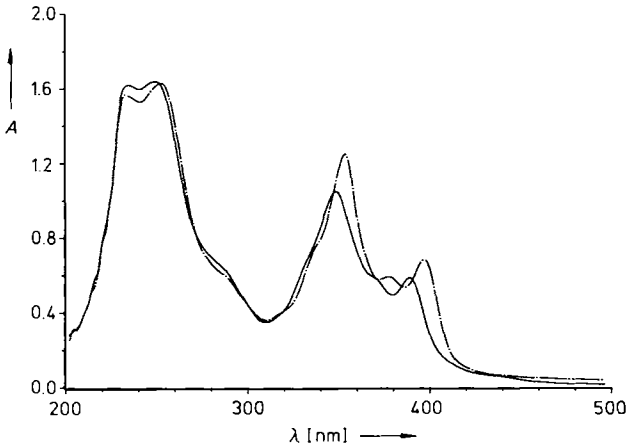

Fig. 1. UV/VIS spectra of receptor **4** in CH_2Cl_2 (1.5×10^{-5} M) before (solid line) and after addition of guanidinium chloride (broken line). A = absorbance.

UV absorption spectra of torand **3** and guanidinium complex **9** are nearly identical, whereas absorption maxima of **4** intensify and shift to longer wavelengths upon formation of **10** (Fig. 1). This result is consistent with the increased conjugation expected by modeling the "induced fit" of helical receptor **4** to guanidinium salts.

In summary, expedient synthesis of a geometrically ideal macrocycle by trimerization suggests that oligomerization approaches might be more generally applied to the preparation of complex unnatural products[11] and designed materials.[7] Exquisite preorganization of hydrogen bonding sites in **3** should result in molecular recognition of guanidinium salts. In contrast, the transduction of optical signals by flexible analogue **4** illuminates a path for the development of selective chemical sensors.[12]

Experimental

8: Ozone was bubbled through a yellow-orange solution of 0.92 g (2 mmol) of **7** in 110 mL of CH_2Cl_2 and 40 mL of methanol at −78 °C until the color of the solution changed to a pale greenish-yellow. Nitrogen was bubbled through the resulting solution for 5 min, then 1 mL of dimethyl sulfide was added and the reaction mixture was allowed to warm to room temperature. Solvents were removed by rotary evaporation. The residue was washed with 100 mL of ether, then dried to yield 0.78 g (100%) of crude **8**, which was suitably pure for direct conversion into **3**. Washing with $CHCl_3$ gave an analytically pure sample, m.p. 160 °C (dec). ^{1}H NMR (300 MHz, [D$_6$] DMSO): $\delta = 9.98$ (s, 1H; CHO), 8.73 (bs, 2H; NH_2), 8.60 (s, 1H; ArH), 3.11 (m, 4H; $ArCH_2CH_2Ar$), 3.00 (m, 2H; CH_2CO), 2.76 (m, 4H; $ArCH_2$-*n*-Pr, $CH_2CH_2CH_2CO$), 2.14 (m, 2H; $ArCH_2CH_2CH_2CO$), 1.45 (m, 4H; $ArCH_2CH_2CH_2CH_3$), 0.95 (t, ^3J(H, H) = 7 Hz, 3H; CH_3). ^{13}C NMR (75 MHz, [D$_6$]DMSO): $\delta = 195.7$, 191.8, 152.5, 151.0, 150.7, 146.1, 144.0, 143.0, 142.1, 137.7, 121.8, 117.5, 30.2, 27.9, 25.8, 23.3, 23.0, 22.6, 22.5, 21.6, 13.8. IR(KBr): $\tilde{\nu}$[cm^{-1}] = 3424, 3365 (NH), 1706 (C = O).

3: A mixture of **8** (0.35 g, 1 mmol), CsOH (0.2 mL of aq. solution, 1.1 mmol) and 150 mL of ethanol was stirred at room temperature under nitrogen for 30 min. Solvent was removed by rotary evaporation and 5 mL of $CHCl_3$ was added to the residue. The resulting mixture was cooled to 0 °C and filtered. The solid was recrystallized from 95% ethanol, then boiled in 25 mL of water for 3 h. The resulting mixture was cooled to room temperature and filtered to give **3** as a yellow solid (89 mg, 28%), m.p. 310 °C (decomp.). ^{1}H NMR (CD_2Cl_2): $\delta = 8.08$ (s, 6H, NaphH), 3.20 (m, 12H; $NaphCH_2CH_2Py$), 3.13 (m, 12H; $NaphCH_2CH_2Py$), 2.84 (m, 6H; $PyCH_2$-*n*-Pr), 1.55 (m, 12H; $PyCH_2CH_2CH_2CH_3$), 1.01 (t, ^3J(H, H) = 7 Hz, 9H; CH_3). ^{13}C NMR (CD_2Cl_2): $\delta = 156.0$, 150.6, 147.1, 135.8, 134.4, 134.3, 133.6, 123.0, 31.9, 28.9, 28.6, 24.8, 23.4, 14.0. UV/VIS (CH_2Cl_2): λ_{max} [nm](ε) = 226 (63000), 254 (130000), 290sh (40000), 370 (100000). FABMS (Xe$^{\oplus}$, 6–8 kV): m/z 940 ($M^{\oplus}$ + 1, 100%). Correct C, H, N analysis.

4: A solution of 0.59 g (1.0 mmol) of **2** and 0.3 g (2.5 mmol) of 2-aminonicotinaldehyde [13] in 25 mL of ethanol was heated to reflux, then 0.01 mL of 15% methanolic KOH was added. The resulting mixture was stirred at reflux under nitrogen for 24 h then cooled to room temperature. The crude product was collected by vacuum filtration and dissolved in 60 mL of CH_2Cl_2. The resulting solution was filtered to remove insoluble impurities. Ethanol (20 mL) was added to the filtrate, then the product was crystallized by slow evaporation at room temperature. Filtration gave 0.53 g (70%) of analytically pure **4** as a yellow solid, m.p. 220–240 °C (decomp.). ^{1}H NMR (CD_3OD): $\delta = 8.94$ (m, 4H; H-2,5,18,21), 8.77 (d, $^3J = 8$ Hz, 2H; H-4,19), 8.70 (s, 2H; H-11,12), 7.89 (dd, $^3J = 4$, 8 Hz, 2H; H-3,20), 3.49 (m, 16H, CH_2-6, 7, 9, 10, 13, 14, 16, 17), 3.11 (m, 4H, CH_2-*n*-Pr), 1.67 (m, 8H, $CH_2CH_2CH_3$), 1.09 (t, $^3J = 7$ Hz, 6H; CH_3). ^{13}C NMR (CD_3OD): $\delta = 156.3$, 155.8, 153.2, 151.6, 150.6, 146.7, 143.9, 142.5, 141.1, 140.8, 140.5, 139.2, 138.9, 136.2, 135.2, 126.7, 126.1, 126.0, 31.9, 30.0, 27.4, 26.9, 24.7, 24.3, 24.1, 14.2. UV/VIS (CH_2Cl_2): λ_{max} [nm] (ε) = 390 (32000), 349 (50000). FABMS: m/z 757 ($M^{\oplus}$ + 1, 100%).

Received: April 17, 1990 [Z 3917 IE]
German version: *Angew. Chem. 102* (1990) 931

CAS-Registry-Numbers:
2, 114301-17-6; **2** (benylidene instead of ketone), 114301-22-3; **3**, 128445-68-1; **4**, 128445-70-5; **5**, 105282-71-1; **6**, 114301-20-1; **7**, 128445-71-6; **8**, 128445-72-7; **9**, 128445-69-2; **10**, 128445-73-8; 4-aminopyrimidine-5-carboxaldehyde, 16357-83-8; 2-aminonicotinaldehyde, 7521-41-7.

[1] J. E. B. Ransohoff, H. A. Staab, *Tetrahedron Lett. 26* (1985) 6179.
[2] T. W. Bell, A. Firestone, *J. Am. Chem. Soc. 108* (1986) 8109; T. W. Bell, A. Firestone, L.-Y. Hu, F. Guzzo, *J. Inclusion Phenom. 5* (1987) 149; T. W. Bell, A. Firestone, R. Ludwig, *J. Chem. Soc. Chem. Commun. 1989*, 1902.
[3] J. Rebek, Jr., *Top. Curr. Chem. 149* (1988) 189; *Pure Appl. Chem. 61* (1989) 1517; *J. Heterocycl. Chem. 27* (1990) 111.
[4] T. W. Bell, J. Liu, *J. Am. Chem. Soc. 110* (1988) 3673.
[5] T. W. Bell, A. Firestone, *J. Org. Chem. 51* (1986) 764; T. W. Bell, Y.-M. Cho, A. Firestone, K. Healy, J. Liu, R. Ludwig, S. Rothenberger, *Org. Synth. 69* (1990), in press.
[6] A cycloarene is a polycyclic aromatic compound composed of angularly and linearly fused benzene rings such that one or more C–H bonds are directed into the central cavity. See: H. A. Staab, F. Diederich, *Chem. Ber. 116* (1983) 3487; H. A. Staab, F. Diederich, C. Krieger, D. Schweitzer, *ibid. 116* (1983) 3504; H. A. Staab, F. Diederich, V. Caplar, *Liebigs Ann. Chem. 1983*, 2262; D. J. H. Funhoff, H. A. Staab, *Angew. Chem. 98* (1986) 757; *Angew. Chem. Int. Ed. Engl. 25* (1986) 742.
[7] F. H. Kohnke, J. P. Mathias, J. F. Stoddart, *Angew. Chem. Adv. Mater. 101* (1989) 1129; *Angew. Chem. Int. Ed. Engl. Adv. Mater. 28* (1989) 1103; *Adv. Mater. 1989*, 275; P. R. Ashton, N. S. Isaacs, F. H. Kohnke, J. P. Mathias, J. F. Stoddart, *Angew. Chem. 101* (1989) 1266; *Angew. Chem. Int. Ed. Engl. 28* (1989) 1258; P. R. Ashton, N. S. Isaacs, F. H. Kohnke, G. S. D'Alcontres, J. F. Stoddart, *Angew. Chem. 101* (1989) 1269; *Angew. Chem. Int. Ed. Engl. 28* (1989) 1261.
[8] W. H. Kruizinga, R. M. Kellogg, *J. Am. Chem. Soc. 103* (1981) 5183, and references therein.
[9] T. J. Meade, D. H. Busch, *Prog. Inorg. Chem. 33* (1985) 59; T. J. McMurray, K. N. Raymond, P. H. Smith, *Science (Washington, D.C.) 244* (1989) 938.
[10] The macrocyclization intermediate, like **4**, is expected to have a helical minimum-energy conformation resulting from a 15–20° twist across each 2,2-bipyridyl linkage. Binding of Cs$^{\oplus}$ would stabilize conformations in which the heterocyclic dipoles converge. This effect can be significant despite the inexact match between the cavity radius of **3** (2.3–2.5 Å) and the ionic radius of cesium (1.7–1.9 Å, R. D. Shannon, *Acta Crystallogr. A 32* (1976) 751).
[11] J. F. Stoddart, *Nature (London) 334* (1988) 10.
[12] T. E. Edmonds (Ed.): *Chemical Sensors*, Chapman & Hall, New York 1988; R. W. Murray, R. E. Dessy, W. R. Heineman, J. Janata, W. R. Seitz (Eds.): *Chemical Sensors and Microinstrumentation*, American Chemical Society, Washington, 1989.
[13] T. G. Majewicz, P. Caluwe, *J. Org. Chem. 39* (1974) 720.

Topologically Interesting Cages for Negative Ions with Extremely High "Coordination Number": An Unusual Property of V-O Clusters**

By *Achim Müller,* Michael Penk, Ralf Rohlfing, Erich Krickemeyer*, and *Joachim Döring*

Dedicated to Professor Edwin Hengge on the occasion of his 60th birthday

Although the inclusion of molecules in oxidic solids, e.g. zeolites, has been known for some time and finds wide application, the first soluble oxide inclusion complex has only recently been obtained in the form of $[V_{12}O_{32}(CH_3CN)]^{4\ominus}$.[1a] Moreover, very little is known about other discrete inorganic host-guest systems. Mixed valence V^{IV}/V^{V}-O and V^{IV}-O clusters are, according to the results of our investigations, remarkable regarding their molecular and electronic structure, since, on the one hand, V^{IV}- and V^{V}-centers are present in almost any desired ratio, and, on the other, the coordination of the vanadium can be widely varied.[1] The formation of "hollow spheres" with unusual "cryptand properties" and interesting topology is possible by the linking of VO_5 pyramids.

The spherical cluster shells $\{V_{18}O_{42}\}$ **1** and $\{V_{15}O_{36}\}$ **2**, which deserve special mention here because of their topological properties, have in the compounds **1a, b** and **2a, b** (**2c** is included only for the discussion of the type of bonding) the

$Cs_9[H_4V_{18}O_{42}(X)] \cdot 12H_2O$ **1a**, X = Br; **1b**, X = I

$(NMe_4)_6[V_{15}O_{36}(Y)] \cdot 4H_2O$ **2a**, Y = Cl; **2b**, Y = Br

$Li_7[V_{15}O_{36}(CO_3)] \cdot$ ca. $39H_2O$ **2c**

remarkable and hitherto virtually unknown property of being able to encapsulate *negatively* charged ions, and even *such ions with significantly different radii.*

The characterization of the clusters was achieved by elemental analysis (including manganometric titration of V^{IV}), magnetic measurements, IR spectroscopy, thermogravimetry (for determination of the content of water of crystallization), and single-crystal X-ray structure analysis.[2] **1** is also present in the corresponding potassium salts containing water of crystallization (e.g. in $K_9[H_4V_{18}O_{42}(Cl)] \cdot 16H_2O$) with encapsulated $Cl^{\ominus}$ (**1c**), $Br^{\ominus}$ (**1d**), and $I^{\ominus}$ ions (**1e**); the complete X-ray crystallographic characterization, however, is more difficult than that of the cesium compounds,[3] which are less stable.

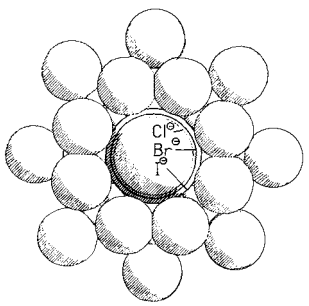

Fig. 1. Structure of a hemisphere of the inclusion compound of **1** with effective ionic radii (see text) and view along the virtual S_8 axis. Range of distances [pm] and mean values in brackets: $Hal^{\ominus}\cdots V$ 367.5–385.1 (374.7, **1a**), 368.3–386.4 (375.3, **1b**); $Hal^{\ominus}\cdots(\mu\text{-O})$ 363.6–370.1 (366.8, **1a**), 365.3–371.5 (368.2, **1b**).

In the inclusion compounds **1a, b** the distance from the center of the cluster to the O-atoms of the periphery is 367.5 pm and to the V-atoms 375.0 pm (mean value; cf. Fig. 1). A "close packing" of O-atoms and halide ions is therefore only possible in **1b** (effective ionic radii: $Cl^{\ominus} = 181$, $Br^{\ominus} = 196$, $I^{\ominus} = 220$, $O^{2\ominus} = 136$ pm;[4] formal consideration because of the covalently bound oxygen). **1**, with approximate D_{4d} symmetry, can be formally converted into $\{V_{18}O_{42}\}$ (**3**) by a 45° rotation of one hemisphere perpendicular to the S_8 axis[5] (Fig. 2), which, despite its size still has T_d symmetry and can be regarded as an enlarged Keggin shell.[6] **3** is formed in aqueous solution when only tetrahedral ions such as $SO_4^{2\ominus}$ or $VO_4^{3\ominus}$ are present, whereas **1** is formed in the presence of spherically symmetrical anions such as $Cl^{\ominus}$, $Br^{\ominus}$ or $I^{\ominus}$.

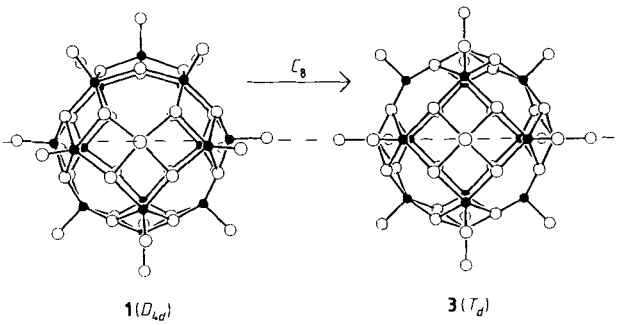

Fig. 2. Comparison of the structures of **1** and **3** (V = black, O = white), which can be interconverted by a C_8 rotation of a hemisphere (marked by a dotted line). The O-atoms of the shell in **1** form the "14th Archimedean solid" (cf. [9b]) and in **3** a distorted rhombicuboctahedron.

2 could be isolated with an encapsulated $Cl^{\ominus}$[1b] or $Br^{\ominus}$ ion, but also as the first heteropolyanion containing a $CO_3^{2\ominus}$ group (Fig. 3). **2** has crystallographic (**2a, b**) or approximate (**2c**) D_{3h} symmetry and formally contains eight V^{IV} centers and seven V^{V} centers. The atoms of the spherical shell in the anions containing **2** are at a distance of 323.6–388.2 pm from the center (cf. Fig. 3.), and the mean value (344.3 pm) corresponds approximately to the sum of the effective ionic radii of $Br^{\ominus}$ and $O^{2\ominus}$. In **2a** the $Cl^{\ominus}$ ion, despite its smaller radius, is, like the $Br^{\ominus}$ ion in **1a**, not disordered.

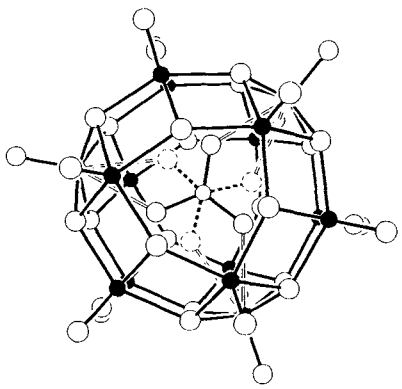

Fig. 3. Structure of the anion in **2c** in the crystal (V = black, O and C = white). The central $CO_3^{2\ominus}$ group is disordered at two positions one of which is dotted. Ranges of the distances [pm] and mean values in brackets for species containing **2**: center$\cdots$V 333.1–352.6 (343.0, **2a**), 335.6–354.6 (345.2, **2b**), 323.6–350.0 (342.6, **2c**); center$\cdots(\mu_3\text{-O})$ 333.4–339.2 (335.3, **2a**), 335.9–340.8 (337.5, **2b**), 329.6–347.0 (341.2, **2c**); center$\cdots(\mu_2\text{-O})$ 388.2 (**2a**), 383.6 (**2b**) 381.6–384.2 (383.3, **2c**).

[*] Prof. Dr. A. Müller, Dipl.-Chem. M. Penk, Dipl.-Chem. R. Rohlfing, E. Krickemeyer, Dipl.-Chem. J. Döring
Fakultät für Chemie der Universität
Postfach 8640, D-4800 Bielefeld 1 (FRG)

[**] We thank Professor *K. Wieghardt*, Bochum, for carrying out the magnetic measurements.

In anions containing **1**, the central ion is surrounded by 18 V-atoms and 24 O-atoms (a grouping which seems to be crucial for inclusions,[7]), and in those containing **2** by 15 V-atoms and 21 O-atoms. Apparently, despite the large distances between the central halide ion and the V-atoms in the species containing **1** and **2** there are probably very weak covalent bonds which are decisive for the stability. Such interactions have hitherto never been discussed. In the case of classical covalent bonds, as in **2c**, where the three O-atoms of the central $CO_3^{2\ominus}$ group each form an O–V bond (225.6 to 232.5 pm), the distance of these three V-atoms from the center is significantly diminished (325.1 instead of 344.1 pm) and the O_{term}–V–(μ-O) angle is also reduced (101.4 instead of 106.8° in **2a** and **2b**).

In all compounds the metal centers are coupled antiferromagnetically, whereby some V^{IV}-centers in the mixed valence V_{15}-species are localized, as shown by the values of the valence bond sums.[8]

The 24 oxygen atoms of the spherical shells of **1** and **3** form (idealized) the corners of convex polyhedra having sides of equal length.[9] In **1** the so-called "fourteenth Archimedean solid" is present,[9b] in which all corners are equivalent. It can be easily converted into the rhombicuboctahedron (one of the usual Archimedean solids) by rotation of the upper hemisphere by 45° (cf. Fig. 2). This solid is formed by the corresponding 24 O-atoms of **3** with a strong "tetrahedral distortion". The basic solid of **2** cannot be attributed to a polyhedron with sides of equal length.

The reason for **1** and **2** being able to encapsulate species of different size, traces back to the preferred linking of tetragonal pyramids and the *trans* effect of the $V=O_{term}$ groups. In the case of polymolybdates and polytungstates the formation of hollow spheres is *not* observed because these elements prefer the MO_6 octahedral linking.

Experimental

1a: A stirred solution of $CsVO_3$ (1.16 g, 5.0 mmol) in H_2O (100 mL) was treated in a 100-mL Erlenmeyer flask (wide-necked) at 90 °C with 180 μL (3.7 mmol) of hydrazinium hydroxide (100%). Stirring was continued for 1 min, and then the flask and its contents (covered with a clock glass) were transferred to an oil bath and heated at 90–95 °C for 1 h. The dark brown solution (pH ≈ 8.2) was adjusted to a pH value of 7.9–8.0 by dropwise addition of a 47% aqueous HBr solution until the pH value remained constant. Then the flask and its contents were again placed in an oil bath at 90–95 °C for 1.5 h and finally cooled slowly within 5 h to 20 °C. The black crystals which precipitated were filtered off, washed with 50% aqueous 2-propanol, and dried on filter paper. Yield 0.2 g.

1b was prepared analogously to **1a** using a 57% aqueous HI solution. Yield: 0.2 g. The more stable potassium salts **1c**–**1e** were prepared analogously to the cesium salts **1a** and **1b** using KVO_3.

2b: A solution of $(NMe_4)Br$ (5.0 g, 32.5 mmol) in H_2O (75 mL) was treated at 60 °C with $(NH_4)_3[VS_4]$ (1.0 g, 4.3 mmol) in a 100-mL Erlenmeyer flask (wide-necked; covered with a clock glass); the flask and its contents were then placed on a hot plate (temperature of reaction mixture 60–65 °C) for 16 h. The color of the mixture changed from reddish-violet to dark brown. After filtration, the solution was allowed to stand for a further 5 d on the hot plate at 60–65 °C. The precipitated black crystals of **2b** were filtered off from the almost colorless supernatant solution, washed with H_2O, 2-propanol, CS_2 and diethyl ether, and dried in air. Yield 0.5 g.

2c: A suspension of Li_2CO_3 (5.88 g, 79.6 mmol) in H_2O (150 mL) was treated portionwise with stirring with 12 g (66 mmol) of V_2O_5 (evolution of CO_2) and stirring continued for 5 min. After filtration, the solution was treated portionwise with stirring at 90 °C in a 300-mL Erlenmeyer flask with 1.5 g (11.5 mmol) of hydrazinium sulfate and finally allowed to stand (covered with a clock glass) on a hot plate at 90 °C for 1 h. After renewed filtration the greenish-black solution was cooled to 20 °C in a sealed flask and treated with shaking with 50 mL of 2-propanol. The black crystals which precipitated out within 2–3 d at 5–7 °C were filtered off, washed with 50% aqueous 2-propanol, and dried on filter paper. Yield: 2.5 g. Characteristic IR absorption bands (solid: CsI pellet) for all compounds containing the cages **1** and for **2a, b**: $\tilde{\nu}$[cm^{-1}] = ca. 965 (vs) ($\tilde{\nu}(V=O_{term})$), 700, 615 (s) ($\tilde{\nu}_{as}$(V–O-V), **1**); 980 (vs) ($\tilde{\nu}(V=O_{term})$), 720 (m), 655 (s) ($\tilde{\nu}_{as}$(V–O–V), **2**); magnetic measurements (Faraday balance, microcrystalline solids): e.g. **1e**: μ_{eff} = 4.5 μ_B (293 K), 3.4 μ_B (81 K); comparable values for the remaining compounds.

Received: February 21, 1990 [Z 3813 IE]
German version: *Angew. Chem. 102* (1990) 927

[1] a) V. W. Day, W. G. Klemperer, O. M. Yaghi, *J. Am. Chem. Soc. 111* (1989) 5959, and references cited therein; b) A. Müller, E. Krickemeyer, M. Penk, H.-J. Walberg, H. Bögge, *Angew. Chem. 99* (1987) 1060; *Angew. Chem. Int. Ed. Engl. 26* (1987) 1045; c) A. Müller, M. Penk, E. Krickemeyer, H. Bögge, H.-J. Walberg, *ibid. 100* (1988) 1787 and *27* (1988) 1719; A. Müller, J. Döring, *ibid. 100* (1988) 1789 and *27* (1988) 1721; d) A. Müller, J. Döring, H. Bögge, E. Krickemeyer, *Chimia 42* (1988) 300.

[2] **1a**: *C2/c*, $a = 2237.7(5)$, $b = 1296.8(3)$, $c = 2333.3(5)$ pm, $\beta = 111.54(2)°$, $V = 6298.2 \times 10^6$ pm^3, $\mu = 82.8$ cm^{-1}, $Z = 4$, $\varrho_{calcd} = 3.25$ g cm^{-3}, $R = 0.081$ for 3886 reflections ($F_0 > 4\sigma(F_0)$). **1b**: *C2/c*, $a = 2239.1(5)$, $b = 1296.0(2)$, $c = 2335.2(5)$ pm, $\beta = 111.41(1)°$, $V = 6308.9 \times 10^6$ pm^3, $\mu = 81.2$ cm^{-1} $Z = 4$, $\varrho_{calcd} = 3.30$ g cm^{-3}, $R = 0.056$ for 4063 reflections ($F_0 > 4\sigma(F_0)$). **1c**: $P\bar{1}$, $a = 1249.0(4)$, $b = 1306.5(5)$, $c = 1889.4(7)$ pm, $\alpha = 88.45(3)$, $\beta = 83.65(3)$, $\gamma = 73.56(3)°$. **1d**: $P\bar{1}$, $a = 1251.5(3)$, $b = 1307.0(3)$, $c = 1887.2(3)$ pm, $\alpha = 88.65(2)$, $\beta = 83.72(2)$, $\gamma = 73.57(2)°$. **1e**: $P\bar{1}$, $a = 1253.1(4)$, $b = 1307.4(4)$, $c = 1890.7(8)$ pm, $\alpha = 88.23(3)$, $\beta = 83.40(3)$, $\gamma = 73.42(3)°$ (complete X-ray structure analyses also carried out on **1c**–**1e**). **2b**: $P6_3/mmc$, $a = 1394.3(4)$, $c = 2020.4(8)$ pm, $V = 3401.6 \times 10^6$ pm^3, $\mu = 25.6$ cm^{-1}, $Z = 2$, $\varrho_{calcd} = 1.89$ g cm^{-3}, $R = 0.100$ for 1056 reflections ($F_0 > 4\sigma(F_0)$). **2c**: $P2_1/m$, $a = 1240.8(4)$, $b = 2110.3(6)$, $c = 1366.9(5)$ pm, $\beta = 110.81(2)°$, $V = 3346.0 \times 10^6$ pm^3, $\mu = 20.7$ cm^{-1}, $Z = 2$, $\varrho_{calcd} = 2.15$ g cm^{-3}, $R = 0.079$ for 4749 reflections ($F_0 > 3.92\sigma(F_0)$).—Siemens R3m/V (**1a**–**2b**) and Syntex $P2_1$ (**2c**) diffractometer. $Mo_{K\alpha}$ radiation, graphite monochromator.—The protons of the anions in **1a** and **1b** could not be localized. The powder diffractograms calculated from single crystal data are in good agreement with the measured data.—Further details of the crystal structure investigations are available on request from the Fachinformationszentrum Karlsruhe, Gesellschaft für wissenschaftlich-technische Information mbH, D-7514 Eggenstein-Leopoldshafen 2 (FRG) on quoting the depository number CSD-54498, the names of the authors, and the journal citation.

[3] Also in $K_{12}[V_{18}O_{42}(Z)] \cdot 16H_2O$ [G. K. Johnson, E. O. Schlemper, *J. Am. Chem. Soc. 100* (1978) 3645] the positions of two $K^{\oplus}$ ions and five H_2O molecules could not be determined because of disorder problems, and the encapsulated species could not be unequivocally indentified (cf. [6]).

[4] Taken from R. D. Shannon, *Acta Crystallogr. Sect. A32* (1976) 751.

[5] In $(NH_4)_8[V^{IV}_{12}V^{V}_{6}O_{42}(SO_4)] \cdot 25H_2O$ (**3a**, formal consideration) **3** has crystallographic and in $Na_6[H_9V^{IV}_{18}O_{42}(VO)_4] \cdot 21H_2O$ (**3b**) approximate T_d symmetry ([1 d]).

[6] M. T. Pope: *Heteropoly and Isopoly Oxometalates (Inorg. Chem. Concepts 8)* Springer, Berlin 1983.

[7] A similar constellation for an encapsulated $Cl^{\ominus}$ ion is surprisingly present in the solid state structure of a polyoxocuprate (R. Kipka, Hk. Müller-Buschbaum, *Z. Naturforsch. B32* (1977) 121, 124). Further investigations indicate that some $V=O_{term}$ groups in **3** can each be formally replaced by an As-O-As unit with retention of the 24-O coordination (A. Müller, J. Döring, unpublished).

[8] The sums of the bond valences for the V atoms $\sum_i (d(V\text{-}O_i)/178)^{-5.15}$ are 4.25–4.68 (**2a**), 4.01–4.67 (**2b**), 4.08–4.96 (**2c**; (cf. I. D. Brown, Kang Kun Wu, *Acta Crystallogr. Sect. B32* (1976) 1957).

[9] a) D. L. Kepert: *Inorganic Stereochemistry (Inorg. Chem. Concepts 6)* Springer, Berlin 1982; b) N. W. Johnson, *Can. J. Math. 18* (1966) 169.

A 1,6-Diphospha-1,2,4,5-hexatetraene, Synthesis and Ring Closure Reactions to Cyclobutenes

By *Gottfried Märkl,* Peter Kreitmeier, Heinrich Nöth,* and *Kurt Polborn*

We recently reported on the preparation of trimethylsilylethynylphosphane **1**[1] and its metalation to the lithium compound **2**, as well as on the importance of the latter for the

[*] Prof. Dr. G. Märkl, Dipl.-Chem. P. Kreitmeier
Institut für Organische Chemie der Universität
Universitätsstrasse 31, D-8400 Regensburg (FRG)
Prof. Dr. H. Nöth, Dr. K. Polborn
Institut für Anorganische Chemie der Universität
Meiserstrasse 1, D-8000 München (FRG)

synthesis of phosphacumulenes. Thus, the phosphabutatrienes **3**, for example, were synthesized by reaction of **2** with carbonyl compounds in a Wittig-Peterson reaction.[2]

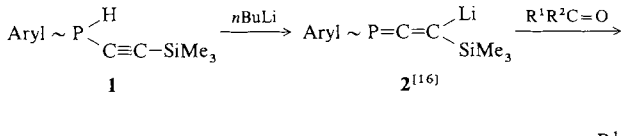

1 **2**[16]

Aryl = 2,4,6-tBu$_3$C$_6$H$_2$

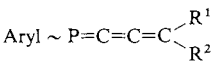

3

We have now found that **2** can be formally coupled oxidatively with Cu_2Cl_2 at $-78\,^{\circ}C$ in THF in the sense of the reaction of vinyl-carbenoids with $Ag^{\oplus}$, $Cu^{2\oplus}$, $Fe^{3\oplus}$ (formation of butatrienes) described by *G. Köbrich*.[3] Three products, **4** (colorless crystals, m.p. 131–133 °C, ^{31}P NMR (101.26 MHz, C_6D_6/C_6H_6): $\delta = 45.07$), **5** (yellow crystals, m.p. 145–147 °C (decomp), ^{31}P NMR: $\delta = 164.91$), and **6** (red needles, m.p. 187 °C (decomp), ^{31}P NMR: $\delta = 131.9$) are obtained, which, according to the mass spectra (m/z = 747.2), have the empirical formula $C_{46}H_{76}P_2Si_2$ of the primarily expected coupling product **A** (numbering arbitrary). That **4**, **5** and **6** are closely related is also indicated by their almost identical mass spectra (EI-MS, 70 eV).

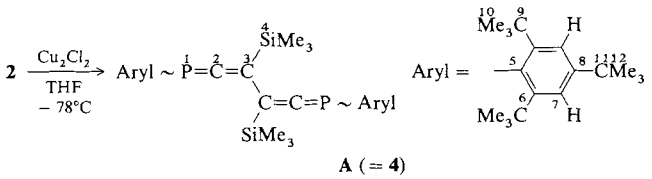

A (= **4**)

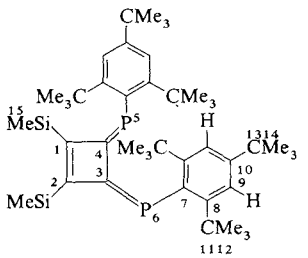

5

According to an X-ray structure analysis (Fig. 1; note: numbering different from the likewise arbitrary numbering in the formula),[4] the yellow compound is the unsymmetrical bis(arylphosphanediyl)cyclobutene **5**.[5] The cyclobutene ring of **5** is almost planar, the folding angle at the C1–C3 axis is 1.5°. The two phenyl rings (C5–C10 and C23–C28) are almost perpendicular to the four-membered ring (86.7, 95.6°).

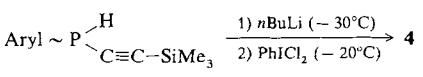

1

The 1,6-diphospha-1,2,4,5-hexatetraene **4**, whose spectroscopic data[7] are consistent with the proposed constitution,

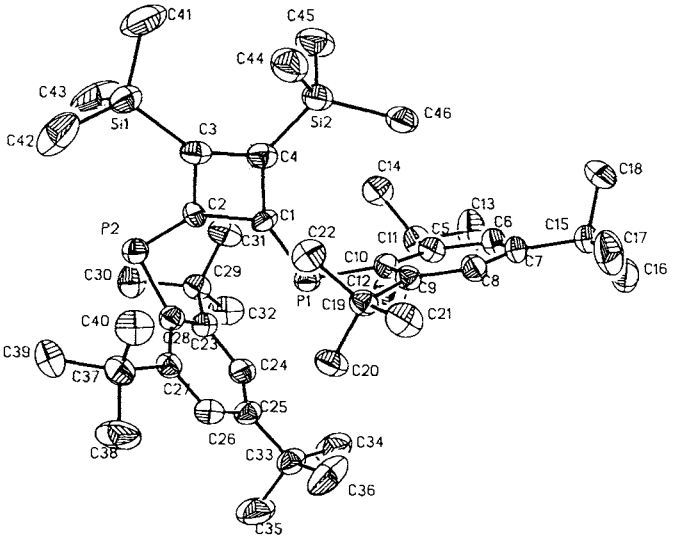

Fig. 1. Structure of the bis(arylphosphanediyl)cyclobutene **5** in the crystal(ORTEP). Selected bond lengths [pm] and angles [°]: P1-C1 166.8(4), P2-C2 166.8(3), Si1-C4 188.0(4), Si2-C3 188.3(4), C1-C2 151.3(5), C2-C3 148.5(5), C1-C4 150.7(5), C3-C4 139.0(5); C1-P1-C10 108.8(2), C2-P2-C28 102.6(2), P1-C1-C2 125.4(2), P1-C1-C4 147.0(3), P2-C2-C3 129.9(3), P2-C2-C1 142.3(3), C1-C2-C3 87.7(3), C1-C4-C3 91.6(3), C2-C3-C4 93.1(3).

is also accessible by reaction of the lithium compound **2** with $PhICl_2$ at $-20\,^{\circ}C$ in an ionic coupling reaction.[6]

The colorless coupling product **4** slowly transforms into **5** in $CHCl_3$ solution at room temperature. The following interpretation provides for the correlation of **4** with **5** and **6**: the radical coupling of **2** with Cu_2Cl_2 leads statistically to three stereoisomeric (axially chiral allenes) hexatetraenes **4a** (*meso* form) and **4b** (racemate: *R,R* and *S,S*).

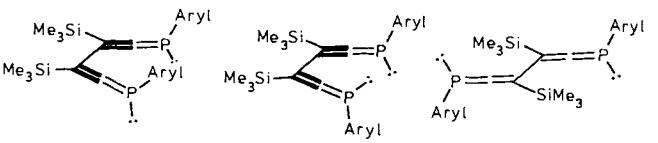

meso-**4 a**(s-*cis*) *rac*-**4 b**(s-*cis*) *meso*-**4 a**(s-*trans*)

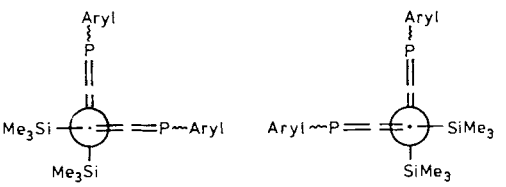

M-**4** *P*-**4**

Furthermore, the *meso*-form as well as the racemate are not planar, but are present in the two mirror image orthogonal helical conformations *M*-**4** and *P*-**4**, whose interconversion can only take place via the energy-rich planar s-*trans* or s-*cis* transition states.[9]

The electrocyclic reactions of **4** to **5** and **6** are only possible via the planar s-*cis* conformations of **4**; the energy barrier for rotation of *M,P*-**4** to s-*cis*-**4** should be markedly higher than that for the rotation to s-*trans*-**4**. The conrotatory ring closure reaction of the 1,3-diene system of *meso*-**4a** (s-*cis*) affords **5**. The cyclization of *rac*-**4b** (s-*cis*) must lead to the bis(phosphanediyl)cyclobutenes **6a, b**; the steric hindrance in **6b**, however, would suggest that exclusively the red isomer **6a**[10] is formed.

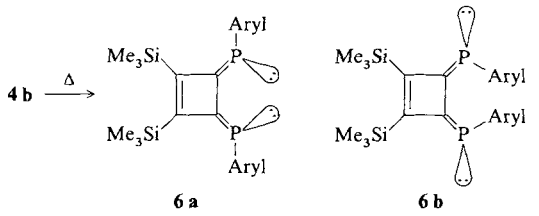

Because of the *trans* arrangement of the sterically very demanding aryl residues, *rac*-**4b** can rotate more easily into the s-*cis* conformation, i.e. *rac*-**4b** cyclizes quantitatively to **6a** under the reaction conditions. In *meso*-**4a**, s-*cis* geometry is sterically more strongly hindered because of the *cis*-arrangement of the aryl residues. Hence, the isolable, colorless coupling product **4** ought to be s-*trans*-*meso*-**4a**, which—due to the stability of the substituents at the phosphorus atoms toward inversion—converts only slowly and exclusively into **5** in solution (e.g. in $CHCl_3$). A slow electrocyclic ring opening of **5** to give the open-chain hexatetraene **4** is observed at 120 °C, whereas **6a** remains unchanged upon heating to 150 °C.

Received: March 26, 1990 [Z 3877 IE]
German version: *Angew. Chem. 102* (1990) 958

[1] a) G. Märkl, S. Reithinger, *Tetrahedron Lett. 29* (1988) 463; b) G. Märkl, P. Kreitmeier, *ibid. 30* (1989) 3939.

[2] See, e.g., E. Colvin: *Silicon in Organic Synthesis*, Butterworths, London 1981, p. 142–152.

[3] See, e.g., G. Köbrich, *Angew. Chem. 84* (1972) 557; *Angew. Chem. Int. Ed. Engl. 11* (1972) 473.

[4] X-ray structure analysis of **5**: CAD-4 four-circle diffractometer, graphite monochromator, $Mo_{K\alpha}$ ($\lambda = 0.71069$ Å), $C_{46}H_{76}P_2Si_2$, $M = 747.24$, space group $P2_1/c$, $a = 19.124(5)$, $b = 12.431(5)$, $c = 21.369(6)$ Å, $\beta = 106.39(2)°$, $V = 4873.6$ Å^3, $Z = 4$, $\varrho_{calcd} = 1.018$ g cm^{-3}. Data collection: single crystal: $0.3 \times 0.32 \times 0.5$ mm^3, ω scan, measured 2θ range: 4–50° in $\pm hkl$, 9245 measured reflections, 7168 symmetry independent, and 5350 observed ($I \geq 2\sigma(I)$). Structure solution: direct methods (SHELXS 86), anisotropic description of the non-hydrogen atoms, H atoms isotropic, 451 parameters, $R = 0.0519$, $R_w = 0.0559$, $\varrho \leq 0.29$ eÅ^{-3}. Further details of the crystal structure investigation are available on request from the Fachinformationszentrum Karlsruhe, Gesellschaft für wissenschaftlich-technische Information mbH, D-7514 Eggenstein-Leopoldshafen 2 (FRG), on quoting the depository number CSD-54659, the names of the authors, and the journal citation.

[5] **5**: 21%; recrystallization from benzene/CH_3CN; ^{1}H NMR (60 MHz, $CDCl_3$): $\delta = -0.33$ (s; $SiMe_3$), 1.34 (s; *p*-*t*Bu), 1.59 (s; *o*-*t*Bu), 7.44 (d, $^4J(P/H) = 2$ Hz; phenyl-H); ^{13}C NMR (22.64 MHz, $CDCl_3$): $\delta = 183.9$ (dd, $^1J(P/C) = 16.9$ Hz; $^2J(P/C) = 15.6$ Hz; C-3, C-4), 176.1 (pt, $J = 4.6$ Hz; C-1), 136.7 (pt, $^1J(P/C) = 29.2$ Hz; C-7), 0.40 (s; C-15); UV (*n*-hexane): $\lambda_{max} = 210$ nm ($\lg \varepsilon = 4.71$), 250 (4.46), 296 (4.64), 305 (4.61), 367 (3.91).

[6] S. Reithinger, *Dissertation*, Universität Regensburg 1990.

[7] **4**: 25%, recrystallization from EtOH; ^{1}H NMR: $\delta = 0.17$ (s; $SiMe_3$), 1.41 (s; *p*-*t*Bu), 1.49 (s; *o*-*t*Bu), 7.32 (br. s; phenyl-H); ^{13}C NMR (C_6D_6): $\delta = 234.02$ (br. d, $^1J(P/C) = 37.6$ Hz; C-2), 115.60 (dd, $^2J(P/C) = 18.7$ Hz, $^3J(P/C) = 13.2$ Hz; C-3), 0.45 (s; C-4), 130.16 (d, $^1J(P/C) = 66.3$ Hz; C-5), 154.77 (d, $^2J(P/C) = 2.6$ Hz; C-6), 122.04 (s; C-7), 149.59 (s; C-8); UV (*n*-hexane): $\lambda_{max} = 218$ nm ($\lg \varepsilon = 4.69$), 260 (4.54), 310 (sh, 4.01) [8].

[8] The phosphaallenes Aryl–P=C=CHR absorb at 220 nm, the molar extinctions $\varepsilon = 20\,000$–$25\,000$ are about half that of **4**.

[9] a) The G^* values of the thermal s-*cis*/s-*trans* racemization were determined for several 2,3-hexadienes. For the structural element =CCl–CCl=, G^* values of 68–70 were found [9b], for =CBr–CBr=, values of 102–104 [9c, d], and for =CMe–CMe=, values of 58–73 kJ mol^{-1} [9e]. b) H.-O. Bödecker, V. Jonas, B. Kolb, A. Mannschreck, G. Köbrich, *Chem. Ber. 108* (1975) 3497; c) M. Rösner, G. Köbrich, *Angew. Chem. 86* (1974) 775; *Angew. Chem. Int. Ed. Engl. 13* (1974) 741; d) G. Becher, A. Mannschreck, *Chem. Ber. 114* (1981) 2365; e) *ibid. 116* (1983) 264.

[10] **6a**: 15%, recrystallization from benzene/CH_3CN; ^{1}H NMR: $\delta = -0.25$ (s; $SiMe_3$), 1.39 (s; *p*-*t*Bu), 1.70 (s; *o*-*t*Bu), 7.47 (br. s; phenyl-H); ^{13}C-NMR ($CDCl_3$): $\delta = 180.9$ (pt, $J = 6.6$ Hz; C-3), 177.8 (pt, $J = 6.2$ Hz; C-1), 127.9 (pt, $J = 8.8$ Hz; C-7), −0.40 (s, C-15); UV (*n*-hexane): $\lambda_{max} = 230$ nm ($\lg \varepsilon = 4.40$), 289 (4.51), 306 (4.42), 360 (sh, 3.97).

[11] Thus, the fact that all NMR signals appear only singly in **5**, despite the unsymmetrical structure, cannot be explained in terms of a rapid ring-opening **5** → **4** and renewed conrotatory ring closure. The mechanism required from the

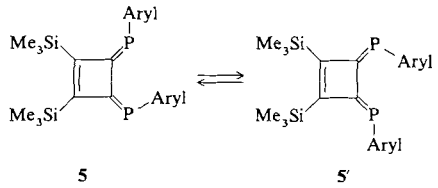

(a)

NMR data, rapid degenerated rearrangement (a)—with exclusion of a synchronous inversion at the phosphorus atoms—is still unclear.

The Azide Homologues Et–PPP and Ph–AsAsAs as Bifacially Coordinated Ligands in Tripod-Cobalt Complexes: Synthesis, Structure and Molecular Dynamics**

By *Annette Barth, Gottfried Huttner,* Martin Fritz,* and *Laszlo Zsolnai*

Dedicated to Professor Luigi Sacconi

It is already known from the works of *L. Sacconi* et al.[1] that tripod-metal complex fragments (tripod)M (tripod = $CH_3C(CH_2PPh_2)_3$) are especially suitable for the stabilization of unusual ligands. On attempting to exploit tripod-cobalt complex fragments for the synthesis of arsinidene complexes[2, 3] we at first unexpectedly obtained complexes of the type $[(tripod)Co\text{-}\mu_2\text{-}(\eta^3\text{-}PhAs_3)Co(tripod)]^{2\oplus}$ **1**, which contain the azide-homologous fragment $PhAs_3$.

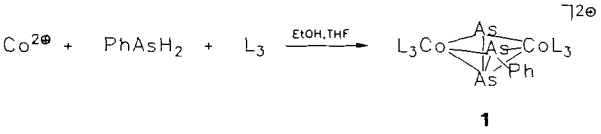

1

$CH_3C(CH_2PPh_2)_3$ = L_3

The cationic complex **1** is formed upon reaction of $Co(BF_4)_2 \cdot 6H_2O$ with $PhAsH_2$ in the presence of tripod. The reaction is accompanied by evolution of gas. After evaporation of the black reaction solution to dryness, **1** crystallizes as the $BF_4^\ominus$ salt in yields of 50% within three days.

The field desorption mass spectrum of **1**-$(BF_4)_2$ shows the signal with $m/2z = 834$ expected for the dication **1**. In the ^{1}H-NMR spectrum of **1**-$(BF_4)_2$ the signals corresponding to the organic building blocks are observed in the expected intensity ratio. In the ^{31}P-NMR spectrum, a broad signal appears at $\delta = 25.4$ for the tripod ligands. Proof of the identity of **1** was afforded by an X-ray structure analysis[4] (Fig. 1).

The As–As distances confirm that there is no direct bonding between the terminal arsenic centers As1 and As3. The bonding As–As distances in **1** are large in comparison to those in the recently described monofacially coordinated

[*] Prof. Dr. G. Huttner, Dipl.-Chem. A. Barth, Dipl.-Chem. M. Fritz, Dr. L. Zsolnai
Institut für Anorganische Chemie der Universität
Im Neuenheimer Feld 270, D-6900 Heidelberg (FRG)

[**] This work was supported by the Fonds der Chemische Industrie and the Deutsche Forschungsgemeinschaft (SFB 247).

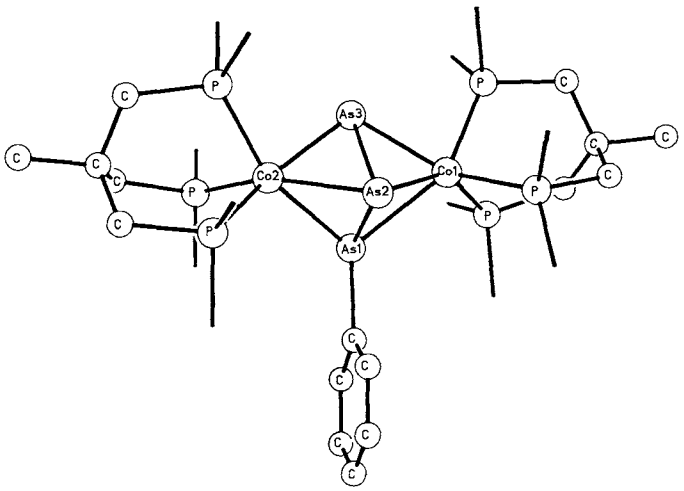

Fig. 1. Structure of **1**-$(BF_4)_2$ in the crystal (phenyl rings of the tripod ligand not shown). Selected bond lengths [pm] and angles [°]: Co–P 220.3–228.5, Co1–As1 261.3, Co2–As1 255.5, Co1–As2 242.3, Co2–As2 245.0, Co1–As3 238.1, Co2–As3 234.4, As1–As2 240.3, As2–As3 247.6, As1···As3 283.0; As1–As2–As3 72.0 (deviation maximally 0.7 units referred to the last decimal place).

Ph_2As_3 in $[Cp^*(CO)_2Mo(\eta^3\text{-}Ph_2As_3)]$ (As–As distances 236 pm).[5] In spite of the bifacial coordination of the $PhAs_3$ ligand in **1**, the mean value of the As–As distances is shorter than an As–As single bond.[6]

Attempts to prepare the phosphorus compound analogous to **1** with $PhPH_2$ as source of PhP_3 ligand have so far met without success. The dication **4** $[(tripod)Co\text{-}\mu_2\text{-}(\eta^3\text{-}EtP_3)Co(tripod)]^{2\oplus}$ analogous to **1** could, however, be synthesized via a circuitous route. The reaction of **2**[7] with $Me_3O^\oplus$ leading to $[(tripod)Co(\eta^3\text{-}MeP_3)]^\oplus$ is already well known.[8] **2** reacts analogously with $Et_3O^\oplus$ to give **3**. This, in turn, reacts with $Co(BF_4)_2 \cdot 6H_2O$ and tripod to give **4**-$(BF_4)_2$, which initially precipitates as microcrystalline, analytically pure solvent adduct **4**-$(BF_4)_2 \cdot 2EtOH$. Crystals

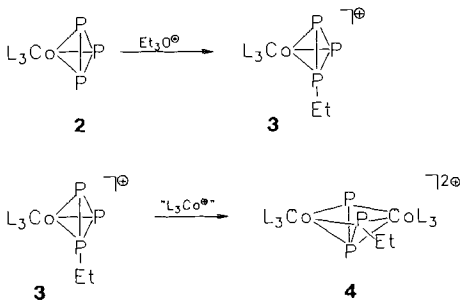

suitable for an X-ray structure analysis were obtained by recrystallization as the solvent-adduct **4**-$(BF_4)_2 \cdot 0.5$ THF from $THF/CH_2Cl_2/Et_2O$. The X-ray structure analysis verifies the analogous structure of **1** and **4**.[4]

The P1–P3 distance (262 pm) confirms the open structure of the EtP_3 unit in **4**. The P–P distances in the EtP_3 ligand are, on average, shorter than a P–P single bond;[9] the distribution of short and of long bond lengths in the EtP_3 unit of **4** does not correspond to the distribution of the As–As bond lengths in the $PhAs_3$ unit of **1** (Fig. 1 and Fig. 2). Hence, it may be assumed that the bifacially coordinated ligands RX_3 (X = As, P) are fluctional systems. This assumption is confirmed by the temperature dependence of the ^{31}P-NMR spectrum of **4**-$(BF_4)_2$. At 293 K, a broad signal is observed for the phosphorus centers of the tripod ligands ($\delta = 17.8$),

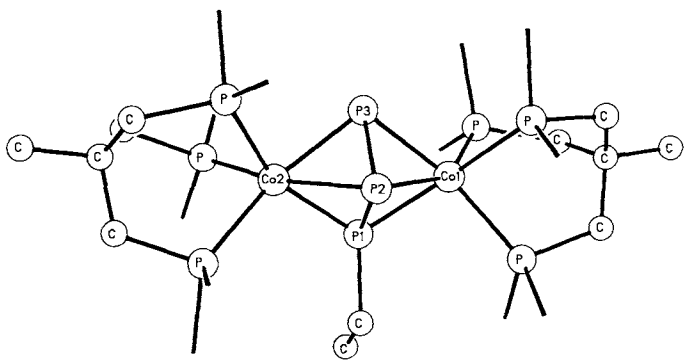

Fig. 2. Structure of **4**-$(BF_4)_2 \cdot 0.5$ THF in the crystal (phenyl rings not shown): selected bond lengths [pm] and angles [°]: Co-P (tripod) 219.0–232.6, Co1-P1 221.4, Co2-P1 218.9, Co1-P2 243.7, Co2-P2 239.3, Co1-P3 228.9, Co2-P3 229.9, P1-P2 222.1, P2-P3 211.0, P1···P3 262.0; P1-P2-P3 74.1 (standard deviations maximally one unit referred to the last decimal place).

which splits at 221 K into three narrowly separated singlets ($\delta = 28.8, 16.4, 8.1$). The broad signal observed at 293 K for the EtP_3 ligand ($\delta = 158$) becomes a broad doublet ($\delta = 178$) at 221 K. In addition, a doublet appears at $\delta = 260$ ($^1J(PP) = 300$ Hz) and a triplet at $\delta = -270$ ($^1J(PP) = 300$ Hz). These two new signals reversibly coalesce on heating the sample, but are not visible at room temperature. The limiting case of the rapid exchange of the two phosphorus centers, which should lead to a sharp signal at $\delta = -5$ cannot be observed, since the sample cannot be heated to the required temperature without decomposition. The low-temperature spectrum corresponds to a static structure of **4** resembling that depicted in Figure 2. The doublet at $\delta = 260$, with two almost identical $^1J(PP)$ coupling constants (300 Hz), can be assigned to the terminal phosphorus P3, the triplet at $\delta = -270$ to the "central" P2, and the doublet at $\delta = 178$ to the ethyl-substituted P1.

Three signals for the phosphorus centers of the tripod ligands correspond to the different environment of these atoms in the static structure (Fig. 2). The coalescence of the signals of P2 and P3 in **4** confirms the dynamic exchange of the two unsubstituted phosphorus centers of the EtP_3 ligand (Scheme 1). The signal assigned to P1 remains virtually unchanged during the coalescence. This means that P1 has, on average, a chemical environment similar to that in the static structure during the exchange.

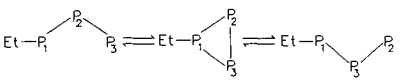

Scheme 1. Exchange of P2 and P3 via a three-membered ring.

The observed dynamics can be explained with a model in which the phosphorus centers P2 and P3 exchange places by intermediate formation of a three-membered ring (Scheme 1). The existence of monofacially coordinated *cyclo*-RP_3 ligands has already been demonstrated;[8] a *cyclo*-EtP_3 ligand is also present in **3**, as follows from the ^{31}P-NMR spectrum (see *Experimental*). The preference for the open geometry of bifacially coordinated RP_3 ligands can be illustrated quite easily using a theoretical approach based on the analysis of triple-decker complexes by *R. Hoffmann* et al.[10] and on the specific analysis of (tripod)M systems by *L. Sacconi* et al.[11]

In a 32-valence-electron triple-decker complex $[(tripod)\text{-}Co\text{-}\mu_2\text{-}(\eta^3\text{-}P_3)Co(tripod)]^\oplus$, with C_3 symmetry of the P_3 unit, the HOMO to be occupied by two electrons is doubly degenerate. The Jahn-Teller distortion to be expected thereby has been confirmed in the case of the isoelectronic system

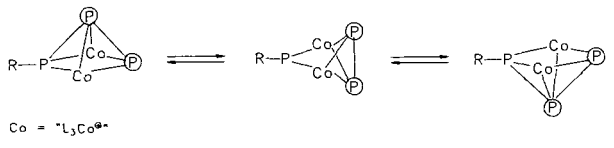

Scheme 2. Skeletal rearrangement of **4**.

[(tripod)Ni-μ_2-(η^3-P_3)Rh(tripod)]$^{2\oplus}$,[11] in which markedly different P–P bonds are observed in the P_3 ring. The idealized square pyramidal structure of **1** and **4** with 14 electrons in the skeleton conforms with the cluster count rule.[12]

The observed dynamics are consistent with a rearrangement of a square pyramidal cluster.[13] The equivalent in organic chemistry is the conversion of a tricyclic carbenium ion $(CH)_5^{\oplus}$ into a square pyramidal carbenium ion.[14]

4 can be formally derived from [(tripod)Co-μ_2-(η^3-P_3)Co(tripod)]$^{\oplus}$ by addition of an $Et^{\oplus}$ group to a free electron pair of *cyclo*-P_3; the two complexes are thus isoelectronic. The symmetry in **4** is, however, disturbed by the ethyl group, so that the orbitals to be occupied by two electrons are no longer degenerate. The lower lying of these two orbitals is so stabilized by complete opening of a P–P bond of the ring that the diamagnetic species with the structure found for **4** results (Scheme 3).

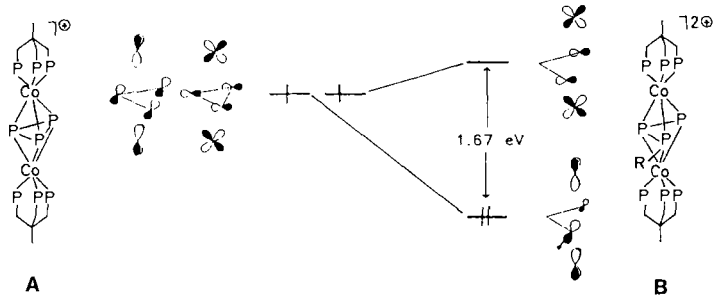

Scheme 3. The geometry of **4** (**B**). The EHT (extended Hückel type) modeling shows the removal of the degeneration of the HOMOs in the 32-electron tripledecker [(tripod)Co-μ_2-(η^3-P_3)Co(tripod)]$^{\oplus}$ **A** by addition of $R^{\oplus}$ (R = H) and opening of the P_3 ring **B** [17]. The geometry of **A** was modeled on [(tripod)Co-μ_2-(η^3-P_3)Co(tripod)]$^{2\oplus}$ [1], that of **B** on that of **4**.

A dynamic process as formulated in Scheme 1 can also take place in **4** if the closed ring with bonds of almost equal length is a transition state and not an intermediate compound. In constrast, a transition state with bonds of equal length cannot occur in the isoelectronic complexes containing *cyclo*-P_3.[15] To our knowledge, nothing has so far been reported about the dynamics of potential Jahn-Teller active *cyclo*-P_3 complexes; however, it is known that the system isoelectronic with **4**, with As_2S instead of EtP_3, contains open As_2S groups in the solid state.[16]

Experimental

All operations were carried out under N_2 in freshly distilled solvents. NMR: solvent $CDCl_2$; ^1H NMR (200 MHz), ^{31}P NMR (81 MHz, standard: $P(OMe)_3$, $\delta = 139$, ext.), Bruker AC-200. Mass spectra: Finnigan MAT 8230.

1: Equimolar amounts of tripod (624 mg, 1 mmol) in 25 mL of THF and $Co(BF_4)_2 \cdot 6H_2O$ (340 mg, 1 mmol) in 15 mL of EtOH were mixed, and the resulting orange-red solution treated dropwise with stirring at room temperature with 0.15 mL (1 mmol) of $PhAsH_2$ in 5 mL of THF. An immediate change in color of the solution to black, with concomitant evolution of gas, was observed. After 2 h, the reaction mixture was filtered over silanized silical gel and the solution evaporated to half of its original volume. Within three days, blackish-green, analytically pure crystals of $\mathbf{4} \cdot (BF_4)_2$ separated out. (It is important that the crystallization vessel be closed with a rubber stopper, which by slow swelling further reduces the amount of solvent.) $M = 1842.3$ g/mol $C_{88}H_{83}P_6Co_2As_3B_2F_8$, yield 460 mg (50% based on consumed $Co^{2\oplus}$). FD mass spectrum: m/z 1536 [$M^{\oplus} - CH_3C(CH_2)_2$, $-Ph$], $m/2z$ 834 ($M^{2\oplus}$). ^1H NMR (293 K): $\delta = 1.76$ (CH_3, 6H), 2.76 (CH_2, 12H), 6.8–7.35 (Ph, 66H); ^{31}P NMR (293 K): $\delta = 25.4$.

3: A suspension of **2** [7] (340 mg) in CH_2Cl_2 (50 mL) was treated with excess $[Et_3O]BF_4$. The color changed within 2 h from yellow to deep-red, and **2** went completely into solution. After removal of solvent there remained an oily-red residue; this was washed three to four times with 10 mL of EtOH and finally with petroleum ether. Upon drying in a high vacuum **3** was obtained as an analytically pure red powder. $M = 892.3$ g/mol $C_{43}H_{44}P_6CoBF_4$, yield: 310 mg (79% based on **1**). FD mass spectrum: m/z 805 ($M^{\oplus}$). ^1H NMR (293 K): tripod: $\delta = 2.58$ (CH_2 6H), 1.82 (CH_3 3H), 7.1–7.3 (Ph, 3OH); ethyl: 1.34 (CH_3 dt, $^3J(PH) = 25$ Hz, 3H); 2.80 (CH_2, $^2J(PH) = 4.7$ Hz, 2H); ^{31}P NMR (293 K): 33.1 (s, 3P), -103 (t, $^1J(PP)$) 360 Hz), -339.4 (d, $^1J(PP) = 360$ Hz).

4: A solution of **3** (300 mg, 0.33 mmol) in CH_2Cl_2 (30 mL) was treated with stirring with a mixture of equimolar amounts of $[Co(BF_4)_2 \cdot 6H_2O]$ (113 mg, 0.33 mmol) in EtOH (10 mL) and tripod (205 mg, 0.33 mmol) in THF (10 mL). The initially red solution slowly turned dark brown. After one hours' stirring the solution was filtered over silanized silica gel and the solution then covered with a layer of 30 mL of Et_2O. After 14 h at room temperature a microcrystalline precipitate of **4** as adduct with EtOH had formed. Yield 260 mg (39% based on **3**). $M = 1754.9$ g/mol, $C_{88}H_{95}P_9O_2Co_2B_2F_8$. Correct C, H, P analysis. FD mass spectrum m/z 1488 ($M^{\oplus}$, ($tripod_2Co_2EtP_3)^{\oplus}$), m/z 1460 ($M^{\oplus} - C_2H_4$), $m/2z$ 744 ($M^{2\oplus}$). ^1H NMR (293 K): tripod: $\delta = 1.65$ (CH_3, 6H); 2.53 (CH_2, 12H), 7.0–7.3 (Ph, 60H); ethyl: $\delta = -0.16$ (CH_2, 2H), 1.79 (CH_3, 3H). ^{31}P NMR (293 K): tripod: $\delta = 17.8$, ($b_{1/2} = 70$ Hz), EtP_3: $\delta = 158$; (221 K): tripod: $\delta = 28.8$, 16.4, (8.1 $b_{1/2} = 100$ Hz), EtP_3: $\delta = 260$ ($b_{1/2} = 120$ Hz; d, $^1J(PP) = 300$ Hz), $\delta = 178$ ($b_{1/2} = 180$ Hz; d, $^1J(PP) = 280$ Hz), $\delta = -270$ ($b_{1/2} = 100$ Hz); (t, $^1J(PP) = 300$ Hz). Crystals suitable for an X-ray structure analysis were obtained by recrystallization as $4\text{-}(BF_4) \cdot 0.5$ THF from $THF/CH_2Cl_2/Et_2O$.

Received: February 15, 1990 [Z 3800 IE]
German version: *Angew. Chem. 102* (1990) 956

[1] M. Di Vaira, L. Sacconi, *Angew. Chem. 94* (1982) 338; *Angew. Chem. Int. Ed. Engl. 21* (1982) 330.
[2] The name arsinides is used here, instead of the IUPAC name arsanediyl.
[3] G. Huttner, *Pure Appl. Chem. 58* (1986) 585; G. Huttner, K. Evertz, *Acc. Chem. Res. 19* (1986).
[4] [**1** · $(BF_4)_2$]: $a = 14.091(6)$, $b = 23.099(7)$, $c = 28.326(9)$ Å, $\beta = 108.25(3)°$, space group $P2_1/c$, $Z = 4$, $R_1 = 12.26$, $R = 10.3$. [**4** · $(BF_4)_2$ · 0.5 THF]: $a = 14.202(6)$, $b = 14.901(6)$, $c = 23.491(8)$ Å, $\alpha = 96.36(3)$, $\beta = 102.43(3)$, $\gamma = 109.32(3)°$, space group $P1$, $Z = 2$, $R_1 = 13.18$, $R_2 = 12.43$. Measurement on a Nicolet(Syntex) P3 diffractometer, graphite monochromator, $Mo_{K\alpha}$ radiation, solution and refinement (rigid group refinement of Ph and BF_4) of the structures with the program system SHELXTL (G. Sheldrick, *SHELXTL Plus*, Göttingen 1988). The structure could only be refined to the quoted *R* values because of the poor quality of the crystals, and disorder, both of the anions as well as of the solvent, in the case of **4**. Further details of the crystal structure investigations are available on request from the Fachinformationszentrum Karlsruhe, Gesellschaft für wissenschaftlich-technische Information mbH, D-7514 Eggenstein-Leopoldshafen 2 (FRG), on quoting the depository number CDS-54433, the names of the authors, and the journal citation.
[5] J. R. Harper, M. E. Fountain, A. L. Rheingold, *Organometallics 8* (1989) 2316.
[6] K. Hedberg, E. W. Hughes, J. Waser, *Acta Crystallogr. 14* (1961) 369.
[7] M. Di Vaira, C. A. Ghilardi, S. Midollini, L. Sacconi, *J. Am. Chem. Soc. 100* (1978) 2550.
[8] G. Cappozzi, L. Chiti, M. Di Vaira, M. Peruzzini, P. Stoppioni, *J. Chem. Soc. Chem. Commun. 1986*, 1799.
[9] J. J. Daly, *J. Chem. Soc. 1965*, 4789.
[10] J. W. Lauher, M. Elian, R. H. Summerville, R. Hoffmann, *J. Am. Chem. Soc. 98* (1976) 3219.
[11] C. Bianchini, M. Di Vaira, A. Meli, L. Sacconi, *J. Am. Chem. Soc. 103* (1981) 1448; see also: H. Brunner, U. Klement, W. Meier, J. Wachter; O. Serhadle, M. L. Ziegler, *J. Organomet. Chem. 335* (1987) 339.
[12] K. Wade, *Adv. Inorg. Chem. Radiochem. 18* (1976) 1.
[13] T. Fässler, G. Huttner, *J. Organomet. Chem. 381* (1990) 391, and references cited therein.
[14] S. Masamune, M. Sahai, U. Oma, A. J. Jonas, *J. Am. Chem. Soc. 94* (1972) 8956; W. Stohrer, R. Hoffmann, *J. Am. Chem. Soc. 94* (1972) 1661.
[15] R. E. Stanton, I. W. McIver, Jr., *Acc. Chem. Res. 7* (1974) 72.
[16] M. Di Vaira, F. Mani, S. Moneti, M. Peruzzini, L. Sacconi, P. Stoppioni, *Inorg. Chem. 24* (1985) 2230.
[17] R. Hoffmann, *J. Chem. Phys. 39* (1963) 1397; R. Hoffmann, W. N. Lipscomb, *ibid. 36* (1962) 2179; *ibid. 36* (1962) 483; *ibid. 37* (1963) 2872. Coefficients for C, H, O, P, Co: J.-F. Halet, R. Hoffmann, J.-Y. Saillard, *Inorg. Chem. 24* (1985) 1695; J. W. Lauher, M. Elian, R. H. Summerville, R. Hoffmann, *J. Am. Chem. Soc. 98* (1976) 3219.

A Novel Synthesis of 2-Aminomethyl-1,3-butadienes from *N,O*-Acetals

By *Thomas Arenz* and *Herbert Frauenrath**

Dedicated to Professor Hans-Dieter Scharf on the occasion of his 60th birthday

Despite the importance of the Mannich reaction in the synthesis of natural products, so far only few diastereo- and enantioselective Mannich reactions have been described in the literature.[1-3] We have therefore investigated to what extent *N,N*-dialkyl-*O*-vinyl acetals **2** are suitable as starting compounds for the stereoselective synthesis of Mannich bases **4**, in analogy to the stereoselective synthesis of aldol ethers by acid-catalyzed rearrangement of alkyl vinyl acetals.[4, 5] The compounds required should be readily accessible from **1** by base-catalyzed C=C isomerization.[6]

N,N-Dialkyl-*O*-allyl acetals **1** can be synthesized in good yields by known methods[7, 8] from secondary amines, allyl alcohols, and aldehydes, usually formaldehyde ($R^3 = H$) (Table 1).

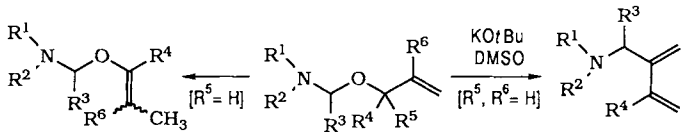

2 **1** **3**

However, in our first investigations concerning the C=C isomerization of **1** ($R^3 = H$) with KO*t*Bu in dimethyl sulfoxide (DMSO), we could only isolate the 2-aminomethyl-substituted butadiene derivatives **3** (Table 1) in 50–70% yield.

Table 1. *N,N*-Dialkyl-*O*-allyl acetals **1** und 2-(*N,N*-dialkylaminomethyl)-1,3-butadienes **3** [9].

	R^1/R^2	R^3	R^4	R^5	R^6	Yield [%] **1**	Yield [%] **3**
a	C_2H_5	H	H	H	H	82	52
b	$-(CH_2)_5-$	H	H	H	H	79	65
c	$CH(CH_3)_2$	H	H	H	H	84	70
d	$CH(CH_3)_2$	H	CH_3	H	H	78	63
e	$CH(CH_3)_2$	H	CH_3	CH_3	H	78	–
f	$CH(CH_3)_2$	H	H	H	CH_3	75	–
g	C_2H_5	C_6H_5	H	H	H	83	–

This, initially unexpected finding, could be resolved by using substituted allyl alcohols for the synthesis of **1** and the use of [D$_6$]DMSO. For example, starting from 1-buten-3-ol, the 3-methyl-substituted diene **3d** is obtained from **1d**. From **1c**, the dideuteriated diene **3h** is formed upon reaction with [D$_6$]DMSO.

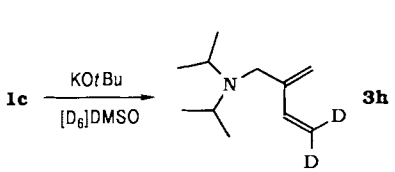

[*] Priv.-Doz. Dr. H. Frauenrath, Dipl.-Chem. T. Arenz
Institut für Organische Chemie der Technischen Hochschule
Professor-Pirlet-Strasse 1, D-5100 Aachen (FRG)

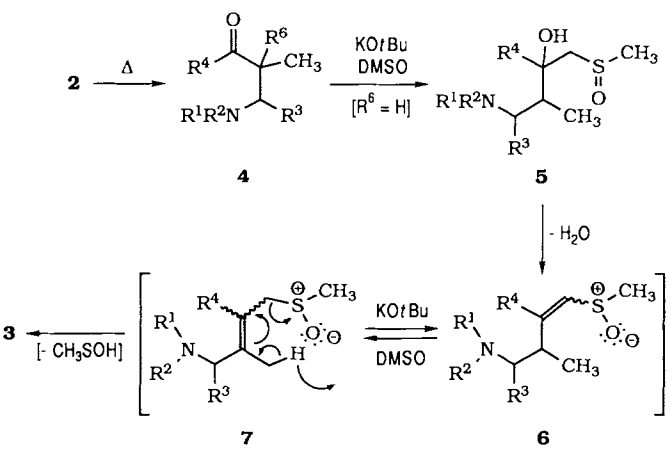

4 **5** **7** **6**

We assume, therefore, that the C=C isomerization leading to **2** and the rearrangement of **2** to give the Mannich bases **4** proceed in the desired way, and that the dienes **3** are formed under the reaction conditions by further reaction of **4** with DMSO.

After nucleophilic addition of the methylsulfinylmethide anion to the Mannich base **4** ($R^6 = H$), subsequent dehydration to give the vinyl sulfoxide **6** and isomerization of **6** should lead to formation of the allyl sulfoxide **7**. Such reactions of carbonyl compounds are already well documented.[10] The allyl sulfoxide **7** could then immediately react further to give the diene **3**. This assumption finds further support from the reaction of conventionally synthesized Mannich bases with DMSO, whereupon the dienes **3** have also been obtained, albeit in poor yields so far.[11]

As expected, with *N,O*-acetals of type **1e** the synthesis of **3** does not succeed, since the double-bond isomerization to give **2** cannot take place. In the same way, no diene can be obtained on using **1f**, since, in this case, no isomerization of **6** to give the allyl sulfoxide **7** is possible.

Table 2. Some physical data of the compounds **3**.

3a: b.p. 56 °C/18 torr; ^{1}H NMR (300 MHz, $CDCl_3$): $\delta = 6.38$ (dd, $J = 11$, 18 Hz, 1H; $H_2C=CH$), 5.48 (d, $J = 18$ Hz, 1H; $HCH=CH$, *trans*), 5.20, 5.10 (each br. s, 2H; $H_2C=C-CH_2$), 5.03 (d, $J = 11$ Hz, 1H; $HCH=CH$, *cis*), 3.15 (br. s, 2H; $H_2C-NR^1R^2$), 2.55 (q, $J = 7$ Hz, 4H; $N(CH_2-CH_3)_2$), 0.98 (t, $J = 7$ Hz, 6H; $N(CH_2-CH_3)_2$); ^{13}C NMR (75 MHz, $CDCl_3$): $\delta = 144.3$ ($C-CH_2$), 138.0 ($H_2C=CH$), 116.9, 113.9 ($H_2C=CH$, $C=CH_2$), 47.2, 45.1 ($N(CH_2-CH_3)_2$, $H_2C-NR^1R^2$), 12.1 ($N(CH_2-CH_3)_2$

3b: b.p. 79 °C/15 torr; ^{1}H NMR: $\delta = 6.35$ (dd, $J = 11$, 18 Hz, 1H; $H_2C=CH$), 5.46 (d, $J = 18$ Hz, 1H; $HCH=CH$, *trans*), 5.13, 5.08 (each br. s, 2H; $H_2C=C-CH_2$), 5.00 (d, $J = 11$ Hz, 1H; $HCH=CH$, *cis*), 3.05 (br. s, 2H; $H_2C-NR^1R^2$), 2.41 (t, $J = 6.5$ Hz, 4H; piperidyl-H), 1.55 (m, $J = 6.5$ Hz, 6H; piperidyl-H); ^{13}C NMR: $\delta = 143.5$ ($C-CH_2$), 137.9 ($H_2C=CH$), 116.9, 114.1 ($H_2C=CH$, $C=CH_2$), 54.4, 53.0 ($H_2C-NR^1R^2$, piperidyl-C), 26.1, 25.9 (piperidyl-C)

3c: b.p. 74 °C/15 torr; ^{1}H NMR: $\delta = 6.40$ (dd, $J = 11$, 18 Hz, 1H; $H_2C=CH$), 5.37 (d, $J = 18$ Hz, 1H; $HCH=CH$, *trans*), 5.36, 5.08 (each br. s, 2H; $H_2C=C-CH_2$), 4.98 (d, $J = 11$ Hz, 1H; $HCH=CH$, *cis*), 3.20 (t, $J = 1.2$ Hz, 2H; $H_2C-NR^1R^2$), 3.02 (sept, $J = 6.5$ Hz, 2H; isopropyl-CH), 0.98 (d, $J = 6.5$ Hz, 12H; isopropyl-CH_3); ^{13}C NMR: $\delta = 145.9$ ($C-CH_2$), 138.2 ($H_2C=CH$), 116.2, 112.6 ($H_2C=CH$, $C=CH_2$), 48.1 (isopropyl-CH), 46.5 ($H_2C-NR^1R^2$), 20.6 (isopropyl-CH_3)

3d: b.p. 83 °C/15 torr; ^{1}H NMR: $\delta = 5.44$ (br.s, 1H; $HCH=C-CH_3$), 5.17, 5.16 (each br.s, 2H; $H_2C=C-CH_2$), 4.9 (br. s, 1H; $HCH=C-CH_3$), 3.25 (t, $J = 6$ Hz, 2H; $H_2C-NR^1R^2$), 3.03 (sept, $J = 6$ Hz, 2H; isopropyl-CH), 1.93 (s, 3H; H_3C-C), 1.00 (d, $J = 6$ Hz, 12H; isopropyl-CH_3); ^{13}C NMR: $\delta = 142.9$, 139.4 ($C-CH_2$, $H_2C=C-CH_3$), 112.9, 111.4 ($H_2C=C-CH_3$, $C=CH_2$), 48.2 (isopropyl-CH), 47.7 ($H_2C-NR^1R^2$), 20.7 (isopropyl-CH_3), 14.0 ($H_2C=C-CH_3$)

3h: b.p. 74 °C/15 torr; ^{1}H NMR: $\delta = 6.4$ (br.s, 1H; $D_2C=CH$), 5.36, 5.08 (je br. s, 2H; $H_2C=C-CH_2$), 3.20 (br. s, 2H; $H_2C-NR^1R^2$), 3.05 (sept, $J = 6.5$ Hz, 2H; isopropyl-CH), 0.98 (d, $J = 6.5$ Hz, 12H; isopropyl-CH_3); ^{13}C NMR: $\delta = 146.0$ ($C-CH_2$), 138.0 ($D_2C=CH$), 116.2, 115.5 ($D_2C=CH$, $C=CH_2$), 48.1 (isopropyl-CH), 46.5 ($H_2C-NR^1R^2$), 20.6 (isopropyl-CH_3)

 © VCH Verlagsgesellschaft mbH, D-6940 Weinheim, 1990 0570-0833/90/0808-0932 $ 3.50+.25/0 Angew. Chem. Int. Ed. Engl. 29 (1990) No. 8

The dienes **3** can be unequivocally characterized ^{1}H- and ^{13}C-NMR spectroscopically (Table 2). In contrast to 1-aminomethyl-1,3-butadiene derivatives, which have proven to be effective antimycotics,[12] very little is known about compounds of type **3**.[13–16] So far, we have been unable to observe dimer formation as has been described for 2-aminomethyl-1,3-butadiene[13] and its quaternary ammonium salt.[16] We are presently investigating whether other dienes **3** can be synthesized by substitution of **1** (e.g. **1g**), and whether the base-catalyzed reaction of DMSO with carbonyl compounds involves a generally applicable principle for the synthesis of dienes.

Experimental

A solution of KO*t*Bu (5.9 g, 52 mmol) in DMSO (50 mL) was treated slowly with 52 mmol of **1** and the resulting mixture stirred for 12 h at 80 °C. After cooling to room temperature the mixture was poured into ice-water, the organic phase separated off, and the aqueous phase extracted several times with ether. The combined organic phases were washed with saturated NaCl solution to remove residual DMSO and then dried over K_2CO_3. After removal of the solvent, the dienes **3a–d** were isolated by distillation in vacuo.

Received: March 22, 1990 [Z 3869 IE]
German version: *Angew. Chem. 102* (1990) 929

CAS-Registry-Numbers:
1a, 24045-54-3; **1b**, 24045-57-6; **1c**, 128328-73-4; **1d**, 128328-74-5; **1e**, 128328-75-6; **1f**, 128328-76-7; **1g**, 128328-77-8; **3a**, 128328-68-7; **3b**, 128328-69-8; **3c**, 128328-70-1; **3d**, 128328-71-2; **3h**, 128328-72-3.

[1] D. Seebach, C. Betschart, M. Schiess, *Helv. Chim. Acta 67* (1984) 1593.
[2] Interim communication on stereoselective Mannich-reactions: N. Risch, U. Billerbeck, A. Esser in: *Vortragsreferate der Chemiedozententagung 1988*, Mainz 1988, p. 31.
[3] H. Kunz, W. Pfrengle, *Angew. Chem. 101* (1989) 1041; *Angew. Chem. Int. Ed. Engl. 28* (1989) 1067.
[4] H. Frauenrath, J. Runsink, *J. Org. Chem. 52* (1987) 2709.
[5] H. Frauenrath, *Synthesis 1989*, 721.
[6] C. C. Price, W. H. Snyder, *J. Am. Chem. Soc. 83* (1961) 1773.
[7] T. D. Stewart, W. E. Bradley, *J. Am. Chem. Soc. 54* (1932) 4172.
[8] A. T. Stewart, C. R. Hauser, *J. Am. Chem. Soc. 77* (1955) 1098.
[9] All the new compounds gave correct elemental analyses and spectra (IR, MS; ^{1}H- and ^{13}C-NMR-spektroscopic data, see Table 2).
[10] R. W. Hoffmann, S. Goldmann, N. Maak, R. Gerlach, F. Frickel, G. Steinbach, *Chem. Ber. 113* (1980) 819, and references cited therein.
[11] For example 1-diisopropylamino-2-methyl-butan-3-one gives the diene **3d**.
[12] A. Stütz, *Angew. Chem. 99* (1987) 323; *Angew. Chem. Int. Ed. Engl. 26* (1987) 320.
[13] C. Mannich, O. Salzmann, *Ber. Dtsch. Chem. Ges. 72* (1939) 506.
[14] D. R. Coulson, *J. Org. Chem. 38* (1973) 1483.
[15] I. M. Zel'dis, S. S. Zhukovskii, A. M. Taber, I. V. Kalechits, V. E. Vasserberg, *Izv. Akad. Nauk SSSR, Ser. Khim. 5* (1983) 1119.
[16] G. D. Jones, W. C. Meyer, *J. Polym. Sci., Part A-1 8* (1970) 2123.

Imidazo[1,2-*e*][1,3,5]triazepine Derivatives: First Representatives of a New Heterocyclic System**

By *Gerd Kaupp** and *Klaus Sailer*

Dinuclear heterocycles containing four nitrogen atoms play an important role in living Nature. Thus, the biological activities of purines, pteridines and related classes of substances are unimaginably diverse.[1] We report here on a simple synthesis of a novel tetraazaheterocyclic system in which a five-membered ring is coupled to a seven-membered ring.[2]

Reaction of methylamine or ethylamine with 2-chloromethylbenzimidazole **1** in dichloromethane leads to direct formation of **3a** (60%) and **3b** (53%; in this case together with 34% **2b**), respectively.

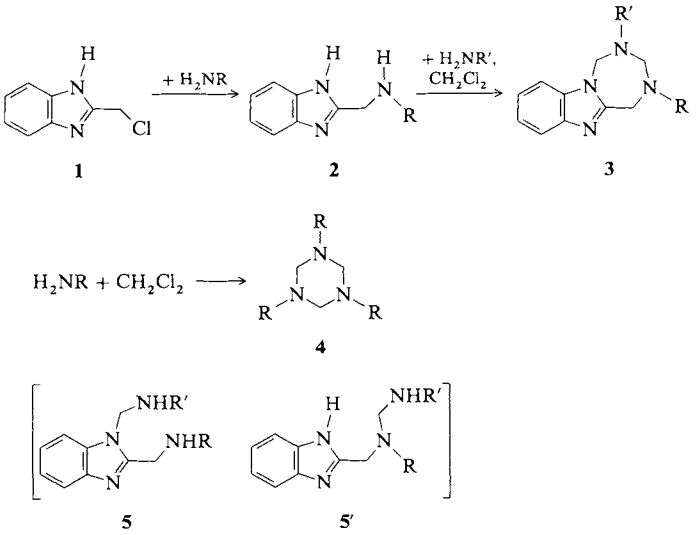

a: R = R′ = CH_3; **b**: R = R′ = C_2H_5; **c**: R = C_2H_5, R′ = CH_3; **d**: R = H, R′ = CH_3; **e**: R = C_6H_5, R′ = CH_3

In these complex reactions, two equivalents of primary amine and two equivalents of dichloromethane are so incorporated into **1** without rearrangement and with multiple HCl elimination that a seven-membered ring is formed as part of the previously unknown heterocyclic system **3**. The high tendency of formation of **3** is surprising and points to high stability.

As expected, the synthesis can be carried out in two steps, if **2** is first synthesized in diethyl ether or chloroform. This procedure, however, is preferred only when different residues R and R′ are to be inserted, as in **3c** (54%), **3d** (57%), and **3e** (88%). Possible intermediates are **5** or **5′**, which, after reaction with dichloromethane, cyclize to **3**.

The readiness with which anhydrous dichloromethane undergoes substitution with primary amines is remarkable. According to the literature dimethylamine, as secondary amine, does not react with dichloromethane below 70 °C in a pressure vessel (to give tetramethylenediamine), cyclic bases such as pyrrolidine react at room temperature in the presence of NaOH.[3] Under our very mild reaction conditions we observed the formation of small amounts of **4a**, **b** as byproducts, which apparently are formed from dichloromethane and primary alkylamines without the assistance of further reagents.[4] This is consistent with the mechanistic concepts.

In the case of starting materials such as the theophylline derivative **6**,[5] the question of the regioselectivity arises, since the reaction should lead to intermediates analogous to **5** or **5′** via the deprotonated imidazole system. In the case of **6**, only a cyclization to N-7 with formation of **7** and not a cyclization to N-9 (of **6**) was observed. This is consistent with semiempirical AM1 and PM3 calculations,[6] according to which **7** is 8.3 and 6.2 kcal mol^{-1}, respectively, more stable

[*] Prof. Dr. G. Kaupp, Dipl.-Chem. K. Sailer
Fachbereich Chemie—Organische Chemie I—der Universität
Postfach 2503, D-2900 Oldenburg (FRG)

[**] This work was supported by the Deutsche Forschungsgemeinschaft, the Fonds der Chemischen Industrie, and the Bundesminister für Forschung und Technologie (Project 10 IVS 325). We thank *Sven Krüger* for the synthesis of **3e**, and BASF, Ludwigshafen, for supplying gaseous amines.

than the analogous product of cyclization to N-9 (of **6**), and which indicate that the latter would be strongly sterically hindered.

The structure **7** can be unequivocally established ^{13}C-NMR spectroscopically by the signal at $\delta = 65.4$, which is due to the aminal carbon atom bound to the imidazole-N, and for which the C13-NMR/IR data bank[7] predicts a value of $\delta = 67.7 + 3.7$ (for the alternative structure 58.9 + 2.1).

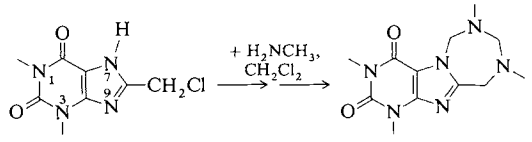

6 **7**

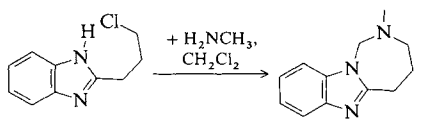

8 **9**

Table 1. Important physical and spectroscopic data of the compounds **2**, **3**, **6**, **7**, and **9**. UV spectra in CH_3OH; 300-MHz ^{1}H-NMR and 75-MHz ^{13}C-NMR spectra in $CDCl_3$, 25 °C, TMS internal; 70 eV mass spectra.

2a: m.p. = 128 °C (CH_2Cl_2/Et_2O); UV: λ_{max} = 243, 269(sh), 274, 280 nm; ^{1}H NMR: δ = 7.55–7.49 (2H, AA'BB'), 7.3(2NH, s, br), 7.22–7.16(2H,BB'AA'), 4.00(2H,s), 2.40(3H,s); ^{13}C-NMR: δ = 151.59, 138.09(2C), 122.43(2C), 114.82(2C), 47.99, 34.93; MS: *m/z* 161 ($M^{\oplus}$, 2%), 160(14), 148(6), 132(100), 131(34), 119(16), 118(10), 104(6); dihydrochloride cf. Ref. [10]

2b: m.p. = 98 °C (CH_2Cl_2/Et_2O); dihydrochloride cf. Ref. [10]

2d: m.p. = 91° (CH_2Cl_2/Et_2O); dihydrobromide cf. Ref. [11]

2e: m.p. = 163 °C (EtOAc/Et_2O) ([12]: 162 °C)

3a: m.p. = 162 °C (CH_2Cl_2/Et_2O); UV: λ_{max} = 248.5, 269(sh), 275, 282 nm; ^{1}H NMR: δ = 7.77–7.70(1H), 7.38–7.21(3H), 5.18(2H,s), 4.10(2H,s), 3.98 (2H,s), 2.46(3H,s), 2.40(3H,s); ^{13}C-NMR (exp./simulated [7]): δ = 154.08/156.7, 142.04/141.4, 136.05/134.4, 122.62/123.5, 121.71/122.9, 119.80/119.9, 108.47/111.0, 80.72/77.4 ± 3.9, 63.94/57.8 ± 8.3, 54.83/47.1 ± 8.1, 42.65/39.7, 38.19/39.7; MS: *m/z* 217 ($M^{\oplus}$, 4%), 216(28), 173(88), 172(32), 158(4), 145(10), 132(100), 131(60), 104(9), 103(28)

3b: m.p. = 123 °C (CH_2Cl_2/Et_2O); ^{1}H NMR: δ = 7.75–7.70(1H), 7.38–7.20(3H), 5.08(2H,s), 4.07(2H,s), 4.02(2H,s), 2.54(2H,q, *J* = 7.2 Hz), 2.50(2H,q, *J* = 7.0 Hz), 1.07(3H,t, *J* = 7.0 Hz), 1.03(3H,t, *J* = 7.2 Hz); ^{13}C NMR: δ = 154.44, 142.02, 135.86, 122.45, 121.50, 119.70, 108.40, 77.49, 61.10, 51.78, 48.17, 43.48, 13.08, 13.02

3c: m.p. = 103 °C (CH_2Cl_2/Et_2O); ^{1}H NMR: δ = 7.73–7.69(1H), 7.35–7.20(3H), 5.12(2H,s), 4.15(2H,s), 4.07(2H,s), 2.63(2H,q, *J* = 7.2 Hz), 2.38(3H,s), 1.13(3H,t, *J* = 7.2 Hz)

3d: m.p. = 136 °C (CH_2Cl_2); ^{1}H NMR: δ = 7.75–7.70(1H), 7.29–7.16(3H), 5.19(2H,s), 4.28(2H,s), 4.20(2H,s), 2.19(3H,s)

3e: m.p. = 184 °C (CH_2Cl_2); UV: λ_{max} = 245, 274, 280 nm; ^{1}H NMR: δ = 7.82–7.74(1H), 7.32–7.22(3H), 7.09–7.21(4H), 6.78–6.71(1H), 5.24(2H,s), 4.89(2H,s), 4.85(2H,s), 2.15(3H,s); ^{13}C NMR: δ = 154.45, 142.27, 135.78, 129.28(2C), 122.73, 121.81, 119.83, 118.84, 114.39(2C), 108.63, 73.34, 64.66, 49.28, 37.53; MS: *m/z* 278 ($M^{\oplus}$, 8%), 236(13), 235(74), 234(19), 223(3), 147(5), 132(88), 131(15), 117(5), 105(100), 104(42)

6: m.p. = 248 °C (CH_2Cl_2) ([5]: 241 °C)

7: m.p. = 179 °C (CH_2Cl_2); UV: λ_{max} = 276 nm; ^{1}H NMR: δ = 5.52(2H,s), 3.96(2H,s), 3.92(2H,s), 3.60(3H,s), 3.40(3H,s), 2.51(3H,s), 2.47(3H,s); ^{13}C NMR: δ = 155.04, 153.27, 151.37, 146.90, 108.08, 80.80, 65.47, 54.36, 40.03, 37.92, 29.54, 27.69; MS: *m/z* 278 ($M^{\oplus}$, 11%), 235(100), 220(3), 206(4), 194(52),

9: m.p. = 153 °C (CH_2Cl_2/Et_2O); UV: λ_{max} = 248,269.5(sh), 275,282 nm; ^{1}H NMR: δ = 7.72–7.66(1H), 7.30–7.14(3H), 5.06(2H,s), 3.27–3.18(2H), 3.18–3.09(2H), 2.08(3H,s), 1.86–1.72(2H); ^{13}C NMR: δ = 156.62, 142.22, 136.22, 122.13, 121.55, 119.27, 108.31, 76.90, 64.26, 58.00, 36.50, 29.29; MS: *m/z* 201 ($M^{\oplus}$, 100%), 186(5), 173(5), 158(45), 157(43), 145(10), 132(22), 131(6), 119(6), 103(4), 101(6)

Compound **7** is the first derivative of a 1,3-dimethyl[1,3,5]-triazepino[7,1-*f*]xanthine. Like **3**, it contains the partially hydrogenated imidazo[1,2-*e*][1,3,5]triazepine subunit. No doubt further examples of the new heterocyclic system can be synthesized, and interesting regioselectivities studied in the case of unsymmetrical substitution.

The advantage of dichloromethane over formaldehyde/hydrochloric acid[8] (avoidance of water and strong acid) is also clearly demonstrated by the synthesis of **9** from **8** (45%).

The structure of the compounds **3**, **7**, and **9** is supported by analytical as well as spectroscopic data (Table 1) and is confirmed by ^{13}C-NMR spectral simulation,[7] so that alternative structures can be ruled out with certainty.[9] Also helpful here is a comparison of **3** and **9**.

The novel heterocycles **3**[2] and **7**[2] can be expected to exhibit interesting biological activities: imidazo[1,2,-*e*]-[1,3,5]triazepines are related to the pteridines in the same way as azulene to naphthalene. By further development of the synthetic route, derivatives **3** with R = R′ = H ought to be accessible, whose oxidation should lead to tetraazaazulene cations.

Experimental

2a: A weak stream (150 mL min^{-1}) of methylamine was passed into a mixture of 500 mg (3.0 mmol) of **1** and 50 mL of anhydrous chloroform or diethyl ether for 30 min at 0 °C and the resulting solution allowed to stand for 10 h at room temperature. The still clear solution was then heated under reflux for 30 min for complete separation of methylamine hydrochloride; the solvent was then removed by evaporation, and the compound **2a** extracted from the residue with diethyl ether. Yield 450 mg (93%), m.p. 128 °C (Et_2O). **2b** [10], **2c** [13] and **2e** [12] were obtained analogously with ethylamine (0°), ammonia (− 35 °C), and aniline (62 °C), respectively.

3a, **b**, **7**: A weak stream (150 mL min^{-1}) of methylamine (ethylamine in the case of **3b**) was fed from a steel cylinder into a slurry of 500 mg (3.0 mmol) of **1** or 1.73 g (7.6 mmol) of **6** in 50 mL of anhydrous ($CaCl_2$) dichloromethane at − 30 °C for 30 min. The resulting solution was allowed to stand at room temperature for 10 h and then heated under reflux for 30 min, whereby excess amine was distilled off and amine hydrochloride was deposited. The reaction solution was then, evaporated to dryness in vacuo and **3a** (390 mg, 60%), **3b** (390 mg, 53%) or **7** (723 mg, 34%) [besides 180 mg (34%) **2b** and 390 mg (23%) of the amine **6** with $NHCH_3$ instead of Cl corresponding to **2a**], respectively extracted from the yellow paste with diethyl ether; adherent **4a**, **b** (100–200 mg) was removed by evaporation in vacuo. When the synthesis was carried out with **2a** as starting material, **3a** was obtained in 92% yield. In the same way, **3c** (54%), **3d** (57%), and **3e** (88%) were obtained from **2b**, **2d**, and **2e**, respectively, and **9** (45%) from **8** [14].

Received: January 26, 1990;
supplemented: May 5, 1990 [Z 3760 IE]
German version: *Angew. Chem. 102* (1990) 917

CAS-Registry-Nummern:
1, 4857-04-9; **2a**, 98997-01-4; **2b**, 127855-46-3; **2c**, 5805-57-2; **2e**, 5805-59-4; **3a**, 127855-47-4; **3b**, 127855-48-5; **3c**, 127855-50-9; **3d**, 127855-51-0; **3e**, 127855-52-1; **6**, 64398-14-7; **7**, 127855-49-6; **8**, 127855-54-3; **9**, 127855-53-2.

[1] See, for example, D. T. Hurst: *An Introduction to the Chemistry of Pyrimidines, Purines and Pteridines*, Wiley, Chichester 1980; T. W. Stone (Ed.): *Purines: Pharmacology and Physiological Role*, VCH, Weinheim 1985; J. A. Blair (Ed.): *Chemistry and Biology of Pteridines—Pteridines and Folic Acid Derivatives*, deGruyter, Berlin 1983.

[2] Substructure searches with CAS-ONLINE and BEILSTEIN yielded no examples of optional degrees of substitution, hydrogenation, annelation and bridging for imidazo [1,2-*e*][1,3,5]triazepines.

[3] L. W. Jones, H. F. Whalen, *J. Am. Chem. Soc. 47* (1925) 1343; H. F. Whalen, L. W. Jones, *ibid. 47* (1925) 1351; J. E. Mills, C. A. Maryanoff, R. M. Cosgrove, L. Scott, D. F. McComsey, *Org. Prep. Proced. Int. 16* (1984) 97; in the meantime prolinamide has been cyclized with CH_2Cl_2 and NH_3 at 50 °C: H. J. Federsel, E. Könberg, L. Lilljequist, B. M. Swahn, *J. Org. Chem. 55* (1990) 2254.

[4] The compounds **4** are usually synthesized from primary amine and formaldehyde: see, for example, Merck-Schuchardt MSInfo 86-10; D. D. Reynolds, B. C. Cossar, *J. Heterocycl. Chem. 8* (1971) 597.

[5] H. Bredereck, E. Siegel, B. Föhlisch, *Chem. Ber. 95* (1962) 403.
[6] QCPE-MOPAC-Version 5.01, scalar version by *D. Gerson* for IBM 3090, adaptation to IBM 4381 for VM/SP by *M. Woyd* and *D. Spingat*, Universität-Gesamthochschule Essen.
[7] C13-NMR/IR-Information-System: BASF AG; on-line from Fachinformationszentrum Karlsruhe via STN International, January 1990. We are grateful for the granting of a generous academic discount.
[8] Compounds containing the heterocyclic system of **9** have been synthesized by this method: R. I. Fryer, J. V. Earley, *J. Heterocycl. Chem. 14* (1977) 1435.
[9] All the compounds isolated gave satisfactory elemental analyses, ^{1}H-NMR, ^{13}C-NMR, and mass spectra.
[10] A. Bloom, A. R. Day, *J. Org. Chem. 4* (1939) 14.
[11] M. Mengelberg, *Chem. Ber. 92* (1959) 977.
[12] G. K. Hughes, F. Lions, *J. Proc. R. Soc. N.S.W. 71* (1938) 209; *Chem. Abstr. 32* (1938) 58309.
[13] W. Ried, F. Grüll, *Chem. Ber. 96* (1963) 130.
[14] R. C. de Selms, *J. Org. Chem. 27* (1962) 2167.

BOOK REVIEWS

Book Reviews are written by invitation from the editor. Suggestions for books to be reviewed and for book reviewers are welcome. Publishers should send brochures or (better) books to the following address: Redaktion Angewandte Chemie, Postfach 101161, D-6940 Weinheim, Federal Republic of Germany. The editor reserves the right of selecting which books will be reviewed. Uninvited books not chosen for review will not be returned.

One and Two Dimensional NMR Spectroscopy. By *Atta-ur-Rahman*. Elsevier, Amsterdam 1989. xix, 578 pp., hard cover, HFl 355.00. – ISBN 0-444-87316-3

This book makes an attempt at providing a comprehensive overview of modern high resolution NMR techniques. The principles of many of the latest generation one- and two-dimensional (1D and 2D) NMR techniques are described in a manner that makes the book easy to read. Descriptions of the tremendous number of pulse sequences contained in this book rely entirely on the popular vector picture approach. As a drawback of this oversimplified approach, explanation of many of the techniques relying on multiple quantum phenomena suffers.

The book starts with a chapter that introduces many of the commonly used concepts in modern NMR. Topics vary from a simplified description of spectrometer hardware to data acquisition and dynamic range, Fourier transformation, phase cycling, solvent suppression, nuclear Overhauser enhancement, and advanced concepts such as coherence transfer and multiple quantum filtration. This chapter includes a brief description of the operator formalism which has played a crucial role in the development of modern pulsed NMR, but the author does not use this formalism in later chapters. A more detailed description of the operator formalism is presented in the last chapter (Chapter 14).

Chapters 2, 3 and 4 are concerned with modern 1D NMR techniques. Chapter 2 starts with an explanation of the "spin-echo" phenomenon in homo- and heteronuclear spin systems, and spectral editing using the large number of different pulse schemes, including all of the "Sørensen variations." Chapter 3 is devoted to the once-popular 1D INADEQUATE technique, again including many of its variations. Chapter 4 gives a very qualitative but useful description of common relaxation mechanisms with emphasis on the NOE effect and its use in structural chemistry.

Starting with a simple introduction of the concept of 2D Fourier transformation in Chapter 5, the remainder of the book describes the tremendous variety of different pulse schemes that have been developed in the past decade. The first "real" 2D chapters deal with heteronuclear and homonuclear *J*-resolved spectroscopy.

Chapter 8 treats homonuclear *J*-correlation techniques such as COSY and its relay derivatives. The chapter includes a description of phase-sensitive COSY without multiple quantum filtration, but remarkably, the multiple quantum filtered E. COSY experiment is briefly discussed. The much simpler P. E. COSY technique is not described. Among a variety of SECSY and Super-SECSY experiments, I was very surprised to find a section on TOSCY spectroscopy, whereas, without any cross-referencing, a later chapter (Ch. 11) is devoted to this topic.

Chapter 9 deals with techniques for delineating cross-relaxation and chemical exchange pathways. Although critical for macromolecular structure analysis, NOE studies of smaller substances are usually carried out more efficiently in a one-dimensional manner, and the description is correspondingly brief. This chapter also includes a brief discussion of the rotating frame NOE experiment, but without any mention of the theoretical basis of this technique.

Heteronuclear shift correlation techniques are treated in Chapter 10. Most of this chapter is related to the low-γ detected variety, including experiments such as HETCOR and COLOC, but their more sensitive ^{1}H-detected counterparts, HMQC and HMBC, are also discussed. Chapter 12 deals with multiple quantum spectroscopy, including the 2D INADEQUATE experiment and multiple quantum filtration of regular homonuclear 2D experiments such as COSY. Chapter 13 provides advice for the practising structural NMR spectroscopist with regard to what set of experiments may typically be most useful for problems concerning natural products. In this respect, Appendix 2 provides a very valuable summary of the most popular experimental techniques currently available, including their strong and weak points.

I noted several (minor) errors in pulse sequences, which may make it necessary to consult the original literature. Also the discussion of quadrature detection and folding applies only to older Bruker spectrometers, and owners of instruments with simultaneous detection of complex data may get

confused. The main weakness of the book is that the author has not been able to get hands-on experience with all the hundreds of techniques described. As a consequence, statements in the book often reflect the subjective and optimistic views of the inventors of such techniques.

This book is most valuable for NMR spectroscopists who are primarily dealing with relatively small molecules for which the tremendous variety of 1D and 2D NMR pulse sequences may be applicable. The absence of any serious mathematics makes the book easy to read, but necessarily makes it lacking in depth. At the end of most chapters, a problem and answer section is included which should be helpful to many readers. The book includes a list of commonly used acronyms plus a substantial number of valuable references.

Ad Bax [NB 1077 IE]
National Institutes of Health
Bethesda, MD 20205 (USA)

Compact Wörterbuch der exakten Naturwissenschaften und der Technik. Band 1. Englisch-Deutsch. By *A. Kučera*. Oscar Brandstetter Verlag, Wiesbaden 1989. xxxi, 1460 pp., hard cover, DM 130.00.—ISBN 3-87097-146-0

As a German-speaking student one spends many years glued to school and lecture theatre benches; after this one continues to pursue one's subject, then suddenly it becomes necessary to work on specialist texts in English, containing words such as primer, multitasking, solenoid valve, drybox, puckering, dose rate, weathering, backing, or plane-polarized. Depending on what specialized training one has had, a few of the words may be familiar, and in some cases one may have an idea of their meaning. But where can one look up completely unknown words or find out their meanings with certainty? Even with a good English dictionary one quickly comes up against its limitations, as there is not space in such a work to include all specialist words or specialist meanings attached to everyday words. One therefore needs a specialist dictionary such as that reviewed here, which was published last year in its second, revised edition. The entries, totalling about 117400, are mainly drawn from monographs and specialist encyclopedias which are listed in the introduction. However, with regard to chemistry and chemical technology it is a little surprising that, although "Römpp" has been referred to in compiling the dictionary, "Ullmann" has not. The introduction also includes a glossary of the abbreviations used and an alphabetical list of the specialist fields used as a basis for classifying the words. These two lists are also summarized on a plastic card in the form of a bookmark; unfortunately most of this information can only be read when the card is not inside the book, since otherwise everything is upside-down. There is an appendix consisting of an addendum ("carrier" and compound expressions containing this word) and a short comparison of how scientific and technical words are formed in English and German.

However, I would have liked to see detailed explanations of the conventions used in the entries, e.g. what is the significance of double vertical slashes (‖), oblique slashes (/) and dots (e.g. in "plasma··sprayed"), and where is it explained that in an entry such as "wrap jack"..."~mode" the wavy line ~ stands for "wrap", not for "wrap jack"? Also it is not quite clear why, for example, there need to be three independent English entries corresponding to the German "Spiegeleisen" (namely "spiegel", "spiegeleisen" and "spiegel iron"), nor why, for abbreviated terms, the (very welcome) explanation of the meaning is not reinforced by also giving the complete English expression. For example, I would find it quite interesting to discover why fuel made from refuse is known in English as RDF. Again, it is surprising that although "work electrode", "working electrode" and "reference electrode" are all included, the abbreviations WE and RE are not, nor is "counter electrode", which is the third type of electrode.

The question of whether or not the German translations are always exact is one on which I cannot give an opinion, but it seemed to me that a few of the chemical expressions did not quite correspond to the most common usage, e.g. "dihedral angle:Dihedralwinkel" (instead of Diederwinkel), "methacrylic acid:Methakrylsäure" (instead of Methacrylsäure), "methyltert-butyl ether" (an unfortunate way of linking the parts of the word!): "Butylmethylether (tertiäres)" (instead of *tert*-Butylmethylether). Whether "impact strength" should be translated as "Kerbschlagfestigkeit", as given here, or as "Kerbschlagzähigkeit", as I have been assured by polymer experts, is something which I cannot decide.

Unfortunately the quality of the printing in this dictionary is not very good. For example, the first few pages distinctly show shadows caused by double printing, and the top entry on page 1137, "shock", appears as "shock". It has, of course, not been possible to completely avoid typesetting errors, but at least those which seriously alter the meaning should have been noticed. Or would you immediately understand the explanation given for "landfall": "Punkt, an dem der MFK nach Flug über Sei die Küste erreicht"? First fault: the abbreviation is not explained (Marschflugkörper); second fault: "Sei" should have read "See". Again, "Wiener filtering", a technique used in electronic reconstruction of images, involves not "Wideraufbau" but Wiederaufbau.

Despite these critical comments I did find the dictionary quite useful when I used it (sporadically) over a period of several months, specifically for looking up specialist words in technological fields. Finally, then, for each of the English terms mentioned at the beginning of this review I list here at least one of the German equivalents given, although one cannot avoid a slight furrowing of the brow here and there: Starter, Multitasking (explained as the simultaneous execution of several tasks by a digital computer), Elektroventil, Trockenschrank, Fältelung (!?), Dosisleistung, Freiluftbewitterung, Schutzschicht and linear polarisiert.

Elisabeth Weber [NB 1071 IE]
Angewandte Chemie, Weinheim (FRG)

Bimolecular Collisions. (Series: Advances in Gas-Phase Photochemistry and Kinetics). Edited by *M. N. R. Ashfold* and *J. E. Baggott*. VCH Verlagsgesellschaft, Weinheim 1989. xvii, 416 pp., hard cover, £ 85.00.—ISBN 0-85186-393-0

The study of bimolecular collision processes at a molecular level has been extended into new areas in the last few years, in particular through the development of sensitive laser spectroscopic techniques capable of identifying excited states. It has become possible to obtain detailed information on the dynamics of chemical reactions and energy transfer processes, and on topics at research frontiers such as the gas-solid transition in metal clusters and the gas-liquid transition in solvent clusters, at a level which enables one to test results from *ab initio* calculations.

The first chapter of the book already provides an excellent example of the progress that has been achieved. Here *Valen-*

 © VCH Verlagsgesellschaft mbH, D-6940 Weinheim, 1990 0570-0833/90/0808-0936 $ 3.50+.25/0

tini and *Phillips* show how laser spectroscopic techniques such as multiphoton resonance ionization and coherent anti-Stokes Raman scattering (CARS) allow one to study the classical hydrogen-deuterium exchange reaction $H + D_2 \rightarrow HD + D$ under single collision conditions for selected states, and to measure rotational and vibrational excitations of the H_2 product molecule for different collision energies. The agreement between the results thus obtained and the populations of the states as predicted by *ab initio* calculations is impressive. New measurements of the partial cross-sections for the reaction $H + p\text{-}H_2(v = 0,\ j = 0,\ 2) \rightarrow o\text{-}H_2(v = 1,\ j) + H$ give sharp maxima for the formation of $o\text{-}H_2(v = 1,\ j)$ at collision energies which, according to quantum dynamics calculations, correspond to vibrational levels of the linear H_3 transitional state. *Valentini* describes this as a "vibrational spectrum of the transition state".

In Chapter 2 *Smith* describes the influence of vibrational excitations of the reactants on bimolecular reactions, with examples which again include the hydrogen-deuterium exchange reaction. Other examples are the reactions of F, $O(^3P)$ and $O(^1D)$ atoms with H_2 and of $O(^3P)$ with HCl and HBr, reactions with four atoms, e.g. $OH + H_2$, OH + HBr, CN + HCl or OH + CO, four-center reactions, and radical-radical reactions. One expects to find large increases in reaction rates following vibrational excitations, especially for endothermic and direct reactions with "late" energy barriers, and this is confirmed to some extent. The transition state theory assuming adiabatic behavior as regards vibrational energy has proved to be a useful theoretical framework for understanding the observed effects.

In Chapter 3 *Davies* and *Pilling* describe the association reactions $H + C_2H_4 \rightarrow C_2H_5$, $CH_3 + CH_3 \rightarrow C_2H_6$, $CH_3 + H \rightarrow CH_4$, $O + OH \rightarrow HO_2$ and $HO_2 + HO_2 \rightarrow H_2O + O_2$; here again the transition state theory of the kinetics provides the theoretical background, as discussed in Chapter 4 by *Hase* and *Wardlaw*. Since reactions of this type often take place via potential wells as opposed to barriers, one cannot assume a transition state at the position of the barrier, but must instead use alternative definitions.

Energy transfer by non-reactive collisions is treated in Chapter 5 by *Hippler* and *Troe*. Here the experimentally measured quantities are the average energy transfered per collision $<\Delta E>$ and the factors that influence $<\Delta E>$. The measured values can be compared with the corresponding values obtained from quasi-classical trajectory calculations and quantum scattering calculations. More detailed information about the dependence of the average collisional energy transfer on the excitation state of the molecule can be obtained from other experimental methods, especially from newer techniques such as "hot" UV absorption spectroscopy, time-resolved multiphoton IR spectroscopy, and multiphoton ionization measurements. Most of the experimental methods used up to now give averaging over sequences of collisions, whereas there have been very few state-specific single collision experiments on highly excited polyatomic molecules. Such experiments would allow a more direct comparison with theory.

In Chapter 6 *Husain* and *Roberts* describe laser spectroscopic techniques which enable one to excite lanthanoid metal atoms to particular states and then to follow their decay by reactive and inelastic collisions in a time-resolved manner. Reactions with oxidizing agents especially are often accompanied by strong chemiluminescence, and this can be used to identify different reaction pathways. By comparing these results with those from *ab initio* calculations and with adiabatic correlation diagrams it is often possible to deduce detailed reaction mechanisms.

In Chapter 7 *Jarrold* deals with the preparation, characterization and reactivity of metal clusters. From this it appears that clusters of certain sizes are particularly inert. Very little is yet known about the effects of electronic and molecular structure on the reactivity of clusters. The aim of these studies is to gain a deeper understanding of chemisorption and catalysis at a molecular level.

In Chapter 8 *Leone* summarizes results from experimental and theoretical studies on bimolecular collision processes for ions in drift fields. Using laser spectroscopy it is now possible to make detailed measurements of state populations and spatial orientation of the ions. A correspondingly detailed form of spectroscopy for investigating simple ion-molecule reactions now seems to be within reach.

The book provides a critical appreciation of some current areas of research in kinetics, together with much useful background material. In the areas with which I am most familiar I found no gaps, inaccuracies or unreliable material. However, it is regrettable that there is scarcely any mention of the extensive studies that have been made of inelastic and reactive scattering in crossed molecular beams. The high price of DM 260.00 is also a drawback. To summarize, the book can be recommended to chemists with interests in this special field.

Karl Kleinermanns [NB 1041 IE]
Physikalisch-Chemisches Institut
der Universität Heidelberg (FRG)

VCH TransDict, Übersetzersoftware, Version 2.2. By *Ulrich Hellinger*. VCH Verlagsgesellschaft, Weinheim 1988. DM 780. ISBN 3-527-26873-1

Translation is an exacting process. Some call it an art, some a craft, some a boring task. At one extreme is the translation of, say, *Paul Celan*'s poetry. *Celan*, himself a polyglot and a prolific translator of other poets, including *Emily Dickinson* and *Robert Frost*, wrote in German. His poems are often difficult to understand in the original and, with their layers of allusion and borrowings from other languages, they are a challenge to translate. At the other extreme is the translation of the experimental protocol of a chemical synthesis. Here, what the linguist *Leonard Bloomfield* termed "operationally equivalent wordings" are required. The translation should merely allow repetition of the synthesis. However, the scientist who wants to publish in a foreign language, usually English, most likely confronts problems lying between these two extremes. The translation has to be accurate, that is, free of scientific ambiguity: a *Hydrierung* in German must be translated as a hydrogenation in English and not as a hydration (*Hydratisierung*). At the same time, the translation should do justice to the author's style of writing. *VCH TransDict* is a potentially useful tool for scientists and translators in meeting both requirements.

No, *TransDict* is not one of those computer programs that translates between several languages at the stroke of the return key. High-quality computer translation is a tantalizing goal. But not even Japan's Fifth Generation Computer Project, now in its ninth year, has been able to fulfill all the needs of the scientist publishing in a foreign language.

TransDict is basically a word-processing program that also allows rapid searching of electronic dictionaries and card files. It requires a computer operating with MS-DOS (version 2.1 or later), having at least a 640-kilobyte main memory, and equipped with a hard disk (20 megabytes or more) and a graphics card. The pull-down menus enable the user to

load, save, and print documents, to work simultaneously with several documents ("windows"), to mark, format, and move within the text, to search for and replace text elements, to make tables, to specify the parameters of the display screen and printer, to perform simple calculations, to create macros (sequences of commands performed together), and to access the disk operating system—in short, to carry out the essential operations of word processing. Simple keyboard codes (consisting of the control key plus a letter or number) are shown conveniently in the upper left-hand corner of the screen when the menus are activated. They allow most commands to be performed more quickly directly from the keyboard. Finally, a Help command provides an explanation of each function.

The dictionary menu, activated by pressing the Alt-W (for *Wörterbuch*) combination, provides access to electronic dictionaries, which can be searched for a particular word or according to phonetic criteria (for example, Hofman, Hofmann, Hoffman, and Hoffmann are treated identically). The user can also leaf—or, in computer jargon, scroll—through the dictionaries. Several German–English dictionaries are currently available on diskette, including a *Langenscheidt* dictionary and the *parat Dictionary of Information Technology*. One of these is included in the price of *TransDict*. In addition, file cards, containing up to ten lines with maximally 60 characters per line and 255 characters per card, can be created and searched in a similar fashion. Lists of words can also be saved under the dictionary function; they are stored chronologically but may be alphabetized by a subprogram. The individualized lists and file cards offer considerable leeway in establishing a personal style of writing in a foreign language.

TDRES, a subprogram containing only the dictionary and file-card functions, allows these to be used with many common word-processing programs such as *Microsoft Word* and *Wordstar*. This feature is especially valuable for writers accustomed to a particular program and should be offered separately at a lower price. An English version of *TransDict*, as well as a version suitable for the widely used Macintosh computer, should also be made available.

Of course, *TransDict* does not absolve the user from learning the grammar and syntax of a language, nor does it guarantee good usage. Only by reading as widely and as attentively as possible in a particular language is it possible to develop a good feel for what constitutes effective writing. Moreover, the electronic dictionaries eventually offered must be accurate and up-to-date. However, *TransDict* does facilitate the process of scientific translation by providing, at the touch of a finger, essential words, phrases, and concepts. Scientists writing the first version of their manuscript in a foreign language will find the software particularly useful.

Greater insight into the process of translation is provided by a recent book, *The Craft of Translation* (University of Chicago Press, Chicago, 1989), edited by *John Biguenet* and *Rainer Schulte*. This excellent collection of articles on the problems facing translators of literary texts includes an essay on the translation of *Celan*'s poetry. The author, *John Felstiner*, notes that "translating Celan—translating any poet, in fact—appropriates all the resources of interpretive criticism." There is a little of the poet in every scientist. Keeping this in mind will make the task of translating a scientific paper no less exacting, but certainly more interesting.

David I. Loewus [NB 1099 IE]
Angewandte Chemie, Weinheim (FRG)

Correspondence

Re: $[H_2Ru_6(CO)_{16}(\mu\text{-}C_6H_4O)]$: Binding of Five Metal Atoms to a Phenol Molecule by D. S. Bohle and H. Vahrenkamp, *Angew. Chem. 102* (1990) 202, *Angew. Chem. Int. Ed. Engl. 29* (1990) 198. We regret having overlooked that the compound mentioned in the title and its molecular structure had already been described previously by S. Bhaduri, K. Sharma, and P. G. Jones (*J. Chem. Soc. Chem. Commun. 1987*, 1769).

D. S. Bohle, H. Vahrenkamp
Institut für Anorganische und Analytische Chemie
der Universität Freiburg (FRG)

Registered names, trademarks, etc. used in this journal, even when not marked as such, are not to be considered unprotected by law.

© VCH Verlagsgesellschaft mbH, D-6940 Weinheim, 1990. – Printed in the Federal Republic of Germany by Konrad Triltsch Druck- und Verlagsanstalt Würzburg.

All rights reserved (including those of translation into foreign languages). No part of this issue may be reproduced in any form — by photoprint, microfilm, or any other means — nor transmitted or translated into a machine language without written permission from the publishers. Only single copies of contributions, or parts thereof, may be made for personal use. This journal was carefully produced in all its parts. Nevertheless, authors, editors and publisher do not warrant the information contained therein to be free of errors. Readers are advised to keep in mind that statements, data, illustrations, procedural details or other items may inadvertently be inaccurate.

Valid for users in the USA: The appearance of the code at the bottom of the first page of an article (serial) indicates the copyright owner's consent that copies of the article may be made for personal or internal use, or for the personal or internal use of specific clients. This consent is given on the condition, however, that the copier pay stated per-copy fee through the Copyright Clearance Center, Inc. (CCC), for copying beyond that permitted by Sections 107 or 108 of the U.S. Copyright Law. This consent does not extend to other kinds of copying, such as copying, for general distribution, for advertising or promotional purposes, for creating new collective works, or for resale. For copying from back volumes of this journal see 'Permissions to Photo-Copy: Publisher's Fee List' of the CCC.

Editorial office: Postfach 10 11 61, D-6490 Weinheim, Federal Republic of Germany, Telephone (06201) 60 22 55, Telex 465 516 vchwh d, Telefax (06201) 602 328.

Editor: *Peter Gölitz*

Associate editors: *D. I. Loewus, A. Stimson.* **Editorial assistant:** *E. Schweikart*

Publishers: VCH Verlagsgesellschaft mbH. (Managing Director: *Hans Dirk Köhler*), Pappelallee 3, D-6940 Weinheim, Federal Republic of Germany.

Advertising office (Advertising Manager *R. J. Roth*): Postfach 10 11 61, D-6940 Weinheim, Federal Republic of Germany, Telephone (0 62 01) 60 61 30, Telex 4 67 155, Telefax (0 62 01) 606 156.

ANGEWANDTE CHEMIE
International Edition in English
Volume 29 · Number 9
September 1990
Pages 939–1076

Gas Chromatographic Separation of Enantiomers on Cyclodextrin Derivatives**

New Analytical Methods (42)

By Volker Schurig* and Hans-Peter Nowotny

In investigations concerned with the phenomenon of molecular chirality, the use of gas chromatography for the enantiomeric analysis of stable, volatile compounds is a technique of steadily growing importance.[1] In the last three years an important breakthrough in gas-chromatographic separation of enantiomers has been achieved by using alkylated cyclodextrins (α, β, and γ) as chiral stationary phases in high-resolution capillary columns. In academic and commercial practice two different and complementary strategies have been adopted up to now. In the first, alkylated cyclodextrins are diluted with polysiloxanes and coated on glass or fused silica capillary columns. In the second, lipophilic per-*n*-pentylcyclodextrins and hydrophilic di-*n*-pentyl- and hydroxyalkylpermethylcyclodextrins are coated directly in the form of liquid phases onto suitably pretreated glass or fused silica surfaces. These techniques permit enantiomer separations not only for polar diols and alcohols, derivatized hydroxycarboxylic acids, amino acids, sugars, and alkyl halides, but also for nonpolar alkenes, cyclic saturated hydrocarbons, and metal π complexes. An important aspect for practical applications is that in many cases the enantiomers can be separated without previous derivatization. Whereas the resolution of racemates of unfunctionalized hydrocarbons is attributed to an enantioselective host–guest inclusion complex, some observations indicate that for polar guest molecules additional enantioselective interactions are also involved. The new chiral stationary phases can be used over a wide range of temperatures (25 to 250 °C). The technique described is likely to become widely adopted as a simple, accurate and highly sensitive method for the enantiomeric analysis of chiral compounds that can be vaporized without decomposition. It will also stimulate future research aimed at finding universal cyclodextrin phases and elucidating the mechanisms of enantioselectivity.

1. Introduction

The problem of determining enantiomeric compositions (enantiomeric excess, *ee*) is central to all contemporary research concerned with the synthesis, characterization, and use of chiral compounds.[1] Gas chromatography offers an accurate and reliable modern analytical method for separating enantiomers of compounds that can be vaporized without decomposition. Its inherent advantages include simplicity, speed, reproducibility, and sensitivity.[2–5]

The availability of high-resolution capillary columns—that is, wall-coated open-tubular (WCOT) columns—and the use of highly sensitive chromatographic detectors allow analyses to be carried out on nanogram quantities of sample, often without the need for tedious sample pretreatment.

[*] Prof. Dr. V. Schurig, Dr. H.-P. Nowotny [+]
Institut für Organische Chemie der Universität
Auf der Morgenstelle 18, D-7400 Tübingen (FRG)
[+] Present address: F. Hoffmann-La Roche
CH-4002 Basel (Switzerland)

[**] Gas Chromatographic Separation of Enantiomers on Optically Active Metal-Complex-Free Stationary Phases, Part 2: Part 1. [7].

Mixtures of different enantiomers can be separated simultaneously (e.g., all proteinogenic amino acids). By combining the method with ancillary techniques such as multidimensional chromatography and/or coupling to spectrometric methods, one can analyze enantiomers even in complex biological matrices. The use of an inert gas as the mobile phase avoids complications due to solvent effects and other variables, such as gradient elution and the use of buffers, modifiers, and additives, which influence liquid-chromatographic enantiomer separation.

The chiral stationary phases that have become particularly important in gas-chromatographic enantiomer separation belong to three classes:

1. amino acid derivatives which form hydrogen bonds[3] (e.g., the commercially available phases Chirasil-Val[4] and XE-60-L-Val(R)-α-pea)[5]
2. carbohydrate derivatives, notably cyclodextrins with a propensity to form inclusion complexes
3. metal complexes ("complexation gas chromatography")[6]

Stationary phases derived from amino acids have already been reviewed;[7] the present article deals with the use of cyclodextrin derivatives for gas-chromatographic separation of enantiomers.

In contrast to the stationary phases of classes 1 and 3, cyclodextrins have only been applied for routine enantiomer separation by high-resolution capillary gas chromatography during the last three years.

2. Cyclodextrins

Cyclodextrins—cycloamyloses, cycloglucans, or cyclomaltooligoses—were isolated as degradation products of starch by *Villiers* as long ago as 1891,[8] but it was not until 1904 that they were characterized by *Schardinger* as cyclic oligosaccharides (the "Schardinger dextrins").[9] Almost two decades before *Pedersen*'s synthesis of crown ethers,[10] *Freudenberg* and *Cramer* in 1948 recognized the ability of cyclodextrins to form molecular inclusion complexes.[11] Cyclodextrins are a homologous series of nonreducing cyclic oligosaccharides made up of six or more (α)-D-glucopyranose units linked together by α-1,4-glycoside bonds[12, 13] (Fig. 1[14]).

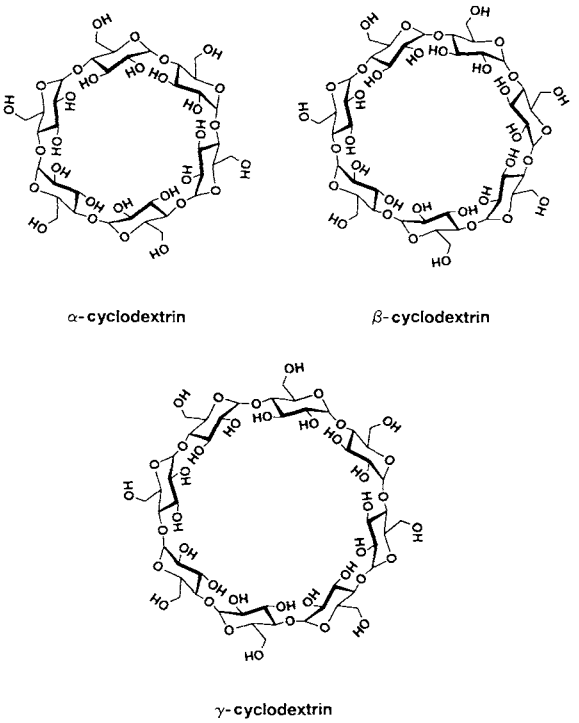

Fig. 1. α-Cyclodextrin (cyclohexaamylose), β-cyclodextrin (cycloheptaamylose), and γ-cyclodextrin (cyclooctylamylose) [14].

Cyclodextrins are obtained biotechnologically via enzymatic degradation of the glucose units of the polysaccharide starch by cyclodextrin glycosyltransferases of *Klebsiella pneumonia*, *Bacillus macerans*, or other types of bacillus. This reaction results in detachment of a turn from the starch helix accompanied by cyclization. The relative quantities of the individual cyclodextrins depend on the type of enzyme employed and can be influenced by the addition of organic compounds.[15]

So far, α-, β-, γ-, and δ-cyclodextrins with six to nine glucopyranose units have been isolated and characterized. Cyclodextrins with up to twelve glucopyranose units have been observed,[15, 16] but only the three lowest members of

Volker Schurig was born in 1940 in Dresden and began studies in chemistry in 1959 at the Universität Tübingen, where he received his doctorate under Ernst Bayer in 1968. He then spent two years in Israel as a postdoc at the Weizmann Institute of Science, where he began his work on the gas-chromatographic separation of enantiomers with Gil-Av. After pursuing this work at the University of Houston, he completed his "Habilitation" in Tübingen with work on complexation gas chromatography. He has been a guest professor at the Université Paris-Sud and the Weizmann Institute. His areas of interest include homogeneous catalysis with soluble polymeric metal compounds, the formation of highly ordered solid-state structures by chiral control, enzymatic epoxidations, chiral NMR shift reagents, chromatographic enantiomer separations, and the stereochemical analysis and synthesis of flavors and pheromones.

Hans-Peter Nowotny was born in Herrenberg in 1959 and began studies in chemistry in 1979 at the Universität Tübingen, where he received his doctorate under Volker Schurig in 1989 on enantiomer separation by inclusion gas chromatography on peralkylated cyclodextrins. He is presently employed by Hoffmann–La Roche in Basel.

the homologous series are at present commercially available (α, β, γ). Strained cyclodextrins with less than six glucopyranose units have not been observed up to now.

Each of the chiral glucose units of the cyclodextrins possesses a rigid $^4C_1$ chair conformation. The macrocyclic conformation of the cyclodextrins corresponds to a torus in both the solid state and in solution; the wider opening is occupied exclusively by secondary hydroxyl groups (C2-OH and C3-OH), while the opposite, narrower opening is occupied exclusively by primary hydroxyl groups (C6-OH). Table 1 lists some molecular dimensions and physical properties of the cyclodextrins.

Table 1. Molecular dimensions and physical data for cyclodextrins.

	Cyclodextrin		
	α	β	γ
Number of glucose units	6	7	8
Number of chiral centers	30	35	40
Molecular mass	972.86	1135.01	1297.15
External diameter [pm]	1370–1460	1530–1540	1690–1750
Internal diameter [pm]	470–520	600–650	750–850
Volume of cavity [nm^3]	0.176	0.346	0.510
pK_a of hydroxyl groups		12.1–12.6 (all)	
Solubility in water [g per 100 mL, 25 °C]	14.50	1.85	23.20
Molarity of saturated solution [M]	0.114	0.016	0.179
Melting and decomposition point [K]	551	572	540

It can be seen that the height of the molecular cavity is constant, whereas its diameter varies. The inside face of the torus comprises two sets of C-H groups (C3 and C5) and, between them, sets of glycoside ether linkages (C1 and C4). The cavity has a high electron density due to the lone pairs of the oxygen atoms. Because of the absence of hydroxyl groups directed inward, the cavity is both hydrophobic and nonpolar.[17] The outer hydroxyl groups at the cavity openings make the underivatized cyclodextrins hydrophilic. The macrocycle derives additional rigidity from the formation of stable intramolecular hydrogen bonds between secondary hydroxyl groups, O3-H···O'2 and O3···H-O'2.

The complexing properties of cyclodextrins, which can be regarded as empty molecular cavities of different sizes, have been thoroughly studied.[12–20] Hydrophobic interactions favor the formation of inclusion complexes. The propensity of cyclodextrins to form complexes with guest molecules is employed in many different technological applications.[15, 21] The observation that, by formation of inclusion complexes, the stability, solubility, bioavailability, residence time, toxicity, and odor properties of guest molecules are beneficially altered commands particular interest for the pharmaceutical and food industries.[14–16, 22]

Numerous X-ray structural studies have been carried out on a variety of inclusion complexes of β-cyclodextrin.[23, 24] In addition to 1:1 inclusion complexes, 2:1 host–guest complexes, in which the cyclodextrin molecules are linked by hydrogen bonds between the secondary hydroxyl groups, can also be formed. Studies on heptakis-(2,6-*O*-dimethyl)-β-cyclodextrin showed that protection of the free hydroxyl groups prevents the formation of cyclodextrin dimers and also that the presence of the methoxy groups can slightly increase the space available to a hydrophobic guest molecule compared with that of the cyclodextrin cavity itself.[24] This example illustrates that the conformation and complexing ability of cyclodextrins can be tailored by chemical modification.

In addition to host–guest selectivity, cyclodextrins exhibit some catalytic properties related to those of enzymes (competitive inhibition and Michaelis–Menten kinetics).[15, 16] Cyclodextrins have therefore been studied as enzyme models for α-chymotrypsin, carbonic anhydrase, and ribonuclease.[25]

A total synthesis of α-cyclodextrin has been achieved.[26] Derivatizations of cyclodextrins, such as alkylations and acylations, can be carried out regioselectively at the hydroxyl groups.[27] Monofunctionalizations,[28] a specific bifunctionalization,[29] and bridging across the cavity (yielding "capped cyclodextrins") have also been reported.[30]

The inherent molecular asymmetry of cyclodextrins, which arises from the fact that the cyclooligomers contain only D-glucose units, widens considerably the scope of potential applications. As a consequence of their biotechnological origin from natural starch, only the dextrorotatory enantiomers of cyclodextrins are known; the racemic forms and the levorotatory antipodes are not available. In many cases, the inclusion of chiral guest molecules into cyclodextrins represents an enantioselective process. Thus, different complex formation constants were found for the two fenchone enantiomers in ESR studies on the formation of inclusion complexes of β-cyclodextrin with (+)- and (−)-fenchone via the competitive displacement of a paramagnetic species from the cyclodextrin cavity.[3] Cyclodextrins have also been used as chiral auxiliary reagents in NMR spectroscopy. In the cyclodextrin complex of 2,2,2,-trifluoro-1-phenylethanol, for example, the CF_3 resonance of the (*S*)-(+) enantiomer appears at higher field than that of the (*R*)-(−) enantiomer.[32] A direct proof of the *enantioselective* complexation of (*R*)- and (*S*)-2-(3-phenoxyphenyl)-propanoic acids (fenoprofen) with β-cyclodextrin has recently been accomplished by crystal structure analysis.[33] The inclusion of optically inactive compounds in cyclodextrins can lead to a measurable circular dichroism, caused by the induction of chiral conformations.[18, 34, 35] Furthermore, diastereomers formed in β-cyclodextrin by the inclusion of a *prochiral* compound were distinguished by ENDOR measurements.[36] Numerous asymmetric catalytic reactions using cyclodextrins have also been described.[16, 37] Kinetic studies on the cyclodextrin-catalyzed hydrolysis of racemic oxazolones provided evidence for enantioselectivities that were of opposite senses for α- and β-cyclodextrins.[38]

An obvious method for separating racemic mixtures using enantioselective complexation in cyclodextrins is to carry out a fractional crystallization on the diastereomeric inclusion complexes. Indeed, racemic carboxylic acid esters, menthol and several carboxylic acids,[39, 40] *O*-alkyl alkylphosphinates,[41] sulfoxides,[42] *O*-alkyl alkylsulfinates,[43] and 2-bromo-2-chloro-1,1,1-trifluoroethane (halothane)[44] have been separated into their enantiomers in this way. However, the enantiomeric purity (*ee*) of the products was low in most cases. The highest reported value was *ee* = 84% for *O*-isopropyl methylphosphinate,[41] but this was only achieved after repeating three times the cycle of complexation, fractional crystallization, and release of the enriched

product. This cumbersome procedure is avoided when the reversible enantioselective inclusion reaction is coupled to a chromatographic (i.e., a multistage) separation process.[45-47]

3. Chromatographic Separation of Enantiomers on Cyclodextrins

Cyclodextrins are used in many chromatographic procedures for selective separations of compounds, including enantiomers.[47, 48] Table 2 gives a summary of representative applications.

Table 2. Applications of cyclodextrins in chromatography [47, 48]. S = in the stationary phase, M = in the mobile phase. Electrokinetic methods: electroosmosis, electrophoresis, isotachophoresis.

	Type of chromatography					
	Thin layer (TLC)	Gas-solid and gas-liquid (GSC, GLC)	Gel inclusion (GIC)	High-pressure liquid (HPLC)	Affinity (AFC)	Electrokinetic (EKC)
Cyclodextrins	M	S		M	M	M
Modified cyclodextrins	M	S		M/S		M
Soluble cyclodextrin polymers	M					
Insoluble cyclodextrin polymers		S	S			
Immobilized cyclodextrins	S			S	S	

In thin layer chromatography (TLC) cyclodextrins can be used as either the stationary or the mobile phase.[49] For example, aqueous solutions of α-cyclodextrin, dimethyl-β-cyclodextrin, γ-cyclodextrin, and soluble polymers of β-cyclodextrin have been used as chiral mobile phases.[47] β-Cyclodextrin itself is not suitable, since it is only sparingly soluble in water. However, its hydrophilicity can be improved by adding urea[50] or by partial derivatization to hydroxyethyl- or hydroxypropyl-β-cyclodextrin.[51] β-Cyclodextrins chemically bound to silica gel have also been used for separating enantiomers.[52, 53] Furthermore, cyclodextrins have been employed for separating enantiomers in electrokinetic chromatographic techniques such as capillary isotachophoresis (CITP)[54] and high-performance capillary zone electrophoresis (HPCZE).[55] Especially noteworthy is the use of cyclodextrins with singly charged substituents in inverse micellar electrokinetic chromatography, as described by *Terabe* et al.[57] In gel inclusion chromatography (GIC)[58] mandelic acid derivatives and indole alkaloids have been separated into their enantiomers both analytically and on a preparative scale on insoluble polymers of β-cyclodextrin.[46, 47, 59]

The use of cyclodextrins for separating enantiomers in high-pressure liquid chromatography (HPLC) has proved especially successful.[60-62] Unlike many of the well-known chiral stationary phases, the cyclodextrin stationary phases described so far are compatible with aqueous and strongly polar mobile phases in the reversed phase mode of operation. The cyclodextrin stationary phases can also be used with subcritical carbon dioxide (subFC) as the mobile phase.[63] Enantiomer separations by liquid chromatography on acetyl and carbamoyl derivatives of β-cyclodextrin have also been recently reported.[64, 65]

In HPLC, as in thin layer chromatography, cyclodextrins were initially used not as immobilized stationary phases but as additives in the mobile phase in conjunction with conventional reversed phases (RP-18).[45, 66] An important advantage of this approach is that the formation of the inclusion complex enhances the fluorescence,[67] giving an appreciable reduction in the lower limit of detection when a fluorescence detector is used. This principle has also been employed in a method whereby β-cyclodextrin as a chiral stationary phase is combined with β-cyclodextrin as an additive in the mobile phase.[68] Partially and fully methylated α- and β-cyclodextrins have also been applied as additives in the mobile phase.[69]

The use of cyclodextrins for gas-chromatographic separation of enantiomers will be described in Section 4.2.

4. Cyclodextrins in Gas Chromatography

4.1. Gas Chromatographic Separation of Achiral Compounds

As long ago as the early sixties, peracylated α- and β-cyclodextrins were used above their melting point (i.e., above 220 °C) as stationary phases in packed columns for the selective separation of fatty acid esters.[70] The analysis of the retention data did not provide conclusive evidence for the formation of inclusion complexes in this case. However, permethylated α- and β-cyclodextrins, when used above their melting point or as solutions in polysiloxane (DC-710) in packed columns, gave retention times that were greater for *iso*-alkanes than for *n*-alkanes, and this was attributed to the formation of inclusion complexes.[71] In gas-solid chromatography (GSC) α- and β-cyclodextrin polyurethane resins,[72] α-, β-, and γ-cyclodextrins,[73, 74] hexakis(2,6-di-*O*-methyl)-α-cyclodextrin, and heptakis(2,6-di-*O*-methyl)-β-cyclodextrin[75] were applied for the selective separation of positionally isomeric arenes (e.g., xylene and lutidine isomers); β-cyclodextrin polymers were found to be unsuitable for this purpose.[76] The packed columns used have low efficiencies, and consequently it was not possible to observe separation of enantiomers.[77] For applications in gas-liquid chromatography (GLC) the hydrophilic nature of underivatized cyclodextrins proved to be a disadvantage, since these require highly polar solvents as achiral stationary phases. This difficulty can be avoided by using peralkylated cyclodextrins, which are lipophilic and low-melting. The first breakthrough was obtained with permethyl-β-cyclodextrin and perpropanoyl-β-cyclodextrin, the latter being covalently bonded onto a polysiloxane.[78] Underivatized α- and β-cyclodextrins, dissolved in formamide or ethylene glycol allowed the separation of positional isomers of xylene, diethylbenzene,[79] and dimethylcyclohexane, as well as *cis*- and *trans*-decalin.[80] Even more remarkable is that with these packed columns the first gas-chromatographic separations of enantiomers on cyclodextrin phases were observed for pinenes and pinanes.[81, 82]

4.2. Gas Chromatographic Separation of Enantiomers of Chiral Compounds

Although numerous gas-chromatographic studies had already been carried out with cyclodextrin stationary phases, notably the pioneering experiments of *Smolková-Keulemansová* et al.,[73, 79, 83] the important breakthrough in enantiomer separation was only achieved quite recently through the use of high-resolution capillary columns. Thus, in a 1987 monograph on the practice of enantiomer separation by capillary gas chromatography, the great potential of cyclodextrins for separating enantiomers of nonpolar molecules is mentioned only in the preface by *Gil-Av*.[84] The attempts by *Kim* in 1981 to separate enantiomers of saturated aliphatic hydrocarbons with the general formula $CR^1R^2R^3R^4$ (R = alkyl), such as 2,2,3-trimethylheptane, on stainless steel capillaries coated with a solution of permethyl-β-cyclodextrin in polysiloxane (20% in OV-101) were unsuccessful, although the retention data led to the conclusion that inclusion complexes were formed.[85a] Finally, *Kościelski* et al., from 1983 onwards, achieved enantiomer separations of some chiral bicyclic alkenes (α- and β-pinene and carene) and bicyclic alkanes (*cis*- and *trans*-pinane) on packed columns in which the supporting material was coated with a solution of α-cyclodextrin in formamide (Fig. 2).[81, 82]

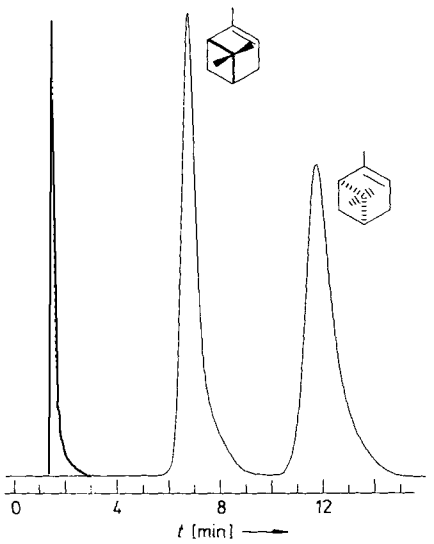

Fig. 2. Separation of the enantiomers of α-pinene on α-cyclodextrin in formamide solution supported on Celite at 44 °C. Packed column, 2 m × 4 mm. The chromatogram shown as a broken line was obtained on pure formamide (without cyclodextrin) supported on Celite. Carrier gas: helium, 2.75 bar [82].

As mentioned earlier, although these columns give large separation factors α for the enantiomers, they have very low efficiencies. Thus, the peak shapes are unusually broad, even for packed columns, as is evident from the low theoretical plate numbers of about 950–1250 for columns two meters long.[79] These columns therefore have lower efficiencies than cyclodextrin columns in HPLC, which give about 8000 theoretical plates for a length of 25 cm.[61] The method is also found to have other disadvantages, namely, the limited temperature range (maximum 70 °C), the short lifetime of the columns owing to the continual loss of solvent and water molecules, which are necessary for separation,[85b] by bleeding, and the fact that the method cannot be adapted for use with capillary columns. This has led to a considerable growth of interest in the development of thermally stable cyclodextrin phases for use in high-resolution capillary columns.

4.3. The Choice of Cyclodextrin Derivatives as Chiral Stationary Phases for High-Resolution Gas Chromatographic Separation of Enantiomers

Because of the physical properties of *underivatized* cyclodextrins, especially their decomposition on melting and their insolubility in polysiloxanes, they appear to be unsuitable for coating capillary columns. On the other hand, many cyclodextrin derivatives with more favorable melting points and/or solubilities are known.[27] Owing to the lability of cyclic oligosaccharides in acid media, only derivatizations carried out in alkaline media can be considered. Peracylated and partially or fully methylated cyclodextrins have already been used as stationary phases in gas chromatography on packed columns.[70, 71] It is essential that the C–O bonds at the chiral centers C2 and C3 remain intact during the acylation or alkylation of the hydroxyl groups in order to avoid epimerizations. In planning the derivatization strategy one must take into account the fact that the newly introduced groups at the wider end of the cyclodextrin torus may participate in the chiral recognition process.[62, 86]

Alkylation offers a number of advantages over acylation:

1. Since the ether group is more stable than the ester group, alkylated derivatives are chemically and thermally more stable and less susceptible to hydrolysis. It can be assumed that the alkoxy groups at the periphery of the cyclodextrin molecule have thermal stabilities similar to those of the glycoside ether linkages in the cyclodextrin skeleton, and the maximum temperature for use as a stationary phase is therefore limited solely by the stability of the cyclodextrin skeleton.

2. Per-*O*-alkyl derivatives are less polar than per-*O*-acyl derivatives. Consequently, the former have lower melting points and are more soluble in nonpolar polysiloxanes.

The C2 hydroxyl group is more acidic and the C6 hydroxyl group is less sterically hindered than the C3 hydroxyl group. Consequently peralkylations do not always proceed to completion. However, this fact can be used advantageously for regioselective derivatization.[87]

In the first enantiomer separations performed by high-resolution capillary gas chromatography, molten permethylated β-cyclodextrin was used, initially by *Juvancz, Alexander*, and *Szetjtli*[88, 89] and later by *Venema* and *Tolsma*.[90] On the other hand, *Schurig* and *Nowotny*[91, 92] employed a solution of permethylated β-cyclodextrin in a moderately polar polysiloxane (e.g., OV-1701) as enantioselective stationary phase. The following cyclodextrin derivatives have successfully been used in solution as stationary phases for gas-chromatographic separation of enantiomers (see Section 5):[91–98]

heptakis(2,3,6-tri-*O*-methyl)-β-cyclodextrin (**1**)
hexakis(2,3,6-tri-*O*-methyl)-α-cyclodextrin (**2**)

octakis(2,3,6-tri-*O*-methyl)-γ-cyclodextrin (**3**)
heptakis(2,6-di-*O*-methyl-3-*O*-trifluoroacetyl)-β-cyclodextrin (**4**)
octakis(2,6-di-*O*-methyl-3-*O*-trifluoroacetyl)-γ-cyclodextrin (**5**)
heptakis(3-*O*-heptafluorobutanoyl-2,6-di-*O*-methyl)-β-cyclodextrin (**6**).

The following derivatives have also been investigated, and, although they can be used, they exhibit lower separation factors α:[92]

heptakis(2,6-di-*O*-methyl)-β-cyclodextrin (**7**)
heptakis(2,3,6-tri-*O*-ethyl)-β-cyclodextrin (**8**)
heptakis(2,3,6-tri-*O*-*n*-propyl)-β-cyclodextrin (**9**)
heptakis(2,3,6-tri-*O*-*n*-butyl)-β-cyclodextrin (**10**)
heptakis(2,3,6-tris-*O*-(*S*)-2′-methylbutyl)-β-cyclodextrin (**11**)
heptakis(2,3,6-tris-*O*-trimethylsilyl)-β-cyclodextrin (**12**)

The high melting points of undiluted permethylated cyclodextrins are found to be a disadvantage. Only one of these, **1**, is liquid over a relatively broad range of temperatures and is suitable in the molten state as a stationary phase. Values for the melting point given in the literature vary from 83 to 175 °C.[71, 78, 88, 89] These discrepancies may be explained by the presence of inhomogeneous, incompletely methylated products. *Venema* and *Tolsma*,[90] on the basis of calorimetric measurements, arrived at a melting point of 150 °C for **1**. However, on cooling, **1** did not crystallize but instead gave a supercooled melt, which afforded very good chromatographic results at temperatures above 76 °C. Commercially available **1** can contain 2,6-di-*O*-methyl-β-cyclodextrin.[99]

König and *Wenz*[100] found that per-*n*-pentylated cyclodextrins are liquids even below room temperature. They employed the following cyclodextrin derivatives very successfully for separating enantiomers of many different racemic mixtures on deactivated glass capillary columns (see Section 6):[100–117]

hexakis(2,3,6-tri-*O*-*n*-pentyl)-α-cyclodextrin (**13**)
hexakis(3-*O*-acetyl-2,6-di-*O*-*n*-pentyl)-α-cyclodextrin (**14**)
heptakis(2,3,6-tri-*O*-*n*-pentyl)-β-cyclodextrin (**15**)
heptakis(3-*O*-acetyl-2,6-di-*O*-*n*-pentyl)-β-cyclodextrin (**16**)
octakis(2,3,6-tri-*O*-*n*-pentyl)-γ-cyclodextrin (**17**)
octakis(3-*O*-butanoyl-2,6-di-*O*-*n*-pentyl)-γ-cyclodextrin (**18**)

Armstrong et al.[118–123] used the following partially alkylated, liquid cyclodextrin derivatives as stationary phases on untreated fused silica capillary columns for gas-chromatographic separation of enantiomers:

hexakis(*O*-(*S*)-2-hydroxypropyl-per-*O*-methyl)-α-cyclodextrin (PMHP-α-CD, **19**)
heptakis(*O*-(*S*)-2-hydroxypropyl-per-*O*-methyl)-β-cyclodextrin (PMHP-β-CD, **20**)
hexakis(2,6-di-*O*-*n*-pentyl)-α-cyclodextrin (dipentyl-α-CD, **21**)
heptakis(2,6-di-*O*-*n*-pentyl)-β-cyclodextrin (dipentyl-β-CD, **22**)
heptakis(2,6-di-*O*-*n*-pentyl-3-*O*-trifluoroacetyl)-β-cyclodextrin (DPTFA-β-CD, **23**)

Compounds **19**–**22** all have free hydroxyl groups which make these moderately polar derivatives hydrophilic. As has been shown by ^{252}Cf mass spectrometry, the derivatives are present as partially alkylated mixtures, which give rise to the desired liquid consistency. For many racemic mixtures, the order in which the enantiomers are eluted is reversed if the stationary phase is changed from **19** to **20** or from **21** to **22**.[118]

5. Gas Chromatographic Separation of Enantiomers on Diluted Cyclodextrin Derivatives

Solutions of peralkylated cyclodextrins in moderately polar polysiloxanes, either in packed columns as described by *Casu* et al.[71] or in capillary columns as described by *Schurig* and *Nowotny*,[91, 92] are useful for the gas-chromatographic separation of enantiomers for the following reasons:

1. The diluted phase can be used over a wide range of temperatures. The essential requirement is that the cyclodextrin derivatives must be soluble in polysiloxanes; their melting points and phase transitions are unimportant. In principle, it is also possible to employ mixtures of different cyclodextrins (α, β, and γ) simultaneously and to incorporate suitable additives for competitive inclusion.
2. Coating the solutions onto glass or fused silica capillary columns, whose surfaces can be deactivated by high-temperature silylation to give very inert columns,[124] results in separations with high efficiency, even for strongly polar substrates.
3. The choice of appropriate solvents allows the polarity of the stationary phase to be varied over a wide range, independently of the nature of the derivatization of the cyclodextrins.
4. Only small quantities of the substances in solution are needed, allowing the economical use of cyclodextrins that are difficult to obtain (γ and δ cyclodextrins).
5. The low concentrations of cyclodextrins give short analysis times, and experience so far indicates that this does not reduce the separation factors α.
6. Thermodynamic parameters involved in enantiomer discrimination ($\Delta_{R,S}(\Delta G^\circ)$, $\Delta_{R,S}(\Delta H^\circ)$, and $\Delta_{R,S}(\Delta S^\circ)$) can readily be determined from relative retention data using the concept of the retention increase R' derived for complexation gas chromatography.[6, 125]

Peralkylated cyclodextrins of low molecular mass are preferred because, for example in *n*-pentylated cyclodextrins, the conformationally flexible *n*-pentyl groups probably do not contribute to chiral recognition, and they also shield the cavity to some extent.

The polydimethylsiloxane OV-101 (100% methyl groups) has proved to be a versatile solvent for optically active metal chelates in complexation gas chromatography.[6] On suitably prepared glass or fused silica capillary columns it forms stable films. Glass capillary columns coated with a solution of **1** in OV-101 can separate enantiomers of many chiral compounds above 80 °C;[92] below this temperature, peak broadening occurs. It appears that at low temperatures the limit of the solubility of cyclodextrins in the highly nonpolar polysiloxane is reached. Compound **1** is soluble in the poly-

methylphenylsiloxanes DC-550 (75% methyl, 25% phenyl) and OV-17 (50% methyl, 50% phenyl) even at room temperature, thus allowing enantiomer separations to be performed also at low temperatures; however, these phases do not form stable films on glass surfaces.

5.1. Heptakis(2,3,6-tri-*O*-methyl)-β-cyclodextrin (1) in OV-1701

OV-1701 is a polysiloxane of higher viscosity (a "gum" phase, with 5% cyanopropyl groups, 7% phenyl groups, and 88% methyl groups). It has a polarity comparable to that of OV-17 and forms very stable films on suitably pretreated glass or fused silica capillary columns. Solutions of **1** in OV-1701 are ideal for gas-chromatographic separation of selected enantiomers between 25 and 200 °C.[91–93] Enantiomer separations can be performed for the following classes of compounds: cyclic ethers such as 2,5-dimethyltetrahydrofuran, underivatized cyclic and acyclic ketones, γ-lactones, terpene ketones (e.g., pulegone), underivatized *secondary* aliphatic alcohols, aromatic alcohols, terpene alcohols (e.g., 3-menthanols), underivatized aliphatic diols, esters of 2-bromopropanoic acid, 1,3-dioxolanes, aliphatic and aromatic oxiranes such as phenyloxirane, bicycloalkenes (α- and β-pinene), and bicycloalkanes (*cis*- and *trans*-pinane). Selected examples of the first enantiomer separations achieved are shown in Figure 3.

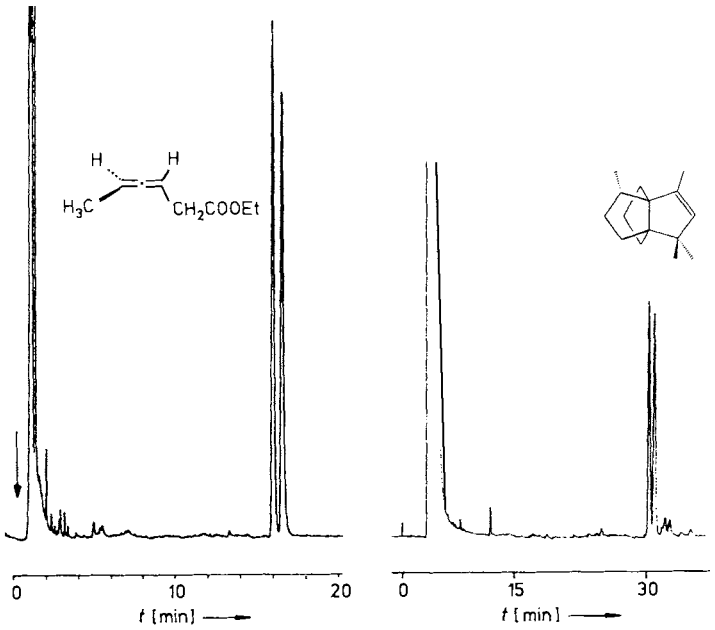

Fig. 4. Separation of the enantiomers of the allene ethylhexa-3,4-dienoate (left) and of the propellane modhephene (right) on **1** in OV-1701 (0.07 M) at 105 °C (left) and 65 °C (right). Deactivated fused silica capillary columns, 40 m × 0.25 mm I.D. (left) and 25 m × 0.25 mm I.D. (right). Carrier gas: H_2, 0.7 bar (left) and 1 bar (right).

Enantiomer separations of particular interest are those for an allene and for an unsaturated propellane (see Fig. 4), as well as the enantiomer separation of unfunctionalized saturated monocyclic hydrocarbons (Fig. 5).[94]

The high degree of deactivation of the fused silica capillary columns used can be seen from the enantiomer separation of underivatized polar diols;[98] no adsorption effects are pres-

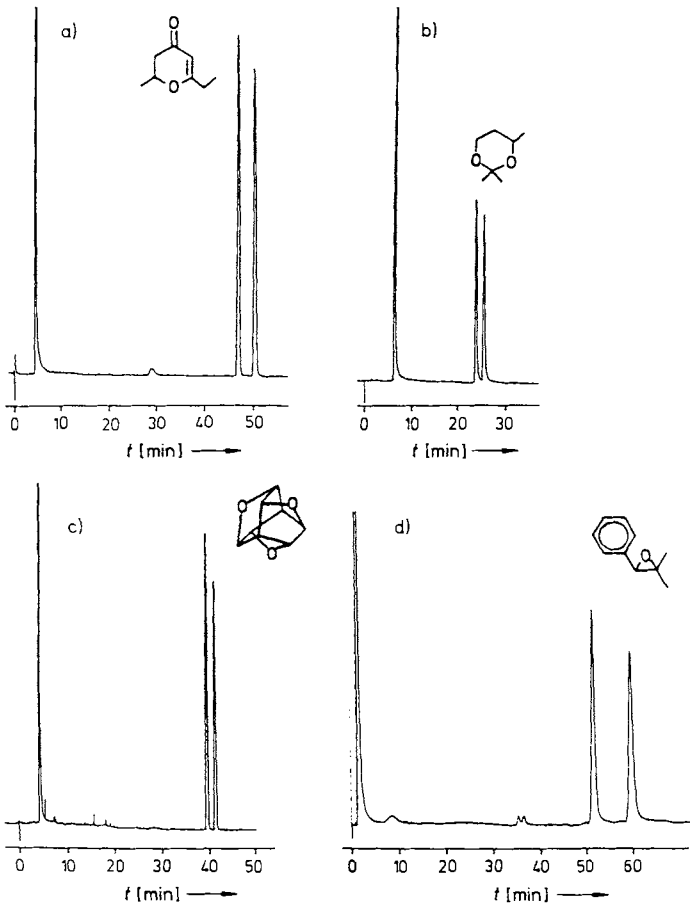

Fig. 3. Separation of the enantiomers of a) 2-ethyl-6-methyl-5,6-dihydro-γ-pyrone, b) 2,2,4-trimethyl-1,3-dioxane, c) 4,7,11-trioxapentacyclo-[6.3.0.$0^{2,6}$.$O^{3,10}$.$O^{5,9}$]undecane [126], and d) 2,2-dimethyl-3-phenyloxirane on **1** in OV-1701 (0.07 M) at 100 °C (a), 60 °C (b and e), 125 °C (c), and 50 °C (d). Glass capillary column, 40 m × 0.25 mm I.D. Carrier gas: 1 bar N_2(a), 0.7 bar N_2(b), 1 bar He (c and d) [93].

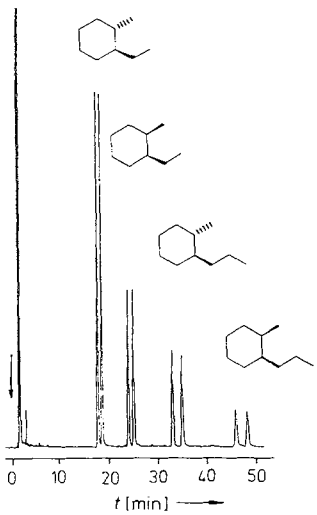

Fig. 5. Separation of the enantiomers of *cis*/*trans*-1-ethyl-2-methylcyclohexane and of *cis*/*trans*-1-methyl-2-*n*-propylcyclohexane on **1** in OV-1701 (0.07 M) at 50 °C. Deactivated fused silica capillary column, 30 m × 0.25 mm I.D. Carrier gas: H_2, 1.5 bar [94].

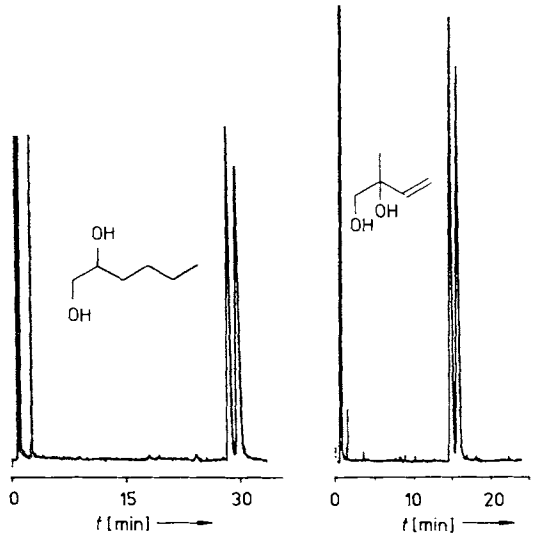

Fig. 6. Separation of the enantiomers of *n*-hexan-1,2-diol and 2-methyl-3-buten-1,2-diol on **1** in OV-1701 (0.07 M) at 75 °C. Deactivated fused silica capillary column, 25 m × 0.25 mm I.D. Carrier gas: H_2, 1 bar [97].

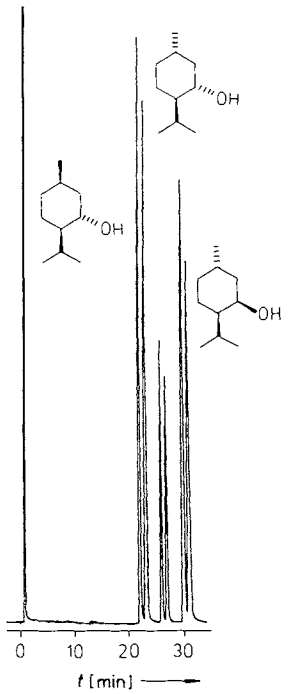

Fig. 7. Separation of the enantiomers of neomenthol, menthol, and isomenthol on **1** in OV-1701 (0.07 M) at 85 °C. Deactivated fused silica capillary column, 25 m × 0.25 mm I.D. Carrier gas: H_2, 1 bar [97].

ent, as is evident from the symmetrical shape of the peaks and the high efficiency of separation (Fig. 6).

Besides enantioselectivity, **1** in OV-1701 shows a pronounced diastereoselectivity, which can be exploited for analytical purposes, as illustrated by the separation of the diastereomeric 3-menthanols (Fig. 7).[97]

5.2. Hexakis(2,3,6-tri-*O*-methyl)-α-cyclodextrin (2) and Octakis(2,3,6-tri-*O*-methyl)-γ-cyclodextrin (3) in OV-1701

It was thought that altering the dimensions of the cyclodextrin cavity would offer a way of influencing the observed enantioselectivity. This assumption was only partly verified in practice,[92] since the enantioselectivities of **1** and **2** are found to overlap. However, **2** shows a distinct selectivity for phenyloxiranes.[92]

The molecular cavity in **3** is large enough to accommodate compounds such as the spiroketals *trans*-2,3-dimethyl-1,4-dioxaspiro[4.4]nonane (Fig. 8) and 2-ethyl-1,6-dioxaspiro-

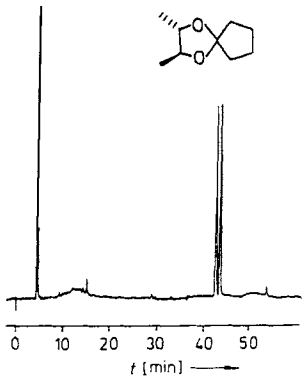

Fig. 8. Separation of the enantiomers of *trans*-2,3-dimethyl-1,4-dioxaspiro[4.4]nonane on **3** in OV-1701 (0.07 M) at 60 °C. Glass capillary column, 40 m × 0.25 mm (I.D.). Carrier gas: 1 bar H_2 [92].

[4.4]nonane and to separate them into their enantiomers.[92] For many of the enantiomers that can be separated on **3**, overlapping was observed with **1** and **2**.[92] Surprisingly, however, **3** showed no enantioselectivity for chiral saturated cyclic hydrocarbons.

5.3. Higher Alkylated Cyclodextrin Derivatives in OV-1701

Peralkylated cyclodextrins with longer *n*-alkyl groups are also soluble in OV-1701 and are suitable for gas-chromatographic separation of enantiomers, giving enantioselectivities that are in some cases different.[92] Since these cyclodextrin derivatives have greater molar masses (with 21 alkyl groups per β-cyclodextrin molecule), their solutions must contain a larger mass fraction of the cyclodextrin to give the same molar concentration. Thus, a 0.07 M solution of permethyl-β-cyclodextrin (**1**) corresponds to 10 wt%, whereas 0.07 M solutions of perethyl-β-cyclodextrin (**8**), per-*n*-propyl-β-cyclodextrin (**9**), and per-*n*-butyl-β-cyclodextrin (**10**) correspond to 12, 14, and 16 wt%, respectively.

Enantiomer separations using diluted per-*n*-pentyl-β-cyclodextrin (**15**) have also been described recently.[127] Surprisingly, blocking of the wider opening of the cyclodextrin torus in **11** by (*S*)-configurated *sec*-pentyl groups did not result in a change in enantioselectivity.[92]

5.4. Heptakis(2,6-di-*O*-methyl-3-*O*-trifluoroacetyl)-β-cyclodextrin (4), Octakis(2,6-di-*O*-methyl-3-*O*-trifluoroacetyl)-γ-cyclodextrin (5), and Heptakis(2,6-di-*O*-methyl-3-*O*-heptafluorobutanoyl)-β-cyclodextrin (6) in OV-1701

The β-cyclodextrin derivatives **4**–**6**,[93,95] derived from heptakis(2,6-di-*O*-methyl)-β-cyclodextrin by selective per-

fluoroacylation at the 3-position, give different enantioselectivities in some cases. This is attributed to the fact that the perfluoroacyl groups are able to form additional hydrogen bonds and to induce dipole–dipole interactions. The separation factors for γ-lactones are considerably greater on **4** (Fig. 9) than on **1**, and the increase in size of the cyclodextrin cavity in **5** gives favorable enantioselectivities for δ-lactones. On the other hand, these perfluoroacylated cyclodextrin derivatives cannot be employed for enantiomer separations of chiral monocyclic alkenes and alkanes. Compound **6** is particularly suitable for separating enantiomers of cyclic and acyclic ketones.[95, 96]

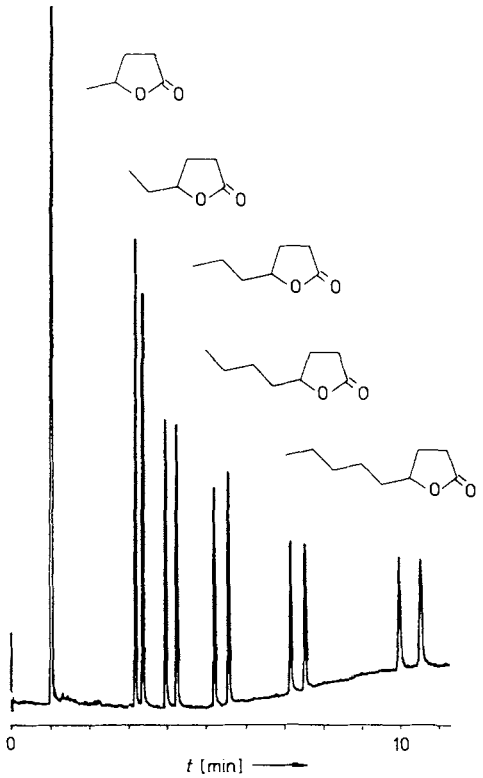

Fig. 9. Separation of the enantiomers of γ-lactones on **4** in OV-1701 (0.07 M) at 160 °C (4 °C min^{-1}). Deactivated fused silica capillary column, 25 m × 0.25 mm I.D. Carrier gas: H_2, 1.3 bar [97].

A dimeric cyclodextrin derivative, bis(permethyl-β-cyclodextrin)glutarate, showed no enantiomer separating properties,[96] despite the fact that this compound was expected to exhibit *cooperative* inclusion behavior.[128, 129]

6. Gas Chromatographic Separation of Enantiomers on Undiluted Liquid Cyclodextrin Derivatives

By introducing *n*-alkyl groups with longer chains (pentyl, hexyl, lauryl), *König* et al. were able to obtain liquid cyclodextrin derivatives preferentially suited for gas-chromatographic separation of many types of compounds on deactivated glass capillary columns.[100–117] These are prepared from α-, β-, or γ-cyclodextrin: for example, regioselective reaction of the cyclodextrin with *n*-pentyl bromide in the presence of a threefold excess of NaOH in dimethyl sulfoxide yields the 2,6-di-*n*-pentylated derivatives.[130] The 3-hydroxyl groups are then further alkylated (in this example, with *n*-pentyl bromide/NaOH) or are acylated using an acyl halide. Per-*n*-pentylcyclodextrins are thermally stable, viscous liquids, which are colorless at room temperature and can be coated onto appropriately deactivated glass surfaces.

The results of *König* et al.[105] more than confirmed the prediction made in 1987 by *Szejtli*,[48] one of the pioneers of cyclodextrin research, who wrote: "It is expected that good complex forming low-melting derivatives of cyclodextrins in capillary columns will result in excellent chiral recognition and resolution of many racemates."

Indeed, the regioselective alkylation and acylation open up the way to a wide variety of possible cyclodextrin stationary phases for gas-chromatographic separation of enantiomers. The range of enantiomer-separation applications

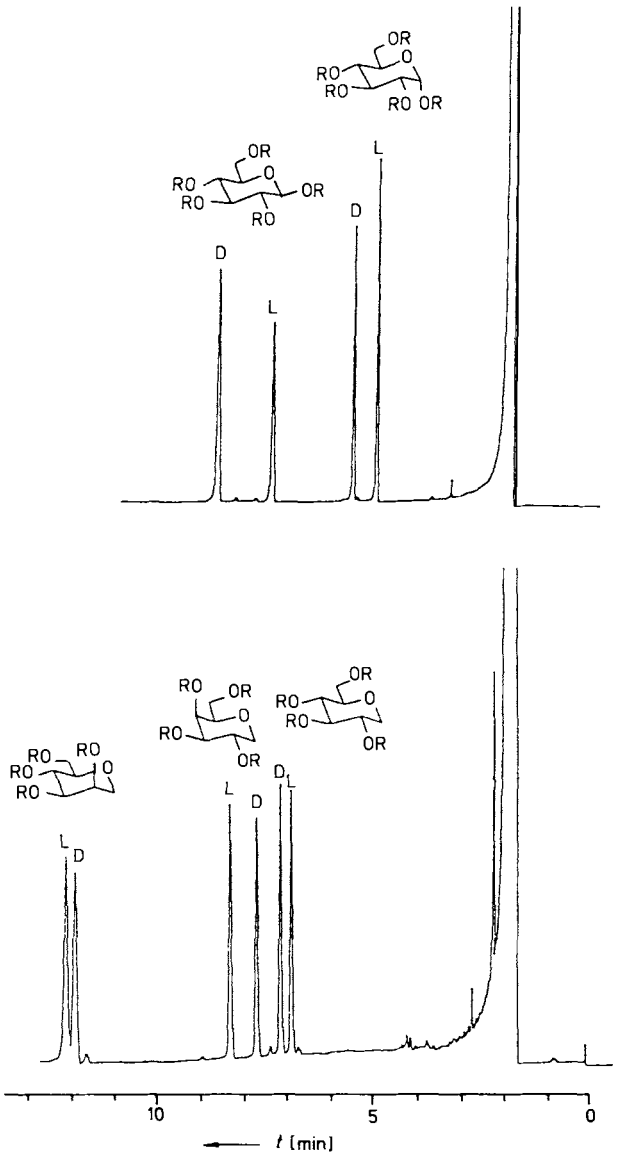

Fig. 10. Separation of the enantiomers of pertrifluoroacetylated carbohydrates and anhydroalditols on **13** at 115 °C and 120 °C. Glass capillary column, 40 m. Carrier gas: H_2, 1 bar. Top: α- and β-glucopyranose. Bottom: 1,5-anhydroglucitol, -galactitol, and -mannitol (R = CF_3CO) [108].

extends from trifluoroacetylated amino and hydroxyl compounds, including carbohydrates, derivatized amino acids, olefins, alkyl halides, and spiro- and bicyclic acetals to diolefin π complexes of metal carbonyls.

6.1. Hexakis(2,3,6-tri-*O*-*n*-pentyl)-α-cyclodextrin (13)

This *lipo*philic cyclo*dex*trin (Lipodex A) stationary phase, which is soluble in dichloromethane, can be used on glass capillary columns to separate racemates of trifluoroacetylated alcohols,[102] epoxy alcohols,[112] diols, triols, carbohydrates (Fig. 10),[108] underivatized 4-methyl-3-heptanone,[106] alkyl halides,[110] spiroacetals,[110] and glycerol derivatives. This phase, or its per-*n*-hexylated analogue, has also been used to resolve enantiomers of *N*-alkylated barbiturates.[116]

6.2. Hexakis(3-*O*-acetyl-2,6-di-*O*-*n*-pentyl)-α-cyclodextrin (14)

This lipophilic cyclodextrin (Lipodex B) stationary phase is particularly effective for separating racemic five-membered heterocycles such as γ-lactones, cyclic carbonates of 1,2-diols, and succinimides.[107] High separation factors are also achieved with this phase for racemic trifluoroacetylated carbohydrates and hydroxy compounds such as aldols, cyanohydrins, and amino alcohols.[106]

6.3. Heptakis(2,3,6-tri-*O*-*n*-pentyl)-β-cyclodextrin (15)

This lipophilic cyclodextrin (Lipodex C) stationary phase allows trifluoroacetylated alcohols, trifluoroacetylated carbohydrates, lower homologues of hydroxycarboxylic acid esters, and cyanohydrins to be separated into their enantiomers.[113] Especially noteworthy is the separation of the enantiomers of the pheromone grandisol, which succeeded despite the fact that the trifluoroacetylated hydroxyl group is separated from the chiral center by two carbon atoms (Fig. 11).

This phase can also be used to resolve the enantiomers of acyclic, monocyclic, and bicyclic olefins and dienes.[109, 113] Here, the enantioselective inclusion process was found to be sensitive to small changes in the structure of the substrate. Thus, 4-methyl-1-hexene and 4-methylcyclohexene could not be separated, in contrast to the 3-methyl isomers. This phase also showed enantioselectivity for cyclic and acyclic alkyl halides with up to eight carbon atoms.[113] For example, racemic mixtures of the 2-chloroalkanes from 2-chlorobutane up to 2-chlorooctane have been resolved (Fig. 11). In contrast to the higher homologues 1,2-dibromoheptane and 1,2-dibromooctane, 1,2-dibromohexane could also be separated into its enantiomers.

6.4. Heptakis(3-*O*-acetyl-2,6-di-*O*-*n*-pentyl)-β-cyclodextrin (16)

This lipophilic cyclodextrin (Lipodex D) stationary phase, whose acetyl groups are capable of forming hydrogen bonds,[106] allows enantiomer separations to be carried out

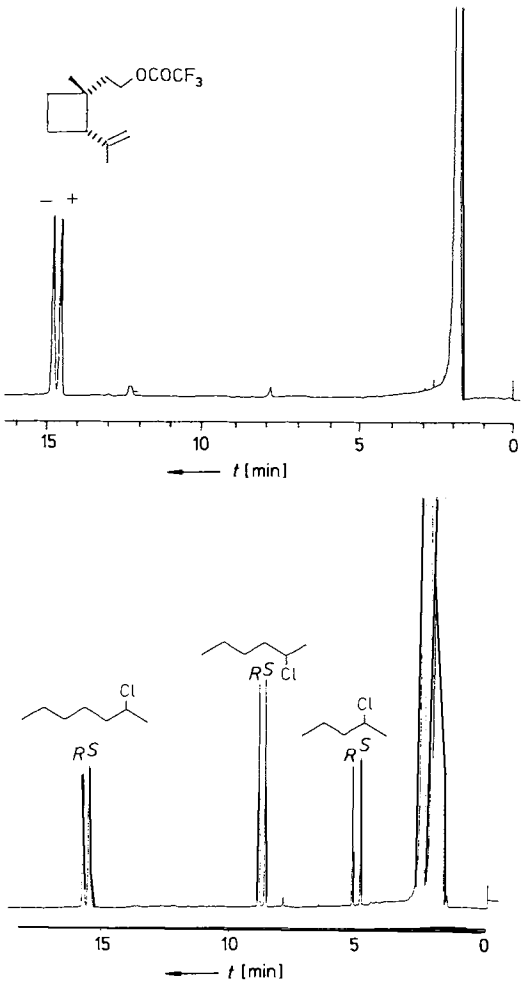

Fig. 11. Separation of the enantiomers of grandisol (top) and alkyl halides (bottom) on **15** at 90 °C and 50 °C, respectively. Glass capillary column, 42 m. Carrier gas: H_2, 1 bar [113].

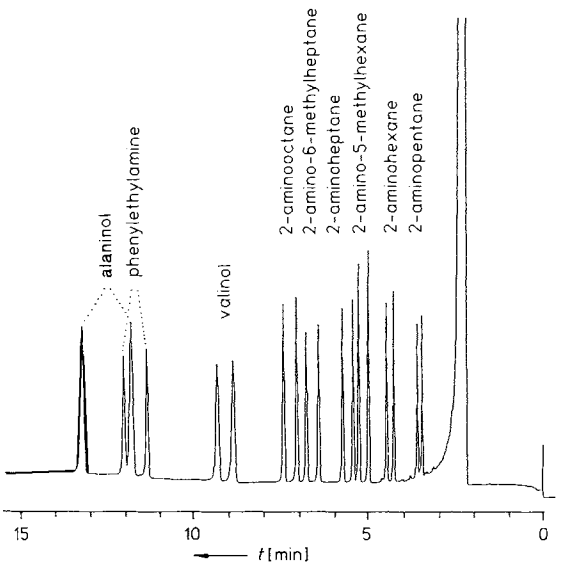

Fig. 12. Separation of the enantiomers of trifluoroacetylated amines and amino alcohols on **16** at 140 °C (2 °C min^{-1}). Glass capillary colum, 45 m. Carrier gas: H_2, 1 bar [103].

on polar compounds such as trifluoroacetylated amines with α- and β-chirality, amino alcohols, esters of β-amino acids, and cyclic *trans*-diols[103] (Figs. 12 and 13).

The presence of the acetyl group gives particularly high separation factors α for trifluoroacetylated amines and amines containing additional functional groups. Many of these derivatized amines could not previously be separated into their enantiomers on amino acid derivatives as stationary phases. Separation of the enantiomers of the methyl ester of α-lipoic acid can also be achieved using **16**.[115]

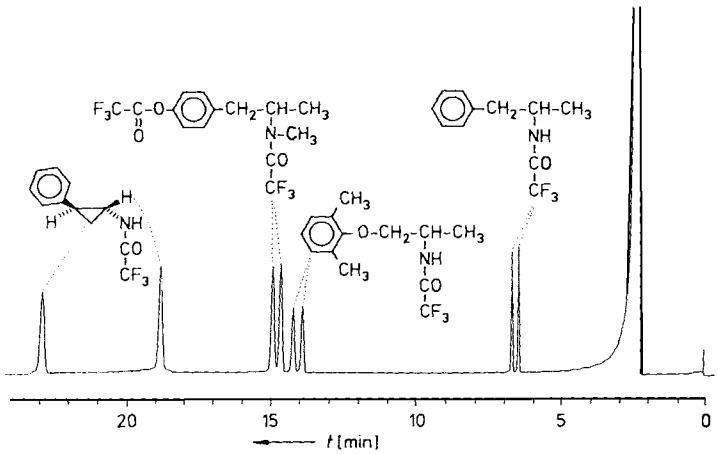

Fig. 13. Separation of the enantiomers of trifluoroacetylated amphetamine, mexiletine, pholedrin, and tranylcypromin (from right to left) on **16** at 175 °C. Glass capillary column, 45 m. Carrier gas: H_2, 1 bar [103].

6.5. Octakis(2,3,6-tri-*O*-*n*-pentyl)-γ-cyclodextrin (17) and Octakis(3-*O*-butanoyl-2,6-di-*O*-*n*-pentyl)-γ-cyclodextrin (18)

For γ-cyclodextrins the greater diameter of the cavity, the increased conformational flexibility of the macrocycle, and the fact that these compounds have been found to form unstable inclusion complexes[49] lead one to expect a reduction in enantioselectivity. Instead, *König* et al.[114, 115] found that **17** and **18** were suitable for separating enantiomers of various types of compounds, giving large separation factors in some cases. Especially noteworthy is the separation of enantiomers of nonpolar substrates such as alkenes with β-chirality: for example, 2,4-dimethyl-1-heptene, the planar-chiral alkene *trans*-3,3,8,8-tetramethylcyclooctene, and the planar-chiral metal carbonyl π complexes tricarbonyl (η^4-2-methylene-1,3-butanediyl)iron(0), and tricarbonyl(η^4-2-methyl-1,3-butadiene)iron(0) have been separated on the hydrophobic liquid **17** (Fig. 14).[115]

Racemic α-alkyl and *N*-methyl α- and β-amino acids in the form of *N*-trifluoroacetyl-*O*-methyl derivatives have also been resolved into their enantiomers on **18**.[114] Except in the case of proline, the D enantiomers of α-amino acids are eluted before the L antipodes, thus facilitating determination of the enantiomeric purity of naturally occurring L-amino acids. However, histidine, tyrosine, and arginine have so far turned out to be unsuitable for analysis.

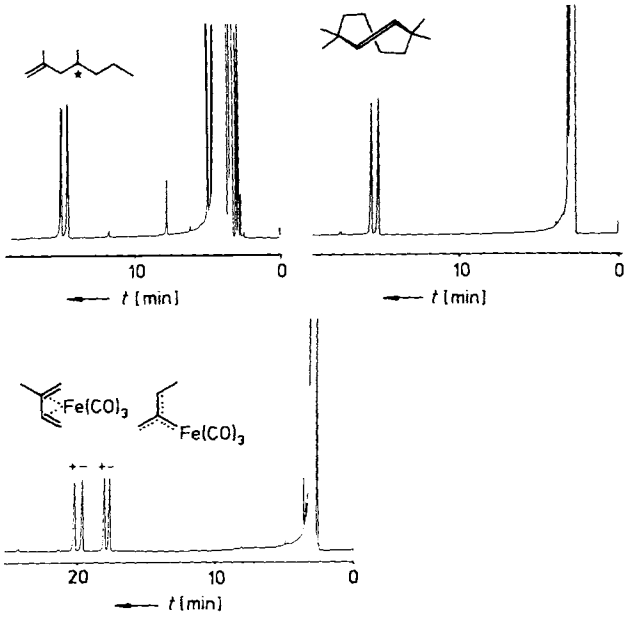

Fig. 14. Separation of the enantiomers of 2,4-dimethyl-1-heptene (top left), *trans*-3,3,8,8-tetramethylcyclooctene (top right), and tricarbonyl(η^4-2-methylene-1,3-butanediyl)iron(0) and tricarbonyl(η^4-2-methyl-1,3-butadiene)iron(0) [117] (bottom) on **17** at 60 °C, 95 °C, and 80 °C, respectively. Deactivated glass capillary column, 50 m. Carrier gas: H_2, 1 bar [115].

O-trifluoroacetylated esters of α- and β-hydroxycarboxylic acids can also be resolved, including the esters of tartaric, malic, and mandelic acid.

Racemic alcohols and diols have been resolved in derivatized form as trifluoroacetyl esters, and a number of terpene ketones such as fenchone, menthone, isomenthone, and camphor have been resolved without derivatization (Fig. 15).

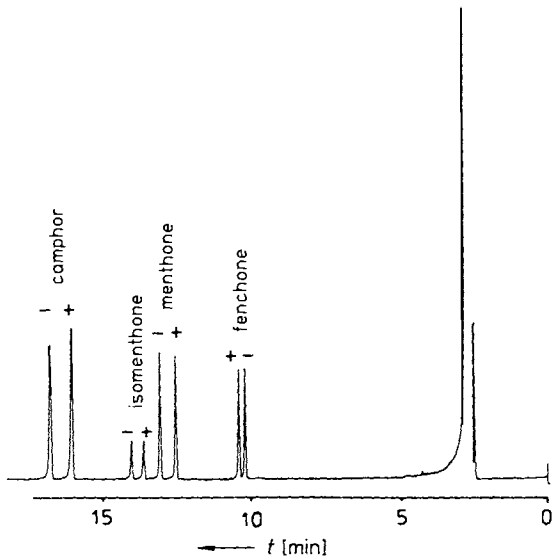

Fig. 15. Separation of the enantiomers of underivatized fenchone, menthone, isomenthone, and camphor on **18** at 100 °C (2 °C min^{-1}). Deactivated glass capillary column, 45 m × 0.25 mm I.D. Carrier gas: H_2, 1 bar [114].

Bicyclic and tricyclic acetals (bark beetle pheromones such as frontalin, *exo*- and *endo*-brevicomin, and lineatin), which were previously separated by complexation gas chromatog-

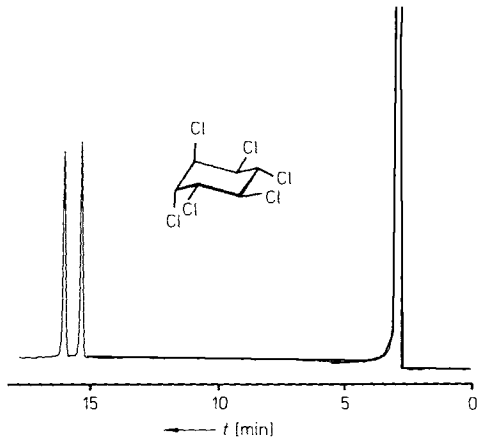

Fig. 16. Separation of the enantiomers of α-hexachlorocyclohexane on **17** at 190 °C. Deactivated glass capillary column, 50 m × 0.25 mm I.D. Carrier gas: H_2, 1 bar [114].

raphy,[2] give large separation factors α with these stationary phases, as also do γ-, δ-, and ε-lactones. Of particular interest is the separation of the enantiomers of α-hexachlorocyclohexane at 190 °C (Fig. 16).[114]

6.6. Heptakis(*O*-(*S*)-2-hydroxypropyl-per-*O*-methyl)-β-cyclodextrin (PMHP-β-CD, 20)

This viscous liquid, which is hydrophilic, relatively polar, and water-soluble, is a suitable enantioselective stationary phase for coating onto fused silica capillary columns.[120] Mass-spectrometric analysis has indicated that the product is a mixture of partially alkylated derivatives. Various types of compounds have been separated into their enantiomers on this phase, including trifluoroacetylated secondary amines, trifluoroacetylated amino alcohols, epoxides, β- and γ-lactones, derivatives of norbornene and norbornane, and monocyclic acetals with five- and six-membered rings. Surprisingly, introducing an additional chiral center via the 2-hydroxypropyl substituent has no effect on the observed enantioselectivity for a wide range of guest molecules, as was shown by comparative experiments using derivatives with substituents having the (*S*) and (*R*) configurations.[120] Apart from some isolated cases, no advantages resulted from using the corresponding α- (**19**) or γ-cyclodextrin derivatives.[120]

6.7. Hexakis(2,6-di-*O*-*n*-pentyl)-α-cyclodextrin (Dipentyl-α-CD, 21) and Heptakis(2,6-di-*O*-*n*-pentyl)-β-cyclodextrin (Dipentyl-β-CD, 22)

These stationary phases, which are more polar than the per-*n*-pentyl cyclodextrin derivatives, can easily be coated onto fused silica capillary columns.[122] For these phases the liquid consistency is again attributed to the presence of a mixture of partially alkylated derivatives. In experiments with 65 racemic compounds, striking differences were found between the enantioselectivities obtained with the α-, β-, and γ-cyclodextrin derivatives.[122] The range of compound types that can be separated on **21** and **22** is similar to that for per-*n*-pentylated cyclodextrins.

6.8. Heptakis(2,6-di-*O*-*n*-pentyl-3-*O*-trifluoroacetyl)-β-cyclodextrin (DPTFA-β-CD, 23)

This phase is especially suitable for separating racemic trifluoroacetylated carbohydrates into their enantiomers.[123] For α-DL-galactose (pyranose) the separation factor α at 120 °C is 2.14.

7. Applications

The main area of application of chiral cyclodextrin phases at present is in *enantiomer analysis* by gas chromatography of chiral compounds that can be vaporized without decomposition. Such applications include the determination of the enantiomeric purity of products obtained by enantioselective reactions and elucidation of the enantiomeric composition of natural substances (e.g., pheromones and flavors) and of pharmaceutical products.[131] An advantage of the method is that many compounds can be analyzed directly without derivatization or sample pretreatment. A few representative examples are briefly mentioned here.

The enantioselective telomerization of butadiene and formaldehyde to *cis*- and *trans*-2,5-divinyltetrahydropyran and the enantiomeric analysis of the products has been described.[127, 132] The stereochemistry of the rhodium(I)-catalyzed hydrogenation of 1-ethyl-2-methylcyclohexene to 1-ethyl-2-methylcyclohexane has been investigated; no enantioselectivity was observed in this case.[96] An analysis of the flavor constituent of hazel nuts, (*E*)-5-methylhept-2-en-4-one (filbertone), revealed a mixture with a preponderance of the *S* antipode.[133]

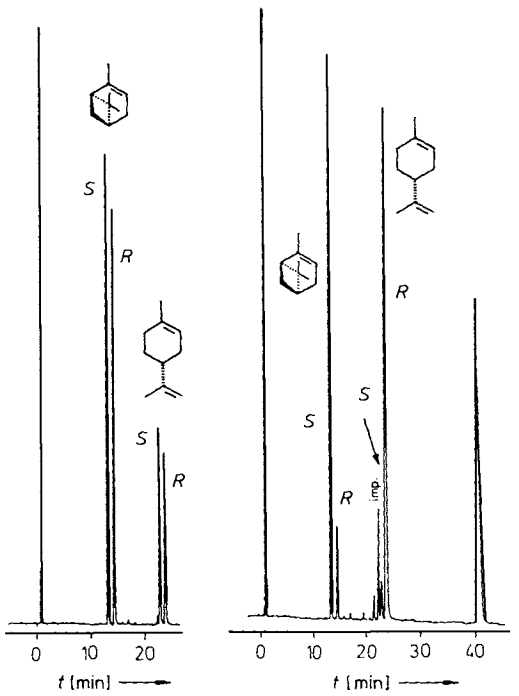

Fig. 17. Separation of the enantiomers of α-pinene and dipentene (limonene) on **1** in OV-1701 at 50 °C. Fused silica capillary column, 25 m × 0.25 mm I.D. Carrier gas: H_2 0.9 bar. Left: racemic mixtures. Right: determination of the enantiomeric purity of the alkenes in a pharmaceutical formulation by headspace analysis [134].

Enantiomeric excesses *ee* differing considerably from 100% were found for optically active α-pinene and limonene in commercial samples and in a pharmaceutical preparation (Fig. 17).[134] The enantiomeric composition of γ-lactones in foodstuffs has been determined by multidimensional gas chromatography.[135]

The absolute configuration of α-damascone and α-ionone in black tea has been investigated (Fig. 18).[136] A number of

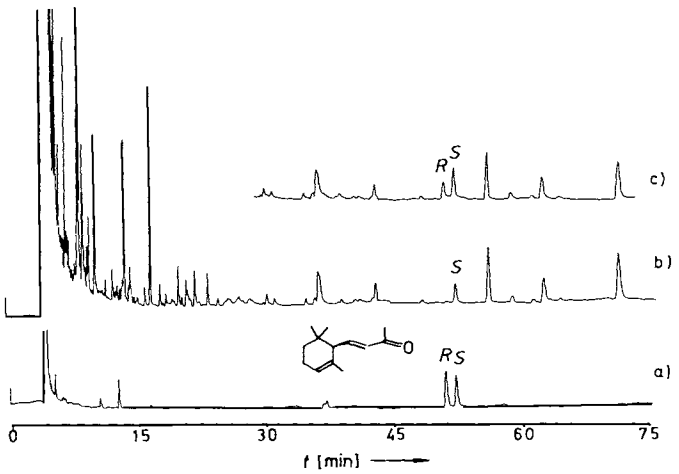

Fig. 18. a) Separation of the enantiomers of α-ionone on octakis(3-*O*-methyl-2,6-di-*O*-*n*-pentyl)-γ-cyclodextrin. b) Gas chromatogram of a fraction from an extract of black tea. c) Coinjection of a) and b). Deactivated glass capillary column, 60 m, 115 °C. Carrier gas: H_2, 1 bar [136].

olefinic algal pheromones (multifidene, aucantene) were separated into their enantiomers using cyclodextrin derivatives, thus laying the basis for clarifying their stereochemical interrelationships.[137] The determination of the enantiomeric composition of chiral *cis*- and *trans*-2,3-epoxy alcohols, which can be prepared by asymmetric epoxidation and have numerous applications, was achieved using per-*n*-pentylated α-cyclodextrin.[12] A particularly interesting application is the gas-chromatographic determination of the enantiomeric purity of tricarbonyl(η^4-2-methylene-1,3-butanediyl)iron(0) and tricarbonyl(η^4-2-methyl-1,3-butadiene)iron(0).[115]

8. Remarks on the Separation Mechanism

As early as 1952, *Cramer*, in a pioneering study of the resolution of racemates on cyclodextrins,[39] wrote: "From this we have discovered a relationship between molecular shape and biochemical activity. Here the cyclodextrin molecule exerts its effect solely as a result of its geometrical shape, not by means of functional groups. However, only those reagents that can enter the molecular cavity can be considered. Thus, striking parallels with the lock and key relationships of biochemical processes are revealed here." On the basis of thermodynamic parameters obtained for cyclodextrin inclusion complexes, *Saenger*[15] concluded that "the inclusion process does not depend primarily on the (chemical) nature of the guest molecule".

The results obtained so far on the gas-chromatographic separation of enantiomers on cyclodextrin derivatives show a remarkably wide range in the types of racemates which can be resolved. They include strongly polar chiral diols, free carboxylic acids, derivatized amino acids and carbohydrates, metal coordination compounds, allenes, propellanes, planar-chiral cycloalkenes, and unfunctionalized monocyclic hydrocarbons. In all cases, molecules that are identical in constitution but differ in their configurations (incongruent mirror-image structures) are discriminated by means of an *aracemic* chiral stationary phase, thereby allowing chromatographic enantiomer separation. The interaction necessary for this to occur can be strong or weak[6] and can consist of an inclusion process and/or other chemical interactions.

With regard to the nature of the host–guest interaction in cyclodextrins, a number of different contributions have been considered:[12, 13, 15, 16, 20] (1) steric fit by conformational change of the guest molecule and/or of the cyclodextrin molecule (induced fit) during the molecular inclusion process,[138–140] (2) hydrogen bonding,[24, 141] (3) van der Waals interactions (London dispersion forces and dipole–induced-dipole interactions), (4) hydrophobic interactions, (5) dipole–dipole interactions, (6) charge-transfer interactions, (7) electrostatic interactions, (8) release of "high-enthalpy" water molecules from the cyclodextrin cavity, (9) release of solvent molecules from the cyclodextrin cavity with a gain in entropy, (10) relief of the ring strain of the macrocycle.

To achieve enantiomer separation by the inclusion process, the molecular geometry should play an important role (shape selectivity and size selectivity). For polar guest molecules chemical interactions can also be important (chemical functionality selectivity). The results obtained so far surprisingly show that the molecular shape of the guest can be varied over a wide range. Thus, in addition to cyclic compounds, branched acyclic molecules such as underivatized ketones, haloalkanes, olefins, and allenes can be separated into enantiomers. Moreover, the molecular size does not appear to be a crucial factor. *Armstrong* et al. have even questioned the importance of the inclusion process, since certain guest molecules do not exhibit selectivity with respect to the diameter of the cyclodextrin cavity (α, β, or γ).[120] Furthermore, peak broadening, which often occurs with inclusion mechanisms due to delayed mass transfer, is not observed here.

Whereas the enantiomer separation of saturated cyclic hydrocarbons such as *trans*-1,2-dimethylcyclohexane can be unambiguously attributed to a molecular inclusion process,[94] for polar substrates one must also take into account additional enantioselective interactions (e.g., hydrogen bonding with cyclodextrins having acyl groups at the 3-position). In this connection it is significant that *Schurig* et al. have also observed enantiomer separations (e.g., of racemic cyclic ethers and aromatic oxiranes) using open-chain per-*n*-pentylated amylose.[142] Thus, enantiomer discrimination can also presumably occur at the outer surface of the cyclodextrin molecule. Surprisingly, modifying the cyclodextrin cavity opening by incorporating chiral anchoring groups has no effect on the enantioselectivity of the host molecule. For example, heptakis(2,3,6-tri-*O*-(*S*)-2′-methylbutyl)-β-cyclodextrin (**11**) does not allow enantiomer separation,[92]

and the configuration of the 2-hydroxypropyl group in derivatives of **19** and **20**[118] does not affect the observed enantioselectivity.[120] On the other hand, the separation of the enantiomers of acylated alcohols and amines on polar cyclodextrin derivatives is dependent on the nature of the acyl group (Fig. 19).[119] Since the acetyl and trifluoroacetyl groups are similar in size and shape, the difference in enantioselectivity is attributed to the different electronic properties of these two acyl groups (polarity and propensity to form hydrogen bonds).[119]

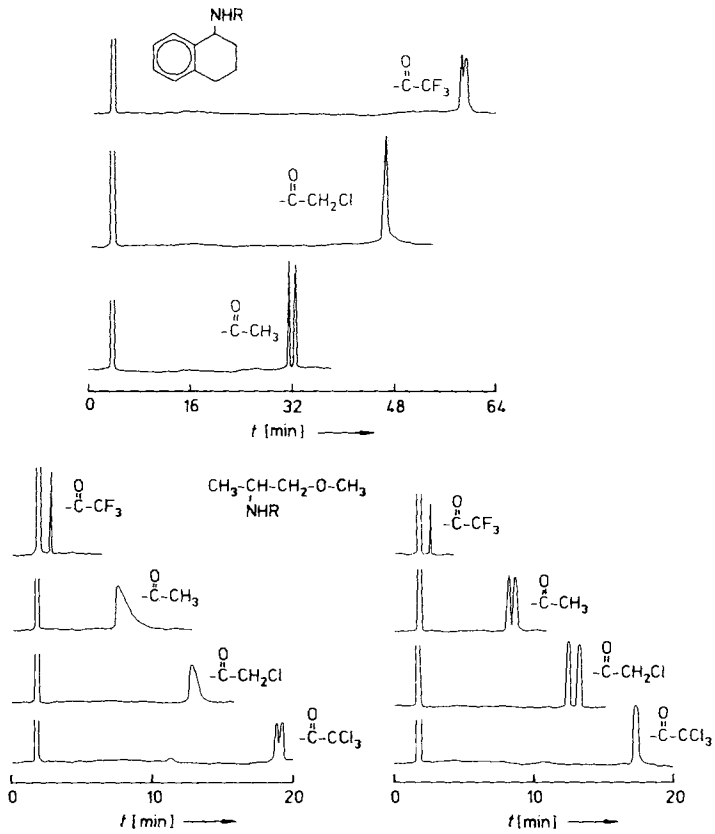

Fig. 19. Effect of derivatization on the separation of the enantiomers of acylated amines. Top: 1,2,3,4-tetrahydro-1-naphthylamine on **22**. Bottom left: 2-amino-1-methoxy-propane on **22**. Right: 2-amino-1-methoxy-propane on **20** [119].

In many cases, minor structural differences in the guest molecules can have dramatic effects on chiral recognition.[92] For example, a comparison of different alkyl-substituted γ-butyrolactones showed that, whereas the chain lengths of alkyl substituents at the γ-position (Fig. 9) and additional substituents at the β-position have only slight effects on the separation factor α, introducing a methyl group at the α-position relative to the carbonyl group leads to inferior separation.[92] Again, whereas 3,3,5-trimethylcyclohexanone was successfully separated quantitatively into its enantiomers on **1**, no separation was obtained for the 2,2,6 isomer.[92]

Methylation of cyclodextrins increases the depth of the molecular cavity (to about 1000–1100 pm) and enhances its conical shape, since the larger opening containing the secondary methoxy groups is increased while the opposite smaller opening containing the primary methoxy groups is narrowed.[138] *Harata* et al. therefore predicted that permethylated cyclodextrins should have a greater propensity for enantiomer differentiation than the corresponding underivatized compounds.[138–140] Contrary to this prediction it is found that, compared with underivatized cyclodextrins in formamide solution (cf. Fig. 2),[81, 82] the separation factors α for pinenes (Fig. 17) and pinanes, for example, on the alkylated and acylated cyclodextrins investigated so far, both in their undiluted and diluted forms, are very small. It is only the very high efficiency of the high-resolution capillary columns used that allows quantitative enantiomer separation in these cases with α values of 1.02 and above. This corresponds to a value of only about 20 cal mol^{-1} for the difference in the free energies for enantiomer discrimination $\Delta_{R,S}(\Delta G^{\circ})$.[7] Enantiomer separations based on such small free energy differences are thus attributed to a rather unpredictable "random effect",[93] which is unlikely to lead to mechanistic conclusions. Accordingly, the observation that minor changes in the host structure can result in reversals of the elution order of enantiomers (Fig. 20)[118] does not seem surprising.

It is known from X-ray crystal structure studies that hydrogen bonding can occur between the host molecule and suitable guest molecules.[24, 86, 141] Crystal structures of inclusion complexes formed by the enantiomer of mandelic acid indicate that such hydrogen bonds can make a crucial contribution to enantiomer differentiation even for permethylated cyclodextrins. Thus, the complex formed between permethyl-α-cyclodextrin and D-mandelic acid contains a hydrogen bond between host and guest which is not present in the complex with L-mandelic acid.[140] It is not clear to what extent the structure in the solid state can be extrapolated to that in solution (packing effects). That some free alcohols undergo enantiomer separation, whereas the corresponding acetates do not,[91–93] may be due to the contribution of hydrogen bonding to chiral recognition. Permethylated cyclodextrins, in contrast to the underivatized compounds, can only act as acceptors for hydrogen bonding to compounds with protic groups.

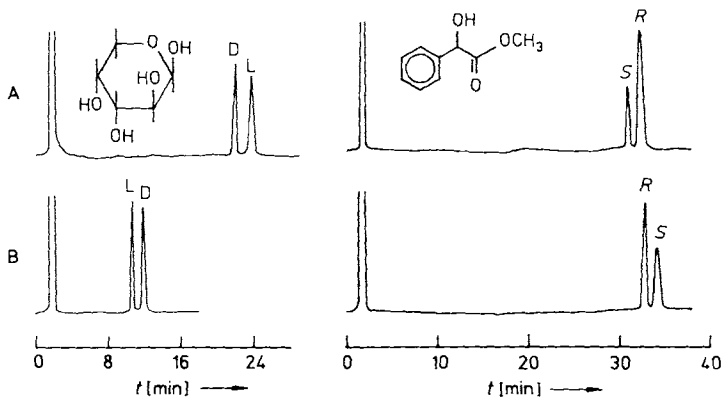

Fig. 20. Reversal of the order of elution of enantiomers on polar cyclodextrin derivatives. Separation of the enantiomers of pertrifluoroacetyl-β-D,L-arabinose (left) and mandelic acid methyl ester (right) on A) **20** and B) **22** at 80 °C and 120 °C, respectively. Fused silica capillary column, 10 m. Carrier gas: N_2 [118].

The so-called classical hydrophobic interactions are mainly caused by entropy effects. Although the formation of the host–guest complex is accompanied by a decrease in entropy, the removal of the hydration shell from the guest molecule and the release of solvent molecules from the cyclodextrin cavity can result in an overall increase in entropy. It will be shown later that the latter type of hydrophobic interaction could also be important for cyclodextrin derivatives diluted in polysiloxane, whereas the effect of any dehydration can be neglected, since water molecules should be completely removed during the conditioning of the gas-chromatographic columns and the injection of the substrate at high temperatures.

Since the formation of the inclusion complex is largely independent of the chemical properties of the guest molecule, it has been suggested that one of the driving forces for the inclusion process is the removal of high-enthalpy water molecules from the molecular cavity, where they reside in an unfavorable, hydrophobic environment.[15] According to the argument above, this contribution should be negligible under the conditions of the gas-chromatographic experiment.

Enantioselective interactions between chiral and prochiral guest molecules and cyclodextrins have been detected by a number of methods.[18, 31, 32, 34] Since the use of cyclodextrins for enantiomer separation in gas chromatography only began quite recently, no theoretical models for the mechanism of chiral recognition have yet been put forward. On the other hand, for the separation of racemates by fractional crystallization with cyclodextrins,[43] for cyclodextrin-catalyzed reactions,[143] and for liquid chromatography (HPLC) on cyclodextrin stationary phases, a three-point interaction model analogous to the models of *Easson* and *Stedman*[144] and of *Dalgliesh*[145] has been proposed.[61, 62] According to this model, a lipophilic, and preferably aromatic, part of the molecule is included in the cyclodextrin cavity, and two polar substituents interact with the secondary hydroxyl groups at the wider opening of the cyclodextrin cavity (e.g., by hydrogen bonding). This model is an appropriate one to account for enantiomer differentiation of arenes with a chiral center in the side-chain and several polar groups at the chiral center (e.g., mandelic acid derivatives and propanolol). However, it is not suitable for alicyclic compounds with chiral centers in the ring, nor for compounds that have no functional groups capable of forming hydrogen bonds. The necessity for an "aromatic presence", as observed in liquid-chromatographic enantiomer separations on carbohydrate stationary phases, is not found in the gas-chromatographic counterpart.

Although van der Waals forces have only a short range (being proportional to r^{-6}), the close contact between host and guest molecules can cause these forces to contribute appreciably to the selective inclusion process. The quantitative enantiomer separation observed for chiral alkanes on **1** (cf. Fig. 5),[82, 94] where other interactions can be excluded, shows that on cyclodextrin phases van der Waals interactions alone are sufficient for differentiating between enantiomers. In a molecular modeling study,[146] force field calculations and molecular dynamics simulations were applied to the inclusion complexes formed by the enantiomers of *cis*- and *trans*-1-ethyl-2-methylcyclohexane with **1**. From Figure 21 (left) it can be seen qualitatively that there is indeed a close contact between the van der Waals surfaces in the complex of *trans*-1-ethyl-2-methylcyclohexane (blue) with **1** (red). The complex is viewed from the side of the secondary methoxy groups, that is, from the wider end of the cavity. Although the guest molecule is completely enclosed by the host, it was not possible on the basis of such a small free energy difference to make predictions about the diastereo- and enantioselectivities, and the calculated values for the stabilities of the complexes were not in agreement with the experimentally observed gas-chromatographic elution order of the *cis* and *trans* isomers (cf. Fig. 5).[92] As already mentioned, carrying out molecular calculations on the basis of crystal structure data and of thermodynamic parameters ($\Delta_{R,S}(\Delta G^\circ)$, $\Delta_{R,S}(\Delta H^\circ)$, $\Delta_{R,S}(\Delta S^\circ)$), determined by gas chromatography for highly enantioselective host–guest complexes, is a worthwhile task for the future.

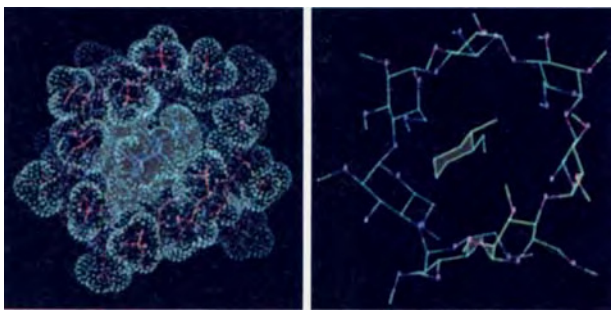

Fig. 21. Molecular modeling study of the inclusion complex of *trans*-1-ethyl-2-methylcyclohexane (one enantiomer) with **1** [146]. Left: with van der Waals radii. Right: without van der Waals radii.

Gas-chromatographic separation of enantiomers is a thermodynamically controlled process. The enantiomer discrimination involving a racemic guest and an aracemic (enantiomerically pure) host is described by the Gibbs–Helmholtz equation (a) and corresponds to the sum of the enthalpy

$$-\Delta_{R,S}(\Delta G^\circ) = -\Delta_{R,S}(\Delta H^\circ) + T\Delta_{R,S}(\Delta S^\circ) \qquad \text{(a)}$$

and entropy differences in the complexation of the enantiomers with the chiral stationary phase. The process is temperature-dependent, and it has recently been observed that the order of elution of the enantiomers on a given chiral phase (amino acid derivatives or metal complexes) is reversed above the "isoenantioselective temperature" T_{iso}.[147]

For a thermodynamic characterization of the mechanism of enantiomer discrimination it is useful to distinguish between the total interaction, as described by $-\Delta G^\circ$, and the difference in free energy between the complexes of the two enantiomers, $-\Delta_{R,S}(\Delta G)^\circ$.[6] One can assume that for a given interaction between host and guest, which can be strong or weak, small additional interactions are sufficient to produce enantiomer discrimination. Accordingly, for the cyclodextrin inclusion process the crucial factor is the competitive behavior of the enantiomers, as determined by the enthalpy and entropy contributions to chiral recognition at a given temperature. Thermodynamic data on enantiomer discrimination have been determined for *cis*-1-ethyl-2-methylcyclo-

hexane and *cis*-pinane on **1** in OV-1701 (0.07 M) (cf. Table 3).[95, 96] The thermodynamic parameters were obtained from relative retention data, using the concept of the retention increase R' adopted from complexation gas chromatography.[6, 125]

Table 3. Thermodynamic parameters for the separation of the enantiomers of *cis*-1-ethyl-2-methylcyclohexane and *cis*-pinane on **1** in OV-1701 (0.07 M) obtained from temperature-dependent measurements between 30 °C and 70 °C using *n*-octane and *n*-decane as standards [95, 96].

Substrate	Standard	$\Delta\Delta H$ [kJ mol^{-1}]	$\Delta\Delta S$ [J K^{-1} mol^{-1}]
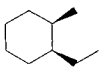	C_8H_{18}	−0.2	0.3
	$C_{10}H_{22}$	−0.2	0.3
	C_8H_{18}	−0.2	0.7
	$C_{10}H_{22}$	−0.2	0.8

Surprisingly, $\Delta_{R,S}(\Delta H^\circ)$ and $\Delta_{R,S}(\Delta S^\circ)$ have opposite signs for the cycloalkanes investigated. It follows from this that no (positive) isoenantioselective temperature exists, and therefore no peak inversions are expected in this system (see also Ref. [118]). The increase in entropy, which is unusual for an association process, may be explained by the fact that the solvent (polysiloxane) molecules released from **1** on inclusion of the hydrocarbon molecules gain individual degrees of freedom. Both $-\Delta_{R,S}(\Delta H^\circ)$ and $\Delta_{R,S}(\Delta S^\circ)$ thus contribute to the enantiomer discrimination, as described by $-\Delta_{R,S}(\Delta G^\circ)$, and a quantitative enantiomer separation occurs even for small entropy and enthalpy differences. A low value of $\Delta_{R,S}(\Delta H^\circ)$ implies that the enantiomer separation shows only a slight temperature dependence, and quantitative separation is obtained even at high temperatures (e.g., 250 °C), as is generally found using cyclodextrin stationary phases.

A systematic search for enantioselective host–guest systems with high separation factors ($\alpha > 2$) is not only a prerequisite for the preparative applications of racemate separation, but is also warranted in order to optimize model systems that can be used for mechanistic studies, thermodynamic measurements of enantioselectivity, crystal structure studies, and computer-aided calculations on the different diastereomeric association complexes.

9. Practical Aspects and Outlook

High-resolution gas-chromatographic separations of enantiomers using cyclodextrin derivatives are achieved at present only with analytical capillary columns. Separations on a semipreparative scale can therefore only be expected in rare cases with the separation factors α that are currently obtained. Enantiomer separations can be performed in the usual temperature range of 25 to 250 °C. For special applications it is also possible to use lower temperatures (−25 °C). The enantioselective phases have a long lifetime if oxygen-free carrier gases are employed (e.g., nitrogen, helium, hydrogen). For samples diluted in solvents the quantities injected should be minimized by using the split injection technique (1:100). The successful coating of glass or fused silica capillary columns with undiluted or diluted cyclodextrin derivatives requires some expertise and can only be carried out satisfactorily on pretreated, deactivated surfaces.[124] Established methods of treatment are leaching, persilylation, or Carbowax deactivation.[124] Capillary columns coated with cyclodextrins are commercially available from well-known chromatography suppliers, including Chrompack (Middelburg, Netherlands) (diluted cyclodextrin **1** on fused silica capillary columns, cf. Section 5),[98] Macherey-Nagel (Düren, FRG) (undiluted *n*-pentylated/acylated cyclodextrin phases **13**–**16** (Lipodex) on glass capillary columns, cf. Sections 6.1–6.5;[105] see also Ref. [127] for the same on fused silica capillary columns), and Astec, Advanced Separation Technologies (Whippany, NJ, USA), and ICT (Frankfurt/Main, FRG) (undiluted polar cyclodextrin phases **19**–**23** on fused silica capillary columns, cf. Sections 6.6–6.8).[120]

For the enantioselective cyclodextrin phases described up to now the user must distinguish between the following factors: availability, performance, reproducibility, long-term stability. The inspection of chromatograms, insofar as they are available, often provides the expert with decisive information. The use of cyclodextrins as solutions in polysiloxanes has resulted in columns of high efficiency, even for strongly polar substrates such as diols (Fig. 6)[97, 98] and alcohols.[127] Thus, for the first eluted peak of *trans*-2,3-dimethyl-1,4-dioxaspiro[4.4]nonane (Fig. 8), the number of effective plates was measured as $N = 79\,400$. For a column length of 40 m this corresponds to a height equivalent theoretical plate (HETP) of 0.50 mm. Accordingly, despite the small separation factor ($\alpha = 1.02$), an almost complete resolution of the peaks ($R = 1.33$) is achieved. For capillary columns with **1** in the molten state at 140–150 °C, HETP values of only 1.6 and 1.4 mm were obtained, and a comparable efficiency (0.3 mm) was only reached at 200 °C.[89] On undiluted polar cyclodextrin derivatives, peak resolution is not always ideal either (Fig. 19).[119] Poorer HETP values were measured for packed columns with β-cyclodextrin in formamide solution (1.8 mm;[79] cf. also Fig. 2) and for gas-solid packed columns with β-cyclodextrin on Chromosorb W (10.8 mm).[74]

Chemically binding the cyclodextrin derivatives to polysiloxanes, in a manner analogous to "Chirasil-Val"[5] or "Chirasil-Metal",[125] is expected to further increase the efficiency and lifetime of the columns.[*] The immobilization of such "Chirasil-Dex" stationary phases on the capillary surface is required for using supercritical gases for enantiomer separation (supercritical fluid chromatography, SFC) or for employing electrically driven chromatographic systems. As mentioned before, the low separation factors α observed up to now render it unlikely that the cyclodextrin phases available at present can generally be used for preparative-scale gas-chromatographic enantiomer separations. Also, there is at present no universal enantioselective cyclodextrin station-

[*] Note added in proof: Successful experiments have been reported recently [148]: e.g., "Chirasil-Dex" [149].

ary phase available, and unsuccessful separation attempts are, regrettably, hardly ever reported in the literature. In our experience, the success rate for quantitative enantiomer separations with a given cyclodextrin phase such as **1** lies well below 50%. Minor changes in the structure of the guest molecules often have a great effect on the enantioselectivity. Even for compounds that are structurally related, often only certain isomers or members of a homologous series can be separated into their enantiomers on cyclodextrin phases. It is therefore difficult to make predictions.

The objective for the future is to discover enantioselective stationary phases based on cyclodextrins that will have as wide a range of applications as possible. A further development still awaited is the preparation of phases with inverse configuration by total synthesis;[26] they are required for carrying out enantiomeric analyses on highly enriched substrates in cases where the trace component is eluted *after* the major component, making integration difficult. Owing to the lack of such inversely configurated phases, in no case has a formal proof of successful enantiomer separation on cyclodextrins, in contrast to phases consisting of amino acids[3] or metal complexes,[150] been possible. Such proof is normally provided by using the racemic form, which gives rise to peak coalescence, or the mirror-image stationary phase, which causes peak inversion.

In the next few years a steady growth of interest in chiral stationary phases based on cyclodextrins for capillary gas chromatography can be expected. Selective achiral separations (of geometrical isomers, diastereomers, positional isomers, etc.), as well as methods for modifying complex elution profiles, will also play an important role. However, cyclodextrin stationary phases are not expected to entirely replace or supersede the amino acid or metal complex stationary phases mentioned in the introduction. Instead, they represent a considerable extension to the range of techniques available to the enantiomer analyst, in accordance with the comment by *Gil-Av*, the pioneer of gas-chromatographic enantiomer separation, that "every phase, whether low or high molecular, will be recognized as suiting best a certain niche of applications".[84]

The authors thank the Deutsche Forschungsgemeinschaft and the Fonds der Chemischen Industrie for supporting this work. We are indebted to Professor Berson (New Haven) for providing a sample of ethyl hexa-3,4-dienoate and to Professor Fitjer (Göttingen) for providing a sample of modhephene. We thank Dipl.-Chem. Dieter Schmalzing, Michael Schleimer, and Martin Jung for their valuable contributions to the gas-chromatographic enantiomer separation on cyclodextrin stationary phases. V. S. thanks Professor König (Hamburg), Professor Armstrong (Rolla, Missouri), and Professor Smolková-Keulemansová (Prague) for reprints and preprints of recent work, and especially Professor Gil-Av (Rehovoth) and Professor Bayer (Tübingen) for fruitful scientific exchange over the years.

Received: March 1, 1990 [A 780 IE]
German version: *Angew. Chem. 102* (1990) 969
Translated by Dr. *Jack Becconsall*, Pwllheli (UK)

[1] a) J. D. Morrison (Ed.): *Asymmetric Synthesis, Vol. 1*, Academic, Orlando 1985; b) J. D. Morrison in [1a], p. 1.
[2] V. Schurig in [1a], p. 87; *Kontakte (Darmstadt) 1986 No. 1*, p. 3.
[3] E. Gil-Av, B. Feibush, R. Charles-Sigler, *Tetrahedron Lett. 1966*, 1009; *J. Mol. Evol. 6* (1975) 131; R. H. Liu, W. W. Ku, *J. Chromatogr. 271* (1983) 309.
[4] H. Frank, G. J. Nicholson, E. Bayer, *J. Chromatogr. Sci. 15* (1977) 174; Angew. *Chem. 90* (1978) 396; Angew. *Chem. Int. Ed. Engl. 17* (1978) 363; B. Koppenhöfer, E. Bayer, *J. Chromatogr. Libr. 32* (1985) 1.
[5] W. A. König: *The Practice of Enantiomer Separation by Capillary Gas Chromatography*, Hüthig, Heidelberg 1987.
[6] V. Schurig, W. Bürkle, *J. Am. Chem. Soc. 104* (1982) 7573; V. Schurig, *J. Chromatogr. 441* (1988) 135.
[7] V. Schurig, Angew. *Chem. 96* (1984) 733; Angew. *Chem. Int. Ed. Engl. 23* (1984) 747.
[8] A. Villiers, *C.R. Acad. Sci. 112* (1891) 536.
[9] F. Schardinger, *Wien. Klin. Wochenschr. 17* (1904) 207; *Zentralbl. Bakteriol. Parasitenkd. Infektionskrankh. Hyg. Abt. 2 29* (1911) 188.
[10] C. J. Pedersen, *J. Am. Chem. Soc. 89* (1967) 2495, 7017.
[11] K. Freudenberg, F. Cramer, *Z. Naturforsch. B3* (1948) 464.
[12] F. Cramer: *Einschlußverbindungen*, Springer, Berlin 1954.
[13] R. J. Clarke, J. H. Coates, S. F. Lincoln, *Adv. Carbohydr. Chem. Biochem. 46* (1988) 205.
[14] J. Szejtli, *Kontakte (Darmstadt) 1988 Nr. 1*, p. 31.
[15] W. Saenger, *Angew. Chem. 92* (1980) 343; *Angew. Chem. Int. Ed. Engl. 19* (1980) 344, and references cited therein.
[16] M. L. Bender, M. Komiyama: *Cyclodextrin Chemistry*, Springer, Berlin 1978, and references cited therein.
[17] S. P. Jones, J. W. Grant, J. Hadgraft, G. D. Parr, *Acta Pharm. Technol. 30* (1984) 213, 263.
[18] F. Cramer, H. Hettler, *Naturwissenschaften 54* (1967) 625.
[19] W. Saenger in J. L. Atwood, J. E. D. Davies, D. D. MacNicol (Eds.): *Inclusion Compounds, Vol. 2*, Academic, London 1984.
[20] J. F. Wojcik, *Bioorg. Chem. 12* (1984) 130.
[21] J. Szejtli: *Cyclodextrins and their Inclusion Complexes*, Akad. Kiadó, Budapest 1982; *Cyclodextrin Technology*, Reidel, Dordrecht 1988; D. Duchêne (Ed.): *Cyclodextrins and their Uses in Various Industries*, Les Editions de Santé, Paris 1987; J. S. Pagington, *Chem. Br. 23* (1987) 455.
[22] J. Szejtli, *Staerke 29* (1977) 26.
[23] K. Harata, *Bull. Chem. Soc. Jpn. 49* (1976) 1493; K. Harata, H. Uedaira, J. Tanaka, *ibid. 51* (1978) 1627; J. J. Stezowski, K. H. Jogun, E. Eckle, K. Bartles, *Nature (London) 274* (1978) 617; K. H. Jogun, J. J. Stezowski, *ibid. 278* (1979) 667; M. M. Harding, J. M. Maclennan, R. M. Paton, *ibid. 274* (1978) 612; J. A. Hamilton, M. N. Sebesan, L. K. Steinrauf, A. Geddes, *Biochem. Biophys. Res. Commun. 73* (1976) 659.
[24] J. J. Stezowski, M. Czugler, E. Eckle, *Proc. Int. Symp. Cyclodextrins* 1st *1981*, 151; R. Tokuoka, T. Fujiwara, K. Tomita, *Acta Crystallogr. Sect. B37* (1981) 1158.
[25] R. Breslow, *Science (Washington D.C.) 218* (1982) 532; D. Hilvert, R. Breslow, *Bioorg. Chem. 12* (1984) 206; I. Tabushi, Y. Kuroda, *J. Am. Chem. Soc. 106* (1984) 4580; D. W. Griffiths, M. L. Bender, *Adv. Catal. 23* (1973) 209; M. L. Bender in M. I. Page, A. Williams (Eds.): *Enzyme Mechanisms*, Royal Soc. Chem., London 1987, p. 56.
[26] Y. Takahashi, T. Ogawa, *Carbohydr. Res. 164* (1987) 277.
[27] A. P. Croft, R. A. Bartsch, *Tetrahedron 39* (1983) 1417.
[28] L. D. Melton, K. N. Slessor, *Carbohydr. Res. 18* (1971) 29.
[29] I. Tabushi, K. Shimokawa, K. Fujita, *Tetrahedron Lett. 1977*, 1527.
[30] I. Tabushi, K. Shimokawa, N. Shimizu, H. Shirakata, K. Fujita, *J. Am. Chem. Soc. 98* (1976) 7855.
[31] J. Michon, A. Rassat, *J. Am. Chem. Soc. 101* (1979) 995.
[32] D. D. MacNicol, R. S. Rycroft, *Tetrahedron Lett. 1977*, 2173.
[33] J. A. Hamilton, L. Chen, *J. Am. Chem. Soc. 110* (1988) 5833.
[34] K. Harata, H. Uedaira, *Bull. Chem. Soc. Jpn. 48* (1975) 375.
[35] H. Yamaguchi, M. Ata, J. F. W. McOmie, J. W. Barton, H. Baumann, *J. Chem. Soc. Faraday Trans. 2 1983*, 599.
[36] E. G. Janzen, Y. Kotake, *J. Am. Chem. Soc. 110* (1988) 7912.
[37] A. Ohno, S. Ushida: *Mechanistic Models of Asymmetric Reductions*, Springer, Berlin 1986, p. 53.
[38] V. Daffe, J. Fastrez, *J. Am. Chem. Soc. 102* (1980) 3601.
[39] F. Cramer, *Angew. Chem. 64* (1952) 136.
[40] F. Cramer, W. Dietsche, *Chem. Ber. 92* (1959) 378.
[41] H. P. Benschop, G. R. Van den Berg, *J. Chem. Soc. Chem. Commun. 1970*, 1431.
[42] M. Mikolajczyk, J. Drabowicz, F. Cramer, *J. Chem. Soc. Chem. Commun. 1971*, 317.
[43] M. Mikolajczyk, J. Drabowicz, *Tetrahedron Lett. 23* (1972) 2379; *J. Am. Chem. Soc. 100* (1978) 2510.
[44] J. Knabe, N. S. Agarwal, *Dtsch. Apoth. Ztg. 113* (1973) 1449.
[45] J. Dębowski, D. Sybilska, J. Jurczak, *Chromatographia 16* (1982) 198; *J. Chromatogr. 237* (1982) 303; *ibid. 282* (1983) 83; D. Sybilska, J. Zukowski, J. Bojarski, *J. Liq. Chromatogr. 9* (1986) 591.
[46] B. Zsadon, L. Décsei, M. Szilasi, F. Tüdos, J. Szejtli, *J. Chromatogr. 270* (1983) 127.

[47] E. Smolková-Keulemansová, S. Krýsl, *J. Chromatogr. 184* (1980) 347; W. L. Hinze, Separ. *Purif. Methods 10* (1981) 159.
[48] J. Szejtli, B. Zsadon, T. Cserháti, *ACS Symp. Ser. 342* (1987) 200, and references cited therein; W. L. Hinze, D. W. Armstrong, *Anal. Lett. 13* (1980) 1093; D. W. Armstrong, F.-Y. He, S. M. Han, *J. Chromatogr. 448* (1988) 345; J. Szejtli, *Starch Staerke 39* (1987) 357.
[49] J. Szejtli, T. Cserháti, B. Bordás, J. Bojarski, *Kontakte (Darmstadt) 1988 Nr. 2*, p. 30.
[50] W. L. Hinze, D. Y. Pharr, Z. S. Fu, W. G. Burkert, *Anal. Chem. 61* (1989) 422.
[51] D. W. Armstrong, J. R. Faulkner, Jr., S. M. Han, *J. Chromatogr. 452* (1988) 323.
[52] A. Alak, D. W. Armstrong, *Anal. Chem. 58* (1986) 582.
[53] T. J. Ward, D. W. Armstrong, *J. Liq. Chromatogr. 9* (1986) 407.
[54] M. Tazaki, M. Takagi, K. Ueno, *Chem. Lett. 1982*, 639.
[55] S. Terabe, H. Ozaki, K. Otsuka, T. Ando, *J. Chromatogr. 332* (1985) 211.
[56] J. Snopek, I. Jelinek, E. Smolková-Keulemansová, *J. Chromatogr. 452* (1988) 571; *ibid. 472* (1989) 308; S. Fanali, *ibid. 474* (1989) 441; A. Guttmann, A. Paulus, A. S. Cohen, N. Grindberg, B. L. Karger, *ibid. 448* (1988) 41.
[57] S. Terabe, *Trends Anal. Chem. 8* (1989) 129; cf. also [55].
[58] N. Wiedenhof, *Staerke 21* (1969) 163.
[59] A. Harada, M. Furue, S. Nozakura, *J. Polym. Sci. 16* (1978) 189.
[60] K. Fujimura, T. Ueda, T. Ando, *Anal. Chem. 55* (1983) 446; Y. Kawaguchi, M. Tanaka, M. Nakae, K. Funazo, T. Shono, *ibid. 55* (1983) 1852; D. W. Armstrong, *J. Liq. Chromatogr. 7* (1984) 353; D. W. Armstrong, W. J. DeMond, *J. Chromatogr. Sci. 22* (1984) 411; D. W. Armstrong, T. J. Ward, R. D. Armstrong, T. E. Beesley, *Science (Washington D.C.) 232* (1986) 1132.
[61] W. L. Hinze, T. E. Riehl, D. W. Armstrong, W. DeMond, A. Alak, T. Ward, *Anal. Chem. 57* (1985) 237.
[62] K. Fujimura, M. Kitagawa, H. Takayanagi, T. Ando, *J. Liq. Chromatogr. 9* (1986) 607.
[63] P. Macaudiere, M. Caude, R. Rosset, A. Tambute, *J. Chromatogr. 405* (1987) 135; *ibid. 450* (1988) 255.
[64] T. J. Ward, D. W. Armstrong, *J. Liq. Chromatogr. 9* (1986) 407.
[65] M. Tanaka, T. Shono, D.-Q. Zhu, Y. Kawaguchi, *J. Chromatogr. 469* (1989) 429.
[66] D. Sybilska, *ACS Symp. Ser. 342* (1987) 218; Y. Nobuhara, S. Hirano, Y. Nakanishi, *J. Chromatogr. 258* (1983) 276; M. Gazdag, G. Szepesi, L. Huszar, *ibid. 351* (1986) 128; *ibid. 371* (1986) 227; K. Cabrera, G. Schwinn, *Kontakte (Darmstadt) 1989 Nr. 3*, p. 3.
[67] S. Scypinski, L. J. Cline Love, *Anal. Chem. 56* (1984) 322; G. Patonay, M. E. Rollie, I. M. Warner, *ibid. 57* (1985) 569.
[68] A. Cepeda-Saez, P. Prognon, G. Mahuzier, J. Blais, *Anal. Chim. Acta 211* (1988) 333.
[69] M. Tanaka, T. Miki, T. Shono, *J. Chromatogr. 330* (1985) 253; J. Zukowski, D. Sybilska, J. Bojarski, *ibid. 364* (1986) 225.
[70] D. M. Sand, H. Schlenk, *Anal. Chem. 33* (1961) 1624; H. Schlenk, J. L. Gellerman, D. M. Sand, *ibid. 34* (1962) 1529.
[71] B. Casu, M. Reggiani, G. R. Sanderson, *Carbohydr. Res. 76* (1979) 59.
[72] Y. Mizobuchi, M. Tanaka, T. Shono, *J. Chromatogr. 194* (1980) 153.
[73] E. Smolková, H. Kralová, S. Krysl, L. Feltl, *J. Chromatogr. 241* (1982) 3; E. Smolková-Keulemansová, *ibid. 251* (1982) 17; T. Kościelski, D. Sybilska, L. Feltl, E. Smolková-Keulemansová, *ibid. 286* (1984) 23; S. Krysl, E. Smolková-Keulemansová, *ibid. 349* (1985) 167.
[74] E. Smolková-Keulemansová, E. Neumannová, L. Feltl, *J. Chromatogr. 365* (1986) 279, 289.
[75] J. Mraz, L. Feltl, E. Smolková-Keulemansová, *J. Chromatogr. 286* (1984) 17.
[76] T. Cserhati, A. Dobrovolszky, E. Fenyvesi, J. Szejtli, *HRC & CC, J. High Resolut. Chromatogr. Chromatogr. Commun. 6* (1983) 442.
[77] E. Smolková-Keulemansová, L. Sojak, *ACS Symp. Ser. 342* (1987) 247.
[78] M. Tanaka, S. Kawano, T. Shono, *Fresenius' Z. Anal. Chem. 316* (1983) 54.
[79] D. Sybilska, T. Kościelski, *J. Chromatogr. 261* (1983) 357; T. Kościelski, D. Sybilska, L. Feltl, E. Smolková-Keulemansová, *ibid. 286* (1984) 23; E. Smolková-Keulemansová, S. Pokorna, L. Feltl, K. Tešarik, *HRC & CC, J. High Resolut. Chromatogr. Chromatogr. Commun. 11* (1988) 670.
[80] T. Kościelski, D. Sybilska, *J. Chromatogr. 349* (1985) 3; T. Kościelski, D. Sybilska, J. Lipkowski, A. Miediok-Ritskaja, *ibid. 351* (1986) 512.
[81] T. Kościelski, D. Sybilska, J. Jurczak, *J. Chromatogr. 280* (1983) 131; *ibid. 364* (1986) 299.
[82] T. Kościelski, D. Sybilska, S. Belniak, J. Jurczak, *Chromatographia 19* (1984) 292; *ibid. 21* (1986) 413.
[83] L. Anděra, E. Smolková-Keulemansová, *J. Inclusion Phenom. 5* (1987) 397; L. Feltl, P. Tajovská, E. Smolková-Keulemansová, *J. Chromatogr.*, in press.
[84] E. Gil-Av, preface to [5].
[85] a) Y. H. Kim, Universität Tübingen 1981, unpublished; b) J. Roeraade, personal communication.
[86] R. D. Armstrong, *ACS Symp. Ser. 342* (1987) 272.
[87] J. Boger, R. Corcoran, J.-M. Lehn, *Helv. Chim. Acta 61* (1978) 2190.
[88] Z. Juvancz, G. Alexander, J. Szejtli, *HRC & CC, J. High Resolut. Chromatogr. Chromatogr. Commun. 10* (1987) 105; G. Alexander, Z. Juvancz, J. Szejtli, *ibid. 11* (1988) 110.
[89] Z. Juvancz, Z. Racz, G. Alexander, J. Szejtli, *Proc. Int. Symp. Cyclodextrins, 4th 1988*, 479.
[90] A. Venema, P. J. A. Tolsma, *J. High Resolut. Chromatogr. 12* (1989) 32.
[91] V. Schurig, H.-P. Nowotny in A. Zlatkis (Ed.): *Proceedings of Advances in Chromatography 1987*, Berlin, 8.–10. September 1987; *J. Chromatogr. 441* (1988) 155.
[92] H.-P. Nowotny, *Dissertation*, Universität Tübingen 1989.
[93] H.-P. Nowotny, D. Schmalzing, D. Wistuba, V. Schurig, *J. High Resolut. Chromatogr. 12* (1989) 383.
[94] V. Schurig, H.-P. Nowotny, D. Schmalzing, Angew. *Chem. 101* (1989) 785; Angew. *Chem. Int. Ed. Engl. 28* (1989) 736.
[95] V. Schurig, M. Jung in D. Stevenson, I. D. Wilson (Eds.): *Chiral Separations 1989, Proceedings of the International Meeting on Chromatography*, University of Surrey, Guildford, 12.–15. September 1989, Plenum, in press.
[96] M. Jung, *Diplomarbeit*, Tübingen 1989.
[97] V. Schurig, M. Jung, D. Schmalzing, M. Schleimer, J. Duvekot, J. C. Buyten, J. A. Peene, J. Lips, *Proc. Int. Symp. Capillary Chromatogr. 11th 1990*, p. 14; *HRC & CC, J. High Resolut. Chromatogr. Commun. 13* (1990) 470.
[98] J. Duvekot, J. C. Buyten, J. A. Peene, J. Lips, V. Schurig, H.-P. Nowotny, *Proc. Int. Symp. Capillary Chromatogr. Chromatogr. 11th 1990*, p. 147.
[99] Sigma Chemical Compounds, Catalogue 1989, p. 693.
[100] W. A. König, G. Wenz, S. Lutz, E. von der Bey, *Offenlegungsschrift*, DE-A 3 810 737, (1989).
[101] W. A. König, S. Lutz, P. Mischnick-Lübbecke, B. Brassat, G. Wenz, *J. Chromatogr. 447* (1988) 193.
[102] W. A. König, S. Lutz, G. Wenz, *Angew. Chem. 100* (1988) 989; *Angew. Chem. Int. Ed. Engl. 27* (1988) 979.
[103] W. A. König, S. Lutz, G. Wenz, E. von der Bey, *HRC & CC, J. High Resolut. Chromatogr. Chromatogr. Commun. 11* (1988) 506.
[104] W. A. König, R. Krebber, G. Wenz, *J. High Resolut. Chromatogr. 12* (1989) 641.
[105] A. Nehrings, *GIT Supplement – Chromatogr. 1989 Nr. 3*, p. 14; W. A. König, *Nachr. Chem. Tech. Lab. 37* (1989) 471.
[106] W. A. König, *Carbohydr. Res. 192* (1989) 51.
[107] W. A. König, S. Lutz, C. Colberg, N. Schmidt, G. Wenz, E. von der Bey, A. Mosandl, C. Günther, A. Kustermann, *HRC & CC, J. High Resolut. Chromatogr. Chromatogr. Commun. 11* (1988) 621.
[108] W. A. König, P. Mischnick-Lübbecke, B. Brassat, S. Lutz, G. Wenz, *Carbohydr. Res. 183* (1988) 11.
[109] J. Ehlers, W. A. König, S. Lutz, G. Wenz, H. tom Dieck, *Angew. Chem. 100* (1988) 1614; *Angew. Chem. Int. Ed. Engl. 27* (1988) 1556.
[110] W. A. König, S. Lutz, G. Wenz, *Proc. Int. Symp. Cyclodextrins 4th 1988*, 465 (cf. p. 145).
[111] W. A. König, S. Lutz, P. Mischnick-Lübbecke, B. Brassat, E. von der Bey, G. Wenz, *Starch Staerke 40* (1988) 472.
[112] W. A. König, S. Lutz, G. Wenz, G. Görgen, C. Neumann, A. Gäbler, W. Boland, *Angew. Chem. 101* (1989) 180; *Angew. Chem. Int. Ed. Engl. 28* (1989) 179.
[113] W. A. König, S. Lutz, M. Hagen, R. Krebber, G. Wenz, K. Baldenius, J. Ehlers, H. tom Dieck, *J. High Resolut. Chromatogr. 12* (1989) 35.
[114] W. A. König, R. Krebber, P. Mischnick, *J. High Resolut. Chromatogr. 12* (1989) 732.
[115] W. A. König, R. Krebber, G. Wenz, *J. High Resolut. Chromatogr. 12* (1989) 790.
[116] W. A. König, S. Lutz, P. Evers, J. Knabe, *J. Chromatogr. 503* (1990) 256.
[117] D. Kappes, H. Gerlach, P. Zbinden, M. Dobler, W. A. König, R. Krebber, G. Wenz, *Angew. Chem. 101* (1989) 1744; *Angew. Chem. Int. Ed. Engl. 28* (1989) 1657.
[118] D. W. Armstrong, W. Y. Li, J. Pitha, *Anal. Chem. 62* (1990) 217.
[119] D. W. Armstrong, H. L. Jin, *J. Chromatogr. 502* (1990) 154.
[120] D. W. Armstrong, W. Y. Li, C. D. Chang, J. Pitha, *Anal. Chem., 62* (1990) 914.
[121] D. W. Armstrong, W. Y. Li, A. M. Stalcup, J. I. Seeman, H. V. Secor, *Anal. Chim. Acta*, in press.
[122] D. W. Armstrong, W. Y. Li, A. M. Stalcup, H. V. Secor, R. R. Izak, J. I. Seeman, unpublished.
[123] W. Y. Li, H. L. Jin, D. W. Armstrong, *J. Chromatogr. 509* (1990) 303.
[124] E. Schulte: *Praxis der Kapillar-Gaschromatographie*, Springer, Berlin 1983; K. Grob: *Making and Manipulating Capillary Columns for Gas Chromatography*, Hüthig, Heidelberg 1986.
[125] V. Schurig, R. Link in D. Stevenson I. D. Wilson (Eds.): *Chiral Separations, Proc. Int. Meet. Chromatogr.*, University of Surrey, Guildford, 3.–4. September 1987; Plenum, London 1988, p. 91.
[126] C. Weitemeyer, A. de Meijere, *Angew. Chem. 88* (1976) 721; *Angew. Chem. Int. Ed. Engl. 15* (1976) 686.
[127] A. Köhnes, H. Römer, *Chemie in Labor und Biotechnik 41* (1990) 70.

[128] R. L. Van Etten, G. A. Clowes, J. F. Sebastian, M. L. Bender, *J. Am. Chem. Soc. 89* (1967) 3253.
[129] A. Harada, M. Furue, S. Nozakura, *Polymer J. (Tokyo) 12* (1980) 29.
[130] I. Ciucanu, F. Kerek, *Carbohydr. Res. 131* (1984) 209.
[131] W. Kitching, J. A. Lewis, M. V. Perkins, R. Drew, C. J. Moore, V. Schurig, W. A. König, W. Francke, *J. Org. Chem. 54* (1989) 3893; C. Everaerts, O. Bonnard, J. M. Pasteels, Y. Roisin, W. A. König, *Experientia 46* (1990) 227; W. Francke, S. Schulz, V. Sinnwell, W. A. König, Y. Roisin, *Liebigs Ann. Chem. 1989*, 1195; G. Takeoka, R. A. Flath, T. R. Mon, R. G. Buttery, R. Teranishi, M. Güntert, R. Lautamo, J. Szejtli, *J. High Resolut. Chromatogr. 13* (1990) 202.
[132] W. Keim, W. Meltzow, A. Köhnes, T. Röthel, *J. Chem. Soc. Chem. Commun. 1989*, 1151.
[133] J. Jauch, D. Schmalzing, V. Schurig, R. Emberger, R. Hopp, M. Köpsel, W. Silberzahn, P. Werkhoff, *Angew. Chem. 101* (1989) 1039; V. Schurig, J. Jauch, D. Schmalzing, M. Jung, W. Bretschneider, R. Hopp, P. Werkhoff, *Z. Lebensm. Unters. Forsch.*, in press.
[134] V. Schurig, M. Schleimer, H.-P. Nowotny, *Naturwissenschaften 77* (1990) 133.
[135] A. Mosandl, A. Kustermann, U. Palm, H. Dorau, W. A. König, *Z. Lebensm. Unters. Forsch. 188* (1989) 517; A. Mosandl, A. Kustermann, *ibid. 189* (1989) 212; A. Bernreuther, N. Christoph, P. Schreier, *J. Chromatogr. 481* (1989) 363; E. Guichard, A. Kustermann, A. Mosandl, *ibid. 498* (1990) 396.
[136] W. A. König, P. Evers, R. Krebber, S. Schulz, C. Fehr, G. Ohloff, *Tetrahedron 45* (1989) 7003.
[137] W. Boland, W. A. König, R. Krebber, D. G. Müller, *Helv. Chim. Acta 72* (1989) 1288.
[138] K. Harata, K. Uekama, M. Otagiri, F. Hirayama, *Bull. Chem. Soc. Jpn. 55* (1982) 3904; *ibid. 56* (1983) 1732.
[139] K. Harata, K. Uekama, M. Otagiri, F. Hirayama, *J. Inclusion Phenom. 1* (1984) 279; *ibid. 2* (1985) 583; K. Harata, F. Hirayama, T. Imai, K. Uekama, M. Otagiri, *Chem. Lett. 1984*, 1549; K. Harata, K. Uekama, M. Otagiri, F. Hirayama, Y. Sugiyama, *Bull. Chem. Soc. Jpn. 55* (1982) 3386.
[140] K. Harata, K. Uekama, M. Otagiri, F. Hirayama, *Chem. Lett. 1983*, 1807.
[141] M. Czugler, E. Eckle, J. J. Stezowski, *J. Chem. Soc. Chem. Commun. 1981*, 1291.
[142] V. Schurig, H.-P. Nowotny, M. Schleimer, D. Schmalzing, *J. High Resolut. Chromatogr. 12* (1989) 549.
[143] V. Daffe, J. Fastrez, *J. Chem. Soc. Perkin Trans. 2 1983*, 789.
[144] L. Easson, E. Stedman, *Biochem. J. 27* (1933) 1257.
[145] C. E. Dalgliesh, *J. Chem. Soc. 3* (1952) 3940.
[146] H. Karfunkel, Firma Ciba-Geigy AG, Basel, Switzerland, unpublished.
[147] K. Watabe, R. Charles, E. Gil-Av, *Angew. Chem. 101* (1989) 194; *Angew. Chem. Int. Ed. Engl. 28* (1989) 192; V. Schurig, J. Ossig, R. Link, *ibid. 101* (1989) 197 and *28* (1989) 194.
[148] P. Fischer, R. Aichholz, U. Bölz, M. Juza, S. Krimmer, *Angew. Chem. 102* (1990) 439; *Angew. Chem. Int. Ed. Engl. 19* (1990) 427.
[149] V. Schurig, D. Schmalzing, U. Mühleck, M. Jung, M. Schleimer, P. Mussche, J. Duvekot, J. C. Buyten, *J. High Resolut. Chromatogr.*, in press.
[150] V. Schurig, *Angew. Chem. 89* (1977) 113; *Angew. Chem. Int. Ed. Engl. 16* (1977) 110.

The Myelin Membrane of the Central Nervous System—Essential Macromolecular Structure and Function

By Wilhelm Stoffel

The neural sheaths that surround the nerve fibers (axons) are composed of myelin-specific complex lipids and are assembled during the myelination phase either by the oligodendrocytes in the central nervous system (CNS) or by the Schwann cells in the peripheral nervous system. These multilayered myelin membranes insulate the axons and permit a rapid, saltatory conduction of excitation and a reduced axon diameter in comparison with noninsulated axons. Myelination was hence the decisive evolutionary event in miniaturization of the central nervous system (brain and spinal cord). The morphology of the myelin membrane has been studied in detail mainly by electron microscopy. Most of its biochemistry has been elucidated in recent years by molecular-level analysis of both the lipid components (cholesterol, phospholipids and sphingolipids) and the constituent proteins. The multilamellar system is distinguished by a characteristic periodicity due to the 5-nm-thick bilayer formed by the myelin-specific lipids. The bilayer interacts with the myelin basic protein (MBP) on the cytosolic side of the plasma membrane process, while the integral membrane protein proteolipid protein (PLP) has hydrophilic domains exposed on both the cytosolic and extracytosolic faces of the bilayer. Numerous protein-chemical and -immunotopochemical findings have been summarized in a model of the myelin membrane. Through molecular biological studies, the genetic structure and chromosomal location of the myelin proteins have been determined. By employing techniques of molecular and cell biology together, it is now possible to analyze the process of myelinogenesis, the time- and location-specific expression of myelin-specific genes in the brain. Gene-technological methods have been used to define the mutations in the models jimpy mouse and myelin-deficient rat. These are animal models that correspond to genetically determined myelin defects (dysmyelinoses) in humans. Using them, it will be possible to study the cell death of oligodendrocytes on a molecular level; this process is the result of expression of mutant myelin proteins and is incompatible with life. Oligodendrocytes and the myelin structures they synthesize are the target structures of cytotoxic lymphocytes (T_c). In the course of the demyelination process in multiple sclerosis, these cause the breakdown of the myelin sheaths, in gradually appearing inflammations. T_c lymphocytes recognize myelin structures as epitopes and destroy them. The picture of the myelin membrane's molecular composition, which we are now perfecting, will also lead to a better understanding of demyelination on a molecular level, and hence to new therapeutic possibilities.

1. Introduction

In the course of evolution, organisms steadily increased in complexity, and a series of mechanisms arose which allowed them to act and react promptly to external influences. The central and peripheral nervous systems (CNS and PNS) were of great importance here, since they allowed information to be transmitted at high speed between the nerve cells (neurons) and the target organs via the nerve fibers (axons). In addition to the neurons, the neuroglia also developed; these form supportive tissue for the neurons and include the astroglia and the oligodendrocytes. The development of an electrical insulation system for the neural fibers, in the form of a myelin sheath constructed by the oligodendrocytes, was a decisive step in evolution. For naked axons, the speed of excitation transmission is proportional to the diameter of the axon. In a myelinated axon transmission occurs up to 100 times faster than in the absence of myelin; the diameter of the axon can hence be significantly decreased, while maintaining the same performance. Apart from the increase in pulse transmission speed, myelination makes room for a far greater number of axons, which makes possible the exceedingly compact structure of the CNS. If the axons of the spinal cord were not myelinated, then in order to achieve the same results the spinal cord would need to have the diameter of an oak tree several hundred years old, and the optic nerve would require a diameter not of 2–4 mm, but of 10–15 cm.

The fatty covering of the CNS axons, which is particularly obvious in the white matter of a brain section (Fig. 1), was first described by *Virchow* in 1854[1] and named myelin (Greek *myelos*, marrow). In 1871, under the light microscope, *Ranvier*[2] observed breaks in the myelin sheath at intervals of 1–2 μm, which today are called the nodes of Ranvier. Here, the axons are bare and carry higher concentrations of the $K^{\oplus}/Na^{\oplus}$ pumps needed to restore the action potential. The high speed of excitation transmission is not achieved by continual depolarization, as in naked axons, but in jumps from one node to the next over the internodal region. This is know as saltatory excitation.[3] Since depolar-

[*] Prof. Dr. Dr. W. Stoffel
Institut für Biochemie
Medizinische Fakultät der Universität
Joseph-Stelzmann-Strasse 52, D-5000 Köln 41 (FRG)

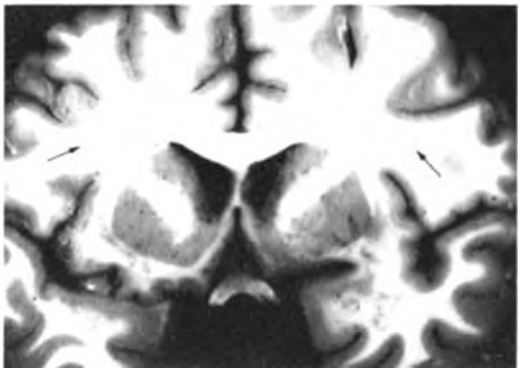

Fig. 1. Macroscopic section through the human brain. The cortex and the white matter (arrows) can be clearly seen.

ization only occurs locally, at the nodes, considerable energy is saved in repolarization.

2. Myelination

Myelin-like neural sheaths first appeared in the evolutionary step that led to the vertebrates (bony fish).[4] The formation of myelin sheaths around the axon gave three advantages; faster information flow, compact organization of the CNS, and energy savings in restoration and maintenance of the resting potential.

Myelination (myelogenesis) takes place in the CNS in a strictly programmed manner, both in when and where it occurs. The program is begun at a characteristic point in time for each species by the precursor cells to O2A astrocytes, which differentiate into oligodendrocytes. In mice and rats this occurs about ten days after birth, in humans at the sixth month of pregnancy. Development of the myelin sheath around the neural fibers of the brain and spinal cord is largely completed in rats and mice by the thirtieth day after birth and in humans by the end of the second to fourth year.[5] During this phase, the oligodendrocyte synthesizes two to three times its own weight in myelin components, lipids and proteins, daily.[6] The oligodendrocytes of the CNS form extended processes of their plasma membranes (Fig. 2A), which approach up to 50 axons and wrap themselves spirally around them. In this process, the cytoplasm is almost entirely squeezed out of the membrane processes. The interior (cytoplasmic) faces lie closely pressed together and appear under the electron microscope as the "main dense line" (MDL), because of their high electron density. In the course of wrapping around the axon, the exterior surfaces of these plasma membrane processes (extracytosolic face) also come into close contact with each other. The contact zone appears as the "intraperiod dense line" (IDL). Figure 2A shows schematically the development of the myelin membrane from the plasma membrane of the oligodendrocytes, Figure 2B the spiral wrapping process, and Figure 2C the

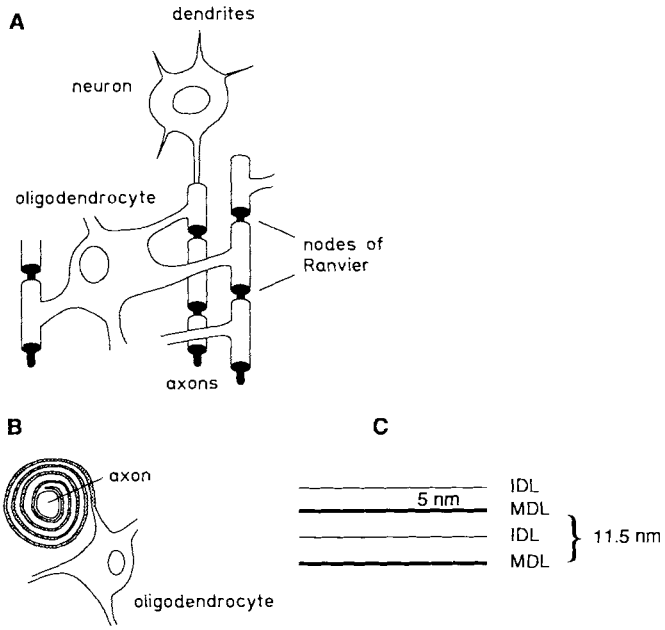

Fig. 2. A) Schematic diagram of plasma membrane processes extending from one oligodendrocyte to many axons, with formation of the nodes of Ranvier. B) Schematic diagram of the spiral winding process in myelination. C) Schematic diagram of myelin periodicity observed under the electron microscope. (see also Fig. 3).

periodicity of the myelin membrane, as seen in the electron microscopic image of a myelinated axon (section in Fig. 3).

The myelin membrane displays a periodicity of 11.5 nm. Each lipid bilayer is about 4–5 nm thick (Fig. 2C) and is therefore significantly larger than the plasma membrane of liver or connective tissue cells (2.5–3 nm). These large di-

Wilhelm Stoffel studied medicine from 1947 to 1952 in Cologne and obtained his doctorate with E. Klenk in physiological chemistry in Cologne. He studied chemistry in Bonn from 1952 to 1957 and received his Diplom with B. Helferich and his doctorate with L. Craig, Rockefeller University, New York, and E. Klenk, Cologne. After postdoctoral study with L. Craig and E. H. Ahrens, Rockefeller University, and C. Martius, ETH Zürich, he habilitated in physiological chemistry in Cologne in 1962 and took up the Chair of Physiological Chemistry in 1967 (now Biochemistry, Medical Faculty of Cologne University). His current research interests include neurochemistry and molecular neurobiology, analysis of atherogenesis (arteriosclerosis research), and structure and function analysis of serum lipoproteins.

Fig. 3. Electron microscopic image of a section through a myelinated axon. The electron-dense main dense line (MDL), corresponding to the cytosolic cleft, can be distinguished, as can the intraperiod dense line (IDL), which results from the extracytoplasmic sides of two myelin membranes packed together. The radial components are also visible.

Table 1. Comparison of the components of oligodendrocyte plasma membranes with those of myelin.

Components	Oligodendrocyte plasma membrane [mol %]	Myelin [mol %]
Proteins	54	21
Lipids	46	79
Cholesterol	36.4	40.9
Cerebrosides	9.4	15.7
Sulfatides	3.0	4.0
Sphingomyelin	5.4	4.7
Phosphatidylcholine	25.4	10.9
Phosphatidylethanolamine	7.3	13.6
Phosphatidylinositol (di)phosphate	7.1	4.7
Phosphatidylserine	5.1	5.0
Gangliosides	0.9	0.5

mensions are the direct result of the various chemical structures of the lipids that form the bilayer, which will be described in the next section.

In the peripheral nervous system, the role of the oligodendrocyte in the CNS is filled by the Schwann cell. Although the PNS myelin is very similar to that of the CNS in its morphological architecture (periodicity), each Schwann cell forms only one internodal sheath.

In the following, four questions concerning the biochemistry and molecular biology of the macromolecular components of the myelin membrane of the central nervous system will be discussed:

1. Which chemical structures are responsible for the compact layering of the myelin lamellae and hence for the insulating effect on the axon, and how is the extraordinary periodicity of the myelin membrane determined?
2. How can the winding of oligodendrocyte plasma membrane processes around the axons be understood?
3. How do the slightest changes in protein structures through mutations lead to complete dysfunction and death?
4. What significance does a knowledge of myelin structures have for the understanding of pathogenic dys- and demyelinating diseases?

3. The Lipid Bilayer of the Myelin Membrane

Myelin may be isolated in homogeneous form for analysis by simple centrifugation steps. The myelin membrane is the most lipid-rich in any animal tissue. About 80% of its dry weight consists of cholesterol and complex sphingo- and phospholipids and only 20% is protein. Table 1 shows the components of myelin, compared with those of the plasma membrane of oligodendrocytes. The lipid bilayer has a very unusual composition in that it has an extraordinarily high cholesterol content of 40 mol%. Hence, for every phospholipid, one molecule of cholesterol is present (sphingomyelin is included with the phospholipids here because it has an identical zwitterionic head group to the phosphatidylcholines); relative to the sphingolipids cerebroside and sulfatide, the proportion is 1:2.

Complete extraction of the myelin lipids from the myelin is only possible with acidic chloroform/methanol (e.g., chloroform–methanol–acetic acid, 2:1:0.1), since the acidic phospholipids and sulfatides form strong ionic bonds to the myelin proteins. The amphiphilic complex lipids are made up of a hydrophobic group—the alkane chains of the fatty acids and of sphingosine, the alkenyl ethers of plasmalogens—which forms the central or core region of the bilayer, and the polar head group, which makes up the surface and faces the aqueous myelin (Figs. 4 and 5).

The hydrophobic portions of sphingolipids (cerebroside and sulfatide) are made up of extremely long fatty acids, from C_{18} (stearic acid) to C_{24} (lignoceric acid). These are present in their saturated, α-D-hydroxy or unsaturated ω-9-monoene forms and are bound to the sphingosine (sphingenine, (2*S*,3*R*,4*E*)-2-amino-1,3-dihydroxyoctadecene) by an amide linkage to give the ceramide. The alkane chains of the fatty acid and sphingosine base portions of the ceramide are hence variable in length. The all-*trans* structure of the long-chain acyl residues ($>C_{24}$) dictates a length of 3.6–4.0 nm. This explains the unusual thickness of the bilayer, 4.5–5.0 nm; the "sticky ends" of the alkane chains overlap in the fluid center of the bilayer.

On the edge of the hydrophilic head group one finds the free hydroxy groups of the sphingosine and of the long-chain α-hydroxy fatty acids. Like the hydroxy group of cholesterol and the amide group of the ceramide, these can undergo hydrogen bonding to the carbonyl groups of the phospho- and sphingolipids. Hydrogen bonds reduce the distance between the groups that form them. The number of free protons available for hydrogen-bond formation allows a cross-linking of all the carbonyl groups in the lipid bilayer and, consequently, its stabilization by a two-dimensional layer of hydrogen bonds (Fig. 4). The acyl groups of the ceramides—sphingomyelin only contains long-chain, saturated, C_{18} and C_{24} fatty acids—would exist in crystalline form at 37 °C, but are converted into a fluid phase by intercalation of cholesterol molecules and of the acyl groups of the phospholipids, which are in part highly unsaturated. Though their function is unknown, the 1-alkenyl ether groups in the phosphatidylethanolamine class are also worth mentioning here.

Regarding the polar head groups of myelin membrane lipids at the water interphase, one finds not only the ubiquitous membrane phospholipids phosphatidylcholine and phosphatidylethanolamine, but also extensive amounts of phosphatidylserine and phosphatidylinositol. Together with

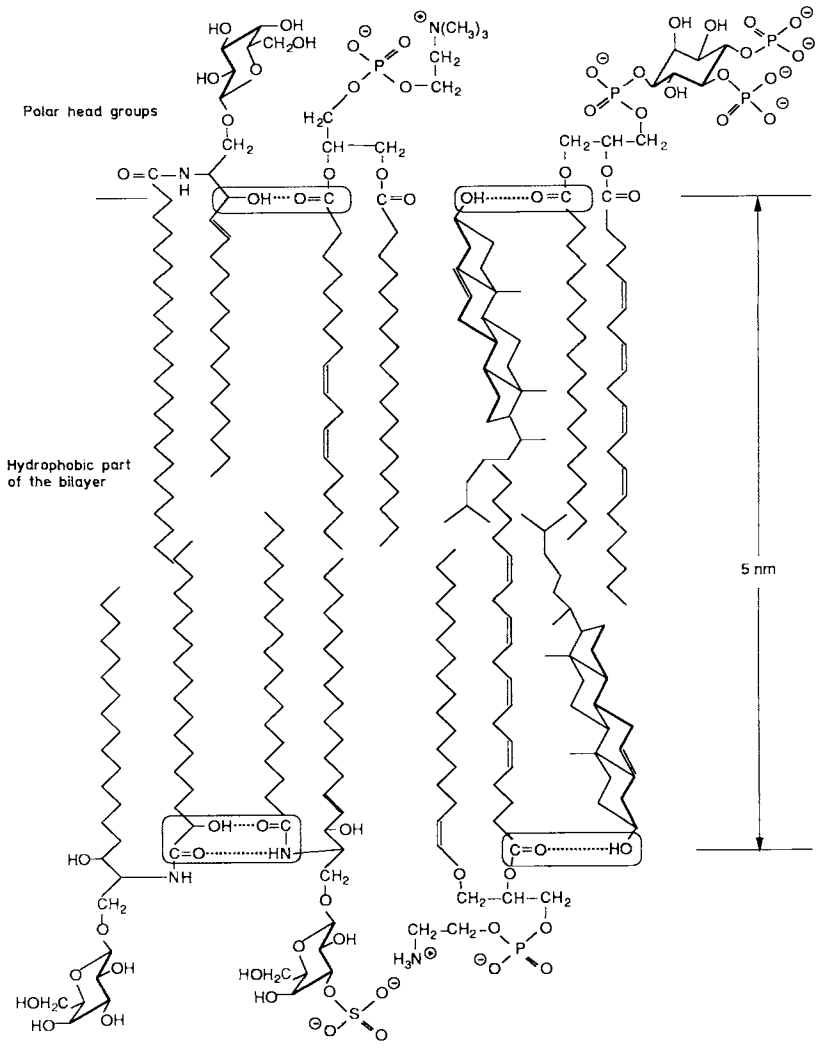

Fig. 4. Diagram of a model lipid bilayer, with cholesterol, the myelin-specific sphingolipids cerebroside and sulfatide, and the acidic phospholipids. The four possible types of hydrogen bonding are emphasized. The chemical structures of myelin lipid species are presented in more detail in Figure 5.

the sulfatides, this means that on average every fourth polar head group of the complex phospho- or sphingolipid type contributes an anionic group to the membrane surface. The gangliosides, which are present as trace lipids in myelin membranes, too, have not been included here (Fig. 5).

At present we know little about the symmetry or asymmetry of lipid distribution in the bilayer. Labeling of the oligodendrocyte plasma membrane and the myelin membrane with anti-galactosylceramide or anti-sulfatide antibodies, however, reveals their dense distribution in the external layers of the membrane sandwich structure.

Because of the zwitterionic head groups of the phospholipids, the hydrophilic, uncharged galactose residues of the cerebroside, and above all the anionic groups, the surfaces of the myelin membrane bilayer have many and varied possibilities for interaction with complementary molecules on both the cytosolic and extracytoplasmic faces of the membrane. These may well be important for compact packing and for the spiral folding process in myelination.

The significance of the relatively high content of phosphatidylinositols, especially with regard to their importance as a "second messenger system", is quite unknown.

4. Myelin Proteins of the CNS

Although the myelin lipids of the PNS and CNS are very similar in composition, significant differences are found for the proteins. Sodium dodecyl sulfate polyacrylamide gel electrophoresis (SDS-PAGE) separates the myelin protein mixture into a few components (Fig. 6).

The bands can be assigned to proteolipid protein (PLP), also called lipophilin, to DM20, an isoprotein derived from PLP, and to the myelin basic protein (MBP) and its isoforms. The latter are lower-molecular-weight forms of MBP, which arise by alternative splicing (see Section 5, Fig. 8). The remaining bands correspond to glycoproteins, Wolfgram proteins (W), and myelin-associated glycoproteins (MAG). Together, PLP and MBP make up about 90% of the total protein.

4.1. Myelin Basic Protein

Myelin basic proteins constitute some 30–40% of the total protein in myelin and can be purified by acid extraction

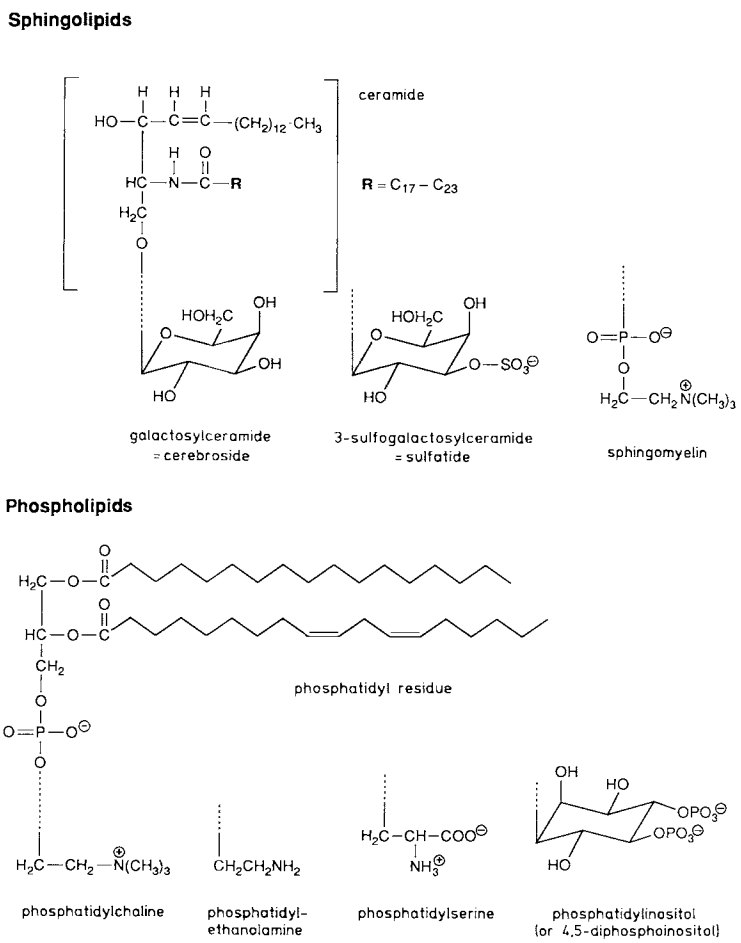

Fig. 5. Structural formulas of the most important classes of lipid in the myelin membrane.

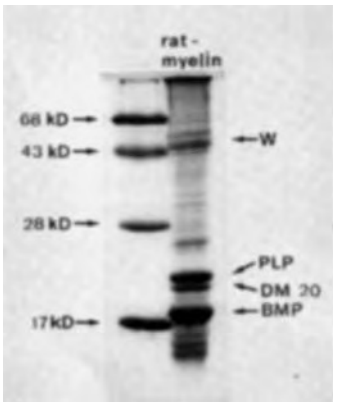

Fig. 6. Right: SDS-polyacrylamide gel electrophoresis of rat myelin proteins. Left: standards. W, Wolfgram proteins; PLP, proteolipid protein; DM 20, isoform of PLP; BMP, myelin basic protein (otherwise abbreviated MBP in this article).

of the myelin with subsequent ion-exchange chromatography and gel filtration.[7] The main component in humans and cattle is an 18.5-kDa MBP with 169 amino acids (bovine) or 170 amino acids (human, with 24% basic amino acids).[9] In humans there are two isoforms, 17.2 kDa and 21.5 kDa in size,[10] while rodents have four isoforms of 14, 17, 18.5, and 21.5 kDa. Here,[10,11] as in humans,[12] these arise by alternative splicing of *one* primary transcript of the MBP gene,[11] which will be discussed in detail with the description of the MBP gene structure (Section 5). MBP shows all the characteristics of a peripheral membrane protein. It has been localized in the cytoplasmic space (visible as the MDL under the electron microscope) with the aid of specific antibodies[13] and by enzymatic degradation of myelin proteins.[14] Because of its high basicity, MBP undergoes ionic interactions with the acidic polar head groups of lipids on the cytoplasmic side of the lipid bilayers, and brings about their compact packing.

In aqueous solution, circular dichroism measurements have shown that MBP occurs predominantly in a random coil conformation.[15] *Stoner*,[16] on the other hand, has proposed a secondary pleated sheet structure, on the basis of secondary-structure parameter weightings in computer calculations.

4.2. Proteolipid Proteins

The proteolipid fraction was first isolated by *Folch* and *Lees* in 1951 from a chloroform–methanol extract of the white matter of the brain.[17] It is the largest protein fraction in myelin, making up 50–55% of the dry weight. SDS-PAGE separates it into two bands, of 26 kDa (PLP) and 20 kDa (DM20). PLP and DM20 are isoproteins, which, because of their high hydrophobicity, are water-insoluble. The principal reason why 30 years elapsed between their discovery and the elucidation of their primary structure in my group in Cologne (1982–1983) was the necessity to develop new separation methods for hydrophobic peptides. These peptides were obtained by chemical cleavage (cyanogen bromide cleavage at methione residues and bromosuccinimide–dimethyl sulfoxide (DMSO) cleavage at tryptophan residues) and enzymic degradation of the PLP; their separation was followed by Edman degradation of the purified peptides.

We studied human and bovine brain. PLP is a polypeptide with 276 amino acids and a molecular mass of 29 891 Da. Surprisingly, we found that the sequences of human and bovine PLP differ at only two positions: Ala 188 and Thr 198 in bovine PLP are replaced by Phe 188 and Ser 198 in human PLP (Fig. 7, top), The sequence is clearly divided into one short and four long hydrophobic sequences, connected by hydrophilic "loops". If one arranges these domains separately (Fig. 7, bottom) and calculates their three-dimensional size, the structures typical of an integral membrane protein emerge. Three domains have just the right size to span the 5-nm bilayer (*trans* helices), while two are present in *cis* configuration, since one domain (40 amino acids) is too long to span the membrane, and the other (12 amino acids) is too short. In addition, both of these contain proline residues in the center of the sequence; proline is an α-helix breaker and leads to a bend and a reversal in the direction of the α-helix. PLP contains 14 cysteine residues, four of them as free cysteines. A disulfide bond is found between Cys 227 and the amino-terminal Cys 5. The hydrophobicity of the polypeptide is increased still further by acylation with a long-chain fatty acid on Thr 198.

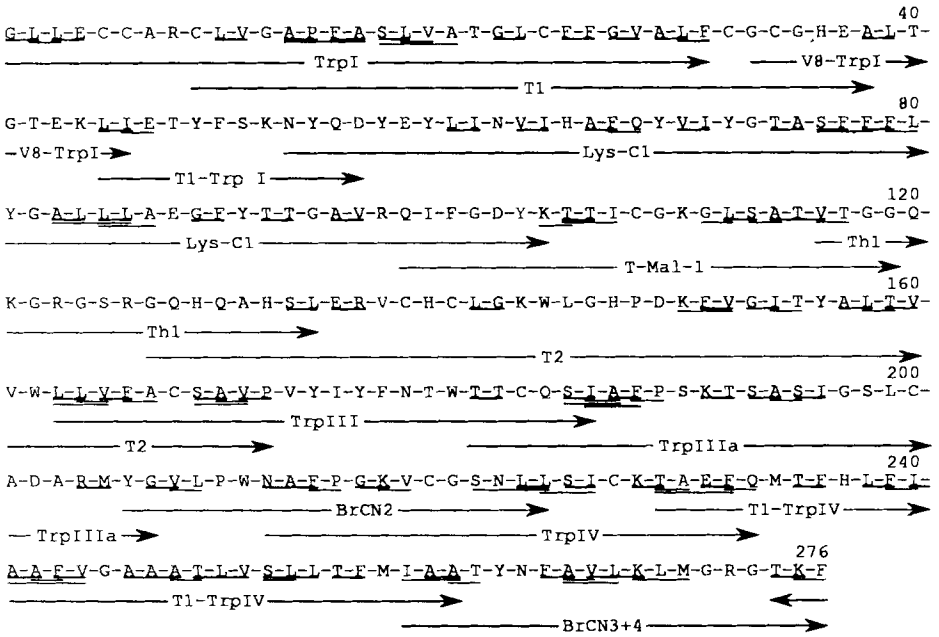

Fig. 7. Top: Amino-acid sequence and sequencing strategy for human proteolipid protein of the central nervous system. Trp, tryptophan fragments I–IV; V8, V8 staphylococcus protease; Lys-C, Lys-C protease; T-Mal, trypsin fragment after maleoylation; Th, thermolysin fragment; T, tryptic peptides; BrCN, cyanogen bromide fragments I–IV. Bottom: Hydrophobic (bold) and hydrophilic domains of the proteolipid protein. Above the sequences are the amino-acid numbers, the number of turns in the α-helix they form (3.6 amino acids per turn), and the length of the resulting helix (0.5 nm per turn).

27 amino acids; 7.5 turns; 4.05 nm

29 amino acids; 8 turns; 4.35 nm

40 amino acids; 11 turns; 6.00 nm

12 amino acids; 3 turns; 1.65 nm

30 amino acids; 8.3 turns; 4.50 nm

4.2.1. Configuration of the Proteolipid Protein in the Myelin Membrane

From the strict division of the PLP polypeptide chain into hydrophobic and hydrophilic domains, a model was proposed for its integration into the myelin lipid bilayer. This was then confirmed by biochemical and immunotopochemical studies. Figure 8 (top) illustrates our current view. On the extracytoplasmic side, one finds a short, hydrophilic, N-terminal sequence, which continues into the first transmembrane α-helix. This, in turn, leads into a hydrophilic domain with two excess negative charges on the cytoplasmic side and folds back onto itself into the second transmembrane helix. The largest, strongly positively charged, hydrophilic sequence (Arg 97 to Arg 150) is found on the extracellular surface. The two *cis* domains also dip into the membrane bilayer from this side, while the C-terminal hydrophobic domain traverses the membrane again, so that the highly positively charged C-terminus of the sequence is oriented towards the cytoplasmic space. The hydrophobic segments are bounded by anionic or cationic amino-acid side chains or by ionic side chains of zwitterionic nature.

In our model, ten cysteine residues lie in the hydrophilic domains on the extracytoplasmic surface and four are found in α-helical domains. On the basis of the disulfide bridge between Cys 5 and Cys 227, and possible disulfide linkages between the *trans* and *cis* helices, we assume a cylindrical aggregation of the hydrophobic helices, as depicted in Figure 8 (bottom). On limited proteolysis of the myelin membrane, we observe facile release of the small hydrophilic domain between Arg 204 and Lys 217 and its ready dissociation from the lipid bilayer. It is quite possible that this domain performs a flip-flop motion into a myelin membrane packed above it, and through intercalation into the lipid bilayer it may hence play a role in fixation and tight apposition to the neighboring membrane, like the long-chain acyl group. These two structural elements could also be important in the dynamics of the spiral winding process.

This model has been substantiated experimentally in two ways. (1) The myelin membrane layers were dissociated by osmotic shock, subjected to tryptic digestion, and separated to give three large polypeptides. On sequencing these, we discovered that the endoprotease had attacked the PLP in the positions indicated by arrows in Figure 8 (top); since the enzyme cannot penetrate the lipid bilayer, this indicates that these sites are accessible on the external surface. Figure 9

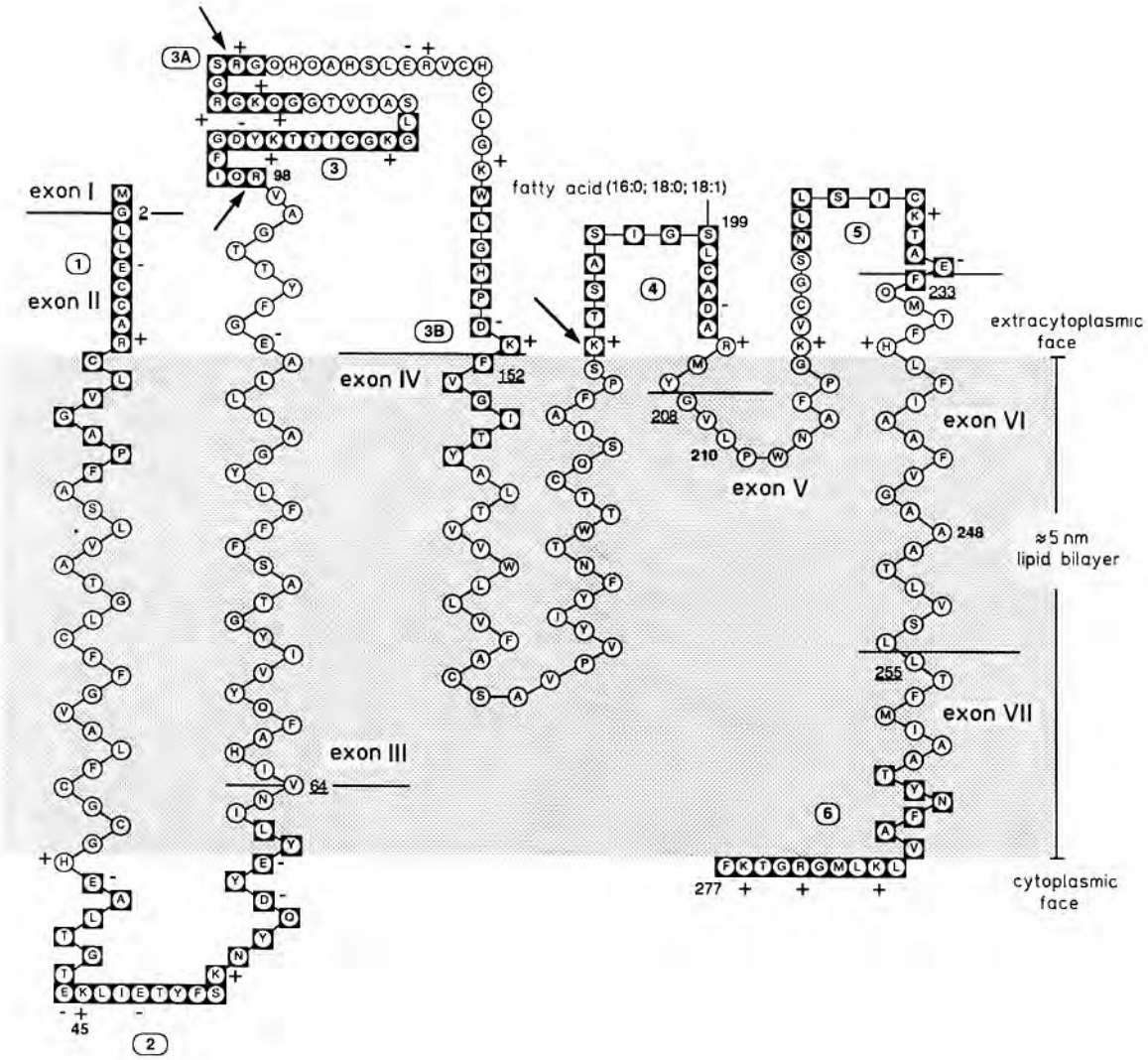

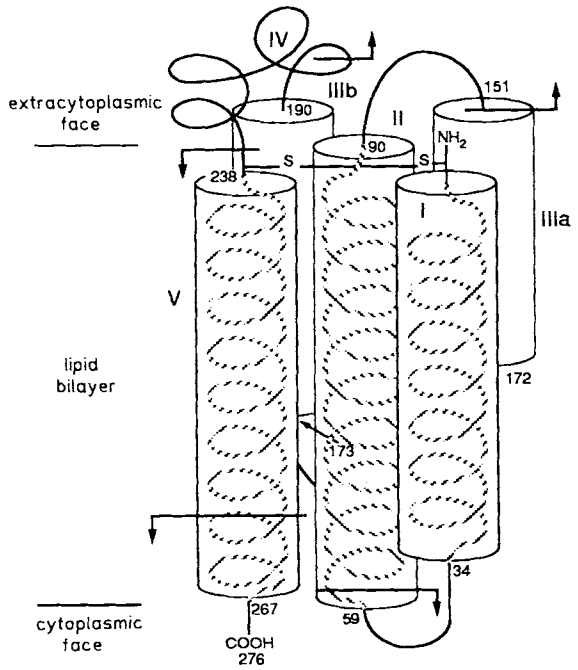

Fig. 8. Top: Model of the membrane integration of proteolipid protein, based on its hydrophobic and hydrophilic domains and on biochemical and immunotopochemical evidence. The peptide sequences framed in black (1, 2, 3, 3A, 3B, 4, 5, and 6) are epitopes which were obtained by solid-phase synthesis and used to generate antibodies. Bars demarcate the exons (Section 5); arrows show points of proteolytic attack by trypsin on intact myelin whose compact layering has been loosened by hyposmotic treatment. Bottom: Suggested association of the intermembrane α-helices within the lipid bilayer, by extracytoplasmic disulfide bonds. The arrows indicate the start of each new exon.

shows the SDS-polyacrylamide gel after proteolytic treatment of the myelin. The PLP band has disappeared, giving smaller polypeptides between 7 and 10 kDa. In contrast, MBP is completely protected from proteolysis, which can only be explained by its localization in the cytoplasmic cleft, shielded by the lipid bilayers. This finding is biochemical evidence for the location of MBP in myelin.

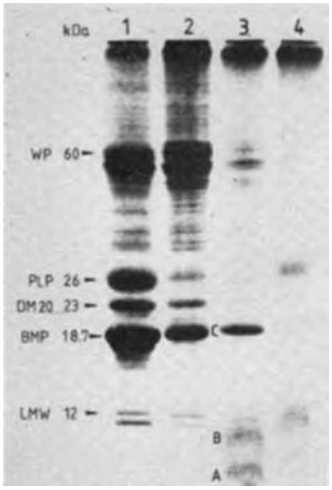

Fig. 9. SDS-polyacrylamide gel electrophoresis of myelin proteins after trypsin treatment of the intact myelin membrane. The PLP band has vanished and is replaced by proteolysis fragments. The cleavage sites are indicated by arrows in Fig. 8 above.

(2) If we accept that it is possible to generate antibodies against synthetic peptide sequences from the various domains of the PLP sequence that are marked as black boxes in Figure 8 (top) and to use them as markers of the nonpermeabilized membrane, then the orientation of PLP should be measurable histologically. For this purpose, we used primary cultures of rat brain oligodendrocytes, taken into culture, 18 days after birth. The expression of myelin proteins is similar in these cells to that in the myelinating rat. The PLP in the plasma membrane should have the final orientation

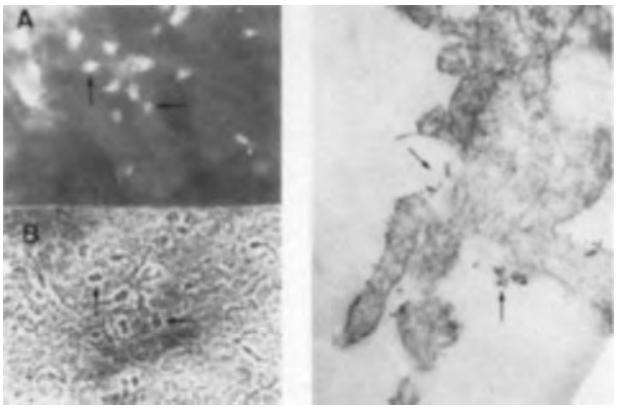

Fig. 10. Immunocytochemical localization of the PLP domains with the aid of antipeptide antibodies. Left: A) Fluorescence labeling, B) phase contrast image. Right: Gold labeling of the oligodendrocyte plasma membrane processes in tissue culture (8150× magnification, electron microscope).

that it will have before it segregates into the growth cone of the oligodendrocyte and on into the myelin membrane process.

Figure 10 (left) shows that only antibodies against peptides in the hydrophilic loop Arg97–Arg150 gave an immunofluorescent labeling of the oligodendrocyte plasma membranes. The same result was obtained with gold-labeled antibodies against this peptide (Fig. 10, right). Hence, both these findings agree with the proposed model for the PLP configuration in the membrane.

Surprisingly, further secondary-structure studies using the rules of *Chou* and *Fasmann*, *Nagano*, and others revealed that all the hydrophilic domains, except for the first third of the largest domain (Arg97–Lys120), are folded as amphipathic helices. These additional secondary structures are included schematically in Figure 11. This result could be of great importance for the packing of the myelin membrane layers.

4.3. Wolfgram and Other Proteins

Further protein components, which are expressed in very low concentrations, are the Wolfgram proteins and the

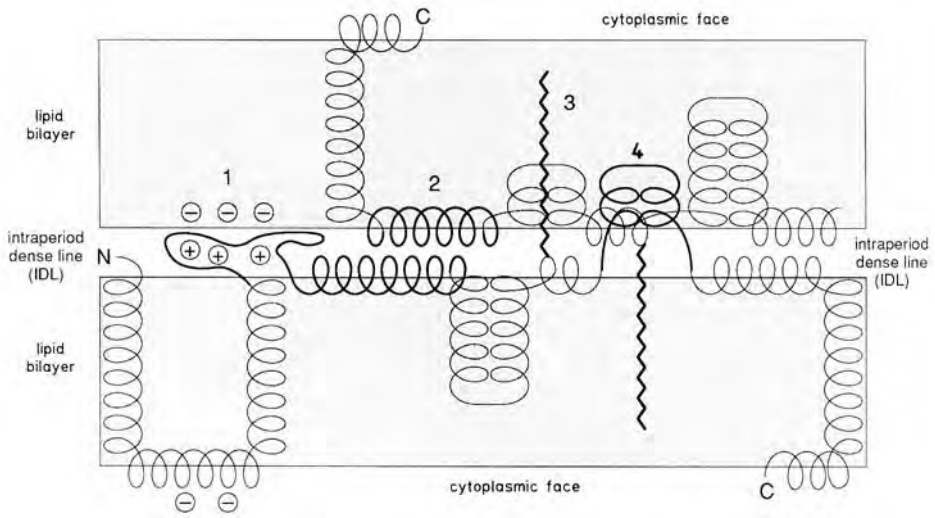

Fig. 11. Contributions to spiral winding and compact packing of the myelin layers by the interaction of (1) charged sequences, (2) the amphipathic helices of extracytoplasmic hydrophilic domains, (3) fatty acid chains, and (4) hydrophobic flip-flop loops of PLP.

"myelin-associated glycoprotein" (MAG, Fig. 6). In 1966, *Wolfgram*[18] isolated a protein fraction from the acidic (pH 5) chloroform–methanol extract. This fraction showed three bands on SDS-PAGE, with molecular masses between 45 and 55 kDa. Of these, the 55-kDa component is α-tubulin, which reacts with specific α-tubulin antibodies in a Western blot, while the 45- and 50-kDa bands can be assigned to the enzyme 2′,3′-cyclic-nucleotide 3′-phosphodiesterase.

Myelin-associated glycoprotein (MAG) is a glycoprotein with a molecular mass of 100 kDa, which is present as a trace protein (1% of total myelin protein). Its amino-acid sequence has recently been deduced from the cDNA; the sequence contains 626 amino acids (100 kDa) and in many regions is homologous to the neural cell adhesion molecule (N-CAM).[19] Its localization in the periaxonal region of the myelin of adult rat points to possible interactions between neurons and oligodendrocytes in myelogenesis.

5. Molecular Biology of Myelin Proteins

5.1. Construction of cDNA Libraries from the RNA of Myelinating Rat Brains and the Isolation of MBP- and PLP-specific Clones

The synthesis of myelin proteins and lipids is at its greatest 18 days after birth.[20] We isolated brain RNA from 18-day-old rats and enriched the poly(A)$^+$-RNA by affinity chromatography on oligo(dT) cellulose.[21] We then synthesized cDNA (complementary or copy DNA) with the aid of reverse transcriptase, by a modified Gubler–Hoffmann method[22] (Fig. 12). Size fractionation by gel electrophoresis in 1% agarose afforded copies of 550- to >6000-bp double-stranded cDNA, which were cloned into the *Pst* I restriction site of the pBR 322 vector. Clones showing specificity for the proteolipid and myelin basic proteins were isolated from this bank by screening colonies by Southern-blot hybridization with labeled oligonucleotides. These nucleotides were derived from the N-terminal, C-terminal, and central regions of our PLP amino-acid sequence and from the C-terminal region of the 18.5-kDa MBP. Of these clones, the 612-bp, MBP-specific cDNA clone contained the entire coding region of the 14.5-kDa MBP isoprotein, while the longest PLP-specific clone was missing about 310 bp of the N-terminal coding sequence.[23] The steps leading to PLP- and MBP-specific clones are summarized in the flow chart shown in Figure 12.

Using these cDNA clones, the size of the mRNA transcripts for PLP and MBP was determined by Northern-blot hybridization. Two strong, PLP-specific RNA bands corresponding to 3.2 and 1.6 kb lengths in a ratio of 2:1, as well as a weak band corresponding to 2.4 kb, were detected in 18-day-old rat brain. The mRNA's do not differ in the coding region, but contain three different 3′-nontranslated sequences; 2062 bases for the longest, 3.2-kb mRNA, 1319 bp for the 2.4-kb mRNA, and 430 bp for the 1.6-kb mRNA in the 3′ direction from the stop codon. Three polyadenylation signals (AATAAA) are present, which are responsible for the varying lengths of the transcripts (Fig. 13). The second sequence required for efficient polyadenylation, TGTGTCTT,

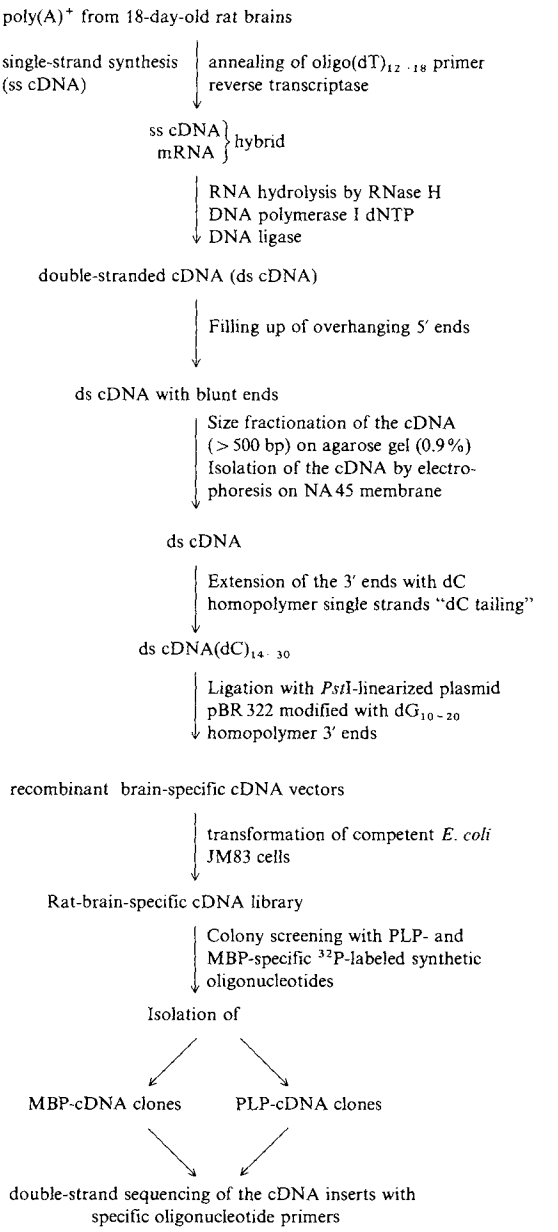

Fig. 12. Flow diagram for preparation of modified, brain-specific cDNA [22] from the brain poly(A)$^+$-RNA of 18-day-old rats and for the isolation of PLP- and MBP-specific clones for DNA sequencing.

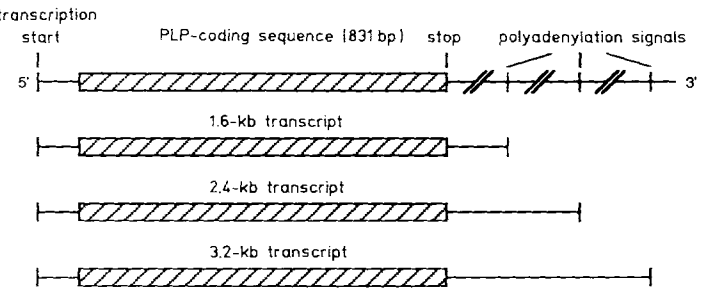

Fig. 13. Layout of the three PLP-specific transcripts. The polyadenylation signals (AATAAA) located 430 bp (1.4-kb transcript), 1310 bp (2.4 kb) and 2062 bp (3.2 kb) in the 3′ direction from the stop codon are used in posttranscriptional modification.

is also present, about 30 bp downstream of the polyadenylation signal.[24] In humans, only the 3.2- and 1.6-kb transcripts are made.

5.2. Genetic Structure of Human Proteolipid Protein and Myelin Basic Protein

With the PLP- and MBP-cDNA clones in hand, we were able to investigate the organization of the two human genes and their chromosomal localization. To do this, we screened human genome libraries in the vectors EMBL-3 and Charon 8, using cDNA probes and oligonucleotides for the coding region and for the 5'- and 3'-noncoding ends of the exons of PLP and MBP.

Analysis of a gene, and in general of large DNA segments, is begun with the preparation of a restriction map, using type II endonucleases, which recognize specific (hexa)nucleotide sequences. With the help of hybridization probes both from the cDNA (restriction fragments) and from synthetic oligonucleotides, the position of the coding sequences (exons) and the segments between them (introns) can be determined. Further, if the 5' and 3' ends of the mRNA have been ascertained with corresponding probes, the map affords information about the size of the sought gene.

5.2.1. *Exon–Intron Structure of the PLPs*[25]

Two overlapping clones were found which contained the entire human PLP gene. Complete digestion with individual restriction enzymes and combinations of two enzymes gave characteristic fragments; logical matching up of the two genomic PLP-specific λ-phage EMBL-3 clones gave the required restriction map.

Figure 14 shows the restriction map, which was drawn up by restriction analysis and Southern-blot hybridization with [^{32}P]-labeled *Pst*I fragments from the PLP clone and 5'-labeled oligonucleotides. It was a great advantage at this stage that we were able to use double-stranded or supercoil sequencing[26,27] and, further, that the time-consuming process of sequencing could be cut short with the aid of synthetic primers from known genomic sequences. Thus, subcloning of small, overlapping restriction fragments of the DNA sequence to be screened (cDNA or genomic DNA) into the

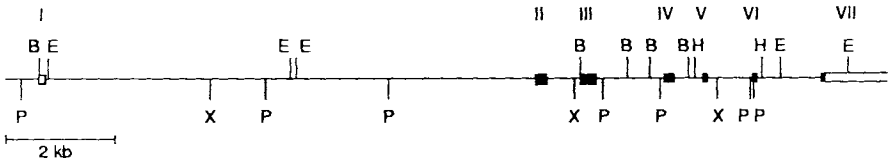


```
I AACAAAATGA AACAATTGCC AGTGAAAGGC AGAAAGAGAA GATGGAGCCC TTAGAGAAGG GAGTATCCCT GAGTAGGTGG GGAAAAGGGG AGGAGAAGGG GAGGAGGAGA GGAGCAGCAA      -205
  AGCAGGCCTA TCCCTTTAAG GGCGTTGGCT GTCAATCAGA AAGCCCTTTT CATTGCAGGA GAAGAGGACA AAGATACTCA GACAGAAAAA GTAAAAGACC GAAGAAGGAG GCTGGAGAGA      -85
                                                                                                    Met G(ly)                          1
  CCAGCATCCT TCCAGCTGAA CAAAGTCAGC CACAAAGCAG ACTACCCAGC CGGCTACAAT TGGAGTCAGA GTCCCAAAGA C ATG G gtaagtttcaaaaactttag...                +1

II                    (G)ly Leu Leu Glu Cys Cys Ala Arg Cys Leu Val Gly Ala Pro Phe Ala Ser Leu Val Ala Thr Gly Leu Cys Phe Phe Gly Val Ala    29
  ...ttcccctattcttcccccag  GC TTG TTA GAG TGC TGT GCA AGA TGT CTG GTA GGG GCC CCC TTT GCT TCC CTG GTG GCC ACT GGA TTG TGT TTC TTT GGG GTG GCA   +87

  Leu Phe Cys Gly Cys Gly His Glu Ala Leu Thr Gly Thr Glu Lys Leu Ile Glu Thr Tyr Phe Ser Lys Asn Tyr Gln Asp Tyr Glu Tyr Leu Ile Asn Val(1)     63
  CTG TTC TGT GGC TGT GGA CAT GAA GCC CTC ACT GGC ACA GAA AAG CTA ATT GAG ACC TAT TTC TCC AAA AAC TAC CAA GAC TAT GAG TAT CTC ATC AAT GT gtaa  +188

  gtacctgccctcccac...                                                    75                md
                                                                         Pro
III                   (Va)l Ile His Ala Phe Gln Tyr Val Ile Tyr Gly Thr GGA ACT Ala Ser Phe Phe Phe Leu Tyr Gly Ala Leu Leu Leu Ala Glu Gly Phe Tyr    91
  ...ttgtctacctgttaatgcag  G ATC CAT GCC TTC CAG TAT GTC ATC TAT                GCC TCT TTC TTC TTC CTT TAT GGG GCC CTC CTG CTG GCT GAG GGC TTC TAC  +273
                                                                         C
                                                                        Ava II
                                                                                                  DM-20
  Thr Thr Gly Ala Val Arg Gln Ile Phe Gly Asp Tyr Lys Thr Thr Ile Cys Gly Lys Gly Leu Ser Ala Thr Val Thr Gly Gly Gln Lys Gly Arg Gly Ser Arg   126
  ACC ACC GGC GCA GTC AGG CAG ATC TTT GGC GAC TAC AAG ACC ACC ATC TGC GGC AAG GGC CTG AGC GCA ACG GTA ACA GGG GGC CAG AAG GGG AGG GGT TCC AGA  +378

  Gly Gln His Gln Ala His Ser Leu Glu Arg Val Cys His Cys Leu Gly Lys Trp Leu Gly His Pro Asp Lys                                            150
  GGC CAA CAT CAA GCT CAT TCT TTG GAG CGG GTG TGT CAT TGT TTG GGA AAA TGG CTA GGA CAT CCC GAC AAG gtgatcatcctcaggatttt...                  +450

IV                      Phe Val Gly Ile Thr Tyr Ala Leu Thr Val Val Trp Leu Leu Val Phe Ala Cys Ser Ala Val Pro Val Tyr Ile Tyr Phe Asn Thr   179
  ...acccatgtcaatcattttag TTT GTG GGC ATC ACC TAT GCC CTG ACC GTT GTG TGG CTC CTG GTG TTT GCC TGC TCT GCT GTG CCT GTG TAC ATT TAC TTC AAC ACC  +537

  Trp Thr Thr Cys Gln Ser Ile Ala Phe Pro Ser Lys Thr Ser Ala Ser Ile Gly Ser Leu Cys Ala Asp Ala Arg Met Tyr G(ly)                        207
  TGG ACC ACC TGC CAG TCT ATT GCC TTC CCC AGC AAG ACC TCT GCC AGT ATA GGC AGT CTC TGT GCT GAT GCC AGA ATG TAT G  gtgagttagggtacgggtgc...     +619

V                     (G)ly Val Leu Pro Trp Asn Ala Phe Pro Gly Lys Val Cys Gly Ser Asn Leu Leu Ser Ile Cys Lys Thr Ala Glu               231
  ...gctttttgtgtcttacttag GT GTT CTC CCA TGG AAT GCT TTC CCT GGC AAG GTT TGT GGC TCC AAC CTT CTG TCC ATC TGC AAA ACA GCT GAG gtgagtgggttattt  +693
  gggtt...      ji /
                g
VI                      Phe Gln Met Thr Phe His Leu Phe Ile Ala Ala Phe Val Gly Ala Ala Ala Thr Leu Val Ser Leu                           253
                      Gly Pro Asn Asp Leu Pro Pro Val Tyr Cys Cys Ile Cys Gly Gly Cys Ser Tyr Thr Gly Phe Pro
  ...ctcttttcattttcctgcag TTC CAA ATG ACC TTC CAC CTG TTT ATT GCT GCA TTT GTG GGG GCT GCA GCT ACA CTG GTT TCC CTG gtgagttgactttgaatgat...     +759

VII                     Leu Thr Phe Met Ile Ala Ala Thr Tyr Asn Phe Ala Val Leu Lys Leu Met Gly Arg Gly Thr Lys Phe Stop                  276
                      Ser His Leu His Asp Cys Cys His Leu Gln Leu Cys Arg Pro Stop
```

Fig. 14. Top: Restriction map and exon–intron organization of the human PLP gene. The exons are indicated by rectangles. Solid rectangles represent coding regions, open ones 5'- and 3'-nontranslated sequences. Bottom: Nucleotide sequence of the PLP exon and the adjacent intron regions. The DM-20 isoprotein and the mutation sites for jimpy mouse and md rat are shown. Restriction enzymes: B, *Bam*H1; E, *Eco*R1; H, *Hind*III; P, *Pst*1; X, *Xba*1.

M 13-phage system for dideoxynucleotide chain-termination sequencing became unnecessary. The newly obtained sequence data afforded the information needed for the oligonucleotide required as a sequencing primer.

The nucleotide sequences for the coding regions agree with the derived amino-acid sequences from the glycine in position 2 of the PLP onwards. For the glycine, however, only two of the three nucleotides were correct.

At its N-terminus, the rat cDNA sequence contains only an additional Met, compared with the mature PLP.[28, 29] It follows that for the one amino-acid presequence of the PLP primary transcript, a further exon must exist, carrying the Met codon ATG and the first base of the glycine triplet. Downstream, GT should serve as the signal for the 5'-donor splicing sequence for the intervening intron. On the basis of the unusually high homology between the PLP sequences of human and rat, we synthesized a 24-mer oligonucleotide with 18 bases of rat cDNA and the base sequence ATGGGT, and used it as a hybridization probe. The missing exon I was identified in this way on a *Pst*I-*Eco*R1 fragment 8.8 kb upstream of exon II.

Together with the restriction map, the sequencing results yield the following picture. The human PLP gene stretches over 17 kb and consists of seven exons and six introns (Fig. 14, top). Exon I contains the 5'-untranslated region, the triplet of the Met presequence, and the first base of the glycine triplet, the N-terminus of the mature protein. From the bases following the start codon, it is clear that human PLP does not possess a signal sequence. Hence, an internal signal sequence for the primary step of integration into the membrane of the rough endoplasmic reticulum is present. The following sequences lie in the 5' region (Fig. 14, bottom): CAAT box at -174 to -170 (Met $= +1$), Hogness box at -115, and transcription start at -80. Exons II–VII are made up of amino acids 1–63, 64–150, 151–206, 207–231, 232–253, and 254–276. The codons for amino acids 1, 63, and 207 include the exon–intron boundaries and are hence divided between two exons, severely limiting the possibilities for alternative splicing. The entire gene is 17 kb long—since the mRNA resulting from transcription is about 3 kb, the calculated intron/exon length ratio is 4.7:1. However, since only 831 bp contain coding sequences, the ratio is 119:1. The exon–intron transition sequences described by *Breathnach* and *Chambon* (GT-AG) are also strictly conserved in the PLP gene.[30]

5.2.2. *Correlation between Exons and Protein Domains*

The most interesting result arises from the position of the PLP amino-acid sequence coded in exons II–VII, not least with respect to our proposed model for integration into the lipid bilayer. Each *cis* and *trans* membrane domain and the adjoining hydrophobic regions are coded in a single exon. The C-terminal domain is an exception, being coded by two exons (VI and VII). These divisions are indicated in Figure 8 (top) by arrows.

In evolution, a variety of proteins arise by recombination of DNA sequences coding for other proteins, giving rise to special, new functions (exon shuffling).[31] An example of this is the receptor gene for low-density lipoprotein (LDL).[32] To date, no polypeptide sequence with high homology to PLP has been found.

5.2.3. *Alternative Splicing of PLP mRNA*

Alternative splicing of primary transcripts is very pronounced in oligodendrocytes. Through the exon loss that this involves, isoforms of the myelin proteins arise. This is also true for the PLP primary transcript. The DM-20 isoform of PLP is approximately 4.5 kDa smaller than normal PLP. The detection of specific DM-20 RNA in mouse brain and the sequencing data for DM-20 mRNA indicate that 105 bp are lacking, corresponding to 35 amino acids.[33, 34] The 212-bp-long exon III contains a cryptic splice donor sequence (G*GT*AAC, Fig. 14, bottom). Activation of this sequence leads to deletion of the 3' end of exon III and hence of amino acids 115–150. Nothing is yet known about how the activation of this splicing site is regulated.

5.2.4. *Localization of the Human PLP Gene on the X Chromosome.*

The assignment of human genes to eukaryotic chromosomes was made possible by the fusion of human and rodent cells (mouse, hamster) to give somatic cell hybrids. These contain the entire set of rodent chromosomes, plus additional human chromosomes or parts of chromosomes.[35] The

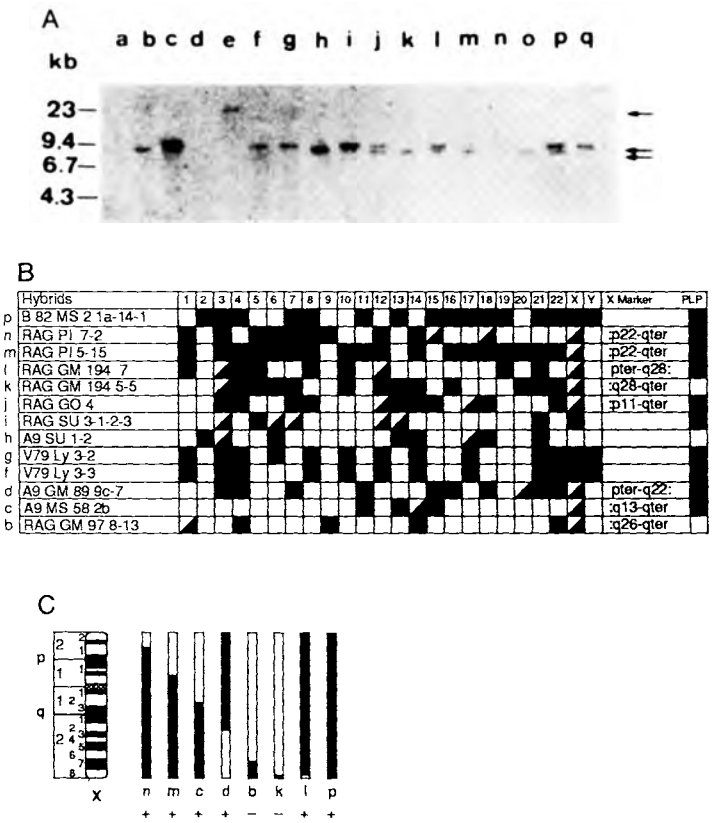

Fig. 15. Determination of the chromosomal localization of the PLP gene. A) Southern-blot hybridization of genomic human–mouse cell hybrid DNA with human-PLP-specific sequences. B) Assignment of the human chromosomes to the cell hybrids and their behavior on hybridization. C) Assignment of the PLP gene to the Xq12–Xq22 region. For details, see text.

```
  Gly Leu Leu Glu Cys Cys Ala Arg Cys Leu Val Gly Ala Pro Phe Ala Ser Leu Val Ala   20
H GGC TTG TTA GAG TGC TGT GCA AGA TGT CTG GTA GGG GCC CCC TTT GCT TCC CTG GTG GCC   60
R   T                       T

  Thr Gly Leu Cys Phe Phe Gly Val Ala Leu Phe Cys Gly Cys Gly His Glu Ala Leu Thr   40
H ACT GGA TTG TGT TTC TTT GGG GTG GCA CTG TTC TGT GGC TGT GGA CAT GAA GCC CTC ACT  120
R                           A                       A                   T

  Gly Thr Glu Lys Leu Ile Glu Thr Tyr Phe Ser Lys Asn Tyr Gln Asp Tyr Glu Tyr Leu   60
H GGC ACA GAA AAG CTA ATT GAG ACC TAT TTC TCC AAA AAC TAC CAA GAC TAT GAG TAT CTC  180
R   T               T                                       G

  Ile Asn Val Ile His Ala Phe Gln Tyr Val Ile Tyr Gly Thr Ala Ser Phe Phe Phe Leu   80
H ATC AAT GTG ATC CAT GCC TTC CAG TAT GTC ATC TAT GGA ACT GCC TCT TTC TTC TTC CTT  240
R   T           T       T

  Tyr Gly Ala Leu Leu Leu Ala Glu Gly Phe Tyr Thr Thr Gly Ala Val Arg Gln Ile Phe  100
H TAT GGG GCC CTC CTG CTG GCT GAG GGC TTC TAC ACC ACC GGC GCA GTC AGG CAG ATC TTT  300
R                           C                               T

  Gly Asp Tyr Lys Thr Thr Ile Cys Gly Lys Gly Leu Ser Ala Thr Val Thr Gly Gly Gln  120
H GGC GAC TAC AAG ACC ACC ATC TGC GGC AAG GGC CTG AGC GCA ACG GTA ACA GGG GGC CAG  360
R

  Lys Gly Arg Gly Ser Arg Gly Gln His Gln Ala His Ser Leu Glu Arg Val Cys His Cys  140
H AAG GGG AGG GGT TCC AGA GGC CAA CAT CAA GCT CAT TCT TTG GAG CGG GTG TGT CAT TGT  420
R
B                                   |

  Leu Gly Lys Trp Leu Gly His Pro Asp Lys Phe Val Gly Ile Thr Tyr Ala Leu Thr Val  160
H TTG GGA AAA TGG CTA GGA CAT CCC GAC AAG TTT GTG GGC ATC ACC TAT GCC CTG ACC GTT  480
R                                                               T
B

  Val Trp Leu Leu Val Phe Ala Cys Ser Ala Val Pro Val Tyr Ile Tyr Phe Asn Thr Trp  180
H GTG TGG CTC CTG GTG TTT GCC TGC TCT GCT GTG CCT GTG TAC ATT TAC TTC AAC ACC TGG  540
R   A                                                           T
B                                                   A           T

  Thr Thr Cys Gln Ser Ile Ala Phe Pro Ser Lys Thr Ser Ala Ser Ile Gly Ser Leu Cys  200
H ACC ACC TGC CAG TCT ATT GCC TTC CCC AGC AAG ACC TCT GCC AGT ATA GGC AGT CTC TGT  600
R                               T                                               C
B                           T GC                        A               C
                              Ala                                       Thr

  Ala Asp Ala Arg Met Tyr Gly Val Leu Pro Trp Asn Ala Phe Pro Gly Lys Val Cys Gly  220
H GCT GAT GCC AGA ATG TAT GGT GTT CTC CCA TGG AAT GCT TTC CCT GGC AAG GTT TGT GGC  660
R
B                                                               G

  Ser Asn Leu Leu Ser Ile Cys Lys Thr Ala Glu Phe Gln Met Thr Phe His Leu Phe Ile  240
H TCC AAC CTT CTG TCC ATC TGC AAA ACA GCT GAG TTC CAA ATG ACC TTC CAC CTG TTT ATT  720
R                                   C
B

  Ala Ala Phe Val Gly Ala Ala Ala Thr Leu Val Ser Leu Leu Thr Phe Met Ile Ala Ala  260
H GCT GCA TTT GTG GGG GCT GCA GCT ACA CTG GTT TCC CTG CTC ACC TTC ATG ATT GCT GCC  780
R                   T           C       A
B       G                       C

  Thr Tyr Asn Phe Ala Val Leu Lys Leu Met Gly Arg Gly Thr Lys Phe                  276
H ACT TAC AAC TTT GCC GTC CTT AAA CTC ATG GGC CGA GGC ACC AAG TTC                  828
R
B                           G
```

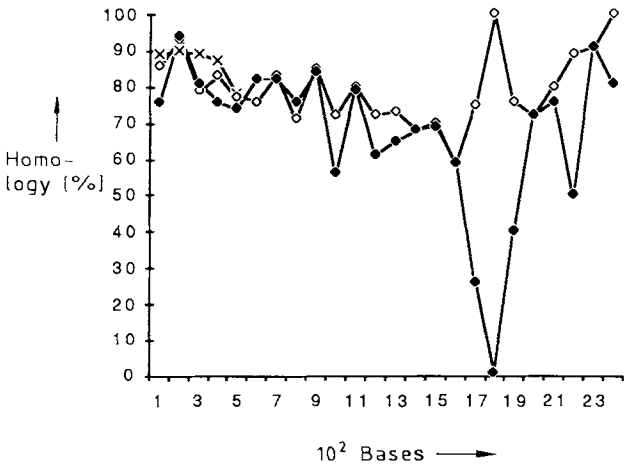

Fig. 16. Top: Comparison of human, rat, and bovine (H, R, and B) amino-acid and nucleotide-coding sequences for PLP. Bottom: Graphic illustration of homology in the 3'-untranslated region. ×, bovine; ○, rat; ◆, mouse.

human chromosomes in each hybrid cell line are defined with the aid of marker gene loci.

The genomic DNA from 15 somatic hybrid cell lines (Fig. 15A, a–q), containing all 23 chromosome pairs, was completely digested with *Bam*H1 (collaboration with Prof. *Grzeschik*, University of Marburg). The fragments were separated by agarose gel electrophoresis and hybridized by Southern-blot hybridization to the ^{32}P-labeled, 1200-bp-long C-terminal *Eco*R1 fragment of the genomic PLP clone. In Figure 15A, the human PLP-specific 9.3-kb *Bam*H1 band in the Southern blot can be distinguished (right-hand arrow, man). The smaller band (right-hand arrow, mouse) is the mouse-specific PLP band. The grid in Figure 15B shows which human chromosomes (1–22, X, Y, upper row) are present in which hybrid, either as complete chromosomes (squares) or in part (triangles). Chromosomes 2, 4, 5, 6, 7, 9, 10, 12, 13, 14, 18, 20, 21, and 22 could be excluded, since the DNA from these cell lines, in tracks b, h, and k, did not

hybridize with the PLP probe. Chromosomes 1, 3, 8, 11, 15, 17, 19, and Y were also eliminated, since hybridization occurred with DNA from cell lines which did not contain them. Hence, the X chromosome remained the sole candidate for the PLP gene locus. The assignment to the X chromosome was supported by hybridization to *Bam*H1 fragments of cell lines with four X chromosomes; strong, PLP-specific signals were clearly visible.

Narrowing down of the PLP locus to the q 13–q 22 region of the X chromosome was possible with the aid of somatic cell hybrids containing only part of the X chromosome. The diagram in Figure 15 C shows the regions of the X chromosome contained in each cell line. Hybridizing cell lines are marked with a (+). Bars c and d reveal the smallest overlapping region between q 13 and q 22. The third phosphoglycerate kinase (PGK) gene is also located in this region. As confirmation, the *Bam*H1 blot was hybridized with a ^{32}P-labeled PGK cDNA. Parallel to our studies, the same result was obtained by *Willard* and *Riordan*[36] and by *Mattei* et al.[37]

5.2.5. *Conservation of PLP during Evolution*

A comparison of the amino-acid sequence and the corresponding coding nucleotide sequence for PLP from species far apart in evolution emphasizes the high level of sequence conservation. A comparison between rat, mouse, human, and, as far as possible, bovine sequences (Fig. 16, top) shows that between human and rat there are no amino-acid exchanges and only 22 nucleotide substitutions out of 831 coding bases. In mouse there are 28 base-pair exchanges, with two conservative amino-acid replacements (Ser → Thr, Tyr → Cys). This extremely high degree of conservation demonstrates the narrow range within which the protein can function. The same is also true for the 3′-noncoding sequence, where very high homology prevails around the potential polyadenylation recognition sequences (Fig. 16, bottom).

5.3. Organization of Human Myelin Basic Protein

The peripheral membrane protein myelin basic protein (MBP) occurs in several isoforms in man, mouse, and rat.[38, 39] Thus, in rat and mouse myelin, the dominant forms are the 18.5-kDa and 14-kDa MBPs. The latter differs from the larger isoform by a deletion of forty amino acids in the C-terminal region. In the mouse, one finds a 21.5-kDa and a 17-kDa form, both with an insertion of 28 amino acids in the N-terminal region.[10, 40]

The relative proportions of the four MBP isoforms change during mouse or rat development.[10, 41, 42] The myelin of the human central nervous system contains three dominant isoforms, the 21.5-kDa, 18.5-kDa, and 17.2-kDa forms. The latter results from a 41-amino-acid deletion in the C-terminal region (140–180 of the 21.5-kDa form).

In Section 5.1 the isolation of a complete MBP-cDNA clone from rat brain cDNA was described. Studies in the laboratories of *Hood*[11, 43] had revealed that the mouse MBP gene is distributed over seven exons, is 30 kb long, and is located on the distal arm of chromosome 18. We isolated the human MBP gene by screening with labeled MBP-cDNA probes from genomic cosmid banks (pcos2 EMBL and Charon 4 A) and analyzed its exon–intron organization. Just as for the human PLP gene, here we also carried out restriction analysis to map the MBP gene. It is distributed over seven exons and 32–34 kb.[44] Figure 17 illustrates its structure and the sequencing strategy.

A comparison of the coding sequence of human and mouse MBP genes makes it clear that though homology in the nucleotide sequence is high, it is not as great as in PLP. Three potential transcription start sites were found by the primer extension method, at −55, −82 and −183 bp in the 5′ direction from the translation start. In the 5′-noncoding region there is neither a TATA box, which is often found in eukaryotic genes, nor a CAAT box. However, there are three direct "repeats", a nonameric sequence and two octameric nucleotide sequences. A decameric sequence at −256 to −265 is absolutely homologous to one in the regulatory region of the PLP gene. Further studies will show whether these motifs are important in transcriptional regulation. The isoforms of MBP arise by alternative splicing. The exons involved here are basically exons II, V, and VI. Figure 18 summarizes the splicing process and the isoforms that result.

6. Animal Models in the Study of Normal and Genetically Defective Myelin Membranes of the CNS (Dysmyelinoses)

Animal models possessing a genetically determined defect in myelin membrane synthesis are extremely useful in (1) investigation of membrane structure and the function of membrane components, especially proteins, (2) analysis of the differentiation process in myelogenesis, and (3) studies of pathogenesis on a molecular level. Myelin mutants of mouse, rat, rabbit, and spaniel are known; two sex-chromosome-linked mutations of mouse and rat will be described.

6.1. Sexually Inherited (X-Chromosomal) Defects

6.1.1. *Jimpy (ji) Mouse*

In 1952, *Falconer* described the Tabby (Ta) marker in mouse.[45] Heterozygous females are distinguished by horizontal stripes on the back, while homozygous males have a light brown coat. The jimpy gene is linked to the Ta marker; it leads to a complete absence of myelin in the affected male mouse and to an early death with symptoms of tremors in the entire striated muscle and of cramps. Females carrying the ji gene display a mosaic pattern, since expression of the X-chromosomal gene is dependent on inactivation of either the mutant or the normal X chromosome.[46, 47] While hypomyelination is compensated for with increasing age in heterozygous females, protein chemical analysis of the brain of affected males shows a marked reduction in PLP and MBP.[48, 49]

The primary effect of the ji mutation was sought first in PLP expression. Southern blots of genomic DNA from ji and

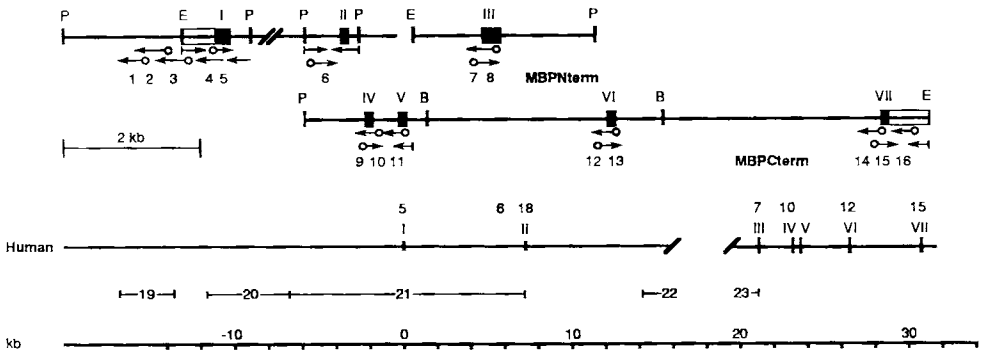

I

```
...tgggtaggtgggtgtgtgtatggatggatggatagatggatggatgggtaaatggactgttatgtggatggatggatggatggatagagagatagatggatgactggtattacagg
gatatgtgagtgaatcctgtttttctgtagataagtaatagagtttggagaggaaactaactaaatgatatttatttaaacctaacactctaacttgaaagcaaaatggattcattgccc
ttcgtgacagaaatgtggtatttttttggagaaagctatgagatgctggtatacaacatgaaatatctcaatcccacttcagatttctaattgtttctgcttccagaggagaagccaagt
caaaatgtcctgaataagcagttctctattgtgagaggcctcttgtggaatctgggattgaaacaattctaaatgccccacttctttcatgcatgaattgcaaaaagatgtggcaagtt
ttgtttctaccaagaaaactaaaaacacctttttgtcaaataaatgctccttgcatatttaacttatgcaccagtggcctttaaacagtcaatgtcccatcaaggtgcctgcacatctg
ggctctccgggagcagccatggcagcacccgggaagaaacgctgatgtggctgctctgcatgctcagatgacttcatcgggaagcctgggtgcattttacgctgggtgccaaatctgag
taactgaggaattcccagagccttctgaaacacagagctgcaataaggctgctccatccaggttagctccatcctaggccaagggctttatgaggactgcacatattctgtgggtttta
taggagacagctaggtcaagacccctcagagaaagctgctttgtccggtgctcagctttgcacaggcccgtattcatatctcattgttgtttgcaggagaggcagatgcgaaccagaac
aatgggacctcctctcaggacacagcggtgactgactccaagcgcacagcggacccgaagaatgcctggcaggatgccacccagctgacccagggagccgccccacttgatccgcctc
ttttcccgagatgccccgggagggaggacaacaccttcaaagacaggccctctgagtccgacgagctccagaccatccaagaagacagtgcagccacctccgagagcctggatgtg

Met Ala Ser Gln Lys Arg Pro Ser Gln Arg His Gly Ser Lys Tyr Leu Ala Thr Ala Ser Thr Met Asp His Ala Arg His Gly Phe Leu   29
ATG GCG TCA CAG AAG AGA CCC TCC CAG AGG CAC GGA TCC AAG TAC CTG GCC ACA GCA AGT ACC ATG GAC CAT GCC AGG CAT GGC TTC CTC   87

Pro Arg His Arg Asp Thr Gly Ile Leu Asp Ser Ile Gly Arg Phe Phe Gly Gly Asp Arg Gly Ala Pro Lys Arg Gly Ser Gly Lys       58
CCA AGG CAC AGA GAC ACG GGC ATC CTT GAC TCC ATC GGG CGC TTC TTT GGC GGT GAC AGG GGT GCG CCC AAG CGG GGC TCT GGC AAG gtga 174

gctctgaggagtagaggagttttagtttaaatggaaaaagcaaaggagaaatcagtaggtgaactcagccattagaggaagaactggcacgtagcctcttgctgtctaaggtctcgttcc
gtgctggagaatgcatatgagcccaagagtgtgggcctgagaggctgcttaggacgttttcgtttaactcacccctcttttcctcacaagggatggtggccggggtgtggctcaggaat
gtaaggacatgctgaattc...
```

II

```
...ctgcagaaaatcggaaaaggtccgtcctcggttcactgaaccttcacagagcagaaaaagctttaacctgctaaatccaatgcagaagataacacacttgctataaaagaaaaaat
acaactctgcaagtaaagtggaatgtaaaatttatccattccatggtagacgtcaaaaaaccctttagtgcactttgctccagactgggaaaggccttctgcactggatcctagaaat
ctttcacagctggtgcctgctgccatattaagaactcttggtcccattgtttgatacagggcctcagaatagacttggaggagagaattcttccctaaactttccttttgctctcgat
ttcctgagtccttcagggcgcatgctgccctctgacctcccatcacctcttgctcttccttccatcatccatcatctgcacatgccttcttctctccctgtcgtccttcatcctccacc
ccccgctcactcctcctcactctgggctcttgccaagccagctctagaggagatttgctggaggactttggggcattgccggcggcgcccacccggactcacgcagcccactctgtgtc

          Val Pro Trp Leu Lys Pro Gly Arg Ser Pro Leu Pro Ser His Ala Arg Ser Gln Pro Gly Leu Cys Asn Met Tyr Lys          84
ccccggcag GTA CCC TGG CTA AAG CCG GGC CGG AGC CCT CTG CCC TCT CAT GCC CGC AGC CAG CCT GGG CTG TGC AAC ATG TAC AAG gtaag  252

acgccggcgggtcctcacccatcggggccaggggtgacctgccgtttcctgagctctcagccgactgtccctcggggcaggtagtgtcactgccaggggcccaccccagcct...
```

III

```
                                                                  Asp Ser His His Pro Ala Arg Thr Ala His Tyr Gly   96
...ttccctgaggaggacaagccgcagggactgtggacttgtcctgaggtcaccgcgcctctgtgtttcag GAC TCA CAC CAC CCG GCA AGA ACT GCT CAC TAC GGC  288

Ser Leu Pro Gln Lys Ser His Gly Arg Thr Gln Asp Glu Asn Pro Val Val His Phe Phe Lys Asn Ile                          119
TCC CTG CCC CAG AAG TCA CAC GGC CGG ACC CAA GAT GAA AAC CCC GTA GTC CAC TTC TTC AAG AAC ATT gtaagtgacgatcgatgggaagaggta  357

gcaactgtgaggggggaggagggg...
```

IV und V

```
                          Val Thr Pro Arg Thr Pro Pro Pro Ser Gln Gly Lys                                           131
...gccagggttctctgtgccttttcag GTG ACG CCT CGC ACA CCA CCC CCG TCG CAG GGA AAG gtaagaccttggaatgttttgattgatcatcactttttctgata  393

gaccttctctaaaatcccataatgtaccaaagagagagttaggctccgagctaccagaatccatcccaaaacgtgttgccaggcagctcccaagtagaacaggtcggagatccatgcac
ccctcctgtccctcccgcacctgcacagccgctgtggccctagctgcggccccctcggagctccgggtggaacctgtttttaccacctcagctccactgtgctttgactgtgtttcct

                                                                Gly Arg Gly Leu Ser Leu Ser Arg Phe Ser Trp           142
gttgattgaaaggactttccctcactgaccaccatgtcattatttctctgtcttcctcatgcag GGG AGA GGA CTG TCC CTG AGC AGA TTT AGC TGG gtaggtgac  426

gaacgcacttccatcggcttcctcttccgtcccagtcctcacagccccgcaacttttgtgttctgctctgtttcggttgcttcctggcctccttttctctcctctcga...
```

VI

```
...cctcagcgtggtgctggcccgtggctcctgaaccactcaccagtccagtccgggcctgggcccttccccggggccctggtggcagctcccagtggctcaagcagcgtgcccagcac

                                    Gly Ala Glu Gly Gln Arg Pro Gly Phe Gly Tyr Gly Gly Arg Ala Ser Asp Tyr Lys Ser   162
cgcgggtggaggttgagctccgtggtcttctcttgcag GGG GCC GAA GGC CAG AGA CCA GGA TTT GGC TAC GGA GGC AGA GCG TCC GAC TAT AAA TCG   486

Ala His Lys Gly Phe Lys Gly Val Asp Ala Gln Gly Thr Leu Ser Lys Ile Phe Lys Leu                                    182
GCT CAC AAG GGA TTC AAG GGA GTC GAT GCC CAG GGC ACG CTT TCC AAA ATT TTT AAG CTG gtaaggtaccctctgctcagctccactga...      546
```

VII

```
...agaaaatgctcatcaaagcaaagcaatggagcggctgcacttcacccacagaatgcacttgtttgcagagcatggttatgccaggcaccactccctggggcctgggaatccgattc
cagttctctctcacagaactggaaattcattagcatttgctgagggaggtcgggagaaatggaatgaaaagaccagctctccggggtgccatttctattagcagatgagagagacaccc

                                                                Gly Gly Arg Asp Ser   187
aatggctcagcatggacccgggaccacagaagaggggatgctggtgtgggaggaccctgcggcactctcgtcctaactcctctctcttcctttttcag GGA GGA AGA GAT AGT   561

Arg Ser Gly Ser Pro Met Ala Arg Arg Stop                                                                          196
CGC TCT GGA TCA CCC ATG GCT AGA CGC TGA aaacccacctggttccggaatcctgtcctcagcttcttaatatatactgccttaaaactttaatcccacttgcccctgtt  588

acctaattagagcagatgaccccttcccctaatgcctgcggagttgtgcacgtagtagggtcaggccacggcagcctaccggcaatttccggccaacagttaaatgagaacatgaaaaca  607
gaaaacggttaaaactgtccctttctgtgtgaagatcacgttccttcccccgcaatgtgcccccagacgcacgtgggtcttcaggggccaggtgcacagacgtccctccacgttcacc  726
cctccacccttggactttcttttcgccgtggctcggcaccctgcgcttttgctggtcactgccatggaggcacacagctgcagagacagagaggacgtgggcggcagagaggactgtt  845
gacatccaagcttcctttgttttttttcctgtccttctctcacctcctaaagtagacttcatttttcctaacaggattagacagtcaaggagtggcttactacatgtgggagcttttt  964
ggtatgtgacatgcgggctgggcagctgttagagtccaacgtggggcagcacagagaggggccacctcccaggccgtggctgcccacacacccccaattagctgaattc...      1074
```

Fig. 17. Top: Exon–intron organization of human MBP gene. Bottom: Nucleotide sequence of the exons and extensive sections of the introns of the MBP gene. Enzymes as in Fig. 14.

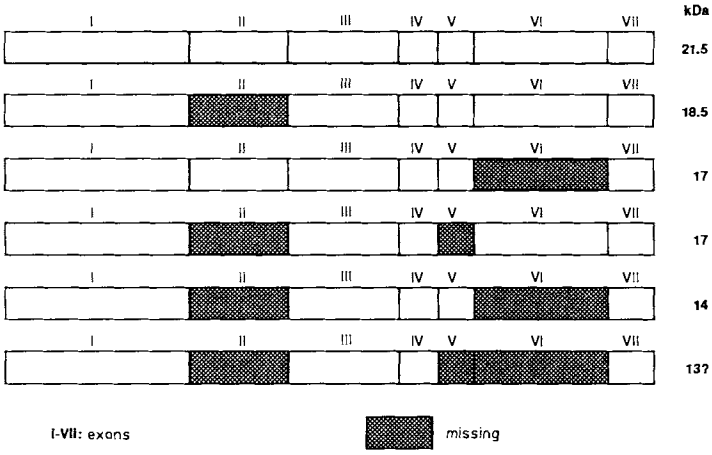

Fig. 18. Isoforms of myelin basic protein arise by alternative splicing. The molecular masses are given in kDa on the right; the exons eliminated by splicing are hatched.

normal mice with PLP cDNA proved to be identical.[34, 37, 50, 51] Exact determination of the ji defect in the mRNA was furnished by isolation and analysis of ji-PLP cDNA.[50] A 74-base-pair deletion was discovered, with a shift in reading frame at the C-terminus of PLP.

A glance at the exon–intron structure of the human PLP gene shows that the 74-base deletion corresponds exactly to the nucleotide sequence of exon V. The most obvious interpretation was an alternative splicing (Fig. 14, bottom). Indeed, there is a transition at the splice acceptor site (AG → GG), which eliminates exon V, intron IV, and intron V. Exon V ends on the first nucleotide of the glycine (G). Since exon VI starts with the triplet TTC (Phe), a frameshift occurs, leading to synthesis of a missense protein. The result

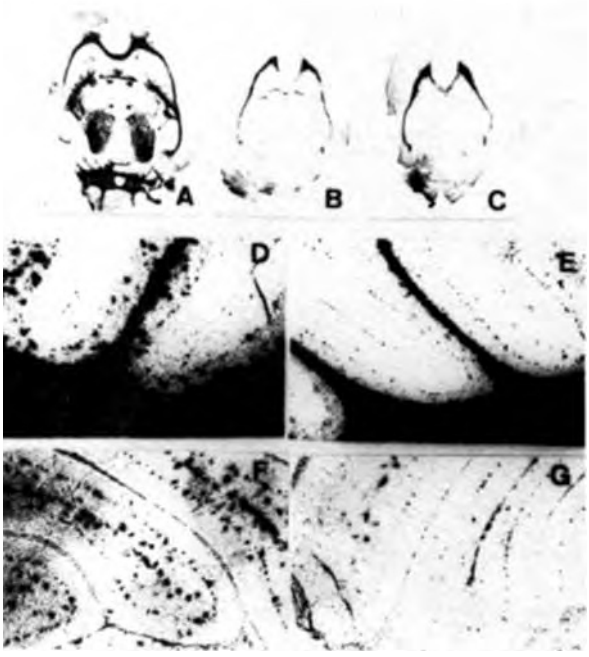

Fig. 19. In situ hybridization of horizontal cryosections of normal and md rat, and of jimpy mouse, with antisense PLP and MBP RNA. A, rat; B, md rat; C, jimpy mouse; D, normal rat hybridized with antisense PLP RNA; E, hybridized with anti-MBP RNA; F, md rat hybridized with antisense PLP RNA; G, hybridized with anti-MBP RNA.

is the loss of myelinated oligodendrocytes and the appearance of immature oligodendrocytes. This is easily recognizable on comparative in situ hybridization of normal, md-rat, and ji brain sections, using antisense PLP and MBP mRNA (Fig. 19).

The disease takes a less dramatic course in the myelin synthesis deficient (msd) mouse, which is phenotypically very closely related to the ji mouse.[52, 53] This mutation is an X-chromosome-linked defect as well. It consists of a single base transition (C → T) in exon IV leading to a homologous amino-acid substitution (alanine → valine) in PLP.[69]

6.1.2. Myelin-Deficient (md) Rat

The md rat is a mutant of the Wistar rat, which in phenotype is very closely related to the ji mouse. The endoplasmic reticulum of the CNS oligodendrocytes is expanded, and fluffy precipitates appear in the cytoplasm.[54] The mRNA of PLP and MBP, and of MAG and CNP, is greatly reduced. Figure 19 compares the in situ hybridizations we performed on brain sections of normal rat, md rat, and jimpy mouse, using [^{35}S]UDPS-labeled antisense PLP and MBP RNA.[55] The markedly reduced number of oligodendrocytes in md and ji brain is recognizable from the insignificant labeling by the specific hybridization probes.

In order to investigate the genetic defect on a molecular level, Southern blots of normal PLP DNA and of md rat were compared. No size differences were observed; the sequences of the 5′-regulatory region and those of exons IV to VII and introns IV to VI were identical. We isolated nucleotide sequences coding for exons I, II, and III from the md-rat-brain-specific cDNA library by the polymerase chain reaction (PCR) method and, at the same time, amplified exon II, intron II, and exon III with suitable oligonucleotide primers. Sequencing of the PCR fragments of the md cDNA revealed a point mutation (A → C transversion), leading to the mutation of Thr 75 into Pro. The point mutation lies in exon III, the sequence coding for the second transmembrane α-helical segment. This transversion generates an *Ava*II restriction site (GGACC), and the resultant *Ava* polymorphism in exon III constitutes a rapid diagnostic test for the md allele (Fig. 20). What are the consequences of this point mutation for the protein structure? Proline, with its preceding glycine, breaks the α-helix structure and leads to a bend and a partial β-turn structure in the helix. This conformation clearly hinders the integration of the C-terminal PLP sequence into the lipid bilayer of the myelin. On a cell biological level, this A → C transversion (i.e., the mutation of one out of 17 000 bases) finds expression in the loss of oligodendrocytes. Myelination does not take place, and this leads to the early death of the affected male animal. We are investigating this pathogenetically important chain of reactions very intensively at the moment.

6.2. Autosomally-Recessively Inherited Dysmyelinoses

One recessively inherited dysmyelinosis is the shiverer defect in mouse (shi). This defect arises from the deletion of five of the seven exons of the MBP gene, which is located on chromosome 18, q 22–qter.[43, 56, 57] The loss of MBP still

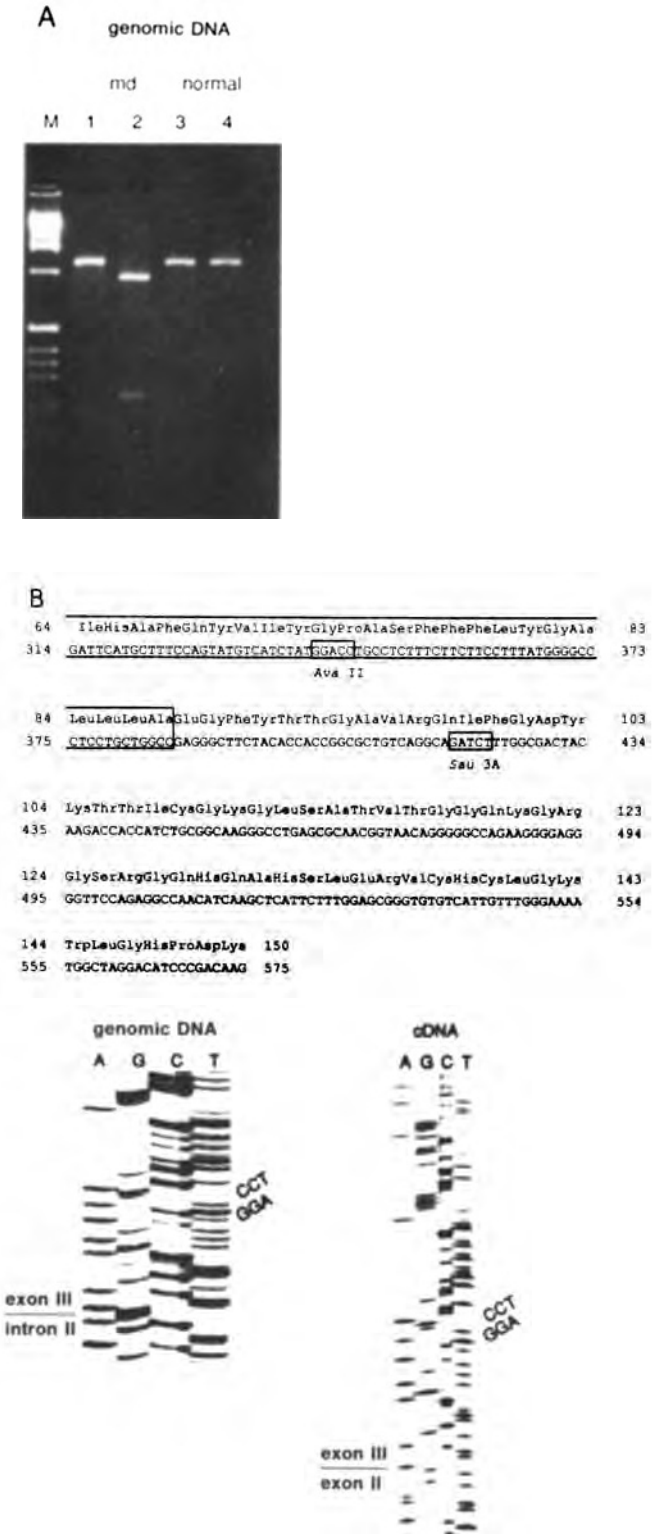

Fig. 20. A) Amplification of exon II–intron II–exon III by the polymerase chain reaction (PCR), using genomic DNA of wild-type and md rat as template (md 1 and normal 3). Restriction of the resulting 1180-bp fragment with *AvaII*. An *AvaII* restriction fragment length polymorphism is apparent. *AvaII* cleaves the fragment derived from the genomic DNA of the md rat into a 960-bp and a 220-bp fragment (md 2), but does not attack the fragment from the genomic DNA of the normal rat (normal 4). B) Nucleotide sequence and derived amino-acid sequence of exon III of the md-rat PLP gene (see also Fig. 16). Sequencing gels of genomic and cDNA from md rat.

permits myelin formation, but the compact cytosolic gap visible under the electron microscope as the main dense line (MDL, Fig. 3) does not develop.[58] This myelination defect was overcome by implanting the intact MBP gene into the germ cells of the mouse in a transgenic model.[59]

A further autosomal mouse mutant is the myelin-deficient mouse. *Hood*'s group has found that, due to an MBP gene duplication and inversion, regulation of gene expression is disturbed, yielding a phenotype similar to that of the shiverer mutant. Here, too, it was possible to generate transgenic mice which made myelin to different extents, by introducing the normal MBP gene into the cells.[60]

The quaking mouse (qk) is the result of a defect linked to chromosome 17. Phenotypically, one sees a much relaxed myelin structure under the electron microscope, with greatly reduced expression of both the PLP and MBP genes. MBP does not seem to be built into the myelin membrane. A molecular biological explanation of this mutation is still awaited.[49, 61]

6.3. Sex-linked Recessive Human Dysmyelinoses

Demyelination leads to the degradation of the existing, intact myelin by inflammatory or toxic agents. In contrast, a series of dysmyelinoses, the leucodystrophies, are the result of genetically conditioned functional disorders in the oligodendrocytes. Human dysmyelinoses with X-chromosomal recessive inheritance (e.g., adrenoleucodystrophy (ALD) and "familial diffuse scleroses", also known as Pelizaeus–Merzbacher disease) are of special importance in this context.[62] In homozygous, male descendants, the severe form, adrenoleucodystrophy, leads to early mental retardation, motor disorders, demyelination of the optic nerve, and blindness, and to death at an age of four to eight years. Characteristic here is the accumulation of very long chain fatty acids ($>C_{24}-C_{26}$) in almost all the tissues, usually as their cholesterol esters.[63] This is used as a diagnostic aid. Gas-chromatographic determination of the long-chain fatty acids in the lipids of leucocytes, skin fibroblasts and cells obtained by amniocentesis is at present the diagnostic method of choice, especially prenatally.[64] The ALD locus on the X chromosome is not yet exactly determined, but a DNA probe specific for the Xq 28 band contains a restriction fragment length polymorphism (RFLP) which is said to be characteristic for the defective allele.[65] However, as long as the exact distance between this probe and the ALD locus is unknown, an uncertainty factor is attached to this RFLP because of possible recombination.

Pelizaeus–Merzbacher disease is a rare form of leucodystrophy. Mental and physical decay begins in infancy and leads to death in the first years of life. The phenotype is very similar to that of ji mouse or md rat. The disease is histologically characterized by a complete lack of white matter in the CNS. Astrocytes in the dysmyelination region reveal fat globules. The defect postulated in phospholipid metabolism[66] is certainly only a peripheral symptom in the complex phenotype of this genetically determined dysmyelinosis. The X-chromosomal linkage, coupled with the complete absence of proteolipid protein[67] and the great immunocytochemical changes in marker enzymes for myelin, points to a mutation in the PLP gene. Cloning and analysis of the Pelizaeus–Merzbacher PLP gene has led to an understanding of the mutation and the pathogenesis of the disease

in four different families: a C → T transition in exon IV leading to a threonine 155 exchange by isoleucine[7a] and proline 14 → leucine,[71] tryptophan 162 → arginine,[72] and proline 216 → serine[73] substitutions.

6.4. Demyelinating Diseases

The commonest and most serious inflammatory disease of the CNS, which very often takes a gradual course, is encephalomyelitis disseminata, also known as multiple sclerosis (MS). Its etiology is still quite unclear, although viral infections—more than twenty have by now been described—are regularly cited as the triggering event. This is especially true of the chicken pox, German measles, and mumps viruses, and, most recently, the human retrovirus HIV-1.[68] An autoimmune reaction plays a significant part in pathogenesis. In animal models it is possible to generate a symptomatically related demyelination experimentally by immunizing rabbits or rats with myelin basic protein. In addition to the sites of inflammatory degeneration that appear in this experimental allergic encephalitis (EAE), T lymphocytes with MBP specificity are activated in the test animal. Transfer of the T lymphocytes to a healthy animal can trigger symptoms of multiple sclerosis. The cerebrospinal fluid of MS patients also contains MBP-specific T lymphocytes, analogously to the animal model.

Independently of the etiology, one can ask whether MBP is the primary antigen for triggering the autoimmune process. In trying to understand pathogenetic events, it is a great help to know the molecular architecture of structures involved in the process. MBP is quite clearly located within the cytoplasmic space of the myelin membrane, where it is shielded from protease attack by the dense lipid bilayers, as has been shown experimentally.[14] If one looks at the myelin membrane model (Fig. 8A), it becomes clear that the proteolipid protein (PLP) has large, hydrophilic domains exposed at the membrane surface, where they are directly accessible as a primary point of attack for the proteases of macrophages, lymphocytes, and leucocytes. Fragmentation of PLP would severely disrupt the membrane organization of the myelin, and this could expose phospholipids to phospholipase attack and, as a result, the myelin basic protein to proteases. The high antigenicity of MBP and its peptide fragments play a dominant role in the autoimmunization process, but only a secondary one in this hypothetical sequence of events, and at a later stage in the pathogenetic process. A knowledge of the crucial epitopes that are recognized primarily by activated T lymphocytes in the demyelination process could be of great importance in understanding the pathogenesis of multiple sclerosis and in its therapy, even if the etiology is not yet fully explained.

7. Summary and Perspectives for Membrane Research in Neurobiology

Because of its relatively small number of components, the CNS myelin membrane is one biological membrane whose morphology and function on a molecular level have largely been described. Chemical and biochemical analysis has revealed that the simple and complex myelin lipids that make up the 5-nm-thick bilayer are the decisive factor in the insulating characteristics of the myelin sheath around the axons. The dense lateral packing of the sphingolipid long-chain fatty acids and the cholesterol in the lipid bilayer is stabilized by a network of hydrogen bonds, described here for the first time. This network is built up between the polar groups at the interphase between the hydrophobic core of the bilayer and the polar heads of the lipids.

The conspicuously high content of acidic polar head groups—one anionic to four polar or zwitterionic—leads to a polyanionic cytoplasmic and extracytoplasmic surface. Both will be involved in ionic interactions. Biochemical and immunotopochemical studies have further revealed that the myelin basic protein in the cytoplasmic space is not accessible from the exterior. Through ionic interactions of the side chains of its basic amino acids with the anionic polar head groups of sulfatides and phospholipids, but also with an anionic domain of proteolipid protein, the MBP causes a compact layering of the oligodendrocyte plasma membrane processes. This is seen in the electron-dense main dense line (MDL) under the electron microscope. Ionic interactions between polar head groups of the lipid bilayer and domains of proteolipid protein must be responsible for the dense packing on the extracytoplasmic side, between the external surfaces of the tightly wrapped myelin processes. This narrow cleft appears in the electron microscope as the intraperiod dense line (IDL). In addition, hydrophobic interactions may occur between opposing membrane surfaces, due to long-chain fatty acid residues. For example, they form an ester bond to Thr/Ser 198 of PLP and can intercalate into the hydrophobic phase. The hydrophobic sides of amphipathic helices could also affect the pattern of outer membrane adhesion surfaces, as could the flip-flop dynamics of a small hydrophobic *cis* loop in the poorly understood spiral winding process (Fig. 2B). Either of these could be a significant stabilizing factor in formation of the dense, multilamellar membrane system. This system is not only responsible for myelin's insulating function, but also for saltatory excitation along the nodes of Ranvier, which proceeds by depolarization of only small areas of the axonal membrane.

The myelination of the CNS axons is a fascinating process of development and differentiation within brain maturation. Following a program that is regulated both in time and in space within the individual regions of the brain, the mass of lipids and myelin proteins is synthesized within a short time span (2–3 weeks in rodents, 1–2 years in humans).

Using the molecular-biological techniques described here, we can now analyze the course and regulation of myelinogenesis and resolve both the controlling elements and factors and the expression of genes coding for myelin membrane proteins and enzymes responsible for synthesis of the complex myelin lipids. In situ hybridization techniques will play a large role here, as will analysis of DNA–protein interactions in the regulatory regions of the genes described. Thus, we will be able to tell whether the gene activity for myelin proteins is "switched on" simultaneously and in conjugation with lipid synthesis, how the myelin building blocks are transported to the axon, where the segregated membrane components of the oligodendrocyte plasma membrane

myelin process are combined. In vitro protein synthesis of PLP and MBP and integration of PLP into the lipid bilayer are currently under experimental investigation, in order to gain understanding of the in vivo process.

Analysis of the genetically determined myelin defects (dysmyelinoses) described here, the jimpy mouse and md rat, furnish convincing evidence of the far-reaching possibilities for molecular biological techniques. They can be used for elucidation not only of defects at the DNA level and their chromosomal locations, but also of the cell biological basis for the pathogenetic process arising from the mutation. Thus, we will soon know why erroneous expression of a structural protein such as PLP causes death of the oligodendrocyte, failure to myelinate, and the early death of the individual. The animal models studied are of eminent importance in explaining analogous dysmyelinoses based on defective myelin synthesis in humans.

A large number of genetically determined myelin defects in animals and in man await the elucidation of the relevant mutations. Transgenic animal models will be indispensable in understanding the pathogenic process in these brain diseases. Elucidation of the myelin membrane topochemistry and the availability of the protein structures has given an important thrust to research on demyelinating diseases, with multiple sclerosis (encephalomyelitis disseminata) the primary example. This is true above all for the autoimmunological aspects of this disease. The antigenic epitopes of the myelin target structures can now be determined, opening up extensive therapeutic possibilities.

The results that have been achieved in biochemical and molecular biological research in recent years in the field of neurobiology, as documented here for the CNS myelin membrane, provide impressive evidence that a solid chemical and biochemical knowledge of macromolecular structure is first required. With the aid of molecular and cell biological techniques and reasoning, it is possible to learn to understand the normal functions linked to these structures and their pathological alterations. The "new biology", in the widest sense, makes molecular neurobiology one of the most exciting fields in biology today.

Our research described in this review article was generously supported by the Deutsche Forschungsgemeinschaft (SFB 74), the Bundesministerium für Wissenschaft und Forschung (Gene Centre, Cologne), and the Fritz-Thyssen-Stiftung. My special thanks go to all the co-workers mentioned and to Dr. B. Tunggal and Dipl.-Chem. K. Hofmann for fruitful and enthusiastic collaboration in a field of neurochemistry that requires a high level of experimental skill. I am grateful to Jochen Teufel for help in preparing the diagrams and the manuscript.

Received: November 17, 1989;
revised: February 13, 1990 [A 779 IE]
German version: *Angew. Chem. 102* (1990) 987
Translated by *Michael Kertesz*, Zürich

[1] R. Virchow, *Virchows Arch. Pathol. Anat. Physiol. 6* (1854) 562–572.
[2] M. L. Ranvier: *Leçons sur l'Histologie du Systeme Nerveux*, Librarie F. Savy, Paris 1878.
[3] A. L. Hodgkin, A. F. Huxley, *J. Physiol. 117* (1952) 500–544.
[4] T. V. Waehneldt, J. M. Matthieu, G. Jesrich, *Neurochem. Int. 9* (1986) 463–474.
[5] P. I. Yakolev, A.-R. Lecours in A. Minkowski (Ed.): *Regional Development of the Brain in Early Life*, Blackwell, Oxford 1967, pp. 3–70.
[6] W. T. Norton, W. Crammer in P. Morell (Eds.): *Myelin*, Plenum Press, New York 1984, pp. 147–195.
[7] Y. Oshiro, E. H. Eylar, *Arch. Biochem. Biophys. 138* (1970) 392–396.
[8] E. Eylar, pp. W. Brostoff, G. Hashim, J. Coccam, P. Burnett, *J. Biol. Chem. 246* (1971) 5770–5784.
[9] P. R. Carnegie, *Biochem. J. 123* (1971) 57–67.
[10] E. Barbarese, P. E. Braun, F. H. Carson, *Proc. Natl. Acad. Sci. USA 74* (1977) 3360–3364.
[11] N. Takahashi, A. Roach, D. B. Taplow, S. B. Prusiner, L. Hood, *Cell 42* (1985) 139–148.
[12] J. Kamholz, F. de Ferra, C. Puckett, R. A. Lazzarini, *Proc. Natl. Acad. Sci. USA 83* (1986) 4962–4966.
[13] P. E. Braun in P. Morell (Ed.): *Myelin*, Plenum Press, New York 1984, pp. 97–106.
[14] W. Stoffel, H. Hillen, H. Giersiefen, *Proc. Natl. Acad. Sci. USA 81* (1984) 5012–5016.
[15] W. Stoffel, unpublished results.
[16] G. L. Stoner, *J. Neurochem. 43* (1984) 433–447.
[17] J. Folch, M. Lees, *J. Biol. Chem. 191* (1951) 807–817.
[18] F. Wolfgram, *J. Neurochem. 13* (1966) 461–470.
[19] M. Arquini, J. Roder, L. S. Chia, J. Down, D. Wilkinson, H. Bayley, P. Braun, R. Dunn, *Proc. Natl. Acad. Sci. USA 84* (1987) 600–604.
[20] W. T. Norton, S. E., *J. Neurochem. 21* (1973) 759–773.
[21] M. V. Norgard, M. J. Tocci, J. J. Monahan, *J. Biol. Chem. 255* (1980) 7665–7672.
[22] U. Gubler, B. J. Hoffman, *Gene 25* (1983) 263–269.
[23] M. Schaich, R.-M. Budzinski, W. Stoffel, *Biol. Chem. Hoppe-Seyler 367* (1986) 825–834.
[24] J. McLauchlan, D. Gaffney, J. L. Whitton, J. B. Clements, *Nucleic Acids Res. 13* (1985) 1347–1368.
[25] H.-J. Diehl, M. Schaich, R.-M. Budzinski, W. Stoffel, *Proc. Natl. Acad. Sci. USA 83* (1986) 9807–9811.
[26] E. J. Chen, P. H. Seeburg, *DNA 4* (1985) 165–170.
[27] P. Heinrich: *Guidelines for Quick and Simple Plasmid Sequencing*, Boehringer Mannheim GmbH, Mannheim 1986.
[28] A. Dautigny, P. M. Alliel, L. d'Auriol, D. Pham-Dinh, J. L. Nussbaum, F. Galibert, P. Jollès, *FEBS Lett. 188* (1985) 33–36.
[29] R. J. Milner, C. Lai, K. A. Nave, D. Lenoir, J. Ogata, J. G. Sutcliffe, *Cell 42* (1985) 931–939.
[30] R. Breathnach, P. A. Chambon, *Annu. Rev. Biochem. 50* (1981) 349–383.
[31] W. Gilbert, *Science 228* (1985) 823–824.
[32] T. C. Südhof, J. L. Goldstein, M. L. Brown, D. H. Russell, *Science 228* (1985) 815–822.
[33] D. Morello, A. Dautigny, D. Pham-Dinh, P. Jollès, *EMBO J. 5* (1986) 3489–3493.
[34] L. D. Hudson, J. A. Bendt, C. Puckett, C. A. Kozak, R. A. Lazzarini, *Proc. Natl. Acad. Sci. USA 84* (1987) 1454–1458.
[35] F. A. Ruddle, *Nature 242* (1971) 165–169.
[36] H. F. Willard, J. R. Riordan, *Science 230* (1985) 940–942.
[37] A. Dautigny, M. G. Mattei, D. Morello, P. M. Alliel, D. Pham-Dinh, L. Amar, D. Arnaud, D. Simon, J. F. Mattei, J. L. Guenet, P. Jollès, P. Avner, *Nature 321* (1986) 867–869.
[38] P. R. Dunkley, P. R. Carnegie, *Biochem. J. 141* (1974) 243–255.
[39] F. de Ferra, H. Engh, L. Hudson, J. Kamholz, C. Puckett, S. Molineaux, R. A. Lazzarini, *Cell 43* (1985) 721–727.
[40] R. E. Mårtenson, G. E. Deibler, M. W. Kies, S. S. McKneally, R. Shapira, R. F. Kibler, *Biochim. Biophys. Acta 263* (1972) 193–203.
[41] C. W. Campagnoni, G. D. Carey, A. T. Campagnoni, *Arch. Biochem. Biophys. 190* (1978) 118–125.
[42] J. H. Carson, M. L. Nielson, E. Barbarese, *Dev. Biol. 96* (1983) 485–492.
[43] A. Roach, N. Takahashi, D. Pravtcheva, F. Ruddie, L. Hood, *Cell 42* (1985) 149–155.
[44] R. Streicher, W. Stoffel, *Biol. Chem. Hoppe-Seyler 370* (1989) 503–510.
[45] D. S. Falconer, *Nature 169* (1952) 664–665.
[46] M. F. Lyon, *Nature 190* (1961) 372–373.
[47] S. M. Gartler, A. D. Riggs, *Annu. Rev. Genet. 17* (1983) 155–190.
[48] A. L. Kerner, J. H. Carson, *J. Neurochem. 43* (1984) 1706–1715.
[49] B. J. A. Sorg, D. Agrawal, H. C. Agrawal, A. T. Campagnoni, *J. Neurochem. 46* (1986) 379–387.
[50] L. A. Nave, C. Kai, F. E. Bloom, R. J. Milner, *Proc. Natl. Acad. Sci. USA 84* (1986) 1454–1458.
[51] M. V. Gardiner, W. B. Macklin, A. J. Diniak, P. L. Deininger, *Mol. Cell. Biol. 6* (1986) 3755–3762.
[52] A. Meier, A. D. MacPike, *Exp. Brain Res. 10* (1970) 512–528.
[53] S. Billings-Gagliardi, L. H. Adcock, M. K. Wolf, *Brain Res. 194* (1980) 325–328.
[54] K. Yanagisawa, I. D. Duncan, J. P. Hammang, R. H. Quarles, *J. Neurochem. 47* (1986) 1901–1907.
[55] D. Boison, W. Stoffel, *EMBO J. 8* (1989) 3295–3302.
[56] D. F. Saxe, N. Takahashi, L. Hood, M. I. Simon, *Cytogenet. Cell. Genet. 39* (1985) 246–249.

[57] P. S. Sparkes, T. Mohandas, C. Heiman, H. J. Roth, I. Klissak, A. T.-Campagnoni, *Hum. Genet. 75* (1987) 147–150.
[58] J. M. Matthieu, J. M. Roach, F. X. Omlin, I. Rauboldt, G. Almanzan, P. E. Braun, *J. Cell. Biol. 103* (1986) 2673–2682.
[59] C. Readhead, B. Popko, N. Takahashi, H. D. Shine, R. Saavedra, R. L. Sidman, L. Hood, *Cell 48* (1987) 703–712.
[60] B. Popko, C. Puckett, E. Lai, H. D. Shine, C. Readhead, N. Takahashi, S. W. Hunt, R. L. Sidman, L. Hood, *Cell 48* (1987) 713–721.
[61] E. L. Hogan, S. Greenfield in P. Morell (Ed.): *Myelin*, Plenum Press, New York 1984, pp. 489–534.
[62] G. Neuhäuser in P. J. Vinken, C. W. Bryott (Eds.): *Handbook of Clinical Neurology*, North Holland, Amsterdam 1979, pp. 498–500.
[63] N. Igahashi, H. Schaumburg, J. Power, Y. Kishimoto, E. Kolodemy, K. Suzuki, *J. Neurochem. 26* (1976) 851–860.
[64] J. Boué, I. Oberlé, R. Heilig, J. L. Mandel, A. Moser, W. Larsen, Y. Dumez, A. Boué, *Hum. Genet. 69* (1985) 272–274.
[65] I. Oberlé, D. Drayna, G. Camerino, R. White, J. L. Mandel, *Proc. Natl. Acad. Sci. USA 82* (1985) 2824–2828.
[66] F. Seitelberger in P. J. Vinken, C. W. Bryott (Eds.): *Handbook of Clinical Neurology*, North Holland, Amsterdam 1979, pp. 150–202.
[67] A. H. Koeppen, N. A. Ronca, E. A. Greenfield, M. B. Hans, *Ann. Neurol. 21* (1987) 159–170.
[68] E. P. Reddy, M. Sandberg-Wollheim, R. V. Mettus, P. E. Ray, E. De Freitas, H. Koprowski, *Science 243* (1989) 529.
[69] S. Gencic, L. D. Hudson, *J. Neurosci. 10* (1990) 117–124.
[70] W. Stoffel, T. Weimbs, T. Dick, E. Boltshauser, unpublished.
[71] J. A. Trofatter, S. R. Dlouky, W. De Myer, P. M. Conneally, M. E. Hodes, *Proc. Natl. Acad. Sci. (USA) 86* (1989) 9427–9430.
[72] L. D. Hudson, C. Puckett, J. Berndt, J. Chan, S. Gencic, *Proc. Natl. Acad. Sci. (USA) 86* (1989) 8128–8131.
[73] S. Gencic, D. Abuelo, M. Ambler, L. D. Hudson, *Am. J. Hum. Genet. 45* (1989) 435–443.

The Directed Synthesis of Biaryl Compounds: Modern Concepts and Strategies

New Synthetic Methods (82)

By Gerhard Bringmann,* Rainer Walter, and Ralf Weirich

The preparation and utilization of specific biaryl systems, particularly those which suffer hindered rotation, is a demanding goal not only in the synthesis of natural products and pharmaceuticals, but also for example in the discovery of new reagents for asymmetric synthesis. This article will attempt to provide a topical review of modern, efficient processes for the specific preparation of biaryls. This appears to be of particular urgency, since, under the pressure of continually increasing demand, a wealth of new or modified synthetic approaches to the ever more important biaryl systems has been realized in recent years. The high standard which has been reached in this field is impressively demonstrated by regio- and stereoselective syntheses of important biaryl natural products such as steganone, ancistrocladine, ancistrocladisine, and dioncophylline A. Besides the utilization of asymmetric induction in the actual coupling step, the thermodynamically or kinetically controlled torsion of biaryl axes belongs to the most important concepts discussed.

1. Introduction

The biaryl axis is the central building block in a very large number of natural products of differing structure, biological activity, and biosynthetic origin, including for example polyketides, terpenes, lignans, coumarins, flavonoids, tannins, peptides, and alkaloids[1] (Fig. 1).

Because of their interesting properties—not only as pharmacologically active natural products, but also as chiral reagents[11] and crown ethers,[12] as chiral host molecules for inclusion compounds,[13] as the basis of chiral phases for chromatography,[14] as inflexible "spacers" between two halves of a molecule[15,16] or also as the basis of chiral liquid crystals[17]—natural and unnatural biaryls constitute attractive synthetic goals. The key step in such syntheses is almost always the coupling of the two aromatic halves of the molecule. This review is not intended to give an all-embracing, encyclopedic list of all the more recent aryl coupling processes but to compare the different *strategies* used. Of particular importance in this direction will be the (still not very numerous) processes which are capable of solving the problems of (in increasing order of priority) "specific cross-coupling/regioselectivity", "stereoselectivity" and finally "chiral economy" and which can then also be applied to the synthesis of actual (when necessary functionalized and sterically hindered) biaryl natural products. The importance of the strategic concept used, for example whether the reaction is carried out in an inter- or intramolecular manner, is demonstrated by the fact that it has recently become possible to separate the two formal goals of stereoselective biaryl synthesis (i.e. C–C bond formation and asymmetric induction) both temporally and methodically (see Section 6.3). This opens up completely novel possibilities which have until now hardly been realized.

We shall however also discuss the most important of those processes which may perhaps not satisfy *all* the criteria presented above (e.g. they may not be stereoselective), but which because of their simplicity are often the methods of choice for the construction of uncomplicated systems (e.g. biaryls that are *not* rotationally hindered) and which have until now dominated the literature.

Because of the large amount of material available we shall deal in this article only with the convergent coupling of pre-

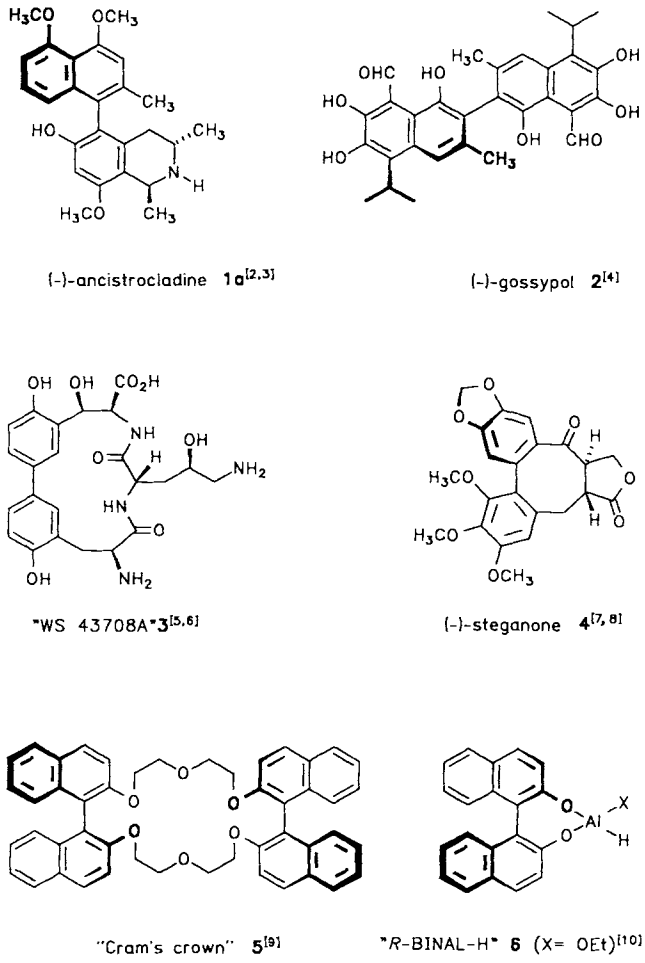

Fig. 1. Some natural and unnatural biaryls.

[*] Prof. Dr. G. Bringmann, Dipl.-Chem. R. Walter, Dipl.-Chem. R. Weirich
Institut für Organische Chemie der Universität
Am Hubland, D-8700 Würzburg (FRG)

formed (*iso*cyclic) aromatic compounds; (linear) biaryl systems obtained by subsequent construction of ring systems will be excluded. As the previous comprehensive[18,19] review on modern methods of biaryl synthesis was written ten years ago,[20] the line of demarcation for the synthetic methods covered in the present survey was drawn at about 1980, also because of the fact that up until then almost[21] no *stereoselective* aryl coupling reactions were known.

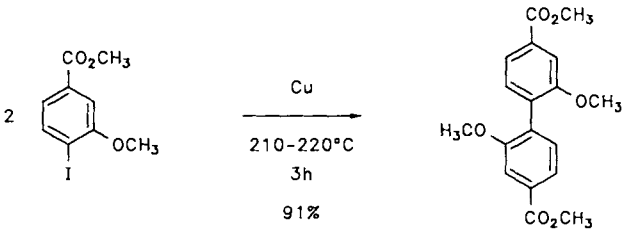

Scheme 1.

7

2. Intermolecular (Dimerizing) Aryl Coupling to Give Constitutionally Symmetrical Biaryls

2.1. The Classical Ullmann Reaction and Other Reductive Processes

The reductive dimerization of aryl halides is one of the oldest methods[22] for the preparation of constitutionally symmetrical biaryl compounds. The classical Ullmann reaction[23] using copper bronze as a reducing agent affords the highest yields in the case of *electron-poor* aryl iodides. Thus, nitro groups (even in *ortho* position) are particularly advantageous, but also aldehyde-, ester-, and lactone-functions are tolerated.[24] However, free primary or secondary amine functions or phenolic hydroxyl groups undergo *N*- or *O*-arylation to give biarylamines[25] and biaryl ethers[26], respectively—a behavior that can also be exploited rationally in synthesis (the "Ullmann condensation").

Since the course of the Ullmann reaction is determined by the position of the halogen, it is specific with regard to the *site* of the coupling: the regioselectivity problem is thus shifted to the preceding halogenation step. As the reaction is heterogeneous, it can be accelerated considerably by the use of ultrasound.[27] The yields are also high for non-benzenoid systems such as azulenes.[28] This *classical* variation is thus even today the method of choice for simpler, sterically not too congested[29] target molecules such as 7[30] (Scheme 1).

In order to avoid the often very high reaction temperatures required by this method, a number of new modifications have been introduced recently, based on work by *Semmelhack*.[31] In these, Ni^0 complexes such as $[Ni(cod)_2]$ used in stoichiometric amounts replace copper. In this way aryl halides can be reacted cleanly and in high yields in homogeneous solution at temperatures as low as 40–50 °C. Various substituents such as nitrile or even free amine functionalities are tolerated. Nitro groups, however, are not compatible with this or other nickel-mediated processes, probably because of the formation of nitrosonickel(0) complexes.[32] It must also be taken into account that proton donors change the course of the reaction dramatically, leading to hydrodehalogenation.[31] Instead of the sometimes sensitive Ni^0 complexes, also activated nickel powder can be used under similarly mild reaction conditions.[33,34]

More modern methods, which until now have been applied merely to simple substrates, use only catalytic amounts of nickel reagents. The reactive low-valent nickel species can be regenerated either electrochemically[35,36] or by co-reductants such as zinc[37,38] or sodium hydride.[39] These methods make it possible to use harder halides (aryl chlorides react most rapidly[38]) and more convenient solvents such as THF.[39]

2.2. "Biomimetic" Phenolic Couplings and Related Oxidative Methods

Complementary to the Ullmann reaction, the oxidative phenolic coupling requires the use of *electron-rich* aromatic

Gerhard Bringmann (born 1951) completed his formal education in 1970. He then studied chemistry (and biology) at the Universities of Giessen and Münster (Diploma in 1975, and Doctorate in 1978 under the supervision of Prof. Dr. B. Franck). After a postdoctoral fellowship with Prof. Sir Derek H. R. Barton in Gif-sur-Yvette, France, he returned to Münster (1979) and, following his habilitation (1984), he was offered professorships at the University of Vienna (1986) and the University of Würzburg (1987). His areas of interest cover synthetic and analytical natural product chemistry (isoquinoline alkaloids from tropical herbs, endogenous alkaloids in mammalian organisms, N-containing synthetic building blocks, biaryls). For his outstanding work in these areas, Professor Bringmann has received several awards, including the Otto-Klung-Preis für Chemie in 1988.

Reiner Walter (born 1963) started his studies in chemistry at the Technische Hochschule in Darmstadt. He then moved to Würzburg, where he gained his Diploma (1989) and is presently studying for his doctorate, the theme of which relates to the development of new concepts concerning stereoselective biaryl syntheses.

Ralf Weirich (born 1963) studied chemistry at the Universities of Düsseldorf and Würzburg. He is presently doing research for his doctorate; his thesis concerns the total synthesis of axially chiral natural products.

compounds with free phenolic groups. Although this type of reaction has a long tradition[40] because of its biomimetic character,[41] it is often of only limited preparative use, even when applied to the construction of constitutionally *symmetrical* biaryls. A reason for this is that frequently a number of unwanted side products are formed if the aromatic substrate has several sterically and electronically comparable positions.[42] In addition, side reactions such as the formation of phenyl ethers[43] and attack at benzylic positions often compete with the desired coupling process. In spite of these problems, isolated examples worthy of mention have been reported even recently, in part with excellent yields, as for example the synthesis of the gossypol analogue **8**[44] (Scheme 2).

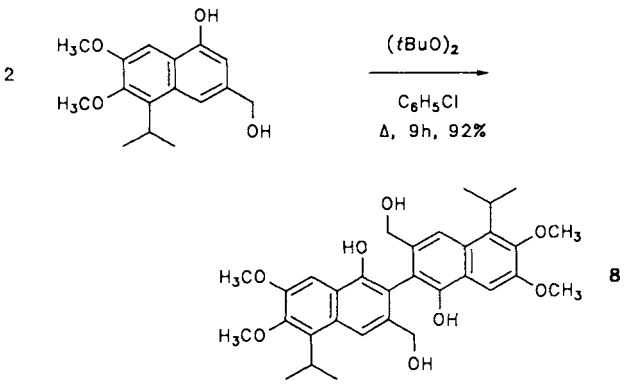

Scheme 2.

Apart from the often-used "classical" oxidizing agents such as $FeCl_3$[45] (which can be handled quite readily when absorbed on silica gel[46]) and potassium hexacyanoferrate(III),[40] also silver oxide,[47] *tert*-butyl peroxide,[43] iodosobenzene diacetate[48] and potassium dichromate[49] have been used, as well as $Mn(acac)_3$.[50] A further class of reagents such as vanadium oxyfluoride (VOF_3), thallium(III) trifluoroacetate (TTFA) etc. also makes possible a "*non-phenolic*" dehydrodimerization of electron-rich aromatic compounds[51] (see also Section 3.1.).

3. Intramolecular Aryl Coupling (the "Bridge" being Part of the Target Molecule)

3.1. Oxidative Methods

The main problems when applying the above-mentioned *inter*molecular methods to the construction of biaryl axes (the lack of regioselectivity and the often-observed formation of *homo*-coupling products when cross-coupling is required) can in principle be solved by the use of *intra*molecular reaction processes. This is true in particular for oxidative aryl coupling methods involving cyclization,[52] as used for the synthesis of aporphine alkaloids and lignans.[53] In spite of its interesting biomimetic connections,[54, 55] the *classical* phenolic oxidation has only seldom achieved far-reaching preparative importance in alkaloid synthesis because of the usually low yields and the numerous side reactions—with only few important exceptions to this rule.[56]

A better approach to, e.g., the aporphine alkaloids first became feasible after the introduction of new efficient oxidizing agents; these, such as vanadium(V) oxidants[48a, 57] (the most "popular" of which is at present VOF_3[58–61]) make possible the oxidative coupling of phenol *ethers* ("*non-phenolic*" coupling). Recently, the more selective reagent TTFA has been used,[62–67] since nearly no by-products are

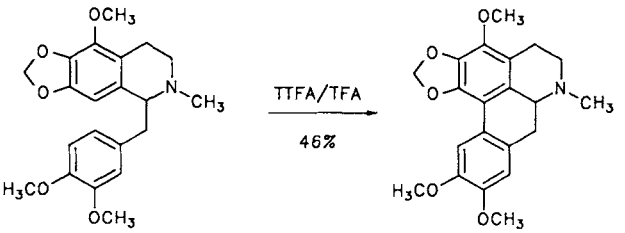

Scheme 3.

formed (Scheme 3).[62] If TTFA is prepared *in situ* from thallium(III) oxide and trifluoroacetic acid,[68] the yields can often be increased while the danger of hydrolysis is considerably reduced.

Results comparable to those obtained with such standard reagents can also be achieved using ruthenium(IV) tetrakis(trifluoroacetate),[69, 70] which is prepared *in situ* from RuO_2 and trifluoroacetic acid. In the area of non-phenolic coupling, iron(III) complexes are rather "exotic" oxidizing agents, although in isolated cases very good yields can be obtained.[71] Anodic electrochemical oxidation is less important in natural product synthesis.[72]

For a successful coupling, at least one of the rings of the substrate to be oxidized, e.g. **9** (Scheme 4), must bear oxygen

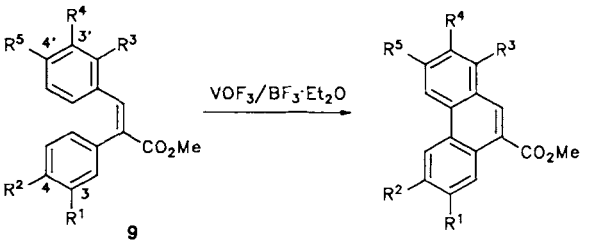

	R^1	R^2	R^3	R^4	R^5	Yield [%]
a	OMe	OMe	H	OMe	OMe	96%
b	OMe	OMe	H	H	H	81%
c	H	H	OMe	OMe	H	-
d	OMe	H	H	OMe	H	-

Scheme 4.

substituents in positions 3 and 4 with respect to the biaryl bridge; this is shown both in systematic studies by *Halton* et al.[58] and by a perusal of the numerous examples in the area of aporphine and lignan synthesis (see Section 6.1.).

The other ring is then not subject to such constraints and can even be oxygen-free (see **9b**). Benzylic oxygen functionalities which may interfere in the coupling must be introduced subsequently[73] (e.g. in the bisbenzocyclooctadiene skeleton of steganone **4**). Amine nitrogens, as long as they are tertiary or acylated, have no effect.

Apart from its function as an integral element of the target molecule, the bridge between the two aromatic rings to be coupled also induces good yields in cross-coupling and reliable regioselectivities (particularly when the bridge is short) because of the intramolecular nature of the reaction. The loss of regioselectivity observed for larger rings such as eight-membered rings with two equivalent coupling positions can sometimes be compensated by using an additional (auxiliary) bridge, the size of which must be varied according to the particular synthetic problem (Scheme 5).[60]

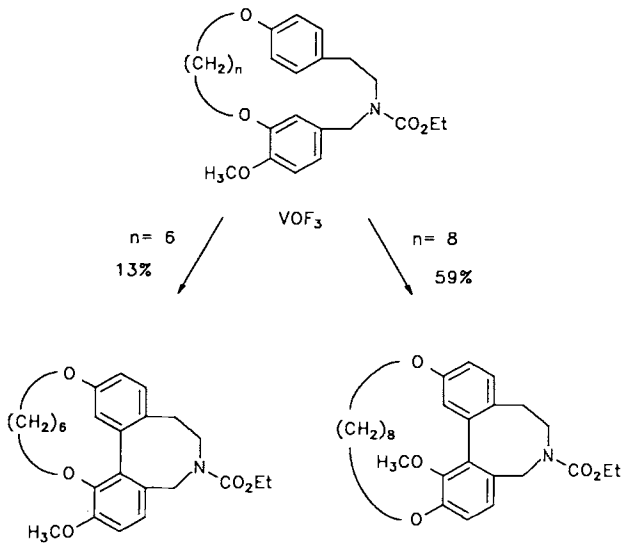

Scheme 5.

Couplings can also be carried out successfully for analogous seven-membered ring systems (e.g. homoaporphines and colchicine analogues);[62,63] even eleven-membered rings can be obtained in this manner, though with considerably lower coupling yield and regiocontrol (Scheme 6).[74]

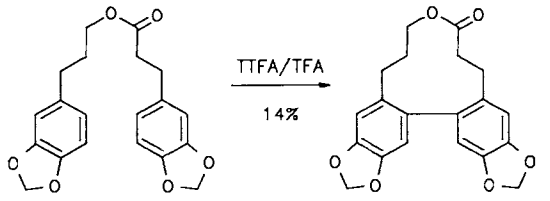

Scheme 6.

3.2. Reductive Processes

*Intra*molecular variants have also proved useful for Ullmann couplings and related reactions, though until now there are only few examples[31,75,76] (cf. also Section 6.2).

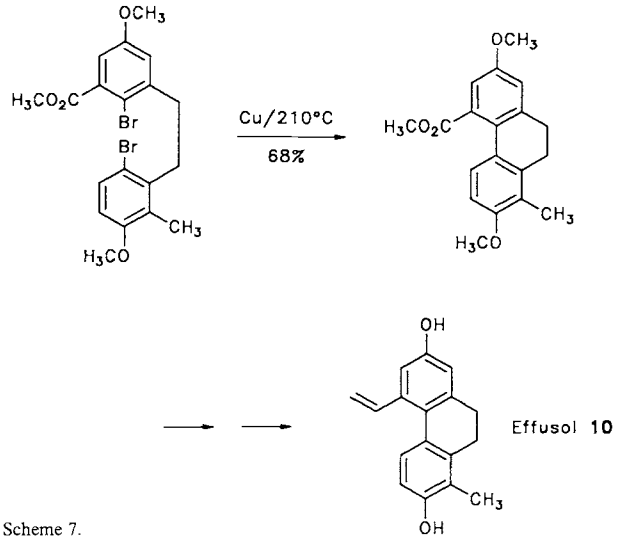

Scheme 7.

The coupling of two different aromatic rings is even possible when these are relatively electron-rich, as in the synthesis of effusol (**10**), a dihydrophenanthrene from marsh grasses (Scheme 7).[77]

3.3. Redox-Neutral Processes

In simple, regiochemically non-problematic cases (e.g. when only *one* free *ortho* position is present next to the bridge) the intramolecular coupling reaction can also be carried out under redox-neutral conditions, e.g., by palladium-catalyzed,[78,79] free radical[80] or photochemical[81] dehydrohalogenation; in some cases it has been possible to obtain unusually large ring systems in surprisingly good yields by intramolecular aryl coupling (Scheme 8).[82]

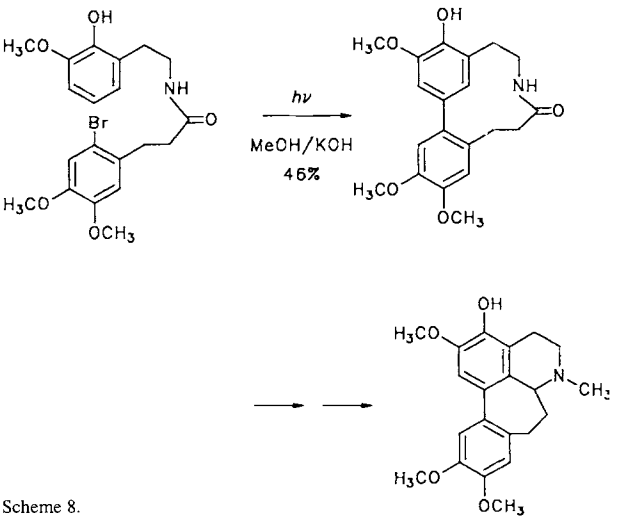

Scheme 8.

A very important disadvantage of the redox-neutral coupling reaction is that hydrodehalogenation without coupling is almost always observed. Since the by-products so formed can generally not be reintroduced into the reaction process by regioselective halogenation, they are no longer available for the required synthesis.

4. Intermolecular Cross-Coupling to Give Constitutionally Unsymmetrical Racemic Biaryls

Crossed and, furthermore, regioselective couplings between two different aromatic rings can thus be forced to occur by utilizing *intra*molecular reactions, as shown in the previous section. In *inter*molecular processes, however, satisfactory yields of cross-coupled products can only be obtained if the two aromatic compounds used are functionally or electronically very different. Thus, both in reductive[83-85] and oxidative[86] processes electron-rich compounds must be allowed to react with electron-poor partners in order to shift the normally statistical product distribution towards the crossed products.

It is however much more effective to use the two aromatic compounds in the form of an electrophile/nucleophile pair. This can be done even within the framework of a formal Ullmann coupling in which an arylcopper compound is *first prepared separately* and then allowed to react with an aryl iodide.[87] Another possibility used with success is the reaction of electron-rich aromatic compounds with quinol acetates.[88]

4.1. Ni- and Pd-Catalyzed Grignard Coupling Reactions

A preparatively favorable combination of electrophilic and nucleophilic aromatic molecules is provided by the pairing of aryl halides with arylmetal compounds. Since the discovery that reactions of aryl-Grignard compounds with organic halides (the "Kharash reaction"[89]) can be accelerated by nickel or palladium derivatives,[90] this method has often been used for C–C bond formation.[91,92]

In order to avoid unwanted addition reactions to carbonyl groups, recourse has sometimes been taken to using the less aggressive zinc analogues of the reactive Grignard compounds; such organozinc derivatives can readily be obtained by transmetalation of the corresponding lithium compounds, as in the steganone synthesis reported by *Larson* and *Raphael*.[93] Here, the key step is the regioselective coupling between the organozinc compound **11** and the aryl halide **12** (Scheme 9)—a reaction that poses no steric problems in this

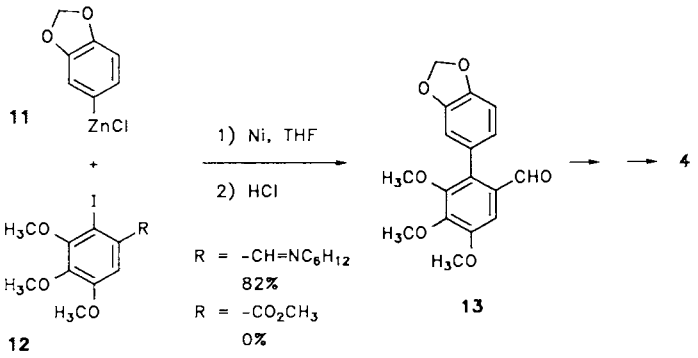

Scheme 9.

formation of the biaryl **13** which has only two substituents in the *ortho* position with respect to the biaryl axis.

When sterically more demanding reactants are used, however, almost no coupling products are obtained: thus even the presence of one *ortho* substituent on *each* of the two aromatic compounds causes the yield to fall dramatically.[94] Organocopper[95] and organomercury[96,97] derivatives are also capable of undergoing analogous palladium-catalyzed cross-coupling reactions, although such reactions have as yet hardly been applied.

4.2. Coupling Reactions Involving Other Metal(loid)s

The presence of carbonyl groups can lead to the formation of by-products under the conditions used for the above "Grignard coupling";[98] this disadvantage can be avoided by the use of organic derivatives of the less electropositive metal(loid)s boron, silicon or tin[99] because of their reduced nucleophilicity.[96] These arylation reagents can be prepared and purified separately, since they are relatively insensitive towards atmospheric oxygen.[100]

One method which has become of widespread use in organic synthesis is the palladium-catalyzed coupling of the readily available arylboronic acids with aryl halides in the presence of auxiliary bases such as potassium carbonate;[98] examples are the functionalization of an aromatic ring by *ortho*-metalation in the stepwise synthesis of teraryls[101] or the preparation of derivatives of the cyclopeptide **3** (see Fig. 1) via **14**[102] (Scheme 10).

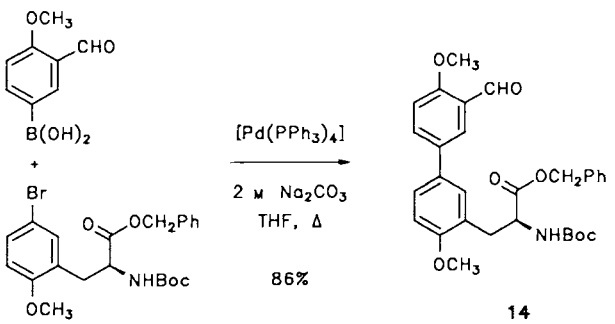

Scheme 10. Boc = *tert*-butoxycarbonyl.

However, steric hindrance of the coupling position by *ortho* substituents, particularly in the boronic acid fragment, has a very negative effect on the yields of coupling product when this method is used.[103]

Phenolic hydroxyl groups can also be exchanged for aryl substituents by palladium-catalyzed reaction of the corresponding aryl triflates with aryltin compounds,[104-106] as in the synthesis of 4-acetylbiphenyl **15**[107] (Scheme 11).

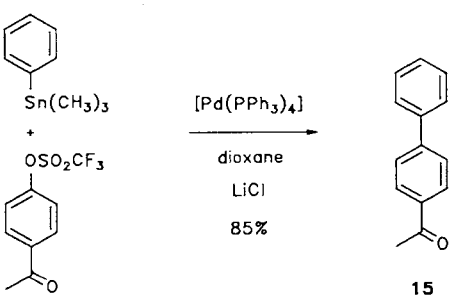

Scheme 11.

Recent reports have dealt with the fluoride-induced cross-coupling of arylfluorosilanes (such as **16**, Scheme 12) with aryl iodides.[108] The palladium-catalyzed synthesis of the biphenyl **17** in a yield of no less than 67% shows that this reaction even tolerates the presence of free hydroxyl groups.

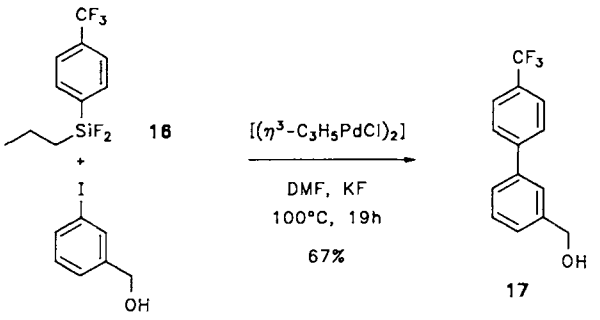

Scheme 12. DMF = dimethylformamide.

4.3. The "Meyers Oxazoline Method"

The process for achieving regioselective cross-coupling between two different aromatic compounds which is at present most generally used is, no doubt, the oxazoline method developed by *Meyers*—an efficient route to constitutionally unsymmetrical biaryls.[109]

The aryl residue is introduced in the form of a Grignard reagent by nucleophilic aromatic substitution of a methoxy group bound to an aromatic nucleus. In contrast to the coupling with aryltins described in the previous section, this uncatalyzed reaction requires the activating influence of an oxazoline moiety in the *ortho* position; this increases the electrophilicity at the reaction center and functions at the same time as an additional directing complex ligand for the attacking Grignard species (Scheme 13).

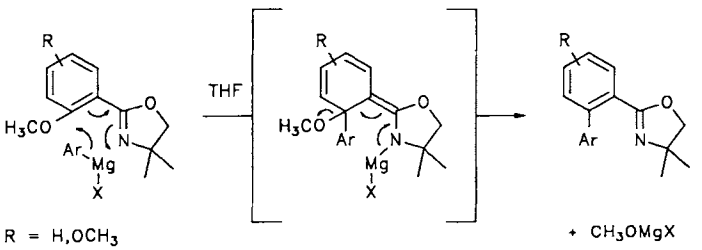

Scheme 13.

The auxiliary group can subsequently undergo hydrolysis to give the biarylcarboxylic acid either under alkaline conditions (after quaternization of the nitrogen with methyl iodide) or under (very harsh) acid conditions; it can also be converted by reductive processes[110, 111] into the corresponding alcohol or aldehyde. In spite of some disadvantages of this method (with respect to the degree of steric hindrance which it tolerates,[110] the sometimes difficult or even impossible preparation of the aryl Grignard reagent,[112] the limitation to certain substitution patterns, etc.: see also Section 5.2.), its popularity can best be seen from the large number of applications in the preparation of biaryl natural products reported in the literature.[113, 114] Thus, besides *rac*-desertorine C[115] and cannabifuran,[116] also the biaryloxazoline **18** has been synthesized; under the reaction conditions used,[117] the latter is directly cyclized to the antimicrobially active lactone defucogilvocarcine V **19**[118] (Scheme 14).

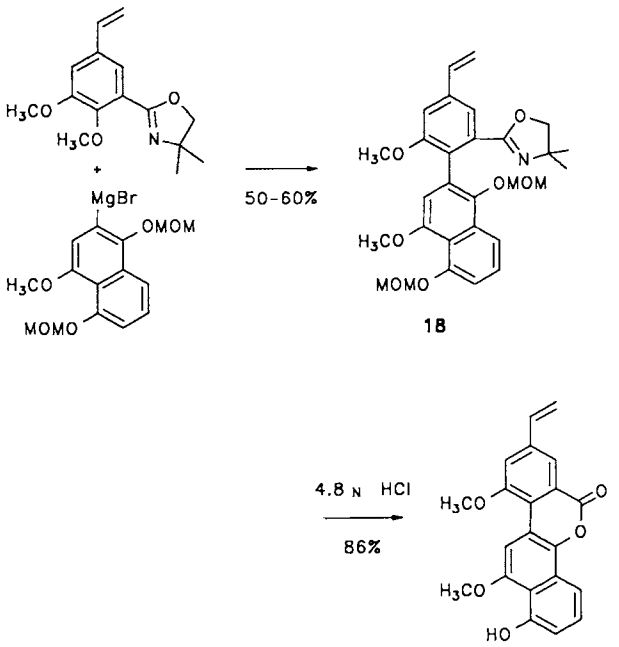

Scheme 14. MOM = CH_3OCH_2-.

5. Intermolecular Atropisomer-Selective Aryl Coupling

5.1. On the Stereochemistry at the Biaryl Axis

In many of the natural or synthetic biaryls bulky *ortho* substituents next to the coupling position lead to hindrance of free rotation around the biaryl axis and thus to the existence of more or less stable atropisomers, sometimes even when only three *ortho* substituents are present,[119] while in extreme cases only two *ortho* substituents may suffice.[120]

The directed synthesis of such axially chiral compounds requires the unambiguous assignment of the configuration of a biaryl unit thus formed. Certainly the most important method for the direct determination of the *absolute* configuration at the axis is the measurement of circular dichroism (CD)[121]—if necessary after "planarization" of potentially disturbing stereogenic *centers*.[6, 119] X-ray crystal structure determinations will provide information on the *absolute* stereochemistry at the axis less frequently, but will at least afford very reliable statements regarding the axial-chiral situation *relative* to stereocenters likewise present in the molecule.[122, 123] An unambiguous assignment of the relative configuration can also be obtained chemically, by means of an atropisomer-differentiating ring closure reaction to give *ansa*-like macrocycles.[124]

5.2. Nucleophilic Aromatic Substitution

The method of nucleophilic aromatic substitution referred to in Section 4.3[125] can also be carried out in an atropisomer-selective manner when enantiomerically pure chiral oxazolines are used.[110, 111] Very high atropisomeric excess is however generally only obtained with aromatic compounds in which the *ortho* substituents next to the coupling position are very different in size (as for example hydrogen vs. alkyl in **20**, see Scheme 15), i.e. in the synthesis of biaryls which bear only three *ortho* substituents.[110] In biaryls of this type however, in which free rotation is only slightly hindered, a racemization-free removal of the chiral auxiliary is often very difficult because of the low atropisomerization barrier, and can only be carried out by reductive means.

It appears that the only biaryl *natural product* which has been prepared by stereoselective coupling using the oxazoline method is steganone (**4**)[126] (Scheme 15); however, even

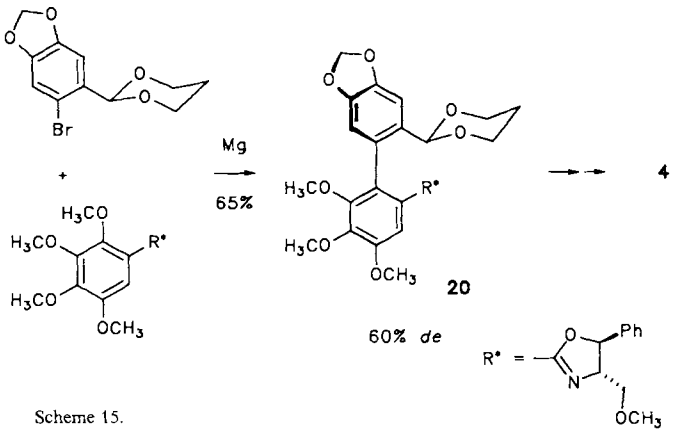

Scheme 15.

in this synthesis the information on axial chirality thus generated is lost at a later stage by epimerization at the axis (to give a 1:1 mixture of atropisomers).

Noticeably lower chemical yields and much poorer asymmetric inductions are often observed in reactions which lead to fourfold *ortho*-substituted biphenyls.[110] One exception is provided by the efficient stereoselective synthesis of the binaphthalene **21** (Scheme 16).[111]

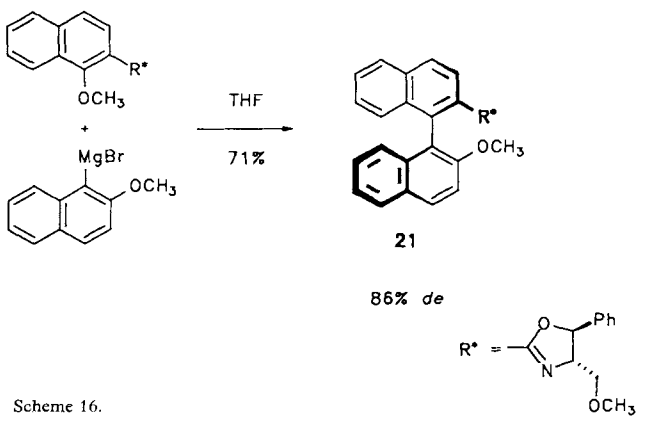

Scheme 16.

Other problems can arise due to the commercial availability of only one of the two enantiomers of the chiral auxiliary as well as due to the limitation of the method to particular biaryl substitution patterns.

A decisive influence on *stereoselection* in these nucleophilic substitutions is suggested to be exerted by the metal cation, since the geometry of the primarily formed addition product is determined by the more favorable mode of complexation[111] (Fig. 2).

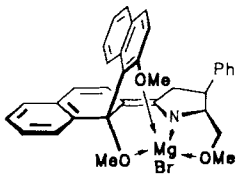

Fig. 2. Presumed intermediates in the arylation to **21** according to *Meyers* et al. [111].

This is also true for the procedure due to *Cram*, in which the required asymmetric induction is obtained by means of a chiral nucleofuge.[127, 128] However, while the use of chiral oxazolines affords diastereomeric mixtures, which can readily be separated by chromatography, the *Cram* procedure may make it necessary to separate the undesired atrop-*enantiomer*. The highest "chirality transfer efficiency" was observed in sterically strongly hindered systems in the reaction

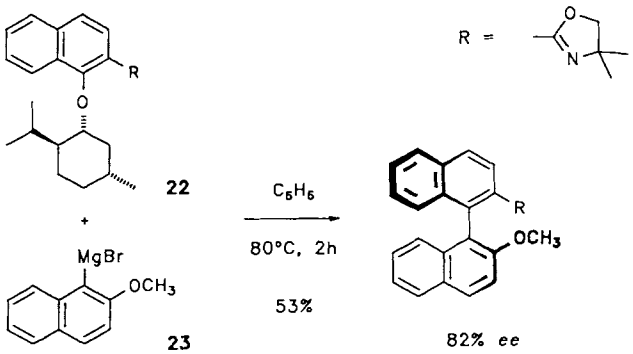

Scheme 17.

of the (−)-menthoxynaphthalene **22** (Scheme 17) with the naphthyl Grignard reagent **23**.[127]

5.3. Coupling with Chiral Copper Complexes

But also when starting from arenes that have not been chirally modified, stereoselective aryl couplings may be carried out, for example by copper complex-mediated phenolic oxidations.[129, 130] Thus, β-naphthol can for example be converted in very good chemical and optical yields into the binaphthol **24** in the presence of a chiral copper-(*S*)-amphetamine complex[129] (Scheme 18). More exact studies, however, show that the excess obtained here does not result from a *kinetic* control, but a subsequent equilibration, i.e. a

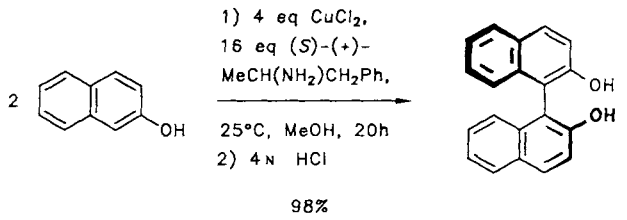

Scheme 18. **24** (96% *ee*)

thermodynamically controlled atropisomer-selective synthesis is involved (see Section 6.3.2). This type of reaction has even been extended to the stereoselective cross-coupling to give teraryls.[131] A disadvantage of this method is the need to have a *more than stoichiometric* amount of chiral auxiliary (up to 16 equivalents of chiral amine per biaryl formed!).

5.4. Coupling with Chiral Catalysts

The development of more economic processes is thus becoming continually more important. Latest results reported by *Hayashi* et al.[132] are a guiding light in the area of *catalytic atrop-enantioselective* crossed Grignard couplings; the catalysts used here are nickel complexes with chiral ferrocenyl ligands such as **25** (Scheme 19).

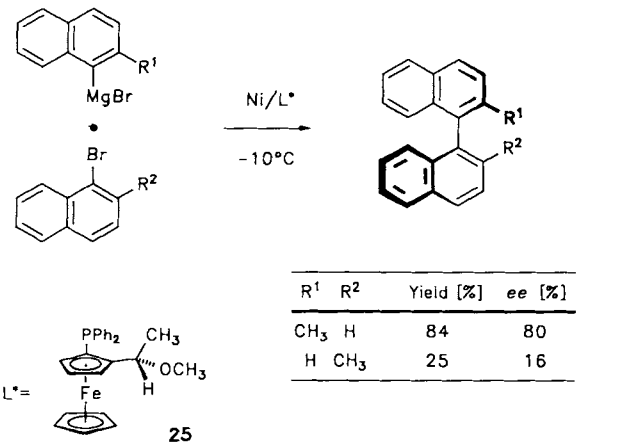

R^1	R^2	Yield [%]	*ee* [%]
CH_3	H	84	80
H	CH_3	25	16

Scheme 19.

As a comparison of the two reactions presented shows, only certain substrate combinations are possible. Thus, in order to obtain good optical yields the aryl Grignard component must generally have two *ortho* substituents, while in order for the chemical yields to be good only a slight steric hindrance is tolerated for the halide. This method has since been used for the synthesis of a chiral binaphthyl(cyclopentadienyl)titanium complex[133].

The process can also be employed in the stereoselective synthesis of ternaphthyls.[134] However, an application to the coupling of complex functionalized aromatic compounds, for example for the preparation of particular biaryl *natural products*, is still awaited.

6. Intramolecular Atropisomer-Selective Aryl Coupling

Recently, powerful methods for intramolecular aryl coupling have been increasingly elaborated. Not only does the bridge (as in the examples discussed in Section 3) lead to an improvement in the yield and a reliable regioselectivity due to the intramolecular nature of the reaction, but it also influences the barrier to atropisomerization and can be the site of the chirality from which the asymmetric induction emanates. After coupling has been carried out, the bridge can either completely or in part remain within the molecule (eventually leaving "bridgeheads" behind) or it can be completely removed.

6.1. Using Bridges which are Naturally Present in the Target Molecule

In many oxidative intramolecular coupling reactions to give lignans[68, 135–138] (see Section 3.1) the "bridge" is not only a constituent part of the target molecule but at the same time it determines the steric course of the coupling reaction. Thus, for example, the reaction of **26** (Scheme 20) with VOF_3 gives under kinetic control solely the unwanted atropisomer **27b** (of the "isostegane type"),[139] which on heating can undergo equilibration[140] to yield the atropisomer mixture **27a/b** (ca. 2:3[141], from which the natural rotational isomer **27a** of the "stegane type" can be isolated in 39% yield.

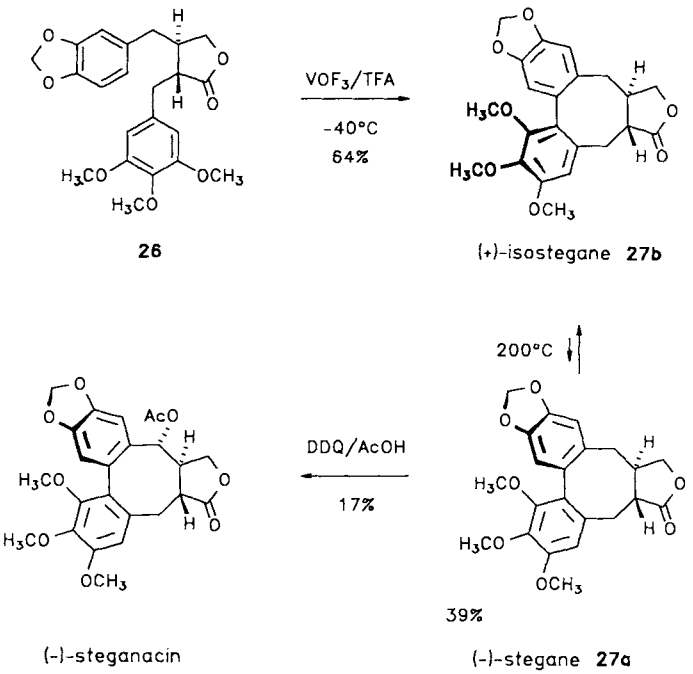

Scheme 20. DDQ = 2,3-dichloro-5,6-dicyanobenzoquinone.

The barrier to atropisomerization as well as the kinetically controlled preferred formation of the isostegane-type isomer is here determined mainly by the configurational inflexibility of the cyclooctadiene system, so that analogous couplings

lead to the isostegane type even when only two substituents *ortho* to the biaryl axis are present[120]—as long as the eight-membered ring formed is kept rigid, for example by an annelated five-membered lactone ring. Without this additional stabilization the barrier to atropisomerization sinks dramatically, and thermodynamically controlled rotational isomer mixtures are formed.[120]

Many of the reactions discussed in Section 3.1 very probably also occur in a stereoselective manner, but unfortunately most publications do not report the configuration at the biaryl axis or even mention the possible existence of atropisomers. Many examples of this type, which could perhaps have been included in this section if a more exact stereochemical study had been carried out, can thus only be treated in this section.

6.2. Coupling in the Presence of Artificial Chiral Auxiliary Bridges

However, even when the target molecule does not contain a "bridge" as an integral part of its structure it is possible to take advantage of an intramolecular stereoselective reaction pathway—by pre-fixing the two aromatic moieties by means of an *artificial* chiral bridge. Thus, *Miyano* developed a process for an atrop-diastereoselective (and if necessary also crossed) intramolecular Ullmann reaction with the help of optically active auxiliary bridges.[142] By far the best results are obtained in this case by using the rigid template formed by a further biaryl, (*R*)-2,2'-binaphthol (*ent*-**24**). Here, complete asymmetric induction is observed, and the product **29** has the same enantiomeric purity as the auxiliary bridge used (Scheme 21).[143]

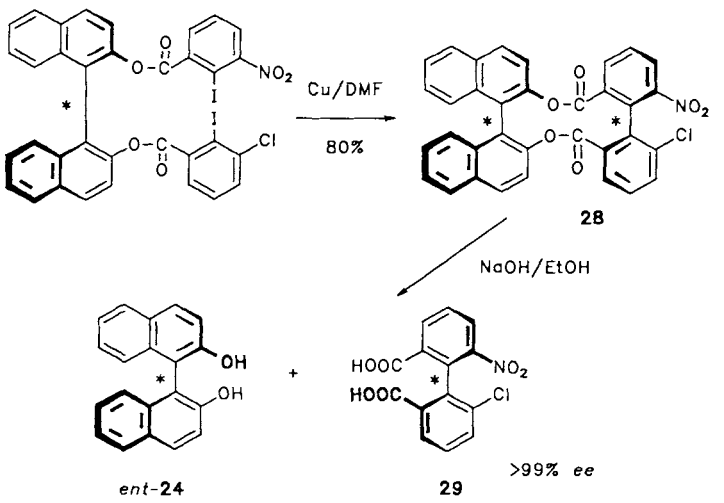

Scheme 21. DMF = dimethylformamide.

The disadvantage of the high price of the chiral biaryl **24**, which must be used in stoichiometric amounts, is partially compensated by the possibility of its reuse. The asymmetric induction is considerably poorer when other, cheaper chiral diols are used as bridges.[144] The reason for the high degree of stereoselectivity achieved when the binaphthol bridge is used has been suggested to be a double helix-like arrangement of the twelve-membered ring **28**, which represents the energetically most favorable conformation of the coupling product.[145] The generation of the corresponding diastereomeric product can be excluded because of the unfavorable geometrical arrangement required.

However, a more general use of this method, for example in natural product synthesis, is hampered by the often poor yields and by its limitation to electron-poorer coupling substrates and to particular substitution patterns.

6.3. Coupling in Presence of Artificial Auxiliary Bridges without Stereogenic Centers

6.3.1. The General Principle

Recently, a new method has been developed for the regio- and stereoselective construction of even highly substituted biaryls for the synthesis of natural products and pharmaceuticals;[7, 124, 146–149] in this procedure the two aromatic residues are brought together at a suitable distance by means of an *achiral* auxiliary chemical bridge and then linked in an intramolecular manner by a coupling proceeding with cyclization. The auxiliary bridge does not need to be an integral part of the target molecule, but is constructed from "bridgeheads" *already present*.

Because of the arrangement of substituents in **30**, which is often found in biaryl natural products, such a prefixation of the two aromatic moieties **33** and **34** was carried out by an ether- or ester-type bridge (as in **32**), which subsequent to the aryl coupling to give **31** can readily be cleaved reductively to yield the final product **30** (Scheme 22).

In this case the auxiliary bridge leads not only to very good coupling yields and to a reliable *ortho* regiospecificity because of the *intra*molecular mode of reaction; in addition there is a dramatic lowering of the atropisomerization barrier in the bridged biaryls **31** in comparison with the ring-opened products **30**.

This effect can be used in a specific manner, since according to the degree of steric hindrance at the biaryl axis the bridged biaryls **31** are either still helically stable (see Section

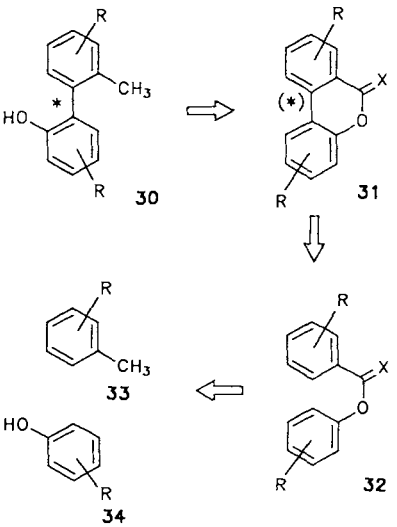

Scheme 22.

6.3.2) and can undergo ring-opening with retention of configuration at the biaryl axis, or they are stereochemically not yet differentiated, but "*axially prostereogenic*";[146] they can then be ring-opened under kinetic control atrop-diastereoselectively (see Section 6.3.3.1) or *atrop-enantioselectively* (see Section 6.3.3.2)—by stereoselective twisting of an already present but on a time average still planar biaryl system.

6.3.2. *Coupling via Helically Twisted Bridged Biaryls*

The power of this new arylation concept is shown particularly clearly in the regio- and stereoselective total synthesis[147] of ancistrocladine (**1a**), the most well-known representative of the naphthylisoquinoline alkaloids,[7] which is configurationally stable at its rotationally hindered axis up to over 200 °C. The ester-type pre-fixation of the two halves of the molecule as in **35** now makes it possible to carry out the (*intermolecularly* not realized[112]) aryl coupling in high yield and with a high regioselectivity (Scheme 23). Because of the steric hindrance at the axis, the bridged biaryl precursor (the lactone **36**) is here not planarized but split into *helicene-like distorted atropisomers* **36a/b**, which can be converted into ancistrocladine (**1a**) and its naturally occurring atropisomer hamatine (**1b**)—with a clear atropisomer excess (e.g. 4.7:1 when $R=CH_2Ph$) in favor of the ancistrocladine type, which is also found more frequently in plants.[7]

This atropisomeric excess depends strongly on the conformational rigidity of the tetrahydroisoquinoline ring (and also of the bridge). Thus, the introduction of the *N*-trifluoroacetyl group in **35** shifts the helimer distribution greatly in favor of the ancistrocladine precursor **36a** ("100:0" for $R=COCF_3$);[124] the ring opening can then be carried out under mild conditions with retention of the configuration at the axis—a *thermodynamically controlled atrop-diastereoselective biaryl synthesis*.

In contrast to the situation in the intermolecular atropisomer-selective cross coupling with the aid of chiral copper complexes described in Section 5.2, where the isomer equilibrium is influenced by an *external* chiral auxiliary (the amine ligands on the copper), the reaction is directed here by *internal* asymmetric induction due to the chirality already present in the substrate (stereogenic centers at C-1 and C-3).

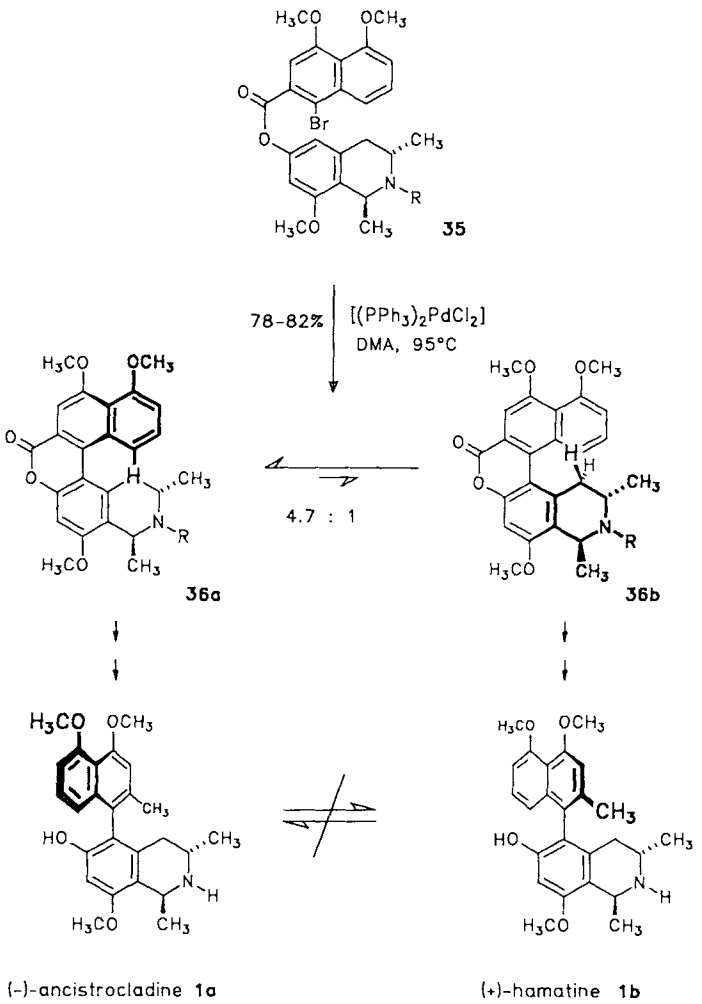

Scheme 23. DMA = *N*,*N*'-dimethylacetamide.

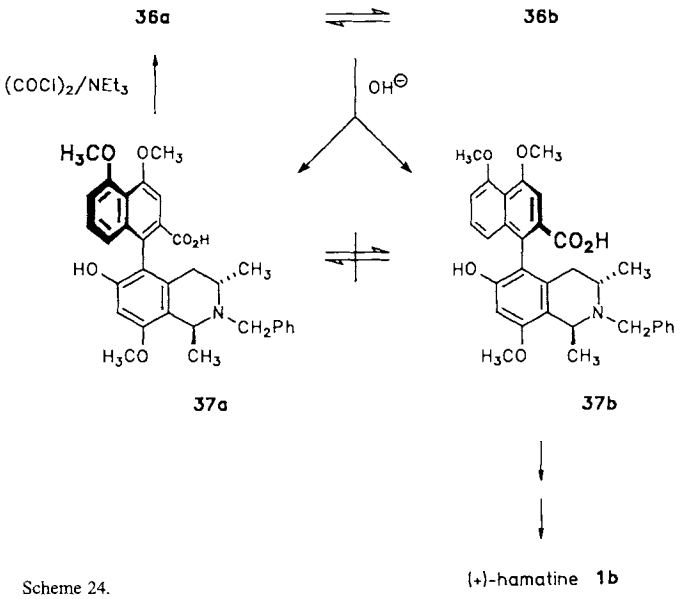

Scheme 24.

A specific synthesis of the minor isomer hamatine (**1b**) by means of isomer separation at the stage of the lactones **36a/b** is made difficult by the fact that these atropisomers interconvert at room temperature with a "half-life" of less than one minute; this is due to the short and planarizing bridge. It is much simpler to open the lactone mixture **36a/b** by means of base-catalyzed ester hydrolysis to give the stable and thus readily separable acids **37a/b** (Scheme 24).[124] Subsequent to the separation, each required atropisomer (e.g. **37b**) can be converted into the corresponding alkaloid (in this case hamatine (**1b**)), while the unwanted stereoisomer (in this case **37a**) can be reintroduced into the reaction process in the sense of "*axially chiral economy*"[124]—a *recycling through recyclization*.

Still more simply, without recourse to the hydrolysis/lactonization cycle, hamatine (**1b**) can be synthesized, via the conformationally more stable and thus readily separable cyclic ethers **38a/b** (Scheme 25)[148] by ring-opening of the

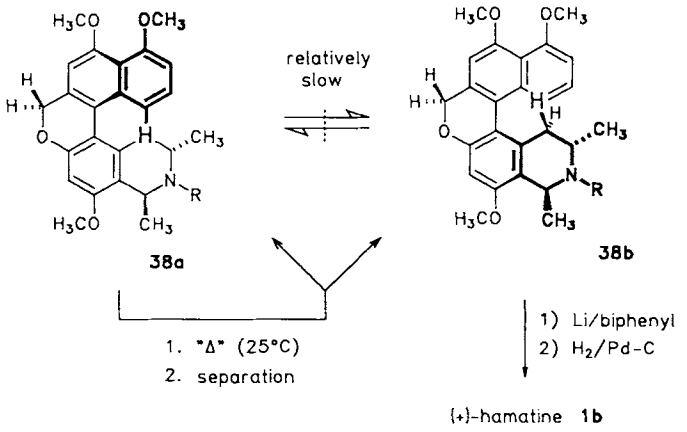

Scheme 25.

now required stereoisomer **38b** and recycling of the unrequired *M*-helical isomer (the "*M*-helimer"[148]) **38a** by equilibration at room temperature and repetition of the procedure thus have possibilities for the synthesis of either of the two atropisomers, hamatine (**1b**) or (in a more direct manner, as described above) ancistrocladine (**1a**), starting from identical precursors.

6.3.3. Coupling via Planarized ("Axially Prostereogenic") Bridged Biaryls

6.3.3.1. By Means of Internal Asymmetric Induction

Stereochemically still not defined, however, is the planarized, "*prostereogenic*" axis, e.g. in the alkaloid precursor **40**,[149] which can also be obtained in very good yields by coupling. The selection of suitable reaction conditions makes it possible to control the cleavage of the auxiliary bridge to give the configurationally stable ring-opened biaryls **41a** and **41b** stereoselectively, by making use of *internal* asymmetric induction (Scheme 26):[124] by reduction of **40** with *Lewis acid* hydride transfer reagents (or corresponding combinations) the ring-opened product **41a**, a precursor to (−)-dioncophylline A (**42**), is formed practically exclusively (*ds* > 95%), whereas the use of *basic* hydride transfer reagents (e.g. "Red-Al") instead gives the atropisomer **41b** in good atropisomeric excess; the latter is also found in nature in the form of **43**[150, 151]—a new principle for the (kinetically controlled) atropisomer-selective biaryl synthesis by *diastereoselective twisting and ring-opening of axially prostereogenic lactone precursors* with the help of achiral H-nucleophiles.

The mechanistic concept[124] used here requires that the following three conditions be fulfilled in order that an already present but initially flat biaryl axis undergoes twisting in such a directed manner:

1) The diastereofacial attack of the hydride transfer reagent on the lactone function of **40** must occur from only *one* direction (e.g. merely from below, Scheme 27) with formation of for example only the (metal) lactolate diastereomer **44** with an α-hydrogen; this can be explained in terms of blockage of the upper side of the molecule by the bulky, strongly complexing aluminum reagent, so that attack of the nucleophile can only occur from below.[152]

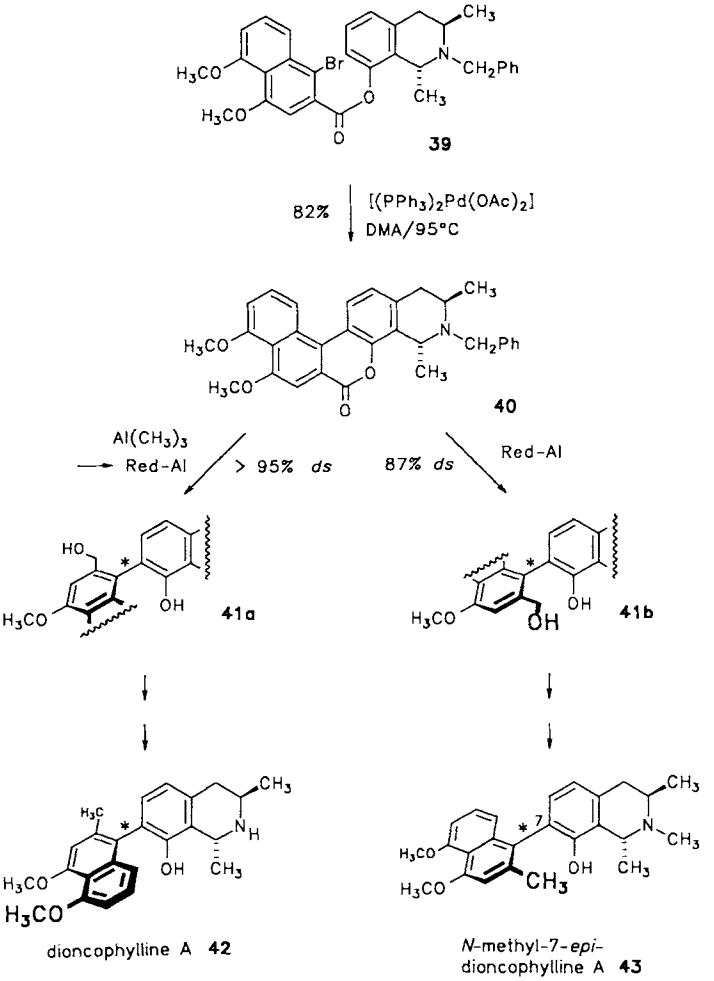

Scheme 26.

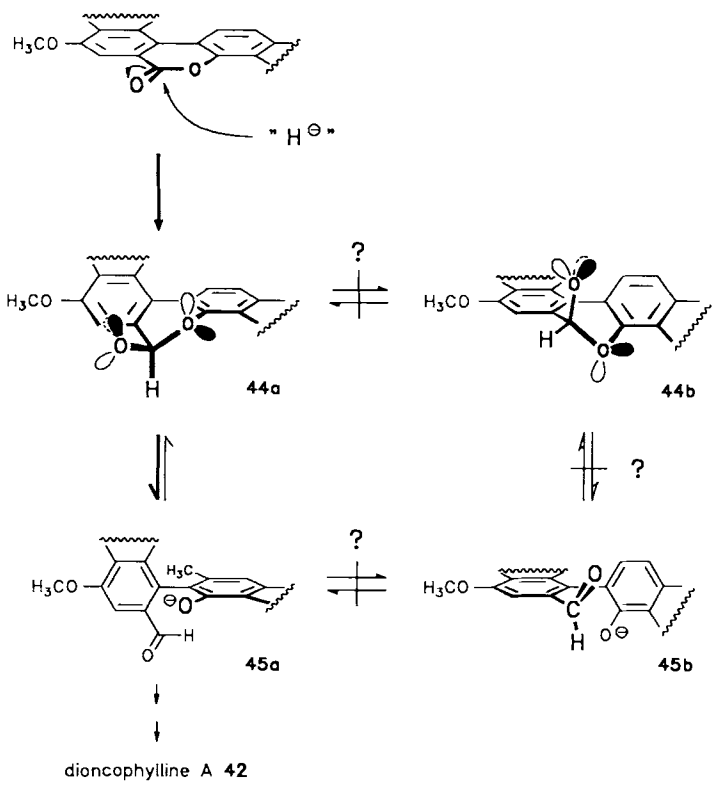

Scheme 27.

2) Preferred ring opening of the (metal) lactolate **44** (possibly stereoelectronically controlled) starting from only *one* of the two possible conformations **a**/**b**; this opening, e.g. of **44a** to give **45a**, would cause the conformation preformed in the lactol to become the final axial "configuration" at the biphenyl axis.
3) The resulting aldehyde **45a** must be reduced rapidly enough to give the configurationally stable alcohol **41a** (see Scheme 26) before it loses its inherent axial chirality information by subsequent recyclization and isomerization processes.

This stereocontrolled synthesis of dioncophylline A (**42**) and (if required) of its atropisomer is at the same time a promising first step in the direction of a general strategy for the specific transformation of a readily-constructed, stereochemically still undefined axis into a stereogenic axis with any required configuration by stereoselective reaction at a coupled stereogenic center (in this case the carbonyl group) followed by a chirality transfer from "centro-chiral" to "axially chiral".

For the stereoselective torsion of the still flat biaryl axis, oxygen nucleophiles can also be used if sufficient steric hindrance is present (see Scheme 28).[153] Thus, the preparative-

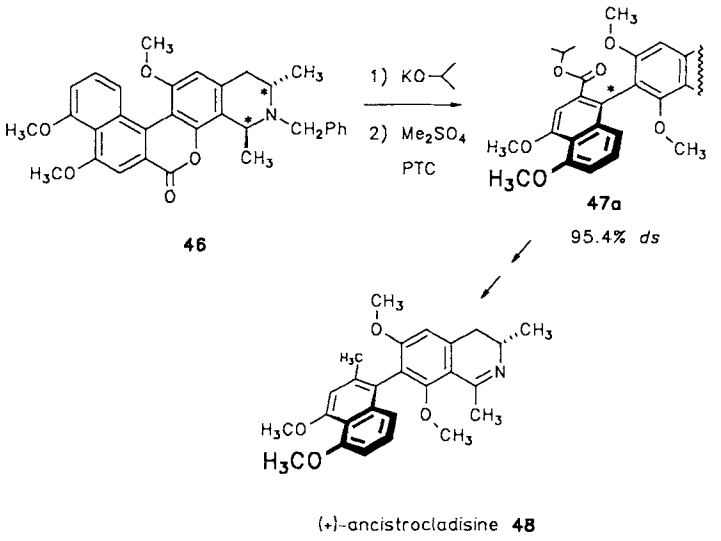

Scheme 28. PTC = phase transfer catalysis with benzyl-tri-*n*-butylammonium chloride.

ly facile ring-opening of the related lactone **46** gives very high atropisomeric excesses even when using potassium isopropoxide; these can be increased by the use of (+)-mentholates, while the use of (−)-mentholates (the "mismatch" case) causes them to be reversed to a small extent. The ring-opened ester **47a** is converted with retention of the configuration at the biaryl axis into the alkaloid (+)-ancistrocladine (**48**) (prepared here for the first time), while the other, unwanted isomer can again be recyclized to the axially prostereogenic lactone **46** in the sense of "axially chiral economy".[146]

This example demonstrates an important practical aspect of the new synthetic principle: it is the first example of an atropisomer-selective synthesis of an axially chiral natural product with two identical *ortho* substituents ($2 \times OCH_3$) next to the biaryl axis[154]—a still unsolved problem for all other methods of stereoselective aryl coupling. In such cases it makes no difference energetically whether a locally symmetrical aromatic compound (i.e. one with two identical *ortho* substituents) approaches to form one or the other atropisomer, even when in a *more distant sphere* there are differences with respect to the substituents: *here* this goal is reached without any difficulty whatsoever, since this stereoselective ring opening is subject to completely different control mechanisms (see above).

6.3.3.2. By Means of External Asymmetric Induction

In the case of the alkaloid syntheses described above it was possible to establish the axial chirality by taking advantage of an *internal* asymmetric induction exerted by stereogenic centers already present in the molecule. In view of the large number of important biaryl natural products which contain no further stereogenic elements apart from their chiral axis it is of particular preparative importance that this principle can now also be extended to include atrop-*enantioselective* biaryl synthesis—by stereocontrolled torsion of completely flat, *achiral* lactone precursors by means of optically active ring-opening nucleophiles.

Thus, the stereoselective ring opening of the benzocoumarin-like lactone **49** (Scheme 29)—a model precursor for a

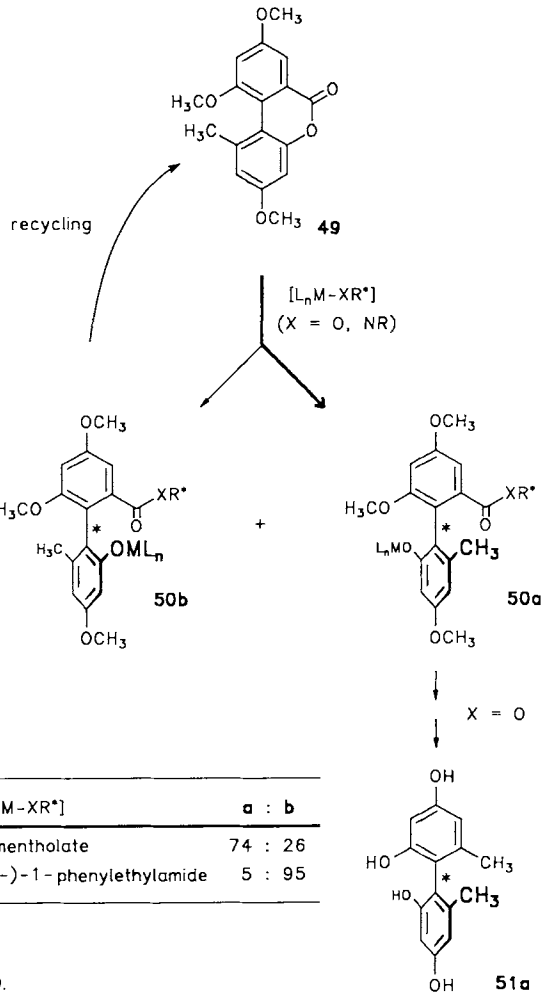

$[L_nM\text{-}XR^*]$	a : b
K-(+)-mentholate	74 : 26
K-(S)-(-)-1-phenylethylamide	5 : 95

Scheme 29.

large number of axially chiral natural products which have similar substitution patterns next to the biaryl axis (e.g. gossypol (**2**))—occurs "right away" in quite good atropisomer ratios with such simple, inexpensive and sterically not particularly differentiating oxygen nucleophiles as (−)-mentholate; it is of mechanistic importance that the best results are always obtained with potassium alcoholates.[155]

The required atropdiastereomer (e.g. **50a**) can be converted into the target molecule (in this case the enantiomerically pure dimeric orcin **51a**) with retention of configuration at the biaryl axis, while the unwanted atropdiastereomer can be reintroduced into the process by recyclization, whereby again the chiral alcohol is reobtained. This method is thus chirally economical with respect to both substrate *and* reagent.

Ring-opening reactions occur in an even more stereoselective manner using the simple nucleophile (*R*)-1-phenylethylamine, which is available cheaply in both enantiomeric forms; again the same surprising tendency is observed for the best results (*dr* 95:5) to be obtained in each case with the corresponding *potassium* amide.[156]

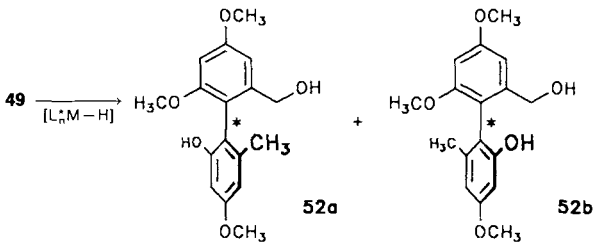

[L*nM−H]	a	:	b
6 (X = H)	10	:	90
53	88	:	12

Scheme 30.

These (overall) *enantioselective* biaryl syntheses starting from achiral bridged biaryl precursors naturally occur in an atrop-*diastereo*selective manner in the actual ring-opening step, since they first lead to diastereomeric products (as in the aforementioned reactions of chiral substrates). The advantage here is the easier subsequent separation (followed by re-use) of the unwanted lesser isomer, while the price to be paid lies in the necessity to remove the chiral auxiliary by cleavage of the previously formed C–O or C–N bond. These additional reactions can be avoided by the use of ring-opening reactions which are actually atrop-*enantio*selective (Scheme 30), e.g. with chiral hydride transfer reagents such as **6** or **53**, which give quite high asymmetric inductions.[157]

7. Summary and Future Prospects

This account clearly shows that, in spite of the great efforts made by different research groups in the last few years, the *single* generally applicable aryl coupling method which can be applied to each individual coupling problem and which satisfies all regio- and stereochemical demands has not yet been found. However, remarkable and powerful new methods have been reported very recently which a) have been shown to be applicable not only to model substances but to the first stereoselective syntheses of actual, functional natural products, in some cases with sterically strongly hindered biaryl axes, b) take account of chiral-economic aspects (e.g. recycling of unwanted isomers, specific syntheses of *both* atropisomers starting from the same precursor, catalytic reaction manner), and c) can even be used successfully when in the target molecule or its precursors the *ortho* substituents next to the biaryl axis are very similar or even *identical*, as for example in ancistrocladisine (**48**).

Further exciting progress can be expected in this field in the future.

We thank the Deutsche Forschungsgemeinschaft (Normalverfahren and Sonderforschungsbereich No. 1373 "Selective Reactions of Metal-Activated Molecules") and the Fonds der Chemischen Industrie for their generous support of our work. Particular thanks are due to the co-workers who have actively taken part in our own aryl coupling concept: Dipl.-Chem. H. Reuscher, Ch. Ewers, B. Schöner, T. Hartung, M. Rübenacker, H. Busse and above all Dr. J. R. Jansen. We also thank Frau L. Kinzinger for valuable technical assistance and Frau M. Lehrmann for producing the typescript.

Received: March 26, 1990 [A 777 IE]
German version: *Angew. Chem. 102* (1990) 1006
Translated by Professor *T. N. Mitchell*, Dortmund (FRG)

[1] a) K.G.B. Torssell: *Natural Product Chemistry*, Wiley, Chichester 1983; b) P. Manitto: *Biosynthesis of Natural Products*, Ellis Horwood, Chichester 1981; c) R.H. Thomson: *The Chemistry of Natural Products*, Blackie and Son, Glasgow 1985; d) G.A. Cordell: *Introduction to Alkaloids, A Biogenetic Approach*, Wiley, New York 1981.
[2] T. Govindachari, K. Nagarajan, P.C. Parthasarathy, T.G. Rajagopalan, H.K. Desai, G. Kartha, S.L. Chen, K. Nakanishi, *J. Chem. Soc. Perkin Trans. 1 1974*, 1413.
[3] G. Bringmann in A. Brossi (Ed.): *The Alkaloids, Vol. 29*, Academic, New York 1986, p. 141.
[4] See also L. Huang, Y.-K. Si, G. Snatzke, D.-K. Zheng, J. Zhou, *Collect. Czech. Chem. Commun. 53* (1988) 2664.
[5] I. Uchida, M. Ezaki, N. Shigematsu, M. Hashimoto, *J. Org. Chem. 50* (1985) 1341.
[6] R. Kannan, D.H. Williams, *J. Org. Chem. 52* (1987) 5435.
[7] S.M. Kupchan, R.W. Britton, M.F. Ziegler, C.J. Gilmore, R.J. Restivo, R.F. Bryan, *J. Am. Chem. Soc. 95* (1973) 1335.
[8] K. Tomioka, T. Ishiguro, K. Koga, *Tetrahedron Lett. 21* (1980) 2973.
[9] D.J. Cram, J.M. Cram, *Science (Washington D.C.) 183* (1974) 803.
[10] R. Noyori, I. Tomino, Y. Tanimoto, M. Nishizawa, *J. Am. Chem. Soc. 106* (1984) 6709.
[11] R. Noyori, *Chem. Soc. Rev. 18* (1989) 187.
[12] D.J. Cram, *Angew. Chem. 100* (1988) 1041; *Angew. Chem. Int. Ed. Engl. 27* (1988) 1009.
[13] E. Weber, *J. Mol. Graphics 7* (1989) 12.
[14] F. Mikes, G. Boshart, *J. Chromatogr. 149* (1978) 455.
[15] V. Brandmeier, M. Feigel, M. Bremer, *Angew. Chem. 101* (1989) 466; *Angew. Chem. Int. Ed. Engl. 28* (1989) 486.
[16] I. Tabushi, K. Yamamura, T. Nabeshima, *J. Am. Chem. Soc. 106* (1984) 5267.
[17] a) K. Yamamura, S. Ono, I. Tabushi, *Tetrahedron Lett. 29* (1988) 1797; b) K. Yamamuro, S. Ono, H. Ogoshi, H. Masuda, Y. Kuroda, *Synlett 1989*, 18.

[18] For a more recent survey: H.-J. Altenbach, *Nachr. Chem. Tech. Lab. 36* (1988) 1324.
[19] Related topic: R.A. Abramowitch, D.H.R. Barton, J.-P. Finet, *Tetrahedron 44* (1988) 3039; P. Kovacic, M.B. Jones, *Chem. Rev. 87* (1987) 357.
[20] M. Sainsbury, *Tetrahedron 36* (1980) 3327.
[21] See also R.E. Damon, R.H. Schlessinger, J.F. Blount, *J. Org. Chem. 41* (1976) 3772.
[22] F. Ullmann, J. Bielecki, *Chem. Ber. 34* (1901) 2174.
[23] P.E. Fanta, *Synthesis 1974*, 9.
[24] E. Brown, J.-P. Robin, R. Dhal, *Tetrahedron 38* (1982) 2569.
[25] S. Gauthier, J.M.J. Frechet, *Synthesis 1987*, 383.
[26] A. Rodriguez de Lera, R. Suau, L. Castedo, *J. Heterocycl. Chem. 24* (1987) 313.
[27] J. Lindlay, T.J. Mason, J.P. Lorimer, *Ultrasonics 25* (1987) 45; *C. A. 107* (1987) 96106r.
[28] T. Morita, K. Takase, *Bull. Chem. Soc. Jpn. 55* (1982) 1144.
[29] For exceptions see e.g. [24]; F. Dallacker, M.-T. Sommer, *Chem.-Ztg. 108* (1984) 329.
[30] M.A. Rizzacasa, M.V. Sargent, *Aust. J. Chem. 41* (1988) 1087.
[31] M.F. Semmelhack, P. Helquist, L.D. Lones, L. Keller, L. Mendelson, L. Speltz Ryono, J. Gorzynski Smith, R.D. Stauffer, *J. Am. Chem. Soc. 103* (1981) 6460.
[32] R.S. Berman, J.K. Kochi, *Inorg. Chem. 19* (1980) 248.
[33] H. Matsumoto, S. Inaba, R.D. Rieke, *J. Org. Chem. 48* (1983) 840.
[34] H. Lam, S.M. Marcuccio, P.I. Svirskaya, S. Greenberg, A.B.P. Lever, C.C. Leznoff, R.L. Cerny, *Can. J. Chem. 67* (1989) 1087.
[35] Y. Rollin, M. Troupel, D.G. Tuck, J. Perichon, *J. Organomet. Chem. 303* (1986) 131.
[36] C. Amatore, A. Jutand, *Organometallics 7* (1988) 2203.
[37] K. Takagi, N. Hayama, K. Sasaki, *Bull. Chem. Soc. Jpn. 57* (1984) 1887.
[38] I. Colon, D.R. Kelsey, *J. Org. Chem. 51* (1986) 2627.
[39] R. Vanderesse, J.-J. Brunet, P. Caubere, *J. Organomet. Chem. 264* (1984) 263.
[40] W.I. Taylor, A.R. Battersby: *Oxidative Coupling of Phenols*, Dekker, New York 1967.
[41] D.H.R. Barton, T. Cohen, *Festschrift Prof. A. Stoll zum siebzigsten Geburtstag*, Birkhäuser, Basel 1957.
[42] D.A. Young, E. Young, D.G. Roux, E.V. Brandt, D. Ferreira, *J. Chem. Soc. Perkin Trans. 1 1987*, 2345.
[43] D.R. Armstrong, R.J. Breckenridge, C. Cameron, D.C. Nonhebel, P.L. Pauson, P.G. Perkins, *Tetrahedron Lett. 24* (1983) 1071.
[44] V.I. Ognyanov, O.S. Petrov, E.P. Tiholov, N.M. Mollov, *Helv. Chim. Acta 72* (1989) 353; see also M.C. Venuti, *J. Org. Chem. 46* (1981) 3124.
[45] F. Toda, K. Tanaka, S. Iwata, *J. Org. Chem. 54* (1989) 3007.
[46] a) T.C. Jempty, L.L Miller, Y. Mazur, *J. Org. Chem. 45* (1980) 749; b) T.C. Jempty, K.A.Z. Gogins, Y. Mazur, L.L. Miller, *ibid. 46* (1981) 4545.
[47] H. Laatsch, *Liebigs Ann. Chem. 1985*, 2420.
[48] Previously however only intramolecular: a) M.A. Schwartz, P.T.K. Pham, *J. Org. Chem. 53* (1988) 2318; b) D.G. Vanderlaan, M.A. Schwartz, *ibid. 50* (1985) 743.
[49] F.R. Hewgill, J.M. Stewart, *J. Chem. Soc. Perkin Trans. 1 1988*, 1305.
[50] F. Diederich, M.R. Hester, M.A. Uyeki, *Angew. Chem. 100* (1988) 1775; *Angew. Chem. Int. Ed. Engl. 27* (1988) 1705.
[51] A. McKillop, A.G. Turrell, D.W. Young, E.C. Taylor, *J. Am. Chem. Soc. 102* (1980) 6504.
[52] For a very good account of the literature up to 1979 see: O.P. Dhingra in W.S. Trahanovsky (Ed.): *Oxidation in Organic Chemistry, Part D*, Academic, New York 1982, p. 207.
[53] S. Nishyama, S. Yamamura, *Yuki Gosei Kagaku Kyokaishi 46* (1988) 192.
[54] T. Kametani, K. Fukumoto, *Synthesis 1972*, 657.
[55] B. Franck, *Angew. Chem. 91* (1979) 453; *Angew. Chem. Int. Ed. Engl. 18* (1979) 429.
[56] B. Franck, L.F. Tietze, *Angew. Chem. 79* (1967) 815; *Angew. Chem. Int. Ed. Engl. 6* (1967) 799.
[57] M.A. Schwartz, M.F. Zoda, *J. Org. Chem. 46* (1981) 4623.
[58] B. Halton, A. Maidment, D.L. Officer, J.M. Warnes, *Aust. J. Chem. 37* (1984) 2119.
[59] A. Gunasekaran, K. Balasubramanian, *Ind. J. Chem. Sect. B27* (1988) 308.
[60] M. Murase, T. Takeya, S. Tobinaga, *Heterocycles 15* (1981) 709.
[61] G.E. Schneiders, R. Stevenson, *J. Org. Chem. 46* (1981) 2969.
[62] E.C. Taylor, J.G. Andrade, G.J.H. Rall, A. McKillop, *J. Am. Chem. Soc. 102* (1980) 6513.
[63] J. S. Sawyer, T.L. Macdonald, *Tetrahedron Lett. 29* (1988) 4839.
[64] P. Magnus, J. Schultz, T. Gallagher, *J. Am. Chem. Soc. 107* (1985) 4984.
[65] P. Magnus, J. Schultz, T. Gallagher, *J. Chem. Soc. Chem. Commun. 1984*, 1179.
[66] R.C. Cambie, M.G. Dunlop, P.S. Rutledge, P.D. Woodgate, *Synth. Commun. 10* (1980) 827.
[67] A.A. Adesomoju, W.A. Davis, R. Rajaraman, J.C. Pelletier, M.P. Cava, *J. Org. Chem. 49* (1984) 3220.
[68] R.C. Cambie, G.R. Clark, P.A. Craw, P.S. Rutledge, P.D. Woodgate, *Aust. J. Chem. 37* (1984) 1775.
[69] Y. Landais, A. Lebrun, V. Lenain, J.-P. Robin, *Tetrahedron Lett. 28* (1987) 5161.
[70] Y. Landais, D. Rambault, J.P. Robin, *Tetrahedron Lett. 28* (1987) 543.
[71] a) M. Murase, E. Kotani, K. Okazaki, S. Tobinaga, *Chem. Pharm. Bull. 34* (1986) 3159; b) T. Takeya, T. Okubo, S. Nishida, S. Tobinaga, *ibid. 33* (1985) 3599.
[72] a) A.J. Majeed, P.J. Patel, M. Sainsbury, *J. Chem. Soc. Perkin Trans. 1 1985*, 1195; b) P. Bird, M. Powell, M. Sainsbury, D.I.C. Scopes, *ibid. 1983*, 2053.
[73] J. Quick, R. Ramachandra, *Tetrahedron 36* (1980) 1301.
[74] S. Nishiyama, S. Yamamura, *Chem. Lett. 1981*, 1511.
[75] a) C.F. Carvalho, M.V. Sargent, *J. Chem. Soc. Perkin Trans. 1 1984*, 2573; b) *ibid 1984*, 1621.
[76] M. Kihara, S. Vangveravong, K. Ohnischi, Y. Imakura, S. Kobayashi, *Chem. Pharm. Bull. 37* (1989) 1744.
[77] C.F. Carvhalo, M.V. Sargent, E. Stanojevic, *Aust. J. Chem. 37* (1984) 2111.
[78] D.E. Ames, A. Opalko, *Tetrahedron 40* (1984) 1919.
[79] R.F. Heck: *Palladium Reagents in Organic Syntheses*, Academic, London 1985.
[80] N.S. Narasimhan, I.S. Aidhen, *Tetrahedron Lett. 29* (1988) 2987.
[81] G. Bringmann, J.R. Jansen, *Tetrahedron Lett. 25* (1984) 2537.
[82] O. Hoshino, H. Ogasawara, A. Takahashi, B. Umezawa, *Heterocycles 23* (1985) 1943; *ibid. 25* (1987) 155.
[83] P.J. Wittek, T.K. Liao, C.C. Cheng, *J. Org. Chem. 44* (1979) 870.
[84] D.L. Coffen, B. Schaer, F.T. Bizzarro, J.B. Cheung, *J. Org. Chem. 49* (1984) 296.
[85] a) M. Lourak, R. Vanderesse, Y. Fort, P. Caubere, *Tetrahedron Lett. 29* (1988) 545; b) *J. Org. Chem. 54* (1989) 4844.
[86] M. Hovorka, J. Günterová, J. Závada, *Tetrahedron Lett. 31* (1990) 413.
[87] F.E. Ziegler, I. Chliwner, K.W. Fowler, S.J. Kanfer, S.J. Kuo, N.D. Sinha, *J. Am. Chem. Soc. 102* (1980) 790.
[88] O. Hoshino, H. Hara, M. Ogawa, B. Umezawa, *Chem. Pharm. Bull. 23* (1975) 2578.
[89] M.S. Kharasch, E.K. Fields, *J. Am. Chem. Soc. 63* (1941) 2316.
[90] B.M. Trost, T.R. Verhoeven in G. Wilkinson (Ed.): *Comprehensive Organometallic Chemistry, Vol. 8*, Pergamon, Oxford 1982, p. 799.
[91] E. Negishi, *Acc. Chem. Res. 15* (1982) 340.
[92] M. Kumada, *Pure Appl. Chem. 52* (1980) 669.
[93] E.R. Larson, R.A. Raphael, *J. Chem. Soc. Perkin Trans. 1 1982*, 521.
[94] D.A. Widdowson, Y.-Z. Zhang, *Tetrahedron 42* (1986) 2111.
[95] See also a) J. Cornforth, A.F. Sierakowski, T.W. Wallace, *J. Chem. Soc. Perkin Trans. 1 1982*, 2299; b) S.D. Carter, T.W. Wallace, *J. Chem. Res. (S) 1985*, 136; c) G.W. Ebert, R.D. Rieke, *J. Org. Chem. 53* (1988) 4482.
[96] I.P. Beletskaya, *J. Organomet. Chem. 250* (1983) 551.
[97] N.A. Bumagin, I.O. Kalinowskii, I.P. Beletskaya, *J. Organomet. Chem. 267* (1984) C1.
[98] N. Miyaura, T. Yanagi, A. Suzuki, *Synth. Commun. 11* (1981) 513.
[99] Recently also intramolecularly: T.R. Kelly, Q. Li, V. Bhushan, *Tetrahedron Lett. 31* (1990) 161.
[100] See, e.g., J.K. Stille, *Angew. Chem. 98* (1986) 504; *Angew. Chem. Int. Ed. Engl. 25* (1986) 505.
[101] a) M.J. Sharp, W. Cheng, V. Snieckus, *Tetrahedron Lett. 28* (1987) 5093; b) W. Cheng, V. Snieckus, *ibid. 28* (1987) 5097.
[102] U. Schmidt, R. Meyer, V. Leitenberger, A. Lieberknecht, *Angew. Chem. 101* (1989) 946; *Angew. Chem. Int. Ed. Engl. 28* (1989) 929.
[103] W.J. Thompson, J. Gaudino, *J. Org. Chem. 49* (1984) 5237.
[104] D. Milstein, J.K. Stille, *J. Am. Chem. Soc. 101* (1979) 4992.
[105] G.T. Crisp, S. Papadopoulos, *Aust. J. Chem. 41* (1988) 1711.
[106] T.R. Bailey, *Tetrahedron Lett. 27* (1986) 4407.
[107] A.M. Echavarren, J.K. Stille, *J. Am. Chem. Soc. 109* (1987) 5478.
[108] Y. Hatanaka, S. Fukushima, T. Hiyama, *Chem. Lett. 1989*, 1711.
[109] a) A.I. Meyers, E.D. Mihelich, *J. Am. Chem. Soc. 97* (1975) 7383; b) A.I. Meyers, R. Gabel, E.D. Mihelich, *J. Org. Chem. 43* (1978) 1372.
[110] A.I. Meyers, K.A. Lutomski, *J. Am. Chem. Soc. 104* (1982) 879.
[111] A.I. Meyers, R.J. Himmelsbach, *J. Am. Chem. Soc. 107* (1985) 682.
[112] M.A. Rizzacasa, M.V. Sargent, B.W. Skelton, A.H. White, *Aust. J. Chem. 43* (1990) 79.
[113] M.A. Rizzacasa, M.V. Sargent, *J. Chem. Soc. Chem. Commun. 1989*, 301.
[114] A.B. Hughes, M.V. Sargent, *J. Chem. Soc. Perkin Trans. 1 1989*, 1787.
[115] M.A. Rizzacasa, M.V. Sargent, *J. Chem. Soc. Perkin Trans. 1 1988*, 2425.
[116] J. Novak, C.A. Salemink, *Tetrahedron Lett. 24* (1983) 101.
[117] A.D. Patten, N.H. Nguyen, S. Danishefsky, *J. Org. Chem. 53* (1988) 1003.
[118] J.A. Findlay, A. Daljeet, P.J. Murray, R.N. Rej, *Can. J. Chem. 65* (1987) 427.
[119] See, e.g., G. Bringmann, M. Rübenacker, J.R. Jansen, D. Scheutzow, L. Aké Assi, *Tetrahedron Lett. 31* (1990) 639.
[120] J.S. Buckleton, R.C. Cambie, G.R. Clark, P.A. Craw, C.E.F. Rickard, P.S. Rutledge, P.D. Woodgate, *Aust. J. Chem. 41* (1988) 305.
[121] N. Harada, K. Nakanishi: *Circular Dichroic Spectroscopy – Exciton Coupling in Organic Stereochemistry*, Oxford University Press, Oxford 1983.
[122] P.C. Parthasarathy, G. Kartha, *Ind. J. Chem. Sect. B22* (1983) 590.

[123] N. Ruangrungsi, V. Wongpanich, P. Tanativatana, H.J. Cowe, P.J. Cox, S. Funayama, G.A. Cordell, *J. Nat. Prod. 48* (1985) 529.
[124] G. Bringmann, J.R. Jansen, A. Hille, H. Reuscher: *The Stereocontrolled Total Synthesis of Naphthyl Isoquinoline Alkaloids: Symposia in print of the "6ème Colloque International, consacré aux Plantes Médicinales et Substances d'Origine Naturelle"*, Angers, France 1988, p. 181.
[125] In the case of very electron-poor aromatic compounds (such as oxazoline-substituted quinolines) the electrophilic coupling partner does not require a nucleofugal group; it can subsequently be oxidatively rearomatized with chirality transfer by removal of the hydrogen atom to be substituted: A.I. Meyers, D.G. Wettlaufer, *J. Am. Chem. Soc. 106* (1984) 1135.
[126] A.I. Meyers, J.R. Flisak, R.A. Aitken, *J. Am. Chem. Soc. 109* (1987) 5446.
[127] J.M. Wilson, D.J. Cram, *J. Org. Chem. 49* (1984) 4930.
[128] J.M. Wilson, D.J. Cram, *J. Am. Chem. Soc. 104* (1982) 881.
[129] J. Brussee, J.L.G. Groenendijk, J.M. te Koppele, A.C.A. Jansen, *Tetrahedron 41* (1985) 3313.
[130] K. Yamamoto, H. Fukushima, M. Nakazaki, *J. Chem. Soc. Chem. Commun. 1984*, 1490.
[131] K. Yamamoto, H. Yumioka, Y. Okamoto, H. Chikamatsu, *J. Chem. Soc. Chem. Commun. 1987*, 168.
[132] T. Hayashi, K. Hayashizaki, T. Kiyoi, Y. Ito, *J. Am. Chem. Soc. 110* (1988) 8153.
[133] S.L. Colletti, R.L. Halterman, *Tetrahedron Lett. 30* (1989) 3513.
[134] T. Hayashi, K. Hayashizaki, Y. Ito, *Tetrahedron Lett. 30* (1989) 215.
[135] R.C. Cambie, P.A. Craw, P.S. Rutledge, P.D. Woodgate, *Aust. J. Chem. 41* (1988) 897.
[136] J.K. Burden, R.C. Cambie, P.A. Craw, P.S. Rutledge, P.D. Woodgate, *Aust. J. Chem. 41* (1988) 919.
[137] Y. Landais, J.-P. Robin, *Tetrahedron Lett. 27* (1986) 1785.
[138] J.-P. Robin, Y. Landais, *J. Org. Chem. 53* (1988) 224.
[139] K. Tomioka, T. Ishiguro, Y. Itaka, K. Koga, *Tetrahedron 40* (1984) 1303.
[140] In another example, an unnatural but biologically more active aza-analogous dibenzocyclooctadiene, the thermodynamic equilibrium even lies at only 1:40; K. Tomioka, Y. Kubota, H. Kawasaki, K. Koga, *Tetrahedron Lett. 30* (1989) 2949.
[141] K. Tomioka, H. Mizuguchi, T. Ishiguru, K. Koga, *Chem. Pharm. Bull. 33* (1985) 121.
[142] a) S. Miyano, M. Tobita, M. Nawa, S. Sato, H. Hashimoto, *J. Chem. Soc. Chem. Commun. 1980*, 1233; b) S. Miyano, K. Shimizu, S. Sato, H. Hashimoto, *Bull. Chem. Soc. Jpn. 58* (1985) 1345; c) S. Miyano, S. Handa, M. Tobita, H. Hashimoto, *ibid. 59* (1986) 235.
[143] S. Miyano, H. Fukushima, S. Handa, H. Ito, H. Hashimoto, *Bull. Chem. Soc. Jpn. 61* (1988) 3249.
[144] S. Miyano, S. Handa, K. Shimizu, K. Tagami, H. Hashimoto, *Bull. Chem. Soc. Jpn. 57* (1984) 1943.
[145] S. Miyano, M. Tobita, H. Hashimoto, *Bull. Chem. Soc. Jpn. 54* (1981) 3522.
[146] G. Bringmann, H. Reuscher, *Tetrahedron Lett. 30* (1989) 5249.
[147] G. Bringmann, J.R. Jansen, H.-P. Rink, *Angew. Chem. 98* (1986) 917; *Angew. Chem. Int. Ed. Engl. 25* (1986) 913.
[148] G. Bringmann, J.R. Jansen, *Heterocycles 28* (1989) 137.
[149] G. Bringmann, J.R. Jansen, H. Reuscher, M. Rübenacker, K. Peters, H.G. von Schnering, *Tetrahedron Lett. 31* (1990) 643.
[150] a) G. Bringmann, F. Pokorny, H. Reuscher, D. Lisch, L. Aké Assi, *Planta med. 56* (1990), in press; b) G. Bringmann, D. Lisch, H. Renscher, L. Aké Assi, K. Günther, *Phytochemistry*, in press.
[151] A further advantage of this process is that apart from **42** and **43** hydroxymethyl compounds of type **41** and lactones of type **40** are found as natural products in the same plants and can thus be included synthetically without additional effort: G. Bringmann, M. Rübenacker, J. R. Jansen, T. Gender, L. Aké Assi, *Planta med. 56* (1990), in press.
[152] In contrast, precomplexation of the alkali metal cation of *basic* hydride transfer reagents at nitrogen and attack of the anionic hydride part of the reagent from the same side (i.e. from above) should lead to the other lactolate diastereomer (not shown in Scheme 27), which bears the hydrogen in β-position; this isomer should react in an analogous manner to give **45b**.
[153] G. Bringmann, H. Reuscher, *Angew. Chem. 101* (1989) 1725; *Angew. Chem. Int. Ed. Engl. 28* (1989) 1672.
[154] See for example the non-stereoselective synthesis of a (probably not separable) mixture of all four possible stereoisomeric ancistrocladisines [113].
[155] G. Bringmann, M. Berndsen, R. Walter, unpublished.
[156] G. Bringmann, C. Ewers, unpublished.
[157] G. Bringmann, T. Hartung, unpublished.

Computer Simulation of Molecular Dynamics: Methodology, Applications, and Perspectives in Chemistry

By Wilfred F. van Gunsteren* and Herman J. C. Berendsen*

During recent decades it has become feasible to simulate the dynamics of molecular systems on a computer. The method of molecular dynamics (MD) solves *Newton*'s equations of motion for a molecular system, which results in trajectories for all atoms in the system. From these atomic trajectories a variety of properties can be calculated. The aim of computer simulations of molecular systems is to compute *macroscopic* behavior from *microscopic* interactions. The main contributions a microscopic consideration can offer are (1) the understanding and (2) interpretation of experimental results, (3) semiquantitative estimates of experimental results, and (4) the capability to interpolate or extrapolate experimental data into regions that are only difficultly accessible in the laboratory. One of the two basic problems in the field of molecular modeling and simulation is how to efficiently search the vast configuration space which is spanned by all possible molecular conformations for the global low (free) energy regions which will be populated by a molecular system in thermal equilibrium. The other basic problem is the derivation of a sufficiently accurate interaction energy function or force field for the molecular system of interest. An important part of the art of computer simulation is to choose the unavoidable assumptions, approximations and simplifications of the molecular model and computational procedure such that their contributions to the overall inaccuracy are of comparable size, without affecting significantly the property of interest. Methodology and some practical applications of computer simulation in the field of (bio)chemistry will be reviewed.

1. Introduction

Computational chemistry is a branch of chemistry that enjoys a growing interest from experimental chemists. In this discipline chemical problems are resolved by computational methods. A model of the real world is constructed, both measurable and unmeasurable properties are computed, and the former are compared with experimentally determined properties. This comparison validates or invalidates the model that is used. In the former case the model may be used to study relationships between model parameters and assumptions or to predict unknown or unmeasurable quantities.

Since chemistry concerns the study of properties of substances or molecular systems in terms of atoms, the basic challenge facing computational chemistry is to describe or even predict

1. the structure and stability of a molecular system,
2. the (free) energy of different states of a molecular system,
3. reaction processes within molecular systems

in terms of interactions at the atomic level. These three basic challenges are listed according to increasing difficulty. The first challenge concerns prediction of which state of a system has the lowest energy. The second challenge goes further; it involves prediction of the relative (free) energy of different states. The third challenge involves prediction of the dynamic process of change of states.

Chemical systems are generally too inhomogeneous and complex to be treated by analytical theoretical methods. This is illustrated in Figure 1. The treatment of molecular systems in the gas phase by quantum mechanical methods is straightforward; if a classical statistical mechanical approximation is permitted the problem becomes even trivial. This is due to the possibility of reducing the many-particle problem to a few-particle one based on the low density of a system in the gas phase. In the crystalline solid state, treatment by quantum mechanical or classical mechanical methods is made possible by a reduction of the many-particle problem to a few-(quasi)particle problem based on symmetry properties of the solid state. Between these two extremes, that is, for liquids, macromolecules, solutions, amorphous solids, etc., one is faced with an *essentially* many-particle system. No simple reduction to a few degrees of freedom is possible, and a full treatment of many degrees of freedom is required in order to adequately describe the properties of molecular systems in the fluid-like state. This state of affairs has two direct consequences when treating fluid-like systems.

1. One has to resort to numerical *simulation* of the behavior of the molecular system on a computer, which
2. produces a *statistical ensemble* of configurations representing the state of the system.

If one is only interested in static equilibrium properties, it suffices to generate an ensemble of equilibrium states, which

[*] Prof. Dr. W. F. van Gunsteren[+]
Department of Physical Chemistry
University of Groningen
Nijenborgh 16, NL-9747 AG Groningen (The Netherlands)
Department of Physics and Astronomy
Free University
De Boelelaan 1081, NL-1081 HV Amsterdam (The Netherlands)
Prof. Dr. H. J. C. Berendsen
Department of Physical Chemistry
University of Groningen
Nijenborgh 16, NL-9747 AG Groningen (The Netherlands)
[+] Present address:
Eidgenössische Technische Hochschule
ETH Zentrum
Universitätstrasse 6, CH-8092 (Switzerland)

may lack any temporal correlations. To obtain dynamic and non-equilibrium properties dynamic simulation methods that produce trajectories in phase space are to be used. The connection between the microscopic behavior and macroscopic properties of the molecular system is governed by the laws of *statistical mechanics*.

Figure 1 also shows the broad applicability of computer simulation methods in chemistry. For any fluid-like, essentially many-particle system, it is the method of choice.

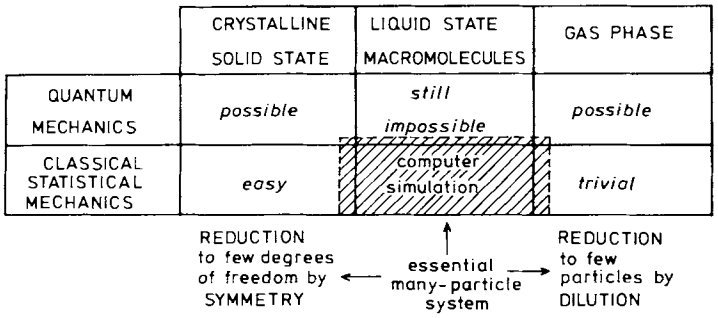

Fig. 1. Classification of molecular systems. Systems in the shaded area are amenable to treatment by computer simulation.

The expanding role of computational methods in chemistry has been fueled by the steady and rapid increase in computing power over the last 40 years, as is illustrated in Figure 2. The ratio of performance to price has increased an order of magnitude every 5–7 years, and there is no sign of any weakening in this trend. The introduction of massive parallelism in computer architecture will easily maintain the present growth rate. This means that more complex molecular systems may be simulated over longer periods of time, or that it will be possible to handle more complex interaction functions in the decades to come.

The present article is concerned with computer simulation of molecular systems. In Section 2 the two basic problems are formulated, a brief history of dynamic computer simulation is presented, the reliability of current simulations is discussed, and the usefulness of simulation studies is considered. Section 3 deals with simulation methodology: choice of computational model and atomic interaction function (Section 3.1), techniques to search configuration space for low energy configurations (Section 3.2), boundary conditions (Section 3.3), types of dynamical simulation methods (Section 3.4), algorithms for integration of the equations of motion (Section 3.5), and finally equilibration and analysis of molecular systems (Section 3.6). In Section 4, a number of applications of computer simulation in chemistry are discussed and examples are given. Finally, future developments are considered in Section 5. For other relatively recent monographs on computer simulation the reader is referred to the literature (see Refs. [1–9]).

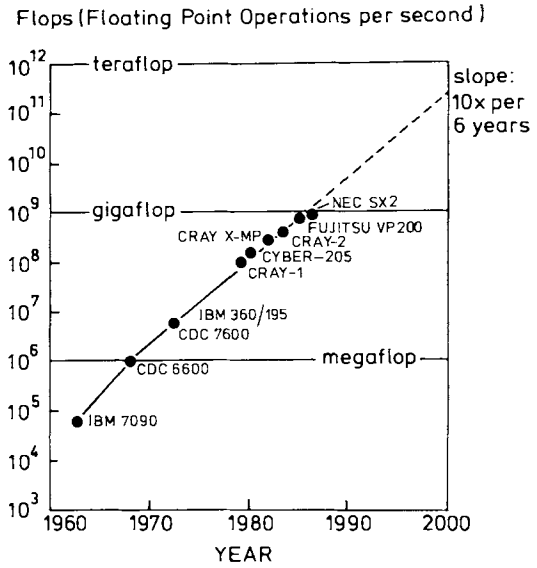

Fig. 2. Development of computing power of the most powerful computers.

2. Computer Simulation of Molecular Systems

2.1. Two Basic Problems

Two basic problems are encountered in the computer simulation of fluid-like molecular systems:

1. *the size of the configurational space* that is accessible to the molecular system, and
2. the *accuracy* of the molecular model or atomic interaction function or force field that is used to model the molecular system.

Wilfred F. van Gunsteren was born in 1947 in Wassenaar (The Netherlands). In 1968 he gained a B.Sc. in physics at the Free University of Amsterdam; in 1976 he was awarded a "Meester" in Law, and in 1976 a Ph.D. in nuclear physics. After postdoc years at the University of Groningen (1976–1978) and at Harvard University (1978–1980) he was, from 1980 until 1987, senior lecturer and, until August 1990, Professor for Physical Chemistry at the University of Groningen. Since September 1987 he has also been Professor of Computer Physics at the Free University Amsterdam. In 1990 he was offered and accepted a professorship of Computer Chemistry at the ETH Zürich. He is holder of a gold medal for research of the Royal Netherlands Chemical Society; in 1988 he was Degussa Guest Professor at the University of Frankfurt. His main interests center on the physical fundamentals of the structure and function of biomolecules.

Table 1. Models at different levels of approximation.

Model	Degrees of freedom left	Degrees of freedom removed	Example of predictable property	Example of force field	
- quantum mechanical	nuclei, electrons	nucleons	reactions	Coulomb	increasing: simplicity, speed of computation, search power, time scale
- all atoms, polarizable	atoms dipoles	electrons	binding charged ligand	ionic models [10]	
- all atoms	solute + solvent atoms	dipoles	hydration	OPLS [11] GROMOS [12]	
- all solute atoms	solute atoms	solvent	gas phase conformation	MM2 [13]	decreasing: complexity, accuracy of atomic properties
- groups of atoms as balls	atom groups	individual atoms	folding topology of macromolecule	LW [14]	

2.1.1. *Size of the Configurational Space*

The simulation of molecular systems at non-zero temperatures requires the generation of a statistically representative set of configurations, a so-called *ensemble*. The properties of a system are defined as ensemble averages or integrals over the configuration space (or more generally phase space). For a many-particle system the averaging or integration will involve many degrees of freedom, and as a result can only be carried out over part of the configuration space. The smaller the configuration space, the better the ensemble average or integral can be approximated. When choosing a model from which a specific property is to be computed, one would like to explicitly include only those degrees of freedom on which the required property is dependent.

In Table 1 a hierarchy of models is shown, in which specific types of degrees of freedom are successively removed. Examples are given of properties that can be computed at the different levels of approximation. If one is interested in chemical reactions, a quantum mechanical treatment of electronic degrees of freedom with the nuclear coordinates as parameters is mandatory. The intranuclear degrees of freedom (nucleon motion) are left out of the model. The computing power required for a quantum mechanical treatment scales at least with the third power of the number of electrons N_e that are considered. Such a treatment is only possible for a limited number of degrees of freedom. At a next level of approximation the electronic degrees of freedom are removed from the model and approximated by (point) polarizabilities. Such a model, allowing for motions of polarizable atoms, could, e.g., be used to compute the binding properties of polar or charged ligands which will polarize the receptor. At this level of modeling the computing effort scales with the square of the number of atoms N_a. This means that many more atoms can be considered than at the quantum level. Removal of the polarizability of the atoms yields a next level of approximation, in which only atomic positional degrees of freedom are considered and the mean polarization is included in the effective interatomic interaction function. Such a model allows for the study of solvation properties of molecules. When studying solutions, a next level of approximation is reached by omitting the solvent degrees of freedom from the model and simultaneously adapting the interaction function for the solute such that it includes the mean solvent effect. When studying protein folding, the configuration space spanned by all protein atoms is still far too large to be searched for low energy conformations. In this case a further reduction in it can be obtained by representing whole groups of atoms, for example an amino acid residue, as one or two balls (3 or 6 degrees of freedom).

From this discussion it is clear that the level of approximation of the model that will be used in the simulation will depend on the specific property one is interested in. The various force fields that are available correspond to different levels of approximation, as is illustrated in the right half of Table 1. There is a hierarchy of force fields.

Once the level of approximation has been chosen, that is, the types of degrees of freedom in the model, one must decide how many degrees of freedom (electrons, atoms, etc.) are to be taken into account. How small a system can be chosen without seriously affecting a proper representation of the property of interest? The smaller the size of the system the better its degrees of freedom can be sampled, or in dynamic terms, the longer the time scale over which it can be simulated.

We may summarize the first basic problem in the computer simulation of molecular systems as follows: the level of approximation of the model should be chosen such that those degrees of freedom that are essential to a proper evaluation of the quantity or property of interest can be sufficiently sampled. In practice any choice involves a compromise between type and number of degrees of freedom and extent of the simulation on the one hand, and the available computing power on the other.

2.1.2. *Accuracy of Molecular Model and Force Field*

When the degrees of freedom are infinitely dense or long sampled the accuracy by which various quantities are predicted by a simulation will depend solely on the quality of the assumptions and approximations of the molecular model and interatomic force field. At the level (Table 1) of quantum mechanical modeling the basic assumption is the validity of the Born-Oppenheimer approximation separating electronic and nuclear motion. The interaction between point atoms and electrons is described by Coulomb's law and the Pauli exclusion principle. When excluding chemical reactions, low temperatures or details of hydrogen atom motion, it is relatively safe to assume that the system is governed by the laws of classical mechanics. The atomic interaction function is called an *effective interaction* since the average effect of the

omitted (electronic) degrees of freedom has been incorporated in the interaction between the (atomic) degrees of freedom explicitly present in the model. To each level of approximation in Table 1 there corresponds a type of effective interaction or force field. For example, a pair potential with an enhanced dipole moment (enhanced atomic charges) may be used as an effective potential that mimics the average effect of polarizability.

In view of the different levels of approximation of molecular models it is not surprising that the literature contains a great variety of force fields. They can be classified along different lines:

- type of compound that is to be mimicked, e.g. carbohydrates, sugars, polypeptides, polynucleotides;
- type of environment of the compound of interest; e.g. gas phase, aqueous or nonpolar solution;
- range of temperatures covered by the effective interaction;
- type of interaction terms in the force field; e.g. bond stretching, bond angle bending, torsional terms, two-, three- or many-body nonbonded terms;
- functional form of the interaction terms; e.g. exponential or 12th power repulsive nonbonded interaction;
- type of parameter fitting, that is, to which quantities are parameters fitted, and are experimentally or ab-initio theoretically obtained values used as target values.

We note that the choice of a particular force field should depend on the system properties one is interested in. Some applications require more refined force fields than others. Moreover, there should be a balance between the level of accuracy or refinement of different parts of a molecular model. Otherwise the computing effort put into a very detailed and accurate part of the calculation may easily be wasted due to the distorting effect of the cruder parts of the model.

2.1.3. *Assumptions, Approximations and Limitations*

When using a particular model to predict the properties of a molecular system, one should be aware of the assumptions, simplifications, approximations and limitations that are implicit in the model. Below, we list the four most important approximations and limitations of classical computer simulation techniques which should be kept in mind when using them.

2.1.3.1. *Classical Mechanics of Point Masses*

A molecular system is described as a system of point masses moving in an effective potential field, which is generally a conservative field, i.e. it only depends on the instantaneous coordinates of the point masses. The motion of the point masses is with a sufficient degree of accuracy governed by the laws of classical mechanics. These assumptions imply the following restrictions to modeling:

- low-temperature (0–10 K) molecular motion is not adequately described;
- detailed motion of light atoms such as hydrogen atoms is not correctly described even at room temperature;
- description of chemical reactions lies outside the scope of classical simulation methods.

For a short discussion of the inclusion of quantum corrections to a classical treatment or of the quantum (dynamical) simulation techniques that are presently under development, we refer to Section 5.1.

2.1.3.2. *System Size or Number of Degrees of Freedom to be Included*

Only a rather limited number of atoms can be simulated on a computer. Simulations of liquids typically involve 10^2–10^3 atoms, simulations of solutions or crystals of macromolecules about 10^3–2×10^4 atoms. Generally, the system size is kept as small as possible in order to allow for a sufficient sampling of the degrees of freedom that are simulated. This means that those degrees of freedom that are not essential to the property one is interested in should be removed from the system. The dependence of the property of interest on the size of the system may give a clue to the minimum number of degrees of freedom required for an adequate simulation of it. The larger the spatial correlation length of the property of interest, the more atoms are to be included in the simulation.

2.1.3.3. *Sufficiency of Sampling of Configuration Space or Time Scale of Processes*

Computer simulation generates an ensemble of configurations of the system. Whether the generated set of configurations is representative for the state of the system depends on the extent to which the important (generally low energy) parts of the configuration space (or, more generally formulated, phase space) have been sampled. This depends in turn on the sampling algorithm that is applied. This should be able to overcome the multitude of barriers of the multidimensional energy surface of the system. In dynamic simulations, the time scale of the process that is mimicked is limited. Presently, molecular simulations cover time periods of 100–1000 picoseconds. In the case of activated processes longer time scales can be reached by using special tricks.[15, 16] Essentially slow processes, like the folding of a protein, are still well out of reach of computer simulation. We note that the observation that a property is independent of the length of a simulation is a necessary but *not* a sufficient condition for adequate sampling. The system may just reside for a period longer than the simulation time in a certain area without being effected by a nearby region of much lower energy from which it is separated by a large energy barrier.

2.1.3.4. *Accuracy of the Molecular Model and Force Field*

As is illustrated in Table 1, there exists a variety of molecular models and force fields, differing in the accuracy by which different physical quantities are modeled. The choice of a particular force field will depend on the property and level of accuracy one is interested in.

When studying a molecular system by computer simulation three factors should be considered (cf. Fig. 3).

1. The properties of the molecular system one is interested in should be listed and the configuration space (or time scale) to be searched for relevant configurations should be estimated.

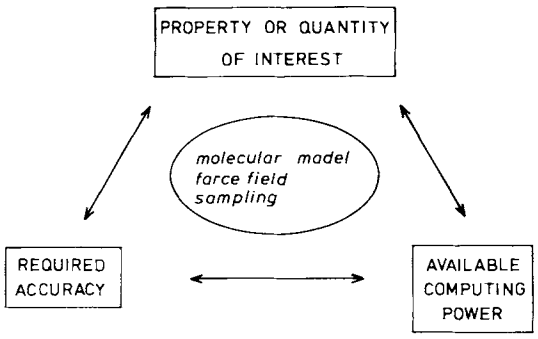

Fig. 3. Choice of molecular model, force field and sample size depends on 1) the property one is interested in (space to be searched), 2) required accuracy of the prediction, 3) the available computing power to generate the ensemble.

2. The required accuracy of the properties should be specified.
3. The available computer time should be estimated.

Given these three specifications the molecular model and force field should be chosen. As is indicated in Table 1 there is a trade off between accuracy of the force field on the one hand and the searching power or time scale that can be attained on the other. We note that in many practical cases one should abandon the idea of trying to simulate the system of interest, since the available computing power will not allow for a sufficiently accurate simulation.

2.2. History of Dynamic Computer Simulation

The growth in the number of applications of computer simulation methods in chemistry and physics is directly caused by the rapid increase in computing power over the last four decades (Fig. 2). Table 2 shows the development of the application of molecular dynamics simulation in chemistry. *Alder* and *Wainwright* pioneered the method using 2-dimensional hard disks. *Rahman*, who can really be considered the father of the field, simulated liquid argon in 1964, liquid water in 1971, and superionic conductors in 1978.[27] He also made many contributions to the methodology, and stimulated the dissemination of the technique in the scientific community. In the seventies, the transition from atomic to molecular liquids was made: rigid molecules like water (1971), flexible alkanes (1975), and a small protein, trypsin inhibitor (1977). The application to molten salts (1971) required the development of methods to handle long-range Coulomb interactions. The eighties brought simulations of biomolecules of increasing size in aqueous solution. For a more thorough review of the past and present of dynamic computer simulation in chemistry and physics we refer to the monographs of *McCammon* and *Harvey*[5] and *Allen* and *Tildesley*.[6]

Table 2. History of computer simulation of molecular dynamics.

Year	System	Length of simulation [s]	Required cpu time on supercomputer [h]
1957	hard two-dimensional disks [17]		
1964	monatomic liquid [18]	10^{-11}	0.05
1971	molecular liquid [19]	5×10^{-12}	1
1971	molten salt [20]	10^{-11}	1
1975	simple small polymer [21]	10^{-11}	1
1977	protein in vacuo [22]	2×10^{-11}	4
1982	simple membrane [23]	2×10^{-10}	4
1983	protein in aqueous crystal [24]	2×10^{-11}	30
1986	DNA in aqueous solution [25]	10^{-10}	60
1989	protein-DNA complex in solution [26]	10^{-10}	300
	large polymers	10^{-8}	10^{3}
	reactions	10^{-4}	10^{7}
	macromolecular interactions	10^{-3}	10^{8}
	protein folding	10^{-1}	10^{9}

From Table 2 it is also clear that a supercomputer is still many orders of magnitude slower than nature: a state of the art simulation is about 10^{15} times slower than nature. Many interesting systems and processes still fall far outside the reach of computer simulation. Yet, with a growth rate of a factor 10 per 5–7 years for (super)computing power the speed of simulation will have caught up with that of nature in about 100 years.

2.3. Accuracy and Reliability of Computer Simulation

The reliability of predictions made on the basis of computer simulation will basically depend on two factors: 1) whether the molecular model and force field are sufficiently accurate, and 2) whether the configuration space accessible to the molecular system has been sufficiently thoroughly searched for low-energy configurations. Although the accuracy of a prediction may be estimated by considering the approximations and simplifications of the model and computational procedure, the final test lies in a comparison of theoretically predicted and experimentally measured properties. In order to provide a firm basis for the application of computer simulation methods the results should be compared with experimental data whenever possible.

In this context we would like to stress that good agreement between calculated and experimental data does *not* necessarily mean that the theoretical model underlying the calculation is correct. Good agreement may be due to any of the following reasons:

1. The model is correct, that is, any other assumption used to derive the model, or any other choice of parameter values would give bad agreement with experiment.
2. The property that is compared is insensitive to the assumptions or parameter values of the model, that is, whatever parameter values are used in the model calculation, the agreement with experiment will be good.
3. Compensation of errors occurs, either by chance or by fitting of the model parameters to the desired properties.

A number of examples of the last case, viz. good agreement for the wrong reason, are given in Ref. [28]. Here, we would only like to remind the reader that it is relatively easy, when modeling high-dimensional systems with many parameters, to choose or fit parameters such that good agreement is obtained for a limited number of observable quantities. On the other hand, disagreement between simulation and experiment may also have different causes: 1) the simulation is *not* correct, the experiment *is*, 2) the simulation *is* correct, the experiment is *not*.

With these cautionary remarks in mind we would like to turn to an evaluation of the accuracy of current simulation studies by comparing simulated with experimental quantities. Table 3 contains a scheme of the atomic quantities of molecular systems for which comparison between simulated and experimental values is feasible. Four phases are distinguished. The most interesting phase from a chemical point of view is that of a molecule in solution. For this phase only few accurately measured *atomic* properties are available for comparison, leaving thermodynamic system properties like the free energy of solvation as a test ground for the simulation. Considerably more atomic data are available from crystallographic diffraction experiments: atomic positions and mobility, although the accuracy of the latter is much lower than that of the former, due to the simplifying approximations (harmonic isotropic motion) used in the crystallographic refinement process.

Table 3. Possible comparison of simulated properties with experimental ones for complex molecules.

Atomic properties	Experimental method	Phase: gas	solution	membrane	crystal
Structure					
- positions	X-ray diffraction				×
	neutron diffraction				×
- distance	NMR		×		
- orientations	NMR			×	
Mobility					
- *B*-factors	X-ray diffraction				×
	neutron diffraction				×
- occupancy factors	X-ray diffraction				×
	neutron diffraction				×
Dynamic properties					
- vibrational frequencies	infrared spectroscopy	×			
- relaxation rates	various NMR optical techniques		×		
- diffusion	NO spin label		×	×	
Thermodynamic properties					
- density			×		×
- free energy			×		
- viscosity, conductance			×		

In the following subsections examples will be given of a comparison of various atomic and system properties for different compounds. The examples are taken from our own work, and so are all based on the GROMOS force field.[12] They only serve as an indication of the degree of accuracy that can be obtained for different properties using current modeling methods.

2.3.1. *Atomic Properties: Positions and Mobilities in Crystals*

From a simulation the average molecular structure can be easily calculated and compared with experiment. Table 4 contains the deviation between simulated and measured atomic positions for a number of molecular crystals. The structural deviation depends on the size of the molecule and ranges from 0.2 Å to 1.2 Å. The numbers are an average over part or over all atoms in the molecules. This means that parts of the molecule will deviate more and other parts will deviate less from the experimental structure. This is illustrated in Figure 4, which shows the deviation for the backbone C_α atoms as a function of residue number averaged over all four BPTI (bovine pancreatic trypsin inhibitor) molecules in the crystal unit cell. Most of the atoms deviate less than 1 Å. Figure 5 shows the root mean square (rms) atomic positional fluctuations calculated from the MD simulation and from the crystallographic *B*-factors. The largest discrepancy is still rather small, about 0.3 Å.

Table 4. Comparison of MD time-averaged structures with experimental X-ray or neutron diffraction structures.

Molecule	Size (number of glucose units or amino acid residues)	Root mean square (RMS) difference in atomic positions [Å]: C_α or C'_3 atoms	all atoms excl. H atoms
cyclodextrin (α/β) [29]	6	0.13/0.35	0.25/0.51
cyclosporin A [30]	11	0.3	0.6
trypsin inhibitor [31]	58	1.0	1.5
subtilisin [32]	275	1.0	1.2

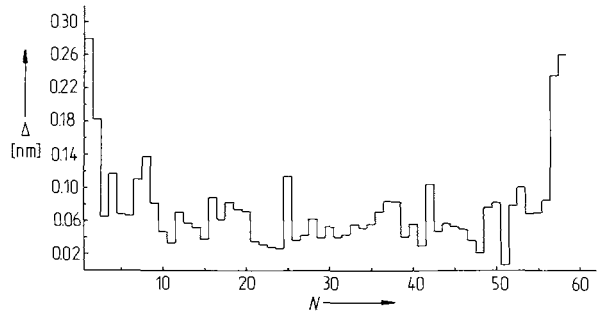

Fig. 4. Root mean square difference between the trypsin inhibitor simulated time- and molecule-averaged C_α atomic positions and the X-ray positions according to [31]. Δ = root mean square deviation, N = aminoacid residue number.

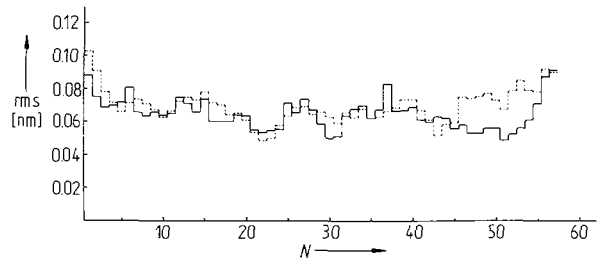

Fig. 5. Root mean square positional fluctations for the trypsin inhibitor atoms averaged over the backbone atoms of each residue according to [31]. Solid line: simulated results. Broken line: fluctuations derived from a set of X-ray temperature factors. rms = root mean square fluctuation, N = amino acid residue number.

A more stringent test of the simulation is to check whether partially occupied atomic sites are reproduced. The neutron diffraction work on β-cyclodextrin shows that 16 hydrogen atoms occupy two alternative sites. In the crystal simulation a non-zero occupancy is observed for 84% of the hydrogen sites, and for 62% of the hydrogen atoms the relative occu-

pancy of the two alternative sites is qualitatively reproduced.[29]

The molecular structure can also be described in terms of hydrogen bonds. Generally the experimentally observed hydrogen bonds are also observed in the simulation. Again cyclodextrin crystals form a sensitive test case for the simulations, since peculiar geometries such as three-center hydrogen bonds, and dynamic processes such as flip-flop hydrogen bonds have been experimentally observed. Almost all experimentally observed three-center hydrogen bonds in crystals of α- and β-cyclodextrin are reproduced in MD simulation, even as far as the detailed asymmetric geometry is concerned.[33] In a so-called flip-flop hydrogen bond the directionality is inverted dynamically. In a MD simulation of β-cyclodextrin, 16 of the 18 experimentally detected flip-flop bonds are reproduced.[34]

2.3.2. Atomic Properties: Distances in Solution

Structural data of solutions can be obtained by two-dimensional nuclear magnetic resonance spectroscopy (2D-NMR) with exploitation of the nuclear Overhauser (NOE) experiments.[35] The data come in the form of a set of upper bounds or constraints to specific proton-proton distances. This affords the possibility of comparing these proton-proton distances as predicted in a simulation with the experimentally measured NOE bounds. In the literature,[25] such a comparison is given for a set of 174 NOE's in an eight base-pair DNA fragment in aqueous solution: 80% of the NOE distances are satisfied by the simulation within experimental error, the mean deviation is 0.22 Å, and the maximum deviation amounts to 2.9 Å.

2.3.3. Atomic Properties: Orientation of Molecular Fragments in Membranes

The degree of order in a membrane or lipid bilayer can be measured selectively along the aliphatic chain by deuterium NMR spectroscopy.[36] In Figure 6[37] both experimental and MD order parameters are displayed for all CH_2 units in a sodium ion/water/decanoate/decanol bilayer system as a function of the position of the carbon atom in the aliphatic chain. The experimentally observed plateau in the order parameters is well reproduced.

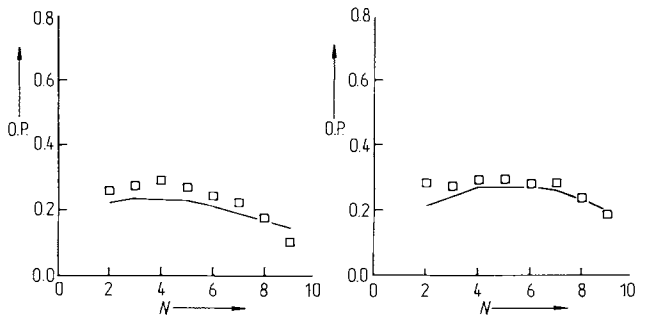

Fig. 6. Carbon-deuterium order parameters as a function of carbon atom number along the aliphatic chain of decanol (upper panel) and decanoate (lower panel) [37]. The head group has number zero. Solid line: simulated result. Squares: experimental values. O.P. = order parameter, N = carbon atom number.

2.3.4. Atomic Properties: Diffusion in Solutions and in Membranes

The dynamic properties of simulations of molecular systems are hard to test by comparison with experiment. An exception is the diffusion constant. Its calculation and comparison with experiment is a standard test for models of liquid water. The diffusion constant of the simple three-point charge (SPC) water model is 4.3×10^{-5} cm^2 s^{-1} compared with an experimental value of 2.7×10^{-5} cm^2 s^{-1} at 305 K.[38] Inclusion of a correction term for self-polarization in the SPC model led to a reparametrization, to the SPC/E (extended simple point charge) model, which yields a considerably smaller diffusion constant of 2.5×10^{-5} cm^2 s^{-1}.[39]

In the bilayered sodium ion/water/decanoate/decanol system mentioned in the previous section the simulated diffusion constants are: 2.7×10^{-6} cm^2 s^{-1} (decanoate) and 5.2×10^{-6} cm^2 s^{-1} (decanol), which values are to be compared with the value of 1.5×10^{-6} cm^2 s^{-1} measured with nitroxide spin labels.

2.3.5. System Properties: Thermodynamic Quantities

Instead of atomic properties, thermodynamic system properties like the density or free energy of solvation can be calculated from a simulation and compared to experimental values.

For a crystal of a cytidine derivative X-ray diffraction data and MD simulation data were compared at two different temperatures.[40] Upon raising the temperature from 113 K to 289 K the volume of the unit cell increased by 2.5% in the simulation at constant pressure, which value is to be compared with an experimentally determined increase of 3.7%. At 289 K the simulated density was only 1.3% too large. A slightly larger discrepancy was found in a MD simulation of crystalline cyclosporin A: the simulated density of 1.080 g cm^{-3} was 3.6% larger than the experimental value of 1.042 g cm^{-3}.[30] Comparable deviations have been found for other systems: the SPC/E model yields 0.998 g cm^{-3} at 306 K, compared with an experimental value of 0.995 g cm^{-3} at 305 K.[39]

Finally, we quote an example of a free energy of hydration. For the solvation of methanol in water the standard GROMOS parameters yield a free enthalpy of 7 kJ mol^{-1} compared with an experimental value of 5 kJ mol^{-1}.[28] However, when charged moieties are involved the accuracy by which free energy of solvation can be calculated is no better than about 10–20 kJ mol^{-1}.[28,41]

2.4. Is Computer Simulation Useful?

The prediction of properties by computer simulation of complex molecular systems is certainly not accurate enough to justify abandoning the measurement of properties. If a measurement is not too difficult it is always to be preferred over a prediction by simulation. The utility of computer simulation studies does not lie in the (still remote) possibility of *replacing* experimental measurement, but rather in its ability to *complement* experiments. Quantities that are inaccessible to experiment can be monitored in computer simulations.

We consider the computer simulation of complex molecular systems to be useful for the following reasons.

1. It provides an *understanding* of the *relation* between *microscopic* properties and *macroscopic* behavior. In a computer a microscopic molecular model and force field can be changed at will and the consequences for the macroscopic behavior of the molecular system can be evaluated.
2. During the last few years computer simulation has become a standard tool in the *determination* of *spatial molecular structure* on the basis of X-ray diffraction or 2D-NMR data.
3. Under favorable conditions computer simulation can be used to obtain *quantitative estimates* of quantities like binding constants of ligands to receptors. This is especially useful where the creation of the ligand or the measurement of its binding constant is costly or time-consuming.
4. Finally we mention the possibility of carrying out simulation under extreme (unobservable) conditions of temperature and pressure.

3. Methodology

Here we briefly describe the methodology of classical computer simulation as it is applied to complex molecular systems.

3.1. Choice of Molecular Model and Force Field

3.1.1. Current Force Fields for Molecular Systems

A typical molecular force field or effective potential for a system of N atoms with masses m_i ($i = 1,2,\ldots,N$) and cartesian position vectors $\boldsymbol{r}_i$ has the form (1).

$$\begin{aligned} V(\boldsymbol{r}_1, \boldsymbol{r}_2, \ldots, \boldsymbol{r}_N) = & \sum_{\text{bonds}} \tfrac{1}{2} K_b [b - b_0]^2 + \sum_{\text{angles}} \tfrac{1}{2} K_\theta [\theta - \theta_0]^2 \\ & + \sum_{\substack{\text{improper} \\ \text{dihedrals}}} \tfrac{1}{2} K_\xi [\xi - \xi_0]^2 \\ & + \sum_{\text{dihedrals}} K_\varphi [1 + \cos(n\varphi - \delta)] \\ & + \sum_{\text{pairs}(i,j)} [C_{12}(i,j)/r_{ij}^{12} - C_6(i,j)/r_{ij}^6 \\ & + q_i q_j / (4\pi\varepsilon_0 \varepsilon_r r_{ij})] \end{aligned} \tag{1}$$

The first term represents the covalent bond stretching interaction along bond b. It is a harmonic potential in which the minimum energy bond length b_0 and the force constant K_b vary with the particular type of bond. The second term describes the bond angle bending (three-body) interaction in similar form. Two forms are used for the (four-body) dihedral angle interactions: a harmonic term for dihedral angles ξ that are not allowed to make transitions, e.g. dihedral angles within aromatic rings, and a sinusoidal term for the other dihedral angles φ, which may make 360 degree turns. The last term is a sum over all pairs of atoms and represents the effective nonbonded interaction, composed of the van der Waals and the Coulomb interaction between atoms i and j with charges q_i and q_j at a distance r_{ij}.

There exists a large number of variants of expression (1).[11-13,42-53] Some force fields contain mixed terms like $K_{b\theta}[b-b_0][\theta-\theta_0]$, which directly couple bond-length and bond-angle vibrations.[42] Others use more complex dihedral interactions terms.[43,44] The choice of the relative dielectric constant ε_r is also a matter of dispute. Values ranging from $\varepsilon_r = 1$[11,12] to $\varepsilon_r = 8$[45] have been used, while others take ε_r proportional to the distance r_{ij}.[22,46,47] Sometimes the Coulomb term is completely ignored.[44] Although hydrogen bonding can be appropriately modeled using expression (1),[11,12,48,49] in some force fields special hydrogen bonding potential terms are used to ensure proper hydrogen bonding.[43-47] Another way to refine expression (1) is to allow for non-atomic interaction centers or virtual sites, that is, interactions between points (e.g. lone pairs) not located on atoms.[50] For solvents, especially water, a variety of molecular models is available,[19,38,51] of which a few have been developed explicitly for use in mixed solute-water systems.[11,49] Models for nonpolar solvents like carbon tetrachloride are also available.[52]

When determining the parameters of the interaction function (1) there are essentially two routes to take. The most elegant procedure is to fit them to results (potential or field) of ab-initio quantum calculations on small molecular clusters. However, due to various serious approximations that have to be made in this type of procedure, the resulting force fields are in general not very satisfactory. The alternative is to fit the force field parameters to experimental data (crystal structure, energy and lattice dynamics, infrared, X-ray data on small molecules, liquid properties like density and enthalpy of vaporization, free energies of solvation, nuclear magnetic resonance data, etc.). In our opinion the best results have been obtained by this semi-empirical approach.[11,53]

We wish to stress that one should fit force field parameters to properties of small molecules, which may be considered as building blocks of larger molecules such as proteins and DNA, and subsequently apply them to these larger molecules as a test without any further adaptations to improve the test results.

The choice of a particular force field should depend on the type of system for which it has been designed. The MM2 force field[13] is based on gas phase structures of small organic compounds. The AMBER[47] and CHARMM[46] force fields are aimed at a description of isolated polypeptides and polynucleotides, in which the absence of a solvent (aqueous) environment is compensated by the use of a distance-dependent dielectric constant ε_r. The ECEPP[43,54] and UNICEPP[55] force fields use $\varepsilon_r = 4$, whereas the GROMOS[12,49] force field uses $\varepsilon_r = 1$, since it has been set up for simulation of biomolecules in aqueous environment. This also holds for the OPLS[11] force field which is aimed at a proper description of solvation properties. Force fields that are applicable to a more restricted range of compounds like ions,[56] liquid metals,[57] salts,[6] or carbohydrates,[58] are manifold. The quality of the various force fields should be judged from the literature concerning their application to molecular systems.

3.1.2. Inclusion of Polarizability

The term in the interaction function (1) representing the nonbonded interactions consists only of a summation over

all pair interactions in the system. Nonbonded many-body interactions are neglected. Yet, inclusion of polarizability of atoms or bonds will be inevitable if one would like to simulate, e.g., the binding of a charged ligand, which will polarize the part of the receptor to which it is binding (Table 1). About 10% (4 kJ mol^{-1}) of the energy of liquid water is polarization energy. The infinite frequency dielectric constant of water is $\varepsilon_\infty = 5.3$, its effective dipole moment changes from 1.85 D in the gas phase to 2.4 D in the liquid. An analysis of the contribution of polarizability to local fields in proteins is given in Ref. [59].

Inclusion of polarizability in the molecular model is not too difficult, as can be observed from the following simple outline.[60] We consider a system of N point dipoles with cartesian position vectors $\boldsymbol{r}_i$, dipole moments $\boldsymbol{p}_i$ and polarizabilities α_i (constant, isotropic). The induced dipoles $\Delta\boldsymbol{p}_i$ obey a field equation (2), where $\boldsymbol{E}_i$ denotes the electric field

$$\Delta\boldsymbol{p}_i = \alpha_i \boldsymbol{E}_i = \alpha_i \sum_{\substack{j=1 \\ \neq i}}^{N} \boldsymbol{T}_{ij}[\boldsymbol{p}_j + \Delta\boldsymbol{p}_j] \tag{2}$$

at position $\boldsymbol{r}_i$ and the field tensor $\boldsymbol{T}_{ij}$ is given by Equation (3). The field equation can be solved for $\Delta\boldsymbol{p}_i$ either by the inver-

$$\boldsymbol{T}_{ij} = (4\pi\varepsilon_0)^{-1}[3\,\boldsymbol{r}_i\boldsymbol{r}_j/r_{ij}^2 - 1]\,r_{ij}^{-3} \tag{3}$$

sion of a matrix of size $3N \times 3N$, or by iteration. The former method is impractical for a molecular system containing thousands of atoms. The latter method is well suited for use in MD simulations, since the induced dipoles at the previous MD integration time step, $\Delta\boldsymbol{p}_i(t - \Delta t)$, will be an excellent starting point for the iterative solution of the field equation (2) at time t, which yields $\Delta\boldsymbol{p}_i(t)$. In this way inclusion of polarizability may increase simulation times by only 20–100%.

Computer simulations that include polarizability have only been performed for a limited number of molecular systems, such as ionic liquids,[10, 61] water,[62] and a single protein.[63, 64] Many aspects of the treatment of polarizability in MD simulations are still under investigation. What is the most practical way to model polarizability?

(1) By inducing point dipoles, as sketched above,
(2) by changing the magnitudes of (atomic) charges,
(3) by changing the positions of (atomic) charges.

How should the size of the atomic polarizabilities α_i be chosen, etc?

3.1.3. Treatment of Long Range Coulomb Forces

The summation of the last term in the interaction function (1) covering the nonbonded interaction runs over all atom pairs in the molecular system. It is proportional to N^2, the square of the number of atoms in the system. Since the other parts of the calculation are proportional to N, computational efficiency can be much improved by a reduction of this summation.The simplest procedure is to apply a cut-off criterion for the nonbonded interaction and to use a list of neighbor atoms lying within the cut-off, which is only updated every so many simulation steps. The cut-off radius R_C usually has a value between 6 Å and 9 Å and the neighbor list is updated about every 10 or 20 MD time steps. This procedure does not introduce any errors as long as the range of the nonbonded interaction is smaller than R_C. However, the Coulomb term in (1) is proportional to r^{-1}, which makes it long-ranged. If the molecular model does not involve bare (partial) charges on atoms, but only dipoles or higher multipoles, the electrostatic interaction term becomes proportional to r^{-3}, which makes it of much shorter range. However, when dipoles are correlated over larger distances, as is the case for secondary structure elements like α-helices in proteins, their interactions again become long-ranged.[65]

In the following subsections we briefly discuss a variety of methods for the treatment of long-range electrostatic interactions in molecular systems.[66, 67]

3.1.3.1. Distance Dependent Dielectric Constant

A simple way to reduce the range of the Coulomb interaction is to introduce a relative dielectric constant proportional to r, viz. $\varepsilon_r = r$ (in Å). The interaction becomes proportional to r^{-2}. It is difficult to find a physical argument in favor of this approximation. Its overall effect is to effectively reduce all types of long-ranged interactions. Due to its simplicity it has been incorporated into a number of current force fields.[46, 47] Nevertheless, we think this approximation is too crude for practical applications.

3.1.3.2. Cut-off Radius and Neutral Groups of Atoms

When applying a cut-off radius R_C, the discontinuity of the interaction at a distance $r = R_C$ will act as a noise source in a MD simulation, and this will artificially increase the kinetic energy of the atoms and thus the temperature of the system. A possible way to reduce the noise is to multiply the nonbonded interaction term in (1) with a so-called switching function (4), which satisfies the conditions $S(R_S) = 1$,

$$S(r) = \begin{cases} 1 & r < R_S \\ (R_C - r)^2(R_C + 2r - 3R_S)/(R_C - R_S)^3 & R_S < r < R_C \\ 0 & r > R_C \end{cases} \tag{4}$$

$\mathrm{d}S/\mathrm{d}r(R_S) = 0$, $S(R_C) = 0$, $\mathrm{d}S/\mathrm{d}r(R_C) = 0$. Its effect is to smoothen the interaction on the interval (R_S, R_C), but there is no physical argument for its use. An empirical evaluation of the use of switching functions can be found in Ref. [68].

When the (partial) atomic charges of a group of atoms add up to exactly zero, the leading term of the electric interaction between two such groups of atoms is of dipolar character, that is, proportional to r^{-3}. For larger r the sum of the r^{-1} monopole contributions of the various atom pairs to the group–group interaction will become zero. Therefore, the range of the electric interaction can be considerably reduced when atoms are assembled in neutral groups, so-called *charge groups*, which have a zero net charge, and for which the electric interaction with other (groups of) atoms is either calculated for all atoms of the charge group or for none.[12, 69] When using the charge group concept the cut-off criterion should be applied to the distance between groups, and a switching function like (4) must *not* be used, since it distorts in the interval (R_S, R_C) the proper r^{-1} weighting of atom–atom monopole interactions.

3.1.3.3. *Cut-off Radius plus Multipole Expansion*

The technique of using neutral groups of atoms is based on the more general fact that a charge distribution of a finite group of atoms can be approximated by a multipole expansion (monopole, dipole, quadrupole, etc.). The electric interaction between two groups of atoms can be formulated as the product of the two multipole expansions. The terms in the resulting expression can be grouped according to their distance dependence: monopole–monopole (r^{-1}), monopole–dipole (r^{-2}), monopole–quadrupole and dipole–dipole (r^{-3}), etc. At long distance only the leading terms in the series need to be taken into account. Application of this multipole expansion approximation in MD simulations was suggested by *Ladd*.[70] It is also used in combination with the "cut-off plus atom pair list" technique in Ref. [46].

3.1.3.4. *Twin Range Method*

The twin range method[66] is illustrated in Figure 7. Two cut-off radii are used. The atoms j lying within a distance R_C^1 from atom i are stored in a neighbor list of atom i. The interaction of the atoms j for which $R_C^1 < r_{ij} < R_C^2$ with atom i, is stored in the form of a so-called long-range force F_i^{lr} on atom i. At each MD time step the nonbonded interaction consists of two contributions: (1) the short-range part which is calculated from the neighbor list using the actual atom positions, and (2) the long range part $\boldsymbol{F}^{lr}$ which is kept fixed during N_C^1 time steps. Neighbor list and long range force $\boldsymbol{F}^{lr}$ are simultaneously updated every N_C^1 (10–100) time steps.

This twin range method is based on the assumption that the high-frequency components of the long range force may be safely neglected. For example, the mean and low frequency field of the correlated peptide dipoles of the long α-helix are accurately accounted for, only the fast ($\lesssim$0.2 ps) vibrations are neglected (see Fig. 7). The twin range method can also be applied using charged groups instead of atoms.[112]

3.1.3.5. *Continuum Approximations to the Reaction Field*

In the previous subsections approximations to the long-range interaction between atoms were discussed that are explicitly taken into account as degrees of freedom in the system that is simulated. If parts of the system are homogeneous, like the bulk solvent surrounding a solute, the number of atoms or degrees of freedom can be reduced considerably by modeling of the homogeneous part as a continuous medium, e.g. a continuous dielectric. In this type of approximation the system is divided into two parts: (1) an inner region where the atomic charges q_i are explicitly treated (dielectric constant ε_1), and (2) an outer region which is treated as a continuous medium with dielectric constant ε_2 and ionic strength I (see Fig. 8). The potential in the inner region

$$\psi_1(\boldsymbol{r}) = \psi_C(\boldsymbol{r}) + \psi_R(\boldsymbol{r}) \tag{5}$$

[Eq. (5)] consists of two terms. The first one [Eq. (6)] is a direct Coulomb term due to the charges in the inner region,

$$\psi_C(\boldsymbol{r}) = (4\pi\varepsilon_0\varepsilon_1)^{-1} \sum_{i=1}^{N} q_i/|\boldsymbol{r} - \boldsymbol{r}_i| \tag{6}$$

which is a solution to the Poisson equation (7) for the inner

$$\vec{\nabla}^2\psi(\boldsymbol{r}) = -\varepsilon_1^{-1} \sum_{i=1}^{N} q_i\delta(\boldsymbol{r} - \boldsymbol{r}_i) \tag{7}$$

region. The second term is the reaction field potential $\psi_R(\boldsymbol{r})$, which satisfies the Poisson equation with zero source terms (no charges), that is, the Laplace equation (8). This means

$$\vec{\nabla}^2\psi(\boldsymbol{r}) = 0. \tag{8}$$

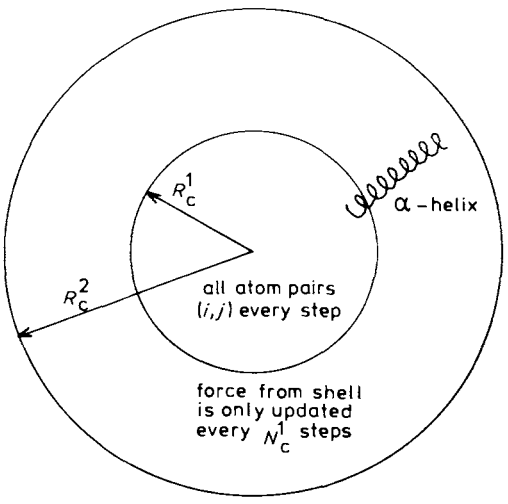

Fig. 7. Twin range method. High-frequency components of the force on the central atom exerted by atoms between R_C^1 and R_C^2 are neglected.

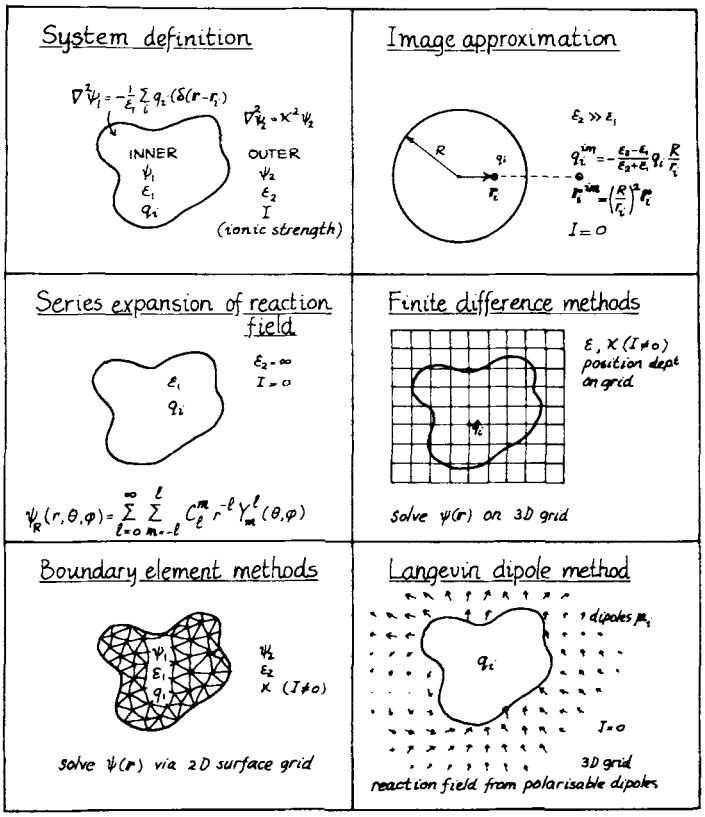

Fig. 8. Non-periodic methods for computing long-range Coulomb forces.

that $\psi_1(\boldsymbol{r})$ is also a solution of (7). The potential in the outer region is denoted by $\psi_2(\boldsymbol{r})$. If the outer region continuum has a finite ionic strength I, the potential $\psi_2(\boldsymbol{r})$ must be a solution of the Poisson-Boltzmann equation (9) with inverse Debye

$$\vec{\nabla}^2\psi(\boldsymbol{r}) = \kappa^2\psi(\boldsymbol{r}) \tag{9}$$

length $\kappa = 2IF^2/(\varepsilon_2 RT)$ in which F is Faraday's constant, R is the gas constant, and T the temperature. For zero ionic strength, (9) reduces to (8). The boundary condition at infinity is given by (10), and at the boundary between the inner

$$\lim_{r\to\infty}\psi_2(\boldsymbol{r}) = 0 \tag{10}$$

and outer regions the potential $\psi(\boldsymbol{r})$ [Eq. (11)] and the dielectric displacement $\varepsilon\vec{\nabla}\psi(\boldsymbol{r})$ [Eq. (12)] must be continuous:

$$\psi_1(\boldsymbol{r}) = \psi_2(\boldsymbol{r}) \qquad \boldsymbol{r} = \text{boundary} \tag{11}$$

$$\varepsilon_1\nabla_n\psi_1(\boldsymbol{r}) = \varepsilon_2\nabla_n\psi_2(\boldsymbol{r}) \qquad \boldsymbol{r} = \text{boundary} \tag{12}$$

where the component of the gradient normal to the boundary is denoted by ∇_n.

The exact form of $\psi(\boldsymbol{r})$ will depend on the shape of the boundary, the values of ε_2 and κ, and the computational method that is used to solve the field equations (7)–(12).

3.1.3.6. Continuum Methods: Image Charge Approximation to the Reaction Field

When the boundary is a sphere of radius R the reaction field due to a charge q_i located at position $\boldsymbol{r}_i$ with respect to the origin of the sphere can be approximated (dipolar approximation, $\varepsilon_2 \gg \varepsilon_1$) by the field that is generated by a so-called image charge $q_i^{\text{im}} = -(\varepsilon_2 - \varepsilon_1)(\varepsilon_2 + \varepsilon_1)q_i R/r_i$ that is located at position $\boldsymbol{r}_i^{\text{im}} = (R/r_i)^2\boldsymbol{r}_i$[71] (see Fig. 8). The name of this approximation is due to the mirror type of behavior of the spherical boundary: if q_i approaches the boundary, q_i^{im} will do likewise, causing a pole in the potential at the boundary. This means that the image approximation breaks down for charges close to the boundary. The other limitations of the method are the requirement of a spherical boundary, and the conditions that $I = 0$ and $\varepsilon_2 \gg \varepsilon_1$.

3.1.3.7. Continuum Methods: Series Expansion of the Reaction Field

When the boundary is of irregular shape the reaction field potential cannot be written in a closed form, but must be approximated numerically. If we assume that $I = 0$ and $\varepsilon_2 = \infty$, the following approach is possible. Since the reaction field potential $\psi_R(\boldsymbol{r})$ must satisfy the Laplace equation (8) it may be expanded in Legendre polynomials, which also satisfy Equation (8) [Eq. (13)]. If $\varepsilon_2 = \infty$, we have $\psi_2(\boldsymbol{r}) = 0$

$$\psi_R(\boldsymbol{r}, \theta, \varphi) = \sum_{l=0}^{\infty}\sum_{m=-l}^{+l} C_l^m r^{-l} Y_m^l(\theta, \varphi). \tag{13}$$

at the boundary, or using (11) and (5) Equation (14), at the boundary, with $\psi_C(\boldsymbol{r})$ fixed by (6). The expansion coefficients

$$\psi_R(\boldsymbol{r}) = -\psi_C(\boldsymbol{r}) \tag{14}$$

C_l^m can be determined numerically by performing a least squares fit of $\psi_R(\boldsymbol{r})$ to the given $-\psi_C(\boldsymbol{r})$ at a chosen number of points on the boundary.

The method works (Berendsen and Zwinderman, private communication), but is rather expensive due to the matrix inversion inherent in the least squares fit procedure. Close to the boundary the approximation is poor. The other limitations are that $I = 0$ and $\varepsilon_2 = \infty$.

3.1.3.8. Continuum Methods: Three-dimensional Finite Difference Techniques

Another numerical approach is to compute the electric potential on a three-dimensional (3D) grid using finite difference methods (Fig. 8). The atomic charges q_i are distributed over grid points. To each grid point a position-dependent dielectric constant ε_1 is assigned. Then the field equations (7)–(12) can be numerically solved.[72] This involves the solution of a set of linear equations for the potential at grid points. The method is too time-consuming to be used in MD simulations, since the density of grid points must be sufficient to adequately represent the atomic charge distribution. The use of a position-dependent dielectric constant introduces an arbitrary element into the method.

3.1.3.9. Continuum Methods: Two-dimensional Boundary Element Techniques

A recent development is the application of Green's function techniques to the electric field problem.[73] The Green's

$$G_1(\boldsymbol{r}|\boldsymbol{r}_0) = \frac{1}{4\pi|\boldsymbol{r} - \boldsymbol{r}_0|} \tag{15}$$

function (15) for the inner region satisfies Equation (16) (a Poisson equation with charge ε_0 at $\boldsymbol{r}_0$). The Green's func-

$$\vec{\nabla}^2 G_1(\boldsymbol{r}|\boldsymbol{r}_0) = -\delta(\boldsymbol{r} - \boldsymbol{r}_0) \tag{16}$$

tion for the outer region [Eq. (17)] satisfies Equation (18) (a Poisson-Boltzmann equation with charge ε_0 at $\boldsymbol{r}_0$).

$$G_2(\boldsymbol{r}|\boldsymbol{r}_0) = \frac{e^{-\kappa|\boldsymbol{r} - \boldsymbol{r}_0|}}{4\pi|\boldsymbol{r} - \boldsymbol{r}_0|} \tag{17}$$

$$\vec{\nabla}^2 G(\boldsymbol{r}|\boldsymbol{r}_0) = \varkappa^2 G(\boldsymbol{r}|\boldsymbol{r}_0) - \delta(\boldsymbol{r} - \boldsymbol{r}_0) \tag{18}$$

The next step is to integrate the following integrand over the

$$[G_1 \times \text{expression (7) for } \psi_1 - \psi_1 \times \text{expression (16) for } G_1] \tag{19}$$

inner region and to convert it by Green's theorem into an integral over the surface of the boundary region. This yields Equation (20), consisting of a surface term and a source term.

$$\psi_1(\boldsymbol{r}) = \int_{\text{surface}} [G_1(\boldsymbol{r}'|\boldsymbol{r})\nabla_n\psi_1(\boldsymbol{r}') - \psi_1(\boldsymbol{r}')\nabla_n G_1(\boldsymbol{r}'|\boldsymbol{r})\,d\sigma + \sum_{i=1}^{N}\frac{q_i}{4\pi\varepsilon_0|\boldsymbol{r} - \boldsymbol{r}_i|} \tag{20}$$

By integrating (21) and conversion we obtain equation (22).

$$[G_2 \times \text{expression (9) for } \psi_2 - \psi_2 \times \text{expression (18) for } G_2] \quad (21)$$

$$\psi_2(\boldsymbol{r}) = \int_{\text{surface}} [G_2(\boldsymbol{r}'|\boldsymbol{r}) \nabla_n \psi_2(\boldsymbol{r}') - \psi_2(\boldsymbol{r}') \nabla_n G_2(\boldsymbol{r}'|\boldsymbol{r})] \mathrm{d}\sigma \quad (22)$$

Application of the boundary conditions (11) and (12) yields two linear integral equations in ψ_1 and $\nabla_n \psi_1$ on the boundary surface. These equations can be solved numerically by discretization on a surface net, and subsequently solved by matrix inversion. The (large) matrix that is to be inverted only depends on the shape and position of the boundary surface, *not* on the positions of the charges in the inner region. This means that in a MD simulation the time-consuming matrix inversion can be avoided as long as the boundary remains fixed.

The promise of this method lies in the reduction of a 3D problem to a 2D problem. On the boundary surface a charge density is generated which produces the proper reaction field. Also the methods of *Shaw*,[74] and of *Zauhar* and *Morgan*[75] transform the problem from a three-dimensional one into a two-dimensional one.

3.1.3.10. Langevin Dipole Model

The Langevin dipole model of *Warshel*[63, 67] uses a 3D-grid, but it is not a continuum method. The medium in the outer region is mimicked by polarizable point dipoles $\boldsymbol{\mu}_i$ on the grid points i of a 3D grid. The dipoles may be thought of as representing the molecular dipoles of the solvent molecules forming the outer region, so the spacing of the grid points corresponds to the size of the solvent molecules. The size and direction of a dipole $\boldsymbol{\mu}_i$ is determined by the electric field $\boldsymbol{E}_i$ at the grid point according to the Langevin formula [Eq. (23)]. Here, μ_0 is the magnitude of the dipole moment

$$\mu_i = \mu_0 \left[\frac{\mathrm{e}^{+C\mu_0 E_i/kT} + \mathrm{e}^{-C\mu_0 E_i/kT}}{\mathrm{e}^{+C\mu_0 E_i/kT} - \mathrm{e}^{-C\mu_0 E_i/kT}} - \frac{1}{C\mu_0 E_i/kT} \right] \frac{\boldsymbol{E}_i}{E_i} \quad (23)$$

of a solvent molecule, and C is a parameter representing the molecular resistance to reorientation. The model has been applied to protein simulations.[64] Questionable features of this model are the representation of the field in the outer region and the discreteness near the boundary.

3.1.3.11. Periodic Lattice Summation Methods

In computer simulations of liquids or solutions, periodic boundary conditions are often used to minimize the boundary effects. The computational box containing the molecular system is surrounded by an infinite number of copies of itself (see Fig. 9). In this way an infinite periodic system is simulated.

The electric interaction in a periodic system is obtained by a summation over all atom pairs in the central box (Fig. 9) and over all atom pairs of which one atom lies in the central box and the other is a periodic image [Eq. (24)].

$$E = (4\pi\varepsilon_0)^{-1} \frac{1}{2} \sum_{\boldsymbol{n}=0}^{\infty} \sum_{\substack{i=1 \\ i \neq j \text{ if } \boldsymbol{n}=0}}^{N} \sum_{j=1}^{N} \frac{q_i q_j}{|\boldsymbol{r}_{ij} + \boldsymbol{n}|} \quad (24)$$

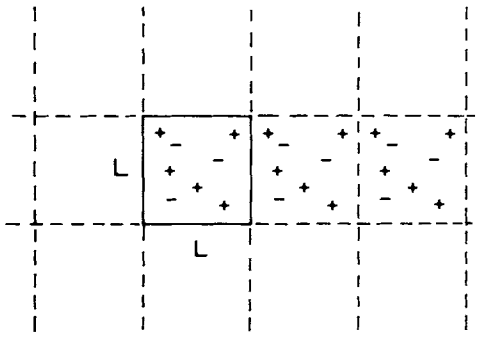

Fig. 9. Periodic cubic system. Central computational box (solid line) with two of the infinite number of periodic image boxes.

The sum over $\boldsymbol{n}$ is a summation over all simple cubic lattice points $\boldsymbol{n} = (n_x L, n_y L, n_z L)$ with n_x, n_y, n_z integers. The infinite sum of point charges must be converted into a form which converges faster than Equation (24).

3.1.3.12. Periodic Methods: the Ewald Sum

The Ewald sum is a technique for computing the interaction of a charge and all its periodic images.[6, 76-78] The charge distribution $\varrho(\boldsymbol{r})$ in the system is an infinite set of point charges, mathematically represented as delta functions [Eq. (25)].

$$\varrho_i(\boldsymbol{r}) = q_i \delta(\boldsymbol{r} - \boldsymbol{r}_i) \quad (25)$$

Each point charge q_i is now surrounded by an isotropic Gaussian charge distribution of equal magnitude and opposite sign [Eq. (26)].

$$\varrho_i^{\mathrm{G}}(\boldsymbol{r}) = -q_i (\alpha/\sqrt{\pi})^3 \mathrm{e}^{-\alpha^2 |\boldsymbol{r} - \boldsymbol{r}_i|^2} \quad (26)$$

This smeared charge screens the interaction between the point charges, so that the interaction calculated using the screened charge distribution (27) becomes short-ranged [Eq. (28)] due to the appearance of the complementary error function (29).

$$\varrho_i^{\mathrm{s}}(\boldsymbol{r}) \equiv \varrho_i(\boldsymbol{r}) + \varrho_i^{\mathrm{G}}(\boldsymbol{r}) \quad (27)$$

$$E^{\mathrm{s}} = (4\pi\varepsilon_0)^{-1} \frac{1}{2} \sum_{\boldsymbol{n}=0}^{\infty} \sum_{\substack{i=1 \\ i \neq j \text{ if } \boldsymbol{n}=0}}^{N} \sum_{j=1}^{N} \frac{q_i q_j}{|\boldsymbol{r}_{ij} + \boldsymbol{n}|} \operatorname{erfc}(\alpha |\boldsymbol{r}_{ij} + \boldsymbol{n}|) \quad (28)$$

$$\operatorname{erfc}(x) = 2\pi^{-1/2} \int_x^{\infty} \mathrm{e}^{-y^2} \mathrm{d}y \quad (29)$$

Thus, E^{s} can be well approximated using a finite summation in (28). Of course a purely Gaussian charge distribution $-\varrho_i^{\mathrm{G}}(\boldsymbol{r})$ must be added to $\varrho_i^{\mathrm{s}}(\boldsymbol{r})$ in order to recover the original charge distribution $\varrho_i(\boldsymbol{r})$. The interaction of these Gaussian distributions is expressed as a lattice sum in reciprocal space minus a self term [Eq. (30)], where

$$E^{\mathrm{G}} = (4\pi\varepsilon_0)^{-1} 2\pi L^{-3} \sum_{k \neq 0}^{\infty} k^{-2} \mathrm{e}^{-k^2/(4\alpha^2)} \left| \sum_{j=1}^{N} q_j \mathrm{e}^{-i\boldsymbol{k} \cdot \boldsymbol{r}_j} \right|^2 - (4\pi\varepsilon_0)^{-1} \pi^{-1/2} \alpha \sum_{j=1}^{N} q_j^2 \quad (30)$$

$\boldsymbol{k} = 2\pi L^{-1}(l_x, l_y, l_z)$ and l_x, l_y, l_z are integers. Due to the presence of the exponential factor the infinite lattice sum can be well approximated by a finite one. The parameter α should be chosen such as to optimize the convergence properties of both sums (28) and (30) which contribute to $E = E^S + E^G$.

The Ewald sum technique is routinely used in simulations of ionic systems. When applied to non-crystalline systems such as liquids or solutions it has the disadvantage of enhancing the artifact of the application of periodic boundary conditions.

3.1.3.13. Periodic Methods: Fourier Techniques

The Poisson equation (31) for the potential $\psi(\boldsymbol{r})$ is a sec-

$$\vec{\nabla}^2 \psi(\boldsymbol{r}) = -\varepsilon_0^{-1} \varrho(\boldsymbol{r}) \tag{31}$$

ond-order partial differential equation in $\boldsymbol{r}$-space. However, when transformed into reciprocal space ($\boldsymbol{k}$-space) it becomes a simple algebraic equation (32) with the solution (33).

$$-k^2 \hat{\psi}(\boldsymbol{k}) = -\varepsilon_0^{-1} \hat{\varrho}(\boldsymbol{k}) \tag{32}$$

$$\hat{\psi}(\boldsymbol{k}) = (\varepsilon_0 k^2)^{-1} \hat{\varrho}(\boldsymbol{k}) \tag{33}$$

Here, the 3D Fourier transformation is defined according to Equation (34), and likewise for the charge density $\varrho(\boldsymbol{r})$. The inverse transform of Equation (33) yields (35).

$$\hat{\psi}(\boldsymbol{k}) \equiv F\{\psi(\boldsymbol{r})\} \equiv (2\pi)^{-3/2} \int \psi(\boldsymbol{r}) e^{-i\boldsymbol{k}\cdot\boldsymbol{r}} d\boldsymbol{r} \tag{34}$$

$$\psi(\boldsymbol{r}) = F^{-1}\{(\varepsilon_0 k^2)^{-1} F\{\varrho(\boldsymbol{r})\}\} \tag{35}$$

Due to the availability of fast Fourier transform techniques Equation (35) is a fast method to solve the Poisson equation on a periodic three-dimensional grid. For a practical implementation of the method we refer to Ref. [1]. It has been employed in the simulation of salts.[1]

3.1.4. Summary

The choice of molecular model and force field is essential to a proper prediction of the properties of a system. Therefore, it is of great importance to be aware of the fundamental assumptions, simplifications and approximations that are implicit in the various types of models used in the literature. When treating molecular systems in which Coulomb forces play a role one should be aware of the way these long-ranged forces are handled. Since these forces play a dominant role in many molecular systems we have tried to give an overview of the different methods—and so the different approximations—that are in use.

From Table 1 and the discussions in the previous sections it should be clear that a "best" force field does *not* exist. What will be the best choice of model and force field will depend on the type of molecular system and the type of property one is interested in. This means that the molecular modeler must have a picture of the strengths and weaknesses of the variety of force fields that are available in order to make a proper choice.

3.2. Searching Configuration Space and Generating an Ensemble

Once the molecular model and force field $V(\boldsymbol{r})$ have been chosen, a method to search configuration space for configurations with low energy $V(\boldsymbol{r})$ has to be selected. Various methods are available, each with their particular strength and weakness, which depend on

- the form and type of the interaction energy function $V(\boldsymbol{r})$,
- the number of degrees of freedom (size of the system),
- the type of degrees of freedom, viz. cartesian coordinates versus other coordinates (e.g. bond lengths, bond angles, torsional angles plus center of mass coordinates of a molecule).

3.2.1. Systematic Search Methods

If the molecular system contains only a small number of degrees of freedom (coordinates) and if $V(\boldsymbol{r})$ does not have too many (relevant) minima upon variation of the degrees of freedom, it is possible to systematically scan the complete configuration space of the system. For example, one can describe conformations of *n*-alkanes in terms of C–C–C–C torsional angles, each of which has three conformational minima, *trans* (0°), *gauche*$^+$ (120°) and *gauche*$^-$ ($-120°$). To find the lowest energy conformation of *n*-decane (seven torsional angles) one would have to compute $V(\boldsymbol{r})$ for $3^7 = 2187$ combinations of torsional angles. The relative weight of the different conformations in the ensemble representing this molecule at temperature T is given by the Boltzmann factor (36).

$$e^{-V(\boldsymbol{r})/k_B T} \tag{36}$$

The computing effort required by a systematic search of the degrees of freedom of a system grows exponentially with their number. Only very small molecular systems can be treated by systematic search methods.[79, 80] The number of degrees of freedom that still can be handled within a reasonable computing time strongly depends on the complexity of the function $V(\boldsymbol{r})$, that is, the time required to compute $V(\boldsymbol{r})$ for each configuration. A possibility for speeding up the calculation is to split the selection of low $V(\boldsymbol{r})$ configurations into different stages. In a first stage a simplified low computing cost energy function $V_{\text{simple}}(\boldsymbol{r})$ is used to quickly discard high $V_{\text{simple}}(\boldsymbol{r})$ configurations. In a second stage the complete $V(\boldsymbol{r})$ is only to be evaluated for the remaining configurations. This type of filtering procedure has been used to predict the loop structure in proteins[81] and to predict the stable conformation of small peptides (five amino acid residues),[82] for example. The basic problem of filtering using simplified forms of $V(\boldsymbol{r})$ is to ensure that the simplified $V_{\text{simple}}(\boldsymbol{r})$ is a correct projection of the complete function $V(\boldsymbol{r})$: when $V_{\text{simple}}(\boldsymbol{r})$ is large, $V(\boldsymbol{r})$ should also be large, otherwise a configuration with low energy $V(\boldsymbol{r})$ might be discarded in the first stage due to a high energy $V_{\text{simple}}(\boldsymbol{r})$.

3.2.2. Random Search Methods

If a system contains too many degrees of freedom, straightforward scanning of the complete configuration space is impossible. In that case a collection of configura-

tions can be generated by random sampling. Such a collection becomes an ensemble of configurations when each configuration is given its Boltzmann factor [cf. Eq. (36)] as weight factor in the collection. Two types of random search methods can be distinguished:

- Monte Carlo methods, in which a sequence of configurations is generated by an algorithm which ensures that the occurrence of configurations is proportional to their Boltzmann factors [Eq. (36)].
- Other methods which produce an arbitrary (non-Boltzmann) collection of configurations, which can be transformed into a Boltzmann ensemble by applying the weight factors from Equation (36).

3.2.2.1. *Monte Carlo Simulation*

The Monte Carlo (MC) simulation procedure by which a (canonical) ensemble is produced consists of the following steps.

1. Given a starting configuration $\boldsymbol{r}_S$ a new configuration $\boldsymbol{r}_{S+1} = \boldsymbol{r}_S + \Delta\boldsymbol{r}$ is generated by random displacement of one (or more) atoms. The random displacements $\Delta\boldsymbol{r}$ should be such that in the limit of a large number of successive displacements the available cartesian space of all atoms is uniformly sampled. This does not mean that the actual sampling must be carried out in cartesian space. It can be done, e.g., in internal coordinate space (r, θ, φ), but since the equivalent volume element is $r^2 \sin\theta \, dr d\theta d\varphi$, the sampling in internal coordinate space must be non-uniform in order to produce a uniform sampling in terms of cartesian coordinates.
2. The newly generated configuration $\boldsymbol{r}_{S+1}$ is either accepted or rejected on the basis of an energy criterion involving the change $\Delta E = V(\boldsymbol{r}_{S+1}) - V(\boldsymbol{r}_S)$ of the potential energy with respect to the previous configuration. The new configuration is accepted when $\Delta E \leq 0$, or if $\Delta E > 0$ when $e^{-\Delta E/k_B T} > R$, where R is a random number taken from a uniform distribution over the interval (0,1).
   Upon acceptance, the new configuration is counted and used as a starting point for the next random displacement. If the criteria are not met, the new configuration $\boldsymbol{r}_{S+1}$ is rejected. This implies that the previous configuration $\boldsymbol{r}_S$ is counted again and used as a starting point for another random displacement.

It is relatively easy to understand that this procedure will generate a Boltzmann ensemble. We consider two configurations $\boldsymbol{r}_1$ and $\boldsymbol{r}_2$ with energies $E_1 = V(\boldsymbol{r}_1) < V(\boldsymbol{r}_2) = E_2$. The probability of stepping from configuration $\boldsymbol{r}_2$ to $\boldsymbol{r}_1$ equals 1, the reverse step has a probability $\exp(-(E_2 - E_1)/k_B T)$. When the populations p_1 and p_2 of the two configurations are in equilibrium, one has detailed balance conditions (37) or (38).

$$p_2 \cdot 1 = p_1 \cdot e^{-(E_2 - E_1)/k_B T} \tag{37}$$

$$p_1/p_2 = e^{-E_1/k_B T}/e^{-E_2/k_B T} \tag{38}$$

Each configuration occurs with a probability proportional to its Boltzmann factor [Eq. (36)].

The advantage of this (Metropolis) Monte Carlo or Boltzmann sampling over random sampling is that most sampled configurations are relevant (low energy), while with random sampling much computational effort is likely to be spent on irrelevant (high energy) configurations. In order to obtain high computational efficiency, one would like to combine a large (random) step size with a high acceptance ratio. This is possible when applying MC techniques to simulate simple atomic or molecular liquids.[6] However, for complex systems involving many covalently bound atoms, a reasonable acceptance ratio can only be obtained for very small step size.[83] This is due to the fact that a random displacement will inevitably generate a very high bond energy of the bonds of the displaced atom. This makes MC methods rather inefficient for (macro)molecular systems.

3.2.2.2. *Distance Geometry Methods*

Distance geometry (DG) is a general method for converting a set of bounds on distances between atoms into a configuration of these atoms that is consistent with these bounds. The emergence of 2D-NMR techniques has spurred a renewed interest in techniques to obtain three-dimensional molecular structures from atom–atom distance information.[84–86] The DG method is also applied in pharmacophore modeling[87] or enzyme substrate docking [*J. M. Blaney*, private communication] to generate a collection of ligand structures compatible with a set of atom–atom distance bounds.

In distance geometry a molecular structure is described in terms of the set of all pairwise interatomic distances, which can be written in the form of a so-called (symmetric) distance matrix. By entering maximum distances between atoms of pairs in the upper right-hand triangle, and minimum distances in the lower left-hand triangle of the distance matrix it becomes a distance bounds matrix. Such a matrix describes the complete configuration space accessible to the molecule within the specified bounds. In a distance geometry calculation a set of random configurations is generated by choosing atom–atom distances at random within the specified bounds, and subsequently converting the resulting distance matrix into a structure in three-dimensional cartesian space using a so-called embedding algorithm.[84–86]

The DG method is a powerful method for generating a set of configurations compatible with a set of atom–atom distances, but also has a number of limitations. It is not possible to apply an energy function $V(\boldsymbol{r})$ like Equation (1) in a DG calculation. The energy function has to be converted into a function of atom–atom distances only, and subsequently it must be simplified to a set of bounds on these distances, by which procedure much of the information present in $V(\boldsymbol{r})$ will be lost. As a consequence the DG method cannot properly handle solvent configurations, since a limited-distance description of a liquid lacks the ability to give proper statistical weight to the great variety of possible configurations. Another problem is the characterization of the distribution of generated three-dimensional configurations. Since the conversion from distance space into three-dimensional cartesian space is non-linear, a uniform sampling of distances between the lower and upper bounds will certainly not produce a set of configurations uniformly distributed in cartesian space.

3.2.2.3. Other Random Search Techniques

There exist infinitely many ways for generating a set of molecular configurations in a random manner. Whether the set of generated configurations may be considered to form an ensemble that can be used for statistical mechanical evaluation of quantities will depend on the sampling properties of the method that is used. It should sample the important (low energy) regions of configuration space and the configurations should occur according to their Boltzmann weight factors. Otherwise the set of configurations can only be viewed as such, not as an ensemble representative of the state of the system that is considered.

3.2.3. Dynamic Simulation Methods

Another way to generate an ensemble of configurations is to apply Nature's laws of motion for the atoms of a molecular system. This has the additional advantage that dynamical information about the system is obtained as well. The two major simulation techniques of this type are Molecular Dynamics (MD), in which Newton's equations of motion are integrated over time, and Stochastic Dynamics (SD), in which the Langevin equation of motion for Brownian motion is integrated over time.

3.2.3.1. Molecular Dynamics Simulation

In the Molecular Dynamics (MD) method a trajectory (configurations as a function of time) of the molecular system is generated by simultaneous integration of Newton's equations of motion (39) and (40) for all the atoms in the

$$\mathrm{d}^2\boldsymbol{r}_i(t)/\mathrm{d}t^2 = m_i^{-1}\boldsymbol{F}_i \tag{39}$$

$$\boldsymbol{F}_i = -\partial V(\boldsymbol{r}_i, \ldots \boldsymbol{r}_N)/\partial \boldsymbol{r}_i \tag{40}$$

system. The force on atom i is denoted by $\boldsymbol{F}_i$ and time is denoted by t. MD simulation requires calculation of the gradient of the potential energy $V(\boldsymbol{r})$, which therefore must be a differentiable function of the atomic coordinates $\boldsymbol{r}_i$. The integration of Equation (39) is performed in small time steps Δt, typically 1–10 fs for molecular systems. Static equilibrium quantities can be obtained by averaging over the trajectory, which must be of sufficient length to form a representative ensemble of the state of the system. In addition, dynamic information can be extracted. Another asset of MD simulation is that non-equilibrium properties can be efficiently studied by keeping the system in a steady non-equilibrium state, as is discussed in Section 5.4. Viewed as a technique to search configuration space, the power of MD lies in the fact that the kinetic energy present in the system allows it to surmount energy barriers that are of order of $k_B T$ per degree of freedom. By raising the temperature T a larger part of conformation space can be searched, as has been shown by *DiNola* et al.,[88] who generated a series of different conformations of the hormone somatostatin by applying MD at $T = 600$ K and at 1200 K. At the elevated temperature the total energy and potential energy are monitored for conspicuous fluctuations which may signal a possibly significant conformational change. When minima in the total energy occur, the system is cooled down and equilibrated at normal temperature (300 K). In this way different conformations with comparable free energy were obtained. We note however that the search at elevated temperature favors selection of higher entropy conformations.

Searching conformation space by MD is expected to be efficient for molecules up to about 100 atoms. For larger molecules, which may and are likely to show a particular topological fold, MD methods will not be able to generate major topological rearrangements. Even when the barriers separating two topologically different low energy regions of conformation space are of the order of $k_B T$, the time needed for traversing them may be much too long to be covered in a MD simulation of 10–100 ps.

3.2.3.2. Stochastic Dynamics Simulation

The method of stochastic dynamics (SD) is an extension of MD. A trajectory of the molecular system is generated by integration of the stochastic Langevin equation of motion (41).

$$\mathrm{d}^2\boldsymbol{r}_i(t)/\mathrm{d}t^2 = m_i^{-1}\boldsymbol{F}_i + m_i^{-1}\boldsymbol{R}_i - \gamma_i \mathrm{d}\boldsymbol{r}_i(t)/\mathrm{d}t \tag{41}$$

Two terms are added to Equation (39), a stochastic force $\boldsymbol{R}_i$ and a frictional force proportional to a friction coefficient γ_i. The stochastic term introduces energy, the frictional term removes (kinetic) energy from the system, the condition for zero energy loss being that given in Equation (42), where

$$\langle \boldsymbol{R}_i^2 \rangle = 6 m_i \gamma_i k_B T_{\mathrm{ref}} \tag{42}$$

T_{ref} is the reference temperature of the system.

SD can be applied to establish a coupling of the individual atom motion to a heat bath,[89] or to mimic a solvent effect.[90, 91] In the latter case the stochastic term represents collisions of solute atoms with solvent molecules and the frictional term represents the drag exerted by the solvent on the solute atom motion. An introduction to SD simulation techniques is given in Refs. [90, 92].

3.2.4. Other Search Methods

There exists a variety of other methods for searching configuration space which are variants of the basic types discussed in the previous subsections.

The method of simulated annealing[93] is a MC or a MD simulation in which the temperature is gradually lowered to 0 K. In this way the system generally ends up in a lower energy state than when an ordinary gradient energy minimizer is used.

In a MD simulation the atomic velocities are large when the system explores the low energy regions of the potential energy function $V(\boldsymbol{r})$, and small when it crosses barriers at higher energy. For an efficient searching of configuration space one would like to invert this behavior: the atoms should move slowly in the valleys of $V(\boldsymbol{r})$. A search algorithm developed along this line seems to perform well for certain systems.[94] Within the framework of MD the ability of atoms to cross barriers can be greatly enhanced by keeping their kinetic energy nearly constant by a tight coupling to a heat bath.

Another possibility is the combination of different techniques; Monte Carlo simulation, gradient minimization, etc. in one computational scheme.[95,96]

3.2.5. *Summary*

The various methods for searching configuration space can be classified as follows:

A. Systematic search methods, which scan the complete configuration space of the molecular system.
B. Methods which aim at generating a representative set of configurations. These may be divided into two types.
   1. Non-step methods, such as the DG method, which generate a (at least in principle) uncorrelated series of random configurations.
   2. Step methods, such as MC, MD and SD, which generate a new configuration from the previous one.

Most search techniques fall in this class. They can be distinguished by the way the step direction and the step size are chosen:

- according to the gradient $-\vec{\nabla}V(\boldsymbol{r})$,
- according to a memory of the path followed so far, or
- at random.

For example, in the MC method, the step direction is chosen at random, the actual step size is determined by the change in energy ΔE (gradient) and a random element in case $\Delta E > 0$. In a MD simulation both step size and direction are determined by the force (gradient) and the velocity (memory). In general a search algorithm will make a step which is a linear combination of the gradient, previous steps (memory) and a random contribution. It will depend on the energy surface $V(\boldsymbol{r})$ which is the optimal linear combination of these three ingredients.

Another classification of algorithms which generate a set of configurations is whether they produce an ensemble or not. Of the schemes discussed above only MC, MD and SD generate a Boltzmann weighted ensemble.

3.3. Boundary Conditions

When simulating a system of finite size, some thought must be given to the way the boundary of the system will be treated. The simplest choice is the vacuum boundary condition. When simulating a liquid, solution or solid rather than a molecule in the gas phase, it is common practice to minimize edge or wall effects by the application of periodic boundary conditions. If the irregularity of the system is incompatible with periodicity, edge or wall effects may be reduced by treating part of the system as an extended wall region in which the motion of the atoms is partially restricted.

3.3.1. *Vacuum Boundary Condition*

Simulation of a molecular system in vacuo, that is, without any wall or boundary, corresponds to the gas phase at zero pressure. When the vacuum boundary is used for a solid or a molecule in solution, properties of atoms near or at the surface of the system will be distorted.[97] The vacuum boundary condition may also distort the shape of a (non-spherical) molecule, since it generally tends to minimize the surface area. Moreover, the shielding effect of a solvent with high dielectric permittivity, like water, on the electric interaction between charges or dipoles in a molecule is lacking in vacuo. We note that the water molecules do *not* need to be positioned between the charges or dipoles in order to produce a screening of the interaction between these. Therefore, simulation of a charged extended molecule like DNA in vacuo is a precarious undertaking. Solvation of DNA in a sphere with solvent molecules will shift the boundary effects from the DNA–vacuum interface to the water–vacuum interface and so improve the treatment of the DNA.[98] The best results in vacuo are obtained for relatively large globular molecular systems.

3.3.2. *Periodic Boundary Conditions*

The classical way to minimize edge effects in a finite system is to use periodic boundary conditions. The atoms of the system that is to be simulated are put into a cubic, or more generally into any periodically space-filling shaped box, which is treated as if it is surrounded by 26 ($= 3^3 - 1^3$) identical translated (over distances $\pm R_{box}$ in the x-, y-, z-directions) images of itself. The next layer of neighbor images of the central computational box contains $5^3 - 3^3 - 1^3 = 98$ boxes, and so on. When an infinite lattice sum of the atomic interactions is to be performed (Sections 3.1.3.11–13), the interactions of an atom in the central computational box with *all* its periodic images are computed. In most cases this is not desirable. Then only interactions with nearest neighbors are taken into account. The black atom in the central computational box in Figure 10a will only interact with atoms or images of atoms that lie within the dashed line (nearest image, NI, or minimum image, MI, approximation). The anisotropy of the interaction due to the cubic shape of the nearest image box can be avoided by the application of a spherical cut-off (radius R_C). The periodic boundary condition affects not only the computation of the forces, but also the positions of the atoms. It is common practice (though not necessary) to keep the atoms together, that is, in the central computational box: when an atom leaves the central box on one side, it enters it with identical velocity at the opposite side at the translated image position.

Application of periodic boundary conditions means that in fact a crystal is simulated. For a liquid or solution the periodicity is an artifact of the computation, so the effects should be minimized. An atom should not simultaneously interact with another atom and a periodic image of that atom. Consequently the length R_{box} of the edge of the periodic box should exceed twice the cut-off radius R_C. Possible distorting effects of the periodic boundary condition[99–102] may be traced by simulation of a system in differently shaped boxes (see below) of different size.

When simulating a spherical solute, use of a more spherically shaped computational box instead of a cubic or rectangular one may considerably reduce the number of solvent molecules that is needed to fill the remaining (after insertion of the solute) empty space in the box. A more spherically shaped space-filling periodic box is a truncated octahedron, (Fig. 10b).[103] It is obtained by cutting off the corners of a cube in such a way that the symmetry of the cube is main-

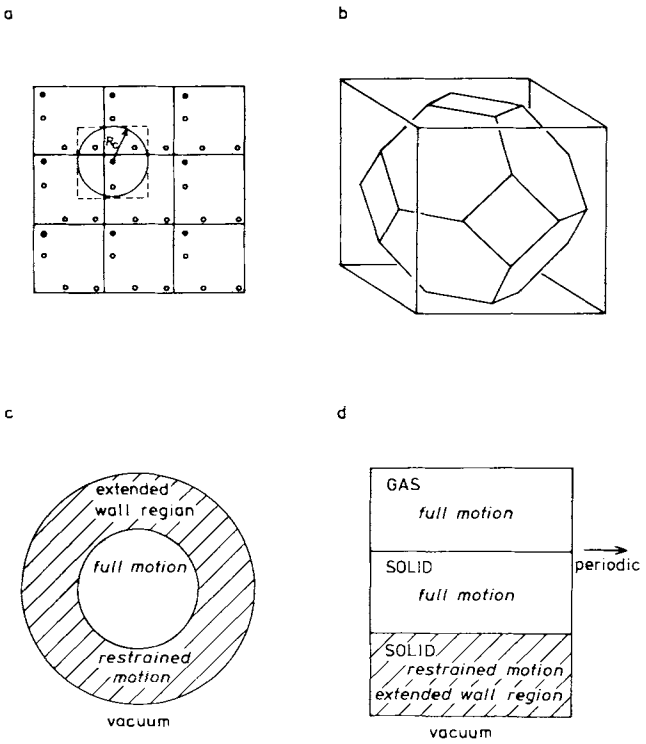

Fig. 10. Types of boundary conditions: a) cubic periodic, b) truncated octahedron periodic, c) spherical extended wall region, d) flat extended wall region for a gas-solid simulation.

tained, and such that the distance between opposite hexagonal planes equals $\frac{1}{2}\sqrt{3}$ times the distance between opposite square planes. In this way half the volume of the original cube is cut away. The ratio of the inscribed-sphere volume to total volume of the truncated octahedron is 0.68, whereas it is only 0.52 for a cube. Use of a truncated octahedron instead of a rectangular periodic box may yield a sizeable reduction of the system to be simulated. For example, the small protein bovine pancreatic trypsin inhibitor (BPTI) (58 amino acid residues) consists of 568 atoms (hydrogen atoms bound to carbons excluded), and its dimensions are 28 Å by 28 Å by 40 Å. If we approximate it by a sphere of radius 16 Å and put it into a cube with a minimum solvent layer thickness of 6 Å to the walls, about 2300 water molecules (6900 atoms) are needed to fill the non-protein part of the cube of volume $[2\times(16+6)]^3$ Å^3. To fill the non-protein part of a truncated octahedron of volume $\frac{1}{2}[4\times(16+6)/\sqrt{3}]^3$ Å^3 takes about 1600 water molecules (4800 atoms). This means a reduction of the system size by at least one quarter of the number of atoms.

3.3.3. Extended Wall Region Boundary Condition

If a molecular system is irregular, i.e. not nearly translationally periodic, periodic boundary conditions cannot be applied. In this case the distorting effect of the vacuum outside the molecular system may be reduced by designating a layer of atoms of the system to be an extended wall region, in which the motion of the atoms is restrained in order to avoid the deforming influence of the nearby vacuum (Fig. 10c, d). The atoms in the extended wall region can be kept fixed[89] or harmonically restrained to stationary positions. Their motion may be coupled to a heat bath, e.g. by applying stochastic dynamics[89] in order to account for exchange of energy with the surroundings. In any case the type of force applied to these atoms should be chosen such that their motion in the finite system resembles as closely as possible the true motion in an infinite system. The extended wall region forms a buffer between the fully unrestrained part of the system and the (unrealistic) vacuum surrounding it.

This extended wall region technique has been applied in the simulation of solids,[104] liquids[105,106] and proteins.[107,108] Although the technique yields considerable savings in computing time, it should be carefully analyzed how far the restraining of the motion of the atoms in the wall region will affect the motion of the freely simulated atoms in the system.

3.4. Different Types of Molecular Dynamics

When Newton's equations of motion (39) and (40) are integrated the total energy is conserved (adiabatic system) and if the volume is held constant the simulation will generate a microcanonical ensemble. For various reasons this is not very convenient and a variety of approaches has appeared in the literature to yield a type of dynamics in which temperature and pressure are independent variables rather than derived properties. When MD is performed in non-equilibrium situations in order to study irreversible processes, catalytic events or transport properties, the need to impress external constraints or restraints on the system is apparent. In such cases the temperature should be controlled as well in order to absorb the dissipative heat produced by the irreversible process. But also in equilibrium simulations the automatic control of temperature and pressure as independent variables is very convenient. Slow temperature drifts that are an unavoidable result of force truncation errors are corrected, while also rapid transitions to new desired conditions of temperature and pressure are more easily accomplished.

3.4.1. Constant-Temperature Molecular Dynamics

Several methods for performing MD at constant temperature have been proposed, ranging from ad-hoc rescaling of atomic velocities in order to adjust the temperature, to consistent formulation in terms of modified Lagrangian equations of motion that force the dynamics to follow the desired temperature constraint. Different types of methods can be distinguished.

1. *Constraint methods*, in which the current temperature $T(t)$ at time point t is exactly equal to the desired reference temperature T_0. This can be achieved by rescaling the velocities at each MD time step[20] by a factor $[T_0/T(t)]^{1/2}$, where the temperature $T(t)$ is defined in terms of the kinetic energy through equipartition [Eq. (43)]. The number of degrees of freedom in the system is N_{df}.

$$E_{kin}(t) = \sum_{i=1}^{N} \frac{1}{2} m_i v_i^2(t) = \frac{1}{2} N_{df} k_B T(t) \tag{43}$$

The same result can be obtained in a more elegant way by a modification of the equations of motion (39),[109-111] such

that the kinetic energy instead of the total energy becomes a constant of motion. This method has two disadvantages. First, numerical inaccuracy of the algorithm may produce a drift in temperature that is not stabilized, since the reference temperature T_0 does not appear in the equations to be integrated. Second, although the system is modeled by a Hamiltonian, this Hamiltonian does not represent a physical system, for which fluctuations in the kinetic energy are characteristic. In practical applications which are aimed at realistically simulating a physical system, the use of a non-physical Hamiltonian is questionable, even though mathematically consistent equations of motion are obtained.

2. *Extended system methods,*[112] in which an extra degree of freedom s representing a heat bath is added to the atomic degrees of freedom of the molecular system. A kinetic and a potential energy term involving this extra degree of freedom are added to the Hamiltonian and the simulation is carried out for the $N_{df}+1$ degrees of freedom of this extended system. Due to the presence of a kinetic term $\frac{1}{2}m_s(ds/dt)^2$ in the Hamiltonian, energy is flowing dynamically from the heat bath to the system and back, the speed being controlled by the inertia parameter m_s. A disadvantage of this type of second-order coupling to a heat bath is the occurrence of spurious energy oscillations, the period of which depends on the value of the adjustable coupling parameter m_s.

3. *Weak coupling methods,*[113] in which the atomic equations of motion are modified such that the net result on the system is a first-order relaxation of the temperature towards the reference value T_0 [Eq. (44)].

$$dT(t)/dt = \tau_T^{-1}[T_0 - T(t)] \tag{44}$$

The kinetic energy can be changed by ΔE_{kin} in a MD time step Δt by scaling all atomic velocities $\vec{v}_i$ with a factor λ. Using (43) we get (45).

$$\Delta E_{kin} = (\lambda^2 - 1)\tfrac{1}{2}N_{df}k_B T(t) \tag{45}$$

If the heat capacity per degree of freedom of the system is denoted by c_V^{df} the change in energy [Eq. (45)] leads to a

$$\Delta T = [N_{df}c_V^{df}]^{-1}\Delta E_{kin} \tag{46}$$

change in temperature [Eq. (46)], which should be equal to ΔT as determined by (44). Solving Equations (44)–(46) for λ we obtain equation (47).

$$\lambda = [1 + c_V^{df}(k_B/2)^{-1}\Delta t\,\tau_T^{-1}(T_0/T(t) - 1)]^{1/2} \tag{47}$$

The heat capacity per degree of freedom c_V^{df} may not be accurately known for the system. This has no consequence for the dynamics since the temperature relaxation time τ_T is an adjustable parameter. This aperiodic coupling to a heat bath through a first-order process has the advantage over the extended system methods that the response to temperature changes is non-oscillatory and that it is rather easy to implement through a simple velocity scaling using Equation (47). The coupling can be chosen sufficiently weak (sufficiently large τ_T) to avoid disturbance of the system and sufficiently strong (small τ_T) to achieve the desired result.

4. *Stochastic methods,* in which the individual atomic velocities $\vec{v}_i$ are changed stochastically. *Andersen*[114] proposed a Maxwellian re-thermalization procedure by stochastic collisions, in which the mean time between collisions plays the role of adjustable parameter determining the strength of the coupling to the heat bath. *Heyes*[115] has suggested a Monte Carlo type technique for selection of new velocities. Others[116] used the Langevin equation (41) to achieve the coupling to a heat bath, the strength of the coupling being determined by the value of the atomic friction coefficients γ_i.

3.4.2. Constant-Pressure Molecular Dynamics

For an isotropic system the pressure is a scalar defined by Equation (48), where V denotes the volume of the computational box and the virial Ξ is defined as in Equation (49).

$$P = 2/(3V)[E_{kin} - \Xi] \tag{48}$$

$$\Xi = -\frac{1}{2}\sum_{\text{pairs }(i,j)}^{N} \boldsymbol{r}_{ij} \cdot \boldsymbol{F}_{ij} \tag{49}$$

Here, $\boldsymbol{r}_{ij} = \boldsymbol{r}_i - \boldsymbol{r}_j$ and $\boldsymbol{F}_{ij}$ is the force on atom i due to atom j. For molecular systems, forces within a molecule may be omitted together with kinetic energy contributions of intramolecular degrees of freedom. A pressure change can be achieved by scaling of the volume of the box and by changing the virial through a scaling of interatomic distances.

The various methods for carrying out MD at constant pressure are based on the same principles as the constant temperature scheme with the role of the temperature played by the pressure and the role of the atomic velocities played by the atomic positions. The following methods can be distinguished.

1. *Constraint methods,*[117] in which the equations of motion are modified such that the pressure instead of the volume becomes a constant of motion. This type of method has the same two disadvantages as its constant temperature counterpart.

2. *Extended system methods,*[114, 118–121] in which an extra degree of freedom V, the volume of the box, is added to the atomic degrees of freedom of the system. A kinetic energy term, $\frac{1}{2}m_v(dV/dt)^2$ and a potential energy term, PV, involving the extra degree of freedom are added to the Hamiltonian, and the simulation is carried out for the $N_{df}+1$ degrees of freedom of the extended system. The rate of volume change is governed by the inertia parameter m_v. A disadvantage of this second-order coupling method is the occurrence of spurious volume oscillations, the period of which depends on the size of the adjustable parameter m_v.

3. *Weak coupling methods,*[113] in which the atomic equations of motion are modified such that the net result on the system is a first-order relaxation of the pressure towards a reference value P_0 [Eq. (50)].

$$dP(t)/dt = \tau_p^{-1}[P_0 - P(t)] \tag{50}$$

Scaling the atomic coordinates $\boldsymbol{r}_i$ and the edges of the computational box by a factor μ leads to a volume change [Eq. (51)].

$$\Delta V = (\mu^3 - 1)V \tag{51}$$

The pressure change ΔP due to this change in volume is given by Equation (52), where the isothermal compressibility of

$$\Delta P = -(\beta_T V)^{-1} \Delta V \tag{52}$$

the system is denoted by β_T. Solving Equations (50)–(52) for μ we get Equation (53).

$$\mu = [1 - \beta_T \Delta t \tau_p^{-1} (P_0 - P(t))]^{1/3} \tag{53}$$

Since the pressure relaxation time τ_p is an adjustable parameter, an accurate value for the compressibility of the system is not required. This first-order pressure coupling method has advantages corresponding to those of the weak temperature coupling method [cf. Eqs. (44)–(47)]. The expressions (48)–(53) can easily be modified to apply to a general anisotropic triclinic system. Virial, kinetic energy, pressure, and the scaling factor μ will become cartesian tensors, and the volume V becomes the determinant of the matrix formed by the vectors $\boldsymbol{a}$, $\boldsymbol{b}$ and $\boldsymbol{c}$ representing the edges of the computational box.

4. *Stochastic methods* for constant-pressure MD have not yet been proposed. They would involve random changes of the box volume.

3.5. Algorithms for Molecular and Stochastic Dynamics

3.5.1. Integration Schemes for Molecular Dynamics

Newton's equation of motion (39), a second-order differential equation, can be written as two first-order differential equations (54) and (55) for the particle positions $\boldsymbol{r}_i(t)$ and

$$\mathrm{d}\boldsymbol{v}_i(t)]\mathrm{d}t = m_i^{-1} \boldsymbol{F}_i(\{\boldsymbol{r}_i(t)\}) \tag{54}$$

$$\mathrm{d}\boldsymbol{r}_i(t)/\mathrm{d}t = \boldsymbol{v}_i(t) \tag{55}$$

velocities $\boldsymbol{v}_i(t)$ respectively. The forces $\boldsymbol{F}_i$ are obtained from the potential energy function through Equation (40); they therefore depend on the configuration $\{\boldsymbol{r}_i(t)\}$ of the system. A simple algorithm for integration of Equations (54) and (55) in small time steps Δt is obtained as follows.

Taylor expansion of $\boldsymbol{v}_i(t)$ at time point $t = t_n$ yields the expression (56) when Equation (54) is used.

$$\begin{aligned}\boldsymbol{v}_i(t_n + \Delta t/2) &= \boldsymbol{v}_i(t_n) + \mathrm{d}\boldsymbol{v}_i/\mathrm{d}t]_{t_n} \Delta t/2 \\ &\quad + \mathrm{d}^2\boldsymbol{v}_i(t)/\mathrm{d}t^2]_{t_n} (\Delta t/2)^2/2! + \mathrm{O}(\Delta t^3) \\ \boldsymbol{v}_i(t_n - \Delta t/2) &= \boldsymbol{v}_i(t_n) - \mathrm{d}\boldsymbol{v}_i/\mathrm{d}t]_{t_n} \Delta t/2 \\ &\quad + \mathrm{d}^2\boldsymbol{v}_i(t)/\mathrm{d}t^2]_{t_n} (\Delta t/2)^2/2! + \mathrm{O}(\Delta t^3)\end{aligned}$$

$$\boldsymbol{v}_i(t_n + \Delta t/2) = \boldsymbol{v}_i(t_n - \Delta t/2) + m_i^{-1} \boldsymbol{F}_i(\{\boldsymbol{r}_i(t_n)\}) \Delta t + \mathrm{O}(\Delta t^3) \tag{56}$$

Using the same procedure for Taylor expansions of $\boldsymbol{r}_i(t)$ at time point $t = t_n + \Delta t/2$ and using Equation (55) we obtain Equation (57).

$$\boldsymbol{r}_i(t_n + \Delta t) = \boldsymbol{r}_i(t_n) + \boldsymbol{v}_i(t_n + \Delta t/2) \Delta t + \mathrm{O}(\Delta t^3). \tag{57}$$

Equations (56)–(57) form the so-called leap-frog scheme. Its name is illustrated in Figure 11. It is one of the most accurate, stable, and yet simple and efficient algorithms available for molecular dynamics of fluid-like systems. Our

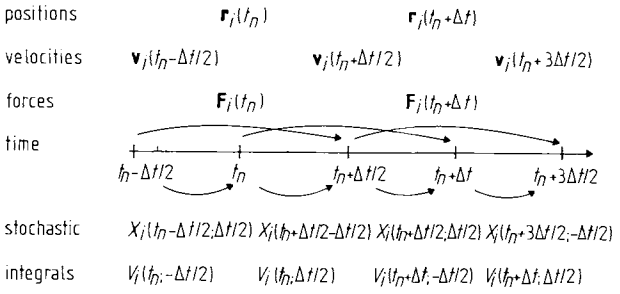

Fig. 11. The leap-frog scheme for integration of Newton's equations of motion and Langevin's equations of motion.

preference for using the leap-frog scheme instead of other algorithms such as those of *Runge-Kutta*,[122] *Gear*,[123] *Verlet*[124] or *Beeman*[125] is a result of performance evaluations[28, 69, 126, 127] and of the following considerations.

1. *Number of force evaluations per time step.* By far the most expensive part of a MD simulation is the force calculation [cf. Eq. (40)], which therefore should not be carried out more than once per integration time step Δt. This rules out algorithms of the Runge-Kutta type.

2. *Order of the algorithm.* It can be shown[69, 127] that the leap-frog, Verlet and Beeman algorithms generate exactly the same trajectory, and are of 3rd-order accuracy in the time step Δt. The application of higher-order, more accurate algorithms like those of *Gear*,[123] which involve the use of higher-order derivatives of the function to be integrated, is of no use as long as this function is a non-harmonic, noisy one. For example, in simulations of polar liquids or macromolecular solutions noise due to the cut-off applied to the long-range Coulomb forces prohibits an increase in accuracy beyond 3rd order.[126] However, if the highest-frequency motions in the molecular system are highly harmonic, as in solids, the higher-order function derivative will possess predictive power, which may lead to improved accuracy by applying higher-order algorithms. Algorithms that are of lower than third order are not efficient in the MD of molecular systems.[127] This is because molecular potential energy functions V generally have positive second derivatives, requiring third- or higher-order algorithms.

3. *Representation of the algorithm.* The much used Verlet algorithm can be obtained from the leap-frog scheme [(56)–(57)] by eliminating the velocities $\boldsymbol{v}_i(t_n + \Delta t/2)$ and $\boldsymbol{v}_i(t_n - \Delta t/2)$ from Equations (56) and (57) and replacement of t_n by $t_n - \Delta t$ in Equation (57).

$$\begin{aligned}\boldsymbol{r}_i(t_n + \Delta t) &= 2\boldsymbol{r}_i(t_n) - \boldsymbol{r}_i(t_n - \Delta t) \\ &\quad + m_i^{-1} \boldsymbol{F}_i(\{\boldsymbol{r}_i(t_n)\}) (\Delta t)^2 + \mathrm{O}(\Delta t^4)\end{aligned} \tag{58}$$

The atomic velocity does not occur explicitly in this algorithm, which makes a coupling of the system to a heat bath by velocity scaling as described in Section 3.4 impossible.

4. *Memory and computational requirements.* In some studies the Beeman algorithm [Eqs. (59) and (60)] is advocated.

$$\boldsymbol{r}_i(t_n + \Delta t) = \boldsymbol{r}_i(t_n) + \boldsymbol{v}_i(t_n)\Delta t + m_i^{-1}[4\boldsymbol{F}_i(t_n) - \boldsymbol{F}_i(t_n - \Delta t)](\Delta t)^2/6 \quad (59)$$

$$\boldsymbol{v}_i(t_n + \Delta t) = \boldsymbol{v}_i(t_n) + m_i^{-1}[2\boldsymbol{F}_i(t_n + \Delta t) + 5\boldsymbol{F}_i(t_n) - \boldsymbol{F}_i(t_n - \Delta t)]\Delta t/6 \quad (60)$$

[44] Although Equations (59) and (60) are much more complicated than Equation (58), the latter follows directly from the former: replace t_n by $t_n - \Delta t$ in Equations (59) and (60), multiply the latter by Δt and subtract the former from it, and add the resulting equation to Equation (59). Reshuffling of terms then gives Equation (58). Since the Beeman, Verlet and leap-frog algorithms generate identical trajectories, we prefer to use the latter because of its minimal computer memory storage and computational requirements.

3.5.2. Integration Schemes for Stochastic Dynamics

Langevin's equation of motion (41) differs from Newton's equation (54) by the occurrence of a stochastic force $\boldsymbol{R}_i(t)$ and a frictional force $m_i\gamma_i\boldsymbol{v}_i(t)$ [Eq. (61)].

$$d\boldsymbol{v}_i(t)/dt = m_i^{-1}\boldsymbol{F}_i(\{\boldsymbol{r}_i(t)\}) + m_i^{-1}\boldsymbol{R}_i(t) - \gamma_i\boldsymbol{v}_i(t) \quad (61)$$

The solution of this equation around $t = t_n$ is formulated in Equation (62).

$$\boldsymbol{v}_i(t) = \boldsymbol{v}_i(t_n)e^{-\gamma_i(t-t_n)} + m_i^{-1}e^{-\gamma_i(t-t_n)}\int_{t_n}^{t} e^{-\gamma_i(t_n-t')}[\boldsymbol{F}_i(t') + \boldsymbol{R}_i(t')]dt' \quad (62)$$

Since the stochastic properties of $\boldsymbol{R}_i(t')$ are given, the integral over $\boldsymbol{R}_i(t')$ can be obtained directly. The integral over the systematic force $\boldsymbol{F}_i(t')$ is, as in the previous section, obtained by expanding $\boldsymbol{F}_i(t')$ in a Taylor series around $t = t_n$ and omitting all terms beyond third order in Δt in the positions, beyond second order in the velocities, and beyond second order in the forces. The SD equivalent of the leap-frog velocity formula (56) then becomes:[128]

$$\boldsymbol{v}_i(t_n + \Delta t/2) = \boldsymbol{v}_i(t_n - \Delta t/2)e^{-\gamma_i\Delta t} + m_i^{-1}\boldsymbol{F}_i(t_n)[1 - e^{-\gamma_i\Delta t}]/(\gamma_i\Delta t) + \boldsymbol{V}_i(t_n; \Delta t/2) - e^{-\gamma_i\Delta t}\boldsymbol{V}_i(t_n; -\Delta t/2) \quad (63)$$

with

$$\boldsymbol{V}_i(t_n; \Delta t/2) \equiv m_i^{-1}e^{-\gamma_i\Delta t/2}\int_{t_n}^{t_n+\Delta t/2} e^{-\gamma_i(t_n-t')}\boldsymbol{R}_i(t')\,dt' \quad (64)$$

When γ_i goes to zero, Equation (63) reduces to Equation (56). The SD equivalent of the leap-frog position formula (57) is obtained by integrating Equation (55) using the expression (62) for the velocity[128] [Eqs. (65), (66)].

$$\boldsymbol{r}_i(t_n + \Delta t) = \boldsymbol{r}_i(t_n) + \boldsymbol{v}(t_n + \Delta t/2)\Delta t[e^{+\gamma_i\Delta t/2} - e^{-\gamma_i\Delta t/2}]/(\gamma_i\Delta t) + \boldsymbol{X}_i(t_n + \Delta t/2; \Delta t/2) - \boldsymbol{X}_i(t_n + \Delta t/2; -\Delta t/2) \quad (65)$$

$$\boldsymbol{X}_i(t_n; \Delta t/2) \equiv (m_i\gamma_i)^{-1}\int_{t_n}^{t_n+\Delta t/2}[1 - e^{-\gamma_i(t_n+\Delta t/2-t')}]\,\boldsymbol{R}_i(t')\,dt' \quad (66)$$

When γ_i goes to zero, Equation (65) reduces to Equation (57).

When using the SD leap-frog algorithm (63–66) it must be noted that $\boldsymbol{V}_i(t_n; -\Delta t/2)$ is correlated with $\boldsymbol{X}_i(t_n - \Delta t/2; \Delta t/2)$, since they are different integrals of $\boldsymbol{R}_i(t)$ over the time interval $(t_n - \Delta t/2;\ t_n)$ (see Fig. 8). The same observation holds for $\boldsymbol{X}_i(t_n + \Delta t/2; -\Delta t/2)$ and $\boldsymbol{V}_i(t_n; \Delta t/2)$ [cf. Eqs. (65) and (63)]. These are different integrals of $\boldsymbol{R}_i(t)$ over the time interval $(t_n, t_n + \Delta t/2)$. This means that these correlated quantities must be sampled in a correlated manner,[128] which makes the SD leap-frog algorithm more complicated than the MD one.

Integration schemes for the generalized Langevin equation involving time-dependent friction coefficients γ_i can be found in Refs. [129, 130].

3.5.3. Application of Constraints in Molecular Dynamics

In Section 3.4 methods to exactly constrain the temperature and pressure of a molecular system were briefly mentioned. Here, methods to constrain molecular bond lengths or bond angles in dynamic simulations will be discussed. They are used to save computing time. The length of the time step Δt in a MD or SD simulation is limited by highest frequency (ν_{max}) motions occurring in the system [Eq. (67)].

$$\Delta t \ll \nu_{max}^{-1}. \quad (67)$$

By freezing the generally uninteresting high-frequency internal vibrations, such as bond-length or possibly bond-angle vibrations, ν_{max}^{-1} is increased, which allows for a longer time step Δt. The application of constrained dynamics makes sense physically and computationally when

1. the frequencies of the frozen (constrained) degrees of freedom are (considerably) higher than those of the remaining ones, thereby allowing a (considerable) increase of Δt,
2. the frozen degrees of freedom are only weakly coupled to the remaining ones, i.e. when the molecular motion is not significantly affected by application of constraints,
3. so-called metric tensor effects[131] play a minor role,
4. the algorithm by which the constraints are imposed on the molecular system does not require excessive mathematical or computational effort.

In molecular simulations typically a factor of 3 in computer time can be saved by application of constraints.[126] The application of constraints implies that the atoms move on a hypersurface in configuration space. While in the full Cartesian configuration space each configuration has equal weight in the partition function, the weighting on the hypersurface will in general depend on its form. The metric tensor defining the hypersurface in terms of Cartesian coordinates will determine these weights. Therefore, when simulating using constraints, metric tensor corrections must be taken into account. Their significance depends on the type of constraint. A discussion of metric tensor effects is given in Refs. [131, 132].

3.5.3.1. Classification of Methods

Several methods exist for integrating the equations of motion of a molecular system in the presence of constraints. They can be classified as follows:

1. *Formulation in terms of generalized coordinates.* In this case the constrained degrees of freedom (e.g. bond lengths, bond angles) are treated as fixed parameters, not as degrees of freedom. For example, a macromolecule may be modeled by only torsional angle degrees of freedom, as is often done in static modeling studies. Two cases can be distinguished.
   a. When dealing with *rigid molecules*, center of mass coordinates and Euler angles can be used as degrees of freedom, leading to the Newton-Euler equations of rigid body motion. A variety of algorithms have been proposed for the integration of these equations.[19, 133–135]
   b. For the more general case of *flexible molecules*, especially when the number of internal degrees of freedom becomes larger than a few, and when inertial terms are not neglected, it is a tedious task to write down explicitly the appropriate equations of motion in generalized coordinates.[136, 137] The reason is that the base vectors of the coordinate system become dependent on time, which has a number of unpleasant consequences.[136] So we think that the use of generalized coordinates, such as torsional angles, is highly unpractical for describing the dynamics of macromolecules.
2. *Formulation in terms of Cartesian coordinates.* Two methods are available for integrating the Cartesian equations of motion of flexible molecules subject to holonomic scleronomous constraints, that is, constraints that are only dependent on atomic coordinates, not on time.
   a. *Matrix methods*[138] bear their name because they involve the (costly) inversion of a matrix of dimension equal to the number of constraints. Thus, these methods are not well suited for application to macromolecular systems.
   b. *Iterative methods*, like the so-called SHAKE method,[138] are especially appropriate for macromolecules, since they treat the constraints in an iterative way.

3.5.3.2. Algorithms for Constraint Dynamics in Cartesian Coordinates

Molecular constraints have the form (68) for the case of

$$\sigma_k(\boldsymbol{r}_1, \ldots, \boldsymbol{r}_N) = 0 \qquad k = 1, \ldots N_c \tag{68}$$

N_c constraints in a molecule consisting of N atoms. Bond-length and bond-angle constraints can be put in the form of distance constraints between atoms k_1 and k_2, as in (69) where the constraint distance is given by $d_{k_1k_2}$.

$$\boldsymbol{r}_{k_1k_2}^2 - d_{k_1k_2}^2 = 0 \tag{69}$$

When applying constraints in MD or SD, the $3N$ equations of motion (39) or (41) have to be integrated while satisfying the N_c constraints. This can be accomplished by applying Lagrange's method of undetermined multipliers.[122] A zero term (68) is added to the potential energy function V in Equation (40), which yields (70) as the equation of motion.

$$m_i d^2\boldsymbol{r}_i(t)/\mathrm{d}t^2 = -\frac{\partial}{\partial \boldsymbol{r}_i}\left\{V(\{\boldsymbol{r}_i(t)\}) + \sum_{k=1}^{N_c} \lambda_k(t)\,\sigma_k(\{\boldsymbol{r}_i(t)\})\right\} \tag{70}$$

The time-dependent multipliers $\lambda_k(t)$ are determined such that the constraints σ_k are satisfied. The physical interpretation of Equation (70) becomes clear by rewriting it in terms of forces [Eq. (71)]:

$$m_i d^2\boldsymbol{r}_i(t)/\mathrm{d}t^2 = \boldsymbol{F}_i(t) + \boldsymbol{G}_i(t) \tag{71}$$

The total unconstrained force $\boldsymbol{F}_i(t)$ derived from the potential energy function is the first term in Equation (70), while the constraint force $\boldsymbol{G}_i(t)$, which compensates the components of $\boldsymbol{F}_i(t)$ that act along the directions of the constraints, is the second term.

The leap-frog scheme [(56)–(57)] for integration of Equation (71) becomes Equations (72) and (73).

$$\boldsymbol{v}_i(t_n + \Delta t/2) = \boldsymbol{v}_i(t_n - \Delta t/2) + m_i^{-1}\{\boldsymbol{F}_i(t_n) + \boldsymbol{G}_i(t_n)\}\,\Delta t \tag{72}$$

$$\boldsymbol{r}_i(t_n + \Delta t) = \boldsymbol{r}_i(t_n) + \boldsymbol{v}_i(t_n + \Delta t/2)\,\Delta t \tag{73}$$

Separating contributions from $\boldsymbol{F}_i(t_n)$ and $\boldsymbol{G}_i(t_n)$ we find

$$\boldsymbol{r}_i(t_n + \Delta t) = \boldsymbol{r}_i' + \delta\boldsymbol{r}_i \tag{74}$$

with

$$\delta\boldsymbol{r}_i = m_i^{-1}\,\boldsymbol{G}_i(t_n)(\Delta t)^2 \tag{75}$$

where $\boldsymbol{r}_i'$ are the positions after a MD or SD step disregarding all constraints, and $\delta\boldsymbol{r}_i$ are the positional corrections to be made as a result of the constraints. Using the definition of $\boldsymbol{G}_i$ we find

$$\delta\boldsymbol{r}_i = -\,m_i^{-1}(\Delta t)^2 \sum_{k=1}^{N_c} \lambda_k(t_n)\,\frac{\partial}{\partial \boldsymbol{r}_i}\,\sigma_k(\{\boldsymbol{r}_i(t_n)\}) \tag{76}$$

or when using the explicit form (69) for σ_k:

$$\delta\boldsymbol{r}_i = -\,2m_i^{-1}(\Delta t)^2 \sum_{\substack{k=1 \\ (k_1,k_2)=(i,j)}}^{N_c} \lambda_k(t_n)\,\boldsymbol{r}_{ij}(t_n) \tag{77}$$

where the summation extends only over constraints involving atom i. This implies that corrections due to the distance constraint between atoms i and j must be applied in the directions of the vector $\boldsymbol{r}_{ij}$. Corrections to $\boldsymbol{r}_i'$ and $\boldsymbol{r}_j'$ are in opposite directions and weighted by the inverse mass of atoms i and j, as is illustrated in Figure 12. Since the positions $\boldsymbol{r}_i(t_n + \Delta t)$ must satisfy the constraints (68, 69) using (74) we have for each constraint:

$$[\boldsymbol{r}_{k_1}' + \delta\boldsymbol{r}_{k_1} - \boldsymbol{r}_{k_2}' - \delta\boldsymbol{r}_{k_2}]^2 = d_{k_1k_2}^2 \tag{78}$$

These form a set of N_c quadratic equations from which the N_c Lagrangian multipliers λ_k can be determined. After linearization of Equation (78) by neglecting the terms quadratic

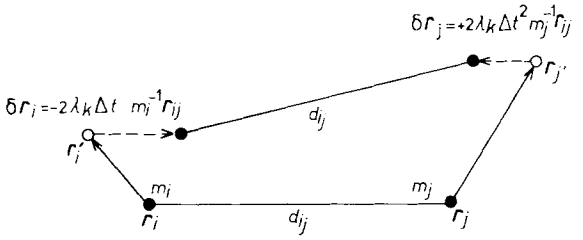

Fig. 12. Application of distance constraints. Atomic coordinate resetting using Lagrangian multipliers λ_k.

in λ_k, a set of linear equations is obtained. The above mentioned matrix methods solve these by a matrix inversion.[138] The iterative methods solve them by treating all constraints in succession, and iterating this procedure until all constraints are satisfied within a specific geometric tolerance.

The so-called SHAKE method, which is much used, is of the iterative type.[138] Its application in various algorithms is denoted by Equation (79). This means that the positions

$$\text{SHAKE}\ (\boldsymbol{r}_i(t_n),\ \boldsymbol{r}_i'(t_n + \Delta t),\ \boldsymbol{r}_i(t_n + \Delta t)) \tag{79}$$

$\boldsymbol{r}_i'(t_n + \Delta t)$ resulting from a non-constraint time step will be reset to give the constrained positions $\boldsymbol{r}_i(t_n + \Delta t)$. When necessary the constraint forces can be determined from Equation (80) and the constrained velocities from Equation (81).

$$\boldsymbol{G}_i(t_n) = m_i[\boldsymbol{r}_i(t_n + \Delta t) - \boldsymbol{r}_i'(t_n + \Delta t)]/(\Delta t)^2 \tag{80}$$

$$\boldsymbol{v}_i(t_n + \Delta t/2) = [\boldsymbol{r}_i(t_n + \Delta t) - \boldsymbol{r}_i(t_n)]/\Delta t \tag{81}$$

3.5.3.3. *Effect of the Application of Constraints*

The effect of constraining bond lengths and bond angles in molecular systems has been evaluated.[126, 139] It turns out that the application of bond-length constraints saves about a factor of 2 in computing effort when bonds to hydrogen atoms are constrained and about a factor of 3 when all covalent bonds are constrained. No evidence was found for a distortion of the physical properties by the rigidity of the bonds.[139] When the bond angles undergo limited variation, which is generally true for molecular systems, metric tensor corrections play an insignificant role when bond-length constraints are applied.[132]

The use of bond-angle constraints is not allowed, since it considerably affects the molecular motion. Macromolecular flexibility and entropy are halved, and the number of torsional angle transitions is dramatically reduced.[139] Moreover, it has been shown that in case of application of bond angle constraints metric tensor corrections, which are nearly impossible to calculate for all but the smallest flexible molecules, are of significant size and may not be ignored.[132] This means that MD or SD of molecular systems should not be performed in torsional space while treating bond lengths and angles as fixed quantities.

3.5.3.4. *Disadvantages of the Application of Constraints*

The advantage of the application of bond-length constraints is clear: at the expense of about 10% extra computing time, longer, time steps Δt can be taken. When simulating macromolecular systems without constraints, a value of $\Delta t = 0.5$ fs is appropriate, whereas with bonds to hydrogen atoms constrained $\Delta t = 1.0$ fs, and with all bonds constrained $\Delta t = 2.0$ fs is appropriate. So, a factor of 2 to 4 in computing effort is saved.

Yet, the application of constraints also has its disadvantages.

1. *Convergence problems for large planar groups.* In practice, procedures like the SHAKE method sometimes fail to converge to a molecular configuration satisfying all constraints. This is often due to the fact that the constraint forces act along the bond directions in the previous MD step (Fig. 12). For a planar group of atoms the constraint forces will act along vectors in the plane. So, when the other forces, e.g. due to charge repulsion, act orthogonally to the plane, it is nearly impossible for the constraint forces to counteract these, since they act orthogonally to each other. A solution to this problem has been proposed in Ref. [140], where virtual atoms lying outside the plane of the planar group are used to obtain constraint forces with sizeable components orthogonal to the plane of the group of real atoms. The implementation of this virtual atom technique would require definition of virtual atoms for each possible type of planar group. This makes this technique not very attractive for application in macromolecules.

2. *Free energy of creation or annihilation of atoms.* When free energy differences are computed using the coupling parameter approach, the application of constraints is a complicating factor. The Hamiltonian, or the potential energy function, is made a function of a coupling parameter λ, which is smoothly changed in the course of a simulation in order to obtain the work done by the system over a reversible change of λ. The problem now is that a constrained bond length cannot be removed from the system as a smooth function of λ. When computing the free energy of breaking a bond one faces the fact that the removal of a constraint is a discontinuous process. Even when only the length of a bond is changed (not removed) as a function of λ, computation of the free energy change due to the work done by the constraint forces is not simple, as is shown in Ref. [141].

3. *Computational bottleneck for parallelization of algorithms.* The constraint forces are generally computed after the other forces have been calculated and an unconstrained integration time step is performed. This makes the application of constraints a computational bottleneck: all other computations have to wait for its termination. Moreover, the most efficient methods for application of constraints, such as the SHAKE method, are of an iterative nature which makes them unsuitable for parallelization on a computer.

4. *Physical model of frozen bonds.* Although no significant effects due to freezing of bonds have been observed for molecular systems in equilibrium, it remains to be seen whether in non-equilibrium situations the finite flexibility of bonds may play a role in the dynamics, e.g. as an energy reservoir.

3.5.4. *Multiple Time Step Algorithms*

An alternative to the application of bond length constraints is the use of a multiple time step (MTS) integration

algorithm.[6, 142] The length of the integration time step is limited by the oscillation or relaxation time of the forces [see Eq. (67)]. In a molecular system three frequency ranges can be distinguished, as shown in Table 5: high-frequency bond-stretching forces $\boldsymbol{F}^{hf}$, low-frequency long-range Coulomb forces $\boldsymbol{F}^{lf}$, and the remaining intermediate frequency forces $\boldsymbol{F}^{if}$. The contribution of the different forces to the atomic trajectories may be integrated using different time steps. An example is the twin range method discussed in Section 3.1.3.4, in which the long-range Coulomb force is kept constant during k time steps Δt, where k lies in the range 5–100.

Table 5. Various relaxation times in macromolecular systems, and force components to be used in multiple time step algorithms.

Type of force	Approximate oscillation or relaxation time (fs)	Force: Application at step $n' = 0,1,2,\ldots$	Force: Update at step	Force: Size of force to be applied
1. high frequency: $\boldsymbol{F}^{hf}$ covalent bond stretching	10	$t_n + n'\Delta t'$	$t_n + n'\Delta t'$	$\boldsymbol{F}_i^{hf}$
2. intermediate frequency: $\boldsymbol{F}^{if}$ bond-angle bending, dihedral angle torsion, van der Waals, shortrange Coulomb	40	$t_n + n'm\Delta t'$	$t_n + n'm\Delta t'$	$m\boldsymbol{F}_i^{lf}$
3. low frequency: $\boldsymbol{F}^{lf}$ long-range Coulomb	1000	$t_n + n'm\Delta t'$	$t_n + n'mk\Delta t'$	$m\boldsymbol{F}_i^{lf}$

A multiple time step scheme could also be applied to the bond-stretching forces.[143] The conventional MD or SD time step Δt is subdivided into m (m = odd) smaller substeps $\Delta t'$, so $\Delta t = m\Delta t'$. The covalent bond forces $\boldsymbol{F}^{hf}$ are evaluated at each time step $t_n + n'\Delta t'$, with $n' = 0,1,2,\ldots$ When n' is a multiple of m, the other forces $\boldsymbol{F}^{if} + \boldsymbol{F}^{lf}$ are applied, but multiplied by a factor m in order to compensate for their omission at the substeps. Application of this MTS algorithm to macromolecules shows that for $m = 3$ or 5 the integration is as accurately performed as when bond-length constraints are used. Since the bond frequencies are about four times the other ones, a value of $m = 4$ would be expected to be large enough to ensure proper integration of the bond forces.

We note that the physical quantities one is interested in should only be evaluated at the conventional time steps Δt, not at the substeps $\Delta t'$. Since the bond stretching forces can be rapidly computed, application of this MTS algorithm is as efficient as the use of the SHAKE method, but it avoids the disadvantages of the latter method which were discussed in the previous section.

3.5.5. *Searching Neighbors*

The bulk (approximately 90%) of the computer time required by a MD or SD simulation is used for calculating the nonbonded interactions, that is, for finding the nearest neighbor atoms and subsequently evaluating the van der Waals and Coulomb interaction terms for the atom pairs obtained. Various schemes for performing this task as efficiently as possible have been proposed.[6, 144]

1. *Neighbor list techniques.* Once the neighbors have been found, either by scanning of all possible atom pairs (operation proportional to N^2), or by using grid-search techniques (proportional to N), the pairs are stored in a neighbor list which is only updated every so many steps, typically every 5 to 100 steps. At each time step the neighbor list is used to calculate the interactions (operation proportional to N).
2. *Grid search techniques.* The computational box is filled with a grid or mesh, and for each grid cell it is determined which atoms lie in it. This operation is proportional to N. The nearest neighbors of an atom can easily be found in the grid cells surrounding the grid cell containing the atom.

An evaluation of the different schemes can be found in Ref. [144]. For small systems ($N \lesssim 1000$) the use of neighbor list techniques will reduce finding the neighbors to a small part of the calculation. For large systems ($N \gtrsim 1000$) the application of grid search techniques will become advantageous.

3.6. Initial Conditions, Equilibration, and Analysis of Simulations

A simulation starts with initial atomic positions and velocities. The results should be independent of these. The initial configuration for a molecular system can be obtained from different sources: X-ray structure, model building, distance geometry calculation, random search techniques, etc. The initial velocities are either taken from a Maxwellian distribution or chosen to be zero, in which case strain in the molecule that is converted into kinetic energy may generate non-zero velocities.

The equilibration period that is required will depend on the relaxation time of the property one is interested in. Some properties, such as the kinetic energy, require short (picoseconds) equilibration times, whereas others, such as dielectric properties, may require longer times of the order of tens of picoseconds. During a simulation a number of quantities, such as the potential and kinetic energy, or the diffusion from the initial structure, are generally monitored to obtain a picture of the stability of the simulation.

The results are generally analyzed by taking time averages or averages over simulations with different initial conditions of the quantities of interest. Fluctuations and correlation functions may be calculated to analyze the mobility and dynamic behavior of the system.[6]

4. Application of Simulations

4.1. Understanding in Terms of Atomic Properties

The obvious utility of computer simulation is the possibility of analyzing molecular processes at the atomic level. Many examples can be found in the literature.[1–9] Here, we briefly mention two recent examples, the atomic interpretation of biochemical data on repressor-DNA operator binding,[26] and the atomic interpretation of biophysical measurements on membrane properties.[37]

4.1.1. Interpretation of Biochemical Data on Repressor-Operator Binding by MD Computer Simulation

In Ref. [26] a 125-ps MD simulation of a Lac repressor headpiece (51 amino acid residues) complexed with its DNA operator (14 base pairs) in aqueous solution was reported. The starting structure for the simulation was obtained from model building and energy minimization based on 169 proton–proton distances for the headpiece and 24 headpiece–DNA proton–proton distances which were available from 2D-NMR measurements.[145] When analyzing the repressor-operator contacts, no evidence was found that a so-called "direct readout" mechanism[146] for recognition is based on direct repressor side-chain–base hydrogen bonds, which is the common view on recognition. The simulation suggested that direct readout occurs rather through non-polar contacts and water-mediated hydrogen bonds. The repressor-operator contacts as observed in the simulation are compatible with the available biochemical data on base-pair or amino acid residue substitution,[147, 148] but do not support the usual interpretation in terms of side-chain–base hydrogen bonds. This illustrates the usefulness of computer simulation studies to obtain an interpretation of biochemical data at the atomic level.

4.1.2. Interpretation of Biophysical Data on Membrane Properties by MD Computer Simulation

In Ref. [37] a 180-ps MD simulation of a bilayered system of 52 sodium ions, 52 decanoate, 76 decanol and 526 water molecules was reported. A detailed analysis of the lipid–water interface was made. The charged (decanoate) head groups lie well within the water layer, but the alcoholic groups are situated more on the lipid side of the interface, which appears to be very diffuse and extends over almost 10 Å. Unexpectedly, the overlap of sodium ion and carboxylic acid distributions suggests a charge compensation rather than an electric double layer as pictured in most textbooks. Water molecule orientation is such that the remaining ion charge distribution is compensated.

Lateral diffusion constants of the lipid molecules as measured in the simulation ($3 \times 10^{-6}\ cm^2\ s^{-1}$) compare well with experiment ($2 \times 10^{-6}\ cm^2\ s^{-1}$) as measured using nitroxide spin labels.[149] Analysis shows that the hydrodynamic interaction of the head groups with the aqueous layer determines the diffusion constant of the lipid molecules, rather than interactions within the lipid layer. This illustrates the usefulness of computer simulation studies to obtain an interpretation of biophysical data at the atomic level.

4.2. Determination of Spatial Molecular Structure on the Basis of 2D-NMR, X-Ray or Neutron Diffraction Data

During the last few years computer simulation has become a standard tool in the determination of spatial molecular structure on the basis of X-ray or neutron diffraction or 2D-NMR data.[150] The goal of structure determination based on experimental NMR or diffraction data is to find a molecular structure that

1. satisfies the experimental data, such as a set of atom–atom distance constraints $\{r_{ij}^0\}$ or torsional angle constraints $\{\varphi_{ij}^0\}$ in the case of NMR, or a set of observed structure factor amplitudes $F_{obs}(hkl)$ and, if available, phases $\alpha(hkl)$ in the case of diffraction data, *and*
2. has a low energy in terms of a molecular potential energy function $V_{phys}(\{r_i\})$ [Eq. (1)].

In order to optimize a structure simultaneously with respect to both criteria, the experimental information is cast into the form of a penalty function or restraining potential V_{restr}, the value of which increases the more an actual structure violates the experimental data. The most simple choice of a function taking into account maximum values for the interatomic distances $\{r_{ij}^{ub}\}$ would be Equation (82), where the force constant is denoted by K_{dr}.

$$V_{restr} = V_{dr} \equiv \tfrac{1}{2} K_{dr} \sum_{\text{all constraints } (ij)} [\max(0, r_{ij} - r_{ij}^{ub})]^2 \qquad (82)$$

The corresponding function which restrains the calculated structure factor amplitudes $F_{calc}(hkl)$ to the observed ones is defined in (83).

$$V_{restr} = V_{sf} \equiv \tfrac{1}{2} K_{sf} \sum_{hkl} [F_{calc}(hkl) - F_{obs}(hkl)]^2 \qquad (83)$$

The optimization problem is to find a molecular structure for which the energy function (84) attains the global

$$V_{opt} = V_{phys}(\{r_i\}) + V_{restr}(\{r_i\}) \qquad (84)$$

minimum. As discussed in Section 3.2, MD simulation is a very powerful method to search configuration space for low energy configurations, due to its ability to surmount energy barriers of the order of $k_B T$ per degree of freedom. Therefore, the application of MD computer simulation in spatial structure refinement of 2D-NMR or X-ray diffraction data has become widespread in recent years.

4.2.1. Refinement of Structures Based on NMR Data

After introduction of the method of MD refinement[151] it has been applied to a variety of molecules using different refinement protocols.[150–154] The penalty function V_{restr} may be chosen in different ways.[154] The relative weight of the restraining term in Equation (84), that is the value of K_{dr}, may be chosen so large as to reduce the distance violations, at the expense of increasing the intramolecular energy V_{phys}. Too large a K_{dr} value will generally lead to a strained (unphysical) molecular structure.[28] The searching of configuration space may be performed at high temperature in order to more easily cross energy barriers.

The standard procedure is to start with a number of distance geometry (DG) type calculations to generate a collection of starting structures, which are subsequently refined by MD simulation. In Ref. [153] it was shown that the best DG structure in terms of distance violations is generally not the best structure after MD refinement. This is due to the crude energy function used in DG which has to be cast in the form of distances, and so favors geometries which are unfavored by more sophisticated energy functions used in simulations.

When the NMR data contain contributions from different molecular conformations it will be impossible to find *one* conformation satisfying the experimental data.[155] This observation led to the introduction of time-dependent constraints[156] which do not force the molecule to satisfy the distance constraints at each time point of the simulation, but only forces the distance constraints to be satisfied on average. This forms a better representation of the measured data.

4.2.2. Refinement of Structure Based on Crystallographic X-Ray or Neutron Diffraction Data

Since its introduction the method of MD refinement of crystallographic data[157] has been applied mainly in protein crystallography. Again, different penalty functions (83) and refinement protocols are used. Generally speaking MD refinement saves a few months work over conventional refinement when applied to proteins. A survey of recent developments is given in Ref. [158].

As in the NMR case, the use of time-dependent structure factor restraints will be a much better representation of the experimental information, which is an average over time and over molecules. Preliminary results (*P. Gros*, private communication) indicate that lower R values and better searching of conformational space are obtained.

4.3. Prediction of Structural Changes by MD Simulation

No reliable approaches are as yet available for the prediction of de novo (macro)molecular structures, and there is no real alternative to experimental structure determination. When structural information on homologous molecules is available, a molecular structure may be predicted starting from the homologous molecules and subsequently changing it to the required composition, either by model building on a graphic device or by more automatic simulation techniques. When additional experimental information from X-ray diffraction or NMR is available the chance of success is greatly increased. An example is the structure determination of the 279-residue protein thermitase, starting from the known structure of subtilisin (275 amino acids).[158,159] These proteins show only 47% homology; residues had to be changed, deleted and inserted when changing subtilisin into thermitase. Subsequent MD refinement using crystallographic X-ray data on thermitase made numerous atoms move over more than 4 Å. Some parts showed a structural change of more than 8 Å.

If only one or a few amino acid side chains in a protein are changed (mutated), the structural change may be predicted by MD simulation without the extra help of X-ray data. In Figure 13 the conformation of the Met-222 → Phe mutant of subtilisin resulting from a MD simulation in which Met-222 was gradually changed into Phe-222[32] is compared with the conformation as obtained from an X-ray diffraction determination of this subtilisin mutant.[160] The predicted conformation is correct. However, this is not always true; especially when hydrogen bond networks, involving bound water molecules, have to be rearranged, the simulation period may be too short compared to the hydrogen bond network relaxation time.[32]

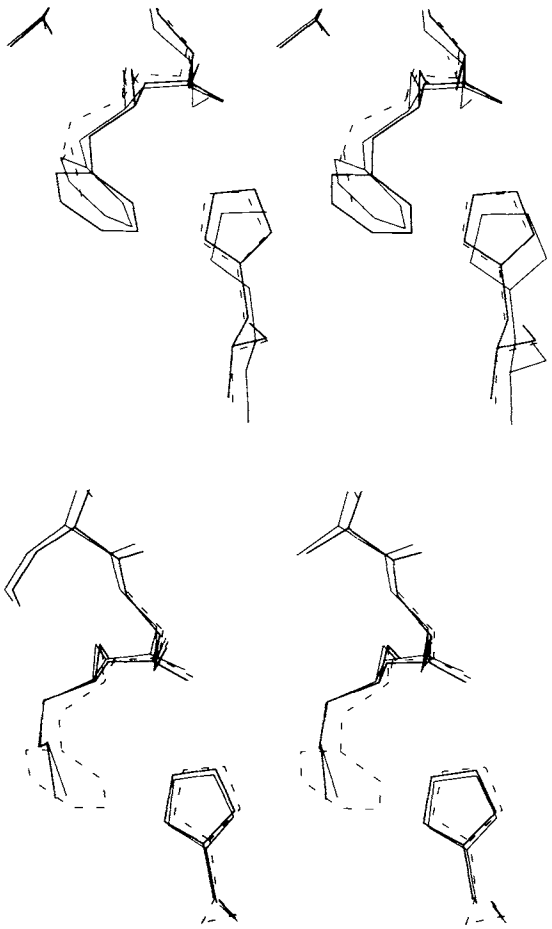

Fig. 13. Stereoview of the hydrophobic binding pocket of subtilisin. Upper part: forward 222 Met → Phe mutation; dashed line: 222 Met (native) starting structure; thick solid line: 222 Phe (mutant) MD predicted structure; thin solid line: 222 Phe (mutant) X-ray structure. Lower part: backwards 222 Phe → Met mutation; dashed line 222 Phe (MD) starting structure; thick solid line: 222 Met MD predicted structure (from 222 Phe mutant); thin solid line 222 Met (native) MD structure (from X-ray).

It is also possible by MD simulation to determine the conformation of a molecule as a function of the type of environment, viz. crystalline, nonpolar solution, aqueous solution, etc. Studies of this type have been performed for different molecules.[161-164] For the immuno suppressive drug cyclosporin A (CPA) the conformational differences found between its crystal conformation and its conformation in a chloroform solution were exactly reproduced by two MD simulations in the corresponding environments (Figure 16).[164]

This application illustrates the power of MD simulation when studying conformational properties of flexible molecules or mutants. However, when large conformational changes are to be expected the length (typically 10^1-10^2 ps) of a MD simulation may be too short to bring these about in the limited time available to surmount possible energy barriers.

4.4. Prediction of Free Energy Changes by MD Simulation

From an MD trajectory the statistical equilibrium averages can be obtained for any desired property of the molec-

ular system for which a value can be computed at each point of the trajectory. Examples of such properties are the potential and kinetic energy of relevant parts of the system, structural properties and fluctuations, electric fields, diffusion constants, etc. A number of thermodynamic properties can be derived from such averages. However, two important thermodynamic quantities, the entropy and the (Gibbs or Helmholtz) free energy, generally cannot be derived from a statistical average. They are global properties that depend on the extent of phase (or configuration) space accessible to the molecular system. Therefore, computation of the absolute free energy of a molecular system is virtually impossible. Yet, the most important chemical quantities like binding constants, association and dissociation constants, solubilities, adsorption coefficients, chemical potentials, etc., are directly related to the free energy. Over the past decade statistical mechanical procedures have evolved by means of which *relative* free energy differences may be obtained. For recent reviews of methodology and applications see Refs. [8, 165].

The most powerful method is the so-called thermodynamic cycle integration technique. The free energy difference between two states A and B of a system is determined from a MD simulation in which the potential energy function $V(\{\boldsymbol{r}_i\})$ [Eq. (1)] is slowly changed such that the system slowly converts from state A into state B. In principle the free enthalpy difference $\Delta G_{BA} = G(B) - G(A)$ is determined as the work necessary to change the system from state A to state B via a reversible path. An example is given in Figure 14, where the free enthalpy of changing one water molecule (state A) in a cube with 216 water molecules into a methanol molecule (state B) is illustrated. The change is carried out over a period of 20 ps and yields $\Delta G_{BA} = 6.1$ kJ mol^{-1}, as compared with an experimental value of 5.2 kJ mol^{-1}.

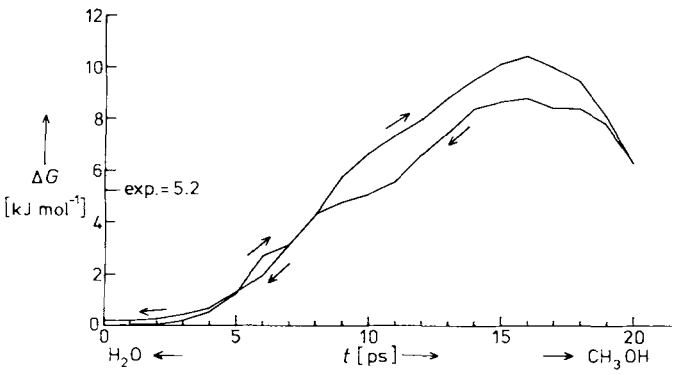

Fig. 14. Free enthalpy change ΔG on changing H_2O into CH_3OH and back again.

The basis on which the thermodynamic cycle approach rests is the fact that the free enthalpy G is a thermodynamic state function. This means that as long as the system is changed in a reversible way the change in free enthalpy ΔG will be independent of the path. Therefore, along a closed path or cycle one has $\Delta G = 0$. This result implies that there are two possibilities of obtaining ΔG for a specific process; one may calculate it directly using the technique sketched above along a path corresponding to the process, or one may design a cycle of which the specific process is only a part, and calculate the ΔG of the remaining part of the cycle. The power of this thermodynamic cycle technique lies in the fact that on the computer also non-chemical processes such as the conversion of one type of atom into another type (H into CH_3, see Fig. 14) may be performed.

The method is outlined in Figure 15 for the process of binding of two different inhibitors, trimethoprim (TMP) and its triethyl analogue (TEP), to the enzyme dihydrofolate reductase (DHFR) from chicken liver[166, 167] in the presence of coenzyme (NADPH) and water. The appropriate thermodynamic cycle is given in Figure 15. The relative

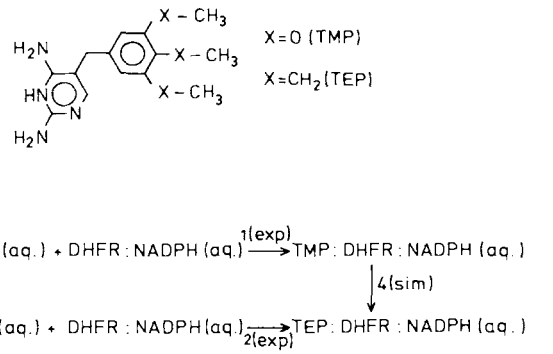

Fig. 15. Thermodynamic cycle for computation of the relative free enthalpy of binding of two inhibitors, trimethoprim (TMP) and its triethyl analogue (TEP), to the enzyme dihydrofolate reductase (DHFR) in the presence of coenzyme (NADPH) in aqueous solution. Complexation is denoted by the symbol ":".

binding constant of the two inhibitors equals $K_2/K_1 = \exp[-(\Delta G_2 - \Delta G_1)/RT]$. However, simulation of processes 1 and 2 is virtually impossible, since it would involve the reversible removal of many solvent molecules from the active site of the enzyme to be substituted by the inhibitor. Since the processes in Figure 15 form a cycle, one has $\Delta G_2 - \Delta G_1 = \Delta G_4 - \Delta G_3$, and the processes 3 and 4 can easily be simulated since they involve the change of three oxygen atoms (TMP) into three CH_2 groups (TEP). MD simulation of process 3 yields $\Delta G_3 = -61 \pm 0.2$ kJ mol^{-1} and of process 4 yields $\Delta G_4 = -65 \pm 10$ kJ mol^{-1}. So, the computed difference in free enthalpy of binding between TEP and TMP is $+4 \pm 10$ kJ mol^{-1} to be compared with an experimental value of $+7$ kJ mol^{-1}.

Although this result seems reasonable, the computed value may only be considered as an order-of-magnitude estimate. This is due to various assumptions and approximations that underlie this type of free energy calculation. Since these have been discussed elsewhere,[141] the most important ones will only be summarized here.

1. *Adequate sampling, or the relaxation time of the environment.* The change from state A to state B has to be carried out in a reversible way, which means that the time period of the change must be much longer than the relaxation time of the environment which has to adapt to the change. The rotational correlation time of a water molecule is about 2 ps and the dielectric relaxation time of water is about 8 ps. This means that a MD simulation of the change from A to B over 20 ps or more is long enough to obtain reasonably accurate ΔG values (see Fig. 14). How-

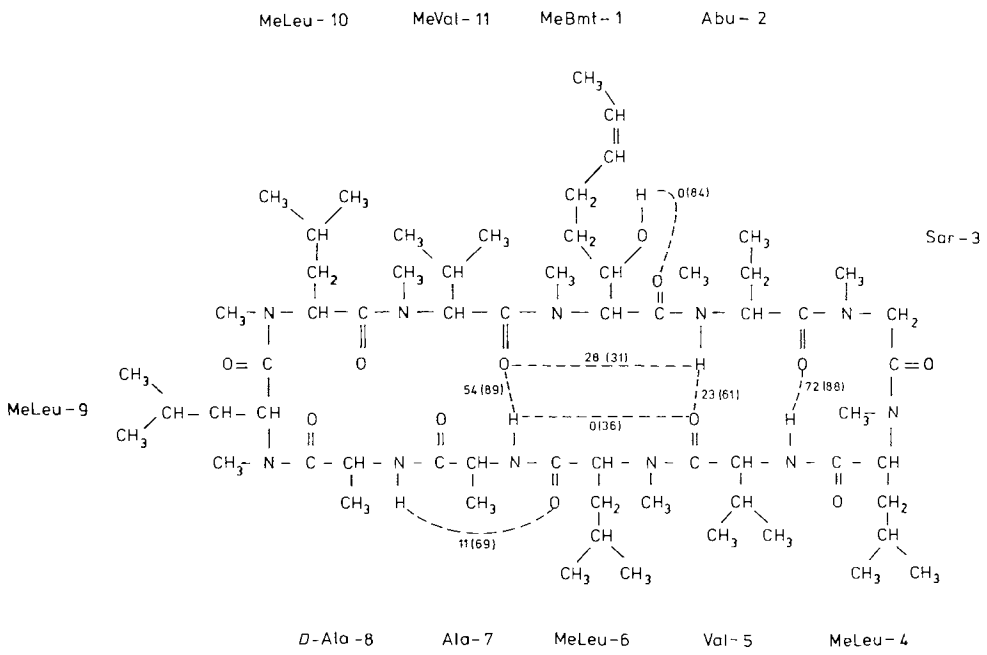

Fig. 16. Hydrogen bonds (dashed lines) occurring in two MD simulations of cyclosporin A. Percentage of occurrence is given, both for a MD simulation in aqueous solution and (in parentheses) for a MD simulation in vacuo.

ever, in process 4 (Fig. 15) the relaxation time of the (protein) environment of the inhibitor is much longer, which results in a large uncertainty of 10 kJ mol^{-1}.

2. *Effect of long-range Coulomb interactions.* Free energy computation involving the creation or annihilation of (full) atomic charges is very dependent on a proper treatment of the Coulomb interaction, which has an r^{-1} distance dependence. For example, when creating an ion in aqueous solution, the contribution of the hydration shell between 9 Å and 12 Å to the free energy of solvation is about 40 kJ mol^{-1},[41] which means that the cut-off radius must be very large to obtain accurate ΔG values. When only dipolar changes play a role, as in the case of Figures 14 and 15, the interaction has an r^{-3} distance dependence, which considerably reduces the need to use a large cut-off radius.
3. *Sensitivity to force field parameters.* Not unexpectedly, the free energy of a molecular system is rather sensitive to the interaction function (1) that is used in the simulation. For example, in the relatively simple case of the free enthalpy of solvation of methanol in water (see Fig. 14), application of force field parameters of established force fields yields values ranging from 0 to 14 kJ mol^{-1},[28] a spread of 2–3 kT around G_{exp} = 5.2 kJ mol^{-1}.

The techniques for computation of (relative) free energy are in many applications not yet sufficiently accurate. However, they are still being improved and are in principle widely applicable in the study of molecular systems.

4.5. Static versus Dynamic Representation of a Molecular System

The common approach to modeling a molecular system on a computer is a static one. For example, quantum calculations yield an equilibrium charge distribution, molecular mechanics calculations one or a few minimum energy conformations of a molecule; on a graphics device, molecules are studied in terms of fixed conformations. However, a molecular system at room temperature is by no means of static character. It should be described in terms of a multidimensional distribution function of all atomic coordinates and its development in time. An example of a dynamic equilibrium between different hydrogen bond patterns is given in Table 6 for crystalline cyclodextrin. The O61 atom is involved in different, mutually exclusive hydrogen bonds. The ones that do exist more than about 20% of the MD simulation are also observed, as expected, in the neutron diffraction

Table 6. Dynamic equilibrium between various hydrogen bond patterns involving the O61 atom in crystalline α-cyclodextrin [a]

Donor [a]	Acceptor	%	MD simulation distance [Å] D···A	MD simulation angle [°] D-H···A	Neutron diffraction distance [Å] D···A	Neutron diffraction angle [°] D-H···A
O61-H61	O63	79	2.79	160	2.81	177
	O65	2	3.04	158		
	O56	1	2.99	158		
	OW3	6	3.04	146		
	OWA	+ 2	2.08	156		
		90				
O21-H21	O61	14	3.06	156		
O63-H63		3	2.84	161		
OWA-HWA1		36	2.97	156	2.97	173
OWA-HWA2		5	3.01	154		
OW3-HW31		8	3.07	153	3.33	107
OW3-HW32		11	3.04	153		
OWB-HWB1		+ 2	2.94	156		
		79				

[a] Abbreviations. D = donor, A = acceptor, W = water atoms [29].

experiment.[168] It is also observed that the lower the occurrence of a hydrogen bond is in the simulation, the more deformed its geometry is when described in terms of one static hydrogen bond, as is the case for the neutron diffraction data (see Table 6).

4.6. The Role of a Solvent in Molecular Simulations

Many (macro)molecular modeling studies involve an isolated molecule without any solvent. This means that solvent effects are completely ignored. The molecular surface will be distorted by the vacuum boundary condition, and certainly no meaningful free energy estimates can be obtained. When a molecular complex is formed, solvent molecules may play a bridging role, as is observed in the repressor–operator complexes.[26, 169] Even intramolecular hydrogen bonding is affected by the competitive presence of water molecules surrounding a solute in aqueous solution. An example is given in Figure 16, where the occurrence of intramolecular hydrogen bonds is given for cyclosporin A, on the one hand simulated in vacuo and on the other in aqueous solution.[164] It is clear that omission of the solvent results in too high a percentage of intramolecular hydrogen bonds. Proper treatment of solvent effects is a necessary condition for a reliable simulation of molecular properties.

4.7. Other Applications of Computer Simulation in Chemistry and Physics

The field of computer simulation of molecular systems has grown so rapidly that a review of all possible applications is hardly feasible. In this section we have chosen examples, mostly of our own work, to illustrate specific aspects of simulation studies. Many other applications may be found in a number of reviews and monographs on computer simulation in physics and chemistry.[1–9] We would like to mention a few recent studies which may lead the reader to areas of application that were not mentioned here. Computer simulation has been applied to the study of electrolytes,[170] ionic conductors,[171] ionic crystals,[172] ionic salts,[10] and, inter alia, to processes like adsorption,[173] sputtering[174] and melting.[175, 176]

5. Future Developments in Computer Simulation

5.1. Quantum Simulations

Classical computer simulation implies a number of restrictions, as mentioned in Section 2.1.3, which are due to the assumption that quantum effects play a minor role. A proper description of low-temperature or light-atom (hydrogen) motion or chemical reactions requires a quantum mechanical treatment. Various quantum methods for application in the area of simulation have been developed and recent years have shown an increasing activity in the area of quantum simulations. Here, we briefly mention a few methods. Quantum effects can be incorporated in simulations in different ways.

A. *Quantum corrections to the results of classical simulations* can be made. Expansion of the partition function in powers of $\hbar$, Planck's constant, leads to correction formulas for thermodynamic quantities like the free energy[177] or structural quantities like the radial distribution function $g(r)$.[178] *Berens* et al. propose a correction formula based on a harmonic approximation of the atomic motion.[179] Also for time-dependent equilibrium quantities, quantum correction formulas are known.[180]

B. *Quantum mechanical treatment of a few degrees of freedom in an otherwise classical simulation* can be implemented in different ways.

1. The *path-integral simulation method*[181–183] yields a quantum mechanical equilibrium distribution. Its name originates from its derivation by a discretization of the path-integral form of the density matrix. A recent application is the treatment of electron transfer reactions.[184]
2. The *Gaussian wave packet method*[185–187] constituted an early attempt to solve the time-dependent Schrödinger equation by computer simulation. A problem inherent in this method is that of arriving at an adequate description of the interaction between a wave packet and its classical environment.
3. In the *density functional dynamic method*[188] an energy functional, as used in density-functional theory, is added to the Lagrangian of the molecular system, and the Lagrangian equations of motion are subsequently integrated using MD techniques. Static and dynamic properties of crystalline silicon were obtained in terms of a self-consistent pseudo potential.[188]
4. In the *adiabatic quantum molecular dynamics method*[189] the time-dependent Schrödinger equation for the excess electrons and Newton's equation of motion for the nuclei plus core electrons are integrated in the Born–Oppenheimer approximation. Electronic states and dynamic properties of dilute liquid K–KCl solutions were studied.[189]

The potential of the different methods has not yet been fully explored, which means that a best methodology has not as yet crystallized. The field is in a state of rapid development and holds much promise for a proper dynamic treatment of quantum degrees of freedom in the future.

5.2. System Size and Time Scale of Simulations

The number of particles in a computer simulation typically lies in the range of 10^2-10^4, although simulations involving more than 10^4 atoms are nowadays feasible.[173] Relatively complex systems like a protein embedded in a membrane will also contain about 10^5 atoms. In practical applications limited system size is much less a concern than the finite time scale of a computer simulation. Due to large energy barriers in the potential energy surface, it may take a molecular system a very long time to cross these barriers and so to sample configuration space efficiently. Typical simulation periods are 10^1-10^2 psec, which is much too short for a proper description of properties which show a much longer relaxation time. Therefore, possibilities to lengthen the time

scale of MD simulations are continuously investigated. Here we mention a few.

1. *Freezing of degrees of freedom.* The basic problem of removing degrees of freedom is that of defining an appropriate interaction function for the remaining degrees of freedom. Moreover, the degrees of freedom removed should play a minor role in the processes one is interested in. Application of bond-length constraints and the twin range method to handle long-range forces fall in this class. An alternative to freezing of degrees of freedom is the use of multiple time step integration methods.
2. *Stochastification of degrees of freedom.* Explicit treatment of degrees of freedom may be replaced by the application of a mean force plus a stochastic force which represent the average effect of the removed or stochastified degrees of freedom on the remaining explicitly treated ones. An example is the use of the Langevin equation to model the solvent or solid-state environment of a molecule.
3. *Scaling of system parameters.* Assume that we are interested in a quantity Q which has a relaxation time τ that is longer than the time period that could be covered by a MD simulation. It may be possible to identify one or more system parameters p for which τ is a (rapidly) changing function $\tau(p)$ of p. In that case the physically correct value of $p = p_{phys}$ can be changed to p_{short} such that $\tau(p_{short})$ becomes shorter than the length of a MD simulation, which can then be carried out to obtain $Q(p_{short})$. Extrapolation of $Q(p)$ for p from p_{short} to p_{phys} will yield an estimate $Q(p_{phys})$. The risk associated with the application of this technique is that by scaling of system parameters, the physical processes are changed such that a process at p_{short} may have nothing to do with one at p_{phys}. For example, when studying the relaxation of vibrational energy of an HCl molecule in an Ar lattice, the relaxation time may be shortened from the μs time scale to the ns time scale by reducing the HCl bond-stretching force constant. This will, however, certainly influence the balance between various relaxation mechanisms that are feasible for this process.
4. *Activated barrier crossing.* In the case of an activated process, methods exist to avoid a full simulation of the rare event of barrier crossing.[115] The procedure consists of three steps: 1) The location of the barrier must be determined. 2) The likelihood that the system will be at the top of the barrier is computed using umbrella sampling techniques. 3) The transition probability is computed by running MD trajectories from the top of the barrier. This technique has been applied to simulate ring flips in proteins.[116]
5. *Mass tensor dynamics.* In the classical partition function the integration over the momenta of the particles can be carried out separately from that over the coordinates, when no constraints are applied. The atomic masses do not appear in the configurational integral, which means that the equilibrium properties of a system will be independent of the masses in the system. The technique of mass tensor dynamics[190] exploits this freedom by choosing the atomic masses such that the high-frequency motions of the molecular system are slowed down, which allows a longer simulation time step to be taken.

None of the above-mentioned methods for lengthening the time scale of a simulation is really satisfactory. Most of the progress in this respect will probably result from the ever increasing power of computers. Yet, a combination of the different techniques mentioned above may yield a considerable reduction of the required computing power in suitable cases.

5.3. Accuracy of Molecular Model and Force Field

As was discussed in Section 3.1.1, there is no best molecular model or force field for all possible applications. The reliability of a particular force field will depend on the type of system and physical quantity it is applied to. Improvement of the quality and extension of the range of applicability is a continual concern in the area of computer simulation. Yet, the improvement of a force field is not a simple exercise for the following reasons.

1. When applying complicated force fields like (1), the exact *relationship* between a *force field parameter* and a *molecular property* is *often not known*. For example, how will the free enthalpy of solvation of methanol in water depend on the geometry and nonbonded interaction parameters?
2. *Force field parameters may be correlated.* For example, the actual barrier for a torsional rotation will depend on the combined effect of the dihedral angle potential energy term in (1) and the third neighbor nonbonded interaction between the first and the last atom defining the torsional angle.
3. There may be *conflicting requirements for improvement.* For example, the van der Waals radii of third neighbor atoms must not be too large in order that the energy of a gauche conformation is not too high in the case of a hydrocarbon chain. However, to obtain the correct density for a hydrocarbon liquid the van der Waals radius must be chosen larger. This conflict may be solved by a separate treatment of third-neighbor and other van der Waals interactions.
4. There is some conflict between the wish to stick to conceptual simplicity of a force field on the one hand, and the wish to extend its range of applicability and accuracy by allowing the force field to become more complex.
5. Approximations inherent in certain force fields may block substantial improvement by changing of the parameters. For example, when applying a cut-off radius to long-range Coulomb forces, it is impossible to obtain a proper representation of electrostatic effects.

The inclusion of polarizability will be essential for an accurate modeling of processes like the binding of charged ligands. Polarizability only allows for a local displacement of charge, not for a transfer of charge. This can be achieved by combining static ab initio or semi-empirical quantum methods to compute charge densities with classical MD simulation in an adiabatic way: the quantum charge density is converted into atomic charges which are used in a number of classical simulation steps, and the new atomic positions are subsequently used to generate a new quantum charge distribution, and so on.[191] This type of treatment is only an improvement over conventional simulation when (i) the quantum Hamiltonian includes the long-range electrostatic

field, and (ii) the classical Hamiltonian accounts in a consistent way for the changing charge distribution.

In view of the limited accuracy of currently available force fields it may be wise in practical applications to check whether the results obtained are force field dependent.

5.4. Non-Equilibrium Molecular Dynamics

In this paper we have considered the computer simulation of systems in equilibrium. It is also possible to change the equations of motion and boundary conditions such that the system is kept in a non-equilibrium state. In such a non-equilibrium molecular dynamics (NEMD) simulation, a non-equilibrium ensemble is sampled. NEMD simulation is an efficient technique to obtain transport coefficients, like viscosity, thermal conductivity, and mobility of molecular systems. An example is the study of the molecular viscosity of *n*-alkanes as a function of the intramolecular interaction function.[192] For an introduction to NEMD methods and their applications see Refs. [6, 7]. It is a rapidly developing field, which is still almost unexplored, with prospects in the area of practical rheology.

5.5. Development of Computing Power

The growth of the field of computer simulation of fluid-like systems has been made possible by the steady and rapid increase of computing power over the last couple of decades. Figure 2 suggests an increase of an order of magnitude every 5–7 years. This trend will continue in the near future, since the present growth of computing power is based on the introduction of massive parallelism. The possibilities of parallel computation can be exploited rather easily in MD simulations, since the most time-consuming part is the force calculation, which can be carried out in parallel for all atoms in the system. Also the integration step can easily be performed in parallel. The required computing time for a MD simulation depends linearly on the simulation period and the number of particles (in case of forces of finite range). Therefore this type of calculation can optimally benefit from the continuous growth of computing power. In contrast, quantum mechanical calculations extend their range much more slowly, due to the fact that the required computing power is approximately proportional to N_e^3 in the case of semi-empirical or local density functional calculations, to N_e^4 in the case of Hartree-Fock calculations, or even to N_e^5 in the case of configurational interaction calculations. Here, N_e is the number of *electronic* degrees of freedom. In classical simulations the required computing power is proportional to N_a, or in the case of inclusion of long-range forces or polarizability to at most N_a^2, where N_a denotes the number of *atomic* degrees of freedom.

6. Summary and Outlook

Dynamic computer simulation is just a branch of computational chemistry and physics in which a mathematical model of the real world is formulated and its consequences for the various physical or chemical quantities are evaluated

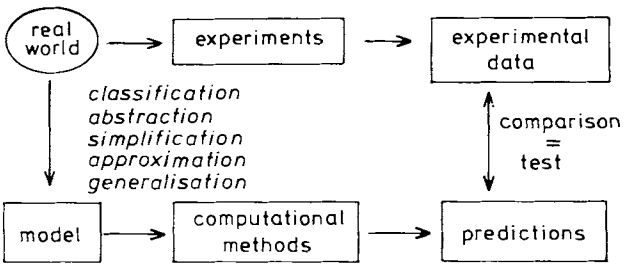

Fig. 17. Computational physics and chemistry involve formulation and testing of a (mathematical) *model* of the *real world*.

by numerical methods. This is illustrated in Figure 17. In this paper much attention has been devoted to methodology, because the core of any model is the approximations, assumptions and simplifications that are used in its formulation. Only an understanding of the basics of a particular model may lead to sensible application or improvement of its performance. Secondly, attention has been focussed on comparison of model predictions with experimental data, which may reveal flaws in the model (or experiment). Due to the complexity of the systems of chemical interest, theoretical methods only became of practical interest with the advent and development of computers. With the continuous progress of methodology and computing power, computational methods, especially computer simulation methods, will find wider and wider application in the different areas of chemistry.

In Table 7 we have listed our thoughts about the possible development of various aspects of (molecular dynamics)

Table 7. Development of various aspects of molecular dynamics computer simulation methods in chemistry.

Aspect	Past (1980)	Present (1990)	Future (2000)
accuracy			
– atomic positions	≈3 Å	≈1 Å	≈0.5 Å
– free energy	–	≈4 k_BT	≈2 k_BT
force field	united atoms	all atoms	polarizability
environment	vacuo	solvents	membranes
time scale	≈10 ps	≈100 ps	≳1 ns
system size	≈1000 atoms	≈10 000 atoms	≈100 000 atoms
quantum (MD) degrees of freedom	–	simple models	enzyme reactions
non-equilibrium simulations	atomic fluids	simple polymers	rheology of molecular mixtures

computer simulation methodology and application in chemistry. From the contents of this paper it will be clear that there are still a number of very difficult problems, such as protein folding or crystallization, which are well beyond the reach of simulation methods owing to the size of the configurational space involved, the time scale of the process, and the small free energy differences between folded and unfolded state or between crystalline and liquid state.

We would like to thank all our co-workers and colleagues who contributed to the work described here. This work was

supported by the Netherlands Foundation for Chemical Research (SON) with financial aid from the Netherlands Organisation for Scientific Research (NWO). The GROMOS (GROningen MOlecular Simulation) program library, which can be used for applying the methods discussed here, is available at nominal cost from the authors.

Received: January 10, 1990 [A 776 IE]
German version: *Angew. Chem. 102* (1990) 1020

[1] R. W. Hockney, J. W. Eastwood: *Computer Simulation using Particles*, McGraw-Hill, New York 1981.
[2] J. Hermans (Ed.): *Molecular Dynamics and Protein Structure*, Polycrystal Book Service, Western Springs, IL, USA 1985.
[3] G. Ciccotti, W. G. Hoover (Eds.): *Molecular-Dynamics Simulation of Statistical-Mechanical Systems (Proc. Int. School Phys. "Enrico Fermi", Course 97)*, North-Holland, Amsterdam 1986.
[4] D. L. Beveridge, W. L. Jorgensen (Eds.): *Computer Simulation of Chemical and Biomolecular Systems (Ann. N.Y. Acad. Sci. 482* (1986)).
[5] J. A. McCammon, S. C. Harvey: *Dynamics of Proteins and Nucleic Acids*, Cambridge University Press, London 1987.
[6] M. P. Allen, D. J. Tildesley: *Computer Simulation of Liquids*, Clarendon, Oxford 1987.
[7] G. Ciccotti, D. Frenkel, I. R. McDonald (Eds.): *Simulation of Liquids and Solids*, North-Holland, Amsterdam 1987.
[8] W. F. van Gunsteren, P. K. Weiner (Eds.): *Computer Simulation of Biomolecular Systems*, Escom, Leiden 1989.
[9] C. R. A. Catlow, S. C. Parker, M. P. Allen (Eds.): *Computer Modelling of Fluid Polymers and Solids (NATO ASI Ser. C 293* (1990)).
[10] M.-L. Saboungi, A. Rahman, J. W. Halley, M. Blander, *J. Chem. Phys. 88* (1988) 5818.
[11] W. L. Jorgensen, J. Tirado-Rives, *J. Am. Chem. Soc. 110* (1988) 1657.
[12] W. F. van Gunsteren, H. J. C. Berendsen: *Groningen Molecular Simulation (GROMOS) Library Manual*, Biomos, Groningen 1987.
[13] N. L. Allinger, *J. Am. Chem. Soc. 99* (1977) 8127; U. Burkert, N. L. Allinger: *Molecular Mechanics*, American Chemical Society, Washington D.C. 1982.
[14] M. Levitt, A. Warshel, *Nature (London) 253* (1975) 694.
[15] B. J. Berne in: J. U. Brackbill, B. I. Cohen (Eds.): *Multiple Time Scales*, Academic, New York 1985, p. 419.
[16] J. A. McCammon, M. Karplus, *Proc. Natl. Acad. Sci. USA 76* (1979) 3585; *Biopolymers 19* (1980) 1375.
[17] B. J. Alder, T. E. Wainwright, *J. Chem. Phys. 27* (1957) 1208; *ibid. 31* (1959) 459.
[18] A. Rahman, *Phys. Rev. 136* (1964) A 405.
[19] A. Rahman, F. H. Stillinger, *J. Chem. Phys. 55* (1971) 3336.
[20] L. V. Woodcock, *Chem. Phys. Lett. 10* (1971) 257.
[21] J. P. Ryckaert, A. Bellemans, *Chem. Phys. Lett. 30* (1975) 123.
[22] J. A. McCammon, B. R. Gelin, M. Karplus, *Nature (London) 267* (1977) 585.
[23] P. van der Ploeg, H. J. C. Berendsen, *J. Chem. Phys. 76* (1982) 3271.
[24] W. F. van Gunsteren, H. J. C. Berendsen, J. Hermans, W. G. J. Hol, J. P. M. Postma, *Proc. Natl. Acad. Sci. USA 80* (1983) 4315.
[25] W. F. van Gunsteren, H. J. C. Berendsen, R. G. Geurtsen, H. R. J. Zwinderman, *Ann. N.Y. Acad. Sci. 482* (1986) 287.
[26] J. de Vlieg, H. J. C. Berendsen, W. F. van Gunsteren, *Proteins 6* (1989) 104.
[27] G. Jacucci, A. Rahman, *J. Chem. Phys. 69* (1978) 4117.
[28] W. F. van Gunsteren in C. Troyanowsky (Ed.): *Modelling of Molecular Structures and Properties*, Elsevier, Amsterdam 1990.
[29] J. E. H. Koehler, W. Saenger, W. F. van Gunsteren, *Eur. Biophys. J. 15* (1987) 197; *ibid. 15* (1987) 211.
[30] J. Lautz, H. Kessler, R. Kaptein, W. F. van Gunsteren, *J. Comput. Aided Mol. Des. 1* (1987) 219.
[31] H. J. C. Berendsen, W. F. van Gunsteren, H. R. J. Zwinderman, R. G. Geurtsen, *Ann. N.Y. Acad. Sci. 482* (1986) 269.
[32] A. P. Heiner, R. R. Bott, H. J. C. Berendsen, W. F. van Gunsteren, unpublished.
[33] J. E. H. Koehler, W. Saenger, W. F. van Gunsteren, *J. Biomol. Struct. Dyn. 6* (1988) 181.
[34] J. E. H. Koehler, W. Saenger, W. F. van Gunsteren, *Eur. Biophys. J. 16* (1988) 153.
[35] R. R. Ernst, G. Bodenhausen, A. Wokaun: *Principles of Nuclear Magnetic Resonance in One and Two Dimensions*, Clarendon, Oxford 1987.
[36] J. Seelig, *Q. Rev. Biophys. 10* (1979) 353.
[37] E. Egberts, H. J. C. Berendsen, *J. Chem. Phys. 89* (1988) 3718.
[38] H. J. C. Berendsen, J. P. M. Postma, W. F. van Gunsteren, J. Hermans in B. Pullman (Ed.): *Intermolecular Forces*, Reidel, Dordrecht 1981, p. 331.
[39] H. J. C. Berendsen, J. R. Grigera, T. P. Straatsma, *J. Phys. Chem. 91* (1987) 6269.
[40] W. F. van Gunsteren, H. J. C. Berendsen in J. Hermans (Ed.): *Molecular Dynamics and Protein Structure*, Polycrystal Book Service, Western Springs, IL, USA 1985, p. 5.
[41] T. P. Straatsma, H. J. C. Berendsen, *J. Chem. Phys. 89* (1988) 5876.
[42] P. Dauber-Osguthorpe, V. A. Roberts, D. J. Osguthorpe, J. Wolff, M. Genest, A. T. Hagler, *Proteins 4* (1988) 31.
[43] F. A. Mommany, R. F. McGuire, A. W. Burgess, H. A. Scheraga, *J. Phys. Chem. 79* (1975) 2361.
[44] M. Levitt, *J. Mol. Biol. 168* (1983) 595.
[45] Z. I. Hodes, G. Nemethy, H. A. Scheraga, *Biopolymers 18* (1979) 1565.
[46] B. R. Brooks, R. E. Bruccoleri, B. D. Olafson, D. J. States, S. Swaminathan, M. Karplus, *J. Comput. Chem. 4* (1983) 187.
[47] S. J. Weiner, P. A. Kollman, D. T. Nguyen, D. A. Case, *J. Comput. Chem. 7* (1986) 230.
[48] A. T. Hagler, E. Huler, S. Lifson, *J. Am. Chem. Soc. 96* (1974) 5319.
[49] J. Hermans, H. J. C. Berendsen, W. F. van Gunsteren, J. P. M. Postma, *Biopolymers 23* (1984) 1513.
[50] E. Platt, B. Robson, *J. Theor. Biol. 96* (1982) 381.
[51] W. L. Jorgensen, J. Chandrasekhar, J. D. Madura, R. W. Impey, M. L. Klein, *J. Chem. Phys. 79* (1983) 962.
[52] D. W. Rebertus, B. J. Berne, D. Chandler, *J. Chem. Phys. 70* (1979) 3395.
[53] S. Lifson, A. T. Hagler, P. Dauber, *J. Am. Chem. Soc. 101* (1979) 5111.
[54] G. Nemethy, M. S. Pottle, H. A. Scheraga, *J. Phys. Chem. 87* (1983) 1883.
[55] L. G. Dunfield, A. W. Burgess, H. A. Scheraga, *J. Phys. Chem. 82* (1978) 2609.
[56] K. Heinzinger in C. R. A. Catlow, S. C. Parker, M. P. Allen (Eds.): *Computer Modelling of Fluid Polymers and Solids (NATO ASI Ser. C 293* (1990)) p. 357.
[57] A. Paskin, A. Rahman, *Phys. Rev. Lett. 16* (1966) 300.
[58] S. N. Ha, A. Giammona, M. Field, J. W. Brady, *Carbohydr. Res. 180* (1988) 207.
[59] D. van Belle, I. Couplet, M. Prevost, S. Wodak, *J. Mol. Biol. 198* (1987) 721.
[60] F. J. Vesely, *J. Comput. Phys. 24* (1977) 361.
[61] B. J. Alder, E. L. Pollock, *Annu. Rev. Phys. Chem. 32* (1981) 311.
[62] P. Barnes, J. L. Finney, J. P. Nicholas, J. E. Quinn, *Nature (London) 282* (1979) 459.
[63] A. Warshel, H. Levitt, *J. Mol. Biol. 103* (1976) 227.
[64] S. T. Russell, A. Warshel, *J. Mol. Biol. 185* (1985) 389.
[65] W. G. J. Hol, P. T. van Duynen, H. J. C. Berendsen, *Nature (London) 273* (1978) 443.
[66] H. J. C. Berendsen in J. Hermans (Ed.): *Molecular Dynamics and Protein Structure*, Polycrystal Book Service, Western Springs, IL, USA 1985, 18.
[67] A. Warshel, S. T. Russel, *Q. Rev. Biophys. 17* (1984) 283.
[68] B. R. Brooks in K. F. Jensen, D. G. Truhlar (Eds.): *Supercomputer Research in Chemistry and Chemical Engineering (ACS Symp. Ser. 353* (1987) 123).
[69] J. Aqvist, W. F. van Gunsteren, M. Leijonmarck, O. Tapia, *J. Mol. Biol. 183* (1985) 461.
[70] A. J. C. Ladd, *Mol. Phys. 33* (1977) 1039; *ibid. 36* (1978) 463.
[71] H. L. Friedman, *Mol. Phys. 29* (1975) 1533.
[72] J. Warwicker, H. C. Watson, *J. Mol. Biol. 157* (1982) 671.
[73] J. P. van Eerden in W. Olson (Ed.): *Nucleic Acid Conformation and Dynamics (Rep. NATO/CECAM Workshop)*, CECAM, Orsay 1983, p. 61.
[74] P. B. Shaw, *Phys. Rev. A 32* (1985) 2476.
[75] R. J. Zauhar, R. S. Morgan, *J. Mol. Biol. 186* (1985) 815; *J. Comput. Chem. 9* (1988) 171.
[76] P. Ewald, *Ann. Phys. (Leipzig) 64* (1921) 253.
[77] S. W. de Leeuw, J. W. Perram, E. R. Smith, *Proc. R. Soc. London A 373* (1980) 27.
[78] D. M. Heyes, *J. Chem. Phys. 74* (1981) 1924.
[79] K. B. Wiberg, R. H. Boyd, *J. Am. Chem. Soc. 94* (1972) 8426.
[80] M. Lipton, W. C. Still, *J. Comput. Chem. 9* (1988) 343.
[81] J. Moult, M. N. G. James, *Proteins 1* (1986) 146.
[82] K. D. Gibson, H. A. Scheraga, *J. Comput. Chem. 8* (1987) 826.
[83] S. H. Northrup, J. A. McCammon, *Biopolymers 19* (1980) 1001.
[84] G. M. Crippen in D. Bawden (Ed.): *Chemometric Research Studies Series*, Wiley, New York 1983.
[85] T. Havel, I. D. Kuntz, G. M. Crippen, *Bull. Math. Biol. 45* (1983) 665.
[86] T. Havel, K. Wüthrich, *Bull. Math. Biol. 46* (1984) 673.
[87] R. P. Sheridan, R. Nilakantan, J. S. Dixon, R. Venkataraghavan, *J. Med. Chem. 29* (1986) 899.
[88] A. DiNola, H. J. C. Berendsen, O. Edholm, *Macromolecules 17* (1984) 2044.
[89] M. Berkowitz, J. A. McCammon, *Chem. Phys. Lett. 90* (1982) 215.
[90] W. F. van Gunsteren, H. J. C. Berendsen, J. A. C. Rullmann, *Mol. Phys. 44* (1981) 69.
[91] Shi Yun-yu, Wang Lu, W. F. van Gunsteren, *Mol. Simulation 1* (1988) 369.
[92] T. Akesson, B. Jönsson, *Mol. Phys. 54* (1985) 369.

[93] S. Kirkpatrick, C. D. Gelatti Jr., M. P. Vecchi, *Science (Washington D.C.) 220* (1983) 671.
[94] R. A. Donnelly, J. W. Rogers, Jr., *Int. J. Quantum Chem.: Quantum Chem. Symp. 22* (1988) 507.
[95] Z. Li, H. A. Scheraga, *Proc. Natl. Acad. Sci. USA 84* (1987) 6611.
[96] W. Braun, N. Go, *J. Mol. Biol. 186* (1985) 611.
[97] W. F. van Gunsteren, M. Karplus, *Biochemistry 21* (1982) 2259.
[98] G. L. Seibel, U. C. Singh, P. A. Kollman, *Proc. Natl. Acad. Sci. USA 82* (1985) 6537.
[99] K. Remerie, W. F. van Gunsteren, J. B. F. N. Engberts, *Chem. Phys. 101* (1986) 27.
[100] M. J. Mandell, *J. Stat. Phys. 15* (1976) 299.
[101] L. R. Pratt, S. W. Haan, *J. Chem. Phys. 74* (1981) 1864, 1873.
[102] S. Gupta, J. M. Haile, *Chem. Phys. 83* (1984) 481.
[103] D. J. Adams, *Chem. Phys. Lett. 62* (1979) 329.
[104] J. B. Gibson, A. N. Goland, M. Milgram, G. H. Vineyard, *Phys. Rev. 120* (1960) 1229.
[105] C. L. Brooks III, M. Karplus, *J. Chem. Phys. 79* (1983) 6312.
[106] A. T. Brünger, C. L. Brooks III, M. Karplus, *Chem. Phys. Lett. 105* (1984) 495.
[107] C. L. Brooks III, A. Brünger, M. Karplus, *Biopolymers 24* (1985) 843.
[108] A. T. Brünger, C. L. Brooks III, M. Karplus, *Proc. Natl. Acad. Sci. USA 82* (1985) 8458.
[109] W. G. Hoover, D. J. Evans, R. B. Hickman, A. J. C. Ladd, W. T. Ashurst, B. Moran, *Phys. Rev. A 22* (1980) 1690.
[110] D. J. Evans, *J. Chem. Phys. 78* (1983) 3297.
[111] J. M. Haile, S. Gupta, *J. Chem. Phys. 79* (1983) 3067.
[112] S. Nosé, *Mol. Phys. 52* (1984) 255.
[113] H. J. C. Berendsen, J. P. M. Postma, W. F. van Gunsteren, A. DiNola, J. R. Haak, *J. Chem. Phys. 81* (1984) 3684.
[114] H. C. Andersen, *J. Chem. Phys. 72* (1980) 2384.
[115] D. M. Heyes, *Chem. Phys. 82* (1983) 285.
[116] T. Schneider, E. Stoll, *Phys. Rev. B17* (1978) 1302; *ibid. B18* (1978) 6468.
[117] D. J. Evans, G. P. Morriss, *Chem. Phys. 77* (1983) 63; *Comput. Phys. Rep. 1* (1984) 297.
[118] J. M. Haile, H. W. Graben, *J. Chem. Phys. 73* (1980) 2421.
[119] M. Parrinello, A. Rahman, *Phys. Rev. Lett. 45* (1980) 1196; *J. Appl. Phys. 52* (1981) 7182; *J. Chem. Phys. 76* (1982) 2662.
[120] M. Parrinello, A. Rahman, P. Vashishta, *Phys. Rev. Lett 50* (1983) 1073.
[121] S. Nosé, M. L. Klein, *Mol. Phys. 50* (1983) 1055.
[122] W. H. Press, B. P. Flannery, S. A. Teukolsky, W. T. Vetterling: *Numerical Recipes*, Cambridge University Press, Cambridge, England 1986.
[123] C. W. Gear, *Numerical Initial Value Problems in Ordinary Differential Equations*, Prentice-Hall, Englewood Cliffs, NJ, USA 1971.
[124] L. Verlet, *Phys. Rev. 159* (1967) 98.
[125] D. Beeman, *J. Comput. Phys. 20* (1976) 130.
[126] W. F. van Gunsteren, H. J. C. Berendsen, *Mol. Phys. 34* (1977) 1311.
[127] H. J. C. Berendsen, W. F. van Gunsteren in G. Ciccotti, W. G. Hoover (Eds.): *Molecular-Dynamics Simulation of Statistical-Mechanics Systems*, North-Holland, Amsterdam 1986, p. 43.
[128] W. F. van Gunsteren, H. J. C. Berendsen, *Mol. Simulation 1* (1988) 173.
[129] G. Ciccotti, M. Ferrario, J.-P. Rijckaert, *Mol. Phys. 46* (1982) 875.
[130] F. J. Vesely, *Mol. Phys. 53* (1984) 505.
[131] H. J. C. Berendsen, W. F. van Gunsteren in J. W. Perram (Ed.): *The Physics of Superionic Conductors and Electrode Materials* (*NATO ASI Ser. B92* (1983)) 221.
[132] W. F. van Gunsteren, *Mol. Phys. 40* (1980) 1015.
[133] J. Barojas, D. Levesque, B. Quentrec, *Phys. Rev. A 7* (1973) 1092.
[134] P. S. Y. Cheung, *Chem. Phys. Lett. 40* (1976) 19.
[135] D. J. Evans, S. Murad, *Mol. Phys. 34* (1977) 327.
[136] M. Fixman, *J. Chem. Phys. 69* (1978) 1527.
[137] J. Wittenburg: *Dynamics of Systems of Rigid Bodies*, Teubner, Stuttgart 1977.
[138] J. P. Ryckaert, G. Ciccotti, H. J. C. Berendsen, *J. Comput. Phys. 23* (1977) 327.
[139] W. F. van Gunsteren, M. Karplus, *Macromolecules 15* (1982) 1528.
[140] G. Ciccotti, M. Ferrario, J. P. Ryckaert, *Mol. Phys. 47* (1982) 1253.
[141] W. F. van Gunsteren in W. F. van Gunsteren, P. K. Weiner (Eds.): *Computer Simulation of Biomolecular Systems*, Escom, Leiden 1989, p. 27.
[142] W. B. Street, D. J. Tildesley, G. Saville, *Mol. Phys. 35* (1978) 639.
[143] O. Teleman, B. Jönsson, *J. Comput. Chem. 7* (1986) 58.
[144] W. F. van Gunsteren, H. J. C. Berendsen, F. Colonna, D. Perahia, J. P. Hollenberg, D. Lellouch, *J. Comput. Chem. 5* (1984) 272.
[145] R. Boelens, R. M. Scheek, J. H. van Boom, R. Kaptein, *J. Mol. Biol. 193* (1987) 213.
[146] B. W. Matthews, *Nature (London) 335* (1988) 294.
[147] M. H. Caruthers, *Acc. Chem. Res. 13* (1980) 155.
[148] J. H. Miller, *J. Mol. Biol. 180* (1984) 205.
[149] H. Schindler, J. Seelig, *J. Chem. Phys. 59* (1973) 1841.
[150] R. Kaptein, R. Boelens, R. M. Scheek, W. F. van Gunsteren, *Biochemistry 27* (1988) 5389.
[151] W. F. van Gunsteren, R. Kaptein, E. R. P. Zuiderweg in W. K. Olson (Ed.): *Nucleic Acid Conformation and Dynamics* (*Rep. NATO/CECAM Workshop*) CECAM, Orsay 1984, p. 70.
[152] G. M. Clore, A. M. Gronenborn, *Protein Eng. 1* (1987) 275.
[153] J. Lautz, H. Kessler, J. M. Blaney, R. M. Scheek, W. F. van Gunsteren, *Int. J. Pept. Protein Res. 33* (1989) 281.
[154] M. Nilges, G. M. Clore, A. M. Gronenborn, *FEBS Lett. 239* (1988) 29.
[155] H. Kessler, C. Griesinger, J. Lautz, A. Müller, W. F. van Gunsteren, H. J. C. Berendsen, *J. Am. Chem. Soc. 110* (1988) 3393.
[156] A. E. Torda, R. M. Scheek, W. F. van Gunsteren, *Chem. Phys. Lett. 157* (1989) 289.
[157] A. T. Brünger, J. Kuriyan, M. Karplus, *Science (Washington D.C.) 235* (1987) 458.
[158] P. Gros, M. Fujinaga, A. Mattevi, F. M. D. Vellieux, W. F. van Gunsteren, W. G. J. Hol in J. Goodfellow, K. Henrick, R. Hubbard (Eds.): *Molecular Simulation and Protein Crystallography* (*Proc. Joint CCP4/CCP5 Study Weekend*) SERC, Daresbury 1989, p. 1.
[159] P. Gros, M. Fujinaga, B. W. Dijkstra, K. H. Kalk, W. G. J. Hol, *Acta Crystallogr. B45* (1989) 488.
[160] R. R. Bott, *World Biotech. Rep. 2* (1985) 51.
[161] W. F. van Gunsteren, H. J. C. Berendsen, *J. Mol. Biol. 176* (1984) 559.
[161] P. Krüger, W. Strassburger, A. Wollmer, W. F. van Gunsteren, *Eur. Biophys. J. 13* (1985) 77.
[163] J. E. H. Koehler, W. Saenger, W. F. van Gunsteren, *J. Mol. Biol. 203* (1988) 241.
[164] J. Lautz, H. Kessler, W. F. van Gunsteren, H. P. Weber, R. M. Wenger, *Biopolymers* (1990), in press.
[165] D. L. Beveridge, F. M. DiCapua, *Ann. Rev. Biophys. Biophys. Chem. 18* (1989) 431.
[166] D. A. Matthews, J. T. Bolin, J. M. Burridge, D. J. Filman, K. W. Volz, J. Kraut, *J. Biol. Chem. 260* (1985) 392.
[167] D. A. Matthews, J. T. Bolin, J. M. Burridge, D. J. Filman, K. W. Volz, B. T. Kaufman, C. R. Beddell, J. N. Champness, D. K. Stammers, J. Kraut, *J. Biol. Chem. 260* (1985) 381.
[168] B. Klar, B. Hingerty, W. Saenger, *Acta Crystallogr. B36* (1980) 1154.
[169] Z. Otwinowski, R. W. Schevitz, R. G. Zhang, C. L. Lawson, A. Joachimiak, R. Q. Marmorstein, B. F. Luisi, P. B. Sigler, *Nature (London) 335* (1988) 321.
[170] V. Vlachy, D. J. Haymet, *J. Chem. Phys. 84* (1986) 5874.
[171] J. Tallon, *Phys. Rev. Lett. 57* (1986) 2427.
[172] R. W. Impey, M. Sprik, M. L. Klein, *J. Chem. Phys. 83* (1985) 3638.
[173] F. F. Abraham, W. E. Rudge, D. J. Auerbach, S. W. Koch, *Phys. Rev. Lett. 52* (1984) 445.
[174] D. M. Heyes, M. Barber, J. H. R. Clarke, *Surf. Sci. 105* (1981) 225.
[175] V. Rossato, G. Ciccotti, V. Pontikis, *Phys. Rev. B33* (1986) 1860.
[176] U. Landman, W. D. Luedtke, R. N. Barnett, C. L. Cleveland, M. W. Ribarsky, E. Arnold, S. Ramesh, H. Baumgart, A. Martinez, B. Khan, *Phys. Rev. Lett. 56* (1986) 155.
[177] J. G. Powles, G. Rickayzen, *Mol. Phys. 38* (1979) 1875.
[178] W. G. Gibson, *Mol. Phys. 28* (1974) 793.
[179] P. H. Berens, D. H. J. Mackay, G. M. White, K. R. Wilson, *J. Chem. Phys. 79* (1983) 2375.
[180] B. J. Berne, G. D. Harp, *Adv. Chem. Phys. 17* (1970) 63.
[181] J. A. Barker, *J. Chem. Phys. 70* (1979) 2914.
[182] D. Chandler, P. G. Wolynes, *J. Chem. Phys. 74* (1981) 4078.
[183] B. de Raedt, M. Sprik, M. Klein, *J. Chem. Phys. 80* (1984) 5719.
[184] C. Zheng, J. A. McCammon, P. G. Wolynes, *Proc. Natl. Acad. Sci. USA 86* (1989) 6441.
[185] E. J. Heller, *J. Chem. Phys. 62* (1975) 1544 and *64* (1976) 63.
[186] N. Corbin, K. Singer, *Mol. Phys. 46* (1982) 671.
[187] K. Singer, W. Smith, *Mol. Phys. 57* (1986) 761.
[188] R. Carr, M. Parrinello, *Phys. Rev. Lett. 55* (1985) 2471.
[189] A. Selloni, P. Carnevali, R. Carr, M. Parrinello, *Phys. Rev. Lett. 59* (1987) 823.
[190] C. H. Bennett, *J. Comput. Phys. 19* (1975) 297.
[191] P. A. Bash, M. J. Field, M. Karplus, *J. Am. Chem. Soc. 109* (1987) 8092.
[192] J. H. R. Clarke, D. Brown, *J. Chem. Phys. 86* (1987) 1542.

Communications may be submitted in English *or* in German. Further details regarding the submission of communications can be found in the "Notice to Authors" reproduced in the January issue of the journal. Copies thereof may be obtained from the editorial office upon request.

Building Blocks for the Synthesis of Enantiomerically Pure Jasmonoids: Synthesis of (+)-Methyl Epijasmonate**

By *Günter Helmchen,* Andreas Goeke, Gilbert Lauer, Matthias Urmann*, and *Jürgen Fries*

Jasmonoids of type **1** (n = 1,3,5) and their reduction products are widespread in the plant world.[1a] The best-known compound is ester **1**, n = 1, X = OCH_3, a valued fragrance,[1b] found in jasmine and rosemary oil. This ester and the corresponding carboxylic acid (**1**, n = 1, X = OH) are endogenous growth regulators in plants.[1a]

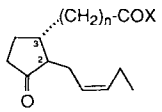

1

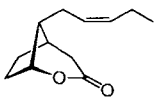

2

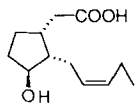

3

a: n = 1, X = OCH_3, 2,3 - *cis*

b: n = 1, X = OCH_3, 2,3 - *trans*

Recent investigations raised the question as to the relative configuration of the biologically active substances. Thus, *Acree* and *Nishida* et al. obtained the pure stereoisomers **1a,b** and their enantiomers by tedious separation procedures.[2] Only **1a** (methyl epijasmonate), which readily isomerizes to **1b** (methyl jasmonate), is fragrant.[2] The above-mentioned plant oils contain only 5% of **1a** together with **1b** (equilibrium mixture). Furthermore, **1a** acts as a pheromone, whereas **1b** is inactive.[3] Finally, cyclopentanes with *cis* configuration have been shown to be the biogenetic precursors of jasmonoids;[4] notably, this also holds true for all reduced compounds such as lactone **2**[5] and cucurbic acid (**3**),[6] neither of which can undergo epimerization at C-2. We have now developed a synthetic strategy that makes available large quantities of enantiomerically pure, structurally diverse *cis* jasmonoids in a stereoselective fashion. Although several syntheses of nonracemic compounds of the *trans* series are known,[7a] only two unselective syntheses of *rac*-**1a** have been described.[7b]

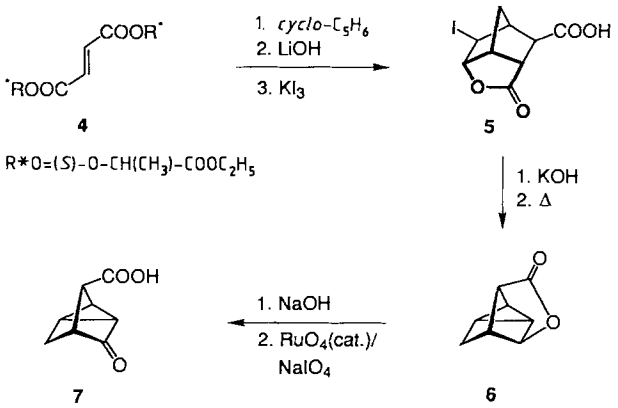

Our starting point is the asymmetric Diels–Alder reaction. Several years ago, we found that the uncatalyzed reactions of the fumarates of (*S*)-ethyl lactate and (*R*)-pantolactone proceed with high diastereoselectivity.[8] For example, ester **4**, readily available in kilogram quantities, and cyclopentadiene react with a diastereoselectivity of 98:2. The crude product is hydrolyzed with LiOH in THF/water to give the salt of 5-norbornene-2,3-dicarboxylic acid, which is then converted directly, without purification, into the iodolactone **5**. Recrystallization affords enantiomerically pure[9] **5** in 70–80% yield. Heating a solution of the dried K salt of **5** in dimethyl sulfoxide (DMSO) (9 h, 175 °C) gives lactone **6** in 84% yield. We assume that this new cyclization is a decarboxylative 1,3 elimination.

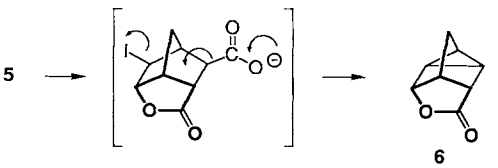

Conversion of **6** to the ketocarboxylic acid **7** [m.p. 123.5–124.5 °C, $[\alpha]_D^{20}$ = 95.5 (*c* = 3, 95% EtOH)] is accomplished in 91% yield by oxidation with RuO_4 (cat.)/$NaIO_4$.[10] In analogy to the C-7 epimer, a key intermediate in prostaglandin synthesis,[11] **7** can be selectively opened at the cyclopropane ring with mineral acids.[12] Heating with concentrated hydrogen iodide leads to 5-iodonorbornanecarboxylic acid (**8a**, 84%), which can be reduced with zinc (THF/KH_2PO_4 buffer) to give the ketocarboxylic acid **8b** (93%).

Whereas C-3 undergoes migration in norbornanones with *syn* (relative to the carbonyl group) halogen or alkyl substituents at position 7,[13] C-1 migrates when the carboxylic acid **8b** is treated with *m*-chloroperbenzoic acid (MCPBA)[14] or peracetic acid. Reaction of the resulting lactone **9** (83%) with oxalyl chloride followed by Rosenmund reduction and treatment of the resulting aldehyde with the phos-

[*] Prof. Dr. G. Helmchen, Dipl.-Chem. A. Goeke, Dipl.-Chem. G. Lauer, Dipl.-Chem. M. Urmann, Dipl.-Chem. J. Fries
Organisch-chemisches Institut der Universität
Im Neuenheimer Feld 270, D-6900 Heidelberg (FRG)

[**] This work was supported by the Deutsche Forschungsgemeinschaft and the Fonds der Chemischen Industrie. The results were presented at the 11th International Symposium Synthesis in Organic Chemistry (Oxford, June 26, 1989). We thank Dr. *J. Weetman* and *T. Lobreyer* for preliminary studies and Prof. *K. Weinges*, whose group independently carried out a synthesis of (+)-**1a**, for exchanging information.

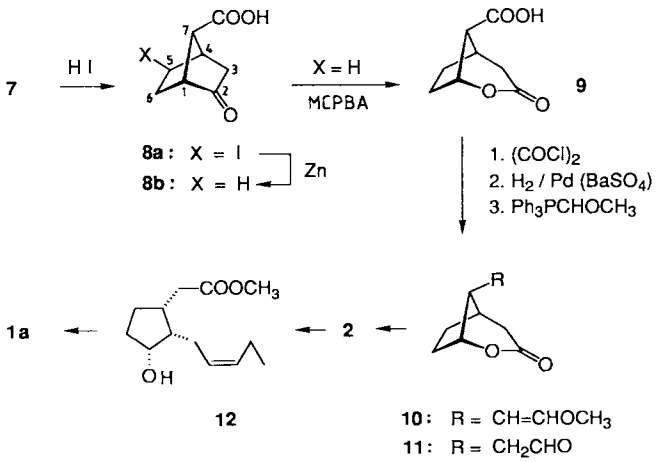

phorane PPh_3CHOCH_3 affords enol ether **10** (66%) as a *Z*/*E* mixture. Hydrolysis of **10** ($THF/H_2O/CH_3COOH$ 1:1:3) leads to aldehyde **11**. Reaction of unpurified **11** with propylidenetriphenylphosphorane in a "salt-free" Wittig reaction results in highly selective[15] formation of lactone **2**, $[\alpha]_D^{20} = -73.0$ ($c = 3.0$, $CHCl_3$),[16] in 72% yield.

Hydrolysis (NaOH) of **2** followed by esterification of the resulting hydroxy acid (CH_2N_2) gives ester **12** (95%). The absence of epimerization had to be ensured for both the oxidation of **12** to the target compound **1a** and the subsequent analysis. HPLC analysis using silica gel columns[17] proved suitable, but gas chromatography on capillary columns did not.[18] The best oxidation results were obtained with pyridinium dichromate in CH_2Cl_2 (**1a**:**1b** = 99.4:0.6, 70% yield). The optical rotation $[\alpha]_D^{20} = 57.3$ ($c = 2.5$, CH_3OH) of HPLC-pure **1a** agrees with the literature value.[2] Whereas a very intense, typical "jasmonate fragrance" is found for **1a**, HPLC-pure **1b** is odorless (cf. Ref. [7a]). The method described here allows methyl epijasmonate (**1a**) to be prepared on a multigram scale and thus makes it available for investigations in plant physiology. Furthermore, intermediates **8** and **11** are building blocks for the EPC synthesis of almost all jasmonoids (about 20 compounds).

Received: December 29, 1989 [Z 3711 IE]
German version: *Angew. Chem. 102* (1990) 1079

CAS Registry numbers:
1a, 95722-42-2; **2**, 54595-10-7; **4**, 111293-23-3; **5**, 128777-68-4; **6**, 6169-95-5; **7**, 128777-69-5; **8a**, 128777-70-8; **8b**, 60133-54-2; **9**, 128685-21-2; **10** (isomer 1), 128685-22-3; **10** (isomer 2), 128777-73-1; **11**, 128777-71-9; **12**, 128777-72-0; *cyclo*-C_5H_6, 542-92-7; $Ph_3PCHOMe$, 20763-19-3; propylidenetriphenylphosphorane, 16666-78-7.

[1] a) G. Sembdner, C. Klose, *Biol. Rundsch. 23* (1985) 29–40; b) E. Demole in E. T. Theimer (Ed.): *Fragrance Chemistry*, Academic, New York 1982, pp. 349–396.
[2] T. E. Acree, R. Nishida, H. Fukami, *J. Agric. Food Chem. 33* (1985) 425–427.
[3] T. C. Baker, R. Nishida, W. L. Roelofs, *Science (Washington D. C.) 214* (1981) 1359–1361.
[4] L. Crombie, K. M. Mistry, *J. Chem. Soc. Chem. Commun. 1988*, 539.
[5] This compound, called "δ-Jasmonsäurelacton" by its discoverers, was isolated from the oil of jasmine flowers: R. Kaiser, D. Lamparsky, *Tetrahedron Lett. 1974*, 3413–3416. However, this paper gives the formula of the enantiomer of **2** (presumably arbitrarily).
[6] H. Fukui, K. Koshimizu, Y. Yamazaki, S. Usuda, *Agric. Biol. Chem. 41* (1977) 189–194.
[7] a) *Synform 1* (1983) 33–63; *ibid. 3* (1985) 125–133; recent work: K. Weinges, H. Gethöffer, U. Huber-Patz, H. Rodewald, H. Irngartinger, *Liebigs Ann. Chem. 1987*, 361–366; F.-P. Montforts, I. Gesing-Zibulak, W. Grammenos, M. Schneider, K. Laumen, *Helv. Chim. Acta 72* (1989) 1852–1859 (these authors generated, via **2**, a 6:4 mixture of **1a** and **1b** and isomerized it to **1b**); b) H. Tanaka, S. Torii, *J. Org. Chem. 40* (1975) 462–465; T. Kitahara, K. Miura, Y. Warita, Y. Takagi, K. Mori, *Agric. Biol. Chem. 51* (1987) 1129–1133.
[8] H. Hartmann, A. F. Abdel Hady, K. Sartor, J. Weetman, G. Helmchen, *Angew. Chem. 99* (1987) 1188–1189; *Angew. Chem. Int. Ed. Engl. 26* (1987) 1143–1145.
[9] In order to determine the enantiomeric purity, **5** was treated with 1(1-naphthyl)ethylamine to give diastereomeric amides, which were analyzed by HPLC.
[10] R. M. Moriarty, C. C. Chien, T. B. Adams, *J. Org. Chem. 44* (1979) 2206–2210.
[11] a) N. R. A. Beeley, R. Peel, J. K. Sutherland, J. J. Holohan, K. B. Mallion, G. J. Sependa, *Tetrahedron 37 (Supplement No. 1)* (1981) 411–420; b) J. S. Bindra, A. Grodski, T. K. Schaaf, E. J. Corey, *J. Am. Chem. Soc. 95* (1973) 7522–7523.
[12] Analogous derivatives **8**, X = Cl, Br, OH, are also readily available in yields of about 80% by heating with aqueous mineral acids.
[13] G. R. Krow, *Tetrahedron 37* (1981) 2697–2724.
[14] Particularly good results were obtained with a "solid-phase variant": F. Toda, M. Yagi, K. Kiyoshige, *J. Chem. Soc. Chem. Commun. 1988* 958–959.
[15] A *Z*/*E* selectivity of ≥96:4 was achieved. Pure *Z* isomer, isolated by MPLC, was used in all further reactions.
[16] Ref. [5] gives a value of $[\alpha]_D^{20} = -47.4$ ($c = 0.775$, $CHCl_3$) for natural material of only 85% purity.
[17] 50-cm column, Merck silica gel 60, 5 μ; eluent, *n*-hexane/ethyl acetate 9:1; refractometer detector.
[18] Capillary columns, Hewlett Packard HP-5 (25 m) and HP-1 (5 m); temperature of injector, 220 and 180 °C, respectively; temperature of column, 120–180 and 80 °C, respectively.

Peptide Synthesis under High Pressure

By *Joachim Gante,* Ulrike Kalthof, Frank-Gerrit Klärner,** and *Thomas Weber*

Dedicated to Professor Wolfgang Kirmse on the occasion of his 60th birthday

A long-cherished wish of peptide chemists is to carry out peptide couplings with nonactivated amino acid alkyl esters as partners in the reaction **1** + **2** → **3** (Scheme 1). The advantages of this reaction would include a simplified procedure, more readily accessible and more inexpensive starting materials, and the easy removal of byproducts (volatile alcohols).

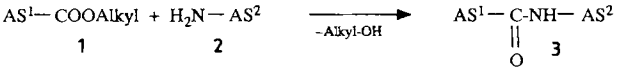

Scheme 1. AS^1, AS^2 = amino acid residues.

Up to now, a practical procedure of this kind could not be developed owing to the low degree of activation of the alkyl esters.[1] Only the addition of large amounts of activating substances—like imidazole as solvent (80 °C!)[2] or complex-forming metal salts[3, 4]—has made possible such a reaction, which requires considerable preparative work.

We have now found a solution to this problem by the use of high pressure (10-kbar range). High pressure has already proved useful in many areas of organic chemistry and has allowed reactions that, under normal conditions, can be carried out only inadequately or not at all.[5] The preparation of

[*] Priv.-Doz. Dr. J. Gante, T. Weber
E. Merck, Pharmaforschung
Frankfurter Strasse 250, D-6100 Darmstadt (FRG)
Prof. Dr. F.-G. Klärner, Dipl.-Chem. U. Kalthof
Fakultät für Chemie der Universität
Postfach 10 21 48, D-4630 Bochum 1 (FRG)

[**] This work was supported by the Deutsche Forschungsgemeinschaft and the Fonds der Chemischen Industrie.

peptides in this way has not yet been described. The only example of a powerful pressure-induced enhancement of the rate and yield of a reaction known to us in amino acid chemistry deals with the reaction of *N*-protected amino acid hydroxysuccinimide esters (that is, "conventionally" activated esters) with poorly reactive imino bis(carboxylic esters) at 10 kbar.[6]

Reaction of various *N*-protected L-amino acid methyl esters **4** with L-amino acid Na salts **5** in methanol[7] at room

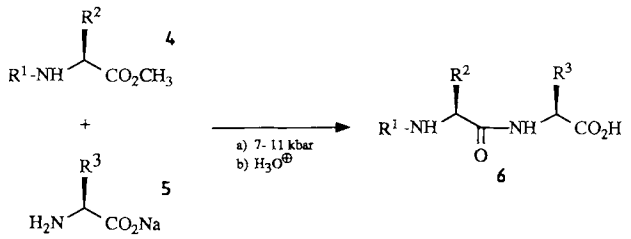

temperature and a pressure of 7–11 kbar leads to formation of the corresponding dipeptide derivatives **6** with loss of methanol (Table 1).

Table 1. High-pressure synthesis of dipeptide derivatives **6** from protected amino acid methyl esters **4** at room temperature.

6	R^1	R^2	R^3	Reaction time [h]	Pressure [kbar]	Yield [%]	M.p. [°C]	$[\alpha]_D^{20}$ ($c = 1$, MeOH)
a	Ph-CO	CH_3	H	17	10	64	178–180	−6.7
b	Ph-CO	CH_3	CH_3	66	10.5	76	201	−13.0
c	Boc[a]	Ph-CH_2	H	66	7	42	158	−4.3
d	Z[b]	Ph-CH_2	CH_3	19	10.6	47	174	−7.3

[a] Boc = *t*Bu-O-CO. [b] Z = Ph-CH_2-O-CO.

The reaction of the methyl esters is also feasible with other amino acid derivatives, as shown by the 1:1 reaction of **4d** with H-Gly-NH_2 (7) to give the protected dipeptide derivative **8** (m.p. 123–124 °C, $[\alpha]_D^{20} = -3.2$ ($c = 1$, MeOH)).

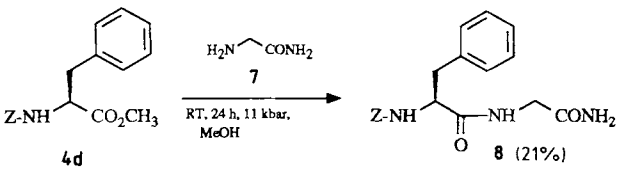

^{1}H NMR and GC analysis of peptides **6a–d**[8] established that, for the benzoylated derivatives **6a** and **6b**, 5 to 8% racemization occurred in the ester-derived component during coupling (corresponding to the tendency also observed in conventional coupling methods), whereas the carbamate-protected products **6c**, **6d**, and **8** were formed without detectable racemization.

The high-pressure method described here thus allows peptide coupling between *N*-terminal-protected amino acid methyl esters and simple amino acid derivatives. The use of amino acid Na salts **5** as "amine component" is a further advantage of the method, since this obviates the additional steps (esterification, saponification) required in the usual techniques involving ester protecting groups.[9]

General Experimental Procedure

A solution of 1.0 mol each of **4** and **5** in 10 mL of dry MeOH was compressed in a sealed polytetrafluoroethylene (PTFE) shrinkage tube according to the conditions given in Table 1[10]. The solution was then evaporated and the residue dissolved in 10 mL of water. The resulting solution was extracted with ethyl acetate, the aqueous phase was acidified to pH ≈ 1 with diluted hydrochloric acid very carefully (since the Boc group is acid labile), and the product **6** was extracted with ethyl acetate. After drying over Na_2SO_4, the organic extract was evaporated and/or petroleum ether was added to give **6** in pure form. The reaction times and yields given in Table 1 are not optimized.

Received: April 12, 1990 [Z 3910 IE]
German version: *Angew. Chem. 102* (1990) 1081

CAS Registry numbers:
4a, 7244-67-9; **4c**, 51987-73-6; **4d**, 35909-92-3; **5** (R^3 = H), 6000-44-8; **5** (R^3 = CH_3), 16480-55-0; **6a**, 71485-48-8; **6b**, 71448-05-0; **6c**, 25616-33-5; **6d**, 21881-18-5; **8**, 598-41-4; **9**, 17187-05-2.

[1] G. Wendlberger, *Methoden Org. Chem. (Houben-Weyl) 4th Ed., Vol. XV/2 1974*, p. 3.
[2] T. Wieland, K. Vogeler, *Justus Liebigs Ann. Chem. 680* (1964) 125–132.
[3] M. Wagatsuma, S. Terashima, S. Yamada, *Chem. Pharm. Bull. 21* (1973) 422–427.
[4] C. R. Clark, R. F. Tasker, D. A. Buckingham, D. R. Knighton, D. R. K. Harding, W. S. Hancock, *J. Am. Chem. Soc. 103* (1981) 7023–7025; D. R. Knighton, D. R. K. Harding, M. J. Friar, W. S. Hancock, G. D. Reynolds, C. R. Clark, R. F. Tasker, D. A. Buckingham, *ibid. 103* (1981) 7025–7026.
[5] Reviews: F. G. Klärner, *Chem. Unserer Zeit 23* (1989) 53–63; R. van Eldik, T. Asano, W. J. le Noble, *Chem. Rev. 89* (1989) 549.
[6] T. Yamada, Y. Manabe, T. Miyazawa, S. Kuwata, A. Sera, *J. Chem. Soc. Chem. Commun. 1984*, 1500–1501.
[7] Working under water-free conditions avoids saponification of the ester.
[8] Diastereomer determination by ^{1}H NMR spectroscopy as well as by gas chromatography on ChirasilVal® (see H. Frank, G. J. Nicholson, E. Bayer, *J. Chromatogr. 167* (1978) 187–196).
[9] Up to now, amino acid Na salts could be used as coupling components only for a few "conventionally" activated esters, see K.-H. Deimer, *Methoden Org. Chem. (Houben-Weyl) 4th Ed., Vol. XV/1 1974*, p. 405.
[10] The pressure experiments were carried out in a 14-kbar apparatus (autoclave volumes 36 mL) built by *A. W. Birks*, Department of Medicinal and Manufacturing Engineering, Queen's University of Belfast, Northern Ireland.

How Do Two C–C Double Bonds Add to One M–M Triple Bond? Structure and Bonding in Bis(η^2-ethylene)hexakis(neopentoxy)ditungsten **

By *Roger H. Cayton, Stephanie T. Chacon, Malcolm H. Chisholm,** and *John C. Huffman*

Dedicated to Professor F. A. Cotton on the occasion of his 60th birthday

The symmetry rules that are so powerful in predicting forbidden reactions in organic chemistry[1] are not as straightforward in inorganic and organometallic chemistry. Thus, [2+2] cycloaddition reactions may be thermally allowed in certain instances. For example, the reversible coupling of two $[W_2(O\mathit{i}Pr)_6]$ to give $[W_4(O\mathit{i}Pr)_{12}]$ occurs with an enthalpy of activation of 10 kcal mol^{-1} and is predicted by a theoretical analysis to be a symmetry-allowed $[\pi_s^2 + \pi_s^2]$ cycloaddition reaction.[2] *Norton* et al.[3] have observed the facile reversible elimination of ethylene from $[Os_2(CO)_8(\mu\text{-}\eta^1\text{:}\eta^1\text{-}C_2H_4)]$ and shown that the stereochemistry at carbon is maintained during this *formal* [2+2] addition/elimination reaction involving C–C and Os–Os double bonds and a 1,2-

[*] Prof. M. H. Chisholm, Dr. R. H. Cayton, Dr. J. C. Huffman, S. T. Chacon
Department of Chemistry and Molecular Structure Center
Indiana University
Bloomington, IN 47405 (USA)

[**] This work was supported by the Department of Energy, Office of Basic Sciences, Chemistry Division, and the National Science Foundation.

diosmacyclobutane. In our studies of the reactions of $[W_2(OR)_6]$ with ethylene we have observed facile ($T < 22$ °C, $p < 1$ bar) C–C bond formation and subsequent C–H activation [Eq. (a)].[4]

$$[W_2(OR)_6] + 3C_2H_4 \longrightarrow [W_2(OR)_6(\mu\text{-}CCH_2CH_2CH_2)] + C_2H_6 \qquad (a)$$

In the specific reaction between $[W_2(OCH_2tBu)_6]$ and ethylene we observed an *initial* reversible equilibrium involving a bisethylene adduct, $[W_2(OCH_2tBu)_6(\eta^2\text{-}C_2H_4)_2]$ (**1**). From considerations of the ^1H and ^{13}C NMR data, we proposed one of two structures for the $W_2O_6(C_2)_2$ skeleton of **1** (Fig. 1), either **I** or **II**.[5] We have now determined the structure in the solid state[6] and find that, contrary to our predictions, **1** adopts the unprecedented structure **III** (Scheme 1).

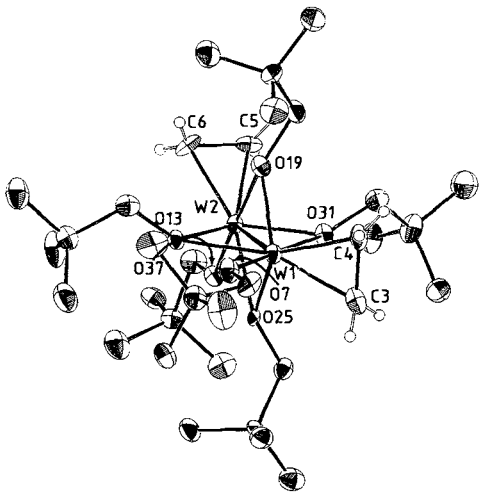

Fig. 1. ORTEP drawing of **1** emphasizing the presence of the four alkoxide bridges and the relative orientation of the ethylene ligands. Important distances [Å]: W-W 2.5331(9), W1-O7 1.89(1), W1-O13 2.28(1), W1-O19 2.00(1), W1-O25 2.31(1), W1-C3 2.13(1), W1-C4 2.14(1), W2-O13 1.98(1), W2-O19 2.32(1), W2-O25 2.32(1), W2-O31 2.00(1), W2-O37 1.88(1), W2-C5 2.15(1), W2-C6 2.15(1), C3-C4 1.45(2), C5-C6 1.45(2).

Complex **1** has a virtual but not crystallographically imposed C_2 axis of symmetry and thus the NMR data obtained in solution (previously reported[4]) are consistent with the solid-state structure. Note that all the methylene protons of the OCH_2tBu ligands are diastereotopic and all four ethylene protons are inequivalent. The W–C and C–C distances associated with the $W(\eta^2\text{-}C_2H_4)$ structural unit imply extensive $W(d_\pi)$-to-$C_2(\pi^*)$ bonding and conform to the metallacyclopropane valence bond description for a coordinated ethylene. The W–W distance (2.533(1) Å) is notably longer than that in $[W_2(OR)_6]$ compounds[7] (ca. 2.30 Å, average), implying that $W(d_\pi)$-to-$C_2(\pi^*)$ bonding has occurred at the expense of $W(d_\pi)$-$W(d_\pi)$ bonding. It is, however, the presence of the four bridging ligands and the specific orientation of the terminal ligands that require most attention. Note, too, the gross asymmetry in the W–O distances to the bridging OR ligands. Each tungsten has two short (2.00(1) Å, average) and two long (2.31(1) Å average) W–O bonds. If the ethylene is considered as a monodentate ligand, the structure of **1** bears a resemblance to the $S_2V(\mu\text{-}S)_4VS_2$ skeleton seen in $[V_2(edt)_4]^{2\ominus}$ (edt = ethylenedithiolate), though the latter has more symmetrical V–μ-S bridges.[8–10]

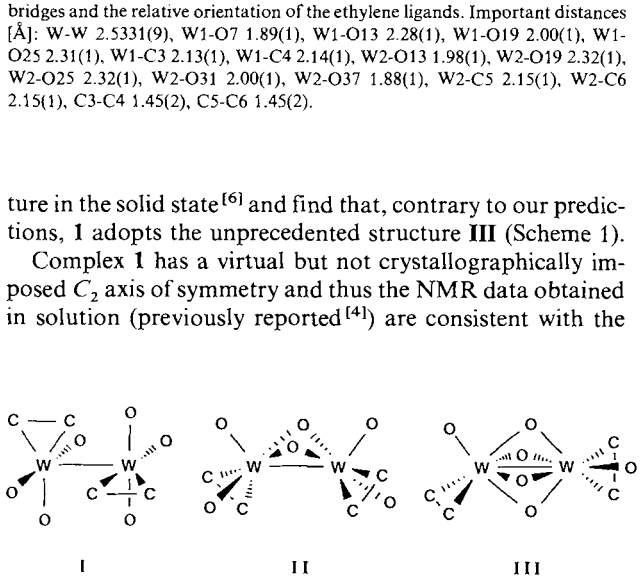

Scheme 1. Possible structures for **1**.

The bonding in **1** can be most easily understood by a Hoffmann frontier molecular orbital approach.[11] Two pseudotetrahedral d^3-$W(OR)_3(C_2H_4)$ fragments are brought together in the manner shown in Scheme 2. As the W–OR bridges are formed, the long W–O bridging distances are *trans* to the terminal OR and η^2-C_2H_4 ligands. The d-orbital splitting for a tetrahedral ML_4 fragment is t_2 above e. Replacement of one L by the single-faced π-acceptor ligand C_2H_4 to give a d^3-$ML_3(C_2H_4)$ fragment will remove the degeneracy of the e orbitals, since one is stabilized by $W(d_\pi)$-to-$C_2(\pi^*)$ bonding. If the d_{z^2} orbital is not allowed to interact with the ethylene, it will be available for M–M bonding (Scheme 2).

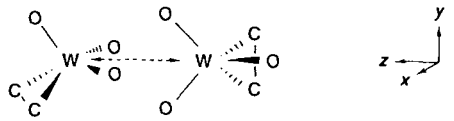

Scheme 2. Formation of **1** from two d^3-$W(OR)_3(C_2H_4)$ fragments.

We have carried out Fenske–Hall MO calculations[12] on the model compound $[W_2(OH)_6(\eta^2\text{-}C_2H_4)_2]$ with metric

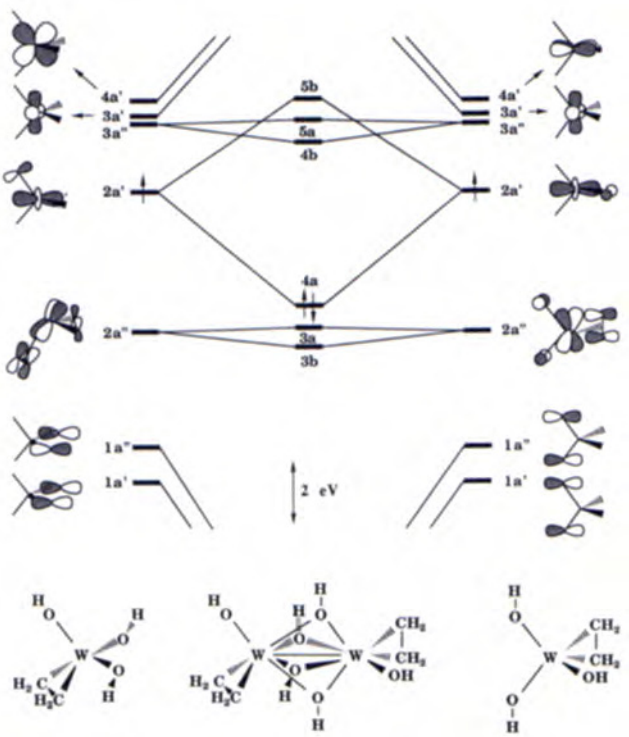

Fig. 2. Frontier molecular orbital diagram for $[W_2(OH)_6(\eta^2\text{-}C_2H_4)_2]$ viewed as the sum of two pseudotetrahedral d^3-$W(OH)_3(C_2H_4)$ fragments (see Scheme 2).

parameters taken from the observed structure of **1**. Although there is additional π bonding involving $W(d_\pi)$ and $O(p_\pi)$ orbitals, the essential features of the bonding are as anticipated from the above considerations. The frontier molecular orbitals are shown in Figure 2. The HOMO is the W–W σ bond formed from the d_z^2–d_z^2 interaction. The M–M δ and δ* orbitals (3a and 3b) are lower in energy and filled, but these orbitals have in reality little M–M bonding character, being essentially localized $M(d_\pi)$-to-$C_2(\pi^*)$ orbitals. The electronic barrier to olefin rotation and the specific orientation of the ethylene ligands arise because M–M and $M(d_\pi)$-to-$C_2(\pi^*)$ bonding compete for use of d_z^2 and d_{xy} orbitals (with the axes shown in Scheme 2).

The relative instability and kinetic lability of a monoethylene intermediate in the reversible reaction between $[W_2(OR)_6]$ and ethylene can also be understood in terms of the competitive nature of M–M d_π–d_π and $M(d_\pi) \rightarrow C_2(\pi^*)$ bonding. Addition of ethylene to one tungsten center effectively activates the other tungsten center by generating a $W(d_\pi)$ electron pair that is poised for uptake of the second ethylene. Schematically, this is shown in Equation (b). Loss of one ethylene from **1** triggers the reverse reaction in

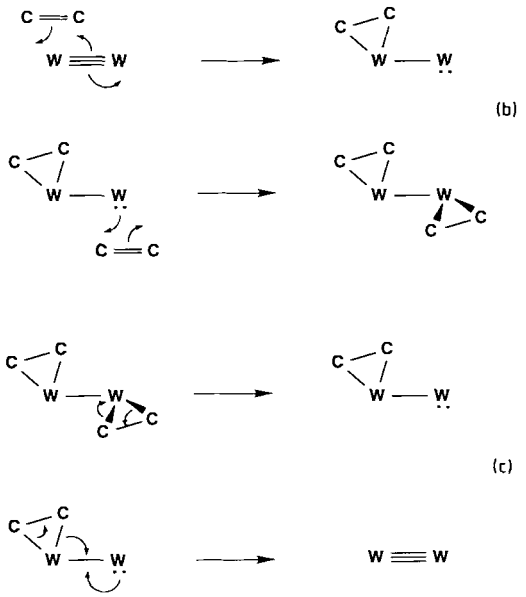

which M–M and C–C π bonds are reformed as shown in Equation (c).

Received: March 9, 1990 [Z 3810 IE]
German version: *Angew. Chem. 102* (1990) 1056

[1] R. B. Woodward, R. Hoffmann, *Angew. Chem. 81* (1969) 797; *Angew. Chem. Int. Ed. Engl. 8* (1969) 781.
[2] M. H. Chisholm, D. L. Clark, M. J. Hampden-Smith, *J. Am. Chem. Soc. 111* (1989) 574.
[3] R. J. Hembre, C. P. Scott, J. R. Norton, *J. Am. Chem. Soc. 109* (1987) 3468.
[4] M. H. Chisholm, J. C. Huffman, M. J. Hampden-Smith, *J. Am. Chem. Soc. 111* (1989) 5284.
[5] M. H. Chisholm and M. J. Hampden-Smith, *Angew. Chem. 99* (1987) 936; *Angew. Chem. Int. Ed. Engl. 26* (1987) 903.
[6] Crystal data for **1** at −155 °C: $a = 11.754(4)$, $b = 21.405(14)$, $c = 11.274(4)$ Å, $\beta = 104.96(2)°$, $Z = 4$, $\varrho_{calcd} = 1.564\ g\,cm^{-3}$, space group $P2_1/c$. Of 5494 reflections collected ($Mo_{K\alpha}$, $6° < \theta < 45°$), 5274 were unique and the 4412 with $F > 2.33\sigma(F)$ were used in the least-squares refinement leading to $R(F) = 0.043$ and $R_w(F) = 0.042$. All hydrogen atoms were refined isotropically and all other atoms anisotropically. Further details of the crystal structure investigation may be obtained from the Fachinformationszentrum Karlsruhe, Gesellschaft für wissenschaftlich-technische Information mbH, D-7514 Eggenstein-Leopoldshafen 2 (FRG), on quoting the depository number CSD-54518, the names of the authors, and the journal citation.
[7] M. H. Chisholm, *Angew. Chem. 99* (1987) 25; *Angew. Chem. Int. Ed. Engl. 26* (1987) 25.
[8] J. R. Dorfman, R. H. Holm, *Inorg. Chem.22* (1983) 3179; C. P. Rao, J. R. Dorfman, R. H. Holm, *ibid. 25* (1986) 428.
[9] R. W. Wiggins, J. C. Huffman, G. Christou, *J. Chem. Soc. Chem. Commun. 1983*, 1313.
[10] D. Szeymies, B. Krebs, G. Henkel, *Angew. Chem. 95* (1983) 903; *Angew. Chem. Int. Ed. Engl. 22* (1983) 885.
[11] R. Hoffmann, *Angew. Chem. 94* (1982) 725; *Angew. Chem. Int. Ed. Engl. 21* (1982) 711.
[12] M. B. Hall, R. Fenske, *Inorg. Chem. 11* (1972) 768.

Perchlorinated and Highly Chlorinated *meso*-Tetraphenylporphyrins **

By *Tilak Wijesekera, Akiteru Matsumoto, David Dolphin,** and *Doris Lexa*

meso-Tetraphenylporphyrins (TPPs) are widely used to study metalloporphyrin chemistry because they are usually readily prepared by simple synthetic sequences. However, since their phenyl and porphyrin rings are sterically constrained to lie essentially perpendicular to each other, the electronic effects of substituted phenyl rings can only be inductively transmitted to the porphyrin ring. Thus, the redox potentials (for the one-electron reduction of the porphyrin ring) for a diverse group of phenyl-substituted TPPs vary by only 130 mV.[1] The effect on a coordinated metal is even less. When directly substituted on the porphyrin ring itself, however, electron-withdrawing groups can have a more pronounced effect on the porphyrin redox chemistry. Indeed, with β-tetracyano-*meso*-tetraphenylporphyrin[2] and *meso*-tetranitro-β-octaethylporphyrin,[3] the anodic shifts resulting from substitution are almost 1 V. In order to expand the versatility of the tetraphenylporphyrins, we have examined β-chlorination reactions and report here on the synthesis and electrochemistry of the iron complexes of TPP and phenyl-ring-chlorinated TPPs.

Although β-polybromination of *meso*-tetraphenylporphyrin derivatives has been successfully accomplished using *N*-bromosuccinimide,[4, 5] the analogous chlorinations using *N*-chlorosuccinimide produced mainly the monosubstituted product.[6] Our attempts to polychlorinate *meso*-tetra(2,6-dichlorophenyl)porphyrin[7] (Cl_8TPPH_2) or its Zn^{II} or Fe^{III} complexes using excess *N*-chlorosuccinimide failed, the starting material being recovered even after heating for 5 h at 140 °C. However, in the presence of anhydrous $FeCl_3$, the Fe^{III} complex **3** in *o*-dichlorobenzene underwent facile perchlorination of the porphyrin ring when treated with chlorine gas. The reaction mixture was maintained at 140 °C following an initial slow bubbling of Cl_2 gas for 5 min and

[*] Prof. D. Dolphin, Dr. T. Wijesekera, Dr. A. Matsumoto
Department of Chemistry, University of British Columbia
2036 Main Mall, Vancouver, B. C., V6T 1Y6 (Canada)
Dr. D. Lexa
Laboratoire D'Electrochimie, Université de Paris 7
2, place Jussieu, F-75230 Paris 05 (France)

[**] This work was supported by the Canadian Natural Scienes and Engineering Research Council, the U. S. National Institutes of Health (DK 17989), and the French C. N. R. S.

parameters taken from the observed structure of **1**. Although there is additional π bonding involving $W(d_\pi)$ and $O(p_\pi)$ orbitals, the essential features of the bonding are as anticipated from the above considerations. The frontier molecular orbitals are shown in Figure 2. The HOMO is the W–W σ bond formed from the d_z^2–d_z^2 interaction. The M–M δ and δ* orbitals (3a and 3b) are lower in energy and filled, but these orbitals have in reality little M–M bonding character, being essentially localized $M(d_\pi)$-to-$C_2(\pi^*)$ orbitals. The electronic barrier to olefin rotation and the specific orientation of the ethylene ligands arise because M–M and $M(d_\pi)$-to-$C_2(\pi^*)$ bonding compete for use of d_z^2 and d_{xy} orbitals (with the axes shown in Scheme 2).

The relative instability and kinetic lability of a monoethylene intermediate in the reversible reaction between $[W_2(OR)_6]$ and ethylene can also be understood in terms of the competitive nature of M–M d_π–d_π and $M(d_\pi) \rightarrow C_2(\pi^*)$ bonding. Addition of ethylene to one tungsten center effectively activates the other tungsten center by generating a $W(d_\pi)$ electron pair that is poised for uptake of the second ethylene. Schematically, this is shown in Equation (b). Loss of one ethylene from **1** triggers the reverse reaction in

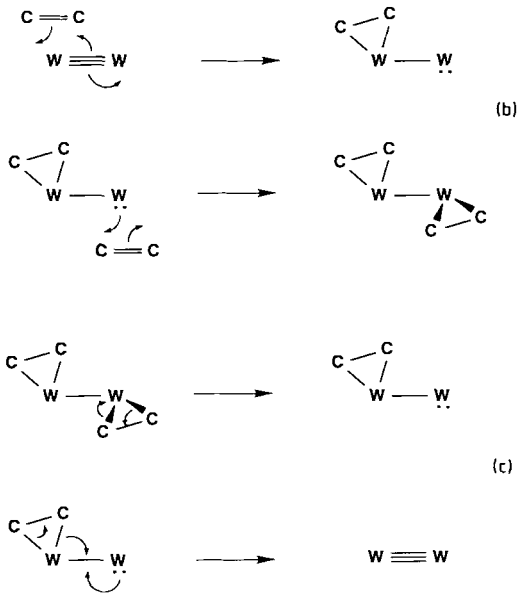

which M–M and C–C π bonds are reformed as shown in Equation (c).

Received: March 9, 1990 [Z 3810 IE]
German version: *Angew. Chem. 102* (1990) 1056

[1] R. B. Woodward, R. Hoffmann, *Angew. Chem. 81* (1969) 797; *Angew. Chem. Int. Ed. Engl. 8* (1969) 781.
[2] M. H. Chisholm, D. L. Clark, M. J. Hampden-Smith, *J. Am. Chem. Soc. 111* (1989) 574.
[3] R. J. Hembre, C. P. Scott, J. R. Norton, *J. Am. Chem. Soc. 109* (1987) 3468.
[4] M. H. Chisholm, J. C. Huffman, M. J. Hampden-Smith, *J. Am. Chem. Soc. 111* (1989) 5284.
[5] M. H. Chisholm and M. J. Hampden-Smith, *Angew. Chem. 99* (1987) 936; *Angew. Chem. Int. Ed. Engl. 26* (1987) 903.
[6] Crystal data for **1** at −155 °C: $a = 11.754(4)$, $b = 21.405(14)$, $c = 11.274(4)$ Å, $\beta = 104.96(2)°$, $Z = 4$, $\varrho_{calcd} = 1.564\ g\,cm^{-3}$, space group $P2_1/c$. Of 5494 reflections collected ($Mo_{K\alpha}$, $6° < \theta < 45°$), 5274 were unique and the 4412 with $F > 2.33\sigma(F)$ were used in the least-squares refinement leading to $R(F) = 0.043$ and $R_w(F) = 0.042$. All hydrogen atoms were refined isotropically and all other atoms anisotropically. Further details of the crystal structure investigation may be obtained from the Fachinformationszentrum Karlsruhe, Gesellschaft für wissenschaftlich-technische Information mbH, D-7514 Eggenstein-Leopoldshafen 2 (FRG), on quoting the depository number CSD-54518, the names of the authors, and the journal citation.
[7] M. H. Chisholm, *Angew. Chem. 99* (1987) 25; *Angew. Chem. Int. Ed. Engl. 26* (1987) 25.
[8] J. R. Dorfman, R. H. Holm, *Inorg. Chem.22* (1983) 3179; C. P. Rao, J. R. Dorfman, R. H. Holm, *ibid. 25* (1986) 428.
[9] R. W. Wiggins, J. C. Huffman, G. Christou, *J. Chem. Soc. Chem. Commun. 1983*, 1313.
[10] D. Szeymies, B. Krebs, G. Henkel, *Angew. Chem. 95* (1983) 903; *Angew. Chem. Int. Ed. Engl. 22* (1983) 885.
[11] R. Hoffmann, *Angew. Chem. 94* (1982) 725; *Angew. Chem. Int. Ed. Engl. 21* (1982) 711.
[12] M. B. Hall, R. Fenske, *Inorg. Chem. 11* (1972) 768.

Perchlorinated and Highly Chlorinated *meso*-Tetraphenylporphyrins **

By *Tilak Wijesekera, Akiteru Matsumoto, David Dolphin,** and *Doris Lexa*

meso-Tetraphenylporphyrins (TPPs) are widely used to study metalloporphyrin chemistry because they are usually readily prepared by simple synthetic sequences. However, since their phenyl and porphyrin rings are sterically constrained to lie essentially perpendicular to each other, the electronic effects of substituted phenyl rings can only be inductively transmitted to the porphyrin ring. Thus, the redox potentials (for the one-electron reduction of the porphyrin ring) for a diverse group of phenyl-substituted TPPs vary by only 130 mV.[1] The effect on a coordinated metal is even less. When directly substituted on the porphyrin ring itself, however, electron-withdrawing groups can have a more pronounced effect on the porphyrin redox chemistry. Indeed, with β-tetracyano-*meso*-tetraphenylporphyrin[2] and *meso*-tetranitro-β-octaethylporphyrin,[3] the anodic shifts resulting from substitution are almost 1 V. In order to expand the versatility of the tetraphenylporphyrins, we have examined β-chlorination reactions and report here on the synthesis and electrochemistry of the iron complexes of TPP and phenyl-ring-chlorinated TPPs.

Although β-polybromination of *meso*-tetraphenylporphyrin derivatives has been successfully accomplished using *N*-bromosuccinimide,[4, 5] the analogous chlorinations using *N*-chlorosuccinimide produced mainly the monosubstituted product.[6] Our attempts to polychlorinate *meso*-tetra(2,6-dichlorophenyl)porphyrin[7] (Cl_8TPPH_2) or its Zn^{II} or Fe^{III} complexes using excess *N*-chlorosuccinimide failed, the starting material being recovered even after heating for 5 h at 140 °C. However, in the presence of anhydrous $FeCl_3$, the Fe^{III} complex **3** in *o*-dichlorobenzene underwent facile perchlorination of the porphyrin ring when treated with chlorine gas. The reaction mixture was maintained at 140 °C following an initial slow bubbling of Cl_2 gas for 5 min and

[*] Prof. D. Dolphin, Dr. T. Wijesekera, Dr. A. Matsumoto
Department of Chemistry, University of British Columbia
2036 Main Mall, Vancouver, B. C., V6T 1Y6 (Canada)
Dr. D. Lexa
Laboratoire D'Electrochimie, Université de Paris 7
2, place Jussieu, F-75230 Paris 05 (France)

[**] This work was supported by the Canadian Natural Scienes and Engineering Research Council, the U. S. National Institutes of Health (DK 17989), and the French C. N. R. S.

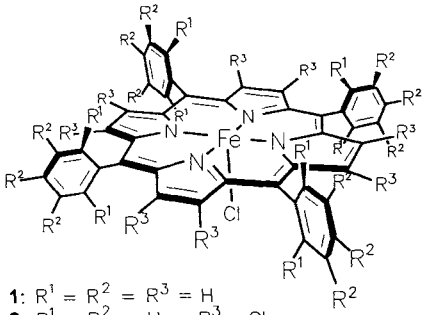

1: $R^1 = R^2 = R^3 = H$
2: $R^1 = R^2 = H$, $R^3 = Cl$
3: $R^1 = Cl$, $R^2 = R^3 = H$
4: $R^1 = R^3 = Cl$, $R^2 = H$
5: $R^1 = R^2 = Cl$, $R^3 = H$
6: $R^1 = R^2 = R^3 = Cl$

Fig. 1. *meso*-Tetraphenylporphyrin (**1**) and chlorinated porphyrins **2**–**6**.

the progress of the reaction was monitored by UV spectroscopy (Soret shifts from 420 to 442 nm in approximately 30 min). The product (**4**)[8] was isolated in 85% yield after chromatography and recrystallization.

meso-Tetra(pentachlorophenyl)porphinatoiron(III) chloride[7] (**5**) was chlorinated under the conditions described above to give perchloro-TPP (**6**) in 70% yield. However, attempted chlorination of the unsubstituted hemin, **1**, with $Cl_2/FeCl_3$ resulted in destruction of the macrocycle. When *N*-chlorosuccinimide was used as the chlorinating agent, the hemin as well as the free-base porphyrin $TPPH_2$ could only be partially chlorinated prior to decomposition. The Ni^{II} complex (TPPNi), on the other hand, reacted with 10–12 equivalents of *N*-chlorosuccinimide in *o*-dichlorobenzene (140 °C) to give *meso*-tetraphenyl-β-octachloroporphinatonickel(II) (β-Cl_8TPPNi), isolated in 75% yield. Demetalation with concentrated H_2SO_4 gave the free-base porphyrin β-Cl_8TPPH_2 (90%), which was converted into the corresponding hemin (**2**) in 85% yield by the standard $FeCl_2$/DMF procedure.[9] Attempted chlorination of Zn- or CuTPP gave several products including ring-opened materials, indicating that the centrally coordinated metal exerts an influence on peripheral electrophilic substitution.[10]

Three successive reductions and two oxidations were observed for the porphyrin chloroiron(III) complexes. In order to determine the effect of the counterion on the redox potential,[11] $E_{1/2}$ measurements were also carried out in the presence of $AgClO_4$ ($Cl^\ominus$ removed as AgCl). In general, the electron-withdrawing chloro substituent produced anodic shifts of potentials, but the effect was more pronounced for pyrrolic substitution (Table 1). For the first reduction of **3** (reversible wave obtained with added $Cl^\ominus$), the positive shift of $E_{1/2}$ compared with that for **1** was marginal, whereas for **2** the corresponding shift was 0.41 V. A shift of similar magnitude was also observed when comparing **3** with **4**, but the largest change (0.64 V) from that of **1** was observed for the perchloro system **6**.

The second reduction of the chloroiron(III) complexes of β-octachlorinated porphyrins **2**, **4**, and **6** produced reversible waves only when the counterion was removed with $AgClO_4$. Observed shifts of $E_{1/2}$ due to β-octachlorination (0.45 V for E_{2-1} and 0.47 V for E_{4-3}) were comparable with that reported for the corresponding redox couple of the tetracyano derivative β-$(CN)_4$TPPFe[12] ($\Delta E = 0.51$ V) but significantly higher than the value reported for the β-tetrabromo analogue β-Br_4TPPFe[13] ($\Delta E = 0.174$ V). As shown in Table 1, addition of $Ag^\oplus$ made no change in the $E_{1/2}$ values for the third reduction, suggesting that in no case is the [Fe-TPP]$^\ominus$

Table 2. Physical data for the iron complexes in PhCN.

Compound	$K_A(M^{-1})$ [15]	Soret bands λ_{max} [nm] ($\varepsilon \times 10^{-5}$)	Visible bands λ_{max} [nm] ($\varepsilon \times 10^{-3}$)
$TPPFe^{II}Cl$	1.8×10^2 [16]	444(1.7)	530(3.2), 571(7.5), 612(6.5)
$TPPFe^{III}Cl$		419(0.99)	510(12), 573(0.37), 656(0.28), 692(3.2)
$Cl_8TPPFe^{II}PF_6$ [a]		412(sh), 431(2.7)	534(19.5), 568(sh)
$Cl_8TPPFe^{II}Cl$	4.0	424(sh), 446(2.6)	528(sh), 570(17.6)
β-$Cl_8Cl_8TPPFe^{II}PF_6$ [a]		452(1.3)	554(14), 586(9.0), 650(sh)
β-$Cl_8Cl_8TPPFe^{II}Cl$	$\sim 10^5$ [b]	374(0.3), 414(0.36), 472(0.98)	550(5.6), 592(12.3), 634(3.4)
β-$Cl_8Cl_8TPPFe^{III}Cl$		398(0.65), 448(0.79)	556(sh), 710(3.0)
β-$Cl_8TPPFe^{II}PF_6$[a]		449(1.6)	
β-$Cl_8TPPFe^{II}Cl$	$> 10^6$ [c]	468(1.6)	590
β-$Cl_8TPPFe^{III}Cl$		408(0.74), 450(0.91)	528(sh), 564(sh), 778(3.8)
β-$Cl_8Cl_{20}TPPFe^{III}Cl$		402(0.65), 448(0.83)	554(sh), 680(3.9)

[a] $Fe^{II}PF_6^\ominus$ species measured in the presence of $TBAPF_6$ (0.1 M). [b] Dilution method used for determination. [c] Accurate determination not possible due to competition with $OH^\ominus$ at low concentration.

Table 1. Summary of half-wave potentials [V] (vs. SCE) of (Porph)FeCl in PhCN (0.1 M $TBAPF_6$) at 21 °C. All potentials were measured versus a $Ag/AgNO_3$ (10^{-2} M) electrode.

Compound	Ligand	c [M]	Reduction			Oxidation	
			[Fe-TPP]$^\oplus$/[Fe-TPP]	[Fe-TPP]/[Fe-TPP]$^\ominus$	[Fe-TPP]$^\ominus$/[Fe-TPP]$^{2\ominus}$	[Fe-TPP]$^\oplus$/[Fe-TPP]$^{2\oplus}$	[Fe-TPP]$^{2\oplus}$/[Fe-TPP]$^{3\oplus}$
TPPFeCl **1**	$Cl^\ominus$	5.0×10^{-4}	−0.37	−1.13	−1.76	1.11	1.47
	$+Ag^\oplus$		−0.028 [a]	−1.12	−1.79	[b]	[b]
β-Cl_8TPPFeCl **2**	$Cl^\ominus$	6.3×10^{-4}	0.044	[c]	−1.26	1.22	1.58
	$+Ag^\oplus$		[b]	−0.67	−1.27	[b]	[b]
Cl_8TPPFeCl **3**	$Cl^\ominus$	5.7×10^{-4}	[c]	−1.05	−1.77	1.33	1.63
	$+Ag^\oplus$		0 [a]	−1.04	−1.77	[b]	[b]
	$+Cl^\ominus$	6.5×10^{-2}	−0.34	−1.04	−1.77	wall $Cl^\ominus$/Cl	
β-Cl_8Cl_8TPPFeCl **4**	$Cl^\ominus$	5.25×10^{-4}	0.10	[c]	−1.31	0.8	1.53
	$+Ag^\oplus$		[b]	−0.57	−1.30	[b]	[b]
Cl_{20}TPPFeCl **5**	$Cl^\ominus$	1.0×10^{-5}	[c]	−0.82	[d]	1.43	1.68
β-Cl_8Cl_{20}TPPFeCl **6**	$Cl^\ominus$	1.0×10^{-5}	0.27	[c]	−1.00	1.71	[d]

[a] Irrversible wave. [b] Quasi-irreversible wave, very close to the reduction of $Ag^\oplus$. [c] Peaks ill-defined. [d] Due to the high concentration of $AgNO_3$ used, the large $Ag^\oplus/Ag$ wave masked that of the metalloporphyrin.

complexed by axial $Cl^{\ominus}$. The anodic shifts observed for β-octachlorination were once again on the order of 0.5 V.

Analysis of current–voltage curves and half-wave potentials,[11] as well as spectroelectrochemistry,[14] have shown that ferrous TPPs can complex with anions. The highly electron-deficient systems described here have been examined spectroelectrochemically. The weak binding of $Cl^{\ominus}$ to Cl_8TPPFe^{II} compared to unsubstituted $TPPFe^{II}$ (K_A; Table 2) may be due to steric effects of the bulky *ortho*-chloro substituents. The β-chlorinated porphyrins, on the other hand, exhibited high stability constants, suggesting that the electronegativity of the β-substituents far outweighs the steric effects of phenyl substitution.

Preliminary studies have shown that these highly electronegatively substituted hemins are robust and effective catalysts for cytochrome-P450-related biomimetic studies.

Received: March 12, 1990 [Z 3848 IE]
German version: *Angew. Chem. 102* (1990) 1073

[1] P. Worthington, P. Hambright, R. F. X. Williams, J. Reid, C. Burnham, A. Shamin, J. Turay, D. M. Bell, R. Kirkland, R. G. Little, N. Datta-Gupta, U. Eisner, *J. Inorg. Biochem. 12* (1980) 281.
[2] A. Giraudeau, H. J. Callot, M. Gross, *Inorg. Chem. 18* (1979) 201.
[3] L.-C. Gong, D. Dolphin, *Can. J. Chem. 63* (1985) 401.
[4] H. J. Callot, *Bull. Soc. Chim. Fr. 1974*, 1492.
[5] T. G. Taylor, S. Tsuchiya, *Inorg. Chem. 26* (1987) 1338.
[6] A. Giraudeau, H. J. Callot, J. Jordan, I. Ezhar, M. Gross, *J. Am. Chem. Soc. 101* (1979) 3857.
[7] P. S. Taylor, D. Dolphin, T. G. Taylor, *J. Chem. Soc. Chem. Commun. 1984*, 279.
[8] All polychlorinated hemins gave satisfactory elemental analysis for C, H, N, and Cl and parent peaks in the mass spectrum in agreement with the calculated values.
[9] A. D. Adler, F. R. Longo, F. Kampos, J. Kim, *J. Inorg. Nucl. Chem. 32* (1970) 2443.
[10] M. M. Catalano, M. J. Crossley, M. M. Harding, L. G. King, *J. Chem. Soc. Chem. Commun. 1984*, 1535.
[11] L. A. Bottomley, K. M. Kadish, *Inorg. Chem. 20* (1981) 1348.
[12] K. M. Kadish, B. Boisselier-Cocolios, B. Simonet, D. Chang, H. Ledon, P. Cocolios, *Inorg. Chem. 24* (1985) 2148.
[13] R. J. Donohoe, M. Atamian, D. F. Bocian, *J. Am. Chem. Soc. 109* (1987) 5593.
[14] K. M. Kadish, R. K. Rhodes, *Inorg. Chem. 22* (1983) 1090.
[15] $K_A = \frac{[TPPFe^{II}Cl]}{[TPPFe^{II}][Cl^{\ominus}]}$ for $TPPFe^{II} + Cl^{\ominus} \rightleftarrows TPPFe^{II}Cl$
[16] C. Gueutin, D. Lexa, M. Momenteau, J.-M. Saveant, F. Xu, *Inorg. Chem. 25* (1986) 4294.

2,3-Diboratabutadienes and 2-Borataallenes**

By *Monika Pilz, Jürgen Allwohn, Peter Willershausen, Werner Massa*, and *Armin Berndt**

Dedicated to Professor Karl Dimroth on the occasion of his 80th birthday

The methyleneborane **1a**[1] reacts with lithium (powder containing 2% sodium) in toluene at 25 °C to give the 2,3-diboratabutadiene **3a**, the symmetrical dimer of its radical anion **2a**. Under the same conditions, **1b** yields the 2-boratraallene **4b**, the unsymmetrical dimer of **2b**, as major product together with **3b** as minor product.[2] The structure[3] of **3a** is shown in Figure 1.

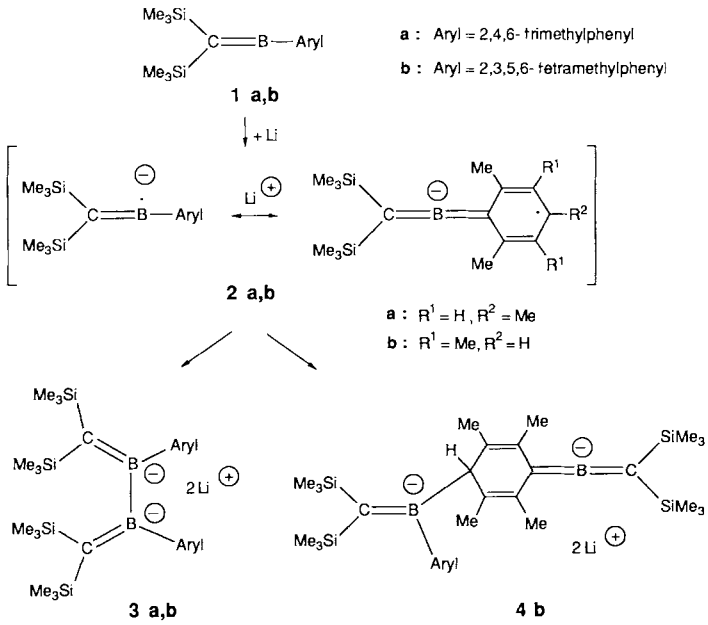

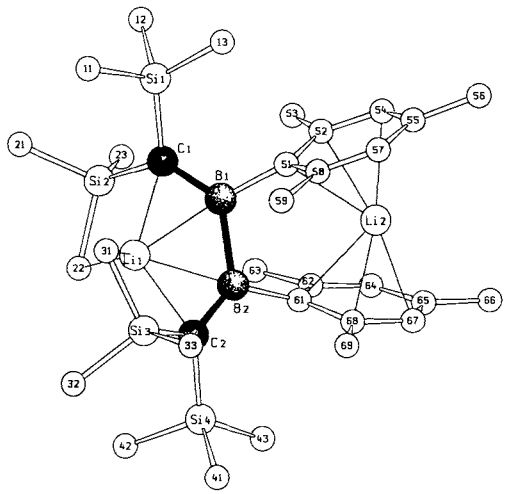

Fig. 1. Schakal drawing of the molecular structure of **3a**. Projection onto the plane B1, B2, Li1, Li2. Important distances [pm] and angles [°]: B1-B2 185.9(8), C1-B1 150.9(8), C2-B2 147.5(8), Li1-C1 213(1), Li1-B1 217(1), Li1-B2 217(1), Li1-C2 214(1), Li1-C22 235(1), Li1-C31 234(1), Li2-C61 238(1), Li2-C68 227(1), Li2-C67 229(1), Li2-C51 234(1), Li2-C52 224(1), Li2-C54 232(1); C1-B1-B2 129.5(5), C2-B2-B1 130.1(5), Si1-C1-B1 119.1(4), Si3-C2-B2 128.4(4), C51-B1-B2 108.7(4), C61-B2-B1 107.4(4); C1-B1-B2-C2 −45.3(8), C1-B1-B2-C61 135.9(5), C2-B2-B1-C51 138.1(5), C51-B1-B2-C61 −40.7(5), Si1-C1-B1-B2 159.1(4), Si1-C1-B1-C51 −24.7(6), Si2-C1-B1-B2 −34.9(8), Si2-C1-B1-C51 141.3(4), Si3-C2-B2-B1 −35.4(8), Si3-C2-B2-C61 143.2(4), Si4-C2-B2-B1 158.7(4), Si4-C2-B2-C61 −22.6(7).

In **3a**, only one lithium ion (Li1) is coordinated to the charge-bearing framework atoms C1, B1, B2, and C2; the other lithium ion (Li2) is found between the mesityl substituents. Li1 displays remarkably short[4] distances to B1 and B2 (217 pm) and short distances to C1 and C2 (213 and 214 pm) as well as to C22 and C31 (235 and 234 pm). Li2 exhibits three short distances to the *ipso*, *ortho*, and *meta* C

[*] Prof. Dr. A. Berndt, Dr. M. Pilz, J. Allwohn, P. Willershausen, Prof. Dr. W. Massa
Fachbereich Chemie der Universität
Hans-Meerwein-Strasse, D-3550 Marburg (FRG)

[**] This work was supported by the Deutsche Forschungsgemeinschaft and the Fonds der Chemischen Industrie.

atoms of the mesityl rings. The 2,3-diboratabutadiene dianion is twisted at the C–B bonds by about 30 and 29° and at the B–B bond by about 43°.

The C1–B1 and C2–B2 bonds (151 and 148 pm, respectively) are longer than the C–B bond in planar **5** (144 pm),[5]

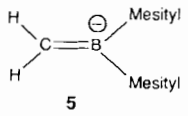

5

and the B1–B2 bond (186 pm) is markedly longer than the B–B bond in uncharged diborane(4) derivatives (171–175 pm).[6] This is presumably due to the electrostatic repulsion of the π charges on the boron atoms. The twisting of the

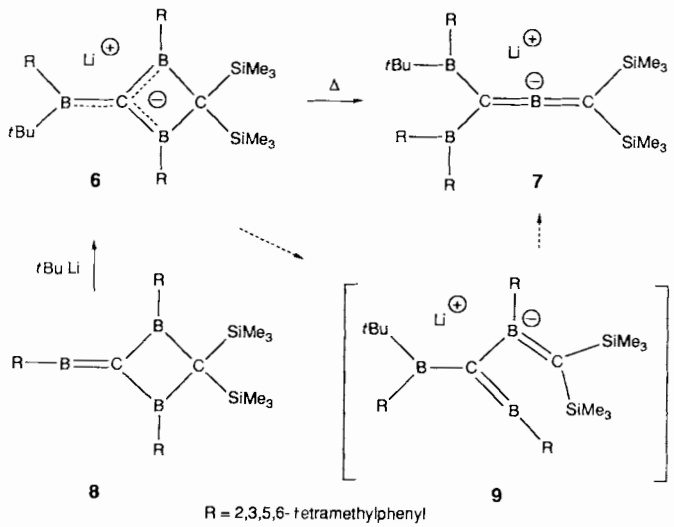

heterobutadiene framework and the resulting chirality[7] explain the diastereotopism of the groups bonded to the *ortho* and *meta* C atoms[8] (see Table 1).

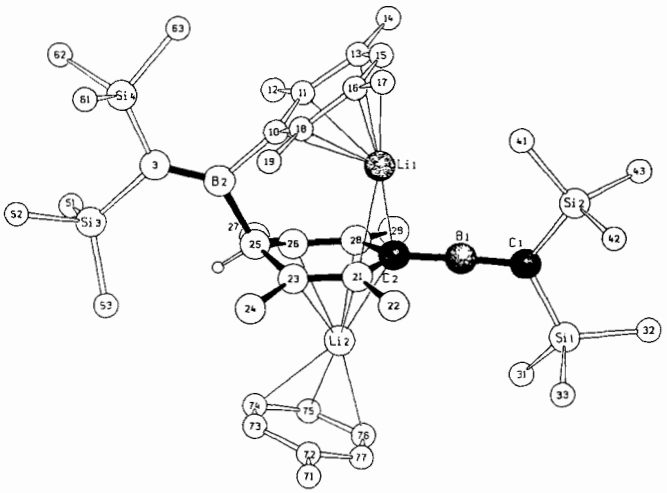

Fig. 2. Schakal drawing of the molecular structure of **4b** · toluene. Projection by 45° onto the plane C1,B1,C2,B2,C3. Important distances [pm] and angles [°]: C1-B1 139(2), C2-B1 142(2), C3-B2 140(2), B2-C25 166(2), B2-C10 163(2), C2-Li1 211(2), C2-Li2 224(2), C10-Li1 232(2), C11-Li1 242(3), C13-Li1 249(2), C15-Li1 243(2), C16-Li1 240(2), C18-Li1 233(2), C21-Li2 226(2), C28-Li2 228(2), C23-Li2 244(2), C26-Li2 237(2); Si1-C1-Si2 117.7(6), C1-B1-C2 177(1), C3-B2-C10 123(1), C3-B2-C25 132(1), C10-B2-C25 105.1(9); Si3-C3-B2-C25 6(2); Si1, Si2, C1-C2, C21, C28 86.4(12).

The structure of **4b** is discussed together with that of the 2-borataallene **7**, formed by heating the 2-boryl-1,3-diboretanide **6** at 200 °C. Presumably, this reaction initially involves a ring-opening to give **9**, a process typical of 1,3-diboretanes.[1] Then, one aryl group undergoes a 1,3-migration from a tri- to the dicoordinated boron atom.[9] Compound **6** is accessible from the methyleneborane **8**[10] and *tert*-butyllithium.

The lithium ions Li1 in **4b** (Fig. 2),[3] which crystallizes with one molar equivalent of toluene, and in **7** (Fig. 3)[3] display short distances to the ring C atoms of the aryl ring on B2 (**4b**, 232–249 pm; **7**, 233–240 pm) and to C2 (211 pm) and C1 (217 pm). In **4b**, Li2 is coordinated by C2 (224 pm), the other sp^2 C atoms of the cyclohexadienyl ring (226–244 pm), and the C atoms C74–C76 (247–253 pm) of the toluene molecule.

The 2-borataallene frameworks in **4b** and **7** are nearly linear (177 and 176°, respectively); the plane Si1, C1, Si2 forms angles of 86 and 85° with the planes C21, C2, C28 and B2, C2, B3, respectively. The C–B distances in the 2-borataallene framework (139 and 145 pm) lie in the range found for the B–C double bonds of the isoelectronic

Table 1. Selected physical data for compounds **3a**, **b**, **4b**, **6**, and **7**. Standard for ^1H and ^{13}C NMR spectra, TMS; for ^{11}B NMR spectra, $BF_3 \cdot OEt_2$.

3a: bright yellow crystals, m.p. 158 °C, yield 5%, ca. 80% according to NMR spectroscopy. ^1H NMR (300 MHz, [D$_8$]toluene, 25 °C): $\delta = 0.00$, 0.51 (s each, 18 H each, $Si(CH_3)_3$), 1.55, 2.30, 2.33 (s each, 6 H each, *o*- and *p*-CH_3), 5.97, 6.16 (s each, 2 H each, *m*-H). ^{13}C NMR (100 MHz, [D$_8$]toluene, −20 °C): $\delta = 5.9$, 6.2 (q each, 6 C each, $Si(CH_3)_3$), 19.6, 22.3, 26.5 (q each, 2 C each, *o*- and *p*-CH_3), 85.3 (br. s, 2 C, C_2B_2), 125.4, 126.5 (d each, 2 C each, *m*-C), 132.5, 143.1 (s each, 2 C each, *o*-C), 138.4 (s, 2 C, *p*-C), 160.2 (br. s, 2 C, *i*-C) ^{11}B NMR (96 MHz, [D$_8$]toluene, 25 °C): $\delta = 57$ ($\nu_{1/2} \approx 1000$ Hz)

3b: ca. 16% yield according to NMR spectroscopy. ^1H NMR (300 MHz, C_6D_6, 25 °C): $\delta = 0.22$, 0.63 (s each, 18 H each, $Si(CH_3)_3$), 1.62, 1.81, 2.17, 2.22 (s each, 6 H each, *o*- and *m*-CH_3), 6.11 (s, 2 H, *p*-H) ^{13}C NMR (75 MHz, C_6D_6, 25 °C): $\delta = 6.2$, 6.6 (6 C each, $Si(CH_3)_3$), 19.7, 19.9, 20.0, 23.2 (2 C each, *o*- and *m*-CH_3), 82.4 (br., 2 C, C_2B_2) 126.2 (2 C, *p*-C), 133.0, 133.1 (2 C each, *o*- and *m*-C), 163.7 (br., 2 C, *i*-C). ^{11}B NMR (96 MHz, [D$_8$]toluene 25 °C): $\delta = 58$ ($\nu_{1/2} \approx 700$ Hz)

4b: bright yellow crystals, m.p. 165 °C, yield 56%. ^1H NMR (300 MHz, [D$_8$]toluene, 25 °C): $\delta = -0.04$, 0.00, 0.09, 0.61 (s each, 9 H each, $Si(CH_3)_3$), 1.25, 1.54 (s each, 6 H each, cyclohexadienyl CH_3), 1.80, 2.12 (s each, 6 H each, *o*- and *m*-CH_3), 2.02 (s, 3 H, CH_3 of toluene), 3.12 (s, 1 H, cyclohexadienyl H), 6.42 (s, 1 H, *p*-H), 6.86–7.02 (m, 5 H, arom. H of toluene), ^{13}C NMR (100 MHz, [D$_8$]toluene, −40 °C): $\delta = 4.9$, 5.2, 6.5, 8.8 (q each, 3 C each, $Si(CH_3)_3$), 18.2, 19.8 (q each, 2 C each, cyclohexadienyl CH_3), 20.7, 21.9 (q each, 2 C each, *o*- and *m*-CH_3), 31.3 (q, 1 C, CH_3 of toluene), 49.8 (d, 1 C, BCH, ^1J (^{13}C, ^1H) = 124.3 Hz), 56.9, 76.5, 80.4 (br. s each, 1 C each, BC), 119.7, 121.6 (s each, 2 C each, cyclohexadienyl sp^2 C), 125.5 (d, 1 C, *p*-C of toluene), 128.4 (d, 2 C, *m*-C of toluene), 128.9 (d, 1 C, *p*-C), 129.2 (d, 2 C, *o*-C of toluene), 132.1, 139.9 (s each, 2 C each, *o*- and *m*-C), 137.7 (d, 1 C, *i*-C of toluene), 157.2 (br. s, 1 C, *i*-C). ^{11}B NMR (96 MHz, [D$_8$]toluene, 90 °C): $\delta = 41$, 63 (1:1, $\nu_{1/2} = 340$, 425 Hz, CB and CBC)

6: white solid, m.p. > 230 °C, yield 20%. ^1H NMR (300 MHz, [D$_8$]toluene, 25 °C): $\delta = 0.00$ (s, 18 H, $Si(CH_3)_3$), 0.81 (s, 9 H, $C(CH_3)_3$), 1.77, 1.92 (s each, 6 H each, *o*- and *m*-CH_3), 2.07, 2.20 (s each, 12 H each, *o*- and *m*-CH_3), 6.34 (s, 1 H, *p*-H), 6.52 (s, 2 H, *p*-H). ^{13}C NMR (100 MHz, [D$_8$]toluene, 25 °C): $\delta = 6.6$ (q, 6 C, $Si(CH_3)_3$), 19.9, 21.2 (q each, 2 C each, *o*- and *m*-CH_3), 20.4, 23.5 (q each, 4 C each, *o*- and *m*-CH_3), 27.1 (br. s, 1 C, $C(CH_3)_3$), 31.2 (q, 3 C, $C(CH_3)_3$), 39.5 (br. s, 1 C, Si_2CB_2), 127.1 (d, 1 C, *p*-C), 127.7 (d, 2 C, *p*-C), 130.7, 132.5 (s each, 2 C each, *o*- and *m*-C), 153.1 (br. s, 2 C, *i*-C), 155.3 (br. s, 1 C, *i*-C), 159.8 (br. s, 1 C, CB_3). ^{11}B NMR (96 MHz, [D$_8$] THF, 25 °C): $\delta = 47$ with broad low-field shoulder at 65 ($\sum \nu_{1/2} \approx 2000$ Hz)

7: colorless crystals, m.p. > 220 °C, yield 70%. ^1H NMR (300 MHz, [D$_8$]THF, 25 °C): $\delta = 0.00$ (s, 18 H, $Si(CH_3)_3$), 1.25 (s, 9 H, $C(CH_3)_3$), 1.90, 1.95, 2.12, 2.38 (s each, 6 H each, *o*- and *m*-CH_3), 2.00 (s, 12 H, *o*- and *m*-CH_3), 6.38, 6.46, 6.76 (s each, 1 H each, *p*-H). ^{13}C NMR (100 MHz, [D$_8$] THF, 25 °C): $\delta = 5.6$ (q, 6 C, $Si(CH_3)_3$), 19.8, 20.7, 21.0, 21.3, 22.09, 22.14 (q each, 2 C each, *o*- and *m*-CH_3), 27.7 (br. s, 1 C, $C(CH_3)_3$), 33.2 (q, 3 C, $C(CH_3)_3$), 39.9 (br. s, 1 C, Si_2CB), 108.1 (br. s, 1 C, CB_3), 127.3, 128.8, 129.0 (d each, 1 C each, p-C), 130.6, 130.7, 131.0, 132.3, 136.0, 136.3 (s each, 2 C each, *o*- and *m*-C), 153.8, 154.6, 155.9, (br. s each, 1 C each, *i*-C). ^{11}B NMR (96 MHz, toluene, 90 °C): $\delta = 75$, 71 ($\sum \nu_{1/2} \approx 1700$ Hz)

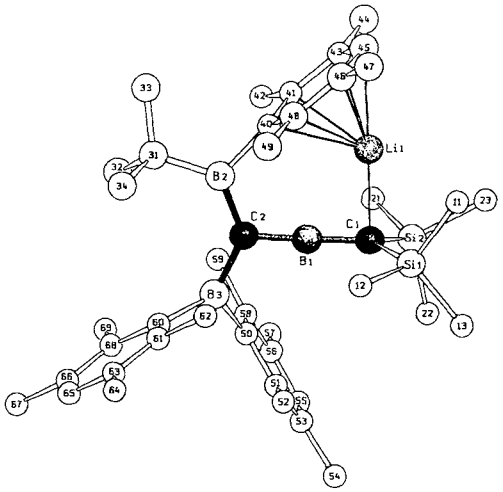

Fig. 3. Schakal drawing of the molecular structure of **7**. Projection onto the plane C1,B1,C2,B2,B3. Important distances [pm] and angles [°]: C1-B1 142(1), C2-B1 145(1), C2-B2 153(1), C2-B3 156(1), B2-C40 162(1), B2-C31 161(1), B3-C50 160(1), B3-C60 160(1), C1-Li1 217(2), C40-Li1 233(2), C41-Li1 237(2), C43-Li1 240(2), C45-Li1 237(2), C46-Li1 240(2), C48-Li1 236(2), B1-Li1 255(2); Si1-C1-Si2 116.8(4), C1-B1-C2 175.7(8), B1-C2-B2 115.5(7), B1-C2-B3 110.9(6), B2-C2-B3 133.7(6), C2-B2-C40 115.6(6), C2-B3-C50 117.4(7); B1-C2-B2-C31 176.3(7), B1-C2-B2-C40 1(1), B1-C2-B3-C50 −32.7(9), B1-C2-B3-C60 140.5(8); Si1,C1,Si2–B2,C2,B3 85.1(10).

aminomethyleneboranes **10** (139–142 pm).[11] A B–C distance of 143.5 pm was calculated for the parent compound **11**.[12]

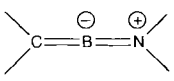

10

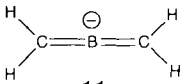

11

Table 1 contains selected physical data for compounds **3a, b**, **4b**, **6**, and **7**.

Received: March 12, 1990;
revised: May 31, 1990 [Z 3851/3852 IE]
German version: *Angew. Chem. 102* (1990) 1085

CAS Registry numbers:
1a, 120638-17-7; **1b**, 120638-21-3; **3a**, 128779-84-0; **3b**, 128779-85-1; **4b**, 128779-86-2; **4b** · PhMe, 128802-18-6; **6**, 128779-87-3; **7**, 128779-88-4.

[1] M. Pilz, M. Stadler, R. Hunold, J. Allwohn, W. Massa, A. Berndt, *Angew. Chem. 101* (1989) 761; *Angew. Chem. Int. Ed. Engl. 28* (1989) 784.

[2] After reduction of **1a, b** with lithium in diethyl ether, no dimers could be detected by NMR spectroscopy.

[3] X-ray structure analyses: four-circle diffractometer (CAD4, Enraf-Nonius) with $Cu_{K\alpha}$ radiation: **3a**: $C_{32}H_{58}Li_2B_2Si_4$, space group $P\bar{1}$, $Z = 2$, $a = 1191.6(3)$, $b = 1207.7(3)$, $c = 1552.3(3)$ pm, $\alpha = 78.44(2)$, $\beta = 73.02(2)$, $\gamma = 62.98(2)°$, 4035 unique reflections with $F_o > 3\sigma(F_o)$ measured at −80 °C; no absorption correction ($\mu = 15.8\ cm^{-1}$), hydrogen atoms included at calculated positions with groupwise common isotropic temperature factors. Anisotropic temperature factors were used for all other atoms, except lithium. Full-matrix refinement. 373 parameters, $R = 0.062$, $R_w = 0.063$ (weighting $w = 1/\sigma^2(F_o)$). **4b** · toluene: $C_{41}H_{70}B_2Si_4Li_2$, space group $Pca2_1$, $Z = 4$, $a = 1773.3(2)$, $b = 1255.2(2)$, $c = 2078.0(1)$ pm, 3831 unique reflections with $F_o > 3\sigma(F_o)$ measured at −80 °C; no absorption correction ($\mu = 13.6\ cm^{-1}$), hydrogen atoms included at calculated positions with groupwise common isotropic temperature factors. Anisotropic temperature factors were used for all other atoms, except lithium, boron, and C31. Full-matrix refinement. 418 parameters. $R = 0.090$, $R_w = 0.051$ (weighting $w = 1/\sigma^2(F_o)$). The refinement of the "correct" enantiomer was shown by an R value that was 0.4% better. The moderate reliability factors are due to the poor quality of the crystals. **7**: $C_{42}H_{66}B_3Si_2Li$, space group $P2_1$, $Z = 2$, $a = 1173.9(3)$, $b = 1603.7(2)$, $c = 1186.3(3)$ pm, $\beta = 108.45(1)°$, 2569 unique reflections with $F_o > 3\sigma(F_o)$ measured at −75 °C; no absorption correction ($\mu = 9.2\ cm^{-1}$), hydrogen atoms included at calculated positions with groupwise common isotropic temperature factors. Anisotropic temperature factors used for all other atoms, except lithium. Block-diagonal matrix refinement with threefold blocking. 452 parameters. $R = 0.064$, $R_w = 0.057$ (weighting $w = 1/\sigma^2(F_o)$). The refinement of the "correct" enantiomer was shown by an R value that was 0.1% better. Further details of the crystal structure investigations may be obtained from the Fachinformationszentrum Karlsruhe, Gesellschaft für wissenschaftlich-technische Information mbH, D-7514 Eggenstein-Leopoldshafen 2 (FRG), on quoting the depository numbers CSD-320091 (**3a**), CSD-320092 (**4b**), and CSD-320090 (**7**), the names of the authors, and the journal citation.

[4] Shortest B-Li distance reported previously: 224 pm; G. Schmidt, G. Baum, W. Massa, A. Berndt, *Angew. Chem. 98* (1986) 1123; *Angew. Chem. Int. Ed. Engl. 25* (1986) 1111.

[5] M. M. Olmstead, P. P. Power, K. J. Weese, R. J. Doedens, *J. Am. Chem. Soc. 109* (1987) 2541.

[6] A. Krämer, H. Pritzkow, W. Siebert, *Angew. Chem. 100* (1988) 963; *Angew. Chem. Int. Ed. Engl. 27* (1988) 926, and references cited therein.

[7] Cf. G. Köbrich, A. Mannschreck, R. A. Misra, G. Rissmann, M. Rösner, W. Zündorf, *Chem. Ber. 105* (1972) 3794.

[8] In **3a**, the *o*- and *m*-C atoms also have different chemical shifts.

[9] Such aryl migrations readily occur in borylmethyleneboranes: J. Allwohn, R. Hunold, M. Pilz, R. G. Müller, W. Massa, A. Berndt, *Z. Naturforsch. B45* (1990) 290.

[10] R. Hunold, M. Pilz, J. Allwohn, M. Stadler, W. Massa, P. von R. Schleyer, A. Berndt, *Angew. Chem. 101* (1989) 759; *Angew. Chem. Int. Ed. Engl. 28* (1989) 781.

[11] B. Glaser, H. Nöth, *Angew. Chem. 97* (1985) 424; *Angew. Chem. Int. Ed. Engl. 24* (1985) 416; B. Glaser, E. Hanecker, H. Nöth, H. Wagner, *Chem. Ber. 120* (1987) 659; R. Boese, P. Paetzold, A. Tapper, *ibid. 120* (1987) 1069.

[12] J. C. Sheldon, G. J. Currie, J. H. Bowie, *J. Am. Chem. Soc. 110* (1988) 8266. Attempts to generate substituted bismethyleneborates are mentioned in B. Glaser, H. Nöth, *Chem. Ber. 119* (1986) 3253.

Compounds with a Boron–Carbon Triple Bond **

By *Jürgen Allwohn, Monika Pilz, Ralf Hunold, Werner Massa*, and *Armin Berndt**

Dedicated to Professor Karl Dimroth on the occasion of his 80th birthday

The *partial* boron–carbon triple bond present in the borylborataalkyne **1a** according to crystal structure data[1] was recently confirmed for unsubstituted **3** by ab initio calcula-

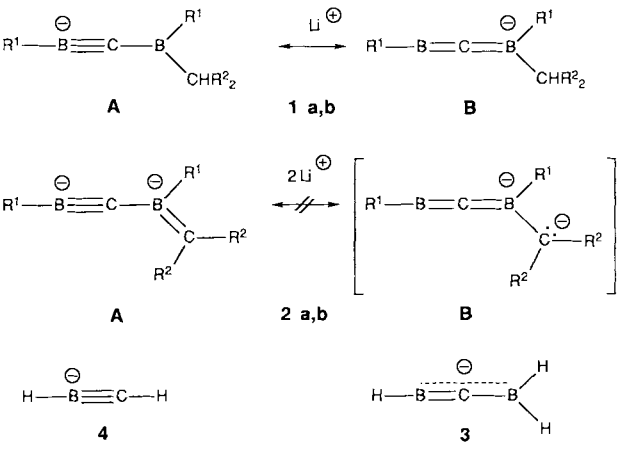

a: R^1 = 2,4,6-trimethylphenyl **b**: R^1 = 2,3,5,6-tetramethylphenyl $R^2 = SiMe_3$

[*] Prof. Dr. A. Berndt, J. Allwohn, Dr. M. Pilz, Dr. R. Hunold, Prof. Dr. W. Massa
Fachbereich Chemie der Universität
Hans-Meerwein-Strasse, D-3550 Marburg (FRG)

[**] This work was supported by the Deutsche Forschungsgemeinschaft and the Fonds der Chemischen Industrie.

tions on the highest level.[2] Here we present evidence supporting a true boron–carbon triple bond in the deprotonated borylborataalkynes **2**.[1, 3]

The molecular structure of the bis(diethyl ether) adduct of **2b** is shown in Figure 1. The B1–C2 bond (132.3(9) pm) is exactly as long as that calculated on the highest level for the unsubstituted borataalkyne **4** (132.3 pm).[2, 5] However, be-

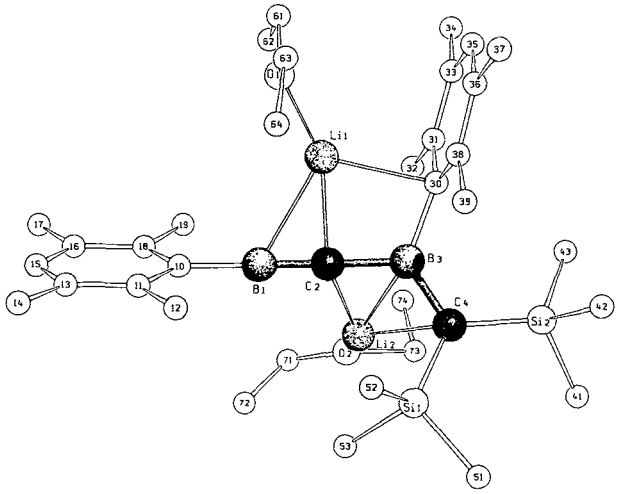

Fig. 1. Schakal drawing of the molecular structure of **2b** · $2Et_2O$. Projection roughly onto the plane C2-C4-C30. Important distances [pm] and angles [°]: B1-C2 132.3(9), C2-B3 154.6(9), B1-C10 156(1), B3-C4 150.5(9), B3-C30 162.8(9), B1-Li1 245(1), C2-Li1 210(1), C30-Li1 228(1), C2-Li2 215(1), B3-Li2 228(1), C4-Li2 226(1); B1-C2-B3 177.2(6), C2-B1-C10 176.3(7), C2-B3-C4 121.9(5), C2-B3-C30 111.7(5), C4-B3-C30 126.3(5), B1-C2-Li1 88.5(5), B3-C2-Li1 91.3(5), C2-Li1-O1 154.1(6), B1-C2-Li2 104.3(5), B3-C2-Li2 74.2(4), C2-Li2-O2 140.4(6) Li1-C2-Li2 142.4(5); C2-B3-C4-Si1 −32.6(8), C2-B3-C4-Si2 169.3(5), C30-B3-C4-Si1 146.5(5), C30-B3-C4-Si2 −11.6(8), Li1-C2-B3-C30 −6.2(6), Li2-C2-B3-C30 138.6(6).

cause of the relatively large standard deviation and the small difference in the B_{sp}–C_{sp} bond lengths in **2b** (132.3 pm) and **1a** (133.9 pm)[1] as well as in **4** (132.3 pm)[2] and **3** (133.8 pm),[2] this agreement alone is not sufficient to prove the existence of a boron–carbon triple bond in **2b**. Also necessary is to show that a delocalization involving resonance structure **B**, which characterizes **1a** as a system with only *partial* B–C triple bond, does not play a significant role in **2b**. This is established by the bond lengths and NMR shifts.

The C2–B3 distance in **2b** (154.6(9) pm) is significantly longer than the corresponding distance in **1a** (149.2(6) pm). In **5a**, whose bond lengths show no evidence of delocalization,[6] the C_{sp}–B_{sp^2} distance is 152.9(6) pm. Furthermore, a delocalization in **2b** should lead to a weakening of the π bond between B3 and C4. The B3–C4 bond in **2b** (150.5(9) pm), however, is relatively short and exhibits only a small twisting (22°), as observed for the B–C double bonds in **6a** (150.9(8) and 147.5(8) pm, 30 and 29°).[7] Additional evidence disfavoring localization of negative π charge on C4, which would be expected for **2B**, is provided by the chemical shifts of C4 (δ = 58.3 for **2a** and 57.9 for **2b**), which are similar to the shift of the corresponding sp^2 C atom in the borataalkene **7b** (δ = 65.3).[8] For *localized* π charge, as in **8**, a value of $\delta(^{13}C)$ = 10.2 is found for the tricoordinated C atoms.[9] The absence of significant delocalization in **2** is also indicated by the greater shielding ($\Delta\delta$ = 15) of the sp boron atoms in **2a, b** (δ = 26) compared with that in **1a, b** (δ = 41).

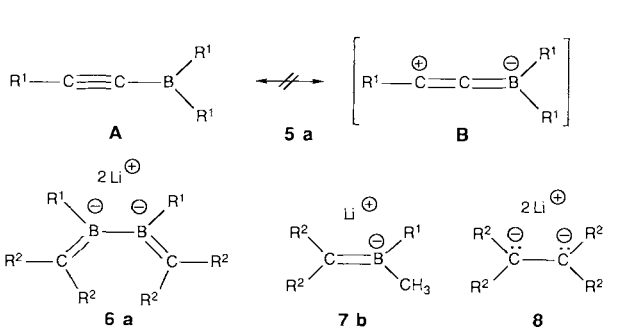

Received: March 29, 1990 [Z 3885 IE]
German version: *Angew. Chem. 102* (1990) 1084

CAS Registry number:
2b · $2Et_2O$, 128659-91-6.

[1] R. Hunold, J. Allwohn, G. Baum, W. Massa, A. Berndt, *Angew. Chem. 100* (1988) 961; *Angew. Chem. Int. Ed. Engl. 27* (1988) 961.
[2] I. L. Alberts, H. F. Schaefer III, *Chem. Phys. Lett. 165* (1990) 250.
[3] R. Hunold, M. Pilz, J. Allwohn, M. Stadler, W. Massa, P. von R. Schleyer, A. Berndt, *Angew. Chem. 101* (1989) 759; *Angew. Chem. Int. Ed. Engl. 28* (1989) 781.
[4] X-ray structure analysis of **2b** · $2Et_2O$: $C_{36}H_{64}B_2Li_2O_2Si_2$, space group $P2_1/c$, $Z = 4$, $a = 1010.6(2)$, $b = 2893.6(8)$, $c = 1450.3(2)$ pm, $\beta = 107.32(1)°$; 3548 unique reflections with $F_o > 3\sigma(F_o)$ measured at −100 °C on a CAD4 Enraf-Nonius diffractometer with $Cu_{K\alpha}$ radiation; no absorption correction ($\mu = 9.06\ cm^{-1}$); methyl groups refined as rigid groups, H atoms included with groupwise common isotropic temperature factors. Anisotropic temperature factors were used for all other atoms. Disorder in the region of one of the two diethyl ether ligands. Full-matrix refinement, 420 parameters, $R = 0.083$, $R_w = 0.053$ (weighting $w = 1/\sigma^2(F_o)$). Further details of the crystal structure investigation may be obtained from the Fachinformationszentrum Karlsruhe, Gesellschaft für wissenschaftlich-technische Information mbH, D-7514 Eggenstein-Leopoldshafen 2 (FRG), on quoting the depository number CSD-320125, the names of the authors, and the journal citation.
[5] At the 6th International Meeting on Boron Chemistry (IMEBORON) in Bechyně, CSSR, 1987, *P. von R. Schleyer* gave the following calculated distances [pm] for **4**: 130.5 (6-31G*), 132.0 (6-31+G*), 132.9 (MP2/6-31G*), 134.1 (MP2/6-31+G*).
[6] J. J. Eisch, B. Shafii, J. D. Odom, A. L. Rheingold, *J. Am. Chem. Soc. 112* (1990) 1847.
[7] M. Pilz, J. Allwohn, P. Willershausen, W. Massa, A. Berndt, *Angew. Chem. 102* (1990) 1085; *Angew. Chem. Int. Ed. Engl. 29* (1990) 1030.
[8] M. Pilz, M. Stadler, R. Hunold, J. Allwohn, W. Massa, A. Berndt, *Angew. Chem. 101* (1989) 761; *Angew. Chem. Int. Ed. Engl. 28* (1989) 784.
[9] A. Sekiguchi, T. Nakanishi, C. Kabuto, H. Sakurai, *J. Am. Chem. Soc. 111* (1989) 3748.

A Compound with a Boron–Arsenic Double Bond**

By *Mark A. Petrie, Steven C. Shoner, H. V. Rasika Dias,* and *Philip P. Power**

In comparison to boron–nitrogen compounds, species with bonds between boron and the heavier elements of the fifth main group are relatively poorly studied. Nonetheless, recent results have suggested that the variety of boron–phosphorus compounds is potentially as great as that found for their boron–nitrogen counterparts.[1] These new developments have not, however, encompassed heavier congeners with B–As, B–Sb, or B–Bi bonds. In fact, well-characterized compounds having such moieties are extremely rare. Apart

[*] Prof. P. P. Power, Dr. H. V. Rasika Dias, M. A. Petrie, S. C. Shoner
Department of Chemistry, University of California
Davis, CA 95616 (USA)

[**] This work was supported by the National Science Foundation (USA).

from boron arsenide, BAs,[2] the structures of only two compounds having B–As bonds have been reported to date.[3, 4] Here we describe the synthesis and structural characterization of **1** (Mes = mesityl) and the ion pair **2** (tmeda = *N,N,N',N'*-tetramethylethylenediamine). Both **1** and **2** have a B–As double bond and dynamic ^{1}H NMR studies demonstrate that the B–As rotation barrier is about 21 kcal mol^{-1}.

$[Li(thf)_3PhAsBMes_2]$ **1**

$[Li(tmeda)_2][PhAsBMes_2]$ **2**

The structures of **1** (Fig. 1) and **2** (Fig. 2) were determined by X-ray crystallography.[5] They are interesting for a number of reasons. For example, they are the first structures

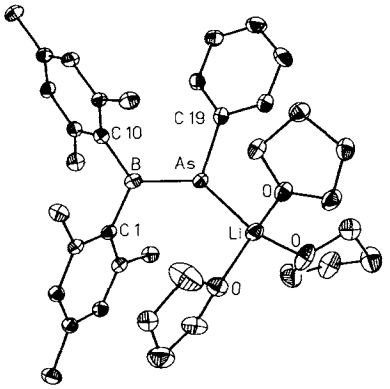

Fig. 1. View of the crystal structure of **1** (H atoms are omitted for clarity). Important bond distances [A°] and angles [°]: B–As 1.926(6), As–C19 1.957(5), As–Li 2.670(9), B–C1 1.613(7), B–C10 1.588(7), Li-O 1.939(9)–1.945(10); 1.945(9), B–As–C19 107.8(2), B–As–Li 122.7(2), Li–As–C19 110.9(2), C1–B–C10 120.3(4), C1–B–As 115.1(3), C10–B–As 124.6(4).

involving bonds between three-coordinate planar boron and approximately sp^2-hybridized arsenic centers. In this respect they resemble their phosphorus counterparts.[6] The B–As bond lengths are 1.926(6) Å (**1**) and 1.936(11) Å (**2**), which

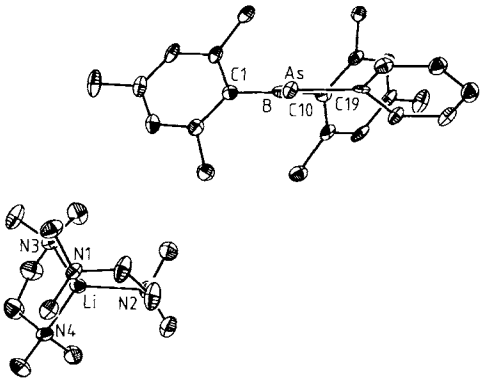

Fig. 2. View of the crystal structure of **2** (H atoms are omitted for clarity). Important bond distances [Å] and angles [°]: B–As 1.936(11), As–C19 1.925(9), B–C1 1.612(16), B–C10 1.595(13), Li–N 2.085–2.146(19), B–As–C19 107.1(4), C1–B–C(10) 118.7(8), C1–B–As 114.8(6), C10–B–As 126.4(8).

are considerably shorter than the previously reported B–As distances in boron arsenide (2.069 Å)[2] and in the cyclic species **3** (2.063(4) Å).[3] They are longer, however,

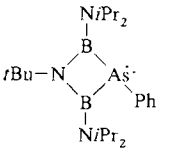

3

than the B–As bonds in the Zintl compound K_3BAs_2 wherein the boron is two coordinate in the linear array [As–B–As]$^{3\ominus}$ and the B–As bonds are 1.868 Å long.[4] The difference between this value and those in **1** and **2** can be accounted for mainly in terms of the dissimilarity in the hybridization (sp vs. sp^2) and coordination number of boron (2 vs. 3). The longer distances (ca. 2.06–2.07 Å) in boron arsenide and **3** are consistent with a bond order of 1 since the sum of the radii of B and As is about 2.06–2.07 Å.[7]

Other aspects of the structures of **1** and **2** support B–As double bonding. In both compounds the empty boron p orbital is aligned (interplanar angle between the B-C10-C1 and As–B–C19 planes = 1.1°) with the arsenic p orbital bearing the lone pair so that overlap is maximized. In **1**, although the arsenic center has a nonplanar coordination (sum of angles at arsenic = 341.4°), the As–C19 bond is in the eclipsed configuration with respect to the BC_2 array and it is the Li–As vector which deviates from the molecular plane. The long Li–As distance and the ease with which the $Li^{\oplus}$ ion may be removed to give **2** suggest that the Li–As interaction is mainly ionic. Furthermore, the B–As bond length is virtually unaffected by the removal of the $Li^{\oplus}$ ion and the ^{11}B NMR chemical shift also remains unchanged. This picture of the bonding receives support from theoretical calculations[8] on the related phosphorus species $LiPHBH_2$ in which the $Li^{\oplus}$ cation is also out of the $[PHBH_2]^{\ominus}$ plane.

Variable-temperature ^{1}H NMR data afforded conclusive proof of the multiple-bond nature of the B–As bond. The ^{1}H NMR spectra[9] of **1** and **2** in $[D_{10}]$xylene at ca. 297 K clearly displayed two distinct sets of peaks attributable to the mesityl hydrogens.[10] Heating of this solution, in the case of **1**, to higher temperatures resulted in the coalescence of the *m*-H resonances at 400 K and of the *o*–Me H resonances at 421 K. Substitution of these values and the values for the peak separations measured 10 °C below coalescence ($\Delta\nu$ = 13.8 Hz for *m*–H and 64 Hz for *o*–Me) into an approximate formula[11] afforded the consistent result of 20.9 kcal mol^{-1} for the energy barrier to the dynamic process. This unexpectedly high value is comparable to those found in aminoboranes.[12] The barriers for the corresponding boron phosphorus species—for example, **4**[6]—are not yet accurately known. However, variable-temperature ^{1}H NMR studies[13]

$[Li(Et_2O)_2PhPBMes_2]$ **4**

indicate that the rotation barrier at the B–P bond in **4** is at least 24 kcal mol^{-1}. Work on these and other compounds containing multiple bonds between boron and elements of the fifth main group is continuing.

Experimental Procedure

Compound **1** was prepared, under anaerobic and anhydrous conditions, by the addition of Mes_2BF[14] (1.00 g, 3.72 mmol) to a solution of Li_2AsPh[15] (0.617 g, 3.72 mmol) in THF (50 mL). The red solution was stirred for 3 h and the solvent was removed under reduced pressure. The residue was dissolved in Et_2O (25 mL); the solution was filtered and the filtrate cooled in a −20 °C freezer over 10 h. The resulting orange-red crystals of **1** were isolated by filtration. Yield 59%; m.p. 111–114 °C. ^{11}B NMR: δ = 74.6. Compound **2** was prepared, also under anaerobic and anhydrous conditions, by the addition of two equivalents of TMEDA (0.815 g, 0.24 mL, 3.2 mmol) to an Et_2O (20 mL) solution of **1** (0.99 g, 1.59 mmol). After stirring for 5 min, a finely divided

yellow precipitate appeared. Addition of THF (3–4 mL) resulted in a clear solution and cooling in a −20 °C freezer for 10 h gave the product **2** as orange-red crystals. Yield 0.37 g, 36%; m.p. 140 °C (dec. slow). ^{11}B NMR: $\delta = 74.9$.

Received: May 2, 1990 [Z 3940 IE]
German version: *Angew. Chem. 102* (1990) 1061

[1] P. P. Power, *Angew. Chem. 102* (1990) 527; *Angew. Chem. Int. Ed. Engl. 29* (1990) 449.
[2] J. A. Perri, S. La Placa, B. Post, *Acta Crystallogr. 11* (1958) 310.
[3] K.-H. van Bonn, P. von R. Schreyer, P. Paetzold, R. Boese, *Chem. Ber. 121* (1988) 1045.
[4] H.-G. von Schnering, M. Somer, M. Hartweg, K. Peters, *Angew. Chem. 102* (1990) 63; *Angew. Chem. Int. Ed. Engl. 29* (1990) 65.
[5] Crystal data for **1** and **2** ($T = 130$ K, $Cu_{K\alpha}$ radiation, ($\lambda = 1.54178$ Å): **1**: $a = 21.911(3)$, $b = 15.974(3)$, $c = 19.768(4)$ Å, orthorhombic, *Pbcn*, $Z = 8$, 3817 unique reflections observed ($I > 2\sigma(I)$), $R = 0.069$. **2**: $a = 18.398(8)$, $b = 9.276(3)$, $c = 22.868(8)$ Å, $\beta = 106.12(1)^{\circ}$, monoclinic, $P2_1/c$, $Z = 4$, 4873 unique reflections observed ($I > 2\sigma(I)$), $R = 0.097$. Further details of the crystal structure investigations may be obtained from the Fachinformationszentrum Karlsruhe, Gesellschaft für wissenschaftlich-technische Information mbH, D-7514 Eggenstein-Leopoldshafen 2 (FRG), on quoting the depository number CSD-54662, the names of the authors, and the journal citation.
[6] R. A. Bartlett, X. Feng, P. P. Power, *J. Am. Chem. Soc. 108* (1986) 6817.
[7] Covalent radii estimated from homonuclear bond lengths: L. Sutton (Ed.): *Tables of Interatomic Distances and Configuration in Molecules and Ions (Spec. Publ.-Chem. Soc. 11* (1958); *ibid. 18* (1965); J. C. Slater, *J. Chem. Phys. 41* (1964) 3199.
[8] T. L. Allen, A. C. Scheiner, H. F. Schaefer III, *Inorg. Chem. 29* (1990) 1930.
[9] ^{1}H NMR (in [D_{10}]xylene, 27 °C): **1**: $\delta = 1.4$ (m, THF), 2.25 (s, *p*-Me), 2.57 (s, *o*-Me), 2.73 (s, *o*-Me), 3.45 (m, THF), 6.77 (s, *m*-H), 6.9 (m, Ph), 7.42 (m, Ph). **2**: $\delta = 1.86$ (s, Me_2N), 1.896 (s, CH_2N), 2.24, 2.25 (s, *p*-Me), 2.663, 2.868 (s, *o*-Me), 6.87, 6.93 (m-CH), 7.06 (m, Ph), 7.76 (d, Ph).
[10] It is possible to propose that the inequivalence of the mesityl resonances could be due to a restricted rotation around the B–C bonds. Thus, if the mesityls were locked into a position perpendicular to the boron-C10-C1 plane and if the As–C bond were in the mirror plane (i.e., no B–As π interaction), inequivalent *ortho*-H and *meta*-H resonances would also be observed. This scenario is unlikely because (1) related studies [1] with B–P compounds fail to show any locking in of the mesityl orientations until a very low temperature (−80 °C) is reached, (2) the barrier observed, 20.9 kcal mol^{-1}, is extremely high and incompatible with a rotation barrier around a B–C bond, (3) two *para* peaks are observed for the mesityl groups in the ^{1}H NMR spectrum of **2**, and (4) the X-ray structure supports π interaction.
[11] D. Kost, E. H. Carlson, M. Raban, *J. Chem. Soc. Chem. Commun.* 656.
[12] P. A. Barfield, M. F. Lappert, J. Lee, *Trans. Faraday Soc. 64* (1968) 2571.
[13] D. C. Pestana and P. P. Power, unpublished results.
[14] Mes_2BF was synthesized by method of *Pelter*. The synthesis is identical to that described for $(2,6\text{-}Me_2C_6H_3)_2BF$: H. Chen, R. A. Bartlett, M. M. Olmstead, P. P. Power, S. C. Shoner, *J. Am. Chem. Soc. 112* (1990) 1048.
[15] A. Tzschach, G. Pacholke, *Chem. Ber. 97* (1964) 419.

Synthesis and NMR Spectra of 2,3-Dihydro-1,3-methanoindene Derivatives and 1,2,3,5-Tetrahydro-1,3-methanopentalene**

By *Manfred Christl** and *Horst Reuchlein*

1,3-Bridged cyclobutanes are interesting models for theoretical[1] and spectroscopic[1b, c, 2] studies as well as for comparisons of reactivity.[1c, 3] Nonetheless, little is known about bicyclo[2.1.1]hexene and its derivatives, since they are accessible only with difficulty. The benzo derivative **1** (2,3-dihydro-1,3-methanoindene) is formed as minor product in the reaction of bicyclo[1.1.0]butane with dehydrobenzene[4a] and has also been synthesized in seven steps from benzonorbornadiene.[4b] Its ^{13}C NMR data are still unknown; however, they were recently calculated.[5]

Here we report a route to this system and to 1,2,3,5-tetrahydro-1,3-methanopentalene (**2**). The relatively readily accessible bicyclo[2.1.1]hexan-2-one (**3**)[6] can be converted, via 2-vinylbicyclo[2.1.1]hexene (**6**), into the dimethyl dicarboxylate **1a**, as shown in Scheme 1. The key intermediate is 2-lithiobicyclo[2.1.1]hexene (**4**), formed by reaction of the 2,4,6-triisopropylbenzenesulfonyl hydrazone of **3** with *n*-butyllithium.[7]

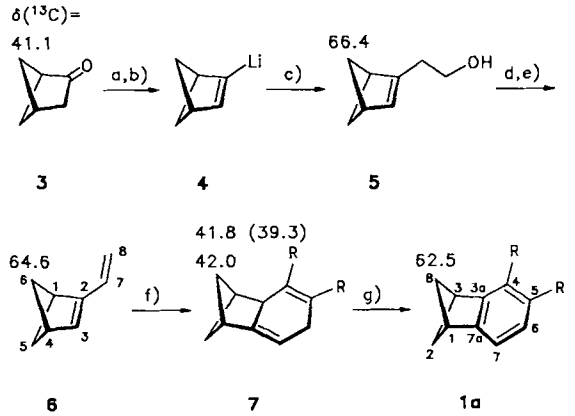

Scheme 1.[8] a) 2,4,6-(iPr)$_3$C$_6$H$_2$SO$_2$NHNH$_2$, MeOH, HCl (cat.), 20 °C, 54%. b) 2 equiv. nBuLi, hexane/tetramethylethylenediamine (1:1), −55 to 20 °C. c) 1 equiv. ethylene oxide, 0–20 °C, 49% based on the hydrazone. d) TosCl, pyridine, 90%. e) KOtBu, DMSO, 75 °C, 20 Torr, 82%. f) R-C≡C-R (R = CO_2CH_3), $CHCl_3$, 20 °C, 75%. g) 1 equiv. 2,3-dichloro-5,6-dicyano-1,4-benzoquinone, C_6H_6, 80 °C, 89%.

To synthesize **2**, we first added dibromocarbene to **6** ($CHBr_3$, KOtBu, pentane, −30 °C, 90%; endocyclic: exocyclic addition 1:3) and obtained the rearranged product **8** together with unrearranged **9**.[8] As expected,[9a] reaction of **9** (containing **8**) with methyllithium in ether resulted in a Skattebøl rearrangement to give **2**[8] (4% yield, isolation by preparative gas chromatography).

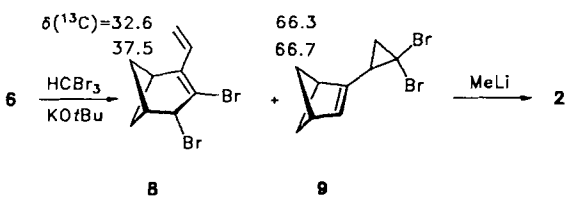

If the behavior of isodicyclopentadiene and related compounds[9b] can be extrapolated to **2**, then 1,4 additions to the 1,3-cyclopentadiene system of **2** should lead to polycyclic

[*] Prof. Dr. M. Christl, Dr. H. Reuchlein
Institut für Organische Chemie der Universität
Am Hubland, D-8700 Würzburg (FRG)

[**] This work was supported by the Deutsche Forschungsgemeinschaft and the Fonds der Chemischen Industrie.

olefins with a strongly pyramidalized double bond between two bridgehead C atoms. An interplanar angle of 145°, instead of 180° as found for normal olefin geometry, was calculated for the parent hydrocarbon of **10**.[10] The hope that, owing to steric hindrance of [2 + 1] cycloaddition by the CH_2 groups of the bicyclohexane system, **2** and dibromocarbene (CBr_4, MeLi, −78 °C) might undergo rare, but known,[11] [4 + 1] cycoladdition to **10** was not fulfilled. Instead, we isolated the bromo derivative **1b**[8] in 23% yield. Compound **1b** is presumably formed by [2 + 1] cycloaddition and ring expansion of the resulting dibromocyclopropane derivative followed by elimination of HBr. Compound **2** also undergoes 1,2 addition with 4-methyl-1,2,4-triazole-3,5(4*H*)-dione (MTAD) (**2** → **11**)[8] as well as with tetracyanoethylene. However, (*E*)-1,2-bisphenylsulfonylethylene undergoes slow Diels–Alder reaction with **2** to give **13**, which, because of its lability, could not be isolated and was only characterized by an ^1H NMR spectrum.

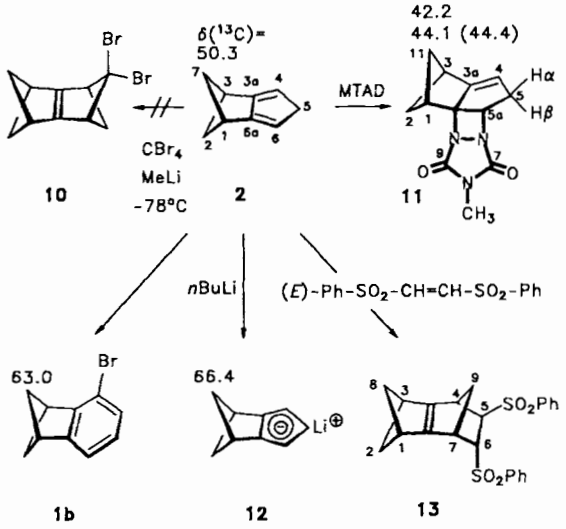

Of particular interest is the ^{13}C NMR spectrum of the cycopentadienyl anion **12**, which we generated by treatment of **2** with *n*-butyllithium. C-2,7 ($\delta = 66.4$) absorb at lower field than C-2,7 of **2** ($\Delta\delta = 16.1$) and than C-2, C-11 of **11** ($\Delta\delta = 22.3$ and 24.2). The latter effect resembles that observed for the C-2, C-8 signals when **7** is converted into **1a**. Remarkably, the methylene C atoms of the tropylium ion **14** ($\delta = 69.0$[12]) are only slightly more deshielded than those of **12** despite the difference in two units of charge.

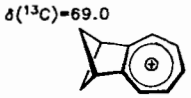

14 [12]

The annelation of arenes to bicyclo[2.1.1]hexane (C-5: $\delta = 39.4$[2b]) thus causes the methylene C atoms to be strongly deshielded by an amount similar to the difference between the chemical shifts of C-5 in bicyclo[2.1.1]hexane and -hexene ($\Delta\delta = 28.7$).[2b] This effect is correctly reproduced by calculations using the IGLO method.[13] The result of the above-mentioned calculation for the value of C-2 in **1**[5] is 30% too small if **1a**, **b** are accepted as models.

Table 1. Selected physical data for **1a**, **2**, **6**, and **11**–**13**; 200- or 400-MHz ^1H NMR spectra and 50- or 100-MHz ^{13}C NMR spectra (δ values, coupling constants in Hz). H*a* = H*anti*, H*s* = H*syn*, H*c* = H*cis*, H*t* = H*trans*.

1a: oil. ^1H NMR ($CDCl_3$): 2.32 (AA' part of an AA'XX' spectrum, $J(2syn,8syn) = -10.0$, $J(2,2) = -6.1$, $J(2syn,8anti) = +0.6$; 2,8-H*s*) 2.73 (m; 2,8-H*a*), 3.17 (dt, $J(1,3) = 7.2$, $J(2anti,3) = 2.5$; 3-H), 3.33 (br.dt, $J(1,2anti) = 2.5$; 1-H), 3.78, 3.82 (s each; 2 CH_3), 7.19 (br.d, $J(6,7) = 7.3$; 7-H), 7.46 (d; 6-H). ^{13}C NMR ($CDCl_3$): 44.9, 45.7 (d each; C-1, 3), 52.2, 52.3 (q each; 2 CH_3), 62.5 (t; C-2,8), 119.8, 127.0 (d each; C-6, 7), 124.9, 125.5 (s each; C-4, 5), 152.8, 158.1 (s each; C-3a, 7a), 167.5, 168.6 (s each; 2 C=O)

2: oil. MS (70 eV): *m/z* (%) 118 (35, $M^{\oplus}$), 117 (100), 116 (11), 115 (48), 103 (14), 91 (32), 77 (10), 65 (11), 51 (11), 39 (18). ^1H NMR ($CDCl_3$): 1.80 (AA' part of an AA'XX' spectrum, $J(2syn,7syn) = -9.8$, $J(2,2) = -5.9$, $J(2syn,7anti) = +0.4$; 2-H*s*), 2.54 (m; 2-Ha), 3.18 (br.t, $J(1,2anti) = 2.7$; 1-H), 3.32 (pseudo-qui, line separation 1.7 Hz; 5-H); 5.65 (br. pseudo-t, line separation 1.7 Hz; 4-H)[a]. ^{13}C NMR ($CDCl_3$): 42.2 (d;C-1,3), 46.1 (t; C-5), 50.3 (t; C-2,7), 111.5 (d; C-4,6), 155.6 (s; C-3a, 6a)

6: oil. MS (70 eV): *m/z* (%) 106 (30, $M^{\oplus}$), 105 (36), 91 (100), 79 (41), 78 (43), 77 (34), 65 (22), 51 (24), 39 (35), 27 (23). ^1H NMR ($CDCl_3$): 2.28 (m; 5,6-H*s*), 2.62 (m; 5,6-H*a*, 4-H), 2.97 (m; 1-H), 4.99 (ddd, $J(7,8cis) = 10.6$, $J(8,8) = 1.5$, $J(3,8cis) = 0.6$; 8-H*c*), 5.18 (ddd, $J(7,8trans) = 17.4$, $J(3,8trans) = 0.9$; 8-H*t*), 6.54 (dd; 7-H), 6.69 (br.s; 3-H)[a]. ^{13}C NMR ($CDCl_3$): 42.2 (d; C-1), 43.2 (d; C-4), 64.6 (t; C-5,6), 111.1 (t; C-8), 131.8 (d; C-7), 139.3 (d; C-3), 156.2 (s; C-2); assignment based on a ^{13}C–^1H correlation

11: m.p. 74–76 °C. ^1H NMR ($CDCl_3$): 0.95 (dd, $J(2syn,11syn) = 10.3$, $J(11,11) = 6.7$; 11-H*s*), 2.25 (br.dt, $J(1,11anti) = J(3,11anti) = 3.2$; 11-H*a*), 2.30 (dt, $J(2,2) = 7.4$, $J(1,2anti) = J(2anti,3) = 2.7$; 2-H*a*), 2.63 (dd; 2-H*s*), 2.90 (dddd, $J(5,5) = 19.1$, $J(5\alpha,5a) = 7.9$, $J(4,5\alpha) = 3.4$; $J(3,5\alpha$ or $11anti,5\alpha) = 0.9$;5-H$_\alpha$), 3.00 (m; 3-H), 3.03 (s; CH_3), 3.12 (dt, $J(1,3) = 5.9$; 1-H), 3.32 (br.dt, $J(4,5\beta) \approx 2$; 5-H$_\beta$), 4.86 (dd; $J(5\beta,5a) = 1.9$; 5a-H), 5.64 (br.d; 4-H). ^{13}C NMR ($CDCl_3$): 25.9 (q; CH_3), 42.2, 44.1, 44.4 (t each; C-2,5,11), 43.1, 44.1 (d each; C-1,3), 66.8 (d; C-5a), 94.0 (s; C-10a), 121.9 (s; C-4), 152.7 (s; C-3a), 161.2, 161.9 (s each; C-7,9)

12: ^{13}C NMR ([D_{10}]-1,2-dimethoxyethane): 43.5 (d; C-1,3), 66.4 (t; C-2,7), 94.9 (d; C-5), 96.1 (d; C-4,6), 133.9 (s; C-3a, 6a)

13: ^1H NMR ($CDCl_3$): 1.65 (dq, $J(9,9) = 9.0$, $J(4,9syn) \approx J(7,9syn) \approx 1.7$; 9-H*s*), 2.18 (br.d; 9-H*a*), 2.31 (dd, $J(2syn,8syn) = 10.0$, $J(2,2$ or $8.8) = 5.1$), 3.19 (dd, $J(8,8$ or $2,2) = 6.1$) (2, 8-H*s*), 2.68, 2.87 (dt, each $J(1,3) = 7.1$, $J(1,2anti) = J(1,8anti) = J(2anti,3) = J(3,8anti) = 2.3$; 1, 3-H), 2.82 (dt, $J(2,2$ or $8,8) = 5.1$), 3.05 (br.dt, $J(8,8$ or $2,2) = 6.1$) (2, 8-H*a*), 3.64 (br.s; 4-H), 3.66 (m; 7-H), 3.72 (dd, $J(5,6) = 5.6$, $J(5,9syn) = 2.0$; 5-H), 4.35 (dd, $J(6,7) = 3.1$; 6-H), 7.50-7.90 (m; 2 C_6H_5)

[a] Assignment on the basis of NOE measurements.

Received: April 17, 1990 [Z 3915 IE]
German version: *Angew. Chem. 102* (1990) 1090

CAS Registry numbers:
1a, 128600-87-3; **1b**, 128600-95-3; **2**, 128600-88-4; **3**, 5164-64-7; **4**, 128600-89-5; **5**, 128600-90-8; **6**, 128600-91-9; **7**, 128600-92-0; **8**, 128600-93-1; **9**, 128600-94-2; **11**, 128600-96-4; **12**, 128600-97-5; **13**, 128600-98-6; CBr_4, 558-13-4; $HCBr_3$, 75-25-2; $CH_3CO_2C{\equiv}CCO_2CH_3$, 762-42-5.

[1] a) W. L. Jorgensen, W. T. Borden, *J. Am. Chem. Soc. 95* (1973) 6649; b) R. Gleiter, P. Bischof, K. Gubernator, M. Christl, L. Schwager, P. Vogel, *J. Org. Chem. 50* (1985) 5064, and references cited therein; c) L. A. Paquette, J. Dressel in A. de Meijere, S. Blechert (Eds.): *Strain and its Implications in Organic Chemistry*, Kluwer, Dordrecht 1989, p. 77, and references cited therein.

[2] a) M. Christl, R. Herbert, *Chem. Ber. 112* (1979) 2022; b) M. Christl, C. Herzog, *ibid. 119* (1986) 3067, and references cited therein.

[3] a) R. Huisgen, P. H. J. Ooms, M. Mingin, N. L. Allinger, *J. Am. Chem. Soc. 102* (1980) 3951; b) F. Lanzendörfer, M. Christl, *Angew. Chem. 95* (1983) 896; *Angew. Chem. Int. Ed. Engl. 22* (1983) 871, and references cited therein.

[4] a) M. Pomerantz, R. N. Wilke, G. W. Gruber, U. Roy, *J. Am. Chem. Soc. 94* (1972) 2752; b) Y. Hata, H. Tanida, *ibid. 91* (1969) 1170.

[5] C. F. Wilcox, Jr., R. Gleiter, *J. Org. Chem. 54* (1989) 2688.

[6] F. T. Bond, H. L. Jones, L. Scerbo, *Org. Photochem. Synth. 1* (1971) 33; W. Trautmann, *Dissertation*, Universität Karlsruhe 1976.

[7] For the method, see: A. R. Chamberlin, E. L. Liotta, F. T. Bond, *Org. Synth. 61* (1983) 141; R. M. Adlington, A. G. M. Barrett, *Acc. Chem. Res. 16* (1983) 55.

[8] The structures of the new compounds are in agreement with the analytical and spectroscopic data.
[9] a) L. A. Paquette, M. Gugelchuk, M. L. McLaughlin, *J. Org. Chem. 52* (1987) 4732; b) L. A. Paquette, C.-C. Shen, *J. Am. Chem. Soc. 113* (1990) 1159, and references cited therein.
[10] C. A. Johnson, *J. Chem. Soc. Chem. Commun. 1983*, 1135.
[11] H. Mayr, U. W. Heigl, *Angew. Chem. 97* (1985) 567; *Angew. Chem. Int. Ed. Engl. 24* (1985) 579; L. W. Jenneskens, W. H. de Wolf, F. Bickelhaupt, *ibid. 97* (1985) 568 and *24* (1985) 585.
[12] K. Komatsu, H. Akamatsu, K. Okamoto, *Tetrahedron Lett. 28* (1987) 5889.
[13] W. Kutzelnigg, U. Fleischer, M. Schindler in P. Diehl, E. Fluck, H. Günther, R. Kosfeld, J. Selig (Eds.): *NMR – Basic Principles and Progress, Vol. 23*, Springer, Berlin, in press. We thank Dr. *Schindler* for providing us with these results before publication.

(3,3-Diphenylallenylidene)trimethylphosphanetitanocene: The First Titanocene Carbene Complex with Three Cumulative Double Bonds

By *Paul Binger,* Patrik Müller, Regine Wenz,* and *Richard Mynott*

Titanocene carbene complexes are of interest in organic synthesis, especially for carbonyl olefination. Their use is limited, however, by a lack of suitable syntheses for substituted titanocene carbene complexes.[1] We recently reported a novel method for preparing the titanocene vinylcarbene complexes **1a–c** from 3,3-disubstituted cyclopropenes and bis(trimethylphosphane)titanocene.[2]

On attempting to carry out a one-pot synthesis of **1a** by treating $[Cp_2TiCl_2]$ with two equivalents of *n*-butyllithium at $-78\,^{\circ}C$ and then allowing the solution to warm up in the presence of PMe_3 and 3,3-diphenylcyclopropene, we found that, in addition to the vinylcarbene complex **1a**, (3,3-diphenylallenylidene)trimethylphosphanetitanocene (**2**) is also formed.[3]

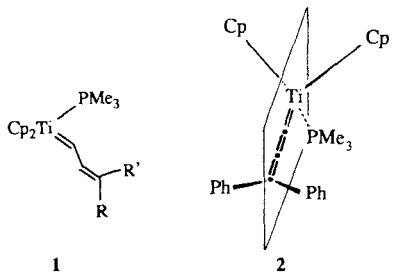

1 **2**

a: R = R' = Ph, **b**: R = Ph, R' = Me, **c**: R = R' = CH_3

Closer examination of this result showed that *n*-butyllithium lithiates 3,3-diphenylcyclopropene under the conditions chosen.[4] Reaction of the two starting materials in a molar ratio of 2:1 at 0 °C for 1 h gives a mixture of the two dilithiated compounds **3** and **4** in a ratio of 14:86. At 25 °C, only the immediate formation of **4** (90% purity) is observed; **4** slowly decomposes at room temperature to unidentified products. Apparently, the dilithiocyclopropene derivative **3** rapidly rearranges to the dilithioallene derivative **4**. The lithium derivatives **3** and **4** have not yet been isolated as pure substances; they were trapped by reaction with trimethylchlorosilane to give the corresponding trimethylsilyl derivatives **5** and **6**, which were then characterized.

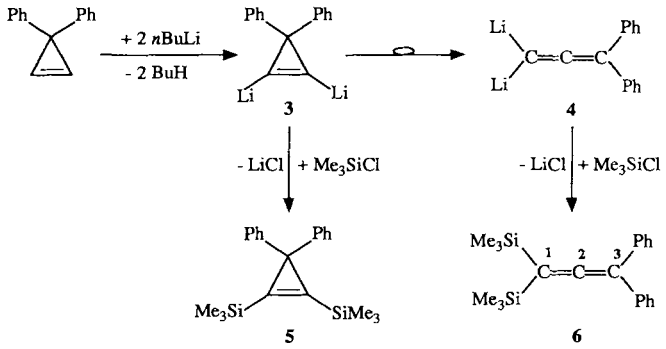

1,1-Dilithio-3,3-diphenylallene (**4**), prepared at 0 °C, reacts at this temperature with titanocene dichloride and trimethylphosphane to give the (3,3-diphenylallenylidene)-titanocene complex **2** in 71% yield. The route of formation of complex **2** is thereby elucidated. At the same time, these results open up a way of synthesizing as yet unknown allenylidenetitanocene complexes.

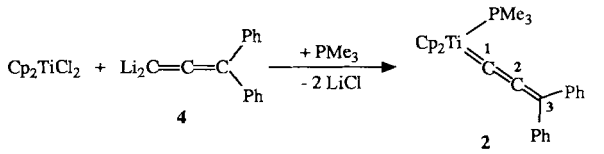

Also new is the selective rearrangement of a 1,2-dilithiocyclopropene to the corresponding 1,1-dilithiopropadiene. Previously, it was known only that both acidic olefinic hydrogen atoms undergo ready lithiation, although almost all preparative applications have used the monometalated cyclopropene.[4, 5] Dilithiated 3,3-dimethylcyclopropene, prepared from 3,3-dimethylcyclopropene and lithium diisopropylamide/tetramethylethylenediamine (LDA/TMEDA) at $-60\,^{\circ}C$ to $+20\,^{\circ}C$, can be trapped as 3,3-dimethyl-1,2-bis(trimethylsilyl)cyclopropene by reaction with trimethylchlorosilane,[6] even though calculations show that, for the parent compound, structure **B** is 51.3 kcal mol^{-1} more stable than 1,2-dilithiocyclopropene (**A**).[7, 8]

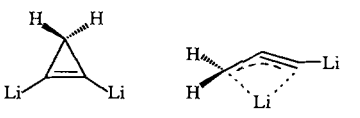

A **B**

Rearrangements of tetrasubstituted cyclopropenes to allenes occur upon irradiation[9] or upon heating at about 150 °C.[5]

The structures of allenylidene derivatives **2** and **6** were established unambiguously by spectroscopy. The IR spectra show strong bands characteristic of both organic[10]

[*] Prof. Dr. P. Binger, Dr. P. Müller, Dipl.-Chem. R. Wenz, Dr. R. Mynott
Max-Planck-Institut für Kohlenforschung
Kaiser-Wilhelm-Platz 1, D-4330 Mülheim-Ruhr (FRG)

and organometallic allene systems (**2**, $\tilde{\nu} = 1870$; **6**, $\tilde{\nu} = 1895\ cm^{-1}$).[11] The ^{13}C NMR spectrum of **2** contains three signals for the three C atoms of the cumulene system: $\delta = 264.9$ (C1, $J_{PC} = 31.4$ Hz); 168.3 (C2, $J_{PC} = 7.8$ Hz), 94.0 (C3, $J_{PC} = 13.2$ Hz). C3 was identified by observation of ^3J (C3, H_{ortho}) in the proton-coupled spectrum, whereas C1 and C2 were assigned by taking into consideration the chemical shifts and J_{PC}. Cooling the sample to $-105\,^{\circ}C$ results in no significant changes in the spectrum, thereby excluding dynamic processes The appearance of only one cyclopentadienyl signal (40 °C, $\delta_C = 103.3$., $J_{CH} = 173$ Hz; $\delta_H = 5.66$) and just one set of phenyl signals is consistent with a tetrahedral arrangement of the ligands around the metal atom, such that the molecule has C_s symmetry with P, Ti, and the three C atoms of the cumulene system lying in the mirror plane. The allene resonances of **6** at $\delta = 93.7$ (C1, $^1J_{SiC} = 48.6$ Hz), 210.6 (C2), and 98.0 (C3, $^3J_{SiC} = 5.7$ Hz) lie in the expected range.

Transition-metal allenylidene complexes have so far been described only for metals of the 6th (M = Cr, W),[11] 7th (M = Mn),[12a] and 8th (M = Ru)[12b] subgroups. All these metal complexes have been synthesized via other routes, however. The existence of a 1,1-dilithioallene derivative has not yet been demonstrated unequivocally; for example, dilithiation of allene gives a dilithium derivative, which, after derivatization with trimethylchlorosilane, affords 1,3-bis(trimethylsilyl)propyne.[13] Reaction of dilithiated 3-methylbutyne with trimethylchlorosilane yields 1,3-bis(trimethylsilyl)-3-methylbutyne.[14] We are currently studying the synthetic possibilities offered by the new compounds **2** and **4**.

Experimental Procedure

2: 11 mL (1.8 mmol) of a 0.16 M solution of *n*-butyllithium in hexane was added to a solution of 3,3-diphenylcyclopropene (0.17 g, 0.9 mmol) in 10 mL of THF at −45 °C. The orange solution was allowed to warm to 0 °C and stirred at this temperature for 1 h. Trimethylphosphane (0.2 mL; 0.27 g, 3.5 mmol) and a solution of titanocene dichloride (0.22 g, 0.9 mmol) in 10 mL of THF were then added in succession. The violet reaction solution was stirred at 13 °C for 6 h, the solvent mixture removed at 10^{-3} torr, the residue dissolved in 25 mL of toluene, the LiCl removed by filtration, and the filtrate concentrated to dryness at 10^{-3} torr. Washing the product with pentane and drying at 10^{-3} torr afforded 0.28 g (71%) of **2** as a dark violet powder (dec. above ca. 70 °C).

6: In analogy to the above procedure, a solution of 3,3-diphenylcyclopropene (96 mg, 0.5 mmol) in 10 mL of THF at 0 °C was allowed to react with 7 mL (1.1 mmol) of a 0.16 M solution of *n*-butyllithium in hexane for 1 h. The resulting orange-yellow solution was then treated with trimethylchlorosilane (120 mg, 1.1 mmol) in 5 mL of THF. The reaction mixture was stirred for 1 h and the solvent then removed at 10^{-3} torr. The product consisted of 269 mg (80%) of a yellow oil having the following composition (GC): **5** (13%), **6** (80%), and six unidentified compounds (7%).

Received: May 28, 1990 [Z 3984 IE]
German version: *Angew. Chem. 102* (1990) 1070

CAS Registry numbers:
2, 128685-26-7; **5**, 128685-25-6; **6**, 116507-70-1; 3,3-diphenylcyclopropene, 22825-21-4.

[1] Reviews: a) W. A. Nugent, J. M. Mayer: *Metal-Ligands Multiple Bonds*, Wiley, New York 1988; b) A. Aguero, A. Osborn, *New J. Chem 12* (1988) 111; c) D. Lenoir, *Synthesis 1989*, 883; d) G. Erker, *Angew. Chem. 101* (1989) 411; *Angew. Chem. Int. Ed. Engl. 28* (1989) 397.

[2] P. Binger, P. Müller, R. Benn, R. Mynott, *Angew. Chem. 101* (1989) 647; *Angew. Chem. Int. Ed. Engl. 28* (1989) 610.

[3] Under these conditions but in the absence of 3,3-diphenylcyclopropene, the reaction of $[Cp_2TiCl_2]$ with PMe_3 and two moles of *n*-butyllithium affords bis(trimethylphosphane)titanocene: P. Binger, P. Müller, R. Benn, A. Rufińska, B. Gabor, C. Krüger, P. Betz, *Chem. Ber. 122* (1989) 1035.

[4] N. I. Yakushkina, G. R. Zhurina, L. S. Surmina, Y. K. Grishin, D. V. Bazhenov, V. V. Plemenkov, I. G. Bolenov, *Zh. Obshch. Khim. 52* (1982) 1604; *J. Gen. Chem. USSR (Engl. Transl.) 52* (1982) 1417.

[5] a) B. Ceskis, A. M. Moiseenkov, T. Y. Rudashevskaya, O. N. Nesmeyanova, A. V. Semenovskii, *Izv. Akad. Nauk. SSSR, Ser. Khim. 1982*, 1084; *Bull. Acad. Sci. USSR Div. Chem. Sci. (Engl. Transl.) 1982*, 965; b) M. A. Kirms, H. Primke, M. Stuhlmeier, A. de Meijere, *Rec. Trav. Chim. Pays-Bas 105* (1986) 462.

[6] R. Walsh, S. Untiedt, M. Stuhlmeier, A. de Meijere, *Chem. Ber. 122* (1989) 637.

[7] a) E. D. Jemmis, J. Chandrasekhar, P. von R. Schleyer, *J. Am. Chem. Soc. 101* (1979) 2848; b) P. von R. Schleyer, E. Kaufmann, G. W. Spitznagel, R. Janoschek, G. Winkelhofer, *Organometallics 5* (1986) 79.

[8] Ab initio calculations give an activation barrier of ca. 7 kcal mol^{-1} for the rearrangement of **3** to **4**. N. J. R. van Eikema Hammes, P. von R. Schleyer, P. Binger, unpublished.

[9] A. Padwa, K. E. Krumpe, L. W. Terry, M. W. Wannamaker, *J. Org. Chem. 54* (1989) 1635.

[10] R. M. Silverstein, G. C. Bassler, T. C. Morill: *Spectrometric Identification of Organic Compounds*, 3rd ed Wiley, New York 1974, p. 88.

[11] a) E. O. Fischer, H. J. Kalder, A. Frank, F. H. Köhler, G. Huttner, *Angew. Chem. 88* (1976) 683; *Angew. Chem. Int. Ed. Engl. 15* (1976) 623; b) H. Berke, P. Härter, G. Huttner, L. Zsolnai, *Chem. Ber. 115* (1982) 695.

[12] a) H. Berke, *Angew. Chem. 88* (1976) 684; *Angew. Chem. Int. Ed. Engl. 15* (1976) 624; b) J. P. Selegue, *Organometallics 1* (1982) 217.

[13] F. Jaffe, *J. Organomet. Chem. 23* (1970) 53.

[14] W. Priester, R. West, T. Ling Chwang, *J. Am. Chem. Soc. 98* (1976) 8413.

An Efficient Route to Linear Conjugated Triepoxides: *allo-*, *galacto-*, and *altro*-Type Trianhydrohexitols **

By *Jürgen Kammerer*, *Grety Rihs*, and *Horst Prinzbach**

The *cis/trans*-isomeric tris-σ-homobenzenes, like the benzene trioxides **1**[1,2] and **2**,[3,4] differ in their thermal stability, that is, in their propensity to undergo [σ2 + σ2 + σ2] cycloreversion.[5] For the mechanistically relevant assessment of kinetic parameters, the thermochemical data[6] for **1** and **2**, as well as those for the linear conjugated 3,4-*cis*-triepoxyhexanes **3**–**5**, 1,2:3,4:5,6-trianhydro derivatives of *meso*-allitol, *meso*-galactitol (dulcitol), and *rac*-altritol,[7] are of interest.

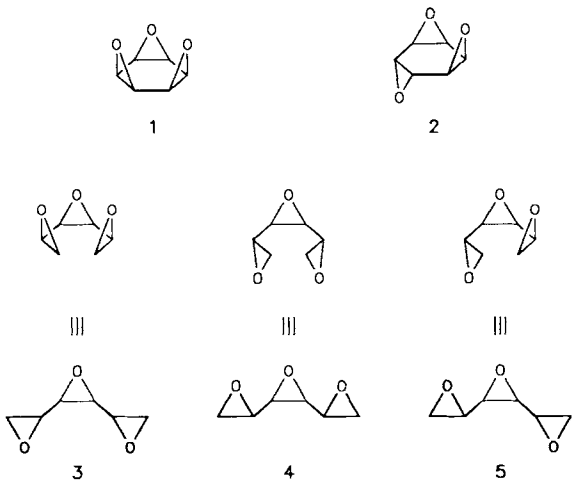

[*] Prof. Dr. H. Prinzbach, Dipl.-Chem. J. Kammerer
Chemisches Laboratorium der Universität,
Institut für Organische Chemie und Biochemie
Albertstrasse 21, D-7800 Freiburg (FRG)
Grety Rihs
Ciba-Geigy AG
CH-4002 Basel (Switzerland)

[**] This work was supported by the Deutsche Forschungsgemeinschaft, the Fonds der Chemischen Industrie, and BASF AG. We thank Dr. *D. Hunkler* and Prof. Dr. *H. Fritz* for NMR measurements and Dr. *J. Wörth* for MS measurements, as well as Dr. *L. Knothe* for stimulating discussions.

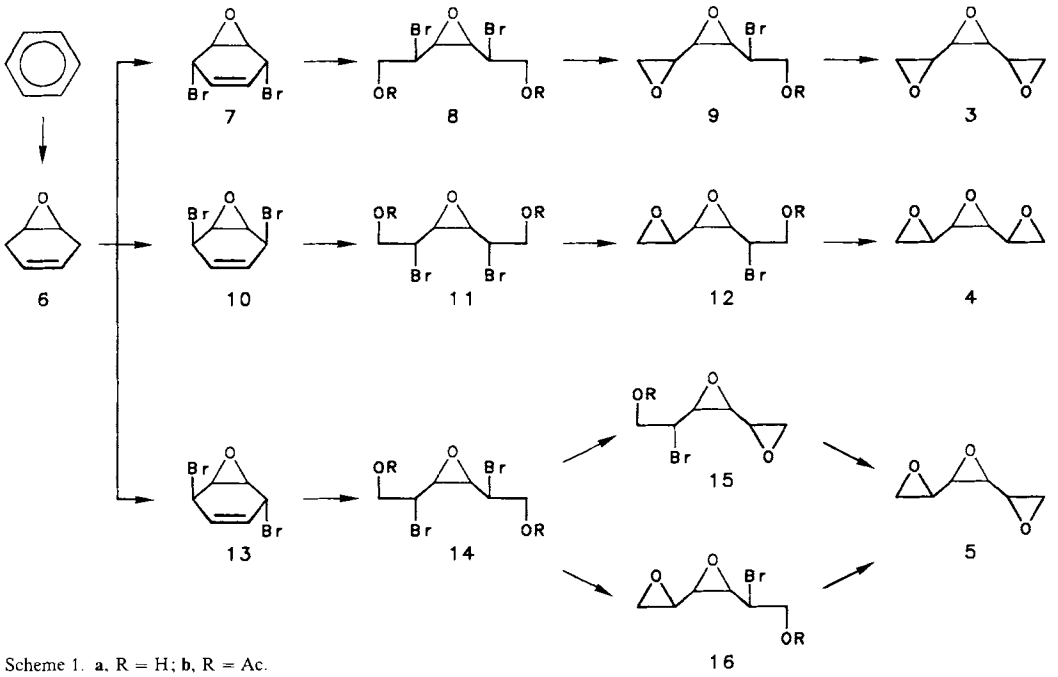

Scheme 1. a, R = H; b, R = Ac.

Triepoxides **3**–**5**, which, like **1**,[5, 8] are attractive as C_6 building blocks, are not yet accessible from sugar precursors. We prepared them in close analogy to the synthesis of **1**[1] (Scheme 1).[9, 10] Starting materials are the dibromides **7**, **10**, and **13**, interconvertible by equilibration and thus directly and efficiently accessible from epoxycyclohexene (**6**).[11] Their oxidative cleavage with ozone (**13** reacts only slowly) leads, after reductive workup,[12] to consistently high yields (85–92%) of the 2,5-dibromo-3,4-epoxy-1,6-hexanediols **8a** (*meso-galacto*, m.p. 97–99 °C, $J_{2,3(4,5)} = 7$ Hz, $CDCl_3$), **11a** (*meso-allo*, m.p. 115°–117 °C, $J_{2,3(4,5)} = 9$ Hz), and **14a** (*rac-altro*, m.p. 78 °C, $J_{1,2} = 5.3$, $J_{1',2} = 4.5$, $J_{2,3} = 9.8$, $J_{3,4} = 3.9$, $J_{4,5} = 9.8$, $J_{5,6} = J_{5,6'} = 4.8$ Hz); they were also characterized as diacetates **8b**, **11b**, and **14b**.

In carrying out the epoxide cyclizations to **3**–**5**, competing cyclizations (including 6-*exo*-pyran formation) and, above all, the reactivity of the intermediates and end products must be considered a priori. Indeed, reaction of **8a**, **11a**, and **14a** in protic solvents in the presence of various bases leads to very complex mixtures of products. However, in aprotic medium (ca. 10^{-2} M THF solutions) with NaH as base and at a reaction temperature of 0–20 °C or under phase-transfer conditions (CH_2Cl_2, nBu$_4$NBr, KOH, room temperature), the epoxide cyclizations proceed with almost no competing reactions; continuous TLC and ^{1}H NMR monitoring reveals no products other than 2-bromo-3,4:5,6-diepoxy-1-hexanols **9a** (*altro*),[14] **12a** (*talo*), **15a** (*galacto*), and **16a** (*allo*), formed with inversion, as well as triepoxyhexanes **3** (*allo*), **4** (*galacto*), and **5** (*altro*). The use of 2.1 equivalents of NaH results in practically exclusive formation of triepoxides **3** (m.p. ca. 30 °C), **4** (m.p. 74 °C), and *rac*-**5** (oil) (0.1 M runs, yields 82–95%). On the other hand, the direct preparation of the diepoxy intermediates is, as expected, problematic: only in the case of **8a** does the use of 1.0 equivalent of NaH lead to selective formation of the diepoxide (**9a**, 90%, oil; $J_{2,3} = 9.5$, $J_{4,5} = 5.5$ Hz);[9] from **11a** or **14a**, however, ca. 1:1 mixtures containing **4** and **12a** or **5** and **15a**/**16a** are obtained. The kinetic and thermodynamic details of these reactions are not known.

Unlike **1** and **2**, triexpoxides **3**–**5** are readily soluble in chloroform, dichloromethane, water, acetonitrile, ethanol, acetone, and tetrahydrofuran; they are sparingly soluble in benzene and tetrachloromethane and nearly insoluble in petroleum ether. The ^{1}H and ^{13}C NMR spectra, which are invariant between +30 and −65 °C (Fig. 1), indicate (average) C_s symmetry for **3** and **4**. Moreover, the hardly differing ^{1}H and ^{13}C NMR chemical shifts and $J_{2,3(4,5)}$ coupling constants (5–6 Hz) are an indication that the "open" unsymmetrical conformations (H–C2(5)–C3(4)–H torsion angle of >150°) generally predominate. The ^{1}H NMR spectra—unlike those of **1**[15]—are not significantly affected by addition of metal ions. The X-ray structure analysis of **4** reveals only approximate C_s symmetry in the crystal (Fig. 2)[16] and manifests, especially with respect to the C–C bond lengths, overall agreement between the linear conjugated triepoxide **4** (average *exo*/*endo* 1.473/1.461 Å) and the cyclic conjugated **1** (*exo*/*endo* 1.487/1.471 Å[17]).

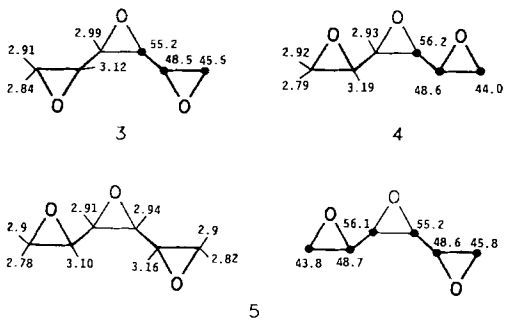

Fig. 1. ^{1}H and ^{13}C NMR chemical shifts for **3**–**5** (400 MHz, $CDCl_3$, ca. 30 °C).

The preparative potential of these linear conjugated triepoxides as C_6 building blocks was demonstrated by the following model reactions. Terminal S_N2 nucleophilic addition to **3** gives the dianhydrohydroxylates **17**. The 5-*exo* ring closure of **17** to give **18** was expected in principle to be highly favored kinetically over the main competing reactions, epoxide migrations (Payne rearrangements). Indeed, in buffered

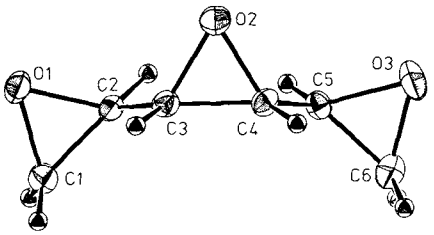

Fig. 2. Molecular structure of **4**. Selected bond lengths [Å] and angles [°]: C1-C2 1.460(6), C2-C3 1.481(5), C3-C4 1.468(5), C4-C5 1.465(5), C5-C6 1.455(6), C1-O1 1.443(6), C2-O1 1.450(4), C3-O2 1.444(5), C4-O2 1.451(5), C5-O3 1.441(4), C6-O3 1.434(6); C1-C2-O1 59.5(2), C1-O1-C2 60.6(2), O1-C1-C2 59.9(3), C3-C4-O2 59.3(2), C3-O2-C4 61.0(3), O2-C3-C4 59.7(3), C5-C6-O3 59.8(2), C5-O3-C6 60.8(3), O3-C5-C6 59.4(3); H2-C2-C3-H3 171.3(4.3), H4-C4-C5-H5 −178.2(2.9), O1-C2-C3-O2 −96.5(0.4), O2-C4-C5-O3 96.0(0.3).

aqueous solution (pH 7–8, 50 °C, Na_2HPO_4/KH_2PO_4), exclusively diol **18a** is formed; reaction with 1.0 equivalent each of NaN_3 (70 min), $NaSCH_2C_6H_5$ (3.5 h), or NaCN (5 h) affords derivatives **18b–d**, respectively (>90%). Even a very large excess of nucleophile (50.0 equivalents) does not result in significant double terminal addition (C1, C6); instead, **18** increasingly undergoes subsequent reaction.

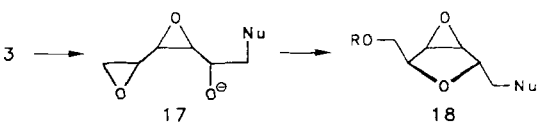

R = H: **a**, Nu = OH; **b**, Nu = N_3; **c**, Nu = $SCH_2C_6H_5$; **d**, Nu = CN

The conformational situation for furan formation (**20**) is predictably less favorable for the primary hydroxylates **19** (obtained from **4**) than for **17**. As a result, an increase in the concentration of nucleophile and the reaction time (under otherwise identical conditions) allows 1,6-bis (**21**) and 1,3,6-

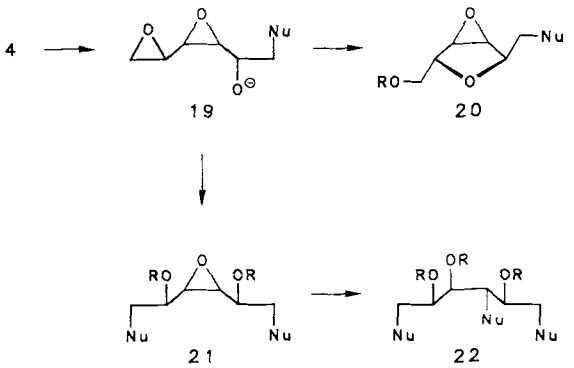

R = H: **a**, Nu = N_3; **b**, Nu = NH_2

tris (**22**) adducts to be prepared directly. For example, reaction with 1.0 equivalent of NaN_3 (3 h) results in a mixture of 70% **20a** and 30% **21a**; with 10.0 equivalents of NaN_3 (40 min), 10% **20a**, 85% **21a**, and 5% **22a** are obtained; with 50.0 equivalents of NaN_3 (70 h), **22a** is formed quantitatively. The latter can be reduced catalytically to give exclusively triaminotriol **22b**.

Received: April 17, 1990 [Z 3913 IE]
German version: *Angew. Chem. 102* (1990) 1087

CAS Registry numbers:
3, 128899-62-7; **4**, 105929-82-6; **5**, 128899-63-8; **7**, 39573-55-2; **8a**, 128823-71-2; **8b**, 128823-79-0; **9a**, 128823-72-3; **10**, 56084-54-9; **11a**, 128899-64-9; **11b**, 128899-71-8; **12a**, 128899-65-0; **13**, 128945-84-6; **14a**, 128899-66-1; **14b**, 128899-72-9; **15a**, 128899-67-2; **16a**, 128899-68-3; **18a**, 128899-69-4; **18b**, 128899-70-7; **18c**, 128823-77-8; **18d**, 128823-78-9; **20a**, 128823-73-4; **21a**, 128823-74-5; **22a**, 128823-75-6; **22b**, 128823-76-7.

[1] R. Schwesinger, H. Prinzbach, *Angew. Chem. 84* (1972) 990; *Angew. Chem. Int. Ed. Engl. 11* (1972) 942; R. Schwesinger, H. Fritz, H. Prinzbach, *Chem. Ber. 112* (1979) 3318.
[2] E. Vogel, H.-J. Altenbach, C.-D. Sommerfeld, *Angew. Chem. 84* (1972) 986; *Angew. Chem. Int. Ed. Engl. 11* (1972) 939.
[3] R. Keller, R. Schwesinger, W. Fritsche, H.-W. Schneider, D. Hunkler, H. Prinzbach, *Chem. Ber. 112* (1979) 3347.
[4] C. H. Foster, G. A. Berchtold, *J. Am. Chem. Soc. 94* (1972) 7939; *J. Org. Chem. 40* (1975) 3743.
[5] B. Zipperer, K.-H. Müller, B. Gallenkamp, R. Hildebrand, M. Fletschinger, D. Burger, M. Pillat, D. Hunkler, L. Knothe, H. Fritz, H. Prinzbach, *Chem. Ber. 121* (1988) 757, and references cited therein.
[6] Thermochemical studies: H.-D. Beckhaus, J. Kammerer, H. Prinzbach, unpublished.
[7] The 3,4-*trans* triepoxides with D-*ido*, D-*manno*, and *rac*-*gluco* configuration were prepared by (unselective) oxidation of the (*E*)-1,2:5,6-dianhydrohex-3-enitols: J. Kuszmann, P. Sohár, *Carbohydr. Res. 83* (1980) 63. A very small amount (2%) of a complex trioxide mixture, obtained by oxidation of a ca. 7:3 mixture of (*E*/*Z*)-1,3,5-hexatriene, probably has structure **4** according to the NMR spectrum: P. Köll, M. Oelting, J. Kopf, *Angew. Chem. 96* (1984) 222; *Angew. Chem. Int. Ed. Engl. 23* (1984) 242; P. Köll, J. Kopf, J. O. Metzger, W. Schwarting, M. Oelting, *Liebigs Ann. Chem. 1987*, 199.
[8] R. Schwesinger, W. Fritsche, H. Prinzbach, *Chem. Ber. 115* (1982) 946; W.-D. Braschwitz, T. Otten, C. Rücker, H. Fritz, H. Prinzbach, *Angew. Chem. 101* (1989) 1383; *Angew. Chem. Int. Ed. Engl. 28* (1989) 1348.
[9] The new compounds were characterized by spectroscopy (^1H, ^{13}C NMR, IR) and elemental analyses; the alcohols were generally characterized as their acetates (R = Ac).
[10] J. Kammerer, *Dissertation*, Universität Freiburg 1990.
[11] Compare the use of this dibromide for the synthesis of anhydroconduritols and anhydroinositols in [3].
[12] Attempts to transform the ozonides into the corresponding 1,6-dialdehydes or 1,6-dicarboxylic acids failed owing to competing processes. Yet, the 2,3:4,5-dianhydrohexitols **24a** (*meso-allo*)/**27a** (*rac-manno*) were accessible by ozonolysis of the *syn*-/*anti*-benzene dioxides **23** and **26**[13] followed by reductive workup. These products can be transformed into the *rac*-1,4:2,3-anhydrohexitols **25a** (*gluco*)/**28a** (*altro*) and 1,4:3,6-dianhydroiditol (**29a**, "isoiditol")[10].

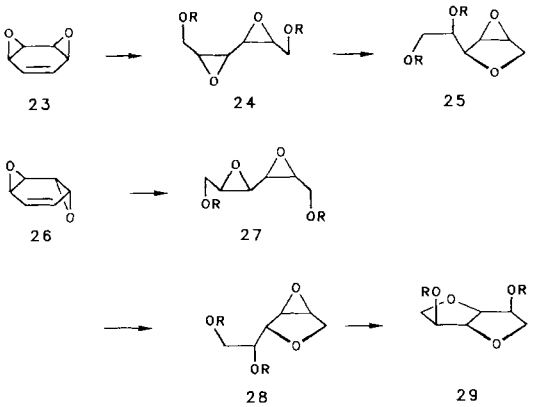

a, R = H, **b**, R = Ac

[13] H.-J. Altenbach, E. Vogel, *Angew. Chem. 84* (1972) 985; *Angew. Chem. Int. Ed. Engl. 11* (1972) 937; E. Vogel, H.-J. Altenbach, E. Schmidbauer, *Angew. Chem. 85* (1973) 862; *Angew. Chem. Int. Ed. Engl. 12* (1972) 838; H. Prinzbach, H.-W. Schneider, *Tetrahedron Lett. 16* (1975) 3073.
[14] K. Bock, I. M. Castilla, I. Lundt, C. Pedersen, *Acta Chem. Scand. 43* (1989) 264; vgl. J. G. Buchanan, A. R. Edgar, *Carbohydr. Res. 10* (1969) 295.

[15] R. Schwesinger, K. Piontek, W. Littke, O. Schweikert, H. Prinzbach, *Tetrahedron Lett. 23* (1982) 2427; R. Schwesinger, K. Piontek, W. Littke, H. Prinzbach, *ibid. 26* (1985) 1201; R. Schwesinger, *Inorg. Chim. Acta 155* (1989) 145.

[16] Crystal structure data for **4**: The structure was solved by direct methods (SDP MULTAN 82). Space group $P2_12_12_1$ (No. 19), $a = 4.780(1)$, $b = 9.407(1)$, $c = 13.640(1)$ Å, $V = 613.3$ Å^3, $Z = 4$, $\varrho = 1.387$ gcm^{-3}, NONIUS diffractometer CAD4 with $Cu_{K\alpha}$ radiation, $2\theta = 4°-150°$, 782 reflections were measured, 692 were considered as observed ($I > 2\sigma(I)$). $R = 0.054$. Further details of the crystal structure investigation may be obtained from the Fachinformationszentrum Karlsruhe, Gesellschaft für wissenschaftlich-technische Information mbH, D-7514 Eggenstein-Leopoldshafen 2 (FRG), on quoting the depository number CSD-54522, the names of the authors, and the journal citation.

[17] W. Littke, U. Drück, *Angew. Chem. 86* (1974) 557; *Angew. Chem. Int. Ed. Engl. 13* (1974) 539.

On the other hand, 1,3-diphenyl-1,3-propanedione (**1a**) is known to react smoothly with **2a** in diethyl ether to give 4-benzoyl-2,3-dioxo-5-phenyl-2-3-dihydrofurans **4a**.[2] Under the same conditions, we obtained 5-*tert*-butyl-2,3-dioxo-4-pivaloyl-2,3-dihydrofuran (**4b**) from **1b** and **2a** (Table 1).

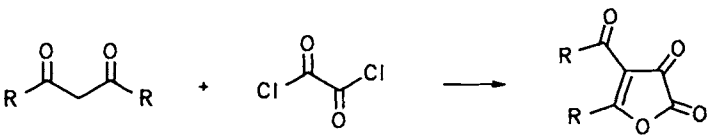

1a: R = Ph
1b: R = *t*Bu

2a

4a: R = Ph
4b: R = *t*Bu

Facile Synthesis of 4-Acyl-5-alkyl-2,3-dioxo-2,3-dihydrofurans and Alkylidenebutenolides**

By *Rolf W. Saalfrank** and *Thomas Lutz*

Dedicated to Professor Hans Jürgen Bestmann on the occasion of his 65th birthday

Earlier we obtained the tetranuclear metal chelate complexes **3** by reaction of diethyl malonate with methylmagnesium iodide or the system methyllithium/metal dichloride and with oxalyl chloride (**2a**) at −78 °C in tetrahydrofuran followed by workup with aqueous ammonium chloride solution.[1] Our attempts to generalize this concept have failed so far. Under the conditions employed, α, γ-dicarbonyl compounds with alkyl or aryl substituents do not undergo *spontaneous self-assembly* to form *adamantanoid* chelate complexes of type **3**.

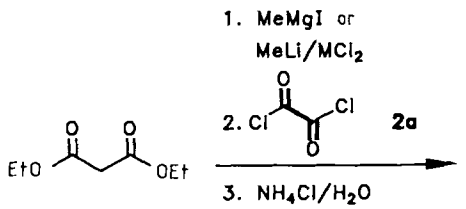

1. MeMgI or MeLi/MCl$_2$
2. **2a**
3. NH_4Cl/H_2O

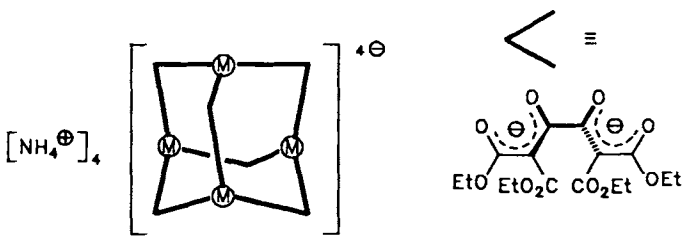

3

3	a	b	c	d
Ⓜ	$Mg^{2\oplus}$	$Mn^{2\oplus}$	$Co^{2\oplus}$	$Ni^{2\oplus}$

Apparently, the situation is completely different for α,γ-diketones **1c–f** containing at least one α-hydrogen in R^1 and/or R^2. *Ziegler* et al.[2] have reported that they were unsuccessful in preparing the analogous furan-2,3-diones **4** by reaction of acetylacetone (**1c**), benzoylacetone (**1f**), etc, with **2a**. In principle, however, it should be possible for the reaction of such α,γ-diketones and **2a** either to give tetranuclear chelate complexes of type **3** via template coupling or to afford furan-2,3-diones **4** via intramolecular ring-closure.

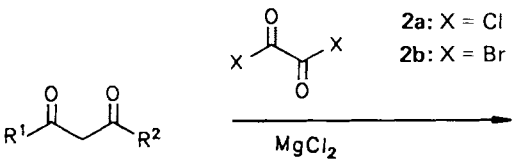

2a: X = Cl
2b: X = Br

$MgCl_2$

1c-f

4c-f ⇌ **5**

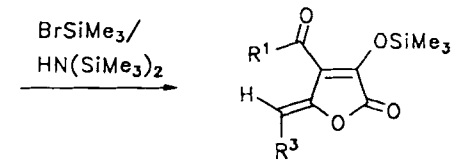

$BrSiMe_3/HN(SiMe_3)_2$

6

1, 4	c	d	e	f
R^1	Me	Me	Me	Me
R^2	Me	Et	CH_2CHMe_2	Ph

5, 6	a	b	c
R^1	Me	Me	Me
R^3	H	Me	$CHMe_2$

[*] Prof. Dr. R. W. Saalfrank, Dipl.-Chem. T. Lutz
Institut für Organische Chemie der Universität Erlangen-Nürnberg
Henkestrasse 42, D-8520 Erlangen (FRG)

[**] 4-Acyl-5-alkyl-2,3-dioxo-2,3-dihydrofurans, Part 1. This work was supported by the Deutsche Forschungsgemeinschaft and the Fonds der Chemischen Industrie.

Our experience with metal-assisted synthesis of tetranuclear chelate complexes **3** made it reasonable to attempt the reaction of α,γ-diketones containing an α-hydrogen with **2a** in diethyl ether in the presence of magnesium chloride.[3] Under these conditions, we obtained the previously unknown compound 4-acetyl-5-methyl-2,3-dioxo-2,3-dihydrofuran (**4c**) from **1c** and **2a**. According to the ^{1}H NMR spectrum, **4c** exists exclusively in the keto form in deuterochloroform at −55 °C (Table 1). At 27 °C, however, **4c** is in equilibrium with approximately 10% of the corresponding enol **5a**.

Surprisingly, the magnesium chloride-induced reaction of the unsymmetrically substituted diketones **1d, e** with **2a** proceeds both *regio-* and *stereospecifically* and affords exclusively enols **5b, c** (Table 1). The information provided by an *NOE* difference spectrum of the silyl enol ether **6b** supports the *Z* configuration proposed for the alkylidenebutenolides **5b, c**. Enols **5a–c** react readily with bromotrimethylsilane in the presence of hexamethyldisilazane to give the corresponding silyl enol ethers **6a–c**; compound **6a** is very sensitive, whereas **6b** and **6c** can be easily purified by kugelrohr distillation (Table 1).

Table 1. Data for the compounds **4b, c, f, 5b, c**, and **6a–c**[a].

4b: 7.7 g (65%), m.p. 94 °C (from $CHCl_3$). IR: $\tilde{\nu}$ = 1740, 1670, 1645 (C=O), 1590 cm^{-1} (C=C). ^{1}H NMR: δ = 1.24, 1.32 (s each, 9H each, 2 $(CH_3)_3$). ^{13}C NMR: δ = 27.32, 27.58 ($(CH_3)_3$), 36.64, 44.81 (C_q), 119.66, 152.71 (=C), 177.49, 189.31, 206.31 (C=O). MS: *m/z* 238 ($M^{\oplus}$)

4c: 4.8 g (62%), m.p. 68 °C (dec.; from ether/hexane (2/1)). IR: $\tilde{\nu}$ = 1780, 1680 (C=O), 1600 cm^{-1} (C=C). ^{1}H NMR (−55 °C): δ = 2.55, 2.88 (s each, 3H each, 2 CH_3). ^{13}C NMR (−55 °C): δ = 17.77, 30.66 (CH_3), 116.56, 152.26 (=C), 175.68, 192.24, 192.59 (C=O). MS: *m/z* 154 ($M^{\oplus}$)

4f: 7.4 g (68%), m.p. 69 °C (dec.; from ether/hexane (2/1)). IR: $\tilde{\nu}$ = 1755, 1685, 1645 (C=O), 1590 cm^{-1} (C=C). ^{1}H NMR: δ = 2.08 (s, 3H, CH_3), 7.60–8.05 (m, 5H, C_6H_5). ^{13}C NMR: δ = 29.66 (CH_3), 92.32, 128.02 (=C), 129.21, 129.85, 134.37, 137.84 (phenyl-C), 144.40, 165.14, 189.13 (C=O). MS: *m/z* 216 ($M^{\oplus}$)

5b: 6.9 g (82%), m.p. 111 °C (dec.; from $CHCl_3$). IR: $\tilde{\nu}$ = 1765, 1740 (C=O), 1640 cm^{-1} (C=C). ^{1}H NMR: δ = 1.98 (d, 3H, CH_3), 2.55 (s, 3H, CH_3), 5.96 (q, 1H, =CH), 9.95 (s, br, OH). ^{13}C NMR: δ = 11.50, 30.70 (CH_3), 110.52, 116.94, 143.20, 149.95 (=C), 164.22, 195.64 (C=O). MS: *m/z* 168 ($M^{\oplus}$)

5c: 7.6 g (78%), m.p. 73 °C (dec.; from $CHCl_3$). IR: $\tilde{\nu}$ = 1780, 1740 (C=O), 1640 cm^{-1} (C=C). ^{1}H NMR: δ = 1.18 (d, 6H, CH_3), 2.58 (s, 3H, CH_3), 3.06 (m, 1H, CH), 5.66 (d, 1H, =CH), 9.87 (s, br, 1H, OH). ^{13}C NMR: δ = 22.66, 30.81 (CH_3), 26.06 (CH), 117.82, 122.81, 141.01, 149.13 (=C), 164.46, 195.34 (C=O). MS: *m/z* 196 ($M^{\oplus}$)

6a: 1.8 g (78%); because of the low stability, only an 1H NMR spectrum was recorded. ^{1}H NMR (60 MHz): δ = 0.37 (s, 9H, $Si(CH_3)_3$), 2.46 (s, 3H, CH_3), 5.08, 5.57 (d each, 1H each, 2=CH)

6b: 2.1 g (86%), b.p. 87 °C/0.04 Torr. IR: $\tilde{\nu}$ = 1770, 1690 (C=O), 1615 cm^{-1} (C=C). ^{1}H NMR: δ = 0.37 (s, 9H, $Si(CH_3)_3$), 1.85 (d, 3H, CH_3), 2.46 (s, 3H, CH_3), 6.03 (q, 1H, =CH). ^{13}C NMR: δ = 0.63 ($Si(CH_3)_3$), 11.18, 31.02 (CH_3), 111.00, 122.46, 143.30, 145.56 (=C), 164.77, 192.98 (C=O). MS: *m/z* 240 ($M^{\oplus}$)

6c: 2.4 g (91%), b.p. 91 °C/0.04 Torr. IR: $\tilde{\nu}$ = 1760, 1680 (C=O), 1600 cm^{-1} (C=C). ^{1}H NMR: δ = 0.18 (s, 9H, $Si(CH_3)_3$), 1.18 (d, 6H, CH_3), 2.45 (s, 3H, CH_3), 2.85 (m, 1H, CH), 5.88 (d, 1H, =CH). ^{13}C NMR: δ = 0.82 ($Si(CH_3)_3$), 22.67, 31.72 (CH_3), 25.72 (CH), 122.67, 123.36, 141.12, 145.75 (=C), 164.95, 193.21 (C=O). MS: *m/z* 268 ($M^{\oplus}$)

[a] IR spectra: IR-5 instrument (Beckman), in KBr, except for **6b, c** (neat) ^{1}H/^{13}C NMR spectra: JNM GX-400 instrument (Jeol); solvent, $CDCl_3$, TMS int., except for **4f** ([D_6]acetone). Mass spectra: Varian MAT-CH-4B, direct inlet, 70 eV.

The reaction of benzoylacetone (**1f**) with **2a** in the presence of magnesium chloride is much more complicated and gives a mixture of substances that is very difficult to separate. On the other hand, reaction with oxalyl bromide (**2b**) under otherwise identical conditions smoothly leads to 4-acetyl-2,3-dioxo-5-phenyl-2,3-dihydrofuran (**4f**) (Table 1). Moreover, we found that the use of the more reactive **2b** obviates the necessity of activating **1f** by addition of magnesium chloride. The new procedure is a considerable extension of the methods previously used for the synthesis of 2,3-dioxo-2,3-dihydrofurans[2, 4] and is strikingly simple to carry out.

Experimental Procedure

4b: A solution of **2a** (6.35 g, 50 mmol) in 20 mL of *n*-hexane was added dropwise over 0.5 h to a solution of **1b** (9.2 g, 50 mmol) in 30 mL of diethyl ether. Yellow crystals of **4b** were collected after 3 d.

4c, 5b, c: Magnesium chloride (1.2 g) was added to a solution of **1c–e** (50 mmol) in 50 mL of diethyl ether and the resulting mixture was added over 0.5 h to a vigorously stirred solution of **2a** (6.35 g, 50 mmol) in 25 mL of *n*-hexane at 0 °C (−10 °C for **4c**). After a reaction time of 3 h at 20 °C (−10 °C for **4c**), 25 mL of *n*-hexane was added, the reaction solution was filtered, the filtrate was concentrated to 30% using a rotory evaporator (water bath temperature 20 °C for **4c**), and the crystals were isolated (in the dark for **4c**).

Compound **4f** was obtained analogously (addition of magnesium chloride was not necessary) from **1f** (8.11 g, 50 mmol) and **2b** (10.79 g, 50 mmol).

6b, c: Hexamethyldisilazane (1.78 g, 11 mmol) and bromotrimethylsilane (1.84 g, 12 mmol), each in 5 mL of diethyl ether, were added in succession to a solution of **5b, c** (10 mmol) in 30 mL of diethyl ether at −78 °C. The resulting reaction mixture was allowed to warm over 20 h to 20 °C and filtered. The solvent was removed with a rotory evaporator and the product distilled.

Received: April 19, 1990 [Z3923 IE]
German version: *Angew. Chem. 102* (1990) 1064

CAS Registry numbers:
1b, 1118-71-4; **1c**, 123-54-6; **1d**, 3002-24-2; **1e**, 3002-23-1; **1f**, 93-91-4; **2a**, 79-37-8; **2b**, 15219-34-8; **4b**, 128751-99-5; **4c**, 128732-08-1; **4f**, 128732-09-2; **5a**, 128732-15-0; **5b**, 128732-10-5; **5c**, 128732-11-6; **6a**, 128732-12-7; **6b**, 128732-13-8; **6c**, 128732-14-9.

[1] R. W. Saalfrank, A. Stark, M. Bremer, H.-U. Hummel, *Angew. Chem. 102* (1990) 292; *Angew. Chem. Int. Ed. Engl. 29* (1990) 311.
[2] E. Ziegler, G. Kollenz, H. Igel, *Monatsh. Chem. 102* (1971) 1769.
[3] A general discussion on the increase in acidity due to metal complexation is found in R. P. Houghton, *Metal Complexes in Organic Chemistry*, Cambridge University Press, Cambridge 1979, pp. 114–116; cf. also M. W. Rathke, P. J. Cowan, *J. Org. Chem. 50* (1985) 2622; M. W. Rathke, M. A. Nowak, *Synth. Commun. 15* (1985) 1039; J. Skarzewski, *Tetrahedron 45* (1989) 4593; S. Shambayati, W. E. Crowe, S. L. Schreiber, *Angew. Chem. 102* (1990) 273; *Angew. Chem. Int. Ed. Engl. 29* (1990) 256.
[4] S. Muria, K. Hasegawa, N. Sonoda, *Angew. Chem. 87* (1975) 668; *Angew. Chem. Int. Ed. Engl. 14* (1975) 636; H. Alper, G. Vasapollo, *Tetrahedron Lett. 30* (1989) 2617.

Tetraphenylallylsodium Diethyl Ether: A Contact Ion Pair with an Intramolecular $Na^{\oplus}$ Sandwich**

By *Hans Bock,* Klaus Ruppert, Zdenek Havlas*, and *Dieter Fenske**

Dedicated to Professor Paul von Ragué Schleyer on the occasion of his 60th birthday

The successful growth of a single crystal of the paramagnetic contact ion pair $[(fluorenone^{\bullet\ominus})\{Na^{\oplus}(dme)_2\}]_2$ (dme = dimethoxyethane)[2] has been our starting point in the use of MNDO energy hypersurface calculations to discover other organic salts in which positive or negative charges bring about similarly amusing perturbations, such as the twisting of the two molecular halves in ethene di-

[*] Prof. Dr. H. Bock, Dipl.-Chem. K. Ruppert, Dr. Z. Havlas
Institut für Anorganische Chemie der Universität
Niederurseler Hang, D-6000 Frankfurt am Main 50 (FRG)
Prof. Dr. D. Fenske
Institut für Anorganische Chemie der Universität
Engesserstrasse, D-7500 Karlsruhe (FRG)

[**] Structures of Perturbed π Systems, Part 4, and Electron Transfer and Ion Pair Formation, Part 19. This work was supported by the Deutsche Forschungsgemeinschaft, the Fonds der Chemischen Industrie, the Alexander von Humboldt-Stiftung (*Z. H.*), and the State of Hesse. Parts 3 and 18: [1a] and [1b].

cations $((H_3C)_2N)_2^{\oplus}C\text{–}C^{\oplus}(N(CH_3)_2)_2$[3] and dianions $(H_5C_6)_2{}^{\ominus}C\text{–}C^{\ominus}(C_6H_5)_2$.[1a] For molecular anions, one observes, in addition, that infinite contact-ion-pair strings[1a] or even three-dimensional networks[4] are formed around the countercations with their usually high-coordination-number dimers;[2] these structures may contain rather surprising connecting links, such as intermolecular "dibenzene sodium sandwich" double cones.[1a]

Our procedure for semiempirical "molecule screening" will be illustrated by the twisted π-hydrocarbon allene, for which MNDO calculations[5] support the sequence of electron transfers and protonation shown in Figure 1 as a speculative redox pathway for formation of contact ion pairs. Obviously, the gas-phase structure of allene[2] is satisfactorily reproduced by the lowest-energy MNDO structure and the single electron transfer to its radical anion should reduce the dihedral angle by about half. The second reduction to the dianion should require considerably more energy (Fig. 1: $\Delta\Delta H_f^{MNDO}$ $(D_2 \rightarrow C_{2v}) \approx 660$ kJ mol^{-1}) and cause dramatic

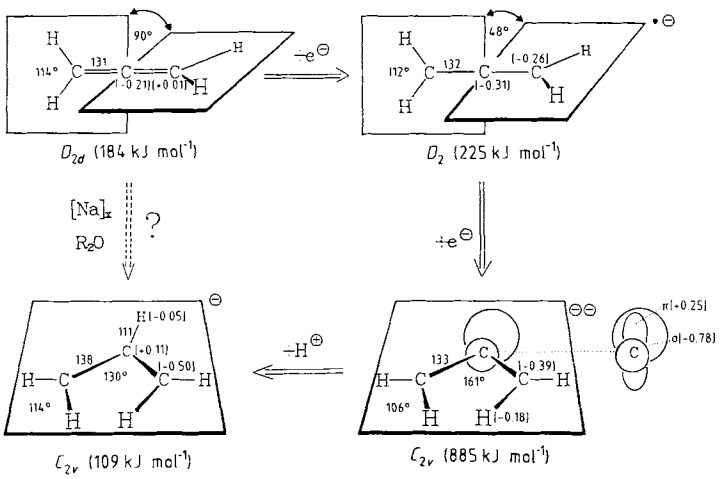

Fig. 1. MNDO geometry-optimized structures of allene, its radical anion and dianion, and the protonation product of the latter, allyl anion, together with MNDO enthalpies of formation ΔH_f° [kJ mol^{-1}] and MNDO charge distributions q_μ (bond lengths in pm).

structural changes: thus, the molecular skeleton should be flattened and bent (Fig. 1: $\sphericalangle$ CCC = 161°), thereby forming a nonstabilized and therefore extremely basic carbon σ lone pair (Fig. 1: $q_{C,\sigma}^{MNDO} = -0.78$). Its protonation (e.g., by the ether solvent) may then result in an allyl anion with each half of the negative charge at the outer carbon centers (Fig. 1: $q_C^{MNDO} = -0.50$).

Well invented? Reacting tetraphenylallene in diethyl ether, which had been dried over Na/K ($c_{H^{\oplus}} < 1$ ppm), at room temperature and under Ar with a sodium mirror produced by vacuum distillation[7] (cf. Ref. [1a]) generates a dark red solution,[8] from which black crystals with a metallic luster deposit.[9] The crystal structure of tetraphenylallylsodium diethyl ether (**1**) (Fig. 2) largely corresponds to that calculated for the allyl anion (Fig. 1): C–C distances of approximately 139 pm and a C–C–C bending angle of approximately 130° are found.

A striking feature of the structure of **1** (Fig. 2) is the intramolecular cage of the two phenyl rings facing each other: it encapsulates the $Na^{\oplus}$ countercation and is sealed by a "solvate plug" consisting of a coordinated diethyl ether in W conformation. A literature search for analogous compounds with a similar "intramolecular alkali-metal-cation sandwich" proved fruitless.

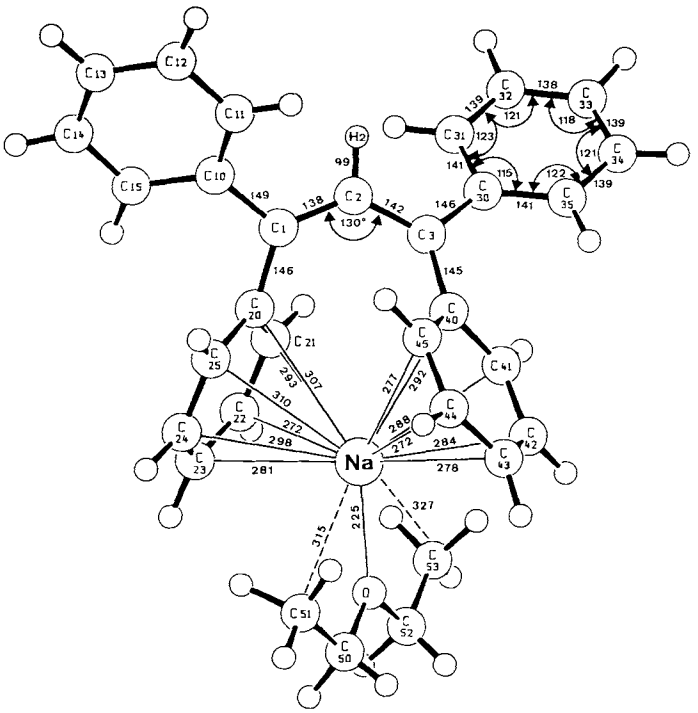

Fig. 2. Molecular structure of **1** [9]. Significant distances [pm, ±0.8] and angles [°, ±0.3]: C1-C2 138, C2-C3 142, C2-H2 99, C1-C(ring) 145, C3-C(ring) 149, C-C(ring) 139, Na···C(ring) 272–310, Na-O 225, O-C50 144; C1-C2-C3 130, C10-C1-C20 117, C30-C3-C40 120, (C50-O-C52 113, C10-C1-C20)/(C30-C3-C40) 46, (C11-C10-C15)/CC1-C2-C3) 40, (C31-C30-C35)/(C1-C2-C3) 49, (C21-C20-C25)/(C1-C2-C3) 58, (C41-C40-C45)/(C1-C2-C3) 55.

Extensive MNDO energy hypersurface calculations for the model compound diphenylallylsodium diethyl ether,[5, 11] the energy minimum of which is represented by the computed structure in Figure 3a, plausibly explain the formation of the intramolecular sodium sandwich: the diphenylallyl anion in its energy-favored C_2 structure, with the opposing phenyl rings each turned around their C_{allyl}–C_{phenyl} axes by 41°, exhibits a total negative charge of $\Sigma q_C = -0.47$ at the five "outer" ring carbons; this charge exceeds that calculated for one of the allyl carbons (−0.36) (Fig. 3b). If the $Na^{\delta\oplus}$ countercation is fixed in the calculations at one of the charge-bearing allyl anion centers, therefore, it moves along a barrier-free path on the MNDO hypersurface to the point of maximum contact-ion-pair interaction between the two phenyl rings facing each other at an acute angle (Fig. 3b). The calculated total charge at the Na center amounts to +0.34; that is, for the $Na^{\oplus}$ allyl anion salt described here, predominantly covalent complexation is predicted. The largest single contribution to the MNDO enthalpy of formation is made by the ether solvate plug in W conformation.

Altogether, the structure determination of carefully grown single crystals of organic salts is of current interest for two reasons.[1] Novel bonding possibilities,[1] such as the intramolecular $Na^{\oplus}$ sandwich, are discovered and hints con-

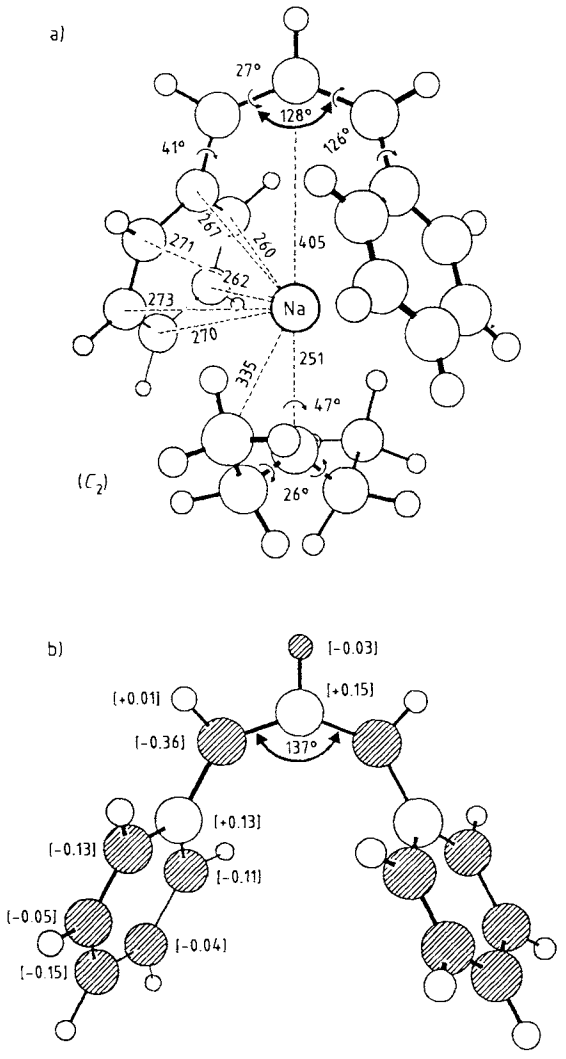

Fig. 3. MNDO energy hypersurface model calculations [5, 11]. a) Structure of diphenylsallylsodium diethyl ether (bond lengths in pm); b) structure and charge distribution of diphenylallyl anion.

cerning microscopic pathways[12] of complicated redox reactions via or to contact ion pairs[1b] are suggested.

Received: April 27, 1990 [Z 3936 IE]
German version: *Angew. Chem. 102* (1990) 1095

[1] a) H. Bock, K. Ruppert, D. Fenske, *Angew. Chem. 101* (1989) 1717; *Angew. Chem. Int. Ed. Engl. 28* (1989) 1685; b) H. Bock, P. Hänel, H.-F. Herrmann, *Z. Naturforsch. B 45* (1990), in press.

[2] H. Bock, H.-F. Herrmann, D. Fenske, H. Goesmann, *Angew. Chem. 100* (1988) 1125; *Angew. Chem. Int. Ed. Engl. 27* (1988) 1067, and references cited therein.

[3] H. Bock, K. Ruppert, K. Merzweiler, D. Fenske, H. Goesmann, *Angew. Chem. 101* (1989) 1715; *Angew. Chem. Int. Ed. Engl. 28* (1989) 1684, and references cited therein.

[4] Cf., e.g., $[(NC)_2C{=}C(CN)_2^{\ominus}K^{\oplus}(H_3CO\text{-}CH_2CH_2\text{-}OCH_3)]_x$, H. Bock, K. Ruppert, D. Fenske, H. Goesmann, unpublished.

[5] For the MNDO calculations cf. [11]; Na parameters: $U_{ss} = -4.611$ eV; $U_{pp} = -2.3643$ eV; $\xi_s = 0.73384$ a.u.; $\xi_p = 0.82957$ a.u.; $\beta_s = 1.14529$ eV; $\beta_p = 1.14101$ eV; $\alpha = 1.26194$ Å^{-1}; $g_{ss} = 7.20$ a.u.; $g_{sp} = 5.18$ a.u.; $g_{pp} = 4.233$ a.u.; $h_{sp} = 0.6428$ a.u. These data have been optimized analogously to the parameters for Li already included in the program and those additionally derived for K (Z. Havlas, unpublished).

[6] Y. Ohshima, S. Yamamoto, N. Nakata, K. Kuchiku, *J. Phys. Chem. 91* (1987) 4696, and references cited therein. For tetraphenylallene we determined the following parameters by single-crystal structure analysis: C=C 132 pm, ∢ C=C=C 173.5°, w ($C_2C\cdots CC_2$) 87.1° (H. Bock, K. Ruppert, unpublished).

[7] Vacuum distillation of Na (120 mg, 5.2 mmol) in a Schlenk trap produces a sodium mirror, which reacts with tetraphenylallene (900 mg, 2.6 mmol) in 25 mL of diethyl ether, distilled over Na/K alloy under Ar at room temperature, in 0.5 h to give a dark red solution. After several days, black, extremely air- and moisture-sensitive crystals separate, which have to be handled under a flow of purified N_2.

[8] For NMR investigations of the reduction of tetraphenylallene with Li, Na, or K in ether, cf. A. Rajca, L. M. Tolbert, *J. Am. Chem. Soc. 109* (1987) 1783; *ibid. 107* (1985) 2971, and references cited therein; accompanying calculations: A. Rajca, A. Streitwieser, Jr., L. M. Tolbert, *ibid. 109* (1987) 1790. Cf. also the literature review by G. Fraenkel, A. Chow, W. R. Winchester, *ibid. 112* (1990) 1382, 2582.

[9] Crystal structure analysis: $C_{27}H_{21}Na \cdot O(C_2H_5)_2$, $a = 898.1(6)$, $b = 1666.8(19)$, $c = 1660.6(9)$ pm, $\beta = 92.41(3)°$, $V = 2483.7 \times 10^6$ pm^3 (200 K), space group $P2_1/n$, $Z = 4$, $\mu(Mo_{K\alpha}) = 0.7$ cm^{-1}, STOE STADI IV four-circle diffractometer, 2θ region: 3–56°, ω scan, 5955 reflections found, of which 3364 are independent with $I > 2\sigma(I)$, structure determination by Patterson methods, SHELXS-86, SHELX-76, SCHAKAL, $R = 0.066$, $R_w = 0.042$; C, O, Na positions anisotropically refined, all H positions found and isotropically improved. Further details of the crystal structure investigation may be obtained from the Fachinformationszentrum Karlsruhe, Gesellschaft für wissenschaftlich-technische Information mbH, D-7514 Eggenstein-Leopoldshafen 2 (FRG), on quoting the depository number CSD-54698, the names of the authors, and the journal citation.

[10] Known are numerous "alkali-cation half-sandwich" compounds (cf. the reviews by W. N. Setzer, P. von R. Schleyer, *Adv. Organomet. Chem. 24* (1985) 353; C. Schade, P. von R. Schleyer, *ibid. 27* (1987) 169) as well as our *inter*molecular "$Na(C_6H_5)_2$ complex" between each two tetraphenylethene dianion–$Na^{\oplus}$ contact ion pairs [1a]. *Intra*molecular bis(μ^3-benzylidene)phosphonium complexes of $Na^{\oplus}$ and $K^{\oplus}$ are reported by H. Schmidbaur, U. Deschler, B. Milewski-Mahrla, B. Zimmer-Gasser, *Chem. Ber. 115* (1981) 608. Also important in this context is the structure determination of $C_3H_5Li \cdot$ pmdta by E. Weiss, U. Schürmann, H. Dietrich, W. Mahdi, *J. Organomet. Chem. 332* (1987) 299, $C_3H_5Li \cdot$ tmeda by H. Köster, E. Weiss, *Chem. Ber. 115* (1982) 3422, and of 1,3 diphenylallyllithium diethyl ether by G. Boche, H. Etzrodt, M. Marsch, W. Massa, G. Baum, H. Dietrich, W. Mahdi, *Angew. Chem. 98* (1986) 84; *Angew. Chem. Int. Ed. Engl. 25* (1986) 104.

[11] The MNDO calculations have been performed using the program SCAMP IV/1 kindly provided by *T. Clark* (Universität Erlangen-Nürnberg) and the VAX 11/750 of our group; the Na parameters used are specified in [5]. From the experimentally determined structure only the data of the phenyl rings have been adopted, all other bond lengths and angles are optimized. The MNDO enthalpies of formation ΔH_f° [kJ mol^{-1}] are: diphenylallyl anion, +211; diphenylallylsodium, −218; diphenylallylsodium diethyl ether, −539. Experimental (Fig. 2) and calculated structure data (Fig. 3b) agree satisfactorily with the exception of the too short Na–C_{phenyl} distances and the exaggerated Na–O coordination bond length, resulting from the accompanying steric overcrowding.

[12] Cf. "How Do Medium-Sized Molecules React?" by H. Bock, *Abh. Math.-Naturwiss. Kl. Akad. Wiss. Lit. Mainz 1986*, No. 2, pp. 1–35; *Polyhedron 7* (1988) 2429; *Öster. Chem. Z. 90* (1989) 142.

Thermal Decomposition of the Nonmetal Octahedron $(ClB)_4P_2$ by Elimination of Its PP Octahedral Edge

By *Bahman Solouki, Hans Bock,* Wolfgang Haubold,** and *Willi Keller*

Dedicated to Professor Rolf Huisgen on the occasion of his 70th birthday

How do medium-sized molecules containing between 4 and 20 centers react?[1, 2] Their relevant reaction dynamics

[*] Prof. Dr. H. Bock, Dr. B. Solouki
Institut für Anorganische Chemie der Universität
Niederurseler Hang, D-6000 Frankfurt am Main 50 (FRG)
Prof. Dr. W. Haubold, Dr. W. Keller
Institut für Chemie der Universität Hohenheim
Garbenstrasse 30, D-7000 Stuttgart 70 (FRG)

[**] Gas-Phase Reactions, Part 79. This work was supported by the Deutsche Forschungsgemeinschaft, the Fonds der Chemischen Industrie, and the States of Hesse and Baden-Württemberg. Part 78: H. Bock, M. Bankmann, *Phosphorus, Sulfur, Silicon Relat. Elem.* (1990), in press; cf. also Part 77, *ibid. 49* (1990) 3.

can presently neither be imagined nor rationalized, owing to the prohibitive number of internal degrees of freedom $(3n-6)$,[1, 2b] according to which a 10-center molecule fills a 24-dimensional hyperspace. Nevertheless, chemists can contribute partial solutions to this fundamental problem, for example, by synthesizing suitable precursors for thermolytic fragmentations, which allow the identification of short-lived[2c] and sometimes "chemically activated"[2d] intermediates. Based on the experimental data, additional energy hypersurface calculations along selected molecular-dynamics coordinates afford approximative insight into the microscopic reaction pathways.

The title compound, $(ClB)_4P_2$, a *closo*-1,2-diphosphahexaborane, recently prepared by copyrolysis of Cl_2BBCl_2 and PCl_3,[3a] is selected as a model, because electron-deficient clusters can be transformed in competing thermal reactions by either rearrangement [Eq. (a)] or elimination of "leaving molecules" [Eq. (b)], thereby improving the electronic configuration. Textbook examples are the *ortho* → *meta* → *para* isomerization of the icosahedral carborane $B_{10}C_2H_{12}$ and the pyrolytic dehydrogenation of B_2H_6 to $B_{10}H_{14}$.[3b] Upon gas-phase thermolysis under close to unimolecular conditions in a white-hot flow-pyrolysis tube (Fig. 1: $p \approx 10^{-4}$ mbar, $T > 1200$ K, PE-spectroscopic real-time analysis[2]), the nonmetal octahedron investigated here, **1**, chooses selective expulsion of the diphosphorus molecule, P≡P [Eq. (b)], analogous to N_2. The dimerization to the phosphorus tetrahedron, $2P_2 \rightleftarrows P_4$, has already been investigated by PE spectroscopy under similar flow conditions[4a] and becomes quantitative only below 1100 K. The other fragmentation product, the B_4Cl_4 tetrahedron,[4b] disproportionates largely to BCl_3 and boron[4] at these rather high pyrolysis temperatures (Fig. 1).

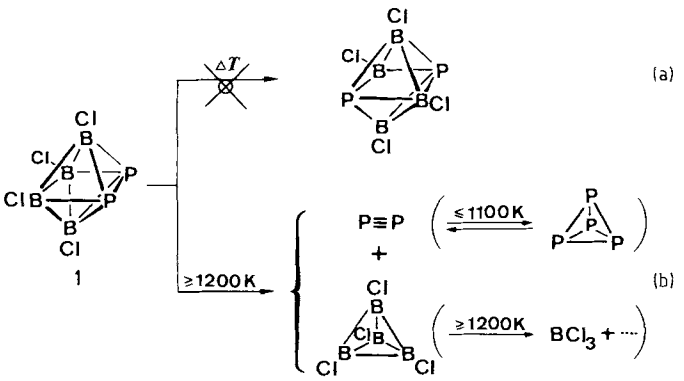

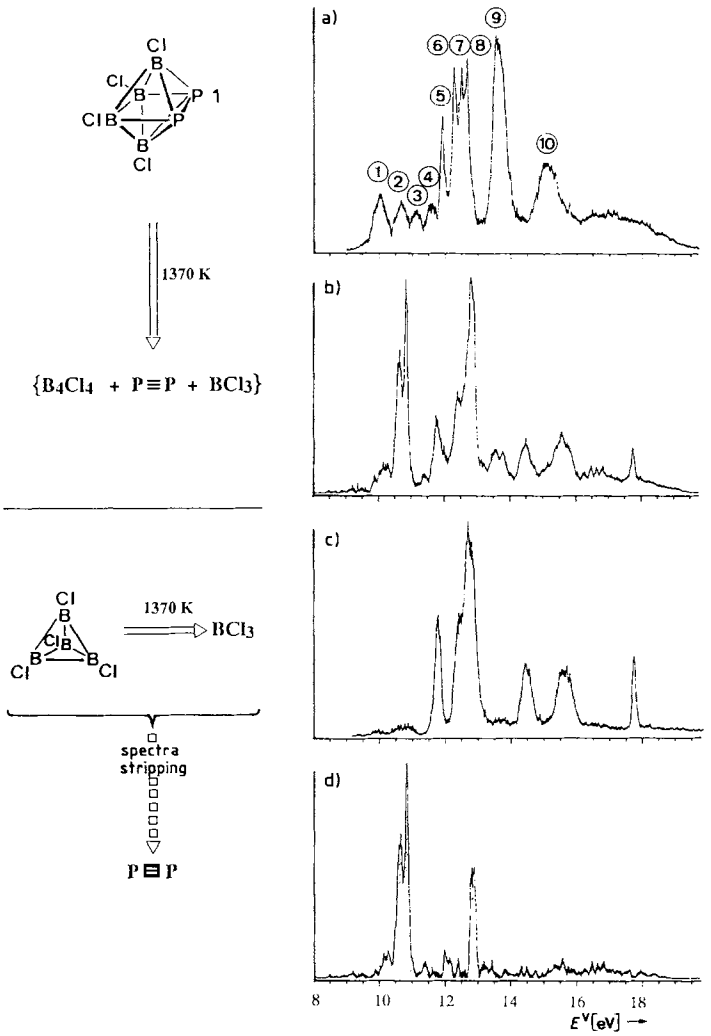

Fig. 1. He(I) PE spectra of $(ClB)_4P_2$, **1** (a), and its 1370 K pyrolysis mixture (b) as well as that of B_4Cl_4 (c) at the same temperature and the one resulting after digital subtraction (d) [2c], which satisfactorily resembles that of P_2 [4a]. E^V = vertical ionization energy. For the assignment of ①–⑩, see [5].

The selective thermal expulsion of an octahedral edge to give a tetrahedron [Eq. (b)] is surprising and novel. Topologically, six bonds have to be broken—as also on fragmentation into two three-membered ring radicals, $(ClB_2)P^{\bullet}$—that is, two more than on elimination of an octahedral center, for example, of BCl to yield the presumably trigonal-bipyramidal *closo*-$(ClB)_3P_2$. An energetically favored decomposition of **1** into B_4Cl_4 and P_2 is in accord with the assumed distribution of the 14 skeletal electrons over one σ_{pp}, two σ_{BBB}, and four σ_{BBP} bonds[5] as well as with the prediction that the reaction pathway, starting from the known C_{2v} molecular structure of **1**[3a] and proceeding in the direction of an internal a_2 coordinate, should be allowed by (orbital) symmetry.[6] These arguments are further supported by a MNDO enthalpy of formation hypersurface (cf. Ref. [2] and especially Ref. [4a]), although its calculation is based on the rather risky assumption that the essential dynamic coordinates for the reaction pathway (b) of the 10-center molecule with altogether 24 internal degrees of freedom[6] may be approximated by the distance changes $\Delta d_{(B_4)(P_2)}$ and Δd_{PP}.

The extensive approximative calculations predict an activation barrier of about 300 kJ mol^{-1} for reaction (b), qualitatively corresponding to the rather high pyrolysis temperature necessary. The reaction products, B_4Cl_4 and P_2, are located in a shallow minimum only about 60 kJ mol^{-1} below the saddle point; that is, in decomposition equilibrium (b), the subsequent thermal disproportionation $B_4Cl_4 \rightarrow BCl_3 + (B)_\infty$ will be responsible for the irreversible process. The geometry-optimized MNDO calculations suggest that the structure at the saddle point is a slightly bent B_4 ring, which only later on forms a tetrahedron along coordinate ζ. The elimination of the relatively electron-rich P_2 donor from the B_4P_2 cluster dramatically changes the charge distribution, especially at the axial B centers (from −0.25 to +0.16; Fig. 2).

The thermal elimination of the P_2 octahedral edge from the nonmetal octahedron **1**, as well as the experimental details such as the high pyrolysis temperature and the at first

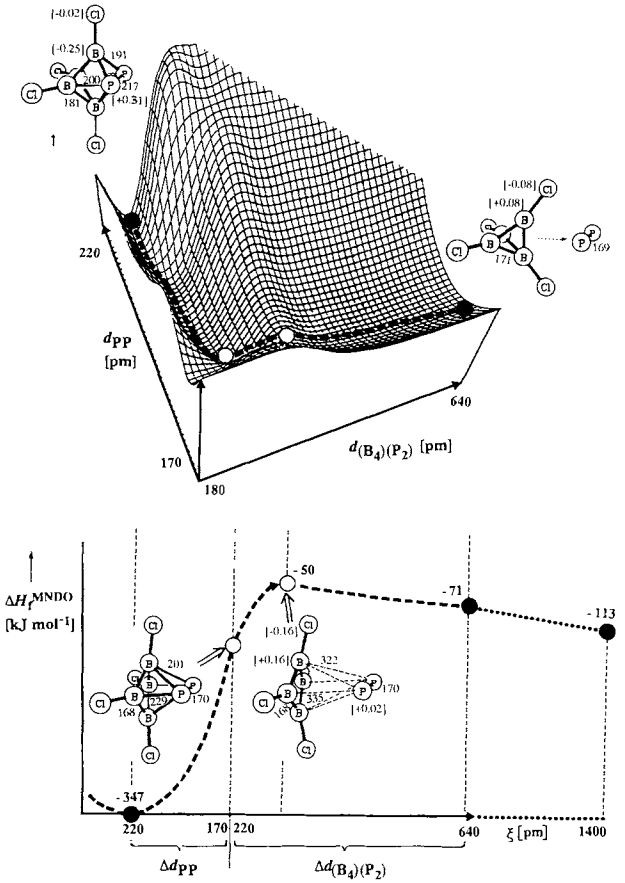

Fig. 2. Top: Simplified ΔH_f^{MNDO} hypersurface along the coordinates $d_{(B_4)(P_2)}$ and d_{PP}, containing the structural data of educts and products reported in the literature [3] (●, local minima; ○, coordinate change as well as saddle point). Bottom: The reaction profile along the hypersurface cut (– – –) defined by the selected coordinates ζ together with the calculated structures at points ○ (bond lengths in pm; representative MNDO charge distribution in brackets).

sight surprising selectivity of the decomposition, can be plausibly rationalized by the calculated MNDO hypersurface—despite the drastic approximations used. Obviously, a potential fracture site is introduced by the P_2 donor group into the otherwise rather electron-poor octahedral borane and constitutes a potentially interesting synthesis principle for the preparation of unknown strained nonmetal tetrahedra.

Received: May 21, 1990 [Z 3969 IE]
German version: *Angew. Chem. 102* (1990) 1099

CAS Registry numbers:
P≡P, 12185-09-0; tetrachloro-*closo*-1,2-diphosphahexaborane, 112897-10-6; B_4Cl_4, 17156-85-3.

[1] a) Cf. the following Nobel Prize lectures: Y. T. Lee, *Angew. Chem. 99* (1987) 967; *Angew. Chem. Int. Ed. Engl. 26* (1987) 939; J. C. Polanyi, *ibid. 99* (1987) 981 and *26* (1987) 952; b) cf. also Y. T. Lee, *Chem. Rev. 87* (1987) 7A; R. D. Levine, R. B. Bernstein: *Molecular Reaction Dynamics and Chemical Reactivity*, Oxford University Press 1987, and references cited in these publications.

[2] a) H. Bock, *Polyhedron 7* (1988) 2429 *Österr. Chem. Z. 90* (1989) 142; *Abh. Naturwiss. Kl. Akad. Wiss. Lit. Mainz 1986*, No. 2, pp. 1–35; *Actual. Chim. 1986*, 33; *Nova Acta Leopold. 59* (1985) 93; b) H. Bock, R. Dammel, B. Roth, *ACS Symp. Ser. 232* (1985) 93; c) H. Bock, B. Solouki, S. Aygen, M. Bankmann, O. Breuer, R. Dammel, J. Dörr, M. Haun, T. Hirabayashi, D. Jaculi, J. Mintzer, S. Mohmand, H. Müller, P. Rosmus, B. Roth, J. Wittmann, H. P. Wolf, *J. Mol. Struct. 173* (1988) 31; d) H. Bock, R. Dammel, *Angew. Chem. 99* (1987) 503; *Angew. Chem. Int. Ed. Engl. 26* (1987) 481; *J. Am. Chem. Soc. 110* (1988) 5261; H. Bock, M. Bankmann, *Angew. Chem. 101* (1989) 950; *Angew. Chem. Int. Ed. Engl. 28* (1989) 911, and references cited in these publications.

[3] a) W. Haubold, W. Keller, G. Sawitzki, *Angew. Chem. 100* (1988) 958; *Angew. Chem. Int. Ed. Engl. 27* (1988) 925. b) Cf., e.g., N. Wiberg: *Hollemann-Wiberg: Lehrbuch der Anorganischen Chemie, 91.–100. Aufl.*, de Gruyter/Berlin 1985, p. 820ff; J. J. Ott, C. A. Brown, B. M. Gimarc, *Inorg. Chem. 28* (1989) 4269, references cited therein.

[4] a) PE spectrum of P≡P: H. Bock, H. Müller, *Inorg. Chem. 23* (1984) 4365. For the equilibrium $P_4 \rightleftarrows 2P_2$, the temperature dependence of the equilibrium constant was determined by PE spectroscopy and amounts to $\ln K_p = -27870\,(1/T) + 12.90$; $R = 0.995$; the dissociation energy is calculated to be $\Delta\Delta H_f^{MNDO} \approx 177$ kJ mol^{-1}; b) PE spectrum of B_4Cl_4: P. R. LeBreton, S. Krano, M. Shahbaz, S. L. Emery, J. A. Morrison, *J. Am. Chem. Soc. 108* (1986) 3937, and references cited therein; thermolysis: B. Solouki, H. Bock, W. Haubold, unpublished results; c) PE spectrum of BCl_3: cf. the review by H. Bock in *Gmelin: Handbuch der Anorganischen Chemie Band 8/23, Teil 5*, Springer, Berlin 1975, p. 170f.

[5] Within the He(I) measuring region, according to the rule of thumb $\Sigma(1s_H + np_F)/2$ (cf. [2c, 3]), about 15 of a total of 25 valence ionizations are expected; these generate the respective radical-cation states of irreducible representations $\Gamma(C_{2v}) = 10a_1 + 3a_2 + 6b_1 + 6b_2$. This is based on the assumption that the formal skeletal electrons of the cluster $(4 \times 2(B) + 2 \times 3(P) = 14)$ are approximately distributed over one σ_{PP} two-center bond and two σ_{BBB} and four σ_{BBP} three-center bonds. The PE-spectroscopic ionization bands of **1** (Abb. 1a) are assigned by Koopmans' correlation with MNDO eigenvalues as follows: ①, 10.1 eV (σ_{BP}, $3A_2$); ②, 10.6 eV (n_P, $6B_1$); ③, 11.2 eV (n_P, $10A_1$); ④, 11.6 eV (σ_{BP}, $6B_2$); ⑤, 11.9 eV (σ_P, $9A_1$); ⑥, 12.3 eV (n_{Cl}, $5B_1$ and $2A_2$); ⑦, 12.5 eV (n_{Cl}, $5B_2$); ⑧, 12.7 eV (n_{Cl}, $8A_1$ and $4B_2$); ⑨, 13.6 eV (n_{Cl}, $4B_1/1A_2/3$ B_1 and $7A_1$); ⑩, 15.1 eV (σ_{BP}, $6A_1$ and $3B_2$); 17.3 eV (σ_{BCl}, $5A_1$).

[6] For the orbital correspondence analysis in maximum symmetry (OCAMS), see E. A. Halevi, *Angew. Chem. 88* (1976) 664; *Angew. Chem. Int. Ed. Engl. 15* (1976) 593. For analogous OCAMS arguments for the D_{3d} symmetry-forbidden dimerization $2P_4 \rightleftarrows P_8$, cf. E. A. Halevi, H. Bock, B. Roth, *Inorg. Chem. 23* (1984) 4376. For the reaction discussed here, one simplifingly proceeds as follows: Comparison of the localized [5] orbitals of $(HB)_4P_2$ ($\Gamma(C_{2v}) = 5a_1 + 2a_2 + 3b_1 + 3b_2$) with those of B_4H_4 ($\Gamma(C_{2v}) = 3a_1 + 1a_2 + 2b_2$) and P_2 ($\Gamma(C_{2v}) = 3a_1 + 1b_1 + 1b_2$) results in the difference $a_1 \times a_2 = a_2$. Correspondence, therefore, can be accomplished along an internal a_2 coordinate, which reduces the symmetry to that of the subgroup C_2. The $3n-6 = 24$ internal symmetry coordinates of $(HB)_4P_2$ transform in C_{2v} according to $(10a_1 + 2a_2 + 5b_1 + 7b_2)$; that is, they also contain the irreducible representation $a_2(R_z)$ and, therefore, the dissociation into $B_4H_4 + P_2$ is (orbital) symmetry allowed.

The Proton Catalyzed Transformation of a Cobaltacyclopentadiene into a η^4-Cyclobutadiene Complex**

By *Lutz Brandt, Michael Green,*and Adrian W. Parkins*

Metallacyclopentadienes of the transition metals have been implicated in both the cyclotrimerization of alkynes and in the cyclocotrimerization of nitriles, and other unsaturated molecules.[1] Kinetic studies[2] with **1** (Me instead of Ph) suggest that an initial dissociative loss of PPh_3 is important. A similar loss of PPh_3 is involved in the reaction of **1** with B_2H_6[3] or N_2CHCO_2Et[4] forming respectively $[Co(\eta^5\text{-}C_4Ph_4BH)(\eta^5\text{-}C_5H_5)]$ and $[Co(\eta^4\text{-}C_4Ph_4\text{-}CHCO_2Et)(\eta^5\text{-}C_5H_5)]$, an excess of the Lewis acid serving to scavenge the triphenylphosphane. In attempting to gain access to the coordinatively unsaturated cobaltacyclopentadienes implicated in these reactions we have examined the reaction of **1** with strong proton acids. However, this has led to

[*] Prof. M. Green, [+], L. Brandt, Dr. A. W. Parkins
Department of Chemistry,
King's College London,
Strand, London WC2R 2LS. (UK).

[+] Present address:
School of Chemistry
University of Bath
Cleverton Down, Bath BA2 7AY (UK)

[**] This work was supported by an EC twinning grant between King's College and the University of Würzburg, and we wish to thank Professor *H. Werner* for his valuable support.

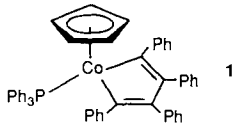

1

the discovery of unusual ring-opening and ring-closure reactions.

Rapid protonation occurred on addition (−78 °C, CH_2Cl_2) of a slight excess of $HSbF_6$ or CF_3CO_2H to **1**,[5] column chromatography (silicagel, CH_2Cl_2/THF, −30 °C) affording 70% yield of the thermolabile green cation **2** (Scheme 1), which can be precipitated from CH_2Cl_2 by addition of Et_2O. Examination of the ^{1}H-, ^{13}C- and ^{31}P-NMR spectra[6] as well as chemical evidence suggested that protonation proceeds with stereofacial selectivity on a carbon of the metallacycle, probably from the face opposite to the η^5-C_5H_5 ligand, to form a cationic species whose structure in solution can be represented by contributions[7–10] from the resonance forms **2** and **2'**. Interestingly, treatment of **2** with triethylamine in CH_2Cl_2 at low temperature results in the quantitative regeneration of **1**.

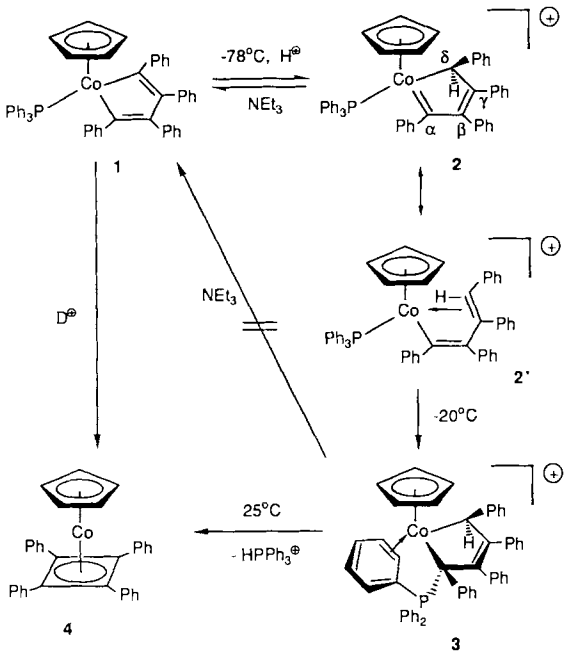

Scheme 1. Counterions of the cationic complexes **2**, **2'** and **3**: $SbF_6^\ominus$ or $CF_3CO_2^\ominus$.

The cation **2** rearranges irreversibly in CH_2Cl_2 on warming to −20 °C to form the cation **3**, which can be purified by column chromatography (silica gel, CH_2Cl_2/THF, −30 °C) as a red-brown, moderately air and moisture sensitive salt (78% yield). Salts of **3** are reasonably thermally stable and their composition has been confirmed by elemental analysis. This new isomeric cation cannot be deprotonated to regenerate **1**, and examination of the NMR spectra[11] of **3** suggested that the triphenylphosphane ligand has migrated from the cobalt to the original α-carbon of the butadienyl fragment to form a metallacyclopent-3-ene with the hydrogen and phosphorus substituents adopting a relative *cis*-configuration. Thus, the ^{13}C-NMR spectra of **3** reveals the disappearance of the carbenoid character associated with the metallacyclic moiety in **2** as indicated by the absence of any low field signals in the spectrum. The presence of a phosphorus coupled doublet at $\delta = 44.7$ (d, J(CP) = 36.6 Hz) is consistent with the proposed structure. The signals due to the three remaining carbon atoms of the metallacyclic moiety are likewise shifted to higher field. Two of these three signals [δ = 99.8(s), 96.9(s)] indicate the presence of two vinylic carbon centers whilst the remaining signal at $\delta = 58.9$(s) correlates with a ^{1}H resonance at $\delta = 2.96$ (d, J(HP) = 2.9 Hz) confirming the presence of a CoCH(Ph) moiety. The ^{1}H-NMR spectrum of the cation **3** also shows unusual signals at $\delta = 5.44$ (d, $J = 7.8$ Hz) and 5.86(d) each integrating for a single proton. Both signals correlate to resonances at $\delta = 134.2$(d, J(CP) = 4.2 Hz) and $\delta = 131.0$(s) in the arene region of the spectrum, and it is suggested that these high field ^{1}H shifts, which are also seen with η^2-bonded arene complexes,[12, 13] are due to a phenyl group of the migrated triphenylphosphane becoming bonded in a η^2-mode to the cobalt center. Connectivity data obtained from a 2D-COSY spectrum and an examination of models support this argument and suggest the illustrated site of coordination of the arene ring (Scheme 1), although coordination involving a different arene C–C bond cannot be ruled out.

When a solution of **3** is allowed to warm to room temperature a further unexpected reaction occurs. The products (6 h, CH_2Cl_2) are the corresponding phosphonium salt [$HPPh_3$]X and the η^4-cyclobutadiene complex **4** previously prepared by thermolysis (194 °C) of **1**.[14] Of particular interest is the observation that in contrast with **2**, treatment of **3** with Et_3N does not regenerate **1**, but instead accelerates the formation of **4**. This implies that the rate determining step in this process corresponds to the deprotonation step. In agreement with the reaction path shown in Scheme 1, when **1** was protonated in the presence of D_2O and allowed to transform into **4** there was no evidence of deuterium incorporation.

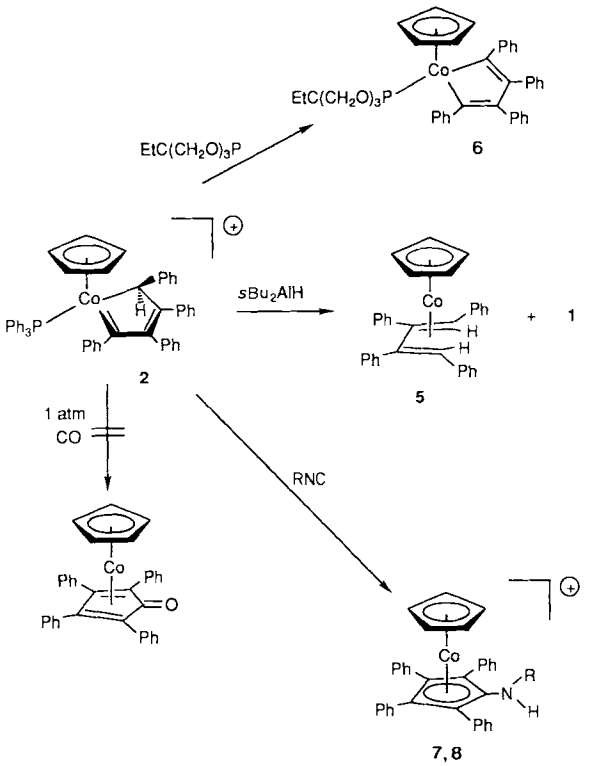

Scheme 2. RNC: R = 2,6-$Me_2C_6H_3$ or *t*Bu. **7**: R = 2,6-$Me_2C_6H_3$. **8**: R = H. Counterion in **7** and **8**: $SbF_6^\ominus$.

The cation **2** undergoes a number of other interesting reactions (Scheme 2). Thus, treatment with a slight excess of sBu_2AlH (CH_2Cl_2, $-78\,^{\circ}C$) affords a 2:3 mixture of the starting material and the known[15] η^4-buta-1,3-diene complex **5**, which could be separated by column chromatography (Al_2O_3 grade II, benzene/hexane, 25 °C). This finding can be rationalized in terms of a competitive reaction involving delivery of "$H^{\ominus}$" to the carbenoid or α-carbon of **2** and proton abstraction from the δ-carbon. In contrast, reaction of **2** (CH_2Cl_2, $-78\,^{\circ}C$) with $EtC(CH_2O)_3P$ does not lead to nucleophilic attack on the α-carbon, but instead deprotonation occurs and the triphenylphosphane is replaced by the cage phosphite to form (column chromatography, silica, MeCN, $-30\,^{\circ}C$) the pink solid **6**.[16]

Although **2** does not react with carbon monoxide, treatment (CH_2Cl_2/THF, $-78\,^{\circ}C$ to $+25\,^{\circ}C$ and chromatography on silica/MeCN) with a two-fold excess of the isocyanides RNC (R = 2,6-$Me_2C_6H_3$, *t*Bu) resulted in the formation of red-orange **7** and yellow **8** respectively as slightly air-sensitive solids. Compound **7** was identified as the hexafluoroantimonate salt by comparison of the ^{1}H-NMR and IR spectra with those of the fluoroborate species described by *Yamazaki*.[17] The corresponding spectroscopic data[18] for **8** suggested that an unexpected reaction had occurred involving loss of the *t*Bu substituent, and this has now been confirmed[19] by single crystal X-ray crystallography. Such a fragmentation reaction has not been previously obtained.

Received: April 2, 1990 [Z 3892 IE]
German version: *Angew. Chem. 102* (1990) 1062

CAS-Registry numbers:
1, 12124-09-3; **2** · SbF_6, 128732-31-0; **2** · CF_3CO_2, 128819-87-4; **3**, 128732-32-1; **4**, 1278-02-0; **5**, 128732-33-2; **6**, 128732-34-3; **7**, 128732-35-4; **8**, 128732-37-6; $EtC(CH_2O)_3P$, 824-11-3; 2,6-$Me_2C_6H_3NC$, 2769-71-3; *t*BuNC, 7188-38-7.

[1] a) P. Hong, Y. Yamazaki, *J. Organomet. Chem. 373* (1989) 133–142; b) H. Bönnemann, W. Brijoux, *Aspects Homogeneous Catal. 5* (1984) 75–196; c) H. Bönnemann, *Angew. Chem. 97* (1985) 264; *Angew. Chem. Int. Ed. Engl. 24* (1985) 248–262; d) P. Cioni, P. Diversi, G. Ingrosso, A. Lucherini, P. Ronca, *J. Mol. Catal. 40* (1987) 337–357; K. Jonas *Angew. Chem. 97* (1985) 292; *Angew. Chem. Int. Ed. Engl. 24* (1985) 295–311; f) K. Abdulla, B. L. Booth, C. Stacey, *J. Organomet. Chem. 293* (1985) 103–114; g) Y. Wakatsuki, H. Yamazaki, *J. Chem. Soc. Dalton Trans. 1978*, 1278–1282; h) S. T. Flynn, S. E. Hasso-Henderson, A. W. Parkins, *J. Mol. Catal. 32* (1985) 101–105; i) E. Lindner, R. M. Jansen, H. A. Mayer, W. Hiller, R. Fawzi, *Organometallics 8* (1989) 2355–2360.

[2] D. R. McAllister, J. E. Bercaw, R. G. Bergman, *J. Am. Chem. Soc. 99* (1977) 1666–1668.

[3] F. E. Hong, C. W. Eigenbrot, T. P. Fehlner, *J. Am. Chem. Soc. 111* (1989) 949–956.

[4] J. M. O'Connor, L. Pu, R. Uhrhammer, J. A. Johnson, *J. Am. Chem. Soc. 111*, (1989) 1889–1891.

[5] H. Yamazaki, N. Hagihara, *J. Organomet. Chem., 7* (1967) p. 22; *Bull. Chem. Soc. Jpn. 44* (1971) 2260–2261.

[6] **2**: ^{1}H NMR (360 MHz, CD_2Cl_2, $-20\,^{\circ}C$): δ = 7.9–6.4 (m, 35 H, C_6H_5), 5.17 (s, 5H, C_5H_5), 3.31 (s, 1H, C*H*Ph); $^{13}C\{^1H\}$ NMR (90 MHz, CD_2Cl_2, $-20\,^{\circ}C$): δ = 176.9 [d, C_α, J(CP) 25.7 Hz], 143.0–125.0 (C_β and C_γ), 141.0–123.0 (aryl), 90.9 (C_5H_5), 75.8 (C_δ); $^{31}P\{^1H\}$ NMR (101 MHz, CD_2Cl_2, $-20\,^{\circ}C$): δ = 35.7.

[7] a) M. Crocker, M. Green, A. G. Orpen, H. P. Neumann, C. J. Schaverien, *J. Chem. Soc. Chem. Commun. 1984*, 1351–1353; b) M. Crocker, M. Green, K. R. Nagle, A. G. Orpen, H. P. Neumann, C. E. Morton, C. J. Schaverien, *Organometallics 9* (1990) 1422–1434.

[8] L. Brammer, M. Crocker, B. J. Dunne, M. Green, C. E. Morton, K. R. Nagle, A. G. Orpen, *J. Chem. Soc. Chem. Commun. 1986*, 1226–1228.

[9] D. C. Brower, K. R. Birdwhistell, J. L. Templeton, *Organometallics 5* (1986) 94–98.

[10] G. C. Conole, M. Green, M. McPartlin, C. Reeve, C. M. Woolhouse, *J. Chem. Soc. Chem. Commun. 1988*, 1310–1313.

[11] **3**: ^{1}H NMR (360 MHz, CD_2Cl_2, $-20\,^{\circ}C$): δ = 7.9–5.4 (overlapping signals) 35H, C_6H_5, η^2-C_6H_5), 5.00 (s, 5H, C_5H_5), 2.96 (d, 1H, C*H*Ph, J(HP) = 2.9 Hz); $^{13}C\{^1H\}$ NMR (90 MHz, CD_2Cl_2, $-20\,^{\circ}C$): δ = 140.3–126.1 (aryl), 99.8(s), 96.9(s) (C_β,C_γ), 88.2 (C_5H_5), 58.9 (C_δ), 44.7 [d, C_α, J(CP) = 36.6 Hz]; $^{31}P\{^1H\}$ NMR (101 MHz, CD_2Cl_2, $-20\,^{\circ}C$): δ = 23.3.

[12] W. D. Jones, L. Dong, *J. Am. Chem. Soc. 111* (1989) 8722–8723.

[13] a) W. D. Harman, H. Taube, *J. Am. Chem. Soc. 110* (1988) 5403–5407; b) W. D. Harman, M. Sekine, H. Taube, *ibid. 110* (1988) 5725–5731; c) W. D. Harman, H. Taube, *ibid. 110* (1988) 7555–7557; d) K.-B. Shui, C.-C. Chou, S.-L. Wang, S.-C. Wei *Organometallics 9* (1990) 286–288.

[14] a) A. Nakamura, N. Hagihara, *Bull. Chem. Soc. Jpn. 34* (1961) 452–453; b) M. D. Rausch, G. F. Westover, E. Mintz, G. M. Reisner, I. Bernal, A. Clearfield, J. M. Troup, *Inorg. Chem. 18* (1979) 2605–2615.

[15] H. Yamazaki, K. Yasufuku, Y. Wakatsuki, *Organometallics 2* (1983) 726–732.

[16] **6**: ^{1}H NMR (360 MHz, $CDCl_3$, 25 °C): δ = 7.3–6.6 (m, 20 H, C_6H_5), 4.58 (s, 5H, C_5H_5), 4.30 [d, 6H, OCH_2, J(HP) = 5.2 Hz], 1.26 [q, 2H, CCH_2, J(HH) = 7.7 Hz], 0.87 [t, 3H, CH_3, J(HH) = 7.7 Hz]; $^{13}C\{^1H\}$ NMR (90 MHz, $CDCl_3$, 25 °C): δ = 162.7 [d, C_α, $C_{\alpha'}$, J(CP) = 18.5 Hz) 156.7–123.3 (aryl), 142.3 [d, C_β, $C_{\beta'}$, J(CP) = 1.3 Hz], 89.4 (C_5H_5), 74.6 [d, OCH_2, J(CP) = 2.9 Hz], 35.5 [*C*Et, J(CP) = 11.5 Hz], 23.4 (CH_2), 7.3 (CH_3); $^{31}P\{^1H\}$ NMR (101 MHz, $CDCl_3$, 25 °C): δ = 143.5.

[17] H. Yamazaki, Y. Wakatsuki, *Bull. Chem. Soc. Jpn. 52* (1979) 1239–1240.

[18] **8**: ^{1}H NMR (360 MHz, CD_2Cl_2, 25 °C): δ = 7.6–6.9 (m, 20 H, C_6H_5), 5.39 (s, 5H, C_5H_5), 4.76 (bs, 2H, NH_2); $^{13}C\{^1H\}$ NMR (90 MHz, CD_2Cl_2, 25 °C): δ = 131.9–128.2 (aryl), 122.7 (C-NH_2), 96.2 (C_α,$C_{\alpha'}$), 88.1 (C_5H_5), 84.0 (C_β,$C_{\beta'}$): IR: ν_{NH}(cm^{-1})(CH_2Cl_2) 3474 m, 3381 m.

[19] S. C. Nyburg, A. W. Parkins, M. Green, unpublished.

The Structure of Vicinal Pentaketones—X-Ray Structure Investigations and Calculations**

By *Rolf Gleiter,* Edwin Litterst, Thomas Oeser,* and *Hermann Irngartinger**

Dedicated to Professor Tetsuo Nozoe on the occasion of his 88th birthday

The recently prepared vicinal pentaketones[1] are ideally suited as models for describing the electronic and steric requirements of a keto group. Each CO moiety possesses a strong local dipole moment and provides two lone pairs at the oxygen as well as a π- and a π^*-orbital. So far, only a few structural data on open chain vicinal di-,[2] tri-[3,4] and tetraketones[3,4] are available. Empirical calculations (MM2[5]) predict the dihedral angles of α-diketones[6] and triketones but fail to do so for those of tetra- and pentaketones. Older semiempirical methods,[7] as well as more recent ones[8] and ab initio calculations with a minimal basis (STO 3G),[9] give unsatisfactory results with respect to the torsional angles of vicinal CO groups in polyketones.[8] In this communication we report on the structural parameters of vicinal pentaketones and present a simple model which reproduces the torsional angles properly.

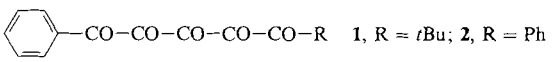

1, R = *t*Bu; **2**, R = Ph

In Figure 1 we show the conformation and most significant bond lengths of *tert*-butylphenylpentaketone (**1**).[10] An X-ray investigation on single crystals of diphenylpentake-

[*] Prof. Dr. R. Gleiter, Prof. Dr. H. Irngartinger, Dr. E. Litterst, Dipl. Chem. T. Oeser
Organisch-Chemisches Institut der Universität
Im Neuenheimer Feld 270, D-6900 Heidelberg (FRG)

[**] This work was supported by the Deutsche Forschungsgemeinschaft, the Fonds der Chemischen Industrie, the German-Israeli Foundation for Scientific Research and Development, and the BASF Aktiengesellschaft. We are grateful to Frau U. Huber-Patz, Frau U. Wiesinger, Herrn S. Gries and Herrn U. Reifenstahl for experimental help.

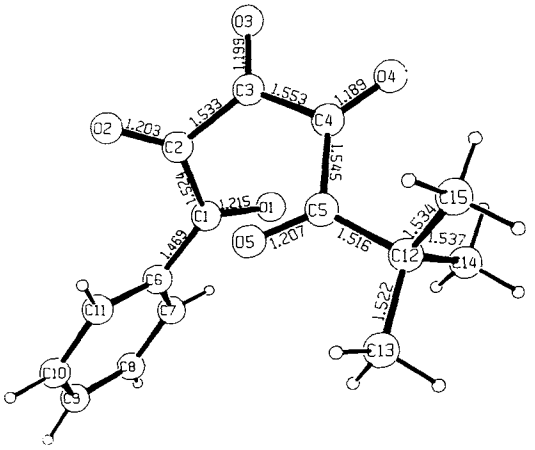

Fig. 1. Structure of **1** in the crystal, with bond lengths (standard deviations 0.002 to 0.003 Å).

tone (**2**)[10] yielded similar torsional angles and bond lengths (see Table 1) as for **1**. In both cases the three central CO groups are arranged cisoid to each other while the outer ones

Table 1. Most relevant bond lengths of **2** [Å].

C1–C6	C1–C2	C2–C3	C3–C4	C4–C5	C5–C12
1.459(3)	1.529(4)	1.522(3)	1.530(3)	1.533(3)	1.467(3)
C1–O1	C2–O2	C3–O3	C4–O4	C5–O5	
1.215(2)	1.204(2)	1.196(3)	1.195(2)	1.219(2)	

show a transoid conformation. The recorded torsional angles for **1** and **2** are given in Table 2.

It is interesting to note that the distances between O5 and C1 and C2 are relatively short (see Table 2). This interaction leads to a slight pyramidalization of the keto groups at C1 and C2. The deviation of C1 and C2 in **1** and **2** from the plane defined by its three neighbor atoms amounts to 0.014 Å/0.063 Å in **1** and 0.006 Å/0.064 Å in **2**. This deviation occurs

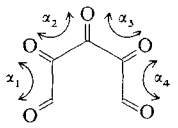

Scheme 1. Definition of the torsional angles in Table 2.

Table 2. Torsional angles α [°] between the CO groups of **1** and **2** and selected distances [Å] between O1, O5 and carbon centers. For the definition of α_1–α_4 see Scheme 1.

	α_1	α_2	α_3	α_4	O5···C1	O5···C2	O1···C4	O1···C5
1	158.4	−52.1	−11.4	172.9	2.738(2)	2.578(2)	2.953(2)	3.195(2)
2	155.8	−55.4	−30.7	−151.0	2.775(3)	2.519(3)	3.036(3)	3.587(3)

in the direction of O5. Corresponding changes at the other side of the molecule cannot be detected since the C···O distances are larger (see Table 2). The proximity of the terminal CO groups is also in line with the finding that the reduction of **2** gives exclusively 3,5-dihydroxy-2,6-diphenyl-4*H*-pyran-4-one (**3**).[11]

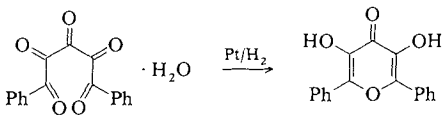

1 · H_2O **3**

On applying current force field methods to calculate the torsional angles between the CO groups by assuming the usual dipole–dipole forces as well as torsional and van der Waals forces, we were unable to reproduce the geometry of the pentaketones satisfactorily. However, upon neglecting torsional and van der Waals forces, assuming the dipole moment of each CO group to be 2.3 D,[5b] the bond distances between the adjacent carbon atoms to be fixed at 1.54 Å, and those between C and O at 1.20 Å, as well as bond angles of 120°, we were able to reproduce the torsional angles between CO groups of vicinal polyketones. The minima found on the corresponding hypersurface show remarkable agreement with experimental data: For 1,2-diketones a dihedral angle of 180° results, for 1,2,3-triketones both dihedral angles are 127°. For vicinal tetraketones we find one broad minimum with two *trans* 1,2-diketone units ($\alpha_1 \approx 180°$, $\alpha_2 \approx 90°$, $\alpha_3 \approx 180°$). A helical structure with $\alpha_1 \approx \alpha_2 \approx \alpha_3 \approx 130°$ also fits well into this minimum.

In Figure 2 we show the dipole-energy of a vicinal pentaketone as a function of α_2 and α_3. For each point of the

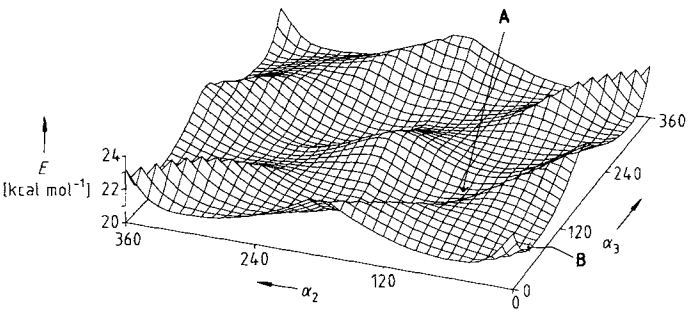

Fig. 2. Dipole energy hypersurface for five vicinal CO groups as a function of α_2 and α_3.

surface the energy was minimized for α_1 and α_4. The surface is symmetrical with respect to the diagonal $\alpha_2 = \alpha_3$. Two nearly equal minima are found at **B** ($\alpha_2 \approx \alpha_3 \approx 25°$, $\alpha_1 \approx 180°$, $\alpha_4 \approx 180°$) at 20.9 kcal mol^{-1} and at **A** ($\alpha_2 \approx \alpha_3 \approx 129°$, $\alpha_1 \approx \alpha_4 \approx 140°$) at 20.0 kcal mol^{-1}. Minimum **B** corresponds to the structures found for **1** and **2**. An analysis of the interactions between the CO groups in **B** shows that the unfavorable cisoid arrangement of the central $(CO)_3$ unit allows the peripheral CO groups to come into a conformation so that their dipole moments are nearly compensated (see Fig. 1). Semiempirical calculations on **1** and **2** suggest an electron transfer from the lone pairs at O5 and—to a lesser extent—from O1 to the π^* level. A further stabilization of minimum **B** with respect to **A**, which is not included in our simple model, is due to the better overlap between the CO groups in **B**. Our simple model suggests that the dipole moment determines the conformation of the $(CO)_x$ moiety. In the current force fields the interplay between torsional, van der Waals and dipole-dipole forces of CO groups is not treated properly.

Experimental

The synthesis of **1** was carried out analogously to that of **2** [1]. **1**: ^{1}H NMR (200 MHz, $CDCl_3$): δ = 7.9–8.0 (m, 2H), 6.8–7.15 (m, 3H), 1.15 (s, 9H); ^{13}C NMR (66, MHZ, $CDCl_3$): δ = 205.6 (s), 191.0 (s), 189.1 (s), 183.3 (s), 182.7 (s), 136.7 (d), 131.8 (s), 131.3 (d), 129.9 (d), 43.5 (s), 25.8 (q); IR (CH_2Cl_2): $\tilde{\nu}$ = 3148 (w), 1728 (s), 1664 (s), 1594 (s) cm^{-1}; UV (CH_2Cl_2): λ_{max} (ε): 431 (207), 542 (136) nm.

The reduction of **2** (hydrate) was carried out with PtO_2/H_2 in ethanol at room temperature (32% yield) or in ethanol/water (3:1) with L-ascorbinic acid (55% yield). **3**: m.p. 249 °C; IR (cm^{-1}): $\tilde{\nu}$ 3250 (br), 1572 (s), 1390 (s); ^{1}H NMR (300 MHz, d_8THF): δ = 7.37–7.56 (6H, m), 8.2–8.7 (4H, m), 8.93 (2H, br); ^{13}C NMR (200 MHz, [D_6]DMSO): δ = 126.97 (d), 128.59 (d), 129.34 (d), 131.35 (s), 140.96 (s), 144.44 (s), 169.45 (s). The structure of **3** was confirmed by an X-ray investigation on the 3,5-bisacetyl-derivative of **3**.[11]

Received: March 14, 1990 [Z 3857 IE]
German version: *Angew. Chem. 102* (1990) 1071

CAS-Registry numbers:
1, 128731-90-8; **2**, 104779-80-8; **3**, 128731-91-9.

[1] R. Gleiter, G. Krennrich, M. Langer, *Angew. Chem. 98* (1986) 1019; *Angew. Chem. Int. Ed. Engl. 25* (1986) 999.
[2] C. J. Brown, R. Sadanaga *Acta Crystallogr. 18* (1965) 158; E. J. Gabe, Y. Le Page, F. L. Lee, L. R. C. Barclay, *Acta Crystallogr. Sect. B37* (1981) 197; K. Eriks, T. D. Hayden, S. Hsi Yang, I. Y. Chan, *J. Am. Chem. Soc. 105* (1983) 3940.
[3] M. B. Rubin, *Chem. Rev. 75* (1975) 177.
[4] R. L. Beddoes, J. R. Cannon, M. Heller, O. S. Mills, V. A. Patrick, M. B. Rubin, A. H. White, *Aust. J. Chem. 35* (1982) 543; M. Kaftory, M. B. Rubin, *J. Chem. Soc. Perkin Trans. 2 1983*, 149.
[5] a) U. Burkert, N. L. Allinger: *Molecular Mechanics (ACS Monogr. 177*, (1982)); b) MMX: consistent of the routines MM2 + MMPI [5a], written by J. J. Gajewski, K. E. Gilbert, Serena Software, Bloomington, IN, USA.
[6] R. Isaksson, T. Liljefors, *J. Chem. Soc. Perkin Trans. II*, (1983) 1351.
[7] J. Kroner, W. Strack, *Angew. Chem. 84* (1972) 210; *Angew. Chem. Int. Ed. Engl. 11* (1972) 220; S. Wolfe, J. E. Berry, M. R. Peterson, *Can. J. Chem. 54* (1976) 210.
[8] E. Litterst, *Dissertation*, Universität Heidelberg, 1990.
[9] W. J. Hehre, L. Radom, P. von R. Schleyer, J. A. Pople: Ab initio Molecular Orbital Theory, Wiley, New York 1986.
[10] **1**: a = 6.347(1), b = 10.175(3), c = 11.686(2) Å, α = 111.41(1), β = 93.90(1), γ = 95.46(2)°, V = 695.1(5) [Å^3], Z = 2, space group $P\bar{1}$, crystal size 0.5 × 0.35 × 0.4 [mm^3], independent reflexions 3337, observed 2072 ($I \geq 2.5\sigma(I)$], R/R_w = 0.038/0.049 ($w = 1/\sigma(F_0)^2 = (4 \times F_0^2)/\sigma(F_0^2)^2$).—**2**: a = 19.187(5), b = 8.880(2), c = 18.582 Å, α = 90°, β = 117.06(3)., γ = 90°, V = 2819.4 (3) [Å^3], Z = 8, space group $C2/c$, crystal size 0.5 × 0.45 × 0.3 [mm^3], independent reflexions: 3373, observed 1325 ($I \geq 2.5\sigma(I)$), R/R_w = 0.038/0.042 ($w = 1/\sigma(F_0^2) = (4 \times F_0^2)/\sigma(F_0^2)^2$).—The data were collected on an automatic diffractometer (CAD4–Enraf Nonius, Mo_{K_α} radiation, graphite monochromater, $\omega - 2\theta$ scan). The structures were solved by direct methods and refined by full matrix procedure (anisotropic thermal parameters for C and O, positions of the H atoms localized according to difference Fourier synthesis and isotropically refined). A final difference Fourier map revealed no peaks greater than 0.17 e/Å^3 (**1**) and 0.19 e/Å^3 for **2**. Further details of the crystal structure investigations are available on request from the Fachinformationszentrum Energie, Physik, Mathematik GmbH, D-7514 Eggenstein-Leopoldshafen 2 (FRG), on quoting the depository number CSD 54658, the names of the authors and the journal citation.
[11] M. Langer, *Dissertation*, Universität Heidelberg, 1987.

Synthesis of a β-Mannosyl-Chitobiosyl-Asparagine Conjugate—a Central Core Region Unit of the *N*-Glycoproteins**

By *Wolfgang Günther* and *Horst Kunz**

N-Glycoproteins are widespread in living organisms as membrane and serum constituents; some, e.g. the immunoglobulins and transferrin, carry functionalities important for biological selectivity.[1] As a rule, *N*-glycoproteins are characterized by an *N*-glycosidic bond between an *N*-acetylglucosamine unit and the amide function of an asparagine unit. On the carbohydrate side there follow a further *N*-acetylglucosamine unit and a mannose unit as building blocks. The linkages are β(1 → 4) glycosidic, so that this section of the core region and binding region has the structure Manβ1 → 4GlcNAcβ1 → 4GlcNacβ1 → Asn **1**.

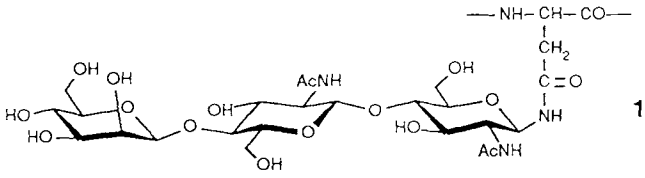

1

The β-glycosidically linked mannose unit in **1** is a central element in the oligosaccharide side chains of the *N*-glycoproteins, since it is the starting point of branching in the antennary saccharide side chains via binding of α-mannoside units.

The especially difficult synthesis of β-mannosides (neighboring group participation and thermodynamic control strongly favor the formation of α-mannosides) was effectively achieved by use of silver silicate catalysts[2] or via oxidation/reduction at the C-2 center of glucosides.[3] In both cases, however, undesirable anomers or epimers are obtained as by-products, which must be separated. In 1988 we developed a directed synthesis of β-mannosides which was based on the inversion of the configuration at C-2 of glycosides (Scheme 1).[4] The β-mannosylglucosamine **3** was obtained in an overall yield of 85% via the glucosylglucosamine **2** by intramolecular nucleophilic substitution.

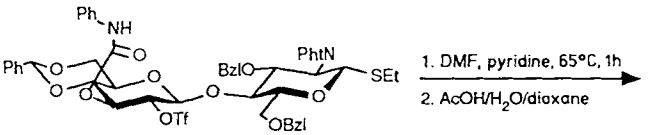

2

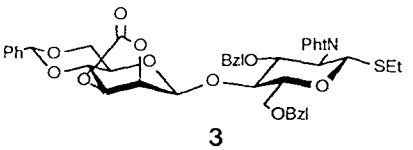

3

Scheme 1. DMF = dimethylformamide. Pht = phthaloyl.

The thioglucoside **3** was now activated according to the method described by *Lönn*[5] using phenylselenyl triflate[6], and coupled with the glucosamine **4** (Scheme 2).

The carbonate group was removed from the β-mannosyl-chitobiose derivative **5**, obtained in 76% yield after chromatographic purification, by treatment with sodium methoxide/methanol, and then the *N*-phthaloyl protecting groups were removed by treatment with hydrazine/ethanol. After acetylation of the deblocked amino and hydroxy functions to give the trisaccharide **6**, the benzylic protecting groups were removed hydrogenolytically. Further acetyla-

[*] Prof. Dr. H. Kunz, Dipl.-Chem. W. Günther
Institut für Organische Chemie der Universität
Joh.-Joachim-Becher-Weg 18–20, D-6500 Mainz (FRG)

[**] This work was supported by the Deutsche Forschungsgemeinschaft and the Fonds der Chemischen Industrie.

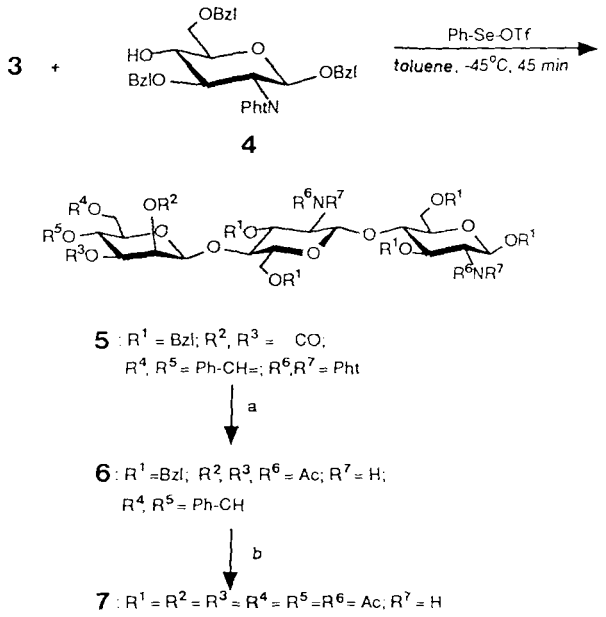

Scheme 2. a) 1. NaOMe, MeOH, 2. H_2N-NH_2, EtOH; 3. Ac_2O/pyridine. b) 1. H_2/Pd-C; 2. Ac_2O/pyridine.

tion then furnished the peracetylated trisaccharide **7** as an anomeric mixture in 85% yield based on **5**.

Reaction of **7** with trimethylsilyl trifluoromethanesulfonate, or even with acetyl chloride/HCl and other activating agents, led exclusively to the dihydrooxazole **8**.[7] All attempts to convert **8** into the anomeric azide with trimethylsilyl azide/$SnCl_4$ according to the procedure of *Jeanloz* et al.[8] met without success. Even the phase transfer procedure, known to be productive in the case of the corresponding chitobiosyl chloride,[9] did not afford the desired trisaccharide. Nevertheless, in order to achieve the coupling of the trisaccharide **7** with asparagine, **8** was first converted into the trisaccharide isothiocyanate **9** in 85% yield by reaction with potassium rhodanide/HBF_4 in the presence of [18]crown-6 as catalyst[10] (Scheme 3).

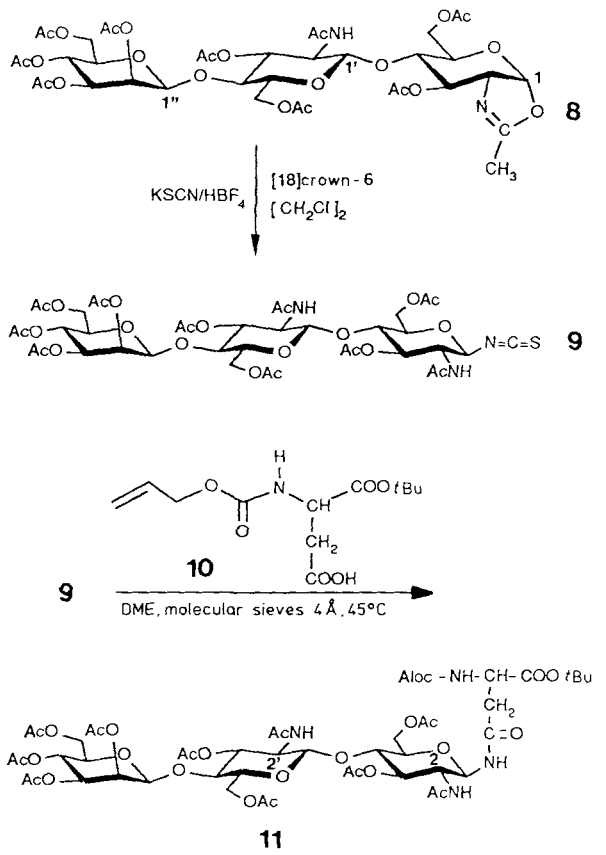

Scheme 3.

This reaction led initially to the anomeric rhodanide, which then rearranged to **9**. Reaction of the isothiocyanate **9**[11] with α-*tert*-butyl *N*-allyloxycarbonyl-L-asparaginate requires strict exclusion of water. Nevertheless, the interfering formation of *N,N'*-bisglycosylthiourea cannot be completely avoided. The target compound, the β-mannosyl-chitobiosyl-asparagine derivative **11**, is obtained in 75% yield.[12] Thus, for the first time, a core region unit of the *N*-glycoproteins which contains the hitherto problematic coupling of the β-mannoside unit to the chitobiosyl-asparagine unit in correct stereochemistry, was synthesized.

Received: May 14, 1990 [Z 3955 IE]
German version: *Angew. Chem. 102* (1990) 1068

[1] Reviews: J. Montreuil, *Adv. Carbohydr. Chem. Biochem. 37* (1980) 157; H. Paulsen, *Angew. Chem. 102* (1990) 851; *Angew. Chem. Int. Ed. Engl. 29* (1990) 823.
[2] H. Paulsen, O. Lockhoff, *Chem. Ber. 114* (1981) 3102.
[3] C. Auge, C. D. Warren, R. W. Jeanloz, *Carbohydr. Res. 82* (1980) 85.
[4] H. Kunz, W. Günther, *Angew. Chem. 100* (1988) 1118; *Angew. Chem. Int. Ed. Engl. 27* (1988) 1086.
[5] H. Lönn, *Carbohydr. Res. 139* (1985) 105.
[6] Y. Ito, T. Ogawa, *Tetrahedron Lett. 29* (1988) 1061.
[7] **8**: $[\alpha]_D^{23} = -24.7$ ($c = 1$, $CHCl_3$); ^{1}H NMR (400 MHz, $CDCl_3$): $\delta = 5.86$ (d, $J(1,2) = 7.3$ Hz, 1H; 1-H), 4.51 (d, $J(1',2') = 8.5$ Hz, 1H; 1'-H), 4.64 (s, 1H; 1''-H).
[8] S. Nakabayashi, C. D. Warren, R. W. Jeanloz, *Carbohydr. Res. 174* (1988) 279.
[9] H. Kunz, H. Waldmann, *Angew. Chem. 97* (1985) 855; *Angew. Chem. Int. Ed. Engl. 24* (1985) 883.
[10] W. P. Stöckl, H. Weidmann, *J. Carbohydr. Chem. 8* (1989) 169.
[11] For analogous reactions of glycosyl isothiocyanates with carboxylic acids see A. Y. Khorlin, S. E. Zurabyan, R. G. Macharadze, *Carbohydr. Res. 85* (1980) 201.
[12] **11**: $[\alpha]_D^{23} = -25.4$ ($c = 1$, $CHCl_3$); ^{1}H-NMR (400 MHz, $CDCl_3$): $\delta = 7.2$ (d, $J = 8.1$ Hz, 1H; γ-NH_{Asn}), 6.60 (d, J(NH; 2) = 7.5 Hz, 1H; 2-NHAc), 6.44 (s, 1H; 2'-NHAc), 4.65 (s, 1H; 1''-H), 2.73 (dd, J(gem) = 16, J(Vic) = 3.8 Hz, 1H; β-CH_2^a-Asn), 1.36 (s, 9H, *t*Bu).

A Novel Type of Ring Contraction as Non-Enzymatic Step in the Later Stages of the Biosynthesis of Urdamycin H**

By *Jürgen Rohr**

The biosynthesis of secondary metabolites is generally characterized by an enzymatic anabolism of highly complex molecules from compounds that stem from the primary metabolism.[1,2] Unsuccessful screening attempts for special biosynthetic enzymes, as well as the small size of certain enzymes which are assumed to be responsible for a great

[*] Dr. J. Rohr
Institut für Organische Chemie der Universität
Tammannstrasse 2, D-3400 Göttingen (FRG)

[**] This work was supported by the N.A.T.O. (Grant No. 0368/88) and the Fonds der Chemischen Industrie (Grant No. 635050).

number of reaction steps,[3] are reasons for the speculation that non-enzymatic steps are more involved in natural product formation than generally accepted. Our investigations on the later steps of the biosynthesis of the angucycline antibiotic[4] urdamycin complex support this hypothesis. Recently we reported on the involvement of non-enzymatic reactions in the later stages of the biosynthesis of the urdamycins C, D, and E.[5] This communication deals with another non-enzymatic reaction step, which is responsible for the formation of urdamycin H **1**.

Urdamycin H **1** was discovered as the latest congener of the urdamycin family[6] during a screening for intermediates between urdamycin A and urdamycins C/D before the non-enzymatic interconversion mechanisms could be deduced.[5] Its structure resembles urdamycin C **2**; only the tetracyclic ring frame of this angucycline is enlarged by a (4-hydroxyphenyl)furan moiety instead of the (4-hydroxyphenyl)-δ-lactone moiety of urdamycin C. Thus, **1** is smaller by one C=O than **2**.[7]

Preliminary biosynthetic studies showed that the 4-hydroxyphenyl moiety of **1**, like that of **2**, derives from tyrosine and not from (4-hydroxyphenyl)glycine. This finding and the structure of **1** rule out **1** being the biosynthetic intermediate between urdamycin A and **2**. Even the converse, namely the possibility of **2** being a precursor of **1**, was probable, but no obvious rearrangement mechanism for the excision of a C=O-unit from **2** to give **1** could support the latter hypothesis.[7]

Based on the observation that the fermentation of the urdamycin H-producing mutant shifted earlier into the alkaline than the wild strain, it was evident that the initiation of the rearrangement cascade could be the opening of the δ-lactone moiety of urdamycin C **2**. An intramolecular nucleophilic attack of the liberated 12-OH group at the olefinic carbon in the α-position of the 4-hydroxyphenyl ring (formerly C-3″ of **2**), followed by synchronic H-rearrangements and an oxidative decarboxylation, completes the formation of urdamycin H **1** (Scheme 1). That the reaction described by this mechanism is non-enzymatic, could be proven in vitro by stirring urdamycin C **2** in 0.1 M phosphate buffer/DMSO (1:1) at pH 8.0 for 24 h at 28 °C in an open Erlenmeyer flask; this yielded, besides unchanged **2**, about 30% of urdamycin H **1**, which, with respect to all physicochemical data, is identical with **1** obtained from *Streptomyces fradiae*.[7] An intermediate such as **3** (Scheme 1) could not be isolated. Since DMSO can be replaced by THF or methanol as solvent, and since no reduced **2** can be found in the reaction mixture, molecular oxygen remains the best oxidizing agent for the reaction.

Since a weak alkaline pH and atmospheric oxygen are essential for the formation of **1** under conditions comparable to the last 24 hours of the fermentation process (pH 7–8), one could assume urdamycin H **1** as being an artifact. Obviously its formation can be limited by a pH barrier if the fermentation were to be carried out in a fermentor. Since Erlenmeyer flasks in a shaker are used for the normal fermentation process of *Streptomyces fradiae*, i.e. without pH control, the formation of **1** cannot be avoided. This is in complete contrast to avoidable artifacts which are due to the working-up procedure, as was recently described, e.g., for the vasodilator FK 409.[8] Independently of whether urdamycin H **1** might be considered being an artifact or not, the discovered ring contraction from an arene δ-lactone into a furan is unusual and novel, and is certainly dependent on the quinomethane system of the chromophore which enables the H-rearrangements and oxidation processes shown in Scheme 1.

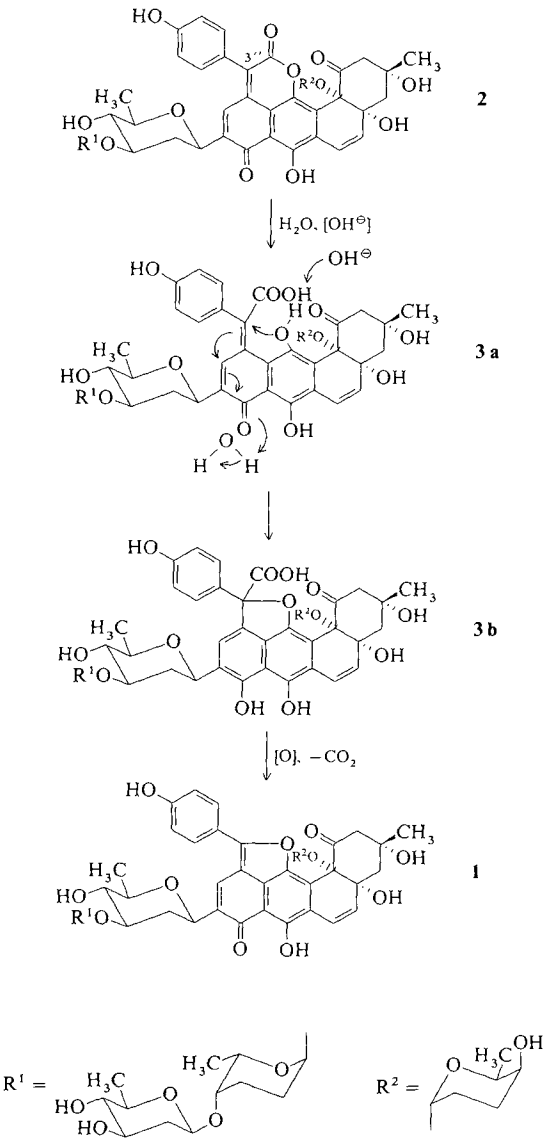

Scheme 1. Mechanism of the non-enzymatic interconversion of urdamycin C **2** into urdamycin H **1**. R^1 = L-rhodinose-D-olivose; R^2 = L-rhodinose.

The formation of urdamycin H **1** from urdamycin C **2** is the third non-enzymatic interconversion reaction which was discovered during investigations on the later steps of the biosynthesis of the urdamycin complex. Thus, this reaction lends further support to the above mentioned hypothesis, namely the involvement of important non-enzymatic reactions in the biosynthesis of natural products. This should always be considered in future biosynthetic studies and increased interest should be shown in the later biosynthetic steps, since one can also discover unexpected new reactions. There is some evidence in the literature for non-enzymatic reactions in the biosynthesis of other antibiotic complexes, e.g., some ansamycins,[9] some naphthocyclinones,[10] and the esmeraldins[11]

Received: April 27, 1990 [Z 3935 IE]
German version: *Angew. Chem. 102* (1990) 1091

CAS-Registry numbers:
urdamycin H, 126121-78-6; urdamycin C, 104443-43-8.

[1] H. G. Floss, J. M. Beale, *Angew. Chem. 101* (1989) 147–179; *Angew. Chem. Int. Ed. Engl. 28* (1989) 146–178.

[2] J. Rohr, A. Zeeck in P. Präve (Ed.): *Jahrbuch der Biotechnologie 1988/89*, Carl Hanser Verlag, München 1988, p. 263.
[3] T. Widlanski, S. L. Bender, J. R. Knowles, *J. Am. Chem. Soc. 111* (1989) 2299–2300.
[4] H. Drautz, H. Zähner, J. Rohr, A. Zeeck, *J. Antibiot. 39* (1986) 1657–1669.
[5] J. Rohr, *J. Chem. Soc. Chem. Commun. 1989* 492–493; J. Rohr, *ibid. 1990* 113–114.
[6] J. Rohr, A. Zeeck, *J. Antibiot. 40* (1987) 459–467; J. Rohr, J. M. Beale, H. G. Floss, *ibid. 42* (1989) 1151–1157; J. Rohr, A. Zeeck, H. G. Floss, *ibid. 41* (1988) 126–129.
[7] J. Rohr, *J. Antibiot. 42* (1989) 1482–1488.
[8] M. Hino, M. Iwami, M. Okamoto, K. Yoshida, H. Haruta, M. Okuhara, J. Hosoda, M. Koshaka, H. Aoki, H. Imanaka, *J. Antibiot. 42* (1989) 1578–1583; M. Hino, T. Ando, S. Takase, Y. Itoh, M. Okamoto, M. Koshaka, H. Aoki, H. Imanaka, *ibid. 42* (1989) 1584–1588; M. Hino, S. Takase, Y. Itoh, I. Uchida, M. Okamoto, M. Koshaka, H.Aoki, H. Imanaka, *ibid. 42* (1989) 1589–1592.
[9] T. Okabe, B. D. Yuan, F. Isono, I. Sato, H. Fukazawa, T. Nishimura, N. Tanaka, *J. Antibiot. 38* (1985) 230–235; T. Okabe, K. Suzuki, H. Suzuki, Y. Inouye, S. Nakamura, N. Tanaka, *ibid. 39* (1986) 316–317.
[10] B. Krone, A. Zeeck, H. G. Floss, *J. Org. Chem. 42* (1982) 4721–4724.
[11] W. Keller-Schierlein, A. Geiger, H. Zähner, M. Brandl, *Helv. Chim. Acta 71* (1988) 2058–2070; A. Geiger, W. Keller-Schierlein, M. Brandl, H. Zähner, *J. Antibiot. 41* (1988) 1542–1551.

Direct Electron Transfer between Carbon Electrodes, Immobilized Mediator and an Immobilized Viologen-accepting Pyridine Nucleotide Oxidoreductase**

By *Helmut Günther, Antonios S. Paxinos, Michael Schulz, Cees van Dijk*, and *Helmut Simon**

Dedicated to Professor Ivar Ugi on the occasion of his 60th birthday

Electrons from an electrode constitute an inexpensive, residue-free reagent for redox reactions whose redox potential can be adjusted over wide ranges to the desired reaction. They could be especially valuable in combination with specific redox enzymes. However, the direct transfer of electrons between redox active prosthetic groups of oxidoreductases and electrodes is far too slow for preparative conversions. Usually recourse to synthetic redox mediators, for example viologens or metallo cage complexes, has to be made in order to achieve satisfactory rates for the electron transfer. Preparative electromicrobial and electroenzymatic systems with dissolved mediator and dissolved enzyme[1] have been reported, as have also systems in which either the mediator or the enzyme was immobilized on the electrode surface.[2, 3] For analytical purposes, a ferrocene derivative was deposited on a graphite electrode and subsequently covalently bound to glucose oxidase.[4] We have now tried to bind both the mediator as well as the enzyme covalently to a functionalized carbon surface in order to check whether electrons flow from the cathode via the mediator, acting as "molecular wire," to the prosthetic group of the enzyme.

For the immobilization, an enzyme discovered by us in thermophilic bacilli was chosen which transfers redox equivalents between viologens [Eq. (1); V = viologen] or Co-cage complexes [Eq. (2); Co-diamser, cf. Fig. 1] and pyridine nucleotides.[5] Viologen-accepting pyridine nucleotide oxidoreductases (VAPORs) are present in numerous cells.

$$2V^{\cdot\oplus} + NAD(P)^{\oplus} + H^{\oplus} \rightleftharpoons NAD(P)H + 2V^{2\oplus} \quad (1)$$

$$2Co^{2\oplus}\text{-diamsar} + NAD(P)^{\oplus} + H^{\oplus} \rightleftharpoons NAD(P)H + 2Co^{3\oplus}\text{-diamsar} \quad (2)$$

The VAPOR from the thermophilic *Bacillus spec.* DSM 466 was immobilized together with viologen, and then the reactions shown in Scheme 1 were carried out. It was not

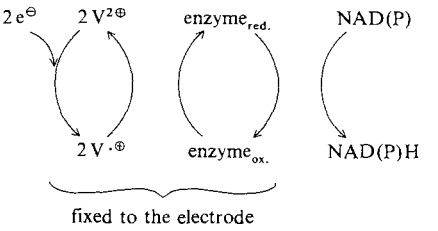

Scheme 1. Flow of electrons via immobilized viologens to an immobilized enzyme that reduces soluble NAD.

our main concern to generate NAD(P)H in this way, but to demonstrate the flow of electrons. The mediators employed are shown in Figure 1. An NAD(P)H or NAD(P) consuming reaction can be coupled on.

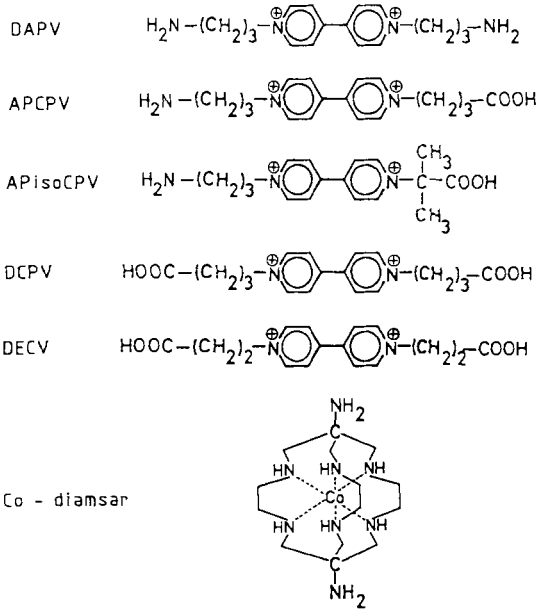

Fig. 1. Mediators employed.

Two routes were used for the immobilization: 1) covalent binding of the mediator to the enzyme followed by covalent binding of the modified enzyme to the functionalized carbon electrode, and 2) covalent binding of the enzyme to an electrode modified with covalently bound bifunctional viologen.

DAPV was covalently bound to VAPOR from *Bacillus spec.* DSM 466 (route 1) under various reaction conditions using the carbodiimide method, and the activity of the so

[*] Prof. Dr. H. Simon, Dr. H. Günther, Dr. A. S. Praxinos, Dipl.-Chem. M. Schulz
Lehrstuhl für Organische Chemie und Biochemie der Technischen Universität München
Lichtenbergstraße 4, D-8046 Garching (FRG)
Dr. C. van Dijk
Agrotechnical Research Institute
NL-6700 AA Wageningen (The Netherlands)

[**] This work was supported by the European Community (Biotechnology Action Program, Contract BAP 250 D).

modified VAPOR was then checked in an optical test (Table 1). Upon covalent binding of DAPV to the enzyme with carbodiimide, not only is the enzyme activity retained, or even increased under certain conditions, but also the K_m value for the binding of NAD changes only negligibly compared to the unmodified enzyme from 0.054 mM to 0.07 mM (80 mol DAPV per mol VAPOR).

Table 1. Enzyme activity in dependence of method of immobilization. EDC = *N*-ethyl-*N'*-(3-dimethylaminopropyl)carbodiimide. HCl. Solutions of DAPV in 10–100 µL of 0.1 N NaOH and of EDC in 100–500 µL of H_2O were added to 5–8 mL VAPOR in TRIS/HCl buffer [TRIS = tris(hydroxymethyl)aminomethane] (0.02 M, pH 7.0) and adjusted to the respective pH with 0.1 N HCl, which was kept constant during the reaction time of 6 min. Finally, unbound DAPV and other low-molecular substances were removed by repeated ultrafiltration.

VAPOR *c* [µM]	DAPV *c* [mM]	EDC *c* [mM]	pH	Spec. Act. [a] [%]	mol DAPV bound per mol VAPOR
0.43	4.7	1.0	4.6	107	10
0.43	4.7	1.0	4.6	71 [b]	6.1
0.43	4.7	1.0	5.5	135	11.1
0.43	4.7	1.0	6.2	108	15.9
3.0	10.0	10.0	4.6	61	80 [c]

[a] Specific activity of the modified VAPOR compared to the native enzyme. [b] With additional 8.6 µmol *N*-hydroxysuccinimide. [c] The reaction time in this case was 2.5 h.

Similar results are to be expected upon immobilization of VAPOR on a carbon surface modified with viologens according to the carbodiimide method (route 2). This was also indicated by experiments in which the stability of such immobilizates was checked. The respective viologen was first covalently bound to carbon felt and thereafter a monomolecular layer of the enzyme was applied. A solution of NAD and $MV^{\bullet\oplus}$ (MV = *N*,*N'*-dimethyl-4,4'-bipyridinium) was now pumped through the carbon felt and the NADH formed was measured samplewise in an optical test with L-lactate dehydrogenase (L-LDH, E.C 1.1.1.27) and pyruvate. The results for various viologens are shown in Figure 2. The non-linearity of the reaction rate is in this case mainly determined by the progressive consumption of the starting materials and the increasing concentration of the products.

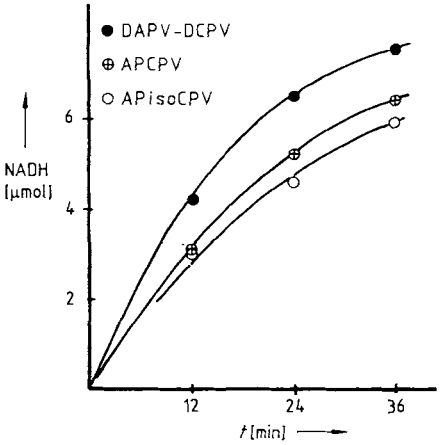

Fig. 2. NADH formation of the immobilized VAPOR as a function of time. DAPV-DCPV, APCPV or APisoCPV was bound covalently to 50 mg carbon felt (ca. 12 cm^2, Type RVG 4000, Carbone Lorraine); a monomolecular layer of VAPOR was then immobilized on the modified felt. For the test, a solution of NAD (10 µmol) and $MV^{\bullet\oplus}$ (25 µmol) in potassium phosphate buffer (0.1 M, pH 7.0) was circulated through the felt at 2.7 mL min^{-1} for about 40 min.

The immobilizates are, after a rapid drop to ca. 50% of the initial activity, very stable. The starting activity is ca. 40% of the activity of the dissolved enzyme.

The functionalization of the glassy carbon electrode and the covalent coating of the electrode surface with a bifunctional viologen will be described elsewhere.[6] By varying the sequence of the immobilization steps for viologen and VAPOR, differently coated electrode surfaces can be prepared (Fig. 3). The electrodes were tested as cathodes in potentiostatically-controlled, electrochemical cells as shown in Scheme 1. All experiments were carried out with strict exclusion of oxygen; anolyte and catholyte were therefore separated by a diaphragm. The initial rate of NADH formation was determined by the bioluminescence method[7] using a calibration curve (Fig. 4). The following conclusions can be drawn: 1) all electrodes without VAPOR (a, b) or without mediator (c, d) show no NADH formation (measured values in the region of that of the blank). 2) Monomolecular layers of VAPOR on a cathode with viologen layer reduce NAD to NADH (e–g). 3) In the case of electrodes modified with DAPV and coated with a multilayer of enzyme (h), the enzyme layers reachable by the substrate no longer have ample electronic contact with the electrode. 4) If, however, DAPV is covalently incorporated in the enzyme layer in the case of such an electrode, a modified electrode (i) is formed which reduces NAD to biologically active NADH). 5) Charge and bonding conditions influence the rate of reaction (e–i).

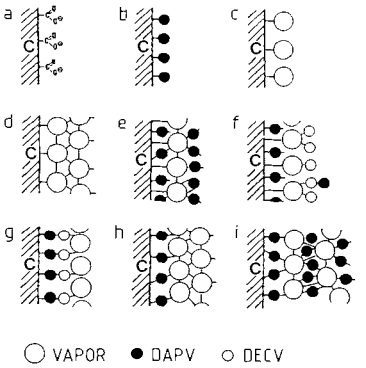

Fig. 3. Schematic representation of the various electrode surfaces. Electrode: glassy carbon (SIGRADUR G), area 1 cm^2. a) Functionalized surface. b) DAPV layer bound via the carboxy groups of (a). c) Monomolecular VAPOR layer: the carboxy groups on an electrode of type (a) were activated by 2 µmol *N*-cyclohexyl-*N'*-[2-(*N*-methylmorpholino)ethyl]carbodiimide · *p*-toluenesulfonate (CMC) in 100 µL 0.1 M potassium phosphate buffer pH 4.5 for 2 h and the so modified electrode treated with 1 U VAPOR in 100 µL 0.05 M TRIS/HCl buffer pH 7.0. d) Multimolecular layer of VAPOR: as (c), but treated simultaneously with 1 µmol CMC in 50 µL 0.1 M potassium phosphate buffer pH 5.5 and the enzyme. e) Monomolecular layer of VAPOR, doped with DAPV: as (c), then both the carboxy groups still available at the electrode surface as well as the enzyme were re-activated and DAPV immobilized thereon. f) Monomolecular layer of VAPOR, doped with DECV: as (c), then DECV was activated with EDC in the molar ratio 1:1.2 and transferred onto the enzyme layer. After 7 min this solution was treated with an additional 2 µmol of DAPV. g) Monomolecular layer of VAPOR, immobilized on a DAPV-DECV layer: as (b), then DECV was treated with EDC analogously to (f) and, after renewed activation of the resulting DAPV-DECV layer with EDC, VAPOR was added. h) Multimolecular layer of VAPOR on DAPV: as (b), then 1 U VAPOR in 100 µL 0.05 M TRIS/HCl buffer pH 7.0 and 1 µmol CMC in 50 µL 0.1 M potassium phosphate buffer pH 5.5 added simultaneously. i) Multimolecular layer of VAPOR and DAPV, cross-linked by DAPV: as (b), then 1 U VAPOR in 100 µL 0.05 M TRIS/HCl buffer pH 7.0, 1 µmol EDC, and 1 µmol DAPV each in 50 µL 0.1 M potassium phosphate buffer pH 5.5 added simultaneously.

The rate of NADH formation decreases significantly over a period of 20 h. The coupling of a reaction rapidly consuming NADH (Scheme 1) increases the rate and stabilizes the reaction, even over a longer period of time. The coupled reaction was the reduction of pyruvate to L-lactate (catalyzed by L-LDH). The lactate formation at the electrode of type (i) was 148 nmol cm^{-2} in 20 h compared to 13.5 nmol cm^{-2} NADH in 19.5 h with a comparable electrode without coupling of an NADH-consuming reaction. In control experiments it was established that all the lactate originates

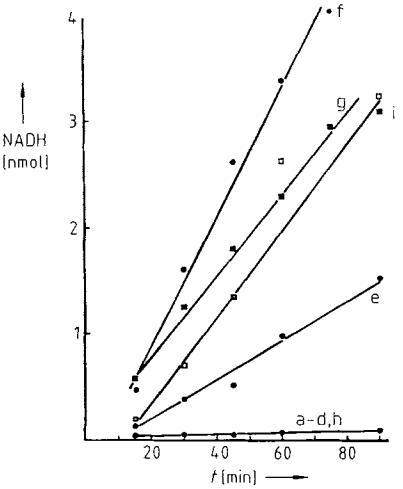

Fig. 4. Time course of NADH formation at carbon electrodes modified as described in Figure 3. Electrode surface: 1 cm^2 (glassy carbon), potential: −407 mV vs. NHE, 6 mL oxygen-free catholyte (TRIS/HCl buffer, 0.1 M, pH 7.0); 18 μmol NAD. (a)–(i) as in Fig. 3). Bioluminescence-NADH test: 250 μL potassium phosphate buffer (25 mM, pH 7.0) contained 25 μmol dithiothreitol, 1.25 μg luciferase EC 1.14.14.3, 9.5 mU flavin mononucleotide (FMN) oxidoreductase EC 1.6.8.1, 0.6 μmol FMN, 10 μg TRITON X-100, 5 μmol myristinaldehyde, 150 μmol NAD, and 50 μL sample. Apparatus: BIOLUMAT LB 9500 T, Berthold, D-7547 Wildbad (FRG).

from the NADH-dependent LDH-catalyzed reaction. A further experiment was carried out with such an electrode in order to clarify the influence of the NADH decomposition during the 19.5 h. First the NADH formation was measured over 90 min according to the bioluminescence method, then, after addition of pyruvate (20 μmol) and L-LDH (7 U), the increase in lactate was determined after a further 17 h. The NADH formation slowed down in the first 30 min from 3.6 nmol cm^{-2} h^{-1} to 1.2 nmol cm^{-2} h^{-1}, but the lactate formation was 9 nmol cm^{-2} h^{-1} over 17 h. In a further analogous experiment with the same electrode the lactate formation was 8.4 nmol cm^{-2} h^{-1} after 2 days.

The higher lactate formation compared to the NADH formation in the absence of an NADH-consuming reaction can be explained in terms of the pyrurate/lactate diffusing more rapidly than NAD/NADH and of an absorption of LDH at the electrode.[8] The NAD concentration in the reaction layer is also increased through the dehydrogenation of the NADH.

According to the above results, current densities lying in the lower range of the current densities of industrial processes can be expected on using carbon felts with larger internal surfaces (referred to the macroscopic surface).[9]

Received: May 17, 1990 [Z 3963 IE]
German version: *Angew. Chem. 102* (1990) 1075

[1] H. Simon, J. Bader, H. Günther, S. Neumann, J. Thanos, *Angew. Chem. 97* (1985) 541–555; *Angew. Chem. Int. Ed. Engl. 24* (1985) 539–553.
[2] C. van Dijk, T. van Eijs, J. W. van Leeuwen, C. Veeger, *FEBS Lett. 166* (1984) 76–80.
[3] C. Bourdillon, R. Lortie, J. M. Laval, *Biotechnol. Bioeng. 31* (1988) 553–589, and references cited therein.
[4] A. E. G. Cass, G. Davis, G. D. Francis, H. A. O. Hill, W. J. Aston, I. J. Higgins, E. V. Plotkin, L. D. L. Scott, A. P. F. Turner, *Anal. Chem. 56* (1984) 667–671.
[5] S. Nagata, R. Feicht, W. Bette, H. Günther, H. Simon, *Eur. J. Appl. Microbiol. Biotechnol. 26* (1987) 263–267.
[6] A. S. Paxinos, H. Günther, D. J. M. Schmedding, H. Simon, unpublished.
[7] J. W. Hastings, *Methods Enzymol. 57* (1978) 125–134; P. E. Stanley, *ibid. 57* (1978) 215–222.
[8] T. Eguchi, T. Iizuka, T. Kagotani, J. H. Lee, I. Urabe, H. Okada, *Eur. J. Biochem. 155* (1986) 415–421.
[9] C. H. Hamann, W. Vielstich: *Elektrochemie II, Elektrodenprozesse, Angewandte Elektrochemie*, Verlag Chemie, Weinheim 1981, p. 265.

Dependence of the Magnetic Superexchange on the Cr···Cr Distance in Dinuclear Chromium(II) Complexes**

By *Ursula Bossek, Karl Wieghardt,* Bernhard Nuber,* and *Johannes Weiss*

The spins of the unpaired electrons of a transition metal ion in a dinuclear complex can be oriented intramolecularly parallel (ferromagnetism) or antiparallel (antiferromagnetism) through the mediation of bridged, non-magnetic anions. This phenomenon is referred to as superexchange.[1] Generally speaking, the extent of this spin-spin coupling is satisfactorily described by the isotropic Heisenberg–Dirac–vanVleck model (HDVV model), whereby the form of the isotropic spin-Hamilton operator is given by $H = -2JS_1S_2$, where J is the exchange coupling constant (in cm^{-1}) and S_1 and S_2 give the total spin of the metal ions **1** and **2**, respectively; J is negative in the case of antiferromagnetic and positive in the case of ferromagnetic spin coupling. The question of whether J is a function of the distance r between the two paramagnetic centers in a bridged, dinuclear complex is still a matter of controversy.[2] Experimentally most convincing is such a dependence with $-J \approx r^{-12}$ in the case of solid-state structures of the type XMF_3 and X_2MF_4 (X = K, Rb, Tl; M = Mn^{II}, Co^{II}, Ni^{II}).[2b] However, the M···M distances vary only by ca. 0.020 Å. Such a dependence on distance has not been observed for the intramolecular spin coupling in dinuclear complexes, since the distance between the metal ions changes with changing type of bridge ligand, and this results in the superexchange mechanism changing.

We have now synthesized dinuclear $Cr^{III}(d^3)$ complexes containing H-bridges as common structural feature:

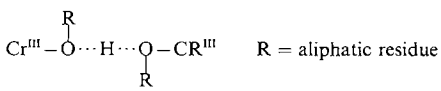

R = aliphatic residue or H

The Cr···Cr distance varies because two octahedrally coordinated Cr^{III} ions are coupled intramolecularly to each

[*] Prof. Dr. K. Wieghardt, U. Bossek
Lehrstuhl für Anorganische Chemie I der Universität
Postfach 10 21 48, D-4630 Bochum 1 (FRG)
Dr. B. Nuber, Prof. Dr. J. Weiss
Anorganisch-chemisches Insitut der Universität
Im Neuenheimer Feld 270, D-6900 Heidelberg (FRG)

[**] This work was supported by the Fonds der Chemischen Industrie.

other via one, two or three such bridges. The Cr···Cr distance varies between 4.46 and 5.64 Å. The temperature-dependent susceptibilities of these compounds were measured on powdered solid samples in the range 4–298 K with a Faraday balance[3] and then fitted to the isotropic HDVV model.[4]

In the complex $[L(acac)CrOH]PF_6 \cdot H_2O$ **1** (L = 1,4,7-trimethyl-1,4,7-triazacyclononane; acac = 2,4-pentanedionate(1−)) the octahedrally coordinated Cr^{III} ions are not coupled to each other (Fig. 1).[5] The Cr–OH group is bound via

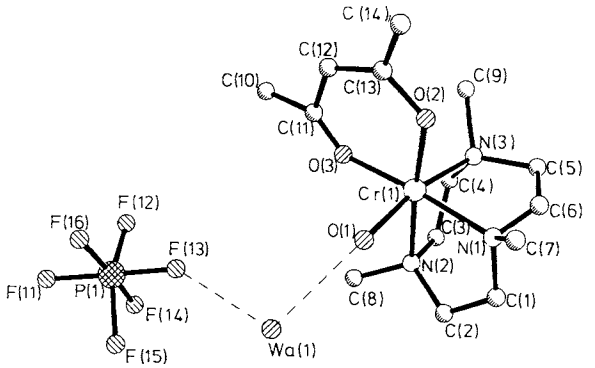

Fig. 1. Structure of **1** in the crystal. Important distances [Å]: Cr1–O1 1.90(2), O1–Wa1 2.66(3), F13···Wa1 2.87(3); Wa = water.

a strong H-bridge to a water molecule; the shortest intermolecular Cr···Cr distance is 8.38 Å. A temperature-independent magnetic moment of 3.79 μ_B was found (Curie behavior), which corresponds to the spin-only value of three unpaired electrons of a Cr^{III} ion. That is **1** shows no spin coupling; an effective superexchange mechanism is lacking.

Crystals of $[(L(acac)Cr)_2(\mu\text{-}H_3O_2)](PF_6)_3$ **2** were obtained from aqueous solutions of **1** at pH = 5. The crystal structure analysis[5] shows that two $[L(acac)Cr\text{-}OH]^{\oplus}$ units are coupled via a strong (O-H···O)-bridge (Fig. 2). Complexes with $(H_3O_2^{\ominus})$-bridges have been the subject of intensive studies in the past few years.[6] Measurements of the temperature-dependent susceptibility of **2** indicate that the spins of the two Cr^{III} ions are coupled weakly antiferromagnetically (Table 1).[7]

Ardon et al.[8] have recently observed a somewhat stronger coupling in two dinuclear Cr^{III} complexes, in each of which there are two $(H_3O_2^{\ominus})$-bridges, namely in β-*cis*-$[(bispictn)_2Cr_2(H_3O_2)_2]I_4 \cdot 4H_2O$ **3** and α-*cis*-$[(pico)_4Cr_2(H_3O_2)_2]I_4 \cdot H_2O$ **4**. The Cr···Cr distances in **3** and **4** are shorter than those in **2**.

Finally, we have obtained the dinuclear, triply bridged complex $[Cr_2^{III}L'_2H_3](PF_6)_3$ **5**[9] by reaction of 1,4,7-tris(2-hydroxyethyl)-1,4,7-triazacyclononone[12] (L′) with $CrCl_3 \cdot 6H_2O$ in ethanol. The structure analysis[5] clearly shows that three O atoms of one ligand are bound via very

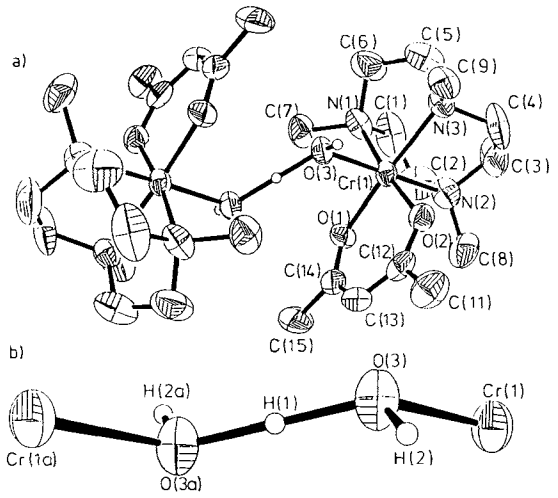

Fig. 2. Structure of the trication of **2** in the crystal. Important distances [Å] and angles [°]: Cr(1)-O(3) 1.969(4), O(3)···O(3)′ 2.496(6), Cr···Cr 5.583(2); O(3)-H(1)-O(3)′ 180.0, Cr(1)-O(3)-H(2) 107.4(2), H(1)-O(3)-H(2) 115.2(3), H(1)-O(3)-Cr(1) 118.8(3). b) structure of the Cr-OH(H)HO-Cr-bridge.

short H-bridges (O···O ≈ 2.47 Å) with the corresponding O atoms of a second ligand (Fig. 3). The Cr···Cr distance could be determined quite reliably as 4.458(6) Å. The temperature dependence of the susceptibility of **5** is typical for an antiferromagnetic spin coupling (Table 1).

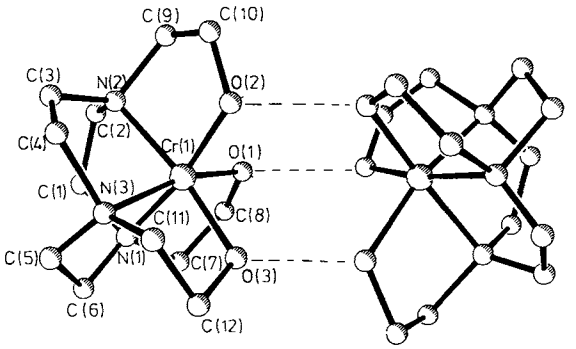

Fig. 3. Structure of the trication of **5** in the crystal. Important distances [Å]: mean O···O distance: 2.47, Cr···Cr 4.458(6), mean Cr-O distance 1.95.

Thus, in each of the complexes **2**–**5** two Cr^{III} ions are coupled via one, two or three O–H···O bridges to give dinuclear units, and the spins are intramolecularly coupled antiferromagnetically. The plot of log $|2J|$, where $-2J$ gives the energy difference between the singlet and the triplet state, versus the logarithm of the Cr···Cr distance yields a straight line of slope −12.1(2) (Fig. 4). That is $-J$ varies proportionally with r^{-12}. Interestingly, the O–H···O distance[13]

Table 1. Structural data and magnetic properties of the μ(ROHOR)-bridged complex. L = 1,4,7-trimethyl-1,4,7-triazacyclononane; acac = 2,4-pentanedionate; bispictn = *N*,*N*′-bis(2-pyridylmethyl)-1,3-propanediamine; pico = 2-picolylamine; L′ = 1,4,7-tris(2-hydroxyethyl)-1,4,7-triazacyclononane(−3H).

Complex	Cr···Cr [Å]	O···O [Å]	Cr-O(H_3O_2) [Å]	J [cm^{-1}]
$[L_2(acac)_2Cr_2(H_3O_2)](PF_6)_3$ **2**	5.583	2.496(2)	1.969(3)	−0.30(10)
β-*cis*-$[(bispictn)_2Cr_2(H_3O_2)_2]I_4 \cdot 4H_2O$ [8] **3**	4.797(1)	2.472(5)	1.906(3) 1.961(4)	−2.29(1)
α-*cis*-$[(pico)_4Cr_2(H_3O_2)_2]I_4 \cdot 2H_2O$ [8] **4**	5.118(2)	2.50(1) 2.48(1)	1.934(7) 1.932(7)	−1.14(1)
$[L'_2Cr_2H_3](PF_6)_3$ **5**	4.458(6)	2.47	1.95	−5.3(5)

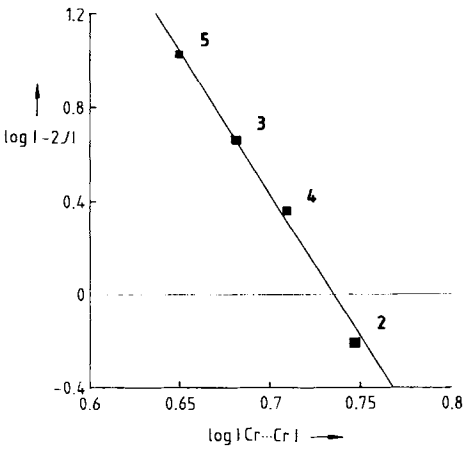

Fig. 4. Plot of log $|-2J|$ versus log |Cr···Cr|.

and the mean Cr–O distance do not correlate with the strength of the spin-exchange coupling; both quantities are about constant in the series **2**–**5**. It has already been experimentally observed that a superexchange mechanism can be facilitated via H-bridges.[10]

It must be pointed out that the straight line in Figure 4 is no limiting function for the dependence of the antiferromagnetic superexchange on the distance between the metal ions, like that suggested by *Coffman* and *Buettner*.[2d] It is possible, of course, that strong intramolecular couplings occur over considerably greater Cr···Cr distances than would be implied by Figure 4 if other bridge ligands bind the magnetic orbitals symmetry allowed with larger overlap constants. Indeed, in the case of $[LCu^{II}(H_2O)(\mu\text{-terephthalato})Cu^{II}L(H_2O)](ClO_4)_2$, for example, there is a strong spin coupling over 11.25 Å.[11] The correlation found here thus implies that, with unchanging superexchange mechanism but with differing distances between the paramagnetic centers in a series of complexes, the strength of the spin coupling decreases with the twelth power of the distance between the metal ions.[14]

Experimental

1: A suspension of $LCrBr_3$ (2.0 g) in H_2O (50 mL) and sodium acetylacetonate (2.0 g) was stirred for 1 h at 70 °C until a clear solution was obtained. After addition of 1.0 g of KPF_6 and cooling to 5 °C, violet crystals of **1** (0.90 g) separated.

2: When the above reaction solution was treated with HPF_6 until the pH was 5, after subsequent addition of 1 g of KPF_6 red crystals of **2** precipitated (1.2 g), which were recrystallized from a minimum of H_2O (pH = 5).

5: A solution of $CrCl_3 \cdot 6H_2O$ (0.27 g) in ethanol (10 mL) was treated under an argon atmosphere with granulated zinc (2–3 pieces). After 15 minutes' stirring at 45 °C an Ar-purged solution of 1,4,7-tris(2-hydroxyethyl)-1,4,7-triazacyclononane(L') (0.26 g) in ethanol (10 mL) was added dropwise and stirring continued for another further 45 min at 45 °C (dark violet solution). After removal of solvent the residue was dissolved in 20 mL of H_2O and the resulting solution treated with 0.55 g of KPF_6 and a few drops of HPF_6 (pH 4). Within a few hours, violet crystals of **5** separated out. Recrystallization from a CH_3CN/H_2O mixture (4:1) furnished single crystals suitable for an X-ray structure analysis.

All the complexes gave correct elemental analyses (C,H,N,Cr); the UV-VIS spectra are typical for octahedral Cr^{III} complexes.

Received: April 30, 1990 [Z 3937 IE]
German version: *Angew. Chem. 102* (1990) 1093

[1] a) P. W. Anderson, *Phys. Rev. 115* (1959) 2; b) J. B. Goodenough, *ibid. 100* (1955) 564; *J. Phys. Chem. Solids 6* (1958) 287; c) J. Kanamori, *J. Phys. Chem. Solids 10* (1959) 87. For an excellent review see: W. E. Hatfield in E. A. Boudreaux, L. N. Mulay (Eds.): *Theory and Applications of Molecular Paramagnetism*, Wiley, New York 1976, p. 349; A. P. Ginsberg, *Inorg. Chim. Acta. Rev. 1971*, 45; P. W. Anderson in F. Seitz, D. Turnbull (Eds.): *Solid State Physics*, Academic, New York 1963, p. 99.

[2] a) D. Bloch, *J. Phys. Chem. Solids 27* (1966) 881; b) L. J. de Jongh, R. Block, *Physica 79 B* (1975) 568; c) D. N. Hendrickson in R. D. Willett, D. Gatteschi, O. Kahn (Eds.): *Magneto-Structural Correlations in Exchange Coupled Systems, NATO Adv. Study Inst. Ser. Ser. C 140* (1983) 523; d) R. E. Coffman, G. R. Buettner, *J. Phys. Chem. 83* (1979) 2387.

[3] We thank Herrn Dipl.-Chem. *Romstedt* and Prof. Dr. *P. Gütlich* (Mainz) as well as Herrn Dr. *P. Fleischhauer* and Prof. Dr. *W. Haase* (Darmstadt) for the temperature-dependent measurements of the susceptibilities of the complexes **1**, **2** and **5**.

[4] C. J. O'Connor, *Prog. Inorg. Chem. 29* (1982) 203.

[5] Crystal structure analysis: **1**: orthorhombic, space group $Pbn2_1$ (C_{2v}^9), $a = 8.378(7)$, $b = 16.73(1)$, $c = 15.81(1)$ Å, $V = 2216$ Å^3, $Z = 4$, $\varrho_{calcd} = 1.51$ g cm^{-3}, $Mo_{K\alpha}$ radiation; $R = 0.106$, $R_w = 0.093$ for 787 independent reflections with $I > 2.5\sigma(I)$ and 121 parameters. **2**: triclinic, space group $P\bar{1}$, $a = 10.588(6)$, $b = 10.752(6)$, $c = 11.569$ (7 Å, $\alpha = 72.72(5)$, $\beta = 80.16(5)$, $\gamma = 65.16(4)°$, $V = 1139.6$ Å^3, $Z = 1$, $\varrho_{calcd} = 1.62$ g cm^{-3}, $Mo_{K\alpha}$ radiation; $R = 0.052$; $R_w = 0.044$ for 2730 independent reflections with $I > 2.5\sigma(I)$ and 286 parameters. The H-atoms of the Cr–OH(H)HO–Cr group were located in the difference Fourier synthesis and refined with isotropic, fixed $U = 0.08$ Å^2; all other H-atoms in calculated positions. **5**: orthorhombic, space group $Pnn2$, $a = 13.748(2)$, $b = 15.357(3)$, $c = 10.184(2)$ Å, $V = 2150.1$ Å^3, $Z = 4$. The structure could not be refined owing to the quality of the crystals and the high degree of disorder of the $PF_6^{\ominus}$ anions. The atomic coordinates were therefore not deposited. Attempts are presently being made to prepare crystals of better quality. We thank Dr. *U. Flörke* and Prof. *H.-J. Haupt* (Paderborn) for the present data. Further details of the crystal structure investigations of **1** and **2** are available on request from the Fachinformationszentrum Karlsruhe, Gesellschaft für wissenschaftlich-technische Information mbH, D-7514 Eggenstein-Leopoldshafen 2 (FRG), on quoting the depository number CSD-54661, the names of the authors, and the journal citation.

[6] M. Ardon, A. Bino, *Struct. Bonding (Berlin) 65* (1987) 1, and references cited therein.

[7] The Hamilton operator $\boldsymbol{H} = -2JS_1S_2 - j(S_1S_2)^2$ is frequently used for the modeling of the magnetic properties of dinuclear Cr^{III} complexes. Attempts to fit x_m curves of **2** and **5** with this operator did not lead to any significant improvement in the fit, but led to almost identical numerical values for J.

[8] M. Ardon, A. Bino, K. Michelsen, E. Pedersen, *J. Am. Chem. Soc. 109* (1987) 5855.

[9] A similarly structured Co^{III} complex has been described recently: A. A. Belal, L. J.Farrugia, R. D. Peacock, J. Robb, *J. Chem. Soc. Dalton Trans. 1989*, 931.

[10] a) J. W. Culvahouse, C. L. Francis, *J. Chem. Phys. 66* (1977) 1079; b) J. A. Bertrand, F. T. Helm, *J. Am. Chem. Soc. 95* (1973) 8184; c) J. A. Bertrand, T. D. Black, P. G. Eller, F. T. Helm, R. Mahmood, *Inorg. Chem. 15* (1976) 2965; d) W. Estes, W. E. Hatfield, *ibid. 17* (1978) 3226; e) H. Muhonen, *ibid. 25* (1986) 4692.

[11] P. Chaudhuri, K. Oder, K. Wieghardt, S. Gehring, W. Haase, B. Nuber, J. Weiss, *J. Am. Chem. Soc. 110* (1988) 3657.

[12] B. A. Sayer, J. P. Michael, R. D. Hancock, *Inorg. Chim. Acta 77* (1983) L63.

[13] In a recent theoretical analysis a linear dependence of $-2J$ on the O···O distance in dimeric, H-bridged Cu^{II} complexes was postulated: F. Nepveu, S. Gehring, L. Walz, *Chem. Phys. Lett. 128* (1986) 300. This, however, has not been verified experimentally.

[14] The dependence of J on r can also be described by the exponential function $J = J_0 e^{-\alpha r}$ [2d]; the plot of $\ln|-2J|$ versus r is likewise linear. A value of 2.6(1) was determined for a.

Ring-Opening of a Bicyclo[3.2.0]hepta-1,3-dienylcobalt(I) Complex Followed by Cycloaddition**

By *Holger Butenschön**

"Ring slippage" reactions of cyclopentadienyl complexes, that is a change in hapticity from η^5 to η^3, were first pro-

[*] Dr. H. Butenschön
Max-Planck-Institut für Kohlenforschung
Kaiser-Wilhelm-Platz 1, D-4330 Mülheim an der Ruhr 1 (FRG)

[**] *H. B.* thanks the Verband der Chemischen Industrie e.V. for a Liebig fellowship, Prof. Dr. *G. Wilke* for generous support, and Herrn *G. Schroth* for help with the NMR investigations. The results of this work were delivered in a lecture at the Chemiedozenten-Tagung 1990 in Ulm.

posed by *Basolo* et al. to explain associative ligand exchange processes.[1] Since then, η^3-cyclopentadienyl complexes have often been postulated as intermediates.[2] *Brintzinger* et al. were the first to succeed in isolating and structurally characterizing an η^3-cyclopentadienyl complex.[3] Herein we report the first case of a ring slippage reaction in which the η^5-cyclopentadienyl ligand being used is altered by breakage and reformation of C–C bonds.

The DSC analysis (differential scanning calorimetry) of the η^5-bicyclo[3.2.0]hepta-1,3-dienylcobalt(I) complex **1** shows a reaction above 200 °C, which, however, does not involve the desired opening of the four-membered ring, but cleavage of the electroneutral cycloocta-1,5-diene (COD).[4] Apparently, the opening of the four-membered ring requires a higher activation energy than the COD cleavage. Therefore COD must be replaced by a less easily cleavable ligand. **1** reacts with diphenylethyne in boiling *ortho*-xylene to give the tetraphenylcyclobutadiene complex **2**, cleavage of which is first expected to take place at higher temperatures.[5, 6] The DSC analysis of **2** also shows a reaction above 200 °C. In order to check whether it involves thermal opening of the four-membered ring, **2** was allowed to react with dimethyl fumarate at 200 °C for 13 h. The cycloadduct **3** was obtained in 65% yield (C_4Ph_4 = tetraphenylcyclobutadiene, E = $COOCH_3$).

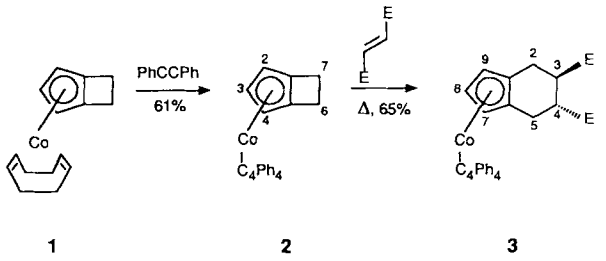

1 **2** **3**

This result suggests formation of an η^3-(4,5-dimethylenecyclopentenyl)cobalt(I) complex[7] (see Scheme 1), an analogue of an *ortho*-quinodimethane complex, as intermediate. Replacement of dimethyl fumarate by dimethyl maleate leads to a less clear result, which nevertheless permits further insights into the course of the reaction.

3 (rel. amount 0.9) and the *cis*-substituted complexes **4** (0.6) and **5** (1.0) are obtained in an overall yield of 90%. The assignment of the structures followed from the spectroscopic data of the mixture (IR, ^1H NMR, ^{13}C NMR, MS) and, in the case of **4** and **5**, also from NOE measurements (irradiation at OCH_3 shows NOE of the *ortho*-H in the case of **5**, and vice versa).

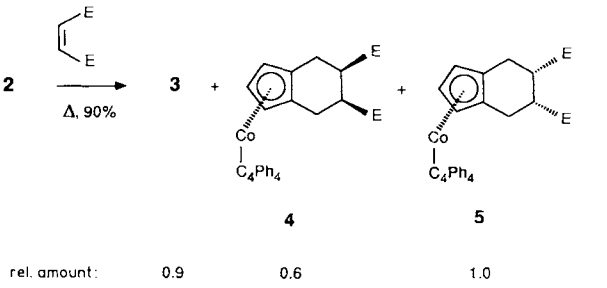

2 **3** **4** **5**

rel. amount: 0.9 0.6 1.0

Some further observations must be taken into consideration in order to explain the course of the reaction: The dimethyl maleate employed contains 0.3% of dimethyl fumarate before the reaction, whereas the dimethyl maleate recovered by distillation after the reaction contains 3.9% of dimethyl fumarate (GC). Apparently an isomerization takes place,[8] as has already been observed previously in the reaction of **1** with dimethyl maleate. In the absence of **2** under otherwise unchanged reaction conditions a comparable isomerization is not observed, and not up to 180 °C even in the presence of **2**. Nor does a comparable isomerization take place under the same conditions with η^5-(cyclopentadienyl)-η^4-(tetraphenylcyclobutadene)cobalt(I).[6] It may therefore be concluded that the *cis-trans* isomerization is transition-metal-catalyzed at a vacant coordination site during the course of opening of the four-membered ring.

These findings would suggest a reaction as depicted in Scheme 1. As a result of the thermal ring-opening, which is best described in therms of an allyl-ene structure such as **6**, the η^5-bicyclo[3.2.0]hepta-1,3-dienyl complex **2** is converted into an η^3-4,5-dimethylenecyclopentenyl complex **7**, which reacts with dimethyl maleate with reformation of the stable η^5-coordination to give the cycloadducts **4** and **5**. Besides the direct cycloaddition, dimethyl maleate can coordinate to the free coordination site and subsequently be isomerized to dimethyl fumarate; from **7**, the complexes **8** and **9** could be formed, which then react with the coordinated dimethyl fumarate or with the dimethyl fumarate present in the reaction mixture (according to *Sauer* this should be more reactive than dimethyl maleate[9]) to give the *trans*-cycloadduct **3** as a stable η^5-cyclopentadienyl complex. That the formation of the *cis-endo* cycloadduct **5** is favored over that of **4**, could be due to an intramolecular transfer of the coordinated dimethyl maleate in **8** to the diene unit.

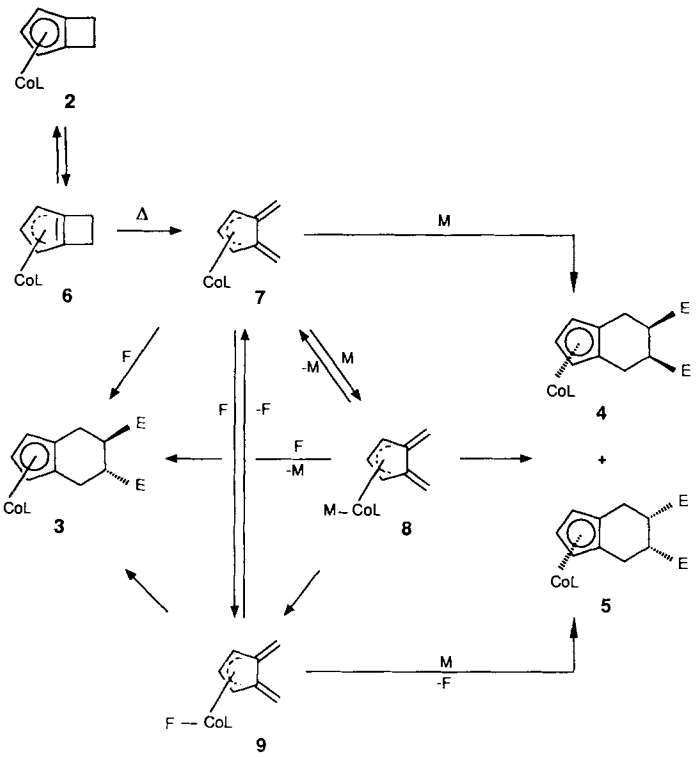

2 **3** **4** **5** **6** **7** **8** **9**

Scheme 1. L = C_4Ph_4; E = $COOCH_3$; F = dimethyl fumarate; M = dimethyl maleate.

Since the course of the reaction with dimethyl maleate was largely influenced by its coordination and the isomerization to dimethyl fumarate, **2** was also allowed to react with the cyclic, poorly coordinating *N*-methylmaleimide. The reaction carried out in *n*-dodecane gave as sole product (93%) the *exo*-cycloadduct **10** corresponding to **4**,[5] whose *exo*-

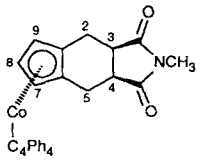

10

configuration was confirmed by an NOE experiment. Apparently, the attack of the non-coordinating dienophile takes place exclusively from the side of the diene away from the metal atom, which is consistent with the postulated reaction course (Scheme 1).

The reactions of the cobalt complex **2** presented here represent the first cases in which a ring-slippage reaction ($\eta^5 \rightarrow \eta^3 \rightarrow \eta^5$) leads to breakage of one, and formation of two new C–C bonds. The driving force behind this reaction could be the ring strain in the educt and the individual transformations of π-bonds into σ-bonds of each Diels-Alder reaction. The similarity to the chemistry of cyclobutabenzene is unmistakable; an essential difference lies, however, in the breaking of a symmetry plane in the educt and in the *ortho*-quinodimethane-analogous intermediates by coordination to a transition metal. Recent findings by *Kündig* et al. are also of interest in this connection.[10]

Received: April 17, 1990 [Z 3914 IE]
German version: *Angew. Chem. 102* (1990) 1058

CAS-Registry numbers:
1, 128382-90-1; **2**, 128632-33-7; **3**, 128632-34-8; **4**, 128706-21-8; **5**, 128706-22-9; **10**, 128632-35-9; dimethyl fumarate, 624-49-7; dimethyl maleate, 624-48-6.

[1] H. G. Schuster-Woldan, F. Basolo, *J. Am. Chem. Soc. 88* (1966) 1657.
[2] J. M. O'Connor, C. P. Casey, *Chem. Rev. 87* (1987) 307, and references cited therein.
[3] G. Huttner, H. H. Brintzinger, L. G. Bell, P. Friedrich, V. Bejenke, D. Neugebauer, *J. Organomet. Chem. 145* (1978), 329.
[4] H. Butenschön, P. Betz, *J. Chem. Soc. Chem. Commun. 1990*, 500.
[5] Consistent spectroscopic data and correct elemental analyses were obtained. **2**: ^{1}H-NMR (200 MHz, $CDCl_3$): $\delta = 2.30$, 2.68 (AA'BB' system, 4H, *endo*-6(7)-H, *exo*-6(7)-H, $\sum J_{3,4} = 9.6$ Hz), 4.34 (t, 1H, 3-H, $^3J_{3,2(4)} = 2.2$ Hz), 4.48 (d, 2H, 2(4)-H), 7.23 (m, 12H, *meta*-H, *para*-H), 7.44 (m, 8H, *ortho*-H).—**3**: (200 MHz, C_6D_6): $\delta = 2.08$ (m, 1H, *exo*-5-H, $^2J_{endo\ 5,exo\ 5} = -15.9$ Hz, $^3J_{4,exo\ 5} = 12.4$ Hz), 2.20 (m, 1H, *endo*-2-H, $^2J_{endo\ 2,exo\ 2} = -15.8$ Hz, $^3J_{endo\ 2,3} = 11.9$ Hz), 2.38 (m, 1H, *exo*-2-H, $^3J_{exo\ 2,3} = 6.1$ Hz), 2.54 (m, 2H, 4-H, *endo*-5-H, $^3J_{4,endo\ 5} = 4.9$ Hz, $^3J_{3,4} = 11.6$ Hz), 2.76 (m, 1H, 3-H), 3.27 (s, 3H, *exo*-$COOCH_3$), 3.29 (s, 3H, *endo*-$COOCH_3$), 4.24 (m, 1H, 7-H o. 9-H, $^3J_{7,8} = {}^3J_{8,9} = 2.5$ Hz, $^4J_{7,9} = 1.5$ Hz), 4.30 (m, 1H, 7-H o. 9-H), 4.36 (dd, 1H, 8-H), 7.1 (m, 12H, *meta*-H, *para*-H), 7.56 (m, 8H, *ortho*-H).—**10**: (200 MHz, $CDCl_3$): $\delta = 2.14$ (m, 1H, *endo*-2(5)-H, $J_{endo\ 2(5),3(4)} \approx 7.3$ Hz, $^2J_{endo\ 2(5),exo\ 2(5)} = -15.1$ Hz), 2.60 (dd, 1H, *exo*-2(5)-H, $J_{exo\ 2(5),3(4)} \approx 3.1$ Hz), 2.73 (m, 1H, 3(4)-H), 2.76 (s, 3H, CH_3), 4.32 (t, 1H, 8-H, $^3J_{7(9),8} = 2.6$ Hz), 4.57 (d, 2H, 7(9)-H), 7.23 (m, 12H, *meta*-, *para*-H), 7.41 (m, 8H, *ortho*-H).
[6] A. Nakamura, N. Hagihara, *Bull. Chem. Soc. Jpn. 34* (1961) 452; G. A. Ville, K. P. C. Vollhardt, M. J. Winter, *Organometallics 3* (1984) 1177; A. Efraty, *Chem. Rev. 77* (1977) 691, and references cited therein.
[7] Cf. J. W. Pattiasina, C. E. Hissink, J. L. de Boer, A. Meetsma, J. H. Teuben, *J. Am. Chem. Soc. 107* (1985) 7758; F. G. N. Cloke, J. C. Green, M. L. H. Green, C. P. Morley, *J. Chem. Soc. Chem. Commun. 1985*, 945.
[8] Taking into account the 100-fold excess of dimethyl maleate used compared to **2**, this corresponds to approximately three catalytic cycles.
[9] J. Sauer, D. Lang, H. Wiest, *Chem. Ber. 97* (1964) 3208.
[10] E. P. Kündig, G. Bernardinelli, J. Leresche, P. Romanens, *Angew. Chem. 102* (1990) 421; *Angew. Chem. Int. Ed. Engl. 29* (1990) 407.

Azadiboriridine-Borane: a Non-Classical Acid-Base Adduct**

By *Peter Paetzold,* Burkhard Redenz-Stormanns, Roland Boese,* Michael Bühl*, and *Paul von Ragué Schleyer**

In the reaction of the azadiboriridine **1a**[1] with THF · BH_3 we expected the Lewis acid BH_3 to add at the N atom. Surprisingly, however, **1a** displays its Lewis basicity across the B–B bond, and as a consequence the bicyclic **2**, a colorless liquid, was obtained in accordance with Equation (a).

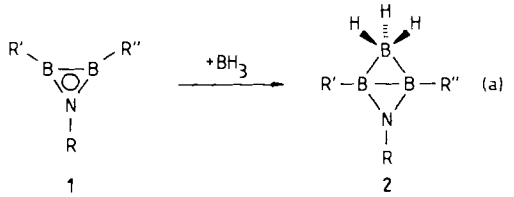

1 **2**

a, R = R' = R'' = *t*Bu
b, R = R' = *t*Bu, R'' = *i*Pr
c, R = R' = R'' = H
d, R = H, R' = R'' = Me

The constitution of **2a** in solution follows from the NMR spectra.[2] The ^{11}B-NMR signal at $\delta = 51.9$ would have been shifted to lower field if the ring π-electron pair had been employed for the formation of a B-N adduct, but actually a high field shift to $\delta = 32.9$ was observed with retention of the equivalence of both B-atoms. Moreover, it can be concluded from the 2D-COSY-^{11}B-^{11}B-NMR spectrum that the B atom of the BH_3 group directly interacts with each of the two other B atoms. A notable feature of **2a** is the rigid conformation of the BH_3 group, which leads to two quartets (1:1:1:1) in the ^{1}H-NMR spectrum and to a doublet/triplet pattern with coupling constants of 131 Hz (BH) and 68 Hz (BH_2) in the ^{11}B-NMR spectrum. The 2:1 non-equivalence of the BH_3 protons is retained even at 90 °C in toluene. The NMR findings in solution are also confirmed for the solid state by an X-ray structure analysis at 120 K (Fig. 1).[3]

The almost equilateral triangles B1–B2–B3 and N–B2–B3 enclose an angle of 42.6°. The markedly large ring angle of 78.1° at the N atom provides optimal clearance for the bulky ligands. The NB_3 skeleton can be regarded as a *nido*-fragment of a trigonal bipyramid, and, indeed, **2a** fulfills the electron count rules for a *nido*-compound. The B1–H12 and B1–H13 distances (each 1.16 Å) are significantly greater than B1–H1 (1.10 Å), but the B2–H12 and B3–H13 distances (ca. 1.67 Å) are too large to assume a bridge position of H12 and H13. The structure of **2a** is, in principle, reminiscent of that of the anion $[Fe(CO)_4B_7H_{12}]^{\ominus}$, which is formed by the addition of BH_3 to a B–B bond of the anion $[Fe(CO)_4B_6H_9]^{\ominus}$ in the pentagonal base of the pyramidal B_6 structure.[4]

[*] Prof. Dr. P. Paetzold, B. Redenz-Stormanns
Institut für Anorganische Chemie der Technischen Hochschule
Templergraben 55, D-5100 Aachen (FRG)
Dr. R. Boese
Institut für Anorganische Chemie der Universität-Gesamthochschule
Universitätsstrasse 5–7, D-4300 Essen (FRG)
Prof. Dr. P. von R. Schleyer, M. Bühl
Institut für Organische Chemie der Universität Erlangen-Nürnberg
Henkestrasse 42, D-8520 Erlangen (FRG)

[**] This work was supported by the Deutsche Forschungsgemeinschaft.

The azadiboriridine **1b** can be prepared analogously to **1a** from Cl–B(*t*Bu)–N(*t*Bu)–B(*i*Pr)–Cl[11] by dehalogenation with Na/K if the reaction is carried out at −78 °C; on allowing to warm to room temperature, **1b** dimerizes to the *nido*-cluster compound $N_2B_4tBu_4iPr_2$.[11] If, however, **1b** is treated with THF · BH_3 at −78 °C, **2b** can be isolated in 34% yield as a colorless liquid, and can be characterized NMR spectroscopically.[5] The ^{11}B-NMR signal of the BH_3 group, at room temperature a doublet-triplet pattern at $\delta = -17.8$ ($J = 131$ and 69 Hz, respectively), is converted into a quartet at $\delta = -17.2$ ($J = 88$ Hz) upon heating to 90 °C in toluene, an indication that the conformational rigidity of the BH_3 group in **2a** has, inter alia, steric origin.

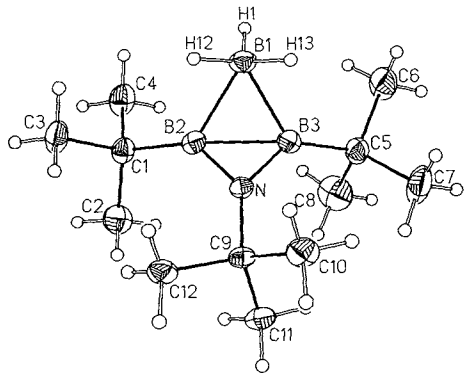

Fig. 1. Molecular structure of **2a** in the crystal. Selected bond lengths, angles, and torsion angles ([Å] and [°], resp., standard deviations in brackets): B1–B2 1.770(2), B1–B3 1.752(2), B2–B3 1.785(2), B1–N 2.484(2), B2–N 1.412(2), B3–N 1.421(2), B2–C1 1.590(2), B3–C5 1.592(2), N–C9 1.480(2), B1–H1 1.098(17), B1–H12 1.158(17), B1–H13 1.155(15), B2–H12 1.686(18), B3–H13 1.653(17); B2–B1–B3 60.9(1), B1–B2–B3 59.1(1), B1–B3–B2 60.0(1), N–B2–B3 51.2(1), N–B3–B2 50.7(1), B2–N–B3 78.1(1), B1–B2–C1 120.9(1), N–B2–C1 136.9(1), B1–B3–C5 120.9(1), N–B3–C5 135.8(1), B2–N–C9 140.8(1), B3–N–C9 140.3(1), H1–B1–B2 127.2(8), H1–B1–B3 124.8(8), H1–B1–H12 119.6(11), H1–B1–H13 118.3(11); H1–B1–B2–N 142.4, H1–B1–B3–N −145.9, H1–B1–B2–B3 113.5, H1–B1–H12–B2 120.8, H1–B1–H13–B3 −117.9, C1–B2–B3–C5 −2.7, C1–B2–N–C9 27.7, C5–B3–N–C9 −33.2, H12–B2–B3–B1 −25.8, H13–B1–B2–B3 −44.2.

Table 1. Comparison of measured (**2a**) and calculated (**2c, d**) distances and ^{11}B-NMR chemical shifts.

	Distances [Å] [a]				δ (^{11}B) [b]	
	B1-B2 B1-B3	B2-B3	B2-N B3-N	B2-H12 B3-H13	B1	B2/B3
2a	1.770 1.752	1.785	1.421 1.412	1.653 1.686	−14.1	32.9
2c	1.716	1.758	1.421	1.599	−15.5	22.1
2d	1.724	1.766	1.424	1.627	−18.9	28.8

[a] MP2/6-31G*-optimized (**2c, d**). [b] IGLO (Individual Gauge for Localized Orbitals) [8]; Double-Zeta Basis (**2c, d**).

Ab initio calculations[6] on the model systems **2c** and **2d** confirm the experimental findings. Optimizations in C_s symmetry satisfactorily reproduce both the geometry[7] as well as the ^{11}B-NMR chemical shifts of **2a** (Table 1). The influence of the alkyl substituents on the ^{11}B-NMR signals of B2/B3 is made clear on going from **2c** ($\delta = 22$) to **2d** ($\delta = 29$).—Based on the calculated bond order of 0.19 a weak B2···H12 interaction becomes apparent in **2c**, in spite of the relatively long distance of more than 1.6 Å.[6] This may be a further explanation for the observed conformational rigidity of the complexed BH_3 group in addition to steric reasons. The enthalpy of formation of −45.7 kcal mol^{-1} for the formation of **2c** from BH_3 and NB_2H_3 is significantly greater than the value of −28.5 kcal mol^{-1} calculated for the formation of H_3B–NH_3 from BH_3 and NH_3 [calculated for both at MP4sdtq(FC)/6-31G**//MP2//(Full)/6-31G* + ZPE(6-31G*) level]. Hence, azadiboriridines are stronger bases towards BH_3 than amines, but the weak B–B bond[9] and not the nitrogen represents the basic center. This is also true for the protonation: the proton affinity of −211.5 kcal mol^{-1} calculated for NB_2H_3 (with formation of a three-center B–H–B bond) is greater than that for ammonia, with a value of −206.8 kcal mol [calculated for both at MP4sdtq(FC)/6-31 + G**//6-31G* + ZPE(6.31G*) level].

Experimental

1,2,3-Tri-*tert*-butyl-*nido*-1-azatetraborane(6) (tri-*tert*-butylazadiboriridineborane) **2a**: A solution of **1a** (1.08 g) in THF (15 mL) was treated at 0 °C with 5.9 mL of a 0.83 M solution of BH_3 in THF. The mixture was stirred for 30 min at room temperature. After removal of solvent and distillation at 45 °C (0.3 torr) we obtained 1.10 g (95%) of **2a**, m.p. −10 °C.

Received: May 2, 1990 [Z 3939 IE]
German version: *Angew. Chem. 102* (1990) 1059

CAS-Registry numbers:
1a, 109976-00-3; **1b**, 128497-14-3; **2a**, 128497-15-4; **2b**, 128497-16-5; **2c**, 128497-17-6; **2d**, 128497-18-7; BH_3, 13283-31-3.

[1] R. Boese, B. Kröckert, P. Paetzold, *Chem. Ber. 120* (1987) 1913.
[2] **2a**: NMR ($CDCl_3$): $\delta(^1H) = 0.92$ (2H), 1.04 (18H), 1.36 (9H), 2.03 (1H); $\delta(^{11}B) = -14.1$ (1B), 32.9 (2B). MS: $m/z = 207$ (21%, $M^{\oplus} - BH_3$), 164 (100, $M^{\oplus} - C_4H_9$), 150 (91, $M^{\oplus} - BH_3 - C_4H_9$), 108 (32, $M^{\oplus} - C_4H_9 - C_4H_8$).
[3] Single crystal from the melt in a measuring tube; $a = 12.143(2)$, $b = 8.644(1)$, $c = 15.637(3)$, $\beta = 103.79(1)°$, $V = 1594.0(4)$ Å^3, $Z = 4$, $\varrho_{calc} = 0.920$ g cm^{-3}, $P2_1/n$ (No. 14); crystal size $d = 0.3$ mm; measuring range: $3 \le 2\theta \le 50°$; 2770 independent reflections, 2268 observed with $F_o \ge 4\sigma(F)$; anisotropic temperature factors for the non-hydrogen atoms; 160 refined parameters; $R = 0.042$, $R_w = 0.048$. Further details of the crystal structure investigation are available on request from the Fachinformationszentrum Karlsruhe, Gesellschaft für wissenschaftlich-technische Information mbH, D-7514 Eggenstein-Leopoldshafen 2 (FRG), on quoting the depository number CSD-54561, the names of the authors, and the journal citation.
[4] O. Hollander, W. R. Clayton, S. G. Shore, *J. Chem. Soc. Chem. Commun. 1974*, 604; M. Mangion, W. R. Clayton, O. Hollander, S. G. Shore, *Inorg. Chem. 16* (1977) 2110.
[5] **2b**: NMR ($CDCl_3$): $\delta(^1H) = 0.70$ (2H), 0.90 (d, $J = 7.0$ Hz, 6H), 1.03(9H), 1.33(9H), 1.64(sept, $J = 7.0$ Hz, 1H) 1.79 (1H); $\delta(^{11}B) = -17.8$ (1B), 32.4 (1B), 34.4 (1B). MS: $m/z = 193$ (28%, $M^{\oplus} - BH_3$), 178 (4, $M^{\oplus} - BH_3 - CH_3$), 150 (92, $M^{\oplus} - C_4H_9$), 136 (100, $M^{\oplus} - BH_3 - C_4H_9$).
[6] Standard procedures and basis sets were used, see, e.g., W. Hehre, P. von R. Schleyer, J. A. Pople, *Ab Initio Molecular Orbital Theory*, Wiley, New York 1986. The scaled 6-31G* frequencies were used for the zero-point correction.
[7] From a population analysis of the natural orbitals (6-31G* basis set); for a review see. A. E. Reed, L. A. Curtiss, F. Weinhold, *Chem. Rev. 88* (1988) 899.
[8] W. Kutzelnigg, *Isr. J. Chem. 19* (1980) 193; M. Schindler, W. Kutzelnigg, *J. Chem. Phys. 76* (1982) 1919; review: W. Kutzelnigg, U. Fleischer, M. Schindler, *NMR Basic Princ. Prog.*, in press.
[9] P. H. M. Budzelaar, P. von R. Schleyer, *J. Am. Chem. Soc. 108* (1986) 3967.

Mechanism of the Cycloaddition of Bicyclo[2.1.0]pent-2-ene: a Non-concerted Homo-Diels-Alder Reaction**

By *Frank-Gerrit Klärner** and *Manfred Naumann*

Dedicated to Professor Wolfgang R. Roth on the occasion of his 60th birthday

Roth and *Martin*[1] have interpreted the *endo*-stereospecific course of the $[_\sigma2+_\pi2]$-cycloaddition of 4-phenyl-4*H*-1,2,4-triazole-3,5-dione **9a** to the bicyclo[2.1.0]pentane derivative **1** as characteristic of a two-step process. As first step, the authors postulate, in line with MO considerations,[2] an electronically favored backside attack of **9a** at the strained, central cyclopropane bond of **1** with formation of the reactive diradical intermediate **2**, which then closes in the second step to give the stable cycloadduct **3**. An analogous *endo*-stereospecificity is also observed in the addition of olefins such as maleic anhydride, fumaronitrile and maleonitrile to bicyclo[2.1.0]pentane,[3] of **9a** to tricyclo[3.2.0.0^{2,4}]heptane,[4] and of **9b** to bicyclo[1.1.0]butane.[5] In contrast, *exo*-stereospecificity is observed in the case of the homo-Diels-Alder reaction of tetracyanoethylene **10**, *N*-phenylmaleimide or fumaronitrile with the 6-methylhomofurans **4a**, **b**,[6] in which a concerted $[(_\sigma2_s + _\pi2_s) + _\pi2_s]$-cycloaddition could be involved due to the stereospecific *cis*-addition of the dienophiles (fumaro- and maleonitrile). Bicyclo[2.1.0]pent-2-ene **6** reacts with **10** predominantly in the sense of a homo-Diels-Alder reaction to give an adduct of type **7**[7] and with **9a**, **b** in the sense of a $[_\sigma2+_\pi2]$-cycloaddition to give adducts of type **8**.[8] We report here on the surprising stereochemical

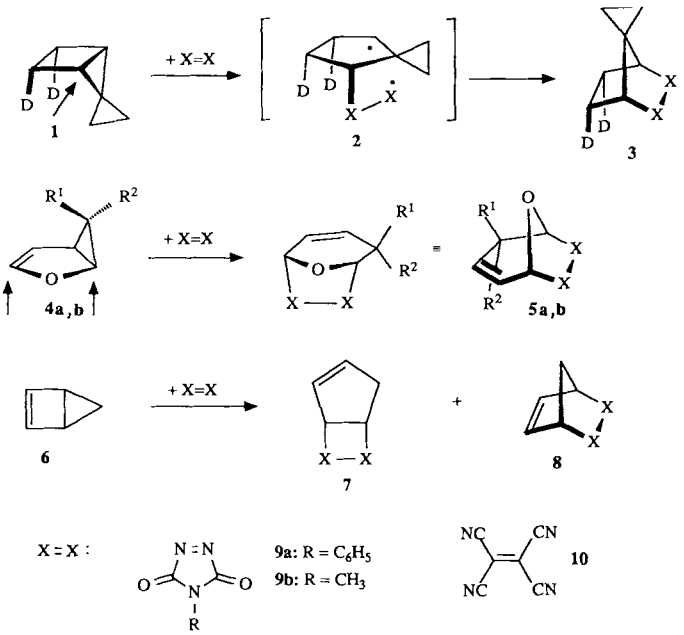

4a, **5a**: $R^1=CH_3$, $R^2=H$; **4b**, **5b**: $R^1=H$, $R^2=CH_3$

course of the bicyclo[2.1.0]pentene cycloaddition, which shows that the homo-Diels-Alder reaction also takes place in two steps in this case.

[*] Prof. Dr. F.-G. Klärner, Dipl.-Chem. M. Naumann
Fakultät für Chemie der Universität
Postfach 102148, D-4630 Bochum 1 (FRG)

[**] This work was supported by the Deutsche Forschungsgemeinschaft and the Fonds der Chemischen Industrie.

We have solved the problem of which side the dienophile attacks the bicyclo[2.1.0]pentene system by using the known bicyclopentene esters **6a**, **b**[9] as model compounds. The separated diasteromers **6a** and **6b** each react quantitatively and stereospecifically with **10**, even at 3 °C (overnight in toluene), to give the formal homo-Diels-Alder adducts **7a** and **7b** respectively. The structure and the stereochemical arrangement of the substituents on C-4 in the diastereomers **7a**, **b** could be determined ^{1}H-NMR spectroscopically. With the given assignment[10] the hydrogen atom 5-H *cis* to the methyl group on C-4 of **7b** absorbs at higher field ($\delta = 3.81$) than the corresponding *trans* hydrogen atom 5-H of **7a** ($\delta = 4.30$), in agreement with the hydrogen atoms 1,4-H_2 *cis* and *trans* to the methyl group on C-5 of **6b** ($\delta = 2.03$) and **6a** ($\delta = 2.38$).[9] This assignment can be checked independently by means of NOE ^{1}H-NMR difference spectra. Upon irradiation of the resonance frequency of the 4-methyl signal, the increase in intensity of the signal of 5-H (relative to 3-H) in the spectrum of **7b** brought about by the nuclear Overhauser effect is, as a result of the smaller steric $\{CH_3\cdots H\}$ distance (2.90 Å), about double that of the corresponding signal in the spectrum of **7a**, in which 5-H and the 4-CH_3 group are *trans* to each other, and their steric separation is 3.84 Å.[11]

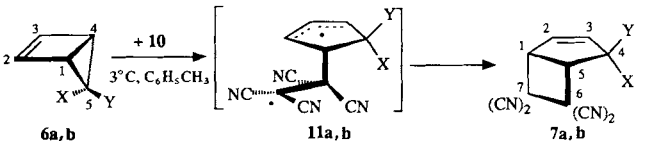

a: X = CH_3, Y = CO_2CH_3; **b**: X = CO_2CH_3, Y = CH_3

The cycloaddition of **10** to the bicyclo[2.1.0]pentenes **6a**, **b** proceeds stereospecifically *endo* with respect to the cyclopropane ring. Thus, the stereochemical course of this reaction is exactly the opposite to that of the homo-Diels-Alder reaction of the homofurans **4a**, **b** and consistent with that of the $[_\sigma2+_\pi2]$-cycloaddition of the bicyclo[2.1.0]pentane system (e.g. **1**). It may be assumed therefore that the formal homo-Diels-Alder reaction of the bicyclo[2.1.0]pentene proceeds, just like the cycloaddition of the bicyclo[2.1.0]pentane, in two steps via a diradical intermediate **11a**, **b**.[12]

To check this assumption we have investigated the stereochemical course of the reaction with respect to the olefinic components using the dicyanofumaric and maleic acid esters **12a**, **c**[13] as model compounds. Reaction of a 93:7 mixture of bicyclopentene **6** and 1,3-cyclopentadiene with **12a** (3 h, 0 °C, THF) led to the formation of three products in the ^{1}H-NMR spectroscopically determined ratio of 55:30:15. The by-product formed in 15% yield is identical with the Diels-Alder adduct **14a** of 1,3-cyclopentadiene and **12a**. The two main products, of which the isomer formed in 55% yield could be enriched by fractional crystallization to 80%, could, according to a comparison of their spectral data[10] with those of the tetracyanoethylene adduct 7,[7] be the bicyclo[3.2.0]heptene derivatives **13a**, **b**. An unequivocal stereochemical assignment of the substituents on C-6 and C-7 is not possible here. The reaction of **6** (purity > 99%) with **12c** leads at 0 °C (48% conversion of **12c** after 15 min) to a mixture of seven products in the ratio 31:22:19:11:10:5:3. Of the three main products, two, which are formed in 31 and 19% yield, are identical with **13a** and **13b**, the products of the reaction of **6** with **12a**. The spectral data of three by-products (formed in 5, 10 and 3% yield) are identical with those of **14a**, **c** and **d**, the Diels-Alder adducts of 1,3-cy-

clopentadiene and **12a** and **12c** respectively.[14] We assign to the remaining products (22 and 11%) the structures of the still missing *cis*-diastereomers **13c, d**. No significant *cis-trans* isomerization **12c** → **12a** (<5%) takes place under the reaction conditions.[15] It is demonstrated therefore, that the cycloaddition of bicyclo[2.1.0]pentene **6** proceeds non-stereospecifically, as expected in the case of a two-step process.

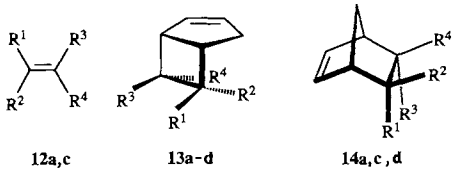

12a,c **13a-d** **14a,c,d**

a: $R^1=R^4=CN$, $R^2=R^3=CO_2CH_3$; **b**: $R^1=R^4=CO_2CH_3$, $R^2=R^3=CN$; **c**: $R^1=R^3=CO_2CH_3$, $R^2=R^4=CN$; **d**: $R^1=R^3=CN$, $R^2=R^4=CO_2CH_3$

Finally, there remains the question of which factors are responsible for the different course of the homo-Diels-Alder reaction of homofuran **4** and bicyclopentene **6**. The two systems have very different strain energies. In the homofuran **4**, the strain energy is essentially determined by the cyclopropane ring, whereas in the bicyclopentene **6** it is composed of the three- and four-membered ring strain as well as the negative resonance energy, which is attributed to the antiaromatic character of **6** as homocyclobutadiene.[16] In the transition state of the two-step process, the central cyclopropane bond could be opened further than in the concerted homo-Diels-Alder reaction. The reaction of **6** profits in particular from this bond opening, since the total strain of the bicyclopentene is released in one step.

Received: April 4, 1990 [Z 3894 IE]
German version: *Angew. Chem. 102* (1990) 1097

CAS-Registry numbers:
6, 5164-35-2; **6a**, 71215-51-5; **6b**, 71276-51-2; **7a**, 128575-90-6; **7b**, 128657-24-9; **12a**, 35234-87-8; **12c**, 101342-44-3; **13a**, 128575-91-7; **13b**, 128657-25-0; **13c**, 128657-26-1; **13d**, 128657-27-2; **14a**, 128575-92-8; **14c**, 128657-28-3; **14d**, 128657-29-4; 1,3-cyclopentadiene, 542-92-7.

[1] W. R. Roth, M. Martin, *Tetrahedron Lett. 1967*, 4695.
[2] F. S. Collins, J. K. George, C. Trindle, *J. Am. Chem. Soc. 94* (1972) 3732.
[3] Review: P. G. Gassman, *Acc. Chem. Res. 4* (1971) 128.
[4] W. R. Roth, F.-G. Klärner, W. Grimme, H. G. Köser, R. Busch, B. Muskulus, R. Breuckmann, B. P. Scholz, H.-W. Lennartz, *Chem. Ber. 116* (1983) 2717.
[5] M. H. Chang, D. A. Dougherty, *J. Am. Chem. Soc. 104* (1982) 1131.
[6] F.-G. Klärner, D. Schröer, *Chem. Ber. 122* (1989) 179.
[7] J. E. Baldwin, R. K. Pinschmidt, Jr., *Tetrahedron Lett. 1971*, 935.
[8] W. Adam, A. Beinhauer, O. De Lucchi, R. J. Rosenthal, *Tetrahedron Lett. 24* (1983) 5727.
[9] F.-G. Klärner, F. Adamsky, *Chem. Ber. 116* (1983) 299.
[10] ^{1}H NMR (400 MHz, $CDCl_3$) of **7a**: $\delta = 1.77$ (s, 3H; 4-CH_3), 3.75 (s, 3H; OCH_3), 4.15 (dt, 1H; 1-H, $J(1,5) = 6.0$, $J(1,2) = J(1,3) = 2.0$ Hz), 4.30 (d, 1H; 5-H), 6.12 (dd, 1H; 2-H, $J(2,3) = 5.5$ Hz), 6.29 (ddd, 1H; 3-H, $J(3,5) < 1$ Hz); of **7b**: $\delta = 1.40$ (s, 3H; 4-CH_3), 3.81 (dt, 1H; 5-H, $J(1,5) = 6.5$, $J(2,5) = J(3,5) = 0.5$ Hz), 3.85 (s, 3H; OCH_3), 4.15 (dt, 1H; 1-H, $J(1,2) = J(1,3) = 2.0$ Hz), 5.98 (ddd, 1H; 2-H, $J(2,3) = 6.0$ Hz), 6.58 (ddd, 1H; 3-H). ^{1}H NMR (400 MHz, [D$_6$]acetone) of **13a**: $\delta = 2.78$ (m, 2H; 4,4-H_2), 3.90, 3.94 (2s, 6H; 6,7-$(CO_2CH_3)_2$), 3.96 (m, 2H; 1,5-H_2), 5.89, 6.14 (2m, 2H; 2,3-H_2); of **13b**: $\delta = 2.78$ (m, 2H; 4,4-H_2), 3.78 (td, 1H; 5-H, $J(1,5) = J(4,5) = 7.6$, $J(4',5) = 2.6$ Hz), 3.89, 3.97 (2s, 6H; 6,7-$(CO_2CH_3)_2$), 4.21 (m, 1H; 1-H), 5.79, 6.11 (2m 2H; 2,3-H_2); in the ^{1}H-NMR spectrum of the mixture in the reaction of **6** with **12c**, the new signals at $\delta = 6.25$, 5.91 and 6.05, 6.03 can be assigned to the olefinic hydrogens 2,3-H; of **14a**: $\delta = 1.92$, 2.20 (2m, 2H, 7,7-H_2, $J = 10.0$ Hz), 3.70 (m, 2H; 1,4-H_2), 3.88, 3.96 (2s, 6H; 2,3-$(CO_2CH_3)_2$), 6.45, 6.61 (2dd, 2H; 5,6-H_2); of **14c**: $\delta = 1.91$, 2.01 (2m, 2H; 7,7-H_2), 3.75 (m, 2H; 1,4-H_2), 3.77 (s, 6H, 2,3-$(CO_2CH_3)_2$), 6.33 (m, 2H; 5,6-H_2); of **14d**: $\delta = 1.81$, 2.40 (2m, 2H; 7,7-H_2), 3.72 (m, 2H; 1,4-H_2), 3.85 (s, 6H; 2,3-$(CO_2CH_3)_2$), 6.67 (m, 2H; 5,6-H_2).
[11] The average $CH_3\cdots H$ distances were taken from MMX force field calculations: J. J. Gajewski, K. E. Gilbert, Serena Software 1988.
[12] Owing to the high polarity of the olefins **10** and **12a, c** the reactive intermediates of type **11** could also have dipolar structures.
[13] C. J. Ireland, K. Jones, J. S. Pizey, S. Johnson, *Synth. Commun. 6* (1976) 185; T. Gotoh, A. B. Padias, H. K. Hall, Jr., *J. Am. Chem. Soc. 108* (1986) 4920.
[14] Since the Diels-Alder reaction of 1,3-cyclopentadiene with **12c** (0°C, 3 h, THF) yields only the *cis*-adducts **14c** and **14d** in the ratio 87:13, the *trans*-adduct **14a** must be formed directly from **6** in the reaction of **6** with **12c**. This result indicates that the $[_\pi 2 + _\pi 2]$-cycloaddition also proceeds non-stereospecifically and thus, as expected, in two steps.
[15] After 2 h the ratio of unchanged **12c** to **12a** is 90:10 and after 3 h 77:23. In a control experiment the extent of *cis-trans* isomerization **12c** → **12a** without addition of **6** was determined as 28% after 3 h at 0°C. It can therefore be ruled out that **6** catalyzes the *cis-trans* isomerization **12c** → **12a**. From the time-dependence of seven measurements (between 15 and 180 min) the product ratio of the reaction of **6** with **12c** was extrapolated to the time $t = 0$: $[\mathbf{13a}:\mathbf{13b}:\mathbf{13c}:\mathbf{13d}:\mathbf{14a}:\mathbf{14c}:\mathbf{14d}]_{t\to 0} = 29:18:24:12:3:11:4$.
[16] W. R. Roth, F.-G. Klärner, H.-W. Lennartz, *Chem. Ber. 113* (1980) 1818.

Nickel-Catalyzed Cyclodimerization of Hexapentaenes: [4]Radialenes and [5]Radialenones with Cumulated Double Bonds**

By *Masahiko Iyoda,* Yoshiyuki Kuwatani, Masaji Oda, Yasushi Kai,* Nobuko Kaneshisa*, and *Nobutami Kasai**

Although cumulenic double bonds[1] have a wide variety of potential reactive sites, which can lead to novel cyclic dimers, trimers, and oligomers, great difficulty in controlling the reactivity has prevented the utilization of cumulenes in organic synthesis. We recently reported the nickel-catalyzed cyclooligomerization of [3]cumulenes (butatrienes)[2] and the cyclodimerization of [5]cumulenes (hexapentaenes)[3] to give various types of radialenes, and demonstrated the synthetic utility of this type of reaction. We report here the nickel-mediated synthesis of novel [4]radialenes and [5]radialenones[4] based on the same synthetic strategy.

Tetramethyl- and tetra-*tert*-butyl[5]cumulenes dimerize thermally to give octamethylcyclododeca-1,3,7,9-tetrayne[6] and tetrakis(di-*tert*-butylvinylidene)cyclobutane.[7] However, nickel-catalyzed cyclodimerization of tetraarylhexapentaene yields 1,2-bis(diarylmethylene)-3,4-bis(diarylpropadienylidene)cyclobutane as the head-to-head dimer.[3] Thus, the known thermal and nickel-catalyzed dimerizations of [5]cumulenes occur regioselectively. In order to investigate the difference in the reactivity of these double bonds, we carried out reactions of the [5]cumulenes **5** with nickel catalysts.

The [5]cumulenes **5a-c** were prepared according to the procedure outlined in Scheme 1. Ethynylation of the ketones

[*] Prof. Dr. M. Iyoda, Y. Kuwatani, Prof. Dr. M. Oda
Department of Chemistry, Faculty of Science
Osaka University
Toyonaka, Osaka 560 (Japan)
Prof. Dr. Y. Kai, Prof. Dr. N. Kasai, N. Kanehisa
Department of Applied Chemistry, Faculty of Engineering
Osaka University
Yamadaoka, Suita, Osaka 565 (Japan)

[**] This work was supported by CIBA-GEIGY Foundation (Japan) for the Promotion of Science and by the Ministry of Education, Science and Culture, Japan. (Grant-in-Aid for Scientific Research No. 63540396).

1a and **1b** with lithium acetylide in THF gave **2a** and **2b** in 91 and 89% yields, respectively. The oxidative coupling of **2a** and **2b** with $Cu(OAc)_2 \cdot H_2O$ in pyridine-methanol at 55 °C afforded the diols **3a** (90%) and **3b** respectively[8]. Treatment of **3a** with conc. hydrobromic acid in acetic acid furnished the corresponding dibromide **4a** (90%). Reduction of **4a** with zinc in THF gave the desired [5]cumulene **5a** (95%). The conversion of **3b** into **5b** was carried out by a previously reported method.[8] The cumulene **5c** was prepared according to the procedure shown in Scheme 1 [a) 88.5%; b) 89%; d) 84%; e) 81%].[9]

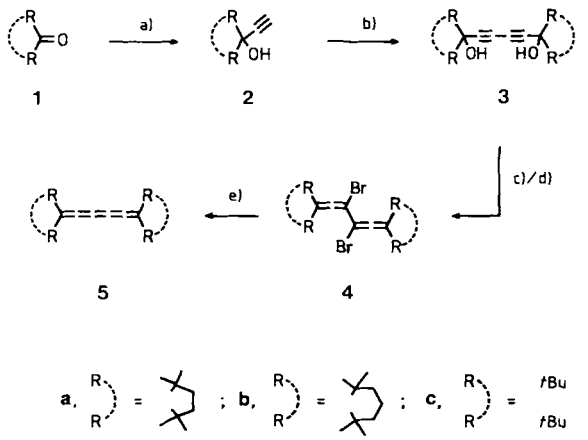

Scheme 1. a) $LiC \equiv CH$, THF, −78 °C → RT. b) $Cu(OAc)_2 \cdot H_2O$, pyridine-methanol (1:1), 55 °C. c) HBr, AcOH, RT. d) PBr_3, benzene, 50 °C. e) Zn, THF, sonication.

Although **5a–c** are less reactive than tetraarylhexapentaenes, which react smoothly with $[Ni(CO)_2(PPh_3)_2]$ **6** in refluxing benzene to afford the dimers, their reactions with stoichiometric amounts of **6** in benzene at the same temperature lead very slowly to the cyclic dimers. Thus, treatment of **5a** with 0.5 equivalents of **6** in refluxing benzene under argon for 24 h gave the head-to-tail dimer **7** in 82% yield. Interestingly, the reaction of the more bulky-substituted **5b** with 1 equivalent of **6** in refluxing benzene for 2 days resulted in the formation of the [5]radialenone **8** in 32% yield, together with the corresponding [4]radialene **9** in 36% yield. The difference in the reactivity of **5a** and **5b** towards the nickel(0) complex may be due to steric factors. Furthermore, treatment of the most bulkily-substituted **5c** with 1 equivalent of **6** in the presence of 3 equivalents of triphenylphosphane in refluxing benzene for 8 days gave the [5]radialenone **10** as the main product (74%), together with a small amount of **11** (6%). Since the starting [5]cumulenes **5** described here can be prepared easily by the route shown in Scheme 1, the [4]radialenes **7** and **9** and the [5]radialenones **8** and **10** can be synthesized in only a few steps.

The *[4]radialenes and [5]radialenones* reported here are very stable towards light and air. Molecular models show that **7** can have a planar structure with D_{2h} symmetry. The ^1H- and ^{13}C-NMR spectra (Table 1) reflect its highly symmetrical structure. The electronic spectra of **7** show absorptions up to 450 nm, indicating elongation of π-conjugation, whereas the electronic spectrum of **9** shows absorption only up to 350 nm, corresponding to its spiro-oriented allenic π bonds. The ^1H- and ^{13}C-NMR spectra of the [5]radialenones **8** and **10** show symmetrical structures. The IR spectra contain two characteristic bands for α,β,γ-unsaturated ketones

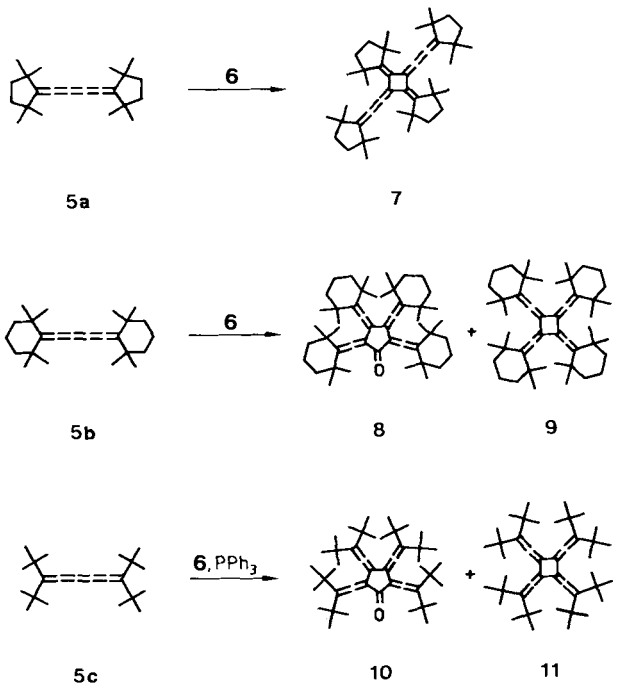

Scheme 2. **6** = $[Ni(CO)_2(PPh_3)_2]$.

at 1940–1910 cm^{-1} (C=C=C) and 1690 cm^{-1} (C=O). The adsorption of the ketones **8** and **10** on silica gel results in a bright yellow coloration, and the electronic spectra of **8** and **10** in CF_3COOH show a marked bathochromic shift tailing up to 700 nm with a deep violet coloration.

Table 1. Selected physical data of compounds 7–**10**.

7: Yellow needles (from CH_2Cl_2-hexane), m.p. = 281–282 °C; MS (70 eV): *m/z* 592 ($M^{\oplus}$); ^1H NMR (400 MHz, $CDCl_3$, 30 °C, TMS): δ = 1.23 (s, 24H; CH_3), 1.45 (s, 24H; CH_3), 1.65 (s, 8H; CH_2), 1.68 (s, 8H; CH_2); ^{13}C NMR (100 MHz, $CDCl_3$, 30 °C, TMS): δ = 27.8(q), 30.3(q), 40.6(s), 41.6(s), 46.1(t), 48.0(t), 118.5(s), 136.7(s), 145.2(s), 148.9(s), 155.2(s), 155.9(s); UV/VIS (cyclohexane): λ_{max} [nm] (log ε) = 253 (4.46), 260 sh (4.42), 285 (4.22), 323 sh (4.73), 334 (4.98), 406 (3.93), 431 sh (3.82); Raman (KBr): $\tilde{\nu}$ [cm^{-1}] = 2005 (C=C=C=C), 1637, 1610 (C=C).

8: Yellow needles (from EtOH), m.p. = 226–227 °C; MS: *m/z* 676 ($M^{\oplus}$); ^1H NMR (400 MHz, $CDCl_3$): δ = 1.12 (s, 12H; CH_3), 1.14 (s, 12H; CH_3), 1.17 (s, 12H; CH_3), 1.19 (s, 12H; CH_3), 1.34–1.47 (m, 16H; CH_2), 1.58–1.69 (m, 8H; CH_2); ^{13}C NMR (100 MHz, $CDCl_3$): δ = 19.0(t), 19.3(t), 30.8(q), 30.9(q), 31.4(q), 31.5(q), 35.7(t), 35.9(t), 40.8(s), 41.7(s), 101.4(s), 107.7(s), 126.9(s), 128.1(s), 191.9 (s, CO), 196.7(s), 202.4(s); UV/VIS (cyclohexane): λ_{max} [nm] (log ε) = 215 (4.78), 246 (4.70), 263 sh (4.22), 298 (3.64), 313 (3.47), 378 (3.39), 408 sh (3.26); IR (KBr): $\tilde{\nu}$ [cm^{-1}] = 1941, 1919 (C=C=C), 1691 (C=O).

9: Colorless needles (from Et_2O-EtOH), m.p. = 315 °C (sublimed); MS: *m/z* 648 ($M^{\oplus}$); ^1H NMR (90 MHz, $CDCl_3$): δ = 1.12 (s, 48H; CH_3), 1.25–1.80 (m, 24H; CH_2); ^{13}C NMR (22.5 MHz, $CDCl_3$): δ = 19.2(t), 31.7(q), 35.5(t), 40.9(s), 109.4(s), 127.6(s). 192.5(s); UV/VIS (cyclohexane): λ_{max} [nm] (log ε) = 215 (5.13), 252 sh (4.27), 259 (4.28), 268 sh (4.19), 300 (3.38), 318 (3.42); IR (KBr): $\tilde{\nu}$ [cm^{-1}] = 1957, 1917 (C=C=C).

10: Yellow prisms (from Et_2O-MeOH), m.p. = 220 °C (sublimed); MS: *m/z* 628 ($M^{\oplus}$); ^1H NMR (400 MHz, $CDCl_3$): δ = 1.24 (s, 36H, *t*-Bu), 1.25 (s, 36H; *t*-Bu); ^{13}C NMR (100 MHz, $CDCl_3$): δ: 32.2(q), 32.5(q), 36.6(s), 36.7(s), 100.7(s), 107.0(s), 129.0(s). 130.6(s), 192.2 (s, CO), 199.2(s), 205.1(s); UV/VIS (THF): λ_{max} [nm] (log ε) = 244 (4.67), 270 sh (4.15), 300 sh (3.75), 315 sh (3.36), 378 (3.36), 408 (3.27); IR (KBr): $\tilde{\nu}$ [cm^{-1}] = 1908 (C=C=C), 1691 (C=O).

In order to elucidate the unique molecular structure of [5]radialenone **10**, its crystal structure was determined by X-ray diffraction analysis.[10] The crystal lattice contains two crystallographically independent molecules, which are found to have essentially the same structure, including the

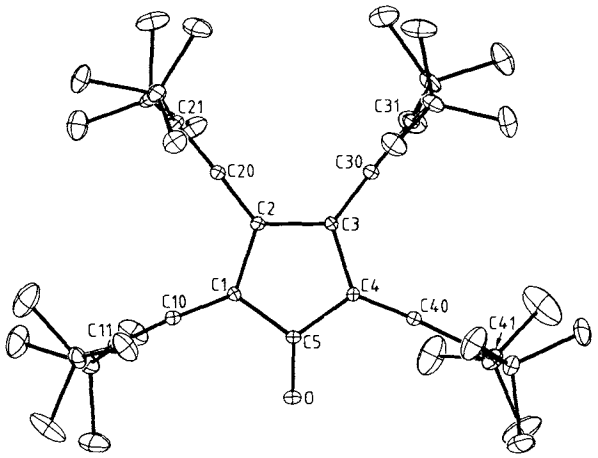

Fig. 1. Molecular structure of **10** in the crystal (ORTEP) with the thermal ellipsoids at the 10% probability level for the non-hydrogen atoms. The estimated standard deviations are 0.009–0.011 Å and 0.7–0.8° for bond distances and angles: C1-C2 1.492, C2-C3 1.483, C3-C4 1.490, C4-C5 1.488, C5-C1 1.476, C5-O 1.206, C1-C10 1.322, C10-C11 1.302, C2-C20 1.318, C20-C21 1.312, C3-C30 1.320, C30-C31 1.310, C4-C40 1.325, C40-C41 1.286; C1-C2-C3 107.8, C2-C3-C4 107.8, C3-C4-C5 108.1, C4-C5-C1 107.7, C5-C1-C2 108.4, C1-C2-C20 123.9, C20-C2-C3 128.4, C2-C3-C30 126.4, C30-C3-C4 125.7, C40-C4-C5 122.0, C4-C5-O 126.2, C2-C1-C10 129.2, C3-C4-C40 129.9, O-C5-C1 126.0, C5-C1-C10 122.4, C1-C10-C11 175.4, C2-C20-C21 177.7, C3-C30-C31 179.2, C4-C40-C41 175.4.

conformations of the *tert*-butyl groups. Figure 1 shows the molecular structure of **10** in the crystal; particularly noteworthy is the high coplanarity of the cyclopentanone ring, the maximum atomic deviation from the least-squares plane of the central five-membered ring being 0.03 Å. The planar structure extends to the exocyclic allenic bonds with a maximum deviation of 0.24 Å. The bond distances in the carbonyl and allene moieties of the molecule are normal, while the bond angles C(2)–C(1)–C(10) [129.2(6)°] and C(3)–C(4)–C(40) [129.9(7)°] are significantly larger than the expected value of 126° in spite of the large distance between the methyl groups of the neighboring *tert*-butyl substituents. A similar angular deformation was found in tetrakis(1,3-dithiaindanylidene)cyclopentanone[11] due to significant non-bonded repulsion between the substituents of exocyclic bonds. In comparison with the half-chair conformation of the molecule, the planar structure of **10** may be due to the absence of steric strain between the *tert*-butyl substituents as a result of the extension of the exocyclic bonds by a cumulenic structure.

Nickel-catalyzed reactions provide the possibility of preparing highly unsaturated compounds containing functional groups.[12] The results reported here demonstrate the utility of nickel-catalyzed cyclooligomerization for the synthesis of highly unsaturated unique molecules.

Received: March 21, 1990 [Z 3864 IE]
German version: *Angew. Chem. 102* (1990) 1077

CAS Registry numbers:
1a, 4541-35-9; **1b**, 1195-93-3; **1c**, 815-24-7; **2a**, 128923-68-2; **2b**, 104850-85-3; **2c**, 33420-19-8; **3a**, 128923-69-3; **3b**, 128923-70-6; **3c**, 54622-15-0; **4a**, 128923-71-7; **4b**, 128923-72-8; **4c**, 54622-16-1; **5a**, 128949-77-9; **5b**, 60004-33-3; **5c**, 7171-72-4; **6**, 13007-90-4; **7**, 128923-73-9; **8**, 128923-74-0; **9**, 128923-75-1; **10**, 128923-76-2; **11**, 7200-90-0.

[1] Synthesis and properties of cumulenes, see, H. Fischer in S. Patai (Ed.): *The Chemistry of Alkenes*, Wiley-Interscience, New York 1964, p. 1025 ff; H. Hopf in S. Patai (Ed.): *The Chemistry of Ketenes, Allenes, and Related Compounds*, Wiley-Interscience, New York 1980, p. 779 ff.

[2] M. Iyoda, S. Tanaka, M. Nose, M. Oda, *J. Chem. Soc. Chem. Commun. 1983*, 1058; M. Iyoda, S. Tanaka, H. Otani, M. Nose, M. Oda, *J. Am. Chem. Soc. 110* (1988) 8494.

[3] M. Iyoda, Y. Kuwatani, M. Oda, *J. Am. Chem. Soc. 111* (1989) 3761.

[4] (n-1)Methylene n-membered ketones are an interesting class of compounds, for which we propose the generic name [n]radialenone. For example, tetraisopropyridenecyclopentanone reported by *Stehling* and *Wilke* [5] is octamethyl[5]radialenone.

[5] L. Stehling, G. Wilke, *Angew. Chem. 97* (1985) 505; *Angew. Chem. Int. Ed. Engl. 24* (1985) 496.

[6] L. T. Scott, G. J. DeCicco, *TetrahedronLett. 1976*, 2663; C. Santiago, K. N. Houk, G. J. DeCicco, L. T. Scott, *J. Am. Chem. Soc. 100* (1978) 692.

[7] H. D. Hartzler, *J. Am. Chem. Soc. 88* (1966) 3155; *93* (1971) 4527.

[8] F. Bohlmann, K. Kieslich, *Chem. Ber. 87* (1954) 1363.

[9] T. Negi, T. Kaneda, H. Mizuno, T. Toyoda, Y. Sakata, S. Misumi, *Bull. Chem. Soc. Jpn. 47* (1974) 2398.

[10] Crystal data of **10**: $C_{45}H_{72}O$, $m = 629.1$, monoclinic, space group $P2_1/n$, $a = 16.400(2)$, $b = 21.176(1)$, $c = 28.087(3)$ Å, $\beta = 116.07(1)°$, $V = 8762.0(16)$ Å^3, $Z = 8$, $D_x = 0.953$ g cm^{-3}. The transformation $100/0\bar{1}0/\bar{1}0\bar{1}$ gives a reduced cell of $P2_1/c$. X-Ray intensity data were measured on a Rigaku four-circle diffractometer with nickel-filtered $Cu_{K\alpha}$ radiation using a $0.3 \times 0.3 \times 0.3$-mm crystal. A collodion coating was necessary to prevent decomposition of the crystal. 11 023 reflections were collected up to $2\theta = 120°$, of which 7355 had $|F_o| > 3\sigma(F_o)$ and were used in the refinement. The intensity data were corrected for Lorentz and polarization effects but not for absorption [$\mu(Cu_{K\alpha}) = 3.8$ cm^{-1}]. The crystal structure was solved by direct method (SHELXS-86) and refined by full-matrix least-squares (XRAY-76). Anisotropic refinement revealed the abnormally large thermal vibration of the *tert*-butyl substituents, all the hydrogen atoms connecting to those methyl carbons were difficult to locate in the difference Fourier maps. The weighting scheme used was $w = [\sigma^2(F_o) + 0.003(F_o)^2]^{-1}$. The final R and R_w indices were 0.118 and 0.161, respectively. Further details of the crystal structure investigation are available on request from the Director of the Cambridge Crystallographic Data Centre, University Chemical Laboratory, Lensfield Road, GB-Cambridge CB21EW (UK), on quoting the full journal citation.

[11] T. Sugimoto, Y. Misaki, Y. Arai, Y. Yamamoto, Z. Yoshida, Y. Kai, N. Kasai, *J. Am. Chem. Soc. 110* (1988) 628.

[12] G. Wilke, *Angew. Chem. 100* (1988) 189; *Angew. Chem. Int. Ed. Engl. 27* (1988) 185.

Golfomycin A, a Novel Designed Molecule with DNA-Cleaving Properties and Antitumor Activity**

By *K. C. Nicolaou,** *Golfo Skokotas, S. Furuya, H. Suemune*, and *D. Colette Nicolaou*

Due to their fascinating structures and biological activities, natural products have been capturing the interest and imagination of isolation, synthetic, and medicinal chemists for a very long time.[1] Designed molecules with predefined chemical and biological properties could enrich and compliment this arsenal of substances and sharpen the capability of chemistry to deliver biologically and therapeutically useful compounds. Described herein are the design, synthesis, and chemical and biological activities of a novel agent with DNA-cleaving[3] and antitumor properties, golfomycin A(**1**).[2]

Detailed in Scheme 1 is the mechanistic rationale that led to the design of compound **1** as a potential DNA-cleaving

[*] K. C. Nicolaou, Golfo Skokotas, S. Furuya, [+]
H. Suemune, D. Colette Nicolaou,
Department of Chemistry
Research Institute of Scripps Clinic
10666 N. Torrey Pines Road, La Jolla, CA 92037 (USA)
and
Department of Chemistry
University of California
San Diego, La Jolla, CA 92093 (USA)

[+] Visiting scientist from Takeda Chemical Industries, Ltd, Japan, 1989–90.

[**] We wish to thank Drs *Dee H. Huang* of the Research Institute of Scripps Clinic and *Raj Chadha* of the University of California, San Diego for their help with the NMR and X-ray crystallographic investigations, respectively. We also wish to thank Professor *B. Snider* of Brandeis University for valuable discussions regarding the chemistry of conjugated allenes.

molecule. Two alternative modes of action were considered plausible: A nucleophilic attack (e.g., from a cofactor or DNA) on the ynone function would lead to the allene-ene-yne structure **2**, which was expected, on the basis of previous results,[4] to undergo a facile cyclization to the diradical **3**. Species **3** was then expected to cleave DNA by a radical mechanism (path a, Scheme 1). Alternatively, nucleophilic addition by DNA on **1** could generate species **4**, which was projected to undergo chemistry leading to DNA cleavage via a nucleophilic mechanism (path b, Scheme 1). The highly strained nature of **1** was expected to facilitate the postulated reactions shown in Scheme 1.

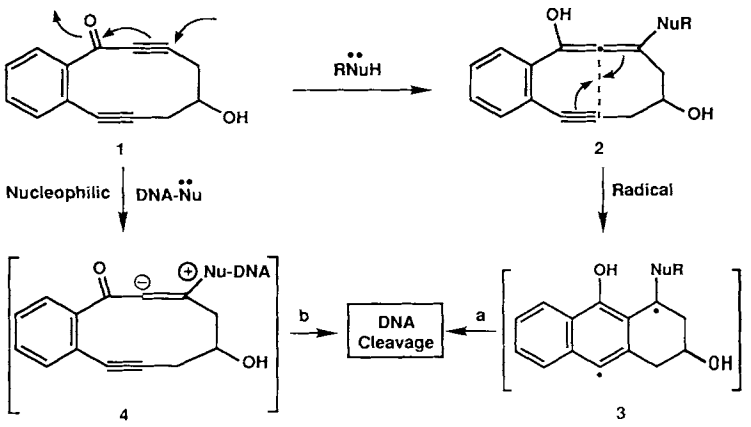

Scheme 1. Mechanism-based design of molecule **1**. Plausible mechanism of DNA cleaving action of **1**, a: radical mechanism, b: nucleophilic mechanism.

The synthesis of golfomycin A (**1**) is detailed in Scheme 2. Thus, reaction of excess Grignard reagent **5** with ethyl formate led to the diacetylenic compound **6**[5] (80%), which was silylated to afford compound **7** (95%). Coupling of **7** with aromatic iodide **8** under the catalytic influence of $Pd(PPh_3)_4$-CuI[6] gave compound **9** (70%), which was oxidized with MnO_2 to furnish the acetylenic aldehyde **10**

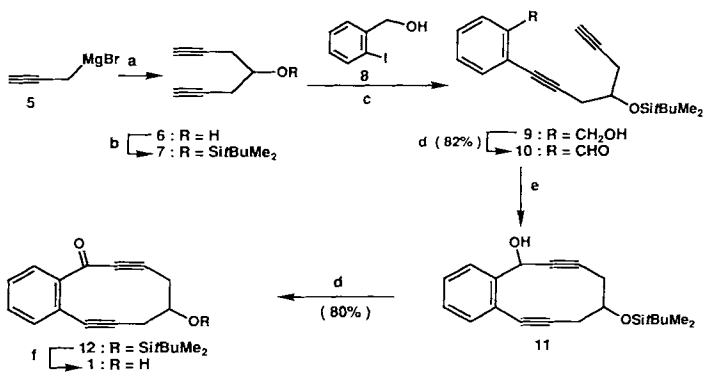

Scheme 2. Synthesis of golfomycin A(**1**). Reagents and conditions. (a) 1.0 eq HCOOEt, THF, 0 °C, 2 h, 80%; (b) 1.2 eq tBuMe$_2$SiCl, 1.2 eq imidazole, DMF, 25 °C, 8 h, 95%; (c) 0.6 eq **5**, 0.03 eq $(Pd(PPh_3)_4$, 0.1 eq CuI, nBuNH$_2$ 0 °C, 3 h, 70%; (d) excess MnO_2, CH_2Cl_2, 25 °C, 4 h, 82%; (e) 1.0 eq $KN(SiMe_3)_2$, THF, −78 °C, 45 min, 51%; (f) 4.0 eq HF-CH_3CN, 25 °C, 3 h, 89%.

(82%). Intramolecular addition of the acetylide derived from **10** and $KN(SiMe_3)_2$ to the aldehyde function led to the ten-membered ring alcohol **11** (51%) which was smoothly oxidized (80%) and desilylated (89%) to afford the desired product **1** via its silyl ether **12**.

Golfomycin A(**1**) was found to cleave DNA in a pH-dependent manner as shown in Figure 1. Addition of methyl

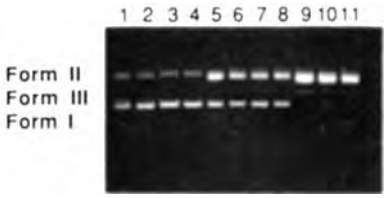

Fig. 1. DNA cleavage by golfomycin A(**1**) at various pH's. $\Phi \times 174$ form I DNA (50 μM per base pair) was incubated for 20 h at 37 °C with golfomycin A(**1**) 1000 μM) in various pH buffers and analyzed by electrophoresis (1% agarose gel, ethidium bromide stain). Lane 1, DNA alone at pH 8.5; lanes 2-11 correspond to pH 5.0, 6.0, 7.0, 7.4, 8.0, 8.5, 9.0, 9.5, 10.0 and 10.7 respectively. Forms I, II and III correspond to supercoiled, relaxed, and linear DNA respectively. Control experiments at the above pH's in the absence of agent demonstrated no DNA cleavage.

thioglycolate as a cofactor inhibited, rather than enhanced the activity of **1**, whereas, the presence of catalase did not have any measurable effect on the cleavage.

The chemistry of **1** was then investigated in order to gain insight into its mode of action. Thus, **1** was swiftly converted by 1,8-diazabicyclo[5.4.0]undec-7-ene(DBU) into an intensely fluorescent compound (75%) whose structure was assigned as **15** (coined golfomycin B, Scheme 3) on the basis of its spectral and chemical properties. Golfomycin B(**15**) reacted rapidly with $NaBH_4$ at 0 °C, leading quantitatively to compound **16** whose structure was confirmed by X-ray crystallographic analysis[7] on its p-bromobenzoate **17** (prepared from **16** in 80% yield).

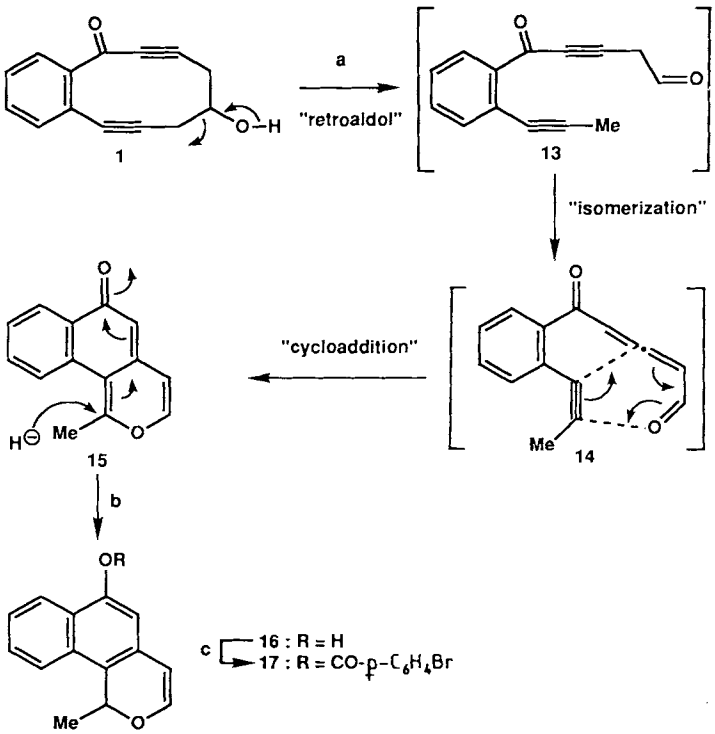

Scheme 3. Chemistry of golfomycin A (**1**). (a) 1.0 eq DBU, benzene-THF, 25 °C, 0.5 h, 75%; (b) 4.0 eq $NaBH_4$, MeOH, 0 °C, 15 min, 97%; (c) 1.5 eq p-bromobenzoyl chloride, 2.0 eq Et_3N, CH_2Cl_2, 25 °C, 2 h, 80%.

To explain the formation of **15** from **1** under the basic conditions, the following events were assumed: a) retroaldol reaction (**1** → **13**); b) base-induced isomerization (**13** → **14**); and c) intramolecular [4+2]-cycloaddition (**14** → **15**).[8] Low temperature ^{1}H-NMR studies revealed the transient presence of **13** [−20 → 25 °C, δ = 9.77 (t, J = 2.5 Hz, C*H*O)] in the reaction mixture, but no signals corresponding to **14** were detected under those conditions (presumably due to the fast nature of the cycloaddition reaction).

The chemistry of golfomycin A(**1**) and B(**15**) towards nucleophiles was then investigated using methyl thioglycolate as a model reagent (Scheme 4). Thus, the silyl ether **12** reacted smoothly with excess reagent at 10 °C under basic conditions to afford compounds **19** (55%, single isomer, stereochemistry unassigned) and **20** (20%), presumably via the intermediacy of the initially formed adduct **18**.[9] Under similar conditions compound **15** furnished the 1,6-adduct **21** in 67% yield and with opposite regioselectivity[10] from the hydride reduction of **15** to **16** (Scheme 3). The propensity of both **12** and **15** to undergo facile nucleophilic attack is presumably due to strain relief (for **12** and **15**) and aromaticity gains (for **15**). Indeed, an open chain analog of **1** did not show the same reactivity, nor did it cleave DNA under the same conditions. The results presented above strongly support a nucleophilic mechanism (path b, Scheme 1) rather than a radical mechanism (path a, Scheme 1) for DNA cleavage by golfomycin A(**1**) [similarly for golfomycin B(**15**)].

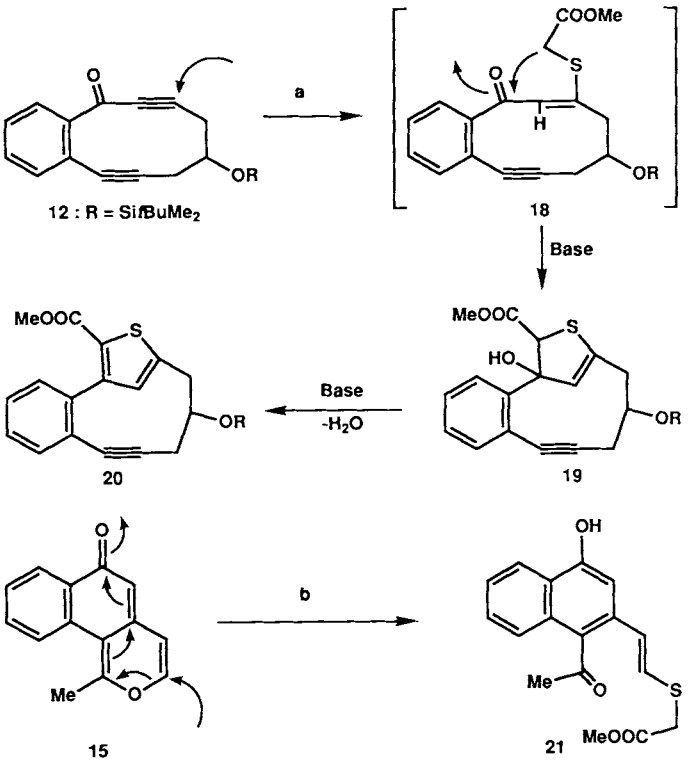

Scheme 4. Addition of methyl thioglycolate to golfomycins A (**1**) and B (**15**). (a) 5.0 eq $HSCH_2COOMe$, 5.0 eq DBU, THF, 10 °C, 75%; (b) 5.0 eq $HSCH_2COOMe$, 1.5 eq DBU, THF, 25 °C, 67%.

The properties of golfomycins A(**1**) and B(**15**) prompted us to test the hypothesis that they might show antitumor activity. Indeed, preliminary in vitro tests show that golfomycin A(**1**) inhibits the growth of MB49 murine bladder carcinoma cells with IC_{50} of 3.4 μmol L^{-1} during 4 days of exposure (37 °C, 7% CO_2).[11, 12]

The described chemistry and biology of golfomycin A(**1**) demonstrate the power of design and synthesis in the preparation of molecules with specific chemical and biological properties. In vivo antitumor studies with golfomycin A(**1**) and further studies in the area of designed molecules are continuing.

Received: April 23, 1990 [Z 3929 IE]
German version: *Angew. Chem. 102* (1990) 1066

[1] For some general references, see a) E. J. Corey, X.-M. Cheng, *The Logic of Chemical Synthesis*, Wiley, New York 1989; b) A.-U. Rahman, P. W. LeQuesne, (Eds.): *Natural Products Chemistry III*, Springer, Berlin 1989; c) K. Hostettmann, P. J. Lea, (Eds.): *Biologically Active Natural Products*, Oxford University Press, Oxford 1987.

[2] The name "golfomycin" was coined for compound **1** from the Greek name "Golfo" of *G. S.* who synthesized it first.

[3] For some recent examples of designed DNA-cleaving molecules, see a) K. C. Nicolaou, Y. Ogawa, G. Zuccarello, H. Kataoka, *J. Am. Chem. Soc. 110* (1988) 7247; b) K. C. Nicolaou, G. Skokotas, P. Maligres, G. Zuccarello, E. J. Schweiger, K. Toshima, S. Wendeborn, *Angew. Chem. 101* (1989) 1255, *Angew. Chem. Int. Ed. Engl. 28* (1989) 1272; c) T. J. Povsic, P. B. Dervan, *J. Am. Chem. Soc. 111* (1989) 3059; d) R. P. Hertzberg, P. B. Dervan, *ibid. 104* (1982) 313; e) H. E. Moser, P. B. Dervan, *Science 238* (1987) 645; f) D. R. Corey, P. G. Schultz, *J. Am. Chem. Soc. 111* (1989) 8523; g) A. M. Pyle, E. C. Long, J. K. Barton, *ibid. 111* (1989) 4520; D. S. Sigman, *ibid. 111* (1989) 4941; i) M. Ohno, M. Otsuka, *ibid. 112* (1990) 838; j) N. B. Mantlo, S. J. Danishefsky, *J. Org. Chem. 54* (1989) 2781.

[4] For some elegant work relating to this mechanism see a) A. G. Myers, E. Y. Kuo, N. S. Finney, *J. Am. Chem. Soc. 111* (1989) 8057; b) A. G. Myers, P. S. Dragovich, *ibid. 111* (1989) 9130.

[5] All new compounds exhibited satisfactory spectral and analytical and/or exact mass data. Yields refer to spectroscopically and chromatographically homogeneous materials. Selected physical data of the most important compounds (Ar = aryl). **1**: pale yellow solid, decomposes upon heating; R_f = 0.36 (silica, 70% ether in petroleum ether); ^{1}H NMR (500 MHz, $CDCl_3$): δ = 8.17 (1H, d, J = 8.7 Hz, Ar), 7.46 (3H, m, Ar), 4.16 (1H, m, C*H*-OH), 2.92 (4H, m, propargylic), 2.58 (1H, d, J = 8.5 Hz, O *H*); IR ($CHCl_3$): $\tilde{\nu}_{max}$ = 3607, 3556, 3019, 2255, 2227, 1630, 1592, 1280, 1216, 668 cm^{-1}; ^{13}C NMR (125 MHz, $CDCl_3$): δ = 176.06 (-*C*=O), 136.30 (Ar), 133.07 (Ar), 132.67 (Ar), 129.19 (Ar), 128.13 (Ar), 124.44 (Ar), 95.80 (acetylenic), 93.83 (acetylenic), 85.12 (acetylenic), 83.21 (acetylenic) 65.14 (*C*-OH), 28.96 (propargylic), 28.69 (propargylic); UV (MeOH): λ_{max} = 330 ($\varepsilon = 0.5 \times 10^4$ M^{-1} cm^{-1}), 274 (1.4×10^4), 240 (5.9×10^4) nm; HRMS calcd for $C_{14}H_{10}O_2$ ($M^{\oplus}$) 211.0759, found 211.0791. **15**: yellow solid, m.p. = 172.3 °C; R_f = 0.33 (silica, EtOAc); ^{1}H NMR (500 MHz, $CDCl_3$): δ = 8.53 (1H, d, J = 7.9 Hz, Ar), 8.02 (1H, d, J = 7.9 Hz, Ar), 7.66 (1H, t, J = 7.9 Hz, Ar), 7.60 (1H, t, J = 7.9 Hz, Ar), 7.34 (1H, d, J = 5.4 Hz, CH=C*H*-O), 6.61 (1H, d, J = 5.4 Hz, C*H*=CH-O), 6.29 (1H, s, C=C*H*-C=O), 2.86 (3H, s, *Me*); IR ($CHCl_3$): $\tilde{\nu}_{max}$ 1650, 1615, 1590, 1550, 1325, 1260, 1215, 933, 883, 845, 670 cm^{-1}; ^{13}C NMR (125 MHz, $CDCl_3$) δ 181.71 (-*C*=O), 159.15 (*C*=C(Me)O), 144.76 (C=*C*H-O), 140.31 (*C*=C-C=O), 134.36 (Ar), 132.02 (Ar), 129.97 (Ar), 127.71 (Ar), 126.81 (Ar), 126.16 (Ar), 113.17 (*C*=C(Me)O), 112.39 (C=*C*H-C=O), 112.18 (*C*H=CH-C=O), 23.02 (Me); UV (CH_3CN): λ_{max} = 370 ($\varepsilon = 1.8 \times 10^4$ M^{-1} cm^{-1}), 278 (0.9×10^4), 240 (2.5×10^4), 212 (2.5×10^4) nm; HRMS calcd for $C_{14}H_{10}O_2$ ($M^{\oplus}$) 210.0681, found 210.0666. **16**: pale yellow oil; R_f = 0.54 (silica, 50% ether in petroleum ether); ^{1}H NMR (300 MHz, $CDCl_3$): δ = 8.15 (1H, d, J = 8.4 Hz, Ar), 7.65 (1H, d, J = 8.4 Hz, Ar), 7.48 (1H, t, J = 8.4 Hz, Ar), 7.38 (1H, t, J = 8.4 Hz, Ar), 6.52 (1H, d, J = 5.6 Hz, CH=C *H*-O), 6.48 (1H, s, C(OH)=C*H*), 6.06 (1H, q, J = 6.6 Hz, O-C*H*-CH_3), 5.69 (1H, d, J = 5.6 Hz, C*H*=CH-O), 1.50 (3H, d, J = 6.6 Hz, *Me*); IR ($CHCl_3$): $\tilde{\nu}_{max}$ = 3596, 1616, 1595, 1420, 1309, 1228, 1218, 1119, 1069, 1048, 847, 765 cm^{-1}; UV ($CHCl_3$): λ_{max} = 336, 280, 270, 248 nm; HRMS calcd for $C_{14}H_{10}O_2$ ($M^{\oplus}$) 212.0837, found 212.0813. **19**: yellow solid, m.p. 87.6 °C; R_f = 0.19 (silica, 20% ether in petroleum ether); ^{1}H NMR (500 MHz, $CDCl_3$): δ = 7.80 (1H, d, J = 7.9 Hz, Ar), 7.28 (3H, m, Ar), 5.77 (1H, s, C=C-*H*), 4.63 (1H, s, O*H*), 4.20 (1H, m, C*H*-OSi), 3.75 (3H, s, COO*Me*), 3.47 (1H, s, C*H*-COOMe), 2.95 (1H, m, C=C-C*H*), 2.65 (3H, m, C=C-C*H*, propargylic), 0.92 (9H, s, Si-*tBu*), 0.13 (6H, s, Si-*Me*); IR ($CHCl_3$): $\tilde{\nu}_{max}$ = 3580, 2955, 2898, 2253, 1736, 1463, 1260, 1089, 838 cm^{-1}; UV (MeOH): λ_{max} = 276, 248, 214 nm; HRMS calcd for $C_{23}H_{30}O_4SSi$ ($M^{\oplus}$) 431.1712, found 431.1645. **20**: yellow oil; R_f = 0.47 (silica, 20% ether in petroleum ether); ^{1}H NMR (300 MHz, $CDCl_3$): δ = 7.74 (1H, d, J = 7.4 Hz, Ar), 7.59 (1H, s, C=C-*H*), 7.37 (1H, m, Ar), 7.25 (2H, m, Ar),

3.80 (1H, m, C*H*-OSi), 3.73 (3H, s, COO *Me*), 3.28 (1H, dd, J = 14.2, 8.3 Hz, C≡C-C*H*), 2.97 (1H, dd, J = 14.2, 2.5 Hz, C≡C-C*H*), 2.72 (1H, dd, J = 17.6, 9.5 Hz, propargylic), 2.49 (1H, J = 17.6, 3.0 Hz, propargylic), 0.90 (9H, s, Si-*t*Bu), 0.13 (6H, s, Si-*Me*); IR ($CHCl_3$): $\tilde{\nu}_{max}$ = 2954, 2858, 2246, 1714, 1472, 1282, 1097, 865, 723; UV (MeOH): λ_{max} = 288, 256, 234, 222 nm; HRMS calcd for $C_{23}H_{28}O_3SSi$ ($M^{\oplus}$) 413.1606, found 413.1587. **21**: colorless oil; R_f = 0.27 (silica, 50% ether in petroleum ether); ^{1}H NMR (300 MHz, $CDCl_3$): δ = 8.19 (1H, m, Ar), 7.61 (1H, m, Ar), 7.48 (2H, m, Ar), 6.83 (1H, s, C*H*=C-OH), 6.72 (1H, d, J = 15.4 Hz, CH=C*H*-S), 6.56 (1H, d, J = 15.4 Hz, C*H*=C-HS), 3.80 (3H, s, COO*Me*), 3.53 (2H, s, SCH_2COOMe), 2.62 (3H, s, CO*Me*); IR ($CHCl_3$): $\tilde{\nu}_{max}$ = 3590, 1737, 1692, 1621, 1595, 1517, 1438, 1389, 1357, 1289, 1209, 1141, 1078, 1010 nm; UV ($CHCl_3$): λ_{max} = 362(s), 316, 290, 246 nm; HRMS calcd for $C_{17}H_{16}O_4S$ ($M^{\oplus}$) 317.0847, found 317.0879.

[6] a) R. D. Stevens, C. E. Castro, *J. Org. Chem. 28* (1963) 3313; b) K. Sonogashira, Y. Tohda, N. Hagihara, *Tetrahedron Lett. 1975* 4467; c) V. Ratovelomana, G. Linstrumelle, *Synth. Commun. 11* (1981) 917.

[7] Details of the crystallographic analysis will be given elsewhere.

[8] The observed second wave of DNA cleavage at pH ≥9 may signal the initiation of this reaction cascade.

[9] Apparently the -SH group from methyl thioglycolate is adding to the acetylene in a *trans* fashion giving **18**, otherwise the following step **18** → **19** would be geometrically impossible. In accordance with this observation, MM 2 calculations revealed that **18** is ca. 4.9 kcal/mol less strained than its geometrical isomer. The stereochemistry of **19** was not assigned.

[10] This striking difference in regioselectivity may be the result of combined steric effects (nucleophile size and electrophilic center environment).

[11] Golfomycin B(**15**) also exhibited DNA-cleaving properties and antitumor activity although with lower potency (ca. 10 times less) than golfomycin A(**1**). These studies were carried out in collaboration with Dr. *D. Rideout* of the Research Institute of Scripps Clinic.

[12] Although it is tempting to relate DNA cleavage with cytotoxic activity this relationship must be viewed with caution pending further investigations.

Synthesis and Cycloadditions of Monomeric Selenobenzophenone **

By *Gerhard Erker,* Regina Hock, Carl Krüger, Stefan Werner, Frank-Gerrit Klärner,* and *Uwe Artschwager-Perl*

Dedicated to Professor Wolfgang R. Roth on the occasion of his 60th birthday

The higher homologues of the aldehydes and ketones are concomitantly more nucleophilic ("higher" HOMO) and more electrophilic ("lower" LUMO) than the normal organic carbonyl compounds,[1] and therefore exhibit a different reaction behavior.[2] Whereas the chemistry of the thiocarbonyl compounds is well documented,[3] only few stable selenoketones are known; all of these carry *tert*-alkyl substituents on the carbonyl carbon atom.[4] Simple selenoketones, e.g. selenobenzophenone **2**, as well as seleno- and telluroaldehydes were considered to be so reactive that they were previously only generated in situ and were detected by the formation of characteristic trapping products.[5] We have now prepared selenobenzophenone **2** and spectroscopically characterized it as the monomeric compound in solution. The stereochemistry of the [4 + 2]-cycloaddition to conjugated dienes frequently used as trapping reaction could be elucidated for the first time with this simple selenoketone. The result was surprising.

[*] Prof. Dr. G. Erker, Dipl.-Chem. R. Hock
Organisch-Chemisches Institut der Universität
Orléans- Ring 23, D-4400 Münster (FRG)
Prof. Dr. C. Krüger, Dipl.-Chem. St. Werner
Max-Planck- Institut für Kohlenforschung
Kaiser-Wilhelm-Platz 1, D-4330 Mülheim an der Ruhr (FRG)
Prof. Dr. F.-G. Klärner, Dr. U. Artschwager-Perl
Fakultät für Chemie der Universität
Universitätsstrasse 150, D-4630 Bochum (FRG)

[**] This work was supported by the Fonds der Chemischen Industrie, the Deutsche Forschungsgemeinschaft, and the Alfried-Krupp-von-Bohlen-und-Halbach Foundation.

2 is formed in the Staudinger chalcogenation[5c, 6] of the phosphorus ylide $Ph_3P{=}CPh_2$ **1** with elemental selenium in toluene at 85 °C (2 h). After sublimation (75 °C, $< 10^{-3}$ bar) and recrystallization, the cyclodimer **3** of the selenobenzophenone **2** can be isolated in two yellow-green crystal modifications **3a**, **3b**. Crystal structure analyses were carried out on both modifications.[7] 2,2,4,4-Tetraphenyl-1,3-diselenacyclobutane with planar C_2Se_2 ring is present, both in the triclinic form **3b** with two independent molecules in the unit cell, as well as in the monoclinic form **3a** (Fig. 1) (Z = 2). The molecules differ only in the interplanar angles between the phenyl rings and the four-membered ring. The averaged data from all independent molecules were as follows: Se–C 2.002(9), Se···Se* 2.901(6) Å; Se–C–Se* 92.9(8), C–Se–C* 87.1(8)°.

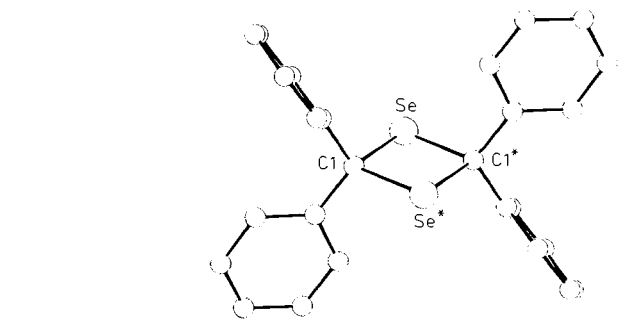

Fig. 1. Structure of the diselenacyclobutane **3** in the crystal (modification **3a**).

In solution, **3** rapidly dissociates with formation of monomeric selenobenzophenone **2**. The transformation **3** → **2** can be monitored quite well on the basis of characteristic NMR spectra.[7] **2** is intense green in solution[7] (λ_{max} = 741 nm, $n \rightarrow \pi^*$[1b]). The cleavage of **3** with formation of **2** is acid-catalyzed in many solvents. In the presence of traces of $H^{\oplus}$ and at concentrations of **3** of ca. 0.1 mol L^{-1} an equilibrium is rapidly established between **3** and **2** (3:2 ≈ 1.9 at room temperature). We have measured the rate of the uncatalyzed, thermally induced cleavage of **3** ^{1}H-NMR spectroscopically at 323 K in C_6D_6 (which was distilled with ca. 1% tetramethylenediamine to remove traces of acid). With an initial concentration of **3** of c = 0.13 mol L^{-1} a first-order rate of $k(\mathbf{3} \rightarrow \mathbf{2}) = 1.73 \times 10^{-4}\ s^{-1}$ [$\Delta G^{\neq}$(323 K) = 24.4 ± 0.3 kcal mol^{-1}] was measured.

Like the reactive selenoaldehydes and selenoketones generated in situ, selenobenzophenone **2** forms [4 + 2]-cycloaddition products with conjugated dienes.[5] With 2,3-dimethylbutadiene, 2,3-dimethoxybutadiene, cyclopentadiene or 1,3-cyclohexadiene the addition compounds **4** and **5** are obtained in good yields at room temperature.[8]

4a, R = CH_3
4b, R = OCH_3

2

5a, n = 1
5b, n = 2

To check whether these cycloadditions are concerted hetero-Diels-Alder reactions we have investigated their stereochemistry by allowing **2** to react with *trans,trans*-hexa-2,4-diene in toluene at room temperature. The reaction was monitored ^{1}H-NMR spectroscopically. A single product was formed and was isolated in 82% yield. According to the spectroscopic data the product is *cis*-3,6-dimethyl-2,2-diphenyl-3,6-dihydro-2*H*-selenapyran *cis*-**6**.[9a] Only *cis*-**6** is found as product also in the analogous reaction of **2** with *cis, trans*-hexa-2,4-diene. That is, the selenapyran is formed with loss of the stereochemical information of the conjugated diene.

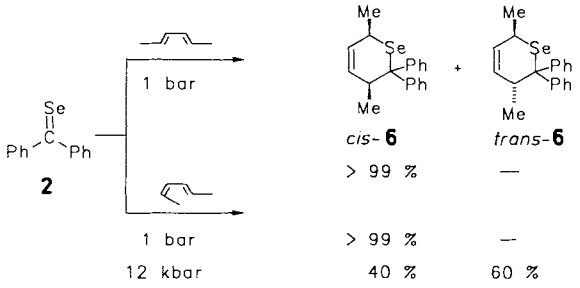

Concerted [4 + 2]-cycloadditions are characterized by strongly negative activation volumes. Consequently, at higher pressures they are favored over the alternative multistep reaction paths.[10] We therefore carried out the reaction of **2** with *cis, trans*-hexa-2,4-diene in toluene at room temperature again but this time at a pressure of 11–12 kbar; we now obtained, besides *cis*-**6**, the stereoisomeric *trans*-**6**[9b] (ratio ca. 40:60). Apparently, in the case of the [4 + 2]-cycloaddition of **2**, the alternative reaction routes — concerted and multistep process — are energetically so widely separated that kinetic acceleration by high pressure is necessary for the concerted hetero-Diels-Alder reaction to be competitive with the multistep addition sequence. We assume that this is true for many of the "Diels-Alder reactions" of non-stabilized chalcogeno-ketones and -aldehydes.[5]

Received: March 21, 1990 [Z 3863 IE]
German version: *Angew. Chem. 102* (1990) 1082

CAS-Registry numbers:
1, 4214-38-4; **2**, 119579-98-5; **3**, 128632-60-0; **4a**, 116897-07-5; **4b**, 128632-63-3; **5a**, 116897-08-6; **5b**, 128632-64-4; **6**-*cis*, 128632-61-1; **6**-*trans*, 128632-62-2; Se, 7782-49-2; 2,3-dimethyl-1,3-butadiene, 513-81-5; 2,3-dimethoxy-1,3-butadiene, 3588-31-6; Cyclopentadiene, 542-92-7; 1,3-Cylohexadiene, 592-57-4; (Z, E)-2,4-hexadiene, 5194-50-3.

[1] a) H. Bock, S. Aygen, P. Rosmus, B. Solouki, E. Weissflog, *Chem. Ber. 117* (1984) 187; V. P. Rao, J. Chandrasekhar, V. Ramamurthy, *J. Chem. Soc. Perkin Trans. 2 1988* 647; b) R. H. Judge, D. C. Moule, *J. Am. Chem. Soc. 106* (1984) 5406; D. J. Clouthier, D. C. Moule, *Top. Curr. Chem. 150* (1989) 167.

[2] P. Beak, J. W. Worley, *J. Am. Chem. Soc. 94* (1972) 597; H. Viola, H. Hartenhauer, R. Mayer, *Z. Chem. 28* (1988) 269, and references cited therein; E. Vedejs, T. H. Eberlein, R. G. Wilde, *J. Org. Chem. 53* (1988) 2220.

[3] See for example J. E. Baldwin, R. C. G. Lopez, *Tetrahedron Lett. 39* (1983) 1487; E. Vedejs, D. A. Perry, R. G. Wilde, *J. Am. Chem. Soc. 108* (1986) 2985, and references cited therein.

[4] Stable selenoketones and -aldehydes: T. G. Back, D. H. R. Barton, M. R. Britten-Kelly, F. S. Guziec, Jr., *J. Chem. Soc. Chem. Commun. 1975*, 539; *J. Chem. Soc. Perkin Trans. 1 1976*, 2079; E. Schaumann, F.-F. Grabley, *Tetrahedron Lett. 21* (1980) 1251; E. R. Cullen, F. S. Guziec, Jr., C. J. Murphy, T. C. Wong, K. K. Andersen, *J. Chem. Soc. Perkin Trans. 2 1982*, 473; A. Ishii, R. Okazaki, N. Inamoto, *Bull. Chem. Soc. Jpn. 61* (1988) 861; R. Okazaki, N. Kumon, N. Inamoto, *J. Am. Chem. Soc. 111* (1989) 5949.

[5] R^1R^2C = Se generated in situ and trapped: a) K. Okuma, J. Sakata, Y. Tachibana, T. Honda, H. Ohta, *Tetrahedron Lett. 28* (1987) 6649; P. T. Meinke, G. A. Krafft, *J. Am. Chem. Soc. 110* (1988) 8679; b) G. Erker, R. Hock, R. Nolte, *ibid. 110* (1988) 624; c) W. Ando, Y. Kumamoto, H. Ishizuka, N. Tokitoh, *Tetrahedron Lett. 28* (1987) 4707; J. Nakayama, K. Akimoto, J. Niijima, M. Hoshino, *ibid. 28* (1987) 4423; P. T. Meinke, G. A. Krafft, J. T. Spencer, *ibid. 28* (1987) 3887; G. W. Kirby, A.N. Trethewey, *J. Chem. Soc. Perkin Trans. 1 1988*, 1913; P. T. Meinke, G. A. Krafft, *J. Am. Chem. Soc. 110* (1988) 8671; M. Segi, T. Nakajima, S. Suga, S. Murai, I. Ryu, A. Ogawa, N. Sonoda, *ibid. 110* (1988) 1976; *Tetrahedron Lett. 29* (1988) 6965; *ibid. 30* (1989) 2095; J. Grobe, D. L. Van, J. Welzel, *J. Organomet. Chem. 340* (1988) 153; Y. Nishiyama, S. Hamanaka, A. Ogawa, N. Kambe, N. Sonoda, *J. Org. Chem. 53* (1988) 1326; R. J. Adrien, R. W. Gable, B. F. Hoskins, D. Dakternieks, *J. Organomet. Chem. 359* (1989) 33; Y. Takikawa, A. Uwano, H. Watanabe, M. Asanuma, K. Shimada, *Tetrahedron Lett. 30* (1989) 6047; d) tellurocarbonyl compounds: G. Erker, R. Hock, *Angew. Chem. 101* (1989) 181; *Angew. Chem. Int. Ed. Engl. 28* (1989) 179; M. Segi, T. Koyama, Y. Takata, T. Nakajima, S. Suga, *J. Am. Chem. Soc. 111* (1989) 8749; e) for metal complexes see e.g.: C. E. L. Headford, W. R. Roper, *J. Organomet. Chem. 244* (1983) C53; W. Paul, H. Werner, *Angew. Chem. 95* (1983) 333; *Angew. Chem. Int. Ed. Engl. 22* (1983) 316; H. Fischer, S. Zeuner, *J. Organomet. Chem. 252* (1983) C63; H. Fischer, *ibid. 345* (1988) 65 and references cited therein.

[6] H. Staudinger, J. Meyer, *Helv. Chim. Acta 2* (1919) 635; H. Tokunaga, K. Akiba, N. Inamoto, *Bull. Chem. Soc. Jpn. 45* (1972) 506.

[7] **3**: 76% isolated, m.p. 109 °C, correct elemental analysis. X-ray structure analysis: monoclinic modification **3a**: space group $P2_1/a$, $a = 7.529(1)$, $b = 17.937(3)$, $c = 7.893(1)$ Å, $\beta = 97.08(1)°$, $V = 1057.8$ Å^3, $Z = 2$, $\varrho_{calcd} = 1.54$ g cm^{-3}, $\lambda = 0.70930$ Å, $\mu = 34.67$ cm^{-1}, $R = 0.030$, $R_w = 0.027$, 3073 unique reflections, 1934 observed ($I > 2\sigma(I)$), 157 refined parameters, residual electron density 0.23 e Å^{-3}; triclinic modification **3b**: space group $P\bar{1}$, $a = 9.928(2)$, $b = 10.244(2)$, $c = 10.837(1)$ Å, $\alpha = 101.51(1)$, $\beta = 104.05(1)$, $\gamma = 96.19(2)°$, $V = 1033.3$ Å^3, $Z = 2$, $\mu = 35.48$ cm^{-1}, $R = 0.055$, $R_w = 0.034$, 7756 independent reflections, 5376 observed ($I > 2\sigma(I)$), 313 refined parameters, residual electron density 1.26 e Å^{-3}. Further details of the crystal structure analyses are available on request from the Fachinformationszentrum Karlsruhe, Gesellschaft für wissenschaftlich-technische Information mbH, D-7514 Eggenstein-Leopoldshafen 2, on quoting the depository number CSD-54466, the names of the authors, and the journal citation. ^{1}H NMR (C_6D_6, 200 MHz): $\delta = 6.80-7.04$ (m, 12H, *p-m*-H), 7.48 (m, 8H, *o*-H). ^{13}C NMR ($CDCl_3$, 50 MHz): $\delta = 126.7$, 127.9, 128.8 (p-*o*-*m*-C), 129.4 (CSe_2), 147.6 (*i*-C).-**2**: UV (toluene): $\lambda = 741$ ($\varepsilon = 80$), 355 (2840), 336 nm (3240). ^{1}H NMR (C_6D_6, 200 MHz): $\delta \approx 7.0$ (m, 4H, *m*-CH), 7.23 (m, 2H, *p*-CH), 7.61 (m, 4H, *o*-CH). ^{13}C NMR ($CDCl_3$, 50 MHz):$\delta = 128.2$, 128.4, 131.4 (*m-o-p*-C), 155.1 (*i*-C), 245.9 (C=Se).

[8] **4a**: 90% isolated. ^{1}H NMR ($CDCl_3$, 200 MHz): $\delta = 1.6$ (s, 6H, 4-, 5-CH_3), 2.80, 2.89 (2s, each 2H, 3-H,H', 6-H,H'), 7.1–7.3 (m, 10H, Ph). ^{13}C NMR ($CDCl_3$, 50 MHz): $\delta = 19.9$, 20.6 (4-,5-CH_3), 24.5 ($^1J_{CH} = 137$, $J_{CSe} = 62$ Hz, C6), 47.5 ($^1J_{CH} = 128$ Hz, C3), 51.7 (C2), 126.3, 127.8, 128.1 (p-*o*-*m*-CH), 124.4, 128.5 (C4, C5), 146.9 (*i*-C); cf. [5a].—**4b**: 88% isolated, m.p. 93–94 °C, correct C,H analysis. ^{1}H NMR ($CDCl_3$, 200 MHz): $\delta = 2.82$ (m, 2H, $^5J_{HH} = 1.8$, $^2J_{SeH} = 14.6$ Hz, 6-H,H'), 3.21 (m, 2H, $^5J_{HH} = 1.8$ Hz, 3-H,H'), 3.38, 3.55 (2s, each 3H, 4-, 5-OCH_3), 7.09–7.33 (m, 10H, Ph). ^{13}C NMR ($CDCl_3$, 50 MHz): $\delta = 17.5$ ($^1J_{CH} = 142$ Hz, C6), 43.7 ($^1J_{CH} = 129$ Hz, C3), 51.0 (C2), 57.6, 58.1 (4-, 5-OCH_3), 126.7, 128.0, 131.3 (*o-m-p*-C), 138.5, 142.0 (C4, C5), 145.2 (*i*-C).—**5a**: 90% isolated, m.p. 140–141 °C. ^{1}H NMR (C_6D_6, 200 MHz): $\delta = 1.77$, 2.17 (2m, each 1H, 7-H,H'), 3.43, 4.03 (2s, each 1H, 1-H, 4-H), 5.24, 6.12 (2m, each 1H, 5-H, 6-H), 6.9–7.4 (m, 10H, Ph). ^{13}C NMR ($CDCl_3$, 50 MHz): $\delta = 50.7$ ($^1J_{CH} = 133$ Hz, C4), 52.2 ($^1J_{CH} = 132$ Hz, C7), 54.9 ($^1J_{CH} = 145$ Hz, C1), C3 under solvent signal, 125.8, 126.0, 127.7, 128.1, 128.4, 129.6 (*σ-, m-, p*-C), 132.7, 139.1 (C5, C6), 145.8, 148.9 (*i*-C); cf. [5a].—**5b**: 70% isolated, m.p. = 188–190 °C (decomp.), satisfactory C,H analysis ^{1}H NMR (C_6D_6, 200 MHz): $\delta = 1.13$, 1.63, 1.90, 2.08 (4m, je 1H, 7-H,H', 8-H,H'), 3.23, 3.36 (2m, each 1H, 1-H, 4-H) 5.82, 6.11 (2m, each 1H, 5-H, 6-H), 6.9–7.1, 7.4–7.5 (m, 10H, Ph). ^{13}C NMR ($CDCl_3$, 50 MHz): $\delta = 21.4$, 29.8 (C7, C8), 30.8 (C3), 32.0, 39.5 (C1, C4), 125.7, 126.2, 127.7, 127.8, 128.9, 129.1 (*σ-, m-, p*-C), 132.7, 134.7 (C5, C6), 146.5, 148.3 (*i*-C).

[9] a) *cis*-**6**: 69% isolated, viscous oil, satisfactory C,H analysis. MS (EI, 70 eV): *m/z* 328 (8%, $M^{\oplus}$), 246 (100%); exact mass: $M^{\oplus}$ (^{80}Se) calcd. 328.0730, obs. 328.0726. ^{1}H NMR (C_6D_6, 200 MHz): $\delta = 0.94$ (d, 3H, 3-CH_3), 1.09 (3H, $^3J_{HH} = 7.4$, $^3J_{SeH} = 17.3$ Hz, 6-CH_3), 2.61 (m, 1H, 3-H), 2.85 (m, 1H, 6-H), 5.34 (dt, 1H, 4-H), 5.68 (ddd, 1H, 5-H), 6.9-7.2, 7.5-7.6 (m, 10H, Ph). ^{13}C NMR ($CDCl_3$, 50 MHz):$\delta = 19.3$ (3-CH_3), 19.9 ($^1J_{CH} = 128$, ^2JSeC = 22 Hz, 6-CH_3), 28.8 ($^1J_{CH} = 143$, $^1J_{SeC} = 59$ Hz, C6), 38.2 (C3), 58.6 (C2), 125.7, 126.4, 127.0, 128.0, 128.2, 129.1 (*σ-, m-, p*-C), 130.7, 135.4 (C4,C5), 146.9, 147.8 (*i*-C). b) *trans*-**6**: ^{1}H NMR ($CDCl_3$, 200 MHz): $\delta = 0.91$, 0.96 (2d, 3-CH_3, 6-CH_3), 3.16, 3.35 (2m, each 1H, 3-H, 6-H), remaining signals of *cis*-**6** masked. ^{13}C NMR ($CDCl_3$, 50 MHz): $\delta = 18.1$, 21.2 (3-CH_3, 6-CH_3), 30.3, 40.0 (C6, C3), 59.1 (C2), remaining signals as in the case of *cis*-**6**.

[10] Reviews: F.-G. Klärner, *Chem. Unserer Zeit 23* (1989) 53; R. van Eldik, T. Asano, W. J. le Noble, *Chem. Rev. 89* (1989) 549; W. J. le Noble (Ed.) *Organic High Pressure Chemistry*, Elsevier, Amsterdam 1988.

Book Reviews are written by invitation from the editor. Suggestions for books to be reviewed and for book reviewers are welcome. Publishers should send brochures or (better) books to the following address: Redaktion Angewandte Chemie, Postfach 101161, D-6940 Weinheim, Federal Republic of Germany. The editor reserves the right of selecting which books will be reviewed. Uninvited books not chosen for review will not be returned.

Serendipity: Accidental Discoveries in Science. By *R. M. Roberts*. Wiley, New York 1989. xviii, 270 pp., paperback $ 12.95.—ISBN 0-471-60203-5

Serendipity is a relatively old word; it was coined in 1754 by the English writer *Horace Walpole* to describe accidental discoveries that are not the result of a deliberate search, but which nevertheless often have far-reaching consequences. An example of serendipity par excellence is the discovery of America by *Columbus*, who, as is well known, began his voyage in a search for a new sea route to India. Not far from India lies Serendip—now called Sri Lanka—where, according to an oriental tale with which *Walpole* was familiar, many centuries ago three princes continually made accidental discoveries of this sort during their extensive journeyings.

For over 200 years serendipity remained a word used only in learned literary circles—for example, *Merton* uses it frequently in his guide through the labyrinth of learned writings "On the Shoulders of Giants"—until about 1970 when a writer who was probably looking for another word at the time came across this one (through serendipity?), and initiated its rapid climb to the status of a fashionable word, though one which is already showing the first signs of being worn out—such is the nature of these things.

That chance discoveries, luck, a "golden hand", or whatever else one may call it, have played a major role in the development of knowledge and continue to do so, is well known. *R. M. Roberts*, Professor of Chemistry at Austin, Texas, has for many years collected stories of lucky chances of this kind, and from these has produced a collection of anecdotes from many different fields of science and technology, from the Rosetta stone to the Velcro fastener, with a definite emphasis on chemical discoveries (ranging from *Wöhler*'s synthesis of urea through *Pasteur*'s separation of racemates and *Perkin*'s mauve dye to *Ziegler*'s synthesis of polyethylene, the determination of the DNA structure, the crown ethers, etc.)—anecdotes whose quality varies between wide extremes. The truth content of such stories can hardly be checked, and to try to do so would perhaps be pointless—one recalls the endless controversy about *Kekulé*'s dreams, which is of course referred to by the author.

However, whether accurate or not, the stories are in every case well told, and they therefore stick in one's memory. And for this reason it may be that their value is often more pedagogic than historical in nature, in view of their usefulness as colorful gems to include in a lecture, or to illustrate to a layman that scientists are anything but rational and "cold" in their thinking, apart from the planning of experiments which is always precise and detailed. Also the anecdotes demonstrate again and again the extent to which "chance favors the prepared mind" (*Pasteur*), thus giving at least a partial answer to the question "Why didn't *I* make that discovery?". "The essential part of any discovery comes by chance, but chance passes most people by" (*F. Nietzsche*). Unfortunately the pleasure of reading the book is slightly marred by a great number of printing and other errors; one could well do without serendipity of this sort in a revised edition.

Henning Hopf [NB 1075 IE]
Institut für Organische Chemie
der Universität Braunschweig (FRG)

Inorganic Chemistry. By *D. F. Shriver, P. W. Atkins* and *C. H. Langford*. Oxford University Press, Oxford 1990. xiii, 706 pp., paperback, £ 16.50.—ISBN 0-19-855231-9

"Inorganic Chemistry" is a typical anglo-american textbook. It is intended to be used mainly as a text in undergraduate courses in Canada, Great Britain and the USA and it is constructed accordingly. The individual chapters are treated briefly but precisely, with a generous quantity of clear and lucid illustrations. In addition, the reader is offered a large number of exercise problems, the solutions to which are given in the book.

As noted by the authors in the preface, the book cannot enter into as detailed a treatment of inorganic chemistry as the well-known textbooks "Cotton and Wilkinson", "Holleman and Wiberg", or "Greenwood and Earnshaw".

In five sections with altogether 19 subchapters, the authors do justice to the objectives of the book in an outstanding fashion. New research results as well as the application of modern spectroscopic methods are also included.

In the first main section the structures of atoms, molecules and solids are discussed. Notable features are the early introduction to symmetry analysis, the related classification of point-groups and the application of MO theory and of isolobal analogies. Physico-chemical methods of analysis are described using illustrative examples at appropriate places in the text. Even a section on one-dimensional conductors and superconductivity is included.

The second main section is entitled "Reactions". Four sections treat the concepts of Brønsted acids and bases, the Lewis acid-base principle, complexes of the d-metals and redox reactions. Here again the linking-up of basic knowledge and the physico-chemical background has succeeded remarkably well.

The third main section which concerns the s- and p-block elements is a successful introduction to the organometallic chemistry of main group elements. Included here are H, B, C, N, the halogens and the noble gases as well as compounds of these elements. Topics discussed include the preparation and structures of organometallic compounds, of compounds with element–element multiple bonding and of boranes. Polyanions and -cations, band gaps and conductivity, and "Chemical Vapour Deposition" are treated in shorter chapters. Two display boxes on manipulations under inert atmospheres are an original contribution.

The fourth main section is devoted to transition metal complexes of the d- and f-block elements. Term diagrams, UV-VIS spectroscopy, luminescence phenomena, EPR spec-

troscopy, reaction mechanisms of the d-block transition metal complexes and the organometallic chemistry of the transition metals are discussed here.

In the last main section entitled "Interdisciplinary Topics" the reader will find those aspects of inorganic chemistry which in the last few years have grown in importance and which have for the most part already developed into their own areas of activity: homogeneous and heterogeneous catalysis, the structure and properties of solids (crystal defects, ionic conduction, structure and magnetic characteristics) and not least bioinorganic chemistry.

The work is rounded off with an appendix which also includes character tables and information on the symmetry of orbital groups, as well as a formula and key-word index. For further reading there are ample references to the current literature; however, all these are English language journals and books.

Only a few errors could be found. The figure referring to $Cl_2B{=}N(iPr)_2$ (p. 338) is incomplete. On p. 340 a method for the preparation of Ga^{II} halides is cited, whereas only on the next page is it correctly pointed out that "$Ga^{II}Cl_2$" is in reality $Ga^{I}[Ga^{III}Cl_4]$. The comparison of a 3z, 2e-bond in the Al_2CH_3 bridge of $Al_2(CH_3)_6$ with the 3z,4e-bond in an Al_2Cl bridge of $(CH_3)_2AlCl_2Al(CH_3)_2$ (p. 316, Fig. 10.3) is also confusing, as the latter is described as a 2z,2e-bridge.

Nonetheless these minor defects cannot tarnish my overall positive impression of the book. Its approach, which differs from that of traditional textbooks, and the fact that new areas of inorganic chemistry are included (even though the choice is subjective), makes it a valuable supplement for students after their prediploma or first degree. It can also be recommended for diplomands and doctorate (graduate) students. Also worth mentioning is the pleasing appearance of the paperback version; it is very good value for the price.

Bernhard Neumüller [NB 1081 IE]
Fachbereich Chemie
der Universität Marburg (FRG)

The Chemistry of Enones. Parts 1 and 2. Edited by *S. Patai* and *Z. Rappoport*. Wiley, Chichester 1989. xvi, 1267 pp., hard cover, £ 285.00.—ISBN 0-471-91563-7 (Part 1)/ 0-471-92289-7 (Part 2)

α,β-Unsaturated carbonyl compounds are among the most important functional groups of organic chemistry, a fact which has now been recognized by the publication of the book "The Chemistry of Enones", edited by *S. Patai* and *Z. Rappoport*, in the series "The Chemistry of Functional Groups". The authors of the 22 individual contributions which make up this two-part work have not assumed an unduly narrow definition of the term "enone", and where the context is appropriate they have also included unsaturated aldehydes, esters or ketenes. In accordance with the aims of the "Patai" series, the authors have not attempted an exhaustive treatment of their individual topics; instead there is a clear emphasis on reviewing recent results. However, the topics are in most cases introduced in such a general way as to result in self-contained, easily readable, chapters that have the character of monographs. To give just one example, Chapter 17 on oxygenation reactions is introduced by a general description of active oxygen-containing species. The resulting unavoidable instances of overlapping between chapters are generally kept within acceptable limits.

In contrast to other handbooks such as "Houben and Weyl", the pattern generally adopted by *Patai* is to present the chemistry of the functional groups in a broad framework ranging from theory through spectroscopic properties to synthetic applications. Accordingly the first chapter by *A. Y. Meyer* (Jerusalem) deals with the general and theoretical aspects of enones. There have been very few recent quantum chemical studies concerned exclusively with enones, and the author therefore takes the opportunity to include in his article a number of his own unpublished studies, and presents a general discussion of the relationships between conformational and spectroscopic properties. The next two chapters, on structural chemistry (*B. Schweizer*, Zürich) and on conformational and optical rotational properties (*J. K. Gawronski*, Poznán) follow logically after the theoretical chapter. The many structural formulas with bond lengths and angles are useful, even though half a page each on cyclobutenone and cyclopentenone (pp. 39, 40) seems rather excessive. In the following review of the thermochemistry (*J. F. Liebman* and *R. M. Pollack*, Baltimore), the most important parts are the tables. The chapter on NMR spectroscopy (*H. E. Gottlieb*, Ramat Gan, Israel) includes detailed conformational analyses as a central topic, and the comparison with the theoretical predictions of the preceding chapters is very instructive. The next article, on the chemistry of ionized enones in the gas phase (*F. Turecek*, Prague), contains a good discussion of the rules governing the mass-spectrometric fragmentation behavior. In this context quinones are also mentioned as an important related class of compounds, which also have a separate volume devoted to them in the *Patai* series.[*]

However, the main emphasis of the work (occupying about 1000 of the 1200 pages) is on the various aspects of chemical reactivity, which are covered in the following 14 chapters. There is not space here to discuss every chapter in detail, but the wide range of subjects provides clear evidence of the many-faceted reactivity of the enones as ambidentate functional groups (Ch. 7, synthesis: *C.* and *Y. Thebtaranonth*, Bangkok; Ch. 8, general synthetic applications: *G. V. Boyd*, Jerusalem; Ch. 9, acid-base behavior: *R. I. Zalewski*, Poznán; Ch. 10, nucleophilic attack: *D. Duval* and *S. Géribaldi*, Nizza; Ch. 11, addition of electrons or radicals: *G. A. Russell*, Ames; Ch. 12, reactions with electrophiles: *K. Müllen* and *P. Wolf*, Mainz; Ch. 13, enzymic transformations: *R. M. Pollack, P. L. Bounds* and *C. L. Bevins*, Baltimore; Ch. 14, electrochemistry: *R. D. Little* and *M. M. Baizer*, Santa Barbara; Ch. 15, photochemistry: *D. I. Schuster*, New York; Ch. 16, radiation chemistry: *P. Neta* and *M. Dizdaroglu*, Maryland; Ch. 17, oxygenation reactions: *A. A. Frimer*, Ramat Gan, Israel; Ch. 18, reductions: *E. Keinan* and *N. Greenspoon*, Haifa; Ch. 19. organometallic derivatives: *J. A. S. Howell*, Keele; Ch. 20, enolizations: *B. Capon*, Hongkong; Ch. 21, asymmetric syntheses: *M. R. Peel* and *C. R. Johnson*, Detroit; Ch. 22, dimerizations and polymerizations: *C. R. Theocharis*, Uxbridge).

The detailed sub-division of the extensive subject matter enables the reader to easily find the topic of immediate interest. Overlapping occurs in some areas, however; thus, for example, the reader looking for information on asymmetric syntheses would be well advised not to limit his attention to Chapter 21. Again, important oxygenation reactions are found not only in Chapter 17 but also under reactions with electrophiles (Chapter 12).

The authors have, without exception, aimed to cover work published up to the beginning of 1988, but the overwhelming

[*] Cf. *Angew. Chem. 101* (1989) 649; *Angew. Chem. Int. Ed. Engl. 28* (1989) 933.

majority of the references are to papers from earlier years. Some random checks showed that modern developments in, for example, enantioselective *cis*-hydroxylation using osmium tetraoxide, polarity reversal of the reactivity in enones and enals, free radical addition to enones (e.g. for synthesizing *C*-glycosides) and modern variants of the Khand-Pauson, Sakurai and Nazarov reactions are all included. It is true that in several of these areas there have been further rapid advances since the volume appeared, but the reader will nevertheless find here a good introduction to these topics. This reviewer was disappointed to note that some important contributions to enones chemistry from the carbohydrates field were not included. The neglect of this aspect is regrettable in view of the use now being made of renewable raw materials for synthesizing enantiomerically pure natural substances.

There is now an increasing level of interest in the safety and toxicity aspects of chemical substances and reagents, and editors of comprehensive handbooks will probably need to give more thought to this in the future. In the present volume such information is only rarely included, e. g. the warning about the possible explosive risk with some molybdenum oxodiperoxy complexes (p. 548).

Now some comments regarding the formulas. The convenient small page format used in "Patai" has advantages for the user, but occasionally, for typographical reasons, it necessitates moving a formula scheme on to the next page. The formulas are generally clear and well set out (except for the fact that the stereo-arrows are too thick, especially in the representation of cyclopentene on p. 255).

The idea of constructing the handbook as a collection of self-contained monographs means that it is particularly important to have comprehensive author and subject indexes. It would perhaps have been useful to make the subject index even a little more comprehensive, at the expense of some duplication. To give just one example, the Sakurai reaction cannot be found in the index under this name; it is (very correctly) indexed as the Hosomi-Sakurai reaction.

No library which already contains parts of the *Patai* series can afford to be without this volume. Because of the importance of the functional groups that it deals with, it will also be a useful and worthwhile addition to the private collections of preparative organic chemists.

Karsten Krohn [NB 1059 IE]
Institut für Organische Chemie
der Technischen Universität Braunschweig (FRG)

The Chemistry of Linear Oligopyrroles and Bile Pigments. By *H. Falk*. Springer, Vienna 1989. xii, 261 pp., hardcover, DM 270.00.—ISBN 3-211-82112-0

There is hardly another class of compounds in organic chemistry that has held more fascination for investigators of successive generations than the pyrrole pigments. Since the pioneering work of *Hans Fischer* and his school, pyrrole derivatives in the widest sense have for several decades been the subject of studies by many renowned laboratories throughout the world. One recalls, for example, such celebrated studies as that which led to the determination of the structure of the vitamin B_{12} coenzyme (*D. C. Hodgkin*), those on the total syntheses of chlorophyll *a* (*R. B. Woodward*) and of cyanocobalamine (*A. Eschenmoser* and *R. B. Woodward*), the biosynthesis of the corrinoids (*A. Battersby, A. I. Scott* and others), the development of models for oxygen fixation (*J. P. Collman, J. E. Baldwin* and others), and many more. However, whereas the chemistry and biology of the macrocyclic pyrrole pigments and the chemistry of pyrrole and its derivatives have been reviewed more than once during the past fifteen years, since the publication of the classic work by *R. Lemberg* and *J. W. Legge* ("Hematin Compounds and Bile Pigments") and of the mainly medically orientated book by *T. B. With* ("Bile Pigments", 1968) there has been no comparable monograph covering the bile pigments and the related linear oligopyrroles. This is probably due to the fact that bile pigments occur as breakdown products of the biologically important porphyrin chromophores, and consequently in the past it is their clinical significance that has been emphasized. Although *Lemberg* discovered as long ago as 1933 that the substances responsible for the colors of cyanobacteria and red algae belong to the class of bile pigments, the renaissance in the chemistry of these compounds did not occur until the early 1950s, following the pioneering work of *H. Fischer* and his school, when a chromophore of the bile pigment type was also shown to be present in phytochrome, the photoreceptor which controls plant morphogenesis. Since then there have been some important milestones in the new era of bile pigment chemistry, such as the elucidation of the structures of the chromophores mentioned above (*J. J. Katz, H. Rapoport, W. Rüdiger, H. W. Siegelman* and others) and of a bioluminescent bile-type pigment found in marine organisms (*Y. Kishi* et al., 1988), and particularly the recently published X-ray structural analysis of the photoreceptor proteins of cyanobacteria (*R. Huber* et al., 1986), and these successes have stimulated a continued growth in activity in this area.

The book "The Chemistry of Linear Oligopyrroles and Bile Pigments", by *H. Falk*, thus closes the existing gap in the literature at an opportune moment, and it does this admirably. The eight chapters of this 534-page work deal exhaustively with the physical and chemical properties of the various members of this class of compounds. After a short introductory chapter, the troublesome question of the nomenclature of linear oligopyrroles is critically discussed in Chapter 2, and suggestions for a rational system of nomenclature are offered. Since moves to resolve this problem at an international level are still in their beginnings, the reader is strongly recommended to read this chapter right at the start. The account in Chapter 3 of the occurrence, formation and importance of linear tetrapyrroles in nature is rather brief (20 pp.), although it is true that further information on these topics is given in the chapters that follow (for example, the latest papers on the enzymic synthesis of tetrapyrroles are cited on p. 352, and the structures of the bile pigments present in butterfly wings are given on pp. 203–205, 231, 318 etc.). The reader whose main interest concerns the clinical aspects of bile pigments is referred to several relevant recent monographs. Chapter 4 collects together some very instructive information about the historical development of pyrrole chemistry; the connection between this and the human intellect is illustrated by drawings from the *papyrus Ebers* of the 17th century B.C., and by the oboe passages of *Mozart*'s Magic Flute (which is even cited in the index).

Chapter 5 covers more than half the book (293 pp.), and deals with the structure and stereochemistry of pyrroles (including MO methods). The majority of the work described here comes from the author's own scientific papers, and the reader thus has the benefit of getting the required information directly from the present leading chemist in this area of research. Non-specialists will also appreciate the short general description in Section 5.1.3 of the physical methods used for the structural analysis of pyrroles, and the references to relevant literature. Chapter 6 describes the synthetic meth-

ods used for preparing linear oligopyrroles with two to six units in the chain, using the "synthone approach", and these are illustrated by appropriate examples. Chapter 7 deals with the physical (mainly spectroscopic) properties of oligopyrroles. Although there is some overlapping here with the contents of Chapter 5, the reader is unlikely to consider this as a disadvantage. Finally, in Chapter 8, the reactivity of oligopyrroles and bile pigments is discussed under the different types of reactions (photochemical rearrangements, the formation of metal chelates, substitution and addition reactions, etc.). The bibliography and the author and subject indexes, which have been very carefully compiled, reinforce the excellent impression obtained from this book. The figures, which have been prepared using an Apple-Macintosh computer program, are excellent and essentially error-free. In the few exceptions to this (Figs. 3.17, 5.96, 6.197–198) the attentive reader should have no difficulty in correcting the mischief of the "printer's devil". Altogether this is an excellent book, which will be indispensable to every chemist working in this field, and to those wishing to become involved.

Albert Gossauer [NB 1028 IE]
Department of Organic Chemistry
University of Fribourg (Switzerland)

Carbon-13 NMR of Flavonoids. (Series: Studies in Organic Chemistry, Vol. 39). Edited by *P. K. Agrawal*. Elsevier, Amsterdam 1989. 564 pp., hardcover, DFl 350.00.—ISBN 0-444-87449-6

Flavonoids occur widely in plants as pigments and other constituents, and are very important not only in food technology, pharmacology and chemotherapy, but also as key substances in the chemotaxonomy of plants. Because of their wide variety of structures their identification and structural elucidation requires unambiguous spectroscopic methods. To the earlier monograph and data compilation *The Flavonoids*, edited by *J. B. Harbone* and *T. J. Mabry* and published in 1975, is now added this volume by *P. K. Agrawal* and coauthors on the ^{13}C NMR data, which supplements and updates the earlier work.

The introduction briefly describes and compares the most important spectroscopic methods that have been used to determine flavonoid structures (IR, UV, MS, ^{1}H NMR), then leads into the subject of the book by revising the structures of a few well-known flavonoids on the basis of their ^{13}C NMR spectra. A useful guide is provided by tables listing typical ^{1}H and ^{13}C NMR chemical shift ranges and coupling constants. Chapter 2 deals very briefly with the most important one- and two-dimensional NMR techniques, including decoupling procedures and correlation spectroscopy and with chemical aids for assigning ^{13}C NMR signals (shift reagents, labeling methods, derivatizations). Even the off-resonance decoupling method, now completely superseded by more sensitive and unambiguous methods for determining CH multiplicities (notably DEPT), is revived yet again.

Chapters 3 to 9 (altogether 414 pp.) constitute the largest and most useful part of the book, in which over 800 literature references are reviewed. These chapters provide a survey, in the form of tables accompanied by a concise commentary, of ^{13}C chemical shifts for flavonoids and anthocyanidines (Chapter 3), isoflavonoids, coumarins, pterocarpanoids and rotenoids (Chapter 4), neoflavonoids, auronoides and homoisoflavonoids (Chapter 5), flavonoid-glycosides (Chapter 6), chalconoides (Chapter 7), and flavanoids and flavanoid-glycosides (Chapter 9). The final chapter of the book gives useful advice on using ^{13}C chemical shift data to distinguish between the different classes of flavonoids, and to recognize functional groups and determine their position. Regrettably, though, the chapter omits to explain that, by analyzing contour diagrams from two-dimensional correlation experiments such as CH-COSY and CH-COLOC, a complete and precise structure elucidation can be obtained even with only a small amount of substance.

The literature up to 1987 is covered. Unfortunately the clarity of the presentation is marred by the fact that the formulas (usually without numbering of the carbon nuclei) are widely separated from the data tables, necessitating constant leafing back and forth. A more user-friendly arrangement would have been to give the chemical shift values directly alongside the carbon nuclei in the formulas, a form of presentation that could have been achieved by using commercially available text-graphics software. This would also have enabled the $\delta(^{1}H)$ values to be clearly shown as complementary data, especially as it is nowadays possible to rapidly determine $\delta(^{13}C)$ and $\delta(^{1}H)$ values in a single correlation experiment (CH-COSY). It would also have been useful to include details of the use of $^{3}J_{CH}$ values for determining substitution patterns (pp. 509f).

The subject and compound indexes have been badly printed in a 9-point matrix format. In the compound index it would have been better to use the Chemical Abstracts method of classification (basic skeleton and substituents). Lastly, the formulas have evidently been reproduced from the authors' hand-drawings; the use of such technically inferior methods is inappropriate in such a highly priced book. Nevertheless, the book is a useful work of reference for all those concerned with identifying flavonoids and elucidating their structures.

Eberhard Breitmaier [NB 1066 IE]
Institut für Organische Chemie und Biochemie
der Universität Bonn (FRG)

Chemistry of Tin. Edited by *P. J. Harrison*. Blackie, Glasgow 1989. xi, 461 pp., hardcover, £ 75.00—ISBN 0-216-92496-0.

Organotin Chemistry. (Series: Journal of Organometallic Chemistry Library, Vol. 21). By *I. Omae*. Elsevier, Amsterdam 1989, viii, 356 pp., hardcover, DFl 270.00.—ISBN 0-444-87456-9

Organotin Compounds in Organic Synthesis. Edited by *Y. Yamamoto*. Tetrahedron Symposia-in-Print 36, Vol. 45, No. 4, pp. 909–1230. Pergamon, Oxford 1989.—ISBN 0040-4020

"Tin for organic synthesis" is the best way of describing the rapid developments that have occurred in organotin chemistry. These developments were initiated by acknowledged masters of the art of dealing with complex organic molecules and their subtle stereochemistry, chemists such as *E. J. Corey, D. H. R. Barton, G. Stork* and *J. K. Stille*. The irony of this development is that most of the basic organotin reactions now used had been known in the literature for twenty years or more, though without having been exploited to such an extent. The rift that had developed between "pure" organic chemistry and organometallic chemistry, and had almost become a tradition—although such a rift did not yet exist in the days of *Victor Grignard, Karl Ziegler* and *Georg Wittig*—was only closed again when the great "back to synthesis" movement began.

Thus we now have four books on the subject. The first, by *Pereyre, Quintard* and *Rahm*, which was reviewed by the unforgettable *J. K. Stille* (*Angew. Chem. 100* (1988) 314; *Angew. Chem. Int. Ed. Engl. 27* (1988) 445), had the misfortune to appear just at the beginning of the phase of most rapid development (it covered literature up to early 1985). Important advances occurred soon afterwards, and a thoroughly revised new edition would be welcome.

The book edited by *Phil Harrison*, covering the literature up to 1987, has the encyclopedic layout of a classic monograph. It contains good thorough compilations of relevant material on the spectroscopy, structure, formation and breakdown of tin compounds, on the basic reactions involving tin, and on its biochemistry, industrial applications, etc. A great deal of information has been carefully compiled and critically evaluated with clear figures and tables. Printing errors are rare, except possibly in the names of authors, e.g. in the preface (*Poller*), while on page 17 two references have become jumbled together under (i), and the name of this reviewer got lost. The formulas are easily legible, and the presentation is attractive. The main emphasis is on structural chemical aspects, in accordance with the interests of the editor. Preparative applications, on the other hand, are relegated to the background. In some places the editor has not succeeded in fully coordinating the contributions of the different authors, as often happens in works of this kind, despite the fact that all are British. For example, overlapping occurs between Chapter 9 (Radical Chemistry of Tin, *A. G. Davies*) and Chapter 10 (The Uses of Organotin Compounds in Organic Synthesis, *J. L. Wardell*), despite the fact that these contain only 20 and 43 pages respectively. One could have wished for both these authors to be given more space, but it is not obvious to the reviewer where economies of space could be made elsewhere in the book without a sacrifice of information that would detract from the encyclopedic value of the book. Thus it is fortunate for readers interested in preparative aspects (and the number of these has increased in the last few years) that there also exist the two other books discussed below.

The book by *I. Omae* covers the literature up to 1987, and partly that of 1988. Although it deals with the classical principles of syntheses and reactions involving the tin atom (including, for example, a good treatment of the direct synthesis of organotin compounds from elemental tin), greater emphasis is put on the important developments of the last few years, e.g. palladium catalyzed reactions using organotin reagents are covered in detail. However, aspects that can be criticized are a degree of unevenness in the treatment, and some arbitrariness in the choice of topics emphasized. For example, whereas free radical reactions using R_3SnH are adequately covered in total in Sections 5.3 and 5.4 of Chapter 5 ("Reactions of Organotin Compounds") and 6.9 of Chapter 6 ("Organic Synthesis with Organotin Compounds", meriting a full chapter of 47 pages), intramolecular coordination in β-carbonylstannanes is given a disproportionately large amount of space in Chapters 3, 6 and 7, despite the fact that a book on this topic by the same author appeared in the same series of monographs in 1986. This leads to quite a lot of repetition. In Chapter 6 under aryl stannanes one fails to find the early electrophilic scission reactions (studied by *C. Eaborn* and others) which are the foundation of modern syntheses. In view of current public concerns it is surprising not to find the keyword "toxicity", even though there are individual mentions of this scattered through the book, e.g. under "Biological Activities". Under environmental aspects the outstanding analytical studies by *F. Brinckman* deserved to be mentioned. However, these comments should not be allowed to detract from the author's achievement in having provided a lucid survey of the rapidly growing knowledge in this field. The book is mainly intended for organic, organometallic, pharmaceutical and industrial chemists involved in research, and is also suitable for advanced students.

However, the publishers must be reproached for the poor standard of production at such an inflated price. The presentation of the text in typescript form, unedited and without any emphases, variations of typography, or bold or italic type, and the clumsy formulas etc., are not reader-friendly. The user will find the book reminiscent of a hand-produced doctoral thesis of 30 years ago. And this in a book which is also recommended for use by students! Any modern program for printing text and formulas on a standard desk computer offers better readability than this.

The Tetrahedron Symposium-in-Print edited by *Yoshinori Yamamoto* is devoted entirely to the use of organotin compounds in organic synthesis, and covers the literature up to 1988. An excellent treatment of the subject is given, with original laboratory recipes, under a number of very well chosen sub-areas. There are 28 articles by expert authors, most of whom are leading participants in the current rapid developments in the field. To meet ideal criteria the book should perhaps also have included contributions by *M. Reetz* and *G. E. Keck*—and from the editor himself! However, this is a very good, timely and relevant report on a rapidly expanding field.

Which of these books ought one to buy? In most cases two are needed. No true student textbook is available. *Harrison*'s book is the encyclopedia of the subject, but is too short on detail for organic synthetic purposes. The book by *Omae* is better in this respect, but contains less information of a general nature. *Yamamoto*'s book is aimed especially at synthetic chemists. One must choose according to one's point of view and objectives.

Wilhelm Paul Neumann [NB 1064 IE]
Institut für Organische Chemie
der Universität Dortmund (FRG)

Leukotrienes and Lipoxygenases. Chemical, Biological and Clinical Aspects. (Series: Bioactive Molecules, Vol. 11). Edited by *J. Rokach*. Elsevier, Amsterdam 1989. xxxii, 518 pp., hardcover, DFl 360.00.—ISBN 0-444-87464-X

The importance that the arachidonic acid derivatives have earned as highly effective, physiologically and pharmacologically active mediators of intercellular communication has led to the coining of the collective term "eicosanoids". Whilst the initial main interest was in the prostaglandins, the new eicosanoid research has shifted to the area of lipoxygenases and leukotrienes. The elucidation of their chemical structures and the biochemical characterization of their biosynthesis and mode of action provided the key for the development of inhibitors for which high hopes are held out, since the lipoxygenase products are involved in the activation of the immune system. Pioneering studies have mainly been carried out by three groups (Harvard, Quebec and Stockholm). Of their publications, this one by *J. Rokach* (Merck Frosst, Canada), in Volume 11 of the "Bioactive Molecules" series, has attempted to collect and critically review all the information obtained to date.

This first attempt at the task has been an outstanding success. Together with 15 coauthors, *Rokach* has systematically brought together all aspects of this material, from

chemical to medical. The main emphasis is on the structural elucidation and chemical syntheses of the lipoxygenase products, tasks which have proved very demanding due to the complex stereochemistry. The many structural formula schemes that are needed are clearly set out, and for the essential syntheses are almost of textbook style, being additionally provided with literature references. A second strong point of the book is the full explanation of the analytical methods, which spares the newcomer in this area from the troublesome study of the primary literature. The biochemistry, pharmacology and pathophysiology of the leukotrienes are also discussed in the light of the latest knowledge. Evidence that the area is still scientifically expanding is apparent from the chapter by *Ford-Hutchinson*, in which only fifteen pages are devoted to the association of the leukotrienes with various illnesses, even though the conditions covered, in which leukotrienes are responsible for many symptoms, include inflammations, asthma, allergies, shock and cardiovascular diseases. A chapter about inhibitors and antagonist receptors is modestly placed at the end of the book. It does not yet include the success of the Merck-Frosst group, who have discovered the most promising 5-lipoxygenase inhibitor to date, which operates by a new principle and is likely to replace the antioxidant type inhibitors that were previously tested. This has demonstrated at the same time how broadly-structured chemical and pharmacological research has consistently led to results both for clinical practice and biochemical theory. When in addition such a book results as a spin-off, both the company and the authors should be equally congratulated.

As this is the first book of its kind on the subject, and against the background of the increasing importance of the leukotrienes in pathophysiology, it is indispensible for researchers in medicine. The book is typographically excellent, but its price (DM 360.—) means that students of chemistry, pharmacy, medicine or biochemistry must be satisfied with only borrowing it.

Volker Ullrich [NB 1088 IE]
Fakultät für Biologie
der Universität Konstanz (FRG)

Transition Metal Oxides: Surface Chemistry and Catalysis. (Series: Studies in Surface Science and Catalysis, Vol. 45). By *H. H. Kung*. Elsevier, Amsterdam 1989. x, 282 pp., hardcover, DFl 215.00.—ISBN 0-444-87394-5

At a time when transition metal oxides are becoming increasingly important, especially in high technology applications such as superconductors, high performance ceramics, microelectronics and sensors, this book on one of the longer-established applications of these oxides is particularly welcome. *Harold H. Kung* here deals with the heterogeneous catalysis and surface chemistry of transition metal oxides, a field in which he has been engaged for many years. The amount of fundamental research that has been carried out in this area during the last two decades is so large that to cover every aspect would appear impossible. This book restricts itself to new developments in the preparation and characterization of catalysts, their reaction mechanisms and catalytic functions, and a limited selection of reactions. Thermodynamic and kinetic aspects are not treated.

Following a short introduction (Chapter 1 and part of Chapter 2), the author continues Chapter 2 with a discussion of the structures of metal oxides. Chapter 3 deals with the physical and electronic properties of metal oxides and their surfaces. The actual charges on the metal ions in the oxides can show considerable differences from those corresponding to their formal oxidation states. A discussion of the importance of the electronic structure at the surface in relation to catalysis leads into the next chapter, which highlights the role of coordinative unsaturation at the surface. *Kung* points out that most studies up to now have been concerned with the electronic structure of clean surfaces, and relatively little is known about the interaction of these surfaces with adsorbed molecules.

The following chapter discusses how the free coordination sites of the surface metal ions depend on the orientation of the surface and on the extent of dehydration. The possibilities for coordinative, dissociative, reductive or abstractive adsorption are explained, taking as examples small molecules such as H_2, CO, NO_x and alkenes.

An important characteristic for heterogeneous catalysis by metal oxides is the surface acidity due to Lewis and Brønsted sites. For adsorbed molecules on metal oxide surfaces the acidity scale for their aqueous solutions can be used. Many mixed metal oxides have strongly acidic surface sites and detailed studies of such materials are described. Methods for the qualitative and quantitative characterization of surface acidity, such as pyridine and ammonia adsorption measurements, determination of the isoelectric point, or the use of indicators, are discussed.

Chapter 6 deals with the reduction of metal oxides, an important pretreatment process for their use as catalysts. In many cases the catalytically active sites are not formed until the surface reduction is carried out. Here it is argued that this involves not only the generation of free coordination sites by reductive removal of surface oxygen atoms, but also a cooperative effect between the metallic and oxide regions of the surface. The effect of the support material on the reducibility of the surface is also discussed. However, the picture given here is not fully up-to-date, since much new knowledge has been gained on this subject in the last four years (e.g. the concept of "strong metal support interaction", SMSI).

Chapter 7 describes the characterization of the various oxygen species and their reactivities at metal oxide surfaces; regrettably, however, there is no corresponding chapter on hydrogen species.

The description of the constitutions and structures of oxide catalysts and their surfaces concludes with Chapter 8, which deals with the preparation of metal oxide catalysts. The different preparative methods are summarized at the beginning of the chapter, and the influence of the choice of method on the activity and morphology of the catalysts is clearly and concisely described. Catalysts consisting of a single component, mixed catalysts and supported catalysts are each discussed separately. However, the micro-, meso- and macroscopic pore distribution in these metal oxide catalysts, which are often of crucial importance to the activity and stability of the catalyst, are not mentioned. The remaining chapters are concerned with a number of reactions that are catalyzed by transition metal oxides.

The catalysts mainly used for the metathesis of olefins are reduced oxides of Mo, W and Re, while the isomerization of olefins is catalyzed by a wide variety of metal oxides through cationic and anionic mechanisms.

For the dehydrogenation and dehydration of alcohols the most common catalysts are oxides of Zn, Cr, Cu, Ti and Ni. The decomposition of N_2O and the reduction of NO are catalyzed by many different metal oxides. This chapter also includes accounts of some relatively old and frequently cited results on hydrogenation and H/D exchange in hydrocarbons on oxide catalysts.

Some representative selective oxidation reactions are briefly discussed from various angles in Chapters 11 and 12. Chapter 13 deals with aspects of CO and CO_2 hydrogenation reactions, ranging from the synthesis of methanol through hydrocarbons synthesis to the water-gas reaction, although there is no mention of the Fischer-Tropsch reaction.

In the final chapter photocatalytic processes, which are observed particularly on oxides of Mo, Ti and W, are again discussed. Reactions whose rates are increased by irradiating with photons of the correct energy include the catalytic oxidation of hydrocarbons, alcohols, CO and NH_3, as well as H_2/D_2 and other isotope exchange reactions.

Although the book appeared as recently as 1989, it corresponds essentially to the state of knowledge in the literature up to 1986. The inclusion of literature references in several different forms is confusing—as well as being listed at the end of each chapter, they also appear in tables with separate numbering or in alphabetical order. Methods for characterizing metal oxide surfaces, particularly surface physics and surface chemistry techniques, are not treated in enough detail, and are usually only mentioned as abbreviations (NEXAFS, HREEL etc.).

The book contains important information for specialists, but its structure makes it also entirely suitable for beginners and students as an introduction to transition metal oxide catalysts.

Wilhelm F. Maier [NB 1067 IE]
Institut für Technische Chemie
der Universität-Gesamthochschule Essen (FRG)

Calixarenes. By *C. D. Gutsche*. Edited by *J. F. Stoddart*. Royal Society of Chemistry, London 1989. xii, 222 pp., hardcover, £ 39.50.—ISBN 0-85186-916-5

This book inaugurates the "Monographs in Supramolecular Chemistry", a series edited by *J. F. Stoddart*. To deal with calixarenes the editor has chosen one of the experts in this field, Professor *C. D. Gutsche*; his fundamental and numerous contributions in the development of calixarene chemistry are widely recognized. The book is subdivided into seven chapters.

The first one describes in detail the long history (covering more than a century) of phenol-formaldehyde chemistry. It is fascinating to notice: i) how many first class scientists have been involved in this area (*Baeyer, Baekeland, Zinke, Cornforth,* to mention just a few); ii) the wealth of reaction possibilities between two rather simple reactants; iii) that the structures of many compounds isolated in the old days have been elucidated only in the last few decades (due to the introduction of improved X-ray and NMR techniques) and revealed to be of primary importance for the development of the calixarenes field.

Chapter 2 deals with the syntheses of calixarenes. The two main procedures, the one-step and the multi-step processes, are thoroughly discussed and exemplified. Syntheses of compounds closely related to calixarenes (homocalixarenes, oxacalixarenes, etc.) are also described.

The third chapter is devoted to the characterization and properties of calixarenes. The X-ray crystallography of several calix[*n*]arenes ($n = 4-6, 8$) is described and discussed. All the typical features of this class of compounds are mentioned: melting points, solubilities, dissociation constants of the OH groups, IR, UV, NMR, MS.

The large fourth chapter focusses on the conformation of calixarenes in both solid state and solution. It starts with the conformational studies of the flexible calixarenes, and goes on to describe the various methods capable of freezing some conformations, so as to obtain compounds with a definite and permanent cavity able to accept guest molecules.

Chapter 5 gives an account of the rich chemistry of calixarenes. The presence of several OH groups allows the preparation of many functionalized derivatives. Thus by appropriate chemical tailoring the simple calixarene can be transformed into a sophisticated compound containing both a binding site, the cavity, and a reactive entity able to react with a bound substrate.

Chapter 6 describes the formation of calixarene complexes. This fundamental aspect of supramolecular chemistry concerns a large variety of substrates. In the solid state, X-ray studies support the existence of complexes with many simple guests (chloroform, benzene, toluene, methanol, anisole, etc.). In some cases formation of these types of complexes is also observed in solution. Calixarenes also form complexes with metal cations, chiefly with the group I cations; extractions and transport are also described. Several water soluble sulfonatocalixarenes form very stable and highly selective complexes with $UO_2^{2\oplus}$. Complexation of organic cations is discussed in this chapter.

The last chapter concentrates on calixarene patents and industrial applications or potential uses of these compounds. At present there does not appear to be a large involvement of calixarenes in the industrial sector, but this is sure to change in the future.

The book is eloquently written and *C. D. Gutsche* has the talent to attract the reader in the calixarenes saga; he is particularly attentive to the history of this field and he has accomplished his preface purpose "by taking the reader inside the house of one small family". Thus all the major contributors in this field are acknowledged by a short biographical note and a picture. However, the most important feature of the book is its account of the state-of-the-art in calixarene chemistry. Since the *Gutsche* review in 1984 (*Topics in Current Chemistry 127*, 1) the number of groups working in this area has greatly increased; this expansion appears in the literature citations (about half of the references are form the period after 1984). The bibliography is large and the literature reviewed is up-to-date (through late 1988) and in addition many unpublished studies and observations are mentioned. The book is well illustrated with many figures (some in colour) and it contains three copious indexes (subject index; phenol-derived and resorcinol-derived calixarenes).

I warmly recommend this book as an excellent work of reference for the chemists actively engaged in this field. For scientists who are preparing to undertake research in calixarene chemistry the reading of this monograph is essential.

B. Dietrich [NB 1086 IE]
Institut de Chimie
Université Louis Pasteur
Strasbourg (France)

Computer-Aided Molecular Design. Edited by *W. G. Richards*. IBC Technical Services, London 1989. vii, 266 pp., hardcover, £ 95.00.—ISBN 1-85271-054-3

Computer-aided design of protein molecules is a topic in which there has been much interest both in industry and the academic world in the last few years. Fascinating possibilities are opened up here, both in applications ("drug design") and in basic research (aimed at understanding structure-activity relationships). While there has up to now been no

book that deals with the topic as a whole, there are already several reports on relevant symposia, although their coverage is necessarily incomplete and selective. In this book an attempt is made to treat the subject comprehensively by means of articles by various authors drawn from several "European Conferences on Computer-Aided Molecular Design" organized by IBC, However, this approach means that quite a number of the articles are several years old and do not include the latest developments.

It is stated in the preface that the book is intended both for newcomers to the field and for experienced scientists who wish to broaden the scope of their work. This is an oblique reference to the fact that the authors of the articles have adopted widely differing approaches. Whereas in some of the contributions (e.g. Chapters 1 and 2) the aim is to give an overview of a particular sub-area, others (e.g. Chapters 9 and 11) deal with specialized topics in a way which is far from comprehensive. The same applies to the literature citations in the individual articles, which in some cases extend only slightly beyond the authors' own publications, whereas in others they give a representative overview.

The book's 21 chapters do in fact cover quite large areas of the subject of molecular design. Thus Chapter 1 (*Murray-Rust*) gives a survey of the structural data banks that exist throughout the world, and in Chapter 2 the reader finds an excellent introduction to force field methods of calculation. Applications of quantum mechanical methods, especially for simulating activated enzyme complexes, are described in Chapter 3, and Chapter 4 describes applications of "free energy perturbation" methods.

Chapter 5 gives a brief sketch summarizing the "distance geometry" method, which is nowadays often used in connection with NMR spectroscopic studies of proteins to develop an initial structure model. Chapter 17 (*Clore, Gronenborn* et al.) gives a general survey of the applications of NMR spectroscopy for determining three-dimensional structures of proteins, and special aspects of this are described in the short Chapter 16 (*Wüthrich* et al.).

Chapter 6 discusses some aspects of the methods, at present only used by a relatively small number of research groups, based on the symbolic description and analysis of molecular conformations.

In Chapter 8 *Marshall* gives an excellent review of the main approaches being used in drug design, while in Chapter 10 *Müller* et al. describe an interesting alternative approach to this problem. Methodological aspects are also discussed in Chapter 12 by *Goodford*.

In the prediction of structures and in the design of proteins, which must still at present be based on already known three-dimensional structures of homologous proteins, the problems encountered are entirely different from those that apply for small molecules. In this regard the book has large gaps. Unfortunately the methods used are only described incompletely and in summary form in Chapter 13. Some aspects of displaying protein structures using fast graphics workstations are discussed in Chapter 14, and a procedure for identifying and classifying antigen sites in proteins is described in Chapter 15.

The last few articles deal with applications of molecular design in areas where the use of this method is very recent, namely in materials science (microporous materials, Chapter 18, and materials in general, Chapter 21) and catalytic research (zeolites, Chapter 19, and heterogeneous catalysis, Chapter 20).

At the end of the book, disconnected from the articles to which they belong, are 16 pages of color plates. Although this arrangement is no doubt more economical from a printing standpoint, it is rather awkward for the reader.

The articles that have not been mentioned here, Chapters 7, 9 and 11, really do not fit into the overall scheme of the book, as they describe specialized applications and software that is not generally available.

The book is certainly not the thorough treatment according to a standard pattern that this subject deserved; some of the articles are no longer fully up-to-date, some important aspects, such as the determination of molecular structures by X-ray crystallography and certain sub-areas of protein design, are not included, but on the other hand many topics are treated comprehensively by experts. Taking into account also the fact that there is virtually no other book which reviews such a wide range of molecular design topics, the present book can be recommended to everyone who wishes to learn about this systematic modern method for developing substances with new properties.

Dietmar Schomburg [NB 1065 IE]
Gesellschaft für Biotechnologische Forschung,
Braunschweig (FRG)

Registered names, trademarks, etc. used in this journal, even when not marked as such, are not to be considered unprotected by law.

© VCH Verlagsgesellschaft mbH, D-6940 Weinheim, 1990. – Printed in the Federal Republic of Germany by Konrad Triltsch Druck- und Verlagsanstalt Würzburg.

All rights reserved (including those of translation into foreign languages). No part of this issue may be reproduced in any form – by photoprint, microfilm, or any other means – nor transmitted or translated into a machine language without written permission from the publishers. Only single copies of contributions, or parts thereof, may be made for personal use. This journal was carefully produced in all its parts. Nevertheless, authors, editors and publisher do not warrant the information contained therein to be free of errors. Readers are advised to keep in mind that statements, data, illustrations, procedural details or other items may inadvertently be inaccurate.

Valid for users in the USA: The appearance of the code at the bottom of the first page of an article (serial) indicates the copyright owner's consent that copies of the article may be made for personal or internal use, or for the personal or internal use of specific clients. This consent is given on the condition, however, that the copier pay stated per-copy fee through the Copyright Clearance Center, Inc. (CCC), for copying beyond that permitted by Sections 107 or 108 of the U.S. Copyright Law. This consent does not extend to other kinds of copying, such as copying, for general distribution, for advertising or promotional purposes, for creating new collective works, or for resale. For copying from back volumes of this journal see 'Permissions to Photo-Copy: Publisher's Fee List' of the CCC.

Editorial office: Postfach 10 11 61, D-6490 Weinheim, Federal Republic of Germany, Telephone (06201) 60 22 55, Telex 465 516 vchwh d, Telefax (06201) 602 328.

Editor: *Peter Gölitz*

Associate editors: *D. I. Loewus, A. Stimson.* **Editorial assistant:** *E. Schweikart*

Publishers: VCH Verlagsgesellschaft mbH. (Managing Director: *Hans Dirk Köhler*), Pappelallee 3, D-6940 Weinheim, Federal Republic of Germany.

Advertising office (Advertising Manager *R. J. Roth*): Postfach 10 11 61, D-6940 Weinheim, Federal Republic of Germany, Telephone (0 62 01) 60 61 30, Telex 4 67 155, Telefax (0 62 01) 606 156.

ANGEWANDTE CHEMIE
International Edition in English
Volume 29 · Number 10
October 1990
Pages 1077–1176

Complexes of Carbon Monoxide and Its Relatives: An Organometallic Family Celebrates Its Birthday**

By Helmut Werner*

Dedicated to Professor Max Schmidt on the occasion of his 65th birthday

Nickel tetracarbonyl was discovered one hundred years ago. Its hundredth birthday deserves to be celebrated not only by metal carbonyl chemists. The pioneering work of *Mond, Langer*, and *Quincke* has led to developments which, particularly in the last 30 years, have had consequences in many areas outside that of metal carbonyl chemistry. The parent ligand of the family, CO, has been joined by a series of relatives which are isoelectronic with it and which in some cases are even more effective as π acceptors. These are in the main extremely reactive molecules such as CS, CNH, and $C{=}CH_2$, which, though very short-lived in the free state, form very stable complexes with transition metals. This article documents the family relationships by structure and reactivity comparisons; attention is also drawn to the synthetic potential of the metal carbonyl analogues, which is still virtually untapped. The final section ventures a look towards the next 100 years, which promise to be just as exciting as the past century.

1. Introduction

An organometallic family celebrates its hundredth birthday this year. In August 1890 an article by *Ludwig Mond, Carl Langer*, and *Friedrich Quincke* appeared in the *Journal of the Chemical Society* with the title "Action of Carbon Monoxide on Nickel"; in this paper the authors described the synthesis of nickel tetracarbonyl.[1] Although this compound, isolated as a colorless, clear, extremely toxic liquid, was not the first metal compound containing carbonyl ligands—the first, $[Pt(CO)_2Cl_2]$, had already been synthesized by *Schützenberger* in 1868[2]—its remarkable properties and its industrial applicability to the preparation of ultrapure nickel were immediately recognized by *Mond*. This serendipitous discovery[3] started a development which reached its first peak in the work of *Walter Hieber*[4] and which, during the last 40 years, has played a very important role in the often-cited "renaissance of inorganic chemistry".

This review will not focus, however, on the chemistry of metal carbonyls, which remains just as fascinating and as topical as it has always been (see Fig. 1). Nickel tetracarbonyl and other stable binary carbonyls, some of them already described by *Ludwig Mond*,[3] have been joined in recent years by very labile carbonyls such as $[Cu_2(CO)_6]$, $[Ag_2(CO)_6]$, $[Pt(CO)_4]$, and $[Ti(CO)_6]$.[5] Thanks in great part to the pioneering work by *Chini, Longoni, Dahl* et al.[6] and *Lewis* et al.,[7] carbonylmetal clusters have achieved a degree of importance undreamed of twenty years ago, in particular as cage frameworks for both smaller and larger metal and nonmetal atoms.[8] Moreover, carbonyl metalates have found an important place in synthetic chemistry—not only because of the importance of *Collman*'s reagent, $Na_2[Fe(CO)_4]$.[9] There are still unmarked areas on the metal carbonyl map, however, as shown, for example, by the fact that the synthesis of salts of the hexacarbonyltitanate dianion, $[Ti(CO)_6]^{2\ominus}$, the first stable binary carbonyl compound

[*] Prof. Dr. H. Werner
Institut für Anorganische Chemie der Universität
Am Hubland, D-8700 Würzburg (FRG)

[**] An extended version of a plenary lecture presented at the IVth European Symposium on Inorganic Chemistry, 12–15 September 1988, Freiburg (FRG).

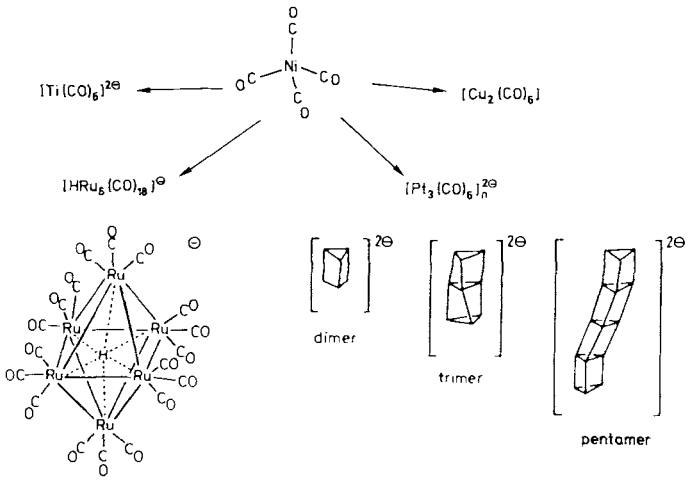

Fig. 1. $[Ni(CO)_4]$ and other, much later synthesized metal carbonyls.

of titanium, was described by *Ellis* only in 1988, that is, almost 100 years after the discovery of nickel tetracarbonyl.[10]

The metal carbonyls have meanwhile been joined by "relatives", which are the subject of this article. Remarkably, their history is almost as long as that of their "ancestor". Soon after the publication of *Mond*'s results,[11] *Sabatier* et al. in Toulouse attempted to bond NO, NO_2, C_2H_4, and C_2H_2 to nickel and similar metals; although they were unsuccessful, their attempts did in fact lead to the discovery that nickel could be used as a catalyst in hydrogenation.[11] There was then a gap of 75 years before *Wilke* et al. were successful in preparing $[Ni(C_2H_4)_3]$,[12] a compound similar to $[Ni(CO)_4]$ although structurally different. It was then used in the synthesis of further nickel(0) complexes, some of which are catalytically extremely active.[13]

Here, however, ethylene will not be regarded as a relative of carbon monoxide. Although there are indeed close relationships between metal carbonyls such as $[Ni(CO)_4]$ and compounds such as $[Ni(C_2H_4)_3]$,[12] $[Ni(PCl_3)_4]$,[14] $[Ni(PPh_3)_4]$,[15] and $K_4[Ni(C\equiv CH)_4]$,[16] only those molecules or fragments that are valence-isoelectronic with CO will be considered relatives. Such ligands resemble CO not only formally but also in their coordination properties and thus form a family with it. For example, the bonding of the parent molecule to one or several metal atoms can be either end-on or via μ_2 or μ_3 bridges (Fig. 2). This is also true for the relatives.

The family of CO-like molecules has two separate branches: the first includes the molecules formed from CO by substitution of the *carbon atom* by a homologous element of the fourth main group or by an isoelectronic ion ($B^{\ominus}$, $N^{\oplus}$). The second contains the molecules derived from CO by replacing

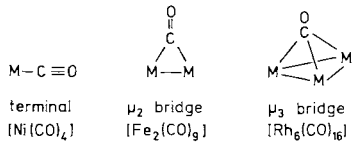

Fig. 2. Coordination possibilities for CO.

the *oxygen atom* by S, Se, or Te or by an isoelectronic fragment such as NH or CH_2. The corresponding classes of compounds will not be discussed in detail; instead, this article will make clear the relationships within the family as well as the particular features of the various members of the family.

2. The Relatives of the Type [X≡O]: Known and Unknown Examples

The closest relative of CO, at least from the point of view of the preparative chemist dealing with this type of molecule, is surely SiO (Scheme 1). This molecule is formed when SiO_2 is heated with Si under vacuum at 1250 °C and can be detected both in the gas phase and at low temperatures in a suitable matrix. The Si–O bond length of 1.51 Å agrees well with the theoretical value of 1.50 Å and shows that SiO is isosteric with CO.[17]

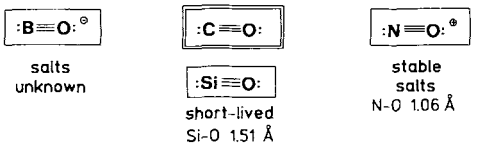

Scheme 1.

Helmut Werner was born in 1934 in Mühlhausen (Thüringen). He studied chemistry at Jena, where he received his "Diplom" under Franz Hein, and at the Technische Hochschule in Munich, where he received his doctorate under E. O. Fischer. After postdoctoral research under J. H. Richards at the California Institute of Technology in Pasadena (1962–1963), he completed his "Habilitation" at the end of 1966 on kinetic investigations of substitution reactions of organometallic complexes. In 1968, he began work in inorganic chemistry at the Universität Zürich, where he became a full professor in 1970. At the end of 1975, he moved to the Universität Würzburg. Helmut Werner has received numerous prizes and honors, including the Alfred-Stock-Gedächtnispreis of the German Chemical Society; since 1988, he has been a full member of the Deutsche Akademie der Naturforscher Leopoldina.

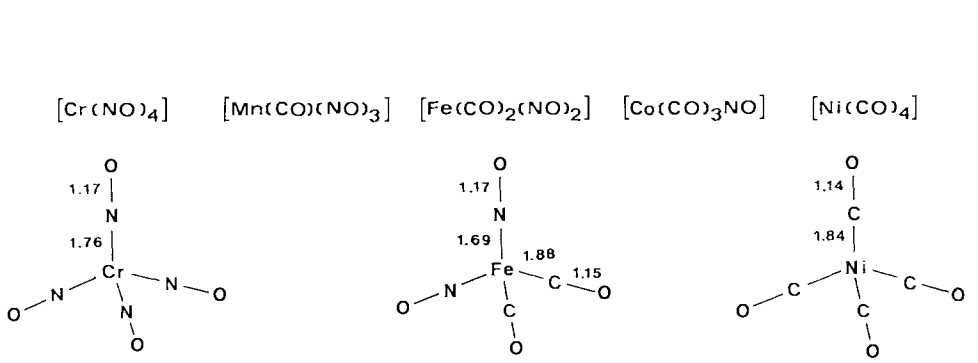

Fig. 3. The $[M(CO)_n(NO)_{4-n}]$ family (n = 0–4).

Metal complexes with SiO as a ligand are still unknown. Although it has been possible during the last 30 years, starting with the synthesis of the first metal cyclobutadiene complexes by *Criegee* et al.[18] and *Hübel* et al.,[19] to bind many molecules that are extremely short-lived in the free state ("nonexistent" molecules) within the coordination sphere of a metal and thus to investigate them, corresponding attempts to isolate or detect complexes of the type $[M(SiO)L_n]$ have so far been unsuccessful. Even matrix studies have provided no evidence for their existence.[20]

The situation with regard to the anion $BO^{\ominus}$ is similar. The protonated molecule HBO has been detected experimentally;[21] however, salts derived from it such as MBO (M = Na, K, etc.) still do not exist. *Rosmus*[22] recently showed from SCF calculations that the potential energy functions of KBO and KCN are very similar, so that the molecule would probably be quasi-linear. This structural prediction also applies to methyl boroxide, which is formally derived from $BO^{\ominus}$ by methylation; this molecule was first prepared as an intermediate by *Paetzold* et al.[23] and was characterized very recently by its PE spectrum.[24] In view of the vast scope of the chemistry of metal carbene complexes $[M(=CXY)L_n]$ it seems remarkable that only very little is known about comparable (isoelectronic or isosteric) compounds of the type $[M'(=BXY)L_n]$.[25]

The picture becomes completely different on moving to the right of CO, that is, to $NO^{\oplus}$. Not only are many salts of this cation known (the N–O distance of 1.06 Å corresponds exactly to that of a triple bond, as in CO) but a great deal is also known about its coordination properties.[26] In fact, the first nitrosyl complex, the dication $[Fe(NO)(H_2O)_5]^{2\oplus}$, was discovered in 1790 by *Priestley*! Although carbonyl and nitrosyl metal compounds have many similarities, very little is known about species of the type $[M(NO)_n]$ or about the corresponding cations or anions. Only $[Cr(NO)_4]$ has been characterized: *Herberhold* and *Razavi* obtained this complex as a brown, low-melting solid by photolysis of $[Cr(CO)_6]$ in an NO atmosphere.[27] The species $[Co(NO)_3]$ has also been reported;[28] however, clear evidence for the existence of this compound is still wanting. Binary metal nitrosyl clusters are still an unknown class of substances; they would be of general interest in connection with the bonding of NO at metal surfaces.

Mixed carbonyl-nitrosyl metal complexes are better known. As early as 1922, *Robert Mond* (the son of *Ludwig Mond*) et al. described the compound $[Co(CO)_3(NO)]$;[29] *Hieber* et al. and later *Lewis* et al. prepared the isoelectronic molecules $[Fe(CO)_2(NO)_2]$[30] and $[Mn(CO)(NO)_3]$.[31] The formal analogy between such compounds, which was later confirmed on a structural basis (Fig. 3), prompted *Seel* in 1942 to propose the "nitrosyl shift relationship",[32] which is still of importance today as a heuristic principle. According to this postulate, it is possible to replace Ni in $[Ni(CO)_4]$ by Co when one of the CO ligands (two-electron donor) is simultaneously replaced by the three-electron donor NO. The metal atoms in the ML_4 series (Fig. 3) thus act as "pseudonickel atoms". Only one analogue of iron pentacarbonyl, the manganese complex $[Mn(CO)_4(NO)]$,[33] has been described; the remaining members of the ML_5 series, $[Cr(CO)_3(NO)_2]$, $[V(CO)_2(NO)_3]$, and $[Ti(CO)(NO)_4]$ still remain to be discovered.

$NO^{\oplus}$ is a stronger π acceptor than CO, as can be seen both from the stretching vibration frequencies in the IR spectra and from the bond distances determined by *Hedberg* and co-workers[34] (see Fig. 3). In particular, the differences in the Fe–C and Fe–N bond distances in the compound $[Fe(CO)_2(NO)_2]$ confirm that the nitrosyl ligands are more strongly bound; this is also documented by the easier exchange of CO (e.g., for PR_3) in substitution reactions of carbonyl–nitrosyl metal complexes.

Although, as already mentioned, binary metal nitrosyl *clusters* do not yet exist, bi- and polynuclear compounds with NO as a ligand are already known;[26] they show the same possibilities for coordination of NO (or, to be more precise, $NO^{\oplus}$) as for CO in the corresponding metal carbonyl complexes (see Fig. 4). When cyclopentadienyl is used

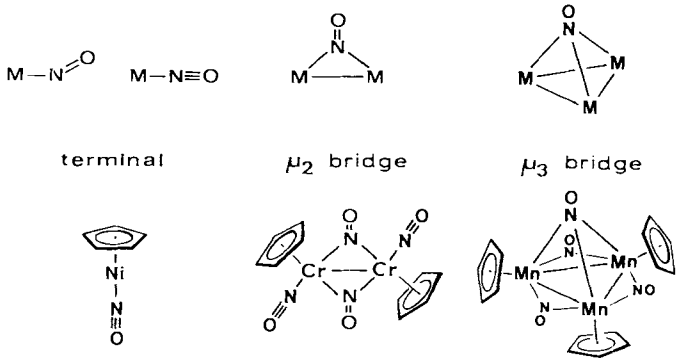

Fig. 4. Coordination possibilities for NO.

as the coligand, an end-on (linear) M–N–O arrangement is found in [CpNi(NO)],[35] whereas μ_2 and μ_3 bridges exist in $[Cp_2(NO)_2Cr_2(\mu\text{-}NO)_2]$[36] and $[Cp_3Mn_3(\mu_2\text{-}NO)_3(\mu_3\text{-}NO)]$,[37] respectively. The structural relationship with CO is extremely obvious here.

Until a few years ago almost nothing was known about analogies in reaction behavior between CO and NO in the coordination sphere of a metal. In particular, it was unclear whether one of the most typical reactions of coordinated CO, insertion into a M–C bond in the presence of an alkyl or aryl ligand (which is also the key step in important catalytic processes such as the oxo process or the Monsanto acetic acid process[38]) is also possible for NO. *Bergman* et al.[39] were the first to show that an alkyl(nitrosyl)metal complex, formed in the same way as an alkyl(carbonyl) compound by alkylation of the corresponding anion, reacts with PPh_3 to give a nitrosoalkane derivative via N–C bond formation (Fig. 5). The coordination number of the metal remains unchanged. In a very similar manner the same group has synthesized and structurally characterized the complex $[C_5Me_5Ru(N(O)Et)(Ph)PMe_2Ph]$ starting from PMe_2Ph and $[C_5Me_5Ru(NO)(Et)Ph]$.[40] On the basis of mechanistic studies,[39b] there is no doubt that the "NO insertion" is in fact an alkyl migration to the nitrosyl ligand, as is the case for the "CO insertion".[41] *Legzdins* et al.[42] and *Vollhardt* et al.[43] have shown very recently that this process occurs not only with neutral donors such as tertiary phosphanes but also with $NO^{\oplus}$ itself.

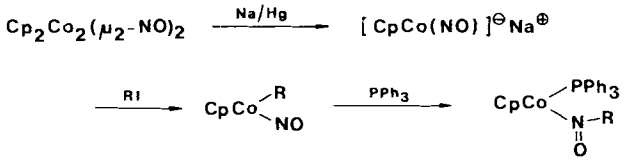

Fig. 5. NO insertion. R = alkyl.

3. The CO Homologues CS, CSe, and CTe: Unstable Molecules with a Rich Coordination Chemistry

Whereas CO and CO_2 are both thermodynamically stable, for the homologous sulfur compounds this is only true for CS_2. The molecule CS, which can be formed from CS_2 by photolysis, thermolysis, or cold electrical discharge, is stable only below −160 °C (Scheme 2) and polymerizes very rapidly at higher temperatures;[44] this process can occur in an explosive manner. In spite of its extreme reactivity, the spectroscopic data for CS are known very precisely, and clear evidence on the mechanism of its formation from CS_2 is available.[44c] Much less is known about CSe,[45] and practically nothing about CTe; the latter has so far resisted all attempts to detect it, so that it still belongs to the group of "nonexistent" diatomic molecules.

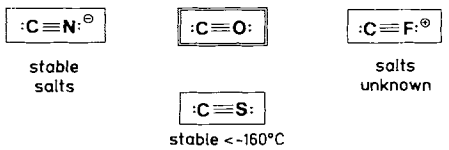

Scheme 2.

The extreme tendency of CS to polymerize makes it understandable that so far almost all attempts to synthesize thiocarbonyl metal complexes from *free* CS and a metal or metal compound have been unsuccessful. Only the cocondensation of CS with nickel atoms in an argon matrix at 10 K gives a product whose IR spectrum indicates it to be $[Ni(CS)_4]$.[46] In contrast to $[Ni(CO)_4]$, it is unstable at room temperature, decomposing to give a black solid which is difficult to characterize.

In the case of iron and chromium, whose carbonyl complexes $[Fe(CO)_5]$ and $[Cr(CO)_6]$ are much more stable than $[Ni(CO)_4]$, the corresponding binary metal thiocarbonyls $[M(CS)_n]$ are still unknown. Mixed carbonyl-thiocarbonyl complexes are however known (Fig. 6). In the 1970s *Angelici* et al. and *Butler* et al. synthesized the $[Cr(CO)_6]$ analogues $[Cr(CO)_5(CS)]$ and $[Cr(CO)_5(CSe)]$,[47] and somewhat later *Petz* reported the preparation of the $[Fe(CO)_5]$ analogue $[Fe(CO)_4(CS)]$.[48] These complexes, which are stable under normal conditions, are volatile and can even be handled in air; their other properties are also very similar to those of the parent compounds $[M(CO)_n]$.

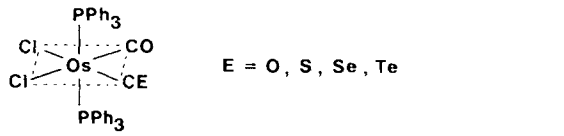

Fig. 6. Metal carbonyls and mixed CO–CE metal complexes.

The characterization of a complete series of the general composition $[M(CE)L_n]$ with E = O, S, Se, and Te was carried out by *Roper* and co-workers, who obtained the complexes $[OsCl_2(CE)(CO)(PPh_3)_2]$ by reaction of $[OsCl_2(CCl_2)(CO)(PPh_3)_2]$ with $EH^{\ominus}$.[49] Exact structural data are available for all the members of the series; $[OsCl_2(CTe)(CO)(PPh_3)_2]$ was the first metal tellurocarbonyl compound to be described.

Since free CS, CSe, and CTe are not available as starting materials, it is necessary to find suitable precursors for the synthesis of complexes with carbon monochalcogenides as ligands. As is shown in Figures 7–9 for CS, three routes for the preparation of compounds of the type $[M(CS)L_n]$ have so far proved generally applicable.[50] In each case, the thiocarbonyl ligand is generated *at the metal* and remains without exception strongly bonded to it.

The oldest and with hindsight most obvious synthetic method starts from CS_2; its discovery is, so to speak, a "by-product" of the trailblazing work of the *Wilkinson* school on the catalytic abilities of $[RhCl(PPh_3)_3]$. When studying the behavior of this compound in various solvents, *Baird* and *Wilkinson* noticed that it reacted with CS_2 to give the square-planar complex *trans*-$[RhCl(CS)(PPh_3)_2]$ via an unstable intermediate with a presumably π-bonded and a σ-bonded CS_2 ligand.[51] In a similar manner (see Fig. 7) *Butler* and co-workers were able several years later to obtain the manganese thiocarbonyl compound $[CpMn(CO)_2(CS)]$, which is

homologous to $[CpMn(CO)_3]$, and also to isolate the intermediate $[CpMn(CO)_2(\eta^2\text{-}CS_2)]$.[52] It reacts with PPh_3 to give $SPPh_3$ and $[CpMn(CO)_2(CS)]$; presumably, the phosphane attacks the sulfur atom bound to the metal and not the exocyclic sulfur atom. The same principle has been applied to prepare further thiocarbonyl and selenocarbonyl complexes (the latter starting from CSe_2),[50] whereby the isolation of $[CpMn(CO)(CS)_2]$ as the first compound with *two* CS ligands deserves particular mention.[52]

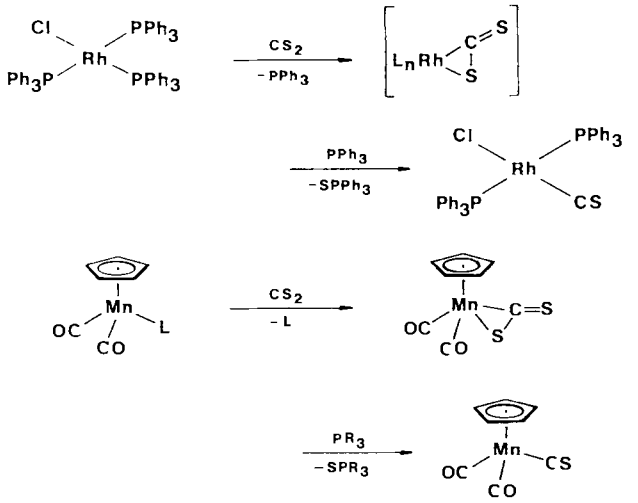

Fig. 7. Synthesis of metal thiocarbonyl complexes from CS_2.

The second likely source for thiocarbonyl ligands is thiophosgene. As shown in Figure 8, its reaction with $[Fe(CO)_4]^{2\ominus}$ and $[M_2(CO)_{10}]^{2\ominus}$ (M = Cr, Mo, W) gives the complexes $[Fe(CO)_4(CS)]$ and $[M(CO)_5(CS)]$, although the yields are not particularly good.[47a, 48] Another synthesis of $[Cr(CO)_5(CS)]$ starts from the metal arene compounds $[(C_6H_5R)Cr(CO)_2(CS)]$ (R = H, CO_2Me), which can be formed from $[(C_6H_5R)Cr(CO)_2(thf)]$ and CS_2; the aromatic ring ligand is then displaced by CO.[47b]

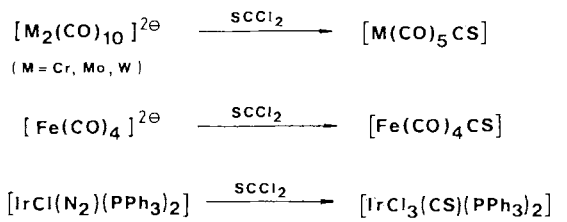

Fig. 8. Synthesis of metal thiocarbonyl complexes from $SCCl_2$.

$SCCl_2$ reacts with square-planar rhodium(I) and iridium(I) complexes such as $[RhCl(PPh_3)_3]$ and $[IrCl(N_2)(PPh_3)_2]$ via oxidative addition to give the corresponding thiocarbonylrhodium(III) and -iridium(III) compounds.[53] The presumed intermediate contains the unit M[C(=S)Cl](Cl), which forms the stable final product via a 1,2 shift of chlorine from carbon to the metal. Treatment of $[Ru_3(CO)_{12}]$ with thiophosgene followed by fragmentation of the cluster results in a similar reaction, leading to $[RuCl_2(CS)(CO)_3]$.[54]

A third method for the synthesis of CS complexes starts from heteroallenes such as CSSe (Fig. 9). In the course of our initial work on the coordination chemistry of CS_2, we found that the compounds $[CpM(PMe_3)(\eta^2\text{-}CS_2)]$ (M = Co, Rh) are formed readily and in good yields starting from $[CpCo(PMe_3)_2]$ and $[CpRh(PMe_3)(C_2H_4)]$; however, the former do not undergo sulfur abstraction with PR_3.[55] At the same time we observed that the reaction of $[CpCo(PMe_3)_2]$ with COS gives the carbonyl complex $[CpCo(PMe_3)(CO)]$, so that we expected that reaction with CSSe would form the thiocarbonyl compound $[CpCo(PMe_3)(CS)]$. This is in fact the case, although, depending on the reaction conditions, its formation may be accompanied by that of the corresponding thiocarbonylselenide complex $[CpCo(PMe_3)(\eta^2\text{-}CSSe)]$.[56] The latter reacts quantitatively with PPh_3 to give $[CpCo(PMe_3)(CS)]$. In the case of rhodium, the conversion of $[Rh](C_2H_4)$ to $[Rh](\eta^2\text{-}CSSe)$ and [Rh](CS), where [Rh] = $[CpRh(PMe_3)]$, can be readily carried out stepwise; here, as for the case where cobalt is the central atom, the reaction of $[Rh](\eta^2\text{-}CSSe)$ with PPh_3 leads solely to [Rh](CS) and not to [Rh](CSe).[56]

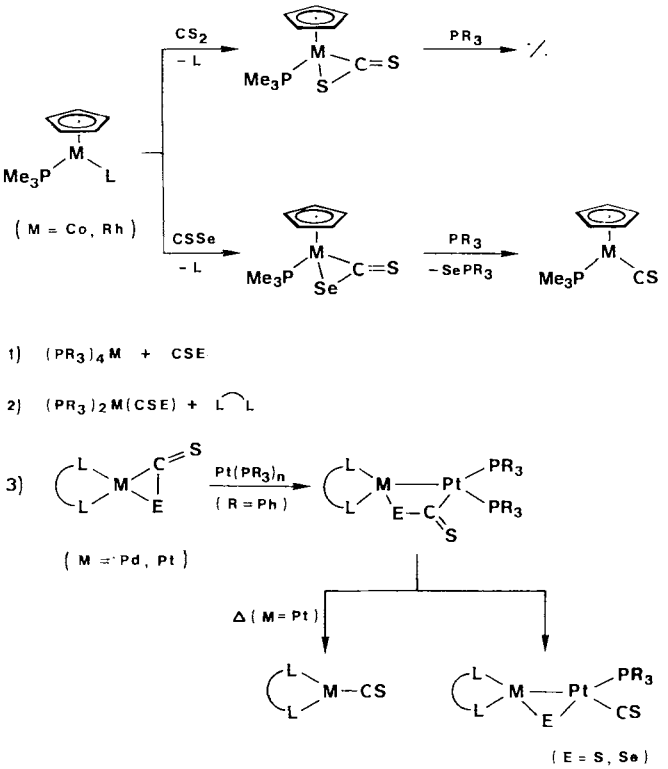

Fig. 9. Synthesis of metal thiocarbonyl complexes from heteroallenes.

A fragmentation of coordinated CS_2 to give CS and S or of CSSe to give CS and Se can be caused not only by PR_3 but also by nucleophilic metal complexes. In earlier studies we had already observed that the cobalt compound $[CpCo(PMe_3)(\eta^2\text{-}CS_2)]$ reacts with the metal base $[CpCo(PMe_3)_2]$ to give the trinuclear cluster $[(CpCo)_3(\mu_3\text{-}CS)(\mu_3\text{-}S)]$ in almost quantitative yield.[57] A similar metal-initiated cleavage of CS_2 or CSSe takes place when either $[Pt(PPh_3)_4]$ or $[Pt(C_2H_4)(PPh_3)_2]$ is allowed to react with the chelate phosphane complexes [(L-L)M(η^2-CSE)] (M = Pd, Pt; E = S,

Se; L-L = $Ph_2PC_2H_4PPh_2$, o-$C_6H_4(CH_2PPh_2)_2$).[58] The products (Fig. 9) are the binuclear sulfido- or selenido-bridged thiocarbonyl compounds [(L-L)M(μ-E)Pt(CS)-(PPh_3)]; it seems likely that the complexes [(L-L)M(μ-CSE)Pt(PPh_3)$_2$] are formed as intermediates. In the case where L-L = o-$C_6H_4(CH_2PPh_2)_2$, M = Pd or Pt, and E = S or Se, products with this composition can be isolated.[58b] Surprisingly, the addition of the ligands $Ph_2PC_2H_4PPh_2$ or o-$C_6H_4(CH_2PPh_2)_2$ to the complexes [(L-L)M(μ-E)Pt(CS)-(PPh_3)] leads not only to the displacement of PPh_3 but also to a recombination of the fragments CS and E to give CSE, so that the final product is an unsymmetrical binuclear complex of the type [(L-L)M(μ-CSE)Pt(L-L)] with two chelating phosphane ligands. There are no other known examples of such a process (fragmentation of a triatomic molecule and its re-formation under the influence of the same metal). The thermolysis of [$(PPh_3)_2$Pt(μ-CS_2)Pt(PPh_3)$_2$] and [(L-L)Pt(μ-CS_2)Pt(PPh_3)$_2$] (L-L = o-$C_6H_4(CH_2PPh_2)_2$) leads to the formation of the compounds [Pt(CS)(PPh_3)$_2$] and [Pt(CS)(L-L)]; these are the first *mono*nuclear thiocarbonyl complexes of platinum(0).[59]

There are only small differences between the modes of coordination adopted by CS and CO. As shown in Figure 10,

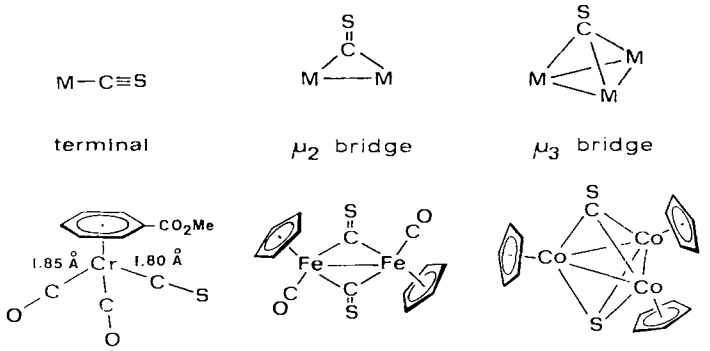

Fig. 10. Coordination possibilities for CS.

the thiocarbonyl ligand can be coordinated both end-on or in a bridging manner (between two or three metal atoms); it should be noted that, when CO and CS are both present in the same molecule (as, for example, in [$Cp_2Fe(CO)_2$-$(CS)_2$][60]), the formation of CS rather than CO bridges is observed.

CS is a stronger π acceptor than CO; this is shown not only by MO calculations[61] but also by the structural data of mixed carbonyl thiocarbonyl metal complexes. For example, the Cr–CS distance in [($C_6H_5CO_2Me$)Cr($CO)_2$(CS)] is shorter by 0.05 Å than the Cr–CO distance (mean value)[62], and a similar difference is observed in the cation [Ir-($CO)_2$(CS)(PPh_3)$_2$]$^{\oplus}$ (as the PF_6 salt).[63] This behavior indicates a stronger synergistic interaction between the metal and the thiocarbonyl ligand. Interestingly, the sulfur atom is clearly nucleophilic in all coordination modes of CS; it can not only undergo alkylation but also add 16-electron fragments such as [$Cr(CO)_5$] or [$CpMn(CO)_2$]. The resulting complexes have a bent arrangement for $(M)_nC$-S-M′, the exact structure of which has been determined for both n = 1 (e.g., in [(C_6H_5Me)Cr($CO)_2$CSCr($CO)_5$][64]) and n = 2 and 3 (e.g., in [Cp(PMe_3)Co(μ-CO){μ-CSMn($CO)_2$Cp}Mn(CO)-Cp][65] and [($CpCo)_3$(μ_3-S){μ_3-CSCr($CO)_5$}], respectively)[57] by X-ray structural analyses. Thus, CS is considerably superior to the parent molecule CO with respect to this additional bonding type and offers a synthetic potential for heterometal multinuclear complexes which has so far hardly been used.

4. Isocyanides as Ligands: CO Analogues with Advantages and Disadvantages

The molecule CNH is strictly isoelectronic with CO; like CS, it is extremely labile in the free state, isomerizing very rapidly to HCN.[66] However, it can be readily generated in the coordination sphere of a metal, where it is stable (a further analogy to CS). The formation of a CNH ligand can be carried out most simply by protonation of anionic cyano complexes; for example, treatment of [$M(CO)_5(CN)$]$^{\ominus}$ with HCl or [(C_5H_4R)Mn($CO)_2$(CN)]$^{\ominus}$ with H_3PO_4: in this manner, the neutral compounds [$M(CO)_5$(CNH)] (M = Cr, Mo, W)[67] and [(C_5H_4R)Mn($CO)_2$(CNH)] (R = H, Me)[68] are formed. Both the spectroscopic properties and the behavior of the complexes [$M(CO)_5$(CNH)] (M = Cr, W) leave no doubt that the M–CNH bond is considerably stronger than the M–NCH bond in the corresponding isomers [$M(CO)_5$(NCH)], which are formed by allowing [$M(CO)_5$(thf)] to react with HCN.[67b]

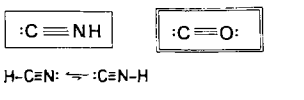

Scheme 3.

Alkyl and aryl isocyanides, which can be prepared in various ways, are much more stable than the parent compound CNH.[69, 70] They are generally stronger σ donors than CO; as a consequence, numerous binary ("homoleptic") *cationic* complexes can be isolated as the corresponding salts (see Table 1): examples are [$M(CNR)_7$]$^{2\oplus}$ (M = Cr, Mo, W), [$Fe(CNR)_6$]$^{2\oplus}$, [$Ni(CNR)_4$]$^{2\oplus}$, [$Ag(CNR)_2$]$^{\oplus}$, and [$Co_2(CNR)_{10}$]$^{4\oplus}$.[71] Comparable carbonyl metal compounds are not yet known.

Table 1. Metal isocyanide complexes of 3d transition metals.

[$Cr(CNR)_6$]	[$Fe(CNR)_5$]	[$Co_2(CNR)_8$]	[$Ni(CNR)_4$]	[$Cu(CNR)_4$]$^{\oplus}$
[$Cr(CNR)_6$]$^{\oplus}$	[$Fe_2(CNR)_9$]	[$Co(CNR)_5$]$^{\oplus}$	[$Ni_4(CNR)_7$]	
[$Cr(CNR)_6$]$^{2\oplus}$	[$Fe(CNR)_6$]$^{2\oplus}$	[$Co(CNR)_5$]$^{2\oplus}$	[$Ni(CNR)_4$]$^{2\oplus}$	
[$Cr(CNR)_7$]$^{2\oplus}$		[$Co_2(CNR)_{10}$]$^{4\oplus}$		

Like CO, isocyanides (CNR) are good π acceptors; not only have various metal(0) complexes of the type [$M(CNR)_n$] (n = 6, M = Cr, Mo, W; n = 5, M = Fe, Ru, Os; n = 4, M = Ni) been synthesized,[71] but also very recently the first *anionic* complex, [$Co(CNR)_4$]$^{\ominus}$ (R = 2,6-$Me_2C_6H_3$)[72] (i.e., an analogue of [$Co(CO)_4$]$^{\ominus}$). Binuclear complexes such as [$Co_2(CNR)_8$] and [$Fe_2(CNR)_9$], which resemble the corre-

sponding metal carbonyls not only in molecular formula but also structurally, are also known.[71] As a historical reminiscence, we may mention that the most direct relatives in this series to the parent $Ni(CO)_4$), the compounds $[Ni(CNR)_4]$ ($R = C_6H_5$, p-$EtOC_6H_4$), were obtained exactly 40 years ago in the same city (Munich) by two groups working fully independently of one another, in both cases via ligand substitution reactions starting from $[Ni(CO)_4]$.[73]

$$[Ni(CO)_4] \xrightarrow[-4\,CO]{4\,CNR} [Ni(CNR)_4]$$

In the case of L = CNR, however, this synthetic method (formation of $[ML_n]$ from $[M(CO)_n]$ and L) is extremely unusual and can only be used in the absence of a catalyst when a labile starting material is available. Under purely thermal conditions, the reaction of metal hexacarbonyls, $[M(CO)_6]$ (M = Cr, Mo, W), and of iron pentacarbonyl, $[Fe(CO)_5]$, with isocyanides often leads only to monosubstitution even at higher temperatures and with long reaction times.[71e] The use of phase-transfer catalysts can improve the situation.[74] However, it is even more favorable to carry out the reaction of $[M(CO)_6]$ or $[Fe(CO)_5]$ with CNR in the presence of a *heterogeneous* catalyst such as $CoCl_2$, activated carbon, or metallic platinum on an oxide support. This method, developed by *Coville* and co-workers,[75] has made it possible to replace *all* the CO ligands in the otherwise inert $Fe(CO)_5$ by CNR and also to substitute more than half of the carbonyl groups in metal clusters such as $[Ir_4(CO)_{12}]$. Apart from metal carbonyls, arene and cyclodi- and -triene complexes have been used as starting materials for reactions with isocyanides; the synthesis of $[Cr(CNR)_6]$ from bis(naphthalene)chromium and CNR ($R = n$Bu, C_6H_{11}) is a good example.[76]

$$[Cr(\eta^6\text{-}C_{10}H_8)_2] \xrightarrow[-2\,C_{10}H_8]{6\,CNR} [Cr(CNR)_6]$$

The coordination properties of CO and isocyanides are similar. The most generally encountered bonding situations are compared in Figure 11, top; it should be mentioned that,

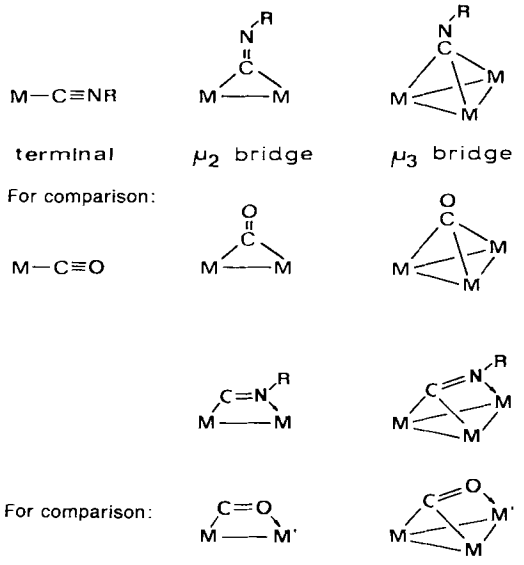

Fig. 11. Coordination possibilities for CNR.

in some cases, terminally bonded isocyanide ligands can be bent at the N atom.[71]

The ligand CNR can also bridge two or three metal atoms, in the manner shown in Figure 11, bottom. A good example of the μ_2-C,N form is the nickel cluster $[Ni_4(CNtBu)_7]$ described by *Muetterties* et al.[77] A comparable interaction of CO with two or three metallic centers has been discussed for the adsorption of carbon monoxide at surfaces;[78] the possible threefold bridging seems particularly likely when M is a transition metal and M′ an electropositive metal such as K, Mg, or Al.

CO and CNR are also closely analogous in their reactions. Both isocyanide and carbonyl ligands are able to undergo insertion into M–C σ bonds; this process can take place either spontaneously or in the presence of a Lewis base L (see Fig. 12). Whether the acyl or imidoyl residue formed is bonded in a mono- or bidentate manner depends ultimately on the electronic configuration and the required coordination geometry of the metal.

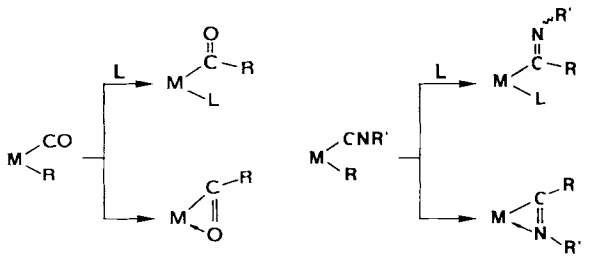

Fig. 12. Insertion of CO and CNR into M–C σ bonds.

There is one interesting reactivity difference between structurally analogous acyl and imidoylcobalt complexes of the half-sandwich type formed by CO and CNR insertion, respectively (see Fig. 13). While the compound [CpCoMe(CO)(PMe_3)]I, obtained from [CpCo(CO)(PMe_3)] and methyl iodide in toluene, undergoes only isomerization to [CpCo{C(O)Me}(PMe_3)I] when acetone is added,[79] a cycloaddition reaction takes place when the corresponding methyl isocyanide complex is dissolved in this solvent. A five-membered metallaheterocycle is formed, probably via an intermediate with the partial structure Co-C(Me) = NCH_3; the final product has been characterized by an X-ray structural analysis.[80] Furthermore, [3 + 2] cycloaddition reactions occur with acetaldehyde and benzaldehyde as well as with a number of nitriles R′CN (R′ = Me, Ph, *cyclo*-C_3H_5, $CH=CH_2$, $CMe=CH_2$, $CH=CHMe$, NH_2, NMe_2, SMe); the five-membered ring of the type [Co]-$C(CH_3)$=NR-CR′=N shown in Figure 13 is thermodynamically unstable and isomerizes to [Co]-$C(=CH_2)$-NR=CR′-NH, independent of the nature of the group R′.[81] With CS_2 it is even possible to realize a *double* cycloaddition, leading to the dimetallaspiroheterocycle depicted in Figure 13; this compound has been structurally characterized.[82] The difference in behavior between coordinated CO and CNR documented by this and other results[83] is probably due to the basicity of the CNR nitrogen atom being higher than that of the oxygen in CO; moreover, the building block [M]-C(Me) = NR formed by a methyl shift is a better 1,3 dipole than the corresponding unit [M]-C(Me) = O.

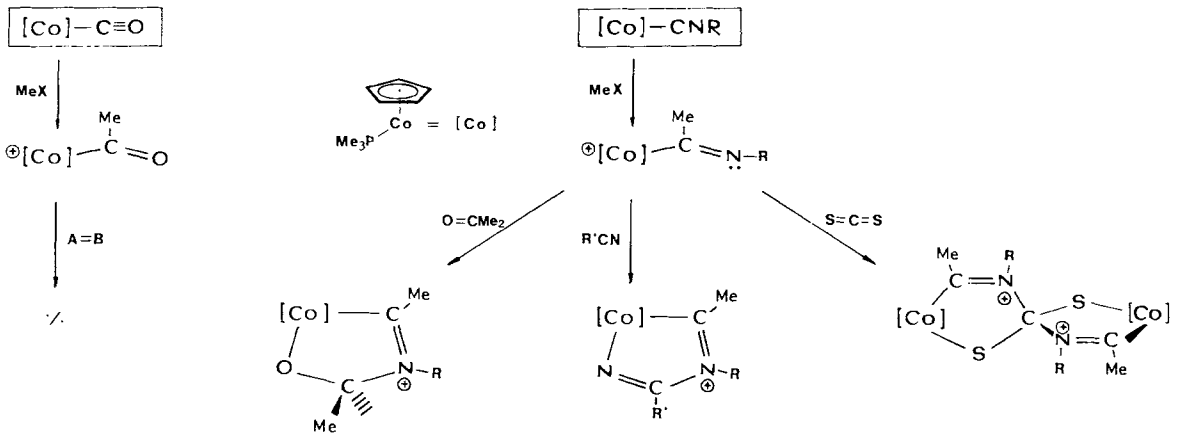

Fig. 13. Reactivity of [CpCo(CO)(PMe$_3$)] and the CNR analogue.

The greater polarity of the C≡NR bond compared with the C≡O bond causes metal isocyanide compounds to be suitable starting materials for the formation of aminocarbene complexes. The pioneering work in this area was done by *Chatt* and co-workers[84], who showed that platinum(II) isocyanide compounds of the type *cis*-[PtX$_2$(L)(CNR)] (X = Cl, Br, I; R = Me, Et, Ph, *p*-Tol; L = PMe$_2$Ph, PEt$_3$, PEt$_2$Ph) react with primary alcohols and amines even under very mild conditions to give *cis*-[PtX$_2$(L){C(NHR)(OR')}] and *cis*-[PtX$_2$(L){C(NHR)(NHR')}], respectively. Somewhat later, this synthetic principle was extended to isocyanide complexes of iron,[85] nickel,[86] palladium,[87] rhodium,[88] ruthenium,[89] osmium,[90] and gold;[91] a large number of carbene complexes of these metals could thus be obtained.[92] The observations (confirmed by kinetic studies) that both primary and secondary amines react faster than alcohols and that electron-withdrawing groups R at the isocyanide nitrogen atom accelerate the reaction indicate that the formation of the carbene ligands C(NHR)(NHR') and C(NHR)(OR') occurs via an initial attack of the amine or alcohol at the carbon atom of the isocyanide.

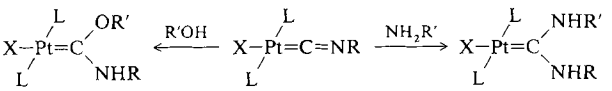

A similar conversion of a coordinated carbonyl group to an amino(hydroxy)carbene ligand C(OH)(NHR) or C(OH)(NR$_2$) is not known; the nucleophilicity of a primary or secondary amine is apparently not sufficient to make this possible. However, *Fischer* and *Kollmeier* showed almost simultaneously with the work carried out by *Chatt* and coworkers (see Fig. 14) that lithium dialkylamides do undergo

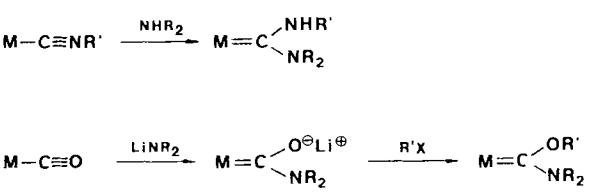

Fig. 14. Nucleophilic addition to CNR and CO metal complexes.

nucleophilic attack at a CO group bound to a metal (e.g., in [Cr(CO)$_6$]); subsequent alkylation gives an alkoxy(amino)-carbene ligand.[93] This variation of the classical Fischer method for the formation of metal carbene complexes has found further application[92] and has proved useful in organic synthesis.[94]

5. The Completion of the Series CO, CNH, CCH$_2$: Vinylidenes as Building Blocks for Metal Complexes

Like CNH, vinylidene (CCH$_2$) is in a strict sense isoelectronic with CO; in addition, it is similarly labile in the free state, in analogy to its nitrogen relative. The energy barrier for the conversion of C=CH$_2$ to its isomer acetylene HC≡CH has been calculated by *Schaeffer* et al. to be only ca. 4 kcal mol^{-1} and could in fact be even lower because of zero point energy effects.[95] The lifetime of C=CH$_2$ can thus be estimated to be 10^{-11} to 10^{-12} s; this is in good agreement with the results of trapping experiments.[96]

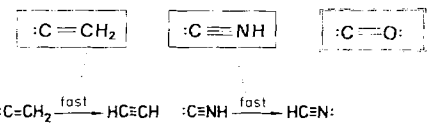

Scheme 4.

In contrast to isocyanides (CNR), vinylidene derivatives of the general type C=CHR and C=CR$_2$ are also unstable and thus not available as starting materials for synthesis of complexes. It is therefore *absolutely necessary* to generate the ligand C=CH$_2$, C=CHR, or C=CR$_2$ at the metal; as will be shown below there are various methods for doing so.

The first results in this direction were obtained only two years after the discovery of the carbene complexes; again, as so often, luck played an important role. *Mills* and *Redhouse*[97] had attempted to prepare an iron carbene complex by irradiating a benzene solution of [Fe(CO)$_5$] and diphenylketene; however, they obtained a product with the molecular formula [Fe$_2$(CO)$_8$(C$_2$Ph$_2$)], the X-ray structural analysis of which showed it to be a bridged vinylidene complex. The first *mononuclear* compound with a vinylidene ligand was de-

scribed in 1972 by *King* and *Saran*, who isolated the compounds $[CpM\{C=C(CN)_2\}L_2Cl]$ (M = Mo, W; L = PPh_3, $AsPh_3$, $SbPh_3$, etc.) in the course of studies on the reactivity of 1-chloro-2,2-dicyanovinyl complexes of molybdenum and tungsten.[98] The extremely high thermodynamic stability of the vinylidene–metal bond observed by them has also been confirmed for many other examples; it is thus not surprising that today vinylidene complexes of almost all the transition metals are known.[99]

Very exact information on the structures and bonding modes of these complexes is available. As can be seen from the comparison in Figure 15, not only vinylidene and carbonyl complexes but also vinylidene and isocyanide com-

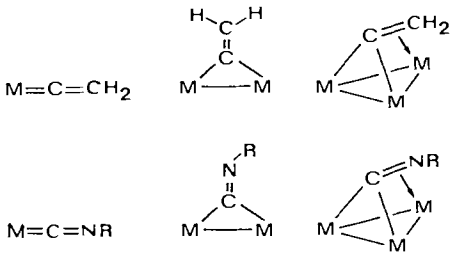

Fig. 15. Coordination possibilities for $C=CH_2$.

plexes show common structural features. The vinylidenes as terminally bonded ligands have excellent π-acceptor properties, which according to a comparative spectroscopic investigation are better than those of CO and only a little worse than those of CS and SO_2.[100] It is remarkable that the rotational barrier for the M=C bond is very small for both isocyanide and vinylidene complexes,[101] so that optical isomers have not yet been detected for allene analogues of the type [LL'M=C=CRR'].[102]

A large number of compounds with doubly bridging vinylidene ligands are known; these can be obtained both directly (see the iron complex $[Fe_2(CO)_8(\mu\text{-}C=CPh_2)]$ already mentioned)[97] and stepwise via addition of a coordinatively unsaturated metal compound to an M=C=CRR' unit.[99] The latter method is important for the formation of binuclear complexes with *two different* metal atoms. The μ_3-C,C bridges (Fig. 15) are also by no means unusual and are found in particular in ruthenium and osmium trinuclear clusters.[103]

The aforementioned extraordinary lability of the compounds C=CRR' leads naturally to the question *how* complexes containing the structural unit M=C=CRR' can be prepared. Two methods have so far proved generally useful; these start either from alkynylmetal compounds or from coordinatively unsaturated or substitution-labile metal complexes and 1-alkynes. Other methods, which employ vinylidene sources such as ketenes,[97] 1,1-dichloroolefins,[104] diazoolefins,[106] and α-(chlorovinyl)silanes,[107] can be used in special cases but have not attained general importance.[99]

The road to vinylidene complexes starting from alkynylmetal compounds was opened in particular by *Davison* and co-workers[108] and *Bruce* and co-workers[109] (see Fig. 16). Cyclopentadienyl iron and ruthenium compounds of the general composition $[CpML_2(C\equiv CR)]$ can undergo not only protonation but also alkylation [using $MeOSO_2F$ or $[OR_3]BF_4$ (R = Me, Et)]; the yields are practically quantitative, indicating that the β-C atom of the alkynyl ligand and not the metal is the preferred site for attack by the electrophile (even for $L=PMe_3$). The observation that anionic alkynyl compounds can undergo electrophilic addition reactions even more readily than neutral compounds corresponds to expectations; it has been used by *Berke* and coworkers, in particular, for the synthesis of the vinylidene manganese complexes $[CpMn(CO)_2(C=CRR')]$.[110]

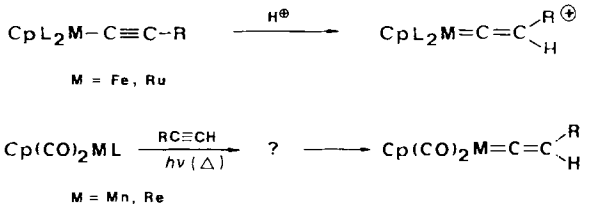

Fig. 16. Synthesis of vinylidenemetal complexes from alkynylmetal compounds and 1-alkynes.

The pioneering work on the conversion of the thermodynamically much more stable 1-alkynes (HC≡CR) into the isomeric vinylidenes (C=CHR) in the coordination sphere of a metal was done by *Antonova, Kolobova*, and their coworkers.[100, 111] They found that the photochemical reaction of $[CpM(CO)_3]$ (M = Mn, Re) with phenylacetylene does not give the expected alkyne metal compounds $[CpM(CO)_2(\eta^2\text{-}PhC\equiv CH)]$ but instead the isomeric vinylidene complexes $[CpM(CO)_2(C=CHPh)]$. The IR spectra recorded during the reaction indicated that the alkyne is first coordinated, but attempts to isolate the intermediate $[CpM(CO)_2(\eta^2\text{-}PhC\equiv CH)]$ in an analytically pure form were unsuccessful[100, 111]. Similar results were obtained later in the reactions of the systems $[CpML_2]^{\oplus}$ (M=Ru, Os), $[Cr(CO)_5]$, and $[W(CO)_3(R_2PC_2H_4PR_2)]$ (all of which are related to $[CpM(CO)_2]$ (M=Mn, Re)) with 1-alkynes reported by *Bruce*,[109b, 112] *Berke*,[113] and *Templeton*[114] and their co-workers. In each case vinylidene rather than 1-alkyne complexes were formed.

The question thus raised regarding the *mechanism* of the conversion of 1-alkynes to metal-bound vinylidenes could at first be answered only in a speculative manner. The suggestion made by various authors, in particular by *Antonova* and co-workers[111] (see Fig. 17), was that subsequent to the coordination of the alkyne an intramolecular oxidative addition takes place, the alkynyl(hydrido) intermediate then un-

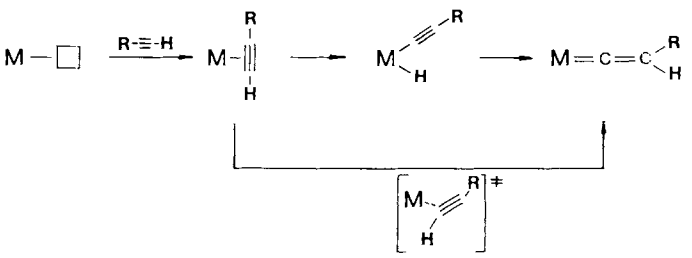

Fig. 17. Proposed mechanisms for vinylidene formation from 1-alkynes.

dergoing a 1,3-H shift to give the vinylidene complex. Although this appeared plausible, there was at first no experimental evidence for it. In addition, a very detailed study by *Silvestre* and *Hoffmann*[115] showed that the isomerization of $[L_nMH(C\equiv CR)]$ to $[L_nM(C=CHR)]$ would have a very high activation energy, so that the stepwise conversion of the alkyne to the vinylidene complex shown in the upper part of Figure 17 would be improbable. They suggested that a slippage of the 1-alkyne into a position in which only *one* carbon atom of the triple bond interacts with the metal should be more favorable; this is reminiscent of the bonding situation in a vinylcarbenium ion (see Fig. 17).

Evidence that a stepwise interconversion is possible after all and that, with the correct choice of ligands, the *three possible isomers* can be isolated was produced in the course of our own work on the reactivity of coordinatively unsaturated triisopropylphosphane rhodium and iridium complexes. In the initial stages we were able (see Scheme 5) to trans-

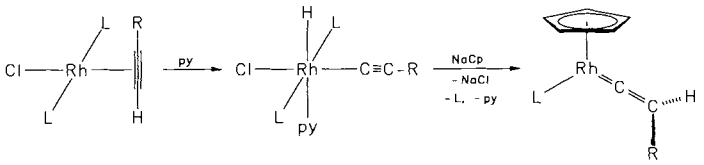

Scheme 5. L = $P\mathit{i}Pr_3$.

form the square-planar alkyne compounds *trans*-$[RhCl(RC\equiv CH)(P\mathit{i}Pr_3)_2]$ into the octahedral alkynyl(hydrido) complexes $[RhHCl(C\equiv CR)(P\mathit{i}Pr_3)_2(py)]$ by adding pyridine and to treat these with CpNa to give the half-sandwich compounds $[CpRh(C=CHR)(P\mathit{i}Pr_3)]$;[116] a little later, using iridium as the central atom, we were able to synthesize the complete series of isomers shown in Scheme 6.[117] According to more recent studies, there is no doubt that an analogous stepwise conversion of $HC\equiv CR$ to $C=CHR$ also occurs for rhodium.[102, 118]

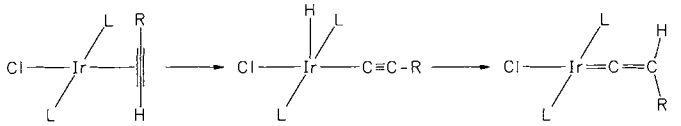

Scheme 6. L = $P\mathit{i}Pr_3$. Middle: $\delta(IrH) \approx -43$.

These results seem at first to be in complete disagreement with the MO calculations of *Silvestre* and *Hoffmann*.[115] However, these authors started from complex building blocks $[ML_n]$ such as $[CpMn(CO)_2]$ (or more simply $[MnH_5]^{4\ominus}$) in which the metal has a 16-electron configuration; thus, addition of the alkyne gives a filled shell with 18 electrons. This requirement is not met, however, by the fragment $[MCl(P\mathit{i}Pr_3)_2]$ (M = Rh, Ir): here, the metal has only a 14-electron configuration, so that a free coordination site is still present after addition of the alkyne. For this reason the hydride transfer from the metal to the β-C atom of the alkynyl ligand in the intermediate $[MHCl(C\equiv CR)(P\mathit{i}Pr_3)_2]$ could occur *inter*molecularly; this is in agreement with preliminary kinetic data (for the example M = Ir).[119]

The final reaction products shown in Schemes 5 and 6 behave in part very similarly to their CO relatives. For example, reaction of both the compounds *trans*-$[IrCl(C=CHR)(P\mathit{i}Pr_3)_2]$ and the Vaska complex *trans*-$[IrCl(CO)(PPh_3)_2]$ with HBF_4 results in protonation at the metal,[120] whereas the half-sandwich compounds $[CpRh(C=CHR)(P\mathit{i}Pr_3)]$ (R = H, Me, Ph) and $[CpRh(CO)(PMe_3)]$ react with benzoyl azide to give the same type of five-membered metallaheterocycles.[121]

The parallels in reactivity are even closer for *isocyanide* and *vinylidene* complexes, however. The method discovered by *Chatt* and co-workers for the preparation of metal alkoxy(amino)- and diaminocarbene compounds (see Section 4), which is based on the nucleophilic attack of a Lewis base such as ROH or RNH_2 on the carbon atom of the isocyanide,[84] can readily be extended to vinylidene complexes, in particular when these are cationic. The α-carbon atom of the vinylidene ligand is then even more electrophilic than in comparable neutral compounds, so that, for example, starting from $[CpFe(C=CH_2)(CO)(PPh_3)]^{\oplus}$ and alcohols, amines, mercaptans or hydrogen halides, it is possible to obtain various types of iron carbene complexes. Figure 18 contains a summary of the results described by *Hughes* et al.[122]

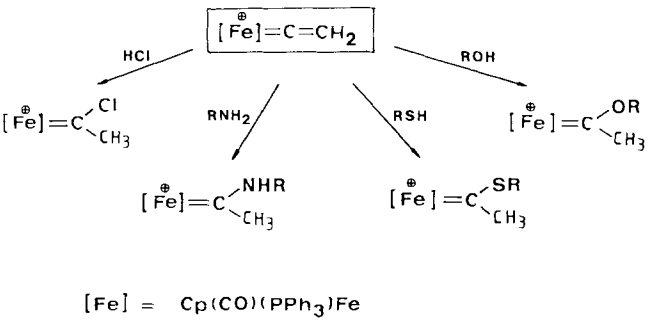

Fig. 18. Reaction of $[CpFe(C=CH_2)(CO)(PPh_3)]^{\oplus}$ with nucleophiles.

Another feature common to the parent compound CO and its near relatives CS and $C=CH_2$ should be mentioned. Since the beginning of this century it has been known that metal carbonyls react with thermally or photochemically generated 16-electron complex fragments to give binuclear compounds in which the CO acts as a bridge; the prototype of this reaction is the formation of $[Fe_2(CO)_9]$ from $[Fe(CO)_5]$ and $[Fe(CO)_4]$.[123] Using the isostructural series $[CpRh(CX)(PR_3)]$ with X = O, S and CH_2 as an example, we were able to show that these three complexes react in exactly the same way with the 16-electron species $[CpMn(CO)_2]$ generated by irradiation of $[CpMn(CO)_3]$ and stabilized by THF (Fig. 19).[65, 124] It is remarkable that not only

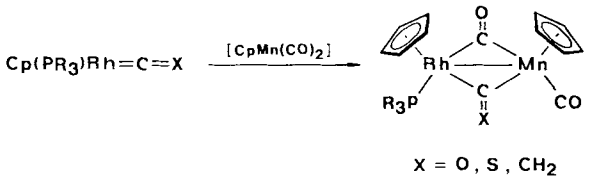

Fig. 19. Reaction of the isostructural compounds $[CpRh(CX)(PR_3)]$ with $[CpMn(CO)_2]$.

the CO but also the CS and $C=CH_2$ bridges occupy an unsymmetrical position between the two metal atoms; this is presumably due to the dissimilar electron configurations at rhodium and manganese.

6. On to the Second Century: The Search for the Missing Relatives

What does the future look like? Will the organometallic family which is now celebrating its birthday increase in size, and in which direction could this perhaps take place? Which will be the next metal-bonded relative of CO?

One very promising candidate is certainly SiO. On the basis of earlier work by *Schmid* et al.,[125] *Zybill* et al. have very recently shown that dichlorosilylene, $SiCl_2$, can be generated at a 16-electron complex fragment just as can a carbene and that the M–$SiCl_2$ bond can be stabilized by means of adduct formation with suitable Lewis bases such as hexamethylphosphoric triamide (HMPT).[126] The X-ray structural analyses of $[(CO)_5CrSiCl_2(hmpt)]$ and $[(CO)_4FeSiCl_2(hmpt)]$ show that the M–Si distance is relatively short and that the HMPT molecule is only weakly bonded.[126] If it were possible to displace the HMPT molecule and replace it by H_2O and thus to eliminate two molecules of HCl, one could generate the CO analogue SiO. A very similar conversion of CCl_2 coordinated at osmium to CO has been described by *Roper* and co-workers.[49] In order to fix the silicon monoxide ligand it may be necessary to use an electron-richer complex building block such as $[C_5Me_5Re(PR_3)_2]$, $[Os(PMe_3)_4]$, or $[C_5Me_5Ir(PMe_3)]$ rather than $[Cr(CO)_5]$ or $[Fe(CO)_4]$; such building blocks could stabilize the M–SiO bond by means of stronger π back-bonding.

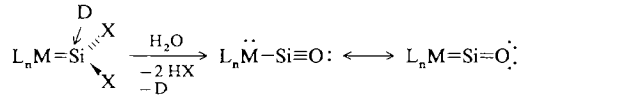

If it were possible to fix SiO, then why not also $BO^{\ominus}$? In Section 2, we referred to the existence of the extremely short-lived species CH_3BO, which is isoelectronic with BH_3CO; the former can be thought to be built up from $CH_3^{\oplus}$ and $BO^{\ominus}$. According to *Hoffmann*,[127] $CH_3^{\oplus}$ is isolobal with $[Mn(CO)_5]^{\oplus}$ and $[Co(CO)_4]^{\oplus}$, so that compounds such as $[Mn(CO)_5(BO)]$ and $[Co(CO)_4(BO)]$ (i.e., analogues of $[Cr(CO)_6]$ and $[Fe(CO)_5]$) would be plausible synthetic goals. Attempts to synthesize these complexes could build on the work of *Nöth* and *Schmid*, who reported the preparation of the readily decomposing compound $[(CO)_4CoBCl_2]$ as early as 1966.[128] Addition of a Lewis base such as HMPT would give an intermediate similar to that formulated above for SiX_2. Careful protolysis could then convert an ElX_2 ligand into an ElO ligand (El = B). Boron compounds with a coordination number of two are no longer curiosities today, as has been shown clearly in the last decade, in particular by *Nöth, Parry, Paetzold*, and *Berndt*.[129]

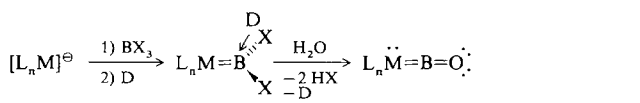

What other possibilities are there apart from SiO and $BO^{\ominus}$? What is the situation regarding $CF^{\oplus}$, which we have already mentioned in Scheme 2, or BF, which is also isoelectronic with CO? Is it realistic to think of such ligands becoming available? If intuition is not deceiving, a compound of the type $L_nM(CF)$ will soon be described in the literature. The question will then be only whether this molecule is better described as a carbyne complex $[L_nM\equiv C-F]$ than as a carbonyl analogue $[L_nM=C=F]$; this question can only be answered by an X-ray structural analysis, together with MO calculations. The signposts on the way to $[L_nM(CF)]$ have probably already been set up by *Roper*, who, during the course of extremely interesting studies, has been able to synthesize several compounds containing the fragments $M(CCl_2)$ and $M(CF_2)$.[130] Although compounds such as $[RuCl_2(CF_2)(CO)(PPh_3)]$ and $[Os(CF_2)(CO)_2(PPh_3)_2]$ have not yet led to products containing an OsCF unit,[131] the compound $[OsCl(CPh)(CO)(PPh_3)_2]$ obtained by the same group[132] shows that the goal of synthesizing a neutral complex $[OsCl(CF)(CO)(PPh_3)_2]$ or a cation $[Os(CF)(CO)_2(PPh_3)_2]^{\oplus}$ is quite realistic. The existence of trinuclear clusters with μ_3-CF bridges such as $[\{(CO)_3Co\}_3(\mu\text{-}CF)]$[133] and $[\{(CO)_3Fe\}_3(\mu_3\text{-}CF)_2]$[134] is also encouraging in this respect. These complexes resemble the corresponding carbonyl compounds with triply bridging CO ligands in both their structure and their bonding features.

A complex such as $[Fe(CO)_4(BF)]$ or $[(C_6R_6)Os(L)(BF)]$ also seems attainable. *Schmid, Petz*, and *Nöth*[135] described compounds of the formula $[Fe(CO)_4(BNR_2)]$ (R = Me, Et) as early as 1970; while these are extremely thermally labile, there is no doubt that they do exist. Although the road from $[Fe(CO)_4(BNR_2)]$ to $[Fe(CO)_4(BF)]$ will not be an easy one, it does appear passable. Reactions at osmium also appear feasible; the building blocks $[C_6H_6Os(PR_3)]$,[136] $[C_6H_6Os(CO)]$,[137] and $[(C_6H_3Me_3)Os(CO)]$,[138] used by us, could well prove suitable for the attachment of a BF ligand.

One hundred years have passed and a new era lies before us. One does not really need to be a prophet to forecast that the second century will also be an exciting one, that further surprises await us, and that the present survey will certainly not be the last occasion on which the serendipitous discovery made by *Ludwig Mond* will be remembered with reverence.

I thank Heinrich Vahrenkamp for suggesting this subject and Ernst Otto Fischer for valuable information regarding the material to be consulted. Oliver Nürnberg helped in the preparation of the reaction schemes, figures, etc., and I thank him heartily for this help.

Received: February 14, 1990 [A 781 IE]
German version: *Angew. Chem. 102* (1990) 1109
Translated by Prof. *T. N. Mitchell*, Dortmund

[1] L. Mond, C. Langer, F. Quincke, *J. Chem. Soc. 1890*, 749.
[2] M. P. Schützenberger, *Annales (Paris) 15* (1868) 100.
[3] Obituary of *L. Mond*: C. Langer, *Ber. Dtsch. Chem. Ges. 43* (1910) 3671; see also W. A. Herrmann, *Chem. Unserer Zeit 22* (1988) 113.
[4] Review: H. Behrens, *J. Organomet. Chem. 94* (1975) 139.
[5] Reviews: a) E. P. Kündig, M. Moskovits, G. A. Ozin, *Angew. Chem. 87* (1975) 314; *Angew. Chem. Int. Ed. Engl. 14* (1975) 292; b) G. A. Ozin, *Acc. Chem. Res. 10* (1977) 21.
[6] a) P. Chini, G. Longoni, V. G. Albano, *Adv. Organomet. Chem. 14* (1976) 285; b) R. W. Broach, L. F. Dahl, G. Longoni, P. Chini, A. J. Schultz,

J. M. Williams, *Adv. Chem. Ser. 167* (1978) 93; c) P. Chini, *J. Organomet. Chem. 200* (1980) 37.
[7] a) B. F. G. Johnson, J. Lewis, *Adv. Inorg. Chem. Radiochem. 24* (1981) 225; b) J. Lewis, B. F. G. Johnson, *Pure Appl. Chem. 54* (1982) 97.
[8] a) V. G. Albano, S. Martinengo, *Nachr. Chem. Tech. Lab. 28* (1980) 654; b) J. S. Bradley, *Adv. Organomet. Chem. 22* (1983) 1; c) W. A. Herrmann, *Angew. Chem. 98* (1986) 57; *Angew. Chem. Int. Ed. Engl. 25* (1986) 56.
[9] J. P. Collman, *Acc. Chem. Res. 8* (1975) 342.
[10] K. M. Chi, S. R. Frerichs, S. B. Philson, J. E. Ellis, *J. Am. Chem. Soc. 110* (1988) 303.
[11] P. Sabatier, *Bull. Soc. Chim. Fr. V. Sér. 6b* (1939) 1261.
[12] K. Fischer, K. Jonas, G. Wilke, *Angew. Chem. 85* (1973) 620; *Angew. Chem. Int. Ed. Engl. 12* (1973) 565.
[13] G. Wilke, *Angew. Chem. 100* (1988) 189; *Angew. Chem. Int. Ed. Engl. 27* (1988) 185.
[14] J. W. Irvine, G. Wilkinson, *Science (Washington D.C.) 113* (1951) 742.
[15] a) G. Wilke, E. W. Müller, M. Kröner, *Angew. Chem. 73* (1961) 33; b) H. Behrens, A. Müller, *Z. Anorg. Allg. Chem. 341* (1965) 124.
[16] R. Nast, *Z. Naturforsch. B 8* (1953) 381.
[17] N. Wiberg: *Lehrbuch der Anorganischen Chemie,* 91st–100th ed., de Gruyter, Berlin 1985, p. 754.
[18] R. Criegee, G. Schröder, *Justus Liebigs Ann. Chem. 623* (1959) 1.
[19] W. Hübel, E. H. Braye, A. Clauss, E. Weiss, U. Krüerke, D. A. Brown, G. S. D. King, C. Hoogzand, *J. Inorg. Nucl. Chem. 9* (1959) 204.
[20] a) J. S. Anderson, J. S. Ogden, *J. Chem. Phys. 51* (1969) 4189; b) M. Auwärter, *Angew. Chem. 87* (1975) 227; *Angew. Chem. Int. Ed. Engl. 14* (1975) 207.
[21] a) E. R. Lory, R. F. Porter, *J. Am. Chem. Soc. 93* (1971) 6301; b) Y. Kawashima, Y. Endo, K. Kawaguchi, E. Hirota, *Chem. Phys. Lett. 135* (1987) 441; c) D. C. Frost, C. Kirby, W. M. Lau, A. McDowell, N. P. C. Westwood, *J. Mol. Struct. 100* (1983) 87.
[22] P. Rosmus, *Angew. Chem. 100* (1988) 1376; *Angew. Chem. Int. Ed. Engl. 27* (1988) 1329.
[23] P. Paetzold, P. Bohm, A. Richter, E. Scholl, *Z. Naturforsch. B 31* (1976) 754.
[24] H. Bock, L. S. Cederbaum, W. von Niessen, P. Paetzold, P. Rosmus, B. Soulouki, *Angew. Chem. 101* (1989) 77; *Angew. Chem. Int. Ed. Engl. 28* (1989) 88.
[25] a) G. Schmid, *Angew. Chem. 82* (1970) 920; *Angew. Chem. Int. Ed. Engl. 9* (1970) 819; b) K. B. Gilbert, S. B. Boocock, S. G. Shore in G. Wilkinson, F. G. A. Stone, E. W. Abel (Eds.): *Comprehensive Organometallic Chemistry, Vol. 6,* Pergamon, Oxford 1982, p. 879.
[26] Reviews: a) B. F. G. Johnson, J. A. McCleverty, *Prog. Inorg. Chem. 7* (1966) 277; b) W. P. Griffith, *Adv. Organomet. Chem. 7* (1968) 211; c) J. H. Enemark, R. D. Feltham, *Coord. Chem. Rev. 13* (1974) 339; d) R. Eisenberg, C. D. Meyer, *Acc. Chem. Res. 8* (1975) 26; e) K. G. Caulton, *Coord. Chem. Rev. 14* (1975) 317; f) J. A. McCleverty, *Chem. Rev. 79* (1979) 53; g) R. D. Feltham, J. H. Enemark, *Top. Stereochem. 12* (1981) 155.
[27] M. Herberhold, A. Razavi, *Angew. Chem. 84* (1972) 1150; *Angew. Chem. Int. Ed. Engl. 11* (1972) 1092.
[28] I. H. Sabherwal, A. B. Burg, *J. Chem. Soc. Chem. Commun. 1970,* 1001.
[29] R. L. Mond, A. E. Wallis, *J. Chem. Soc. 1922,* 32.
[30] J. S. Anderson, W. Hieber, *Z. Anorg. Allg. Chem. 208* (1932) 238.
[31] C. G. Barraclough, J. Lewis, *J. Chem. Soc. 1960,* 4842.
[32] F. Seel, *Z. Anorg. Allg. Chem. 249* (1942) 308.
[33] P. M. Treichel, E. Pitcher, R. B. King, F. G. A. Stone, *J. Am. Chem. Soc. 83* (1961) 2593.
[34] a) L. Hedberg, K. Hedberg, S. K. Satija, B. I. Swanson, *Inorg. Chem. 24* (1985) 2766; b) K. Hedberg, L. Hedberg, K. Hagen, R. R. Ryan, L. H. Jones, *ibid. 24* (1985) 2771.
[35] a) E. O. Fischer, O. Beckert, W. Hafner, H. O. Stahl, *Z. Naturforsch. B 10* (1955) 598; b) T. S. Piper, F. A. Cotton, G. Wilkinson, *J. Inorg. Nucl. Chem. 1* (1955) 165; c) structure: A. P. Cox, L. F. Thomas, J. Sheridan, *Nature (London) 181* (1958) 1157.
[36] a) R. B. King, M. B. Bisnette, *Inorg. Chem. 3* (1964) 791; b) structure: J. L. Calderon, S. Fontana, E. Frauendorfer, V. W. Day, *J. Organomet. Chem. 64* (1974) C 10.
[37] a) R. C. Elder, F. A. Cotton, R. A. Schunn, *J. Am. Chem. Soc. 89* (1967) 3645; b) structure: R. C. Elder, *Inorg. Chem. 13* (1974) 1037.
[38] a) R. L. Pruett, *Adv. Organomet. Chem. 17* (1979) 1; b) D. Forster, *ibid. 17* (1979) 257; c) G. W. Parshall: *Homogeneous Catalysis,* Wiley-Interscience, New York 1980.
[39] a) W. P. Weiner, M. A. White, R. G. Bergman, *J. Am. Chem. Soc. 103* (1981) 3612; b) W. P. Weiner, R. G. Bergman, *ibid. 105* (1983) 3922.
[40] J. Chang, M. D. Seidler, R. G. Bergman, *J. Am. Chem. Soc. 111* (1989) 3258.
[41] a) A. Wojcicki, *Adv. Organomet. Chem. 11* (1973) 87; b) F. Calderazzo, *Angew. Chem. 89* (1977) 305; *Angew. Chem. Int. Ed. Engl. 16* (1977) 299; c) E. J. Kuhlmann, J. J. Alexander, *Coord. Chem. Rev. 33* (1980) 195; d) T. C. Flood, *Top. Stereochem. 12* (1981) 37.
[42] a) P. Legzdins, B. Wassink, F. W. B. Einstein, A. C. Willis, *J. Am. Chem. Soc. 108* (1986) 317; b) P. Legzdins, G. B. Richter-Addo, B. Wassink, F. W. B. Einstein, R. H. Jones, A. C. Willis, *ibid. 111* (1989) 2097.
[43] A. Goldhaber, K. P. C. Vollhardt, E. C. Walborsky, M. Wolfgruber, *J. Am. Chem. Soc. 108* (1986) 516.
[44] a) R. Steudel, *Z. Anorg. Allg. Chem. 361* (1968) 180; b) G. Gattow, W. Behrendt, *Top. Sulfur Chem. 2* (1977) 197; c) E. K. Moltzen, K. J. Klabunde, A. Senning, *Chem. Rev. 88* (1988) 391; d) K. J. Klabunde, E. K. Moltzen, K. Voska, *Phosphorus, Sulfur Silicon Relat. Elem. 43* (1989) 47.
[45] a) R. K. Laird, B. F. Barrow, *Proc. Phys. Soc. London Sect. A 66* (1953) 836; b) R. Steudel, *Angew. Chem. 79* (1967) 649; *Angew. Chem. Int. Ed. Engl. 6* (1967) 635.
[46] L. W. Yarbrough II, G. V. Calder, J. G. Verkade, *J. Chem. Soc. Chem. Commun. 1973,* 705.
[47] a) B. D. Dombek, R. J. Angelici, *J. Am. Chem. Soc. 95* (1973) 7516; b) A. M. English, K. R. Plowman, I. S. Butler, G. Jaouen, P. LeMaux, J. Y. Thepot, *J. Organomet. Chem. 132* (1977) C1.
[48] W. Petz, *J. Organomet. Chem. 146* (1978) C23.
[49] a) G. R. Clark, K. Marsden, W. R. Roper, L. J. Wright, *J. Am. Chem. Soc. 102* (1980) 1206; b) G. R. Clark, K. Marsden, C. E. F. Rickard, W. R. Roper, L. J. Wright, *J. Organomet. Chem. 338* (1988) 393.
[50] Reviews: a) I. S. Butler, A. E. Fenster, *J. Organomet. Chem. 66* (1974) 161; b) I. S. Butler, *Acc. Chem. Res. 10* (1977) 359; c) P. V. Yaneff, *Coord. Chem. Rev. 23* (1977) 183; d) S. Rajan, *J. Sci. Ind. Res. 38* (1979) 648; e) P. V. Broadhurst, *Polyhedron 4* (1985) 1801.
[51] a) M. C. Baird, G. Wilkinson, *J. Chem. Soc. Chem. Commun. 1966,* 267; b) M. C. Baird, G. Wilkinson, *J. Chem. Soc. A 1967,* 865.
[52] a) A. E. Fenster, I. S. Butler, *Inorg. Chem. 13* (1974) 915; b) I. S. Butler, N. J. Coville, D. Cozak, *J. Organomet. Chem. 133* (1977) 59.
[53] M. Kubota, C. J. Curtis, *Inorg. Chem. 13* (1974) 2277.
[54] F. Faraone, P. Piraino, V. Marsala, S. Sergi, *J. Chem. Soc. Dalton Trans. 1977,* 859.
[55] a) H. Werner, K. Leonhard, C. Burschka, *J. Organomet. Chem. 160* (1978) 291; b) H. Werner, O. Kolb, R. Feser, U. Schubert, *ibid. 191* (1980) 283.
[56] a) H. Werner, O. Kolb, *Angew. Chem. 91* (1979) 930; *Angew. Chem. Int. Ed. Engl. 18* (1979) 865; b) O. Kolb, H. Werner, *J. Organomet. Chem. 268* (1984) 49.
[57] a) H. Werner, K. Leonhard, *Angew. Chem. 91* (1979) 663; *Angew. Chem. Int. Ed. Engl. 18* (1979) 627; b) H. Werner, K. Leonhard, O. Kolb, E. Röttinger, H. Vahrenkamp, *Chem. Ber. 113* (1980) 1654.
[58] a) M. Ebner, H. Otto, H. Werner, *Angew. Chem. 97* (1985) 522; *Angew. Chem. Int. Ed. Engl. 24* (1985) 518; b) H. Werner, M. Ebner, H. Otto, *J. Organomet. Chem. 350* (1988) 257.
[59] M. Ebner, H. Werner, *Chem. Ber. 121* (1988) 1449.
[60] J. W. Dunker, J. S. Finer, J. Clardy, R. J. Angelici, *J. Organomet. Chem. 114* (1976) C49.
[61] a) M. A. Andrews, *Inorg. Chem. 16* (1977) 496; b) J. Y. Saillard, D. Grandjean, P. Caillet, A. Le Beuze, *J. Organomet. Chem. 190* (1980) 371.
[62] J. Y. Saillard, G. Le Borgne, D. Grandjean, *J. Organomet. Chem. 94* (1975) 409.
[63] J. S. Field, P. J. Wheatley, *J. Chem. Soc. Dalton Trans. 1972,* 2269.
[64] S. Lotz, R. R. Pille, P. H. van Rooyen, *Inorg. Chem. 25* (1986) 3053.
[65] H. Werner, O. Kolb, P. Thometzek, *J. Organomet. Chem. 347* (1988) 137.
[66] N. V. Sidgwick: *The Chemical Elements and Their Compounds,* Oxford Univ. Press, London 1950, p. 699.
[67] a) R. B. King, *Inorg. Chem. 6* (1967) 25; b) J.-F. Guttenberger, *Chem. Ber. 101* (1968) 403.
[68] a) E. O. Fischer, R. J. J. Schneider, *J. Organomet. Chem. 12* (1968) P27; b) J. A. Dineen, P. L. Pauson, *ibid. 71* (1974) 91.
[69] L. Malatesta, F. Bonati: *Isocyanide Complexes of Metals,* Wiley-Interscience, New York 1969.
[70] I. Ugi (Ed.): *Isonitrile Chemistry,* Academic, New York 1971.
[71] More recent reviews on metal isocyanide complexes (see also [69]): a) P. M. Treichel, *Adv. Organomet. Chem. 11* (1973) 21; b) F. Bonati, G. Minghetti, *Inorg. Chim. Acta 9* (1974) 95; c) S. J. Lippard, *Prog. Inorg. Chem. 21* (1976) 91; d) Y. Yamamoto, *Coord. Chem. Rev. 32* (1980) 193; e) E. Singleton, H. E. Oosthuizen, *Adv. Organomet. Chem. 22* (1983) 209.
[72] G. F. Warnock, N. J. Cooper, *Organometallics 8* (1989) 1826.
[73] a) F. Klages, K. Mönkemeyer, *Chem. Ber. 83* (1950) 501; b) W. Hieber, E. Böckly, *Z. Anorg. Allg. Chem. 262* (1950) 344.
[74] J. Chatt, G. J. Leigh, N. Thankarajan, *J. Organomet. Chem. 29* (1971) 105.
[75] a) M. O. Albers, N. J. Coville, T. V. Ashworth, E. Singleton, H. E. Swanepoel, *J. Organomet. Chem. 199* (1980) 55; b) N. J. Coville, M. O. Albers, T. V. Ashworth, E. Singleton, *J. Chem. Soc. Chem. Commun. 1981,* 408; c) M. O. Albers, N. J. Coville, C. P. Nicolaides, R. A. Webber, T. V. Ashworth, E.Singleton, *J. Organomet. Chem. 217* (1981) 247; d) M. O. Albers, N. J. Coville, E. Singleton, *J. Chem. Soc. Dalton Trans. 1982,* 1069; e) *J. Organomet. Chem. 326* (1987) 229.
[76] E. P. Kündig, P. L. Timms, *J. Chem. Soc. Dalton Trans. 1980,* 991.
[77] V. W. Day, R. O. Day, J. S. Kristhoff, F. J. Hirsekorn, E. L. Muetterties, *J. Am. Chem. Soc. 97* (1975) 2571.
[78] a) E. L. Muetterties, *Angew. Chem. 90* (1978) 577; *Angew. Chem. Int. Ed. Engl. 17* (1978) 545; b) T. N. Rhodin, G. Ertl (Eds.): *The Nature of the Surface Chemical Bond,* North-Holland, Amsterdam 1979; c) C. K. Rofer-DePoorter, *Chem. Rev. 81* (1981) 447.

[79] A. Spencer, H. Werner, *J. Organomet. Chem. 171* (1979) 219.
[80] H. Werner, B. Heiser, U. Schubert, K. Ackermann, *Chem. Ber. 118* (1985) 1517.
[81] B. Heiser, A. Kühn, H. Werner, *Chem. Ber. 118* (1985) 1531.
[82] U. Schubert, B. Heiser, L. Hee, H. Werner, *Chem. Ber. 118* (1985) 3151.
[83] H. Werner, B. Heiser, C. Burschka, *Chem. Ber. 115* (1982) 3069.
[84] a) E. M. Badley, J. Chatt, R. L. Richards, G. A. Sim, *J. Chem. Soc. Chem. Commun. 1969,* 1322; b) E. M. Badley, J. Chatt, R. L. Richards, *J. Chem. Soc. A 1971,* 21.
[85] a) R. J. Angelici, L. M. Charley, *J. Organomet. Chem. 24* (1970) 205; b) J. S. Miller, A. L. Balch, J. H. Enemark, *J. Am. Chem. Soc. 93* (1971) 4613; c) A. L. Balch, J. S. Miller, *ibid. 94* (1972) 417; d) D. J. Doonan, A. L. Balch, *Inorg. Chem. 13* (1974) 921; e) R. J. Angelici, P. A. Christian, B. D. Dombek, G. A. Pfeffer, *J. Organomet. Chem. 67* (1974) 287.
[86] C. H. Davies, C. H. Game, M. Green, F. G. A. Stone, *J. Chem. Soc. Dalton Trans. 1974,* 357.
[87] a) F. Bonati, G. Minghetti, T. Boschi, B. Crociani, *J. Organomet. Chem. 25* (1970) 255; b) B. Crociani, T. Boschi, M. Nicolini, U. Belluco, *Inorg. Chem. 11* (1972) 1292; c) B. Crociani, T. Boschi, G. G. Troilo, U. Croatto, *Inorg. Chim. Acta 6* (1972) 655; d) J. S. Miller, A. L. Balch, *Inorg. Chem. 11* (1972) 2069; e) G. A. Larkin, R. P. Scott, M. G. H. Wallbridge, *J. Organomet. Chem. 37* (1972) C 21.
[88] a) P. R. Branson, M. Green, *J. Chem. Soc. Dalton Trans. 1972,* 1303; b) P. R. Branson, R. A. Cable, M. Green, M. K. Lloyd, *J. Chem. Soc. Chem. Commun. 1974,* 364.
[89] D. J. Doonan, A. L. Balch, *J. Am. Chem. Soc. 95* (1973) 4769.
[90] J. Chatt, R. L. Richards, G. H. D. Royston, *J. Chem. Soc. Dalton Trans. 1973,* 1433.
[91] a) F. Bonati, G. Minghetti, *Synth. Inorg. Met. Org. Chem. 1* (1971) 299; b) F. Bonati, G. Minghetti, E. Maionica, *Gaz. Chim. Ital. 102* (1972) 731; c) F. Bonati, G. Minghetti, *J. Organomet. Chem. 59* (1973) 403.
[92] Reviews: K. H. Dötz, H. Fischer, P. Hofmann, F. R. Kreissl, U. Schubert, K. Weiss: *Transition Metal Carbene Complexes,* Verlag Chemie, Weinheim 1983.
[93] E. O. Fischer, H. J. Kollmeier, *Angew. Chem. 82* (1970) 325; *Angew. Chem. Int. Ed. Engl. 9* (1970) 309.
[94] K. H. Dötz, *Angew. Chem. 96* (1984) 573; *Angew. Chem. Int. Ed. Engl. 23* (1984) 587.
[95] Y. Osamura, H. E. Schaeffer III, S. K. Gray, W. H. Miller, *J. Am. Chem. Soc. 103* (1981) 1904.
[96] P. S. Skell, F. A. Fagone, K. J. Klabunde, *J. Am. Chem. Soc. 94* (1972) 7862.
[97] a) O. S. Mills, A. D. Redhouse, *J. Chem. Soc. Chem. Commun. 1966,* 444; b) *J. Chem. Soc. A 1968,* 1282.
[98] R. B. King, M. S. Saran, *J. Chem. Soc. Chem. Commun. 1972,* 1052.
[99] Reviews: a) M. I. Bruce, A. G. Swincer, *Adv. Organomet. Chem. 22* (1983) 59; b) A. B. Antonova, A. A. Johansson, *Usp. Khim. 58* (1989) 1197.
[100] N. E. Kolobova, A. B. Antonova, O. M. Khitrova, M. Yu. Antipin, Yu. T. Struchkov, *J. Organomet. Chem. 137* (1977) 69.
[101] N. M. Kostic, R. F. Fenske, *Organometallics 1* (1982) 974.
[102] a) H. Werner, J. Wolf, F. J. Garcia Alonso, M. L. Ziegler, O. Serhadli, *J. Organomet. Chem. 336* (1987) 397; b) H. Werner, U. Brekau, *Z. Naturforsch. B 44* (1989) 1438.
[103] a) A. J. Deeming, S. Hasso, M. Underhill, *J. Chem. Soc. Dalton Trans. 1975,* 1614; b) C. R. Eady, B. F. G. Johnson, J. Lewis, *ibid. 1977,* 477; c) M. Green, A. G. Orpen, C. J. Schaverien, *J. Chem. Soc. Chem. Commun. 1984,* 37; d) T. Albiez, W. Bernhardt, C. von Schnering, E. Roland, H. Bantel, H. Vahrenkamp, *Chem. Ber. 120* (1987) 141.
[104] R. B. King, M. S. Saran, *J. Am. Chem. Soc. 95* (1973) 1811.
[105] D. F. Marten, E. V. Dehmlow, D. J. Hanlon, M. B. Hossain, D. van der Helm, *J. Am. Chem. Soc. 103* (1981) 4940.
[106] W. A. Herrmann, C. Weber, M. L. Ziegler, O. Serhadli, *J. Organomet. Chem. 297* (1985) 245.
[107] U. Schubert, J. Grönen, *Chem. Ber. 122* (1989) 1237.
[108] a) A. Davison, J. P. Solar, *J. Organomet. Chem. 155* (1978) C 8; b) A. Davison, J. P. Selegue, *J. Am. Chem. Soc. 100* (1978) 7763; c) *ibid. 102* (1980) 2455.
[109] a) M. I. Bruce, R. C. Wallis, *J. Organomet. Chem. 161* (1978) C 1; b) M. I. Bruce, F. S. Wong, B. W. Skelton, A. H. White, *J. Chem. Soc. Dalton Trans. 1982,* 2203.
[110] a) H. Berke, *Z. Naturforsch. B 35* (1980) 86; b) *Chem. Ber. 113* (1980) 1370; c) H. Berke, P. Härter, G. Huttner, J. von Seyerl, *J. Organomet. Chem. 219* (1981) 317.
[111] a) A. N. Nesmeyanov, G. G. Aleksandrov, A. B. Antonova, K. N. Anisimov, N. E. Kolobova, Yu. T. Struchkov, *J. Organomet. Chem. 110* (1976) C 36; b) A. B. Antonova, N. E. Kolobova, P. V. Petrovsky, B. V. Lokshin, N. S. Obezyuk, *ibid. 137* (1977) 55.
[112] M. I. Bruce, R. C. Wallis, *Aust. J. Chem. 32* (1979) 1471.
[113] H. Berke, P. Härter, G. Huttner, L. Zsolnai, *Z. Naturforsch. B 36* (1981) 929.
[114] K. R. Birdwhistell, S. J. Nieter Burgmayer, J. L. Templeton, *J. Am. Chem. Soc. 105* (1983) 7789.
[115] J. Silvestre, R. Hoffmann, *Helv. Chim. Acta 68* (1985) 1461.
[116] J. Wolf, H. Werner, O. Serhadli, M. L. Ziegler, *Angew. Chem. 95* (1983) 428; *Angew. Chem. Int. Ed. Engl. 22* (1983) 414.
[117] a) F. J. Garcia Alonso, A. Höhn, J. Wolf, H. Otto, H. Werner, *Angew. Chem. 97* (1985) 401; *Angew. Chem. Int. Ed. Engl. 24* (1985) 406; b) A. Höhn, H. Otto, M. Dziallas, H. Werner, *J. Chem. Soc. Chem. Commun. 1987,* 852; c) A. Höhn, H. Werner, *J. Organomet. Chem., 382* (1990) 255.
[118] H. Werner, F. J. Garcia Alonso, H. Otto, J. Wolf, *Z. Naturforsch. B 43* (1988) 722.
[119] A. Höhn, unpublished; see also [117c].
[120] A. Höhn, H. Werner, *Angew. Chem. 98* (1986) 745; *Angew. Chem. Int. Ed. Engl. 25* (1986) 737.
[121] a) H. Werner, A. Höhn, R. Weinand, *J. Orgamomet. Chem. 299* (1986) C 15; b) A. Höhn, H. Werner, *Chem. Ber. 121* (1988) 881.
[122] B. E. Boland-Lussier, R. P. Hughes, *Organometallics 1* (1982) 635.
[123] J. Dewar, H. O. Jones, *Proc. R. Soc. London Ser. A 76* (1905) 573.
[124] H. Werner, F. J. Garcia Alonso, H. Otto, K. Peters, H. G. von Schnering, *Chem. Ber. 121* (1988) 1565.
[125] G. Schmid, E. Welz, *Angew. Chem. 89* (1977) 823; *Angew. Chem. Int. Ed. Engl. 16* (1977) 785.
[126] a) C. Zybill, G. Müller, *Angew. Chem. 99* (1987) 683; *Angew. Chem. Int. Ed. Engl. 26* (1987) 669; b) *Organometallics 7* (1988) 1368; short review: C. Zybill, *Nachr. Chem. Tech. Lab. 37* (1989) 248.
[127] R. Hoffmann, *Angew. Chem. 94* (1982) 725; *Angew. Chem. Int. Ed. Engl. 21* (1982) 711.
[128] H. Nöth, G. Schmid, *Allg. Prakt. Chem. 17* (1966) 610; see also [25a].
[129] Review: H. Nöth, *Angew. Chem. 100* (1988) 1664; *Angew. Chem. Int. Ed. Engl. 27* (1988) 1603.
[130] Review: W. R. Roper, *J. Organomet. Chem. 300* (1986) 167.
[131] W. R. Roper, personal communication (September 1988).
[132] G. R. Clark, K. Marsden, W. R. Roper, L. J. Wright, *J. Am. Chem. Soc. 102* (1980) 6570.
[133] a) W. T. Dent, L. A. Duncanson, R. G. Guy, H. W. Reed, B. L. Shaw, *Proc. Chem. Soc. London 1961,* 169; b) B. R. Penfold, B. H. Robinson, *Acc. Chem. Res. 6* (1973) 73.
[134] D. Lentz, I. Brüdgam, H. Hartl, *Angew. Chem. 97* (1985) 115; *Angew. Chem. Int. Ed. Engl. 24* (1985) 119.
[135] G. Schmid, W. Petz, H. Nöth, *Inorg. Chim. Acta 4* (1970) 423.
[136] a) H. Werner, H. Kletzin, A. Höhn, W. Paul, W. Knaup, M. L. Ziegler, O. Serhadli, *J. Organomet. Chem. 306* (1986) 227; b) K. Roder, H. Werner, *ibid. 362* (1989) 321.
[137] K. Roder, H. Werner, *Chem. Ber. 122* (1989) 833.
[138] a) A. McCamley, R. N. Perutz, S. Stahl, H. Werner, *Angew. Chem. 101* (1989) 1721; *Angew. Chem. Int. Ed. Engl. 28* (1989) 1690; b) S. Stahl, H. Werner, *Organometallics 9* (1990) 1876.

Aspartic and Glutamic Acid as Ligands to Alkali and Alkaline-Earth Metals: Structural Chemistry as Related to Magnesium Therapy

By Hubert Schmidbaur,* Hans Georg Classen, and Joachim Helbig

Dedicated to Professor Max Schmidt on the occasion of his 65th birthday

Magnesium and other alkaline-earth and alkali metals play an important role in the biochemistry of virtually all living organisms. In contrast to "trace elements", these "common metals" are distributed in most cells and tissues, often in considerable concentrations, and a constant supply is indispensable for unrestricted performance of biological functions. In contemporary medicine, various forms of magnesium therapy are recommended in order to compensate for magnesium deficiency due to certain dysfunctions as well as to loss from excessive transpiration. In addition, there are numerous indications for prophylaxis. Magnesium is usually administered orally in the form of "complexes" with "natural" anions derived from L-aspartic, L-glutamic, L-pyroglutamic (pidolic), citric, and orotic acid. Analytical, electrochemical, and spectroscopic investigations of aqueous solutions of these pharmaceuticals, together with X-ray diffraction studies of crystalline samples, have given a detailed knowledge of these coordination compounds. Only certain combinations can be addressed as magnesium complexes, whereas others are only present as aquo complexes both in aqueous solutions and in the solid state. Thus, a delicate balance of metal complexation and hydrogen bonding exists for the components of the drugs, which is relevant for the metal carrier functions of the organic ligands. Compared with the more flexible stereochemistry of Ca, Sr, Ba, Mn^{II}, Zn, Li, Na, and K complexes, which have coordination numbers between 4 and 9, octahedral hexacoordination is found exclusively for magnesium, the most stereoselective of these metals.

1. Introduction

Terms like "inorganic biochemistry" or "bioinorganic chemistry" have been coined for an area of interdisciplinary research where interest is focused largely on the role of metals in biological systems.[1-7] It was recognized very early that a deficiency of common minerals or mineral components in food and drink may greatly affect the health of animals and humans,[8,9] with "salt" (sodium chloride) perhaps being the most prominent example in the history of mankind. Regular uptake of demineralized water is an injurious diet not only due to, for example, the lack of buffer anions like (bi)carbonate, phosphate, or sulfate, but also owing to depletion of the concentrations of standard metals in the body, leading to a breakdown of most osmotic systems and to mal- or dysfunction of most enzymes, biological signal processing, and biomineralization.

For many body functions some of the "essential metals" are required in relatively high quantities and have to be provided by a regular intake in order to secure standard performance. Bioinorganic chemists classify these elements as "common metals", as opposed to "trace elements" for which only minute quantities are required, and for which a constant supply is less mandatory owing to, for example, storage capabilities of the body (which is particularly true for first-row transition metals like iron). The rest of the metals in the periodic table are biologically "nonessential metals", whose absence appears to be of little or no immediately obvious consequence, but for which concentrations above certain limits may be found to be either toxic or, in certain cases, of therapeutic use.

In biological systems, the most prominent common metals are the alkali and alkaline-earth metals sodium, potassium, magnesium, and calcium (Table 1).[9-16] On the other hand, lithium[15] is considered a nonessential metal, but with considerable therapeutic value and low toxicity. The bioinor-

Table 1. Distribution and significance of some alkali and alkaline-earth metals in biological systems and recommended daily intake.

Element	Total (adult)	Serum (plasma level)	Essential	Recommended daily intake (adults)
Li	2–3 mg	2–3 μmol L^{-1}	no	–
Na	85 g	134–141 mmol L^{-1}	yes	2 g
K	120–150 g	3.8–4.5 mmol L^{-1}	yes	3–4 g
Mg	24–26 g	0.76–1.10 mmol L^{-1}	yes	0.3–0.45 g
Ca	750–1100 g	2.15–2.55 mmol L^{-1}	yes	0.8–1.2 g
Sr	140–1000 mg	1.6–5.0 μmol L^{-1}	questionable	–
Mn	10–40 mg	1.8–20 μmol L^{-1} [a]	yes	2–5 mg
Zn	1.4–2.1 g	12–17 μmol L^{-1}	yes	15–25 mg

[a] The higher value applies to infants.

[*] Prof. Dr. H. Schmidbaur
Anorganisch-chemisches Institut der Technischen Universität München
Lichtenbergstrasse 4, D-8046 Garching (FRG)

Prof. Dr. H. G. Classen
Institut für Biologische Chemie und Ernährungswissenschaft,
Fachgebiet Pharmakologie und Toxikologie der Universität Hohenheim
Postfach 70 05 62, D-7000 Stuttgart 70 (FRG)

[*] Dr. Joachim Helbig
Klinische Forschung und Entwicklung
Verla-Pharm Arzneimittelfabrik GmbH KG
Von-Kühlmann-Strasse 7, D-8132 Tutzing (FRG)

ganic chemistry of the very rare elements rubidium and cesium has remained largely unexplored.[4, 5, 9] Beryllium is considered highly toxic, at least in respiratory uptake, but less so when administered orally.[17–19] Strontium is rated nontoxic, and traces of it appear to be "essential", though the reason for this is not yet known. Barium causes typical "heavy-metal poisoning" even at low concentrations if soluble compounds are applied.[4]

Apart from diseases involving resorptive, storage, or excretion malfunction, deficiency syndromes associated with the most common metal cations in humans and animals, $Na^{\oplus}$, $K^{\oplus}$, $Mg^{2\oplus}$, and $Ca^{2\oplus}$, have been rare phenomena for many years. Virtually all standard diets appeared to guarantee a sufficient supply of these cations owing to their high abundance. This situation has changed in modern society, where, for example, animals are raised in a controlled environment with special growth-regulating diets, and humans may be subject to rapid loss of electrolyte due to stress, excessive recreational activities, or highly irregular and selective eating and drinking habits. Food processing and conservation, which result in depletion of some elements, are other origins. This is particularly true for *magnesium*, which is most likely to be deficient owing to its somewhat lower abundance compared with that of sodium, potassium, or calcium. Magnesium therapy has therefore become an important issue in contemporary medicine, including veterinary medicine. The enormous increase in the consumption of mineral water from bottles labeled with a complete analytical inventory probably also reflects contemporary attitudes and concern.

One of the most relevant questions arising in this context is the optimum administration of magnesium, that is, the selection of compounds (salts or complexes) which lead to rapid and efficient resorption without upsetting the pH or the ionic equilibria in body fluids. If possible, side effects from the anionic and/or ligand components should be negligible or, if possible, therapeutically beneficial.

Among the many possibilities for a "magnesium formulation", the natural amino acids and their derivatives are preferred candidates. The acidic members of the amino acid series, L-aspartic and L-glutamic acid as well as L-pyroglutamic acid (pidolic acid), were therefore chosen at an early stage of the development of magnesium drugs, though only preliminary information was available on pertinent acid/base and complex equilibria in aqueous media resembling the situation in body fluids. The present article summarizes the results of more recent research in this area and also deals with other "common" and "trace elements".

Hubert Schmidbaur was born in Landsberg/Lech in 1934 and studied chemistry at the University of Munich from 1953 to 1960 (Dissertation with Max Schmidt). He became a lecturer at the University of Marburg in 1964 and was Professor of Inorganic Chemistry at the University of Würzburg from 1965 to 1973, when he was appointed Professor of Inorganic and Analytical Chemistry at the Technical University of Munich. Hubert Schmidbaur has received many honors and is a member of the Göttingen Academy of Sciences and the Leopoldina Academy in Halle. He currently has research interests in the chemistry of silicon and germanium (as related to solar cell and sensor technology), the chemistry of gold (as related to microelectronics and electrical engineering), the coordination chemistry and organometallic chemistry of the p-block metals (e.g., gallium), the synthetic and structural chemistry of organophosphorus compounds, and the bioinorganic chemistry of magnesium (magnesium therapy).

Joachim Helbig was born in Rabenstein near Chemnitz in 1929 and studied biology at the University of Dresden and veterinary medicine at the Humboldt University in Berlin. He received his doctorate degree (med. vet.) at the Free University of Berlin in 1957 and worked for the Spitzner Company (Ettlingen) and for Grünenthal Inc. as a research associate. Since 1962, he has been head of the Clinical Research and Development Division of Verla-Pharm (Tutzing). Joachim Helbig is a member of numerous national and international scientific societies and editor of "Magnesium Bulletin".

Hans Georg Classen was born in Schatensen near Uelzen in 1936 and studied medicine at the University of Göttingen from 1955 to 1960 (Dr. med. in 1962). In 1964 he started as a research assistant at the Institute for Experimental Therapy of the University of Freiburg and became a lecturer in toxicology and pharmacology there in 1971. Since 1976, Hans Georg Classen has been head of the division of Pharmacology and Toxicology of Nutrition at the University of Hohenheim. His main research interests are the metabolism of magnesium, cadmium, and nitrate/nitrite, mainly as related to stress conditions and their pharmacological treatment.

1.1. The Role of Magnesium and Other Alkaline-Earth Metals in Biological Systems

Magnesium is one of the most important elements in biological systems. The many facets of its action can therefore only be summarized here very briefly. Magnesium is present solely as the solvated or complexed dication $Mg^{2\oplus}$, basically as part of the osmotic equilibria in- and outside of cells and in all tissues.[20, 21] It is readily transported through membranes, including the blood/brain barrier.[22] In purely "inorganic" form it is accumulated (stored) in invertebrate "granules" as the carbonate, phosphate, or citrate, mostly along with the calcium salt as the main matrix constituent, from which it can be remobilized.[23-25] In vertebrate bone and teeth it plays only a minor role (again next to calcium). Magnesium cations available from these sources or from direct intake bind to various sites on protein (or pectin) surfaces to induce or stabilize tertiary structures (e.g., membranes[22]) or to enhance certain functionalities. This is particularly true for enzyme activities, with ATP and ADP hydrolysis perhaps being one of the most significant examples. For example, $Mg^{2\oplus}$ and $K^{\oplus}$ are indispensable cofactors of ribonuclease activity.[22] Careful investigation of the magnesium (or calcium) binding sites on proteins has shown that the acidic groups of L-aspartic and L-glutamic acid are the key anchoring positions for these cations.[23-25]

In the above processes, magnesium competes successfully for certain coordination sites with the other common metal ions, some of which are antagonists through a different specificity. Since ion–ion and ion–dipole interactions are the main binding forces, this specificity is predominantly governed by the charge and size of the individual cation, as well as by the resulting effective coordination number and geometry. An improved understanding of the function of biological cations is thus to be expected from a detailed study of the coordinating properties of the metals competing for the ligand sites of a given matrix. However, the specific contributions from cation- and anion-based Coulomb forces may be obscured, for example, by the effect of ubiquitous hydrogen bonding, which energetically can be of the same order of magnitude. Thus, only a complete picture of the structural situation allows individual contributions to be distinguished.

Table 2. Oral toxicity of M(L-AspH)Cl (M = Mg, Ca, Sr, Mn, Zn); Sprague–Dawley rats, empty stomach. Except for the insoluble Mg(L-Asp) · $3H_2O$ reference, all compounds were dissolved in water. LD_{50}: dosis resulting in the death of 50% of the animals.

Compound	% Weight		LD_{50} [g kg^{-1}]
	M	Cl	(95% reliability)
Mg(L-AspH)Cl	9.55	14.26	10.69 (9.82–11.70)
Mg(L-Asp) · $3H_2O$	8.68	–	36.01 (22.70–57.15)
Ca(L-AspH)Cl	18.35	15.90	6.04 (4.96–7.37)
Sr(L-AspH)Cl	31.50	12.94	ca. 14
Mn(L-AspH)Cl	22.80	14.80	3.42 (2.28–5.15)
Zn(L-AspH)Cl	28.39	14.77	1.91 (1.50–2.42)

The (oral) toxicity of alkaline-earth metals, like that of other metals, is strongly dependent on the anions present in the drug. This dependence may be due to different "bioavailability", as well as to the specific effects of the anions. As pertinent examples, the oral toxicities of M(L-AspH)Cl (M = Mg, Ca, Sr, Mn^{II}, Zn) are listed for comparison in Table 2.[14, 26] Since the same anions are present in all cases, these data reflect relative metal toxicities for the given system. Magnesium toxicity is recognized to be a minimum in this series. LD_{50} values as high as 10 g kg^{-1} (!) are tolerated.

1.2. The Metal-Binding Role of L-Aspartic and L-Glutamic Acid in Biological Systems

As already pointed out, the common metals become attached predominantly to the carboxylate groups of L-aspartate and L-glutamate residues. Particularly striking cases are the matrices for biomineralization in general and for shell, bone, and dental growth in particular. For example, aspartic acid, along with (phospho)serine, is the main component of the calcium carbonate biomineralization matrices of mollusks and of phosphophoryns in dentin fractions.[23]

In polysaccharide and other matrices the cations become primarily associated with sulfonate or phosphate groups, but carboxylate coordination via L-aspartic acid is also retained. Soluble glycoproteins were found to become attached to the surface of common metal carboxylates like fumarate or maleate through their aspartate residues, and intercrystalline proteins of biomineralized material ($CaCO_3$, $Ca_5(PO_4)_3OH$, CaC_2O_4, $CaSO_4$, $SrSO_4$, $BaSO_4$) were invariably shown to contain extremely high concentrations of L-aspartate.[23]

Whereas the key role of L-aspartate and, to a lesser extent, L-glutamate in the binding of metals to polymeric biomatrices is thus well established, the metal-cation affinity of low-molecular-weight peptides and free amino acids in aqueous solutions is much less well documented. Only very few complexes have been isolated, and—owing to the complexity of the equilibria involved—other physical measurements in vitro and in vivo have not always given conclusive results.

2. Dissociation Equilibria of Aspartic and Glutamic Acid in Aqueous Solution

Aspartic acid ($AspH_2$) and glutamic acid ($GluH_2$) can dissociate in aqueous solution [Eqs. (1), (2), (4), and (5)] to form monoanions ($AspH^{\ominus}$, $GluH^{\ominus}$) and dianions ($Asp^{2\ominus}$, $Glu^{2\ominus}$).

$$AspH_2 + H_2O \rightarrow AspH^{\ominus} + H_3O^{\oplus} \quad (1)$$

$$AspH^{\ominus} + H_2O \rightarrow Asp^{2\ominus} + H_3O^{\oplus} \quad (2)$$

$$AspH_2 + H_3O^{\oplus} \rightarrow AspH_3^{\oplus} + H_2O \quad (3)$$

$$GluH_2 + H_2O \rightarrow GluH^{\ominus} + H_3O^{\oplus} \quad (4)$$

$$GluH^{\ominus} + H_2O \rightarrow Glu^{2\ominus} + H_3O^{\oplus} \quad (5)$$

$$GluH_2 + H_3O^{\oplus} \rightarrow GluH_3^{\oplus} + H_2O \quad (6)$$

At very low pH, both acids can be further protonated [Eqs. (3) and (6)] to give the species $AspH_3^{\oplus}$ and $GluH_3^{\oplus}$, but these two cations (with both carboxylate groups and the amino group protonated) are of very limited biological relevance. By contrast, all four anionic species have to be considered, since the corresponding equilibrium constants suggest

significant concentrations in neutral and weakly basic media: $pK = 1.88$ ($AspH_3^{\oplus}$), 3.65 ($AspH_2$), 9.60 ($AspH^{\ominus}$); 2.16 ($GluH_3^{\oplus}$), 4.32 ($GluH_2$), 9.96 ($GluH^{\ominus}$).

Figure 1 shows the distribution of the three species derived from L-$AspH_2$ as a function of pH. The monoanion $AspH^{\ominus}$ is clearly the dominant species in the biologically most relevant pH range 5–9.[25]

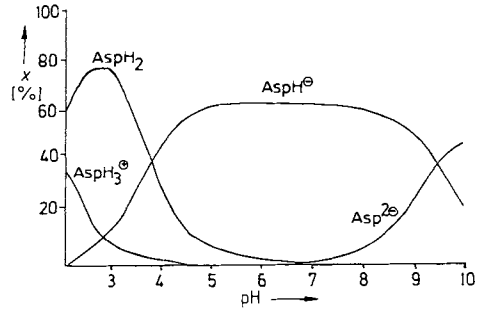

Fig. 1. Dissociation of L-aspartic acid in water as a function of pH.

The monoanions $AspH^{\ominus}$ and $GluH^{\ominus}$ (with protonated amino groups) are potentially bidentate ligands with either two carboxylate groups or the amino group together with one of the two (nonequivalent) carboxylate groups as the donor sites. For pure, dilute aqueous solutions, the amino group is assumed to be protonated, but, in the presence of metal ions, a proton transfer from N to O (α or β/γ) can generate N,O(α) or N,O(β/γ) chelate ligands. Upon coordination, these ambidentate aspartate and glutamate monoanions can form five-, six/seven-, and seven/eight-membered rings and are therefore very adaptable to the conditions of size and charge imposed by the metal.

The dianions are potential N,O(α),O(β) tripod ligands. In such mononuclear complexes, the resulting bicyclic systems have the ring sizes mentioned above.

The free acids $AspH_2$ and $GluH_2$ feature only one carboxylate group; in the protonated forms, no basic sites are left. However, more than one oxygen atom per carboxylate group may be involved in coordination in condensed solid-state structures, where even oxygen bridging of metals may occur (see below). In aqueous solutions, the high donor ability of water molecules generally overrules the donor capacity of carbonyl oxygen atoms (C=O), but not necessarily of the carboxylate oxygen atoms ($C-O^{\ominus}$).

3. Metal-Ion Complexation by Aspartate and Glutamate Ligands in Aqueous Solution

Aspartate and glutamate anions are known to coordinate with many metals, but characterization of these complexes is often still not satisfactory. This is particularly true for those metals whose complexation is "weak", meaning that the complexes are strongly dissociated in dilute aqueous solution. The stability constants of a number of complexes have been determined, largely by potentiometric titration.[27–32]

Although the values indicate relatively stable complexes for the later first-row transition metals (e.g., divalent Fe, Co, Ni, and Cu), this is not true for the common metals (e.g., Mg, Ca, Sr, and Zn or the alkali metals).

The values $\lg K = 2.45$ for Mg(L-AspH)$^{\oplus}$ and $\lg K = 1.90$ for Mg(L-GluH)$^{\oplus}$, as determined in classical studies by *Martell* et al. for dilute aqueous solutions, are a measure of the extensive dissociation of the two basic magnesium complexes. Figure 2 shows the distribution of magnesium aspartate complexes in water as a function of pH.[33]

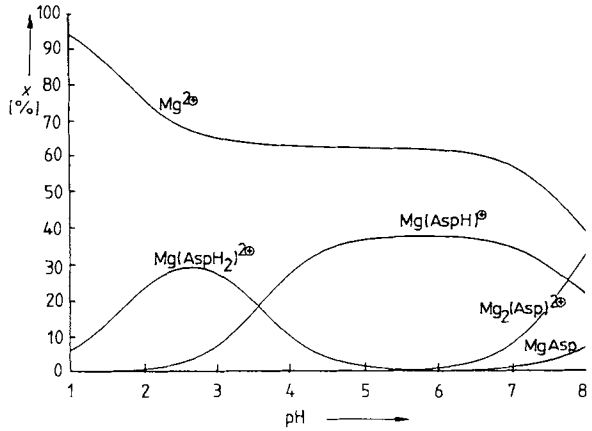

Fig. 2. Distribution of magnesium L-aspartate complexes in water as a function of pH.

These data have recently been confirmed by titrations using ion-sensitive electrodes with ion-selective membranes. The $Mg^{2\oplus}$ concentrations detected over the most important pH range are in good agreement with those calculated from previous measurements.[34]

This dissociation does not mean that these complexes are inherently unstable, but rather indicates that water molecules are able to compete favorably with the amino acids for metal complexation. The energy balance in the system is maintained by a redistribution of hydrogen bonding between the amino and carboxylate functions and the water molecules. The resulting reversibility makes aspartate and glutamate amenable as carriers, or auxiliary carriers, for metals in biological systems. Methods for the determination of structural features of the species present in solution are discussed below.

4. Influence of Aspartate and Glutamate on Transport and Distribution of Magnesium and the Effect of Auxiliary Anions

To compensate for loss of magnesium by structural incorporation (cells, skeleton, etc.) and excretion (perspiration, urine, feces), the body is dependent on regular uptake of magnesium. Should a deficiency arise, as easily revealed by lower magnesium concentrations in serum and tissue, the uptake has to be increased. Moreover, an increase in the magnesium concentration beyond the standard level can also be therapeutically useful in conditions as different as premature labor, eclampsia, or heart attack, where antagonism with $Ca^{2\oplus}$ is important.[20, 35]

The kind of administration (enteral or parenteral) is determined by the galenic form, the dose, and the specific indications. For parenteral administration of a magnesium compound (intramuscular, intravenous), high solubility (no oxide, carbonate, oxalate, orotate) and tissue compatibility (no magnesium chloride!) are of prime importance. For oral administration, maintenance of the acid/base equilibrium is particularly critical if larger doses of magnesium are necessary: anions of weak acids are strong buffers, which lead to a rapid increase in gastrointestinal pH.[20, 36]

Although neutralization of stomach acid by oxides, hydroxides, or carbonates is a standard procedure in gastroenterology, alkalotic metabolic conditions may arise with large quantities of these magnesium compounds. On the other hand, acidosis may occur in treatment with $MgCl_2$. Shifts of the acid/base equilibria are biologically very significant: the action of catecholamines, typical stress hormones, is greatly enhanced under alkalotic conditions, whereas it is reduced under acidotic conditions.[37] Secondary shifts in the electrolyte equilibria (e.g., hypopotassemia under alkalosis) are likely to aggravate the symptoms. Aspartic and glutamic acid have intermediate acid/base properties and therefore do not seriously affect the proton equilibria in the stomach or in body fluids.

Aspartic acid is converted into oxaloacetate through metabolic transamination or oxidative deamination and then fed into the citric acid cycle.[10] Together with glutamic acid, it is thus classified as a glucoplastic amino acid. Glutamic acid plays a key role in transamination processes and in the formation of urea. In the brain, the neurotransmitter γ-aminobutyric acid (GABA) is generated. Drugs based on magnesium complexes of the two acidic amino acids are therefore designed in such a way that both cationic and anionic components play active roles in therapy.

Monitoring of serum and bone magnesium levels, which are transport and storage indicators, in animal tests with rats and cats have shown that enteral availability of magnesium is clearly greater for Mg(L-AspH)Cl than for $Mg(L\text{-}AspH)_2$ or $MgSO_4$. $MgCl_2$ turned out to be significantly more toxic, probably owing to accompanying acidosis.[38] Administration of the complex $Mg(L\text{-}AspH)Cl \cdot 3H_2O$ was more effective than simultaneous administration of $Mg(L\text{-}AspH)_2$ and KCl.[39a] The magnesium uptake was even more rapid using Mg(L-AspH)Br, but interfering bromism makes application for magnesium supplementation inappropriate. In therapeutical dosage, the compound can be used as a daytime seditive showing tranquilizing and thymoleptic effects. In long-term experiments, no bromide intoxication could be observed for this medication, in clear contrast to inorganic bromides.[39b, c]

In agreement with the resorption studies, Mg(L-AspH)Cl proved to be superior to $MgSO_4$ in the treatment of experimental animal heart necrosis models, in that it also lowered adrenalin-induced high blood pressure.[40] These positive effects are ascribed to high magnesium availability, the absence of a dependence on acid/base equilibria,[36, 40] and inhibition of the hypothalamus–hypophysis–adrenalin gland axis activated in acute stress.[41]

The results of the initial animal experiments have been confirmed in tests with livestock.[41, 42] A pronounced protective effect against transport-induced stress, secondary sterility, and cannibalism was observed for a community of 6000 hogs, and stress reactions were also greatly reduced in groups of 1500 cattle and horses. Similar results are to be expected for the corresponding glutamate. However, since resorption processes from the gastrointestinal tract are exceedingly complex (pH range as wide as 2.0–9.5, active and passive mechanisms, liver clearance, enterohepatic cycles, etc.), no detailed knowledge can be claimed as yet regarding the individual mechanistic steps for either the aspartate or the glutamate complex.

5. Approaches to Structure Elucidation of Species in Solution and Matrices

Colligative properties, as measured, for example, by electrochemical methods (potentiometry, conductivity) or by osmometry, can serve to determine stoichiometry, charge, and distribution of species in solution (cf. Figs. 1 and 2), but give no clue as to the structure of the individual components. Other approaches therefore had to be chosen in order to clarify the mode of complexation of metals by aspartate and glutamate.

IR and Raman studies met with only limited success owing to the complexity of the system; the difficulties encountered are mainly due to the comparable effects of metal complexation and hydrogen bonding on molecular vibrations. Similar problems arose in the evaluation of optical rotation and circular dichroism.[43]

NMR spectroscopy is a more promising technique, at least for the elucidation of the aspartate and glutamate conformations through the determination of chemical shifts, coupling constants, and relaxation times as a function of pH, concentration, and temperature.[44] Three ground-state conformations have been proposed for the two amino acids and their complexes[45] (Fig. 3). When acid titrations of magnesium

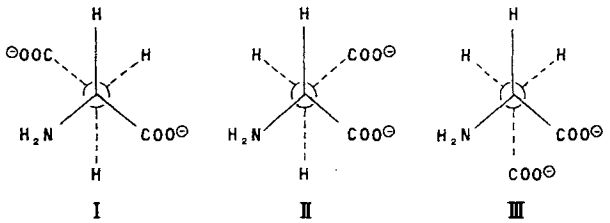

Fig. 3. Proposed ground-state conformations of L-aspartic (L-glutamic) acid, determined by NMR spectroscopy. I, N,O chelate; II, O,O chelate; III, N,O,O tripod.

aspartate (glutamate) solutions are monitored by ^1H and ^{13}C NMR spectroscopy, the resulting curves for the δ and J values are in good agreement with potentiometric measurements. The transition from one prevailing species to the other (cf. Fig. 2) is shown by similar inflections in the curves. NMR spectroscopy is a "slow" method, however, and only yields time-averaged parameters for all species present in solution.

Nevertheless, for pH ranges where one species is dominant in solution, the J values can give a clear indication as to the

structure of the ligand. For magnesium aspartate and glutamate solutions at pH = 8, conformation **III** (Fig. 3) appears to prevail; at lower pH, conformation **I** becomes important.[34] This result indicates that the dianion $Asp^{2\ominus}$ functions as a tripod ligand for $Mg^{2\oplus}$, whereas $AspH^{\ominus}$ is N,O(α)-bidentate.

For other metals, with an even more extensive dissociation (e.g., the alkali metals), evaluation of the spectra is less straightforward. ^{7}Li NMR spectroscopy shows differences in the δ values and line widths for lithium aspartate and glutamate solutions, but the pH dependence is not very pronounced. Although the variations in the line widths indicate differences in the environment of the metal, no detailed information can be deduced.[34] This situation is not unlike the results of related NMR studies with the quadrupolar nucleus ^{23}Na.[46]

By contrast, NMR studies using the nucleus ^{113}Cd have recently attracted considerable interest. The δ values of Cd are strongly dependent on the metal environment and thus a good indicator of the coordination number and/or geometry. Since $Cd^{2\oplus}$ can replace $Ca^{2\oplus}$ ions in their specific binding sites, this technique can also be used to probe the coordination sphere of $Ca^{2\oplus}$. X-ray results seem to confirm the assignments made on the basis of NMR experiments.[47–49] It is no coincidence that, in the proteins investigated in this important study, aspartate groups are the main contact sites for the metals!

6. The Structures of Crystalline Materials

Crystal structure studies of metal aspartate and glutamate complexes have recently been renewed and intensified for several reasons: (1) Investigations of aqueous solutions of the compounds have not yielded fully satisfactory information on the mode of coordination of the amino acids. (2) Solid-state structures may give at least a clue regarding the structures to be expected in solution. (3) In the light of the low equilibrium constants, it had been questioned whether the species present in solution and/or isolated as solids were true coordination compounds of the amino acid and not just aquo complexes with aspartate or glutamate as the counterions. (4) For economical and galenic reasons the formulations for magnesium therapy are often amorphous binary or ternary compositions (e.g., $Mg(L\text{-}AspH)_2 \cdot 4H_2O$ or $Mg(L\text{-}AspH)Cl \cdot 3H_2O$), with the stoichiometry adjusted by spray-drying of solutions with the desired quantities of the components; it was therefore of prime importance to prove that the latter products, for example, were not just mixtures of $Mg(L\text{-}AspH)_2 \cdot aq$ and $MgCl_2 \cdot aq$, but discrete ternary phases.

Unfortunately, many metal aspartate and glutamate phases are extremely difficult to crystallize. Prolonged (literally year-long) efforts were often required to isolate suitable single crystals. But for some phases this has never been possible, and therefore there are still gaps in the systematics of these complexes. The following inventory covers the literature until early 1990, when structural studies were still under way in several laboratories; the results of these studies may make important additions to the present picture of metal binding by amino acids.

Most of the studies refer to species derived from the L-amino acids, which are the dominant species in biological systems and are used exclusively for medication. Although the crystal structures of the D forms would only be mirror images, the racemic compounds have entirely different crystal structures, with serious implications for biological matrices.

6.1. Magnesium Aspartates and Glutamates

6.1.1. *Magnesium L-Aspartate Trihydrate*

A compound of the composition $Mg(L\text{-}Asp) \cdot 3H_2O$ is isolated from strongly alkaline solutions (pH > 10) of magnesium aspartate (cf. Fig. 2), regardless of the initial composition.[50] Crystal growth from concentrated solutions (containing KOH) may require several months. The structure of the material consists of chains composed of individual mononuclear complexes, where the $Asp^{2\ominus}$ dianion acts as an N,O(α),O(β) tripod ligand. The environment of the magnesium atom is octahedral with two (of the three) hydrate water molecules and a carbonyl oxygen atom of a neighboring unit occupying the remaining three vertices (Fig. 4). The strands of complex units are interconnected by hydrogen bonds involving the third hydrate water molecule.

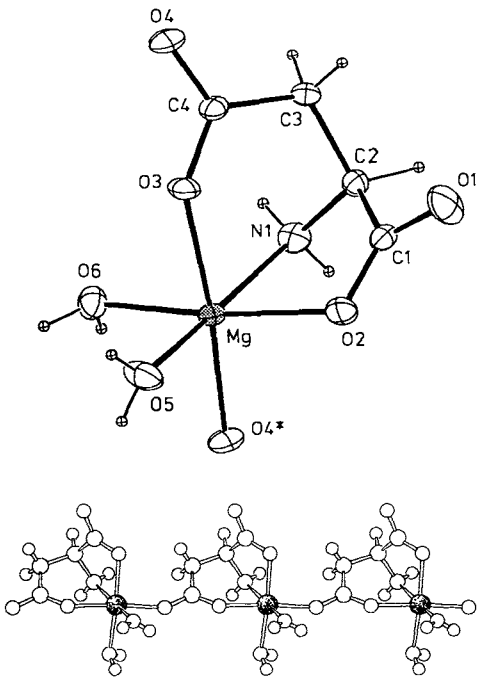

Fig. 4. Crystal structure of $Mg(L\text{-}Asp) \cdot 3H_2O$. Top: Individual complex unit. Bottom: Coordination polymer. (Interstitial water molecules are not shown.)

The crystal structure of $Mg(L\text{-}Asp) \cdot 3H_2O$ clearly shows the chelating ability of the aspartate dianion for $Mg^{2\oplus}$ ions and the preference of the latter for octahedral coordination. The compound dissolves only slowly in cold water. It is tempting to propose that, in this solvation process, individual complexes are released from the chains through substitution of the carbonyl oxygen donor by a water molecule. Further hydrolysis may remove one of the three donor func-

tions from the metal, converting the tripod into a bidentate ligand. Such a process would account for the alkaline reaction of the compound (pH = 9), since protonation of the liberated functional group leads to an increase in the $OH^{\ominus}$ concentration.

6.1.2. *Magnesium L-Glutamate Tetrahydrate*

From alkaline (KOH) solutions of magnesium glutamate, the species Mg(L-Glu) can be obtained as the dihydrate or the tetrahydrate, depending on the reaction conditions. The crystal structure of the tetrahydrate[51] has been determined, since, owing to its higher water content, it should resemble more closely the solution state of the complex. Crystalline Mg(L-Glu) · $4H_2O$ is built from individual complex units, in which the magnesium atom is N,O(α)-chelated by the L-$Glu^{2\ominus}$ dianion. The γ-carboxylate function is not engaged in metal coordination, and the remaining four vertices of the octahedron are occupied by water molecules (Fig. 5). Hence,

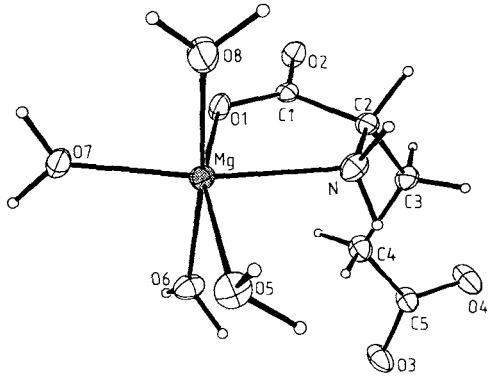

Fig. 5. Crystal structure of Mg(L-Glu) · $4H_2O$.

whereas all three possible ring systems, including a seven-membered heterocycle, are present in the tripod of the aspartate analogue, the largest (eight-membered) chelate ring is avoided in the glutamate complex. Instead, the "dangling" γ-carboxylate group is engaged in hydrogen bonding with water molecules of neighboring complexes.

6.1.3. *Magnesium Bis(Hydrogenaspartate) and Bis(Hydrogenglutamate) Hydrates*

Neutralization of MgO, $Mg(OH)_2$, or $MgCO_3$ with aspartic acid or glutamic acid yields the bis(hydrogenaspartates) or bis(hydrogenglutamates) in quantitative yield.[52] The products generated from the pure L or D forms of aspartic or glutamic acid have to date only been obtained in microcrystalline form, and their structures are unknown. By contrast, racemic aspartic acid yields the complex Mg(D,L-$AspH)_2$ · $4H_2O$, which can be readily crystallized from aqueous methanol. This product is also formed in the racemization of Mg(L-$AspH)_2$ in basic medium at elevated temperature.

In the crystal lattice the compound again shows octahedral coordination around magnesium, with four water molecules occupying equatorial positions and β-carboxylate oxygen atoms of the two anions in the (*trans*) axial positions (Fig. 6). The two amino acids are optical antipodes and structurally related by a center of symmetry (at Mg). The structure of the tetrahydrate is a caveat in that it shows that the aspartate monoanions, unlike the dianions, do not necessarily act as bidentate ligands towards magnesium, their interactions with the metal being reduced in this case to a single, monodentate contact. In the dihydrate, the aspartate will have to coordinate in a multidentate fashion, of course, owing to the reduced number of hydrate water molecules available. In dilute aqueous solution, however, the aspartate anions may even fully dissociate from the magnesium center, as indicated by the dissociation equilibria.

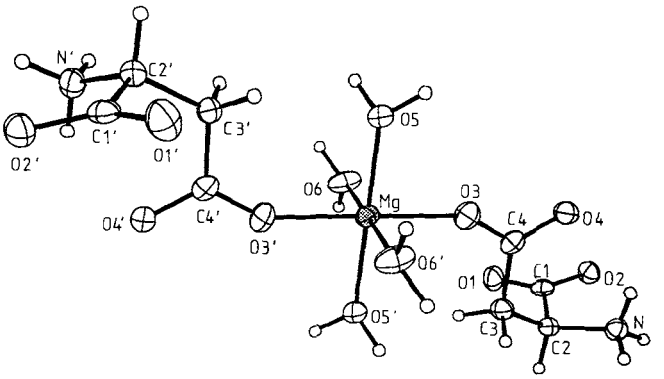

Fig. 6. Crystal structure of Mg(L, D-$AspH)_2$ · $4H_2O$.

Clearly, the delicate balance between enthalpy and entropy terms related to metal coordination/solvation and aspartate protonation (in hydrogen bonds), already advanced in the discussion of the colligative properties of the solutions, also shows up in the structural features of the crystalline compounds.

6.1.4. *Magnesium L-Hydrogenaspartate Chloride Trihydrate*

A compound of the stoichiometry Mg(L-AspH)Cl · $3H_2O$ is produced by spray-drying of aqueous solutions containing the components $Mg^{2\oplus}$, $AspH^{\ominus}$, $Cl^{\ominus}$ in the molar ratio 1:1:1. This preparation must be carried out under carefully controlled conditions in order to avoid racemization of the amino acid, condensation with formation of diketopiperazines, and other side reactions leading to contamination of the product. Mg(L-AspH)Cl is an established drug for magnesium therapy. The spray-dried trihydrate material is X-ray amorphous. In very tedious experiments it has recently been possible to crystallize the compound and to determine its structure.[53]

Mg(L-AspH)Cl · $3H_2O$ has a layer structure, where the chloride anions and one of the three water molecules are found between sheets of the composition $[Mg(L\text{-}AspH)(H_2O)_2^{\oplus}]_n$. The layers represent cationic coordination polymers with the magnesium atoms in an octahedral environment. The hydrogen aspartate anions function as O(α),O(β)-chelating ligands through their α- and β-carboxylate groups; the amino group is protonated and has no metal contact

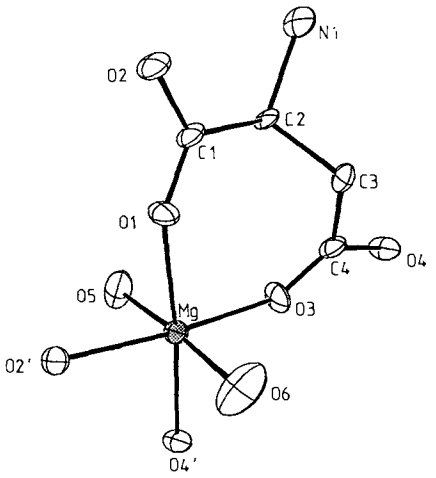

Fig. 7. Crystal structure of Mg(L-AspH)Cl · $3H_2O$; one of two crystallographically independent, but similar moieties.

(Fig. 7). Two hydrate water molecules and two carbonyl oxygen atoms of neighboring complex units occupy the remaining coordination sites of the octahedron. A network of hydrogen bonds connects the layers and the interstitial water molecules. The chlorides form distinct hydrogen bonds to the ammonium groups. Two adjacent layers are crystallographically nonequivalent, but the structural differences are almost negligible. Figure 8 shows a projection of one of these layers and the corresponding chloride ions and hydrate water molecules.

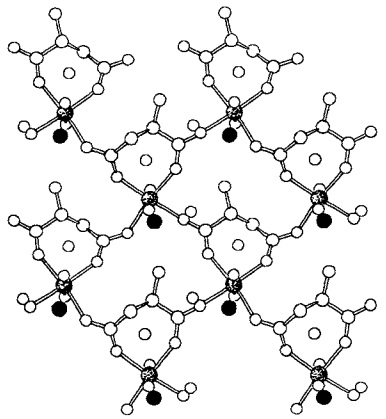

Fig. 8. Layer structure of Mg(L-AspH)Cl · $3H_2O$. Filled circles, Cl; small empty circles, interstitial water; dotted circles, Mg.

Mg(L-AspH)Cl · $3H_2O$ is thus a discrete phase and not a mixture of two or more components. Its special structure shows yet another mode of coordination between magnesium and aspartate ions as far as the individual complex units are concerned (cf. Fig. 7). In addition, the bulk structure suggests novel features in the degradation (hydration, hydrolysis) and resorption (ion complexation and transport) of the compound. Layer structures of this kind are likely to exhibit ion-exchange properties until the (slow) degradation of the sheets leads to a breakdown of the framework. Moreover, the degradation need not lead immediately to mononuclear complex units; instead, it can yield di- or polynuclear species with differing transport behavior. Probably, therefore, the distinct pharmacological properties of this compound are partly of structural origin. Ca(L-GluH)Cl · H_2O has a similar structure (see Section 6.2).

6.2. The Structures of Crystalline Calcium, Strontium, and Barium Analogues

Aspartates and glutamates of the heavier alkaline-earth metals were found to crystallize more readily than their magnesium analogues. Roughly the same number of structures with calcium has been determined, but most of the results were available earlier than for magnesium.

Like magnesium, calcium forms crystalline complexes of the types Ca(L-Asp), Ca(L-AspH)$_2$, and Ca(L-AspH)Cl. Depending on the reaction conditions, Ca(L-Asp) is obtained in the form of two hydrates. A tetrahydrate is generated on neutralization of $Ca(OH)_2$ with L-$AspH_2$. On the other hand, $CaCO_3$ and $AspH_2$ first yield the hydrogen aspartate Ca(L-AspH)$_2$, which can be converted into Ca(L-AspH)Cl in a redistribution reaction with $CaCl_2$. In strong alkali (KOH), the latter finally affords a precipitate of the dihydrate of Ca(L-Asp). Calcium L-glutamate, Ca(L-Glu), obtained like Ca(L-Asp) · $4H_2O$, was found to crystallize as the trihydrate.

Aspartate and glutamate structures have also been determined for strontium and barium. Sr(L-Glu/L-Asp) and Ba(L-Glu/L-Asp) are available from the metal dihydroxides and glutamic/aspartic acid and are crystallized as tetra- and hexahydrates, respectively.

6.2.1. Calcium L-Aspartate Tetrahydrate and Dihydrate

In Ca(L-Asp) · $2H_2O$, the aspartate anion functions as an N,O(α),O(β) tripod ligand. The individual complex units (Fig. 9) are arranged in double strands with a peculiar pattern of metal bridging by carbonyl oxygen atoms (Fig. 10).[54] The coordination number of the calcium atoms is eight: apart from the tripod ligand, two hydrate water molecules and three O(β) oxygen atoms of two neighboring complex units are part of the inner coordination sphere. The polymeric strands are cross-linked by hydrogen bonds.

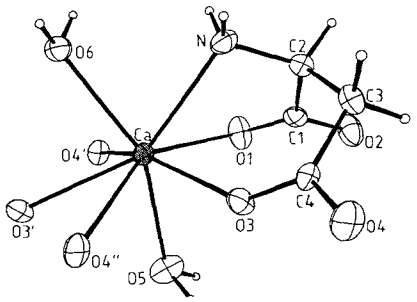

Fig. 9. Crystal structure of Ca(L-Asp) · $2H_2O$.

In Ca(L-Asp) · $4H_2O$, the aspartate anion is present only as an N,O(α) chelate ligand in the individual complex unit

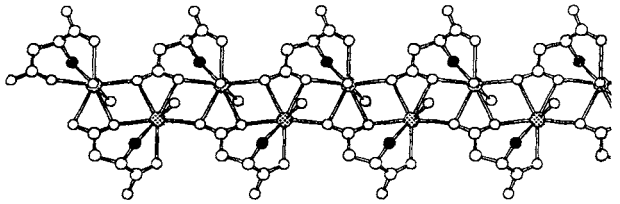

Fig. 10. Double-chain structure of Ca(L-Asp) · $2H_2O$. Dotted circles, Ca; filled circles, N.

(Fig. 11), but the β-carboxylate group is coordinated to a neighboring unit. Through these contacts, the complexes are again associated into chains, which, however, feature a single

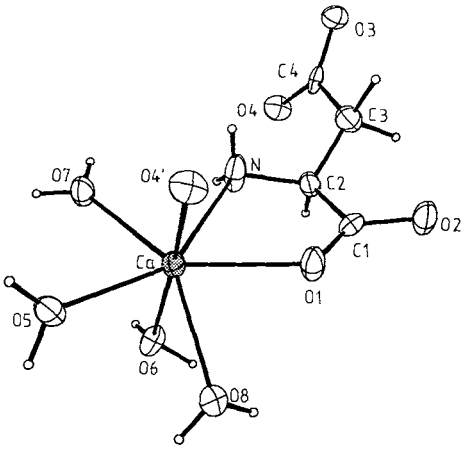

Fig. 11. Crystal structure of Ca(L-Asp) · $4H_2O$.

metal strand (Fig. 12). The coordination number of the calcium atoms is again eight, with all four hydrate water molecules attached to the metal. There are two crystallographically independent complex units in the crystal, but with only minor geometrical differences. Hydrogen-bonding connects the polymeric strands into a three-dimensional network.

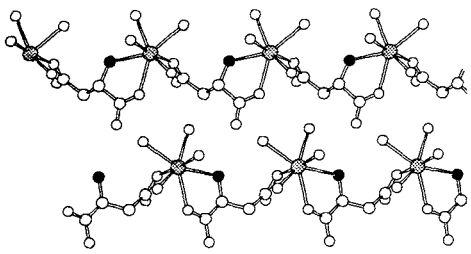

Fig. 12. Chain structure of Ca(L-Asp) · $4H_2O$.

6.2.2. *Calcium* L-*Glutamate Trihydrate*

The individual units of crystalline Ca(L-Glu) · $3H_2O$[55] closely resemble those in the aspartate dihydrate. The amino acid is N,O(α)-chelating, and the γ-carboxylate groups of two neighboring molecules, together with two hydrate water molecules, are part of the inner coordination sphere. Since both oxygen atoms of each of the γ-carboxylate groups have about the same Ca–O(γ) distance, the coordination number of the calcium atom is again eight. The bulk structure is a true three-dimensional coordination polymer, not only based on hydrogen bonding as in the chain and layer structure of the aspartate analogues.

6.2.3. *Strontium and Barium* L-*Aspartate Trihydrates and* L-*Glutamate Hexahydrates*

The strontium and barium aspartates, as well as the two glutamates, are isomorphous.[51, 56] Differences arise from the lengthening of the chain by one CH_2 group on going from aspartate to glutamate; surprisingly, this change is simply compensated for by inclusion of three more interstitial water molecules for the glutamates. Owing to the difference in the atomic radii of Sr and Ba, there are small deviations in the bond distances and angles, but the general features are the same. The metals are nine-coordinate (Fig. 13), with four

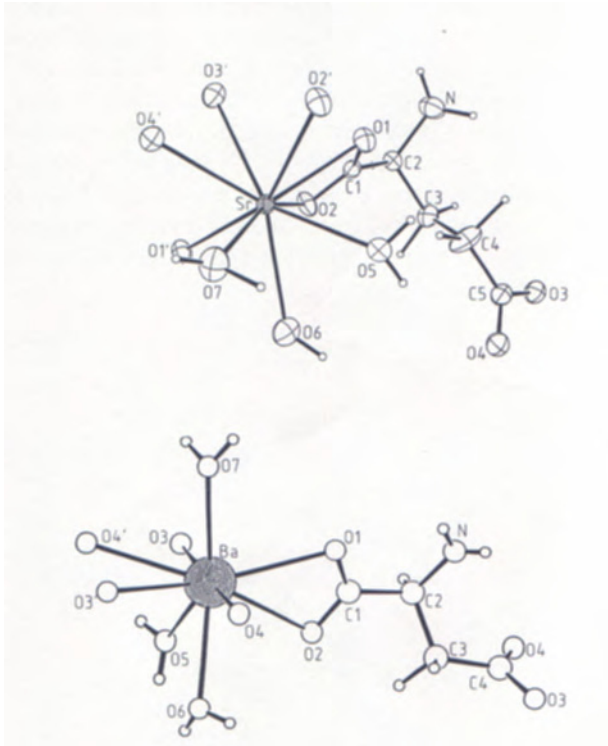

Fig. 13. Crystal structures of Sr(L-Glu) · $6H_2O$ (top) and Ba(L-Asp) · $6H_2O$ (bottom).

α-carboxylate and two β/γ-carboxylate oxygen atoms (of three different anions) and three water molecules as nearest neighbors. The metals are arranged in double strands and bridged via the O(α) atoms. These double strands are bridged by the O(β/γ) contacts to give the layer structures (Fig. 14). In the glutamate structure, the remaining three crystal water molecules are part of the hydrogen-bonding system connecting the layers.

High coordination numbers, as found for the aspartate and glutamate complexes of strontium and barium, are rare in the coordination chemistry of amino acids. Important parallels are found with the large cations from the lanthanoid series, however. A typical example is Ho(L-AspH)-Cl_2 · $6H_2O$. Here, the Ho atoms are eight-coordinate. In the

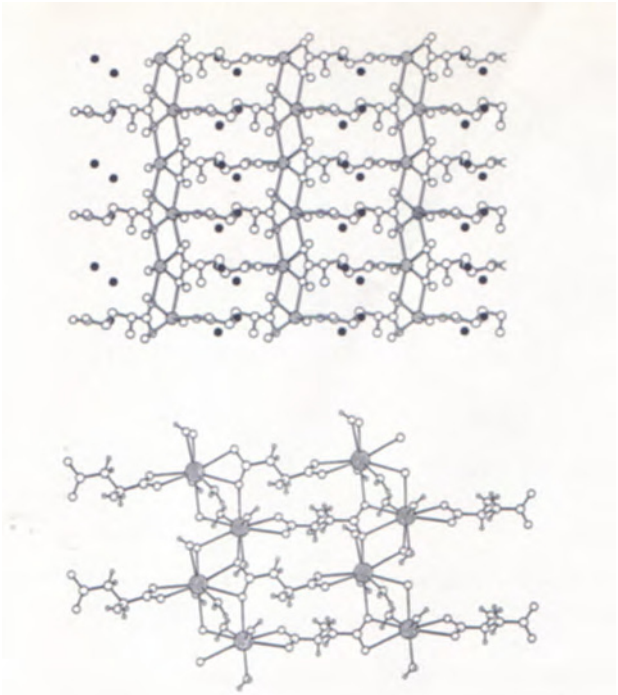

Fig. 14. Layer structures of Sr(L-Glu) · $6H_2O$ (top; filled circles, H_2O) and Ba(L-Asp) · $6H_2O$ (bottom); interstitial water molecules not shown.

binuclear praseodymium complex Pr_2(L-GluH)$_2(ClO_4)_4 \cdot 11H_2O$, the metal atoms are even nine-coordinate.[57, 58]

6.2.4. Calcium Bis(L-Hydrogenglutamate) Tetrahydrate and Calcium L-Hydrogenglutamate Chloride Monohydrate

The compounds Ca(L-GluH)Cl · H_2O and Ca(L-GluH)$_2$ · $4H_2O$ are readily obtained by following a procedure similar to that used for the magnesium hydrogen aspartate chloride and magnesium hydrogen aspartate complexes.

Ca(L-GluH)Cl · H_2O again features a layer structure. The chloride ions are eclipsed between sheetlike cationic coordination polymers of the composition $[Ca(L\text{-}GluH)^{\oplus}(H_2O)]_n$. In the complex unit the calcium atoms are hexacoordinate with five oxygen atoms from five different $(L\text{-}GluH)^{\ominus}$ anions and the water molecule directly attached to the metal. There are thus no chelating interactions. The amino group is protonated and hydrogen-bonded to the chloride counterion.

Ca(L-GluH)$_2$ · $4H_2O$ has a structure with a three-dimensional coordination network consisting of alternating layers of $GluH^{\ominus}$ anions and $Ca^{2\oplus}$ cations. The calcium atoms are hexacoordinate with four equatorial contacts to carboxylate oxygen atoms of four different anions [$2 \times O(\alpha)$, $2 \times O(\gamma)$] and two axial water molecules. The amino groups are protonated and, together with the remaining two interstitial water molecules, are engaged in hydrogen-bonding.

6.3. Beryllium, the Missing Link

Very surprisingly, there is very little information on the structural chemistry of beryllium complexes of amino acids. No beryllium aspartates or glutamates have been isolated in the crystalline state, and information on the nature of their aqueous solutions is very limited.[61–63] The known structural chemistry of beryllium complexes indicates that $Be^{2\oplus}$ ions will probably strictly adhere to coordination number four in amino acid complexes. On this basis alone, the coordination chemistry of beryllium with aspartate and glutamate anions will be entirely different from that of its heavier alkaline-earth congeners. It is also tempting to suggest that beryllium toxicity is directly associated with this change in coordination chemistry towards amino acids, peptides, and proteins, as well as polysaccharides and related natural polyfunctional ligands. Work in this direction is in progress. Parallels in the coordination chemistry of lithium, which also has a very small ionic radius, should be noted.

6.4. Structural Relations with Complexes of the First-Row Transition Metals

Divalent first-row transition elements form aspartate and glutamate complexes with a stoichiometry similar to that of the alkaline-earth metals. In the intermediate pH range (5–9), the composition M(L-Asp/L-Glu) prevails. Structurally, the aspartate compounds are found to be isomorphous for M = Mn, Fe, Co, Ni, and Zn.[64–66] The complex units contain the $(L\text{-}Asp)^{2\ominus}$ dianion as an N,O(α),O(β) tripod to the hexacoordinated metals. These units are arranged in chains with a connectivity pattern not unlike that found for Mg(L-Asp) · $3H_2O$ (cf. Fig. 3), except for a difference in the positioning of the carbonyl oxygen atom originating from a neighboring molecule. In the magnesium complex, this occurs *trans* to O, whereas it is *trans* to N in transition-metal complexes (Fig. 15).

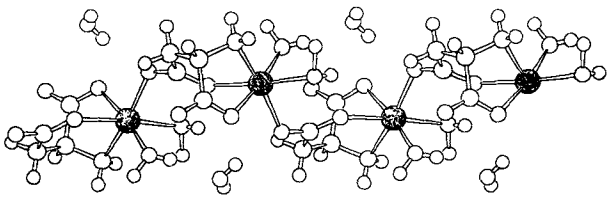

Fig. 15. Chain structure of Mn(L-Asp) · $3H_2O$.

Hydrogen aspartate and glutamate complexes of first-row transition metals are less well represented. The product obtained from ZnO and L-glutamic acid was shown not to be the expected Zn(L-GluH)$_2$, but to contain zinc associated with two L-pyroglutamate anions.[67] In Zn(L-pGlu)$_2$ ·

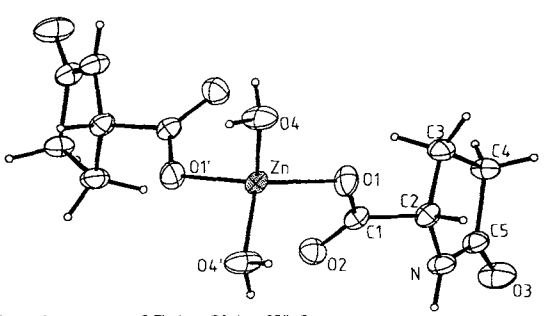

Fig. 16. Crystal structure of Zn(L-pGlu)$_2$ · $2H_2O$.

$2H_2O$, zinc has coordination number four and the two L-pGlu units are related by a twofold axis (Fig. 16).

Zinc bis(L-hydrogenaspartate) and zinc dichloride form a crystalline ternary phase, Zn(L-AspH)Cl, which contains no hydrate water.[68] The structure of the compound features a three-dimensional network in which the zinc atoms are again tetracoordinate. Three oxygen atoms (of three different hydrogen aspartate anions) and the chloride anion are ligands to the metal (Fig. 17). This situation is unique in comparison to the structures of the corresponding compounds of Mg or

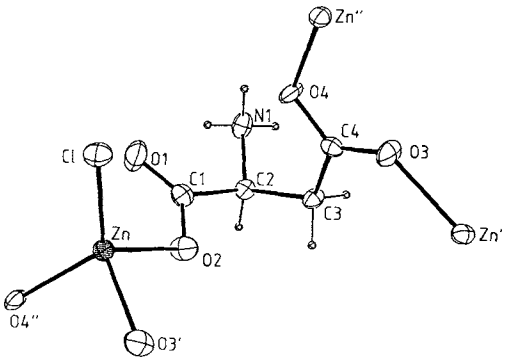

Fig. 17. Environment of the zinc and aspartate units in the three-dimensional network of Zn(L-AspH)Cl.

Ca, where coordination numbers are six or seven and the chloride counterions are not part of the inner coordination sphere of the metals. Though higher coordination numbers are known, the obvious preference of zinc for low coordination and for halide contacts is noteworthy and probably reflects the completely different biochemical activity of the metal.

6.5. Alkali Aspartate and Glutamate Complexes

A few representative aspartate and glutamate complexes of lithium, sodium, and potassium have been structurally characterized by X-ray diffraction studies. A comparison of the results shows variations similar to those encountered with the alkaline-earth analogues. With the small lithium cation, the coordination number is restricted to four, whereas sodium and potassium allow higher coordination numbers, but are obviously less selective.

6.5.1. *Lithium L-Hydrogenaspartate Monohydrate*

Neutralization of LiOH or Li_2CO_3 with L-$AspH_2$ yields a crystalline monohydrate, which has a layer structure.[69] The four-coordinate lithium centers are arranged in double strands with carboxylate oxygen atoms as bridging units (Fig. 18). The amino group is protonated and not coordinated to lithium. Together with the interstitial water molecule, it is responsible for extensive hydrogen bonding between the layers.

The compounds Li_2(L-Asp) · $2H_2O$, Li(L-GluH), and Li_2(L-Glu) have also been prepared, but their structures are unknown.

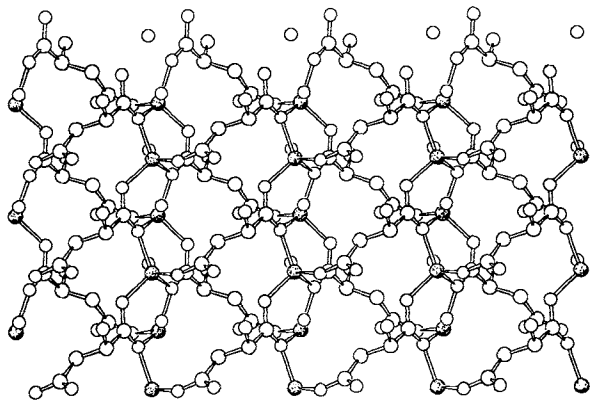

Fig. 18. Three-dimensional network of Li(L-AspH) · H_2O.

6.5.2. *Sodium and Potassium L-Hydrogenaspartates and -glutamates*

For crystalline sodium aspartates and glutamates only limited and preliminary information is available. Sodium L-hydrogenglutamate is reported to crystallize as a monohydrate, Na(L-GluH) · H_2O, in which sodium is hexacoordinate. Carboxylate oxygen atoms bridge adjacent metal atoms.[70]

Potassium L-hydrogenaspartate,[69] obtained as the dihydrate K(L-AspH) · $2H_2O$ upon neutralization of KOH with L-$AspH_2$, has a chain structure reminiscent of the structures of Sr/Ba(L-Glu) · $6H_2O$. The metal atoms are arranged in double strands, bridged by carboxylate oxygen atoms. As a special feature, the potassium compound also shows metal-bridging water molecules. The coordination number of the potassium atoms is only seven, since the α-carboxylate and the amino groups are not coordinated to the metal (Fig. 19).

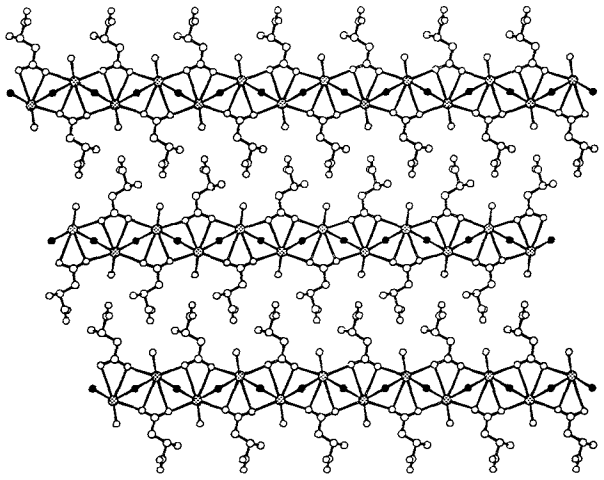

Fig. 19. Double-chain structure of K(L-Asp) · $2H_2O$; shaded circles, K; filled circles, H_2O.

Potassium L-hydrogenglutamate,[71] obtained similarly as a monohydrate, K(L-GluH) · H_2O, has a layer structure in which the potassium atoms are arranged in parallel strands and interconnected by the hydrogenglutamate anions (Fig. 20). The potassium atoms are hexacoordinate with the

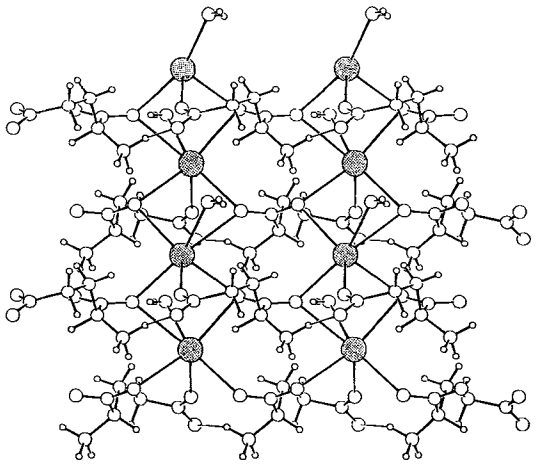

Fig. 20. Layer structure of K(L-GluH) · H_2O.

coordination polyhedron in the form of a distorted trigonal prism. The L-$GluH^{\ominus}$ anion is O(α),O(γ)-chelating, giving rise to an eight-membered ring, with carboxylate atoms also in a metal-bridging position. The amino group of the ligand is protonated and hydrogen-bonded, but not metal-coordinated.

No stoichiometric or structural data are available on related rubidium or cesium compounds.

7. "Complexation" of Magnesium and Other Cations by Related Counterions

Among formulations used for magnesium therapy, the orotates also have a special position.[72] For these compounds, in particular, it had remained an open question whether the (hydrogen)orotate anions would really form complexes with magnesium or just function as counterions for the hexaaquamagnesium cation.

The magnesium salt $Mg(OrH)_2$ of 6-uracilic acid (orotic acid, OrH_2) can be crystallized in the form of several hydrates. Of these, the octahydrate, with the highest number of water molecules, was chosen for structural studies, since its structural situation would perhaps most closely resemble the solution structure.[73] The *octa*hydrate was also found to crystallize from solutions obtained from samples with a smaller number of hydrate water molecules in the stoichiometric unit.

7.1. Magnesium Bis(Hydrogenorotate) Octahydrate

$Mg(OrH)_2 \cdot 8H_2O$[73] is generated by neutralization of MgO, $Mg(OH)_2$, or $MgCO_3$ with orotic acid or by metathesis of magnesium salts and alkali orotates, followed by crystallization. Single-crystal X-ray diffraction studies showed the compound to consist of hexaaquamagnesium dications and two hydrogenorotate anions, which are associated through hydrogen-bonding (Fig. 21). Crystallographically, the two anions are related by a center of symmetry (at Mg). This rules out the classification of magnesium orotates as "complexes", since it is extremely unlikely that, upon dissolution in water, the orotate anions would enter the magnesium coordination sphere by substitution of water molecules. For a rationalization of the therapeutic effects of the magnesium orotate drugs, an auxiliary or independent anion-based mechanism must be considered.

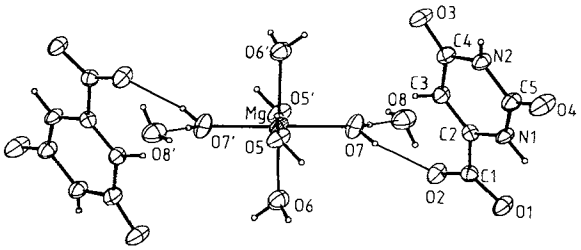

Fig. 21. Stoichiometric unit $Mg(OrH)_2 \cdot 8H_2O$.

The structures of ammonium hydrogenorotate monohydrate,[74] nickel(II) orotate tetrahydrate,[75] and *cis*-diaminoplatinum(II) orotate[76] were determined earlier. With the transition metals nickel and platinum, true complexes are formed, whereas the ammonium salt is a hydrogen-bonded network.

Lithium hydrogenorotate was recently found to crystallize as the monohydrate, which has a very simple layer structure (space group $P\bar{1}$). The lithium atoms are tetracoordinated to three orotate oxygen atoms and one water oxygen atom (Fig. 22).

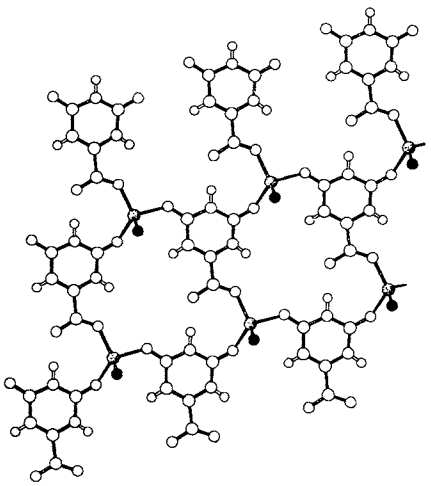

Fig. 22. Layer structure of lithium hydrogen orotate monohydrate.

Electrochemical studies have also shown that alkaline-earth orotates are "weak" complexes with β values decreasing in the series Mg (2.41), Ca (2.34), Sr (1.91), and Ba (1.62) under standard conditions.[77]

7.2. Magnesium Citrate and L-Pyroglutamate Compounds

Apart from the aspartate/glutamate and orotate complexes described above, magnesium citrate and L-pyroglutamate hydrates (pidolates) have been employed in magnesium ther-

apy. Some years ago X-ray diffraction studies on the citrate complex (as a decahydrate) showed the magnesium atoms to be only partially present as part of a true citrate complex: one of the three magnesium ions is found as part of a hexaaquo complex (Fig. 23).[78a]

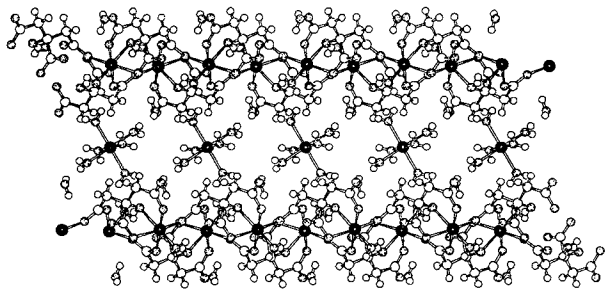

Fig. 23. Stoichiometric unit of $[Mg(H_2O)_6][MgC_6H_5O_7(H_2O)]_2 \cdot 2H_2O$.

The whole structure can be described as a coordination polymer network composed of triple strands of metal complexes and hydrates. The citrate anion acts as a multidentate ligand with tripod and bridging functions. The constitution can be best accounted for by the formula $[Mg(H_2O)_6]^{2\oplus}$ $2[MgC_6H_5O_7(H_2O)]^{\ominus} \cdot 2H_2O$.

Magnesium bis(L-pyroglutamate) hydrates, also known as magnesium pidolates, can be obtained either by dehydration of magnesium bis(L-hydrogenglutamate) or by metathesis reactions with L-pyroglutamates. These methods have recently turned out to be very efficient processes.[78b]

The structures of the magnesium derivatives are still unknown, but a zinc[67] (Fig. 16) and a sodium[78c] complex have been characterized, as already mentioned above. They show totally different coordinative features.

8. Scope and Problems of "Magnesium Therapy"

The therapeutic advantages of parenteral administration of magnesium for compensation of a deficiency or as a $Ca^{2\oplus}$ antagonist are unquestionable for treatment of disorders such as eclampsia, preeclampsia, or premature labor. In several placebo-controlled studies, positive effects in the treatment of acute myocardial infarction (reduction in mortality and in frequency of arrhythmias) and digitalis intoxication have been demonstrated.[21, 79] Other indications, such as ethanol withdrawal symptoms, extracellular calcification, angina pectoris, and asthma, need further study.

Oral administration would of course be the preferred form of medication, especially for lighter, nonacute forms of magnesium deficiency. Since these are difficult to monitor by standard laboratory techniques—cellular deficiency may not necessarily be associated with hypomagnesemia—and often are accompanied by secondary shifts of Na, K, and/or Ca levels, leading to complex clinical symptoms, the success of an oral therapy has to be cross-checked very thoroughly against placebos. Particular attention should again be given to the fact that different magnesium compounds may lead to entirely different results.

The following indications appear to be amenable to magnesium therapy at least for oral application of higher doses, predominantly of Mg(L-AspH)Cl preparations:

- Hypomagnesemia (< 0.76 mmol L^{-1} serum), caused by Mg-deficient diet, disturbances of enteral absorption, high (mainly renal) loss, or increased demand for magnesium and accompanied by corresponding symptoms
- Constipation, in particular with spastic symptoms.[80]
- Tetanic syndrome, with or without hypomagnesemia[21, 81]
- Premature labor and nocturnal calf cramps during pregnancy[82, 83]
- Diuretic-induced disorder associated with treatment of arterial hypertension[84–86]
- Stress-induced hypertension[87]
- Cardiac arrhythmias[88, 89]

Positive effects on other indications need further confirmation, and pertinent studies are in progress.[90–92]

G. B. Weiss has summarized the present knowledge (1986) as follows: "Thus, the possible therapeutic applications of an orally effective magnesium salt like magnesium (hydrogen)-aspartate chloride include established indications in frank hypomagnesemic states. In addition, Mg(AspH)Cl has a potentially broad range of therapeutic activity as an orally effective $Ca^{2\oplus}$-like membrane stabilizer and a physiological cellular $Ca^{2\oplus}$ antagonist."[93]

Because of this medical interest, basic research in the area of alkaline-earth and alkali aspartate and glutamate chemistry has been given renewed attention in recent years, with a focus mainly on magnesium complexes. It is to be expected, however, that similar therapeutic perspectives will emerge for the corresponding calcium compounds, for example, since availability, distribution, and biological effects depend so strongly on the nature of the individual chemical and its galenic formulation. In addition, there is the advantage that no "artificial" auxiliary carrier ligand needs to be introduced with a completely unknown spectrum of side effects.

The research reported in this article has been supported by the Deutsche Forschungsgemeinschaft (Leibniz-Programm), the Fonds der Chemie und Biologischen Chemie, and the Alexander von Humboldt-Stiftung (D.L.W.). Synthetic and analytical studies have been carried out mainly by Dr. Ina Bach, Dipl.-Chem. Patrizia Mikulcik, and Dr. Annette Schier (TU München), as well as by Dr. G. Manninger and G. Hopf (Verla-Pharm). The structural studies were performed, in the X-ray laboratory of TU München, by Prof. Dr. G. Müller, Dr. D. L. Wilkinson, J. Riede, Dipl.-Chem. P. Mikulcik, and, last but not least, Dipl.-Chem. O. Kumberger, who also has been particularly helpful in providing the drawings of the structures. Their cooperation is gratefully acknowledged.

Received: March 26, 1990 [A 783 IE]
German version: *Angew. Chem. 102* (1990) 1122

[1] H. C. Freeman in G. L. Eichhorn (Ed.): *Inorganic Biochemistry, Vol. 1*, Elsevier, Amsterdam 1964, Chapter 4.
[2] M. A. Fiabane, D. R. Williams: *The Principle of Bioinorganic Chemistry*, Chem. Soc., London 1977.
[3] R. J. P. Williams, *Adv. Chem. Ser. 11* (1976) 1.
[4] H. Sigel (Ed.): *Metal Ions in Biological Systems*, a multivolume series, Dekker, New York 1974-present.
[5] T. G. Spiro: *Metal Ions in Biology, Vol. 3, Vol. 5*, Wiley-Interscience, New York 1981, 1983.

[6] T. Doyne, *Adv. Protein Chem. 22* (1966) 600.
[7] R. J. P. Williams, *Q. Rev. Chem. Soc. 24* (1970) 331.
[8] H. H. Ussing: *Handbuch der Experimentellen Pharmakologie*, Springer, Berlin 1960.
[9] A. S. Prasad (Ed.): *Essential and Toxic Trace Elements in Human Health and Disease*, Liss, New York 1988.
[10] K. Lang: *Biochemie der Ernährung*, 4th ed., Steinkopff, Darmstadt 1979.
[11] Deutsche Gesellschaft für Ernährung: *Empfehlungen für Nährstoffzufuhr*, Umschau, Frankfurt 1985.
[12] H. G. Seiler, H. Sigel, A. Sigel: *Handbook on Toxicity of Inorganic Compounds*, Dekker, New York 1988.
[13] P. Brätter, P. Schramel (Eds.): *Trace Element Analytical Chemistry in Medicine and Biology, Vol. 4*, de Gruyter, Berlin 1987.
[14] H. G. Classen, P. S. Elias, W. P. Hammes: *Toxikologisch-hygienische Beurteilung von Lebensmittelinhalts- und -zusatzstoffen sowie bedenklicher Verunreinigungen*, Parey, Berlin 1987, p. 26.
[15] See [4], *Vol. 14* (1982): *Lithium*.
[16] See [4], *Vol. 17* (1984): *Calcium*.
[17] D. N. Skilleter, *Chem. Br. 26* (1990) 26.
[18] *Gmelin Handbook of Inorganic Chemistry, Beryllium, Suppl. Bd. A 1*, Springer, Berlin 1987, p. 300 ff.
[19] G. Petzow, H. Zorn, *Chem.-Ztg. 98* (1974) 236.
[20] H. G. Classen in [4], *Vol. 26* (1990), Chapter 29.
[21] J. Durlach: *Le Magnesium en Pratique Clinique*, Bailliere, Paris 1985.
[22] P. von Sengbusch: *Molekular- und Zellbiologie*, Springer, Berlin 1979.
[23] S. Mann, J. Webb, R. J. P. Williams (Eds.): *Biomineralization*, VCH, Weinheim 1989.
[24] G. Krampitz, G. Graser, *Angew. Chem. 100* (1988) 1181; *Angew. Chem. Int. Ed. Engl. 27* (1988) 1145.
[25] H. D. Jakubke, H. Jeschkat: *Aminosäuren, Peptide, Proteine*, Verlag Chemie, Weinheim 1982, p. 38 ff.
[26] G. Krieger, H. G. Classen, *Magnesium-Bull. 1* (1979) 191.
[27] A. E. Martell, R. M. Smith: *Critical Stability Constants*, Plenum, New York 1974; L. G. Sillen, A. E. Martell: *Stability Constants of Metal Ion Complexes, Chem. Soc. Spec. Publ. No. 17*, London 1963.
[28] A. E. Martell, M. Calvin: *Chemistry of the Metal Chelate Compounds*, Prentice-Hall, NJ-Englewood Cliffs 1952.
[29] A. E. Martell, R. J. Motekaitis: *Determination and Use of Stability Constants*, VCH, Weinheim 1988.
[30] A. McAuley, J. Hill, *Q. Rev. Chem. Soc. 23* (1969) 18.
[31] A. Albert, *Biochem. J. 50* (1953) 441.
[32] L. Tmozik, A. Wojciechowska, M. Jaskolski, *Monatsh. Chem. 114* (1983) 1185.
[33] C. Blaquiere, G. Berthon, *Inorg. Chim. Acta 135* (1987) 179.
[34] I. Bach, *Dissertation*, Technische Universität München 1989.
[35] H. G. Classen, W. Achilles, G. M. Bachem, A. Conradt, R. Fehlinger, H. H. Gossmann, T. Günther, K. J. Münzenberg, K. Paschen, G. Schreiber, A. Schroll, L. Spätling, A. Wischnik, H. Zumkley, *Magnesium-Bull. 8* (1986) 117.
[36] H. F. Schimatschek, H. G. Classen, H. Thöni, W. Haubold, *Magnesium-Bull. 9* (1987) 161.
[37] A. Fleckenstein: *Calcium Antagonism in Heart and Smooth Muscle*, Wiley, New York 1983, p. 148.
[38] H. G. Classen, P. Marquardt, M. Späth, H. Ebel, *Arzneim.-Forsch. 23* (1973) 267; H. G. Classen, P. Marquardt, M. Späth, K.-A. Schumacher, B. Gräbling, *Arzneim.-Forsch. 28* (1978) 807.
[39] a) H. G. Classen, P. Marquardt, M. Späth, H. Ebel, K.-A. Schumacher, J. Helbig, B. Gräbling, *Arzneim.-Forsch. 26* (1976) 249; b) S. Borelli, H. Gehrken, *Der informierte Arzt 3* (1975) 103; c) H. Leube, P. Schmidt, *Ärztl. Prax. 28* (1976) 2063.
[40] H. G. Classen, P. Marquardt, H. Ebel, K.-A. Schumacher, M. Späth, J. Helbig in M. Cantn, M. S. Seelig (Eds.): *Magnesium in Health and Disease*, Spectrum Publ., New York 1980, p. 521.
[41] H. G. Classen, G. Fischer, J. Marx, H. F. Schimatschek, C. Schmid, C. Stein, *Magnesium 6* (1987) 34.
[42] H. G. Classen, *Artery (Fulton Mich.) 9* (1981) 182.
[43] G. Wünsch, E. Jäger, H. Fischer, J. Helbig, unpublished results.
[44] S. Fujiwara, Y. Arasta, *Bull. Chem. Soc. Jpn. 37* (1964) 344.
[45] K. G. R. Pachler, *Fresenius Z. Anal. Chem. 224* (1967) 211.
[46] K. G. R. Pachler, *Spectrochim. Acta 19* (1963) 2580.
[47] A. L. Swain, E. L. Amma, *Inorg. Chim. Acta 163* (1989) 5.
[48] R. H. Kretsinger, *CRC Crit. Rev. Biochem. 1* (1980) 174.
[49] K. B. Seamon, R. H. Kretsinger in T. G. Spiro (Ed.): *Calcium in Biology*, Wiley, New York 1983, p. 1 ff.
[50] H. Schmidbaur, G. Müller, J. Riede, G. Manninger, J. Helbig, *Angew. Chem. 98* (1986) 1014; *Angew. Chem. Int. Ed. Engl. 25* (1986) 1013.
[51] H. Schmidbaur, I. Bach, D. L. Wilkinson, G. Müller, *Chem. Ber. 122* (1989) 1433.
[52] H. Schmidbaur, I. Bach, D. L. Wilkinson, G. Müller, *Chem. Ber. 122* (1989) 1445.
[53] H. Schmidbaur, D. L. Wilkinson, G. Müller, G. Manninger, J. Helbig, unpublished results.
[54] H. Schmidbaur, I. Bach, D. L. Wilkinson, G. Müller, *Chem. Ber. 122* (1989) 1439.
[55] H. Einspahr, C. E. Bugg, *Acta Crystallogr. Sect. B30* (1974) 1037.
[56] H. Schmidbaur, P. Mikulcik, G. Müller, *Chem. Ber. 123* (1990) 1599.
[57] I. Csöregh, P. Kierkegaard, J. Legendziewicz, E. Huskowska, *Acta Chem. Scand. 43* (1989) 636.
[58] I. Csöregh, P. Kierkegaard, J. Legendziewicz, E. Huskowska, *Acta Chem. Scand. Ser. A 41* (1987) 453.
[59] H. Einspahr, C. E. Bugg, *Acta Crystallogr. Sect. B35* (1979) 316.
[60] H. Einspahr, G. L. Gartland, C. E. Bugg, *Acta Crystallogr. Sect. B33* (1977) 3385.
[61] F. Bertin, G. Thomas, *Bull. Soc. Chim. Fr. 1971*, 3467.
[62] G. Duc, F. Bertin, G. Thomas-David, *Bull. Soc. Chim. Fr. 1976*, 414.
[63] G. Duc, F. Bertin, G. Thomas-David, *Bull. Soc. Chim. Fr. 1974*, 793.
[64] H. Schmidbaur, I. Bach, J. Riede, G. Müller, J. Helbig, G. Hopf, *Chem. Ber. 121* (1988) 795.
[65] T. Doyne, R. Pepinsky, T. Watanabe, *Acta Crystallogr. 10* (1957) 438.
[66] L. Kryger, S. E. Rasmussen, *Acta Chem. Scand. 27* (1973) 2674.
[67] H. Schmidbaur, I. Bach, D. L. Wilkinson, G. Müller, *Chem. Ber. 121* (1988) 1441.
[68] H. Schmidbaur, I. Bach, J. Riede, G. Müller, J. Helbig, G. Hopf, *Chem. Ber. 120* (1987) 867.
[69] H. Schmidbaur, I. Bach, D. L. Wilkinson, G. Müller, *Chem. Ber. 122* (1989) 1427.
[70] S. T. Rao, M. Mallikarjunan, *Acta Crystallogr. Sect. A 31* (1975) 48.
[71] H. Schmidbaur, P. Mikulcik, G. Müller, *Chem. Ber. 123* (1990) 1001.
[72] Orotate: *Apothekenpraxis 9* (1987) 11.
[73] H. Schmidbaur, I. Bach, O. Kumberger, unpublished results.
[74] J. Solbakk, *Acta Chem. Scand. 25* (1971) 3006.
[75] M. Sabat, D. Zglinska, *Acta Crystallogr. Sect. B36* (1980) 1187.
[76] T. Solin, K. Matsumoto, K. Fuwa, *Bull. Chem. Soc. Jpn. 54* (1981) 3731.
[77] J. Maslowska, A. Dorabialski, *Pol. J. Chem. 57* (1983) 1089.
[78] a) C. K. Johnson, *Acta Crystallogr. 18* (1965) 1004; b) H.-P. Krimmer, K. Drauz, H. Klenk, *Chem.-Ztg. 114* (1990) 117; c) O. Kumberger, J. Riede, H. Schmidbaur, *New. J. Chem.*, in press.
[79] M. Shechter, *Magnesium-Bull. 12* (1990) 1; H. S. Rasmussen, P. Norregard, O. Lindenberg, P. Mcnair, V. Backer, S. Balslev, *The Lancet 1* (1986) 234.
[80] O. Kinnunen, J. Salokannel, *Ann. Clin. Res. 19* (1987) 321.
[81] R. Fehlinger, L. Franke, E. Glatzel, E. Meyer, M. Michalik, S. M. Rapopo, M. Ruston, Ch. Schulz, G. Schumann, *Magnesium-Bull. 3* (1981) 298; R. Fehlinger, C. Kemnitz, K. Seidel, T. Günther, *ibid. 9* (1987) 115; R. Fehlinger, C. Kemnitz, A. Stephan, D. Vank, C. Franke, R. Fehlinger, E. Glatzel, *Curr. Ther. Res. 43* (1988) 160.
[82] L. Spätling, G. Spätling, *Br. J. Obstet. Gynaecol. 95* (1988) 120.
[83] L. Kovacs, B. G. Molnar, E. Huhn, L. Bodis, *Geburtshilfe Frauenheilkd. 48* (1988) 595.
[84] T. Dyckner, P. O. Wester, *Br. Med. J. 286* (1983) 1847.
[85] T. Dyckner, P. O. Wester, L. Widman, *Int. J. Cardiol. 19* (1988) 81.
[86] M. B. Zemel, J. Green, P. C. Zemel, F. Douglas, R. Greiser, J. R. Sowers, *Nutr. Res. (N.Y.) 9* (1989) 1285.
[87] H. Rüddel, R. Schmieder, W. Langewitz, W. Schulte, *J. Hum. Hypertension 1* (1988) 259.
[88] D. H. Antoni, M. Engel, N. Gumpel, *Magnesium-Bull. 11* (1989) 125; R. Mletzko, W. Jung, M. Manz, T. Kamradt, F. Vogel, B. Lüderitz, *Z. Kardiol. 78* (1989) 602; M. Manz, R. Mletzko, W. Jung, B. Lüderitz, *Dtsch. Med. Wochenschr. 115* (1990) 386; T. Gustafson, K. Boman, E. Moberg, I. Ringqvist, P. O. Wester, *Magnesium Res. 3* (1990) 73.
[89] B. S. Krasner, R. Girdwood, H. Smith, *Can. Anaesth. J. 28* (1981) 329.
[90] R. Meysing, *Ther. Ggw. 118* (1979) 3; S. W. Golf, H. Riedinger, S. Matthes, D. Kuhn, C. Baumgärtner, V. Graef, H. Temme, N. Katz, L. Roka, J. Ceske, *Magnesium Res. 3* (1990) 70.
[91] H. Kühr, W. Rüther, J. Helbig, K. J. Münzenberg, *Magnesium-Bull. 8* (1986) 276.
[92] O. Classen, H. Fischer, H. G. Classen, *Der Kinderarzt 17* (1986) 1565.
[93] G. B. Weiss, V. M. Traina, F. L. Douglas in A. Scrabine (Ed.): *New Cardiovascular Drugs*, Raven, New York 1986, p. 243.

Complexes with Substituent-free Acyclic and Cyclic Phosphorus, Arsenic, Antimony, and Bismuth Ligands

By Otto J. Scherer*

Dedicated to Professor Max Schmidt on the occasion of his 65th birthday

Until recently, phosphorus, arsenic, antimony and bismuth ligands were nearly always understood to be molecules such as R_3E, $R_2E(CH_2)_nER_2$, and $RC[(CH_2)_nER_2]_3$(E = P, As, Sb, Bi) in which the lone pair of the atom E functions as a 2e donor. Current research interests, however, increasingly involve substituent-free E_n ligands (n = 1–6), the various types of which are mainly accessible via EX_3 (X = F,Cl,Br,Ph), $E(SiMe_3)_3$, $(RAs)_n$, P_4S_3, As_4S_4, gray arsenic, and especially P_4 and As_4; these ligands can be stabilized in the coordination spheres of certain transition metal fragments. P_1, As_1 and Sb_1 units with multiple M–E bonds are found in bi- and trinuclear complexes; E_1 units can also be encapsulated (partially or completely) in cavities of a variety of metal cluster frameworks. Metallatetrahedranes with up to three E atoms are especially common. Besides E_1 units, the greatest variety of coordination modes is exhibited by E_4 ligands, which are found as intact tetrahedra and also as parts of chains, polycycles, cubes and a trigonal prism. The phosphorus and arsenic species *cyclo*-E_n, isoelectronic to the carbocyclic $(CH)_n$ species, are suitable ligands for forming sandwich complexes (n = 3, 4, 5) and triple-decker sandwich complexes (n = 3, 5, 6). In addition to the wide variety of chemical reactions, remarkable parallels are found in organic chemistry as well as in solid-state chemistry for many of these substance classes. Some of the molecules have received lively interest from theoretical chemists.

1. Introduction

In a fascinating review article "Homonuclear Bonds Involving Main Group Elements" published in 1981,[1] *H. G. von Schnering* pointed out that insights into general chemical principles can be hindered by too narrow a view of demarcated research interests. Links between the various chemical disciplines of inorganic (solid state, main group, transition metal chemistry), organic, and theoretical chemistry have been forged as a result of two breakthroughs: first, the successful isolation in the 1980s of an unexpectedly wide variety of molecules with (p–p)π multiple bonds (both between elements of the first octet of main group elements and heavier elements, and among the heavier elements alone), and secondly the concept of isolobal analogy (published by *R. Hoffmann* in 1982[2]) and its applications in organometallic chemistry.[3] Such unifying concepts have proved ever more powerful and have facilitated views of chemistry as an indivisible whole. A further useful heuristic principle is the diagonal relationship between carbon and phosphorus (C ↘ P); the expertise of *Baudler* and co-workers[4] was applied in the synthesis of polyphosphanes P_nH_{n+2} and $(PH)_n$, the analogues of alkanes C_nH_{2n+2} and cycloalkanes $(CH_2)_n$, and the structurally impressive polycyclic organophosphanes with P- and PR-units, which are in turn isoelectronic and isolobal to the fragments CH and CH_2 ($CH_3 \triangleq PH_2$).

Since the N_2 analogue P_2 ($P{\equiv}P \triangleq HC{\equiv}CH$) had been well-known and spectroscopically characterized and the first kinetically stabilized diphosphene derivative, *trans*-R–P=P–R (R = 2,4,6-tBu$_3$C$_6$H$_2$), had been isolated by *Yoshifuji* et al.,[5] and since *cyclo*-E_3 (E = P,As) had been stabilized in sandwich complexes by *Sacconi*'s group in Florence,[6] and *cyclo*-P_6 (hexaphosphabenzene) in similar fashion by *H. Sitzmann* in this Institute,[7] hope was nourished that other E_n units (E = P,As,Sb,Bi), in particular E_n rings isoelectronic to carbocyclic π systems $(CH)_n$, could be stabilized in the coordination spheres of transition metal fragments. This review article describes the properties of ligands composed of "naked" acyclic and cyclic E_n structural units (E = N homologues) and aims to give an impression of the momentum of research[8] in this novel and multidisciplinary area.

2. E_1 Ligands

2.1. Terminal Coordination (η^1-E)

Phosphaalkynes R–C≡P have been isolated and thoroughly studied.[9] In contrast, there is only indirect evidence and speculation to support the existence of molecules with a metal–phosphorus (or arsenic) triple bond (coordination type **I**).

$L_nM{\equiv}E$ **I** (E = P, As)

The trimetallaphosphatetrahedrane $[W_3(\mu_3\text{-P})(\mu\text{-OR})_3(OR)_6]$ (**10c**), R = CH_2tBu, may be formed from $W_2(OR)_6$ and $(RO)_3W{\equiv}P$.[10a] The co-photolysis of the Mo_3As tetrahedrane $[As\{Mo(CO)_2Cp\}_3]$ (**10d**) and $[CpM(CO)_2]$, M = Co,[10b] Rh[10c] (cf. Section 2.2.2.3) allows the identification of, inter alia, the products $[Cp(CO)_2Mo{\equiv}Mo(CO)_2Cp]$ and

[*] Prof. Dr. O. J. Scherer
Fachbereich Chemie der Universität
Erwin-Schrödinger-Straße, D-6750 Kaiserslautern (FRG)

$[Cp_2(CO)_4Mo_2(\mu,\eta^2\text{-}As_2)]$ (**33g**). The formation of **33g** has been postulated to be the result of a fragmentation of **10d** into the two triple bond systems $LMo \equiv MoL$ ($L = Cp(CO)_2$) and $LMo \equiv As$ ($LMo \leftrightarrow CH,P,As$), isolobal to acetylene. $LMo \equiv As$ could then give the isolated Mo_2As_2 tetrahedrane **33g** by dimerization.[10b,c]

2.2. Bridging Coordination

2.2.1. *Doubly Bridging (μ-E, Allene-like)* [*]

The unusual linear two-coordination of type **II** was recently reported for the first time by *Huttner* et al.[11]

$[L_nM{=}E{=}ML_n]^{\oplus}$ **II** (E=P, As)

The extremely hydrolysis-sensitive dimetallaphospha- and -arsacumulenes **2a**[11a] and **2b**[11b] are obtained from the phosphinidene or arsinidene complexes **1a** and **1b** by removal of hydride or chloride.

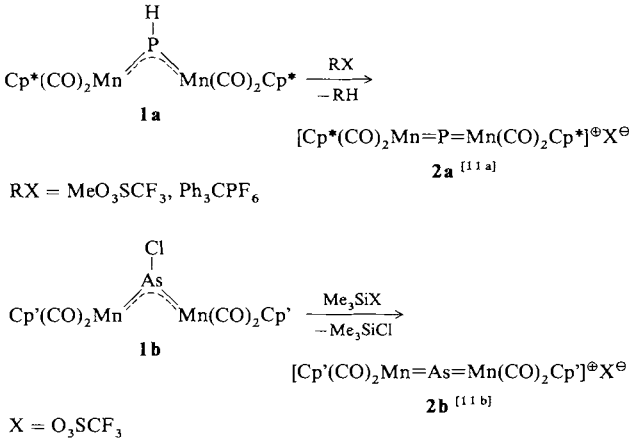

Substances **2** are typified by a shift of the π–π* transition of starting material **1** to lower wavelength (**1a** → **2a**: 522 → 411 nm,[11a] **1b** → **2b**: 512 → 380 nm[11b]). Parallel to this, one observes a drastic high-field shift in the ^{31}P-NMR spectrum (**1a** → **2a**: $\delta = 816 \rightarrow \delta = 172$[11a]). Both observations point to a strengthening of the Mn–E π-bond on going from **1** to **2**. The X-ray structure analysis of the Cp* derivative of **2b**[11b] confirms both the stronger bond ($\bar{d}$(Mn–As) for **1b**(Cp′) → **2b**(Cp*) = 2.223 → 2.147 Å) and the linear geometry (Mn–As–Mn = 176.3(1)°), and thus, also the formulation of the cation as an allene analogue, the $Cp^*(CO)_2Mn$ moieties of which are rotated by 88.5° from each other with respect to the Mn–As–Mn axis.

2.2.2. *Triply Bridging (μ_3-E)*

2.2.2.1. *Trigonal Planar EM_3 Framework*

The trigonal planar geometry at an E_1 atom (E = P,As,Sb) has been found in complexes of coordination type **III** and **IV**.

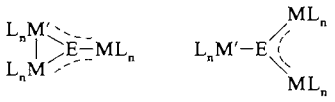

III (E = P, As) **IV** (E = As, Sb)

Characteristic for this bonding mode is an sp^2-hybridized E atom and ML_n moieties capable of π bonding. Ideal starting compounds, which satisfy these conditions, are the halogen-containing phosphinidene, arsinidene, and stibinidene complexes **3a–c**, which give complexes of classes **4** and **5** by substitution of the halogen on reaction with an organometallic nucleophile.[12]

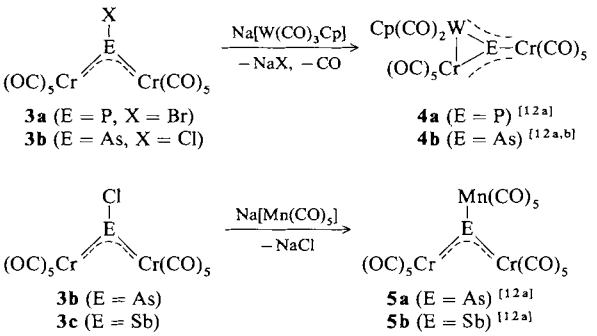

The five valence electrons of the E atom (E = P,As,Sb) in the cyclic trinuclear clusters **4a, b** are involved in bonding

[*] Abbreviations: Cp = η^5-C_5H_5, Cp* = η^5-C_5Me_5, Cp′ = η^5-C_5H_4Me, Cp″ = η^5-C_5HiPr_4 Cp‴ = η^5-1,3-$tBu_2C_5H_3$, Cp^x = η^5-C_5Me_4Et, triphos = $MeC(CH_2PPh_2)_3$, np_3 = $N(CH_2CH_2PPh_2)_3$, py = pyridine; VE = valence electrons, SEP = skeletal electron pairs.

Otto J. Scherer, born 1933 in Amberg (Bavaria), studied chemistry from 1955 through 1959 at the Technische Hochschule Aachen and at the Universität München, where he gained his doctorate in 1962 under the supervision of Max Schmidt. He then went as scientific assistant with his supervisor to Marburg and to Würzburg. After his habilitation in 1967 at the Universität Würzburg there followed an appointment as dozent (1968) and the offer of a chair at the newly founded Universität Kaiserslautern. His research activities center on the study of the ligand properties of lower coordinated phosphazenes and the coordinative stabilization of "naked" phosphorus and arsenic ligands.

with two 16e fragments and one 15e fragment. To satisfy the 18e rule, a W–Cr bond is formed and CO eliminated. In the acyclic complexes **5**, the five electrons are distributed amongst two 16e fragments and one 17e fragment. Complexes **5** correspond to a classical methylarsinidene or -stibinidene complex[13] in which the CH_3 group is replaced by the isolobal $Mn(CO)_5$ fragment. The extreme low-field shift of the ^{31}P-NMR signal ($\delta = 945$[12a]), induced by the planar μ_3-coordination of the phosphorus by three metal atoms, is characteristic of **4a**. X-ray structure analysis confirms for **4a, b**[12a,b] and **5a**[12a] that the strongest E–M bonds (**4a, b**: d(E–W) $\approx d$(E–Cr_{exo}) < d(E–Cr_{endo}); **5a**: d(As–Cr) = 2.44/2.42 Å, d(As–Mn) = 2.52 Å) are those between E = P,As and the less electron-rich ML_n fragment. In solution, **5a** forms the cyclic trinuclear cluster **6** by decarbonylation, slowly at room temperature but rapidly at 80 °C.[12a]

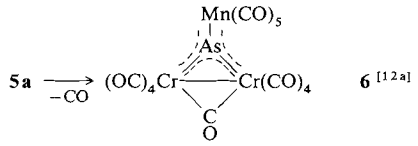

If **3c** is allowed to react with the decacarbonyldimetalates $Na_2[M_2(CO)_{10}]$ of the sixth subgroup (Group 6) in CH_2Cl_2, the extremely air-sensitive salts **7** are obtained on removal of the solvent and treatment with tetrahydrofuran.[12a]

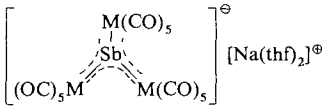

7 (M = Cr, Mo, W) [12a]

The structural parameters of the chromium compound, together with the intense color of the complexes **7**,[12a] show the existence of a Sb–M(d − p)π-multicenter interaction.

The same planar μ_3-E coordination with E–M π-bonding is observed in the E_2M_2 butterfly frameworks of complexes **8a**[14] and **8b**,[12a] obtained from $[Cp(CO)_2Mn(PBr_3)]$ and $Fe_2(CO)_9$ or photochemically from the Cp′ derivative of complex **42**,[27h] respectively (see Section 3.3).

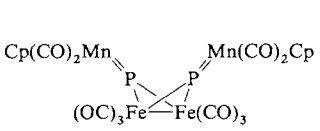

8a [14]

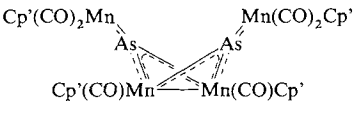

8b [12a]

A comparison of the X-ray structures of the isoelectronic molecules **8a** and **8b**, which contain different 14e ML_n-fragments along the hinge, shows that the π-bonding component in **8a** is clearly more strongly localized in the exocyclic double bond ($\bar{d}$(P–Mn) = 2.10, $\bar{d}$(P–Fe) = 2.18 Å). Like **4a**, **8a** also shows a ^{31}P-NMR signal shifted to extremely low field ($\delta = 977$).[14]

2.2.2.2. *Trigonal Pyramidal EM_3 Framework*

This geometrical variant of μ_3-E coordination can be subdivided into complexes with or without metal–metal bonding between the ML_n fragments. If each CH_3 group of the main group molecules $E(CH_3)_3$ (E = P,Sb,Bi) is formally replaced by an isolobal 17e ML_n fragment, then the substance class **9** is obtained.

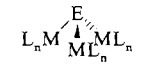

9 (E = P, Sb, Bi)

9	E	ML_n (17e)	Ref.
a	P	$Mo(CO)_3Cp$	[15a]
b	Sb	$Mo(CO)_3Cp$	[15b]
c[*]	Sb	$Fe(CO)_2Cp$	[15b, c]
d[*]	Bi	$Mo(CO)_3Cp(')$	[15d]
e	Bi	$Mn(CO)_5$	[15e]
f	Bi	$Fe(CO)_2(PPh_3)(NO)$	[15f]
g[*]	Bi	$Fe(CO)_2Cp(')$	[15g]
h[*]	Bi	$Co(CO)_4$	[15f, h]

[*] X-ray structure analysis

The preferred synthesis of **9**[15] involves the reaction of EX_3 (X = F, most commonly Cl, or Br) with the corresponding carbonylmetalates Na(K) $[ML_n]$. In isolated cases,[15f,h] the binuclear complexes $L_nM–ML_n$ (e.g. $Co_2(CO)_8$) can be used as the source of the 17e ML_n fragment. The remaining lone pair on *E* in **9** can react with S_8, $BF_3 \cdot OEt_2$[15a] and $M(CO)_5$(thf) (M = Cr,W[15c]). Photochemical[15g] or thermal CO elimination[16h] can convert the "open" Bi clusters **9g** and **9h** into the closed clusters **10**, involving tetrahedrane geometry and 15e ML_n fragments.

$$[Bi\{Fe(CO)_2Cp^{(')}\}_3] \xrightarrow[-3\,CO]{h\nu} [Bi\{Fe(\mu\text{-}CO)Cp^{(')}\}_3]$$

9g → **10g** [15g]

$$[Bi\{Co(CO)_4\}_3] \xrightarrow[-3\,CO]{\Delta} [Bi\{Co(\mu\text{-}CO)(CO)_2\}_3]$$

9h → **10h** [16h]

2.2.2.3. *Tetrahedranes with EM_3 Core*

All clusters of coordination type **10** possess 50 VE (valence electrons) and can be formally derived either from the tetrahedral 60 VE molecule $[Ir(CO)_3]_4$ or from the $P_4(E_4)$ tetrahedron (20 VE) by exchange of the isolobal units $P(E) \leftrightarrow Ir(CO)_3$ (in general a 15e ML_n fragment).

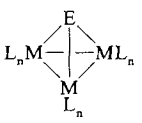

10 (E = P, As, Sb, Bi)

10	E	ML_n(15e)	Ref.
a	P	$Ir(PF_3)_3$	[16a]
b	P	$Co(CO)_3$	[16b]
c[*]	P	$W(OCH_2tBu)_3$	[10a]
d	As	$Co(CO)_3$	[16c]
e[*]	As	$Mo(CO)_2Cp$	[16d]
f[*]	Bi	$Ir(CO)_3$	[16g]
h[*]	Bi	$Fe(CO)Cp(')$	[15g]
g[*]	Bi	$Co(CO)_3$	[16h, i]

[*] X-ray structure analysis

The preparation of clusters **10** (for **10g** and **10h** see substance class **9**) involves the use of PF_3,[16a] P_4, or EX_3 (X = Cl,Br,I; E = P,[10a,16b] As,[16c] Bi[16g]) or grey arsenic[16d] as the source of the element E. The 15e ML_n fragments are obtained from $IrCl_3$,[16a] $[Ir(CO)_4]^{\ominus}$,[16g] $Co_2(CO)_8$ or $[Co(CO)_4]^{\ominus}$,[16b,c] $[Cp(CO)_3Mo]_2$[16d] or $[W_2(OCH_2tBu)_6(HNMe_2)_2]$.[10a] With antimony, only anionic complexes of type **10** are known, such as $[(OC)_4Fe \leftarrow Sb\{Fe(CO)_3\}_3(\mu\text{-}H)]^{2\ominus}$ (**10i**),[16e] in which the Sb lone pair is additionally coordinated to an $Fe(CO)_4$ fragment. Starting materials for this synthesis are $[Sb\{Fe(CO)_4\}_4]^{3\ominus}$ (**16a**) and CF_3SO_3H.[16e] The structurally related 50 VE cluster anion $[Bi\{Fe(CO)_3\}_3(\mu_3\text{-}CO)]^{\ominus}$ (**10j**),[16f] which displays an extra μ_3-CO cap, is formed from $NaBiO_3$ and $Fe(CO)_5$ in methanol; its alkylation with $CH_3SO_3CF_3$ gives $[Bi\{Fe(CO)_3\}_3(\mu_3\text{-}COCH_3)]$, an uncharged $BiFe_3$ tetrahedrane with a μ_3-methoxyalkylidyne ligand as 3e donor.[17a] A large number of complexes **10** have been studied with respect to an extension of their coordination to the μ_4 type $[(L_nM)_3E \rightarrow M'L_n]$.[16b,17b-f] Such clusters can be constructed in completely different ways, namely by reaction of $[Cp(CO)_2Mn(PBr_3)]$ with $Co_2(CO)_8$ or of $[\{(OC)_5Cr\}_2AsCl]$ with $Na[Co(CO)_4]$; the products are the trimetallatetrahedranes $[\{(OC)_3Co\}_3E \rightarrow M'L_n]$, E = P, $M'L_n = Mn(CO)_2Cp$ and E = As, $M'L_n = Cr(CO)_5$.[17e] A slight alteration of the reaction conditions between the arsinidene complex and $Na[Co(CO)_4]$ leads to the cluster **11**, for which the idealized square-pyramidal geometry of the As_2Co_2Cr core was confirmed by X-ray crystallography[17e] (cf. complex **14**).

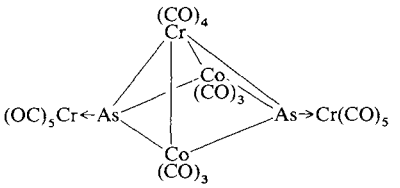

11 [17e]

In the anion $[(\mu\text{-}CO)\{Fe(CO)_3\}_3P \rightarrow Fe(CO)_4]^{\ominus}$, prepared from $[Fe_4(CO)_{13}]^{2\ominus}$ and PCl_3, the 50 VE of the tetrahedrane core are provided by three 14e $Fe(CO)_3$ fragments, one bridging CO, the P atom, and the negative charge.[17f]

10b[16b] and **10d**[16c] tend to cyclotrimerize, retaining the tetrahedral EM_3 core and eliminating three molecules of CO. **10e**[16d] gives the cluster **12a, b**, which has a trigonal bipyramidal core, on co-thermolysis with $CpM(CO)_2$ (M = Co,Rh).[10b,c]

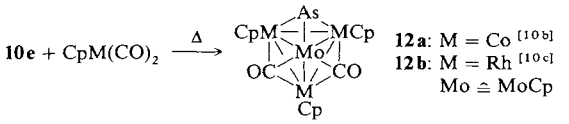

12a: M = Co [10b]
12b: M = Rh [10c]
Mo ≙ MoCp

12b additionally contains a CpRh(CO) fragment coordinated to the As lone pair.

2.2.2.4. *Trigonal Bipyramids with EM_3E Core*

The M_3 plane of the *closo* cluster type **13**[18a] is generally composed of three 14e $Fe(CO)_3$ fragments. In order to introduce the μ_3-E caps (E = As and Sb as well as P) into the clusters **13**,[18a] compounds **3** are treated with $Na_2[Fe(CO)_4]$; only in the case of **13a** is a terminal $Cr(CO)_5$ ligand replaced by $Fe(CO)_4$.

$$[\{(OC)_5Cr\}_2ECl] \xrightarrow{Na_2[Fe(CO)_4]} \mathbf{13}$$

3a–c
(E = P, As, Sb)

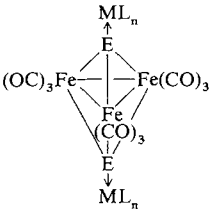

13 [18]

13	E	ML_n	Ref.
a	P	$Cr(CO)_5$ (1 × $Fe(CO)_4$)	[18a]
b	P	$Mo(CO)_5$	[18a]
c	P	$W(CO)_5$	[18a]
d[*]	P	$Mn(CO)_2Cp$	[18a]
e	As	$Cr(CO)_5$	[18a]
f[*]	As		[18b,c]
g	Sb	$Cr(CO)_5$	[18a]
h[*]	Bi		[18d]

[*] X-ray structure analysis

13a–c are obtained in better yield from $(OC)_5M(PX_3)$ (M = Cr,Mo,W; X = Cl,Br) and $Fe_2(CO)_9$.[18a] The remarkable conversion of trigonal planar coordinated μ_3-P into μ_4-P is observed in the formation of **13d**[18a] from **8a** and $Fe_2(CO)_9$. **13d** can be formally derived from **8a** by bridging the two butterfly wingtips with an $Fe(CO)_3$ fragment and forming two additional Fe–Fe bonds. The ML_n-free compound **13f** has been known for a long time; it is obtained from AsF_3 and $Fe(CO)_5$ or from AsX_3 (X = Cl,Br)[18c] and $Na_2[Fe(CO)_4]$. Starting materials for the cluster **13h**,[18d] isoelectronic with **13f**, and also for $[Bi\{M(CO)_3\}_3Bi]$ (M = Ru,Os),[18e] are $NaBiO_3$ and $Na[HFe(CO)_4]$ or $M_3(CO)_{12}$ (M = Ru,Os).

The reaction between $[Bi\{Fe(CO)_3\}Bi]$ (**13h**)[18d] and $[Fe(CO)_4]^{2\ominus}$ leads to opening of an Fe–Fe bond and formation of $[Bi_2Fe_4(CO)_{13}]^{2\ominus}$ **14**,[18f] a cluster anion of the *nido* type (cf. complex **11**) with a square-pyramidal Bi_2Fe_3 core (by X-ray analysis) and a terminal $Fe(CO)_4$ group.

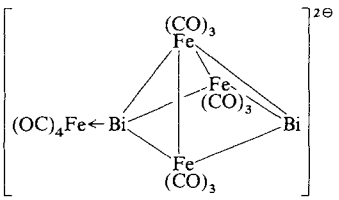

14 [18f]

2.2.2.5. *Cubanes with E_4M_4 Core*

Molecules whose core corresponds to a cubane (slightly or considerably distorted) occupy a key position among transition metal clusters.[19] With elements of the fifth main group (group 15), cubanes of the type A_4B_4 are preponderant (substance class **15**).

Such molecules were discovered in 1970 by *Dahl* et al.,[20c] who prepared **15e** from $Co(OAc)_2 \cdot 4H_2O$ and $SbCl_3$ in methanol under CO/H_2 pressure. **15d**[78d] and **15f**[20d] are

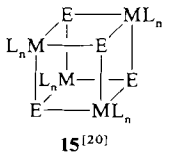

15[20]

15	E	ML_n	Ref.
a	P	CoCp	[20a]
b	P	NiCp′	[20b]
c	As	NiCp′	[20b]
d	As	MoCp	[78d]
e	Sb	$Co(CO)_3$	[20c]
f	Bi	$Co(CO)_3$	[20d]

formed in the thermolysis of $[\{CpMo(CO)_2\}_2\{\mu\text{-}(AsMe)_5\}]$ or $[Bi\{Co(CO)_4\}_3]$ (**9h**); **15a**[20a] and **15b, c**[20b] in the co-thermolysis of $CpCo(CO)_2$ or $[Cp'Ni(CO)]_2$ (Cp′ = C_5H_4Me) with E_4 (E = P,As). 15e fragments isolobal to E are the preferred ML_n fragments. Of the cubanes characterized by X-ray structure analysis (**15a**,[20a] **15e**,[20c] **15f**[20d]), **15a** with its 14e CoCp fragment shows, as expected, the most pronounced distortion. Four short P···P distances (av. 2.57 Å) are observed in addition to the two very short Co···Co distances (av. 2.50 Å).[20a]

2.2.3. *Quadruply Bridging (μ_4-E)*

2.2.3.1. *Tetrahedral EM_4 Core*

This coordination type can be subdivided into polynuclear complexes without (substance class **16**) or with M–M bonds (spirocyclic complexes, **17**).

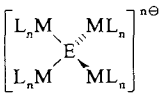

16

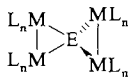

17

In the case of the anionic complexes **16**, in the examples known so far E is restricted to Sb and Bi, and ML_n to $Fe(CO)_4$ and $Co(CO)_4$. $[Sb\{Fe(CO)_4\}_4]^{3\ominus}$ (**16a**)[16e] can be prepared from, e.g., $SbCl_3$ or $SbCl_5$ and $Na_2[Fe(CO)_4]$, $[Bi\{Fe(CO)_4\}_4]^{3\ominus}$ (**16b**)[21a] from $NaBiO_3$ and $Fe(CO)_5$ in methanolic KOH. $[Bi\{Co(CO)_4\}_4]^{\ominus}$ (**16c**)[21b] is formed from $BiCl_3$ and $[Co(CO)_4]^{\ominus}$ and in the reaction of $[Cp_2Co][Co(CO)_4]$ with $[Bi\{Co(CO)_4\}_3]$ (**9h**) to form $[Cp_2Co][Bi\{Co(CO)_4\}_4]$ (**16d**),[21c] a paramagnetic complex with ten electrons at bismuth. The tetrahedral environment of Sb and Bi in **16a–16d** was proved by X-ray structure analysis. The structures of the cationic complexes[15f] $[Sb\{Fe(CO)_2(NO)(PPh_3)\}_4]^{\oplus}$ and $[Sb\{Co(CO)_3(PPh_3)\}_4]^{\oplus}$, however, have not yet been determined.

Preferred ML_n fragments in the substance class **17** are $Fe(CO)_n$ units. Thus, PX_3 (X = Cl, Br), $AsCl_3$, and *i*Pr(H)PCH_2PH_2 react with $Fe_2(CO)_9$ to form the spirocyclic complexes **17a–d**.

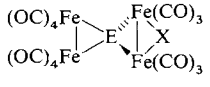

17a–d

17	E	X	Ref.
a[*]	P	Cl	[22a]
b[*]	P	Br	[18a]
c	P	PMe*i*Pr	[22b]
d[*]	As	Cl	[22a]

[*] X-ray structure analysis

If the pnicogen E is replaced by its heaviest homologues Sb and Bi, complexes with different structures are obtained. The reaction of $SbCl_3$ with $[Fe(CO)_4]^{2\ominus}$ or $[Fe_2(CO)_8]^{2\ominus}$ leads to the multinuclear bispiro cluster $[\{(OC)_8Fe_2(\mu_4\text{-}Sb)\}_2\{Fe(CO)_3\}_2]$ (**17e**),[22c] the structure of which can be formally derived from that of **17a** by replacing the 3e ligand X of the latter by another 3e donor fragment, $\{(OC)_4Fe\}_2Sb$. **17e** possesses an $SbFe_2Sb$ core with butterfly geometry. The spirocyclic core is also preserved in the Bi multinuclear cluster $[\{(OC)_8Ru_2\}(\mu_4\text{-}Bi)(\mu\text{-}H)Ru_3(CO)_{10}]$ (**17f**),[22d] which is synthesized from $Bi(NO_3)_3 \cdot 5H_2O$ and $Na[Ru_3H(CO)_{11}]$ in methanol. The role of 3e bridging donor is here assumed by μ-H and an $Ru(CO)_4$ fragment of the original Ru_3 starting material.[22d]

The uncharged arsa-spirocycles **18a, b** arise in the co-photolysis of $[\{Cp(CO)_2Mo\}_3(\mu_3\text{-}As)]$ (**10e**)[16d] and $[CpM(CO)_2]$ (M = Co,Rh),[10b,c] the related cation **18c** in the reaction of $[CpCo(CO)_2]$ with AsF_3.[22e] In these inorganic

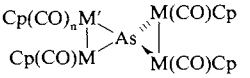

18

18a: M = Co, M′ = Mo, n = 2 [10b]
18b: M = Rh, M′ = Mo, n = 2 [10c]
[18c]$^{\oplus}$: M = M′ = Co, n = 1 [22e]

spiropentane analogues, characterized by X-ray analysis, the "extra" electron of **18a, b** at the spiro junction (As instead of C) can be removed to the 15e molybdenum fragment; the symmetric cation **18c** has an $As^{\oplus}$ spiro junction isoelectronic and isolobal to C.

2.2.3.2. *Square Bipyramidal EM_4E Core*

If the *trans* positions of an octahedron with six 14e ML_n fragments are replaced by Sb or Bi atoms, the *closo* cluster **20b** is obtained; this is the prototype of square pyramidal μ_4-E coordination and possesses 7 SEP (skeletal electron pairs).

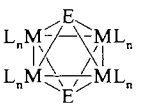

20

20a: E = Sb, ML_n = $Fe(CO)_3$; dianion [23a]
20b: E = Bi, ML_n = $Ru(CO)_3$ [18e, 23b]

The dianion **20a**, with additional terminal coordination at Sb, is formed, inter alia, photochemically from **19**, the μ_4-Sb atom of which is coordinated by four Fe atoms in a distorted tetrahedron.

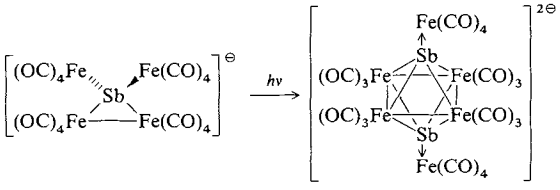

19[23a] **20a**[23a]

Whereas the four ruthenium atoms of **20b**, synthesized from $Bi(NO_3)_3 \cdot 5H_2O$ and $Ru_3(CO)_{12}$, lie in a plane,[18e,23b]

the electron-richer anion **20a** (8 SEP = n + 2 type) displays a folded Fe_4 ring.[23a] The *cis* isomer of substance class **20** can be realized for the heaviest homologue of group 8.[18e]

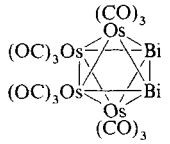

20c [18e]

The cluster core of **20c** consists of an Os_4 butterfly bridged by a Bi_2 unit (d(Bi–Bi) = 3.017(2) Å, cf. Section 3). In the cubic body-centered clusters **21a**, **b** (characterized by X-ray analysis) all the faces are capped by μ_4-As ligands.[24a,b]

The starting materials for the syntheses are $[NiCl_2(PPh_3)_2]$ and $PhAs(SiMe_3)_2$ or $[Pd_3(\mu_3\text{-}S)_2Cl_2(PPh_3)_4]$ and $As(SiMe_3)_3$, respectively.

$[Ni_9(\mu_4\text{-}As)_6(PPh_3)_5Cl_3]$ **21a** [24a]

$[Pd_9(\mu_4\text{-}As)_6(PPh_3)_8]$ **21b** [24b]

In the structurally more complicated macroclusters **22a**, **b**, not only μ_4-As coordination but also face-linking μ_5-As and connected tetrahedra with μ_6-As are observed.

$[Pd_8\{\mu\text{-}Pd(PPh_3)\}_{12}(\mu_5\text{-}As)_{12}]$ **22a** [24b]

$[Co_8\{\mu_6\text{-}As)(\mu_4\text{-}As)(\mu_4\text{-}AsPh)_2(CO)_{16}]_2$ **22b** [24c]

The source of the "naked" As atom is $As(SiMe_3)_3$ for **22a** and $(PhAs)_6$ for **22b**, which are allowed to react with $[PdCl_2(PPh_3)_2]$ or $[Co_2(CO)_8]$, respectively.

2.2.4. *Clusters with Semi-interstitial P and Interstitial E Atom (E = P,As,Sb)*

The partial or complete incorporation of E_1 structural units into open or closed metal polyhedra leads in the case of P_1 to the clusters **23**–**32**, which display a fascinating structural diversity (Scheme 1). If P_1 is replaced by its larger homologues (covalent radii: P 110, As 121, Sb 141, Bi 146 pm), then sufficient space is only available for As_1 in the singly or doubly capped square antiprism of Rh atoms (complexes **30b**, **31b**) and for Sb_1 in the distorted Rh_{12} icosahedron (complex **32**). In all clusters with semi-interstitial P, butterfly fragments are present.

The solid-state structures of metal-rich phosphides[26] offer many parallels to the coordination polyhedra of **27**–**31**. X-ray structure analysis of the clusters $[Os_6(CO)_{18}(\mu_6\text{-}P)(\mu\text{-}AuPPh_3)]$ (**27a**)[25d] and $[Os_6(CO)_{18}(\mu_6\text{-}P)(\mu\text{-}Cl)]$ (**27b**),[25k] prepared from **27** and $Ph_3PAu^{\oplus}$ or $FeCl_3$ respectively, reveals that an intact triangle edge of **27** is bridged in **27a**, but in **27b** an opened edge. Fenske–Hall calculations on Ru model analogues of **27** and **27b** show the interaction of the tangential Cl atomic orbital with the antibonding Ru–Ru LUMO of $[Ru_6(CO)_{18}P]^{\ominus}$ to be crucial; the cluster electron count of **27b** is raised to 92.[25k] The longer metal–phosphorus bonds, as determined by X-ray methods, are indicated by dotted lines in the diagrams of clusters **23**–**26**. In **30** and **31**, these are the Rh–P bonds to the caps.[25g–i] Temperature-dependent multinuclear NMR studies[25l] show that both the CO ligands and the polyhedral core are subject to fluxional processes; for **32** in solution, these dynamic processes are rapid even at − 97 °C.

Sources of the E_1 units are: $[Cp(CO)_2MnPCl_3]$ (for **23**),[18a] $[Ru_3(CO)_n(PPh_2)(H)]$ (for **24**, **26**),[25a,c] PCl_3 (for **25**),[25b] $[Os_6H_2(CO)_{21}(PH)]$ (for **27**),[25d] red phosphorus (for **28**),[25e] $HPPh_2$ (for **29**)[25f] and Ph_3E (E = P,As,Sb) (for **30**–**32**).[25g–j]

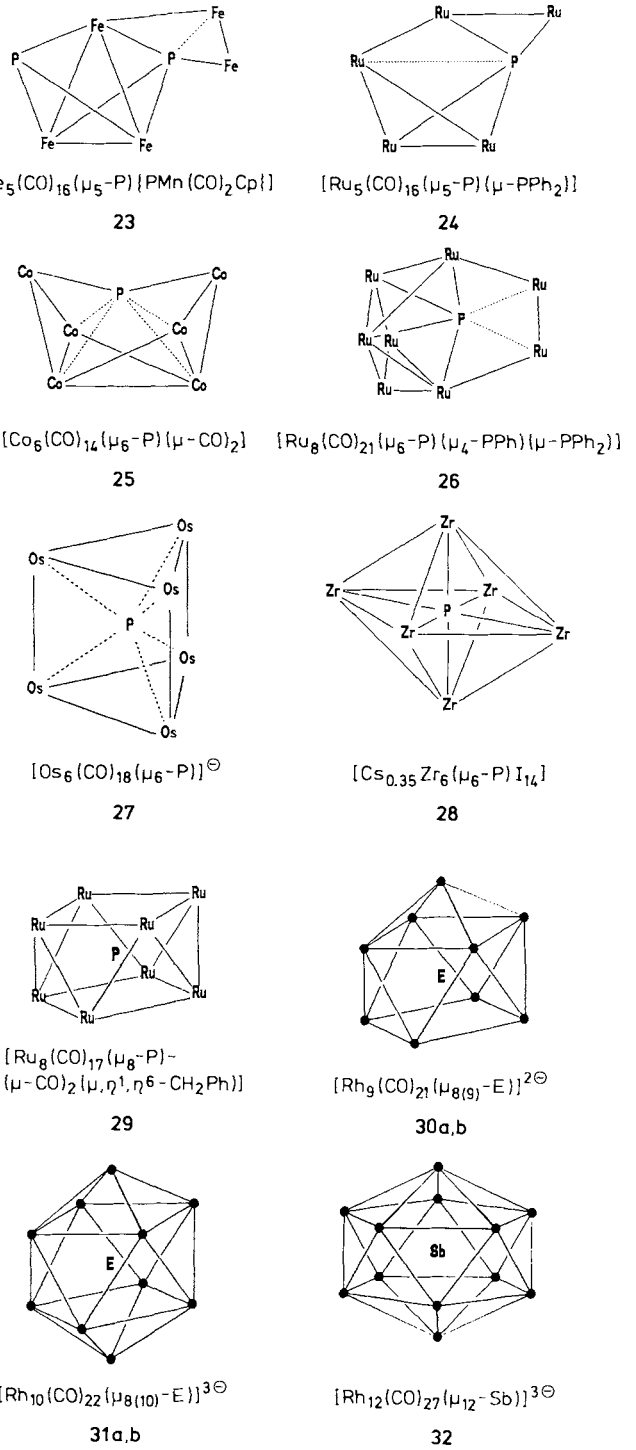

Scheme 1. Schematic representations of the polyhedral skeletons of clusters with semi-interstitial P(**23**–**26**) and interstitial P, As, and Sb atom (**27**–**32**).

3. E_2 Ligands

3.1. μ,η^2 Coordination (4e Donor)

3.1.1. Tetrahedranes with E_2M_2 Core

The E_2 ligands P_2, As_2 and Bi_2 (isoelectronic to acetylene $HC\equiv CH$) tend to form the tetrahedral clusters **33** with side-on coordinated E_2 ligands and 15e L_nM fragments.

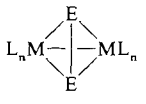

33 (E = P, As, Bi)

33	E	ML_n	Ref.
a	P	$Co(CO)_3$	[16b, 27a]
b	P	$Cr(CO)_2Cp$	[27b]
c	P	$Mo(CO)_2Cp$	[27c]
d	P	$W(CO)_2Cp$	[84]
e[*]	P	$W(OiPr)_3$	[27d]
f	As	$Co(CO)_3$	[27e, f]
g	As	$Mo(CO)_2Cp(*)$	[27g, h, i]
h	As	$W(CO)_2Cp$	[27g, h]
i	Bi	$Mo(CO)_2Cp(')$	[27j]

[*] Contains another py ligand

$[\{(OC)_3Co\}_2(\mu,\eta^2\text{-}As_2)]$ (**33f**), the first representative of this substance class, was prepared as early as 1969 from $[Co_2(CO)_8]$ and $AsCl_3$[27e] and characterized by X-ray structure determinations of its derivatives $[Co_2(CO)_{6-n}(PPh_3)_n(\mu,\eta^2\text{-}As_2)]$ (**33f'**, n = 1, **33f''**, n = 2) (Table 1).[27f] The sources of E_2 were (for phosphorus) P_4[16b, 27b, c] and PX_3 (X = Cl,Br,I)[16h] and (for arsenic) *cyclo*-$(PhAs)_6$,[27g] the μ_3-As trinuclear clusters **4b, c**[12a, b] (in **4c**, W is replaced by Mo) and As_4S_4.[27i] **33i** is formed photochemically from $[Bi\{Mo(CO)_3Cp'\}_3]$ (**9d**).[15d] The 15e ML_n fragments of Cr, Mo, and W can conveniently be obtained by the following thermolysis reactions:

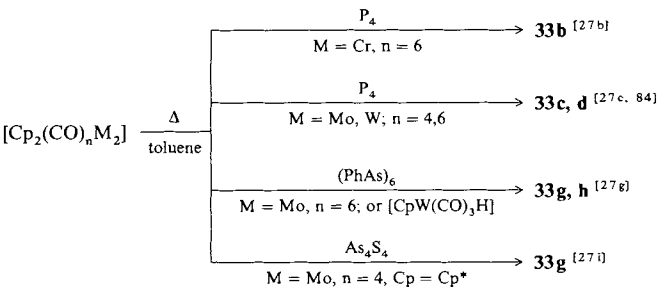

The transfer of an E_2 unit of **33** is a remarkable reaction type, for which only one example is known.[27d]

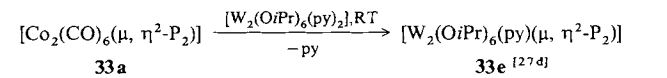

If the trigonal bipyramidal cluster **13h** is allowed to react with $[Co(CO)_4]^{\ominus}$, the edge-bridged tetrahedrane anion **34** is obtained, formally by replacing an $Fe(CO)_3$ fragment by $Co(CO)_4$ and simultaneously forming a Bi–Bi bond[18f] (cf. complex **14**).

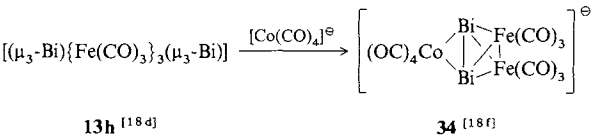

13h [18d] **34** [18f]

A tetrahedrane with two capped faces constitutes the Bi_2Co_4 core of the paramagnetic anion **35**,[16i] which is obtained, inter alia, by reaction of $BiCl_3$ with $[Co(CO)_4]^{\ominus}$.

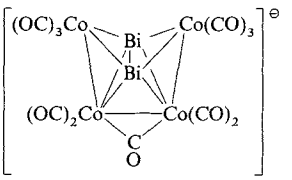

35 [16i]

The characteristic valence electron count of 40 for tetrahedranes **33** (*nido* type with n + 2 SEP) is attained in **34** with the help of two electrons from the $[Co(CO)_4]^{\ominus}$.

3.1.2. Compounds with E_2M_2 Butterfly Cores

14e and 16e ML_n fragments are typical of this type of E_2M_2 core **36**.

36 (E = P, As)

36	E	ML_n	Ref.
a	P	$Ni(Et_2PCH_2)_2$	[28a]
b	P	$Ni(PEt_3)_2$	[28b]
c	P	$Pt(PEt_3)_2$	[28c]
d	As	$Pd(PPh_3)_2$	[24b]
e	As	$Mn(CO)_2Cp^*$	[28d]

Whereas **36e** is formed by thermolysis of the arsinidene complex $[\{Cp^*(CO)_2Mn\}_2AsH]$,[28d] other representatives of this substance class are synthesized from $[Cl_2M(PR_3)_2]$ (M = Ni,Pt; R = Et;[28b, c] M = Pd, R = Ph[24b]) or $[Cl_2Ni(Et_2PCH_2)_2]$[28a] and $E(SiMe_3)_3$ (E = P,As) or $LiP(SiMe_3)_2$.[28b, c]

3.2. 6e-Donor E_2-Ligands

As well as the complexes **37**, with additional terminal coordination of an E_2M_2 tetrahedrane **33**, star-shaped molecules **38** are known, in which the unusual μ_3-η^2-E_2 coordination type has been verified.

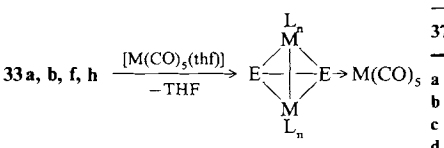

37

37	E	M	ML_n	Ref.
a	P	Cr	$Co(CO)_3$	[29a]
b	P	Cr	$Cr(CO)_2Cp$	[29b]
c	As	Cr	$Co(CO)_3$	[29c]
d	As	W	$W(CO)_2Cp$	[27h]

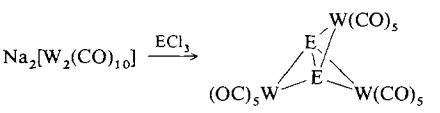

38

38a: E = As[30a]; **b**: E = Sb[30b]; **c**: E = Bi[30c]

38c is formed in the reaction of $(Me_3Si)_2CHBiCl_2$ with $Na_2[W(CO)_5]$; this reaction also gives rise to the edge-bridged Bi_2W_2 tetrahedrane **39a**.[30d] The related As_2W_2 cluster **39b** (d(As–As) = 2.305(10) Å), with an iodine bridge, is obtained from **38a** and iodine.[27h]

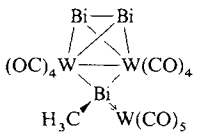

39a [30d]

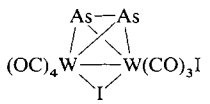

39b [27h]

3.3. 8e-Donor E_2 Ligands

Numerous complexes of type **40** are known; some examples are shown in the diagrams. The E_2M_2 core coordinates additionally through both E atoms to terminal transition metal fragments. The complexes **40** can either be obtained from the tetrahedrane precursor **33**, or can be formed directly in the coordination sphere of the transition metals.

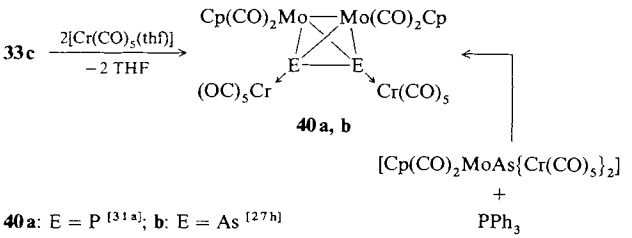

40a: E = P [31a]; **b**: E = As [27h]

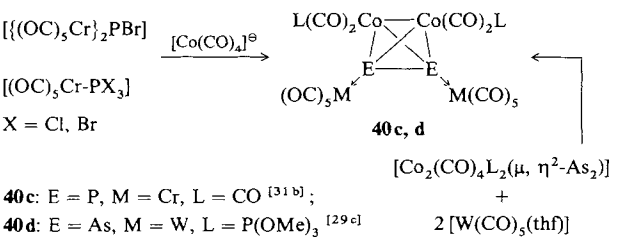

40c: E = P, M = Cr, L = CO [31b];
40d: E = As, M = W, L = $P(OMe)_3$ [29c]

The variant with bridging coordination is so far confined to complex **41**.

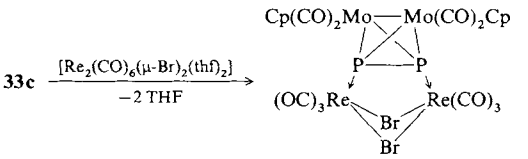

41 [31a]

Complex **42**, in which an As_2 ligand is coordinated to four 16e fragments, is formed by reductive coupling.[27h, 28d]

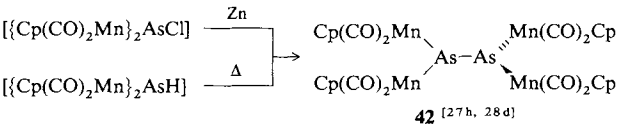

42 [27h, 28d]

X-ray structure analysis of **42** shows that both 3c,4e-Mn⋯As⋯Mn halves are rotated by 75.9° with respect to each other and are thus incapable of conjugation. The As–As bond length of 2.445(4) Å (single bond) (cf. Table 1) and the planar geometry at As indicate the presence of a diarsinidene ligand ⋮As–As⋮.[27h]

3.4. Structural and Theoretical Aspects

The X-ray data (Table 1) show clearly that the E–E and M–M bond lengths of the E_2M_2 tetrahedrane unit undergo only slight changes on going from a 4e(μ,η^2)- to an 8e(μ,$\eta^{2:1:1}$)-E_2 donor ligand (e.g. **33a'**/**40c**, **33c**/**41** and **33g**/**40b**). The Bi–Bi bond becomes appreciably longer on going from the uncharged tetrahedranes **33i** (2.838(1) Å)[27j] and **39a** (2.796(1) Å)[30d] to the anions **34** (3.092(2) Å)[18f] and **35** (3.088(1) Å)[16i].

The side-on coordination of an E≡E ligand leads, as expected (and as was shown by EH calculations on N_2 com-

Table 1. $^{31}P\{^1H\}$-NMR data (δ values, J in Hz, 85% H_3PO_4 ext.) and E–E and M–M bond lengths [Å] of selected examples with E_2M_2 core.

Compound		^{31}P	E–E	M–M	Ref.
33a'	$[(CO)_5(PPh_3)Co_2P_2]$		2.019(9)	2.574(3)	[27a]
33c	$[\{Cp(CO)_2Mo\}_2P_2]$	−42.9(s)	2.079(2)	3.022(1)	[27c]
33e	$[(^iPrO)_6(py)W_2P_2]$		2.154(4)	2.695(1)	[27d]
33f'	$[(CO)_5(PPh_3)Co_2As_2]$		2.273(3)	2.594(3)	[27f]
33g	$[\{Cp(CO)_2Mo\}_2As_2]$[a]		2.311(3)	3.039(2)	[27g, h]
33i	$[\{Cp'(CO)_2Mo\}_2Bi_2]$		2.838(1)	3.167(2)	[27j]
36a	$[\{(Et_2PCH_2)_2Ni\}_2P_2]$[a]	133(q), ^2J(PP)33.0	2.121(6)	2.908(3)	[28a]
36d	$[\{(Ph_3P)_2Pd\}_2As_2]$		2.274	3.46(M···M)	[24b]
36e	$[\{Cp^*(CO)_2Mn\}_2As_2]$		2.225(1)	4.02(M···M)	[28d]
37b	$[\{Cp(CO)_2Cr\}_2(P_2)\{Cr(CO)_5\}]$		2.052(2)	2.996(1)	[29c]
38a	$[\{(CO)_5W\}_3As_2]$		2.279(4)		[30a]
38b	$[\{(CO)_5W\}_3Sb_2]$		2.663(3)		[30b]
38c	$[\{(CO)_5W\}_3Bi_2]$		2.818(3)		[30c]
40b	$[\{Cp(CO)_2Mo\}_2(As_2)\{Cr(CO)_5\}_2]$		2.310(3)	3.064(3)	[27h]
40c	$[\{(CO)_3Co\}_2(P_2)\{Cr(CO)_5\}_2]$		2.060(5)	2.565(3)	[31b]
40d	$[\{(CO)_2(MeO)_3PCo\}_2(As_2)\{W(CO)_5\}_2]$		2.28(1)	2.59(2)	[29c]
41	$[\{Cp(CO)_2Mo\}_2(P_2)\{Re_2(CO)_6(\mu\text{-}Br)_2\}]$	−78.5(s)	2.093(8)	3.077(2)	[31a]
42	$[\{Cp(CO)_2Mn\}_4As_2]$		2.445(4)		[27h]

[a] Two independent molecules in the unit cell.

plexes)[32] to a lengthening of the E–E bond. In the tetrahedrane **33e** (Table 1) the P–P bond is 0.26 Å longer than in uncomplexed P≡P [d(P≡P)$_{exp}$ = 1.894, d(P≡P)$_{calc}$ = 1.896 Å[33]]. The corresponding bond length in metal phosphides with $P_2^{4\ominus}$ "dumbbells" is ca. 2.23 Å.[34]

By means of EH calculations on the model substance types $[Co_2(CO)_6E_2]$ (E = P,PH and $PCr(CO)_5$), the criteria determining the choice of tetrahedrane or various butterfly geometries were analyzed (compare **36** with **8a**).[35] Analogous calculations for $(L_5W)_3As_2$, L = CO, suggest plausibly that the E_2 ligand in complexes of type **38** uses its σ bond pair as well as the 4π electrons in bonding to transition metals.[30a]

4. E_3 Ligands

4.1. Mononuclear Complexes with *cyclo*-E_3 Ligands

The substance class **43**, the least metal-rich respresentative of the tetrahedrane series $[(L_nM)_{4-n}E_n]$ (n = 1,2,3), contains a *cyclo*-E_3 unit. The complexes **43a–h** represent typical examples with widely differing ML_n fragments (mostly 15e).

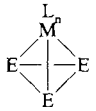

43 (E = P, As)

43	E	ML_n	Ref.
a	P	$Mo(CO)_2Cp$	[27c]
b	P	$W(OCH_2tBu)_3(HNMe_2)$	[10a, 36a]
c	P	$Co(CO)_3$	[16b]
d	P	Co(triphos)	[6, 36b]
e	P	Ni(triphos) [a]	[6, 36b]
f	P	NiCp*	[20b]
g	As	$Mo(CO)_2Cp^*$	[27i]
h	As	$Co(CO)_3$	[36c]

[a] Cation

As with the E_2M_2 tetrahedranes, it was *Dahl*'s group that succeeded in the pioneering studies of this type of complex; they synthesized $[(OC)_3Co(\eta^3\text{-}As_3)]$ (**43h**)[36c] from $(MeAs)_5$ and $[Co_2(CO)_8]$ at 200 °C under high CO pressure. **43a, c, g**. **43b**[10a] and **10c** are products of the thermolysis of $[W_2(OCH_2tBu)_6(HNMe_2)_2]$ with P_4, which is also (along

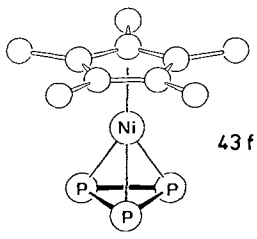

43f

with P_4S_3) the source of P_3 for **43d, e**; the (triphos)M moieties are obtained from $[M(H_2O)_6][BF_4]_2$ (M = Co,Ni) and triphos.[6, 36b] Starting materials for the classical sandwich complex **43f**[20b] are $[Cp^*Ni(\mu\text{-}CO)]_2$ and P_4.

4.1.1. *Reactivity of the cyclo-P_3 Ligand*

The lone pair of each atom of the P_3 ring is, as expected, capable of further coordination.[37a, b]

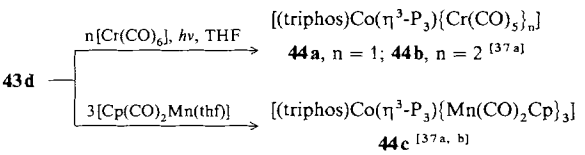

$[Cp^*(CO)_2W(\eta^3\text{-}P_3)\{Mn(CO)_2Cp\}_3]$ **44d**[37c]

$[Cp^*Ni(\eta^3\text{-}P_3)\{Cr(CO)_5\}_3]$ **44e**[20b]

In the complex $[Cp^*(CO)_2W(\eta^3\text{-}P_3)\{Mn(CO)_2Cp\}_3]$ (**44d**) (analogous to **44c**), restricted rotation of the *cyclo*-P_3 disk ($T_c \approx 330$ K, $\Delta G^{\neq}_{T_c}$ = ca. 56 kJ/mol) was demonstrated by ^{31}P-NMR spectroscopy.[37c] Complex **43f** reacts with excess $[Cr(CO)_5(thf)]$ to form $[Cp^*Ni(\eta^3\text{-}P_3)\{Cr(CO)_5\}_3]$ (**44e**).[20b] While the P_3 ring remains intact when **43d** is alkylated,[38a] one P–P edge is opened when the cationic complex **43e** reacts with $L_2Pt(C_2H_4)$.[38b]

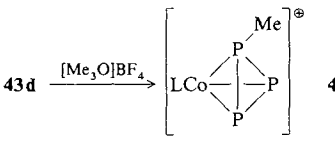

L = triphos

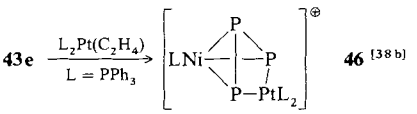

L = triphos

If the ethyl derivative of **45** is allowed to react with $Co^{2\oplus}$ and triphos, the binuclear product **47** contains EtP_3, the phosphorus analogue of ethyl azide, stabilized by coordination.[38c]

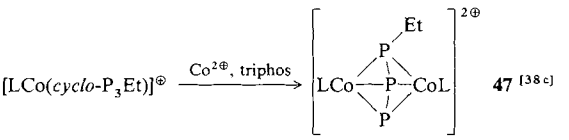

L = triphos

47 shows a certain parallel to **48**, which is formed (together with $[Cp^*(CO)_2Mo(\eta^3\text{-}P_3)]$, $[\{Cp^*(CO)_2Mo\}_2(\mu,\eta^2\text{-}P_2)]$

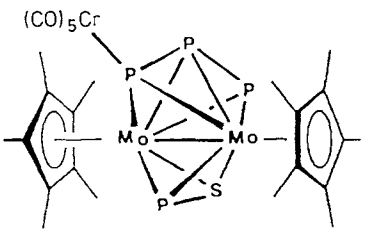

48

and $[Cp^*_2Mo_2P_2S_3]$) during the co-thermolysis of $[Cp^*(CO)_2Mo]_2$ and P_4S_3.[39]

Characteristic for complexes **45**–**48** are the marked differences (as shown by X-ray methods) in the P–P and M–P bond lengths (Table 2). The EtP_3 ligand displays a remarkable dynamic ring opening and closing behavior, as shown by temperature dependent ^{31}P-NMR spectroscopy.

A particularly striking example of a cluster assembly reaction is seen in the reaction of [(triphos)Co(η^3-P_3)] (**43d**) with CuBr, which results in the impressive multilayer sandwich structure **49**.[40] The Cu_6P_6 core, which may also be regarded as a cuboctahedron, consists of a Cu_6 central deck and two *cyclo*-P_3 decks ($\bar{d}$(P–P) = 2.03(1) Å).[40]

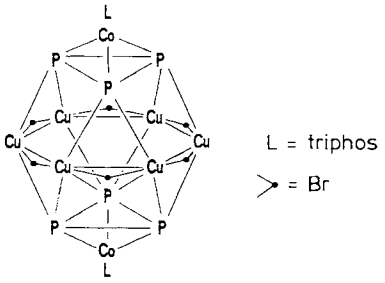

49

4.2. Binuclear Complexes with *cyclo*-P_3 Ligands

The discovery by *Sacconi* et al. of the triple-deckers **50**, with a central *cyclo*-E_3 deck (E = P,As) was a milestone in the studies of complexes with "naked" E_n ligands.[6] Typical examples are **50a**–**f**.[6]

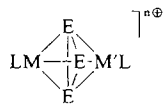

50: E = P, As, L = triphos

50	E	M	M'	n	VE	Ref.
a	P	Co	Co	2	31	[6]
b	P	Ni	Ni	2	33	[6]
c	P	Pd	Pd	1	34	[6, 41]
d[a]	P	Co	Fe	2	30	[6]
e	P	Co	Ni	2	32	[6]
f	As	Co	Co	2	31	[6]

[a] L = $MeC(CH_2PEt_2)_3$ to the Fe

The homonuclear representatives **50a**, **b**, **c**, **f** are prepared from $[M(H_2O)_6]^{2\oplus}$ (M = Co,Ni) or $[PdCl_2(PBu_3)_2]$, triphos and E_4 (E = P,As)[6] or As_4S_3.[42] [(triphos)Co(η^3-P_3)] (**43d**) can be extended to a triple-decker sandwich **50e** by reaction with the $[(triphos)Ni]^{2\oplus}$ moiety (generated as just described); this is an impressive demonstration of the π-donor properties of the *cyclo*-P_3 ligand. Some of these complexes can be reduced to the monocation with $NaBH_4$.[6] Complex **50a** can be oxidized (30 VE) or reduced (32,33 VE) cyclovoltammetrically.[6] Complexes with 31 to 33 VE are[6], with the exception of $[(triphos)Ni(P_3)Rh(triphos)]^{2\oplus}$, a 32 VE complex with a strongly distorted P_3 central deck [d(P–P) = 2.15–2.31 Å[6]], paramagnetic. In this complex and the edge-opened 32 VE binuclear complex **47**,[38c] the double degeneracy of the HOMO is removed by a Jahn–Teller distortion, changing the ground state from a triplet to a singlet state.[6, 38c]

If the Wade–Mingos electron counting rules for *closo* deltahedra[44] are applied to the triple-deckers **50** (which conform to the classical 30/34e rule[43]), then it is obvious that only the 30e species **50d** possesses the necessary 6 SEP for a trigonal bipyramid (n + 1 type).

Cyclo-As_3 can also form part of a polynuclear cluster. In $[Co_4(\mu_3\text{-}As)_3(\mu_3,\eta^3\text{-}As_3)L_4]$ (**51**), synthesized from [Co-

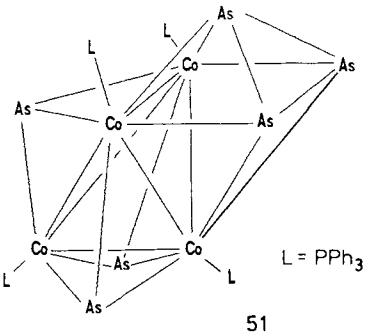

51

Cl_2L_2] and $PhAs(SiMe_3)_2$,[46] the cluster core consists of a Co_4 tetrahedron with three faces capped by As atoms and with the fourth face extended to an octahedron by an As_3 ligand [d(As–As) = 2.463(2) Å].

4.3. Spectroscopic, Structural, and Theoretical Aspects

In the mononuclear complexes **43**, the strongest deshielding of the ^{31}P-NMR signal is observed for **43f** (Table 2) and [(triphos)Pd(η^3-P_3)]BF_4 (**43i**), δ = – 132.9(q).[36b] The signal is shifted by ca. 200 ppm to high field in the binuclear complex **50c** (Table 2). The very small ^1J(MP) coupling constants [**43b**: $^1J(^{183}W^{31}P)$ = 16 Hz,[10a] [(triphos)Rh(η^3-P_3)] (**43j**): $^1J(^{103}Rh^{31}P)$ = 13 Hz[36b]] indicate an essentially π-bonded η^3-P_3 ligand.

The X-ray structure analyses show that the average P–P bond lengths of the mononuclear complexes **43** lie in a narrow range, 2.100–2.155 Å, and that the extension of the clusters to triple-deckers with a μ,η^3-P_3 central deck leads only to a small increase in the bond length; this trend is also recognizable in the few values available for the As complexes (Table 2). The P–P bond length (2.183 Å) in the bent, symmetric P_3 chain of the 19e radical anion $P_3^{4\ominus}$ (in K_4P_3[47]) does not differ greatly (in contrast to the P–P–P angle) from the average P–P bond length of the P_3 ligand in **47** (2.16 Å[38c]) and **48** (2.20 Å[39]). The M···M distances of the binuclear complexes **50**, with a central E_3 deck, lie in the non-bonding range (Table 2).

Ab initio calculations for the 16e anion $P_3^{\ominus}$ (an analogue of azide, $N_3^{\ominus}$) indicate that the bent isomer is only slightly less stable than the linear form.[48]

EH calculations,[6, 49a] carried out for the model systems $[LM(\mu,\eta^3\text{-}P_3)ML]^{n\oplus}$, suggest that the interactions between the xz and yz metal orbitals (e″ combinations of the LM···ML system) and the z orbitals of the phosphorus (e″ set of the *cyclo*-P_3 fragment) are crucial. Analogous calculations were also carried out for the 32 VE model compounds $[(H_3P)_3M(E_2S)M(PH_3)_3]^{n\oplus}$ (E = P,As).[50]

Table 2. $^{31}P\{^1H\}$-NMR data (δ values, J in Hz, 85% H_3PO_4 ext.) and E–E and M–M bond lengths [Å] of selected examples with $E_3M_{1(2)}$ core.

Compound		^{31}P	E–E [a]	M–M	Ref.
43a	$[Cp(CO)_2MoP_3]$[b]	−351.5(s)	2.127		[27c, 45]
43b	$[(Me_2NH)(tBuCH_2O)_3WP_3]$	−205.2(s), ^1J(WP)16	2.155		[10a, 36a]
43d	$[(triphos)CoP_3]$	−276.2(m)	2.141		[6, 36b]
43e	$[(triphos)NiP_3]BF_4$	−155.7(q), ^2J(PP)14	2.122		[6, 36b]
43f	$[C\overset{*}{p}NiP_3]$	−141.8(s)	2.100		[20b]
43g	$[C\overset{*}{p}(CO)_2MoAs_3]$		2.375		[27i]
43h	$[(CO)_3CoAs_3]$		2.372		[36c]
44d	$[C\overset{*}{p}(CO)_2WP_3\{Mn(CO)_2Cp\}_3]$	−154.5(t), −234.0(d) (243K), ^1J(PP)248	2.139		[37c]
45	$[(triphos)Co(P_3Me)]BF_4$	−121.0(t), −342.2(d) ^1J(PP)362	2×2.08(2) 1×2.17(2)		[38a]
46	$[(triphos)Ni(P_3PtL_2)]BPh_4$	−103.5(m)	2.17, 2.53(P···P)		[38b]
47	$[\{(triphos)Co\}_2(P_3Et)](BF_4)_2$	317(d) 339(d), −131(t) (221K) J(PP)280/300	2.21, 2.11[c] 2.62(P···P)		[38c]
48	$[\{C\overset{*}{p}Mo\}_2(PS)\{P_3Cr(CO)_5\}]$	[d]	2.109(7), 2.286(6)	2.676(1)	[39]
50a	$[\{(triphos)Co\}_2P_3](BPh_4)_2$		2.18[c]	3.86[c]	[6]
50c	$[\{(triphos)Pd\}_2P_3]BPh_4$	−334.0(sept) ^2J(PP)20	2.14[c]	4.33[c]	[6, 41]
50f	$[\{(triphos)Co\}_2As_3](BPh_4)_2$		2.43[c]	3.91[c]	[6]

[a] Average value (exceptions: **45**, **47**, **48**). [b] Two independent molecules in the unit cell. [c] Standard deviations < 0.01 Å. [d] ABMX spin system for the starting material $[Cp^*_2Mo_2P_4S)]$.

5. E_4 Ligands

5.1. E_4 Tetrahedra (E = P,Bi) as Ligands

Of the three conceivable coordination modes of an E_4 tetrahedrane, the terminal η^1-P_4 and edge-bridging (side-on) η^2-P_4 coordination have been realized for phosphorus and the face-capped variant η^3-Bi_4 for bismuth. Starting materials for **52**[6] and **53**[51] (apart from P_4) are the complexes $[(np)_3Ni]$ and $[ClRh(PPh_3)_3]$; **54** is formed in the reaction between $[Bi\{Fe(CO)_3\}_3(\mu_3\text{-}CO)]^{\ominus}$ (**10j**)[16f] and CO.[52]

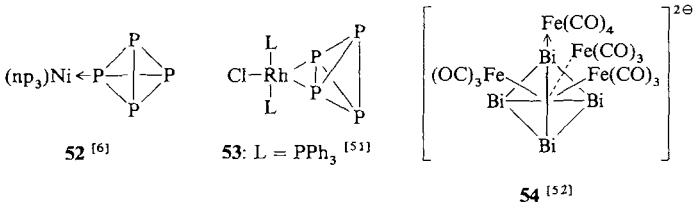

52 [6] **53**: L = PPh_3 [51] **54** [52]

X-ray structure analysis reveals characteristic differences in the E–E bond lengths. Whereas the average $P_{ap.}$–$P_{bas.}$ bond length in **52** is 2.20 Å, 0.1 Å longer than the mean $P_{bas.}$–$P_{bas.}$,[6] the difference in **54** is as high as 0.3 Å (mean $Bi_{ap.}$–$Bi_{bas.}$ 3.47, $Bi_{bas.}$–$Bi_{bas.}$ 3.16 Å). This trend is consistent with the results of EH calculations for $[Bi_4(\mu_3\text{-}FeL_3)_3]^{2\ominus}$.[52] The side-on coordination of the P_4 edge in **53**, almost perpendicular to the $[(Ph_3P)_2ClRh]$ plane, leads to an increased bond length of 2.462 Å, while the opposite bond is significantly the shortest (2.188 Å), and the others (mean P–P 2.21 Å) correspond to those of the P_4 molecule.[51] EH calculations for the model complexes $[(H_3P)_3Ni(\eta^1\text{-}P_4)]$[6] and $[(H_3P)_2ClRh(P_4)]$[51,53] do not allow a clear distinction between an intact η^2-P_4 edge or one opened by oxidative addition (cf. complexes **55** and **56**).[53]

The cluster-like particles M_6Sb_4 (M = Na,Cs), detected in the gas phase, are suggested to possess a tetrahedral Sb_4 core, surrounded by an alkali metal octahedron.[54]

5.2. E_4 Ligands Formally Derived by Opening Edges of an E_4 Tetrahedron

If one imagines three edges of an E_4 tetrahedron being successively opened by 2e reduction, then the Zintl ions[1,55] $E_4^{n\ominus}$ (n = 2,4,6) are formally obtained (E = P,As,Sb,Bi).

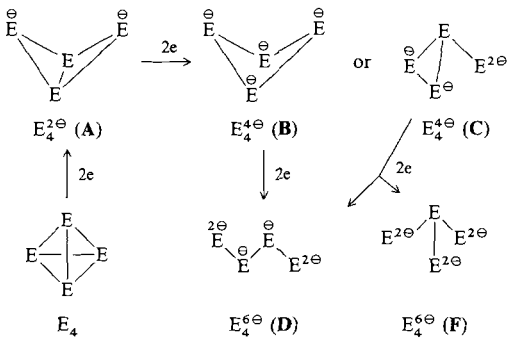

$E_4^{2\ominus}$ **(A)** $E_4^{4\ominus}$ **(B)** $E_4^{4\ominus}$ **(C)** E_4 $E_4^{6\ominus}$ **(D)** $E_4^{6\ominus}$ **(F)**

Scheme 2. $E_4^{n\ominus}$ units derived from the E_4 tetrahedron. ≡E denotes one, $=E^{\ominus}$ two, and $-E^{2\ominus}$ three lone pairs.

If covalent bonding is assumed, the successive homolytic bond cleavage of an E_4 tetrahedron leads to the uncharged species corresponding formally to **A**–**F** ($=\ddot{E}\cdot$ forming two bonds, $-\ddot{\underset{\cdot}{E}}\cdot \triangleq -\ddot{\underset{\cdot}{\ddot{E}}}$ forming one bond).

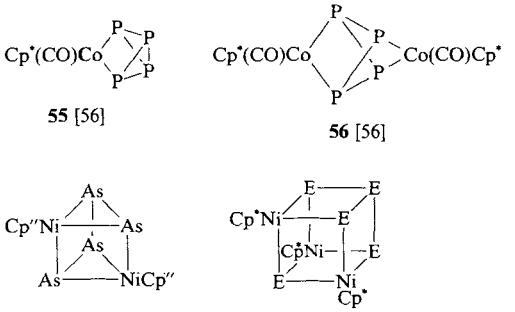

55 [56] **56** [56]

57 [57] **58a**: E = P [20b] **58b**: E = As [20b]

Of the $E_4^{n\ominus}$ units in Scheme 2, it has so far proved possible to stabilize **A**, **B**, **D** and **F** in the coordination compounds **55** (**A**),[56] **56** (**B**),[56] **57** (**D**),[57] and **58** (**F**).[20b] According to the principle of isolobal analogy[2] the complexes **56**–**58** can be formally derived from tricyclo[2.2.0.$0^{2,5}$]hexane and the hypothetical molecules hexaarsaprismane and E_8-cubane (E = P,As) respectively [Cp(CO)Co $\leftrightarrow\sigma\rightarrow$ CH_2, P $\leftrightarrow\sigma\rightarrow$ CH; CpNi $\leftrightarrow\sigma\rightarrow$ P,As].

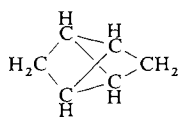

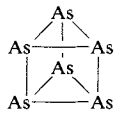

As_6

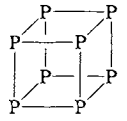

P_8

The ^{31}P-NMR[56] and X-ray data for the cobaltatetraphosphatricycloalkanes **55** [$\bar{d}$(P···P) = 2.61 Å] and **56** [$\bar{d}$(P···P) = 2.58 Å] show, in comparison with **53**,[51] that a single (to $P_4^{2\ominus}$) or double oxidative addition (to $P_4^{4\ominus}$) of P_4[56] has taken place. The suggested $P_4^{2\ominus}$ butterfly structure (**A** in Scheme 2) for K_2P_4 (detected by mass spectroscopy)[58a] was proved for $HP_4^{\ominus}$[58b] by ^{31}P-NMR spectroscopy.

The mean As–As bond length of 2.40 Å in the distorted dinickelatetraarsaprismane **57**[57] is slightly shorter than the value of 2.44 Å in the distorted trinickelapentaarsacubane **58b**.[20b] The most remarkable feature of the structures of the cubanes **58** is the tripod-like E_4 ligand, corresponding to an E_4 tetrahedron with three bonds broken. This leads, as expected, to a widening of the E–E–E angle from 60° to ca. 82°; the mean E–E bond lengths of 2.21 (**58a**) and 2.44 Å (**58b**)[20b] are however identical to those of P_4 or As_4 respectively. **58a** displays an interesting similarity to the solid-state structure of $La_6Ni_6P_{17}$,[59] in which sixteen P atoms formally constitute four trigonal pyramidal $P_4^{6\ominus}$ units and the seventeenth functions as $P^{3\ominus}$. The relevant Ni–P and P–P distances in both structures are essentially identical. The chemical bonding topology of binary and ternary transition metal polyphosphides has been studied on the basis of edge-localized models.[60]

The synthesis of **56**–**58** is achieved by thermolysis of $[Cp^*M(\mu\text{-}CO)]_2$ (M = CO,[56] Ni[20b]) and $[Cp''Ni(\mu\text{-}CO)]_2$[57] with P_4 or As_4.

The only fragment so far capable of coordinatively stabilizing tetraphospha- or tetraarsacyclobutadienes is the 14e fragment $Cp^*Nb(CO)_2$. The Wade–Mingos electron counting rules[44] for the slightly distorted square pyramid E_4Nb in **59** lead to the necessary number of SEP (n + 2 = 7) for the *nido* structure; the average E–E bond lengths (**59a** 2.16 Å,[61a] **59b** 2.38 Å[61b]) lie in the expected range for a *cyclo*-E_4 ligand with sandwich-like coordination.

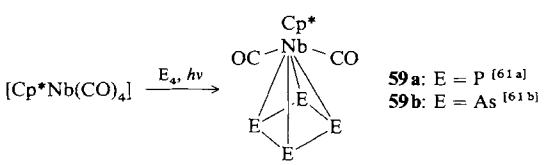

59a: E = P [61a]
59b: E = As [61b]

The analogy to cyclobutadiene,[62] C_4H_4, and to the allyl-like distortion of the dianion,[63] $C_4H_4^{2\ominus}$, would lead one to postulate the structures **F** and **G** for $E_4^{0/2\ominus}$ (E = P,As $\leftrightarrow\sigma\rightarrow$ CH) (Scheme 3).

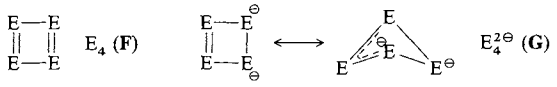

E_4 (**F**) $E_4^{2\ominus}$ (**G**)

Scheme 3. E = CH,P,As.

A slight distortion of the planar P_4 base of **59a** to a kite shape is observed (the two P–P bonds approximately parallel to the CO groups are slightly shorter).[61] It is not clear whether this is evidence for a formulation as *cyclo*-$P_4^{2\ominus}$ ligand **G** (d^2-Nb), because the distortion of an uncharged *cyclo*-P_4 ligand **F** (d^4-Nb) could be caused by the different ligands at the Nb atom.

Theoretical investigations suggest[64] that *cyclo*-P_4, the "antiaromatic" phosphorus analogue of cyclobutadiene, should prefer the square arrangement with a P–P bond length (6-31G* value) of 2.143 Å (average value in **59a** 2.16 Å[61a]).

In the series of square planar Zintl anions *cyclo*-$E_4^{2\ominus}$ (E = As,[65] Sb and Bi[66]), an As–As bond length of 2.35 Å was found[65] for *cyclo*-$As_4^{2\ominus}$ (characterized by EXAFS studies), which is in equilibrium with *cyclo*-$As_6^{4\ominus}$ (cf. 2.38 Å mean As–As in **59b**[61b]). Similar planar *cyclo*-E_4 units are found in the solid-state structures of (e.g.) CoE_3 (E = P,As; skutterudite-type),[67] where the E_4 rectangles display appreciably longer E–E bonds (CoP_3,[67a] 2.24/2.34 Å, $CoAs_3$,[67b] 2.47/2.56 Å). This type of molecule can be described either as an ionic or a covalent form.

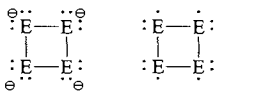

$(Co^{3\oplus})_4(E_4^{4\ominus})_3 \equiv CoE_3 \equiv Co_4(E_4)_3$

If $[Cp^xRh(CO)_2]$ and P_4 are thermolyzed, then **61**[68b] and the binuclear complex **60**[68a] are formed; in the latter, the

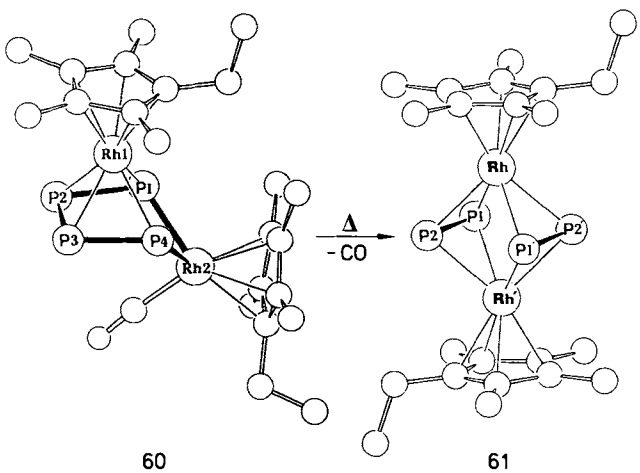

60 61

Scheme 4. Conversion of **60** into **61** at elevated temperature.

metallatetraphosphacyclopentadiene moiety itself acts as an η^4 ligand. **60** can be converted at 150 °C in xylene with cleavage of CO into **61** (Scheme 4).

The X-ray structure analysis of **60** shows that the planar P_4 unit and the top Cp^x deck are arranged parallel to each other, as in a sandwich.[68a] The almost equal P–P distances (av. 2.15 Å) contrast with those of the P_4 rectangle in the binuclear sandwich complex **61**,[68b] with a short (2.052(2) Å; cf. Table 1) and a very long (2.845(2) Å P···P) P–P distance (Rh···Rh = 3.324(1) Å).

The mononuclear complex **62**, prepared from $[Co(H_2O)_6]^{2\oplus}$, P_4 and $R_2PCH_2PR_2$,[69] contains a zig-zag-shaped η^4-tetraphosphabutadiene central ligand moiety with P–P bond lengths in the range 2.171–2.197(3) Å.

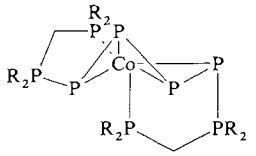

62 [69]: R = Ph

White phosphorus undergoes a ready insertion into the Zr–P bonds of a bis(phosphido)zirconium complex under very mild conditions, leading to the complex **63**.[70] The four remaining edges of the original P_4 tetrahedron have bond

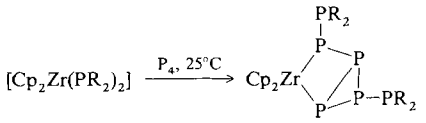

63 [70]

R = $SiMe_3$

lengths of 2.213 Å (mean value for the P_3 triangle) and 2.241(4) Å.[70]

5.3. $(E_2)_2$ Ligands (E = P,As)

As well as the rectangular arrangement of two P_2 units already discussed for the sandwich complex **61**,[68b] the alternative trapezium form of $(E_2)_2$ has been realized in the binuclear molybdenum complexes **62**. Single crystals of **62a** suitable for an X-ray structure determination were obtainable

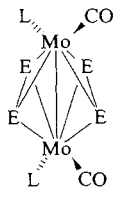

62

62	E	L	Ref.
a	P	Cp*	[7]
b	As	Cp*	[71a, 85]
c	As	Cp′	[71b]

only in the case of the derivative **62a′**, $[Cp^*(CO)MoP_2\{Cr(CO)_5\}]_2$.[71a] In **62a′** and **62c**[71b] the plane of the E_4 trapezium is perpendicular to the Mo–Mo axis [d(Mo–Mo) = 2.905(1) (**62a′**), 2.950(1) Å (**62c**)], which forms the common edge of two Mo_2E_2 tetrahedranes. The E_2 units [d(P–P) = 2.063(5)/2.071(5), d(As–As = 2.279(2)/2.300(2) Å, cf. Table 1] approach each other in the phosphorus compound to within 2.849(5) Å and in the arsenic complex **62c** to 3.051(2) Å. The bonding and nonbonding P–P distances of **62a′** and **61** are thus comparable. The structure of **62** throws light on the synthesis[71a] of the triple-decker complex $[\{Cp^*Mo\}_2(\mu,\eta^6\text{-}P_6)]$ (**68a**)[7] from **62a** and white phosphorus (see Section 7.1).

62a–c are formed together with other products in the thermolysis of $[Cp^*(CO)_2Mo]_2$ or $[Cp'(CO)_3Mo]_2$ and E_4 (E = P, **62a**[7] As **62b**[71a, 85]) or *cyclo*-$(MeAs)_5$ **62c**.[71b]

6. *cyclo*-E_5 Ligands (E = P,As)

6.1. Sandwich Complexes

In 1987 the pentaphosphacyclopentadienide ion *cyclo*-$P_5^\ominus$, isoelectronic to the classical cyclopentadienide ion $C_5H_5^\ominus$, was synthesized from white phosphorus P_4 and stabilized in the sandwich complex $[Cp^*FeP_5]$ (**63a**)[72a]

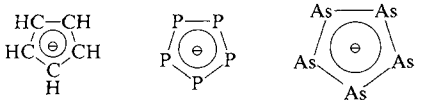

At about the same time[73a] *Baudler* et al. succeeded in preparing stable solutions of MP_5 (M = Li,Na) from P_4 and sodium in diglyme or from P_4 and $LiPH_2$ in THF (NaP_5/[18]crown-6/THF[73a, c]). The products were characterized by ^{31}P-NMR and UV spectroscopy and by negative-ion mass spectroscopy[73b] (the same method demonstrated the presence of $P_5^\ominus$ in the spectrum of red phosphorus at 325 °C[74]) and by conversion into **63a**[73b].

The anion *cyclo*-$As_5^\ominus$, prepared from yellow arsenic As_4, is to date the largest known 6π five-membered ring ligand, and is suitable for constructing the sandwich complexes **63**.[75]

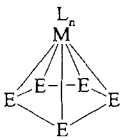

63

63	E	ML_n	Ref.
a	P	FeCp*	[72a, 73b]
b	P	$FeCp^x$	[72b]
c	P	RuCp*	[72b]
d	P	$RuCp^x$	[72b]
e	As	FeCp*	[75a]
f	As	$FeCp^x$	[75a]
g	As	RuCp*	[75b]
h	As	$RuCp^x$	[75b]

The metallocenes **63**, with a *cyclo*-E_5 deck, are mostly stable thermally and towards air; like ferrocene, they are typical *nido* compounds (n + 2 = 8 SEP) with a pentagonal pyramidal core.

63a reacts with $[Cr(CO)_5(thf)]$ or $[CpMn(CO)_2(thf)]$ in such a way as to utilize two (in **64**[76]) or even four (in **65**[76]) of its lone pairs for further coordination.

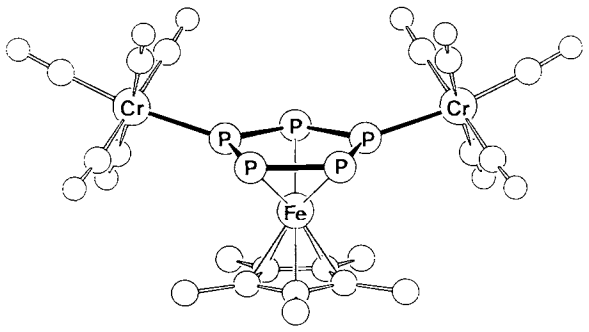

64

65: $[Cp^*FeP_5\{Mn(CO)_2Cp\}_4]$

The decamethylferrocene stacking reaction, discovered by *Rybinskaya* et al. for the synthesis of the 30 VE triple-decker sandwich complex $[(C_5H_5)Fe(C_5Me_5)Fe(C_5Me_5)]PF_6$[77] can also be applied to **63b** and **63e**.

63b, e $\xrightarrow[-C_6H_6]{[CpFe(C_6H_6)]PF_6,\ h\nu}$ $[CpFe(E_5)Fe(C_5Me_4R)]PF_6$

66g: E = P, R = Et [76]
66h: E = As, R = Me [75a]

The mixed sandwich complexes **63** are formed by cothermolysis of E_4 (E = P,[72] As[75]) with $[\eta^5\text{-}C_5Me_4R)M(CO)_2]_2$ (M = Fe,Ru) or $[(\eta^5\text{-}C_5Me_4R)Ru(CO)_2Br]$ (R = Me,Et).

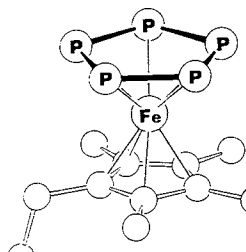

63b

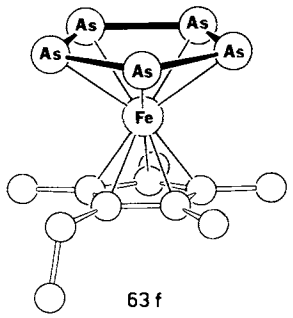

63f

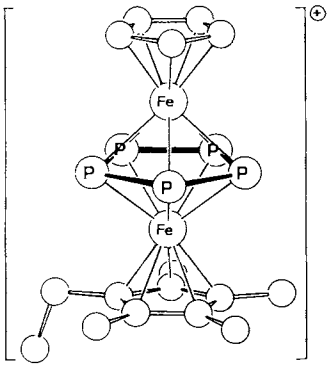

66g

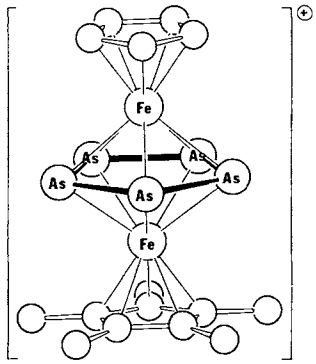

66h

The reaction of the Me_2Si-bridged binuclear complex $[\{(C_5Me_4)_2SiMe_2\}Fe_2(CO)_2(\mu\text{-}CO)_2]$ with P_4 in decalin (12 h, 190 °C) leads to the "double sandwich" structure **67**, which can also, analogously to **66g**, be further "stacked up" at both P_5 rings.[79]

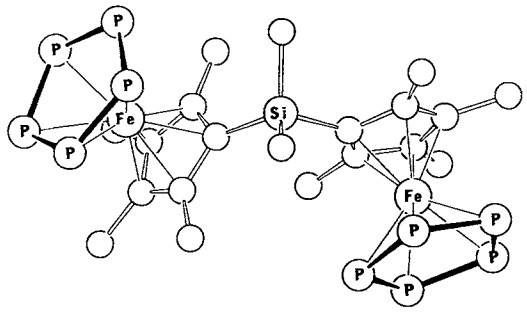

67

6.2. Triple-Decker Sandwich Complexes

Whereas the stacking up of **63** leads to the cationic, diamagnetic 30 VE complexes, the synthetic approach according to the following methods has so far only yielded the

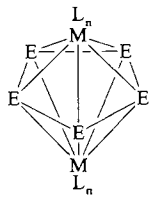

66

66	E	ML_n	Ref.
a	P	CrCp*	[78a]
b	P	CrCp	[78a]
c	P	CrCp′	[78a]
d	As	CrCp′	[78b]
e	As	$CrCp^\times$	[78c]
f	As	MoCp	[78d]

27 VE species **66a–f**. Possibly the preparation of **66f**,[78d] the only molybdenum compound of the series, depends on the use of *cyclo*-$(MeAs)_5$ instead of P_4[78a] and As_4,[78b,c] which served as sources for the E_5 deck in the chromium complexes (cf. the triple-decker complexes with *cyclo*-P_6 middle deck). In both cases different Cp-substituted binuclear complexes of the type $[CpM(CO)_3]_2$ (M = Cr,Mo) are used to generate the ML_n fragments of **66** in the thermolysis reaction. The photochemical conversion of $[Cp^\times(CO)_2Cr(\eta^3\text{-}As_3)]$ into **66e**[78c] is also known.

Cyclovoltammetric studies[78a] show that the mixed-valence (d^4/d^5-Cr), paramagnetic (μ = 2.07 μB[78e]) 27 VE triple-decker complex **66a** can readily be reversibly reduced (28 VE species, E_{red} = − 0.97 V) and oxidized (26 VE species, E_{ox} = + 0.07 V); the latter is possible even on the preparative scale with $[Cp_2Fe]^\oplus$.[78f]

6.3. Spectroscopic, Structural, and Theoretical Aspects

^{31}P-NMR studies show that the signal for the *cyclo*-P_5 ring undergoes a continuous high-field shift upon conversion of LiP_5[73a,b] (δ = 470) into the sandwich and triple-decker sandwich complexes (Table 3; e.g. **63a**, **b** and **66g**). The average P–P bond lengths (see Table 3; determined by electron diffraction in the gas phase for $[Cp^*Fe(P_5)]$ (**63a**),[80] by X-ray methods for all other *cyclo*-P_5 sandwich complexes) are all very similar and agree well with values from ab initio calculations for *cyclo*-$P_5^\ominus$ [2.081 Å (3-21 G*), 2.093 Å (DZ + P)][81a,b] and NaP_5 [2.093 Å (3-21 G*)].[81a] EH calculations for the model complexes $(C_6H_6)_2Cr$, $(C_6H_6)CrP_6$, $[(C_5H_5)_2Cr]^{2\ominus}$, $[(C_5H_5)CrP_5]^{2\ominus}$, $(C_5H_5)_2Fe$ and (C_5H_5)-

Table 3. $^{31}P\{^1H\}$-NMR data (δ values, 85% H_3PO_4 ext.) and selected bond lengths [Å] and angles [°] for sandwich and triple-decker complexes with a *cyclo*-E_5-ligand.

Compound		^{31}P	E–E [a]	M–M	$M–E_{5(center)}$	$M–C_{5(center)}$	M–E–M [a]	VE	Ref.
63a	$[C\overset{\bullet}{p}FeP_5]$[b]	153.0(s)	2.12		1.55	1.75($C\overset{\bullet}{p}$)		18	[72a, 80]
63b	$[C\overset{\times}{p}FeP_5]$	152.8(s)	2.10		1.53	1.71($C\overset{\times}{p}$)		18	[72b]
67	$[\{(C_5Me_4)_2SiMe_2\}\{FeP_5\}_2]$	156.6(s)	2.07		1.54	1.71(C_5Me_4)		18	[79]
			2.09		1.54	1.71			
63d	$[C\overset{\times}{p}RuP_5]$	84.8(s)	2.10		1.65	1.85($C\overset{\times}{p}$)		18	[72b]
64	$[C\overset{\bullet}{p}Fe(P_5)\{Cr(CO)_5\}_2]$	[c]	2.10		1.58	1.72($C\overset{\bullet}{p}$)		18	[76]
66g	$[CpFe(P_5)FeC\overset{\times}{p}]PF_6$[d]	−15.5(s)	2.11	3.043(2)	1.52	1.69(Cp)	80.6	30	[78a]
					1.52	1.71($C\overset{\times}{p}$)			
66a	$[C\overset{\bullet}{p}Cr(P_5)CrC\overset{\bullet}{p}]$	−290.5(s)	2.19	2.727(5)	1.36[a]	1.86[a]	72.5	27	[78a]
63f	$[C\overset{\times}{p}FeAs_5]$		2.32		1.54	1.715($C\overset{\times}{p}$)		18	[75a]
66h	$[CpFe(As_5)FeC\overset{\bullet}{p}]PF_6$		2.33	3.074(3)	1.53	1.68(Cp)	75.6	30	[75a]
					1.54	1.71($C\overset{\bullet}{p}$)			
66d	[Cp'Cr(As$_5$)CrCp']		2.42	2.776(4)	1.39[a]	1.84[a]	68.0	27	[78b]
66e	$[C\overset{\times}{p}Cr(As_5)CrC\overset{\times}{p}]$		2.42	2.773(2)	1.39[a]	1.85[a]	67.8	27	[78c]
66f	[CpMo(As$_5$)MoCp]		2.389(2)–2.762(3)	2.764(2)				27	[78d]

[a] Average value. [b] Electron diffraction. [c] AMM'XX' spin system. [d] Values for one of the two independent molecules in the unit cell. VE = number of valence electrons.

FeP_5 indicate that the compounds with *cyclo*-$P_{5(6)}$ ligands are at least as stable as their carbocyclic analogues;[82] this result has so far only been confirmed for $[Cp^*FeP_5]$ (**63a**) and other P_5 metallocenes with highly alkylated Cp ligands (Table 3).

In all the sandwich and triple-decker sandwich complexes, the five-membered rings are planar and parallel to each other. $[Cp^\times FeP_5]$ (**63b**) and $[Cp^\times FeAs_5]$ (**63f**) display nearly identical pairs of distances from the iron atom to the centers of the five-membered rings (Table 3). The appreciably shorter M–M distances (ca. 2.73–2.78 Å) in the less electron-rich 27 VE triple-deckers (cf. ca. 3.05 Å in the 30 VE species) lead to a compression of the pentagonal bipyramidal ME_5M framework (the angles M–E–M are ca. 8° narrower), accompanied by a lengthening of the average E–E bond length by ca. 0.09 Å (cf. **66g** with **66a**, and **66h** with **66d**, **e** in Table 3).

EH calculations for triple-decker compounds $[CpM(\mu,\eta^n\text{-}E_n)MCp]$ (n = 5, E = P,As; n = 6, E = P) with bonding M–M distances suggest[49] that 28 VE should be the magic number (cf. the 30/34e rule[43]). If the electron count is increased to 30, then two electrons must occupy the antibonding a_2'' (σ^*) orbital,[49] which explains the experimentally established lengthening of the M–M bond length by ca. 0.3 Å (see Table 3).

$[CpMo(As_5)MoCp]$ (**66f**)[78d] occupies a special position among the triple-decker complexes **66d–f** with a central As_5 deck. The distortion **H** of the As_5 ring to an "allyl–ene" system, of which this is surprisingly the only known example, can be attributed to Jahn–Teller effects, as shown by EH calculations.[49] In the 28 VE triple-decker $[(CpMo)_2(\mu,\eta^3\text{-}As_3)(\mu,\eta^2AsS)]$ (**67**),[83] the As_4S middle deck (the AsS

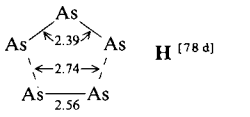

H [78d]

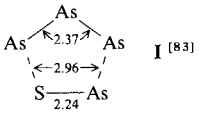

I [83]

part is disordered) displays the distortion in **I**, also consistent with theory[49a] (cf. the analogous triple-decker **48**[39] with a central P_4S deck).

If the Wade–Mingos electron-counting rules[44] are applied to substance class **66**, then only the 30 VE triple-deckers **66g**[76] and **66h**[75a] have the necessary number of skeletal electron pairs for a pentagonal bipyramid (n + 1 = 8 SEP).

7. *cyclo*-E_6 Ligands (E = P,As)

7.1. Triple-Decker Sandwich Complexes

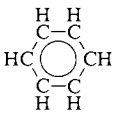

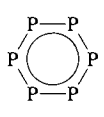

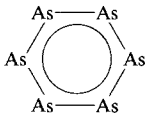

The molecules *cyclo*-P_6 (hexaphosphabenzene) and *cyclo*-As_6 (hexaarsabenzene), isoelectronic to benzene (CH ≙ P,As) were first coordinatively stabilized in 1985[7] and 1989[85] respectively, as the central decks of the triple-decker sandwich complexes **68a** and **68i**.

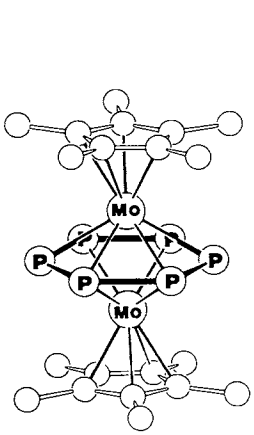

68a

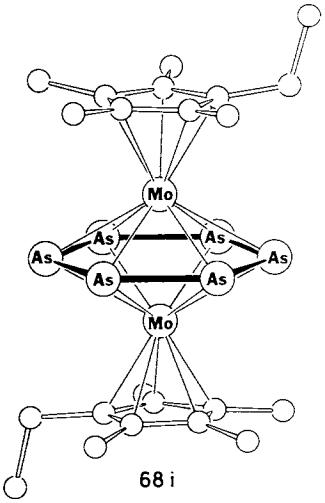

68i

The synthesis of **68** can involve the thermolysis of E_4 (E = P,As) with $[Cp_2^{*(x)}M_2(CO)_n]$ (n = 4,6; M = Mo,[7, 85] W[84]) or $[Cp^{*(x)}M(CO)_4]$ (M = V,[84] Nb,[61a, 87]) or the photolysis of $[Cp^{*(x)}(CO)_2Mo(\eta^3\text{-}E_3)]$ (E = P,[86] As[85]).

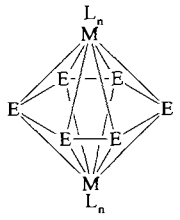

68

68	E	ML_n	Ref.
a	P	MoCp*	[7, 86]
b	P	WCp*	[84]
c	P	VCp*	[84]
d	P	VCp^x	[84]
e	P	NbCp*	[61a]
f	P	$NbCp^x$	[61a]
g	P	NbCp'''	[87]
h	As	MoCp*	[85]
i	As	$MoCp^x$	[85]

For group 4 metals, the synthesis of **69**[88] involves not only CO elimination but also the removal of a Cp* ligand from the mononuclear Ti complex.

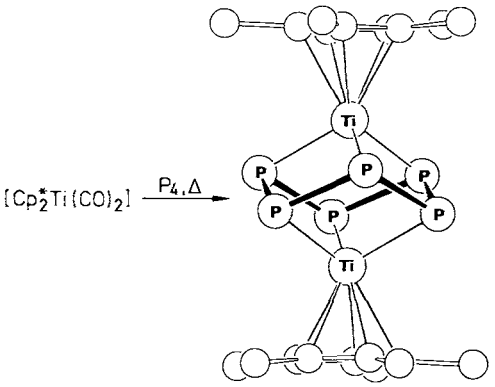

69

68 and **69** are thermally very stable and can be handled in air.

Cyclovoltammetric studies[84] show that the triple-decker complexes **68a–c**, with 28 or 26 VE, have a strong tendency to form 27 VE complexes (open-shell configuration) by reduction (V complex **68c**) or oxidation (W complex **68b**). The 24 VE complex **69** is irreversibly oxidized to the 23 VE cation and reversibly reduced to the 25 VE anion.[88]

Attempts to prepare cubic P_8 from **69** and two moles of PX_3 (X = Cl,Br) have proved unsuccessful.[88]

7.2. Spectroscopic, Structural, and Theoretical Aspects

The lowering of the valence electron number from 28 to 24 leads to an increasing low-field shift in the ^{31}P-NMR signals of the *cyclo*-P_6 group in **68** and **69** (Table 4). Parallel to this, an increasing distortion of the *cyclo*-P_6 ligand is observed by X-ray methods. The separation of the benzene π system into two allyl-like 3e units, just observable in the 26 VE triple-decker $[CpV(C_6H_6)VCp]$,[89] is particularly marked in the *cyclo*-P_6 ligand of **68g**; the central deck here (**J**) shows four short (2.104(2)–2.116(3) Å) and two very long (2.345(3) Å) P–P bonds (Table 4; cf. complex **68f**[61a]). The presence of a *cyclo*-$P_6^{2\ominus}$ ligand is also formally conceivable (resonance forms **K** and **L**). LCAO-MO calculations[90] for the series *cyclo*-$P_6^{n\ominus}$ (n = 0,2,4,6) with idealized symmetry 6/*mmm* indicate the greatest stability for *cyclo*-$P_6^{2\ominus}$.

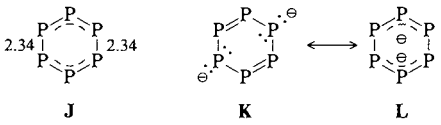

J **K** **L**

The 28 VE triple-deckers **68a**, **b** and **68i** display within experimental error regular phosphorus or arsenic hexagons; the average E–E bond lengths are only slightly different from those of the polyphosphides M_4P_6[90] (M = K,Rb 2.15 Å; Cs 2.14 Å) and the polyarsenide Rb_4As_6[1] (2.37 Å), which also possess a regular hexagonal ring, $E_6^{4\ominus}$ (10π system). The marked enlargement of the central E_6 deck on going from E = P (**68a**, **b**) to E = As (**68i**), coupled with the almost constant Mo–Mo distance (Table 4), causes a flattening (decrease of Mo–E–Mo angle) of the hexagonal bipyramidal $Mo(E_6)Mo$ framework.

If the chair-shaped P_6 ring in the distorted Ti_6P_6 cubane framework of **69**[88] is attributed the formal charge *cyclo*-$P_6^{6\ominus}$ (isoelectronic with *cyclo*-S_6), an interesting analogy to the μ,η^3,η^3-*cyclo*-$P_6^{6\ominus}$ moiety of Th_2P_{11}[91] arises; the average P–P bond length and P–P–P angles of the latter compound are essentially the same as in **69** (2.23 Å, 105.9°).[88]

EH calculations[49] for the model compound [CpMo(P_6)MoCp], as for the triple-decker complexes with a central P_5 deck, indicate that the magic number of electrons should be 28; the HOMO–LUMO gap (ca. 0.7 eV) is much smaller here. The crystallographically determined average P–P bond length of **68a**, **b** (Table 4) is ca. 0.07 Å longer

Table 4. $^{31}P\{^1H\}$-NMR data (δ values, 85% H_3PO_4 ext.) and selected bond lengths [A] and angles [°] for triple-decker complexes with a central *cyclo*-E_6-deck.

Compound		^{31}P	E–E [a]	M–M	M–$E_{6(center)}$	M–$C_{5(center)}$	M–E–M [a]	VE	Ref.
68a	[Cp*Mo(P_6)MoCp*]	−315,6(s)	2.17	2.647(1)	1.32	2.00(Cp*)	62.8	28	[7, 86]
68b	[Cp*W(P_6)WCp*]	−338.2(s)	2.17	2.639(1)	1.32	1.99(Cp*)	62.5	28	[84]
68d	[$Cp^xV(P_6)VCp^x$]	160.3(s) $\Delta\nu_{1/2}$ = 543 [b]	2.13	2.627(2)	1.31[a]	1.94[a] (Cp^x)	63.2	26	[84]
68f	[$Cp^xNb(P_6)NbCp^x$]	126.0(s)	2.140(9)–2.243(9)	2.791(2)	1.395 1.40	2.08(Cp^x) 2.07(Cp^x)	65.1	26	[61a]
68g	[Cp'''Nb(P_6)NbCp''']	113.4(s)	2.104(2)–2.345(3)	2.818(1)	1.41	2.10(Cp''')	66.4	26	[87]
69	[Cp*Ti(P_6)TiCp*]	386.7(s)	2.23	3.187(4)(M···M)		2.00(Cp*)		24	[88]
68i	[$Cp^xMo(As_6)MoCp^x$]		2.35	2.639(1)	1.32	1.98(Cp^x)	58.7	28	[85]

[a] Average value. [b] ^{51}V-NMR ($VOCl_3$ ext.): δ = 60(sept), $^1J(^{51}V^{31}P)$ = 56 Hz.

than indicated by ab initio calculations (6-31G*, 2.096 Å)[64, 81b, 92a, b] for uncoordinated hexaphosphabenzene, *cyclo*-P_6. Whereas *cyclo*-$P_5^{\ominus}$ proves in every respect to be the all-phosphorus analogue of $C_5H_5^{\ominus}$, *cyclo*-P_6 differs from benzene mainly in the σ framework properties (rather than the π electronic effects).

8. Prospects

The coordinative stabilization of numerous substituent-free E_n units of phosphorus, arsenic, antimony and bismuth has proved in some cases to be surprisingly simple. This has led to a rapid growth of the interdisciplinary research area within a short time. Parallel to these developments is an increase in the number of examples that support the original hopes of forging links to organic and solid-state chemistry.

It remains to be seen whether suitable synthetic strategies can be developed (a) to stabilize *cyclo*-P_6 in sandwich complexes and *cyclo*-$P_{7(8)}$ analogously or in triple-decker complexes and (b) to prepare polydecker sandwich complexes[93] or to stabilize coordinatively the uncharged As building blocks of the interesting anions $[As_7Cr(CO)_3]^{3\ominus}$[94] and $^1_\infty[Rb\{NbAs_8\}]^{2\ominus}$.[95] It is not too wild a prediction that clusters and cage molecules with cyclic and acyclic E_n frameworks will soon be discovered with ever increasing frequency. The attempts to illuminate the mechanistic aspects[27b] should be continued, the cyclovoltammetric and magnetic measurements intensified, and the study of catalytic properties taken in hand. The continued active interest of the theoreticians will be a great advantage.

My particular thanks are due to the proficient and dedicated co-workers, whose names are given in the references, and who have worked in this (for us) new research area. We also thank Prof. Kaim (Stuttgart) for spontaneously assenting to collaboration and Dr. G. Wolmershäuser for constant and rapid assistance, readily given, in determining the many X-ray structures. Both have decisively influenced the progress of our research. The Deutsche Forschungsgemeinschaft and the Fonds der Chemischen Industrie gave generous financial assistance.

Received: March 29, 1990 [A 782 IE]
German version: *Angew. Chem. 102* (1990) 1137
Translated by Professor *P. G. Jones*, Braunschweig (FRG)

[1] H. G. von Schnering, *Angew. Chem. 93* (1981) 44; *Angew. Chem. Int. Ed. Engl. 20* (1981) 33.
[2] R. Hoffmann, *Angew. Chem. 94* (1982) 725; *Angew. Chem. Int. Ed. Engl. 21* (1982) 711.
[3] F. G. A. Stone, *Angew. Chem. 96* (1984) 85; *Angew. Chem. Int. Ed. Engl. 23* (1984) 89.
[4] M. Baudler, *Angew. Chem. 94* (1982) 520; *Angew. Chem. Int. Ed. Engl. 21* (1982) 492; *ibid. 97* (1987) 429 and *26* (1987) 419.
[5] M. Yoshifuji, I. Shima, N. Inamoto, K. Hirotsu, T. Higuchi, *J. Am. Chem. Soc. 103* (1981) 4587; *ibid. 104* (1982) 6167.
[6] Review article: M. Di Vaira, L. Sacconi, *Angew. Chem. 94* (1982) 338; *Angew. Chem. Int. Ed. Engl. 21* (1982) 330.
[7] O. J. Scherer, H. Sitzmann, G. Wolmershäuser, *Angew. Chem. 97* (1985) 358; *Angew. Chem. Int. Ed. Engl. 24* (1985) 351.
[8] In the last five years alone, more or less extensive review articles have dealt with several aspects of this field: O. J. Scherer, *Angew. Chem. 97* (1985) 905; *Angew. Chem. Int. Ed. Engl. 24* (1985) 924; W. A. Herrmann, *ibid. 98* (1986) 57 *and 25* (1986) 56; O. J. Scherer, *Comments Inorg. Chem. 6* (1987) 1; M. Di Vaira, P. Stoppioni, M. Peruzzini, *Polyhedron 6* (1987) 351; D. Fenske, J. Ohmer, J. Hachgenai, K. Merzweiler, *Angew. Chem. 100* (1988) 1300; *Angew. Chem. Int. Ed. Engl. 27* (1988) 1277; K. H. Whitmire, *J. Coord. Chem. 17* (1988) 95; N. C. Norman, *Chem. Soc. Rev. 17* (1988) 269; A.-J. Di Maio, A. L. Rheingold, *Chem. Rev. 90* (1990) 169. Most recent comprehensive review: M. Scheer, E. Hermann, *Z. Chem. 30* (1990) 41.
[9] Review article: M. Regitz, P. Binger, *Angew. Chem. 100* (1988) 1541; *Angew. Chem. Int. Ed. Engl. 27* (1988) 1484; M. Regitz, *Chem. Rev. 90* (1990) 191.
[10] a) M. H. Chisholm, K. Folting, J. W. Pasterczyk, *Inorg. Chem. 27* (1988) 3057; b) M. L. Ziegler, H. P. Neumann, *Chem. Ber. 122* (1989) 25; c) H. P. Neumann, M. L. Ziegler, *J. Organomet. Chem. 377* (1989) 255.
[11] a) A. Strube, J. Heuser, G. Huttner, H. Lang, *J. Organomet. Chem. 356* (1988) C9; b) A. Strube, G. Huttner, L. Zsolnai, *Angew. Chem. 100* (1988) 1586; *Angew. Chem. Int. Ed. Engl. 27* (1988) 1529.
[12] a) G. Huttner, U. Weber, B. Sigwarth, O. Scheidsteger, H. Lang, L. Zsolnai, *J. Organomet. Chem. 282* (1985) 331; b) G. Huttner, B. Sigwarth, J. von Seyerl, L. Zsolnai, *Chem. Ber. 115* (1982) 2035.
[13] Review article: G. Huttner, K. Evertz, *Acc. Chem. Res. 19* (1986) 406; see also: G. Huttner, K. Knoll, *Angew. Chem. 99* (1987) 765; *Angew. Chem. Int. Ed. Engl. 26* (1987) 743.
[14] H. Lang, L. Zsolnai, G. Huttner, *Angew. Chem. 95* (1983) 1016; *Angew. Chem. Int. Ed. Engl. 22* (1983) 976; *Angew. Chem. Suppl. 1983*, 1451.
[15] a) V. Grossbruchhaus, D. Rehder, *Inorg. Chim. Acta 141* (1988) 9; b) W. Malisch, P. Panster, *Z. Naturforsch. B30* (1975) 229; A. M. Barr, M. D. Kerlogue, N. C. Norman, P. M. Webster, L. J. Farrugia, *Polyhedron 8* (1989) 2495; c) W. Malisch, P. Panster, *Angew. Chem. 88* (1976) 680; *Angew. Chem. Int. Ed. Engl. 15* (1976) 618; d) W. Clegg, N. A. Compton, R. J. Errington, N. C. Norman, A. J. Tucker, M. J. Winter, *J. Chem. Soc. Dalton Trans. 1988*, 2941; e) J. M. Wallis, G. Müller, H. Schmidbaur, *Inorg. Chem. 26* (1987) 458; f) W. R. Cullen, D. J. Patmore, J. R. Sams, *ibid. 12* (1973) 867; g) J. M. Wallis, G. Müller, H. Schmidbaur, *J. Organomet. Chem. 325* (1987) 159; W. Clegg, N. A. Compton, R. J. Errington, N. C. Norman, *Polyhedron 6* (1987) 2031; *J. Chem. Soc. Dalton Trans. 1988*, 1671; h) G. Etzrodt, R. Boese, G. Schmid, *Chem. Ber. 112* (1979) 2574.
[16] a) T. Kruck, G. Sylvester, J. P. Kunau, *Z. Naturforsch. B28* (1973) 38; b) A. Vizi-Orosz, G. Pályi, L. Markó, *J. Organomet. Chem. 60* (1973) C25; A. Vizi-Orosz, *ibid. 111* (1976) 61; c) A. Vizi-Orosz, V. Galamb, G. Pályi, L. Markó, G. Bor, G. Natile, *ibid. 107* (1976) 235; d) K. Blechschmitt, H. Pfisterer, T. Zahn, M. L. Ziegler, *Angew. Chem. 97* (1985) 73; *Angew. Chem. Int. Ed. Engl. 24* (1985) 66; e) S. Luo, K. H. Whitmire, *Inorg. Chem. 28* (1989) 1424; f) K. H. Whitmire, C. B. Lagrone, M. R. Churchill, J. C. Fettinger, L. V. Biondi, *ibid. 23* (1984) 4227; g) W. Kruppa, D. Bläser, R. Boese, G. Schmid, *Z. Naturforsch. B37* (1982) 209; h) K. H. Whitmire, J. S. Leigh, M. E. Gross, *J. Chem. Soc. Chem. Commun. 1987*, 926; i) S. Martinengo, G. Ciani, *ibid. 1987*, 1589.
[17] a) K. H. Whitmire, C. B. Lagrone, A. L. Rheingold, *Inorg. Chem. 25* (1986) 2472; b) A. Vizi-Orosz, V. Galamb, G. Pályi, L. Markó, *J. Organomet. Chem. 216* (1981) 105; c) R. Lal De, H. Vahrenkamp, *Z. Naturforsch. B40* (1985) 1250; d) A. Vizi-Orosz, V. Galamb, I. Ötrös, G. Pályi, L. Markó, *Transition Met. Chem. (Weinheim, Ger.) 4* (1979) 294; e) H. Lang, G. Huttner, B. Sigwarth, I. Jibril, L. Zsolnai, O. Orama, *J. Organomet. Chem. 304* (1986) 137; f) A. Gourdon, Y. Jeannin, *ibid. 304* (1986) C1.
[18] a) H. Lang, G. Huttner, L. Zsolnai, G. Mohr, B. Sigwarth, U. Weber, O. Orama, I. Jibril, *J. Organomet. Chem. 304* (1986) 157; b) L. T. J. Delbaere, L. J. Kruczynski, D. W. Mc Bride, *J. Chem. Soc. Dalton Trans. 1973*, 307; c) T. Zimler, A. Vizi-Orosz, L. Markó, *Transition Met. Chem. (Weinheim, Ger.) 2* (1977) 97; d) M. R. Churchill, J. C. Fettinger, K. H. Whitmire, *J. Organomet. Chem. 284* (1985) 13; e) H. G. Ang, C. M. Hay, B. F. G. Johnson, J. Lewis, P. R. Raithby, A. J. Whitton, *ibid. 330* (1987) C5, see also [23b]; f) K. H. Whitmire, K. S. Raghuveer, M. R. Churchill, J. C. Fettinger, R. F. See, *J. Am. Chem. Soc. 108* (1986) 2778; K. H. Whitmire, M. Shieh, C. B. Lagrone, B. H. Robinson, M. R. Churchill, J. C. Fettinger, R. F. See, *Inorg. Chem. 26* (1987) 2798.
[19] C. D. Garner in B. F. G. Johnson (Ed.): *Transition Metal Clusters*, Wiley, New York 1980, p. 265.
[20] a) G. L. Simon, L. F. Dahl, *J. Am. Chem. Soc. 95* (1973) 2175; b) O. J. Scherer, J. Braun, G. Wolmershäuser, *Chem. Ber. 123* (1990) 471; see also: O. J. Scherer, T. Dave, J. Braun, G. Wolmerhäuser, *J. Organomet. Chem. 350* (1988) C20; c) A. S. Foust, L. F. Dahl, *J. Am. Chem. Soc. 92* (1970) 7337; d) G. Ciani, M. Moret, A. Fumagalli, S. Martinengo, *J. Organomet. Chem. 362* (1989) 291.
[21] a) M. R. Churchill, J. C. Fettinger, K. H. Whitmire, C. B. Lagrone, *J. Organomet. Chem. 303* (1986) 99; b) S. Martinengo, A. Fumagalli, G. Ciani, M. Moret, *ibid. 347* (1985) 413; c) J. S. Leigh, K. H. Whitmire, *Angew. Chem. 100* (1988) 399; *Angew. Chem. Int. Ed. Engl. 27* (1988) 396.
[22] a) G. Huttner, G. Mohr, B. Pritzlaff, J. von Seyerl, L. Zsolnai, *Chem. Ber. 115* (1982) 2044; b) D. J. Brauer, S. Hiefkamp, H. Sommer, O. Stelzer, *Z. Naturforsch. B40* (1985) 1677; c) A. L. Rheingold, S. J. Geib, M. Shieh, K. H. Whitmire, *Inorg. Chem. 26* (1987) 463; A. M. Arif, A. H. Cowley, M. Pakulski, *J. Chem. Soc. Chem. Commun. 1987*, 622; d) B. F. G. Johnson, J. Lewis, P. R. Raithby, A. J. Whitton, *ibid. 1988*, 401; e) C. F. Campana, L. F. Dahl, *J. Organomet. Chem. 127* (1977) 209.

[23] a) S. Luo, K. H. Whitmire, *J. Organomet. Chem. 376* (1989) 297; b) C. M. Hay, B. F. G. Johnson, J. Lewis, P. R. Raithby, A. J. Whitton, *J. Chem. Soc. Dalton Trans. 1988*, 2091.

[24] a) D. Fenske, K. Merzweiler, J. Ohmer, *Angew. Chem. 100* (1988) 1572; *Angew. Chem. Int. Ed. Engl. 27* (1988) 1512; b) D. Fenske, H. Fleischer, C. Persau, *ibid. 101* (1989) 1740 and *28* (1989) 1665; c) A. L. Rheingold, P. J. Sullivan, *J. Chem. Soc. Chem. Commun. 1983*, 39.

[25] a) S. A. Mc Laughlin, N. J. Taylor, A. J. Carty, *Inorg. Chem. 22* (1983) 1409; b) P. Chini, G. Ciani, S. Martinengo, A. Sironi, L. Longhetti, B. T. Heaton, *J. Chem. Soc. Chem. Commun. 1979*, 188; G. Ciani, A. Sironi, *J. Organomet. Chem. 241* (1983) 385; c) F. Van Gastel, N. J. Taylor, A. J. Carty, *Inorg. Chem. 28* (1989) 384; d) S. B. Colbran, C. M. Hay, B. F. G. Johnson, F. J. Lahoz, J. Lewis, P. R. Raithby, *J. Chem. Soc. Chem. Commun. 1986*, 1766; e) G. Rosenthal, J. D. Corbett, *Inorg. Chem. 27* (1988) 53; f) L. M. Bullock, J. S. Field, R. J. Haines, E. Minshall, D. N. Smit, G. M. Sheldrick, *J. Organomet. Chem. 310* (1986) C47; g) J. L. Vidal, W. E. Walker, R. L. Pruett, R. C. Schoening, *Inorg. Chem. 18* (1979) 129; h) J. L. Vidal, *ibid. 20* (1981) 243; i) J. L. Vidal, W. E. Walker, R. C. Schoening, *ibid. 20* (1981) 238; j) J. L. Vidal, J. M. Troup, *J. Organomet. Chem. 213* (1981) 351; k) S. B. Colbran, C. E. Housecroft, B. F. G. Johnson, J. Lewis, S. M. Owen, P. R. Raithby, *Polyhedron 7* (1988) 1759; l) B. T. Heaton, L. Strona, R. D. Pergola, J. L. Vidal, R. C. Schoening, *J. Chem. Soc. Dalton Trans. 1983*, 1941.

[26] D. E. C. Corbridge: *The Structural Chemistry of Phosphorus*, Elsevier, New York 1974.

[27] a) C. F. Campana, A. Vizi-Orosz, G. Pályi, L. Markó, L. F. Dahl, *Inorg. Chem. 18* (1979) 3054; b) L. Y. Goh, C. K. Chu, R. C. S. Wong, T. W. Hambley, *J. Chem. Soc. Dalton Trans. 1989*, 1951; c) O. J. Scherer, H. Sitzmann, G. Wolmershäuser, *J. Organomet. Chem. 268* (1984) C9; d) M. H. Chisholm, K. Folting, J. C. Huffman, J. J. Koh, *Polyhedron 4* (1985) 893; e) A. S. Foust, M. S. Foster, L. F. Dahl, *J. Am. Chem. Soc. 91* (1969) 5633; f) A. S. Foust, C. F. Campana, J. D. Sinclair, L. F. Dahl, *Inorg. Chem. 18* (1979) 3047; g) P. J. Sullivan, A. L. Rheingold, *Organometallics 1* (1982) 1547; h) G. Huttner, B. Sigwarth, O. Scheidsteger, L. Zsolnai, O. Orama, *ibid. 4* (1985) 326; i) I. Bernal, H. Brunner, W. Meier, H. Pfisterer, J. Wachter, M. L. Ziegler, *Angew. Chem. 96* (1984) 428; *Angew. Chem. Int. Ed. Engl. 23* (1984) 438; j) W. Clegg, N. A. Compton, R. J. Errington, N. C. Norman, *Polyhedron 7* (1988) 2239.

[28] a) H. Schäfer, D. Binder, D. Fenske, *Angew. Chem. 97* (1985) 523; *Angew. Chem. Int. Ed. Engl. 24* (1985) 522; b) H. Schäfer, D. Binder, *Z. Anorg. Allg. Chem. 546* (1987) 55; c) H. Schäfer, D. Binder, *ibid. 560* (1988) 65; d) W. A. Herrmann, B. Koumbouris, T. Zahn, M. L. Ziegler, *Angew. Chem. 96* (1984) 802; *Angew. Chem. Int. Ed. Engl. 23* (1984) 812; W. A. Herrmann, B. Koumbouris, A. Schäfer, T. Zahn, M. L. Ziegler, *Chem. Ber. 118* (1985) 2472.

[29] a) A. Vizi-Orosz, G. Pályi, L. Markó, R. Boese, G. Schmid, *J. Organomet. Chem. 288* (1985) 179; b) L. Y. Goh, R. C. S. Wong, T. C. W. Mak, *ibid. 373* (1989) 71; c) M. Müller, H. Vahrenkamp, *ibid. 252* (1983) 95.

[30] a) B. Sigwarth, L. Zsolnai, H. Berke, G. Huttner, *J. Organomet. Chem. 226* (1982) C5; b) G. Huttner, U. Weber, B. Sigwarth, O. Scheidsteger, *Angew. Chem. 94* (1982) 210; *Angew. Chem. Int. Ed. Engl. 21* (1982) 215; c) G. Huttner, U. Weber, L. Zsolnai, *Z. Naturforsch. B37* (1982) 707; d) A. M. Arif, A. H. Cowley, N. C. Norman, M. Pakulski, *Inorg. Chem. 25* (1986) 4836.

[31] a) O. J. Scherer, H. Sitzmann, G. Wolmershäuser, *Angew. Chem. 96* (1984) 979; *Angew. Chem. Int. Ed. Engl. 23* (1984) 968; b) H. Lang, L. Zsolnai, G. Huttner, *ibid. 95* (1983) 1017 and *22* (1983) 976.

[32] K. I. Goldberg, D. M. Hoffman, R. Hoffmann, *Inorg. Chem. 21* (1982) 3863.

[33] For example R. Ahlrichs, S. Brode, C. Ehrhardt, *J. Am. Chem. Soc. 107* (1985) 7260, and references cited therein.

[34] Review article: H. G. von Schnering, W. Hönle, *Chem. Rev. 88* (1988) 243.

[35] J.-F. Halet, J.-Y. Saillard, *J. Organomet. Chem. 327* (1987) 365.

[36] a) M. H. Chisholm, J. C. Huffman, J. W. Pasterczyk, *Inorg. Chim. Acta 133* (1987) 17; b) M. Di Vaira, L. Sacconi, P. Stoppioni, *J. Organomet. Chem. 250* (1983) 183; c) A. S. Foust, M. S. Foster, L. F. Dahl, *J. Am. Chem. Soc. 91* (1969) 5631.

[37] a) C. A. Ghilardi, S. Midollini, A. Orlandini, L. Sacconi, *Inorg. Chem. 19* (1980) 301; b) C. Mealli, S. Midollini, S. Moneti, L. Sacconi, *Cryst. Struct. Commun. 9* (1980) 1017; c) O. J. Scherer, J. Schwalb, G. Wolmershäuser, *New J. Chem. 13* (1989) 399.

[38] a) G. Capozzi, L. Chiti, M. Di Vaira, M. Peruzzini, P. Stoppioni, *J. Chem. Soc. Chem. Commun. 1986*, 1799; b) M. Di Vaira, P. Stoppioni, M. Peruzzini, *Polyhedron 6* (1987) 351; c) A. Barth, G. Huttner, M. Fritz, L. Zsolnai, *Angew. Chem. 102* (1990) 956; *Angew. Chem. Int. Ed. Engl. 29* (1990) 929.

[39] H. Brunner, U. Klement, W. Meier, J. Wachter, O. Serhadle, M. L. Ziegler, *J. Organomet. Chem. 335* (1987) 339.

[40] F. Cecconi, C. A. Ghilardi, S. Midollini, A. Orlandini, *J. Chem. Soc. Chem. Commun. 1982*, 229.

[41] P. Dapporto, L. Sacconi, P. Stoppioni, F. Zanobini, *Inorg. Chem. 20* (1981) 3834.

[42] P. Stoppioni, M. Peruzzini, *J. Organomet. Chem. 262* (1984) C5.

[43] J. W. Lauher, M. Elian, R. H. Summerville, R. Hoffmann, *J. Am. Chem. Soc. 98* (1976) 3219.

[44] For example K. Wade, *Adv. Inorg. Chem. Radiochem. 18* (1976) 1; D. M. P. Mingos, *Acc. Chem. Res. 17* (1984) 311.

[45] O. J. Scherer, H. Sitzmann, G. Wolmershäuser, *Acta Crystallogr. Sect. C 41* (1985) 1761.

[46] D. Fenske, J. Hachgenei, *Angew. Chem. 98* (1986) 165; *Angew. Chem. Int. Ed. Engl. 25* (1986) 175.

[47] H. G. von Schnering, M. Hartweg, U. Hartweg, W. Hönle, *Angew. Chem. 101* (1989) 98; *Angew. Chem. Int. Ed. Engl. 28* (1989) 56.

[48] J. K. Burdett, C. J. Marsden, *New J. Chem. 12* (1988) 797.

[49] a) W. Tremel, R. Hoffmann, M. Kertesz, *J. Am. Chem. Soc. 111* (1989) 2030; b) E. D. Jemmis, A. C. Reddy, *Organometallics 7* (1988) 1561.

[50] M. Di Vaira, F. Mani, S. Moneti, M. Peruzzini, L. Sacconi, P. Stoppioni, *Inorg. Chem. 24* (1985) 2230.

[51] A. P. Ginsberg, W. E. Lindsell, K. J. Mc Cullough, C. R. Sprinkle, A. J. Welch, *J. Am. Chem. Soc. 108* (1986) 403.

[52] K. H. Whitmire, T. A. Albright, S. K. Kang, M. R. Churchill, J. C. Fettinger, *Inorg. Chem. 25* (1986) 2799.

[53] S. K. Kang, T. A. Albright, J. Silvestre, *Croat. Chem. Acta 57* (1984) 1355.

[54] A. Hartmann, K. G. Weil, *Angew. Chem. 100* (1988) 1111; *Angew. Chem. Int. Ed. Engl. 27* (1988) 1091, and references cited therein.

[55] Review article: H. Schäfer, B. Eisenmann, W. Müller, *Angew. Chem. 85* (1973) 742; *Angew. Chem. Int. Ed. Engl. 12* (1973) 694.

[56] O. J. Scherer, M. Swarowsky, G. Wolmershäuser, *Organometallics 8* (1989) 841.

[57] O. J. Scherer, J. Braun, G. Wolmershäuser, unpublished.

[58] a) T. P. Martin, *Angew. Chem. 98* (1986) 197; *Angew. Chem. Int. Ed. Engl. 25* (1986) 197; b) M. Baudler, C. Adamek, S. Opiela, H. Budzikiewicz, D. Ouzounis, *ibid. 100* (1988) 1110 and *27* (1988) 1059.

[59] D. J. Braun, W. Jeitschko, *Acta Crystallogr. Sect. B 34* (1978) 2069.

[60] R. B. King, *Inorg. Chem. 28* (1989) 3048.

[61] a) O. J. Scherer, J. Vondung, G. Wolmershäuser, *Angew. Chem. 101* (1989) 1395; *Angew. Chem. Int. Ed. Engl. 28* (1989) 1355; b) O. J. Scherer, J. Vondung, G. Wolmershäuser, *J. Organomet. Chem. 376* (1989) C35.

[62] Most recent review article: G. Maier, *Angew. Chem. 100* (1988) 317; *Angew. Chem. Int. Ed. Engl. 27* (1988) 309.

[63] B. A. Hess Jr., C. S. Ewig, L. J. Schaad, *J. Org. Chem. 50* (1985) 5869.

[64] G. Ohanessian, P. C. Hiberty, J.-M. Lefour, J.-P. Flament, S. S. Shaik, *Inorg. Chem. 27* (1988) 2219.

[65] J. Rozière, A. Seigneurin, C. Belin, A. Michalowicz, *Inorg. Chem. 24* (1985) 3710.

[66] Most recent review article: J. D. Corbett, *Chem. Rev. 85* (1985) 383.

[67] a) S. Rundqvist, N. O. Ersson, *Ark. Kemi 30* (1968) 103; b) A. Kjekshus, T. Rakke, *Acta Chem. Scand. A28* (1974) 99.

[68] a) O. J. Scherer, M. Swarowsky, H. Swarowsky, G. Wolmershäuser, *Angew. Chem. 100* (1988) 738; *Angew. Chem. Int. Ed. Engl. 27* (1988) 694; b) O. J. Scherer, M. Swarowsky, G. Wolmershäuser, *ibid. 100* (1988) 423 and *27* (1988) 405.

[69] F. Cecconi, C. A. Ghilardi, S. Midollini, A. Orlandini, *Inorg. Chem. 25* (1986) 1766.

[70] E. Hey, M. F. Lappert, J. L. Atwood, S. G. Bott, *J. Chem. Soc. Chem. Commun. 1987*, 597.

[71] a) O. J. Scherer, H. Sitzmann, G. Wolmershäuser, *J. Organomet. Chem. 309* (1986) 77; b) A.-J. Di Maio, A. L. Rheingold, *J. Chem. Soc. Chem. Commun. 1987*, 404.

[72] a) O. J. Scherer, T. Brück, *Angew. Chem. 99* (1987) 59; *Angew. Chem. Int. Ed. Engl. 26* (1987) 59; b) O. J. Scherer, T. Brück, G. Wolmershäuser, *Chem. Ber. 121* (1988) 935.

[73] a) M. Baudler, D. Düster, D. Ouzounis, *Z. Anorg. Allg. Chem. 544* (1987) 87; b) M. Baudler, S. Akpapoglou, D. Ouzounis, F. Wasgestian, B. Meinigke, H. Budzikiewicz, H. Münster, *Angew. Chem. 100* (1988) 288; *Angew. Chem. Int. Ed. Engl. 27* (1988) 280; c) M. Baudler, D. Ouzounis, *Z. Naturforsch. B44* (1989) 381.

[74] J. T. Snodgrass, J. V. Coe, C. B. Freidhoff, K. M. Mc Hugh, K. H. Bowen, *Chem. Phys. Lett. 122* (1985) 352.

[75] a) O. J. Scherer, C. Blath, G. Wolmershäuser, *J. Organomet. Chem. 387* (1990) C21; b) O. J. Scherer, C. Blath, G. Wolmershäuser, unpublished.

[76] O. J. Scherer, T. Brück, G. Wolmershäuser, *Chem. Ber. 122* (1989) 2049.

[77] A. R. Kudinov, M. I. Rybinskaya, Y. T. Struchkov, A. I. Yanovskii, P. V. Petrovskii, *J. Organomet. Chem. 336* (1987) 187.

[78] a) O. J. Scherer, J. Schwalb, G. Wolmershäuser, W. Kaim, R. Gross, *Angew. Chem. 98* (1986) 349; *Angew. Chem. Int. Ed. Engl. 25* (1986) 363; b) O. J. Scherer, W. Wiedemann, G. Wolmershäuser, *J. Organomet. Chem. 361* (1989) C11; c) O. J. Scherer, W. Wiedemann, G. Wolmershäuser, *Chem. Ber. 123* (1990) 3; d) A. L. Rheingold, M. J. Foley, P. J. Sullivan, *J. Am. Chem. Soc. 104* (1982) 4727; e) W. Bronger, private communication; f) J. Schwalb, *Dissertation*, Universität Kaiserslautern, 1988.

[79] O. J. Scherer, A. Schneider, unpublished.

[80] R. Blom, T. Brück, O. J. Scherer, *Acta Chem. Scand. 43* (1989) 458.

[81] a) T. P. Hamilton, H. F. Schaefer III, *Angew. Chem. 101* (1989) 500; *Angew. Chem. Int. Ed. Engl. 28* (1989) 485; b) R. Janoschek, *Chem. Ber. 122* (1989) 2121.

[82] M. C. Kerins, N. J. Fitzpatrick, M. T. Nguyen, *Polyhedron 8* (1989) 1135.
[83] A.-J. DiMaio, A. L. Rheingold, *Inorg. Chem. 29* (1990) 798.
[84] O. J. Scherer, J. Schwalb, H. Swarowsky, G. Wolmershäuser, W. Kaim, R. Gross, *Chem. Ber. 121* (1988) 443.
[85] O. J. Scherer, H. Sitzmann, G. Wolmershäuser, *Angew. Chem. 101* (1989) 214; *Angew. Chem. Int. Ed. Engl. 28* (1989) 212.
[86] P. Jutzi, R. Kroos, *Chem. Ber. 121* (1988) 1399.
[87] O. J. Scherer, R. Winter, unpublished.
[88] O. J. Scherer, H. Swarowsky, G. Wolmershäuser, W. Kaim, S. Kohlmann, *Angew. Chem. 99* (1987) 1178; *Angew. Chem. Int. Ed. Engl. 26* (1987) 1153.
[89] K. Angermund, K. H. Claus, R. Goddard, C. Krüger, *Angew. Chem. 97* (1985) 241; *Angew. Chem. Int. Ed. Engl. 24* (1985) 237, and references cited therein.
[90] H. G. von Schnering, T. Meyer, W. Hönle, W. Schmettow, U. Hinze, W. Bauhofer, G. Kliche, *Z. Anorg. Allg. Chem. 553* (1987) 261, and references cited therein.
[91] H. G. von Schnering, M. Wittmann, R. Nesper, *J. Less-Common Met. 76* (1980) 213.
[92] a) S. Nagase, K. Ito, *Chem. Phys. Lett. 126* (1986) 43; b) M. T. Nguyen, A. F. Hegarty, *J. Chem. Soc. Chem. Commun. 1986*, 383. For MNDO-calculations see: N. C. Baird, *Can. J. Chem. 62* (1984) 341.
[93] Review article: W. Siebert, *Angew. Chem. 97* (1985) 924; *Angew. Chem. Int. Ed. Engl. 24* (1985) 943.
[94] B. W. Eichhorn, R. C. Haushalter, J. C. Huffman, *Angew. Chem. 101* (1989) 1081; *Angew. Chem. Int. Ed. Engl. 28* (1989) 1032.
[95] H. G. von Schnering, J. Wolf, D. Weber, R. Ramirez, T. Meyer, *Angew. Chem. 98* (1986) 372; *Angew. Chem. Int. Ed. Engl. 25* (1986) 353.

Communications may be submitted in English *or* in German. Further details regarding the submission of communications can be found in the "Notice to Authors" reproduced in the January issue of the journal. Copies thereof may be obtained from the editorial office upon request.

An *N*-Phosphino *C*-Thiophosphinoyl Nitrilimine as a Formal 1,4 Dipole: Synthesis of 1,2,3λ^5-Diaza- and 1,2,4,3λ^5-Triazaphosphinines**

By *Michel Granier, Antoine Baceiredo, Martin Nieger,* and *Guy Bertrand**

Compared to the other known nitrilimines,[1, 2] the stability of the *N*-phosphino *C*-thiophosphinoyl nitrilimine **1** (m.p. 100 °C)[3] was striking. Thus, the question arose as to whether it was possible to use the tricoordinated trivalent phosphorus as a second center of functionality of the molecule. Here, we report that reactions specific to $\sigma^3\lambda^3$ phosphorus can occur and that the phosphorus center can even react faster than the nitrilimine moiety with dipolarophiles, affording new families of heterocycles.

One of the classic reactions of phosphanes is sulfurization with S_8. When **1** was treated with an excess of elemental sulfur at 20 °C, a clean reaction took place and was complete after a few minutes. After workup, 1,3,4,2λ^5-thiadiazaphosphole **2a** was isolated in 85% yield. The disappearance of the nitrilimine skeleton was obvious from the IR spectrum and the cyclic structure was established from the NMR spectra.[4] Addition of selenium led to a similar product **2b**,[4] in 84% yield. The coupling constants $^1J_{P(ring)Se} = 474.7$ Hz and $^2J_{PSe} = 61.7$ Hz provided strong evidence for the structural assignment. Reaction of phenyl azide with **1** resulted in evolution of nitrogen and formation of the 1,2,4,3λ^5-triazaphosphole **2c**[4] in 74% yield.

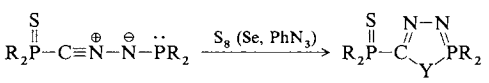

1: R = iPr$_2$N

2a, Y = S
2b, Y = Se
2c, Y = NPh

Although adducts **2** formally result from a [4 + 1] cycloaddition process, a two-step mechanism is most likely involved: electrophilic attack of sulfur, selenium, or phenyl azide on the phosphorus lone pair, activated by the electron-rich nitrilimine skeleton, leads to intermediates **3**, which undergo 1,5 electrocyclization.[5] The formation of 1,3,4-thiadiazoles and 1,3,4-triazoles from unstable *N*-thiocarbonyl[6] and *N*-imino nitrilimines,[7] respectively, has already been reported.

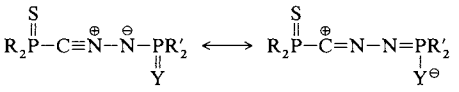

3

Definitive proof for primary attack on the phosphorus lone pair was provided by the reaction of **1** with a stoichiometric amount of methyl triflate. A clean reaction led to the new nitrilimine **4**, which was isolated as white crystals (m.p. 100–102 °C, 87% yield) after recrystallization from a THF–ether solution. In contrast with **1**, nitrilimine **4** is poorly soluble in nonpolar solvents and therefore presumably has an ionic structure. The presence of the methyl group at phosphorus was obvious from the ^{1}H NMR spectrum ($\delta = 2.12$, d, $J_{PH} = 13.3$ Hz, 3H) and the ^{13}C NMR spectrum ($\delta = 16.71$, d, $J_{PC} = 87.9$ Hz). The rather high-field ^{31}P NMR chemical shift of the λ^5 phosphorus ($\delta = 28.75$),[3c] the small phosphorus–phosphorus coupling constant ($^4J_{PP} = 6.7$ Hz), and the ^{13}C NMR signal of the quaternary carbon ($\delta = 69.83$, dd, $J_{PC} = 90.3$ and 17.7 Hz) were consistent with the nitrilimine structure.

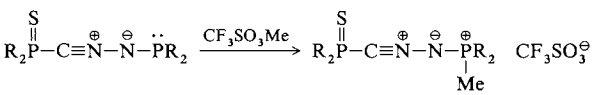

1 **4**

R = iPr$_2$N

With all the reagents mentioned above, the nitrilimine moiety was not able to compete with the phosphorus lone pair. In contrast, a dipolarophile such as dimethyl acetylenedicarboxylate should react with the 1,3 dipole. In fact, the reaction of **1** with a stoichiometric amount of this alkyne afforded the 1,2,3λ^5-diazaphosphinine **5** as orange crystals (m.p. 147 °C, 90% yield).[4] Although the synthesis of 1,2,4λ^5-diazaphosphinines was recently described[8] and several examples of 1,3,2λ^5-diazaphosphinines are known,[9] no derivatives of type **5** have yet been reported. Thus, an X-ray crystal study was carried out (Fig. 1).[10]

Particularly interesting are the bond lengths in the ring, all of which have a value halfway between a single and a double bond. Moreover, the ring is nearly planar as shown by the values of the deviations from the best plane: P1, 0.078; N2, −0.064; N3, −0.009; C4, 0.064; C5, −0.025; C6, −0.043 Å. The six-membered ring **5** formally results from a [4 + 2] cycloaddition process. However, as mentioned above, an alternative mechanism involving an electrophilic attack of the electron-poor reagent on the phosphorus lone pair of **1**, followed by a 1,6 ring closure of intermediate **6**, seems more likely. Although no examples of 1,6 electrocyclization involving nitrilimine are known, it has been shown that electron-poor alkynes react with phosphanes to give 1,3 dipolar species,[11] and this hypothesis

[*] Dr. G. Bertrand, M. Granier, Dr. A. Baceiredo
Laboratoire de Chimie de Coordination du CNRS
205, Route de Narbonne, F-31077 Toulouse Cédex (France)
Dr. M. Nieger
Anorganisch-chemisches Institut der Universität
Gerhard-Domagk-Strasse 1, D-5300 Bonn 1 (FRG)

[**] We thank Prof. Edgar Niecke for providing *M. Nieger* with X-ray facilities.

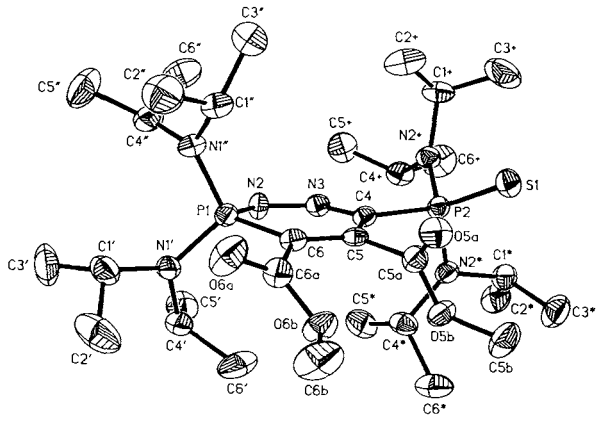

Fig. 1. Molecular structure of **5**. Important bond lengths [Å] and angles [°]: P1-N2 1.650 (4), N2-N3 1.316 (5), N3-C4 1.353 (6), C4-C5 1.421 (6), C5-C6 1.377 (6), C6-P1 1.765 (5), P1-N1' 1.640 (3), P1-N1'' 1.642 (3), C4-P2 1.829 (4), C5-C5a 1.510(7), C6-C6a 1.475 (7); C6-P1-N2 104.8 (2), N1'-P1-C6 115.0 (2), N1''-P1-C6 113.0 (2), N1'-P1-N2 105.9 (2), N1''-P1-N2 110.0 (2), N1''-P1-N1' 107.8 (2), P1-N2-N3 124.3 (3), N2-N3-C4 124.3 (4), N3-C4-C5 123.5 (4), N3-C4-P2 109.6 (3), P2-C4-C5 126.7 (3), C4-C5-C6 123.0 (4), C4-C5-C5a 120.3 (4), C5a-C5-C6 116.7 (4), C5-C6-P1 118.7 (3), C5-C6-C6a 123.1 (4), C6a-C6-P1 117.7 (3).

well rationalizes the difference in reactivity observed between dimethyl acetylenedicarboxylate and methyl acetylenecarboxylate, the latter of which led to **7** via a classical cycloaddition process.[3a]

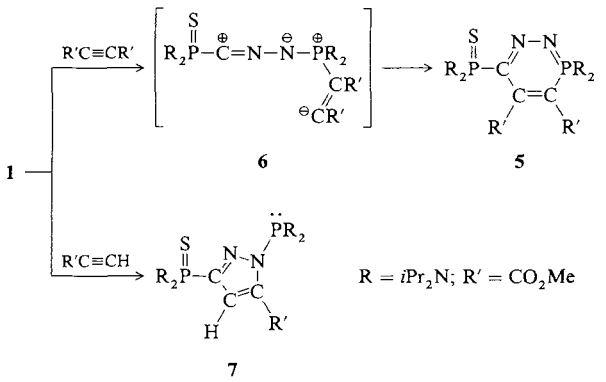

Another example of a reaction where the phosphorus lone pair reacts faster than the 1,3 dipole is the reaction of **1** with tetracyanoethylene (TCNE). Moreover, although addition and cycloaddition reactions of tetracyanoethylene usually proceed with high selectivity at the carbon–carbon double bond,[12] we did not obtain the expected adduct **8** but instead the 1,2,4,3λ⁵-triazaphosphinine **9** (80% yield).[4] This six-membered ring formally results from a [4 + 2] cycloaddition reaction involving a nitrile group of the reagent. Very few examples of [3 + 2][13] and [4 + 2][14] cycloaddition with the carbon–nitrogen triple bond of this electron-poor olefin have been reported. On the other hand, the attack of the phosphorus lone pair on the nitrogen of the nitrile, instead of at carbon, can be explained by the structure of intermediate **10**, where the negative charge can be delocalized. The only previous examples of triazaphosphinines were the 1,3,5,2λ⁵-triazaphosphinines.[15]

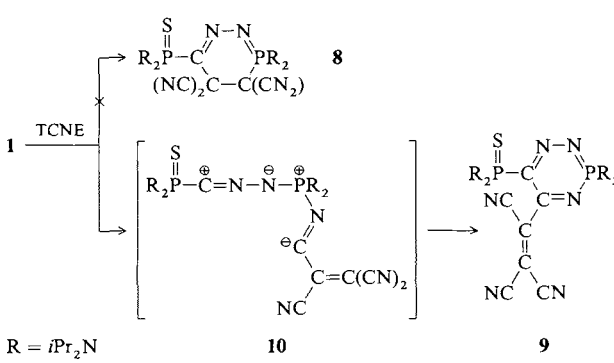

It is clear from these results and those of *Regitz* et al.[8] that the scope of application of dipoles having nitrilium betaine structure can be enlarged enormously by introducing the phosphanyl group.

Received: May 21, 1990;
revised: July 9, 1990 [Z 3967/3968 IE]
German version: *Angew. Chem. 102* (1990) 1185

[1] Reviews on transient nitrilimines: a) R. Huisgen, *Angew. Chem. 75* (1963) 604, 742; *Angew. Chem. Int. Ed. Engl. 2* (1963) 565, 742. b) P. Caramella, P. Grünanger in A. Padwa (Ed.): *1,3 Dipolar Cycloaddition Chemistry*, Wiley Interscience, New York 1984.

[2] Apart from P-substituted nitrilimines [3], only one other has been isolated: F. Castan, A. Baceiredo, G. Bertrand, *Angew. Chem. 101* (1989) 1253; *Angew. Chem. Int. Ed. Engl. 28* (1989) 1250.

[3] a) G. Sicard, A. Baceiredo, G. Bertrand, *J. Am. Chem. Soc. 110* (1988) 2663; b) M. Granier, A. Baceiredo, G. Bertrand, *Angew. Chem. 100* (1988) 1397; *Angew. Chem. Int. Ed. Engl. 27* (1988) 1350; c) M. Granier, A. Baceiredo, Y. Dariguenave, M. Dartiguenave, M. J. Menu, G. Bertrand, *J. Am. Chem. Soc. 112* (1990) 6277.

[4] Selected spectroscopic data: **2a**: ^{31}P NMR ($CDCl_3$):δ = + 86.4 and + 54.3, J(PP) = 7.2 Hz. ^{13}C NMR ($CDCl_3$): δ = 145.9 (dd, J(PC) = 163.8 and 65.7 Hz, C=N). **2b**: ^{31}P NMR ($CDCl_3$):δ = + 91.6 and + 55.7 J(PP) < 1 Hz. ^{13}C NMR ($CDCl_3$):δ = 149.0 (dd, J(PC) = 154.7 and 70.2 Hz, C=N). **2c**: ^{31}P NMR ($CDCl_3$): δ = + 57.3 and + 37.9, J(PP) = 8.2 Hz. ^{13}C NMR ($CDCl_3$): δ = 122.6 (s, *o*-C), 128.8 (s, *p*-C), 129.0 (s,*m*-C), 145.1 (dd, J(PC) = 171.1 and 66.7 Hz, C=N), 148.5 (s, *i*-C). **5**: ^{31}P NMR (C_6D_6): δ = + 68.6 and + 14.5, J(PP) = 4.4 Hz. ^{1}H NMR (C_6D_6) 3.30 and 3.75 (s, OMe). ^{13}C NMR ($CDCl_3$): δ = 52.3 and 52.4 (s, OMe), 92.2 (dd, J(PC) = 107.5 and 11.7 Hz, NPC), 138.7 (d, J(PC) = 31.7 Hz, PC*C*), 141.6 (dd, J(PC) = 171.7 and 54.7 Hz, C = N), 166.6 (s, C=O). IR (KBr):$\tilde{\nu}$ = 1705 and 1740 cm^{-1}, C=O). **9** : ^{31}P NMR ($CDCl_3$) δ = + 50.7 and + 22.4, J(PP) < 1 Hz. ^{13}C NMR ($CDCl_3$): δ = 89.9 (d, J(PC) = 8.3 Hz, *C*(CN)$_2$), 106.7 (s, CN), 107.1 (d, J(PC) = 1.5 Hz, CN), 108.1 (s, CN), 149.2 (d, J(PC) = 4.5 Hz, PCC*C*), 153.2 (dd, J(PC) = 10.6 and 8.3 Hz, PC*C*), 168.0 (dd, J(PC) = 158.1 and 14.0 Hz, PC).

[5] For a review on 1,5 electrocyclization see: E. C. Taylor, I. J. Turchi, *Chem. Rev. 79* (1979) 181.

[6] R. Huisgen, H. J. Sturm, M. Seidel, *Chem. Ber. 94* (1961) 1555.

[7] a) R. Huisgen, J. Sauer, M. Seidel, *Chem. Ber. 93* (1960) 2885. b) H. Reimlinger, J. J. M. Vandewalle, G. S. D. King, W. R. F. Lingier, R. Merenyi, *ibid. 103* (1970) 1918; c) H. Reimlinger, J. J. M. Vandewalle, W. R. F. Lingier, *ibid. 103* (1970) 1960; d) M. S. Gibson, *Tetrahedron 19* (1963) 1587.

[8] T. Facklam, O. Wagner, H. Heydt, M. Regitz, *Angew. Chem. 102* (1990) 316; *Angew. Chem. Int. Ed. Engl. 29* (1990) 314.

[9] a) P. P. Kornuta, L. S. Kuz'menko, L. N. Markovski, *Zh. Obshch. Khim. 49* (1979) 2201; b) E. A. Romanenko, V. V. Pen'kovski, Yu. P. Egorov, A. V. Kirsanov, *Dokl. Akad. Nauk. SSSR 214* (1974) 821; c) V. P. Kukhar, A. P. Boiko, *Zh. Obshch. Khim. 46* (1976) 2132; d) A. P. Boiko, V. P. Kukhar, *ibid. 51* (1981) 400; e) P. P. Kornuta, A. I. Kalenskaya, V. I. Shevchenko, *ibid. 41* (1971) 993.

[10] Crystal data for **5**: $C_{31}H_{62}N_6O_4P_2S$, monoclinic, a = 9.859 (4), b = 24.543 (9), c = 16.474(6) Å, β = 104.82 (3)°, V = 3.854 nm^3, space group $P2_1/n$, Z = 4. Nicolet R3m diffractometer ($Mo_{K\alpha}$ radiation, graphite monochromator), 3° < 2θ < 45°, ω scan. 5038 unique reflections were collected with 3630 used in refinement ($F > 4\sigma(F)$). The structure was solved by direct methods (SHELXS 86). All non-hydrogen atoms were refined anisotropically. Hydrogen atoms were localized by difference electron density determination and refined using a "riding" model. At final convergence, R = 0.058; R_w = 0.057. Further details of the crystal structure investigation are available on request from the Fachinformationszentrum Karlsruhe, Gesellschaft für wissenschaftlich-technische Information mbH, D-7514

Eggenstein-Leopoldshafen 2 (FRG), on quoting the depository number CSD-54756, the names of the authors, and the journal citation.
[11] R. Luckenbach: *Dynamic Stereochemistry of Pentacoordinated Phosphorus and Related Elements*, Thieme, Stuttgart 1973.
[12] For a review on cycloaddition reactions of tetracyanoethylene see: A. J. Fatiadi, *Synthesis 1987*, 749.
[13] Examples: a) J. E. Franz, R. K. Howe, H. K. Pearl, *J. Org. Chem. 41* (1976) 620; b) M. Brown, R. E. Benson, *ibid. 31* (1966) 3849; c) Y. D. Samuilov, S. E. Soloveva, A. I. Konovalov, *Zh. Obshch. Khim. 50* (1980) 138; d) K. Burger, H. Schickaneder, M. Prinzel, *Liebigs Ann. Chem. 1976*, 30.
[14] a) K. Burger, H. Goth, *Angew. Chem. 92* (1980) 836; *Angew. Chem. Int. Ed. Engl. 19* (1980) 810. b) K. Burger, H. Goth, W. Schöntag, J. Firl, *Tetrahedron 38* (1982) 287.
[15] Examples: a) G. Shöning, O. Glemser, *Chem. Ber. 109* (1976) 2960; b) *ibid. 110* (1977) 1148. c) V. P. Kukhar, T. N. Kasheva, *Zh. Obshch. Khim. 46* (1976) 239. d) M. Meyer, U. Klingebiel, *Chem. Ber. 121* (1988) 1119.

Synthesis of Two Tl^{III} Diacetonyl Compounds and Crystal Structure of $[Tl\{CH_2C(O)Me\}_2(\mu\text{-}CF_3SO_3)(bpy)]_2$ **

By *José Vicente,* José-Antonio Abad, Gabriel Cara,* and *Peter G. Jones**

Despite the interest in thallation reactions in organic chemistry,[1] those involving ketones have only recently been studied;[2] the synthesis in aqueous solutions of Tl^{III} monoketonyl species, $[Tl\{CH_2C(O)R\}X_2]$, was reported, but not their structures. Diketonyl species, $[Tl\{CH_2C(O)R\}_2]^{\oplus}$, could also be detected in solution, but they were always accompanied by the monoketonyl species.

During our work on the synthesis of Tl^{III} monoaryl compounds,[3] some evidence was obtained for the formation of Tl acetonyl(aryl) compounds; this prompted us to attempt to isolate acetonyl derivatives starting from Tl^{III} salts. We had already obtained Au^{III} acetonyl complexes by C–H activation of acetone with Au^{III} 2-(phenylazo)phenyl complexes.[4] There is, as far as we are aware, only one previous report (which did not involve an X-ray structure) of the isolation of a metal diacetonyl complex.[5–7] We report here the isolation of two Tl^{III} diacetonyl derivatives and the X-ray structural characterization of one of them, a diacetonyl complex. An additional unusual structural feature is the presence of coordinated triflate ions.

Addition of trifluoromethanesulfonic acid to a solution of thallium(III) trifluoroacetate in acetone (1.25:1) at room temperature results in formation of the diacetonyl complex **1**,[8] which reacts with 2,2′-bipyridine (bpy) to give **2**.[9] The solid-state IR spectra of the two complexes show bands at similar wave numbers in the regions expected for ν(CO), $\nu(CF_3)$, and $\nu(SO_3)$.[8–10] The ^1H NMR spectra show a singlet (Me) and a doublet (CH_2), the latter coupled with ^{203}Tl and ^{205}Tl nuclei with $^2J(Tl, H)$ values consistent with the presence of two acetonyl groups C-bonded to the Tl atom.[2] Both complexes behave as 1:1 electrolytes in acetone solution, probably because of formation of the solvent complexes $[Tl\{CH_2C(O)Me\}_2(Me_2CO)_n](CF_3SO_3)$ and $[Tl\{CH_2C(O)Me\}_2(bpy)(Me_2CO)_n](CF_3SO_3)$.

$$Tl(CF_3CO_2)_3 + CF_3SO_3H + 2\,Me_2CO \rightarrow 3\,CF_3COOH + [Tl\{CH_2C(O)Me\}_2(CF_3SO_3)]\quad \mathbf{1}$$

$$\mathbf{1} + bpy \rightarrow [Tl\{CH_2C(O)Me\}_2(\mu\text{-}CF_3SO_3)(bpy)]_2\quad \mathbf{2}$$

The crystal structure of **2** reveals distorted six-coordination of the thallium atom (Fig. 1). The ligand sphere may conveniently be regarded as consisting of three components: (1) strong, almost linear (160.8°) coordination by the acetonyl carbons [Tl-C4 216.1(8), Tl-C1 217.1(7) pm] in a manner reminiscent of dimethylthallium(III), (2) longer contacts to the N atoms of the bipy ligand [Tl-N1 245.6(5), Tl-N2 250.0(4) pm], and (3) weak coordination by the oxygen atoms of two triflate ions [Tl-O3 273.9(6), Tl-O5′ 280.6(4) pm]. These weak contacts involve the formation of centrosymmetric dimers. The bond lengths in the acetonyl groups [C=O 122.2, 122.7(8) pm, H_3C-C 148.6(10), 151.1(9) pm, H_2C-C 147.4(9), 148.1(8) pm] strongly indicate the C-bonded nature of the ligand, and this was confirmed by direct location of all H atoms except those at C3. The more usual type of ketone–metal interactions involve metal–oxygen bonds.[12]

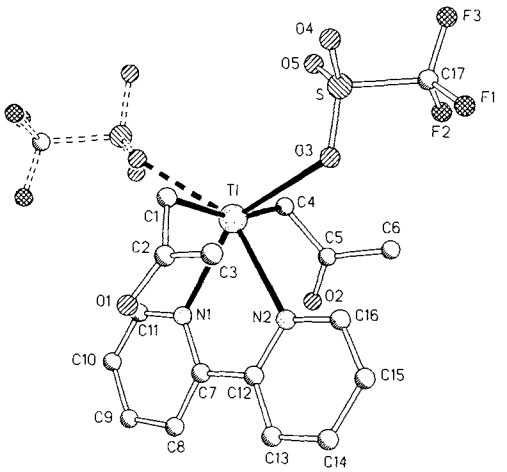

Fig. 1. The structure of **2** in the crystal. Radii are arbitrary; H atoms omitted for clarity. The coordination sphere at thallium is completed by a symmetry-generated triflate ion (indicated by dashed bonds).

The similar IR spectra of **1** and **2** indicate that the triflate ligand also acts as a bridging ligand in **1**.

Experimental Procedure

1: A solution of $Tl(CF_3CO_2)_3$ (500 mg, 0.92 mmol) in acetone (8 mL) was stirred with CF_3SO_3H (2 drops, ca. 1.15 mmol) at room temperature for 1 h. On partial evaporation of the solvent and addition of diethyl ether, **1** precipitated as a white solid (satisfactory elemental analyses). Yield 320 mg (76%).
2: 2,2′-bipyridine (26 mg, 0.16 mmol) was added to **1** (75 mg, 0.16 mmol) in acetone (8 mL). The resulting mixture was stirred at room temperature for 15 min and the solution evaporated to ca. 2 mL. Addition of diethyl ether resulted in precipitation of complex **2** as a white solid (satisfactory elemental analyses). Yield 83 mg (81%).

[*] Prof. Dr. J. Vicente, Dr. J. A. Abad, Mr. G. Cara
Departamento de Química Inorgánica, Facultad de Ciencias Químicas
Universidad de Murcia, Campus de Espinardo
E-30171 Espinardo, Murcia (Spain)
Prof. Dr. P. G. Jones
Institut für Anorganische und Analytische Chemie
der Technischen Universität
Hagenring 30, D-3300 Braunschweig (FRG)

[**] This work was supported by DGICT (Spain), the Fonds der Chemischen Industrie, and an Acción Integrada Hispano-Alemana (94B).

Received: May 29, 1990 [Z 3989 IE]
German version: *Angew. Chem. 102* (1990) 1184

[1] a) A. McKillop, E. C. Taylor, *Adv. Organomet. Chem. 11* (1973) 147; b) A. McKillop, E. C. Taylor in F. G. A. Stone, E. Abel (Eds.): *Comprehensive Organometallic Chemistry, Vol. 7*, Pergamon, Oxford 1982, p. 499.
[2] B. Györi, A. Sánchez, J. Glaser, *J. Organomet. Chem. 361* (1989) 1.
[3] J. Vicente, J. A. Abad, J. F. Gutiérrez-Jugo, P. G. Jones, *J. Chem. Soc. Dalton Trans. 1989*, 2241.
[4] J. Vicente, M. D. Bermúdez, M. T. Chicote, M. J. Sánchez-Santano, *J. Chem. Soc. Chem. Commun. 1989*, 141.
[5] The only other diacetonyl derivative of which we are aware is $[Hg\{CH_2C(O)Me\}_2]$, obtained by the reaction of $[(Me_3Si)_2N]_2Hg$ with acetone [6]. The mercuriation of acetone in aqueous solutions leads to mono- and polymercuriation of the acetone molecule [7].
[6] I. B. Fedot'eva, O. A. Kruglaya, B. V. Fedot'ev, N. S. Vyazankin, *Zh. Obskch. Khim. 48* (1978) 2387; *Chem. Abstr. 90* (1979) 72293d.
[7] F. A. Johnson, W. D. Perry, *Organometallics 8* (1989) 2646.
[8] M.p. 165 °C (dec.); $\Lambda_M = 103\,\Omega^{-1}\,cm^2\,mol^{-1}$. ^1H NMR (200 MHz, [D$_6$]DMSO, TMS): $\delta = 2.12$ (s, 6H; Me), 2.58 (d, br, $^2J(Tl; H) = 756$ Hz, 4H; CH_2). IR (Nujol): $\tilde{\nu}[cm^{-1}] = 1670, 1650$ (C=O); 1280 [SO_3(E)], 1030 [$SO_3(A_1)$] 1225 or 1240 [$CF_3(A_1)$], 1170 or 1180 [CF_3(E)], all very strong.
[9] M.p. 162 °C (dec.); $\Lambda = 98\,\Omega^{-1}\,cm^2\,mol^{-1}$. ^1H NMR (200 MHz, $CDCl_3$, TMS): $\delta = 1.98$ (s, 6H; Me), 2.99 (d, br, $^2J(Tl; H) = 692$ Hz, 4H; CH_2). IR (Nujol): $\tilde{\nu}[cm^{-1}] = 1675, 1655$ (C=O), 1285 [SO_3(E)], 1025 [$SO_3(A_1)$] 1225(br) [$CF_3(A_1)$], 1155 or 1165 [CF_3(E)], all very strong. Single crystals of **2** were obtained by slow diffusion of diethyl ether into a solution of **2** in acetone.
[10] G. A. Lawrance, *Chem. Rev. 86* (1986) 17.
[11] Crystal data for **2** at −95 °C: $C_{17}H_{18}N_2O_5F_3STl$ (monomer), $M = 623.8$. Triclinic, space group $P\bar{1}$, $a = 848.2(3)$, $b = 1008.4(4)$, $c = 1288.5(5)$ pm, $\alpha = 102.73(3)$, $\beta = 94.45(3)$, $\gamma = 106.63(3)°$, $V = 1.0183$ nm^3, $Z = 1$ dimer, $\varrho_{calcd} = 2.034$ Mg m^{-3}. The final R value was 0.031 for 3167 reflections $> 4\sigma(F)$. Further details of the crystal structure investigation may be obtained from the Fachinformationszentrum Karlsruhe, Gesellschaft für wissenschaftlich-technische Information mbH, D-7514 Eggenstein-Leopoldshafen 2 (FRG), on quoting the depository number CSD-54696, the names of the authors, and the journal citation.
[12] D. Seebach, *Angew. Chem. 100* (1988) 1685; *Angew. Chem. Int. Ed. Engl. 27* (1988) 1624.

Organometallic Host–Guest Systems Representing Novel Charge-Transfer "Ion Pairs" with Three-Dimensional Electron-Donor Networks**

By *Stefan Eller, Martin Adam*, and *R. Dieter Fischer**

Dedicated to Professor Helmut Behrens on the occasion of his 75th birthday

Recently, we described several examples of compounds of type A, a widely variable new class of three-dimensional (3D) host–guest systems involving guest cations $G^{\oplus}$ like

$$[(G^{n\oplus})_{1/n}(Me_3Sn^{IV})_3M^{II}(CN)_6]_\infty \quad M = Fe, Ru \quad \text{(type A)}$$

$NR_4^{\oplus}$ (R = alkyl), $[(C_5H_5)_2Co]^{\oplus}$, and even $Me_3Sn^{\oplus}$.[1] Here, we wish to present the first type-A[2] systems with $G^{2\oplus}$ = methyl- and benzylviologen ($MV^{2\oplus}$ and $BV^{2\oplus}$, respectively), as well as with their reduced forms $G^{\oplus} = MV^{\bullet\oplus}$ and $BV^{\bullet\oplus}$.[3] Rod-shaped $MV^{n\oplus}$, and even more $BV^{n\oplus}$ (n = 1,2), requires a maximum of space in just *one* direction. Moreover, $MV^{2\oplus}$ and $BV^{2\oplus}$ display notable electron affinities and thus a tendency to form charge-transfer (CT) adducts with numerous anionic[4] and uncharged[5] electron donors.[3b]

Compounds **1** ($G^{2\oplus} = MV^{2\oplus}$) and **2** ($G^{2\oplus} = BV^{2\oplus}$) are accessible in high yields via ion exchange[1, 6] according to Equation (a). The "alloyed" host–guest systems **3** may be

$$[(Me_3Sn)_4M(CN)_6]_\infty \xrightarrow[-[Me_3Sn(H_2O)_2]^{\oplus}]{0.5\,G^{2\oplus}/H_2O} \underset{\mathbf{1,\ 2}}{[(G^{2\oplus})_{0.5}(Me_3Sn)_3M(CN)_6]_\infty} \quad \text{(a)}$$

a, M = Fe; **b**, M = Ru; **c**, M = Os

prepared correspondingly from the well-characterized precursors $[(Me_3Sn)_4Fe_{1-x}Ru_x(CN)_6]_\infty$.

$$[(MV^{2\oplus})_{0.5}(Me_3Sn)_3Fe_{1-x}Ru_x(CN)_6]_\infty \quad \mathbf{3a},\ x = 0.50;\ \mathbf{3b},\ x = 0.25$$

Suspension of **1** and **2** in an aqueous $Na_2S_2O_4$ solution affords within a few minutes the likewise insoluble, pure type-A systems **4** and **5**, respectively, containing $G^{\bullet\oplus}$ guest ions [Eq. (b)].[6, 8] Alternatively, **4** and **5** may be prepared by

$$2\underset{\mathbf{1,\ 2}}{[(G^{2\oplus})_{0.5}(Me_3Sn)_3M(CN)_6]_\infty} \xrightarrow[-7\,HSO_3^{\ominus}]{7/2\,S_2O_4^{2\ominus}} \underset{\mathbf{4,\ 5}}{[(G^{\bullet\oplus})(Me_3Sn)_3M(CN)_6]_\infty} + [M(CN)_6]^{4\ominus} + 3\,Sn^{2\oplus} + \text{organic products} \quad \text{(b)}$$

"ion exchange"[6] starting from $[(G^{\oplus})(Me_3Sn)_3M(CN)_6]_\infty$ (G = NH_4, Et_4N, Me_3Sn,[1] and even 1/2 MV) and $MV^{\bullet\oplus}$ or $BV^{\bullet\oplus}$ radical ions generated in situ. The NIR/VIS absorption spectra of **4** and **5** strongly resemble those of $(MV^{\bullet\oplus})(PF_6)$ and $(BV^{\bullet\oplus})(PF_6)$, respectively (Table 1). The ESR spectrum of polycrystalline **4b**[9] reflects the involvement of only *one* type of radical ion. Exposure of pure **4a** and **4b** to air results in less abrupt changes[10] than for the apparently more sensitive, blue host–guest system "{zeolite Y/$MV^{\bullet\oplus}$}".[11]

A single-crystal X-ray study of **1b**,[12] the first well-crystallizing type-A species,[13, 14] indicates that all $MV^{2\oplus}$ guest ions are encapsulated in equally shaped cavities of "finite dimensions" spanned by a 3D network of nonlinear $\{Ru-C\equiv N-Sn-N\equiv C\}_\infty$ chains regularly interlinked by the octahedrally coordinated Ru^{II} ions (Fig. 1). The short-

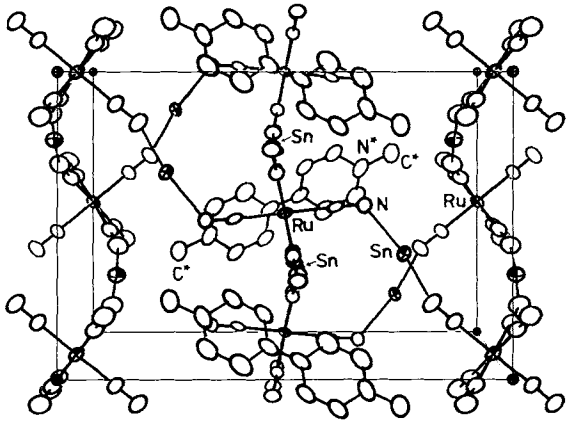

Fig. 1. Unit cell [12] of **1b** (ORTEP). Some atoms of the $MV^{2\oplus}$ guest ion have been marked by an asterisk; the CH_3 groups of all Sn atoms have been omitted.

[*] Prof. Dr. R. D. Fischer, Dipl.-Chem. S. Eller, Dipl.-Chem. M. Adam
Institut für Anorganische und Angewandte Chemie der Universität
Martin-Luther-King-Platz 6, D-2000 Hamburg 13 (FRG)

[**] This work was supported by the Deutsche Forschungsgemeinschaft and the Fonds der Chemischen Industrie. We thank *S. Schaugsdat* for her assistance, for example, in the growing of single crystals, Prof. *J. Voß* for measuring an ESR spectrum, and Prof. *U. Behrens* for critical discussion of the X-ray analysis.

est host···guest separations may be deduced from the smallest interatomic distances found, that is, 2.5 ± 0.2 Å for C(CN)···C(MV) and N(CN)···C(MV) (Sn···C(MV) and Ru···C(MV) > 3.5 Å). In view of the different spatial demands of $MV^{n\oplus}$ and $BV^{n\oplus}$ and the variable host/guest ratio (2 for **1** and **2**, but 1 for **4** and **5**), the architecture of the polymeric host network of **1**, **2**, **4**, and **5** is expected to undergo characteristic variations.

Whereas the host–guest system "{zeolite Y/$MV^{2\oplus}$}" has been reported[5] to incorporate spontaneously various π-electron-rich arenes D to form "{zeolite Y/($MV^{2\oplus}$·D)}" with colored CT complexes $MV^{2\oplus}$ · D as guests, **1** and **2** do not react in a corresponding fashion. The pronounced tendency of dissolved $MV^{2\oplus}$ and $[Fe(CN)_6]^{4\ominus}$ ions, for example, to associate to give comparatively stable CT "ion pairs"[4] suggests that the strikingly colored solids **1**–**3** (Table 1) are indeed genuine CT complexes.

Table 1. Properties of the solids **1**–**5** and of some dissolved samples of spectroscopic relevance.

Compd	$G^{n\oplus}$	M	Color	CT maximum [a, b] $\tilde{\nu}$ [cm^{-1}]	System for comparison	CT maximum [a] $\tilde{\nu}$ [cm^{-1}]
1a	$MV^{2\oplus}$	Fe	blue	15870		18870 [4]
1b	$MV^{2\oplus}$	Ru	brick-red	21740		24040 [4]
1c	$MV^{2\oplus}$	Os	violet	20000	$G^{2\oplus}$/	22730
2a	$BV^{2\oplus}$	Fe	lime green	17860	$[M(CN)_6]^{4\ominus}$/	18180
2b	$BV^{2\oplus}$	Ru	red violet	22220	H_2O [c]	22730 [e]
2c	$BV^{2\oplus}$	Os	bright violet	21050		22220
3a	$MV^{2\oplus}$	Fe/Ru	violet	20410	[d]	23530
3b	$MV^{2\oplus}$	Fe/Ru	violet	20410		
4a	$MV^{\cdot\oplus}$	Fe	dark blue	25000 and		25320 and
4b	$MV^{\cdot\oplus}$	Ru	dark blue	16000	$G^{\cdot\oplus}$ (PF_6)	16540
5a	$BV^{\cdot\oplus}$	Fe	dark violet	26670 and	/$NCCH_3$	25420 and
5b	$BV^{\cdot\oplus}$	Ru	dark violet	17860		16260

[a] **1**–**3**, *inter*molecular electron transfer; **4**–**5**, *intra*molecular excitations of $G^{\cdot\oplus}$ (principal bands). [b] Solid samples (KBr pellets). [c] Solution of $(MV)Cl_2 \cdot H_2O$ or $(BV)Br_2$ and $K_4[M(CN)_6]$ (1/1) in H_2O. [d] Solution of $(MV)Cl_2 \cdot H_2O$, $K_4[Fe(CN)_6]$, and $K_4[Ru(CN)_6]$ (1/1/1) in H_2O. [e] Salt **6b** dissolved in H_2O.

Actually, the NIR/VIS absorption spectra of **1a**–**1c** (Fig. 2), as well as those of **2a**–**2c** (Table 1), display one distinct potential CT band which is absent in the spectra of their components. The λ_{max}(CT) values of **1** and **2** may reasonably be correlated with the oxidation/reduction potentials of the couples $[M^{II}(CN)_6]^{4\ominus}/[M^{III}(CN)_6]^{3\ominus}$ [15a] and $G^{\cdot\oplus}/G^{2\oplus}$,[15b] respectively. However, the *bathochromic* shift of λ_{max}(CT) of **1** and **2** (compared with λ_{max}(CT) of corresponding ion pairs in aqueous solution[4]) is surprising. It is well documented[16] that, for example, the Lewis acid/base neutralization shown in Equation (c) causes a notable de-

$$[M^{II}(CN)_6]^{4\ominus} + 6L^q \rightarrow [M^{II}(CNL)_6]^{6q-4} (0 \le q \le 1) \quad (c)$$

crease in the electron-donor strength of the central d^6 metal ion. The influence of the Lewis acid L^q present in **1** and **2** (formally, L = 1/2 $Me_3Sn^{\oplus}$ with $q = 1/2$) should thus favor a *hypso*chromic shift of λ_{max}(CT). Further insight has so far been hampered by the poorly structured solid-state absorption spectra[17] of the easily accessible new salts $(BV^{2\oplus})_2[M^{II}(CN)_6] \cdot 3H_2O$ (**6a**–**c**), and the appearance of no more than one broad CT absorption band also in the spectra of the "alloyed" systems **3** (Table 1, Fig. 2).

Interestingly, the transition from the "CT sandwich" "bis(*p*-phenylene)-[34]crown-10/$MV^{2\oplus}$" ≙ {DAB/$MV^{2\oplus}$/DAB} (DAB = *p*-dialkoxybenzene)[18] to the "inverted" (with respect to the donor and acceptor components) CT sandwich {$MV^{2\oplus}$/DAB/$MV^{2\oplus}$}(i.e., "cyclobis(methylviologen-*p*-phenylene)/DAB" with DAB = *p*-dimethoxybenzene[19]) is also accompanied by a strong *bathochromic* shift of the main CT band (436 vs. 478 nm[20]). Possibly, *collective phenomena* may operate not only in the latter cyclodimer[21] but likewise in the 3D polymers **1**–**3**, strengthening both the acceptor (coupled pair of $MV^{2\oplus}$ ions) and donor (coupled $[M^{II}(CN)_6]^{4\ominus}$ units) capacity. One illustrative example of an ensemble of six arene units that can be *collectively* oxidized in spite of the "isolation" of each individual π system by CH_2 and $(CH_2)_3$ bridges is "spheric cryptophane".[22] The *spontaneously* occurring ion exchange[6] [Eq. (d), see

$$\mathbf{1}(\text{solid}) + MV^{\cdot\oplus} \xrightarrow{H_2O} \mathbf{4}(\text{solid}) + 0.5\ MV^{2\oplus} \quad (d)$$

above[6, 23]] suggests some extra stabilization of the $MV^{\cdot\oplus}$ ions encapsulated in **4**.[24] This feature is also likely to contribute to the bathochromic shift of the CT excitation (e).

$$\mathbf{1} \xrightarrow{x\,h\nu} [(MV^{\cdot\oplus})_x(MV^{2\oplus})_{0.5-x}(Me_3Sn)_3M^{III}_xM^{II}_{1-x}(CN)_6]_\infty \quad (e)$$

$x \ll 0.5$.

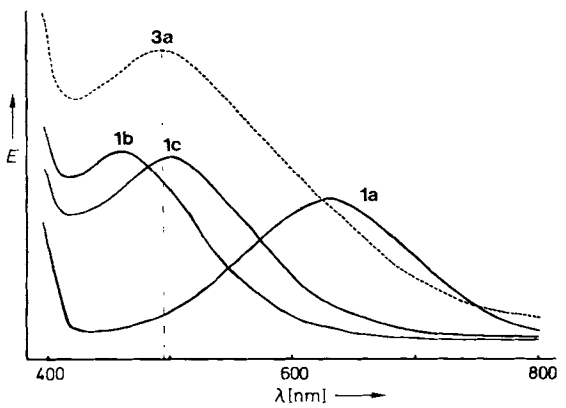

Fig. 2. Absorption spectra of **1a**–**1c** and of **3a** within the range of their CT bands (samples, KBr pellets; Cary 17 spectrophotometer). E = extinction.

Experimental Procedure

1–**3** (typical procedure): 0.3 mmol of $[(Me_3Sn)_4M(CN)_6]_\infty$ (cf. [1]) was suspended in a solution of 0.3 mmol of $(MV)Cl_2 \cdot H_2O$ (Fluka) or $(BV)Br_2$[7] in 40 mL of H_2O. After stirring (room temperature, 12 h), filtration, washing with H_2O, and drying under high vacuum, analytically pure products were obtained (correct elemental analyses for C, H, N, Sn, and Fe in all cases). Yields between 82 (**1a**) and 90% (**2b**, **2c**); decomposition temperatures between 200 (**1a**) and 245 °C (**2b**).

$[(Me_3Sn)_4Fe_{0.5}Ru_{0.5}(CN)_6]_\infty$ (**3a**): Addition of a solution of Me_3SnCl (0.85 g, 4.26 mmol) in 10 mL of H_2O to a solution of $K_4[Fe(CN)_6]$ (0.19 g, 0.53 mmol) and $K_4[Ru(CN)_6]$ (0.22 g, 0.53 mmol) in 15 mL of H_2O; after stirring (5 h), filtration, washing with H_2O, and drying (high vacuum, room temperature), 0.90 g (0.93 mmol) of analytically pure product was obtained (correct elemental analyses for C, H, N, Sn, and Fe; yield 87%; decomposition temperature, 230 °C).

4 and **5** (typical procedure): Suspension of 0.3 mmol of **1** or **2** in a solution of ca. 3.0 mmol of $Na_2S_2O_4$ (Merck-Schuchardt) in 30 mL of O_2-free H_2O under an atmosphere of N_2 resulted in a color change to dark blue and dark violet, respectively, within a few minutes. Analytically pure products were isolated in practically quantitative yields (when referred to $MV^{\cdot\oplus}$ and $BV^{\cdot\oplus}$, respectively) after prolonged stirring (3 h, room temperature), filtration, washing with a small amount of H_2O, and drying (high vacuum, 8 h); correct elemental analyses for C, H, N, Sn and Fe. The filtrate, which still contained $S_2O_4^{2\ominus}$ anions, was free of any $MV^{\cdot\oplus}$ or $BV^{\cdot\oplus}$ ions, but not of the anions $[Fe(CN)_6]^{4\ominus}$ or $[Ru(CN)_6]^{4\ominus}$.

$(BV^{2\oplus})_2[Ru(CN)_6] \cdot 3H_2O$, **6b**: A solution of $(BV)Br_2$ (0.24 g, 0.48 mmol) [7] in 15 mL of H_2O was added to a solution of $K_4[Ru(CN)_6]$ (0.10 g, 0.24 mmol) in 5 mL of H_2O. The instantaneously resulting violet precipitate was separated from the filtrate, washed with a small amount of H_2O, and dried (high vacuum, 8 h). Yield, 74%; correct elemental analyses for C, H, N, and O.

Received: May 25, 1990 [Z 3977 IE]
German version: *Angew. Chem. 102* (1990) 1157

[1] S. Eller, P. Brandt, A. K. Brimah, P. Schwarz, R. D. Fischer, *Angew. Chem. 101* (1989) 1274; *Angew. Chem. Int. Ed. Engl. 28* (1989) 1263.
[2] All host-guest compounds related to **1**–**3**, but involving also covalent host–guest linkages (including hydrogen bonding), are here referred to as type-B systems; see [1] and M. Adam, A. K. Brimah, X.-F. Li, R. D. Fischer, *Inorg. Chem. 29* (1990) 1595, as well as the structure of $[(Me_3Sn)_4Fe^{II}(CN)_6 \cdot 4H_2O]_\infty$ (U. Behrens, A. K. Brimah, R. D. Fischer, unpublished results).
[3] a) $MV^{n\oplus}$ = 1,1'-dimethyl-4,4'-bipyridinium; $BV^{n\oplus}$ = 1,1'-dibenzyl-4,4'-bipyridinium (n = 1,2); an alternative name for methylviologen is paraquat; b) For some other host–guest systems with $MV^{2\oplus}$, see, e.g., footnote 1 of [19].
[4] See H. E. Toma, *Can. J. Chem. 57* (1979) 2079.
[5] Donor = mesitylene, durene, as well as some naphthalene and anthracene derivatives; see K. B. Yoon, J. K. Kochi, *J. Am. Chem. Soc. 110* (1988) 6586.
[6] Increasing experimental evidence suggests that these and some related reactions intermediately involve partial cleavage of the initial polymer, followed by spontaneous self-assembly of the new polymer: cf. S. Eller, P. Schwarz, P. Brandt, R. D. Fischer, unpublished results; S. Eller, S. Dülsen, R. D. Fischer, *J. Organomet. Chem. 390* (1990) 309.
[7] Prepared according to W. Geuder, S. Hünig, A. Suchy, *Tetrahedron 42* (1986) 1665.
[8] The stability of all Me_3Sn^{IV} building blocks remaining in the resulting 3D coordination polymer is unexpected in view of the presence of strongly reducing $S_2O_4^{2\ominus}$ and $G^{\cdot\oplus}$ ions; however, all Me_3Sn^{IV} units liberated according to Equation (b) undergo reductive decomposition.
[9] Appearance of only *one* symmetrical signal (T = 22 °C; g = 2.0416, line width ca. 2.3 G).
[10] When exposed to air, a KBr pellet of **4b** does not show any notable changes in its absorption spectrum after at least 24 h, and the color of finely powdered, *pure* **4a** turns green only after several days (the two principal absorptions of the $MV^{\cdot\oplus}$ ion merging below 550 nm to *one* very broad signal).
[11] K. B. Yoon, J. K. Kochi, *J. Am. Chem. Soc. 111* (1989) 1128.
[12] X-ray structure analysis of **1b**: SYNTEX $P2_1$ four-circle diffractometer with graphite monochromator ($Mo_{K\alpha}$ radiation, λ = 0.709261 Å). Orthorhombic cell, space group *Pmna* with a = 11.248(1), b = 16.459(2), c = 17.648(3) Å, V = 3267 Å^3, Z = 4. Partial disorder involving one of the CNSnNC fragments was accounted for to arrive at the solution of the structure presented in Figure 1. Use of 3159 symmetry-independent reflections with $F \geq 4\sigma(F)$; after refinement of 181 parameters, convergence at R = 0.068, R_w = 0.076 with w = 1.9346 $[\sigma^2(F) + 0.0005\,F^2]^{-1}$. The final structure of **1b** will be published elsewhere in detail, taking into consideration an apparent superlattice (doubling of the number of parameters).
[13] For the structures of two type-B compounds, see [2].
[14] One remotely related type-A system is the recently described 3D polymer $[(NMe_4)Cu^{I}_{0.5}Zn^{II}_{0.5}(\mu\text{-}CN)_4]_\infty$: see B. F. Hoskins, R. Robson, *J. Am. Chem. Soc. 112* (1990) 1546.
[15] a) E^0 (vs. SCE) = 0.19 (Fe), 0.70 (Ru), and 0.40 (Os) V; cf. J. C. Curtis, T. J. Meyer, *Inorg. Chem. 21* (1982) 1562; b) E^0 = −0.69 (MV) and −0.58 (BV) V; cf. Z. Li, C. M. Wang, L. Persaud, T. E. Mallouk, *J. Phys. Chem. 92* (1988) 2592.
[16] See D. F. Shriver, *Structure and Bonding 1* (1966) 32.
[17] As a rule, λ_{max}(CT) of a solid sample turns out to exceed λ_{max} (CT) of a corresponding solution; cf. H. Kuroda, M. Kobayaschi, M. Kinoshita, S. Takemoto, *J. Chem. Phys. 36* (1962) 457.
[18] B. L. Allwood, N. Spencer, H. Shariari-Zavareh, J. F. Stoddart, D. J. Williams, *J. Chem. Soc. Chem. Commun. 1987*, 1064.
[19] B. Odell, M. V. Reddington, A. M. Z. Slawin, N. Spencer, J. F. Stoddart, D. J. Williams, *Angew. Chem. 100* (1988) 1605; *Angew. Chem. Int. Ed. Engl. 27* (1988) 1547.
[20] Even concentrated solutions of $(MV)Cl_2$ and *p*-dimethoxybenzene in $NCCH_3$ (2:1) do not show any clear CT band.
[21] In the former cyclodimer, the two DAB units are linked via fairly long, and thus optimally "isolating", $(CH_2)_n$ bridges.
[22] A. Renault, D. Talham, J. Canceill, P. Batail, A. Collet, J. Lajzerowicz, *Angew. Chem. 101* (1989) 1251; *Angew. Chem. Int. Ed. Engl. 28* (1989) 1249.
[23] For M = Ru (**1b** → **4b**), the reaction is accompanied by the following color changes: red → blue (suspended solid) and blue → colorless (aqueous solution).
[24] The redox potential E° of the pair $MV^{\cdot\oplus}/MV^{2\oplus}$ is also known to vary with the solvent: see C. L. Bird, A. T. Kuhn, *Chem. Soc. Rev. 10* (1981) 49.

Isomerization of Benzoylalkylidene Sulfur Tetrafluorides C_6H_5-CO-CR=SF_4 to Dihydrooxathietes**

By *Thomas Henkel, Thomas Krügerke*, and *Konrad Seppelt**

Of the six known alkylidene sulfur tetrafluorides RR'C=SF_4, only F-CO-CH=SF_4 bears a C-functional group.[1] In the crystal at −168 °C, this compound has a fully planar molecular framework with C–S and C–O double bonds arranged in a *cis* fashion.[2] Like most alkylidene sulfur tetrafluorides, it exhibits considerable stability. In attempts to prepare the benzoyl-substituted compounds C_6H_5-CO-CR=SF_4 (**1**), however, they could only be detected as intermediates by ^{19}F NMR (R = H) or were not observed at all (R = Br), since they isomerize immediately to the isolable oxathietes **2**. Because the ^{19}F NMR spectra of

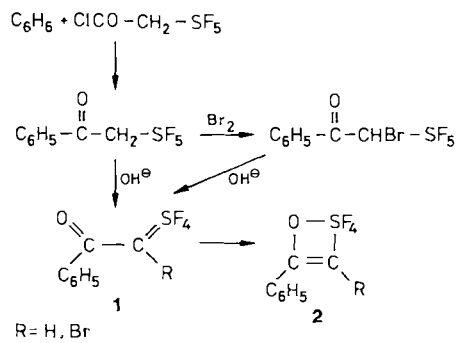

isomers **1** and **2** reveal an A_2BC system in each case, signal assignment requires plausible assumptions regarding the chemical shifts and coupling constants. This is possible for the alkylidene sulfur tetrafluorides, but reference spectra are lacking for the new *S*-tetrafluorodihydrooxathietes. The X-ray structure analysis (Fig. 1) unambiguously established the presence of the unsaturated four-membered ring.[3]

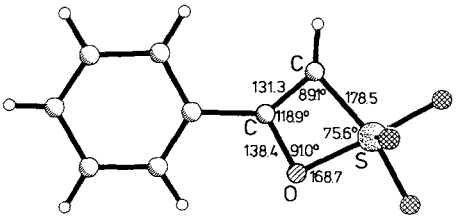

Fig. 1. Molecular structure of **2**, R = H, at −153 °C (XP plot).

Owing to the special geometry of alkylidene sulfur tetrafluorides such as **1**, where the substituents at carbon lie in the plane defined by the sulfur and the axial fluorines, an approach of the carbonyl oxygen to the sulfur requires that one axial fluorine be pushed aside. The necessary twisting around the C–S double bond can occur in three ways (Scheme 1): rotation, pseudorotational[4] pairwise interchange of axial and equatorial positions, or a combination of

[*] Prof. Dr. K. Seppelt, Dipl.-Chem. T. Henkel, Dr. T. Krügerke
Institut für Anorganische und Analytische Chemie der Freien Universität
Fabeckstrasse 34–36, D-1000 Berlin 33

[**] This work was supported by the Deutsche Forschungsgemeinschaft and the Fonds der Chemischen Industrie.

both mechanisms. The last possibility is assumed in unsubstituted $H_2C{=}SF_4$ for the methylene torsion, which, owing to the high barrier of 100 kJ mol^{-1}, cannot be observed by NMR spectroscopy.[1]

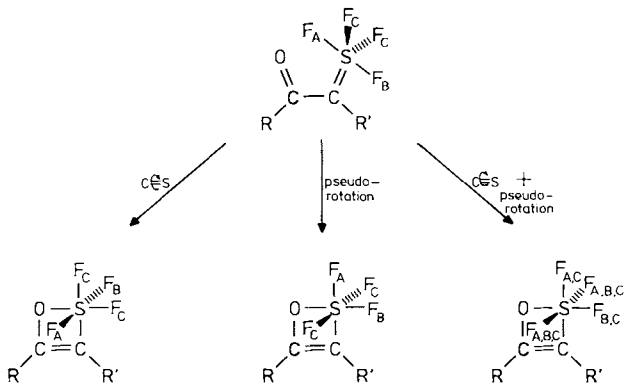

Scheme 1. Possible mechanism for the isomerization **1** → **2**. The displacement of the axial fluorine can occur by twisting around the C–S double bond (left), by Berry pseudorotation of the fluorines (middle), or by a combination of the two mechanisms (right). The mechanisms could be distinguished if labeling of fluorine were experimentally possible.

The ready isomerization **1** → **2** contrasts with the fact that the butadiene–cyclobutene isomerization, which almost always occurs in the opposite direction, proceeds by conrotatory twisting around the two double bonds for symmetry reasons and therefore requires a high activation energy (130–155 kJ mol^{-1}).[5, 6] 1,2-Dithiones undergo reversible

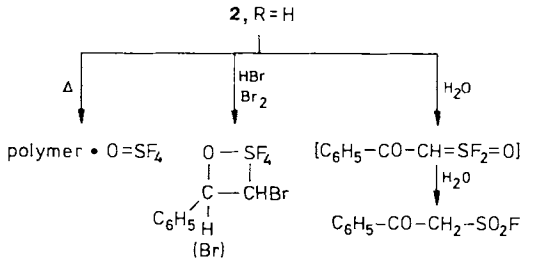

transformation to dihydro-1,2-dithietes without any symmetry change and with about half of this activation energy.[7]

The four-membered ring is not opened upon addition of HBr or Br_2 to **2**, but it is cleaved by water. Thermolysis of **2** results in elimination of SOF_4.

Experimental Procedure

C_6H_5-CO-CH_2-SF_5: $AlCl_3$-catalyzed acylation of C_6H_6 with ClCO-CH_2-SF_5 at 0 °C followed by classical workup, distillation at 63 °C/0.6 mbar, sublimation under high vacuum at −30 °C; 38% yield, colorless solid, m.p. 38 °C. ^{19}F NMR (84.25 MHz, $CFCl_3$): AB_4X_2 spectrum, δ = 82.2(A), 73.8(B), ^2J(AB) = 153.0, ^3J(BX) = 7.4 Hz. ^1H NMR (90 MHz, TMS): δ = 5.4(CH_2), 7.7–8.6 (C_6H_5).

C_6H_5-CO-CHBr-SF_5: Bromination of C_6H_5-CO-CH_2-SF_5 at 30 °C in CCl_4 under UV irradiation in Pyrex; yield 23%, colorless solid, m.p. 52 °C. ^{19}F NMR: AB_4Xspectrum, δ = 77.4(A), 65.1(B), ^2J(AB) = 148.7, ^3J(BX) = 5.5 Hz. ^1H NMR: δ = 7.0(CH), 7.8–8.6(C_6H_5).

2: C_6H_5-CO-CHR-SF_5 (1 g) in 50 mL of pentane was stirred with NaOH (5 g) at room temperature for 2–3 d. The reaction was monitored by ^{19}F NMR spectroscopy. For R = H, **1** was detected as an intermediate (A_2BCX spectrum: δ = 63.3(A), 58.2(B), 57.8(C), ^2J(AB) = 166.1, ^2J(AC) = 168.5, ^2J(BC) = 9.9, ^3J(AX) = 8.8, ^3J(BX) = −39.4, ^3J(CX) = −13.3 Hz). After complete reaction, the mixture was filtered, the filtrate cooled to −78 °C, and the pentane removed under oil-pump vacuum. **2**, R = H: Colorless solid, which slowly decomposes at 0 °C; recrystallized from ether. IR(CH_2Cl_2): $\tilde{\nu}$ [cm^{-1}] = 1636 (C=C), 877, 810, 788 (S-F). ^{19}F NMR: A_2BCX spectrum, δ = 66.9 (A), 70.2 (B), 57.5 (C), ^2J(AB) = 137.4, ^2J(AC) = 112.1, ^2J(BC) = 135.4, ^3J(AX) = 1.7, ^3J(CX) = 4.7 Hz. ^1H NMR: δ = 7.1(CH), 8.0 (C_6H_5). **2**, R = Br: Colorless solid. ^{19}F NMR: A_2BC spectrum, δ = 61.8(A), 66.5(B), 39.5(C), ^2J(AB) = 147.5, ^2J(AC) = 119.2, ^2J(BC) = 133.1 Hz. MS (80 eV, EI): *m/z* 304, 306 ($M^{\oplus}$, 21%), 105 ($C_7H_5O^{\oplus}$, 27), 89 ($SF_3^{\oplus}$, 100) and smaller fragments.

C_6H_5-CO-CH_2-SO_2F: **2**, R = H, was hydrolyzed by heating it in aqueous acetone at 56 °C. An ^{19}F NMR spectrum assignable to C_6H_5-CO-CH=SF_2=O was recorded during the reaction (δ = 59.7 (S-F), ^3J(HF) = 2.7 Hz). Removal of the solvent and recrystallization from CCl_4 gave C_6H_5-CO-CH_2-SO_2F in quantitative yield. Colorless solid, m.p. 83–86 °C. IR (KBr): $\tilde{\nu}$ [cm^{-1}] = 689(C=O), 1413, 1201 (S=O) 801 (S-F). MS (80 eV, EI): *m/z* 202 ($M^{\oplus}$, 31%), 105 ($C_7H_5O^{\oplus}$, 100) and smaller fragments. ^{19}F NMR: δ = 64.0 (S-F), ^3J(HF) = 2.4 Hz. ^1H NMR: δ = 5.5(CH_2), 7.9–8.6 (C_6H_5)

Received: June 5, 1990 [Z 3997 IE]
German version: *Angew. Chem. 102* (1990) 1171

CAS Registry numbers:
2 (R=H), 129421-50-7; **2** (R=Br), 129421-51-8; C_6H_6, 71-43-2; $ClCOCH_2SF_5$, 2353-88-0; $C_6H_5COCH_2SF_5$, 129421-48-3; $C_6H_5COCHBrSF_5$, 129421-49-4.

[1] Review: K. Seppelt, *Angew. Chem. 103* (1991), in press; *Angew. Chem. Int. Ed. Engl.* in press.
[2] T. Krügerke, J. Buschmann, G. Kleemann, P. Luger, K. Seppelt, *Angew. Chem. 99* (1987) 808; *Angew. Chem. Int. Ed. Engl. 26* (1987) 799.
[3] **2**, R = H: $P2_1/c$, a = 725.57(8), b = 563.56(9), c = 2114.03(11) pm, β = 93.63(5)°, Z = 4. 1816 measured, 796 unique, 424 reflections with $I \geq 3\sigma(I)$, SHELX, full matrix. R_w = 0.079. The relatively poor R value is due to a notorious twinning. Only the reflection intensities of the larger individual were measured. Analysis using a program for twins failed. Further details of the crystal structure investigation may be obtained from the Fachinformationszentrum Karlsruhe, Gesellschaft für wissenschaftlich-technische Information mbH, D-7514 Eggenstein-Leopoldshafen 2 (FRG), on quoting the depository number CSD-54808, the names of the authors, and the journal citation.
[4] R. S. Berry, *J. Chem. Phys. 32* (1960) 933.
[5] R. Criegee, D. Seebach, R. E. Winter, B. Börretzen, H.-A. Brune, *Chem. Ber. 98* (1965) 2339.
[6] H. M. Frey, *Adv. Phys. Org. Chem. 4* (1966) 183.
[7] W. Küsters, P. de Mayo, *J. Am. Chem. Soc. 95* (1973) 2383; *ibid. 96* (1974) 3502.

Stereospecific Insertion of the Carbene Ligand of a Fischer Carbene Complex into Olefinic C–H Bonds**

By *Anette Wienand* and *Hans-Ulrich Reissig**

The addition of the C(OMe)Ph ligand of **1** to α,β-unsaturated esters **2** to give cyclopropanes **3** was first described 20 years ago.[1] The synthetic potential of donor–acceptor-substituted cyclopropanes,[2] like **3**, prompted us to investigate the scope of this cyclopropanation method[3] as well as the mechanism of the carbene transfer.[4] We have found that, in

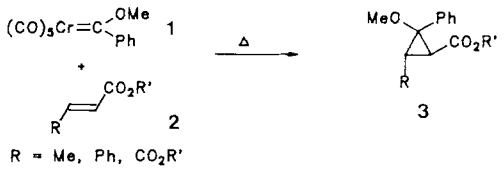

[*] Prof. Dr. H.-U. Reissig, Dr. A. Wienand
Institut für Organische Chemie der Technischen Hochschule
Petersenstrasse 22, D-6100 Darmstadt (FRG)

[**] This work was supported by the Volkswagen-Stiftung, the Fonds der Chemischen Industrie, and the Vereinigung von Freunden der Technischen Hochschule zu Darmstadt.

reactions of **1** with *E*- and *Z*-crotononitrile, *E*-**4** and *Z*-**4**, respectively, the carbene ligand of **1** undergoes unprecedented stereospecific[5] insertion into the β-C–H bond of the olefin with inversion of double-bond configuration.

Heating a solution of **1** and *E*-**4** in cyclohexane (80 °C, 23 h) affords a mixture of four products (yield 71 %). More than 90 % of the mixture consists of the insertion product *E*-**6**,[6] whereas *Z*-**6** and the expected cyclopropanes **5** and **7**

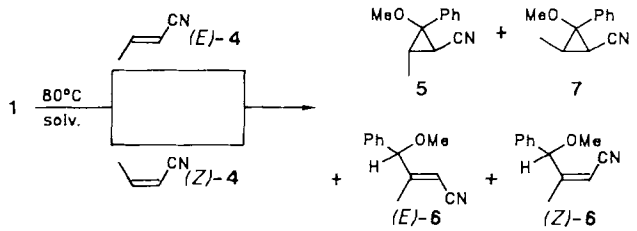

are only formed in small amounts (Table 1). On the other hand, use of *Z*-**4** gives *Z*-**6**[6] as the main product (60 % of the mixture). The remaining products consist of only 4 % of the configurationally isomeric insertion product *E*-**6** and, according to NMR spectroscopy, 15 and 21 % of the cyclopropanes **5** and **7**, respectively.

Table 1. Reactions of chromium carbene complex **1** with the crotononitriles *E*-**4** and *Z*-**4** in cyclohexane or acetonitrile (80 °C, 13–28 h, nitrogen atmosphere, ca. 0.5 M[a]).

Olefin	Solvent[b]	Product distribution [%] 5	*E*-6	*Z*-6	7	Overall yield [%]
E-4	C_6H_{12}	3	92	2	3	71
E-4	CH_3CN	77	16	–	7	35
Z-4	C_6H_{12}	15	4	60	21	67
Z-4	CH_3CN	24	2	9	65	32

[a] The product distribution was determined by ^1H NMR spectroscopy (300 MHz; estimated error ± 3 %); the components were separated or enriched by HPLC, so that an unambiguous structural assignment could be made from the ^1H and ^{13}C NMR spectra. Only one of the possible isomers of **5** is formed; **7** is obtained as a mixture of diastereomers (position of Ph/OMe); all chiral products are racemic mixtures. [b] When **1** is allowed to react with *E*-**4** or *Z*-**4** in the absence of solvent (ca. 4 h, 90 °C), the resulting product distribution lies between those found in C_6H_{12} and CH_3CN. No fundamental changes are found with respect to the stereospecificity of the formation of **6**.

The insertion of the carbene ligand into the olefinic β-C–H bond is also highly stereospecific in acetonitrile as solvent: *E*-**6** is obtained preferentially from *E*-**4**, and *Z*-**6** from *Z*-**4**. However, the proportion of cyclopropanes obtained in this solvent is much greater and the overall yield much lower (Table 1). Control experiments established that, under the reaction conditions, (1) the olefins are practically configurationally stable (maximally 5 % $Z \rightarrow E$ isomerization), (2) cyclopropanes **5** and **7** are not transformed into their acyclic isomers *E*/*Z*-**6**, and (3) no hydrogen is abstracted from the solvent (no D incorporation from C_6D_{12} as solvent).

The product distribution in Table 1 clearly shows that the insertion reaction is stereospecific with > 90 % inversion of the olefin configuration, whereas the cyclopropane formation is largely nonstereospecific. Therefore, these two reactions of **1** presumably proceed via different pathways. We will describe elsewhere a cyclopropanation mechanism that is consistent with these findings.[4] Here, we wish to make a (speculative) proposal regarding the mechanism of the stereospecific carbene insertion reaction. Loss of a CO ligand from **1** gives **8**, which reacts with *E*-**4**—presumably via a metal–olefin complex—to afford the chromacyclobutane **9**. Rearrangement of **9** to give the hydridochromium complex **10** may be regarded as a syn elimination of the β-H atom[7] and results in the observed inversion of olefin configuration. Finally, reductive elimination affords *E*-**6**.

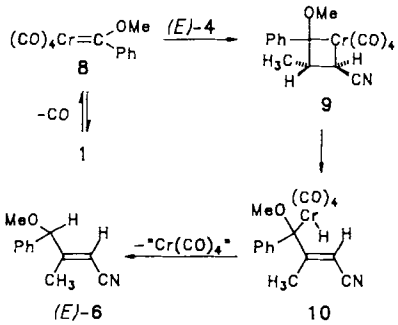

Semmelhack and *Tamura* postulated a corresponding mechanism for the reactions of the iron carbene complexes $[(CO)_4FeC(OEt)R]$, which are analogous to **1**, with methyl acrylate and styrene.[8] However, neither their examples nor the observation of CH insertion products as minor compounds in previously reported reactions of olefins with **1** or other chromium carbene complexes[9] allow a prediction of the stereochemical course of the reaction. The inversion of olefin configuration described here is a strong indication for the involvement of metallacyclobutanes such as **9** and for a β-syn elimination. If the formation of the insertion product **6** occurred by direct attack of **8** on the C–H bond, then retention of the olefin configuration would have been expected.[10] Still unanswered is the question why insertion of the carbene ligand of **1** into the crotononitriles *E*/*Z*-**4** so strongly predominates over cyclopropanation. Presumably, the nitrile group plays a decisive, yet still unexplained, role.

Table 2. ^1H and ^{13}C NMR data (300 and 75.5 MHz, respectively, $CDCl_3$) for *E*-**6** and *Z*-**6**.

E-**6**: ^1H NMR: $\delta = 7.42-7.27$ (m, 5H; Ph), 5.74 (q, $J \approx 1$ Hz, 1H; 2-H), 4.61 (s, 1H; 4-H), 3.31 (s, 3H; OMe), 1.89 (d, $J \approx 1$ Hz, 3H; 3-Me). ^{13}C NMR: $\delta = 162.9$ (s; C-3), 137.7, 128.8, 128.7, 127.5 (s, 3d; Ph), 117.0 (s; CN), 95.4 (d; C-2), 85.7 (d; C-4), 56.8 (q; OMe), 17.8 (q; 3-Me)

Z-**6**: ^1H NMR: $\delta = 7.46-7.30$ (m, 5H; Ph), 5.36 (s, 1H; 4-H), 5.28 (q, $J = 1.4$ Hz, 1H; 2-H), 3.40 (s, 3H; OMe), 1.77 (d, $J = 1.4$ Hz, 3H; 3-Me). ^{13}C NMR: $\delta = 163.7$ (s; C-3), 138.1, 128.3, 127.9, 125.6 (s, 3d; Ph), 116.1 (s; CN), 96.9 (d; C-2), 82.7 (d; C-4), 56.6 (q; OMe), 16.9 (q; Me)

Received: June 1, 1990 [Z 3993 IE]
German version: *Angew. Chem. 102* (1990) 1156

CAS Registry numbers:
1, 27436-93-7; (*E*)-**4**, 627-26-9; (*Z*)-**4**, 1190-76-7; **5**, 129421-46-1; (*E*)-**6**, 129421-45-0; (*Z*)-**6**, 129421-47-2; **7** (isomer 1), 129518-52-1; **7** (isomer 2), 129518-53-2.

[1] K. H. Dötz, E. O. Fischer, *Chem. Ber. 103* (1970) 1273; *ibid. 105* (1972) 1356.
[2] H.-U. Reissig, *Top. Curr. Chem. 144* (1988) 73.
[3] a) A. Wienand, H.-U. Reissig, *Tetrahedron Lett. 29* (1988) 2315; b) M. Buchert, H.-U. Reissig, *ibid. 29* (1988) 2319; c) H.-U. Reissig in H. Werner, G. Erker (Eds.): *Organometallics in Organic Synthesis*, Springer, Berlin 1989; see also d) J. W. Herndon, S. Tumer, *Tetrahedron Lett. 30* (1989) 4771; *J. Org. Chem.*, in press.

[4] [3c]; A. Wienand, H.-U. Reissig, unpublished.
[5] We use the term stereospecificity as described by *Eliel*: E. L. Eliel: *Stereochemie der Kohlenstoffverbindungen*, Verlag Chemie, Weinheim 1966, p. 517.
[6] The configurations of *E*-**6** and *Z*-**6** were established by determination of the C–H coupling constants between 2-H and 3-CH_3: the values are 8.0 Hz for *E*-**6** and 5.4 Hz for *Z*-**6**. Cf. R. V. Dubs, W. von Philipsborn, *Org. Magn. Reson. 12* (1979) 326. The chemical shifts are also consistent with this assignment. For further NMR data, see Table 2.
[7] For β-H elimination in metallacycles, see J. B. Collman, L. S. Hegedus, J. R. Norton, R. G. Finke: *Principles and Applications of Organotransition Metal Chemistry*, University Science Books, Mill Valley, CA, USA 1987, p. 459.
[8] M. F. Semmelhack, R. Tamura, *J. Am. Chem. Soc. 105* (1983) 6750. The use of other olefins, besides acrylic esters and styrene, gave acyclic compounds with a different position of the double bond.
[9] Corresponding insertion products are found in smaller amounts (< 10 %) in the reactions of **1** with methyl acrylate, but not with acrylonitrile or *E*/*Z*-methyl crotonate. See also M. D. Cooke, E. O. Fischer, *J. Organomet. Chem. 56* (1973) 279; [3a, d].
[10] For competition between π-complex formation and CH insertion in the reaction of olefins with coordinatively unsaturated metal complexes, see P. O. Stoutland, R. G. Bergman, *J. Am. Chem. Soc. 107* (1985) 4581; M. V. Baker, L. D. Field, *ibid. 108* (1986) 7433, 7436.

Catalytic Hydrosilylation or Hydrogenation at One Coordination Site of [Cp'Fe(CO)(X)] Fragments**

By Henri Brunner and Konrad Fisch*

The mechanisms proposed for the hydrosilylation of olefins and ketones require that the catalytically active transition-metal complex have three coordination sites, two for oxidative Si–H addition and one for binding of the unsaturated substrate.[1–3] These reactions often result in formation of byproducts, for example, silyl enol ethers from enolizable ketones.[4, 5] Here we describe the use of iron complexes as homogeneous catalysts for the hydrosilylation of acetophenone with diphenylsilane. The reaction takes place at one coordination site and does not lead to byproducts.

The acetyl complexes (+)- and (−)-**1**/**2**,[6] the methyl complexes (+)- and (−)-**3**–**5**,[7] and $[CpFe(CO)_2(CH_3)]$ were used as catalysts.[8]

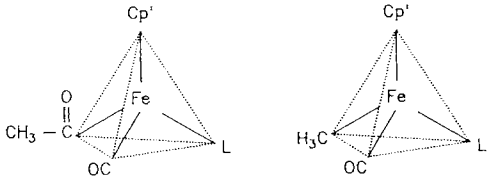

1,2 **3-5**

1,3: Cp' = cyclopentadienyl (Cp)
2,4: Cp' = indenyl (Ind)
5: Cp' = 1-*t*Bu-indenyl
L = (*S*)-(+)-$(C_6H_5)_2P-N(CH_3)-CH(CH_3)C_6H_5$

When equimolar amounts of acetophenone and diphenylsilane are heated in the presence of 0.5–1.0 mol % of the iron complex, the hydrosilylation begins after an induction period.[9] The temperatures at which the reaction proceeds at a measurable rate differ considerably, depending on the catalyst. Surprisingly, they correlate with the temperatures necessary for the epimerization at the Fe atom of the catalyst (80 and 60 °C for acetyl complexes **1** and **2**,[10] respectively; 70 and 50 °C for methyl complexes **3** and **4**,[11] respectively). Reaction for 24 hours at these temperatures always results in quantitative formation of the silylated 1-phenylethanol **6**. In no case was silylated enol **7** detected.

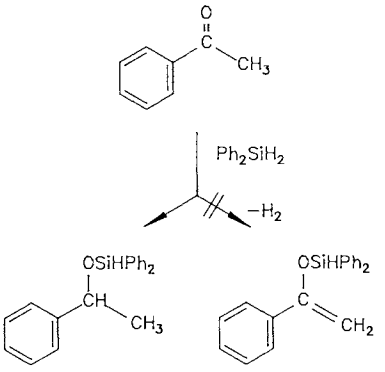

6 **7**

Presumably, loss of the phosphane ligand from complexes **1**–**4** is the rate-determining step for both the epimerization and the formation of the catalytically active species.[13] This assumption is supported by the fact that small trialkylphosphanes inhibit the reaction. On the other hand, the complex $[CpFe(CO)_2(CH_3)]$ is activated by methyl group migration,[14] which results in formation of the same intermediate, $[CpFe(CO)(COCH_3)]$, as that obtained by loss of the phosphane ligand from **1**. In the presence of 1.0 mol % of $[CpFe(CO)_2(CH_3)]$ at 70 °C, the catalytic hydrosilylation is also complete within 24 hours.

The acetyl complexes **1** and **2** can be recovered at the end of the catalytic reaction by chromatography on Al_2O_3 with pentane/diethyl ether (4/1) as eluent. The complex $[CpFe(CO)_2(CH_3)]$, however, is consumed during the catalysis.

A possible mechanism for the catalytic hydrosilylation involves initial addition of diphenylsilane to the 16-electron fragment formed by thermal loss of the phosphane ligand or methyl migration. The adduct then reacts with acetophenone to form coordinated **6**, release of which re-forms the 16-electron fragment. There are two possibilities for the addition of silane to the coordinatively unsaturated complex fragment: (1) oxidative addition with cleavage of an Si–H bond and (2) formation of an M–Si–H three-center bond, like that already found for $[CpMn(CO)_2(silane)]$ complexes.[15–17]

We rule out addition of the Si–H bond to the acetyl group of the complexes, since this addition would require additional catalysts[18] and since the methyl complexes **3** and **4** also catalyze the hydrosilylation. We explain the absence of silyl enol ether **7** by a hydrosilylation mechanism involving an Fe–Si–H three-center bond rather than an Fe–H species. By contrast, the hydrosilylation of acetophenone with diphenylsilane catalyzed by hydridorhodium complexes always affords enol ether **7** (in varying amounts) in addition to silyl ether **6**.[4, 5] The different induction periods found for the catalysts are presumably due to deactivation of the catalytically active species at the start of the reaction by traces of impurities.

[*] Prof. Dr. H. Brunner, Dipl.-Chem. K. Fisch
Institut für Anorganische Chemie der Universität
Universitätsstrasse 31, D-8400 Regensburg (FRG)

[**] Optically Active Transition-Metal Complexes, Part 101. This work was supported by the Deutsche Forschungsgemeinschaft, the Fonds der Chemischen Industrie, and BASF AG, Ludwigshafen. Part 100: H. Brunner, H. Peter, *J. Organomet. Chem.*, in press.

The lack of optical induction when the optically active catalysts **1**–**4** are used is the result of rapid racemization of the catalytically active species. Surprisingly, optical induction is still not observed with the optically active complex **5**, whose planar chiral structure does not isomerize even at 200 °C. We interpret this result to mean that acetophenone attacks the coordinated diphenylsilane from the side not facing the complex. The newly formed asymmetric center is thus too far from the planar chiral group.

The complex $[CpFe(CO)_2(CH_3)]$ and also the complex $[IndFe(CO)_2(CH_3)]$ can be used as hydrogenation catalysts. For example, they catalyze the hydrogenation of α-methylstyrene to isopropylbenzene at 100 °C under H_2 (50 bar) in THF.[19] However, owing to rapid deactivation of the complexes employed—formation of the dimeric compounds $[Cp'Fe(CO)_2]_2$, which are catalytically inactive—only a few catalytic cycles are achieved. The phosphane complexes **3** and **4** decompose during hydrogenation of α-methylstyrene (90 °C, bar H_2, THF) so rapidly that only a few percent of hydrogenated product is formed. We explain the catalytic hydrogenation by formation of an η^2-H_2 complex from the unsaturated intermediate $[Cp'Fe(CO)(COCH_3)]$ under the reaction conditions; this complex, formed in competition with THF and olefin complexes, reacts with α-methylstyrene similarly to the reaction of the Fe-bonded SiH group with acetophenone. Such η^2-H_2 complexes have also been postulated to be formed during decomposition of $[CpFe(CO)_2(CH_3)]$ and $[IndFe(CO)_2(CH_3)]$ in the presence of hydrogen.[20]

The majority of the reactions of organometallic compounds proceed via intermediates containing a free coordination site at the metal. It should be possible to use these free coordination sites for catalysts of known structure.[21]

Received: May 23, 1990 [Z 3975 IE]
German version: *Angew. Chem. 102* (1990) 1189

CAS Registry numbers:
(−)-**1**, 67375-04-6; (+)-**1**, 67291-26-3; (−)-**2**, 74984-64-8; (+)-**2**, 74945-73-6; (−)-**3**, 59727-90-1; (+)-**3**, 59568-04-6; (−)-**4**, 123075-70-7; (+)-**4**, 123163-87-1; (−)-**5**, 129286-99-3; (+)-**5**, 129388-44-9; **6**, 51276-65-4; $CpFe(CO)_2CH_3$, 12080-06-7; Ph_2SiH_2, 775-12-2; acetophenone, 98-86-2; α-methylstyrene, 98-83-9; isopropylbenzene, 98-82-8.

[1] J. L. Speier, *Adv. Organomet. Chem. 17* (1979) 407.
[2] I. Ojima, K. Hirai in J. D. Morrison (Ed.): *Asymmetric Synthesis, Vol. 5*, Academic Press, Orlando, FL, USA 1985, p. 103.
[3] F. Seitz, M. S. Wrighton, *Angew. Chem. 100* (1988) 281; *Angew. Chem. Int. Ed. Engl. 27* (1989) 289.
[4] K. Yamamoto, T. Hayashi, M. Kumada, *J. Organomet. Chem. 46* (1972) C65.
[5] H. Brunner, U. Obermann, *Chem. Ber. 122* (1989) 499.
[6] H. Brunner, H. Vogt, *J. Organomet. Chem. 191* (1980) 181.
[7] H. Brunner, H. Vogt, *J. Organomet. Chem. 210* (1981) 223.
[8] The structural formulas show the forms of **1**–**5** that are levorotatory at $\lambda = 436$ nm. The Fe center has the *R* configuration, the C center, the *S* configuration.
[9] 1.0 mL (8.0 mmol) of acetophenone, 1.6 mL (8.0 mmol) of diphenylsilane, 0.5–1.0 mol % of catalyst. The hydrosilylation can be monitored by ^1H NMR spectroscopy. The induction period can be from several minutes to a few hours.
[10] A simple rate law cannot be formulated for the epimerization, which occurs over hours[14].
[11] The half-lives for epimerization of **3** and **4** in $[D_6]$benzene are 70 min at 70 °C and 37 min at 50 °C[12].
[12] H. Brunner, K. Fisch, P. G. Jones, J. Salbeck, *Angew. Chem. 101* (1989) 1558; *Angew. Chem. Int. Ed. Engl. 28* (1989) 1521.
[13] Replacement of the aminophosphane L by PPh_3 in complexes **1**–**4** does not affect the catalytic activity.
[14] H. Brunner, H. Vogt, *Chem. Ber. 114* (1981) 2186.
[15] D. L. Lichtenberger, A. Rai-Chaudhuri, *Inorg. Chem. 29* (1990) 975.
[16] H. Rabaa, J.-Y. Saillard, U. Schubert, *J. Organomet. Chem. 330* (1987) 397.
[17] The $[CpMn(CO)_2(silane)]$ complexes do not catalyze the hydrosilylation of acetophenone with diphenylsilane; we have obtained evidence for a stoichiometric reaction.
[18] E. J. Crawford, P. K. Hanna, A. R. Cutler, *J. Am. Chem. Soc. 111* (1989) 6891.
[19] 1.50 mL (11.6 mmol) of α-methylstyrene, 0.50 g (2.6 mmol) of $[CpFe(CO)_2(CH_3)]$ in 5 mL of THF, 50 bar H_2, 110 °C; degree of hydrogenation 90% (^1H NMR integration).
[20] T. C. Forschner, A. R. Cutler, *Inorg. Chim. Acta 102* (1985) 113.
[21] Reports have appeared describing the use of $[(arene)Cr(CO)_2(\eta^2\text{-}HSiHPh_2)]$ complexes as catalysts for the activation of the Si–H bond of diphenylsilane in thermal reactions: O. B. Afanasova, E. Zubarev, T. M. Sokolova, E. A. Chernyshew, *Zh. Obshch. Khim. 57* (1987) 1909. E. Matarasso-Tchiroukhine, *J. Chem. Soc. Chem. Commun. 1990*, 681.

Electrostatic Control of the Molecular and Crystal Structure of an Olefinic Double Betaine **

By *Robert Weiss,* Reinhardt Roth, Rainer H. Lowack,* and *Matthias Bremer*

Dedicated to Professor Hans Jürgen Bestmann on the occasion of his 65th birthday

E/*Z*-isomeric olefinic double betaines of the type **1**/**2** were previously unknown. The quadrupole system **2**, which has an alternating charge pattern, should be significantly more stable than system **1**, because of the more favorable electrostatic interactions between the charged substituents in **2**. Model calculations have shown that, depending on the substituents, this difference in stability can be up to 40 kcal mol^{-1}.[1] Here we describe the first synthesis of a stable compound of type **1** as well as its unusual molecular and crystal structure.

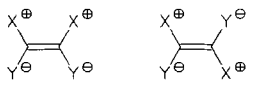

1 **2**

The starting point of the synthesis was our observation that, in structure-determined analogy to *p*-chloranil,[2] dichloromaleic anhydride (**3**) can be substituted in a bis-onio fashion by 4-dimethylaminopyridine (DMAP, **6**). The yellow

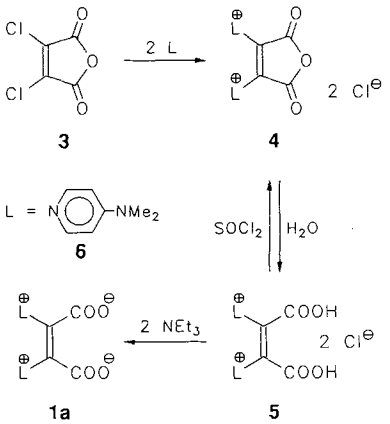

3 **4** **6** **1a** **5**

[*] Prof. Dr. R. Weiss, Dr. R. Roth, Dipl.-Chem. R. H. Lowack, Dr. M. Bremer
Institut für Organische Chemie der Universität
Henkestrasse 42, D-8520 Erlangen (FRG)

[**] This work was supported by the Fonds der Chemischen Industrie. *R. H. L.* thanks the Studienstiftung des deutschen Volkes for a doctoral fellowship.

dication salt **4**, obtained in good yields as an analytically pure CH_2Cl_2 adduct, was fully characterized.[3]

The salt **4** can be converted, without loss of an onio substituent, into the corresponding maleic acid **5** by treatment with a small excess of H_2O in CH_2Cl_2.[3] Reconversion of **5** to anhydride **4** by reaction with $SOCl_2$ confirms that the energetically unfavorable *Z* configuration of the two onio moieties is not affected by the hydrolysis. Double deprotonation of **5** finally yields the dihydrate of the *Z* double betaine **1a**.[4] Recrystallization from boiling H_2O affords the hexahydrate of **1a** as crystals suitable for X-ray analysis.[5] Figure 1 shows the molecular structure of **1a** · $6H_2O$ in the crystal.

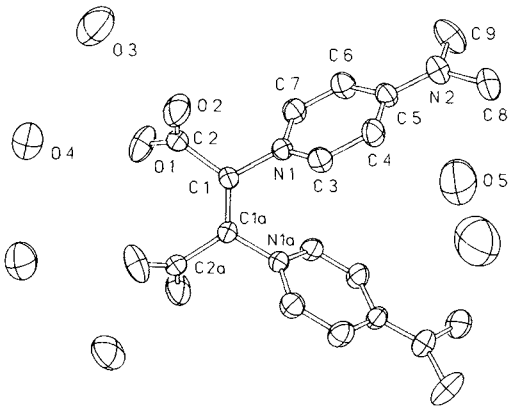

Fig. 1. Structure of **1a** · $6H_2O$ in the crystal. Selected distances [pm], angles [°], and torsion angles [°]: C1-C1a 133.4(7), C1-C2 151.3(5), C2-O2 125.1(5), C2-O1 122.8(5), C1-N1 144.8(4), N1-C3 136.0(5), N1-C7 136.5(5), C3-C4 135.9(6), C6-C7 135.4(6), C4-C5 140.6(6), C5-C6 142.1(6), C5-N2 133.1(5), N2-C8 146.8(6), N2-C9 146.8(6); C1a-C1-C2 125.2(2), C1a-C1-N1 120.1(2), C2-C1-N1 114.5(3); C1a-C1-C2-O2 125.5, C1a-C1-C2-O1 52.4, C3-N1-C1-C1a 62.9, C7-N1-C1-C1a 118.6, C8-N2-C5-C6 174.3, C9-N2-C5-C4 175.5, N1-C1-C1a-N1a −3.8, C2-C1-C1a-C2a 4.7.

The two carboxylate and the two pyridinium substituents are twisted in a *conrotatory* fashion from coplanarity with the central double bond. The torsion angles of the pyridinium moieties (e.g., C3-N1-C1-C1a) are 63°, those of the carboxylate moieties (e.g., C1a-C1-C2-O1) 52°. The molecule has overall C_2 symmetry (twofold axis perpendicular to the double bond in the plane of the double bond). Thus, the double betaine is *chiral* in the crystalline state. Undoubtedly, the electrostatic repulsion of the identically charged substituents in *Z* arrangement is responsible for the observed deconjugation. X-ray structure analyses of alkali-metal maleates show that, in those cases, one carboxylate group remains coplanar with the double bond, while the other is oriented almost orthogonally.[6] AM1 calculations, performed by us, predict that all substituents in **1a** should be twisted by 90° from coplanarity. The flattened form of this double betaine observed in the crystal, however, is presumably the result of a compromise between intramolecular minimization of charge repulsion and intermolecular maximization of charge attraction in the crystal lattice.

Owing to this electrostatic attraction of oppositely charged substituent pairs, **1a** forms a novel stacked structure in the crystal lattice. The basic motif is shown in Figure 2.

The structure displays the following characteristic features:

1. The asymmetric structural units form a racemate by *alternating* stacking of enantiomers along the *c* axis.
2. The charged ligands are each located within the electrostatic attraction region of an oppositely charged ligand of the neighbor in the stack.
3. The midpoints of the central double bonds are separated by 481 pm in the stack. Along the *c* axis, the projection of each of these double bonds relative to the two identically positioned neighboring systems is shifted parallel to the *b* axis by 94 pm (cf. also Fig. 3). A direct interaction of the olefinic double-bond moieties is not expected for this spatial arrangement.
4. The shortest intrastack contacts (225 pm) are formed between two carboxylate oxygen atoms of a given quadrupole **1a** and a partially positively charged DMAP α-H atom of each of the two nearest neighbors in the stack. Both the short distances and the spatial arrangement of the interacting centers (linear O···H-C sequence, C–O···H angle) show that these contacts must involve hydrogen bonds.[7] As revealed in Figure 2, each molecule of **1a** in the stack is anchored by four H-bond systems. As shown by more detailed analysis using molecular models, this favorable situation for interaction is due to the alternating stacking of enantiomers of **1a** to form the racemate.

In the projection along the *c* axis, the stacks of **1a** are approximately X-shaped. In the crystal, these structural units, containing lipophilic end groups (methyl groups of the NMe_2 substituents) are joined together as shown in Figure 3. The remarkable novel solid-state structure thereby resulting contains as structural elements both an undulating layer lat-

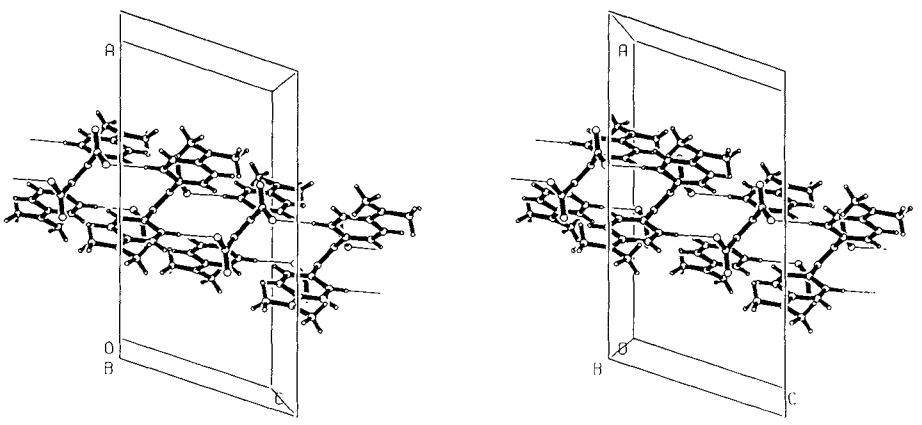

Fig. 2. Hydrogen bonding and stacking of four molecules of **1a** in the crystal (stereoview, projection along the *b* axis).

tice (distance between layers 0.33 nm) and rhomboidal channels (shorter diameter 0.7 nm, longer diameter 1.4 nm).

In the present case, as shown in Figure 3, the cavities are filled with H_2O molecules. Thus, it appears that this intriguing host lattice should be able to accept other polar and ionic guest molecules as well. Corresponding investigations have already been initiated.

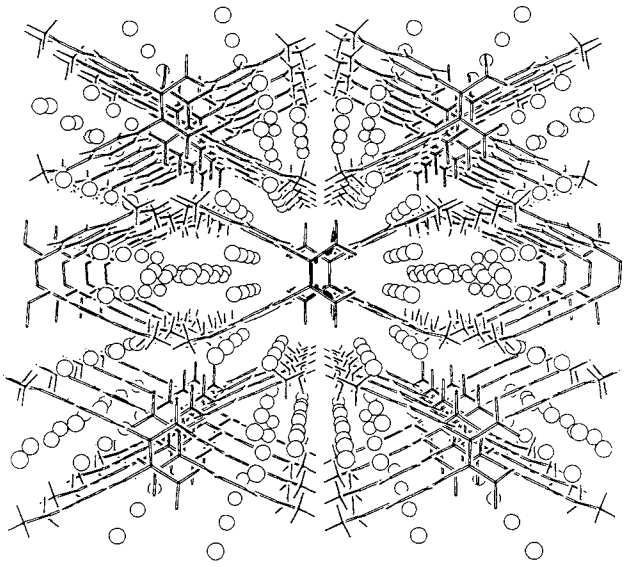

Fig. 3. Perspective drawing of the packing of the stacks of **1a** (projection along the *c* axis) with the oxygen atoms of the molecules of crystal water.

Received: March 9, 1990 [Z 3846 IE]
Publication delayed at authors' request
German version: *Angew. Chem. 102* (1990) 1164

CAS Registry numbers:
1 (Y = CO_2H, X = NH_2), 128191-80-0; **1a** · $6H_2O$ (L = DMAP), 128191-78-6; **1a** (L = DMAP), 128191-79-7; **4** (L = DMAP), 128191-81-1; **5** (L = DMAP), 128191-82-2.

[1] The following reaction enthalpies were calculated for the isomerization of **1** to **2** by using the MNDO and AM1 methods: for Y = COO and X = DMAP, −26.7 (MNDO) or −27.6 (AM1); for Y = COO and X = NH_3, −37.7 (MNDO) or −51.1 kcal mol^{-1} (AM1).

[2] R. Weiss, N. J. Salomon, G. E. Miess, R. Roth, *Angew. Chem. 98* (1986) 925; *Angew. Chem. Int. Ed. Engl. 25* (1986) 917.

[3] For further details, see R. Roth, *Dissertation*, Universität Erlangen-Nürnberg 1989.

[4] Colorless crystals, m.p. 170–173 °C (dec.). IR (Nujol): $\tilde{\nu}$ (cm^{-1}) = 3400 (br, m), 1650(sh), 1625(vs), 1570(m), 1210(m), 1190(m), 1070(w), 1030(w), 950(w), 930(w), 825(m), 780(w), 760(m). ^{13}C NMR (100.6 MHz, D_2O): δ = 41.06, 109.25, 138.65, 141.72, 157.62, 166.35.

[5] Crystal structure data for **1a** · $6H_2O$: M_r = 464.48, monoclinic, space group *C2/c*, *a* = 1773.5(7), *b* = 1479.7(5), *c* = 942.8(3) pm, β = 108.75(3)°, *V* = 2.3428 nm^3, *Z* = 4, ϱ_{calcd} = 1.32 g cm^{-3}, $Mo_{K\alpha}$ radiation (*T* = 293 K), graphite monochromator, Nicolet R3m/V diffractometer. 2310 unique reflections ($4 < 2\Theta < 52°$), 1290 with $F > 5\sigma(F)$ observed, 147 parameters refined. The structure was solved by direct methods (SHELXTL PLUS). Non-hydrogen atoms were refined anisotropically. Hydrogen atoms of the water molecules were not included, the other hydrogen atoms were incorporated using a rigid model. R = 0.072, R_w = 0.085 [$w^{-1} = \sigma^2(F) + 0.015\,F^2$]. Further details of the crystal structure investigation may be obtained from the Fachinformationszentrum Karlsruhe, Gesellschaft für wissenschaftlich-technische Information mbH, D-7514 Eggenstein-Leopoldshafen 2 (FRG), on quoting the depository number CSD-54565 the names of the authors, and the journal citation.

[6] W. G. Town, R. W. H. Small, *Acta Crystallogr. Sect. B 29* (1973) 1950.

[7] R. Taylor, O. Kennard, *J. Am. Chem. Soc. 104* (1982) 5063.

Phenyl-Linked Quinone-Substituted Porphyrin Trimers **

By *Jonathan L. Sessler** and *Vincent L. Capuano*

Long-distance photoinduced electron-transfer (ET) reactions have attracted considerable attention due to their importance in many biological processes as well as their significance in solar energy conversion devices.[1] Of notable interest are those ET reactions which occur upon photoexcitation of the bacterial photosynthetic reaction centers (RC's).[2] However, the complexity surrounding the reactive components in the RC's poses a significant challenge to the understanding of the mechanisms operating throughout the charge separation process.

While experiments performed on native RC's[2–4] and on model systems[5, 6] have helped to clarify those factors, such as distance, orientation, energetics, and medium, which control long-distance ET reactions, the unification of experiment with theory[7, 8] has proven problematic. A particular area of ambiguity concerns the role, if any, of the intermediate monomeric bacteriochlorophyll (BChl) in mediating the initial ET step from the photoexcited special pair (SP*) donor to the bacteriopheophytin (Bph) acceptor.[7] An attractive, but as yet experimentally unconfirmed, mechanism casts this BChl prosthetic group in the role of a "superexchange" mediator, facilitating the long-range (17-Å center-to-center) SP*-to-Bph ET process.[7–9]

Given the controversial nature of this hypothesis we have over the past few years sought to develop a series of acceptor-substituted porphyrin-type model systems which contain a variety of chromophores held in well-defined rigid arrangements. We have recently reported the synthesis and study of several elaborated quinone-substituted porphyrin dimers in which evidence for apparent porphyrin-based "superexchange"-mediated ET behavior was obtained.[6] More sophisticated systems, however, might allow for a further probing of this behavior as well as other related mechanistic questions. We have recently turned our attention, therefore, to the development of model systems containing more than two porphyrin subunits.

In this communication we wish to report the synthesis and photophysical properties of the bis-quinone phenyl-linked trimeric porphyrin **1**, which, to the best of our knowledge, represents the first acceptor-substituted porphyrin trimer.[10] In addition, we report the synthesis of the quinone-free control system **2**.[11]

The syntheses of the title compounds **1** and **2** are based on the condensation between the α-unsubstituted dipyrrylmethane **7** and the functionalized porphyrins **9** and **11**, respectively, using a modified procedure for formation of porphyrin trimers.[12] The central porphyrin is constructed in the final bond-forming sequence. The starting materials **7**, **9**, and **11** were prepared using modifications of methods which we and others have recently reported.[5, 6] Specifically, dipyrrylmethane **3** was prepared by the acid-catalyzed condensation of 4-(hydroxymethyl)benzaldehyde (introduced in the form of its diethyl acetal)[13] with ethyl 3-ethyl-4-methyl-2-pyrrolecarboxylate (75% yield) and was saponified and decarboxylated in boiling ethylene glycol to give **4** as a pale tan solid (m.p. 149–151 °C, 95% yield).[14] Compound **4** was

[*] Prof. J. L. Sessler, V. L. Capuano
Department of Chemistry, University of Texas at Austin
Austin, TX 78712 (USA)

[**] This work was supported by The Robert A. Welch Foundation, the Camille and Henry Dreyfus Foundation (Teacher-Scholar Award to *J.L.S.*), and The National Institutes of Health (GM 41657 to *J.L.S.*)

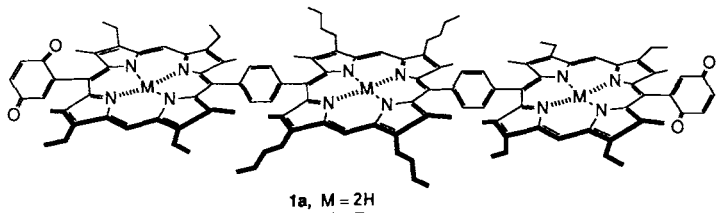

1a, M = 2H
1b, M = Zn

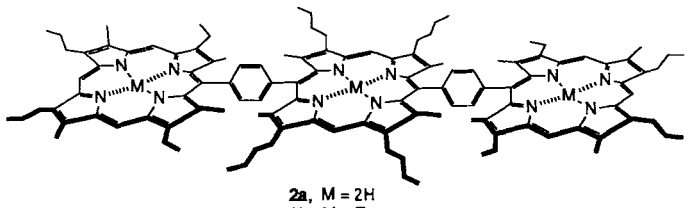

2a, M = 2H
2b, M = Zn

then condensed with the known di(formylpyrryl)methanes **5** and **6** under conditions of acid catalysis in THF/MeOH (2/1) to give the hydroxymethylphenyl-substituted porphyrin monomers **8** (λ_{max} ($CHCl_3$) = 410, 507, 540, 574, 625 nm)[14] and **10** (λ_{max} ($CHCl_3$) = 404, 502, 537, 571, 623 nm),[14] the direct precursors to **9** and **11**, in 50 and 55% yield, respectively, following *o*-chloranil oxidation and chromatographic purification (silica gel, 2% MeOH in $CHCl_3$). The key formylphenyl-substituted monomers **9** (λ_{max}($CHCl_3$) = 410, 507, 538, 572, 624 nm)[14] and **11** (λ_{max} ($CHCl_3$) = 407, 504, 539, 572, 624 nm)[14] were then obtained from **8** and **10** in almost quantitative yield as bright violet crystals following oxidation with pyridinium dichromate in CH_2Cl_2 and subsequent recrystallization from chloroform/hexanes.

The acid-catalyzed trimer-forming condensation between **11** and **7**, which gave, after *o*-chloranil oxidation, the control compound **2a**, was found to be highly sensitive to the reaction conditions, particularly to the choice of catalyst and reactant concentration. The best yields, roughly 50%, were obtained using reactant concentrations of exactly 1.0×10^{-2} M in CH_2Cl_2 with trifluoroacetic acid (10^{-3} M) as the acid catalyst. These conditions are quite similar to those recently reported by *Lindsey* for use in an optimized porphyrinogen-based tetraphenylporphyrin-forming procedure,[15] suggesting that in this case the critical yield-determining step also involves the formation of an intermediate porphyrinogen-like species. In fact, the use of dipyrrylmethanes and aryl aldehydes requires the formation of half the number of C–C bonds as the Lindsey procedure, which involves monomeric pyrroles.

Using the same conditions as above, the condensation of **9** and **7** gave the bis(hydroquinone methyl ether) trimer **12** (λ_{max}($CHCl_3$) = 409, 507, 541, 573, 625 nm)[14] in over 60% yield after chromatographic purification (silica gel, 2% MeOH in $CHCl_3$) and recrystallization ($CHCl_3$/hexanes). The conversion of **12** to the diquinone trimer **1a** (obtained as a pale burgundy solid[14]) was then accomplished in roughly 40% yield by deprotecting the methyl ethers with BI_3 in CH_2Cl_2[16] (to give **13**[14]) and subsequently oxidizing with dichlorodicyano-*p*-benzoquinone (DDQ) in CH_2Cl_2.

As is true for the 1,4-phenyl-linked dimers **16** and **17**,[6] the phenyl-linked trimers **1** and **2** show evidence for intersubunit excitonic interactions in the ground-state absorption spectra. In the case of the free-base systems **1a** (λ_{max}($CHCl_3$) = 415, 509, 535, 572, 626 nm) and **2a** (λ_{max}($CHCl_3$) = 412, 508, 538, 574, 624 nm), this is only apparent in terms of a slight broadening of the Soret band in the trimers as compared to monomeric, phenyl-substituted porphyrins (e.g., 5,15-diphenylporphyrin[17] (λ_{max}($CHCl_3$) = 408, 506, 541, 573, 624 nm)). However, in the case of the trizinc complexes **1b** and **2b** (obtained by treatment of **1a** and **2a** with excess $Zn(OAc)_2$ in MeOH/$CHCl_3$), which possess strong absorption bands, this excitonic coupling is manifest in terms of a significant bathochromic shifting of the Soret transition along with a dramatic splitting of the absorption into two equally intense peaks. On the basis of simple exciton theory calculations performed on these systems and earlier 1,4-phenyl-linked dimers,[18] such shifts can be readily explained in terms of a point dipole approximation.

The steady-state fluorescence spectrum of **1a** recorded in benzene solution shows substantial quenching relative to **2a** (λ_{max} = 630, 695 nm) upon irradiation at 410 nm. From quantitative analyses, the ratio of the emission intensities of

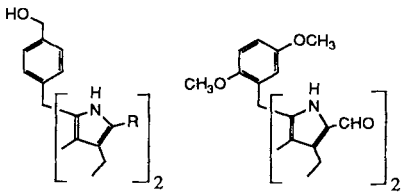

3, R = CO_2Et
4, R = H

5

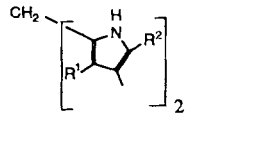

6, R^1 = $CH_2CH_2CH_3$, R^2 = CHO
7, R^1 = $CH_2CH_2CH_2CH_3$, R^2 = H

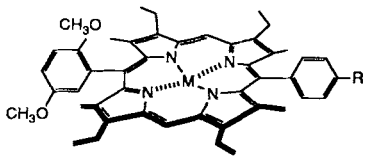

8, R = CH_2OH, M = 2H
9, R = CHO, M = 2H

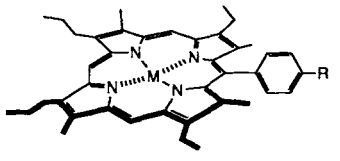

10, R = CH_2OH, M = 2H
11, R = CHO, M = 2H

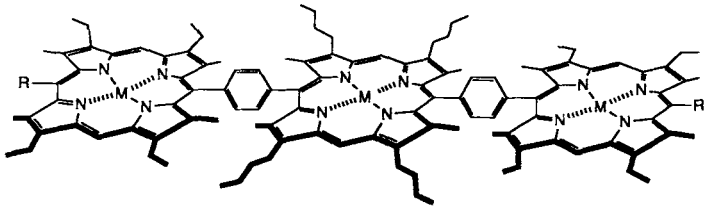

12, R = hqe, M = 2H
13, R = hq, M = 2H
1a, R = bq, M = 2H

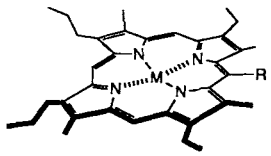

14, M = 2H, R = bq
15, M = 2H, R = hqe

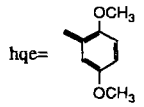

hqe=

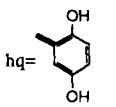

hq=

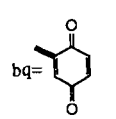

bq=

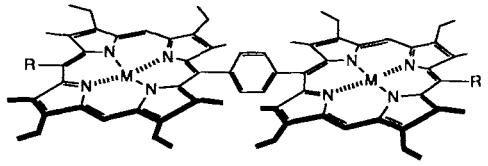

16, M = 2H, R = bq
17, M = 2H, R = hqe

1a and **2a** was found to be ≤ 0.02. This suggests that the various porphyrin excited states in **1a** are quenched by electron transfer to the quinone acceptors.[5, 6, 19] The excited singlet-state behavior of **1a** is thus very different from that of the simpler quinone-substituted monomeric and dimeric systems **14** and **16**, which show no detectable fluorescence ($\Phi_f < 10^{-5}$) when irradiated under identical conditions.[6] Therefore, the residual fluorescence observed for **1a** can be ascribed to the central porphyrin. However, the fluorescence quantum yield of **1a** ($\Phi_f \leq 0.002$[20]), although substantially higher than that of **14** and **16**, is still considerably reduced relative to the acceptor-free systems **2a**, **15**, and **17**. This indicates that the excited singlet state of the central porphyrin in **1a** is quenched by the presence of the distant "outer" quinones. This in turn indicates that a very efficient porphyrin-to-quinone electron-transfer process is occurring for the inner porphyrin subunit as well as for the outer two porphyrin components. From the measured fluorescence lifetime for the unsubstituted system **2a** (9.09 ns) and standard data analyses,[6c] a lower limit of $5 \times 10^9\ s^{-1}$ for the overall rate of ET from the porphyrin trimer **1a** to the quinones may be determined.[21]

The efficiency with which the net ET process in **1a** occurs over what is a distance nearly comparable to that found in the natural photosynthetic reaction centers, suggests that systems such as **1** and **2** may be well suited for studying long-range ET mechanisms in multicomponent systems. Accordingly, the syntheses of more elaborate analogues in which the acceptor is bound to only one terminus of the system and where metal cations are selectively complexed into two or fewer porphyrin subunits are currently under way.

Experimental Procedure

12: A 50-mL three-necked, round-bottomed flask equipped with an argon inlet, reflux condensor, and septum port was charged with **9** (212 mg, 0.295 mmol, 10^{-2}M), **7** (85 mg, 0.297 mmol, 10^{-2}M), and 30.0 mL of CH_2Cl_2. The solution was then bubbled with argon for 15 minutes. Trifluoroacetic acid (22.7 μL) was added via syringe and the reaction was allowed to stir in the dark for 3.5 h under a blanket of argon. *o*-Chloranil (109 mg, 0.449 mmol) was added and the reaction was placed in a preheated 40 °C oil bath and allowed to stir for an additional 3 h. Thin layer chromatography (2% MeOH/$CHCl_3$, silica gel) indicated the complete absence of the starting porphyrin aldehyde and the appearance of a new spot at lower R_f ascribed to the porphyrin trimer. The solvent was removed in vacuo and the trimeric porphyrin was purified by chromatography on silica gel (2% MeOH/$CHCl_3$, eluent) and recrystallization from $CHCl_3$/hexanes to yield 201 mg (0.0892 mmol, 60.4%) of **12** as a pale purple solid. UV-VIS ($CHCl_3$): λ_{max} (ε) = 409 (630 000), 507 (54 600), 541 (16 200), 573 (20 100), 625 (4010) nm). ^{1}H NMR (300 MHz, $CDCl_3$): $\delta = -1.84$ (3H, br. s, NH), $-1,47$) (3H, br. s, NH), 1,24 (12H, t, $J = 7.26$ Hz, $CH_2CH_2CH_2CH_3$), 1.86 (8H, m, $CH_2CH_2CH_2CH_3$), 1.93 (12H, t, J = 7.59 Hz, 12″,18″-CH_2CH_3), 1.96 (12H, t, J = 7.33 Hz, 2″,8″-CH_2CH_3), 2.37 (8H, m, $CH_2CH_2CH_2CH_3$), 2.68 (12H, s, 13″,17″-CH_3), 3.22 (12H, s, 3,7,13,17-CH_3), 3.23 (12H, s, 3″,7″-CH_3), 3.73 (6H, s, OCH_3), 3.89 (6H, s, OCH_3), 4.11 (16H, m, CH_2CH_3), 4.21 (8H, m, $CH_2CH_2CH_2CH_3$), 7.29 (6H, m, aryl), 8.17 (8H, dd, aryl), 10.34 (4H, s, 10″,20″-H), 10.47 (2H, s, 10,20-H). ^{13}C NMR (125 MHz, $CDCl_3$): δ = 13.64, 14.41, 17.33, 17.45, 17.69, 17.78, 20.02, 20.16, 23.61, 26.82, 35.72, 56.05, 56.12, 96.61, 97.34, 111.89, 113.68, 115.12, 117.89, 118.06, 120.25, 131.66, 133.30, 133.41, 133.47, 135.38, 135.74, 135.98, 140.77, 141.22, 143.37, 144.51, 144.56, 144.67, 145.55, 145.66, 146.04, 153.70, 153.93. MS (FAB, 79 eV): *m/z* 2255 ($M^{\oplus}$), 2118 ($M^{\oplus} - 137$).

1a: The protected dihydroquinone trimer **12** (50 mg, 0.022 mmol) was dissolved in 10 mL of freshly distilled CH_2Cl_2 and bubbled with Ar for 15 min. A freshly prepared solution of BI_3 (1.3 mL of a 0.81 M solution in CH_2Cl_2) was then added dropwise over 30 s at 0 °C. The reaction was allowed to stir in the dark at 0 °C for an additional 15 min. The vessel was then removed from the ice bath and allowed to warm to room temperature over the course of 30 min. The excess BI_3 was quenched with H_2O and the reaction neutralized with dilute ammonia and extracted with $CHCl_3$ (3 × 30 mL). The organic layer was separated and dried over Na_2SO_4 and the solvent was removed under reduced pressure to give a final volume of approximately 50 mL. DDQ (25 mg, 0.11 mmol) was added and the reaction stirred at room temperature, in the dark, for 2.5 h. The reaction mixture was washed with aqueous Na_2CO_3 and H_2O and dried over Na_2SO_4. The product **1a** was purified by column chromatography on silica gel (2% MeOH/$CHCl_3$) to yield 18 mg (0.0095 mmol, 43.2%). UV-VIS ($CHCl_3$): λ_{max} (ε) = 415 (501 000), 510 (41 700), 535 (13 000), 572 (16 800), 627 (5910) nm. ^{1}H NMR (300 MHz, $CDCl_3$): $\delta = -1.99$ (2H, s, NH), -1.88 (2H, s, NH), $-1,46$ (2H, s, NH), 1.28 (12H, t, $CH_2CH_2CH_2CH_3$), 1.88–1.97 (32H, m, 2,8,12,18-$CH_2CH_2CH_2CH_3$, 2″,8″,12″,18″-CH_2CH_3), 2.39 (8H, q, $CH_2CH_2CH_2CH_3$), 3.09 (24H, s, 3,7,13,17-CH_3, 3″,7″-CH_3), 3.17 (12H, s, 13″,17″-CH_3), 4.14–4.23 (24H, m, 2″,8″,12″,18″-CH_2CH_3, 2,8,12,18-$CH_2CH_2CH_2CH_3$), 7.34 (8H, dd, H_{phenyl}), 8.42 (6H, m, $H_{quinone}$), 10.39 (4H, s, 10″,20″-H_{phenyl}), 10.49 (2H, 10,20-$H_{quinone}$). ^{13}C NMR (125 MHz, $CDCl_3$): δ = 14.39, 16.37, 17.33, 17.49, 17.71, 20.04, 20.11, 23.60, 26.82, 29.70, 35.71, 97.23, 97.39, 110.23, 117.94, 119.28, 133.31, 133.38, 133.50, 135.92, 136.13, 137.17, 137.93, 139.53, 141.17, 141.33, 141.96, 142.26, 143.46, 144.67, 144.90, 145.71, 146.05, 187.34, 189.00. MS (FAB, 70 eV): *m/z* 1913 ($M^{\oplus}$ + 3), 1912 ($M^{\oplus}$ + 2), 1911 ($M^{\oplus}$ + 1).

Received: April 17, 1990;
supplemented: July 5, 1990 [Z 3918 IE]
German version: *Angew. Chem. 102* (1990) 1162

[1] M. A. Fox, M. Chanon (Eds.): *Photoinduced Electron Transfer*, Elsevier, Amsterdam 1988.

[2] a) R. A. Marcus, N. Sutin, *Biochim. Biophys. Acta 810* (1985) 265; b) M. W. Windsor, *J. Chem. Soc. Faraday Trans. 2 1986*, 2237; c) C. Kirmaier, D. Holten, *Photosynth. Res. 13* (1987) 225; d) G. Feher, J. P. Allen, M. Y. Okamura, D. C. Rees, *Nature (London) 339* (1989) 111; e) R. Huber, *Angew. Chem. 101* (1989) 849; *Angew. Chem. Int. Ed. Engl. 28* (1989) 848.

[3] a) J. Deisenhofer, O. Epp, K. Miki, R. Huber, H. Michel, *J. Mol. Biol. 180* (1984) 385; b) *Nature (London) 318* (1985) 618; c) C.-H. Chang, M. Schiffer, D. Tiede, U. Smith, J. Norris, *J. Mol. Biol. 186* (1985) 201; d) J. P. Allen, G. Feher, T. O. Yeates, H. Komiya, D. C. Rees, *Proc. Natl. Acad. Sci. USA 84* (1987) 5730, 6162.

[4] a) N. W. Woodbury, M. Becker, D. Middendorf, W. W. Parsons, *Biochemistry 24* (1985) 7516; b) J. Breton, J.-L. Martin, G. R. Fleming, J.-C. Lambry, *ibid. 27* (1988) 8276; c) R. A. Goldstein, L. Takiff, S. G. Boxer, *Biochim. Biophys. Acta 934* (1988) 253; d) M. R. Gunner, P. L. Dutton, *J. Am. Chem. Soc. 111* (1989) 3400; k) J. von Gersdorff, M. Huber, H. Schubert, D. Niethammer, B. Kirste, M. Plato, K. Möbius, H. Kurreck, R. Eichberger, R. Kietzmann, F. Willig, *Angew. Chem. 102* (1990) 690; *Angew. Chem. Int. Ed. Engl. 29* (1990) 670.

[5] a) J. R. Miller, T. L. Calcaterra, G. L. Closs, *J. Am. Chem. Soc. 106* (1984) 3047; b) Y. Sakata, S. Nishitani, N. Nishimizu, S. Misumi, A. R. McIntosh, J. R. Bolton, Y. Kanda, A. Karen, T. Okada, N. Mataga, *Tetrahedron Lett. 26* (1985) 5207; c) A. D. Joran, B. A. Leland, P. M. Felker, A. H. Zewail, J. J. Hopfield, P. B. Dervan, *Nature (London) 327* (1987) 508; d) M. R. Wasielewski, *Photochem. Photobiol. 47* (1988) 923; e) H. Oevering, J. W. Verhoeven, M. N. Paddon-Row, E. Costaris, N. S. Hush, *Chem. Phys. Lett. 143* (1988) 488; f) D. Gust, T. A. Moore, A. L. Moore, D. Barrett, L. O. Bensasson, M. Rougee, *J. Am. Chem. Soc. 110* (1988) 321; g) D. Mauzerall, J. Weiser, H. A. Staab, *Tetrahedron 45* (1989) 4807; h) M. D. Johnson, J. R. Miller, N. S. Green, G. L. Closs, *J. Phys.* (1989) 1173; i) A. Osuka, K. Maruyama, I. Yamazaki, N. Tamai, *Chem. Lett. 165* (1990) 392; j) H. Meier, Y. Kobuke, S.-i. Kugimiya, *J. Chem. Chem. Commun. 1989*, 923; k) J. von Gersdorff, M. Huber, H. Schubert, D. Niethammer, B. Kirste, M. Plato, K. Möbius, H. Kurreck, R. Eichberger, R. Kietzmann, F. Willig, *Angew. Chem. 102* (1990) 690; *Angew. Chem. Int. Ed. Engl. 29* (1990) 670.

[6] a) J. L. Sessler, M. R. Johnson, *Angew. Chem. 99* (1987) 679; *Angew. Chem. Int. Ed. Engl. 26* (1987) 678; b) J. L. Sessler, M. R. Johnson, T.-Y. Lin, S. E. Creager, *J. Am. Chem. Soc. 110* (1988) 3659; c) J. L. Sessler, M. R. Johnson, T.-Y. Lin, *Tetrahedron 45* (1989) 4767; d) J. L. Sessler, M. R. Johnson, S. E. Creager, J. Fettinger, J. A. Ibers, J. Rodriguez, C. Kirmaier, D. Holten in E. Riklis, (Ed.): *Photobiology: The Science ant its Applications*, Plenum, New York, in press.

[7] a) Y. Won, R. A. Friesner, *Biochim. Biophys. Acta 975* (1988) 9; b) *ibid. 977* (1989) 99.

[8] a) R. A. Marcus, *Chem. Phys. Lett. 133* (1987) 471; b) S. F. Fischer, P. O. Scherer, *J. Chem. Phys. 115* (1987) 151; c) S. Creughton, J. K. Hwang, A. Warshel, W. W. Parson, J. Norris, *Biochemistry 27* (1988) 774.

[9] a) M. Bixon, J. Jortner, M. E. Michel-Beyerle, A. Ogrodnik, W. Lersch, *Chem. Phys. Lett. 140* (1987) 626; b) M. E. Michel-Beyerle, M. Bixon, J. Jortner, *J. Chem. Phys. 115* (1988) 188; c) M. Plato, K. Mobius, M. E. Michel-Beyerle, M. Bixon, J. Jortner, *J. Am. Chem. Soc. 110* (1988) 7279; d) M. Bixon, J. Jortner, *Chem. Phys. 159* (1989) 17; e) S. G. Boxer, R. A. Goldstein, D. J. Lockhart, R. Middendorf, L. Takiff, *J. Phys. Chem. 93* (1989) 8280.

[10] First communicated at the *4th Int. Conf. Bioinorg. Chem.* (Boston, MA, USA 1989).

[11] Subsequent to the submission of this manuscript, the synthesis of an acceptor-free trimer analogous to **2** was reported: T. Nataga, A. Osuka, K. Maruyama, *J. Am. Chem. Soc. 112* (1990) 3054. For other reports of

acceptor-free oligomeric tetrapyrrolic systems see: A. Osuka, K. Matuyama, H. Tomita, *Chem. Lett. 1988*, 1243; A. Osuka, K. Maruyama, *J. Am. Chem. Soc. 110* (1988) 4454; S. Chardon-Noblat, J.-P. Sauvage, P. Mathis, *Angew. Chem. 101* (1989) 631; *Angew. Chem. Int. Ed. Engl. 28* (1989) 593; G. M. Dubowchik, A. D. Hamilton, *J. Chem. Soc. Chem. Commun. 1987*, 293; *ibid. 1986*, 665, 1391; L. R. Milgrom, *J. Chem. Soc. Perkin. Trans. 1 1983*, 2535.

[12] I. Abdalmuhdi, C. K. Chang, *J. Org. Chem. 50* (1985) 411.

[13] Prepared by the reduction of terephthaldehyde mono(diethyl acetal) with $LiAlH_4$ in THF.

[14] All new compounds gave ^1H NMR, ^{13}C NMR, and mass spectrometric data consistent with their proposed structure.

[15] a) J. S. Lindsey, R. W. Wagner, *J. Org. Chem. 54* (1989) 828; b) J. S. Lindsey, I. C. Schreiman, H. C. Hsu, P. C. Kearney, A. M. Marguerettaz, *J. Org. Chem. 52* (1987) 827.

[16] J. M. Lansinger, R. C. Ronald, *Synth. Commun. 9* (1979) 341.

[17] The diphenylporphyrin control compound 2,8,12,18-tetrabutyl-3,7,13,17-tetramethyl-5,15-diphenylporphyrin was prepared by the condensation of 7 with benzaldehyde [14].

[18] a) Y. Won, R. A. Friesner, M. R. Johnson, J. L. Sessler, *Photosynth. Res. 22* (1989) 201; b) J. Ha, R. A. Friesner, J. L. Sessler, unpublished results.

[19] Importantly, as expected on the basis of considerable prior work [1], at the concentrations employed (ca. 10^{-5} M) a 1:1 mixture of **2** and benzoquinone does not result in a significant quenching of the porphyrin fluorescence.

[20] Calculated relative to tetraphenylporphyrin ($\Phi_f = 0.11$).

[21] This result is supported by direct picosecond transient absorption studies: The lifetime of the excited singlet state for **1a** was found to be ≤ 75 ps, which represents the temporal resolution limit for our available apparatus. We thank *Stefan Hubig* and *Anthony Harriman* at the Center for Fast Kinetics Research (an NIH user-shared facility at the University of Texas) for assistance in carrying out these static and dynamic spectral experiments.

$[(Ph_3P)_2N]_2[Os_{18}Hg_2C_2(CO)_{42}]$ a Photochemically Generated High-Nuclearity Cluster Which Reversibly Incorporates Metallic Mercury into Its Metal Core**

By *Eleni Charalambous, Lutz H. Gade, Brian F. G. Johnson, Thomas Kotch, Alistair J. Lees, Jack Lewis,** and *Mary McPartlin**

The majority of studies into the photochemical properties of transition-metal cluster compounds have so far been conducted in the context of ligand activation or substitution in triatomic clusters,[1] while investigations of light-induced transformations of the metal core are comparatively rare.[2] Mixed-metal clusters incorporating transition or main-group metals with significantly different electronic properties to those of the principal core metal, and consequently containing polar metal–metal bonds, have intrinsic sites where bond cleavage may preferentially occur, either by chemical or photochemical means. The latter, in particular, would permit the generation of metal-frame structures which are inaccessible via conventional synthetic routes.

An ideal model system for the study of these anticipated properties of large mixed-metal clusters is the dianion $[Os_{18}Hg_3C_2(CO)_{42}]^{2\ominus}$ (**1**), which we recently reported along with a variety of other high-nuclearity Os-Hg clusters.[3] Cluster **1** contains a triangular Hg_3 subcluster, sandwiched by two tricapped-octahedral $Os_9C(CO)_{21}$ fragments and therefore clear-cut interfaces between different metallic domains. In the course of our investigation of the chemical reactivity of **1**, we have found that, when the deep purple solution of $[PPN]_2 \cdot$ **1** [PPN = $(Ph_3PNPPh_3)^{\oplus}$] was exposed to light, the compound underwent a clean photochemical conversion to an unknown burgundy red product **2**, which is markedly less deeply colored than **1**. Simultaneously, metallic mercury was generated and precipitated. The light-induced loss of Hg was confirmed by the negative-ion FAB mass spectrum (FAB = fast atom bombardment) of the product **2**, which displayed the same basic pattern as the spectrum of **1** but was shifted by $\Delta(m/z)$ 200 to lower mass.[4] The similarity of the IR absorption band patterns of **1** and **2** in the CO stretching region and the signal patterns in the ^{13}C NMR spectra of both compounds[5] suggested similar overall symmetries. The reaction product **2** was therefore formulated as $[Os_{18}Hg_2C_2(CO)_{42}]^{2\ominus}$, with a metal core consisting of an Hg_2 fragment fusing the two $Os_9C(CO)_{21}$ units already present in the starting material.[6]

In order to substantiate this proposal and to obtain detailed information about the structural environment of the two remaining Hg atoms, a single-crystal X-ray structure analysis of the PPN salt of **2** was carried out.[7] It revealed that the open Os_3 triangles of the $Os_9C(CO)_{21}$ units are staggered, with each of the two Hg atoms linking an edge of one triangle with the corner of the other, the two halves of the molecule being related by a crystallographic center of symmetry at the midpoint of the Hg–Hg vector (Fig. 1). The Hg–Hg distance of 2.744(5) Å is considerably shorter than

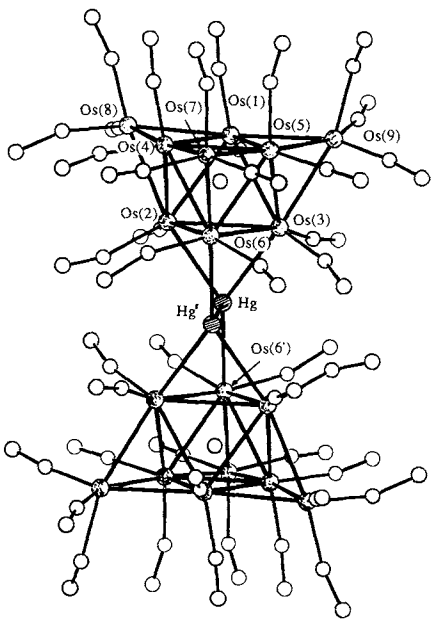

Fig. 1. Molecular structure of **1**. Principal bond distances [Å] (maximum standard deviation 0.005 Å): Os(1)-Os(2) 2.872, Os(1)-Os(3) 2.870, Os(1)-Os(4) 2.862, Os(1)-Os(5) 2.855, Os(1)-Os(8) 2.755, Os(1)-Os(9) 2.772, Os(2)-Os(3) 3.009, Os(2)-Os(4) 2.875, Os(2)-Os(6) 3.038, Os(2)-Os(8) 2.816, Os(3)-Os(5) 2.877, Os(3)-Os(6) 3.001, Os(3)-Os(9) 2.792, Os(4)-Os(5) 2.841, Os(4)-Os(6) 2.842, Os(4)-Os(7) 2.778, Os(4)-Os(8) 2.743, Os(5)-Os(6) 2.836, Os(5)-Os(7) 2.761, Os(5)-Os(9) 2.755, Os(6)-Os(7) 2.798, Os(2)-Hg 2.822, Os(3)-Hg 2.907, Os(6')-Hg 2.636, Hg-Hg' = 2.744(5).

[*] Prof. Lord J. Lewis, L. H. Gade, Dr. B. F. G. Johnson
University Chemical Laboratory
Lensfield Road, GB-Cambridge CB2 1EW (UK)
Prof. M. McPartlin, E. Charalambous
School of Chemistry, The Polytechnic of North London
Holloway Road, GB-London, N7 8DB (UK)
Prof. A. J. Lees, T. Kotch
Department of Chemistry, State University of New York
Binghamton, NY 13901 (USA)

[**] We acknowledge the award of an SERC studentship (*E. C.*) and an Foreign and Commonwealth Office (FCO) Kurt Hahn Scholarship (*L. H. G.*). *A. J. L.* thanks the donors of the Petroleum Research Fund for support of this research.

the mean Hg–Hg distance in the triangular mercury unit of **1** (2.918(5) Å), but comparable to that in the recently described $(Hg_3)^{4/3\oplus}$ clusters in $[Hg_3(dppm)_3(SO_4)_2]$ (d(Hg-Hg) = 2.764–2.802 Å, dppm = diphenylphosphinomethane)[8] or the mineral terlinguaite, $Hg_4Cl_2O_2$ (2.703 Å).[9] The Hg_2 fragment is embedded in the metal frame in a uniquely compact way in comparison to other examples of mixed-metal compounds containing Hg_2 units.[10]

The ^{13}C NMR spectrum of **2**, recorded at 295 K, has four sharp carbonyl resonances, which correspond to a higher symmetry (C_{3v}) with respect to a molecular axis through the centers of both Os units than that displayed in the solid-state structure. We attribute this to a fast rotation of the two Os_9 subclusters relative to each other on the NMR time scale in solution. This is not unexpected, since fluxional cores are commonly observed in high-nuclearity Os-Hg clusters.[11]

If, under exclusion of light, **2** is exposed to metallic mercury, thermal reinsertion of an Hg atom into the structure occurs, regenerating **1** almost quantitatively. This means that the photoreaction from **1** to **2** is thermally fully reversible.

The observed retention of sharp isosbestic points in a sequence of UV-VIS spectra, recorded after successive irradiation of the solution of **1** in CH_2Cl_2 with the 458-nm line of an Ar-ion laser, suggests that the photochemical Hg extrusion proceeds without interference from secondary photoprocesses (Fig. 2). The intensity of the absorption band

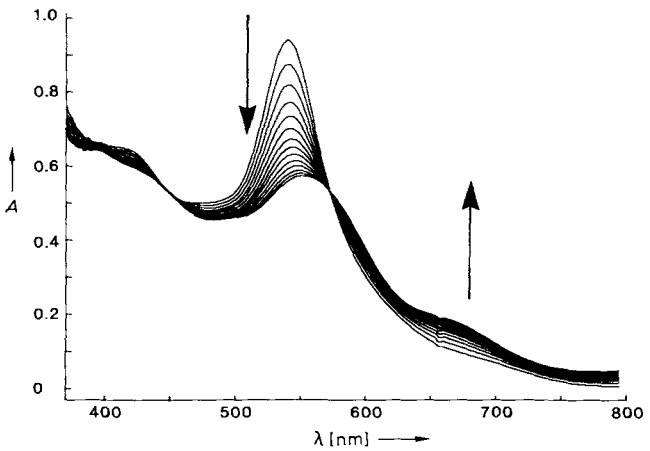

Fig. 2. UV spectra obtained after 458-nm photolysis (Ar-ion laser) of 2.15×10^{-5} M solutions of $[PPN]_2 \cdot$ **1** in deoxygenated CH_2Cl_2 at 20 °C. Spectra were recorded at irradiation intervals of 30 s. A = absorbance. The arrows indicate the direction of spectral change.

of the starting material at 540 nm ($\varepsilon = 4.38 \times 10^4$ L mol^{-1} cm^{-1}) decreases significantly during the reaction with a concomitant shift of the maximum by ca. 10 nm to longer wavelengths. The initial step in this reaction is thought to be a metal-to-metal charge-transfer (MMCT) transition, which is then followed by the extrusion of an Hg atom and subsequent rearrangement of the metal core. The low quantum efficiency of 0.004–0.005 for this process on irradiation in the range of 458–514 nm[12] is probably a consequence of the large number of nonreactive deactivation pathways for the cluster, but it may also reflect the efficiency of the thermal back-reaction that regenerates the starting material during the period of irradiation.

The dianions **1** and **2** can be oxidized by silver salts, yielding the corresponding radical monoanions $[Os_{18}Hg_3C_2(CO)_{42}]^{\ominus}$ (**3**) and $[Os_{18}Hg_2C_2(CO)_{42}]^{\ominus}$ (**4**), which are extremely air-sensitive and immediately regenerate the dianions when exposed to moist air.[5a] Both monoanions are related to each other by a set of similar photochemical Hg extrusion and thermal reinsertion reactions as found for **1** and **2**. Thus, the clusters **1**–**4** are part of a reversible redox and photochemical cycle (Fig. 3).

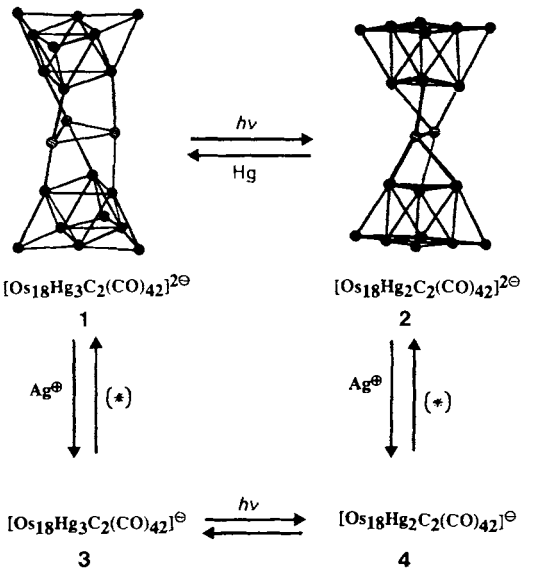

Fig. 3. The photo- and redox chemical cycle linking **1**–**4**. (*): standing in moist air.

Received: June 6, 1990 [Z 4001 IE]
German version: *Angew. Chem. 102* (1990) 1172

[1] a) M. A. Gallop, B. F. G. Johnson, J. Lewis, A. McCamley, R. N. Perutz, *J. Chem. Soc. Chem. Commun. 1988*, 1071; b) J. L. Graff, M. S. Wrighton, *Inorg. Chim. Acta 63* (1982) 63; c) J. Malito, S. Markiewicz, A. J. Poe, *Inorg. Chem. 21* (1982) 4335; d) J. G. Bentsen, M. S. Wrighton, *J. Am. Chem. Soc. 109* (1987) 4518; e) J. G. Bentsen, M. S. Wrighton, *ibid. 109* (1987) 4530; f) M. F. Desrosiers, D. A. Wink, R. Trautmann, A. E. Friedmann, P. C. Ford, *ibid. 108* (1986) 1917.

[2] H. Bantel, B. Hansert, A. K. Powell, M. Tasi, H. Vahrenkamp, *Angew. Chem. 101* (1989) 1084; *Angew. Chem. Int. Ed. Engl. 28* (1989) 1059.

[3] L. H. Gade, B. F. G. Johnson, J. Lewis, M. McPartlin, H. R. Powell, *J. Chem. Soc. Chem. Commun. 1990*, 110. The Ru analogue has also been synthesized and is under current investigation: see P. J. Bailey, B. F. G. Johnson, J. Lewis, M. McPartlin, H. R. Powell, *ibid. 1989*, 1513.

[4] The negative-ion FAB mass spectra of the salts of dianionic clusters display a characteristic peak pattern: dianion, monoanion, {dianion + cation}, and, in exceptional cases {dianion + 2 × cation}. For **1** and **2** the most abundant isotopomers for the cluster anions were found at: **1** dianion m/z 2615 (simulated 2615), monoanion m/z 5228 (simulated 5230), **2** dianion m/z 2514 (simulated 2514.5), monoanion m/z 5028 (simulated 5029).

[5] a) IR (CH_2Cl_2) [cm^{-1}]: **1**: $\tilde{\nu}$ = 2072 (m), 2057 (s), 2005 (s); **2**: 2064 (s), 2057 (vs), 2007 (s). **3**: $\tilde{\nu}$ = 2085 (m), 2072 (s), 2022 (s); **4**: $\tilde{\nu}$ = 2081 (s), 2073 (vs), 2022 (s). b) ^{13}C NMR (50% ^{13}C enriched Samples, CD_2Cl_2, 295 K): **1**: δ = 185.7 (6 CO), 184.9 (6 CO), 177.7 (12 CO, $^2J(^{199}Hg^{13}C)$ = 56 Hz), 175.6 (18 CO, the carbonyls on the Os(CO)$_3$ vertices are equivalent on the NMR time scale at 295 K) **2**: δ = 185.8 (6 CO), 185.7 (6 CO), 179.7 (12 CO, $^2J(^{199}Hg^{13}C)$ not resolved), 176.0 (18 CO), 411 (interstitial carbide).

[6] *Experimental Procedure*: A stirred solution of $[PPN]_2 \cdot$ **1** (50 mg, 0.0082 mmol) in CH_2Cl_2 was irradiated with a 250-W tungsten lamp, the reaction vessel being cooled externally with water. After ca. 10 min, precipitation of metallic mercury was observed and the reaction was complete after 40–50 min as judged by IR spectroscopy. During this time, the color of the solution changes from deep purple to a much less intense burgundy red. After separation of the mercury by filtration, the solvent volume was reduced to 20 mL and the product crystallized by slow vapor diffusion with diethyl ether. Black crystals, yield 45.5 mg (92%).

[7] Crystal data for $[PPN]_2 \cdot 2$: ($C_{116}H_{60}O_{42}Hg_2N_2Os_{18}P_4$) triclinic, space group $P\bar{1}$ (No. 2), $a = 18.711(4)$, $b = 16.379(3)$, $c = 11.724(2)$ Å, $\alpha = 111.242(2)$, $\beta = 84.284(1)$, $\gamma = 105.994(2)°$, $M = 6102.41$, $V = 3220.08$ Å^3, $Z = 1$, $\varrho_{calcd} = 3.147$ g cm^{-3}, $F(000) = 2694$, $R = 0.0938$ for 3537 reflections with $I/\sigma(I) > 3.0$ corrected for absorption [$\mu(Mo_{K\alpha}) = 201.6$ cm^{-1}]. The only crystals which could be obtained diffracted rather weakly due to marked disorder of the [PPN] counterions. Relatively high thermal parameters for Os(9) and Hg appear to be due to slight disorder of the cluster dianion, which could not be resolved. Nonetheless, the structural features of the cluster are well established. Further details of the crystal structure investigations are available on request from the Director of the Cambridge Crystallographic Data Centre, University Chemical Laboratory, Lensfield Road, Cambridge CB2 1EW (UK), on quoting the full journal citation.

[8] B. Hämmerle, E. P. Müller, D. L. Wilkinson, G. Müller, P. Peringer, *J. Chem. Soc. Chem. Commun. 1989*, 1527.

[9] K. Brodersen, G. Göbel, G. Liehr, *Z. Anorg. Allg. Chem. 575* (1989) 145.

[10] a) C. A. Ghilardini, S. Midollini, S. Moneti, *J. Chem. Soc. Chem. Commun. 1981*, 865; b) A. Albinati, A. Moor, P. S. Pregosin, L. M. Venanzi, *J. Am. Chem. Soc. 104* (1982) 7672.

[11] L. H. Gade, B. F. G. Johnson, J. Lewis, unpublished results.

[12] L. H. Gade, B. F. G. Johnson, T. Kotch, A. J. Lees, J. Lewis, publication in preparation.

Selective Deamidation of Peptide Amides**

By *Dörte Steinke* and *Maria-Regina Kula**

The choice of protecting groups is crucial in the synthesis of peptides.[1, 2] The selective removal of certain protecting groups is often desirable, but difficult to realize. For example, the selective cleavage of the amide bond of peptide amides has not yet been accomplished without at least partial hydrolysis of the chemically similar peptide bonds. For this reason, the amide function has found little use as a C-terminal protecting group in peptide synthesis, even though it offers several advantages, including a lower pK_i value than for the corresponding free amino acids, increased solubility of the peptide, and good chemical stability. We have now isolated and characterized an enzyme which can be used to hydrolyze peptide amides of apparently any length to give peptides having a free C terminus without cleavage of peptide bonds. A highly selective C-terminal deprotection is thus possible (Scheme 1).

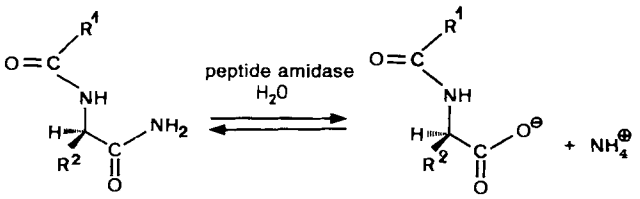

Scheme 1. Amide cleavage by the peptide amidase. R^1 = amino acid residue, peptide residue, or N-terminal protecting group of an amino acid amide. R^2 = side chain of an amino acid.

[*] Prof. Dr. M.-R. Kula, Dipl.-Biol. D. Steinke
Institut für Enzymtechnologie der Universität Düsseldorf
Forschungszentrum Jülich
Postfach 2050, D-5170 Jülich (FRG)

[**] This work was supported by the Bundesministerium für Forschung und Technologie (project No. 031 900 713) and by Degussa AG. We thank Dr. *Drauz* (Degussa AG) and Dr. *Berndt* (Deutsches Wollforschungsinstitut, Aachen) for providing substrates.

The peptide amidase was isolated and characterized from the flavedo of oranges. The pH dependence of the enzymatic hydrolysis of Z-Gly-Tyr-NH_2, for example, is shown in Figure 1. The broad pH optimum from pH 6.8 to 8.4, as well as the broad range of substrates (see Table 1), makes the enzyme universally applicable. The peptide amidase accepts both N-terminal protected peptides and peptides with a free N terminus as substrates. The side chains of the C-terminal amino acids appear to be of secondary importance. Of the forty peptide amides so far investigated, only those with C-terminal D-amino acids were not converted by the peptide amidase. Table 1 lists a selection of substrates employed.

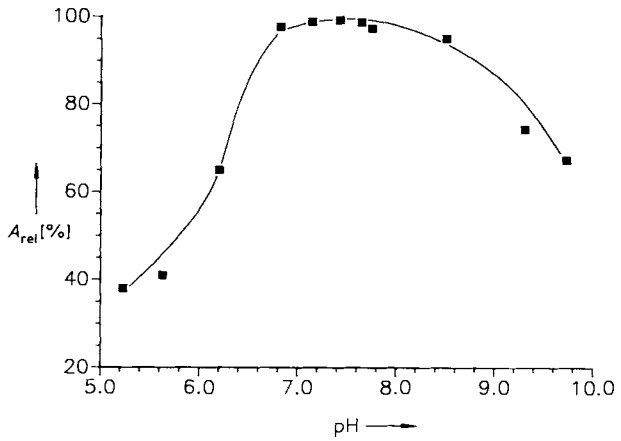

Fig. 1. The pH dependence of the enzymatic deamidation of Z-Gly-Tyr-NH_2. Reaction conditions: 10 mM Z-Gly-Tyr-NH_2, 50 mM Na citrate, Na phosphate, or Na carbonate buffer, 40 μg mL^{-1} peptide amidase, 30 °C. A_{rel} = relative activity of the peptide amidase.

The enzyme is therefore markedly nonspecific with respect to the amino acid side chains of the peptide, and its stereose-

Table 1. Substrate spectrum of the peptide amidase.

Substrate [a]	Conversion [%] after 6 h	Separation conditions TBA [b]/acetonitrile	Retention time Amide	Retention time Acid
Ac-Trp-NH_2	100	65/35	3.30	4.0
Bz-Arg-NH_2	100	90/10	3.5	6.8
Bz-Tyr-NH_2	100	60/40	9.24	21.2
H-Val-Phe-NH_2	100	80/20	11.54	27.3
H-Asp-Phe-NH_2	100	80/20	12.12	12.9
H-Ala-Phe-NH_2	100	80/20	4.8	8.1
H-Arg-Met-NH_2	100	80/20	6.7	5.4
H-Phe-Leu-NH_2	100	80/20	17.5	22.1
Z-Gly-Tyr-NH_2	100	65/35	4.16	5.16
Bz-Tyr-Thr-NH_2	100	60/40	3.15	3.56
Bz-Tyr-Ser-NH_2	100	60/40	2.99	3.35
Bz-Tyr-Ala-NH_2	100	60/40	3.33	4.0
Boc-Leu-Val-NH_2	20	60/40	7.1	11.4
Trt-Gly-Leu-Val-NH_2	80	80/20	3.6	10.6
Z-Pro-Leu-Gly-NH_2	100	60/40	4.9	6.3
Z-Gly-Gly-Leu-NH_2	100	60/40	3.9	5.0
H-Gly-D-Phe-Tyr-NH_2	100	80/20	6.9	13.7
H-Gly-Phe-D-Phe-NH_2	0 [c]	80/20	7.3	11.4
H-Arg-Pro-D-Ala-NH_2	0 [c]	99/1	2.4	
Z-Arg-Arg-*p*Na	0 [c]			

[a] The substrates were supplied by Bachem, Heidelberg, or by Dr. *Drauz* or Dr. *Berndt*. [b] TBA = $Bu_4N(HSO_4)$. [c] No conversion in 12 h (no decrease in the area of the amide peak). Ac = acetyl, Bz = benzoyl, Boc = *tert*-butyloxycarbonyl, Z = benzyloxycarbonyl, *p*Na = *para*-nitroanilide, Trt = trityl. Unless otherwise indicated, the amino acids had L configuration (2*S*-amino acids).

lectivity appears to be restricted to the C-terminal amino acid: the substrate H-Gly-D-Phe-Tyr-NH_2 is deamidated, whereas H-Gly-Phe-D-Phe-NH_2 and H-Arg-Pro-D-Ala-NH_2 do not react.

Amino acid amides with free α-amino groups are not hydrolyzed, whereas N-protected amino acid amides are accepted as substrates (see the first three entries in Table 1). Substituted amides, such as peptide anilides, which are frequently used in analysis of proteases, are not cleaved.

The enzyme can be readily used in enzymatic peptide syntheses, since it does not cleave the amino acid amides preferentially used as nucleophiles.[1, 3, 4] Therefore, these are always available for reaction, whereas the resulting peptide amide is deamidated. Thus, a peptide synthesis with simultaneous deamidation of the product is possible.[5]

When amino acid amides are used instead of esters as nucleophiles in enzymatic peptide syntheses, a much lower excess of nucleophile is required,[2] thereby facilitating workup of the peptide. For some carboxypeptidases, amides are obligatory substrates as nucleophiles for peptide synthesis.[6]

Because of the poor solubility of many peptide substrates in water, the effect of water-miscible organic solvents on the stability of the peptide amidase was investigated. The results are shown in Figure 2. The least loss of activity was observed

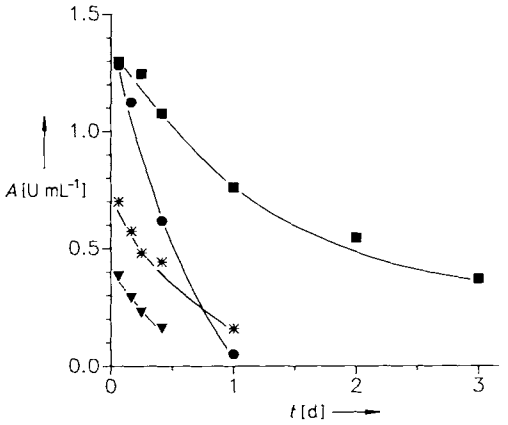

Fig. 2. Effect of organic solvents on the stability of the peptide amidase. Reaction conditions: 40 μg mL^{-1} enzyme was preincubated at 30 °C in 50 mM Tris buffer (pH 7.5) containing 30% organic solvent. The reaction was started at $t = 0$ by addition of substrate (Z-Gly-Tyr-NH_2). In the corresponding control (enzyme in 50 mM Tris/HCl, pH 7.5, without organic solvent), the activity remained unchanged. ■ = DMF, ● = acetone, * = ethanol, ▼ = acetonitrile.

with dimethylformamide (DMF): after three days of incubation in DMF/H_2O (30/70) at 30 °C, 30% of the original activity was still present.

Experimental Procedure

The enzyme preparation was obtained from the flavedo of oranges, that is, from the outermost colored layer of the peel, by a two-step purification involving fractionating salt precipitation and ion exchange chromatography. The peptide amidase had an activity of 2 to 100 U mg^{-1}, depending on the substrate, whereby an activity of 1 U corresponds to the formation of 1 μmol of product per minute at 30 °C and pH 7.5. Unless otherwise stated, 10–50 mM peptide amide in 50 mM Tris/HCl buffer at pH 7.5 was treated with 20–40 μg mL^{-1} of the peptide amidase. The determination and quantification of the peptide was accomplished by HPLC on an RP-18 column, which was eluted isocratically with various compositions of TBA/acetonitrile at a rate of 1.0 mL min^{-1}. The UV detector was set to the absorption maximum of the respective substrate. The eluent compositions are given in Table 1. In all experiments, only one new peak was observed in the chromatogram; its area remained unchanged even after 24–48 h of incubation and its retention time was identical with that of a reference sample (if available). The following reference substances, obtained from Bachem, Heidelberg, were used for product identification: Ac-Trp-OH, Bz-Arg-OH, Z-Gly-Tyr-OH, H-Asp-Phe-OH, H-Ala-Phe-OH, H-Arg-Met-OH, H-Val-Phe-OH, Z-Pro-Leu-Gly-OH, Z-Gly-Gly-Leu-OH, and H-Gly-Phe-Phe-OH.

Received: July 17, 1990 [Z 4071 IE]
German version: *Angew. Chem. 102* (1990) 1204

[1] V. Kasche, *Enzyme Microb. Technol. 8* (1986) 4–15.
[2] A. Schwarz, D. Steinke, M.-R. Kula, C. Wandrey, *Biotechnol. Appl. Biochem. 12* (1990) 188–195.
[3] H. D. Jakubke in S. Udenfriend, J. Meienhofer (Eds.): *The Peptides, Analysis, Synthesis, Biology*, Academic Press, London 1987, pp. 103–165.
[4] T. Oka, K. Morihara, *J. Biochem. 82* (1977) 1055–1062.
[5] D. Steinke, M.-R. Kula, A. Schwarz, C. Wandrey: *Peptidamidase und deren Verwendung*, Patentanmeldung P 4014 564.6-41.
[6] D. Steinke, M.-R. Kula, *Enzyme Microb. Technol.*, in press.

Novel Bonding Mode for a Cyanometalate Ligand: Synthesis and Crystal Structure of the Mn_4Pd_4 Cluster $[(OC)Pd(\mu\text{-}NC)Mn(\eta\text{-}C_5H_4Me)(CO)_2]_4$ Containing an Orthogonal Arrangement of Helical Units**

By *Pierre Braunstein,* Benoît Oswald, Antonio Tiripicchio,* and *Marisa Tiripicchio Camellini*

Cyanide complexes attract increasing interest in synthetic and physical chemistry owing to the ability of the cyanide ligand to link different organometallic units, to stabilize unusual electron counts and mixed-valence systems, to act as a charge-transfer mediator,[1] and to form catalytically active transition-metal complexes.[2] The fact that the cyanide ligand is isosteric with CO has also made it a model for CO chemistry,[3] though it is a poorer π acceptor and better σ donor than CO. Although the donor strength of the cyanide ion is the dominant property of this ligand in $[Cp'Mn(CN)(CO)_2]^{\ominus}$ ($\mathbf{1}^{\ominus}$, Cp' = η-C_5H_4Me), the title complex represents the first example of a polynuclear complex displaying both direct metal–metal bonding and M–CN–M' bridge formation, which result in a novel molecular architecture.

Here we compare the reactivity of $\mathbf{1}^{\ominus}$ [5] with that of the isosteric[6] anion $[CpMo(CO)_3]^{\ominus}$ ($\mathbf{2}^{\ominus}$) towards palladium complexes. The reaction of *trans*-$[PdCl_2(PPh_3)_2]$ with two equivalents of Na · **1** (THF, 0.5 h, 25 °C) led to chloride substitution and formation of the red-violet complex *trans*-$[Pd\{(\mu\text{-}NC)Mn(CO)_2Cp'\}_2(PPh_3)_2]$ (**3**) in 89% yield.

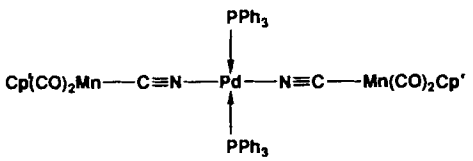

3

[*] Dr. P. Braunstein, B. Oswald
Laboratoire de Chimie de Coordination, URA 416 CNRS
Université Louis Pasteur
4 rue Blaise Pascal, F-67070 Strasbourg Cédex (France)
Prof. A. Tiripicchio, Prof. M. Tiripicchio Camellini
Istituto di Chimica Generale ed Inorganica
Università di Parma
Centro di Studio per la Strutturistica Diffrattometrica del CNR
Viale delle Scienze, I-43100 Parma (Italy)

[**] Financial support from the CNRS (Paris) and the Commission of the European Communities (Contract No. ST2J-0347-C) is gratefully acknowledged.

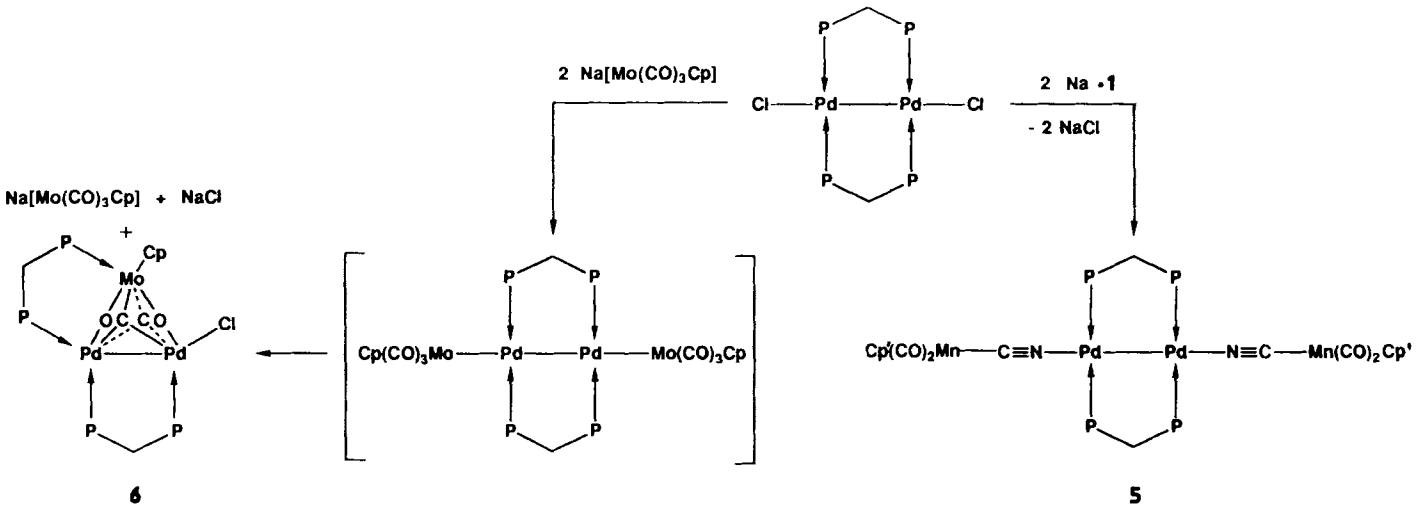

Scheme 1.

Under similar conditions, Na · **2** afforded the planar cluster $[Pd_2Mo_2Cp_2(CO)_6(PPh_3)_2]$ (**4**), in which the metal atoms form two edge-sharing triangles and Pd^{II} has been reduced to Pd^{I}.[6] This difference is steric in origin, since the *trans*-Mo–Pd–Pd–Mo chain structure is not stable when two PR_3 ligands are bonded to Pd.[6]

The reaction of the Pd^{I}–Pd^{I} dinuclear complex $[Pd_2Cl_2(\mu\text{-}CO)(PPh_3)_3]$ with $\mathbf{1}^{\ominus}$ (toluene, 5 h, 0 to 25 °C) led to disproportionation to **3** (44% yield) and Pd metal, but reaction with $\mathbf{2}^{\ominus}$ gave **4**.[7] The reasons for the instability of the primary reaction product resulting from simple substitution of the chloride ligand by $\mathbf{1}^{\ominus}$ or $\mathbf{2}^{\ominus}$ must be electronic in the first case and again steric in the second since one Pd–Mo bond would be *cis* with respect to the two PPh_3 ligands.

The dppm-stabilized dinuclear complex $[Pd_2(\mu\text{-}dppm)_2Cl_2]$ (dppm = $Ph_2PCH_2PPh_2$) reacted with two equivalents of $\mathbf{1}^{\ominus}$ (THF, 1 h, 25 °C) to form the stable eight-atom chain complex $[Pd_2(\mu\text{-}dppm)_2\{(\mu\text{-}NC)Mn(CO)_2Cp'\}_2]$ (**5**) in 91% yield (Scheme 1). The spectroscopic data for **5** are consistent with the symmetrical structure shown: the singlet observed in the $^{31}P\{^1H\}$ NMR spectrum has a chemical shift of $\delta = -5.33$, similar to that of other $[Pd_2(\mu\text{-}dppm)_2X_2]$ complexes,[8] and the IR $\tilde{\nu}$(CN) and $\tilde{\nu}$(CO) absorptions are, as in **3**, similar to those observed when this or analogous fragments are bonded through nitrogen to a metal center.[1,4] In a formal sense, **3** and **5** may also be viewed as "isocyano" Pd complexes[9] stabilized by the 16-electron fragment $Cp'Mn(CO)_2$. In contrast, $\mathbf{2}^{\ominus}$ reacted with $[Pd_2(\mu\text{-}dppm)_2Cl_2]$ to give the *triangulo* cluster $[Pd_2MoClCp(CO)_2(\mu\text{-}dppm)_2]$ (**6**), formed by phosphorus migration from Pd to an adjacent Mo atom in the sterically crowded and therefore unstable Mo–Pd–Pd–Mo intermediate chain complex $[Pd_2(\mu\text{-}dppm)_2\{Mo(CO)_3Cp\}_2]$[10] (Scheme 1).

The tetranuclear Pd^{I} complex $[Pd_4(CO)_4(OAc)_4](AcOH)_2$ reacted quantitatively with four equivalents of Na · **1** (toluene, 3 h, −40 to 25 °C) to form a deep violet solution of the new, air-stable cluster **7** ("Mn_4Pd_4"). The structure of the ethanol solvate **7** · C_2H_5OH has been fully elucidated by an X-ray study.[11] Neglecting the Cp' ligands, this cluster has approximate S_4 symmetry. It consists of two nearly orthogonal, bent Mn–Pd–Pd–Mn metal chains, *s-trans* connected by four Mn–(μ-CN)–Pd bridges (Figs. 1 and 2). A terminal CO completes the approximately square-planar coordination of each Pd atom. One of the Mn-bound CO ligands is semibridging, as indicated by the rather short contact with the Pd atom (Pd–C distances in the range 2.35(3)–2.41(3) Å) and by the slightly bent Mn–C–O angle (in the range 162(3)–165(3)°). Of note is that each μ-CN ligand also makes short contacts with a Pd atom in the neighboring Mn–Pd–Pd–Mn chain: the Pd–C distances are in the range 2.49(2)–2.56(3) Å, while the corresponding Pd–N distances (3.09(2)–3.14(2) Å) are in a range consistent with the weak interactions between the filled π orbitals of the nitrile functions and the empty 5p orbitals of the palladium atoms.[13]

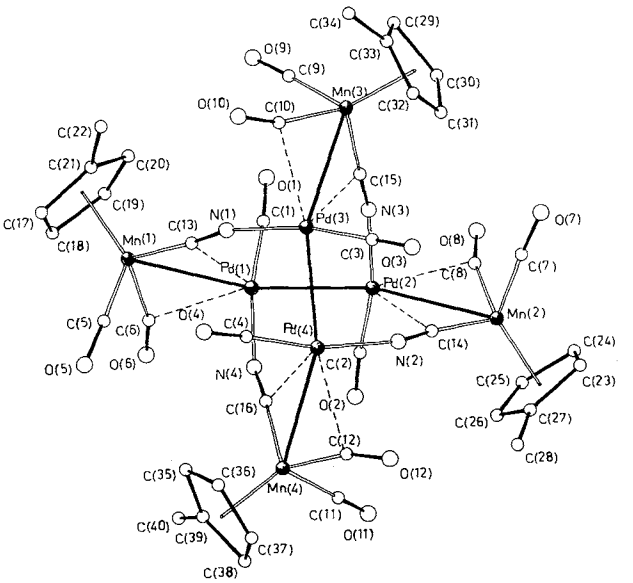

Fig. 1. View of the molecular structure of **7**. Selected bond distances [Å] and angles [°]: Pd(1)-Pd(2) 2.591(3), Pd(3)-Pd(4) 2.612(3), Pd(1)-Mn(1) 2.791(4), Pd(2)-Mn(2) 2.810(4), Pd(3)-Mn(3) 2.788(5), Pd(4)-Mn(4) 2.800(5), Pd(1)-C(1) 1.78(4), Pd(1)-C(6) 2.39(2), Pd(1)-C(13) 2.49(2), Pd(1)-N(4) 2.05(3), Pd(2)-C(2) 1.82(3), Pd(2)-C(8) 2.35(3), Pd(2)-C(14) 2.50(3), Pd(2)-N(3) 2.01(2), Pd(3)-C(3) 1.81(3), Pd(3)-C(10) 2.38(2), Pd(3)-C(15) 2.56(3), Pd(3)-N(1) 2.06(2), Pd(4)-C(4) 1.87(2), Pd(4)-C(12) 2.41(3), Pd(4)-C(16) 2.52(3), Pd(4)-N(2) 2.05(2), Mn(1)-C(13) 1.90(3), Mn(2)-C(14) 1.93(3), Mn(3)-C(15) 1.97(2), Mn(4)-C(16) 1.97(3), C(13)-N(1) 1.18(3), C(14)-N(2) 1.16(3), C(15)-N(3) 1.15(3), C(16)-N(4) 1.12(4); Mn(1)-Pd(1)-Pd(2) 161.6(2), Pd(1)-Pd(2)-Mn(2) 161.1(2), Mn(3)-Pd(3)-Pd(4) 153.3(2), Pd(3)-Pd(4)-Mn(4) 154.9(2), Pd(1)-Mn(1)-C(13) 60.5(7), Pd(2)-Mn(2)-C(14) 60.3(7), Pd(3)-Mn(3)-C(15) 62.3(8), Pd(4)-Mn(4)-C(16) 61.0(8), Mn(1)-C(13)-N(1) 173(2), C(13)-N(1)-Pd(3) 160(2), Mn(2)-C(14)-N(2) 173(2), C(14)-N(2)-Pd(4) 161(2), Mn(3)-C(15)-N(3) 175(2), C(15)-N(3)-Pd(2) 164(2), Mn(4)-C(16)-N(4) 173(2), C(16)-N(4)-Pd(1) 162(2).

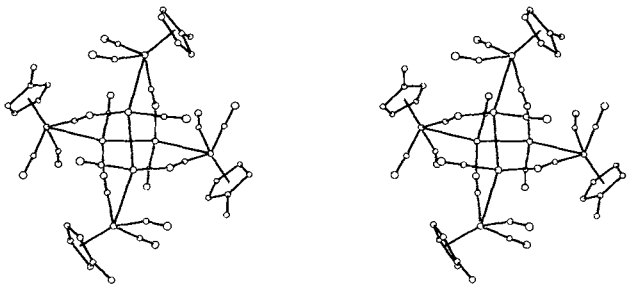

Fig. 2. Stereoview of the structure of 7.

No redox reaction has occurred in the course of the synthesis, and it could be considered that $1^{\ominus}$ has formally replaced an acetate ligand of the precursor complex, thus acting as an overall four-electron donor ligand. Of note is that the Pd_4 core of **7** contains two short metal–metal bonds (2.591(3) and 2.612(3) Å), as in the rectangular, 60-electron, Pd^I clusters $[Pd_4(CO)_4(OAc)_4]$ (2.663(1) Å) and $[Pd_4(\mu\text{-}Cl)_2(\mu\text{-dppm})_4](PF_6)_2$ (2.594(2) Å).[14] The topology of the $Pd_4Mn_4(CN)_4$ core is that of a tetrahedron, which is colored (the Pd–Pd edges are different from the Pd–Mn–CN–Pd ones) and oriented (through the Mn–CN–Pd vector) (Fig. 3).[15] The structure may be viewed as formed by two helices of opposite chirality whose axes are orthogonal, thus resulting in an overall *meso* structure.[16] The shape is largely

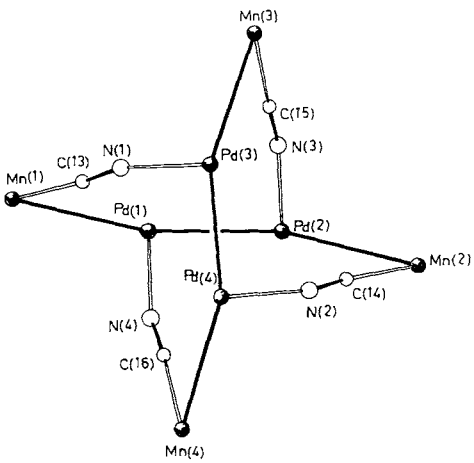

Fig. 3. Top: Core structure of 7 showing the Pd(1)N(4)C(16)Mn(4)Pd(4)Pd(3)-Mn(3)C(15)N(3)Pd(2) and Pd(3)N(1)C(13)Mn(1)Pd(1)Pd(2)Mn(2)C(14)N(2)Pd(4) *M* and *P* whorls of helices whose axes are orthogonal to each other, resulting in a *meso* arrangement [21]. Bottom: Schematic drawing of the structure.

controlled by the coordination geometry about the metals, in particular with $Pd–Mn–C_{cyanide}$ angles ranging from 60.3(7) to 62.3(8)°. Cluster **7** remained the only product observed when the stoichiometry of the reaction was changed, thus providing an interesting example of molecular self-assembly.

The Pd-bound CO ligands of **7** (Pd^I) are readily displaced by, for example, PPh_3, resulting in quantitative disproportionation to **3** (Pd^{II}) and Pd^0. The reaction of $[Pd_4(CO)_4(OAc)_4]\cdot(AcOH)_2$ with $2^{\ominus}$ was recently shown[17] to afford the anionic cluster $[Pd_4\{MoCp(CO)_3\}_4]^{2\ominus}$, in which each $MoCp(CO)_3$ fragment bridges a Pd–Pd edge of the central Pd_4 square in a manner similar to that encountered in **4**.[6] The latter reaction occurs with formal reduction of Pd^I to $Pd^{1/2}$. Whereas the ability of $[CpMo(CO)_3]^{\ominus}$ to act as a bridging metallo ligand is now well documented,[18] the first examples of $1^{\ominus}$ acting as a bridging ligand via the N atom have only recently been reported.[4b]

Reactions with $1^{\ominus}$ afford di-, tri-, and tetranuclear mixed-metal complexes, in which the metals are only linked by M–(μ-NC)–Mn bridges (CN-centered donor ability), and the octanuclear title cluster, the first cyanometalate complex with additional metal–metal interactions. Whereas most of the electron density in $1^{\ominus}$ is localized on the nitrogen atom, sufficient electron density must remain at the metal for further metal–metal bonding. These results provide an interesting contrast with the bonding behavior of $2^{\ominus}$, where metal–metal bond formation is usual (metal-centered donor ability) and M–(μ-OC)–Mo bridge formation much less common.[19] It is noteworthy that the metal-centered basicity of $CpCo(CO)_2$ was recently found to account for the formation of the Lewis acid–base complexes $[Cp(OC)_2Co \rightarrow HgX_2]$, whereas, with the stronger base $[CpCo(CN)(CO)]^{\ominus}$, the corresponding complex is unstable with respect to further electron transfer and elemental mercury is formed.[20]

Experimental Procedure

Reactions were performed under purified nitrogen, using standard Schlenk-type techniques. All compounds have been fully characterized by elemental analysis and spectroscopy. Unless otherwise noted, IR spectra were measured (Bruker IFS 66 spectrometer) in CH_2Cl_2 and ^1H and $^{31}P\{^1H\}$ NMR spectra in C_6D_6 (δ values in ppm relative to TMS) and THF/C_6D_6 (δ values in ppm relative to external H_3PO_4), respectively. Selected data: **3**: deep red crystals. IR: $\tilde{\nu}$(CN) = 2074 s, $\tilde{\nu}$(CO) = 1918 vs, 1865 vs cm^{-1}. IR (Nujol): $\tilde{\nu}$(CN) = 2070 vs, $\tilde{\nu}$(CO) = 1918 vs, 1909 vs, 1849 vs, br cm^{-1}. ^1H NMR: δ = 7.83–7.11 (m, 30H, C_6H_5), 3.71–3.66 (m, 8H, CH_3-C_5H_4), 1.54 (*s*, 6H, CH_3-C_5H_4). $^{31}P\{^1H\}$ NMR: δ = 19.17 (s). **5**: IR: $\tilde{\nu}$(CN) = 2067 s, $\tilde{\nu}$(CO) = 1913 vs, 1846 vs cm^{-1}. IR (Nujol): $\tilde{\nu}$(CN) = 2075 vs, $\tilde{\nu}$(CO) = 1916 vs, 1905 vs, 1834 vs cm^{-1}. ^1H NMR: δ = 7.43–7.07 (m, 40H, C_6H_5), 4.26–3.66 (m, 8H, CH_3-C_5H_4), 3.68 (m, 4H, ^{2+4}J(P,H) = 5 Hz, PCH_2), 1.71 (s, 6H, CH_3-C_5H_4). $^{31}P\{^1H\}$ NMR: (THF/C_6H_6): δ = − 5.33 (s). **7**: Deep violet crystals. IR: $\tilde{\nu}$ = 2055 w, 2018 s, 1932 vs, 1876 w cm^{-1}. IR (Nujol): $\tilde{\nu}$(CO) = 2061 m, 2048 m, 2023 w, 1938 vs, 1925 vs, 1870 m, 1855 m, br cm^{-1}. ^1H NMR: δ = 4.37–4.14 (m, 16H, CH_3-C_5H_4), 1.65 (s, 12H, CH_3-C_5H_4).

Received: May 25, 1990 [Z 3979 IE]
German Version: *Angew. Chem. 102* (1990) 1206

[1] a) A. Christofides, N. G. Connelly, H. J. Lawson, A. C. Loyns, *J. Chem. Soc. Chem. Commun. 1990*, 597; b) C. Carini, C. Pelizzi, G. Pelizzi, G. Predieri, P. Tarasconi, F. Vitali, *ibid. 1990*, 613; c) G. A. Carriedo, N. G. Connelly, M. C. Crespo, I. C. Quarmby, V. Riera, *ibid. 1987*, 1806; d) M. Adam, A. K. Brimah, R. D. Fischer, L. Xing-Fu, *Inorg. Chem. 29* (1990) 1595; e) A. Burewicz, A. Haim, *ibid. 27* (1988) 1611; f) A. J. Deeming, G. P. Proud, H. M. Dawes, M. B. Hursthouse, *J. Chem. Soc. Dalton Trans. 1988*, 2475; *Polyhedron 7* (1988) 651; g) F. Calderazzo, U. Mazzi, G. Pampaloni, R. Poli, F. Tisato, P. F. Zanazzi, *Gazz. Chim. Ital. 119* (1989) 241; h) W. F. McNamara, E. N. Duesler, R. T. Paine, *Organometallics 7* (1988) 384; i) E. Bär, W. P. Fehlhammer, *J. Organomet. Chem. 353* (1988) 197; j) H. Behrens, G. Landgraf, P. Merbach, M. Moll, K.-H. Trummer, *ibid. 253* (1983) 217; k) J. A. Davies, F. R. Hartley, S. G. Murray, M. A. Pierce-Butler, *J. Chem. Soc. Dalton Trans. 1983*, 1305; l) D. M. Duggan, R. G. Jungst, K. R. Mann, G. D. Stucky, D. N. Hendrickson, *J. Am. Chem. Soc. 96* (1974) 3443, and references cited therein.

[2] See, for example: a) I. Hashimoto, N. Tsuruta, M. Ryang, S. Tsutsumi, *J. Org. Chem. 35* (1970) 3748; b) M. Iguchi, *Nippon Kagaku Kaishi (1921–47) 63* (1942) 1752; c) T. Funabiki, S. Yoshida, K. Tarama, *J. Chem. Soc. Chem. Commun. 1978*, 1059.
[3] G. J. Baird, S. G. Davies, S. D. Moon, S. J. Simpson, R. H. Jones, *J. Chem. Soc. Dalton Trans. 1985*, 1479.
[4] a) E. O. Fischer, R. J. J. Schneider, *J. Organomet. Chem. 12* (1968) P27; b) B. Oswald, A. K. Powell, F. Rashwan, J. Heinze, H. Vahrenkamp, *Chem. Ber. 123* (1990) 243.
[5] F. A. Holleman, N. Wiberg: *Lehrbuch der Anorganischen Chemie*, W. de Gruyter, Berlin 1985, p. 130. In the narrow sense, $1^{\ominus}$ is isosteric with $[CpCr(CO)_3]^{\ominus}$, but the latter anion was shown to afford compounds isostructural with their Mo analogues[6].
[6] R. Bender, P. Braunstein, J.-M. Jud, Y. Dusausoy, *Inorg. Chem. 22* (1983) 3394.
[7] R. Bender, P. Braunstein, A. Tiripicchio, M. Tiripicchio Camellini, *J. Chem. Soc. Chem. Commun. 1984*, 42.
[8] C. T. Hunt, A. L. Balch, *Inorg. Chem. 20* (1981) 2267; *ibid. 21* (1982) 1242.
[9] Md. N. I. Khan, C. King, J.-C. Wang, S. Wang, J. P. Fackler, Jr., *Inorg. Chem. 28* (1989) 4656.
[10] a) P. Braunstein, M. Ries, C. de Méric de Bellefon, Y. Dusausoy, J.-P. Mangeot, *J. Organomet. Chem. 355* (1988) 533; b) P. Braunstein, C. de Méric de Bellefon, M. Ries, J. Fischer, *Organometallics 7* (1988) 332.
[11] Crystal structure determination of $7 \cdot C_2H_5OH$: $C_{40}H_{28}Mn_4N_4O_{12}Pd_4 \cdot C_2H_5OH$, $M = 1448.10$, triclinic, space group $P\bar{1}$, $a = 13.324(6)$, $b = 18.377(8)$, $c = 10.954(6)$ Å, $\alpha = 101.90(2)$, $\beta = 109.90(2)$, $\gamma = 90.98(2)°$, $V = 2457(2)$ Å^3, $Z = 2$, $\varrho_{calcd} = 1.958$ g cm^{-3}, graphite-monochromated, $Mo_{K\alpha}$ radiation, $\lambda = 0.71073$ Å, $\mu = 24.28$ cm^{-1}. The intensity data were collected on a Philips PW 1100 diffractometer, using the ω-2θ scan technique at room temperature. A decay of about 30% of the initial intensity of a standard reflection, measured after 50 reflections, was observed during the data collection and corrected. 7135 unique reflections, $3 < \theta < 25°$, 2635 with $I > 2\sigma(I)$ used in the refinement. The structure was solved by Patterson and Fourier methods and refined by full-matrix least-squares fit procedures, with anisotropic thermal parameters in the last cycles of refinement for all the non-hydrogen atoms except the carbon atoms of the methylcyclopentadienyl rings and the atoms of the molecule of solvation. The hydrogen atoms were introduced in calculated positions, but their parameters were not refined. The SHELX-76 and SHELXS-86 system of computer programs was used[12]. The R and R_w values were 0.0578 and 0.0852, respectively. Further details of the crystal structure analysis may be obtained from the Fachinformationszentrum Karlsruhe, Gesellschaft für wissenschaftlich-technische Information mbH, D-7514 Eggenstein-Leopoldshafen 2 (FRG), on quoting the depository number CSD-54 697, the names of the authors, and the journal citation.
[12] G. M. Sheldrick, *„SHELX-76", Program for Crystal Structure Determination*, University of Cambridge (UK) 1976. *„SHELXS-86", Program for Crystal Structure Solution*, Universität Göttingen 1986.
[13] For related interactions with Cu^{I}: M. J. Begley, P. Hubberstey, P. H. Walton, *J. Chem. Soc. Chem. Commun. 1989*, 502; with Ir^{I}: P. A. Chetcuti, C. B. Knobler, M. F. Hawthorne, *Organometallics 7* (1988) 650; and with Mo^{II}: T. C. Wright, G. Wilkinson, M. Motevalli, M. B. Hursthouse, *J. Chem. Soc. Dalton Trans. 1986*, 2017.
[14] P. Braunstein, M. A. Luke, A. Tiripicchio, M. Tiripicchio Camellini, *Angew. Chem. 99* (1987) 802; *Angew. Chem. Int. Ed. Engl. 26* (1987) 768.
[15] D. M. Walba, *Tetrahedron 41* (1985) 3161.
[16] There is an obvious and aesthetically pleasing topological relationship between the core structure of 7 and that of tricyclo[3.3.0.0^{3,7}]octane (bisnoradamantane). For bisnoradamantane, see: P. K. Freeman, V. N. M. Rao, G. E. Bigam, *Chem. Commun. 1965*, 511; B. R. Vogt, S. R. Suter, J. R. E. Hoover, *Tetrahedron Lett. 1968*, 1609.

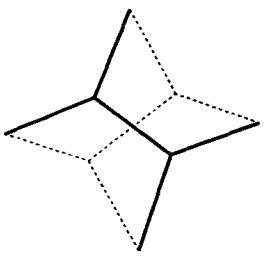

8

[17] T. A. Stromnova, I. N. Busygina, S. B. Katser, A. S. Antsyshkina, M. A. Porai-Koshits, I. I. Moiseev, *J. Chem. Soc. Chem. Commun. 1988*, 114.
[18] R. Bender, P. Braunstein, C. de Méric de Bellefon, *Polyhedron 7* (1988) 2271, and references cited therein.
[19] C. P. Horwitz, D. F. Shriver, *Adv. Organomet. Chem. 23* (1984) 219.
[20] S. J. Carter, L. S. Stuhl, *Organometallics 7* (1988) 1909.
[21] The authors are grateful to *J.-P. Mage* and *P. Verley* (Groupe IAO, Centre de calcul du CNRS, Strasbourg) for the computer-generated color drawing of 7 in Figure 3, which was obtained by using the actual atomic coordinates of the Pd, Mn, C, and N atoms and the CATIA software.

2,3,4,5-Tetramethyl-1-sodiopyrrole: An Azacyclopentadienyl Ligand in a Novel Bridging Function**

By *Norbert Kuhn,* Gerald Henkel,* and *Jörg Kreutzberg*

Dedicated to Professor Max Schmidt on the occasion of his 65th birthday

The structure and reactivity of pyrrolides (**1**) exhibit features of cyclopentadienides as well as of pyridines and amides. These similarities are reflected in the coordination of structure **2** and **3**, which have been identified in dimeric carbazolides of the alkali metals (**4** and **5**)[1, 2] (Scheme 1).

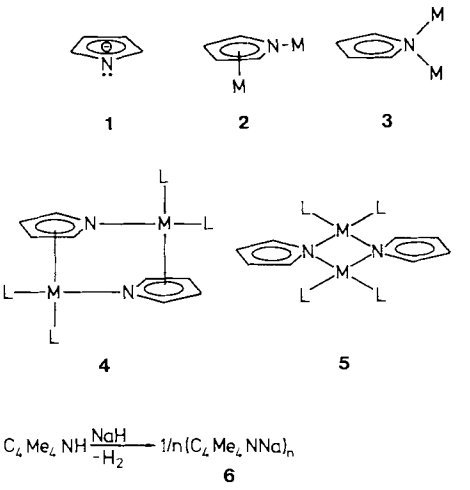

1 2 3 4 5

6

Scheme 1.

The structure of 2,3,4,5-tetramethyl-1-sodiopyrrole (**6**)[3] combines the characteristic features of amide bridges[4] with the π coordination of dienyl ligands.[5] In Figure 1, the double chain structure, consisting of alternating sodium and nitrogen atoms, shows that each pyrrolyl ligand[6] bridges three sodium atoms; the unusual coordination numbers 7 and 5 are thereby attained for sodium and nitrogen, respectively. As observed for lithiocarbazole,[1a] the two Na–N bonds involving η^1 bonding are of different lengths (Na-N^j 2.411(2), Na-N^k 2.351(1) Å); however, since the two η^1-bonded sodium atoms in **6** lie outside the plane of the linking pyrrolyl ligand to the same extent (the angle Na^i-N-Na^l is roughly bisected by the ring plane), a differentiation between σ and π bonding makes no sense in this case. On the other hand, the Na-N bond involving η^5 bonding (2.694(1) Å) is clearly longer and lies in the range observed for π bonding.[7] A comparison of the Na–C bonds (Na-C1 2.660(2), Na-C2 2.631(2), Na-C3 2.635(2), Na-C4 2.666(2) Å), also lying in the expected range,[5] shows that the sodium atom is displaced toward the carbon atoms in β position; this finding is in agreement with the structure calculated for lithiopyrrole.[1a] The bond lengths in the pyrrole ring (N-C1 1.387(2), N-C4 1.384(2), C1-C2 1.386(2), C2-C3 1.432(2), C3-C4 1.387(2) Å) are markedly longer than those of noncoordinat-

[*] Prof. Dr. N. Kuhn, Prof. Dr. G. Henkel, Dipl.-Chem. J. Kreutzberg
Fachbereich 6 (Chemie) der Universität-Gesamthochschule
Lotharstrasse 1, D-4100 Duisburg 1 (FRG)

[**] Heterocycles as Ligands, Part 6. This work was supported by the Fonds der Chemischen Industrie. We thank Prof. Dr. *P. Sartori* for his support. Part 8: N. Kuhn, E.-M. Lampe, *J. Organomet. Chem. 385* (1990) C9–C12.

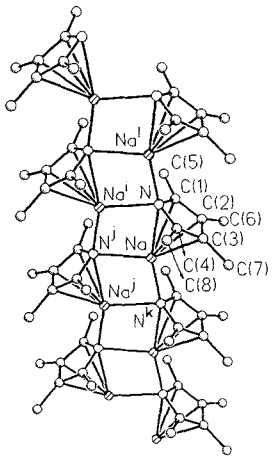

Fig. 1. Structure of **6** in the crystal (hydrogen atoms omitted). Selected interatomic distances [Å] and bond angles [°]: N···N^j 3.724(2), Na···Na^i 3.229(1); Na^i-Na-Na^j 101.3(1), N-Na-N^k 163.6(1), N-Na-N^j 93.5(1), N^k-Na-N^j 102.9(1), Na-N-Na^l 163.6(1), Na-N-Na^j 78.2(1), Na^l-N-Na^i 85.4(1).

ed tetramethyl pyrrole, but not as long as those in the fragment $(\pi\text{-}C_4Me_4N)Fe$.[8, 9] The Na_2N_2 quadrilaterals formed by the double chains (interatomic distances and bond angles shown in Fig. 1) are planar within the limits of experimental error and form angles of 0.8° with each other, resulting in a layer structure resembling a distorted rope ladder.

Unlike the analogous lithium compound, **6** is readily soluble in THF and is present in solution as a dimer. In the ^{13}C NMR spectrum, the signals of the ring carbon atoms (δ = 124.84 and 111.77) are only slightly shifted compared with those of tetramethylpyrrole (δ = 119.96 and 113.33); this finding indicates that the π bonding is disrupted upon dissolution with formation of structure type **5** (L = THF).

The unique structural features of 2,3,4,5-tetramethyl-1-sodiopyrrole confirm that the azacyclopentadienyl ligand displays versatile coordination properties, which were until now only presumed. In view of the rich structural chemistry of cyclopentadienyl compounds of the main-group elements,[10] the coordination chemistry of this heteroarene should offer promising applications.

Experimental Procedure

6: NaH (0.57 g, 23.7 mmol) and 2,3,4,5,-tetramethylpyrrole (2.93 g, 23.7 mmol) were allowed to react in 100 mL of refluxing THF for 18 h. The reaction mixture was then filtered, the solvent removed, and the residue extracted with 30 mL of diethyl ether. Yield after recrystallization of the residue from THF/diethyl ether: 1.28 g (43%) of colorless crystals. ^{13}C NMR (75.43 MHz, [D_8]THF, TMS int.): δ = 124.84 (C2,5), 111.77 (C3,4), 13.70 (C2,5-CH_3), 10.43 (C3,4-CH_3). MS (70 eV): *m/z* 145 ($M^{\oplus}$, 1%), 122 ($M^{\oplus}$ − Na], 100%). Molecular mass: found 265 (vapor pressure osmometry in THF at 45 °C), calcd 145.2 (monomeric formula unit).

Received: April 9, 1990 [Z 3903 IE]
German version: *Angew. Chem. 102* (1990) 1179

CAS Registry number:
2,3,4,5-tetramethyl-1-sodiopyrrole, 128191-83-3.

[1] a) R. Hacker, E. Kaufmann, P. von R. Schleyer, W. Mahdi, H. Dietrich, *Chem. Ber. 120* (1987) 1533–1538; b) K. Gregory, M. Bremer, P. von R. Schleyer, P. A. A. Klusener, L. Brandsma. *Angew. Chem. 101* (1989) 1261–1264; *Angew. Chem. Int. Ed. Engl. 28* (1989) 1224–1226.

[2] Structure type **2** has been identified for transition metals in the chemistry of azaferrocene[11a], 1,1'-diazaferrocene[11b], and azacymantrene[12]. The linking of two molybdenum centers to form a structure like **3** has not been confirmed by structure analysis[13].

[3] **6** (150 K): Monoclinic $P2_1/n$, a = 11.090(4), b = 4.994(1), c = 15.705(5) Å, β = 106.60(2)°, V = 833.55 Å^3, Z = 4, ϱ_{calcd} = 1.157 g cm^{-3}, $Mo_{K\alpha}$ radiation, scan range $4° \le 2\theta \le 54°$, 1834 unique reflections, 1548 observed ($I \ge 1.96\sigma(I)$), R = 0.034, R_w = 0.043, $w = [\sigma^2(F_0) + (0.01 \cdot F_0)^2]^{-1}$. Further details of the crystal structure investigation may be obtained from the Fachinformationszentrum Karlsruhe, Gesellschaft für wissenschaftlich-technische Information mbH, D-7514 Eggenstein-Leopoldshafen 2 (FRG), on quoting the depository number CSD-54660, the names of the authors, and the journal citation.

[4] Cf., e.g., R. Grünig, J. L. Atwood, *J. Organomet. Chem. 137* (1977) 101–111; D. J. Brauer, H. Bürger, W. Geschwandtner, G. R. Liewald, C. Krüger, *ibid. 248* (1983) 1–15.

[5] Cf., e.g., R. D. Rogers, J. L. Atwood, M. D. Rausch, D. W. Macomber, W. P. Heist, *J. Organomet. Chem. 238* (1982) 79–85; T. Aoyagi, H. M. M. Shearer, K. Wade, G. Whitehead, *ibid. 175* (1979) 21–31.

[6] The linking of three Os centers by the ligand $C_4H_3N^{2\ominus}$ was recently demonstrated: M. W. Day, K. I. Hardcastle, A. J. Deeming, A. J. Arce, Y. De Sanctis, *Organometallics 9* (1990) 6–12.

[7] Cf. K. Jonas, D. J. Brauer, C. Krüger, P. J. Roberts, Y.-H. Tsay, *J. Am. Chem. Soc. 98* (1976) 74–81.

[8] N. Kuhn, E.-M. Horn, R. Boese, N. Augart, *Angew. Chem. 100* (1988) 1433–1435; *Angew. Chem. Int. Ed. Engl. 27* (1988) 1368–1369.

[9] A similar finding results from comparison of the ring bond lengths in the fragments C_5H_5Na and C_5H_5Fe, cf. [5] as well as C. Krüger, B. L. Barnett, D. Brauer in E. A. Koerner von Gustorf, F. W. Grewels, I. Fischler (Eds.): *The Organic Chemistry of Iron, Vol. 1*, Academic Press, New York 1978, pp. 1–112.

[10] Cf. review: P. Jutzi, *Adv. Organomet. Chem. 26* (1986) 217–295; P. *Pure Appl. Chem. 61* (1989) 1731–1736.

[11] a) N. Kuhn, M. Schulten, E. Zauder, N. Augart, R. Boese, *Chem. Ber. 122* (1989) 1891–1896; b) N. Kuhn, E.-M. Horn, R. Boese, D. Bläser, *ibid. 122* (1989) 2275–2277.

[12] W. A. Herrmann, I. Schweitzer, P. S. Skell, M. L. Ziegler, K. Weidenhammer, B. Nuber, *Chem. Ber. 112* (1979) 2423–2435; V. G. Andrianov, Y. T. Struchkov, N. I. Pyshnograeva, V. N. Setkina, D. N. Kursanov, *J. Organomet. Chem. 206* (1981) 177–184, and references cited therein.

[13] W. Dell, M. L. Ziegler, *Z. Naturforsch. B 37* (1982) 7–12; cf. [6].

α-Umpolung of Ketones via Enol Radical Cations: A Mechanistic Study**

By *Michael Schmittel,* Ahmed Abufarag, Olaf Luche,* and *Michael Levis*

Numerous MO calculations[1] and mass-spectrometric studies[2] have confirmed that simple enol radical cations are much more stable than the tautomeric keto ions in the gas phase, in distinct contrast to the order of stability of the neutral species[3] (Fig. 1).

Reversal of the thermodynamics of the keto/enol equilibrium by one-electron oxidation is also found in solution, as exemplified by studies on stable enols.[4] For example, the radical cations of β,β-dimesityl-substituted enols are up to 25 kcal mol^{-1} more stable than those of the tautomeric ketones in acetonitrile.

This finding opens up interesting possibilities for new synthetic procedures. Starting from the ketone, the small amount of enol present in equilibrium can be selectively oxidized by suitable choice of oxidizing agent and the resulting radical cation can be trapped by nucleophiles. If enolization is sufficiently fast (acid or base catalysis), the carbonyl com-

[*] Dr. M. Schmittel, A. Abufarag, O. Luche, Dipl.-Chem. M. Levis
Institut für Organische Chemie und Biochemie der Universität, Albertstrasse 21, 7800 Freiburg (FRG)

[**] Enol Radical Cations in Solution, Part 2. This work was supported by the Deutsche Forschungsgemeinschaft, the Land Baden-Württemberg (Fr-NW 31), and the Fonds der Chemischen Industrie (Liebig-Stipendium for *M. S.*). We thank Prof. *C. Rüchardt* for supporting our work and *D. Morat* for her dedicated assistance. Part 1: [4].

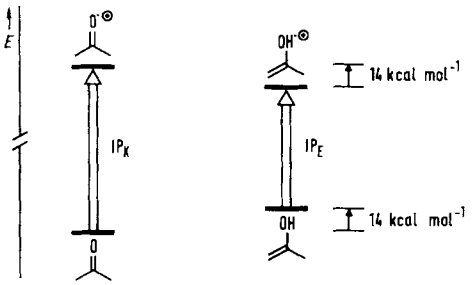

Fig. 1. Relative energies of acetone and the tautomeric propen-2-ol as neutral molecules and as radical cations in the gas phase [2].

pound could react quantitatively via enol radical cation intermediates.

To investigate this possibility, we first studied the reaction of 1-(*p*-methoxyphenyl)propan-2-one (**1**), which has an enol content of only about 10^{-4}% 1-(*p*-methoxyphenyl)propen-2-ol,[5] with tris(*p*-bromophenyl)ammoniumyl hexachloroantimonate ($\mathbf{2}^{\bullet\oplus}$). The direct one-electron oxidation of **1** (E_p = 1.67 V[6]) by $\mathbf{2}^{\bullet\oplus}$ (**2**: $E_{1/2}$ = 1.06 V[7]) is so strongly endergonic that, even for rapid subsequent reactions of $\mathbf{1}^{\bullet\oplus}$, reactions should occur only slowly. On the other hand, the oxidation potential of the enol of **1** should be less than 1 V,[8] ensuring its rapid oxidation by $\mathbf{2}^{\bullet\oplus}$. Reaction of **1** with 200 mol% of $\mathbf{2}^{\bullet\oplus}$ in acetonitrile/methanol (9:1) for 14 min gave **3**[9] (56%) [Eq. (a)]. In addition, *p*-anisaldehyde (<9%) and 1-(*p*-methoxyphenyl)propane-1,2-dione (<5%) were formed.

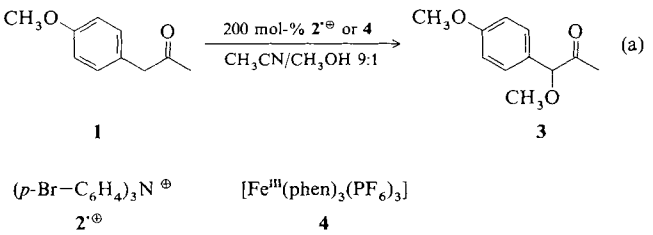

Comparable yields of **3** (49%) are obtained when 200 mol% of tris(*o*-phenanthroline)iron(III) tris(hexafluorophosphate) (**4**) is used. This finding supports the assumption of one-electron oxidation steps in the reaction mechanism, since **4** ($E_{1/2}$ = 1.09 V) is known to be an outer-sphere oxidizing agent according to the work of *Kochi* et al.[10]

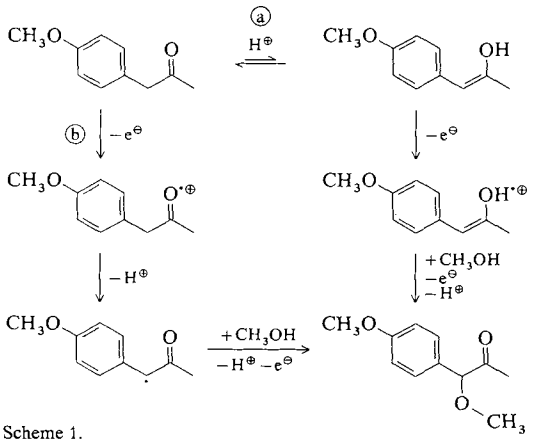

Scheme 1.

The products obtained are consistent with the assumed course of the reaction. The acid released during the reaction catalyzes the enolization of **1** and the enol is selectively oxidized and then trapped by methanol (Scheme 1, path a). Also plausible would be the route involved in oxidative functionalization of alkylarenes[11] (path b). This reaction is known to proceed effectively despite strongly endergonic electron-transfer steps.

Control experiments allow a distinction to be made between the two reaction hypotheses. According to path b, a strongly endergonic electron-transfer step is followed by deprotonation of the keto radical cation. The rate of the overall reaction should therefore increase, or at least remain constant, upon addition of a base. In fact, however, the reaction of **1** with $\mathbf{2}^{\bullet\oplus}$ proceeds much slower in the presence of 200 mol% of 2,6-di-*tert*-butylpyridine: after 5 h, only 8% of **3**, together with 58% of unreacted **1**, is obtained.[12] This finding rules out path b but is consistent with path a, since the acid-catalyzed enolization should be suppressed by addition of base.[13]

Additional arguments against path b are provided by the reaction of 3-(*p*-methoxyphenyl)butan-2-one (**5**, E_p = 1.69 V) with ammoniumyl salts. The direct oxidation of **5** can be suppressed or enhanced relative to acid-catalyzed enolization by the use of ammoniumyl salts having various oxidizing strengths (Table 1) [Eq. (b)].

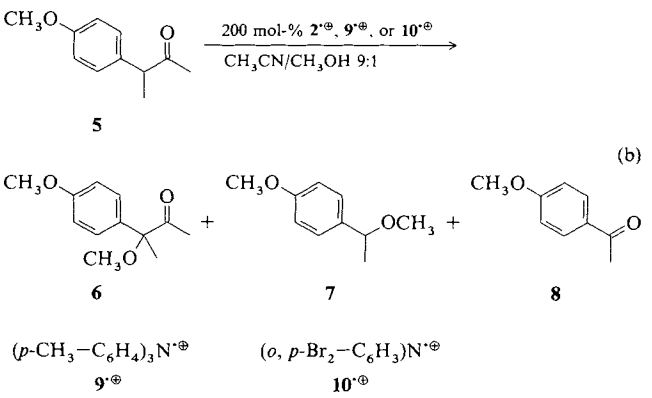

Table 1. Products of the reaction of **5** with ammoniumyl salts (200 mol%) in acetonitrile/methanol (9:1) at room temperature. The yields and reaction times are average values from at least three independent experiments.

Ammoniumyl salt	$E_{1/2}$ (SCE)[14] [V]	**6** [%]	**7** [%]	**8** [%]	**5** [%]	*t* [12]
$\mathbf{9}^{\bullet\oplus}$ [a]	0.76	78	<1	<1	5	33 h
$\mathbf{2}^{\bullet\oplus}$ [a]	1.06	30	10	6	29	153 min
$\mathbf{10}^{\bullet\oplus}$ [a]	1.50	<1	7	6	41	25 s

[a] As hexachloroantimonate.

The product analysis clearly shows that the use of strong ammoniumyl salts results in a large decrease in the amount of **6** and an increase in the formation of cleavage products such as **7** and **8**.[9, 15] Apparently, $\mathbf{5}^{\bullet\oplus}$ is not deprotonated under the reaction conditions, as required according to path b, but instead undergoes C–C bond cleavage. On the other hand, the use of a weakly oxidizing ammoniumyl salt leads to high yields of **6**; in this case, the direct oxidation of **5** can no longer compete with the acid-catalyzed enolization and subsequent oxidation of the enol.

The use of alcohols as nucleophiles necessitates the consideration of further reaction pathways in addition to those discussed above, since, besides ketones and tautomeric enols, small equilibrium concentrations of enol ethers and acetals may also be present.[16] However, acetals and enol ethers need not be intermediates in the umpolung reaction, as shown by treatment of 2-(*p*-methoxyphenyl)cyclohexanone (**11**, E_p = 1.63 V) with 200 mol% of $\mathbf{9}^{\bullet\oplus}$ in pure acetonitrile: **12** is formed in 74% yield [Eq. (c)].

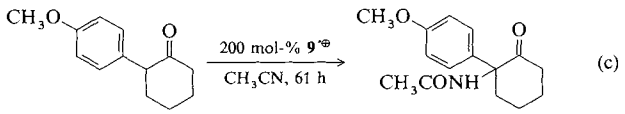

11 **12** (c)

The investigations show that ketones such as **1** and **5**, which exhibit a low tendency toward enolization, can be methoxylated in the α position via their enol radical cations. It is still unclear how the enol radical cations react further to give the products.[17] Elucidation of the mechanistic details and scope of application of this novel umpolung reaction of ketones, especially in comparison with known methods,[18] is in progress.

Received: May 11, 1990 [Z 3950 IE]
German version: *Angew. Chem. 102* (1990) 1174

CAS Registry numbers:
1, 122-84-9; $\mathbf{2}^{\bullet\oplus}$, 24964-91-8; **3**, 21165-40-2; **4**, 28277-57-8; **5**, 7074-12-6; **6**, 104741-73-3; **7**, 77525-91-8; $\mathbf{9}^{\bullet\oplus}$, 65644-87-3; $\mathbf{10}^{\bullet\oplus}$, 58047-17-9; **11**, 37087-68-6; **12**, 128973-49-9.

[1] N. Heinrich, F. Louage, C. Lifshitz, H. Schwarz, *J. Am. Chem. Soc. 110* (1988) 8183; N. Heinrich, W. Koch, G. Frenking, H. Schwarz, *ibid. 108* (1986) 593; W. J. Bouma, J. K. MacLeod, L. Radom, *ibid. 101* (1979) 5540.
[2] J. L. Holmes, F. P. Lossing, *J. Am. Chem. Soc. 102* (1980) 1591; *ibid. 104* (1982) 2648.
[3] J. Toullec, *Adv. Phys. Org. Chem. 18* (1982) 1; F. Turecek, L. Brabec, J. Korvola, *J. Am. Chem. Soc. 110* (1988) 7984.
[4] M. Schmittel, U. Baumann, *Angew. Chem. 102* (1990) 571; *Angew. Chem. Int. Ed. Engl. 29* (1990) 541.
[5] J. R. Keeffe, A. J. Kresge, Y. Yin, *J. Am. Chem. Soc. 110* (1988) 8201.
[6] The oxidation potentials given here refer to the saturated calomel electrode (SCE); they were measured in acetonitrile (100 mV s^{-1}): 2–3 mM **1** or **5**, 0.1 M tetra-*n*-butylammonium hexafluorophosphate, ferrocene as reference.
[7] W. Schmidt, E. Steckhan, *Chem. Ber. 113* (1980) 577.
[8] The oxidation potentials of β,β-dimesityl-substituted enols [4] are about 1 V below those of the tautomeric ketones. Assuming identical differences in oxidation potential for **1** in enol and keto form, E_p (enol) should be much less than 1 V (SCE).
[9] A 30 mM solution of the ketone in acetonitrile/methanol (9:1) was stirred with 20 mol% of $\mathbf{2}^{\bullet\oplus}$ at room temperature until the blue color of the ammoniumyl salt vanished. The products were characterized by spectroscopy and by comparison with authentic substances.
[10] C. L. Wong, J. K. Kochi, *J. Am. Chem. Soc. 101* (1979) 5593.
[11] E. Baciocchi, A. Dalla Cort, L. Eberson, L. Mandolini, C. Rol, *J. Org. Chem. 51* (1986) 4544; C. J. Schlesener, J. K. Kochi, *ibid. 49* (1984) 3142; L. Eberson, *J. Am. Chem. Soc. 105* (1983) 3192; E. Baciocchi, C. Rol, G. V. Sebastiani, B. Serena, *Gazz. Chim. Ital. 113* (1983) 853.
[12] As a measure of the reaction rate, the time required for color change from blue (color of $\mathbf{2}^{\bullet\oplus}$) to brown was determined.
[13] Addition of 200 mol% of trifluoromethanesulfonic acid to the reaction mixture gave **3** in 78% yield after 10 min.
[14] E. Steckhan, *Top. Curr. Chem. 142* (1987) 1.
[15] The low conversion of **5** upon oxidation with $\mathbf{10}^{\bullet\oplus}$ is due to rapid reaction of $\mathbf{10}^{\bullet\oplus}$ with the solvent mixture. Furthermore, competition experiments showed that, when $\mathbf{10}^{\bullet\oplus}$ was used as oxidizing agent, **6** did not react faster than **5**.
[16] M. Gaudry, A. Marquet, *Tetrahedron 26* (1970) 5617.
[17] Here, too, several reaction hypotheses are plausible (e.g., attack of methanol on the enol radical cation or deprotonation of the enol radical cation). Some of these reactions have already been described for the electrochemical oxidation of enol acetates to α-acetoxy ketones or of enol ethers to α-alkoxy acetals: see S. Torii: *Electroorganic Syntheses—Methods and Applications, Part 1: Oxidations*, Kodansha, Tokio 1985, pp. 230, 234.
[18] R. M. Moriarty, O. Prakash, M. P. Duncan, R. K. Vaid, H. A. Musallam, *J. Org. Chem. 52* (1987) 150; R. M. Moriarty, O. Prakash, *Acc. Chem. Res. 19* (1986) 244.

Isomerization versus Decarboxylation of Protonated Oxetanone: Comparison between Experimental Results and Theoretical Calculations

By *Gregorio Asensio,* Miguel A. Miranda,* Julia Perez-Prieto, Maria J. Sabater,* and *Antonio Simón-Fuentes*

Decarboxylation of 2-oxetanones is a general and useful method for the stereospecific synthesis of olefins, proceeding with complete stereoretention in neutral organic solvents.[1] Conversely, upon addition of an acid catalyst, *cis*-3,4-disubstituted 2-oxetanones undergo carbon dioxide elimination with almost total inversion of configuration and a marked increase in the reaction rate.[2] Recent theoretical calculations[3] on the decarboxylation of 2-oxetanone protonated at the carbonyl oxygen atom ($\mathbf{1H}^{\oplus}$) as a model for the acid-catalyzed thermolysis appear to support the intermediacy of a carbenium ion ($\mathbf{2H}^{\oplus}$), which is assumed to undergo fragmentation affording ethylene and protonated carbon dioxide. Hence, we decided, as a part of our work on the thermolysis of protonated carbonyl compounds,[4] to study the behavior of the parent 2-oxetanone (**1**) in concentrated sulfuric acid in order to determine the role of cationic species in the decarboxylation and to check the feasibility of the suggested C3–C4 fragmentation of $\mathbf{2H}^{\oplus}$ to ethylene and protonated carbon dioxide.

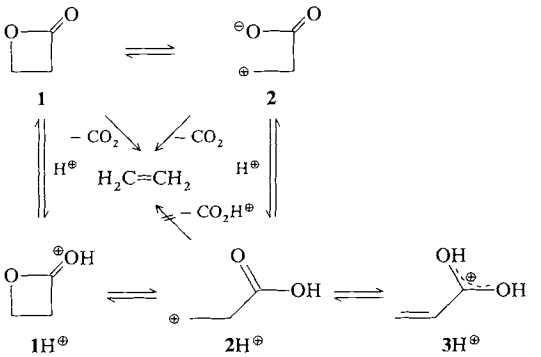

The protonated lactone $\mathbf{1H}^{\oplus}$ [5] was studied over a temperature range of 30 to 150 °C, during a period of up to several days, by keeping the corresponding sulfuric acid solutions in thermostated baths and recording periodically the ^{1}H NMR

[*] Prof. Dr. G. Asensio, Prof. Dr. M. A. Miranda, Dr. J. Perez-Prieto, M. J. Sabater, Dr. A. Simón-Fuentes
Departamento de Química Orgánica, Facultad de Farmacia
Avda. Blasco Ibañez, 13, E-46010 Valencia (Spain)

[**] We thank the Direccion General de Investigación Cientifica Y Técnica (DGICYT, Grant No. PB87-0989) for financial support.

spectra. Surprisingly, formation of ethylene could not even be detected.[6] Instead, an equilibrium[7] was established between O-protonated 2-oxetanone ($1H^{\oplus}$) and O-protonated acrylic acid ($3H^{\oplus}$).[8] Alternatively, $3H^{\oplus}$, generated directly by protonation of **3** in concentrated sulfuric acid, was heated in the same temperature range to afford equilibrium mixtures of $1H^{\oplus}$ and $3H^{\oplus}$ with the same composition as starting from $1H^{\oplus}$. Even after prolonged heating at 150 °C, the transformations were clean[9] in that no polymers were formed, as shown by adding a known amount of methanesulfonic acid as internal standard for ^1H NMR integration. These results strongly suggest the intermediacy of the cation $2H^{\oplus}$, which does not decarboxylate at all, in clear disagreement with theoretical calculations.[3]

To rule out the possibility of alternative reaction pathways not involving the intermediacy of $2H^{\oplus}$ (i.e., E_2 elimination from $1H^{\oplus}$ or conjugate addition to $3H^{\oplus}$), we studied the *tert*-butyl-substituted oxetanone **5** and its β-hydroxy acid precursor **4**.[10] We anticipated that the corresponding C-protonated species $6H^{\oplus}$, if formed, would rearrange to the more stable tertiary cation $7H^{\oplus}$. As expected, compounds **4** and **5**, when dissolved in sulfuric acid at room temperature, gave O-protonated 4,5,5-trimethyl-γ-butyrolactone ($8H^{\oplus}$)[11] in quantitative yield.

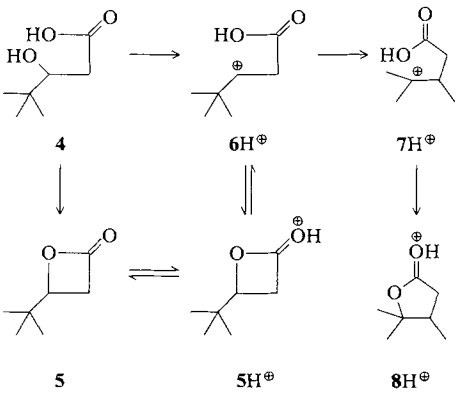

Since the value of ΔG° for the conversion of O-protonated oxetanone ($1H^{\oplus}$) to O-protonated acrylic acid ($3H^{\oplus}$) is very small,[7] it is easy to understand why the observed isomerization $1H^{\oplus} \rightleftharpoons 3H^{\oplus}$ takes place. On the other hand, the predicted fragmentation of $1H^{\oplus}$ to ethylene and protonated CO_2 would be strongly endothermic.[3]

Nonetheless, it must be taken into account that our results have been obtained in solution, whereas the theoretical calculations refer to the gas phase. For this reason, we recorded the CI mass spectrum of **1**, since fragmentation of the $(M+1)$ peak, corresponding to the protonated molecule, is highly relevant in terms of gas-phase ion chemistry.[4] In this spectrum, the peak with *m/z* 73, resulting from the isobaric ions $1H^{\oplus}$ and $3H^{\oplus}$, was most intense. Dehydration of $3H^{\oplus}$ to the corresponding acylium ion would account for the presence of a fragment with *m/z* 55 (5%). A minor peak with *m/z* 45 (5%), assignable to protonated carbon dioxide, was observed, thus indicating that the predicted cleavage of $1H^{\oplus}$ can indeed occur to a small extent under the very energetic conditions inherent to mass spectrometry. Moreover, the alternative pathway for the formal [2+2] cycloreversion, involving formation of protonated ketene (*m/z* 43 (21%)), appears to be more important. This fragmentation was also detected in solution.[9]

In summary, we have shown that the only significant process undergone by protonated 2-oxetanone ($1H^{\oplus}$) in concentrated sulfuric acid solution is the isomerization to O-protonated acrylic acid ($3H^{\oplus}$) via the C-protonated intermediate $2H^{\oplus}$, which does not decarboxylate as predicted earlier.[3] These results might be interesting in connection with the reported inverted stereospecificity and rate enhancement in the decarboxylation of 3,4-disubstituted 2-oxetanones in the presence of catalytic amounts of acid.[2] Under these conditions, $2H^{\oplus}$ (or the corresponding substituted species) would be in equilibrium with the zwitterion **2**. It is reasonable to assume, therefore, that a fast rotation around the C–C bond will occur in $2H^{\oplus}$, where 1,4 interactions are weaker, whereas decarboxylation should take place from **2**, as postulated for the neutral compound **1**.[1b,c]

Received: August 11, 1998;
revised: June 8, 1990 [Z 3492 IE]
German version: *Angew. Chem. 102* (1990) 1187

[1] a) W. Adam, J. Baeza, J. C. Liu, *J. Am. Chem. Soc. 94* (1972) 2000; b) J. Mulzer, M. Zippel, *Tetrahedron Lett. 21* (1980) 751; c) J. Mulzer, M. Zippel, G. Brüntrup, *Angew. Chem. 92* (1980); *Angew. Chem. Int. Ed. Engl. 19* (1980) 465; d) W. Adam, L. A. Arias Encarnación, *Synthesis 1979*, 388; e) W. Adam, G. Martinez, J. Thompson, F. Yany, *J. Org. Chem. 46* (1981) 3359; f) N. S. Isaacs, A. N. Laila, *Tetrahedron Lett. 24* (1983) 2897.
[2] J. Mulzer, M. Zippel, *J. Chem. Soc. Chem. Commun. 1981*, 891.
[3] A. Moyano, M. A. Pericàs, E. Valentí, *J. Org. Chem. 54* (1989) 573.
[4] a) A. M. Amat, G. Asensio, M. J. Castelló, M. A. Miranda, A. Simón-Fuentes, *J. Org. Chem. 52* (1987) 4790; b) A. M. Amat, G. Asensio, M. A. Miranda, M. J. Sabater, A. Simón-Fuentes, *ibid. 53* (1988) 5480.
[5] Spectral data for $1H^{\oplus}$: ^1H NMR (96% H_2SO_4, 80 MHz, 30 °C): $\delta = 3.2$ (t; 2H), 4.5 (t; 2H). ^{13}C NMR (96% H_2SO_4, 20 MHz): $\delta = 187.5$(s), 67.3(t), 34.1(t).
[6] Under these conditions, ethylene is trapped as (2-hydroxyethyl)sulfonic acid: W. Adam, M. A. Miranda, *J. Org. Chem. 52* (1987) 5499.
[7] The measured values of the equilibrium constants were nearly 1.0 and showed a very small variation within the studied temperature interval. The equilibrium was reached after ca. 80 h at 60 °C or 1 h at 150 °C.
[8] G. A. Olah, M. Calin, *J. Am. Chem. Soc. 90* (1968) 405. In separate experiments, no interconversion between $1H^{\oplus}$ and $3H^{\oplus}$ was observed to take place below 30 °C. This is in agreement with *Olah*'s observation of $3H^{\oplus}$ as a stable species in magic acid at −78 °C.
[9] Besides $1H^{\oplus}$ and $3H^{\oplus}$, small amounts (ca. 4%) of protonated acetic acid were also detected by ^1H NMR spectroscopy.
[10] T. H. Black, J. A. Hall, R. G. Sheu, *J. Org. Chem. 53* (1988) 2371.
[11] Spectral data for $8H^{\oplus}$: ^1H NMR (96% H_2SO_4, 80 MHz): $\delta = 3.5$–2.5 (m; 3H), 1.7 (s; 3H), 1.5 (s; 3H), 1.1 (d; 3H). ^{13}C NMR (96% H_2SO_4, 20 MHz): $\delta = 195.2$ (s), 113.1 (s), 39.9 (t), 38.8 (d), 26.2 (q), 20.7 (q), 13.0 (q).

A Novel Palladium-Catalyzed Carbonylation of Aromatic *N*-Chlorosulfonamidates to Arylsulfonyl Isocyanates**

By *Gábor Besenyei, Sándor Németh*, and *László I. Simándi**

Catalytic hydroformylation and related carbonylations at carbon atoms affording aldehydes, carboxylic acids and esters are well known and widely used in laboratory and industry. Other important types of carbonylation are those occurring at the nitrogen atoms of aromatic amines and nitro compounds, leading to the formation of isocyanates and their derivatives like ureas and carbamates,[1,2] which find

[*] Prof. Dr. L. I. Simándi, Dr. G. Besenyei, Dr. S. Németh,
Central Research Institute for Chemsitry
Hungarian Academy of Sciences
P.O. Box 17, H-1525 Budapest (Hungary)
[**] This work was supported by Nitrokèmia, Balatonfüzfö, Hungary.

application as components of polyurethane resins and plant protecting agents. Owing to the drastic conditions, expensive catalysts, and sometimes inadequate selectivities the best methods of isocyanate synthesis remain those based on the phosgenation of amines.

In the course of searching for new possibilities concerning the synthesis of arylsulfonyl isocyanates, we have discovered that sodium and potassium salts of aromatic *N*-chlorosulfonamidates (**1**) can be catalytically carbonylated to arylsulfonyl isocyanates (**2**) at 20–100 °C and a CO pressure of 20–50 bar in CH_2Cl_2 or 1,2-dichloroethane as solvent [Eq. (a), M = Na, K]. Suitable catalysts are palladium salts and complexes like $[PdCl_2(CH_3CN)_2]$, $[PdCl_2(PhCN)_2]$, $[PdCl_2(Ph_3As)_2]$ and $[Pd_2(dba)_3]$ (dba = dibenzylideneacetone). The starting compounds **1a–e** are listed in Table 1 together with typical yields of the product isocyanates **2a–e**. The latter were identified by the strong N=C=O stretching

$$\underset{\textbf{1a-e}}{[ArylSO_2NCl]M} + CO \xrightarrow{\text{Pd-catalyst}} \underset{\textbf{2a-e}}{ArylSO_2NCO} + MCl \qquad (a)$$

Table 1. Yields of arylsulfonyl isocyanates **2** by catalytic carbonylation of *N*-chloroarylsulfonamidates ($p(CO)$ = 40 bar; solvent CH_2Cl_2). Right-hand column: molecular masses of the corresponding arylsulfonylureas **3** determined by FAB-MS.

1 Aryl	M	*T* [°C]	Catalyst/Additive	Yield of **2** [%]	($M^{\oplus}$ + H) of **3**
a Phenyl	$K^{\oplus}$	20	$[PdCl_2(Ph_3As)_2]$	76	311
a Phenyl	$Na^{\oplus}$	20	$PdCl_2/CH_3CN$	71	311
b 4-Methylphenyl	$K^{\oplus}$	55	$[Pd_2(dba)_3]$	80	325
b 4-Methylphenyl	$Na^{\oplus}$	20	$[PdCl_2(PhCN)_2]/CH_3CN$	72	325
c 2-Chlorophenyl	$K^{\oplus}$	20	$PdCl_2/CH_3CN$	76	345
d 2-Bromophenyl	$K^{\oplus}$	80	$PdCl_2/CH_3CN$	72	389
e 2-Naphthyl	$K^{\oplus}$	20	$[PdCl_2(PhCN)_2]/CH_3CN$	76	361

band at $\tilde{\nu}$ = 2250–2230 cm^{-1} readily observed in the diluted product mixture. Upon addition of some ethanol, the N=C=O band disappears and new bands appear at $\tilde{\nu}$ = 3600 and 1750 cm^{-1}, which are due to excess ethanol and ethyl *N*-arylsulfonylcarbamate. The yields in Table 1 were determined by treating the reaction mixture with the theoretical amount of 2-chloroaniline (2-CA), followed by isolation of the *N*-arylsulfonyl-*N'*-(2-chlorophenyl)ureas **3a–e** formed [Eq. (b)], which were identified by FAB-MS, IR spectroscopy, and elemental analysis.

$$\underset{\textbf{2a-e}}{ArylSO_2NCO} + 2\text{-CA} \longrightarrow \underset{\textbf{3a-e},\ Aryl' = 2\text{-chlorophenyl}}{ArylSO_2NHC(O)NHAryl'} \qquad (b)$$

Currently the best method available for the synthesis of arylsulfonyl isocyanates involves phosgenation of *N*-arylsulfonyl-*N'*-butylureas.[3] Reaction (a) constitutes a new and convenient phosgene-free route to arylsulfonyl isocyanates, which are important intermediates in the synthesis of sulfonylurea type herbicides and pharmaceuticals.

Two kinds of mechanisms are conceivable for reaction (a), namely those involving an arylsulfonylcarbamoyl chloride and those involving an arylsulfonylnitrene as intermediate. To our knowledge the only N-Cl carbonylation reported thus far is the reaction of *N*-chloroamines with CO, resulting in the formation of substituted carbamoyl chlorides.[4] We could not detect a carbamoyl band ($\tilde{\nu}$ = 1760–1810 cm^{-1}) in the reaction mixture, which rules out accumulation of a carbamoyl chloride intermediate. If this intermediate is formed, it should immediately decompose with elimination of the alkali metal chloride to give the isocyanate. The possibility of a nitrene intermediate receives some support from a claim that *N*-chloro-*p*-toluenesulfonamidate may be a potential source of tosylnitrene.[5] It is reasonable to assume that nitrene, if involved, should coordinate to the palladium ion, which may also bind a carbonyl ligand, thus providing a path for nitrene carbonylation in the coordination sphere. Work is in progress in our laboratory to elucidate the mechanism of this new reaction.

Experimental

A 45-mL stainless steel reactor (Parr Model 4712) was charged with 10 mL of dry CH_2Cl_2, 2.7 g (0.01 mol) of potassium *N*-chloro-2-chlorobenzenesulfonamidate **1c** [6], 70 mg of $PdCl_2$ and 1 mL of CH_3CN. After flushing with CO, the reactor was pressurized to 40 bar with CO. The mixture was stirred for 6 h at ambient temperature. The pressure was released, and 0.5 mL of the reaction solution was diluted with CH_2Cl_2 to 20 mL for the IR measurement. The intense band observed at 2230 cm^{-1} disappeared upon treatment with EtOH. The rest of the mixture was treated dropwise with 1.2 g (0.01 mol) of 2-chloroaniline under N_2. A violent reaction took place, which required external cooling. Evaporation to dryness afforded 3.54 g of a pale yellow crude product, which, besides KCl and the catalyst, contained 76% of *N*-(2-chlorophenylsulfonyl)-*N'*-(2-chlorophenyl)urea (**3c**), and 10% 2-chlorobenzenesulfonamide, as shown by HPLC. IR (KBr) (cm^{-1}): **2c**: $\tilde{\nu}$ = 2230 (ν_{as}NCO); **3c**: $\tilde{\nu}$ = 1690 (νCO), 1535(amide II), 1435, 1335(ν_{as} SO_2), 1155(ν_s SO_2), 755(γCH), 745(γCH); the 3370–2820 region is dominated by free and associated νNH vibrations. MS (FAB): *m/z* 345 ($M^{\oplus}$ + H, 10%).

Received: July 12, 1990 [Z 4010 IE]
German version: *Angew. Chem. 102* (1990) 1168

CAS Registry numbers:
1a · K, 17338-33-9; **1a** · Na, 127-52-6; **1b** · K, 125069-32-1; **1b** · Na, 127-65-1; **1c** · K, 125069-33-2; **1d** · K, 125069-36-5; **1e** · K, 129678-24-6; **2a**, 2845-62-7; **2b**, 4083-64-1; **2c**, 64900-65-8; **2d**, 127528-17-0; **2e**, 21926-42-1; **3a**, 129678-25-7; **3b**, 53855-79-1; **3c**, 125069-25-2; **3d**, 125069-31-0; **3e**, 129678-26-8; $[PdCl_2(Ph_3As)_2]$, 14126-26-2; $PdCl_2$, 7647-10-1; $[Pd_2(dba)_3]$, 51364-51-3; $[PdCl_2(PhCN)_2]$, 14220-64-5; o-$ClC_6H_4NH_2$, 95-51-2.

[1] W. B. Hardy, R. P. Bennett, *Tetrahedron Lett. 1967*, 961–962.
[2] S. Cenini, M. Pizzotti, C. Crotti in R. Ugo (Ed.): *Aspects of Homogeneous Catalysis, Vol. 6*, Reidel, Dordrecht, 1988, Vol. 6, pp. 97–198; *Methoden der Organischen Chemie (Houben-Weyl) 4th Edit. Vol. E4, 1983*, pp. 189–192, 365–367, and references therein.
[3] H. Ulrich, A. A. R. Sayigh, *Angew. Chem. 78* (1966) 761–768; *Angew. Chem. Int. Ed. 5* (1966) 704–712.
[4] T. Saegusa, T. Tsuda, Y. Isegawa, *J. Org. Chem. 36* (1971) 858.
[5] D. Carr, T. P. Seden, R. W. Turner, *Tetrahedron Lett. 13* (1969) 477.
[6] For the synthesis of aromatic *N*-chlorosulfonamidates, see *Methoden der Organischen Chemie (Houben-Weyl) 4th Edit. Vol. IX, 1955*, pp. 641–648; M. M. Campbell, G. Johnson, *Chem. Rev. 78* (1978) 65–79; D. H. Bremner: *Chloramine T*, in J. S. Pizey (Ed.): *Synthetic Reagents, Vol. 6*, Wiley, New York, pp. 9–59.

Cooperative Interactions in Molecular Recognition—the Binding of Diamines to a Tetracarboxylic Acid**

By *Frank Ebmeyer* and *Julius Rebek, Jr.**

One of the paradigms of molecular recognition studies that have emerged over recent years is the concept of preorganization. It is generally agreed that binding selectivity and

[*] Prof. J. Rebek, Jr., Dr. F. Ebmeyer
Department of Chemistry,
Massachusetts Institute of Technology
Cambridge, MA 02139 (USA)

[**] This work was supported by the National Institutes of Health; *F. E.* is grateful for a postdoctoral fellowship from the Fonds der Chemischen Industrie. We thank Dr. *J. Schroeder* and Dr. *P. Ballester* for carrying out the NMR measurements.

high affinities result when the conformation of the free host approaches that of the complex.[1] However, it has been hard to dissect the enthalpic contributions of ground state destabilization from those involving entropic factors, such as restricted motions. In this work, we use an allosteric effect as a means of preorganization and provide a measure of what enhanced affinity may be expected from such remote interactions.

The system involves the Kemp triacid derivative **1**, in which the acidic OH bonds of up to four carboxy groups can converge toward the center of the structure.

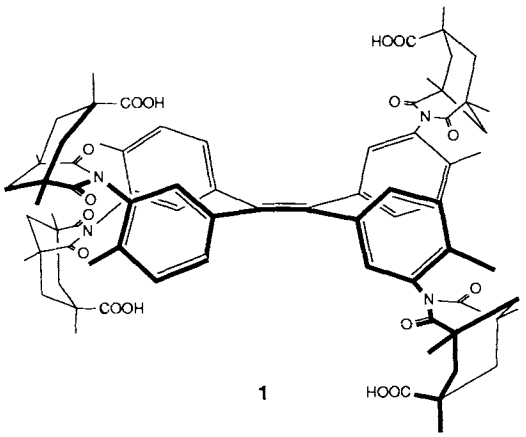

1

1 was synthesized from the dinitrobenzophenone **2**[2] via its hydrazone. Oxidation of the hydrazone with $Pb(OAc)_4$ in CH_2Cl_2 gave the diazo compound **4**, which was decomposed in hot benzene using $Cu(acac)_2$ as a catalyst to give the tetraphenylethylene derivative **3**, along with the corresponding ketazine and the ketone **2** as side products. Reduction of **3** with Raney nickel in dioxane gave the tetramine from which **1** was prepared by condensation with four equivalents of Kemp's triacid (Scheme 1).[3]

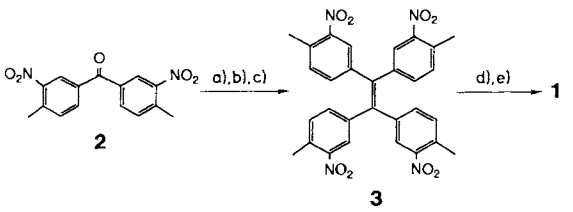

Scheme 1. a) hydrazine, ethanol, 82%; b) $Pb(OAc)_4$, CH_2Cl_2, 96%; c) $Cu(acac)_2$, benzene, 35%; d) H_2, Raney-Ni, dioxane, 3 bar, 95%; e) anhydride acid chloride of Kemp's triacid, pyridine, dimethylaminopyridine (DMAP), 30%.

Molecular modeling suggested that several diamines would be suitable guests for **1**. Hydrazine, ethylenediamine, 1,4-diazobicyclo[2.2.2]octane (DABCO) and 2-aminopyrimidine were selected for study and proton NMR titrations of **1** with these diamines in $CDCl_3$ were performed. The downfield shifts ($\delta = 0.15-0.60$) of the aromatic host protons in the 2,2',2'' and 2''' positions were followed. The titration curves obtained showed the formation of a 1:2 complex; 1:1 models such as Eadie-Hofstee-plots[4] did not fit the experimental data, but Hill plots gave appropriate sigmoid shapes. While rapid exchange was observed at room temperature, the DABCO complex showed slow exchange at 213 K in $CDCl_3/CD_2Cl_2$ mixtures. Signals for the 1:1, the 1:2 complex and the free host were resolved. Further, irradiation of the DABCO resonance in a 1:2 mixture of **1** and DABCO in $CDCl_3$ results in a homonuclear intermolecular NOE effect of +30% for the aromatic host protons near the imide groups (2,2',2'',2'''-positions). The results are consistent with the structure shown in Scheme 2. FAB mass spectra (matrix: *m*-nitrobenzyl alcohol, 8 kV-Xe-bombardment) of mixtures of **1** with the chosen guest molecules show intense signals for the 1:1 complexes; signals for the 1:2 complexes could not be observed. The statistically corrected association constants (Table 1) were obtained from Hill plots.[5]

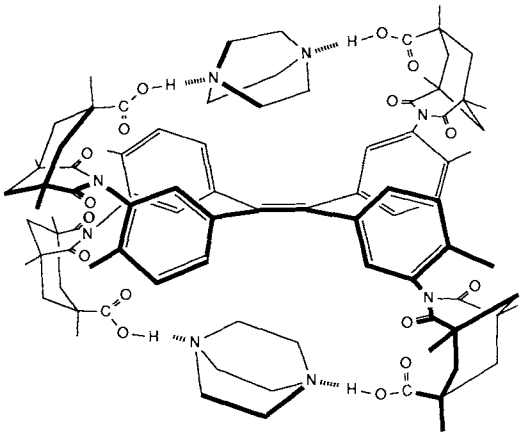

Scheme 2. Proposed structure of the 1:2 complex of **1** with DABCO.

Table 1. Statistically corrected association constants for the 1:1 and 1:2 complexes of **1** with various diamines[a].

Guest	$K(1:1)$ [L mol^{-1}]	$K(1:2)$ [L mol^{-1}]
Hydrazine	630	35000
Ethylendiamine	9	1700
DABCO	150	360
2-Aminopyrimidine	1400	90

[a] $T = 25\,^{\circ}C$; $c_{host} = 1 \times 10^{-3}$ mol L^{-1}, $c_{guest} = 5 \times 10^{-3}$ mol L^{-1}. Errors are estimated to be 10%.

Hydrazine and ethylenediamine show extensive positive cooperativity. DABCO shows reduced cooperativity, whereas 2-aminopyrimidine features negative cooperativity. It is likely that intramolecular hydrogen bonds between adjacent carboxy groups stabilize the unbound state. Chelation of one molecule of either hydrazine or ethylenediamine by nonadjacent acid groups of **1** forces the remaining acid groups to the other side of the ethylene planes in a conformation where they are poised (preorganized) for chelation of a second amine. This could lead to the 55 to nearly 200-fold increase of the association constants for the second binding event. DABCO has a somewhat longer N–N distance (2.6 Å) than is ideal for the cavity, and binding on one site could result in buttressing effects that reduce the cooperativity of the system. The chelation of 2-aminopyrimidine probably involves two adjacent sites, but we are unable to distinguish just which isomer this is. If a third carboxy group makes binding contact in the 1:1 complex, negative cooperativity would be the result.

In conclusion, the results show that binding cooperativity in these systems is much larger than those previously ob-

served with crown ether derivatives;[6] whether they arise from lost rotational degrees of freedom or exposure of buried sites is a matter for future research.[7]

Received: June 8, 1990 [Z 4005 IE]
German version: *Angew. Chem. 102* (1990) 1191

[1] D. J. Cram, *Angew. Chem. 98* (1986) 1041, *Angew. Chem. Int. Ed. Engl. 25* (1986) 1039; D. J. Cram, K. N. Trueblood in F. Vögtle, E. Weber (Eds.): *Host Guest Complex Chemistry—Macrocycles*, Springer, Berlin 1985, p. 125.
[2] G. Errera, *Gazz. Chim. Ital. 21* (1891) 94.
[3] D. S. Kemp, K. S. Petrakis, *J. Org. Chem. 46* (1981) 5140. The triacid is commercially available from Aldrich Chemical Co.; for a convenient synthesis see: J. Rebek, Jr., B. Askew, M. Killoran, D. Nemeth, F. T. Liu, *J. Am. Chem. Soc. 109* (1987) 2426. All the new compounds were characterized by ^{1}H- and ^{13}C-NMR spectroscopy, mass spectrometry, and elemental analysis.
[4] G. S. Eadie, *J. Biol. Chem. 146* (1942) 85.
[5] A. Levitzki, *Quantitative Aspects of Allosteric Mechanisms*, Springer, Berlin 1978.
[6] J. Rebek, Jr., R. V. Wattley, T. Costello, R. Gadwood, L. Marshall, *Angew. Chem. 93* (1981) 584, *Angew. Chem. Int. Ed. Engl. 20* (1981) 584.
[7] For a discussion of enthalpic vs. entropic origins of preorganization see: J. Rebek, Jr., *Acc. Chem. Res.*, in press.

Synthesis and Structure of a Diphosphadigalletane: A Novel Base-Stabilized Ga_2P_2 Ring System**

By *Alan H. Cowley,* Richard A. Jones,* Miguel A. Mardones, Jaime Ruiz, Jerry L. Atwood,** and *Simon G. Bott*

The search for new semiconductor precursors provides much of the impetus for a rekindled interest in the synthetic chemistry of the heavier group 13 and 15 elements. Apart from Lewis acid-base adducts, most of the current emphasis has been placed on compounds of the general type $(R_2MER'_2)_n$ (M = Ga,In; E = P,As,Sb).[1] However, we have recently turned our attention to species of empirical composition RMER'. Such compounds are of interest because of the potentially rich variety of structural forms and the possibility of novel bonding modes. Previous examples of compounds of the type $(RMER')_n$ have been confined to cases where M = B, Al and E = N.[2] We report the first instance in which both M and E are heavier main group elements.

Our initial attempts to prepare the desired compounds focussed on base-promoted dehydrochlorination reactions of $[t$Bu(Cl)GaP(H)Ar'$]_2$ which, in turn, was prepared via the methathetical reaction of $(t$BuGaCl$_2)_2$ with Ar'PHLi (Ar' = 2,4,6-tBu$_3$C$_6$H$_2$).[3] However, these efforts were thwarted by the strong Lewis acidity of Ga. As a consequence, we decided to explore the possibility of intramolecular Lewis base stabilization of the desired structure. The monoanionic ligand $[2,6\text{-}(Me_2NCH_2)_2C_6H_3]^{\ominus}$ seemed well suited for this purpose because of its demonstrated ability to stabilize unusual transition metal intermediates.[4]

[*] Prof. A. H. Cowley, Prof. R. A. Jones, M. A. Mardones, Dr. J. Ruiz
Department of Chemistry
University of Texas at Austin
Austin, TX 78712 (USA)
Prof. J. L. Atwood, Dr. S. G. Bott
Department of Chemistry
University of Alabama
Tuscaloosa, AL 35486 (USA)

[**] This work was supported by the National Science Foundation, The Robert A. Welch Foundation, and the U.S. Army Research Office.

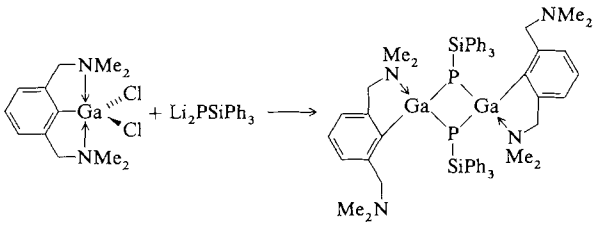

1 2

Treatment of $Li[2,6\text{-}(Me_2NCH_2)_2C_6H_3]$[5] with an equimolar quantity of $GaCl_3$ in toluene solution at −78 °C affords **1** which was characterized spectroscopically[6] and by an X-ray analysis.[7] The geometry around Ga in **1** is approximately trigonal bipyramidal (Fig. 1): the two N atoms

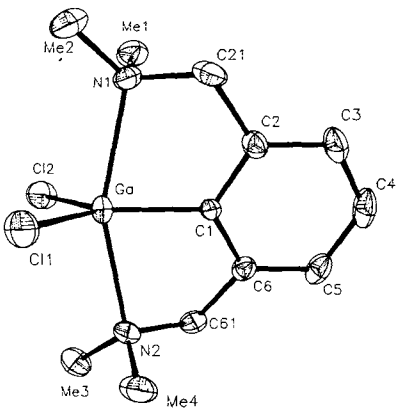

Fig. 1. The structure of **1** in the crystal. Selected bond lengths [Å] and bond angles [°]: Ga-Cl1 2.189(1), Ga-Cl2 2.189(2), Ga-N1 2.359(4), Ga-N2 2.351(4), Ga-C1 1.924(4), Cl11-Ga-Cl2 111.01(8), N1-Ga-N2 158.2(1), Cl1-Ga-C1 124.5(1), Cl2-Ga-C1 124.4(1).

adopt axial sites while the equatorial positions are occupied by two Cl atoms and the aryl group. There is, however, considerable distortion from the ideal angles, for example Cl-Ga-Cl = 110.01(8)° and N-Ga-N = 158.2(1)°.

Treatment of Ph_3SiPH_2[8] with 2.0 equivalents of tBuLi in Et_2O affords Li_2PSiPh_3 which, in turn, reacts with **1** at −78 °C to give **2**. The ^{1}H- and ^{13}C{^{1}H}-NMR data for **2**[6] establish equal abundances for the aryl and Ph_3Si substituents, and the high-resolution mass spectrum for the most intense $M^{\oplus}$ peak (found 1102.295630, calculated for $C_{60}H_{68}{}^{69}Ga^{71}GaN_4P_2Si_2$ 1102.296064) corresponds to a dimer of composition $[\{(Me_2NCH_2)_2C_6H_3\}GaPSiPh_3]_2$. Detailed structural information was provided by an X-ray analysis (Fig. 2). The central Ga_2P_2 core of **2** comprises a rhombus which resides on a center of symmetry. The bond angle at Ga (94.25(5)°) is somewhat larger than at P (85.75(5)°). The Ga–P bond length (2.338(1) Å) is over 0.1 Å shorter than those found in dimers or trimers of empirical composition RR'GaPR"R"'.[1] While it is tempting to suggest a modicum of P → Ga dative π-bonding, it should be noted that the phosphorus geometry is pyramidal (sum of angles at P = 325.52°). Clearly if there is any delocalization in the Ga_2P_2 ring, it is considerably less than that in diazadiboretidines[2] which are therefore much closer analogues of cyclobutadiene. Note also that each Ga is tetracoordinate due to the coordination of one dimethylamino group on each aryl ligand. In solution at ambient temperature there is evidently an exchange between free and coordinated Me_2N moieties since only one set of resonances is apparent in the

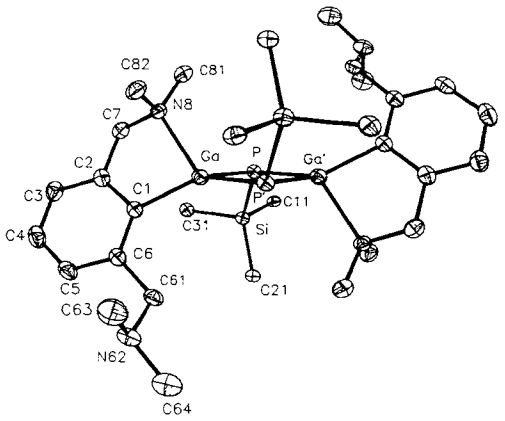

Fig. 2. The structure of **2** in the crystal. Selected bond lengths [Å] and bond angles [°]: Ga-P 2.388(1), P-Si 2.210(2), Ga-N8 2.139(4), Ga-C1 1.982(4), P'-Ga-P 94.25(5), P'-Ga-C1 129.4(1), P-Ga-N8 119.1(1), Ga'-P-Ga 85.75(5), Ga-P-Si 125.21(6), Ga'-P-Si 114.56(6), C1-Ga-N8 84.2(2), P-Ga-N8 119.1(1).

^{1}H- and ^{13}C{^{1}H}-NMR spectra.[6] No significant spectral changes were detectable down to −78 °C.

The thermolysis of **2** has been examined by temperature-programmed EI and CI mass spectrometry. When the temperature of the sample is increased at 20 °C/minute, a cluster of peaks appear at ca. 130 °C which are attributable to the monomer, e.g. at 200 °C for $C_{30}H_{34}{}^{69}GaN_2PSi$, found 550.147365, calculated 550.148472. No peaks corresponding to the dimer are evident at this temperature.

Experimental

1: A solution of 7.38 mmol of Li[2,6-$(Me_2NCH_2)_2C_6H_3$] [5] in 30 mL of toluene was added dropwise to a cooled (−78 °C) solution of $GaCl_3$ (1.3 g, 7.38 mmol) in 25 mL of toluene. The reaction mixture was allowed to warm to ambient temperature, after which it was stirred for a further 24 h. Filtration, followed by solvent evaporation, afforded a turbid liquid from which colorless crystals of **1** (m.p. 58 °C) were obtained in 61% yield by the addition of benzene. MS(EI, 70 eV): 332 ($M^{\oplus}$, 32.20%), 297 ($M^{\oplus}$ − Cl, 8.76%), 289 ($M^{\oplus}$ − NMe_2, 42.14%), 191 ($M^{\oplus}$ − $GaCl_2$, 99.71%), 105 (GaCl, 26.32%), 58 (CH_2NMe_2, 100%).
2: A suspension of Li_2PSiPh_3 was prepared by the addition of 1.8 mL of *t*BuLi (1.7 M in pentane) to a cooled (−78 °C) suspension of Ph_3SiPH_2 [8] (0.44 g, 1.5 mmol) in 25 mL of Et_2O. The stirred suspension was allowed to warm to ambient temperature, following which it was added to the suspension of **1** (0.73 g, 1.5 mmol) in 25 mL of Et_2O at −78 °C. The reaction mixture was allowed to reach ambient temperature and stirring was continued for 3 h. After filtration and concentration of the filtrate, colorless crystals of **2** (m.p. 234–237 °C), formed in 43% yield by cooling to −20 °C. Compound **2** is soluble in Et_2O, THF and toluene, but only slightly soluble in *n*-hexane.

Received: June 10, 1990 [Z 4021 IE]
German version: *Angew. Chem. 102* (1990) 1169

[1] For a review, see A. H. Cowley, R. A. Jones *Angew. Chem. 101* (1989) 1235; *Angew. Chem. Int. Ed. Engl. 28* (1989) 1208.
[2] For representative examples, see P. Paetzold, *Adv. Inorg. Chem. 31* (1987) 123; H. Nöth, *Angew. Chem. 100* (1988) 1664; *Angew. Chem. Int. Ed. Engl. 27* (1988) 1603; K. M. Waggoner, H. Hope, P. P. Power, *ibid. 100* (1988) 1765 and *27* (1988) 1699; P. B. Hitchcock, J. D. Smith, K. M. Thomas, *J. Chem. Soc. Dalton Trans. 1976*, 1433.
[3] A. H. Cowley, R. A. Jones, M. A. Mardones, unpublished.
[4] G. van Koten, J. Terheijden, J. A. M. van Beek, I. C. M. Wehman-Ooyevaar, R. Muller, C. H. Stam, *Organometallics 9* (1990) 903.
[5] G. van Koten, A. Leusink, J. G. Noltes, *J. Chem. Soc. D. 1970*, 1107.
[6] ^{1}H NMR (300 MHz, 295 K, C_6D_6, TMS ext.): **1**: δ = 2.12 (s, 12H, $(CH_3)_2N$), 3.03 (s, 4H, CH_2N), 6.95 (m, 3H H-aryl). **2**: δ = 2.32 (s, 24H, $(CH_3)_2N$), 3.52 (s, 8H, CH_2N), 7.20 (m, 18H, *m* + *p*-H, Si-Ph), 7.29 (m, 6H, *m* + *p*-H, Ga-aryl), 7.49 (m, 12H *o*-H, Si-Ph). ^{13}C{^{1}H} NMR (75.48 MHz, 295 K, C_6D_6, TMS ext.). **1**: δ = 46.0 ($(CH_3)_2N$), 63.5 (CH_2N), 124.7 (broad, *C*-Ga), 129.9 (*p*-C, Ga-aryl), 130.1 (*m*-C, Ga-aryl) 143.3 (*o*-C, Ga-aryl). **2**: δ = 46.0 ($(CH_3)_2N$), 66.1 (CH_2N), 125.3 (broad, C-Ga), 127.6 (*m* + *p*-C, Ga-aryl), 128.9 (broad, *o*-C, $SiPh_3$), 136.2 (broad, C-Si), 144.8 (*o*-C, Ga-aryl). ^{31}P{^{1}H} NMR (121.5 MHz 295 K, C_6D_6, 85% H_3PO_4 ext.): **2**: δ = −205, s.
[7] Crystal structure data for **1** · C_6H_6: $C_{18}H_{25}Cl_2GaN_2$, triclinic, space group $P\bar{1}$ (No. 2), Z = 2, a = 8.2851(3), b = 9.4420(3), c = 14.5120(5) Å, α = 85.505(3), β = 79.723(3), γ = 63.981(3)°, V = 1004(1) Å^3, ϱ_{calcd} = 1.361 g cm^3, ($Cu_{K\alpha}$, λ = 1.5418 Å, μ = 43.80 cm^{-1}), 2530 unique data collected ($\theta/2\theta$ scan technique, 2.0 ≤ 2θ ≤ 110.0°), of which 2255 had $I > 3\sigma(I)$ and were used for structure solution and refinement.—**2** · 2$C_6H_5CH_3$: $C_{74}H_{84}Ga_2N_4P_2Si_2$ triclinic, space group $P\bar{1}$ (No. 2), Z = 1, a = 11.3298(8), b = 12.1100(7), c = 14.7970(9) Å, α = 66.342(5), β = 68.596(6), γ = 77.947(5)° V = 1727(4) Å^3, ϱ_{calcd} = 1.242 g/cm^3, ($Cu_{K\alpha}$, λ = 1.5418 Å, μ = 20.56 cm^{-1}), 3411 unique data collected ($\theta/2\theta$ scan technique, 2.0 ≤ 2θ ≤ 110.0°), of which 3271 had $I > 3\sigma(I)$ and were used for structure solution and refinement. Both data sets were collected on an Enraf-Nonius CAD 4 diffractometer at 293 K, and were corrected for Lorentz, polarization, crystal decay, and X-ray absorption (empirical Ψ-scan method). Both structures were solved by direct methods (SHELX 86). Refinement (full-matrix, least-squares) gave R = 0.0512 and R_w = 0.0544 for **1** and R = 0.0418 and R_w = 0.0457 for **2**. Further details of the crystal structure investigations can be obtained from the Fachinformationszentrum Karlsruhe, Gesellschaft für wissenschaftlich-technische Information mbH D-7514, Eggenstein-Leopoldshafen 2 (FRG), by quoting the depository number CSD-54759, the names of the authors, and the journal citation.
[8] A. H. Cowley, P. C. Knüppel, C. M. Nunn, *Organometallics 8* (1989) 2490.

Facile Hydrogenation of the Central Cyclohexatriene of Tris(benzocyclobutadieno)benzene: Synthesis, Structure, and Thermal and Photochemical Isomerization of all-*cis*-Tris(benzocyclobuta)cyclohexane **

By *Debra L. Mohler, K. Peter C. Vollhardt,** and *Stefan Wolff*

We describe the first chemical reaction of hydrocarbon **1**,[1] namely its facile and stereoselective hydrogenation to **2**, whose X-ray structural analysis reveals the presence of an unusually bond-fixed, planar cyclohexane ring. The latter undergoes stereospecific thermal retrocyclization exclusively to the hexaene **3**, a feature that, in conjunction with the associated kinetic data, suggests the occurrence of an unprecedented all-disrotatory process.[2] In contrast, irradiation of **2** effects the rearrangement to the new hydrocarbon **4** and, ultimately, phenanthrene and naphthalene, whereas **3** photoisomerizes to **5** (Scheme 1). The reported chemistry expands significantly the range of the transformations recorded for the benzocyclobutene nucleus and the tribenzo-$(CH)_{12}$-manifold.

The hydrogenation of **1** to **2a** proceeded under extraordinarily mild conditions,[3] a finding ascribable to the high degree of bond localization and strain in the system. On the other hand, the 2,3,6,7,10,11-hexakis(trimethylsilyl) derivative of **1**[1] was inert even at elevated hydrogen pressures (80 atm, THF, Pd-C).

The stereochemistry of **2a** was first assigned on the basis of its ^{1}H-NMR spectrum, particularly the signal for the central ring hydrogens (a singlet at δ = 4.19), the ^{13}C-NMR spectrum (4 lines) and the analogous behavior of the related angular and linear [3]phenylenes.[4] Because of its novelty and unexpected chemistry (see below), and also for comparison with **1**, an X-ray structural investigation was carried out

[*] Prof. Dr. K. P. C. Vollhardt, D. L. Mohler, Dr. S. Wolff
Department of Chemistry, University of California at Berkeley,
and the Materials and Chemical Sciences Division,
Lawrence Berkeley Laboratory, Berkeley, CA 94720 (USA)

[**] This work was supported by the Director, Office of Energy Research, Office of Basic Energy Sciences, Materials Science Division of the U. S. Department of Energy (Contact No. DE-AC03-76 SF 00098). S. W. acknowledges a Postdoktoranden-Stipendium of the Deutsche Forschungsgemeinschaft (1989–1990).

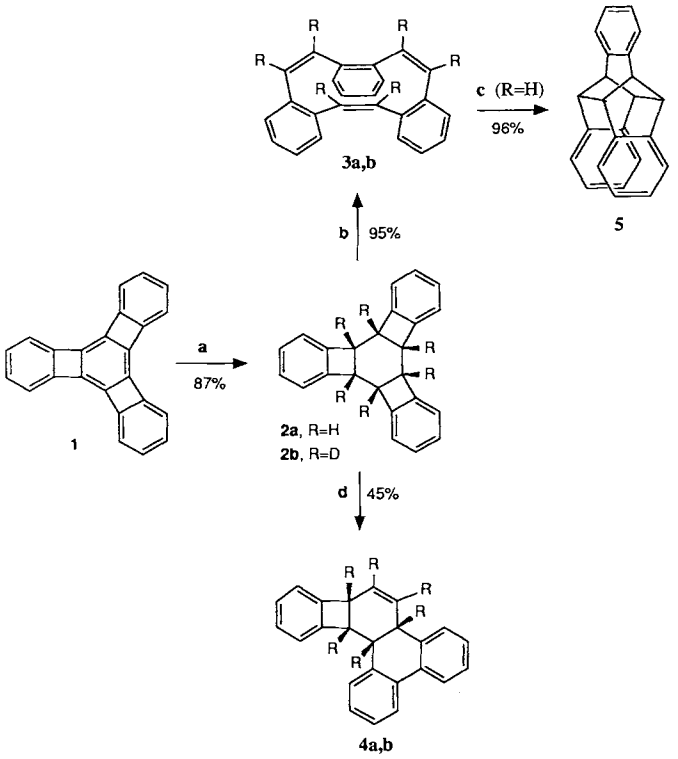

Scheme 1. (a) H_2 or D_2 (1 atm), Pd-C, THF, 18 h; (b) C_6D_6, sealed tube, 125 °C–160 °C; (c) Et_2O, *hv* 254 nm, – 22 °C, 4.5 h; (d) Et_2O, *hv* 254 nm, – 2 °C, 3.5 h.

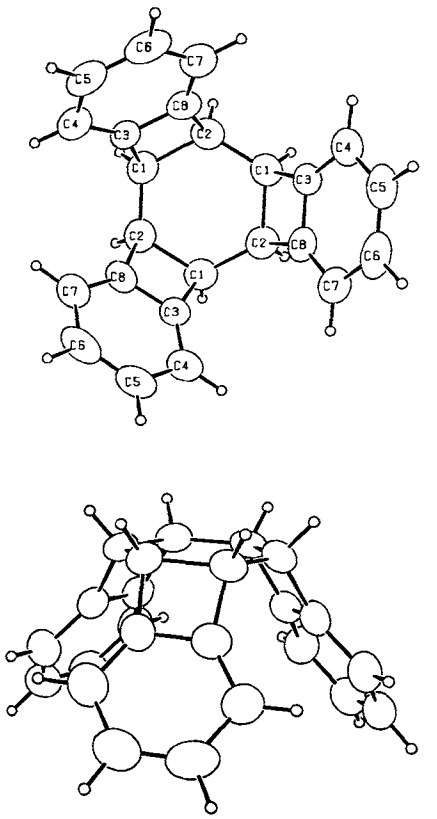

Figure 1. ORTEP drawings of the top and side views of **2a**. Ellipsoids are scaled to represent the 50% probability surface and hydrogen atoms are given as arbitrary small spheres. Selected bond lengths [Å] and angles [°]: C1-C2 1.599(4), C1-C2′ 1.511(4), C1-C3 1.516(3), C2-C8 1.526(3), C3-C4 1.393(4), C3-C8 1.379(4), C4-C5 1.394(4), C5-C6 1.379(5), C6-C7 1.391(4), C7-C8 1.376(3); C2-C1-C2′ 119.8(2), C2-C1-C3 85.6(2), C1-C2-C8 86.0(2), C4-C5-C6 122.2(3), C5-C6-C7 121.9(2), C6-C7-C8 116.1(3), C2-C8-C3 93.5(2), C3-C8-C7 122.5(2).

(Fig. 1).[5] The central cyclohexane ring is planar, a geometry enforced by the three fused benzocyclobutenes. The average dihedral angle between the plane of the former and those of the latter is 54.5°, giving rise to a strongly cup-shaped molecule. Most remarkable are two features: 1) There is strong bond alternation in the cyclohexane frame (C1–C2, 1.60 Å; C1–C2′, 1.51 Å), to a degree that is unprecedented,[6] and 2) the geometry of the benzene rings is changed very little relative to those of its precursor **1**,[1, 7] both comparing well to those of model benzocyclobutenes,[8] an aspect also reflected in the ^{1}H- and ^{13}C-NMR data. The first characteristic could be a trigger to the thermal chemistry of **2** (see below), the second may further corroborate recent theoretical findings that σ-effects play an important role in the bond-fixation observed in **1** (and, presumably, other benzenoid hydrocarbons of this type).[9]

Hydrocarbon **2** may be viewed as a trishomolog of the extensively investigated all-*cis*-tris-σ-homobenzenes[10] and as being endowed with sufficient ring strain (>100 kcal mol^{-1})[11] to undergo an analogous retro-[2+2+2]cycloaddition unraveling the cyclohexane moiety. However, the tenuous nature of this notion becomes apparent when one considers that the benzofusion in **2** renders (a least strained) disrotatory four-ring opening unfavorable on the basis of orbital symmetry considerations,[12] that any concerted path may be inhibited by the development of the antiaromatic circuit of a [12]annulene system, and that the saturated debenzo relative of **2**, *cis*-tris[2.2.2]-σ-homobenzene **6**, is stable to high temperatures, when it decomposes through radical intermediates to a complex mixture of products.[13d] These caveats notwithstanding, on heating (C_6D_6, sealed tube, 125–160 °C, several days), **2a** was isomerized cleanly and stereospecifically to **3a**,[3] following first order kinetics [$\Delta H^{\neq}$ = 29.4 (4.7) kcal mol^{-1}, $\Delta S^{\neq}$ = – 12.7(11.3) cal K^{-1} mol^{-1}]. NMR, in particular, highlighted not only the symmetrical nature of the product but also its dissimilarity to the corresponding *E,E,E* form,[14] including J_{cis} = 12 Hz for the former vs. J_{trans} = 18 Hz for the latter (obtained from the respective ^{13}C-satellite ^{1}H-NMR signals). The ease and specifity of the formation of **3a** from **2a** provide strong evidence for the occurrence of a concerted, all-disrotatory mechanism. For comparison, Table 1 summarizes the activation parameters of some model systems.

Table 1. Activation energies E_a (kcal mol^{-1}) for thermal ring-opening reactions of selected model compounds [a].

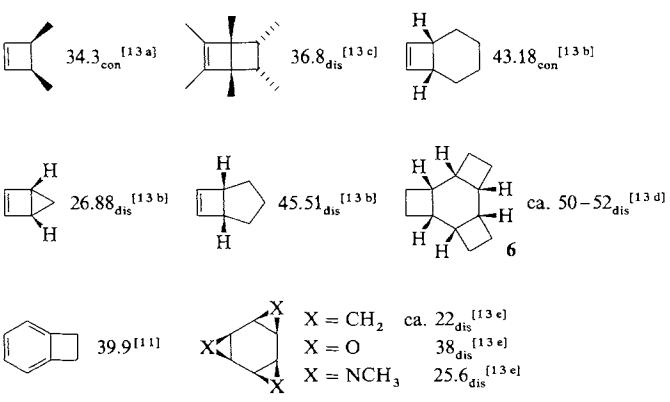

[a] Stereochemistry of the reaction indicated by subscripts.

Support for the two cornerstones of this claim was assembled as follows. Stereochemistry: **3** cannot be preceded by one of its double bond isomers, as those with either *E,E,E*[14] or *E,Z,Z* configuration[2] are inert to the reaction conditions, while that containing the *E,E,Z* structure has been convincingly demonstrated to furnish stable **5** through homo-Diels-Alder cycloaddition of the *cis*-π-bond to the other two (see also below).[14] Concertedness: both directly competitive and independent kinetic runs, employing **2a** and its hexadeuterated relative **2b** [$k_H(125\,°C) = 3.11(\pm 0.08) \times 10^{-6}\,s^{-1}$; $k_D(125\,°C) = 1.98(\pm 0.06) \times 10^{-6}\,s^{-1}$] revealed the same α-secondary deuterium isotope effect of $k_H/k_D(D_6) = 1.57$! This figure translates into $k_H/k_D(D_1) = 1.08$, the same as that observed for concerted cyclobutene openings.[15] The absence of any relatively long-lived intermediates was ascertained by transforming **2a** into **3a** in molten *cis*-2-butenedioic anhydride (160 °C, 7 d) without change in the outcome of the reaction.

In view of the above findings, one might (naively) expect that photochemical activation of **2** would, by an all-conrotatory pathway (producing initially either or both of the *E,E,E* or *E,Z,Z* isomers of **3**) result in **5**.[14] However, upon photolysis of **2a** (or **2b**) with 254-nm UV lamps (Rayonet, Et_2O, − 2 °C, 3.5 h), **4a** (or **4b**) was formed in 45% yield, together with starting material (32%) and small amounts of phenanthrene (or 9,10-dideuteriophenanthrene) and naphthalene (or [D_4]naphthalene, the position of the label was not ascertained). The new compound **4a** was characterized by spectroscopy[3] and X-ray analysis (Fig. 2).[16]

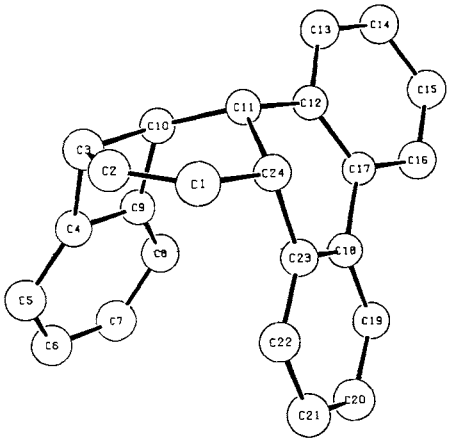

Fig. 2. ORTEP drawing of **4a**. Ellipsoids are scaled to represent the 50% probability surface and hydrogen atoms are given as arbitrary small spheres. Selected bond lengths [Å] and angles [°]: C1-C2 1.351(5), C1-C24 1.526(6), C2-C3 1.512(6), C3-C4 1.542(6), C3-C10 1.590(6), C4-C5 1.392(5), C4-C9 1.376(5), C5-C6 1.426(6), C6-C7 1.413(6), C7-C8 1.407(6), C8-C9 1.401(5), C9-C10 1.539(5), C10-C11 1.527(5), C11-C12 1.514(5), C11-C24 1.549(5), C12-C17 1.386(5), C17-C18 1.482(5), C18-C23 1.415(6), C23-C24 1.525(5); C2-C1-C24 123.1(4), C1-C2-C3 122.3(4), C2-C3-C4 112.9(3), C2-C3-C10 116.2(3), C4-C3-C10 85.8(3), C3-C4-C5 142.3(4), C3-C4-C9 94.1(3), C5-C4-C9 123.6(4), C4-C5-C6 114.8(4), C5-C6-C7 121.2(4), C6-C7-C8 122.6(4), C7-C8-C9 114.7(4), C4-C9-C8 123.1(4), C4-C9-C10 93.8(3), C8-C9-C10 143.1(4), C3-C10-C9 86.2(3), C3-C10-C11 113.9(3), C9-C10-C11 122.7(3), C10-C11-C12 113.2(3), C10-C11-C24 113.8(3), C12-C11-C24 109.2(3), C11-C12-C13 118.4(4), C11-C12-C17 121.3(4), C12-C17-C18 119.4(4), C17-C18-C19 121.5(4), C17-C18-C23 118.9(4), C18-C23-C24 117.8(4), C22-C23-C24 122.5(4), C1-C24-C11 110.6(3), C1-C24-C23 113.3(4), C11-C24-C23 110.9(3).

A control experiment revealed that irradiation of **3a** with 254-nm UV lamps at − 22 °C for 4.5 h leads to **5** almost quantitatively. It is therefore clear that the photochemistry of **2** is associated with a new mechanistic manifold.[14] While delineation of its details are premature, there are topologically analogous transformations in the literature.[12b, c, 17]

Received: June 29, 1990 [Z 4046 IE]
German version: *Angew. Chem. 102* (1990) 1200

[1] R. Diercks, K. P. C. Vollhardt, *J. Am. Chem. Soc. 108* (1986) 3150.

[2] The conversion of **1** into **2a** and subsequently **3a** was first communicated April 6, 1987, at the 193rd ACS National Meeting (April 5-10, 1987), Denver, Colorado. While this work was in progress, an alternative synthesis of **2a** and its thermal conversion into **3a** was reported, lacking, however, the essential structural and mechanistic and photochemical studies delineated here: M. Iyoda, Y. Kuwatani, T. Yamauchi, M. Oda, *J. Chem. Soc. Chem. Commun. 1988*, 65.

[3] All compounds gave satisfactory analytical and spectral data. For example, **2a**: colorless crystals, m.p. 192–195 °C; MS (70 eV): *m/z* 306 ($M^{\oplus}$, 100), 305(86), 191(61); ^{1}H NMR (250 MHz, $CDCl_3$): δ = 4.19 (s, 6H), 6.84 (AA'm, 6H), 6.92 (BB'm, 6H); ^{13}C NMR (75 MHz, $CDCl_3$): δ = 40.6, 123.7, 126.4, 147.2; IR (KBr): $\tilde{\nu}$ = 2930, 1455, 1210, 1110 cm^{-1}; UV (hexane) λ_{max} (log ε) = 268 (3.27), 274 (3.24) nm. **2b**: MS (70 eV): *m/z* 312 ($M^{\oplus}$, 84), 311(63), 194(72). **3a**: colorless crystals, m.p. 185–186 °C; MS (70 eV): *m/z* 306 ($M^{\oplus}$, 100), 305(52), 191(55); ^{1}H NMR (250 MHz, C_6D_6): δ = 6.56 (s, 6H), 6.77 (AA'm, 6H), 7.08 (BB'm, 6H); ^{13}C NMR (75 MHz, C_6D_6): δ = 126.1, 130.1, 132.5, 136.6; IR (KBr): $\tilde{\nu}$ = 2990, 2920, 1460, 1440, 1260, 1085, 800, 740, 650 cm^{-1}; UV (hexane): λ_{max} (log ε) = 218 (4.43), 268 (3.43) nm. **3b**: MS (70 eV): *m/z* 312 ($M^{\oplus}$, 100). **4a**: colorless crystals, m.p. 145–147 °C; MS (70 eV): *m/z* 306 ($M^{\oplus}$, 70), 305 (47), 178 (100), 128 (75); ^{1}H NMR (400 MHz, $CDCl_3$): δ = 3.24 (dd, *J* = 5.8, 5.8 Hz, 1H), 3.81 (dd, *J* = 6.2, 6.2 Hz, 1H), 3.87 (dd, *J* = 5.3, 5.3 Hz, 1H), 4.03 (dd, *J* = 5.2, 5.2 Hz, 1H), 5.96 (dd, *J* = 7.4, 1 Hz, 1H), 6.37 (dd, *J* = 10.1, 6.7 Hz, 1H), 6.44 (dd, *J* = 10.1, 5.5 Hz, 1H), 6.48 (ddd, *J* = 7.4, 7.4, 2 Hz, 1H), 6.70–6.80 (m, 2H), 6.99 (dddd, *J* = 7.0, 7.0, 2, 1 Hz, 1H), 7.29–7.41 (m, 3H), 7.55 (bd, *J* = 7.7 Hz, 1H), 7.84 (bd, *J* = 7.4 Hz, 1H). ^{13}C NMR (100 MHz, $CDCl_3$) δ = 36.86, 41.59, 42.61, 46.82, 120.08, 123.09, 123.42, 123.51, 125.70, 126.03, 126.24, 126.53, 127.23, 127.36, 127.65, 128.88, 129.25, 129.72, 133.70, 134.56, 138.01, 138.35, 145.83, 146.15; IR (KBr): $\tilde{\nu}$ = 3063, 3028, 2913, 2838, 1482, 1450, 1243, 747 cm^{-1}; UV (hexane): λ_{max} (log ε) = 234 sh (3.13), 269 (3.12), 305 (2.65) nm.

[4] a) B. C. Berris, G. H. Hovakeemian, Y.-H. Lai, H. Mestdagh, K. P. C. Vollhardt, *J. Am. Chem. Soc. 107* (1985) 5670; b) R. Diercks, K. P. C. Vollhardt, *Angew. Chem. 98* (1986) 268; *Angew. Chem. Int. Ed. Engl. 25* (1986) 266.

[5] Crystal size 0.19 × 0.22 × 0.27 mm^3, trigonal Laue symmetry, space group *R*3, 2θ scan range 3°–45°, *a* = 14.9760(18) Å, *b* = 14.9760(18) Å, *c* = 6.1680 (6) Å, α = 90.0°, β = 90.0°, γ = 120.0°, *V* = 1198.0(4) Å^3, *Z* = 3, ϱ_{calcd} = 1.27 g cm^{-3}, μ = 0.7 cm^{-1}, reflections collected at room temperature, 1034, of which 346 were taken as observed [$F^2 > 3\sigma(F^2)$], without absorption correction, *R* = 0.0395, R_w = 0.0556. Hydrogen atoms were assigned idealized locations. The ideal positions of the hydrogens on the strained carbons were adjusted based on residual peaks in the difference Fourier map during the last cycles of refinement [18].

[6] G. McMullen, M. Lutterbeck, H. Fritz, H. Prinzbach, C. Krüger, *Isr. J. Chem. 22* (1982) 19.

[7] We are juxtaposing the X-ray structural features of **2a** to those of hexasilylated **1**. The (minor) perturbation caused by the substituents in the latter can be assessed by comparing the analogous data for 4,5-bis(trimethylsilyl)-1,2-dihydrocyclobutabenzene [K. P. Moder, E. N. Duesler, N. J. Leonard, *Acta Crystallogr. B 37* (1981) 289] with those for 1,2-dihydrocyclobutabenzene [8].

[8] R. Boese, D. Bläser, *Angew. Chem. 100* (1988) 293; *Angew. Chem. Int. Ed. Engl. 27* (1988) 304.

[9] A. Stanger, K. P. C. Vollhardt, *J. Org. Chem. 53* (1988) 4889.

[10] a) W.-D. Braschwitz, T. Otten, C. Rücker, H. Fritz, H. Prinzbach, *Angew. Chem. 101* (1989) 1383; *Angew. Chem. Int. Ed. Engl. 28* (1989) 1348; b) D.-R. Handreck, D. Hunkler, H. Prinzbach, *ibid. 101* (1989) 1386 and *28* (1989) 1351, and references cited therein.

[11] a) W. R. Roth, M. Biermann, H. Dekker, R. Jochems, C. Mosselman, H. Hermann, *Chem. Ber. 111* (1978) 3892; b) W. R. Roth, B. P. Scholz, *ibid. 114* (1981) 3741.

[12] a) J. F. Liebman, A. Greenberg: *Structure and Reactivity*, VCH Publishers, New York 1988; b) J. J. Gajewski: *Hydrocarbon Thermal Isomerizations*, Academic Press, New York 1981; c) A. Greenberg, J. F. Liebman: *Strained Organic Molecules*, Academic Press, New York 1978.

[13] a) R. Srinivasan, *J. Am. Chem. Soc. 91* (1969) 7557; b) D. S. Weiss, *Tetrahedron Lett. 1975*, 4001; c) F. v. Rantwijk, H. v. Bekkum, *ibid. 1976*, 3341; d) M. Maas, M. Lutterbeck, D. Hunkler, H. Prinzbach, *Tetrahedron Lett. 24* (1983) 2143; e) B. Zipperer, K.-H. Müller, B. Gallenkamp, R. Hildebrand, M. Fletschinger, D. Burger, M. Pillat, D. Hunkler, L. Knothe, H. Fritz, H. Prinzbach *Chem. Ber. 121* (1988) 757.

[14] a) M. W. Tausch, M. Elian, A. Bucur, E. Cioranescu, *Chem. Ber. 110* (1977) 1744; b) H. A. Staab, F. Graf, K. Doerner, A. Nissen, *Chem. Ber. 104* (1971) 1159.

[15] a) J. J. Gajewski in E. Buncel, C. C. Lee (Eds): *Isotopes in Organic Chemistry, Secondary and Solvent Isotope Effects, Vol. 7*, Elsevier, New York 1987, pp. 160–162; b) see also: J. J. Gajewski, K. B. Peterson, J. R. Kagel, Y. C. J. Huang, *J. Am. Chem. Soc. 111* (1989) 9078.

[16] Crystals dimensions $0.25 \times 0.30 \times 0.40$ mm^3, orthogonal Laue symmetry, space group *Pbca*, 2θ scan range 3°–45°, $a = 7.522(2)$ Å, $b = 15.009(3)$ Å, $c = 28.858(7)$ Å, $\alpha = 90.0^\circ$, $\beta = 90.0^\circ$, $\gamma = 90.0^\circ$, $V = 3257.7(23)$ Å^3, $Z = 8$, $\varrho_{calcd} = 1.25$ g cm^{-3}, $\mu = 0.7$ cm^{-1}, reflections collected at room temperature, 2474, of which 1312 were taken as observed [$F^2 > 3\sigma(F^2)$], without absorption correction, $R = 0.104$, $R_w = 0.123$ [18].

[17] G. I. Fray, R. G. Saxton: *The Chemistry of Cyclooctatetraene and Its Derivatives*, Cambridge University Press, New York 1978; J. D. Coyle (Ed.): *Photochemistry in Organic Synthesis*, The Royal Society of Chemistry, London 1986. See also: J. J. McCullough, *Acc. Chem. Res. 13* (1980) 270.

[18] Further details of the crystal structure investigation may be obtained from the Fachinformationszentrum Karlsruhe, Gesellschaft für wissenschaftlich-technische Information mbH, D-7514 Eggenstein-Leopoldshafen 2 (FRG), on quoting the depository number CSD-54806, the names of the authors, and the journal citation.

Structure of a Synthetic Trefoil Knot Coordinated to Two Copper(I) Centers**

By *Christiane O. Dietrich-Buchecker, Jean Guilhem, Claudine Pascard,** and *Jean-Pierre Sauvage**

Although knotted forms of DNA are relatively common, as shown by recent results of molecular biology,[1, 2] knotted compounds in chemistry have only been envisaged and discussed as hypothetical objects.[3–5]. A year ago, the first synthetic trefoil knot was reported.[6] The preparation of this topologically novel molecular system was made possible by the use of a double three-dimensional template effect. Two coordinating molecular threads were interlaced on two copper(I) centers, forming a double helix, the precursor of a knotted system.

Although convincing evidence for the knotted topology of the molecule was obtained from mass and ^{1}H-NMR studies, in particular by taking advantage of the chirality of a trefoil knot, it was of utmost importance to obtain an X-ray structure of the molecule. In the meantime this has been achieved, and we now report the molecular structure of the compound. This study removes the last uncertainty regarding the knotted structure of the molecule obtained. It also provides interesting data on the fine structure and conformation. Moreover, it demonstrates that the knotted compound undergoes spontaneous resolution, which is very encouraging for a future separation into right- and left-knotted enantiomers.[7]

The chemical representation of the molecule is given in Figure 1. The organic skeleton is made up of a single 86-membered molecular chain, whose ends are tied with formation of a trefoil knot. The molecule still contains the two copper(I) centers used as templating species during the synthesis.

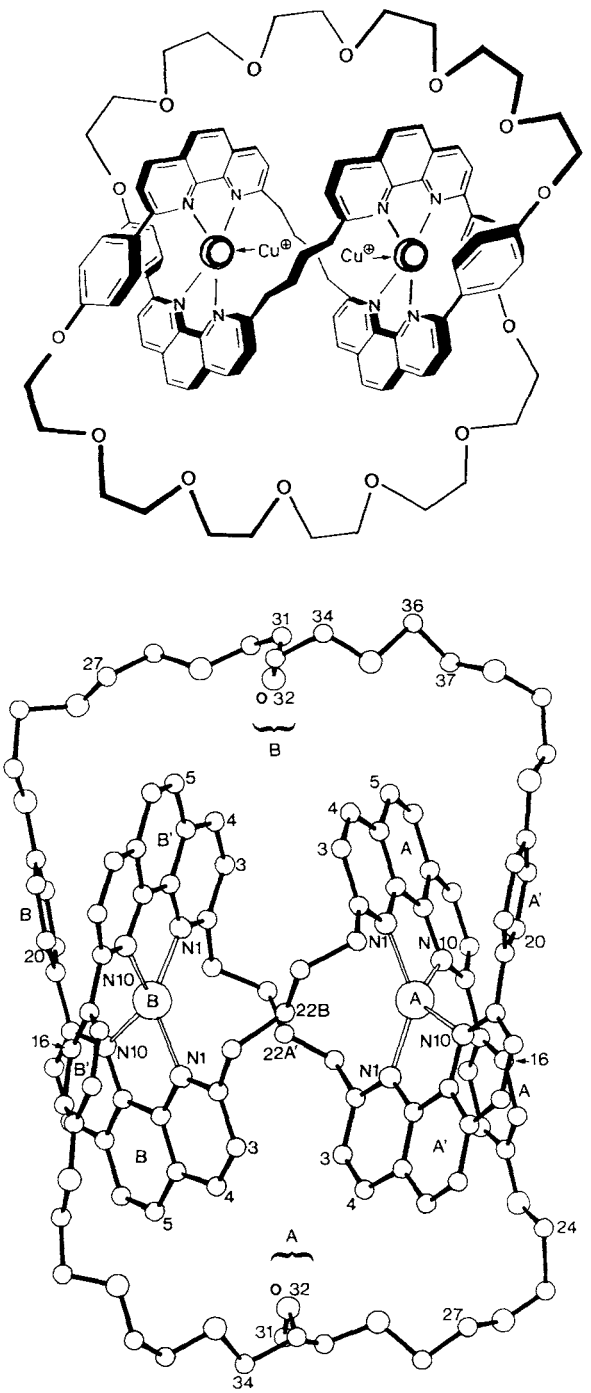

Fig. 1. Structural formula (top) and ORTEP of the knotted compound. For sake of clarity, the written symbols corresponding to the crystallographic numbering have all been omitted, those of O partly omitted. A denotes CuA and B denotes CuB.

The X-ray crystallographically determined molecular structure is shown in Figure 1 (bottom).[8] The molecule has effective D_2 symmetry, with three mutually perpendicular pseudo-twofold axes, one joining the two copper cations, one passing through the middle of the two $(CH_2)_4$ bridges, and the third one passing through the central oxygens of the two polyoxyethylene chains. The symmetry places the two complexes around CuA and CuB, with their respective 1,10-phenanthroline rings (CuA with phen A and phen A′ and CuB with phen B and phen B′) in superimposed fashion: A over B′, and A′ over B. Starting from phen A, the molecular

[*] Dr. C. Pascard, Dr. J. Guilhem
Laboratoire de Cristallochimie
Institut de Chimie des Substances Naturelles, CNRS
F-91198 Gif-sur-Yvette (France)
Dr. J. P. Sauvage, Dr. C. O. Dietrich-Buchecker
Laboratoire de Chimie Organo-Minérale, UA 422 du CNRS
Institut de Chimie, Université Louis Pasteur
F-67008 Strasbourg (France).

[**] This work was supported by the Centre National de la Recherche Scientifique (CNRS).

ribbon goes along the $(CH_2)_4$ bridge joining phen A to phen B, turns around CuB with phen B, follows the long oxy chain B back to phen A', turns around CuA with phen A', goes along the second $(CH_2)_4$ bridge to phen B', and, following the oxy chain A, ends up at the starting point phen A.

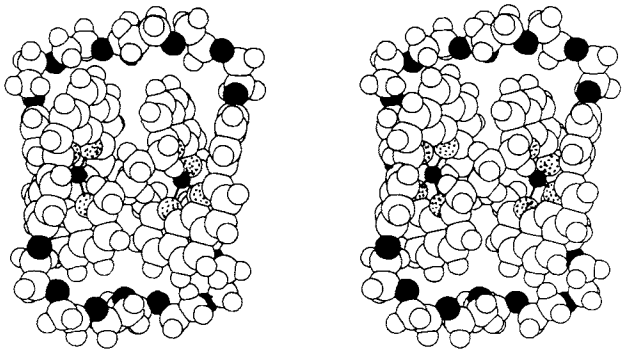

Fig. 2. Stereoview of the knotted compound.

The stereoview (Fig. 2) shows how the two metal atoms are located 6.3 Å apart inside a double helix. The two complexes, around CuA and CuB face each other with similar coordination angles (see Table 1), the wider angle (141° average) opening towards the center of the knot.

Table 1. Structural data of the Cu centers

Cu A environment		Cu B environment	
Distances [Å]			
Cu-N1A	2.00(3)	Cu-N1B	2.08(2)
Cu-N10A	2.14(2)	Cu-N10B	2.06(3)
Cu-N1A'	1.95(2)	Cu-N1B'	2.11(2)
Cu-N10A'	2.11(2)	CuN10B'	2.13(3)
Angles [°] ($\sigma \approx 1°$)			
N1A-Cu-N10A	83	N1B-Cu-N10B	80
N1A'-Cu-N10A'	83	N1B'-Cu-N10B'	79
N10A-Cu-N10A'	128	N10B-Cu-N10B'	135
N10A-Cu-N1A'	113	N10B-Cu-N1B'	112
N1A-Cu-N10A'	114	N1B-Cu-N10B'	120
N1A-Cu-N1A'	143	N1B-Cu-N1B'	140

The general molecular shape of the knotted complex can be compared with that of the chemically related dicopper(I) [3]-catenate consisting of two peripheral 30-membered rings separately interlocked with a central 44-membered ring.[9, 10] In the [3]-catenate, the Cu···Cu distance is noticeably longer than in the knot (8.0 Å instead of 6.3 Å), although better π-stacking is observed in the [3]-catenate than in the knot (see Table 2). In the [3]-catenate[10] the superimposed

Table 2. Relevant dihedral angles [°] between aromatic rings.

	Phenyl A	phen A'	Phenyl A'	phen B	Phenyl B	phen B'	Phenyl B'
phen A	43	64	29	60	19	24	45
Phenyl A		25	37	16	26	52	23
phen A'			43	20	46	60	22
Phenyl A'				50	20	18	22
phen B					42	67	32
Phenyl B						28	38
phen B'							39

phenanthroline rings are roughly parallel (dihedral angle 7°), whereas in the knotted compound they are inclined toward each other (24° and 20°) with their tip ends in proximity: average distance between H3 and H4 of each pair of phenanthrolines (A–B' and A'–B): 3.5 Å. On the other hand, the coordination sphere of each copper(I) ion in the knotted compound is only very slightly distorted compared to that in the [3]-catenate.

Within the complex units of the knotted compound, the dihedral angle between the two phenanthroline rings is 64 and 67° respectively, which reflects the strong distortion of each coordination polyhedron from a tetrahedral geometry. Furthermore, each phenyl ring forms a dihedral angle of approximately 42° with its bonded phenanthroline.

All the oxygen atoms of the polyoxyethylene chains are turned inward, and the molecule has a rectangular hydrophobic feature. The chains are actually a little too long, as can be seen by the folded fragments around the central oxygens O32A and O32B.

The centers of the short $(CH_2)_4$ bridges are very close together, with short distances between the hydrogens of the methylenic carbon atoms C22B and C22A'. Many other short distances exist, in particular between the hydrogen atoms of the hexaethyleneoxy chains and the aromatic groups. The most important data have been collected in Table 3.

Table 3. Shortest intramolecular H-H distances [Å] ($\sigma \approx 0.1$ Å).

Between superimposed phenanthroline rings	*Between phenyl rings*
	H16A-H20A' 2.4
H4A-H4B' 3.5	H16B'-H20B 2.5
H4B-H4A' 3.4	*Between $(CH_2)_4$ bridges*
H4B-H3A' 3.4	H_a22B-H_b22A' 2.3
Between phenanthroline rings and polyoxyethylene chains [a]	*Between the methylene groups in a chain* [a]
H5A-H_b37B 2.8	H_b24A-H_a27A 2.4
H4A'-H_a27A 2.6	H_b31A-H_b34A 2.2
H5B-H_a31A 2.7	H_a31B-H_b34B 2.2
H5B'-H_b27B 2.4	H_a31B-H_b36B 2.5

[a] H_a and H_b are the two H atoms of a given CH_2 group.

Further, the X-ray structure analysis revealed that the chiral dicopper(I) knotted compound crystallizes as a conglomerate of enantiomers, i.e. a given crystal contains only one enantiomer: Figure 3 shows a stereoview of the unit cell with two left knotted enantiomers.

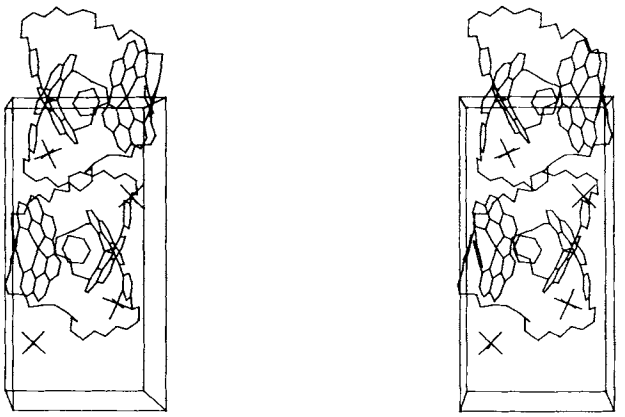

Fig. 3. Stereoview of the unit cell. Shown are two complexes, four anions ($PF_6^{\ominus}$), and two solvent molecules (benzene).

Experimental

Crystals of $[C_{104}H_{104}N_8O_{14}Cu_2](PF_6)_2 \cdot C_6H_6$ were grown from CH_2Cl_2/C_6H_6 by vapor diffusion of benzene. The dark-red, well-shaped crystals obtained ($0.8 \times 0.3 \times 0.1$ mm) were sealed in a capillary tube. Intensity data were collected at 1.1 Å resolution ($\theta_{max} = 45°$) with an automatic Philips PW1100 diffractometer, wavelength $Cu_{K\alpha}$ ($\lambda = 1.5418$ Å), graphite monochromator. From 7925 unique measured reflections, only 2967 independent reflections with $I \geq 2\sigma(I)$ were kept in the calculations. $M = 2183$, monoclinic, space group $P2_1$, $a = 13.462(6)$, $b = 27.841(14)$, $c = 13.912(7)$ Å $\beta = 93.66(4)°$, $V = 5204$ Å^3 $Z = 2$. $\varrho_{calc} = 1.39$ g cm^{-3}. Structure solved by direct methods [11]. High pseudo symmetry rendered the crystallographic study very difficult. Low resolution and thermal agitation led to rigid block refinement of the aromatic parts (except in the last refinement cycle) and constraints in the long chains. The final R factor is 12.8%. Further details of the crystal structure will be published elsewhere and will be available from the Director of the Cambridge Crystllographic Data center, University Chemical Laboratory, Lensfield Road, Cambridge CB2 IEW (UK), on quoting the names of the authors and the journal citation.

Received: May 23, 1990 [Z 3974 IE]
German version: *Angew. Chem. 102* (1990) 1202

[1] M. A. Krasnow, A. Stasiak, S. J. Spengler, F. Dean, T. Koller, N. R. Cozzarelli, *Nature (London) 304* (1983) 559.
[2] J. D. Griffith, H. A. Nash, *Proc. Natl. Acad. Sci. USA 82* (1985) 3124.
[3] H. F. Frisch, E. Wasserman, *J. Am. Chem. Soc. 83* (1961) 3789.
[4] G. Schill, L. Tafelmair, *Synthesis 1971*, 546; J. Boeckmann, G. Schill, *Tetrahedron 30* (1974) 1945; G. Schill, G. Doerjer, E. Logemann, H. Fritz, *Chem. Ber. 112* (1979) 3603.
[5] D. M. Walba, *Tetrahedron 41* (1985) 3161; D. M. Walba, J. D. Armstrong, III, A. E. Perry, R. M. Richards, T. C. Homan, R. C. Haltiwanger, *ibid. 42* (1986) 1883.
[6] C. O. Dietrich-Buchecker, J.-P. Sauvage, *Angew. Chem. 101* (1989) 192; *Angew. Chem. Int. Ed. Engl. 28* (1989) 189.
[7] A. Collet, M.-J. Brienne, J. Jacques, *Chem. Rev. 80* (1980) 215.
[8] C. K. Johnson, ORTEP: Report ORNL 3794. Oak Ridge National Laboratory, Oak Ridge, TN, USA 1976.
[9] C. O. Dietrich-Buchecker, A. Khemiss, J.-P. Sauvage, *J. Chem. Soc. Chem. Commun. 1986*, 1376.
[10] C. O. Dietrich-Buchecker, J. Guilhem, A. K. Khemiss, J.-P. Kintzinger, C. Pascard, J.-P. Sauvage, *Angew. Chem. 99* (1987) 711; *Angew. Chem. Int. Ed. Engl. 26* (1987) 661.
[11] G. M. Sheldrick SHELX86 program for crystal structure determination, Göttingen 1986 (FRG).

Synthesis, Structure, and Catalase-Type Activity of a Novel Oxo-Bridged Tetranuclear Manganese Aggregate Exhibiting Short O···O Interactions

By *Robert T. Stibrany* and *Sergiu M. Gorun**

Dedicated to Professor Stephen J. Lippard on the occasion of his 50th birthday

Due to their relevance to the catalytic center of the photosynthetic water splitting apparatus of green plants and cyanobacteria, tetranuclear manganese aggregates have become a subject of intensive research.[1] A Mn_4 unit is essential for the coupling of two water molecules and liberation of dioxygen [Eq. (a)] in photosystem II (PSII).[2]

$$2H_2O \rightarrow O_2 + 4H^{\oplus} + 4e^{\ominus} \qquad (a)$$

During this process the Mn_4 aggregate passes through five oxidation states, S_0 to S_4, S_0 representing the most reduced state.[3] The S_0 state is believed to comprise one Mn^{II} and three Mn^{III} centers.[1] EXAFS and EPR spectroscopy suggest that the Mn ions are primarily ligated by O donor atoms.[1, 2] Oxo, hydroxo or alkoxo groups are believed to bridge the metals. Two hydroxo groups (to be evolved as O_2 after deprotonation and coupling) have been postulated to be present in the S_0 state.[4] Calcium has also been shown to be essential for activity but its function is not understood.[5] Interestingly, in the absence of light the PSII reaction center can evolve O_2 when H_2O_2 is added as a substrate, a process believed to involve the S_0 and S_2 states [Eq. (b)].[6]

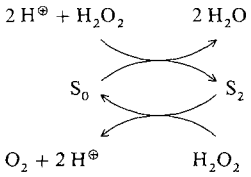

(b)

Despite great efforts no structurally characterized model for the S_0 state exists.[1c, 7] Furthermore, tetranuclear manganese aggregates associated with the biologically relevant calcium ions are not known, and, to our knowledge, biomimetic activity has not been reported thus far for the inorganic models.

We report here the synthesis and structural characterization of the mixed valence $Mn^{II}Mn^{III}_3$ complex **1**,[8] which contains an unprecedented $(Mn_4O_2H)^{8\oplus}$ core. We also report the catalytic biomimetic decomposition of H_2O_2 by **1**.

$(Ba,Ca)_2[Mn_4(\mu\text{-}O)(\mu\text{-}OH)(O_2CCH_3)_2L_2]$ **1**

L = 1,3-Diamino-2-hydroxypropane-*N*,*N*,*N'*,*N'*-tetraacetic acid.

In the anion of **1**, shown in Figure 1, the four manganese ions describe a trapezoid. A crystallographically imposed

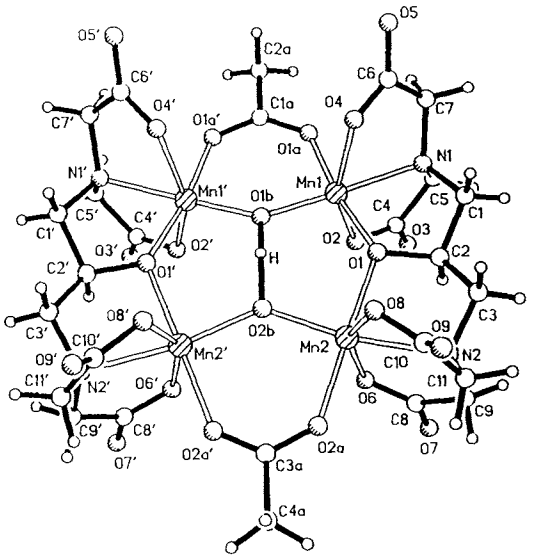

Fig. 1. Structure of the anion of **1** in the crystal. Selected bond lengths [Å] and angles [°]: Mn1-Mn1' 3.379(2), Mn2-Mn2' 3.584(2), Mn1-Mn2 3.718(1), Mn1-O1b 1.817(2), Mn1-O1a 1.961(4), Mn1-O4 2.217(4), Mn1-N1 2.120(4), Mn1-O2 2.152(4), Mn1-O1 1.954(3), Mn2-O2b 1.925(3), Mn2-O2a 2.078(5), Mn2-O8 2.169(5), Mn2-N2 2.190(4), Mn2-O6 2.140(4), O1b-H 1.2(2), O2b-H 1.3(1); Mn1-O1b-Mn1' 136.8(3), Mn2-O2b-Mn2' 137.2(4), Mn1-O1-Mn2 132.5(2), O1b-H-O2b 156(10).

[*] Dr. S. M. Gorun, R. T. Stibrany
Exxon Research & Engineering Company
Corporate Research Science Laboratories
Annandale, N. J. 08801 (USA)

mirror plane intersects the atoms C2a, C1a, O1b, H, O2b, C3a and C4a. The structure can be viewed as a dimer of dimers. The unique Mn1 and Mn2 are bridged by the alkoxo groups of the ligand and the $(O_2H)^{3\ominus}$ unit. Reflection across the mirror plane gives the symmetry-related Mn1′, Mn2′ dimer. The two dimers are linked by the $(O_2H)^{3\ominus}$ and acetato groups. Alternatively, Mn1 and Mn1′ bridged by O1b and one carboxylate could define one dinuclear fragment while Mn2 and Mn2′ bridged by O2b and another carboxylate could form another one. The two dinuclear fragments are linked covalently, by alkoxo groups, and by hydrogen bonding interactions via the hydrogen atom H.

The bridging $(O_2H)^{3\ominus}$ unit is of special interest. The hydrogen atom H, located in the difference Fourier map and subsequently refined (its position was not fixed), is shared by the two bridging oxo groups. The unusually short O1b···O2b contact, 2.467(5) Å, indicates a strong hydrogen bond.[9] We suggest that this unit could represent an intermediate stage in the deprotonation and coupling of two water molecules at the metal center [see Eq. (a)]. The stability of **1** would be enhanced by the formation of two six-membered metallocycles by the $(O_2H)^{3\ominus}$ core, the manganese ions and the bridging alkoxo groups.

The stoichiometry of **1** requires that the average charge per Mn atom be + 2.75, suggesting most likely one Mn^{II} and three Mn^{III} ions in the complex. Furthermore, redox titration of **1** with $KI/Na_2S_2O_3$ indicates a 2.9 ± 0.1 electron reduction process per manganese aggregate, i.e., complete reduction from the $Mn^{II}Mn^{III}_3$ oxidation level to the Mn^{II}_4 level.[10, 12]

The average Mn1–ligand distance, 2.037 Å, is typical for Mn^{III};[13] the average Mn2–ligand distance, 2.102 Å, is longer. The Mn–OR bridges are asymmetric: Mn1–O1 = 1.954(3) Å, is within the 1.88–1.96 Å range found for Mn^{III}–OR; Mn2–O1 = 2.108(3) Å, falls short of the 2.120–2.386 Å range known for the Mn^{II}–OR bond length. This asymmetry is typical for localized mixed valence dinuclear complexes.[1a] The symmetry and interatomic distances argue against the presence of oxidation states > III. Thus, **1** is formulated as a $Mn^{II}Mn^{III}_3$ complex.

Based on the above metrical parameters, we assign Mn1 as Mn^{III}. A Jahn-Teller compression of the axial O1b–Mn1–N1 bonds is observed: $Mn–X_{axial} = 1.969$ Å vs. $Mn–X_{eq} = 2.071$ Å. This compression is somewhat alleviated by the *trans* oxo π donation of O1b along the Mn1–N1 vector. A similar phenomenon encountered in dinuclear Mn^{III} complexes has been discussed recently.[14] The Mn1–O1b bond (1.817(2) Å) is slightly longer than 1.78 ± 0.02 Å, the range known for oxo-bridged dinuclear Mn^{III} complexes, but lower than ≃1.95 Å, a typical value encountered for μ-OH and μ-OR bridges.[1, 15] This intermediate value may reflect the presence of partial H-bonds in the O···H···O group since it is known that protonation of μ-oxo bridges results in elongation of the metal–oxygen bonds.

The average + 2.5 oxidation state of the Mn2/Mn2′ pair could arise from valence delocalization or crystallographic disorder. The thermal ellipsoids of Mn2 are equal to or larger than their Mn1 counterparts. In particular, B_{eq} for O2a (80(2)) is clearly different, namely twice as large as B_{eq} for O1a, (36(1)). Also, B_{eq} for O2b (49(2)) is significantly larger than B_{eq} for O1b (33(2)). Moreover, the Mn2–O1 bond length is intermediate between Mn^{II}–OR and Mn^{III}–OR (see above). These observations can be rationalized if the Mn2 site is disordered, half of the time Mn^{II} and the other half Mn^{III}.

The spatial relationship between the Mn_4 complex anion and the barium/calcium ions is shown in Figure 2. Interestingly, the smaller $Ca^{2\oplus}$ ions are located on the Mn^{III} side of the aggregate, the larger $Ba^{2\oplus}$ ions on the $Mn^{II,III}$ side.[16] The water molecules present in the coordination spheres of $Ba^{2\oplus}$ and $Ca^{2\oplus}$ are hydrogen bonded to the carboxylic groups of the ligand.

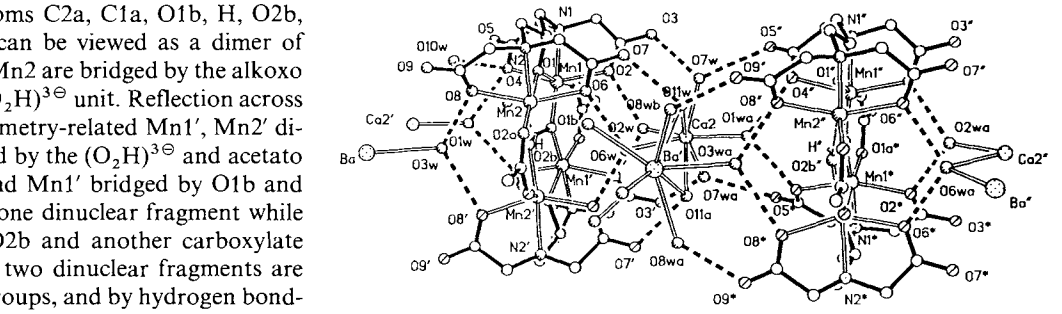

Fig. 2. Section of the structure of the crystal assembly of **1** showing alternating Mn_4 aggregates and bridging calcium and barium ions. View along the O1b–O2b axis. Hydrogen bonds between carboxylate oxygens and calcium/barium bound waters are represented by dashed lines. Only the non-hydrogen atoms are shown.

The above results demonstrate for the first time that a Mn-Ca aggregate can be assembled outside a protein environment and suggest that hydrated Ca ions could play both structural (protein side chains binding) and functional (facilitation of H_2O access to the Mn site) roles in PSII.

The biomimetic activity of our S_0 state model was tested by using H_2O_2 as substrate [see also Eq. (b)]. Complex **1** decomposes H_2O_2 catalytically at high rates.[17] This activity suggests that **1** may be a *functional* model for the S_0 state of PSII. The decomposition of H_2O_2 by **1** lends further support to the "dimers of dimers" view of **1**, since dinuclear Mn^{III} centers (unknown coordination) are present at the active sites of catalases and pseudo-catalases whose main function in vivo is H_2O_2 decomposition.[1a, 18]

Experimental

A solution of the ligand L (268 mg, 0.83 mmol) in H_2O (15 mL) was adjusted to pH 7.0 with an equimolar amount of $Ba(OH)_2$ and $Ca(OH)_2$. After addition of 406 mg (1.66 mmol) of $Mn(OAc)_2 \cdot 4H_2O$ dissolved in 1 mL methanol the pH of the stirred solution was adjusted to 8.5. Bubbling of air through the solution or addition of 1 mL of 25% H_2O_2 (**caution:** heat and gas evolution) resulted in a dark brown coloration. Crystalline products were obtained upon addition of DMF and subsequent slow evaporation of the mixture.

Received: May 28, 1990 [Z 3985 IE]
German version: *Angew. Chem. 102* (1990) 1195

[1] Only the most recent reviews are quoted; a) K. Wieghardt, *Angew. Chem. 101* (1989) 1179; *Angew. Chem. Int. Ed. Engl. 28* (1989) 1153; b) J. B. Vincent, G. Christou, *Adv. Inorg. Chem. 33* (1989) 197; c) G. Christou, *Acc. Chem. Res. 22* (1989) 328; d) G. W. Brudvig, R. H. Crabtree, *Prog. Inorg. Chem. 37* (1989) 99.

[2] a) C. F. Yocum, C. T. Yerkes, R. E. Blankenship, R. R. Sharp, G. T. Babcock, *Proc. Natl. Acad. Sci. USA 78* (1981) 7507; b) J. Amesz, *Biochim. Biophys. Acta. 726* (1983) 1; c) G. C. Dismukes in U. L. Schramm, F. C. Welder (Eds): *Manganese in Metabolism and Enzyme Function*, Academic Press, London 1986, p. 275; d) G. Renger, *Angew. Chem. 99* (1987) 660; *Angew. Chem. Int. Ed. Engl. 26* (1987) 643; e) G. W. Brudvig, *J. Bioenerg. Biomemb. 19* (1987) 91.

[3] B. Kok, B. Forbush, M. McGloin, *Photochem. Photobiol 11* (1970) 457.

[4] H. T. Witt, O. Saygin, K. Brettel, E. Schlodder, *Prog. Photosynth. Res. 1* (1987) 523.

[5] A Boussac, A. W. Rutherford, *Chem. Scr. 28A* (1988) 123, and references cited therein.

[6] W. D. Frasch, R. Mei, *Biochem. Biophys. Acta 891* (1987) 8.

[7] J. B. Vincent, C. Christmas, H.-R. Chang, Q. Li, P. D. W. Boyd, J. C. Huffman, D. N. Hendrickson, G. Christou, *J. Am. Chem. Soc. 11* (1989) 2086.

[8] **1**: $C_{26}H_{33}N_4O_{22}(Ba,Ca)_2Mn_4 \cdot xH_2O$. The red-brown crystals readily lose water upon exposure to air. x = 10, elemental analysis, calculated (observed) [%]: Ca: 2.94(2.99); C: 22.93(22.70); H: 3.85(3.79), N: 4.11(4.19). Single crystal $0.3 \times 0.3 \times 0.6$ mm, space group $P_{2_1/m}$ (No. 11), $a = 11.203(2)$, $b = 20.506(4)$, $c = 11.741(2)$ Å, $\beta = 98.12(1)°$, $V = 2670(1)$ Å^3, $Z = 2$; 6326 independent reflections ($3° < 2\theta < 55°$), 3622 "observed" with $I > 3\sigma(I)$, $R = 0.050$, $R_w = 0.062$, 427 parameters. Non-hydrogen atoms were refined anisotropically; anion hydrogen H and some of the hydrogens from the waters of crystallization were located from the difference Fourier maps and refined as independent isotropic atoms. The first cation position is partly occupied by barium and calcium. The second cation position is occupied exclusively by calcium. Further details of the crystal structure investigation are available on request from the Director of the Cambridge Crystallographic Data Centre, University Chemical Laboratory, Lensfield Road, GB-Cambridge, CB2 1EW (UK), on quoting the full journal citation.

[9] Short O···O separations, 2.5 ± 0.1 Å, are known for hydroxy bridged polynuclear iron complexes; a) F. A. Cotton, G. Wilkinson: *Advanced Inorganic Chemistry*, Wiley, New York 1988, p. 90; b) N. V. Gerbeleu, A. S. Batsanov, G. A. Timko, Y. T. Struchkov, K. M. Indrichan, G. A. Popovich, *Dokl. Akad. Nauk SSSR 293* (1986) 364; c) D. L. Jameson, C.-L. Xie, D. N. Hendrickson, J. A. Potenza, H. J. Schugar, *J. Am. Chem. Soc. 109* (1987) 740; d) W. Micklitz, S. J. Lippard, *Inorg. Chem. 27* (1988) 3069; e) A. S. Batsanov, Y. T. Struchkov, G. A. Timko, *Koord. Khim. 14* (1988) 266.

[10] This method was also used for a tetranuclear (μ-oxo)(μ-acetato)$Mn^{II}_2Mn^{III}_2$ complex. A 1.9 ± 0.2 electron reduction process was observed (versus 2.0 calculated)[11].

[11] R. J. Kulawiec, R. H. Crabtree, G. W. Brudvig, G. K. Schulte, *Inorg. Chem. 27* (1988) 1311.

[12] The possibility of a second proton on the (Mn_4O_2H) core has been considered; in this case **1** would most likely comprise two Mn^{II} and two Mn^{III} ions. A comparison of bond distances and angles with those of known di- and trinuclear mixed valence complexes indicates that this is very unlikely. Also, two, not three electrons should have been obtained by redox titration. Nevertheless, a neutron diffraction study is planned in order to locate the exact position(s) of the core proton(s).

[13] Bond distances are frequently used to establish the + 3 oxidation state of manganese. See, for example, B. Chiswell, E. D. McKenzie, L. F. Lindoy in G. Wilkinson (Ed): *Comprehensive Coordination Chemistry*, Pergamon Press, New York 1987 Vol. 4, p. 1.

[14] U. Bossek, K. Wieghardt, B. Nuber, J. Weiss, *Inorg. Chim. Acta. 165* (1989) 123.

[15] M. Suzuki, T. Sugisawa, H. Senda, H. Oshio, A. Uehara, *Chem. Lett. 1989*, 1091.

[16] In order to investigate the role of counter ions, the more biologically relevant analogue of **1**, the pure calcium complex **2**, has been prepared. Single crystal, $0.1 \times 0.1 \times 0.3$ mm, quasi isomorphous to **1**: $a = 11.336(3)$; $b = 20.710(3)$, $c = 11.559(3)$ Å, $\beta = 98.51(4)°$.

[17] Rates of O_2 evolution [mL s^{-1}]: $MnCl_2$ 0.01; $Mn(OAc)_2$ 0.1; Mn(TPP)(OAc) [TPP = tetraphenylporphyrinato dianion] 0.05; **1** 4.00. For comparison the rate for solid MnO_2 is 0.25.

[18] a) Y. Kono, I. Fridovich, *J. Biol. Chem. 258* (1983) 6015; b) G. S. Allgood, J. J. Perry, *J. Bacteriol. 168* (1986) 563.

The Tri-μ-amidobis[triamminecobalt(III)] Cation: The First Triply Amido-bridged Complex**

By *Walter Frank,* Klaus Hoffmann*, and *Ludwig Heck**

Shortly after the turn of the century, *A. Werner* succeeded in synthesizing the triply OH-bridged binuclear complexes ("triols") **I** via partial deprotonation of *fac*-triaqua complexes.[1] X-ray studies later confirmed his ideas on their structure. [2]Grimm-isosteric, triply amido-bridged structural units have been discussed by *Schmitz-DuMont* in connection with speculations on the structure of the amides of chromium(III) and cobalt(III).[3] In systematic studies, on the deprotonation of ammine complexes and on complex condensation with the formation of NH_2 bridges ("ammine olation")[4] it has now been possible for the first time to detect a corresponding complex **II** with NH_2 instead of OH.

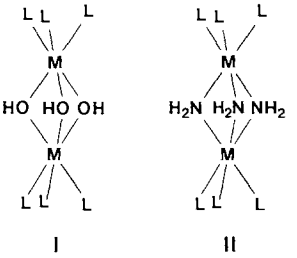

Upon reaction of hexaamminecobalt(III) perchlorate with one equivalent of potassium amide in liquid ammonia we obtained tri-μ-amidobis[triamminecobalt(III)] perchlorate **1**. From its remarkably stable aqueous solution the bromide **2** can be precipitated with potassium bromide. The crystal structure analysis of **2**,[5] together with the analytical, spectroscopic and crystal data of **1** and **2**, unequivocally confirm the tri-μ-amido structure of the cations in these compounds.

$[(NH_3)_3Co(NH_2)_3Co(NH_3)_3](ClO_4)_3$ **1** $[(NH_3)_3Co(NH_2)_3Co(NH_3)_3]Br_3$ **2**

The cations in the crystal of **2** exhibit a high crystallographic point group symmetry (D_{3h}) (Fig. 1). The amido bridges

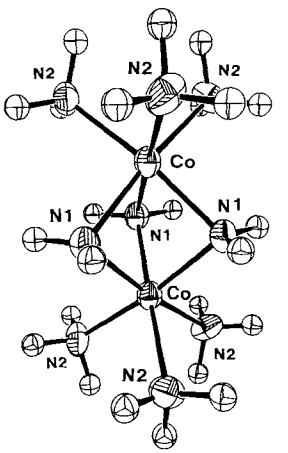

Fig. 1. Structure of the tri-μ-amidobis[triamminecobalt(III)] cation in the crystal of **2**. The ellipsoids of the thermal vibrations are drawn at the 50% probability level; the hydrogen atoms are not labeled, their radius was chosen arbitrarily. Bond lengths [pm] and angles [°]: Co-N1 193.9(5), Co-N2 199.9(5); N1-Co-N1′ 79.8(2), N1-Co-N2 173.1(2), N2-Co-N2′ 89.9(2), Co-N1-Co′ 84.4(3).

force the two cobalt atoms 260 pm apart. The Co–N bonds in the bridges are slightly shorter, the terminal Co–N bonds slightly longer than the mean value of 196.9(3) pm, which agrees with the value in $[Co(NH_3)_6]^{3\oplus}$ (196.6(3) pm).[6] Based on the concept of two face-sharing octahedra the angles observed can be understood as resulting from an elongation along the threefold axis, which only concerns the trigonal bipyramidal core of the cation. The angles between terminally bound N atoms are almost exactly 90°. The observed geometry can thus be understood in terms of a Co–Co

[*] Dr. W. Frank, Prof. Dr. L. Heck, K. Hoffmann
Fachrichtung Anorganische Chemie der Universität
Im Stadtwald, D-6600 Saarbrücken (FRG)

[**] This work was supported by the Fonds der Chemischen Industrie.

repulsion and restoring force as a result of the angular deformation at the μ-N-atoms.

The crystal structure of **2** can be described in terms of the similarity between the cation substructure and a hexagonal closest packing (hcp): All the cavities in an arrangement of hexagonally packed layers of cations according to the stacking sequence AB,AB...(*h*) are occupied by $Br^{\ominus}$ ions.[7]

Experimental

1: A mixture of hexamminecobalt(III) perchlorate (1.0 g, 2.18 mmol) and potassium amide (0.104 g, 2.61 mmol) in liquid ammonia (15 mL) was heated in a pressure tube for 24 h at 100 °C. After removal of the ammonia by evaporation, all by-products were extracted from the remaining mixture with 10 × 2 mL of water. There remained 0.220 g (35.6% based on $[Co(NH_3)_6](ClO_4)_3$) of rosered **1**.

Correct elemental analysis (Co,N); IR (KBr): $\tilde{\nu}$ [cm^{-1}] = 3333, 3304, 3252, 3215, 2023, 1615, 1471, 1247, 1142, 1109, 1086, 940, 927, 793, 636, 627, 542, 432, 338; UV/VIS (H_2O): λ_{max} [nm] (ε) = 298 (1740).

2: 100 mL of a saturated solution of **1** (0.188 g, 0.331 mmol) was treated with 25 mL of a saturated potassium bromide solution. A red precipitate of **2** was recrystallized from water (0.129 g, 76.7%).

IR (kBr): $\tilde{\nu}$ [cm^{-1}] = 3333, 3304, 3251, 3215, 1615, 1468, 1245, 927, 793, 542, 432, 338; UV/VIS (H_2O): λ_{max} [nm] (ε) = 298 (1740).

Received: June 5, 1990 [Z 3996]
German version: *Angew. Chem. 102* (1990) 1178

CAS-Registry-Numbers:
1, 129493-01-2; **2**, 129493-02-3; $[Co(NH_3)_6](ClO_4)_3$, 13820-83-2.

[1] A. Werner, *Ber. Dtsch. Chem. Ges. 40* (1907) 4834.
[2] M = Co, L = NH_3: P. Andersen, *Acta Chem. Scand. 21* (1967) 243; U. Thewalt, *Z. Anorg. Allg. Chem. 412* (1975) 29. M = Cr, L = NH_3: P. Andersen, A. Dossing, S. Larsen, E. Pedersen, *Acta Chem. Scand., Ser. A 41* (1987) 381. M = Co, Rh, Cr, L = N atoms of tridentate ligands: K. Wieghardt, P. Chaudhuri, B. Nuber, J. Weiss, *Inorg. Chem. 21* (1982) 3086; K. Wieghardt, M. Guttmann, D. Ventur, W. Gebert, *Z. Anorg. Allg. Chem. 527* (1985) 33.
[3] O. Schmitz-Du Mont, J. Pilzecker, H. F. Piepenbrink, *Z. Anorg. Allg. Chem. 248* (1941) 175.
[4] M. Kretschmer, L. Heck, *Z. Anorg. Allg. Chem. 490* (1982) 215; L. Heck, M. Ardon, A. Bino, J. Zapp, *J. Am. Chem. Soc. 110* (1988) 2691.
[5] Crystal structure analysis of **2**: M_r = 507.82, hexagonal, a = 723.7(3), c = 1696(1) pm, Z = 2, space group $P6_3/mmc$, four-circle diffractometer, $Mo_{K\alpha}$ radiation, 347 independent reflections with $I > 0$, numerical absorption correction, 23 refined parameters, R = 0.051, R_w = 0.032. Further details of the crystal structure investigation are available on request from the Fachinformationszentrum Karlsruhe, Gesellschaft für wissenschaftlich-technische Information mbH, 2 (FRG), on quoting the depository number CSD-54807 the names of the authors, and the journal citation. Crystal data of **1** determined via film methods: hexagonal, a = 801(2), c = 1803(3) pm, space group $P6_3mc$, $P\bar{6}2c$ or $P6_3/mmc$.
[6] G. J. Kruger, E. C. Reynhardt, *Acta Crystallogr. Sect. B 33* (1978) 915.
[7] A corresponding arrangement is not realized in the case of compounds with spherically-shaped ions owing to the proximity of each of the two tetrahedral cavities in the undistorted hcp assemblage.

A Synthetic Allosteric System with High Cooperativity between Polar and Hydrophobic Binding Sites**

By *Hans-Jörg Schneider** and *Dieter Ruf*

Characteristic of allosteric systems is that the occupation of spatially separated binding sites by different or identical effector molecules leads to a mutual influence of the binding sites. Their role in the regulation of biological processes is long known; it rests on conformational couplings, the molecular mechanism of which can be analyzed only with difficulty because of the complexity of the participating proteins. In the few previously described simple synthetic receptor molecules displaying allosteric behavior this depends on the mutual interaction of two metal ion-binding sites.[1] Artificial systems with significant allosteric effects, e.g., between an ionic and a lipophilic binding site[2] have not yet been reported in the literature. We now present a particularly simple and effective model, in which the occupation of a polar site—e.g. by a metal ion—leads to the closing of a hydrophobic pocket. In aqueous medium a hydrophobic binding site is formed in which a lipophilic guest molecule is complexed (Scheme 1).

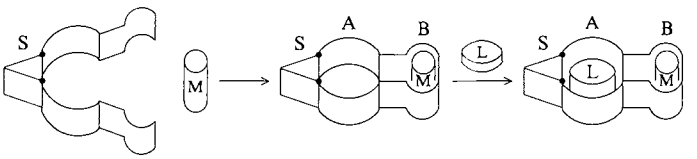

Scheme 1. Schematic outline of the cooperative formation of binding sites. S = hinge, M = metal ion, A = hydrophobic binding site, B = polar binding site, L = lipophilic guest molecule.

To synthesize the model complex, the receptor **4** containing an ethylenediamine as metal binding site B was synthesized from the bis(*p*-anilino)methane **1** via **2** and **3**.[3] The

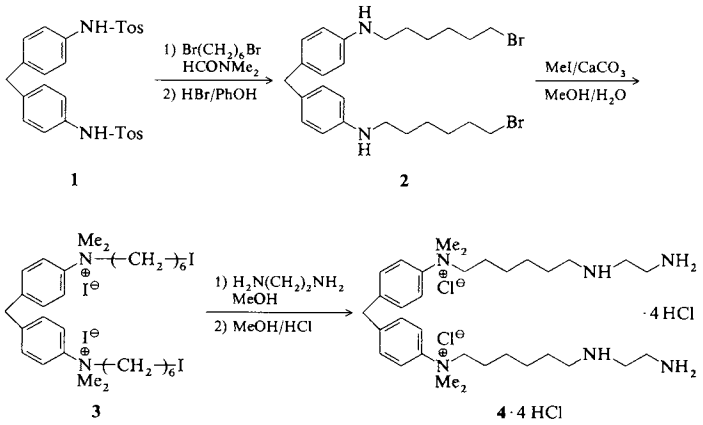

alkane chains in **4** form the lipophilic site A, whose ability to hydrophobically bind aromatic hydrocarbons is enhanced by the ammonium ions on the chains.[4] Furthermore, the presence of doubly charged sites in the receptor **4** makes it sufficiently water soluble to investigate, e.g., the hydrophobic complexation of hydrocarbons. A relatively rigid spacer unit such as diphenylmethane in the hinge S is necessary in order to prevent collapse of the alkane chains and thus also of hydrophobic interaction without substrate intercalation.

At pH 10 in aqueous borate buffer, the receptor **4** shows with copper(II) ions the absorption values λ_{max} = 561 nm, ε_{max} = 112, typical for bidentate ethylenediamine ligands;[5] the UV/VIS titration of **4** with $Cu^{2\oplus}$ indicated formation of a 1:1 complex. Addition of the **4** · $Cu^{2\oplus}$ complex to a solu-

[*] Prof. Dr. H.-J. Schneider, Dipl.-Chem. D. Ruf
Fachrichtung Organische Chemie der Universität
D-6600 Saarbrücken 11 (FRG)

[**] Host-Guest Chemistry, Part 24. This work was supported by the Deutsche Forschungsgemeinschaft and the Fonds der Chemischen Industrie.—Part 23: H.-J. Schneider, R. Kramer, I. Theis, M. Zhou, *J. Chem. Soc. Chem. Commun. 1990*, 276.

tion of naphthalene (0.33×10^{-3} M) in D_2O/CD_3OD at pH 10 leads to increased shielding of the naphthalene α-proton in the NMR spectrum (at $[\mathbf{4} \cdot Cu^{2\oplus}] = 6.6 \times 10^{-3}$ M, e.g., by $\Delta\delta = -0.33$); this is not observed upon addition of **4** or $Cu^{2\oplus}$ alone, and affords proof of intracavity inclusion of the hydrocarbon in the $\mathbf{4} \cdot Cu^{2\oplus}$ complex. The incorporation of naphthalene in the analogously built preformed cavity of the azoniacyclophane **5** manifested itself in an upfield shift of

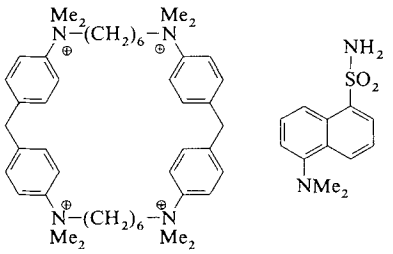

5

6

$\Delta\delta \approx -0.95$ for complete complexation as obtained from computer simulation of the NMR titration curves under the same conditions.[6a] A corresponding titration is not possible in the case of the $\mathbf{4} \cdot Cu^{2\oplus}$ complex because of its sparing solubility; however, if one assumes a CIS value (*C*omplexation *I*nduced *S*hift at 100% complexation) of ca. −0.5 (smaller than in the case of **5**, since $\mathbf{4} \cdot Cu^{2\oplus}$ contains only a half of the shielding arene rings and $N^{\oplus}$ units[6b]), a complex constant of $K \approx 10$ can be estimated.

A further proof of the binding of lipophilic substrates is afforded, for example by a shift in the fluorescence maximum of the fluorscence indicator dansylamide **6** from 520 nm to 510 nm and an increase in intensity of ca. 85% on measuring a solution of **6** (5×10^{-6} M), **4** (10^{-3} M) and a $Zn^{2\oplus}$ salt (6×10^{-4} M) at pH 12 (NaOH/KCl buffer). Here again, the determination of an equilibrium constant is prevented, in this case by too high a self-fluorescence of the acceptor at $[\mathbf{4}] > 10^{-3}$ M; however, by comparison with the fluorescence values of the complete complexation of **6** with **5** a value of $K \approx (0.5 \text{ to } 1) \times 10^3$ can be estimated.

The decrease in the values of the complexation constants K (by a factor of 10–100) of naphthalene and dansylamide (**6**) with $\mathbf{4} \cdot M^{2\oplus}$ (M = Cu, Zn) instead of **5** is consistent with the twofold instead of fourfold $N^{\oplus}$–arene interaction, which is decisive for the binding of aromatic guest molecules.[4] However, the results indicate at least a tenfold to hundredfold stronger complexation of lipophilic substrates by **4** in the presence of metal ions, since NMR or fluorescence control experiments with **4** alone showed no binding of naphthalene or **6**. Thus the allosteric system **4** bears the characteristics of a heterotopic, positive, and especially strong cooperativity.[8] In the case of proteins, systems with a binding constant ratio of ≈10 are already counted as strongly cooperative.[9] Synthetic receptors can be conceived as exhibiting an essentially direct conformational coupling and thus also as being suitable, in principle, as molecular switches.

One of the applications of the systems described here is in the detection of diamagnetic transition metal ions—which, due to their affinity for ethylenediamine units are still bound at concentrations of 10^{-10} to 10^{-20} M—via the fluorescence of suitable dyes in the corresponding ternary complexes. Figure 1 shows the increase in the fluorescence intensity of **6** as a function of the $Zn^{2\oplus}$ concentration. The observed linearity is consistent with the formation of <10% ternary complex $[\mathbf{4} \cdot Zn^{2\oplus} \cdot \mathbf{6}]$. Paramagnetic ions such as $Cu^{2\oplus}$ also bind strongly—also visible by way of NMR line broadening—but lead to quenching of the fluorescence and can therefore be differentiated from diamagnetic ions.

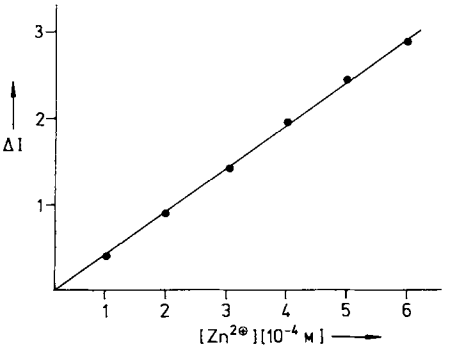

Fig. 1. Increase in fluorescence intensity I of **6** in the presence of **4** as a function of the concentration of added $Zn^{\oplus}$ ions. $[\mathbf{6}] = 5 \times 10^{-6}$ M, $[\mathbf{4}] = 10^{-3}$ M NaOH/KCl buffer, pH 12.

The increase in the binding constants and solubilities of the ternary complexes, as well as the lowering of the self-fluorescence of the receptors should make it possible, with the new principle demonstrated here, to increase the number and variety of known fluorophores.[10]

Received: June 25, 1990 [Z 4034 IE]
German version: *Angew. Chem. 20* (1990) 1192

[1] a) J. Rebek, Jr., *Acc. Chem. Res. 17* (1984) 258; b) J. Rebek, Jr., J. E. Trend, R. V. Wattley, S. Chakravarti, *J. Am. Chem. Soc. 101* (1979) 4333; c) J. Rebek, Jr., R. V. Wattley, *ibid. 102* (1980) 4853; d) P. D. Beer, A. S. Rothin, *J. Chem. Soc. Chem. Commun. 1988*, 52; cf. also e) J.-C. Chembron, J.-P. Sauvage, *Tetrahedron Lett. 27* (1986) 865. For a corresponding system with metal-activated DNA ligands cf. J. H. Griffin, P. B. Dervan, *J. Am. Chem. Soc. 109* (1987) 6840.

[2] F. Diederich, M. R. Hester, M. A. Uyeki, *Angew. Chem. 100* (1988) 1775; *Angew. Chem. Int. Ed. Engl. 27* (1988) 1705.

[3] All the new compounds showed ^1H- and ^{13}C-NMR spectra consistent with the quoted structures without indication of impurities. **4** × 4HCl has a decomposition point of 190 °C; elemental analyses were not possible owing to their hygroscopic character, ^1H-NMR spectroscopic determinations of concentration gave ≧ 95% purity in each case.

[4] a) H.-J. Schneider, T. Blatter, *Angew. Chem. 100* (1988) 1211; *Angew. Chem. Int. Ed. Engl. 27* (1988) 1163; b) H.-J. Schneider, T. Blatter, S. Simova, I. Theis, *J. Chem. Soc. Chem. Commun. 1989*, 580.

[5] Cf., e.g. H. Ojima, K. Sone, *Bull. Chem. Soc. Jpn. 35* (1962) 298 (for $[Cu\{PrNHCH_2)_2\}_2]^{2\oplus}$: $\lambda_{max} = 563$ nm, $\varepsilon_{max} = 101$).

[6] a) H.-J. Schneider, K. Philippi, J. Pöhlmann, *Angew. Chem. 96* (1984) 907; *Angew. Chem. Int. Ed. Engl. 23* (1984) 908; b) H.-J. Schneider, J. Pöhlmann, *Bioorg. Chem. 15* (1987) 183.

[7] H.-J. Schneider, R. Kramer, S. Simova, U. Schneider, *J. Am. Chem. Soc. 110* (1988) 6442.

[8] A series of effective artificial ditopic receptors owe their cooperativity not to allosteric effects but to the direct interaction between two effector guest molecules, which must therefore be in contact within the ternary complex: a) C. J. van Staveren, D. E. Fenton, D. N. Reinhoudt, J. van Eerden, S. Harkema, *J. Am. Chem. Soc. 109* (1987) 3456; b) F. C. J. M. van Veggel, D. N. Reinhoudt in H.-J. Schneider, H. Dürr (Ed.): *Perspectives in Supramolecular Chemistry and Photochemistry*, VCH, Weinheim 1990; c) I. Willner, Z. Goren, *J. Chem. Soc. Chem. Commun. 1983*, 1469.

[9] Cf. G. H. Czerlinski, *Biophys. Chem. 34* (1989) 169, and references cited therein.

[10] a) F. Vögtle: *Supramolekulare Chemie*, Teubner, Stuttgart 1989, p. 82 f; see also b) A. W. Czarnik in H.-J. Schneider, H. Dürr (Eds.): *Perspectives in Supramolecular Chemistry und Photochemistry*, VCH, Weinheim 1990, in press.

Host-Guest Complexes with Closed, Half-open, and Stretched Receptors: Hydrophobic Cavity Effects and Induced Pole-Dipole Interactions**

By *Hans-Jörg Schneider,* Thomas Blatter,* and *Patrick Zimmermann*

Lipophilic receptor cavities are an essential element for molecular recognition and the binding of unpolar substrates in aqueous solution.[1] We report here on the experimental differentiation of the underlying hydrophobic effects and van-der-Waals interactions by binding studies with closed, half-open, and stretched host compounds (Scheme 1). These studies also emphasize the exceptional properties of water,

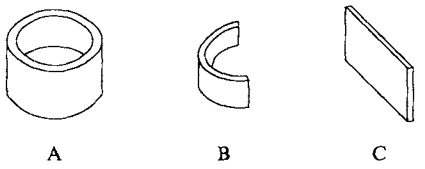

Scheme 1. Schematic diagram of closed (A), half-open(B), and stretched host compounds (C).

which can scarcely give rise to entropically determined interactions in complexes with the open structures **2** (≙ B) and **3** (≙ C).[1]

The marked complexation of aromatic hydrocarbons compared to aliphatic substrates by azoniacyclophanes of type **1**[2, 3] and the pronounced decrease in binding upon removal of positively charged nitrogen atoms from the cavity[3b] can be explained both by electrostatic interactions between the $N^{\oplus}$ units and the quadrupoles of aromatic substrates as well as by the induction of a dipole in the complexed arene system.[4] The observation that diiodomethane **8**, in contrast to dichloromethane **9**, forms a complex with **1** (Table 1) now reveals the dominance of the second effect, for iodine has an especially easily polarizable electron cloud. The dependence of the complexation constants of **1** and lipophilic substrates on the water content of the solution gave values which approach those observed in corresponding studies with cyclodextrins:[3a] the hydrophobic effect in the case of the dominating $N^{\oplus}$-arene interactions discussed here is thus due to the fact that the polarizability of water is much lower than that of substrates such as **4**–**8**.[5]

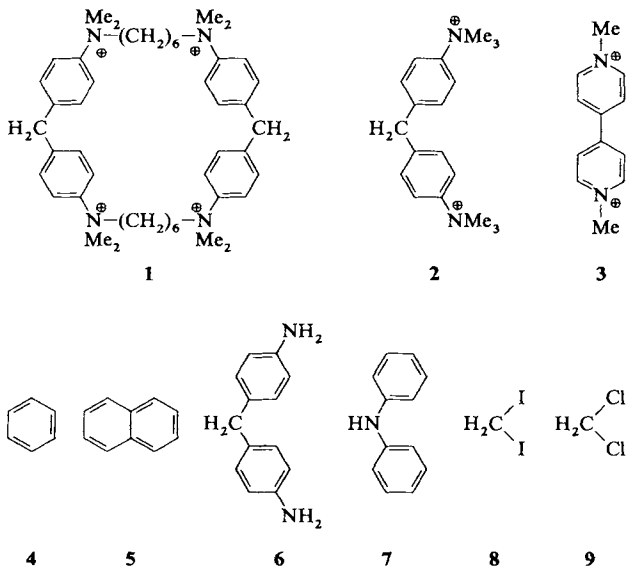

Table 1. Free complexation enthalpies $\Delta G°$ [kJmol^{-1}] at 25 °C for complexes of **1**–**3** with **4**–**9**. Standard deviation ±0.2 kJmol^{-1}.

	4 [a]	**5** [b]	**6** [a]	**7** [c]	**8** [b]	**9** [b]
1	10.0	17.3	14.5	14.5	7.5	<1
2	2.7	–	6.9	6.0	1.7	<1
3	–	4.6	4.7	–	–	–

[a] In CD_3OD/D_2O (5/95, vol/vol). [b] In $CD_3OD:D_2O$ (10/90, vol/vol). [c] In CD_3OD/D_2O (20/80, vol/vol).

With the host compound **2**, a complexation with a half-open receptor is observed—to our knowledge for the first time—which is analogous to that of a macrocyclic host (Table 1). Molecular mechanics simulations demonstrate that the polarizable substrate moieties can, especially in the complexes with **6**, **7** and **8**, assume an almost ideal position with respect to the inducing $N^{\oplus}$-pole (Fig. 1a, b). From the measured complexation enthalpies an average value of $\Delta G_{N^{\oplus}/\pi} \approx 3$ kJmol^{-1} can be calculated for the interaction between a phenyl ring and an $N^{\oplus}$-charge. This value is in satisfactory agreement with previously assumed values.[3] A similar order of magnitude is found for the complexation enthalpy even with the stretched receptor **3** (Table 1). The somewhat lower values can be explained in terms of a rather poor fit (cf. Fig. 1c) (charge transfer contributions to these complexes are relatively small, as shown by a comparison of structurally similar ion-pair complexes[6]).

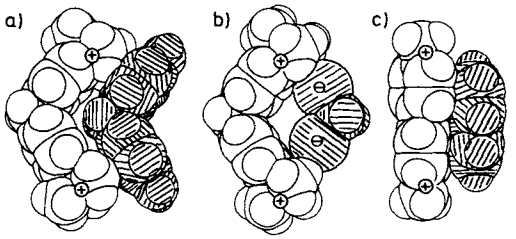

Fig. 1. Space-filling models (from CHARMM/QUANTA simulations) of the complexes **2** · **6** (a), **2** · **8** (b) and **3** · **5** (c). The optimum position of the polarized phenyl ring (a) and iodine atoms (b) with respect to the inducing $N^{\oplus}$ of the receptor **2** is clearly recognizable.

The enthalpies of free binding the substrates **4** and **6**–**8** in the macrocyclic host **1** are in each case about 7 kJmol^{-1} higher than in the half-open analogue **2** (Table 1). The reason for this surprisingly constant difference can be entropic effects, or the unfavorable enthalpy of water molecules, which can form fewer hydrogen bridges inside than outside of the receptor cavity.[7] Molecular mechanics simulations of **1** in a water box using the CHARMM program[8] show that the azoniacyclophane **1** in fact contains about five water molecules in or near the cavity, which altogether participate in only about five hydrogen bridges (Fig. 2); water molecules

[*] Prof. Dr. H.-J. Schneider, Dipl.-Chem. T. Blatter, P. Zimmermann
Fachrichtung Organische Chemie der Universität
D-6600 Saarbrücken 11 (FRG)

[**] Host-Guest Chemistry, Part 25. This work was supported by the Deutsche Forschungsgemeinschaft and the Fonds der Chemischen Industrie.—Part 24: H.-J. Schneider, D. Ruf, *Angew. Chem. 102* (1990) 1192; *Angew. Chem. Int. Ed. Engl. 29* (1990) 1159.

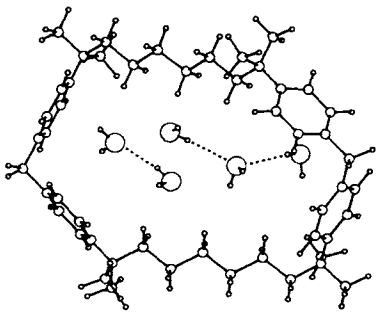

Fig. 2. Molecular structure obtained from CHARMM/QUANTA simulations for the azoniacyclophane **1** with five water molecules in the cavity; hydrogen bridges in the cavity are indicated by dotted lines.

outside of the cavity, on the other hand, are stabilized by an average of four bridges per molecule.

Received: June 25, 1990 [Z 4035 IE]
German version: *Angew. Chem. 102* (1990) 1194

[1] See, e.g., W. P. Jencks: *Catalysts in Chemistry and Enzymology*, McGraw-Hill, New York 1969.
[2] Cf. K. Odashima, K. Koga in P. M. Kuhn, S. M. Rosenfeld (Eds.): *Cyclophanes, Vol. 2*, Academic Press, New York 1983, pp. 629–677.
[3] a) H.-J. Schneider, R. Kramer, S. Simova, U. Schneider, *J. Am. Chem. Soc. 110* (1988) 6442; b) H.-J. Schneider, T. Blatter *Angew. Chem. 100* (1988) 1211; *Angew. Chem. Int. Ed. Engl. 27* (1988) 1163; c) H.-J. Schneider, T. Blatter, S. Simova, I. Theis *J. Chem. Soc. Chem. Commun. 1989*, 580.
[4] Cf. a) S. K. Burley, G. A. Petsko, *Adv. Protein Chem. 39* (1988) 125; b) J. Sunner, K. Nishizawa, P. Kebarle, *J. Phys. Chem. 85* (1981) 1814; c) C. A. Deakyne, M. Meot-Ner, *J. Am. Chem. Soc. 107* (1985) 474; d) M. A. Petti, T. J. Shepodd, R. E. Barrans, Jr., D. A. Dougherty, *ibid. 110* (1988) 6825; e) D. A. Stauffer, D. A. Dougherty, *Tetrahedron Lett. 29* (1988) 6039, and references cited therein.
[5] Examples of average polarizabilities [10^{-24} cm^3]: H_2O 1.45 (D_2O 1.26), $CHCl_3$ 9.5, benzene 10.5 (*Handbook of Chemistry and Physics*, E66-E75, 67th edit., CRC Press, Boca Raton, FL, USA 1986/1987).
[6] a) Cf. H.-J. Schneider, I. Theis, *Angew. Chem. 101* (1989) 757; *Angew. Chem. Int. Ed. Engl. 28* (1989) 753; and references cited therein; b) H.-J. Schneider, T. Schiestel, P. Zimmermann, unpublished results.
[7] Such an effect had already been postulated for cyclodextrin complexes: a) D. W. Griffith, M. L. Bender, *Adv. Catal. 23* (1973) 209; b) W. Saenger, *Angew. Chem. 92* (1980) 343; *Angew. Chem. Int. Ed. Engl. 19* (1980) 344. c) *Diederich* et al. have on many occasions emphasized the role of cohesive forces in the formation of apolar complexes: D. B. Smithrud, F. Diederich, *J. Am. Chem. Soc. 112* (1990) 339, and references cited therein.
[8] See, for example C. L. Brooks, M. Karplus, *Methods, Enzymol. 127* (1986) 369.

Macrocyclically Fixed Diarylhexatrienes**

By *Fritz Vögtle** and *Carlo Thilgen*

Open-chain and cyclic polyenes have been the subject of intensive research in organic chemistry for many years.[1] 1,6-diphenyl-1,3,5-hexatriene (DPH), for example, is a commonly used fluorescence indicator in investigations concerning the arrangement of molecules in vesicle and cell membranes, in liquid crystal phases, and in polymer films. Our studies in this context are currently directed to the synthesis of novel organic materials with specific properties by incorporating classical structural building blocks into macrocyclic systems, and we now report on the configurationally and conformationally stiffened cyclopolyenes **1** and **2**.

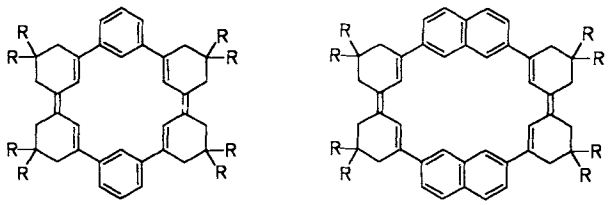

1 **2**

a: R=H; **b**: R=CH_3

Although the McMurry reaction has found wide application,[2] so far it has rarely been employed for the directed cyclodimerization of dicarbonyl compounds in one step.[3] The one-pot synthesis of the hydrocarbons **1** and **2**, which proceeds in comparatively good yields (**1a**: 36% after optimized coupling of **5a**[4]) makes this method attractive for the synthesis of macrocycles.

In order to work out optimal reaction conditions, but also for comparative purposes, we first prepared the "open chain" triene **4a** from **3a**.

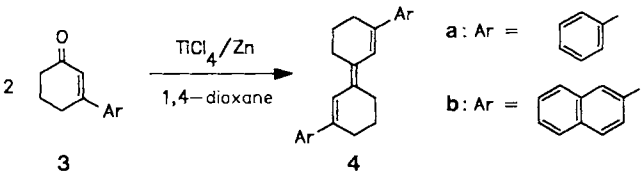

3 **4**

The cyclization to **1** or **2** was best achieved under moderate dilution conditions; we assume that the principle of rigid groups plays a role thereby. The synthetic concept is widely applicable. Thus, in addition to **1a** and **4a**, the macrocycles **1b** (20%), **2a** (20%), and **2b** (4% yield), as well as the triene **4b** could be prepared.

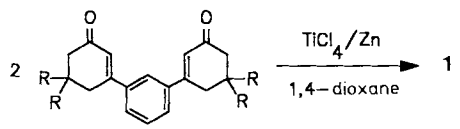

5

The yellowish, sparingly soluble microcrystals of the cycloalkene **1**, which precipitated in analytically pure form on recrystallization from pyridine, melt in an evacuated tube at 385–388 °C (decomp). Besides the peaks for $M^{\oplus}$ [m/z = 468.2817(calcd); 468.2814(obs), base peak] and $M^{2\oplus}$ [m/z = 234], the mass spectrum of **1a** also exhibits peaks of graduated intensity for all the dehydrogenation products down to m/z = 456, which corresponds to the especially stable hexa-*m*-phenylene[6a] (same carbon framework). The ^{1}H-NMR spectrum (200 MHz, $CDBr_3$) shows the following signals: δ = 1.93 (m, 8H; CH_2), 2.51 (m, 8H; CH_2), 2.60 (m, 8H; CH_2), 7.20–7.38 (m, 6H; Ar-CH), 7.57 (s, 4H; vinyl-CH), 8.08 (s, 2H; Ar-CH). A striking feature is the down-

[*] Prof. Dr. F. Vögtle, Dipl.-Chem. C. Thilgen
Institut für Organische Chemie und Biochemie der Universität
Gerhard-Domagk-Strasse 1, D-5300 Bonn 1 (FRG)

[**] This work was supported by the Volkswagen-Stiftung. We thank Prof. Dr. *E. Steckhan*, Universität Bonn, for measuring and evaluating the cyclovoltammograms, and Dipl. Chem. *P. M. Windscheif*, Universität Bonn, for carrying out calculations.

field shift of the olefinic and aromatic protons oriented to the center of the molecule, as has also been observed for hexa-*m*-phenylene[6a] and kekulene.[6b]

The fully aromatized hydrocarbon **6** containing two naphthalene units could be detected for the first time after treatment of the cyclopolyene **2a** with 2,3-dichloro-5,6-dicyano-*p*-benzoquinone (DDQ) [MS: m/z = 556.2185 ($M^{\oplus}$ obs), 556.2191 ($M^{\oplus}$ calcd); 278 ($M^{2\oplus}$)].

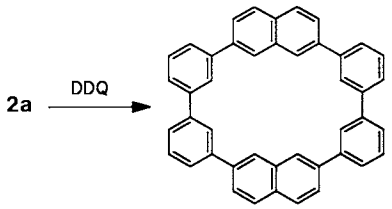

6

1a contains two diphenylhexatriene units with a fixed geometry, in which the double bonds are (1*E*, 3*Z*, 5*E*)-configurated, and the free rotation of the benzene rings is suppressed. In the "open-chain" triene **4a**, however, there is still the possibility of (*E*)/(*Z*)-isomerization with regard to the exocyclic double bond.

The diarylhexatrienes **1**, **2** and **4** allow the consequences of configurational and confirmational fixation of the respective chromophore on the electronic excitation to be investigated by UV/VIS spectroscopy. The maxima of the absorption bands of the trienes **4a**, **b** are unstructured, and hypochromic in comparison to those of DPH and DNH (1,6-di[2-naphthyl]-1,3,5-hexatriene), and in each case they exhibit a bathochromic shift of 14–16 nm.[7a, b]

The red shift due to the more extended chromophore in the dinaphthylhexatriene **4b** already manifests itself in its deeper yellow tone when compared to that of the diphenylhexatriene **4a**, whose bright yellow platelet-shaped crystals get a green tinge by the blue fluorescence in incident light (Fig. 1).

Whereas *Zechmeister* et al.[8] found a hypsochromic shift of only 1–2 nm for the longest wavelength absorption maximum of (3*Z*)-DPH in comparison to its all-(*E*)-isomer, the corresponding difference between the "open-chain" all-(*E*)-triene **4a** and its cyclic counterpart **1a** with the fixed double (3*Z*)-configuration amounts to 23 nm.[7a] In the case of (*E*)- and (*Z*)-stilbene the difference of 15.5 nm is attributed to a hindrance of the conjugation in the no longer planar (*Z*)-isomer.[10] In **1a**, a rotation of the benzene rings out of the plane of conjugation may contribute to the observed shift.

The absence of an absorption band at even longer wavelength in the UV/VIS spectra of **1a** and **2a** confirms the assumption that the macrocycles contain two isolated diphenylhexatriene systems instead of a single chromophore extended over the whole ring.[11]

The most outstanding difference between the spectra of **1a**, **2a** and those of the "open chain" analogues **4a**, **b** is the occurrence of an additional band in the former at λ = 273 and 286 nm respectively. From a theoretical viewpoint, this is due to the absence of a symmetry center[12] and has proven to be characteristic of the presence of a (*Z*)-double bond within a polyene chain. The "*cis*-peaks" of the macrocycles **1** and **2** are striking, not only by their high extinction coefficient but also by the sole fact of their occurrence, since **1a** shows an inversion center in the energetically most favorable conformation, as is predicted by calculations.[13] This observation also suggests a division of the molecules into two separate chromophores.

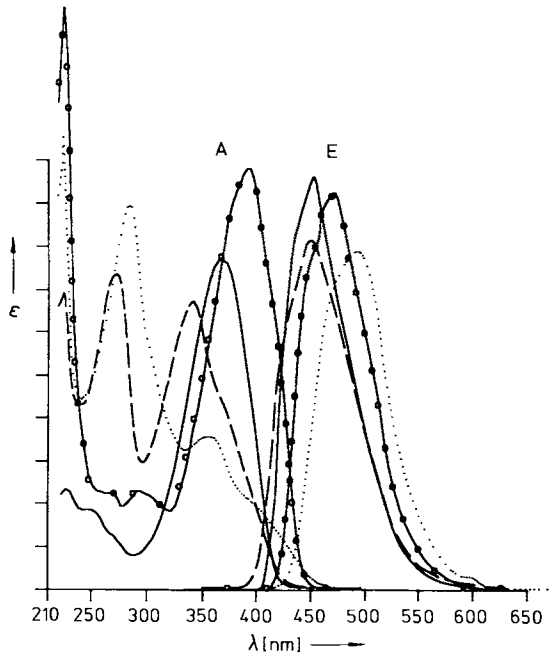

Fig. 1. Absorption (A) and emission (E) spectra (in 1,4-dioxane, T = 292 K, excitation at 380–400 nm) of the diarylhexatrienes **4a** (——) and **4b** (⊖⊖⊖) and of the cyclopolyenes **1a** (– – –) and **2a** (···). ε in relative units.

Whereas the emission maxima[7c] of the diphenylhexatrienes DPH, **4a** and **1a** are located at almost the same λ (blue spectral region), a pronounced bathochromic shift characterizes the transition to the dinaphthylhexatriene **4b** (blue-green) and further to the cyclic dinaphthylpolyene **2a** (green). The difference between absorption and emission maxima is significantly larger in the case of the cyclic compounds **1a** and **2a** than in the case of the "open chain" analogues **4a**, **b**[7a, c] (Fig. 1).

Diphenylpolyenes form cations in sufficiently concentrated sulfuric acid.[15, 16] Those of **4a**, **b**, **1a** and **2a** (in 96% H_2SO_4) are deep-colored, and in each case their absorption spectra exhibit two intense bands.[7b] From the fact that the solutions of the cyclic ions no longer show bands of the hydrocarbons **1a** or **2a** it may be assumed that both chromophoric units of the molecules are protonated.

Deep-blue/violet solutions of anions were obtained on treatment of the diphenylpolyenes **1a** and **4a** with sodium metal in THF. The structural variety observed for the anions of 1,n-diphenylpolyenes[17] should be strongly reduced in the case of the species described here by the additional clamping. Cyclovoltammetric measurements in pyridine afforded the first reduction potentials of the polyenes **1a** and **4a**, which are superimposed to the reduction of the base electrolyte: they have nearly the same value for "open chain" (**4a**) and cyclic triene (**1a**).[18] Unlike **1a**, **4a** displays a quasi-reversible behavior: at potential scanning rates of $\geq$100 mVs^{-1} the reoxidation of its radical anion can be observed, indicating that the chemical stability of $\mathbf{4a}^{\odot\ominus}$ is significantly higher than that of $\mathbf{1a}^{\odot\ominus}$.

Hydrocarbon rings of the type described here—particularly when substituted with eight solubilizing long-chain residues R—provide means for further manipulations of light absorption and emission.

Received: May 30, 1990 [Z 3991 IE]
German version: *Angew. Chem.* *102* (1990) 1176

[1] H. A. Staab: *Einführung in die theoretische organische Chemie*, Verlag Chemie, Weinheim 1964; B. M. Krasovitskii, B. M. Bolotin: *Organic Luminescent Materials*, VCH, Weinheim 1988.
[2] Review: J. E. McMurry, *Chem. Rev. 89* (1989) 1513.
[3] a) D. Tanner, O. Wennerström, E. Vogel, *Tetrahedron Lett. 23* (1982) 1221; b) K. Yamamoto, S. Kuroda, M. Shibutami, Y. Yoneyama, J. Ojimo, S. Fujita, E. Ejiri, K. Yamigihara, *J. Chem. Soc. Perkin Trans. 1 1988*, 395; c) E. Vogel, I. Grigat, M. Köcher, J. Lex, *Angew. Chem. 101* (1989) 1687; *Angew. Chem. Int. Ed. Engl. 28* (1989) 1653, and references cited therein; cf. also: d) J. E. McMurry, G. J. Haley, J. R. Matz, J. C. Clardy, G. Van Duyne, R. Gleiter, W. Schäfer, D. H. White, *J. Am. Chem. Soc. 108* (1986) 2932; e) H. F. Grützmacher, E. Neumann, F. Ebmeyer, K. Albrecht, P. Schelenz, *Chem. Ber. 122* (1989) 2291.
[4] M. Bennett, N. B. Sunshine, G. F. Woods, *J. Org. Chem. 28* (1963) 2514.
[5] As described by: a) T. Mukaiyama, T. Sato, J. Hanna, *Chem. Lett. 1973*, 1041; b) D. Lenoir, *Synthesis 1977*, 553.
[6] a) H. A. Staab, F. Binnig, *Chem. Ber. 100* (1967) 293; b) F. Diederich, H. A. Staab, *Angew. Chem. 90* (1978) 383; *Angew. Chem. Int. Ed. Engl. 17* (1978) 372.
[7] a) λ_{max} (absorption) [nm]: **1a** 344, **2a** 360, **4a** 367, **4b** 395, in 1,4-dioxane; DPH 351, in *n*-hexane[8]; DNH 381, in THF[9]; b) ε_{max} [cm^2mol^{-1}]: **4a** 46000, **4b** 59000, in 1,4-dioxane; DPH ca. 78000, in *n*-hexane[8]; DNH 95000, in THF[9]; c) λ_{max} (emission) [nm]: **1a** 448, **3a** 490, **4a** 447, **4b** 470, in 1,4-dioxane; DPH 450, in *n*-heptane[14]; d) λ_{max} (absorption) [nm] of the cations of **1a** 443, 492 (deep orange), **2a** 445, 482 (red-brown), **4a** 419, 475 (orange), **4b** 447, 504 (red).
[8] K. Lunde, L. Zechmeister, *J. Am. Chem. Soc. 76* (1954) 2308.
[9] K. Mandal, T. N. Misra, *Bull. Chem. Soc. Jpn. 49* (1976) 975.
[10] A. Smakula, A. Wassermann, *Z. Phys. Chem. Abt. A 155* (1931) 353.
[11] Cf. J. Dale, *Acta Chem. Scand. 11* (1957) 971; cf. also [6a].
[12] a) L. Zechmeister, A. L. LeRosen, W. A. Schroeder, A. Polgár, L. Pauling, *J. Am. Chem. Soc.* 65 (1943) 1940; b) R. S. Mulliken, *J. Chem. Phys. 7* (1939) 203.
[13] MM2(86)/MMP2 calculations (on HP 9000/825S SRX) afforded σ-strain energies of 130 (**1a**), 52 ((3*E*)-**4a**), and 59 $kJmol^{-1}$ ((3*Z*)-**4a**; not isolated); semiempirical calculations with SCF-MNDO [MNDO 89 Version 2.3 (W. Thiel, Wuppertal 1989), on CONVEX C220 in the scope of the special research project SFB 334 (closed shell, singlet, RHF)] afforded SCF bond enthalpies of 469 (**1a**) and 279 $kJmol^{-1}$ (**4a**), respectively.
[14] A. N. Nikitina, M. D. Galanin, G. S. Ter-Sarkisyan, B. M. Mikhailov, *Opt. Spektrosk. 6* (1959) 354; *Opt. Spectrosc. (Engl. Transl.) 6* (1959) 226.
[15] R. Kuhn, A. Winterstein, *Helv. Chim. Acta 11* (1928) 87.
[16] S. Dähne, F. Schob, *J. Prakt. Chem. 315* (1973) 810.
[17] R. Schenk, W. Huber, P. Schade, K. Müllen, *Chem. Ber. 121* (1988) 2201.
[18] $E_1^{red} = 2.1$ V versus normal hydrogen electrode (NHE), pyridine, Bu_4NBF_4 (0.1 M) as supporting electrolyte, $T = 293$ K, scanning rate 100 mVs^{-1}, potentials measured versus $Ag/AgNO_3$ (0.1 M in CH_3CN), ferrocene calibration (converted to NHE). This potential is correlated with the value of −1.85 V found for DPH (versus SCE; Δ −1.61 V versus NHE; 96% aqueous 1,4-dioxane): G. J. Hoijtink, J. Van Schooten, E. De Boer, W. I. Aalbesberg, *Recl. Trav. Chim. Pays-Bas 72* (1954) 895.

Stable Azirinimines? A Structural Corrigendum**

By *Klaus Banert,* Elisabeth Reissaus, Hans-Jörg Deiseroth, Claus Peter Kluge,* and *Eva-Maria Peters*

Dedicated to Professor Wolfgang Kirmse on the occasion of his 60th birthday

W. Meyer zu Reckendorf and *N. Schultz* recently reported on abortive attempts to convert the sulfonate **1** (Ts = *p*-toluenesulfonyl) with cyanide ions into the chain-lengthened product **2**.[1] They obtained instead a product with melting point 130–131 °C in 15% yield, which is said to have the surprising structure **3a**. This novel azirinimine was said to be converted into the geometrical isomer **3b** (m.p. 180–182 °C) upon treatment with bases ($NaHCO_3$ in aqueous acetone). As evidence in support of the structures the authors quote spectroscopic data and secondary reactions of **3a**: reaction of **3a** with sodium methoxide in methanol is reported to give mainly **3b** and, in a side reaction, **4**. The product **3b** is likewise described as being formed from **4** under the same reaction conditions, while layer-chromatographic work-up is reported to lead to **5**.

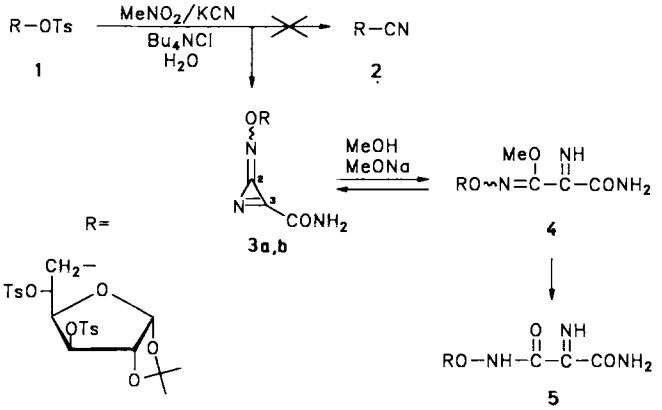

The report[1] on the synthesis and reactions of the first azirinimines[2, 3] is contrary to the hitherto known chemistry of the 2*H*-azirines.[4] The strained heterocycles **3a, b** are said to be surprisingly stable, which is in sharp contrast to the instability which is postulated for the azirinones **6**[5] and has been demonstrated in the case of the methyleneazirines **7**.[6] Usually, 2*H*-azirines show a ^{13}C-NMR signal for C-3 in the range $\delta = 157–173$;[4] in the case of **7** this signal is shifted downfield ($\delta = 185–188$), which points to the participation of a dipolar resonance form.[6] The ^{13}C-NMR spectra[1] of **3a** (C3: $\delta = 133.5$) and **3b** (C3: $\delta = 127.2$) therefore appear to be hardly reconcilable with azirinimine structures. Furthermore, one would also expect the signals for C2 to appear at much lower field (**3a**: $\delta = 112.3$; **3b**: $\delta = 106.8$) if one compares the data quoted in the literature for aziridinimines.[7] In the present communication we present corrected structures for the substances **3a, b, 4** and **5**.

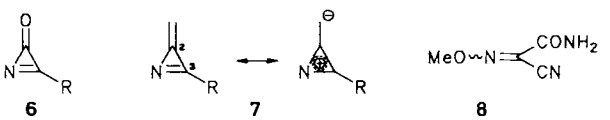

In the case of the model compound **8**[8] it is not a three-membered ring, but the anisotropic effect of the cyano group[9] which gives rise to an upfield shift of the oxime signal in the ^{13}C-NMR spectrum. The ^{13}C-NMR and the ^{15}N-NMR data of **8** resemble those of the reputed azirinimines (Table 1) to which the structures **9** and **11** should accordingly be assigned. In order to confirm this, **11** was synthesized independently from **10**,[10] sodium hydroxide and **1**[11] in dimethyl sulfoxide (DMSO) (16 h, 50 °C, yield 91%).[12] When **1** was allowed to react—as described in the literature[1]—with potassium cyanide and tetrabutylammo-

[*] Dr. K. Banert, E. Reissaus
Fachbereich 8, Organische Chemie II
der Universität-Gesamthochschule
Adolf-Reichwein-Strasse, D-5900 Siegen (FRG)
Prof. Dr. H.-J. Deiseroth[+], C. P. Kluge[+]
Fachbereich 8, Anorganische Chemie II
der Universität-Gesamthochschule
Adolf-Reichwein-Strasse, D-5900 Siegen (FRG)
E.-M. Peters[+]
Max-Planck-Institut für Festkörperforschung
Heisenbergstrasse 1, D-7000 Stuttgart 80 (FRG)

[+] X-ray structure analysis.

[**] This work was supported by the Deutsche Forschungsgemeinschaft. We thank Prof. Dr. *H. Quast* (Würzburg) for stimulating discussions.

Table 1. Selected physical data of the compounds **8**, **9**, **11**, **12**, and **14**[a].

8: m.p. 170–172 °C (water); ^{1}H NMR ([D$_6$]DMSO): δ = 4.20 (s; OMe), 7.93 (br. s; NH$_2$); ^{13}C-NMR ([D$_6$]DMSO): δ = 65.4 (q; OMe), 108.3 (s; C≡N), 127.5 (s; C=N), 158.7 (s; CONH$_2$); ^{15}N NMR ([D$_6$]DMSO): δ = −278.5 (t, $^1J \approx 90$ Hz; NH$_2$), −102.8 (s; C≡N), +45.3 (s; NOMe); IR (KBr): $\tilde{\nu}$ [cm^{-1}] = 3400 (NH$_2$), 3200 (NH$_2$), 2240 (vw; C≡N), 1700, 1600, 1555

9: m.p. 130.5–132 °C (ether); ^{1}H NMR (CDCl$_3$): δ = 1.28 (s; OC*Me*), 1.43 (s; OC*Me*), 2.49 (s; aryl *Me*), 2.52 (s; aryl *Me*), 4.38 (t, ^3J = 3.1 Hz; H4), 4.57 (m, 2H; H6), 4.75 (d, ^3J = 3.7 Hz; H2), 4.83 (m; H5), 4.87 (d, ^3J = 3.1 Hz; H3), 5.86 (d, ^3J = 3.7 Hz; H1), 6.45 (br. s; NH), 7.28 (br. s; NH), 7.35 (br. d, 2H), 7.48 (br. d, 2H), 7.65 (br. d, 2H), 7.88 (br. d, 2H); ^{13}C NMR (CDCl$_3$): δ = 21.72 (q; aryl *Me*), 21.78 (q; aryl *Me*), 26.08 (q; OC*Me*), 26.44 (q; OC*Me*), 75.15(d), 76.60 (t; C6), 78.99(d), 81.04(d), 82.28(d), 104.48 (d; C1), 111.78 (s; C≡N), 112.94 (s; OC*Me*$_2$), 127.86(d), 128.12(d), 130.30(d), 130.36(d), 131.84(s), 132.21(s), 132.59(s), 146.20(s), 146.24(s), 155.92 (s; CONH$_2$); IR (CHCl$_3$): $\tilde{\nu}$ [cm^{-1}] = 3480 (NH$_2$), 3370 (NH$_2$), 1695 (CONH$_2$), 1590 (CONH$_2$), 1370

11: m.p. 180–183 °C (chloroform/ether); ^{1}H NMR (CDCl$_3$): δ = 1.21 (s; OC*Me*), 1.47 (s; OC*Me*), 2.45 (s; aryl *Me*), 2.51 (s; aryl *Me*), 4.14 (d, ^3J = 3.7 Hz; H2), 4.52 (dd, ^2J = 13.5 Hz, ^3J = 2.6 Hz; H6), 4.56 (dd, ^2J = 13.5, ^3J = 7.8 Hz; H6), 4.81 (dd, ^3J = 3.0, 1.5 Hz; H4), 5.03 (ddd, ^3J = 7.8, 2.6, 1.5 Hz; H5), 5.09 (d, ^3J = 3.0 Hz; H3), 5.83 (d, ^3J = 3.7 Hz; H1), 6.14 (br. s; NH), 6.93 (br. s; NH), 7.36 (br. d, 2H), 7.46 (br. d, 2H), 7.81 (br. d, 2H), 7.83 (br. d, 2H); ^{13}C NMR (CDCl$_3$): δ = 21.46 (q; aryl *Me*), 21.65 (q; aryl *Me*), 26.09 (q; OC*Me*), 26.46 (q; OC*Me*), 75.52 (t; C6), 76.15(d), 80.28(d), 81.78(d), 82.87(d), 104.54 (d; C1), 106.80 (s; C≡N), 112.99 (s; OC*Me*$_2$), 127.25 (s; C=N), 127.67(d), 128.30(d), 130.40(d), 130.45(d), 131.67(s), 131.98(s), 145.86(s), 146.35(s), 158.46 (s; CONH$_2$); ^{15}N NMR ([D$_6$]DMSO, 60 °C): δ = −280.6 (t, $^1J \approx 90$ Hz; NH$_2$), −99.9 (s; C≡N), +36.8 (s; C=N); IR (CHCl$_3$): $\tilde{\nu}$ [cm^{-1}] = 3490 (NH$_2$), 3370 (NH$_2$), 1700 (CONH$_2$), 1590 (CONH$_2$), 1370

12: ^{1}H NMR (CDCl$_3$): δ = 1.21 (s; OC*Me*), 1.43 (s; OC*Me*), 2.43 (s; aryl *Me*), 2.50 (s; aryl *Me*), 4.27 (d, ^3J = 3.7 Hz; H2), 4.39 (m, 2H; H6), 4.62 (br. t, $^3J \approx 2.5$ Hz; H4), 4.98 (d, ^3J = 3.0 Hz; H3), 5.18 (m; H5), 5.49 (br. s; NH), 5.81 (d, ^3J = 3.7 Hz; H1), 6.92 (br. s; NH), 7.34 (br. d, 2H), 7.41 (s; NH), 7.45 (br. d, 2H), 7.80 (br. d, 2H), 7.86 (br. d, 2H)

14: m.p. 142–143 °C (ether/methanol/pentane); ^{1}H NMR (CDCl$_3$): δ = 1.21 (s; OC*Me*), 1.37 (s; OC*Me*), 2.45 (s; aryl *Me*), 2.50 (s; aryl *Me*), 4.33 (m, 2H; H2, H4), 4.43 (dd, ^2J = 13.5, ^3J = 8.0 Hz; H6), 4.50 (dd, ^2J = 13.5, ^3J = 2 Hz; H6), 4.78 (d, ^3J = 3.1 Hz; H3), 5.15 (br. dt, ^3J = 8.0, ca. 2 Hz; H-5), 5.75 (br. s; NH), 5.79 (d, ^3J = 3.6 Hz; H1), 6.12 (br. s; NH), 6.71 (br. s; NH), 7.11 (br. s; NH), 7.35 (br. d, 2H), 7.44 (br. d, 2H), 7.77 (br. d, 2H), 7.85 (br. d, 2H); ^{13}C NMR (CDCl$_3$): δ = 21.42 (q; aryl *Me*), 21.55 (q; aryl *Me*), 25.95 (q; OC*Me*), 26.22 (q; OC*Me*), 73.67 (t; C6), 76.21(d), 78.91(d), 81.79 (d, 2C), 104.24 (d; C1), 112.60 (s; OC*Me*$_2$), 127.75(d), 127.78(d), 129.93(d), 130.25(d), 131.78(s), 132.38(s), 145.53(s), 146.09(s), 146.68(s), 161.27 (s; CONH$_2$), 162.07 (s; CONH$_2$); ^{15}N NMR ([D$_6$]DMSO): δ = −280.8 (t, $^1J \approx 90$ Hz; NH$_2$), −268.3 (t, $^1J \approx 90$ Hz; NH$_2$), −2.5 (s; C=N); IR (CHCl$_3$): $\tilde{\nu}$ [cm^{-1}] = 3490 (NH$_2$), 3370 (NH$_2$), 1700 (CONH$_2$), 1680 (CONH$_2$), 1595 (CONH$_2$), 1575 (CONH$_2$), 1370

[a] ^{1}H NMR spectra at 80 and 400 MHz, position of the NH signals concentration-dependent; ^{13}C NMR spectra at 100.6 MHz; ^{15}N NMR spectra at 40.5 MHz, CH_3NO_2 as external standard.

nium chloride in nitromethane/water (two-phase system, 2–4 d, 50 °C), after work-up and column chromatographic separation of the starting material (SiO_2, ether/pentane 9:1) a substance (designated **9** in the following) was obtained which was converted into **11** by base-catalyzed isomerization[1] ($NaHCO_3$ in acetone/water 10:1, 3 d, 60 °C). This proves that the reputed azirinimines **3a**, **b** are in fact the substances **9** and **11**.[13] γ-Effects in the ^{13}C-NMR spectroscopy[9, 14] plausibly suggest the *Z*-configuration for **9** and the *E*-configuration for **11**: the signal of the amide C-atom appears at higher field in the case of **9** than in the case of **11**, whereas in the case of the cyanide C-atom the behavior is reversed. In the IR spectrum, **10** shows, just like the model compound **8**, an extremely weak nitrile band. It is not surprising, therefore, that the cyano groups in **9** and **11** cannot be detected IR spectroscopically. Final doubts about the structure of **9** are cleared by a single-crystal X-ray diffraction analysis[15] (Fig. 1).

Reaction of **9** with sodium methoxide in methanol (0.015 M, 4 d, 37 °C) yielded mainly **11** and the carboximide

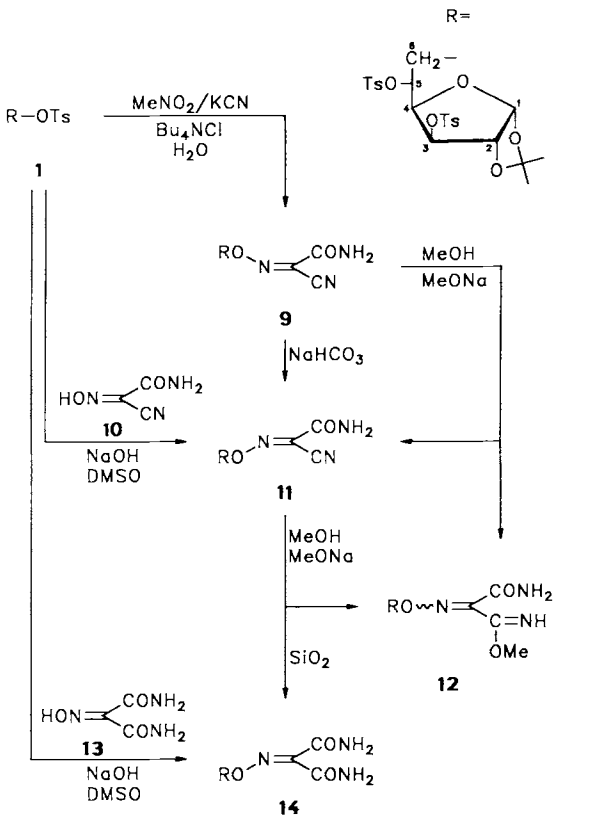

ester[16] **12** as by-product. After only 24 h reaction time a further by-product could be detected whose amount decreased again on prolonged treatment with the methoxide, and which was completely decomposed upon chromatographic work-up (SiO_2, ether/dichloromethane). ^{1}H-NMR and ^{13}C-NMR spectra of the crude product indicated that it was a geometrical isomer of the carboximide ester **12** listed in Table 1. Very slow reaction of **11** with sodium methoxide (0.015 M, 14 d, 37 °C) furnished the addition product **12**. This could be separated chromatographically (SiO_2, ether/dichloromethane) from unreacted **11**, whereby a further compound was formed which was not contained in the crude product. This new compound was the diamide **14**, which could also be prepared independently from **13**,[17] sodium hydroxide and **1** in DMSO (2 d, 50 °C, yield 88%). The spectroscopic data of **12** and **14** (Table 1) reveal that the

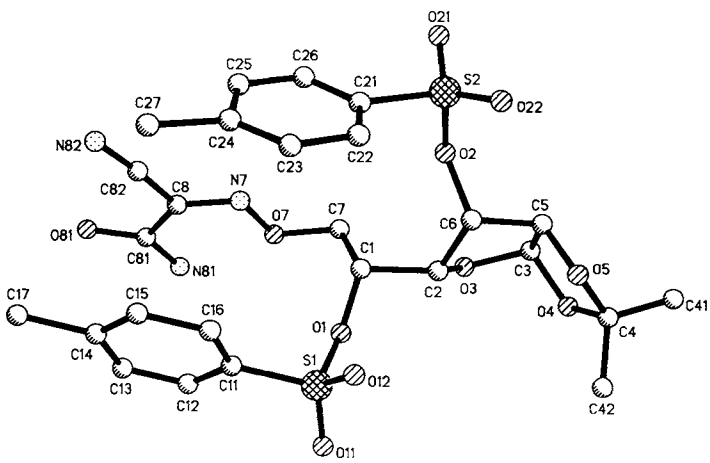

Fig. 1. Structure of **9** in the crystal (H atoms not shown)[15].

structures **4** and **5** were erroneously assigned to the two substances.[1] As the ^{15}N-NMR spectrum shows, **14** has two NH_2 groups and one further nitrogen atom, which is not reconcilable with structure **5**.

$^{\ominus}O-N=CH-CH-NO_2^{\ominus}$ **15**

As has already been suggested,[1] in the reaction of **1** with potassium cyanide and tetrabutylammonium chloride in nitromethane/water the condensation product **15**[18] could be formed initially. Possibly subsequent *O*-alkylation by the sulfonate **1**, nucleophilic attack by cyanide at the neighboring carbon atom and formal double elimination and addition of water (sequence variable) could lead to **9**.

Received: November 17, 1989;
revised: July 17, 1990 [Z 3638 IE]
German version: *Angew. Chem. 102* (1990) 1166

[1] W. Meyer zu Reckendorf, N. Schultz, *Angew. Chem. 100* (1988) 1094–1096; *Angew. Chem. Int. Ed. Engl. 27* (1988) 1075–1077.
[2] Concerning abortive attempts to detect the azirinimines cf.: G. L'abbé, F. Godts, *J. Chem. Soc. Chem. Commun. 1983*, 748–750; G. L'abbé, *Bull. Soc. Chim. Belg. 93* (1984) 579–592.
[3] Azirinimines have been discussed as intermediates and in theoretical studies: J. H. Boyer, J. Dunn, J. Kooi, *J. Chem. Soc. Perkin Trans. 1 1975*, 1743–1747; J. B. Moffat, *J. Chem. Soc. Chem. Commun. 1975*, 888–890; *J. Mol. Struct. 94* (1983) 261–265.
[4] V. Nair, in A. Hassner (Ed.): *Small Ring Heterocycles Part 1*, in *The Chem. Heterocycl. Comp.* (A. Weissberger, E. C. Taylor, Eds.) Vol. *42*, Wiley, New York 1983 pp. 215–332, and references cited therein.
[5] A. Hassner, R. J. Isbister, R. B. Greenwald, J. T. Klug, E. C. Taylor, *Tetrahedron 25* (1969) 1637–1641; A. Padwa, J. K. Rasmussen, A. Tremper, *J. Am. Chem. Soc. 98* (1976) 2605–2614.
[6] K. Banert, M. Hagedorn, *Angew. Chem. 102* (1990) 90–92; *Angew. Chem. Int. Ed. Engl. 29* (1990) 103–105.
[7] H. Quast, L. Bieber, G. Meichsner, *Chem. Ber. 121* (1988) 2117–2120.
[8] O. Diels, E. Borgwardt, *Ber. Dtsch. Chem. Ges. 54* (1921) 1334–1343; H. Junek, M. Mittelbach, *Z. Naturforsch. B 34* (1979) 280–282.
[9] H.-O. Kalinowski, S. Berger, S. Braun: *^{13}C-NMR-Spektroskopie*, Thieme, Stuttgart 1984, p. 220–222, 227.
[10] J. M. Ross, W. C. Smith, *J. Am. Chem. Soc. 86* (1964) 2861–2868.
[11] W. P. Shyluk, J. Honeyman, T. E. Timell, *Can. J. Chem. 33* (1955) 1202–1206; H. Ohle, H. Wilcke, *Ber. Dtsch. Chem. Ges. 71* (1938) 2316–2327.
[12] For the alkylation of **10** by sulfonates see: M. M. Safta, Rom. RO 80887 (1982) Intrepinderea Chimica Turda; *Chem. Abstr. 101* (1984) P 6639r.
[13] The corrected structures are also consistent with the catalytic hydrogenation [1] of **9** and the reaction **1** → **9** using labeled reagents [1] ($KC^{15}N$ or $^{13}CH_3NO_2$).
[14] The configurations of oximes were determined on the basis of the ^{13}C-NMR data: G. E. Hawkes, K. Herwig, J. D. Roberts, *J. Org. Chem. 39* (1974) 1017–1028; G. C. Levy, G. L. Nelson, *J. Am. Chem. Soc. 94* (1972) 4897–4901.
[15] $C_{26}H_{29}N_3O_{11}S_2$: (Enraf-Nonius CAD4 diffractometer, $Mo_{K\alpha}$ radiation, $\lambda = 0.71069$ Å, $T = 293$ K, crystal system: orthorhombic space group $P2_12_12_1$ (No. 19), $a = 7.9291(59)$, $b = 14.2810(9)$, $c = 27.9100(34)$ Å, $V = 3160(3)$ Å^3. Data range $-9 \le h \le 9$, $0 \le k \le 17$, $0 \le l \le 33$, 5897 measured reflections, 2397 symmetry-independent with $I > 3\sigma(I)$, $R_{conv} = 0.117$, $R_w = 0.092$ (refinement with isotropic temperature coefficients and without hydrogen atoms). Structure solution by SHELXTL-PLUS. Further details of the crystal structure determination are available on request from the Fachinformationszentrum Karlsruhe, Gesellschaft für wissenschaftlich-technische Information mbH, D-7514 Eggenstein-Leopoldshafen 2 (FRG), on quoting the depository number CSD-54805, the names of the authors, and the journal citation.
[16] The base-catalyzed addition of alcohols to electron-deficient nitriles has already been studied in detail: F. C. Schaefer, G. A. Peters, *J. Org. Chem. 26* (1961) 412–418, and references cited therein.
[17] M. Conrad, A. Schulze, *Ber. Dtsch. Chem. Ges. 42* (1909) 729–735.
[18] S. Brownstein, *J. Org. Chem. 28* (1963) 2919–2921; P. A. S. Smith: *The Chemistry of Open-Chain Nitrogen Compounds, Vol. II*, Benjamin, New York 1966, p. 402–403.

Epoxidation of the P=C Double Bond of Phosphaalkene Complexes: X-Ray Crystal Structure Analysis of a Stable Oxaphosphirane Complex

By *Siegfried Bauer, Angela Marinetti, Louis Ricard*, and *François Mathey**

The oxaphosphirane ring is of special interest because of its analogy to the oxirane ring. However, until now, only one oxaphosphirane, which was obtained by [2 + 1] cycloaddition of hexafluoroacetone to a bulky aminoiminophosphane, has been characterized by spectroscopy.[1] The direct epoxidation of the P=C double bond of phosphaalkenes would provide a far better access to oxaphosphiranes. Unfortunately, however, free phosphaalkenes are preferentially oxidized at the phosphorus.[2] It was thus logical to block the lone pair at phosphorus and to investigate the oxidation of a series of phosphaalkene P-complexes.

Complex **1**, readily obtained from the corresponding aldehyde via the "phospha-Wittig" reaction,[3] was directly oxidized by *m*-chloroperbenzoic acid in THF to give a quantitative yield of the corresponding oxaphosphirane **3**[4] [Eq. (a)].

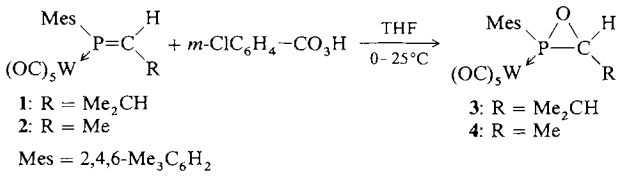

1: R = Me_2CH
2: R = Me
Mes = 2,4,6-$Me_3C_6H_2$

3: R = Me_2CH
4: R = Me

The X-ray crystal structure analysis of **3**[5] confirmed the presence of a three-membered oxaphosphirane ring. The intracyclic C1–P–O2 angle [50.9(2)°] is close to that found in a phosphirane *P*–$W(CO)_5$ complex,[6] whereas the intracyclic

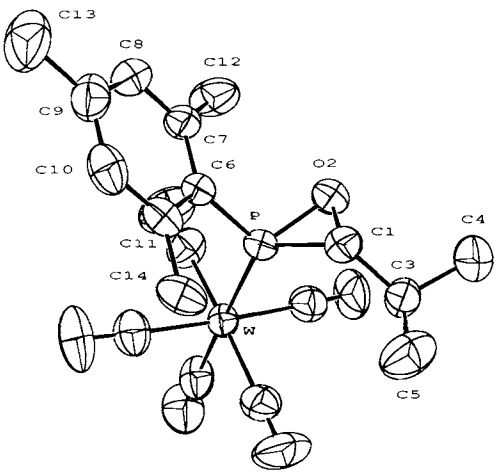

Fig. 1. Structure of **3** in the crystal [5]. Ellipsoids are scaled to enclose 50% of the electronic density. Hydrogen atoms are omitted for clarity. Important bond distances [Å] and angles [°]: W-P 2.443(1), P-O2 1.657(4), P-C1 1.778(6), P-C6 1.819(5), O2-C1 1.480(7), C1-C3 1.505(8); W-P-O2 120.7(2), W-P-C1 128.7(2), W-P-C6 122.1(2), O2-P-C1 50.9(2), O2-P-C6 106.3(2), C1-P-C6 106.5(3), P-O2-C1 68.8(3), P-C1-O2 60.3(3), P-C1-C3 125.7(4), O2-C1-C3 114.9(5).

[*] Prof. Dr. F. Mathey, Mr. S. Bauer, Dr. A. Marinetti, Dr. L. Ricard
Laboratoire de Chimie du Phosphore et des Métaux de Transition
DCPH, Ecole Polytechnique
F-91128 Palaiseau Cedex (France)

P–O2–C1 angle is less acute than in epoxides.[7] The most interesting feature of this structure is that it keeps the "memory" of its phosphaalkene precursor. The sum of the W–P–C6, W–P–C1, and C1–P–C6 angles (357.3°) is close to 360°, as in the parent phosphaalkene complex.[3b] The plane of the oxaphosphirane ring is almost orthogonal to the WPC1C6 mean plane [90.3(0.2)°]. The phosphorus atom appears to retain its initial sp^2 hybridization. Even the P–C1 bond [1.778(6) Å] is shorter than expected for a normal P–C single bond. The structure of **3** also shows that the epoxidation of the P=C double bond takes place with retention of the initial *trans* stereochemistry of **1** [C3–P–C1–C6 dihedral angle 161.3(5)°]. However, with the less hindered phosphaalkene complex **2**, this retention is not complete. Indeed, the epoxidation of **2** mainly leads to **4**.[8] The ^{1}H-NMR spectrum of **4**, like that of **3** shows no *H*–C1–*P* coupling.[4] Thus, **4** probably has the same *trans* stereochemistry as **3**. However, besides **4** ($\delta^{31}P = +2.9$ in C_6D_6), another compound **5** ($\delta^{31}P = +6.2$) is produced in minor amounts (ca. 10%). This compound is probably the *cis* isomer corresponding to **4**. Finally, the main decomposition path of the oxaphosphiranes **3** and **4** in the mass spectrometer involves splitting of the ring into the terminal phosphinidene complex [Mes–P=W(CO)$_5$] and the aldehydes RCHO. This process is exactly the reverse of the first described synthesis of this ring.[1]

Experimental

A solution of *m*-chloroperbenzoic acid (1.9 g, 1.1×10^{-2} mol) in THF (10 mL) was added dropwise to a solution of the phosphaalkene complex **1** (5.3 g, 1×10^{-2} mol) in THF (30 mL). The reaction was slightly exothermic. After evaporation of THF, the residue was extracted with hexane. The extract after removal of hexane was recrystallized from pentane/CH_3CN. 5.0 g of **3** (~86%), colorless crystals: m.p. 68–69 °C. The same procedure with **2** gave **4** in 40% yield after recrystallization; m.p. 61–64 °C (along with *ca* 10% of the *cis* isomer).

Received: June 5, 1990 [Z 3999 IE]
German version: *Angew. Chem. 102* (1990) 1188

[1] G.-V. Röschenthaler, K. Sauerbrey, R. Schmutzler, *Chem. Ber. 111* (1978) 3105; see also: E. Niecke, D. Gudat, W. W. Schoeller, P. Rademacher, *J. Chem. Soc. Chem. Commun.* (1985) 1050.

[2] Th. A. van der Knaap, Th. C. Klebach, R. Lourens, M. Vos, F. Bickelhaupt, *J. Am. Chem. Soc. 105* (1983) 4026. A stable phosphaalkene *P*-oxide has been characterized by X-ray crystal structure analysis: R. Appel, F. Knoch, H. Kunze, *Angew. Chem. 96* (1984) 159; *Angew. Chem. Int. Ed. Engl. 23* (1984) 157.

[3] a) A. Marinetti, F. Mathey, *Angew. Chem. 100* (1988) 1435; *Angew. Chem. Int. Ed. Engl. 27* (1988) 1382; b) A. Marinetti, S. Bauer, L. Ricard, F. Mathey, *Organometallics 9* (1990) 793.

[4] **3**: m.p. 68–69 °C (pentane/acetonitrile); ^{31}P NMR (C_6D_6): $\delta = +3.8$, $^1J(^{31}P^{183}W) = 300$ Hz; ^{1}H NMR (C_6D_6): $\delta = 0.96$ (d, ^3J(HH) = 6.8 Hz, 3H, Me_2C), 0.99 (dd, ^{3}J(HH) = 6.3 Hz, ^4J(HP) = 1.15 Hz, 3H, Me_2C), 1.73 (m, 1H, C*H* Me_2), 1.95 (s, 3H, Me), 2.30 (s, 3H, Me), 2.40 (d, ^3J(HH) = 9.9 Hz, 1H, OCH), 2.61 (s, 3H, Me), 6.51 (s. br., 2H, arom. C*H*); ^{13}C NMR (C_6D_6): $\delta = 19.15$ (s, Me), 19.57 (d, J(CP) = 12.2 Hz, Me), 20.44 (d, J(CP) = 9.4 Hz, Me), 20.87 (d, J(CP) ≃ 8.5 Hz, Me), 20.96 (s, Me), 31.32 (s, *C*H Me_2), 69.78 (d, ^1J(CP) = 28.1 Hz, OCH), 194.96 (d, ^2J(CP) = 7.9 Hz, *cis* CO); The isopropyl substituent displays two nonequivalent diastereotopic methyl groups (^{1}H and ^{13}C NMR). Both show small ^4J(HP) couplings but only the larger one could be measured at 200 MHz. MS (70 eV, ^{184}W): *m/z* 546 ($M^{\oplus}$, 4%), 474 ($M^{\oplus}$ – C_4H_8O, 36%), 446 (474 – CO, 36%), 418 (474 – 2 CO, 19%, 390 (474 – 3 CO, 100%). Correct elemental analysis.

[5] X-ray structure determination of **3**: crystals of **3**, $C_{18}H_{15}O_6PW$ were grown at 4 °C from acetonitrile. Data were collected at 18° ± 1 °C on an Enraf Nonius CAD4 diffractometer. The crystal structure was solved and refined using the Enraf Nonius SDP package. The compound crystallizes in space group $C2/c$, $a = 32.539(3)$ Å, $b = 7.164(1)$ Å, $c = 21.984(2)$ Å, $\beta = 125.79(1)°$; $V = 4156.8(1.9)$ Å^3; $Z = 8$; $\varrho_{calcd} = 1.740$ g/cm^3; $Mo_{K\alpha}$ radiation ($\lambda = 0.71073$ Å) graphite monochromator; $\mu = 58.0$ cm^{-1}; $F(000) = 2080$. A total of 6030 unique reflections were recorded in the range $2° \le 2\theta \le 60.0°$, of which 3248 were considered as observed ($F^2 < 3.0\sigma(F^2)$). The structure was solved by Patterson methods. The hydrogen atoms were included as fixed contributions in the final stages of refinement (non-H atoms anisotropic). A non-Poisson weighting scheme was applied with a p factor of 0.05. The final R factors were $R = 0.029$, $R_w = 0.037$, G. O. F. = 1.03. Further details of the crystal structure investigation are available on request from the Fachinformationszentrum Karlsruhe, Gesellschaft für wissenschaftlich-technische Information mbH, D-7514 Eggenstein-Leopoldshafen 2 (FRG), on quoting the depository number CSD-54755, the names of the authors, and the journal citation.

[6] B. Deschamps, L. Ricard, F. Mathey, *Polyhedron 8* (1989) 2671.

[7] C-O-C Intracyclic angle close to 61°: E. G. Lewars in: *Comprehensive Heterocyclic Chemistry*, A. R. Katritzky, C. W. Rees Eds, Pergamon, Oxford, vol. 7 (1984) p. 98.

[8] **4**: ^{31}P NMR (C_6D_6): $\delta = +2.9$; ^{1}H NMR (C_6D_6): $\delta = 1.28$ (dd, ^3J(HH) = 5.8 Hz, ^3J(HP) = 16.6 Hz, 3H, *Me*-CH), 1.94 (s, 3H, Me), 2.22 (s, 3H, Me), 2.59 (s, 3H, Me), 2.76 (q, ^3J(HH) = 5.8 Hz, 1H, OCH), 6.49 (m, 2H, arene C*H*); ^{13}C NMR (C_6D_6): $\delta = 16.46$ (s, *Me*-CH), 20.24 (d, J(CP) = 9.2 Hz, Me), 20.85 (d, J(CP) = 10.5 Hz, Me), 20.96 (s, Me), 60.71 (d, ^1J(CP) = 30.8 Hz, OCH), 194.89 (d, ^2J(CP) = 8.5 Hz, *cis* CO); MS (70 eV, ^{184}W): *m/z* 518 ($M^{\oplus}$, 4%), 474 ($M^{\oplus}$ – C_2H_4O, 32%), 446 (474 – CO, 30%), 418 (474 – 2 CO, 13%), 390 (474 – 3 CO, 100%).

Nonradioactive Assay of DNA Hybridization by DNA-Template-Mediated Formation of a Ternary Tb^{III} Complex in Pure Liquid Phase

By *Andreas Oser* and *Günther Valet**

The identification of specific nucleic acid sequences by the hybridization technique[1] is usually carried out in a heterogeneous two-phase system. The nucleic acid material being investigated is immobilized on a solid matrix and then incubated in individual steps (prehybridization, hybridization, washings, detection) with various solutions.[2] Homogeneous hybridizations in pure liquid phase exhibit more favorable hybridization kinetics and, moreover, make the prehybridization and washing steps superfluous. This appreciable simplification is of great interest for the development of automated procedures. However, it requires special labeling of the nucleic acid probes, so that a measurable signal—by fluorescence resonance energy transfer (FRET),[3] for example—is only obtained after hybrid formation with the complementary sequence. Here we describe such a system involving suitable pairs of oligonucleotide probes, chemically modified to form a ternary Tb^{III} complex after hybridization with the template nucleic acids. Upon photoexcitation, the salicylate group of one oligonucleotide, serving as a ligand, transfers the excitation energy to the lanthanide ion of the second oligonucleotide[4] and a $Tb^{3\oplus}$-specific, long-lived fluorescence is then emitted.

The chemical modification involved attachment of the energy donor salicylate (pAS) to the 3′ end of one oligonucleotide (3′ON-pas) and a diethylenetriaminepentaacetate (DTPA) ligand bearing the energy acceptor and fluorescence emitter $Tb^{3\oplus}$ to the 5′ end of the other oligonucleotide (5′ON-DTPA-Tb) (Fig. 1). The oligonucleotide sequences were chosen in such a way that, after hybridization to the complementary DNA strand, the energy donor and acceptor were positioned in direct proximity.[5] Compared with ternary complex formation in free solution, the formation of a complex between DTPA-Tb on the one hand and salicylate on the other is strongly favored on the DNA template (Fig. 1).

The 3′-end labeling of 3′ON with 4-aminosalicylic acid (pAS) was accomplished by established methods of 3′-end

[*] Prof. Dr. G. Valet, Dr. A. Oser
Max-Planck-Institut für Biochemie
D-8033 Martinsried (FRG)

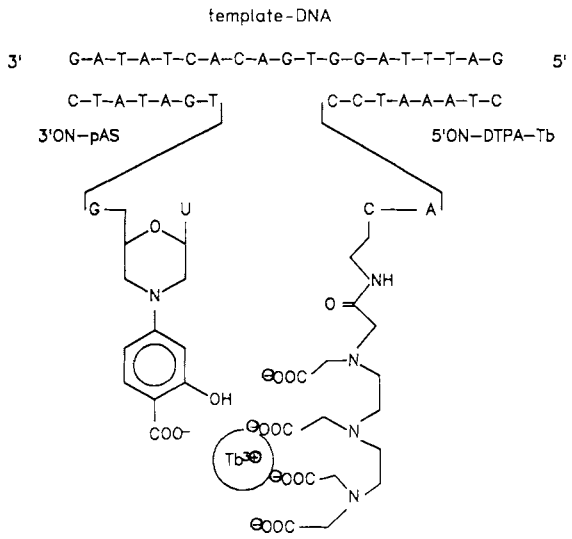

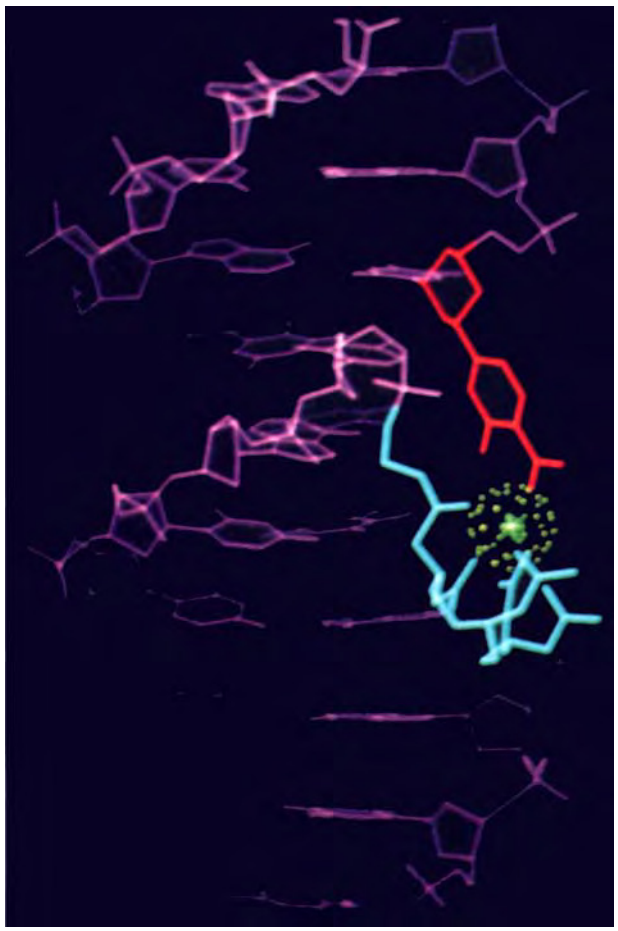

Fig. 1. Schematic (top) and graphic (bottom) drawing of the model system for homogeneous hybridization [6]. The 3'-end label of the 9-mer 3'ON with pAS and the 5'-end label of the 10-mer 5'ON with DTPA-Tb are enlarged. Red, salicylate residue with morpholino moiety; light blue-green, DTPA; yellow, $Tb^{3\oplus}$, magenta, B-DNA helix.

labeling of RNA molecules via periodate oxidation.[7] The extension of this 3' modification to DNA molecules can be performed either enzymatically[8] or—as is the case here—chemically[3b, 9] by the use of a 3'-terminal ribonucleotide moiety. Periodate oxidation affords a dialdehyde group at the 3' ribose moiety. Double reductive amination of this dialdehyde group with pAS in the presence of cyanoborohydride results in conversion of the 3'-terminal ribose moiety to a morpholino moiety containing a salicylate group (Fig. 1, top).

In order to label 5'ON with DTPA-Tb, the oligonucleotide was first synthesized with an aminoethyl linker at the 5' terminus.[10] DTPA dianhydride was then used for covalent coupling of DTPA to the primary amino group of the oligonucleotide[11] and finally made possible the stable complexation of $Tb^{3\oplus}$ ions ($K_a = 10^{23}$[12]).

Figure 2 shows the $Tb^{3\oplus}$-specific fluorescence values after hybridization of the oligonucleotide pair 3'ON-pAS/5'ON-DTPA-Tb, present in constant concentration, with increasing concentrations of the complementary template DNA in solution. The sensitivity of detection is one picomole of template DNA in one milliliter. That the detected ternary complex is indeed formed by binding of the oligonucleotide pair to the complementary DNA was confirmed by the increase in $Tb^{3\oplus}$ fluorescence with increasing concentration of template DNA (Fig. 2). Control measurements showed that the

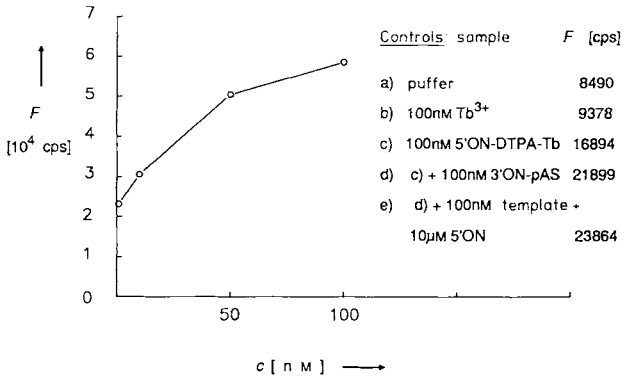

Fig. 2. Delayed $Tb^{3\oplus}$ fluorescence F after hybridization of the oligonucleotide pair with increasing concentrations c of template DNA. The hybridization was carried out for 30 m in 10 mM Tris-HCl/0.5 M NaCl at pH 8.0 in the presence of 100 nM 3'ON-pAS and 100 nM 5'ON-DTPA-Tb at 6 °C. Subsequently, the delayed fluorescence was measured in counts per second (cps) with an Arcus 1230 fluorometer (LKB-Wallac, Turku, Finnland) at 400-μs delay time and 400-μs measuring time (excitation 268–388 nm, emission > 435 nm). Values for the controls are shown on the right-hand side of the figure.

energy transfer can be competitively inhibited by an excess of unlabeled 5' oligonucleotide (control e), thereby demonstrating the specificity of the fluorescence excitation. The control experiments also show that the delayed background fluorescence is not generated by direct excitation of the $Tb^{3\oplus}$ ions (control b) but rather by energy transfer from nucleotide bases of the 5'ON oligonucleotide to the complexed $Tb^{3\oplus}$ ion;[4a] this fluorescence is already measurable before the hybridization (control c).

Further proof for the hybridization-dependent complex formation is provided by the inverse correlation between hypochromicity and increase in the $Tb^{3\oplus}$ fluorescence on cooling of the hybridization solutions—that is, on going from the denatured to the reassociated state of the template/oligonucleotide pair system (Fig. 3). The melting point of the template/3'ON-pAS/5'ON-DTPA-Tb system is about 1 K greater than that of a system containing the same components but without 5'-DTPA-Tb terminal modification. This corresponds to an enthalpy change and therefore a stabilization contribution of about 2.5 kJ mol^{-1}.[13] Accordingly, the positive cooperativity[14] already observed on binding of two directly neighboring oligonucleotides to a complementary template is further increased by the chelate formation.

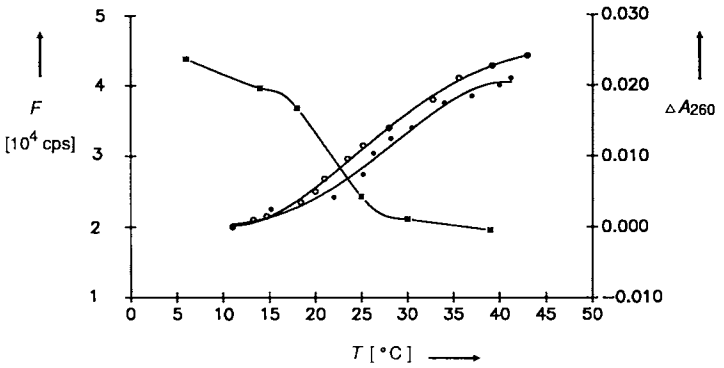

Fig. 3. Time-delayed fluorescence F (■—■) and change of the absorption ΔA_{260} (●—●) for the system template/3'ON-pAS/5'ON-DTPA-Tb (each 100 nM) as a function of temperature T in 10 mM Tris-HCl/0.5 M NaCl at pH 8.0. A T_m value of 27 °C was determined from the variation in hypochromicity; by contrast, the system without 5'-end labeling (template/3'ON-pAS/5'ON, o—o) has a T_m value of 26 °C. The T_m values of 3'ON and 5'ON alone with the template DNA are 19.5 and 20 °C, respectively.

The dependence of the energy-transfer efficiency on the distance of the oligonucleotide pairs was investigated by shortening 5'ON by one nucleotide. The DTPA-Tb label was then located on the adenine residue of 5'ON (see Fig. 1). For the same concentration of template, the hybridization signal thereby decreased by 54%. Lengthening of the spacer between the 5'-phosphate group and the DTPA-Tb chelate from an ethyl to a hexyl arm[15] resulted in restoration of 88% of the original energy-transfer efficiency.

Complex formation between energy donor and acceptor guarantees a more efficient energy transfer in comparison to a system in which energy transfer only occurs owing to spatial proximity of donor and acceptor—as was the case for the earlier described hybridization assays using the FRET principle.[3]

A further advantage of the pAS/Tb donor/acceptor system results from the *long-lived* $Tb^{3\oplus}$ fluorescence with a lifetime of 1.58 ms,[4b] which allows the measurement of delayed fluorescence.[16] The direct donor and acceptor fluorescence emission, which is short-lived and independent of the energy-transfer process, leads to an appreciable, unspecific background fluorescence in the usual FRET systems.[17] Measurement of the delayed fluorescence, however, allows reliable suppression of this background fluorescence. The sensitivity of the DNA-hybridization assay described here might be further increased by a better choice of excitation and emission wavelengths of fluorescence and by the use of other ligand/lanthanide FRET systems.

Besides simplifying the hybridization process compared with two-phase systems, the method described here is of special significance for the rapid identification of mutations, insertions, deletions, chromosome translocations, and splicing sites, since the two oligonucleotide probes must be in direct proximity.

Experimental Procedure

Synthesis of 3'ON-pAS: 16 nmol of 3'ON containing a 3'-ribouridyl residue [3b, 9] was treated for 2 h on ice with $NaIO_4$ (2 μmol) in 0.2 mL of 50 mM sodium acetate buffer at pH 4.75. After addition of ethylene glycol (10 μL, 90 μmol) and Sephadex G-25 chromatography, the oxidized 3'ON was incubated with pAS (4 μmol) and $NaBH_3CN$ (4 μmol) in 0.15 mL of 0.2 M sodium phosphate buffer at pH 8.0 for about 15 h. After Sephadex G-25 purification, 3'ON-pAS was isolated by denaturing polyacrylamide gel electrophoresis (20%, 8 M urea) [18a].

Synthesis of 5'ON-DTPA-pAS: 160 nmol of the 5'-aminolink-functionalized oligonucleotide [10] was treated twice in 50 μL of 0.2 M potassium hydrogen carbonate buffer at pH 8.2 with DTPA dianhydride (4 μmol; 0.2 M solution in anhydrous dimethyl sulfoxide). After Sephadex G-25 purification, the 5'ON-DTPA was isolated by reversed phase HPLC [18b] and then treated with an equimolar amount of $TbCl_3$.

Received: May 25, 1990;
supplemented: August 20, 1990 [Z 3981 IE]
German version: *Angew. Chem. 102* (1990) 1197

[1] a) U. Landegren, R. Kaiser, C. T. Caskey, L. Hood, *Science 242* (1988) 229; b) J. A. Matthews, L. J. Kricka, *Anal. Biochem. 169* (1988) 1.
[2] J. Meinkoth, G. Wahl, *Anal. Biochem. 138* (1984) 267.
[3] a) M. J. Heller, L. E. Morrison in D. T. Kingsburg, S. Falkow (Eds.): *Rapid Detection and Identification of Infectious Agents*, Academic Press, London 1985, p. 245; b) R. A. Cardullo, S. Agrawal, C. Flores, P. C. Zamecnik, D. E. Wolf, *Proc. Natl. Acad. Sci. USA 85* (1988) 8790; c) J. Telser, K. A. Cruickshank, L. E. Morrison, T. L. Netzel, C.-K. Chan, *J. Am. Chem. Soc. 111* (1989) 7226.
[4] a) F. S. Richardson, *Chem. Rev. 82* (1982) 541; b) M. P. Bailey, B. F. Rocks, C. Riley in T. T. Ngo (Ed.): *Nonisotopic Immunoassays*, Plenum, New York 1988, p. 187.
[5] Since we only wanted to show that the FRET detection procedure could work in principle, we chose a model system involving only short oligonucleotides (9- and 10-mers). For practical applications, longer oligonucleotides with higher melting points (T_m) are necessary.
[6] The molecular modeling system consisted of an Evans & Sutherland PS390 Workstation and the graphics programs "Helix" (Dr. U. Heinemann, Institut für Kristallographie, Freie Universität Berlin) and "Insight" (Biosym, München). We gratefully acknowledge the friendly support of Dr. *J. Köhler* (Genzentrum, München).
[7] a) N. K. Kochetkov, E. I. Budovskii (Eds.): *Organic Chemistry of Nucleic Acids. Part B*, Plenum, New York 1972, p. 466; b) T. R. Booker, L. M. Augerer, P. H. Yeu, N. D. Hershey, N. Davidson, *Nucleic Acids Res. 5* (1978) 363.
[8] M. Lemaitre, B. Bayard, B. Lebleu, *Proc. Natl. Acad. Sci. USA 84* (1987) 648.
[9] T. Tanaka, S. Tamatsukuri, M. Ikehara, *Nucleic Acids Res. 14* (1986) 6265.
[10] For the use of the aminolink-1 reagent 2-methoxy-3-trifluoroacetyl-1,3,2-oxaazaphosphacyclopentane, see *Applied Biosystems User Bulletin 38* (1986); Applied Biosystems, Foster City, CA, USA.
[11] A 5'-end labeling of oligonucleotides with metal chelates was first described by: B. C. F. Chu, L. E. Orgel, *Proc. Natl. Acad. Sci. USA 82* (1985) 963.
[12] T. Moeller, D. F. Martin, L. C. Thompson, R. Ferrus, G. R. Feistel, W. J. Randall, *Chem. Rev. 65* (1965) 1.
[13] For the determination of T_m values and enthalpy changes, see K. J. Breslauer, J. M. Sturtevant, I. Tinoco Jr., *J. Mol. Biol. 99* (1975) 549.
[14] I. Tazawa, S. Tazawa, P. O. P. Ts'O, *J. Mol. Biol. 66* (1972) 115.
[15] After functionalization with the aminolink-2 reagent: see *Applied Biosystems User Bulletin 49* (1988).
[16] I. Wieder in W. Knapp, K. Holubar, G. Wick (Eds.): *Immunofluorescence and Related Staining Techniques*, Elsevier/North Holland Biomedical Press, Amsterdam 1978, p. 67.
[17] L. E. Morrison, *Photochem. Photobiol. 45 Suppl.* (1987) 72S.
[18] a) R. Wu, N.-H. Wu, Z. Hanna, F. Georges, S. Narang in M. J. Gait (Ed.): *Oligonucleotide Synthesis. A Practical Approach*, IRL Press, Oxford 1984, p. 135; b) L. W. McLaughlin, N. Piel, *ibid.* p. 117.

Synthesis of D- and L-2-Amino-2-deoxyarabinose and 1,4-Dideoxy-1,4-iminolyxitol by (C_2 + C_3)-Nitroaldol Addition with 2-*O*-Benzylglyceraldehyde**

By *Volkmar Wehner* and *Volker Jäger**

Dedicated to Professor Hans Jürgen Bestmann on the occasion of his 65th birthday

Many of the reported glycosidase inhibitors can be viewed as configurationally analogous, mostly conformationally

[*] Prof. Dr. V. Jäger, Dipl.-Chem. V. Wehner
Institut für Organische Chemie der Universität
Am Hubland, D-8700 Würzburg (FRG)

[**] Nitro Compounds, Part 3. This work was supported by the Volkswagen-Stiftung, the Deutsche Forschungsgemeinschaft, the Fonds der Chemischen Industrie, and Bayer AG. We thank the Freistaat Bayern for a graduate fellowship (*V. W.*), Dr. *D. Häbich*, Bayer AG, for discussions, and *H. Sattler*, Dipl.-Chem. *U. Stahl*, and *C. Hahner* for experimental assistance.—Part 2: [9].

rigid iminosugar derivatives of mono- or bicyclic structure.[1-3] In addition, polyhydroxypyrrolidines such as L- and D-1,4-dideoxy-1,4-iminoarabinitol (LAB and DAB, resp.), polyhydroxypiperidines such as deoxynojirimycin, and indolizidines such as castanospermine have been shown to be (more or less cytotoxic) inhibitors of HIV replication.[2] These findings stimulated syntheses of numerous groups, based, e.g., on the modification of carbohydrates[2]—often involving a sophisticated protecting group strategy—or the use of stereoselective C–C coupling reactions such as the aldolase-catalyzed aldol additions.[3]

We are currently trying to find new and efficient syntheses in this series[4] and report here and in the following communication[5] on various routes to D- and L-*arabino*-configurated dihydroxypyrrolidines of type **A** (Scheme 1). These derivatives are of interest both as target compounds[6] and as intermediates[6b] for syntheses of indolizidines.

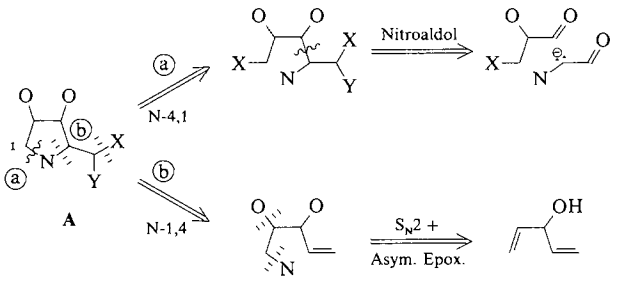

A

Scheme 1. Nitroaldol (this work) and divinylcarbinol route [5] to the dihydroxypyrrolidines **A**.

The key step of the syntheses according to route a presented here is a highly stereoselective case of the often capricious nitroaldol addition (Henry reaction).[7] We have carried out systematic investigations into the conditions and structural variations of more complex components of this reaction.[8, 9] Concerning C_5 products, it emerged that nitroacetaldehyde diethylacetal **2** and 2-*O*-benzylglyceraldehyde, (BGA) **1**[10], developed recently (for that purpose), are best suited. In the presence of tetrabutylammonium fluoride trihydrate at room temperature both combine to afford a mixture of only two of the four possible diastereomers, namely *arabino*- and *ribo*-**3**, in the ratio of 88:12, in 90% yield. Based on cross experiments, this results from a very high 1,2-induction (*erythro*) with regard to the aldehyde **1** (*erythro* configuration referred to C4/C3 in **3**), and subsequent equilibrium epimerization at the nitromethine group (C2) in the adduct **3**. The mixture of the 1,4-protected nitropentoses **3** was reduced[11] and converted into the *N*-acetyl derivative of the acyclic arabinosamine acetal **6** by standard methods[12] (Scheme 2). The epimers could be separated at the stage of the O,N-peracetylation products **5**. L-**6** was obtained in four steps (plus one chromatographic separation) with an overall yield of 51% (D-**6** with 45%).[13] Gratifyingly, **3** survived the reduction to **4** *without* epimerization at C2, and **6** was isolated with an enantiomeric purity of > 99:1 [^{1}H NMR analysis with (+)-Eu(hfc)$_3$]. Once more,[10] this shows that **1** can undergo stereoselective reactions with basic nucleophiles *without* racemization.

The open-chain arabinosamine acetals L- and D-**4** likewise proved suitable intermediates for the synthesis of the iminoarabinitols **13** (*lyxo* configuration when named as 1-deoxysugars). Benzyloxycarbonyl(Z)-protection of the amino group and 5-O-tosylation gave the *N*-Z-protected cyclization precursors **8** which were stable only in basic medium, i.e. in

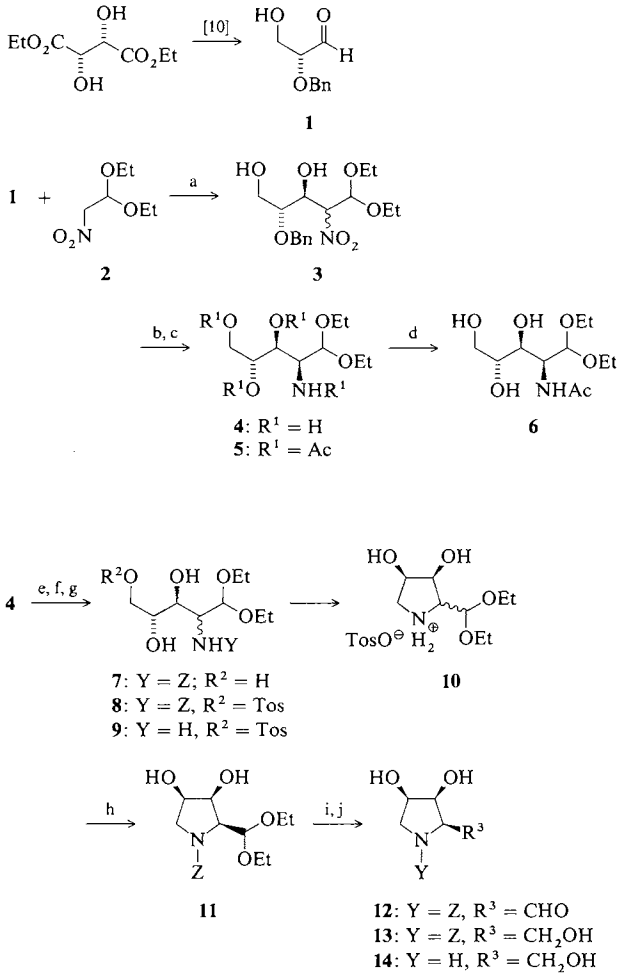

Scheme 2: Synthesis of 2-arabinosamine acetal **6**, *N*-Z-dihydroxyprolinal **12**, and *N*-Z-1,4-dideoxy-1,4-iminolyxitol **13**. The formulas depict the starting materials and products for the case of (*R*)-**3**; all reactions were carried out in both enantiomeric series. In the case of **3**, **5**–**7**, **11**, **13** the structures and configurations are established by complete analytical and spectroscopic data. a) 0.5 $Bu_4NF \cdot 3H_2O$, THF, $-78 \rightarrow -5$ °C, 4 h, then 13 h at -5 °C; 89–92% **3**, pale-yellow syrup, *arabino*/*ribo* 88:12. b) H_2, Pd/C, MeOH, 25 °C, 24 h; yield of **4** quantitative, pale-yellow, sticky solid. c) Ac_2O, pyridine, 0 °C → 25 °C, 22 h, 97–98% **5** as *arabino*/*ribo* mixture 88:12 (± 2); medium-pressure liquid chromatography (MLPC) (LiChroprep Si60, 25–40 μm, ethyl acetate): D-**5** 61%, m.p. 65–66 °C, after recrystallization, colorless needles, m.p. 67 °C, $[\alpha]_D^{21} = +29.7$ ($c = 0.58$, $CHCl_3$); L-**5** 65%, m.p. 63–65 °C, after recrystallization 67–68 °C, $[\alpha]_D^{21} = -30.0$ ($c = 0.58$, $CHCl_3$). d) 25% NH_3 solution in H_2O, MeOH, 25 °C, 22 h; recrystallization (ethyl acetate), 84% D-**6** and 86% L-**6**, colorless flakes, m.p. 142 and 143 °C; D-**6**: $[\alpha]_D^{20} = -7.1$ ($c = 0.51$, ethanol); L-**6**: $[\alpha]_D^{20} = +7.0$ ($c = 0.51$, ethanol); enantiomeric ratio for both > 99:1 according to ^{1}H NMR analyses with 16 mol-% (+)-Eu(hfc)$_3$ and comparison with 4:96 mixed sample: ^{1}H NMR (200.1 MHz, $CDCl_3$): $\delta = 2.11$ ($COCH_3$) for D- and L-**6**; with 16 mol-% (+)-Eu(hfc)$_3$: $\delta = 2.64$ (D-**6**) and 2.46 (L-**6**). e) Z-Cl, $NaHCO_3$, H_2O, 25 °C, 20 h, filtration through silica gel with petroleum ether/ether 3:7 and ethyl acetate; 63 and 60% of **7**, respectively, as 88:12 mixture, colorless solid, m.p. 73–76 and 73–78 °C resp. f) *p*-TosCl, pyridine/ether, 25 °C, 3 d, 76 and 70% of **8**, resp., pale-yellow syrup. g) H_2, Pd/C, MeOH, 25 °C, 17–18 h; 91 and 88% of **10**, resp., colorless foam, melting range 40–80 °C, *arabino*/*ribo* mixture 88:12. h) Z-Cl, $NaHCO_3$, H_2O, 25 °C, 22 h, silica gel filtration; 70–75% pale-yellow oil; LPLC (Lobar LiChroprep Si60, 40–63 μm, $CHCl_3$/MeOH 95:5), colorless oil; D-**11** 50%, $[\alpha]_D^{21} = -45.6$ ($c = 0.76$, $CHCl_3$); L-**11** 57%, $[\alpha]_D^{21} = +44.7$ ($c = 0.76$, $CHCl_3$). i) 0.1N HCl/THF 4:1, 25 °C, 13 h, TLC control (silica gel/Al foil 60F 254, $CHCl_3$/MeOH 9:1), then addition of $NaBH_4$/EtOH, 25 °C, 6 h, flash chromatography (silica gel, $CHCl_3$/MeOH 9:1); **13**: colorless, analytically pure syrup, 86 and 87% respectively; D-**13**: $[\alpha]_D^{22} = -46.3$ ($c = 0.32$, MeOH); L-**13**: $[\alpha]_D^{22} = +46.1$ ($c = 0.32$, MeOH) ([6c] *Joullié* et al.): $[\alpha]_D^{23} = -47.5$ ($c = 0.32$, MeOH) for D-**13**. ^{13}C NMR: at 20 °C two sets of signals in the ratio of 60:40 (carbamate rotamers), at 60 °C in [D_6] DMSO one set, diastereomeric purity > 94:6. j) **13** → **14** cf. Ref. [6a, c] (*Hashimoto* and *Joullié* et al., resp.). We obtained, e.g., L-**14** with H_2, Pd/C in 99% yield; hydrochloride: m.p. 155.156 °C, $[\alpha]_D^{20} = -18.4$ ($c = 0.22$, H_2O); ([**6a**] (*Fleet* et al.): m.p. 157–159 °C, $[\alpha]_D^{20} = +18.8$ ($c = 0.16$, H_2O) for D-**14** (hydrochloride)).

the presence of pyridine. It should be noted that the selective *O*-terminal tosylation **7** → **8**, for which, inter alia, examples with other acyclic triols,[14] diols and pyranose derivatives[15] are known, opens up further possibilities for the synthesis of imino sugars unexploited so far. The Z-tosylate **8** was converted into a mixture of the diastereomeric dihydroxyprolinal acetals **10** (as hydrotosylates) on catalytic hydrogenation (Pd/C) which liberated the NH_2 group (in **9**), in turn effecting intramolecular OTos substitution. The separation of the diastereomers was accomplished after conversion of **10** into the Z derivatives **11**, by low-pressure liquid chromatography (LPLC). The acetal **11** (prepared in gram amounts) was hydrolyzed (acid-catalysis) to furnish the aldehyde **12**. TLC control and NMR analysis showed the *cis*-aldehyde **12** to be formed first; this then in part epimerized to the *trans*-derivative (*ribo*). When the reaction was stopped after ca. 13 h and the crude product **12** reduced with $NaBH_4$, the all-*cis*-triol **13** (1,4-dideoxy-1,4-imino-D-lyxitol or *cis*-L-dihydroxyprolinol) was secured in analytically pure form. The overall yield for both D- and L-**13** from **1** after eight steps was 17% (from diethyl tartrate 12%/eleven steps).

The synthesis of **13** described here requires only two chromatographic steps and is, in our opinion, more efficient than the previously reported ones starting from D-mannose,[6a] D-glucose[6c] and L-glutaminic acid,[6b] respectively. Several novel acyclic 2-aminoarabinose derivatives with further potential applications are intermediates; in addition, the synthesis is not limited to one enantiomeric series, as is generally the case with carbohydrate educts. The *N,O,O*-tribenzylated aldehyde analogous to **12** was recently converted into (−)-swainsonine in five steps.[6b]

Received: June 13, 1990 [Z 4011 IE]
German version: *Angew. Chem. 102* (1990) 1180

[1] D. A. Winkler, G. Holand, *J. Med. Chem. 32* (1989) 2084.
[2] a) G. W. J. Fleet, A. Karpas, R. A. Dwek, L. E. Fellows, A. S. Tyms, S. Petursson, S. K. Namgoong, N. G. Ramsden, P. W. Smith, J. C. Son, F. Wilson, D. R. Witty, G. S. Jacob, T. W. Rademacher, *FEBS Lett. 237* (1988) 128; b) G. W. J. Fleet, *Top. Med. Chem. 65* (1988) 149.
[3] See, for example, T. Ziegler, A. Straub, F. Effenberger, *Angew. Chem. 100* (1988) 737; *Angew. Chem. Int. Ed. Engl. 27* (1988) 716; C. H. von der Osten, A. J. Sinskey, C. F. Barbas, III, R. L. Pederson, Y.-F. Wang, C.-H. Wong, *J. Am. Chem. Soc. 111* (1989) 3924, and references cited therein.
[4] V. Jäger, V. Wehner, W. Hümmer, R. Öhrlein, U. Burkhardt, T. Franz, U. Stahl, 22. GDCh-Hauptversammlung, Bonn, September 18–22, 1989, Abstr. OCH 3, p. 345.
[5] V. Jäger, W. Hümmer, following communication: *Angew. Chem. 102* (1990) 1182; *Angew. Chem. Int. Ed. Engl. 29* (1990) 1171.
[6] Syntheses of D-**14** or derivatives from a) D-mannose: G. W. J. Fleet, S. J. Nicholas, P. W. Smith, S. V. Evans, L. E. Fellows, R. J. Nash, *Tetrahedron Lett. 26* (1985) 3127; B. P. Bashyal, G. W. J. Fleet, M. J. Gough, P. W. Smith, *Tetrahedron 42* (1986) 5685; H. Setoi, K. Kayakiri, H. Takeno, M. Hashimoto, *Chem. Pharm. Bull. 35* (1987) 3395; b) L-glutamic acid: N. Ikota, A. Hanaki, *ibid. 35* (1987) 2140; c) D-glucose: G. N. Austin, P. D. Baird, G. W. J. Fleet, J. M. Peach, P. W. Smith, D. J. Watkin, *Tetrahedron 43* (1987) 3095; S.-Y. Han, P. A. Liddell, M. M. Joullié, *Synth. Commun. 18* (1988) 275; cf. A. Gateau, A.-M. Sepulchre, A. Gaudemer, S. D. Gero, *Carbohydr. Res. 24* (1972) 474; J. Defaye, D. Horton, *ibid. 14* (1970) 128.
[7] Reviews: D. Seebach, E. W. Colvin, F. Lehr, T. Weller, *Chimia 33* (1978) 1; G. Rosini, R. Ballini, *Synthesis 1988*, 833; K. B. G. Torssell: *Nitrile Oxides, Nitrones, and Nitronates in Organic Synthesis*, VCH, Weinheim 1988; M. Eyer, D. Seebach, *J. Am. Chem. Soc. 107* (1985) 3601.
[8] R. Öhrlein, *Dissertation*, Universität Würzburg 1988; cf. [9]; V. Wehner, *Dissertation*, Universität Würzburg 1990; G. Schnabel, *Dissertation*, Universität Würzburg 1990.
[9] R. Öhrlein, V. Jäger, *Tetrahedron Lett. 29* (1988) 6083.
[10] From diethyl tartrate in three steps in ca. 70% yield: V. Jäger, V. Wehner, *Angew. Chem. 101* (1989) 512; *Angew. Chem. Int. Ed. Engl. 28* (1989) 469. In the meantime D- and L-**1** have become available from E. Merck (Darmstadt).
[11] F. W. Lichtenthaler, H. P. Albrecht, *Chem. Ber. 102* (1969) 964.
[12] A. C. Richardson, H. O. L. Fischer, *J. Am. Chem. Soc. 83* (1961) 1133.
[13] Earlier syntheses (selection): I. Drivas, D. Picq, D. Anker, H. Pacheco, *J. Carbohydr. Chem. 3* (1984) 243 (from D-arabinose, 10 steps, 17% overall yield); M. Wolfrom, S. Otami, *Carbohydr. Res. 153* (1986) 150, and references cited therein (from D- and L-arabinose).
[14] B. Häfele, D. Schröter, V. Jäger, *Angew. Chem. 98* (1986) 89; *Angew. Chem. Int. Ed. Engl. 25* (1986) 87.
[15] See examples given by S. Hanessian: *Total Synthesis of Natural Products: The 'Chiron' Approach*, Pergamon, Oxford 1983.

Cyclization of *N*-Protected 1-Amino-4-pentene-2,3-diols to *lyxo*-Configurated Deoxyimino Sugars (*cis*-Dihydroxypyrrolidines); Synthesis of Potential Glycosidase Inhibitors**

By *Volker Jäger** and *Walter Hümmer*

Dedicated to Professor Hans Jürgen Bestmann on the occasion of his 65th birthday

The inhibition of α-mannosidases[1] by swainsonine **A** and the imino-D-mannitols **B** and **C** (IC_{50} 1.75 to 8,[1a] 0.5,[1b] and 0.6[1c] μM, resp.) is attributed to the topographical equivalence of the respective 1,4-dideoxy-1,4-imino-D-lyxitol fragment **D** with the mannopyranosyl cation **E**.[1a] The individual OH groups are assigned different roles (influence on "binding", "potency", "specificity"); the 4-CHOH group of the mannoside appears to be dispensable.[1a] The iminolyxitol **D**, for which in the preceding communication we present a novel synthesis of both enantiomers via nitroaldol reaction,[2] displays moderate activity as an α-mannosidase inhibitor, but strongly inhibits α-galactosidase [IC_{50} 14 and 0.2 μM, resp].[1b] Compared with the α-D-galactosides **F**, **D** can be regarded as an analogue now lacking the 2-CHOH equivalent.

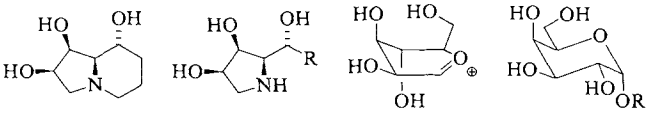

A **B**: R = CH_2OH **C**: R = CH_3 **D**: R = H **E** **F**

Syntheses of mono- and bicyclic glycosidase inhibitors with modified structure (and configuration) are therefore of particular relevance, and even more attractive when providing novel pathways to this series.[3] The following simple routes to variants of **D** – to the 5-deoxy-5-halo derivatives **3** and **4**, the 2,5-anhydro compound **6**, and the homologue **12**—are based on 1-amino-4-pentenediol **1**. This starting material is equally well accessible in the D- and the L-*erythro* form by Sharpless epoxidation of 1,4-pentadiene-3-ol[4] and

[*] Prof. Dr. V. Jäger, Dipl.-Chem. W. Hümmer
Institut für Organische Chemie der Universität
Am Hubland, D-8700 Würzburg (FRG)

[**] This work was supported by the Fonds der Chemischen Industrie, by the Bundesministerium für Forschung und Technologie (AIDS-Forschungsförderung im Bundesgesundheitsamt), and by Bayer AG. We thank Dr. *D. Häbich* and Dr. *B. Junge*, Bayer AG, for discussions, and Ms. *S. Blumbach* and Mr. *H. Sattler* for experimental assistance. Thanks are also due to Mrs. *E.-M. Peters*, Dr. *K. Peters*, and Prof. Dr. *H. G. von Schnering*, Max-Planck-Institut für Festkörperforschung, Stuttgart, for the crystal structure analysis of **5**.—Presented at the 22nd GdCh-Hauptversammlung, Bonn, September 18–22, 1989, Abstr. OCH 3, p. 345.

subsequent aminolysis[5] (Scheme 1). Following the strategy outlined previously (route b in Ref. [2]), we attempted to extend some of the known cyclizations[6] of unsaturated racemic amines or amino alcohols to *N*-protected derivatives of optically active **1** *bearing two free OH groups*.

Haloamidations[7] were successful with the *p*-toluenesulfonamide **2a** both using *N*-bromosuccinimide (NBS) and iodine/sodium hydrogencarbonate. In each case the crude product contained a mixture (ca. 90:10) of the *cis*/*trans* cyclization products, from which the pure diastereomers **3** and **4**, respectively, could be isolated in ca. 60% yield. Upon reaction with bases such as silver(I) oxide/water or 2N sodium hydroxide the bicyclic species **5** was formed. After reductive detosylation with naphthalene sodium[7b] crude, impure **6** was obtained, which was purified via the Z-derivative **7** and isolated in pure form after subsequent catalytic reduction (Scheme 1). The structure and (relative) configuration of the novel anhydro-iminolyxitol **6** {(1*R*, 4*R*, 7*S*)-7-hydroxy-2-oxa-5-azabicyclo[2.2.1]heptane} are confirmed by a crystal structure analysis of **5**.[8]

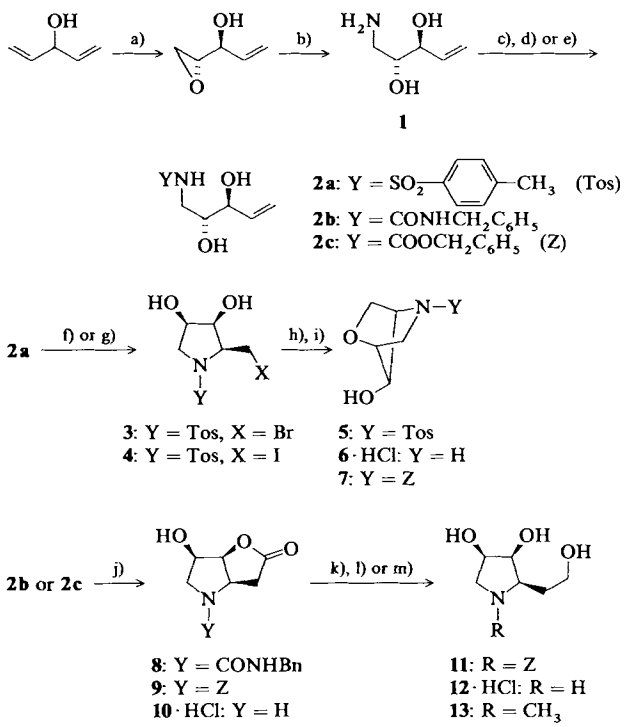

Scheme 1. Synthesis of D-*lyxo*-configurated deoxyimino sugars from 1,4-pentadien-3-ol. Structure and configuration of the compounds prepared are confirmed by spectroscopic data and correct elemental analyses. a) Asymmetric Sharpless epoxidation, 60–70% [4]; b) NH_3, quant. [5]; c) **2a**: Tos-Cl, pyridine, 79%, m.p. 69–70 °C, $[\alpha]_D^{20} = +9.3$ ($c = 0.607$, $CHCl_3$); d) **2b**: BnNCO, $CHCl_3$, 67%, m.p. 133.5 °C, $[\alpha]_D^{26} = -5.6$ ($c = 0.35$, MeOH); e) **2c**: Z-Cl, $NaHCO_3$, 0–25 °C, 89%, m.p. 91–92 °C, $[\alpha]_D^{20} = +0.50$ ($c = 1.45$, MeOH); f) NBS, DME/H_2O (4:1), 0 °C, 2 h, crude diastereomer ratio *dr* 91:9, after crystallization (ethyl acetate/petroleum ether) 62% with *dr* > 95:5, m.p. 151 °C, $[\alpha]_D^{20} = -142.7$ ($c = 0.287$, MeOH); g) I_2, $NaHCO_3$, Et_2O/H_2O, −5 °C, 4 h, crude *dr* = 90:10, after crystallization (ethyl acetate/petroleum ether) 61% with *dr* > 95:5, m.p. 158 °C, $[\alpha]_D^{22} = -181.3$ ($c = 0.705$, MeOH); h) **3** or **4** → **5**: 2N NaOH, 25 °C, 2 d, quant., m.p. 134 °C, $[\alpha]_D^{22} = -13.8$ ($c = 0.345$, MeOH); monoclinic, space group $P2_1$ [8]; i) **5** → **6** → **7** → **6**·HCl: Na/naphthalene, DME, 25 °C, 1 h, then Z-Cl, $NaHCO_3$/DMAP (cat.), 25 °C, 2 d, column chromatography (SiO_2, etbyl acetate), pale yellow oil, 31% **7**; H_2/Pd-C, CH_3OH/HCl, 25 °C, 12 h; **6** quant., colorless solid, m.p. 151–152 °C, $[\alpha]_D^{20} = +46.9$ ($c = 0.215$, MeOH); j) CO, $PdCl_2$ (0.1 equiv.), $CuCl_2$ (3.0), NaOAc (3.0), HOAc, 25 °C (analogous to [10]), 2–4 d, in each case colorless solid; **8**: 58%, m.p. 73 °C, $[\alpha]_D^{26} = -45.0$ ($c = 0.350$, MeOH), **9**: 83%, m.p. 108–109 °C, $[\alpha]_D^{22} = -71.6$ ($c = 0.666$, $CHCl_3$), ^{13}CNMR (50.3 MHz, [D_6]DMSO, 70 °C): $\delta = 35.7$ (CH_2), 50.2 (CH_2N), 56.0 (*C*HN), 66.3 (OCH_2), 68.8 (*C*HOH), 82.0 (*C*HO), 127.4, 127.7, 128.3, 136.7 (C_6H_5), 153.8 (NCO), 175.5 (OCO), purity > 95% (no other signals visible). **10**·HCl: from **9** with H_2/Pd-C in EtOH/HCl to give mixture with ethyl ester (ca. 30:70), recrystallization therefrom (CH_3OH/ethyl acetate) 14% of **10**·HCl colorless solid, m.p. 164–165 °C, $[\alpha]_D^{22} = +19.7$ ($c = 0.299$, MeOH) ([12a]: m.p. 178–179 °C, $[\alpha]_D = +20$ ($c = 0.009$, EtOH)); k) **11**: $LiBH_4$, THF, 25 °C, 3 d, 74%, colorless, viscous oil (2 rotamers, in [D_6]DMSO at 80 °C one signal set in the ^1H- and in the ^{13}C-NMR spectrum), $[\alpha]_D^{22} = -29.4$ ($c = 0.277$, MeOH); l) **12**·HCl: from **11** with H_2/Pd-C, CH_3OH/HCl, 84%, colorless crystals, m.p. 137–138 °C, $[\alpha]_D^{24} = -7.0$ ($c = 0.193$, MeOH); m) **11** → **13**: $LiAlH_4$, Et_2O, reflux, 10 h, pale yellow, gel-like oil, 71%, $[\alpha]_D^{22} = -70.3$ ($c = 0.270$, MeOH).

For the synthesis of **12** (1,4,5-trideoxy-1,4-imino-D-*lyxo*-hexitol, "*cis*-dihydroxyhomoprolinol"), homologous to **D**, the Pd^{II}-catalyzed bicyclization **2b** → **8** (or **2c** → **9**) proved the key step (an intramolecular amidocarboxylation). This reaction was first performed with unsaturated amines,[9] and recently extended to racemic monohydroxy derivatives. For the latter, urea and methylurethane derivatives were found suitable for optimal adjustment of the *N*-nucleophilicity in order to favor the cyclization step over the competing N-Pd complexation.[10] In the present study we introduced benzyl derivatives, i.e. the *N*-benzylaminocarbonyl and benzyloxycarbonyl compounds **2b** and **2c**: this should guarantee simplified reaction control (by UV detection/TLC analysis) and, in particular, facilitate cleavage of the *N*-protecting group, which is essential for the following transformations. The urea variant (starting compound **2b**) indeed furnished the diastereomerically pure pyrrolidinolactone **8** (58%); with the Z-derivative **2c**, after optimizing the reaction time and work-up, we obtained the desired product **9** chemo-, regio-, and stereoselectively in 83% yield. Thus, a highly selective homologation of an unsaturated aminodiol can be achieved with minimal employment of protecting groups. Moreover, this is the shortest and most efficient synthesis of the pyrrolidinolactone **9**[11,12] (four steps/51% total yield from 1,4-pentadiene-3-ol; previously reported syntheses of **9**, or corresponding derivatives, require 9 to 15 steps to give 1.5–42% overall yields[12]). The diastereomeric purity of the lactones **8** and **10** was found to be > 95:5 (NMR); the enantiomeric purity of **9** proved satisfactory as verified at the stage of the hydrochloride of **10** (obtained rather by accident, see caption to Scheme 1): $[\alpha]_D^{22} = +19.7$ ($c = 0.299$, MeOH), compared to $[\alpha]_D = +20°$ ($c = 0.009$, EtOH) for a product obtained from L-hydroxyproline.[12a]

Upon reduction with $LiBH_4$ the pyrrolidinolactone **9** was converted into the iminotriol **11**, and further, on catalytic hydrogenation, into the previously unknown imino-D-*lyxo*-hexitol (L-dihydroxyhomoprolinol) **12**. Since the *N*-alkylated derivatives of deoxyimino sugars in many cases show increased glycosidase inhibition,[13] the *N*-Z-protected lactone **9** was also reduced to the *N*-methyl derivative **13** using lithium aluminum hydride.[14]

In addition to the novel entries to various dihydroxypyrrolidines as analogues of **D**, these results show that the halogen- as well as the Pd^{II}- induced intramolecular amidation may be extended to substrates with *two (and more?) free hydroxy groups*. Whether the stereochemical course of the addition to the C=C bond to afford *cis* products is solely directed by the α-OH group, should become evident by submitting substrates of the *threo* series to this process. We shall report separately on analogous studies in the C_6 series and related alkoxycarboxylations[9c] with alkene polyols (alkenitols).

Received: June 13, 1990 [Z 4012 IE]
German version: *Angew. Chem. 102* (1990) 1182

[1] a) D. A. Winkler, G. Holan, *J. Med. Chem. 32* (1989) 2084, and references cited therein; b) G. W. J. Fleet, S. J. Nicholas, P. W. Smith, S. V. Evans, L. E. Fellows, R. J. Nash, *Tetrahedron Lett. 26* (1985) 3127; G. N. Austin,

P. D. Baird, G. W. J. Fleet, J. M. Peach, P. W. Smith, D. J. Watkin, *Tetrahedron 43* (1987) 3095; c) M. J. Eis, C. J. Rule, B. A. Wurzburg, B. Ganem, *Tetrahedron Lett. 26* (1985) 5397; d) cf. also D. C. Montefiori, W. E. Robinson, W. M. Mitchell, *Proc. Natl. Acad. Sci. USA 85* (1989) 9248; J. G. Buchanan, K. W. Lumbard, R. J. Sturgeon, D. K. Thompson, R. H. Wightman, *J. Chem. Soc. Perkin Trans. 1 1990*, 699.

[2] V. Wehner, V. Jäger, preceding communication: *Angew. Chem. 102* (1990) 1181; *Angew. Chem. Int. Ed. Engl. 29* (1990) 1169.

[3] See, e.g. [1d] and references in [2] and [13].

[4] B. Häfele, D. Schröter, V. Jäger, *Angew. Chem. 98* (1986) 89; *Angew. Chem. Int. Ed. Engl. 25* (1986) 87; B. Koppenhoefer, M. Walser, D. Schröter, B. Häfele, V. Jäger, *Tetrahedron 43* (1987) 2059; V. Jäger, D. Schröter, B. Koppenhoefer, *ibid.*, in press; cf. S. Hatakeyama, K. Sakurai, S. Takano, *J. Chem. Soc. Chem. Commun. 1985*, 1759.

[5] W. Hümmer, T. Gracza, V. Jäger, *Tetrahedron Lett. 30* (1989) 1517.

[6] Reviews on electrophilic heterocyclizations: P. A. Bartlett in J. D. Morrison (Ed.): *Asymmetric Synthesis, Vol. 3*, Academic, New York 1984; p. 411 ff; G. Cardillo, M. Orena, *Tetrahedron 46* (1990) 3321.

[7] a) Y. Tamaru, S. Kawamura, T. Bando, K. Tanaka, M. Hojo, Z. Yoshida, *J. Org. Chem. 53* (1988) 5491; b) J. G. Kim, J. K. Cha, *Tetrahedron Lett. 30* (1989) 5721; c) cf. intramolecular amino- und amidomercurations: R. C. Bernotas, B. Ganem, *ibid. 25* (1984) 165; *ibid. 26* (1985) 1123; L. J. Liotta, R. C. Bernotas, D. B. Wilson, B. Ganem, *J. Am. Chem. Soc. 111* (1989) 785; H. Takahata, M. Tajima, Y. Banba, T. Momose, *Chem. Pharm. Bull. 37* (1989) 2550.

[8] K. Peters, E.-M. Peters, H. G. von Schnering, *Z. Kristallogr.*, in press.

[9] a) L. S. Hegedus, G. F. Allen, D. J. Olsen, *J. Am. Chem. Soc. 102* (1980) 3583; b) Y. Tamaru, M. Hojo, H. Higashimura, Z. Yoshida, *ibid. 110* (1988) 3994; c) review: L. S. Hegedus, *Tetrahedron 40* (1984) 2415; d) cf. intramolecular alkoxycarboxylations: M. F. Semmelhack, C. Bodurow, *J. Am. Chem. Soc. 106* (1984) 1496; M. F. Semmelhack, N. Zhang, *J. Org. Chem. 54* (1989) 4483; M. McCormick, R. Monahan III, J. Soria, D. Goldsmith, D. Liotta, *ibid. 54* (1989) 4485; and references cited therein.

[10] Y. Tamaru, T. Kobayashi, S. Kawamura, H. Ochiai, Z. Yoshida, *Tetrahedron Lett. 26* (1985) 4479; Y. Tamaru, M. Hojo, Z. Yoshida, *J. Org. Chem. 53* (1988) 5741.

[11] **9** and derivatives have been used as intermediates for optically active Geissman-Waiss lactone (deoxy derivative of **10**) and for syntheses of pyrrolizidines (crotanecine, retronecine),[13] but few experimental details have been reported so far (cf. caption to Scheme 1, j).

[12] Syntheses of **9** and derivatives: a) V. K. Yadav, H. Rüeger, M. Benn, *Heterocycles 22* (1984) 2735; H. Rüeger, M. Benn. *ibid. 19* (1982) 23; b) J. G. Buchanan, G. Singh, R. H. Wightman, *J. Chem. Soc. Chem. Commun. 1984*, 1299; J. G. Buchanan, A. R. Edgar, B. D. Hewitt, V. B. Jigajinni, G. Singh, R. H. Wightman in D. Horton, L. D. Hawkins, G. J. McGarvey (Eds.): *Trends in Synthetic Carbohydrate Chemistry, ACS Symp. Ser. 386*, ACS, Washington D.C. 1989, p. 107–116; c) M. K. Gurjar, V. J. Patil, S. M. Pawar, *Indian J. Chem. Sect. B 26* (1987) 1115.

[13] G. W. J. Fleet, A. Karpas, R. A. Dwek, L. E. Fellows, A. S. Tyms, S. Petursson, S. K. Namgoong, N. G. Ramsden, P. W. Smith, J. C. Son, F. Wilson, D. R. Witty, G. S. Jacob, T. W. Rademacher, *FEBS Lett. 237* (1988) 128.

[14] The results of the tests concerning glycosidase inhibitors with the hydroxypyrrolidines described here and in [2] shall be published together with the experimental details of this work.

Fluorescence "Off–On" Signalling upon Linear Recognition and Binding of α,ω-Alkanediyldiammonium Ions by 9,10-Bis{(1-aza-4,7,10,13,16-pentaoxacyclooctadecyl)methyl}anthracene**

By *A. Prasanna de Silva** and *K. R. A. Samankumara Sandanayake*

In memoriam Sylvia Innocence

We demonstrate the fluorescence 'off-on' signalling of a linear recognition and binding phenomenon.[1] This opens the way to molecular digital devices which display sensitive, fast and remote signalling[2] upon selecting a molecular length with atomic resolution.[3] *Bouas-Laurent, Lehn* et al. have very recently reported an elegant case of 'monomer-excimer' fluorescence switching upon linear recognition.[4] A length-selective absorptiometric sensor was reported recently by *Misumi* et al.,[5] while *Schmidtchen* et al.[6] and *Sutherland* et al.[7] have employed absorptiometric changes in the guest and host respectively to signal the linear recognition by ditopic hosts.[8] The fluorescence of several polytopic polyether hosts have already been examined, though in other contexts.[9] In another case, contrary to expectation the system did not signal the recognition of guest length.[10] Photoswitchable recognition of length is an interesting counterpoint to the phenomenon discussed here.[11] A further impetus to the present work is that α,ω-alkanediammonium ions, the present guests, are important biological species (e.g. putrescine, cadaverine) as also are higher polyammonium ions (e.g. spermine).

The ditopic co-receptor **1**, which is easily synthesized,[12] is designed as a fluorescent PET (Photoinduced Electron Transfer) sensor.[2b, 13] The fluorescence quantum yield of guest-free **1**, $\Phi_{F\,min}$ is 0.0021 in $CHCl_3$:CH_3OH (1:1, v/v). Its fluorescence is 'switched on' only when both nitrogen lone electron pairs are blocked,[14] causing a significant increase in the oxidation potential. Ethyl ammonium ions **2** achieve this via two $[N\cdots H\cdots N]^{\oplus}$ hydrogen bonds.[15] The 2:1 complex of **2** and **1** has a fluorescence quantum yield ($\Phi_{F\,max}$) of 0.13, which is a 62-fold enhancement (Fig. 1). Ammonium ion-azacrown ether binding is known to involve $[N\cdots H\cdots N]^{\oplus}$ bonds.[16–18]

α,ω-Alkanediammonium ions **3** 'switch on' the fluorescence of **1** much more effectively than **2**, since the blocking

$[H_3N(CH_2)_nNH_3]^{2\oplus}$ **3** n = 3–8

of the second nitrogen electron pair is a pseudo-intramolecular cyclization.[19] The effective concentrations for **3**,

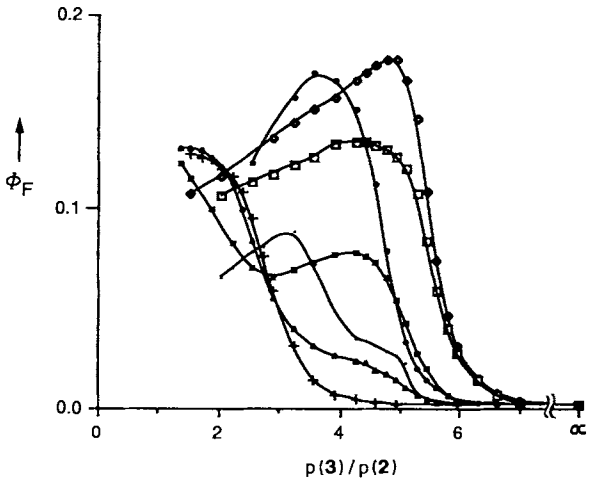

Fig. 1. Fluorescence quantum yield (Φ_F) of **1** (10^{-6} M in $CHCl_3$:CH_3OH (1:1, v/v)) as a function of the concentration of **3**, n = 3–8 or **2** (perchlorate salts). p(**3**) = − lg [**3**]. λ_{em} = 404 (0,0), 427 (0,1), 452 (0,2) ± 2 nm in all cases where measurable. λ_{ex} = 376 nm. λ_{abs} = 396 (0,0), 376 (0,1), 358 (0,2) ± 2 nm in all cases. These constant spectral parameters facilitate the calculation of quantum yields from measured intensities. The quantum yields were calibrated by comparison of spectra with that of 9,10 dimethylanthracene in deaerated C_2H_5OH [25]. The similarity of the spectra obviated the need to correct spectra for instrumental response. Complexed ammonium ion: + = **2**; ▪ = **3**, n = 3; ◇ = **3**, n = 4; □ = **3**, n = 5; ■ = **3**, n = 6; ● = **3**, n = 7; ▲ = **3**, n = 8.

[*] Dr. A. P. de Silva, Dr. K. R. A. S. Sandanayake
School of Chemistry, Queen's University
Belfast BT9 5AG (Northern Ireland)

[**] This work was supported by the Science and Engineering Research Council and Queen's University. We thank Dr. *H. Q. N. Gunaratne* and *Irene Campbell* for their help.

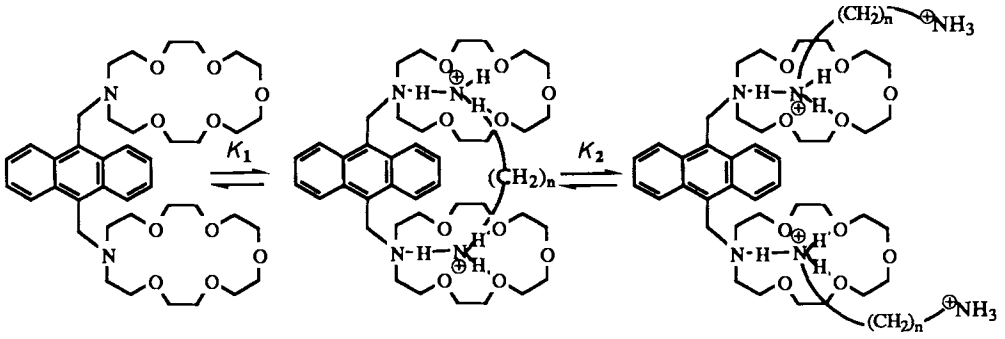

1 **1 · 3** **1 · 3_2**

n = 4,5 are smaller than that for **2** by ca. three orders of magnitude while the fluorescence enhancements are similar (as seen by the $\Phi_{F\,max1}$ values).

Such binding of **1** and **3** is confirmed by NMR paramagnetic shielding effects (Fig. 2) in agreement with previous studies of linear recognition.[7, 18, 20–22] In those cases of **3** (n = 3,6,8) where 1:1 binding results in moderate fluorescence enhancements (indicated by moderate $\Phi_{F\,max1}$ values), higher concentrations of **3** allow the fluorimetric observation of 2:1 interaction via $\Phi_{F\,max2}$ values. The $\Phi_{F\,max1}$ values are so high in **3**, n = 4,5,7 that the 2:1 interaction at higher concentrations of **3** does not result in any further fluorescence increase, i.e., $\Phi_{F\,max2}$ is unobservable.

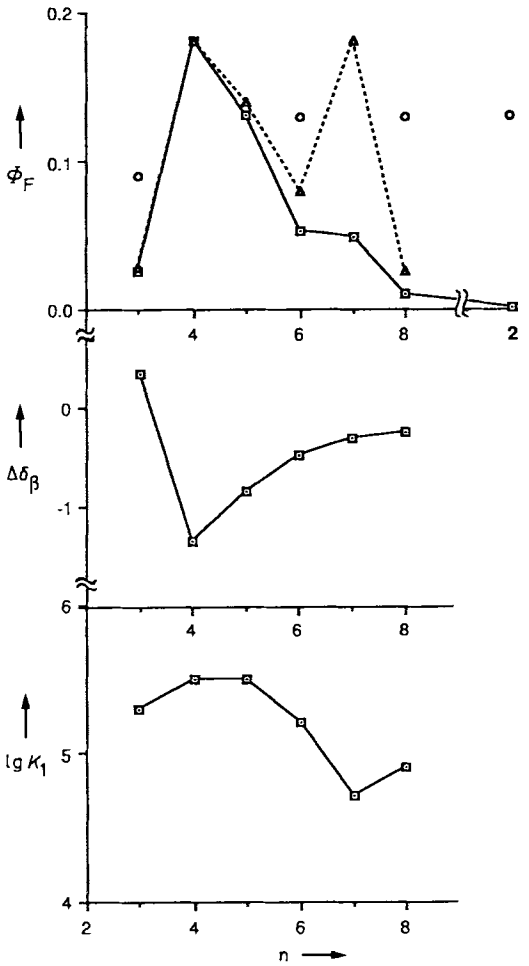

Fig. 2. Fluorescence quantum yield (Φ_F) of **1 · 3** (top), NMR shift displacement, $\Delta\delta$, of the β protons of **3** upon complexation (middle), and binding constant (lg K_1) of **1 · 3** in $CHCl_3$, CH_3OH (1:1, v/v) as a function of carbon chain length of **3**. Three types of Φ_F are shown: Φ_F at p(**3**) = 5 (□), $\Phi_{F\,max1}$ (△) and $\Phi_{F\,max2}$ (○). $\Phi_{F\,max1}$ and $\Phi_{F\,max2}$ values are the first and second maxima or inflexions respectively in the Φ_F/p(**3**) profiles (Fig. 1) as p(**3**) is progressively lowered. Lg K_1 values (bottom) are obtained from the midpoint of the first step in the Φ_F/p(**3**) profiles. A more accurate analysis is deferred since it is hampered by the non-unity activity coefficients of highly-charged species in the rather apolar medium.

From the viewpoint of operational devices, the fluorescence signal (expressed as Φ_F) shows good selectivity in favor of **3**, n = 4 and 5 at p(**3**) = 5 (Fig. 2) due to the presence of the rigid 9,10-dimethylanthracenyl 'spine' in **1**. The sharp fall-off on either side of **3**, n = 4 and 5 in Figure 2 demonstrates that atomic resolution of linear recognition is attainable. It is notable that the electronic emission/absorption spectral parameters of **1** (except Φ_F) are virtually unaffected by **2** or **3**. The more fundamental selectivity patterns are found in the parameters lg K_1 and $\Phi_{F\,max1}$ (Fig. 2). Lg K_1 values are determined by three-point hydrogen bonding of each of the two ammonium groups in **3** to the two azacrown ether units in **1**, among other possible interactions. On the other hand, $\Phi_{F\,max1}$ values are controlled principally by the length and angle of only two of these bonds, i.e. the pair of $[N\cdots H\cdots N]^{\oplus}$ hydrogen bonds. Inspection of molecular models (CPK) of the **1 · 3** complex reveals two points: a) There are repulsions between the methylene hydrogens of **3**, n = 3 and the π-cloud of **1**. However, it is noted that 1:1 complexation is not observed for **3**, n = 3 in the NMR $\Delta\delta$ values (Fig. 2) because the high concentrations (0.05 M **1** and 0.05 M **3**, n = 3) employed encourages alternating copolymerization[23] rather than cyclization.[19] The latter is favored at the lower concentrations (10^{-6} M **1** and 10^{-7}–10^{-2} M **3**, n = 3) used for fluorimetry.

b) There are intrachain repulsions between methylene hydrogens (a type of transannular effect[19]) of **3**, n = 6,8 and (to a lesser extent) 7.

This rationalizes (i) the selectivity of lg K_1 values for **3**, n = 4 and 5, and (ii) the low $\Phi_{F\,max1}$ values for **3**, n = 3,6 and 8, whereas **3**, n = 4,5 and 7 show an essentially constant value (ca. 0.17) produced by linear $[N\cdots H\cdots N]^{\oplus}$ hydrogen bonds of normal length. Such a view is confirmed by the observation in the 2:1 complexes, which are free of conformational constraints by cyclization, of $\Phi_{F\,max2}$ values which approach this same value (ca. 0.12) where observable. The accumulation of light-absorbing impurities at high concentrations of **3** and **2** is responsible for the fact that $\Phi_{F\,max2}$ is somewhat below 0.17.

It is notable that the anthracene unit has been designed to serve a dual role of fluorescent signalling site and rigid spacer between the azacrown ether moieties. The latter is the major contributor to the length selectivity. Selective fluorescent signalling of guest species with various chosen geometries

should be achievable by employing other multisubstitutional patterns as receptor arrays on anthracene and other rigid fluors within the constraints of our design logic.[2b] Related diammonium ion receptors with higher levels of preorganization and other ditopic receptors with rigid and fluorescent spacers are accessible for several laboratories[7, 9, 17, 18, 20, 21, 24] and may be suitable candidates for similar studies.

Received: May 22, 1990 [Z 3973 IE]
German version: *Angew. Chem. 102* (1990) 1159

[1] K. R. A. S. Sandanayake, *Ph.D. Thesis*, Queen's University of Belfast 1989.
[2] These are common characteristics of molecular fluorescence processes. a) A. S. Waggoner in D. L. Taylor, F. Lanni, R. Murphy, and A. S. Waggoner (Eds.): *Applications of Fluorescence in the Biomedical Sciences*, Liss, New York 1986, p. 3; b) A. J. Bryan, A. P. de Silva, R. A. D. D. Rupasinghe, and K. R. A. S. Sandanayake, *Biosensors 4* (1989) 169. For a general account pertaining to molecular devices, see; V. Balzani, L. Moggi, F. Scandola in V. Balzani (Ed.): *Supramolecular Photochemistry*, Riedel, Dordrecht 1987, p. 1.
[3] 'Spectroscopic rulers' (L. Stryer, *Annu. Rev. Biochem. 47* (1978) 819; C. F. Meares, T. G. Wensel, *Acc. Chem. Res. 17* (1984) 202) which are based on energy transfer, are different in that they measure various distances (with less resolution) around the Forster distance as opposed to selecting a particular, predefined length.
[4] F. Fages, J.-P. Desvergne, H. Bouas-Laurent, J.-M. Lehn, J.-P. Konopelski, P. Marsau, Y. Barrans, *J. Chem. Soc. Chem. Commun. 1990*, 655.
[5] T. Kaneda, Y. Ishizaki, S. Misumi, Y. Kai, G. Hirao, N. Kasai, *J. Am. Chem. Soc. 110* (1988) 2970; S. Misumi, *Pure Appl. Chem. 62* (1990) 493.
[6] F. P. Schmidtchen, *J. Am. Chem. Soc. 108* (1986) 8249; F. P. Schmidtchen, A. G. Leich, A. Schummer, *Pure Appl. Chem. 61* (1989) 1535.
[7] I. O. Sutherland, *Pure Appl. Chem. 62* (1990) 499.
[8] A related recent case is; Y. Aoyama, M. Asakawa, A. Yamagishi, H. Toi, H. Ogoshi, *J. Am. Chem. Soc. 112* (1990) 3145.
[9] V. Thanabal, K. Krishnan, *J. Am. Chem. Soc. 104* (1982) 3643; U. Herrmann, B. Tummler, G. Maass, P. K. T. Mew, F. Vögtle, *Biochemistry 23* (1984) 4059; M. Gubelmann, A. Harriman, J.-M. Lehn, J. L. Sessler, *J. Chem. Soc. Chem. Commun. 1988*, 77.
[10] N. M. Richardson, I. O. Sutherland, P. Camilleri, J. A. Page, *Tetrahedron Lett. 26* (1985) 3739. For a weak linearly selective fluorescence effect in a monocrown ether, see; S. Shinkai, Y. Ishikawa, H. Shinkai, T. Tsuno, H. Makishima, K. Ueda, O. Manabe, *J. Am. Chem. Soc. 106* (1984) 1801.
[11] S. Shinkai, Y. Honda, Y. Kusano, O. Manabe, *J. Chem. Soc. Chem. Commun. 1982*, 848.
[12] Prepared by reacting monoaza[18]crown-6 (H. Maeda, Y. Nakatsuji, M. Okahara, *J. Chem. Soc. Chem. Commun. 1981*, 471) with 9,10-bis(chloromethyl)anthracene (G. M. Badger, J. W. Cook, *J. Chem. Soc. 199* (1939) 802) according to a procedure available in the literature (A. H. Beckett, J. Walker, *Tetrahedron 19* (1963) 545). m.p. 92–95 °C (ethyl acetate pretroleum ether (60–80 °C) 1:1), satisfactory C,H,N analysis for $C_{40}H_{60}N_2O_{10}$. ^{1}H NMR (300 MHz, $CDCl_3$, 25 °C, TMS): $\delta = 2.90$ (t, 8H; NCH_2CH_2O), 3.58–3.67 (m, 40H; OCH_2CH_2O, OCH_2CH_2N), 4.60 (s, 4H; Aryl CH_2), 7.47–8.61 (m, 8H; Aryl).
[13] A. P. de Silva, K. R. A. S. Sandanayake, *J. Chem. Soc. Chem. Commun. 1989*, 1183; See also, M. A. Fox, M. Chanon (Eds.): *Photoinduced Electron Transfer, Parts A–D*, Elsevier, Amsterdam, 1988.
[14] For recent examples, see: M. E. Huston, K. W. Haider, A. W. Czarnik, *J. Am. Chem. Soc. 110* (1988) 4460; F. Fages, J.-P. Desvergne, H. Bouas-Laurent, P. Marsau, J.-M. Lehn, F. Kotzyba-Hibert, A.-M. Albrecht-Gary, M. Al-Joubbeh, *ibid. 111* (1989) 8672; M. E. Huston, E. U. Akkaya, A. W. Czarnik, *ibid. 111* (1989) 8735; A. P. de Silva, H. Q. N. Gunaratne, *J. Chem. Soc. Chem. Commun. 1990*, 186; C. Munkholme, D. R. Parkinson, D. R. Walt, *J. Am. Chem. Soc. 112* (1990) 2608; E. U. Akkaya, M. E. Huston, A. W. Czarnik, *ibid. 112* (1990) 3590. For a case with reverse action, see; A. P. de Silva, S. A. de Silva, A. S. Dissanayake, K. R. A. S. Sandanayake, *J. Chem. Soc. Chem. Commun. 1989*, 1054.
[15] Akkaya, Huston and Czarnik (Ref [14]) have employed a [N···H···O] hydrogen bond to successfully operate a fluorescent PET sensor for $HPO_4^{2\ominus}$.
[16] See, e.g., J.-M. Lehn, P. Vierling, *Tetrahedron Lett. 21* (1980) 1323; E. Graf, J.-M. Lehn, J. Le Moigne, *J. Am. Chem. Soc. 104* (1982) 1672.
[17] J.-M. Lehn, *Angew. Chem. 100* (1988) 91; *Angew. Chem. Int. Ed. Engl. 27* (1988) 89.
[18] I. O. Sutherland, *Chem. Soc. Rev. 15* (1986) 63.
[19] M. A. Winnik, *Chem. Rev. 81* (1981) 491; *Acc. Chem. Res. 18* (1985) 173.
[20] I. O. Sutherland, *Pure Appl. Chem. 61* (1989) 1547 and earlier papers, including; R. Mageswaran, S. Mageswaran, I. O. Sutherland, *J. Chem. Soc. Chem. Commun. 1979*, 722.
[21] F. Kotzyba-Hibert, J.-M. Lehn, P. Vierling, *Tetrahedron Lett. 21* (1980) 941, and other papers collected in Ref. [17].
[22] K. Saigo, N. Kihara, Y. Hashimoto, R. J. Lin, H. Fujimura, Y. Suzuki, M. Hasegawa, *J. Am. Chem. Soc. 112* (1990) 1144; Y. Tanaka, Y. Kato, Y. Aoyama, *ibid. 112* (1990) 2807.
[23] M. R. Johnson, I. O. Sutherland, R. F. Newton, *J. Chem. Soc. Chem. Commun. 1979*, 306; *J. Chem. Soc. Perkin Trans. 1 1980*, 586.
[24] J. Rebek, *J. Mol. Recognit. 1* (1988) 1; *Angew. Chem. 102* (1990) 261; *Angew. Chem. Int. Ed. Engl. 29* (1990) 245.
[25] R. L. Barnes, J. B. Birks, *Proc. R. Soc. A 291* (1966) 570.

BOOK REVIEWS

Book Reviews are written by invitation from the editor. Suggestions for books to be reviewed and for book reviewers are welcome. Publishers should send brochures or (better) books to the following address: Redaktion Angewandte Chemie, Postfach 101161, D-6940 Weinheim, Federal Republic of Germany. The editor reserves the right of selecting which books will be reviewed. Uninvited books not chosen for review will not be returned.

Metal-DNA Chemistry. (ACS Symp. Ser. 402). Edited by *T. D. Tullius*. American Chemical Society, Washington, DC 1989. x, 213 pp., hardcover, $ 59.95.—ISBN 0-8412-1660-6

The assertion by the editor *Thomas D. Tullius* in his preface to this volume is probably correct: not very long ago a book with a title such as this would have been considered quite exotic, and would probably even have evoked a pitying smile. All that has changed. In fact, transition metal complexes are now important tools of molecular biology and nucleic acids chemistry, whether used directly or as a means of inducing certain chemical behavior. An American Chemical Society symposium was held in Toronto in 1988 with the

objective of improving the understanding of these developments and indicating new directions of research. Some of the papers are collected together in this Volume 402 of the *ACS Symposium Series*, together with several chapters which appear to have been written at the editor's invitation.

The book has been prepared with the degree of care that is usual for ACS symposium volumes, the price is reasonable even without the dollar discount, the literature references are up-to-date and correspond to the current state of knowledge, and the index is helpful. The scientist interested in this subject may well buy the book without seeing it beforehand, only to be a little disappointed, like the present reviewer, with the choice of topis and the treatment. Although the introductory chapter (by *Thomas D. Tullius*) concisely reviews in a few pages the strategies adopted and the potential uses for metal complexes in nucleic acids chemistry, some vitally important details must of necessity be left out here. It would have been desirable to have some more detailed original contributions by authors such as, for example, *P. B. Dervan, J. K. Barton* and *S. J. Lippard*, especially as some of these were participants in the symposium according to the program. The absence of such contributions reduces the overall usefulness of the book as a source of information on the current state of research in this fascinating area. Also the role of OsO_4 as a chemical probe would certainly have merited a chapter. A further criticism is that the treatments of the two highly topical matters "Zinc Fingers" (Chapter 6, *J. M. Berg*) and "Mercury Metalloregulatory Proteins" (Chapter 7, *B. Frantz* and *T. V. O'Halloran*) are inexcusably short. To get a true insight into these topics the interested reader must turn to other monographs (*Prog. Inorg. Chem. 37* (1989); *Met. Ions Biol. Syst. 25* (1989)), where these topics are comprehensively treated by the same authors.

The eleven chapters may be roughly divided into three subject areas: i) applications of metal complexes, especially those with nuclease activity, to studies of nucleic acids, ii) three-component interactions in the protein/metal/nucleic acid system in relation to gene regulatory processes, and iii) fundamental aspects of the interactions of main- and subgroup metals with nucleic acids. The majority of the chapters (1 to 5, 10) are concerned with the first of these areas. Thus in Chapter 1 *T. D. Tullius* describes some elegant studies on the question of the helical periodicity and folding of DNA, based on results from scission reactions using OH radicals generated from the non-coordinating $[Fe^{II}(edta)]^{2\ominus}$ complex and H_2O_2. Chapters 2 (*D. S. Sigman* and *C.-H. B. Chen*) and 3 (*R. Tamilarasan, D. R. McMillin* and *F. Liu*) describe both applications and mechanistic aspects of the activity of Cu(1,10-phenanthroline) complexes, which were the first synthetic metal- containing nucleases discovered. In particular Chapter 2 provides a very good insight into the philosophy underlying the development from agents with little or no selectivity to those that are highly specific. Chapters 4 (*R. F. Pasternack* and *E. J. Gibbs*) and 5 (*G. Raner, J. Goddisman* and *J. C. Dabrowiak*) deal with porphyrins and metalloporphyrins as DNA intercalators and groove-binding species, and with the effect of the metal atom on the bonding behavior and the hierarchy of preferred bonding sites. Finally, in Chapter 10 *J. W. Scuggs, J. D. Higgins III, R. W. Wagner* and *J. T. Millard* report on the nuclease activity of a cyclometallated Pd complex. From the standpoint of an orderly arrangement of subject matter this article would perhaps have fitted in better immediately after Chapter 5.

The slim middle section of the book, consisting of Chapters 6 to 8, is concerned with the role of metals (Zn, Hg, Fe) in gene regulation processes. The shortness of Chapters 6 and 7 has already been mentioned. Chapter 8 (*K. Nakamura, V. de Lorenzo* and *J. B. Neilands*) describes the complex interaction between free Fe^{II}, the siderophore gene and its regulator protein Fur.

The work is completed by two comprehensive and well written chapters (which are the longest in the book) on the fundamentals of metal-nucleic acid interactions. The first (*L. G. Marzilli, T. Page Kline, D. Live* and *G. Zon*) describes ^{31}P NMR studies on the reactions of Pt^{II} coordination compounds with oligonucleotides, and in the second *H. Sigel* discusses the formation of metal-nucleotide complexes. One might well wish that one or two other chapters of the book could have had something of the amount of detail and breadth of these two chapters.

In summary, the book indicates some directions of progress in this topical field of research. In this reviewer's opinion the breadth of the subjects covered leaves something to be desired, but despite this it is recommended that libraries and all chemists and biologists interested in nucleic acids should buy the book.

Bernhard Lippert [NB 1063 IE]
Fachbereich Chemie
der Universität Dortmund (FRG)

Registered names, trademarks, etc. used in this journal, even when not marked as such, are not to be considered unprotected by law.

© VCH Verlagsgesellschaft mbH, D-6940 Weinheim, 1990. – Printed in the Federal Republic of Germany by Konrad Triltsch Druck- und Verlagsanstalt Würzburg.

All rights reserved (including those of translation into foreign languages). No part of this issue may be reproduced in any form — by photoprint, microfilm, or any other means — nor transmitted or translated into a machine language without written permission from the publishers. Only single copies of contributions, or parts thereof, may be made for personal use. This journal was carefully produced in all its parts. Nevertheless, authors, editors and publisher do not warrant the information contained therein to be free of errors. Readers are advised to keep in mind that statements, data, illustrations, procedural details or other items may inadvertently be inaccurate.

Valid for users in the USA: The appearance of the code at the bottom of the first page of an article (serial) indicates the copyright owner's consent that copies of the article may be made for personal or internal use, or for the personal or internal use of specific clients. This consent is given on the condition, however, that the copier pay stated per-copy fee through the Copyright Clearance Center, Inc. (CCC), for copying beyond that permitted by Sections 107 or 108 of the U.S. Copyright Law. This consent does not extend to other kinds of copying, such as copying, for general distribution, for advertising or promotional purposes, for creating new collective works, or for resale. For copying from back volumes of this journal see 'Permissions to Photo-Copy: Publisher's Fee List' of the CCC.

Editorial office: Postfach 10 11 61, D-6490 Weinheim, Federal Republic of Germany, Telephone (06201) 60 22 55, Telex 465 516 vchwh d, Telefax (06201) 602 328.

Editor: *Peter Gölitz*

Associate editors: *D. I. Loewus, A. Stimson.* **Editorial assistant:** *E. Schweikart*

Publishers: VCH Verlagsgesellschaft mbH (Managing Directors: *Hans Dirk Köhler, Dr. Hardy G. Sehrt*) Pappelallee 3, D-6940 Weinheim, Federal Republic of Germany.

Advertising office (Advertising Manager *R. J. Roth*): Postfach 10 11 61, D-6940 Weinheim, Federal Republic of Germany, Telephone (0 62 01) 60 61 30, Telex 4 67 155, Telefax (0 62 01) 606 156.

ANGEWANDTE CHEMIE
International Edition in English
Volume 29 · Number 11
November 1990
Pages 1177–1370

Chemistry for the Future—State of the Art and Perspectives

By Hans-Jürgen Quadbeck-Seeger*

A particularly close relationship exists between chemistry, the science of the transformation of matter, and developments in human living conditions. Though little more than 150 years old, chemical technology has had a greater influence on our civilization than any other technological discipline. Its roots lie not in the crafts, but in scientific research. Relationships derived from the laws of nature were taken as a basis for the systematic solution of practical problems. It is to this strategy that chemistry owes its success. New opportunities arise from new discoveries. These result from basic research at universities, research institutes, and industrial laboratories. Applied research in turn transforms the discoveries into innovative solutions to problems on an industrial scale. The objectives of applied research are oriented toward the marketplace and to the needs of mankind. Our knowledge of scientific interrelationships has been growing with unabated vigor for decades, but so too has our insight into the enormous complexity of the material world. Many of the problems that civilization faces result from the fact that our knowledge is still inadequate. Intensive research and development offer the only hope for progress. Scientists must of course act responsibly with the knowledge they acquire, and they must provide the information necessary to establish public confidence in their methods and products. This is the prerequisite for broad acceptance of technological progress, and given the extent of the world's population no alternative to progress exists. The shape of that progress is also subject to influences outside the realm of science, however, including social norms and political activities. A country that is not rich in raw materials, like the Federal Republic of Germany, must pay particular attention to these factors as well if it is to maintain its innovative strength.

1. Introduction

"Everything changes except change". *Arthur Schopenhauer* could never have anticipated how well the twentieth century would confirm his formulation of this piece of folk wisdom. The dramatic political, economic, and social changes we are seeing today, especially in Germany, will be recognized by future historians to be just as "revolutionary" as the technological upheavals in the last century that we now describe as the First Industrial Revolution. Most of today's basic industries came into being at that time, among them the chemical industry, which has increasingly evolved into the driving force behind change.

The chemical industry was not a product of the traditional crafts, but arose through the deliberate application of scientific conclusions for industrial purposes. Developments generally followed rapidly in the wake of new scientific discoveries, often by great leaps. Chemistry as the science of the transformation of matter was then, and remains today, particularly closely associated with the conditions of human life. Human beings dependent exclusively on the products of nature were capable of reacting only within very narrow limits

[*] Prof. Dr. H.-J. Quadbeck-Seeger
Member of the Executive Board
BASF Aktiengesellschaft
D-6700 Ludwigshafen

to such threats as food shortages or epidemics. Only with the help of the methods of chemistry did it become possible to create materials lacking in nature, or ones available only to a limited extent, such as fertilizers or effective drugs.

The early successes of the chemical industry were greeted with enthusiasm and wonder, although by today's standards most of the solutions provided were actually inadequate. Today, however, in a period characterized by high standards of living, the chemical industry has been placed in a fundamentally different position with respect to society, and this despite major advances in technology.

The chemical industry with its products has brought lasting improvement to the conditions of human life while at the same time undergoing radical change as the level of understanding has risen. The development of BASF, which this year looks back on 125 years of corporate history, provides a striking example.

2. The Beginnings of Modern Chemistry

The scientific pursuit of chemistry in Germany began with *Justus von Liebig*. His pupils often put their newly acquired knowledge to practical use, thereby giving birth to the chemical industry. The first step was the commercial production of synthetic dyes. A rash of new dye factories quickly sprang into being, though most of them proved short-lived. In fact, Bayer (1863), Hoechst (1863), and BASF (1865) were all latecomers on the scene. Why, then, did these particular companies turn out to be more successful and viable than so many of their contemporary competitors?

The first industrially produced and commercially successful dyes, including mauveine, fuchsin, and methyl violet, had already reached their limits in terms of application, and demand was beginning to lag behind supply. This resulted in the demise of the simplistic but at first highly successful notion of straightforward economic exploitation of a single scientific discovery. A new entrepreneurial strategy was needed, one that emphasized corporate research as the key to increasing scientific knowledge. Companies began to carry out their own research. Two years after the founding of BASF an in-house laboratory began the search for additional dyes and new synthetic routes, a quest that also took into account basic starting materials and intermediates. However, this also entailed an increasing demand for capital, an insight that induced the founder of BASF, *Friedrich Engelhorn*, to choose from the outset the legal form of the joint stock company, a novelty among dye manufacturers in those days. A cooperative relationship involving both scientists and businessmen in management positions proved to be a highly successful formula for developing the innovative powers of the young chemical companies. It also led to an early acceptance of the crucial role of research in ensuring a company's long-term success. From the very beginning there was an awareness of the close interactive role of basic research as well. This early vision on the part of chemical companies proved to be the key to their success and to the overall significance of the chemical industry today.

A research-oriented attitude on the part of chemical companies meant that they were not content with merely improving their existing product lines; they also branched out into new fields based on new discoveries. At BASF, dyes were joined by such diverse product lines as fertilizers, fibers, plastics, pesticides, information systems, vitamins, and pharmaceuticals (Fig. 1). Today it is precisely this breadth of corporate activities, together with extensive integration, that constitutes an important factor in the company's success.

The essential prerequisites for the development of a new field of activity have often emerged from pioneering achievements in basic scientific research. These have then served as the foundation for applied research leading to marketable products and cost-effective processes. Such a division of labor seems at first rather straightforward, but it actually requires some explanation.

3. Basic Research and Applied Research: A Changing Relationship

In all of the sciences, including chemistry, we make a distinction between two types of research: basic research and applied research. How do they differ? The English terms "pure science" and "applied science" actually embody more value judgement than explanation. Among the many possible definitions, the following is particularly incisive, reflecting as it does the Platonic principle of exploring the underlying idea: "The aim of basic research is to understand the world, while the aim of applied research is to improve it."

In *Liebig*'s day, no such distinction was made. The wide range of his personal activities shows him to have been a leading figure in both types of research. *Liebig*'s achievements range from investigating the nutritional requirements of plants (the basis of modern fertilizer theory) to the commercial production of meat extract. When did the distinction first arise between basic and applied research, and what were the reasons for it?

There can be little doubt that applied chemical research first saw the light of day when chemists were hired to study in a scientific way specific problems that were deemed important to companies. Through their involvement with company objectives these researchers soon found themselves confronted with circumstances quite unlike those experienced by their university colleagues. If anything, this trend has become even more marked today.

Basic research, consistent with the precept of scientific freedom, is regulated only by a few fundamental laws and principles, whereas applied research has become entangled in a network of determining factors (Fig. 2). Its principal stimuli come from the demands of the marketplace, which in turn derive from the needs of the populace, both basic and sophisticated. These needs can be subdivided broadly into nutrition, health, shelter, and clothing, as well as communication and leisure. In meeting these needs through new products, industrial research is subjected to regulatory influences of social standards, set down, for example, in laws and ordinances. The competitive situation, including a company's know-how, patent rights, and the strength of its market position, also has an influence on applied research. It is these interrelationships that are evaluated when a decision must be made as to whether research should be undertaken in a specific case, and if so in what directions. With respect to individual research projects, the current state of scientific

1895 Foundation of the company by *Friedrich Engelhorn* of Mannheim.

1867 Two years after the foundation of the company the first plant laboratory for the synthesis of new dyes is erected, and a year later central research is introduced.

1870 Process for the industrial production of the dye alizarin. Further important dyes such as fast red, auramin and eosin follow.

1877 The first German patent application in the field of coal tar dyes is filed for methylene blue. Later, *Robert Koch* succeeds in making bacteria visible in the microscope with the aid of methylene blue.

1888 *Robert Knietsch* develops the process for producing sulfuric acid from roaster gases. The sulfuric acid contact process is the first catalytic process on a large industrial scale.

1897 Under the direction of *Heinrich von Brunck*, indigo is synthesized industrially at BASF after 17 years of development work. Indigo, the "king of dyes", thus becomes available in large quantities and at low price.

1913 After wide-ranging research work in the catalysis and engineering fields, the production of ammonia by the Haber-Bosch process can be started. This provides the raw material base for the production of nitrogenous fertilizers. The further development of high-pressure technology leads to the large-scale synthesis of methanol and urea (1922).

1924 With alkylated naphthalene sulfonic acids BASF establishes a new basis for synthetic detergents and textile auxiliaries (Nekal®).

1928 *Walter Reppe* discovers a process for safely using acetylene in reactions under pressure. Starting in 1938, this chemistry is extended to the reaction of acetylene or olefins and carbon monoxide, using metal carbonyls as catalysts (Reppe chemistry).

1929 With the first industrial synthesis of styrene, the plastics era begins: polymeric acrylic compounds (1929), polystyrene (1930), polyvinyl chloride (1931), polyisobutylene (1931), polyvinyl ether (1928/1934), polyethylene (1937). These are followed by urea/formaldehyde condensation products (e.g. Kaurit® glue) and numerous other polymers with special material properties.

1935 The BASF Magnetophon tape, developed in cooperation with AEG, is presented to the public for the first time at the Radio Exhibition in Berlin.
Start of the production of phthalocyanine dyes: Heliogen® Blue B, followed in 1936 by Heliogen Green G.

1951 Styropor® foam plastic. High-impact polystyrene.

1956 The synthesis of hydroxylamine by catalytic hydrogenation of nitric oxide with hydrogen opens up an economical production route for caprolactam, and thus for the polyamide plastic Perlon®.

1960 New lines of dispersion (Palanil®) and cationic dyes (Basacryl®) extend the range of application for new textile fibers.

1963 New industrial vitamin A syntesis.

The novel, selectively acting pyridazone derivative, chloridazon (Pyramin®), ensures the competitiveness of sugarbeet growing in Europe.

1968 The nyloprint® plate, a photopolymer material developed by BASF for the printing industry, is launched onto the market. Single-stage production of high-purity melamine in a fluidized-bed reactor.

1971 A new foam (Neopolen®) having a wide variety of applications is obtained on the basis of polyethylene. The morpholine derivative tridemorph (Calixin®) has a systemic action on powdery mildew species.

1974 Basagran®, a substituted thiadiazinone dioxide, has a selective action on weeds in the large-scale crops rice, soybean, and cereals.
Kali und Salz AG, a BASF Group company, obtains magnesium sulfate fertilizers for the first time by a dry method by electrostatic separation of raw salts; this is an environmentally friendly and energy-saving production process.

1977 Isotactic polypropylene obtained by a novel BASF gas phase process. Production is started at Rheinische Olefinwerke in Wesseling.

1980 Acrylic acid-based polycarboxylates as additives for detergents allow a reduction in, or replacement of, phosphates.

1982 Citral, a terpene building block for vitamins, carotenoids, and fragrances, is produced by a new process from petrochemical raw materials.

1983 BASF develops the grass herbicide sethoxydim (Poast®) to market maturity for soybean and cotton crops; it allows sowing without plowing in cultivation zones that are susceptible to erosion.
Styrolux®, a glass-clear high-impact polystyrene material for high-grade packaging and medical instruments.

1989 A newly developed, environmentally friendly process for methyl methacrylate, the monomer for plastic glass materials.

1990 Tumor Necrosis Factor (TNF), an endogenous active protein, becomes accessible by a genetic engineering process. It proves to be effective for the treatment of malignant ascites and cancer of the kidneys.

Biotechnological production of vitamin B_2 from renewable raw materials.
The production of the Ultrason® high temperature-resistant thermoplastics with polysulfone and polyethersulfone units widens the range of applications of polymeric materials.

Fig. 1. Milestones in 125 years of BASF research. The development of the chemical industry from its beginnings to its present-day significance has been substantially shaped by chemical research. The history of BASF provides a typical example.

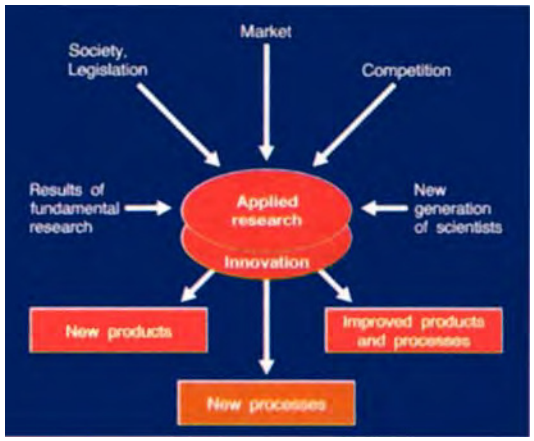

Fig. 2. Environment of applied chemical research. A close interactive relationship exists between applied research and a variety of general parameters that affect not only the selection of research projects but also their course.

knowledge, one's own understanding, and the influx of new methods—particularly through the younger generation of scientists—together with the ideas, skills, and commitment of those associated with the project, all play decisive roles in shaping the way toward innovative problem-solving. Because existing infrastructures and internal know-how are involved, the specific form this path takes can vary greatly from company to company.

Nevertheless, the operating procedures applicable to basic research and applied research are very similar. This is what led *R. B. Woodward* to observe that he recognized no distinction between pure and applied science, only between good and bad research. Changes have occurred, however, particularly in recent decades, and these changes have affected both types of research as well as the relationship between them. In applied research, for example, development has become an increasingly important factor. What is development? Whereas the objective of research, by definition, is to make new discoveries, the objective of development is to use existing knowledge to find new solutions to problems, or to use known methods to answer precisely defined technical questions.

The change in the relationship between basic research and applied research is best depicted with a few outstanding examples. Well over a hundred years ago, *Adolf von Baeyer* determined the constitutional formula of indigo. Proof of the structure was still lacking, however, and this he accomplished through total synthesis. For the basic researcher the problem was thereby solved. But for his friend *Heinrich Caro* at the Badische Anilin- & Soda-Fabrik, the problem had just begun. An industrial synthesis had to be developed, and sixteen years elapsed before the task was completed: the first synthetic indigo came on the market in 1897.

In the case of the ammonia synthesis the step from solving the problem theoretically to implementing the solution in practice was even larger. *Fritz Haber* succeeded in demonstrating at the beginning of this century that atmospheric nitrogen reacts with hydrogen under pressure and in the presence of suitable catalysts to give ammonia. His impressively simple apparatus can be seen today in Munich's Deutsches Museum. But this potential solution to one of mankind's major problems—supplying agriculture with sufficient nitrogenous fertilizer—had been demonstrated only in principle. Building an ammonia factory on the basis of *Haber*'s discoveries called for immense efforts on the part of BASF's applied research team. It became strikingly clear for the first time that additional disciplines were urgently needed for the solution of technical problems; in this specific case above all engineering science. High-pressure technology introduced a completely new approach to the transformation of matter. When the world's first ammonia factory came on stream at Ludwigshafen in 1913 the groundwork had been laid for a fundamental improvement in the world's food supply situation. At the same time this achievement marked the beginning of the development of process engineering, a development that will certainly still continue far into the future, and one whose multi-faceted applications have had an undreamed-of impact on living standards. The ammonia example also points up clearly the difference between invention and innovation. An invention or discovery demonstrates the theoretical potential for solving a problem; innovation, by contrast, constitutes the development of a complete solution to a problem on an industrial scale.

The two examples cited demanded all the strength available to the company at the time, and they consumed many years of development effort. Both represented true pioneering projects. Today the time-span has become significantly longer, even for projects that have more of the character of "further development". The realization of a new product or an industrial-scale process often entails fifteen or more years—and this despite tremendous advances in scientific knowledge. Why is this the case?

As knowledge in every field increases, our understanding of relationships becomes deeper, but so does our insight into their complexity. The result is that research has become increasingly multi-disciplinary. Even problems that appear simple prove on closer analysis to be multi-factorial, and it has become generally accepted that solutions can be reached only through the interaction of several disciplines. In the case of applied research this trend began to be established very early. Scaling up the synthesis of ammonia for industrial application required that chemists and engineers be joined by physical chemists and physicists. And that was only the beginning. Once the synthesis of ammonia had provided access to new "artificial fertilizers" it then became necessary to learn how to handle these synthetic materials. This meant seeking the cooperation of biologists and agronomists. Here we see already a multi-disciplinary team at work, and the trend has continued. The development of modern drugs, for example, requires the joint efforts of natural scientists from virtually every discipline, together with doctors, engineers, and even lawyers and marketing experts.

But it is not only applied research and development that have become more complex; the same applies even to certain areas of basic research. For example, research institutes dealing with the structure of matter or nuclear fusion have long since grown to industrial dimensions. One effective response to increasing complexity has been the growth of international cooperation in research. The "scientific community" represents a model for a true world community. It is therefore only logical that science, and particularly basic research, should take up questions that affect the whole of mankind. Today we are forced to recognize that problems such as

dying forests, the greenhouse effect, or the hole in the ozone layer have their origins in extremely complex cause-and-effect networks. Human concerns such as the assurance of adequate food supplies and the long-term availability of energy are bound to be involved as well. Basic research is confronted by multi-layered challenges that are very similar in their complexity to the problems facing applied research, even though the dimensions are different.

In this context, attention should be drawn to one characteristic of scientific and technological progress that is generally overlooked. As our level of knowledge rises, the tools for recognizing and examining undesirable effects become progressively more efficient. This mechanism of self-monitoring is certainly welcome, yet it has one fatal side effect. The inconceivably low limits of detection associated with modern methods of analysis are being increasingly perceived by some sectors of the public as threats. Politicians in turn often succumb to the temptation to define the ultimate detectable limit as a new *legal* limiting value. This can easily result in the misapplication of resources, or even deflect attention entirely from the real problems. For example, the central problem facing us in the next few decades is the virtually unrestricted increase in world population. From the scientific and medical standpoints this problem has long since been solved. It is now up to individuals, politics, and religion to devise answers.

It has become almost a fad to hold scientific and technological progress responsible for everything. *C. P. Snow* in the 1960s defined the notion of "the two cultures". Now there is an irrepressible demand to recognize the birth of a third, one for which there is no such thing as progress, only difficulties. It finds everything to be "difficult", and might therefore be appropriately designated as the "difficulture". Advances in communication technology have made it easier and easier to influence large numbers of people, so this phenomenon must be taken seriously. It is of particular concern to chemistry (both as an industry and as a science), which is increasingly seen as the cause of problems. By contrast, chemistry's capacity to *identify* problems and find technical solutions to them is virtually ignored.

Regaining public confidence is a challenge confronting both basic and applied research, one that requires cooperation transcending the boundaries of all the subdisciplines. The concept of interdisciplinarity needs to be extended even beyond the various scientific circles, although it also requires further development within them.

4. Interdisciplinary Effort—A Characteristic of Applied Research

Within applied research itself, a division of labor into research and development, each comprising interdisciplinary teams, has become indispensable. Two developments have brought this about. First, the tremendous increase in knowledge means that the individual scientist is no longer able to master and evaluate more than a trickle out of the flood of new information. If the number of papers covered by Chemical Abstracts is a measure of the growth of knowledge, a massive upward trend is apparent, especially since about 1950 (Fig. 3).

This deluge can be dealt with in university research by restricting oneself to an in-depth exploration of some specialized field. In industrial research, however, the current problems are never conveniently tailored to the expertise of a single specialist. Only a team is capable today of approaching the literature and filtering out the essentials for a particular task.

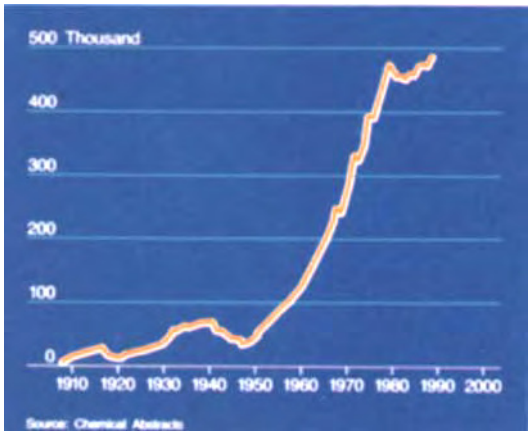

Fig. 3. Papers, patents, and books abstracted in Chemical abstracts. The number of chemical publications, and hence the store of chemical knowledge, is increasing exponentially. Scientists need to specialize more and more while at the same time maintaining contact with other disciplines in order to filter out those advances that are essential for a research project.

In the second place, projects in applied research become more and more complex as their level of development progresses, because they begin to interact increasingly with various limiting factors (availability of raw materials, market situation, production facilities, approvals, etc.), requiring suitable adaptations. Therefore the path from idea to product no longer leads directly from laboratory to production plant. Instead a wide variety of specialists is required to work in parallel on the project, all at different levels, until it is ripe for a final decision. Once applied research leaves the laboratory stage it is virtually always pursued today by a team. Where a few dominant personalities were formerly in a position to place their stamp on the course of development, today this role is filled by coordinated expertise, which can fully develop only within the framework of a cooperative team spirit.

The increasing complexity of the problems has led to research in the chemical industry demanding not only a growth in the number of active personnel but also full coverage of the entire spectrum of scientific disciplines. If we examine the ranks of scientists and engineers in the German chemical industry since 1964 we find that their numbers have more than doubled over that period (Fig. 4). There has been a constant rise in the number of chemists and engineers, but scientists from other disciplines have been added at a disproportionately high rate. The changing tasks facing applied research are reflected in greatly increased numbers of biologists, physicists, and mathematicians, revealing the growing importance of the life sciences, instrumentation technology, and data processing. Agronomists, on the other hand, have always worked closely with chemists in the agrochemical sector, so the increase in their numbers has been less striking.

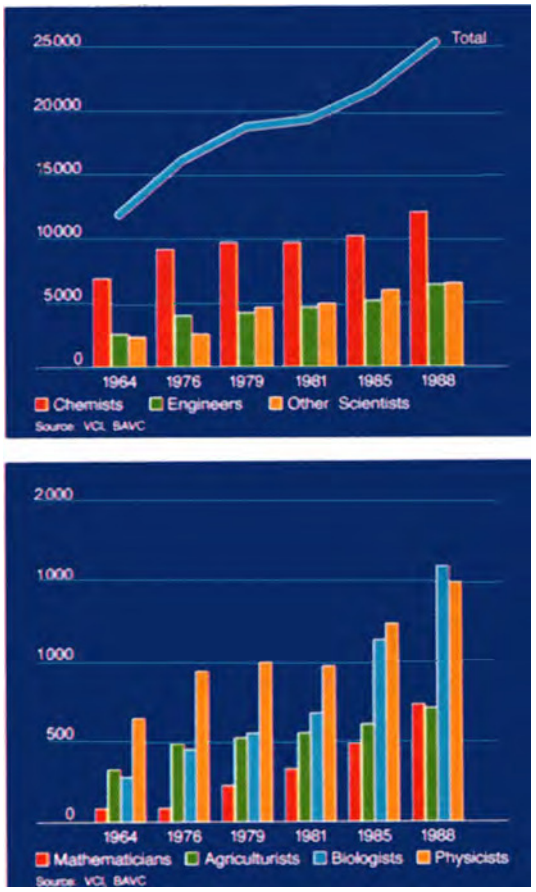

Fig. 4. Scientists and engineers in the German chemical industry. Since 1964, the number of scientists and engineers in the West German chemical industry has more than doubled. The number of chemists and engineers has grown steadily, while there has been a disproportionately large increase in the number of other scientists from other disciplines, in particular biologists, physicists, and mathematicians.

5. Applied Research in a Changing Environment

Apart from changes in the scientific realm, economic, social, and political trends have a critical influence on applied research. In particular, the effort required increases steadily as a result of constantly rising legislative demands. The industrial researcher in Germany is confronted by a rising tide of laws, ordinances, and regulations (Fig. 5). The last 20 years in particular have witnessed a breathtaking escalation. Chemical companies now devote large departments exclusively to the task of ensuring that the right documents reach the right authorities at the right time.

One dubious effect of the numerous statutory requirements, which often start with a justifiable question but end in bureaucratic perfectionism, is a shift in the emphasis of research activity. The innovative content of research—the pursuit of new discoveries—is becoming ever smaller relative to the effort to demonstrate that a problem has been solved responsibly—testing for potential side effects, for example, or confirming environmental compatibility. Innovative research, the quest for new solutions to problems, is today almost matched by "defensive" research aimed at satisfying statutory requirements. In the case of research related to active compounds, this aspect now accounts for well over three-quarters of all expenditures.

Although legal requirements are usually targeted at industrial production, they nevertheless have a direct influence on innovative research as well. Obstacles placed in the path of new products or processes increase the costs, and development times are drastically lengthened. One result is that even advances entailing environment-friendly production and disposal methods, or improved application characteristics, suffer unwarranted delays. Installations aimed directly at improving the state of the environment, such as waste incinerators, waste air filters, exhaust gas scrubbers, or effluent pretreatment units, have become subject to increasingly time-consuming approval procedures. This is a case where environmental legislation often proves to be self-defeating.

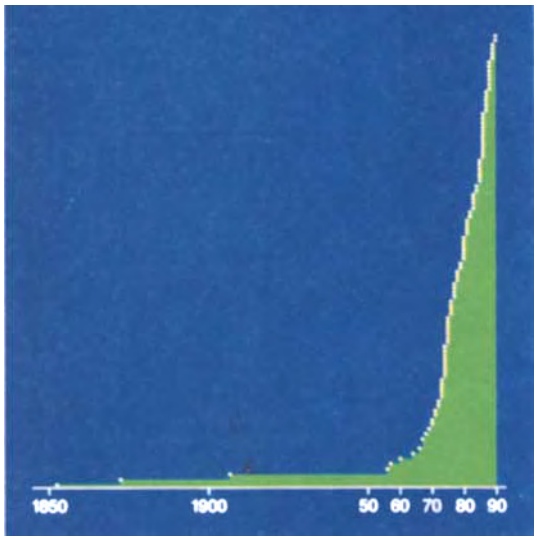

Fig. 5. Changes in environmental legislation (FRG). In the period since about 1960 environmental legislation in the Federal Republic of Germany has escalated to take on crippling proportions. Not a year passes without a further increase in the number of laws, regulations, and amendments. Each dot in the graph represents a newly adopted law or ordinance. In many of these cases, what began as a legitimate question has developed more and more into a bureaucratic obstacle race tying up substantial personnel resources in both industry and government.

In fact, the chemical industry seized the initiative long before the environmental debate began, dramatically tightening the demands for cost-effectiveness and safety in its processes and products, in both research and production. There is a long tradition in the chemical industry of seeking ways to use inexpensive raw materials or previously wasted by-products. The first chemical manufacturers owed their very existence to the utilization of a by-product of energy generation in coking plants: coal tar provided the raw materials for synthetic dyes. Increasing reaction yields, utilizing by-products, and reducing energy consumption have always represented effective responses to the pressure to improve competitiveness. Today, when the emphasis is on environmentally compatible design of our industrial production processes, these same endeavors continue to enjoy top priority. An additional factor is the obligation to ensure proper disposal of those residues that cannot be physically recycled or utilized to generate energy. Alongside continuous im-

provements in landfill technology, the chemical industry has also made notable advances in reducing the amount of waste that needs to be consigned to a landfill. The chemical industry has also expended considerable effort jointly with the recycling industry to develop further the whole concept of recycling.

The energy input required to produce chemical products has undergone a steady decline thanks to advances in process development. In the first ammonia plant of 1913, the production of ammonia still required the introduction of several times the energy content of the NH_3 molecule. Consistent improvement in the process has reduced this today to a factor of 1.3.

The development of crop protection agents provides an impressive illustration of the way in which chemical products have been forced to meet higher and higher standards for safe application and specificity. As recently as the 1960s, the development of one new pesticide entailed the synthesis of about 4 000 new substances. Today the figure has risen to 15–20 000 (Fig. 6). This lower success rate is a consequence

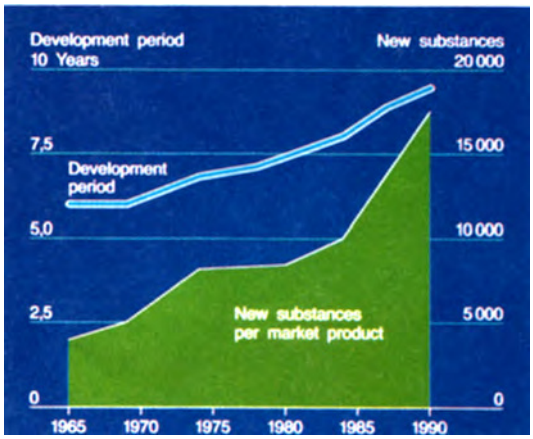

Fig. 6. Development period and success rate in crop protection research. The number of syntheses necessary for the market launch of a single crop protection agent has increased during the past 25 years from 4,000 to more than 15,000. This reduced success rate reflects the requirements products now must meet with respect to efficacy, ecological acceptability, and steadily decreasing dosages. As a consequence, the development period has risen from six years to almost ten.

of searches directed increasingly toward specific activity and minimal dosage. In particular, however, toxicological and ecotoxicological acceptability continue to move into the foreground. Toxicological studies now account for about one third of development costs. As expenditures have risen, so too have development times (Fig. 7), which now stretch out over nearly 10 years in the case of pesticides. In the pharmaceutical sector 12–15 years are already usual. Because of these long development times and the associated high costs, the search for active substances has become a financial risk, which leads to predictable consequences. In addition, the gap is becoming ever narrower between the time required to develop a new market product and the patent term of 20 years, expiration of which means that the product is open to manufacture and marketing by imitators. The latter incur no significant expenses for research and development, so they are able to undercut significantly the prices set for the original products. The German Health Reform Act with its fixed price regulations will make it virtually impossible to recover development costs in the Federal Republic of Germany. This is certain to have medium-term consequences on the Federal Republic as a site for research.

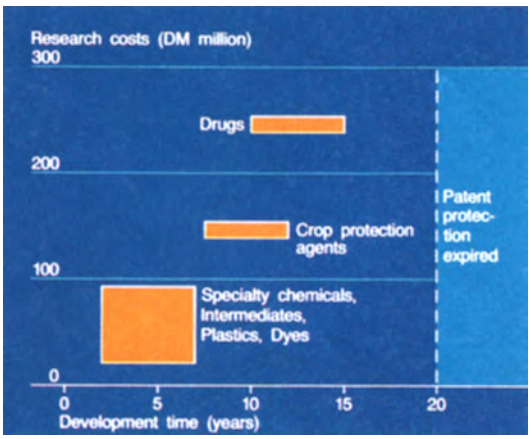

Fig. 7. In general, there has been a substantial rise in both research expenditures and development times for new products or processes. The development of a new drug takes longest of all, and is fast approaching the protection period afforded by a patent. As a result, in precisely those areas with the highest development costs, cost recovery has become virtually impossible. The period of patent protection is soon to be extended, a change that is vital if we are to maintain the power of innovation in these areas.

Applied research is also being influenced more strongly today than in the past by the idiosyncrasies of particular markets. Increasing specificity of customer demands and varying but generally more stringent requirements with respect to the properties and quality of products, together with legislative restrictions, mean that research remains intimately linked with a product or process until well into the production phase. This has always been the case for pharmaceuticals and pesticides, where research is responsible for the so-called "monitoring" of a product throughout its entire life cycle. But in other sectors, such as coatings and paints, specialty plastics, or process chemicals for the paper and leather industries, research is becoming more and more enmeshed in production and marketing.

It is only through intensive cooperation between research, technical services, and production that market stimuli can be rapidly absorbed and transformed into new or improved products. As a result, the local industrial environment generally is becoming more and more important in determining the quality of a research site.

In a country like the Federal Republic of Germany, which is not rich in raw materials, prosperity is essentially a function of innovative skill. The first requirement for innovation is knowledge, and knowledge is acquired through research. We have attained our current standard of living on the basis of convincing research efforts and efficient structures for production. The general environment that prevailed in the past has also played a role. We must be vigilant in the future so that we do not relinquish this high standard. It is certainly nice to enjoy prosperity, but effort is required to maintain it.

6. Applied Research and Technological Change—Reciprocal Influences

Of the most important raw materials used in the chemical industry—oil, natural gas, and rock salt—the Federal Republic of Germany has adequate resources only of the latter. It is for this reason that we are obligated to develop superior technologies and exploit synergies available within our established integrated system of production and our infrastructures, since only in this way can we maintain our competitive edge in the long term over those who do possess raw materials.

These essential raw materials are now the basis worldwide of some 300 important primary products and intermediates, which are in turn converted by a highly diversified chemical processing industry into about 20–30 000 different products that eventually find their way into a wide variety of finished goods (Fig. 8). The chief distinguishing feature of primary

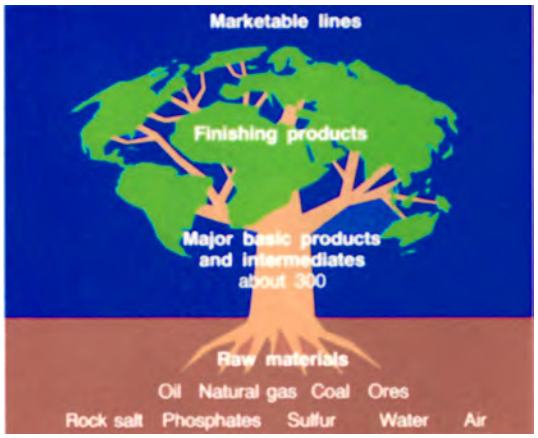

Fig. 8. The spectrum of chemical products begins with a few raw materials and extends through a set of basic products and intermediates up to the wide variety finished products. Only the latter experience a life cycle, and are constantly replaced by better products.

products and intermediates is the diversity of their chemistry. Unlike many end products, which in the course of time are subject to replacement by others, these materials are themselves not subject to the phenomenon known as a "life cycle". The processes involved in their preparation do undergo change, however. Change of this kind is sometimes brought about by new technologies and advances derived from research, but it may also be dictated by the raw materials outlook. At the beginning of this century, most product lines were geared to coal as a raw material, but a shift occurred after about 1940 in the direction of oil. More recently, oil has increasingly been supplemented by natural gas, and the future will witness the growing significance of biomass as a raw material.

Change affects entire areas of operation, not simply isolated product groups or individual products. Products do experience a life cycle, which can be described in terms of an initial phase, a growth phase, and a period of maturity. For this reason, the product portfolio of a single company or of an entire industrial sector will at any given time include operations and products characterized by various stages of development.

Detergents and cleansers provide a particularly interesting example of a change occurring within an essentially mature area of operation, and brought about by an interaction of the conditions of life with consumer demands. Cleansing agents can be regarded as a sensitive indicator of the state of civilization, at the same time reflecting the problems that go hand in hand with a higher standard of living. A few years ago, our rivers and lakes were threatened with eutrophication caused by a high influx of phosphates from detergents. Finding an immediate substitute for sodium polyphosphate proved difficult, however, since this substance is a source of a rich combination of essential characteristics. The replacement of phosphates by zeolites was recognized as a step that would halt the overfertilization of surface waters, but it would also have led to the formation of deposits on textile fibers and on the heating elements of washing machines. Only the development of supplementary polymeric additives (polycarboxylates) by BASF actually made it feasible to effect the replacement of phosphates in detergents without any sacrifice in familiar washing characteristics.

This example clearly illustrates the way demands of the market and of the environment can trigger innovation. Detergents and cleansers also serve as a useful example of a trend currently apparent within applied research generally. Development is moving increasingly from individual substances toward combinations of ingredients. These can then be regarded as *molecular systems*, all the components of which must be carefully matched. Use of such a system permits a set of properties to be varied within rather broad limits by custom-tailoring the blend of components. For example, neutralized polyacrylic acid can be adapted simply by adjusting the molecular weight to such divergent fields of application as dispersion and flocculation, e.g. for water treatment purposes, as a raw material for detergents, or as a thickener for establishing the proper viscosity in cleansing agents (cf. Fig. 9). This principle of optimizing a molecular system has also become extremely important in the finishing of textiles and leather, in electroplating, in the printing sector, and in the design of new polymeric materials, an application with particular significance for the future.

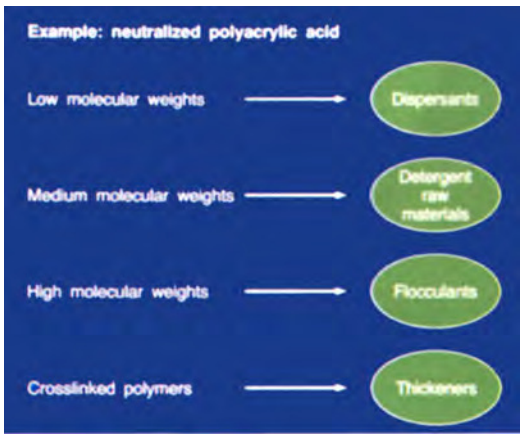

Fig. 9. So far as most consumer products are concerned, individual substances are no longer able to meet today's more demanding standards. Instead, molecular systems are invoked. These are tailored to specific uses, for example by way of special formulations or grades.

One of the distinguishing characteristics of a mature field is the fact that basic innovations result only rarely from fundamentally new discoveries. More often, new products or technical solutions are introduced because of disadvantages associated with the application of conventional market products. By contrast, in an operation passing through its growth phase progress derived from new discoveries and opportunities tends also to shape the market for new applications.

Polymeric materials represent a case in point. Despite more than half a century of development no end is yet in sight. At the same time, various classes of polymers have achieved very different levels of maturity (Fig. 10). The commodity plastics (green) are characterized by a rather high degree of maturity, and their many applications are responsible for a significant market volume. The market segment for engineering plastics (yellow) is smaller, since these are more often restricted to specific applications. During the early stages of product development, markets are generally so limited that development costs outweigh earnings. Thus, a balanced product portfolio is especially important in strengthening the potential for further development.

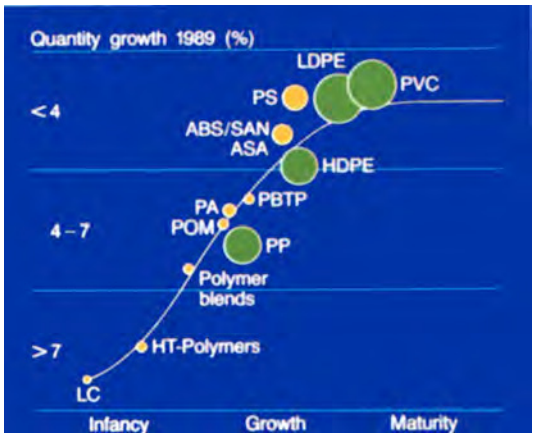

Fig. 10. Levels of maturity of various polymeric materials. The product groups labeled in green are commodity plastics, while those labeled in yellow are engineering plastics. The area of the circle signifies the market volume. LC = liquid crystalline polymers; HT polymers = high-temperature resistant polymers; POM = polyoxymethylene; PA = polyamide; PBTP = polybutylene terephthalate; ASA, SAN, ABS = styrene copolymers; PS = polystyrene; PP = polypropylene; HDPE, LDPE = high density/low density polyethylene.

7. New Opportunities from New Materials

Recent advances in connection with new materials have been made possible by new insights into the relationship between morphology and properties. Use is made here of a characteristic of matter that has given impressive evidence of its value over the course of evolution: the capacity for self-organization under a specific, defined set of molecular circumstances.

The properties of polymeric materials are not only dependent on chemical composition but are also critically related to structure in the molecular and supramolecular ranges, i.e., to morphological factors. In the case of the first-generation plastics there was little recognition of this fact. Today, internal structure can be predetermined to a considerable extent, and it is subject to almost unlimited modification. To this end, polymers are combined in the form of blends, just as metals are combined to produce alloys. The properties of individual components are not simply additive; what instead results is often an entirely new profile of characteristics. Polymer blends are generally not homogeneous single-phase materials, but are made up of microscopically small zones with differing chemical composition and corresponding in some cases even to different physical states. The key to the effectiveness of such a morphology lies in the structures of the individual microphases and in the firm anchoring of the microphases to one another.

A polymer blend consisting of polyamide, polyphenylene ether, and rubber (Fig. 11) displays characteristics that cannot be deduced directly from the property profiles of the components: a very high heat distortion temperature ($> 150\,^{\circ}C$), exceptional impact strength, and, not least, greatly reduced capacity for absorbing water, thereby eliminating a major disadvantage of polyamide as an engineering material.

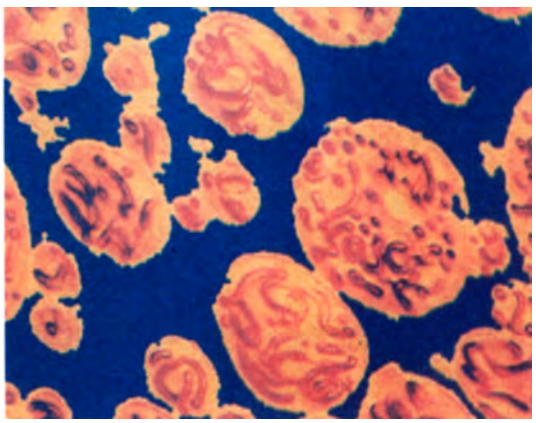

Fig. 11. This electron micrograph shows a blend of polyamide, polyphenylene ether, and rubber. The blue region represents the polyamide matrix. Polyphenylene ether is shown in yellow. The rubber (red areas) is included within the polyphenylene ether particles.

One of the ambitious aims of research into polymeric materials was, and still is, to challenge the supremacy of metals in their ability to absorb energy under conditions of very high stress. The structural principle underlying high-performance composites requires that continuous fibers which can serve as load-bearing elements are embedded within a polymeric resin. This principle is quite familiar from nature. The role assigned to the ribs in leaves or the cellulose fibers in plant stems is assumed in the case of composites by carbon or glass fibers. The fibers must be so oriented in the finished components that they can absorb forces applied along almost any axis. For this reason, components usually consist of several layers, with fibers crossing at specific, precalculated angles. A structure of this type can be achieved, for example, with the aid of computer-controlled winding units (Fig. 12). Particularly when carbon fibers are used, the result is a composite whose ability to absorb stress rivals even that of conventional steel from the standpoint of rigid-

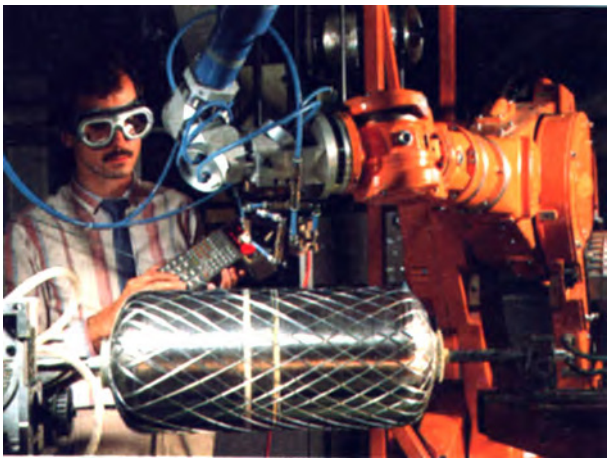

Fig. 12. Winding unit for the manufacture of high-performance composite materials. A robot carries out laser welding of plastic-impregnated glass fibers to form a highly stress-resistant wound article.

ity, tensile strength, and fatigue strength. All these advantages are present in a system that also offers a much lower weight, high corrosion resistance, and absolute dimensional stability. These are properties of considerable value in the aerospace industry, where a reduction in weight is especially critical since it translates into lower fuel consumption or increased payload.

Polymer blends and high-performance composites are just two illustrations of developments in the field of engineering polymers that hold great promise for the future. A whole series of new products has emerged in recent years in this field, offering combinations of unusual properties that cannot be duplicated with conventional materials (Fig. 13). Ex-

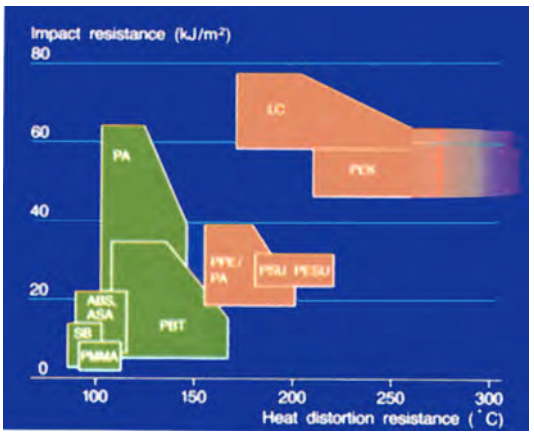

Fig. 13. Novel thermoplastics combine high heat distortion resistance with high mechanical strength. They include, for example, polymer blends of polyphenylene ether and polyamide (PPE/PA), polysulfones (PSU), polyether sulfones (PESU), polyether ketones (PEK), and liquid crystalline polymers (LC). SB = high-impact polystyrene; PMMA = poly(methyl methacrylate); ABS, ASA = styrene copolymers; PA = polyamide; PBT = polybutylene terephthalate.

amples of such properties are increased temperature resistance, toughness, strength, dimensional stability, low flammability, corrosion resistance, specific optical properties, or electrical conductivity. In the case of conventional organic polymers, advantage is taken of only about 5% of the potential to withstand mechanical stress that is actually present in the chemical bonds. Modern developments like carbon fibers already permit more than 50% of this potential to be exploited, and the resistance of such materials to stress is increased correspondingly. Further developments are aimed in two directions. First, it is hoped that improved production techniques will minimize the occurrence of weak spots that reduce product strength. Second, even more advantage is to be taken of the potential residing in chemical bonds, permitting the elimination, for example, of extreme anisotropic behavior with respect to physical properties (e.g., graphite layers in carbon fibers) through chemical cross-linking of adjacent layers.

This trend toward use-oriented specialization in plastics development will, in the future, permit even more rapid progress in electrical engineering, electronics, vehicle and aircraft manufacture, mechanical engineering, and information and communications technology. Because of the leading position Germany has attained in plastics technology—both as a science and in production and application—we expect to play a crucial role in helping to shape the future. The situation looks rather different, however, in another sector currently undergoing dramatic changes and promising to bring substantial improvements in the conditions of life.

8. Genetic Engineering—A Biotechnological Method of the Future

The use of biotechnology is as old as mankind itself. Microorganisms have always played a part in alcoholic fermentation and in the preparation of sour dough or cheese. Specific microorganisms have been selected, now and in the past, on the basis of the effectiveness of their adaptation to the processes in question. A modern example is provided by a new biotechnological process for the production of vitamin B_2 that was commercialized this year by BASF. The process leads directly to vitamin B_2 itself, and it utilizes a renewable raw material, vegetable oil, taking advantage of a microorganism that has been carefully optimized, though not modified by genetic engineering. Alternative chemical processes invariably involve a large number of intermediate steps.

Recently, genetic engineering has provided us with methods for obtaining more rapidly than in the past very high levels of synthetic performance from microorganisms. The secret is discriminate modification of the target organism's genetic information. On the one hand this makes it possible to prepare substances more economically than by the methods of conventional chemistry, but it also opens the way to products obtainable *only* by this route. The advantages of genetic engineering are particularly apparent with respect to a number of new pharmaceutical agents based on endogenous proteins. According to a survey by the World Health Organization (WHO), of about 30 000 discrete diseases only about one third are amenable to cure through drugs. This amply documents the need for further therapeutic advances. Cardiovascular disorders, viral infections, rheumatism, and cancer are widespread diseases with fateful consequences for the victims. There is thus an urgent need for new substances

that might be able to contribute to therapeutic progress. At present, twelve therapeutic agents derived from genetic engineering are commercially available worldwide. These include antibodies, enzymes from the coagulation series such as the tissue plasminogen activator tPA or factor VIII, vaccines (e.g., for hepatitis B), endogenous modulators of the immune system such as interferons, and peptide hormones such as insulin. The number of projects currently at the preclinical and clinical stages of development is about 100, underscoring the dynamic growth of a technology barely 20 years old.

With tumor necrosis factor (TNF), a mediator of the immune system, BASF now possesses a genetic engineering product that is at an advanced stage of clinical trials. TNF was first identified in 1975. The year 1984 witnessed the successful cloning of the TNF gene, the elucidation of its amino acid sequence, and the preparation of the active substance itself by genetic engineering using E. coli bacteria. Since then the protein has also been crystallized and its structure determined in a joint effort with a team of scientists at Oxford (Fig. 14). This means that the active centers can now

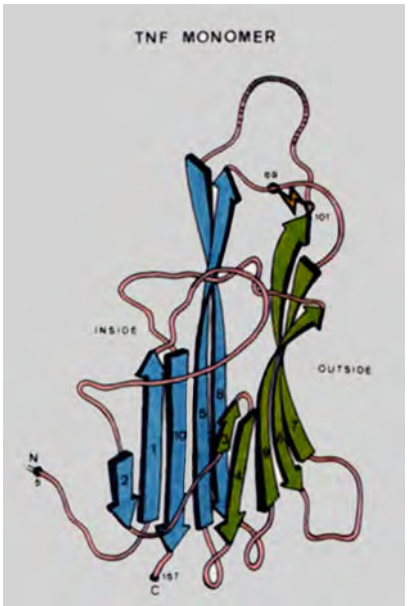

Fig. 14. Structure of tumor necrosis factor (TNF). After BASF had succeeded in obtaining tumor necrosis factor (TNF) in crystalline form, the structure was elucidated in a joint project with Oxford University. In its active form, TNF consists of three identical subunits, each containing 157 amino acids.

be identified and characterized pharmacologically. Clinical trials have demonstrated that TNF is an efficacious agent against malignant ascites. This is a condition that arises in the abdominal cavity as a consequence of cancer, leading to an excessive accumulation of fluid, and it has hitherto not proven amenable to treatment with drugs. A further success has even more recently been recorded: invocation of a combination of TNF and α-interferon as a treatment for metastasizing kidney cell carcinoma led to tumor recession in 50% of the patients tested. Although an industrial-scale synthesis of TNF has already been developed, and the necessary tests—including clinical trials—are well advanced, securing the required approval for production under the German Federal Air Pollution Control Act is proving to be incredibly difficult. The stack of documents prepared to obtain authorization for a TNF production facility with a fermenter volume of 200 L and an annual output of 0.5 kg now exceeds the height of the reactor (Fig. 15). This clearly illustrates the extent of the legal uncertainty at this time in the Federal Republic of Germany in the field of genetic engineering.

Fig. 15. The TNF production plant, now in the approval stage, has a fermentation volume of 200 liters. Annual production is to be 0.5 kg. It is being erected in an existing building and will use existing infrastructures. The picture shows the fermenter and, alongside it, the documents prepared for obtaining official approval for production.

It is therefore a welcome development that the Genetic Engineering Act came into force in July of this year. Binding legal parameters now circumscribe genetic engineering research and the construction and operation of genetic engineering plants. Nevertheless, this act and the regulations associated with it still do not guarantee that approval proceedings will advance smoothly. The mandatory hearings at safety review stages 2–4 are still subject to the influence of "refusal experts". It is to be hoped that practical implementation of the regulations will be governed by an understanding of the subject and not by ideology.

In view of the opportunities opened up by genetic engineering, particularly for medicine but also for food production, one would have anticipated a greater degree of acceptance on the part of the public. Unfortunately such has not been the case in the Federal Republic of Germany, in contrast to the USA or Japan. This may be due in part to the fact that the public and political debates have failed to draw a sufficiently clear distinction between genetic engineering on the one hand and, on the other, reproductive biology with all its ethical, moral, and legal ramifications. The latter falls clearly within the domain of medicine. The chemical and pharmaceutical industries are not active in these areas.

9. The Responsibility of the Chemical Industry for Our Future Society

Growth of knowledge in the field of genetic engineering is occurring at a tremendous rate, and Europe, far from setting the pace, is having trouble keeping up. Extending our understanding of the molecular dimension of life's processes is a challenge to scientists the world over. Practical application of newly acquired knowledge will bring many blessings, but abuse of this knowledge cannot be excluded. We repeatedly see evidence of the fact that although knowledge widens our opportunities it also increases our responsibility. Being aware of this responsibility and behaving accordingly legitimizes the freedom of action to which basic research and applied research lay claim and indeed require. We must continuously demonstrate to the public that we are conscious of our responsibility; only in this way can trust be regained.

The tasks facing applied research grow out of problems that confront our civilization, and these in turn arise from one basic source: unchecked population growth. Indeed, this is the origin not merely of the tasks that face us, but also of our responsibility to continue making technical advances in the interest of mankind. The chemical industry plays the key role, since it alone is able to open up new solutions through the transformation of matter. Its importance relative to other industries will continue to grow, and the fields it encompasses will become ever more complex. This of course has direct consequences for chemical research. Above and beyond areas traditionally associated with chemical operations, interdisciplinary development of new aspects of technology is becoming more and more critical to successful problem-solving. At the same time, the individual scientist will be constantly under obligation to examine the consequences of his actions. For his part, however, he must also insist that his expertise be taken into account in the decision-making process.

Received: August 9, 1990 [A796 IE]
German version: Angew. Chem. 102 (1990) 1213

The Integrating Effect of the Research Policy of the European Communities

By Karl-Heinz Narjes*

The research and development policy of the European Community (EC) was raised to a more solid legal basis by means of an extension of the treaties—the Single European Act—30 years after the enactment of the treaties of Rome. Today, the EC has succeeded in creating an independent, successful continent-wide research und development community despite rather limited budgetary means. The reasearch activities of the EC were originally restricted to EURATOM, which takes care of problems concerning civil nuclear research. EURATOM brought many experiences in the course of time, and also yielded many successes. We have learned above all how community research and national research are to be coordinated in the most efficient way. After the energy crisis of the seventies, and after many national R & D failures in various fields, high priority was given to the improvement and safeguarding of the technological competitivity of the community and the effective strengthening of its innovation potential. It was more and more generally accepted that all R & D resources had to be concentrated throughout the community in order to enable it to compete successfully, especially with the U.S. and Japan. In order to fulfill this objective a research policy with a strong integrating effect was requested in addition to the national R & D research policies. Cohesion and know-how transfer inside the EC belong therefore to the central issues of the R & D policy of the community, as do special efforts to include small and medium-sized institutes and enterprises (SMEs). Framework programs were introduced in the eighties in order to ensure a medium-term disposability of the budgetary means for R & D and to secure a certain continuity. The third framework program has been agreed upon, and it provides research funding until 1994. In 1987 approximately 1 Bill. Ecu/year were spent for R & D. Today, 1,5 Bill. Ecu/year are available, and this amount will further grow to provide approximately 2 Bill. Ecu/year in 1992/93. Issues like the difference between basic and applied research under inclusion of industry-political viewpoints are also included in this report. Furthermore, cooperation with and delimitation to other countries or communities such as the U.S. and Japan or the EFTA and the Comecon member states will be discussed. Finally, perspectives for R & D policies of the European Community in the nineties will be presented.

1. Introduction

The research and development policy of the European Community is not an isolated function, but an integral part of the overall objectives of the European Union. Since 1950, the Union has been endeavoring to create an irreversible, democratically legitimated European forum with a decision-making procedure anchored in the same manner as a constitution in order to fulfill various tasks and achieve the aims that the six founding states have helped to set in motion when they allocated it appropriate powers. The political circumstances of the 1950s did not enable us to approach all these tasks simultaneously and comprehensively. It was advisable to start with those areas of integration in which the need for union is irrefutable and the consensus needed to bring it about appeared to be solid and lasting. By electing to move toward integration the founding states abandoned the formerly customary systems of national law, and particularly the machinery of cooperation, since these—bilaterally or collectively—had all failed to pass their actual historic test, the preservation of peace in Europe, since the rise of the national state, in other words since the Congress of Vienna. After two terrible world wars, both of which had begun as European civil wars, Europe in 1945 stood on the very brink of the abyss. To assert itself, it needed a radical change of methods and paradigms. This was the origin of the community concept, supranationality, integration, and the endeavor to solve community problems and resolve conflicts jointly, in other words by applying the methods of domestic politics. This actually represents the only real political innovation of the post-war era.

The correctness of this approach has become apparent, not least in the last two years. The successes of the community and its methods have exerted their full effect as a model and catalyst in the historic revolutionary events in Central and Eastern Europe.

2. Research Policy of the European Communities

2.1. Historical Development and the Situation Today

Research and development played only a minor role in the first community founded after 1950, the European Coal and Steel Community (ECSC). Under the influence of the massive American superiority in technology, European public opinion changed very rapidly, so that the European Atomic

[*] Dr. K.-H. Narjes
Avenue de la Renaissance 1, Bte. 1
B-1040 Brussels (Belgium)

Energy Community came into existence in March 1957, at the same time as the European Economic Community. EURATOM established a communal responsibiity for virtually every function of the peaceful use of nuclear sciences. Its later development, dictated principally by factors associated with power politics, cannot be described here. However, it has brought about many important events and successes, from matters concerned with the efficiency and limitations of community large-scale research installations to sounding out the correct distance between the Community and industry. This task was influenced by the views of the member states regarding economic systems, which originally differed considerably. In particular, there were variations in attitudes toward the functions of the state in the process of innovation and toward the delimitation of those functions from the duties of individual companies. EURATOM also created an "esprit de corps" among the researchers and engineers involved, reestablishing something akin to European self-confidence—the awareness that this continent, once it succeeds in concentrating its resources, is capable of achievements that will guarantee it a seat at the top table in every sphere of world events. Whether the point at issue relates to the high standards of European reactor safety or the development of new types of reactors, the concentration of efforts and of human and economic resources has paid off every time. The same is true today, if we recall for example the important role played throughout the world by the European Community and its effective coordination of European research into thermonuclear fusion, in concert with the United States, Japan, and the Soviet Union.

But the limitations on power and political constraints also became apparent if we think, for example, of the thorny question of the demarcation into nuclear and non-nuclear powers in the European Atomic Energy Community, or the labors that were necessary in order to ensure the autonomy of EURATOM from the Vienna Agency in the world system of the non-proliferation treaty.

Under the influence of the first oil crisis and the substantial technological advances achieved by the United States in the subsequent 15 years, the Community then began, after 1973, to formulate its own research and development policy beyond the spheres of competence of EURATOM and the ECSC. Not only did it progress toward supplying the new demand for research and development in the sector of non-nuclear energy generation and consumption, but it also began to encourage the flagging competitiveness of European industry. Increasingly, the restoration of industry became a political challenge to all member states, as well as to the Community itself. There was no mistaking the loss of the innovative spirit and global competitiveness in key industrial sectors, if one takes as a basis the indices for the Community as a whole rather than restricting oneself to a comparison with the Federal Republic, which in many respects occupies a leading position.

Among the weak points that required action at that time, one important example was the fragmentation of European markets. The almost explosive increase in research and development costs gave rise to an irresistible compulsion to establish a major economic area, one large-scale market, since it was only in an enlarged domestic market that there was any prospect of recovering the high R & D expenditure through the market price, taking full advantage of the scaled-up returns. It immediately became apparent, however, that increasing research projects called for a level of expenditure which exceeded the capabilities of the individual member states. Only by pooling resources was it possible to guarantee that development could keep pace with that in the United States or Japan. Experience with the European Center for Nuclear Research (CERN), the European Space Administration (ESA) and also the European Molecular Biology Organization (EMBO) confirmed this insight, and led the member states to adopt Community initiatives and finance them from the budget.

In 1983, after a great preparatory effort, an initial outline program for research and development was approved, running from 1984 to 1987. In many ways it is in the nature of a compromise, exploiting the experience of the past 30 years and endeavoring, successfully, to initiate a research and development policy with continuity over a number of years and independent of the annual budget disputes. The occurrence of these program compromises in the negotiations of the Council of Ministers made it clear that it was essential to adopt the form of an outline program, which is synonymous with a "negotiation package", in which the various interests are combined. Such an arrangement need not be a political burden if—as in a well-managed company—all those involved cooperate constructively, and if there is the appropriate political will, unity, and mutual trust.

Against this background, it became possible in 1985 to contemplate a first substantive change in the Treaties of Rome and to take advantage of the opportunity presented by the incorporation of the 1992 single-market program to introduce into the amended treaty an express Community responsibility for a number of other policies. This amendment to the treaty took place in 1985 through the Single European Act, which came into force in 1987.

It also lays down that the outline program is to be implemented through specific programs, these specific programs differing from the outline program in that decisions can be taken by means of a qualified majority vote. The effect of this difference is that the member states try insofar as possible to introduce into the outline programs themes and standpoints that reflect their specific interests, since the only way in which they can influence the content of the outline program is by their veto. In addition to this, the Single European Act envisages coordinating the research policy of the member states, though this has hitherto been achieved only to an unsatisfactory extent, principally because the early availability of information necessary for effective ex ante coordination can rarely be anticipated. What is now happening in this area—the comparative assessment of national research and development programs, known as COPOL (*Co*nfrontation de *Pol*itiques nationales)—is nevertheless of considerable interest to some member states, particularly those that have not hitherto developed any procedure for a national R & D policy extending over a number of years.

Experience shows that the other possibility, that of resolving upon additional programs in which only some member states participate, has not been very enthusiastically received. To put it crudely, if there is no money available from Brussels, then neither is there any reason why the Community should be involved at all in cooperation between individu-

al member states—except perhaps for purposes of a joint defense against nuclear attack.

More interesting in the long-term is another possibility, namely involvement in large-scale research installations as a way of ensuring research facilities even for those member states of the Community which, through their own efforts, could neither participate in such an installation nor, as outsiders, negotiate opportunities for jobs and training there for their citizens.

Even today, in the light of our brief experience with research policy since 1986/87, two areas have become apparent in which political efforts should be made to introduce corrections: First, the rigorous nature of the five-year plan should be loosened, preferably by adopting a budgeting procedure based on rolling programming, which would make it possible every 24 or 36 months to change the emphasis and incorporate new themes or abandon obsolete ones. Second, an effort should be made to put an end to the requirement of unanimity for the outline programs. Experience with the single market project has produced highly favorable results as regards decisions taken by means of the qualified majority vote. The mere possibility of being outvoted compels all delegations to formulate their positions from the outset in such a way as to at least achieve a blocking minority and thereby avoid isolation. Since all partners operate in this way, the whole business of negotiation and argument is facilitated and a higher common denominator for constructive decisions is achieved than would be possible if delegations persistied in extreme positions, without perceptiveness or common sense, trusting in the veto option. Since a governmental conference is meeting as early as December of this year to draft institutional improvements to the Treaties of Rome and decisive steps toward European union, I regard it as not inconceivable that such a change in the voting method could be approved before the end of next year.

As regards the budget resources available for Community research and development, I shall confine myself to observing that the actual sum available in the year 1987/88 was about one billion ECUs, that this sum will be increasing to about 2 billion ECUs per year for the years 1989 to 1991/92 (1 ECU currently being equivalent to DM 2.06), and that an annual sum of 3 billion ECUs can be expected by the mid 1990s. This is quite a small budget for a large fraction of a continent. However, it does not include direct payments by the member governments to other European research organizations (especially ESA and CERN), which are not funded from the Community budget. Nor does it include Community military research and development under the *I*ndependent *E*uropean *P*rogramme *G*roup (IEPG), which is now in its early stages.

The present annual expenditure of about 2 billion compares with the Community's gross domestic product of about 4 trillion ECUs. The upper limit of the total Community budget is about 1.2% of this gross domestic product, which means at present about 50 billion ECUs. Of this, the Community's common agricultural policy swallows up more than 50% or, in round figures, at least 15 times the figure for its research and development policy.

This budget situation forces the Community to husband its scarce resources with extreme care if it hopes to make a significant contribution to the Community's research aims.

2.2. Heterogeneous Interests of the Member States

A political, economic, social, and cultural heterogeneity of the member states, to which I have already referred, is also reflected in their relative interests in research policy. Three quarters of the total Community expenditure on research is contributed by the United Kingdom, France, and the Federal Republic of Germany. In addition, there are wide differences in the proportions of the respective total national research expenditures devoted to military research and development. Whereas this percentage was about 50% in the United Kingdom, the figure for military research in the Federal Republic was generally in the vicinity of 10%. The other nine member states did not begin systematic development of a research policy until the 1980s. Also, many of even the larger industrial companies in smaller countries did not have their own research operations (or at most supported a limited development department) with a responsibility to work on innovative products and processes. All of the states recognized, however, that the competitiveness of their national economies, just like that of the Community as a whole, are critically dependent on the efficiency of their research and development potential, and that this in turn is substantially shaped by the quality of university education in the member states, or in those states to which their scientists are sent for training. There was a repeated demand for top performance, "centres d'excellence". In terms of the gross national product, the Federal Republic succeeded some years ago in increasing its R & D expenditure into the range of 2.8–2.9% of the gross national product, thus reaching a level which corresponds to that achieved in Japan. The other member states are also constantly striving, with rates of increase greater than those of their budget and national product, gradually to bring their budgets to a comparable level.

Whatever their individual positions, however, all the countries have an interest in using the route through the Community to expedite the development of their R & D and innovation potentials and bring them to the highest possible qualitative levels, even though focal points and traditions may vary.

In particular, however, great importance is attached to transferring to Community level those research and development projects that call for a greater input of capital expenditures and resources than can be afforded even by the largest of the individual member states. Civil nuclear research within EURATOM was an earlier example, and fusion research is now the most expensive large-scale research sector at nearly 200 billion ECUs per year (JET installation at Oxford).

Similarly, there are no differences of opinion over whether, for example, problems in climatology and broad areas of environmental research should be solved at the national level alone, and whether Community efforts are of universal benefit.

So far as the distinction between military and civil research is concerned, I see fewer problems at Community level than in the member states. Whereas the Community pursues everything for which a civil demand exists, at the national level there often seems to be a concern to find, or even invent, some military use so that the corresponding R & D can be financed from the military research budgets. These budgets offer more generous conditions, exercise less

strict control, and also seem to be more accommodating with respect to deadlines than civil programs, which adopt more stringent yardsticks. The Pentagon's "cost plus" contracts proved almost a guarantee of effortless revenue.

2.3. Research Sectors—Distribution of Budgetary Means

As regards the selection of the specific EC program, this is governed by the distribution of resources and the program description in the framework program. The latter incorporates eight research sectors which, with their sub-sectors and specific allocations of resources for these sub-sectors, are generally defined so extensively and in such detail that little freedom of action remains with respect to specific program decisions and their "quantitative framework". For example, of the approximately 5.4 billion ECUs of the second framework program, 375 million ECUs are allocated to the research sector "Quality of life" (health, radiation protection, environment), 2275 million for the key sector of information and communications technologies, including associated new services, 845 million to the modernization of the industrial sector (not just development of production processes and advanced materials but also prenormative research as part of the preparation of standards, methods, and reference materials), and 280 million for the exploration of biological resources, including agro-industrial technologies and methods of improving competitiveness in rural areas. 1173 million ECUs were provided for energy research, 80 million for science and technology in the field of development aid, and another 80 million for the development of sea bed and marine resources. Finally, for the improvement of European scientific and technological cooperation—which includes basic research—the provision is 288 million ECUs.

In order to understand this allocation of resources, and also in order to follow their use in detail, it is worthwhile pointing out that the Commission can for this purpose call upon a comprehensive consultancy structure, aimed at establishing a consensus, with extensive consultation of the member states and the various research milieus involved. A committee with the acronym CODEST (*Co*mmittee for the *De*velopment of *S*cience and *T*echnology) provides the cooperative link between the Commission and top scientific organizations behind national research policies, such as the Max-Planck Institutes and the German Research Association, to name German examples, or—in other member states—with the personal scientific advisers of the heads of government. This commission, which operates at the highest level, also has a program of its own (SCIENCE) that enables it to refer appropriate short-term assistance to valuable high-level projects provided they involve researchers from a number of member states. Several Nobel prize winners are regular members of CODEST. It exercises a lasting effect on the Community's research activities, and promotes their reputation and standing throughout the world. Another committee, *C*omité de la *re*cherche *s*cientifique et *t*echnique (CREST) was brought into being in order to ensure the closest possible consultation with the basic research departments of the national research ministries or administrations, which in Germany means the current Ministerial Director at the Federal Ministry for Research and Technology who is responsible for these matters. Then there is the very active *I*ndustrial *R*esearch and *D*evelopment *A*dvisory *C*ommittee (IRDAC) committee, currently under the chairmanship of a research manager from Shell. Here leading representatives of industrial research cooperate in order to contribute to the design and implementation of Community research policy. Current German representatives are Prof. Danielmeyer from Siemens and Prof. Dörfel, head of research at BASF until mid 1990. The interaction of these three advisory committees achieves a considerable degree of consensus, and so ensures that the Commission's research initiatives generally arouse interest and approval within the Council of Ministers and the European Parliament—at least so long as purely political motives within the Council or Parliament do not give rise to contradiction, opposition, or even obstruction.

Over and above this, there is a process of "inhouse" agreement within the Commission, because a number of general directorates, as customers for research results, also have a natural interest in exercising an early influence on research. This applies, for example, to environment policy, transport policy, and also fisheries and development policy.

In purely organizational terms, research and development is divided between two general directorates within the Commission, GD XII and XIII. The reasons for this are partly historical, though it is also attributable to the fact that it was expedient to have an independent organizational unit for information and communications technologies, currently the largest key area, which includes the major microelectronic programs ESPRIT and RACE, to which more than DM 800 million are allocated each year. In both general directorates, the officers responsible for project direction and management are recruited primarily from the sciences. The number of appointments falling to lawyers or economists is small. The officers come from all member states and are independently recruited by the Commission either for life or on the basis of 5-year restricted contracts. They are divided in such a way that today, for example, following the expansions, approximetely one officer in 7 holds German citizenship.

The consultancy procedures themselves, largely oriented towards consensus, create what amounts to a special awareness of the Community as the crystallization point of an independent European technological association. The tendency is further underlined by the widespread call for the Community to be given complementary tasks that are as closely dovetailed as possible, and to extend the principle of subsidiarity, an element of constitutional policy, into the field of R & D policy as well. This again is less easy to accomplish in practice than to call for politically; for example, the number of research tasks that Germany can undertake with its own resources is far greater than what would be possible for Portugal, Ireland, Denmark, Greece, or Luxembourg. If German efficiency and capability were to be taken as the yardstick for subsidiarity decisions, all the other 11 states would sooner or later fall out of the running and be deprived of the opportunity for full participation in Community R & D endeavors. Consequently, when it comes to a practical determination of what "subsidiary" means in specific terms, the only choice is to seek compromises. This in turn is accomplished, or at any rate facilitated, by the consensus procedure I have described. However, complementarity and

subsidiarity do not mean that the Community must stand ineffectively aside until all the member states have become aware of the relevance and wealth of opportunity offered by new research areas. On the contrary, the Commission has always endeavored, with considerable assistance from its consultancy structures, to adopt new themes at an early stage, conduct broadly based discussions of new problems, and, above all, pursue new objectives. It is precisely the smaller member states that are grateful for this effort by the Commission, because their own limited conceptual powers means that they are often not in a position to obtain a reliable overview and assessment of the global research landscape in all its ramifications. Interpretive aid and evaluation from Brussels are extremely welcome as they reach their own decisions.

2.4. Precompetitive Research and Shared-Cost-Contracts

In the implementation of the Community's specific programs both direct independent research and contractual research are possible, but there is a clear trend toward the latter. The Joint Research Center (JRC) taken over by EURATOM is in many ways developing into a European edition of the research institute of the American National Bureau of Standards (NBS). In particular, there is an ever-increasing emphasis on environmental and safety research at JRC.

In contractual research, the dominant element is the shared-cost contract, which as a whole has proven very valuable for many reasons. Cost-sharing means first and foremost that neither the Community's research bureaucracy nor technocratic research in Brussels can prescribe what is to be done and what is to be left undone. The process is neither top-down nor bottom-up: mutual agreement is obligatory in the sense of the constructive compromise.

Next, cost-sharing means that research institutes involved must make a high individual contribution: 50%. This prevents any tendency to foist particularly high-risk or less promising projects onto the Community while "hoarding" the supposedly better ones.

Another factor involved in shared-cost contracts is the requirement that projects must be concerned with pre-competitive research; that is to say, with the development of marketable products or processes. To promote direct product development would amount to an inadmissible subsidy of industry. By contrast, pre-competitive research proves successful it should provide sufficient data and "know-how" to finance further development of products and processes through normal commercial channels, relying on the independent responsibility of the company and the researchers involved. Finally, the only projects permitted are those in which at least two partners from different members states participate. The Commission is specifically required to assist international, integrative research.

So far as access to projects is concerned, there is no question of any restriction to industry, universities, or independent research institutes, nor to particular orders of magnitude. The conditions in the Community-wide invitations to tender are decisive, and a system of competitive tendering is in force. There is also a strictly anonymous selection system—peer review—and, consequently no national quotas but only opportunities based on merit. This merit system also means there is no room for the ominous law of the "juste retour", the classical nationalist rule of cooperation whereby each member state must receive from a transnational budget every last cent that it has paid in, if not more.

Another contractual principle is the obligation of all those involved in a project to conduct a mutual exchange of results from prior research that have a bearing on the project at hand. The intention here is to propagate and elevate the level of European achievement, although there is also no mistaking the fact that this obligation also deters one or another highly advanced member from pursuing the route of the European shared-cost contract. If a given member has already acquired precious know-how and valuable knowledge through its own efforts, and it would prefer not to pass these along to others without charge, then it is free to continue going it alone or to find partners on some other basis. Naturally, there are also EC regulations governing the propagation and use of jointly acquired knowledge.

Shared-cost contracts are used primarily in the field of the ESPRIT information technology program and the RACE communications program, as well as in the BRITE and EURAM industrial research programs. Feedback and success rates are very good. Most programs are between six and ten times oversubscribed. The level of projects is also assessed as very high. The quality of researchers assigned to these programs by the participants is described as good to very good. The younger participants in particular very quickly become accustomed to working together with researchers from other countries. The practical effect and range of the joint research efforts in the key areas are very far-reaching despite the limited resources, thanks largely to the shared-cost contracts. Thus the ESPRIT program, for example, embraces and coordinates about 30% of all pre-competitive research and development work done in the Community by all participants, and in this way also exerts an influence on the remaining 70%. Particularly successful and popular are the annual conferences for those involved in these large-scale programs. For example, as many as 1500–2000 researchers, engineers, and assignees of the involved institutions participate in the ESPRIT week. About 1000 pages of working papers are presented, critical masses are formed and synergistic effects discovered, results are discussed, and valuable stimuli are produced for all the institutions and companies involved. Statistics show, incidentally, that these programs are by no means the preserve of large companies or research institutes. Important contributions are noted every year from projects involving small and medium-size enterprises and institutions. Nor are the institutions in the peripheral member states disadvantaged. For example, every Greek university today takes part in at least one ESPRIT project, one of the reasons being that the EC's stimulation of opportunities for research and development in Greece has led to a new research surge there, and even to interesting reimmigration trends, particularly from the United States.

The principle reason why I have described in considerable detail this system of shared-cost programs in the Community's research and development policy is to indicate the high degree to which, in these key areas, integration of the research community is already taking place, leading to an independent European R & D identity. Those familiar with the

American situation have several times assured me that any such development would be inconceivable there. Experience in America, particularly with the Pentagon programs, has apparently demonstrated that shared-cost programs—however they might be individually organized, and whatever the cost-sharing arrangement might be—are rarely staffed by the very best researchers from the institutions and companies involved. The researchers assigned are sufficiently qualified to understand everything in the way of new knowledge that might be contributed by their project partners and competitors, but they are not sufficiently familiar with their own achievements, so they fail to report everything from their home bases that might be relevant to the communal project. It is hardly surprising, then, that the large national laboratories in America retain a lead in quality relative to contractural research.

Naturally, another element of every shared-cost project is the regular check on the performance status. This is paired with a readiness to put a rapid end to projects that prove unpromising for any reason. For example, about 10 to 15% of all ESPRIT projects fail to be carried through to the end.

3. Contribution of the R & D Policy of the European Communities to European Integration

3.1. Complementarity of the Single Market and the European Technological Community

When I referred initially to the encouragement of competitiveness as being one of the essential aims of Community research and development policy, I also observed that the rapidly increasing costs of research and development could no longer be recovered on the basis of safe, accessible foreign markets without a large-scale base or home market. Fragmented markets entail such a competitive disadvantage on the more remote world markets that there is rarely any real chance to win back lost market shares in the high-tech sector. Consequently, the 1992 single-market project, which is likely to be completely implemented on schedule in less than 30 months, is also having a considerable effect on innovation and research policy. It offers European industry a home market which, from the standpoint of its dimensions and buying power, is far superior to the Japanese market and matches the American market. This advantage of magnitude enjoyed by the European single market will become still more pronounced if, as is hoped, it expands economically to embrace the EFTA states in the near future and the former COMECON states at a later stage. A Europe of 400 million consumers is an entirely feasible expectation for the period shortly after the turn of the century. The full opening-up and development of the inherent technological potential of that market is a priority task for the European technological community.

The elements that have opened up an opportunity to Europe's generally successful research and development policy also include a strict refusal to reproduce traditional research policy "dog fights" at European level: basic research versus applied research, university research versus industrial research, research in the humanities and social sciences versus scientific research, large-scale research versus decentralized research, etc. The EC Commission and European Parliament endeavor over the years not only to recognize all cases where there is a justified demand for promising international research and development, but also, in cooperation with the member states, to supply that demand at Community level insofar as possible.

In these efforts, the Commission has had no problem whatsoever in reaching a constructive arrangement and division of labor with other respected European organizations, such as the European Science Foundation or EUREKA. Indeed, all are making every effort to achieve a permanent strengthening of European R & D potential, and to set in motion the scientific renaissance of a continent that has so often been pronounced dead.

3.2. Acceptance of Scientific R & D in Europe

All responsible institutions are conscious of the need to defend the position of the sciences against a public at times unjustifiably inclined to mistrust and reject them, and to wage a common struggle for greater overall acceptance of scientific research and development. The world "struggle" here is no exaggeration. Problems of acceptance are not simply the result of deliberate political interference and repeated attempts to split scientific research in the universities away from that in industry. They are also due to a rapidly widening gap between the accelerating advance of science, and the depth of understanding of public opinion and those who shape that opinion. Particularly in an age like this, in which it has even become possible to drop scientific disciplines before taking one's school leaving examinations, it is hardly surprising if the considerable vacuum in elementary knowledge and understanding of scientific relationships is being filled, and dangerously abused, from another quarter. In such a situation, the precise nature of which varies from one member state to another, a representative European voice of science developed at Community level (perhaps in the form of an academy or a scientific assembly) could make an essential contribution to the restoration, relaxation, and normalization of the necessary public dialog on the progress of science.

One thing, however, does seem to me important: the sciences must recognize that their accountability to the public regarding what they are doing, how much it costs, what they are achieving, and how their results can be put to beneficial use will become more and more urgent and more and more extensive. For example, we will need to consider how the scientist who ventures to portray his field in generally comprehensible terms, without the customary quotable scientific apparatus, is to be protected against professional disadvantages. This may sound banal. Yet my experience suggests that this relationship represents an understandable but avoidable obstacle to acceptance, since every individual career depends on the number and quality of scientific publications. For this very reason, it should be possible to separate without disadvantage publications for non-scientific purposes from those specialist publications that advance a scientist's career. This function cannot be entirely left to the media, since they themselves have enormous personnel prob-

lems in trying to find good writers with appropriate scientific qualifications and available on terms they can offer. Great efforts will be necessary to close the gap in understanding, and the EC should be of assistance here.

Another aspect—or, if you like, a hangover from 1968—also in urgent need of correction seems to me to be a kind of emotional prejudice against scientists, irrespective of whether they work in industry or are involved, for example, in constantly widening the limits of human knowledge in fields such as molecular biology or microbiology. I believe it is intolerable that scientists, collectively and a priori, should be treated as somewhat unstable individuals, believed to be unable and unwilling to take responsibility for their actions, or to regard them as "obsessed" or "infatuated" characters to be closely watched by, for example, sociologists. This is another area where a representative and powerful voice speaking for European scientists generally could make a more balanced contribution to advancing the overdue process of correction.

A comparable benefit to Community development would be a de-emotionalization of environmental policy. The protection of nature and the environment is far too important a task to be left to the vociferous emotions of certain scientists who pursue eclectic lines of argument and selective lines of work. But this task, too, presupposes a great willingness for personal public commitment. It is not only in the media that one rarely encounters individuals who are equally talented in science and in the various forms of communication; the same is true in politics, which ultimately has the last word in any decision regarding the use of public R & D resources. The Community, incidentally, with its nine official languages, is itself under an obligation to produce texts that can be universally read and believed.

3.3. Community Programs for Promoting the Mobility of Scientists and Cooperation with States Outside the Community

Parallel to the various aspects of the common research and development policy, the Community also operates a number of backup programs intended to help integrate young scientists and researchers. The Commission discovered some years ago that only 1% of all students in the Community spend at least one term at university in another member state at some point during their studies. The remaining 99%, then, are ignorant of universities in other states. This situation, alongside the political aim of integrating the Community's citizens, was the essential reason for launching a comprehensive scholarship program which you may already have encountered under the name "Erasmus". The aim of this program is to make increasing use of resources to enable 10% of all the Community's students to benefit from terms abroad by the mid-1990s. The numbers doing so are already increasing sharply, but there are not yet sufficient resources to satisfy the demand immediately. Moreover, the popular universities can only absorb limited numbers of extra students. Even so, we are favorably placed to achieve the ambitious target on time. Another program that serves the same purpose is the *Com*munity action program in *E*ducation and *T*raining for *T*echnology (COMETT) which is more concerned with the exchange of senior colleagues between industries, universities and research institutions from the member states. In some cases, this involves researchers working abroad for periods of several years. Well over 1000 projects have now been accepted, and about 15000 soldiers and civilian workers are now benefiting from these opportunities. Another special program, TEMPUS (*T*rans *E*uropean *M*obility Scheme of *U*niversity *S*tudents), is also to be launched in the near future to assist with the reintegration into the West of academic circles in Poland and Hungary.

Apart from these measures to integrate European human resources, there are other programs whose aim is to use resources from the regional structural fund to enable the basic technological equipment of the more peripheral member states of the Community to be brought rapidly in line with the state of the art (STRIDE and BRIDGE, to cite only the acronyms). In addition, every effort is being made, particularly on the information and communications side, to create a broadly based data infrastructure by extensive networking of the dataflow within the continent.

Up to this point, my remarks have dealt only with the Community. The first necessity was for its formative process and its methods and objectives to be understood. But is also endeavors unceasingly to make its activities available to the other European states that are not members, or not yet members, on a basis of strict mutuality. This applies to the OECD countries (the COST program), the EFTA states (first bilateral cooperative agreement) and all those involved in EUREKA. The most graphic example of this expansion exists in Germany, where the accession of the German Democratic Republic will cause research in that country to be fully integrated with Community research. In addition, R & D relations with the former COMECON states will grow rapidly in intensity and scope. Another effect of these processes will be to bridge political gaps and to restore the integrity of the European cultural and scientific realms. Researchers in all countries are once again to be fully involved in the flow and exchange of information, and they will again be able to take advantage of all the opportunities offered by professional contacts free of frontiers and obstacles, with exchanges and meetings and whatever else benefits the integration of research and researchers, extending to successful joint efforts or unfettered participation in free and undistorted competition. Everyone knows that differences in gross national product do not necessarily reflect similar differences in individual or collective scientific talent.

4. Conclusion

Naturally this EC development has its critics, who focus principally on the way in which it portrays itself, and its organizational proportions, which are not always understood in the broader context. Another adverse factor is that, in contrast to the United States and Japan, nine different languages are spoken within the Community today. Moreover, many protagonists are relatively unfamiliar with EC procedures. The size of the Community necessarily means that a Community authority seems more anonymous than the familiar faces in the R & D Ministry back home in a country of 5 or 10 million inhabitants.

Disappointments, of course, often lead to reproaches. The Commission constantly endeavors to investigate the factual content of such reproaches, and to correct weaknesses. It knows from its own experience, better than others perhaps, that all those involved in the planning of research and development at the European Community level are undergoing a major learning process, a process governed in part by the principle of trial and error.

Despite all this, the inescapable need for communal R & D endeavors must not be forgotten. It is a necessary corollary of the formation of the European home market. Communal endeavors alone make possible the concentration of financial resources needed for the construction of industrial-scale plants of all kinds, now or in the future. Similarly, they permit more effective use to be made of human resources, which are in short supply, and an end to avoidable duplication of effort arising, for example, from unnecessary fragmentation in the pre-competitive R & D sector.

In short, the technological community, too, offers opportunities for the self-assertion and renaissance of a continent that has so often been written off; aims that have ranked second only to the safeguarding of peace as the crucial reasons for integration policies since 1950, and will remain so in future. Their necessity and current relevance has been repeatedly confirmed by the developments of the last 15 months. Our prospects for the 21st Century do not necessarily have to be poor!

Received: August 16, 1990 [A 798 IE]
German version: *Angew. Chem. 102* (1990) 1225

References

Apart from numerous descriptions of the R & D policy of the European Community in the literature relating to legal, economical or political affairs is the newly emerging literature relating to research politics. The initiative lies with the commission. Their proposals as well as their decisions are published in the offical gazette of the EC.

A useful introduction into the daily affairs of the available programs is contained in the following guide: L. Krickau-Richter, O. von Schwerin: *Sponsoring Research and Technology in the EC; GD XII of the Commission of the European Community*, 2nd edition, Economica Verlag, Bonn 1990.

The commission is obliged to report periodically to the European Parliament about the state of research and technology in Europe. The first report has been published in 1988: Commission of the European Community: *First report on the state of research and technology in Europe*, rue de la loi 200, B-1049 Brussels (Belgium).

Useful information can also be found in:

J. von Freyand, H. H. Eberstein, C. Kreklau: *BDI Handbook of Supporting Research and Innovation*, Verlagsgruppe Deutscher Wirtschaftsdienst, Cologne 1980.

The various proposals can also be obtained as seperate documents from the office for publications of the European Communities, rue mercier 2, L-2984 Luxembourg. The final reports, requests, and debates of the European Parliament can be obtained from its general secretariat. In addition special information is available for the various research fields and programmes, e.g. IRDAC News, rue defacqz 1, Box 12, B-1050 Brussels (Belgium); EURO TECNET, Centre Européen "Travail et Societé", Hoogbrugstraat 43, POB 3073, NL-6202 NB Maastricht (Netherlands).

Misconceptions on Pollution and the Causes of Cancer**

By Bruce N. Ames* and Lois Swirsky Gold

The public has numerous misconceptions about the relationship between environmental pollution and human cancer. Underlying these misconceptions is an erroneous belief that nature is benign. In this article we highlight eight of these misconceptions and describe the scientific information that undermines each one.

1. Misconception No. 1: Cancer Rates Are Soaring

According to the latest update from the National Cancer Institute (February 1988), "the age adjusted mortality rate for all cancers combined except lung cancer has been declining since 1950 for all individual age groups except 85 and above."[1] That represents a 13-percent decrease overall, 44 000 deaths below expected, and a 0.1-percent increase in the over-85 group (unless otherwise noted, all statistics given in this article refer to the USA.)

The types of cancer deaths that have been decreasing during this period are primarily stomach (by 75 percent, 37 000 deaths below expected), cervical (by 73 percent, 11 000 deaths below expected), uterine (by 60 percent, 9000 deaths below expected), and rectal (by 65 percent, 13 000 deaths below expected). The types of cancer deaths that are increasing are primarily lung cancer (by 247 percent, 91 000 deaths above expected), which is due to smoking (as are 30 percent of all U.S. cancer deaths), and non-Hodgkin's lymphoma (by 100 percent, 8000 deaths above expected).

Changes in incidence rates and effects of treatment are also relevant in interpreting the changes in mortality rates.[1, 2] Incidence rates have been increasing for some types of cancer.

In their definitive study on cancer trends,[2] Sir *Richard Doll* and *Richard Peto* point out that, although incidence rates are of interest, they should not be taken in isolation, because trends in the recorded incidence rates are biased by improvements in the level of registration and diagnosis. Even if particular types of cancer can be shown to be increasing or decreasing, establishing a causal relation among the many changing aspects of our lives is difficult.[3-15] There is no persuasive evidence that life in the modern industrial world has in general contributed to cancer deaths.[2, 10, 13]

Cancer is fundamentally a degenerative disease of old age, although exogenous factors can increase cancer rates (e.g., cigarette smoking in humans) or decrease them (e.g., caloric restriction in rodents).[16-18] For mammalian species, cumulative cancer risk increases with approximately the fourth power of age, both in short-lived species such as rats and mice (about 30% have cancer by the end of their 2-year life span) and in long-lived species such as humans (about 30% have cancer by the end of their 85-year life span).[2, 13, 19-21]

Life expectancy is steadily increasing in the United States and other industrial countries. Infant mortality is decreasing. Although the statistics are less adequate on birth defects, there is no evidence that they are increasing. Conclusion: Americans, Japanese, and Western Europeans are healthier now than they have been in their history.

2. Misconception No. 2: Cancer Risks to Humans Can Be Assessed by Testing Chemicals at High Doses in Rodents

Results from animal cancer tests, which are conducted at near toxic doses of the test chemical, cannot predict the cancer risk to humans at the usually low levels of human exposures. Knowledge of the mechanisms of carcinogenesis is necessary for prediction and is now progressing rapidly. Recent understanding of these mechanisms undermines many of the assumptions of current regulatory policy towards rodent carcinogens and necessitates a rethinking of the utility and meaning of routine animal cancer tests. The following summarizes our current understanding of these mechanisms and how they relate to animal cancer tests.

2.1. Mutagenesis Can Cause Cancer, and Normal Rates of Mutagenesis Are High

Mutagens cause cancer by mutating the DNA of cells in ways that cause cells to proliferate in an uncontrolled manner. It is generally agreed that several mutations are necessary to convert a normal cell into a cancer cell capable of uncontrolled growth.[22, 23] Mutagens are often assumed to be exogenous agents (coming from outside the body), such as synthetic chemicals; however, many endogenous mutagens (coming from inside the body) are formed naturally during normal metabolic processes like oxygen utilization, which produces DNA-damaging oxidants. These oxidants are the same as those produced by radiation, which itself is an oxidative mutagen. Thus, in a sense, breathing oxygen is equivalent to irradiating the body. Normal metabolism causes chronic, oxidative DNA damage: we estimate that the number of oxidative hits to DNA per cell per day is about 100 000 in rats and 10 000 in humans.[21, 24, 25] Endogenous rates of DNA damage are thus so high that it may be difficult for exogenous mutagens to increase this damage significantly at the normal levels of human exposure. All mammals have numerous defenses to counter this damage, such as enzymes

[*] Prof. B. N. Ames, L. S. Gold
Division of Biochemistry and Molecular Biology
and
Lawrence Berkeley Laboratory
Barker Hall
University of California
Berkeley, CA 94720 (USA)

[**] The names of compounds in this article are not always in accordance with IUPAC nomenclature.

that repair damaged DNA.[20, 21, 26] Nevertheless, this damage appears to be a major contributor to aging and to many of the degenerative diseases associated with aging, including cancer.

2.2. Chronic Cell Division Increases Mutagenesis and Carcinogenesis

"Promoters" of carcinogenesis have been recognized for many years, but the concept of "promotion" and its role in carcinogenesis have been fuzzy compared to the concept of mutagenesis and its role in carcinogenesis. This is primarily because the mechanisms of carcinogenesis have in the past not been well understood. Cell division (cell proliferation) promotes carcinogenesis by increasing the vulnerability of the DNA to mutation. A dividing cell is much more at risk from mutagens (either endogenous or exogenous) than is a nondividing, quiescent cell.[26-32] Agents that cause chronic cell division are therefore indirectly mutagenic (and commonly carcinogenic).[28-33] Saccharin, for example, is not itself a mutagen, but high doeses of saccharin given to rodents cause sufficient cell division to be carcinogenic.[32] Low doses, however, would be expected to have no carcinogenic effect. Agents that cause chronic cell division (e.g., by irritation and inflammation of tissues) appear to be important in many of the known causes of human cancer: hepatitis B or C viruses or alcohol in liver cancer, high salt or *Helicobacter* (*Campylobacter*) bacteria in stomach cancer,[34-43] hormones in breast cancer, papilloma virus in cervical cancer,[44] asbestos or tobacco smoke in lung cancer,[45] and excess animal fat and low calcium in colon cancer.[46] For the chemicals associated with occupational cancer, worker exposures usually have been at near-toxic doses that would be likely to cause cell proliferation.

2.3. Animal Cancer Tests Are Primarily Measuring the Effects of Massive Cell Division

Animal cancer tests of chemicals are conducted at near-toxic, chronic doses—the maximum tolerated dose (MTD). (Such high doses are used in order to increase the sensitivity of the test to detect a carcinogenic effect among small numbers of animals, because the tests are very expensive to conduct.) Such high doses often cause chronic cell death and a consequent chronic cell division of neighboring cells that replace the dead cells. Chronic dosing at the MTD can be thought of as chronic wounding, which is known to be both a promoter of carcinogenesis in animals and a risk factor for cancer in humans.[31, 47-49] Thus, by causing chronic cell division, a high percentage of all chemicals might be expected to be carcinogenic at chronic, near-toxic doses. This is exactly what is found (see Section 3). About *half* of all chemicals tested chronically at the MTD are carcinogens.[3, 50-55] The fact that about 40% of rodent carcinogens are not mutagens is consistent with our understanding of the important role of cell division in carcinogenesis.

Although toxicity at or near the MTD often induces cell division, below a certain dose no such effect is observed. Therefore, if animal cancer tests are primarily measuring the effects of cell division, then the dose–response curve would be expected to curve steeply upward rather than be linear.[3, 30-32, 56-58] This means that a tenfold reduction in dose in a rodent experiment would produce much more than a tenfold reduction in cancer risk. This prediction is confirmed by several recent analyses.[32, 59-61]

3. Misconception No. 3: Most Carcinogens and Other Toxins Are Synthetic

About 99.99% of all pesticides in the human diet are natural pesticides from plants.[62] All plants produce toxins to protect themselves against fungi, insects, and animal predators such as man.[62-71] Tens of thousands of these natural pesticides have been discovered, and every species of plant contains its own set of different toxins, usually a few dozen. When plants are stressed or damaged (e.g., during a pest attack), they increase the levels of natural pesticides manyfold, occasionally to levels that are acutely toxic to humans. We estimate that Americans eat about 1500 mg per person

Table 1. Forty-nine natural pesticides (and metabolites) in cabbage. See [a] for remarks on the numbered compounds.

Glucosinolates
prop-2-en-1-yl glucosinolate (sinigrin, **1**)
3-methylthiopropyl glucosinolate
3-methylsulfinylpropyl glucosinolate
but-3-en-1-yl glucosinolate
2-hydroxy-but-3-en-1-yl glucosinolate
4-methylthiobutyl glucosinolate
4-methylsulfinylbutyl glucosinolate
4-methylsulfonylbutyl glucosinolate
benzyl glucosinolate
2-phenylethyl glucosinolate
propyl glucosinolate
butyl glucosinolate

Indole glucosinolates and related indoles
3-indolylmethyl glucosinolate (glucobrassicin)
1-methoxy-3-indolylmethyl glucosinolate (neoglucobrassicin)
indole-3-carbinol (**2**)
indole-3-acetonitrile (**3**)
3,3'-diindolylmethane

Isothiocyanates and goitrin
allyl isothiocyanate (**4**)
3-methylthiopropyl isothiocyanate
3-methylsulfinylpropyl isothiocyanate
3-butenyl isothiocyanate
5-vinyloxazolidine-2-thione (goitrin, **5**)
4-methylthiobutyl isothiocyanate
4-methylsulfinylbutyl isothiocyanate
4-methylsulfonylbutyl isothiocyanate
4-pentenyl isothiocyanate
benzyl isothiocyanate
phenylethyl isothiocyanate

Cyanides
1-cyano-2,3-epithiopropane
1-cyano-3,4-epithiobutane
1-cyano-3,4-epithiopentane
threo-1-cyano-2-hydroxy-3,4-epithiobutane
erythro-1-cyano-2-hydroxy-3,4-epithiobutane
2-phenylpropionitrile
allyl cyanide (**6**)
1-cyano-2-hydroxy-3-butene
1-cyano-3(methylsulfinyl)propane
1-cyano-4(methylsulfinyl)butane

Terpenes
menthol
neomenthol
isomenthol
carvone (**7**)

Phenols
2-methoxyphenol
3-caffoylquinic acid (chlorogenic acid, **8**)
4-caffoylquinic acid (**9**)
5-caffoylquinic acid (neochlorogenic acid, **10**)
4-*p*-coumaroylquinic acid
5-*p*-coumaroylquinic acid
5-feruloylquinic acid

[a] *Clastogenicity:* Chlorogenic acid (**8**) [160] and allyl isothiocyanate (**4**) are positive [75]. Compound **8** and its metabolite caffeic acid are also mutagens [161-163], as is **4** [77]. *Carcinogenicity:* Allyl isothiocyanate (**4**) induced papillomas of the bladder in male rats (a neoplasm that is unusually rare in control rats) and was classified by the National Toxicology Program (NTP) as carcinogenic. There was no evidence of carcinogenicity in mice: however, NTP indicated "the mice probably did not receive the MTD" [164, 165]. Sinigrin (**1**; the glucosinolate, that is, thioglycoside of **4**) is cocarcinogenic for the rat pancreas [166]. Carvone (**7**) is negative in mice [167]. Indoleacetonitrile (**3**) has been shown to form a carcinogen, nitrosoindoleacetonitrile, in the presence of nitrite [168]. Caffeic acid is a carcinogen [169, 170] and clastogen [160] and is a metabolite of its esters **8**–**10**. *Metabolites:* Sinigrin (**1**) gives rise to **4** on eating raw cabbage (e.g., coleslaw); in cooked cabbage it also is metabolized to **6**, which is untested. Indolecarbinol (**2**) forms dimers and trimers on ingestion, which mimic dioxin (TCDD) (see Section 4.2) [71]. *Occurrence* [65, 68, 124, 171], *Toxicology:* The mitogenic effects of **5** (which is goitrogenic) and various organic cyanides from cabbage suggest that they may be potential carcinogens [172, 173]. Aromatic cyanides related to those from cabbage have been shown to be mutagens and are metabolized to hydrogen cyanide and potentially mutagenic aldehydes [174].

per day of natural pesticides, which is 10 000 times more than they eat of synthetic pesticide residues.[62] The concentration of natural pesticides is usually measured in parts per million (ppm), rather than parts per billion (ppb), which is the usual concentration of synthetic pesticide residues or of water pollutants. We also estimate that a person ingests annually about 5000 to 10 000 different natural pesticides and their breakdown products.[62] Table 1 lists 49 natural pesticides (and breakdown products) ingested on eating cabbage and indicates which ones have been tested for carcinogenicity or clastogenicity (the ability to break chromosomes). Lima beans contain a different array of 23 natural toxins that, in stressed plants, range in concentration from 0.2 to 33 parts per thousand fresh weight: none appears to have been tested for carcinogenicity or teratogenicity (the ability to cause birth defects).[66] A large literature has examined the toxicity of many of these compounds to herbivorous animals, such as humans and domestic animals.[63–68]

Surprisingly few plant toxins have been tested in animal cancer tests, but among those tested in at least one species, about half (27/52) are carcinogenic.[62] A search in plant foods for the presence of just these 27 natural-pesticide rodent carcinogens indicates that they occur naturally in the following foods (those at concentrations greater than 10 000 ppb of a single carcinogen are listed in italics): *anise, apple*, banana, *basil*, broccoli, *Brussels sprouts, cabbage*, cantaloupe, *caraway, carrot, cauliflower, celery, cherry*, cinnamon, cloves, cocoa, *coffee (brewed), comfrey tea, dill, eggplant, endive, fennel, grapefruit juice, grape, honey*, honeydew melon, *horseradish*, kale, *lettuce, mace, mango, mushroom, mustard (brown), nutmeg, orange juice, parsley, parsnip*, peach, *pear, pepper (black)*, pineapple, *plum, potato*, radish, raspberry, *rosemary, sage, sesame seeds (heated)*, strawberry, *tarragon, thyme*, and turnip (Table 2).

Thus, it is probable that almost every plant product in the supermarket contains natural carcinogens. The ppm levels of the known natural carcinogens in the above plants are commonly thousands of times higher than the ppb levels of man-made pesticides. The occurrence in the diet of natural pesticides that are rodent carcinogens should be interpreted cautiously. We need not be alarmed by the presence of low doses of synthetic toxins and a plethora of natural toxins in our food. As will be discussed in Section 5.1, humans are well protected against low doses of toxins by many layers of inducible, general defenses that do not distinguish between synthetic and natural toxins.

Dietary exposures to natural toxins are not necessarily of much relevance to human cancer. Indeed, a diet rich in fruit and vegetables is associated with lower cancer rates.[72, 73] This may be because anticarcinogenic vitamins and antioxidants come from plants.[72, 73] What is important in our analysis is that chronic exposures to natural rodent carcinogens may cast doubt on the relevance of far lower levels of exposures to synthetic rodent carcinogens.

Table 2. Concentrations of some natural pesticides that are rodent carcinogens. 1 ppm = 1000 ppb.

Plant food	Rodent carcinogen	Concentration [ppm]
Parsley	5- and 8-methoxypsoralen	14
Parsnip, cooked		32
Celery		0.8
Celery, new cultivar		6.2
Celery, stressed		25
Mushroom, commercial	*p*-hydrazinobenzoate	11
Mushroom, commercial	glutamyl-*p*-hydrazinobenzoate	42
Cabbage	sinigrin **1** (allyl isothiocyanate, **4**) [a]	35–590
Collard greens		250–788
Cauliflower		12–66
Brussels sprouts		110–1560
Mustard (brown)		16 000–72 000
Horseradish		4500
Orange juice	limonene	31
Mango		40
Pepper, black		8000
Basil	*estragole*	3800
Fennel		3000
Nutmeg	safrole	3000
Mace		10 000
Pepper, black		100
Pineapple	ethyl acrylate	0.07
Sesame seeds (heated oil)	sesamol	75
Cocoa	α-methylbenzyl alcohol	1.3
Basil	benzyl acetate	82
Jasmine tea		230
Honey		15
Coffee (roasted beans)	catechol	100
Apple, carrot, celery, cherry, eggplant, endive, grapes, lettuce, pear, plum, potato	caffeic acid	
Absinthe, anise, basil, caraway, dill, marjoram, rosemary, sage, savory, tarragon, thyme		> 1000
Coffee (roasted beans)		1800
Apricot, cherry, peach, plum	chlorogenic acid **8** (caffeic acid) [b]	50–500
Coffee (roasted beans)		21 600
Apple, apricot, broccoli, brussels sprouts, cabbage, cherry, kale, peach, pear, plum	neochlorogenic acid **10** (caffeic acid) [b]	50–500
Coffee (roasted beans)		11 600

[a] Sinigrin (**1**) is a cocarcinogen [166] and is metabolized to the rodent carcinogen **4**, although no adequate test has been done on **1** itself. The proportion of **1** converted into **4** or into allyl cyanide (**6**) depends on food preparation [123, 124, 171]. Chlorogenic acid (**8**) and neochlorogenic acid (**10**) are metabolized to the carcinogens caffeic acid and catechol (a metabolite of quinic acid), but have not been tested for carcinogenicity themselves. The clastogenicity and mutagenicity of the above compounds are discussed in Table 1.

3.1. Teratogens and Clastogens Are Common

It is also reasonable to assume that a sizable percentage of both natural and synthetic chemicals will be reproductive toxins at high doses because a high proportion of positives is reported for rodent teratogenicity tests. One-third of the 2800 chemicals tested in laboratory animals have been shown to cause reproductive damage in the standard, high-dose protocol.[74]

Results from other types of tests also indicate that the natural world should not be ignored and that positive results are commonly observed in high-dose tests. *Ishidate* et al.[75] reviewed experiments on the clastogenicity (chromosome breakage) of 951 chemicals in mammalian cell cultures. Of these 951 chemicals, we identified 72 as natural plant pesticides. Among these, 48% (35/72) were positive for clastogenicity in some or all tests. This is similar to the results of

the remaining chemicals; 53% (467/879) were positive in some or all tests. Thus, about half of the chemicals tested—whether synthetic or natural—have been shown to break chromosomes at high dose. These in vitro experiments do not necessarily simulate in vivo conditions, and chromosome breakage is probably much less extensive in tissues of the body than in laboratory tissue cultures.

Of particular interest are the levels at which some of the carcinogenic plant toxins in Table 2 were clastogenic:[75] (1) Allyl isothiocyanate (**4**) was clastogenic at a concentration of 0.0005 ppm, which is about 200 000 times less than the concentration of its glucosinolate, sinigrin (the parent compound **1**), in cabbage. Allyl isothiocyanate (**4**) was among the most potent chemicals in the compendium[75] and is also effective at unusually low levels in transforming[76] and mutating animal cells.[77] (See also the discussion of cancer tests in the legend to Table 1.) (2) Safrole was clastogenic at a concentration of about 100 ppm, which is 30 times less than the concentration in nutmeg, and roughly equal to the concentration in black pepper. The rodent carcinogens safrole and estragole, and a number of other related dietary natural pesticides that have not been tested in animal cancer tests, have been shown to produce DNA adducts (damaged DNA bases) in mice.[78] (3) Caffeic acid was clastogenic at a concentration of 260 and 500 ppm, which is less than its concentration in roasted coffee beans and close to its concentration in apples, lettuce, endive, and potato skin. Chlorogenic acid (**8**), a precursor of caffeic acid, was clastogenic at a concentration of 150 ppm, which is 100 times less than its concentration in roasted coffee beans and similar to its concentration in apples, pears, plums, peaches, cherries, and apricots. Chlorogenic acid (**8**) and its metabolite caffeic acid are also mutagens (Table 1). The toxicity of coffee to the DNA in mammalian cells has been demonstrated.[79]

3.2. Cooking Food

The cooking of food is also a major dietary source of potential rodent carcinogens. Cooking produces about 2000 mg per person per day of mostly untested burnt material that contains many rodent carcinogens.[3, 69, 70, 80–85] Roasted coffee, for example, is known to contain about 825 volatile chemicals.[69] Only 21 have been tested, and 16 are rodent carcinogens.[51–54] In addition, roasted coffee also contains hundreds of nonvolatile chemicals: caffeic acid has been tested and is a carcinogen. With just these few chemicals tested, the carcinogens total 9 mg per cup of coffee (40 000 ppb). (There is some, but not sufficient evidence to conclude that coffee causes cancer in humans.)[72, 80] When proteins or amino acids are heated, certain mutagens known as heterocyclic amines are sometimes produced. Thus far, ten of these heterocyclic amines have been shown to be carcinogens in rodents, and many others are in the process of being isolated and tested.[86, 87] In addition, cooked food contains a plethora of other mutagens as well as rodent carcinogens (polycyclic hydrocarbons, furfural, and nitrosamines).[3, 69, 70, 80–85]

The total amount of browned and burnt material consumed per person in a typical day is at least several hundred times more than that inhaled in a day

air pollution.[71] Three mutagenic nitropyrenes present in diesel exhaust have now been shown to be rodent carcinogens,[88] but the intake of these carcinogenic nitropyrenes has been estimated to be much higher from grilled chicken than from air pollution.[86, 87, 89] Gas flames generate NO_2, which can form both carcinogenic nitropyrenes[3] and nitrosamines in foods that are cooked in gas ovens. Food cooked in gas ovens may be a major source of dietary nitropyrenes and nitrosamines.

3.3. Residues of Man-made Pesticides

By contrast, human exposures to man-made pesticide residues are minuscule. The Food and Drug Administration (FDA) assayed food for residues of the 200 synthetic compounds thought to be of greatest importance, including most synthetic pesticides and a few industrial chemicals.[90] The FDA estimates that the intake of these residues averages about 0.09 mg per person per day and other analyses are similar.[91] For comparison, we estimate that the intake of natural pesticides averages about 1500 mg per person per day.[62] About half of the intake of synthetic residues is composed of four chemicals (ethylhexyl diphenyl phosphate, dicloran, malathion, and chlorpropham)[90] that were not carcinogenic in rodent tests.[51, 92] Thus, the intake of carcinogens from synthetic residues (0.05 mg a day, if one assumes that all the other residues are carcinogenic, which is unlikely) is extremely tiny relative to the background of natural substances; this 0.05 mg intake is equivalent to about 60 ppb of synthetic residues in plant food consumed daily.

4. Misconception No. 4: Synthetic Toxins Pose Greater Risks than Natural Toxins

The possible carcinogenic hazards from synthetic pesticides (at normal exposures) are minimal compared with the background hazards of nature's pesticides. Even though an overwhelming number of the chemicals that humans eat are natural, the natural world of chemicals has never been tested systematically. Synthetic chemicals account for 350 (82%) of the 427 chemicals tested chronically at high doses in both rats and mice.[3, 50–55] Of the 77 *natural* chemicals tested, the proportion carcinogenic is about *half* (37/77), that is, similar to that of synthetic chemicals (212/350).[3, 50–54] It is unlikely that the high proportion of carcinogens in rodent studies is due simply to selection of suspicious chemical structures: while some synthetic or natural chemicals were selected precisely because of suspect structures, most chemicals were selected because they were widely used industrially; for example they were high-volume chemicals, pesticides, drugs, dyes, or food additives.[50] The natural world of chemicals has never been looked at systematically.

In recent years, we have tried to formulate a method of setting priorities among possible carcinogenic hazards.[3] The potencies of different carcinogens vary more than 10^7-fold in rodent tests, and the comparison of possible hazards

is

Table 3. Ranking possible carcinogenic hazards [a].

Possible hazard HERP [%] [b]	Daily human exposure	Carcinogen dose for a 70-kg human
Environmental pollution		
0.001*	Tap water, 1 liter	Chloroform, 83 μg (U.S. average)
0.004*	Well water, 1 liter contaminated (worst well in Silicon Valley, CA, USA)	Trichloroethylene (TCE), 2800 μg
0.0004*	Well water, 1 liter contaminated (Woburn, MA, USA)	Trichloroethylene, 267 μg
0.0002*		Chloroform, 12 μg
0.0003*		Tetrachloroethylene (perc), 21 μg
0.008*	Swimming pool, 1 hour (for child)	Chloroform, 250 (average pool) μg
0.6	Conventional home air (14 h per day)	Formaldehyde, 598 μg
0.004		Benzene, 155 μg
2.1	Mobile home air (14 h per day)	Formaldehyde, 2.2 mg
Pesticides and other residues [c]		
0.0002*	PCBs: daily dietary intake	PCBs, 0.2 μg (U.S. average)
0.0003*	DDE/DDT: daily dietary intake	DDE, 2.2 μg (U.S. average)
0.0004	1,2-dibromoethane (EDB): daily dietary intake (from grains and grain products)	EDB, 0.42 μg (U.S. average)
Natural pesticides and dietary toxins		
0.003	Bacon, cooked (100 g)	Dimethylnitrosamine 0.3 μg
0.006		Diethylnitrosamine, 0.1 μg
0.003	Sake (250 mL)	Urethane, 43 μg
0.03	Comfrey herb tea, 1 cup	Symphytine, 38 μg (750 μg pyrrolizidine alkaloids)
0.03	Peanut butter (32 g; one sandwich)	Aflatoxin, 64 ng (U.S. average, 2 ppb)
0.06	Dried squid, broiled in gas oven (54 g)	Dimethylnitrosamine, 7.9 μg
0.07	Brown mustard (5 g)	Allyl isothiocyanate (**4**), 4.6 mg
0.1	Basil (1 g of dried leaf)	Estragole, 3.8 mg
0.1	Mushroom, one raw (15 g) (*Agaricus bisporus*)	Mixture of hydrazines, etc.
0.2	Natural root beer (12 oz; 354 mL) (now banned)	Safrole, 6.6 mg
0.008	Beer, before 1979 (12 oz; 354 mL)	Dimethylnitrosamine, 1 μg
2.8*	Beer (12 oz; 254 mL)	Ethanol, 18 mL
4.7*	Wine (250 mL)	Ethanol, 30 mL
6.2	Comfrey-pepsin tablets (nine daily)	Comfrey root, 2700 mg
1.3	Comfrey-pepsin tablets (nine daily)	Symphytine, 1.8 mg
Food additives		
0.0002	AF-2: daily dietary intake before banning	AF-2 (furylfuramide), 4.8 μg
0.06*	Diet cola (12 oz; 354 mL)	Saccharin, 95 mg
Drugs		
[0.3]	Phenacetin pill (average dose)	Phenacetin, 300 mg
[5.6]	Metronidazole (therapeutic dose)	Metronidazole, 2,000 mg
[14]	Isoniazid pill (prophylactic dose)	Isoniazid, 300 mg
16*	Phenobarbital, one sleeping pill	Phenobarbital, 60 mg
17*	Clofibrate (average daily dose)	Clofibrate, 2,000 mg
Occupational exposure		
5.8	Formaldehyde: Workers' average daily intake	Formaldehyde, 6.1 mg
141	EDB: Workers's daily intake (high exposure)	EDB, 150 mg

[a] We have tried to use average or reasonable daily intakes to facilitate comparisons [3]. In several cases, such as contaminated well water or factory exposure to EDB, this is difficult to determine, and we give the value for the worst exposure found. The calculations assume a daily dose for a lifetime; where drugs are normally taken for only a short period, we have bracketed the HERP value. [b] The asterisk means that the HERP value is from carcinogens thought to be nogenotoxic. [c] PCBs = polychlorinated biphenyls, DDE = 1,1-dichloro-2,2-bis(4-chlorphenyl)ethylene, DDT = 1,1,1-trichloro-2,2-bis(4-chlorphenyl)ethane.

into account. We have analyzed animal cancer tests from our Carcinogenic Potency Database[51-54] and, for each chemical, have calculated the TD_{50} (*T*umorigenic *D*ose 50), which is essentially the daily dose of the chemical estimated to give half of the animals tumors. We have constructed an index to rank possible carcinogenic hazards: first, we estimate a reasonable daily lifetime human exposure to each chemical and express that as milligrams (of the chemical) per kilogram of body weight. Then, that mg kg^{-1} human exposure is expressed as a percentage of the rodent TD_{50} dose (mg kg^{-1}) for each carcinogen. We call this percentage the HERP value (*H*uman *E*xposure dose/*R*odent *P*otency dose). Because rodent data are all calculated on the basis of lifetime exposure at the indicated daily dose rates,[8, 51] the human exposure data are similarly expressed as lifelong daily exposure rates, even though the human exposure is likely to be less than daily for a lifetime (Table 3).

The HERP values do not estimate human risk directly, because it is impossible to extrapolate to low doses (see Section 1), but they do offer a way of comparing possible hazards and thus of putting exposures into a relative context so that priorities can be more reasonably set. (Carcinogens clearly do not all work in the same way, and as we learn more about mechanisms, HERP comparisons can be refined, as can risk assessments.) Our results suggest that alcohol at moderate doses should be high on our priority list for epidemiological studies on cancer. The HERP analysis further suggests that the possible carcinogenic hazard of synthetic chemicals that humans ingest from pesticide residues or water pollution appears to be trivial relative to the background of carcinogenic hazards from natural chemicals and chemicals formed by cooking food.[3, 71, 93]

4.1. Water Pollution

The possible hazards from carcinogens in contaminated well water in places like California's Santa Clara ("Silicon")

Valley or Woburn, Massachusetts,[94-99] should be compared with the possible hazards of ordinary tap water.[3] Of the 35 wells that were shut down in Santa Clara Valley because of a supposed carcinogenic hazard to humans (low traces of trichloroethylene), only two were of a possible hazard greater than ordinary tap water. Well water is not usually chlorinated and therefore lacks the 83 ppb of chloroform present in average chlorinated tap water in the U.S.[3] Water from the most polluted well in the Santa Clara Valley had a relative hazard that was orders of magnitude less than that for an equal volume of coffee, beer, or wine.[3] The consumption of tap water is only about one or two liters per day, and animal evidence[3] provides no good reason to expect that either the chloroform produced in water by chlorination or the current levels of synthetic pollutants in water would pose a significant carcinogenic hazard.[3] Natural arsenic appears to be the most significant carcinogen in both well water and tap water and is often present at quite high levels.[100] Arsenic is a known human carcinogen.

The trace amounts of chemicals found in polluted wells are likely to be a negligible cause of birth defects, in comparison to the background level of known teratogens such as alcohol. The important risk factors for birth defects and reproductive damage in humans are the age of the mother, her consumption of alcohol, her smoking habits, and her exposure to the rubella virus.

4.2. TCDD (Dioxin) Compared with Broccoli and Alcohol

Cabbage and broccoli contain a chemical whose breakdown products bind to the body's Ah receptor, induce enzymes, and possibly cause cell division—just as does dioxin (TCDD), one of the most feared industrial contaminants. TCDD is of great public concern because it is carcinogenic and teratogenic in rodents at extremely low doses. The doses humans ingest, however, are far lower than the lowest doses that have been shown to cause cancer and reproductive damage in rodents.

TCDD exerts many or all of its harmful effects in mammalian cells through binding to the Ah receptor.[101] A wide variety of natural substances also bind to the Ah receptor (e.g., tryptophan oxidation products[102]) and, insofar as they have been examined, they have similar properties to TCDD. A cooked steak, for example, contains polycyclic hydrocarbons that bind to the Ah receptor and mimic TCDD. In addition, a variety of other plant substances in the diet also bind to the Ah receptor. Indole carbinol (**2**), for example, is present in large amounts in broccoli (500 ppm), cabbage,[103] cauliflower, and other members of the *Brassica* family. At the pH of the stomach, **2** forms chemical structures (known as dimers and trimers) that induce the same set of detoxifying enzymes as TCDD.[104-106] Like TCDD, **2** protects against carcinogenesis when given *before* aflatoxin or other carcinogens.[106-108] However, when given *after* aflatoxin or other carcinogens, **2**, like TCDD, stimulates carcinogenesis.[105] This stimulation of carcinogenesis has also been shown for cabbage itself.[109] These derivatives of **2** appear to be much more of a potential hazard than TCDD. The Environmental Protection Agency's human "reference dose" (formerly "acceptable dose limit") of TCDD is 6 femtograms per kilogram per day. This should be compared with 50 mg of **2** per 100 g of broccoli (one portion) (see also cabbage).[62, 103] Although the affinity of the indole derivatives in binding to Ah receptors is less than that of TCDD by a factor of about 8000, the effective dose to the Ah receptor from a portion of broccoli would be about 15000 times higher than that of TCDD, taking into account another factor of 1000 for the very long lifetime of TCDD in the body (several years) and assuming that the lifetime of the hydrophobic indole dimers is as short as one day. However, it is not clear whether, at the low doses of human exposure, *either* **2** or TCDD is hazardous. It seems likely that many more of these natural "dioxin simulators" will be discovered in the future.

If TCDD is compared with alcohol, it seems of minor interest as a teratogen or carcinogen. Alcohol is the most important known human chemical teratogen.[72] In contrast, there is no persuasive evidence that TCDD is either carcinogenic or teratogenic in humans, although it is both at near-toxic doses in rodents. If one compares the teratogenic potential of TCDD to that of alcohol for causing birth defects (after adjusting for their respective potency as determined in rodent tests), then a daily consumption of the EPA reference dose of TCDD (6 fg) would be equivalent in teratogenic potential to a daily consumption of alcohol from 1/3000000 of a beer. That is equivalent to drinking a single beer (15 g of ethanol) over a period of 8000 years.

In humans alcoholic beverages are carcinogenic[110] as well as teratogenic. A comparison of the rodent carcinogenic potential of TCDD with that of alcohol (adjusting for the potency in rodents) shows that ingesting the TCDD reference dose of 6 fg per kilogram per day is equivalent to a man ingesting one beer every 345 years. Since the average consumption of alcohol in the United States is equivalent to more than one beer per person per day, and since five drinks a day are a carcinogenic risk in humans, the experimental evidence does not of itself seem to justify the great concern over TCDD at levels in the range of the reference dose.

5. Misconception No. 5: The Toxicology of Man-made Chemicals Is Different from That of Natural Chemicals

It is often assumed that, because plants are part of human evolutionary history, whereas industrial chemicals are not, the mechanisms that animals have evolved to cope with the toxicity of natural chemicals will succeed in protecting them against natural chemicals, yet will fail to protect against synthetic chemicals: "For the first time in the history of the world, every human being is now subjected to contact with dangerous chemicals, from the moment of conception until death" (Rachel Carson: *Silent Spring*, 1962). We find this assumption flawed for several reasons.

5.1. Defenses That Animals Have Evolved Are Mostly of a General Type

Since the number of natural chemicals that might have toxic effects is so large, general defenses offer protection not

only against natural but also against synthetic chemicals, making humans well buffered against toxins.[3, 7, 103, 111] These defenses include the following: (1) The continuous shedding of cells exposed to toxins: the surface layers of the mouth, esophagus, stomach, intestine, colon, skin, and lungs are discarded every few days. (2) The induction of a wide variety of general detoxifying enzymes, such as antioxidant enzymes[20, 21, 112] or the glutathione transferases for detoxifying alkylating agents:[113] human cells that are exposed to small doses of an oxidant, such as radiation or hydrogen peroxide, induce antioxidant defenses and become more resistant to higher doses.[114–118] These defenses can be induced by both synthetic oxidants (e.g., the herbicide paraquat) and natural oxidants and are effective against both. (3) The active excretion of planar hydrophobic molecules (natural or synthetic) out of liver and intestinal cells.[119] (4) DNA repair: this is effective against DNA adducts formed from both synthetic and natural chemicals and is inducible in response to DNA damage.[26] (5) Animals' olfactory and gustatory perception of bitter, acrid, astringent, and pungent chemicals: these defenses warn against a wide range of toxins and could possibly be more effective in warning against some natural toxins that have been important in food toxicity during evolution than against some synthetic toxins. However, it seems likely that these stimuli are also general defenses and are monitoring particular structures correlated with toxicity; some synthetic toxic compounds are also pungent, acrid, or astringent. Even though mustard, pepper, garlic, onions, etc., have some of these attributes, humans often ignore the warnings.

The fact that defenses are usually general, rather than specific for each chemical, makes good evolutionary sense. Predators of plants evolved general defenses against toxins presumably to be prepared to counter a diverse and ever-changing array of plant toxins in an evolving world; if a herbivore had defenses only against a set of specific toxins it would be at a great disadvantage in obtaining new plant foods when favored plant foods became scarce or evolved new toxins.

5.2. Various Natural Toxins, Some of Which Have Been Present throughout Vertebrate Evolutionary History, Nevertheless Cause Cancer in Vertebrates

Mold aflatoxins, for example, have been shown to cause cancer in trout, rats, mice, monkeys, and, possibly, humans.[3, 110] Eleven mold toxins have been reported to be carcinogenic[103] and nineteen mold toxins have been shown to be clastogenic.[75] Many of the common elements are carcinogenic (e.g., salts of lead, cadmium, beryllium, nickel, chromium, selenium, and arsenic) or clastogenic[75] at high doses, despite their presence throughout evolution.

Furthermore, epidemiological studies from various parts of the world show that certain natural chemicals in food may be carcinogenic risks to humans: the chewing of betel nuts with tobacco around the world has been correlated with oral cancer.[110, 120] The phorbol esters present in the Euphorbiacea, some of which are used as folk remedies or herb teas, are potent mitogens (inducers of cell proliferation) that are thought to be a cause of nasopharyngeal cancer in China and esophageal cancer in Curacao.[121, 122] Pyrrolidizine toxins are mutagens that are found in comfrey tea, various herbal medicines, and some foods; they are hepatocarcinogens in rats and may cause liver cirrhosis and other pathologies in humans.[120]

Plants have been evolving and refining their chemical weapons for at least 500 million years and incur large fitness costs in producing these chemicals. If these chemicals were not effective in deterring predators, plants would not have been naturally selected to produce them.

5.3. Humans Have Not Had Time to Evolve into a "Toxic Harmony" with All of the Plants in Their Diet

Indeed, very few of the plants that humans eat would have been present in an African hunter-gatherer's diet. The human diet has changed drastically in the last few thousand years, and people are eating many recently introduced plants that their ancestors did not, for example, coffee, cocoa, tea, potatoes, tomatoes, corn, avocados, mangoes, olives, and kiwi fruit. In addition, cruciferous vegetables such as cabbage, broccoli, kale, cauliflower, and mustard were used in ancient times "primarily for medicinal purposes" and were spread as foods across Europe only in the Middle Ages.[123, 124] Natural selection works far too slowly for humans to have evolved specific resistance to the food toxins in these newly introduced plants.

5.4. Poisoning from Plant Toxins in the Milk of Foraging Animals Was Quite Common in Previous Centuries

In nonindustrial societies, cow or goat milk and other ingested dairy products were contaminated by the natural toxins from plants that were eaten by foraging animals, because toxins that are absorbed through the animal's gut are often secreted in the milk. Since the plants foraged by cows vary from place to place and are usually inedible for human consumption, the plant toxins that are secreted in the milk are, in general, not toxins to which humans could have easily adapted. *Abraham Lincoln*'s mother, for example, died from drinking cow's milk that had been contaminated with toxins from the snakeroot plant.[125] When cows and goats forage on lupine, their offspring may have teratogenic abnormalities, such as "crooked calf" syndrome caused by the anagyrine in lupine.[126–128] Such significant amounts of these teratogens can be transferred to the animals' milk that drinking the milk during pregnancy is teratogenic for humans:[126–128] in one rural California family, a baby boy, a litter of puppies, and goat kids all had a "crooked" bone birth defect. The pregnant woman and the pregnant dog had both been drinking milk obtained from family goats that had been foraging on lupine, the main forage in winter.[126–128]

5.5. Anticarcinogenic Chemicals in the Diet May Help to Protect Humans Equally Well against Synthetic and Natural Carcinogens

Although plants contain anticarcinogenic chemicals (e.g., antioxidants) that may protect against carcinogens,[129, 130]

these anticarcinogens *do not distinguish* whether carcinogens are synthetic or natural in origin.

5.6. Although Synergism between Synthetic Carcinogens Could Multiply Hazards, This Is Also True of Natural Chemicals

Natural chemicals are by far the major source of chemicals in the diet.

5.7. Although the Synthetic Pesticide DDT Bioconcentrates in the Food Chain Due to Its Unusual Fat Solubility, Natural Toxins Can Also Bioconcentrate

DDT is often viewed as the typically dangerous synthetic pesticide because it persists for years; it was representative of a class of chlorinated pesticides. Natural pesticides, however, also bioconcentrate if fat-soluble: the teratogens solanine (and its aglycone solanidine) and chaconine, for example, are found in the tissues of potato eaters.[131-133] Although DDT was unusual with respect to bioconcentration, it was remarkably nontoxic to mammals, saved millions of lives, and has not been shown to cause harm to humans.[134] To a large extent DDT, the first major synthetic insecticide, replaced lead arsenate, a major carcinogenic pesticide used before the modern era; lead arsenate is even more persistent than DDT. When the undesirable bioconcentration and persistence of DDT and its lethal effects on some birds were recognized, it was prudently phased out and less persistent chemicals were developed to replace it. Examples of these newer chemicals are the synthetic pyrethroids that disrupt the same sodium channel in insects as DDT,[135] are degraded rapidly in the environment, and can often be used at a concentration as low as a few grams per acre.

6. Misconception No. 6: Storks Bring Babies and Pollution Causes Cancer and Birth Defects

The number of storks in Europe has been decreasing for decades. At the same time, the European birth rate also has been decreasing. We would be foolish to accept this high correlation[136] as evidence that storks bring babies. The science of epidemiology tries to sort out the meaningful correlations from the numerous chance correlations. That is, epidemiology attempts to determine correlations that may indicate cause and effect. However, it is not easy to obtain persuasive cause-and-effect evidence by epidemiological methods, because of inherent methodological difficulties.[10] There are many sources of bias in observational data, and chance variation is also important. For example, because there are so many different types of cancer and birth defects, by chance alone one might expect some of them to occur at a high frequency in a small community here and there. Toxicology provides evidence that can help us decide whether an observed correlation might be causal or accidental.

There is no persuasive evidence from epidemiology or toxicology that pollution is a significant cause of birth defects or cancer. For example, the epidemiological studies of the Love Canal toxic waste dump in Niagara Falls, New York, or of dioxin in Agent Orange,[137, 138] or of pollutants produced by the refineries in Contra Costa County, California,[139, 140] or of the contaminants in the wells of Silicon Valley[141] or Woburn, Massachusetts,[94-99] or of the now-banned pesticide DDT, provide no persuasive evidence that pollution was the cause of human cancer in any of these well-publicized exposures. At Love Canal, where people were living next to a toxic waste dump. the epidemiological evidence for an effect on public health is equivocal. Analyses of the toxicology data on many of these cases suggest that the amounts of the chemicals involved were much too low relative to the background of naturally occurring carcinogens and carcinogens from cooking food to be credible sources of increased cancer in humans.[3] With respect to birth defects, a comparative analysis of teratogens using a HERP-type index, which would express the human exposure level as a percentage of the dose level known to cause reproductive damage in rodents, would be of interest. Such an analysis has not been done in a systematic way.

Environmental exposures to industrial chemical pollutants are thousands of times lower than some occupational exposures to these same agents.[3, 8] Thus, if ppb levels of these pollutants were causing cancer or birth defects, one might expect to see an effect in the workplace. So far, however, epidemological studies on these chemicals do not suggest an association with cancer.[142]

Historically, for chemicals that have been shown to increase cancer in the workplace, exposures were at high levels. For example, in California the levels of the fumigant ethylene dibromide (EDB) that workers were allowed to breathe in were once shockingly high.[3] We testified in 1981 that our calculations showed that the workers were allowed to breathe in a dose higher than the dose that gave half of the test rats cancer. California lowered the permissible worker exposure more than a hundredfold. Despite the fact that the epidemiology on EDB in highly exposed workers does not show any significant effect, the uncertainties of our knowledge make it important to have strict rules about workers, because they can be exposed chronically to extremely high doses.

7. Misconception No. 7: Trade-offs Are Not Necessary in Eliminating Pesticides

Since no plot of land is immune to attack by insects, plants need chemical defenses—either natural or synthetic—in order to survive pest attack. "It has been suggested that one consequence of crop plant domestication is the deliberate or inadvertent selection for reduced levels of secondary compounds that are distasteful or toxic. Insofar as many of these chemicals are involved in the defense of plants against their enemies, the reduction due to artificial selection in these defenses may account at least in part for the increased susceptibility of crop plants to herbivores and pathogens..."[143] Thus, there is a trade-off between natural pesticides and man-made pesticides.

Cultivated plant foods commonly contain fewer natural toxins than do their wild counterparts. For example, the wild potato, the progenitor of cultivated strains of potato, has a glycoalkaloid content about three times that of cultivated strains and is more toxic.[144, 145] The leaves of the wild cabbage (the progenitor of cabbage, broccoli, and cauliflower) contain about twice as many glucosinolates as cultivated cabbage.[146] The wild bean contains about three times as many cyanogenic glucosides as does the cultivated bean.[147] Similar reductions in toxicity through agriculture have been reported in lettuce, lima bean, mango, and cassava.[65]

One consequence of disproportionate concern about synthetic pesticide residues is that some plant breeders are currently developing plants that are more insect-resistant and, thus, higher in natural toxins. Two recent cases illustrate the potential hazards of this approach to pest control. (1) When a major grower introduced a new variety of highly insect-resistant celery into commerce, a flurry of complaints were made to the Centers for Disease Control from all over the country, because people who handled the celery developed rashes when they were subsequently exposed to sunlight. Some detective work found that the pest-resistant celery contained 6200 ppb of carcinogenic (and mutagenic) psoralens instead of the 800 ppb present in normal celery (Table 2).[64, 103, 148, 149] It is not known whether other natural pesticides in the celery were increased as well. The celery is still on the market. (2) A new potato, developed at a cost of millions of dollars, had to be withdrawn from the market because of its acute toxicity to humans when grown under particular soil conditions—a consequence of higher levels of the natural toxins solanine and chaconine. Solanine and chaconine inhibit cholinesterase, thereby blocking nerve transmission, and are known rodent teratogens. They were widely introduced into the world diet about 400 years ago with the dissemination of the potato from the Andes. Total toxins are present in normal potatoes at a level of 15 mg per 200-g potato (75 ppm), which is less than a tenfold safety margin from the measurably toxic daily dose level for humans.[144] Neither solanine nor chaconine has been tested for carcinogenicity. In contrast, the cholinesterase inhibitor malathion, the main synthetic organophosphate pesticide residue in our diet (0.006 mg per day), has been tested and is not a carcinogen in rats or mice. Common cultivars of plants differ widely in the level of particular natural toxins (Table 2),[103] and other factors in the plant also play a part in pest resistance. Breeding or genetic engineering can be used to increase or decrease specific chemicals or other factors.

Certain cultivated crops have become popular in developing countries because they thrive without costly synthetic pesticides. However, the trade-offs of cultivating some of these naturally pest-resistant crops are that they are highly toxic and require extensive processing to detoxify them. For example, cassava root, a major food crop in Africa and South America, is quite resistant to pests and disease; however, it contains cyanide at such high levels that only a laborious process of washing, grinding, fermenting, and heating can make it edible; ataxia due to chronic cyanide poisoning is endemic in many of the cassava-eating areas of Africa.[150] In one part of India, the pest-resistant grain *Lathyrus sativus* is cultivated to make some types of dahli. Its seeds contain the neurotoxin β-*N*-oxalylaminoalanine, which causes a crippling nervous system disorder, neurolathyrism.[151]

As an alternative to synthetic pesticides, it is legal for "organic farmers" to use the natural pesticides from one plant species against pests that attack a different plant species: for example, rotenone (which Indians used to poison fish) or the pyrethrins from chrysanthemum plants. These naturally derived pesticides have not been tested as extensively for carcinogenicity (rotenone is negative, however), mutagenicity, or teratogenicity as have synthetic pesticides; therefore, their safety compared to synthetically derived pesticides should not be prematurely assumed.

There is a tendency for nonscientists to think of *chemicals* as being only synthetic and to characterize synthetic chemicals as toxic, as if every natural chemical were not also toxic at some dose. Even a recent National Research Council report[152] states: "Advances in classical plant breeding ... offer some promise for nonchemical pest control in the future. Nonchemical approaches will be encouraged by tolerance revocations. ..." The report was concerned with pesticide residues in tomatoes, but ignored the natural pesticides in tomatoes. Tomatine, one of the natural toxins in tomatoes, is a recent chemical, too, since it was introduced to the world diet from Peru 400 years ago. Neither tomatine nor its aglycone, tomatidine, an antifungal steroidlike molecule, has been tested in rodent cancer bioassays. Tomatine is present at 36 mg per 100-g tomato (360 ppm), a concentration that is much closer to the acutely toxic level in humans than are the concentrations of man-made pesticide residues.[144]

Efforts to prevent hypothetical carcinogenic risks of 1 in a million could be counterproductive if the risks of the alternatives are worse. For example, Alar was withdrawn from the market after the EPA proposed cancellation hearings on it and after the Natural Resources Defense Council (NRDC) went to the media to get the process accelerated.[93] However, we incur various risks by withdrawing Alar, and these risks should be addressed. Alar is a growth regulator that delays ripening of apples so that they do not drop prematurely, and it also delays overripening in storage. Alar plays a role in reducing pesticide use on some types of apples, particularly in the Northeast.[153] Without Alar, the danger of fruit fall from the pests known as leafminers is greater, and more pesticides are required to control pests. When fruit falls prematurely, pests on the apples remain in the orchard to attack the crop the next summer, and more pesticides must be used. Since Alar produces healthier apples that stay on the trees, Alar-treated fruit is less susceptible to molds. Therefore, it is likely that the amounts and variety of mold toxins present in apple juice (e.g., patulin[154–157]) will be higher in juice made from untreated apples. The carcinogenicity of patulin has not been adequately examined.[158] Another trade-off of eliminating Alar is decreasing the availability of domestically grown, fresh apples throughout the year and increasing the price of apples, which might lead consumers to substitute less healthy foods.

Synthetic pesticides have markedly lowered the cost of plant food, thus promoting increased consumption. Eating more fruits and vegetables, and less fat, may be the best way to lower risks of cancer and heart disease (other than giving up smoking).

8. Misconception No. 8: Technology Is Harmful to Public Health

Modern technologies are almost always replacing older, more hazardous technologies. Billions of pounds of trichloroethylene (TCE), one of the most important nonflammable, industrial solvents, and perchloroethylene (perc), the main drycleaning solvent in the United States, are used because they are low in toxicity and are not flammable. Chlorinated solvents replaced flammable solvents in industry and in dry cleaning; this was a major advance in fire safety, with a minor trade-off of an occasional ppb contamination in water.

Eliminating a carcinogen may have unwanted effects. For example, 1,2-dibromoethane (ethylene dibromide, EDB), the main fumigant in the United States before it was banned in 1984, was present in trivial amounts (about 0.4 ppb) in our food: the average daily intake was a possible carcinogenic hazard, about one-tenth that of the aflatoxin in the average peanut butter sandwich, itself a minimal possible hazard (Table 3).[3] It is possible that the elimination of EDB fumigation will result in greater insect infestation and contamination of grain by carcinogen-producing molds. This would result in a reduction in public health, not an advance, and would greatly increase costs. Furthermore, alternative fumigants to replace EDB do not appear satisfactory and may be more hazardous and expensive.

Similarly, modern synthetic pesticides replaced more hazardous substances, such as lead arsenate, one of the major pesticides before the modern era. Lead and arsenic are both natural, highly toxic, and carcinogenic. Pesticides have increased crop yields and have brought down the price of foods, a major public health advance. Each new generation of synthetic pesticides is more environmentally and toxicologically benign.

Every living thing and every industry "pollutes" to some extent. The fact that scientists have developed methods to measure part per billion levels of chemicals and are developing methods to measure parts per trillion, makes us more aware of toxicity, but does not mean that exposure to toxins is necessarily increasing or that detected chemicals are causing human disease. Minimizing pollution is clearly desirable for other reasons, but is a separate issue from cancer prevention; getting the most pollution reduction for the lowest economic cost is, of course, important.[159]

Focusing on minor rather than major health risks is counterproductive. If we divert too much of our attention to traces of pollution as a public health concern we do not improve public health—and, in the confusion, the important hazards may be neglected: for example, smoking (400 000 deaths per year), alcohol (100 000 deaths per year), eating unbalanced diets) such as too much saturated fat and cholesterol and too few fruits and vegetables), AIDS, radioactive radon released from the soil into homes, and high-dose occupational exposures to chemicals.

It is the inexorable progress of modern technology and scientific research that is likely to lead to a decrease in cancer death rates, a decrease in the incidence of birth defects, and an increase in the average human life span.

This work was supported by the National Cancer Institute (Outstanding Investigator Grant CA39910), by the National Institute of Environmental Health Sciences Center (Grant ES01896), and by the U.S. Environmental Protection Agency (Grant No. DE-AC03-76SF00098). This article has been partially adapted from Refs. [3, 36, 62] and the following references: B. N. Ames, "What Are the Major Carcinogens in the Etiology of Human Cancer? Environmental Pollution, Natural Carcinogens, and the Causes of Human Cancer: Six Errors" (in V. T. De Vita, Jr., S. Hellman, S. A. Rosenberg (Eds.): Important Advances in Oncology 1989, Lippincott, Philadelphia 1989, pp. 237–247); B. N. Ames, L. S. Gold: "Dietary Carcinogens, Environmental Pollution, and Cancer: Some Misconceptions" (Med. Oncol. Tumor Pharmacother. 7 (1990) 69–85).

Received: August 9, 1990 [A 794 IE]
German version: *Angew. Chem. 102* (1990) 1233

[1] National Cancer Institute: *1987 Annu. Cancer Statistics Rev. Including Cancer Trends 1950–1985*, NIH Publ. No. 88-2789, National Institutes of Health, Bethesda, MD, USA 1988.
[2] R. Doll, R. Peto: *The Causes of Cancer*, Oxford Univ. Press, Oxford 1981.
[3] B. N. Ames, R. Magaw, L. S. Gold, *Science (Washington D.C.) 236* (1987) 271–280.
[4] B. N. Ames, R. Magaw, L. S. Gold, *Science (Washington D.C.) 237* (1987) 235.
[5] B. N. Ames, R. Magaw, L. S. Gold, *Science (Washington D.C.) 237* (1987) 1283–1284.
[6] B. N. Ames, R. Magaw, L. S. Gold, *Science (Washington D.C.) 237* (1987) 1399–1400.
[7] B. N. Ames, L. S. Gold, *Science (Washington D.C.) 238* (1987) 1634.
[8] L. S. Gold, G. M. Backman, N. K. Hooper, R. Peto, *Environ. Health Perspect. 76* (1987) 211–219.
[9] B. N. Ames, L. S. Gold, *Science (Washington D.C.) 240* (1988) 1045–1047.
[10] J. Higginson, *Cancer Res. 48* (1988) 1381–1389.
[11] B. E. Henderson, R. Ross, L. Bernstein, *Cancer Res. 48* (1988) 246–253.
[12] M. Lipkin, *Cancer Res. 48* (1988) 235–245.
[13] R. Peto in A. D. Woodhead, C. J. Shellabarger, V. Pond, A. Hollaender (Eds.): *Assessment of Risk from Low-Level Exposure to Radiation and Chemicals*, Plenum, New York 1985, pp. 3–16.
[14] C. S. Yang, H. L. Newmark, *CRC Crit. Rev. Oncol./Hematol. 7* (1987) 267–287.
[15] B. C. Pence, F. Buddingh, *Carcinogenesis (London) 9* (1988) 187–190.
[16] R. Holliday, *Bio Essays 10* (1989) 125–127.
[17] F. Roe: *Toxicological Aspects of Food*, Elsevier, Amsterdam 1987, pp. 59–72.
[18] E. Lok, F. W. Scott, R. Mongeau, E. A. Nera, S. Malcolm, D. B. Clayson, *Cancer Lett. 51* (1990) 67–73.
[19] R. Peto, S. E. Parish, R. G. Gray in A. Likhachev, V. Anismov, R. Montesano (Eds.): *Age-Related Factors in Carcinogenesis*, IARC Sci. Publ., No. 58, Lyon 1985, pp. 43–53.
[20] B. N. Ames, *Environ. Mol. Mutagen. 14* (1989) 66–77.
[21] B. N. Ames, *Free Radical Res. Commun. 7* (1989) 121–128.
[22] R. A. Weinberg: *Oncogenes and the Molecular Origins of Cancer*, Cold Spring Harbor Lab., Cold Spring Harbor 1990.
[23] R. A. Weinberg, *Cancer Res. 49* (1989) 3713.
[24] C. G. Fraga, M. K. Shigenaga, J.-W. Park, P. Degan, B. N. Ames, *Proc. Natl. Acad. Sci. USA 87* (1990) 4533–4537.
[25] M. K. Shigenaga, C. J. Gimeno, B. N. Ames, *Proc. Natl. Acad. Sci. USA 86* (1989) 9697–9701.
[26] B. E. Butterworth, T. Smith-Oliver, L. Earle, D. J. Loury, R. D. White, D. J. Doolittle, P. K. Working, R. C. Cattley, R. Jirtle, G. Michalopoulos, S. Strom, *Cancer Res. 49* (1989) 1075–1084.
[27] C. Tong, M. Fazio, G. M. Williams, *Proc. Natl. Acad. Sci. USA 77* (1980) 7377–7389.
[28] H. C. Pitot, T. L. Goldsworthy, S. Moran, W. Kennan, H. P. Glauert, R. R. Maronpot, H. A. Campbell, *Carcinogenesis (London) 8* (1987) 1491–1499.
[29] E. Farber, *Environ. Health Perspect. 75* (1987) 65–70.
[30] B. E. Butterworth, T. Slaga (Eds.): *Chemically Induced Cell Proliferation: Implications for Risk Assessment*, Wiley, New York 1990, in press.
[31] B. N. Ames, L. S. Gold, *Proc. Natl. Acad. Sci. USA 87* (1990) 7772–7776.
[32] S. M. Cohen, L. B. Ellwein, *Science (Washington D.C.) 249* (1990) 1007–1011.
[33] H. A. Dunsford, S. Sell, F. V. Chisari, *Cancer Res. 50* (1990) 3400–3407.
[34] J. V. Joossens, J. Geboers, *Nutr. Cancer 2* (1981) 250–261.

[35] C. Furihata, Y. Sato, M. Hosaka, T. Matsushima, F. Furukawa, M. Takahashi, *Biochem. Biophys. Res. Commun. 121* (1984) 1027–1032.
[36] A. J. Tuyns, *Nutr. Cancer 11* (1988) 229–232.
[37] J.-B. Lu, Y.-M. Qin, *Int. J. Epidemiol. 16* (1987) 171–176.
[38] C. Furihata, K. Sudo, T. Matsushima, *Carcinogenesis (London) 10* (1990) 2135–2137.
[39] D. Coggon, D. J. P. Barker, R. B. Cole, M. Nelson, *JNCI J. Natl. Cancer Inst. 81* (1989) 1178–1182.
[40] G. Charnley, S. R. Tannenbaum, *Cancer Res. 45* (1985) 5608–5616.
[41] T. Karube, H. Katayama, K. Takemoto, S. Watanabe, *Jpn. J. Cancer Res. 80* (1989) 698–701.
[42] B. J. Rathbone, R. V. Heatley (Eds.): *Campylobacter pylori and gastroduodenal disease*, Blackwell, Oxford 1989.
[43] M. J. Blaser (Ed.): *Campylobacter pylori in gastritis and peptic ulcer disease*, Igaku/Shoin, New York 1989.
[44] R. Peto, H. zur Hausen (Eds.): *Banbury Rep. 21, Viral Etiology of Cervical Cancer*, Cold Spring Harbor Lab., New York 1986.
[45] J. Petruska, J. P. Marsh, E. Kagan, B. T. Mossman, *Am. Rev. Respir. Dis. 137* (1988) 403.
[46] H. L. Newmark, M. Lipkin, N. Maheshwari, *JNCI J. Natl. Cancer Inst. 82* (1990) 491–496.
[47] H. B. Demopoulos, D. D. Pietronigro, E. S. Flamm, M. L. Seligman, *J. Environ. Pathol. Toxicol. 3* (1980) 273–303.
[48] A. Templeton, *J. Environ. Pathol. Toxicol. 3* (1980) 387–397.
[49] J. G. Lewis, D. O. Adams, *Environ. Health Perspect. 76* (1987) 19–27.
[50] L. S. Gold, L. Bernstein, R. Magaw, T. H. Slone, *Environ. Health Perspect. 81* (1989) 211–219.
[51] L. S. Gold, C. B. Sawyer, R. Magaw, G. M. Backman, M. de Veciana, R. Levinson, N. K. Hooper, W. R. Havender, L. Bernstein, R. Peto, M. C. Pike, B. N. Ames, *Environ. Health Perspect. 58* (1984) 9–319.
[52] L. S. Gold, M. de Veciana, G. M. Backman, R. Magaw, P. Lopipero, M. Smith, M. Blumenthal, R. Levinson, J. Gerson, L. Bernstein, B. N. Ames, *Environ. Health Perspect. 67* (1986) 161–200.
[53] L. S. Gold, T. H. Slone, G. M. Backman, R. Magaw, M. Da Costa, P. Lopipero, M. Blumenthal, B. N. Ames, *Environ. Health Perspect. 74* (1987) 237–329.
[54] L. S. Gold, T. H. Slone, G. M. Backman, S. Eisenberg, M. Da Costa, M. Wong, N. B. Manley, L. Rohrbach, B. N. Ames, *Environ. Health Perspect. 84* (1990) 215–285.
[55] L. S. Gold, T. H. Slone, L. Bernstein, *Environ. Health Perspect. 79* (1989) 259–272.
[56] D. G. Hoel, J. K. Haseman, M. D. Hogan, J. Huff, E. E. McConnell, *Carcinogenesis (London) 9* (1988) 2045–2052.
[57] D. G. Hoel, C. J. Portier, unpublished.
[58] J. A. Swenberg, F. C. Richardson, J. A. Boucheron, F. H. Deal, S. A. Belinsky, M. Charbonneau, B. G. Short, *Environ. Health Perspect. 76* (1987) 57–63.
[59] R. Peto, R. Gray, P. Brantom, P. Grasso, *Cancer Res.* (1990), in press.
[60] R. Peto, R. Gray, P. Brantom, P. Grasso, *Cancer Res.* (1990), in press.
[61] R. Gray, R. Peto, P. Brantom, P. Grasso, *Cancer Res.* (1990), in press.
[62] B. N. Ames, M. Profet, L. S. Gold, *Proc. Natl. Acad. Sci. USA 87* (1990) 7777–7781.
[63] D. H. Janzen, *Annu. Mo. Bot. Gard. 64* (1977) 706–736.
[64] R. C. Beier in G. W. Ware (Ed.): *Reviews of Environmental Contamination and Toxicology*, Springer, New York 1990, pp. 47–137.
[65] G. A. Rosenthal, D. H. Janzen (Eds.): *Herbivores: Their Interaction With Secondary Plant Metabolites*, Academic Press, New York 1979.
[66] M. B. Green, P. A. Hedin (Eds.): *Natural Resistance of Plants to Pests: Roles of Allelochemicals (ACS Symp. Ser. 296,* (1986)).
[67] H. D. VanEtten, D. E. Matthews, P. S. Matthews, *Annu. Rev. Phytopathol. 27* (1989) 143–165.
[68] D. H. Watson (Ed.): *Natural Toxicants in Food*, VCH, Weinheim 1987.
[69] H. Maarse, C. A. Visscher (Eds.): *Volatile Compounds in Foods, Vol. I, II, III*, TNO-CIVO Food Anal. Inst., Zeist, The Netherlands 1989.
[70] J. Stofberg, F. Grundschober, *Perfum. Flavor. 12* (1987) 27.
[71] B. N. Ames, *Science (Washington D.C.) 221* (1983) 1256–1264.
[72] National Research Council: *Diet and Health, Implications for Reducing Chronic Disease Risk*, NAS, Washington D.C., USA 1989.
[73] National Research Council: *Diet, Nutrition, and Cancer*, NAS, Washington D.C., USA 1982.
[74] J. L. Schardein, B. A. Schwetz, M. F. Kenal, *Environ. Health Perspect. 61* (1985) 55.
[75] M. Ishidate, Jr., M. C. Harnois, T. Sofuni, *Mutat. Res. 195* (1988) 151–213.
[76] A. Kasamaki, T. Yasuhara, S. Urasawa, *J. Toxicol. Sci. 12* (1987) 383–396.
[77] D. B. McGregor, A. Brown, P. Cattanach, I. Edwards, D. McBride, C. Riach, W. J. Caspary, *Environ. Mol. Mutagen. 12* (1988) 85–154.
[78] K. Randerath, E. Randerath, H. P. Agrawal, R. C. Gupta, M. E. Schurdak, V. Reddy, *Environ. Health Perspect. 62* (1985) 57–65.
[79] J. D. Tucker, R. T. Taylor, M. L. Christensen, C. L. Strout, M. L. Hanna, *Mutagenesis 4* (1989) 343–348.
[80] R. J. Clarke, R. Macrae (Eds.): *Coffee, Vol. 1–3*, Elsevier, New York 1988.
[81] C. Furihata, T. Matsushima, *Annu. Rev. Nutr. 6* (1986) 67–94.
[82] T. Sugimura, *Mutat. Res. 205* (1988) 33–39.
[83] S. Takayama, Y. Nakatsuru, S. Sato, *Gann. 78* (1987) 1068–1072.
[84] B. Beije, L. Möller, *Mutat. Res. 196* (1988) 177–209.
[85] *Dietary Mutagens (Environ. Health Perspect. 67* (1986), special issue).
[86] T. Sugimura, S. Sato, H. Ohgaki, S. Takayama, M. Nagao, K. Wakabayashi in I. Knudsen (Eds.): *Genetic Toxicology of the Diet*, Liss., New York 1986, pp. 85–107.
[87] T. Sugimura, *Science (Washington D.C.) 233* (1986) 312–318.
[88] H. Ohgaki, H. Hasegawa, T. Kato, C. Negishi, S. Sato, T. Sugimura, *Cancer Lett. 26* (1985) 239.
[89] T. Kinouchi, H. Tsutsui, Y. Ohnishi, *Mutat. Res. 171* (1986) 105.
[90] E. L. Gunderson, *J. Assoc. Off. Anal. Chem. 71* (1988) 1200–1209.
[91] H. N. Nigg, R. C. Beier, O. Carter, C. Chaisson, C. Franklin, L. Lavy, R. Lewis, P. Lombardo, J. F. McCarthy, K. Maddy, M. Moses, D. Norris, C. Peck, K. Skinner, R. G. Tardiff in S. Baker, C. Wilkinson (Eds.): *Pesticides: Health Effects*, Princeton Univ. Press, Princeton, NJ, USA 1990.
[92] J. Treon, F. Dutra, F. Cleveland, *AMA Arch. Ind. Health 8* (1953) 170–184.
[93] B. N. Ames, L. S. Gold, *Science (Washington D.C.) 244* (1989) 243–244.
[94] S. W. Lagakos, B. J. Wessen, M. Zelen, *J. Am. Stat. Assoc. 81* (1986) 583.
[95] B. MacMahon, *J. Am. Stat. Assoc. 81* (1986) 597.
[96] R. L. Prentice, *J. Am. Stat. Assoc. 81* (1986) 600.
[97] S. H. Swan, J. M. Robbins, *J. Am. Stat. Assoc. 81* (1986) 604.
[98] A. S. Whittemore, *J. Am. Stat. Assoc. 81* (1986) 609.
[99] S. W. Lagakos, B. J. Wessen, M. Zelen, *J. Am. Stat. Assoc. 81* (1986) 611.
[100] A. H. Smith, C. Hopenhayn-Rich, M. Bates, H. Goeden, I. Hertz, H. Allen, R. Wood, M. Kosnett, M. Smith, unpublished.
[101] J. C. Knutson, A. Poland, *Cell 30* (1982) 225–234.
[102] A. Rannug, U. Rannug, H. S. Rosenkranz, L. Winqvist, R. Westerholm, E. Agurell, A.-K. Grafstrom, *J. Biol. Chem. 262* (1987) 15422–15427.
[103] B. N. Ames, M. Profet, L. S. Gold, *Proc. Natl. Acad. Sci. USA 87* (1990), in press.
[104] C. A. Bradfield, L. F. Bjeldanes, *J. Agric. Food Chem. 35* (1987) 46–49.
[105] C. A. Bradfield, L. F. Bjeldanes, *J. Toxicol. Environ. Health 21* (1987) 311–323.
[106] J. J. Michnovicz, H. L. Bradlow, *JNCI J. Natl. Cancer Inst. 82* (1990) 947–949.
[107] R. H. Dashwood, D. N. Arbogast, A. T. Fong, J. D. Hendricks, G. S. Bailey, *Carcinogenesis (London) 9* (1988) 427–432.
[108] G. S. Bailey, J. D. Hendricks, D. W. Shelton, J. E. Nixon, N. E. Pawlowski, *JNCI J. Natl. Cancer Inst. 78* (1987) 931–934.
[109] D. F. Birt, J. C. Pelling, P. M. Pour, M. G. Tibbels, L. Schweickert, E. Bresnick, *Carcinogenesis (London) 8* (1987) 913–917.
[110] *IARC Monographs on the Evaluation of Carcinogenic Risk of Chemicals to Humans: Overall Evaluations of Carcinogenicity, An Updating of IARC Monogr. Vol. 1–44, Suppl. 7*, IARC, Lyon, France 1988.
[111] W. B. Jakoby (Ed.): *Enzymatic Basis of Detoxification, Vol. I, II*, Academic Press, New York 1980.
[112] G. Storz, L. A. Tartaglia, B. N. Ames, *Science (Washington D.C.) 248* (1990) 189–194.
[113] B. Mannervik, U. H. Danielson, *CRC Crit. Rev. Biochem. 23* (1988) 283–337.
[114] S. Wolff, V. Afzal, J. K. Wiencke, G. Olivieri, A. Michaeli, *Int. J. Radiat. Biol. Relat. Stud. Phys. Chem. Med. 53* (1988) 39–48.
[115] R. S. Yalow in M. E. Burns (Ed.): *Low-Level Radioactive Waste Regulation: Science, Politics, and Fear*, Lewis, Chelsea 1988, pp. 239–259.
[116] S. Wolff, G. Olivieri, V. Afzal in A. T. Natarajan, G. Obe (Eds.): *Chromosomal Aberrations: Basic and Applied Aspects*, Springer, New York 1989.
[117] L. Cai, S. Liu, *Int. J. Radiat. Biol. Relat. Stud. Phys. Chem. Med. (1989)*, in press.
[118] S. Wolff, J. K. Wiencke, V. Afzal, J. Youngblom, F. Cortés, K. F. Baverstock, J. W. Stather (Eds.): *Low Dose Radiation: Biological Bases of Risk Assessment*, Taylor & Francis, London 1989.
[119] W. D. Klohs, R. W. Steinkampf, *Cancer Res. 48* (1988) 3025–3030.
[120] I. Hirono (Ed.): *Naturally Occurring Carcinogens of Plant Origin: Toxicology, Pathology and Biochemistry, Bioactive Molecules, Vol. 2*, Elsevier, Amsterdam 1987.
[121] T. Hirayama, Y. Ito, *Prev. Med. 10* (1981) 614–622.
[122] E. Hecker, *J. Cancer Res. Clin. Oncol. 99* (1981) 103–124.
[123] G. R. Fenwick, R. K. Heaney, W. J. Mullin, *CRC Crit. Rev. Food Sci. Nutr. 18* (1983) 123–201.
[124] R. McDanell, A. E. M. McLean, A. B. Hanley, G. R. Fenwick, *Food Chem. Toxicol. 26* (1988) 59–70.
[125] R. C. Beier, J. O. Norman in W. C. Keller, V. R. Beasley, J. F. Robens (Eds.): *Public Health Significance of Natural Food Toxicants in Animal Feeds, Veterinary and Human Toxicology*, in press.
[126] W. W. Kilgore, D. G. Crosby, A. L. Craigmill, N. K. Poppen, *Calif. Agric. 35* (1981) 6.
[127] D. G. Crosby, *Chem. Eng. News 61* (1983) No. 15, p. 37.

[128] C. D. Warren, *Chem. Eng. News 61* (1983) No. 24, p. 88.
[129] L. W. Wattenberg, *Proc. Nutr. Soc.*, in press.
[130] Y. Kuroda, D. M. Shankel, M. D. Waters (Eds.): *Antimutagenesis and Anticarcinogenesis Mechanisms II*, Plenum, New York 1990.
[131] J. A. Matthew, M. R. A. Morgan, R. McNerney, H. W.-S. Chan, D. T. Coxon, *Food Chem. Toxicol. 21* (1983) 637–640.
[132] M. H. Harvey, B. A. Morris, M. McMillan, V. Marks, *Hum. Toxicol. 4* (1985) 503–512.
[133] W. D. B. Claringbold, J. D. Few, J. H. Renwick, *Xenobiotica 12* (1982) 293–302.
[134] T. H. Jukes, *Naturwissenschaften 61* (1974) 6–16.
[135] T. A. Miller, V. L. Salgado in J. P. Leahey (Ed.): *The Pyrethroid Insecticides*, Taylor & Francis, London 1985, pp. 43–97.
[136] H. Sies, *Nature (London) 332* (1988) 495.
[137] G. D. Lathrop, S. G. Machado, P. G. Karrison, W. D. Grubbs, W. F. Thomas, W. H. Wolfe, J. E. Michalek, J. C. Miner, M. R. Peterson, R. W. Ogerskok: *Air Force Health Study: Epidemiologic Investigation of Health Effects in Air Force Personnel Following Exposure to Herbicides. First Follow-Up Examination Results*, U.S. Air Force, Brooks Air Force Base, TX, USA 1987.
[138] M. Gough: *Dioxin, Agent Orange: The Facts*, Plenum, New York 1986.
[139] D. F. Austin, V. Nelson, B. Swain, L. Johnson, S. Lum, P. Flessel: *Epidemiological Study of the Incidence of Cancer as Related to Industrial Emissions in Contra Costa County, CA*, NTIS Publ. No. PB84-199785, Washington, D.C., USA 1984.
[140] A. H. Smith, K. Waller: *Air Pollution and Cancer Incidence in Contra Costa County: Review and Recommendations*, Contra Costa County Dep. Health Serv., CA, USA 1985.
[141] Epidemiological Studies and Services Section: *Pregnancy Outcome in Santa Clara County, 1980–1985*, Calif. Dep. Health Serv., Berkeley, CA, USA 1988.
[142] *IARC Monographs on the Evaluation of Carcinogenic Risk of Chemicals to Humans: Overall Evaluations of Carcinogenicity, An Updating of IARC Monogr., Vol. 1–42, Suppl. 7*, IARC, Lyon, France, 1987.
[143] M. R. Berenbaum, A. R. Zangerl, J. K. Nitao, *Phytochemistry 23* (1984) 1809–1810.
[144] S. J. Jadhav, R. P. Sharma, D. K. Salunkhe, *CRC Crit. Rev. Toxicol. 9* (1981) 21–104.
[145] P. E. Schmiediche, J. G. Hawkes, C. M. Ochoa, *Euphytica 29* (1980) 685–704.
[146] R. F. Mithen, B. G. Lewis, R. K. Heaney, G. R. Fenwick, *Phytochemistry 26* (1987) 1969–1973.
[147] B. Lucas, A. Sotelo, *Nutr. Rep. Int. 29* (1984) 711–719.
[148] S. F. Berkley, A. W. Hightower, R. C. Beier, D. W. Fleming, C. D. Brokopp, G. W. Ivie, C. V. Broome, *Ann. Intern. Med. 105* (1986) 351–355.
[149] P. J. Seligman, C. G. T. Mathias, M. A. O'Malley, R. C. Beier, L. J. Fehrs, W. S. Serrill, W. E. Halperin, *Arch. Dermatol. 123* (1987) 1478–1482.
[150] R. Cooke, J. Cock, *New Sci. 122* (1989) 63–68.
[151] K. S. Jayaraman, *Nature (London) 339* (1989) 495.
[152] National Research Council Board on Agriculture: *Regulating Pesticides in Food*, NAS, Washington, D.C., USA 1987.
[153] R. J. Prokopy: *Fruit Notes 53*, Univ. Mass. Coop. Ext., Amherst 1988, p. 7.
[154] C. F. Jelinek, A. E. Pohland, G. E. Wood, *J. Assoc. Off. Anal. Chem. 72* (1989) 225.
[155] D. M. Wilson in J. V. Rodricks (Ed.): *Mycotoxins and Other Fungal Related Food Problems*, ACS, Washington, D.C., USA 1976, pp. 90–109.
[156] G. M. Ware, C. W. Thorpe, A. E. Pohland, *J. Assoc. Off. Anal. Chem. 57* (1974) 1111.
[157] J. L. Wheeler, M. A. Harrison, P. E. Koehler, *J. Food Sci. 52* (1987) 479.
[158] *IARC Monographs on the Evaluation of the Carcinogenic Risk of Chemicals to Humans: Some Naturally Occurring and Synthetic Food Components, Furocoumarins and Ultraviolet Radiation, Vol. 40*, IARC, Lyon, France, 1986, pp. 83–98.
[159] A. S. Blinder: *Hard Heads, Soft Hearts*, Addison-Wesley, Reading, MA, USA 1987.
[160] H. F. Stich, M. P. Rosin, C. H. Wu, W. D. Powrie, *Mutat. Res. 90* (1981) 201–212.
[161] R. R. Ariza, G. Dorado, M. Barbancho, C. Pueyo, *Mutat. Res. 201* (1988) 89–96.
[162] V. A. Fung, T. P. Cameron, T. J. Hughes, P. E. Kirby, V. C. Dunkel, *Mutat. Res. 204* (1988) 219–228.
[163] A. F. Hanham, B. P. Dunn, H. F. Stich, *Mutat. Res. 116* (1983) 333–339.
[164] *Carcinogenesis Bioassay of Allyl Isothiocyanate (CAS No. 57-06-7) in F344/N Rats and B6C3F$_1$ Mice (Gavage Study), Natl. Toxicol. Program Tech. Rep. Ser. 234*, NIH Publ. No. 83-1790, Research Triangle Park, N.C., USA 1982.
[165] J. E. Huff, S. L. Eustis, J. K. Haseman, *Cancer Metastasis Rev. 8* (1989) 1–21.
[166] M. A. Morse, C.-X. Wang, S. G. Amin, S. S. Hecht, F.-L. Chung, *Carcinogenesis (London) 9* (1988) 1891–1895.
[167] *Draft Technical Report: Toxicology and Carcinogenesis Studies of d-Carvone in B6C3F$_1$ Mice and Toxicology Studies in F344/N Rats, Natl. Toxicol. Program Tech. Rep. Ser. 381*, NIH Publ. No. 90-2836, Research Triangle Park, N.C., USA 1989.
[168] K. Wakabayashi, M. Suzuki, T. Sugimura, M. Nagao, *Proc. 48th Annu. Meet. Jpn. Cancer Assoc.* (Nagoya, October 1989), Abstr. No. 284.
[169] N. Ito, M. Hirose, *Gann. 78* (1987) 1011–1026.
[170] M. Hirose, S. Fukushima, T. Shirai, R. Hasegawa, T. Kato, H. Tanaka, E. Asakawa, N. Ito, *Gann. 81* (1990) 207–212.
[171] C. H. VanEtten, H. L. Tookey in G. A. Rosenthal, D. H. Janzen (Eds.): *Herbivores: Their Interaction with Secondary Plant Metabolites*, Academic Press, New York 1979, pp. 471–500.
[172] K. Nishie, M. E. Daxenbichler, *Food Cosmet. Toxicol. 18* (1980) 159–172.
[173] K. Nishie, M. E. Daxenbichler, *Food Chem. Toxicol. 20* (1982) 279–280.
[174] I. M. Villasenor, C. Y. Lim-Sylianco, F. Dayrit, *Mutat. Res. 224* (1989) 209–212.

What Will Chemistry Do in the Next Twenty Years?

By George Whitesides*

The path of chemistry in the future will be determined both by its participation in solving large-scale societal problems and by its generation of new ideas through basic research. This article sketches four of the areas of societal "pull" in which chemistry will play a role in solving applied problems—national security, health care, the environment, and energy—and four areas in which basic research will be especially fruitful—materials chemistry, biological chemistry, computational chemistry, and chemistry exploring the limits of size and speed in chemical phenomena.

1. Introduction

Chemistry advances on two feet: one is utility, one curiosity. A prediction of its future path can only be a guess, based on its past progress and its present position. The *most* interesting and important directions to come—those that represent radical departures from the present—I cannot predict. What I *can* identify are societal concerns that seem certain to require solutions that are (at least in part) technical, and scientific ideas that seem equally certain to drive basic research for at least some time. What are these societal problems and scientific ideas?

I propose to organize this discussion in terms of the "pull" of societal concerns and the "push" of science and technology. I suggest four topics in each category (Table 1). A fifth topic under "pull"—globalization— is probably equally important as a determinant of societal concerns. The technical aspects of globalization (as opposed to its political or commercial aspects) are, however, largely subsumed in the other topics. I start with a discussion of the four current societal issues, not because they are more important than the four scientific themes driving basic research, but because they provide the context for discussions of applications of the basic research.

Table 1. The "pull" of societal concerns and the "push" of basic research set the direction of chemistry.

Pull	Push
National Security	*Materials Chemistry*
Economic competition as the equivalent of war	Polymers
	Surfaces and interfaces
	Functional and "smart" materials
Health Care	Materials for manufacturing
An aging population	Environmentally compatible materials
Global epidemics	
Cost containment	*Biological Chemistry*
Drugs	Molecular recognition
	Evolution and self-assembly
The Environment	Bioenergetics
Global change	
Waste management	*Computational Chemistry*
Toxicology	Increasing power
	New architectures: massively parallel machines and neural nets
Energy	
Alternatives to fossil fuels	
Electricity	*Small Basic Science*
	Exploring the limits: very small; very fast; very large
Globalization	

2. Societal Concerns That Will "Pull" Chemistry

2.1. National Security

Concern for national security is a major determinant of the allocation of resources. ("National" will, undoubtedly, be replaced by "regional" as globalization proceeds, but the concern remains the same.) National security concerns (largely meaning, in the past, military concerns) have been a major source of motivation, developmental capital, and markets for new technology. Development of nuclear power, high-octane gasoline, penicillin, computers, the jet airplane, and satellite communications, for example, all had roots in military problems.

For an interval (and perhaps permanently), we can hope that the probability of large-scale war between major powers will be small. What, if anything, will take the place of war as the ultimate expression of national and regional competition? As concerns with military technology decline, what will the consequences be for the development of new technology?

One form of competition that seems certain to intensify is economic. The future success or failure of nations—as judged by their ability to pay for essential public services for their citizens—may be based largely on their ability to compete in global markets. This competition will, I believe, emphasize an ability to produce and sell products with very high quality and acceptable cost for consumer markets. Chemistry will certainly play a key role in manufacturing and economic competitiveness, because it supplies key materials to virtually all manufacturing sectors of the economy.[1] Further, as the manufacturing process becomes more highly integrated—with, for example, designers of plastic automobile body parts ultimately specifying the detailed molecular weight distribution of the polymers from which these parts are made, to ensure the quality and reproducibility of their injection-molding processes—chemistry will necessarily be more heavily involved in materials, design, and manufacturing issues. *Simply making chemical compounds will not suffice for economic success.*

The shift in focus of national security from national defense to economic competitiveness will probably foster a

[*] Prof. G. M. Whitesides
Department of Chemistry, Harvard University
12 Oxford Street, Cambridge, MA 02138 (USA)

shift in emphasis from very high performance materials to materials for manufacturing. At the same time, national subsidies for materials-related research will decline, and an increasing share of these research and development expenses will fall upon corporations. In effect, until or unless there are changes in national policies that will make manufacturing a government priority (unlikely, in most countries, in a world in which capitalism has emerged triumphant), the shift from military to economic defense will represent a form of privatization of national security.

One other, smaller, area of national competition (and, perhaps, cooperation) seems likely to influence the allocation of resources in technology and science—namely, "big science" projects. The motivations for these projects are complex, but a decision to pursue the manned exploration of the planets, the superconducting supercollider (SSC), or the human genome project would represent a major choice in setting national priorities in science and technology. Each of these projects has a specific molecular component, but this component can range from moderately large (for the genome project) to insignificantly small (for the SSC).

2.2. Health Care

Health care remains a central societal concern (Table 2). Four issues in health care will be important in the next years: all have implications for chemistry.

Table 2. Prevalence in USA of selected conditions [prevalence in millions]. The list of human infirmities is, depending on one's viewpoint, a sorrow or a shopping list of opportunities for biomedical research. (Adapted from *In Vivo*, January 1990; Source: Mattson Jack).

Condition	Prevalence	Condition	Prevalence
Periodontal disease	45.0	Polyps (colon/rectum)	7.0
Obesity	34.0	Diabetes sequelae	6.0
Chronic sinusitis	28.1	Insomnia	6.0
Arthritis	25.9	Cancer	4.8
Hypertension	23.7	Congestive heart failure	4.0
Osteoporosis	18.0	Ulcers	3.8
High cholesterol	17.8	Stroke	2.2
Heart conditions	16.4	Alzheimer's disease	2.0
Allergy	15.6	Emphysema	2.0
Lower back pain	15.0	Psoriasis	2.0
Depression	11.1	Benign prostatic hypertrophy	1.0
Migraine	7.7	AIDS and AIDS-related conditions (ARC)	0.7

One is an aging population. The great majority of health care costs pay for treatment of the diseases of old age—heart disease, cancer, stroke, diabetes, arthritis, and others. As the population ages, the number of individuals subject to and concerned with these diseases increases. In addition, new concerns arise—most recently, Alzheimer's disease and related neurological conditions. The importance of chemistry in developing drugs to treat these conditions, and the importance for chemistry (and for society) of forming effective interactions with biology and medicine in order to solve these medical problems, increases. The majority of drugs will continue to be chemical entities, made by chemical syntheses.

A second health-care issue is the emergence of global epidemics. Rapid, large-scale movement of people and materials between countries makes it likely that new diseases will emerge and spread rapidly: AIDS, antibiotic-resistant bacterial disease, and new strains of influenza represent current examples. There will be an increased need to respond rapidly to these epidemics with analytical and clinical tests, drugs, and vaccines.

A third health-care issue is cost. Although no one will argue that health care is not an essential component of a high standard of living, many will argue that even now health care costs too much. There will be intense pressure from both government and insurers, and as a result of competition among companies, to decrease the cost of developing and producing new drugs. The fact that many of these costs are mandated by regulatory requirements will not decrease these pressures and will, in fact, provide competitive advantage to the companies able to meet them. To meet these challenges will require the fusion of chemical and biological sciences to improve all phases of the process of drug development: screening, targeted drug design, optimization, demonstration of safety and efficacity, manufacturing, formulation, and distribution.

A fourth issue related to health care is drug abuse. The direct impact of drug use on the standard of living, especially in large cities, is large and increasing. The indirect impact—through spread of disease, damage to children born to women using drugs, loss of individuals from the work force—is perhaps even larger. Curiously, chemistry has, so far, played a relatively modest part in dealing with drug abuse: it has contributed primarily through development of clinical assays and a small number of drugs used in treating addiction. As neuropharmacology advances, chemistry may have a more active role in this area.

2.3. The Environment

The environment promises to be a major societal concern for many years (Table 3). It is based simultaneously on heartfelt popular concern and interest, inadequate scientific evidence, and exceptionally difficult matters of public policy requiring international cooperation and agreement.[2, 3] Both analysis of the problem and the technical component of its solution will require essential contributions from chemistry and active cooperation between chemistry and other fields.

Global warming is of intense current interest and will remain so until the implications of large-scale climatic change caused by human activities—especially combustion of fossil fuels and farming—have been resolved (Fig. 1). If, in fact, it is possible to establish that human activities are responsible for global warming and that this warming is undesirable, it may then be possible (or necessary) to ameliorate the climatic change by modifying these activities or by supplying corrective solutions. The role of chemistry in these activities will be crucial. The analytical methods necessary to establish the stable and reactive chemical entities in oceans and atmospheres are still incomplete; understanding the kinetics of the reactions of these chemical entities is a necessary part of global modeling; development of alternative methods of

Table 3. Public concern with environmental problems corresponds only approximately to the seriousness of these problems, as characterized by the US Environmental Protection Agency (EPA). (From L. Roberts, *Science (Washington, D.C.) 249* (1990) 616.)

EPA's top environmental problems (not in rank order)	Public concerns (in rank order)
Ecological risks	1. Active hazardous waste sites (67%)
Global climate change	2. Abandoned hazardous waste sites (65%)
Stratospheric ozone depletion	3. Water pollution from industrial wastes (63%)
Habitat alteration	4. Occupational exposure to toxic chemicals (63%)
Species extinction and biodiversity loss	5. Oil spills (60%)
	6. Destruction of the ozone layer (60%)
Health risks	7. Nuclear power plant accidents (60%)
Criteria air pollutants (e.g., smog, O_3, SO_2, NO_x)	8. Industrial accidents releasing pollutants (58%)
	9. Radiation from radioactive wastes (58%)
Toxic air pollutants (e.g., benzene)	10. Air pollution from factories (56%)
Radon	11. Leaking underground storage tanks (55%)
Indoor air pollution	12. Coastal water contamination (54%)
Drinking water contamination	13. Solid waste and litter (53%)
Occupational exposure to chemicals	14. Pesticide risks to farm workers (52%)
Application of pesticides	15. Water pollution from agricultural runoff (51%)
Stratospheric ozone depletion	16. Water pollution from sewage plants (50%)
	17. Air pollution from vehicles (50%)
	18. Pesticide residues in foods (49%)
	19. Greenhouse effect (48%)
	20. Drinking water contamination (46%)
	21. Destruction of wetlands (42%)
	22. Acid rain (40%)
	23. Water pollution from city runoff (35%)
	24. Nonhazardous waste sites (31%)
	25. Biotechnology (30%)
	26. Indoor air pollution (22%)
	27. Radiation from X-rays (21%)
	28. Radon in homes (17%)
	29. Radiation from microwave ovens (13%)

producing energy or fuels that do not generate CO_2—electricity from nuclear-, solar-, or wind-powered generators, dihydrogen from nuclear thermal cycles—will require the development of relevant materials technologies. The biochemistry of CO_2 consumption and methane generation is incompletely understood. Dramatic large-scale ideas—promoting CO_2 fixation by marine algae by adding iron to the polar seas—would require detailed modeling. We may yet be called on to produce a chemical consumer of CO_2 that is the equivalent of the Amazonian rain forest!

The management of industrial and urban waste is a second economically and technically demanding environmental problem. Cleanup of existing waste will require innovative technology, particularly if some value is to be recovered from this waste by the separation of its components. Minimization of future industrial waste will be a key part of the development of new processes, of redesigning or replacing old ones, and of integrating production of basic starting materials with manufactured products. The cost of waste management will make "yield" an increasingly important parameter and may require the large-scale modification of catalysts and processes for the largest-volume chemicals. The minimization of the quantity, environmental impact, and unfavorable public reception of industrial waste (including byproducts of chemical production such as scrap and solvents/materials used in manufacturing, packaging, use, and disposal—that is, overall production and life-cycle waste) will increasingly determine the cost of products. Minimization of costs—especially costs of waste management—is not as exciting as generating new materials and products, but will be an essential (and probably heavily regulated) part of any business that uses chemicals or materials.

The impact of requirements for waste management will, in due course, probably also strongly influence the course of basic research. University laboratories are even less well equipped to handle the costs of disposal of chemicals and treatment of effluents than are industrial laboratories—there are no customers to whom to pass on the cost! The environmental costs of a university laboratory involved in biochemistry, for example, are intrinsically less than those of a laboratory doing exploratory synthesis in organoselenium chemistry. The difference will inevitably encourage some types of research relative to others, influence the rates at which new ideas are generated in different fields, and determine the numbers of trained professionals that are produced in these fields.

A final, constant theme in concern about the environment is understanding the toxicology of chemicals and materials, both products and waste (Fig. 2). Developing truly rational

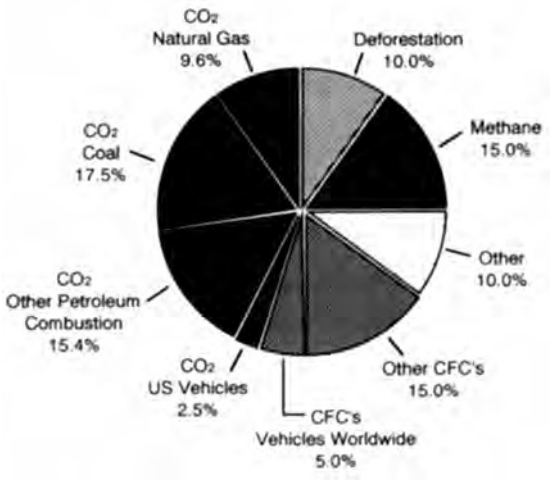

Fig. 1. Currently identified, major worldwide contributors to global warming include combustion of fossil fuels, agricultural practices, and release of chlorofluorocarbons. The contribution associated with each is uncertain.

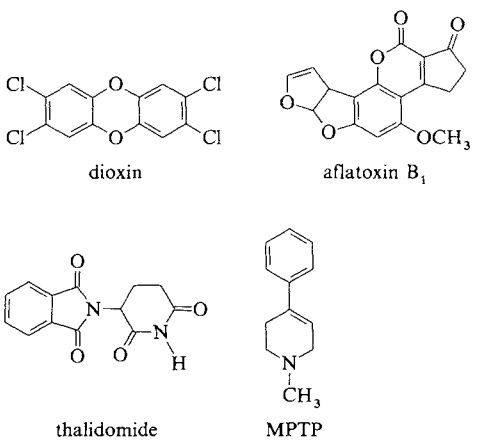

Fig. 2. The hazard associated with many prominent chemical substances (dioxin, aflatoxin, thalidomide, MPTP) was discovered only retrospectively: in most cases, this hazard could not have been predicted based on knowledge of metabolism. Accurate *prediction* of toxicity for new compounds requires much deeper understanding of metabolism and molecular biology.

bases for regulating release of chemicals into the environment or the workplace during manufacture, use, disposal, or accident may be too much to hope for, but wildly *irrational* bases for regulation are guaranteed unless we acquire a firm understanding of metabolism and toxicology of chemicals and materials and of their transformations during processing and in the environment.

2.4. Energy

The fourth major societal concern will continue to be energy. In the next 20 years the cost of energy will rise as the most readily available of the world's petroleum reserves are depleted. Whether significant new opportunities will arise for application of chemistry in enhanced oil production and exploitation of other fossil fuels, in developing technologies that promote conservation or increase fuel efficiency, or in rationally or irrationally mandated alternative fuels such as methanol and ethanol, remains to be seen.

The only technology capable of replacing fossil fuel combustion in very large-scale power generation is, of course, nuclear. If nuclear generation does reemerge as a politically acceptable source of power, the replacement of liquid hydrocarbons by electricity as an energy source for vehicles will create a myriad of opportunities in batteries and electrically functional materials (such as conductors, insulators, and dielectrics) (Fig. 3). Even if the transition from fossil-fuel-based to nuclear power is slow, regulations designed to control urban air pollution now seem certain to force the development of electric and hybrid-combustion electric automobiles. This process of regulation is most clear and most advanced in southern California. In this matter, with high probability, "As goes Los Angeles, so goes the world!"

Fig. 3. The General Motors "Impact" prototype electric vehicle. Environmental issues and a declining availability of petroleum are forcing serious consideration of electric and hybrid automobiles. These vehicles will require new materials and technologies for electrical storage and use, for lightweight, aerodynamic construction, and for safe operation.

The development of small, safe nuclear reactors might, in the longer term, make electrochemistry and high-temperature chemistry attractive for new chemical processes.

3. Four Scientific Themes That Will Push Chemistry

One reason for pursuing scientific research is to solve problems; another is to understand how nature functions. Three scientific themes in chemistry—materials chemistry, biochemistry, and computational chemistry—have captured the interest and imagination of many chemists, because these areas offer important problems in basic science, rapidly advancing analytical technology to use in addressing these problems, and opportunities for applications. Each of these three themes will remain strong for years to come.

A broad range of other areas in basic research are also being explored on smaller scale. From these many exploratory efforts, I have arbitrarily selected one representative theme that seems certain to produce important new science: research involving phenomena occurring at scales of size, time, or intensity that have historically defined the limits or boundaries of interest of chemistry—that is, phenomena occurring at scales of fractions of atomic dimensions, or faster than bond vibrations.

3.1. The Chemistry of Materials

The chemistry of materials is the first of the major scientific themes that will unite broad areas of research in the future.[4] Chemistry has moved from the study of atoms and small molecules to the study of large molecules and collections of molecules. One focus of this study is the chemistry of materials (an area of ill-defined boundaries, sharing many concerns with polymer and solid-state chemistry, condensed matter physics, and materials science and engineering). Two of the broad objectives of this area are understanding the macroscopic properties of matter based on a knowledge of its microscopic (atomic-scale) structure, and preparing new materials having new properties. Questions representing these objectives would be: "How can one predict the structure and moduli of a organic polymer knowing only the structure of its monomeric units?" and "How can one synthesize a solid that is superconducting at 400 K?" The chemistry of materials is an exceptionally broad field, and I will only touch on a few themes here.

3.1.1. Man-made Polymers

Man-made polymers have historically been the most important of the contributions of chemistry to materials science. It seems unlikely that there will be many new commodity polymers introduced in the future. A new polymer would have to provide fundamentally new properties or significantly lowered cost for existing properties to justify its introduction; neither possibility seems likely. New *processes* for existing monomers and polymers will, however, be important, to minimize byproduct streams and environmental costs and to adapt to changing raw materials. These process improvements for manufacture of large-volume chemicals (and production of hydrocarbon fuels), and development of new processes to produce specialty polymers, will continue to provide important and deeply challenging problems in catalysis.

Heterogeneous systems based on polymers—phase-separated copolymers, alloys, fiber-reinforced composites—provide a field of great interest and utility.[5] The development of fundamental understanding of all aspects of these systems is still at an early stage. Fiber-reinforced composites represent a particularly interesting example. In principle, these systems offer very attractive properties; in practice, their application has been limited by incomplete fundamental understanding of almost every aspect of their behavior: What is the atomic basis of fracture in composites? How are composite properties related to the bulk properties of the matrix, the fiber, and the matrix–fiber interface? How is energy dissipated in the solid at the molecular level? Answering these questions will require a deep understanding of the atomic/molecular behavior of solids under stress.

3.1.2. *Surfaces and Interfaces*

Surfaces and interfaces are ubiquitous in systems from microelectronic devices through heterogeneous catalysts to living tissue.[6] One trend in materials is toward the use of nanostructured materials—that is, materials having components with dimensions of 0.2–100 nm. In nanostructured materials, interfaces may be major determinants of properties and may constitute a significant fraction of the total volume of the system. The interface can be considered, in a certain sense, as a separate phase of matter. Interfaces are regions where gradients in properties can be very steep, and where structure, properties, and reactivity can be very different from those in bulk matter (Fig. 4).

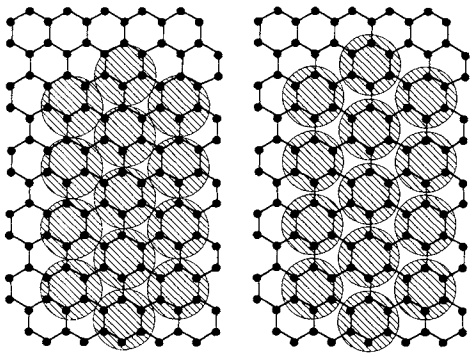

Fig. 4. Monolayers of matter can show behavior distinct from that of bulk matter. For example, krypton on graphite shows two distinct crystalline phases, one commensurate with the underlying graphite lattice, one incommensurate. (Adapted from work of R. Birgenau, *Science (Washington D.C.) 232* (1986) 329.)

New analytical techniques—from X-ray photoelectron spectroscopy (XPS) to scanning tunneling microscopy (STM)—have revolutionized the study of interfaces.[7] Synthetic techniques such as chemical vapor deposition (CVD)[8] and molecular self-assembly make possible a high level of control over the structures of interfaces. Combination of these analytical and synthetic techniques makes interfacial chemistry as tractable now as solution chemistry has been in the past.

Developing structure–property relationships for interfaces will be an extremely rewarding area of condensed matter science and invaluable in the design and applications of materials whose properties are based on phase-separated systems.

3.1.3. *Functional and "Smart" Materials*

A current challenge to materials synthesis is the design and preparation of materials with exceptional properties. Three recent examples are metal oxide high-temperature superconductors,[9] polyaniline-derived organic conductors,[10] and vapor-deposited diamond thin films.[11] The list of candidates for new ideas in design is enough to engage the creativity of those interested in the solid state for the foreseeable future: examples include "room temperature" ($T_c \approx 400$ K) superconductors, materials with very large nonlinear optical coefficients,[12] organic ferromagnets,[13] solids having negative Poisson's ratios,[14] thermally conducting organic solids, and high-temperature elastomers.

The availability of materials with unusual properties leads naturally to what promises to be a major area of materials science in the next years: namely, the development of so-called smart materials and structures—materials and structures that respond to their environment with large changes in one or several of their properties. Examples of smart materials are photochromic glasses (which change color in response to light),[15] ferromagnetic fluids (which change shape in response to magnetic field gradients),[16] and electrorheological fluids (which change viscosity in response to electric fields).[17] These materials often exhibit their interesting properties as reflections of cooperative behaviors—phase changes and aggregation—of central interest in pure chemistry. They offer the basis for new classes of devices (in the examples given, sunglasses, rotary magnetic seals, and clutches).

3.1.4. *Materials for Manufacturing*

The increased emphasis on understanding and controlling manufacturing has highlighted a broad series of problems offering both basic and applied components. For example, understanding the wetting of solids by polymers and the flow of polymers in high shear is central to understanding the manufacturing of composites, injection molding of polymers, and a host of other technologies. These areas have also provided a stimulus to try to rationalize the motion of fluids (especially polymeric fluids) near interfaces.[18] Designing packages for integrated circuits has focused attention on understanding the influence of strain on thin films and on controlling adhesion and the coefficient of thermal expansion in these systems.

Virtually every manufacturing process—molding, machining, welding, coating—contains elements of basic science that have seemed in the past too complicated and too applied to address at the level of basic science (Fig. 5). The combination of new analytical techniques, advanced computational techniques, and practical necessity now makes many of these problems tractable. In the same way that much of the basic research in biochemistry has been supported under the banner of "health care," "manufacturing" (as opposed

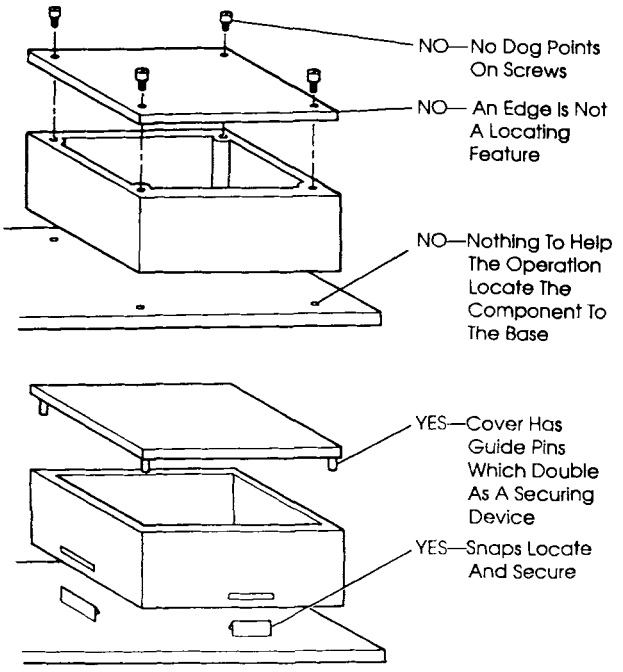

Fig. 5. Design for manufacturing (DFM) introduces complex shapes into molded parts. Successful application of DFM requires close control over materials and process variables. (Adapted with permission from a drawing by Munro and Associates, Inc.)

to "high-performance materials for defense") may provide both the justification and the focus for a broad group of neglected but very interesting problems in the chemistry of materials.

3.1.5. Environmentally Compatible Materials and Processes

The concern of society for the environment has been slow to sink into the chemical consciousness and slower still to be converted into programs leading to new classes of materials *designed* for compatibility with the environment. At least two themes have, however, emerged from this concern to receive increased (although still small) effort in materials science: materials that can be recycled[19] and materials that will biodegrade.[20] Both of these themes are, of course, well recognized, but their ultimate impact in terms of new materials and processes in not yet defined.

3.2. Biological Chemistry

The second major scientific theme dominating current basic chemistry and certain to push chemistry in the future is the study of the substances and reactions relevant to life. Biology has been the center of one of the great intellectual revolutions of the century, and its excitement will continue for many years. Reducing the broad descriptions provided by biology to molecular detail, exploiting the knowledge from these molecular descriptions in pharmacological and agricultural chemistry, and extracting new principles of organization and reaction for development in nonbiological systems are a central occupation of chemistry.

The scope and speed of development of biology and biological chemistry are so broad as to make any short description trivial, but some of the areas of opportunitiy for chemistry are already well established.

3.2.1. Molecular Recognition

A very large number of biological processes share a common event: the selective recognition of one molecule or molecular fragment by another in the very complex mixture present in the cell or organism, as well as the association of these two entities.[21] Although this sort of recognition—of an enzyme for its substrate (and perhaps transition state) or of a receptor for its ligand—is ubiquitous, understanding the basis for molecular recognition in sufficient detail to make successful predictions has proved astonishingly difficult.[22, 23] Chemistry has been very successful in dealing with systems involving single strong bonds—the covalent bond, the hydrogen bond. Biological systems seem to utilize large numbers of relatively weak interactions, occurring over large areas of molecular surface, together with poorly understood contributions from solvent, to achieve selectivity in recognition. A range of techniques—from site-specific mutagenesis through two-dimensional NMR spectroscopy and X-ray analysis to computation—is now being focused on understanding molecular recognition in biological systems. There is every reason to expect rapid progress in this area, but no reason to expect that there will be a single solution to it, or that molecular recognition will ultimately prove to be simple.

An application and extension of molecular recognition is the problem of "rational drug design".[24] The process of drug development is presently slow and expensive, with much time spent in random trial and error. In principle, it should be possible to make this process much more efficient by taking advantage of techniques from molecular biology. The proposed paradigm (much oversimplified) would have three steps: first, through studies of biology, identify a key enzyme or receptor involved in a disease; second, clone the gene for this protein, obtain substantial quantities of it, and determine its structure by X-ray crystallography; third, design and synthesize molecules that bind tightly to its active site (Fig. 6). This process would, of course, only generate tight-binding inhibitors of key target proteins and would

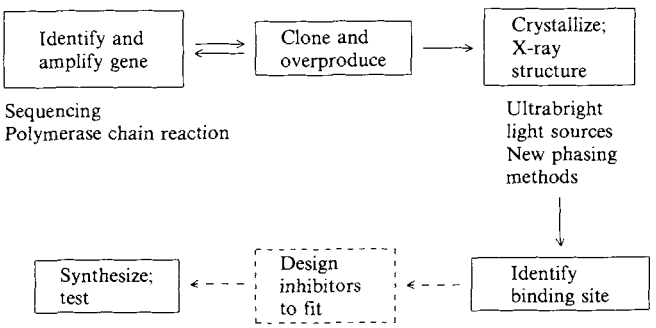

Fig. 6. All phases of the paradigm for rational design of candidate drugs work well, except for that part requiring the design of organic molecules to fit specific sites on proteins.

leave the other parts of the cycle of drug discovery—testing for safety and efficacity, manufacturing—unchanged. It would, nonetheless, shorten and simplify the overall process.

All elements of this process work well except that of designing molecules to fit an active site. This problem in molecular recognition has proved difficult, and, although certain specific systems have yielded impressive results, the difficulty and labor involved in achieving these successes have remained large.[25]

A third aspect of studies of molecular recognition that has increasingly attracted attention focuses on "biodiversity". Nature, so the teleological argument goes, achieves tight binding by randomly generating many structures (for example, polypeptides) and selects from among these, using various strategies, those having biological activity. Can chemistry use the same strategy? Can it generate compounds randomly, and efficiently select desirable activities from this random collection?

It is clear that this approach can sometimes work brilliantly, especially when chemical and biological approaches are coupled. One example is the development of catalytic monoclonal antibodies, by raising antibodies to analogues of transition states.[26] There are, so far, no purely chemical analogues to this type of process, since it is difficult to achieve the type of selection and amplification that characterizes life in nonbiological systems. The challenge of developing practical tactics for generating large numbers of compounds, and for selecting desirable activities from them is, however, being actively studied.

A final theme in molecular recognition is that of binding "simple" molecules to one another[22, 23] and to relatively ordered biological targets such as nucleic acids.[27] Starting from the discovery of crown ethers and proceeding to recognition based on hydrogen-bonding networks, it has been possible to generate satisfyingly specific interactions, often by incorporating and adapting naturally occurring recognition elements. The extension of these systems to self-replicating structures, complex self-assembled molecules, and related topics promises to offer substantial understanding of recognition, to provide guidelines for synthesizing structures based on noncovalent interactions, and to generate new reagents for biochemistry.

3.2.2. *Evolution and Self-assembly*

The origin of life and the nature of evolution are among the great questions in natural science. Early studies showed that it was possible to form simple molecules under plausible prebiotic conditions, but gave no hint of the route from these simple species to complex ones, or to living organisms.[28] Demonstrations of plausible pathways from α-amino nitriles to porphyrins and from glycolaldehyde phosphate to ribose have established a new paradigm for examining this type of problem and offer evidence that the path from simple to complex molecules may be remarkably direct.[29] These studies suggest that a broad range of processes in the early molecular stages of evolution should be reconsidered and perhaps used as the basis for new types of chemical reactions.

These studies open one new door along the corridor leading (perhaps) from an undifferentiated, primordial soup to life; they leave others still closed, or only slightly ajar. The spontaneous assembly of certain classes of molecules into assemblies or structures held together by noncovalent bonds is also central to understanding the procession from molecules to life. "Self-assembly" is clearly relevant to the formation of lipid membranes, to the folding of polypeptides into globular proteins, and to a wide variety of other processes leading to organized assemblies in biological systems.[30 - 32] Self-assembly has also stimulated interest in uncovering the rules for these systems and in using them in nonbiological or quasi-biological systems to form new types of structures (such as ordered monolayer films, liquid crystals, and liposomes).

These advances in a number of separate areas have suggested sections of a pathway from molecules to life. A key part of the path—that dealing with self-replication of the organized ensemble representing a primitive cell—still remains hidden.[33] A major step in understanding self-replicating systems might enable chemistry to begin to make serious proposals concerning the origin of life.

3.2.3. *Bioenergetics*

One of the most interesting unresolved puzzles in biological systems is that surrounding "vectorial" chemistry (Fig. 7). Energy is stored in all organisms (to some extent) in

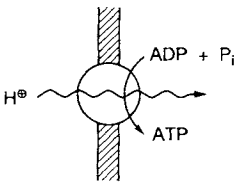

Fig. 7. In biological systems, energy is stored, in part, in concentration gradients across membranes. The discharge of a concentration gradient coupled with the formation of a chemical bond is a ubiquitous process in biology, but poorly understood at the molecular level.

the form of concentration gradients of ions across membranes.[34] Despite its enormous importance, this idea—*Mitchell*'s famous chemiosmotic hypothesis—has virtually no nonbiological model. How is the discharge of the concentration gradient coupled to the formation of ATP from ADP?[35]

The structures of the proteins involved in these vectorial processes are now emerging and will help to solve the puzzle.[36] As with molecular recognition, however, until good models that have predictive power have been developed, the puzzle of how energy is stored in and regenerated from concentration gradients across cell membranes remains unsolved.

3.3. Computation

The use of computation is the third major scientific theme that will push chemistry in the future. Computational power is one of the few items in chemistry that is rapidly becoming more available. Large-scale computation has traditionally

been the province of the "quantum mechanician". Computation (especially in semiempirical forms such as molecular mechanics,[37] molecular dynamics,[38] and large-scale simulation) is now rapidly becoming an indispensable component of experimental programs as well, particularly those concerned with complex systems. The power of computation is such that calculated results may exceed experimental results in their ability to identify trends and to distinguish contributions of individual factors. It is, for example, straightforward by simulation to "mutate" an NH group in a protein into a CH_2 group while leaving other elements of the structure unchanged, or to change the dielectric constant of water.[39, 40] Accomplishing these transformations experimentally is, obviously, more difficult (or impossible!).

Identifying some of the pending changes in the technology of computation is relatively straightforward: chemistry is, in general, a follower rather than a leader in applying computers, and one has only to look at computationally more advanced areas—electrical engineering, fluid dynamics, or computer science—to see what will be available. In addition to an ever lower "price per bit" and "price per flop", the next years will see exploration and application to chemistry of two important new architectures in computers: massively parallel machines and neural networks (Fig. 8). The former

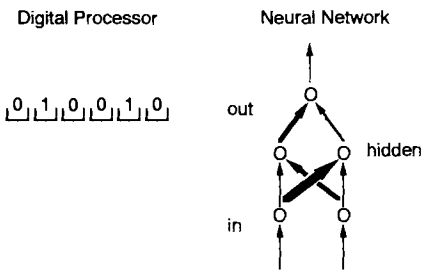

Fig. 8. The information in a digital processor (a conventional computer) is stored in bits (0 or 1) in specified locations. The information in a neural network is stored in connections of different strengths between nodes. Neural networks are particularly useful for analyzing complex nonlinear problems where high numerical precision is not required and for problems in pattern recognition. The fact that chemistry has many such problems suggests that neural networks may be useful here.

should make it possible to handle problems involving very large numbers of atoms (or other components); the latter is presently poor for problems requiring high numerical precision, but may be excellent for certain types of problems involving pattern recognition, highly nonlinear relationships, or relationships in which the functional form connecting input and output is unknown.[41, 42]

To what problems will these new methods of computation be applied? To calculations in molecular and supramolecular structure and reactivity, of course, but also to a range of problems that have historically been outside the realm of chemistry: fracture, complex coupled systems of many reactions in the atmosphere or in a cell, flow of a non-Newtonian polymer, and protein folding. The routine incorporation of large-scale computation into experimental programs has as much potential as any other technique to change the way in which chemistry is practiced.

3.4. Exploring the Limits: Very Small, Very Fast, Very Large

This fourth theme that will push chemistry is one of many that could be identified in basic research. The new capabilities and ideas emerging constantly in chemistry and in related areas of physics and biology are an astonishing testimonial to the vitality of these fields. Chemistry has begun, in certain areas, to push to the limits of what is usually defined as "chemistry". It is, for example, now possible to visualize atoms directly and to study processes occurring more rapidly than a bond vibrates. There is an enormous amount to be learned now, and in the future, by studying phenomena occurring at these boundaries of the intellectual territory named chemistry. Whether chemistry will respond to reaching these boundaries by pushing further (for example, to studies of inner-shell electrons) or whether, more probably, it will turn toward other frontiers (for example, very complex systems and the chemistry of cognition, perception, and memory[43]) remains to be seen. Some of the activities in basic research at the present limits are discussed below.

3.4.1. Very Small

The scanning tunneling microscope (STM) and its many progeny have started a revolution in the visualization of structure.[44] Subatomic-scale resolution—the limit of interest in almost all chemical problems—of nonperiodic structures is routine in many systems, although interpretation of STM images remains a challenge. STM will clearly be a key instrument for high-resolution structure determination in conducting materials; atomic force microscopy provides complementary information, including information concerning insulators.

The phrase "very small" applies to quantity as well as size. The polymerase chain reaction (PCR) has made routine the manipulation of very small numbers of copies of a gene.[45] As chemistry incorporates techniques from biology, the PCR and yet-to-be-discovered techniques for gene identification, amplification, and modification will be indispensable.

3.4.2. Very Fast

Femtosecond IR spectroscopy also reaches the practical limit of interest in chemistry.[46] The ability to follow a characteristic infrared chromophore on scales of time short compared to vibrations is clearly not a general technique, but it makes possible the analysis of bond-forming and bond-breaking processes and of energy transfer with exquisite detail (Fig. 9).

Femtosecond spectroscopy depends on the laser to generate very short pulses of light. A related application of intense photon sources is flash X-ray diffraction—using a synchrotron as a source of X-rays and an array detector to collect diffraction data, it is possible to obtain the information needed to solve the structure of a protein (in favorable cases) in very short intervals.[47]

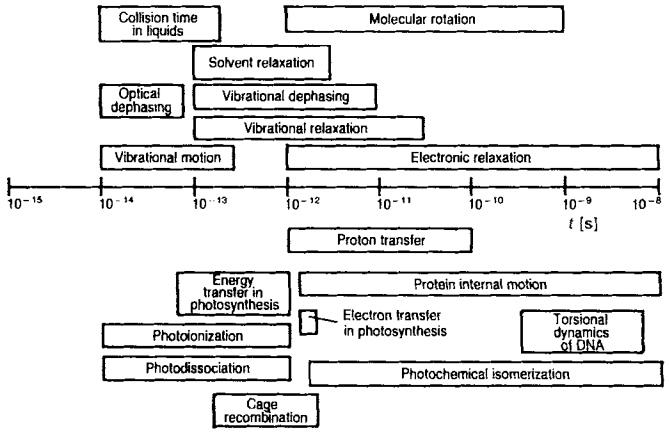

Fig. 9. Fast forms of spectroscopy have opened for investigation areas that encompass the fastest processes that concern chemistry. (From G. R. Fleming, P. G. Wolynes, *Phys. Today 43* (1990) No. 5, p. 36.)

3.4.3. Very Large

The very large electromagnetic fields generated by focused lasers make possible the ordering of particles in new ways ("light matter")[48] and even the trapping and observation of single atoms (in light traps).[49] The synthesis of isotopically pure ^{12}C diamond[50] has confirmed the theoretical prediction that this material has the largest thermal conductivity known and illustrates the coupling of theory and synthesis in materials science.

4. Conclusion

Although the subjects of interest in chemistry have changed dramatically in the last 20 years and will probably change even more in the next 20, its fundamental character remains the same. *Chemistry is the most fundamental of the sciences concerned with perceptible reality*. The affairs of nucleons and of galaxies are extraordinarily interesting, but are removed from everyday experience. Biology ultimately reduces to chemistry. Chemistry combines understanding of the molecules and processes that underlie reality as we experience it directly—from inanimate structures and fire through life—with tools to shape this reality—polymers, fuels, and drugs. It combines curiosity and utility in the direct service of man.

The details of recent changes in chemistry suggest its future. In the commercial sphere, the era of large-scale "simple" chemistry is over as an area of innovation. Discovering processes to new compounds has largely been replaced by the effort to discover sophisticated processes to existing compounds, while meeting increasingly complex boundary conditions: low cost, low capital cost, safety, environmental acceptability. Although new reactions or new catalysts always offer the opportunity to develop new processes, the emphasis has shifted to strategies for adding value to bulk chemicals—by blending or compounding them or by moving downstream to production of complex systems (coatings, multilayer films, components of composites) to meet complex needs. More carefully specified raw materials compatible with high-quality manufacturing will either be offered by chemical producers in the future or be demanded of them by users.

The chemical industry seems determined to move to materials to increase its margins and perhaps to the manufacture of engineered components. Catalysis will remain centrally important in providing economical routes to the precursors and to the final materials (Fig. 10). Although materials and components offer great opportunities, they also require a degree of sophistication in design, manufacturing, and contact with customers that is unfamiliar to many chemical companies.

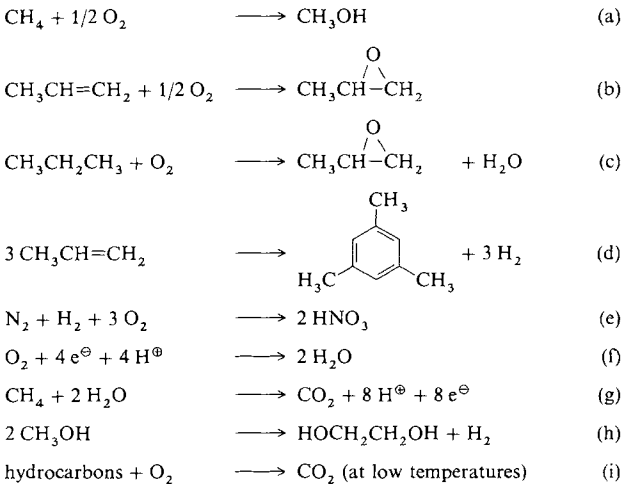

Fig. 10. Catalysis, one of the central disciplines in chemistry, offers a continuing range of challenges. All of these reactions are presently unknown or impractical, and the development of efficient reactions and catalysts to accomplish them would be useful in areas such as commodity synthesis (b, c, d, e, h), fuel transportation (a), fuel cell operation (f, g), and automobile emissions control (i).

The pharmaceutical companies expect, doubtless correctly, a stream of opportunities from biochemistry, biology, and research medicine. Organic synthesis will remain the most important technology in manufacturing drugs.

In basic science also, the focus has shifted from simple chemistry—synthesis of new organic and inorganic compounds (albeit of very great structural complexity), study of the dynamics of basic reactions—to studies of much more complex molecules, molecular ensembles, and processes. The physical-organic chemistry of 20 years ago (solvolysis of norbornyl tosylate) has become the study of factors influencing binding of oligopeptides to proteins using site-specific mutagenesis. Studies of intermolecular potentials using molecular-beam scattering has evolved into studies of two-dimensional phase separation of lipids in supported bilayers.

The problems posed by biology and by the behavior of condensed phases—solids and solutions—offer a host of opportunities for those attracted by complexity. Computers, advanced light sources, and new classes of analytical instruments capable of dealing with very small objects and very fast processes provide new tools for studying these problems. The first hints of answers to certain big questions—the origin of life, the molecular basis of memory—are beginning to appear.

What the unexpected developments will be in the next years is, of course, impossible to predict. The rate of change in chemistry and in the fields surrounding it is, however, sufficiently rapid that there is, fortunately, no doubt but that there *will* be unexpected developments. I will be lucky if the

predictions I have offered here are good for ten years; beyond that, all is conjecture.

Received: August 9, 1990 [A 795 IE]
German version: *Angew. Chem. 102* (1990) 1247

[1] Board on Chemical Science and Technology: *Opportunities in Chemistry*, National Academy Press, Washington, DC, USA 1985.
[2] F. di Castri, *La Recherche 21* (1990) 882.
[3] D. R. Hopper, *Chem. Eng. N.Y. 96* (1989) No. 8, p. 94; B. Hileman, *Chem. Eng. News 67* (1989) No. 11, p. 25. J. H. Seinfeld, *Science 243* (1989) 745; M. B. McElroy, R. J. Salawitch, *ibid. 243* (1989) 763. S. H. Schneider, *ibid. 243* (1989) 771. D. E. Gushee *CHEMTECH 19* (1989) 470.
[4] Committee on Materials Science and Engineering: *Materials Science and Engineering for the 1990s*, National Academy Press, Washington, DC, USA 1989; P. A. Psaras, H. D. Langford (Eds.): *Advancing Materials Research*, National Academy Press, Washington, DC, USA 1987.
[5] H. Ishida: *Interfaces in Polymer, Ceramic and Metal Matrix Composites*, Elsevier, New York 1988.
[6] A. Adamson: *Physical Chemistry of Interfaces*, 4th ed., Wiley-Interscience, New York 1982; J. N. Israelachvili: *Intermolecular and Surface Forces*, Academic Press, New York 1985.
[7] L. C. Feldman, J. W. Mayer: *Fundamentals of Surface and Thin Film Analysis*, North-Holland, New York 1986; D. Griggs, M. P. Seah: *Practical Surface Analysis by Auger and X-ray Photoelectron Spectroscopy*, Wiley, New York 1988.
[8] G. S. Girolami, J. E. Gozum in T. M. Besmann, B. M. Gallois (Eds.): *Chemical Vapor Deposition of Refractory Metals and Ceramics, Vol. 168*, Proc. Mater. Res. Soc., Pittsburgh, PA, USA 1990, p. 319; D. P. Stinton, T. M. Besmann, R. A. Lowden, *Am. Ceram. Soc. Bull. 67* (1988) 350.
[9] M. B. Maple, *MRS Bull. 15* (1990) 31.
[10] Polyaniline: J. M. Ginder, A. J. Epstein, A. G. MacDiarmid, *Synth. Met. 29* (1989) E 395. Polyacetylene: T. M. Swager, R. H. Grubbs, *J. Am. Chem. Soc. 111* (1989) 4413.
[11] W. A. Yarbrough, R. Messier, *Science 247* (1990) 688; J. C. Angus, F. A. Buck, M. Sunkara, T. F. Groth, C. C. Hayman, R. Gat, *MRS Bull. 14* (1989) 38; J. C. Angus, C. C. Hayman, *Science 241* (1988) 913.
[12] D. Pugh, J. N. Sherwood, *Chem. Br. 24* (1988) 544; Y. R. Shen, *Nature 337* (1989) 519.
[13] A. Izuoka, S. Murata, T. Sugawara, H. Iwamura, *J. Am. Chem. Soc. 109* (1987) 2531; W. E. Broderick, J. A. Thompson, E. P. Day, B. M. Hoffman, *Science 249* (1990) 401; J. S. Miller, A. J. Epstein, W. M. Reiff, *ibid. 240* (1988) 40; *Acc. Chem. Res. 21* (1988) 114.
[14] J. Cherfas, *Science 247* (1990) 630.
[15] K. Bange, T. Gambke, *Adv. Mater. 2* (1990) 10. G. C. Basak, *Trans. Indian Ceram. Soc. 42* (1983) 135. "Photochemical hole burning" is also of interest here: W. E. Woerner, *Top. Curr. Phys. 44* (1988); J. Friedrich, D. Haarer, *Angew. Chem. 96* (1984) 96; *Angew. Chem. Int. Ed. Engl. 23* (1984) 113.
[16] T. A. Witten, *Phys. Today 43* (1990) No. 7, p. 21; S. A. Safran, N. Clark (Eds.): *Physics of Complex and Supermolecular Fluids*, Wiley, New York 1987; K. Kendall, *Contemp. Phys. 21* (1980) 277.
[17] N. Webb, *Chem. Br. 26* (1990) 338.
[18] F. Heslot, A. M. Cazabat, P. Levinson, N. Fraysse, *Phys. Rev. Lett. 65* (1990) 599; F. Heslot, A. M. Cazabat, P. Levinson, *ibid. 62* (1989) 1286; F. Heslot, N. Fraysse, A. M. Cazabat, *Nature 338* (1989) 1289; P. G. De Gennes, *Rev. Mod. Phys. 57* (1985) 827.
[19] R. B. Seymour, *Rev. Plast. Mod. 55* (1990) 759, 765.
[20] J. D. Evans, S. K. Sikdar, *CHEMTECH 20* (1990) 38; F. Rodriguez, *ibid. 20* (1990) 409.
[21] A. Fersht: *Enzyme Structure and Mechanism*, Freeman, New York 1987; J. Darnell, H. Lodish, D. Baltimore: *Molecular Cell Biology*, Freeman, New York 1986.
[22] J. Rebek, Jr., *Angew. Chem. 102* (1990) 261; *Angew. Chem. Int. Ed. Engl. 29* (1990) 245.
[23] J.-M. Lehn, *Angew. Chem. 100* (1988) 91; *Angew. Chem. Int. Ed. Engl. 27* (1988) 89; D. J. Cram, *ibid. 100* (1988) 1041 and *27* (1988) 1009.
[24] W. G. J. Hol, *Angew. Chem. 98* (1986) 765; *Angew. Chem. Int. Ed. Engl. 25* (1986) 767; T. J. Perun, C. L. Propst (Eds.): *Computer-Aided Drug Design: Methods and Applications*, Marcel Dekker, New York 1989; N. C. Cohen, J. M. Blaney, C. Humblet, P. Gund, D. C. Barry, *J. Med. Chem. 33* (1990) 883; P. M. Dean: *Molecular Foundations of Drug-Receptor Interaction*, Cambridge University Press, Cambridge, UK, 1987.
[25] O. W. Woltersdorf, Jr., H. Schwam, J. B. Bicking, S. L. Brown, S. J. deSolms, D. R. Fishman, S. L. Graham, P. D. Gautheron, J. M. Hoffman, R. D. Larson, W. S. Lee, S. R. Michelson, C. M. Robb, N. N. Share, K. L. Shepard, A. M. Smith, R. L. Smith, J. M. Sondey, K. M. Strohmaier, M. F. Sugrue, M. P. Viader, *J. Med. Chem. 32* (1989) 2486; S. L. Graham, K. L. Shepard, P. S. Anderson, J. J. Habecker, J. M. Hoffman, P. A. Lyle, S. R. Michelson, G. S. Ponticello, C. M. Robb, H. Schwam, A. M. Smith, R. L. Smith, J. M. Sondey, K. M. Strohmaier, M. F. Sugrue, S. L. Varga, *ibid. 32* (1989) 2548; M. Sandler, H. J. Smith: *Design of Enzyme Inhibitors as Drugs*, Oxford Science Publications, Oxford 1989.
[26] P. G. Schultz, *Angew. Chem. 101* (1989) 1336; *Angew. Chem. Int. Ed. Engl. 28* (1989) 1283; S. J. Pollack, P. G. Schultz, *J. Am. Chem. Soc. 111* (1989) 129; S. J. Pollack, P. Hsiun, P. G. Schultz, *ibid. 111* (1989) 5961; A. W. Schwabacher, M. I. Weinhouse, M.-T. M. Andotor, R. A. Lerner, *ibid. 111* (1989) 2344; K. D. Janda, M. I. Weinhouse, D. M. Schloeder, R. A. Lerner, S. J. Benkovic, *ibid. 112* (1990) 1274; see also C. Tuerk, L. Gold, *Science 249* (1990) 505; L. Abelson, *ibid. 249* (1990) 488.
[27] L. C. Griffin, P. B. Dervan, *Science 245* (1989) 967; L. J. Maher, P. Wold, P. B. Dervan, *ibid. 245* (1989) 725.
[28] M. Eigen, W. Gardiner, P. Schuster, R. Winkler-Oswatitsch, *Sci. Am. 244* (1981), No. 4, p. 88; *Spektrum Wissensch. 1981*, No. 6, p. 36.
[29] G. Ksander, G. Bold, R. Lattmann, C. Lehmann, T. Fruh, Y. B. Xiang, K. Inomata, H. P. Buser, J. Schreiber, E. Zass, A. Eschenmoser, *Helv. Chim. Acta 70* (1987) 1115; S. Drenkard, J. Ferris, A. Eschenmoser, *ibid. 73* (1990) 1373; E. Wagner, Y.-B. Xiang, K. Baumann, J. Glück, A. Eschenmoser, *ibid. 73* (1990) 1391; D. Müller, S. Pitsch, A. Kittaka, E. Wagner, C. F. Wintner, A. Eschenmoser, *ibid. 73* (1990) 1410; A. Eschenmoser, *Angew. Chem. 100* (1988) 5; *Angew. Chem. Int. Ed. Engl. 27* (1988) 5.
[30] L. R. Faulkner, *Chemtracts: Anal. Phys. Chem. 1* (1989) 169; C. D. Bain, G. M. Whitesides, *Angew. Chem. Adv. Mater. 101* (1989) 522; *Angew. Chem. Int. Ed. Engl. Adv. Mater. 28* (1989) 506; *Adv. Mater. 1* (1989) 110.
[31] N. Boden, *Chem. Br. 26* (1990) 345; J. H. Fendler: *Membrane Mimetic Chemistry*, Wiley-Interscience, New York 1982.
[32] T. E. Creighton: *Proteins, Structures and Molecular Principles*, Freeman, New York 1983; P. Friedrich: *Supramolecular Enzyme Organization*, Pergamon, Oxford 1984.
[33] T. Tjivikua, P. Ballester, J. Rebek, Jr., *J. Am. Chem. Soc. 112* (1990) 1249; S. A. Strobel, P. B. Dervan, *Science 249* (1990) 73; see also G. von Kiedrowski, *Angew. Chem. 98* (1986) 932; *Angew. Chem. Int. Ed. Engl. 25* (1986) 932.
[34] W. A. Hamilton, D. F. Niven, *Biochem. Soc. Trans. 2* (1974) 797; G. D. Greville, *Curr. Top. Bioenerg. 3* (1969) 1; P. Mitchell, *Biochem. J. 116* (1970) 5P.
[35] V. P. Skulachev, P. C. Hinkle: *Chemiosmotic Proton Circuits in Biological Membranes*, Addison-Wesley, Reading, MA, USA 1981.
[36] L. J. Stern, P. L. Ahl, T. Marti, T. Mogi, M. Dunach, S. Berkowitz, K. J. Rothschild, H. G. Khorana, *Biochemistry 28* (1989) 10035; C. G. Brouillette, R. B. McMichens, L. J. Stern, H. G. Khorana, *Proteins: Struct. Funct. Genet. 5* (1989) 38.
[37] F. Mohamadi, N. G. Richards, W. C. Guida, R. Liskamp, M. Lipton, C. Caufield, G. Chang, T. Hendrickson, W. C. Still, *J. Comput. Chem. 11* (1990) 440; U. Burkert, N. L. Allinger: *Molecular Mechanics* (ACS Monogr. 177) American Chemical Society, Washington, DC, USA 1982.
[38] J. McCammon, S. C. Harvey: *Dynamics of Proteins and Nucleic Acids*, Cambridge University Press, Cambridge, UK 1987; W. F. van Gunsteren, H. J. C. Berendsen, *Angew. Chem. 102* (1990) 1020; *Angew. Chem. Int. Ed. Engl. 29* (1990) 992.
[39] P. A. Bartlett, C. K. Marlowe, *Science 235* (1987) 569.
[40] B. Jayaram, R. Fine, K. Sharp, B. Honig, *J. Phys. Chem. 93* (1989) 4320.
[41] D. E. Rumelhart, J. L. McClelland (Eds.): *Parallel Distributed Processing*, MIT Press, Cambridge, MA, USA 1986; S. F. Zornetzer, J. D. Davis, C. Lau (Eds.): *An Introduction to Neural and Electronic Networks*, Academic Press, San Diego, CA, USA 1990; T. Poggio, S. Edelman, *Nature 343* (1990) 263; C. Mead: *Analog VLSI and Neural Systems*, Addison-Wesley, Reading, MA, USA 1989.
[42] L. H. Holley, M. Karplus, *Proc. Natl. Acad. Sci. USA 86* (1989) 152.
[43] M. Barinaga, *Science 248* (1990) 1603; R. A. Zalutsky, R. A. Nicoll, *ibid. 248* (1990) 1619; D. L. Alkon, *Sci. Am. 261* (1989) No. 1, p. 42.
[44] G. Binnig, H. Rohrer, *Angew. Chem. 99* (1987) 622; *Angew. Chem. Int. Ed. Engl. 26* (1987) 606; P. K. Hansma, J. Tersoff, *J. Appl. Phys. 61* (1987) No. 21; J. A. Golovchenko, *Science 232* (1986) 48; D. Rugar, P. K. Hansma, *Phys. Today 43* (1990) 23; H. K. Wikramasinghe, *Sci. Am. 261* (1989), No. 4, p. 98; R. J. Hamers, *Annu. Rev. Phys. Chem. 40* (1990) 531; J. E. Griffith, G. P. Kochanski, *Annu. Rev. Mater. Sci. 20* (1990) 219.
[45] B. I. Eisenstein, *New Engl. J. Med. 322* (1990) 178; S. P. Watson, W. James, *Trends Pharmacol. Sci. 10* (1989) 346; K. B. Mullis, *Sci. Am. 262* (1990) No. 4, p. 56.
[46] J. H. Glownia, J. Misewich, P. P. Sorokin, *Chem. Phys. Lett. 139* (1987) 491; P. A. Anfinrud, C.-H. Han, P. A. Hansen, J. N. Moore, R. M. Hochstrasser, *Ultrafast Phenomena VI* (1988) 442; P. A. Anfinrud, C.-H. Han, R. M. Hochstrasser, *Proc. Natl. Acad. Sci. USA 86* (1989) 8387; M. Gruebele, A. H. Zewail, *Phys. Today 43* (1990) 24; G. R. Fleming, P. G. Wolynes, *ibid. 43* (1990) 36.
[47] C. T. Prewitt, P. Coppens, J. C. Phillips, L. W. Finger, *Science 238* (1987) 312.
[48] M. M. Burns, J.-M. Fournier, J. A. Golovchenko, *Phys. Rev. Lett. 63* (1989) 1233; M. M. Burns, J.-M. Fournier, J. A. Golovchenko, *Science*, in press.
[49] R. Pool, *Science 248* (1990) 1076.
[50] T. R. Anthony, W. F. Banholzer, J. F. Fleischer, L. Wei, P. K. Kuo, R. L. Thomas, R. W. Pryor, *Phys. Rev. B 42* (1990) 1104.

Elementary Steps in Heterogeneous Catalysis**

By Gerhard Ertl*

Despite the great importance of heterogeneous catalysis, research in this field has long been characterized by its empiricism. Now, however, thanks to the rapid development of methods in surface physics, the elementary steps can be identified at the atomic level and the underlying principles understood. Defined single crystal surfaces are employed as models, based on the analysis of the surfaces of 'real' catalysts. Direct images, with atomic resolution, can be obtained using scanning tunneling microscopy, while electron spectroscopic methods yield detailed information on the bonding state of adsorbed species and the influence of catalyst additives (promotors) upon them. The successful application of this approach is illustrated with reference to the elucidation of the mechanism of ammonia synthesis. The catalyst surface is usually transformed under reaction conditions, and, as the processes involved are far-removed from equilibrium, such transformations can lead to intrinsic spatial and temporal self-organization phenomena. In this case, the reaction rate may not remain constant under otherwise invariant conditions but will change periodically or exhibit chaotic behavior, with the formation of spatial patterns on the catalyst surface.

1. Introduction

The term 'catalysis,' originally coined by *Berzelius* in 1835 was itself occasionally the subject of considerable controversy up to the end of the 19th century, until *W. Ostwald* was finally able to clarify its relationship to the rate of chemical reaction. How exactly a catalyst works remains, however, something of a mystery to this day. It is for this reason that the strategy of extensive catalyst screening for technical applications, introduced by *A. Mittasch* around 1909, still finds widespread use today. Between 1909 and 1912 *Mittasch* carried out about 6500 activity determinations on around 2500 different catalysts, as part of the development of the Haber-Bosch process.[1] His endeavors met with striking success—the catalyst composition he developed is still being used industrially today, in largely unaltered form. For *Fritz Haber* the catalyst question had been solved with the discovery of the catalytic activity of osmium and uranium. It soon became evident, however, that the large-scale application of such materials was hardly a realistic proposition.

Mittasch was inspired by the idea "in the catalytic production of ammonia some kind of intermediate nitrides are formed, even if of very labile nature."[2] Following the discovery of the increased activity of mixed catalysts (promotor effect), first described in a patent dated January 9, 1910,[3] he speculated, "that the nitrogen is taken up by one component and the hydrogen by another in a labile form and activated. As a result of the intimate association of both components, the strongly reactive nitrogen then unites with the similar form of the hydrogen, thus readily forming ammonia, which is then emitted". He admitted, somewhat meekly, however, "that this is just a rough model, which in theoretical terms leaves us somewhat out on a limb."[4]

Apart from the intellectual curiosity expressed in this statement, *Mittasch* had recognized that, despite the success achieved, the situation would remain unsatisfactory in practical terms as long as a better comprehension of the fundamental atomic processes was lacking. Only such an approach would one day enable an optimal catalyst to be 'tailored' for a desired application.

Nevertheless, one should always bear in mind that, for practical purposes, not only the intrinsic chemical activity but also other properties, such as the diffusive behavior, the strength, mechanical stability etc., can be decisive factors. This further complicates the situation and ensures that for a given reaction *the* catalyst is usually a pipe dream.

Thanks to the development of powerful techniques in the area of surface physics and the accompanying theoretical advances, considerable progress has been made in the last few years towards answering the major questions concerning the characterization of the elementary processes underlying a catalytic reaction. This paper will report some aspects of the advances which have been achieved as examples.

Since industrial reactions proceed on complex catalysts and under conditions, e.g. high pressure, that rule out the direct in-situ application of most of the experimental methods mentioned, the following stepwise approach has proved both expedient and successful:

1. The surface properties, especially chemical composition and the distribution of various elements, may deviate considerably from those of the bulk. It is thus first necessary to characterize the surface, and in particular the 'active centers' of a catalyst, in as much detail as possible. The so-called 'pressure gap' mentioned before can present special difficulties, as an examination under actual reaction conditions is problematical. Simplified model systems for the structure and chemical composition are therefore enlisted, above all to permit the systematic variation of these parameters. The most convenient systems for this purpose are well-defined, single crystal surfaces. Their use naturally introduces a 'materials gap', meaning one subsequently has to check, in each case, the extent to which the properties of the 'real' catalyst agree with those of the model system.

2. The essence of the surface science approach is the study of the energetics and dynamics of the interactions between the molecules participating in the reaction and the model

[*] Prof. Dr. G. Ertl
Fritz-Haber-Institut der Max-Planck-Gesellschaft
Faradayweg 4-6, 1000 Berlin 33

[**] From a paper presented at the awarding of the A.-Mittasch Medal during a colloquium celebrating the 125th. anniversary of the founding of BASF on September 24, 1990 in Ludwigshafen (FRG).

surfaces mentioned and structures of the chemisorbed phases formed thereby. On this basis, one determines the microscopic reaction mechanism and the kinetics of the elementary steps.

3. Information on the reaction mechanism, which should be as complete as possible, enables one, in principle, to develop a kinetic scheme for calculating the steady state reaction rate as a function of external parameters, such as temperature, partial pressure, etc. When translating the results to industrial conditions, the agreement between the calculated (i.e. predicted) and experimental conversions is the yardstick for success.

Although the strategy outlined has up to now only been realized thoroughly and successfully in two instances (CO oxidation and ammonia synthesis), these have demonstrated its basic soundness. Quite apart from this, even clarification of individual aspects can provide a rich vein of important data relevant to practical applications.

2. From "Real" Catalysts to Single Crystal Surfaces

Industrial catalysts are, as a rule, very complex systems in terms of the structure and chemical composition of their surfaces. This is evident in Figure 1, which depicts a scanning

Fig. 1. Scanning electron microscope image of the surface topography of a commercial ammonia synthesis catalyst [5].

electron microscope image of the BASF ammonia synthesis catalyst S6-10.[5] The topography exhibits a labyrinth of catalyst material and pores with a diameter of typically several hundred angstroms, which is reflected in the relatively high specific area of around 15 $m^2 g^{-1}$. The source material, magnetite (Fe_3O_4), which is reduced to metallic iron during the activation process, contains low concentrations of Al_2O_3 (+ CaO) and K_2O as additives. As *Mittasch* discovered,[3] these 'promotors' make an important contribution toward raising the activity. During the course of complex solid-state chemical reactions associated with catalyst activation,[6] aluminum, in the form of its ternary oxides fabricates a kind of framework, which prevents the Fe particles from sintering together, and thus plays the role of a 'structural' promotor.

The rather inhomogeneous distribution of the various elements over the catalyst surface can be seen from Figure 2 in the series of Auger electron spectra taken at different locations. In the case of No. 1, a catalytically active site with

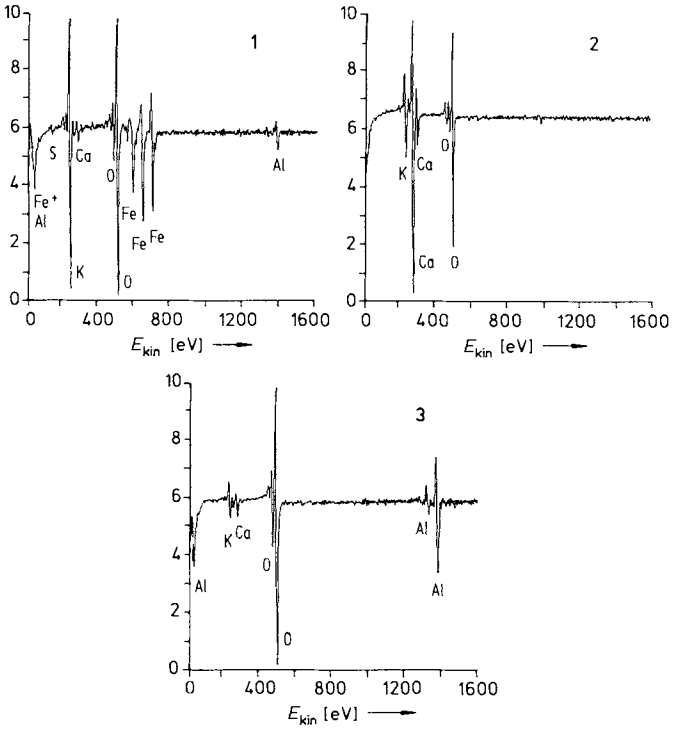

Fig. 2. Auger electron spectra from various locations on the surface of an ammonia synthesis catalyst [5]. E_{kin} = kinetic energy of the electrons.

considerable concentrations of Fe and K (+ O) is analyzed, while No. 2 largely consists of CaO, and No. 3 of Al_2O_3. The laterally resolved chemical composition of the surface is illustrated in 'Auger maps' in Figure 3. Remarkably, potassi-

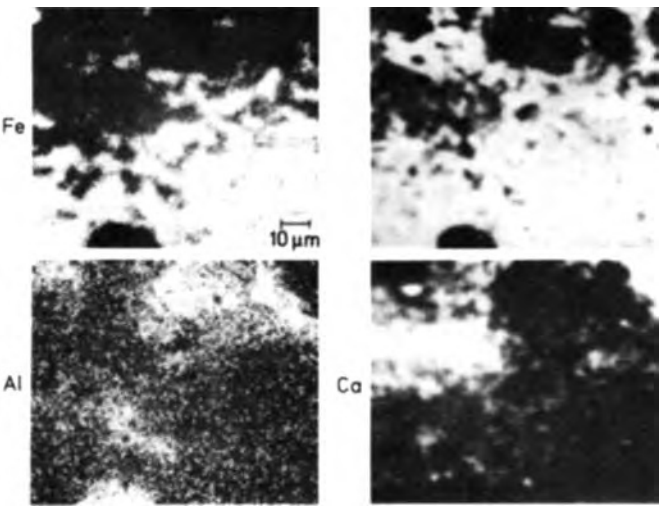

Fig. 3. 'Auger maps' showing the lateral distribution of the elements Fe, K, Al and Ca on the surface of an ammonia catalyst [5].

um is always found at locations where iron is also present. Although the total potassium concentration is only around 0.5%, its strong tendency to segregate out of the bulk leads to it covering about 30% of the metallic iron surface, where it serves as an 'electronic' promotor. More precisely, the catalytically active surface consists of metallic iron onto which a sub-monolayer amount of a two-dimensional K + O

phase (with a stoichiometry of about 1:1) is chemisorbed. This is certainly not one of the known bulk compounds of potassium, since these would be unstable under the reaction conditions.

Figure 4 depicts a high resolution transmission electron microscope (TEM) image of an activated catalyst particle, together with an electron diffraction pattern, at a selected location. The latter illustrates the single crystal character,

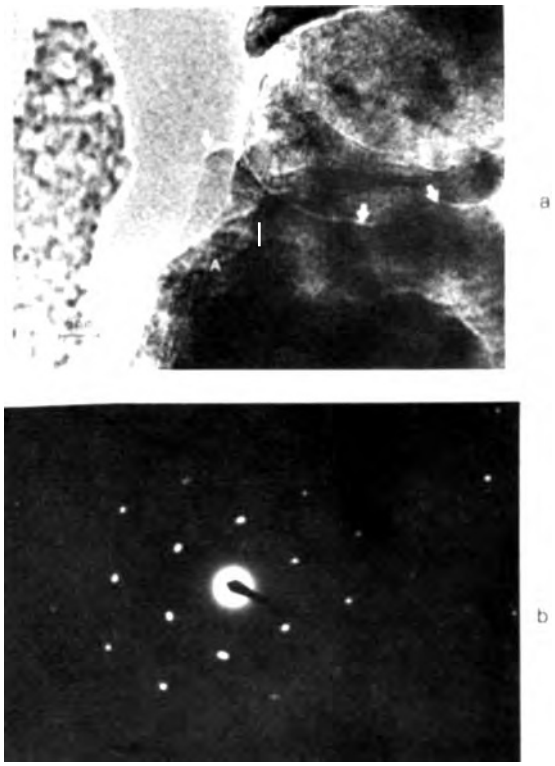

Fig. 4. a) Transmission electron microscope (TEM) image of an ammonia catalyst. Region A shows the lattice planes of a α-Fe lamella with (111) orientation. The arrows indicate the boundaries of this lamella within a stack of others having different orientations. The region on the left-hand side is amorphous carbon from the mounting support. b) Corresponding electron diffraction image, which can be identified as an iron single crystal (111) orientation [6].

which can be identified unambiguously as the (111) plane of α iron.[6] Closer inspection of the TEM image reveals the individual network layers and indicates that the catalyst primarily consists of small single crystallite particles of iron, the external surface of which, as we have previously seen, is partially covered with a K + O adsorption layer.

It therefore makes sense to use clean single crystal surfaces of iron with different orientations as a suitable model system for studying the influence of the atomic structure of the surface. The effect of electronic promotors can then be investigated via deliberate dosing with potassium.

Such samples have areas of at most 1 cm^2, so that measuring the conversion of a catalytic reaction represents a considerable experimental challenge. Despite this, *Somorjai* et al. were able to conduct such measurements successfully for a stoichiometric N_2:H_2 mixture at a pressure of 20 bar and a temperature of 500 °C.[8] They found that the activity varied between the various surface orientations by two orders of magnitude in the sequence (111) > (100) > (110), that is to say it was strongly influenced by the surface structure. However, even the Fe(111) surface exhibits only relatively low activity: the probability that a nitrogen molecule arriving at the surface will leave it as ammonia is only of the order of magnitude of one in a million.

The direct determination of chemisorbed complexes bound on the surface using the techniques of surface physics, requires, as mentioned above, a shift to much lower pressures ($\leq 10^{-3}$ mbar). Whether or not the surface species formed at high pressures remain stable under high vacuum depends on the temperature and the strength of the chemisorption bonding, and this has to be checked for each case individually. Provided one proceeds with adequate caution, however, surmounting the 'pressure gap' presents no problems in principle.

3. Elementary Processes in the Interaction between Molecules and Surfaces

Conceptually, a chemical reaction can be envisaged in its general form as the motion of a system of atoms along a 'reaction coordinate', in the course of which the energy changes in the manner shown in Figure 5. The local minima

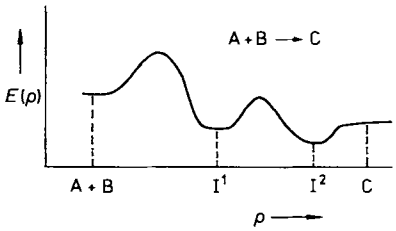

Fig. 5. Schematic diagram of the energy changes along the reaction coordinate ϱ for a chemical reaction (A + B → C). I = intermediate.

denote the nuclear configurations of intermediate compounds, while the maxima, representing the transition states, have to be overcome by summoning up the associated activation energy. Knowledge of the intermediates' properties and the rates of the respective transformations furnishes the reaction mechanism and, moreover, enables one to predict the total rate of the reaction. With the exception of the simplest gas phase reactions, a complete a priori theoretical evaluation is, however, still a long way off and one still has to rely on detailed experimental data.

The elementary processes in heterogeneously catalyzed reactions are as shown schematically in Figure 6: a molecule arriving at the surface can be bound (chemisorbed) there; the

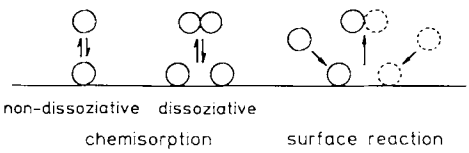

Fig. 6. Elementary processes in the interaction between molecules and a solid surface.

bonding process can be reversed and the molecule desorbed as a result of thermal activation. The surface bonding can also lead to bond rupture within the molecule (dissociative chemisorption), in which case desorption occurs via recombination of the fragments on the surface. Finally, the formation of new bonds can take place on the surface and, as a consequence of this, different molecules will then be desorbed.

It is obvious that the determination of the chemisorption complexes, together with the dynamics of their formation and transformation, is the key to understanding the elementary processes in a heterogeneously catalyzed reaction. Nowadays there is a whole variety of experimental methods available for such work.[9] These have recently been augmented in a spectacular fashion by the invention of scanning tunneling microscopy (STM) by *Binnig* and *Rohrer*.[10] Figure 7 illustrates the direct imaging of an Al(111) surface with

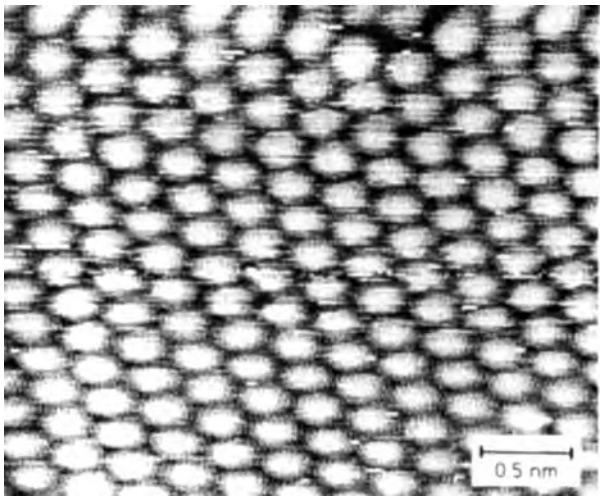

Fig. 7. Image of an Al(111) surface with atomic resolution obtained with the help of scanning tunneling microscopy [11].

atomic resolution as obtained by this technique.[11] Figure 8 shows the same surface with three chemisorbed C atoms.[12] One can see that these favor a coordination with three neighboring substrate atoms, i.e. they occupy defined adsorption sites.

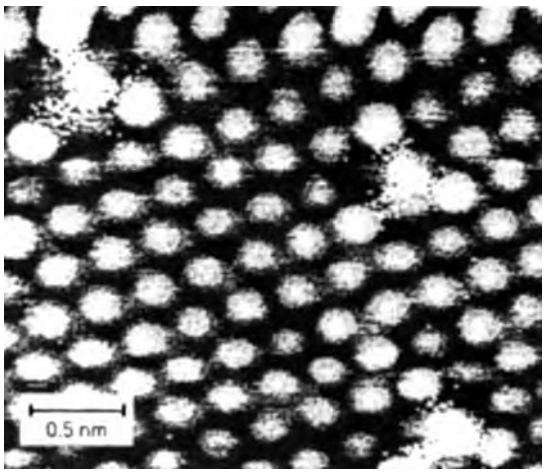

Fig. 8. Scanning tunneling microscope image of an Al(111) surface with three chemisorbed C atoms, which are discernible as diffuse light spots over a triangle of neighboring substrate atoms [12].

Generally, neighboring chemisorbed particles interact with each other, and this commonly gives rise to the formation of ordered two-dimensional phases. As an example, a sequence of STM images of a Cu(110) surface with increasing coverage of chemisorbed oxygen atoms is shown in Figure 9.[13] At low surface concentrations, small islands of a

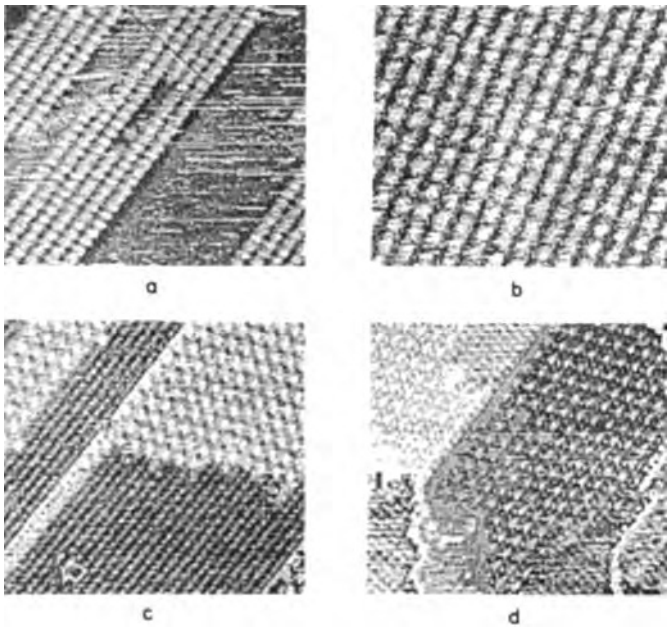

Fig. 9. Series of scanning tunneling microscope images of a Cu(110) surface with increasing O coverage [13]. a) Coverage $\theta < 1/2$: domains of a 2×1 phase together with patches of surface free from adsorbate. b) Fully developed 2×1 structure at $\theta = 1/2$. c) For $\theta > 1/2$: domains of a $c(6 \times 2)$ phase are formed in addition to the 2×1 phase (depicted as parallel streaks). d) Fully developed $c(6 \times 2)$ phase on terraces whose levels are separated by monatomic steps as differentiated by the gray scale.

2×1 phase are formed (a), which at higher concentrations cover the entire surface (b). Further increasing the degree of coverage leads to the formation of domains of an additional $c(6 \times 2)$ phase (c), rich in oxygen, which ultimately marks the saturation of the chemisorption phase (d) before the transition to three-dimensional oxide formation.

The actual structure of ordered surface phases can be determined by low-energy electron diffraction (LEED), a method which is analogous to X-ray diffraction for the determination of three-dimensional crystal structures. As an example, Figure 10 shows the structure of a 2×1 phase of chemisorbed oxygen atoms on a Ni(110) surface ascertained in this way[14] (this represents the counterpart to the previously depicted tunneling microscope image of the O-(2×1)/Cu(110) phase). The formation of chemisorption bonds has a profound influence on the substrate surface: every second row of atoms in the [001] direction is removed ('missing row' structure), that is to say the surface is reconstructed, and there is also an effect on the positions of atoms in deeper layers. Since the strength of the chemisorption bond is usually comparable to that between substrate atoms, it is entirely plausible that the most favorable overall atomic configuration may deviate considerably from that of the clean, i.e.

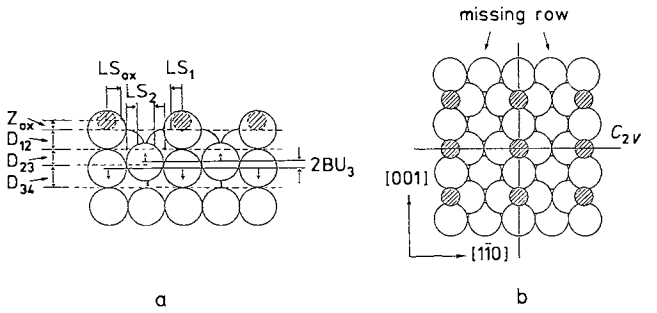

Fig. 10. Structural model of the 2×1 phase formed upon chemisorption of O atoms (shaded circles) on a Ni(110) surface [14]. Structural parameters: $Z_{ox} = 0.2$, $LS_{ox} = 0.1$, $LS_1 = 0.0$, $LS_2 = 0.0$, $D_{12} = 1.30$, $D_{23} = 1.23$, $D_{34} = 1.25$, $2BU_3 = \pm 0.05$ Å. a) Profile. b) Bird's-eye view.

adsorbate-free, surface. Conversely, there are a number of cases in which already the structure of clean surfaces deviates from the ideal bulk termination.[15]

In the above examples, the chemisorption phase was produced via the dissociative chemisorption of oxygen molecules, rather than by the action of oxygen atoms on the surface. This process is of decisive importance for catalysis, and can be rationalized with the aid of the schematic potential diagram shown in Figure 11. A molecule approaching

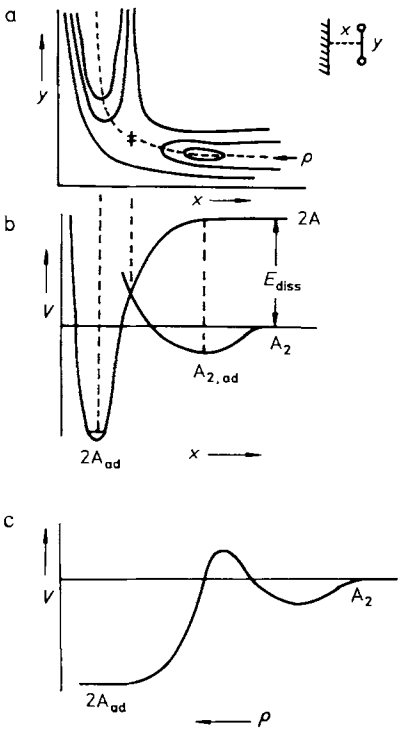

Fig. 11. Schematic potential diagram for dissociative chemisorption of a diatomic molecule A_2. a) Contour plot as a function of the distances x from surface and y between the two atoms. b) One-dimensional Lennard-Jones potential. c) Variation of potential along the reaction coordinate.

the surface experiences an initial decrease in its energy, can be weakly bound to the surface in the form of a molecular 'precursor', and will subsequently undergo dissociation when the activation barrier is surmounted. Since the formation of two bonds between the surface and the resultant two atoms more than compensates for the dissociation energy, the overall process involves a net energy gain. The course of the potential along the reaction coordinate and, in particular, the height of the activation barrier, determine the sticking coefficient, i.e. the probability that a molecule arriving at the surface will be chemisorbed dissociatively rather than bouncing back into the gas phase. Surface structure and coadsorbed particles, acting either as promotors or poisons, exert an appreciable influence at this juncture. As the rate constants of chemical reactions exhibit an exponential dependence on the activation energy, even slight energetic changes have a substantial effect on the kinetics.

4. Mechanism of Ammonia Synthesis

Let us now return to the problem of catalytic ammonia synthesis for a while. Figure 12 illustrates the increase in the surface concentration of atomically adsorbed nitrogen as a function of the nitrogen supply in the gas phase for the three low-index single-crystal surfaces of iron.[16] 1 L =

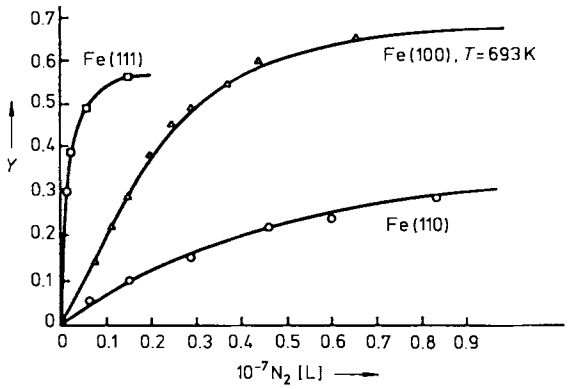

Fig. 12. Increase in surface concentration of chemisorbed N atoms (Y, in relative units) on Fe(111), (100), and (110) surfaces at 420 °C as a function of the exposure to N_2 molecules from the gas phase [16].

10^{-6} mbar s is a convenient unit for the gas exposure, because it suffices for the saturation of a surface with adsorbed particles if the sticking coefficient equals unity. Two features can be recognized from Figure 12: 1) the rate of dissociative nitrogen chemisorption depends strongly on the surface structure according to the sequence (111) > (100) > (110); 2) since typically not 1 L but $> 10^6$ L N_2 are necessary to achieve saturation, the sticking coefficient must be very low, i.e. of the order of 10^{-6}. Both findings are in full agreement with the results mentioned above concerning the catalytic activity of iron single crystal surfaces in ammonia formation, and demonstrate that the rate of ammonia synthesis is limited by the dissociative chemisorption of nitrogen. The agreement is all the more remarkable when one considers that the reaction conversions were measured at 20 bar and the chemisorption at 10^{-7} bar—the 'pressure gap' thus presents no serious hurdle in this case.

As the Fe(111) surface exhibits the highest activity, the interaction of nitrogen on this surface has been examined in

greatest detail. It has been shown that three different forms of adsorbed nitrogen can arise in this case, which may be characterized using the differing 'fingerprints' in the N_{1s}-photoelectron spectrum[17] (Fig. 13a): 1) a very weakly bound molecular state (γ), with terminal coupling[18] and a N-N stretching vibration at 2100 cm^{-1}, close to the value for the free molecule;[19] 2) under mild thermal activation, the γ-state is transformed into another molecular form (α), which is also directly populated from the gas phase and represents the actual 'precursor' for dissociative chemisorption.[20] The frequency of N-N stretching is much reduced (ca. 1500 cm^{-1}) signaling a pronounced weakening of the N–N bond.[17, 19, 21] The molecular axis is tilted with respect to the surface, so that an interaction with both nitrogen atoms occurs;[17, 18] 3) from the above state, the final dissociation ensues upon surmounting a modest activation barrier, yielding the strongly bound, atomic β form, as illustrated schematically in the potential diagram in Figure 13b.

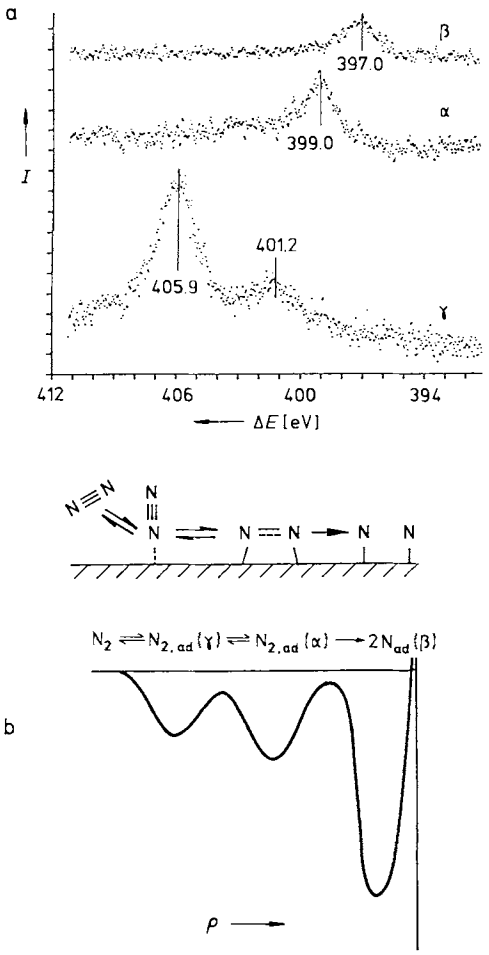

Fig. 13. N-1s photoelectron spectra of the various adsorbed N species on a Fe(111) surface (a) and the corresponding schematic potential (b) [17]. I = intensity; α,γ = molecular states; β = atomic state; $\Delta E = E - E_{Fermi}$; ϱ = reaction coordinate.

An example of a structure formed by chemisorbed N atoms on a Fe(100) surface is illustrated in Figure 14.[22] The nitrogen atoms occupy sites with fourfold coordination and, additionally, exhibit a strong interaction with the Fe atoms of the second layer. In other cases, the formation of the chemisorbed nitrogen phase is associated with considerable reconstruction of the substrate (see Section 3). Such phases can generally be denoted as 'surface nitrides' (the familiar bulk nitrides are thermodynamically unstable under the conditions of the ammonia synthesis!). *Mittasch*'s speculation that "in the catalytic formation of ammonia some kind of intermediate nitrides" arise, is thus entirely vindicated in its essence.

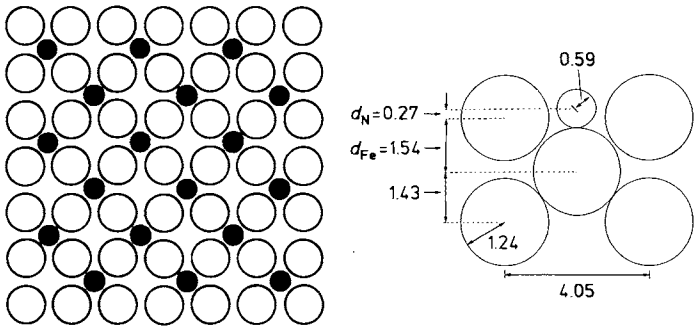

Fig. 14. Structural model of the c(2 × 2) phase formed by chemisorbed N atoms on an Fe(100) surface [22]. d = layer separation.

The role played by 'electronic' promotors can be studied by application of sub-monolayer amounts of potassium to pure iron surfaces. In this manner, it was shown that the sticking coefficient for dissociative nitrogen chemisorption could be raised dramatically.[23] This is essentially due to the increased substrate electron density in the vicinity of an adsorbed $K^{\delta\oplus}$ atom, which leads to a stabilization of the molecular α-state through increased π-back donation. This state (α_2) has a higher adsorption energy and the frequency of the N-N vibration is further lowered, thus facilitating dissociation.[21, 23–25]

The occurrence of various binding states for nitrogen on a potassium doped Fe(111) surface is manifested also in the thermal desorption spectrum, which exhibits maxima at the respective desorption temperatures (Fig. 15, curve a).[19] For

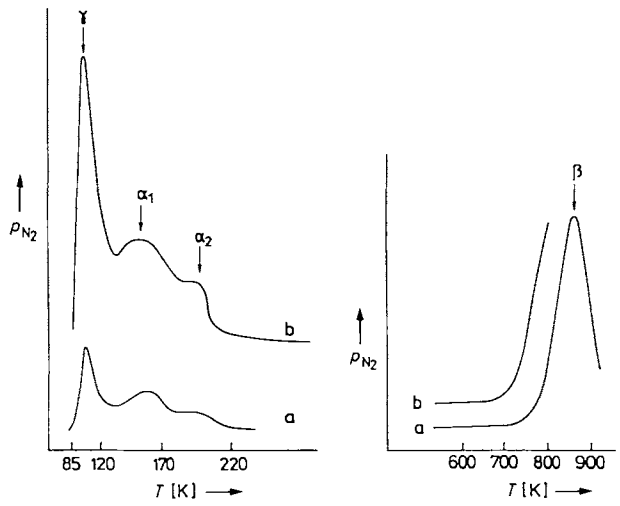

Fig. 15. Thermal desorption of N_2 from a K covered Fe(111) surface (curve a) and from a commercial ammonia catalyst (curve b) [19]. Left: desorption from the molecular states γ,α_1 and α_2. Right: Desorption following recombination of the atomic state β.

comparison, this figure depicts (curve b) data determined upon heating a nitrogen covered industrial catalyst.[26] It is notable that the temperature maxima, i.e. the respective bond energies, are in full agreement with one another. This demonstrates that the adsorption behavior of the commercial catalyst is simulated really well by the model system (Fe(111) surface, covered with around 1.2×10^{14} K atoms/cm^2). It further shows that the 'materials gap' mentioned above can be overcome in this case, and thus that the information obtained from surface science studies can form a basis for the *quantitative* modeling of 'real' catalysis in its own right.

The quintessential features of the results obtained from a large number of detailed studies on the individual steps of the catalytic ammonia synthesis are summarized in the energy diagram shown in Figure 16:[7, 27] the homogeneous reac-

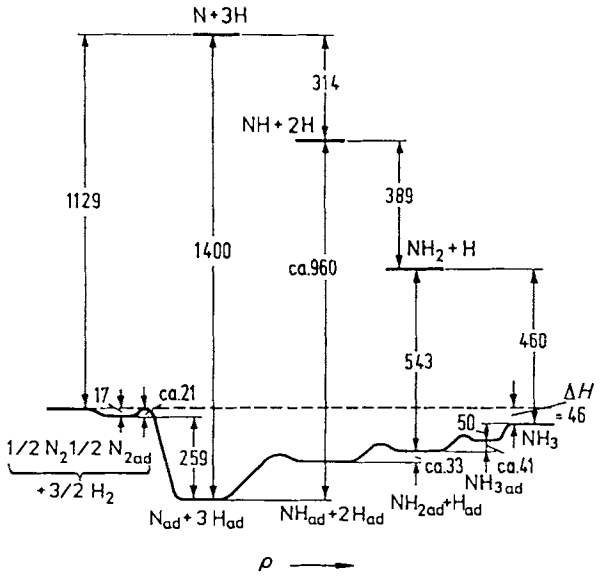

Fig. 16. Schematic potential diagram for the course of catalytic ammonia synthesis along the reaction coordinate in comparison to the energy differences for the corresponding non-catalytic steps (energy in kJ mol^{-1}) [7, 27].

tion in the gas phase would require a prohibitive amount of energy for the dissociation of the H_2 and N_2 molecules. In the presence of the catalyst, on the other hand, this process may be achieved by overcoming only relatively low energy barriers, the formation of chemisorbed nitrogen and hydrogen atoms actually even producing surplus energy. The further reaction steps comprise the successive recombination of N_{ad} and H_{ad}, ending with the desorption of NH_3. The corresponding energy demands of these elementary processes are easily met by virtue of the high reaction temperature ($\geq 400\,^{\circ}C$).

The attempt to predict the conversion in high-pressure industrial reactors using commercial catalysts on the basis of detailed information about the kinetic parameters for the individual steps, as obtained from the single-crystal model systems under the high vacuum conditions described, has been tackled by several research groups employing differing approaches.[28-29] As is evident from Figure 17, the agreement, e.g. in the analysis by *Stoltze* and *Nørskov*,[28] is really surprisingly good. This example illustrates that catalysis is

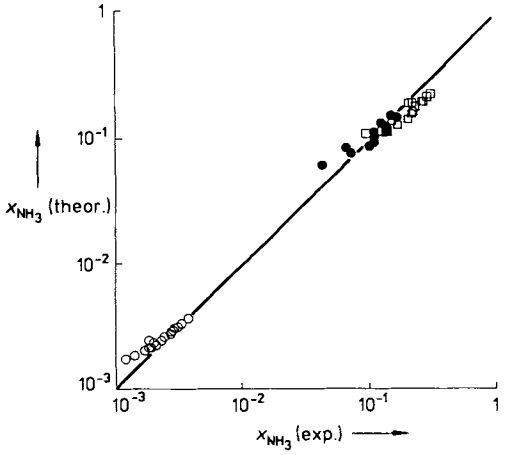

Fig. 17. Comparison of the ammonia yields determined experimentally under industrial conditions with theoretical values calculated with the help of model studies on a single surface. Taken from *Stoltze* and *Norskov* [28]. x = mol fraction. ○ = 1 atm, ● = 150 atm, □ = 300 atm.

by no means a 'black art', and that even complex technical systems can be described quantitatively via an analysis of the underlying elementary processes.

5. Nonlinear Dynamics: Temporal and Spatial Intrinsic Organization

The possibility of being able to calculate exactly the rate of a chemical reaction from a detailed knowledge of the kinetic parameters (i.e. reaction order and rate constants) for the individual steps, can admittedly, in certain cases, come up against fundamental limitations having their origins in the mathematical structure of the underlying equations.

For a catalytic reaction taking place in a continuous flow reactor, an open system well-removed from equilibrium is involved, the temporal behavior of which can be described by a series of coupled, nonlinear differential equations for the individual concentration variables (in our case the coverages by the various species), hence the expression 'nonlinear dynamics'. Systems of this kind need not behave in a stationary (i.e. time-independent) manner, even when external parameters (temperature, pressure) are maintained at constant levels, but can undergo transitions to temporal and spatial self-organization. Such phenomena were classified as 'dissipative structures' by *Prigogine* et al.[30] and were later incorporated into the general area of synergetics by *Haken*.[31]

Temporally oscillating reaction rates were observed early on in detail, e.g. with the Belousov-Zhabotinsky (BZ) reaction in homogeneous solution[32] and with electrochemical systems.[33] Such effects were first described for a heterogeneously catalyzed reaction, CO oxidation on supported Pt catalysts, by *Wicke* et al. about twenty years ago.[34] Here too, the reaction mechanism could be clarified using the strategy described.

For Pt(100) and Pt(110) single crystal surfaces at low partial pressures and under strictly isothermal conditions, the presence of CO triggers a structural transformation of the surface, with an associated increase in the sticking coefficient

for oxygen. In this way, the adsorbed CO is removed by reaction with a high probability and the surface reverts to its original structural modification. Under certain conditions, the surface can thus alternate between two states with high and low activities, giving rise to corresponding oscillations in the reaction rate. As an example, Figure 18 shows for a Pt(110) surface the development of regular oscillations following a rapid change of the O_2 partial pressure to a new value at the point marked by the arrow.[37]

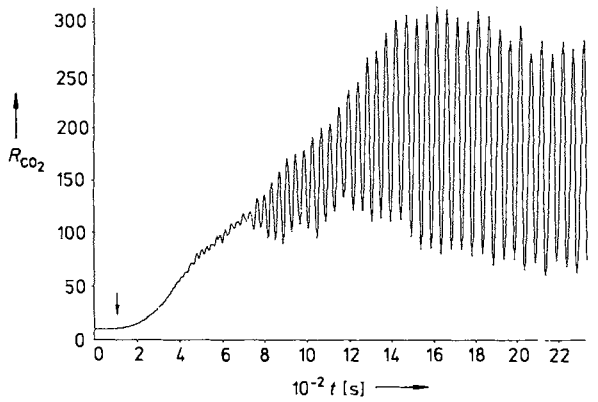

Fig. 18. Rate R_{CO_2} of catalytic CO_2 formation on a Pt(110) surface (in arbitrary units) as a function of time under steady-state flow conditions [37]. $T = 470$ K, $p_{CO} = 3.0 \times 10^{-5}$ mbar, at the point indicated by the arrow, p_{O_2} was raised from 2.0×10^{-4} to 2.6×10^{-4} mbar.

The occurrence of such oscillations is usually restricted to a certain range of values for the external parameters. In the example shown in Figure 19, small amplitude oscillations commence upon adopting a particular value of the CO partial pressure ($p_{CO} = 5.6 \times 10^{-5}$ mbar) (a). The amplitude initially grows upon further reduction of p_{CO}, while the frequency remains unchanged (b); this signals the occurrence of a so-called Hopf bifurcation. Reducing the CO partial pressure still further leads to a doubling of the period (i.e. with alternating large and small amplitudes) (c), which is then itself superseded by a further doubling (not shown here). Finally, at $p_{CO} = 5.2 \times 10^{-5}$ mbar, irregular dynamic behavior is observed. A detailed analysis[38] indicated that this reflects a transition to deterministic chaos via the so-called Feigenbaum route.[39] In contrast to the regular oscillations, the dynamic behavior is no longer predictable, hence the term 'chaos'. This effect occurs *despite the fact* that the external conditions, and thus also the mathematical formulation, are well defined (apart from small stochastic fluctuations, which can never be eliminated entirely), hence the adjective 'deterministic'.

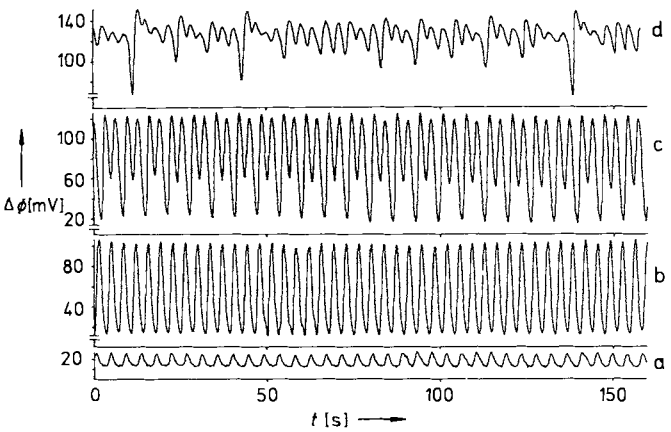

Fig. 19. Various forms of oscillation encountered during the catalytic oxidation of CO on a Pt(110) surface under steady state conditions. $T = 530$ K, $p_{O_2} = 1.1 \times 10^{-4}$ mbar, p_{CO} was varied between 5.6×10^{-5} (a) and 5.2×10^{-5} mbar (d) [37].

Chaotic phenomena occur in totally different areas and have shaken the scientific credo of being able, in principle anyway, to predict the temporal behavior of *macroscopic* systems.

The system under consideration exhibits a further peculiarity: the manifestation of temporal variations in the reaction rate integrated over the entire surface of 30 mm^2 necessitates some form of communication between different locations, i.e. an additional, spatial self-organization. For the Belousov-Zhabotinsky reaction mentioned earlier, local variations in concentration can be rendered visible by means of color differences, and manifest themselves, for example, as expanding concentric rings or spirals[40]. With the system just described, corresponding differences in CO and O coverages can be visualized using a recently developed photoemission electron microscope for which the contrast is determined by variations in the (local) work function associated with the dipole moments of the adsorbates. Two examples of the numerous different patterns formed (the phenomenology of which is dictated uniquely by temperature and partial pressure) are shown in Figure 20, corresponding to the rings and spirals of the BZ reaction mentioned earlier. It should once again be stressed that these patterns are truly two-dimensional. The contrast is created only by local differences in the coverage on an initially homogeneous surface (dark: O_{ad} coverage; bright CO_{ad} coverage). The patterns change on a time scale of about 1 s (sometimes much more rapidly too); when conditions are no longer suitable (e.g. one of the gases is cut off) the patterns disappear immediately and the surface once again assumes a fully uniform appearance.

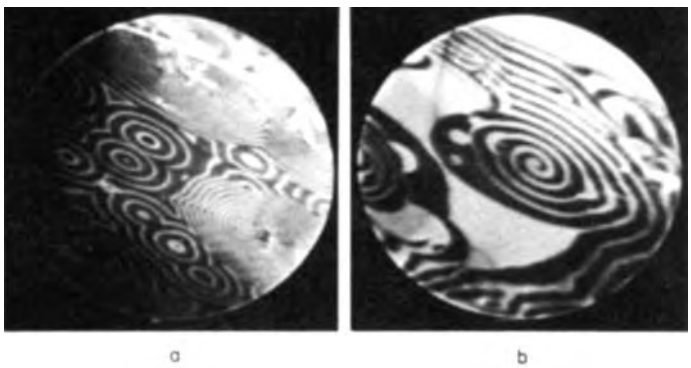

Fig. 20. Spatio-temporal pattern formation on a Pt(110) surface during the oscillatory CO oxidation. Both figures depict a section of the surface with a diameter of approximately 0.5 mm as imaged by photoemission electronmicroscopy [41]. a) $T = 430$ K, $p_{O_2} = 3.2 \times 10^{-4}$ mbar, $p_{CO} = 3.0 \times 10^{-5}$ mbar. b) $T = 435$ K, $p_{O_2} = 3.0 \times 10^{-4}$ mbar, $p_{CO} = 2.8 \times 10^{-5}$ mbar.

6. Conclusion

In this paper, an attempt has been made to show how, even for a phenomenon as complex as heterogeneous catalysis, basic research can enable one to proceed to underlying fundamental principles. This route and its likely future relevance for practical applications was formulated by *Mittasch* several decades ago as follows:[41]

"When one considers that catalysis is truly a 'land of unlimited possibilities', one cannot exclude the likelihood that continued experimental research will not only provide complete theoretical explanations, but could also become of importance in the further refinement of commercial processes."

Received: April 18, 1990 [A 785 IE]
German version: *Angew. Chem. 102* (1990) 1258

[1] a) Mittasch: *Geschichte der Ammoniaksynthese*, Verlag Chemie, Weinheim 1951; b) [1a], p. 116.
[2] [1a], p. 92.
[3] C. Bosch, A. Mittasch, G. Stern, H. Wolf, DRP 249447 (1910) with additions DRP 258146 and 262823, BASF.
[4] [1a], p. 111/112.
[5] G. Ertl, D. Prigge, R. Schlögl, M. Weiss, *J. Catal. 79* (1983) 359.
[6] R. Schlögl in: J. R. Jennings (Ed.): *Catalytic Ammonia Synthesis*, Plenum, New York 1990, in press (Chapter 2).
[7] G. Ertl in [6], Chapter 5.
[8] a) N. D. Spencer, R. C. Schoonmaker, G. A. Somorjai, *J. Catal. 74* (1982) 129; b) D. D. Strongin, J. Carrazza, S. R. Bare, G. A. Somorjai, *ibid. 103* (1987) 213.
[9] a) G. Ertl, J. Küppers: *Low Energy Electrons and Surface Chemistry*, 2nd Edit., VCH, Weinheim 1985; b) D. P. Woodruff, T. A. Delchar: *Modern Techniques of Surface Science*, Cambridge University Press, Cambridge 1986; c) A. Zangwill: *Physics at Surfaces*, Cambridge University Press, Cambridge 1988.
[10] See, e.g., H. Rohrer, N. Garcia, R. J. Behm (Eds.): *Basic Concepts and Applications in Scanning Tunneling Microscopy*, Kluver, Dordrecht 1990; b) G. Binnig, H. Rohrer, *Angew. Chem. 99* (1987) 622; *Angew. Chem. Int. Ed. Engl. 26* (1987) 606.
[11] J. Wintterlin, J. Wiechers, H. Brune, T. Gritsch, H. Höfer, R. J. Behm, *Phys. Rev. Lett. 62* (1988) 59.
[12] H. Brune, J. Wintterlin, R. J. Behm, G. Ertl, *Europhys. Lett. 13* (1990) 123.
[13] D. Coulman, J. Wintterlin, R. J. Behm, G. Ertl, *Phys. Rev. Lett. 64* (1990) 1761; *Surf. Sci.*, in press.
[14] G. Kleinle, J. Wintterlin, G. Ertl, R. J. Behm, F. Jona, W. Moritz, *Surf. Sci. 225* (1990) 171.
[15] K. Müller, *Ber. Bunsen-Ges. Phys. Chem. 90* (1986) 184.
[16] a) F. Boszo, G. Ertl, M. Grunze, M. Weiss, *J. Catal. 49* (1977) 18; b) F. Boszo, G. Ertl, M. Weiss, *ibid. 50* (1977) 519.
[17] M. Grunze, M. Golze, W. Hirschwald, H. J. Freund, H. Pulm, U. Seip, M. C. Tsai, G. Ertl, J. Küppers, *Phys. Rev. Lett. 53* (1984) 850.
[18] H. J. Freund, B. Bartos, R. P. Messmer, M. Grunze, H. Kuhlenbeck, M. Neumann, *Surf. Sci. 185* (1987) 187.
[19] L. J. Whitman, C. E. Bartosch, W. Ho, G. Strasser, M. Grunze, *Phys. Rev. Lett. 56* (1986) 1984.
[20] G. Ertl, S. B. Lee, M. Weiss, *Surf. Sci. 114* (1982) 515.
[21] M. C. Tsai, U. Seip, I. C. Bassignana, J. Küppers, G. Ertl, *Surf. Sci. 155* (1985) 387.
[22] R. Imbihl, R. J. Behm, W. Moritz, G. Ertl, *Surf. Sci. 123* (1982) 129.
[23] G. Ertl, S. B. Lee, M. Weiss, *Surf. Sci. 114* (1982) 527.
[24] L. J. Whitman, C. E. Bartosch, W. Ho, *J. Chem. Phys. 85* (1986) 3688.
[25] a) N. D. Lang, S. Holloway, J. K. Nørskov, *Surf. Sci. 150* (1985) 24; b) J. K. Nørskov, in H. P. Bonzel, A. M. Bradshaw, G. Ertl, (Eds.): *Alkali Metal Adsorption*, Elsevier, Amsterdam 1989, p. 253.
[26] R. Schlögl, R. C. Schoonmaker, M. Muhler, G. Ertl, *Catal. Lett. 1* (1988) 237.
[27] G. Ertl in J. R. Anderson, M. Boudart (Eds.): *Catal. Sci. Technol. Vol. 4*, Springer, Berlin 1983, p. 209.
[28] P. Stoltze, J. K. Nørskov, *Phys. Rev. Lett. 55* (1985) 2502; *Surf. Sci. 117* (1988) L230; *J. Catal. 110* (1988) 1.
[29] a) M. Bowker, I. Parker, K. Waugh, *Appl. Catal. 14* (1985) 101, with revision in *Surf. Sci. 197* (1988) L223; b) J. A. Dumesic, A. A. Trevino, *J. Catal. 116* (1989), 119.
[30] G. Nicolis, I. Prigogine: *Self-Organisation in Nonequilibrium Systems*, Wiley, New York 1977, See also I. Prigogine, *Angew. Chem. 90* (1978) 704.
[31] H. Haken: *Synergetics. An Introduction*, Springer, Berlin 1982; *Advanced Synergetics*, Springer, Berlin 1983.
[32] See, e.g., A. M. Zhabotinsky, *Ber. Bunsen-Ges. Phys. Chem. 84* (1980) 303.
[33] See, e.g., U. F. Franck, *Ber. Bunsen-Ges. Phys. Chem. 84* (1980) 334.
[34] a) P. Hugo, *Ber. Bunsen-Ges. Phys. Chem. 74* (1970) 121; b) H. Beusch, P. Fieguth, E. Wicke, *Chem. Ing. Techn. 44* (1972) 445.
[35] M. Eiswirth, K. Krischer, G. Ertl, *Appl. Phys. A 51* (1990) 79.
[36] G. Ertl, *Adv. Catal. 37* (1990), in press.
[37] M. Eiswirth, G. Ertl, *Surf. Sci. 177* (1986) 90.
[38] M. Eiswirth, K. Krischer, G. Ertl, *Surf. Sci. 202* (1988) 565.
[39] a) H. G. Schuster: *Deterministic Chaos*, Physik-Verlag, Weinheim 1984; b) J. M. T. Thompson, H. B. Stewart: *Nonlinear Dynamics and Chaos*, Wiley, New York 1987; c) S. Wiggins: *Global Bifurcations and Chaos*, Springer, Berlin 1988.
[40] R. J. Field, M. Burger (Eds.): *Oscillations and Travelling Waves in Chemical Systems*, Wiley, New York 1985.
[41] a) H. H. Rotermund, W. Engel, M. Kordesch, G. Ertl, *Nature (London) 343* (1990) 355; b) H. H. Rotermund, W. Engel, S. Jakubith, A. von Oertzen, G. Ertl, unpublished.
[42] A. Mittasch: *Chemische Grundlegung der industriellen Ammoniak-Katalyse – BASF-Versuche 1909–1912*. Printed as manuscript, Ludwigshafen 1953.

What Does the Chemical Industry Expect from Physical and Industrial Chemistry?

By Wolfgang Jentzsch*

Process innovation—the systematic optimization of raw materials, energy consumption and product yields—is a constant challenge for those operating plants producing vital basic and intermediate chemicals. The production processes, rather than the products themselves, exhibit life cycles and determine the profitability of downstream manufacturing. The ongoing task of interdisciplinary teams of experts is not just to develop new process routes, but, more commonly, to improve individual process steps. The impulse for this innovation arises from changes in the price and availability of raw materials, economic and environmental considerations and, last but not least, scientific and technological progress. This paper illustrates the opportunities available using examples which have already been put into practice as well as problems not yet resolved. Questions such as the use of alternative feedstocks and the switch to catalytic processes are addressed and used to suggest novel ideals for basic research. Worthwhile projects are identified in the area of industrial oxidation, both catalytic and non-catalytic. A highly developed, systematic, computer-based method for optimizing the integration of energy flows within a plant is presented and novel measurement techniques for efficient production control and product quality are discussed. The successful realization of such concepts requires the ability and the willingness to think in terms of new approaches to problem solving, making this an important objective for university education geared to future needs.

1. Innovation as a Basic Corporate Element

From the very beginning, the basic entrepreneurial idea behind the chemical industry was to commercialize innovations in chemical technology. Scientific advances have always provided the basis for strategic planning.

We always have to ask ourselves which factors are responsible for success, and so ascertain the future importance of innovation and the possible contribution of basic research.

Even in the early days, the chemical industry was involved not only in the synthesis of the desired final products, but also in the necessary preliminary processing. For example, BASF manufactured not only fuchsin and Hofmann-violet, but also the aniline, sulfuric acid and soda from which they were produced. Then as now, the aim was to ensure that production costs were kept below the added value by means of extensive vertical integration, as opposed to operating just a couple of synthesis steps. In this manner, the well-known "family trees" of products arose. These are synonymous with intelligent integration of production, often yielding synergies which are decisive for success (Fig. 1).

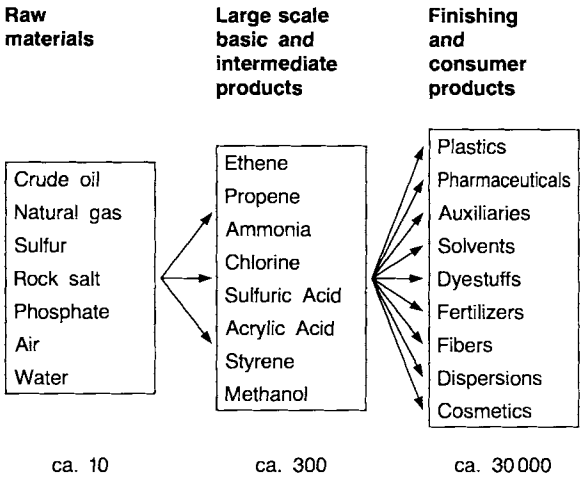

Fig. 1. From raw material to finishing and consumer products.

2. Product and Process Innovation

The various "family trees" demand different types of innovation. The relatively few commercial products marketed by the chemical industry in its infancy have since been supplanted and supplemented by several generations and many thousands of new products. In this evolutionary process, product innovation has played the dominant role, supported by progress in synthesis development. The basic stimulus has been provided by man's need for nutrition and health, clothing and housing, communication, leisure and, last but not least, mobility.

Nevertheless, the basic products have remained the same, and their total number has only increased to several hundred individual chemicals in the course of time. New final products are almost always based, for whatever reason, on existing precursors. As each precursor is converted into hundreds of commercial derivatives, one is concerned exclusively with the large-scale inorganic and organic basic chemicals, produced worldwide in thousands to millions of tons annually. There are, in all, little more than 300 such key products, and they are largely independent of changes in the range of mar-

[*] Dr. W. Jentzsch
Deputy Chairman of the Board of Executive Directors
BASF Aktiengesellschaft, E100
D-6700 Ludwigshafen

ket products. It therefore makes no sense to categorize such products as "fledgling" or "mature". The production process rather than the chemical itself exhibits a life cycle curve, as illustrated for acrylic acid in Fig. 2.

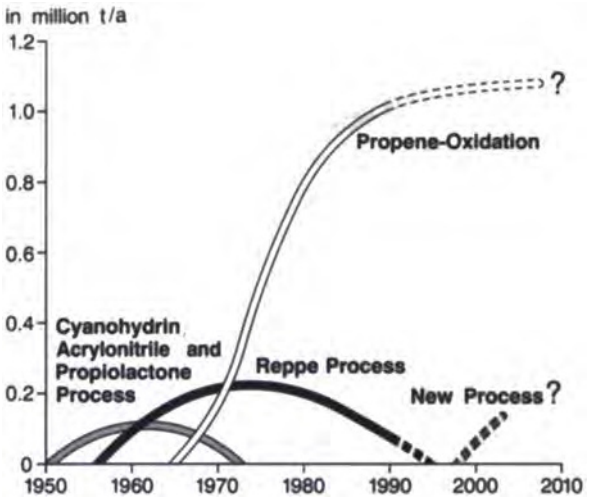

Fig. 2. Life cycles of processes for manufacturing acrylic acid.

The first three processes have already passed through their life cycles. Their demise was ushered in by the emergence of the Reppe process. This acetylene-based process too, however, has long passed its zenith and been superseded by propene oxidation. The question whether this synthesis will pass the baton on to a new process is presently unresolved. A fundamental principle in the production of such basic chemicals is evident: each innovative impulse improves the production economics, thus expanding the spectrum of applications and increasing demand. The resultant capacities, expressed in tons per annum, are almost always considerably higher than those for the preceding generation of plants.

There is virtually no room for product innovation in this area; instead, process innovation becomes the decisive factor for success. Every material, energetic, technological, or ecological advantage achieved in the large-scale synthesis propagates itself via an intricate network of chemical processing steps through to the products sold.

There is a series of entrepreneurial questions which needs to be answered in connection with every process innovation: the efficient integration of the individual process into the production network of a site and thus into the entire global strategy of production locations; whether a large-scale product should be processed internally or sold externally, and the extent to which one might profit from the success of the customer, who could also be a competitor, in the market. The detailed treatment of such questions is beyond the scope of this paper.

3. Interplay between Industrial and Academic Research

Research and development for the systematic, innovative optimization of production processes and production integration is usually carried out entirely in industry. It is here that one has access to the nucleus of know-how and where the processes are actually operated. Economic necessity thus determines both the underlying nature and methods of technical chemistry, compelling one to use simple cheap molecules as feedstocks and to exploit the most effective process parameters: catalysts, temperature, and pressure. On the other hand, the results from research in the many specialist disciplines at universities are indispensable tools for industry, and often serve to trigger innovation. Nowadays, an exceptional degree of broadly based, interdisciplinary work is the prerequisite for successful process research.

The demand for such scientific contributions is clearly increasing. If I were to attempt to illustrate this with concrete examples, I would have to anticipate future research results. Not being in a position to do this, I will try to demonstrate, using topical examples, that older process can also possess considerable potential for improvement and thus still profit from innovation. By means of some historical examples, I wish to show just how enormous the actual repercussions of an innovative impulse can be.

3.1. An Example: The Synthesis of Ammonia

I would like to use the historical development of the ammonia synthesis as an example of the interdisciplinary interplay and the contribution of fundamental research (Fig. 3). More than 80 years ago, in Karlsruhe, *Haber* managed to synthesize ammonia from its elements. The work was prompted by basic research on the law of mass action and chemical equilibrium. The technical realization of the process, however, only became possible thanks to the systematic catalyst development pursued by *Mittasch* and the elegant solution of the materials problems devised by *Bosch*—both success stories of BASF development work.

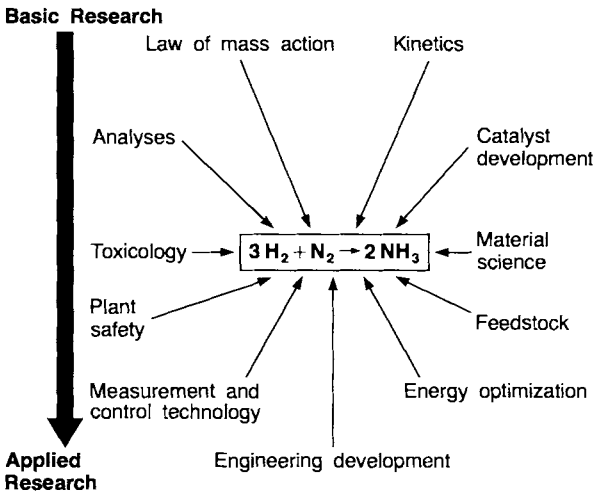

Fig. 3. Development of a basic process, using as an example the synthesis of ammonia.

The constant technological development of this process in industry and engineering firms is a model example of process innovation for a large-scale basic product: the switch from coal, via naphtha, to natural gas feedstocks and the transfor-

mation from purely thermal processing of raw materials to the present day synthesis-gas manufacture in seven catalytic stages. One should also mention the advances in mechanical and equipment technologies that have led to giant single-train plants, the development of hydrogen-resistant steels, progress in measurement, control, and process control techniques, and the systematic integration of energy flows. All these measures have brought energy consumption in the present process down very close to the theoretical level (Fig. 4).

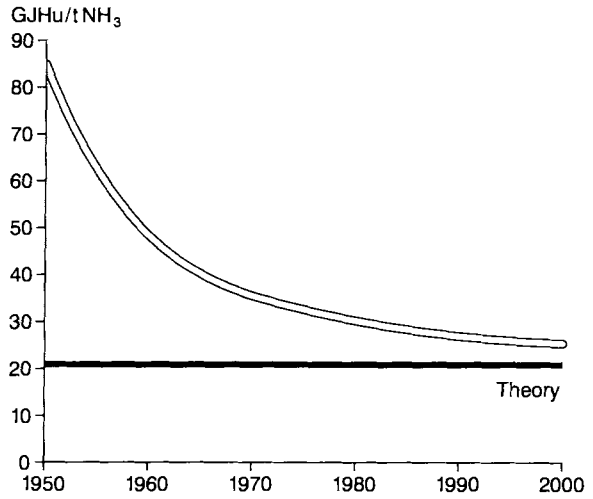

Fig. 4. Specific energy consumption of ammonia synthesis plants.

The extent of technological change is evident from a comparison of the resources required for the old and the new synthesis routes (Table 1). In contrast to the modern single-train plants, restrictions on the size of equipment and mechanical units meant that earlier plants comprised parallel batteries of production lines. Even though such plants had less than half the capacity of today's "worldscale" plants, they required twice as much area and materials. Moreover, manning was at several times present levels to cope with the time-consuming maintenance and manual plant operation and control.

Table 1. Comparison of ammonia synthesis on the basis of coke and methane.

	Multi-train plant 1940	Single-train plant 1990
Capacity [t/d]	800	1800
Plant area [m^2]	35000	18000
Steel [t]	30000	13000
Personnel	1800	50
Investment [a] [10^6 DM]	1000	300
Energy consumption [GJ/t/NH_3]	88	28

[a] Price basis 1990

Dyestuffs, fertilizers, synthetic fibers, plastics, pharmaceuticals, and plant protection agents were all beneficiaries of this gigantic improvement. It was brought about by technological and scientific progress just in the peripheral areas of process technology and by a switch in feedstocks without, however, a change in the product or chemistry of the underlying synthesis step.

4. Raw Materials as the Driving Force behind Technological Change

This leads us to another stimulus for technological change, namely variation in the price and/or availability of raw materials. The transition from coal to petrochemicals following the Second World War, in conjunction with fundamental advances in process technology, resulted in an unprecedented impulse for innovation; the era of plastics would not have been possible without this switch. The key technology involved, steam cracking, still suffers from a basic flaw, despite its technological maturity (Fig. 5). While it has proved possible to attain feedstock flexibility on the input side, an important factor for profitability, the product mix can at most be varied within narrow limits. One is thus confronted with the awkward problem of large-scale coupled production. Ethene is always the major product, and even a change of feedstock only alters the product spectrum to a slight extent. A constellation in which propene, for example, constitutes the primary product has so far proved elusive. Theoretical solutions, such as a flexible-output cracker and the functionalization of alkanes in order to produce individual products independent of the cracker mix are still hampered by lack of suitable techniques for their realization.

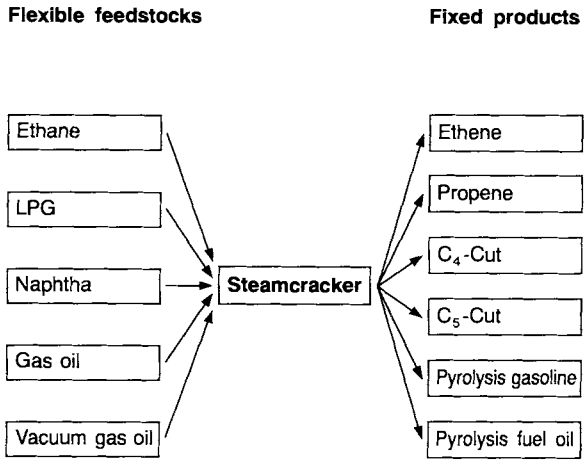

Fig. 5. Production of basic petrochemical products by steam cracking.

A topical example of a new, industrially feasible, synthesis route for an intermediate which has been important for decades is that for methacrylic acid, the monomer building block for perspex and a component of many other plastics and polymer dispersions. The conventional process (Fig. 6) is characterized by the use of chemical "auxiliaries", such as sulfuric and prussic acids, and the unavoidable formation of 2 tons of ammonium sulfate by-product for every ton of methyl methacrylate. Although not previously active in this sector, BASF developed a process (Fig. 7) based on C_1 buildung blocks in the form of synthesis gas, methanol, and formaldehyde and the C_2 component ethene. Our expertise in oxo-chemistry and with oxidation reactions proved especially valuable with the compact, purely catalytic, reaction scheme.

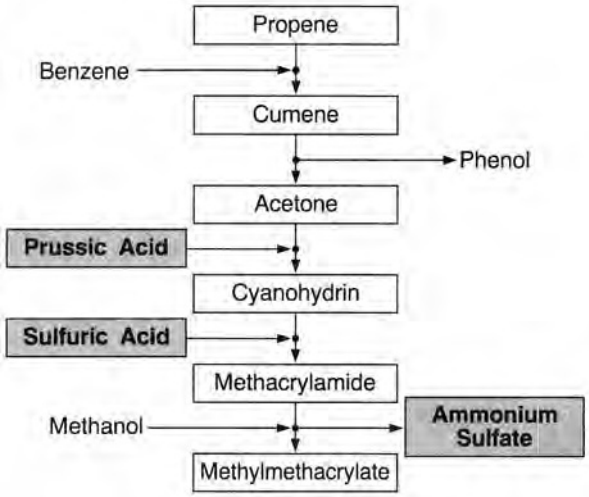

Fig. 6. Methyl methacrylate synthesis: the cyanohydrin process.

This example demonstrates the entrepreneurial and economic importance of process innovation: existing supplier structures could be broken up to the advantage of the innovator. The new process offers market benefits, providing fresh quantitative and qualitative impulses for the derived product lines. As with every new process, it contains the

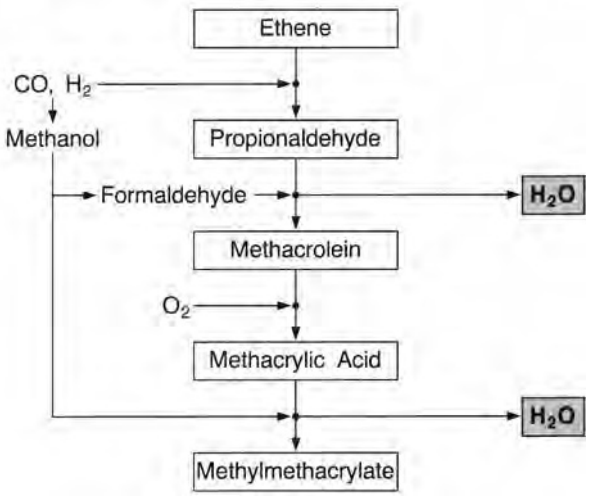

Fig. 7. Methyl methacrylate synthesis: the BASF process.

potential for further improvements. The spectrum of BASF intermediates was complemented by three important monomers: methacrolein, methacrylic acid and methyl methacrylate, thus opening new avenues for the creative synthesis chemist. Bifunctional methacrolein became available on a large scale for the first time.

5. The Potential for Improvements in Long-Established Processes

The rationalization of existing processes is of the greatest importance, and there are plenty of starting points even for well-established processes. Experts know just how difficult it is to raise the yield in the oxidation of *o*-xylene to phthalic acid anhydride even by tenths of a percent. Nobody, however, would dispute that a yield of 78% leaves considerable room for improvement. Further examples are ethene oxide, with a conversion of around 80%, and acrylic acid with 85%, all of which, it can be seen, involve oxidation reactions.

Hydrogenations, even those with exacting demands on structural selectivity and where methanization can occur, generally yield good results. In the final analysis, this could be due to the fact that with catalytic hydrogenations one can fall back on a much greater accumulation of know-how than with catalytic oxidations. Chemists were already carrying out hydrogenations with the most diverse catalyst systems at a time when they were still carrying out oxidations with chromic and nitric acids. Selective catalytic oxidations remain a challenge for the practitioner and basic science alike. The molecular processes are every bit as complex as the structure and composition of the catalysts themselves.

The material optimization of a process is always the highest priority, closely followed by the energetic aspects. Increases in yield and selectivity correlate directly to higher feedstock utilizations and lower by-product formation levels. The economic advantage of an increase in selectivity of just 1% is not just a matter of small change, but involves annual savings of millions, owing to the scale of production.

The economic advantage of an improvement in the process always goes hand in hand with environmental benefits. Higher selectivities minimize the environmental impact by saving raw materials and cutting by-products and residues for disposal.

6. The Great Importance of Catalyst Research

Catalyst optimization usually necessitates a simultaneous adaptation of process parameters in the broadest sense. The chemical reaction controlled by the catalyst, which is being studied at ever deeper levels, must be correlated with the chemistry and physics of the catalyst itself. In many cases, our knowledge of the function and the influence of promotors on the reaction is incomplete, as is the information on the structure of active and deactivated phases.

A purely empirical approach to the fine optimization of catalysts is no longer sufficient. The deeper insight into the structure of the catalytically active centers afforded by various surface analysis techniques is now indispensable. In this area, a whole new field is opening up for finding out more about the relational interaction between the nature and function of a catalyst. The characterization of a catalyst is often carried out on oxidized precursors in atypical operating atmospheres. Setting up experimental possibilities for studying the idealized situation with simulation of the operating conditions, including the material environment, would dramatically expand the horizons of our knowledge.

An oxidation process urgently in need of improvement is the air oxidation of cyclohexane to so-called anolone, a mixture of cyclohexanol and cyclohexanone (Fig. 8). Around 4 million tons of anolone are produced annually worldwide via this route. Although the yield has been increased considerably over the years, the conversion is still less than 4%. As

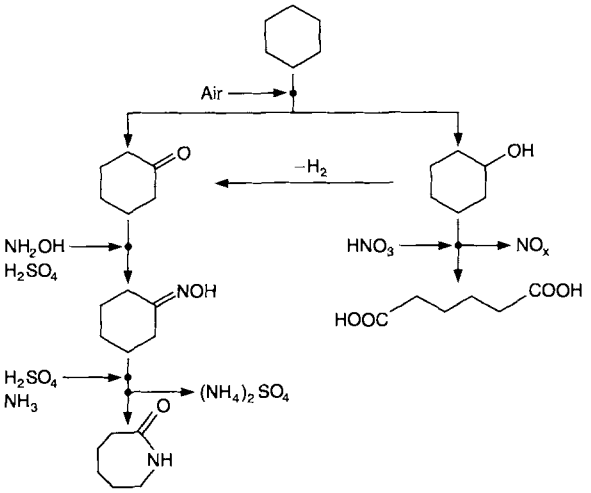

Fig. 8. Manufacture of caprolactam and adipic acid starting with cyclohexane.

a consequence, a huge amount of cyclohexane has to be recycled—a safety problem as well as one of economics.

Anolone is either oxidized to adipic acid by mixing with nitric acid, (i.e., a conventional chemical oxidation with ring cleavage) or converted to caprolactam via cyclohexanone oxime following catalytic dehydrogenation of the cyclohexanol present. New synthesis routes were developed, above all to avoid the unsatisfactory two-stage oxidation synthesis for the adipic acid fraction.

Rhone-Poulenc has patented a process whereby diacetoxybutene, which can be obtained on a large scale via the acetoxylation of butadiene, is carbonylated to the 3-hexene dicarbonic acid diester. Subsequent hydrogenation and saponification yields adipic acid. The successful technical realization of this process would offer a synthesis route for adipic acid based on butadiene.

BASF has also developed a novel synthesis for adipic acid (Fig. 9). The direct carbonylation of butadiene means that

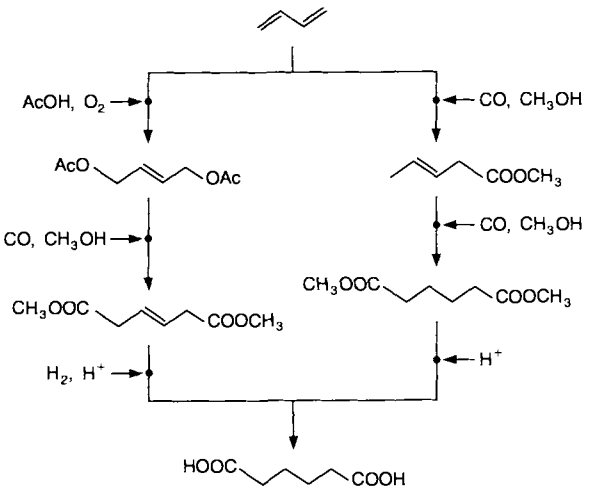

Fig. 9. Manufacture of adipic acid from butadiene.

one pays the price of a two-stage synthesis for adipic acid diester, the isomers formed being recycled after cleavage, but the process has the advantage that the C_4 cut can be drawn directly from the steam cracker. Chemical extraction of the butadiene is thus carried out concurrently with its further processing.

This provides two basic insights:

- even for large-scale products of more than 40 years standing, competition between innovations can arise, the outcome of which is by no means certain
- the raw material source for the new competitive process is a by-product from the C_4 fraction in olefin synthesis, one that has not previously been fully exploited.

The intrinsic possibilities for butadiene are by no means exhausted, and the C_5 fraction from the steam cracker is similarly not being optimally exploited. These are just a few of the many conceivable indications of the treasures which remain to be unearthed sooner or later.

7. Reduction of Energy Input

While the material rationalization remains an ongoing objective, something of an end-point has been reached in the area of energy integration down to temperatures of about 100 °C. In the 1980s, BASF made great efforts in this direction and was able to achieve considerable energy savings by the systematic application of heat integration methods in individual plants and processes. Investment in measures for saving energy by means of more intensive use of process heat not only obviated the need for a new power station, it also saved 700 tons per hour of steam. This success was reflected in a significant reduction in specific energy expenditure (Fig. 10). Despite an increase of 60% in production from

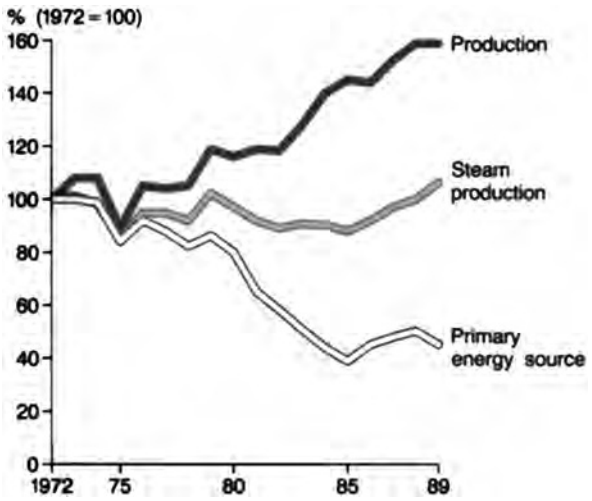

Fig. 10. Changes in production and energy consumption between 1972 and 1989.

1972, the consumption of primary energy sources was cut to 40% of its previous value. The substantial reduction in the past decade is due to the systematic implementation of the program for saving energy.

Since a reduction in the energy inputs always entails lower CO_2 and pollutant discharges, such measures have a considerable positive impact on the environment (Table 2). BASF

Table 2. Environmental advantages of energy savings.

Energy Savings	
Fuel Oil	600000 t/a
Reduction in emissions	
Carbon dioxide	1900000 t/a
Sulfur dioxide	12000 t/a
Nitrogen oxides	6000 t/a
Ash	180 t/a

has thus already made a major contribution towards cutting CO_2 emissions. This is an exceptionally successful, recent example of how innovation can be initiated by theoretical work at universities, in this case by Professor *Linnhoff* at Manchester University. The collective expertise and specific technical knowledge available in industry then enable such methods to be put into practice in production plants.

8. Further Development of Process Analysis and Control: Fascinating Opportunities

We see further innovation shortfall in electrical, measurement, and control technologies. Detailed knowledge of the individual process steps through to modelling and simulation of the entire process are a sine qua non for the further expansion of process control using advanced control systems. The increasing computer-supported application of these techniques will benefit above all those large-scale processes with varying raw materials and feedstock quality due to the resultant minimizing of energy and material inputs. Minimization of the off-specification production between charges is a further plus.

For many applications, however, a more thorough realization is impeded by a principal shortcoming: electronic data processing can combine manifold and diverse measurement data for process control; the main problem, however, lies in the determination of these data. Although the in-situ determination of temperature, pressure, flows, and certain material properties presents no real problems, sensors for on-line, or better still, in-line measurement of concentrations are, as a rule, missing. In particular, low concentrations of chemically similar substances are still elusive in terms of direct, exact determinations. This is especially true for heavy or non-volatile compounds, which cannot be monitored using gas chromatography. Even seemingly trivial questions, such as the concentration of nitric acid in sulfuric acid, of metal or salt ions in various oxidation states, or traces of metal in gas streams, can still not be resolved by direct and continuous analysis. This state-of-the-art clamors for the development of suitable sensors and measurement techniques.

Above all in solids processing, the rapid and direct determination of product state and measures to alter it are of vital importance for control and quality assurance. An important characteristic of solids processing is that the product properties depend not only on the chemical compositon but also, to a large extent, on the dispersive properties of the product. The fineness and crystallinity of a product, for example, influence the filtration process and its results to a considerable degree.

The color effect of automobile varnish paint is dictated by both the size of the pigment particles and, for example, the rheological properties of the varnish paint and its treatment. Figure 11 shows the dependency of the desired objective parameters on the measured values. Since both properties depend on particle size in differing ways, and because the color intensity should be strong and the flow limit small, there is only a narrow optimal range (gray in Fig. 11). Matters are complicated by the fact that this characteristic parameter is influenced not only by the synthesis of the pigment, but also by its subsequent treatment, such as drying, confection, or dispersion in the varnish paint resin.

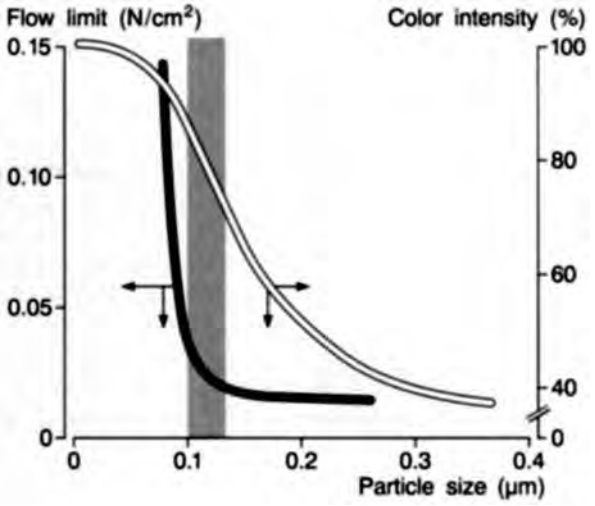

Fig. 11. Influence of particle size on the flow limits of paint dispersions and on the color intensity of pigmented paints.

To control the production process exactly and ensure an appropriate quality, it is necessary to establish which key parameters are suitable indicators for the final quality. Furthermore, one should also be aware of how these quantities depend on the process conditions in the various stages, and be able to monitor changes in them clearly when conditions in the plant are altered. Commonly, however, such objective parameters cannot be established by direct physical measurements. Phenomenological properties of materials, such

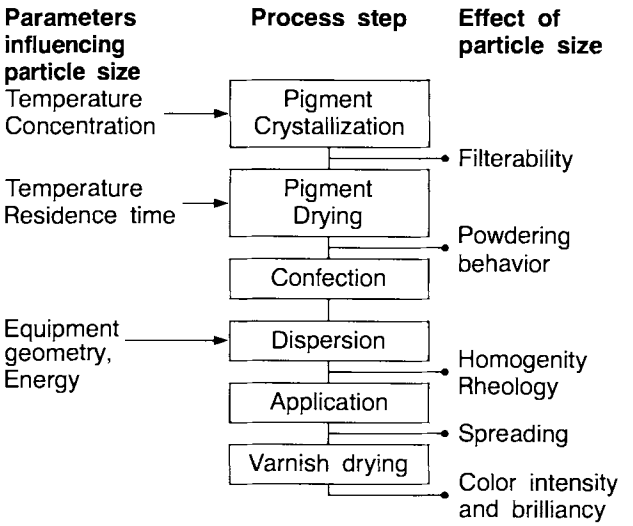

Fig. 12. Manufacture of varnish paint and lacquering.

as cohesive behavior of crystallizates during drying, the brilliance of pigments, or the dust formation of powders, simply cannot be determined using standardized physical measurement techniques. The control of such production processes using analytical data, only possible after time-consuming sample preparation, is empirical and extremely difficult. There is thus a great need here to progress from heuristic models to generally applicable measurement processes, and to correlate the results with the desired product properties and the process operating and equipment parameters.

9. Perspectives

The chemical industry will remain a dynamic growth industry. Modern standards of living and the performance of many other sectors of the economy would be inconceivable without the chemical industry. The innovative momentum of our industry is relentless. Finally, we still need the economic muscle of our traditional activities, to provide the resources for expansion into new areas, be it biotechnology or novel, high performance materials.

Innovation is by no means a unidimensional process, but rather comparable to the intermeshing gears of a clock. Advances are generally the sum total of numerous creative ideas and interdisciplinary cooperation. Figuratively speaking, our diverse operational integration of products and energy flows must have its counterpart in an overlapping "brain trust". Universities should be an active component in this intellectual integration.

Research in process technology will remain the domain of the chemical industry, as it is here—and not in the universities—that one must confront rigorous competition and comply with the demands of economics and environmental compatibility. Such constraints should not apply to the university researcher, for whom the acquisition of knowledge should have precedence. Where their interests coincide, industry and universities have to adopt differing basic positions corresponding to the fundamental differences in their functions within society. Even so, I consider both an intensive dialogue and close cooperation between the two to be indispensable, and not just in the early phase of evolution. The same holds true for other branches of industry, such as mechanical and electrical engineering. Here too, innovative synergies between universities and the corresponding sectors of the economy are vital factors for success, in final analysis for both the economy as a whole and the prosperity and health of the population.

Received: July 17, 1990 [A 791 IE]
German version: *Angew. Chem. 102* (1990) 1267

Mathematical Modeling of Chemical Reactors—Development and Implementation of Novel Technologies

By Yuri Shaevich Matros*

Mathematical modeling is an important tool for rapid and reliable reactor development and design. The models are built up from basic studies of the reaction mechanism and kinetics, the transfer processes, and the interactions within the system. A detailed understanding of the elementary processes enables the construction of powerful and complex models for dynamic and steady-state simulation. With the aid of experimentally determined parameter values one can develop new processes or improve existing ones. Excellent results obtained in experimental work under idealized laboratory conditions can seldom be fully realized in practice. This is due to factors such as transfer resistances, local gradients, fluctuating conditions, and constructional and other limitations which lead to unsatisfactory parameter values and higher costs to compensate for these shortcomings. Some recommendations are made for circumventing these deficiencies.

1. Introduction

This review is mainly concerned with the problems involved in applying the results of mathematical modeling to the design of highly efficient chemical reactors. These will be briefly outlined with the aid of examples. The plethora of excellent books and reviews devoted to chemical reactors[1–8] bears witness to the breadth of the subject matter. It is no easy task to condense a topic of this scope into the limited space available, and for this reason I will concentrate primarily on scale-up discrepancies between small-scale experimental and production plant results. Despite the huge variety of chemical reactors, it is tempting to suggest that there is a certain "something" that thwarts extrapolation of laboratory data and mathematical models to industrial units. The emphasis on catalytic reactors as examples reflects both their complex nature and the research and industrial activities of the author.

2. Mathematical Models

2.1. Application of Mathematical Models

The practical value of mathematical modeling can be best illustrated by two examples: the oxidation of methanol to formaldehyde, and the industrial application of the reverse flow reactor.

2.1.1. Reactor for the Partial Oxidation of Methanol

Mathematical modeling of the oxidation of methanol to formaldehyde has established that reactor productivity can be improved by using tubes with internal diameters of 20–21 mm in conjunction with 3–4 mm pellets of an iron-molybdenum catalyst.[9, 11] To meet industrial demands for further productivity increases, the development of a reactor with a series of adiabatic beds and intermediate removal of the heat of reaction was proposed,[11]—an unworkable solution according to contemporary opinion.[10] A further complication was the presence of spatial inhomogeneities in the system. Initial calculations indeed indicated a high parametric sensitivity (PS), i.e. the outlet temperature was extremely sensitive to inlet parameters, such as temperature, flow rate, and composition. By further mathematical modeling and experimental investigations it was possible: a) to understand why the PS is so high and what can be done to decrease it; b) to significantly reduce the spatial inhomogeneities and their influence; c) to elucidate the formation of and to suppress "hot-spots"; d) to develop an appropriate reactor control system.

An industrial reactor with multiple adiabatic beds of oxide catalyst for the production of 60 000 tons/year of formalin was constructed on the basis of these results and has been operated successfully over the last few years in the Soviet Union (Fig. 1).[11] This was probably the first industrial realization of a partial oxidation process based on such a reactor configuration.

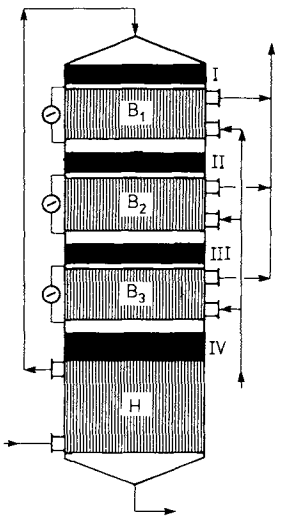

Fig. 1. Basic layout of a reactor for the oxidation of methanol to formaldehyde with adiabatic beds of oxide catalyst (I–IV). B_1, B_2, B_3: boilers, economizers; H: heat exchangers.

[*] Prof. Dr. Y. S. Matros
Institute of Catalysis
Siberian Branch of the Academy of Sciences,
Novosibirsk (USSR)

2.1.2. *Reverse Flow Reactors*

The second example concerns the development and industrial implementation of fixed-bed, reverse flow reactors. Mathematical modeling of unsteady state reactor processes taught us how to set up and control optimal temperature and concentration profiles in a catalyst bed operating under forced periodic conditions induced by reversal of the flow regime. We have since proposed reverse flow, catalytic reactors for a variety of industrial problems, such as the oxidation of SO_2 to SO_3 in the production of sulfuric acid,[12] the removal of CO, nitrogen oxides[14] and organic impurities[13] from waste gases, the methanol and ammonia syntheses,[15, 16] the recovery of sulfur by the Claus process,[17] and the production of synthesis gas.[18] The advantages that a reverse flow reactor offers over a traditional one in terms of constructional simplicity are illustrated in Figure 2. The reverse flow reactor (Fig. 2a) has no heat exchangers, fewer valves, and a single catalyst bed.

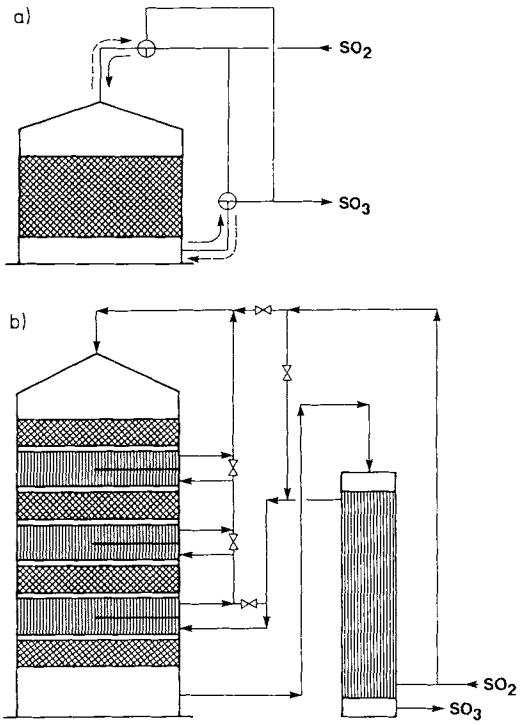

Fig. 2. Catalytic reactors for SO_2 oxidation under a) steady-state and b) unsteady-state conditions.

2.2. Formulation of Mathematical Models

We should first note that scale-up procedures based on similarity theory belong to the past. For many years the development and improvement of chemical processes mostly depended on a hit-and-miss approach to theoretical and experimental studies. Assuming that sufficient data are available to formulate a kinetic model of the process which quantitatively describes the rate of chemical transformation as a function of concentration, temperature, and pressure in the system with adequate precision, one can derive the reactor's present state from its past history. The generalized representation of a kinetic model for an unsteady state chemical process is shown in Equations (1)–(5), where $\boldsymbol{W}$ = reaction rate, $\boldsymbol{f}$ = vector of underlying kinetic functions, $\boldsymbol{\varphi}$ = vector characterizing the effect of reaction mixture on catalyst properties, $\boldsymbol{c}$ = vector of gas phase concentrations, $\boldsymbol{\theta}$ = vector of reactant concentrations on the catalyst surface, $\boldsymbol{\alpha}$ = vector of catalyst parameters influenced by reaction medium, T = temperature.

$$\boldsymbol{W} = \boldsymbol{F}(\boldsymbol{f}, \boldsymbol{\varphi}) \tag{1}$$

$$\boldsymbol{f} \equiv \boldsymbol{f}(\boldsymbol{c}, \boldsymbol{\theta}, \boldsymbol{\alpha}, T) \tag{2}$$

$$\boldsymbol{\varphi} \equiv \boldsymbol{\varphi}(\boldsymbol{c}, \boldsymbol{\theta}, \boldsymbol{\alpha}, T) \tag{3}$$

$$\frac{d\boldsymbol{\theta}}{dt} \equiv \boldsymbol{F}_1(\boldsymbol{c}, \boldsymbol{\theta}, \boldsymbol{\alpha}, T) \tag{4}$$

$$\frac{d\boldsymbol{\alpha}}{dt} \equiv \boldsymbol{F}_2(\boldsymbol{c}, \boldsymbol{\theta}, \boldsymbol{\alpha}, T) \tag{5}$$

Modern kinetic studies are characterized by a trend toward models extending right down to the molecular level. They thus enable one to predict the rules governing the formation of compounds with the required properties and structural features.

The model is a means to an end, but not a solution in its own right. The suitability of the model is thus primarily dictated by the extent to which it solves the problem under consideration. The more we know about a process, the easier it becomes to describe it. On the other hand, as Einstein put it, "everything should be made as simple as possible but no simpler".

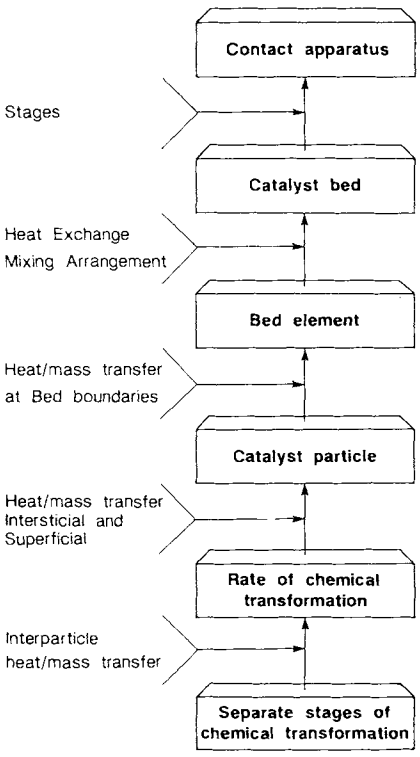

Fig. 3. Structure of a mathematical model for a fixed-bed catalytic reactor.

Reactors are complex systems but generally have a repetitive, multistage structure. Mathematical models are thus often assembled from and embody several constituent submodels derived from a preliminary analysis, a procedure illustrated in Figure 3. The fundamental principles of model formulation depend on the uniform scale of reactor elements and their invariance with time.[11] This basis permits the prediction of dynamic reactor performance for reactors of all shapes and sizes.

2.3. Limitations of Mathematical Models

The satisfactory agreement of experimental data with model calculations is a necessary, but not sufficient, condition for model acceptability. It is easy to envisage a situation in which two different models describe the same set of data equally well. Under conditions deviating from the experimental ones, however, models selected according to empirical or intuitive criteria can lead to serious errors.

An example of this is the model of a porous catalyst particle covered by a liquid film of uniform thickness, used for a long time to simulate gas–liquid–solid systems with low heat evolution. For systems such as the hydrogenation of benzene, β-methylacrolein, α-methylstyrene, cyclohexene etc., this model proved to be totally inadequate. The particle surface was actually found to be only partially wetted with the liquid.[19] Shortly thereafter, data were obtained showing a "strong" dependence of the chemical reaction rate on the wetted surface area fraction and "weak" dependence on gas and liquid velocities.[20] A model which took into account the presence of liquid velocity pulsations in the vicinity of the wetted surface was able to explain these "anomalies". Further investigations showed that, in the case of strongly exothermic reactions, it was also necessary to consider the partial wetting of the pore network within the particle.[21] This detailed model was ultimately able to account for the significant gradients across the particle radius and multiple steady state behavior.

The imperfect mixing often encountered in reactors offers a further example. The traditional solution is to develop ever more detailed models, e.g. cell models with stagnant zones and by-pass routes. Sooner or later, one derives a model which reasonably matches the experimental residence time distribution function for the reaction mixture in the reactor. Due to the non-linear dependence of the kinetics and other properties on composition, temperature, and pressure, however, it is almost always impossible to use such models to calculate reactor processes with any degree of precision.

Consider a mathematical model describing unsteady state reactor processes in an adiabatic catalyst bed [Eqs. (6)–(15)].

$$(C_g + \varepsilon_g C_p)\frac{\partial T_g}{\partial t} = \lambda \frac{1}{r^2}\frac{\partial}{\partial r}\left(r^2 \frac{\partial T_g}{\partial r}\right) + QW(T_g, y) \qquad 0 \leqq r \leqq R_g,\ 0 \leqq \tau \leqq \tau_L \quad (6)$$

$$\varepsilon_g \frac{\partial y}{\partial t} = D\frac{1}{r^2}\frac{\partial}{\partial r}\left(r^2 \frac{\partial y}{\partial r}\right) + W(T_g, y)\frac{1}{c_0} \qquad 0 \leqq r \leqq R_g,\ 0 \leqq \tau \leqq \tau_L \quad (7)$$

$$\varepsilon \frac{\partial T}{\partial t} = \frac{\lambda_M + \lambda_B}{C_p u^2}\frac{\partial^2 T}{\partial \tau^2} - \frac{\partial T}{\partial \tau} + \frac{\alpha S}{C_p}(T_g - T) \qquad r = R_g,\ 0 \leqq \tau \leqq \tau_L \quad (8)$$

$$\varepsilon \frac{\partial x}{\partial t} = \frac{D_M + D_B}{u^2}\frac{\partial^2 x}{\partial \tau^2} - \frac{\partial x}{\partial \tau} + \beta S(y - x) \qquad r = R_g,\ 0 \leqq \tau \leqq \tau_L \quad (9)$$

$$-S\lambda \frac{\partial T_g}{\partial r} = S\alpha(T_g - T) - \frac{\lambda_r}{u^2}\frac{\partial^2 T_g}{\partial \tau^2} \qquad r = R_g,\ 0 \leqq \tau \leqq \tau_L \quad (10)$$

$$SD\frac{\partial y}{\partial r} = S\beta(y - x) \qquad r = R_g,\ 0 \leqq \tau \leqq \tau_L \quad (11)$$

$$\frac{\partial T_g}{\partial \tau} = 0;\ \frac{\lambda_M + \lambda_B}{C_p u^2}\ \frac{\partial T}{\partial \tau} = T - T_0;\ \frac{D_M + D_B}{u^2}\ \frac{\partial x}{\partial \tau} = x - x_0 \qquad r = R_g,\ \tau = 0 \quad (12)$$

$$\frac{\partial T_g}{\partial \tau} = \frac{\partial T}{\partial \tau} = \frac{\partial x}{\partial \tau} = 0 \qquad r = R_g,\ \tau = \tau_L \quad (13)$$

$$\frac{\partial T_g}{\partial r} = \frac{\partial y}{\partial r} = 0 \qquad r = 0,\ 0 \leqq \tau \leqq \tau_L \quad (14)$$

$$t = 0;\ x = y = 1;\ T_g = T = T_{in} \quad (15)$$

The model incorporates: mass and heat transfer within the particle, between the catalyst particles and the gas phase, and the axial transfer processes within the gas phase; T = gas temperature; T_0 = initial bed temperature; T_{in} = inlet temperature; T_g = catalyst temperature; x = conversion in gas phase; y = conversion in catalyst; c_0 = reactant inlet concentration; S = specific external surface area of the catalyst per unit bed volume (e.g. for spherical particles: $S = 3(1 - \xi)/R_g$); L = length of the catalyst bed; l = axial bed coordinate; $\tau = l/u$, the gas residence time; $\tau_L = L/u$; u = gas velocity; r = radial catalyst coordinate; R_g = pellet radius; λ = effective radial conductivity of pellet; D = effective diffusivity within the pellet; C_g = heat capacity of pellet; C_p = heat capacity of gas; λ_M and λ_B are the coefficients of molecular and eddy heat transfer in the gas; D_M and D_B are the coefficients of molecular and eddy diffusion in the gas; α and β are the coefficients for heat and mass transfer at the pellet surface; Q = heat of reaction. Prior to formulating the detailed equations, the optimal regime should be established theoretically, using only the kinetic model, regardless of whether it can be realized technically or not. This regime defines theoretical limits for such factors as productivity and selectivity. Simulation work based on mathematical models then makes it possible to determine the main technological parameters of the process and design data for the details of the one or more reactor configurations which could be expected to operate near the theoretical optimum. In most cases, however, the process characteristics observed in this optimal reactor are inferior to those obtained at the theoretical optimum and often in comparison to those obtained in laboratory units too. What can be done about this? Unfortunately we live in an imperfect world!

The deterioration in performance is caused by numerous factors: the balances relating composition and temperature, diffusion limitations, heat exchange in the bed, transfer resistances at phase interfaces, temperature and concentration gradients at various reactor levels, micromixing and microflow regimes within the reactor, instability or autooscillatory behavior, variation in inlet parameters etc. etc.

2.4. Influence of Inhomogeneity on Reactor Operation

Although the results of mathematical modeling may be intrinsically reliable, the pilot or industrial equipment constructed on the basis of them usually exhibits inferior operational indices. A significant reason for this deviation from

ideal behavior is the presence of spatial inhomogeneity in the temperature, concentration, and pressure distributions. Such inhomogeneity in the reactors may arise owing to both external and internal generic factors. Irregular temperature, concentration, velocity and pressure profiles in the reactor inlet belong to the first class. The usual response to non-uniform inputs in practice is to try and compensate for them by changing the reaction mixture residence time in the reactor (MRTR), a mostly unsuccessful approach. For example, due to the thermodynamic equilibrium in a reversible exothermic system, it is impossible to counteract the negative influence of a non-uniform temperature profile in the inlet simply by increasing the MRTR.

2.4.1. Non-Uniform Flow

Internal inhomogeneities are caused, for instance, by irregularities in the distribution of flow permeability within the reactor. In Figure 4 the experimentally measured temperature values in the outlet section of an adiabatic reactor with exothermic reaction are presented by way of an example. The catalyst was charged via hoses at two locations, giving two piles. These were subsequently leveled off carefully, to

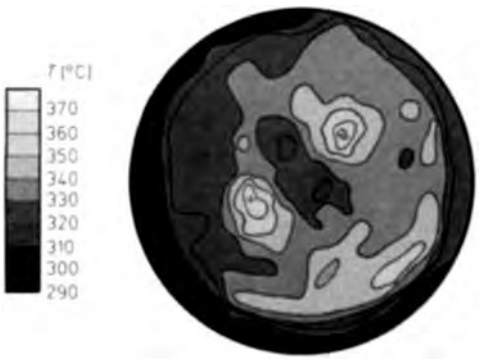

Fig. 4. Isotherms in the outlet of an adiabatic catalyst bed, in which the catalyst was loaded by "piling" from a hose. The crosses indicate the centers of the catalyst piles formed during charging.

yield a bed of uniform depth. Tomographic measurements, however, showed that the bed density at the charging locations was higher than elsewhere, and the "hot-spots" were also found in these zones.[22] It should be noted that variations in MRTR across a reactor can yield unexpected results, with superadiabatic or superequilibrium temperatures. The charging of catalyst by a "rain" technique[23] yielded pratically uniform permeability over the bed section.

Developing suitable, detailed methods for installing catalysts, internals, heat exchangers and intermediate inlets and outlets so as to ensure uniform permeability and heat and mass transfer conditions in the reactor is one of the major challenges facing chemical engineers.

The empty regions before and after the reaction zones function as distinctive collecting points with practically homogeneous static pressure values. The pressure drop between them drives the reaction mixture through the reaction zone. Mathematical modeling commonly asumes that the velocity of the reaction mixture, u, is constant. The correct formulation of the problem, however, is to assume a constant value for Δp over the reactor and treat the u as the unknown parameter.[24–28] This approach describes the effects of positive feedback (for exothermic reactions): decreasing values of u lead to increasing residence times, conversions, and reaction temperatures, the last of which further decreases the value of u and so on. This phenomenon, only recently fully appreciated, explains why a high PS is often observed in practice and how various parts of the reactor can operate under significantly different conditions—a feature demonstrated by the large scatter in some experimental data. Assuming a constant value of Δp allows for the possibility of several steady states under similar inlet conditions (Fig. 5), even for those reactors operating in or around the plug flow regime.

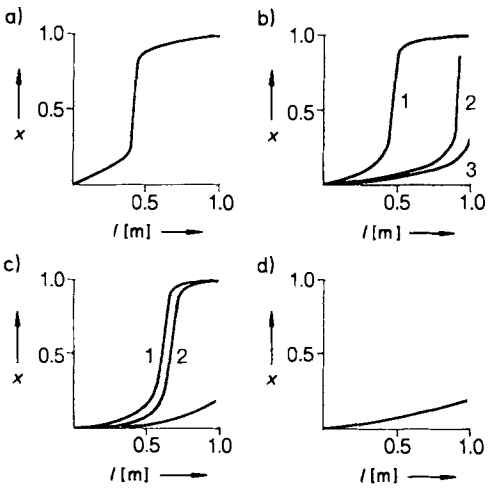

Fig. 5. Profiles of the degree of conversion (X, or temperature, given by $T = \Delta T_{ad} X$) as a function of normalized catalyst bed length (l) in a plug flow, adiabatic reactor. For a single irreversible reaction, the system can exhibit either unique high (a) or a low (d) temperature regimes, or three steady states (1,3 stable, 2 unstable).

The possibility of high- and low-temperature regimes occurring simultaneously was finally able to explain how adiabatic beds can give rise to "hot-spots". This phenomenon is most pronounced for temperature-sensitive reaction rates, for large heats of reaction, and in cases where viscosity is a strong function of temperature and composition. The last criterion is especially important for thermonuclear reactions.

2.4.2. Non-Uniform Inlet Conditions

Two main parameters determine the extent to which the non-uniform inlet conditions influence the hydrodynamic situation within the reactor: the ratio of the distance between inlet and bed to bed diameter, h, and the ratio of bed cross-section to that of the inlet duct divided by the square root of the bed pressure drop coefficient, $A = F_b/[F_{in}\sqrt{\xi}]$, where ξ is the coefficient of the drop in pressure in the bed. The velocity field may be assumed to be uniform prior to entering the bed if $A < 0.2–0.5$.

Novel reactor configurations providing improved hydrodynamic homogeneity are of great practical interest. An example in this context is the concentric spherical flow reactor

in which the feed is introduced via an inner perforated spherical surface and the products are removed through a similar outer shell.

Modern, high-speed computers permit the simultaneous calculation of pressure, velocity, concentration, and temperature profiles in reactors, even for multidimensional problems. Generally, however, the solutions are restricted to idealized geometrical structures. It is still difficult to calculate global and especially local hydrodynamic conditions when the stochastic nature of parameters has to be taken into account.

We should at this juncture perhaps consider the equations that enable us to estimate the effect of spatial inhomogeneities on reactor performance. Let the distribution of a nonuniform parameter P be described by the differential distribution function $\alpha(P)$ [Eq. (16)] with moments given by Equation (18) and assume that a unique outlet parameter

$$\int_{P_{min}}^{P_{max}} \alpha(P)\,dP = 1 \tag{16}$$

$$\bar{P} = P_{average} = \int_{P_{min}}^{P_{max}} P\alpha(P)\,dP \tag{17}$$

$$M_i = \int_{P_{min}}^{P_{max}} (P - \bar{P})^i \alpha(P)\,dP \tag{18}$$

function exists $A(P)$, the derivatives of which with respect to P can be obtained from the mathematical model. The average value of this parameter is then given by Equation (19).

$$\bar{A} \cong A(\bar{P}) + \sum_i \frac{1}{i!} M_i \frac{\partial^i A(P)}{\partial P^i}\bigg|_{P=\bar{P}} \tag{19}$$

3. Optimal Reactor Design

3.1. Economic Factors

Assume that a reactor has been selected with the help of mathematical modeling and that an optimal operating regime has been determined for this configuration (line "e" in Fig. 6). The economics of converting reactants into products in this reactor may still be unfavorable, however. As a rule, simplifications in reactor construction diminish the depreciation while increasing the operating costs. One thus has to balance off the amortization (B_1) and operating costs (B_2) to achieve an economic optimum for production. The optimal point "B_3" can be established using mathematical modeling.

3.2. Technical Factors

The precision with which an optimal regime can be realized depends on the intrinsic reactor properties and the unavoidable external perturbations. The intrinsic reactor behavior is characterized by the values of PS, the number and stability of the various steady states, the margin of stability, the dynamic properties, by the laws governing the variation of certain parameters with time, spatial inhomogeneity etc. The efficiency and stability of the process are determined by intrinsic reactor properties and the nature of the external perturbations. Reactor stability is dictated by the insensitivity to external disturbances and the extent to which one can achieve a given narrow optimal operating regime under varying inlet conditions.

As a rule, increasing efficiency leads to diminishing stability. The problem in mathematical modeling is to provide the maximum efficiency for the process under the constraints imposed by its stability criteria.

The efficiency is given by the specific productivity of the reactor, the selectivity, and the costs of constructing, controlling and operating the reactor.

3.3. Optimization of Tubular Reactor Diameter

Let us now consider a few examples of this, starting with a multitubular reactor in which the reaction takes place within tubes surrounded by a circulating heat transfer medium. The stability of such reactors is determined primarily by the value of the inner tube diameter (IDT). The capacity of the reactor may be increased by enlarging the tubes, but this results in a reduction in heat exchange area, a corresponding drop in cooling-agent temperature, increased PS, and greater dynamic overshoot (Fig. 7).

For an exothermic process, the decisive factors controlling IDT are: PS, the dynamic characteristics, the pressure drop,

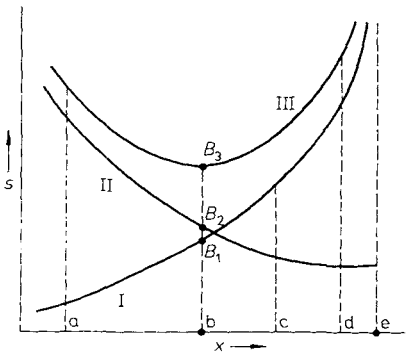

Fig. 6. Dependence of amortization (I), operating (II) costs and total costs (III) on the product yield (X). a) CSTR; b) practical optimum; c) best laboratory results; d) PFR; e) theoretically obtainable maximum yield in an ideal reactor. S = costs.

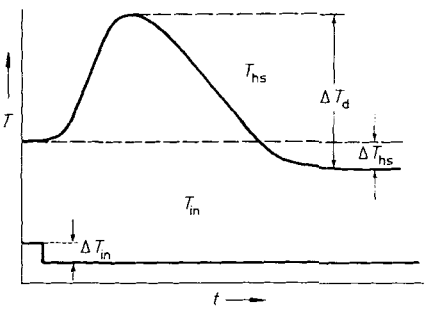

Fig. 7. Variation in "hot-spot" temperature (T_{hs}) in a tubular reactor following a step reduction in inlet temperature (T_{in}) of ΔT_{in}. $\Delta T_{hs}/\Delta T_{in}$ is the parametric sensitivity of "hot-spot" to inlet temperature and $\Delta T_d/\Delta T_{in}$ the dynamic overshoot.

the selectivity, and the potential fluctuation in all inlet parameters when the control system is working satisfactorily. IDT is chosen on the basis of an analysis of the temperature and concentration profiles calculated for a range of tube diameters. The operating conditions—residence time, temperature range, coolant temperature, initial composition, etc.—are chosen so as to achieve conditions close to the optimum, to obtain the desired productivity etc.. The maximum IDT is selected from the variants calculated to fulfill two main criteria:

1) so as to ensure that permissable deviations in the critical sections of the tube are not exceeded for the fluctuation in inlet parameter values which can be expected from the operational precision of the automatic control system, and

2) so that the hydraulic pressure drop Δp does not exceed a given value.

For endothermic processes operating near equilibrium, the parameters determining the choice of IDT are generally the specific capacity of the equipment and the magnitude of the pressure drop Δp. The maximum IDT for the oxidation of methanol to formaldehyde over oxide catalysts is around 25 mm; for the synthesis of vinyl chloride from acetylene 55 mm for concentrated and about 80 mm for dilute streams. For a periodic process manufacturing cyanogen chloride via the trimerization of chlorine cyanide, the IDT is approximately 80 mm.

It should be mentioned that the main reserve for increasing efficiency in tubular reactors lies in raising the effective radial conductivity λ_r, which permits larger IDT values and thus greater specific reactor capacities. To achieve the necessary increase in λ_r one can install special packing elements in the reactor to intensify turbulence. For heterogeneous catalytic processes, one increases λ_r by employing pellets with high voidage, e.g. Raschig rings with internals. Suitable preparation and charging of these pellets decreases both pressure drop and pore diffusion resistance, thus reducing the amount of catalyst needed and often yielding improved selectivity. A very promising area in catalyst design is the development of special catalysts using the tube wall as a catalyst carrier. We have calculated that this technique could permit a reduction in the amount of catalyst by a factor of ten and substantially improve selectivity.

4. Conventional Reactors

4.1. Adiabatic Reactors

High conversion levels or values close to equilibrium lead to very stable reactor operation. For multiphase processes with spatial distribution, the main danger is the possible formation of non-monotonic (see Fig. 7) transient regimes with dramatic dynamic overshoot. If the degree of conversion in the reactor outlet is far from equilibrium, then the PS of the outlet parameters compared to the inlet ones is approximately proportional to $\exp[(T_{out} - T_{in})\ E/RT_{in}]$, with T_{in} and T_{out} being the inlet and outlet temperatures respectively, R the universal gas constant and E the observed activation energy for the reaction. In the case of catalytic processes, for example, the value of E is halved upon going from kinetic to internal diffusive control. This essentially results in lower PS and improves stability. The quality of the automatic control system and the permissible drop in selectivity with increasing pore diffusion resistance were the factors which finally determined the main technological and constructional features of the reactor design for the production of formaldehyde from methanol in adiabatic oxide catalyst beds (see Fig. 1).

Recently, there has been an increasing tendency to employ monolithic (honeycomb) catalysts to carry out large-scale catalytic processes, for instance the catalytic reduction of nitrogen oxides with ammonia. This trend is a consequence of the lower pressure drop characteristics, the feasibility of treating dusty gases, the relative insignificance of pore diffusion resistances, and a number of other advantages inherent in the use of monolithic catalysts.

4.2. Fluidized Bed Reactors

4.2.1. Advantages

This reactor type has several very attractive practical features: 1) very high specific productivity; 2) large and adjustable axial bed conductivity, which, together with suitable distribution of heat exchange surface and partitioning within the reactor, permits near-optimal temperature profiles; 3) simple exchange of fluidized material during operation; 4) quasi-ideal plug flow in the gas phase by structuring the bed with packing elements, partitioning, and other methods; 5) very low external and internal diffusive resistance for the small fluidized particles; 6) the possibility of carrying out unsteady state processes on the internal pore surfaces of the catalyst particles; 7) easy heat removal and temperature control for strongly exothermic systems.

In organic syntheses alone, fluidized bed reactors are employed in the manufacture of vinyl acetate, pthalic anhydride, vinyl chloride, and maleic anhydride.

4.2.2. Shortcomings

In the last ten to fifteen years, however, the initial optimism accompanying the use of fluidized beds has waned somewhat. This can be explained both by the significant advantages often offered by alternative reactor configurations and by the shortcomings of fluidized bed reactors. These include the presence of large bubbles and their detrimental effect on interphase mass transfer, and large-scale particle circulation, often avoided by resorting to partitioning, rotating internals, special geometries or arranging spillover between separate bed sections. The countermeasures, however, result in decreased particle mobility and therefore reduce radial heat transfer, which can lead to hot-spot formation. A further consequence is the increased clogging and sintering of particles, all of which can lead to blockages on the walls or at other locations in the fluidized bed. Some more "generic" disadvantages should be added to those listed above: the high pressure drop, the mechanical erosion of metallic reactor internals, the large reactor volume, reaction in the gas space over the bed and connecting

lines, rapid particle attrition, and the need for dust removal in the product stream. All these factors usually mean that selectivity of the reaction is relatively low.

5. Novel Reactors

Up to now, only the problems involved in the detailed design of optimal reactors have been dealt with. It is, however, probably also worthwhile mentioning several fundamentally new techniques for carrying out chemical reactions, for example plasmochemical and unsteady state processes.

5.1. Plasma Chemistry

This is a new area in chemical technology developed in the 60's and 70's.[29] An essential prerequisite for its application was the availability of plasma generators producing low-temperature, chemically active plasma in either arc, glow, high-frequency or super-high-frequency discharges. Plasma entering the reactor serves both as a heating medium and the initiator for chemical reaction. The main characteristics of such reactors are the extremely low reaction times (10^{-3}–10^{-4} s), the high temperatures (1000–1300 °C), and the need for thorough mixing of streams within the plasma. The mathematical modeling of the process requires the study of simultaneous heat, mass, and momentum transfer. This means that the form and solution of the mathematical model are more complex. Gas mixing is carried out by co-current injection, and utilizes the kinetic energy of both component streams. Perhaps the most efficient mixing technique is to introduce one component into the flow so as to provide jet impact, leading to the formation of a turbulent zone. Examples of plasmochemical processes being developed include the pyrolysis of hydrocarbons (methane, benzene) in a hydrogen plasma for the production of acetylene and ethylene; the pyrolysis of chlorine- and fluorine-containing hydrocarbons, the synthesis of hydrogen cyanide, cyanogen and dicyanogen from hydrocarbons and nitrogen, and the fixation of atmospheric nitrogen. Plasmochemical processes obviously entail a high specific energy consumption.

5.2. Reactor Operation under Forced Unsteady-State Conditions (FUSC)

Under unsteady state conditions it is possible to enhance transfer, sorption, rectification, extraction, separation, grinding, and crystallization processes. Forced pulsing in the combustion of solid fuels improves both oxidation and heat exchange, cuts energy consumption for draught, and permits operation with less surplus air and oxygen. Furthermore, nitrogen oxide levels are lower and the heat exchange surface stays cleaner. Interphase transfer can often be promoted significantly by means of hydrodynamic instability or forced velocity pulsations close to the natural turbulence frequency. Pulsed mixing in the reaction zone by periodic variation of the pressure has been found to be very effective.[30]

FUSC in polymerization systems leads to shifts in the molecular weight distribution function for the resultant polymer and increased reactor productivity.[31, 32] Such an operation can be realized, for example, by periodically changing the hydrogen concentration in the reactor inlet for a free-radical and polycondensation polymerization of olefins. In complex biological systems, it is possible to stabilize two competitive populations dynamically, when under similar steady state conditions one of them would be suppressed.[33]

The effectiveness of FUSC in CSTR reactors can be observed clearly where a chemical reaction of an order greater than unity is occurring.[34] For reactions of second order, for example, the productivity of the reactor increases in proportion to the square of the amplitude of inlet concentration pulsations and attains a maximum value at low frequencies.[35, 36] The productivity can be raised still further if the flow rate and composition are both changed periodically, especially if the pulsations are of large amplitude and out of phase with each other. FUSC has been found to be very efficient in cases where the rate of chemical reaction exhibits extreme sensitivity to process parameters. One of the most effective ways to "excite" a reactor is to use the temperature of the heating medium. For example, a switch to FUSC in gas–solid systems permits one to intensify ore roasting, or some other interaction between the gaseous and solid phases and can improve the efficiency of heterogeneous catalytic processes.[36 - 38]

The application of pulsed voltages in electrochemical reactors used for electroorganic syntheses (amplitude, impulse duration, magnitude of reverse voltage) can give rise to changes in selectivity, producing different products simultaneously from the same feedstocks,[39] or to superior reproducibility in the electrochemical machining of metals.[40] Changing the direction and value of the applied voltage can be used to vary the color of anodic oxide films on metals and the composition and properties of alloys manufactured by electrodeposition.

The examples presented above illustrate that efficiency is improved by exploiting the wider range of concentration, temperature, and pressure profile conditions which can be achieved at unsteady state and which are often unattainable under steady state conditions. In particular, much steeper concentration and temperature gradients are feasible with FUSC. Temporal and spatial shifts in concentration and temperature profiles, non-linear dependence of reaction rates on concentration and temperature, and other factors lead to dynamic overshoots, superadiabatic behavior, oscillating transient regimes, stable limit cycles, and even chaos. Under optimal FUSC conditions, one cannot achieve worse results than at steady state.

The impact of the transition from steady to unsteady state heterogeneous catalysis can be judged according to two major criteria: the influence on catalyst structure and composition and the dynamic properties of the reactor as a whole.

Experimental data presented in the literature confirm that it is possible, in principle, to improve the performance of a variety of catalytic processes by this means: ammonia synthesis on iron or ruthenium catalysts,[41, 42] SO_2 oxidation on vanadium catalysts[43, 44] oxidative dehydrogenation of ethylbenzene to styrene on active carbon,[45] the oxidation of ethylene on silver,[46] the hydrogenation of butadiene on nickel,[47] the Fischer-Tropsch synthesis on supported ruthe-

nium catalyst,[48] CO oxidation on platinum and vanadium catalysts,[49-51] the synthesis of ethyl acetate,[52] etc.

Let us now consider the periodic variation in the inlet conditions of a fixed catalyst bed as a means of increasing the efficiency of reactor performance, using temperature cycling as an example.[53]

In Figure 8, it can be seen that in an unsteady state regime, an almost total conversion can be attained at an average temperature of 160 °C, while steady state operation would require 250 °C. For a reversible, exothermic process a temperature drop of 90 °C over the reactor could result in considerable improvement in conversion. An optimization of ammonia synthesis over iron catalyst, for example, showed that the productivity of the reactor can be increased by a factor of 1.5 by using suitable periodic temperature control in the inlet.[54]

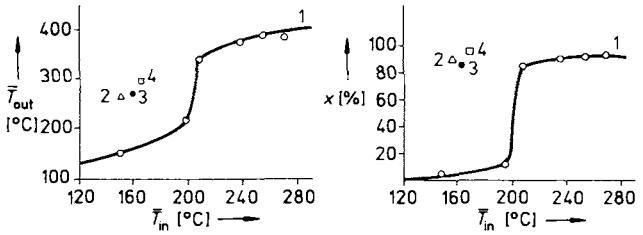

Fig. 8. Influence of average inlet temperature (T_{in}) on the cycle-averaged outlet temperature (T_{out}) and the overall degreee of conversion (x). Oxidation of 0.12% butane under (1) steady- and (2–4) unsteady-state conditions. Steady-state residence time is ca. 4.5 s. Unsteady-state cycles are characterized by t_c, the cycle duration, t_c^{max}, the duration of the maximum temperature phase, and Δ_{in}, the amplitude of the forced temperature pulsing in the inlet, T_{max}-T_{min}. 2: $\Delta_{in} = 200$, $t_c = 3600$ s, $t_c^{max} = 1800$ s; 3: $\Delta_{in} = 230$, $t_c = 2400$ s, $t_c^{max} = 1200$ s; 4: $\Delta_{in} = 255$, $t_c = 3000$ s, $t_c^{max} = 1500$ s.

5.2.1. *Reverse Flow Reactor*

A reverse flow system (Fig. 9) for heterogeneous catalytic processes was proposed in the mid 70's[38,55-57] and has since found widespread industrial application. The basic concept, as described earlier in this paper, comprises the periodic reversal of the cold feed gas being fed to a preheated catalyst bed. The theoretical basis of the reverse flow process is founded on fundamental studies of unsteady state behavior in fixed bed reactors.[11,38] The main advantages of the reverse flow process have been formulated as follows:[57]

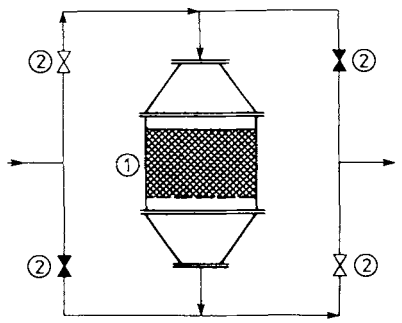

Fig. 9. Basic flowsheet of a reverse flow process in which the flow direction of the reaction mixture through the adiabatic catalytic reactor ① is alternated by appropriate operation of the valves ②.

1. The catalyst fixed bed serves firstly to accelerate the chemical reaction and secondly as a regenerative heat exchanger. It enables one to do without heat exchangers prior to the reactor and additional heat to maintain the reaction.
2. Autothermal operation is feasible even when the reaction mixture is so dilute that the adiabatic temperature rise for complete conversion is only 10–15 °C.
3. Feedstocks with considerable fluctuations in inlet characteristics can be treated.
4. The conditions created in the catalyst bed approach the optimum. Productivity and/or selectivity are often improved and reactor construction simplified. Thus, for a reversible exothermic process it is necessary to decrease the temperature to achieve higher conversions, the exact opposite of what occurs in the normal steady-state arrangement. In the reverse flow process on the other hand, a much more favorable temperature profile is obtained (Fig. 10).

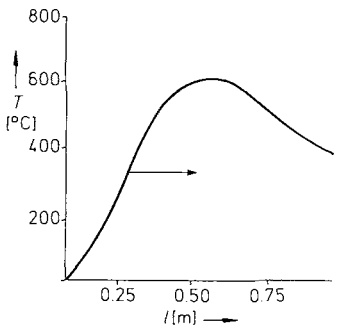

Fig. 10. Typical temperature (T) profiles along the bed length (l) in an exothermic reverse flow process prior to switching the flow direction. The arrow indicates the motion of the temperature wave.

5. The average temperature in the catalyst bed and connecting lines is reduced significantly, which, together with the simplified reactor design, leads to a large decrease in the energy consumption needed to counteract the pressure losses (20–50%).
6. The unsteady state of the catalyst surface may also be beneficial for catalyst performance in comparison to the steady state.
7. Decreasing the average temperatures and sizes of the reactors and the simplified construction combine to cut heat losses.
8. The catalytic oxidation of low energy content reaction mixtures or fuels in a reverse flow process permits the removal of high grade heat at high temperature from the central reaction zone (Fig. 11).[57]

Let us now take stock of some of the industrial applications of the reverse flow process.

Decontamination of Industrial Exhaust Gases: The decontamination of industrial exhaust gases by removing various organic compounds, CO, and nitrogen oxides[13,56-59] (Fig. 12) is one increaslingly important application of the reverse flow reactor. Experience has shown that the new method of operation reduces the capital cost of a detoxifica-

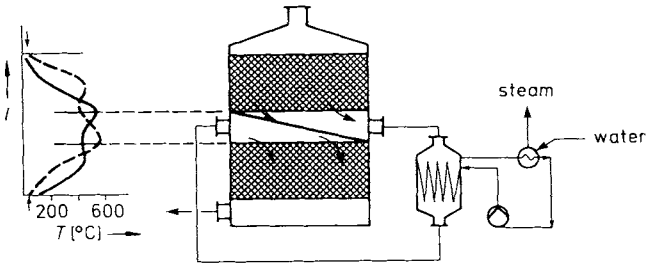

Fig. 11. Basic flowsheet for high-grade heat recovery in a reverse flow process for waste-gas treatment. The temperature profiles prior to flow reversal are shown on the left-hand side.

tion plant by a factor of 1.5 to 3 and cuts operating costs by a factor of 1.5 to 2. The process is able to purify gases with low and varying contents of pollutants, at average concentrations around 0.5 g/m^3 or higher, autothermally. At concentrations above 3 g/m^3, high-grade heat may be extracted. The numerous reverse flow processes that have been developed for waste-gas purification applications are characterized by high levels of removal (99%) for pollutants and for other odoriferous or toxic impurities and by the use of cheap oxide catalysts.

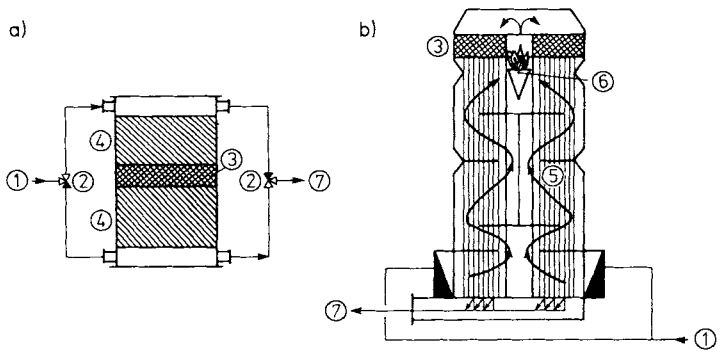

Fig. 12. Technical flowsheet of reactor units for waste gas treatment in a) unsteady-state (cf. Fig. 11) and b) conventional steady-state operation. ① feed to be decontaminated; ② valves; ③ catalyst bed; ④ inert bed; ⑤ recuperative heat exchanger; ⑥ jet burner; ⑦ purified gas.

Sulfur Dioxide Oxidation: Sulfur dioxide oxidation on vanadium oxide catalysts for sulfuric acid production using a reverse flow process[12, 60] has attracted considerable industrial interest. The reverse flow process does not require multiple catalyst beds (Fig. 2). For start-up at low SO_2 concentrations, small quantities of additional energy must be supplied. Depending on the actual conditions encountered in practice, unsteady state operation permits reductions of 50–70% in reactor size (metal weight), 30–50% in pressure drop, 30–80% in total capital cost, 5–20% in the sulfuric acid production costs, as well as simplifying construction. The operating principles of the reverse flow process make it possible to treat "dilute" roasting gases containing 0.5–3% SO_2 or to convert the gases following intermediate absorption with 0.5–1% SO_2 in a double catalyst–double absorption plant, in a simple single stage reactor with no external heat exchangers.

Claus Process: In the Claus process for sulfur production, estimates for reverse flow operation indicate that capital costs could be reduced by 20–30% and the amount of catalyst by 20–35%. Furthermore, it would not be necessary to expend external energy to heat up the feed prior to reaction.

The theoretical principles for the unsteady Claus reactor were developed using an original mathematical model,[62] which took into account sulfur condensation in the low-temperature reactor inlet zone. It could be shown that, with heat removal from the central portion of the bed in combination with sulfur condensation and separation (Fig. 13), sulfur removal rates around 98% were feasible.[61]

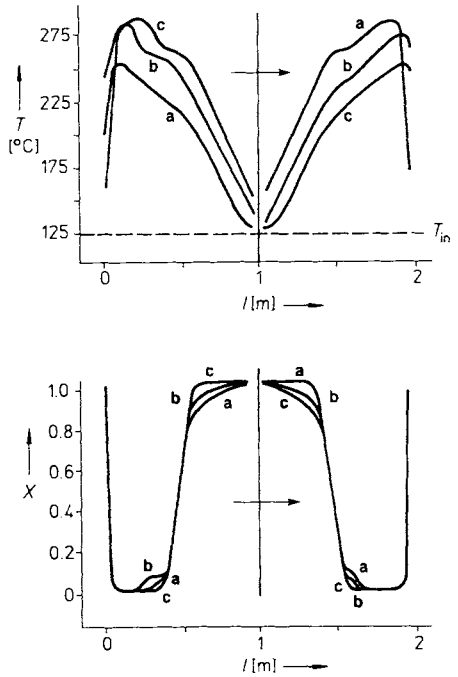

Fig. 13. Calculated profiles of temperature (T) and sulfur content (X) along catalyst bed length (l) in a reverse flow reactor with intermediate gas cooling and sulfur condensation. Curves a, b and c correspond to the beginning, middle, and end of the cycle, respectively. The arrow indicates the flow direction and T_{in} is the inlet temperature of the feed gas.

Recently, a so-called "double" reverse flow Claus process has been proposed,[63] comprising a primary catalytic stage and a subsequent purification step (Fig. 14). In this arrangement, high-temperature gas is fed to the first reactor (1), in

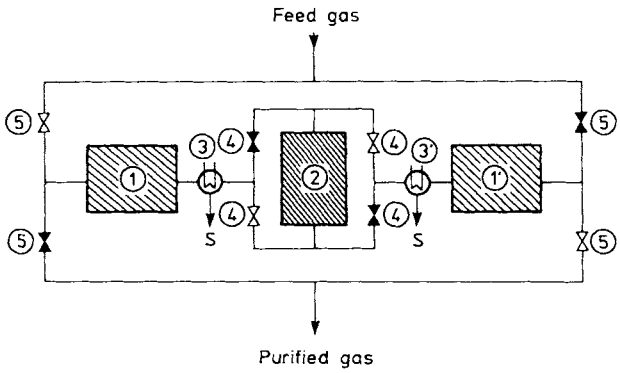

Fig. 14. Three stage, unsteady state Claus process. ①, ①', ② reactors; ③, ③' sulfur condensation; ④ valves for switching flow in intermediate, periodic reactor; ⑤ valves for switching flow through entire system.

which the Claus reaction together with COS and CS_2 hydrolysis take place under steady-state conditions. Following sulfur separation in a condenser (3), the gas, at a temperature of 120–160 °C, is passed into the second reactor (2) which operates in a periodic mode with alternating flow. Sulfur is then once again condensed out (3') and the gas fed to the third reactor (1'), which is operated so as to adsorb the sulfur formed on the catalyst. When this reactor becomes saturated with sulfur, the gas flow in the system is reversed. This configuration is predicted to be capable of achieving average sulfur removal rates of 99.5–99.9% over one cycle.

Due to the limited space available, this review is unable to deal with further fascinating features of reverse flow reactors, such as the development of other processes, the influence of the chemical dynamics of the catalyst on operational efficiency, the formulation of dynamic models, optimization, qualitative and quantitative analyses, control systems, etc.

6. Ideal Reactors—Pitfalls and Perspectives

Despite the availability of reliable experimental data, promising model calculations, and the convincing arguments of experienced engineers, the efficient chemical reactor usually remains an unrealized ideal. Why is this so? In the remainder of the review, we will try to elucidate the difficulties responsible for this shortfall.

1. The absence of unambiguous, reliable kinetic data for chemical processes. Despite the availability of good equipment, kinetic measurements are often either falsified by undesirable transport effects or restricted to too narrow a range of temperature and concentration. It is pointless to try and cut corners and save money in kinetic studies. It is well known that the greedy end up paying twice over!
2. The presence of spatial inhomogeneities due to external factors and internal characteristics. Achieving homogeneous operation within the reactor volume is both complex and costly, but nevertheless worth it. A major problem is the scale-up from pilot plant to industrial level. Adequate theory and reliable mathematical models are a weak link in this chain.
3. Inferior mathematical models and large errors in model parameters leading to poor modeling and design. To circumvent this, engineers who repeat serious mistakes should move on to less demanding jobs!
4. High parametric sensitivity of the system to inlet fluctuations or system parameters, instability or narrow stability margin. All these difficulties can be solved if enough time, care, and qualified personal are invested in the development of the automatic control system. A well-developed theory for automatic control permits one to provide a control system which ensures that the reactor parameters remain within admissible limits. Mathematical modeling methods are a *sine qua non* for the design of optimal chemical reactors operating in the vicinity of an unstable steady state or within a tight stability margin.
5. Explosion and fire hazards. The potential must be evaluated and, if possible, eliminated. In fluidized-bed processes at risk from explosions, the adoption of passive measures, e.g. designing ducts and particle separations so as to extinguish conflagration and hinder flame propagation, are to be recommended. Such conditions need only be fulfilled at the reactor inlet and outlet as these then isolate the reactor system.
6. Poor choice of construction materials. Such problems can almost always be eliminated if cost is no object. But nowadays, who can afford not to think cost-effectively?

General shortcomings, such as poor facilities, inadequately qualified staff, and low quality feedstocks are, naturally, problems confined to the competition!

It is important to notice that the gravity of the problems listed increases with increasing reactor size. Above all, this is a consequence of spatial inhomogeneity, in particular of the generic variety. In addition, difficulties arising with construction, transport, installation, and maintenance become greater. The negative influence of dynamic behavior, especially during start-up and shutdown, and the costs of ensuring a reliable and environmentally acceptable operation are also exacerbated in the case of larger reactors.

For the mathematical modeler there is no greater satisfaction than being able to behold and touch a reactor created with the help of his work. It is a pleasure to record that the expanding potential of modern scientific and engineering disciplines and techniques should enable us to experience such elation more frequently.

Received: May 21, 1990 [A 792 IE]
German version: *Angew. Chem. 102* (1990) 1274

[1] P. Trambouze, H. Van Landeghem, J.-P. Wauquier: *Chemical Reactors (Design, Engineering, Operation)*, Ed. Technip, Paris 1988.
[2] O. Levenspiel: *The Chemical Reactor Omnibook*, OSU Bookstores Inc. Corvallis, OR 97339, USA 1989.
[3] G. F. Froment, R. B. Bischoff: *Chemical Reactor Analysis and Design*, 2nd Edit., Wiley, New York 1990.
[4] L. K. Doraiswamy, R. A. Mashelkar: *Frontiers in Chemical Reaction Engineering, Vol. 1, 2*, Wiley, New York 1984.
[5] B. D. Kulkarni, R. A. Mashelkar, M. M. Sharma: *Recent Trends in Chemical Reaction Engineering, Vol. 1, 2*, Wiley, New York 1987.
[6] J. Villadsen, *Chem. Eng. Sci. 43* (1988) 1725.
[7] M. M. Sharma, *Chem. Eng. Sci. 43* (1988) 1749.
[8] Y. T. Shah: *Gas-Liquid-Solid Reactor Design*, McGraw-Hill, New York 1979.
[9] M. G. Slin'ko, Yu. Sh. Matros, G. S. Yablonskii, V. S. Beskov, B. L. Kamenko, *Khim. Prom. (Moscow) 48* (1972) 451.
[10] P. Mars: *Chimica E Dinamica Della Catalisi*, CNR, Rome 1964, p. 101–117.
[11] Yu. Sh. Matros: *Unsteady Processes in Catalytic Reactors*, Elsevier, Amsterdam 1985.
[12] G. K. Boreskov, Yu. Sh. Matros, A. A. Ivanov, V. P. Volkov: Certificate of Authorship, No. 994400, USSR 1983; GB-Pat. 2085421 B (1984); CA-Pat. 1154933 (1983); FR-Pat. 2514742 (1983); JP-Pat. 6018604 (1985); DD-Pat. 207182 (1984); DOS-A1 3050368 (1980).
[13] G. K. Boreskov, Yu. Sh. Matros, V. I. Lugovskoy: Certificate of Authorship, No. 849594, USSR 1982; G. K. Boreskov, Yu. Sh. Matros, V. S. Lakhmostov, V. S. Puzhilova, V. I. Lugovskoy, Certificate of Authorship, No. 882056, USSR 1982.
[14] L. N. Bobrova, E. M. Slavinskaya, A. S. Noskov, Yu. Sh. Matros,: *React. Kinet. Catal. Lett. 37* (1988) 267.
[15] G. K. Boreskov, Yu. Sh. Matros, I. A. Zolotarskii, V. S. Lakhmostov, I. A. Ryzhak, Yu. V. Lender: Certificate of Authorship, No. 1249010, USSR 1984.
[16] G. K. Boreskov, N. M. Zhavoronkov, O. S. Chekhov, Yu. Sh. Matros, V. N. Orlik, V. A. Chumachenko, V. S. Lakhmostov, A. M. Alekseev, Yu. A. Sokolinskii: Certificate of Authorship, No. 865796, USSR 1981.
[17] G. K. Boreskov, Yu. Sh. Matros, A. I. Oruzheinikov, A. V. Filatov, V. I. Volkov, A. I. Toporovskii, V. A. Orlov, N. N. Kundo: Certificate of Authorship, No. 911852, USSR 1984.

[18] G. K. Boreskov, A. S. Noskov, Yu. Sh. Matros, I. A. Zolotarskii, V. N. Men'shov: Certificate of Authorship, No. 1 188 095, USSR 1985.
[19] F. Berruti, R. R. Hudgins, E. Rhodes, S. Sicardi, *Can. J. Chem. Eng. 62* (1984) 644.
[20] P. L. Mills, M. P. Duducovic, *AIChE/J. 27* (1981) 893.
[21] V. I. Drobyshevich, V. A. Kirillov, *PMTF Zh. Prikl. Mekh. Tekh. Fiz. 1985*, 66.
[22] G. K. Boreskov, Yu. Sh. Matros, O. P. Klenov, V. I. Lugovskoy, V. S. Lakhmostov, *Dokl. Akad. Nauk SSSR 258 6* (1981) 1418.
[23] O. P. Klenov, Yu. Sh. Matros: *Aerodynamics of Fixed Bed Catalytic Reactors*, Nauka, Novosibirsk 1985, p. 4–15.
[24] Yu. Sh. Matros, N. A. Chumakova, *Dokl. Akad. Nauk SSSR 250 6* (1980) 1421.
[25] N. A. Chumakova, Yu. Sh. Matros: *Mathematical modelling of catalytic reactors*, Nauka, Novosibirsk 1989, p. 5–26.
[26] Yu. P. Gupalo, Yu. S. Ryazancev, *PMTF Zh. Prikl. Mekh. Tekh. Fiz. 1969*, 82.
[27] J. P. Lee, V. Balakotaiah, D. Luss, *Chem. Eng. Sci. 41* (1986) 749.
[28] J.-P. Lee, V. Balakotaiah, D. Luss, *AIChEJ. 33* (1987) 1136.
[29] O. V. Onis'kova, E. P. Martsevoi, V. V. Chislovskii: *Modelling of Reactors for Plasmochemical Homogeneous Processes*, Naukova Dumka, Kiev 1982, p. 200.
[30] V. A. Bogomolov, A. N. Zolotnikov, A. D. Kadushkin: *Pulsing Reactors (Abstr. All-Union Conf. Khimreaktor-10, Vol. 1)*, Kuibyshev-Tol'yatti, 1988, p. 168–172.
[31] V. N. Genkin, V. V. Sokolov, *Dokl. Akad. Nauk SSSR 234* 1 (1977) 94.
[32] G. Crone, F. Renken, *Chem. Ing. Tech. 51* (1978) 42.
[33] Yu. P. Gupalo, B. A. Novihev, Yu. S. Ryazancev, *Prikladnaia Mathematika i Mechanika 46* (1982) 254.
[34] G. Stephanopoulos, A. G. Fredrickson, R. Aris, *AIChE J. 25* (1979) 863.
[35] J. M. Douglas, D. W. T. Rippiu, *Chem. Eng. Sci. 21* (1966) 305.
[36] A. Renken, *Chem. Ing. Tech. 54* (1982) 571.
[37] P. L. Silveston, *Sadhana 10* (1987) 217.
[38] Yu. Sh. Matros: *Catalytic Processes under Unsteady-State Conditions*, Elsevier, Amsterdam New York 1989.
[39] L. I. Kheifets, A. B. Gol'dberg, *Electrokhimiya 25* (1989) 3.
[40] V. S. Krylov, A. D. Davydov, *Sov. Chem. Ind. 13* (1981) 1499.
[41] H. D. Wilson, R. G. Rinker, *Chem. Eng. Sci. 37* (1982) 343.
[42] A. K. Jain, R. R. Hudgins, P. L. Silveston, *Can. J. Chem. Eng. 61* (1983) 824.
[43] H. P. Unni, R. R. Hudgins, P. L. Silveston, *Can. J. Chem. Eng. 51* (1973) 623.
[44] J. P. Briggs, R. R. Hudgins, P. L. Silveston, *Chem. Eng. Sci. 32* (1977) 1087.
[45] A. E. Lisovskii, L. I. Kozharov. Yu. A. Ismailov, T. T. Alhazov, *Kinet. Katal. 19* (1978) 760.
[46] A. Renken, M. Müller, C. Wandrey: *Chem. React. Eng. Proc. Int. Symp. 4th, Vol. 1*, DECHEMA Frankfurt am Main 1976, p. 107–116.
[47] A. S. Al-Tail, L. S. Kerschenbaum, *ACS Symp.Ser. 65* (1978) 512.
[48] F. M. Dantzenberg, J. N. Helle, R. A. Van Santen, H. Verbeek, *J. Catal. 50* (1977) 8.
[49] L. L. Hegedus, C. C. Chang, D. J. McEwen, E. H. Sloan, *Ind. Eng. Chem. Fundam. 19* (1980) 367.
[50] M. P. Cutlip, *AIChE J. 25* (1979) 502.
[51] H. K. Abdul-Kareem, P. L. Silveston, R. R. Hudgins, *Chem. Eng. Sci. 35* (1980) 2077.
[52] E. J. Leupold, A. Renken, *Chem. Ing. Tech. 49* (1977) 667.
[53] P. Valko, Yu. Sh. Matros, *Teor. Osn. Khim. Tekhnol. 16* (1982) 33.
[54] A. M. Ahmetzyanov, V. A. Kuzin, Yu. Sh. Matros, A. S. Noskov, *Teor. Osn. Khim. Tekhnol. 20* (1986) 626.
[55] Yu. Sh. Matros. *Zh. Vses. Khim. Ova im. D. I. Mendeleeva. 22* (1977) 576.
[56] G. K. Boreskov, Yu. Sh. Matros, O. V. Kiselev, G. A. Bunimovich, *Dokl. Akad. Nauk SSSR 237* (1977) 160.
[57] Yu. Sh. Matros in *Large Chemical Plants 7*, Bruges 1988, pp. 21–33.
[58] G. K. Boreskov, Yu. Sh. Matros, V. S. Lakhmostov, Certificate of Authorship, No. 1160201, USSR 1989.
[59] L. N. Bobrova, A. S. Noskov, Yu. Sh. Matros, E. M. Slavinskia, *Khim. Tekhnol. (Kiev) 5* (1989) 80.
[60] Yu. Sh. Matros, *Sulphur 183* (1986) 23.
[61] Yu. Sh. Matros, A. N. Zagoruiko, *Dokl. Akad. Nauk SSR 294 6* (1987) 1424.
[62] A. N. Zagoruiko, A. S. Noskov, V. I. Drobyshevich, L. V. Yausheva, I. V. Malakhova, Yu. Sh. Matros, *Teor. Osn. Khim. Tekhnol. 23* (1989) 209.
[63] Yu. Sh. Matros, A. N. Zagoruiko, I. V. Malakhova, O. G. Eremin, GB-Pat. 2206108 (1988).

Molecular Thermodynamics for Chemical Process Design

By John M. Prausnitz*

Thermodynamic properties are essential for quantitative process design to produce chemical products. Caloric properties are required for heat balances, but these properties are usually available or estimated easily. More important—and often much more difficult to estimate—are the chemical potentials of components in mixtures; it is these potentials which determine phase equilibria, as required for separation operations, and chemical equilibria, as required for chemical reactors and for separation operations based on chemical reactions. Molecular thermodynamics is an engineering-oriented science for calculating the desired chemical potentials from a minimum of experimental data. This applied science, based on classical and statistical thermodynamics, yields chemical potentials through models that are based on molecular physics and physical chemistry. Selected examples are cited to illustrate the applicability of molecular thermodynamics: group-contribution methods for obtaining chemical potentials in highly nonideal mixtures as required for distillation-column and process-safety design; equation of state for precipitation of uniform-sized crystals from supercritical fluids; molecular-orbital calculations to guide process development for alternatives to environmentally dangerous chlorofluorohydrocarbons; molecular-simulation calculations for separation of gas mixtures with porous adsorbents; equilibria in two-phase aqueous systems for separation of protein mixtures; and, finally, extended polymer-solution thermodynamics to guide synthesis of hydrogels suitable for protein recovery from soybeans and for novel drug-delivery devices.

1. Introduction

One generation ago, the goal of chemical engineering was stated easily: to establish efficient and economic methods for producing on a large scale what the chemist or material scientist produces in small quantities. Today, that statement is incomplete. Today's chemical engineer does not start where the chemist stops. Increasingly, chemists and chemical engineers work together on product conception and development. Twenty-five years ago, chemists and chemical engineers worked in series: first the chemist, then the chemical engineer. Today they must work in parallel.

If the idea for a new product is to become a reality, then its early development must soon be linked to a process for its production. That process must be concerned not only with production capacity and product quality but, increasingly, with consideration for safety and for environmental protection.

Chemical process design is based on several scientific disciplines, whose relative importance depends on the nature of the product. Only a few of these disciplines are always essential; they are the cornerstones of chemical engineering. One of these is chemical thermodynamics. This article presents some applications of chemical thermodynamics for chemical engineering.

For process design, the first law of thermodynamics gives energy balances which require primarily caloric properties of materials; these properties are usually available from published experimental data or from semiempirical correlations.

[*] Prof. J. M. Prausnitz
Chemical Engineering Department
and
Chemical Sciences Division
Lawrence Berkeley Laboratory
University of California
Berkeley, CA 94720 (USA)

The second law of thermodynamics gives a quantitative framework for calculating phase equilibria and chemical equilibria. These equilibria are essential for the design of separation operations such as distillation and extraction and they are often required for design of chemical reactors and for separation operations based on chemical reactions.

2. The Chemical Potential

For calculation of equilibria in mixtures, the most important thermodynamic property is the chemical potential μ for every component in the mixture, as a function of temperature, pressure, and composition. These chemical potentials are often not readily available.

The essential relations for phase equilibria and chemical equilibria were given by *Gibbs* 115 years ago; they are remarkably simple. When two phases (′ and ″) are in equilibrium, Equation (1) holds for every component i that exists in these phases.

$$\mu_i' = \mu_i'' \tag{1}$$

When a reversible chemical reaction, $A + B \rightleftharpoons C$, attains equilibrium, Equation (2) holds.

$$\mu_C = \mu_A + \mu_B \tag{2}$$

While the Gibbs equations are deceptively simple, it is their reduction to practice which is difficult, especially for multicomponent systems containing complex molecules. For such systems, experimental data are scarce or, as often happens, totally absent.

To apply chemical thermodynamics to chemical process design, it is necessary to relate the abstract, essentially mathematical, chemical potential μ to the physical, measurable

quantities pressure P, temperature T, and composition x. Classical thermodynamics gives only formal relations between the chemical potential and other macroscopic properties. To establish relations between the chemical potential and molecular properties, we must go beyond classical thermodynamics to statistical thermodynamics. But for most realistic situations, present knowledge in statistical thermodynamics is not sufficient. To reduce the Gibbs equations to practice, it is necessary to establish approximate models based on molecular physics or physical chemistry. The parameters that appear in these models are obtained from only a few experimental measurements. These models serve as a bridge between the Gibbs equations and the quantities needed for chemical process design. It is the development and application of these approximate but useful models which we call molecular thermodynamics.[1] Molecular thermodynamics provides essential information for the manufacture of a large variety of chemical products, as illustrated by the examples below.

3. Nonideal Liquid Mixtures: Activity Coefficients from Group Contributions

In the chemical industries many (indeed most) separation methods are based on phase-contacting: at equilibrium, when two phases are in contact, the composition of one phase is not the same as that of the other; well-known examples are distillation, absorption, extraction, crystallization, and adsorption. In chemical technology, separation operations are essential. In the manufacture of numerous chemical products, separation costs are often dominant; it is therefore of direct economic interest to conceive and design efficient separation operations. To achieve that efficiency, it is necessary to know the thermodynamic properties of mixtures, especially liquid mixtures.

Thermodynamic properties are conveniently expressed through models based on the ideal-solution concept; the large advantage of the ideal solution is that properties of mixtures can often be predicted using only experimental data for the pure components. For real solutions, the ideal-solution equations serve as a useful point of departure for constructing a systematic theory; to represent the properties of real solutions, we require activity coefficients γ. For every component i in a liquid mixture, we require its activity coefficient, which, typically, depends strongly on composition, moderately on temperature, and (except for high pressures or critical conditions) weakly on pressure.

There are numerous methods for measuring activity coefficients and the literature is rich with experimental results, especially for binary systems at temperatures near ambient. But the possible number of mixtures (especially multicomponent mixtures) and the extensive variety of conditions (composition, temperature) are so large, that experimental determination of all desired activity coefficients is prohibitive. One task of molecular thermodynamics is to provide a procedure for estimating coefficients for a wide variety of mixtures, using minimum experimental information.

For liquid mixtures containing typical nonelectrolytes (e.g., hydrocarbons, ketones, alcohols, nitriles, ethers, weak organic acids, esters, water), activity coefficients can often be estimated from group contributions.

To illustrate, consider a mixture of toluene and acetone. For each component, there are two contributions to the activity coefficient: the first comes from the difference in molecular size, the second from attractive forces between molecular pairs. In this binary mixture there are three possible pairs: toluene–toluene, acetone–acetone, and toluene–acetone. To characterize these pair interactions, it is useful to introduce the group-contribution concept: each molecule is divided into groups as indicated in Figure 1. The interaction between one molecule and another is given as the sum of the group–group interactions, where each group in the first molecule interacts with each group in the second.

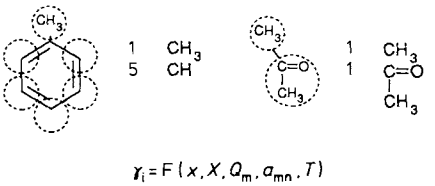

Fig. 1. Activity coefficients γ from group contributions, as exemplified by a mixture of toluene and acetone. γ_i = activity coefficient of toluene or acetone; x = molecular mole fraction; X = group mole fraction; Q_m = size of group m; a_{mn} = energy of interaction between group m and group n.

Contributions to γ_i from differences in molecular size depend on the composition through the usual mole fractions x. But contributions to γ_i from differences in attractive intermolecular forces depend on composition through the *group* mole fractions X. A semiempirical framework for calculating γ_i is provided by a model called UNIFAC.[2–4]

UNIFAC provides a group-contribution method for characterizing molecule–molecule interactions by summing suitably weighted group–group parameters for each group–group interaction. This procedure has a significant advantage: while the number of different molecules of interest in chemical technology is very large, these molecules are composed of a much smaller number of groups that appear over and over again. Nearly all organic molecules of current interest can be characterized by perhaps 40 to 60 groups, depending on how much distinction one allows for steric effects or for the influence of neighboring groups. In the group-contribution method, we replace molecule–molecule interaction parameters by group–group interaction parameters. For a wide variety of fluid mixtures, the number of different group–group interaction parameters is much smaller than the number of different molecule–molecule interaction parameters. Using group–group interaction parameters obtained from published activity-coefficient data, it is possible to predict activity coefficients for mixtures that have not been studied experimentally.

During the last 15 years, there has been a concerted effort to evaluate group–group interaction parameters from experimental data. Thanks to numerous contributors, primarily Prof. *Fredenslund* and Dr. *Rasmussen* and their co-workers at the Technical University of Denmark and Prof. *Gmehling* and his co-workers at the University of Dortmund (now at the University of Oldenburg), we now have a substantial

data bank of group–group interaction parameters; we also have computer programs for calculating activity coefficients based on UNIFAC.

To illustrate applicability, Figure 2 shows a freezing-point diagram for the system benzene–phenol. The lines are predictions; the points show experimental results. With some modifications, UNIFAC has also been applied to polymer solutions.[5–7] Some illustrative results are shown in Figure 3.

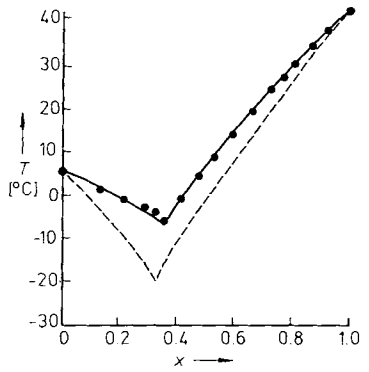

Fig. 2. Solid–liquid equilibria for the system benzene–phenol x = mole fraction of phenol in liquid phase; • = experimental; —— = predicted by UNIFAC; – – – = predicted for an ideal solution.

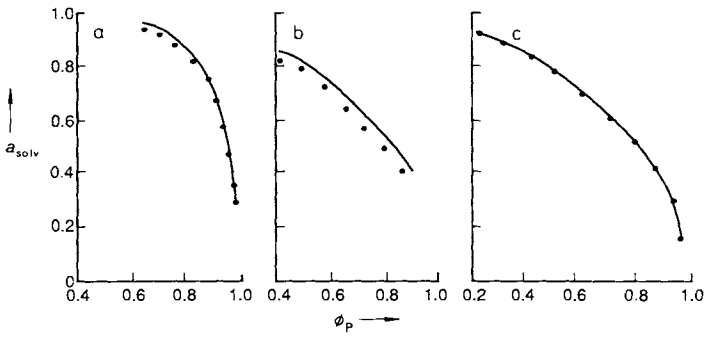

Fig. 3. Activities a of solvents in polymer solutions calculated from group contributions. Φ_p = volume fraction polymer; $\bar{M}$ = number-average molecular weight; • = experimental;—predicted by UNIFAP (UNIFAC for polymers). a) Benzene in polyisobutylene, 25 °C, $\bar{M}$ = 40000; b) ethyl acetate in polyvinyl acetate, 30 °C, $\bar{M}$ = 110000; c) benzene in polyethylene oxide, 70 °C, $\bar{M}$ = 5700.

Flaningham and *Hand*[8] have recently described an application of UNIFAC concerning the manufacture of silicones for specialty polymers, wetting agents, anti-foaming formulations, and numerous other uses in electronics and packaging. A key step in the manufacture of silicones is the synthesis of chlorosilanes, that is, compounds of silicon, hydrogen, and chlorine. In the chemical reactor, where silicon is allowed to react with methyl chloride, many different chlorosilanes are produced. Following synthesis, it is necessary to separate those chlorosilanes desired for a particular silicone from numerous side products. By studying experimentally a few selected binary mixtures of chlorosilanes, *Flaningham* and *Hand* obtained a set of pertinent group–group parameters; using UNIFAC, they are then able to predict activity coefficients in multicomponent mixtures containing many different chlorosilanes.

UNIFAC (or any other group-contribution method) does not eliminate the need for experimental data, but it very much reduces the amount of experimental work that is needed to estimate activity coefficients in multicomponent mixtures. The accuracy of prediction is not very high, but it is often sufficient for preliminary design purposes.

Two additional examples indicate the versatility of the group-contribution method. These examples are not concerned with the usual distillation or extraction applications found in textbooks. Instead, they are concerned with a subject that has always been important but that in recent years has become a major focus of industrial chemistry: safety.

In chemical process design, serious attention must be given to prevention of fires and explosions. Toward that end, a useful design parameter is the flash temperature (also called flashpoint), that is, the temperature where a flame can be propagated when the equilibrium vapor of a liquid is mixed with air at atmospheric pressure, as illustrated in Figure 4. L_i

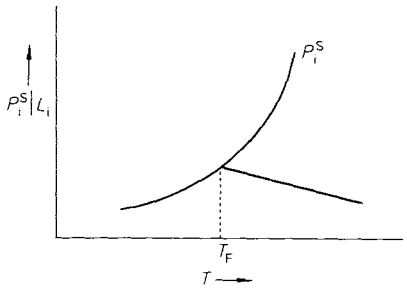

Fig. 4. Flash temperature T_F for a pure substance. P_i^s = partial pressure (vapor pressure) of liquid i; L_i = partial pressure of i at lower flammability limit.

has been obtained experimentally for many liquids using standardized procedures. Figure 4 is for a pure liquid. To calculate the flash temperature for a liquid mixture, we must find the temperature which satisfies relation (3), where p_i is the partial pressure of component i in the liquid mixture.

$$\sum_i p_i/L_i = 1 \tag{3}$$

(Equation (3) is not exact but provides a good approximation.) For finding the flash temperature of a mixture, the essential problem is the calculation of p_i given by Equation (4),

$$p_i = \gamma_i x_i P_i^s \tag{4}$$

where x_i is the mole fraction of component i in the liquid mixture and γ_i is its activity coefficient.

A group-contribution method such as UNIFAC can be used to estimate γ_i. To illustrate, Figure 5 compares UNIFAC predictions with experimental results for the flash temperatures of water–ethanol mixtures.[9] Similarly, Figure 6 shows calculated and experimental flash temperatures for the partially immiscible binary system methanol–heptane.[10] Also shown are predicted results assuming ideal-solution behavior ($\gamma_i = 1$). Figure 6 shows that flash tempera-

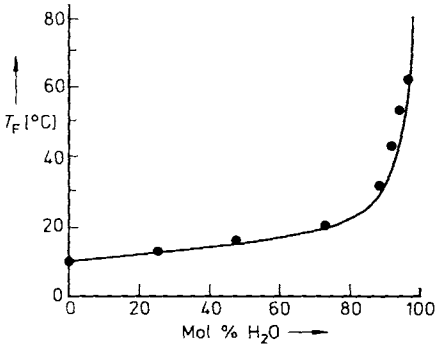

Fig. 5. Predicted and observed flash temperatures T_F for mixtures of ethanol and water. • = experimental (*M. Choe, H. G. Schecker*, 1981); — = predicted using UNIFAC [9].

tures based on ideal-solution behavior are dangerously high because they indicate that the mixtures are safe under conditions where, in fact, they are not safe.

Activity coefficients may also find application in monitoring air quality in chemical plants where solvent mixtures are used. Vapors from these mixtures may be harmful to plant personnel. To monitor air quality, it is often possible to use a chemical sensor which continuously measures the concentration of one key component, but it is not practical to use sensors for every component that may exist in the multicomponent solvent mixture.

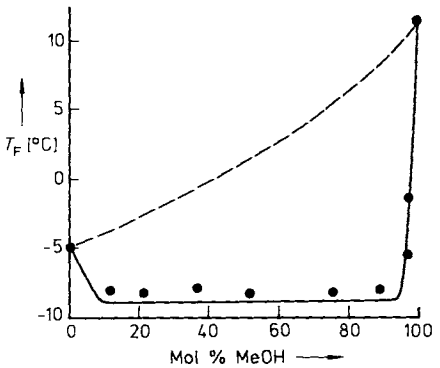

Fig. 6. Predicted and observed flash temperatures for mixtures of methanol and heptane, including the partial-miscibility region. • = experimental (*M. Choe*, 1982); — = predicted using UNIFAC [10]; - - - = predicted for an ideal solution.

In a chemical plant, the composition of the air depends not only on the equilibrium partial pressures of the components in the solvent mixture but also on the extent of ventilation. Suppose the chemical sensor measures Y_j, the moles of component j per liter of air. For typical solvent mixtures, the ratio of Y_i to Y_j can be estimated to a good approximation by Equation (5), where x is the liquid-phase mole fraction,

$$\frac{Y_i}{Y_j} = \frac{\gamma_i x_i P_i^s}{\gamma_j x_j P_j^s}\left(\frac{D_i}{D_j}\right)^k \tag{5}$$

P^s the pure-liquid vapor pressure, γ the activity coefficient, and D the diffusivity in air. Under stagnant conditions (negligible flow of air), $k = 1$. As air velocity rises, k falls. For typical normal ventilation conditions, $k = 0.5$.[11]

Equation (5) provides a simple method for continuous chemical analysis of air pollutants arising from solvent mixtures. Analytical measurement is required for the concentration of only one key component (j); the concentrations of the others (i) are calculated. The estimate provided by Equation (5) requires the liquid-phase composition of the solvent mixture, as well as pure-component vapor pressures and diffusivities in air, which depend only on temperature. But in addition, Equation 5 requires activity coefficients, which often depend strongly on composition; for components at high dilution, γ_i may be of the order of 10 or 100. These activity coefficients can be obtained from a group-contribution method. While the accuracy is not very high, it is often sufficient for maintenance of industrial hygiene. In a chemical production facility where solvent mixtures may present a potential health hazard, a single chemical sensor, coupled with a microprocessor, can produce continuous surveillance of air quality.

4. Crystallization of Uniform Particles from a Supercritical Solvent

For describing the thermodynamic properties of fluids, the classical procedure (dating back more than 100 years to *van der Waals*) is to construct an equation of state, that is, an equation relating the pressure of a system to its temperature, density, and composition. From a equation of state, we can calculate many of the thermodynamic properties required for chemical process design.

A well-known application of equations of state is for calculation of vapor–liquid equilibria as required for design of distillation columns, especially at high pressure.[1] Since that application is well described, we need not discuss it here. Instead, we call attention to a recent application, which is directed at design of a crystallization process for obtaining very small crystals with a narrow size distribution, as required, for example, for pharmaceutical products.

Normally, crystallization is achieved by cooling a solution of the desired solid in a liquid solvent. Since bulk cooling cannot be achieved rapidly, thermal gradients in the solution tend to produce a broad distribution of particle sizes. By contrast, if the liquid solvent is replaced by a dense gas near its critical state, a small, sudden decrease in pressure can precipitate particles of uniform size. The essential advantage is that the solvent power of a dense gas falls very quickly in response to a drop in pressure. To design a pressure-induced crystallization process, we need to know the solubility of the solid component in the dense gas as a function of temperature and pressure; that solubility can be obtained from an equation of state. Further, the rate of crystallization is described by theories which require information on the chemical potential of the dissolved solid in a supersaturated solvent; that chemical potential is also obtained from the same equation of state.

Chang and *Randolph*[12] designed a process for recrystallizing β-carotene from supercritical ethylene; β-carotene is a potentially useful medication for lowering blood cholesterol and for cancer prevention. For optimum pharmaceutical effect, β-carotene particles should be small with a narrow size distribution.

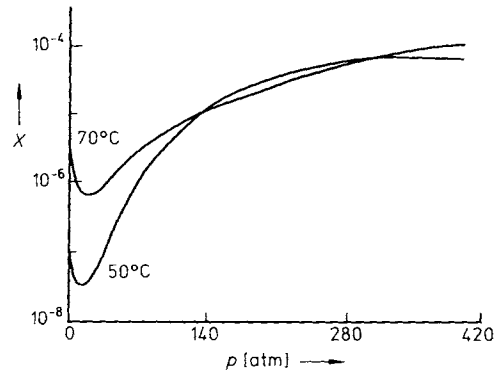

Fig. 7. Solubility of β-carotene in supercritical ethylene. The calculations are based on a modified Peng–Robinson equation of state, using only a few experimental measurements [12]. x = mole faction of β-carotene.

Figure 7 shows the solubility of β-carotene in ethylene, whose critical temperature and pressure are 9 °C and 50 atm. Near critical conditions, a small change in pressure can produce a large change in solubility. The results were obtained using an equation of state coupled with only a few experimental data. Figure 8 shows two size distributions for solid β-carotene particles. The broad distribution is for the feed material, the narrow distribution for the product crystallized from supercritical ethylene.

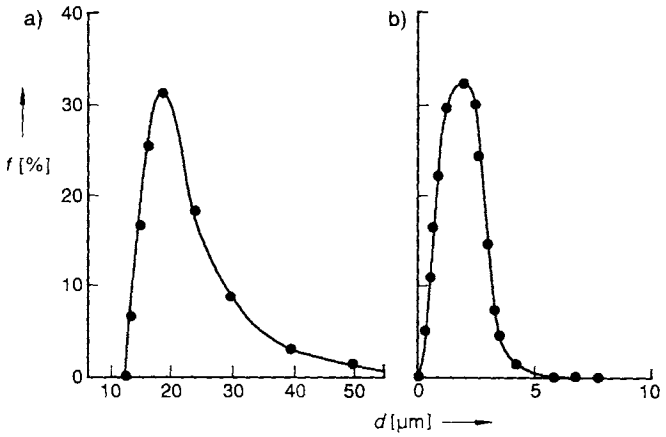

Fig. 8. Crystallization of β-carotene from supercritical ethylene. The product has a much smaller average particle size and a more narrow size distribution. f = differential fraction expressed as per cent; d = particle diameter. a) Experimental data for feed; b) experimental data for product.

Design of a supercritical-fluid crystallization process requires transport data (heat and mass transfer) in addition to thermodynamic information. But the thermodynamic information is primary because, prior to any rate calculations, it addresses the question of feasibility: what conditions are needed to make a process possible? An equation of state, coupled with a few experimental measurements, can quickly answer that question.

5. Thermodynamic Properties from Molecular (Computer) Simulations

The range of thermodynamic applications in industry has been significantly extended by supercomputers which enable calculation of thermodynamic properties by molecular simulations. In such simulations, intra- and intermolecular forces are given by quantum-mechanical or semiempirical equations. The properties of individual molecules or of assemblies of molecules are then obtained by numerical methods which require vast computing power. To illustrate such applications, we briefly discuss two examples.

5.1. Chemical Stabilities of Chlorofluorohydrocarbons (Freons)

Chlorofluorohydrocarbons are used extensively throughout the world as coolants in refrigerators and air conditioners, as blowing agents, and as solvents. But, unfortunately, many commonly used freons destroy ozone in the stratosphere and therefore, to protect the environment, there has been a search for new refrigerants that are useful for technology but that do not decompose ozone.

Ironically, presently used freons are environmentally unacceptable because of their remarkable chemical stability. A typical conventional freon passes through the troposphere without decomposing and then has a long lifetime in the stratosphere, where, ultimately, ultraviolet radiation causes cleavage of C–Cl bonds; the released chlorine atoms catalyze ozone decomposition.

For a compound i, chemical stability is measured by an equilibrium constant K_i given by $K_i = \exp - G_i^f/(RT)$, where R is the gas constant and G_i^f the Gibbs energy of formation of compound i from its stable elements; for example, for CF_2Cl_2, G^f is the change in Gibbs energy for reaction (6). For high stability (large K_i), $G^f/(RT)$ is negative and much larger than unity.

$$C + F_2 + Cl_2 \rightarrow CF_2Cl_2 \qquad (6)$$

The stabilities of conventional freons are so high that they reach the stratosphere where, eventually, they contribute to ozone decomposition; such freons must be rejected. On the other hand, chlorofluorohydrocarbons with very low stability constants are also unsatisfactory because they decompose too easily. To provide guidance in searching for an environmentally acceptable refrigerant, it is desirable to have G^f values for numerous chlorofluorohydrocarbons so that those with very high or very low stability constants can be eliminated from further consideration.

The Gibbs energy of formation is obtained from H^f, the enthalpy of formation, and S^f, the entropy of formation [Eq. (7)].

$$G^f = H^f - T S^f \qquad (7)$$

While H^f can be measured directly using calorimetry, S^f is obtained from the third law of thermodynamics through integration of heat-capacity measurements at low temperatures. The required experimental measurements are tedious and require much patience. Therefore, experimental G^f results are available for only a limited number of chlorofluorohydrocarbons.

Molecular simulation provides an alternative to experimental measurements. The enthalpy of formation can be

...ated using molecular-orbital theory and, for molecules of moderate size at reasonable temperatures, the entropy of formation can be calculated using statistical mechanics with parameters obtained from spectroscopic correlations.[13]

It is therefore possible to use large computers to generate stability constants for a substantial number of refrigerants that *may* be useful for technical application. The stability constant can immediately tell us whether a given chlorofluorohydrocarbon can exist under ordinary conditions and whether it is likely to decompose before it reaches the stratosphere.

In the troposphere, the most common reactive species is the hydroxyl radical ·OH. To estimate if a chlorofluorohydrocarbon is likely to decompose, it is therefore helpful to calculate the equilibrium constant for reaction (8). For that calculation we again require the Gibbs energy of formation of the chlorofluorohydrocarbon in the reaction.

$$\text{chlorofluorohydrocarbon} + {}^{\cdot}\text{OH} \rightarrow \text{products} \qquad (8)$$

While kinetic and other nonthermodynamic properties are also important for assessing a chlorofluorohydrocarbon, molecular-simulation calculations provide a helpful screening procedure; these calculations give guidance concerning which refrigerants are most likely to satisfy requirements for technical applicability as well as for meeting environmental concerns.

5.2. Adsorption of Gas Mixtures

Another industrially oriented example is provided by molecular-simulation calculations for adsorption of gas mixtures in porous media. For a given system of gases and adsorbent at fixed temperature, these calculations give the individual amounts of fluid adsorbed per gram of adsorbent as a function not only of partial pressure, but also of pore size.

Consider adsorption of methane on solid carbon as shown schematically in Figure 9. Because there is a strong energy of

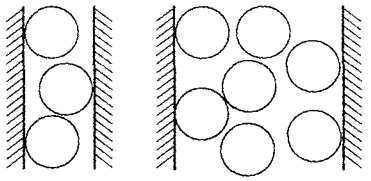

	Small pores	Large pores
Surface area per gram of carbon	High (ΔH is strongly favorable)	Low (ΔH is only weakly favorable)
Accessibility of pores to methane molecules	Low (ΔS is strongly unfavorable)	High (ΔS is only weakly unfavorable)

Fig. 9. Effect of particle size on adsorption of methane on carbon.

attraction between a methane molecule and the carbon atoms of the solid, methane "likes" to adsorb on the carbon surface. To maximize adsorption per gram of carbon, it is desirable to increase the surface area per gram; this increase is achieved by using porous carbon. But now a problem arises: to maximize surface area, we want very small pores; however, if the pores are too small, the methane molecules are not able to move easily into and within the pore. We have here a classical optimization problem directly related to thermodynamics [Eq. (9)].

$$\Delta G(\text{adsorption}) = \Delta H(\text{adsorption}) - T\Delta S(\text{adsorption}) \qquad (9)$$

For strong adsorption, we want ΔG(adsorption) to be large and negative. Because methane is attracted to carbon, ΔH(adsorption) is negative and that is good; we want a large surface area, because ΔH(adsorption) is directly proportional to the accessible surface area. But ΔS(adsorption) is also negative and—because of the minus sign in Equation (9)—that is not good. As pores become smaller, the magnitude of ΔS(adsorption) becomes increasingly larger due to geometrical interference of the methane molecules in the pore; this interference is called the excluded-volume effect. As pore size becomes very small, the total surface area rises but the accessible surface area declines.

For a fixed temperature and partial pressure of methane, there is an optimum pore diameter where methane adsorption is maximized. This optimum can be calculated using molecular simulations.

Instead of methane, consider ethane adsorbing on the same carbon surface. Again, we can use molecular simulation to calculate an optimum pore diameter. The optimum pore diameter for ethane will not be the same as that for methane, because ethane molecules are larger than methane molecules and because the attractive energy for ethane-carbon is not the same as that for methane-carbon.

But now, finally, consider a mixture of methane and ethane. We want to separate the mixture by adsorption using a carbon adsorbent; what is the best pore diameter for achieving this separation? In other words, what pore diameter will give the maximum selectivity β?

The selectivity of component 2 (ethane) relative to component 1 (methane) is defined by Equation (10), where ζ is the mole fraction in the adsorbed phase and y is the mole fraction in the bulk (gas) phase. For efficient separation, we want β_{21} to be as large as possible.

$$\beta_{21} = \frac{y_1(1-\zeta_1)}{\zeta_1(1-y_1)} \qquad (10)$$

Consider a gaseous mixture at 200 K containing 90 mol% methane and 10 mol% ethane; at 18.6 bar, this mixture is near its dew point. We want to remove ethane by selective adsorption on porous carbon. For this mixture, Figure 10 shows selectivities calculated by *Tan* and *Gubbins*[14] as a function of pore diameter. For small pores, the selectivity oscillates as pore size rises, as we might expect since the diameter of methane is about 3.8 Å while that for ethane is only a little larger. For small pores, wall effects are extremely important. As pore size increases, wall effects begin to disappear and eventually the selectivity reaches an asymptotic value where pore size no longer matters.

An economic adsorbent must possess not only good selectivity but also high capacity. The model used by *Tan* and *Gubbins* necessarily gives only an idealized representation of a real porous carbon. A model should never be confused with reality. Nevertheless, computer-generated calculations

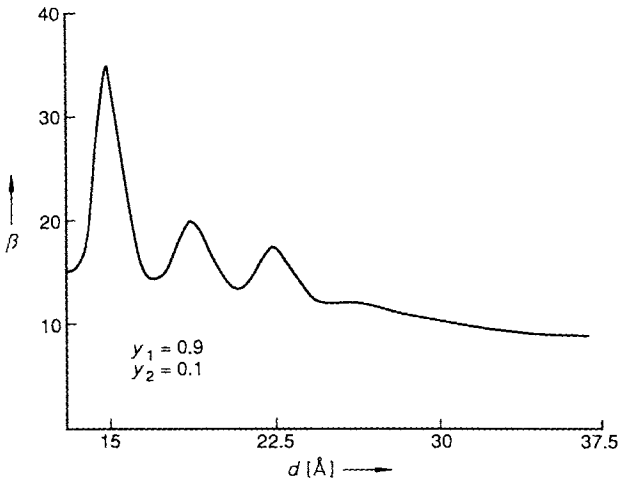

Fig. 10. Molecular simulation of the effect of pore diameter on selectivity in adsorption of a mixture of methane (1) and ethane (2) on carbon [14]. β = selectivity; d = pore diameter; y = mole fraction in the gas phase; $T = 200$ K; $p = 18.6$ bar.

similar to those outlined here can provide guidance for selecting the best absorbent for a desired separation.

6. Separation of a Protein Mixture

The rising importance of biotechnology presents a new challenge: Can molecular thermodynamics be extended to apply also to biotechnical processes? Efforts toward that end are now in progress in many laboratories. An example is provided by applying molecular thermodynamics toward design of an aqueous two-phase extraction process for separation of mixtures containing proteins.

Figure 11 presents a schematic of the extraction system. When two water-soluble polymers are dissolved in an excess

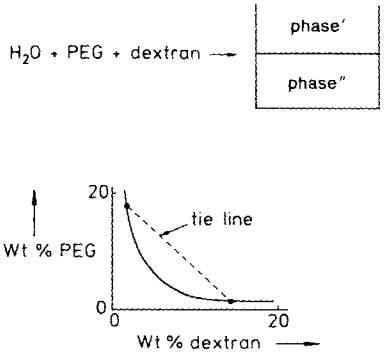

Fig. 11. Formation of a two-phase aqueous mixture for extraction. Phase' = PEG containing a small amount of dextran; phase" = dextran containing a small amount of PEG. Below: Calculated phase diagram.

of water, we obtain two separate phases. Figure 12 indicates the extraction process; when a mixture of proteins is added to the two-phase aqueous system, some proteins prefer to go to the upper phase, others to the lower phase. Therefore, separation can be achieved.

Typical phase-forming polymers are polyethylene glycol (PEG) and dextran. To prevent denaturation and to maintain pH control, small amounts of (buffer) salts may be added. The desired contribution of molecular thermodynamics is to provide a model for predicting the partition coefficient of a protein.

Fig. 12. Separation of a mixture of proteins i, j, k, ... by extraction. For the definition of the partition coefficient K, see Equation (13).

The first task is to calculate the liquid–liquid phase diagram formed by water and the two water-soluble polymers. This calculation is achieved by expressing the chemical potentials of all three components through an osmotic virial expansion in the polymer concentrations; the coefficients in that expansion are obtained from low-angle light-scattering data.[15]

For equilibrium between liquid 1 and liquid 2, Equation (11) holds; μ is the chemical potential; subscript 1 refers to

$$\mu_1' = \mu_1''; \; \mu_2' = \mu_2''; \; \mu_3' = \mu_3'' \tag{11}$$

water and subscripts 2 and 3 refer to the water-soluble polymers. For i = 1, 2 or 3, μ_i is given by Equation (12),

$$\mu_i = \mathscr{J}_i \text{ [concentrations of 2 and 3; } B_{22}; B_{33}; B_{23}] \tag{12}$$

where B_{jk}, the osmotic second virial coefficient, reflects the interaction of solute molecule j with solute molecule k in the aqueous solvent. $\mathscr{J}_i$ is a known function, obtained from the osmotic virial expansion.

With virial coefficients obtained from low-angle laser light-scattering measurements, it is possible to generate a reliable phase diagram, as shown schematically at the bottom of Figure 11.

Consider now a protein component (4) which is distributed between the two aqueous phases. The partition coefficient K is defined by Equation (13).

$$K_4 = \frac{\text{concentration of protein in phase'}}{\text{concentration of protein in phase"}} \tag{13}$$

Depending on pH, the protein may be electrically charged and therefore the presence of ions (salts) must be taken into account. When all proteins in the system are dilute, Equation (14) holds. Here, F is Faraday's constant, Φ the electric

$$\ln K_4 = \ln \frac{\gamma_4''}{\gamma_4'} + \frac{F z_4 (\Phi'' - \Phi')}{RT} \tag{14}$$

potential, z the electric charge (vector), and γ the chemical activity coefficient.

Activity coefficients are found from the osmotic virial expansion with coefficients B_{22}, B_{33}, B_{23}, B_{24}, and B_{34}; addi-

tional terms for protein–salt and polymer–salt interactions are obtained from osmometric data.[16]

The electric-potential difference between the two phases arises because the salt does not partition equally between the two phases. This difference is given by a relation [Eq. (15)] similar to the Nernst equation,

$$\Delta\Phi = \Phi'' - \Phi' = \left(\frac{RT}{F}\right)(z_+ + z_-)^{-1} \ln\left(\frac{\gamma''_-}{\gamma''_+}\right)\left(\frac{\gamma'_+}{\gamma'_-}\right) \qquad (15)$$

where z is the absolute value of the ion's electric charge. Activity coefficients γ_+ and γ_- are again found from the osmotic virial expansion.

In typical cases, the potential difference is small, perhaps a few millivolts. But that small potential difference can have a large effect. In some cases, the effect of the potential difference on K_4 is dominant, much more important than that of the activity coefficients.

Figure 13 compares calculated and experimental partition coefficients for albumin, chymotrypsin, and lysozyme. The horizontal axis of Figure 13 is the tie-line length (Fig. 11, bottom), which provides a measure of how different phase′ is from phase″; when the tie-line length is zero, the two phases are identical.

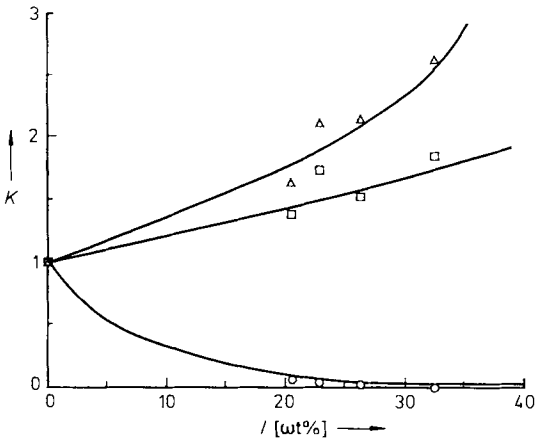

Fig. 13. Predicted and experimental partition coefficients for a protein mixture in an aqueous two-phase system containing PEG 3350, dextran T-70, and 50 mM KCl (overall). l = tie-line length; d = diameter [Å]; z = electric charge; pH = 7.5; 25 °C. ○ = albumin (d = 78; z = −8); □ = chymotrypsin (d = 34; z = 2); △ = lysozyme (d = 22; z = 7).

The molecular-thermodynamic analysis shows that when the protein is charged, the influence of the electric potential is often decisive. This molecular-thermodynamic analysis, therefore, suggests that enhanced partition coefficients for a protein could be obtained by raising the asymmetry of partition of the salt. One method for doing so is provided by adding to the two-phase system a very small amount of α-cyclodextrin and a salt whose cation is strongly adsorbed by that cyclodextrin. Figure 14 shows the effect on the partition coefficient for chymotrypsin when the salt is KI.

We have here a particularly happy example to indicate how molecular thermodynamics can benefit process design. Thermodynamic analysis showed the unexpectedly large influence of salt partitioning on the partition coefficient of a charged protein. Once that influence was identified, the sharpness of separation could be significantly improved by enhancing the electric potential difference between phases′ and ″ through the addition of a suitably chosen entrainer.

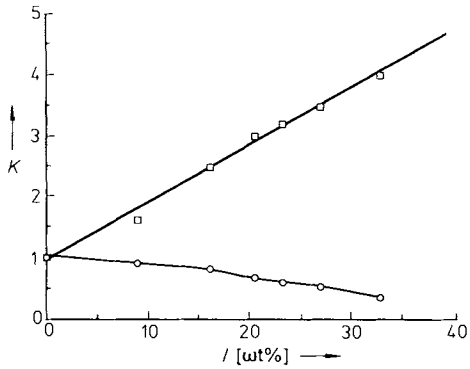

Fig. 14. Effect of electric potential $\Delta\Phi$ on the partition coefficient for chymotrypsin in PEG 3350/dextran T-70/water. z = 5; pH = 7.3; 25 °C. ○ = 1 mM KI; □ = 1 mM KI + 1 mM α-cyclodextrin.

7. Molecular Thermodynamics of Hydrophilic Gels

The traditional domain of chemical thermodynamics has been confined to gases, liquids, and solids. However, especially in recent years, physical chemists and chemical engineers have also applied thermodynamics to partially ordered media such as liquid crystals, micelles, and gels. These partially ordered materials are likely to have numerous applications in different areas of technology including packaging, insulation, extractive metallurgy, and agriculture, as well as medicine and pharmaceutics.

Here we present briefly a few results of recent studies on temperature-sensitive phase transitions in hydrophilic gels made from cross-linked poly(*N*-isopropylacrylamide). When this gel is in contact with water (or with aqueous solutions), it can experience a tremendous increase in volume. That increase depends strongly on temperature.

Figure 15 shows some experimental results by *Hirotsu* et al.[17] where the gel volume is plotted against temperature for different compositions of the aqueous phase. For some temperatures we see large first-order phase transitions; a very small change in temperature can produce either a large

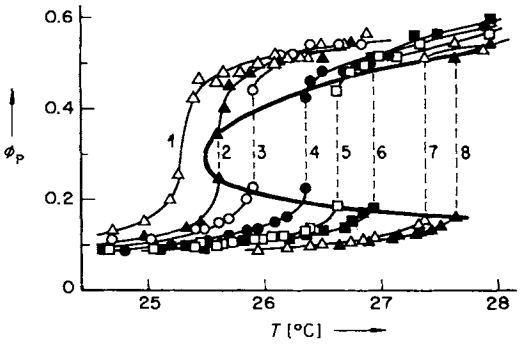

Fig. 15. Swelling of *N*-isopropylacrylamide gels in water–methanol mixtures [17]. Vol% methanol: 18.5 (curve 1), 18.0(2), 17.5(3), 17.0(4), 16.5(6), 15.5(7), 15.0(8). Φ_p = volume fraction of polymer.

swelling of the gel (similar to vaporization of a liquid) or a collapse (similar to condensation). These volumetric properties, including first-order phase transitions, can be described quantitatively using molecular-thermodynamic methods.

Hirotsu's results are for gels in contact with aqueous mixtures. For simplicity, we consider here a gel that is in contact with pure water. For such a gel, the equation of equilibrium is (16), where μ_w is the chemical potential of water. We know the chemical potential of pure water as a function of temperature. However, for the chemical potential of water in the gel phase we must develop an appropriate model.

$$\mu_w(\text{pure liquid}) = \mu_w(\text{gel}) \tag{16}$$

To obtain μ_w (in gel), we need an expression for the Gibbs energy G of the gel phase because μ_w (in gel) is related to G by Equation (17), where n_w = moles of water.

$$\mu_w(\text{in gel}) = \left(\frac{\partial G(\text{gel phase})}{\partial n_w}\right)_{T,p} \tag{17}$$

When water enters a gel phase, there is a contribution to G from mixing; in addition, there is a contribution to G from elastic deformation, because the gel stretches (swells). To calculate the chemical potential of water in the gel, we need one model for mixing water and gel and another for elastic deformation. Fortunately, such models are now available.[18-20] Calculations at two characteristic temperatures are shown schematically in Figure 16. At some unique temperature, when a plot of the second type meets the equal-area criterion (Maxwell construction), we have a first-order phase transition; at that unique temperature, we have three coexisting phases: water, swollen gel, and collapsed gel. Thus, classical thermodynamic methods, coupled with molecular-thermodynamic models, can be used to calculate swelling properties of hydrophilic gels, including phase transitions.

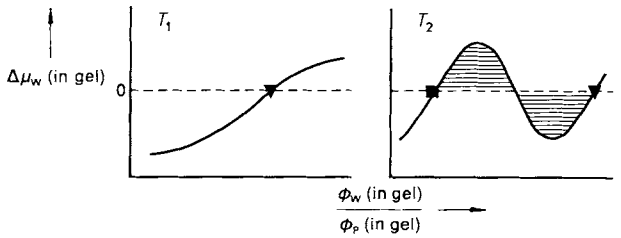

Fig. 16. Phase transition in a temperature-sensitive hydrogel. Φ_w = volume fraction of water. At T_1, water is in equilibrium with swollen gel (▼). At T_2, water is equilibrium with swollen gel (▼) and collapsed gel (■). The shaded areas are equal (Maxwell construction).

Figure 17 shows an application: a continuous extraction process for separating proteins from soybeans, where the extracting agent is a temperature-sensitive gel. By controlling the extent of cross-linking in the gel, water is readily absorbed while protein is not; in effect, the gel acts as a filter. The temperature-sensitive properties of the gel make regeneration possible as required for a continuous process.[21]

Pharmaceutical companies are now giving attention to collapsible gels as devices for drug delivery, shown schematically in Figure 18. For some gels, the collapse can be produced by a small change of temperature; for others, it can be produced by changing the composition or pH of the surrounding liquid. The drug is placed in the fluid-filled gel, which acts as a holding matrix. When the gel collapses, the drug rapidly flows out of the gel by convection. Molecular thermodynamics provides a useful method for correlating and predicting the properties of a gel in response to changing external conditions.[22]

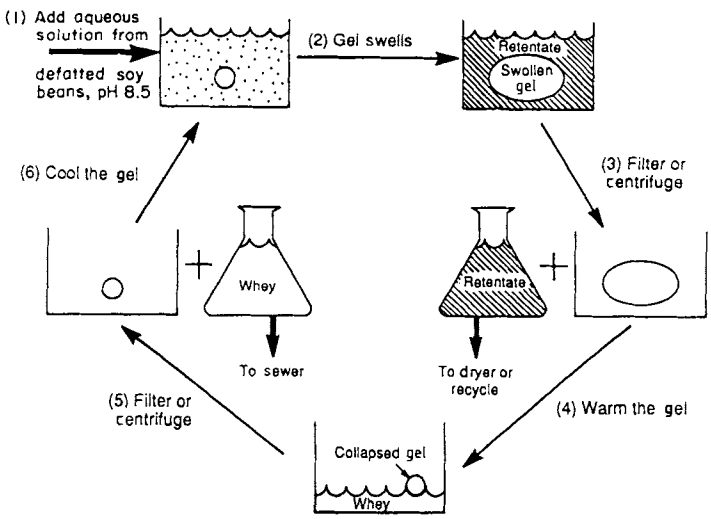

Fig. 17. Purification and concentration of a protein extract (from *Cussler* et al. [21]). Upon swelling, the gel rejects solutes with a molecular weight of about 10^4 or more ("retentate").

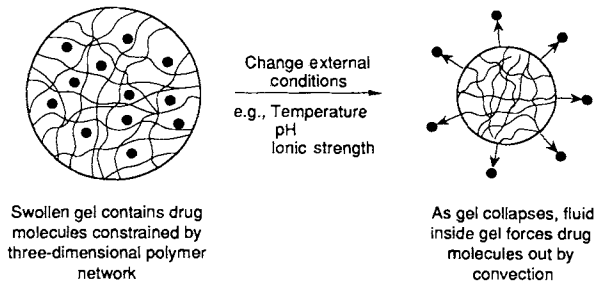

Fig. 18. Gels for controlled drug delivery.

8. Conclusion

The examples presented here show how molecular thermodynamics can contribute toward the development of chemical products and processes. Although the examples indicate a broad variety of applications, they all contain some common characteristics: in every case, there is a combination, a synthesis, of concepts from classical thermodynamics and from molecular physics or physical chemistry. This combination, this synthesis, is expressed through an approximate model that retains the essential physics of the phenomenon but that is also sufficiently simplified so that it can

be used for engineering purposes with a minimum of experimental data.

During the last generation, we have seen two related trends: first, unprecedented advances in science as shown in the exploding scientific literature; second, extensive advances in the quantity and variety of chemical products as shown in the prosperity of our material standard of living. All evidence indicates that these trends will continue and accelerate, subject only to the limits of raw materials and environmental concerns. These trends clearly indicate that there is an ever-growing need for effective communication between fundamental chemical sciences and chemical engineering. This needed communication is one form of what economists call technology transfer, that is, the challenge of bringing new scientific knowledge to the market place. Numerous tools are required to meet that challenge. One of these tools is molecular thermodynamics.

This work was supported, in part, by the Director, Office of Energy Research, Office of Basic Energy Sciences, Chemical Sciences Division of the U.S. Department of Energy. The author is also grateful to the National Science Foundation and to the Donors of the Petroleum Research Fund (administered by the American Chemical Society) for financial support and to Eric Anderson for helpful comments.

Received: April 11, 1990 [A 790 IE]
German version: *Angew. Chem. 102* (1990) 1286

[1] J. M. Prausnitz, R. N. Lichtenthaler, E. G. Azevedo: *Molecular Thermodynamics of Fluid-Phase Equilibria*, 2. ed., Prentice-Hall, Englewood Cliffs NJ, USA 1986.
[2] Aa. Fredenslund, R. L. Jones, J. M. Prausnitz, *AIChE J. 21* (1975) 1086.
[3] Aa. Fredenslund, J. Gmehling, P. Rasmussen: *Vapor-Liquid Equilibria Using UNIFAC*, Elsevier, Amsterdam 1977; R. C. Reid, J. M. Prausnitz, B. E. Poling: *The Properties of Gases and Liquids*, 4th, ed., MC-Graw-Hill, New York 1987, chapter 8.
[4] J. Gmehling, *Fluid Phase Equilib. 30* (1986) 119.
[5] T. Oishi, J. M. Prausnitz, *Ind. Eng. Chem. Process Des. Dev. 17* (1987) 333.
[6] J. Holten-Andersen, P. Rasmussen, Aa. Fredenslund, *Ind. Eng. Chem. Prod. Res. Dev. 26* (1987) 1382.
[7] R. Goydan, R. C. Reid, H. S. Tseng, *Ind. Eng. Chem. Prod. Res. Dev. 28* (1989) 445.
[8] O. L. Flaningham, J. H. Hand: *Application of the UNIFAC Vapor-Liquid Equilibrium Estimation Method to Chlorosilane Compounds* (*Annu. Meet. AIChE*, San Francisco, CA, USA, November 1989).
[9] J. Gmehling, P. Rasmussen, *Ind. Eng. Chem. Fundam. 21* (1982) 186.
[10] M. Choe, J. Gmehling, H. G. Schecker, *Chem. Ing. Tech. 56* (1984) 44.
[11] E. C. Bishop, W. Popendorf, D. Hanson, J. M. Prausnitz, *Am. Ind. Hyg. Assoc. J. 43* (1982) 656.
[12] C. J. Chang, A. D. Randolph, *AIChE J. 35* (1989) 1876.
[13] D. A. Dixon, personal communication, 1989.
[14] Z. Tan, K. E. Gubbins: *Fluid and Fluid Mixture Behavior in Micropores* (*Annu. Meet. AIChE*, San Francisco, CA, USA, November 1989).
[15] R. S. King, H. W. Blanch, J. M. Prausnitz, *AIChE J. 34* (1988) 1585.
[16] C. A. Haynes, H. W. Blanch, J. M. Prausnitz, *Fluid Phase Equilib. 53* (1989) 463.
[17] T. Tanaka: *Gels* (*Encyclopedia of Polymer Science and Engineering, 6*, 2nd ed., 1986, p. 514); S. Hirotsu, *J. Chem. Phys. 88* (1988) 427.
[18] M. Prange, H. H. Hooper, J. M. Prausnitz, *AIChE J. 35* (1989) 803.
[19] H. H. Hooper, J. P. Baker, H. W. Blanch, J. M. Prausnitz, *Macromolecules 23* (1990) 1096.
[20] S. Beltran, H. H. Hooper, H. W. Blanch, J. M. Prausnitz, *J. Chem. Phys. 92* (1990) 2061.
[21] S. J. Trank, D. W. Johnson, E. L. Cussler, *J. Food Sci. 71* (1989) 78.
[22] R. A. Siegel, M. Falamarzian, B. A. Firestone, B. C. Moxley, *J. Controlled Release 8* (1988) 179; R. A. Siegel, B. A. Firestone, *Macromolecules 21* (1988) 32 516.

Advanced Materials: Trends and Possibilities in Liquid Crystalline Polymers

By James Economy*

During the past ten years there has been a sharp increase in interest in the opportunities afforded by R & D in the field of specialty polymers. Interest is mainly being shown in two distinct categories of polymers, namely, a) polymers which are used in very small quantities to fulfill critical needs as a part of device system, and b) high-performance engineering polymers which significantly extend their mechanical and thermal properties for structural applications. The first category ranges from advanced resists and insulating layers for microelectronic devices to membranes for filtration systems. The second category encompasses improved matrices for advanced composites as well as liquid crystalline polymers. In the present paper an overview is first given of the emerging opportunities for advanced materials and particularly specialty polymers. The status of work on liquid crystalline copolyesters is then discussed with special emphasis on one of the major problems confronting this field, namely interpreting the microstructure of the copolyesters.

1. Advanced Materials with a Future

As we look to the future technological possibilities of the 21st century it is generally accepted that the areas of advanced materials, biotechnology and information will represent the cornerstones of the high-technology industries of the future. It is noteworthy that the fields of biotechnology and information will also depend on the development of new materials. And, it quickly becomes apparent that scientific and technological advances in most of the technologies critical to the future (e.g. transportation, infrastructure, environmental control, energy, microelectronics, aerospace, defense) will depend on advanced materials.

One might justifiably question the potential for designing new and improved materials to address the myriad of needs that exist across these fields. In fact, one might also question the feasibility of even educating and training scientists and technologists to undertake R & D which encompasses the field of metals, ceramics and polymers, let alone composites, electronic materials, and biomaterials.

Regarding the first question one has only to look at the discoveries of the past two decades in the area of advanced materials to sense the tremendous opportunities in designing and tailoring new and improved systems for use by the high-tech industries of the future. The field of ceramics is particularly noteworthy when one recounts recent achievements concerning phase transformation toughened ceramics, high-temperature superconductors, ceramic composites, diamond films, and new kinds of ferroelectrics. In the case of polymers one might note recent developments in the areas of liquid crystalline polymers, molecular composites, membranes, thermoplastic matrices, radiation sensitive polymers, and thermally stable polymers.

With respect to the second question concerning the education and training of scientists and technologists in materials science and engineering (MSE) this is clearly a major challenge. We can see some glimmerings of the future from the attempts of educators in MSE who are trying to design a curriculum which will permit the scientists of the future to effectively work at the interfaces of this field. A closer scrutiny of the six major areas of materials science (Table 1) suggests that the field can be described as a matrix in which the fields of metals, ceramics and polymers, and electronic materials, composites and biomaterials are clearly interdependent and share many points in common. Then what remains is to structure a curriculum which provides the student with the skills in synthesis and processing, structure and property relationships and characterization without in any way sacrificing the basics in mathematics, physics and chemistry—a tremendous challenge for the universities!

Table 1. Materials science and engineering. A: There is a critical interdependency. B: There are some areas of overlap.

	Composites	Electronic Materials	Biomaterials
Ceramics	A	A	B
Metals	A	A	B
Polymers	A	A	A

This responsibility cannot be deferred to industry with the expectation that the young scientist will master the key elements of MSE during his first few years in industry. The logical place, in fact the only place where this process can occur is in a university environment. I tend to be very optimistic about the prospect of achieving this goal based on my personal experience in beginning to implement a completely new, integrated curriculum in MSE at the University of Illinois.

2. Possibilities for New Types of Polymers

Let me turn more specifically to the field of polymers, since this represents an area where the BASF Corporation has made many major contributions over the past 50 years.

[*] Prof. Dr. J. Economy
Department of Materials Science and Engineering
1304 West Green Street, Urbana, IL 61801 (USA)

From the period 1930–60 we witnessed the birth and maturation of the field of commodity synthetic plastics. This plastics revolution dramatically changed the field of materials providing far more versatile materials to replace the natural fibers, cellulosic film, phenolic molding compounds and even structural metals. However, by the mid 1960's it became apparent that there were no new commodity polymers left to be discovered and the emphasis began to shift to speciality polymers. Today one could easily argue that the opportunities that exist for research in polymers is greater than ever before (Table 2). These opportunities will be discussed in somewhat more detail in the following sections.

Table 2. Scope of application of specialty polymers.

Structural polymers
● Thermoplastic matrices for advanced composites
● Molecular composites
● Melt processible liquid crystalline polymers
Polymers for electronic applications
● Ultrasensitive resists for submicron lithography
● Thermally stable dielectric insulators
● Substrates and encapsulants
Polymers for pollution control
● Selective adsorption of CO_2, Freons, SO_x
● Removal of trace pollutants from ground water
Membranes
● Biopolymers

In the area of structural polymers significant progress has been achieved in the design of improved matrices for high performance composites. Thus, we have witnessed development of both rubber toughened thermosets as well as thermoplastic matrices. Today both areas are being pursued aggressively in order to further optimize the damage resistance of fiber reinforced composites. These approaches are indicated schematically in Figure 1 along with other related con-

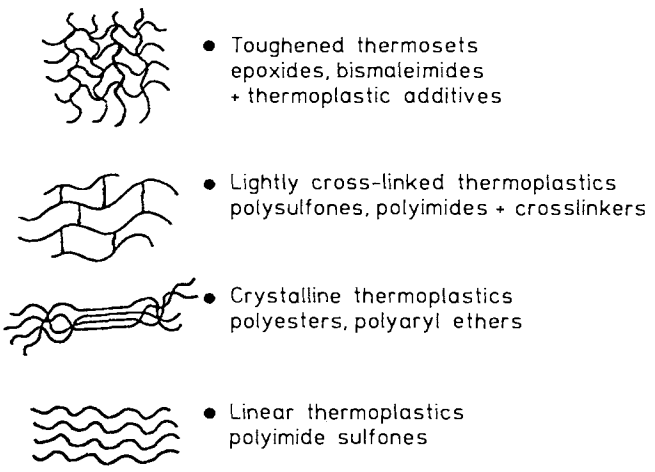

Fig. 1. Molecular approaches to improved matrices for advanced composites

cepts. The concept of molecular composites in which high strength/modulus microfibrils such as polybenzoxazole are dispersed in a high-temperature polymer matrix has also received considerable attention. One should mention however that these microfibrils may have diameters in the range of 1000 Å, hence the teminology "molecular composites" may be somewhat inappropriate. Work on liquid crystalline polymers based on aromatic polyesters has been pursued intensively since the late 1960's; this will be discussed in more detail later.

Turning to electronic materials there is little doubt that the need for new kinds of polymers such as resists, substrates and insulating layers is greater today than at any time in the past 20 years. Thus, progress in going to higher density D-RAM chips and packages requires ultrasensitive resists for use in far-UV, X-Ray and E-Beam lithography. New kinds of photosensitive, high-temperature polymers with very low dielectric constants are required as insulating layers in both the advanced chips and packages. Figure 2 shows the

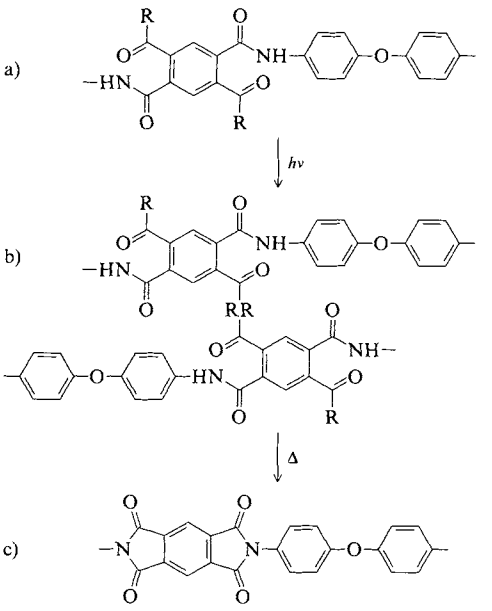

Fig. 2. Chemical steps in the processing of a photosensitive polyimides; R = $-OCH_2CH_2OC(O)C(CH_3)=CH_2$. a) Soluble, photoreactive precursor, b) insoluble photo-crosslinked intermediate, c) heat-resistant final product.

well known chemistry of the photosensitive polyimides developed in the 1970's at Siemens. A more recent approach involves the use of photosensitive diacetylenic oligomers which, on exposure to light and heat, yield a cross-linked structure (Fig. 3). Such systems are inert to moisture and can display significantly lower dielectric constants of less that 3.[1] The increased numbers of interconnects between the chip and substrate result in fatigue problems that can only be resolved by development of substrates that better match the thermal expansion coefficient of silicon. These are some of the needs facing the microelectronics industry which promise to challenge polymer scientists through the next decade.

In the area of pollution control, opportunities for advanced materials have hardly been addressed. In fact, most of the research on the problems of global warming, ozone depletion, acid rain, and urban air pollution have focussed on attempts to quantify the seriousness of the problem. Attempts to design materials for solving these problems have not been pursued in any substantive manner. Undoubtedly, one of the reasons is that many of the government funding agencies have not, as yet, been made aware of the opportuni-

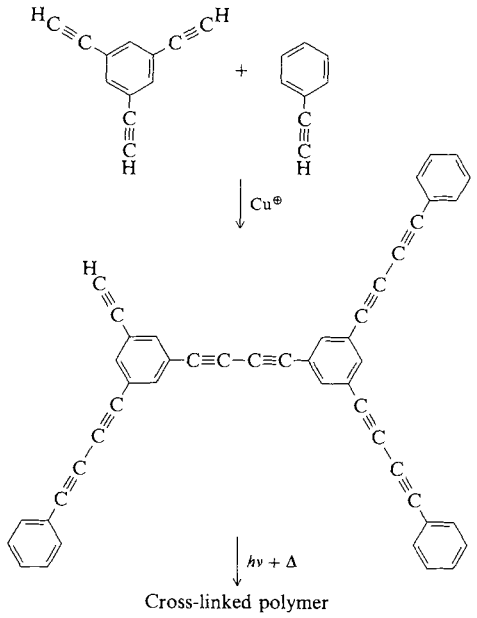

Fig. 3. Design of a photosensitive diacetylene polymer with a low dielectric constant.

ties afforded by the design of advanced materials to quantitatively remove atmospheric impurities from the environment. It would seem that during the next decade we will witness a greatly increased effort in the design of advanced polymers to control both air and water pollutants. One interesting approach to the design of activated carbons uniquely tailored to adsorb specific trace contaminants has been reported recently.[2] In this method the activated carbon surface is locally chemically converted into a range of different surfaces (Fig. 4). Some of the characteristics of these new materials are collected in Table 3.

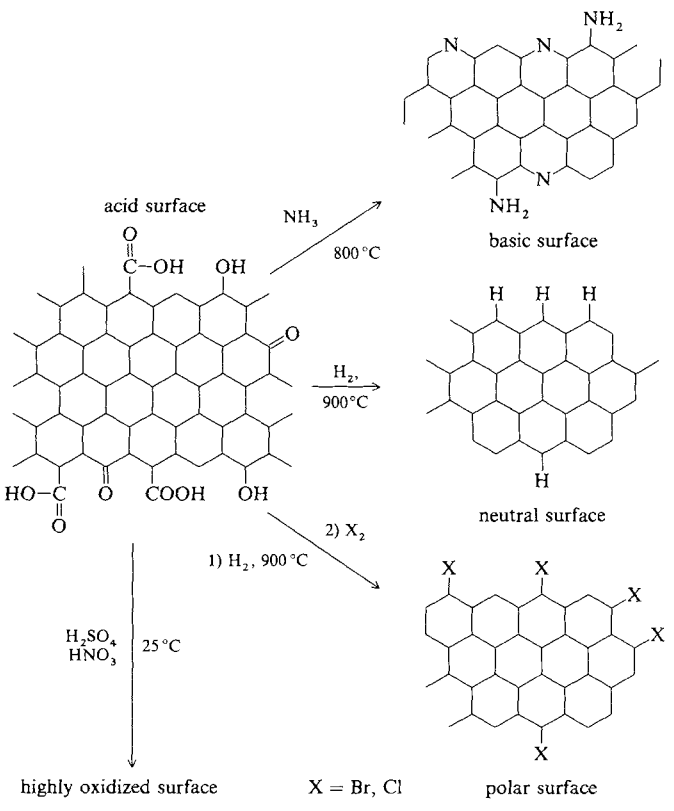

Fig. 4. Preparation of chemically tailored carbon surfaces.

Table 3. Characteristic data of chemically tailored carbon surfaces.

Chemical treatment	T [°C]	Elemental analysis	Surface area [m^2/g]	Weight change [%]
Steam [a]	900	4.1% O	1658	−40
NH_3(gas)	800	6.3% N	2274	−32
H_2(gas)	900	0.5% H	1276	−6.8
Cl_2(gas)	450	25% Cl	891	+8.5
Br_2	25	13% Br	890	+23
H_2SO_4/HNO_3	25	40% O	574	+25

[a] Used as precursor for the preparation of the surface.

For sake of brevity, the opportunities in biopolymers and advanced membranes will not be considered in this paper. However, it should be noted that both of these fields provide tremendous opportunities for basic and applied research, and this is clearly evident from the intense efforts currently underway in the USA, Germany, and Japan. Considerable effort is also being expended on improving the processes and properties of many of the commodity polymers developed in an earlier era. Such efforts continue to pay off handsomely, as with the recent improvements in the manufacture of polypropylene.

One might summarize that the field of materials and especially of polymers afford many opportunities for research. One point that cannot be overemphasized is the importance of carrying out fundamental research associated with the more directed developments in advanced materials. In fact, the discussion which follows on liquid crystalline polymers provides an excellent example of the problems that may arise when technologists get too far ahead of the scientists.

3. Liquid Crystalline Polymers

3.1. Background

The phrase "liquid crystalline polymers" encompasses both lyotropic as well as thermotropic systems. Since many of the questions concerning lyotropics such as the Aramids have been addressed since the early 1970's emphasis here will be placed on the thermotropics and particularly the aromatic copolyesters of *p*-hydroxybenzoic acid (HBA).

This class of polymers was discovered in the Spring of 1963, and in 1970 began the commercialization of homo- and copolymers of HBA.[3] During this early period practically all of the R & D was of a developmental nature and directed at the goals enumerated in Table 4. The significance of these early efforts is illustrated by the fact that the materials which were introduced in 1970 and 1972 are still commercially available today, some 20 years after their original introduction. In the meantime, starting in the late 1970's and continu-

Table 4. Early developmental thrusts on the aromatic polyesters.

Synthesis –	low cost, scaleability, reproducibility
Processing –	injection molding, fiber spinning, metal forming
Characterization –	basic, end-use
Patent protection –	composition, processing, end-use
Customer applicatons –	tailored compositions

ing to the present, a number of companies have introduced their own versions of the liquid crystalline copolyesters of HBA.[4, 5] However, today it appears that further commercial development is gated by our lack of understanding of 1) the microstructure of these copolyesters and 2) the rheological features which control the tendency for these materials to form skin-core and microfibrillar structures (Fig. 5). The

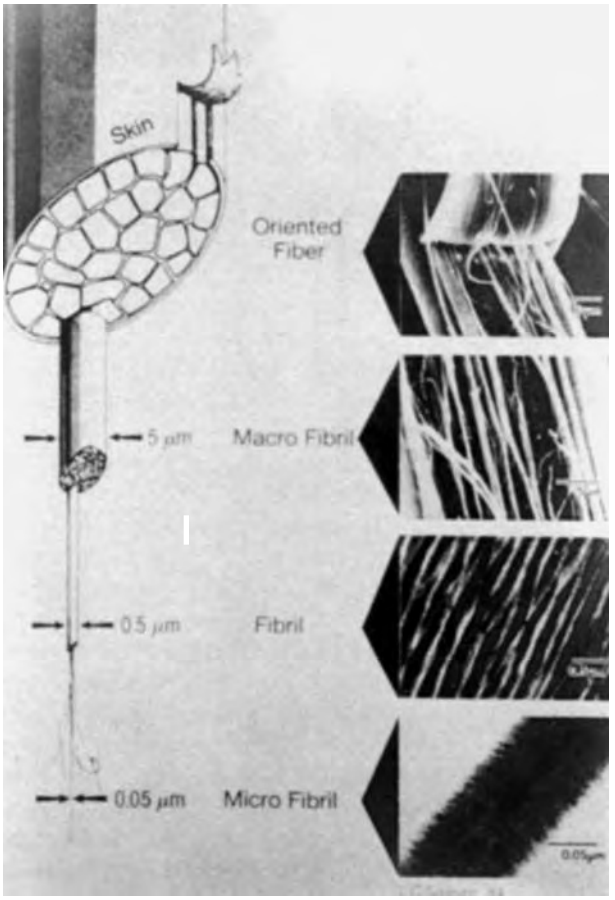

Fig. 5. Structure of liquid crystalline polyesters.

first problem has been identified as the single most important fundamental problem deterring progress in this field, while the second problem has greatly hindered efforts to take advantage of the unique directional properties inherent to thermotropic polymers, both in molded shapes and in films.

In the following, our work on elucidating the nature of the microstructure of the aromatic copolyesters is described, which demonstrates the profound role of chemical processes in influencing and controlling the microstructure of these copolymers. In a more global sense, by taking into account the subtle chemical and physical processes that occur at elevated temperatures one is now able to predict both the nature of the microstructure as well as many of the morphological features of the commercially available liquid crystalline copolyesters of HBA.

3.2. Factors Which Influence the Microstructure of Liquid Crystalline Copolyesters

Undoubtedly, much of the confusion surrounding the nature of the microstructure of the copolyesters of HBA arises from the relative intractability of the copolymers, which greatly reduces the number of analytical techniques which can be used in the characterizations of these systems. Interestingly, there are almost an equal number of publications which describe the respective copolymers of Scheme 1 as being either random or blocklike with respect to their microstructure.[6–10] In considering the behavior of these systems in the nematic melt there is also consideable confusion. Thus, some workers describe these sytems as undergoing a

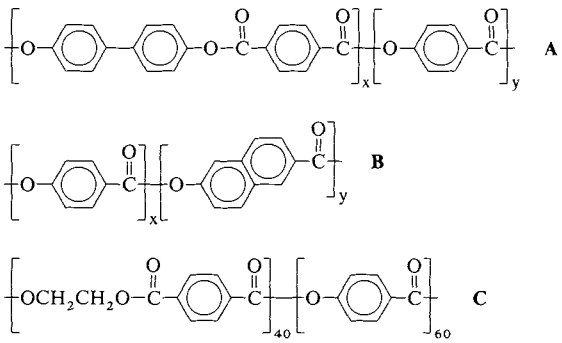

Scheme 1. Commercially available liquid crystalline copolyesters. **A** Amoco (Carborundum), **B** Celanese, **C** Tennessee Eastman.

crystallization-induced ordering[11] or a physical ordering,[12] while others indicate that mixtures of different copolyesters are stable in the nematic melt.[13] In contrast, we point out in a recent publication that, in the nematic melt, mixtures of polyesters will undergo very rapid transesterification reactions to a random microstructure.[14] Clearly, a systematic study was required to examine not only the possible changes that might occur in the microstructure during high-temperature processing, but also to establish the influence of the original synthetic route on the microstructure. The factors that would appear important concerning the microstructure are enumerated in Table 5. In the following the role of the synthetic route on microstructure is considered briefly, followed by a more detailed discussion of the

Table 5. Origin of the microstructure of the liquid crystalline aromatic polyesters.

- Role of the synthetic route
  - Reactivity ratios
  - Interchain transesterification
  - Homogenous vs heterogenous conditions (isotropic or nematic)
- Role of temperature on ordering and randomizing
  - Annealing below $T_{c\rightarrow N}$
  - Heating near $T_{c\rightarrow N}$
  - Processing in the nematic melt

effects of high-temperature processing. Finally, the role of trace impurities, nucleating agents, and the nature of the end groups are briefly mentioned.

With respect to the synthetic route, obviously the reactivity ratios of the monomers as well as the conditions of polymerization will determine the initial microstructure. We decided to focus on the 50/50 HBA/HNA copolymer (HNA = 6-hydroxy-2-naphthoic acid) because of its relative tractability. On stopping the polymerization at a M_n of 2000 we found that the composition was identical to that of the ratio of the starting reactants, indicating that reactivity ratios for the HBA and HNA were identical. To characterize the possible role of a very rapid interchain transesterification we also examined the reaction of ^{13}C enriched HBA* with the dimer of HBA-HNA at the reaction temperature of 245 °C. By use of ^{13}C-NMR techniques we were able to identify 14% of HBA*-HNA in the oligomer with 2000 M_n, indicating interchain transesterification did occur but was not a dominant factor in this process. The temperature dependence of this reaction was also examined and it was found that at 225° and 275 °C the concentration of HBA*-HNA remained the same. This ought not to be surprising, since the concentration of COOH end groups was the same in all three cases and the degree of polymerization was carried out to the same M_n.

Turning now to possible high-temperature processes that might influence the microstructure, it is appropriate to start with those that might occur during annealing (typically 20 h at 50–70 °C below the $T_{C\leftrightarrow N}$). What was found was that the degree of crystallinity of the 50/50 HBA/HNA copolymer increased from ca. 10% to 25–30% based on Differential Scanning Calorimetry (DSC) measurements of transition enthalpies. Analysis of the microstructure by ^{13}C-NMR spectroscopy indicated that there was essentially no change in the dyad sequence. On the other hand, the M_n increased from 10000 to well over 20000 indicating significant mobility of the end groups leading to further polymerization by ester interchange at the end groups. Examination of the DSC curves indicated no shift in the position of the peak of an endothermic reaction of the 50/50 copolymer. These results can only be interpreted on the basis that annealing leads to a higher incidence of the like-ordered units in the defective three-dimensional crystallites. There does not seem to be any tendency for further ordering of the like-ordered sequences via interchain transesterification otherwise one would observe a shift in the DSC peak to a higher C↔N transition temperature. On the other hand, the increased M_n indicates that transesterification processes can occur in the solid state.

Turning to the use of annealing conditions just above or below the $T_{C\leftrightarrow N}$ of the HBA/HNA copolyesters, one observes a completely different behavior. In this case we examined both the 73/27 and 50/50 HBA/HNA polyesters. For the 73/27 polyester the peak at 280 °C corresponding to the crystalline → nematic transition disappears and is replaced by two new peaks for endothermic reactions occurring at 240 and 330 °C; in the case of the 50/50 system the endothermic transformation at 250 °C is replaced by two transformations at 240° and 330 °C and one at 380 °C. In both cases the total increase in transition enthalpy was modest and nowhere near that observed in annealing at 50–70 °C below $T_{C\leftrightarrow N}$. In addition, the annealed samples were almost insoluble in pentafluorophenol, suggesting either a more highly ordered structure, a sharply increased M_n, or both. By use of capping agents such as 2-naphthoic acid it was possible to control the M_n of both compositions down to well under 10000; however, the solubility was still very low. Consequently, these results could only be interpreted as arising from the emergence of a new kind of a more highly ordered sequence distribution. Fortunately, we had available to us DSC scans of the homopolymers of HBA and HNA[15] (both showing strong endothermic transitions at ca. 330–340 °C) and one of the alternating copolyester of (HBA-HNA)$_x$ with endothermic transitions at 240° and 380 °C. Thus, one obvious interpretation of the changes associated with heating near $T_{C\leftrightarrow N}$ is that, within the poorly formed three-dimensional crystallites of the "as-prepared" copolesters, interchain transesterification occurs leading to highly ordered domains of the homopolymers and alternating copolymer. The relative concentrations of these domains is determined by the composition of the original copolyester as well as the approximate starting sequence of the poorly formed crystallites. The driving forces are kinetic and arise from the improved packing and dipole interactions that are obtained. Since it is reasonable to expect a higher concentration of carboxylic acid end groups at the interfaces between the crystalline and nematic phases, there is more than sufficient concentration of end groups to effect the necessary ordering through intermolecular transesterification. Additional evidence in support of such a transformation is obtained from X-ray diffraction analysis of the two materials. Thus, the low-temperature annealed material displays a hexagonal symmetry, while the more ordered system shows an orthorhombic structure consistent with the structures of the homopolymers of HBA and HNA.

The final question that remains is the nature of the processes that may occur well above $T_{C\leftrightarrow N}$. A unique experiment was designed to eliminate the presence of any possible ordering just above $T_{C\leftrightarrow N}$.[14] A 50/50 mixture of the two homopolymers of HBA and HNA was compression molded above 450 °C, ensuring the absence of any three-dimensional order in the melt. It was found that by using relatively low M_n homopolymers the mixture reacted extremely rapidly to form the random 50/50 copolyester. The structure of the copolyester was confirmed by DSC and ^{13}C-NMR measurements showing a high concentration of HBA-HNA dyads. Thus, entropic effects seem to dominate in driving the system toward randomization. The extremely rapid rate of the reaction (completed in less than one minute) is consistent with what one would extrapolate from similar processes carried out at ca. 280 °C[16] and assuming that the Arrhenius process holds.

4. Conclusions

The picture that emerges from the results of this work indicates that both the microstructure and resultant morphology are controlled by subtle chemical and physical processes that very much depend on the thermal history of the materials. As illustrated in Table 6, one can clearly distinguish the chemical and physical processes which are operative in these systems. Thus, at temperatures well above $T_{C\leftrightarrow N}$

Table 6. Chemical and physical processes in liquid crystalline polyesters

Temperature	Dominant processes	Changes in microstructure or morphology
$\gg T_{C\leftrightarrow N}$	Chemical	Randomization
$\sim T_{C\leftrightarrow N}$	Physical	Crystallization
Annealing (near $T_{C\leftrightarrow N}$)	Chemical	Crystal/Ordering
Annealing (below $T_{C\leftrightarrow N}$)	Physical	Further crystallization
T_{NG}	Physical	Nematic glass

chemical processes dominate. The calculated number of interchain transesterification reactions at 450 °C is extremely rapid, i.e. ca. 100 interchanges/chain/second. At the same time M_n increases rapidly, resulting in a sharp reduction in end-group concentration and thus reducing the potential for further reaction. The propensity of randomization in the nematic phase (below $T_{C\leftrightarrow N}$) continues with decreasing temperature, but with correspondingly slower rates until the nematic phase freezes into a glass (e.g., in the HBA-HNA system the nematic glass transitions range from 80–130 °C depending on composition).

As one goes from the nematic melt through the crystal-nematic transition, physical processes dominate and the rod-like random chains match up to produce relatively small concentrations of defective three-dimensional crystallites. If one continues to anneal in this temperature range, chemical processes dominate and within the ordered regions interchain transesterification occurs to yield bimodal crystalline domains of highly ordered sequences. Further polymerization is observed during these annealing experiments.

Finally, if one anneals at 50–70 °C below the $T_{C\leftrightarrow N}$ diffusion processes dominate, resulting in a significant increase in concentration of the defective crystallites. Some chemistry also occurs at the end groups, as shown by the increase in M_n.

From the outline in Table 6 we appear to have a reasonably self-consistent interpretation of the microstructure of the liquid crystalline copolyesters. Most of the earlier confusion can be explained from this model. However, it is important to note that capping of the copolymers will eliminate the ability of the carboxylic acid to effect the randomization, ordering or polymerization reactions. Furthermore, presence of trace impurities and nucleating agents can profoundly influence the course of these processes. Hence, when one is confronted by apparently inexplicable behavior in these copolyesters, one of the first items that should be checked is the possible role of trace impurities.

Received: April 11, 1990 [A 786 IE]
German version: *Angew. Chem. 102* (1990) 1296

[1] D. J. Dawson, W. W. Fleming, J. R. Lyerla, J. Economy, *ACS Symp. Ser. 282* (1985) 63.
[2] H. Jung, J. Economy, *Polym. Prepr. Am. Chem. Soc. Div. Polym. Chem. 31*, (1990) No. 2.
[3] J. Economy, *Mol. Cryst. Liq. Cryst. 169* (1989) 1.
[4] W. J. Jackson, Jr., H. F. Kuhfuss, *J. Polym. Sci. Polym. Chem. Ed. 14* (1976) 2043.
[5] G. W. Calundann, US-Pat. 4 161 407 (1979); US-Pat. 4 184 996 (1980).
[6] J. Blackwell, A. Biswas, *Macromol. Chem. Macromol. Symp. 2* (1986) 21.
[7] L. Quach, E. Hornbogen, W. Volksen, J. Economy, *J. Polym. Sci. Polym. Chem. Ed. 27* (1989) 775.
[8] R. D. Johnson, A. Mühlebach, J. Economy, J. Lyerla, C. Wade, APS Meeting, St. Louis, MO, USA 1989.
[9] A. Mühlebach, R. Johnson, J. Lyerla, J. Economy, *Macromolecules 21* (1988) 315.
[10] S. Z. D. Cheng, *Macromolecules 21* (1988) 2475.
[11] R. W. Lenz, J.-I. Jin, K. A. Feichtinger, *Polymer 24* (1983) 327.
[12] Y. G. Lin, H. H. Winter, *Macromolecules 21* (1988) 2439.
[13] M. T. DeMeuse, M. Jaffé, *Mol. Cryst. Liq. Cryst. Inc. Nonlin. Opt. 157* (1988) 535.
[14] A. Mühlebach, J. Economy, R. D. Johnson, T. Karis, J. Lyerla, *Macromolecules 23* (1990) 1804.
[15] A. Mühlebach, J. Lyerla, J. Economy, *Macromolecules 22* (1989) 3741.
[16] D. W. Wiswe, H-G., Zachmann, K. Hahn, E. W. Fischer, *Macromolecules 20* (1987) 1116.

Perspectives in the Development of High-Temperature Polymers

By Paul M. Hergenrother*

Research on high-temperature organic polymers was initiated in the late 1950s primarily to meet the needs of the aerospace and electronics industry. Since then, many different heat-resistant polymer systems have been reported, of which several are now commercially available. These polymers are used in many diverse applications such as circuitry in microelectronic components, coatings on cookware, binders in brake systems, sealants for fuel tanks in high-speed aircraft, gears in copying machines, structural components in high-speed aircraft, and space vehicles, films and wire coatings for electrical insulation. Worldwide use for high-temperature polymers in 1988 was estimated at 90 million kilograms with a value of $ 2.3 billion. This market is expected to double by the end of this decade. The major polymer classes discussed in the present paper are polyimides and poly(aryl ethers).

1. Introduction

High-temperature organic polymers are often described as polymers that retain useful properties after thousands of hours of exposure at 200 °C in air under static conditions. This definition is misleading and varies considerably depending upon the supplier and user. In many instances, temperature is reported without regard to other important factors that influence the performance of a polymer such as time, thermal cycling, stress, and environmental factors like moisture, or chemical and electrical action. In addition, polymers that can survive high-temperature processing cycles such as high-temperature soldering steps in the fabrication of microelectronic components but are otherwise not exposed to high temperatures are also referred to as high-temperature polymers.

The quest for high-temperature organic polymers began in the late 1950s primarily to meet the demands of the aerospace and electronics industries. Since then, many different high-temperature polymer systems have been reported. Several of these polymers are now commercially available as adhesives, coatings, composite matrices, fibers, films, foams, membranes, and moldings. They are currently already in use or are being considered for use in the following representative applications:

- Electronic and microelectronic components (circuit boards, moldings, flexible cables, insulators, coatings, wire wraps, etc.)
- Gaskets, sealants and tubing
- Binding systems in brake shoes, abrasive wheels and cutting disks
- Structural resins (adhesives, composite matrices, foams) for aircraft, space vehicles, and military items
- Jet engine components (fan blades, flaps, ducting, bushings, cowlings, races, etc.)
- Nuclear reactor components (coolants, insulation, structural parts)
- Conveyor belts for treating and drying materials
- Pipes for chemical processing and energy generators
- Fire-resistant materials (protective clothing)
- Reinforcements (high-modulus and high-strength fibers and ribbons)
- Ablators (thermal protection systems)
- Automotive components (connecting rods, wrist pins, pistons, switches, electrical components)
- Household items (nonstick interior and decorative exterior surfaces on cookware, irons)
- Medical devices (prostheses, circuitry in bio-implants, dental instruments)
- Copying machines (gears and picks)

Unknown to the vast majority of people, these polymers affect our lives in many different ways. For example, commercial airplanes and large traction motors that drive locomotives use high-temperature polymers as insulation for electrical wiring. Their excellent chemical resistance, mechanical properties and ability to survive sterilization cycles have opened applications in the medical field. Household items such as lightweight electric irons, microwave cookware, and other non-stick decorative cookware use high-temperature polymers. These polymers are used in protective, flame-resistant suits for firemen, energy conversion systems, space probes such as communication satellites, and complex computer systems. High-temperature polymers have had and will continue to have a significant impact on mankind. The worldwide market for high-temperature polymers in 1988 was estimated at 90 million kilograms with a value of $ 2.3 billion[1] (Fig. 1). This market is expected to double by the end of this decade.

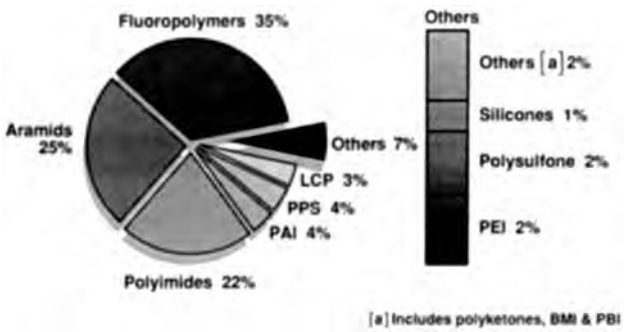

Fig. 1. World market (1988) for high-temperature polymers by polymer type [1]. LCP = liquid crystalline polymers, PPS = poly(phenylene sulfide), PAI = poly(amide imides), PEI = poly(ether imides).

[*] Dr. P. M. Hergenrother
Materials Division,
NASA Langley Research Center
Hampton, VA 23665-5225 (USA)

2. Historical Review

Early work uncovered the many factors that contribute to the thermal stability of polymers. Some of these are primary bond strength, resonance stabilization, secondary bonding forces, rigid intra-chain structure, molecular weight and molecular weight distribution, and stable end-groups on the molecules. Most high-temperature polymers are composed predominantly of aromatic or heteroaromatic units (excluding systems like fluoropolymers and silicones). The chemical structure that makes a polymer thermally stable also makes it difficult to form into useful items because of limited solubility and moldability. Since most of the early high-temperature polymers were virtually intractable, stable flexibilizing groups such as carbonyl, oxygen, sulfone and hexafluoroisopropylidene were incorporated between aromatic rings to improve solubility and moldability. In addition, pendant groups such as phenyl rings and *meta* catenation within the polymer backbone were introduced which further improved the fabricability. These modifications had only minor effects upon the thermal stability of the polymer although the actual utilization temperature was generally compromised (lowering of the glass transition temperature T_g). This work, coupled with control of molecular weight and end-capping, opened the way for the synthesis of many soluble, readily moldable, high-temperature polymers with excellent mechanical properties. Some of these materials are now commercially available. The evolution of the major high-temperature polymers is outlined in Table 1. As is evident from the table, polyimides are of special importance and have received considerable attention. A large number of other important high-temperature polymers have intentionally been omitted from Table 1 to avoid confusion. Information on these polymers can be found in many review articles and books.[26-28]

Table 1. Major high-temperature organic polymers.

Polymers	Year Reported or Introduced	Commercial Availability	Ref.
Poly(phenylene sulfide)	1948	yes	[2]
Polyimide solution (Pyre-ML)	1959	yes	–
Polybenzimidazole	1961	yes	[3]
Polyimide binder (Skygard®)	1962	yes	–
Polyimide	1963	yes	[4,5,6]
Polyquinoxalines	1964	no	[7,8]
Polyimide film (Kapton®, wire coatings, moldings)	1965	yes	–
Polyamideimides	1965	yes	[9]
Polyaryl sulfone (Astrel® 360)	1967	no	[10]
Polyphenylquinoxalines	1967	yes	[11]
Polyimides containing hexafluoroisopropylidene groups (NR 150)	1967	yes	[12]
Polyimides from isocyanates (2080)	1968	yes	[13]
Aromatic polyamides (PRD-49, Kevlar®)	1970	yes	–
Bismaleimide resins	1970	yes	[14]
Norbornene-terminated polyimides (PMR-15)	1972	yes	[15]
Ethynyl-terminated polyimides (Thermid® 600)	1974	yes	[16]
Poly(ether imides) (Ultem®)	1974	yes	[17]
Polyimide-containing indane (Matrimid® 218)	1975	yes	[18]
Liquid crystalline polyester [poly(4-benzoate), Ekonol®]	1976	yes	[19]
Polyketoimide (LARC-TPI)	1976	yes	[20,21]
Rigid rod polybenzazoles (PBT, PBI, PBO)	1981	no	[22,23]
Polyimide film (Upilex® R and S)	1985	yes	–
Semicrystalline polyimides (LARC-CPI, New TPI)	1987	yes	[24]
Poly(aryl sulfone) (Radel® C)	1989	yes	–
Polyimides via Friedel-Crafts reaction	1989	no	[25]

Polyimides and poly(aryl ethers) including poly(aryl ether ketones), more so than other high-temperature polymer systems, have captured the attention of scientists and engineers alike as materials that offer outstanding properties for high-performance applications. Their versatile synthesis permits tailoring of these polymers for specific applications. With this in mind, the remaining discussion in this paper will concentrate on these two polymer systems.

3. Polyimides

Polyimides are generally divided into two types, addition and condensation polymers. Addition polyimides are exemplified by bismaleimides, norbornene-terminated imide oligomers such as PMR-15 and ethynyl-terminated imide oligomers such as the Thermid® series.[29] These cure upon heating to yield brittle resins. In spite of their brittleness, these materials are used as composite matrices in applications such as printed circuit boards and structural composites. Composites are receiving considerable attention for several diverse applications, particularly in airplanes, automobiles, trains, and off-shore oil-drilling platforms. For these applications, composites offer the following benefits over metals:

- better design flexibility
- corrosion resistance
- higher specific strength and stiffness
- lower thermal expansion
- better fatigue resistance

High specific strength and stiffness is extremely important, particularly for commercial airplanes, because this translates into lower weight and thus means better fuel economy and the ability to carry a higher payload. As the cost of fuel increases and the supply decreases, composites will be used more extensively on commercial airplanes. In addition, as the overall cost of composites becomes more competitive with that of a metallic component, more extensive use of composites, particularly in commercial airplanes, will be realized. The high cost of large composite structures today is due primarily to the labor intensive fabrication processes. New ways of fabricating large composite structures such as resin-transfer molding show excellent promise to reduce the manufacturing cost and provide a structure with excellent mechanical performance.

During the last few years, new bismaleimide formulations have evolved which offer good toughness and accordingly damage tolerance [composites that exhibit useable *c*ompression strength *a*fter *i*mpact (CAI) at a stress level of 6.67 $kJ\,m^{-1}$ (1500 pounds per inch)]. Damage tolerance is described as the ability of a structure to sustain damage but still carry a load. Table 2 summarizes the properties of three leading bismaleimide-based composite systems. Although significant improvements, particularly in impact resistance, have been made in bismaleimide-based composites over the last few years, the users desire further improvements. Some of these are better performance at 200 °C wet, higher CAI

Table 2. Composite properties of bismaleimide based matrices.

Properties	BP/U. S. Polymeric V391/HT46-8B [30]	Ciba-Geigy RX130-9/T-300 [31]	BASF/Narmco X5250-4/IM-7 [32]
Flexural strength [MPa] (Ksi)			
room temperature	1764 (256)	1799 (261)	1551 (225)
177 °C, wet	841 (122)	1330 (193)	724 (105)
Flexural modulus [GPa] (Msi) [a]			
room temperature	169 (24.5)	121 (17.5)	157 (22.8)
177 °C, wet	159 (23.0)	119 (17.2)	148 (21.4)
Short beam shear strength			
[MPa] (Ksi) room temperature	124 (18.0)	123 (17.9)	152 (22.1)
177 °C, wet	55 (8.0)	68 (9.9)	60 (8.7)
Open-hole compression			
[MPa] (Ksi) room temperature	400 (58.0)	413 (59.9)	–
177 °C	338 (49.0)	370 (53.7)	–
Compression after impact (6.67 kJ m^{-1}), MPa (Ksi)			
room temperature	238 (34.5)	186 (27.0)	208 (30.1)

[a] Msi = million pounds per square inch.

(comparable to the new toughened epoxy system), no microcracking upon thermal cycling (influenced by prepreg layup) and better tack. One of the better materials that has been developed to meet these new goals is the BASF Structural Materials/Narmco X5260 system.[33] The CAI ranges from 331 to 348 MPa, the highest value reported for a bismaleimide-based system.

Another addition polyimide composite matrix offering higher temperature performance than bismaleimides is PMR-15, a norbornene-terminated imide oligomer formed by the *p*olymerization of *m*onomeric *r*eactants at a calculated molecular weight of 1500 g/mol. The synthetic route is shown in Scheme 1.

PMR-15 cures via a complex thermally induced retro-Diels-Alder reaction to yield a brittle resin. As a result, even unidirectional composites of PMR-15 undergo pronounced microcracking upon thermal cycling. This is accompanied by substantial loss of mechanical properties. Microcracking is significantly more severe in crossply composites. Since PMR-15 is one of the few high-temperature composite matrices with an engineering data base, work has been directed towards toughening PMR-15 to alleviate the microcracking problem. Unidirectional laminates from a blend of a tough, high T_g, polyimide (NR150B2) with PMR-15 showed no microcracking after thermal cycling and mechanical properties equivalent to PMR-15 at 316 °C.[34] No results were reported on crossply composites.

The current interest in PMR-15 composites is primarily due to their anticipated use in jet engines. This market could be quite substantial. As a result, several companies are actively involved in PMR-15 work. For example, BASF Structural Materials has obtained promising results on neat resins from a blend of PMR-15 powder and a high-T_g thermoplastic polyimide powder. Powder impregnation to form prepreg offers certain attractive features such as a means of applying insoluble but fusible polymer, no organic solvents, and drape in the prepreg.

Condensation polyimides can be prepared from a variety of relatively inexpensive monomers by the following synthetic methods. By judicious choice of starting materials, polyimides can be tailor-made for specific applications:

- Aromatic dianhydrides and aromatic diamines (formation of polyamidic acid in solution and subsequent chemical or thermal cyclodehydration.[35]
- Aromatic dianhydrides and aromatic diamines (melt polymerization).[36]
- Aromatic dianhydrides and aromatic diisocyanates.[37]
- Aromatic dianhydrides or tetracarboxylic acids and aromatic or aliphatic diamines in high-boiling solvents, e.g. *N*-methylpyrrolidinone or *m*-cresol (direct to polyimide).[38]
- Esters of aromatic tetracarboxylic acids with aromatic diamines.[39]
- Aromatic tetracarboxylic acid ester chlorides with aromatic diamines.[40]
- Displacement of an activated nitro group by a phenoxide anion, e.g., bis(nitrophthalimide) and bisphenolates.[41]
- Transimidization (amine–imide interchange).[42]
- Friedel-Crafts reaction (dicarboxylic acid chloride and imide monomer)[25]

For example, the glass transition or crystalline melt temperature, toughness, dielectric constant, coefficient of thermal expansion, modulus, melt viscosity, and other properties can be controlled within certain boundaries. This versatility has permitted the development of various commercial products from condensation polyimides. These include adhesives, composite matrices, coatings, films, fibers, foams, moldings, and membranes. The chemistry, physical and mechanical properties, and uses of polyimides have been reviewed recently in a book.[43]

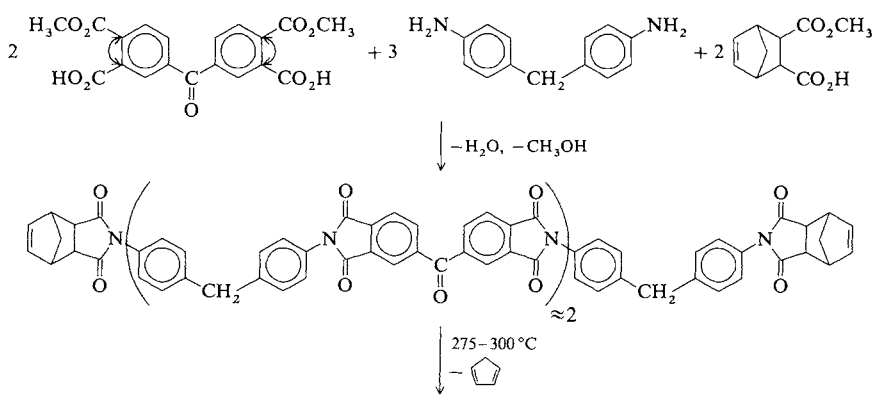

Scheme 1. Reaction route to PMR-15, a thermosetting polyimide used as a composite matrix resin.

Table 3. Properties of polyimide films.

Film (Source)	Strength [MPa] (Ksi)	Tensile Properties [b] Modulus [GPa] (Ksi)	Elongation [%]	Stability in strong bases	Loss in weight [%] [c]
Kapton® (DuPont)	172.4 (25.0)	2.96 (430)	70	poor	4.4
Apical® (Allied-Signal/Kanegafuchi)	193.0 (28.0)	2.79 (405)	90	poor	4.6
Upilex® S (ICI/Ube Chem.)	392.3 (56.9)	8.82 (1280)	30	excellent	1.7
Novax® (Mitsubishi Chem.)	343.3 (49.8)	6.87 (996)	50	good	30.6
LARC-CPI [a] (NASA/Foster-Miller)	448.1 (65.0)	10.34 (1500)	15	excellent	5.9 [d]

[a] Uniaxially oriented, tested in machine direction. All other films biaxially oriented. [b] At 25 °C. [c] After 500 h at 300 °C in air. [d] Unoriented film.

The most popular condensation polyimide, which is available in various forms (e.g. coatings, binders, films, and moldings), is that obtained by reaction of pyromellitic dianhydride with 4,4'-diaminodiphenyl ether (Scheme 2). In film

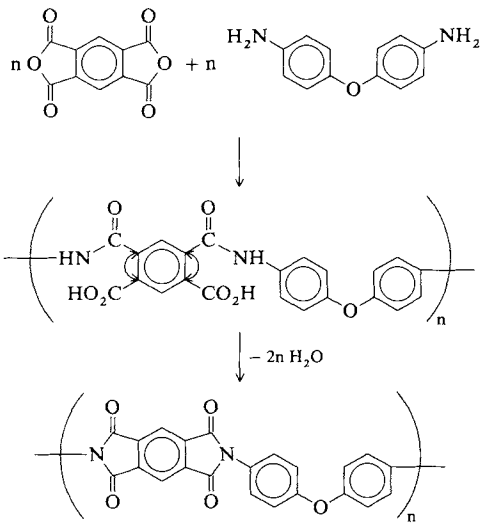

Scheme 2. Reaction route to a polyimide.

form, this material is known as Kapton®[44] and Apical®.[45] The market for polyimide films in 1988 was about $ 150 M with Kapton® comprising about 75%. This market is expected to grow substantially, and to double by 1995. As a result, a few new polyimide films have been introduced within the last few years. The properties of several commercial and experimental polyimide films are presented in Table 3. Although the polyimide film market is relatively large, the market for polyimide compression and injection molded parts is significantly larger.

The material called LARC-CPI (*La*ngley *R*esearch *C*enter-*C*rystalline *P*oly*i*mide) is a relatively new polyimide. The synthetic route is shown in Scheme 3. It exhibits many attractive features such as excellent chemical resistance, fracture energy [critical strain energy release rate (G_{Ic})] of 6600 Jm^{-2} (37.8 psi),[46] adhesive titanium tensile shear strength at 232 °C of 25.9 MPa (3670 psi [*]),[46] AS-4 unidirectional laminate flexural strength and modulus[47] at 232 °C of 1441 MPa (209 Ksi[*]) and 91.7 GPa (13.3 Msi) respectively and high thermooxidative stability at 316 °C in air. Work is underway to develop an optimized, end-capped, controlled molecular weight form that can be more readily compression molded for adhesive and composite components.

Another relatively new polyimide is New-TPI,[48] whose neat resin properties are presented in Table 4. Composites from this material have shown good properties. A drawback, however, is the temperature of about 427 °C necessary for the fabrication of these composites.

Several polyimides have been reported which contain the hexafluoroisopropylidene group located between aromatic rings in the dianhydride and/or diamine portion of the molecule. This group imparts several advantageous features to the polymers such as lower dielectric constant, better solubil-

[*] psi = pounds per square inch; Ksi = thousand pounds per square inch.

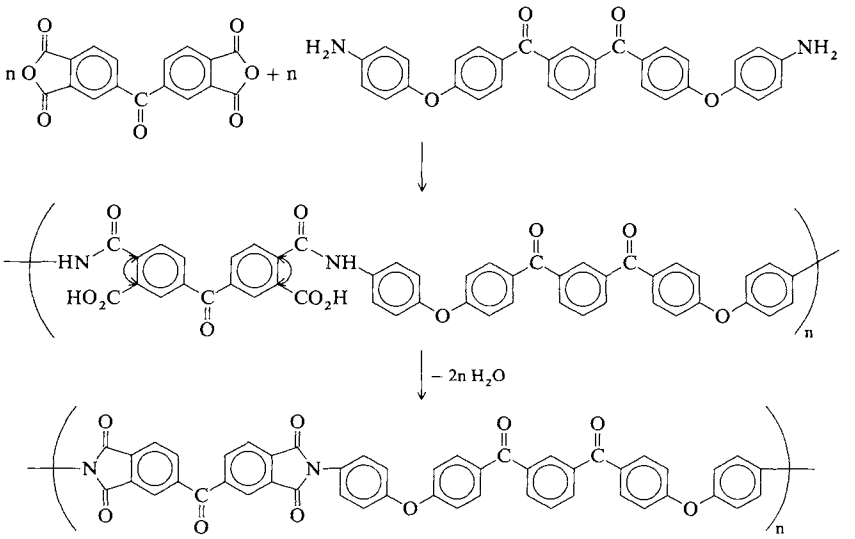

Scheme 3. Reaction route to LARC-CPI, a semicrystalline polyimide.

Table 4. Properties of NEW-TPI injection molded specimens.

Property	Material	
	Unannealed	Annealed
Tensile Strength [MPa] (Ksi)	107.5 (15.6)	–
Tensile Modulus [GPa] (Ksi)	2.06 (299)	3.53 (512)
Elongation [%]	150	10
Flexural Strength [MPa] (Ksi)	118.6 (17.2)	133.1 (19.3)
Flexural Modulus [GPa] (Ksi)	2.86 (415)	3.73 (541)
Heat Deflection Temp. [°C]	236	250

ity, lower pickup of moisture and less color. Some of these properties of a polymer are particularly important in integrated devices in microelectronic applications. More recent work in Japan[49, 50] and the United States[51–54] has involved strategically locating trifluoromethyl groups on the aromatic rings of the dianhydride and/or diamine portion of the polyimide molecule. The trifluoromethyl group imparts properties to the polymer similar to that imparted by the hexafluoroisopropylidene group, but with one notable advantage: In some polyimides, the tensile properties of drawn films and fibers were exceptional. For example, fibers[53] of the polyimide obtained by reaction of 3,3′,4,4′-biphenyltetracarboxylic dianhydride with 2,2′-bis(trifluoromethyl)-benzidine as shown in Scheme 4 which were spun from an

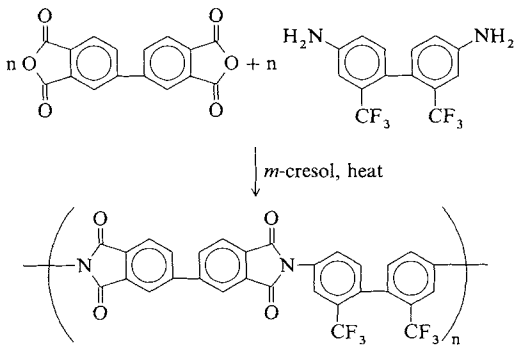

Scheme 4. Reaction route to a polyimide with good fiber properties.

isotropic solution in *m*-cresol and subsequently drawn, gave properties better than that of Kevlar®.[55] Crystalline ordering was observed to occur in this polymer when it was in a gelled state in *m*-cresol at ambient temperature. In addition, this particular polyimide exhibited outstanding stability at 371 °C under 4 atm air pressure, conditions present in some parts in jet engines.

4. Poly(aryl ethers)

Poly(aryl ethers), like polyimides, offer an attractive combination of properties. Many of these polymers are commercially available and find use in diverse applications. Poly(aryl ethers) can be synthesized by the following methods:

- Nucleophilic substitution[56]
- Electrophilic substitution[10, 57]
- Oxidative coupling[58]
- Ullmann ether synthesis[59]

Nucleophilic and electrophilic substitution reactions are the methods commonly used in the preparation of high-performance poly(aryl ethers). In general, amorphous and semicrystalline poly(aryl ethers) are less expensive than polyimides and some display high optical transparency, making them potentially useful in windows and canopies for aerospace vehicles. Poly(aryl ethers) find use in a wide variety of applications primarily in the form of adhesives, coatings, composite matrices, membranes, and moldings. Because of their excellent chemical inertness and mechanical properties, these polymers are under evaluation for use in different medical applications such as prostheses.

Some of the most recent synthetic work on poly(aryl ethers) has involved the incorporation of fluorinated groups[60, 61] and heterocyclic units within the polymer backbone. Poly(aryl ethers) containing quinoxaline,[62–64] imidazole,[65, 66] 1,3,4-oxadiazole,[67] 1,2,4-triazole,[67] and benzoxazole[68] have been prepared. The heterocyclic unit generally brings about an increase in the cohesive energy density which is reflected in an increase of the strength, of the modulus, and of the glass temperature T_g. Polymers can be designed for specific applications and can be readily prepared because of the versatility offered in the polymer synthesis. Properties such as hydrophilicity, T_g, and solubility can be altered considerably by incorporation of pendent groups on the heterocyclic ring. These polymers show promise for use in a variety of applications including membranes for separating gases (e.g. carbon dioxide/methane) and enzymes.

An example of the reaction route to a poly(aryl ether) containing heterocyclic units is shown in Scheme 5. 4,5-

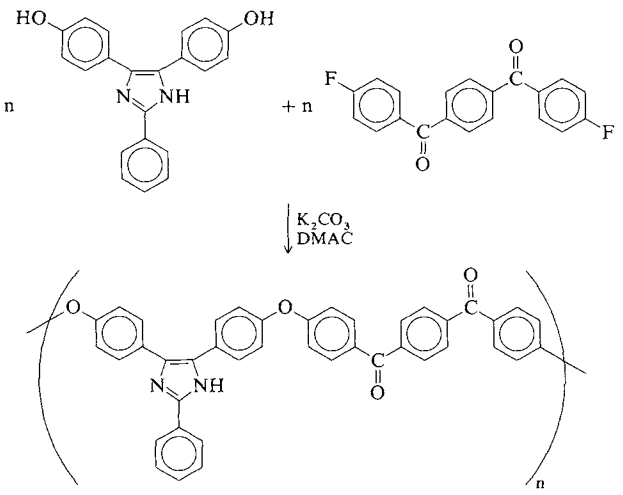

Scheme 5. Reaction route to a poly(aryl ether) containing phenylimidazole units.

Bis(4-hydroxyphenyl)-2-phenylimidazole reacts with 1,4-bis(4-fluorobenzoyl)benzene in the presence of potassium carbonate in *N,N*-dimethylacetamide (DMAC) to yield a high molecular weight polymer. The polymer exhibits an inherent viscosity of 0.89 dL g^{-1}, and an apparent T_g of 248 °C. Thin films showed a tensile strength and modulus of 97.9 MPa (14.2 Ksi) and 2.81 GPa (407 Ksi) respectively at 25 °C, and excellent adhesive properties.[66]

Various poly(aryl ethers) such as poly(ether ketone ketone) (PEKK)[69] are being evaluated as matrices for high-

performance, graphite-filament, reinforced composites. These thermoplastic composites exhibit good flexural, tensile, and CAI properties, but the compressive and interlaminar shear strengths are lower than those of epoxy- and bismaleimide-based systems. Although thermoplastics have been suggested to offer certain advantages over thermosets such as the potential of low-cost composite manufacturing, this has not been fully realized. The fabrication of thermoplastic composites requires higher temperatures and pressures than that of most thermosets. Conventional autoclave fabrication of composites is not cost-effective for thermoplastics. Matched-metal tooling, although expensive initially, can offer lower cost if many of the same composite parts are made. A potential advantage of thermoplastics over thermosets is the thermoforming of flat panels. Although the future of thermoplastic composites is unclear, new innovative prepreg forms and composite fabrication processes will resolve certain problems and make them more competitive with thermosets as composite matrices.

Aryl ether oligomers and polymers have been modified with various reactive groups such as ethynyl, allyl, amino, cyanato, epoxy, maleimido, and norbornenyl. The molecular weight of the oligomer and polymer can easily be controlled stoichiometrically. Several of these end-group-modified oligomers and polymers have been subjected to further thermal treatment to provide cured materials whose properties are governed primarily by the chemical structure, molecular weight of the oligomer or polymer, and curing conditions. This route opens up a method for controlling properties such as solubility, toughness, modulus and T_g of the cured material. An example is a study reported on ethynyl-terminated sulfone oligomers[70] (Scheme 6) where the molecular weight was varied from 4000 to 12000 g mol^{-1}. Upon thermal curing, the ethynyl group undergoes a complex reaction leading to some linear chain extension, branching and cross-linking.[71] Cured resins from low molecular weight oligomers exhibited higher modulus and higher T_g, lower toughness, and less solvent sensitivity than cured resins from high molecular weight oligomers due to increased cross-link density.

Because of their low cost, compatibility with thermosets, high toughness, and other properties, aryl ether oligomers terminated with groups such as amino, epoxy and maleimido have been used as toughening agents with thermosets. Several epoxy-[72, 73] and maleimide-based[30-32] systems presumably modified with functionalized aryl ether oligomers are available in prepreg form. Composites therefrom have provided outstanding properties including high CAI. Although these systems are not classified as true high-temperature materials, it is important to note that this technology is being extended as a means of toughening high-temperature thermosets (e.g. PMR-15 and ethynyl-terminated imide oligomers).

5. Imide/Aryl Ether Copolymers

Since polyimides and poly(aryl ethers) each offer specific attractive properties, it seemed only reasonable to combine these two families of polymers into one via blends or copolymers. The latter approach has been successfully used to obtain the excellent features of each polymer family in one material. For example, by synthesizing block copolymers[74] the high fracture energy and good compression moldability of a specific poly(aryl ether) and the high modulus and excellent solvent resistance of a particular polyimide were incorporated within one material, based upon rule of mixture. This approach has been successfully used with many other polymer families and offers an attractive route for tailoring polymer properties.

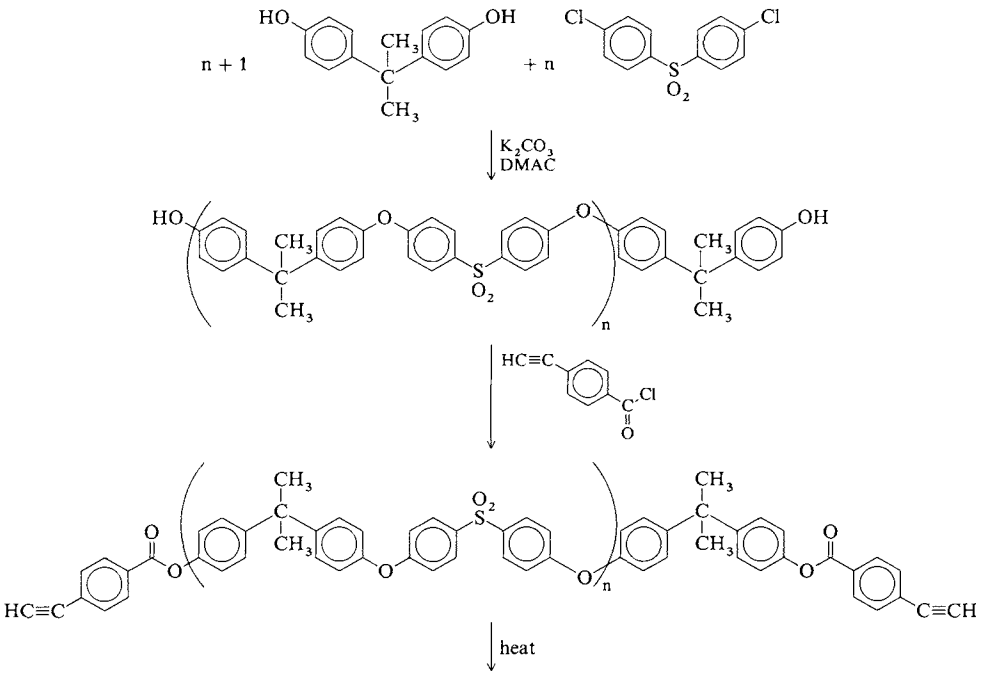

Scheme 6. Reaction route to ethynyl-terminated sulfone oligomers.

6. Concluding Remarks

The thermal performance of high-temperature polymers today and that projected for the year 2000 are presented in Table 5. Only marginal improvements in the thermal stability of organic polymers are anticipated. We are approaching the thermal capability offered by these materials. Advances will be made primarily in developing lower cost, more processable materials with better properties. As a result, the market for high-temperature polymers will grow significantly over the next decade as new and improved materials evolve with a more favorable combination of *price, processability and performance.*

Table 5. Maximum projected use time and temperature for organic polymers in unstressed condition in air.

T [°C]	1990 Use Time Projection	2000 Use Time Projection
760	< 1 min	< 1 min
538	10 min	10 min
427	20 h	20 h
371	200 h	300 h
316	2000 h	3000 h
260	> 20000 h	> 50000 h
232	> 50000 h	> 50000 h

Received: April 11, 1990 [A 788 IE]
German version: *Angew. Chem. 102* (1990) 1302

[1] J. M. Weatherall, A. T. Ono: *Proc. Symp. Recent Adv. in Polyimides and Other High Performance Polymers, Am. Chem. Soc. Div. Polym. Chem.*, San Diego, CA, USA January 1990.
[2] A. D. Macallum, *J. Org. Chem. 13* (1948) 154.
[3] H. Vogel, C. S. Marvel, *J. Polym. Sci. 50* (1961) 511.
[4] J. I. Jones, F. W. Ochynski, F. A. Rackley, *Chem. and Ind.* (1962) 1686.
[5] G. W. Bower, L. W. Frost, *J. Polym. Sci. Part A1* (1963) 3135.
[6] A. L. Endrey, US-Pat. 3179631; US-Pat. 3179633 (1965), DuPont.
[7] G. P. de Gaudemaris, B. J. Sillion, *J. Polym. Sci. Part B2* (1964) 203.
[8] J. K. Stille, J. R. Williamson, *J. Polym. Sci. Part B2* (1964) 209.
[9] D. L. Loncrini, US-Pat. 3182073 (1965), General Electric Co.
[10] H. A. Vogel, *J. Polym. Sci. Part A1 8* (1970) 2035.
[11] P. M. Hergenrother, H. H. Levine, *J. Polym. Sci. Part A1 5* (1967) 1453.
[12] F. E. Rogers, US-Pat. 3356648 (1967), DuPont.
[13] W. J. Farrissey, J. S. Rose, P. S. Carleton, *Polym. Prepr. (Am. Chem. Soc. Div. Polym. Chem.) 9(2)* (1968) 1581.
[14] F. Grundschober, J. Sambeth, US-Pat. 3533996 (1970).
[15] T. T. Serafini, P. Delvigs, G. R. Lightsey, *J. Appl. Polym. Sci. 16* (1972) 905.
[16] A. L. Landis, N. Bilow, R. H. Boschan, R. E. Lawrence, T. J. Aponyi, *Polym. Prepr. (Am. Chem. Soc. Div. Polym. Chem.) 15(2)* (1974) 533, 537.
[17] J. G. Wirth, P. R. Heath, US-Pat. 3838097 (1974), General Electric Co.
[18] J. H. Bateman, W. Geresey, D. S. Neiditch, *Coat. Plast. Prepr. Pap. Meet. (Am. Chem. Soc. Div. Org. Coat. Plast. Chem.) 35(2)* (1975) 77.
[19] J. Economy, B. E. Nowak, S. G. Cotlis, *SAMPE J. 6* (1970) 6.
[20] V. L. Bell, B. L. Stump, H. Gager, *J. Polym. Sci. Polym. Chem. Ed. 14* (1976) 2275.
[21] A. K. St. Clair, T. L. St. Clair, *Sci. Adv. Mater. Process Eng. Ser. 26* (1981) 165.
[22] J. F. Wolfe, F. E. Arnold, *Macromolecules 14* (1981) 909.
[23] J. F. Wolfe, B. H. Loo, F. E. Arnold, *Macromolecules 14* (1981) 915.
[24] P. M. Hergenrother, N. T. Wakelyn, S. J. Havens, *J. Polym. Sci. Polym. Chem. Ed. 25* (1987) 1093.
[25] K. J. Dahl, P. J. Horner, H. C. Gors, V. Jansons, R. H. Whiteley, US-Pat. 4868271 (1989), Raychem Corp.
[26] P. M. Hergenrother: *Heat-Resistant Polymers, Encycl. Polym. Sci. Eng., Vol. 7*, 2nd Edit., Wiley, New York 1987, p. 639.
[27] P. E. Cassidy: *Thermally Stable Polymers*, Dekker, New York 1980.
[28] J. P. Critchley, G. J. Knight, W. W. Wright: *Heat-Resistant Polymers*, Plenum, New York 1983.
[29] National Starch and Chemical Corp., Bridgewater, NJ 08807, USA.
[30] M. Konarski, *Sci. Adv. Mater. Process Eng. Ser. 34* (1989) 505.
[31] V. Ho, *Sci. Adv. Mater. Process Eng. Ser. 34* (1989) 514.
[32] J. Boyd, G. Chang, P. Eisenbarth, W. Webb, *Sci. Adv. Mater. Process Eng. Ser. 34* (1989) 2365.
[33] J. D. Boyd, G. E. C. Chang, V. Altstädt, D. Gerth, W. Heckmann, *Sci. Adv. Mater. Process Eng. Ser. 35* (1990) 994.
[34] R. Pater, C. Morgan, *Proc. SPE 46. Annu. Tech. Conf. Exhibits* (1988) 1639.
[35] G. M. Bower, L. W. Frost, *J. Polym. Sci. Part A1 1* (1963) 3135.
[36] J. P. Critchley, P. A. Grattan, M. A. White, P. S. Pippet, *J. Polym. Sci. Part A1, 10* (1972) 1789.
[37] W. F. Farrisey, J. S. Rose, P. S. Carleton, *Polym. Prepr. (Am. Chem. Soc. Div. Polym. Chem.) 9* (1968) 1581.
[38] M. Dorr, M. Levy, *J. Polym. Sci. Polym. Chem. Ed. 13* (1975) 171.
[39] R. J. Boyce, T. P. Gannett, H. H. Gibbs, A. R. Wedgewood, *Sci. Adv. Mater. Process Eng. Ser. 32* (1987) 169.
[40] S. N. Kharkov, E. P. Krasnov, Z. N. Laurova, S. A. Baranova, U. P. Aksenova, A. S. Chegola, *J. Polym. Sci. USSR 13(4)* (1971) 940.
[41] T. Takekoshi, J. G. Wirth, D. R. Heath, J. E. Kochanowski, J. S. Manello, M. J. Webber, *J. Polym. Sci. Polym. Chem. Ed. 18* (1980) 3069.
[42] T. Takekoshi: *32. IUPAC Int. Symp. Macromol.*, Kyoto, Jpn., August 1989; US-Pat. 3847870 (1974), General Electric Co.
[43] D. Wilson, H. Stenzenberger, P. M. Hergenrother: *Polyimides–Chemistry and Applications*, Blackie, Glasgow 1990.
[44] E. I. DuPont de Nemours and Co., *Ind. Film Div.*, Wilmington, DE 19898, USA.
[45] Kanegafuchi Chemical Ind. Co., Shiga 520-01, Jpn.
[46] P. M. Hergenrother, S. J. Havens, *SAMPE J. 24(4)*(1988) 13.
[47] P. M. Hergenrother, M. W. Beltz, S. J. Havens, *Sci. Adv. Mater. Process Eng. Ser. 34* (1989) 961.
[48] Mitsui Toatsu Chemicals, Inc., Königsallee 92a, 4000 Düsseldorf 1.
[49] T. Matsuura et al., *Polym. Prep. (Am. Chem. Soc. Div. Polym. Chem.) Jpn. 38* (1989) 435.
[50] S. Numata: *Polymers for Microelectronics, Sci. Tech.*, Univ. Tokio, Jpn. Oct. 29–Nov. 2, 1989.
[51] A. J. Beuhler, M. J. Burgess, D. E. Fjare, J. M. Gaudette, R. T. Roginski, *Proc. Mater. Res. Soc.*, Boston, MA, USA November 1989.
[52] W. B. Alston, R. F. Gratz in D. Weber, M. R. Gupta (Eds.): *Recent Adv. Polyimide Sci. Tech., Soc. Plastics Eng.*, Poughkeepsie, NY, USA 1987, p. 1.
[53] M. Gerber, R. Pratt, T. St. Clair, A. St. Clair, *Polym. Prepr. (Am. Chem. Soc. Div. Polym. Chem.) 31(1)* (1990) 340.
[54] F. W. Harris, S. L. Shu, C. C. Tso, *Polym. Prepr. (Am. Chem. Soc. Div. Polym. Chem.) 31(1)* (1990) 342.
[55] E. I. DuPont de Nemours and Co., *Ind. Fibers Div.*, Wilmington, DE 19898, USA.
[56] R. N. Johnson, A. G. Farnham, F. A. Clendinning, W. F. Hale, C. N. Merriam, *J. Polym. Sci. Part A1 5* (1967) 2375.
[57] M. Ueda, M. Sata, *Macromolecules 20* (1987) 2675.
[58] A. S. Hay et al., *J. Am. Chem. Soc. 81* (1959) 6335.
[59] H. M. Vandort et al., *Eur. Polym. J. 4* (1968) 275.
[60] G. L. Tullos, P. E. Cassidy, A. K. St. Clair, *Polym. Mater. Sci. Eng. 60*, (1989) 310.
[61] J. W. Labadie, J. L. Hedrick: *Int. Chem. Congr. Pac. Basin Soc.*, Abstr. No. 321, MACRO 07, Honolulu, HA 1989; *Macromolecules*, in press.
[62] J. L. Hedrick, J. W. Labadie, *Macromolecules 21* (1988) 1883.
[63] J. W. Connell, P. M. Hergenrother, *Polym. Prepr. (Am. Chem. Soc. Div. Polym. Chem.) 29(1)* (1988) 172.
[64] F. W. Harris, J. E. Korleski, *Polym. Mater. Sci. Eng. 61* (1989) 870.
[65] J. W. Connell, P. M. Hergenrother, *Polym. Mater. Sci. Eng. 60* (1989) 527.
[66] J. W. Connell, P. M. Hergenrother, *Sci. Adv. Mater. Process Eng. Ser. 35* (1990) 2175.
[67] P. M. Hergenrother, J. W. Connell, P. Wolf: *Proc. Symp. Recent Adv. in Polyimides and Other High Performance Polymers, Am. Chem. Soc. Div. Polym. Chem.*, San Diego, CA, USA, January 1990; 33rd IUPAC Int. Symp. Macromol., Montreal, Canada, July 1990.
[68] J. G. Hilborn, J. W. Labadie, J. L. Hedrick, *Polym. Mater. Sci. Eng. 60* (1989) 523.
[69] E. I. DuPont de Nemours and Co., *Adv. Composites Div.*, Wilmington, DE 19898, USA.
[70] P. M. Hergenrother, B. J. Jensen, S. J. Havens, *SAMPE J. 20 (5)* (1984) 18.
[71] P. M. Hergenrother: *Acetylene-Terminated Prepolymers, Encycl. Polym. Sci. Eng., Vol. 1*, 2nd. Edit., Wiley, New York 1985, p. 61.
[72] N. Odagiri, T. Muraki, K. Tobukuro, *Sci. Adv. Mater. Process Eng. Ser. 33* (1988) 272.
[73] G. R. Alman, R. K. Maskell, V. Malhotra, M. S. Sefton, P. T. McGrail, S. P. Wilkinson, *Sci. Adv. Mater. Process Eng. Ser. 33* (1988) 979.
[74] B. J. Jensen, P. M. Hergenrother, R. G. Bass, *Polym. Mater. Sci. Eng. 60* (1989) 294; *Polym. Prepr. (Am. Chem. Soc. Div. Polym. Chem.) 30(2)* (1989) 132; *ibid. 31(1)* (1990) 618.

Specific Interactions of Proteins with Functional Lipid Monolayers – Ways of Simulating Biomembrane Processes

By Michael Ahlers, Wolfgang Müller, Anke Reichert, Helmut Ringsdorf* and Joachim Venzmer

The interplay between molecular self-organization and molecular recognition leads to the construction of functional supramolecular systems in which order and mobility are combined and whose function is based on their organization. These fascinating phenomena, for which the living cell is a perfect example, can be understood only if a wide range of scientific disciplines work together. For this purpose, synthetic supramolecular systems can be used to simulate natural biomembrane processes. One example of this is the specific recognition and interaction between membrane-bound ligands and receptor proteins. Thus, the specific interaction of vitamin H (biotin) with the tetrafunctional protein streptavidin in the monolayer leads to 2D crystallization of the protein. Structural analysis shows that the protein is attached to the lipid membrane by two biotin-binding sites, leaving two still free. The opportunity this allows for biotinylated molecules to dock to the protein leads to interesting possibilities for constructing protein-containing functional multilayers. Another example for the simulation of biomembrane processes is the function of enzymes which is coupled to the recognition process. In the interaction of phospholipase A_2 with lecithin monolayers, specific recognition between enzyme and substrate is followed by an active phase of lipid cleavage and then by aggregation of the enzyme to give domains of regular morphology. Fluorescence microscopy can be used to follow this process directly: an enzyme caught in action.

Der Witz ist der Finder und der Verstand der Beobachter.
Georg Christoph Lichtenberg**

1. Steps across Borders?

1.1. There are Many Ways of Solving a Scientific Problem

Steps across borders? Is it going too far to choose such a title for the introduction to a presentation of scientific results? Without a question mark it would be ridiculous. Nevertheless, the question involves one of the essential problems of modern scientific development: the almost worrying one-sidedness of scientific thought. The pressures are great, and specialization has become indispensable. This is why it is necessary to make steps across borders. Can we learn how to do this?

There are various theories relating to the acquisition of scientific knowledge.[2] The emphasis now is on the discursive method, which entails reasoning and drawing causal conclusions, at the expense of the intuitive approach to solving problems. Intuition has been devalued because of the lack of absolute certainty, and it is treated badly in our education system.[3] Part of the reason for this is historical, derived from the predominant aim of epistemology (theory of cognition): the securing of knowledge. *Descartes* and *Kant* made certainty virtually the criterion of truth: only really certain knowledge can be true, which does not leave much room for intuition. Many scientific and technical discoveries demonstrate the increasing success of conclusions drawn by the discursive method from facts and unambiguous concepts. This has led to an overestimation of scientific thinking and to a fundamental devaluation of what is less certain and, especially, of intuition in science. Positivists do not even accept that knowledge which is uncertain actually is cognition and regard it as no more than a leisure time occupation. However, it is demonstrably true that certain knowledge is far from sufficient for breakthroughs in science, to say nothing of coping with existence.[4]

Georg Christoph Lichtenberg, who was an eighteenth century physicist and philosopher in Göttingen, posed the question about steps across borders, and the answer he gave was:[1b] "A really serious examination is necessary of why most inventions come about by chance. The main reason is probably that people view everything in the same way as their teachers and colleagues do. This is why it would undoubtedly be useful to suggest certain rules for departing from the rules." The development of macromolecular chemistry is a good example of this. It arose from steps across borders, preferring intuitive concepts to accepted doctrines. It is of historical interest to see how *Hermann Staudinger*, at the height of his creativity in organic chemistry, dared to leave this "classical" area and go into macromolecular chemistry.[5] There is no doubt that the time was ripe, but he still had to overcome established concepts. This is also an interesting example of what *Leonardo da Vinci* said so long ago: "In a difference of opinion, the person who quotes authorities is using his memory and not his intellect."

1.2. Functionalized Supramolecular Systems

One of the areas of organic chemistry now being intensively studied, on an interdisciplinary basis in many laboratories,

[*] Prof. Dr. H. Ringsdorf, Dr. M. Ahlers,
Dipl.-Chem. W. Müller, Dipl.-Chem. A. Reichert,
Dipl.-Chem. J. Venzmer
Institut für Organische Chemie der Universität
J.-J.-Becherweg 18–20, 6500 Mainz (FRG)

[**] "Wit is the finder and intelligence the observer" [1a].

is that of supramolecular systems. Since classical organic chemistry is now able to construct highly complicated molecules and provide biologists and biochemists with detailed insights into natural processes, the chemists are becoming interested in investigating organic chemistry beyond the covalent bond, as *J. M. Lehn* called it.[6]

In nature, system functioning is achieved by interplay between different functional units. The smallest unit which demonstrates this perfectly is the cell:[7] it is the interplay between molecular self-organization and molecular recognition of its individual constituents (lipids, proteins, nucleic acids...) which leads to the construction of this natural supramolecular system. It combines order and mobility, and its functioning is based on its organization. This fascinating phenomenon can be understood only if a wide range of modern scientific disciplines work together. The special tasks of organic and macromolecular chemistry in this connection involve finding new syntheses and solving structural problems. One of the interesting questions which arises is whether it is possible to develop new materials which simulate natural supramolecular systems in that their functioning is determined by their organization. This will not be possible without going beyond the limits of classical thinking in the individual disciplines.

Where are examples of connecting links between apparently separated disciplines of science? Figure 1 describes common perspectives of life science and materials science relating to functional supramolecular systems.

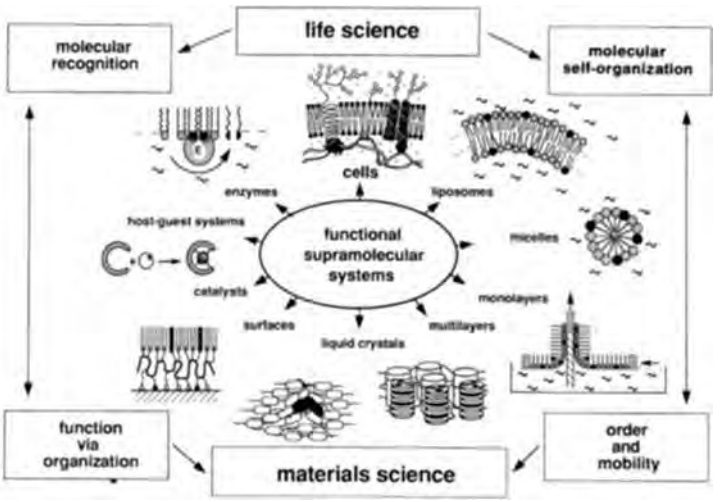

Fig. 1. Functional supramolecular systems—connecting link between life science and materials science.

The cell with its recognition structures on the surface is structured by the lipid membrane and dominantly functionalized by proteins. Its stability is determined both by proteins or lipids which extend through the membrane and by polymer networks, for example the cytoskeleton. Descending in complexity from this perfect natural pattern one finds liposomes[8] with their relatively simple bilayers and finally micelles[9] with their various lyotropic structures.[10] They have long been important in studies of synthetic and natural systems and, in colloid science, determined the course of physical chemistry in the 1920s. Recent developments in monolayers and multilayers (Langmuir and Langmuir-Blodgett systems)[11] have resulted in ultrathin films in which order and mobility can be combined. Of more interest to materials science are liquid crystals[12] which are already of industrial importance, in both low molecular weight and macromolecular forms. Their order is based on their form-anisotropy, and it is possible for rods,[13] disks[14] or boards[15] to self-organize. Too often, it is forgotten that liquid crystals have always been essential in nature. Many of the natural polymers, and cell membranes themselves should be regarded as liquid-crystal systems, although lyotropic not thermotropic.[16]

Besides molecular self-organization, another crucial property of natural supramolecular systems is their capability of molecular recognition, which leads to specific interactions. Many processes on the cell membrane start with recognition and lead on to enzymatic reactions, such as cleavage of lipids by the various phospholipases.[17] The problem of molecular recognition has for some time been an important part of organic chemistry owing to the variety of studies on guest-host systems[18] and their importance for synthetic supramolecular systems. This area also includes the alteration of surfaces and the structuring of ultrathin layers, which are of particular interest in catalyst research, sensor technology and tribology. As Figure 1 indicates, it is also possible to functionalize liquid crystals. The function of such addressable liquid crystals is, in principle, based on their organization, and the molecular recognition is introduced by reactive groups, for example photosensitive groups.[19] Intensive study of this is now in progress in the area of non-linear optics[20] and optical storage.[21]

In this contribution it is not intended to review the field of functional supramolecular systems. Only three examples showing the interplay between molecular self-organization and molecular recognition will be presented in this paper. The techniques employed combine the self-organization of lipids in the monolayer, which can represent half a cell membrane, with the specificity of molecular recognition of proteins and enzymes. This is briefly discussed in the next section.

1.3. Attempts to Simulate Recognition Processes and Protein Functions on Model Membranes

The self-organization of lipids to form the plasma membrane[7] was a crucial step in the evolution of the earliest forms of life—cellular life is impossible without the protection provided by the lipid membrane. However, it is more than just a passive barrier between the cytosol and the surroundings. On the contrary, it is a highly selective, active filter. Moreover, the cell surface plays an essential part in intercellular communication (for example in immune reactions). Whereas the lipid bilayer determines the basic structure of biological membranes, most of their functions, for example specific receptors, enzymes or transport systems, are provided by proteins embedded in the lipid bilayer. However, the structure of the cell membrane is so complex that it is difficult to study specific individual processes in biological systems. This is why it is an advantage to choose model membranes for investigating biomembrane processes be-

cause they can be limited to a few variable factors (see Section 2). Figure 2 outlines various membrane processes whose simulation in monolayers is to be discussed.

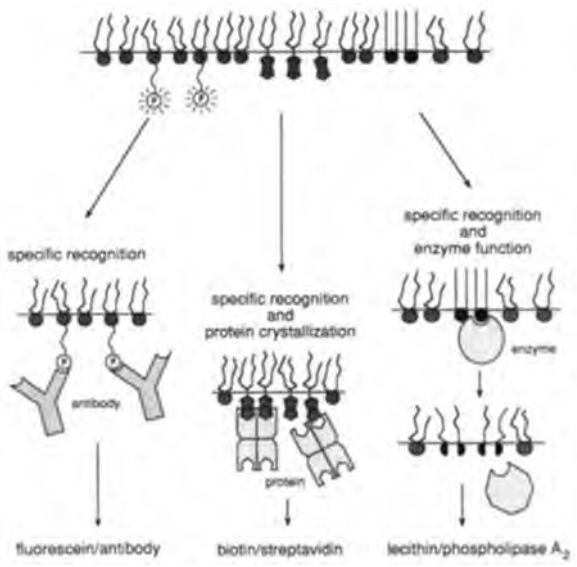

Fig. 2. Examples of the simulation of specific recognition reactions at model membranes: recognition (fluorescein/anti-fluorescein antibody), recognition and protein crystallization (biotin/streptavidin), recognition and enzyme function (lecithin/phospholipase A_2).

The first important step in many surface reactions is the specific recognition taking place between a ligand on the membrane and a receptor protein (for example an antibody). An interaction of this type will be exemplified by fluorescein-lipids and the anti-fluorescein antibody (Section 3). As a consequence of specific recognition different processes can take place on the membrane. One example of this is the 2D crystallization of streptavidin after binding to biotin-lipid monolayers which is described in Section 4. This process is also of interest with a view to potential use in biosensors. If the protein is an enzyme, the specific recognition can be followed by an enzymatic function being carried out. This will be illustrated by the example of phospholipid-monolayer hydrolysis by phospholipase A_2 (Section 5).

Before these membrane processes are discussed in detail, the next section will briefly describe the various model membrane systems and especially the characterization methods for monolayers used in this article.

2. Lipid Monolayers as Simple Models of Biomembranes

2.1. Model Membranes

Single membrane processes are preferably investigated on the four model systems depicted in Figure 3. These model membranes are, like their natural prototype, the cell, composed of lipids which, since they are amphiphilic molecules which are insoluble in water, undergo spontaneous self-organization on contact with water. The force behind this self-organization is the hydrophobic effect.[22] Depending on the

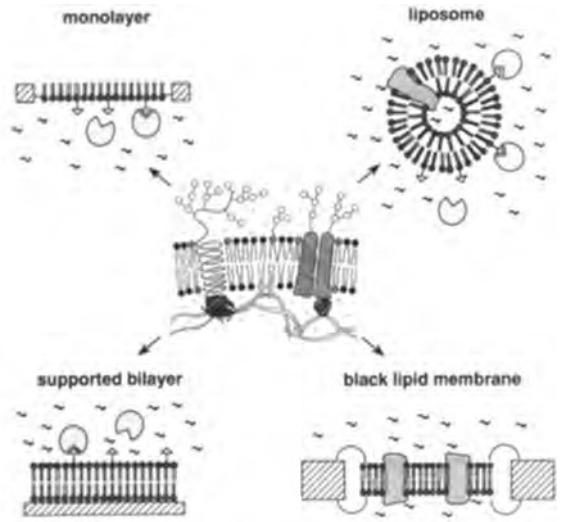

Fig. 3. Simple models for biological membranes: model membranes for studying surface recognition reactions, protein reconstitution and protein functions.

preparation technique, different supramolecular structures are formed, which can be used as model membrane systems.

Liposomes (vesicles)[8] are lipid bilayers which form a closed sphere containing an aqueous compartment in a similar way to the cell membrane. They are used, inter alia, for reconstituting membrane proteins and studying surface recognition reactions.

Black lipid membranes (BLMs)[23] are planar lipid bilayers, which, by covering a hole in a teflon wall, separate two aqueous compartments from one another. It is possible in this way, for example, to study the transport of ions through lipid membranes – passively or actively assisted by incorporated proteins – by conductivity measurements.

Preparation of lipid bilayers on a solid substrate (*supported bilayers*)[24] results in membranes which are considerably more stable than BLMs and can easily be manipulated on the exposed side not facing the substrate. They are therefore particularly suitable for studying surface recognition reactions.

Monolayers[25] are formed when a lipid is spread on a water surface and they correspond formally to one half of the lipid bilayer of a cell membrane. The hydrophilic headgroups of the lipids face towards the water and the hydrophobic alkyl chains face towards the air. There are a number of methods for investigating lipid monolayers and their interaction with substances (for example proteins) dissolved in the water, and those which will be dealt with are the characterization by pressure/area diagrams and fluorescence microscopy.

2.2. Pressure Area Diagrams of Lipid Monolayers[25a]

When the solution of a lipid is spread on the water surface in a Langmuir balance, the tendency of the molecules to self-organization results in spontaneous formation of a two-dimensional lipid phase. This monolayer can be gas-, liquid- or solid-analogous depending on the lipid concentration (molecules/area). Use of a movable barrier to reduce the area available to the lipid allows a two-dimensional phase

diagram (surface pressure/area diagram) to be measured at constant temperature. The packing of the molecules in a monolayer as a function of the surface pressure is shown schematically in Figure 4.

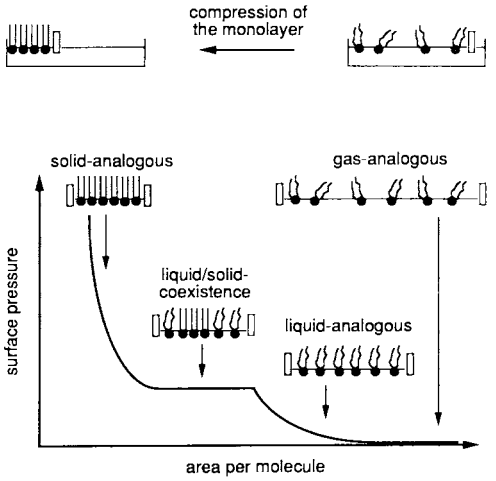

Fig. 4. Pressure/area diagram of a lipid monolayer: representation of the compression behavior and packing in the gas-, liquid-, and solid-analogous phase.

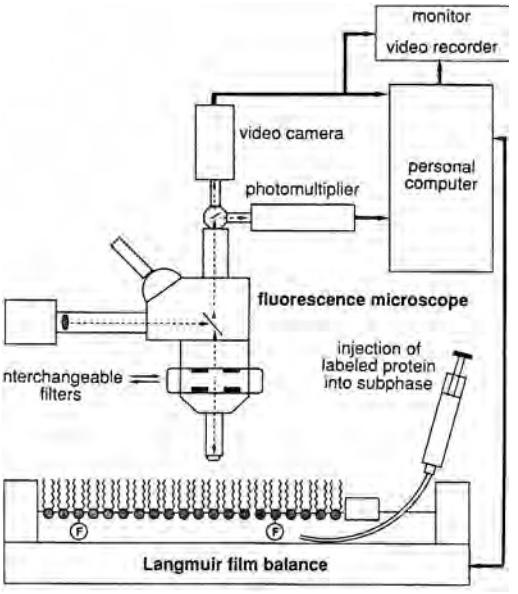

Fig. 5. Schematic representation of a fluorescence film balance (combination of a Langmuir film balance with a fluorescence microscope): the fluorescence microscope is used to observe a monolayer at the gas/water interface. The processes taking place can be recorded by a video system. The fluorescence can be quantified by means of a photomultiplier. The interchangeable filter system can be used for selective observation of the monolayer and the protein by using different fluorescence dyes.

In the gas-analogous phase, there is extensive disorder of the lipid molecules. A reduction in the area leads to the formation of a liquid-analogous phase, and the closer-packing of the amphiphiles becomes evident from an increase in the surface pressure. Further compression results in the monolayer entering the region of solid/liquid coexistence. At this transition, the alkyl chains of the lipids start to form two-dimensional crystals which are solid-analogous in a liquid-analogous lipid matrix. Further compression results in crystallization of the complete monolayer so that its compressibility is now low and there is a steep rise in the isotherm. The shape of the isotherms depends greatly on the structure of the lipids.[27] The pressure/area diagrams allow statements to be made about their orientation, mobility and interactions with compounds dissolved in the subphase.

2.3. Fluorescence Microscopy of Lipid Monolayers

Combination of a Langmuir balance with a fluorescence microscope (Fig. 5) allows processes in or at the monolayer to be observed by using fluorescent dyes as probes.[26] For this, the lipid to be investigated is doped with 0.5 mol% of a fluorescence-labeled lipid (for example the sulforhodamine lipid **1**).

Such a small amount of fluorescent marker does not influence the phase behavior of the monolayer so that direct observation of the lipid phases is possible under the fluorescence microscope. A video camera is used for continuous recording of the processes taking place in the monolayer. A photomultiplier allows the fluorescence emitted by the monolayer to be quantified, which permits the measurement of quenching effects (see also Section 3).

The appearance of a monolayer doped with a fluorescence dye (for example **1**) during measurement of a pressure/area diagram is shown by the images taken at different surface pressures (Fig. 6).

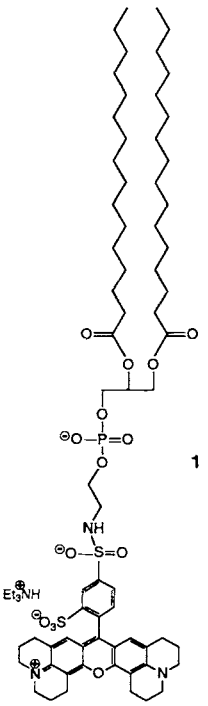

In the liquid-analogous phase, the fluorescence is homogeneous throughout the field of observation. Compression of the lipid film into the phase transition region produces dark, non-fluorescent domains (solid-analogous lipid) in a bright matrix with homogeneous fluorescence (liquid-analogous lipid mixed with a fluorescence dye). The solid-analogous

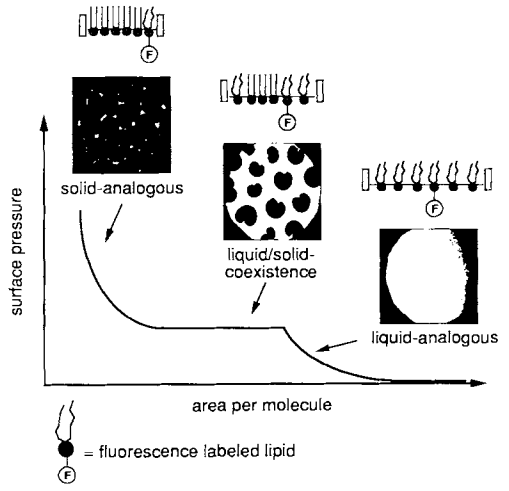

Fig. 6. Phase behavior of a lipid monolayer doped with a fluorescence lipid: diagram and appearance under the fluorescence microscope: in the liquid-analogous phase, the fluorescence dye is homogeneously distributed in the monolayer; in the phase transition region there are solid-analogous lipid domains, which appear dark because the fluorescence dye is not incorporated, in a bright liquid-analogous matrix; the solid-analogous phase is almost completely dark.

domains are dark because the fluorescence dye is not incorporated in the crystalline regions. The morphology of the lipid domains depends greatly on the lipid used. Thus, chiral lipids may form domains with a chiral structure. Finally, in the solid-analogous phase, the lipid has undergone almost complete 2D crystallization and phase separation from the fluorescence dye. Now there are only small fluorescing areas (pure fluorescence dye) in a dark matrix of solid-analogous lipid.

It is advantageous when investigating the interaction of the lipid monolayer with a protein dissolved in the subphase to be able to observe the lipid layer and the protein selectively. This can be achieved by using a suitable filter system and two fluorescence dyes whose absorption and emission spectra do not overlap (for example sulforhodamine: $\lambda_{Ex} = 584$ nm, $\lambda_{Em} = 607$ nm and fluorescein: $\lambda_{Ex} = 497$ nm, $\lambda_{Em} = 521$ nm). One of the two dyes is mixed with the lipid monolayer as described above, while the other is covalently bound to the protein. Thus, for example, it is possible by using a rhodamine filter to excite fluorescence only from the monolayer doped with sulforhodamine in order to follow the changes in the morphology of the lipid layer. On the other hand, with the fluorescein filter fluorescence is excited only from the fluorescein which is attached to the protein, and the lipid layer becomes virtually transparent.

Application of these methods to the investigation of the specific interactions between proteins and monolayers (see Fig. 2) is described in the following sections.

3. Hapten Antibody Interactions on Monolayers: Specific Recognition of Fluorescein by the Anti-Fluorescein Antibody

Intercellular communication in assemblages of cells is based on specific recognition and binding at the molecular level. Recognition reactions of this type are also extremely important for immune processes: the specific interaction between receptor and ligand for binding antibodies to cellular antigens represents a key element in histocompatibility and immunogenicity,[7] Specific recognition reactions also form the basis for developing new drug delivery strategies[27] and for constructing new immunoassays.

The study of such antigen/antibody interactions on model membranes has to date mainly used dinitrophenyl (DNP)-lipid conjugates as haptens.[24, 28] Here, the fluorescein/anti-fluorescein antibody system will be discussed. Their interaction can easily be followed spectroscopically because binding of the antibody causes fluorescence quenching.

3.1. Properties of Fluorescein and Its Antibody

Fluorescein is very suitable as an antigenic determinant because of its aromatic, dianionic nature and space-filling structure.[29] The monoclonal anti-fluorescein antibody used in these studies has the highest known binding constant (3.4×10^{10} M^{-1}) for a synthetic antigen.[30, 31]

Binding leads to almost complete quenching of the fluorescence of fluorescein. This means that fluorescence spectroscopy can be used to monitor and quantify the specific recognition and binding of the antigen by the antibody.[29a]

Figure 7 shows the fluorescence spectra of a fluorescein solution titrated with an antibody solution. The decrease in

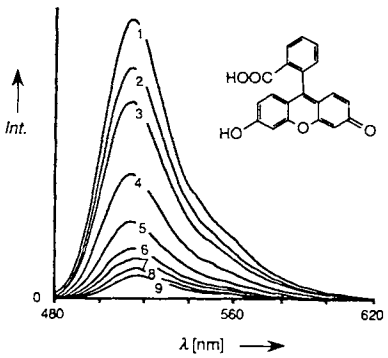

Fig. 7. Fluorescence spectra of fluorescein (2.7×10^{-12} M) before (1) and after (2–9) incubation with the anti-fluorescein antibody: increasing the antibody concentration increases the quenching of the fluorescein fluorescence; antibody concentrations: (2) 8.5×10^{-13} M; (3) 1.7×10^{-12} M; (4) 3.4×10^{-12} M; (5) 5.1×10^{-12} M; (6) 6.8×10^{-12} M; (7) 8.5×10^{-12} M; (8) 1.1×10^{-11} M; (9) 1.5×10^{-11} M.

fluorescence intensity as the antibody concentration increases is evident. F_{AB} fragments of the antibody complexed to fluorescein can be crystallized, which made it possible to determine the spatial structure of the antibody binding site.[32] In the antibody/hapten complex the fluorescein molecule is anchored deep (about 15 Å) in the binding site on the antibody by van der Waals interactions, hydrogen bonding, and charge neutralization (Fig. 8).

On these grounds, it is to be expected that fluorescein attached to a membrane will be available for such binding only if the attachment is via a sufficiently long spacer. This is why the investigations on monolayers were carried out

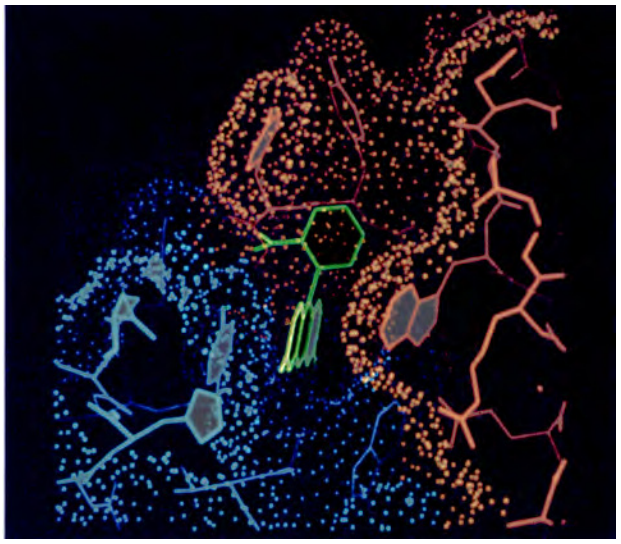

Fig. 8. 3D model of the binding region of the antifluorescein antibody (orange, blue); its hapten fluorescein (green) is anchored deeply in the binding pocket which is accessible only through a narrow channel [32].

with the spacer-containing lipid **2** and lipid **3** which has no spacer.[33a]

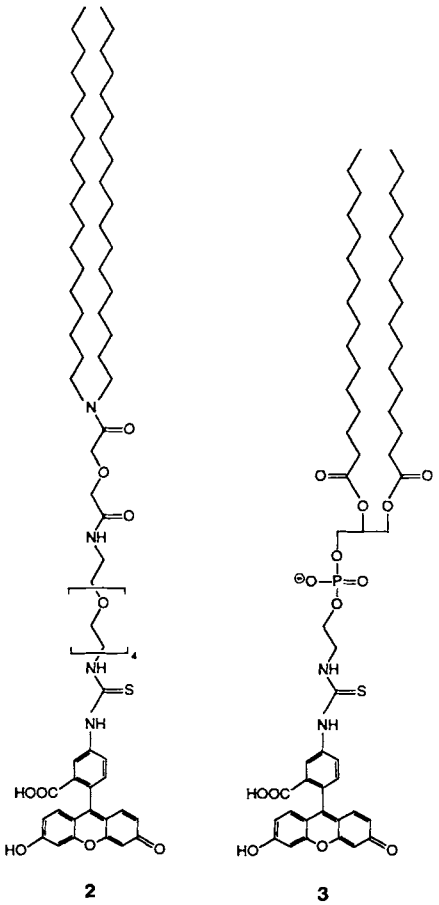
N
O
NH
NH
S
NH
HOOC
HO
O
O
O

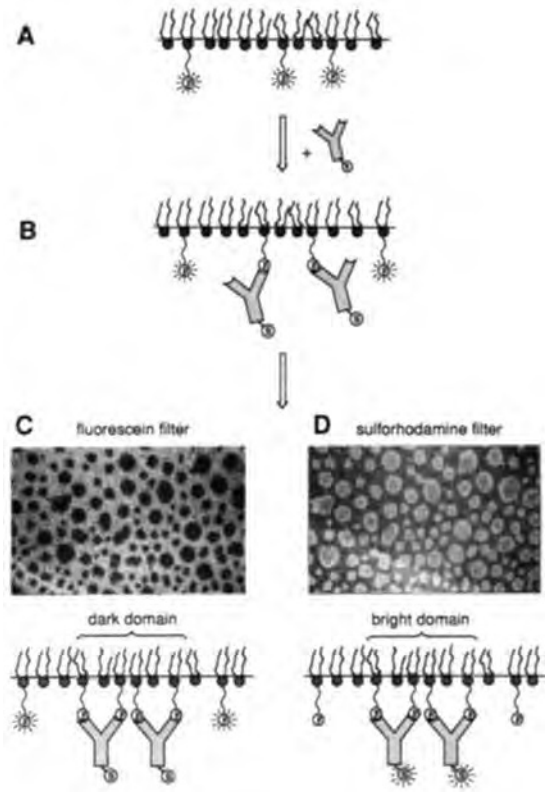

Fig. 10. Schematic representation of the binding of the anti-fluorescein antibody to monolayers doped with fluorescein-lipid: the sulforhodamine-labeled antibody dissolved in the subphase binds specifically to the hapten on the membrane and quenches its fluorescence (A,B); domain formation of the antibody can then be observed under the fluorescence microscope (C,D). These domains appear dark through the fluorescein filter (C) because of the fluorescence quenching, and appear bright through the sulforhodamine filter owing to the labeling of the antibody with sulforhodamine (D); 1% fluorescein-lipid **2** in POPC; $\pi = 5$ mN/m; 5 mm $\triangleq$ 20 μm.

The fluorescence quenching shows that the antibody binds considerably better to the fluorescein-lipid **2** with a spacer than to the lipid **3** without a spacer. A long hydrophilic spacer between the functional group (fluorescein) and the alkyl chains which form the membrane in the case of lipid **2** makes it possible for the antibody to bind to the fluorescein without hindrance from the lipid monolayer. However, the antibody binding is influenced not only by the nature of the lipid but also by the state of the monolayer. Thus, although the extent of quenching is approximately independent of the pressure between 2 mN/m and 30 mN/m, the domain formation as shown in Figure 10 only occurs at low pressure. In this case, the low packing density allows high lateral mobility of the antibody-fluorescein-lipid complexes, which makes the formation of the protein aggregates possible.

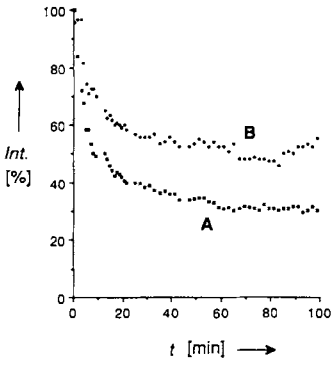

Fig. 11. Quantification of the fluorescence quenching when the antibody binds to fluorescein-lipids in monolayers: (A) the fluorescence of the spacer-containing lipid **2** is quenched by 70%; (B) the fluorescence quenching is only 50% with the lipid **3** without a spacer; 1% fluorescein-lipid in POPC, $\pi = 30$ mN/m.

4. Biotin-Lipid/Streptavidin Interaction in Monolayers: Specific Recognition and 2D Crystallization of Streptavidin

One example of specific protein-lipid interactions in monolayers is the recognition of the fluorescein-lipids **2** and **3** by their antibody which has been discussed in the previous section. Studies by *R. Kornberg* et al. have shown that this type of interaction can lead to 2D crystallization of the protein under certain conditions.[34] The example of the specific recognition between the tetrafunctional protein streptavidin and biotin attached to lipids[35] will be used to show how such processes in monolayers can be studied and possibly utilized in biosensors.

4.1. Importance of the Biotin/Avidin System

Avidin ($M = 68$ kDa) and streptavidin ($M = 60$ kDa) are two homologous water-soluble proteins which differ in molecular weight due to additional oligosaccharide units in the avidin.[36] Each is composed of four identical subunits and each of these four subunits has a specific binding site for biotin **4** (vitamin H) (Fig. 12).[37]

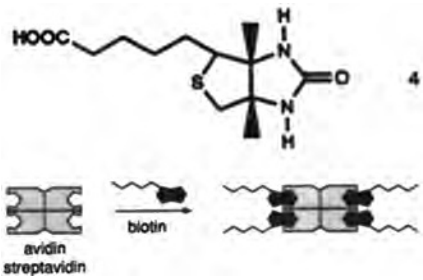

Fig. 12. Schematic representation of the binding of biotin **4** (vitamin H) to the tetrameric proteins avidin and streptavidin.

This recognition reaction has the exceptionally high binding constant of 10^{15} M^{-1}, which corresponds to a binding energy of 20 kcal mol^{-1}. This is only about one order of magnitude less than the energy of a covalent bond.[38] Binding of biotin to avidin/streptavidin is thus virtually irreversible.

The significance of this interaction in nature is not yet clearly known. On the other hand, the function of biotin itself is known in considerably more detail. It is found in all higher organisms and acts as a coenzyme in the fixation of CO_2 by various carboxylases.[39] This function is inhibited by avidin and streptavidin, which bind biotin so strongly so that it is no longer available for the enzymatic carboxylation.

Knowledge of the specific biotin/avidin binding has led to wide use in bioanalytics,[40] molecular biology[41] and immunology.[42] Other advantages of this system are that the protein is very stable and that biotin can be functionalized on its free carboxyl group without impairing its binding properties. This makes it possible to incorporate biotin into lipid head groups and thus to investigate the recognition between biotin and avidin or streptavidin in model membrane systems.

4.2. Specific and Non-specific Interactions between Streptavidin and Biotin-Lipid Monolayers[43]

A number of biotin lipids have been synthesized (**5**–**8**) to study the interaction between biotin and avidin or streptavidin in monolayers. They differ in the length of the hydrophilic spacer between the membrane-forming alkyl chains and the biotin head group which is to be recognized.

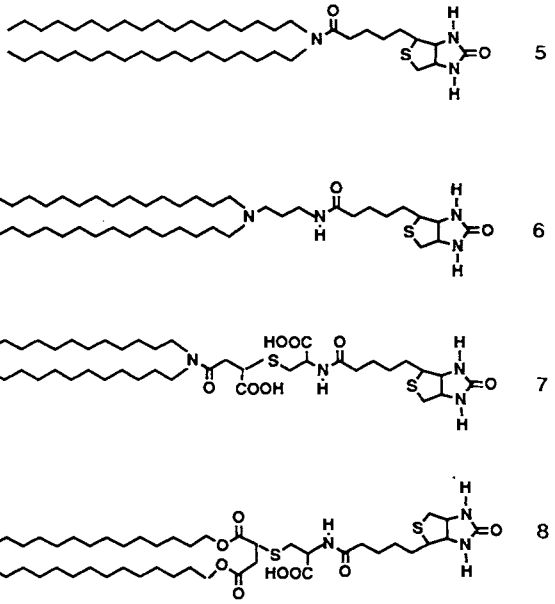

Account has to be taken of the fact that streptavidin and avidin not only interact specifically with membrane-bound biotin but also undergo non-specific adsorption on interfaces. This non-specific adsorption is considerably stronger for the glycoprotein avidin than for streptavidin. Thus, streptavidin was always used for the experiments to be described, since the specific recognition was the reaction of interest.

Specific and non-specific interactions of streptavidin with biotin-lipid monolayers are distinguished by measuring pressure/area diagrams on various protein-containing subphases. The protein used was either active, with four free biotin binding sites, or inactivated, that is saturated with biotin. There were significant differences in the isotherms (Figs. 13 and 14). In the case of spacer lipid **8**, there was a large shift to bigger areas when the subphase contained active protein (Fig. 13). This is explained by strong interaction between the streptavidin and the biotin-lipid monolayer. When inactivated streptavidin was used there was only a small shift in the isotherms. This derives from a non-specific interaction between the protein and the lipids because the protein has no free binding sites for specific recognition of

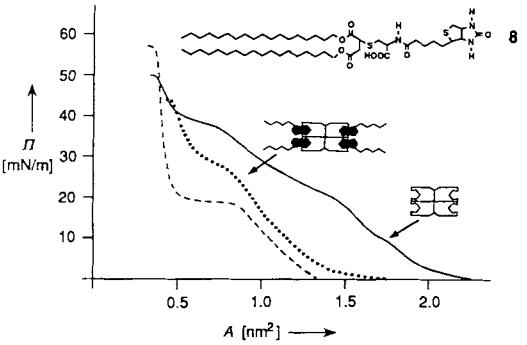

Fig. 13. Distinction between specific and non-specific binding of streptavidin to monolayers of spacer-containing biotin-lipids: specific interaction of the protein with the biotin-lipids (subphase containing active streptavidin) leads to a large expansion of the monolayer, unlike the non-specific interaction (subphase containing inactive, biotin-saturated protein); pressure/area diagram for biotin-lipid **8**: (– – –) subphase without protein; (——) subphase containing active streptavidin; (····) subphase containing inactivated (biotin-saturated) streptavidin.

biotin. Thus there is no doubt that the strong interaction found between the active protein and the biotin-lipid monolayers is an effect deriving from specific recognition.

The effect of the spacer between the biotin head group and the membrane-forming alkyl chains is evident from Figure 14. In this case, the pressure/area diagrams for the

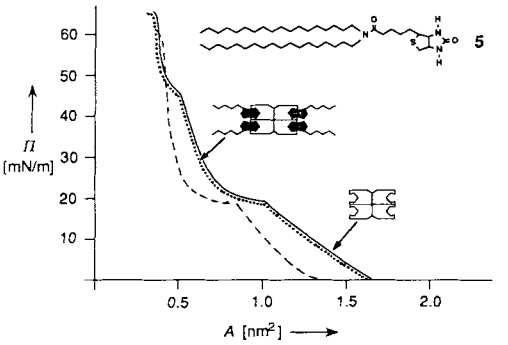

Fig. 14. Interaction of streptavidin with monolayers of spacer-free biotin-lipids: pressure/area diagrams for biotin-lipid **5** show only non-specific adsorption of the protein because the distance of the biotin from the membrane is too short for efficient binding: (– – –) subphase without protein; (——) subphase containing active streptavidin, (····) subphase containing inactivated (biotin-saturated) streptavidin.

spacer-free lipid **5** are identical after addition of streptavidin and of biotin-saturated streptavidin. The biotin thus appears to be too close to the membrane for efficient binding, and the only interaction possible is the non-specific one between the streptavidin and the biotin-lipid monolayer.

4.3. 2D Crystallization of Streptavidin as a Consequence of the Specific Recognition

4.3.1. Observation of Domain Formation by Fluorescence Microscopy

The specific recognition process between biotin and streptavidin was examined using the fluorescence microscopy method described in Section 2.3. A solution of fluorescein-labeled streptavidin was injected under a monolayer of biotin-lipid **8** in the gas-analogous state. Streptavidin domains of a regular shape are formed after a certain time. The explanation of this is that the protein molecules, which are initially homogeneously distributed in the subphase, recognize the ligands presented on the lipid layer (Fig. 15A, B). The protein molecules bind to the monolayer and undergo preliminary orientation and finally aggregate because of the high mobility in the plane of the monolayer (Fig. 15C).

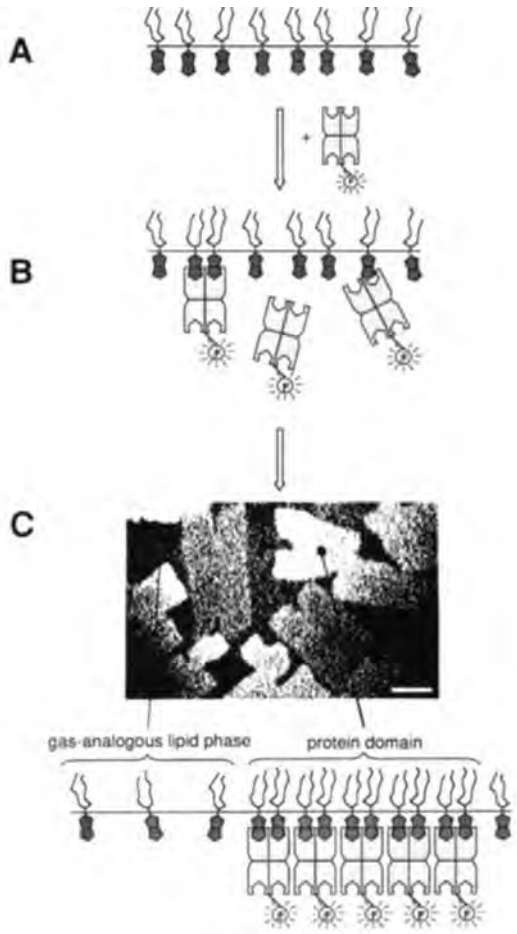

Fig. 15. Diagram representing the binding of streptavidin to monolayers of biotin-lipid **8**: the fluorescein-labeled streptavidin dissolved in the subphase binds specifically to biotin on the membrane (A,B); formation of streptavidin domains can then be observed under the fluorescence microscope (bright areas through the fluorescein filter; C); $\pi = 0$ mN/m; bar $\triangleq$ 20 μm.

The shape of the domains depends greatly on the conditions of preparation. The various morphologies can be described as dendritic, H-shaped, or butterfly-shaped.

Excitation of fluorescence using linearly polarized light results in the relation shown in Figure 16 between the fluorescence intensity of the streptavidin domains and the polarizer setting. The two photos are of an identical area of the monolayer, with the polarizer having been turned through 90° from Figure 16A to Figure 16B. Protein domains which appear light in Figure A are dark in Figure B and vice versa. This optical anisotropy suggests a high degree of order and low mobility of the protein molecules in the domains.

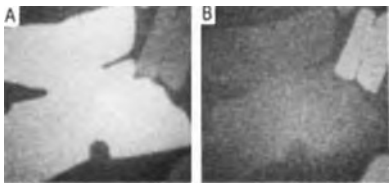

Fig. 16. Optical anisotropy of the streptavidin domains under the fluorescence microscope: the plane of polarization of the exciting light differs by 90° in A and B; domains which appear bright in A are dark in B because of the optical anisotropy, and vice versa; biotin-lipid **8**, 5 mm $\triangleq$ 30 μm.

Control experiments with biotin-saturated streptavidin and with lipid layers incapable of binding, that is biotin-free (for example DPPC) produced no protein domains in any instance. Thus the formation of these domains is a consequence of the specific recognition of biotin by streptavidin.

4.3.2. Structure Determination by Electron Microscopy

The optical anisotropy of the streptavidin domains suggests that they are two-dimensional protein crystals. This prompted detailed investigation of the protein domains by electron microscopy in cooperation with *R. D. Kornberg* et al. (Fig. 17).[33]

Figure 17A shows several protein domains under low magnification, some of which are disrupted by the preparation. Increasing the magnification (Fig. 17B, C) reveals a

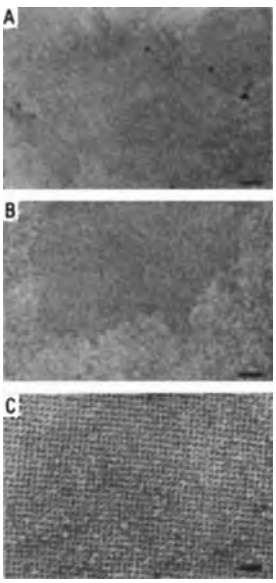

Fig. 17. Electron micrographs of streptavidin crystals with increasing magnification; bar $\triangleq$ (A) 0.5 μm, (B) 125 nm, (C) 25 nm; negative staining with uranyl acetate.

regular pattern with tetragonal ordering. Electron diffraction of these ordered regions showed that they really are two-dimensional streptavidin single crystals. These 2-D crystals could be used to determine the 3-D structure of the streptavidin bound to the biotin-lipid layer with a resolution of 15 Å. At the same time, *Hendrickson* determined the three-dimensional structure of the protein, including the position of the biotin binding sites by X-ray structural analysis with a resolution of 3 Å.[44] When the structure found by *Hendrickson* and that obtained from the 2D crystals are superimposed there is found to be very good agreement. This permits the position of the biotin binding sites to be transferred to the reconstruction of the protein obtained from the 2D crystals (Fig. 18).

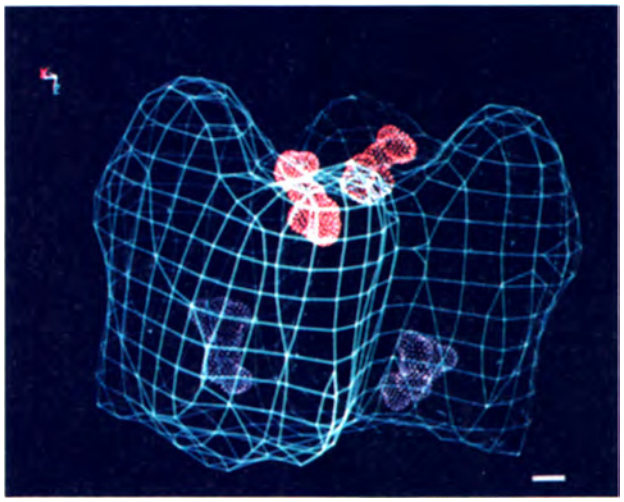

Fig. 18. 3D model of streptavidin (blue contour lines); the four biotin binding sites are indicated (after *Hendrickson* [44]); bar ≙ 4 Å.

These results allow the orientation of the streptavidin bound to the biotin-containing monolayer to be visualized for the first time (Fig. 19).

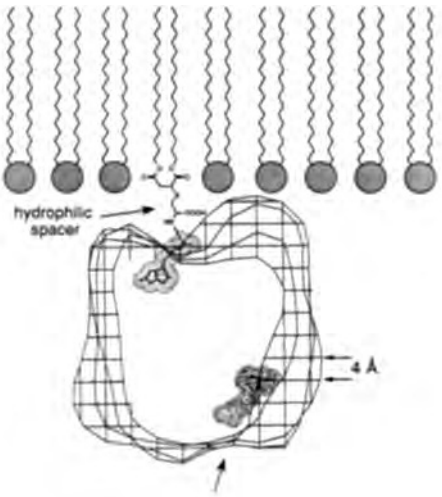

Fig. 19. Section through a monolayer containing biotin-lipids with bound streptavidin: the distance of the upper biotin binding site from the monolayer approximately corresponds to the length of the spacer in the biotin-lipid **8**; the lower free binding site is accessible from the subphase (arrow).

There are two points worthy of note here: the distance between the binding site and the lipid monolayer approximately corresponds to the length of the spacer in the biotin-lipid **8** used. This explains the rapid interaction of the protein with this biotin-lipid and its 2D crystallization. In addition, each streptavidin molecule contains two other free binding sites for biotin which point into the aqueous phase. As will be seen, these are available for further reactions of biotinylated molecules with the protein layer.

4.4. Docking of Biotinylated Molecules to 2D Streptavidin Crystals

Docking of an easily detectable biotinylated molecule can be used to demonstrate that there really are free binding sites for biotin available on the crystallized streptavidin layer. An example of such a molecule is the fluorescein-biotin **9** (Fig. 20).[45]

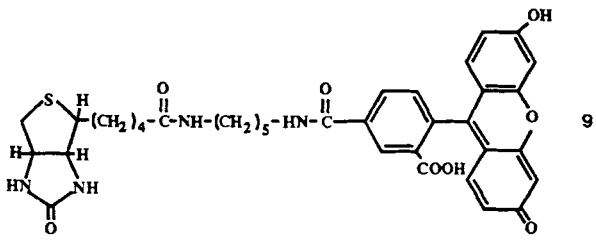

9

The experiment was carried out with streptavidin labeled with sulforhodamine. The protein domains formed as described under a biotin-lipid monolayer appear bright in the sulforhodamine filter. Injection of fluoroscein-labeled biotin under a protein monolayer of this type (**9**), as shown in the

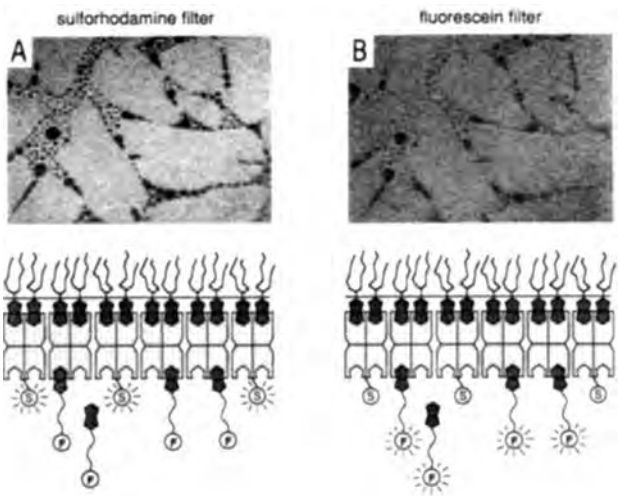

Fig. 20. Docking of biotin-fluorescein **9** to 2D crystals of sulforhodamine-labeled streptavidin: under the fluorescence microscope the streptavidin domains appear bright through both the sulforhodamine filter (marker on protein, A) and the fluorescein filter (fluorescein-biotin, B); 5 mm ≙ 20 μm.

above diagram, results in docking of the biotin to the free binding sites on the streptavidin. This becomes evident from the fact that, after a short incubation time, the protein do-

mains appear bright not only in the sulforhodamine filter but also in the fluorescein filter.

Biotinylated ferritin was chosen as model macromolecule for the docking.[33] The molecular weight of this protein is 600 kDa, which is about ten times that of streptavidin. In addition, it contains iron and thus is easy to detect with the electron microscope. Streptavidin domains were transferred to a solid substrate and incubated with a solution of biotinylated ferritin and then thoroughly washed. Under the electron microscope there are seen to be isolated ferritin molecules bound to the regular crystal structure of the streptavidin layer (Fig. 21). The fact that this is based on the biotin/streptavidin interaction is shown by the comparison experiment with non-biotinylated ferritin, where the 2D streptavidin layer can be washed free of ferritin.

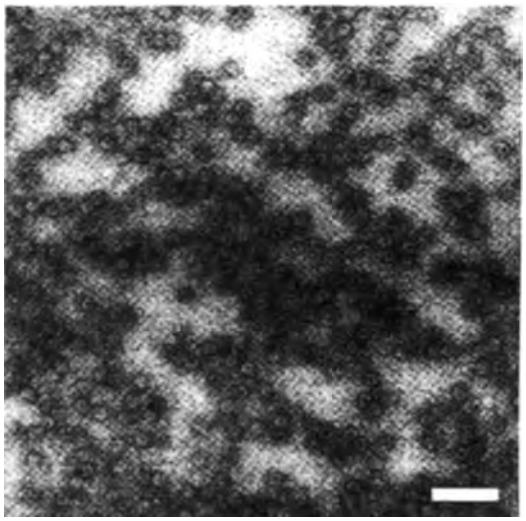

Fig. 21. Electron micrograph of a 2D streptavidin crystal with bound biotinylated ferritin; bar ≙ 50 nm; negative staining with uranyl acetate.

These two examples show unambiguously that the 2D streptavidin crystals represent a matrix which can be further functionalized with biotin.

4.5. Protein-Containing Monolayers in Biosensors?

The highly specific and extremely strong binding of biotin to avidin/streptavidin has found application in affinity chromatography for some time now.[40] There are also a number of immunoassays which utilize this protein/ligand interaction. However, no use has yet been made of the properties of highly ordered monomolecular layers which can be prepared with streptavidin at biotin-lipid layers.

The possibility of functionalizing 2D streptavidin crystals which has been mentioned in the previous section has resulted in a number of ideas which may lead to applications of protein-containing monolayers (Figure 22).

Bifunctional biotin derivatives could conceivably be used to construct very thin well-defined streptavidin multilayer structures. In addition, since the crystalline protein layer is a highly ordered matrix which is compatible with proteins, it might be used for docking of other biotinylated proteins

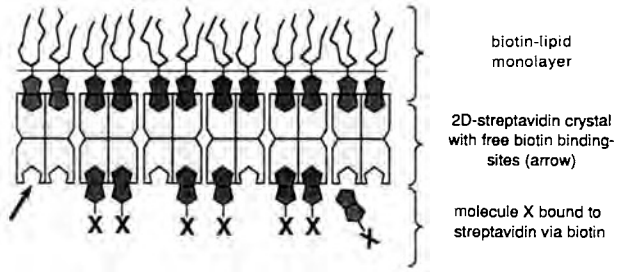

Fig. 22. 2D crystalline streptavidin layer functionalized by binding of biotinylated molecules X to free biotin binding sites: X = protein, functional group, polymer, biotin (bis-biotin compound).

(for example enzymes, antibodies) or nucleic acids (for example RNA, DNA). In these cases, both the function of the coupled proteins and their tendency to crystallize may be of interest.

A stabilized lipid layer to which the streptavidin can bind would be advantageous for such applications. Suitable examples are biotin-containing polymers (for example **10**) or polymerizable biotin-containing amphiphiles such as the diacetylene-biotin-lipids **11**–**14**. Besides high stability, the

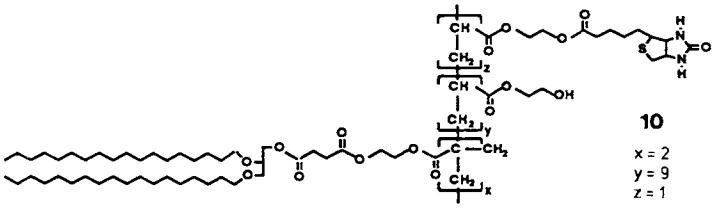

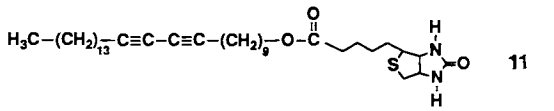

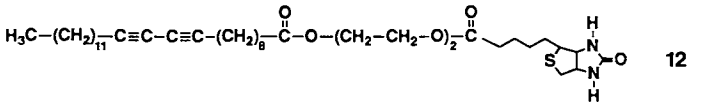

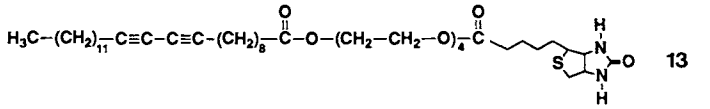

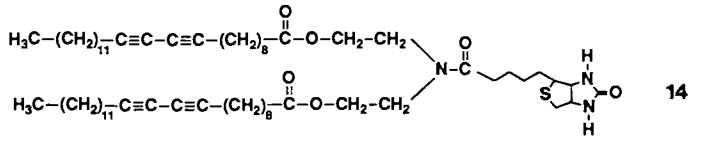

biotin-containing polydiacetylenes have other interesting properties. Thus, tiny changes in the conformation of the polymer backbone can be detected very sensitively by changes in the spectroscopic properties of the polymer (for example UV, Raman[46, 47] and CD[48]) or the conductivity after doping. This might form the basis for the development of a sensitive sensor for the binding of streptavidin to the polymeric lipid layer. Coupling of streptavidin to a molecule to be detected is a conceivable basis for a large number of biosensors.

5. Enzyme Substrate Interaction: Specific Recognition, Function and Domain Formation of Phospholipase A_2 at Lecithin Monolayers

Most of the chemical reactions taking place in an organism and regulating metabolism are enzymatic.[49] The first step in these is, just as it is in the examples discussed in Sections 3 and 4, the specific recognition between a protein and its substrate. The particular feature of an enzyme is that it not only recognizes the bound substrate but also brings about a chemical change in it (formation or breaking of bonds). One example of such a reaction taking place on a membrane is the hydrolytic function of phospholipase A_2. Its interaction with lecithin monolayers will be dealt with in this section.

5.1. Function and Properties of Phospholipase A_2

Phospholipases comprise an important class of enzymes.[17, 50] They catalyze the hydrolysis of ester bonds in membrane-forming phospholipids. The enzyme from this class which has been investigated most thoroughly is phospholipase A_2, which is very widespread.[51] One of its most important functions is to rebuild and modify cell membranes. However, the mechanism for regulating this enzyme is still unknown. The reason why cell membranes are not all destroyed remains to be found. Phospholipase A_2 also induces the release of arachidonic acid which leads to the formation of substances which produce inflammation (prostaglandins, leukotrienes, thromboxanes).[52] Thus, a way of regulating their activity would provide a good method for controlling inflammatory processes.

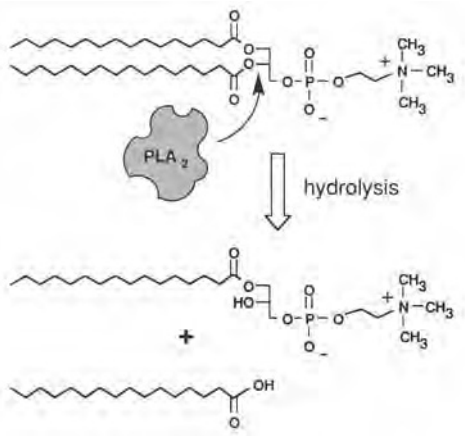

Fig. 23. Cleavage reaction catalyzed by phospholipase A_2 (schematic): the enzyme hydrolyses of the ester bond in C-2 position of a lecithin, resulting in the corresponding lysolecithin and the free fatty acid.

Phospholipase A_2 is relatively small, with a molecular weight of 12–14 kDA, is soluble in water, and is very stable, having a large number of disulfide linkages. It catalyzes ester cleavage at the C-2 position in naturally occurring glycerophospholipids to give the corresponding lysolecithin and the free fatty acid (Fig. 23).

The reaction takes place both regioselectively, that is, only the ester linkage in the C-2 position is cleaved, and stereospecifically, that is only the naturally occurring L form of the lipid can be hydrolyzed – the D form is inert.[53] Phospholipase A_2 activity depends very strongly on the physical state of the substrate.[17, 50, 51, 54] It increases many times over in going from a homogeneous solution to organized substrates such as micelles, liposomes or monolayers. The highest activity in liposomes is found when the lipid is in the phase-transition region.[54g, 55] This property of phospholipase A_2 makes it especially interesting for investigations in monolayers because it is easy to bring about large changes in both the composition and the physical state of the membrane (compare lipid domain formation in Fig. 6 in Section 2.3).

5.2. Hydrolysis of Substrate Lipids of Phospholipase A_2 in Monolayers

The fluorescence film balance described in Section 2.3 was used to investigate the hydrolytic activity of phospholi-

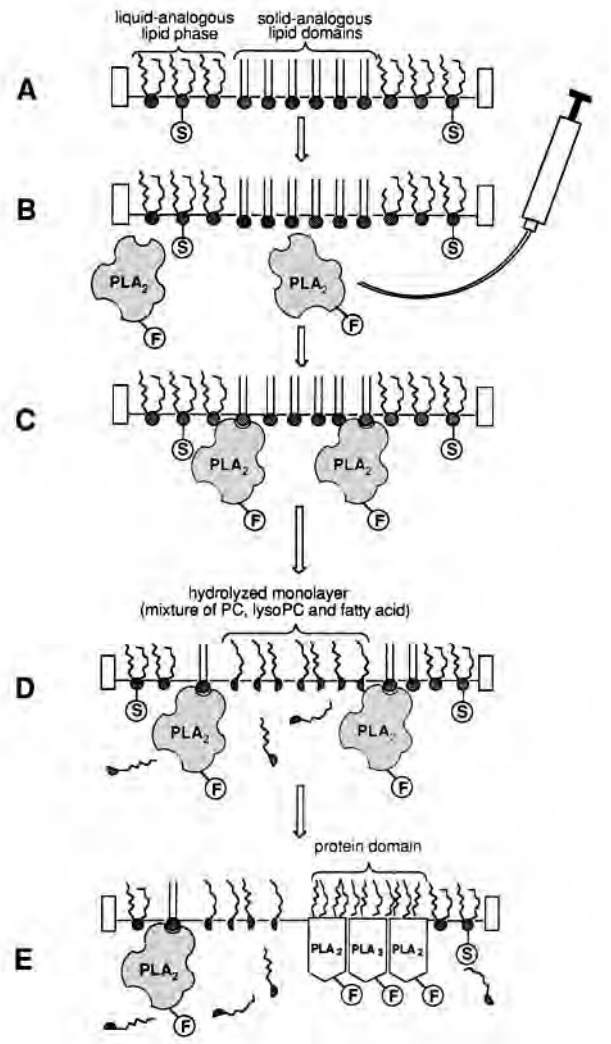

Fig. 24. Hydrolysis of a lipid monolayer by phospholipase A_2 (schematic): (A) monolayer in the phase transition region with solid-analogous lipid domains in a liquid-analogous lipid matrix mixed with a sulforhodamine marker; (B) injection of the FITC-labeled phospholipase A_2; (C) specific recognition of the substrate lipids by the enzyme and preferential attack at the boundaries between liquid- and solid-analogous phase; (D) hydrolysis of the solid-analogous lipid domains and accumulation of the hydrolysis products in the monolayer; (E) aggregation of the enzyme. PC = phosphatidylcholine.

pase A_2. In these experiments the monolayer was doped with a sulforhodamine-lipid, and the phospholipase was labeled with fluorescein isothiocyanate (FITC). These two labels made it possible to observe processes in the lipid monolayer and the behavior of the enzyme separately. An experiment of this type is outlined in Figure 24.

The lipid monolayer is compressed until it is in the phase transition region. This leads to the formation of solid-analogous lipid domains in a liquid-analogous matrix (Fig. 24A; see also Section 2.3). Injection of the labeled phospholipase A_2 into the subphase (Fig. 24B) is followed by specific recognition between the enzyme and its substrate. The attack by the protein takes place preferentially at the boundary between the solid-analogous and the liquid-analogous phase (Fig. 24C).[56] As hydrolysis progresses, the solid-analogous lipid domains are broken down and the hydrolysis products accumulate in the monolayer (Fig. 24D). After a certain time, the phospholipase A_2 starts to aggregate to form domains of its own which have a specific shape (Fig. 24E). This may indicate a change in the conformation of the protein due to interaction with the hydrolyzed monolayer. These processes can be observed directly under the fluorescence microscope,[57] as will be illustrated by the examples of L-α-dipalmitoylphosphatidylcholine (DPPC) and L-α-dimyristoylphosphatidylcholine (DMPC) monolayers.

5.2.1. *Hydrolysis of Solid-Analogous* L-α-*DPPC Domains*[57]

As mentioned above, the enzyme is injected under a monolayer which is in the phase transition region. Viewed through the sulforhodamine filter, dark solid-analogous lipid do-

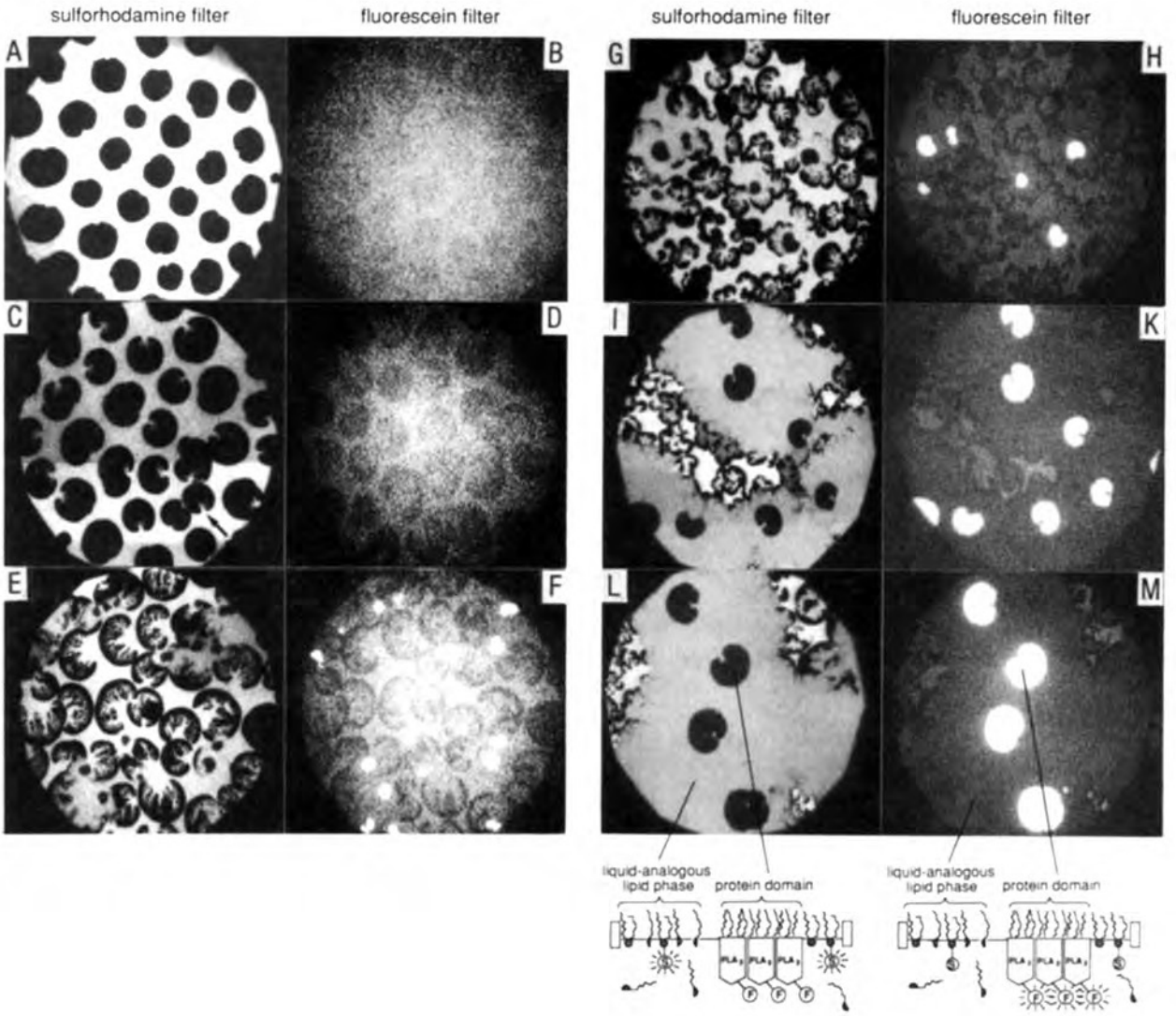

Fig. 25. Hydrolysis of an L-α-DPPC monolayer by phospholipase A_2 observed by fluorescence microscopy; the monolayer is seen through the sulforhodamine filter (on the left) and the enzyme is seen through the fluorescein filter (on the right): (A) dark solid-analogous lipid domains in a bright liquid-analogous matrix; (B) homogeneous fluorescence of the enzyme in the subphase; (C) first signs of hydrolysis of the lipid domains (arrow); (D) homogeneous fluorescence of the enzyme in the subphase; (E), (F) progressive degradation of the lipid domains and first signs of the formation of enzyme aggregates below the monolayer (bright spots through the fluorescein filter) (E), dark spots through the sulforhodamine filter (F)); (G)–(K) further hydrolysis of the lipid domains (G,I) with simultaneous growth of the protein domains (H,K); (L), (M) after almost complete degradation of the lipid domains there are now only protein domains in a fluid matrix composed of the hydrolysis products and DPPC; these enzyme domains have a specific shape and appear dark through the sulforhodamine filter (L) and bright through the fluorescein filter (M); (A), (B) $t = 0$ min (immediately after enzyme injection); (C), (D) $t = 10$ min; (E), (F) $t = 30$ min; (G), (H) $t = 40$ min; (I), (K) $t = 50$ min; (L), (M) $t = 60$ min; $\pi = 22$ mN/m; $T = 30\,^{\circ}C$; 5 mm $\triangleq$ 20 μm.

mains which are typical of L-α-DPPC[58] are seen in the bright matrix of liquid-analogous lipid and sulforhodamine marker (see Fig. 25A and scheme in Figs. 24A, B). With the fluorescein filter, the homogeneous fluorescence of the protein is seen under the monolayer (see Fig. 25B). The first signs that the enzyme has recognized its substrate in the monolayer and started to hydrolyze it appear after 10 minutes. Firstly, areas of erosion form, specifically at the concavities previously present in the lipid domains (see Fig. 25C and scheme in Fig. 24C). The enzyme then starts to degrade the domains inwards from these points (Fig. 25C, E). Once the enzyme has bound to the phase boundary and started to hydrolyze the lipid, there is local accumulation of the acid and lysolecithin, which may lead to autocatalytic activation of the phospholipase A_2 at this point.[59] This would explain why further hydrolysis from an initial point of attack is preferred. After about 60 minutes, only slight remains of the lipid domains are left (Fig. 25E, G, I, L).

Observation through the fluorescein filter reveals small bright dots after 30 minutes (Fig. 25F), which appear dark through the sulforhodamine filter: the protein is starting to aggregate underneath the monolayer.[57, 59a, 60] These bright dots increase in number and size as the reaction progresses (Fig. 25F, H, K) until, at its end (after about 60 minutes), they have a typical kidney shape (see Fig. 25L). The monolayer now consists only of almost completely destroyed solid-analogous lipid domains and the protein domains in a matrix of liquid-analogous lipid (see Fig. 25L, M).

It is noticeable that the domains of phospholipase A_2 are similar in shape to some of the lipid domains present at the start of the reaction (see Fig. 25L, M and Fig. 24A). To examine whether there is a template effect, the hydrolysis experiment was repeated with L-α-DMPC which forms solid-analogous domains of different morphology.

5.2.2. *Hydrolysis of Solid-Analogous L-α-Domains*[57b]

The lipid domains in the phase transition region of a DMPC monolayer differ from those of DPPC in being small and star-shaped (see Fig. 26A and Fig. 25A). 5 minutes after the injection of the FITC-labeled phospholipase A_2, small concavities are evident in these domains in the sulforhodamine filter. With the fluorescein filter, bright dots are seen at the corresponding points, which are the first signs that protein aggregation is starting (see arrows in Fig. 26B and 26C).[57, 59a, 60] These protein aggregates grow as the reaction progresses (Fig. 26D–I), and finally the enzyme domains have the same morphology as in the hydrolysis of an L-α-DPPC monolayer (see Fig. 25L, M). This shows that the shape of the protein domains does not depend on the original shape of the solid-analogous lipid domains.

However, observation of the progress of hydrolysis reveals some differences. Whereas individual domains of L-α-DPPC are specifically attacked and degraded, in the case of L-α-DMPC the enzyme produces large areas containing no solid-analogous lipid. The protein domains then appear in the middle of these areas (Fig. 26D–G). It is not yet clear how this different degradation behavior relates to the mechanism of hydrolysis.

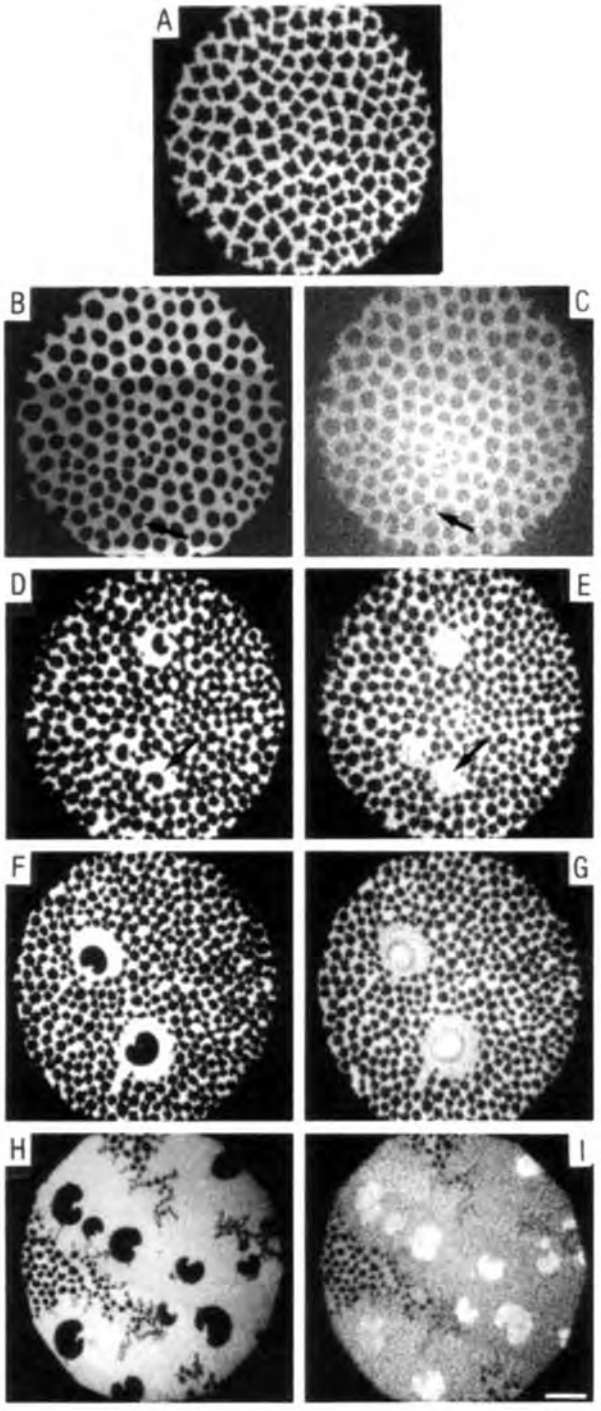

Fig. 26. Hydrolysis of an L-α-DMPC monolayer by phospholipase A_2 observed by fluorescence microscopy; the monolayer is seen through the sulforhodamine filter and the enzyme is seen through the fluorescein filter: (A) dark solid-analogous lipid domains in a bright liquid-analogous matrix; (B), (C) first signs of hydrolysis of the lipid domains; small bright dots are seen at the corresponding sites through the fluorescein filter – these are signs that protein aggregation is starting (arrows in B and C); (D)–(G) progressive hydrolysis leads to circular areas without solid-analogous lipid, in the centers of which the protein domains (arrow) are growing; (H), (I) after almost complete degradation of the lipid domains; there are now only the protein domains in a fluid matrix composed of the hydrolysis products and DMPC; these enzyme domains have specific shapes and appear dark through the sulforhodamine filter (H) and bright through the fluorescein filter (I); (A) $t = 0$ min (immediately after enzyme injection); (B), (C) $t = 10$ min; (D), (E) $t = 20$ min; (F), (G) $t = 30$ min; (H), (I) $t = 50$ min; $\pi = 22$ mN/m; $T = 10$ °C; bar ≙ 20 μm.

5.2.3. *Compression of a Hydrolyzed* L-α-DPPC Monolayer

More information about the nature of the protein in the domains was obtained by changing the surface pressure in a hydrolyzed L-α-DPPC monolayer.[57b] Expansion to the gas-analogous state ($\pi = 0$ mN/m) has no effect on the shape of the protein domains, which indicates that they are very stable. Figure 27 shows the processes observed during compression, both schematically and as they appear under the fluorescence microscope. New solid-analogous lipid domains are formed in the fluid matrix (Fig. 27B). This shows

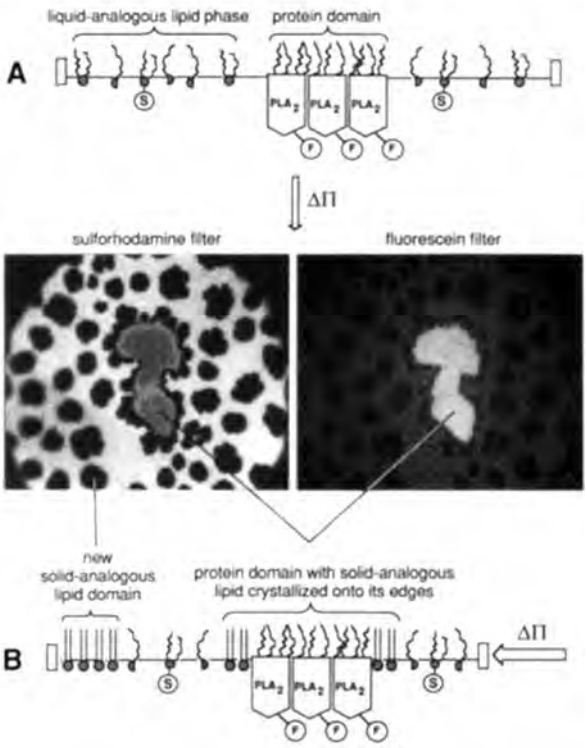

Fig. 27. Compression of an L-α-DPPC monolayer after hydrolysis by phospholipase A_2; (A) schematic representation of a protein domain in a fluid matrix composed of hydrolysis products and DPPC; (B) compression leads to formation of new solid-analogous lipid domains both in the fluid matrix and directly on the edges of the protein domains (appearance under the fluorescence microscope and schematic representation); 5 mm ≙ 20 μm.

that even after complete hydrolysis of the original lipid domains there is still uncleaved lecithin present in the monolayer. However, it is noteworthy that new lipid domains are produced not only in the fluid phase but also directly on the edges of the protein domains (bright through the fluorescein filter). This lipid crystallized onto the protein domains is not attacked and degraded by the enzyme organized in them, which indicates that the aggregated phospholipase A_2 is no longer active.

The first evidence that the lysolecithin and fatty acid produced in the hydrolysis play an important part in the formation of the protein domains was gained from analogous experiments with D-α-DPPC: although the enzyme is able to recognize this lipid it cannot cleave it.[53] Unlike the hydrolysis of an L-α-DPPC monolayer, even after 2 hours there is neither degradation of the solid-analogous lipid domains nor formation of protein domains. Thus, because the existence of the hydrolysis products in the monolayer appears to be a necessary precondition for the formation of protein domains, investigations were carried out using mixed monolayers.

5.3. Phase Behavior of Mixed Lecithin, Lysolecithin and Fatty Acid Monolayers and Their Interaction with Phospholipase A_2

In order to confirm that the existence of the hydrolysis products in the monolayer is crucial for the observed aggregation and inhibition of phospholipase A_2, the effect of the hydrolysis products was investigated separately from the hydrolysis process. This can be achieved by using mixed monolayers composed of lecithin, lysolecithin and fatty acid in various ratios (1:x:x, x = 1–5); such mixtures simulate the situation after a hydrolysis reaction. Assuming that only the cleavage products and not reactions during the hydrolysis (for example acylation[61]) induce domain formation and inhibition of phospholipase A_2, there should be spontaneous development of protein domains when the composition of these mixed monolayers is suitable. The following example shows this.

After spreading of a 1:5:5 mixture of L-α-DPPC, L-α-LysoPPC and palmitic acid, the liquid-analogous monolayer appears homogeneously bright under the fluorescence microscope (Fig. 28A). However, compression leads to phase separation and thus formation of domains of unknown composition[62] (Fig. 28B).

These mixed domains are gray, unlike the black solid-analogous lipid domains described above; thus these domains do not completely exclude the fluorescent dye.

Injection of the FITC-labeled phospholipase A_2 under a mixed monolayer containing these gray domains results in binding of the protein to the domains within two minutes without visible evidence of hydrolysis (Fig. 28C). This is even more noteworthy when it is compared with the relatively slow formation of the protein domains during hydrolysis with phospholipase A_2 (about 60 minutes, see Fig. 25L, M). The mixed domains therefore represent a preferred environment for protein binding. They act directly as templates for the rapidly forming protein domains: the shape of the mixed domains (sulforhodamine filter) is identical to the shape of the protein domains (fluorescein filter). The results are the same when the D form of DPPC is used in the mixing experiments. This is clear evidence that recognition of the headgroup of the lecithin, but not its cleavage, is necessary for rapid aggregation of the protein.

A 1:1 mixture of lysolecithin and fatty acid, without DPPC, shows no domain formation by these hydrolysis products nor protein aggregation. Uncleaved lecithin is thus necessary for inducing protein aggregation.

The results of these monolayer investigations do not yet make a direct contribution to the vigorous discussion in the literature about the mechanism of hydrolysis by phospholipase A_2.[17, 50, 51] Whereas many studies have discussed inhibition of phospholipase A_2,[17, 50, 51, 52] no domain formation of the protein has been observed. The straightforwardness of the described method might not only provide

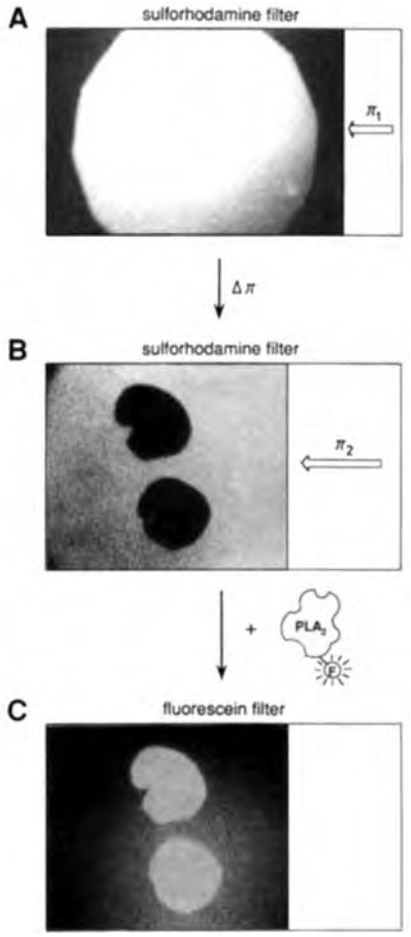

Fig. 28. Interaction of phospholipase A_2 with monolayers composed of a 1:5:5 mixture of lecithin, lysolecithin and fatty acid: (A) homogeneous fluorescence of the liquid-analogous mixed monolayer doped with sulforhodamine-lipid **1**; (B) compression leads to the formation of gray mixed domains of unknown composition; (C) fluorescein-labeled phospholipase A_2 injected under this monolayer binds very quickly to these mixed domains which thus appear bright through the fluorescein filter. 5 mm ≙ 20 μm

new ways of testing inhibitors for phospholipase A_2 but also contribute to providing detailed information on the mechanism of the catalysis by this essential class of enzymes.

6. Conclusion

The experiments with fluorescein/anti-fluorescein antibody and biotin/streptavidin were attempts to use monolayers as systems to model specific recognition reactions at cell membranes. It was possible, by using the relatively new method of fluorescence microscopy on monolayers, to observe other phenomena apart from the expected specific interaction. In both cases there was spontaneous formation of protein domains at the monolayer. In the case of streptavidin, the protein domains proved to be 2D crystals. However, a far more interesting fact is that the highly ordered streptavidin layer provides a matrix which has two further highly active binding sites per protein molecule. This suggests possible uses in biosensors, as already discussed in Section 4.5.

The example of the enzymatic activity at the monolayer, that is the interaction of phospholipase A_2 with lecithin domains, was originally based on ideas about the breaking down ("uncorking") of liposomes by phospholipase A_2.[6c] In the monolayer experiments it was possible for the first time to follow the progress of enzymatic reactions on organized substrates, the lipid domains, by direct visual observation. Once again, enzyme domains with a regular morphology were formed, which indicates inhibition of phospholipase A_2 by the hydrolysis products. This might help to explain why the phospholipases which are widespread in the body do not destroy all cell membranes.

There remains the interesting question of how functional supramolecular systems can be used as a basis for materials science to learn from life science. There are no doubt very many biochemical processes which can be transferred to model membrane systems. Increasing numbers of examples are being provided by affinity chromatography and the new area of biosensors.

Received: June 5, 1990 [Z A 789 IE]
German version: *Angew. Chemie 102* (1990) 1310

[1] G. C. Lichtenberg: *Aphorismen*, Insel-Taschenbuch, Frankfurt 1979, a) p. 202; b) p. 204.
[2] a) P. K. Feyerabend: *Wider den Methodenzwang*, Suhrkamp, Frankfurt 1983; b) *Ausgewählte Schriften, Band 1: Der wissenschaftstheoretische Realismus und die Autorität der Wissenschaften; Band 2: Probleme des Empirismus*, Vieweg, Braunschweig, Wiesbaden 1978, 1981; c) K. R. Popper: *Objective Knowledge. An Evolutionary Approach*, Oxford 1972; d) in I. Lakatos, A. Musgrave (Eds.): *Criticism and the Growth of Knowledge*. Cambridge 1970, p. 51; e) T. S. Kuhn: *Die Struktur wissenschaftlicher Revolutionen*, Suhrkamp, Frankfurt 1967; f) in I. Lakatos, A. Musgrave (Eds.): *Criticism and the Growth of Knowledge*, Cambridge 1970, S. 1; g) W. Stegmüller: *Neue Wege der Wissenschaftsphilosophie*, Springer, Berlin 1980.
[3] *H. Sachsse* has commented on this in a paper entitled: *Die Bedeutung der Intuition. Von der Einseitigkeit unseres wissenschaftlichen Denkens; DABEI-Forum 9* (1986) 1.
[4] L. Wittgenstein said in this connection, almost with resignation: "We feel that even if all possible scientific questions are answered, the problems of living will still not have been touched upon." in *Tractatus logico-philosophicus*, Suhrkamp, Frankfurt 1960, Chapter 6.52.
[5] a) H. Morawetz, *Angew. Chem. 99* (1987) 95; *Angew. Chem. Int. Ed. Engl. 26* (1987) 93; b) C. Preisner: in *H. Staudinger, H. Mark, K. H. Meyer: Thesen zur Größe und Struktur der Makromoleküle: Ursachen und Hintergründe eines akademischen Disputes*, Verlag Chemie, Weinheim 1980; c) H. Staudinger: *Arbeitserinnerungen*, Dr. Alfred Hüthig Verlag, Heidelberg 1961.
[6] a) J.-M. Lehn, *Science (Washington D.C.) 227* (1985) 849; b) *Angew. Chem. 100* (1988) 91; *Angew. Chem. Int. Ed. Engl. 27* (1988) 89; c) H. Ringsdorf, B. Schlarb, J. Venzmer, *ibid. 100* (1988) 117 and *27* (1988) 113 respectively.
[7] B. Alberts, D. Bray, J. Lewis, M. Raff, K. Roberts, J. D. Watson: *Molecular Biology of the Cell*, Garland, New York 1983; *Molekularbiologie der Zelle*, VCH, Weinheim 1986.
[8] a) G. Gregoriadis, A. C. Allison (Eds.): *Liposomes in Biological Systems*, Wiley, Chichester 1980; b) C. G. Knight (Ed.): *Liposomes: From Physical Structure to Therapeutic Applications*, Elsevier, Amsterdam 1981; c) G. Gregoriadis (Ed.): *Liposome Technology, Vol. I–III*, CRC Press, Boca Raton, FL, USA 1984; d) M. J. Ostro (Ed.): *Liposomes*, Dekker, New York 1983; e) M. J. Ostro (Ed.): *Liposomes: From Biophysics to Therapeutics*, Dekker, New York 1987.
[9] J. N. Israelachvili in V. Degiorgio, M. Corti (Eds.): *Physics of Amphiphiles: Micelles, Vesicles and Microemulsions*, North-Holland, Amsterdam 1985, p. 24.
[10] a) G. W. Gray, P. A. Winsor (Eds.): *Liquid Crystals and Plastic Crystals, Vol. I,II*, Horwood, Chichester 1974; b) G. J. T. Tiddy, *Phys. Rep. 57* (1980) 1; c) B. J. Forrest, L. W. Reeves, *Chem. Rev. 81* (1981) 1.
[11] *Thin Solid Films 68* (1980); *ibid. 99* (1983); *ibid. 132–134* (1985); *ibid. 159–160* (1988); *ibid. 178–180* (1989).
[12] a) F. D. Saeva (Ed.): *Liquid Crystals: The Fourth State of Matter*, Dekker, New York 1979; b) H. Kelker, R. Hatz: *Handbook of Liquid Crystals*, Verlag Chemie, Weinheim 1980; c) C. B. McArdle (Ed.): *Side Chain Liquid Crystal Polymers*, Blackie, Glasgow 1989.
[13] V. Percec, C. Pugh in [12c], p. 30.
[14] a) S. Chandrasekhar, B. K. Sadashiva, K. A. Suresh, *Pramana 9* (1977) 471; *Chem. Abstr. 88* (1978) 30566y; b) C. Destrade, P. Foucher, H. Gasparoux, Nguyen Huu Tinh, A.-M: Levelut, J. Malthête, *Mol. Cryst.*

Liq. Cryst. 106 (1984) 121; c) W. Kreuder, H. Ringsdorf, *Makromol. Chem. Rapid Commun. 4* (1983) 807; d) W. Kreuder, H. Ringsdorf, P. Tschirner, *ibid. 6* (1985) 367; e) G. Wenz, *ibid. 6* (1985) 577.

[15] a) H. Ringsdorf, P. Tschirner, O. H. Schönherr, J. H. Wendorff, *Makromol. Chem. 188* (1987) 1431; b) M. Ebert, O. H. Schönherr, J. H. Wendorff, H. Ringsdorf, P. Tschirner, *Mol. Cryst. Liq. Cryst. 7* (1990) 63; c) M. Ballauff, G. F. Schmidt, *Makromol. Chem. Rapid Commun. 8* (1987) 93.

[16] a) J. D. Barnal, *Trans. Faraday Soc. 29* (1933) 1022; b) *The Physical Basis of Life*, Rutledge Kegan, London 1951; c) G. H. Brown, J. J. Wolken: *Liquid Crystals and Biological Systems*, Academic Press, New York 1979.

[17] M. Waite: *The Phospholipases*, Plenum, New York 1987.

[18] a) F. Vögtle, H.-G. Löhr, J. Franke, D. Worsch, *Angew. Chem. 97* (1985) 721; *Angew. Chem. Int. Ed. Engl. 24* (1985) 727; b) F. Vögtle, E. Weber (Eds.): *Host Guest Complex Chemistry, Vol. I–III (Top. Curr. Chem. 98* (1981), *ibid. 101* (1982), *ibid. 121* (1984)); c) *Biomimetic and Bioorganic Chemistry, Vol. I–III (Top. Curr. Chem. 128* (1985), *ibid. 132* (1986), *ibid. 136* (1986)); d) D. J. Cram, *Angew. Chem. 98* (1986) 1041; *Angew. Chem. Int. Ed. Engl. 25* (1986) 1039; e) F. H. Kohnke, J. P. Mathias, J. F. Stoddart, *Angew. Chem. Adv. Mater. 101* (1989) 1129; *Angew. Chem. Int. Ed. Engl. Adv. Mater. 28* (1989) 1103; *Adv. Mater. 1989*, 275.

[19] I. Cabrera, M. Engel, H. Ringsdorf in D. O. Hall, G. Grassi (Eds.): *Photoconversion Processes for Energy and Chemicals, Energy from Biomass 5*, Elsevier, London 1989, p. 68.

[20] W. Groh, D. Lupo, H. Sixl, *Angew. Chem. Adv. Mater. 101* (1989) 1580; *Angew. Chem. Int. Ed. Engl. Adv. Mater. 28* (1989) 1548; *Adv. Mater. 1989*, 366.

[21] a) H. J. Coles, R. Simon, *Polymer 26* (1985) 1801; b) M. Eich, J. H. Wendorff, B. Reck, H. Ringsdorf, *Makromol. Chem. Rapid. Commun. 8* (1987) 59.

[22] C. Tanford: *The Hydrophobic Effect*, Wiley, New York 1980.

[23] a) H. T. Tien: *Bimolecular Lipid Membranes – Theory and Practice*, Dekker, New York 1974; b) P. Läuger, *Angew. Chem. 97* (1985) 939; *Angew. Chem. Int. Ed. Engl. 24* (1985) 905.

[24] H. M. McConnell, T. H. Watts, R. M. Weis, A. A. Brian, *Biochim. Biophys. Acta 864* (1986) 95.

[25] a) G. L. Gaines: *Insoluble Monolayers at Liquid-Gas Interfaces*, Wiley Interscience, New York 1966; b) H. Kuhn, D. Möbius, *Angew. Chem. 83* (1971) 672; *Angew. Chem. Int. Ed. Engl. 10* (1971) 620.

[26] a) V. von Tscharner, H. M. McConnell, *Biophys. J. 36* (1981)409; b) H. Möhwald, M. Lösche, *Rev. Sci. Instrum. 55* (1984) 1968; c) P. Meller, *ibid. 59* (1988) 2225.

[27] L. Gros, H. Ringsdorf, H. Schupp, Angew. *Chem. 93* (1981) 311; Angew. *Chem. Int. Ed. Engl. 20* (1981) 305.

[28] a) K. Uemura, R. A. Nicoletti, H. R. Six, S. C. Kinsky, *Biochemistry 13* (1974) 572; b) H. Bader, *Dissertation*, Universität Mainz 1985; c) E. E. Uzgiris, R. D. Kornberg, *Nature (London) 301* (1983) 125; d) L. K. Tamm, *Biochemistry 27* (1988) 1450; e) H. R. Six, K. Uemura, S. C. Kinsky, *ibid. 12* (1973) 4003; f) S. C. Kinsky, *Biochim. Biophys. Acta 265* (1972) 1.

[29] a) E. W. Voss (Ed.): *Fluorescein Hapten: An Immunological Probe*, CRC Press, Boca Raton, Fl, USA 1984; b) T. W. Athey, R. E. Cathou, *Immunochemistry 14* (1977) 397.

[30] R. M. Bates, D. W. Ballard, E. W. Voss, *Mol. Immunol. 22* (1985) 871.

[31] J. N. Herron, D. M. Kranz, D. M. Jameson, E. W. Voss, *Biochemistry 25* (1986) 4602.

[32] J. N. Herron, X.-M. He, M. L. Mason, E. W. Voss, Jr., A. B. Edmundson, *Proteins 5* (1989) 271.

[33] a) M. Ahlers, *Dissertation*, Universität Mainz 1990; b) S. A. Darst, M. Ahlers, P. H. Meller, E. W. Kubalek, R. Blankenburg, H. O. Ribi, H. Ringsdorf, R. D. Kornberg, *Biophys. J.*, in press.

[34] a) S. A. Darst, H. O. Ribi, D. W. Pierce, R. D. Kornberg, *J. Mol. Biol. 203* (1988) 269; b) E. E. Uzgiris, R. D. Kornberg, *Nature (London) 301* (1983) 125; c) E. E. Uzgiris, *J. Cell. Biochem. 29* (1985) 239; d) E. E. Uzgiris, *Biochem. J. 242* (1987) 293; e) D. S. Ludwig, H. O. Ribi, G. K. Schoolnik, R. D. Kornberg, *Proc. Natl. Acad. Sci. USA 83* (1986) 8585; f) R. A. Reed, J. Mattai, G. G. Shipley, *Biochemistry 26* (1987) 824; g) H. O. Ribi, D. S. Ludwig, K. L. Mercer, G. K. Schoolnik, R. D. Kornberg, *Science (Washington D.C.) 239* (1988) 1272; h) H. O. Ribi, P. Reichard, R. D. Kornberg, *Biochemistry 26* (1987) 7974; i) E. E. Uzgiris, *Biophys. J. 41* (1983) 389a.

[35] a) E. A. Bayer, M. Wilchek, *Biochim. Biophys. Acta 550* (1979) 464; b) K. Hashimoto, J. E. Loader, S. C. Kinsky, *ibid. 901* (1986) 556; c) R. Blankenburg, P. Meller, H. Ringsdorf, C. Salesse, *Biochemistry 28* (1989) 8214; d) M. Ahlers, R. Blankenburg, D. W. Grainger, P. Meller, H. Ringsdorf, C. Salesse, *Thin Solid Films 180* (1989) 93.

[36] a) Y. Hiller, J. M. Gershoni, E. A. Bayer, M. Wilchek, *Biochem. J. 248* (1987) 167; b) K. Hofmann, S. W. Wood, C. C. Brinton, J. A. Montibeller, F. M. Finn, *Proc. Natl. Acad. Sci. USA 77* (1980) 4666.

[37] a) M. Green, *Adv. Protein Chem. 29* (1975) 85; b) R. M. Buckland, *Nature (London) 320* (1986) 557; c) E. A. Bayer, M. Wilchek, *TIBS 14* (1989) 408.

[38] R. K. Garlick, R. W. Giese, *J. Biol. Chem. 263* (1988) 210.

[39] F. Lynen, J. Knappe, E. Lorch, G. Jütting, E. Ringelmann, *Angew. Chem. 71* (1959) 481.

[40] M. Wilchek, E. A. Bayer, *Anal. Biochem. 171* (1988) 1.

[41] E. A. Bayer, M. Wilchek, *Meth. Biochem. Anal. 26* (1980) 1.

[42] M. Wilchek, E. A. Bayer, *Immunol. Today 2* (1984) 39.

[43] R. Blankenburg, *Dissertation*, Universität Mainz 1989.

[44] a) P. C. Weber, D. H. Ohlendorf, J. J. Wendoloski, F. R. Salemme, *Science (Washington D.C.) 243* (1989) 85; b) W. A. Hendrickson, A. Pähler, J. L. Smith, Y. Satow, E. A. Merrit, R. P. Phizackerley, *Proc. Natl. Acad. Sci. USA 86* (1989) 2190.

[45] E. Rump, *Diplomarbeit*, Universität Mainz 1990.

[46] D. Batchelder, D. Bloor in R. J. H. Clark, R. E. Hester (Eds.): *Advances in Infrared and Raman Spectroscopy, Vol. 11*, Wiley, 1984, p. 133.

[47] D. N. Batchelder in H. Bässler (Ed.): *Optical Techniques to Characterize Polymer Systems*, Elsevier, Amsterdam 1989.

[48] A. F. Drake, D. J. Ando, D. Bloor, J. S. Obhi, S. Mann, *Polymer 30* (1989) 1063.

[49] R. F. Doolittle, *Scientific American 253* (1985) No. 10, p. 74.

[50] a) E. A. Dennis in P. D. Boyer (Ed.): *The Enzymes, Vol. 16*, 3rd Edit., Academic Press, New York 1983, p. 307; b) H. Van den Bosch, *Biochim. Biophys. Acta 604* (1980) 191.

[51] a) H. M. Verheij, A. J. Slotboom, G. H. de Haas, *Rev. Physiol. Biochem. Pharmacol. 91* (1981) 91; b) A. Achari, D. Scott, P. Barlow, J. C. Vidal, Z. Otwinowski, S. Brunie, P. B. Sigler, *Cold Spring Harbor Symp. Quant. Biol. 52* (1987) 441; c) J. Drenth, B. W. Dijkstra, R. Renetseder in F. A. Jurnak, A. McPherson (Eds.): *Biological Macromolecules and Assemblies, Vol. 3 – Active Sites of Enzymes*, Wiley, New York 1987, p. 287; d) M. K. Jain, O. G. Berg, *Biochim. Biophys. Acta 1002* (1989) 127.

[52] a) J. Chang, J. H. Musser, H. McGregor, *Biochem. Pharmacol. 36* (1987) 2429; b) P. Vadas, W. Pruzanski, *Lab. Invest. 55* (1986) 391; c) G. C. Liggins, M. D. Wilson, T. Wilson, *Am. J. Perinatol. 6* (1989) 153; d) T. J. Nevalainen, *Z. Med. Laboratoriums diagn. 30* (1989) 299; e) W. Scheuer, *Klin. Wochenschr. 67* (1989) 153.

[53] P. P. M. Bonsen, G. H. De Haas, W. A. Pieterson, L. L. M. Van Deenen, *Biochim. Biophys. Acta 270* (1972) 364.

[54] a) N. Gheriani-Gruszka, S. Almog, R. L. Biltonen, D. Lichtenberg, *J. Biol. Chem. 263* (1987) 11 808; b) T. Thuren, P. Vainio, J. A. Virtanan, P. Somerharju, K. Blomquist, P. K. J. Kinnunen, *Biochemisty 23* (1984) 5129; c) J. N. Israelachvili, S. Marcelja, G. Horn, *Q. Rev. Biophys. 13* (1980) 121; d) P. N. Barlow, J.-C. Vidal, M. D. Lister, E. A. Dennis, P. B. Sigler, *J. Biol. Chem. 263* (1988) 12 954; e) G. Romero, K. Thompson, R. L. Biltonen, *ibid. 262* (1987)13 476; f) R. Sundler, *Chem. Phys. Lipids 34* (1984) 153; g) D. Lichtenberg, G. Romero, M. Menashe, R. L. Biltonen, *J. Biol. Chem. 261* (1986) 5328; h) D. Lichtenberg, G. Romero, M. Menashe, R. L. Biltonen, *ibid. 261* (1987) 5334; i) A. Alsina, O. Valls, G. Rieroni, R. Verger, S. Garcia, *Colloid Polymer Sci. 261* (1983) 923; k) A. Alsina, M. L. Garcia, O. Valls, S. Garcia, *Colloids Surf. 14* (1985) 277; l) A. Alsina, M. L. Garcia, M. Espina, O. Valls, *Colloid Polymer Sci. 267* (1989) 923; m) D. W. Grainger, A. Reichert, H. Ringsdorf, C. Salesse, D. E. Davies, J. B. Lloyd, *Biochim. Biophys. Acta 1022* (1990) 146.

[55] a) J. A. F. Op den Kamp, J. De Gier, L. L. M. Van Deenen, *Biochim. Biophys. Acta 345* (1974) 253; b) D. O. Tinker, A. D. Purdon, J. Wei, E. Mason, *Can. J. Biochem. 56* (1978) 552.

[56] a) J. C. Wilschut, J. Regts, H. Westenberg, G. Scherphof, *Biochim. Biophys. Acta 508* (1978) 185; b) G. C. Upreti, M. K. Jain, *J. Membr. Biol. 55* (1980) 113.

[57] a) D. W. Grainger, A. Reichert, H. Ringsdorf, C. Salesse, *FEBS Lett. 252* (1989) 74; b) D. W. Grainger, A. Reichert, H. Ringsdorf, C. Salesse, *Biochim. Biophys. Acta 1023* (1990) 365.

[58] H. M. McConnell, L. K. Tamm, R. M. Weis, *Proc. Natl. Acad. Sci. USA 81* (1984) 3249.

[59] a) A. Plückthun, E. A. Dennis, *J. Biol. Chem. 260* (1985) 11 099; b) M. K. Jain, D. V. Jahagirdar, *Biochim. Biophys. Acta 814* (1985) 313; c) M. K. Jain, M. R. Egmond, H. M. Verheij, R. Apitz-Castro, R. Dijkman, G. H. De Haas, *ibid. 688* (1982) 341.

[60] a) T. L. Hazlett, E. A. Dennis, *Biochemistry 24* (1985) 6152; b) T. L. Hazlett, E. A. Dennis, *Biochim. Biophys. Acta 961* (1988) 22; c) C. R. Kensil, E. A. Dennis, *J. Biol. Chem. 254* (1979) 5843; d) G. Romero, K. Thompson, R. L. Biltonen, *ibid. 262* (1987) 13 476; e) C. M. Smith, M. A. Wells, *Biochim. Biophys. Acta 663* (1981) 687; f) R. A. Deems, E. A. Dennis, *Methods Enzymol. 71* (1981) 703.

[61] W. Cho, A. G. Tomasselli, R. L. Heinrickson, F. J. Kezdy, *J. Biol. Chem. 263* (1988) 11 237.

[62] For instance, for a phase separation of the hydrolized products in vesicles see B.-Z. Yu, A. Kozubek, M. K. Jain, *Biochim. Biophys. Acta 980* (1989) 23.

Organic Synthesis in the Age of Computers

By James B. Hendrickson*

The computer affords four areas of interest to synthetic chemists: (1) storage and retrieval of information; (2) complex calculations of shape and reaction dynamics; (3) artificial intelligence (AI) to solve synthetic and analytical problems; (4) overall direction of multiple laboratory experiments. Our work began 30 years ago initiating molecular geometry calculations to match experimental results. The explosive growth of computer power since will be illustrated. Synthesis design (as AI) requires an efficient protocol to search huge trees. The SYNGEN program is based on simplification and systematization, first of skeletal dissection, then of structure and reaction characterization, for generation of optimal synthesis routes. The program will be be described and its future development outlined. Finally, a perspective on the future of all four areas will be sketched, noting the necessary attendant growth in systematic use by chemists and in sympathetic interfaces by software designers.

1. Introduction

The overlap of organic synthesis with understanding of computers has traditionally been small. As we stand back to view our science on this celebration of the 125th anniversary of BASF, it may be useful to explore how this has happened and what we may look for in the future for their codevelopment. The impact of computers on science has certainly been dramatic and organic synthesis has a lot to gain by intimate collaboration. Here is a perspective on what computers can do.

1. Complex calculations: molecular properties, reaction dynamics, and molecular modeling.
2. Information storage and retrieval: very large amounts of data stored, with retrieval completely dependent on efficient search systems.
3. Artificial intelligence for intellectual problem solving: synthesis design and structure elucidation.
4. Automation of laboratory experiments: robotics to explore reaction optimization.

The order is roughly historical. Thirty years ago as a natural products chemist at UCLA, I introduced myself to computers because I needed to know the conformations of rings larger than six-membered in order to understand the possibilities for stereocontrol in sesquiterpene synthesis. The problem involves calculating the molecular geometry and may be appreciated by considering the cycloheptane molecule, for which seven bond and seven dihedral angles must be set and then all of the 189 interatomic distances between nonbonded atoms calculated from these, each by a complex formula involving functions of the angles along the connecting bond path. The strain energy corresponding to the overall geometry is calculated from these angles and interatomic distances using individual parameters for each of these three kinds of geometrical measure. The problem then becomes one of closing in on the minimum energy and its corresponding geometry as established experimentally. This requires, in turn, calculating a sequence of these molecular geometries and their energies to establish the correct minimum-energy conformation with the correct energy. Another dimension is added, however, since the whole set must be done with various estimates of the energy parameters, which were only to be extracted from other kinds of physical measurements.

Here is a typical problem involving a huge set of iterative complex calculations. I set out to explore this for the cycloalkanes of ring size 6–10, having available at that time a slide rule, the sine/cosine tables, and pencil and paper! It quickly became clear that this was a problem which could be systematically solved only with a computer, and so I enrolled for an early one-day course in FORTRAN programming and access to the only computer at UCLA—an IBM 709 in the Engineering Department. The procedure was to punch out each line of program on an IBM card with a noisy card-punch typewriter, submit the stack of instructions so obtained to the computer operator, and come back the next day for printed output. The problem would never have been solved without a computer. With it I was able to publish the first paper[1] in an area which has since grown enormously and been designated as molecular mechanics, a full collaboration of computers and organic chemistry.

With the development of great calculation speed and computer graphics presentation, these calculations of molecular shape are now routine and vividly presented in three dimensions on the screen, with energy minimization in real time as you watch. Such calculations are widely used for comparing the shape of a molecule with some model. Pictorially, the presentation is so convincing that it is sometimes hard to remember that the intrinsic weakness of these calculations remains the still-empirical assignment of the parameters in the equations that produce the molecular energy and so direct the conformational preferences. Furthermore, in modeling we are usually really asking for the nature of the interaction of a molecule with some other (e.g., a receptor). By calculating shape we learn something of the molecule as a kind of neutral sponge, increasingly resistant to penetration, but nothing of its electrical "color"—the intermolecular effects of local partial charges and their fields, π electrons, and orbital interactions. In short, we focus in these calculations on steric interactions but not electronic ones.

The problem of molecular nature was approached in the same period from a more secure physical basis with ab initio and semiempirical molecular orbital calculations. Before

[*] Prof. J. B. Hendrickson
Department of Chemistry, Brandeis University
Waltham, MA 02254-9440 (USA)

computers, the solution to the problem of the hydrogen molecule was a proud achievement in the 1930s. Owing to thirty years of rapid growth in computer speed for iterative calculations, this field has also expanded enormously. Not only are larger molecules accessible to more or less full physical description, but also it is possible to assess the reliability of a number of simplifying assumptions and so make possible the solution of much larger molecules to a rougher accuracy which is still usefully predictive. This is the same kind of approach as with the molecular geometry above in altering parameters and calculational details, through numerous individual cases, in order to match experimental fact. It is the huge capacity of computers for this iterative work that makes these developments possible at all.

2. Logical Basis for Synthesis Design

Twenty years ago the area of artificial intelligence, or problem solving, was opened with the Corey–Wipke publication[2] of the OCSS program for synthesis design. They began with the problem of establishing facile communication between man and machine and created the molecular graphics which allow the presentation of material on the terminal screen in familiar structural formulas. This is not a trivial problem, and some detail on its implementation will be shown below, but without structural formulas the synthetic chemist would probably never have paid much attention to computers, since organic chemistry is very little dependent on mathematical calculations.

Corey's approach to synthesis design for the computer was straightforward.[3] The net structural change of a reaction is seen in reverse as a transform, from product to substrate. Thus, all possible transforms can be applied to the target to create the intermediates one step back, and these as subtargets further transformed a second step back to the next level of intermediates, and so forth. The process was called "computer-assisted" and so was set up as interactive with the operator, who pruned the tree down to a few intermediates at each level as he went along. This procedure depended on the presence of a library of general transforms, kept as a database in the computer and keyed to be applied wherever the functionality of the target under consideration matched that of a transform in the library. This was said to be the process by which synthetic chemists designed their syntheses, but curiously the chemical literature was mute on the subject of this design process.

The problem of synthesis design is simply that the number of possible synthetic routes to any target molecule of interest is enormous, much larger than generally appreciated. A view of the synthesis tree in Figure 1 is meant to emphasize this. The points are compounds: target at right, intermediates in the midst, and available starting materials as heavy dots at the left, all more or less diminishing in size to single-carbon materials at the far left. The lines are reactions, directed to the right (or transforms to the left), so that particular synthesis routes may be picked out, as shown in red, from the whole. The intermediates stand in levels, or steps, back from the target, with diminishing overall yields for the routes shown below, assuming 80% per step.

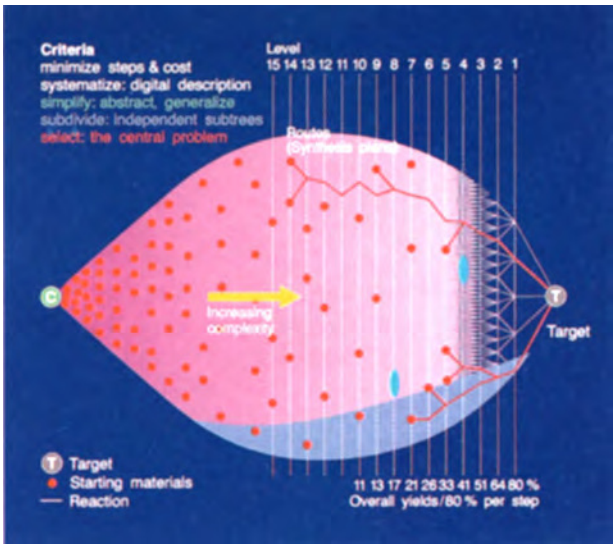

Fig. 1. Synthesis tree.

For the computer it is simple in principle to generate a whole tree; the real problem is one of selecting the optimal routes. It would not be unreasonable to expect 30 reactions which might convert intermediates at the first level into the target. Since each of these 30 intermediates will still be of comparable complexity, each will also have some 30 reactions from level-2 intermediates. To proceed back five levels will therefore produce 30^5, or 24 million, possible routes, and many syntheses are much longer. Now the question is, which is the one route to take in the laboratory?

To create an approach for the computer to this problem,[4] we can apply some principles from large tree searches in other fields. The data in the search space—here, it is structures and reactions—must be *systematically* described in digital format, not only for rapid computer manipulation but also to assure that all possibilities can be derived as simple mathematical combinations, and so none will be missed. The tree is so large that *simplification* is imperative and consists of generalizing the entries by coalescing trivial detail. This makes a much smaller tree, with fewer entries abstracting all the original ones. The digital system used can be designed to facilitate this reduction. This simplification is analogous to maps in that a map of a small area shows far more detail than that of a large area. In practice, we use the latter to find our way to the desired locale and the former to refine the detail as we approach it. The same principle of generalize first and refine later to practical detail is used here to seek optimal routes from the synthesis tree. The simplified, generalized tree is still enormous, but it can be made more manageable by *subdividing* it into subtrees, which are independent and so may be explored separately and sequentially.

The problem remaining is that of *selecting* the few best routes. This requires defining criteria for "optimality", stringent enough to select only a few routes. In our approach to synthesis design we opted for a criterion of economy—the shortest routes with the most efficient assembly from the cheapest starting materials. We also wanted all these best routes to be found by the computer via consistent application of the criteria, rather than leaving the process interactive, at the whim of the operator.

To seek these, we first consider any structure as divisible into two parts: (1) the carbon *skeleton* or backbone (later to include some skeletal heteroatoms as well) and (2) the *functionality*, that is the placement of double bonds and attached heteroatom functional groups on the skeleton. This dichotomy then divides reactions similarly into *constructions*, which create C–C σ bonds and so assemble the skeleton and *refunctionalizations*, which alter functional groups without affecting the skeleton. In this view the assembly of the skeleton is primary and considered first. This leads to an initial and drastic simplification of the tree—by considering only the skeletons. Thus, while there are perhaps 50 000 available starting materials, there are only 13 acyclic starting skeletons of six carbons or less. A survey of published syntheses shows that the average-size starting material for nonaromatic targets is only *three carbons* incorporated into the target skeleton.

3. Focus on Skeleton

The primary importance of the skeleton and its assembly in synthesis is philosophical: *synthesis itself is a skeletal concept*. Synthesis consists of joining small starting molecules to make a large target. Therefore, the central, obligatory reactions are the skeletal constructions, which join those small pieces. In principle, refunctionalizations are not needed at all, despite the observation that the average synthesis has twice as many refunctionalizations as constructions. This leads to a stringent criterion for economy: to seek only *ideal syntheses*, those consisting only of construction reactions, since these—though rare—must be the shortest routes. In an ideal synthesis, the chosen starting materials have the correct functional groups to initiate the constructions joining them, and the subsequent constructions, in direct sequence, lead to the target skeleton with all its correct functional groups in place, as a natural consequence of the chemistry of the construction reaction sequence.

These considerations imply that we need to systematize the structures in the synthesis tree to deal efficiently but separately with the skeleton and the functionality on the skeleton. We need to determine which skeleton bonds of the target will the the best ones to construct, and then what functional groups are required to construct those bonds so as to result in the final target functionality directly.

Even though the focus on skeleton greatly simplifies the tree, there remains an enormous number of possible ways just to assemble a target skeleton. This arises from a combinatorial monster of what pieces to use and what order to join them. We may designate a *bondset* in a target skeleton as a set of λ bonds which are the ones to construct, as in Figure 2 for the estrone skeleton. If we remove all the bondset bonds from the skeleton, we are left with the several smaller skeletons of the starting materials. The bondset defines a family of syntheses which all make just those skeletal bonds. For any bondset, the order, or sequence, in which the bonds are made defines a generalized route, that is, a plan of assembly of the starting skeletons into the target skeleton. The assembly plan in Figure 2 is just a route from the synthesis tree (Fig. 1), but composed only of the construction reactions. Indeed, the simplest gross description of any synthetic route—of its essentials—is this *ordered bondset*, which shows the starting material skeletons and the sequence of target bonds which are constructed to link them.

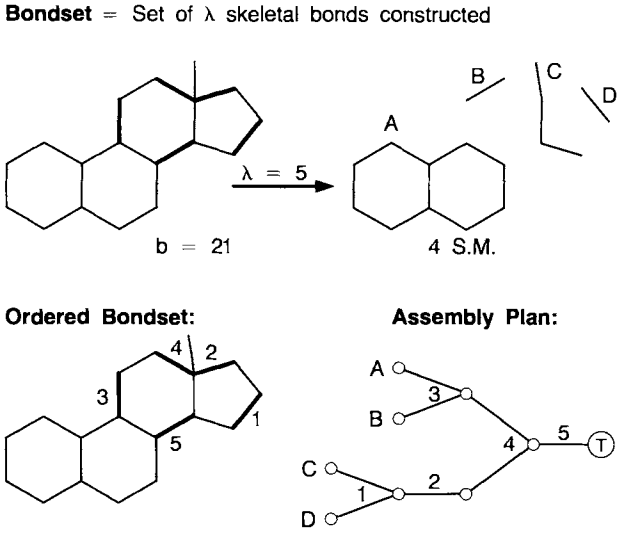

Fig. 2. Skeletal dissection and assembly. λ = number strategic bonds; b = number of CC bonds; S.M. = number of starting materials.

The number of possible ordered bondsets is the number of ways to dissect the skeleton: for a target of b bonds this is $b!/(b-\lambda)!$ Thus, an assembly of the estrone skeleton ($b = 21$ bonds) from pieces averaging three carbons would require a bondset of $\lambda = 9$ bonds and affords 10^{11} assembly plans (ordered bondsets), that is, 100 billion routes, even without considering the detailed chemistry involved. A dramatic realization of these combinatorics may be seen in the total synthesis of cortical steroids from one-carbon units, for which there are 6×10^{23} assembly plans: this means that to make a mole of cortisone one can make every molecule by a different route!

There are two powerful criteria which allow a severe reduction in these numbers. The first is the choice of a *convergent* assembly, which can be shown[5] to be significantly more efficient than a linear plan, in terms of the total weight of starting materials required. The convergent plans can very simply be created by cutting the target skeleton into two pieces and cutting each of these again into two more. The second choice is merely to require that the four starting skeletons so derived each time must be found in a catalog of actual, available starting materials. This implies that a target of twenty carbons will result in starting materials averaging five skeletal carbons each, and our experience with such catalogs shows a sharp drop-off in functional group variety in starting materials above five carbons. This suggests that by applying these criteria we should be able to find real chemistry for at least some of these plans. Not only are these convergent plans the shortest and most efficient syntheses, they are also quite rare and so afford the needed severe reduction in the total bondsets that must be examined.[6]

Here we may pause to look at the problem for the computer in storing these skeletons and comparing them with those in a catalog to find matches.[7] Figure 3A shows a skeleton

of eight atoms, arbitrarily numbered, and an adjacency matrix of its connectivity, which fully defines the structure. This matrix may be strung out to form a linear binary string; this is now just a binary number which can be used as an identification number for this skeleton. However, there are 8! ways to number this skeleton, that is, 40 320 numberings, of which we must pick one which will always be unique. This can be done by finding the one for which its binary string will be the *maximum binary number*. Such a maximal numbering is shown in Figure 3B. The catalog is then a list of maximal

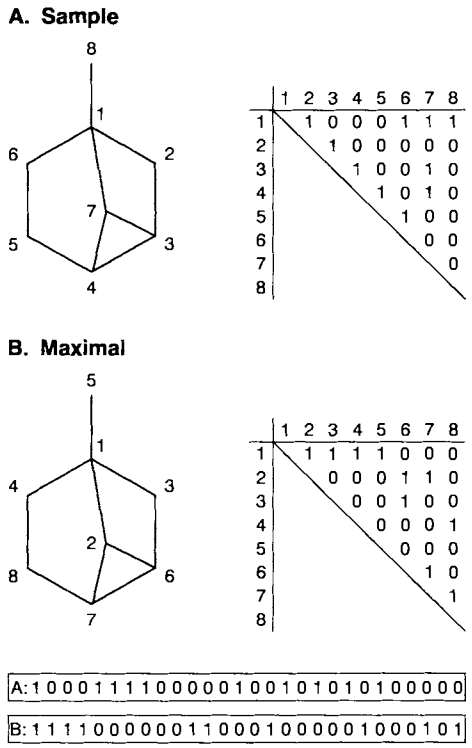

Fig. 3. Maximal canonical numbering. A) Arbitrary canonical numbering; B) maximal canonical numbering. Below: Binary numbers corresponding to the numberings in A and B.

binary numbers of its contained skeletons, arranged in numerical order so that any search for a match with some generated skeleton becomes a simple binary search, very fast in the computer. Also, we created a program to draw the structural formula from its maximal binary number.

4. Systematizing Reactions

To proceed now to the chemistry for synthesis routes, we must first create a system to describe the functional groups on the skeletons and the net structural change they undergo in reactions. Such a system must be digital for the computer, simple but rigorous in its description of chemistry and capable of generalizing and simplifiying by coalescing trivial structural detail. The system[8] summarized in Figure 4 assigns four synthetically important kinds of attachment which any skeletal carbon may have: H for bond to hydrogen, electron pair, or electropositive atom; R for a σ bond to carbon—its skeletal connectivity,[9] Π for a π bond to another skeletal carbon; Z for bond (σ or π) to electronegative atom (O,N,X,S,P). The *number* of bonds to the carbon for each kind of attachment is then given by h,σ,π or z, respectively, with a sum of 4. The oxidation state of any carbon is given by x = z − h, and the change in oxidation state in any reaction is found by summing all the changes in x.

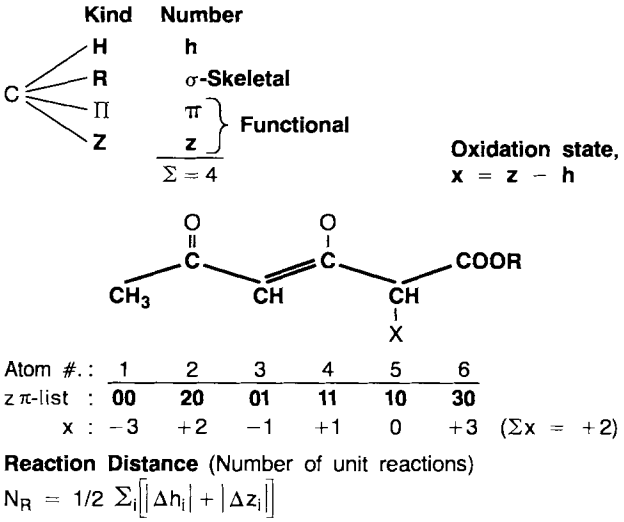

16 Units Reactions (one carbon)

Oxidation	ZH	
Reduction	HZ	
Substitution	HH, ZZ	
Addition	HΠ, ZΠ, RΠ	ΠΠ
Elimination	ΠH, ΠZ, ΠR	ΠΠ
Construction	RH, RZ, RΠ	RR
Fragmentation	HR, ZR, ΠR	RR

Fig. 4. Digital characterization of structures and reactions.

The functionality of a carbon may now be abstracted as its zπ value, contained in the computer with only two bits each for z (= 0–3) and π (0–2). Computer description of a compound then consists first of its skeleton as a maximal binary number followed by the zπ list of the functionality on its numbered carbons in numerical order. The σ value of each carbon comes from the row sums of the adjacency matrix (Fig. 3) and the h value by subtraction of (σ + z + π) from 4. This compound binary list for the skeleton and functionality of any structure may then be compared with any starting material in the catalog for a match, either by skeleton separately or by the whole abstracted structure. The coalescence of detail may be appreciated by noting in the example in

Figure 4 that all carboxylic derivatives are denoted by a $z\pi$ value of 30.

Reactions may also be described using the system presented in Figure 4. Ignoring its mechanism, any reaction may be described by its *net structural change* from substrate to product at each changing skeletal carbon. A unit reaction at any one carbon is just a unit exchange of attachments, for which $4 \times 4 = 16$ unit exchanges are possible. These we denote with a two-letter symbol, the first letter for the bond made, the second for that broken. The possible unit reactions at one carbon fall into familiar chemical categories as shown below in Figure 4. Reactions like elimination, addition, and construction require more than one (adjacent) carbon changing; each carbon will have a symbol.

The value of such a system is that it affords an abstract description of every possible change a carbon may undergo. Hence, it forms a basis for a rigorous organization of all organic reactions.[10] Like the Beilstein system for organic structures, this can create a catalog of organic reactions in which every possible reaction will have a place. Such an organization of all the unit reactions on one to three carbons is presented in Figure 5 and will be seen to include all common reactions.[11]

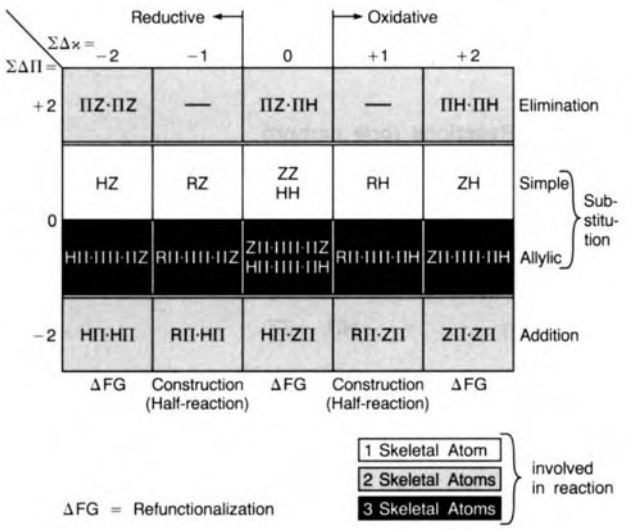

Fig. 5. Reaction characterization for one to three skeletal atoms.

The construction reactions are those with which synthesis design is specially concerned and are the only reactions in an ideal synthesis. A construction may be seen as the combination of two half-reactions, usually one oxidative (nucleophilic) and one reductive (electrophilic); the three possible unit half-reactions of each kind are included in Figure 5. On inspection of the net structural changes depicted, one can see that these represent the common familiar construction half-reactions: for example, formation of carbanions or allylic carbanions, enolates and enamines, alkylations and allylic alkylations, carbonyl addition, acylation, and conjugate addition. With the systems described above, we can see how the computer can quickly generate the substrates from the products (or vice versa) for any given construction, illustrated with an example in Figure 6. Here the bond to construct (heavy line) is dictated by the ordered bondset, and up to

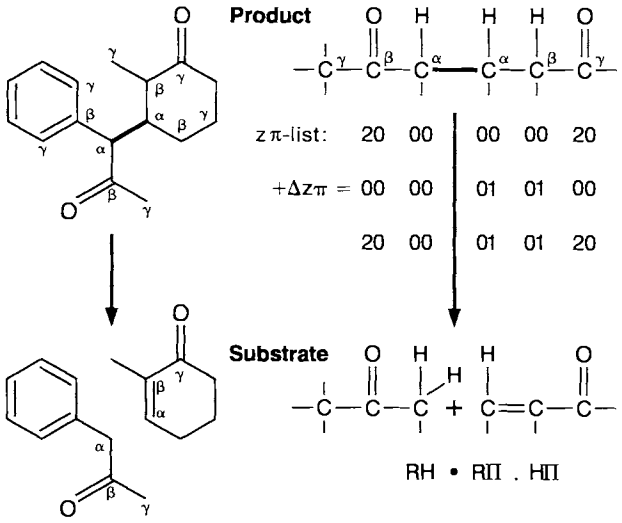

Fig. 6. Rapid generation of reactions in SYNGEN.

three atoms out from each end (labeled α, β, γ) will bear the functionality of a construction product. A combined $z\pi$ list of each αβγ strand across the bond made is called and to it is added a *$\Delta z\pi$-list generator* characteristic of any combination of nucleophilic and electrophilic half-reactions. This directly generates the $z\pi$ list for the possible substrates, shown for one example on the right side of Figure 6. The process is very fast for the computer.

5. The SYNGEN Program

The foregoing exposition of a synthesis design logic for the computer is realized in the SYNGEN program developed in our laboratories over the last ten years.[12] The program is designed to locate and generate all the possible shortest synthetic routes—convergent ideal syntheses—for any target. The program is not interactive and so is independent of the user's preconceptions. An overview of its operation is presented in Figure 7 and has two phases.

First, only the target skeleton is examined; it is cut through two levels to find all the most efficient, convergent modes for its assembly from four (or less) available starting material skeletons found in the catalog (the present catalog contains over 6000 compounds). These modes are the possible ordered bondsets, each of which is an independent subtree of the whole synthesis tree. In Figure 7, one such bondset, consisting of three bonds, is shown for an estrone derivative and leads through two levels to starting skeletons B,C,D (Fig. 7, left).

Second, the program then generates the functionality changes, as in Figure 6, back from the target functionality through the successive bonds of each bondset. When all the bonds in each bondset have been constructed (in the retrosynthetic direction), the functionality required on each starting material is revealed and these structures are then sought in the catalog. Only routes with all of the starting materials found in the catalog are accepted. The three starting materials for Figure 7 are B-2,C-3,D-5, generating the commercial (and ideal) synthesis of estrone, after reduction

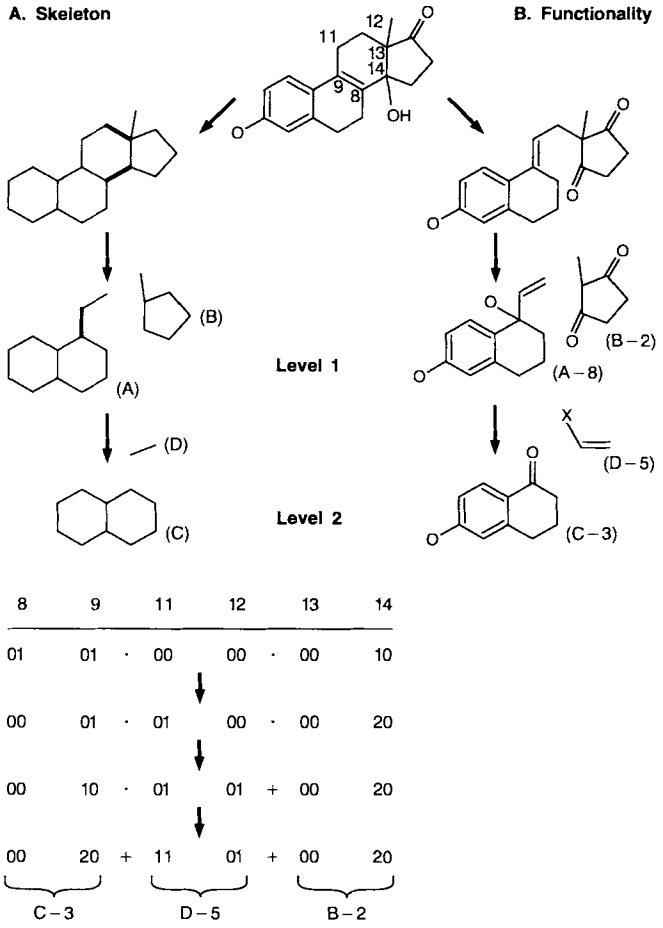

Fig. 7. Overview of SYNGEN protocol (see also Section 6).

of the target shown. At the bottom of Figure 7 are the successive $z\pi$ lists of the changing carbons through the three successive constructions.

In practice the SYNGEN program is very easy. In a facile drawing routine the user enters a crude structure of the target, which the program normalizes; the synthesis routes are then generated without operator interaction in 1–3 minutes. The output is stored in a directory and may be called up at any time for inspection of the results, summarized first on a screen like that of Figure 8 for synthesis of the AIDS drug AZT (3'-azidothymidine). The number of entries for each of four categories is appended for each level below.[13] At the top may be seen the four categories which may be separately accessed for examination: *bondsets, starting materials, intermediates*, and *reactions*. Any entry in any of the categories may be individually retained or deleted, along with its related entries in each other category; for example, if unwanted bondsets are deleted, all related reactions and compounds are also deleted. The totals at the top of the screen automatically adjust for each selection so that the operator may see the scope of his choice.

A sample listing of starting materials (Fig. 9) shows that some starting materials can be made by refunctionalization

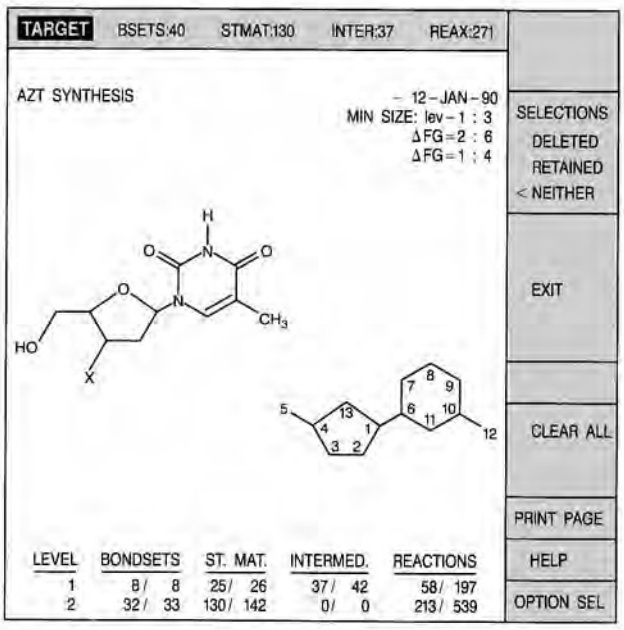

Fig. 8. Application of SYNGEN program to AZT synthesis (x = N_3).

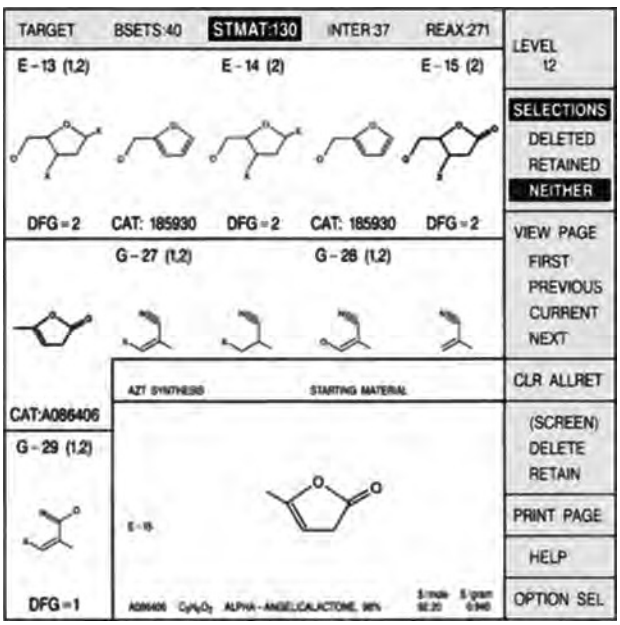

Fig. 9. Sample screen showing starting materials for the synthesis of AZT.

of others if they are not found in the catalog, indicated by DFG and followed by a real starting material with an Aldrich number. The DFG signifies a "reaction-distance"—the number of steps for refunctionalization between the generated material and the nearest one in the catalog. This may be calculated with the formula for N_R (Fig. 4). The insert in Figure 9 shows how an expansion of the listing can be called if desired, here of compound E-15.

A sample listing of reactions (Fig. 10) shows the structure being made at upper left (the target at level 1, intermediates at level 2) and they reactions for it in abstracted form with abbreviated notations of the involved half-reactions for each construction. Again, an expansion of any entry appears, as in the insert for reaction 3-34 of bondset 3, and expands on the abbreviated reaction notations as well.

Even when large numbers of routes are found, there are powerful pruning tools to allow one to focus in quickly on desirable pathways,[14] such as the individual delete/retain

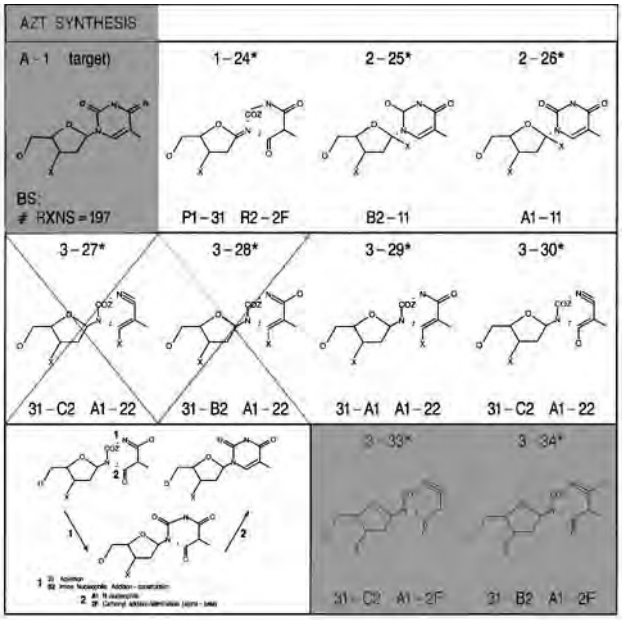

Fig. 10. Sample screen showing reactions for the synthesis of AZT.

options for entries in each category, or the possibility of tracing all reactions involving any single chosen bondset, starting material, or intermediate. Another tool is a set of broad conditions about either compounds or reactions, as in Figure 11. These include starting material cost or the necessity of repairing its functional groups, and regiochemical or other uncertainties or incompatibilities which may be present in the reactions. Selections among these broad options can dramatically reduce the total number of allowed routes; the deletions made on the options screen of Figure 11 have reduced the total reactions from 736 in Figure 8 to only 34.

REACTION / SELECTIONS	RXN-1-	RXN-2-	TOTAL REACTIONS
UNCLEAR REGIO:KETONE	0	0	24 10
UNCLEAR REGIO:PI-BOND	10	0	MOVE CURSOR TO:
MIXED MODE CONSTRUCTION	4	0	LEVEL -1-
TWO-STEP ANNEL: ACID/BASE	0	0	LEVEL -2-
TWO-STEP ANNEL: RED.CYC.	0	0	TEXT FOR 1&2
BALDWIN RULES VIOLATION	24	0	ENTER:
COMPATIBILITY: LEAVING GROUP	10	6	R FOR RETAIN
COMPATIBILITY: KETONE	0	0	D FOR DELETE
COMPATIBILITY: ALDEHYDE	0	0	C FOR CLEAR
EQUIV: SAME CONCEPT	12	2	Clear All Flags
EQUIV: SAME SUBSTRATES	4	2	HELP
EQUIV: SAME REACTIONS	17	2	EXIT

COMPOUND / SELECTIONS	SM-1-	SM-2-	RXN-1-	RXN-2-
COST LIMIT 2S(1) 1S(2)	6	14	24	10
SM NOT REFUNCTIONALIZED	0	8	0	10
SM REFUNCTIONALIZED	6	6	24	10
INTERMEDIATES	4	0	24	0

Fig. 11. Reaction/selections option screen.

The operation of this program has shown it to be a very facile way of finding all the possible shortest syntheses for many targets. It finds known syntheses and suggests many other interesting routes. It has the particular advantage of assuring the operator that he has not missed some short pathways to the synthesis of his choice target.

6. Current Developments

In extension of the SYNGEN program we have now developed an interface to the large commercial databases of organic reactions, REACCS and SYNLIB. This allows close literature precedents to be found for the reactions that are generated by SYNGEN. The databases must first be annotated as in the SYNGEN system to recognize not compound structures but rather just the *net structural change* in the reaction. To do this, we probed the reactant and product structures in the database entries to find C–C bonds made and then listed the $z\pi$-list changes occurring on the $\alpha\beta\gamma$ strands for each half-reaction. These were then ordered into a (nucleophile × electrophile) matrix for rapid retrieval. This allows us to locate all matches for the reactions that are generated by SYNGEN. When there are too many examples of one reaction type, a closer match of the atom types and the σ,z,π values at the construction site is made until the best matches are found. Organizing the reactions this way creates a subset of some 26000 construction reactions accessible from REACCS and SYNLIB. This now constitutes a powerful library of literature precedents of the closest structural matches for any particular reaction generated by SYNGEN and provides the chemist with the practical laboratory details that he needs to execute a chosen synthetic route.

In other variations on the theme of efficient synthesis, we have created two ancillary programs to seek special opportunities for multiple constructions of targets to make their syntheses even shorter.[15] In another area we have built a program to proceed in the forward instead of retrosynthetic direction, from available starting materials to close derivatives of the target. This aims at locating routes which will involve some refunctionalization reactions in the path as well as just constructions of the skeleton and so expands the variety of routes found.

This FORWARD program begins like SYNGEN in first defining the best convergent bondsets and their derived starting skeletons. It then proceeds by pairwise combinations of all the catalog starting materials so designated, accepting only those for which the functional groups converge toward the target. This is possible through calculation of the "reaction distance" (see Fig. 4) of intermediates from target and then massively prunes what would otherwise be an unmanageable combinatorial explosion. This FORWARD program produces not only the target molecule but also all close derivatives which may easily be transformed into it and so offers a much larger selection of short, practical synthetic routes. Thus, the synthesis in Figure 7 is for a derivative of

estrone, not estrone itself (which produces only few and rather poor routes in SYNGEN). In the FORWARD program, however, routes to various close derivatives of estrone are all found when estrone is entered, including that of Figure 7; others are shown in Figure 12, but the program excludes those which are more than two steps from the target.

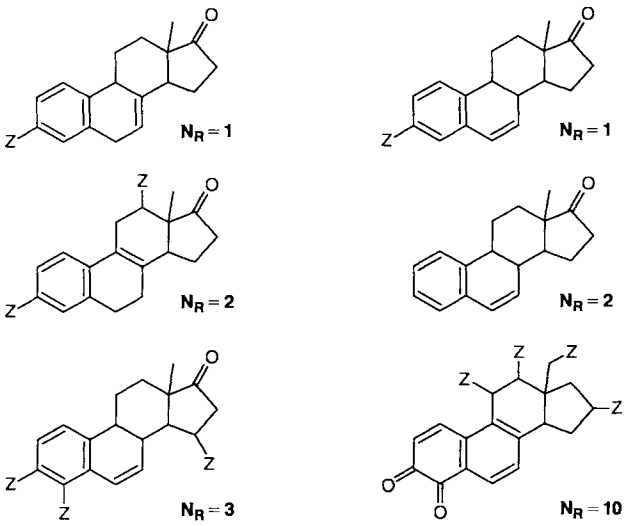

Fig. 12. Estrone derivatives from FORWARD program. N_R = reaction distance (cf. Fig. 4).

These programs are based on a developing logic for synthesis design. In a further search for design logic embedded in published syntheses, we are creating a database of published routes, especially to popular targets which have been synthesized in many ways. These now can be manipulated in the computer to create a number of numerical measures of complexity and similarity which are submitted to multivariate analysis in an effort to see if threads of general logic can be discerned in these routes and so to define some measure of synthesis "optimality".

7. Perspectives on the Future

Looking now to the future prospects for interaction between synthesis and computers, we may address the original four areas of collaboration (see Section 1). In the area of complex calculations the ultimate need is real-time calculation of reaction rates. In generating reactions, SYNGEN uses generalized abstract descriptions. These must be reduced to real prediction for the particular case, specifying rate preferences for solvent, bases, counterions, etc., and comparing them to those of possible competing reactions. At a qualitative mechanistic level, the prediction of possible competing reactions is already well underway in the CAMEO program of *Jorgensen*.[16] Meaningful rate calculations will require more powerful computers.

Here we may look at some hopeful projections from the historical growth of computer capability. In Figure 13, we see the remarkable increase with time of computer speed, measured in floating point operations per second (FLOPS). This certainly implies that the desired rate calculations may be accessible in real time in the very near future. Furthermore, Figure 13 shows that the cost of such capability is coming down at the same logarithmic rate (MIPS = million instructions per second), to become available to practicing chemists.

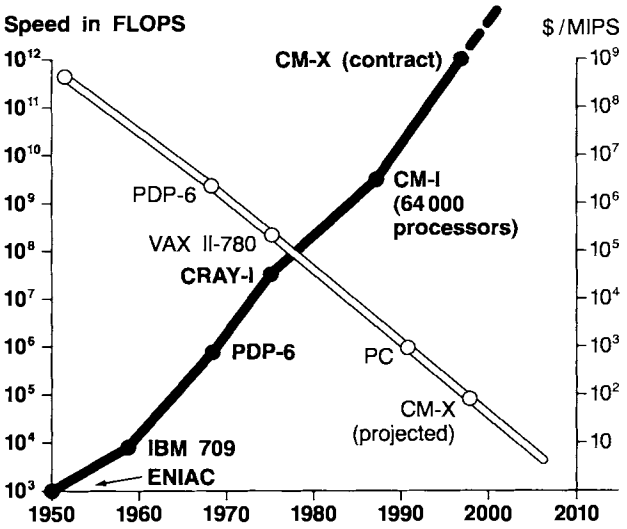

Fig. 13. Speed and cost of computing since 1950. FLOPS = floating point operations per second. MIPS = 1×10^6 instructions per second.

But practicing chemists are also involving themselves in the other direction, developing instead of using the computer. One way to speed up a computer is to make it smaller, and the size of transistors has been inexorably decreasing in proportion to the speed increase. The smallest commercial transistor now is about a micron and the present technology is limited to about 0.1 μm by quantum tunneling. *Wrighton* and *Whitesides* have projected work aimed at making a molecular switch.[17] These molecules are to be covalently attached to vapor-deposited metal conductor strips, and the molecular gap can now be on the order of 0.01 μm. An even greater potential is on the horizon when one considers that such a "switch" molecule may have more than two accessible molecular states and thus be adaptable for a more complex computer logic than one simply based on "on/off" choices.

In the area of information storage we are desperate to reduce the accelerating consumption of paper and library space for journals and books. We use the computer now for searches of references by author, keyword, or structure, but we still require the library of bound volumes to read the primary source. What we want is to be able to dial up a reference on our office terminal and read it from the screen, then to be able to call up all subsequent articles which refer to it as well, to obtain a quick update on the subject.

This source material can be stored as well as searched on a computer as long as a single storage unit could accommodate everything for searching all at once. Like the growth of computing capability (Fig. 13), the evolution of disk storage capacity for digital information continues, more or less doubling every year in the last decade. An optical disk can now store 2×10^{10} bits. Our library at Brandeis contains 1000 meters of chemical and biological journals for the last 15

meters of chemical and biological journals for the last 15 years. If this were all text, it would amount to 10^{12} bits of information. The annual journal input could then be accommodated on four present disks, and a 20-fold increase (perhaps 5 years) in storage capacity would store the whole library on one disk! An even smaller storage unit has been explored[18] with a three-dimensional molecular matrix for optical reading and writing, theoretically capable of storing 10^{12} bits per cubic inch.

The problem of pictures in the text can be confronted by a compression program, operating in reverse on retrieval to decompress for display. At present an hour of television pictures (216000 pictures) can be compressed by such a program onto a single CD. Indeed chemical structures are much less dense than text, since our program for storing structures (Fig. 3) requires only 400 bits to store the AZT structure, while the same journal space in the form of printed text requires 3200 bits.

Accordingly, we can envision a system (Fig. 14) in which the contents of journals are beamed up by the publisher to a satellite which then sends them continuously to library receivers, to be sifted automatically for those subscribed and stored on the library disk (the same sifter can pass on copies to individual subscribers). This would make possible a system in which one could call up on an office terminal any journal article, read it, and make a copy if desired; no paper need be kept except that which is actually read.

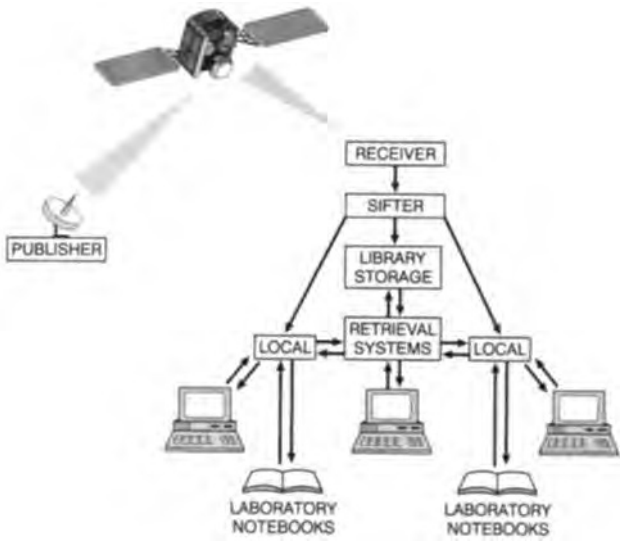

Fig. 14. The computerized library.

The problem of retrieval raises the issue of documentation for retrieval. While we have reasonable means for retrieving authors, references, keywords, and structures, we need a good system for the retrieval of reactions, nested from the general to the particular as in the Beilstein system for structures, to provide a place for every conceivable reaction, whether currently realized or not. Our approach (Fig. 5) from unit reactions is offered in this vein and we are currently exploring reaction databases to locate refunctionalizations as well as constructions in this way, with considerable success. Chemists will have to take a more lively interest in creating these documentation systems if they wish to have really efficient means of finding information.

The third area of artificial intelligence can be applied both to synthesis and to analysis. In synthesis design the SYNGEN program can offer all the shortest generalized reactions; it needs a stereochemical component as well. Linking it to CAMEO would reveal what other reactions might interfere, and a link to a substantive rate prediction program could quantify these. In analysis the chemist needs a master "black box" program to collect data from various analytical instruments and interpret it in structural terms, showing the chemist what he actually obtained in a reaction.

Finally, the computer can be instructed to run the experiments. Utilizing a Zymark computer-directed robotic apparatus, *Fuchs*[19] has demonstrated an integrated system for running series of parallel experiments intended to optimize conditions for a reaction on a scale of 0.1 mmol mL^{-1}. The system centers on an arm programed to move vertically and radially to syringe substrates and solvent into a reactor (and to wash it afterwards!) and, after a programed time and temperature, to filter, extract, and analyze them by chromatography, with analytical spectra taken on the effluents. With eight reactors and two gas chromatographs, he can program the system to perform 400 reactions a day, and he has shown a complex reaction optimized from almost nothing to a yield of over 70%.

These rosy (if dangerous) predictions of the future seem to suggest that synthetic chemists themselves will have little to do except to man their computer terminals! While this is certainly not at all likely, it is clear that they will have to be much more familiar with computers than they are now and use them more intensively. More than that, they will need more appreciation of the importance and nature of the logical systems used to describe and retrieve chemical information, and they must actively assist in the development of clear, useful software for chemical purposes. In short, they will become much more involved with computers than they are at present.

I wish to acknowledge the wonderful spirit, devoted diligence, and remarkable computer skills of my colleagues who have made possible the work I have described here: Glenn Toczko, with me since the inception of SYNGEN ten years ago, David Grier, Zmira Bernstein, Ping Huang, Todd Miller, and Camden Parks.

Received: June 5, 1990 [A 784 IE]
German version: *Angew. Chem. 102* (1990) 1328

[1] J. B. Hendrickson, *J. Am. Chem. Soc. 83* (1961) 4537.
[2] E. J. Corey, W. T. Wipke, *Science (Washington, D.C.) 166* (1969) 178.
[3] E. J. Corey, A. K. Long, S. D. Rubenstein, *Science (Washington D.C.) 228* (1985) 408.
[4] J. B. Hendrickson, *Acc. Chem. Res. 19* (1986) 274.
[5] J. B. Hendrickson, *J. Am. Chem. Soc. 99* (1977) 5439.
[6] The convergent bondsets so created cut no more than two bonds per cut, that is, six bonds ($\lambda = 6$) or less in total. For estrone ($b = 21$) there are 39 million ordered bondsets possible; but the number of fully convergent ones from catalog skeletons is less than 900, and most of these have no acceptable chemistry for ideal syntheses.
[7] J. B. Hendrickson, A. G. Toczko, *J. Chem. Inf. Comput. Sci. 23* (1983) 171.
[8] J. B. Hendrickson, *J. Am. Chem. Soc. 93* (1971) 6847.
[9] Primary carbons have $\sigma = 1$; secondary, $\sigma = 2$; tertiary, $\sigma = 3$, quaternary, $\sigma = 4$.

[10] J. B. Hendrickson, *J. Chem. Inf. Comput. Sci. 19* (1979) 129.
[11] No fragmentations have been shown in Figure 5 in order to make it clearer, but they can easily be incorporated as the reverse of the constructions.
[12] J. B. Hendrickson, Z. Bernstein, T. M. Miller, A. G. Toczko in B. A. Hohne, T. H. Pierce (Eds.): "Expert System Applications in Chemistry," *ACS Symp. Ser. 408* (1989), Chapter 6.
[13] Two numbers are shown for each category and level; the first excludes all equivalent reactions.
[14] J. B. Hendrickson, A. G. Toczko, *J. Chem. Inf. Comput. Sci. 29* (1989) 137.
[15] J. B. Hendrickson, P. Huang, *J. Chem. Inf. Comput. Sci. 29* (1989) 145.
[16] T. D. Salatin, W. L. Jorgensen, *J. Org. Chem. 45* (1980) 2043; G. D. Paderes, W. L. Jorgensen, *ibid. 54* (1989) 2058.
[17] P. E. Laibinis, J. J. Hickmann, M. S. Wrighton, G. M. Whitesides, *Science (Washington, DC) 245* (1989) 845.
[18] D. A. Parthenopoulos, P. M. Rentzepis, *Science (Washington, DC) 245* (1989) 843.
[19] A. R. Frisbee, M. H. Nantz, G. W. Kramer, P. L. Fuchs, *J. Am. Chem. Soc. 106* (1984) 7143.

Catalytic Antibodies: A New Class of Transition-State Analogues Used to Elicit Hydrolytic Antibodies

By Kevan M. Shokat, Marcia K. Ko, Thomas S. Scanlan, Lynn Kochersperger, Shirlee Yonkovich, Suvit Thaisrivongs, and Peter G. Schultz*

The design and generation of selective catalysts is an important aim of chemists and biologists. A number of successful strategies have emerged, including the synthesis and derivatization of synthetic hosts, the chemical modification and site-directed mutagenesis of enzymes, and the attenuation of natural enzyme activities in organic solvents. Since 1986 several laboratories have exploited the immune system to generate selective catalysts capable of catalyzing a wide range of chemical transformations. These include acyl transfer, β-elimination, carbon–carbon bond-forming, carbon–carbon bond-cleaving, porphyrin metalation, peroxidation, and redox reactions. The variety and number of transformations catalyzed by antibodies in this short period of time is testament to the versatility and power of the method in generating selective catalysts for applications in chemistry, biology, and medicine. Here we report the use of a new class of uncharged transition-state analogues for generating antibodies capable of catalyzing ester and carbonate hydrolysis. These antibodies are compared to those raised against tetrahedral phosphate and phosphonate transition-state analogues.

1. Introduction

The immune system has the potential to generate more than 10^{11} unique antibodies.[1] The ability to generate this degree of diversity and to select molecules with the desired biological properties from this enormous pool is unique to biological systems. The mechanism by which the immune system generates and screens this huge collection of antibodies is clonal selection. Each antibody molecule of the primary immunological repertoire is stored on the surface of cells called lymphocytes. When a cell with a unique antibody expressed on its surface encounters an antigen, it undergoes division and differentiation and starts to produce soluble antibody molecules. At the same time, the genes encoding the binding site of the antibody undergo mutation, leading to an increase in affinity for the hapten. Antibodies can be selectively generated against virtually any biopolymer, small synthetic molecule, or natural product of interest. With the ability to generate a binding site for virtually any potential substrate, the challenge becomes one of designing chemical strategies to introduce catalytic activity into these macromolecules. Enzymes utilize a variety of strategies simultaneously, including transition-state stabilization, general acid–general base catalysis, cofactors, and proximity effects to catalyze reactions. Each of these strategies has been successfully applied to the generation of antibody catalysts. Several comprehensive reviews on the design and characterization of catalytic antibodies have been written.[2–5]

The first examples of antibody-catalyzed reactions were based on the notion of transition-state stabilization. *Jenck*'s first proposed over twenty years ago that antibodies raised against a transition-state analogue should bind the transition state of a reaction selectively over the substrate and thereby catalyze the reaction (Fig. 1).[6] In fact, many enzymes have evolved to provide an active site that is sterically and electronically complementary to the rate-determining transition state.[7,8] Hydrolytic enzymes such as the zinc peptidase thermolysin function in part by selectively stabilizing the negatively charged tetrahedral intermediate in peptide hydrolysis.[9] Analogues of the transition-state configuration have been shown to be potent enzyme inhibitors. Such transition-state analogues seek to take advantage of the complementarity of the enzyme to the transition-state configuration to achieve high binding affinities. One of the best inhibitors of thermolysin is phosphonamidate **1**, where a tetrahedral phosphorus is substituted for the scissile carbonyl

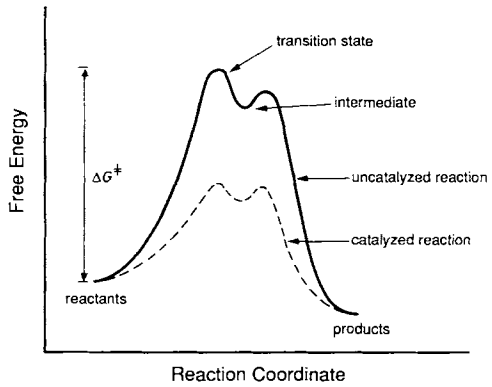

Fig. 1. Reaction coordinate diagram for an antibody-catalyzed and an uncatalyzed reaction.

[*] Prof. P. G. Schultz, K. M. Shokat, M. K. Ko, Dr. T. S. Scanlan
Department of Chemistry, University of California
Berkeley, CA 94720 (USA)
Dr. S. Thaisrivongs
Cardiovascular Diseases Research
The Upjohn Company
Dr. L. Kochersperger, S. Yonkovich
Department of Bioorganic Chemistry
Affymax Research Institute

[**] This work was supported by the Director, Office of Energy Research, Office General Life Sciences, Structural Biology Division of the U. S. Department of Energy (DE-AC03-76SF00098), and the Damon Runyon–Walter Winchell Cancer Research Fund Fellowship (DRG-1016) (*T.S.S.*). We thank Dr. *Jeff Jacobs* for helpful discussions in the early stages of this effort.

carbon in the substrate.[9] Because a typical P–O single bond is 10–15% longer than a C–O single bond, these analogues are quite similar to the tetrahedral transition-state structure which has longer, partially formed bonds.

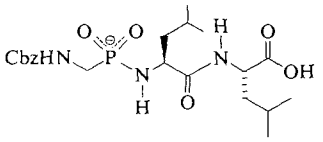

1

Phosphonamidate **1** was shown to be a transition-state analogue inhibitor by the synthesis of a series of analogues of inhibitor **1** and the corresponding substrates with substitutions at the carboxy-terminal amino acid and measurement of K_I and K_M/k_{cat} values, respectively. The K_I values correlated not with K_M values but with K_M/k_{cat} values, suggesting that the factors that influenced binding of inhibitors similarly affected binding of the transition state relative to the substrate.

Another important class of peptidase inhibitors consists of uncharged tetrahedral mimics of the transition state, including hydrated ketones,[10] fluoroketones,[11] and secondary alcohols.[12] One such molecule is pepstatin, an inhibitor of the aspartic protease pepsin.[13] The key feature of this inhibitor is the novel amino acid statine, which contains an uncharged secondary alcohol substituted for the carbonyl of the scissile amide bond in the substrate. An analysis similar to that performed in the case of thermolysin compared a series of inhibitor K_I values and substrate K_M/k_{cat} values for pepsin, but yielded inconclusive results due to the fact that two distinct rate constants contribute to the measured k_{cat} values for this enzyme.[10] The fact that pepstatin K_I values do not correlate with K_M or with K_M/k_{cat} values suggests that these inhibitors do not function exclusively as either transition-state analogue inhibitors or as multisubstrate inhibitors. Since statine-like compounds at least in part resemble the tetrahedral transition state for hydrolysis of an amide bond, we reasoned that antibodies raised against a statine-based inhibitor might catalyze the hydrolysis of the corresponding ester or amide substrates. Antibodies elicited against alcohol **2** do indeed catalyze the hydrolysis of *para*-nitrophenyl acetate and *para*-nitrophenyl methyl carbonate.

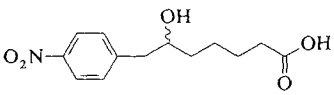

2

This study extends the transition-state stabilization strategy for generating catalytic antibodies to a new class of peptidase inhibitors. The kinetic properties of antibodies elicited toward statine-like inhibitor **2** are comparable with those of the more numerous phosphonate-specific antibodies.

2. Phosphate- and Phosphonate-Specific Antibodies

A large number of antibodies elicited against compounds that contain charged tetrahedral phosphorus and function as analogues of the transition states in hydrolytic reactions have been characterized and several examples are reviewed below.

2.1. Phosphorylcholine-Binding Antibodies MOPC 167 and T15

Two of the first catalytic antibodies characterized, MOPC 167 and T15, were not elicited against a synthetic immunogen but were members of a well-studied class of antibodies binding phosphorylcholine (PC). These antibodies had been previously characterized with regard to ligand-binding specificity,[14, 15] kinetics, and biomolecular structure.[16] Both are specific for *para*-nitrophenyl phosphorylcholine (**3**), which is an analogue of the transition-state **5** in the hydrolysis of *para*-nitrophenyl phosphorylcholine carbonate (**4**). Indeed, MOPC 167 and T15 catalyze the hydrolysis of **4** with kinetics obeying the Michaelis–Menten rate expression.[17, 18] The Michaelis constant K_M is equal to the

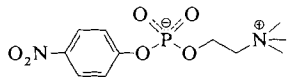

3

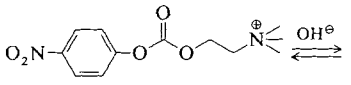

4

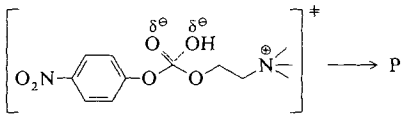

5

concentration of substrate, [S], that produces one-half the maximal catalyzed rate, $k_{cat}[E_T]$, where $[E_T]$ is the total enzyme concentration and k_{cat} is the unimolecular rate constant for the catalytic step. The k_{cat} and K_M values for MOPC 167 and T15 are $k_{cat} = 0.4\ min^{-1}$, $K_M = 208\ \mu M$ and $k_{cat} = 0.32\ min^{-1}$, $K_M = 708\ \mu M$, respectively. The highly specific nature of antibody–antigen recognition leads to highly specific catalysts. For example, *para*-nitrophenyl ethyl carbonate is not hydrolyzed to any appreciable extent by MOPC 167. The inhibition constants measured for MOPC 167 and T15 were 5 μM and 55 μM, respectively. Between pH 6.25 and 8.0, both antibody-catalyzed reactions were shown to be first order with respect to hydroxide ion. Comparison of the $OH^{\ominus}$-catalyzed rate $k_{OH}[OH^{\ominus}]$ (corrected for intramolecular assistance by the tetraalkylammonium ion) with the antibody-catalyzed rate k_{cat} affords rate accelerations of 11 500 for MOPC 167 and 9200 for T15. However, the observed differential binding energy of the transition-state analogue over the substrate (K_M/K_I) does not account for the entire rate acceleration, indicating that other factors must be contributing to the observed rate acceleration.

2.2. X-Ray Crystal Structure of the Phosphorylcholine-Specific Antibody McPC603

The X-ray crystal structure of McPC603, which is an antibody highly homologous to T15, has been solved.[16] This

crystal structure makes possible direct identification of the combining-site residues responsible for catalysis (Fig. 2).[19] Phosphorylcholine is bound in the cavity of McPC603 with the choline group deep in the interior and the phosphate toward the exterior, in contact with aqueous solvent. The heavy-chain residues, Tyr 33H and Arg 52H, which are invariant in all of the phosphorylcholine binding antibodies sequenced to date, bind the phosphate via hydrogen bonding and electrostatic interactions with the phosphoryl oxygen atoms. The X-ray structure demonstrates that the combining

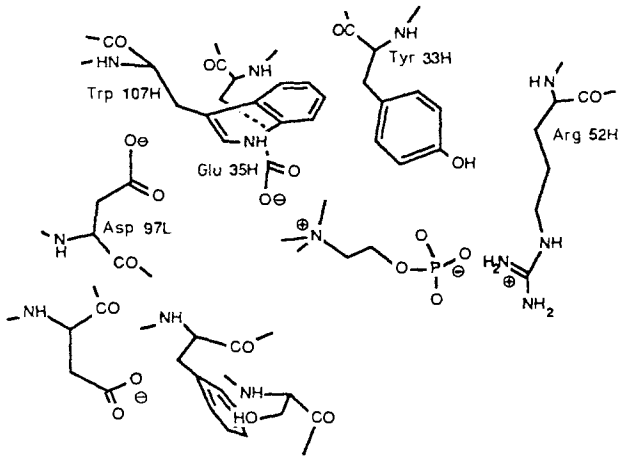

Fig. 2. Schematic representation of binding interactions between phosphorylcholine and amino acid side chains in the combining site of McPC603.

site of McPC603 is both sterically and electronically complementary to the tetrahedral, negatively charged phosphate moiety of phosphorylcholine. Inasmuch as this tetrahedral phosphate mimics the transition state for $OH^{\ominus}$-catalyzed hydrolysis of **4**, the phosphorylcholine antibodies should be capable of polarizing the bound carbonate for attack of hydroxide ion in the rate-determining step. Because the ground-state structure of **4** differs substantially from the transition-state configuration for hydrolysis, **5**, the differential binding affinity of the antibody to these two species is reflected in a lowered free energy of activation for the reaction.

2.3. Site-Directed Mutagenesis of the Phosphorylcholine-Specific Antibody S107

A site-directed mutagenesis study of the PC-specific antibody S107, which has the same heavy-chain variable sequence as T15, has further delineated the catalytic roles of residues Arg 52H and Tyr 33H.[20] Both residues were substituted with a variety of amino acids with no charge, with opposite charge, or with side chains designed to serve specific catalytic functions such as general acid or general base catalysis. One mutant (Tyr→His 33H) displayed increased catalytic activity over the wild-type antibody. The increase in activity is attributed to His 33H functioning as a general base.

The mutant S107 antibodies were expressed in myeloma cells not expressing endogenous antibody. The mutant DNA was introduced into the myeloma cells by electroporation using an azaserine/hypoxanthine selection. Large quantities of the mutants (1–50 mg) were isolated from ascites of immunosuppressed mice injected with the transfected cells.

Tyrosine 33H was mutated to Phe, Glu, Asp, and His in the study. Without exception, all mutants exhibited only slight increases in K_M for **4** compared to wild-type S107. With the exception of the His mutant, the effect of the Tyr mutations on the catalytic activity was small. These results suggest that Tyr 33H is not involved in binding or catalysis of the reaction being studied. By substituting His for Tyr at position 33H, a general base is placed in close proximity to the bound carbonyl carbon of **4** as shown by molecular modeling using the McPC603 crystal structure. Indeed, the His 33H mutant was shown to accelerate the hydrolysis of **4** by a factor of 6700 compared to methylimidazole free in solution. Alternatively, it might have been expected that placement of a general acid in the combining site, such as the β or γ carboxyl group of Asp or Glu, might also lead to enhanced catalysis relative to the wild type. The failure of these substitutions suggests that the formation of the negatively charged transition state in the hydrolysis of **4** is disfavored in the presence of the negatively charged carboxylates, at neutral pH.

Arginine 52H was mutated to Lys, Gln, and Cys. The Lys 52H mutant showed only slightly lowered catalytic efficiency compared to wild type S107. In contrast, the Gln 52H and Cys 52H mutants showed considerably lowered catalytic efficiencies, presumably due to the loss of positive charge necessary for stabilization of the negatively charged oxyanion in the transition state of the reaction. Consistent with this notion, the Gln 52H and Cys 52H mutants bound **3** much more weakly than wild-type S107, whereas the mutants showed little change in binding to the uncharged substrate **4**. The Cys mutation was introduced as a chemical handle to enable derivatization with cofactors or reporter molecules to generate semisynthetic catalytic antibodies.[21, 22] The mutagenesis study of S107 demonstrates the importance of electrostatic interactions in transition-state stabilization and also shows that the catalytic efficiency of a catalytic antibody can be enhanced by rational design.

2.4. Generation of Antibodies to Phosphonate and Phosphonamidate Transition-State Analogues

Besides antibodies that fortuitously bind transition-state analogues for carbonate hydrolysis, catalytic antibodies have been rationally designed to bind transition-state analogues for specific reactions. The hydrolysis of *para*-nitrophenyl methyl carbonate (**6**) proceeds through the tetrahedral negatively charged transition state **7**. The corresponding phosphonate transition-state analogue **8** was synthesized and coupled to protein carrier keyhole limpet hemocyanin (KLH).[23] Small molecules are not immunogenic by themselves and must be covalently attached to a protein in order to elicit an antibody response. Fourteen distinct monoclonal antibodies specific for **8** were isolated in this way and assayed for catalysis of the hydrolysis of *para*-nitrophenyl methyl carbonate (**6**) and *para*-nitrophenyl acetate (**9**). Two of these antibodies catalyzed the reaction and were inhibited

by free hapten **8**. Inhibition by free hapten strongly suggests that the catalysis observed is taking place in the antibody combining site. Antibody 48G7-4A1 catalyzed hydrolysis of ester **9** with $k_{cat} = 7.4\ min^{-1}$ and $K_M = 430\ \mu M$. The kinetic constants for the hydrolysis of the related carbonate **6** were $k_{cat} = 26.2\ min^{-1}$ and $K_M = 360\ \mu M$. The rate enhancements over the uncatalyzed rate are 1600 and 7300 for **9** and **6**, respectively. Inhibition studies demonstrated competitive inhibition by the free hapten **8** with $K_I = 330$ nM.

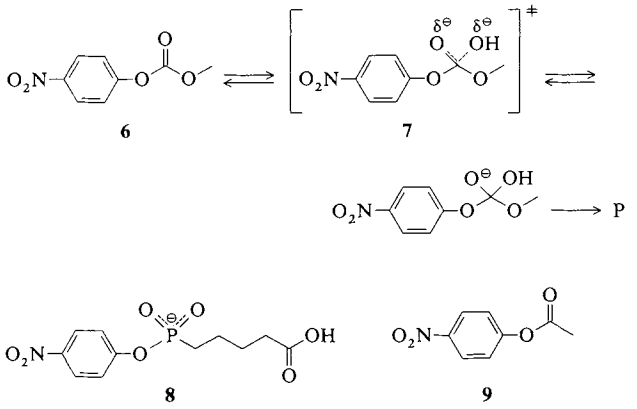

Several possible mechanisms could account for the catalysis observed: direct hydroxide attack, general base catalysis, or acyl-antibody formation followed by hydrolysis (Fig. 3).

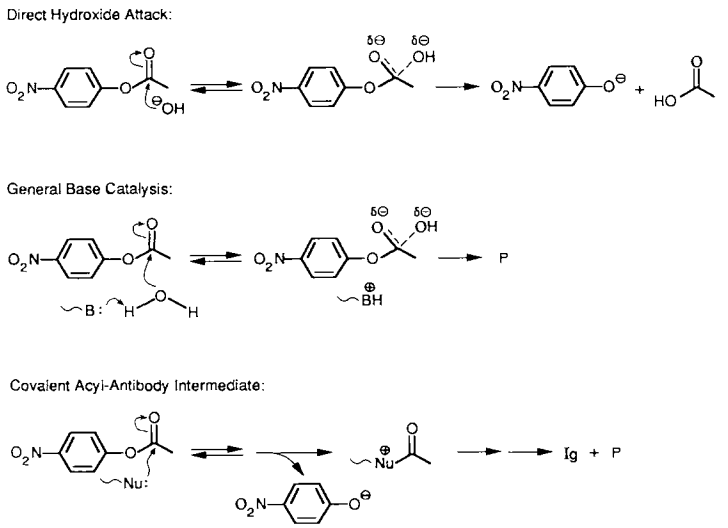

Fig. 3. Possible mechanisms for hydrolysis of **9** by antibody 48G7-4A1. Ig = immunoglobulin, p = product.

The pH dependence of antibody catalysis was shown to be first order with respect to hydroxide between pH 7.5 and 9.4, arguing for direct attack by hydroxide ion in this pH range. If the general base mechanism were responsible for the catalysis observed, the pH dependence of k_{cat} would reflect a dependence on the pK_a of a specific residue in the combining site. Note, however, that a general base could be present but its pK_a cannot lie in the range of 7.5–9.4. Kinetic analyses using high antibody concentrations were not consistent with a pre-steady-state burst of *para*-nitrophenolate and thus ruled out the third mechanism involving acyl-enzyme formation. Chemical modification studies revealed the presence of tyrosine, arginine, and histidine in the combining site of this antibody.[24] Interestingly, antibody S107, which catalyzes the hydrolysis of *para*-nitrophenyl choline carbonate (**4**) also has an arginine and a tyrosine, which were identified by chemical modification studies. Perhaps in analogy to S107, arginine serves to stabilize the oxyanion formed in the transition state for ester or carbonate hydrolysis.

The largest rate acceleration by an esterolytic antibody was achieved using a phosphonate transition-state analogue. *Lerner, Tramontano* et al. isolated twenty antibodies specific for compound **10** and found five which catalyzed the hydrolysis of ester **12**.[25] The kinetic constants measured for the most active antibody were $k_{cat} = 20\ s^{-1}$ and $K_M = 1.5$ mM. The free hapten **11** binds extremely tightly with $K_I = 50$ nM. The large difference in affinity of the antibody for the substrate versus the inhibitor accounts for most of the large rate acceleration achieved by this antibody, $k_{cat}/k_{uncat} = 6.25 \times 10^5$.

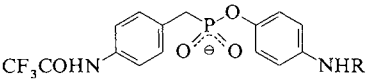

10, R = $(CH_2)_4COON(COCH_2)_2$
11, R = CH_3

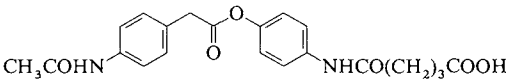

12

Antibodies have been shown to catalyze the stereospecific hydrolysis of unactivated esters. Antibodies elicited toward phosphonates **13** and **15** were shown to catalyze the hydrolysis of **15** and **16**, respectively, in a stereospecific manner. In both cases, antibodies were elicited against a racemic mixture of the hapten. Of eighteen antibodies specific for **13**, nine catalyzed the hydrolysis of (*R*)-**14** and two catalyzed the hydrolysis of (*S*)-**14**.[26] Two antibodies, one of each specificity, were further characterized. The rate acceleration for the hydrolysis of (*R*)-**14** by antibody 2H6 was 80 000, whereas the (*S*)-**14**-specific antibody 21H3 only showed a modest 1600-fold rate acceleration over the uncatalyzed reaction. The *R*/*S* selectivity is greater than 98%.

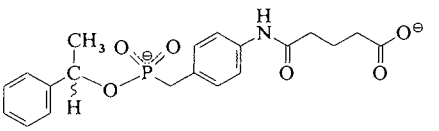

13

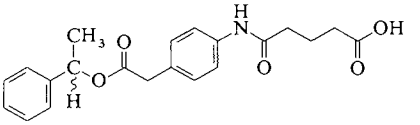

14

Of 25 antibodies isolated that were specific for the tripeptide phosphonate **15**, 18 accelerated the hydrolysis of the

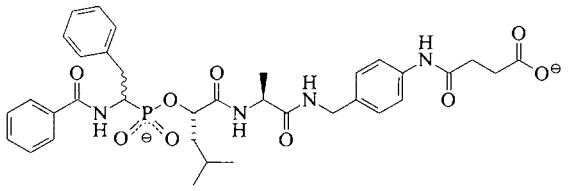

15

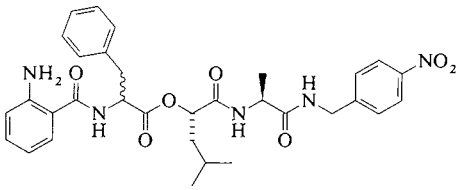

16

corresponding ester substrates.[27] It is interesting that an exclusive preference for antibodies of one specificity was observed. All 18 antibodies were selective for the D-phenylalanyl isomer of **16**. The selectivity for D- over L-phenylalanine at this position was greater than 99.5% for three of the five antibodies characterized. The modest rate accelerations of 50–300-fold may be a result of the size of the immunogen. The tetrahedral phosphonate contributes proportionally less to the overall binding energy of hapten to antibody than it does in smaller haptens. Note that substrate **16** also contains fluorogenic and quenching groups at the amino and carboxy termini, respectively. These groups allow hydrolysis of the substrate to be monitored by observing the fluorescence increase which occurs when the fluorescent 2-aminobenzoyl group is separated from the quenching 4-nitrobenzylamide group in the reaction. This sensitive assay may allow direct screening of ELISA[28] plates or of λ libraries expressing up to 10^6 different F_{ab} fragments,[29] greatly facilitating the production of catalytic antibodies. These two examples suggest that excellent stereoselectivities can be achieved by antibodies with large or small substrates and chiral centers in the alcohol portion or the acyl group portion of the substrate.

An antibody, NPN43C9, elicited against phosphonamidate **17** was shown to catalyze the hydrolysis of the activated amide bond in **18**.[30] A rate acceleration of 2.5×10^5 over

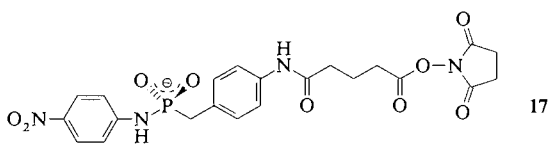

17

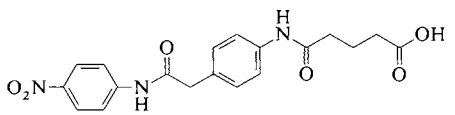

18

the uncatalyzed rate was reported. This rate acceleration is again much higher than the differential binding of the transition state over the substrate for the reaction, $\Delta\Delta G = -2.2$ kcal mol^{-1}. This difference in binding energy only accounts for a 100-fold rate acceleration. Again other factors such as acid/base catalysis must be responsible for the observed rate acceleration. In this context it was found that 150 mM NaCl completely inhibited antibody catalysis. The structural feature of this hapten responsible for induction of such acid/base catalysis is not apparent because the phosphonamidate NH group is not charged in the immunogen.

3. Statine-based Peptidase Inhibitors

In addition to negatively charged phosphonates, a number of uncharged transition-state analogues exist for hydrolytic enzymes. The most well characterized of these is the potent pepsin inhibitor pepstatin, which contains the novel amino acid analogue statine (Fig. 4). The measured K_I of pepstatin

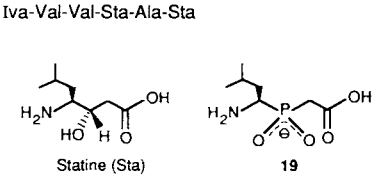

Fig. 4. Structures of pepstatin and the phosphinate analogue **19** of the novel amino acid statine.

for pepsin is 46 pM, making it one of the most potent enzyme inhibitors known. Statine is considered a dipeptide analogue which contains a hydroxyl group substituted for the carbonyl group of the scissile amide bond in pepsin substrates. The hydroxyl group is thought to displace an enzyme-bound water molecule which is contacted by the two catalytically important aspartate residues in pepsin. In the X-ray crystal structure of the complex formed between pepstatin and *Rhizopus chinensis* aspartic protease, the hydroxyl group is within hydrogen-bonding distance of the two aspartate residues.[30] Based on this structure, statine is considered to be a "collected" substrate analogue possessing binding determinants of both the peptide substrate and the enzyme-bound water responsible for addition to the scissile amide bond. The sp^3-hybridized carbon attached to the hydroxyl group mimics the tetrahedral transition state for amide bond hydrolysis.

A comparison between the two classes of inhibitors, phosphorus-based versus statine-based, can be made directly because the phosphinate analogue of statine, **19**, has been synthesized.[31] The K_I of the pepstatin-like peptide, where statine is substituted with the phosphinate analogue **19** is < 70 pM. Thus, the two classes of inhibitors display roughly the same inhibitory potency.

In addition to peptidase inhibitors, uncharged transition-state-analogue inhibitors of enzymes in nucleotide biosynthesis pathways have been isolated. Coformycin (**20**) inhibits the enzyme adenosine deaminase and is one of the most potent inhibitors known for any enzyme ($K_I = 2.5$ pM).[32] The enzyme converts adenosine into inosine, which involves the hydrolysis of the amidine moiety of adenine. Tetrahydrouridine (**21**) is another member of this class of inhibitors.[13] One interesting common feature of this class of inhibitors, which is not understood, is the slow binding nature of the inhibition observed. The rate constant for formation of the tight enzyme–inhibitor complex is exceedingly slow, the half-time for dissociation of coformycin from

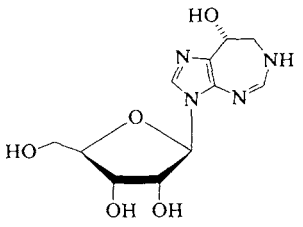

20

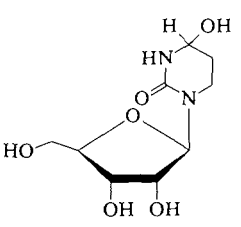

21

adenosine deaminase is 24 h. Based on the tight binding constants of these transition-state analogues, haptens with similar structural features might be expected to elicit catalytic antibodies.

4. Hydrolytic Antibodies Elicited toward an Uncharged Hapten

In this study we have generated five antibodies toward racemic 6-hydroxy-7-(4-nitrophenyl)heptanoic acid (**2**), which is a "statine-like" transition-state-analogue inhibitor for the hydrolysis of *para*-nitrophenyl acetate (**9**) and *para*-nitrophenyl methyl carbonate (**6**). This hapten was chosen because it is an uncharged hydroxyl-containing analogue of hapten **8**.[23] Direct comparison of the catalytic properties of antibodies elicited toward these different haptens is straightforward since they are designed to catalyze the same reactions. Indeed, one antibody, 7K16.2, was isolated which catalyzed the hydrolysis of **6** and **9**. This is the first example of the use of an uncharged hapten to elicit an esterolytic antibody. This is a surprising result considering the importance of charge–charge complementarity between the antibody combining site and the transition state as demonstrated by the mutagenesis study of the PC-binding antibody S107.[20] The hydroxy carboxylic acid **2** was prepared from adipic acid monoethyl ester and ethyl *para*-nitrophenylacetate via **22** and **23** (Scheme 1).

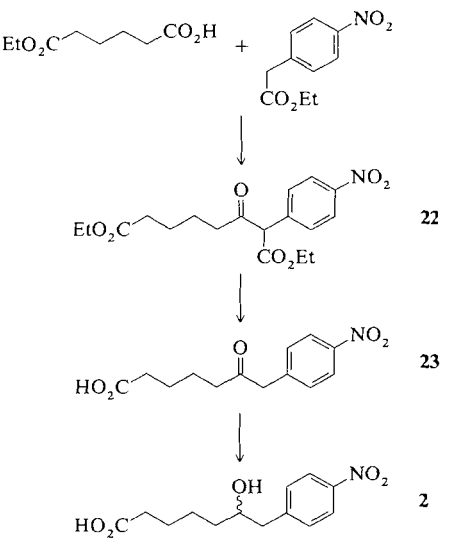

Scheme 1.

Experimental Procedure

22: To a stirred solution of adipic acid monoethyl ester (102.3 mg, 0.59 mmol) in 0.6 mL of tetrahydrofuran was added carbonyldiimidazole (100 mg, 0.62 mmol). The resulting mixture was allowed to stir at room temperature for 45 min. To a stirred solution of 0.62 mL (0.62 mmol) of 1 M sodium hexamethyldisilazide in tetrahydrofuran at −78 °C under argon was slowly added a solution of ethyl 4-nitrophenylacetate (123.3 mg, 0.59 mmol) in 0.5 mL of tetrahydrofuran to give a purple reaction mixture. After 5 min, the above solution of the imidazolide was slowly added. The resulting mixture was allowed to warm to 0 °C. After 30 min, it was allowed to warm to room temperature. After an additional 30 min, the reaction mixture was partitioned between dichloromethane and aqueous NH_4Cl. The organic phase was dried over $MgSO_4$ and then concentrated. The resulting residue was chromatographed on silica gel with 20% ethyl acetate in hexane to give 182 mg (0.5 mmol, 85%) of **22**. IR (thin film): $\tilde{\nu}$ [cm^{-1}] = 3000, 1730, 1650, 1600, 1520, 1350. ^{1}H NMR (250 MHZ, $CDCl_3$) (equilibrium mixture of keto and enol tautomers): δ = 1.20 (m, 6H), 2.2 (m, 4H), 2.55 (m, 3H), 4.15 (m, 4H), 4.81 (s, 1H), 7.33, 7.55 (d, 2H, J = 9 Hz), 8.21, 8.24 (d, 2H, J = 9 Hz). High-resolution FAB MS: m/z 366.1546 (M + H$^{\oplus}$).

23: A solution of **22** (145 mg, 0.4 mmol) in 2 mL of 40% aqueous H_2SO_4 was heated in an oil bath at 100 °C for 15 h. The cooled reaction mixture was diluted with water and then extracted with dichloromethane. The organic phase was washed with saturated aqueous NaCl, dried over $MgSO_4$, and then concentrated. The residue was chromatographed on silica gel with 5% methanol in ethyl acetate to give 44 mg (0.16 mmol, 42%) of **23**. IR (KBr): $\tilde{\nu}$ [cm^{-1}] = 2950, 1710, 1605, 1520, 1340. M.p. 103–105 °C. ^{1}H NMR (250 MHz, $CDCl_3$): δ = 1.63 (m, 4H), 2.36 (t, 2H, J = 7 Hz), 2.55 (t, 2H, J = 7 Hz), 3.83 (s, 2H), 7.36 (d, 2H, J = 9 Hz), 8.19 (d, 2H, J = 9 Hz). High-resolution FAB MS: m/z 266.1021 (M + H$^{\oplus}$).

2: To a stirred solution of **23** (44 mg, 0.16 mmol) in 1 mL of methanol at 0 °C was added sodium borohydride (13 mg, 0.34 mmol). After stirring at 0 °C for 1 h, the reaction mixture was allowed to warm to room temperature and then partitioned between dichloromethane and aqueous $KHSO_4$. The organic phase was dried over $MgSO_4$ and then concentrated to give 44 mg (0.16 mmol, 100%) of **2**. IR (KBr): $\tilde{\nu}$ [cm^{-1}] = 3000, 1710, 1700, 1600, 1510, 1320. M.p. 81–84 °C. ^{1}H NMR (250 MHz, $CDCl_3$): δ = 1.6 (m, 6H), 2.37 (t, 2H, J = 7 Hz), 2.79 (dd, 1H, J = 8, 14 Hz), 2.91 (dd, 1H, J = 4, 14 Hz), 3.90 (m, 1H), 7.38 (d, 2H, J = 9 Hz), 8.16 (d, 2H, J = 9 Hz). High-resolution FAB MS: m/z 268.1195 (M + H$^{\oplus}$).

4.1. Generation and Characterization of Antibody 7K16.2

The racemic hapten **2** was coupled to carrier proteins KLH and bovine serum albumin (BSA) by treatment of the *N*-hydroxysuccinimide-activated ester of **2** with the individual proteins at pH 9.0 in order to derivatize surface ε-amino groups of surface lysine residues.[33] The ratio of hapten to protein carrier, calculated by using UV difference spectroscopy (**2**: ε_{400} = 9100), was 7 per KLH monomer and 3 per BSA monomer.

Five monoclonal antibodies were isolated from the fusion of KLH–**2** conjugate-immunized Swiss Webster mouse spleenocytes with P3X63 myeloma cells.[34] Monoclonal antibodies were produced in vivo and isolated by affinity chromatography on Protein-A-coupled Sepharose 4B.[35] Following Protein A affinity chromatography, the antibodies were further purified by Pharmacia FPLC Mono S 10/10 cation-exchange column chromatography. Antibody was determined to be > 95% pure by 12.5% SDS polyacrylamide gel electrophoresis with Coomasie blue staining.[37] Of these five antibodies one (7K16.2) accelerated the hydrolysis of *para*-nitrophenyl acetate (**9**) and *para*-nitrophenyl methyl carbonate (**6**) and was inhibited by free hapten.

The 7K16.2-catalyzed reactions obeyed classical Michaelis–Menten kinetics. Lineweaver–Burke plots obtained at pH 7.5 were linear with kinetic constants k_{cat}(**9**) = 0.72 min^{-1} K_M(**9**) = 3.65 mM and k_{cat}(**6**) = 0.31 min^{-1}, K_M(**6**) = 3.33 mM (Fig. 5). The uncatalyzed rate constants under the same conditions are k_{uncat}(**9**) = 3.33×10^{-4} min^{-1} and k_{uncat}(**6**) = 3.2×10^{-4} min^{-1}. The antibody is competi-

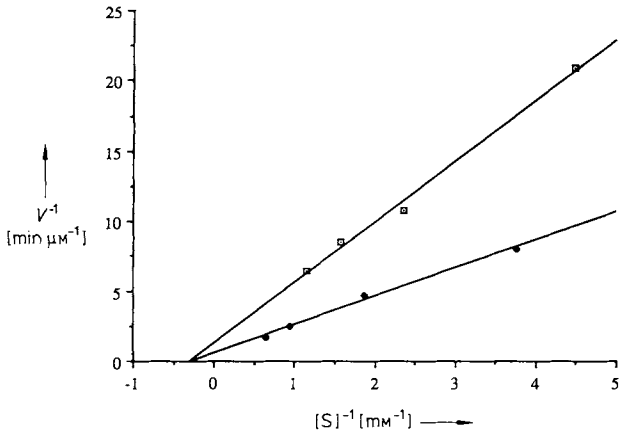

Fig. 5. Lineweaver–Burke plot for the hydrolysis of **6** (□) and **9** (◆) catalyzed by antibody 7K16.2. Velocities were determined spectrophotometrically by measuring the initial absorbance increase at 400 nm (*para*-nitrophenol λ_{max} = 400 nm (ε = 4.05)). The concentration of 7K16.2 was 2.5 μM as determined by absorbance at 280 nm using E(1 cm, 0.1%) = 1.37 and M_r = 150000 for IgG. Antibody 7K16.2 was preincubated at 30 °C in 10 mM sodium phosphate, 100 mM NaCl, pH 7.5. The reaction was initiated by adding 10 μL of a stock solution of **6** or **9** in tetrahydrofuran (THF) to give a final THF concentration of 2%. The uncatalyzed rate was measured under the same conditions, affording k_{uncat} (**6**) = 3.2×10^{-4} min^{-1}, k_{uncat} (**9**) = 3.3×10^{-4} min^{-1}.

tively inhibited by free hapten **2** with a K_I of 140 μM (Fig. 6).[38] As in other examples of hydrolytic catalytic antibodies, the differential binding energy between the substrate and inhibitor, $K_M(\mathbf{6})/K_I = 24$, $K_M(\mathbf{9})/K_I = 26$, found with antibody 7K16.2 does not account for the full rate acceleration observed, $k_{cat}(\mathbf{6})/k_{uncat}(\mathbf{6}) = 930$; $k_{cat}(\mathbf{9})/k_{uncat}(\mathbf{9}) =$

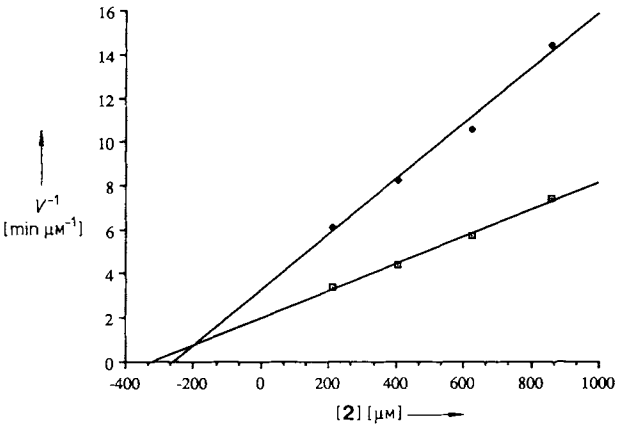

Fig. 6. Dixon plot of inhibition of antibody 7K16.2 by **2**. Antibody concentration was 2.5 μM. Data were obtained at two concentrations of substrate **9**: 500 μM (◆) and 1 mM (□). Buffer conditions are as described in Figure 5.

2250. For the identical reaction catalyzed by antibody 48G7-4A1 raised against phosphonate **8**, the differential binding energy is $K_M(\mathbf{6})/K_I(\mathbf{8}) = 1300$, compared to the observed rate accelerations of $k_{cat}(\mathbf{6})/k_{uncat}(\mathbf{6}) = 7300$. However, the disparity between the two values is much more pronounced in the case of antibody 7K16.2, suggesting that other factors (such as immunological diversity) contributing to the catalysis besides transition-state stabilization are of greater relative importance than was the case for antibody 48G7-4A1. In order to more definitively determine the differences between catalysts elicited toward different classes of inhibitors, large numbers of antibodies must be analyzed. With recent λ-library technology these statistically significant numbers of different antibodies may be accessible.[29]

Catalysis by 7K16.2 of a more energetically demanding hydrolytic reaction was also explored. The rate of hydrolysis of *para*-nitrophenylacetanilide at pH 9.0 was not accelerated by this antibody as determined by an HPLC assay, using *para*-nitrobenzamide as an internal standard. In a separate study, antibodies were elicited against a KLH–coformycin conjugate. None of the eight coformycin-specific antibodies accelerated the conversion of adenosine to inosine ($k_{uncat} = 1.8 \times 10^{-10}$ s^{-1}) as measured by an ammonia release assay.[39] It is possible that further screening of antibodies specific for these haptens will yield catalytic antibodies.

5. Outlook

In the past five years the diversity of the immune system has been exploited to generate catalysts capable of carrying out many different transformations. Moreover, a number of successful strategies have been developed to produce catalytic antibodies. Several strategies have yet to be demonstrated such as the use of strain to destabilize substrates as well as genetic screens and selections to identify more active catalysts generated by random and directed mutagenesis. The efficient and selective hydrolysis of peptides, nucleic acids, and carbohydrates continue to be major targets for catalysis by antibodies. Clearly, the antibody molecule will play an increasingly important role in chemistry. In addition, exciting new approaches for tapping the diversity of biological systems are being developed.[36,40–41] These advances will no doubt lead to new molecules with novel biological properties in much the same fashion as the development of antibody catalysts.

Received: July 24, 1990 [A 793 IE]
German version: *Angew. Chem. 102* (1990) 1339

[1] M. M. Davis, P. J. Bjorkmann, *Nature (London) 334* (1988) 395.
[2] P. G. Schultz, *Angew. Chem. 101* (1989) 1336; *Angew. Chem. Int. Ed. Engl. 28* (1989) 1283.
[3] P. G. Schultz, *Acc. Chem. Res. 22* (1989) 287.
[4] K. M. Shokat, P. G. Schultz, *Annu. Rev. Immunol. 8* (1990) 335.
[5] P. G. Schultz, R. A. Lerner, S. J. Benkovic, *Chem. Eng. News 68* (1990) No. 22, p. 26.
[6] W. P. Jencks: *Catalysis in Chemistry and Enzymology*, McGraw-Hill, New York 1969.
[7] L. Pauling, *Am. Sci. 36* (1948) 51.
[8] R. Wolfenden, *Annu. Rev. Biophys. Bioeng. 5* (1976) 271.
[9] P. A. Bartlett, C. K. Marlowe, *Biochemistry 22* (1983) 4618.
[10] M. W. Holladay, F. G. Salituro, D. H. Rich, *J. Med. Chem. 30* (1987) 374.
[11] K. N. Allen, R. H. Abeles, *Biochemistry 28* (1989) 135.
[12] W. M. Kati, D. T. Pals, S. Thaisrivongs, *Biochemistry 26* (1987) 7621.
[13] D. R. Rich, *J. Med. Chem. 28* (1985) 263.
[14] A. M. Goetze, J. H. Richards, *Biochemistry 16* (1977) 228.
[15] L. G. Bennett, C. P. Glaudemans, *Biochemistry 18* (1979) 3337.
[16] D. M. Segal, E. A. Padlan, G. H. Cohen, S. Rudikoff, D. Potter, D. R. Davies, *Proc. Natl. Acad. Sci. USA 71* (1974) 4298.
[17] S. J. Pollack, J. W. Jacobs, P. G. Schultz, *Science (Washington D.C.) 234* (1986) 1570.
[18] S. J. Pollack, P. G. Schultz, *Cold Spring Harbor Symp. Quant. Biol. 52* (1987) 97.

[19] Y. Satow, G. H. Cohen, E. A. Padlan, D. R. Davies, *J. Mol. Biol. 190* (1986) 593.
[20] D. Y. Jackson, J. R. Prudent, E. P. Baldwin, P. G. Schultz, *Proc. Natl. Acad. Sci. USA 87* (1990), in press.
[21] S. J. Pollack, G. R. Nakayama, P. G. Schultz, *Science (Washington D.C.) 242* (1988) 1038.
[22] S. J. Pollack, P. G. Schultz, *J. Am. Chem. Soc. 111* (1989) 1929.
[23] J. W. Jacobs, P. G. Schultz, R. Sugasawara, M. Powell, *J. Am. Chem. Soc. 109* (1988) 2174.
[24] J. W. Jacobs, *Dissertation*, University of California, Berkeley 1989.
[25] A. Tramontano, A. A. Ammann, R. A. Lerner, *J. Am. Chem. Soc. 110* (1988) 2282.
[26] K. D. Janda, S. J. Benkovic, R. A. Lerner, *Science (Washington D.C.) 224* (1989) 437.
[27] S. J. Pollack, P. Hsuin, P. G. Schultz, *J. Am. Chem. Soc. 111* (1989) 5961.
[28] E. Engvall, P. Perlmann, *J. Immunol. 109* (1972) 129.
[29] W. D. Huse, L. Sastry, S. A. Iverson, A. S. Kang, M. Alting-Mees, D. R. Burton, S. J. Benkovic, R. A. Lerner, *Science (Washington D.C.) 246* (1989) 1275.
[30] K. D. Janda, D. Schloeder, S. J. Benkovic, R. A. Lerner, *Science 241* (1988) 1188.
[31] P. A. Bartlett, W. B. Kezer, *J. Am. Chem. Soc. 106* (1984) 4282.
[32] L. Frick, J. P. Mac Neela, R. Wolfenden, *Bioorg. Chem. 15* (1987) 100.
[33] B. Erlanger, *Methods Enzymol. 70* (1980) 85.
[34] R. Sugasawara, C. Prato, J. Sippel, *Infect. Immun. 42* (1983) 863.
[35] G. Kronvall, H. Grey, R. Williams, *J. Immunol. 105* (1972) 1116.
[36] C. Tuerk, L. Gold, *Science (Washington D.C.) 249* (1990) 505.
[37] U. Laemmli, *Nature (London) 227* (1970) 680.
[38] G. Dixon, *Biochem. J. 55* (1953) 170.
[39] A. L. Chaney, E. P. Marbach, *Clin. Chem. 8* (1962) 130.
[40] J. J. Devlin, L. C. Panganiban, P. E. Devlin, *Science (Washington D.C.) 249* (1990) 404.
[41] J. K. Scott, G. P. Smith, *Science (Washington D.C.) 249* (1990) 386.

Perspectives in Supramolecular Chemistry—From Molecular Recognition towards Molecular Information Processing and Self-Organization

By Jean-Marie Lehn*

The selective binding of a substrate by a molecular receptor to form a supramolecular species involves molecular recognition which rests on the molecular information stored in the interacting species. The functions of supermolecules cover recognition, as well as catalysis and transport. In combination with polymolecular organization, they open ways towards molecular and supramolecular devices for information processing and signal generation. The development of such devices requires the design of molecular components performing a given function (e.g., photoactive, electroactive, ionoactive, thermoactive, or chemoactive) and suitable for assembly into an organized array. Light-conversion devices and charge-separation centers have been realized with photoactive cryptates formed by receptors containing photosensitive groups. Electroactive and ionoactive devices are required for carrying information via electronic and ionic signals. Redox-active polyolefinic chains, like the "caroviologens", represent molecular wires for electron transfer through membranes. Push-pull polyolefins possess marked nonlinear optical properties. Tubular mesophases, formed by organized stacking of suitable macrocyclic components, as well as "chundle"-type structures, based on bundles of chains grafted onto a macrocyclic support, represent approaches to ion channels. Lipophilic macrocyclic units form Langmuir–Blodgett films that may display molecular recognition at the air–water interface. Supramolecular chemistry has relied on more or less preorganized molecular receptors for effecting molecular recognition, catalysis, and transport processes. A step beyond preorganization consists in the design of systems undergoing self-organization, that is, systems capable of spontaneously generating a well-defined supramolecular architecture by self-assembling from their components under a given set of conditions. Several approaches to self-assembling systems have been pursued: the formation of helical metal complexes, the double-stranded helicates, which result from the spontaneous organization of two linear polybipyridine ligands into a double helix by binding of specific metal ions; the generation of mesophases and liquid crystalline polymers of supramolecular nature from complementary components, amounting to macroscopic expression of molecular recognition; the molecular-recognition-directed formation of ordered solid-state structures. Endowing photo-, electro-, and ionoactive components with recognition elements opens perspectives towards the design of programmed molecular and supramolecular systems capable of self-assembly into organized and functional supramolecular devices. Such systems may be able to perform highly selective operations of recognition, reaction, transfer, and structure generation for signal and information processing at the molecular and supramolecular levels.

1. Introduction

Supramolecular chemistry, the chemistry beyond the molecule, is the *designed* chemistry of the intermolecular bond, just as molecular chemistry is that of the covalent bond.[1–3] It is a highly interdisciplinary field of science covering the chemical, physical, and biological features of chemical species held together and organized by means of intermolecular (noncovalent) binding interactions. This relatively young area has been defined, conceptualized, and structured into a coherent system. Its roots extend into organic chemistry and the synthetic procedures for receptor construction, into coordination chemistry and metal-ion–ligand complexes, into physical chemistry and the experimental and theoretical studies of interactions, and into biochemistry and the biological processes that all start with substrate binding and recognition. A major feature is the range of perspectives offered by the cross-fertilization of supramolecular chemical research due to its location at the intersection of chemistry, biology, and physics. Such wide horizons are a challenge and a stimulus to the creative imagination of the chemist.

Earlier research has been thoroughly reported and discussed in numerous books, chapters, reviews (see, for instance, Refs. [1–12]), and publications devoted to the basic aspects of supramolecular chemistry, molecular recognition, reactivity and catalysis, and transport processes. Our own work has been reviewed in recent papers[1–3] which contain references to earlier publications.

Based on the chemical, physical, and biological features of supramolecular systems, novel lines of investigation have developed, concerned with the design of molecular devices and of systems displaying higher forms of molecular and supramolecular behavior such as self-organization, regula-

[*] Prof. J.-M. Lehn
Institut Le Bel, Université Louis Pasteur
4, rue Blaise Pascal, F-67000 Strasbourg (France)
and
Collège de France
11, Place Marcelin Berthelot, F-75005 Paris (France)

tion, cooperativity, communication, and replication. One may note that a common thread of all areas of supramolecular chemistry is the *information*[3, 4] stored in the structural (and eventually temporal) features of molecules and supermolecules. Thus, it is a kind of *molecular information science* or *molecular "informatics"* that is progessively shaping up.

The present article will build on the most recent of the previous reviews,[3] focusing on the lines of development that lead from molecular recognition to the various aspects of handling information and signals at the molecular and supramolecular levels.

2. Molecular Recognition, Information, and Signals: Semiochemistry

The selective binding of a substrate by a molecular receptor to form a supermolecule involves *molecular recognition*, which rests on the *molecular information*[4, 13] stored in the interacting partners. It requires the design of receptors possessing steric and electronic features complementary to those of the substrate to be bound and a balance between rigidity and flexibility suitable for the function to be performed. Such organization of molecular structural and dynamical features has been at the origin of the development of the cryptands[4] and other types[5 - 11] of more or less rigidly built ligand molecules.

Molecular recognition events represent the basis of information processing at the supramolecular level. They may give rise to changes in electronic, ionic, optical, and conformational properties and thus translate themselves into the generation of a signal. A great variety of receptor molecules has been designed for effecting the recognition of numerous and very diverse types of substrates (spherical, tetrahedral, linear or branched, charged or neutral, organic, inorganic or biological, etc.). Structural units have been incorporated that may respond to or be perturbed by external factors. Most investigations have focused on *endo-receptors* in which the binding (information) sites are oriented into a molecular concavity; *exo-receptors*, with outward-directed sites, present "informed" surfaces on which recognition may occur.[3] By making use of the three-dimensional information storage/readout operating in molecular (endo- or exo-) recognition, in combination with substrate transformation and translocation, one may design components for *molecular devices* that would be capable of processing information and signals at the molecular and supramolecular levels. The resulting area of investigation may be termed *semiochemistry* (from the greek σημεῖον: sign, signal), the chemistry of molecular signal generation, processing, transfer, conversion, and detection.[14]

3. Molecular and Supramolecular Devices

Molecular devices have been defined as structurally organized and functionally integrated chemical systems built into supramolecular architectures.[3] They are based on specific components arranged in a suitable manner. The *function* performed by a device results from the integration of the *elementary acts* performed by the components. The components may, for instance, be photoactive, electroactive or ionoactive, depending on whether they operate with photons, electrons, or ions.

Molecular recognition processes may play a role at several key levels: (1) the building up of the device from its components; (2) its incorporation into supramolecular arrays; (3) the selective operation on given species (e.g., ions); (4) the response to external physical or chemical stimuli (light, electrons, ions, molecules, etc.) that may regulate the operation of the device and switch it on or off; (5) the nature of the signals generated and signal conversion effected (photon/photon, photon/electron, electron/electron, electron/ion, ion/ion, etc.)

Recognition-dependent devices, which one may term *informed molecular devices*, represent the molecular and supramolecular entities by which molecular recognition events may be transduced into information and signals. This requires the design of receptor components responding to external stimuli and suitable for incorporation into devices.

Our work has been concerned with various aspects of device chemistry, related in particular to basic device design and to recognition-dependent processes. The present description extends an earlier article in *Angewandte Chemie*.[3]

3.1. Molecular Photonic Devices

Compared to the isolated components, supramolecular entities containing photoactive components may display novel properties, thus defining a *supramolecular photochemistry*.[15 - 17] Various processes may take place within these *photochemical molecular devices*, modulated by the arrangement of the bound units as determined by the organizing receptor: photoinduced energy migration, charge separation by electron or proton transfer, perturbation of optical transitions and polarizabilities, modification of redox potentials in ground or excited states, photoregulation of binding properties, selective photochemical reactions, etc. These processes may depend on recognition events and occur only if the correct selective binding of the complementary active components takes place, as illustrated for a two-component case in Figure 1 (see also Fig. 10 in Ref. [3]).

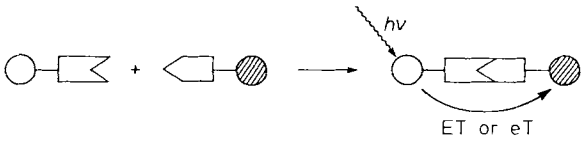

Fig. 1. Molecular-recognition-dependent photochemical molecular devices. Photochemical processes such as energy transfer (ET) or photoinduced electron transfer (eT) may be induced via association of two (or more) complementary units, each bearing a component of the device; the complementary units may be as small as heterocyclic bases or as large as antigen–antibody conjugates.

In principle, molecular photonic devices require a complex organization and adaptation of the components in space, energy, and time, leading to the generation of optical, electronic, protonic, or ionic photosignals.

3.1.1. Light Conversion by Energy Transfer

Conversion of absorbed light into emitted light of another wavelength occurs in any luminescent species. One would like, however, to perform *separately* the various steps of the overall process by means of different components that may be optimized for a given purpose (wavelength of absorbed or emitted light; lifetime of emission, etc.). This is the case for a *light-conversion molecular device* consisting of two components, a *light collector* (or *antenna*) formed by an array of absorbing units and an *emitter*, which allow separate optimization of absorption and emission. In order to function, intercomponent *energy transfer* must occur (as efficiently as possible). Thus, such a device operates in a three-step mode: absorption–energy transfer–emission (A–ET–E, Fig. 2).

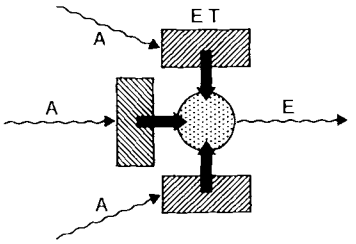

Fig. 2. Light-conversion photochemical molecular device, consisting of two components, a light collector (or antenna, light-absorbing groups A) and a light emitter E, and performing a three-step process: absorption (A), energy transfer (ET), and emission (E).

This has been realized in europium(III) and terbium(III) cryptates of macrobicyclic ligands that incorporate various heterobiaryl groups (2,2'-bipyridine, phenanthroline,[18, 19] bithiazole, biimidazole, bipyrimidine,[20] biisoquinoline,[21] and their *N,N'*-dioxides[21, 22]) serving as light-collecting antenna components. These complexes present a unique combination of features arising from both their cryptate structure and the nature of the emitting species: protection of the included ion from deactivation due to interaction with solvent (water) molecules; very high thermodynamic stability and kinetic inertness; multiple absorbing groups suitable for ET; characteristic long wavelength (for Eu^{III}) and long lifetime of the emission. They display a bright luminescence that results from UV light absorption by the organic groups followed by energy transfer to the included lanthanoid cation which then emits its characteristic visible radiation.[16, 20–24] The corresponding A-ET-E process is shown for the cryptate **1**.

Higher conversion efficiency and stronger luminescence are found for europium cryptates such as **2**[21] containing *N*-oxide ligands.[22] In the solid state, complex **1** exhibits especially high energy-conversion efficiency (about 60%).[25] This is also the case for the corresponding Tb^{III} cryptate up to about 100 K; at higher temperature, energy migration and back-transfer from the ion to the cryptand decreases the emission intensity.[26] Since the nature of the ligand groups strongly influences the photophysical properties, it may be possible to tune them to the desired purposes by suitable structural variations.

Such photoactive cryptates are of interest as novel luminescent materials (in solution or in the solid state) and as labels for biological applications subject to very stringent constraints (labeling of monoclonal antibodies, oligonucleotides, membrane components; cytofluorimetry, etc.). Linked, cascade systems performing very long range energy transfer (VLRET) may be imagined.

3.1.2. Ion-Binding Luminophores

Photosensitive receptor molecules may display marked modifications in their photophysical properties on binding of substrate species, allowing their detection by absorption or emission measurements.[27] They represent molecular devices for *substrate-selective optical signal generation.*

Cryptands such as **3** combine the strong complexing ability of cryptands and the intense fluorescence emission of the anthracene group. They display dramatic changes in fluorescence emission upon complexation of alkali-metal cations and protonation.[28]

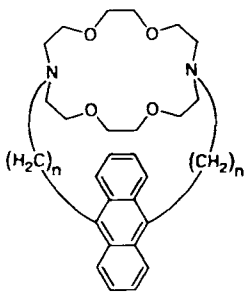

3 (n = 2, 3)

Of special interest is the strong enhancement of the acridine fluorescence observed when adenosine triphosphate binds to a receptor molecule formed by a $[24]N_6O_2$ macrocycle bearing a lateral acridine group.[29] Double recognition

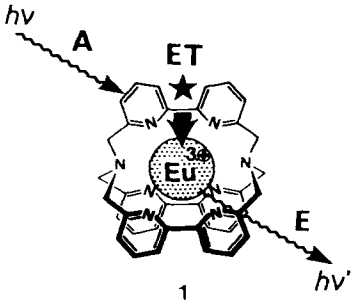

1

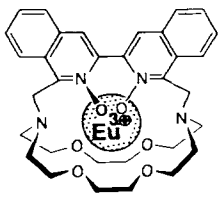

2

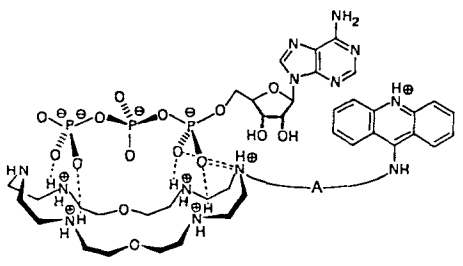

4, A = CH_2-CH_2-CH_2

occurs via binding of the triphosphate group to the protonated macrocycle and stacking of the adenine unit with the dye residue, as shown in **4**. Furthermore, guanosine triphosphate slightly decreases the emission. Thus, this receptor is a *sensitive* and *selective ATP probe* that generates a fluorescence signal on ATP binding.

3.1.3. Photoinduced Electron Transfer in Photosensitive Cryptates

Irradiation of a device containing a photosensitizer (PS) as well as suitable donor (D) and acceptor (A) groups may induce electron transfer, generating the charge-separated state $D^{\oplus}$-PS-$A^{\ominus}$. Such processes are being investigated very actively in view of their interest in photosynthesis and in photocatalysis.[15a]

Our own work has been concerned with photoinduced charge separation in macropolycyclic coreceptors containing both a photosensitive porphyrin group and binding sites for silver(I) ions as acceptor centers. Irradiation leads to transfer of an electron from the porphyrin to Ag^{I}, generating a porphyrinium cation of long lifetime. The efficiency of the charge separation is much higher in these coreceptor species than in the nonlinked model compounds.[16, 30]

Systems undergoing photoinduced electron-transfer processes represent components for *light-to-electron conversion devices*. Of special interest is the design of systems capable of performing long-range electron transfer (see Section 3.2.3), for instance, to generate transmembrane photoelectric signals or to serve as the basis of an electronic shift register memory at the molecular level.[41c]

3.1.4. Photoinduced Reactions in Supramolecular Species

Receptor molecules that contain suitable light-sensitive groups may undergo structural and conformational changes that affect their binding properties.[31a] As a consequence, substrate uptake or release occurs, representing a way to generate protonic or ionic photosignals in *light-to-ion conversion devices* (see also Section 3.3).

Receptor-substrate binding may affect their photochemical reactivity. The recognition process could thus modify the course of a reaction, affecting its rate or the nature of the products. For instance, the binding of cobalt(III) hexacyanide by macrocyclic polyammonium receptors markedly affects their photoaquation quantum yield in a structure-dependent manner.[32] One may imagine a number of other photoreactions whose course could be altered by selective binding.

In this way, recognition is expressed via a chemical transformation, in the nature or the rate of formation of the products, amounting to the generation of a specific molecular signal.

3.1.5. Nonlinear Optical Effects in Supramolecular Species

Highly polarizable molecules may be expected to present marked optical nonlinearities.[33] Novel effects should arise on going from the molecular to the supramolecular level.[34] Incorporation into supramolecular arrangements may influence the properties of the individual molecules by orientation and/or perturbation of their electronic properties.

Of special interest are push-pull polyenes, composed of a polyolefinic chain bearing a donor group on one end and an acceptor on the other end. In the course of our studies on molecular wires of caroviologen type (see below), a number of push-pull carotenoid derivatives were also synthesized in order to investigate their nonlinear optical properties. These are highly polarizable conjugated polyenes that also represent polarized molecular wires (Fig. 3). They have been found to display marked second harmonic generation as powdered samples.[35] The determination of the hyperpolarizabilities in solution gave exceptionally large values for the longer of these compounds.[36] Incorporation of such a compound into Langmuir–Blodgett films yields oriented arrangements of interest for nonlinear optical studies.[37]

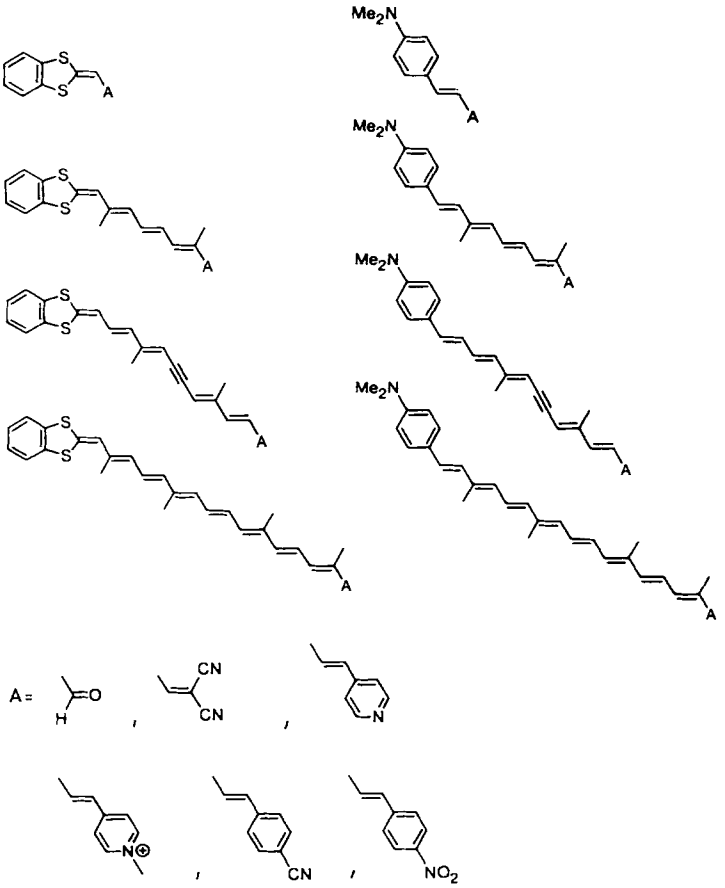

Fig. 3. Structures of a series of donor–acceptor carotenoid (D-C-A) derivatives.

If a highly polarizable group is introduced into a receptor molecule, substrate binding may cause substantial perturbations, so that the recognition event will be converted into a nonlinear optical signal. Such recognition-dependent nonlinear optical probes may be derived from polyenes such as those shown in Figure 3.

All the photochemical and photophysical processes discussed above may be coupled to recognition processes, as already pointed out. Thus emerges the area of recognition-dependent molecular photonics, the transduction of molecular information into photosignals.

3.2. Molecular Electronic Devices

Molecular devices operating on electrons are basic elements for converting molecular recognition events into electronic signals. For example, redox properties may be affected by binding in a structure-dependent manner. This is the case for the complexation of metal hexacyanides by polyammonium macrocycles where the shift in redox potential depends on the binding constant.[38] Such perturbations by complexation lead to an electrochemical characterization of recognition. Electrochemical effects resulting from receptor–substrate binding define a domain of *supramolecular electrochemistry*.

Much interest has been shown in the possibility of designing electronic devices that would operate at the molecular level (for recent discussions see, for instance, Refs. [39–41]). This involves several steps. It is first necessary to imagine a molecule that may possess the desired features, synthesize it, and study its properties. The second step is to incorporate it into supramolecular architectures, such as membranes or other organized structures, and to investigate whether the resulting entity possesses the required properties. The third step requires the connection of the basic unit to other components, in order to address it via relay molecules or with an external physical signal. Of course, the goal of designing molecular electronic circuitry may have many spin-offs along the way, in addition to raising novel questions about the handling of molecules. It is probably premature to try to define clearly the routes to the goal; indeed, the definition of the goal itself may change under the influence of progress made along a given path.

The possibility of designing devices such as molecular rectifiers, transistors, switches, and photodiodes has been envisaged and some of the required features are present in compounds such as metal complexes or D-PS-A systems (see above) that lead to photoinduced charge separation at the level of the isolated molecule.[15a]

3.2.1. Caroviologens as Molecular Wires

Among the various devices and components performing molecular-scale electronic functions that may be imagined, a crucial one is a *molecular wire*, which might operate as a connector permitting electron flow to occur between the different elements of a molecular electronic system.

Our first approach towards the design of molecular wires was based on the *caroviologens* ($CV^{2\oplus}$), long, conjugated polyolefinic chains bearing pyridinium groups at each end, which combine the structural features of carotenoids with the redox properties of methylviologen. Such compounds (e.g., **5a**) were synthesized and shown to be incorporated in a transmembrane fashion into dihexadecyl phosphate (DHDP) vesicles.[42]

The orientation of caroviologens in model lipid membranes was studied by linear dichroism measurements. Dichroic ratios were determined on caroviologens of different lengths solubilized in lyotropic lamellar phases of different thicknesses and macroscopically aligned between quartz plates. The orientation parameters obtained indicated transmembrane arrangement for caroviologens of length compatible with the bilayer thickness of the membrane.[43]

Electron-transfer experiments employing the initial $CV^{2\oplus}$/DHDP vesicle system did not give positive results, perhaps because of the high negative charge of the membrane surfaces, which might reduce interfacial electron transfer rates and modify the redox potential of incorporated $CV^{2\oplus}$.

Zwitterionic caroviologens $CV^{2\oplus}$ such as **5b** were therefore prepared[44] and incorporated into phospholipid vesi-

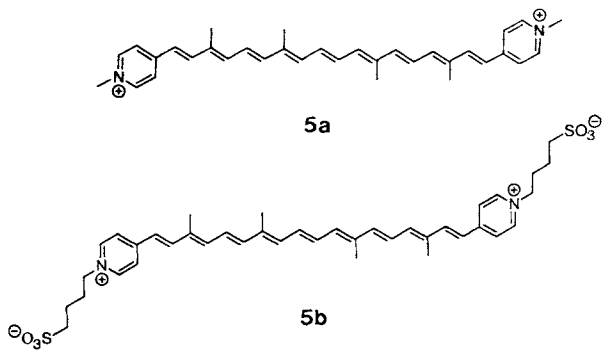

cles.[45] Electron-transfer experiments were performed between an external reducing phase and an internal oxidizing phase, as shown in Figure 4; only a small amount of incorporated $CV^{2\oplus}$ was used in order to be able to study the effect of a few molecules per vesicle.[45] The rate of reduction of the internal oxidant ferricyanide to ferrocyanide was accelerated by a factor of about 4, which, although small, nevertheless clearly indicated that electron conduction did occur. No measurable rate acceleration was produced by lipophilic viologens under the same conditions.

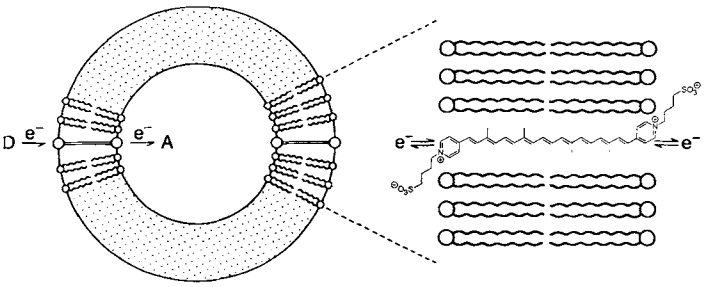

Fig. 4. Schematic representation of transmembrane electron transfer from a reducing agent (such as sodium dithionite) to an oxidizing agent (such as potassium ferricyanide) by a zwitterionic caroviologen such as **5b**, incorporated in the bilayer membrane of a phospholipid vesicle.

Thus, the caroviologen approach does produce *functional molecular wires* that effect electron conduction in a supramolecular-scale system. Incorporation into black lipid bilayer membranes (BLMs) should allow further investigations of the electron-transfer properties of these caroviologens.[46] Other approaches to molecular wires may also be envisaged (see below).

3.2.2. Polarized Molecular Wires

Conjugated polyolefinic chains bearing an electron-acceptor group on one end and a donor on the other end represent

polarized molecular wires that should display preferential *one-way electron transfer* and act as a *rectifying component*.

Such molecules, donor–acceptor carotenoids (cf. Fig. 3), were prepared and shown to possess very pronounced *nonlinear optical properties* in powder form,[35] in solution,[36] or in Langmuir–Blodgett films[37] (see above). Oriented incorporation into vesicles and electron-transfer experiments might reveal one-way conduction by polarized molecules of this or similar type.

3.2.3. *Modified and Switchable Molecular Wires*

Modifications on the original $CV^{2\oplus}$ type of molecular wire may be made on the terminal groups or on the conjugated chain or on both. The carotenoid chain might be replaced, for instance, by extended dye systems, oligopyrroles, or oligothiophenes or strings of redox centers allowing electron "hopping". We first performed variations on the terminal groups.

Carotenoid chains bearing ferrocene, 2,2'-bipyridine, and pyridine as terminal groups have been prepared (see **6** and **7**). Metal complex derivatives, such as **8**, were also obtained.[47a] These *metallocarotenate* type of molecular wires combine the rich electrochemical and photochemical activities of metal complexes with the long-range conjugation properties of carotenoid chains, thus leading the way towards systems capable of performing electro- or photoinduced very long range electron transfer (VLReT).[48] The redox-active ferrocene unit has also been introduced into donor–acceptor type conjugated systems (as in **9a** and **9b** or its metal complexes) to serve as donor center or redox switch.[47b]

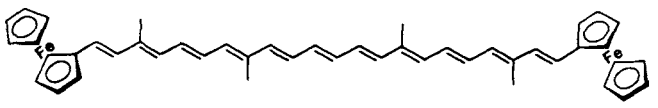

6

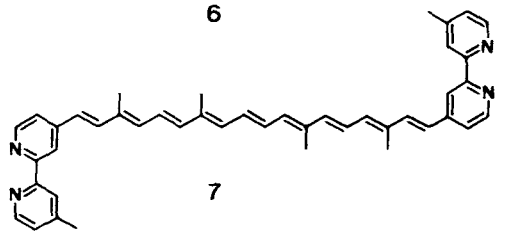

7

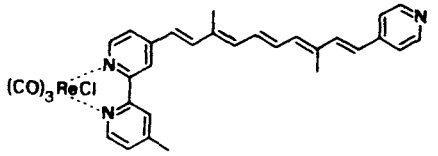

8

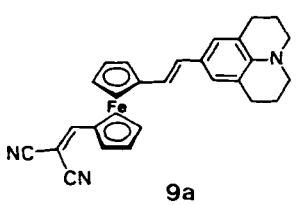

9a

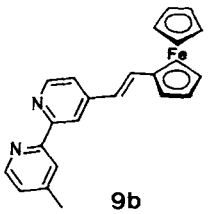

9b

These types of compounds incorporate electro- and photosensitive switches at the end of or inside the conjugated chain and thus represent switchable molecular wires responding to external stimuli.

3.3. Molecular Ionic Devices

The vast amount of data available on selective ion binding and transport by a great variety of ligands and carrier molecules provides the basis for the design of molecular devices handling ionic species. The molecular recognition events involved may be directly related to information and signal processing by means of ions, as is the case in biology. Receptors containing light- or redox-sensitive groups[31] represent photo- or electro-switchable components responding to external physical stimuli and capable, for instance, of generating photoionic pulses.[49] Analytical devices based on ion binding and transport have been developed.[50]

On the basis of our work on ion binding, we have studied extensively ion transport by mobile carriers, together with its regulation by coupling to symport or antiport processes and to physical or chemical gradients.[51]

In addition to transport by mobile carriers, ion transfer may also be performed by selective ion channels. The design of such transmembrane channels has been much less explored, probably because of the inherently larger molecular structures involved, despite the fact that biological transport is thought to occur mainly via channel-type species. We have investigated various approaches to the design of ion channels and ion-responsive membrane systems.

3.3.1. *Tubular Mesophases*

A stack of macrocyclic rings represents a molecular tube through which ions might flow, as illustrated by a solid-state model of such an ion channel.[52] Since in discotic liquid crystals, the spontaneous axial stacking of molecular discs

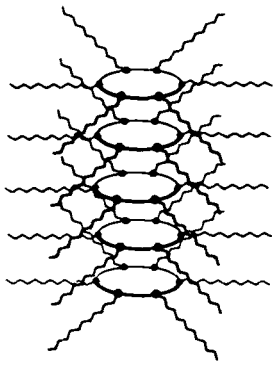

10

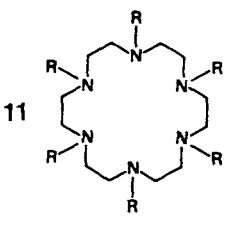

11

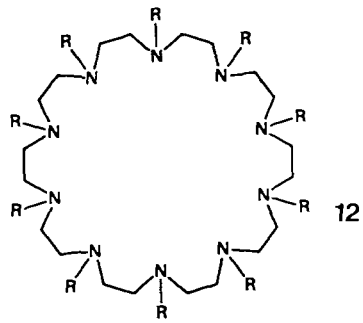

12

R = *p*-*n*-$C_{12}H_{25}O$-C_6H_4-CO

yields columnar mesophases, it appeared that if such phases could be obtained with ring elements, their arrangement in an axial stack would yield a hollow column, that is, a molecular tube (**10**). Macrocyclic polyamines bearing suitable side chains, such as **11** and **12**, indeed give *tubular mesophases* that contain stacks of macrocycles forming tubes.[53] Although the macrocyclic elements used at present are not well suited for ion binding, further elaboration could lead to ion channels that are phase (temperature) dependent.

3.3.2. *Ion-Responsive Monolayers*

Deposition of macrocycles bearing lipophilic side chains at the air–water interface could form Langmuir monolayers, thus yielding ion-responsive molecular films.

Indeed, macrocycles **11** and **12** form such monolayers.[53b, 54] Comparison of measured surface areas with molecular models indicated that the macrocycles were lying flat on the water surface while the aliphatic chains were tilted upright in the compressed film, as shown in Figure 5.[54]

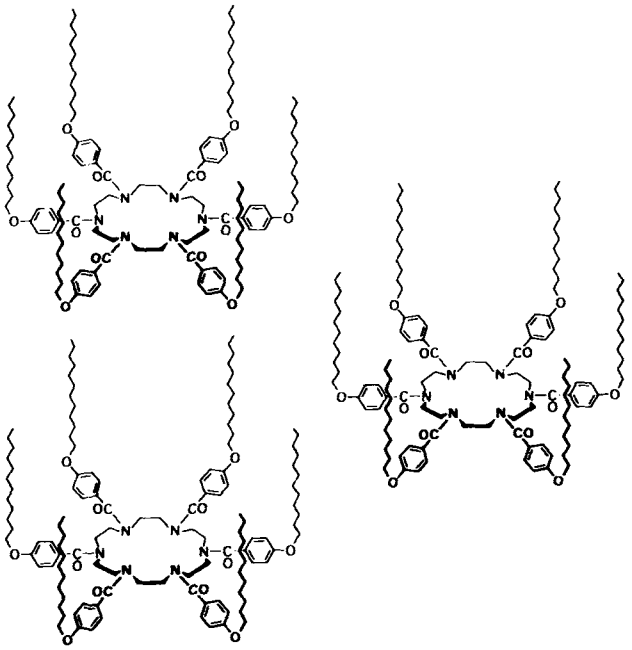

Fig. 5. Schematic representation of the arrangement of macrocycle **11** in a compressed film at the air–water interface; the aliphatic chains are represented in their fully extended form, but some curling may occur.

Such monolayers should be able to interact selectively with ions present in the subphase; this has been shown to be the case for monolayers formed of calixarene derivatives.[55]

Various developments may be envisaged, such as monolayers effecting molecular recognition at an interface (of interest, for instance, for selective detection) or ion-binding, electro- or photoactive films.

3.3.3. *The "Chundle" Approach to Molecular Channels*

A channel may also be defined by a bundle of transmembrane chains, formed either by the spontaneous association of individual molecules (e.g., the polymolecular channel formed by the peptide alamethicin[56–58]) or by grafting several chains onto a supporting unit such as a polyfunctional macrocycle that constitutes the organizing core, as represented by **13a**. This may be termed the *chundle* (or

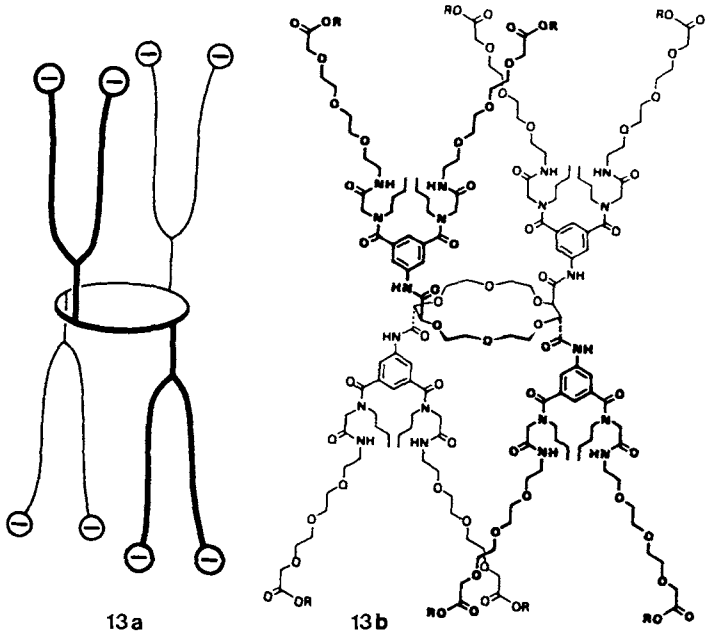

"bouquet") approach to a transmembrane *ch*annel based on a b*undle* of chains. Such an entity should present three main features: (1) two bundles of chains long enough to span half a membrane bilayer, (2) a central annulus serving both as support to maintain the two bundles of chains and as substrate-selection component, and (3) terminal polar groups for anchoring the molecule to each interface in a transmembrane fashion.

The synthesis of a chundle molecule, **13b**, has been realized.[59] Its structural features correspond to those desired for studies of chundle-type molecular channels: (1) the functionalized macrocyclic annulus possesses selective metal-cation binding properties; (2) it bears two axially oriented bundles of four oxygen-containing chains, which provide binding sites for metal cations and are long enough for the molecule to span a typical lipid membrane (the overall length with the chains in an extended state may be estimated to lie in the 45–50-Å range); (3) the eight terminal carboxylate groups allow for anchorage at water–membrane interfaces and transmembrane orientation, as well as for eventual coupling to proton gradients.

The octacarboxylate **13b** has been incorporated into model bilayer membranes.[60] The synthesis and properties of a related molecule based on a similar macrocyclic core have been reported.[61] Whether molecule **13b** is a functional cation channel is being investigated. Structural modifications may be required. In particular, the nature of the central annulus should be critical for rapid and selective ion flow. The alamethicin bundle contains a central annulus of hydrogen-bonded glutamine residues[57] which is much wider than the macrocyclic unit in **13b**, suggesting that a larger macrocycle may be required.

For this reason, a much bigger core was chosen for a second chundle-type molecule: β-cyclodextrin (β-CD), whose cavity diameter is about 6 Å. Selective derivatization by oligooxyethylene units (terminated, for instance, by a carboxylic group) should lead to a species such as that represented schematically by **14**.[62] Such a very large molecule bearing seven chains on each side of the rigid β-CD core has been obtained.[63] It is in itself of interest since, by its size, its internal space, and its chains, it represents a sort of *molecular vesicle*.

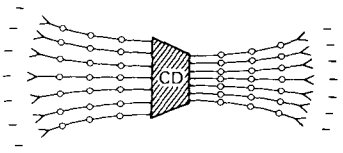

14

Because it is dissymetric, this β-CD chundle could act as an oriented transmembrane device. Its transfer selectivities might have analogies with those of the channel of the acetylcholine receptor. Physical, chemical, membrane-incorporation, and substrate-transfer properties of this and other β-CD derivatives will provide basic information about the handling and the behavior of very large functional molecular species. Whether or not the present or other chundle-type molecules do indeed act as ion channels, they should nevertheless allow the testing of approaches to channel design and to the handling of selective ionic conduction.

Incorporation of the molecular ionic devices described above into supporting structures (such as membranes, layers, and films) will allow the exploration of their functional properties and of their ability to produce ionic signals. Regulation of flow, switching, and coupling to other components will require further structural modifications.

4. Molecular Recognition and Self-Organization. Programmed Molecular Systems

Supramolecular chemistry has relied on more or less rigidly organized,[4, 10] synthetically built up, molecular receptors for effecting molecular recognition, catalysis, and transport processes. Beyond *pre*organization lies the design of systems undergoing *self-organization*, that is, systems capable of *spontaneously* generating a well-defined (functional) supramolecular architecture by *self-assembly* from their components under a well-defined set of conditions.[13b] It is *designed* assembly into a well-defined discrete supramolecular species, as compared to the spontaneous formation of molecular layers, films, membranes, etc. (see, for instance, Sections 3.3.1 and 3.3.2).[64 - 66] Self-assembly requires binding; self-organization additionally implies information. The *information* necessary for the process to take place and the *algorithm* (the "Aufbau" rules) that the process follows must be stored in the components and operate via selective molecular interactions. Thus, these systems may be termed *programmed molecular and supramolecular systems*[67] that generate organized entities following a defined plan based on molecular recognition events.[68] Self-organization represents a basic feature of supramolecular chemistry, since it rests on intermolecular interactions, whereas preorganization makes use of covalent bonding. Note also that it amounts to a (noncovalent) replication process at the supramolecular level.

Self-organization may occur in solution, in liquid crystalline phase, or in the solid state and make use of hydrogen bonding, electrostatic and donor–acceptor effects, or metal-ion coordination as basic interactions between the components, as well as of medium (solvophobic) effects. Multiple binding subunits are required, as present in polytopic coreceptors. The process may display positive cooperativity and lead to *molecular amplification devices*, if, once initiated, the subsequent steps of the assembly are facilitated. This can be the case for polytopic coreceptor molecules in which interaction between the multiple subunits, or substrate binding to them, occurs in such a way that each association step sets the stage for the following one.[3] Cooperativity may also be considered to present features of an *error filter* device.

Numerous biological supramolecular structures result from self-assembly, such as the spontaneous formation of the double helix of nucleic acids,[69] the viral protein coat,[70] and multiprotein complexes.[71]

We have pursued several approaches to self-organizing systems: (1) the formation of double-helical metal complexes, the *helicates*, from two oligobipyridine strands and suitable metal ions; (2) the generation of mesophases and liquid crystalline polymers of supramolecular nature from complementary components; (3) the molecular-recognition-directed formation of ordered solid-state structures.

4.1. Self-Organization of Double-Helical Metal Complexes: Helicates and Deoxyribonucleohelicates (DNH)

Self-organization may occur in repetitive chain ligands, acyclic coreceptors containing several identical binding subunits arranged linearly, if substrate binding to a given site is connected to binding to the other sites so that full site occupation is only compatible with a defined final architecture.

This is the case for the ligands **15**–**18** containing two to five bipyridine (bpy) groups. In the presence of Cu^{I} ions,

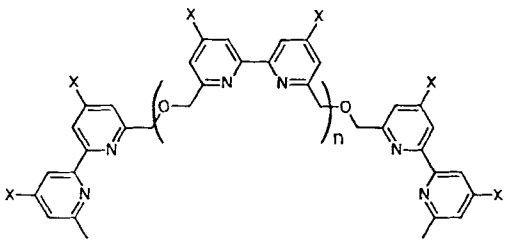

	X = H	X = COOR or $CONR_2$
n = 0	**15**	**24**
n = 1	**16**	**25**
n = 2	**17**	**26**
n = 3	**18**	**27**

spontaneous assembly takes place giving *double-stranded helicates*, ds-$\mathscr{H}$, in which two ligand strands are wrapped around each other in a double-helical fashion with Cu^{I} ions holding them together.[72 - 74] The di- to pentahelicates **19**–

22 have thus been obtained. Their *double-helix* structure rests on the determination of the crystal structures of **19**[75] and **20**[73] and on spectroscopic data. It results from the tetrahedral-like coordination imposed by each $Cu(bpy)_2^{\oplus}$ site and from the design of the ligands, which disfavors binding to only a single strand. These two features make up, respectively, the recognition process (the algorithm) and the molecular steric "program" that leads to preferential formation of the double-helical structures. In other words, helicate formation amounts to a tetrahedral reading of the molecular information stored in the bpy strands. Thus, only metal ions presenting the appropriate coordination features with bpy will yield double helicates. This has also been shown to be the case for Ag^I, which yields the tri-, tetra-, and pentahelicates, as confirmed by determination of the crystal structure of the silver trihelicate **23**.[76] On the other hand, the analogous

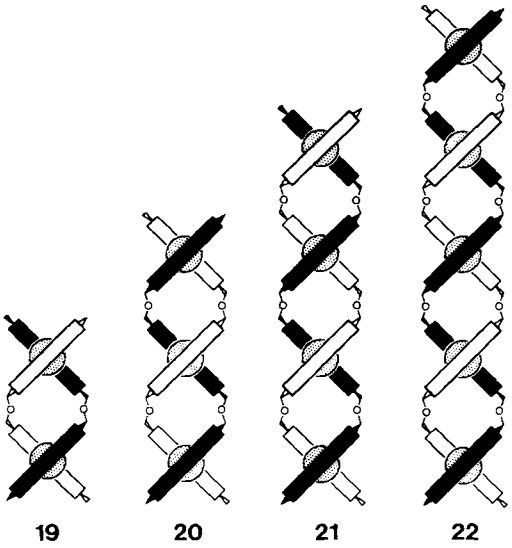

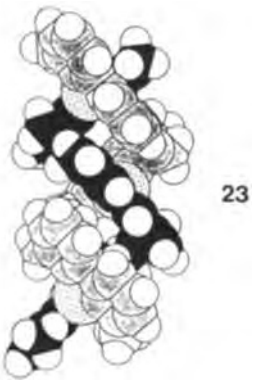

oligobipyridines containing two or three bpy units separated by a CH_2CH_2 group also yield the corresponding Cu^I helicates.[77] The formation of double helicates may be expected to occur only in a narrow range of coordination and structural parameters. Figure 6 shows a molecular model of the pentahelicate **22**.

Of particular interest is the finding that the helicate formation process appears to take place with *positive cooperativity*[73, 78] and with *self-recognition*,[73] a given ligand forming a double helix preferentially with an identical strand if a mixture of ligands is used.

Fig. 6. Molecular model of the pentahelicate **22** formed by self-assembly of two oligobipyridine ligands **18** and five Cu^I cations.

A major feature of this spontaneous generation of a double-helical structure is that it can be employed as an *organization framework*, allowing the arrangement in space in a double-helical fashion of substituents attached to the bpy units. To this end, the oligo-bpy strands **24**–**27**, containing substituents in 4,4′ position on the bpy groups, were synthesized.[79]

Especially attractive was the possibility to connect nucleosides, as has been realized, for instance, with the hexathymidine **28** and with the elongated and alternating strands **29** and **30**.[80] These compounds represent *artificial oligonucleosides*, which may interact with natural polynucleotides or nucleic acids. On treatment with Cu^I, **29** and **30** gave the double-helical complexes **31** and **32**, respectively, inside-out analogues of double-stranded nucleic acids which may be termed *deoxyribonucleohelicates* (DNH).[80] Since these species are positively charged and present the hydrogen-bonding base on the periphery, one may expect them to bind to both single-stranded and double-stranded nucleic acids with formation of mixed natural-artificial triple- and quadruple-stranded species.[81] Such interactions may present selectivities resulting both from the overall shape of the DNHs and from the thymidine groups. The DNH molecules **31** and **32**, which bear outward-oriented recognition sites, represent polytopic variants of exo-receptors of the metallonucleate type.[3] Figure 7 shows molecular models of the deoxyribonucleotrihelicate **31** (left) and its pentahelicate analogue **32** (right).

Of course, it is possible to organize numerous other units by means of the helicate framework, thus bringing together groups capable of conferring, for instance, energy-transfer, electron-transfer, or specific ion-binding features.

Finally, one may note that the dihelicate **19** has features reminiscent of the two homochiral components obtained in the "Coupe du Roi" (Fig. 8, left)[82] rendered in a sculpture by *Max Bill* (Fig. 8, right). The aesthetic features of the double helix have also been widely recognized (Fig. 9)!

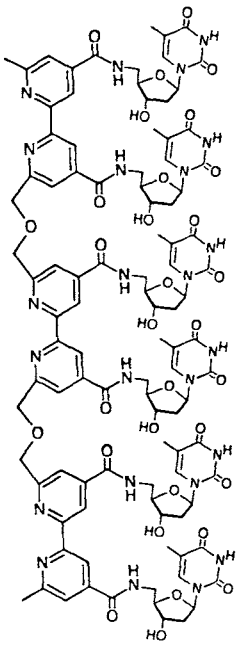

28

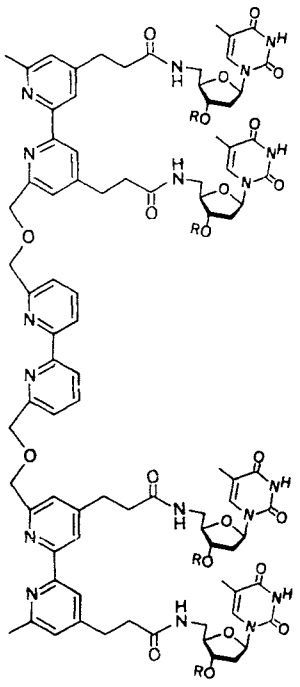

29

R = tBuMe$_2$Si, H

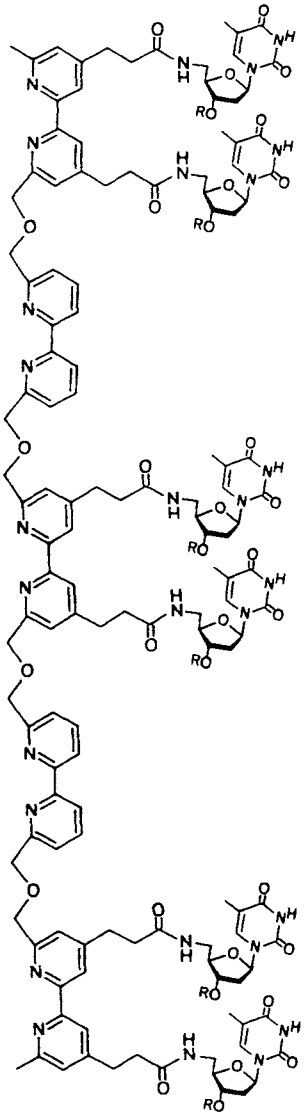

30

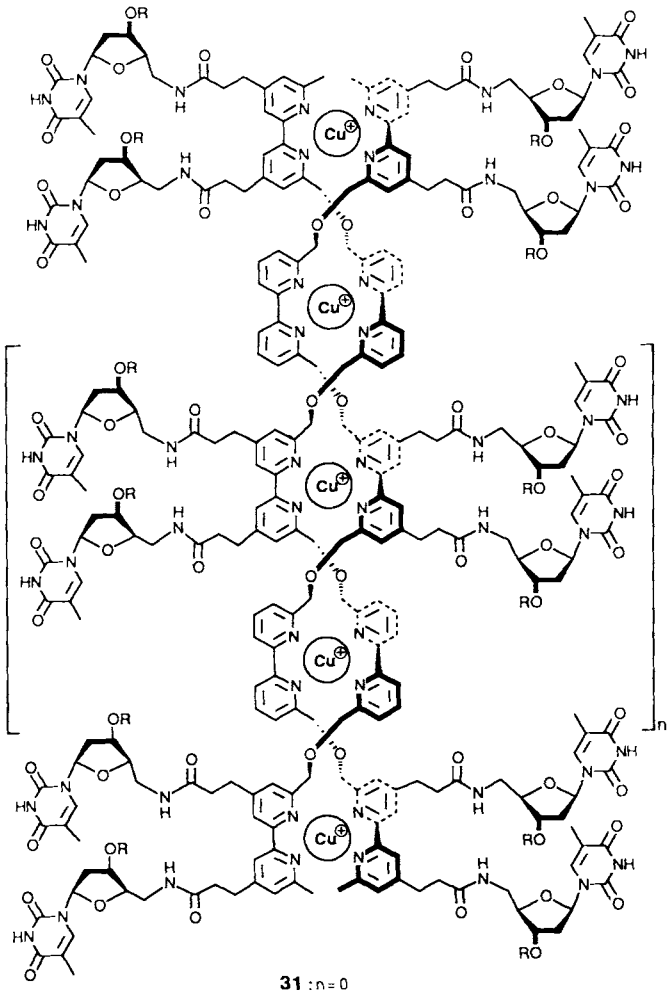

31 : n = 0
32 : n = 1

R = tBuMe$_2$Si, H

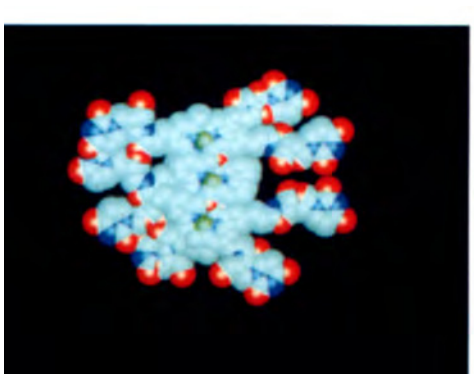

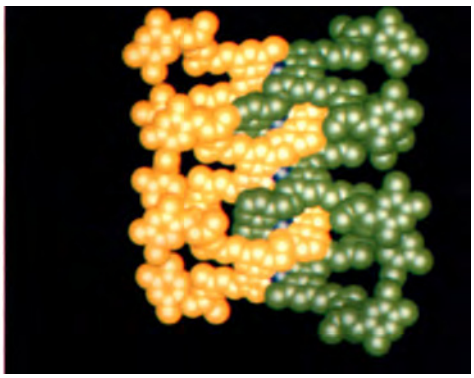

Fig. 7. Left: Computer-generated representation of the deoxyribonucleotrihelicate **31** formed by self-assembling of two tetrathymidine tribipyridine strands (**29**) and three Cu^{I} cations. The disposition of the side chains is arbitrary. Right: Molecular model of the analogue pentahelicate **32**.

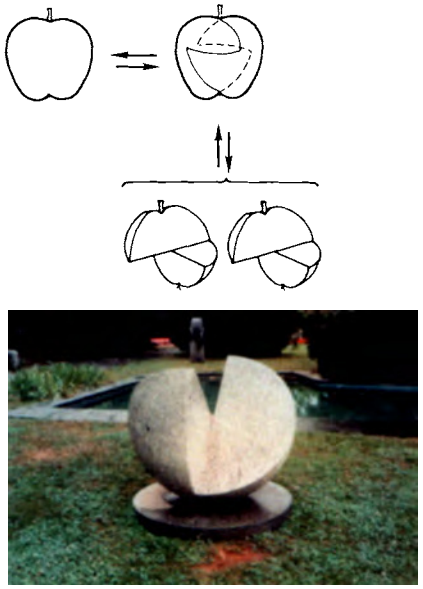

Fig. 8. Left: The "Coupe du Roi" or how to cut an apple into two homochiral components of same helicity[82], as an analogy to the dihelicate **19**. Right: A component of la Coupe du Roi as rendered by the sculptor *Max Bill*.

Fig. 9. A double helix as found on the Cattedrale of Ferrara (courtesy of *F. Scandola*).

4.2. Molecular-Recognition-Directed Assembly of Organized Phases

Molecular processes occurring in a material may induce marked changes in its properties. For instance, the interaction between molecular units that by themselves would not be mesogenic could lead to the formation of a supramolecular species presenting liquid crystalline behavior. If so, it might be possible to take advantage of selective interactions so that the mesogenic supermolecule would form only from complementary components. This would amount to *macroscopic expression of molecular recognition*, since recognition processes occurring at the molecular level would be displayed at the macroscopic level of the material by the induction of a mesomorphic phase that may be termed supramolecular and "in-formed", since it is conditioned by the molecular information present in its components. This has been accomplished in the generation of supramolecular mesophases and liquid crystalline polymers from complementary molecular units.

4.2.1. Mesophases Induced by Association of Complementary Molecular Components

The most common type of molecular species that form thermotropic liquid crystals possess an axial rigid core fitted with flexible chains at each end. One may then imagine a splitting of the central core into two complementary halves $\in$ and $\ni$, whose association would generate the mesogenic supermolecule, as schematically represented in Figure 10.

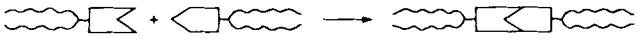

Fig. 10. Formation of a mesogenic supermolecule from two complementary components.

This was realized with derivatives of the complementary heterocyclic groups 2,6-diaminopyridine and uracil bearing long aliphatic chains.[83] Whereas the pure compounds did not show liquid crystalline behavior, 1:1 mixtures gave a metastable mesophase of columnar hexagonal type. Its existence may be attributed to the formation of a mesomorphic supermolecule **33** via molecular-recognition-directed association of the complementary components.

Numerous extensions may be envisaged, such as the introduction of various central cores, in particular those already known to yield molecular liquid crystals, the incorporation of light-sensitive or electrosensitive units, the potential use for detection devices, and the extension to various recognition components of biological nature.

4.2.2. Self-Organization of Supramolecular Liquid Crystalline "Polymers" from Complementary Components

If two (or more) complementary units $\in$ or $\ni$ are grafted on a template T, mixing $T\in_m$ with the complementary $T\ni_m$ may lead to the self-assembling of a linear or cross-linked polymeric supramolecular species ($T\in_m$, $T\ni_m$), whose existence is conditioned by the molecular-recognition-directed association between the $\in$ and $\ni$ groups. Figure 11 represents schematically such a process in the case of two-site (ditopic) complementary components $T\in_2$ and $T\ni_2$. The resulting supramolecular polymeric material, $(T\in_2, T\ni_2)_n$, may present liquid crystalline properties if suitable chains are introduced on the components.

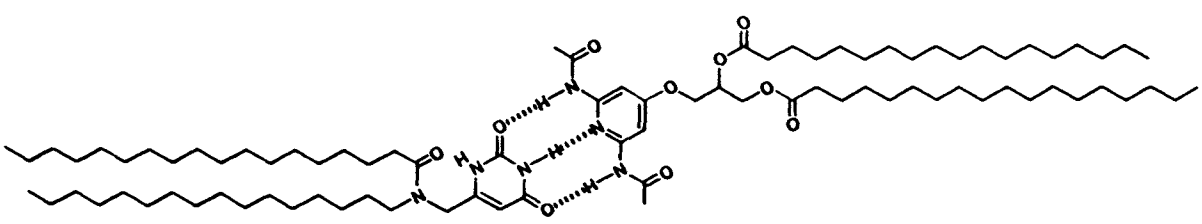

33

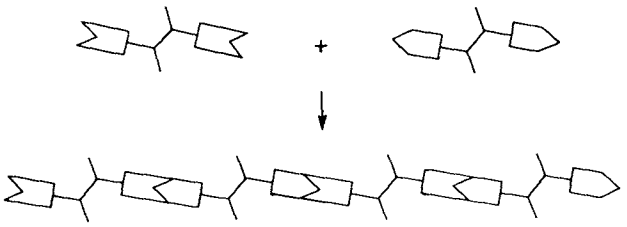

Fig. 11. Formation of a polymeric supramolecular species by association of two complementary ditopic components.

Condensation of the complementary heterocyclic groups 2,6-diaminopyridine (P) and uracil (U) with long-chain derivatives of L-, D-, or *meso*-tartaric acid gave substances LP_2, LU_2, MP_2, MU_2, etc., each containing two identical units capable of undergoing association via triple hydrogen bonding.[84] The pure compounds are solids exhibiting a more or less complex melting behavior due to solid-state polymorphism. In contrast, the 1:1 mixtures (LP_2 + LU_2) and (MP_2 + MU_2) display a *thermotropic mesophase* from below room temperature to above 200 °C. The material has the aspect of a highly birefringent glue that forms fibers under spreading.

It is reasonable to assume that the complementary units will form the expected triply hydrogen-bonded pairs, so that the entirely different behavior of the pure compounds and of the 1:1 mixtures may be attributed to the spontaneous association of the complementary components into a polymolecular entity based on hydrogen bonding. The overall process may then be described as the *self-assembling of a supramolecular liquid crystalline polymer* based on molecular recognition. The resulting species, $(LP_2 + LU_2)_n$, is represented schematically by structure **34**.

The X-ray patterns show that the two materials obtained from the configurational isomers of tartaric acid have different structures. Both are hexagonal columnar mesophases, but, whereas the data for $(LP_2, LU_2)_n$ are consistent with columns formed by three polymeric strands having a triple-helix superstructure (Fig. 12), those for the $(MP_2, MU_2)_n$ mixture fit a model built on three strands in a zigzag conformation. One may note that these species also represent self-assembled molecular tubes. The LD mixture has yet another arrangement. These three materials make clear the profound influence of chirality on the superstructure formed.

The results above show that it is possible to engineer molecular-recognition-dependent liquid crystals based on mesogenic supermolecules formed by association of complementary components.[85] Furthermore, molecular species that may form liquid crystalline *polymers* of *supramolecular* nature (or mesomorphic polymolecular associations)[86] may be obtained by the *self-assembly* of complementary subunits, thus expressing the recognition process occurring on the molecular level via the formation of a macroscopic mesophase.

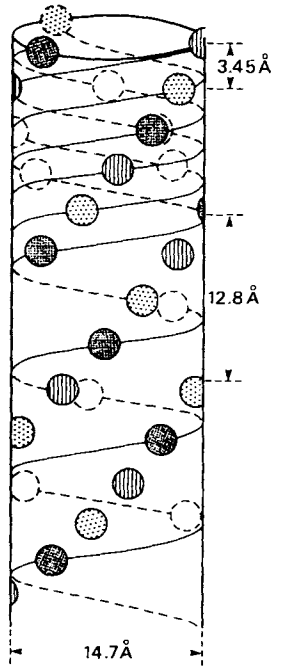

Fig. 12. Schematic representation of the columnar triple-helical superstructure derived from the X-ray data for $(LP_2, LU_2)_n$; each spot represents a PU or UP base pair; spots of the same type belong to the same helical strand of the triple helix; the dimensions are compatible with an arrangement of the PTP and UTU components along the strands indicated (see also **34**); the aliphatic chains stick out of the cylinder, more or less perpendicularly to its axis; a single helical strand and the full triple helix are represented, respectively, on the bottom and at the top of the column.

These effects amount to a macroscopic reading of molecular information via a phase change which, being a highly cooperative process, also corresponds to an *amplification* of molecular recognition and information from the microscopic to the macroscopic level.

4.2.3. Supramolecular Automorphogenesis

Control over the generation of molecular shapes and architectures may rely on covalent bond formation (covalent

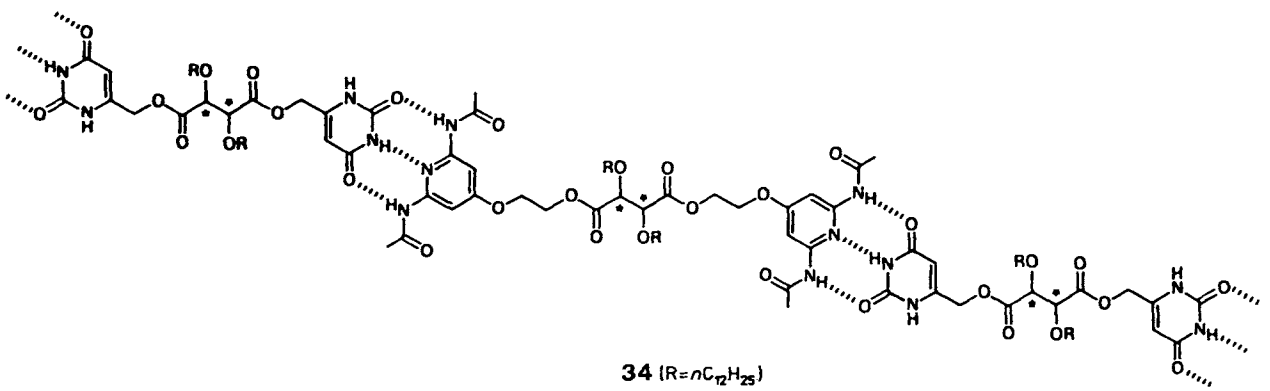

34 (R=$nC_{12}H_{25}$)

or molecular morphogenesis).[3] This is the case for polymeric oriented systems derived from molecular assemblies[87] and for branched structures formed via cascade processes growing from a central core, as realized in "starburst dendrimers"[88] and "arborols".[89]

On the other hand, it may be possible to achieve the spontaneous generation of supramolecular shapes by self-assembly of complementary molecular components. This represents a recognition-dependent *automorphogenesis* of supramolecular nature, based on noncovalent, intermolecular bonding. It should open paths to the controlled self-organization of polymolecular shapes, architectures, and patterns (for instance, in molecular layers).

4.3. Molecular-Recognition-Directed Self-Assembly of Ordered Solid-State Structures

The architectural and functional features of organized supramolecular structures result from the molecular information stored in the components and from the active groups which they bear.

A simple and general concept for generating molecular order is based on the recognition-directed spontaneous assembly of a supramolecular strand from complementary molecular components, each of which presents two identical recognition sites (Fig. 13). The interaction of two such units

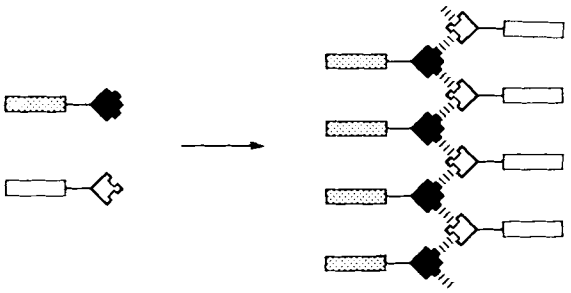

Fig. 13. Schematic representation of the formation of an ordered supramolecular strand by the molecular-recognition-induced association of two different molecular units. Each unit contains a group that possesses two identical binding sites complementary to those of the other unit.

may generate organized polymolecular strands in solution, in a mesomorphic phase, or in the solid state by cocrystallization. In the latter case, recognition-based crystal engineering may allow the structural design of organic solids.[90, 91] All residues of the same type are expected to be located on the same side of the strand (Fig. 13), thus providing spontaneous like/unlike *sorting* (into two substrands) and *orientation* of the molecular components in the supramolecular arrangement.

2,4,6-Triaminopyrimidine and barbituric acid derivatives are complementary components presenting the required features, since they should be able to form *two* arrays of three hydrogen bonds with each other. Mixtures of the two species gave indications for association in solution and formed 1:1 mixed crystals by cocrystallization.

The crystal structure of such a compound showed that the components are arranged in mixed supramolecular strands in which each unit forms six hydrogen bonds with its two complementary neighbors, as schematically represented by structure **35** (Fig. 14). As a consequence of molecular recognition, expressed by the hydrogen-bonding pattern between the two components, *all like residues* A and B are indeed located on the same side of the strand.[92]

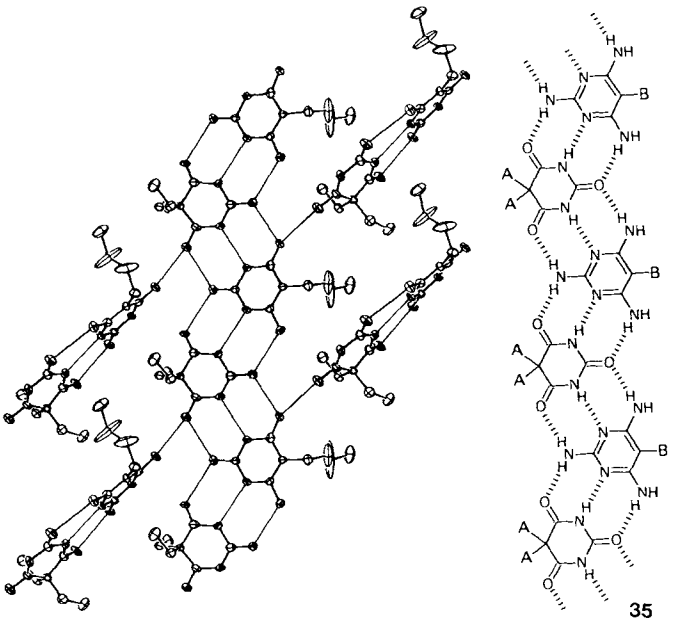

35

Fig. 14. X-ray structure (left) of the cocrystal of the 1:1 species (right) formed by two complementary components derived from barbituric acid (A = ethyl) and 2, 4, 6-triaminopyrimidine (B = butyl).

Thus, the recognition interaction between the present complementary components spontaneously induces molecular sorting of like/unlike species and generates long-range order, orientation, and left/right differentiation at the molecular level. The process may be considered as the operation of a programmed molecular system that contains the information required for the self-organization of precisely this supramolecular architecture. The species formed represents a kind of self-assembled "ladder" polymer of supramolecular nature. The solid is thus a supermolecule, a very large supermolecule indeed (this applies to molecular solids in general).

The arrangement produced may impart specific properties to the material at the macroscopic level. If the barbituric unit is regarded as the "assembler" component, mixing it with a triaminopyrimidine derivative should automatically lead to the generation of an *oriented* arrangement of functional B groups along a strand, thus offering the opportunity of inducing novel properties (optical, electronic, ionic, magnetic, etc.). For instance, such a process may allow the designed engineering of cocrystals of organic molecules exhibiting nonlinear optical, electron-transfer, or energy-transfer properties.

Other basic recognition units could give rise to numerous patterns (ribbons, rings, cylinders, strips, belts, friezes, etc.), leading to a recognition-based "molecular patterning". It is of particular interest that the self-assembly of such supra-

molecular species also occurs in solution, thus providing self-organization in the fluid state.[93]

Molecular-recognition-directed processes thus provide a powerful entry into *solid-state engineering*.[90, 91] Modification of surfaces with recognition units leads to extended exo-receptors that could display selective surface binding on the microscopic level and to *recognition-controlled adhesion* on the macroscopic scale.

The design of molecular-information-dependent, *informed*, and functional self-organizing systems reveals new horizons in supramolecular chemistry. The possibility of *"intelligent"*, functional supramolecular materials, network engineering, and polymolecular patterning makes such systems the subject of increasing activity in chemical research.[3, 94]

5. Chemionics. Outlook

The chemistry of molecular components and devices that operate on photons, electrons, and ions defines areas—molecular photonics, electronics, and ionics—of a broad field which may be termed chemionics.[3]

Substances such as the caroviologens **5**, the chundle **14**, and the helicate **22** are of rather large size, entering the nanometric domain. They are members of the class of *organized and functional nanostructures*, synthetically constructed or self-assembled species possessing features suitable for the design of molecular and supramolecular devices.[95] The increasing size of such molecules and supermolecules leads to species of nanometric dimensions defining a *nanochemistry* that works its way upward towards microlithography and microphysical engineering, which, by further and further miniaturization, strive to produce ever smaller elements.

The processing of molecular information via molecular recognition events implies the passage from the molecular to the supramolecular level. Recognition-directed processes may be expressed at the macroscopic level by the formation of mesophases or of ordered solid-state structures, or by the generation of an optical, electronic, or ionic signal.

The reading of molecular information as well as the operation of molecular devices requires ways and means of *addressing* molecular and supramolecular species. Despite the problems and difficulties that one may apprehend, encouraging perspectives are offered, for instance, by the recent demonstration of tunnel diode effects on an atomic scale,[96] of optical absorption spectroscopy on nanometer dimensions,[97] and of single-atom positioning[98] using scanning tunneling microscopy, or the display of a light source smaller than the optical wavelength.[99]

Endowing photo-, electro-, or ionoactive components with recognition elements leads to programmed molecular systems capable of molecular-recognition-directed self-assembly into organized and functional (photonic, electronic, ionic) supramolecular devices. Cooperative processes display amplification and represent error filters. Thus, *chemionics* is the chemistry of recognition-directed, self-organized, and functional entities of supramolecular nature (Fig. 15), which may eventually be capable of replication. It points to a *molecular information science*, molecular *informatics* and *semiochemistry* involving information and signal processing and communication at the molecular and supramolecular levels.

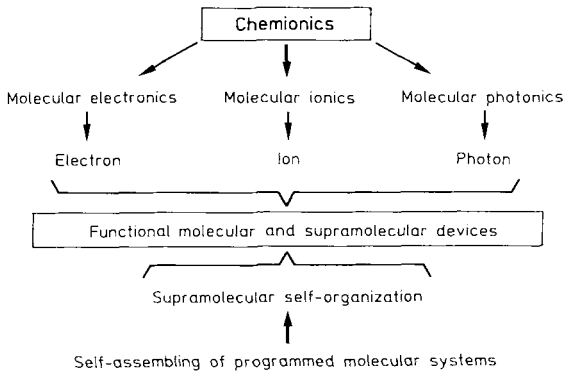

Fig. 15. Chemionics as the chemistry of recognition-directed and self-organized photonic, electronic, and ionic molecular and supramolecular devices.

6. Conclusion

The development of supramolecular chemistry involves a more and more complete control over molecules, supermolecules, and materials. Although many studies are concerned with substances of biological or biomimetic type, the emphasis is definitely on abiotic, non-natural species, figments of the imagination of the chemist, which possess a desired chemical, biological, or physical property.

Such an evolution rests on a definite outlook: the elaboration of *strategies towards properties and functions*[4] rather than towards structures, the goal being to express a desired property in a molecule or a material, whatever the composition and structure of the substance.

This opens wide the door to the creative imagination of the chemist at the meeting point of chemistry with biology and physics, in order not only to discover but above all to *invent*, to *create*: the score of chemistry is not just to be played but to be composed!

The essence of chemical science thus finds its full expression in the words of *Leonardo da Vinci*: "Where nature finishes producing its own species, man begins, using natural things and in harmony with this very nature, to create an infinity of species."

I wish to express my warmest thanks to my collaborators at the Université Louis Pasteur in Strasbourg and the Collège de France in Paris who have performed the work described above.

Received: May 14, 1990 [A 787 IE]
German version: *Angew. Chem. 102* (1990) 1347

[1] J.-M. Lehn, *Pure Appl. Chem. 50* (1978) 871.
[2] J.-M. Lehn, *Science (Washington D. C.) 227* (1985) 849.
[3] J.-M. Lehn, *Angew. Chem. 100* (1988) 91; *Angew. Chem. Int. Ed. Engl. 27* (1988) 89.
[4] J.-M. Lehn, *Struct. Bonding (Berlin) 16* (1973) 1.
[5] See, for example, *Top. Curr. Chem. 98* (1981); *101* (1982); *121* (1984); *128* (1985); *132, 136* (1986); *140* (1987); *149* (1988).
[6] R. M. Izatt, J. J. Christensen (Eds.): *Progress in Macrocyclic Chemistry Vol. 1–3*, Wiley, New York 1979, 1981, and 1987, respectively.
[7] J.-M. Lehn, translated and supplemented by J. Lipkowski, M. Pietraszkiewicz, K. Suwińska, T. Kościelski, M. Kożbial: *Chemia Supramolekularna*, Polskiej Akad. Nauk., Warsaw 1985.

[8] F. Vögtle: *Supramolekulare Chemie*, Teubner, Stuttgart 1989.
[9] H. Dugas: *Bioorganic Chemistry*, Springer, Heidelberg 1989.
[10] D. J. Cram, *Angew. Chem. 98* (1986) 1041; *Angew. Chem. Int. Ed. Engl. 25* (1986) 1039.
[11] C. D. Gutsche: *Calixarenes*, R. Soc. Chem., Cambridge 1989.
[12] a) H.-J. Schneider, H. Dürr (Eds.): *Frontiers in Supramolecular Organic Chemistry and Photochemistry*, VCH, Weinheim, in press; b) J.-M. Lehn in [12a].
[13] For a discussion of molecular information and self-organization in biological systems see a) M. Eigen, L. DeMaeyer, *Naturwissenschaften 53* (1966) 50; b) M. Eigen, *ibid. 58* (1971) 465.
[14] Semiology is the general theory of signs. Semiochemicals are signaling chemicals that an organism can detect in its environment; D. R. Kelly, *Chem. Br. 26* (1990) 24.
[15] a) V. Balzani (Ed.): *Supramolecular Photochemistry*, Reidel, Dordrecht 1987; b) V. Balzani, L. Moggi, F. Scandola in [15a], p. 1.
[16] J.-M. Lehn in [15a], p. 29.
[17] B. Alpha, J.-M. Lehn, G. Mathis, *Angew. Chem. 99* (1987) 259; *Angew. Chem. Int. Ed. Engl. 26* (1987) 266.
[18] J.-C. Rodriguez-Ubis, B. Alpha, D. Plancherel, J.-M. Lehn, *Helv. Chim. Acta 67* (1984) 2264.
[19] B. Alpha, E. Anklam, R. Deschenaux, J.-M. Lehn, M. Pietraszkiewicz, *Helv. Chim. Acta 71* (1988) 1042.
[20] J.-M. Lehn, J.-B. Regnouf de Vains, *Tetrahedron Lett. 30* (1989) 2209; J.-B. Regnouf de Vains, *Thèse de Doctorat-ès-Sciences*, Université Louis Pasteur, Strasbourg 1989.
[21] J.-M. Lehn, M. Pietraszkiewicz, J. Karpiuk, *Helv. Chim. Acta 73* (1990) 106.
[22] J.-M. Lehn, C. Roth, unpublished.
[23] B. Alpha, V. Balzani, J.-M. Lehn, S. Perathoner, N. Sabbatini, *Angew. Chem. 99* (1987) 1310; *Angew. Chem. Int. Ed. Engl. 26* (1987) 1266.
[24] N. Sabbatini, S. Perathoner, V. Balzani, B. Alpha, J.-M. Lehn in [15a], p. 187.
[25] G. Blasse, G. J. Dirksen, D. Van der Voort, N. Sabbatini, S. Perathoner, *Chem. Phys. Lett. 146* (1988) 347.
[26] G. Blasse, G. J. Dirksen, N. Sabbatini, S. Perathoner, J.-M. Lehn, B. Alpha, *J. Phys. Chem. 92* (1988) 2419.
[27] See, for example, H.-G. Löhr, F. Vögtle, *Acc. Chem. Res. 18* (1985) 65.
[28] J. P. Konopelski, F. Kotzyba-Hibert, J.-M. Lehn, J.-P. Desvergne, F. Fages, A. Castellan, H. Bouas-Laurent, *J. Chem. Soc. Chem. Commun. 1985*, 433; F. Fages, J.-P. Desvergne, H. Bouas-Laurent, P. Marsau, J.-M. Lehn, F. Kotzyba-Hibert, A.-M. Albrecht-Gary, M. Al-Joubbeh, *J. Am. Chem. Soc. 111* (1989) 8672; F. Fages, J.-P. Desvergne, H. Bouas-Laurent, J.-M. Lehn, J. P. Konopelski, P. Marsau, Y. Barrans, *J. Chem. Soc. Chem. Commun. 1990*, 655.
[29] M. W. Hosseini, A. J. Blacker, J.-M. Lehn, *J. Chem. Soc. Chem. Commun. 1988*, 596; *J. Am. Chem. Soc.* 112 (1990) 3896; see also E. U. Akkaya, M. E. Huston, A. W. Czarnik, *ibid. 112* (1990) 3590.
[30] M. Gubelmann, A. Harriman, J.-M. Lehn, J. L. Sessler, *J. Chem. Soc. Chem. Commun. 1988*, 77; *J. Phys. Chem. 94* (1990) 308.
[31] a) S. Shinkai, O. Manabe, *Top. Curr. Chem. 121* (1984) 67; b) P. D. Beer, *Chem. Soc. Rev. 18* (1989) 409.
[32] V. Balzani, M. W. Hosseini, J.-M. Lehn, *J. Am. Chem. Soc. 107* (1985) 6888; F. Pina, L. Moggi, M. F. Manfrin, V. Balzani, M. W. Hosseini, J.-M. Lehn, *Gazz. Chim. Ital. 119* (1989) 65.
[33] D. S. Chemla, J. Zyss (Eds.): *Non-linear Optical Properties of Organic Molecules and Crystals, Vol. 1, 2*, Academic Press, New York 1986 and 1987.
[34] J.-M. Lehn in [33], *Vol. 2*, p. 215.
[35] M. Blanchard-Desce, I. Ledoux, J.-M. Lehn, J. Malthête, J. Zyss, *J. Chem. Soc. Chem. Commun. 1988*, 737.
[36] M. Barzoukas, M. Blanchard-Desce, D. Josse, J.-M. Lehn, J. Zyss, *Chem. Phys. 133* (1989) 323.
[37] S. Palacin, M. Blanchard-Desce, J.-M. Lehn, A. Barraud, *Thin Solid Films 178* (1989) 387.
[38] F. Peter, M. Gross, M. W. Hosseini, J.-M. Lehn, *J. Electroanal. Chem. Interfacial Electrochem. 144* (1983) 279.
[39] D. Haarer, *Angew. Chem. Adv. Mater. 101* (1989) 1576; *Angew. Chem. Int. Ed. Engl. Adv. Mater. 28* (1989) 1544; *Adv. Mater. 1* (1989) 362; F. Garnier, *ibid. 101* (1989) 529 and *28* (1989) 513; *Adv. Mater. 1* (1989) 117; H. C. Wolf, *Nachr. Chem. Tech. Lab. 37* (1989) 350.
[40] A. Barraud, O. Kahn, J.-P. Launay, *Sci. Tech. 15* (1989) 54; P. Day, *Chem. Br. 26* (1990) 52.
[41] a) A. Barraud, *J. Chim. Phys. Phys. Chim. Biol. 85* (1988) 1121; b) for approaches toward molecular rectifiers, see R. M. Metzger, C. A. Panetta, *ibid. 85* (1988) 1125; *J. Mol. Electronics 5* (1989) 1; F. R. Ahmed, P. E. Burrows, K. J. Donovan, E. G. Wilson, *Synth. Met. 27* (1988) B 593; c) for an approach to a molecular shift register memory, see J. J. Hopfield, J. N. Onuhic, D. N. Beratan, *J. Phys. Chem. 93* (1989) 6350; d) for molecular switching, see, for example, H. Tachibana, T. Nakamura, M. Matsumoto, H. Komizu, E. Manda, H. Niino, A. Yabe, Y. Kawabata, *J. Am. Chem. Soc. 111* (1989) 3080.
[42] T. S. Arrhenius, M. Blanchard-Desce, M. Dvolaitzky, J.-M. Lehn, J. Malthête, *Proc. Natl. Acad. Sci. USA 83* (1986) 5355.
[43] L. B.-A. Johansson, M. Blanchard-Desce, M. Almgren, J.-M. Lehn, *J. Phys. Chem. 93* (1989) 6751.
[44] M. Blanchard-Desce, J.-M. Lehn, unpublished.
[45] S.-i. Kugimiya, T. Lazrak, J.-M. Lehn, unpublished.
[46] T. S. Arrhenius, J.-M. Lehn, unpublished; M. Blanchard-Desce, J.-M. Lehn, E. Bamberg, unpublished.
[47] a) B. Marczinke, J.-M. Lehn, unpublished; b) K. J. Przibilla, J.-M. Lehn, unpublished.
[48] For a type of photoinduced molecular wire, see P. Seta, E. Bienvenue, A. L. Moore, T. A. Moore, D. Gust, *Electrochim Acta 34* (1989) 1723.
[49] R. Warmuth, E. Grell, J.-M. Lehn, unpublished.
[50] See, for example, D. N. Reinhoudt, E. J. R. Sudhölter, *Adv. Mater. 2* (1990) 23.
[51] J.-M. Lehn in G. Spach (Ed.): *Physical Chemistry of Transmembrane Ion Motions*, Elsevier, Amsterdam 1983, p. 181; J.-M. Lehn, *Ann. N. Y. Acad. Sci. 471* (1986) 41.
[52] J.-P. Behr, J.-M. Lehn, A.-C. Dock, D. Moras, *Nature (London) 295* (1982) 526.
[53] a) J.-M. Lehn, J. Malthête, A.-M. Levelut, *J. Chem. Soc. Chem. Commun. 1985*, 1794; b) see also C. Mertesdorf, H. Ringsdorf, *Mol. Cryst. Liq. Cryst. 5* (1989) 1757; c) for another approach see O. E. Sielcken, L. A. van de Kuil, W. Drenth, J. Schooman, R. J. M. Nolte, *J. Am. Chem. Soc. 112* (1990) 3086.
[54] J. Malthête, D. Poupinet, R. Vilanove, J.-M. Lehn, *J. Chem. Soc. Chem. Commun. 1989*, 1016.
[55] Y. Ishikawa, T. Kunitake, T. Matsuda, T. Otsuka, S. Shinkai, *J. Chem. Soc. Chem. Commun. 1989*, 736.
[56] R. Nagaraj, P. Balaram, *Acc. Chem. Res. 14* (1981) 356.
[57] R. O. Fox, Jr., F. M. Richards, *Nature (London) 300* (1982) 325.
[58] For channels based on model peptides, see J. D. Lear, Z. R. Wasserman, W. F. DeGrado, *Science (Washington D. C.) 240* (1988) 1177.
[59] L. Jullien, J.-M. Lehn, *Tetrahedron Lett. 29* (1988) 3803.
[60] L. Jullien, T. Lazrak, J.-M. Lehn, unpublished.
[61] V. E. Carmichael, P. J. Dutton, T. M. Fyles, T. D. James, J. A. Swan, M. Zojaji, *J. Am. Chem. Soc. 111* (1989) 767; for other approaches, see I. Tabushi, Y. Kuroda, K. Yokota, *Tetrahedron Lett. 23* (1982) 4601; J.-H. Fuhrhop, U. Liman, *J. Am. Chem. Soc. 106* (1984) 4643.
[62] J.-M. Lehn, *Annu. Collège Fr. Paris 1980–1981*, 189.
[63] J. Canceill, L. Jullien, J.-M. Lehn, unpublished.
[64] H. Kuhn, D. Moebius, *Angew. Chem. 83* (1971) 672; *Angew. Chem. Int. Ed. Engl. 10* (1971) 620.
[65] H. Kuhn, *Pure Appl. Chem. 53* (1981) 2105; *Thin Solid Films 178* (1989) 1.
[66] J. H. Fendler: *Membrane Mimetic Chemistry*, Wiley, New York 1982.
[67] J.-M. Lehn *Annu. Collège Fr. Paris 1988–1989*, 221.
[68] Use of a template to produce a given structure is not self-assembly; however, self-assembly may involve templating.
[69] W. Saenger: *Principles of Nucleic Acid Structure*, Springer, New York 1984.
[70] A. Klug, *Angew. Chem. 95* (1983) 579; *Angew. Chem. Int. Ed. Engl. 22* (1983) 565.
[71] See, for example, C. Frieden, *TIBS 14* (1989) 283; R. Jaenicke, *Angew. Chem. 96* (1984) 385; *Angew. Chem. Int. Ed. Engl. 23* (1984) 395.
[72] For an early case of a complex related to the helicate formed by **15**, see J.-M. Lehn, J.-P. Sauvage, J. Simon, R. Ziessel, C. Piccini-Leopardi, G. Germain, J.-P. Declercq, M. Van Meersche, *Nouv. J. Chim. 7* (1983) 413.
[73] J.-M. Lehn, A. Rigault, J. Siegel, J. Harrowfield, B. Chevrier, D. Moras, *Proc. Natl. Acad. Sci. USA 84* (1987) 2565.
[74] J. M. Lehn, A. Rigault, *Angew. Chem. 100* (1988) 1121; *Angew. Chem. Int. Ed. Engl. 27* (1988) 1095.
[75] J. Harrowfield, J.-M. Lehn, B. Chevrier, D. Moras, unpublished.
[76] T. M. Garrett, U. Koert, J.-M. Lehn, A. Rigault, D. Meyer, J. Fischer, *J. Chem. Soc. Chem. Commun. 1990*, 557.
[77] Y. He, J.-M. Lehn, *Acta Chim. Sin.*, in press; J.-M. Lehn, R. Ziessel, unpublished.
[78] T. M. Garrett, J.-M. Lehn, unpublished.
[79] M. M. Harding, J.-M. Lehn, A. Rigault, unpublished.
[80] U. Koert, M. M. Harding, J.-M. Lehn, *Nature 346* (1990) 339.
[81] B. Schoentjes, J.-M. Lehn, unpublished.
[82] F. A. L. Anet, S. S. Miura, J. Siegel, K. Mislow, *J. Am. Chem. Soc. 105* (1983) 1419; K. Mislow, *Croat. Chim. Acta 58* (1985) 353; J. Jacques, *L'Argonaute 17* (1984) 39; M. Cinquini, F. Cozzi, F. Sannicolo, A. Sironi, *J. Am. Chem. Soc. 110* (1988) 4363.
[83] M.-J. Brienne, J. Gabard, J.-M. Lehn, I. Stibor, *J. Chem. Soc. Chem. Commun. 1989*, 1868.
[84] C. Fouquey, J.-M. Lehn, A.-M. Levelut, *Adv. Mater. 2* (1990) 254.
[85] Other complementary units, such as the cytosine–isocytosine pair, may be envisaged: H. Keller, J.-M. Lehn, unpublished.
[86] a) For H-bonded mesophases, see R. Eidenschink, *Angew. Chem. Adv. Mater. 101* (1989) 1454; *Angew. Chem. Int. Ed. Engl. Adv. Mater. 28* (1989) 1424; *Adv. Mater. 1* (1989) 338; b) for supramolecular discotic phases based on H-bonded components, see K. Praefcke, B. Kohne, P. Marquardt, P. Psaras, W. Stephan, A. Eckert, A.-M. Levelut, *18. Freiburger Arbeitstagung Flüssigkristalle 1989, Nr. 22*, IAF, Freiburg, cited in [86a].
[87] H. Ringsdorf, B. Schlarb, J. Venzmer, *Angew. Chem. 100* (1988) 117; *Angew. Chem. Int. Ed. Engl. 27* (1988) 113.

[88] D. A. Tomalia, A. M. Naylor, W. A. Goddard III, *Angew. Chem. 102* (1990) 119; *Angew. Chem. Int. Ed. Engl. 29* (1990) 138.
[89] G. R. Newkome, Z.-q. Yao, G. R. Baker, V. K. Gupta, P. S. Russo, M. J. Saunders, *J. Am. Chem. Soc. 108* (1986) 849.
[90] "Molecular Engineering and Structure Design", *Isr. J. Chem. 25* (1985), special issue.
[91] G. R. Desiraju: *Crystal Engineering, The Design of Organic Solids*, Elsevier, Amsterdam 1989.
[92] J.-M. Lehn, M. Mascal, A. DeCian, J. Fischer, *J. Chem. Soc. Chem. Commun. 1990*, 479; for recent examples of inorganic solid-state engineering, see P. J. Fagan, M. D. Ward, J. C. Calabrese, *J. Am. Chem. Soc. 111* (1989) 1698; B. F. Koskins, R. Robson, *ibid. 112* (1990) 1546.
[93] Such species are of "supramolecular" nature by their constitution and type of bonding; by their extension in space and the large number of components, they may be termed "hypermolecular".
[94] a) For other types of structures see J. F. Stoddart in [12a]; b) for recent interest see, for example, A. Schepartz, J. P. McDevitt, *J. Am. Chem. Soc. 111* (1989) 5976; J. S. Manka, D. S. Lawrence, *Tetrahedron Lett. 1989*, 7341; *J. Am. Chem. Soc. 112* (1990) 2440.
[95] For nanometric linear molecular structures, see, for example, T. M. Dietz, B. J. Stallman, W. S. V. Kwan, J.-F. Penneau, L. L. Miller, *J. Chem. Soc. Chem. Commun. 1990*, 367, and references therein.
[96] I.-W. Lyon, P. Avouris, *Science (Washington D. C.) 245* (1989) 1369; P. Bedrossian, D. M. Chen, K. Mortensen, J. A. Golovdenko, *Nature (London) 342* (1989) 258.
[97] J. M. R. Weaver, L. M. Walpita, H. K. Wickramasinghe, *Nature (London) 342* (1989) 783.
[98] D. M. Eigler, E. K. Schweizer, *Nature (London) 344* (1990) 524.
[99] K. Lieberman, S. Harush, A. Lewis, R. Kopelman, *Science (Washington D. C.) 247* (1990) 59.

Organic Synthesis—Where now?

By Dieter Seebach*

This review article is an attempt to sketch the important developments in organic synthesis during the past 25 years, and to project them into the future.—The primary motivations that once induced chemists to undertake natural product syntheses no longer exist. Instead of target structures themselves, molecular function and activity now occupy center stage. Thus, inhibitors with an affinity for all the important natural enzymes and receptors have moved to the fore as potential synthetic targets.—New synthetic *methods* are most likely to be encountered in the fields of biological and organometallic chemistry. Enzymes, whole organisms, and cell cultures for enantioselective synthesis of specific substances have already been incorporated into the synthetic arsenals of both research laboratories and industry. In addition, designing appropriate analogues to transition states and intermediates should soon make it possible, with the aid of the mammalian immune system and gene technology, to prepare catalytically active monoclonal antibodies for almost any reaction; perhaps more important, such processes will increasingly come to be applied on an industrial scale.—The discovery of truly *new* reactions is likely to be limited to the realm of transition-metal organic chemistry, which will almost certainly provide us with additional "miracle reagents" in the years to come. As regards main group elements ("organoelemental chemistry"), we can surely anticipate further stepwise improvements in experimental procedures and the broader application of special techniques, leading to undreamed of efficiency and selectivity with respect to known procedures. The primary center of attention for all synthetic methods will continue to shift toward catalytic and enantioselective variants; indeed, it will not be long before such modifications will be available with every standard reaction for converting achiral educts into chiral products.—Analysis, spectroscopy, structure determination, theory, and electronic data processing have all become indispensable in organic synthesis. Only with the aid of these "tools" will the methods of organic chemistry permit selective syntheses of ever larger and more complex systems on both the molecular and supramolecular levels.—Examples have been introduced throughout this discourse to illustrate its many themes, and a very comprehensive bibliography should help the interested reader become more familiar with important keywords and authors.[**] This article will have served its intended purpose if it changes the minds of some of those who claim organic chemistry is a *mature science*, and if it causes students to discover the vitality and forcefulness with which organic synthesis is meeting new challenges and attempting to fulfill old dreams.

Er zeigt uns so in seinem wissenschaftlichen Leben, daß die Chemie nicht von einer *Theorie, nicht von* einer *Methode aus zu erschöpfen ist, und daß Erkenntnis und Nutzen in ihr untrennbar verwoben sind.*[***]
R. Koch, writing about Louis Pasteur

1. Introduction—a Difficult Subject!

1.1. On the Problems Associated with Prognostication

One can certainly plan research,
but not the results!
(Addressed to all those engaged in the distribution of research grants!)

The task I have set myself, ten years before the end of the present century, is to take inventory of the field of organic chemistry and attempt to discern the nature of some of the developments that lie ahead.

It is obviously impossible to review such a broad topic in the space available without imposing certain limits. To begin with, all my prognostication is subject to the bounds imposed by one general consideration that arises out of the very nature of scientific progress, which results from a combination of discovery, invention, development, and explanation. By definition, a *discovery* is something totally unexpected—even to the discoverer. Thus, Columbus set out in search of a route to India, but instead *discovered* America. If one accepts the premise that organic chemistry entails discoveries, then one is also compelled to be somewhat wary of predictions. On the other hand, impending inventions, explanations, and especially developments often *can* be foreseen through careful analysis of current trends and application of the time-tested scientific principle of extrapolation.

One additional imponderable is the effect of outside influences on the development of the discipline. No one in the mid-1960s would have anticipated the impending precipi-

[*] Prof. Dr. D. Seebach
Laboratorium für Organische Chemie der Eidgenössischen Technischen Hochschule
ETH-Zentrum, Universitätstrasse 16, CH-8092 Zürich (Switzerland)

[**] The list of references is also available upon request in the form of a Microsoft Word* file on diskette.

[***] "He showed us through his scientific life that chemistry cannot be exploited fully with the aid of a *single* theory or a *single* methodology, and that it is a field in which knowledge and application are inextricably linked." G. Bugge: *Das Buch der großen Chemiker, Vol. 2*, 4th reprint, Verlag Chemie, Weinheim 1974.

tous decline in United States dominance of the field of mechanistic physical organic chemistry, which was in part a consequence of research-political decisions by the National Institutes of Health at the end of the decade to limit funding more strictly to health-related projects. Japan illustrates how quickly a new nation can come onto the playing field and completely change the course of the game. Thus it is tempting to hope that the forthcoming steps toward European unification will eventually produce a system of elite universities like those in the USA, which would be in a position to attract the most talented minds in a population reservoir of nearly 300 million.

There is one other limitation that must be recognized with respect to the present endeavor, and it relates directly to the author himself. I have necessarily treated the subject from my own personal vantage point, which reflects my particular range of experiences. This in turn implies an emphasis on organic *synthesis*, and a time span of direct observation encompassing only 25 years. Nevertheless, a quarter of a century should more than suffice, and synthesis is certainly at the center of the discipline. No matter what the narrow goal of any particular project, whether the work involved is groundbreaking or of a more routine nature, synthesis and analysis are crucial to every chemist's activities.

1.2. Organic Chemistry in Crisis?

The biologists usually pick out the raisins, while the chemists are left to do the foot-work.
(The observation of a young researcher immediately after a postdoctoral experience in a research group concerned with the chemistry of DNA)

We are all very much aware of the fact—and also partly responsible for it!—that chemistry has a rather poor reputation in the media and within the public generally.[1] Even so, it is somewhat surprising to see an educated layman like the editor of *Nature*, *John Maddox*, declaring[2] that chemistry as a discipline has lost its identity, and citing as evidence the fact that the 1985 Nobel Prize for chemistry was actually awarded to two mathematicians.[3] It is also sad to find respected colleagues referring to organic chemistry, and specifically to organic synthesis, as a "mature" science.[4] There is no way this remark can be regarded as anything but an expression of resignation, of self-pitying nostalgia—indeed, as evidence of a "drop-out" mentality. A more accurate diagnosis would focus on the fact that discrete boundaries no longer exist between the various natural sciences (mathematics, physics, chemistry, biology, medicine) and especially between related subdisciplines (in this case inorganic, biological, organic, and physical chemistry). This has been the case for a long time in the world of applications, and it is just as true along the frontlines of research. Chemistry has not lost its identity: it has instead gained important footholds within the domains of other disciplines—albeit rarely at the initiative of chemists. Most of the real advances in the field of biochemistry, and increasingly in medicine as well, result directly from a deeper understanding of the processes of life at the molecular and supramolecular levels, and they must clearly be numbered among the accomplishments of chemistry. What is DNA sequencing[5] if not the structural analysis of a macromolecule? Is a DNA-[6, 7] or peptide-synthesizing machine[8] anything more than an automaton for repetitively carrying out a particular series of high-yield synthetic steps, always relying on the same reagents and very similar subunits? In the field of polymers, block polymerization via O-silyl ketene acetals (intermediates that were developed originally for organic synthetic purposes) has led to materials with very remarkable properties,[9] and careful introduction of "functional groups" has made it possible to use chemical reactions and the resulting covalent bonds as a way of binding surfaces together.[10] It is also appropriate to point to the recent synthesis of palitoxin,[11] a substance with 68 stereogenic units; organic synthesis has been responsible for a number of monumental breakthroughs in the pharmaceutical industry, contributing daily to the saving of countless lives.

In summary, the crass contradiction between the accomplishments and the reputation of chemistry, of which organic synthesis and its industrial applications constitute a significant part, can only be characterized as remarkable.[12, 13]

That which follows is a descriptive look at the current goals of organic synthesis; recently developed approaches to the purification, isolation, and identification of organic substances; key considerations in the development of improved techniques and in research into synthetic methodology; new insights gained through further investigation of classic reactions; and a few industrial applications drawn from the field of pharmaceutical synthesis. The selection is a *very* personal one, based on a much larger pool of potential examples, but it should nevertheless demonstrate quite clearly the vitality and ferment that characterize organic chemistry and organic synthesis in our day.[14]

2. Old and New Target Structures in Organic Synthesis—Not Simply a Matter of Fashionable Trends!

La chimie crée son objet. Cette faculté créatrice, semblable à celle de l'art lui même, la distingue essentiellement des sciences naturelles et historiques.[*]
M. Berthelot (1860)

2.1. From Natural Products to Supramolecular Structures

New synthetic methods have traditionally emerged from one of two sources: a) the deliberate attempt to perfect a known reaction or invent a new one in order to permit the preparation of a specific target molecule, which may be either a natural product or some structure that so far exists only in the imagination, or b) studies of the reactivity of some new class of carbon derivatives (organo*metallic* compounds, perhaps, or the more classical "organo*elemental*" substances). To these traditional sources of innovation we

[*] "Chemistry creates its own object. This creative power, similar to that of the arts, distinguishes it fundamentally from the natural and historical sciences."

must add, thanks to the initiative of *E. J. Corey*,[15, 16] c) the directed search for reactivity, including attempts to realize specific desirable synthetic transformations (an approach that gave birth to the terms *synthon*,[17] *retron*, and *transform*[16]), as well as systematic *umpolung* of known modes of reactivity.[18] A few examples taken from these three distinct breeding grounds are presented in Scheme 1.

The most celebrated aspect of synthesis has been the preparation of ever larger and more complex natural products, an endeavor in which creativity, intelligence, and endurance are prerequisites to success. The masters of the art have been immortalized in classic achievements, and their names can be found not only in the annals of chemistry but also among the ranks of Nobel Prize winners.[36–45] Through their efforts, we have come to believe (like them) that virtually any molecule is amenable to synthesis. Together with non-natural products chemists as well as the pioneers of synthetic methodology and elemental (i.e., "main group") organic chemists generally, they managed to discover almost every reaction there was to find; indeed, only transition-metal organic chemistry can still be regarded as a fertile field for synthetic surprises (see Sec. 6 below). Moreover, almost everything the study of unusual molecules could teach us about the nature of the chemical bond has probably already been learned. In other words, all the most important traditional reasons for undertaking a synthesis—proof of structure, the search for new reactions or new structural effects, and the intellectual challenge and pride associated with demonstrating that "it can be done"—have lost their validity. Exceptions[46–51] only prove the rule (cf. Scheme 2).

Natural target molecule

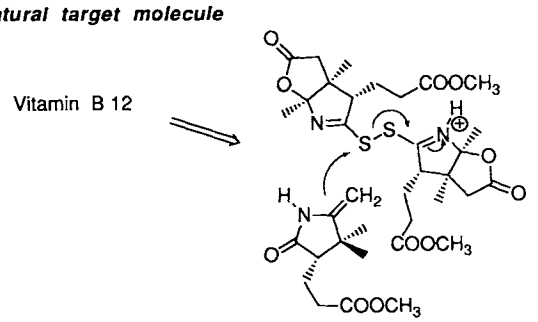

Non-natural target molecules

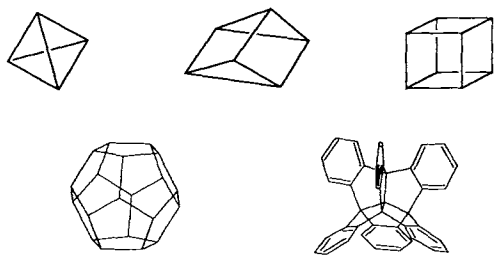

Olefination of a carbonyl compound

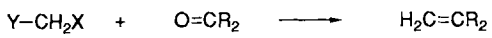

Synthetically equivalent reagents

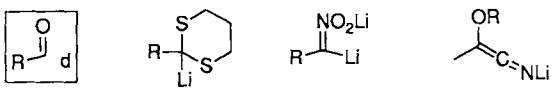

Umpolung of nitroolefin reactivity

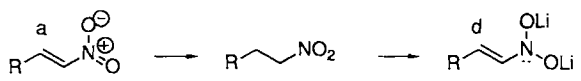

Scheme 1. New synthetic methods have arisen as "by-products" of natural product syntheses (sulfide contraction [19, 20]), as well as in the course of preparing such unusual, non-natural substances as tetrahedrane [21], prismane [22], cubane [23], dodecahedrane [24], and centrohexaindane [25]. Olefinations have resulted from a preoccupation with heteroatom-substituted organometallic reagents [26–30]. Nucleophilic acylation via dithianes [31], doubly metallated nitroalkanes [32] or cyanohydrin derivatives [33, 34], and umpolung of a nitroalkene to a super-enamine [35] all owe their discovery to systematic searches.

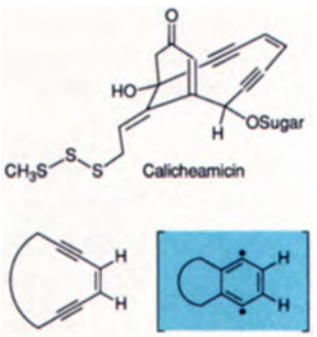

Scheme 2. A novel natural product system containing the *cis*-en-diyne moiety. Several derivatives with this characteristic skeleton have now been isolated (neocarcinostatin [46], esperamycin [47a], calicheamicin [47b], dynemicin A [47c]). The high antitumor activity of these compounds is based [48] on an elegant initiation of the illustrated ring-closure reaction to give an aromatic diradical (1,4-dehydrobenzene [49]), which reacts with a nucleotide unit of DNA to cause chain cleavage. Numerous synthesis-oriented research groups in the USA are busy trying to develop a synthesis of this natural system, and especially of simpler analogues [50].

Attempts are often still made to synthesize natural products with interesting biological properties or pharmacological activity, compounds unavailable from natural sources in quantities sufficient for thorough biological testing, but here there is an important financial motivation: such an effort stands a good chance of attracting research funds, either from government or industry. Multistep syntheses could also be said to provide the broadest possible training for graduate students in organic chemistry, and they certainly represent ideal preparation for jobs in the pharmaceutical industry, but sponsoring a project for this reason amounts to the fulfillment of a teaching responsibility rather than a commitment to the conduct of basic research within a university environment.[52a] In short, it really should come as no surprise that someone not prepared to adapt to new kinds of goals might refer to organic chemistry as a *mature* science.[52b]

How can we characterize the new generation of appropriate target structures for organic synthesis? In answering this

question it is useful to consider an observation of one of my colleagues in Zürich, a theoretical physical chemist who remarked during a 1982 lecture to the local chemical society: "Nowadays, the molecular program of chemistry has arrived at its successful termination" (*H. Primas*). What he meant is that research should no longer be directed primarily toward areas that lend themselves to treatment by simple molecular models. Instead, we should take the risk of attacking more complicated systems, ones whose structures and properties are determined by non-covalent interactions. This is precisely the shift in emphasis that has occurred in organic chemistry. In all aspects of the discipline—target structures, analysis, synthetic methodology, mechanistic investigations—discussions now tend to revolve around topics such as molecular recognition; supramolecular chemistry (or "supermolecules", to use *Lehn*'s terminology);[53] inclusion compounds (clathrates);[54] self-assembly, self-organization,[53, 55] even the self-reproduction or self-replication[56] of structures. Titles of lectures and publications now regularly include expressions like host–guest,[57] intertwining molecular threads,[58] information storage and processing,[53] molecular architecture,[59] molecular hole burning,[60] molecular computers,[60] molecular devices,[53] molecular cybernetics,[61] molecular cavities and clefts,[62] molecular Lego,[60] molecular mechanisms of biomineralization,[63] molecular robots,[12b, 64] molecular slits,[56] molecules within molecules,[57] nanochemistry,[53] programmed molecular systems,[53] spontaneous structure generation,[53] starburst dendrimers (control over size, form, and surface),[65] synzymes,[62, 66] template-associated synthetic proteins,[67] triple-helix formation in the non-enzymatic cleavage of DNA,[68] and van der Waals molecules.[57] The names of some of the key players on this new stage can be identified with the aid of the cited notes and literature references. An impressive example illustrative of the modern approach, particularly from the standpoint of "classical" catenane and rotaxane syntheses,[69] is summarized in Scheme 3. Scheme 4 compares the structure of the recently synthesized homo-DNA with that of normal DNA. Scheme 5 shows two self-orienting double helices in which bipyridyl–metal complex formation assumes the role of the familiar base-pairing interactions in DNA.

The exciting synthetic targets today are no longer molecules to be prepared "for their own sake"; instead, they are systems associated with particular functions or properties (cf. Scheme 6). Organic chemists are busy designing new materials,[10, 73, 74] and not only within the context of polymer chemistry,[9, 75] which—except in the case of certain biopolymers—is concerned largely with the preparation and investigation of products that show a Gaussian distribution in molecular weight. The molecular "design" of a (super)-structure[76] now captures the spotlight, while the synthetic process itself may withdraw into the background. The very simple organic reactions often turn out to be appropriate for the purpose of synthesizing such structures: acetal formation, alkylation, etherification, esterification, the formation of amides and sulfamides, or electrophilic aromatic substitution. Nevertheless, it will still be the chemists skilled in synthesis who will succeed in preparing the most interesting targets and exploring the most challenging themes, also in this area!

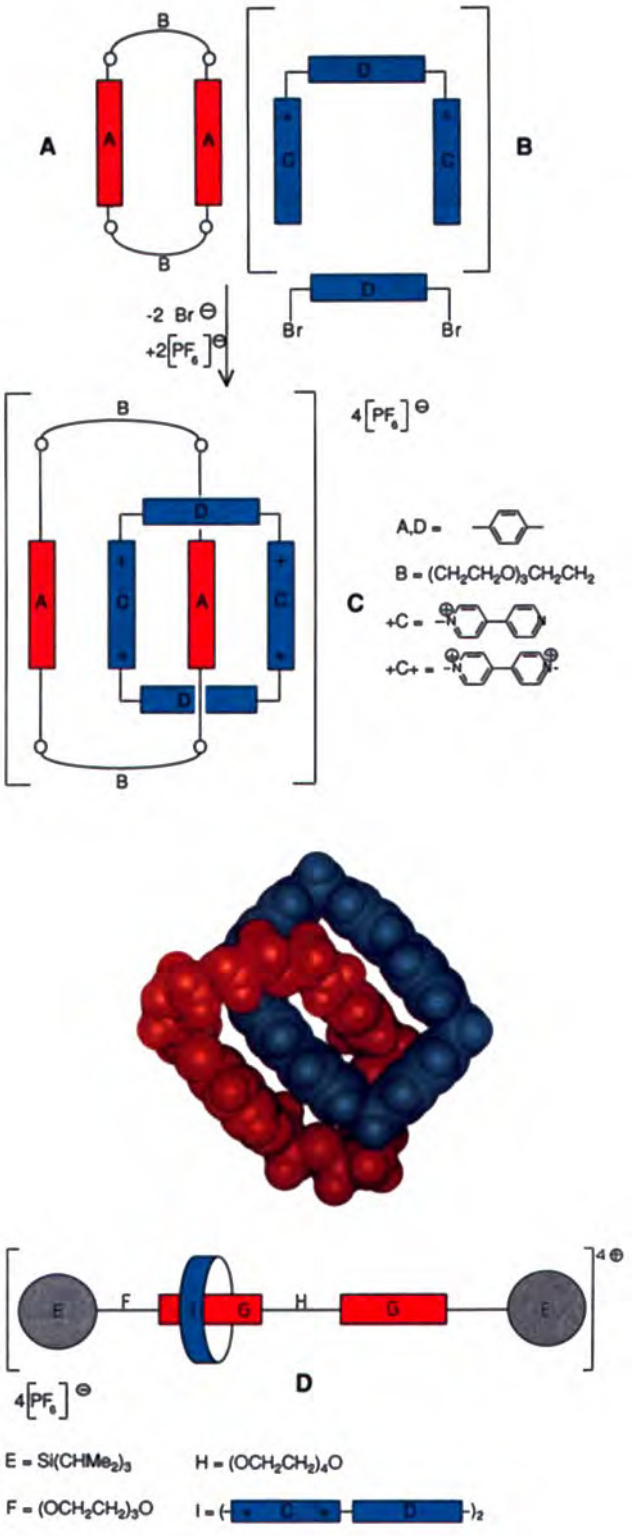

Scheme 3. "Self-assembly" of a catenane and a rotaxane (the authors employ the term *fabrication*) [60]. The O–*p*-phenylene–O units (O–A–O) of the macrocyclic ether **A** "bind" the two *p*-bis(pyridinium) units (+ C) of **B**, one inside the ring and the other outside. This causes the two pyridine nitrogen atoms to be kept in close proximity, so they can be joined using dibromo-*p*-xylene to provide, in 70% yield, the catenane **C**. The crystal structure of **C** displays not only a layer-like packing of donor and acceptor aromatic units but also "edge-to-face" interactions [70] between benzene rings A and benzene rings D. A similar synthesis of a simple catenane was accomplished starting with components held together by metal complexation [58]. Rotaxane **D** [60] was constructed using the same principle that was applied to catenane **C**. Back-and-forth motion of ring **I** [a bis(pyridinium) dication unit] between the *p*-phenylene units **G** has been verified by NMR spectroscopy ($\Delta G^{\neq} = 54.3$ kJ mol^{-1} in [D_6]acetone). The authors [60] call the system a "molecular shuttle".

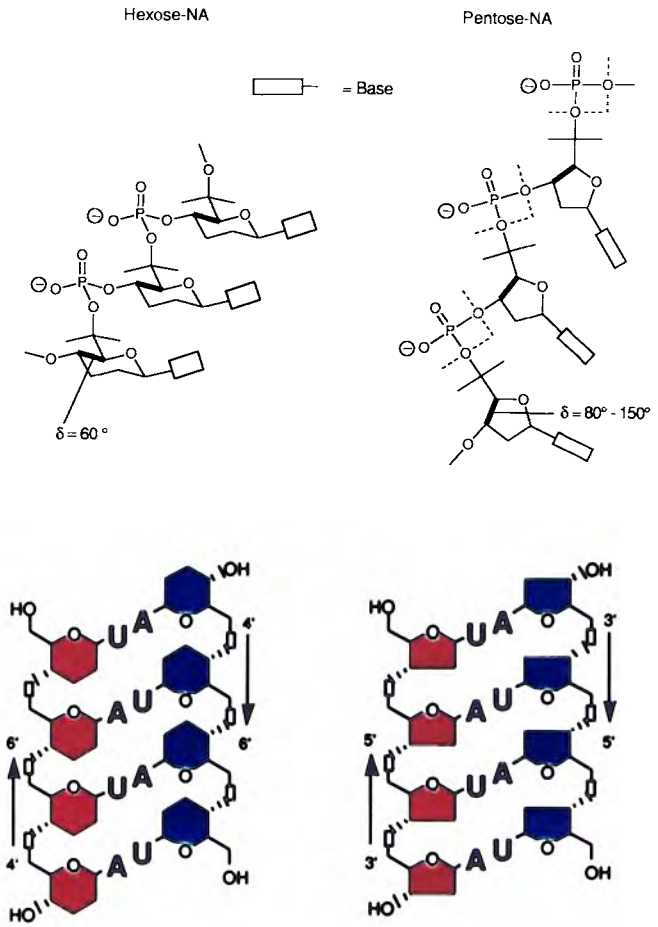

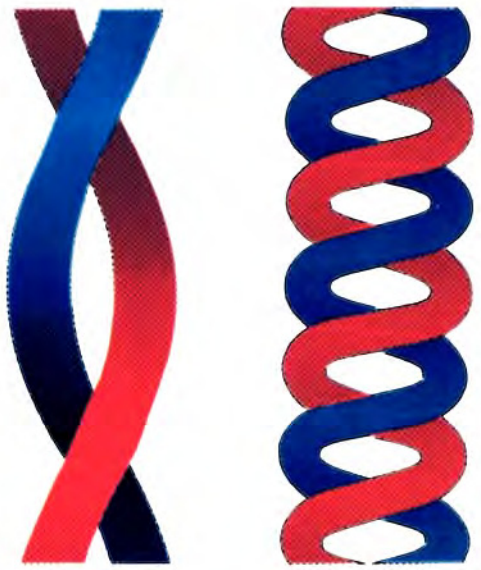

Scheme 4. An oligonucleotide that contains bis(desoxy)glucose (left) in place of the usual desoxyribose (right) carbohydrate units [55]. Perfect staggering about *all* the single bonds in the hexose derivative results in an inherently linear chain, along which the bases are arranged in parallel array. The tetrahydrofuran ring of DNA is characterized by incomplete staggering, leading to an intrinsically helical chain and greater conformational flexibility ("pseudorotation"). The most distinctive features of homo-DNA relative to normal DNA include stronger complexation between the strands, a much longer helix pitch, and pairing rules that differ from the Watson–Crick rules.

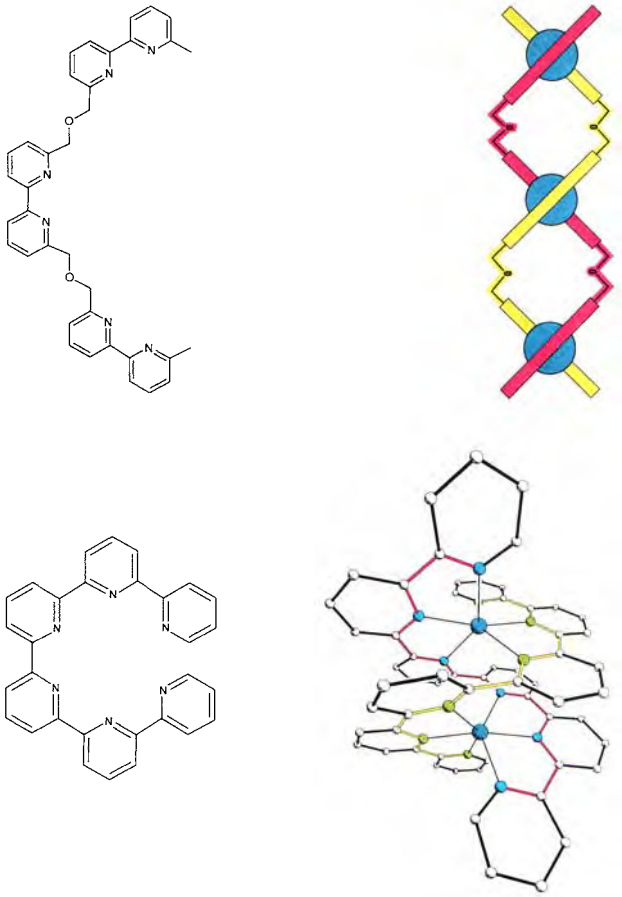

Scheme 5. "Inorganic" double helices constructed from doubly methylated, CH_2–O–CH_2-bridged bipyridine ligands and copper(I) ions (top) [53] or sexipyridine and cadmium(II) ions (bottom) [71]. In the first case it has been shown that (a) complex formation is attributable to positive cooperativity, (b) the mixing of bipyridine ligands with differing numbers of bpy units leads to "self-recognition" (i.e., complexes containing two ligands of the same length are favored), and (c) introduction of chiral substituents into one pyridine ring of a bpy unit causes preferential formation of one of the two possible enantiomeric helices (diastereoselectively!). In the second case, the double helix is probably stabilized by stacking interactions between superimposed pyridine rings. One of the ligands (top) was prepared by etherification, the other (bottom) through a Kröhnke reaction [72].

Molecules with the following

Form:		Function:	
- ball bearings	- knots	- abacuses	- nuts and bolts
- beads and threads	- ladders	- capacitors	- resistors
- belts	- nets	- catalysts	- screws
- cages	- springs	- circuits	- semiconductors
- chains	- stacks	- clocks	- sensors
- chimneys	- strips	- conductors	- shuttles
- clefts	- washers	- dynamos	- superconductors
- coils	- wires	- membranes	- switches
- collars		- motors	

Scheme 6. *Stoddart*'s list of objects and functions that are familiar from everyday life and for which he has proposed equivalents at the molecular level. (Taken from a lecture delivered by Prof. *Stoddart* at the ETH Zürich, 5 February 1990) [60].

2.2. Concerning Inhibitors, Suicidal Substrates, and Flustrates

Für die Biochemie braucht man mindestens so viel organische Chemie wie für die organische Chemie.[*]
L. Ruzicka (1964)

Another important new type of synthetic target is related to the active centers of biological catalysts (enzymes, receptors, transport and channel proteins, ribosomes). Recently there has been an explosive increase in the number of proteins whose structures have been characterized, proteins taken from throughout the realm of nature, beginning with viruses and proceeding through microorganisms, plants, and animals, all the way to man. This development can be attributed primarily to advances in gene technology and to modern methods of structure determination. Sequencing of the human genome is expected to be the key to all the proteins in our bodies, which should then become more readily available through expression in other organisms. Many proteins are already available on short notice and in substantial quantity, and this means that prospects are greatly improved for success in the crystallization experiments that of necessity precede X-ray structural analysis (see below).[77] At the same time, NMR spectroscopy is being used to carry out protein studies in solution, an approach supported by powerful computer modelling and computer dynamics (see Sec. 3). Characterization of an active center, or perhaps a substrate–enzyme complex, is the step that opens the way to further study through organic synthesis. Once the interaction between enzyme and substrate has been clarified, the likelihood is increased that an effective inhibitor can be designed. Medicinal chemistry is on the way to targeted preparation of inhibitors for all the crucial enzymes in the mammalian organism. Even agricultural chemistry is turning increasingly to selective intervention in the cellular chemistry of plants and pests.

Success in these areas demands a great deal of fantasy, considerable knowledge of structure–reactivity relationships, and experience in the efficient assembly of complex molecules—but it also requires a willingness to learn the "languages" of biochemistry, biology, and medicine.[78, 79] The importance of biological chemistry can easily be inferred from what has already been said in this section and from Sections 2.3 and 7.2.1 below. It is also apparent, however, from the number of relevant articles published in the new review journal *Chemtracts (Organic Chemistry)*:[80] in 1988 such articles accounted for 90 of the 500 pages, and by 1989 the proportion had grown to 130 out of 400! Other representative examples can be drawn from recent Nobel Prize lectures.[81, 82] Effects of all this activity on the methodology of organic synthesis are evident, for example, in a series of innovative investigations of compactin and its analogues[83] (useful for reducing cholesterol levels) as well as in syntheses of statin[84] and other rhenin inhibitors (which act to lower the blood pressure).[85] Interest in the latter has resulted in an active demand for novel approaches to non-proteinogenic amino acids,[86] peptides, and their analogues (cf. Sec. 7).[87]

[*] "Biochemistry requires at least as much organic chemistry as does organic chemistry."

Organofluorine compounds frequently play a role in the synthesis of inhibitors, substrate analogues, so-called enzymatic or metabolic probes, antimetabolites, "transition state analogues",[88a] and suicide substrates or inhibitors.[88b] Indeed, there has recently been a real "boom" in this field,[89, 90] producing considerable research activity in both academia and industry. This will certainly lead to improved methods for the synthesis of organofluorine compounds,[91, 92] but it will also provide a deeper understanding

Bond energy *[kJ mol^{-1}]*

C-H 416 C-F 485 C-Cl 328

Bond length *[Å]*

C-H 1.09 C-F 1.38 C-Cl 1.78

Van der Waals radius *[Å]*

CH_3 2.0 CF_3 2.7 CCl_3 3.5 $C(CH_3)_3$ 3.5

Van der Waals volume *(hemisphere [Å^3])*

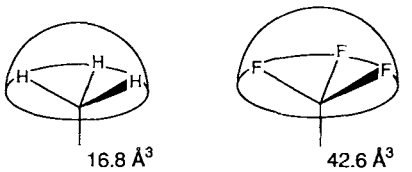

Electronegativity *(according to Pauling)*

H 2.1 C 2.5 Cl 3.0 F 4.0

Polarizability *(for CH_3X [10^{-24} cm^3])*

H 2.59 F 2.97 Cl 4.72 Br 6.03

Magnetic properties *(relative sensitivity)*

^{1}H (Spin 1/2) 1.00 ^{19}F (Spin 1/2) 0.83 ^{13}C (Spin 1/2) 0.016

Competitive inhibition

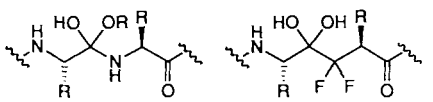

Suicide inhibition

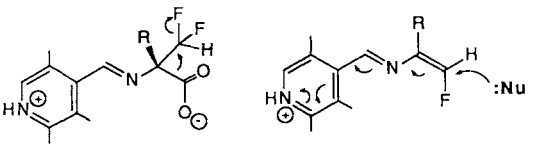

Scheme 7. Characteristic features of organofluorine compounds [91, 92]. The C–F bond is particularly strong; of all the bonds involving carbon, the C–F bond is the shortest apart from C–H; despite the fact that a CF_3 group has nearly twice the van der Waals volume of a CH_3 group, it is still capable of replacing the latter statistically in crystals (solid solutions [94a]); the C–F bond is extremely polar, but is nevertheless stable under most conditions; fluorine has a very high electronegativity, but fluorine compounds are very volatile; and substitution of CH, CH_2, or CH_3 by CF, CF_2, or CF_3 increases the lipophilicity of a compound (low polarizability of the fluorine electrons). On the other hand, fluorine substitution has enormous effects on the characteristics of functional groups: pK_a (C_2H_5OH) 16, (CF_3CH_2OH) 12.4; i.e., the trifluoro alcoholate is stabilized by 21 kJ mol^{-1} [92]; the introduction of F-substituted aromatic rings into pharmaceutical agents usually causes little change in general characteristics, but it leads to inhibition of oxidative metabolism (increased bioaccessibility, reduced dosage, patent "jumping"; the first fluorine-containing drugs were *Fried*'s fluorosteroids [98]); α-CF_2 ketones exist as hydrates in aqueous solution (cf. the similarity between the resulting hydrate and the tetrahedral intermediate of a peptide serinase-cleavage [92, 99]); α-difluoromethyl amino acids [91d] act as irreversible inhibitors ("suicide inhibitors") in that they lead to formation of a Michael acceptor at the active site of the enzyme responsible for pyridoxal phosphate metabolism (by nucleophilic addition to a neighboring group in the protein [100]). The magnetic properties of the ^{19}F nucleus facilitate the investigation of receptors and metabolic phenomena without interference from other magnetic nuclei [101]. (For sources of the data on fluorine compounds generally see [102].)

of the effects of fluorine on physical properties and of the frequently unexpected reactivity of this class of compounds.[91-97] A few aspects of the subject are illustrated in Scheme 7. The hectic state of activity in this field and the surprises that often emerge from what should be the simplest transformations of fluorine derivatives make it hard for me to resist coining a new term: *flustrates* (≡fluorine-containing substrates).

Not quite so well developed, but still subject to similar types of investigation, are nitro- and sila-analogues of physiologically active compounds, a few examples of which are shown in Schemes 8 and 9.

Properties of carboxyl and nitro groups

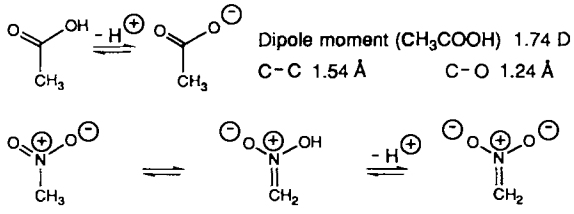

Relative binding constants of carboxylate enzyme substrates and their nitronate analogues

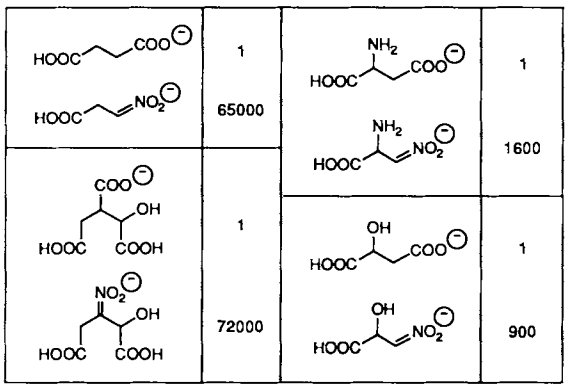

Scheme 8. A comparison of the nitronate group with the carboxylate group. According to [103], nitronate effectively mimics the characteristics of carboxylate with respect to geometry, polarity, and charge. Despite the great polarity of the nitro group [102], nitroaliphatics behave as non-polar compounds—in chromatography over silica gel, for example (NO_2 is a poor candidate for hydrogen bonding; cf. the fluorine derivatives in Scheme 7); references [95, 96, 104, 105] provide access to some of the author's preparative work and recent reviews of the literature. The greatly increased enzyme affinity of nitronate anion analogues compared with carboxylate anion substrates results in (apparently very successful) competitive inhibition [103].

Sila-isosteres of carbon compounds in particular may someday become very important, but within an entirely different context. Although sila derivatives have the same geometries as their carbon counterparts, their van der Waals dimensions are somewhat greater. In certain cases they might therefore serve as transition-state analogues for the preparation of catalytic antibodies, which would then accelerate reactions leading to the corresponding carbon systems. The same principle should apply to other heteroatom deriva-

***Bond lengths** [Å] CX vs. SiX*

C-**H** 1.09	C-**C** 1.54	C-**O** 1.41
Si-**H** 1.48	Si-**C** 1.86	Si-**O** 1.50

***Van der Waals radii** [Å] $C(CH_3)_2$ vs. $Si(CH_3)_2$*

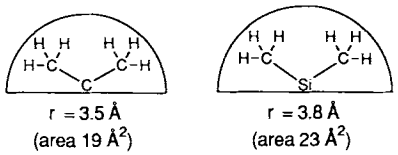

***Bioisosteric relationship** between C/Si analogues*

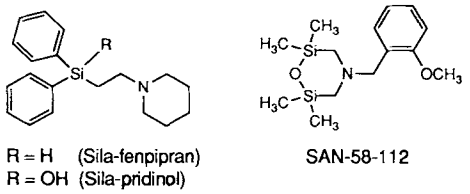

Scheme 9. Comparison of isosteric C and Si compounds. The illustrated Si isosteres of active substances [106] differ in interesting ways from the parent compounds; once again, the spatial arrangements [102, 107b] of the compounds are almost unaffected by incorporation of Si, but the reactivities (metabolizabilities) change considerably, as do electronic properties (possible formation of hypervalent species [107], σ-donor characteristics of the Si–C bond [108, 109]).—Deuterated derivatives have so far not been utilized, although the somewhat reduced size of CD_3 relative to CH_3 [110], for example, should have significant consequences, as should kinetic isotope effects [111] in interactions with receptors and in rates of metabolism (particularly on the physiological time scale).

tives as well, "organoelemental" compounds in which bonds to elements in the first row of the periodic table (such as C–H, C–N, C–C, C–O, R_3N, and R_2O bonds) are replaced by ones to elements displaying similar bonding geometries but greater bond lengths (bonds such as Si–H, Sn–H, C–P, C–Si, C–S, R_3P, R_3As, R_2S, R_2Se, etc.); the point is elaborated in the section that follows and in Schemes 10 and 11.

2.3. Antibodies as Catalysts in Synthetic Reactions: from Abzymes to Diels–Alder-ases

The intended targets of the molecular probes discussed in the preceding section were active centers of enzymes and receptors. Four years ago, two groups[112, 113] in the USA showed that with the aid of the immune system[79] chemists can also prepare selective catalysts that have antibody-type structures (i.e., immunoglobulins, giant protein molecules with molecular weights of ca. 150 000 daltons), substances that have been referred to as "abzymes" (*antibody enzymes*).[112] Work in this area is particularly dependent on the chemist's imagination and knowledge. In *one* of the reported variants, the preparative procedure is essentially[114] as follows (Schemes 10 and 11): first, a molecule is synthesized with a shape resembling as closely as possible either a transition state or a short-lived intermediate in the reaction to be catalyzed. This substance is treated as a hapten and coupled with a carrier molecule (e.g., a protein) to produce a combination with immunogenic properties (an antigen). The antigen is then introduced into the circulatory system of

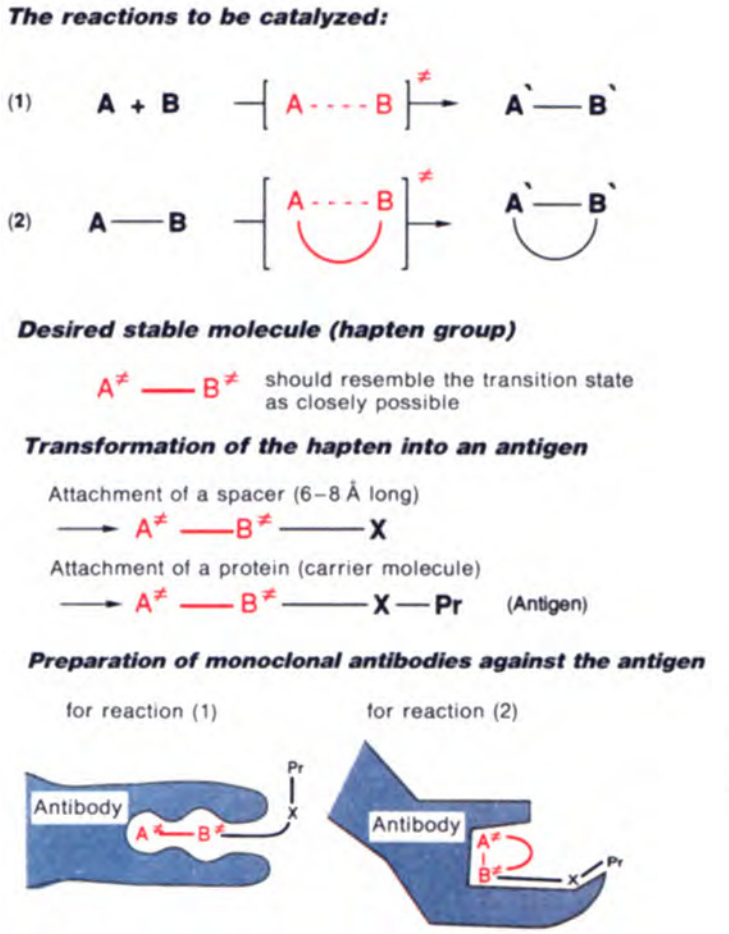

Prerequisites for an antibody effective as an enzyme-like catalyst

The "active center" must have a greater affinity for the transition state or intermediate than for the educt or product

Scheme 10. Preparation of monoclonal antibodies with "recognition potential" for the arrangement of transition states or intermediates; there also exist other methods by which catalytically active antibodies (abzymes) can be prepared [114b].

a mammal,[119] which responds with an immune reaction leading to antibodies. The antibodies are isolated, and those with the highest affinity are separated and replicated monoclonally.[120] Finally, a test is performed for catalytic effectiveness in accelerating the target reaction. Abzymes prepared in this way[114] have been shown to accelerate by factors as great as 10^5 such reactions as ester-,[115, 121] amide-,[114b] and peptide-bond cleavages;[122] lactonizations;[123] and even Claisen rearrangements,[116] Diels–Alder reactions (catalysis by "Diels–Alder-ase"),[118] and redox reactions.[124] All such reactions of course display enantioselectivity.

It would be unreasonable to suggest that synthetic chemists will soon be trying to make an abzyme for "the next step" in a multistep laboratory-scale synthesis. On the other hand, industrial chemists interested in the production of larger amounts of fine chemicals or pharmaceuticals are not likely to shy away from the effort required to prepare such custom-designed catalysts. Indeed, the day may come when attempts will be made to develop entire reaction cascades mediated by multi-abzyme systems, with a final, irreversible step ensuring the smooth operation of a complex sequence of abzyme-catalyzed reactions. Just as has happened with enzymatic transformations,[125] abzyme procedures are likely soon to be extended beyond the constraints of aqueous media, and some abzyme-catalyzed processes will probably prove to be essentially substrate-independent (as in the case, for example, of lipase- and esterase-catalyzed enzymatic reactions;[126] cf. also Section 7.2.1).

We have so far been dealing with considerations that impinge directly on the synthetic organic chemist, but recent developments also have the potential for deepening our over-

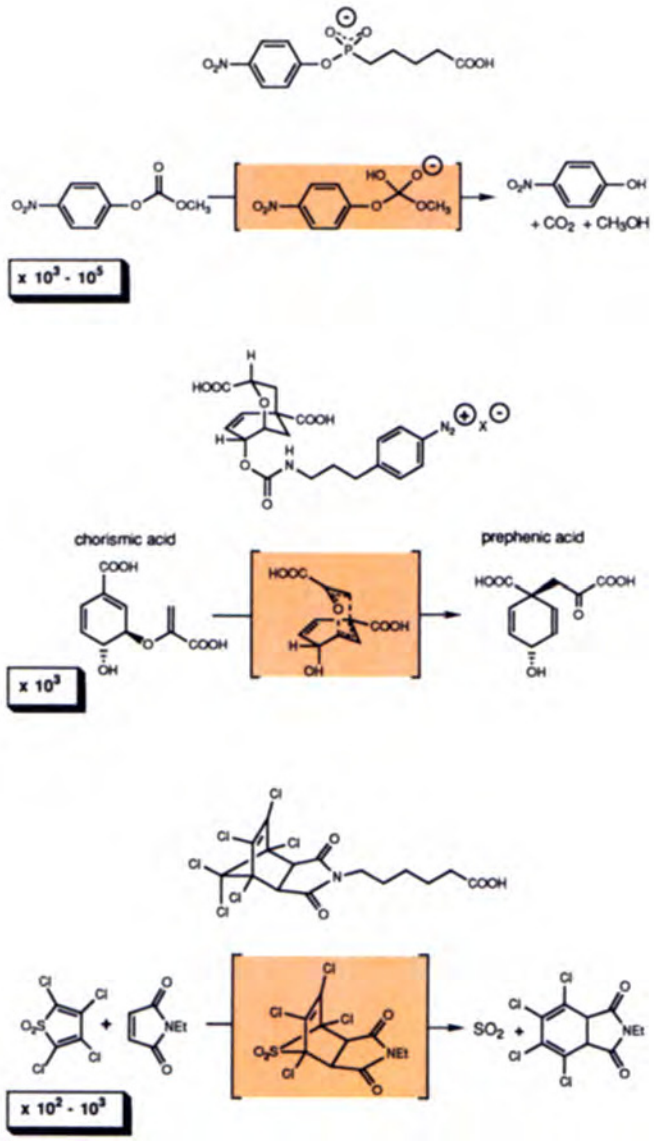

Scheme 11. Three examples of abzyme-catalyzed reactions. The observed rate enhancements in ester hydrolysis [114b, 115] and in the rearrangement of chorismic to prephenic acid [116] are significantly less than those produced by natural enzymes (esterases and chorismate mutase [117]). In the case of the Diels–Alder reaction [118], the antibody—generated in response to the hapten, and replicated monoclonally—must be methylated with $CH_2O/NaCNBH_3$ in order to keep it from reacting with tetrachlorothiophene dioxide (cf. suicide substrates). In each of the three examples, the hapten and the spacer are shown at the top, and directly below is the corresponding catalyzed reaction, including the transition state or intermediate and an indication of the observed extent of rate enhancement.

all understanding of molecular interactions. Examples have already been reported[114b] of structural investigations based on the use of catalytic antibodies and their complexes with transition-state analogues, permitting identification of the interactions that are at the root of hapten affinities. In the future, investigations of this type may compete successfully with the point-mutation methodology in protein studies ("site-specific mutagenesis"), especially since they offer the prospect of a much wider choice of potential substrates ("the whole of organic chemistry"). This potential may soon be further enhanced as a result of recent successes in the biosynthetic, targeted introduction of *non-proteinogenic* amino acids into proteins.[127–131]

3. Analysis, Computers, and Theory—No Progress without Help

—citius, altius, fortius[*]
Pierre de Coubertin, father of the modern Olympic Games

Dramatic progress in organic chemistry has always been closely linked to the introduction of new methods in analytical chemistry generally. The pace of advances increases as a direct function of the speed, sensitivity, and precision of the methods available for following a reaction, for establishing a reaction's outcome, or for determining the constitution of

[*] "Swifter, higher, stronger."

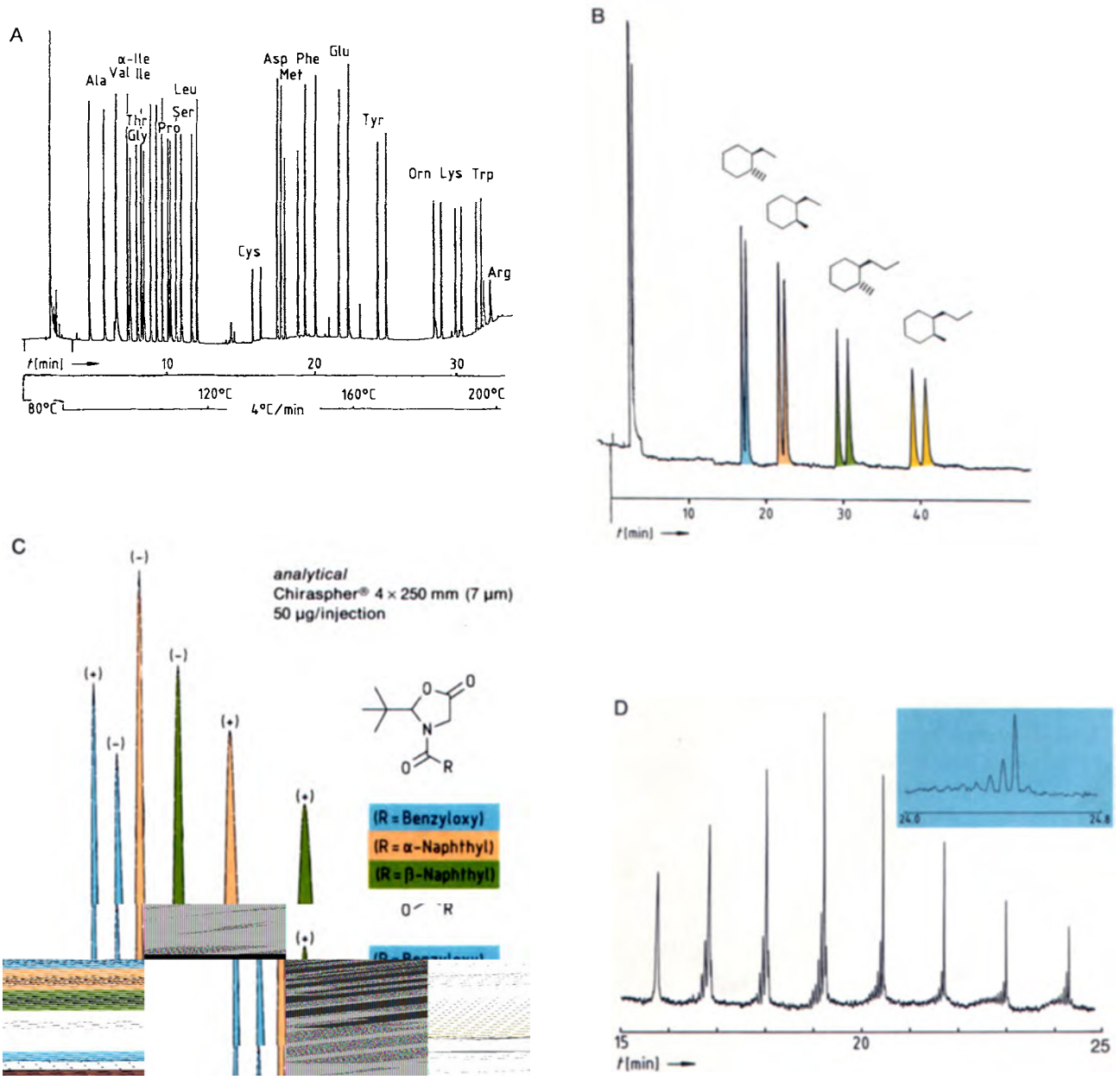

Fig. 1. Selected examples of separations accomplished with the aid of modern analytical methods. A) Gas chromatogram from a mixture of all the proteinogenic amino acids (racemic mixtures, in the form of *N*-pentafluoropropionyl isopropyl esters); Chirasil®-L-Val column containing 5% Kóvats phase [135]. B) Gas chromatogram from a preparation containing racemic *cis*- and *trans*-1-ethyl-2-methyl- and *cis*- and *trans*-1-methyl-2-propylcyclohexane; cyclodextrin column [136]. C) HPLC separation of a mixture of three racemic oxazolidinones for amino acid synthesis; Chiraspher® column [137]. D) HPCE separation of a poly(desoxy)thymidylic acid mixture, with an enlargement of the region near 160 nucleotide units; polyacrylamide gel, 3×10^7 plates [138].

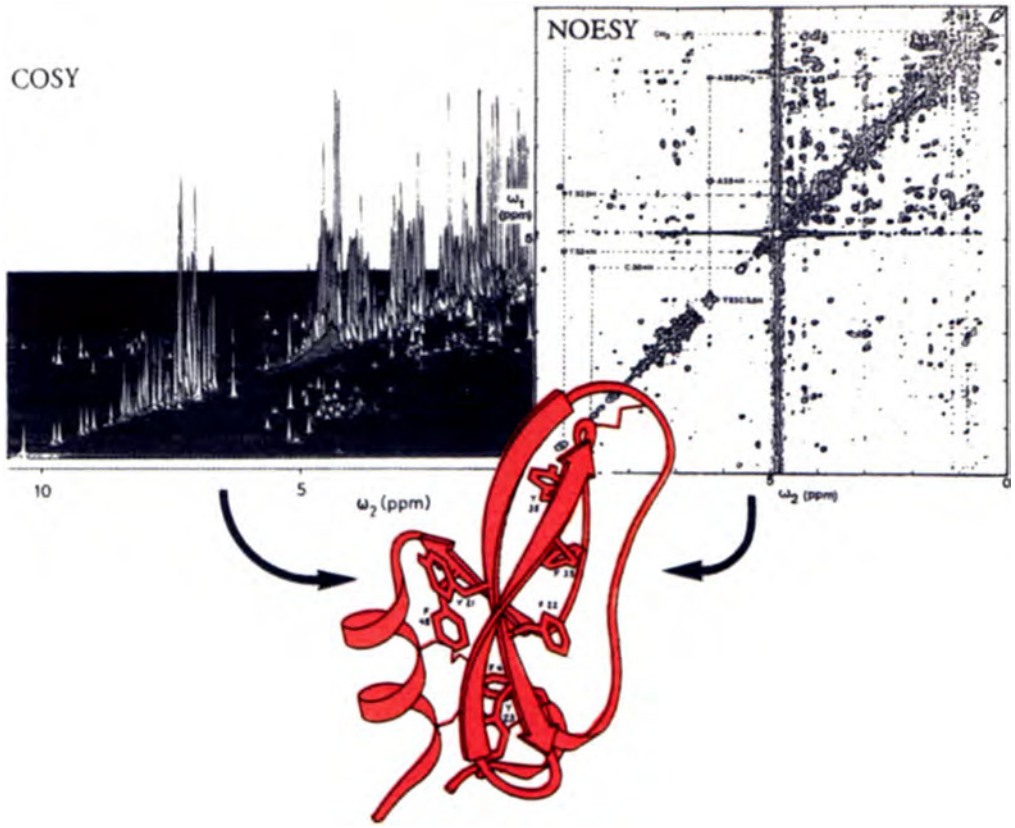

Fig. 2. 2D-NMR spectrum of the basic trypsin inhibitor from the pancreas [143]. A combination of X-ray structure analysis, NMR spectroscopy, and computer-assisted modeling/dynamic calculation on proteins results in detailed information about both their structure and their enzymatic function (see Sec. 3.3 and Fig. 8).

a mixture or the structure of a complex molecule—up to and including antibodies, DNA, or supermolecules held together by non-covalent forces. It would be wrong in a presentation such as this not to acknowledge, at least, the dependency of organic chemistry upon analytical chemistry. Unfortunately, limits of time and space preclude my doing much more than "name-dropping", although I will provide a few key citations and introduce a handful of impressive examples.

3.1. Chromatography, NMR, and Mass Spectroscopy

The last 35 years have witnessed the advent of remarkable new analytical techniques. These can be conveniently separated into three categories: chromatography, spectroscopy, and miscellaneous methods. With respect to the first, thin-layer and gas chromatography[132] appeared in the vanguard, then came HPLC, and finally chiral stationary phases for determining enantiomeric ratios[133, 134] (Fig. 1). Very recent additions include HPCE ("high-performance capillary electrophoresis")[138] and FFF[139] ("field flow fractionation", which actually involves a different principle altogether). Now there is even talk of *neochromatographic* techniques.[139, 140]

The earliest of these developments in chromatography coincided with the introduction of NMR spectroscopy, a technique whose triumphal march through chemistry is far from exhausted. Accustomed originally to small instruments based on permanent magnets and applicable only to ^{1}H measurements, we now take for granted sophisticated high-field spectrometers with magnetic coils fabricated from superconducting materials. Various pulse techniques and Fourier transform capability have been incorporated into versatile devices suitable for routine multi-element analysis. 2D-[141] and 3D-spectroscopy[142] (Fig. 2) as well as the study of

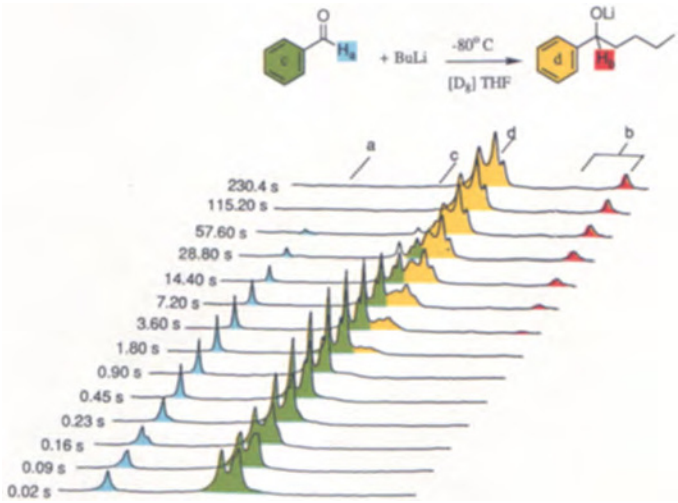

Fig. 3. Rapid-injection ^{1}H-NMR measurement (RI-NMR) [145] during the reaction of butyllithium with benzaldehyde at $-80\,^{\circ}C$ in perdeuteriotetrahydrofuran. A benzaldehyde solution of the substrate (2.3 mg in 250 μL [D_8]THF) and butyllithium (15 μL, 2 M in hexane) were injected into a 5 mm NMR tube (rotation frequency 10 Hz). Pulses and Fourier transforms were applied after the indicated time intervals (Bruker model WH-360) [146]. Further applications of this method involve studies of reactions of other organolithium systems and of organomagnesium compounds [147, 148], and investigations of short-lived cations [149].

dynamic processes have all become possible through the introduction of extremely clever pulse sequences,[144] and accessories have been made available for automatic sampling and for low-temperature analysis of fast chemical processes [RI ("rapid injection") NMR methods, cf. Fig. 3].[145, 147]

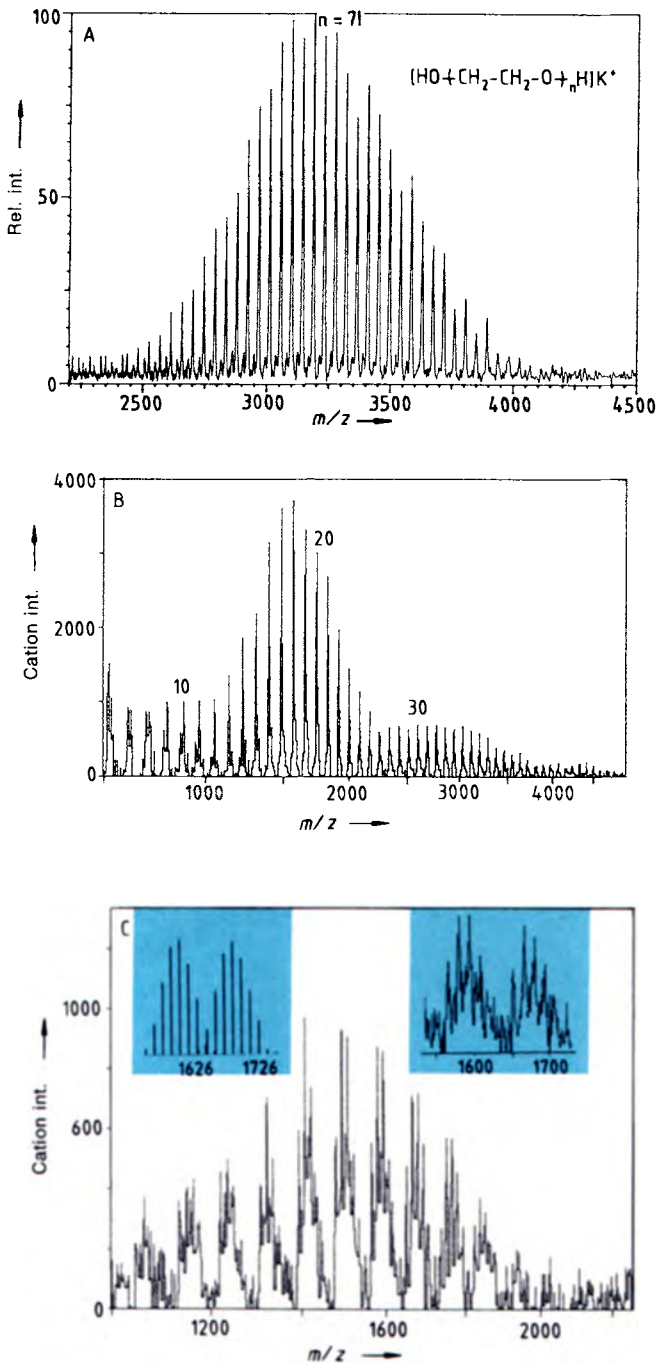

Fig. 4. Analysis of the molecular weight distribution of polymers by mass spectroscopy. A) Laser-desorption Fourier-transform mass spectrum (LD-FTMS) of a poly(ethylene glycol) sample (mean molecular weight 3550 dalton) [155]. B) Plasma-desorption mass spectra (PDMS) of poly[(*R*)-3-hydroxybutyric ester] [PHB, mean molecular weight 2740 dalton (osmometric)] and C) of a copolymer consisting of 78% PHB and 22% poly[(*R*)-3-hydroxyvaleric ester] (BIOPOL®). The inserts show observed intensities and intensities calculated for a statistical distribution of HB and HV [156]. Recently, a special laser-desorption mass-spectroscopic method was used to detect the molecular ion of the protein bovine albumin (67 000 dalton) [157]. Coupled capillary-zone electrophoresis/ion-spray mass spectroscopy permitted the detection of (multiply charged) molecular ions from proteins with molecular weights as high as 150 000 dalton [154c].

Chiral shift reagents now permit the direct determination by NMR spectroscopy of enantiomer ratios,[134] and difference-nuclear Overhauser effect measurements are used routinely as a source of information about configuration, once determined almost exclusively by "wet chemical" methods (i.e., chemical correlations). It seems quite likely that NMR will soon be providing structural resolution at the level of one C–C bond length (1.5 Å) with proteins containing over 100 amino acid residues. Indeed, bets have been placed on the question of whether NMR spectroscopists or X-ray crystallographers will be the first to establish a protein structure with a given degree of precision. The principal differences between the two methods are that NMR deals with structures as they exist in solution rather than in the crystalline phase, and only NMR is capable of probing dynamic processes.[141–152] Solid-state NMR spectroscopy is also well on the way to becoming a routine technique.[153]

Mass spectroscopy has undergone developments comparable in importance to those of NMR. For example, FAB ionization has finally made it possible to apply this technique to the detection and study of molecules of ever-increasing size. Radically new ionization techniques[154] have been introduced very recently, and these are currently undergoing tests (cf. Fig. 4). The combinations GC/MS, HPLC/MS, and HPCE/MS have facilitated analysis of the most complicated mixtures as well as high molecular mass materials—a major advance for chemistry, but one subject to serious abuse by those who ignore *Paracelsus'* still valid definition of a "poison".[158]

The fact that organic synthesis is now preoccupied with increasingly complex systems has effectively brought an end to the days when a synthetic chemist could hope to identify a product with a "quick glance" at a set of IR, NMR, and mass spectra. Today, and even more in the future, such problems warrant the involvement of teams of specialists. The methods available for structural analysis are now so diverse that one can no longer aspire to be both an imaginative chemist who studies a wide range of reactions and an expert at analyzing the resulting products. On the other hand, a "super-spectroscopist" runs the risk of becoming little more than a sterile technician in the absence of contact and collaborative interaction with those in a position to recognize and investigate important chemical problems and isolate species with intriguing new structures.[159]

3.2. X-Ray Structure Analysis—Also Valuable for Probing Reactivity!

The difference between a chemist and a crystallographer can be compared to two people who try to ascertain what furniture is present in a darkened room; one probes around in the dark breaking the china, while the other stays by the door and switches on the light!
J. D. Dunitz (1977)

Among the remaining analytical methods, X-ray structure analysis surely deserves to be mentioned first.[160] It has

become impossible for a synthetic organic chemist to remain competitive without access to this technique. Tears well up in crystallographers' eyes when they hear synthetic chemists assert that X-ray structure analysis is on the verge of becoming a type of spectroscopy. Instruments are indeed being developed that use more powerful X-ray tubes and incorporate faster mechanical devices for more rapid collection of reflections, and increasingly efficient computers and better software[161] are being incorporated for the solution of structures. It is now possible to carry out routine X-ray structural analyses of moderately complex molecules in the same amount of time that used to be set aside for NMR analysis. State-of-the-art technology for the solution of very large structures is soon likely to feature a synchrotron as the source of short-wavelength radiation, and to invoke non-monochromatic radiation (as in the original Laue method, cf. Fig. 5).[162-164] The ability to grow perfect single crystals of pure compounds—one of the most ancient of chemical arts—will once again command respect in the laboratory. Chemists who display a combination of dexterity and devotion as they manipulate their products will stand the greatest chance of success in this endeavor. The foregoing generalization is equally applicable to small and large structures;[165, 166] compounds that are stable and those that are extremely air-sensitive;[167a] and materials subject to decomposition[167b] well below room temperature,[168] loss of solvent,[169] melting,[170] or the development of plastic crystallinity.[171]

It has recently become apparent that X-ray diffraction can be important to the chemist not only for establishing the structures of isolated products, but also as a means of learning something about the structures of reactive intermediates—and therefore about reactivity in general. Many of the idiosyncrasies and imponderables associated with the chemistry of polar organometallic compounds have become better understood, or have even been circumvented entirely, once the corresponding crystal structures were "seen";[167, 171-174] four recent examples are presented in Fig. 6. Other cases show how structural data can be correlated with the reactivity of compounds (the principle of structure–reactivity correlation)[179-181] or with force constants.[182] Three examples are presented in Fig. 7 in which pyramidalization of trigonal carbon atoms, determined in the crystalline phase, has been used to explain reactivities in solution. It is to be hoped that the future will bring more such non-routine applications of structure determination, and it is almost certain that X-ray results will continue to "open the eyes" of synthetic chemists. The crystallographic data bank in Cambridge (CSD)[189] already contains a wealth of uninterpreted information, a veritable treasure trove waiting to be exploited by the initiated!

It is difficult to predict which other analytical techniques will provide valuable information for synthetic chemists in the future.[190] We look with envy, for example, at tunneling electron microscopy,[191] which permits one to probe surfaces with a resolution sufficient to cause pyrrole and benzene rings—even individual xenon atoms—to become "visible",[192a] and capable of revealing a piece of double-stranded DNA as a kind of "molecular braid".[192b]

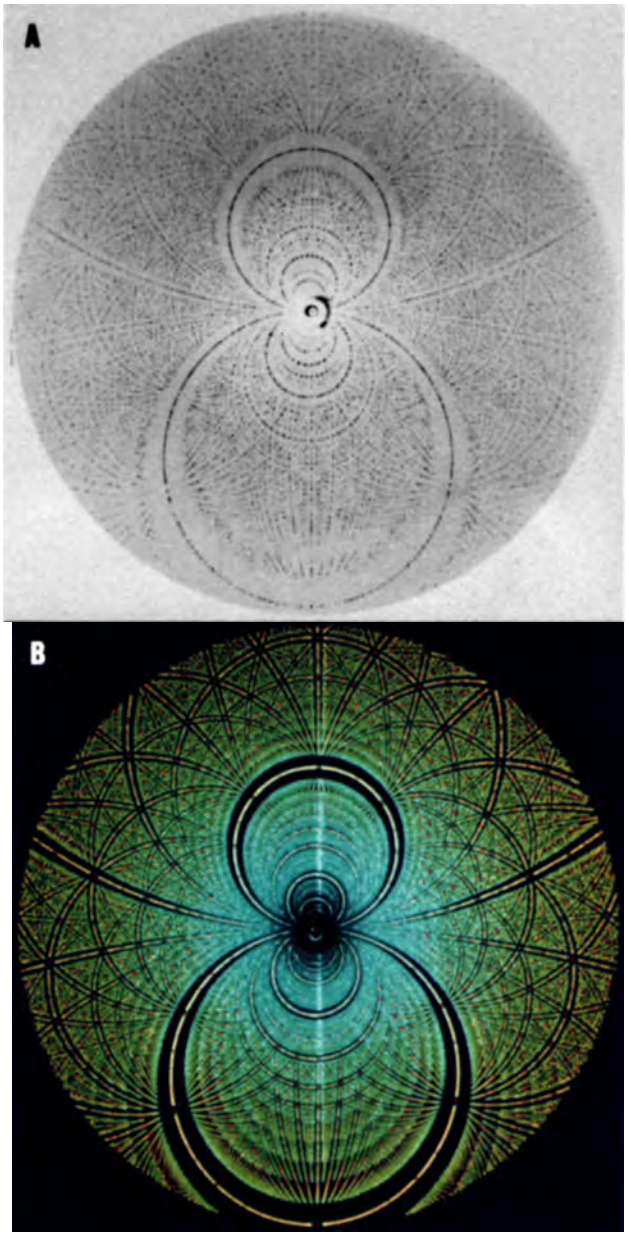

Fig. 5. Laue diffraction pattern of glycogen phosphorylase B. The use of high intensity, non-monochromatic synchrotron irradiation permits the collection within minutes of the data associated with a large protein or nucleic acid molecule—even an entire crystalline virus [162, 163]. Polychromatic irradiation permits a great many planes to fulfill the conditions of reflection, so that a single 100 μs "shot" can produce 150 000 measurable reflections. Employing a video camera as the recording device makes it possible to record the reflections generated by several pulses directed in rapid succession at a rotating crystal. This method is of course equally applicable to crystals of smaller molecules or even typical inorganic solids, although it requires crystals of higher quality than those typically used for monochromatic irradiation. *J. Hajdu* [164] has visions of employing pulse lengths of 10–40 ps, intervals of a few ns, and intensities equivalent to those produced by the highest energy synchrotrons to investigate on the ps time scale reactions occurring in the crystalline state. Nevertheless, enormous problems remain to be overcome (computer programs for the corresponding structural calculations, radiation damage, etc.). A: Laue photograph of glycogen phosphorylase B (space group $P4_32_12$, $a=b=128.8$, $c=116.2$ Å), taken at station 9.7 of the Daresbury synchrotron radiation source. The crystal was rotated 33.75° from the position with a^* antiparallel to the beam and c^* coinciding with the spindle of a one circle camera. Wavelength range: 0.20–2.10 Å; crystal to film distance: 133.8 mm; film radius: 59 mm; exposure time: 1 s; predicted total number of reflections: 49 570.—B: Computer-generated Laue pattern of glycogen phosphorylase B (parameters as above) at 2.4 Å resolution. Reflections were color-coded to their wavelengths: blue signifies 0.20 Å and red is 2.10 Å (other wavelengths shown correspondingly in relation to the visible spectrum; computer program written by *I. J. Clifton*, Laboratory of Molecular Biophysics, Oxford University); total number of reflections: 49 570.

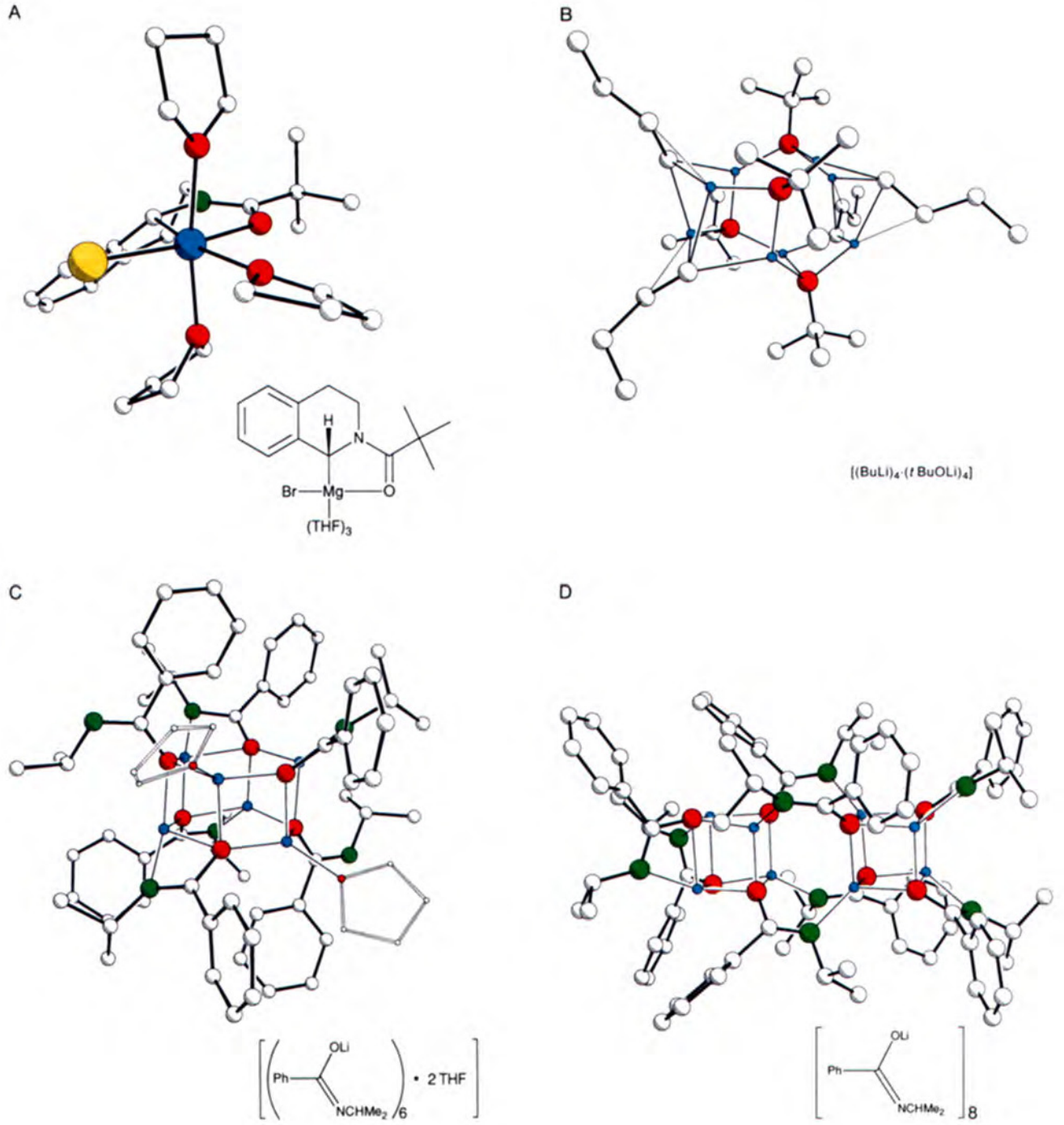

Fig. 6. Four structures of polar organometallic compounds of preparative significance. A) A tetrahydroisoquinoline derivative metallated in the 1-position; in contrast to the Li analogue, the Mg derivative whose crystal structure is shown here [174] adds with high diastereoselectivity to aldehydes [175]; structural data (Mg octahedral, Li tetrahedral; one of the THF solvent molecules is considerably further removed from the metal than the other two) were used in the development of a mechanistic model. B) Crystal structure [176] of an octameroid complex with the composition $[(BuLi)_4 \cdot (t\text{-}BuOLi)_4]$. Complex bases derived from butyllithium and potassium *tert*-butyl alcoholate (Lochmann–Schlosser bases [177]) prove to be much more efficient deprotonating agents than their components; it has been suggested that the uniqueness of such bases is a consequence of their complex structure. C) and D) Hexamer and octamer of lithiated benzoic acid isopropylamide [178]; the existence of such complex structures may be responsible for the remarkably selective reactions of polylithiated oligopeptides [172].

3.3. Quantum Mechanics and Force Fields: Ever Larger Pictures, Increasingly Reliable (a Contribution to Chemistry from Microchips)

Electronic data processing has played an important part in all the dramatic advances in instrumental analysis described above[193]—a contribution of microelectronics to chemistry. The same applies to other areas of considerable interest to the synthetic chemist: literature searching, the organization of information about reactions, retrosynthetic analysis, structural data banks, structural and dynamic modelling of molecules and transition state geometries, and ab initio cal-

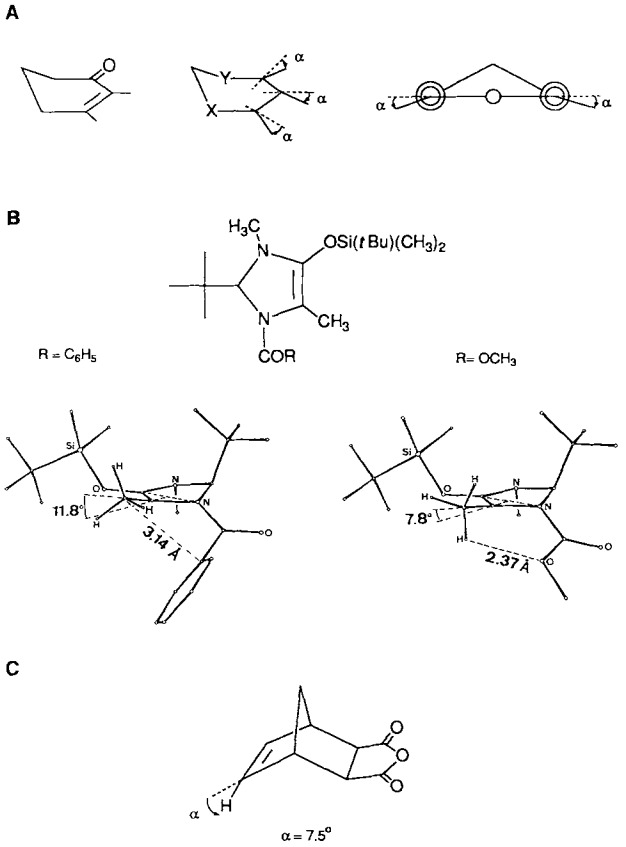

Fig. 7. Pyramidalization and reactivity at trigonal centers. A) In the crystalline state, cyclohexenones and similar derivatives with five atoms nearly in a plane and a sixth atom outside this plane ("sofa" conformation) often display pyramidalization of the trigonal centers in precisely that direction from which attack occurs during reactions transforming the trigonal centers into tetragonal centers [183]. B) Crystal structures of silylenol ethers from imidazolidinones, where $R = C_6H_5$ or OCH_3; the trigonal, methyl-substituted C atoms are displaced by 7.8 or 11.8° ($\Delta = 0.07$, 0.11 Å) from the plane of the five-membered ring, and pyramidalization is in the direction from which reaction occurs with electrophiles for both the Si enol ethers and the corresponding Li enolates [184] (see also Scheme 12). C) The crystal structure of a norbornene derivative (determined using neutron diffraction) displays pyramidalization in the *exo* direction for the trigonal carbon atoms of the C–C double bond [185] (cf. the suggestion made in 1967 that the unexpectedly high *exo* selectivity in reactions of norbornenes might be due to torsional effects [186, 187], as well as *Huisgen*'s "Factor X" [188]).

culations, to name but a few. Computer technology and the advent of instantaneous worldwide data transfer have transformed the everyday life of the chemist, and their importance will certainly continue to grow. Table 1 contains a list of computer programs we have assembled for use in our research group. Most are for the Apple Macintosh computers that are running day and night in our laboratories and offices, serving also as terminals that can be used for tapping the extensive resources of the ETH computer center.

Product and transition-state geometries of increasingly large molecules and even supermolecules can be simulated effectively with the aid of computer programs that are also constantly increasing in their power. The demonstrated reliability of such predictions—judged on the basis of comparisons with structural parameters obtained through spectroscopy or diffraction—has caused even novices to trust computed results for systems that are not (or not yet!) susceptible to experimental verification (cf. the examples in Scheme 12). Virtually all the fundamental reactions of or-

Table 1. Sources of computer information, and computer-based tools useful to the synthetic chemist [194]. Most of the programs and databases listed here are currently available in the organic chemical laboratories of the ETH Zürich. (To be fully effective, the programs must be immediately accessible within the laboratory itself.)

Drawing	ChemDraw [195]	
Literature searching	*Chemical Abstracts* databases Substructure searches [196]	
Retrosynthesis [17b] **and reactivity**	CAMEO	(**C**omputer-**A**ssisted **M**echanistic **E**valuation of **O**rganic Reactions) [197]
	CASP	(**C**omputer **A**ssisted **S**ynthesis **P**lanning) [198]
	CHIRON	("**Chir**al **Syn**thons") [199]
	LHASA	(**L**ogic and **H**euristics **A**pplied to **S**yntheses **A**nalysis) [17b,200]
Reactions [201]	ORAC	(**O**rganic **R**eaction **A**ccess by **C**omputer) [202]
	REACCS	(**Reac**tion **A**ccess **S**ystem) [203]
	SYNLIB	(**Syn**thetic **Lib**rary) [204]
Structures	CSD	(Cambridge Structural Database "Cambridge File") [189]
Modeling	MacMoMo [205] Chem 3 D Plus [206] Macro Model [207] (MM2 [208]) [209]	
ab initio calculations [210]	Monster-Gauss [211] CADPAC [212] GAMESS [213] MOPAC [214]	

ganic synthesis[218]—including nucleophilic addition to carbonyl groups,[219] the Michael addition,[220] the aldol addition,[221] 1,3-dipolar cycloaddition,[222] the Diels–Alder reaction,[223] hydroboration,[224] and addition to double bonds with stereogenic centers at their allyl positions[219, 220–224]—have been subjected to more or less elaborate calculations based on force field and/or ab initio methods. "Theoretical Chemistry en route to a Theory of Chemistry" is a proclamation[225] that pertains not only to very simple systems, and not just to reactants; it even embraces solvents (in modeling,[226] as well as in the context of proteins and nucleic acids;[227] cf. Fig. 8).

4. Experimental Design, Experimental Procedures, Types of Reactions, and Reaction Techniques—a Question of More Than Just the Scale of the Reaction

Necessity is the mother of invention!

Many of the modern techniques for carrying out reactions or purifying products still have a reputation for being somewhat exotic, and certainly inapplicable to large-scale work, but it is easy to foresee the day when these same methods will begin to play a significant role in the manufacture of organic compounds, opening the way to the synthetic reactions that depend on them. Meanwhile, other industrial processes that are now wide-spread will need to be abandoned because they are associated with indefensible levels of risk and the cost of retaining them will prove too high [e.g., reactions in hexamethylphosphortriamide (HMPT), which has mutagenic properties].[228] When I speak here of industry I am really referring to the preparation (usually in several steps) of specialty chemicals—particularly pharmaceutical agents, perfumes, vitamins, and agricultural products—not the bulk manufacture of petrochemicals, solvents, or polymer precur-

A

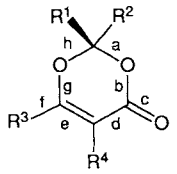

Bond	a	b	c	d
Average value	1.430	1.371	1.202	1.443
Calculated	1.422	1.383	1.195	1.467

Bond	e	f	g	h
Average value	1.336	1.487	1.359	1.427
Calculated	1.322		1.366	1.436

Angle	ab	bc	bd	cd	de
Average value	116.2	118.1	114.5	127.2	121.3
Calculated	118.6	120.0	113.8	126.2	120.5

Angle	eg	ef	fg	gh	ah
Average value	119.9	127.8	112.3	114.4	110.0
Calculated	122.9	124.5	112.6	114.5	111.5

B

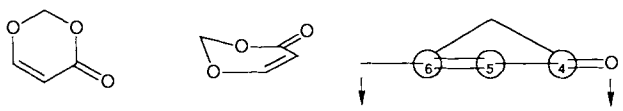

observed and calculated displacement of the substituents in the indicated direction: 0.2–4°

C

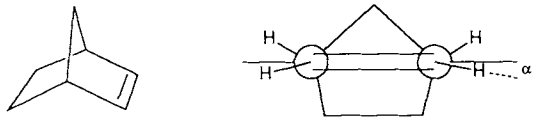

obs. 7.5°, calc. 3.4°

D

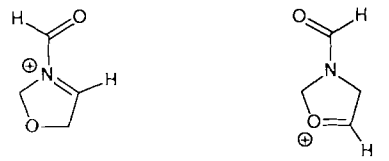

0.00 kJ / mol 44.8 kJ / mol

Scheme 12. A comparison of several structures obtained by crystal structure analysis with predictions based on ab initio calculations. A) Observed and computed (3-21G for the unsubstituted dioxinone $R^1=R^2=R^3=R^4=H$) pyramidalization of the trigonal C atoms of dioxinones (cf. Fig. 7); bond lengths in Å, angles in degrees [183]. B) Pyramidalization at the trigonal centers of norbornene; comparison of observed parameters (Fig. 7) [185] with predictions (STO-3G) made many years earlier [215]. C) The acyliminium ion is found experimentally to be more stable than the oxonium ion, and it is also predicted to be more favorable by ab initio calculations (3-21G) [216]. Perhaps the most ambitious calculations to date (MP3/6-311++G**//6-31G*) are due to *Wiberg* [217], and they have shaken the foundations of our qualitative models of resonance stabilization.

sors. In this context, many methods have already been introduced into large-scale practice that only a few years ago would have classed as truly bizarre ("the stuff of academia"). Consider the following examples, arranged al-

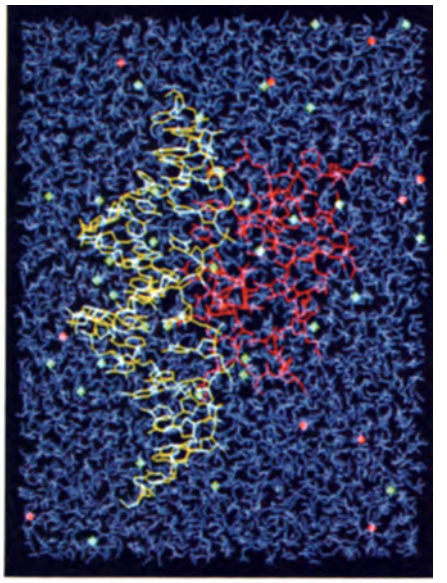

Fig. 8. Modelling in chemistry from the early days to the present. A) Calculations by *van Gunsteren* et al. (a complex of a DNA containing 14 base pairs with the lac-repressor protein from *Escherichia coli* in the presence of 34 $Na^{\oplus}$ ions, 10 $Cl^{\ominus}$ ions, and 3906 H_2O molecules; support provided by NMR data) [227]. B) "Match box" models of *van t'Hoff* (from the chemistry museum in the *Maison de chimie* of the French Chemical Society in Paris).

phabetically and supplemented with illustrations (or at least key literature references).

- *B*iological-chemical reactions (i.e., processes involving microorganisms and enzymes) are a good place to start, although some have actually been in limited use for years (cf. *Reichstein*'s vitamin C synthesis).[229] BASF now prepares (*R*)-lactic acid and various fragrances by fermentative routes; ICI makes tons of poly[(*R*)-3-hydroxybutanoate] by fermentation,[230] and the company has recently developed a process for the production of polyphenylene starting with *cis*-cyclohexa-3,5-dien-1,2-diol, an enzymatic oxidation product of benzene;[231] amino acids are prepared in Japan with immobilized enzymes and microorganisms that display unbelievably long catalytic lifetimes; and enantioselective esterification and saponification with lipases are accepted as standard procedures in both large- and small-scale applications (cf. also "abzymes" and the EPC synthesis, Sections 2.3 and 7.2).
- *C*hromatography over aluminum oxide, silica gel, or ion exchangers has apparently proven to be economically feasible in the purification of products like cyclosporin[232]

and in the bulk isolation of amino acids from protein hydrolyzates.[233] About ten years ago, a synthetic chemist in the pharmaceutical industry reacted to a management directive stating that active ingredients were no longer to be developed as enantiomeric mixtures by exclaiming "Then from now on we'll only study achiral compounds!" A decade later, chromatographic separation (by preparative HPLC) of a kilogram of an enantiomeric mixture is thought to be possible for less than 1000 DM (ca. $600).[133d]

- *C*lays, zeolites, and aluminum oxide have been recommended as catalysts or carriers for synthetic reagents.[234]
- *E*lectrolysis is seeing increasing use both in industry[235, 236] and in the laboratory[237, 238] (cf. Scheme 13).

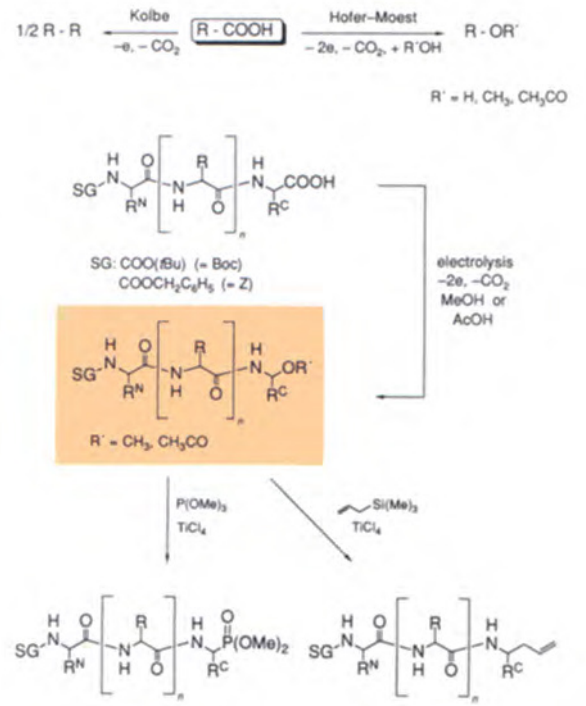

Scheme 13. Electrolysis of carboxylic acids and its application to the modification of peptides [239]. The great advantage of carboxylic acid electrolysis in particular is the fact that no electrolyte is required, and it is not necessary to employ divided cells. Addition of an amine causes the solution to become conductive; CO_2 is formed at the anode, and H_2 at the cathode. Equipment demands are minimal. "Normal" carboxylic acids afford Kolbe coupling products, while α-heterosubstituted acids undergo oxidative decarboxylation [237, 238]. In the case of oligopeptides (with up to six amino acid residues), electrolysis permits straightforward modification of the acid end of the molecule [239]; cf. the formation of phosphonic acid and allyl derivatives (polar vs. lipophilic end groups).

Indirect electrolysis[240] has proven particularly attractive, since it can be regarded as a catalytic process (e.g., an electrochemically generated oxidizing agent undergoes reduction in the course of a "perfectly normal" substrate oxidation, and is then regenerated at an electrode).[241]

- *F*luorination with elemental fluorine is now a subject of active investigation even in industrial laboratories.[92]
- *H*igh- and very-high-pressure conditions (up to 20 kbar) permit the realization of reactions with negative activation volumes ($\Delta V^{\neq}$).[242] For example, Diels–Alder reactions between sterically hindered components become feasible under such conditions, whereas equilibrium considerations preclude the usual approach of simply heating the mixture of starting materials to a high temperature.
- *L*ow and very low temperatures[243] under inert atmosphere have become commonplace even in large reactors—a source of some satisfaction for those who 20 years ago were telling industrial chemists about the remarkable selectivity of reactions with organometallic reagents at −100°C under argon, often to be greeted with smiles reflecting pity for the naiveté of "academic eggheads". To-

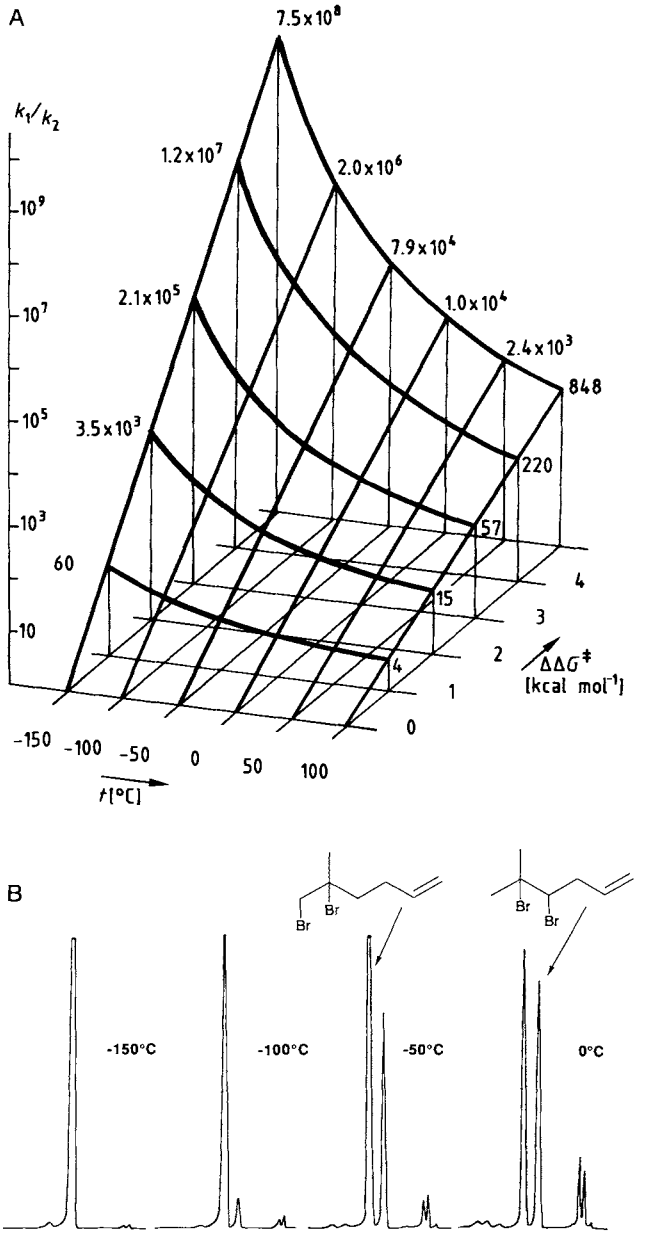

Fig. 9. Increase in the selectivity of reactions at extremely low temperature [243a]. A) 3D diagram showing the relationship between the yields of two products (from competing reactions, both first-order) as a function of difference in enthalpies of activation ($\Delta\Delta G^{\neq}$) and temperature. B) Gas chromatogram of the reaction mixture obtained on treatment of 2-methyl-1,5-hexadiene with bromine; ratios of the principal components at 0°C (in $CH_2Cl_2/CHCl_3$), −50°C (in CHF_2Cl), −100°C (in $CH_2Cl_2/CHCl_3$), and −150°C (in CHF_2Cl) 1:1, 2:1, 200:1, > 500:1. Of course, lower temperatures do not always result in greater selectivity [243b], since selectivity is a function of the relative temperature dependencies of competing reactions, which intersect at the isoselective temperature [243c]. Complex reactions (sequential reactions, pre-equilibria, systems with feedback) also lead to situations much more complicated than that depicted in diagram A [172, 243d–f, 253].

day, when these same "deranged prophets" are invited to tour the "holiest-of-holies", they are likely to encounter a perfectly ordinary-looking 1500 L reaction vessel—cooled by liquid nitrogen!—to which is being added 150 L of butyl lithium solution. The result of such efforts is often a considerable increase in selectivity, achieved despite free energy of activation differences smaller than one kcal mol^{-1}[243] (cf. Fig. 9). An example of a continuous low-temperature process is outlined in Fig. 10.[247] Even C–C bond formation with the aid of lithiated 1,3-dithianes,[18i] now a standard laboratory method but one that requires low temperatures,[31, 248] has been adapted for large-scale application.

- *M*icrowaves are the answer!—or so it would appear from the increasing number of papers in which this approach to introducing energy is described as the "method of choice".[249]
- *O*zonolyses are being used in the manufacture of specialty chemicals.[250] No one would have believed that possible in the days when I was working on my dissertation with *Criegee*!
- *P*hotoreactions (progeny of a venerable family of chemical transformations)[251] now are employed not only for initiating chain reactions, but also under circumstances in which the quantum yield is smaller than 1, especially if they lead in a single step to structural changes that cannot be realized in other ways[252–254] (cf. Table 4G and Scheme 20B).
- *R*adical reactions were viewed with considerable suspicion by synthetic chemists as recently as 10 years ago, attracting favor only among those interested in the study of mechanisms.[255] Today they are securely embedded in the methodology of synthesis,[256–258] and it is likely they will become still more important, especially as tin derivatives relinquish their roles as chain initiators and synthetic reagents generally.[259]
- *S*alt effects are as old as organic chemistry itself. It has recently been discovered, however, that alkali metal and alkaline earth salts in particular have extraordinary solubilizing effects with respect to compounds otherwise insoluble in organic solvents (e.g., polylithiated derivatives[172] and oligopeptides;[260] cf. Table 2 and Fig. 11).
- *S*olid-phase syntheses have been achieved on a wide variety of carriers.[8, 263] Combination of the Merrifield peptide synthesis with modern separation methods has even made it possible to prepare relatively large peptide segments useful in the pharmaceutical industry for the *production* of active ingredients.[264]
- *S*olid–solid reactions are not likely to evoke images that are especially appealing. Nevertheless, close inspection of the abstracts from a conference[265] on the subject[54, 266] reveals astonishing possibilities. A few examples are presented in Scheme 14.
- *S*olvents are more and more becoming the "problem children" in applied organic chemistry. For instance, it is absolutely necessary that new and safer techniques be developed for the use of dichloromethane in those cases where it cannot be avoided, techniques that will guarantee the recycling of over 95% of the solvent. The urgency of finding replacements for the equally unique HMPT has already been noted.[228] Easily recoverable chiral solvents, especially ones available in both enantiomeric forms,[276] would be useful for enhancing stereoselectivity.[277, 278]
- *U*ltrasound has been found to work wonders in many heterogeneous reactions—sometimes in homogeneous systems as well.[249, 279, 280] It is especially effective for activating surfaces (e.g., in virtually any reaction that involves a dissolving metal) and has become a standard

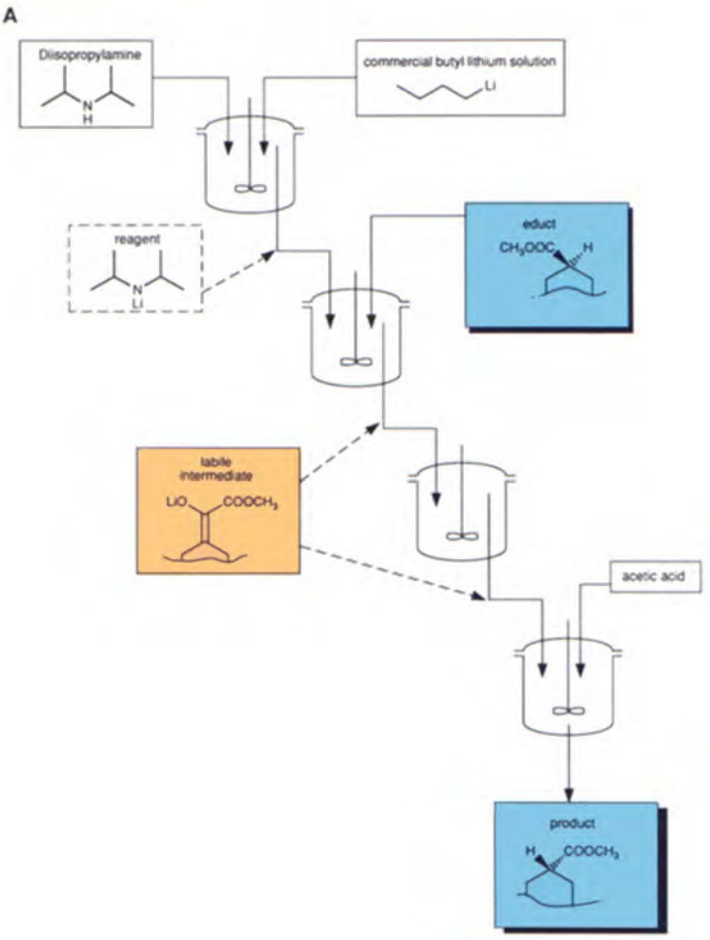

Fig. 10. Example of a low-temperature reaction carried out as a continuous process. Dihydrolysergic acid methyl ester is deprotonated to the Li enolate using lithium diisopropylamide (LDA) generated in situ. Subsequent protonation results in iso-9,10-dihydrolysergic acid methyl ester [245, 246]. A) Schematic representation of the process, and B) photograph of the pilot facility [244]. 1–4 correspond to the stirred reactors in A.

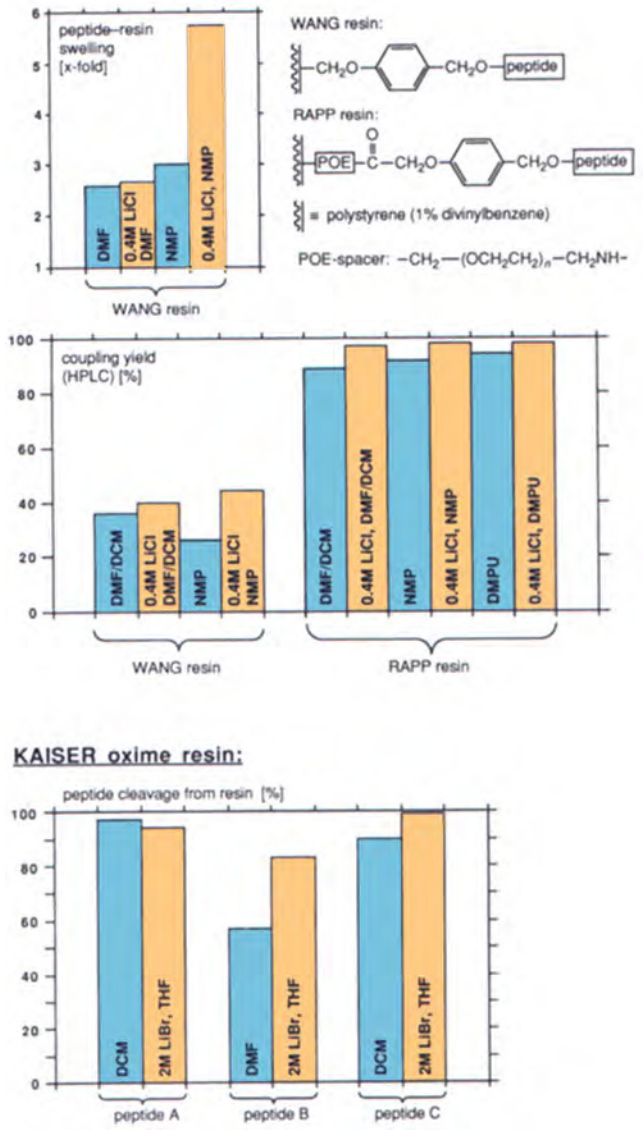

Fig. 11. Use of LiX-containing solvents [260] in Merrifield peptide syntheses involving various anchoring groups and coupling methodologies. The peptides chosen were notorious for a tendency to undergo aggregation (β-pleated sheet!), which normally implies a decrease in yield after a certain chain length has been attained. Experiments with Rapp and Wang resins [261] as well as with Kaiser oxime resin [262]. Polystyrene/1% divinylbenzene was the basis resin in each case. DCM = dichloromethane; NMP = *N*-methylpyrrolidone.

Table 2. Solubilization of oligopeptides in tetrahydrofuran and other organic solvents through the addition of salts and titanates. The reported maximum solubility is often achieved only after redissolving the residue from a much more dilute solution [260]. This method made it possible to obtain solutions of peptides soluble in *no* other solvent (example at the bottom of the table) [262]. For an application involving solid-state synthesis see Fig. 11.

Peptide / Solvent	Solubility [mg mL^{-1}] without	with salt	[mol per mol peptide]
Z-Gly-Gly-Nva-OH			
THF	27	≥ 500	3.0 LiCl
		≥ 470	3.6 LiBr
		≥ 420	2.9 LiI
		≥ 360	3.0 $LiBF_4$
		≥ 340	3.0 $LiClO_4$
		≥ 510	3.0 $Ti(OEt)_4$
		≥ 440	3.0 $Ti(OCHMe_2)_4$
DME	10	> 145	3.2 $LiClO_4$
Z-Ile-Gly-Gly-OH			
THF	23	≥ 340	2.8 LiCl
		≥ 190	3.0 $Ti(OCHMe_2)_4$
Boc-Gly-Gly-Nva-OH			
THF	27		
		≥ 470	2.9 LiBr
H_2N-Asp(OBzl)-Val-Tyr-OBzl·HCl			
THF	1.5	≥ 510	2.9 LiCl
		≥ 520	2.9 $LiClO_4$
		≥ 140	3.0 NaI
		≥ 150	3.0 $MgBr_2 \cdot OEt_2$
		≥ 390	3.1 $ZnCl_2$
Dioxane	2.3	12	3.5 LiCl
DME	0.45	> 27	5.0 LiCl
DMF	≥ 200		
DMPU	≥ 410	70	2.9 LiCl
PEG	≥ 120	≥ 120	3.3 $LiClO_4$
Boc-Ala-Gly-Gly-Gly-OH			
THF	2.0	≥ 300	5.9 LiCl
HCl·H_2N-Lys(Z)-Asp(OBzl)-Val-Tyr-OBzl			
THF	3.8	≥ 380	3.1 LiCl
Z-Arg-Lys(Z)-Asp(OBzl)-Val-Tyr-OBzl·HCl			
THF	0.7	≥ 230	6.0 LiCl
H_2N-Leu-Met-Val-Gly-Gly-Val-Val-Ile-Ala-OH			
THF	insoluble	≥ 100	20 LiBr

These examples have been selected to call attention to a number of unusual or at least (until recently) atypical ways of carrying out reactions. At the same time, they illustrate the principle that the feasibility of extreme conditions is limited in practice only by the value of the product to be synthesized.

5. Reactivity: the Age-Old and Uniquely Chemical Fascination. New reactions—Are Any More Waiting to Be Discovered?

For the great things are not done by impulse, but by a series of small things brought together.
Vincent van Gogh (1888, in a letter to his brother Theo)[*]

A great many synthetic chemists, whether devotees of natural products synthesis or simply interested in synthesis gen-

method in the research laboratory, where an ultrasonic cleaning bath will usually do the job. To the best of my knowledge, however, no technological solution has so far been found to the problem of adapting ultrasound techniques to a large reaction vessel.

- Water has been recommended[281–284] as a medium for organic reactions, even ones involving organometallic intermediates. The advantages of water as a solvent are self-evident.

[*] Quoted from Irving Stone (ed.): *Dear Theo*, Doubleday, New York 1969, p. 164.

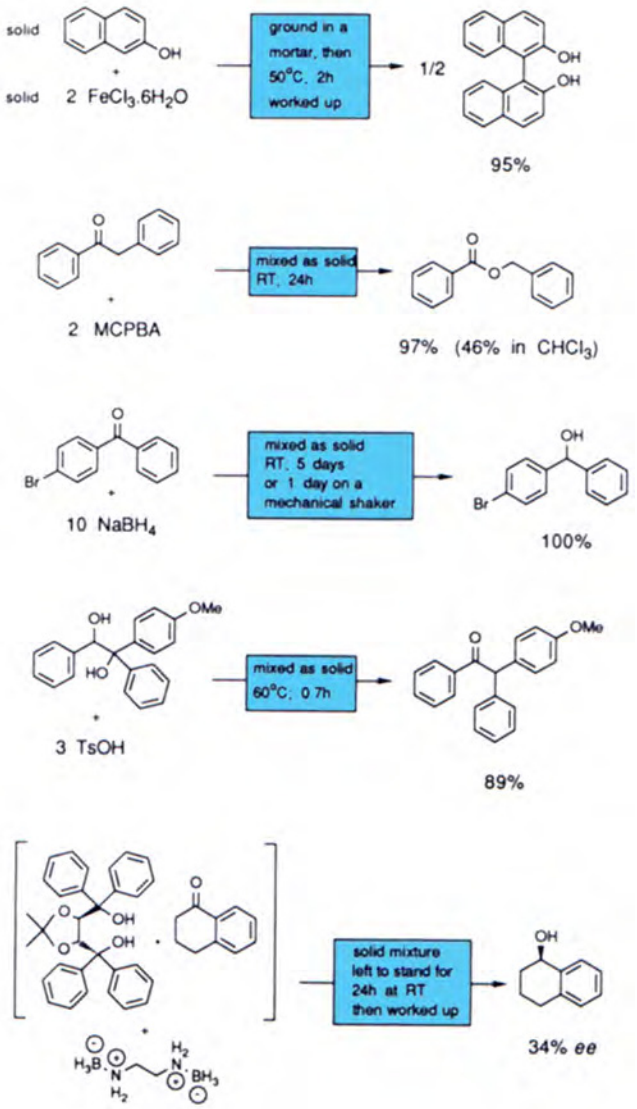

Scheme 14. In certain cases, solid–solid reactions are superior to the corresponding transformations in solution with respect to yield and selectivity. The examples shown come from the laboratory of *Toda* [267], and illustrate a phenol coupling reaction [268a], a Baeyer–Villiger oxidation (MCPBA = *m*-chloroperbenzoic acid) [268b], a $NaBH_4$ reduction [269], a pinacol rearrangement [270], and an enantioselective reduction [271] [by mixing a crystalline clathrate from an achiral ketone and a chiral host [272–275] with the solid complex $(H_3B)_2 \cdot (CH_2NH_2)_2$].—To the best of my knowledge it is not yet known to what extent such reactions represent a safety risk in terms of large-scale adaptation. Nevertheless, it is reasonable to anticipate that a technical solution might be found if the approach proves its superiority in other ways (absence of solvent, high volume-efficiency!).

erally,[285, 286] list one of their areas of specialization as "new synthetic methods". It would be difficult, though, to develop a general consensus on the issue of what a "new" synthetic method really is. It has also become common to find words like *principle*, *strategy*, or even *protocol* linked with the adjectives "new" or "novel" (even "new *and* novel"!). But when one examines the piece of work to which such a description has been applied it often turns out to contain only a minor improvement on a well-known reaction, or a new *application* of an old technique. (Such observations tend to become more frequent as one grows older and wiser!) Years ago, a bet was made between one of my colleagues in Zürich and a chemist in Munich[287] about whether it is possible to find a truly new reaction with the help of a computer program[288] rooted in general principles of reactivity. The challenge is still open! For my part, I am convinced that only in the area of transition-metal organic chemistry are there new reactions waiting to be discovered (see Sections 6 and 7.2.2). In terms of main-group elements, whether metallic (Li through Ca, Be through Ba, Al through Tl, Ge through Pb, or Bi), metalloid (B, Si, As, Sb, Se, Te), or non-metallic (N, P, O, S, the halogens, or the noble gases), carbon derivatives have been examined for so long and with such intensity that no fundamentally new types of reactivity can reasonably be anticipated (see the applications associated with silicon and a few elements from higher periods outlined in Table 3 and

Table 3. Examples for Si-modified reactions from A to U. Most of the cases offer more or less significant advantages relative to the corresponding "normal" procedures. The Si variants can also be implemented at reasonable cost provided commercial silylating agents are utilized. (Numerous silyl compounds are manufactured in bulk for use in the preparation of silicones [314].)

Si-acetalization	of aldehydes and ketones, Si-triflate catalysis (based on *Noyori*) [298–300]
Si-acyloin condensation	Rühlmann variant of the acyloin reaction [301,302]
Si-aldol additions	see Schemes 19 and 26
Si-azide	"the versatile reagent" [303]
Si-Birch reduction	and other Si-modified reactions of dissolving metals [304]
Si-cyanohydrin reaction	see below, Si-umpolung
Si-diazomethane	safer variant of the standard diazomethane reactions [305]
Si-Friedel–Crafts-type acylations	at aromatic, vinylic, and acetylenic C-atoms [109,289]
Si-Mannich	see below, Mannich reactions [336]
Si-Nazarov reaction	five-membered ring annelation [306], cf. also the Si-variant of the Robinson annelation [307]
Si-nitroaldol additions	diastereoselective to give products of *l* or *u* configuration [18f,308]
Si-olefination	Peterson olefination [108,295,309]
Si-ozonolysis	with triethylsilyl-hydrotrioxide [310]
Si-pinacol rearrangements	migrating α-Si-vinyl group [311], see also Scheme 16 and [322] therein
Si-Pummerer rearrangement	from sulfoxides to α-Si-thioethers [312]
Si-radical chain reductions	see above, Scheme 15 **D**, ref. [259]
Si-umpolung	with trimethylsilylcyanide [34] or with Me_3Si-thiazole [313]

Schemes 15–17). This obviously does not mean that in the areas we have long regarded as the true domain of classical organic chemistry there will be no more progress. On the contrary! The achievements of the past 30 years,[330] indeed the past 10 years, have been quite remarkable. To a greater extent than in the past, however, progress has been not the product of solitary, revolutionary discoveries, but rather the cumulative effect of innumerable small steps taken by increasing numbers of researchers throughout the world.

Thus, we have not witnessed the discovery of new aldol,[331] Beckmann,[332] Claisen,[333] Cope,[334] Diels–Alder,[335] Mannich,[336] Michael,[331a, 337] or Wittig[26, 27, 338]

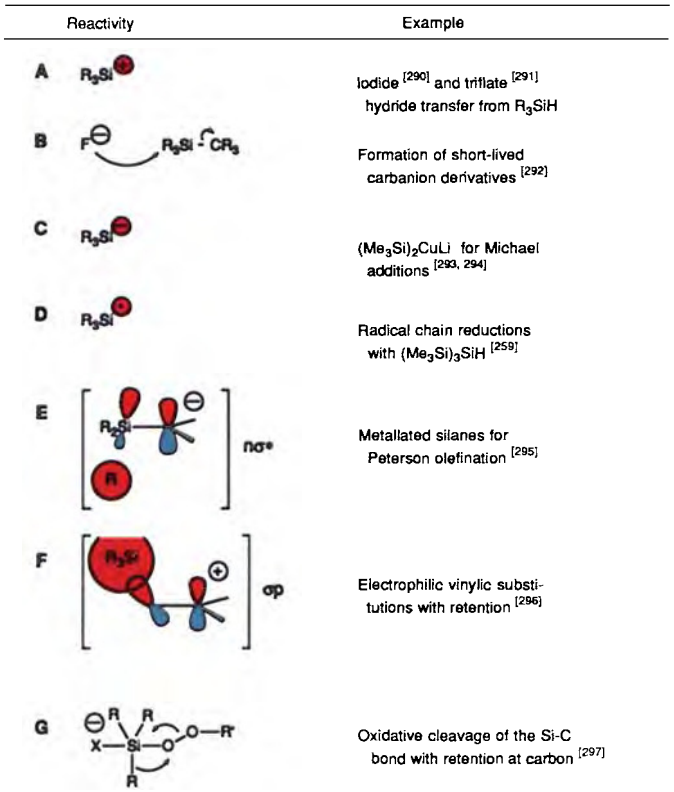

Scheme 15. R_3Si: more than just a "big, fat proton". In most of the organic synthetic applications of R_3Si derivatives, the Si group plays a role identical to that of the proton in analogous classical reactions (cf. A and B, as well as the aldol reactions in Scheme 19) [289]. The Si group can be introduced nucleophilically by way of Li or Cu derivatives (cf. C). Radical hydrogen transfer can be accomplished with SiH compounds in the presence of chain initiators such as AIBN (D). Stabilization by Si of α-anionic charges (E), as well as β-cationic charges (F, cf. Scheme 16) also leads to useful applications of Si derivatives in synthesis. The oxidative cleavage of SiC bonds indicated in G establishes synthetic equivalence between silyl groups and OH.

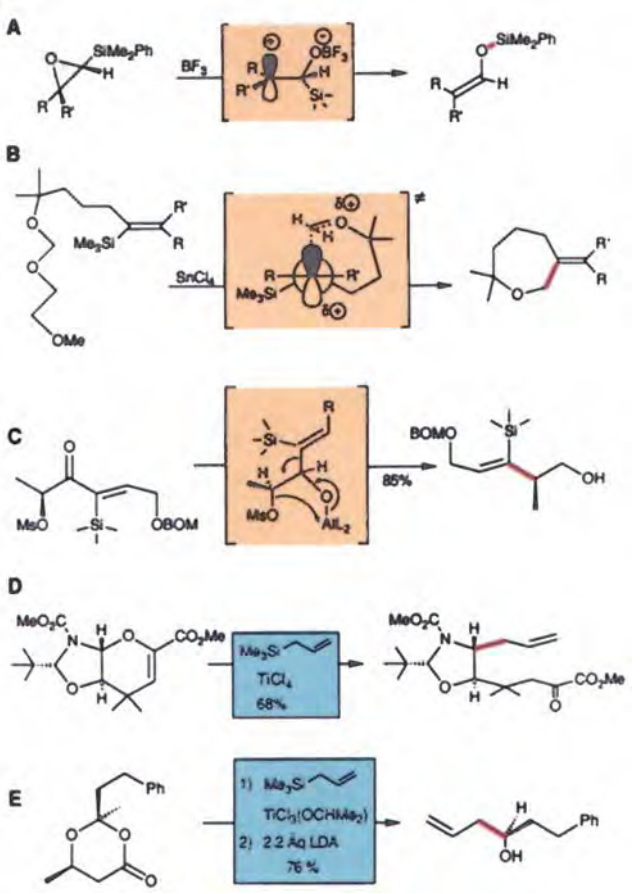

Scheme 16. Transformations facilitated by the stability of β-Si carbocations. The amount of stabilization associated with the β-Si effect has been estimated to be as great as 159 kJ mol^{-1} [315]. Vinyl- [109] and allylsilanes [107, 316] have acquired considerable significance in organic synthesis. Thus, Si groups activate double bonds, control regioselectivity in electrophilic attack, ensure stereoselectivity during reaction (cf. the preference for retention in substitution of vinylic silyl groups [109, 296] and S_E-*anti*-substitution of allylic silyl groups [109, 317, 318]), and function—formally speaking—as leaving groups of the type $R_3Si^{\oplus}$. A) Stereoselective (*cis* → *Z*, *trans* → *E*, ca. 95% *ds*) rearrangement of silyloxiranes to Si enol ethers [319, 320]. B) Attack of an oxonium ion on a vinyl silane, leading to an oxepane via substitution with retention (R = Bu, R′ = H and R = H, R′ = Bu, > 98% *ds*) [321]. C) Migration of an α-silylvinyl group in what amounts to a pinacol rearrangement (retention at the migrating carbon, inversion at the migration terminus; this process may involve a β-Si stabilized cyclopropylmethyl carbocation) [311, 322] (BOM = benzyloxymethyl). D) Allylation with allyltrimethylsilane via an acyliminium ion, accompanied by retention of configuration [323]. E) Allylsilane/$TiCl_3(OCHMe_2)$ used to effect S_N2 ring opening of a dioxanone with the (1*R*,6*R*) configuration, a process that entails subsequent elimination to provide a homoallylic alcohol (overall yield 76%, enantiomeric excess 94% *ee*) [299, 324].

reactions; even the exploitation of strain effects in small rings[339] and the broader application of 1,3-dipolar cycloadditions,[340] dithiane methodology,[18i] ortho metallation ("new arene chemistry"),[341] the acyloin[342a] and pinacol condensations,[274, 342b–d], photochemical[251–254, 343] and radical reactions,[255–259, 344–346] nucleophilic substitution,[347] and "umpolung" of reactivity[18, 31–35, 313, 348] took place without the discovery of new modes of reactivity. Nevertheless, each of the transformations cited[349] has, in a sense, been raised to a much higher level of sophistication. Major thrusts of recent activity have centered around catalytic modifications, diastereoselectivity,[350] enantioselectivity, and the linking together of series of reactions into multistep in situ sequences.[351]

It is obviously quite impossible within the confines of this paper to present an account that even begins to describe the true extent of the efforts and accomplishments of the research groups responsible for these many developments. Instead, I have chosen the following course: First, two Schemes (18 and 19) present selected examples of stepwise improvements to certain standard reactions, and Table 4 highlights some diastereoselective reaction sequences in which a few steps suffice to generate surprisingly complex molecules. These representative samplings are followed by two chapters more directly related to my own interests,[273, 274, 342d, 352–354] illustrating the application of transition-metal derivatives in organic synthesis and the preparation of enantiomerically pure compounds, with an emphasis on catalytic methods. It is my conviction that precisely these two areas will become increasingly important over the next few years.

6. Transition-Metal Derivatives—Always Good for a Discovery

Anyone who has attended one of the biennial conferences on *o*rgano*m*etallic *c*hemistry directed toward *o*rganic *s*ynthesis (OMCOS), and sensed there the atmosphere of excite-

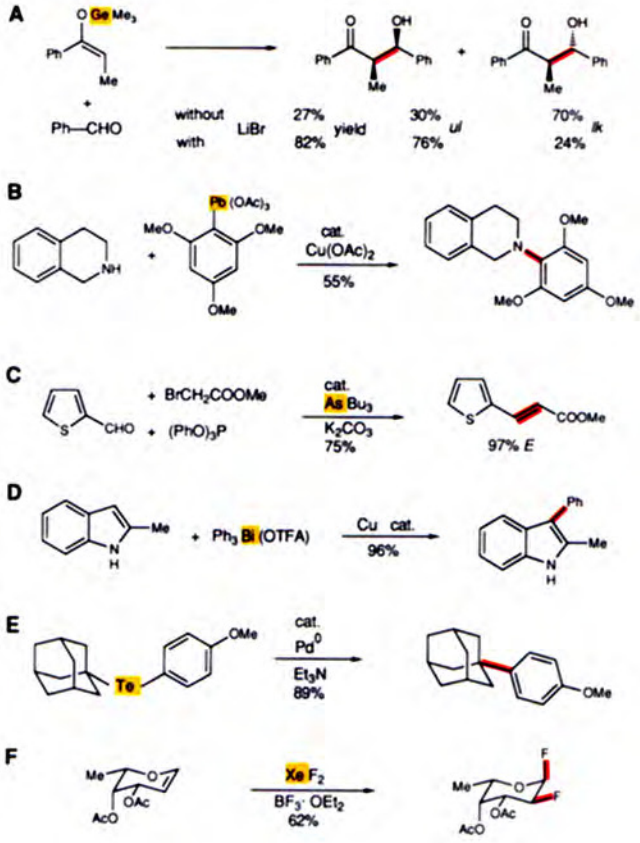

Scheme 17. Synthetic transformations involving organometallic compounds containing main-group elements from higher periods. A) The Li enolate of propiophenone, prepared with the aid of LDA, was transmetallated to give the indicated Ge enolate, which in turn leads preferentially, depending on the reaction conditions, to either an *lk*- or a *ul*-aldol [325]. B) Cu-catalyzed reaction of tetrahydroisoquinoline with aromatic Pb(IV) compounds, resulting in *N*-arylation [326]. C) A first catalytic olefination following the scheme of the Wittig reaction proceeds via an arsenic ylid [327a]. D) Phenylation of an indole with triphenylbismuth trifluoroacetate [327b]. E) A type of mixed Wurtz coupling between adamantyl and *p*-methoxyphenyl, accomplished via a telluride [328]. F) Use of XeF_2 as reagent for the addition of fluorine to a double bond [329] (cf. also Scheme 7). It is worth noting that three of the six reactions shown are catalyzed by transition metals! (cf. also Sections 6 and 7.2).

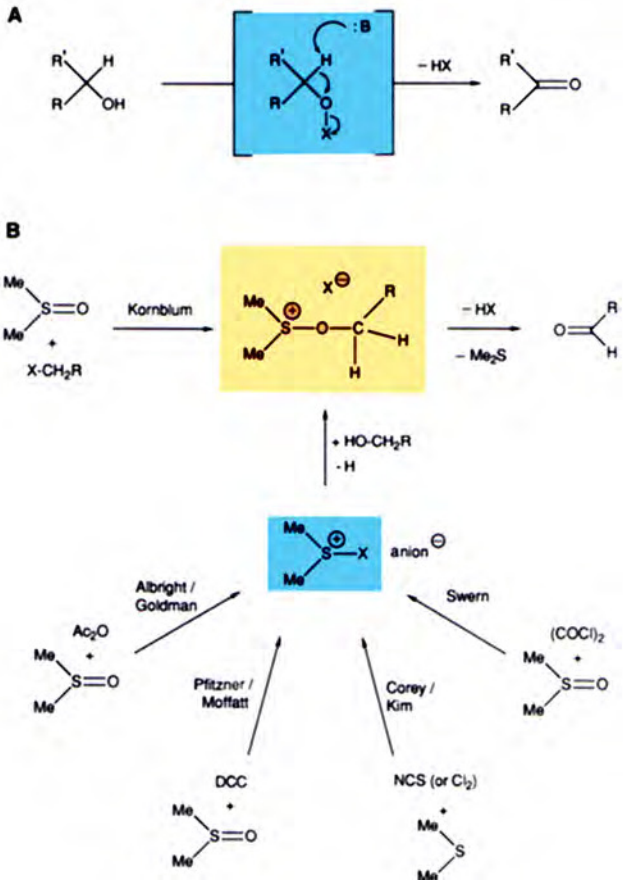

Scheme 18. "Evolution" in the oxidation of an alcohol to a carbonyl derivative [355]. A) A leaving group is first introduced, after which the actual oxidation at carbon takes place by HX elimination. This scheme characterizes, for example, chromic acid oxidation [355], the reaction with hypochlorite [356], corresponding reactions of peroxides [357]—in principle, even the oxidation of amines to carbonyl compounds with the aid of an *o*-quinone [358]. B) Reaction by way of sulfoxonium salts can occur starting with educts of widely varying type [359–363], with the Kornblum oxidation itself [359] serving to convert an alkyl halide into an aldehyde. The currently most popular variant is the Swern oxidation [362], favored because of its mild conditions. There are numerous other possibilities for activating DMSO in the oxidation of alcohols to aldehydes and ketones (cf. the review articles cited under [362, 363]). DCC = dicyclohexylcarbodiimide, NCS = *N*-chlorosuccinimide.

ment enveloping both speakers and audience, will surely find it inconceivable that organic chemistry could be described as a "mature" science. At the last of these OMCOS conferences (in Florence) the air was full of the way "we OMCOS people" would tackle something—and do it better! Many general treatises[388] and reviews, of which only two will be cited here,[389, 390] as well as the even more numerous monographs and articles dealing with specific reactions of the derivatives of particular metals,[391] demonstrate the increasing role of transition metals in the field of organometallic synthesis. Relevant papers may appear in general, inorganic, organic, organometallic, or even more specialized chemical journals, and it is difficult to maintain a satisfactory overview.[392] Furthermore, the reactions themselves are often not easy to classify, and despite great progress in both theory and formalism[393] they do not always lend themselves to detailed formulation, frequently leaving the reader to puzzle over the marvelous transformation of educt into product. One indication of activity in the field is the fact that most of the new organic name reactions of the last decades trace their origins to transition-metal chemistry;[394, 395] a few examples are presented in Table 5. (The author accepts full responsibility for incorrect classifications and missing names!) Scheme 20 illustrates several cyclizations that proceed via carbonyl complexes and are without precedent in classical organic chemistry.

Here, too, there have been significant developments with respect to well-known reaction types;[408–411] for the practitioner, some of them amount to genuine quantum leaps. Thus, by using transmetallation to go from classical Grignard or organolithium reagents to the easily prepared titanium,[273–275, 299, 412] zirconium,[273, 274, 413] or lanthanide derivatives,[414–416] it is possible to experience selectivity increases during carbonyl addition that raise the yield of the desired product from less than 10% to over 90%. Examples of differentiation among several functional groups, preparation of specific diastereoisomers, and the realization of enantioselective transformations are provided in Scheme 21, Fig. 12, and Scheme 22, respectively.

Reductive coupling[301, 342] of carbonyl derivatives and their thio and imino analogues has been greatly facilitated by the advent of low-valent derivatives of titanium, vanadium,

Table 4. In situ sequences [373] of classical reactions leading to the formation of up to five new stereogenic centers. Enthusiasm over successful "complexity-enhancement" has resulted in several dazzling descriptions [351, 374–376]. A) Carbonyl addition, oxy-Cope rearrangement [334b], proton transfer, and selenization leads to a tricyclic product with five stereogenic centers (where the educt contained only two); KHMDS = potassium hexamethyldisilazanide [343c]. B) Two bonds, two rings, and three stereogenic centers are formed in this sequence of radical reactions [377]. C) A C-acylation of 4-methylcyclohexanone enolate with 4-nitrobutyryl chloride, followed by an intramolecular nitroaldol addition, results in a *trans*-decalin derivative [378]. D) Michael addition of the di-enolate of 3,5-dioxohexanoic acid ester to a nitrostyrene, followed by nitroaldol addition, gives a cyclohexanone with four adjacent stereogenic centers [337d]. E) Intermolecular Michael addition (or S_N substitution?), intramolecular Michael addition, and proton transfer accomplishes diastereoselective generation of a total of five stereogenic centers [337e]. F) Iminium salt formation, aza-Cope rearrangement, a Mannich reaction, and condensation between the *ortho* amino group and the newly formed carbonyl function all occur in situ during synthesis of the alkaloid methoxytabersonine [336a, 379]. G) Light truly works wonders in this intramolecular cycloaddition between an olefinic double bond and a benzene ring [380] (Kaplan–Bryce–Smith reaction [254, 381, 382]). H) Ethoxycarbonylmethylation at the nitrogen of a thiazole, ylid formation, cycloaddition to the C–C double bond of an enone, and tetrahydrofuran formation are the steps leading from two achiral educts to a tricyclic system with five centers of chirality [383]. I) Three-fold Michael addition produces four stereogenic centers [384]. K) Enamine acylation, followed by intramolecular Michael and Dieckmann reactions, transforms methacrylyl chloride and a cyclohexanone derivative directly into the adamantane skeleton [385]. L) A 1:2 intermediate trapped along the way toward polymerization [9] in the reaction of cyclohexanone enolate with methacrylic ester [386]. M) Michael addition to methylcyclopentanone, trapping of the resulting enolate with a vinylphosphonium salt, and an intramolecular Wittig reaction—carried out as a one-pot sequence leading to the estrone skeleton, albeit in low yield [387].

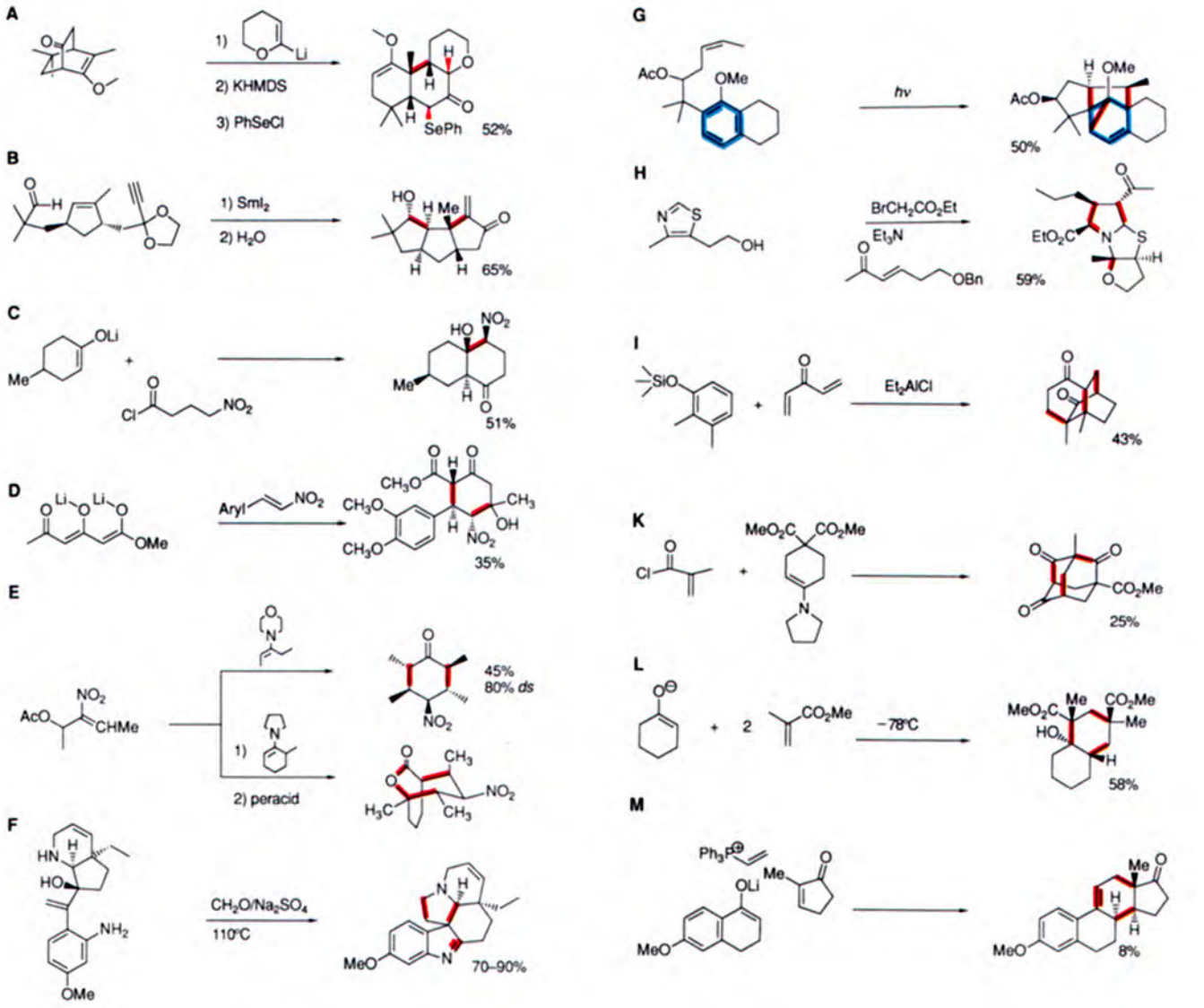

and niobium, and the scope of the reaction has been broadened (e.g., to include nitriles), as shown in Scheme 23.

An application of allyl protective groups in DNA synthesis[430–434] provides a particularly impressive example of what can be achieved with organometallic methodology: Nitrogen atoms in the constituent bases were subjected to allyloxycarbonyl (AOC) protection, and *O*-allyl groups were incorporated into the added phosphoramidite units. In a dramatic final step, with the substrate still attached to the polymeric carrier, all the protective groups were removed at once by treatment with Pd^0/Ph_3P/butyl amine/formic acid in THF. Oligonucleotides resulting from this "Nagoya method" are of unprecedented purity; this is illustrated in Fig. 13, which compares samples of nucleotides containing up to 60 nucleoside units prepared by the conventional method and by the new method.

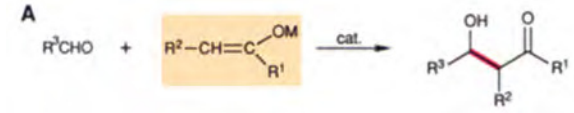

M	Comments and references
H, Na	Acid- or base-catalyzed classical aldol addition
R_3Si	Silyl enol ethers as precursors to Li enolates [109, 172, 364, 365]
	TiX_4-mediated aldol additions or acetal variants [109, 331a, b]
	Trityl cation-catalyzed reactions [331a]
Li	R_2NLi-generation of Li enolates, see the discussion in [172, 331b]
BR_2	Generation [331a, c] of the enolate with R_2BOTf / Hünig base [365]
AlR_2	Provides supplementary thermodynamic control over the aldol addition [331a, c, 367]
SnOTf	Also for enantioselective aldol and Michael additions with chiral additives [331a, 368]

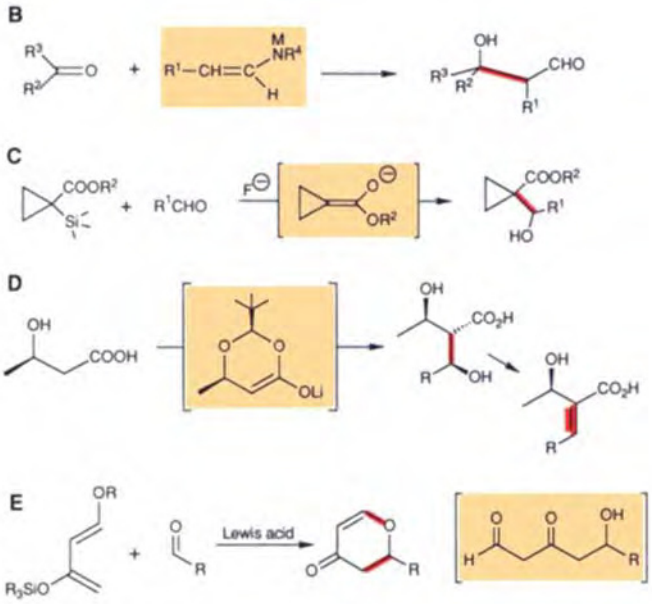

Scheme 19. Aldol addition—from humble origins to undreamed of heights (the enantioselective variant is included in Sec. 7, Scheme 26). A) Development of the aldol reaction from an unselective process in protic solvents to a diastereoselective variant in non-polar medium at low temperature. B) Directed aldol addition (and increased enolate nucleophilicity) with enamides and enhydrazides [369]. C) In situ generation of unstable or highly reactive enolates via α-Si carbonyl compounds, exemplified by a cyclopropanecarboxylic acid derivative [292, 370]. D) Aldol adducts and condensation products from aldols via enolates of (2*R*,6*R*)-dioxanones [371]. E) Aldol addition (or is it a hetero-Diels–Alder reaction?), cyclization, elimination, and desilylation leads to dihydropyran units with synthetic utility. The Lewis acid-induced addition (LACDAC = "*L*ewis *a*cid-catalyzed *d*iene–*a*ldehyde *c*yclocondensation") of a "double enol ether" to an aldehyde (stereoselectively in the case of a 1-substituted diene or a chiral aldehyde) has proven to be a veritable gold mine in the hands of *Danishefsky* and his group [372].

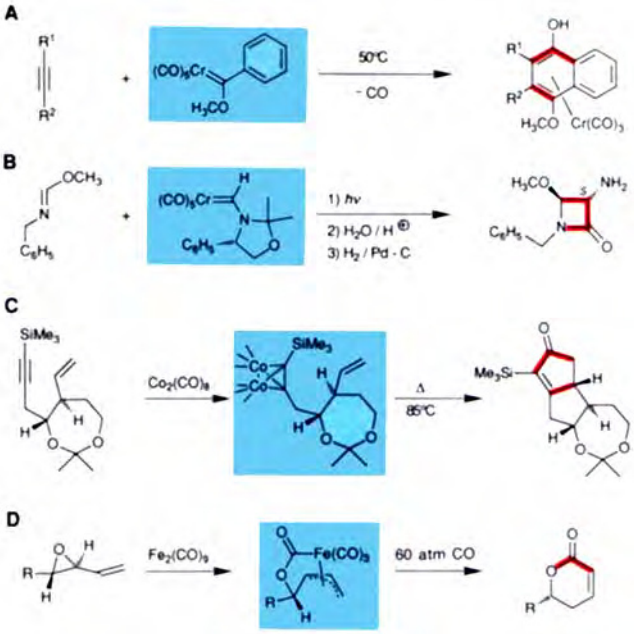

Scheme 20. Four cases of cyclization accompanied by CO insertion and made possible by transition-metal derivatives. A) [3+2+1]-Carbocyclization in the Dötz reaction [397–399]. B) β-Lactam formation through photochemical addition of an aminocarbene complex to an imine (*Hegedus* [390, 394]). C) [2+2+1]-Carbocyclization via a cobalt carbonyl–acetylene complex (*Magnus* [390, 401, 403]). D) Lactone formation by CO insertion into a vinyloxirane (*Ley* [390]).

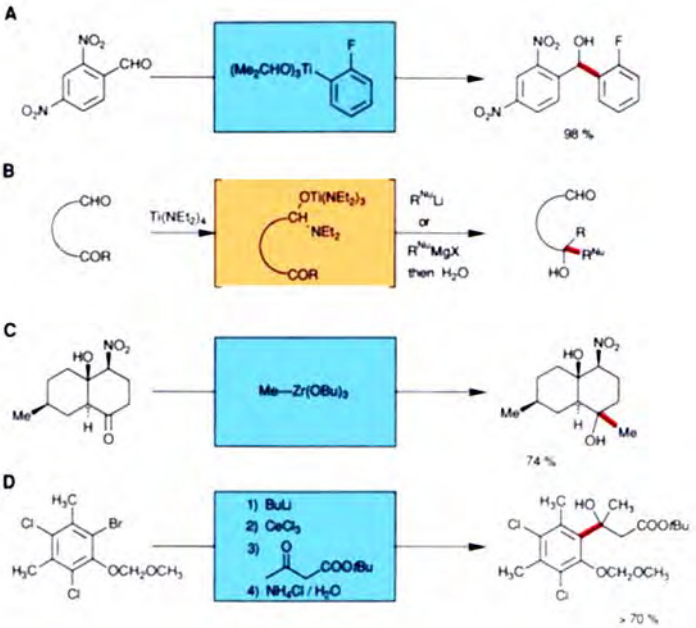

Scheme 21. Highly selective nucleophilic addition of Ti, Zr, and Ce reagents to carbonyl groups (cf. also Fig. 12). A) *o*-Fluorophenyl triisopropoxytitanium, stable at room temperature, adds nearly quantitatively to a dinitrobenzaldehyde [417] (cf. case A in Fig. 12). B) The non-basic reagent tetrakis(diethylamino)titanium (synthesis described in [274]) adds selectively to the aldehyde group in a formyl ketone, leaving only the keto group accessible to attack by a polar nucleophile [412]. C) Neither electron transfer nor base-induced retro-nitroaldol addition interferes with diastereoselective (> 98% *ds*) addition of the methylzirconium reagent (74% yield) [413]. D) If all else fails, or if an absolutely foolproof method is required, then the answer today is transmetallation of a Li or Mg derivative with $CeCl_3$ prior to introduction of a carbonyl compound! [414].

The high price and/or toxicity of many transition metals adds urgency to the ongoing quest for catalytic approaches to such transformations, even on the laboratory scale; this particular problem has recently been addressed in a review article.[435]

Table 5. A few examples of transition-metal *name* reagents or reactions that in the last 20 years have come to be regarded as standard procedures. Excluded from consideration here are primarily industrial methods, such as hydroformylation or the Ziegler–Natta polymerization. Some of the reactions shown require stoichiometric amounts of the organometallic reagents, whereas others are catalytic (in some cases involving polymer-bound catalysts). Enantioselective transformations are discussed further in Sec. 7. The book [394] by *Collman, Hegedus, Norton,* and *Finke* includes pertinent references to all the examples shown.

Birch-Pearson	**Fe** tricarbonyl complexes of cyclohexadiene and other dienes for C,C coupling [390,396]
Crabtree	**Ir** hydrogenation catalyst for C,C double bonds (in the presence of other reducible groups)
Dötz (Scheme 20)	**Cr** carbonyl–carbene complexes for annelation of aromatic rings [397–399]
Heck-Stille	**Pd**-catalyzed arylation, vinylation, and CO insertions [400]
Hegedus (Scheme 20)	**Cr** carbonyl–carbene complexes and imines lead photochemically to β-lactams [390]
Horner-Knowles	**Rh** complexes with chiral phosphanes (Wilkinson catalysts) for enantioselective hydrogenations of C,C double bonds
McMurry (Scheme 23)	Ti^0 ("low-valent" Ti) for the coupling of two carbonyl groups directly to olefins [342b–d]
Mukaiyama (Scheme 19)	TiX_4-mediated reactions of silylenol ethers with aldehydes, acetals, and Michael acceptors [331a,b]
Nicholas-Pettit (Scheme 20)	**Co** carbonyl–acetylene complexes as protective groups and precursors for cyclizations [401]
Noyori	$Fe_2(CO)_9$ for preparing oxallyl cations for use in [3+2]- and [4+3]-cycloadditions
Noyori-Takaya	**Rh**-, **Ru**-catalyzed enantioselective hydrogenations of C,O double bonds [402]
Pauson-Khand (Scheme 20)	**Co** carbonyl complexes for the preparation of cyclopentenones with CO insertion [390,403]
Schwartz-Negishi	**Zr** reagent (Cp_2ZrHCl) for hydrozirconation of C,C double and triple bonds [404]
Sharpless	**Ti**(OR_4) / ROOH / tartrate for enantioselective epoxidation of allyl alcohols
Suzuki	**Pd**-catalyzed coupling of aryl and vinyl boron compounds with halides [405]
Tebbe-Grubbs	**Ti** / Al–carbene complex for methylenation of carbonyl compounds (also esters, amides) [29]
Tsuji-Trost	**Pd** allyl complexes for C,C coupling, especially for cyclizations [406,407]
Vollhardt	**Co** complexes for cyclotrimerization of acetylenes (also with the participation of nitriles) to aromatic systems

7. The Preparation of Enantiomerically Pure Compounds (EPC)

There is nothing faster than the years.
Ovid (43 B. C.–17 A. D.)

At the present time, almost no aspect of organic synthesis is generating as many publications as the preparation of enantiomerically pure compounds.[436–438] It is easy to predict that by the year 2000 this flurry of activity will have provided us with all of the following: a) simple approaches to the synthesis of enantiomerically pure chiral compounds

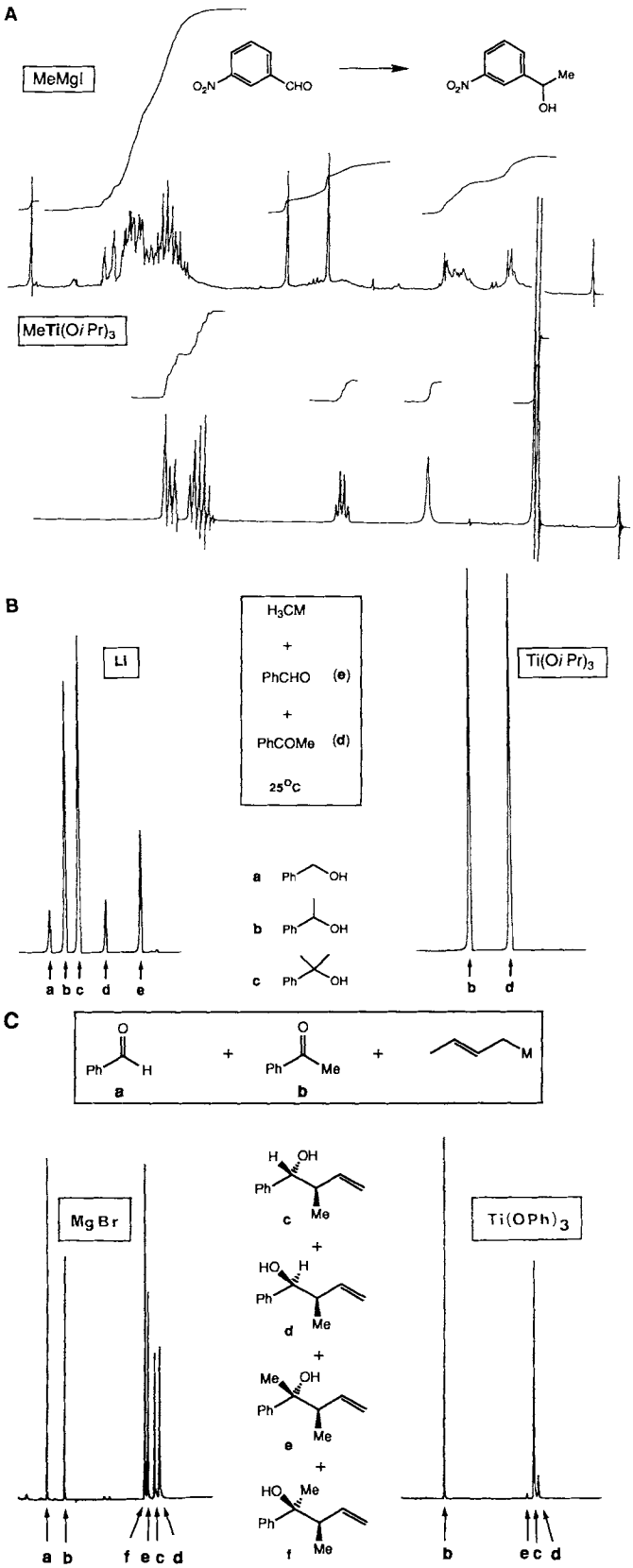

Fig. 12. Three examples of yield and selectivity increases that can be achieved by transmetallation of Li and Mg reagents to Ti derivatives. A) A glance at the NMR spectrum of the crude product betrays the high yield obtained upon addition of the methyltitanium reagent to *m*-nitrobenzaldehyde [418] relative to addition of a Grignard reagent. B) A comparison of crude product gas chromatograms reveals the perfect selectivity of MeTi vs. MeLi with respect to aldehyde/ketone addition. With the Li reagent, the rate of addition at the ketone is comparable to that at the aldehyde [274]. C) Crotyltitanium adds more selectively than the crotyl Grignard reagent to a mixture of benzaldehyde and acetophenone [273a].

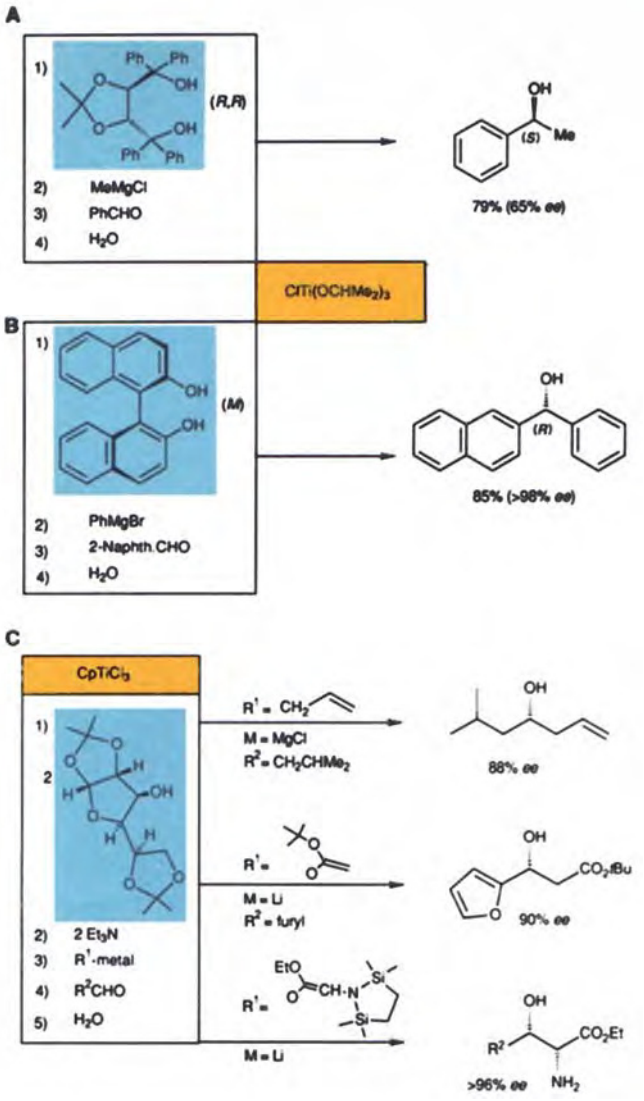

Scheme 22. The in situ generation of chiral alkyl, allyl, aryl, and vinyloxytitanium derivatives bearing $(R^*O)_2$ ligands, followed by addition to aldehydes. A) The chiral diol derived from tartaric acid [272–274] ensures fair-to-good enantiomeric excesses in the addition of alkyl groups to aldehydes (in this example, 79% yield, 65% *ee*) [273a, 275]. B) Particularly useful for the preparation of enantiomerically pure benzhydrol derivatives [419, 420] is the binaphthol ligand (here providing an 85% yield, > 98% *ee*) [402]. C) The use of CpTi derivatives in which the R*O group is derived from glucose offers distinct advantages (recoverability of $CpTiCl_3$; inexpensive, commercially available auxiliary; reproducible results); this method has been successfully utilized for allyl transfer (*lk* combination, cf. Fig. 12c) and aldol additions [421]. The diol shown in A has also been allowed to react with $CpTiCl_3$, providing access to both enantiomers of products of the type illustrated in C [422].

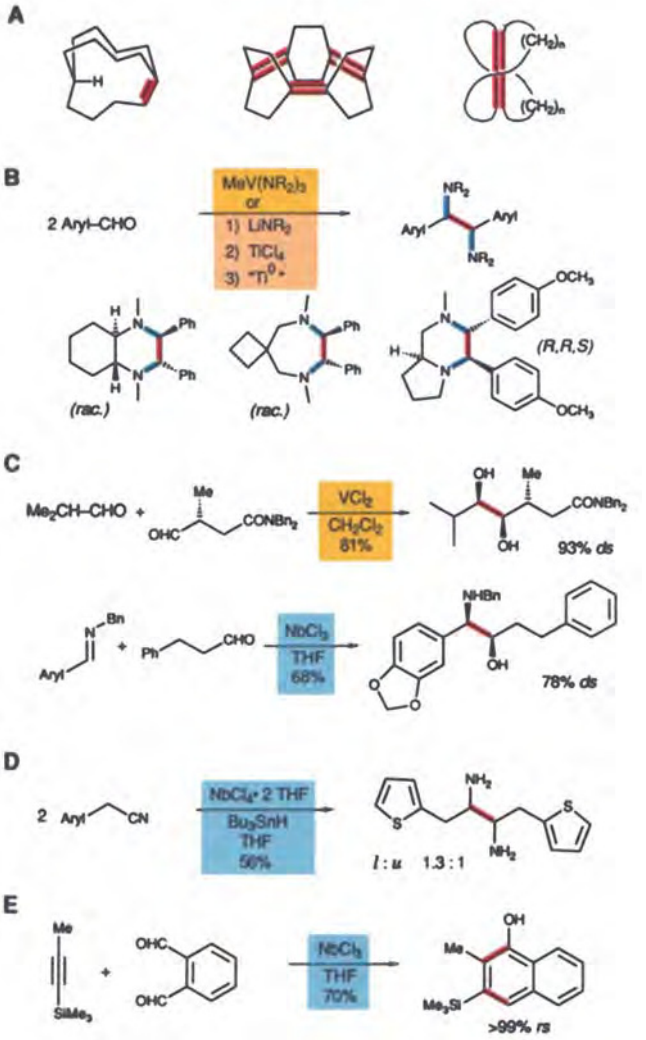

Scheme 23. Reductive coupling of carbonyl compounds and their analogues using derivatives of low-valent metals from the fourth and fifth subgroups. A) Three (attractive!) unsaturated hydrocarbons prepared from the corresponding diketones and a ketoaldehyde via the McMurry reaction (reviews: [342b–d]). B) Reductively aminating one-pot coupling of aromatic aldehydes to 1,2-diarylethan-1,2-diamines using either a vanadium(IV) derivative [423] or "titanium(0)" [342d, 424]. C) Diastereoselective crossed coupling with VCl_2 of two different aldehydes [425], and of an imine and an aldehyde using $NbCl_3$ [426] (cf. also the *like*-selective coupling of aromatic aldehydes with $TiCl_4$/BuLi [427]). D) 1,2-Diamines from nitriles and $NbCl_4$/Bu_3SnH [428]. E) Regioselective reductive [4 + 2]-carbocyclization of *o*-phthalaldehyde with an alkyne to give a naphthol [429] (rs = regioselectivity).

representing all the known classes of substances; b) catalytic variants for every reaction in which achiral precursors lead to at least one element of chirality; c) corresponding methods suitable for industrial use on any desired scale; and d) much wider understanding of intermolecular interactions and the detailed course of reactions.

Why is it that enantiomeric compounds have moved so decisively toward the center of attention? One important factor is certainly the *general* recognition that living systems, which are themselves made up of chiral components,[439] interact with enantiomers in different ways (as a result of diastereomeric relationships). This awareness has led to increasingly restrictive guidelines with respect to the registration of racemic mixtures of active substances (by the FDA, for example),[440] which has in turn forced industry to amend its ways.[435, 441, 442] Anyone who has had the occasion to sniff samples of both enantiomers of certain fragrances will not be surprised to learn that the fragrance industry has been one of the leaders in this development.

Ever since stereochemistry was in its infancy, experts—or perhaps one should say "the educated"—have understood the profound difference between enantiomers and racemates; *Pasteur* himself was able to show that microorganisms have no trouble distinguishing between (*R*,*R*)- and (*S*,*S*)-tartaric acid (Scheme 24).

Actually, there has been nothing fundamentally new discovered in this area during the 140 years since *Pasteur* took the first steps along the three basic paths to pure enan-

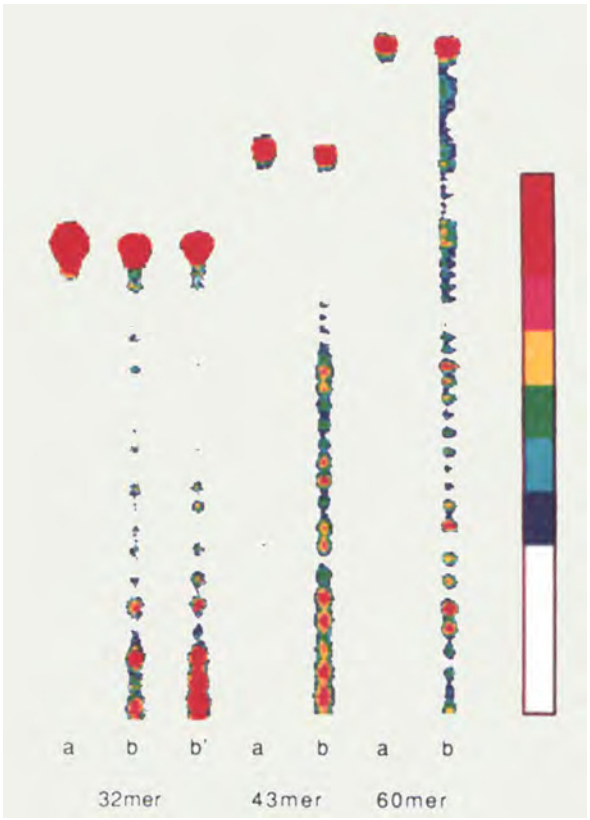

Fig. 13. "Bio-image" chromatogram of oligo-DNA crude products [430–433]. Track a: products prepared via the new (allyl–allyloxycarbonyl) protective group method. Track b: products obtained by what are now the standard routes. Color scale: red (high intensity) to blue (lower intensity) [434].

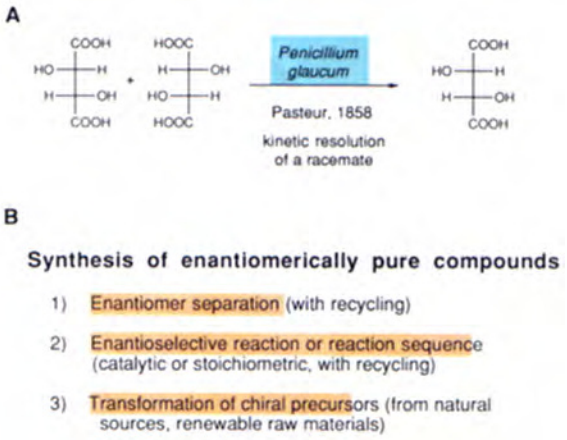

Scheme 24. *Pasteur*'s kinetic separation of the tartaric acid enantiomers with the aid of a microorganism (an enantioselective biological-chemical reaction!), and the three techniques for synthesis of enantiomerically pure compounds. A) If *Penicillium glaucum* is permitted to grow on racemic tartaric acid (*acidum racemicum*), fermentation ceases as soon as the (*R*,*R*)-(+)-tartaric acid has been consumed; *Pasteur* succeeded in isolating residual (−)-enantiomer from the growth medium. B) The following review articles on the three methods of preparing enantiomerically pure compounds (EPCs) have already been cited in Sections 2–5: separation of racemates [133–137, 343a], enantioselective reaction [125, 126, 331a, c, 353, 354, 402, 435], incorporation of chiral building blocks [199, 352–354] (the author of the present article accepts responsibility for the widespread use of the term "chiral pool" [443]—a sin from the days of his youth, of which he first became fully aware in *Vlado Prelog*'s circle [444, 445]; a "readily available supply" cannot be chiral! See the remarks in [436]).

tiomers: separation of a racemic mixture, enantioselective reaction, and synthesis based on chiral starting materials isolated from natural sources. Quite properly, synthetic chemists devoted themselves first to the subject of reactivity in general, and natural products chemists nearly always synthesized their targets in racemic form. After all, a complex synthesis must be seen basically as the struggle to arrive at a correct constitution containing many stereogenic units; enantioselective generation of the first center of chirality, or separation of some intermediate into its enantiomers ("resolution"), represented the least of the worries! Times have changed, however, and interest in this subject has now become so intense that entire conferences have been devoted to it.[442, 446] Some have hailed enantioselective synthesis as *the* challenge,[447] and new publications have been established with titles like *Asymmetry* and *Chirality*.[448] In the present context it will be possible to touch upon only a few highlights.[449] Moreover, the subject itself is such that it precludes the offering of general prescriptions or advice regarding, for example, which of the three general approaches to enantiomerically pure compounds is "the best".

7.1. Separation, Selectivity, or Incorporation—That is the (Gretchen) Question![*]

Which of the three routes one chooses to prepare an enantiomerically pure compound depends essentially upon the task at hand. The substance in question may be required on a tons-per-annum basis (as in the case of phenylalanine, lactic acid, or menthol). On the other hand, a few hundred kilograms per year might suffice for an expensive pharmaceutical agent, and pharmacological screening can be carried out with much smaller amounts. A research laboratory is more likely to need a few grams of one enantiomerically pure substance today and a different one tomorrow. If the problem is one of developing a new stereoselective application, or of completing a mechanistic investigation, a few hundred milligrams of a pure substance will probably serve the purpose. The greater the quantity of material required, the more important it becomes to recycle the unwanted enantiomer after a resolution, to recover an auxiliary introduced in stoichiometric quantities, to choose natural (renewable) chiral building blocks, or to develop efficient catalytic methods. The more limited and diverse the needs, the more flexible must be the methods with respect to product structure and to the chemistry involved; cost is not then an issue, as exemplified by the extreme case of a radioactively labeled material for use in metabolic studies.

The examples shown in Schemes 25–27 have been selected to demonstrate all three of the basic methodologies. Thus, heterocyclic glycine derivatives obtained through separation of enantiomeric mixtures (Scheme 25) facilitate the synthesis of non-proteinogenic amino acids, and this method of preparation is quite competitive with other approaches.[86] By the way, the *tert*-butyl group responsible here for selectivity came from BASF, which supported our work with a gener-

[*] An allusion to Margaret's (Gretchen's) famous query of Faust: "How do you feel about religion?" (Goethe).

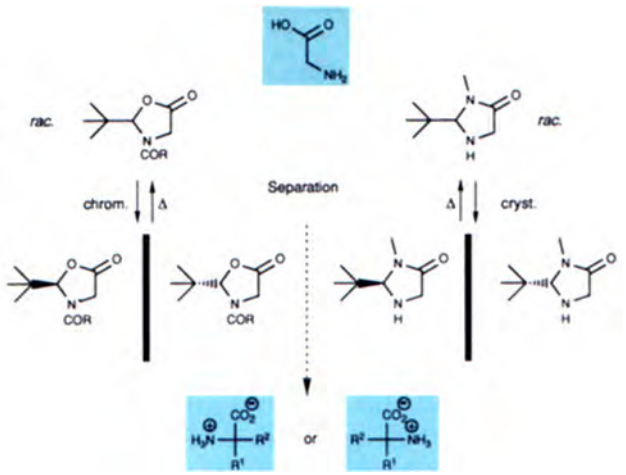

Scheme 25. Glycine derivatives that are readily accessible by the separation of racemates and are useful in the synthesis of (*R*) or (*S*) amino acids. The oxazolidinones (R = OBn, aryl) are obtained by the chromatographic separation of enantiomers [137] (Fig. 1), and the imidazolidinones by crystallization of their mandelic acid salts [450] (recycling by heating). A versatile series of transformations [137, 353, 450, 451] leads ultimately to branched and unbranched nonproteinogenic amino acids with a wide "structural bandwidth".

ous gift of pivalaldehyde (a byproduct in the hydroformylation of isobutylene, previously disposed of by burning!).

The collage of auxiliary groups for stereoselective synthesis shown in Scheme 26 is only a small sample, representing a few of the most successful reagents; most were prepared from inexpensive chiral precursors such as amino acids, ephedrine, 3-amino-3-phenylpropan-1,3-diol, β-hydroxybutyric acid, mandelic acid, tartaric acid, pantolactone, men-

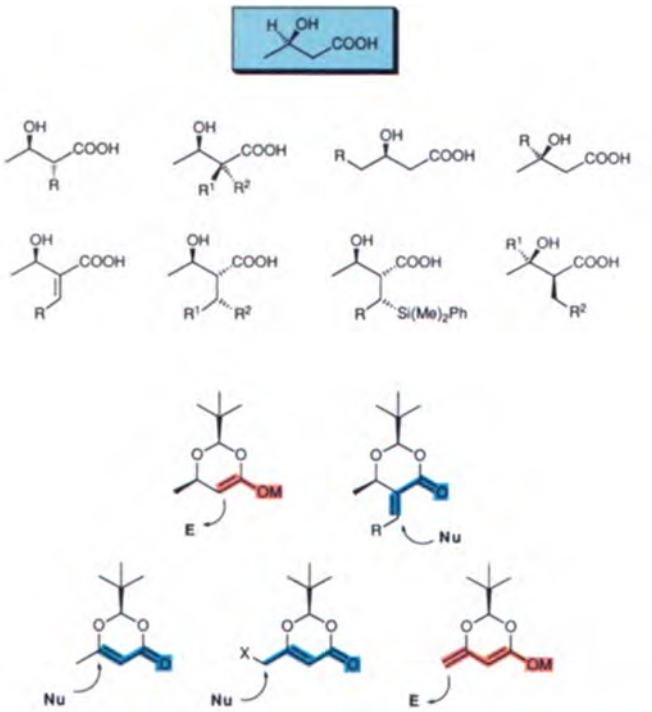

Scheme 27. Products obtained through transformations of (*R*)-3-hydroxybutyric acid derived from the biopolymer PHB. In a formal sense, the β-hydroxy acids shown at the top constitute aldol adducts of aldehydes or ketones with acetic acid, higher acids, or α-branched acids. Directly below these are the nucleophilic and electrophilic intermediates utilized for CC bond formation [183, 294, 353, 354, 371, 474–476]. It is clearly apparent that substituents can also be introduced at C-3 and C-4 of the hydroxybutyric acid without the occurrence of racemization (principle of self-regeneration of a stereogenic center [353, 477, 478]).

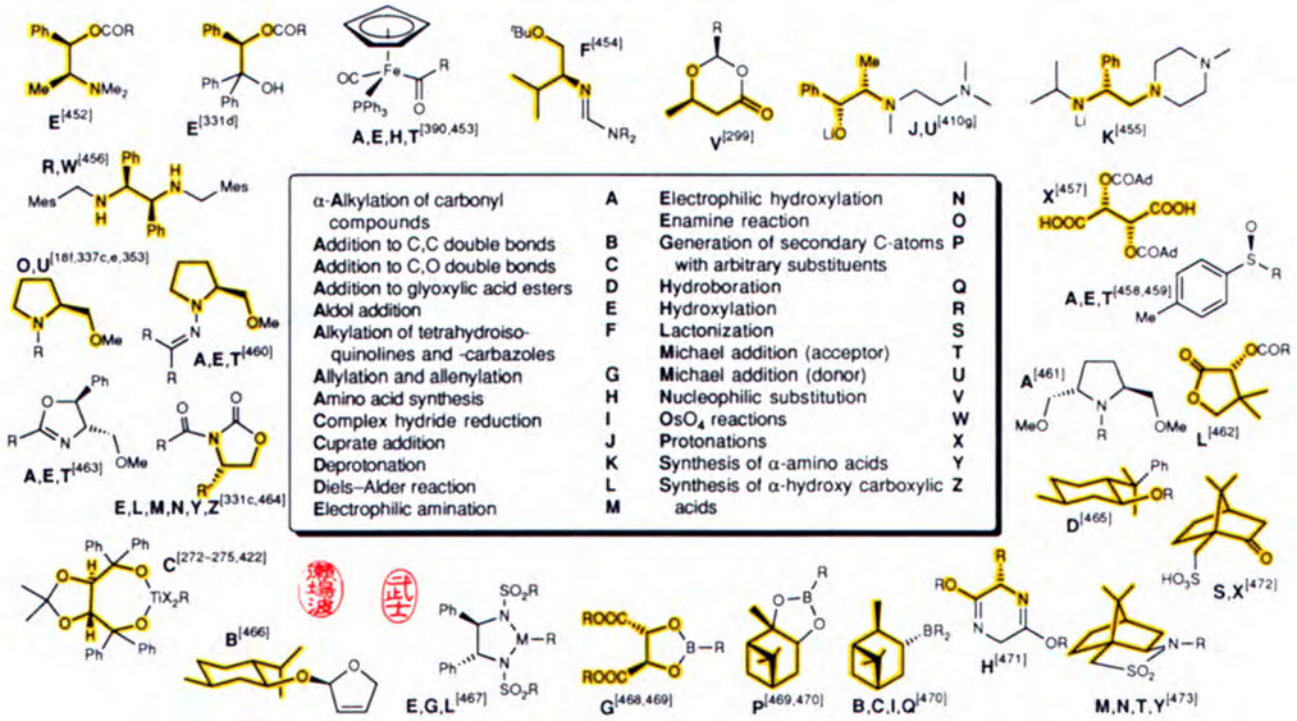

Scheme 26. A selection of chiral auxiliaries for multistep enantioselective syntheses. The chiral auxiliaries included in this collage are attached to the reactive center of an achiral molecule by way of a covalent bond in order to carry out the various transformations A–Z. The point is to ensure that a diastereoselective reaction, followed by removal of the auxiliary, will lead to the isolation of product enriched in a single enantiomer. No attempt has been made to provide a comprehensive list of such auxiliaries. Color has been used to emphasize the sources of the various auxiliary reagents. To the best of my knowledge, those auxiliaries not depicted in color result from the separation of racemic mixtures.

thol, pinene, or camphor. The long list of suggested applications for *Evans*' acyloxazolidinone is testimony to the profound significance of this particular reagent (cf., for example, the total synthesis of fujimycin).[51]

Finally, Scheme 27 illustrates a few transformation products derived from poly[(*R*)-3-hydroxybutyrate], which is prepared on a commercial scale by fermentation. Some of the compounds even contain quaternary centers, rendering them inaccessible in enantiomerically pure form by alternative methods.[479] Other applications of the incorporation method can be mentioned here only in passing.[480–482]

7.2. Catalytic Enantioselective Reactions: from Enzymes to Chemzymes

Even after casting off the phlogiston theory, chemists were (and remain today) fascinated by the synthetic achievements of nature, many of which can now be appreciated at the molecular level. The synthetic organic chemist typically regards nature's achievements not only as a standard to be emulated, but also as a formidable challenge, especially from the standpoint of selectivity (above all enantioselectivity). A single enzyme molecule is capable of supervising the transformation of millions and billions of substrate molecules before it loses its own activity. When an achiral educt is converted enzymatically into a chiral product, the enantiomeric yield is of the order of 10^6–10^9%, at least according to the way some chemists prefer to make calculations of this type!

Lurking between the lines of the following three more or less prosaic utterances is a subtle mixture of anxiety and fascination:

"Lord, I fall upon my knees
And pray that all my syntheses,
May no longer be inferior,
To those conducted by bacteria."[483]

"These new catalysts will be better than enzymes in that they will work under more flexible conditions than biological systems. Also, they don't need to work in water and don't have complicated cofactors and all this other garbage around that has to be gotten rid of when the product is purified."[484]

"Chemzymes are small, soluble organic molecules that can catalyze certain reactions in much the same way that natural enzymes catalyze biochemical reactions. ... Think of a submicroscopic production-line worker: over and over again, the chemzyme grabs a pair of reactant molecules out of the surrounding solution, twists them into position, welds them together into a precise three-dimensional structure, and then tosses the product molecule away to free itself for the next pair of reactants."[64b, 485]

It is no wonder that synthetic chemists have frequently tried to make direct use of biochemical catalysts,[486] and countless standard laboratory methods[487–489] have been perfected for the biological-chemical synthesis of simple compounds. Increasingly, however, various research groups are turning their attention to non-biochemical catalysis.[490] In fact, there is a real atmosphere of discovery surrounding the subject of catalysis in organic synthesis, as evidenced by the recently released collection of essays *Catalysis of Organic Reactions*.[491, 492] It would appear that most of the true sorcerers in this field are located in Japan. The following sections constitute brief discussions of enantioselective catalysis—first with enzymes, and then without.

7.2.1. *Biological-chemical Transformations*

Biological-chemical transformations on both an industrial scale and in the laboratory can be carried out using either whole cells or isolated enzymes. In certain industrial applications it has even proven feasible to "optimize" the required organisms or enzymes, sometimes carrying it to the point of preparing abzymes (Sec. 2.3).[114] Unusual types of reactions or conditions may be invoked (again, after extensive optimization) in the effort to prepare specific products. All the following substances are currently being synthesized on a more or less large scale by fermentation techniques:[493] alkaloids and dyes (in plant cell cultures),[494, 495] *cis*-3,5-cyclohexadien-1,2-diol (using a dioxygenase),[231, 496] cyclosporin (with *Tolypocladium inflatum* Gans),[232] a copolymer based on (*R*)-3-hydroxybutyric and valeric acids (PHB/PHV, Biopol®, with *Hydrogenomonas eutropha*),[230] 2-hydroxypropionic acid (by lactic acid fermentation; used by BASF in the production of an agricultural product), penicillin (and other antibiotics), proteins (such as insulin and interferon, using *Escherichiia coli* modified with the aid of gene technology), hydroxysteroids (using oxygenases),[497] vitamin C (L-sorbose, from D-sorbitol, with *Acetobacter suboxydans*),[229] and tartaric acid.[352] A recently conducted analysis[498] of publications and patents dealing with preparative applications and included in the 1987/1988 "Warwick Biotransformation Abstracts" demonstrated on the one hand that 40% of the reported transformations involved syntheses or reactions of esters, 25% were dehydrogenase-related procedures, and 24% had to do with peptide or oligosaccharide syntheses. Of the ester-cleaving enzymes employed (proteases, esterases, and lipases, enzymes that are available commercially), by far the most prevalent was pig liver esterase. Almost all the applications related to reduction involved whole cells; according to this source, half were carried out[488b] with baker's yeast (*Saccharomyces cerevisiae*). Enzymatic enantioselective esterifications, transesterifications, and saponifications can clearly be regarded today as standard laboratory procedures. The reduction of carbonyl groups requires the presence of NADPH as a hydride donor, and in this case it is more common to take advantage of the metabolic capabilities of whole cells. Yeast for this purpose can be managed successfully without a bioreactor,[499–501] at least with small preparations.[487]

There are, of course, a great many tricks and variations applicable to biological-chemical reaction steps, but this is true for the "classical" methods of organic synthesis as well.[502] For example, simple reductions with yeast alone sometimes fail to produce adequate enantioselectivity, usually because of competition between a number of oxidoreductases.[503] The situation can often be improved by carrying out the reaction in the presence of additives, or by an expedient such as pretreatment of the yeast (e.g., "starving"),[504a]

temporary modification of the substrate (cf. protective group techniques),[503] or switching to an organic medium (e.g., the "microemulsion"[504b] method).[505] Use of the easily cultured thermophilic microorganism *Thermoanaerobium brockii*, which is most comfortable at 70–80 °C, may lead to advantages in both selectivity and convenience (sterilization of the apparatus is not required).[506, 507] Methods have also been devised for improving the yield, selectivity, and isolability of the product in applications involving isolated enzymes or enzyme concentrates (pig liver esterase is often employed as a concentrate[126]); examples appear under the first two entries in the alphabetical list in Chapter 4. Biological-chemical methods are currently used for synthesizing amino acids both on a large[508–510] and a small[511] scale. Here the enzymes themselves are immobilized on a solid phase or trapped within a membrane[509–511] (dialysis tubing or a bag—permeable, for example, to molecules with a molecular weight less than 1000 daltons, i.e., to educts and products). Aqueous medium is not a disadvantage with amino acids—indeed, it is essential—but in other applications of biological-chemical methods insufficient polarity or lack of water solubility on the part of educt and/or product can often be a serious limiting factor. Organic solvents sometimes help, especially in transformations involving isolated enzymes,[125, 512, 513] but this alternative is usually associated with a significant retardation in the reaction rate.

The biological-chemical reactions with the strongest appeal for synthetic chemists are those capable of converting achiral educts (or chiral educts that rapidly equilibrate through achiral intermediates) into a *single* enantiomerically pure product containing as many stereogenic centers and functional groups as possible. It is therefore appropriate to conclude the discussion with a few examples that fall in this category (Schemes 28–30). The easiest to carry out are based on enzymes that require no cofactors (other than metal ions).

Even a cursory examination of the many "unnatural" compounds that have been successfully subjected to biological-chemical transformations[486–489, 496, 512] reveals a remarkable degree of diversity, and one is forced to conclude that enzymes are amazingly "tolerant".[536] Perhaps it is no accident that the most frequently utilized biological reagents have assignments in nature that also demand flexibility.

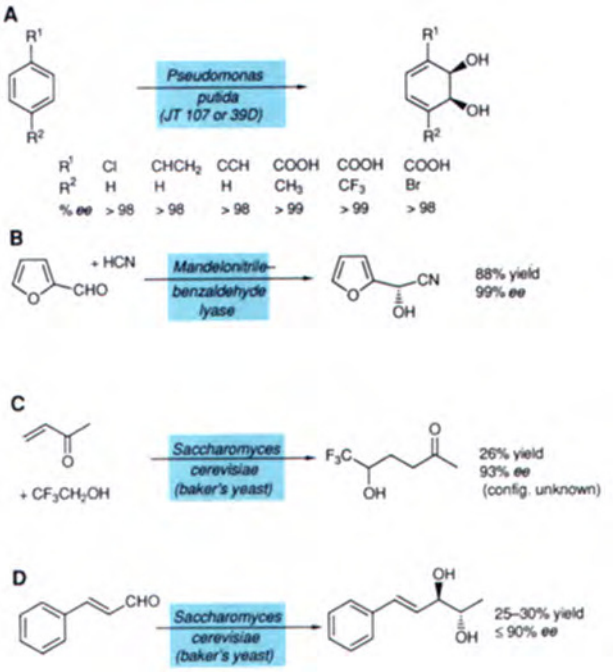

Scheme 28. Biological-chemical reactions involving enantioselective hydroxylation or C–C bond formation. A) The microorganisms capable of hydroxylating arenes to cyclohexadiendiols were discovered in a landfill in which aromatic compounds had been deposited [231, 496, 514]. B) MBL, extracted from almond flour, catalyzes the cyanohydrin reaction to give the nitriles of (*R*)-2-hydroxycarboxylic acids, a procedure that is effective with both aliphatic and aromatic aldehydes [513]. C) Formally speaking, this is a Michael addition of trifluoroethanol (d^1 reactivity [18g]) to methyl vinyl ketone (oxidation of trifluoroethanol to an aldehyde and thiamine pyrophosphate umpolung !?) [515]. D) Analogous reaction involving 1,2-addition of acetaldehyde to cinnamaldehyde [516].

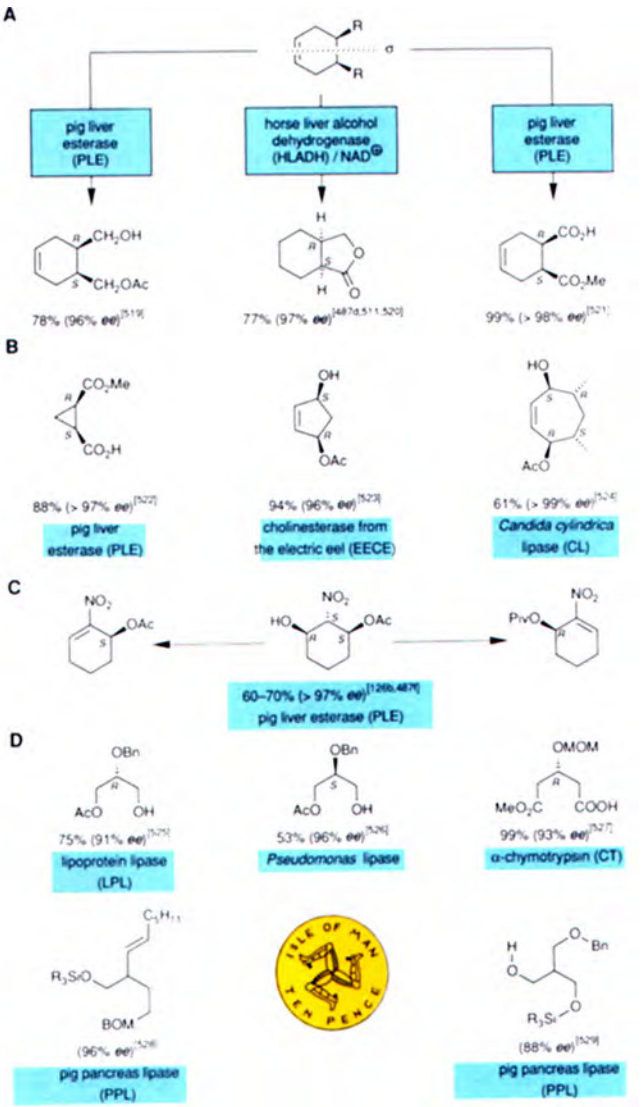

Scheme 29. Compounds with the *meso* configuration [517] and other achiral educts containing enantiotopic groups [518] can be ideal substrates for biological-chemical transformations. Subsequent to the enzymatic reaction it is almost always possible to invoke straightforward synthetic manipulations in order to prepare either enantiomer of the desired product (e.g., C). A) Products derived ultimately from the Diels–Alder adduct of butadiene with maleic ester; in the first case, R = CH_2OAc; in the second, CH_2OH (hydrogenation of the double bond!); in the third, CO_2Me. B) Three-, five-, and seven-membered ring derivatives containing up to four stereogenic centers and prepared from *meso* precursors. C) Three adjacent functional groups and stereogenic centers in a cyclohexane and enantiomeric nitrocyclohexenyl esters. D) Chiral derivatives of compounds with C_s and C_{3v} symmetry—versatile educts!

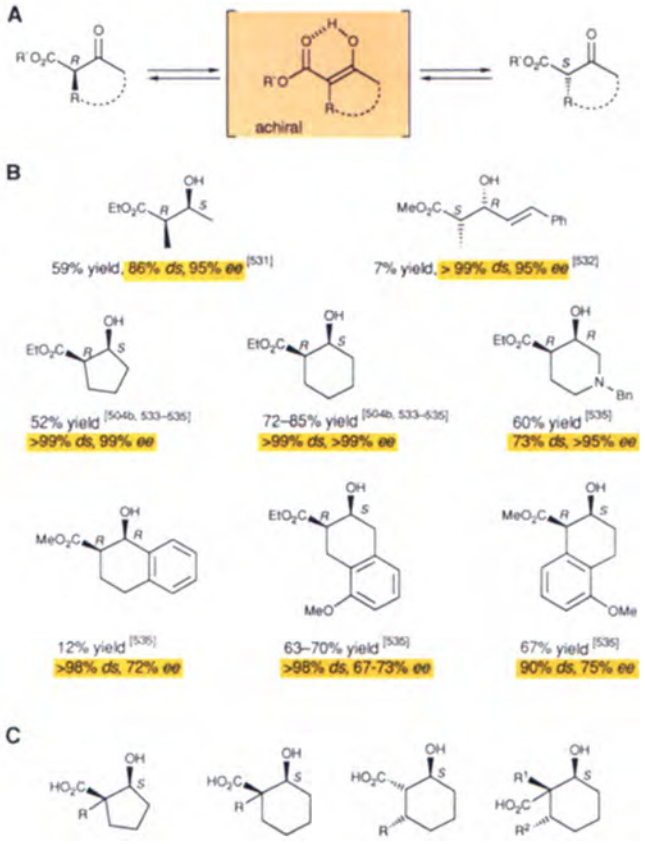

Scheme 30. Baker's yeast will do it [530]! Yeast reduction of 3-oxo esters with stereogenic centers at the 2-position is preceded by keto–enol tautomerization. Yeast reduces the (*R*) enantiomer, thereby removing it from the equilibrium; the process can thus be described as a kinetic resolution of enantiomers with in situ recycling, followed by diastereoselective reduction. The relative topicity [444] of the carbonyl reduction is consistent with the Prelog rule; that is, hydride is transferred from the *Re* side of the trigonal center in $R_L COR_S$ (with the priority $R_L > R_S$; in the case of styryl derivatives the styryl group assumes priority—although with a yield this low it is questionable whether any such consideration is permissible!). A) Equilibrium between enantiomeric 3-oxo esters. B) Yeast reduction products of the corresponding 3-oxo esters. C) Enantiomerically pure hydroxycyclopentane- and hydroxycyclohexanecarboxylic acid derivatives from the corresponding yeast reduction products [534].

Thus, liver esterases come from the mammalian organ most responsible for detoxification, and they have been shown to consist of isoenzyme mixtures; monooxygenases ("hydroxylases") owe their existence in part to the need for making hydrocarbons "metabolizable"; lipases promote cleavage of all types of fatty acid esters; and yeasts have "evolved" in such a way that they grow on a wide variety of culture media and under diverse sets of conditions.

7.2.2. Enantioselective Catalysis: Bases, Phase Transfer, and the Ligand Spheres of Metals

So far, the only popular, standard laboratory reaction that is both enantioselective and catalytic in nature is the Sharpless epoxidation.[537] Not only does it employ inexpensive reagents (*tert*-butylhydroperoxide, titanate, and ethyl tartrate) and involve educts (allyl alcohols) and products (epoxides) that are ubiquitous in organic synthesis, but it also enjoys an unusually wide range of applicability because of insensitivity to many aspects of substrate structure (constitution, configuration, chirality). Selection of the proper chiral form of the starting tartrate ester allows one to establish both the chirality of the product and/or its relative configuration.[538] An example of a simple enantioselective epoxidation is presented in Scheme 31.

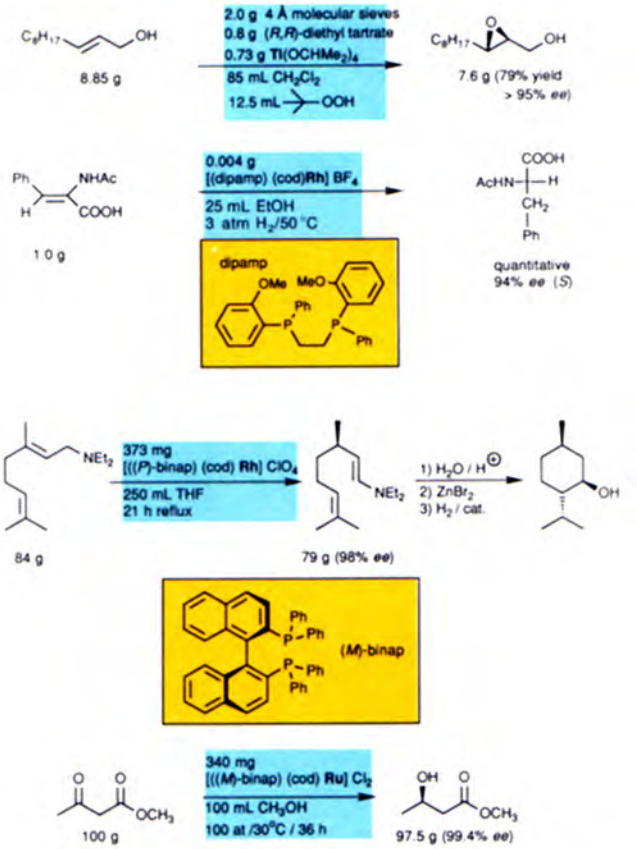

Scheme 31. Four examples of enantioselective transformations catalyzed by transition metals: Sharpless epoxidation of 2-undecen-1-ol [537d], Knowles hydrogenation to phenylalanine [435, 539], the Otsuka synthesis of menthol [540], and Noyori reduction of acetoacetic ester [402a].

Enantioselective hydrogenations and hydrogen shifts catalyzed by phosphane complexes of rhodium and ruthenium[402, 539–541] (Scheme 31) are not quite so straightforward on a laboratory scale, nor are they as easy to reproduce, but they do have broad applicability. Looking at the conditions[402a] required for the reduction of acetoacetic ester to (*R*)-3-hydroxybutyrate (Scheme 31) one cannot help but wonder what process will triumph for large-scale preparation of this important hydroxy acid (useful, for example, in the synthesis of thienamycin): the catalytic transition-metal approach or one of the fermentative methods mentioned previously.[230] The "volume yield" criterion (i.e., mass of product obtained per unit volume of reactor) argues for the non-biological procedure.

Scheme 32 illustrates a few other standard organic reactions[542] that can be induced to proceed in a catalytic and enantioselective way by the addition of transition-metal complexes. Brief mention should also be made of two catalytic processes that do not involve the ligand spheres of metals: a phase-transfer route to enantioselective amino acid synthesis[543a] and the cycloaddition reaction of ketene with α-halogenated aldehydes to give β-lactones, catalyzed by cinchona alkaloids.[543b]

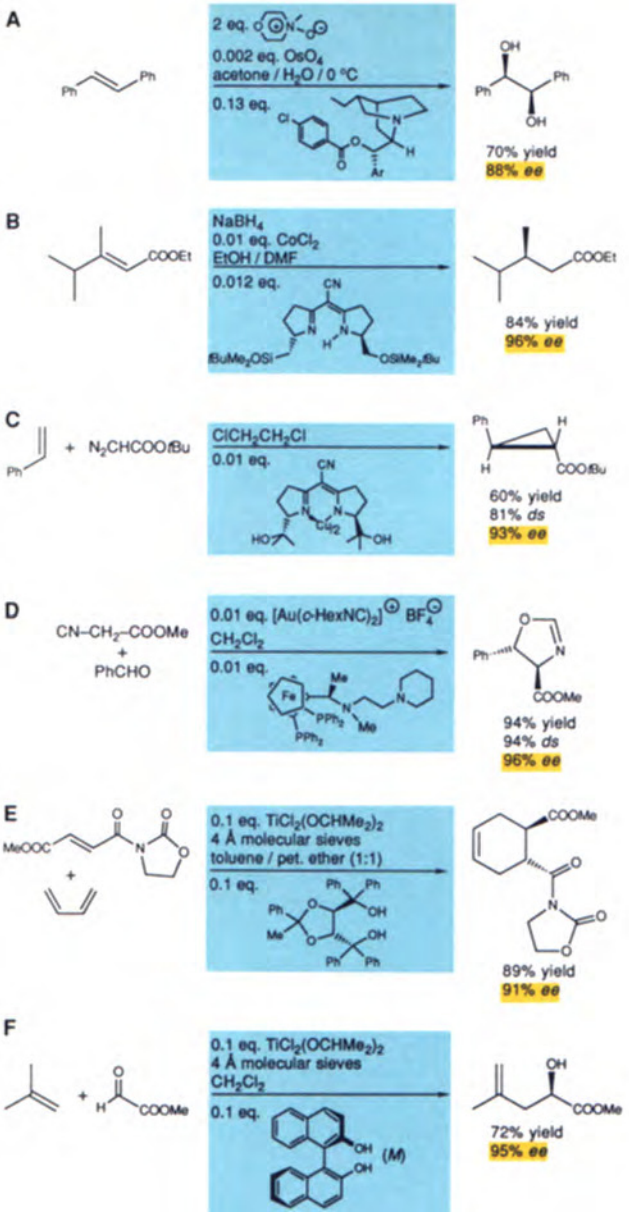

Scheme 32. Some examples of enantioselective reactions catalyzed by transition metals. A) Hydroxylation with osmium tetroxide, accelerated and made enantioselective by the presence of a cinchona alkaloid [544]. B) Hydrogenation of an α,β-unsaturated ester with $NaBH_4$/chiral-Co catalyst (ligand based on pyroglutamic acid) [490e]. C) Cyclopropanation with diazoacetic ester [copper(II)/chiral-semicorrin ligand] [490e]. D) The gold complex of a complicated chiral-ferrocene ligand catalyzes the addition of isocyanoacetic ester to benzaldehyde, leading to a *threo*-phenylserine derivative [545]. E) A ligand derived from tartaric acid [272–275] provides a Ti complex capable of catalyzing the Diels–Alder reaction in an enantioselective way [546, 547]. F) A derivative prepared from binaphthol/$TiCl_2(OCHMe_2)_2$ causes differentiation between the enantiotopic faces of the aldehyde in the ene reaction of isobutylene with glyoxylic ester [548].

It is interesting to note that many reactions called "catalytic" in the literature actually require the addition of rather large amounts of the alleged catalyst. For example, consider a benzylated or benzoylated quinine derivative with a molecular weight of over 400 daltons. If 0.1 mole-equivalent of such a material were to be utilized in a transformation leading to a product with a molecular weight of 120, then the substrate/catalyst relationship would be such that few *true* catalysis chemists would be willing to regard the reaction as belonging to their discipline.[549] It is also remarkable that precisely those enantioselective catalytic reactions that are most successful were either discovered accidentally or resulted from years of effort devoted to optimization. Even though it has sometimes been possible to discern the mechanism of a catalytic reaction[550]—the recently proposed mechanism for the Sharpless epoxidation is a case in point[537f]—the rational design of a structurally defined chiral catalyst is still in its infancy.[551] A noteworthy example of such an effort is mentioned near the end of this discussion.

One group of enantioselective reactions has been the subject of special attention in recent years. I am referring to reactions in which organometallic compounds that are normally unreactive toward aldehydes and ketones can be activated by catalytic amounts of a chiral amino alcohol so that they undergo enantioselective carbonyl addition. Organometallic agents of this type include alkyl zinc[552] and alkyl lead[553] derivatives, but most interesting perhaps are the boranes and borates.[554] The latter have the advantage that their reactions seem to lend themselves best—before or after the fact—to rationalization on the basis of mechanistic models. Alkyl, alkoxy, aryloxy, and dialkylamino groups are kinetically more tightly bound to boron than to other metallic centers, inhibiting dynamic processes that might otherwise result in ligand-exchange reactions. More important, however, one can rely on the fact (thanks to the octet rule!) that boron will never associate with more than four ligands, and that the ligands will be arranged tetrahedrally. With the single exception[555] of beryllium, whose toxicity has so far prevented its application in organic chemistry, all other metals are capable of supporting as many as six (or more!) ligand sites, characterized (depending upon valence and placement in the periodic table) by tetragonal planar, tetrahedral, trigonal bipyramidal, tetragonal pyramidal, or octa-

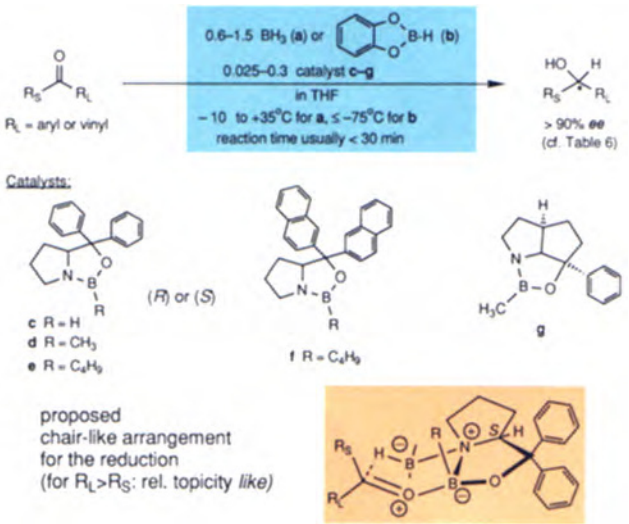

Scheme 33. The catalytic enantioselective reduction due to *Corey* et al. [559]. Several examples and references are collected in Table 6. As suggested by the analogy to an assembly line worker (see text), the authors believe that the bi- or tricyclic boron derivative functions at the boron atom as a Lewis acid, which is capable of activating the ketone that is to be reduced. The neighboring bridgehead nitrogen atom in turn binds to borane, activating it for the hydride transfer. The two achiral reaction partners are brought together in a chiral environment such that one of the enantiotopic sides of the carbonyl group is preferentially directed toward the hydride-transferring boron atom. Nevertheless, it is also important for the catalytic course of the reaction that the product alcoholate group is transferred from the boron atom in the ring to another boron atom, thereby removing it from the catalyst.

Table 6. Reductions of ketones with the boranes **a** and **b** of Scheme 33 and the chiral catalysts **c**–**g** [567]. Even the purely aliphatic substrate cyclohexyl methyl ketone undergoes reduction with an enantioselectivity as high as 95:5. In the last case the borane in question (**b**) contained D in place of H.

Product from the corresponding ketone (or aldehyde)			Borane		Catalyst		Ref.
formula	yield	*ee*		equiv.		equiv.	
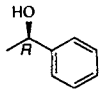	> 99%	97%	**a**	1.2	(*S*)-**c**	0.1	[559]
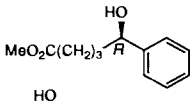	quant.	97%	**a**	0.6	(*S*)-**d**	0.1	[560]
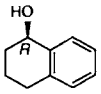	> 90%	95%	**a**	0.6	**g**	0.1	[561]
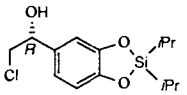	96%	97%	**a**	0.6	(*R*)-**f**	0.1	[562]
	> 95%	93%	**b**	1.5–2.0	(*S*)-**e**	0.1	[563]
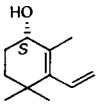	91%	90%	**a**	0.6	(*R*)-**d**	0.2	[564]
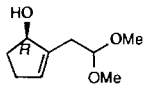	88%	93%	**a**	0.6	(*S*)-**d**	0.1	[565]
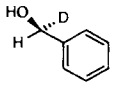	90%	91%	**b**	1.5	(*S*)-**f**	0.3	[566]

hedral geometries. Finally, BC, BO, and BN bonds are shorter than the corresponding bonds to carbon,[556] so that the groups bonded to boron approach each other more closely than in the case of boron-free systems, and considerably more closely than in compounds with other metals, permitting steric (van der Waals repulsion) and polar interactions (Coulomb forces) to play a more effective role.[557] The currently favored mechanistic model for enantioselective borane reduction of aromatic and α,β-unsaturated ketones with various chiral catalysts has been proven so reliable in explaining all the observed experimental results that *Corey* allowed himself to be seduced into inventing the word "chemzyme", a term already alluded to several times in this contribution.[12b, 64, 485, 558] Scheme 33 and Table 6 provide several examples of this type of borane reduction along with the proposed mechanism.

8. Concluding Remarks

Teach me the glorious lesson
that occasionally it is possible
that I may be mistaken
"Prayer of an ageing woman",
ascribed to Teresa of Ávila (1515–1582)

In presenting a paper or a talk, nothing is worse than beginning with a bad title, and the worst titles are ones that promise too much! I hope my contribution does not fit in this category, though I confess that the last part of the title ("Where now?") caused me to lose a certain amount of sleep and suffer several crises of conscience.

The effort will not have been wasted if I have convincingly swept away the one-sided but prevalent notion that organic chemistry and organic synthesis are mature sciences. On the contrary: they are neither stagnating, nor are they on the decline! The general directions I expect our disciplines to take in the future are apparent in the structure of the presentation itself and in the summary at the beginning. The topic treated last—preparing enantiomerically pure compounds, in particular with the aid of enantioselective catalysis—is one I would especially like to have discussed in more detail, but time and space constraints have made this impossible.

My time will also have been well spent if the roughly 1000 literature references prove to be stimulating, especially for my younger colleagues. I hope those readers who find the limited and very personal selection of topics unbalanced, or who regard the mode of presentation as awkward or somewhat "gauche" (Fig. 14), will nevertheless take to heart what

Fig. 14. Color plate based on an ancient Egyptian pattern [and distributed by the Franklin Mint AG, Zug (Switzerland)]. Hunter and huntress are shown with homochiral pairs of left hands, despite which they achieve their goal. The author hopes–despite taking controversial positions, passing judgments, and making difficult decisions regarding the research areas and research groups to be mentioned–that no friendships or feelings have been hurt, and that (unlike the archer in this picture) he has not put his neck into the "noose".

I consider the most important message: that organic synthesis continues to react forcefully and with vitality to new challenges, still ready to pursue old dreams. Considering the

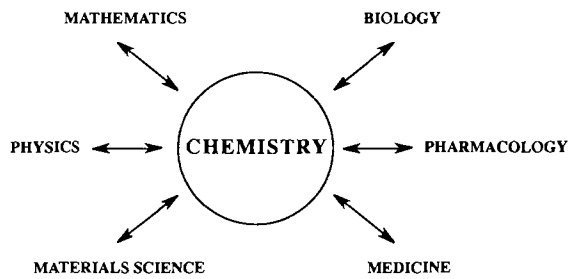

Scheme 34. Chemistry—including organic synthesis—at the center of the natural and technical sciences.

extent of chemical methodology's contributions to other disciplines it is tempting to take the charge that chemistry is in danger of losing its identity[2] and turn it around, proclaiming instead that chemistry—today more than ever before—is "the central science" (Scheme 34).[568] What a change from the days when *Albertus Magnus* (1193–1280) in his tract "De Alchemia" placed at the head of the list of essential characteristics for an alchemist:

He must be taciturn and circumspect,
and should communicate to no one
the results of his operations.

This article could not have been written without the help of a great many coworkers: Albert K. Beck (bibliography); Silvia Sigrist (preparation of the manuscript); Linda Behrendt (figures, schemes, tables); Josef Meienberger (departmental librarian) and Christoph von den Bussche Hünnefeld (literature searches); Bernd Lamatsch and Dietmar Plattner (strucural data); Stefan Blank, Denis Blaser, Richard Breitschuh, Urs Gysel, André Jeanguenat, Axel Neidlein, Christof Schickli, and Adrian Thaler (preparation of drawings and figures); as well as the rest of the group for checking in the library all the names and numbers in the bibliography. I offer all of you my heartfelt thanks; it is a real privilege to be surrounded by such a host of talented and motivated young people.

I also wish to thank those colleagues who have supplied me with information, data, drawings, or figures for use in this article (see also the acknowledgements in the legends and the list of references): E. Bayer (Tübingen), G. Boche (Marburg), Z. Brich (Sandoz, Basel), E. C. Constable (Cambridge, U. K.), R. R. Ernst (Zürich), A. Eschenmoser (Zürich), E. Galantay (Sandoz, Basel), J. Hajdu (Oxford), D. Hilvert (La Jolla), B. L. Karger (Boston), P. T. Lansbury (Boston), R. Noyori (Nagoya), L. E. Overman (Irvine), Sir D. Phillips (Oxford), J. F. Stoddart (Sheffield), W. F. van Gunsteren (Groningen), E. Vedejs (Madison), E. Zass (Zürich).

Received: May 9, 1990 [A 778 IE]
German version: *Angew. Chem.* 102 (1990) 1363
Translated by Dr. *W. E. Russey*, Huntingdon, PA (USA)

[1] *Roald Hoffmann* is currently working on a 26-part television series entitled "The World of Chemistry" for broadcast in the USA in 1991. He has also planned a series of three one-hour broadcasts entitled "The Molecular World"! [S. C. Stinson, *Chem. Eng. News 67* (1989) No. 23, pp. 19–21].

[2] *J. Maddox*, editor of the journal *Nature*, made the following assertion during a speech in Maastricht (Netherlands) in March 1988: "Chemists have done wonders in losing their identity in the rest of science. Some might argue the point, but it is a fact that the Nobel committee awarded its 1985 chemistry prize to a pair of mathematicians.—Meanwhile, the practice of what still passes for chemistry seems to have been largely preempted by outsiders—physicists, quantum theoreticists, computer mavens, statisticians, instrument designers, laser experts, genetic engineers, medical researchers, psychiatrists, astronomers, material specialists and a host of other species. Truly, the science of chemistry has lost its identity." (These sentences have been quoted with Mr. *Maddox*'s permission, cf. also [12b].)

[3] *H. A. Hauptman* and *J. Karle*, for developing the direct methods of solving X-ray structures of molecules containing no heavy atoms. "Direct Methods and Anomalous Dispersion" (Nobel Lecture): H. Hauptman, *Angew. Chem. 98* (1986) 600–610; *Angew. Chem. Int. Ed. Engl. 25* (1986) 603–613; "Recovering Phase Information from Intensity Data" (Nobel Lecture): J. Karle, *ibid. 98* (1986) 611–626 and *25* (1986) 614–629.

[4] It is worth reading in this context an editorial by R. Scheffold with the title "Synthese: Jugendstil oder Postmoderne" [*Chimia 43* (1989) 37]; cf. also the thoughts expressed by B. Giese on the theme "Perspektiven der organischen Chemie" [*Merck-Spektrum (Darmstadt) 1/90* (1990)]. A troubled analysis of the situation of our discipline bears the title "What's wrong with chemistry?" [M. Heylin, *Chem. Eng. News 68* (1990) No. 5, p. 3].

[5] "DNA Sequencing and Gene Structure" (Nobel Lecture): W. Gilbert, *Science (Washington D.C.) 214* (1981) 1305–1312.

[6] Monograph: W. Saenger: *Principles of Nucleic Acid Structure*, Springer, New York 1984.

[7] E.-L. Winnacker: *Gene und Klone*, Verlag Chemie, Weinheim 1984; "Gene Synthesis": J. W. Engels, E. Uhlmann, *Angew. Chem. 101* (1989) 733–752; *Angew. Chem. Int. Ed. Engl. 28* (1989) 716–734.

[8] "Solid Phase Synthesis" (Nobel Lecture): R. B. Merrifield, *Angew. Chem. 97* (1985) 801–812; *Angew. Chem. Int. Ed. Engl. 24* (1985) 799–810; "Solid-phase peptide synthesis: a silver anniversary report": G. Barany, N. Kneib-Cordonier, G. Mullen, *Int. J. Pept. Protein Res. 30* (1987) 705–739; "True automation of peptide synthesis": R. C. Sheppard, *Chem. Br. 24* (1988) 557–562.

[9] O. W. Webster, W. R. Hertler, D. Y. Sogah, W. B. Farnham, T. V. Rajan-Babu, *J. Macromol. Sci. Chem. A21* (1984) 943.

[10] "Size of Alkyl Group R: Principal Factor Determining Wettability of Surface-Functionalized Polyethylenes (PE-CONHR and PE-CO_2R) by Water": M. D. Wilson, G. S. Ferguson, G. M. Whitesides, *J. Am. Chem. Soc. 112* (1990) 1244; see also the article by *Whitesides* in the book by *Roberts* [79b].

[11] R. W. Armstrong, J.-M. Beau, S. H. Cheon, W. J. Christ, H. Fujioka, W.-H. Ham, L. D. Hawkins, H. Jin, S. H. Kang, Y. Kishi, M. J. Martinelli, W. W. McWhorter, Jr., M. Mizuno, M. Nakata, A. E. Stutz, F. X. Talamas, M. Taniguchi, J. A. Tino, K. Ueda, J. Uenishi, J. B. White, M. Yonaga, *J. Am. Chem. Soc. 111* (1989) 7530.

[12] a) A complete description of the situation as seen through American eyes is the so-called *Pimentel Report: Opportunities in Chemistry*, National Academic Press, Washington, D.C. 1985 (ISBN 0-309-03594-5); b) "Something Valuable from Almost Nothing: A Personal View of Synthetic Chemistry", E. J. Corey, *Chemist (Washington, D. C.) July/August 1989*, 3–5.

[13] A recently published book that illustrates how the products of chemistry have transformed everyday life in the past 135 years: E. Bäumler: *Farben Formeln Forscher. Hoechst und die Geschichte der industriellen Chemie in Deutschland*, Piper Verlag, München 1990.

[14] In 1985 the *Pimentel Report* [12a] came to the conclusion that five priorities should be established within the areas of chemistry. The first two are related to synthesis: A) *Understanding Chemical Reactivity* ("We propose an initiative to apply the full power of modern instrumental techniques and chemical theory to the clarification of factors that control the rates of reactions and to the development of new synthetic pathways for chemical change"). B) *Chemical Catalysis* ("We propose an initiative to apply the techniques of chemistry to obtain a molecular-level and coherent understanding of catalysis that encompasses heterogeneous, homogeneous, photo-, electro-, and artificial enzyme catalysis").

[15] "General Methods for the Construction of Complex Molecules": E. J. Corey, *Pure Appl. Chem. 14* (1967) 19–37.

[16] E. J. Corey, X.-M. Cheng: *The Logic of Chemical Synthesis*, Wiley, New York 1989.

[17] a) *Corey*'s original definition of *synthon* [15] was very useful in the context of retrosynthetic analysis, but the expression has now degenerated into one that is applied to synthetic intermediates. As a result, Corey himself no longer employs it at all—in the book cited previously [16], for example, which deals with all of his work to date! b) "Retrosynthetic Thinking—Essentials and Examples" (Robert Robinson Lecture): E. J. Corey, *Chem. Soc. Rev. 17* (1988) 111–133.

[18] Review articles: a) "Methods and Possibilities of Nucleophilic Acylation": D. Seebach, *Angew. Chem. 81* (1969) 690–700; *Angew. Chem. Int. Ed. Engl. 8* (1969) 639–649; b) "Nucleophile Acylierung mit 2-Lithium-1,3-dithianen bzw. 1,3,5-trithianen": D. Seebach, *Synthesis 1969*,17–36; c) "Umpolung (dipole inversion) of carbonyl reactivity": D. Seebach, M. Kolb, *Chem. Ind. (London) 1974*, 687–692; d) "Umpolung of Amine Reactivity. Nucleophilic α-(Secondary Amino)-alkylation *via* Metalated Nitrosamines": D. Seebach, D. Enders, *Angew. Chem. 87* (1975) 1–18; *Angew. Chem. Int. Ed. Engl. 14* (1975) 15–32; e) "Umpolung of the Reactivity of Carbonyl Compounds Through Sulfur Containing Reagents": B.-T. Gröbel, D. Seebach, *Synthesis 1977*, 357–402; f) "Nitroaliphatic Compounds—Ideal Intermediates in Organic Synthesis?": D. Seebach, E. W. Colvin, F. Lehr, T. Weller, *Chimia 33* (1979) 1–18; g) "Methoden der Reaktivitätsumpolung": D. Seebach, *Angew. Chem. 91* (1979) 259–278; *Angew. Chem. Int. Ed. Engl. 18* (1979) 239–258; h) T. A. Hase (Ed.): *Umpoled Synthons*, Wiley, New York 1987; i) "Synthetic Uses of the 1,3-Dithiane Grouping from 1977 to 1988": P. C. Bulman Page, M. B. van Niel, J. C. Prodger, *Tetrahedron 45* (1989) 7643–7677; j) "Ketene Dithioacetals in Organic Synthesis: Recent Developments": M. Kolb, *Synthesis 1990*, 171–190.

[19] "Sulfidkontraktion *via* alkylative Kupplung: eine Methode zur Darstellung von β-Dicarbonylderivaten": M. Roth, P. Dubs, E. Götschi, A.

Eschenmoser, *Helv. Chim. Acta 54* (1971) 710; "Roads to Corrins": A. Eschenmoser, *Q. Rev. Chem. Soc. 24* (1970) 366–415; see also A. Eschenmoser in *23rd Int. Congr. Pure Appl. Chem., Vol. 2*, Butterworth, London 1971, pp. 69–106.

[20] "Organische Naturstoffsynthese heute. Vitamin B_{12} als Beispiel": A. Eschenmoser, *Naturwissenschaften 61* (1974) 513–525; "Natural Product Synthesis and Vitamin B_{12}": A. Eschenmoser, C. E. Wintner, *Science (Washington, D. C.) 196* (1977) 1410–1420.

[21] "Tetrahedrane and Cyclobutadiene": G. Maier, *Angew. Chem. 100* (1988) 317–341; *Angew. Chem. Int. Ed. Engl. 27* (1988) 309–332.

[22] Review: "Synthesen und Reaktionen von Derivaten des Dewar-Benzols und des Prismans": R. Criegee, *Accad. Naz. Lincei, Roma, Mod. Sviluppi Sint. Org., Corso Estivo Chim. 1967*, 165–179.

[23] P. E. Eaton, T. W. Cole, Jr., *J. Am. Chem. Soc. 86* (1964) 3157.

[24] The first dodecahedrane synthesis: L. A. Paquette, J. C. Weber, T. Kobayashi, Y. Miyahara, *J. Am. Chem. Soc. 110* (1988) 8591; the pagodane route to dodecahedranes: H. Prinzbach et al., *Angew. Chem. 101* (1989) 307, 309, 312, 314, 319; *102* (1990) 102, 105; *Angew. Chem. Int. Ed. Engl. 28* (1989) 298, 300, 303, 305, 310; *29* (1990) 92, 95.

[25] D. Kuck, B. Paisdor, *Chemiedozententagung 1990*, Ulm, 26–28 March 1990, Wissenschaftliches Programm und Vortragsreferate, Universitätsverlag Ulm, A 18; D. Kuck, A. Schuster, *Angew. Chem. 100* (1988) 1222; *Angew. Chem. Int. Ed. Engl. 27* (1988) 1192; D. Kuck, H. Bögge, *J. Am. Chem. Soc. 108* (1986) 8107.

[26] G. Wittig, G. Geissler, *Justus Liebigs Ann. Chem. 580* (1953) 44.

[27] L. Horner, W. Klink, H. Hoffmann, *Chem. Ber. 96* (1963) 3133; B. E. Maryanoff, A. B. Reitz, *Chem. Rev. 89* (1989) 863.

[28] D. J. Peterson, *J. Org. Chem. 33* (1968) 780.

[29] F. N. Tebbe, G. W. Parshall, G. S. Reddy, *J. Am. Chem. Soc. 100* (1978) 3611; S. H. Pine, R. Zahler, D. A. Evans, R. H. Grubbs, *ibid. 102* (1980) 3270.

[30] K. Takai, Y. Hotta, K. Oshima, H. Nozaki, *Tetrahedron Lett. 1978*, 2417.

[31] E. J. Corey, D. Seebach, *Angew. Chem. 77* (1965) 1134, 1135; *Angew. Chem. Int. Ed. Engl. 4* (1965) 1075, 1077; see also the review articles listed in [18a, b, e, i].

[32] D. Seebach, F. Lehr, *Angew. Chem. 88* (1976) 540; *Angew. Chem. Int. Ed. Engl. 15* (1976) 505; M. Eyer, D. Seebach, *J. Am. Chem. Soc. 107* (1985) 3601 and references cited therein. See also review article [18f] as well as the work cited under [35].

[33] G. Stork, L. Maldonado, *J. Am. Chem. Soc. 93* (1971) 5286.

[34] K. Deuchert, U. Hertenstein, S. Hünig, *Synthesis 1973*, 777; trimethylsilyl cyanide as an umpolung reagent: S. Hünig, C. Marschner, K. Peters, H. G. von Schnering, *Chem. Ber. 122* (1989) 2131 and intervening papers in this series of publications from the Hünig group.

[35] R. Henning, F. Lehr, D. Seebach, *Helv. Chim. Acta 59* (1976) 2213; D. Seebach, R. Henning, F. Lehr, J. Gonnermann, *Tetrahedron Lett. 1977*, 1161; D. Seebach, R. Henning, F. Lehr, *Angew. Chem. 90* (1978) 479; *Angew. Chem. Int. Ed. Engl. 17* (1978) 458; D. Seebach, R. Henning, J. Gonnermann, *Chem. Ber. 112* (1979) 234; D. Seebach, R. Henning, T. Mukhopadhyay, *ibid. 115* (1982) 1705; U. Brändli, M. Eyer, D. Seebach, *ibid. 119* (1986) 575; cf. also [18f].

[36] The "Habilitationsschrift" of *R. Neier*, Universität Freiburg (Switzerland) 1989, contains an interesting discussion (with extensive bibliography) of the history of natural product synthesis and the role it has played in the discovery of new synthetic methods. I wish to thank Dr. *Neier* for providing me with a copy of this work.

[37] All of *E. J. Corey*'s natural product syntheses are collected in [16].

[38] "Synthesis in Biochemistry": R. Robinson, *J. Chem. Soc. 1936*, 1079.

[39] "Synthesis": R. B. Woodward in A. R. Todd (Ed.): *Perspectives in Organic Chemistry*, Interscience, New York 1956, pp. 155–184. *Woodward* says here: "We do not propose to examine this vast domain in detail, or to *prognosticate* the direction of its advance, in response to the need, desire, and fancy of man. We shall leave it that the evidence is overwhelming that the creative function of organic chemistry will continue to augment nature, with great rewards, for mankind and the chemist in equal measure."

[40] "The Total Synthesis of Strychnine": R. B. Woodward, M. P. Cava, W. D. Ollis, A. Hunger, H. V. Daeniker, K. Scheuber, *Tetrahedron 19* (1963) 247–288.

[41] "Über organische Naturstoffsynthese: von der Synthese des Vitamin B_{12} zur Frage nach dem Ursprung der Corrinstruktur": A. Eschenmoser, *Nova Acta Leopoldina*, Neue Folge, Issue 247, Vol. *55* (1982) pp. 5–47; see also [20].

[42] "Vitamin B_{12}: Experiments Concerning the Origin of Its Molecular Structure": A. Eschenmoser, *Angew. Chem. 100* (1988) 5–40; *Angew. Chem. Int. Ed. Engl. 27* (1988) 5–39.

[43] An important document in this context is an interview with *A. Eschenmoser* and *R. B. Woodward* about Vitamin B_{12} and the situation in organic chemistry, bearing the title "Herr Woodward bedauert, daß die Sache fertig ist": *Nachr. Chem. Techn. 20* (1972) 147–150.

[44] "Organische Synthese—Zukunft und Gegenwart" is the title of an interview with *G. Stork* in *Nachr. Chem. Tech. Lab. 35* (1987) 349–353.

[45] *Kishi*'s palitoxin synthesis [11] must also be mentioned again here.

[46] M. A. Napier, B. Holmquist, D. J. Strydom, I. H. Goldberg, *Biochem. Biophys. Res. Commun. 89* (1979) 635.

[47] a) M. Konishi, H. Ohkuma, K.-I. Saitoh, H. Kawaguchi, J. Golik, G. Dubay, G. Groenewold, B. Krishnan, T. W. Doyle, *J. Antibiot. 38* (1985) 1605; b) A. A. Fantini, J. D. Korshalla, F. Pinho, N. A. Kuck, M. J. Mroczenski-Wildey, M. Greenstein, W. M. Maiese, R. T. Testa, *Progr. Abstr. 26th Intersci. Conf. Antimicrob. Agents Chemother.*, New Orleans, LA, Sept. 1986, Am. Soc. Microbiol., Washington, D.C., Abstr. 227; M. D. Lee, G. O. Morton, T. S. Dünne, D. R. Williams, J. K. Manning, M. Siegel, C. C. Chang, D. B. Borders, *ibid.*, Abstr. 228; c) M. Konishi, H. Ohkuma, K. Matsumoto, T. Tsuno, H. Kamei, T. Miyaki, T. Oki, H. Kawaguchi, G. D. VanDuyne, J. Clardy, *J. Antibiot. 42* (1989) 1449.

[48] N. Zein, A. M. Sinha, W. J. McGahren, G. A. Ellestad, *Science (Washington, D. C.) 240* (1988) 1198.

[49] R. G. Bergman, *Acc. Chem. Res. 6* (1973) 25.

[50] S. L. Schreiber, L. L. Kiessling, *J. Am. Chem. Soc. 110* (1988) 631; S. J. Danishefsky, N. B. Mantlo, D. S. Yamashita, *ibid. 110* (1988) 6890; M. Paz Cabal, R. S. Coleman, S. J. Danishefsky, *ibid. 112* (1990) 3253; P. Magnus, R. T. Lewis, J. C. Huffman, *ibid. 110* (1988) 6921; K. C. Nicolaou, Y. Ogawa, G. Zuccarello, H. Kataoka, *ibid. 110* (1988) 7247; A. S. Kende, C. A. Smith, *Tetrahedron Lett. 29* (1988) 4217; K. Tomioka, H. Fujita, K. Koga, *ibid. 30* (1989) 851.

[51] Another unusual natural product from the standpoint of structure is *fujimycin (FK 506)*, an immunosuppresive agent containing a 1,2,3-tricarbonyl unit, which has attracted the attention of a great many synthetic groups. Isolation and structure determination: a) T. Kino, H. Hatanaka, M. Hashimoto, M. Nishiyama, T. Goto, M. Okuhara, M. Kohsaka, H. Aoki, H. Imanaka, *J. Antibiot. 40* (1987) 1249; H. Tanaka, A. Kuroda, H. Marusawa, H. Hatanaka, T. Kino, T. Goto, M. Hashimoto, *J. Am. Chem. Soc. 109* (1987) 5031; A. W. Thomson, *Immunol. Today 10* (1989) 6; synthesis: b) T. K. Jones, S. G. Mills, R. A. Reamer, D. Askin, R. Desmond, R. P. Volante, I. Shinkai, *J. Am. Chem. Soc. 111* (1989) 1157; T. K. Jones, R. A. Reamer, R. Desmond, S. G. Mills, *ibid. 112* (1990) 2998; additional synthetic contributions: c) E. J. Corey, H.-C. Huang, *Tetrahedron Lett. 30* (1989) 5235; d) R. E. Ireland, P. Wipf, *ibid. 30* (1989) 919; e) A. B. Smith III, K. J. Hale, *ibid. 30* (1989) 1037; f) H. H. Wasserman, V. M. Rotello, D. R. Williams, J. W. Benbow, *J. Org. Chem. 54* (1989) 2785; g) A. B. Jones, M. Yamaguchi, A. Patten, S. J. Danishefsky, J. A. Ragan, D. B. Smith, S. L. Schreiber, *ibid. 54* (1989) 17; A. B. Jones, A. Villalobos, R. G. Linde II, S. J. Danishefsky, *ibid. 55* (1990) 2786; h) D. R. Williams, J. W. Benbow, *ibid. 53* (1988) 4643; i) P. Kocienski, M. Stocks, D. Donald, M. Cooper, A. Manners, *Tetrahedron Lett. 29* (1988) 4481.

[52] a) It is no wonder that one often leaves a lecture or a symposium in which "something else has just been synthesized" with a feeling of boredom coupled with a sense that the same lectures could just as well have been delivered 20 years ago! b) Nowadays the synthetic portion of a lecture is sometimes delivered almost in an apologetic tone: "it has to be done, but it's not exciting, so let's get it over with". Not long ago a well-known young synthetic (organic) chemist observed as part of the introduction to a lecture that people like himself now represent "a dying beast".

[53] "Supramolecular Chemistry—Scope and Perspectives; Molecules, Supermolecules, and Molecular Devices" (Nobel Lecture): J.-M. Lehn, *Angew. Chem. 100* (1988) 91–116; *Angew. Chem. Int. Ed. Engl. 27* (1988) 89–112; "Some Future Aspects of Stereochemistry": J.-M. Lehn in *Euchem Conference on Stereochemistry, Bürgenstock/Switzerland 1965–1989*, Salle + Sauerländer, Aarau 1989, pp. 28–30; "Coordination Compounds as Molecular Devices": J.-M. Lehn, Lecture *OMCOS-V, 1–6 Oct. 1989*, Florence (Italy).

[54] "Molecular Inclusion and Molecular Recognition—Clathrates I and II": E. Weber (Ed.): *Top. Curr. Chem. 140* (1987) and *149* (1988); "New Clathrate Family Based on Small-Ring Compounds": E. Weber, M. Hecker, I. Csöregh, M. Czugler, *ICCOSS IX*, 2–7 July 1989, Como (Italy), Abstr. OC 4.

[55] "Why not Hexosenucleic Acids?": A. Eschenmoser, *25th Euchem Conf. Stereochem.* 30 April–6 May 1989, Bürgenstock (Switzerland); "Warum nicht Hexosenucleinsäuren?": A. Eschenmoser, *Bohlmann-Vorlesung 1989*, 30 Nov. 1989, Technische Universität Berlin. I wish to thank my colleague *Albert Eschenmoser* most warmly for providing me with slide copies and the permission to use them in this article (Scheme 4).

[56] "Molecular Recognition with Model Systems": J. Rebek, Jr., *Angew. Chem. 102* (1990) 261–272; *Angew. Chem. Int. Ed. Engl. 29* (1990) 245–255; "A Self-Replicating System": T. Tjivikua, P. Ballester, J. Rebek, Jr., *J. Am. Chem. Soc. 112* (1990) 1249; "Recognition and Catalysis Using Molecular Clefts": J. Rebek, Jr., *Chemtracts: Org. Chem. 2* (1989) 337–352, cf. also the article by *Rebek* in *Roberts*' book [79b].

[57] "The Design of Molecular Hosts, Guests, and Their Complexes" (Nobel Lecture): D. J. Cram, *Angew. Chem. 100* (1988) 1041–1052; *Angew. Chem. Int. Ed. Engl. 27* (1988) 1009–1020; "Molecules within Molecules": D. J. Cram, J. C. Sherman, J. A. Bryant, K. Paek, *Int. Chem. Congr. Pacific Basin Societies*, 17–22 Dec. 1989, Honolulu, HI, Abstr.

BIOS 319; "Organic Molecules Dimerize with High Structural Recognition When Each Possesses a Large Lipophilic Surface Containing Two Preorganized and Complementary Host and Guest Regions": J. A. Bryant, C. B. Knobler, D. J. Cram, *J. Am. Chem. Soc. 112* (1990) 1254; "Structure and Properties of the Cryptophane-E/$CHCl_3$ Complex, a Stable van der Waals Molecule": J. Canceill, M. Cesario, A. Collet, J. Guilhem, L. Lacombe, B. Lozach, C. Pascard, *Angew. Chem. 101* (1989) 1249; *Angew. Chem. Int. Ed. Engl. 28* (1989) 1246; "Complexation of Neutral Molecules by Cyclophane Hosts": F. Diederich, *ibid. 100* (1988) 372–396 and *27* (1988) 362–386.

[58] "A Topologically Chiral [2]Catenand": D. K. Mitchell, J.-P. Sauvage, *Angew. Chem. 100* (1988) 985; *Angew. Chem. Int. Ed. Engl. 27* (1988) 930; "Interlocking of Coordinating Molecular Threads: From the Statistical Approach to the Templated Synthesis of Catenands": C. O. Dietrich-Buchecker, J.-P. Sauvage, *Chem. Rev. 87* (1987) 795–810.

[59] "Molecular Architecture and Function of Polymeric Oriented Systems: Models for the Study of Organization, Surface Recognition, and Dynamics of Biomembranes": H. Ringsdorf, B. Schlarb, J. Venzmer, *Angew. Chem. 100* (1988) 117–162; *Angew. Chem. Int. Ed. Engl. 27* (1988) 113–158.

[60] "Host–Guest Chemistry": J. F. Stoddart, *Annu. Rep. Prog. Chem. Sect. B 85* (1988) 353–386; "Molecular Lego": F. Stoddart, *Chem. Br. 24* (1988) 1203–1208; "A Polymolecular Donor–Acceptor Stack Made of Paraquat and a 1,5-Dihydroxynaphthalene-Derived Crown Ether": J.-V. Ortholand, A. M. Z. Slawin, N. Spencer, J. F. Stoddart, D. J. Williams, *Angew. Chem. 101* (1989) 1402; *Angew. Chem. Int. Ed. Engl. 28* (1989) 1394; cf. also the article by *Stoddart* in *Roberts*' book [79b]; "Rotaxanes and Catenanes Made to Order": J. F. Stoddart, *Organisch-chemisches Kolloquium*, 5 Feb. 1990, ETH Zürich (Switzerland). I wish to thank Professor *Stoddart* for providing me with certain materials related to this theme, especially for unpublished manuscripts of work that will appear in *J. Am. Chem. Soc.* and in *Angew. Chem.*

[61] F. L. Carter, *Physica (Amsterdam) D10* (1984) 175.

[62] "Main-Chain Chirality and Optical Activity in Polymers Consisting of C–C Chains": G. Wulff, *Angew. Chem. 101* (1989) 22–38; *Angew. Chem. Int. Ed. Engl. 28* (1989) 21–37.

[63] "Stereochemical and Structural Relations Between Macromolecules and Crystals in Biomineralization": L. Addadi, S. Weiner in S. Mann, J. Webb, R. J. P. Williams (Eds.): *Biomineralization*, VCH Verlagsgesellschaft, Weinheim 1989, pp. 133–156; "Molecular Mechanisms of Biomineralization in the Formation of Calcified Shells": G. Krampitz, G. Graser, *Angew. Chem. 100* (1988) 1181–1193; *Angew. Chem. Int. Ed. Engl. 27* (1988) 1145–1156.

[64] a) E. J. Corey, J. O. Link, *Tetrahedron Lett. 30* (1989) 6275, cf. also [552b] and Sec. 7.2.2; b) an article that led to numerous controversies over the concept of *chemzymes*: M. M. Waldrop, *Science (Washington, D. C.) 245* (1989) 354.

[65] "A New Class of Polymers: Starburst-Dendritic Macromolecules": D. A. Tomalia, H. Baker, J. Dewald, M. Hall, G. Kallos, S. Martin, J. Roeck, J. Ryder, P. Smith, *Polym. J. (Tokyo) 17* (1985) 117–132; A. D. Meltzer, D. A. Tirrell, A. A. Jones, P. T. Inglefield, D. M. Downing, D. A. Tomalia, *Polym. Prepr. Am. Chem. Soc. Div. Polym. Chem. 30* (1989) 121; G. R. Newkome, Z. Yao, G. R. Baker, V. K. Gupta, P. S. Russo, M. J. Saunders, *J. Am. Chem. Soc. 108* (1986) 849; "'Starburst-Dendrimere' und 'Arborole'" (Synthese im Blickpunkt): K. Krohn, *Nachr. Chem. Tech. Lab. 35* (1987) 1252–1255; "Starburst Dendrimers: Molecular-Level Control of Size, Shape, Surface Chemistry, Topology, and Flexibility from Atoms to Macroscopic Matter": D. A. Tomalia, A. M. Naylor, W. A. Goddard III, *Angew. Chem. 102* (1990) 119–157; *Angew. Chem. Int. Ed. Engl. 29* (1990) 138–175; theory: "Statistics of 'Starburst' Polymers": P. G. De Gennes, H. Hervet, *J. Phys. Lett. 44* (1983) 351–360.

[66] "Synthetic Polymers with Enzyme-like Activities": I. M. Klotz, *Ann. N. Y. Acad. Sci. 434* (1984) 302–320; "Molecular Imprinting": G. Wulff, *ibid. 434* (1984) 327–333; with respect to template polymerization see also: K. J. Shea, D. Y. Sasaki, *J. Am. Chem. Soc. 111* (1989) 3442.

[67] M. Mutter, S. Vuilleumier, *Angew. Chem. 101* (1989) 551–571; *Angew. Chem. Int. Ed. Engl. 28* (1989) 535–554.

[68] "Design of Sequence-Specific DNA-Binding Molecules": P. B. Dervan, *Science (Washington, D. C.) 232* (1986) 464–471; "Synthetic Sequence Specific-DNA Binding Molecules": P. B. Dervan, R. S. Youngquist, J. P. Sluka in W. Bartmann, K. B. Sharpless (Eds.): *Stereochemistry of Organic and Bioorganic Transformations, Workshop Conferences Hoechst, Vol. 17*, VCH Verlagsgesellschaft, Weinheim 1987, pp. 221–234; K. J. Luebke, P. B. Dervan, *J. Am. Chem. Soc. 111* (1989) 8733.

[69] G. Schill: *Catenanes, Rotaxanes and Knots*, Academic Press, New York 1971; G. Schill, N. Schweickert, H. Fritz, W. Vetter, *Chem. Ber. 121* (1988) 961; "Total Synthesis of the First Molecular *Möbius* Strip": D. M. Walba, R. M. Richards, R. C. Haltiwanger, *J. Am. Chem. Soc. 104* (1982) 3219; D. M. Walba, R. M. Richards, M. Hermsmeier, R. C. Haltiwanger, *ibid. 109* (1987) 7081; theory: "Topological Stereochemistry: Knot Theory of Molecular Graphs": D. M. Walba, *Stud. Phys. Theor. Chem. 51* (1987) 23–42.

[70] E. G. Cox, D. W. J. Cruickshank, J. A. S. Smith, *Proc. R. Soc. London 247* (1958) 1; J. Singh, J. M. Thornton, *FEBS Lett. 191* (1985) 1; S. K. Burley, G. A. Petsko, *J. Am. Chem. Soc. 108* (1986) 7995; A. D. Hamilton, N. Pant, A. Mühldorf, *Pure Appl. Chem. 60* (1988) 533.

[71] E. C. Constable, M. D. Ward, *J. Am. Chem. Soc. 112* (1990) 1256. I wish to thank Dr. *Constable*, University Chemical Laboratory, Cambridge (England), for providing me with the coordinates of the sexipyridine-double helix structure.

[72] Review: "The Specific Synthesis of Pyridines and Oligopyridines": F. Kröhnke, *Synthesis 1976*, 1.

[73] As, for example, conductive organic materials, or even superconductors, liquid crystals, ferroelectrics, materals for non-linear optics and information storage, layers and coatings, fibers, membranes, vesicles, and much besides. A recently published article bears the prognosis-rich title: "Materials for the Next Millenium": E. D. Hondros, E. Bullock, *Angew. Chem. Adv. Mater. 101* (1989) 1114–1123; *Angew. Chem. Int. Ed. Engl. Adv. Mater. 28* (1989) 1088–1097; *Adv. Mater. 1989*, 260–269; for a delightful presentation of "Organische Magnete, Idee und Realität" see L. Dulog, *Nachr. Chem. Tech. Lab. 38* (1990) 445–451; "Materials for Optical Data Storage": M. Emmelius, G. Pawlowski, H. W. Vollmann, *Angew. Chem. 101* (1989) 1475–1502; *Angew. Chem. Int. Ed. Engl. 28* (1989) 1445–1471.

[74] There recently appeared a book full of ideas and encouragement with respect to this theme, including nearly 100 key references: R. Hoffmann, *Solids and Surfaces, A Chemist's View of Bonding in Extended Structures*, VCH Verlagsgesellschaft, Weinheim 1988.

[75] "New Methods for the Anionic Polymerization of α-Activated Olefins": M. T. Reetz, *Angew. Chem. Adv. Mater. 100* (1988) 1026–1030; *Angew. Chem. Int. Ed. Engl. Adv. Mater. 27* (1988) 994–998.

[76] F. Vögtle: *Supramolekulare Chemie*, Teubner, Stuttgart 1989.

[77] "Pharmaceutical Proteins": D. Blohm, C. Bollschweiler, H. Hillen, *Angew. Chem. 100* (1988) 213–231; *Angew. Chem. Int. Ed. Engl. 27* (1988) 207–225.

[78] *Leopold Ruzicka*'s vision with respect to the development of organic chemistry in the direction of biological chemistry has been documented in two recent articles: "Leopold Ruzicka: von der Isoprenregel zur Frage nach dem Ursprung des Lebens": A. Eschenmoser, *Rad Jugosl. Akad. Znan. Umjet. Kem.* [443] *7* (1989) 21–68 and "Leopold Ruzicka—From the Isoprene Rule to the Question of Life's Origin": A. Eschenmoser, *Chimia 44* (1990) 1–21.

[79] a) An excellent introduction, even though more than ten years old, is the monograph by A. Fersht: *Enzyme Structure and Mechanism*, W. H. Freeman & Co., Reading 1977. A more mechanistically oriented book is: C. Walsh: *Enzymatic Reaction Mechanisms*, W. H. Freeman & Co., San Francisco 1979. More "chemical" is: "Stereospecificity in Organic Chemistry and Enzymology": J. Rétey, J. A. Robinson in H. F. Ebel (Ed.): *Monographs in Modern Chemistry*, Verlag Chemie, Weinheim 1982. Probably *the* textbook of molecular biology is: B. Lewin: *Genes III*, 3rd ed., Wiley, New York 1987; b) see also the article about enzymatic reactions in S. M. Roberts (Ed.): *Molecular Recognition: Chemical and Biochemical Problems*, The Royal Society of Chemistry, Cambridge 1989.

[80] *Chemtracts: Organic Chemistry* (ISSN 0895-4445), co-published by Data Trace Inc. and Wiley, New York.

[81] "Drugs from Emasculated Hormones: The Principle of Syntopic Antagonism" (Nobel Lecture): J. W. Black, *Angew. Chem. 101* (1989) 910–919; *Angew. Chem. Int. Ed. Engl. 28* (1989) 886–894.

[82] "Selective Inhibitors of Dihydrofolate Reductase" (Nobel Lecture): G. H. Hitchings, Jr., *Angew. Chem. 101* (1989) 903–909; *Angew. Chem. Int. Ed. Engl. 28* (1989) 879–885.

[83] "Synthetic Studies in the Mevinoid Field. The Total Synthesis of ML236A": S. J. Danishefsky, B. Simoneau, *Pure Appl. Chem. 60* (1988) 1555–1562; "Mevinic Acids": *Synform 5* (1987) 87–124; "The Synthesis of Mevinic Acids": T. Rosen, C. H. Heathcock, *Tetrahedron 42* (1986) 4909–4951.

[84] H.-J. Altenbach, *Nachr. Chem. Tech. Lab. 36* (1988) 756–758, and references cited therein.

[85] J. Boger, N. S. Lohr, E. H. Ulm, M. Poe, E. H. Blaine, G. M. Fanelli, T.-Y. Lin, L. S. Payne, T. W. Schorn, B. I. LaMont, T. C. Vassil, I. I. Stabilito, D. F. Veber, D. H. Rich, A. S. Bopari, *Nature (London) 303* (1983) 81; S. Thaisrivongs, D. T. Pals, S. R. Turner, L. T. Kroll, *J. Med. Chem. 31* (1988) 1369; P. Bühlmayer, A. Caselli, W. Fuhrer, R. Göschke, V. Rasetti, H. Rüeger, J. L. Stanton, L. Criscione, J. M. Wood, *ibid. 31* (1988) 1839; S. H. Rosenberg, K. W. Woods, H. D. Kleinert, H. Stein, H. N. Nellans, D. J. Hoffman, S. G. Spanton, R. A. Pyter, J. Cohen, D. A. Egan, J. J. Plattner, T. J. Perun, *ibid. 32* (1989) 1371; J. S. Kaltenbronn, J. P. Hudspeth, E. A. Lunney, B. M. Michniewicz, E. D. Nicolaides, J. T. Repine, W. H. Roark, M. A. Stier, F. J. Tinney, P. K. W. Woo, A. D. Essenburg, *ibid. 33* (1990) 838; "Synthese hydroxyethylen-isosterer Dipeptide" (Synthese im Blickpunkt): R. Henning, *Nachr. Chem. Tech. Lab. 38* (1990) 460–464.

[86] R. M. Williams: *Synthesis of Optically Active α-Amino Acids*, Pergamon Press, Oxford 1989.

[87] The design of building blocks that mimic the turns in peptides and lead to conformational fixation ("turn mimetics") is subject to a great deal of phantasy; a few recent examples are described in the following publications: M. Kahn, B. Chen, *Tetrahedron Lett. 28* (1987) 1623; D. S. Kemp, W. E. Stites, *ibid. 29* (1988) 5057; M. G. Hinds, N. G. J. Richards, J. A. Robinson, *J. Chem. Soc. Chem. Commun. 1988*, 1447; amino acid isosteres for incorporation into peptides are intended to mimic the geometry and/or functionality of amino acids, but inhibit cleavage by peptidases: "Peptide Backbone Modifications: A Structure–Activity Analysis of Peptides Containing Amide Bond Surrogates, Conformational Constraints, and Related Backbone Replacements": A. F. Spatola in B. Weinstein (Ed.): *Chemistry and Biochemistry of Amino Acids, Peptides, and Proteins, Vol. 7*, Marcel Dekker, New York 1983, pp. 267–357; "The Synthesis of Peptide Analogues with a Modified Peptide Bond": D. Tourwé, *Janssen Chim. Acta 3* (1985) No. 1, pp. 3–18.

[88] a) W. P. Jencks: *Catalysis in Chemistry and Enzymology*, McGraw-Hill, New York 1969; "Analog Approaches to the Structure of the Transition State in Enzyme Reactions": R. Wolfenden, *Acc. Chem. Res. 5* (1972) 10–18; b) S. Ghisla, H. Ogata, V. Massey, A. Schonbrunn, R. H. Abeles, C. T. Walsh, *Biochemistry 15* (1976) 1791.

[89] At the Chemical Congress of Pacific Basin Countries in Honolulu (17–22 Dec. 1989), 12% of all the contributions (lectures and posters) in the Organic Chemistry Section contained the five letters *fluor* in their titles; there were two symposia on organofluorine compounds, with the titles "Symposium on Modern Synthetic Methods in Fluorine Chemistry" and "Symposium on Biologically Active Organofluorine Compounds" (The 1989 International Chemical Congress of Pacific Basin Societies, Book of Abstracts II). The following fluorine symposia were arranged in the course of 1990 ACS conventions: 199th National ACS Meeting, 22–27 April 1990, Boston, MA: Symposium on the Effects of Selective Fluorination on Reactivity, Symposium on Fluorine Containing Polymeric Materials; 200th National ACS Meeting, 21–31 Aug. 1990, Washington, D.C.: Symposium on Mass Spectrometry of Fluorinated Compounds, Symposium on Fluorine Chemistry for Organic Chemists.

[90] The growing interest in fluorine chemistry is documented by the steadily increasing number of publications in the area. The following diagram was constructed on the basis of publications covered by *Chemical Abstracts* in the period from Jan. 1967 to March 1990 (solid bars: total number, in units of 100; dotted bars: publications indexed under "fluorine"; black line: contribution of "fluorine" publications in terms of percent).

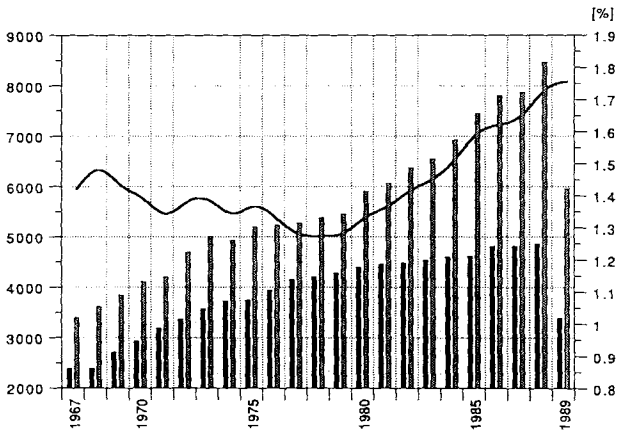

[91] Monographs: a) M. Hudlicky: *Chemistry of Organic Fluorine Compounds, 2nd Edition*, Ellis Horwood, Chichester 1976; b) R. D. Chambers: *Fluorine in Organic Chemistry*, Wiley-Interscience, New York 1973; c) "Fluorinated Organic Molecules": B. E. Smart in J. F. Liebman, A. Greenberg (Eds.): *Molecular Structure and Energetics, Vol. 3*, VCH Publishers, Deerfield Beach 1986, pp. 141–191; d) J. F. Liebman, A. Greenberg, W. R. Dolbier, Jr.: *Fluorine-Containing Molecules—Structure, Reactivity, Synthesis and Applications*, VCH Publishers, New York 1988; e) J. T. Welch, S. Eswarakrishnan: *Fluorine in Bioorganic Chemistry*, Wiley, New York 1990.

[92] Recent review articles with an emphasis on synthetic aspects of the chemistry of organofluorine compounds: a) "Modern Synthetic Procedures for the Fluorination of Organic Molecules": A. Haas, M. Lieb, *Chimia 39* (1985) 134–140; b) "Präparative Fluorierung mit molekularem Fluor": H. Vyplel, *ibid. 39* (1985) 305–311; c) "Fluorination with Diethylaminosulfur Trifluoride and Related Aminofluorosulfuranes": M. Hudlicky, *Org. React. (N. Y.) 35* (1988) 513–637; d) "A Guide to Modern Organofluorine Chemistry": R. E. Banks, J. C. Tatlow, *J. Fluorine Chem. 33* (1986) 227–284; e) "Exploration into Selective Monofluorination Methods and Their Application to the Synthesis of Fluorinated Bio-active Compounds": M. Shimizu, H. Yoshioka, *Yuki Gosei Kagaku Kyokaishi (J. Synth. Org. Chem. Jpn.) 47* (1989) 27–39; f) "Fluor in der organischen Synthese" (Synthese im Blickpunkt): R. Bohlmann, *Nachr. Chem. Tech. Lab. 38* (1990) 40–43; g) "Drucklose Direktfluorierung—eine einfache Methode zur präparativen Synthese von neuen Fluorierungsreagenzien": K. Auer, E. Hungerbühler, R. W. Lang, *Chimia 44* (1990) 120. A few reviews that have appeared since 1987 and which focus on the biological activity of F-derivatives: h) "Modern Methods for the Introduction of Fluorine into Organic Molecules: An Approach to Compounds with Altered Chemical and Biological Activities": J. Mann, *Chem. Soc. Rev. 16* (1987) 381–436; i) "A New Approach to Synthetic Pyrethroids Having a Trifluoromethyl Group": M. Fujita, T. Hiyama, *Yuki Gosei Kagaku Kyokaishi (J. Synth. Org. Chem. Jpn.) 45* (1987) 664–671; j) "New Catalytic Reactions of the Hydrolytic Enzymes in Fluorine Chemistry": T. Kitazume, T. Yamazaki, *ibid. 45* (1987) 888–897; k) "Advances in the Preparation of Biologically Active Organofluorine Compounds": J. T. Welch, *Tetrahedron 43* (1987) 3123–3197; l) "Synthetic Fluoropeptides as Pharmacologically Useful Compounds": B. Imperiali, *Adv. Biotechnol. Processes 10* (1988) 97–129.

[93] As an outsider one has the impression that specialists take it for granted that reactions of "normal" compounds *won't* work with fluorine derivatives; if they do succeed, the astonishing news warrants immediate publication! A few personal experiences would suggest that one should be prepared for anything with even the simplest reactions—a thrilling prospect; see [94–97] (cf. also Chapter 4, "Aliphatic Fluoronitro Compounds", in [105a]).

[94] a) D. Seebach, P. Renaud, W. B. Schweizer, M. F. Züger, M.-J. Brienne, *Helv. Chim. Acta 67* (1984) 1843; b) D. Seebach, P. Renaud, *ibid. 68* (1985) 2342.

[95] D. Seebach, A. K. Beck, P. Renaud, *Angew. Chem. 98* (1986) 96; *Angew. Chem. Int. Ed. Engl. 25* (1986) 98.

[96] "Fluorierte Nitro- und Aminoalkohole": D. Seebach, A. K. Beck, *DOS 3 540 332* (1987), Bayer AG; *Chem. Abstr. 107* (1987) 115 246e; "Verfahren zur Herstellung von fluorierten Nitroalkylverbindungen": D. Seebach, A. K. Beck, *DOS 3 808 276* (1988), Bayer AG; *Chem. Abstr. 112* (1990) 98013k; "Synthesis of Fluorinated Nitro- and Aminoalcohols": B. Baasner, M. J. Negele, A. K. Beck, D. Seebach, *12th Int. Symp. Fluorine Chem.* 7–12 Aug. 1988, Santa Cruz, CA (USA), Abstr. 331.

[97] M. Ács, C. von dem Bussche, D. Seebach, *Chimia 44* (1990) 90; A. K. Beck, M. Gautschi, D. Seebach, *Chimia 44* (1990), 291.

[98] J. H. Fried, E. F. Sabo, *J. Am. Chem. Soc. 75* (1953) 2273; reviews: J. Fried, A. Borman, *Vit. Horm. (N. Y.) 16* (1958) 303; G. Ehrhart, H. Ruschig: *Arzneimittel, Vol. 3*, Verlag Chemie, Weinheim 1972, pp. 402–417.

[99] S. Thaisrivongs, D. T. Pals, W. M. Kati, S. R. Turner, L. M. Thomasco, *J. Med. Chem. 28* (1985) 1553; S. Thaisrivongs, D. T. Pals, W. M. Kati, S. R. Turner, L. M. Thomasco, W. Watt, *ibid. 29* (1986) 2080.

[100] P. Bey, *Actual. Chim. Thér.-16e série* (1989) 111–122.

[101] T. Shimizu, M. Hatano, *Yuki Gosei Kagaku Kyokaishi (J. Synth. Org. Chem. Jpn.) 43* (1985) 371–381.

[102] The physical and spectroscopic data listed here, as well as the bond angles and bond lengths, have been taken from standard textbooks, monographs, and reference works. Bond lengths from X-ray structural data: a) F. H. Allen, O. Kennard, D. G. Watson, L. Brammer, A. G. Orpen, R. Taylor, *J. Chem. Soc. Perkin Trans. 2 1987*, S1–S19; b) A. G. Orpen, L. Brammer, F. H. Allen, O. Kennard, D. G. Watson, R. Taylor, *J. Chem. Soc. Dalton Trans. 1989*, S1–S83; see also [107b].

[103] T. A. Alston, D. J. T. Porter, H. J. Bright, *Acc. Chem. Res. 16* (1983) 418–424.

[104] Examples of recent reviews on nitroaliphatics: a) H. Feuer, A. T. Nielsen (Eds.): *Nitro Compounds—Recent Advances in Synthesis and Chemistry*, VCH Publishers, New York 1990; b) G. A. Olah, R. Malhotra, S. C. Narana: *Nitration—Methods and Mechanisms*, VCH Publishers, New York 1989; c) K. B. G. Torssell: *Nitrile Oxides, Nitrones, and Nitronates in Organic Synthesis—Novel Strategies in Synthesis*, VCH Publishers, New York 1988; d) "Functionalized Nitroalkanes are Useful Reagents for Alkyl Anion Syntheses": G. Rosini, R. Ballini, *Synthesis 1988*, 833–847.

[105] a) "Syntheses and Selected Reductions of Conjugated Nitroalkenes. A Review": G. W. Kabalka, R. S. Varma, *Org. Prep. Proced. Int. 19* (1987) 285–328; b) "Conjugated Nitroalkenes: Versatile Intermediates in Organic Synthesis": A. G. M. Barrett, G. G. Grabowski, *Chem. Rev. 86* (1986) 751–762.

[106] Reviews: "Sila-Substitution of Drugs and Biotransformation of Organosilicon Compounds": R. Tacke, B. Becker, *Main Group Met. Chem. 10* (1987) 169–197; "Historical overview and comparison of silicon with carbon": J. Y. Corey in S. Patai, Z. Rappoport (Eds.): *The Chemistry of Organic Silicon Compounds, Part 1*, Wiley, New York 1989, pp. 1–56; "Steric Influence of the Trimethylsilyl Group in Organic Reactions": J. R. Hwu, N. Wang, *Chem. Rev. 89* (1989) 1599–1615.

[107] a) R. Corriu, *Pure Appl. Chem. 60* (1988) 99–106; A. Hosomi, S. Kohra, Y. Tominaga, *Yuki Gosei Kagaku Kyokaishi (J. Synth. Org. Chem. Jpn.) 47* (1989) 831–842; M. Kira, K. Sato, H. Sakurai, *J. Am. Chem. Soc. 112*

(1990) 257; M. Kira, K. Sato, C. Kabuto, H. Sakurai, *ibid. 111* (1989) 3747; "Selektive Tranformationen mit pentakoordinierten Siliciumverbindungen" (Synthese im Blickpunkt): D. Schinzer, *Nachr. Chem. Tech. Lab. 37* (1989) 28–30; see also the references in Schemes 15 and 16 and in Table 3; b) an extensive collection (*ca.* 2000 literature references) of structures of organosilicon compounds (including pentacoordinate cases) can be found in: E. Lukevics, O. Pudova, R. Sturkovich: *Molecular Structure of Organosilicon Compounds*, Wiley, New York 1989.

[108] "Alkene Synthesis *via* β-Functionalized Organosilicon Compounds": T.-H. Chan, *Acc. Chem. Res. 10* (1977) 442–448.

[109] Excellent monographs on silicon in organic synthesis: a) E. W. Colvin: *Silicon in Organic Synthesis*, Butterworth, London 1981; "Preparation and use of organosilicon compounds in organic synthesis": E. W. Colvin in F. R. Hartley (Ed.): *The Chemistry of the Metal–Carbon Bond, Vol. 4*, Wiley, Chichester 1987, pp. 539–621; E. W. Colvin: *Silicon Reagents in Organic Synthesis*, Academic Press, London 1988; b) W. P. Weber: *Silicon Reagents for Organic Synthesis*, Springer, Berlin 1983; c) J. Y. Corey, E. R. Corey, P. P. Gaspar (Eds.): *Silicon Chemistry*, Ellis Horwood, Chichester 1988; d) S. Patai, Z. Rappoport (Eds.): *The Chemistry of Organic Silicon Compounds, Parts 1 and 2*, Wiley, New York 1989.

[110] K. Mislow, R. Graeve, A. J. Gordon, G. H. Wahl, Jr., *J. Am. Chem. Soc. 86* (1964) 1733; H. Pracejus, *Tetrahedron Lett. 1966*, 3809; S. A. Sherrod, R. L. da Costa, R. A. Barnes, V. Boekelheide, *J. Am. Chem. Soc. 96* (1974) 1565.

[111] L. Melander, W. H. Saunders, Jr.: *Reaction Rates of Isotopic Molecules*, Wiley, New York 1980.

[112] A. Tramontano, K. D. Janda, R. A. Lerner, *Science (Washington, D. C.) 234* (1986) 1566.

[113] S. J. Pollack, J. W. Jacobs, P. G. Schulz, *Science (Washington, D. C.) 234* (1986) 1570.

[114] Review articles on this topic: a) "Enzymes and Abzymes": S. J. Benkovic, *Proc. Robert A. Welch Found. Conf. Chem. Res. 31: Design of Enzymes and Enzyme Models*, 2–4 Nov. 1987, Houston, TX 1987, pp. 113–125; b) "Catalytic Antibodies": P. G. Schultz, *Angew. Chem. 101* (1989) 1336–1348; *Angew. Chem. Int. Ed. Engl. 28* (1989) 1283–1295; c) "Catalytic Antibodies": P. G. Schultz, *Acc. Chem. Res. 22* (1989) 287–294; d) "Observations in the Interface between Immunology and Chemistry": R. A. Lerner, *Chemtracts: Org. Chem. 3* (1990) 1–36; e) "Catalytic Antibodies": R. A. Lerner, A. Tramontano, *Sci. Am. 258* (1988) No. 3, pp. 58–70; *Spektrum Wiss. 1988*, No. 5, pp. 78–87.

[115] S. J. Pollack, P. Hsiun, P. G. Schultz, *J. Am. Chem. Soc. 111* (1989) 5961.

[116] D. Y. Jackson, J. W. Jacobs, R. Sugasawara, S. H. Reich, P. A. Bartlett, P. G. Schultz, *J. Am. Chem. Soc. 110* (1988) 4841; D. Hilvert, S. H. Carpenter, K. D. Nared, M.-T. M. Auditor, *Proc. Natl. Acad. Sci. USA 85* (1988) 4953.

[117] S. D. Copley, J. R. Knowles, *J. Am. Chem. Soc. 107* (1985) 5306.

[118] D. Hilvert, K. W. Hill, K. D. Nared, M.-T. M. Auditor, *J. Am. Chem. Soc. 111* (1989) 9261.

[119] It has recently proven possible to express mouse antibody fragments in *E. coli*: W. D. Huse, L. Sastry, S. A. Iverson, A. S. Kang, M. Alting-Mees, D. R. Burton, S. J. Benkovic, R. A. Lerner, *Science (Washington, D. C.) 246* (1989) 1275.

[120] Gram-quantities of monoclonal antibodies are now accessible. The fundamental work on immunochemistry and monoclonal antibodies is summarized in the following review articles: "The Generative Grammar of the Immune System" (Nobel Lecture): N. K. Jerne, *Angew. Chem. 97* (1985) 813–818; *Angew. Chem. Int. Ed. Engl. 24* (1985) 810–816; "From the Structure of Antibodies to the Diversification of the Immune Response" (Nobel Lecture): C. Milstein, *ibid. 97* (1985) 819–828 and *24* (1985) 816–826; "Derivation and Diversification of Monoclonal Antibodies" (Nobel Lecture): G. Köhler, *ibid. 97* (1985) 829–836 and *24* (1985) 827–833.

[121] K. D. Janda, S. J. Benkovic, R. A. Lerner, *Science (Washington, D. C.) 244* (1989) 437.

[122] B. L. Iverson, R. A. Lerner, *Science (Washington, D. C.) 243* (1989) 1184.

[123] A. D. Napper, S. J. Benkovic, A. Tramontano, R. A. Lerner, *Science (Washington, D. C.) 237* (1987) 1041.

[124] N. Janjic, A. Tramontano, *J. Am. Chem. Soc. 111* (1989) 9109; K. M. Shokat, C. H. Leumann, R. Sugasawara, P. G. Schultz, *Angew. Chem. 100* (1988) 1227; *Angew. Chem. Int. Ed. Engl. 27* (1988) 1172.

[125] "Enzymes that work in organic solvents": A. M. Klibanov, *CHEMTECH 1986*, 354–359; H. Kitaguchi, A. M. Klibanov, *J. Am. Chem. Soc. 111* (1989) 9272; "Asymmetric Transformations Catalyzed by Enzymes in Organic Solvents": A. M. Klibanov, *Acc. Chem. Res. 23* (1990) 114–120.

[126] a) "Chiral Synthons by Ester Hydrolysis Catalyzed by Pig Liver Esterase": M. Ohno, M. Otsuka, *Org. React. (N. Y.) 37* (1989) 1–55; b) For a collection of examples for the application of ester-cleaving enzymes to *meso*-substrates see: M. Eberle, M. Egli, D. Seebach, *Helv. Chim. Acta 71* (1988) 1; c) "Non-Enzymatic Asymmetric Transformations Involving Symmetrical Bifunctional Compounds": R. S. Ward, *Chem. Soc. Rev. 19* (1990) 1–19.

[127] L. B. Shih, H. Bayley, *Anal. Biochem. 144* (1985) 132.

[128] J. R. Roesser, M. S. Chorghade, S. M. Hecht, *Biochemistry 25* (1986) 6361.

[129] C. J. Noren, S. J. Anthony-Cahill, M. C. Griffith, P. G. Schultz, *Science (Washington, D. C.) 244* (1989) 182; M. H. Hopkins, R. B. Silverman, *Chemtracts: Org. Chem. 2* (1989) 302–304.

[130] J. D. Bain, E. S. Diala, C. G. Glabe, T. A. Dix, A. R. Chamberlin, *J. Am. Chem. Soc. 111* (1989) 8013.

[131] The predictions expressed here will come to pass in Germany only if "the thorny path to gene technology for the pharmaceutical industry in the Federal Republic" (headline in the *Neue Zürcher Zeitung* for 20 March 1990, p. 39) is, in the end, traversed successfully. A treatment of the problematics by one who should know: "Biotechnologie aus der Sicht der Industrie": K. H. Büchel in Kernforschungsanlage Jülich GmbH (Ed.): *Festvortrag anläßlich der Einweihung des Biotechnikums der Kernforschungsanlage Jülich GmbH, 15. April 1988*, Jülich (ISBN 3-89336-004-2).

[132] "Pheromones in Nanogram Quantities: Structure Determination by Combined Microchemical and Gas Chromatographic Methods": A. B. Attygalle, E. D. Morgan, *Angew. Chem. 100* (1988) 475–494; *Angew. Chem. Int. Ed. Engl. 27* (1988) 460–478.

[133] a) W. A. König: *The Practice of Enantiomer Separation by Capillary Gas Chromatography*, Hüthig, Heidelberg 1987; "Eine neue Generation chiraler Trennphasen für die Gas-Chromatographie": W. A. König, *Nachr. Chem. Tech. Lab. 37* (1989) 471–476; b) "Enantiomerentrennung von Aminosäuren mittels Dünnschichtchromatographie": J. Martens, R. Bhushan, *Chem.-Ztg. 112* (1988) 367–372; "Dünnschichtchromatographische Enantiomerentrennung mittels Ligandenaustausch": K. Günther, *GIT Suppl.3/86* (1986) 6–12; c) "Considerations of Chiral Recognition Relevant to the Liquid Chromatographic Separation of Enantiomers": W. H. Pirkle, T. C. Pochapsky, *Chem. Rev. 89* (1989) 347–362; d) "Präparative chromatographische Enantiomerentrennung": J. N. Kinkel, K. Reichert, P. Knöll, *GIT Suppl. 3/89* (1989) 104–112; e) "Applications and limitations of commercially available chiral stationary phases for high-performance liquid chromatography": R. Däppen, H. Arm, V. R. Meyer, *J. Chromatogr. 373* (1986) 1–20.

[134] J. D. Morrison (Ed.): *Asymmetric Synthesis, Vol. 1: Analytical Methods*, Academic Press, New York 1983; "Moderne Methoden zur Bestimmung enantiomerer Gemische" (Parts 1–3): V. Schurig, *Kontakte (Darmstadt) 1985*, No. 1, pp. 54–60; *1985*, No. 2, pp. 22–36; *1986*, No.1, pp. 3–22; S. G. Allenmark: *Chromatographic Enantioseparation: Methods and Applications*, Ellis Horwood, Chichester 1988.

[135] "Chirale Erkennung von Naturstoffen an optisch aktiven Polysiloxanen": E. Bayer, *Z. Naturforsch. B 38* (1983) 1281–1291. I wish to thank Professor *Ernst Bayer* for providing me with the gas chromatogram shown in Fig. 1A.

[136] V. Schurig, H.-P. Nowotny, D. Schmalzing, *Angew. Chem. 101* (1989) 785; *Angew. Chem. Int. Ed. Engl. 28* (1989) 736.

[137] D. Seebach, S. G. Müller, U. Gysel, J. Zimmermann, *Helv. Chim. Acta 71* (1988) 1303.

[138] "High-performance capillary electrophoresis in the biological sciences": B. L. Karger, A. S. Cohen, A. Guttman, *J. Chromatogr. 492* (1989) 585–614; A. Guttman, A. S. Cohen, D. N. Heiger, B. L. Karger, *Anal. Chem. 62* (1990) 137; I wish to thank Professor *Karger*, Barnett Institute and Department of Chemistry, Northeastern University, Boston, MA, for placing at my disposal the HPCE spectra; "Kapillarelektrophorese—ein Durchbruch in der Separationstechnik": V. P. Burolla, S. L. Pentoney, R. Zare, *Beckman Rep.* Issue 70, May 1990, pp. 2–3 (with 31 references); a nearly complete review of applicable equipment is provided in: W. Steuer, I. Grant, *Nachr. Chem. Tech. Lab. 38* (1990) M1–M12.

[139] This technique is described in H. M. Widmer, *Chimia 43* (1989) 320, 388.

[140] A lively column, always reflecting the current state of the art, is written by *H. M. Widmer* in *Chimia* (Columna Analytica, since 1986), with individual contributions carrying titles like "Drei Geburtstagsfeiern und ihre Botschaft für die analytische Chemie" [*Chimia 43* (1989) 357] or "Analytische Chemie im Spannungsfeld zwischen dem unendlich Kleinen und unendlich Großen" [*ibid. 44* (1990) 22].

[141] R. R. Ernst, G. Bodenhausen, A. Wokaun: *Principles of nuclear magnetic resonance in one and two dimensions*, Clarendon Press, Oxford 1987; "Two-Dimensional NMR Spectroscopy: A Powerful Tool for the Investigation of Molecular Structure and Dynamics": R. R. Ernst, *Chimia 41* (1987) 323–340; W. R. Croasmun, R. M. K. Carlson (Eds.): *Two Dimensional NMR Spectroscopy*, VCH Verlagsgesellschaft, Weinheim 1987; "Two-Dimensional NMR Spectroscopy: Background and Overview of the Experiments": H. Kessler, M. Gehrke, C. Griesinger, *Angew. Chem. 100* (1988) 507–554; *Angew. Chem. Int. Ed. Engl. 27* (1988) 490–536; "Modern NMR Pulse Experiments: A Graphic Description of the Evolution of Spin Systems": U. Eggenberger, G. Bodenhausen, *ibid. 102* (1990) 392–402 and *29* (1990) 374–383.

[142] 3D-NMR techniques: C. Griesinger, O. W. Sørensen, R. R. Ernst, *J. Magn. Reson. 73* (1987) 574; *J. Am. Chem. Soc. 109* (1987) 7227; H. Oschkinat, C. Griesinger, P. J. Kraulis, O. W. Sørensen, R. R. Ernst, A. M. Gronenborn, G. M. Clore, *Nature (London) 332* (1988) 374.

[143] I wish to thank my colleague *Richard R. Ernst* for providing me with the copy for Fig. 2. The NOESY and COSY spectra are derived from the following two publications: A. Kumar, R. R. Ernst, K. Wüthrich, *Biochem. Biophys. Res. Commun. 95* (1980) 1–6; G. Wagner, K. Wüthrich, *J. Mol. Biol. 155* (1982) 347–366.

[144] R. Brüschweiler, C. Griesinger, R. R. Ernst, *J. Am. Chem. Soc. 111* (1989) 8034.

[145] J. F. McGarrity, J. Prodolliet, T. Smyth, *Org. Magn. Reson. 17* (1981) 59.

[146] Z. Brich, H.-R. Loosli, previously unpublished experiments, Sandoz AG, Basel 1982. I wish to thank Dr. *Brich* for providing the spectra, along with permission to reproduce one of them here.

[147] J. F. McGarrity, J. Prodolliet, *J. Org. Chem. 49* (1984) 4465; J. F. McGarrity, C. A. Ogle, *J. Am. Chem. Soc. 107* (1985) 1805; J. F. McGarrity, C. A. Ogle, Z. Brich, H.-R. Loosli, *ibid. 107* (1985) 1810.

[148] S. V. Frye, E. L. Eliel, R. Cloux, *J. Am. Chem. Soc. 109* (1987) 1862.

[149] T. W. Bentley, W. Kirmse, G. Llewellyn, F. Söllenböhmer, *J. Org. Chem. 55* (1990) 1536.

[150] "Conformation and Biological Activity of Cyclic Peptides": H. Kessler, *Angew. Chem. 94* (1982) 509–520; *Angew. Chem. Int. Ed. Engl. 21* (1982) 512–523.

[151] K. Wüthrich: *NMR of Proteins and Nucleic Acids*, Wiley-Interscience, New York 1986.

[152] "The Development of Nuclear Magnetic Resonance Spectroscopy as a Technique for Protein Structure Determination": K. Wüthrich, *Acc. Chem. Res. 22* (1989) 36–44; Y. Q. Qian, M. Billeter, G. Otting, M. Müller, W. J. Gehring, K. Wüthrich, *Cell 59* (1989) 573.

[153] H. Kuzmany: *Festkörperspektroskopie: eine Einführung*, Springer, Berlin 1990; "Two-Dimensional Solid-State NMR Spectroscopy: New Possibilites for the Investigation of the Structure and Dynamics of Solid Polymers": B. Blümich, H. W. Spiess, *Angew. Chem. 100* (1988) 1716–1734; *Angew. Chem. Int. Ed. Engl. 27* (1988) 1655–1672; "High-Resolution Solid-State ^{13}C-NMR Spectroscopy of Polymers": R. Voelkel, *ibid. 100* (1988) 1525–1540 and *27* (1988) 1468–1483. See also tomography and microscopy with NMR methods: "NMR Microscopy—Fundamentals, Limits and Possible Applications": W. Kuhn, *ibid. 102* (1990) 1–18 and *29* (1990) 1–19.

[154] a) L. Prokai: *Field Desorption Mass Spectrometry*, Marcel Dekker, New York 1990; b) C. B. Lebrilla, D. T.-S. Wang, T. J. Mizoguchi, R. T. McIver, Jr., *J. Am. Chem. Soc. 111* (1989) 8593 and in literature cited in the introduction to this paper; c) "Multiphoton-Ionization-Mass Spectrometry (MUPI-MS)": J. Grotemeyer, E. W. Schlag, *Angew. Chem. 100* (1988) 461–474; *Angew. Chem. Int. Ed. Engl. 27* (1988) 447–459; d) "Capillary Electrophoresis and Ion Spray Mass Spectrometry, New Powerful Methods for Separation and Characterization of Proteins and Nucleotides": E. Bayer in H. Tschesche (Ed.): *Modern Methods in Protein Chemistry, Vol. 4*, Walter de Gruyter, Berlin, in press. I wish to thank Professor *Ernst Bayer* for sending me a copy of the manuscript.

[155] R. S. Brown, D. A. Weil, C. L. Wilkins, *Macromolecules 19* (1986) 1255.

[156] D. Seebach, A. K. Beck, U. Brändli, D. Müller, M. Przybylski, K. Schneider, *Chimia 44* (1990) 112.

[157] M. Karas, F. Hillenkamp, *Anal. Chem. 60* (1988) 2299.

[158] Theophrastus Bombastus Paracelsus von Hohenheim (1493–1541): "Was ist das nit gifft ist? alle ding sind gifft (und nichts ohn gifft). Allein die dosis macht das ein ding kein gifft ist" [*Dosis facit venenum*, 1537; "What is not a poison? All things are poisons (and nothing is without poison). The dose alone keeps a thing from being a poison"]. Cited in F. Lieben: *Geschichte der physiologischen Chemie*, F. Deuticke, Leipzig and Vienna, 1935; see also H. Eilingsfeld: *Der Sanfte Wahn-Ökologismus total*, Südwestdeutsche Verlagsanstalt, Mannheim 1989 (ISBN 3-87804-195-0).

[159] In an article entitled "Ist die Molekülstrukturanalyse durch Röntgenbeugung mehr als Routine?" the question is raised whether the synthetic chemist "has been surrendered over to the data-gathering specialist, or if ... the ... latter has become the measuring servant of the chemist", examined in the context of crystal structure analysis: R. Boese, *Nachr. Chem. Tech. Lab. 37* (1989) 906–911.

[160] J. D. Dunitz: *X-Ray Analysis and the Structure of Organic Molecules*, Cornell University Press, Ithaca 1979.

[161] G. M. Sheldrick: *SHELX76, SHELX86. Program for Crystal Structure Determination*, University Chemical Laboratory, Lensfield Road, GB-Cambridge CB2 1EW, 1986.

[162] "Progress with Laue Diffraction Studies on Protein and Virus Crystals" (Perspectives in Biochemistry): J. Hajdu, L. N. Johnson, *Biochemistry 29* (1990) 1669.

[163] J. Hajdu, P. A. Machin, J. W. Campbell, T. J. Greenhough, I. J. Clifton, S. Zurek, S. Gover, L. N. Johnson, M. Elder, *Nature (London) 329* (1987) 178.

[164] "Structural Studies on Macromolecules and Viruses with Laue Diffraction": J. Hajdu, *Lecture in the Physical-Chemical Colloquium of the ETH Zürich*, 28 March 1990. I wish to thank Dr. *Hajdu* and Professor *Phillips* (Oxford) for stimulating discussions. I am grateful to Dr. *Hajdu* for the Laue diffraction pattern shown in Fig. 5 and the data in the caption.

[165] "Flexibility and Rigidity of Proteins and Protein–Pigment Complexes": R. Huber, *Angew. Chem. 100* (1988) 79–89; *Angew. Chem. Int. Ed. Engl. 27* (1988) 79–88.

[166] To the best of my knowledge, the first crystal structure analysis of a membrane-bound protein complex (the photosynthetic enzyme from a microorganism) was primarily the result of a spectacular piece of work in preparing and isolating a suitable single crystal: "A Structural Basis of Light Energy and Electron Transfer in Biology" (Nobel Lecture): R. Huber, *Angew. Chem. 101* (1989) 849–871; *Angew. Chem. Int. Ed. Engl. 28* (1989) 848–869; "The Photosynthetic Reaction Center from the Purple Bacterium *Rhodopseudomonas viridis*" (Nobel Lecture): J. Deisenhofer, H. Michel, *ibid. 101* (1989) 872–892 and *28* (1989) 829–847.

[167] a) R. Amstutz, T. Laube, W. B. Schweizer, D. Seebach, J. D. Dunitz, *Helv. Chim. Acta 67* (1984) 224; b) D. Seebach, R. Amstutz, T. Laube, W. B. Schweizer, J. D. Dunitz, *J. Am. Chem. Soc. 107* (1985) 5403; c) E. Hahn, T. Maetzke, D. A. Plattner, D. Seebach, *Chem. Ber. 123* (1990), in press.

[168] "Low-Temperature X-Ray Structure Techniques for the Characterization of Thermolabile Molecules": M. Veith, W. Frank, *Chem. Rev. 88* (1988) 81–92.

[169] *E. Hahn* und *S. Rupprecht* (Institut für Anorganische und Analytische Chemie der Technischen Universität Berlin) recently determined the structure of $[(LiCl)_2 \cdot 4THF]$, which begins to lose solvent and decompose above $-60\,^{\circ}C$. Single crystals can only be isolated directly from the mother liquor.

[170] P. Luger, C. Zaki, J. Buschmann, R. Rudert, *Angew. Chem. 98* (1986) 254; *Angew. Chem. Int. Ed. Engl. 25* (1986) 276.

[171] T. Laube, *Angew. Chem. 99* (1987) 580; *Angew. Chem. Int. Ed. Engl. 26* (1987) 560; *J. Am. Chem. Soc. 111* (1989) 9224.

[172] "Structure and Reactivity of Lithium Enolates. From Pinacolone to Selective *C*-Alkylations of Peptides. Difficulties and Opportunities Afforded by Complex Structures": D. Seebach, *Angew. Chem. 100* (1988) 1685–1715; *Angew. Chem. Int. Ed. Engl. 27* (1988) 1624–1654.

[173] "The Structure of Lithium Compounds of Sulfones, Sulfoximides, Sulfoxides, Thioethers and 1,3-Dithianes, Nitriles, Nitro Compounds and Hydrazones": G. Boche, *Angew. Chem. 101* (1989) 286–306; *Angew. Chem. Int. Ed. Engl. 28* (1989) 277–297.

[174] D. Seebach, J. Hansen, P. Seiler, J. M. Gromek, *J. Organomet. Chem. 285* (1985) 1.

[175] D. Seebach, J.-J. Lohmann, M. A. Syfrig, M. Yoshifuji, *Tetrahedron 39* (1983) 1963; D. Seebach, M. A. Syfrig, *Angew. Chem. 96* (1984) 235; *Angew. Chem. Int. Ed. Engl. 23* (1984) 248; D. Seebach, I. M. P. Huber, *Chimia 39* (1985) 233; D. Seebach, I. M. P. Huber, M. A. Syfrig, *Helv. Chim. Acta 70* (1987) 1357; I. M. P. Huber, D. Seebach, *ibid. 70* (1987) 1944.

[176] M. Marsch, K. Harms, L. Lochmann, G. Boche, *Angew. Chem. 102* (1990) 334; *Angew. Chem. Int. Ed. Engl. 29* (1990) 308. I wish to thank Professor *Gernot Boche* for providing the coordinates of the structure shown in Fig. 6.

[177] L. Lochmann, J. Pospisil, J. Vodnansky, J. Trekoval, D. Lim, *Collect. Czech. Chem. Commun. 30* (1965) 2187; M. Schlosser, *Pure Appl. Chem. 60* (1988) 1627.

[178] T. Maetzke, C. P. Hidber, D. Seebach, *J. Am. Chem. Soc. 112* (1990), in press; T. Maetzke, D. Seebach, *Organometallics 9* (1990), in press.

[179] "Stereochemistry of Reaction Paths as Determined from Crystal Structure Data—A Relationship between Structure and Energy": H.-B. Bürgi, *Angew. Chem. 87* (1975) 461–475; *Angew. Chem. Int. Ed. Engl. 14* (1975) 460–473; "From Crystal Statics to Chemical Dynamics": H.-B. Bürgi, J. D. Dunitz, *Acc. Chem. Res. 16* (1983) 153–161; H.-B. Bürgi, J. D. Dunitz, *J. Am. Chem. Soc. 109* (1987) 2924; *Acta Crystallogr. Sect. B 44* (1988) 445; H.-B. Bürgi, K. C. Dubler-Steudle, *J. Am. Chem. Soc. 110* (1988) 4953, 7291.

[180] For discussions regarding the possible relationship between the packing of carbocation counterions in the crystal and their behavior during solvolyses, see [171].

[181] Complexation of metals by the CO groups of carbonyl compounds: "On the Conformation and Structure of Organometal Complexes in the Solid State: Two Studies Relevant to Chemical Synthesis": S. Shambayati, W. E. Crowe, S. L. Schreiber, *Angew. Chem. 102* (1990) 273–290; *Angew. Chem. Int. Ed. Engl. 29* (1990) 256–272.

[182] "Atomic Motions in Molecular Crystals from Diffraction Measurements": J. D. Dunitz, E. F. Maverick, K. N. Trueblood, *Angew. Chem. 100* (1988) 910–926; *Angew. Chem. Int. Ed. Engl. 27* (1988) 880–895.

[183] D. Seebach, J. Zimmermann, U. Gysel, R. Ziegler, T.-K. Ha, *J. Am. Chem. Soc. 110* (1988) 4763.

[184] D. Seebach, T. Maetzke, W. Petter, B. Klötzer, D. A. Plattner, *J. Am. Chem. Soc. 112* (1990), in press.

[185] O. Ermer, P. Bell, S. A. Mason, *Angew. Chem. 101* (1989) 1298; *Angew. Chem. Int. Ed. Engl. 28* (1989) 1239.

[186] P. von R. Schleyer, *J. Am. Chem. Soc. 89* (1967) 701.

[187] "Dynamic stereochemistry of the 5-, 6- and 7-membered rings using the torsion angle notation": E. Toromanoff, *Tetrahedron 36* (1980) 2809–2931.

[188] R. Huisgen, P. H. J. Ooms, M. Mingin, N. L. Allinger, *J. Am. Chem. Soc. 102* (1980) 3951.
[189] CSD, *The Cambridge Structural Database*, Cambridge Crystallographic Data Centre, University Chemical Laboratory, Lensfield Road, GB-Cambridge CB2 1EW; "The Cambridge Crystallographic Data Centre: Computer-Based Search Retrieval, Analysis and Display of Information": F. H. Allen, S. Bellard, M. D. Brice, B. A. Cartwright, A. Doubleday, H. Higgs, T. Hummelink, B. G. Hummelink-Peters, O. Kennard, W. D. S. Motherwell, J. R. Rodgers, D. G. Watson, *Acta Crystallogr. Sect. B 35* (1979) 2331–2339.
[190] "The renaissance of *Raman* spectroscopy": D. A. Long, *Chem. Br. 25* (1989) 589–596.
[191] "Scanning Tunneling Microscopy—from Birth to Adolescence": (Nobel Lecture): G. Binnig, H. Rohrer, *Angew. Chem. 99* (1987) 622–631; *Angew. Chem. Int. Ed. Engl. 26* (1987) 606–614.
[192] a) J. P. Rabe, *Angew. Chem. Adv. Mater. 101* (1989) 1153; *Angew. Chem. Int. Ed. Engl. Adv. Mater. 28* (1989) 1127; *Adv. Mater. 1989*, 299; b) S. M. Lindsay, T. Thundat, L. Nagahara, U. Knipping, R. L. Rill, *Science (Washington, D. C.) 244* (1989) 1063.
[193] The equipment manufacturers (i.e., ultimately the commercial aspects) help to determine which methods actually find entry into the daily practice of the synthetic chemist, and how quickly.
[194] H. R. Collier (Ed.): *Chemical Information—Information in Chemistry, Pharmacology and Patents*, Springer, Berlin 1989; W. A. Warr (Ed.): *Chemical Structure Information Systems—Interfaces, Communication, and Standards*, American Chemical Society, Washington, D.C. 1989; G. Vernin, M. Chanon (Eds.): *Computer Aids to Chemistry*, Ellis Horwood, Chichester 1986.
[195] S. Rubenstein, Cambridge Scientific Computing, Inc., 875 Massachusetts Ave., Suite 41, Cambridge, MA 02139; J. Kintscher, U. Kramer, J. Martens, *Labo 12/1989*, 21; C. K. Gerson, R. A. Love, *Anal. Chem. 59* (1987) 1031A.
[196] "On Searching the Literature—Using the Computer (and your Head) to Retrieve Structures, References, Reactions and Data Online": E. Zass in H. J. E. Loewenthal (Ed.): *A Guide for the Perplexed Organic Experimentalist, 2nd Ed.*, Wiley, New York/Salle + Sauerländer, Aarau 1990, pp. 45–81; Y. Wolman: *Chemical information: a practical guide to utilization, 2nd Ed.*, Wiley, Chichester 1988; H. R. Pichler: *Online-Recherchen für Chemiker*, VCH Verlagsgesellschaft, Weinheim 1986.
[197] T. D. Salatin, W. L. Jorgensen, *J. Org. Chem. 45* (1980) 2043; G. D. Paderes, W. L. Jorgenson, *ibid. 54* (1989) 2058.
[198] H. W. Braun, *Chem. Ind. (Düsseldorf) 40* (1988) No. 5, p. 43.
[199] "Carbohydrates *vs.* non-carbohydrates in organic synthesis": S. Hanessian, J. Streith, H. Prinzbach, G. Schill (Eds.): *Organic Synthesis, an interdisciplinary challenge*, Blackwell Scientific Publications, Oxford 1985, pp. 267–280; S. Hanessian: *Total Synthesis of Natural Products: The "Chiron" Approach*, Pergamon Press, Oxford 1983.
[200] A. K. Long, S. D. Rubenstein, L. J. Joncas, *Chem. Eng. News 61* (1983) No. 19, p. 22.
[201] "Neue Möglichkeiten zur Recherche von organisch-chemischen Reaktionen: Ein Vergleich der 'in-house'-Datenbanksysteme REACCS, SYNLIB und ORAC": E. Zass, S. Müller, *Chimia 40* (1986) 38–50; "Chemical Reaction Searching Compared in REACCS, SYNLIB and ORAC": J. H. Borkent, F. Onkes, J. H. Noordik, *J. Chem. Inf. Comput. Sci. 28* (1988) 148–150.
[202] ORAC Ltd., 18 Blenheim Terrace, Woodhouse Lane, GB-Leeds LS2 9HD; A. P. Johnson, *Chem. Br. 21* (1985) 59.
[203] Molecular Design Ltd., 2132 Farallon Drive, San Leandro, CA 94577; Molecular Design MDA AG, Mühlebachweg 9, CH-4123 Allschwil 2 (Switzerland); A. J. Kos, G. Grethe, *Nachr. Chem. Tech. Lab. 35* (1987) 586.
[204] D. F. Chodosh, Distributed Chemical Graphics, Inc., 1326 Carol Road, Meadowbrook, PA 19046; D. F. Chodosh, W. L. Mendelson, *Drug Inf. J. 17* (1983) 231.
[205] M. Dobler: *MacMoMo–Molecular Modeling Program Version 6.0*, Laboratorium für Organische Chemie, ETH Zürich 1990.
[206] M. Rubenstein, S. Rubenstein, Cambridge Scientific Computing, Inc., 875 Massachusetts Ave., Suite 41, Cambridge, MA 02139.
[207] W. C. Still: *MacroModel*, Columbia University, New York 1986; R. M. J. Liskamp, *Chem. Mag. (Rijswijk, Neth.) 1987*, No. 1, p. 18; "MacroModel–An Integrated Software System for Modeling Organic and Bioorganic Molecules Using Molecular Mechanics": F. Mohamadi, N. G. J. Richards, W. G. Guida, R. Liskamp, M. Lipton, C. Caufield, G. Chang, T. Hendrickson, W. C. Still, *J. Comput. Chem. 11* (1990) 440–467.
[208] "Molecular Mechanics": U. Burkert, N. L. Allinger, *ACS Monogr. 177* (1982).
[209] The use of force field methods with the full set of parameters (MacroModel) requires a high-resolution color graphics terminal (e.g., the Evans–Sutherland Picture System).
[210] W. J. Hehre, L. Radom, P. von R. Schleyer, J. A. Pople: *Ab Initio Molecular Orbital Theory*, Wiley, New York 1986.
[211] M. R. Peterson, R. A. Poirier: *Monster-Gauss*, Departments of Chemistry, University of Toronto, Toronto, and Memorial University of Newfoundland, St. John's (Canada).
[212] R. D. Amos, J. E. Rice: *The Cambridge Analytic Derivatives Package*, Issue 4.1 L, GB-Cambridge.
[213] M. W. Schmidt, J. A. Boatz, K. K. Baldridge, S. Koseki, M. S. Gordon, S. T. Elbert, B. Lam, *QCPE Bull. 7* (1987) 115.
[214] J. J. P. Stewart, *QCPE Bull. 9* (1989) 10.
[215] N. G. Rondan, M. N. Paddon-Row, P. Caramella, K. N. Houk, *J. Am. Chem. Soc. 103* (1981) 2436.
[216] G. Stucky, D. Seebach, *Chem. Ber. 122* (1989) 2365; D. Seebach, G. Stucky, E. Pfammatter, *ibid. 122* (1989) 2377; T.-K. Ha, B. Lamatsch, G. Stucky, D. Seebach, previously unpublished calculations.
[217] "Resonance Interactions in Acyclic Systems": K. B. Wiberg, *Chemtracts: Org. Chem. 2* (1989) 85–93.
[218] W. J. Hehre, C. F. Pau, S. D. Kahn, R. F. Hout, Jr., M. M. Francl: *Molecular Modeling Computer-Aided Descriptions of Molecular Structure and Reactivity*, Wiley, New York, in press (promised in footnote 10b of [220]).
[219] "Regio- and Stereo-Selectivities in Some Nucleophilic Reactions": N. T. Anh, *Top. Curr. Chem. 88* (1980) 145–162; "Theory of stereoselectivity of nucleophilic additions to carbonyl compounds": K. N. Houk, Y. Wu in W. Bartmann, K. B. Sharpless (Eds.): *Stereochemistry of Organic and Bioorganic Transformations, Workshop Conferences Hoechst, Vol. 17*, VCH Verlagsgesellschaft, Weinheim 1987, pp. 247–260; Y.-D. Wu, K. N. Houk, *J. Am. Chem. Soc. 109* (1987) 908; Y.-D. Wu, K. N. Houk, B. M. Trost, *ibid. 109* (1987) 5560.
[220] S. D. Kahn, K. D. Dobbs, W. J. Hehre, *J. Am. Chem. Soc. 110* (1988) 4602 ("Modeling Chemical Reactivity 9"), and the preceding eight papers in this series.
[221] Y. Li, M. N. Paddon-Row, K. N. Houk, *J. Am. Chem. Soc. 110* (1988) 3684; *J. Org. Chem. 55* (1990) 481 and papers cited therein by *N. T. Anh* and *C. Gennari*.
[222] K. N. Houk, H.-Y. Duh, Y.-D. Wu, S. R. Moses, *J. Am. Chem. Soc. 108* (1986) 2754.
[223] M. J. Fisher, W. J. Hehre, S. D. Kahn, L. E. Overman, *J. Am. Chem. Soc. 110* (1988) 4625.
[224] M. N. Paddon-Row, N. G. Rondan, K. N. Houk, *J. Am. Chem. Soc. 104* (1982) 7162.
[225] A. Amann, W. Gans, *Angew. Chem. 101* (1989) 277–285; *Angew. Chem. Int. Ed. Engl. 28* (1989) 268–276.
[226] "Free Energy Calculations: A Breakthrough for Modeling Organic Chemistry in Solution": W. L. Jørgensen, *Acc. Chem. Res. 22* (1989) 184–189.
[227] See the papers of *W. F. van Gunsteren*, in which structural data are used to calculate the docking of a peptide at a DNA molecule located in a sea of several thousand water molecules: "Testing the method of crystallographic refinement using molecular dynamics": M. Fujinaga, P. Gros, W. F. van Gunsteren, *J. Appl. Crystallogr. 22* (1989) 1–8; "Combined procedure of distance geometry and restrained molecular dynamics techniques for protein structure determination from nuclear magnetic resonance data: application to the DNA binding domain of lac repressor from *Escherichia coli*": J. De Vlieg, R. M. Scheek, W. F. van Gunsteren, H. J. C. Berendsen, R. Kaptein, J. Thomason, *Proteins: Struct., Funct., Genet. 3* (1988) 209–218; "Protein structures from NMR": R. Kaptein, R. Boelens, R. M. Scheek, W. F. van Gunsteren, *Biochemistry 27* (1988) 5389–5395; "The role of computer simulation techniques in protein engineering": W. F. van Gunsteren, *Protein Eng. 2* (1988) 5–13; "Dynamic simulation of complex molecular systems": H. J. C. Berendsen, W. F. van Gunsteren, E. Egberts, J. De Vlieg, *ACS Symp. Ser. 353* (1987) 106–122; "Simulation of proteins in water": H. J. C. Berendsen, W. F. van Gunsteren, H. R. J. Zwinderman, R. G. Geurtsen, *Ann. N. Y. Acad. Sci. 482* (1986) 269–286; "A molecular dynamics computer simulation of an eight-base-pair DNA fragment in aqueous solution: comparison with experimental two-dimensional NMR data": W. F. van Gunsteren, H. J. C. Berendsen, R. G. Geurten, H. R. J. Zwinderman, *ibid. 482* (1986) 287–303. The representation in Fig. 8 was kindly provided by Professor *Willem F. van Gunsteren*.
[228] A substitute that is equivalent in many cases is DMPU ("*d*imethyl *p*ropylene *u*rea", *N*,*N*'-dimethyl-3,4,5,6-tetrahydropyrimidin-2(1*H*)-one), manufactured by BASF: T. Mukhopadhyay, D. Seebach, *Helv. Chim. Acta 65* (1982) 385; D. Seebach, *Chem. Br. 21* (1985) 632; *Chimia 39* (1985) 147.
[229] T. Reichstein, A. Grüsser, R. Oppenauer, *Helv. Chim. Acta 16* (1933) 561; T. Reichstein, A. Grüsser, *ibid. 17* (1934) 311; T. Reichstein, A. Grüsser, R. Oppenauer, *ibid. 17* (1934) 510.
[230] P. A. Holmes, L. F. Wright, S. H. Collins, Eur. Pat. Appl. EP 52,459 (1982); Imperial Chemical Industries PLC; *Chem. Abstr. 97* (1982) 143146 r.
[231] D. G. H. Ballard, A. Courtis, I. M. Shirley, S. C. Taylor, *J. Chem. Soc. Chem. Commun. 1983*, 954; S. C. Taylor, Eur. Pat. Appl. EP 76,606 (1983); Imperial Chemical Industries PLC; *Chem. Abstr. 99* (1989) 103704f.
[232] "Synthesis of Cyclosporine and Analogues: Structural Requirements for Immunosuppressive Activity": R. M. Wenger, *Angew. Chem. 97* (1985) 88–96; *Angew. Chem. Int. Ed. Engl. 24* (1985) 77–85, and references cited therein.

[233] Amino acids: K. Drauz, F. Geiger, W. Leuchtenberger in "Stets geforscht ...", *Chemieforschung im Degussa-Forschungszentrum Wolfgang, Vol. 2*, Degussa AG, Frankfurt 1988, pp. 129–148.

[234] "Clays, Zeolites and Other Microporous Solids for Organic Synthesis": J. M. Thomas, C. Theocharis, *Mod. Synth. Methods 5* (1989) 249–304; "*Claycop*, A User-Friendly Oxidizing and Nitrating Reagent": P. Laszlo, A. Cornélis, *Aldrichimica Acta 21* (1988) 97–103; P. Laszlo (Ed.): *Preparative Chemistry Using Supported Reagents*, Academic Press, San Diego 1987; see also the use of Al_2O_3 for nitroaldol additions in [104d] (*Rosini, Ballini*).

[235] "Organic Electrosyntheses in Industry": D. Degner, *Top. Curr. Chem. 148* (1988) 1–95.

[236] "Die Zukunft der Elektrochemie—Einige Betrachtungen aus der Sicht der Industrie": W.-D. Lutz, E. Zirngiebl, *Chem. Unserer Zeit 23* (1989) 151–160.

[237] "Electrochemistry I-IV", *Top. Curr. Chem. 142* (1987); *143* (1988); *148* (1988); *152* (1990).

[238] T. Shono: *Electroorganic Chemistry as a New Tool in Organic Synthesis*, Springer, Berlin 1984; S. Torii: *Electroorganic Syntheses, Part I: Oxidations*, Kodansha, Ltd., Tokyo/VCH Verlagsgesellschaft, Weinheim 1985; "C-C-Verknüpfung und Umfunktionalisierung an der Elektrode (Teil 1 und 2)": H. J. Schäfer, *Kontakte (Darmstadt) 1987*, No. 2, pp. 17–31 and No. 3, pp. 37–49; A. J. Fry: *Synthetic Organic Electrochemistry, 2nd Ed.*, Wiley, New York 1989.

[239] D. Seebach, R. Charczuk, C. Gerber, P. Renaud, H. Berner, H. Schneider, *Helv. Chim. Acta 72* (1989) 401.

[240] "Organic syntheses with electrochemically regenerable redox systems": E. Steckhan, *Top. Curr. Chem. 142* (1987) 1–69.

[241] See also the combination of electrochemical and enzymatic methods: "Chiral Compounds Synthesized by Biocatalytic Reductions": H. Simon, J. Bader, H. Günther, S. Neumann, J. Thanos, *Angew. Chem. 97* (1985) 541–555; *Angew. Chem. Int. Ed. Engl. 24* (1985) 539–553; "*...we are now witnessing a marriage taking place between enzyme biochemistry and electrochemistry*" in K. Thompson, *Chem. Br. 1989*, 1071–1072.

[242] "Chemie unter Hochdruck": F.-G. Klärner, *Chem. Unserer Zeit 23* (1989) 53–63; J. Jurczak, B. Baranowski (Eds.): *High Pressure Chemical Synthesis*, Elsevier, Amsterdam 1989; W. J. Le Noble (Ed.): *Organic High Pressure Chemistry*, Elsevier, Amsterdam 1988; see also the high-pressure chapter in [249].

[243] a) "Synthese bei Temperaturen unter $-80\,^{\circ}C$": D. Seebach, A. Hidber, *Chimia 37* (1983) 449–462, and references cited therein; b) "Asymmetrische Synthesen": H. Pracejus, *Fortschr. Chem. Forsch. 8* (1967) 493–553; c) "Basis and Limitations of the Reactivity-Selectivity Principle": B. Giese, *Angew. Chem. 89* (1977) 162–173; *Angew. Chem. Int. Ed. Engl. 16* (1977) 125–136; d) "Crystal Structures and Stereoselective Reactions of Organic Lithium Derivatives": D. Seebach, *Proc. Robert A. Welch Found. Conf. Chem. Res. 27: Stereospecificity in Chemistry and Biochemistry*, 7–9 Nov. 1983, Houston, TX 1984, pp. 93–141; e) "Autocatalysis—The next generation of asymmetric synthesis": H. Wynberg, *Chimia 43* (1989) 150–152; f) see the "principle of isoinversion" and suggestions for establishing optimal conditions in complex reaction phenomena [253], as well as the Curtin–Hammett principle (textbooks of physical organic chemistry), originally formulated for conformational pre-equilibria.

[244] "Small Scale Continuous Processes": E. Galantay, lecture at the *PMA Spring Symposium*, Charlottesville, VA, 17–20 April 1988 (Bulk Pharmaceutical Operations—the Challenge of the Nineties). I wish to thank Dr. *Galantay* (Sandoz Pharma AG, Basel) for providing the pictures included in Fig. 11.

[245] Z. Brich, H. Mühle, Eur. Pat. Appl. EP 48,695 (1982), Sandoz AG; *Chem. Abstr. 97* (1982) 72651p.

[246] J. Benes, A. Cerny, V. Miller, S. Kudrnac, *Collect. Czech. Chem. Commun. 48* (1983) 1333.

[247] In some experiments that we carried out under argon at temperatures as low as $-140\,^{\circ}C$ [243,276] the volume of the reaction mixture increased—presumably because of argon condensation—without formation of any precipitate or of two layers. In the meantime, xenon has been recommended as a solvent: "Liquid Xenon: An Effective Inert Solvent for C–H Oxidative Addition Reactions": M. B. Sponsler, B. H. Weiller, P. O. Stoutland, R. G. Bergman, *J. Am. Chem. Soc. 111* (1989) 6841.

[248] Lithiation of dithianes is normally carried out at *ca.* $-20\,^{\circ}C$ in THF. The resulting solutions can be kept for some time in the refrigerator.

[249] "Nonconventional Reaction Conditions: Ultrasound, High Pressure, and Microwave Heating in Organic Synthesis": R. J. Giguere in T. Hudlicky (Ed.): *Organic Synthesis—Theory and Applications, A Research Annual, Vol. 1*, JAI Press, Greenwich 1989, pp. 103–172.

[250] Furaneol® (aromatic component of pineapple and strawberries) is prepared by the ozonolysis of 3-hexin-2,5-diol on a 40 t/a scale: L. Re, B. Maurer, G. Ohloff, *Helv. Chim. Acta 56* (1973) 1882 and related patents.

[251] "The Beginnings of Organic Photochemistry": H. D. Roth, *Angew. Chem. 101* (1989) 1220–1234; *Angew. Chem. Int. Ed. Engl. 28* (1989) 1193–1207.

[252] a) "Neuere Anwendungen der Paterno-Büchi-Reaktion" (Synthese im Blickpunkt): M. Braun, *Nachr. Chem. Tech. Lab. 33* (1985) 213–219; b) "(2+2) Photocycloadditions in the synthesis of chiral molecules": S. L. Schreiber, *Science (Washington, D. C.) 227* (1985) 857–863.

[253] "Chiral Induction in Photochemical Reactions. 10. The Principle of Isoinversion: A Model of Stereoselection Developed from the Diastereoselectivity of the *Paternò-Büchi* Reaction": H. Buschmann, H.-D. Scharf, N. Hoffmann, M. W. Plath, J. Runsink, *J. Am. Chem. Soc. 111* (1989) 5367–5373.

[254] a) "Aromatic Compounds: Isomerisation and Cycloaddition": P. A. Wender, T. W. von Geldern in J. D. Coyle (Ed.): *Photochemistry in Organic Synthesis*, The Royal Society of Chemistry, London 1986, pp. 226–256; b) "Photochemically Generated Building Blocks I and II": K. Schaffner, M. Demuth, *Mod. Synth. Methods 4* (1986) 61–124.

[255] ... or should one say "radicalomaniacs"? "Radical anion reactions of nitro compounds": N. Kornblum in S. Patai (Ed.): *The chemistry of amino, nitroso and nitro compounds and their derivatives*, Wiley, Chichester 1982, *Suppl. F*, pp. 361–393; N. Kornblum, P. A. Wade, *J. Org. Chem. 52* (1987) 5301; "Reactivity of Substituted Aliphatic Nitrocompounds with Nucleophiles": W. R. Bowman, *Chem. Soc. Rev. 17* (1988) 283–316; "A Critical Evaluation of Studies Employing Alkenyl Halide 'Mechanistic Probes' as Indicator of Single-Electron–Transfer Processes": M. Newcomb, D. P. Curran, *Acc. Chem. Res. 21* (1988) 206–214; "Single-Electron Transfer, a Major Reaction Pathway in Organic Chemistry. An Answer to Recent Criticisms": E. C. Ashby, *ibid. 21* (1988) 414–421; "Electron Transfer and Charge Transfer: Twin Themes in Unifying the Mechanisms of Organic and Organometallic Reactions": J. K. Kochi, *Angew. Chem. 100* (1988) 1331–1372; *Angew. Chem. Int. Ed. Engl. 27* (1988) 1227–1266.

[256] "Radikalische C-C-Verknüpfung" (Synthese im Blickpunkt): M. Braun, *Nachr. Chem. Tech. Lab. 33* (1985) 298–304; see also [344–346].

[257] B. Giese: *Radicals in Organic Synthesis: Formation of Carbon–Carbon Bonds*, Pergamon Press, Oxford 1986; "The Stereoselectivity of Intermolecular Free Radical Reactions": B. Giese, *Angew. Chem. 101* (1989) 993–1004; *Angew. Chem. Int. Ed. Engl. 28* (1989) 969–980.

[258] "The Design and Application of Free Radical Chain Reactions in Organic Synthesis" (Parts 1 and 2): D. P. Curran, *Synthesis 1988*, 417–439 and 489–513.

[259] C. Chatgilialoglu, D. Griller, M. Lesage, *J. Org. Chem. 53* (1988) 3641; *54* (1989) 2492; B. Giese, B. Kopping, C. Chatgilialoglu, *Tetrahedron Lett. 30* (1989) 681; K. J. Kulicke, B. Giese, *Synlett 1990*, 91.

[260] D. Seebach, A. Thaler, A. K. Beck, *Helv. Chim. Acta 72* (1989) 857.

[261] F. Cardinaux, A. Thaler, D. Seebach, *Helv. Chim. Acta 74* (1991), in press.

[262] J. C. Hendrix, K. J. Halverson, J. T. Jarrett, P. T. Lansbury, Jr., *J. Am. Chem. Soc. 112* (1990), in press. I wish to thank Professor *Peter Lansbury* for providing me with the manuscript prior to the publication of this work, and for permission to mention his results.

[263] a) D. C. Sherrington, P. Hodge: *Syntheses and separations using functional polymers*, Wiley, Chichester 1988; b) "Chiral polymer catalysts in preparative organic chemistry: a critical overview": M. Aglietto, E. Chiellini, S. D'Antone, G. Ruggeri, R. Solaro, *Pure Appl. Chem. 60* (1988) 415–430.

[264] The use of graphite inclusion compounds also makes it possible to carry out certain reactions more selectively than by the classical methods: "Graphite–Metal Compounds": R. Csuk, B. I. Glänzer, A. Fürstner, *Adv. Organomet. Chem. 28* (1988) 85–137; "Synthese mit Graphit-Metall-Verbindungen": R. Csuk, *Nachr. Chem. Tech. Lab. 35* (1987) 828–833.

[265] *ICCOSS IX, 9th International Conference on the Chemistry of the Organic Solid State*, Villa Olmo, Como (Italy), 2–7 July 1989, Abstracts.

[266] G. R. Desiraju (Ed.): *Organic Solid State Chemistry*, Elsevier Science Publishers, Amsterdam 1987.

[267] "Studies of Host–Guest Chemistry. Fundamentals and Applications of Molecular Recognition and their Development to New Organic Solid State Chemistry": F. Toda, *Yuki Gosei Kagaku Kyokaishi (J. Synth. Org. Chem. Jpn.) 47* (1989) 1118–1131.

[268] a) F. Toda, K. Tanaka, S. Iwata, *J. Org. Chem. 54* (1989) 3007; b) F. Toda, M. Yagi, K. Kiyoshige, *J. Chem. Soc. Chem. Commun. 1988*, 958.

[269] F. Toda, K. Kiyoshige, M. Yagi, *Angew. Chem. 101* (1989) 329; *Angew. Chem. Int. Ed. Engl. 28* (1989) 320.

[270] F. Toda, T. Shigemasa, *J. Chem. Soc. Perkin Trans. 1 1989*, 209.

[271] F. Toda, K. Mori, *J. Chem. Soc. Chem. Commun. 1989*, 1245.

[272] Both the dioxolane derivative used here and its enantiomer are accessible in two steps from (*R,R*)- or (*S,S*)-tartaric acid. It was first used as a ligand in the enantioselective addition to aldehydes via alkyl titanium compounds [273,274] and later also for the TiX_4-mediated Diels–Alder reaction [275] (see also Scheme 22, enantioselective catalysis, and Sec. 7). Preparation of the compound has been described in detail [274,275].

[273] a) "Some recent advances in the use of titanium reagents for organic synthesis": D. Seebach, A. K. Beck, M. Schiess, L. Widler, A. Wonnacott, *Pure Appl. Chem. 55* (1983) 1807; b) "Organometallic Compounds of Titanium and Zirconium as Selective Nucleophilic Reagents in Organic Synthesis": B. Weidmann, D. Seebach, *Angew. Chem. 95* (1983) 12–26; *Angew. Chem. Int. Ed. Engl. 22* (1983) 31–45; c) "New Applications of

organometallic derivatives of Li, Mg, B, Al, Si, Ti and V in selective syntheses": D. Seebach in J. Streith, H. Prinzbach, G. Schill (Eds.): *Organic Synthesis: an interdisciplinary challenge*, Blackwell Scientific Publications, Oxford 1985, pp. 77–99.

[274] "Titanium and Zirconium Derivatives in Organic Synthesis": D. Seebach, B. Weidmann, L. Widler, *Mod. Synth. Methods 3* (1983) 217–353.

[275] D. Seebach, A. K. Beck, R. Imwinkelried, S. Roggo, A. Wonnacott, *Helv. Chim. Acta 70* (1987) 954.

[276] W. Langer, D. Seebach, *Helv. Chim. Acta 62* (1979) 1710; D. Seebach, G. Crass, E.-M. Wilka, D. Hilvert, E. Brunner, *ibid. 62* (1979) 2695; D. Seebach, A. Hidber, *Org. Synth. 61* (1983) 42, and references cited therein.

[277] C. H. Heathcock, C. T. White, J. J. Morrison, D. Van Derveer, *J. Org. Chem. 46* (1981) 1296.

[278] Chiral Li amides, used in preparing enolates and for other lithiations, also lead to chiral amines in the reaction mixture, and they can influence the steric course of reactions; see the discussion in [172] (Sec 4.3, ref. [259–278]); also, as a further example, an enantioselective addition of RLi in the 2-position of the naphthalene ring of *N*-(1-naphylmethylene)cyclohexylamine in the presence of (*R*,*R*)-1,2-dimethoxy-1,2-diphenylethane: K. Tomioka, M. Shindo, K. Koga, *J. Am. Chem. Soc. 111* (1989) 8266.

[279] "Ultrasound in Synthesis": K. S. Suslick, *Mod. Synth. Methods 4* (1986) 1–60.

[280] "Sonochemistry—The Use of Ultrasonic Waves in Synthetic Organic Chemistry": C. Einhorn, J. Einhorn, J.-L. Luche, *Synthesis 1989*, 787–813, and references cited therein; "Ultrasound in Organic Synthesis": R. F. Abdulla, *Aldrichimica Acta 21* (1988) 31–42.

[281] "C-C-Verknüpfungen in Wasser" (Synthese im Blickpunkt): H.-U. Reissig, *Nachr. Chem. Tech. Lab. 34* (1986) 1169–1171.

[282] C. Einhorn, J.-L. Luche, *J. Organomet. Chem. 322* (1987) 177; S. R. Wilson, M. E. Guazzaroni, *J. Org. Chem. 54* (1989) 3087.

[283] T. Kauffmann, P. Fiegenbaum, R. Wieschollek, *Angew. Chem. 96* (1984) 500; *Angew. Chem. Int. Ed. Engl. 23* (1984) 532.

[284] P. A. Grieco, D. T. Parker, *J. Org. Chem. 53* (1988) 3325, 3658; E. Brandes, P. A. Grieco, P. Garner, *J. Chem. Soc. Chem. Commun. 1988*, 500; A. Lubineau, E. Meyer, *Tetrahedron 44* (1988) 6065.

[285] *E. Winterfeld* once said: "It has certainly been good for synthetic chemistry that natural product synthesis has consistently set increasingly ambitious goals, thereby subjecting newcomers on the 'methods' market to a swift baptism by fire" (lecture: *25 Jahre Organische Chemie—Entwicklungen und Tendenzen*, 125th anniversary of Hoechst, Scientific Symposium, 19–20 May 1988, Festschrift pp. 42–54).

[286] In June 1990 within the context of the "Joint 45th Northwest/10th Rocky Mountains Regional Meeting—American Chemical Society" in Salt Lake City, UT, there was a symposium with the title "Post-Modern Organic Synthesis—Methods for the 1990s". A glance at the lecture topics failed to provide for me any revealing visions of the future. I wish to thank Dr. *Janet Grissom* for sending me a copy of the program prior to its actual release.

[287] ... *A. E.* and *I. U.*

[288] "Computer assistance in the design of syntheses and a new generation of computer programs for the solution of chemical problems by molecular logic": I. K. Ugi, J. Bauer, R. Baumgartner, E. Fontain, D. Forstmeyer, S. Lohberger, *Pure Appl. Chem. 60* (1988) 1573–1586.

[289] For recent general reviews of Si chemistry in organic synthesis see [109] and: "Organosilicon Chemistry in Organic Synthesis", Tetrahedron Symposia-in-Print Number 32: I. Fleming (Guest Editor), *Tetrahedron 44* (1988) 3761–4292.

[290] "Iodotrimethylsilane—A Versatile Synthetic Reagent": G. A. Olah, S. C. Narang, *Tetrahedron 38* (1982) 2225–2277.

[291] "Trialkylsilyl Perfluoroalkanesulfonates: Highly Reactive Silylating Agents and Lewis Acids in Organic Synthesis": H. Emde, D. Domsch, H. Feger, U. Frick, A. Götz, H. H. Hergott, K. Hofmann, W. Kober, K. Krägeloh, T. Österle, W. Steppan, W. West, G. Simchen, *Synthesis 1982*, 1–26.

[292] "Silyl-Substituted Cyclopropanes as Versatile Synthetic Reagents": L. A. Paquette, *Chem. Rev. 86* (1986) 733–750.

[293] a) I. Fleming, T. W. Newton, *J. Chem. Soc. Perkin Trans. 1 1984*, 1805; b) "Applications of Higher-Order Mixed Organocuprates to Organic Synthesis": B. H. Lipshutz, *Synthesis 1987*, 325–341.

[294] W. Amberg, D. Seebach, *Angew. Chem. 100* (1988) 1786; *Angew. Chem. Int. Ed. Engl. 27* (1988) 1718; *Chem. Ber. 123* (1990), in press.

[295] "α-Neutral Heteroatom-Substituted Organometallic Compounds": D. J. Peterson, *Organomet. Chem. Rev. Sect. A 7* (1971) 295–358.

[296] K. Utimoto, M. Kitai, H. Nozaki, *Tetrahedron Lett. 1975*, 2825.

[297] Oxidative cleavage of Si–C bonds requires an electronegative substituent at Si (see also "hypervalent" Si derivatives [107]): K. Tamao, N. Ishida, T. Tanaka, M. Kumada, *Organometallics 2* (1983) 1694; I. Fleming, P. E. J. Sanderson, *Tetrahedron Lett. 28* (1987) 4229; "Oxidative Spaltung von Silicium–Kohlenstoff-Bindungen" (Synthese im Blickpunkt): D. Schinzer, *Nachr. Chem. Tech. Lab. 37* (1989) 263–266.

[298] T. Tsunoda, M. Suzuki, R. Noyori, *Tetrahedron Lett. 21* (1980) 1357; cf. also A. Eschenmoser, *Chem. Soc. Rev. 5* (1976) 377.

[299] D. Seebach, R. Imwinkelried, G. Stucky, *Helv. Chim. Acta 70* (1987) 448.

[300] D. Seebach, T. Vettiger, H.-M. Müller, D. A. Plattner, W. Petter, *Liebigs Ann. Chem. 1990*, 687.

[301] "Die Umsetzung von Carbonsäureestern mit Natrium in Gegenwart von Trimethylchlorsilan": K. Rühlmann, *Synthesis 1971*, 236–253; "The Acyloin Condensation": J. J. Bloomfield, D. C. Owsley, J. M. Nelke, *Org. React. (N. Y.) 23* (1976) 259–403.

[302] A. Fadel, J.-L. Canet, J. Salaün, *Synlett 1990*, 89.

[303] "Trimethylsilylazid": *Kontakte (Darmstadt) 1987*, No. 2, pp. 14–15, and references cited therein.

[304] Z. Marcinow, D. K. Clawson, P. W. Rabideau, *Tetrahedron 45* (1989) 5441.

[305] "Trimethylsilyldiazomethane": T. Shioiri, T. Aoyama, *Yuki Gosei Kagaku Kyokaishi (J. Synth. Org. Chem. Jpn.) 44* (1986) 149–159.

[306] S. E. Denmark, K. L. Habermas, G. A. Hite, *Helv. Chim. Acta 71* (1988) 168; S. E. Denmark, G. A. Hite, *ibid. 71* (1988) 195; see also the overview of Nazarov-Khand-Pauson methodology [403].

[307] G. Stork, B. Ganem, *J. Am. Chem. Soc. 95* (1973) 6152.

[308] D. Seebach, A. K. Beck, F. Lehr, T. Weller, E. W. Colvin, *Angew. Chem. 93* (1981) 422; *Angew. Chem. Int. Ed. Engl. 20* (1981) 397; D. Seebach, A. K. Beck, T. Mukhopadhyay, E. Thomas, *Helv. Chim. Acta 65* (1982) 1101; see also the book by *Torssell* cited in [104c].

[309] "The Peterson Reaction": D. J. Ager, *Synthesis 1984*, 384–398; "The Peterson Olefination Reaction": D. J. Ager, *Org. React. (N. Y.) 38* (1990) 1–224.

[310] G. H. Posner, K. S. Webb, W. M. Nelson, T. Kishimoto, H. H. Seliger, *J. Org. Chem. 54* (1989) 3252; cf. also the silyloxylation of nucleophilic centers with disilyl peroxides: H. Neumann, D. Seebach, *Chem. Ber. 111* (1978) 2785; L. Camici, P. Dembech, A. Ricci, G. Seconi, M. Taddei, *Tetrahedron 44* (1988) 4197 and other work cited in these papers.

[311] "Highly Selective Acyclic Stereocontrol Based on 1,2-Rearrangement": K. Suzuki, *Yuki Gosei Kagaku Kyokaishi (J. Synth. Org. Chem. Jpn.) 46* (1988) 365–377.

[312] R. D. Miller, D. R. McKean, *Tetrahedron Lett. 24* (1983) 2619; N. Tokitoh, Y. Igarashi, W. Ando, *ibid. 28* (1987) 5903; D. Seebach, A. Jeanguenat, J. Schmidt, T. Maetzke, *Chimia 43* (1989) 314.

[313] "Preparation and Reactivity of Metallated (Silicon and Tin) Thiazoles and Oxazoles with Carbon Electrophiles. New Approaches Towards Heterocyclic and Acyclic Building Blocks": A. Dondoni, G. Fantin, M. Fogagnolo, A. Mastellari, A. Medici, E. Negrini, P. Pedrini, *Gaz. Chim. Ital. 118* (1988) 211–231; cf. also the biochemical umpolung with thiamine pyrophosphate as cofactor [79] and the Stetter variant of thiazole umpolung: "Catalyzed Addition of Aldehydes to Activated Double Bonds—A New Synthetic Approach": H. Stetter, *Angew. Chem. 88* (1976) 695; *Angew. Chem. Int. Ed. Engl. 15* (1976) 639.

[314] "Chemie und Technologie der Silicone I": R. Schliebs, J. Ackermann, *Chem. Unserer Zeit 21* (1987) 121–127; "Chemie und Technologie der Silicone II": J. Ackermann, V. Damrath, *ibid. 23* (1989) 86–99.

[315] S. G. Wierschke, J. Chandrasekhar, W. L. Jorgensen, *J. Am. Chem. Soc. 107* (1985) 1496; M. R. Ibrahim, W. L. Jorgensen, *ibid. 111* (1989) 819.

[316] Overview of the α-, β-, γ-, and δ-effects: "The interaction of silicon with positively charged carbon": J. B. Lambert, *Tetrahedron 46* (1990) 2677–2689; the many publications on allyl silanes are exhaustively covered in the following recent review articles (also in [109]): "Cyclisierung von Allyl- und Vinylsilanen" (Synthese im Blickpunkt): K. Krohn, *Nachr. Chem. Tech. Lab. 35* (1987) 358–362; "Characteristics in the Reactions of Allylsilanes and Their Applications to Versatile Synthetic Equivalents": A. Hosomi, *Acc. Chem. Res. 21* (1988) 200–206; "Intramolecular Addition Reactions of Allylic and Propargylic Silanes": D. Shinzer, *Synthesis 1988*, 263–273; "Metamorphosis of Synthetic Strategies with Allylic Silanes: Tetracoordinated Allylic Silanes into Pentacoordinated Allylic Silicates": H. Sakurai, *Synlett 1989*, 1–8; "The Electrophilic Substitution of Allylsilanes and Vinylsilanes": I. Fleming, J. Dunoguès, R. Smithers, *Org. React. (N. Y.) 37* (1989) 57–575; "Allylsilanes in Organic Synthesis": G. Majetich in T. Hudlicky (Ed.): *Organic Synthesis—Theory and Applications, A Research Annual, Vol. 1*, JAI Press, Greenwich 1989, pp. 173–240; "Allylation of Aldehydes with Etherification by Dialkoxydichlorotitanium/Alkyltrimethylsilane; an Asymmetric Variant of the Sakurai Reaction": R. Imwinkelried, D. Seebach, *Angew. Chem. 98* (1985) 781; *Angew. Chem. Int. Ed. Engl. 24* (1985) 765.

[317] T. Hayashi, K. Kabeta, T. Yamamoto, K. Tamao, M. Kumada, *Tetrahedron Lett. 24* (1983) 5661.

[318] V. G. Matassa, P. R. Jenkins, A. Kümin, L. Damm, J. Schreiber, D. Felix, E. Zass, A. Eschenmoser, *Isr. J. Chem. 29* (1989) 321.

[319] G. Stork, E. Colvin, *J. Am. Chem. Soc. 93* (1971) 2080.

[320] I. Fleming, T. W. Newton, *J. Chem. Soc. Perkin Trans. 1 1984*, 119.

[321] K. Isaac, P. Kocienski, *J. Chem. Soc. Chem. Commun. 1982*, 460.

[322] K. Suzuki, K. Tomooka, E. Katayama, T. Matsumoto, G. Tsuchihashi, *J. Am. Chem. Soc. 108* (1986) 5221; see also [311].

[323] G. Stucky, D. Seebach, *Chem. Ber. 122* (1989) 2365; D. Seebach, G. Stucky, E. Pfammatter, *ibid. 122* (1989) 2377, and references cited therein.

[324] The original Johnson method is much trickier to use and requires, after ring-opening of the dioxane, an oxidation to release the desired alcohol:

P. A. Bartlett, W. S. Johnson, J. D. Elliott, *J. Am. Chem. Soc. 105* (1983) 2088.

[325] Y. Yamamoto, J. Yamada, *J. Chem. Soc. Chem. Commun. 1988*, 802.

[326] a) D. H. R. Barton, D. M. X. Donnelly, J.-P. Finet, P. J. Guiry, *Tetrahedron Lett. 30* (1989) 1377; b) other applications of organolead compounds: T. Kauffmann, G. Ilchmann, R. König, M. Wensing, *Chem. Ber. 118* (1985) 391; Y. Yamamoto, J. Yamada, *J. Am. Chem. Soc. 109* (1987) 4395; J. Yamada, Y. Yamamoto, *J. Chem. Soc. Chem. Commun. 1987*, 1302; see also Sec. 7.2.2, enantioselective carbonyl addition of organolead compounds under the influence of chiral catalysts.

[327] a) L. Shi, W. Wang, Y. Wang, Y.-Z. Huang, *J. Org. Chem. 54* (1989) 2027; "Arsonium Ylides (with some mention also of Arsinimines, Stibonium and Bismuthonium Ylids)": D. Lloyd, I. Gosney, R. A. Ormiston, *Chem. Soc. Rev. 16* (1987) 45–74; b) D. H. R. Barton, J.-P. Finet, J. Khamsi, *Tetrahedron Lett. 29* (1988) 1115.

[328] a) D. H. R. Barton, N. Ozbalik, M. Ramesh, *Tetrahedron Lett. 29* (1988) 3533; b) "Organic Transformations Based on Tellurium Compounds": H. Suzuki, *Yuki Gosei Kagaku Kyokaishi (J. Synth. Org. Chem. Jpn.) 45* (1987) 603–615; "Synthetic Applications of Tellurium Reagents": N. Petragnani, J. V. Comasseto, *Synthesis 1986*, 1–30; "Synthetic Applications of Organotellurium Chemistry": L. Engman, *Acc. Chem. Res. 18* (1985) 274–279; c) First α-Te–C–Li compounds: D. Seebach, A. K. Beck, *Chem. Ber. 108* (1975) 314.

[329] a) W. Korytnyk, S. Valentekovic-Horvath, C. R. Petrie III, *Tetrahedron 38* (1982) 2547; b) an interesting contribution to the history of noble-gas compounds: "One or Several Pioneers? The Discovery of Noble-Gas Compounds": P. Laszlo, G. J. Schrobilgen, *Angew. Chem. 100* (1988) 495–506; *Angew. Chem. Int. Ed. Engl. 27* (1988) 479–489.

[330] a) For this reason it pleases me as a former *Criegee* student on the one hand to see recent papers in which the strain in *small rings* is exploited for synthetic purposes [339]: "Strained Polycyclic Systems Consisting of Three- and Four-Membered Rings": D. Seebach, *Angew. Chem. 77* (1965) 119–129; *Angew. Chem. Int. Ed. Engl. 4* (1965) 121–131; "Methoden zur Herstellung und Umwandlung isocyclischer Vierring-Verbindungen": D. Seebach in E. Müller (Ed.): *Methoden der Organischen Chemie (Houben–Weyl), Vol. IV/4*, Thieme, Stuttgart 1971, pp. 1–444; b) on the other hand, the former *Corey*-coworker *D. S.* [18,31] is fascinated by the host of developments since 1976 [330c] in the area of applications of sulfur and selenium compounds in organic synthesis stemming directly from the laboratories of former *Corey*-group members. A few examples are cited under [330d]; c) "Verwendung von Schwefel- und Selenderivaten in der Organischen Synthese": D. Seebach, K.-H. Geiss, M. Kolb, A. K. Beck, *Mod. Synth. Methods 1* (1976) 173–299; d) "Zwiebelanes": T. Bayer, H. Wagner, E. Block, S. Grisoni, S. H. Zhao, A. Neszmelyi, *J. Am. Chem. Soc. 111* (1989) 3085; "The Chemistry of Mixed Organosulfur–Silicon Compounds": E. Block, M. Aslam, *Tetrahedron 44* (1988) 281–324; T. P. Burkholder, P. L. Fuchs, *J. Am. Chem. Soc. 110* (1988) 2341; see also the review article by *P. Fuchs* et al. in [376]; A. Krief, L. Hevesi: *Organoselenium Chemistry I, Functional Group Transformations*, Springer, Berlin 1988; K. C. Nicolaou, C.-K. Hwang, M. E. Duggan, *J. Am. Chem. Soc. 111* (1989) 6682 and [342a]; "Asymmetric synthesis using α-sulfinyl carbanions and β-unsaturated sulfoxides": G. H. Posner in S. Patai, Z. Rappoport, C. J. M. Stirling (Eds.): *The Chemistry of Sulphones and Sulphoxides*, Wiley, New York 1988, pp. 823–849; "Total Synthesis Mediated by Cyclic Sulfides": E. Vedejs, article for the book by E. Block (Ed.): *Organic Synthesis—Theory and Application*, JAI Press, Greenwich, in press; I wish to thank Professor *Edwin Vedejs* for providing me with a manuscript copy.

[331] a) The following book is an excellent source of information and discussion of the fundamental contributions by *Mukaiyama*: T. Mukaiyama: *Organic Synthetic Reactions*, Tokyo Kagakudojin 1987; English version: *Challenges in Synthetic Organic Chemistry*, Int. Ser. Monographs on Chemistry No. 20, Oxford University Press, Oxford 1990; b) "The Directed Aldol Reaction": T. Mukaiyama, *Org. React. (N. Y.) 28* (1982) 203–331; c) "The Aldol Addition Reaction": C. H. Heathcock in J. D. Morrison (Ed.): *Asymmetric Synthesis, Vol. 3*, Academic Press, Orlando, FL 1984, pp. 111–212. The contributions by *Masamune* are covered in [437]; d) most recent, comprehensive review: "Recent Developments in Stereoselective Aldol Reactions": M. Braun in V. Snieckus (Ed.): *Advances in Carbanion Chemistry*, JAI Press, Greenwich, CT 1990, in press; cf. also "Stereoselective Aldol Reactions with α-Unsubstituted Chiral Enolates": M. Braun, *Angew. Chem. 99* (1987) 24–37; *Angew. Chem. Int. Ed. Engl. 26* (1987) 24–37; M. Braun, D. Waldmüller, H. Sacha, *Chemiedozententagung 1990*, Ulm, 26–28 March 1990, Wissenschaftliches Programm und Vortragsreferate, Universitätsverlag Ulm, A 33; e) for diastereoselective nitroaldol additions see [308].

[332] a) "Selective Reactions Using Organoaluminum Reagents": K. Maruoka, H. Yamamoto, *Angew. Chem. 97* (1985) 670–683; *Angew. Chem. Int. Ed. Engl. 24* (1985) 668–682; b) "The Beckmann Reactions: Rearrangements, Elimination–Additions, Fragmentations, and Rearrangement–Cyclizations": R. E. Gawley, *Org. React. (N. Y.) 35* (1988) 1–420.

[333] Ireland–Claisen variants: R. E. Ireland, R. H. Mueller, A. K. Willard, *J. Am. Chem. Soc. 98* (1976) 2868; "Diastereoselektive Claisen-Umlagerung" (Synthese im Blickpunkt): H.-J. Altenbach, *Nachr. Chem. Tech. Lab. 36* (1988) 520–522; "Esterenolat-Claisen-Umlagerung" (Synthese im Blickpunkt): *ibid. 36* (1988) 644–646; "The Thermal, Aliphatic Claisen Rearrangement": F. E. Ziegler, *Chem. Rev. 88* (1988) 1423–1452.

[334] a) Aza-Cope: "The Hetero-*Cope* Rearrangements in Organic Synthesis": S. Blechert, *Synthesis 1989*, 71–82 and in the reviews of the Mannich reaction cited in [336]; b) oxy-Cope: D. A. Evans, A. M. Golob, *J. Am. Chem. Soc. 97* (1975) 4765; cf. also "carbanion-accelerated" Cope rearrangements: "Carbanion-accelerated Claisen rearrangements. 6": S. E. Denmark, M. A. Harmata, K. S. White, *ibid. 111* (1989) 8878 and previous articles in this series; c) "Carbonyl Group Regeneration with Substantive Enhancement of Structural Complexity": L. A. Paquette, *Synlett 1990*, 67–73.

[335] a) "Intramolecular [4+2] and [3+2] Cycloadditions in Organic Synthesis": W. Oppolzer, *Angew. Chem. 89* (1977) 10–24; *Angew. Chem. Int. Ed. Engl. 16* (1977) 10–23; "Asymmetric Diels–Alder and Ene Reactions in Organic Synthesis": W. Oppolzer, *ibid. 96* (1984) 840–854 and *23* (1984) 876–889; b) "Stereochemical Aspects of the Intramolecular Diels–Alder Reaction": D. Craig, *Chem. Soc. Rev. 16* (1987) 187–238; c) A. J. Gutierrez, K. J. Shea, J. J. Svoboda, *J. Org. Chem. 54* (1989) 4335; d) "Retro-Diels–Alder Strategy in Natural Product Synthesis": A. Ichihara, *Synthesis 1987*, 207–222; e) "Dramatic Acceleration of the Diels–Alder Reaction by Adsorption on Chromatography Adsorbents": B. Ganem, *Chemtracts: Org. Chem. 1* (1988) 192–193; f) hetero-Diels–Alder additions of enol ethers to 2-trichloroacetylacrolein derivatives and corresponding tandem-Knoevenagel/hetero-Diels–Alder reactions: L. F. Tietze, T. Brumby, M. Pretor, G. Remberg, *J. Org. Chem. 53* (1988) 810; L. F. Tietze, H. Meier, H. Nutt, *Chem. Ber. 122* (1989) 643; *Liebigs Ann. Chem. 1990*, 253; see also the enantioselective Diels–Alder reactions in Sec. 7.2.2 and the "all-carbon" Diels–Alder reactions of Danishefsky dienes cited in [372].

[336] a) "Intramolecular Mannich and Related Reactions": L. E. Overman, D. J. Ricca in [349]; b) "*N*-Acyliminium Ions as Intermediates in Alkaloid Synthesis": H. Hiemstra, W. N. Speckamp, *Alkaloids (N. Y.) 32* (1988) 271–339; c) "Elektrophile Cyclisierungen zu Heterocyclen. Teil I: Iminium-Systeme" (Synthese im Blickpunkt): D. Schinzer, *Nachr. Chem. Tech. Lab. 37* (1989) 370–374; d) "Further advances in the chemistry of Mannich bases": M. Tramontini, L. Angiolini, *Tetrahedron 46* (1990) 1791–1837.

[337] a) D. A. Oare, C. H. Heathcoek, *J. Org. Chem. 55* (1990) 157; D. A. Oare, M. A. Henderson, M. A. Sanner, C. H. Heathcock, *ibid. 55* (1990) 132; "Stereochemistry of the Base-Promoted Michael Addition Reaction": D. A. Oare, C. H. Heathcock, *Top. Stereochem. 19* (1989) 227–407; b) Michael additions under the various conditions of the Mukaiyama aldolization are collected in chapters 9 and 13 of [331a]; c) "Diastereoselektive Michael-Additionen an Nitroolefine": D. Seebach, H. F. Leitz, V. Ehrig, *Chem. Ber. 108* (1975) 1924; M. Züger, T. Weller, D. Seebach, *Helv. Chim. Acta 63* (1980) 2005; D. Seebach, J. Golinski, *ibid. 64* (1981) 1413; S. J. Blarer, W. B. Schweizer, D. Seebach, *ibid. 65* (1982) 1637; S. J. Blarer, D. Seebach, *Chem. Ber. 116* (1983) 2250, 3086; R. Häner, T. Laube, D. Seebach, *Chimia 38* (1984) 255; D. Seebach, A. K. Beck, J. Golinski, J. N. Hay, T. Laube, *Helv. Chim. Acta 68* (1985) 162; G. Calderari, D. Seebach, *ibid. 68* (1985) 1592; M. A. Brook, D. Seebach, *Can. J. Chem. 65* (1987) 836; M. Eberle, M. Egli, D. Seebach, *Helv. Chim. Acta 71* (1988) 1; M. A. Brook, R. Faggiani, C. J. L. Lock, D. Seebach, *Acta Crystallogr. Sect. C44* (1988) 1981; see also the papers cited here of investigations by the research group of *Risaliti* and *Valentin* (Trieste) into the reactions of enamines with nitroolefins. For reviews of the reactions of nitroolefins see [105a] (*Kabalka, Barrett*); d) "[4+2]-Carbocyclisierungen, die durch eine konjugierte Addition an ein Nitroolefin eingeleitet werden": V. Ehrig, D. Seebach, *Chem. Ber. 108* (1975) 1961; T. Weller, D. Seebach, *Tetrahedron Lett. 23* (1982) 935; e) "[3+3]-Carbocyclisierungen über doppelte Nitroolefin-Addition": D. Seebach, G. Calderari, W. L. Meyer, A. Merritt, L. Odermann, *Chimia 39* (1985) 183; D. Seebach, M. Missbach, G. Calderari, M. Eberle, *J. Am. Chem. Soc. 112* (1990), 7625.

[338] a) It appears that the mechanism has now been clarified once and for all: E. Vedejs, C. F. Marth, *J. Am. Chem. Soc. 111* (1989) 1519; *ibid. 112* (1990) 3905, and references cited therein; b) cf. also the Peterson [28, 108, 295, 309], Tebbe–Grubbs [29], Nozaki [30] and Julia olefinations: "Recent Sulphone-Based Olefination Reactions": P. Kocienski, *Phosphorus Sulfur 24* (1985) 97–127.

[339] a) "Cyclopropyl building blocks for organic synthesis": A. de Meijere, *Chem. Br. 23* (1987) 865–870; b) "Vinylcyclopropane Rearrangements": Z. Goldschmidt, B. Crammer, *Chem. Soc. Rev. 17* (1988) 229–267; c) "Cyclobutanones and Cyclobutenones in Nature and in Synthesis": D. Bellus, B. Ernst, *Angew. Chem. 100* (1988) 820–850; *Angew. Chem. Int. Ed. Engl. 27* (1988) 797–827; d) A. de Meijere, S. Blechert (Eds.): *Strain and Its Implications in Organic Chemistry*, Kluwer Academic Publishers, Dordrecht 1989 and the articles therein by *L. Ghosez* (pp. 235–254), *H.-U. Reissig* (pp. 51–58) and *B. M. Trost* (pp. 1–23); e) "Strain-Assisted Syntheses": Tetrahedron Symposia-in-Print Number 38: L. Ghosez

(Guest Editor), *Tetrahedron 45* (1989) 2875–3231; f) "Dioxiranes: A New Class of Powerful Oxidants": W. Adam, R. Curci, J. O. Edwards, *Acc. Chem. Res. 22* (1989) 205–211; g) "Applications of oxaziridines in organic synthesis": F. A. Davis, A. C. Sheppard, *Tetrahedron 45* (1989) 5703–5742; h) "Tailoring the Reactivity of Small Ring Building Blocks for Organic Synthesis": A. de Meijere, L. Wessjohann, *Synlett 1990*, 20–32; see also [343a].

[340] a) "The cycloadditive approach to β-hydroxy carbonyls: an emerging alternative to the aldol strategy": D. P. Curran, *Adv. Cycloaddit. 1* (1988) 129–189; b) "Naturstoffe *via* 1,3-dipolare Cycloaddition I und II" (Synthese im Blickpunkt): J. Mulzer, *Nachr. Chem. Tech. Lab. 32* (1984) 882–887 and 961–965; c) Mukaiyama methods for preparing nitrile oxides from nitroalkanes: Chapter 2 in [331a]; d) A. Padwa: *1,3-Dipolar Cycloaddition Chemistry, Vol. 1* and *Vol. 2*, Wiley, New York 1984.

[341] a) "Heteroatom-Facilitated Lithiations": H. W. Gschwend, H. R. Rodriguez, *Org. React. (N. Y.) 26* (1979) 1–360; b) "Neue Wege der aromatischen Substitution" (Synthese im Blickpunkt): M. Braun, *Nachr. Chem. Tech. Lab. 33* (1985) 21–24; c) "Stereo- and Regiocontrol by Complex Induced Proximity Effects: Reactions of Organolithium Compounds": P. Beak, A. I. Meyers, *Acc. Chem. Res. 19* (1986) 356–363; d) "Heteroatom Directed Aromatic Lithiation Reactions for the Synthesis of Condensed Heterocyclic Compounds": N. S. Narasimhan, R. S. Mali, *Top. Curr. Chem. 138* (1987) 63–147; e) "Réaction de métallation *ortho* dirigée des composés aromatiques. Nouvelles méthodologies et applications en synthèse organique": V. Snieckus, *Bull. Soc. Chim. Fr. 1988*, 67–78.

[342] a) K. C. Nicolaou, C.-K. Hwang, M. E. Duggan, P. J. Carroll, *J. Am. Chem. Soc. 109* (1987) 3801; K. C. Nicolaou, S. A. DeFrees, C.-K. Hwang, N. Stylianides, P. J. Carrol, J. P. Snyder, *ibid. 112* (1990) 3029; K. C. Nicolaou, C.-K. Hwang, B. E. Marron, S. A. DeFrees, E. A. Couladouros, Y. Abe, P. J. Carrol, J. P. Snyder, *ibid. 112* (1990) 3040; b) "Carbonyl-Coupling Reactions Using Low-Valent Titanium": J. E. McMurry, *Chem. Rev. 89* (1989) 1513–1524; c) "Reductions promoted by low valent transition metal complexes in organic synthesis": J.-M. Pons, M. Santelli, *Tetrahedron 44* (1988) 4295–4212; d) "Anwendung niedervalenter Titan-Reagentien in der Organischen Synthese": C. Betschart, D. Seebach, *Chimia 43* (1989) 39–49 and [274]; e) "The Application of Low-Valent Titanium Reagents in Organic Synthesis": D. Lenoir, *Synthesis 1989*, 883–897.

[343] a) "Stereoselective Synthesis of Enantiomerically Pure Natural Products—Estrone as Example": G. Quinkert, H. Stark, *Angew. Chem. 95* (1983) 651–669; *Angew. Chem. Int. Ed. Engl. 22* (1983) 637–655; b) G. Quinkert, U.-M. Billhardt, H. Jakob, G. Fischer, J. Glenneberg, P. Nagler, V. Autze, N. Heim, M. Wacker, T. Schwalbe, Y. Kurth, J. W. Bats, G. Dürner, G. Zimmermann, H. Kessler, *Helv. Chim. Acta 70* (1987) 771–861.

[344] "Radical-Mediated Cyclization Processes": G. Stork in W. Bartmann, B. M. Trost (Eds.): *Selectivity—a Goal for Synthetic Efficiency, Workshop Conferences Hoechst, Vol. 14*, Verlag Chemie, Weinheim 1984, pp. 281–298.

[345] "The Captodative Effect": H. G. Viehe, Z. Janousek, R. Merényi, L. Stella, *Acc. Chem. Res. 18* (1985) 148–154.

[346] "Tri-*n*-butyltin Hydride as Reagent in Organic Synthesis": W. P. Neumann, *Synthesis 1987*, 665–683; "New Reactions for Use in Natural Products Chemistry": D. H. R. Barton, S. D. Gero, B. Quiclet-Sire, M. Samadi, N. Ozbalik, J. C. Sarma, M. Ramesh, *Pure Appl. Chem. 60* (1988) 1549–1554; "The Invention of Chemical Reactions": D. H. R. Barton, *Aldrichimica Acta 23* (1990) 3–10.

[347] "The Use of Diethyl Azodicarboxylate and Triphenylphosphine in Synthesis and Transformation of Natural Products": O. Mitsunobu, *Synthesis 1981*, 1–28; mechanism: M. Varasi, K. A. M. Walker, M. L. Maddox, *J. Org. Chem. 52* (1987) 4235.

[348] "Organoalkali Compounds by Radical Anion Induced Reductive Metalation of Phenyl Thioethers": T. Cohen, M. Bhupathy, *Acc. Chem. Res. 22* (1989) 152–161; see also the review article by *E. Block* et al. in [330d].

[349] The most complete up-to-date review of the current state of organic synthesis will be provided by the eight-volume work *Comprehensive Organic Synthesis* (B. M. Trost, Ed.), Pergamon Press, London, which is to be released this year.

[350] Diastereoselectivity is at the heart of a series of seven essays by *E. Winterfeldt* published between 1985 and 1987 in the Merck magazine *Kontakte (Darmstadt)*, which have in the meantime appeared in book form: E. Winterfeldt: *Prinzipien und Methoden der Stereoselektiven Synthese*, Vieweg, Braunschweig 1988. The Diels–Alder reaction, the Claisen–Cope rearrangement, the aldol and Michael additions, stereoselective additions to carbonyl groups, and the utilization of small rings are all subjects of extensive discussion (altogether over 800 references).

[351] ... often referred to as "tandem reactions", "multiple-component coupling", or "multiply convergent reactions".

[352] "Syntheses of Enantiomerically Pure Compounds (EPC Syntheses)—Tartaric Acid, an Ideal Source of Chiral Building Blocks for Synthesis": D. Seebach, E. Hungerbühler, *Mod. Synth. Methods 2* (1980), 91–173.

[353] "EPC Syntheses with C–C Bond Formation *via* Acetals and Enamines": D. Seebach, R. Imwinkelried, T. Weber, *Mod. Synth. Methods 4* (1986) 125–259.

[354] "Biological-Chemical Preparation of 3-Hydroxycarboxylic Acids and Their Use in EPC-Syntheses": D. Seebach, S. Roggo, J. Zimmermann in W. Bartmann, K. B. Sharpless (Eds.): *Stereochemistry of Organic and Bioorganic Transformations, Workshop Conferences Hoechst, Vol. 17*, VCH Verlagsgesellschaft, Weinheim 1987, pp. 85–126.

[355] a) An outstanding book about oxidation of organic compounds in general, with chapters on the oxidation of alcohols, is: A. H. Haines: *Methods for the Oxidation of Organic Compounds. Alcohols, Alcohol Derivatives, Alkyl Halides, Nitroalkanes, Alkyl Azides, Carbonyl Compounds, Hydroxyarenes and Aminoarenes*, Academic Press, London 1988; b) a catalytic variant of the use of CrO_3 for the oxidation of alcohols actually employs peracid as the oxidant: E. J. Corey, E.-P. Barrette, P. A. Magriotis, *Tetrahedron Lett. 26* (1985) 5855.

[356] Utilization of hypochlorite ("swimming-pool chlorine"): R. V. Stevens, K. T. Chapman, H. N. Weller, *J. Org. Chem. 45* (1980) 2030; R. V. Stevens, K. T. Chapman, C. A. Stubbs, W. W. Tam, K. F. Albizati, *Tetrahedron Lett. 23* (1982) 4647.

[357] "Herstellung und Umwandlung von Peroxiden": R. Criegee in E. Müller (Ed.): *Methoden der Organischen Chemie (Houben–Weyl), Vol. VIII, Sauerstoffverbindungen III*, Thieme, Stuttgart 1952, pp. 3–74; "Peroxo-Verbindungen als Reagenzien in der Organischen Chemie": K. P. Zeller in H. Kropf (Ed.): *ibid., Vol. E 13*, Thieme, Stuttgart 1988, pp. 1143–1145, 1150–1160.

[358] E. J. Corey, K. Achiwa, *J. Am. Chem. Soc. 91* (1969) 1429.

[359] N. Kornblum, J. W. Powers, G. J. Anderson, W. J. Jones, H. O. Larson, O. Levand, W. M. Weaver, *J. Am. Chem. Soc. 79* (1957) 6562; N. Kornblum, W. J. Jones, G. J. Anderson, *ibid. 81* (1959) 4113; similar in principle to the Kornblum oxidation is the much older Kröhnke oxidation, in which an alkyl halide is converted into an aldehyde via the pyridinium salt and a nitrone prepared with *p*-dimethylamino(nitroso)benzene: "Über α-Keto-aldonitrone und eine neue Darstellungsweise von α-Keto-aldehyden": F. Kröhnke, E. Börner, *Ber. Dtsch. Chem. Ges. 69* (1936) 2006.

[360] J. D. Albright, L. Goldman, *J. Am. Chem. Soc. 89* (1967) 2416; "Sulfoxide–Carbodiimide and Related Oxidations": J. G. Moffatt in R. L. Augustine, D. J. Trecker (Eds.): *Oxidation, Vol. 2*, Marcel Dekker, New York 1971, pp. 1–64.

[361] E. J. Corey, C. U. Kim, *J. Am. Chem. Soc. 94* (1972) 7586; *Tetrahedron Lett. 1973*, 919.

[362] K. Omura, D. Swern, *Tetrahedron 34* (1978) 1651–1660.

[363] "Activated Dimethyl Sulfoxide: Useful Reagents for Synthesis": A. J. Mancuso, D. Swern, *Synthesis 1981*, 165–185.

[364] H. O. House: *Modern Synthetic Reactions, 2nd Ed.*, W. A. Benjamin, Menlo Park 1972.

[365] G. Stork, P. F. Hudrlik, *J. Am. Chem. Soc. 90* (1968) 4462, 4464.

[366] S. Hünig, M. Kiessel, *Chem. Ber. 91* (1958) 380.

[367] M. Ertas, D. Seebach, *Helv. Chim. Acta 68* (1985) 961.

[368] "Tin(II) compounds as synthetic control elements in organic synthesis": T. Mukaiyama, *Pure Appl. Chem. 58* (1986) 505–512.

[369] See the work of *G. Wittig, G. Stork, A. I. Meyers, E. J. Corey*, and *D. Enders* in chapter 6 of the following review: D. Seebach, K.-H. Geiss in D. Seyfert (Ed.): *Proc. Symp. ACS Natl. Meet. New York City*, 6–9 April 1976; *J. Organomet. Chem. Libr. 1* (1976) 1–92.

[370] For the structure of a cyclopropanecarboxylic ester Li enolate and a discussion of its high reactivity see [167c] and references cited therein.

[371] W. Amberg: *Substituierte β-Hydroxycarbonsäuren aus (2R,6R)-2-tert-Butyl-6-methyl-dioxanonderivaten, Dissertation Nr. 9148*, ETH Zürich 1990; W. Amberg, D. Seebach, *Chem. Ber. 123* (1990), in press.

[372] The history of the discovery, development, and application of Danishefsky dienes is the subject of an excellent recent summary: "Cycloaddition and Cyclocondensation Reactions of Highly Functionalized Dienes: Applications to Organic Synthesis", S. Danishefsky, *Chemtracts: Org. Chem. 2* (1989) 273–297; instructions for the preparation of a Danishefsky diene: S. J. Danishefsky, T. Kitahara, P. F. Schuda, *Org. Synth. 61* (1983) 147; "Totally Synthetic Routes to the Higher Monosaccharides": S. J. Danishefsky, M. P. DeNinno, *Angew. Chem. 99* (1987) 15–23; *Angew. Chem. Int. Ed. Engl. 26* (1987) 15–23.

[373] Trivial steps conducted prior to or following the actual in-situ reaction sequence are implicitly included.

[374] MIMIRC for *M*ichael–*M*ichael *r*ing *c*losure, MIMI-MIRC für *M*ichael–*M*ichael–*M*ichael *r*ing *c*losure, or SMIRC for *s*equential *M*ichael *r*ing *c*losure [375].

[375] "Multicomponent One-Pot Annulations Forming Three to Six Bonds": G. H. Posner, *Chem. Rev. 86* (1986) 831–844.

[376] There are numerous other examples—in [330–350], for example. In place of classical Michael additions like those in Table 4, vinyl sulfoxides or vinyl sulfones can also function as acceptors of nucleophiles in such multi-step processes; see the work of *Fuchs* et al. and *Posner* et al. in [330d], as well as: "Multiply Convergent Syntheses *via* Conjugate-Addition Reactions to Cycloalkenyl Sulfones": P. L. Fuchs, T. F. Braish, *Chem. Rev. 86* (1986) 903–917; cross-linking of proteins: S. J. Brocchini,

M. Eberle, R. G. Lawton, *J. Am. Chem. Soc. 110* (1988) 5211; vinyl sulfones as coupling reagents: P. Auvray, P. Knochel, J. F. Normant, *Tetrahedron 44* (1988) 6095.
[377] T. L. Fevig, R. L. Elliott, D. P. Curran, *J. Am. Chem. Soc. 110* (1988) 5064.
[378] D. Seebach, M. S. Hoekstra, G. Protschuk, *Angew. Chem. 89* (1977) 334; *Angew. Chem. Int. Ed. Engl. 16* (1977) 321; D. Seebach, T. Weller, G. Protschuk, A. K. Beck, M. S. Hoekstra, *Helv. Chim. Acta 64* (1981) 716; T. Weller, D. Seebach, R. E. Davis, B. B. Laird, *ibid. 64* (1981) 736.
[379] L. E. Overman, M. Sworin, R. M. Burk, *J. Org. Chem. 48* (1983) 2685.
[380] P. A. Wender, A. G. Olivero, unpublished experiments, mentioned in [254a].
[381] K. E. Wilzbach, L. Kaplan, *J. Am. Chem. Soc. 88* (1966) 2066.
[382] D. Bryce-Smith, A. Gilbert, B. H. Orger, *J. Chem. Soc. Chem. Commun. 1966*, 512.
[383] G. A. Kraus, J. O. Nagy, *Tetrahedron 41* (1985) 3537; for additional examples of diastereoselective formation of pyrrolidine see [340d].
[384] H. Hagiwara, A. Okano, H. Uda, *J. Chem. Soc. Chem. Commun. 1985*, 1047.
[385] P. W. Hickmott, M. G. Ahmed, S. A. Ahmed, S. Wood, M. Kapon, *J. Chem. Soc. Perkin Trans. 1 1985*, 2559 and additional references cited therein to work by the same group.
[386] G. H. Posner, S.-B. Lu, E. Asirvatham, E. F. Silversmith, E. M. Shulman, *J. Am. Chem. Soc. 108* (1986) 511.
[387] G. H. Posner, J. P. Mallamo, A. Y. Black, *Tetrahedron 37* (1981) 3921.
[388] See especially the nine-volume work by G. Wilkinson, F. G. A. Stone, E. W. Abel (Eds.): *Comprehensive Organometallic Chemistry*, Pergamon Press, Oxford 1982.
[389] "Transition Metals in Organic Synthesis": R. Scheffold (Ed.): *Modern Synthetic Methods 1983, Vol. 3*, Otto Salle Verlag, Frankfurt am Main/Verlag Sauerländer, Aarau 1983.
[390] "The Influence of Organometallic Chemistry on Organic Synthesis: Present and Future. A discussion organized and edited by M. L. H. Green and S. G. Davies", *Phil. Trans. R. Soc. London A 326* (1988) 501–653.
[391] Especially useful are the annual reviews, organized according to metal or by group within the periodic table, appearing as: *Organometallic Chemistry (Specialist periodical report)*, The Royal Society of Chemistry, Burlington House, London W1V 0BN.
[392] Valuable summaries appear in *Cheminform*: H. D. Spanagel, C. Weiske (Eds.), *Fachinformationszentrum Chemie GmbH, Gesellschaft Deutscher Chemiker, Bayer AG*, VCH Verlagsgesellschaft mbH, Weinheim, and especially in the six annual volumes of *Cahiers Bibliographiques de Chimie Organometallique (Bibliographic Notebooks for Organometallic Chemistry)*, Université de Rennes.
[393] "Building Bridges Between Inorganic and Organic Chemistry" (Nobel Lecture): R. Hoffmann, *Angew. Chem. 94* (1982) 725–739; *Angew. Chem. Int. Ed. Engl. 21* (1982) 711–724.
[394] To the best of my knowledge, the best book on OMCOS chemistry, containing extensive chapters (13–20) on applications—and complete with numerous literature references—is: J. P. Collman, L. S. Hegedus, J. R. Norton, R. G. Finke: *Principles and Applications of Organotransition Metal Chemistry*, University Science Books, Mill Valley, CA 1987.
[395] General and specialized experimental procedures are to be found in [389] and in the series by R. B. King, J. J. Eisch (Eds.): *Organometallic Syntheses*, Academic Press, New York 1965 (Vol. 1), 1981 (Vol. 2), and Elsevier, Amsterdam 1985 (Vol. 3), 1988 (Vol. 4); applications of transition-metal derivatives in natural product syntheses: P. J. Harrington: *Transition metals in total synthesis*, Wiley, New York 1990.
[396] "Multiple Stereocontrol Using Organometallic Complexes. Applications in Organic Synthesis and Consideration of Future Prospects": A. J. Pearson, *Synlett 1990*, 10.
[397] "Carbene Complexes in Organic Synthesis": K. H. Dötz, *Angew. Chem. 96* (1984) 573–594; *Angew. Chem. Int. Ed. Engl. 23* (1984) 587–608.
[398] "The Mechanism of the Dötz Reaction: Chromacyclobutenes by Alkyne–Carbene Coupling?": P. Hofmann, M. Hämmerle, *Angew. Chem. 101* (1989) 940; *Angew. Chem. Int. Ed. Engl. 28* (1989) 908.
[399] K. H. Dötz, H. Fischer, P. Hofmann, F. R. Kreissl, U. Schubert, K. Weiss: *Transition Metal Carbene Complexes*, Verlag Chemie, Weinheim 1983; "Fischer-Carben-Komplexe als Schlüsselverbindungen" (Synthese im Blickpunkt): H.-U. Reissig, *Nachr. Chem. Tech. Lab. 22* (1986) 22–24.
[400] "Regio- und stereoselektive Arylkupplungen" (Synthese im Blickpunkt): H. J. Altenbach, *Nachr. Chem. Tech. Lab. 36* (1988) 1324–1327.
[401] K. M. Nicholas, *Acc. Chem. Res. 20* (1987) 207.
[402] a) "Enantioselective Catalysis with Metal Complexes, an Overview": R. Noyori, M. Kitamura, *Mod. Synth. Methods 5* (1989) 115–198; b) "Chemical Multiplication of Chirality: Science and Applications": R. Noyori, *Chem. Soc. Rev. 18* (1989) 187–208; T. Ohta, H. Takaya, R. Noyori, *Inorg. Chem. 27* (1988) 566.
[403] "Nazarov- und Khand-Pauson-Reaktionen" (Synthese im Blickpunkt): K. Krohn, *Nachr. Chem. Tech. Lab. 35* (1987) 606–609.
[404] "Hydrozirconation: A New Transition Metal Reagent for Organic Synthesis": J. Schwartz, J. A. Labinger, *Angew. Chem. 88* (1976) 402–409; *Angew. Chem. Int. Ed. Engl. 15* (1976) 333–340; "Organozirconium Compounds as New Reagents and Intermediates": E. Negishi, T. Takahashi, *Aldrichimica Acta 18* (1985) 31–47.
[405] For applications of the Suzuki coupling see [341e].
[406] "New Synthetic Reactions of Allyl Alkyl Carbonates, Allyl β-Keto Carboxylates, and Allyl Vinylic Carbonates Catalyzed by Palladium Complexes": J. Tsuji, I. Minami, *Acc. Chem. Res. 20* (1987) 140–145; "Cyclizations via Palladium-Catalyzed Allylic Alkylations": B. M. Trost, *Angew. Chem. 101* (1989) 1199–1219; *Angew. Chem. Int. Ed. Engl. 28* (1989) 1173–1192; "Palladium-Catalyzed Cycloisomerizations of Enynes and Related Reactions": B. M. Trost, *Acc. Chem. Res. 23* (1990) 34–42.
[407] See also the Pd-catalyzed 1,4-difunctionalization of dienes and the metallo-ene reaction: "Palladium in Some Selective Oxidation Reactions": J.-E. Bäckvall, *Acc. Chem. Res. 16* (1983) 335–342. "Metal-Mediated Additions to Conjugated Dienes": J.-E. Bäckvall, *Adv. Met.-Org. Chem. 1* (1989) 135–175; "Intramolecular, Stoichiometric (Li, Mg, Zn) and Catalytic (Ni, Pd, Pt) Metallo-Ene Reactions in Organic Synthesis": W. Oppolzer, *Angew. Chem. 101* (1989) 39–53; *Angew. Chem. Int. Ed. Engl. 28* (1989) 38–52.
[408] "Raney-Nickel: Nickel–Aluminium Alloy as a Reducing Agent": L. K. Keefer, G. Lunn, *Chem. Rev. 89* (1989) 459–502.
[409] Organocopper compounds were first investigated almost 70 years ago: M. R. Reich, *C. R. Hebd. Séances Acad. Sci. 177* (1923) 322; H. Gilman, J. M. Straley, *Recl. Trav. Chim. Pays-Bas 55* (1936) 821; M. S. Kharasch, P. O. Tawney, *J. Am. Chem. Soc. 63* (1941) 2308.
[410] Cuprates (Gilman reagents) have undergone developments that have dramatically increased their breadth of application; cf. the previously cited sources [293, 294, 388] and [389] (here the article by *Normant*), [390] (article by *Casey, Normant, Pearson*), [394–396], as well as: a) an outstanding general monograph: G. H. Posner: *An Introduction to Synthesis Using Organocopper-Reagents*, Wiley, New York 1980; see also: "Recent Developments in Organocopper Chemistry", Tetrahedron Symposia-in-Print Number 35: B. H. Lipshutz (Guest Editor), *Tetrahedron 45* (1989) 349–578; b) "Prescriptions and Ingredients for Controlled CC Bond Formation with Organometallic Reagents": M. Schlosser, *Angew. Chem. 86* (1974) 751–756; *Angew. Chem. Int. Ed. Engl. 13* (1974) 701–706; c) BF_3 activation: "Selective Synthesis by Use of Lewis Acids in the Presence of Organocopper and Related Reagents": Y. Yamamoto, *ibid. 98* (1986) 945–957 and *25* (1986) 947–959; "Organocopper–Lewis Acid Complex Reagents. The Past and Present": Y. Yamamoto, *Yuki Gosei Kagaku Kyokaishi (J. Synth. Org. Chem. Jpn.) 44* (1986) 829–845; B. H. Lipshutz, E. L. Ellsworth, T. J. Siahaan, *J. Am. Chem. Soc. 111* (1989) 1351; d) for the use of silylcuprates in the Michael addition of Si-groups see [293, 294]; e) "higher-order" cuprates: "The Evolution of Higher Order Cyanocuprate": B. H. Lipshutz, *Synlett 1990*, 119–128; f) cuprate reactions in the presence of chlorosilanes: C. Chuit, J. P. Foulon, J. F. Normant, *Tetrahedron 36* (1980) 2305; E. J. Corey, N. W. Boaz, *Tetrahedron Lett. 26* (1985) 6015, 6019; S. Matsuzawa, Y. Horiguchi, E. Nakamura, I. Kuwajima, *Tetrahedron 45* (1989) 349; g) enantioselective cuprate additions: E. J. Corey, R. Naef, F. J. Hannon, *J. Am. Chem. Soc. 108* (1986) 7114; R. K. Dieter, M. Tokles, *ibid. 109* (1987) 2040.
[411] Improvements and extensions with respect to the Reformatzky reaction: a) recent review: "Recent Advancements in the Reformatzky Reaction": A. Fürstner, *Synthesis 1989*, 571–590; b) regarding the reaction mechanism and structural aspects: M. J. S. Dewar, K. M. Merz, Jr., *J. Am. Chem. Soc. 109* (1987) 6553; J. Dekker, P. H. M. Budzelaar, J. Boersma, G. J. M. van der Kerk, *Organometallics 3* (1984) 1403; c) "homologous" Reformatzky reagents: Y. Tamaru, H. Tanigawa, T. Yamamoto, Z. Yoshida, *Angew. Chem. 101* (1989) 358; *Angew. Chem. Int. Ed. Engl. 28* (1989) 351; "Carbon–Carbon Bond Forming Reactions *via* Metal Homoenolates": E. Nakamura, *Yuki Gosei Kagaku Kyokaishi (J. Synth. Org. Chem. Jpn.) 47* (1989) 931–938.
[412] "Organotitanium Reagents in Organic Synthesis. A Simple Means to Adjust Reactivity and Selectivity of Carbanions": M. T. Reetz, *Top. Curr. Chem. 106* (1982) 1–54; M. T. Reetz: *Organotitanium Reagents in Organic Synthesis*, Springer, Berlin 1986; "Chelation or Non-Chelation Control in Addition Reactions of Chiral α- and β-Alkoxy Carbonyl Compounds": M. T. Reetz, *Angew. Chem. 96* (1984) 542–555; *Angew. Chem. Int. Ed. Engl. 23* (1984) 556–569.
[413] B. Weidmann, C. D. Maycock, D. Seebach, *Helv. Chim. Acta 64* (1981) 1552.
[414] T. Imamoto, Y. Sugiura, N. Takiyama, *Tetrahedron Lett. 25* (1984) 4233; K. Nagasawa, K. Ito, *Heterocycles 28* (1989) 703.
[415] "Lanthanides in Organic Synthesis": H. B. Kagan, J. L. Namy, *Tetrahedron 42* (1986) 6573–6614.
[416] Cf. also the application of chromium(II) derivatives (e.g., the Hiyama method for diastereoselective allylation and crotylation of aldehydes): "Organo-chromium Reagents for Highly Selective Carbon–Carbon Bond Formation": K. Takai, K. Utimoto, *Yuki Gosei Kagaku Kyokaishi (J. Synth. Org. Chem. Jpn.) 46* (1988) 66–77.
[417] B. Weidmann, L. Widler, A. G. Olivero, C. D. Maycock, D. Seebach, *Helv. Chim. Acta 64* (1981) 357.
[418] R. Imwinkelried, D. Seebach, *Org. Synth. 67* (1988) 180.

[419] A. G. Olivero, B. Weidmann, D. Seebach, *Helv. Chim. Acta 64* (1981) 2485.
[420] D. Seebach, A. K. Beck, S. Roggo, A. Wonnacott, *Chem. Ber. 118* (1985) 3673.
[421] M. Riediker, R. O. Duthaler, *Angew. Chem. 101* (1989) 488; *Angew. Chem. Int. Ed. Engl. 28* (1989) 494; R. O. Duthaler, P. Herold, W. Lottenbach, K. Oertle, M. Riediker, *ibid. 101* (1989) 490 and *28* (1989) 495; G. Bold, R. O. Duthaler, M. Riediker, *ibid. 101* (1989) 491 and *28* (1989) 497; M. Riediker, A. Hafner, U. Piantini, G. Rihs, A. Togni, *ibid. 101* (1989) 493 and *28* (1989) 499; K. Oertle, H. Beyeler, R. O. Duthaler, W. Lottenbach, M. Riediker, E. Steiner, *Helv. Chim. Acta 73* (1990) 353.
[422] G. Bold, R. Duthaler, P. Herold, W. Lottenbach, K. Oertle, M. Riediker, G. Rihs, A. Togni, Lectures at the *Herbstversammlung der Schweizerischen Chemischen Gesellschaft*, Bern, October 1989, Abstract Volume pp. 20, 21, 22.
[423] R. Imwinkelried, D. Seebach, *Helv. Chim. Acta 67* (1984) 1496.
[424] C. Betschart, D. Seebach, *Helv. Chim. Acta 70* (1987) 2215; C. Betschart, B. Schmidt, D. Seebach, *ibid. 71* (1988) 1999.
[425] J. H. Freudenberg, A. W. Konradi, S. F. Pedersen, *J. Am. Chem. Soc. 111* (1989) 8014.
[426] E. J. Roskamp, S. F. Pedersen, *J. Am. Chem. Soc. 109* (1987) 6551.
[427] H. G. Raubenheimer, D. Seebach, *Chimia 40* (1986) 12.
[428] E. J. Roskamp, S. F. Pedersen, *J. Am. Chem. Soc. 109* (1987) 3152.
[429] J. B. Hartung, Jr., S. F. Pedersen, *J. Am. Chem. Soc. 111* (1989) 5468.
[430] Y. Hayakawa, M. Uchiyama, H. Kato, R. Noyori, *Tetrahedron Lett. 26* (1985) 6505; Y. Hayakawa, H. Kato, M. Uchiyama, H. Kajino, R. Noyori, *J. Org. Chem. 51* (1986) 2400.
[431] Y. Hayakawa, H. Kato, T. Nobori, R. Noyori, J. Imai, *Nucleic Acids Res. Symp. Ser. 17* (1986) 97; Y. Mitsuhira, S. Tahara, K. Goto, Y. Hayakawa, R. Noyori, *ibid. 19* (1988) 25; Y. Hayakawa, S. Wakabayashi, R. Noyori, *ibid. 20* (1988) 75.
[432] Y. Hayakawa, S. Wakabayashi, H. Kato, R. Noyori, *J. Am. Chem. Soc. 112* (1990) 1691.
[433] "Organometallic methodologies for nucleic acid synthesis": R. Noyori, M. Uchiyama, H. Kato, S. Wakabayashi, Y. Hayakawa, *Pure Appl. Chem. 62* (1990) 613–622 (manuscript from the *OMCOS Meeting, Florence*, October 1989).
[434] I wish to thank Professor *Ryoji Noyori* most sincerely for providing me with manuscript copies prior to their publication [432,433], as well as for the chromatogram in Fig. 13 and permission to include these findings here.
[435] "Asymmetric catalysis in organic synthesis with industrial perspectives": H. B. Kagan, *Bull. Soc. Chim. Fr. 1988*, 846–853.
[436] We suggested [352] in 1980 use of the abbreviation "EPC synthesis" as a generic term for the preparation of enantiomerically pure compounds. While there might be disagreement over the definition of "purity" (which is dependent above all on the sensitivity of the analytical methods employed), the terminology is otherwise unambiguous. Expressions like "homochiral compounds" [437] or "isochiral compounds" [438] are unfortunate in several respects. Thus, "homochiral" has long been used in comparing the chirality of *two* similar compounds, or a pair of chiral molecules in the unit cell of a crystal, but it is now considered appropriate for describing a flask full of (+)-tartaric acid (10^{23} molecules per mole)! Expressions like "chiral synthesis" and "racemic synthesis" have also become common; while these may be permissible in English (which also tolerates combinations like "married name" and "fishing pond"), they certainly cannot be translated directly into German. The equally correct expression "chiral, not racemic" is more awkward than "enantiomerically pure". Finally, let me urge that the matter not be carried too far; in most cases all that is required is judicious use of *R* or *S*!
[437] *Homochiral:* "Double Asymmetric Synthesis and a New Strategy for Stereochemical Control in Organic Synthesis": S. Masamune, W. Choy, J. S. Petersen, L. R. Sita, *Angew. Chem. 97* (1985) 1–31; *Angew. Chem. Int. Ed. Engl. 24* (1985) 1–30.
[438] *Isochiral:* Under discussion with respect to the preparation of a new edition of the classic textbook of stereochemistry by *E. L. Eliel*.
[439] "The Handedness of the Universe": R. A. Hegstrom, D. K. Kondepudi, *Sci. Am. 262* (1990), No. 1, pp. 98–105; *Spektrum Wiss. 1990*, No. 3, pp. 56–67.
[440] A missionary in this field is *E. J. Ariens* [*Eur. J. Clin. Pharmacol. 26* (1984) 663], who has suggested the terms "eutomer" and "distomer" (the good and the bad isomers) to classify active and inactive enantiomers.
[441] "Enantioselective Synthesis of Non-racemic Chiral Molecules on an Industrial Scale": J. W. Scott, *Top. Stereochem. 19* (1989) 209–226.
[442] "Industrial Application of Asymmetric Synthesis" is the announced theme of the following conference: *2nd Int. IUPAC Symp. Org. Chem.: Technological Perspectives* (Baden-Baden, April 1991).
[443] "Enantiomerenreine Naturstoffe und Pharmaka aus billigen Vorläufern (Chiral Pool). Zur Frage der chiralen ökonomischen und ökologischen Totalsynthese": D. Seebach, H.-O. Kalinowski, *Nachr. Chem. Tech. Lab. 24* (1976) 415–418.
[444] "The Unambiguous Specification of the Steric Course of Asymmetric Syntheses": D. Seebach, V. Prelog, *Angew. Chem. 94* (1982) 696–702; *Angew. Chem. Int. Ed. Engl. 21* (1982) 654–660.
[445] "Basic Principles of the CIP-System and Proposals for a Revision": V. Prelog, G. Helmchen, *Angew. Chem. 94* (1982) 614–631; *Angew. Chem. Int. Ed. Engl. 21* (1982) 567–583.
[446] "Chirality Recognition in Synthesis" (Fine Chemicals Group, Society of Chemical Industry, London 1988). "Synthesis from Natural Homochiral Precursors" (Fine Chemicals Group, Society of Chemical Industry, London 1990). "Second International Symposium on Chiral Discrimination" (Rome 1991).
[447] "Asymmetric Synthesis–Meeting the Challenge" (series of articles in the March issue of *Chemistry in Britain, 1989*).
[448] As if there were not already enough periodicals–and it were not already possible to present every good piece of work on the subject in one of the standard national or international chemical journals!
[449] Twenty years ago everything known about stereoselective reactions could be presented together in the single book by J. D. Morrison and H. S. Mosher: *Asymmetric Organic Reactions*, Prentice Hall 1971 (*ca.* 450 pp.). The new Morrison (*Asymmetric Synthesis*, Academic Press, New York, 1983–1985) consists of five volumes (*ca.* 1800 pp.), and it is already obsolete!
[450] "α-Amino Acid Synthesis", Tetrahedron Symposia-in-Print Number 33: R. Fitzi, D. Seebach, *Tetrahedron 44* (1988) 5277.
[451] D. Seebach, E. Dziadulewicz, L. Behrendt, S. Cantoreggi, R. Fitzi, *Liebigs Ann. Chem. 1989*, 1215.
[452] C. Gennari, A. Bernardi, L. Colombo, C. Scolastico, *J. Am. Chem. Soc. 107* (1985) 5812.
[453] "Chiral auxiliaries": S. G Davies, *Chem. Br. 25* (1989) 268–272; "Synthesis and stereoselective reactions of α,β-unsaturated acyl ligands bound to the chiral auxiliary $[(\eta^5\text{-}C_5H_5)Fe(CO)(PPh_3)]$: A review": S. G. Davies, I. M. Dordor-Hedgecock, R. J. C. Easton, S. C. Preston, K. H. Sutton, J. C. Walker, *Bull. Soc. Chim. Fr. 1987*, 608–630.
[454] "Formamidines as Precursors to α-Amino Carbanions and Their Application to Asymmetric C–C Bond-Forming Reactions": A. I. Meyers, *Aldrichimica Acta 18* (1985) 59–68.
[455] R. Shirai, M. Tanaka, K. Koga, *J. Am. Chem. Soc. 108* (1986) 543; "Asymmetric Synthesis Using Chiral Lithium Amide Bases": N. S. Simpkins, *Chem. Ind.* (London) *1988*, 387–389.
[456] E. J. Corey, P. D. Jardine, S. Virgil, P.-W. Yuen, R. D. Connell, *J. Am. Chem. Soc. 111* (1989) 9243.
[457] "Asymmetric protonations": L. Duhamel, P. Duhamel, J.-C. Launay, J.-C. Plaquevent, *Bull. Soc. Chim. Fr. II 1984*, 421–430.
[458] "Asymmetric Synthesis of Carbon–Carbon Bonds Using Sulfinyl Cycloalkenones, Alkenolides and Pyrones": G. H. Posner, *Acc. Chem. Res. 20* (1987) 72–78; see also *G. H. Posner* in [330d].
[459] "Recent Results in the Field of Asymmetric Synthesis Using Chiral Sulfoxides": G. Solladié, *Pure Appl. Chem. 60* (1988) 1699–1704; "Chirale Sulfoxide zur Synthese enantiomerenreiner Verbindungen" (Synthese im Blickpunkt): K. Krohn, *Nachr. Chem. Tech. Lab. 35* (1987) 22–25.
[460] "Alkylation of Chiral Hydrazones": D. Enders in J. D. Morrison (Ed.): *Asymmetric Synthesis, Vol. 3*, Academic Press, Orlando, FL 1984, pp. 275–339.
[461] S. Ikegami, H. Uchiyama, T. Hayama, T. Katsuki, M. Yamaguchi, *Tetrahedron 44* (1988) 5333.
[462] "Asymmetric Diels–Alder Reactions with Chiral Enolates as Dienophiles": G. Helmchen, R. Karge, J. Weetman, *Mod. Synth. Methods 4* (1986) 261–306.
[463] "Asymmetric Synthesis *via* Chiral Oxazolines": K. A. Lutomski, A. I. Meyers in J. D. Morrison (Ed.): *Asymmetric Synthesis, Vol. 3*, Academic Press, Orlando, FL 1984, pp. 213–274; A. I. Meyers: *Heterocycles in Organic Synthesis*, Wiley, New York 1974.
[464] "Stereoselective Aldol Condensations": D. A. Evans, J. V. Nelson, T. R. Taber, *Top. Stereochem. 13* (1982) 1–115; other transformations of Evans enolates: D. A. Evans, M. M. Morrissey, R. L. Dorow, *J. Am. Chem. Soc. 107* (1985) 4346; D. A. Evans, E. B. Sjogren, A. E. Weber, R. E. Conn, *Tetrahedron Lett. 28* (1987) 39; D. A. Evans, J. A. Ellman, R. L. Dorow, *ibid. 28* (1987) 1123; D. A. Evans, K. T. Chapman, J. Bisaha, *J. Am. Chem. Soc. 110* (1988) 1238; D. A. Evans, T. C. Britton, R. L. Dorow, J. F. Dellaria, Jr., *Tetrahedron 44* (1988) 5525.
[465] "New Perspectives in Asymmetric Induction": J. K. Whitesell, *Acc. Chem. Res. 18* (1985) 280–284.
[466] B. de Lange, F. van Bolhuis, B. L. Feringa, *Tetrahedron 45* (1989) 6799; J. F. G. A. Jansen, B. L. Feringa, *Tetrahedron Lett. 30* (1989) 5481.
[467] a) E. J. Corey, R. Imwinkelried, S. Pikul, Y. B. Xiang, *J. Am. Chem. Soc. 111* (1989) 5493; b) E. J. Corey, C.-M. Yu, S. S. Kim, *ibid. 111* (1989) 5495; c) E. J. Corey, C.-M. Yu, D.-H. Lee, *ibid. 112* (1990) 878.
[468] W. R. Roush, R. L. Halterman, *J. Am. Chem. Soc. 108* (1986) 294; W. R. Roush, L. Banfi, J. C. Park, L. K. Hoong, *Tetrahedron Lett. 30* (1989) 6457 and earlier cited work by the same research group.
[469] "Boronic Esters in Stereodirected Synthesis": D. S. Matteson, *Tetrahedron 45* (1989) 1859–1885; "Asymmetric Synthesis with Boronic Esters": D. S. Matteson, *Acc. Chem. Res. 21* (1988) 294–300; "The Use of Chiral Organoboranes in Organic Synthesis": D. S. Matteson, *Synthesis 1986*, 973–985.
[470] "Development of a Simple General Procedure for Synthesis of Pure Enantiomers *via* Chiral Organoboranes": H. C. Brown, B. Singaram,

Acc. Chem. Res. 21 (1988) 287–293; "Asymmetric Synthesis Made Easy": H. C. Brown, *Chemtracts: Org. Chem.1* (1988) 77–88; A. Pelter, K. Smith, H. C. Brown: *Borane Reagents*, Academic Press, London 1988.

[471] U. Schöllkopf, T. Tiller, J. Bardenhagen, *Tetrahedron 44* (1988) 5293 and earlier cited work related to the bislactim-ether method.

[472] K. Fuji, M. Node, S. Terada, M. Murata, H. Nagasawa, T. Taga, K. Machida, *J. Am. Chem. Soc. 107* (1985) 6404.

[473] "Camphor Derivatives as Chiral Auxiliaries in Asymmetric Synthesis": W. Oppolzer, *Tetrahedron 43* (1987) 1969–2004; "Metal-directed Stereoselective Functionalizations of Alkenes in Organic Synthesis": W. Oppolzer, *Pure Appl. Chem. 60* (1988) 39–48; W. Oppolzer, J. Blagg, I. Rodriguez, E. Walther, *J. Am. Chem. Soc. 112* (1990) 2767.

[474] J. Zimmermann, D. Seebach, T.-K. Ha, *Helv. Chim. Acta 71* (1988) 1143.

[475] Y. Noda, D. Seebach, *Helv. Chim. Acta 70* (1987) 2137.

[476] D. Seebach, U. Mißlitz, P. Uhlmann, *Angew. Chem. 101* (1989) 484; *Angew. Chem. Int. Ed. Engl. 28* (1989) 472.

[477] D. Seebach, R. Naef, *Helv. Chim. Acta 64* (1981) 2704.

[478] "Synthesis of Chiral Non-Racemic Compounds", Tetrahedron Symposia-in-Print Number 15: D. Seebach, R. Naef, G. Calderari, *Tetrahedron 40* (1984) 1313.

[479] "Methodology for the construction of quaternary carbon centers": S. F. Martin, *Tetrahedron 36* (1980) 419–460.

[480] Numerous pheromones have been prepared by *Mori* and coworkers starting with 3-hydroxybutyric acid, as well as with 3-hydroxyvaleric acid, which is also accessible from biopolymers: "Chiral Synthesis: Examples in the Pheromone Field": K. Mori, *Spec. Publ. R. Soc. Chem. 53* (1985) 293–306; "Chiral synthesis of bioactive natural products employing the building blocks of microbial origin": K. Mori, *Stud. Nat. Prod. Chem. 1* (1988) 677–712; "Recent Progress in Pheromone Chemistry": K. Mori, S. Kuwahara, *Yuki Gosei Kagaku Kyokaishi (J. Synth. Org. Chem. Jpn.) 46* (1988) 467–477; "Synthesis of optically active pheromones": K. Mori, *Tetrahedron 45* (1989) 3233–3298.

[481] There continues to be a role for such old standbys as derivatives of glycerol and glyceraldehyde, which remain convenient and versatile sources of a *single* center of chirality: "Der 2,3-Isopropyliden-glycerinaldehyd—eine Modeverbindung" (Synthese im Blickpunkt): *Nachr. Chem. Tech. Lab. 32* (1984) 146–149; "Optisch aktive Glycerinderivate" (Synthese im Blickpunkt): H.-J. Altenbach, *ibid. 36* (1988) 33–38.

[482] Finally, sugars are still "in" as sources for the "pool" of chiral synthetic building blocks: "Chirale Bausteine aus Kohlenhydraten" (Synthese im Blickpunkt): K. Krohn, *Nachr. Chem. Tech. Lab. 35* (1987) 1155–1160; "New Chiral Synthons Derived from D-Glucose": H. Hashimoto, N. Kawaguchi, *Yuki Gosei Kagaku Kyokaishi (J. Synth. Org. Chem. Jpn.) 45* (1987) 408–420; "Synthesis of Versatile Chiral Building Blocks Starting from D-Mannitol": S. Takano, K. Ogasawara, *ibid. 45* (1987) 1157–1170.

[483] "The Microbiological Production of Industrial Chemicals": D. E. Eveleigh, *Sci. Am. 245* (1981) No. 3, p. 120; *Spektrum Wiss. 1981*, No. 11, p. 88.

[484] T. H. Maugh II, *Science (Washington, D. C.) 221* (1983) 351.

[485] Even a general-circulation newspaper like DIE ZEIT (R. Schwerthöffer, *Die Zeit* No. 10, 2 March 1990, p. 96) recently devoted a half page in its science section to the subject *The Art of Catalysis* ("Die Chemie nutzt natürliche Vorbilder"), mentioning among other things *Corey*'s "Chemzymes".

[486] Previously cited books and reviews covering biological-chemical synthetic methods [79, 114, 125, 126, 241, 354]. A few additional, more recent articles: a) "Enzymes in Organic Syntheses": J. B. Jones in *F. E. C. S. Int. Conf. Chem. Biotechnol. Biol. Act. Nat. Prod. (3.)*, VCH Verlagsgesellschaft, Weinheim 1987, pp. 18–39; b) "Microbial and Enzymatic Processes for the Production of Biologically and Chemically Useful Compounds": H. Yamada, S. Shimizu, *Angew. Chem. 100* (1988) 640–661; *Angew. Chem. Int. Ed. Engl. 27* (1988) 622–642; c) "General Aspects and Optimization of Enantioselective Biocatalysis in Organic Solvents: The Use of Lipases": C.-S. Chen, C. J. Sih, *ibid. 101* (1989) 711–724 and *28* (1989) 695–707; d) "Resolution of Enantiomers *via* Biocatalysis": C. J. Sih, S.-H. Wu, *Top. Stereochem. 19* (1989) 63–126; e) "Baker's Yeast as a Reagent in Organic Synthesis": S. Servi, *Synthesis 1990*, 1–25.

[487] The following biological-chemical procedures have so far been incorporated into *Organic Syntheses*: a) yeast reduction of hydroxyacetone to (*S*)-propan-1,2-diol [P. A. Levene, A. Walti, *Coll. Vol. 2* (1943) 545]; b) emulsin-catalyzed dimerization of glucose to gentobiose [B. Helferich, J. F. Leete, *Coll. Vol. 3* (1955) 428]; c) yeast reduction of acetoacetic ester to ethyl (*S*)-3-hydroxybutyrate [D. Seebach, M. A. Sutter, R. H. Weber, M. F. Züger, *Vol. 63* (1985) 1]; d) the lactone from (1*S*,2*R*)-2-hydroxymethylcyclohexane carboxylic acid using horse liver alcohol dehydrogenase/NAD/FMN [J. B. Jones, I. J. Jakovac, *Vol. 63* (1985) 10]; e) yeast reduction of 2,2-dimethylcyclohexan-1,2-dione to (*S*)-3-hydroxy-2,2-dimethylcyclohexanone [K. Mori, H. Mori, *Vol. 68* (1989) 56]; f) (1*S*,2*S*,3*R*)-3-hydroxy-2-nitrocyclohexyl acetate by hydrolysis of the corresponding *meso*-nitrodiacetate with pig liver esterase [M. Eberle, M. Missbach, D. Seebach, *Vol. 69* (1990), 19].

[488] Numerous procedures for carrying out biological-chemical reactions can be found in the articles by *Fischli* as well as *Crout* and *Christen* (*Vol. 2* and *5* in the series *Modern Synthetic Methods*). A comparison reveals the progress in this field between 1980 and 1989: a) "Chiral Building Blocks in Enantiomer Synthesis Using Enzymatic Transformations": A. Fischli, *Mod. Synth. Methods 2* (1980) 269–350; b) "Biotransformations in Organic Synthesis": D. H. G. Crout, M. Christen, *ibid. 5* (1989) 1–114.

[489] A truly outstanding new book treating all the biological-chemical methods of preparative interest: H. G. Davies, R. H. Green, D. R. Kelly, S. M. Roberts: *Biotransformations in Preparative Organic Chemistry (The Use of Isolated Enzymes and Whole Cell Systems in Synthesis)* from the series *Best Synthetic Methods* [A. R. Katritzky, O. Meth-Cohn, C. W. Rees (Eds.)], Academic Press, London 1989.

[490] Previously cited books and reviews on the topic of organometallic catalysis [263b, 388, 390, 394, 400, 402, 405–407, 433, 435], above all the articles by *J. K. Stille, L. S. Hegedus* and *R. Scheffold* in [389] and citations in Scheme 17. A few additional more recent articles: a) "Enantioselective Synthesis with Optically Active Transition-Metal Catalysts": H. Brunner, *Synthesis 1988*, 645–654; b) "Enantioselective Synthesis of Organic Compounds with Optically Active Transition Metal Catalysts in Substoichiometric Quantities": H. Brunner, *Top. Stereochem. 18* (1988) 129–247; c) "Asymmetric homogeneous catalysis": J. M. Brown, *Chem. Br. 25* (1989) 276–280; d) "Recent Advances in Catalytic Asymmetric Reactions Promoted by Transition Metal Complexes": I. Ojima, N. Clos, C. Bastos, *Tetrahedron 45* (1989) 6901–6939; e) A particularly useful review because of the inclusion of representative procedures and numerous citations: "Enantioselective Catalysis with Chiral Cobalt and Copper Complexes": A. Pfaltz, *Mod. Synth. Methods 5* (1989) 199–248.

[491] D. W. Blackburn (Ed.): *Catalysis of Organic Reactions*, Marcel Dekker, New York 1990.

[492] See also the *Journal of Molecular Catalysis*, published since 1975, and a recent review article: "Catalysis from the perspective of an organic chemist: common problems and possible solutions": C. A. Maryanoff, J. E. Mills, R. C. Stanzione, J. T. Hortenstine, Jr., *Chem. Ind. (Dekker) 33* (1988) 359–379.

[493] In other words, biotechnology really *is* just an "old hat with new feathers" (H. Metz in *Merck-Spektrum*, Switzerland, No. 2, 1987).

[494] For example, shikonin from the firm Mitsui Petrochemical Industries, Ltd., Iwakuni, Yamaguchi-ken 740 (Japan).

[495] Recent brief review: "Cultured Plant Cells—the Factory Within": F. DiCosmo, P. J. Facchini, M. M. Kraml, *Chem. Br. 25* (1989) 1001–1004.

[496] See also the preparation of polyphenylene [231] and enantiomerically pure diols of this type from substituted arenes by ICI in England. Recent example: D. W. Ribbons, A. E. G. Cass, J. T. Rossiter, S. J. C. Taylor, M. P. Woodland, D. A. Widdowson, S. R. Williams, P. B. Baker, R. E. Martin, *J. Fluorine Chem. 37* (1987) 299; examples in Scheme 28.

[497] W. Charney, H. L. Herzog: *Microbial Transformations of Steroids*, Academic Press, New York 1967; see also non-steroidal cyclic compounds: K. Kieslich: *Microbial transformations on non-steroid cyclic compounds*, Thieme, Stuttgart 1976.

[498] Only papers of interest to the synthetic chemist have been considered [488b].

[499] B. Wipf, E. Kupfer, R. Bertazzi, H. G. W. Leuenberger, *Helv. Chim. Acta 66* (1983) 485.

[500] The yeast reduction of acetoacetic ester in a "chemostat": M. Rohner, T. Münch, B. Sonnleitner, A. Fiechter, *Biocatalysis 3* (1990) 37.

[501] "Bioreaktoren—Einführung in die Technik": W. F. Hess, M. B. Gatzemeier, *Chem. Ing. Tech. 60* (1988) A554–A559.

[502] One need only consider the many possible conditions for an aldol addition (see [331] and Scheme 26), or for reduction with a complex hydride $M^1(M^2H_{4-n}X_n)_b$, in which M^1 = Li, Na, K, Zn, Bu_4N, M^2 = B, Al, X = RO, RCOO, R_2N with $n = 1-3$ (there are entire books on the subject!).

[503] B. Zhou, A. S. Gopalan, F. VanMiddelsworth, W.-R. Shieh, C. J. Sih, *J. Am. Chem. Soc. 105* (1983) 5925; W.-R. Shieh, A. S. Gopalan, C. J. Sih, *ibid. 107* (1985) 2993.

[504] a) J. Ehrler, F. Giovannini, B. Lamatsch, D. Seebach, *Chimia 40* (1986) 172; b) T. Haag, T. Arslan, D. Seebach, *ibid. 43* (1989) 351, and references cited therein.

[505] For extensive, competent discussions of the subject containing numerous literature citations see [486b,e; 488b].

[506] a) D. Seebach, M. F. Züger, F. Giovannini, B. Sonnleitner, A. Fiechter, *Angew. Chem. 96* (1984) 155; *Angew. Chem. Int. Ed. Engl. 23* (1984) 151; b) D. Seebach, F. Giovannini, B. Lamatsch, *Helv. Chim. Acta 68* (1985) 958; c) C. H. Wong, D. G. Drueckhammer, H. M. Sweers, *J. Am. Chem. Soc. 107* (1985) 4028; d) "Synthetic Applications of Alcohol-Dehydrogenase from *Thermoanaerobium brockii*": E. Keinan, K. K. Seth, R. Lamed, *Ann. N. Y. Acad. Sci. 501* (1987) 130–149.

[507] Cubes of concentrated cell masses of the anaerobic microorganism *Thermoanaerobium brockii* can be kept wrapped in aluminum foil in a freezer—like baker's yeast in a refrigerator—for long periods of time without loss of reductase activity [506b].

[508] Proteinogenic amino acids are produced in Japan either by fermentative techniques or by the enantioselective cleavage of amino acid derivatives with immobilized microorganisms or peptidase enzymes: "Production of

Optically Active Amino Acids Using Immobilized Biocatalysts": T. Tosa, *Int. Chem. Congr. Pacific Basin Societies,* 17–22 Dec. 1989, Honolulu, HI, Abstr. ORGN 615.

[509] Degussa utilizes membrane techniques [233], cf. also [511]. Nevertheless, much of the Degussa amino acid output is derived from protein hydrolyzates (animal skin, hair, horn, hoof, or feathers, or protein-containing material from plants) [233].

[510] α-Branched amino acids are manufactured [for example, by DMS Research, Bio-organic Chemistry Section, Geleen (Netherlands)] through the enantioselective cleavage of amino acids with *Mycobacterium neoaurum*: W. H. Kruizinga, J. Bolster, R. M. Kellogg, J. Kamphuis, W. H. Boesten, E. M. Meijer, H. E. Schoemaker, *J. Org. Chem. 53* (1988) 1826; J. Kamphuis, H. F. M. Hermes, J. A. M. van Balken, H. E. Schoemaker, W. H. J. Boesten, E. M. Meijer in G. Lubec, G. A. Rosenthal (Eds.): *Amino Acids,* Escom, Leiden 1990, pp. 119–125.

[511] Application of membrane techniques (cf. [509]) on a laboratory scale ("*M*embrane-enclosed *e*nzymatic *c*atalysis = MEEC): M. D. Bednarski, H. K. Chenault, E. S. Simon, G. M. Whitesides, *J. Am. Chem. Soc. 109* (1987) 1283.

[512] C. Laane, J. Tramper, M. D. Lilly (Eds.): *Biocatalysis in Organic Media,* Elsevier, Amsterdam 1987.

[513] An entirely different case in which the change to an organic solvent proved crucial is the enantioselective cyanohydrin reaction catalyzed by mandelonitrile benzaldehyde lyase (MBL) and discovered by *Pfeil* [W. Becker, H. Freund, E. Pfeil, *Angew. Chem. 77* (1965) 1139; *Angew. Chem. Int. Ed. Engl. 4* (1965) 1079], a process that was long thought impractical due to its reversibility. Three years ago it was demonstrated that the problem can be circumvented with immobilized enzyme in ethyl acetate, permitting the large-scale preparation of cyanohydrins in > 98% *ee* and high yield: F. Effenberger, T. Ziegler, S. Förster, *ibid. 99* (1987) 491 and *26* (1987) 458; J. Brussee, E. C. Roos, A. Van Der Gen, *Tetrahedron Lett. 29* (1988) 4485; see Scheme 28, B.

[514] J. J. De Frank, D. W. Ribbons, *Biochem. Biophys. Res. Commun. 70* (1976) 1129; *J. Bacteriology 129* (1977) 1356; S. J. C. Taylor, D. W. Ribbons, A. M. Z. Slawin, D. A. Widdowson, D. J. Williams, *Tetrahedron Lett. 28* (1987) 6391; T. Hudlicky, H. Luna, G. Barbieri, L. D. Kwart, *J. Am. Chem. Soc. 110* (1988) 4735.

[515] T. Kitazume, N. Ishikawa, *Chem. Lett. 1984,* 1815.

[516] "Baker's Yeast Mediated Preparation of Carbohydrate-like Chiral Synthons": C. Fuganti in M. P. Scheider (Ed.): *Enzymes as Catalysts in Organic Synthesis,* D. Reidel, Dordrecht 1986, pp. 3–17.

[517] Another case I would prefer to regard as a "youthful sin" (cf. Scheme 24b) is my suggestion [352]–taken up by many others as well–that this process be designated the "*meso* trick". Such expressions really should be confined to the–important!–realm of laboratory jargon.

[518] I now deliberately refrain from using the terms *prochiral* (let alone "pro-prochiral") and *prostereogenic.* They have contributed too much to a state of confusion (e.g., "prochiral hydrogen", "prochiral ketones"), and they are unnecessary. See also the remarks in the caption to Scheme 24B, the comments in [353], and CIP nomenclature [444, 445]. The thoughts expressed on the subject by *Mislow* ["Stereoisomerism and Local Chirality": K. Mislow, J. Siegel, *J. Am. Chem. Soc. 106* (1984) 3319] derive more from fundamental and theoretical considerations than from practical concerns.

[519] G. Guanti, L. Banfi, E. Narisano, R. Riva, S. Thea, *Tetrahedron Lett. 27* (1986) 4639.

[520] H. B. Goodbrand, J. B. Jones, *J. Chem. Soc. Chem. Commun. 1977,* 469; I. J. Jakovac, H. B. Goodbrand, K. P. Lok, J. B. Jones, *J. Am. Chem. Soc. 104* (1982) 4659.

[521] H.-J. Gais, K. L. Lukas, W. A. Ball, S. Braun, H. J. Lindner, *Liebigs Ann. Chem. 1986,* 687.

[522] G. Sabbioni, J. B. Jones, *J. Org. Chem. 52* (1987) 4565.

[523] D. R. Deardorff, A. J. Matthews, D. S. McMeekin, C. L. Craney, *Tetrahedron Lett. 27* (1986) 1255.

[524] A. J. Pearson, H. S. Bansal, Y.-S. Lai, *J. Chem. Soc. Chem. Commun. 1987,* 519.

[525] D. Breitgoff, K. Laumen, M. P. Schneider, *J. Chem. Soc. Chem. Commun. 1986,* 1523.

[526] Y.-F. Wang, C.-H. Wong, *J. Org. Chem. 53* (1988) 3127.

[527] R. Roy, A. W. Rey, *Tetrahedron Lett. 28* (1987) 4935; cf. also the corresponding 3-aminoglutaric acid derivative: M. Ohno, S. Kobayashi, T. Imori, Y.-F. Wang, T. Izawa, *J. Am. Chem. Soc. 103* (1981) 2405 and [126a].

[528] G. Guanti, L. Banfi, E. Narisano, *Tetrahedron Lett. 30* (1989) 2697.

[529] J. Ehrler, D. Seebach, *Liebigs Ann. Chem. 1990,* 379.

[530] The title of a contribution in the series *Synthese im Blickpunkt*: H.-U. Reißig, *Nachr. Chem. Tech. Lab. 34* (1986) 782–84.

[531] R. W. Hoffmann, W. Ladner, K. Steinbach, W. Massa, R. Schmidt, G. Snatzke, *Chem. Ber. 114* (1981) 2786.

[532] H. Akita, H. Koshiji, A. Furuichi, K. Horikoshi, T. Oishi, *Tetrahedron Lett. 24* (1983) 2009.

[533] B. S. Deol, D. D. Ridley, G. W. Simpson, *Aust. J. Chem. 29* (1976) 2459.

[534] B. Herradon, D. Seebach, *Helv. Chim. Acta 72* (1989) 690.

[535] D. Seebach, S. Roggo, T. Maetzke, H. Braunschweiger, J. Cercus, M. Krieger, *Helv. Chim. Acta 70* (1987) 1605.

[536] ... or might one here employ the adjective *promiscuous*? Cf. the classical picture of the "key and keyhole".

[537] a) Discovery: T. Katsuki, K. B. Sharpless, *J. Am. Chem. Soc. 102* (1980) 5974; b) kinetic separation of enantiomers: V. S. Martin, S. S. Woodard, T. Katsuki, Y. Yamada, M. Ikeda, K. B. Sharpless, *ibid. 103* (1981) 6237; c) overviews: "Synthetic Aspects and Applications of Asymmetric Epoxidation": B. E. Rossiter in J. D. Morrison (Ed.): *Asymmetric Synthesis, Vol. 5,* Academic Press, Orlando, FL 1985, pp. 194–246; "Asymmetric Epoxidation of Allylic Alcohols: The Sharpless Epoxidation": A. Pfenninger, *Synthesis 1986,* 89–116; "Die Sharpless-Epoxidierung" (Synthese im Blickpunkt): D. Schinzer, *Nachr. Chem. Tech. Lab. 37* (1989) 1294–1298; d) catalytic variant: R. M. Hanson, K. B. Sharpless, *J. Org. Chem. 51* (1986) 1922; e) cyclic sulfonate esters of 1,2-diols (available from epoxides): Y. Gao, K. B. Sharpless, *J. Am. Chem. Soc. 110* (1988) 7538; f) most recent suggestion regarding the mechanism of the Sharpless epoxidation: "On the Origin of Enantioselectivity in the Katsuki–Sharpless Epoxidation Procedure": E. J. Corey, *J. Org. Chem. 55* (1990) 1693.

[538] This has been designated as "reagent control" [437]–in contrast to "substrate control". In German it would have to be expressed as "durch das Reagens gesteuert". I well remember the sermons on a similar theme by my thesis advisor *Rudolf Criegee,* who was at that time editor of *Chemische Berichte*: "es muß heißen kinetisch oder thermodynamisch *gesteuerte,* nicht kontrollierte Reaktion; Kontrolle hat im Deutschen eine vom Englischen 'control' verschiedene Bedeutung!" From the fact that the term "stereocontrol" is about to replace "stereoselectivity", we must conclude that now everything is "under control".

[539] "Asymmetric Synthesis using Organometallic Catalysts": H. B. Kagan in [388], *Vol. 8,* chap. 53, pp. 463–498, and the original literature cited therein.

[540] "Asymmetric Catalytic Isomerization of Functionalized Olefins": S. Otsuka, K. Tani in J. D. Morrison (Ed.): *Asymmetric Synthesis, Vol. 5,* Academic Press, Orlando, FL 1985, pp. 171–191, and the original literature cited therein.

[541] "Directed Homogeneous Hydrogenation": J. M. Brown, *Angew. Chem. 99* (1987) 169–182; *Angew. Chem. Int. Ed. Engl. 26* (1987) 190–203; see also [490c].

[542] "Synthetic Applications of Enantioselective Organotransition-Metal-Mediated Reactions": S. L. Blystone, *Chem. Rev. 89* (1989) 1663–1679.

[543] a) PTC catalyst is an ammonium ion derived from cinchonine: M. J. O'Donnell, W. D. Bennett, S. Wu, *J. Am. Chem. Soc. 111* (1989) 2353; cf. also the enantioselective allylation of an indanone carried out by Merck Sharp & Dohme: D. L. Hughes, U.-H. Dolling, K. M. Ryan, E. F. Schoenewaldt, E. J. J. Grabowski, *J. Org. Chem. 52* (1987) 4745; b) H. Wynberg, E. G. J. Staring, *J. Am. Chem. Soc. 104* (1982) 166; *J. Org. Chem. 50* (1985) 1977; P. E. F. Ketelaar, E. G. J. Staring, H. Wynberg, *Tetrahedron Lett. 26* (1985) 4665.

[544] E. N. Jacobsen, I. Markó, W. S. Mungall, G. Schröder, K. B. Sharpless, *J. Am. Chem. Soc. 110* (1988) 1968.

[545] Y. Ito, M. Sawamura, T. Hayashi, *J. Am. Chem. Soc. 108* (1986) 6405; Y. Ito, M. Sawamura, M. Kobayashi, T. Hayashi, *Tetrahedron Lett. 29* (1988) 6321.

[546] K. Narasaka, N. Iwasawa, M. Inoue, T. Yamada, M. Nakashima, J. Sugimori, *J. Am. Chem. Soc. 111* (1989) 5340.

[547] a) The most recent essay about stereoselective Diels–Alder reactions contains sections on the following topics: chiral dienophiles and heterodienophiles, chiral dienes, chiral catalysts, and asymmetric intramolecular Diels–Alder reactions: "Asymmetric Diels–Alder Reactions": M. J. Taschner in T. Hudlicky (Ed.): *Organic Synthesis–Theory and Applications, A Research Annual, Vol. 1,* JAI Press, Greenwich 1989, pp. 1–101; b) "Asymmetrische Induktion bei Diels–Alder-Reaktionen" (Synthese im Blickpunkt): K. Krohn, *Nachr. Chem. Tech. Lab. 35* (1987) 836–841; see also the article by *Helmchen* et al. [462]; c) recent example: K. Furuta, S. Shimizu, Y. Miwa, H. Yamamoto, *J. Org. Chem. 54* (1989) 1481.

[548] K. Mikami, M. Terada, T. Nakai, *J. Am. Chem. Soc. 111* (1989) 1940.

[549] One should also note that it has become common to speak of Lewis acid-catalyzed reactions even when equimolar amounts or even large excesses of $SnCl_4$, TiX_4, or BF_3–ether are added, in which case the Lewis acid could be regarded as part of the solvent!

[550] "Asymmetric Catalytic Hydrogenation: Mechanism and Origin of Enantioselection": J. Halpern in J. D. Morrison (Ed.): *Asymmetric Synthesis, Vol. 5,* Academic Press, Orlando, FL 1985, pp. 41–69.

[551] See, for example, the semicorrin ligand proposed for transition-metal-catalyzed reactions by *A. Pfaltz* [490e], as well as B and C in Scheme 32.

[552] So far, the addition of alkylzinc compounds with high enantioselectivity has been successful only with aromatic aldehydes; a) first examples with very high selectivity: M. Kitamura, S. Suga, K. Kawai, R. Noyori, *J. Am. Chem. Soc. 108* (1986) 6071; b) application of pyrrolidine ligands: E. J. Corey, F. J. Hannon, *Tetrahedron Lett. 28* (1987) 5233, 5237; E. J. Corey, P.-W. Yuen, F. J. Hannon, D. A. Wierda, *J. Org. Chem. 55* (1990) 784; c) highly effective (down to 10^{-4} equiv.) catalysts for dialkylzinc additions to benzaldehyde are prepared from tetraisopropyltitanate and the ditri-

flate of (*R,R*)-*trans*-1,2-cyclohexanediamine: M. Yoshioka, T. Kawakita, M. Ohno, *Tetrahedron Lett. 30* (1989) 1657.

[553] Y. Yamamoto, J. Yamada, *J. Am. Chem. Soc. 109* (1987) 4395; J. Yamada, Y. Yamamoto, *J. Chem. Soc. Chem. Commun. 1987*, 1302.

[554] A review article summarizing the results obtained through 1986: "Catalytic Asymmetric Reduction Using Optically Active Amino Alcohol–Borane Complex": S. Itsuno, *Yuki Gosei Kagaku Kyokaishi (J. Synth. Org. Chem. Jpn.) 45* (1987) 101–111.

[555] With few exceptions, lithium also does not exceed the limit of four tetrahedrally oriented ligands; see [172] and references cited therein. Higher coordination numbers with this element appear to result largely from ionic interactions.

[556] Mean lengths for the bonds [Å] between N, C, and O and a number of the metals that are important in synthetic applications.

Li-N	2.11(8)	Li-C	2.214	Li-O	2.0(1)
B-N	1.404	B-C	1.597	B-O	1.367
C-N	1.469	C-C	1.530	C-O	1.426
Mg-N	2.21(7)	Mg-C	2.15	Mg-O	2.11(6)
Al-N	1.94(5)	Al-C	1.97(3)	Al-O	2.04(9)
Ti-N	2.296	Ti-C	see below	Ti-O	2.205
Zn-N	2.159	Zn-C	1.964	Zn-O	2.093
Sn-N	2.24(6)	Sn-C	2.12(2)	Sn-O	2.7(1)

Commentary: The average bond lengths for pure B/C/N/O-compounds are taken from [102a]. Average bond lengths for Ti and Zn compounds are derived from [102b] and apply to compounds containing a metal bonded to a methyl group, or complexes with aliphatic amines or aliphatic ethers. In the case of the Ti-CH_3 group only two widely divergent values have been reported (1.969 and 2.206 Å). The rest of the data resulted from a search in the CSD [189] for comparable bonds (only trimethyl compounds in the case of Al-C and Sn-C). If more than twenty values were found, the average has been supplemented (in parentheses) with the standard deviation applicable to the last reported digit. Since the reported values were obtained on the basis of differing criteria they should be regarded only as points of reference.

[557] The most selective aldol additions with boron enolates [331,437,464]. See also the chiral 2,5-dimethylborolanes, which are of little practical utility but are nonetheless "reliable" in their reactivity and selectivity: R. P. Short, S. Masamune, *J. Am. Chem. Soc. 111* (1989) 1892; "Stereochemical Control of Organic Reactions with Chiral Organoboron Reagents": S. Masamune in W. Bartmann, K. B. Sharpless (Eds.): *Stereochemistry of Organic and Bioorganic Transformations, Workshop Conferences Hoechst, Vol. 17*, VCH Verlagsgesellschaft, Weinheim 1987, pp. 49–72.

[558] E. J. Corey, *Proc. 31st Natl. Org. Symp. Am. Chem. Soc.*, June 1989, pp. 1–14.

[559] E. J. Corey, R. K. Bakshi, S. Shibata, *J. Am. Chem. Soc. 109* (1987) 5551.

[560] E. J. Corey, R. K. Bakshi, S. Shibata, C.-P. Chen, V. K. Singh, *J. Am. Chem. Soc. 109* (1987) 7925.

[561] E. J. Corey, C.-P. Chen, G. A. Reichard, *Tetrahedron Lett. 30* (1989) 5547.

[562] E. J. Corey, J. O. Link, *Tetrahedron Lett. 31* (1990) 601; E. J. Corey, S. Shibata, R. K. Bakshi, *J. Org. Chem. 53* (1988) 2861.

[563] E. J. Corey, R. K. Bakshi, *Tetrahedron Lett. 31* (1990) 611.

[564] E. J. Corey, P. Da Silva Jardine, T. Mohri, *Tetrahedron Lett. 29* (1988) 6409; E. J. Corey, P. Da Silva Jardine, J. C. Rohloff, *J. Am. Chem. Soc. 110* (1988) 3672.

[565] E. J. Corey, A. V. Gavai, *Tetrahedron Lett. 29* (1988) 3201.

[566] E. J. Corey, J. O. Link, *Tetrahedron Lett. 30* (1989) 6275.

[567] The amino alcohols used for preparing the catalysts **c**–**f** were derived from *N*-protected proline esters and phenyl or naphthyl Grignard reagents. The diphenylmethanol group has proven effective as part of a chiral auxiliary in other cases as well (*M. Braun* in [331d], Schemes 14, 22 [275]). For the use of other 2-hydroxymethylpyrrolidine or "prolinol" derivatives in enantioselective synthesis see also Scheme 26, chapters 11 and 14 of [331a], and D. Seebach, H.-O. Kalinowski, B. Bastani, G. Crass, H. Daum, H. Dörr, N. P. du Preez, V. Ehrig, W. Langer, C. Nüssler, H.-A. Oei, M. Schmidt, *Helv. Chim. Acta 60* (1977) 301.

[568] The prophetic observations of *Woodward* in his famous 1956 essay on the subject of "Synthesis" [39] remain just as valid today. On the other hand, it was left to a magician like Stork to propose a time scale: "So it is not surprising that organic synthesis is far from the level that many people assume. Progress is continuing, but there will not be any dramatic developments. It is more like a glacier that gradually moves forward until it has finally covered an entire region, but it will still be *centuries* before synthesis has acquired the status that many people already ascribe to it today" [44].

Book Reviews are written by invitation from the editor. Suggestions for books to be reviewed and for book reviewers are welcome. Publishers should send brochures or (better) books to the following address: Redaktion Angewandte Chemie, Postfach 101161, D-6940 Weinheim, Federal Republic of Germany. The editor reserves the right of selecting which books will be reviewed. Uninvited books not chosen for review will not be returned.

Inorganic Crystal Structures. By *B. G. Hyde* and *S. Andersson*. Wiley, Chichester 1988. xv, 430 pp., hard cover, £ 41.55.—ISBN 0-471-62897-2

In the last few decades the determination of chemical structures—especially of crystal structures—has become more important, is carried out more often, and is more useful as regards the information obtained. A knowledge of the structure of a compound not only gives very important insights into the spatial arrangement of atoms, clusters, and molecules, but also provides the starting point for various, more advanced theoretical studies (e.g. MO or band structure calculations) and experiments (e.g. on structure-property relationships, phase transformations or diffusion processes).

As a result of far-reaching developments in methods for structure determination, such as the work of *J. Karle* and *H. Hauptmann* (as described in their Nobel Prize address: *Angew. Chem. 98* (1986) 600, 611; *Angew. Chem. Int. Ed. Engl. 25* (1986) 603, 614), the majority of crystal structure determinations can now be carried out rapidly and easily. Every year many new structures or new variations of older structural types are described. Consequently it is becoming increasingly difficult to keep track of the whole field of structural chemistry.

To maintain an overview of the field, it is very important to classify crystal structures and to recognize cross-correlations between them. Where can one find information about whether a "new structure" is in fact completely new, or whether and in what way it is related to known structural types? Again and again cases occur where this question is relevant, but is disregarded or simply overlooked. For example, who would guess that $LiGaO_2$, Li_2SiO_3 and Li_3PO_4 are practically isostructural, or that the Fe_2P structure is closely related to that of Li_2ZrF_6?

Despite the existence of some important more or less up-to-date resources for systematizing and standardizing structures (e.g. standardization according to *Parthé*, categorization according to *Pearson*, and data banks), this is still a difficult task, and sometimes only specialists can hope to succeed. An exhaustive treatment of the topic, including new structures, could in fact only be undertaken by a large team of experienced scientists. That such a work is needed, and would remain in demand for a long time if it were available, is shown by the fact that monographs which are partly already quite old, such as those by *Wells, Pearson*, and *Schubert*, to name only a few, are still frequently used. Where else could one find cross-correlations between structures?

The monograph by *B. G. Hyde* and *S. Andersson* is dedicated to this task; the title "Inorganic Crystal Structures" is at the same time both ambitious and modest. In fact the book only treats a selection of inorganic structures, and the authors do not make any claim of completeness. Both authors are old hands at the business of investigating complex crystal structures and analyzing structural relationships. There are many places in the book where it becomes clear that many years of experience are being brought to bear and very interesting aspects are illuminated. Both, especially *S. Andersson*, are known for their extraordinary insights into apparently familiar topics, something which they have often proved in their publications (e.g. *Angew. Chem. 95* (1983) 67; *Angew. Chem. Int. Ed. Engl. 22* (1983) 69). The concepts of "chemical twinning" and of block and shear structures are especially thoroughly explained, and are used widely for elucidating structural correlations. The authors have concentrated throughout on a method of describing structures which uses the coordination polyhedra as basic units. Each of the 15 chapters constructs relationships between simple basic types and structures of increasing complexity, using diagrams which are mostly of excellent quality. Unfortunately though, a few of the diagrams suffer a loss of clarity due to too much scale reduction.

In the first six chapters structures are put into directly comparable forms by the use of suitably chosen projection directions. At the beginning of each chapter the different types of polyhedra are described in the appropriate projections. The variants of these with cubic and hexagonal symmetry having the highest spherical packing densities are then studied in detail in different viewing directions. Combinations of the most densely packed cubic and hexagonal structures are also treated. In these sections the basis structures are discussed in a variety of representations and in different relationships; this procedure is very useful both for beginners and for advanced readers, and it makes the book a valuable learning aid.

Two chapters are also devoted to the derivatives of the cubic and hexagonal primitive arrangements; these include discussions of the large families of structures that have the fluorite and AlB_2 structures as their basis.

Another chapter deals, in a very interesting way throughout, with the steric effects of electron lone pairs and their influence on crystal structures. The authors have themselves developed some interesting models to help in understanding these effects, as well as topological transformations, which are first described for polyhedra and networks, and are then carried over to various structural types. A longer section deals with some selected deformed variants of the perovskite structure.

The next chapter is devoted to crystal forms containing noncommensurate partial structures. The so-called chimney-ladder, layer misfit, and vernier structures are discussed, illustrated by excellent diagrams. A treatment of derivatives of body-centered cubic and cubic primitive structures with tetrahedral stars (Schubert stars) as structural elements leads into the structures of intermetallic phases. Here again the size of the monograph allows only a few structures to be discussed; however, some of the aspects considered are not found in the older treatments by *Schubert* or *Pearson*.

The final chapter is concerned with a selection of silicate structures, but regrettably the discussion is very brief. The diagrams given here compete with those seen in the earlier treatments by *Wells* or *Liebau*. Here, however, the interpre-

tations of complex structures in terms of chemical twinning by translational or rotational operations—one of *Andersson*'s specialities—again provide new insights.

As a whole, the book discusses a selection of compounds which spans the whole of inorganic chemistry, from fluorides to intermetallic phases. At the end one is left with the feeling that the book could have been much more detailed, especially in the last two chapters. This is not so much a criticism of the book's content as of its length, and is an expression of the desire for a modern treatment of inorganic structures which would be, as far as possible, complete.

It is also noticeable that the book appears to have been started several years ago, and in some places the literature coverage is out of date. This shortcoming, together with a few errors, should be corrected in a subsequent edition.

On the other hand there are other parts of the book where one finds "brand-new" information, e.g. on the new high-temperature superconductors. One must also single out for special praise the fact that for most of the structures discussed the complete structural parameters are given. This gives the reader direct access to more advanced studies, and avoids the often tedious searching out of data.

For beginners the "polyhedral" view of structures may at first seem strange and difficult. However, after a little practice the consistent projections used (Chapters 2–6) allow one to recognize correlations quickly. For experienced structural chemists too, polyhedral models are very important; they can even be used as a sort of "analog computer" (*H. G. von Schnering*) for "calculating" ideal structures and structural parameters, as is done frequently in this book.

The book undoubtedly enriches the literature in this field, and it also motivates the reader to look at structures from different points of view, to understand them, and to look for cross-correlations. It is useful both for teaching purposes and for those engaged in structural chemistry research.

Reinhard Nesper [NB 1029 IE]
Max-Planck-Institut für Festkörperforschung,
Stuttgart (FRG)

Houben-Weyl. Methoden der Organischen Chemie. 4th Edition, supplementary volumes. **Carbene(oide), Carbine, Teil 1 und 2.** (Volumes E 19b). Edited by *M. Regitz*. Thieme, Stuttgart 1989. Part 1: xxxvi, pp. 1–1021; Part 2: xxi, pp. 1022–2214; hardcover, DM 2680.00 (subscription price: DM 2412.00).—ISBN 3-13-219704-1

Whereas previously the main emphasis in Houben-Weyl was on functional groups and compound classes, the editors have now also turned their attention to reactive intermediates. A two-volume work on free radicals (E 19a) was followed at the end of 1989 by the present work on carbene(oid)s, which is also in two volumes. As the most recent monograph on carbenes was published in 1975 (reviews since then have treated only parts of the topic), a serious information gap had appeared. This shortcoming was especially felt by the synthetic organic chemist wishing to use carbene(oid)s as building blocks for synthesizing target molecules. A welcome resource in this respect is now available in the amazingly comprehensive, reliable and up-to-date Houben-Weyl volumes.

The introduction (*W. W. Schoeller*, 56 pages) unfortunately does not succeed in clearly presenting the basic principles of carbene chemistry. Instead it describes what the theory of carbenes and their reactions has to offer. The contributions of the theory are treated thoroughly and competently, but the relationship to experiment is often not adequately covered. For example, the four pages of theory on the 1,4-cycloaddition of carbenes are not accompanied by a single practical example. Strangely, the authoritative studies by *Bickelhaupt* and *Mayr* are presented as *unsuccessful* attempts at 1,4-cycloaddition (p. 34). *Schoeller* explains the negative activation energies of some carbene addition reactions as being due to the formation of π-complexes (p. 16), and in support of this cites *Houk*, despite the fact that he is responsible for the much more plausible explanation in terms of entropy control. Other factual errors are on page 49, where the protonation of **I** occurs after the carbene rearrangement of **II**, not before it as stated, and on page 55, where neither the educts (cycloalkylcarbenes) nor their reaction path b are given correctly. Although it contains useful information on the capabilities and limitations of the theory, this article is not a good "calling card" for the work as a whole.

A chapter on carbynes (*H. Heydt*, 36 pages) includes everything that is worth knowing about the R-Ĉ: bonding arrangement, which combines the properties of carbenes and free radicals. The subject matter ranges from the gas phase reactions of methylidyne and halocarbynes to the formation of carbynes from their (transition) metal complexes and by chemisorption.

The entire field of carbene(oid) chemistry is then treated in about 1800 pages. The subject matter is arranged according to the substitution patterns of the intermediates. These main chapters and their authors are as follows: alkylidenecarbenes, alkenylidenecarbenes, etc. (*P. Stang*, 80 pp.); methylene and alkyl- and dialkylcarbenes (*K. P. Zeller, H. Gugel*, 171 pp.); cycloalkylcarbenes and cycloalkylidenes (*U.-H. Brinker* with *J. Arct, J. Backes, W. Erdle, M. Fermann, L. K. Sydnes*, 328 pp.); alkenyl- and alkynylcarbenes (*U. Misslitz, A. de Meijere*, 110 pp.); cycloalkenylcarbenes and cycloalkenylidenes (*H. Dürr*, 48 pp.); aryl-, diaryl- and heteroarylcarbenes (*C. Wentrup*, 198 pp.); acylcarbenes (*G. Maas*, 388 pp.); silylcarbenes, etc. (*H. Tomioka*, 49 pp.); halocarbenes (*E. V. Dehmlov*, 166 pp.); oxycarbenes (*H. Heydt, M. Regitz*, 55 pp.); sulfocarbenes (*K. Schank*, 63 pp.); nitrogen-substituted carbenes (*H. Heydt, M. Regitz*, 77 pp.); phosphocarbenes (*H. Heydt, M. Regitz, G. Bertrand*, 78 pp.). The way in which these chapters are subdivided according to second substituent, complexity, etc. largely prevents overlapping and makes it easy to find a particular carbene without referring to the subject index. An exception: dihalo- and trihaloalkylcarbenes appear in the chapter on acylcarbenes, where they belong according to their oxidation state but not their reaction properties.

All the chapters show a high level of expert knowledge, orientated according to the authors' own fields of research. A few carbene(oid) types that are of preparative importance (e.g. dihalocarbenes) are not given as much space as one would expect, as their reactions are already covered in earlier volumes of the Houben-Weyl series (e.g. 4/3 on cyclopropanes). However, the cross-references are always supplemented by new knowledge and further developments. As the preparation of reactive intermediates is necessarily linked to their further reaction, it is not possible in discussing the various types of carbenes to stick to the traditional Houben-Weyl scheme of presentation (A. Preparation, B. Reactions). Where some of the authors have nevertheless tried to do so, it seems artificial and leads to repetition. The most sensible arrangement, and also the one most often used, is according to the co-reactants, thus: "preparation of ... in the presence of ...". The value of the numerous tables with their detailed information cannot be too highly praised. Sometimes the

tations of complex structures in terms of chemical twinning by translational or rotational operations—one of *Andersson*'s specialities—again provide new insights.

As a whole, the book discusses a selection of compounds which spans the whole of inorganic chemistry, from fluorides to intermetallic phases. At the end one is left with the feeling that the book could have been much more detailed, especially in the last two chapters. This is not so much a criticism of the book's content as of its length, and is an expression of the desire for a modern treatment of inorganic structures which would be, as far as possible, complete.

It is also noticeable that the book appears to have been started several years ago, and in some places the literature coverage is out of date. This shortcoming, together with a few errors, should be corrected in a subsequent edition.

On the other hand there are other parts of the book where one finds "brand-new" information, e.g. on the new high-temperature superconductors. One must also single out for special praise the fact that for most of the structures discussed the complete structural parameters are given. This gives the reader direct access to more advanced studies, and avoids the often tedious searching out of data.

For beginners the "polyhedral" view of structures may at first seem strange and difficult. However, after a little practice the consistent projections used (Chapters 2–6) allow one to recognize correlations quickly. For experienced structural chemists too, polyhedral models are very important; they can even be used as a sort of "analog computer" (*H. G. von Schnering*) for "calculating" ideal structures and structural parameters, as is done frequently in this book.

The book undoubtedly enriches the literature in this field, and it also motivates the reader to look at structures from different points of view, to understand them, and to look for cross-correlations. It is useful both for teaching purposes and for those engaged in structural chemistry research.

Reinhard Nesper [NB 1029 IE]
Max-Planck-Institut für Festkörperforschung,
Stuttgart (FRG)

Houben-Weyl. Methoden der Organischen Chemie. 4th Edition, supplementary volumes. **Carbene(oide), Carbine, Teil 1 und 2.** (Volumes E 19b). Edited by *M. Regitz*. Thieme, Stuttgart 1989. Part 1: xxxvi, pp. 1–1021; Part 2: xxi, pp. 1022–2214; hardcover, DM 2680.00 (subscription price: DM 2412.00).—ISBN 3-13-219704-1

Whereas previously the main emphasis in Houben-Weyl was on functional groups and compound classes, the editors have now also turned their attention to reactive intermediates. A two-volume work on free radicals (E 19a) was followed at the end of 1989 by the present work on carbene(oid)s, which is also in two volumes. As the most recent monograph on carbenes was published in 1975 (reviews since then have treated only parts of the topic), a serious information gap had appeared. This shortcoming was especially felt by the synthetic organic chemist wishing to use carbene(oid)s as building blocks for synthesizing target molecules. A welcome resource in this respect is now available in the amazingly comprehensive, reliable and up-to-date Houben-Weyl volumes.

The introduction (*W. W. Schoeller*, 56 pages) unfortunately does not succeed in clearly presenting the basic principles of carbene chemistry. Instead it describes what the theory of carbenes and their reactions has to offer. The contributions of the theory are treated thoroughly and competently, but the relationship to experiment is often not adequately covered. For example, the four pages of theory on the 1,4-cycloaddition of carbenes are not accompanied by a single practical example. Strangely, the authoritative studies by *Bickelhaupt* and *Mayr* are presented as *unsuccessful* attempts at 1,4-cycloaddition (p. 34). *Schoeller* explains the negative activation energies of some carbene addition reactions as being due to the formation of π-complexes (p. 16), and in support of this cites *Houk*, despite the fact that he is responsible for the much more plausible explanation in terms of entropy control. Other factual errors are on page 49, where the protonation of **I** occurs after the carbene rearrangement of **II**, not before it as stated, and on page 55, where neither the educts (cycloalkylcarbenes) nor their reaction path b are given correctly. Although it contains useful information on the capabilities and limitations of the theory, this article is not a good "calling card" for the work as a whole.

A chapter on carbynes (*H. Heydt*, 36 pages) includes everything that is worth knowing about the R-Ĉ: bonding arrangement, which combines the properties of carbenes and free radicals. The subject matter ranges from the gas phase reactions of methylidyne and halocarbynes to the formation of carbynes from their (transition) metal complexes and by chemisorption.

The entire field of carbene(oid) chemistry is then treated in about 1800 pages. The subject matter is arranged according to the substitution patterns of the intermediates. These main chapters and their authors are as follows: alkylidenecarbenes, alkenylidenecarbenes, etc. (*P. Stang*, 80 pp.); methylene and alkyl- and dialkylcarbenes (*K. P. Zeller, H. Gugel*, 171 pp.); cycloalkylcarbenes and cycloalkylidenes (*U.-H. Brinker* with *J. Arct, J. Backes, W. Erdle, M. Fermann, L. K. Sydnes*, 328 pp.); alkenyl- and alkynylcarbenes (*U. Misslitz, A. de Meijere*, 110 pp.); cycloalkenylcarbenes and cycloalkenylidenes (*H. Dürr*, 48 pp.); aryl-, diaryl- and heteroarylcarbenes (*C. Wentrup*, 198 pp.); acylcarbenes (*G. Maas*, 388 pp.); silylcarbenes, etc. (*H. Tomioka*, 49 pp.); halocarbenes (*E. V. Dehmlov*, 166 pp.); oxycarbenes (*H. Heydt, M. Regitz*, 55 pp.); sulfocarbenes (*K. Schank*, 63 pp.); nitrogen-substituted carbenes (*H. Heydt, M. Regitz*, 77 pp.); phosphocarbenes (*H. Heydt, M. Regitz, G. Bertrand*, 78 pp.). The way in which these chapters are subdivided according to second substituent, complexity, etc. largely prevents overlapping and makes it easy to find a particular carbene without referring to the subject index. An exception: dihalo- and trihaloalkylcarbenes appear in the chapter on acylcarbenes, where they belong according to their oxidation state but not their reaction properties.

All the chapters show a high level of expert knowledge, orientated according to the authors' own fields of research. A few carbene(oid) types that are of preparative importance (e.g. dihalocarbenes) are not given as much space as one would expect, as their reactions are already covered in earlier volumes of the Houben-Weyl series (e.g. 4/3 on cyclopropanes). However, the cross-references are always supplemented by new knowledge and further developments. As the preparation of reactive intermediates is necessarily linked to their further reaction, it is not possible in discussing the various types of carbenes to stick to the traditional Houben-Weyl scheme of presentation (A. Preparation, B. Reactions). Where some of the authors have nevertheless tried to do so, it seems artificial and leads to repetition. The most sensible arrangement, and also the one most often used, is according to the co-reactants, thus: "preparation of ... in the presence of ...". The value of the numerous tables with their detailed information cannot be too highly praised. Sometimes the

tables contain even more than their titles claim; for example, Table 155 (p. 1253) on Wolff rearrangements lists not only heterocyclic but also polycyclic diazoketones. The retro-rearrangement of alkynes to alkylidenecarbenes (*R. F. C. Brown*) and their preparative applications (*A. S. Dreiding*) are to be found in Table 29 (pp. 131–134) but not in the associated text.

The arrangement according to carbene types is useful from the standpoint of the synthetic chemist who comes across a carbene during a retrosynthetic analysis of the molecule in which he is interested, and needs further information on it. However, it is rather inadequate when one is interested in the carbene aspects of particular reactions. "How can one selectively functionalize adamantane by C-H insertion of a carbene at the 1-position?" or "Which carbene(oid)s add preferentially at the lower (or higher) substituted double bond of a diene?"—questions such as these can only be approached in a laborious way by using the 200-page subject index, which is arranged in order of increasing complexity (acyclic, cyclic, bicyclic...). Some carbene(oid)s have their own separate entries, while others appear *after* the corresponding hydrocarbons. The substitutive nomenclature that is used exclusively (e.g. "Carboxycyclopropan" rather than "Cyclopropancarbonsäure") serves the purpose well, although it corresponds to neither the IUPAC nor the Chemical Abstracts rules. Also the bibliography (13 pages) and the author index (100 pages) often give further help; in the latter the aristocracy stay together, and even *Doering* and *Schleyer* appear under V!

How do these volumes measure up to the traditional virtues of Houben-Weyl? *Reliability:* It seems to me that printing errors are more frequent than in earlier volumes, though many of them are not serious (e.g. wrong column titles on pages 59–69 and 103–133), some are comical (e.g. optically acute allenes on p. 51; "Cyclopentanten", p. 1073; yields quoted in °C, p. 1469) and only a few are misleading (p. 848: the rate constant for the S → T interconversion of diphenylcarbene is $3 \times 10^9\ s^{-1}$, not $3 \times 10^{-9}\ s^{-1}$; on p. 878 even a laboratory recipe is given for the wrong product **IV**). Without making a detailed search I found twenty errors in structural formulas (with about ten formulas per page this gives a rate of only 0.1%!). Of about 350 literature references chosen at random, only six contained minor errors. This is an excellent result when compared with the quality of the citations in many original papers. *Completeness of coverage*: For the period 1977–83 my own (selective) literature collection contains 227 papers of preparative importance on carbenes; of these, 178 (78%) are cited in the work. The only gap that I noticed in the systematic coverage was that benzocycloalkenylidenes are not dealt with under either the cycloalk(en)ylidenes or the arylcarbenes. *Up-to-date-ness*: Expressing the cited publications for each year as a percentage of those in my own literature collection, a maximum of 92% is reached for 1987, and the figure for 1988 is still as high as 48%. There are even some references to 1989 papers.

As a penalty for the rapid publication the editors have occasionally had to resort to "reaction paths of lowest energy" (pp. 22, 23). "Aus dieser Sicht müssen auch die Berichte über die [1.4]-Addition eines Triplett-Carbens an einem intermediären Ylid oder über ein Vinylcyclopropan/Cyclopenten-Umlagerung ablaufen" (p. 37)—such grammatical liberties are below the standard of Houben-Weyl (and of most other works).

However, minor defects can have an endearing effect in a book which is otherwise perfect. These volumes will be enthusiastically received by readers with interests in reactive intermediates, and will become their primary information resource. However, it is preparative chemists who will benefit most, as the work will give them a much better overview of the synthetic potential of the carbene(oid)s and enable them to use it more effectively.

Wolfgang Kirmse [NB 1076 IE]
Fakultät für Chemie
der Ruhr-Universität Bochum (FRG)

Registered names, trademarks, etc. used in this journal, even when not marked as such, are not to be considered unprotected by law.

© VCH Verlagsgesellschaft mbH, D-6940 Weinheim, 1990. – Printed in the Federal Republic of Germany by Konrad Triltsch Druck- und Verlagsanstalt Würzburg.

All rights reserved (including those of translation into foreign languages). No part of this issue may be reproduced in any form – by photoprint, microfilm, or any other means – nor transmitted or translated into a machine language without written permission from the publishers. Only single copies of contributions, or parts thereof, may be made for personal use. This journal was carefully produced in all its parts. Nevertheless, authors, editors and publisher do not warrant the information contained therein to be free of errors. Readers are advised to keep in mind that statements, data, illustrations, procedural details or other items may inadvertently be inaccurate.

Valid for users in the USA: The appearance of the code at the bottom of the first page of an article (serial) indicates the copyright owner's consent that copies of the article may be made for personal or internal use, or for the personal or internal use of specific clients. This consent is given on the condition, however, that the copier pay stated per-copy fee through the Copyright Clearance Center, Inc. (CCC), for copying beyond that permitted by Sections 107 or 108 of the U.S. Copyright Law. This consent does not extend to other kinds of copying, such as copying, for general distribution, for advertising or promotional purposes, for creating new collective works, or for resale. For copying from back volumes of this journal see 'Permissions to Photo-Copy: Publisher's Fee List' of the CCC.

Editorial office: Postfach 10 11 61, D-6490 Weinheim, Federal Republic of Germany, Telephone (06201) 60 22 55, Telex 465 516 vchwh d, Telefax (06201) 602 328.

Editor: *Peter Gölitz*

Associate editors: *D. J. Loewus, A. Stimson.* **Editorial assistant:** *E. Schweikart*

Publishers: VCH Verlagsgesellschaft mbH. (Managing Director: *Hans Dirk Köhler, Dr. Hardy G. Sehrt*), Pappelallee 3, D-6940 Weinheim, Federal Republic of Germany.

Advertising office (Advertising Manager *R. J. Roth*): Postfach 10 11 61, D-6940 Weinheim, Federal Republic of Germany, Telephone (0 62 01) 60 61 30, Telex 4 67 155, Telefax (0 62 01) 606 156.

ANGEWANDTE CHEMIE
International Edition in English
Volume 29 · Number 12
December 1990
Pages 1371–1522

CC Bond Formation by Addition of Carbenium Ions to Alkenes: Kinetics and Mechanism

By Herbert Mayr*

Dedicated to Professor Rolf Huisgen on the occasion of his 70th birthday

The addition of carbenium ions to CC double bonds, a key step in many syntheses in organic and macromolecular chemistry, is analyzed using the Lewis acid promoted reactions of alkyl chlorides with alkenes as an example. Stereochemical and kinetic experiments suggest that the transition state is slightly bridged and product-like. Rearrangements of the carbenium ions that result from the electrophilic attack can be minimized by adding salts with nucleophilic counter ions. The thermodynamics of the addition reactions are analyzed, and the conditions necessary in order to observe the back reaction (i.e. the Grob fragmentation) are discussed. Multiparameter equations that predict rate constants are derived from kinetic studies on the reactivities of carbenium ions and alkenes. Reactivity-selectivity relationships over a reactivity range that covers eight orders of magnitude show that the structure of the transition state is only changed by variation of substituents in the immediate vicinity of the reaction center.

1. Introduction

Lewis acid promoted carbon–carbon bond formation reactions have found considerable interest in organic synthesis in recent years.[1] Generally, the function of the Lewis acid is to activate an electrophile so strongly (e.g. by complexation to a carbonyl group or imine or by ionization of acetals and related compounds) that it can attack an electron-rich doubly bonded system such as a silyl enol ether or an allylmetal compound (Scheme 1).

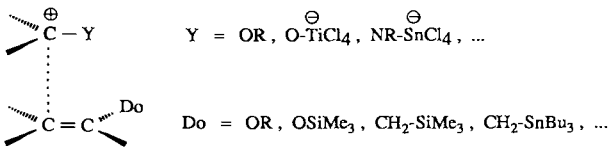

Scheme 1.

[*] Prof. H. Mayr
Institut für Chemie
Medizinische Universität zu Lübeck
Ratzeburger Allee 160, W-2400 Lübeck 1 (FRG)

The prototype for this type of reaction is the addition of a carbenium ion to a normal CC double bond, as exemplified by the Lewis acid induced reaction of alkyl halides with alkenes and dienes (Scheme 2). Now that the conditions necessary to perform such reactions selectively (i.e. to avoid polymerization) are known,[2] it has become possible to investigate their mechanisms.

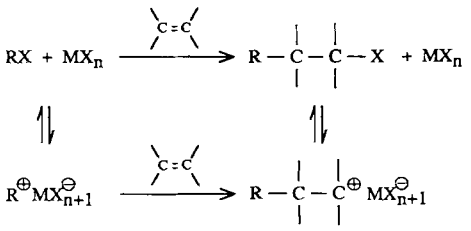

Scheme 2.

para-Substituted diarylcarbenium ions **1** proved to be particularly suitable model compounds, because their reactivity can be varied over a wide range by changing the substituents

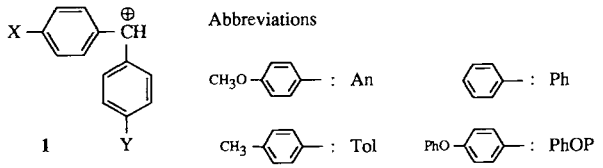

X and Y without affecting the steric environment of the reactive center.

For such studies the carbenium ions **1** can either be used as stable salts or they can be generated as short-lived intermediates in the presence of alkenes.

2. Regio- and Stereoselectivity

Like proton-induced HX additions,[3] additions of carbenium ions to alkenes proceed strictly regioselectively, the orientation being determined by the stability of the intermediate carbenium ions[2,4] according to the Markownikow rule. They differ in this respect from other electrophilic additions, such as sulfenylation or selenylation, in which the orientation is determined by the direction of nucleophilic attack on the bridged intermediate (Scheme 3).

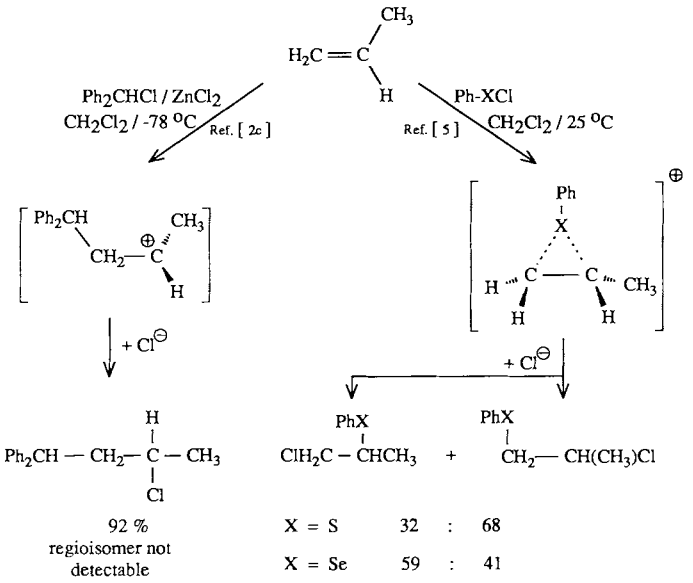

Scheme 3.

Even the sterically crowded olefin **2** is attacked by diarylcarbenium ions **1** exclusively at the *tert*-butyl-substituted vinyl carbon atom,[6] emphasizing the control of the direction of addition by electronic factors in the intermediate carbenium ion.

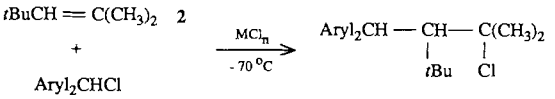

Similarly, the Lewis acid catalyzed addition of alkyl halides to alkyl- and aryl-substituted acetylenes strictly follows the Markownikow rule.[7,8] Alkyl-substituted 1,3-dienes react so that the allyl cation with the highest possible number of terminal alkyl groups is formed, leading to the regioselectivity indicated in Scheme 4.[4,6,9] 1-Butene-3-yne is attacked by C-electrophiles at the 4-position, and the reversal of the direction of addition in 1-hexene-3-yne (Scheme 4) can be explained by the electronic effect of the extra ethyl group on the cationic intermediate.[2d,9]

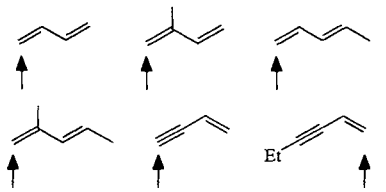

Scheme 4. Sites for attack by carbenium ions on conjugated dienes and enynes.

According to MINDO/3 calculations,[10] the addition of carbenium ions to alkenes should occur via π-complexes. This would explain the high *anti*-stereoselectivity in carbocationic cyclizations.[1b,11] Stereochemical studies on Lewis acid catalyzed intermolecular reactions of diphenylmethyl chlorides with (*Z*)- and (*E*)-2-butene showed that the ratio of the *syn*- and *anti*-addition products depends on the nature of

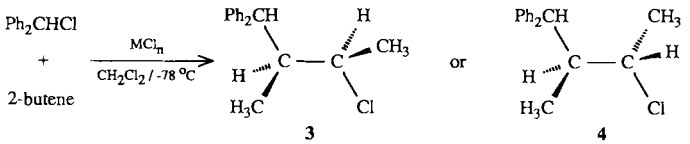

Herbert Mayr was born in Weilheim, Bavaria in 1947 and obtained his doctorate under R. Huisgen at the Universität München in 1974. After one year as postdoc at the Case-Western-Reserve-University in Cleveland/Ohio under G. A. Olah, he returned to Germany in 1976 and joined P. von R. Schleyer in Erlangen, where he completed his "Habilitation" in 1980. In 1984 he took over the direction of the Institute of Chemistry at the "Medizinische Universität zu Lübeck", and in 1990 he was offered a professorship at the "Technische Hochschule Darmstadt". His areas of interest are syntheses via carbocationic intermediates, kinetics of ion-molecule reactions, linear free energy relationships, carbocationic telomerisations and unusual cycloadditions.

the Lewis acid, but that in all cases the formation of the *anti*-products **3** or **4**, respectively, is strongly favored (Table 1).[12]

The data shown in Table 1 have been explained by the occurrence of partially bridged intermediates **5**.[12] Alternatively, it has been suggested that free rotation is hindered by an interaction between the carbenium center and the neighboring aryl ring (see **6**).[13] We consider such a stabilizing interaction to be unlikely, however, because the solvolysis of tertiary alkyl chlorides is not accelerated, but rather slowed down slightly, by a β-diphenylmethyl group.[14]

Table 1. Diastereomeric ratios of the products of Lewis acid catalyzed reactions of diphenylmethyl chloride with (*Z*)- and (*E*)-2-butene (CH_2Cl_2, −78 °C)[a].

Alkene	MCl_n	3:4
(*Z*)-2-Butene	$ZnCl_2$	86:14
	BCl_3	83:17
	$SnCl_4$	91:9
	$TiCl_4$	96:4
(*E*)-2-Butene	$ZnCl_2$	4:96
	BCl_3	12:88
	$SnCl_4$	8:92
	$TiCl_4$	<1:>99

[a] The reaction also produces rearrangement products via H-shifts (see Section 3).

As the electron-donor strength of the substituents on C_α increases, the bridging in **5** becomes less significant. Thus, diastereomer **7** is formed as the major product with both isomers of β-methylstyrene, indicating an almost free rotation in the intermediate. Corresponding changes in stereoselectivity have been observed for brominations of butenes and styrenes.[15]

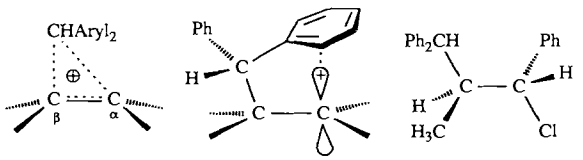

5 **6** **7**

On the other hand, the stereochemical results of Lewis acid induced additions of alkyl chlorides to alkynes can be explained by the intermediacy of non-bridged species.[8] The direction of attack of a nucleophile on the intermediate vinyl cation **8** is determined by the relative sizes of the substituents R and R′ (Scheme 5).

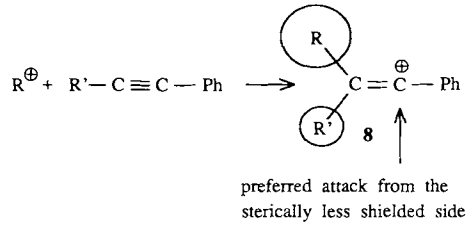

preferred attack from the sterically less shielded side

Scheme 5.

This interpretation is supported by the fact that a 50:50 mixture is isolated from the benzylation of 1,3-diphenylpropyne with labeled benzyl chloride (Scheme 6).[8]

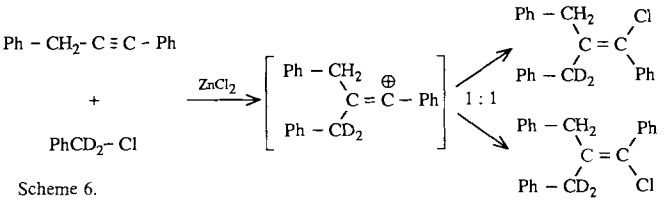

Scheme 6.

There have been very few investigations of the diastereoselectivity of the CC bond-forming step in electrophilic attack of carbenium ions on alkenes. Generally, we found only low stereoselectivity, as shown by the Lewis acid catalyzed addition of 4-chloro-2-pentene ("1,3-dimethylallyl chloride") to (*Z*)-2-butene. The *si,re*-transition state **9** is only slightly favored over the *si,si*- (and *re,re*-) transition state **10** (75:25), and for the corresponding addition to (*E*)-2-butene, the advantage of *si,re* over *si,si* (or *re,re*) sinks to 57:43.[16]

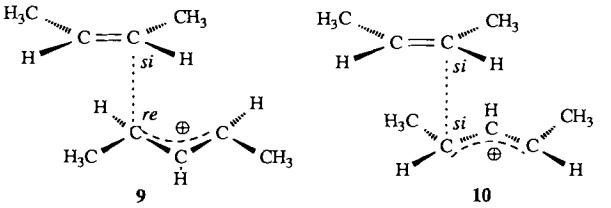

9 **10**

3. Rearrangements

1,2-Alkyl and hydrogen shifts are among the fastest reactions known in organic chemistry.[17] Degenerate 1,2-migrations in persistent carbocations can often not be frozen out on the NMR time scale, even at −120 °C, so that special techniques have been developed to determine the structure of such cations.[17a, b] The barrier for degenerate 1,2-hydrogen and methyl shifts in tertiary carbenium ions is usually about 12–15 kJ mol^{-1}. The barrier decreases if the rearrangement leads to a stabilization of the carbenium ion. Despite these very low barriers, rearrangements of the intermediate cations shown in Scheme 2 often play an astonishingly minor role. Although 1,2-H shifts forming tertiary from secondary carbenium ions occur without activation barriers,[17] the reaction of diphenylmethyl chloride with (*E*)- and (*Z*)-2-butene yields a mixture of the normal addition products **3** and **4** and the product **13** that is derived from the rearranged cation **11** (Scheme 7).[12] Because **12** is partially bridged, the rotation about the original double bond that must precede the 1,2-shift is slow, so that the reaction of **12** with $MCl^{\ominus}_{n+1}$ (yielding **3** and **4**) can compete with the rearrangement to **11**. Thus, the normal addition products **3** and **4** are formed predominantly in the reaction of diphenylmethyl chloride with (*E*)-2-butene (Table 1) and only 20% of the products are derived from the rearranged cation **11** if $ZnCl_2 \cdot OEt_2$,

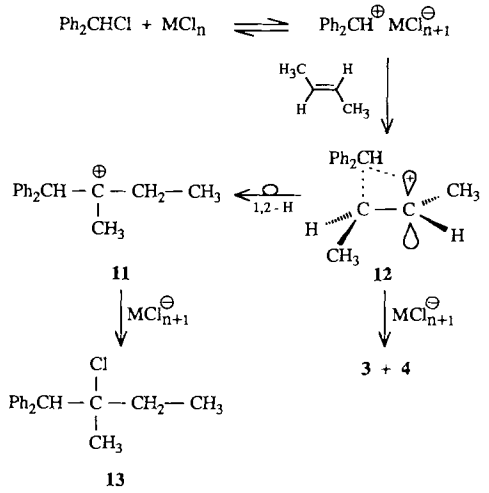

Scheme 7.

BCl_3, or $SnCl_4$ are used as catalysts (CH_2Cl_2, $-78\,^{\circ}C$). The rearrangement can be reduced to 4% with $TiCl_4$. The corresponding reaction with (*Z*)-2-butene yields a higher proportion (up to 65%) of rearranged product. This is, once again, lowest (21%) when $TiCl_4$ is used.[12]

Because electrophilic additions to 1,2-dialkylethylenes always yield secondary carbenium ions that can rearrange to tertiary carbenium ions via 1,2-H shifts, significant amounts of rearrangement products are always formed in reactions with cyclopentene and cyclohexene.[18] In view of these results, it is surprising that no rearrangement occurs when the reaction of *tert*-butyl chloride with ethylene is catalyzed by aluminum chloride.[19] The intermediacy of a primary carbocation can therefore be ruled out and the formation of **14** can be rationalized by assuming the intermediacy of a bridged cation (*tert*-butyl bridged ethylene). Alternatively, the attack of the *tert*-butyl cation at ethylene may be nucleophilically assisted by the $AlCl_4^{\ominus}$ ion because of the low stability of the 3,3-dimethyl-1-butyl cation (Scheme 8).[20]

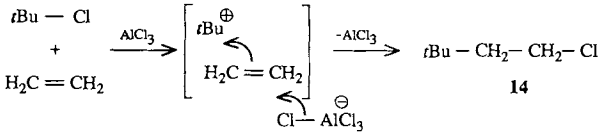

Scheme 8.

Rearrangements that result in little or no stabilization of the carbenium ion (e.g. tertiary → tertiary or secondary → secondary) are observed occasionally, but can be partly or totally suppressed by increasing the rate of ionic recombination (v_1, Scheme 9).

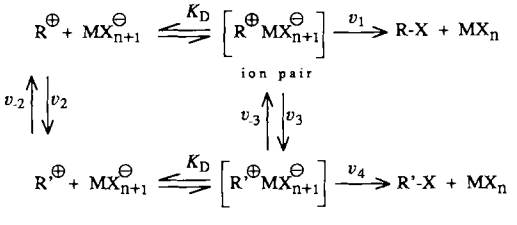

Scheme 9.

Because rearrangements ($R^{\oplus} \rightarrow R'^{\oplus}$) can occur in paired or unpaired ions, their rate ($v_2 + v_3$) depends little ($v_2 \approx v_3$) or not at all ($v_2 = v_3$) on the degree of ion-pairing. The rate of ionic recombination (v_1, v_4), on the other hand, is almost proportional to the concentration of ion pairs and can, for instance, be increased by addition of a quaternary ammonium salt ($R_4N^{\oplus}MX_n^{\ominus}$). Table 2 shows how the yield of **17** relative to that of the cyclization product **18** increases with increasing $BCl_4^{\ominus}$ concentration. The **17**:**18** ratio remains essentially constant, however, once the majority of the ions are paired.[14, 21]

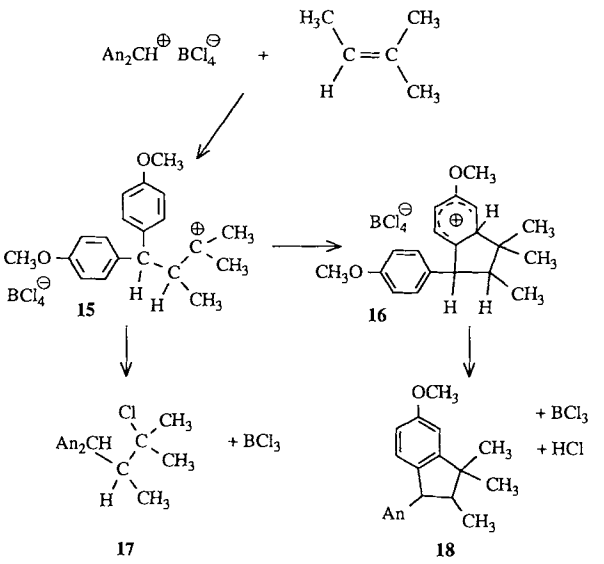

Table 2. The influence of benzyltriethylammonium tetrachloroborate on the product ratio observed in the reaction of bis(*p*-anisyl)carbenium tetrachloroborate with 2-methyl-2-butene in CH_2Cl_2 at $-70\,^{\circ}C$.[14, 21]

$c(An_2CH^{\oplus})$ [mol L^{-1}] [a]	$c\,(BCl_4^{\ominus})$ [mol L^{-1}] [a, b]	Ions paired:unpaired	Product ratio **17**:**18**
5.5×10^{-5}	5.5×10^{-5}	17:83	41:59
5.5×10^{-5}	5.6×10^{-4}	54:46	68:32
5.5×10^{-5}	3.4×10^{-3}	78:22	82:18
5.5×10^{-5}	1.5×10^{-2}	89:11	86:14
5.5×10^{-5}	4.9×10^{-2}	94:6	84:16

[a] Initial concentration [b] Sum of $c\,(An_2CH^{\oplus}BCl_4^{\ominus})$ and $c\,(BzNEt_3^{\oplus}BCl_4^{\ominus})$.

The fact that the $ZnCl_2$-catalyzed reaction of the allyl chloride **19** with styrene yields a 65:35 mixture of **23** and **24**, whereas pure **23** is obtained under the same conditions on addition of benzyltriethylammonium trichlorozincate, can be explained in the same way.[4b, 22] Thus the 1,3-vinyl shift **20** → **21** → **22** can be suppressed by increasing the $ZnCl_3^{\ominus}$ concentration and thereby accelerating the transfer of a chloride ion to **20** (Scheme 10).

As a rule-of-thumb one may assume that reducing the strength of the Lewis acid will also suppress a rearrangement, because a decrease in the stability of $MX_{n+1}^{\ominus}$ will facilitate the transfer of the halide ion $X^{\ominus}$ to a carbenium ion. There is, however, no strict relationship between the tendency to rearrange and the thermodynamic stability of $MX_{n+1}^{\ominus}$,

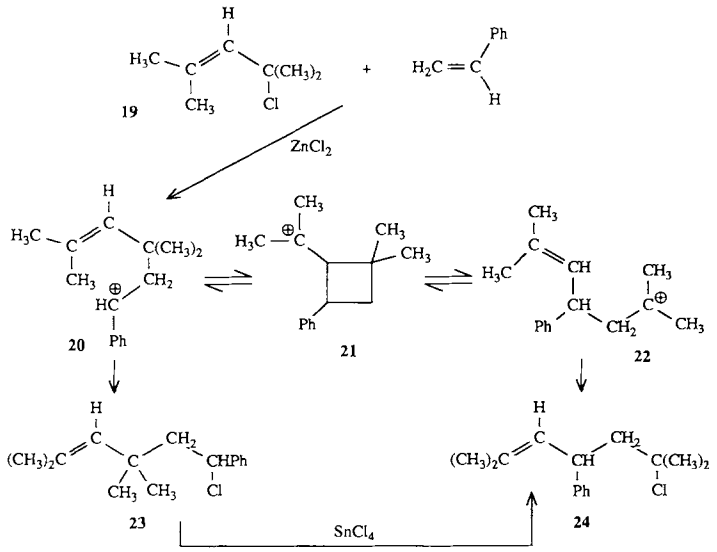

Scheme 10.

as shown by the reaction of benzhydryl chloride with the 2-butenes discussed above. Although $TiCl_4$ is a stronger chloride acceptor than $ZnCl_2 \cdot OEt_2$, less rearrangement product was formed in the presence of $TiCl_4$. We were unable to suppress rearrangement when cations of the cyclopropylcarbinyl, cyclopropyl or norbornyl types are formed by the electrophilic attack. Alkylation of 1-methylethenylcyclopropane,[23] methylenecyclopropane,[24] and norbornene[25] yielded exclusively the rearranged products **25**–**27**, respectively.

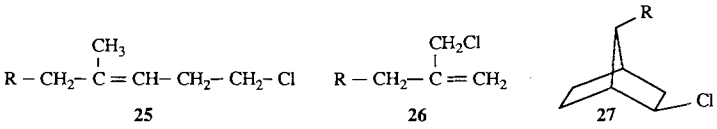

4. Thermodynamics of Addition Reactions: Addition versus Grob-Fragmentation

In order to treat the thermodynamics of addition reactions, we consider four extreme cases that differ in the degree of ionization of reactants and products:

a) Reactants and products are covalent.
b) Reactants and products are ionic.
c) Reactants are covalent, products ionic.
d) Reactants are ionic, products covalent.

The classifications (a–d) are also used in the subscripts ($\Delta G_a^0 \ldots \Delta G_d^0$) in Scheme 11.

Case a: If carbenium ions are only present in small equilibrium concentrations (i.e., the reactants and products are predominantly covalent), ΔH_a^0 is given by the energy gain for the conversion of a π_{cc} into a σ_{cc} bond. This energy is estimated from mean bond energies[26] to be $\Delta H_a^0 = -84$ kJ mol^{-1}, in fair agreement with the calorimetrically determined heats of reaction[27] for the addition of benzhydryl chloride to 2-methyl-1-pentene (−84.5), styrene (−83.4),

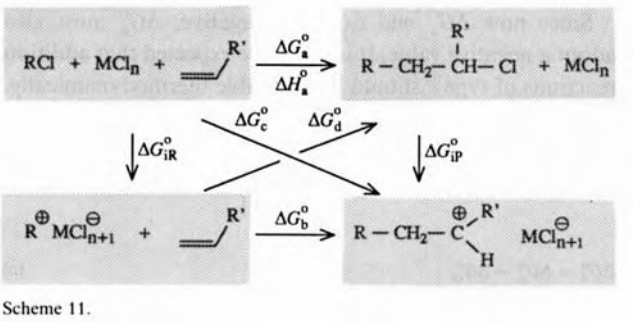

Scheme 11.

2-methyl-2-butene (−78.9), and isoprene (−74.2). Changes in the ground state energy of the π-systems and different degrees of steric strain in the addition products have little effect on the magnitude of the enthalpy of addition. Using reaction entropies of −150 to −175 J mol^{-1} K^{-1} determined from increments,[28] we obtain ΔG_a^0 (−70 °C) ≈ −50 kJ mol^{-1}. ΔG_a^0, which is independent of the Lewis acid, only varies significantly if considerable steric strain is present in the addition products. However, as even the strongly hindered *tris*(*p*-chlorophenyl)methyl chloride **28** reacts with isobutene at −10 °C to give the adduct **29**,[29] we can conclude that ΔG_a^0 only becomes positive in extreme cases.

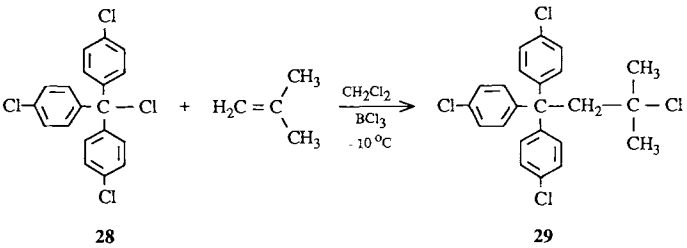

Case b: If the reactants and products are ionic, the standard free energy of reaction according to Scheme 11 is given by Equation (a).

$$\Delta G_b^0 = \Delta G_a^0 - (\Delta G_{iR}^0 - \Delta G_{iP}^0) \quad \text{(a)}$$

Equation (a) shows that ΔG_a^0 must be corrected by the difference in the free energies of ionization of reactants and products in this case. Previously we discussed the fact that for case b the selective formation of 1:1 products is only possible if $\Delta G_{iR}^0 > \Delta G_{ip}^0$, i.e., when $R^{\oplus}$ is less stabilized than the product carbenium ion R–CH_2–$^{\oplus}$CHR′ (addition rate control). If this is not the case, polymers are formed.[2a, 30] Because ΔG_a^0 is usually negative, as discussed above, ΔG_b^0 must also be negative if $\Delta G_{iR}^0 > \Delta G_{iP}^0$. In other words, the addition of a poorly stabilized carbenium ion to a CC double bond leading to a better stabilized carbenium ion is always exergonic at the usual reaction temperatures.

Case c: If ionic products (i.e. $\Delta G_{iP}^0 < 0$) are to be formed from covalent reactants (i.e. $\Delta G_{iR}^0 > 0$), the standard free energy of reaction is given by Equation (b).

$$\Delta G_c^0 = \Delta G_a^0 + \Delta G_{iP}^0 \quad \text{(b)}$$

Since now ΔG_a^0 *and* ΔG_{iP}^0 are negative, ΔG_c^0 must also adopt a negative value. It is therefore expected that addition reactions of type *c* should be favorable thermodynamically.

Case d: If covalent products (i.e. $\Delta G_{iP}^0 > 0$) are to be formed from ionic reactants ($\Delta G_{iR}^0 < 0$), the standard free energy of reaction is given by Equation (c).

$$\Delta G_d^0 = \Delta G_a^0 - \Delta G_{iR}^0 \qquad (c)$$

According to Equation (c), ΔG_d^0 is negative if $\Delta G_a^0 < \Delta G_{iR}^0$. A value of -50 kJ mol^{-1} was estimated for ΔG_a^0 (-70 °C) above, so that carbenium salts can only add to olefins to form covalent products if $\Delta G_{iR}^0 \gtrsim -50$ kJ mol^{-1}. As ΔG_{iR}^0 depends both on the structure of $R^{\oplus}$ and on the Lewis acidity of MCl_n, we can conclude that the thermodynamic driving force for Case *d* increases when the stabilization of $R^{\oplus}$ or the chloride-ion affinity of MCl_n decreases. Correlation (d) can be derived for the ionization of diarylmethyl chlorides with BCl_3.[31]

$$\Delta G_{iR}^0/\text{kJ mol}^{-1} = -6.1\ pK_{R^{\oplus}} - 67.1 \qquad (d)$$

Substituting expression (d) and $\Delta G_a^0 \approx -50$ kJ mol^{-1} in Equation (c) gives:

$$\Delta G_d^0/\text{kJ mol}^{-1} \approx 6.1\ pK_{R^{\oplus}} + 17.1 \qquad (e)$$

Therefore, a positive value for ΔG_d^0 is calculated for the addition of carbenium tetrachloroborates to alkenes to give covalent products (CH_2Cl_2, -70 °C) if carbenium ions with $pK_{R^{\oplus}} \gtrsim -2.8$ are used.[33] If such highly stabilized carbenium ions ($pK_{R^{\oplus}} \gtrsim -2.8$) are to be made to react with olefins, $BCl_4^{\ominus}$ must be replaced by an anion with higher Lewis basicity.

The reverse of the addition reactions discussed here is the Grob fragmentation.[32] In qualitative agreement with Equation (e), fragmentation is observed if the CC bond cleavage yields a well stabilized carbenium ion (large $pK_{R^{\oplus}}$ value), as for instance in the ionization of β-amino-substituted alkyl derivatives (Scheme 12).

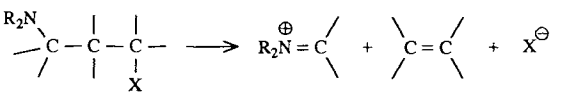

Scheme 12.

Fragmentation to form the aromatic tropylium ion ($pK_{R^{\oplus}} = +4.76$) is observed when **30** (R = H) is treated with sulfuric acid.[34] In order to demonstrate the counter ion effect discussed above, we combined tropylium tetrafluoroborate (**31**·$BF_4^{\ominus}$) with isobutene in *methanol* and isolated **30** (R = CH_3) in 45% yield.[35]

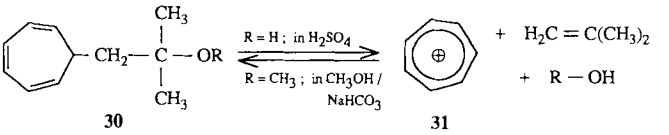

30 **31**

5. Kinetic Studies

5.1. Methods

The relationship between structure and reaction rates has been determined by competition experiments and by measuring absolute rate constants. Because the reaction rates do not depend on the nature of the counter ion (see Section 5.1.2), the results of the two types of experiment can be directly combined.

5.1.1. The Determination of Relative Rate Constants by Competition Experiments

The relative reactivities of alkenes are determined by generating diarylcarbenium ions in situ from diarylmethyl chlorides and Lewis acids in the presence of an excess of two competing olefins.[23, 36] If conditions are chosen under which subsequent reaction of the 1:1 products with excess olefin cannot occur, the reactivity ratio of the two alkenes can be determined from the ratio of the addition products **32** and **33** (Scheme 13).

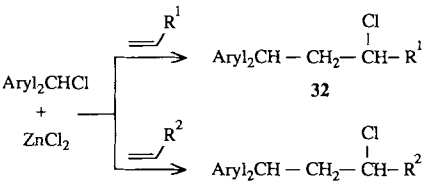

Scheme 13.

Similarly, the relative reactivities of electrophiles are determined from the ratio of the 1:1 adducts **34** and **35** that results when an alkene is added to a mixture of electrophiles (Scheme 14).[30, 37] As will be shown in Section 5.2, the relative electrophilicity is strongly dependent on the type and amount of Lewis acid MX_n.

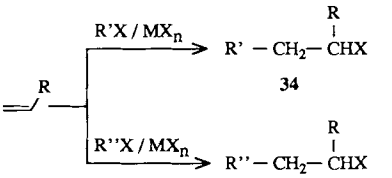

Scheme 14.

5.1.2. Determination of Absolute Rate Constants

Absolute rate constants for the reaction of carbenium ions with alkenes were first determined by observing the decrease

in absorption due to benzhydryl and benzyl cations produced pulse-radiolytically[38] in the presence of alkenes and dienes.[39] This technique is, however, only suitable for very fast reactions ($k_2 > 10^5 - 10^6$ L mol^{-1} s^{-1}).

A considerably broader set of data is based on the fact that many diarylmethyl chlorides can be ionized fully by Lewis acids in dichloromethane to give colored, electrically conducting solutions.[40] If alkenes are added to these solutions, covalent products are often formed (Scheme 15) and the

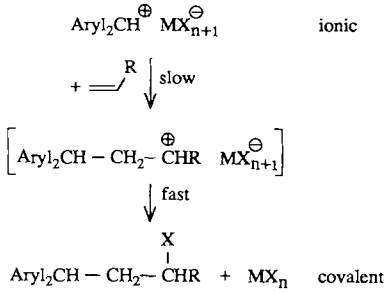

Scheme 15.

reaction can be followed both photometrically and conductimetrically.[41, 14] These are second order reactions according to Eq. (f) in which [Aryl$_2$CH$^\oplus$] represents the sum of the concentrations of paired and unpaired diarylcarbenium ions.

$$d[Aryl_2CH^\oplus]/dt = k_2[Aryl_2CH^\oplus][Alkene] \quad (f)$$

As the ion concentration sinks during the reaction, and the ratio of unpaired to paired ions therefore rises, the validity of Equation (f) implies that unpaired ions and those paired with complex counterions have the same reactivity towards alkenes. In agreement with this conclusion, the reation rate is not changed by the addition of quaternary ammonium salts with the same counter ion.

The fact that, in contrast to the ionization constant K_I (Scheme 16), the dissociation constant K_D is essentially inde-

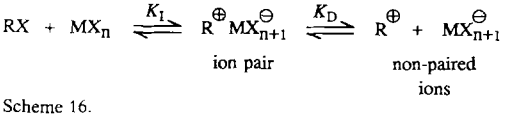

Scheme 16.

pendent of the nature of the ions provides an explanation for this observation. K_D values of about 10^{-4} mol L^{-1} were found in dichloromethane for all combinations of the cations Aryl$_2$ CH$^\oplus$, Aryl$_3$ C$^\oplus$, tropylium, pyrylium, and tetraethyl ammonium with the anions $BCl_4^\ominus$, $SbCl_6^\ominus$, $SbF_6^\ominus$ and $AsF_6^\ominus$ known to us.[40] We can therefore assume that K_D also adopts a similar value for reactants, products and activated complexes of the reaction shown in Figure 1. This leads to a constant population ratio between paired and unpaired ions in ground and transition states. The fact that the reaction

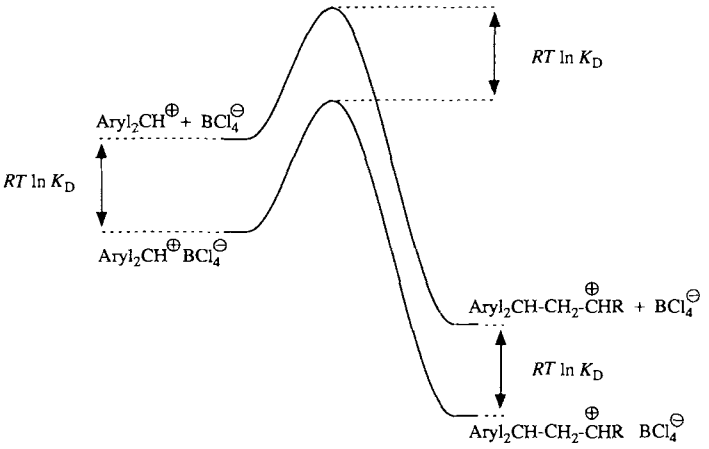

Fig. 1. Energy profiles for the rate-determining steps of the additions of paired and unpaired carbenium ions to alkenes.

rate is independent of the degree of ion-pairing can thus be explained.

It is well known that the dissociation constant K_D for organometallic compounds depends on the nature of the cation and the structure of the anion.[42] In agreement with this observation, large differences in reactivity are found for free and paired carbanions.[43, 44]

In a few cases, the energy profiles for the entire reaction sequence shown in Scheme 15, including the initial ionization step, have been determined.[14] These studies showed that a fast ionic recombination usually follows the slow attack of the carbenium ion on the alkene.

Because one carbenium ion is produced from another in the rate-determining step, it is not surprising that changes in solvent have only a minor effect on the reaction rate. We found a linear correlation of the rate of reaction of An$_2$CH$^\oplus$ with 2-methyl-1-pentene with the solvent parameter E_T (30).[45] The addition occurs 4.8 times faster in nitromethane ($E_T = 46.3$) than in chloroform ($E_T = 39.1$).[14]

Secondary kinetic isotope effects have been measured for the reaction of AnPhCD$^\oplus$ with some olefins. Their magnitude ($k_D/k_H \approx 1.2$) indicates that the rehybridization ($sp^2 \rightarrow sp^3$) of the benzhydryl carbon is very advanced in the transition state.[14]

5.2. Variation of the Carbenium Ion

As expected, decreasing the electron donating power of the *para*-substituent leads to an increase in the reactivity of diarylcarbenium ions. As shown in Table 3, this is due to a decrease in the enthalpy of activation, ΔH^+. The entropy of activation ΔS^+ remains essentially constant within a series of reactions. We have attempted to interpret the negative enthalpy of activation observed in a few cases.[46]

$$Aryl_2CHCl + BCl_3 \xrightarrow[-70\,^\circ C]{\Delta G_1^0} Aryl_2CH^\oplus BCl_4^\ominus \quad (g)$$

$$Aryl_2CH^\oplus BCl_4^\ominus + R^1CH{=}C(CH_3)R^2 \xrightarrow[-70\,^\circ C]{k_2,\ \Delta H^*,\ \Delta S^*} Aryl_2CH{-}CHR^1{-}CR^2Cl{-}CH_3 \quad (h)$$

Table 3. Free ionization enthalpies ΔG_i^0 of diarylmethyl chlorides [Eq. (g)] and kinetics of the additions of diarylcarbenium ions to 2-methyl-1-pentene and 2-methyl-2-butene [Eq. (h)] in dichloromethane [14, 46].

Carbenium ion	ΔG_i^0 (−70 °C) [kJ mol^{-1}]	2-Methyl-1-pentene k_2(−70 °C) [L mol^{-1} s^{-1}]	2-Methyl-1-pentene $\Delta H^{\neq}$ [kJ mol^{-1}]	2-Methyl-1-pentene $\Delta S^{\neq}$ [J mol^{-1} K^{-1}]	2-Methyl-2-butene k_2(−70 °C) [L mol^{-1} s^{-1}]	2-Methyl-2-butene $\Delta H^{\neq}$ [kJ mol^{-1}]	2-Methyl-2-butene $\Delta S^{\neq}$ [J mol^{-1} K^{-1}]
$An_2CH^{\oplus}$	−35.1	2.92×10^{-2}	29.7	−125	8.38×10^{-2}	21.9	−155
An(PhOP)$CH^{\oplus}$	−27.9	1.69×10^{-1}			7.5×10^{-1}		
An(Tol)$CH^{\oplus}$	−22.8	3.38	22.7	−120	1.83×10^{1}	13.6	−151
An(Ph)$CH^{\oplus}$	−16.6	2.58×10^{1}	18.6	−123	2.47×10^{2}	7.5	−159
PhOP(Tol)$CH^{\oplus}$	−15.4	3.30×10^{1}					
PhOP(Ph)$CH^{\oplus}$	−9.2	2.86×10^{2}	15.3	−119	3.92×10^{3}	5.3	−147
$Tol_2CH^{\oplus}$	−7.0	3.40×10^{3}	11.6	−117	6.79×10^{4}	−1.4	−156

The reactivities shown in Table 3 correlate only moderately well with $\Sigma\sigma^+$, because different aryl rings in the diarylcarbenium ions are twisted by different amounts out of the plane, and substituent effects are therefore not additive.[14, 47] Plots of the free energy of activation for the addition ($\Delta G^{\neq}$) against the free energy of ionization of the benzhydryl chlorides (Fig. 2) give linear relationships with gradients between 0.64 and 0.94. This indicates that more than 2/3 of the carbenium ion character of the diarylmethyl fragment has been lost in the addition transition state; i.e. the transition states are product-like.

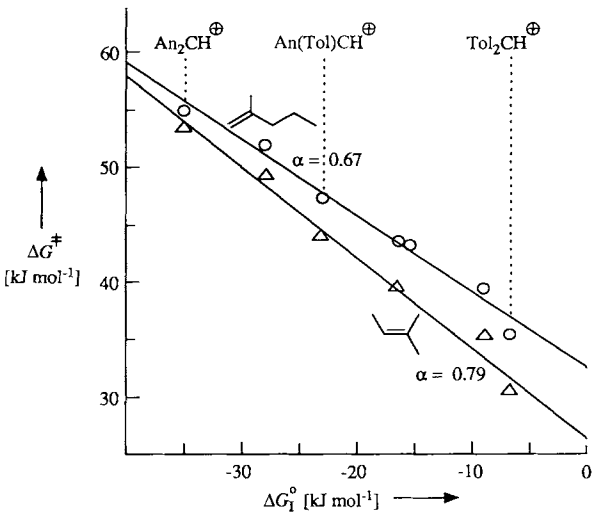

Fig. 2. Correlation between $\Delta G^{\neq}$ for the reactions of diarylcarbenium ions with alkenes [Eq. (h)] and ΔG_i^0 for the ionization of the corresponding diarylmethyl chlorides [Eq. (g)].

Figure 3, in which the energies of the non-ionized benzhydryl chlorides are set at the same level, shows clearly that the order of stability of the benzhydryl cations is retained in the transition states for the additions, but that the separations of the energy levels are much smaller than in the ground states.

The reverse of the reactivity order for the electrophiles discussed above is observed in competition experiments according to Scheme 14, if only catalytic amounts of Lewis acid are used.[2a, 30] Under these conditions, the benzhydryl chloride that forms the better stabilized carbenium ion is more reactive, because according to the Curtin–Hammett principle[48] the relative reactivity is determined solely by the height of the transition state for the CC-coupling step in Figure 3, as long as the equilibrium in the preceding ionization step is established fast compared to the rate of addition. The fact that electrophilicity orders can be inverted by variation of the Lewis acid has been used in synthesis planning.[2a] Although the existing kinetic work has been concerned primarily with diarylcarbenium ions, the conclusions reached can be extended to other systems, as shown in Figure 4. The relative reactivities of benzhydryl, phenethyl, cumyl and propargyl chlorides toward allyltrimethylsilane (which can be regarded as a substituted ethylene, see Fig. 5–7) in the presence of catalytic quantities of zinc chloride are proportional to the rates of ethanolysis of these compounds. As the rates of ethanolysis provide a measure of the "stability" of the intermediate carbenium ions,[50] Figure 4 provides experimental support for the fact that, in the presence of *catalytic amounts* of Lewis acid, the relative electrophilicity of alkyl chlorides increases with the "stability" of the intermediate carbenium ions.

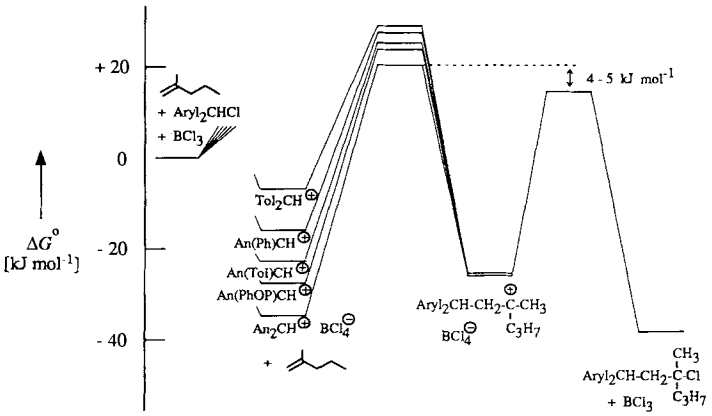

Fig. 3. Free-energy profiles for the boron trichloride induced additions of diarylmethyl chlorides to 2-methyl-1-pentene [14].

The reactivity correlation shown in Figure 4 covers six orders of magnitude and indicates that steric effects are insignificant compared to electronic effects in these systems. The limitations of this approximation become apparent, however, from the fact that triarylcarbenium ions react many times slower than would be expected from their "sta-

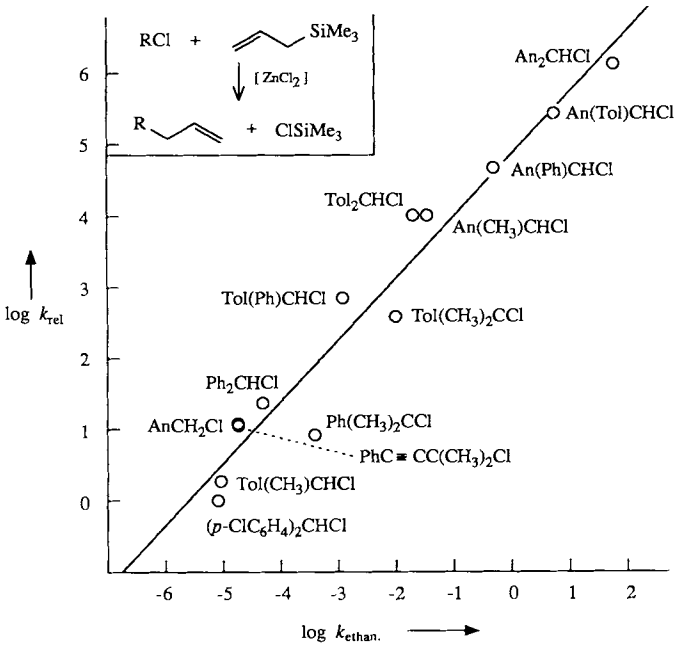

Fig. 4. Plot of the relative reactivities of alkyl chlorides towards allyltrimethylsilane (from competition reactions with $ZnCl_2$ in CH_2Cl_2 at $-70\,^{\circ}C$) [49] vs the logarithms of the ethanolysis rate constants log k_{ethan} (100% EtOH, 25 °C) [50].

bility" ($pK_{R\oplus}$ or solvolysis rates) because of their large steric requirements.[29,49]

5.3. Variation of the Alkene

Stereochemical studies (Section 2) suggest that the attack of carbenium ions on alkenes proceeds via partially bridged transition states, so that different effects can be expected from substituents on the α-carbon atom (the developing carbenium center) and β-carbon atom (the point of attack of the electrophile) (see **36**).

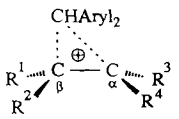

36

5.3.1. α-Effects

The Hammett constant ϱ is often used to characterize the charge distribution in the activated complex.[51] Competition experiments with ditolylcarbenium ions generated in situ (Scheme 17) gave a moderate Hammett correlation with $\varrho^+ = -5.0$ (r = 0.993) and $\varrho = -5.2$ (r = 0.984).[23]

$Tol_2CH^{\oplus}$ + 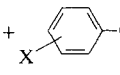 $(ZnCl_2 \cdot OEt_2, CH_2Cl_2, -70\,^{\circ}C)$

X	H	p-F	p-Br	p-Cl	m-NO_2
k_{rel}	1.00	1.14	0.26	0.26	0.00031

Scheme 17. See [23].

The reaction constants are thus in the region of those for the protonation ($\varrho^+ = -3.6$ to -5.4, $\varrho = -4.8$ to -7.0)[52] and bromination ($\varrho^+ = -4.2$)[53] of styrenes and are significantly more negative than those found for NOCl addition ($\varrho = -3.84$, $\varrho^+ = -2.08$)[54] or addition of 2,4-dinitrophenylsulphenyl chloride ($\varrho = -2.33$, $\varrho^+ = -2.03$).[54] These values suggest a high positive charge density on the α-carbon atom in the transition state, which is compatible with the strong dependence of the reaction rate on R shown in Table 4.[6]

Table 4. Rate constants for the reaction of 2-substituted propenes with the *p*-methoxy-substituted diphenylmethyl cation (CH_2Cl_2, $-70\,^{\circ}C$): $An(Ph)CH^{\oplus} + H_2C{=}C(CH_3)R$.

R	k_2[L mol^{-1} s^{-1}]	k_{rel}
$-C{\equiv}CH$	no reaction	< 0.1
H	9.39×10^{-4}	1.0
CH_3	23.3	2.5×10^4
$CH{=}CH_2$	15.6	1.7×10^4
C_6H_5	1.45×10^3	1.5×10^6
Cyclopropyl	5.65×10^3	6.0×10^6

Table 4 shows that the reaction rate increases by a factor of 25 000 when the hydrogen atom in position 2 of propene is replaced by a methyl group (→ isobutene). The $\Delta\Delta G^{\neq}$ value obtained from these data ($\Delta\Delta G^{\neq} = 17$ kJ mol^{-1}) corresponds to about half the difference between the proton affinities of propene and isobutene in the non-nucleophilic solvent SO_2ClF.[36b] Whereas a vinyl group has about the same accelerating effect as methyl (isobutene ≈ isoprene), phenyl and cyclopropyl cause millionfold rate increases. Surprisingly, the ethynyl group is deactivating relative to hydrogen, so that 2-methyl-1-butene-3-yne is inert under conditions in which propene reacts smoothly with electrophiles.

Somewhat different substituent effects are found, however, if variations of R on a secondary carbon are considered (Table 5).[6] Butadiene is 21 times more reactive than propene, showing that in this case a vinyl group exerts a much stronger activating effect than a methyl group. The additional methyl group in *trans*-piperylene causes a 2400 times rate increase relative to butadiene. The activating effect of a phenyl group is also significantly larger than in the example shown in Table 4: whereas α-methylstyrene only reacts 62 times faster than isobutene, styrene is 12 000 times more reactive than propene. Styrene is thus about as nucleophilic towards carbenium ions as isobutene, in agreement with the rule-of-thumb that carbenium ions are stabilized about as

Table 5. Rate constants for the reaction of monosubstituted ethylenes with the *p*-methoxy-substituted diphenylmethyl cation (CH_2Cl_2, $-70\,^{\circ}C$): $An(Ph)CH^{\oplus} + H_2C{=}CHR$.

R	k_2 [L mol^{-1} s^{-1}]	k_{rel}
CH_3	9.39×10^{-4}	1.0
$CH{=}CH_2$	1.93×10^{-2}	21
C_6H_5	10.9	1.2×10^4
$CH{=}CH(CH_3)$	46.2	4.9×10^4

well by two methyl groups as by one phenyl.[55] On the other hand, isobutene may be up to 1000 times more reactive than styrene towards other classes of electrophiles.[56]

Branching of the the α-substituent in the allylic position leads to a moderate decrease in reactivity. The *tert*-butyl-substituted compound in Scheme 18 reacts 19 times slower than isobutene.

$An(Ph)CH^{\oplus} + H_2C = C(CH_3)R$ (CH_2Cl_2, −70 °C)

R	Me	Et	*i*Pr	*t*Bu
k_2 [L mol^{-1} s^{-1}]	23.3	18.4	6.08	1.21

Scheme 18. Effect of methyl groups in an allylic site [6].

In contrast, branching in a homoallylic position actually leads to a small increase in reactivity. In this case, the hyperconjugative effect outweighs the steric effect (Scheme 19).

$An(Ph)CH^{\oplus} + H_2C = C(CH_3)CH_2R$ (CH_2Cl_2, −70 °C)

R	Me	Et	*t*Bu
k_2 [L mol^{-1} s^{-1}]	18.4	25.8	28.6

Scheme 19. Effect of methyl groups in a homoallylic site [6].

5.3.2. β-Effects

Whereas α-effects are predominantly enthalpic in nature, β-effects result from a complex interplay of enthalpic and entropic influences. Furthermore, α-effects are found to be independent of the nature of the reference cation, whereas β-effects vary with different benzhydryl cations (cf. Section 5.4). In general, however, the introduction of a methyl group into the β-position results in a more negative $\Delta S^{\neq}$ and a simultaneous decrease in the enthalpy of activation, $\Delta H^{\neq}$ (*cis*-1-phenylpropene is an exception). A methyl group in the β-position may thus either facilitate or hinder electrophilic attack (Table 6). The discussion of the influence of a second β-methyl group is more difficult, because the CC bond formation step is no longer rate-determining for the reaction of diarylcarbenium ions with tetramethylethylene.[21]

Table 6. The influence of β-methyl groups in alkenes on their reactivities toward the methoxy-substituted benzhydryl cation $An(Ph)CH^{\oplus}$ (CH_2Cl_2, −70 °C).

	$\Delta H^{\neq}$ [kJ mol^{-1}]	$\Delta S^{\neq}$ [J mol^{-1} K^{-1}]	k_2 [L mol^{-1} s^{-1}]	k_{rel}	$\Delta\Delta S^{\neq}$(rel.)
	32.6	−139	9.39×10^{-4}	1.0	0
	31.4	−145	1.01×10^{-3}	1.1	−6
	29.9	−150	1.26×10^{-3}	1.3	−11
	21.1	−112	23.3	1.0	0
	7.5	−159	247	10.6	−47
	(8.0)	(−188)	>5.62	>0.24	−76
	19.3	−127	10.9	1.0	0
	15.5	−154	3.87	0.36	−27
	26.1	−134	0.083	0.0076	−7
	22.4	−99	46.2	1.0	0
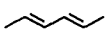	15.1	−124	182	3.9	−25

$An(Ph)CH^{\oplus}$ + RHC = $C(CH_3)_2$ (−70 °C, CH_2Cl_2)

R	CH_3	*t*Bu
k_2 [L mol^{-1} s^{-1}]	247	< 0.247

Scheme 20. See [6].

Very large steric effects are observed when a *tert*-butyl group is introduced into the β-position. Thus, **2** reacts at least 1000 times slower than 2-methyl-2-butene (Scheme 20). As **2** undergoes acid-catalyzed rearrangement to the far more reactive **37**, this value must be considered a lower limit.

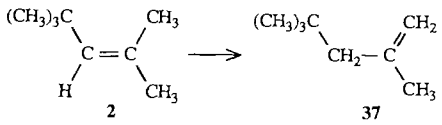

2 **37**

5.3.3. Cyclic Alkenes and Dienes

Cycloalkenes and methylenecycloalkanes sometimes show very different nucleophilicity to their acyclic analogues.[6, 36b] As the reasons for this behavior are still largely unclear, they will not be discussed here. For cycloalkadienes, increasing non-planarity of the π system causes a decrease in the nucleophilicity (Scheme 21).

$An(Ph)CH^{\oplus}$ + (CH_2Cl_2, −70 °C)

n	1	2	3	4
k_2 [L mol^{-1} s^{-1}]	1740	27.5	3.04	0.326

Scheme 21.

5.3.4. Comparison with Other Nucleophilicity Series

Both the kinetic and the stereochemical results indicate that the transition state for the attack of carbenium ions on alkenes is only slightly bridged, so that it is not surprising that the order of reactivity towards carbenium ions does not correlate with those found for bridging electrophiles. Table 7 shows, for instance, the similarity of α- and β-methyl effects in brominations.[57] (*E*)-2-Butene and isobutene are brominated with comparable rates, whereas styrene is significantly less reactive. As in the case of carbenium ion addition, very

different α- and β-effects are observed for protonation (isobutene/(*E*)-2-butene = 10^4; Table 7). However, π-conjugation has a much weaker activating effect in proton addition than in carbenium ion addition. Thus the protonation of isoprene is one and that of styrene three orders of magnitude slower than that of isobutene, although these three compounds are almost equally reactive towards carbenium ions.

Table 7. Relative reactivities of π-nucleophiles toward some electrophiles.

					Ph
$An(Ph)CH^{\oplus}$ (−70 °C) [a]	1.00	1.34	2.48×10^4	1.66×10^4	1.16×10^4
Br_2 (CH_3OH, 25 °C) [b]	1.00	32.3	92.3		3.80
$H_3O^{\oplus}$ (H_2SO_4, 25 °C) [c]	1.00	14.8	1.56×10^5	1.34×10^4	1.01×10^2

[a] Ref. [6]. [b] Ref. [57]. [c] Ref. [58].

A comparison of the reactivity of 20 alkenes and dienes towards $H_3O^{\oplus}$ and $AnPhCH^{\oplus}$ shows that the two data sets are only weakly correlated (r = 0.71),[6] so that there is little chance at present to predict reactivity towards carbenium ions from data for other electrophilic additions. In agreement with the postulated product-like nature of the transition state for carbenium ion addition, however, a reasonable correlation (r = 0.91) was found between addition rates to alkenes and solvolysis rates of the addition products.[6]

5.4. Linear Free Energy Relationships

Better correlations than those shown in Figure 2 result when the reactivities of alkenes towards diarylcarbenium ions are compared with each other (i.e. when the reactivity of these carbenium ions towards a standard nucleophile is used as a reference scale). Figure 5 shows that the reactivity-reactivity correlations thus obtained for terminal alkenes give essentially parallel straight lines, i.e. the relative reactivity of these vinyl compounds is independent of the electrophile.[46]

An alternative representation of this relationship (Fig. 6) shows that the selectivity of the carbenium ions remains constant towards a given pair of nucleophiles, even if the reactivity of the carbenium ion is varied by eight orders of magnitude. This is an example of "constant selectivity correlations", as described by *Ritchie*,[59] even though the usual explanation of these relationships using solvent effects[60] is not applicable here.

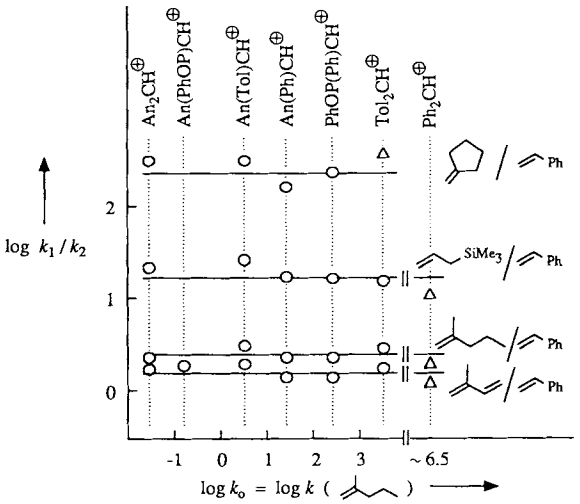

Fig. 6. Constant selectivities of diarylcarbenium ions towards pairs of terminal alkenes (−70 °C, CH_2Cl_2). The selectivities that are plotted as triangles are derived from competition experiments [23, 36b], the others from directly measured rate constants.

We can therefore conclude that structural variations in the reactants remote from the reaction center do not influence the structure of the transition state. This interpretation is all the more attractive, because if alkenes with non-terminal double bonds are included they also give linear reactivity-reactivity relationships, but with corrrelation lines that are no longer parallel (Fig. 7). Changes in the transition state

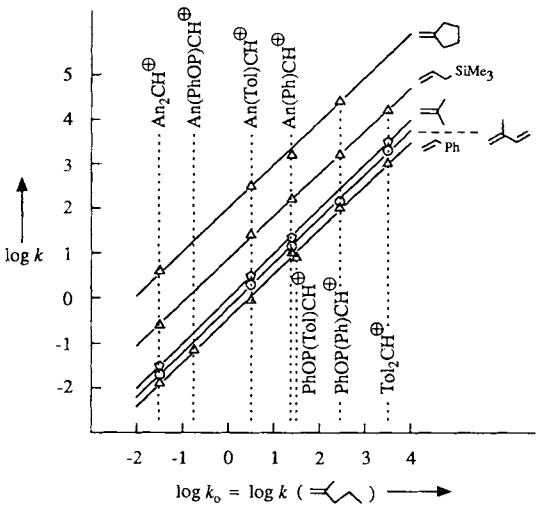

Fig. 5. Reactivities of terminal alkenes towards diarylcarbenium ions (−70 °C, CH_2Cl_2, reference reaction: $Aryl_2CH^{\oplus}$ + 2-methyl-1-pentene) [46].

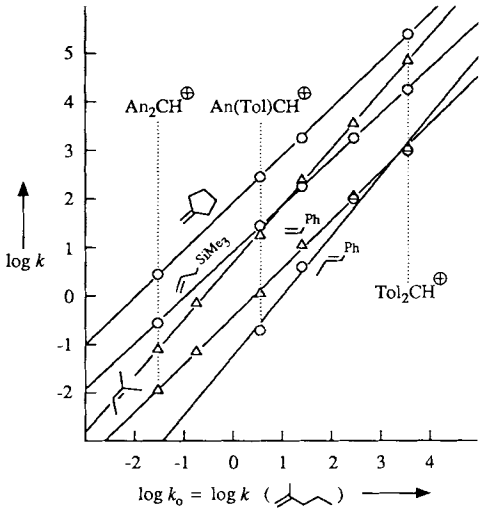

Fig. 7. Reactivities of olefins toward diarylcarbenium ions (−70 °C, CH_2Cl_2, reference reaction: $Aryl_2CH^{\oplus}$ + 2-methyl-1-pentene) [46].

structure caused by variation of substituents at the reaction center are thus indicated. In contrast to Figure 5, the lines now cross, and the nucleophilicity order found for a given carbenium ion is not the same for other electrophiles.

As there is a linear correlation (Fig. 2) between the reactivities of the diarylcarbenium ions and their ground state energies (ΔG_i^0) which in turn are related to the $pK_{R\oplus}$ values by Equation (d), Equation (i) can be derived for the reactivity of diarylcarbenium ions with alkenes. Correspondingly, Equation (j) follows from the correlation between ΔG_i^0 and the ethanolysis rate constants for the benzhydryl chlorides.[46]

$$\log k(CH_2Cl_2,\ -70\,^\circ C) = -7.42 \cdot s - 1.07 \cdot s \cdot pK_{R\oplus} + c \qquad \text{(i)}$$

$$\log k(CH_2Cl_2,\ -70\,^\circ C) = 0.90 \cdot s - 1.26 \cdot s \cdot \log k_{ethan} + c \qquad \text{(j)}$$

Values for c, a nucleophilicity parameter for the alkenes, and for s, a parameter which describes the sensitivity of the rate constant on variation of the carbenium ion, are given in Table 8. $pK_{R\oplus}$ values are listed in reference [61] and ethanolysis rates for the benzhydryl chlorides at 25 °C ($\log k_{ethan}$) in reference [31]. Because the gradients (s) of the reactivity-reactivity correlations (Fig. 7) depend chiefly on the substituents attached to the electrophilically attacked carbon atom, Equations (i) and (j) can also be used to calculate the reactivity of further alkenes that are not included in Table 8. Details for this procedure are given in reference [46]. Because of the correlation shown in Figure 4, it is likely that correlations (i) and (j) can also give approximate values for other classes of carbenium ions, provided that systems with large steric requirements, e.g. triphenylmethyl systems, are excluded.

Table 8. Alkene parameters for the calculation of reactivities toward diarylcarbenium ions according to Equation (i) and (j) [46].

Alkene	s	c
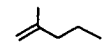	1.000	0.000
	1.000	0.014
	0.948	2.00
	0.978	−0.418
	0.977	−0.174
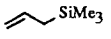	0.950	0.918
	1.164	0.722
	1.106	−0.633
	1.248	−1.26
	1.394	−1.25

5.5. Are SET Processes Important?

An alternative to the mechanisms discussed above is the single electron transfer (SET) shown in Equation (k) to give a diarylmethyl radical and an alkene radical cation followed by combination of these two radicals.[62]

$$Ar_2CH^\oplus + H_2C{=}CH\text{-}R \xrightarrow{\Delta E \approx 2eV} Ar_2\dot{C}H + [H_2C \dot{-} CH\text{-}R]^{\cdot\oplus} \qquad \text{(k)}$$

(Ar = Aryl)

Dorfman et al.[39] ruled out such an electron-transfer step, because of the unfavorable thermodynamics of the process (ionization potentials, $Ph_2CH^\cdot$ 7.32 eV; isobutene 9.23 eV). Although the ionization potentials refer to the gas phase, it is unlikely that solvation will significantly change the energetics because the polarity is little changed by the single electron transfer.

Nevertheless, if we assume that the electron-transfer step shown in Equation (k) is rate-determining in the addition of carbenium ions to alkenes, the reaction rates should be related to the ionization potentials of the alkenes. Table 6 shows, however, that isobutene is 20 000 times more reactive than the 2-butenes, despite its slightly higher ionization potential (9.23 eV vs 9.13 eV).[63] This result speaks against a rate-determining SET step, but steric effects cannot be rigorously ruled out as reason for the discrepancy in reactivity.

In Figure 8 the reactivities of terminal alkenes are plotted against their ionization potentials. It can be seen, for instance, that butadiene and methylenecyclopentane differ by five orders of magnitude in their reactivity despite having similar ionization potentials. On the other hand, isobutene is as reactive as styrene despite a difference of 0.8 eV in their ionization potentials. As we have concluded from Figure 5 that all the transition states for the attack of diarylcarbenium ions on terminal alkenes are structurally very similar, we interpret the lack of correlation between reactivity and ionization potential in Figure 8 as evidence against a rate-determining SET process.

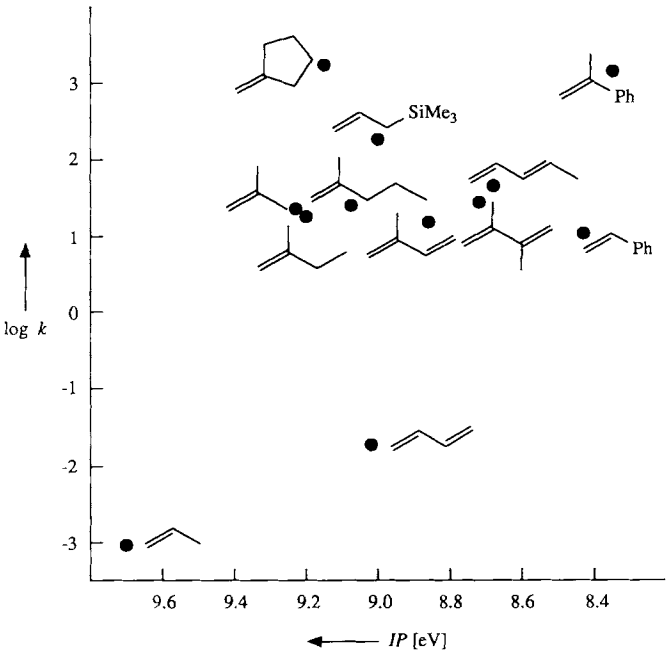

Fig. 8. The reactivities of terminal alkenes toward An(Ph)CH$^\oplus$ plotted against their ionization potentials IP [64].

6. Outlook

As described in the introduction, diarylcarbenium ions **1** were chosen as mechanistic probes, beause their reactivity can be modified by *para*-substituents without changing the steric environment at the reaction center. The principles and relationships thus obtained are, however, transferrable to other electrophiles. Kinetic studies with cyclopentenylium ions have shown, for instance, that the *relative* reactivities of alkenes shown in Tables 4 and 5 change only slightly if allyl cations are used as reference electrophiles instead of benzhydryl cations.[65] It can therefore be expected that the nucleophilicity orders given in Section 5.3 can be used as an approximation for alkylations of alkenes with any carbenium ion. As shown in Figure 4, there is a correlation between the relative electrophilicity and the rate of ethanolysis (S_N1-reactivity). This is not only true for diarylmethyl chlorides, but also for other S_N1-active compounds, including the primary *p*-methoxybenzyl chloride and the tertiary cumyl chloride. The synthetic chemist may therefore predict relative and absolute rates of alkylations on the basis of Figure 4 or Equation (j) if the solvolysis rates of the carbenium ion precursors are known.

Diarylcarbenium ions have therefore shown themselves to be suitable probes for obtaining information about the mechanism of carbenium ion attack on alkenes and about some basic interrelationships between reactivity and selectivity. As these ions can also be produced by laser pulse photolysis in the presence of more reactive olefins (enol ethers etc.),[66] it is possible to extend the reactivity series described here into the region of diffusion-controlled reactions. Kinetic studies on the reactions of diarylcarbenium ions with allyl–element compounds of the fourth main group[67, 68] and with arenes[68] have shown that these nucleophiles obey the same linear free energy relationships as alkenes. It is therefore now possible to describe a wide variety of polar CC bond forming reactions using a consistent mechanistic scheme. Some of the consequences of this work for synthesis planning have been presented in a short summary.[2a]

The majority of the work described here was carried out by Drs. R. Pock, R. Schneider, and C. Schade with the able support of M. Deters (Rubow) and U. Grabis. Only their dedicated and enthusiastic work enabled such a complex reaction sequence to be clarified within a mere few years. This work would not have been possible without a generous initial grant from the Universität Lübeck and the constant unbureaucratic support of the Deutsche Forschungsgemeinschaft. Thanks are also due to the Fonds der Chemischen Industrie and to the Volkswagen-Stiftung for the grant of a Kekulé fellowship to C. Schade.

Received: April 17, 1990 [A 797 IE]
German version: *Angew. Chem. 102* (1990) 1415
Translated by *T. Clark*, Erlangen

[1] a) D. Schinzer (Ed.): *Selectivities in Lewis Acid Promoted Reactions* (NATO ASI Series C, Vol. 289), Kluwer, Dordrecht 1989; for older reviews, see: b) P. A. Bartlett in J. D. Morrison (Ed.): *Asymmetric Syntheses, Vol. 3, Part B*, Academic Press, New York 1984, Chap. 5 and 6; c) G. A. Olah (Ed.): *Friedel-Crafts and Related Reactions*, Wiley-Interscience, New York 1963–1965; d) G. A. Olah: *Friedel-Crafts Chemistry*, Wiley-Interscience, New York 1973; e) R. M. Roberts, A. A. Khalaf: *Friedel-Crafts Alkylation Chemistry*, M. Dekker, New York 1984.

[2] a) H. Mayr in [1a], p. 21; b) *Angew. Chem. 93* (1981) 202; *Angew. Chem. Int. Ed. Engl. 20* (1981) 184; c) H. Mayr, W. Striepe, *J. Org. Chem. 48* (1983) 1159; d) L. Schmerling in [1c], Vol. II, Chap. 26; e) G. A. Olah, S. J. Kuhn, D. G. Barnes, *J. Org. Chem. 29* (1964) 2685; f) H. Stetter, P. Goebel, *Chem. Ber. 95* (1962) 1039; g) A. A. Petrov, K. V. Leets, *J. Gen. Chem. USSR 26* (1956) 1263; h) M. L. Genusov, A. A. Petrov, *ibid. 33* (1963) 2787.

[3] a) P. B. D. De la Mare, R. Bolton: *Electrophilic Additions to Unsaturated Systems*, 2nd Edit., Elsevier, Amsterdam 1982, Chap. 3; b) G. H. Schmid, D. G. Garratt in S. Patai (Ed.): *The Chemistry of Double-Bonded Functional Groups Suppl. A, Part 2*, Wiley, London 1977, Chap. 9, p. 732; c) V. J. Nowlan, T. T. Tidwell, *Acc. Chem. Res. 10* (1977) 252.

[4] a) H. Mayr, H. Klein, *Chem. Ber. 115* (1982) 3528; b) H. Mayr, H. Klein, G. Kolberg, *ibid. 117* (1984) 2555.

[5] See [3b], p. 860.

[6] H. Mayr, R. Schneider, B. Irrgang, C. Schade, *J. Am. Chem. Soc. 112* (1990) 4454.

[7] F. Marcuzzi, G. Melloni, *J. Chem. Soc. Perkin Trans. 2 1976*, 1517.

[8] F. Marcuzzi, G. Melloni, *J. Am. Chem. Soc. 98* (1976) 3295.

[9] H. Groß, E. Höft, *Angew. Chem. 79* (1967) 358; *Angew. Chem. Int. Ed. Engl. 6* (1967) 335.

[10] M. J. S. Dewar, C. H. Reynolds, *J. Am. Chem. Soc. 106* (1984) 1744.

[11] W. S. Johnson, *Angew. Chem. 88* (1976) 33; *Angew. Chem. Int. Ed. Engl. 15* (1976) 9; *Bioorg. Chem. 5* (1976) 51 (cf. [1b]).

[12] R. Pock, H. Mayr, M. Rubow, E. Wilhelm, *J. Am. Chem. Soc. 108* (1986) 7767.

[13] K. Matyjaszewski in G. Allen, J. C. Bevington (Eds.): *Comprehensive Polymer Science, Vol. 4*, Pergamon Press, Oxford 1989, Chap. 41.

[14] H. Mayr, R. Schneider, C. Schade, J. Bartl, R. Bederke, *J. Am. Chem. Soc. 112* (1990) 4446.

[15] a) J. H. Rolston, K. Yates, *J. Am. Chem. Soc. 91* (1969) 1469, 1477; b) M. F. Ruasse, *Acc. Chem. Res. 23* (1990) 87.

[16] E. von der Brüggen, *Dissertation*, Medizinische Universität zu Lübeck 1988.

[17] a) P. Vogel: *Carbocation Chemistry*, Elsevier, Amsterdam 1985, Chap. 8; b) M. Saunders, J. Chandrasekhar, P. von R. Schleyer in P. de Mayo (Ed.): *Rearrangements in Ground and Excited States, Vol. 1*, Academic Press, New York 1980, Chap. 1; c) W. Kirmse, *Top. Curr. Chem. 80* (1979) 125; d) V. G. Shubin, *ibid. 116/117* (1984) 267.

[18] a) M. L. Genusov, A. A. Petrov, *Zh. Org. Khim 1* (1965) 2105; *Chem. Abstr. 64* (1966) 11 098 a; b) H. Klein, *Dissertation*, Universität Erlangen-Nürnberg 1982; c) R. Pock, *Diplomarbeit*, Universität Erlangen-Nürnberg 1981; d) K. Musigmann, *Dissertation*, Medizinische Universität zu Lübeck 1990.

[19] L. Schmerling, *J. Am. Chem. Soc. 67* (1945) 1152.

[20] This suggestion corresponds to a so-called „enforced mechanism": W. P. Jencks, *Acc. Chem. Res. 13* (1980) 161.

[21] R. Schneider, *Dissertation*, Universität Erlangen-Nürnberg 1987.

[22] E. Bäuml, G. Kolberg, H. Mayr, *Tetrahedron Lett. 28* (1987) 387.

[23] R. Pock, H. Mayr, *Chem. Ber. 119* (1986) 2497.

[24] C. Schade, H. Mayr, unpublished results.

[25] R. Pock, H. Klein, H. Mayr, *Chem. Ber. 119* (1986) 929.

[26] A. Streitwieser, Jr., C. H. Heathcock: *Introduction to Organic Chemistry*, 3rd Edit., Macmillan, New York 1985, p. 1153.

[27] C. Schade, H. Mayr, E. M. Arnett, *J. Am. Chem. Soc. 110* (1988) 567.

[28] S. W. Benson, *Thermochemical Kinetics*, 2nd Edit., Wiley-Interscience, New York 1976.

[29] Actually, the salt $(ClC_6H_4)_3C^{\oplus}BCl_4^{\ominus}$ was used for this reaction (case d), so that ΔG_a^0 must be strongly negative in this case: C. Schade, H. Mayr, *Makromol. Chem. Rapid Commun. 9* (1988) 477.

[30] H. Mayr, C. Schade, M. Rubow, R. Schneider, *Angew. Chem. 99* (1987) 1059; *Angew. Chem. Int. Ed. Engl. 26* (1987) 1029.

[31] By combination of Equations 5 and 7 in : C. Schade, H. Mayr, *Tetrahedron 44* (1988) 5761.

[32] a) C. A. Grob, P. W. Schiess, *Angew. Chem. 79* (1967) 1; *Angew. Chem. Int. Ed. Engl. 6* (1967) 1; b) C. A. Grob, *ibid. 81* (1969) 543 and *8* (1969) 535; c) K. G. Becker, C. A. Grob in S. Patai (Ed.): *The Chemistry of Double-Bonded Functional Groups, Suppl. A, Part 2*, Wiley, London 1977, Chap. 8.

[33] This limit naturally changes if the covalent product forms a stable complex with the Lewis acid.

[34] K. Conrow, *J. Am. Chem. Soc. 81* (1959) 5461.

[35] E. Bäuml, C. Schell, H. Mayr, unpublished results.

[36] a) H. Mayr, R. Pock, *Tetrahedron Lett. 24* (1983) 2155; b) H. Mayr, R. Pock, *Chem. Ber. 119* (1986) 2473.

[37] H. Mayr, R. Schneider, *Makromol. Chem. Rapid Commun. 5* (1984) 43.

[38] L. M. Dorfman, R. J. Sujdak, B. Bockrath, *Acc. Chem. Res. 9* (1976) 352.

[39] Y. Wang, L. M. Dorfman, *Macromolecules 13* (1980) 63.

[40] R. Schneider, H. Mayr, P. H. Plesch, *Ber. Bunsenges. Phys. Chem. 91* (1987) 1369, and literature cited therein.

[41] R. Schneider, U. Grabis, H. Mayr, *Angew. Chem. 98* (1986) 94; *Angew. Chem. Int. Ed. Engl. 25* (1986) 89.

[42] J. Smid in M. Szwarc (Ed.): *Ions and Ion Pairs in Organic Reactions, Vol. 1*, Wiley-Interscience, New York 1972, Chap. 3.

[43] a) H. Hostalka, G. V. Schulz, *Z. Phys. Chem. Neue Folge 45* (1965) 286; b) D. N. Bhattacharyya, C. L. Lee, J. Smid, M. Szwarc, *J. Phys. Chem. 69* (1965) 612; c) M. Szwarc in M. Szwarc (Ed.): *Ions and Ion Pairs in Organic Reactions, Vol. 2*, Wiley-Interscience, New York 1974, Chap. 4.
[44] A detailed analysis of the different situations for carbocations and carbanions is given in: H. Mayr, R. Schneider, C. Schade, *Macromol. Chem. Macromol. Symp. 13/14* (1988) 43.
[45] C. Reichardt: *Solvents and Solvent Effects in Organic Chemistry*, 2nd Edit., VCH Verlagsgesellschaft, Weinheim 1988, p. 365.
[46] H. Mayr, R. Schneider, U. Grabis, *J. Am. Chem. Soc. 112* (1990) 4460.
[47] For this reason, the solvolysis rates of methoxy-substituted diphenylmethyl derivatives also correlate poorly with $\sum\sigma^+$: S. Nishida, *J. Org. Chem. 32* (1967) 2692, 2695, 2697.
[48] a) D. Y. Curtin, *Rec. Chem. Progr. 15* (1954) 111; b) L. P. Hammett: *Physical Organic Chemistry*, McGraw-Hill, New York 1970; c) J. I. Seeman, *Chem. Rev. 83* (1983) 83.
[49] J. P. Dau-Schmidt, H. Mayr, unpublished results.
[50] E. M. Arnett, C. Petro, P. von R. Schleyer, *J. Am. Chem. Soc. 101* (1979) 522.
[51] O. Exner: *Correlation Analysis of Chemical Data*, Plenum Press, New York 1988, Chap. 2.4 and literature cited therein.
[52] a) W. M. Schubert, J. R. Keeffe, *J. Am. Chem. Soc. 94* (1972) 559; b) A. D. Allen, M. Rosenbaum, N. O. L. Seto, T. T. Tidwell, *J. Org. Chem. 47* (1982) 4234.
[53] J. H. Rolston, K. Yates, *J. Am. Chem. Soc. 91* (1969) 1483.
[54] G. Collin, U. Jahnke, G. Just, G. Lorenz, W. Pritzkow, M. Röllig, L. Winguth, P. Dietrich, C.-E. Doering, H. G. Hauthal, A. Wiedenhöft, *J. Prakt. Chem. 311* (1969) 238.
[55] A. Streitwieser, Jr., *Solvolytic Displacement Reactions*, McGraw Hill, New York 1962, p. 43.
[56] See Table 3 in [23] for relevant literature.
[57] M. F. Ruasse, J. E. Dubois, A. Argile, *J. Org. Chem. 44* (1979) 1173.
[58] a) W. K. Chwang, V. J. Nowlan, T. T. Tidwell, *J. Am. Chem. Soc. 99* (1977) 7233; b) P. Knittel, T. T. Tidwell, *ibid. 99* (1977) 3408; c) W. K. Chwang, P. Knittel, K. M. Koshy, T. T. Tidwell, *ibid. 99* (1977) 3395.
[59] a) C. D. Ritchie, *Acc. Chem. Res. 5* (1972) 348; b) C. D. Ritchie, *Can. J. Chem. 64* (1986) 2239.
[60] a) A. Pross, *J. Am. Chem. Soc. 98* (1976) 776; b) C. D. Ritchie, *Pure Appl. Chem. 51* (1979) 153.
[61] a) N. C. Deno, J. Jaruzelski, A. Schriesheim, *J. Am. Chem. Soc. 77* (1955) 3044; b) N. C. Deno, A. Schriesheim, *ibid. 77* (1955) 3051.
[62] For reviews on SET-processes, see: a) A. Pross, *Acc. Chem. Res. 18* (1985) 212; b) L. Eberson, F. Radner, *ibid. 20* (1987) 53; c) L. Eberson, *Adv. Phys. Org. Chem. 18* (1982) 79; d) J. K. Kochi, *Angew. Chem. 100* (1988) 1331; *Angew. Chem. Int. Ed. Engl. 27* (1988) 1227.
[63] F. Freeman, *Chem. Rev. 75* (1975) 439.
[64] Ionization potentials were taken from [63] or, if not given there, from: a) D. W. Turner, *Adv. Phys. Org. Chem. 4* (1966) 31; b) Allyltrimethylsilane: A. Schweig, U. Weidner, G. Manuel, *J. Organomet. Chem. 67* (1974) C4.
[65] B. Irrgang, H. Mayr, unpublished results.
[66] a) J. Bartl, S. Steenken, H. Mayr, R. A. McClelland, *J. Am. Chem. Soc. 112* (1990) 6918; b) R. A. McClelland, N. Banait, S. Steenken, *ibid. 108* (1986) 7023.
[67] H. Mayr, G. Hagen, *J. Chem. Soc. Chem. Commun. 1989*, 91.
[68] J. Bartl, G. Hagen, B. Irrgang, H. Mayr, 22nd GDCh-Hauptversammlung, Bonn, 1989, Poster OC46.

Communications may be submitted in English *or* in German. Further details regarding the submission of communications can be found in the "Notice to Authors" reproduced in the January issue of the journal. Copies thereof may be obtained from the editorial office upon request.

Acetylene-Cumulene Porphyrinoids**

By *Norbert Jux, Peter Koch, Hans Schmickler, Johann Lex*, and *Emanuel Vogel**

Dedicated to Professor Günther Wilke on the occasion of his 65th birthday

The aromatic 1,2,8,9-tetradehydro[14]annulene (**1**), discovered accidentally by *Sondheimer* et al. in the course of the synthesis of [14]annulene, is the prototype of the theoretically interesting acetylene-cumulene dehydroannulenes.[1] These annulenes, characterized by the pairwise occurrence of linear $C_{sp^2}C_{sp}C_{sp}C_{sp^2}$ structural units,[2] can be represented by Kekulé resonance structures containing acetylene and cumulene bonds, as exemplified by **1**. Although acetylene-cumulene dehydroannulenes have received much attention owing to the work of *Nakagawa* et al.,[2b,3] the potential usefulness of acetylene-cumulene structural units in the design of "advanced materials" has hitherto not been considered.

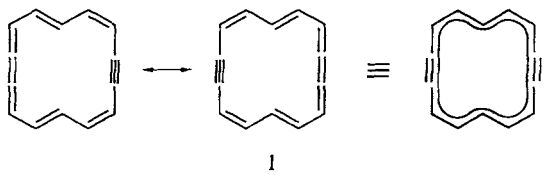

1

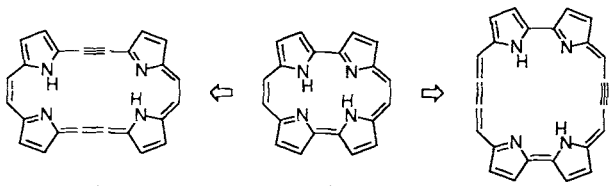

3 2 4

Since porphyrins[4] and porphycenes[5] can be regarded as annulenes in disguise, employment of acetylene-cumulene structural units as building blocks in the development of novel porphyrinoids suggests itself. Assuming that acetylene-cumulene porphycenes should be more readily accessible than the corresponding porphyrins, we turned our initial attention to the former type of compounds. Two structurally isomeric acetylene-cumulene porphycenes, **3** and **4**, may be derived conceptually from porphycene (**2**). Both compounds fulfill the electronic and steric prerequisites for aromaticity, since they possess a main conjugation pathway that involves 22π electrons and is embedded into a planar ring skeleton. The successful synthesis of the octaethyl acetylene-cumulene prophycene **12** (Scheme 1), a porphyrinoid exhibiting high crystallinity and good solubility in organic solvents owing to the presence of the ethyl groups, confirmed this prognosis for the compound of type **3**.

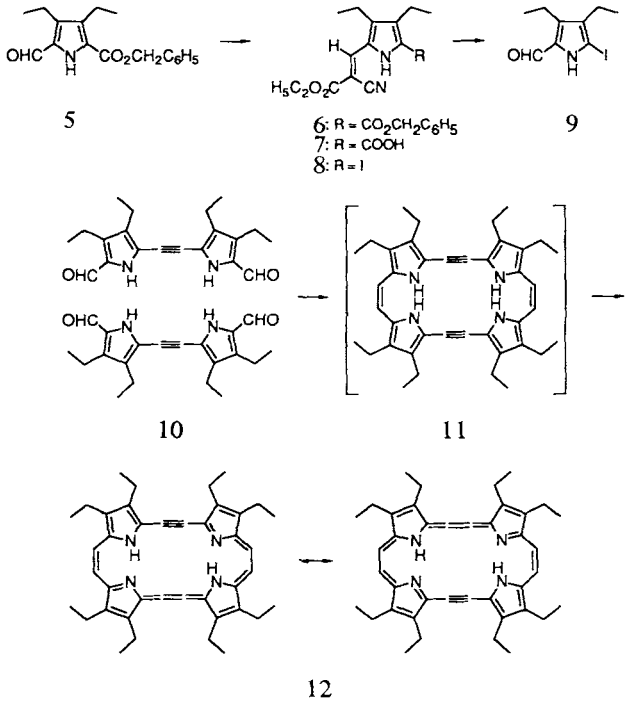

5 6: R = $CO_2CH_2C_6H_5$, 7: R = COOH, 8: R = I 9

10 11

12

Scheme 1. **5** → **6**: $NCCH_2CO_2Et$, EtOH, $MeNH_2$, 5 min, 78 °C, 81%. **6** → **7**: Pd/C, H_2, 1 atm, 4 h, 25 °C, 94%. **7** → **8**: ICl, AcOH, NaOAc, 20 min, 70 °C, 85%. **8** → **9**: NaOH, $MeOH/H_2O$, reflux, 3 h, 70%. **9** → **10**: acetylene, $Pd(PPh_3)_2Cl_2$, CuI, $HNEt_2$, 7 h, 45 °C, 22%. **10** → **12**: $TiCl_4$, Zn, CuCl, THF, reflux, 10 min, 18%.

The synthetic concept for **12** was based on the expectation that the acetylenic dipyrroledialdehyde **10** would undergo reductive coupling in the presence of low-valent titanium[6] to give the true tetrapyrrolic macrocycle **11**, which should show behavior analogous to that of *N,N'*-dihydroporphycene[7] and thus be oxidized spontaneously by air with formation of the acetylene-cumulene porphycene **12**. The actual task would therefore be reduced to synthesis of **10**. To obtain **10**, we first used established methods of pyrrole chemistry[9] to convert the known pyrrolealdehyde **5**,[8] via **6** [yellow needles (ethanol), m.p. 108 °C; yield 81%], 7 [yellow platelets (ethanol), m.p. 184–185 °C (dec.); yield 94%; crude product sufficiently pure for further reaction], and **8** [yellow-orange platelets (ethanol), *E/Z*-isomeric mixture; yield 85%], into iodoaldehyde **9** [bright pink platelets (ethanol/water 1:1), m.p. 105–106 °C; yield 70%]. When acetylene is admitted into a solution of **9** in diethylamine in the presence of bis(triphenylphosphane)palladium(II) chloride and copper(I) iodide,[10] the desired dialdehyde **10** is formed as the nonpolymeric main product. Chromatography on silica gel with ethyl acetate/pentane (1:1) as eluent followed by recrys-

[*] Prof. Dr. E. Vogel, N. Jux, P. Koch, Dr. H. Schmickler, Dr. J. Lex
Institut für Organische Chemie der Universität
Greinstrasse 4, W-5000 Köln 41 (FRG)

[**] This work was supported by the Deutsche Forschungsgemeinschaft and the Stiftung Volkswagenwerk.

tallization from ethanol afforded **10** as yellow-orange cubes [m.p. 255 °C (dec.); yield 22%]. The reductive coupling of **10** to give **12** (via **11**), regarded as the critical step of the synthesis, was carried out as described in the *Experimental Procedure* by a modification of the method used to synthesize **2** and several of its alkyl derivatives.[11]

Table 1. Selected physical data for **6**–**10** and **12**.

6: ^{1}H NMR (300 MHz, $CDCl_3$): δ = 10.26 (br. s, 1H), 8.00 (s, 1H), 7.43, 7.36, 7.31 (m, 5H), 5.35 (s, 2H), 4.33 (q, 2H), 2.73 (q, 2H), 2.59 (q, 2H), 1.36 (t, 3H), 1.13 (t, 3H), 1.12 (t, 3H). MS (EI, 70 eV): *m/z* 380 ($M^{\oplus}$, < 1%), 91 (100). IR (KBr): $\tilde{\nu}$[cm^{-1}] = 3426, 2207, 1714, 1595. UV/VIS (CH_2Cl_2): λ_{max} [nm] (ε) = 239 (17000), 381 (35200).

7: ^{1}H NMR (300 MHz, $CDCl_3$): δ = 11.39 (br. s, 1H), 10.24 (br. s, 1H), 8.03 (s, 1H), 4.34 (q, 2H), 2.76 (q, 2H), 2.62 (q, 2H), 1.37 (t, 3H), 1.16 (t, 3H), 1.15 (t, 3H). MS (EI, 70 eV): *m/z* 290 ($M^{\oplus}$, 64%), 200 (100). IR (KBr): $\tilde{\nu}$[cm^{-1}] = 3419, 2615, 2210, 1724, 1666. UV/VIS (CH_2Cl_2): λ_{max} [nm] (ε) = 239 (15300), 378 (32300).

8: (E/Z-isomeric mixture 58:42): ^{1}H NMR (300 MHz, $CDCl_3$): δ = 12.49 (*Z*, br. s, 1H), 9.62 (*E*, br. s, 1H), 7.81 (*E*, s, 1H), 7.12 (*Z*, s, 1H), 4.32 (*Z*, q, 2H), 4.30 (*E*, q, 2H), 2.61 (*E*, q, 2H), 2.60 (*Z*, q, 2H), 2.40 (*E* and *Z*, q, each 2H), 1.36 (*Z*, t, 3H), 1.33 (*E*, t, 3H), 1.13 (*E*, t, 3H), 1.12 (*Z*, t, 3H), 1.07 (*E* and *Z*, t, each 3H). MS (EI, 70 eV): *m/z* 372 ($M^{\oplus}$, 8%), 157 (100). IR (KBr): $\tilde{\nu}$[cm^{-1}] = 3264, 2205, 1707, 1685. UV/VIS (CH_2Cl_2): λ_{max} [nm] (ε) = 227 (10200), 260 (1000), 306 (3300), 402 (41200).

9: ^{1}H NMR (300 MHz, $CDCl_3$): δ = 9.54 (br. s, 1H), 9.38 (s, 1H), 2.73 (q, 2H), 2.38 (q, 2H), 1.21 (t, 3H), 1.07 (t, 3H). MS (EI, 70 eV): *m/z* 277 ($M^{\oplus}$, 100%), 262 (84). IR (KBr): $\tilde{\nu}$[cm^{-1}] = 3246, 1620, 1367. UV/VIS (CH_2Cl_2): λ_{max} [nm] (ε) = 226 (4100), 313 (19700).

10: ^{1}H NMR (300 MHz, [D_6] dimethyl sulfoxide): δ = 12.30 (br. s, 1H), 9.60 (s, 1H), 2.70 (q, 2H), 2.52 (q, 2H), 1.13 (t, 3H), 1.12 (t, 3H). MS (EI, 70 eV): *m/z* 324 ($M^{\oplus}$, 100%). IR (KBr): $\tilde{\nu}$[cm^{-1}] = 3233, 1614, 1442, 1277. UV/VIS (CH_2Cl_2): λ_{max} [nm] (ε) = 246 (17700), 257 (18700), 283 (20700), 381 (36000), 400 (37200).

12: ^{1}H NMR (300 MHz, CS_2/CD_2Cl_2): δ = 9.99 (s, 4H, H-11,12,23,24), 4.50 (q, 8H, H-3a,8a,15a,20a), 4.16 (q, 8H, H-2a,9a,14a,21a), 2.34 (t, 12H, H-3b,8b,15b,20b), 2.28 (br. s, 2H, NH), 2.03 (t, 12H, H-2b,9b,14b,21b). ^{13}C NMR (75.5 MHz, CS_2/CD_2Cl_2):δ = 143.28, 142.76, 140.82, 126.72, 111.85, 105.75, 22.02, 21.02, 19.43, 18.41. MS (EI, 70 eV): *m/z* 582 ($M^{\oplus}$, 100%), 291 ($M^{2\oplus}$, 6). IR (CsI): $\tilde{\nu}$[cm^{-1}] = 2962, 2067, 1479, 1267, 1216, 1200, 1116, 994, 941, 932. UV/VIS (CH_2Cl_2): λ_{max} [nm] (ε) = 297 (12800), 381 (45600) sh, 405 (188700), 439 (76500), 492 (6200) sh, 619 (4900) sh, 651 (15300) sh, 677 (38900), 724 (73300), 766 (79400).

The structure and aromaticity of **12** are already evident from the spectra of the new tetrapyrrolic macrocycle. The ^{1}H NMR spectrum (300 MHz, CS_2/CD_2Cl_2), for which no temperature dependence has been so far observed (− 100 °C to + 25 °C), consists of a singlet at δ = 9.99 (H-11), two quartets at δ = 4.50 (H-3a) and 4.16 (H-2a), two triplets at δ = 2.34 (H-3b) and 2.03 (H-2b), and a broadened signal at δ = 2.28 (NH). In its general features, this spectrum, which is indicative of a porphyrinoid compound with strong N-H · · · N hydrogen bonds,[12] resembles that of 2,3,6,7,12,13,16,17-octaethylporphycene (**16**),[13] but agrees even better with that of unsubstituted porphycene ($\delta_{H\text{-}9}$ = 9.83; δ_{NH} = 3.15) with respect to the position of the resonances of the vinylic and NH protons.[5] That the NH signal of **16** appears at relatively high field (δ = 0.6) is explained by the increase in the N1N2′ and N1′N2 distances owing to the steric interaction between the inner ethyl groups (weaker N-H · · · N hydrogen bonds). The presence of the $C_{sp} \equiv C_{sp}$ bonds in **12** is revealed by the ^{13}C NMR spectrum, which shows, in addition to the resonances corresponding to those in the spectrum of **16**, a signal at δ = 105.75, typical for C atoms of this kind of compound.[14] The NMR spectroscopic results provide compelling evidence that **12**, like **2**, is a planar molecule exhibiting effective D_{2h} symmetry.

In the UV/VIS spectrum of **12**, the close electronic relationship of **12** with **2** and its alkyl derivatives is very impressively manifested. The spectra of **12** and 2,7,12,17-tetrapropylporphycene (**13**)[11a] (Fig. 1) have almost the same appearance, although in the spectrum of **12** the Soret double band and Q bands exhibit pronounced bathochromic shifts, consistent with the increased length of the main conjugation pathway (22π- instead of 18π-electron system). The mass spectrum (EI, 70 eV) shows the molecular ion (*m/z* 582, 100%) as the base peak and, as additional peak, the doubly charged molecular ion (*m/z* 291, 6%). The presence of strong N-H · · · N hydrogen bonds, as revealed by the position of the NH signal at relatively low field in the ^{1}H NMR spectrum, is further supported in the IR spectrum (CsI) by the absence of a band in the region of 3360–3300 cm^{-1} typical for the NH stretching vibration. An intense absorption at 2067 cm^{-1} corresponds to the asymmetric $C_{sp}C_{sp}$ stretching vibration.

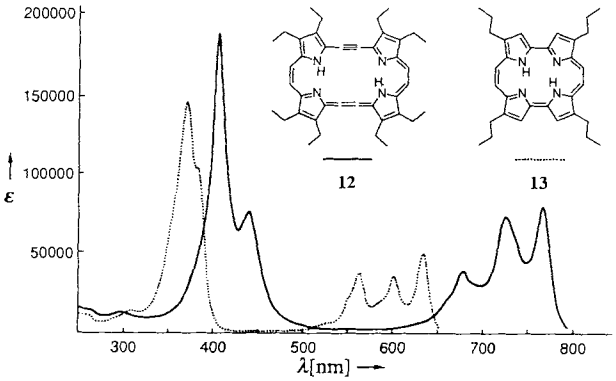

Fig. 1. UV/VIS spectrum of **12** and 2,7,12,17-tetrapropylporphycene (**13**) in dichloromethane.

In the crystal[15] (Fig. 2), the acetylene-cumulene porphycene **12** exists as a centrosymmetric molecule with a prac-

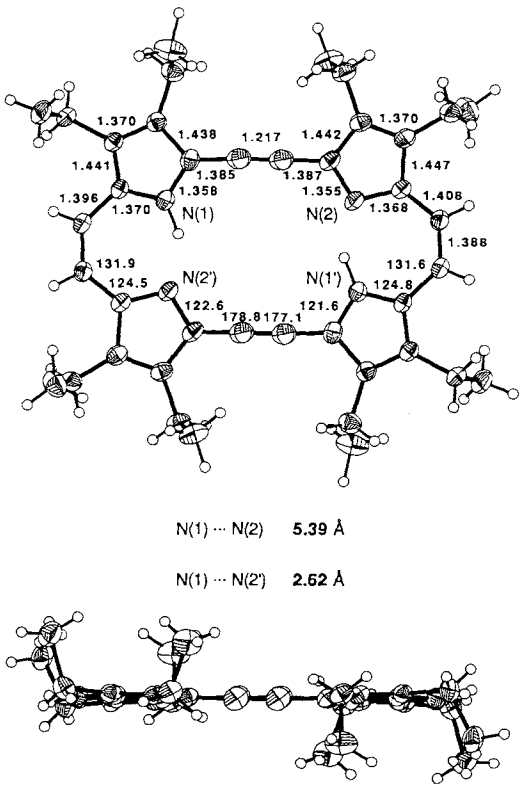

Fig. 2. Molecular structure of **12**. Top: Top view. Bottom: Side view. Selected bond lengths and other distances [Å] and bond angles [°]; standard deviations of ca. 0.002 Å and 0.1°. The thermal ellipsoids are drawn at 40% probability.

tically planar ring framework (maximal distance of the C and N atoms from the mean ring plane: 0.07 Å). As indicated by the symmetry, the $C_{sp^2}C_{sp}C_{sp}C_{sp^2}$ structural units on opposite sides are equivalent; **12** should therefore be formulated as a resonance hybrid. The geometric parameters of these C_4 units are in excellent agreement with those in **1**[2a] and in 3,9,12,18-tetra-*tert*-butyltetradehydro[18]annulene[2b] with respect to the bond angles at the sp-hybridized carbons (178.8 and 177.1°) and the lengths of the $C_{sp^2}C_{sp}$ and $C_{sp}C_{sp}$ bonds (1.385/1.387 Å and 1.217 Å, respectively). Basically, the macrocycle **12** may be viewed as a "stretched" porphycene. The NH hydrogens in **12**, unlike those in **2**, are not disordered, so that assignment to specific nitrogens (which must be N atoms in diagonal positions owing to symmetry) is possible. The cavity of **12** exhibits N1N2′ and N1N2 distances of 2.62 and 5.39 Å, respectively, and therefore has very unfavorable dimensions for complexation of metals. Conceivably, however, the $C_{sp}C_{sp}$ bonds might assist coordination with suitable metal ions.

The small amounts of byproducts formed on reductive coupling of **10** to give **12** were identified as the acetylenic dihydro compound **14** and the tetrahydro compound **15**. Compound **15**, described in the following communication,[16] represents the first [22]porphyrin(2.2.2.2).

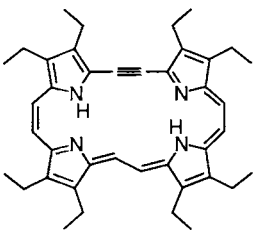

14

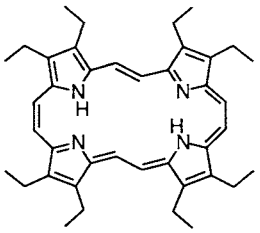

15

Experimental Procedure

12: Activated zinc (650 mg, 10 mmol) and anhydrous copper(I) chloride (65 mg, 0.7 mmol) were suspended in 40 mL of absolute tetrahydrofuran (THF) and treated slowly with titanium tetrachloride (0.54 mL, 5 mmol). The mixture was refluxed for 3 h before dialdehyde **10** (162 mg, 0.5 mmol) was added in small portions. After 10 min of further heating, 40 mL of aqueous ammonia was added in order to hydrolyze the reaction mixture, which was then extracted with chloroform. Chromatography on silica gel with carbon disulfide and subsequent recrystallization from benzene afforded 26 mg (18%) of **12** as blue needles with a metallic luster (dec. above 300 °C). Compounds **14** and **15** were isolated as minor products in up to 5% combined yield.

Received: December 13, 1989 [Z 3685 IE]
Publication delayed at authors' request
German version: *Angew. Chem. 102* (1990) 1429

CAS Registry numbers:
5, 59435-28-8; **6**, 130248-82-7; **7**, 130248-83-8; **8** (isomer 1), 130248-81-6; **8** (isomer 2), 130248-85-0; **9**, 130248-86-1; **10**, 130248-87-2; **12**, 130248-84-9; **13**, 106562-37-2; $NCCH_2CO_2Et$, 105-56-6; acetylene, 74-86-2.

[1] F. Sondheimer, Y. Gaoni, *J. Am. Chem. Soc. 82* (1960) 5765; F. Sondheimer, Y. Gaoni, L. M. Jackman, N. A. Bailey, R. Mason, *ibid. 84* (1962) 4595.
[2] a) N. A. Bailey, R. Mason, *Proc. Chem. Soc. 1963*, 180; b) C. Kabuto, Y. Kitahara, M. Iyoda, M. Nakagawa, *Tetrahedron Lett. 1976*, 2787, 2791.
[3] K. Fukui, T. Nomoto, S. Nakatsuji, M. Nakagawa, *Tetrahedron Lett. 1972*, 3157; M. Iyoda, M. Nakagawa, *ibid. 1972*, 3161; M. Nakagawa, *Pure Appl. Chem. 44* (1975) 885; *Angew. Chem. 91* (1979) 215; *Angew. Chem. Int. Ed. Engl. 18* (1979) 202.
[4] H. Scheer, J. J. Katz in K. M. Smith (Ed.): *Porphyrins and Metalloporphyrins*, Elsevier, Amsterdam 1975, p. 399; M. Gouterman in D. Dolphin (Ed.): *The Porphyrins, Vol. III*, Academic Press, New York 1978, p. 1.
[5] E. Vogel, M. Köcher, H. Schmickler, J. Lex, *Angew. Chem. 98* (1986) 262; *Angew. Chem. Int. Ed. Engl. 25* (1986) 257; E. Vogel, *Pure Appl. Chem. 62* (1990) 557.
[6] J. E. McMurry, M. P. Fleming, *J. Am. Chem. Soc. 96* (1974) 4708; T. Mukaiyama, T. Sato, J. Hanna, *Chem. Lett. 1973*, 1041; S. Tyrlik, I. Wolochowicz, *Bull. Soc. Chim. Fr. 1973, 2147*; recent reviews: J. E. McMurry, *Chem. Rev. 89* (1989) 1513; D. Lenoir, *Synthesis 1989*, 883.
[7] *N,N′*-Dihydroporphycene has so far eluded detection. Its 9,10,19,20-tetrapropyl derivative, however, is sufficiently stable in the absence of air to be characterized; the compound was shown to be a phane by X-ray structure analysis: E. Vogel, I. Grigat, M. Köcher, J. Lex, *Angew. Chem. 101* (1989) 1687; *Angew. Chem. Int. Ed. Engl. 28* (1989) 1655.
[8] J. B. Paine III, R. B. Woodward, D. Dolphin, *J. Org. Chem. 41* (1976) 2826.
[9] J. B. Paine III, D. Dolphin, *J. Org. Chem. 53* (1988) 2787.
[10] H. A. Dieck, F. R. Heck, *J. Organomet. Chem. 93* (1975) 259; K. Sonogashira, Y. Tohda, N. Hagihara, *Tetrahedron Lett. 1975*, 4467.
[11] a) E. Vogel, M. Balci, K. Pramod, P. Koch, J. Lex, O. Ermer, *Angew. Chem. 99* (1987) 909; *Angew. Chem. Int. Ed. Engl. 26* (1987) 928; b) E. Vogel, M. Köcher, J. Lex, O. Ermer, *Isr. J. Chem. 29* (1989) 257.
[12] J. Emsley, *Chem. Soc. Rev. 9* (1980) 91; A. Novak, *Struct. Bonding (Berlin) 18* (1974) 177.
[13] E. Vogel, P. Koch, unpublished.
[14] K. Müllen, *Chem. Rev. 84* (1984) 603.
[15] $C_{40}H_{46}N_4$, dec. > 300 °C, crystals from benzene; triclinic, space group $P\bar{1}$, $Z = 1$; $a = 8.315(1)$, $b = 9.405(1)$, $c = 11.268(2)$ Å, $\alpha = 94.97(1)$, $\beta = 100.81(1)$, $\gamma = 104.15(1)°$; $\varrho_{calcd} = 1.164$ g cm^{-3}; intensities measured on an Enraf-Nonius CAD-4 diffractometer [room temperature, $\lambda_{Mo} = 0.71069$ Å, $\theta_{Mo}(max) = 27°$]; refinement (C, N anisotropic, H isotropic) taking into consideration 2634 reflections with $F > 4\sigma(F_o)$; $R = 0.040$, $R_w = 0.050$. Further details of the crystal structure investigation may be obtained from the Fachinformationszentrum Karlsruhe, Gesellschaft für wissenschaftlich-technische Information mbH, W-7514 Eggenstein-Leopoldshafen 2 (FRG), on quoting the depository number CSD-54912, the names of the authors, and the journal citation.
[16] E. Vogel, N. Jux, E. Rodriguez-Val, J. Lex, H. Schmickler, *Angew. Chem. 102* (1990) 1431; *Angew. Chem. Int. Ed. Engl. 29* (1990) 1387.

Porphyrin Homologues: [22]Porphyrin(2.2.2.2), a "Stretched Porphycene"

By *Emanuel Vogel,* Norbert Jux, Eduardo Rodriguez-Val, Johann Lex*, and *Hans Schmickler*

Dedicated to Professor Rolf Huisgen on the occasion of his 70th birthday

Porphyrin (**1a**), the parent compound of the biologically most important class of natural dyes and pigments, is a tetrapyrrolic macrocycle whose π-electron structure can be described by various models.[1] In the design and synthesis of novel porphyrinoid ring systems,[2] it has proven useful to regard **1a** as an [18]annulene. Accordingly, **1a** should have homologues derived from [4n+2]annulenes with $n > 4$. These homologues, some of which are already known as dicationic *N,N′,N″,N‴*-tetraalkyl derivatives from the elegant biomimetic syntheses of *Franck* et al.,[3] may be represented (together with **1a**) by the generalized formula **1** (leaving stereochemistry aside).[4]

An obvious variation of formula **1** would be to differentiate the four $(CH)_n$ segments as depicted by formula **2**. In **2**, a $(4n+2)\pi$-electron main conjugation pathway is maintained if the sum of the carbons in the segments is a multiple of 4. The porphyrin homologues are thus complemented by a broad spectrum of porphyrin analogues. Representative examples are [18]porphyrin(2.0.2.0) (porphycene), first synthesized in 1986,[2a] and the [22]porphyrin(3.1.3.1) system, the parent structure of the platyrins,[5] the preparation of which was recently reported.[6]

[*] Prof. Dr. E. Vogel, N. Jux, E. Rodriguez-Val, Dr. J. Lex, Dr. H. Schmickler
Institut für Organische Chemie der Universität
Greinstrasse 4, W-5000 Köln 41 (FRG)

Porphyrin homologues Porphyrin analogues Dicationic porphyrinoids

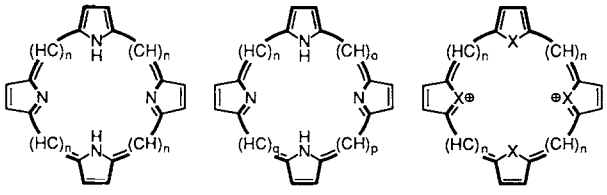

1 2 3

a: n=1
b: n=2
c: n=3

(n+o+p+q) = 4 N
N = 1, 2, 3, etc.

X = NH, NCH_3, O, S, Se

As pointed out earlier,[2c] porphyrin and its homologues bear a close relationship to the dicationic porphyrinoids represented by formula **3**, that is, the *N*,*N*′,*N*″,*N*‴-tetraalkylated porphyrins[2e] and their homologues,[3] and compounds in which the N/NH functions in **1** are replaced by heteroatoms such as oxygen,[2c] sulfur,[2d] and selenium.[2d] A similar relationship linking neutral molecules to charged species applies to the porphyrin analogues **2**.[2b] As regards the charge distribution in the dicationic porphyrinoids, it is not yet clear to what extent resonance structures in which the positive charges reside at the heteroatoms contribute to the hybrid.

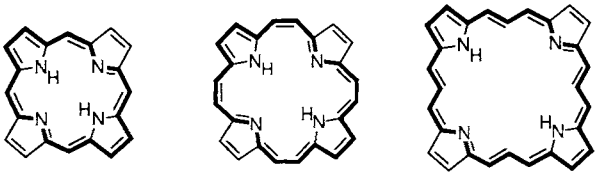

1a 4 5

[18]Porphyrin(1.1.1.1) [22]Porphyrin(2.2.2.2) [26]Porphyrin(3.3.3.3)

Of the porphyrinoids **1**–**3**, the neutral porphyrin homologues **1b**, **1c**, etc., which are of interest as unusual chromophores, potential ligands, and components of supramolecular structures, still pose a challenge for the synthetic chemist. In pursuing the synthesis of such molecules, it must be kept in mind that the transition from porphyrin to its homologues is accompanied by the occurrence of configurational isomerism.[7] Stereochemical considerations indicate that a distinction should be made between porphyrin homologues with odd and even index n (formula **1**). Whereas a porphyrin-like geometry with D_{2h} symmetry should be favored for **1c**, **1e**, etc., as shown by formula **5** for **1c**—that is, $(CH)_n$ segments with all-*trans*-CH=CH bonds—the existence of a D_{2h}-symmetric molecule is rendered difficult, if not ruled out, for **1b**, **1d**, etc., for steric reasons.

The target molecule of the present work is the *next higher homologue of porphyrin*, termed [22]porphyrin(2.2.2.2) (**1b**), for which, besides the isomer **4** containing four *cis*-CH=CH bonds, isomers with *trans*-CH=CH bonds must be considered. In all probability, **4** is nonplanar, since it should have a relatively high strain, which can hardly be compensated for by the resonance energy of the system. As consistently found by both examination of molecular models and force-field calculations,[8] **4a**, the *cis,trans,cis,trans* isomer of [22]porphyrin(2.2.2.2), is energetically favored over **4** and other isomers. Structure **4a** can adopt a planar conformation with only slight skeletal strain and has the additional advantage that it possesses N-H···N hydrogen bonds tending to stabilize a planar arrangement.

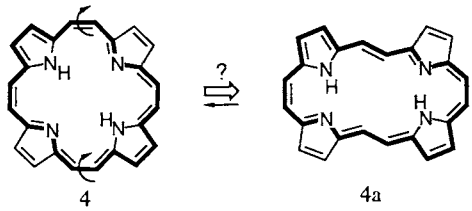

4 4a

Here we describe two syntheses of the porphyrin homologue 2,3,8,9,14,15,20,21-octaethyl[22]porphyrin(2.2.2.2) (**7**), the first one employing the acetylene-cumulene porphyrinoid **6** reported in the preceding communication[9] as starting compound. Hydrogenation of **6** with palladium (Pb-poisoned), carried out until the starting material and dihydro compound were consumed (TLC monitoring), afforded the tetrahydro compound **7** as the major nonpolymeric product.

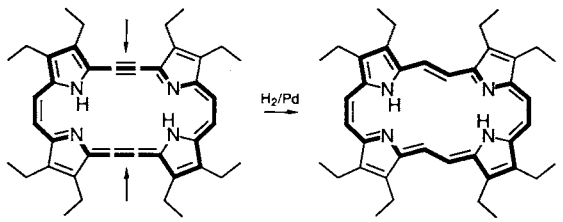

6 7

Chromatography on silica gel with carbon disulfide followed by crystallization from benzene furnished violet crystals (rhombs; dec. above 285 °C; yield 35%), which, in organic solvents, produced green solutions.

The ^{1}H NMR spectrum of **7** (see Fig. 1 and Table 1) is temperature-dependent and consistent with a *cis,trans,-cis,trans* configuration of the compound. The extreme low- and high-field positions of the resonances of the perimeter protons H-5,11,12 and H-6, respectively, convincingly demonstrate the aromatic porphyrinoid nature of **7**, whereas the resonance of the NH protons at relatively low field (porphyrin NH protons: $\delta = -3.76$[10]), due to the presence of strong N-H···N hydrogen bonds,[11] clearly reveals the structural relationship of **7** to porphycene (NH protons: $\delta = 3.15$[2a]). The changes in the spectrum observed above 70 °C (in $C_2D_2Cl_4$) indicate that rapid exchange occurs between H-5 and H-6, H-11 and H-12, the ethyl groups on C-2 and C-9, and the ethyl groups on C-3 and C-8 and thus suggest that [22]porphyrin(2.2.2.2), in *cis,trans,cis,trans* con-

Table 1. Selected physical data for **7** and **9**.

7: ^{1}H NMR (300 MHz, CS_2/CD_2Cl_2, room temperature): $\delta = 11.70$ (d, $^3J_{5,6} = 15.24$ Hz, 2H; H-5,17), 9.88, 9.83 (2 d, $^3J_{11,12} = 11.23$ Hz, 4H; H-11,12,23,24), 4.69, 4.28 (2 q, 8H; H-3a,8a,15a,20a), 4.14 (q, 8H; H-2a,9a,14a,21a), 2.36, 2.14 (2 t, 12H; H-3b,8b,15b,20b), 2.01, 1.99 (2 t, 12H; H-2b,9b,14b,21b), 1.34 (br. s, 2H, NH), −7.50 (d, 2H; H-6,18). ^{13}C NMR (75.5 MHz, CS_2/CD_2Cl_2): $\delta = 147.26$, 145.61, 144.99, 140.48, 140.24, 139.93, 139.85, 139.48, 116.09, 113.84, 111.30, 108.96, 23.10, 20.90, 20.66, 20.46, 19.37, 19.30 (2 C), 16.81. MS (EI, 70 eV): *m/z* 586 ($M^{\oplus}$, 100%), 293 (18). IR (CsI): $\tilde{\nu}$[cm^{-1}] = 2963, 2932, 2871, 1471, 1283, 1195, 1054, 1006, 985, 937, 806, 619. UV/VIS (CH_2Cl_2): λ_{max} [nm] (ε) = 270 (14400), 417 (79800) sh, 440 (207900), 464 (104400), 482 (41600) sh, 579 (2200) sh, 618 (4100) sh, 656 (19500) sh, 672 (38900), 685 (26500) sh, 719 (16600) sh, 726 (17100), 790 (57200).

9: ^{1}H NMR (300 MHz, $CDCl_3$): $\delta = 10.02$ (br.s, 1H), 9.86 (s, 2H), 2.74 (q, 4H), 1.21 (t, 6H). MS (EI, 70 eV): *m/z* 179 ($M^{\oplus}$, 100%). IR (KBr): $\tilde{\nu}$[cm^{-1}] = 3261, 1675, 1649, 1470, 1220. UV/VIS (CH_2Cl_2): λ_{max} [nm] (ε) = 241 (19300), 320 (1400).

figuration, undergoes an isodynamic transformation involving rotation around the *trans*-CH=CH bonds[12]—corresponding to a transition from C_{2h} to effective D_{2h} molecular symmetry. A detailed line-shape analysis of the temperature-dependent spectrum is still being carried out. However, the coalescence temperature of the signals of the methyl protons of the ethyl substituents on C-3 and C-8 already allows the free energy of activation $\Delta G^{\neq}$ of the isodynamic conformational process to be estimated as about 20 kcal mol^{-1}.

The ^{1}H NMR spectrum of **7** may be compared with that of *Franck*'s compound **8**,[6] derived from [22]porphyrin(1.3.1.3), a porphyrinoid isomeric to [22]porphyrin-(2.2.2.2) (**4a**). An astounding analogy is found between the two types of [22]porphyrin with respect to the ring-current effect. In both **7** and **8**, the difference in the chemical shifts of the inner and outer protons is on the order of no less than $\Delta\delta = 20$ (Fig. 1).

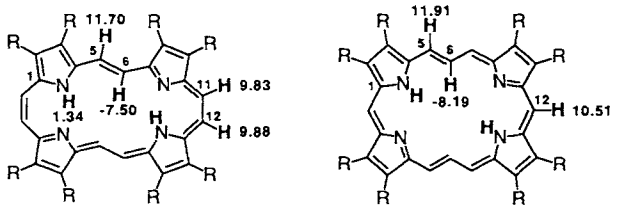

7: R=C_2H_5 8: R=CH_2COOEt

Fig. 1. Comparison of the ^{1}H NMR data (each 300 MHz, room temperature) of **7** (in CS_2/CD_2Cl_2) and **8** (in $CDCl_3$) [6] with respect to the chemical shifts of the protons most influenced by the diamagnetic ring current (no information is available regarding the position of the signal for the NH proton in **8**).

The UV/VIS spectrum of **7** contains a strong Soret band, appearing as a double band at $\lambda = 440/464$ nm ($\varepsilon = 207900/104400$), and Q bands in the region of $\lambda = 672$ to 790 nm. Owing to the shape and position of the bands, this spectrum might be looked upon as a porphycene spectrum shifted to longer wavelength. The IR spectrum of **7** reveals no NH stretching vibration and thus provides an additional argument that this compound, like porphycene, features strong N-H···N hydrogen bonds. In the mass spectrum (EI, 70 eV), the molecular ion (*m/z* 586, 100%) accounts for the base peak and the doubly charged molecular ion (*m/z* 293, 18%) for an additional prominent peak.

An X-ray structure analysis[13] of **7** (Fig. 2) confirms the *cis,trans,cis,trans* configuration of the compound and reveals, in particular, the planarity of the ring framework (maximum distance of the C and N atoms from the mean ring plane: 0.05 Å). Compound **7** is centrosymmetric; accordingly, the imino hydrogens can be assigned to diagonally opposite nitrogens. A parallel observation is that **7** contains two kinds of pyrrolic rings, whose bond lengths and angles agree within the limits of error with those in octaethylporphyrin.[14] Whereas the relationship of **7** to porphyrins is reflected in the structural parameters of the pyrrolic rings, the striking similarities in the partial structures of **7** and porphycene justify regarding **7** as a "stretched porphycene". The presence of strong N-H···N hydrogen bonds in **7** is presumably of decisive importance for the planarity of the ring framework of the molecule as is true for porphycene. The nonbonding interactions between the inner CH hydrogens are too small, in agreement with molecular models, to cause a significant deviation of these hydrogens from the plane of the molecular framework. However, such interactions are reflected by an increase in the CCC angles at C-6

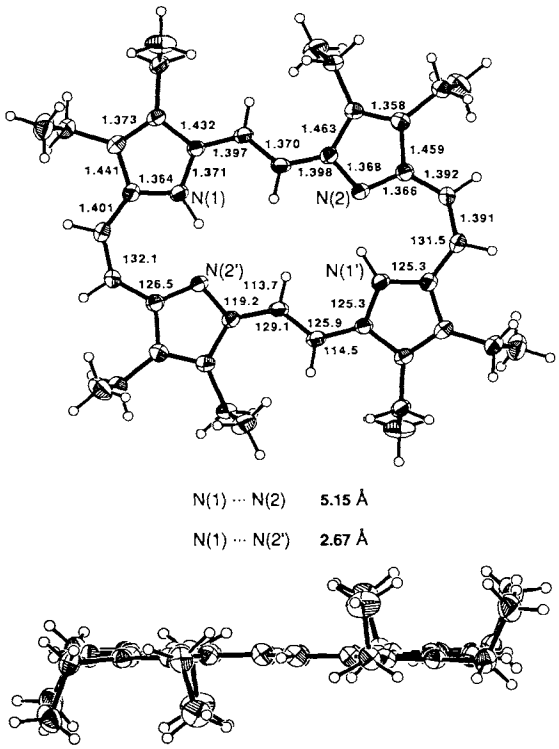

Fig. 2. Molecular structure of **7**. Top: Top view. Bottom: Side view. Selected bond lengths and other distances [Å] and bond angles [°]; standard deviations ca. 0.003 Å and 0.2°. The thermal ellipsoids are drawn at 40% probability.

and C-18. The four N atoms in **7** define a parallelogram (N2-N1-N2′ = 78.1°) owing to the presence of the *trans*-CH=CH segments.

The stability of *cis,trans,cis,trans*-octaethyl[22]porphyrin-(2.2.2.2) (**7**) encouraged us to attempt a one-pot synthesis of the compound—comparable to the biomimetic synthesis of porphyrins[15] from α-hydroxy- or α-aminomethylpyrroles—by reductive coupling of dialdehyde **9**[16] with low-valent titanium.[17] Indeed, reaction of **9** with the coupling reagent generated from titanium tetrachloride and zinc-copper in tetrahydrofuran gave the desired compound **7** as the only low-molecular-weight product, although in a preliminary yield of only 1%. In the meantime, we have also

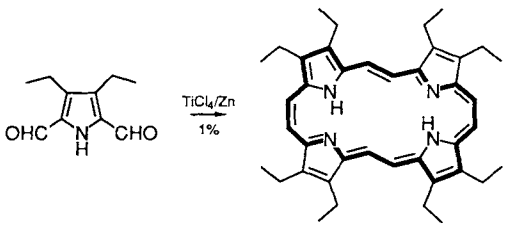

9 **7**

carried out the coupling of 2,5-pyrroledicarbaldehyde under the same conditions to give unsubstituted *cis,trans,cis,trans*-[22]porphyrin(2.2.2.2) (**4a**).[18] In this case, the yield is even lower (0.1–0.2%), presumably owing to solubility problems. A full characterization of the parent compound will therefore require further experimentation.

Received: May 4, 1990 [Z 3944 IE]
Publication delayed at authors' request
German version: *Angew. Chem.* *102* (1990) 1431

CAS Registry Numbers:
4a, 130274-67-8; **6**, 130248-84-9; **7**, 130274-65-6; **9**, 130274-66-7; 2,5-diformylpyrrole, 39604-60-9; 2-(2-cyano-2-ethoxycarbonylvinyl)-3,4-diethyl-5-iodopyrrole), 130274-68-9.

[1] H. Scheer, J. J. Katz in K. M. Smith (Ed.): *Porphyrins and Metalloporphyrins*, Elsevier, Amsterdam 1975, p. 405; T. R. Janson, J. J. Katz in D. Dolphin (Ed.): *The Porphyrins, Vol. IV*, Academic Press, New York 1979, p. 1; J. Michl, *J. Am. Chem. Soc. 100* (1978) 6801; I. Gutman, *Croat. Chem. Acta 58* (1985) 359; M. J. S. Dewar, E. F. Healy, J. Ruiz, *Pure Appl. Chem. 58* (1986) 67; W. Flitsch, *ibid. 58* (1986) 153.

[2] a) Porphycene: E. Vogel, M. Köcher, H. Schmickler, J. Lex, *Angew. Chem. 98* (1986) 262; *Angew. Chem. Int. Ed. Engl. 25* (1986) 257; E. Vogel, *Pure Appl. Chem. 62* (1990) 557; b) Tetraoxaporphycene dication: E. Vogel, M. Sicken, P. Röhrig, H. Schmickler, J. Lex, O. Ermer, *Angew. Chem. 100* (1988) 450; *Angew. Chem. Int. Ed. Engl. 27* (1988) 411; c) Tetraoxaporphyrin dication: E. Vogel, W. Haas, B. Knipp, J. Lex, H. Schmickler, *ibid. 100* (1988) 445 and *27* (1988) 406; W. Haas, B. Knipp, M. Sicken, J. Lex, E. Vogel, *ibid. 100* (1988) 448 and *27* (1988) 409; d) Tetrathiaporphyrin dication: E. Vogel, P. Röhrig, M. Sicken, B. Knipp, A. Herrmann, M. Pohl, H. Schmickler, J. Lex, *ibid. 101* (1989) 1683 and *28* (1989) 1651; e) *N,N',N'',N'''*-Tetramethylporphyrin dication: B. Franck, *ibid. 94* (1982) 327 and *21* (1982) 343; see also [2d].

[3] *N,N',N'',N'''*-Tetramethyl[26]porphyrin(3.3.3.3) dication: M. Gosmann, B. Franck, *Angew. Chem. 98* (1986) 1107; *Angew. Chem. Int. Ed. Engl. 25* (1986) 1100; *N,N',N'',N'''*-Tetramethyl[34]porphyrin(5.5.5.5) dication: G. Knübel, B. Franck, *ibid. 100* (1988) 1203 and *27* (1988) 1170.

[4] Representatives of porphyrinoids that have a $(4n+2)\pi$-electron main conjugation pathway and are not covered by formulas **1** and **2** are the sapphyrins [M. J. Broadhurst, R. Grigg, A. W. Johnson, *J. Chem. Soc. Perkin Trans. 1 1972*, 2111; V. J. Bauer, D. L. J. Clive, D. Dolphin, J. B. Paine III, F. L. Harris, M. M. King, J. Loder, S.-W. Chien Wang, R. B. Woodward, *J. Am. Chem. Soc. 105* (1983) 6429; J. L. Sessler, M. J. Cyr, V. Lynch, *J. Am. Chem. Soc. 112* (1990) 2810], pentaphyrins [H. Rexhausen, A. Gossauer, *J. Chem. Soc. Chem. Commun. 1983*, 275], corroles [A. W. Johnson in K. M. Smith (Ed.): *Porphyrins and Metalloporphyrins*, Elsevier, Amsterdam 1975, p. 732; A. W. Johnson, I. T. Kay, *J. Chem. Soc. 1965*, 1620; A. R. Battersby, G. L. Hodgson, M. Ihara, E. McDonald, J. Saunders, *J. Chem. Soc. Perkin Trans. 1 1973*, 2923], and texaphyrins [J. L. Sessler, M. R. Johnson, V. Lynch, *J. Org. Chem. 52* (1987) 4394; J. L. Sessler, T. Murai, V. Lynch, M. Cyr, *J. Am. Chem. Soc. 110* (1988) 5586].

[5] R. A. Berger, E. LeGoff, *Tetrahedron Lett. 1978*, 4225; E. LeGoff, O. G. Weaver, *J. Org. Chem. 52* (1987) 710.

[6] M. Gosmann, A. Vogt, B. Franck, *Liebigs Ann. Chem. 1990*, 163; see also the communication by *Franck* et al. in this issue: H. König, C. Eickmeier, M. Möller, U. Rodewald, B. Franck, *Angew. Chem. 102* (1990) 1437; *Angew. Chem. Int. Ed. Engl. 29* (1990) 1393; S. Beckmann, T. Wessel, B. Franck, W. Hönle, H. Borrman, H.-G. von Schnering, *ibid. 102* (1990) 1439 and *29* (1990) 1395.

[7] For the stereoisomerism of the furan and thiophene macrocycles structurally analogous to the still unknown *N,N'*-dihydro[22]porphyrin-(2.2.2.2), see J. A. Elix, *Austr. J. Chem. 22* (1969) 1951 and A. Strand, B. Thulin, O. Wennerström, *Acta Chem. Scand. B31* (1977) 521, respectively.

[8] G. Hohlneicher, Universität Köln, personal communication.

[9] N. Jux, P. Koch, H. Schmickler, J. Lex, E. Vogel, *Angew. Chem. 102* (1990) 1429; *Angew. Chem. Int. Ed. Engl. 29* (1990) 1385.

[10] H. Scheer, J. J. Katz in K. M. Smith (Ed.): *Porphyrins and Metalloporphyrins*, Elsevier, Amsterdam 1975, p. 413.

[11] J. Emsley, *Chem. Soc. Rev. 9* (1980) 91.

[12] J. F. M. Oth, *Pure Appl. Chem. 25* (1971) 573; R. Gygax, J. Wirz, J. T. Sprague, N. L. Allinger, *Helv. Chim. Acta 60* (1977) 2522; J.-M. Gilles, J. F. M. Oth, F. Sondheimer, E. P. Woo, *J. Chem. Soc. B 1971*, 2177.

[13] $C_{40}H_{50}N_4$, dec. above 285 °C, crystals from carbon disulfide; triclinic, space group $P\bar{1}$, $Z = 1$; $a = 8.460(2)$, $b = 9.352(2)$, $c = 11.021(3)$ Å, $\alpha = 96.27(2)$, $\beta = 100.19(2)$, $\gamma = 103.40(2)°$; $\varrho_{calcd} = 1.182$ g cm^{-3}; intensities measured on an Enraf-Nonius CAD-4 diffractometer [room temperature, $\lambda_{Mo} = 0.71069$ Å, $\theta_{Mo}(max.) = 25°$]; refinement (C,N anisotropic, H isotropic) taking into consideration 1557 reflections with $F_0 > 4\sigma(F_0)$; $R = 0.043$, $R_w = 0.045$. Further details of the crystal structure investigation may be obtained from the Fachinformationszentrum Karlsruhe, Gesellschaft für wissenschaftlich-technische Information mbH, W-7514 Eggenstein-Leopoldshafen 2 (FRG), on quoting the depository number CSD-54913, the names of the authors, and the journal citation.

[14] K. M. Smith in A. R. Katritzky, C. W. Rees (Eds.): *Comprehensive Heterocyclic Chemistry, Vol. 4*, Pergamon Press, Oxford 1984, p. 377; J. W. Lauher, J. A. Ibers, *J. Am. Chem. Soc. 95* (1973) 5148.

[15] F. R. Longo, E. J. Thorne, A. D. Adler, S. Dym, *J. Heterocycl. Chem. 12* (1975) 1305; J. B. Paine III, W. B. Kirshner, D. W. Moskowitz, D. Dolphin, *J. Org. Chem. 41* (1976) 3857.

[16] The previously unknown pyrrole derivative **9** was obtained from 2-(2-cyano-2-ethoxycarbonylvinyl)-3,4-diethyl-5-iodopyrrole [9] by dehalogenation with zinc in acetic acid [yellow needles (ethanol), m.p. 118 °C, 95%], Vilsmeyer formylation, and removal of the aldehyde protecting group [light brown needles (ethanol), m.p. 105–106 °C, 50%]. The expected formation of the corresponding, previously unknown 1,4:7,10:13,16-trisimino[18]annulene of the same type as *Badger*'s bridged [18]annulenes [G. M. Badger, J. A. Elix, G. E. Lewis, *Austr. J. Chem. 18* (1965) 70; *ibid. 19* (1966) 1221] has not been observed so far.

[17] Recent reviews: J. E. McMurry, *Chem. Rev. 89* (1989) 1513; D. Lenoir, *Synthesis 1989*, 883.

[18] So far obtained as a microcrystalline blue powder with a metallic luster; ^{1}H NMR spectrum (300 MHz, $CDCl_3$, room temperature): $\delta = 11.67$ (H-5), 10.19 (H-3), 9.95 (H-12), 9.86 (H-11), 9.46 (H-8), 9.36 (H-2), 9.30 (H-9), 2.21 (NH), −7.13 (H-6). The couplings of **9** and 2,5-pyrroledicarbaldehyde were carried out by *S. Böhm* and *W. Hennig*.

Isocorroles: Novel Tetrapyrrolic Macrocycles**

By *Stefan Will, Afssaneh Rahbar, Hans Schmickler, Johann Lex*, and *Emanuel Vogel**

Dedicated to Professor Albert Eschenmoser on the occasion of his 65th birthday

Corrole (**2**), which may be regarded as the aromatic basic structure of the ring framework of vitamin B_{12} [1] and which has been investigated extensively by *A. W. Johnson* and his co-workers,[2] is formally derived from porphyrin (**1**) by contraction of the C_{20} perimeter with expulsion of a *meso* carbon atom. Compound **2**, like **1**, exhibits an 18π-electron main conjugation pathway, but differs from **1** in that it contains three pyrrole-like nitrogen atoms, assumed to be responsible for the ready anion formation in the case of **2**. The spectra of corroles display a close relationship with those of porphyrins, even though the ring framework deviates noticeably from planarity, presumably owing to steric interactions between the NH hydrogens.[3] The chemistry of corroles, which have not yet been found in nature, is dominated by their ability to form complexes (metallocorroles) with metal ions.[2, 4]

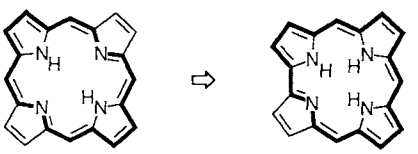

1 2

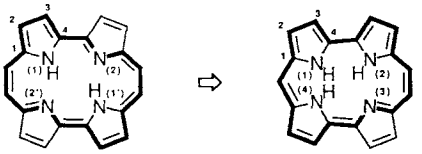

3 4

It occurred to us that the formalism relating **1** and **2** structurally might be extended to the porphyrin isomer porphycene (**3**).[5] Our attention was thereby directed to the previously unknown tetrapyrrolic macrocycle **4**, for which the name isocorrole is proposed. Compound **4**, in a planar conformation, is more strained than **2**, so that it was open to

[*] Prof. Dr. E. Vogel, S. Will, A. Rahbar, Dr. H. Schmickler, Dr. J. Lex
Institut für Organische Chemie der Universität
Greinstrasse 4, W-5000 Köln 41 (FRG)

[**] This work was supported by the Deutsche Forschungsgemeinschaft.

question whether the compound would possess an aromatic ring system. In our exploration of the chemistry of 2,7,12,17-tetrapropylporphycene (**5**),[6] we have now discovered a *porphycene–isocorrole rearrangement*, which leads to a stable isocorrole.

Because of its favorable solubility, compound **5**, accessible on a preparative scale, is a good model compound for the study of electrophilic and other substitutions on the porphycene ring system, although the pyrrole rings in **5** each have only one substitutable hydrogen. The expectation that quantum-mechanical calculations would provide reliable information on the course (substitution pattern) of the reaction of **5** with electrophiles has been frustrated so far, since the relative reactivities of the CHCH bridge carbons and the pyrrole carbons determined by the conventional calculational procedures (PPP, CNDO, AM1, and others) are not consistent.[7] The initially studied bromination of **5** with bromine in carbon tetrachloride had the surprising result that halogen substitution occurred at the four available β-pyrrolic positions to form the 3,6,13,16-tetrabromo compound **6** before substitution at the nonpyrrolic carbons took place.[8] If the product of monobromination, 3-bromo-2,7,12,17-tetrapropylporphycene (**8**), is desired, bromine on a polymeric support is best used as the brominating agent (see *Experimental Procedure*).

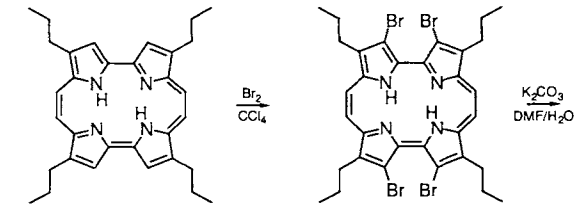

5 6

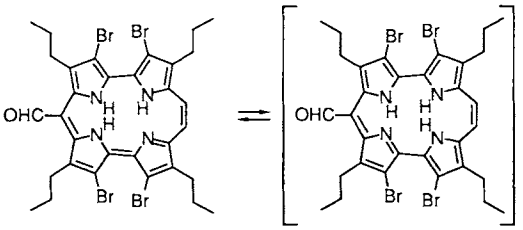

7a 7b

The structural proof for **6** and **8** is based on the ^{1}H and ^{13}C NMR spectra; in addition, an X-ray structure analysis[11] was carried out on **6** (Fig. 1). Compound **6** is a centrosymmetric molecule, whose ring framework practically retains the planarity found for **3** and **5**, but whose bromine atoms are markedly displaced from the plane of the framework owing to nonbonding interactions. Thus, compound **6** strikingly differs from 2,3,6,7,12,13,16,17-octaethylporphycene,[12] which has the same substitution pattern, since, in the latter compound, the substituents in the 3,6- and 13,16-positions cause a pronounced ruffling of the ring framework. The "squeezing" of the bromine atoms, revealed in the relatively short Br ··· Br distance of 3.267 Å (sum of the van der Waals radii: 3.9 Å), causes the pyrrole rings to rotate within the plane of the ring framework and results in angle deformations of up to 6° at the positions where the rings are joined. Moreover, a reversal of the relative distances within the N_4 core (now, N1 ··· N2 < N1 ··· N2′) ensues. Because of partial disorder, the two imino hydrogens are distributed with half occupancy over each of the four possible positions.

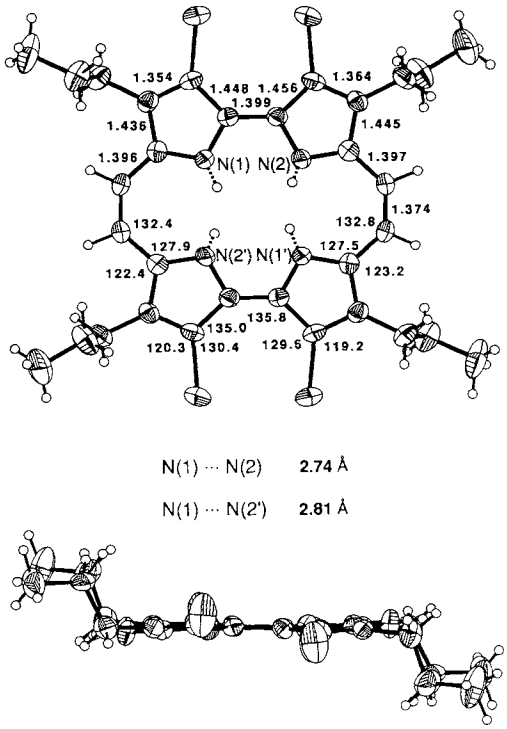

Fig. 1. Molecular structure of **6**. Top: Top view. Bottom: Side view. Selected bond lengths and other distances [Å] and bond angles [°]; standard deviations ca. 0.009 Å and 0.8°. The thermal ellipsoids are drawn at the 40% probability level.

The supposition that steric compression of the bromine atoms in **6** might facilitate nucleophilic substitutions leading to a linkage of C3 and C6 was not borne out. Compound **6** reacts only very sluggishly with nucleophiles, as observed for other halopyrroles.[13] This behavior of **6** allows for the occurrence of a porphycene–isocorrole ring contraction, which requires a basic medium and is apparently associated with the presence of the halogen atoms.[14] When **6** is heated with potassium carbonate in DMF/water (7:1) under argon to 120 °C (4 h) and the resulting products are chromatographed on silica gel (chloroform), two fractions are obtained. The first consists of **6** together with unidentified, decomposable products and the second contains the isocorrole aldehyde **7**. Crystallization from dichloromethane/hexane affords **7** as small black-green needles (dec. above 180 °C; yield 34%).

The ^{1}H NMR spectrum of **7** (Table 1) shows a simple pattern, in agreement with the assumption that **7** undergoes rapid NH tautomerism, which gives the molecule effective C_{2v} symmetry: singlets at $\delta = 11.45$ (aldehyde proton) and 8.77 (H-9,10; $^3J_{9,10} = 12.5$ Hz), six groups of signals in the region of $\delta = 1.0-3.6$ (protons of four pairwise identical propyl groups), and two strongly broadened signals at $\delta = 3.5$ (1 NH; involved in hydrogen bonding) and -2.5 (2 NH), which only become sharp singlets at -50 °C. Consistent with this spectrum, the ^{13}C NMR spectrum shows 17 signals, that at $\delta = 187.72$ (CHO; $^1J_{C,H} = 176.1$ Hz) being assigned to the aldehyde carbon. The aromaticity of the ring system in **7** is apparent from the positions of the resonances for the two perimeter protons and for the two NH protons not involved in hydrogen bonding at relatively low and high field, respectively. The UV/VIS spectrum of **7** contains a moderately intense Soret band at $\lambda = 371$ nm ($\varepsilon = 53\,100$) as well as a relatively complex system of Q bands. In addition, however, there is a short-wavelength band at 260 nm (20 300), which has no counterpart in the spectra of **1**, **3**, and the known corroles. In the IR spectrum, unlike in the corre-

Table 1. Selected physical data for **6**, **7**, and **8**.

6: ^{1}H NMR (300 MHz, $CDCl_3$): δ = 9.48 (s, 4H; H-9,10,19,20), 3.80 (t, 8H; H-2a,7a,12a,17a), 3.60 (br.s, 2H; NH), 2.12 (m, 8H; H-2b,7b,12b,17b), 1.23 (t, 12H; H-2c,7c,12c,17c). ^{13}C NMR (75.5 MHz, $CDCl_3$): δ = 145.55, 142.38, 134.80, 112.38, 111.86, 30.02, 25.22, 14.55. MS (EI, 70 eV): *m/z* 798/796/794/792/790 ($M^{\oplus}$, 23/74/100/73/17%), 769/767/765/763/761 (14/48/77/50/17), 397 ($M^{2\oplus}$, 16), 82(17), 80(18). IR (CsI): $\tilde{\nu}$[cm^{-1}] = 2956, 2922, 2864, 1552, 1523, 1462, 1089, 1047, 986, 922. UV/VIS (CH_2Cl_2): λ_{max} [nm] (ε) = 379 (107 000), 387 (104 000) sh, 591 (36 000), 639 (20 600), 684 (29 000).

7: ^{1}H NMR (300 MHz, $CDCl_3$): δ = 11.45 (s, ^1J(C,H) = 176.1 Hz, 1H; CHO), 8.77 (s, ^3J(H,H) = 12.5 Hz, 2H; H-9,10), 3.55 (t, 4H; H-7a,12a), 3.5 (br. s, 1H; NH), 3.25 (m, 4H; H-2a,17a), 2.02 (m, 4H; H-7b,12b), 1.92 (m, 4H; H-2b,17b), 1.16 (t, 6H; H-7c,12c), 1.05 (t, 6H; H-2c,17c), −2.5 (br. s, 2H; NH). ^{13}C NMR (75.5 MHz, $CDCl_3$): δ = 187.72 (CHO), 142.46, 140.77, 136.14, 129.80, 129.29, 126.59, 111.94, 109.26, 108.82, 107.48, 31.25, 29.28, 25.16, 24.59, 14.53, 14.36. MS (FAB): *m/z* 814/812/810/808/806 ($M^{\oplus}$, 23/65/100/60/15%). IR (CsI): $\tilde{\nu}$[cm^{-1}] = 3415, 2959, 2868, 1659, 1544, 1456, 1318, 1261, 1132, 1072, 1001, 924; UV/VIS (CH_2Cl_2): λ_{max} [nm] (ε) = 260 (20 300), 371 (53 100), 386 (39700) sh, 409 (32700) sh, 632 (30 300) sh, 684 (40 800) sh, 708 (48 300).

8: ^{1}H NMR (300 MHz, $CDCl_3$): δ = 10.11 (s, 1H; H-6), 9.51 (m, 4H; H-9,10,19,20), 9.18 (s, 1H; H-16), 9.08 (s, 1H; H-13), 3.90 (m, 8H; H-2a,7a,12a,17a), 2.32 (m, 9H; H-2b,7b,12b,17b, NH3), 1.98 (br.s, 1H; NH1), 1.31 (m, 12H; H-2c,7c,12c, 17c). ^{13}C NMR (75.5 MHz, $CDCl_3$): δ = 148.50, 147.38, 144.86, 144.69, 143.52, 142.40, 138.98, 138.30, 137.79, 133.09, 131.16, 130.57, 123.84, 122.47, 121.66, 114.64, 112.52, 111.83, 109.51, 108.53, 30.47, 30.39, 30.23, 29.63, 25.70, 25.42, 25.11, 24.99, 14.55, 14.49. MS (EI, 70 eV): *m/z* 558/556 ($M^{\oplus}$, 20/18%), 529/527 (7/7), 82 (95), 80 (100). IR (CsI): $\tilde{\nu}$[cm^{-1}] = 2950, 2918, 2855, 1555, 1455, 1210, 1035, 1012, 936, 803. UV/VIS (CH_2Cl_2): λ_{max} [nm] (ε) = 372 (121 000), 383 (101 000), 565 (34 000), 608 (28 600), 643 (44 000).

sponding spectra of **3**, **5**, and **6**, an NH stretching band (3415 cm^{-1}) is observed and is presumably due to the imino hydrogens not participating in hydrogen bonding. The EI mass spectrum contains only signals of fragment ions of low mass, whereas FAB ionization results in a single peak, due to the molecular ion.

An X-ray structure analysis of **7**[15] (Fig. 2) reveals the nonplanarity of the isocorrole ring framework, which is mainly due to the steric interactions between the imino hydrogens, and, in addition, confirms the porphyrinoid nature of the compound. Whereas pyrrole rings B and C, which, together with C-9 and C-10, form a porphycene partial structure (dipyrroethene structure), lie in the mean plane of the ring framework, rings A and D are each twisted out of this plane by 23° but in opposite directions. A consequence of the torsion of rings A and D is that the N ··· N contact distances are nearly equal (ca. 2.7 Å). The ring framework of **7** thus deviates more strongly from planarity than that of corroles, since a structure analysis of 8,12-diethyl-2,3,7,13,17,18-hexamethylcorrole (**9**)[3] has shown that, in this molecule, pyrrole rings A, B, and C are arranged in a nearly planar fashion and ring D is twisted by only 8–10°. Interestingly, the imino hydrogens in **7** are not statistically disordered over the four nitrogens, as observed for **9** and the porphycenes **3**, **5**, and **6**, but rather can be localized in compliance with the NH tautomer **7a**. As inferred from the situation for **3** and **5**, a strong N-H ··· N hydrogen bond should exist between N2 and N3. The similar bond lengths in the nonpyrrolic perimeter CC bonds, especially in combination with the length relation C_α-C_β > C_β-C_β,[16] observed for the pyrrole rings, support the aromatic character of **7**. The isocorrole system once again corroborates the finding that the ring frameworks of porphyrins and their analogues can be considerably deformed without a serious loss of aromaticity.[17]

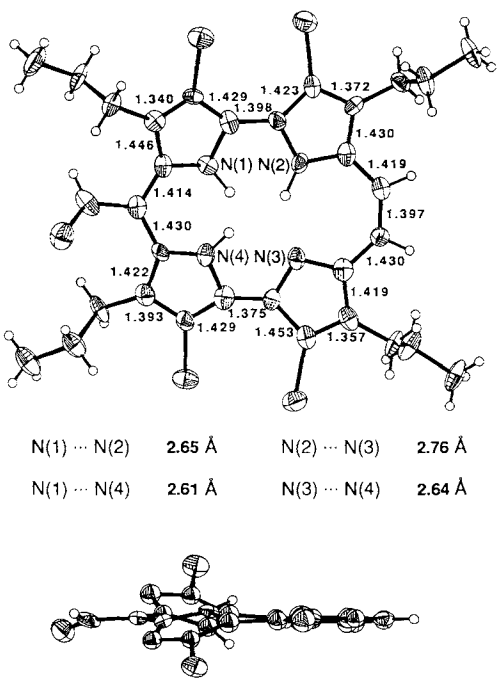

Fig. 2. Molecular structure of **7**. Same projections as in Fig. 1 (standard deviation ca. 0.012 Å). Side view without propyl groups.

Preliminary reactions of **7** with di- and trivalent metal ions led to metal complexes, but these usually decomposed rapidly. An exception was the complex obtained with Co^{II} ions in the presence of pyridine. According to NMR spectroscopic investigations, this complex has the structure of a diamagnetic Co^{III} isocorrole complex with two molecules of coordinatively bound pyridine.

Experimental Procedure

8: Compound **5** (100 mg, 0.2 mmol) in 40 mL of dichloromethane and 40 mL of acetic acid was treated at 0 °C under argon with 260 mg of Amberlyst A-26 (Br_3 form)[9] (corresponding to 0.4 mmol of bromine). The reaction mixture was stirred for 2 h and then filtered. The solvent was removed and the residue chromatographed on silica gel (column: 100 × 5 cm) with hexane/dichloromethane (6:1). The first fraction (also the main fraction) contains the monobromide **8**, which, after crystallization from hexane, was obtained as violet needles with a metallic luster; m. p. 199–200 °C, yield 93 mg (80%).

6: Bromine (225 mg, 1.4 mmol) in 20 mL of carbon tetrachloride was added over 10 min at room temperature to a vigorously stirred mixture of **5** (100 mg, 0.2 mmol) in 40 mL of carbon tetrachloride and a buffer solution (1 g of sodium acetate in 40 mL of water). The resulting reaction mixture was stirred for 1 h. The organic phase was washed with a saturated solution of sodium thiosulfate and with water and then chromatographed on silica gel (column: 100 × 4 cm) with hexane/dichloromethane (6:1). Three fractions were obtained: the first contained a complex mixture of polybromides, the second 3,6,13-tribromo-2,7,12,17-tetrapropylporphycene[10], and the third **6**. Crystallization from hexane/dichloromethane afforded **6** as violet needles with a metallic luster; dec. above 300 °C, yield 67 mg (40%).

Received: July 20, 1990 [Z 4082 IE]
German version: *Angew. Chem. 102* (1990) 1434

CAS Registry numbers:
5, 106562-37-2; **6**, 130670-37-0; **7**, 130670-40-5; **7**·CH_2Cl_2, 130698-79-2; **8**, 130670-39-2; porphycene, 100572-96-1; 2-bromporphycene, 130670-38-1; 3,6,13-tribromo-2,7,12,17-tetrapropylporphycene, 130698-78-1.

[1] A. Eschenmoser, *Angew. Chem. 100* (1988) 5; *Angew. Chem. Int. Ed. Engl. 27* (1988) 5.

[2] A. W. Johnson, I. T. Kay, *J. Chem. Soc. 1965*, 1620; A. W. Johnson, *Pure Appl. Chem. 23* (1970) 375; A. W. Johnson in K. M. Smith (Ed.): *Porphyrins and Metalloporphyrins*, Elsevier, Amsterdam 1975, p. 729; R. Grigg in D. Dolphin (Ed.): *The Porphyrins, Vol. II*, Academic Press, New York 1978, p. 327; N. S. Genokhova, T. A. Melent'eva, V. M. Berezovskii, *Usp. Khim. 49* (1980) 2132 [*Russ. Chem. Rev. 49* (1980) 1056]; T. A. Melent'eva, *ibid. 52* (1983) 1136 [*ibid. 52* (1983) 641].

[3] For the X-ray structure analysis of a corrole, see: H. R. Harrison, O. J. R. Hodder, D. C. Hodgkin, *J. Chem. Soc. B 1971*, 640.

[4] P. B. Hitchcock, G. M. McLaughlin, *J. Chem. Soc. Dalton Trans. 1976*,

1927; Y. Murakami, S. Yamada, Y. Matsuda, K. Sakata, *Bull. Chem. Soc. Jpn. 51* (1978) 123; Y. Murakami, Y. Matsuda, K. Sakata, S. Yamada, Y. Tanaka, Y. Aoyama, *ibid. 54* (1981) 163.

[5] E. Vogel, M. Köcher, H. Schmickler, J. Lex, *Angew. Chem. 98* (1986) 262; *Angew. Chem. Int. Ed. Engl. 25* (1986) 257; P. F. Aramendia, R. W. Redmond, S. Nonell, W. Schuster, S. E. Braslavsky, K. Schaffner, E. Vogel, *Photochem. Photobiol. 44* (1986) 555; E. Vogel, M. Köcher, M. Balci, I. Teichler, J. Lex, H. Schmickler, O. Ermer, *Angew. Chem. 99* (1987) 912; *Angew. Chem. Int. Ed. Engl. 26* (1987) 931; B. Wehrle, H.-H. Limbach, M. Köcher, O. Ermer, E. Vogel, *ibid. 99* (1987) 914 and *26* (1987) 934; H. Levanon, M. Toporowicz, H. Ofir, R. W. Fessenden, P. K. Das, E. Vogel, M. Köcher, K. Pramod, *J. Phys. Chem. 92* (1988) 2429; J. Schlüpmann, M. Huber, M. Toporowicz, M. Köcher, E. Vogel, H. Levanon, K. Möbius, *J. Am. Chem. Soc. 110* (1988) 8566; E. Vogel, M. Köcher, J. Lex, O. Ermer, *Isr. J. Chem. 29* (1989) 257; E. Vogel, *Pure Appl. Chem. 62* (1990) 557.

[6] E. Vogel, M. Balci, K. Pramod, P. Koch, J. Lex, O. Ermer, *Angew. Chem. 99* (1987) 909; *Angew. Chem. Int. Ed. Engl. 26* (1987) 928; M. W. Renner, A. Forman, W. Wu, C. K. Chang, J. Fajer, *J. Am. Chem. Soc. 111* (1989) 8618; L. R. Furenlid, M. W. Renner, K. M. Smith, J. Fajer, *ibid. 112* (1990) 1634.

[7] We thank Prof. *G. Hohlneicher* (Universität Köln) and Prof. *R. Gleiter* (Universität Heidelberg) for performing these calculations.

[8] In the case of the porphycene parent compound, reaction with bromine also leads exclusively to β-pyrrolic bromination, but the bromine substituent is found in the 2-position, which is occupied by a propyl group in **5**. 2-Bromoporphycene is the only isolated monobromination product (unpublished results with *K. Pramod* and *H.-J. Dünnwald*). This substitution pattern for bromination is different from that of porphyrin, for which regioselective substitution at the methine bridge leads to the formation of 5-bromoporphyrin [H. J. Callot, E. Schaeffer, *J. Chem. Res. (S) 1978* 51; L. R. Nudy, H. G. Hutchinson, C. Schieber, F. R. Longo, *Tetrahedron 40* (1984) 2359], even though PPP calculations indicate that electrophilic attack on the β-pyrrolic carbon should have occurred [J. V. Knop, J.-H. Fuhrhop, *Z. Naturforsch. B 25* (1970) 729]. The β-pyrrolic bromination of porphyrin observed earlier by E. Samuels, R. Shuttleworth, and T. S. Stevens [*J. Chem. Soc. C 1968*, 145] could not be reproduced by *F. R. Longo* et al. (cited above).

[9] A. Bongini, G. Cainelli, M. Contento, F. Manescalchi, *Synthesis 1980*, 143.

[10] Like **6**, the tribromo compound (m.p. 269–270 °C), which is currently being investigated in more detail, can be made the main product.

[11] $C_{32}H_{34}Br_4N_4$, dec. > 300 °C, crystals from hexane/dichloromethane; triclinic, space group $P\bar{1}$, $Z = 1$; $a = 5.686(1)$, $b = 10.208(2)$, $c = 13.839(3)$ Å, $\alpha = 96.13(2)$, $\beta = 93.27(2)$, $\gamma = 96.16(2)°$; $\varrho_{calcd} = 1.67$ g cm^{-3}; intensities measured on a four-circle diffractometer [room temperature, $\lambda_{Mo} = 0.71069$ Å, $\theta_{Mo}(max) = 25°$]; empirical absorption correction, refinement (C, N, Br anisotropic, H isotropic) taking into consideration 1677 reflections with $F_0 > 4\sigma(F_0)$; $R = 0.063$, $R_w = 0.073$ [18].

[12] 2,3,6,7,12,13,16,17-Octaethylporphycene is of interest, since it reacts with zinc and several other metals to afford planar complexes that are more stable than the corresponding metal complexes of **3** and **5**: E. Vogel, P. Koch, unpublished results.

[13] A. Gossauer: *Die Chemie der Pyrrole*, Springer, Berlin 1974, p. 326.

[14] The porphycene-isocorrole rearrangement suggests associations with the ring-contraction step in the biosynthesis of the corrin ring of vitamin B_{12} [1]. To the best of our knowledge, a contraction of porphyrins to corroles has not been observed so far.

[15] $C_{32}H_{34}Br_4N_4O{\cdot}CH_2Cl_2$, dec. > 180 °C, crystals from dichloromethane; triclinic, space group, $P\bar{1}$, $Z = 2$; $a = 8.443(2)$, $b = 13.898(3)$, $c = 16.034(4)$ Å, $\alpha = 66.15(2)$, $\beta = 88.01(2)$, $\gamma = 87.02(2)°$; $\varrho_{calcd} = 1.75$ g cm^{-3}; intensities measured on a four-circle diffractometer [room temperature, $\lambda_{Mo} = 0.71069$ Å, $\theta_{Mo}(max) = 25°$]; empirical absorption correction; refinement (C, N, O, Cl, Br anisotropic, H isotropic) taking into consideration 2301 reflections with $F_0 > 4\sigma(F_0)$; $R = 0.074$, $R_w = 0.063$ [18].

[16] K. M. Smith in A. R. Katritzky, C. W. Rees (Eds.): *Comprehensive Heterocyclic Chemistry, Vol. 4*, Pergamon Press, Oxford 1984, p. 386.

[17] Porphyrins: T. P. Wijesekera, J. B. Paine III, D. Dolphin, F. W. B. Einstein, T. Jones, *J. Am. Chem. Soc. 105* (1983) 6747; *N*-protonated porphyrins: N. Hirayama, A. Takenaka, Y. Sasada, E.-I. Watanabe, H. Ogoshi, Z.-I. Yoshida, *J. Chem. Soc. Chem. Commun. 1974*, 330; *N*-substituted porphyrins: D. K. Lavallee: *The Chemistry and Biochemistry of N-Substituted Porphyrins*, VCH Publishers, New York/Weinheim 1987; *N,N',N'',N'''*-tetramethyloctaethylporphyrin dication: B. Franck, *Angew. Chem. 94* (1982) 327, *Angew. Chem. Int. Ed. Engl. 21* (1982) 343; M. Gosmann, *Dissertation*, Universität Münster 1986 (see also following reference); tetrathiaporphyrin dication: E. Vogel, P. Röhrig, M. Sicken, B. Knipp, A. Herrmann, M. Pohl, H. Schmickler, J. Lex, *Angew. Chem. 101* (1989) 1683; *Angew. Chem. Int. Ed. Engl. 28* (1989) 1651.

[18] Further details of the crystal structure investigation may be obtained from the Fachinformationszentrum Karlsruhe, Gesellschaft für wissenschaftlich-technische Information mbH, W-7514 Eggenstein-Leopoldshafen 2 (FRG), on quoting the depository number CSD-54911, the names of the authors, and the journal citation.

Synthesis of a Bisvinylogous Octaethylporphyrin**

By *Hartmann König, Christian Eickmeier, Manfred Möller, Ute Rodewald*, and *Burchard Franck**

In memoriam Hans Fischer

Octaethylporphyrin (OEP, **2**), first synthesized in 1929 by *Hans Fischer* et al.,[1] is one of the most important and most investigated porphyrins.[2] Here we describe an efficient synthesis of the title compound **1**, which is extremely stable and markedly aromatic. Thus, the crystal structure analysis of the bistrifluoroacetate of **1** revealed that the conjugated perimeter is planar and its bonds largely equal in length. The ^{1}H NMR spectrum indicates an intense diamagnetic ring current. Furthermore, **1** is the first annulene for which the protons inside and outside the aromatic system exhibit a large difference in reactivity. According to the nomenclature for vinylogous porphyrins,[7] **1** is named [22]octaethylporphyrin(1.3.1.3).

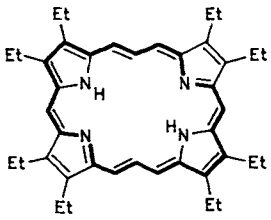

1

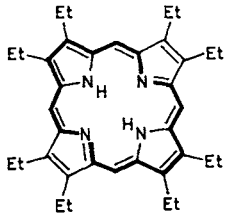

2

An initial synthetic attempt based on the procedure of *MacDonald* et al.[3] was unsuccessful owing to the low stability of the required pyrromethene and pyrropropene intermediates. However, the "biladiene synthesis path",[4] which is of less general use in porphyrin syntheses, proved to be a more efficient route to **1**. The key compound is the previously unknown bisvinylogous biladiene **5**, which was obtained in 81% yield by condensation of **3**[6] and **4**[5b] (Scheme 1), both of which are readily accessible from 3,4-diethylpyrrole.[5] Condensation of biladiene **5** to give porphyrin **1** was accomplished by heating **5** with CH_2O/MeOH followed by in situ oxidation with 2,3-dichloro-5,6-dicyano-1,4-benzoquinone (DDQ) (42% yield based on **5**).[8]

The ^{1}H NMR spectrum of **1** in $CDCl_3$/1% trifluoroacetic acid (TFA) (Table 1) shows that the signals for the inner and outer bridge protons are strongly shifted upfield and downfield, respectively; the spectrum spans an unusually broad

Table 1. ^{1}H NMR data for [22]octaethylporphyrin **1** and for the hexadeuterated [22]octaethylporphyrin **6** in $CDCl_3$/1% TFA.

Proton	**1** δ	**1** J [Hz]	**6** δ
H^a	11.96(s)	–	–
H^b	12.78(d)	13.9	–
H^c	−9.54(t)	13.9	−9.71(s)
NH	−6.61(s)	–	−6.50(s)

[*] Prof. Dr. B. Franck, Dipl.-Chem. H. König, C. Eickmeier
Organisch-chemisches Institut der Universität
Orléansring 23, W-4400 Münster (FRG)
Dr. M. Möller, Dipl.-Ing. U. Rodewald
Anorganisch-chemisches Institut der Universität Münster

[**] Novel Porphyrinoids, Part 10. This work was supported by the Deutsche Forschungsgemeinschaft, the Fonds der Chemischen Industrie, and BASF AG (Ludwigshafen). Part 9: [7a].

range of $\Delta\delta = 20.2$. Thus, according to ^{1}H NMR criteria,[9] **1** is a pronouncedly aromatic porphyrinoid.

The electrophilic deuteration carried out in order to investigate the chemical stability and reactivity of [22]octaethylporphyrin **1** (Scheme 1) gave an interesting result: *exclusively*

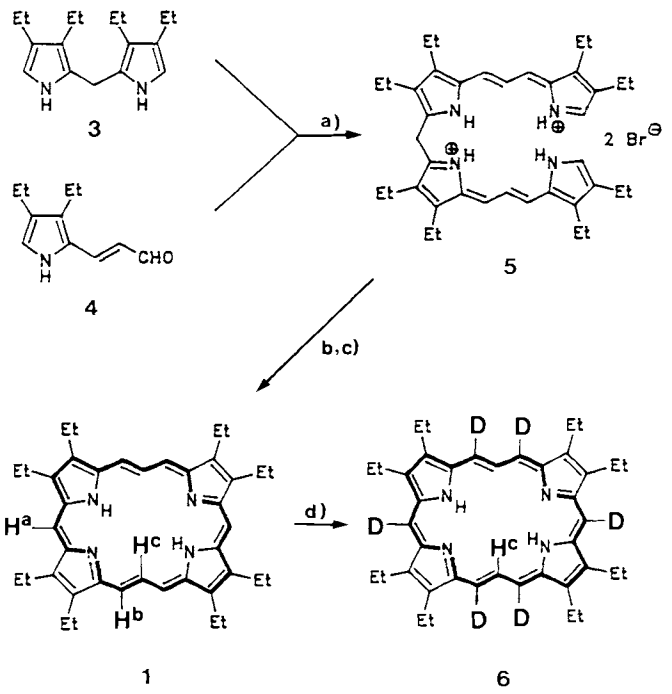

Scheme 1. Synthesis of [22]octaethylporphyrin **1** and its electrophilic deuteration. Reaction conditions: a) HBr, MeOH, −15 °C, 5 min; 81% **5** (dec. above 160 °C); b, c) aqueous CH_2O, MeOH/HBr, reflux, 30 min, then DDQ/CH_2Cl_2, 20 °C, 2 h; 42% **1** as deep green needles (dec. above 280 °C); d) D_2SO_4/D_2O (9:1), 20 °C, 72 h, **6** (see also text).

the outer protons of the C_1 and C_3 bridges of the conjugated perimeter were exchanged and the deuterated product **6** was formed in high yield (90.3%) as determined by mass spectrometry. Thus, the ^{1}H NMR spectrum of the hexadeuterated [22]octaethylporphyrin **6** (Table 1), in contrast to that of **1**, shows only a two-proton singlet for the inner protons H^c at $\delta = -9.71$. Clearly, the outer protons of the 22π-electron system of **1** readily undergo electrophilic substitution, whereas the inner protons are inert.

Since **1** crystallizes from various solvents as small, strongly intergrown needles, a crystal structure determination of the free base was not possible. Finally, however, we obtained dark green single crystals up to 2 mm in length from the bistrifluoroacetate of [22]porphyrin **1** and were able to perform a crystal structure analysis (Fig. 1).[10]

The [22]porphyrin dication **1**-2H$^\oplus$ has—without the β side chains—a practically planar structure (Fig. 1, bottom). The maximum deviation of the C and N framework atoms from the mean plane is 19.5 pm (**2**-2H$^\oplus$ 9.5 pm[11b]). A trifluoroacetate ion above and below the arene plane can be assigned to the porphyrin dication. The bond lengths and angles (Fig. 1, top) in the pyrrole units correspond to those in the OEP dication (**2**-2H$^\oplus$).[11b] The C–C bond lengths in the bridges between the pyrrole rings (137.5–139.1 pm) also lie in the range observed for **2**-2H$^\oplus$ (136.6–138.8 pm). This holds for the monomethine bridges as well as for the trimethine bridges; if "loss of aromaticity" had occurred on going from **1** to OEP (**2**), bond-length alternation would have been expected in the trimethine bridges.[3] The similarity of the

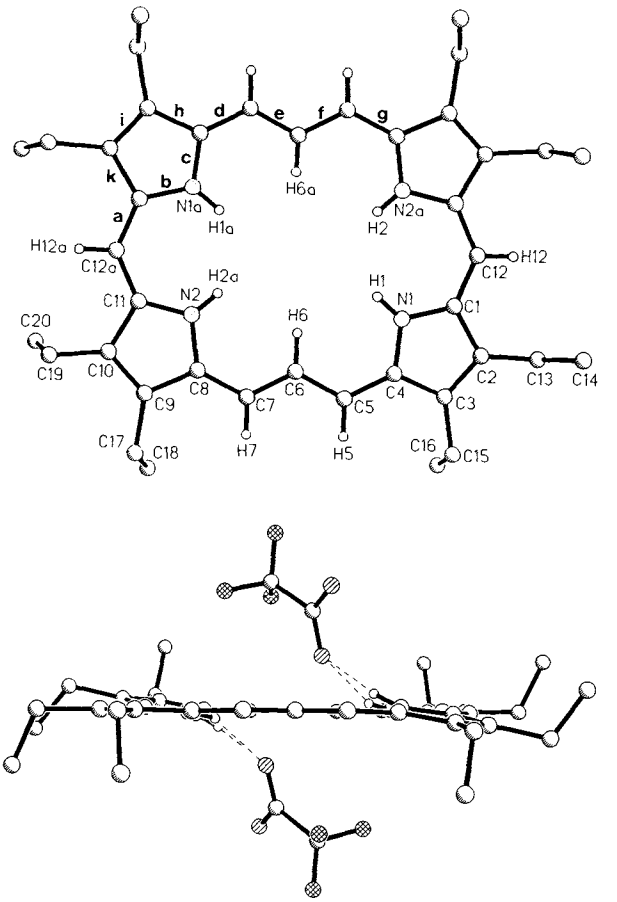

Fig. 1. Molecular structure of the centrosymmetric dication **1**-2H$^\oplus$. Top: View perpendicular to the arene plane. Below: Side view. Important distances [pm]: a = 138.6, b = 136.8, c = 136.7, d = 139.0, e = 138.1, f = 137.5, g = 139.1, h = 143.4, i = 136.7, k = 144.4.

crystal structures of OEP (**2**)[11a] and the OEP dication (**2**-2H$^\oplus$)[11b] justifies the assumption that the structure of the [22]porphyrin dication **1**-2H$^\oplus$ determined here differs only slightly from that of free porphyrin (**1**).

Received: July 5, 1990 [Z 4055 IE]
German version: *Angew. Chem. 102* (1990) 1437

CAS Registry numbers:
1, 130469-04-4; **1**·2F_3CCO_2H, 130495-61-3; **3**, 65858-34-6; **4**, 130469-05-5; **5**, 130469-06-6; **6**, 130469-07-7.

[1] H. Fischer, R. Bäumler, *Justus Liebigs Ann. Chem. 468* (1929) 58–98.
[2] J. B. Kim, A. D. Adler, F. R. Longo in D. Dolphin (Ed.): *The Porphyrins, Vol. I*, Academic Press, New York 1978, p. 88.
[3] G. P. Arsenault, E. Bullock, S. F. MacDonald, *J. Am. Chem. Soc. 82* (1960) 4384–4389.
[4] J. Engel, A. Gossauer, *Justus Liebigs Ann. Chem. 1976*, 1637–1658.
[5] H. W. Whitlock, R. Hanauer, *J. Org. Chem. 33* (1968) 2169–2171.
[6] J. B. Paine, R. B. Woodward, *J. Org. Chem. 41* (1976) 2826–2835.
[7] a) M. Gosmann, A. Vogt, B. Franck, *Liebigs Ann. Chem. 1990*, 163–168; b) M. Gosmann, B. Franck, *Angew. Chem. 98* (1986) 1107–1108; *Angew. Chem. Int. Ed. Engl. 25* (1986) 1100–1101; B. Franck, M. Gosmann, DOS 3 635 820 (vinylogous porphyrins), 28 April 1988, BASF AG; *Chem. Abstr. 109* (1988) 94748u.
[8] The new compounds **1** and **5** were fully characterized by elemental analyses and spectroscopic data. **1**: ^{1}H NMR: see Table 1. FT-IR (KBr): ν[cm^{-1}] = 3034 (= CH), 2963, 2928, 2868 (CH), 1659, 1597 cm^{-1} (conjugated C=C). UV/VIS (CH_2Cl_2): λ_{max} [nm] (lg ε) = 463 (5.62), 489 (4.71), 592 (4.04). UV/VIS (CH_2Cl_2 + 1% TFA): λ_{max} [nm](lg ε) = 434 (4.77), 460 (6.05), 607 (4.10), 621 (4.31), 678 (4.11), 691 (3.90). MS (70 eV): *m/z* 587 ($M^\oplus$+1, 34%), 586 ($M^\oplus$, 42%). **5**: ^{1}H NMR (300 MHz, CD_2Cl_2, 20 °C, TMS): δ = 0.75 (t, *J* = 7.4 Hz, 6H, CH_2CH_3), 1.15–1.23 (m, 18H, CH_2CH_3), 4.62 (s, 2H, bridge CH_2), 9.03 (t, *J* = 13.6 Hz, 2H, CH=CHCH). IR (KBr): ν [cm^{-1}] = 2960, 2920, 2860 (CH), 1570 (s, conjugated C=C). MS (FD): *m/z* 576 ($M^\oplus$ − 2HBr, 100%).

[9] P. J. Garratt: *Aromaticity*, Wiley, New York 1986, p. 52; E. Breitmeier: *Vom NMR-Spektrum zur Strukturformel organischer Verbindungen*, Teubner, Stuttgart 1990, p. 53.

[10] A dark green, cube-shaped crystal of the bistrifluoroacetate of [22]porphyrin **1** suitable for X-ray structure analysis was obtained from CH_2Cl_2/TFA 40:1: CAD4 four-circle diffractometer (Enraf-Nonius), room temperature ($Mo_{K\alpha}$ radiation), 13025 reflections. Crystal data: space group *P*-1, $a = 884.2(4)$, $b = 1112.0(8)$, $c = 1230.4(5)$ pm, $\alpha = 76.22(4)$, $\beta = 74.18(4)$, $\gamma = 67.64(4)°$, $Z = 1$. Further details of the crystal structure investigation may be obtained from the Fachinformationszentrum Karlsruhe, Gesellschaft für wissenschaftlich-technische Information mbH, W-7514 Eggenstein-Leopoldshafen 2 (FRG), on quoting the depository number CSD-54708, the names of the authors, and the journal citation.

[11] a) J. W. Lauher, J. A. Ibers, *J. Am. Chem. Soc. 95* (1973) 5148–5152; b) E. Cetinkaya, A. W. Johnson, M. F. Lappert, G. M. MacLaughlin, K. W. Muir, *J. Chem. Soc. Dalton Trans. 1 1974*, 1236–1243.

[22]Coproporphyrin II for Photodynamic Therapy **

By *Stefan Beckmann, Thomas Wessel, Burchard Franck,* Wolfgang Hönle, Horst Borrmann,* and *Hans-Georg von Schnering*

Dedicated to Professor Albert Eschenmoser on the occasion of his 65th birthday

Hematoporphyrin (**1a**) and related compounds have found application as photosensitizers for photodynamic tumor therapy (PDT)[1] and for deactivation of viruses in transfusion blood (PDV).[2] The disadvantages of these photosensitizers are their chemical instability, the stereoisomerism of the two secondary hydroxyl groups, and the similarity of the UV/VIS absorption with that of the red blood pigment hemin. The latter property makes it difficult to apply photodynamic therapy to the deeper layers of tumors and transfusion blood. Here we describe the total synthesis of the bisvinylogous coproporphyrin II **2a**, which is free of the above-mentioned disadvantages, as well as its properties as a photosensitizer and the crystal structure analysis of its dihydrochloride.

The lower half of the hematoporphyrin **1a** (enclosed in the formula) has more favorable properties for photomedicinal applications than the upper half: it is chemically stable and contains, instead of stereogenic hydroxyethyl groups, two propionic acid moieties, which promote solubility. Therefore, a porphyrin consisting of two of these lower halves should be a more suitable photosensitizer for photodynamic therapy. To improve still further the photomedicinal properties, we chose the *bisvinylogous* porphyrinoid **2** as our synthetic goal, since it absorbs at longer wavelengths than **1a**. Compound **2** is an enlarged derivative of coproporphyrin II and is therefore structurally related to natural porphyrins in terms of its substitution pattern. In accordance with the nomenclature for vinylogous porphyrinoids,[3] **2a** is named [22]coproporphyrin II(1.3.1.3).

The key step in the synthesis of the [22]coproporphyrin II **2a** is the acid-catalyzed condensation of the bis(carbonylvinyl)dipyrrylmethane **3** with the dipyrrylmethane **4** (Scheme 1). Subsequent dehydrogenation in situ with 2,3-dichloro-5,6-dicyano-1,4-benzoquinone (DDQ) gave **2a**, which forms deep green solutions and could be isolated in analytically pure form in 35% yield by column chromatography (silica gel, Merck, 0.063–0.2 mm, ethyl acetate/methanol 10:1).[4] After addition of HCl, the dihydrochloride hydrate **2b** could be crystallized. The synthesis of **3** was carried out by double vinylogous Vilsmeier formylation[3] of the dipyrrylmethane **4** with dimethylaminoacrolein/$POCl_3$.[4] Compound **4**, in turn, was obtained from the known dipyrrylmethanedicarboxylic acid **6**[5] in two steps by

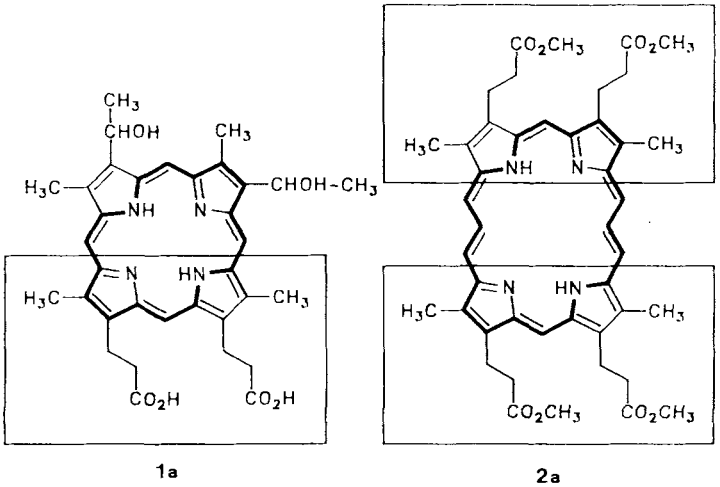

1a

1b: $-CH_2-CH_2OH$ instead of $-CHOH-CH_3$

2a

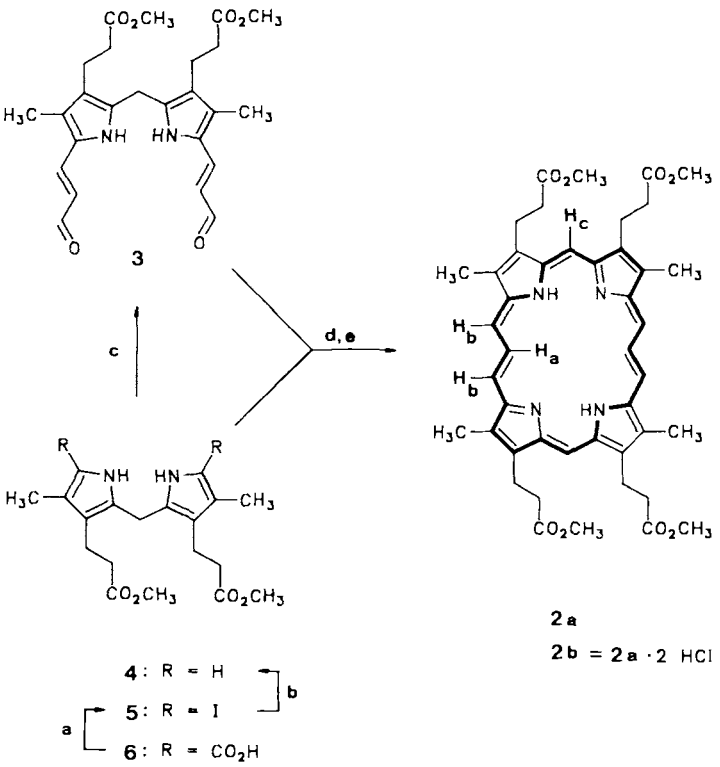

2a

2b = **2a** · 2 HCl

4: R = H

5: R = I

6: R = CO_2H

a, b

Scheme 1. Synthesis of [22]coproporphyrin II tetramethyl ester **2a** [4]. a) I_2/saturated $NaHCO_3$ solution, 20 °C, 1.5 h; 86% **5** (m.p. 114 °C); b) H_2/Pt in MeOH, 4 h; 84%; c) 3-(dimethylamino)acrolein/$POCl_3$, CH_2Cl_2, −78 °C, 15 min; 42% **3** (m.p. 231 °C); c,d) HBr/MeOH, 20 °C, 1 h, then DDQ/CH_2Cl_2, 20 °C, 2 h; 35% **2a** as anthracite-colored needles (dec. above 230 °C).

[*] Prof. Dr. B. Franck, Dipl.-Chem. S. Beckmann, Dipl.-Chem. T. Wessel
Organisch-chemisches Institut der Universität
Orléansring 23, W-4400 Münster (FRG)

[*] Dr. W. Hönle, Dr. H. Borrmann, Prof. Dr. H.-G. von Schnering
Max-Planck-Institut für Festkörperforschung
D-7000 Stuttgart 80 (FRG)

[**] Novel Porphyrinoids, Part 11. This work was supported by the Deutsche Forschungsgemeinschaft, the Fonds der Chemischen Industrie, and BASF AG (Ludwigshafen). Part 10: [10].

mild decarboxylation to give the diiodide **5**, which was then catalytically hydrogenated.

The conjugated 22π-electron perimeter in **2a** results in a strong diamagnetic ring-current effect in the ^{1}H NMR spectrum. The difference between the signals for the inner protons (H_a) and those for the outer protons (H_b, H_c) is remarkably large ($\Delta\delta = 20.27$ and 18.88, respectively)[6] and corresponds to that of [22]octaethylporphyrin.[10]

Of particular importance for photomedicinal application of the [22]coproporphyrin **2a** is its photosensitizing effect as well as its UV/VIS absorptions, which are shifted to longer wavelengths and are of greater intensity than those of the blood pigment hemin or hematoporphyrin (**1a**). Figure 1 shows the UV/VIS absorption of **2a** together with that of the isohematoporphyrin (**1b**). The latter compound has the same UV/VIS spectrum as hematoporphyrin (**1a**), which, because it is unstable, is unsuitable for detailed comparison of the spectra.

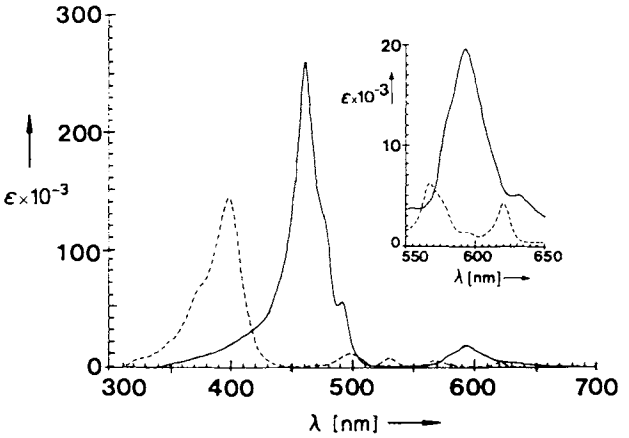

Fig. 1. UV/VIS spectra of [22]coproporphyrin **2a** and the dimethyl ester of isohematoporphyrin (**1b**) in dichloromethane.

A measure of the photosensitizing ability of the [22]coproporphyrin **2a** is singlet oxygen formation, which was determined chemically and compared with that of the excellent photosensitizer Rose Bengal and that of isohematoporphyrin (**1b**). This was accomplished by the cycloaddition of $^1O_2$ to 2,5-dimethylfuran, which is a quantitative reaction, followed by titration of the hydroperoxide formed upon methanolysis.[7, 8] For **2a**, $^1O_2$ formation exceeds that of Rose Bengal and isohematoporphyrin (**1b**) by factors of 1.4 and 1.7, respectively.

The single crystals of the [22]coproporphyrin II dihydrochloride **2b**, in the form of flat parallelepipeds (maximum size $0.26 \times 0.12 \times 0.02$ mm^3), are stable in air and display an anthracite-colored metallic luster even in thin layers. The difficulties in measuring the diffraction intensities were due, on the one hand, to the poor diffractive properties of the crystals and, on the other, to the strong decrease in intensity with θ. Compound **2b** has crystallographic $\bar{1}$ symmetry (Fig. 2). The bond lengths in the 22π-electron perimeter of **2a** (highlighted by bold lines in the formula) are nearly equal and show typical values for porphyrins ($d_{N-C} = 137.8$ pm and $d_{C-C} = 138.6$ pm).[11] The lengths of the C–N and C–C bonds in the conjugated perimeter of **2a** differ by only 0.6%; therefore, **2a**, like the [22]octaethylporphyrin described in the preceding communication,[10] fulfills not only the ring-current criterion but also the second most important criterion for aromaticity.[6] Both [22]porphyrins are thus the largest cyclic π-electron systems so far found in which the largely equal-length bonds prove both aromaticity and the validity of the (4n+2) rule.[12] Further noteworthy is the pronounced planarity of the cyclic conjugated system. Thus, the mean deviation from planarity is only 0.6 pm (Fig. 2).

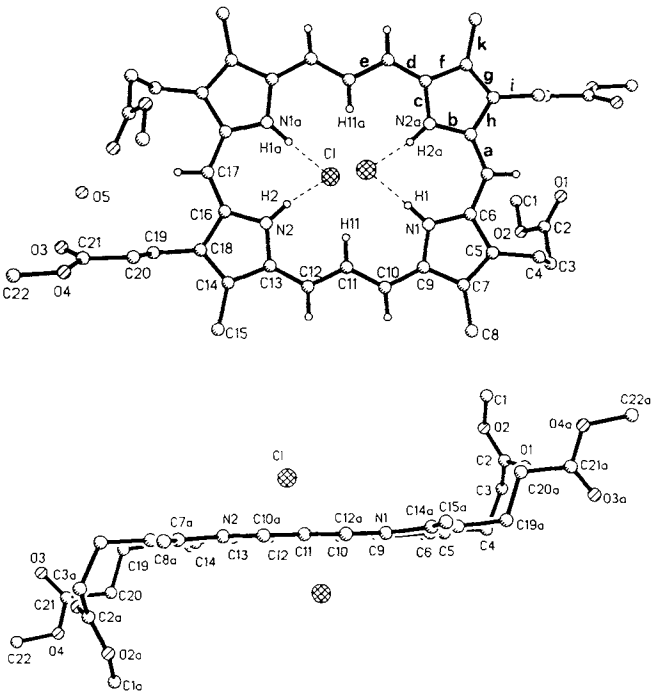

Fig. 2. Structure of **2b** with crystallographic position labeling as viewed from above (top) and from the side (bottom). Important average distances [pm]: a = 138.6, b = 137.9, c = 137.8, d = 139.3, e = 137.9, f = 143.5, g = 137.8, h = 143.1, i = 149.1, k = 148.9.

Received: July 5, 1990 [Z 4056 IE]
German version: *Angew. Chem. 102* (1990) 1439

CAS Registry numbers:
2a, 130495-56-6; **2a**·2HCl, 130468-95-0; **3**, 130468-96-1; **4**, 802-52-8; **5**, 130468-97-2; **6**, 809-27-8; 3-(dimethylamino)acrolein, 692-32-0.

[1] T. J. Dougherty, *Photochem. Photobiol. 45* (1987) 879; *Photosensitizing Compounds: Their Chemistry, Biology and Clinical Use* (Ciba Foundation Symposium 146), Wiley, New York 1989.

[2] J. T. Matthews, J. T. Newman, F. Sogandares-Bernal, M. M. Judy, H. Skiles, J. E. Leveson, A. J. Marengo-Rowe, T. C. Chanh, *Transfusion (Philadelphia) 28* (1988) 81–83.

[3] M. Gosmann, B. Franck, *Angew. Chem. 98* (1986) 1107; *Angew. Chem. Int. Ed. Engl. 25* (1986) 1100.

[4] The new compounds **2**–**4** were fully characterized by elemental analyses and spectroscopic data. **2a**: ^{1}H NMR ($CDCl_3$, TMS): $\delta = -8.43$ (t, J = 13.4 Hz, 2H, inner trimethine-bridge H), 10.45 (s, 2H, monomethine-bridge H), 11.84 (d, J = 13.4 Hz, 4H, outer trimethine-bridge H). UV/VIS (CH_2Cl_2): λ_{max} [nm] (ε) = 463 (277 500), 492 (56 100) 593 (13 500). UV/VIS (CH_2Cl_2 + 1% trifluoroacetic acid): λ_{max} nm (ε) = 461 (961 000). MS (EI): *m/z* 762 ($M^{\oplus}$, 12%) 380 ($M^{2\oplus} - 2H$, 5%).

[5] P. S. Clezy, C. J. R. Fookes, A. J. Liepa, *Austr. J. Chem. 25* (1972) 1979.

[6] P. J. Garratt: *Aromaticity*, Wiley, New York 1986, p. 52.

[7] C. S. Foote, M. T. Wuesthoff, S. Wexler, I. G. Burstain, R. Denny, G. O. Schenck, K.-H. Schulte Elte, *Tetrahedron 23* (1967) 2583–2599.

[8] B. Franck, M. Dust, A. Stange, P. P. Hoppe, *Naturwissenschaften 69* (1982) 401–402; G. Fülling, D. Schröder, B. Franck, *Angew. Chem. 101* (1989) 1550; *Angew. Chem. Int. Ed. Engl. 28* (1989) 1519.

[9] X-ray structure analysis of the [22]coproporphyrin II **2b**: space group $P2_1/n$, $a = 828.1(5)$, $b = 2619.5(6)$, $c = 1028.7(6)$ pm, $\beta = 100.30(2)°$, $Z = 2$, four-circle diffractometer CAD4 (Enraf-Nonius) ($Cu_{K\alpha}$, $\lambda = 154.178$ pm, graphite monochromator), 3561 measured reflections. Further details of the crystal structure investigation may be obtained from the Fachinformationszentrum Karlsruhe, Gesellschaft für wissenschaftlich-technische Information mbH. W-7514 Eggenstein-Leopoldshafen 2 (FRG), on quoting the depository number CSD-54603, the names of the authors, and the journal citation.

[10] H. König, C. Eickmeier, M. Möller, U. Rodewald, B. Franck, *Angew. Chem. 102* (1990) 1437; *Angew. Chem. Int. Ed. Engl. 29* (1990) 1393.

[11] R. Scheidt in D. Dolphin (Ed.): *The Porphyrins, Vol. III a*, Academic Press, New York 1978, p. 500.

[12] Other [22]porphyrins are also described in this issue: E. Vogel, N. Jux, E. Rodriguez-Val, J. Lex, H. Schmickler, *Angew. Chem. 102* (1990) 1431; *Angew. Chem. Int. Ed. Engl. 29* (1990) 1387.

Ge^{II} and Sn^{II} Complexes of [2.2.2]Paracyclophane with Threefold Internal η^6 Coordination**

By *Thomas Probst, Oliver Steigelmann, Jürgen Riede,* and *Hubert Schmidbaur**

During the last few years π complexes of main-group p-block elements have been ordered in a system which now covers the complete triads (Ga,In,Tl), (Ge,Sn,Pb), and (As,Sb,Bi).[1-3] Though the interactions of these metals with neutral aromatic hydrocarbons are relatively weak, the structural features are amazingly consistent. They include the strong centroid (η^6) coordination above the aromatic rings, which is observed for all nine metals in oxidation states corresponding to an $nd^{10}(n+1)s^2$ electronic configuration. Only for antimony(III) is this mode of coordination avoided by a displacement of the metal away from the central position.[4]

At first only *mono*(arene) complexes were found, but later on a series of *bis*(arene) complexes with interplanar angles of about 60° were also discovered.[1,5-7] The [n.n]paracyclophanes (n = 2, 3), in particular, have shown high donor capacities. However, the metal ions in the resulting systems are coordinated to the benzene rings from the outside.[8,9] Attempts to introduce $Ga^{\oplus}$ into the cavity were finally successful when [2.2.2]paracyclophane with its larger interstice was allowed to react with gallium subhalides, $Ga[GaX_4]$ (X = Cl, Br).[10]

We now report the synthesis and structural characterization of the analogous germanium(II) and tin(II) compounds. They are obtained by allowing the cyclophane (p-$C_6H_4CH_2CH_2)_3$ (= $C_{24}H_{24}$) to react in benzene with one equivalent of $GeCl_2$ and $SnCl_2$, respectively, and two to three equivalents of $AlCl_3$. Upon standing, the resulting yellow to red solutions afford colorless crystals. In the case of the Sn^{II} compound, depending on the molar ratios employed, these crystals contain the expected 1:1:2 adduct (**1**, m.p. 63 °C), with two $AlCl_4^{\ominus}$ anions, or a 1:1:3 adduct (**2**, m.p. 225 °C), with one of the anions extended to the $Al_2Cl_7^{\ominus}$ species [Eqs. (a) and (a'), respectively]. Similarities in the IR and ^1H NMR spectra suggest the presence of the same cationic species in both cases.

$$C_{24}H_{24} + SnCl_2 + 2\,AlCl_3 \longrightarrow [\{(C_{24}H_{24})Sn\}(AlCl_4)]^{\oplus}AlCl_4^{\ominus}\ \mathbf{1} \quad (a)$$

$$C_{24}H_{24} + SnCl_2 + 3\,AlCl_3 \longrightarrow [\{(C_{24}H_{24})Sn\}(AlCl_4)]^{\oplus}Al_2Cl_7^{\ominus}\ \mathbf{2} \quad (a')$$

Crystallization of the Ge^{II} compound is much slower. Single crystals of a product are obtained only over a longer period accompanied by unavoidable slow diffusion of water into the solution. The germanium atoms of the cations are still bound to one chlorine ligand and are associated—in the molar ratio 2:1—with the anions $Al_4O_2Cl_{10}^{2\ominus}$ formed by partial hydrolysis [Eq. (b)]. 1:1:1 complexes were not obtained.

$$2\,C_{24}H_{24} + 2\,GeCl_2 + 4\,AlCl_3 + 2\,H_2O \longrightarrow 4\,HCl + [(C_{24}H_{24})GeCl]_2(Al_4O_2Cl_{10})\ \mathbf{3} \quad (b)$$

^1H NMR spectra of solutions of the three complexes in [D_6]acetone (**1**, **2**) or [D_6]dimethyl sulfoxide (**3**) show only two signals in each case, indicating the preservation of the maximum symmetry of the ligand (ψ-D_{3h}) through unperturbed centroid metal coordination in solution. This observation may however be the result of a shift in anion coordination from one side to the other (see below), which is fast on the NMR time scale, or of solvation by the strongly donating solvents.

The tin(II) bis(tetrachloroaluminate) **1** crystallizes with 1.5 equivalents of benzene (m.p. 63 °C). X-ray analysis[11] revealed that the Sn^{II} ion in **1** is indeed located in the interior of the arene "fence" (Fig. 1). The contact to one of the counterions causes a displacement of the metal away from the center of the cavity. This is accompanied by a tilting of the three benzene rings in such a manner that the positioning of the metal ions above the ring centers is largely retained. The distances of the tin atom from the 18 carbon atoms of the rings span a relatively narrow range (2.817(5)–3.075(6) Å). The $AlCl_4^{\ominus}$ counterion, which shows metal contact, is coordinated only via one chlorine atom (Sn-Cl2 = 3.073(2) Å); the second counterion is not engaged in metal bonding.

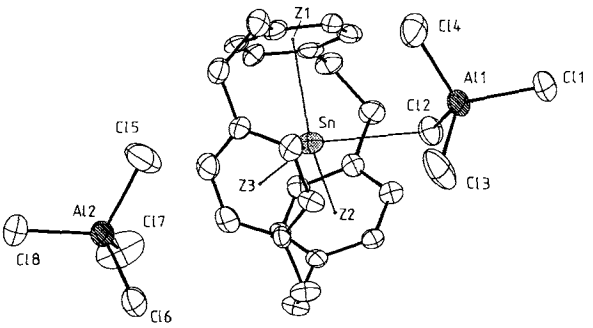

Fig. 1. Structure of **1** (ORTEP, thermal ellipsoids at 50% probability; H atoms omitted).

The distances of the tin atom from the centers of the benzene rings are not exactly the same, but their values (Sn-Z1 = 2.623, Sn-Z2 = 2.666, Sn-Z3 = 2.534 Å) indicate a comparable bonding situation. The sum of the angles Z1-Sn-Z2 = 115.52°, Z1-Sn-Z3 = 119.08°, and Z2-Sn-Z3 = 118.53° is 358.13°. The small deviation from the standard value of 360° for a local trigonal-planar symmetry reflects the only moderate distortional influence of the anion contact.

The germanium(II) compound **3** crystallizes with four molecules of benzene.[11] The anions $Al_4O_2Cl_{10}^{2\ominus}$ do not need any further description, since they are already known as compo-

[*] Prof. Dr. H. Schmidbaur, Dipl.-Chem. T. Probst, Dipl.-Chem. O. Steigelmann[+], J. Riede[+]
Anorganisch-chemisches Institut der Technischen Universität München
Lichtenbergstrasse 4, W-8046 Garching (FRG)

[+] X-ray structure analyses

[**] This work has been supported by the Deutsche Forschungsgemeinschaft (Leibniz-Programm) and the Fonds der Chemischen Industrie.

nents of other salts.[12] As a consequence of the crystallographic center of symmetry, pairs of cations $(C_{24}H_{24})$-$GeCl^{\oplus}$ are structurally equivalent. The geometrical situation in the cations of **1** (Fig. 1) and **3** (Fig. 2) seems to be similar only at first glance. The most important difference is the strong binding of the germanium atom to one chlorine atom, as revealed by the short distance of 2.224(1) Å. Accordingly, a $\tilde{\nu}$(Ge-Cl) vibrational band is found in the IR spectrum at 429 cm^{-1}.

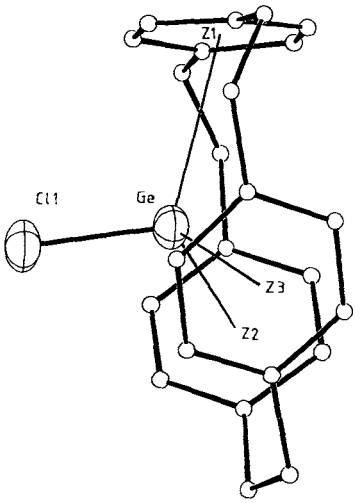

Fig. 2. Structure of the cation in **3** (ORTEP, thermal ellipsoids at 50% probability; arbitrary radii for C atoms, H atoms omitted).

The environment of the germanium atom in **3** can best be described as tetrahedral, consisting of three arene rings and one chlorine atom. The Ge–Z distances (Ge-Z1 = 2.797, Ge-Z2 = 2.722, Ge-Z3 = 2.715 Å) are slightly longer than the Sn–Z distances in **1**, and the Ge–C distances (2.724(7)–3.408(7) Å) are scattered over a broader range than the Sn–C distances in **1**. Tin is thus more strongly coordinated to the arene rings than germanium, which is consistent with the situation met with arsenic and antimony. Stereochemical activity of the lone pair at the metal center is not obvious.

The threefold coordination to neutral aromatic hydrocarbons $(3 \cdot \eta^6)$ found for the compounds **1**–**3** and for the analogous complex of $Ga[GaBr_4]$[10] has not been observed previously for transition metals. The complex $(C_{24}H_{24}) \cdot AgClO_4$[13] is also significantly different, since the metal is coordinated only to one edge of each of three arenes $(3 \cdot \eta^2)$. Centroid (η^6) coordination of transition metals like chromium(0) to [2.2.2]paracyclophane occurs with different stoichiometries and externally.[14] The larger radii of the p-block elements compared to the d-block elements seem to be an essential condition for accomplishing the excessive coordination found with low-valent main-group metals.

Experimental Procedure

1: A slurry of $SnCl_2$ (0.56 g, 2.95 mmol) and [2.2.2]paracyclophane (0.98 g, 2.94 mmol) in 180 mL of benzene was treated with $AlCl_3$ (0.81 g, 6.1 mmol), which was added slowly under reflux conditions via a Soxhlet apparatus. The color of the mixture changed to red. After 30 min the mixture was allowed to cool slowly to room temperature and then filtered. Upon standing at 20 °C, the solution afforded clear colorless crystals (**1**, 2.19 g, 84%), m.p. 63 °C. ^1H NMR ([D_6]acetone): $\delta = 7.36$ (s, 3H, C_6H_6), 6.71 (s, 4H, C_6H_4), 2.94 (s, 4H, CH_2).

2: As described for **1**, reaction of $SnCl_2$ (0.40 g, 2.11 mmol), paracyclophane (0.64 g, 2.05 mmol), and $AlCl_3$ (0.81 g, 6.07 mmol) resulted in a yellow solution above a red oil, which was separated. The solution was heated again, evaporated in vacuo to a volume of 100 mL, and cooled to room temperature. Colorless crystals separated (**2**, 1.59 g, 86%), m.p. 225 °C (dec.). The ^1H NMR spectrum was as observed for **1**.

3: As described for **1**, $GeCl_2$ (0.52 g, 3.62 mmol), cyclophane (0.84 g, 2.69 mmol), and $AlCl_3$ (1.50 g, 11.25 mmol) were allowed to react in 175 mL of benzene under reflux conditions. After 1 h a yellow solution was obtained, which was concentrated to a volume of 85 mL. Upon standing for several weeks, the solution turned green and small colorless crystals separated (**3**, 1.76 g, 44%). (Apparently, some water diffused into the solution during crystallization, though the reasons for this were not obvious.) ^1H NMR ([D_6]DMSO): $\delta = 7.35$ (s, 8H, C_6H_6), 6.65 (s, 4H, C_6H_4), 2.85 (s, 4H, CH_2).

Received: March 26, 1990;
supplemented: July 5, 1990 [Z 3876 IE]
German version: *Angew. Chem. 102* (1990) 1471

CAS Registry numbers:
1, 129813-05-4; **1** · $1\frac{1}{2}C_6H_6$, 129833-12-1; **2**, 129813-07-6; **3**, 129813-10-1; **3** · $4C_6H_6$, 129833-13-2; $C_{24}H_{24}$, 283-80-7; $SnCl_2$, 7772-99-8; $GeCl_2$, 10060-11-4; $AlCl_3$, 7446-70-0.

[1] H. Schmidbaur, *Angew. Chem. 95* (1985) 893; *Angew. Chem. Int. Ed. Engl. 24* (1985) 893.
[2] H. Schmidbaur, T. Probst, B. Huber, G. Müller, C. Krüger, *J. Organomet. Chem. 365* (1989) 53; H. Schmidbaur, T. Probst, O. Steigelmann, G. Müller, *Z. Naturforsch. B44* (1989) 1175; H. Schmidbaur, T. Probst, O. Steigelmann, G. Müller, *Heteroat. Chem. 1* (1990) 161, and references cited therein.
[3] H. Schmidbaur, W. Bublak, B. Huber, G. Müller, *Angew. Chem. 99* (1987) 248; *Angew. Chem. Int. Ed. Engl. 26* (1987) 234; H. Schmidbaur, R. Nowak, B. Huber, G. Müller, *Organometallics 6* (1987) 2266.
[4] H. Schmidbaur, R. Nowak, A. Schier, J. M. Wallis, B. Huber, G. Müller, *Chem. Ber. 120* (1987) 1829; H. Schmidbaur, R. Nowak, J. M. Wallis, B. Huber, G. Müller, *ibid. 120* (1987) 1837; H. Schmidbaur, R. Nowak, O. Steigelmann, G. Müller, *ibid. 123* (1990) 19, and references cited therein.
[5] M. Uson-Finkenzeller, W. Bublak, B. Huber, G. Müller, H. Schmidbaur, *Z. Naturforsch. B41* (1986) 346.
[6] H. Schmidbaur, R. Nowak, B. Huber, G. Müller, *Z. Naturforsch.B43* (1988) 1447; H. Schmidbaur, R. Nowak, B. Huber, G. Müller, *Polyhedron 9* (1990) 283.
[7] H. Schmidbaur, T. Probst, B. Huber, O. Steigelmann, G. Müller, *Organometallics 8* (1989) 1567.
[8] H. Schmidbaur, W. Bublak, B. Huber, G. Müller, *Organometallics 5* (1986) 1647; *Helv. Chim. Acta 69* (1986) 1742; *Z. Naturforsch. B42* (1987) 147.
[9] H. Schmidbaur, W. Bublak, B. Huber, J. Hofmann, G. Müller, *Chem. Ber. 122* (1989) 265.
[10] H. Schmidbaur, R. Hager, B. Huber, G. Müller, *Angew. Chem. 99* (1987) 354; *Angew. Chem. Int. Ed. Engl. 26* (1987) 338.
[11] **1**: Crystal data: $C_{33}H_{33}Al_2Cl_8Sn$, $M_r = 885.91$, monoclinic, space group $P2_1/n$, $a = 17.431(3)$, $b = 12.738(3)$, $c = 17.617(3)$ Å, $\beta = 99.86(1)°$, $V = 3853.8$ Å^3, $Z = 4$, $\varrho_{calcd} = 1.527$ gcm^{-3}, $\mu(Mo_{K\alpha}) = 7.85$ cm^{-1}, $F(000) = 1280$ e, Syntex $P2_1$ diffractometer, $Mo_{K\alpha}$ radiation, $\lambda = 0.71069$ Å, $T = -50$ °C, 5990 independent reflections to $(\sin\theta/\lambda)_{max} = 0.572$ Å^{-1}, 4520 observed with $F_o \geq 4.0\sigma(F_o)$. $R(R_w) = 0.051(0.045)$, $\omega = 1/\sigma^2(F_o)$, [397 refined parameters, anisotropic, H fixed (21 located, 12 calculated)], ($\Delta\varrho_{fin} = +1.10/-1.69$ eÅ^{-3}). **3**: $C_{72}H_{72}Al_4Cl_{12}Ge_2O_2$, $M_r = 1647.92$, monoclinic, space group $P2_1/c$, $a = 12.878(1)$, $b = 12.207(1)$, $c = 24.529(2)$ Å, $\beta = 96.97(1)°$, $V = 3827.5$ Å^3, $Z = 2$, $\varrho_{calcd} = 1.430$ gcm^{-3}, $\mu(Mo_{K\alpha}) = 12.84$ cm^{-1}, $F(000) = 1680$ e, Syntex $P2_1$ diffractometer, $Mo_{K\alpha}$ radiation, $\lambda = 0.71069$ Å, $T = -50$ °C, 6000 independent reflections to $(\sin\theta/\lambda)_{max} = 0.572$ Å^{-1}, 4665 observed with $F_o \geq 4.0\sigma(F_o)$, empirical absorption correction ($T = 0.71$–1.00). $R(R_w) = 0.060(0.068)$, $w = 1/\sigma^2(F_o)$ [415 refined parameters, anisotropic, H calculated at ideal geometrical positions (fixed with $U_{iso} = 0.05$ Å^2)], ($\Delta\varrho_{fin} = +0.59/-0.62$ eÅ^{-3}). Further information on the X-ray structure determinations can be obtained from the Fachinformationszentrum Karlsruhe, Gesellschaft für wissenschaftlich-technische Information GmbH, W-7514 Eggenstein-Leopoldshafen 2 (FRG), on quoting the dispository number CSD-54757, the names of the authors, and the journal citation.
[12] U. Thewalt, F. Stollmaier, *Angew. Chem. 94* (1982) 137; *Angew. Chem. Int. Ed. Engl. 21* (1982) 133.
[13] C. Cohen-Addad, P. Baret, P. Cheautemps, J.-L. Pierre, *Acta Crystallogr. Sect. C 39* (1983) 1346.
[14] C. Elschenbroich, J. Schneider, M. Wünsch, J.-L. Pierre, P. Baret, P. Cheautemps, *Chem. Ber. 121* (1988) 177.

Assembly of the $[CAu_6]^{2\oplus}$ Cluster with a Tailor-made Diphosphane Spanning the Octahedral Edges**

By *Oliver Steigelmann, Peter Bissinger,* and *Hubert Schmidbaur**

Accumulating experimental and theoretical evidence suggesting the existence of hypercoordination at carbon by gold and related d^{10} elements has led to a systematic search for compounds featuring carbon and other elements completely surrounded by gold atoms ("gilded atoms"). The initial series of investigations resulted in the synthesis and characterization of the extremely stable species $[RC(AuL)_4]^{\oplus}$, $[C(AuL)_5]^{\oplus}$, and $[C(AuL)_6]^{2\oplus}$, containing penta- and even hexacoordinate carbon atoms in the center of square pyramids, trigonal bipyramids, or octahedra of gold atoms, respectively (**A**–**C**).[1–4] This chemistry has meanwhile been extended to include the atoms boron, nitrogen, silicon, and phosphorus as nucleation centers for gold. Pertinent results cover not only more classical species like $[RN(AuL)_3]^{\oplus}$ and $[RP(AuL)_3]^{\oplus}$, but also the unprecedented di- and trications $[N(AuL)_5]^{2\oplus}$, $[N(AuL)_6]^{3\oplus}$, and $[P(AuL)_5]^{2\oplus}$ (**D**–**F**).[1, 5–8]

In all compounds obtained to date the ligand L is monodentate triphenylphosphane. The simple question therefore arose whether the novel element-centered gold clusters could also be prepared with other auxiliary donors, especially chelating ligands. Bidentate ligands, for example, could further stabilize the electron-deficient, hypercoordinate clusters and also impose different symmetry properties and chirality. We now report the assembly of the $[CAu_6]^{2\oplus}$ core triply chelated by a new diphosphane, $(1,2\text{-}C_6H_4)(CH_2CH_2PPh_2)_2$, tailor-made to span the edges of the $[CAu_6]^{2\oplus}$ octahedron.

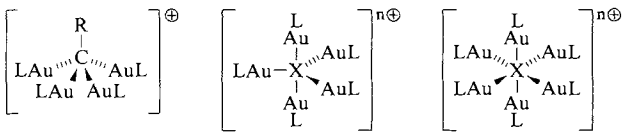

A **B**: X = C, n = 1 **C**: X = C, n = 2
D: X = N, n = 2 **E**: X = N, n = 3
F: X = P, n = 2

Graphical evaluation of models based on the geometry of the $[C(AuL)_6]^{2\oplus}$ cation[3] has shown that a ligand $R_2P(CH_2)_mPR_2$ should contain a chain with m = 6 in order to bridge the vertices of the metal octahedron if the C–Au–P axes are required to be linear. Molecular modeling suggested that a ligand such as **1** should provide the required P···P distance and acceptor orbital orientation at neighboring gold atoms (Scheme 1).

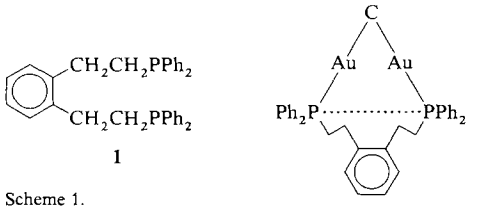

1

Scheme 1.

1,2-Bis(2-diphenylphosphinoethyl)benzene (**1**) [m.p. 71 °C, $\delta(^{31}P) = -15.1$] was prepared starting from 1,2-bis(cyanomethyl)benzene as shown in Scheme 1. Most of the conversions, involving standard procedures, gave satisfactory yields. Treatment of the ligand **1** with tetrachloroauric acid in the presence of a thioether as a reducing and complexing agent[9] finally afforded the pale-yellow dinuclear complex **2** [m.p. 205 °C (dec.), $\delta(^{31}P) = 29.2$] in ca. 65% yield as the key reagent for assembly of the carbon-centered cluster (Scheme 2).

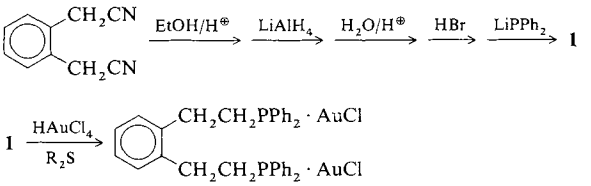

2

Scheme 2. Synthesis of **2**.

Reaction of the gold complex **2** with tetrakis(dimethoxyboryl)methane[3, 10] in hexamethylphosphoric triamide (HMPT) in the presence of cesium fluoride produced an orange solution. After filtration and precipitation with a benzene/pentane mixture, yellow crystals of **3** were obtained in about 10% yield (m.p. 155 °C with decomposition) [Eq. (a)].

$$3\,\mathbf{2} + C[B(OCH_3)_2]_4 + 8\,CsF \rightarrow 6\,CsCl + 2\,B(OCH_3)_3 + 2\,CsOCH_3 + [\{C_6H_4(CH_2CH_2PPh_2Au)_2\}_3C][BF_4]_2 \quad (a)$$

3

Compound **3** was identified by elemental analysis and field desorption mass spectrometry. The parent peak at *m/z* 1350.7 is readily assigned to the dication in **3** (in CH_2Cl_2). The $^{31}P\{^1H\}$ NMR spectrum (in CD_2Cl_2) shows a single resonance at $\delta = 24.3$. Both the ^1H and the ^{13}C NMR spectra exhibit sets of signals indicating not only virtual threefold symmetry of the dication in solution, but also an internal twofold symmetry of the ligand (C_2) which renders the ligand halves equivalent.[11] The resonance of the central carbon atom could not be observed, but the counterions have been detected through their ^{11}B resonance ($\delta = -17.9$, $^1J(BF) = 17.1$ Hz).

The structure of the new cluster cation was determined by X-ray diffraction.[12] Crystals grown from dichloromethane/benzene/pentane solution (monoclinic, space group $C2/c$, $Z = 4$) contain one molecule of crystal benzene per stoichiometric unit. The dication $[CAu_6(\mathbf{1})_3]^{2\oplus}$ does not obey the high point-group symmetry (D_{3d}) suggested by the NMR spectra of the solutions, but exhibits only crystallographic C_2 symmetry with the twofold axis passing through the central carbon atom and through the centers of two C–C bonds on opposite sides of one of the *ortho*-phenylene rings (Fig. 1). Each dication is a chiral entity, which is related with a neighboring enantiomer by a center of symmetry.

The CAu_6 core can be described as a distorted carbon-centered octahedron of gold atoms with Au···Au distances between 2.942(2) and 3.132(2) Å and with C–Au distances of 2.09(3), 2.15(3), and 2.13(3) Å. The three independent Au–P distances and C–Au–P angles are equal within the limits set by the rather large standard deviations for these parameters.

[*] Prof. Dr. H. Schmidbaur, Dipl.-Chem. O. Steigelmann, P. Bissinger
Anorganisch-chemisches Institut der Technischen Universität München
Lichtenbergstrasse 4, W-8046 Garching (FRG)

[**] This work has been supported by the Deutsche Forschungsgemeinschaft (Leibniz-Programm) and the Fonds der Chemischen Industrie and by Hoechst AG, Degussa AG, and W. C. Heraeus GmbH.

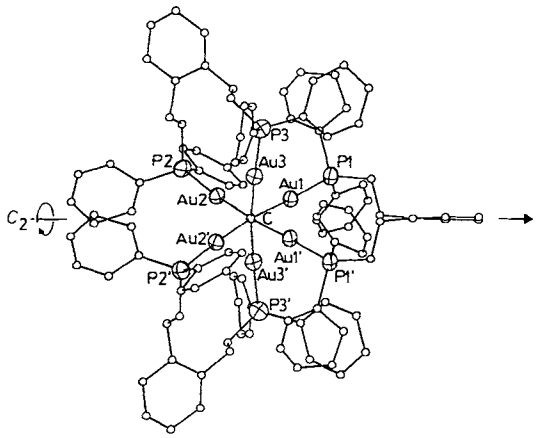

Fig. 1. Structure of the dication of **3** in the crystal [12] (ORTEP, thermal ellipsoids drawn at 50% probability for Au, P; arbitrary radius for C; H atoms omitted for clarity). Selected distances [Å] and angles [°]: Au1-Au1' 2.979(3), Au1-Au2 2.947(2), Au1-Au3 2.942(2), Au1-Au3' 2.985(2) Au2-Au3 3.094(2), Au2-Au3' 2.982(2), Au2-Au2' 3.132(2); C-Au1 2.15(3), C-Au2 2.09(3), C-Au(3) 2.13(3); P1-Au1 2.266(9), P2-Au2 2.267(9), P3-Au3 2.275(9); C-Au1-P1 177.3(3); C-Au2-P2 175.3(9), C-Au3-P3 175.8(9).

The structure of the dication in **3** is thus very similar to that of the parent hexakis(triphenylphosphane) cluster. Though the yields are not really satisfactory, the successful synthesis of the triply chelated cluster **3** and its thermal and chemical stability support the validity of the aurophilicity concept advanced in an attempt to account for formation and bonding of this new type of coordination.[1, 3, 13] It is important to note here that all attempts to prepare clusters of the types $[C(AgL)_6]^{2\oplus}$ and $[C(CuL)_6]^{2\oplus}$ have met with failure, whereas work in progress on other functional or polychelating organophosphane complexes of the $[CAu_6]^{2\oplus}$ unit continue to show promising results.

Experimental Procedure

1 (Scheme 2): a) 1,2-Bis(cyanomethyl)benzene (40.0 g, 0.256 mol) in ethanol (95%, 125 mL) was treated with concentrated H_2SO_4 (100 g) and refluxed for 7 h. Hydrolytic workup afforded the ethyl ester (47.1 g, 73%), b.p. 146–8 °C/1 Torr) [14]. b) This ester (45.0 g, 0.18 mol) in diethyl ether (225 mL) was reduced by $LiAlH_4$ (12.8 g, 0.34 mol, in 850 mL of Et_2O). Workup in aqueous sulfuric acid yielded 10.5 g of the diol (35%, m.p. 61 °C (from benzene)) [15]. c) The diol (5.8 g, 35 mmol) was treated with aqueous HBr (120 mL, 80%) for 5 h at reflux temperature. Extraction with CH_2Cl_2 and distillation gave 7.3 g of the dibromide (72%, b.p. 134 °C/1 Torr) [16]. d) A red solution of $LiPPh_2$ was prepared from Li powder (1.52 g, 220 mmol) and $ClPPh_2$ (11.1 g, 50 mmol) in THF (100 mL) at reflux temperature (30 min) under nitrogen. This solution was treated with the dibromide precursor (7.32 g, 25 mmol) in THF (30 mL) at 0–65 °C. Workup with aqueous HCl (30 mL, 10%) yielded ligand **1** (6.0 g, 48%, m.p. 71 °C (from ethanol)). $^{13}C\{^1H\}$ NMR (CD_2Cl_2): δ = 29.3 (d, J(PC) = 18 Hz), 29.8 (d, J(PC) = 14 Hz; CH_2) C_6H_4: δ = 139.2(d, J(PC) = 14 Hz; C1,C2), 129.4 (C3,C6), 126.6 (C4,C5), C_6H_5: δ = 140.6 (d, J(PC) = 13 Hz; *ipso*-C), 133.0 (d, J(PC) = 19 Hz; *o*-C), 128.9 (d, J(PC) = 13 Hz; *m*-C'), 128.9 (*p*-C). $^{31}P\{^1H\}$ NMR (CD_2Cl_2): δ = − 15.1 [17].

2 and **3**: $HAuCl_4 \cdot 3H_2O$ (3.67 g, 9.3 mmol) was dissolved in ethanol (50 mL) and treated with thiodiglycol (3.41 g, 27.9 mmol) in ethanol (20 mL) at 0 °C [9]. As soon as the yellow color had vanished, ligand **2** (2.34 g, 4.66 mmol) was added in acetone (50 mL). The pale yellow precipitate of **2** was collected after 12 h (2.8 g, 62%, dec. at 205 °C). $^{13}C\{^1H\}$ NMR ($CDCl_3$, see **1** for assignments, J(PC) coupling constants in parentheses): 28.2(4), 29.3(36); 137.3(14), 129.3, 127.6; 128.8(60), 133.2(13), 129.5(11), 132.2. $^{31}P\{^1H\}$ NMR ($CDCl_3$): δ = 29.2.

Complex **2** (2.1 g, 2.17 mmol) and CsF (4.32 g, 28.4 mmol) in HMPT (60 mL) were treated with a solution of $C[B(OCH_3)_2]_4$ (0.220 g, 0.725 mmol) in the same solvent (20 mL) for 48 h at 20 °C under N_2. The orange solution was filtered and the product precipitated with pentane/benzene. Repeated extraction with CH_2Cl_2 and reprecipitation with pentane/benzene afforded yellow crystals of **3** (0.20 g, 10%, dec. at 155 °C). For NMR data see [11].

Received: June 8, 1990 [Z 4000 IE]
German version: *Angew. Chem. 102* (1990) 1473

CAS Registry numbers:
1, 118636-00-3; **2**, 129731-20-0; **3**, 129731-22-2; **3** · C_6H_6, 129756-46-3; 1,2-$C_6H_4(CH_2CH_2CN)_2$, 613-73-0; 1,2-$C_6H_4(CH_2CO_2Et)_2$, 17532-66-0; 1,2-$C_6H_4(CH_2CH_2OH)_2$, 17378-99-3; 1,2-$C_6H_4(CH_2CH_2Br)_2$, 17379-00-9; $ClPPh_2$, 1079-66-9; $HAuCl_4 \cdot 3H_2O$, 16961-25-4; $C[B(OCH_3)_2]_4$, 17936-80-0.

[1] H. Schmidbaur, *Gold Bull. 23* (1990) 11.
[2] F. Scherbaum, B. Huber, G. Müller, H. Schmidbaur, *Angew. Chem. 100* (1988) 1600; *Angew. Chem. Int. Ed. Engl. 27* (1988) 1542.
[3] F. Scherbaum, A. Grohmann, B. Huber, C. Krüger, H. Schmidbaur, *Angew. Chem. 100* (1988) 1602; *Angew. Chem. Int. Ed. Engl. 27* (1988) 1544.
[4] F. Scherbaum, A. Grohmann, G. Müller, H. Schmidbaur, *Angew. Chem. 101* (1989) 464; *Angew. Chem. Int. Ed. Engl. 28* (1989) 453.
[5] A. Grohmann, J. Riede, H. Schmidbaur, *Nature (London) 345* (1990) 140.
[6] J. Strähle et al. (Tübingen), personal communication.
[7] G. Weidenhiller, H. Schmidbaur, unpublished.
[8] For theoretical papers: see D. M. P. Mingos, *Nature (London) 345* (1990) 113, and references cited therein. See also V. Ramamoorthy, P. R. Sharp, *Inorg. Chem. 29* (1990) 3336.
[9] A. K. Al-Sa'Ady, C. A. McAuliffe, R. V. Parish, J. A. Sandbark, *Inorg. Synth. 23* (1985) 191.
[10] R. B. Castle, D. S. Matteson, *J. Am. Chem. Soc. 90* (1968) 2194; *J. Organomet. Chem. 20* (1969) 19.
[11] **3**: ^1H NMR (CD_2Cl_2): δ = 2.57–2.61 (m, 12H), 2.91–2.93 (m, 12H; CH_2), 7.0–7.6 (m, 72H; Aryl). $^{13}C\{^1H\}$ NMR (CD_2Cl_2): C_6H_5: δ = 127.3 (d, J(PC) = 61.6 Hz; *ipso*-C), 133.2 (m, *o*-C), 129.8 (m, *m*-C), 132.5 (s, *p*-C), C_6H_4: 135.2 (d, J(PC) = 12 Hz; C1,C2), 132.2 (s, C3,C6), 129.9 (s, C4,C5), CH_2: δ = 29.3(s), 31.6 (d, J(PC) = 32 Hz). $^{31}P\{^1H\}$ NMR (CD_2Cl_2): δ = 24.3(s).
[12] Crystal data and structure solution for **3** · C_6H_6: $C_{109}H_{102}Au_6B_2F_8P_6$, M_r = 2873.2; monoclinic, space group $C2/c$, a = 14.677(3), b = 36.141(4), c = 20.656(3) Å, β = 97.26(2)°, V = 10868.9 Å^3, Z = 4, ϱ_{calcd} = 1.805 g cm^{-3}, $\mu(Mo_{K\alpha})$ = 78.9 cm^{-1}, Enraf Nonius CAD4 diffractometer, $Mo_{K\alpha}$ radiation, λ = 0.71069 Å, T = 23 °C, 9524 independent reflections, 5239 observed with $F_o \geq 4.0\sigma(F_o)$; empirical absorption correction (T = 0.81–1.00). Solution by direct methods (SHELXS-86), $R(R_w)$ = 0.075(0.088) for 273 refined parameters (Au, P anisotropic; C isotropic, BF_4 calculated in idealized geometry in the region of high residual electron density with U_{iso} = 0.25 for B and F), $\Delta\varrho_{fin}$(max/min) = + 4.43/−2.21 e/Å^3. (The high R values and relatively large standard deviations arise from the poor quality of the crystals.) Further details of the crystal structure investigation are available on request from Fachinformationszentrum Karlsruhe, W-7514 Eggenstein-Leopoldshafen (FRG), on quoting the depository number CSD-54804, the names of the authors, and the journal citation.
[13] N. Rösch, A. Görling, D. E. Ellis, H. Schmidbaur, *Angew. Chem. 101* (1989) 1410; *Angew. Chem. Int. Ed. Engl. 28* (1989) 1357.
[14] R. Adams, A. F. Thal: *Organic Syntheses Collective Volume I*, 2nd ed. Wiley, New York 1941, p. 270.
[15] J. O. Halford, B. Weissman, *J. Org. Chem. 17* (1952) 1646.
[16] C. W. Muth, D. O.: Steininger, Z. B. Panastassiou, *J. Org. Chem. 77* (1955) 1006.
[17] E. Vincent, L. Verdonck, G. P. van der Kelen, *Spectrochim. Acta Part A 36*, (1980) 699; B. E. Mann, *J. Chem. Soc. Perkin Trans 2, 1972*, 30.

Amine-Template-Directed Synthesis of Cyclic Porphyrin Oligomers**

By *Harry L. Anderson* and *Jeremy K. M. Sanders**

The use of guest molecules as templates for directing the assembly of complementary host structures is a recurrent theme in many areas of biochemistry. It is also an approach widely used in the synthesis of coronands,[1] catenanes,[2] zeolites,[3] functionalized polymers,[4] and biomimetic systems such as models for enzymic catalysis[5] and self-replica-

[*] Dr. J. K. M. Sanders, H. L. Anderson
Cambridge Centre for Molecular Recognition
University Chemical Laboratory
Lensfield Road, Cambridge CB2 1EW (UK)

[**] This work was supported by the Science and Engineering Research Council (UK).

tion.[6] Here we describe how this concept can be extended to the ligand-templated synthesis of cyclic porphyrin oligomers. Recently we reported the structure-directed synthesis of a porphyrin trimer.[7] We have now found that, by judicious use of templates, the outcome of this reaction can be directed down either of two quite different pathways (Scheme 1).

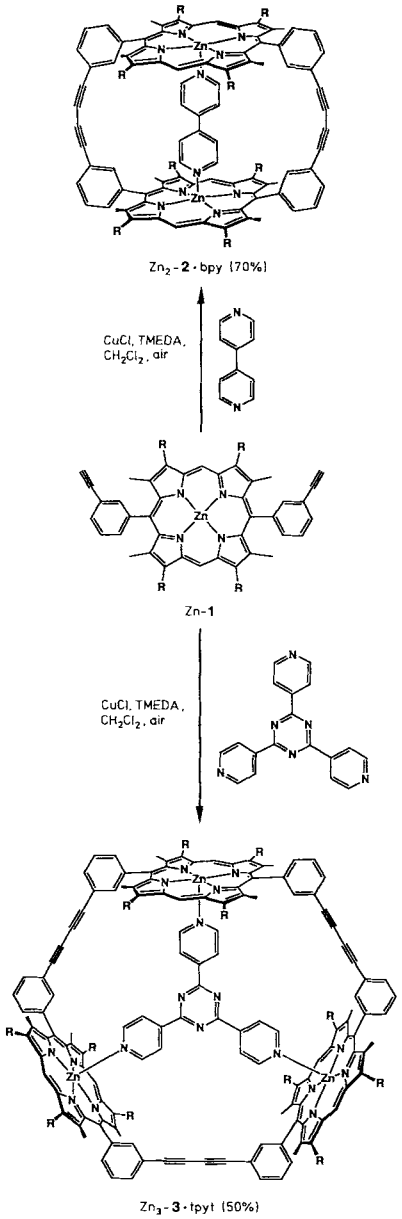

Scheme 1. Control of supermacrocyclization by amine templates (R = $CH_2CH_2CO_2Me$).

The ester-functionalized bisacetylenic porphyrin H_2-**1** was synthesized in 55% yield by condensation of **4**[8] (generated in situ) with 3-ethynylbenzaldehyde. We first prepared the

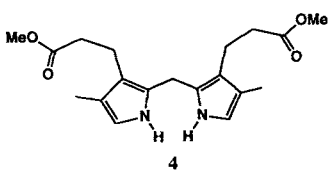

4

functionalized porphyrin dimer and trimer, H_4-**2** and H_6-**3**, by the untemplated oxidative coupling of Zn-**1** using conditions developed for the synthesis of unfunctionalized porphyrin trimer[7] (0.5 mM Zn-**1**/60 mM CuCl/pyridine/air). This reaction yields a mixture of Zn_2-**2** and Zn_3-**3**, which were demetalated, separated by flash chromatography, and isolated in 20–25% and 30–35% yield, respectively.[9] Both cyclic oligomers are readily soluble in chloroform.[10]

Ligands such as 4,4'-bipyridyl (bpy) and s-tri(4-pyridyl)-triazine (tpyt) have no affect on the coupling reaction in coordinating solvents such as pyridine. After screening a wide range of conditions, however, we found that dramatic templating effects are observed in noncoordinating solvents, such as dichloromethane, when air/CuCl/*N,N,N',N'*-tetramethylethylenediamine (TMEDA) is used as the oxidant.[11] This effect is seen most clearly by looking at the *meso* region of the ^{1}H NMR spectra of the crude reaction mixtures after removing copper, bound zinc, and ligands (Fig. 1). The reso-

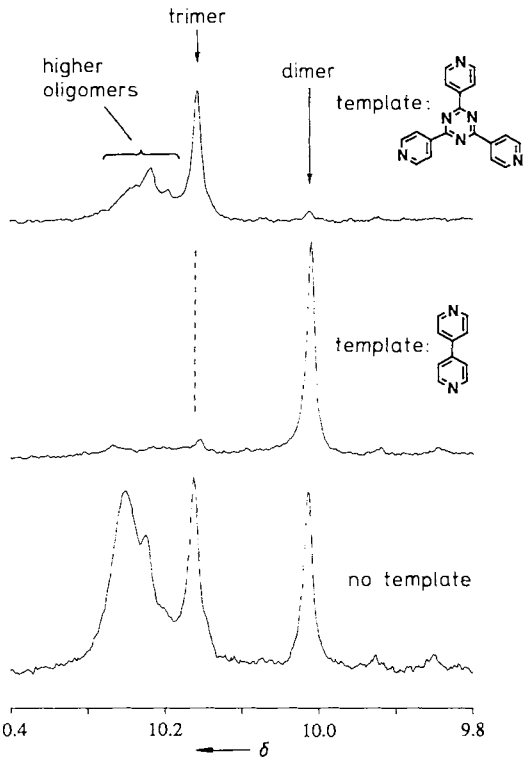

Fig. 1. ^{1}H NMR spectra of crude reaction mixtures demonstrating the effects of amine templates. The conditions used to produce these reaction mixtures differed only in the type of template present.

nances of the *meso* protons of H_6-**3** and H_4-**2** are shifted to progressively lower chemical shift, relative to H_2-**1**, by the ring current effect across the porphyrin cavity, so that the product distribution can be accurately estimated from these spectra. The tpyt ligand clearly enhances formation of Zn_3-**3** and inhibits formation of Zn_2-**2**, whereas bpy has the opposite effect, templating formation of Zn_2-**2**. In our hands, template-directed synthesis is now the most practical preparative route to both **2** and **3**.

The origin of these effects can be understood by comparing the binding properties[12] of a range of ligands with their templating behavior[13] (Table 1). The bpy ligand, which gives a threefold increase in the yield of dimer, shows a remarkable affinity for Zn_2-**2**.[14] The chelation factor (effective molarity) of the Zn_2-**2**·bpy complex (34 M) is higher than

values reported for similar complexes,[15] although it is still much less than the theoretical maximum.[16] The tpyt ligand is the best template for trimer synthesis and binds strongly to Zn_3-**3**, although it appears to be slightly too small to fit this host perfectly and shows an overall chelation factor of only ca. 1 M. The templating and binding properties of 1,3-di(4-pyridyl)propane are almost as effective as those of tpyt; the third binding site of tpyt has only a modest effect on both its binding and its templating. 1,2-Di(4-pyridyl)ethane binds quite strongly to both Zn_2-**2** and Zn_3-**3**, showing little selectivity and exhibiting little template effect.

Table 1. Host affinities and yields for various template ligands[12, 13].

Ligand/Template	lg$K$ Zn-**1**	lg$K$ Zn_2-**2**	lg$K$ Zn_3-**3**	Yield [%] H_4-**2**	Yield [%] H_6-**3**
Pyridine	3.7	3.7	3.6	23	34
4,4'-Bipyridyl	3.9	8.8	4.9[a]	72	4
1,2-Di(4-pyridyl)ethane	4.1	6.1	7.5[a]	27	34
1,3-Di(4-pyridyl)propane	4.2	5.1	8.8[a]	7	43
s-Tri(4-pyridyl)triazine	3.9	3.8	10.0	6	52

[a] These are lgK_1 values. K_2 values were also measured.

In general, there is a close correspondence between the templating properties of each ligand and its trimer/dimer binding selectivity, which indicates that the transition state for acetylene coupling has a geometry closely resembling that of the product. The criteria for an efficient trimer-producing template are more stringent than those for a dimer template: a trimer-producing template must both bind the linear dimer intermediate **5**[17] in a conformation which prevents it from cyclizing and bind linear trimer **6** in the correct conformation for accelerating ring closure; in contrast, a dimer-producing template has only to accelerate the cyclization of linear dimer **5**. The tpyt ligand appears to be very efficient at inhibiting cyclization of **5** but less good at accelerating the closure of **6**.

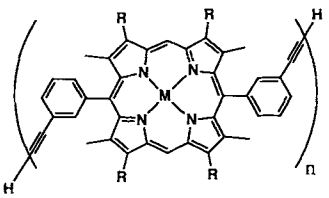

5 (n = 2), **6** (n = 3)

This templating approach not only provides a good practical route to potentially catalytic molecules but also elucidates some of the design principles required. When designing templates for the assembly of more complex hosts, it will be important to remember that the template must be able to bind strongly to early intermediates and prevent them from following undesired pathways, and that it must be able to bind later intermediates and hold them in conformations resembling that of the desired product. Importantly, a good template does not need to show perfect product complementarity.

Experimental Procedure

H_2-**1**: Palladium on carbon (10%, 140 mg) was added to a solution of 5,5'-dibenzyloxycarbonyl-3,3'-di(2-methoxycarbonylethyl)-4,4'-dimethyl-2,2'-dipyrrylmethane [18] (4.0 mmol) in THF (100 mL) containing 1% triethylamine and the mixture was stirred under hydrogen. After 1 h, the catalyst was filtered off and the filtrate was evaporated and redissolved in trifluoroacetic acid (TFA, 25 mL) under argon at 0 °C to generate a solution of **4**[8]. After 20 min, a solution of 3-ethynylbenzaldehyde (4.0 mmol) in methanol (100 mL) was added and the mixture was stirred for 2 h. 2,3-Dichloro-5,6-dicyano-1,4-benzoquinone (6 mmol) in THF (50 mL) was added and the mixture was stirred for a further 2 h and then evaporated. The product was purified by flash chromatography ($SiO_2/CHCl_3$, $R_f = 0.18$) and recrystallized from chloroform/methanol. Yield 55% (1.005 g). ^{1}H NMR (400 MHz, $CDCl_3$): $\delta = -2.48$ (s, 2H), 2.52 (s, 12H, 3.15 (t, 8H), 3.18 (s, 2H), 3.65 (s, 12H), 4.36 (t, 8H), 7.73 (t, 2H), 7.95 (d, 2H), 8.04 (d, 2H), 8.20 (s, 2H), 10.28 (s, 2H). IR ($CHCl_3$): $\tilde{\nu}$[cm^{-1}] = 3304 (C-H), 1732 (C=O). UV/VIS (CH_2Cl_2): λ_{max}[nm] = 408, 506, 539, 574, 627. FAB MS (Xe$^{\oplus}$, 8 KV): m/z 911 ($M^{\oplus}$).

H_4-**2**: A solution of Zn-**1** (0.20 mmol, 200 mg) in anhydrous dichloromethane (500 mL) was treated with copper(I) chloride (14 mmol), TMEDA (14 mmol), and 4,4'-bipyridyl (1.2 mmol) and stirred under dry air. After 24 h, the reaction mixture was washed with water (3 × 500 mL) and treated with methanolic TFA (10%, 100 mL), then washed again with water (4 × 500 mL) and evaporated. (The ^{1}H NMR of the crude material was recorded at this stage.) The product was purified by flash chromatography (SiO_2/1:1 $CH_2Cl_2/CHCl_3$, $R_f = 0.13$ in $CHCl_3$). Yield 65–75% (120–135 mg). ^{1}H NMR: $\delta = -2.63$ (s, 4H), 2.34 (s, 4H), 2.34 (s, 24H), 2.95 (t, 16H), 3.53 (s, 24H), 4.17 (t, 16H), 7.08 (s, 4H), 7.74 (m, 8H), 8.49 (d, 4H), 10.01 (s, 4H). IR: $\tilde{\nu}$[cm^{-1}] = 1732 (C=O). UV/VIS: λ_{max}[nm] = 315, 336, 407, 507, 540, 575, 627. FAB MS: m/z 1818 ($M^{\oplus}$).

H_6-**3**: The procedure was identical to that described above, except that s-tri(4-pyridyl)triazine (1.2 mmol) was used instead of 4,4'-bipyridyl. Yield 50–55% (90–100 mg). $R_f = 0.11$ in $CHCl_3$. ^{1}H NMR: $\delta = -2.66$ (s, 6H), 2.43 (s, 36H), 3.04 (t, 24H), 3.55 (s, 36H), 4.23 (t, 24H), 7.72 (t, 6H), 7.98 (d, 6H), 8.02 (d, 6H), 8.07 (s, 6H), 10.16 (s, 6H). IR: $\tilde{\nu}$[cm^{-1}] = 1733 (C=O). UV/VIS: λ_{max}[nm] = 314, 334, 408, 506, 539, 574, 627. FAB MS: m/z 2727 ($M^{\oplus}$), 1364 ($M^{2\oplus}$).

All products were spectroscopically pure. Free-base porphyrins were metalated with zinc in near quantitative yield by treatment with excess zinc acetate in chloroform.

Received: July 20, 1990 [Z 4080 IE]
German version: *Angew. Chem. 102* (1990) 1478

[1] D. H. Busch, N. A. Stephenson, *Coord. Chem. Rev. 100* (1990) 119; L. F. Lindoy: *The Chemistry of Macrocyclic Ligands*, Cambridge University Press, Cambridge 1989, Chapter 2.
[2] C. O. Dietrich-Buchecker, J.-P. Sauvage, *Tetrahedron 46* (1990) 503; P. R. Ashton, T. T. Goodnow, A. E. Kaifer, M. V. Reddington, A. M. Z. Slawin, N. Spencer, J. F. Stoddart, C. Vincent, D. J. Williams, *Angew. Chem. 101* (1989) 1404; *Angew. Chem. Int. Ed. Engl. 28* (1989) 1396.
[3] S. L. Lawton, W. J. Rohrbaugh, *Science (Washington D. C.) 247* (1990) 1319.
[4] K. J. Shea, D. Y. Sasaki, *J. Am. Chem. Soc. 111* (1989) 3442.
[5] T. R. Kelly, C. Zhao, G. J. Bridger, *J. Am. Chem. Soc. 111* (1989) 3744; M. Hattori, H. Nakagawa, M. Kinoshita, *Makromol. Chem. 181* (1980) 2325.
[6] T. Tjivikua, P. Ballester, J. Rebek, Jr., *J. Am. Chem. Soc. 112* (1990) 1249.
[7] H. L. Anderson, J. K. M. Sanders, *J. Chem. Soc. Chem. Commun. 1989*, 1714.
[8] M. Czurylowski, *Dissertation*, Fribourg University, Switzerland, 1987.
[9] The ester groups of these compounds can be hydrolyzed to give water-soluble hosts.
[10] It appears that some unfunctionalized cyclic porphyrin dimer is also formed during the synthesis[7] of unfunctionalized trimer, but that it is extremely insoluble and is lost during workup.
[11] No reaction occurs in dichloromethane in the absence of TMEDA, but this ligand has no effect on the reaction in pyridine. The use of TMEDA to promote Glaser coupling in noncoordinating solvents was first reported by *A. S. Hay* (*J. Org. Chem. 27* (1962) 3320).
[12] Binding constants were determined by simulation analysis of UV titration curves in CH_2Cl_2 at ambient temperatures: see C. A. Hunter, P. Leighton, J. K. M. Sanders, *J. Chem. Soc. Perkin Trans. 1 1989*, 547. The lgK_1 values are reproducible to within ± 1%, except for values greater than 8 which are only accurate to ± 5%. Zn-**1** and Zn_3-**3** have similar binding constants to those of their unfunctionalized analogues, some of which have already been published [7].
[13] The templated yields of dimer and trimer in Table 1 were determined by integrating the *meso* regions of ^{1}H NMR spectra of crude reaction mixtures obtained using 1.7 mM template (see *Experimental Procedure*).

Yields can be estimated accurately in this way because all the products are soluble and no porphyrin units are destroyed during reaction; values are reproducible within ± 5% and compare well with isolated yields.

[14] The Zn_2-**2**·bpy complex exchanges slowly with excess bpy on the ^1H NMR time scale at ambient temperatures and its ^1H NMR spectrum has been fully assigned using 2D NMR techniques (NOEs are detected between internal *ortho*-aromatic protons of the host and both guest protons). The 1:1 complex can also be observed directly by FAB MS.

[15] I. P. Danks, I. O. Sutherland, C. H. Yap, *J. Chem. Soc. Perkin Trans. 1 1990*, 421.

[16] M. I. Page, W. P. Jencks, *Proc. Natl. Acad. Sci. USA 68* (1971) 1678; W. P. Jencks, *ibid. 78* (1981) 4046.

[17] Linear intermediates such as **5** and **6** have not been isolated. A compound resembling **5** has recently been synthesized: K. Maruyama, S. Kawabata, *Bull. Chem. Soc. Jpn. 63* (1990) 170.

[18] P. S. Clezy, A. J. Liepa, *Aust. J. Chem. 23* (1970) 2443.

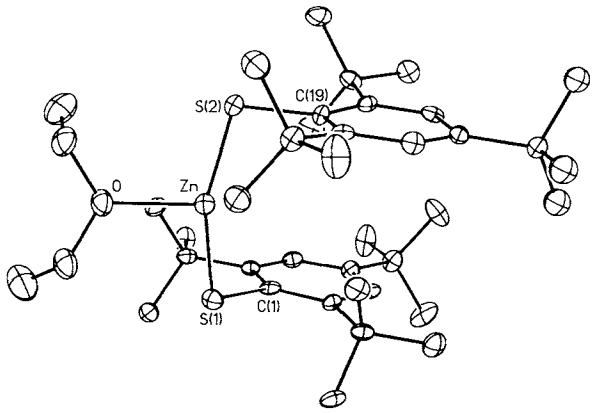

Fig. 1. Molecular structure of **1** (the H atoms are omitted for clarity) [13]. Selected bond distances [Å] and angles [°]: Zn-S1 2.194(2), Zn-S2 2.197(2), Zn-O 2.133(5), S1-C1 1.810(7), S2-C19 1.805(7); S1-Zn-S2 159.6(1), S1-Zn-O 99.6(2), S2-Zn-O 100.8(2), Zn-S1-C1 102.6(2), Zn-S2-C19 103.2(2).

Synthesis and Structure of $[Et_2OZn(SC_6H_2tBu_3)_2]$, the First T-Shaped Zinc Complex**

By *Philip P. Power** and *Steven C. Shoner*

Considerable effort has been devoted to the study of zinc thiolates in the search for structural models for the metal–sulfur bonding in zinc-cysteine metalloproteins.[1–3] In addition, recent results concerning the structure of the so-called zinc finger centers in nucleic acid binding proteins have provided added impetus to this area of research.[4, 5] A characteristic feature of many of the zinc thiolate complexes synthesized to date has been their tendency to form aggregates or cages comprised of $[ZnS_4]$ units.[1–3] It has been shown recently that association can be prevented by the use of bulky ligands, as seen in $[Zn(2,3,5,6\text{-}Me_4C_6HS)_3]^{\ominus}$,[6] a monomeric ion having trigonal-planar coordination at zinc and Zn–S distances near 2.23 Å. In sharp contrast to these data, there is little structural information currently available for neutral zinc thiolate species. Normally, $Zn(SR)_2$ complexes are polymeric with tetrahedrally coordinated zinc linked by SR bridges.[7] Monomeric species are observed only when ancillary or chelating ligands are used, as exemplified by $Zn(SCH_2CH_2NMe_2)_2$, which has four-coordinate zinc.[8] As part of our work on the synthesis of the quasi-aromatic ring systems $(RZnSR')_3$ (R and R′ = bulky alkyl or aryl groups),[9, 10] we have become interested in the reactions of zinc alkyls with bulky thiols. Here we describe the synthesis and structure of the unusual compound $[Et_2OZn(SAr)_2]$ (**1**, Ar = 2,4,6-$tBu_3C_6H_2$), which has approximately T-shaped coordination at zinc.

Compound **1** was synthesized by reaction of $Zn(CH_2SiMe_3)_2$[11] with two equivalents of HSAr in the presence of ether. In the absence of Et_2O, a white precipitate of $Zn(SAr)_2$ (**2**) was formed. This species dissolves in warm toluene and is sparingly soluble in warm hexane. ^1H NMR spectroscopy and cryoscopy indicate a monomeric structure in C_6D_6. Unfortunately, crystals of **2** suitable for X-ray crystallography have not been obtained to date. The apparent monomeric nature of **2** in solution is in agreement with the recently reported solution data for $Cd(EAr)_2$ (E = S or Se).[12] These compounds have dimeric structures in the solid with EAr bridges.

The monomeric structure of **1** (Fig. 1) features a planar, three-coordinate Zn center. The angles observed at zinc justify the description of the coordination as T-shaped. The Zn–S distances (ca. 2.196 Å) are the shortest thus far observed for a Zn–S bond and, in fact, approach the value of 2.133(5) Å observed for the Zn–OEt_2 bond. The short Zn–S bonds suggest that the Zn–S bonding orbitals probably have approximate sp hybridization. The relatively long Zn–O bond (cf. ca. 2.077 Å for Zn-O_{thf} in four-coordinate $[Zn(2,6\text{-}tBu_2C_6H_3O)_2(thf)_2]$[14]) is consistent with this view and is indicative of the involvement of a p-like Zn orbital in the Zn–O bond. The weaker nature of the Zn–O bond is reflected in the relative ease with which Et_2O may be removed under reduced pressure and moderate temperature (100 °C).

The unusual geometry of this molecule is probably the result of a combination of factors. For example, it is notable that the aromatic rings are almost parallel, both to each other and to those of neighboring molecules. The approximately parallel stacking of the Ar groups and the ca. 102.9° Zn–S–C angles result in a S–Zn–S angle of ca. 160°. Owing to its low coordination and relative electron deficiency, the Zn center can behave readily as an acceptor toward one Et_2O molecule.

Coordination of a second ether is disfavored for steric reasons and because it would probably destroy the advantageous packing arrangement. The T-shaped geometry is unknown for Zn species and has only been authenticated in a few transition-metal complexes.[15–17]

Experimental Procedure

Under anaerobic and anhydrous conditions, 2,4,6-$tBu_3C_6H_2SH$ (1.11 g, 4 mmol) [18] in pentane (20 mL) was added dropwise to $Zn(CH_2SiMe_3)_2$ (0.48 g, 2 mmol) [11] in pentane (5 mL). The solution was refluxed for 1 h, and a white precipitate was formed. The volatile materials were removed under reduced pressure and the residue was dissolved in Et_2O (7 mL). Cooling slowly to −25 °C resulted in formation of colorless crystals of **1** in 70–80% yield. ^1H NMR (300 MHz, C_6D_6): δ = 1.08 (t, 6H; Et_2O), 1.33 (s, 18H), 1.65 (s, 36H), 3.26 (q, 4H; Et_2O), 7.45 (s, 4H). The crystals became yellow upon heating above 150 °C. They melt at 202–205 °C. It is possible, however, that the fusible species may not be **1**. Probably, it is **2** or the thioether $S(Ar)_2$.

Received: July 30, 1990 [Z 4105 IE]
German version: *Angew. Chem. 102* (1990) 1484

CAS Registry numbers:
1, 130551-87-0; **2**, 130551-88-1; **3**, 41924-26-9.

[*] Prof. P. P. Power, S. C. Shoner
Department of Chemistry
University of California
Davis, CA 95616 (USA)

[**] This work was supported by the National Science Foundation.

[1] I. G. Dance, *Polyhedron 5* (1986) 1037.

[2] P. J. Blower, J. R. Dilworth, *Coord. Chem. Rev. 76* (1987) 121.

[3] B. Krebs, G. Henkel in H. Roesky (Ed.): *Rings, Clusters and Polymers of Main Group and Transition Elements*, Elsevier, Amsterdam 1989, p. 439.
[4] A. Klug, D. Rhodes, *Trends Biochem. Sci. 12* (1987) 466; R. M. Evans, S. M. Hollenberg, *Cell 52* (1988) 1.
[5] J. M. Berg, *Science 232* (1986) 485.
[6] E. S. Gruff, S. A. Koch, *J. Am. Chem. Soc. 111* (1989) 8762.
[7] F. F. Said, D. G. Tuck, *Inorg. Chim. Acta 59* (1982) 1.
[8] I. Casals, P. Gonzalez-Duarte, C. Lopez, X. Solans, *Polyhedron 9* (1990) 763.
[9] P. P. Power, *J. Organomet. Chem.*, in press.
[10] P. P. Power, S. C. Shoner, *J. Am. Chem. Soc.*, in press.
[11] S. Moorhouse, G. Wilkinson, *J. Chem. Soc. Dalton Trans. 1974*, 2187.
[12] M. Bochmann, K. Webb, M. Karman, M. B. Hursthouse, *Angew. Chem. 102* (1990) 703; *Angew. Chem. Int. Ed. Engl. 29* (1990) 638.
[13] Crystal data at 130 K with Cu_{K_α} radiation ($\lambda = 1.54178$ Å); $a = 20.023(7)$, $b = 10.053(6)$, $c = 40.819(12)$ Å, $\beta = 91.12(1)°$, monoclinic, $C2/c$, $Z = 8$; 3593 unique observed ($I > 2\sigma I$) data, $R = 7.73\%$. Further details of the crystal structure investigation may be obtained from the Fachinformationszentrum Karlsruhe, Gesellschaft für wissenschaftlich-technische Information mbH, W-7514 Eggenstein-Leopoldshafen 2, on quoting the depository number CSD-54894, the names of the authors, and the full journal citation.
[14] R. L. Geerts, J. C. Huffman, K. G. Caulton, *Inorg. Chem. 25* (1986) 1803.
[15] Y. W. Yared, S. L. Miles, R. Bau, C. A. Reed, *J. Am. Chem. Soc. 99* (1977) 7076.
[16] J. Hvoslef, H. Hope, B. D. Murray, P. P. Power, *J. Chem. Soc. Chem. Commun. 1983*, 1438.
[17] T. N. Sorrell, M. R. Malachowski, *Inorg. Chem. 22* (1983) 1863.
[18] W. Rundel, *Chem. Ber. 101* (1968) 2956.

A New Mode of Metal Encapsulation**

By *John S. Bartlett, James F. Costello, Shrock Mehani, S. Ramdas, Alexandra M. Z. Slawin, J. Fraser Stoddart** and *David J. Williams*

Highly organized, synthetically derived molecular architectures, such as those comprising macrocycles,[1] bridged polymacrocycles[2] and cyclophanes,[3] have enjoyed much attention in the investigation of noncovalent bonding interactions in supramolecular systems.[4] By comparison, their acyclic analogues have received only modest attention as they are considered to be poorly preorganized[5] for the recognition event. Nonetheless, interest in noncyclic hosts has resulted in both elegant[6-10] and spectacular[11] examples of the unquestionable potential of such systems. Previous studies[12] on the encapsulation of alkali metal cations by functionalized acyclic oligoethers[13] encouraged us to re-examine this approach towards the design[14] of ligands capable of achieving both kinetically fast and thermodynamically selective complexation of alkaline earth metal dications.[15] We anticipated that the elaboration of both an oligoether *tail* and a pair of nucleophilic *pincers* into the same acyclic molecular framework would generate a new class of ligands capable of exercising both fast and selective formation of strong *scorpion-like*[16] dicationic chelates.

Here we report the synthesis of a series of scorpion-like ligands capable of metal encapsulation and the characterization of their mode of interaction with metal ions, both in solution and in the solid state. Initially **4** and **7b**, based on planar and tetrahedral tripodal constitutions respectively, were chosen as synthetic targets. Important intermediates in the synthesis of scorpion-like ligands such as **5** and **8a–d** are the mesylated monomethyl ethers **1a–d**.

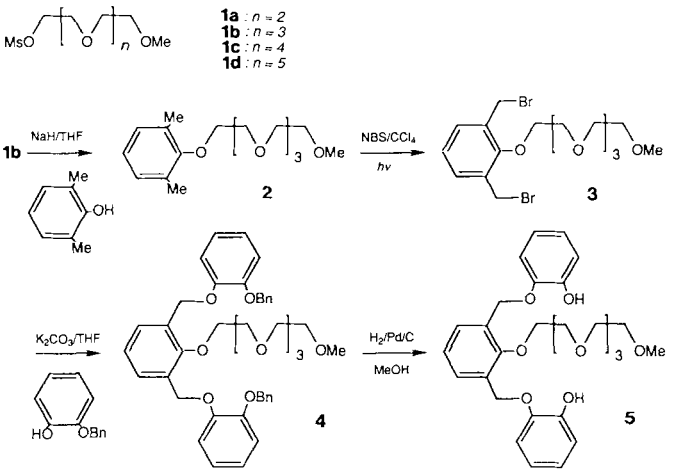

Reaction of **1b** with sodium 2,6-dimethylphenoxide generated **2**, which upon bromination with N-bromosuccinimide (NBS) and subsequent reaction with potassium *o*-benzyloxyphenoxide afforded **4**, the dibenzyl ether of **5**.

Treatment of the sodium alkoxide of **6**[18] with the appropriate mesylate (**1a–d**) produced the range of compounds **7a–d**, the dibenzyl ethers of **8a–d**.

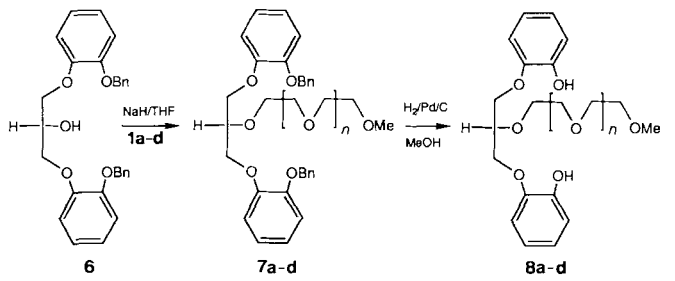

Strong evidence in support of the encapsulation of $Ba^{2\oplus}$ ions came from 250 MHz ^1H NMR spectroscopic studies in [D_6]acetone of **4** · $Ba(SCN)_2$ and **7b** · $Ba(SCN)_2$. Marked ion-induced downfield chemical shifts were observed, which resulted in the dispersion and simplification of certain spin systems, most notably for those attributable to the protons arising from (i) the catechol residues of both **7b** and **4** (especially those protons *ortho* to the oxygen substituents, where $\Delta\delta \approx 0.20$), and (ii) the glycerol residue of **7b** (where the methylene and methine protons have $\Delta\delta$ values of ca. 0.25 and 0.10, respectively). It is apparent that many of the ligand oxygen atoms are participating in the metal ion coordination. Table 1 records the relative affinities of the neutral ligands **4** and **7b**, among others, toward alkali and alkaline

[*] Dr. J. F. Stoddart, J. F. Costello
Department of Chemistry, The University
GB-Sheffield S3 7HF (UK)
Dr. J. S. Bartlett
Belgrave House
BP Chemicals
GB-London SW1W OSU (UK)
Dr. D. J. Williams, A. M. Z. Slawin
Chemical Crystallography Laboratory
Department of Chemistry, Imperial College
GB-London SW7 2AY (UK)
Dr. S. Ramdas, Dr. S. Mehani
Sunbury Research Centre
BP Research
GB-Middlesex TW16 7LN (UK)

[**] This work was supported by a Science and Engineering Research Council CASE Award and by BP Chemicals Limited, UK.

earth metal picrates.[19] As far as selectivity is concerned, it is clear that **7b** and **4** show a size selectivity for ionic radii of about 1.3 Å ($K^{\oplus}$ and $Ba^{2\oplus}$). It is noteworthy that **7b** appears to bind more tightly to $K^{\oplus}$ ions than does **4**. More importantly, the ligand **7b**, which is based on tetrahedral geometry, associates with the harder $Ba^{2\oplus}$ ion approximately 16 times more strongly than does ligand **4** with its planar structure. In order to probe further the mode of association of **7b** with $Ba^{2\oplus}$ ions in solution, the effect of complexation upon the ^1H spin-lattice relaxation time[20] of the ligand was investigated. In the presence of the dication, the rates of relaxation of the protons of the bismethylene and methyl units in the oligoether chain increase by 70–85%. This effect may be the result of a decrease in the mobility of the chain, when it wraps itself about the metal dication.

Table 1. Association constants K_a [M^{-1}] in $CHCl_3$ of a range of neutral acyclic oligoether ligands [a] with alkali metal and alkaline earth metal cations as measured by the picrate extraction technique [19].

Ligand	$Li^{\oplus}$	$Na^{\oplus}$	$K^{\oplus}$	$Rb^{\oplus}$	$Cs^{\oplus}$	$Mg^{2\oplus}$	$Ca^{2\oplus}$	$Sr^{2\oplus}$	$Ba^{2\oplus}$
2	<100	140	360	160	<100	<100	130	340	630
4	160	1300	1600	610	220	140	500	900	1500
7a	200	700	3200	930	500	<100	290	720	12000
7b	670	1100	3800	1100	800	180	700	1700	24000
7c	740	1000	5100	2000	1500	230	610	2500	46000
7d	900	2400	17000	4700	3500	260	800	31000	100000

[a] K_a values $\lesssim 1000\ M^{-1}$ are subject to an uncertainty of ca. 10%

Computer-aided molecular modeling[21] provided an insight into the reasons for the superior complexing ability of **7b** over **4** and the ion selectivity exhibited by the ligands. **7b** resembles a noncyclic[22] cryptand[23] with carbon as bridgehead atoms and as a consequence can define a pseudo-cavity for a metal ion of the appropriate size more efficiently than **4**, which is based on planar geometry. In the presence of a metal ion, **7b** attempts to maximize the number of stabilizing ion–dipole interactions by forming such a pseudo-cavity around the metal ion. Molecular modeling shows that when the metal ion is small (i.e. $Li^{\oplus}$, $Na^{\oplus}$) the severe steric crowding experienced by the oligoether tail and the benzylic moities of **7b** during complexation probably leads to destabilizing intramolecular interactions of a steric nature, and consequently fewer stabilizing electronic interactions result. The lower binding affinities (Table 1) of **4** and **7b** toward the larger ions ($Rb^{\oplus}$, $Cs^{\oplus}$) is possibly a result of the inability of these ligands to satisfy completely the normal coordination number of these softer cations.

In order to investigate further the interplay between ionic size and intramolecular crowding, we synthesized ligands **7a**, **7c** and **7d**, and related trends in selectivity to those of the corresponding diphenols **8a–d**. It is noteworthy (Table 1) that the general affinity for ions of radii around 1.3 Å persists and that the strength of $Ba^{2\oplus}$ ion complexation increases by a factor of two with the sequential addition of an oxygen atom to the homologous series of ligands. Interestingly, **7d** appears to have an anomalously higher affinity towards $Sr^{2\oplus}$ ions than does its lower homologues. One would expect that a scorpion-like complex of **7d** with the smaller (radius 1.1 Å), harder $Sr^{2\oplus}$ ion would be extremely crowded. A different mode of encapsulation may therefore operate in order to avoid intramolecular crowding.

The diphenols **8a–d** were obtained in good yields by catalytic hydrogenolysis (H_2/Pd/C) of the corresponding dibenzyl ethers **7a–d**. Ligand **5** could be obtained in a similar manner from **4**, but only in modest yields because of the presence of two other benzylic centers. In addition to the significant ion-induced chemical shifts, a feature common to the ^1H NMR spectra ([D_6]acetone) of the ligands **8a–d** and **5** in the presence of one equivalent of $Ba(SCN)_2$ is the significant downfield shift ($\Delta\delta \approx 2.5$) of the phenolic protons. We ascribe the observation to a thiocyanate–hydrogen bond, because no such downfield chemical shift is observed when picrate is the counterion.

Removal of the sterically demanding benzyl ether groups is expected to facilitate tighter metal encapsulation, as the intramolecular repulsion involved in such a process would decrease. In an NMR experiment irradiation of the resonance of the oligoether methyl group in the complex **8b** · $Ba(SCN)_2$ resulted in a nuclear Overhauser enhancement of the resonance for the proton *ortho* to the phenolic hydroxyl group. The spatial proximity implied for these nuclei is a direct consequence of encapsulation.

Fortunately, single crystals of **8c** · $Ba(SCN)_2Me_2CO$ which were suitable for X-ray crystallographic analysis[24] were obtained. The solid-state structure (Fig. 1) confirms the

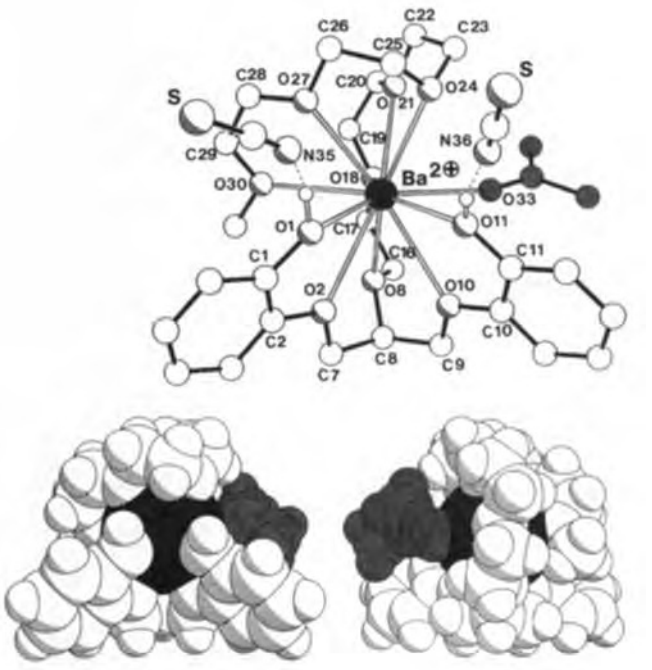

Fig. 1. Ball-and-stick representation of the structure of **8c** · $Ba(SCN)_2.Me_2CO$ in the crystal. Top: Crystal data: orthorhombic, $a = 11.925(2)$, $b = 13.267(2)$, $c = 23.295(5)$ Å, $V = 3685$ Å^3, space group $P2_12_12_1$, $Z = 4$, $\varrho_{calcd} = 1.48$ g cm^{-3}, $\mu(Cu_{K\alpha}) = 101$ cm^{-1}, 2646 independent observed absorption-corrected reflections [$|F_o| > 3\sigma(|F_o|)$, $2\theta \leq 116°$], $R = 0.035$, $R_w = 0.035$. $Ba^{2\oplus}$–O bond lengths [Å]: Ba–O1 2.871(5), Ba–O2 2.985(5), Ba–O8 2.815(5), Ba–O10 2.973(5), Ba–O11 2.860(5), Ba–O18 2.907(5), Ba–O21 2.925(5), Ba–O24 2.816(5), Ba–O27 2.867(6), Ba–O30 2.862(6), Ba–O33 2.762(7). Hydrogen bond lengths [Å]: O1···N35 2.74(1), O11···N36 2.70(1). Torsion angles [°]: O2–C7–C8–C9 70.2(8), C7–C8–C9–O10 −63.4(8), O8–C16–C17–O18 50.5(10), O18–C19–C20–O21 −40.2(12), O21–C22–C23–O24 −50.6(10), O24–C25–C26–O27 48.7(10), O27–C28–C29–O30 −10.5(19). Bottom: Space-filling model, on the left viewed from the same vantage point as the ball and stick model, and on the right viewed from the opposite direction. The $Ba^{2\oplus}$ ion is highlighted in black and the acetone molecule of solvation is featured in gray.

scorpion-like character of the complex in which the barium ion is 11-coordinate. All ten oxygen atoms of **8c** coordinate to the metal at distances ranging between 2.81 and 2.99 Å. The remaining eleventh coordination site is occupied by an acetone molecule of solvation (Ba–O, 2.76 Å). The complexation of the barium ion by all the oxygen atoms of the

polyether chain is achieved—with the exception of the 'flattening' of the terminal bismethylenedioxy unit—without any significant perturbation of the characteristic *gauche*-O–C–C–O- and *anti*-C–C–O–C-conformations. Each phenolic hydroxyl group forms a strong O–H···N hydrogen bond to a thiocyanate counterion.

The results described here have established the superiority of the ligands based on the tetrahedral tripodal constitution (**7a–d** and **8a–d**) over those (**4** and **5**) based on the planar constitution.

Experimental Procedure

2: Reaction of 2,6-dimethylphenol (NaH/THF/66 °C) with the mesylate **1b** (1 mol equiv.) afforded, after chromatography (SiO_2, EtOAc/$CHCl_3$), an oil (62%), which was characterized as **2** (EI-MS): *m/z* 312 ($M^{\oplus}$); ^{1}H NMR ($CDCl_3$): δ = 2.27 (s, 6H), 3.35 (s, 3H), 3.51–3.98 (m, 16H), 6.83–6.92 (m, 3H).

3: A stirred suspension of NBS (12.5 g, 70 mmol) and **2** (10 g, 32 mmol) in CCl_4 (200 mL) was irradiated (Hanovia photochemical reactor) for 1 h. The resulting crude mixture afforded as oils, after chromatography (SiO_2, $CHCl_3$/MeOH) in order of elution, the monobromide and **3**: 3.7 g (24%), CIMS *m/z* 488 ($[M + NH_4]^{\oplus}$); ^{1}H NMR ($CDCl_3$): δ = 3.38 (s, 3H), 3.53–3.59 (m, 2H), 3.64–3.81 (m, 10H), 3.82–3.93 (m, 2H), 4.23–4.31 (m, 2H), 4.64 (s, 4H), 7.14 (t, J = 7 Hz, 1H), 7.52 (d, J = 7 Hz, 2H)].

4: A solution of **3** (0.6 g, 1.2 mmol) in dry THF (50 mL) was added dropwise under reflux to a solution of *o*-benzyloxyphenol (0.61 g, 3 mmol) and K_2CO_3 (1.2 mol equiv.) in dry THF (100 mL) during 2 h under N_2. The solution was heated for a further 72 h, cooled to room temperature and concentrated in vacuo. Chromatography on SiO_2 ($CHCl_3$/Et_2O: 4/1 v/v) afforded 0.42 g (46%) of a clear colorless oil, characterized as **4**: FAB MS *m/z* 731 $[M + Na]^{\oplus}$; ^{1}H NMR ([D$_6$]acetone): δ = 3.23 (s, 3H), 3.39–3.42 (m, 2H), 3.48–3.55 (m, 10H), 3.65–3.69 (m, 2H), 4.17–4.20 (m, 2H), 5.12 (s, 4H), 5.24 (s, 4H), 6.87–6.92 (m, 4H), 7.03–7.07 (m, 2H), 7.12–7.19 (m, 2H), 7.17 (t, J = 7 Hz, 1H), 7.27–7.38 (m, 6H), 7.45–7.49 (m, 4H), 7.55 (d, J = 7 Hz, 2H).

5: Hydrogenolysis (H_2/Pd/C) of **4** (150 mg, 0.2 mmol) in dry MeOH (25 mL) at room temperature afforded, after chromatography on SiO_2 ($CHCl_3$/EtOAc: 4/1 v/v), an oil, which was characterized as **5**: 20 mg (18%) FAB MS *m/z* 551 $[M + Na]^{\oplus}$; ^{1}H NMR ([D$_6$] acetone): δ = 3.23 (s, 3H), 3.39–3.44 (m, 2H), 3.49–3.62 (m, 10H), 3.72–3.81 (m, 2H), 4.12–4.19 (m, 2H), 5.23 (s, 4H), 6.73–6.88 (m, 6H), 7.07–7.20 (m, 2H), 7.15 (t, J = 7 Hz, 1H), 7.54 (d, J = 7 Hz, 2H), 7.73 (br. s, 2H).

7c: A solution of 6 [18] (3.30 g, 7.23 mmol) in dry THF (40 mL) was added dropwise with stirring over 0.5 h to a suspension of NaH (600 mg, 50% dispersion in oil, 12.5 mmol) in dry THF (50 mL) under N_2. The mixture was heated under reflux for a further 2 h. The mesylate **1c** (2.62 g, 7.94 mmol) dissolved in THF (10 mL) was added within 1 h and the mixture was stirred under reflux for a further 16 h. After cooling and subsequent standard work-up, the crude product was subjected to column chromatography (SiO_2, $CHCl_3$/EtOAc: 4/1 v/v) and gave a clear oil, characterized as **7c**: 2.22 g (47%); FAB MS: *m/z* 713 ($[M + Na]^{\oplus}$); ^{1}H NMR ([D$_6$]acetone): δ = 3.26 (s, 3H), 3.41–3.47 (m, 2H), 3.49–3.58 (m, 16H), 3.84–3.89 (m, 2H), 4.12–4.3 (m, 5H), 5.09 (s, 4H), 6.85–6.95 (m, 4H), 6.98–7.07 (m, 4H), 7.24–7.37 (m, 6H), 7.45–7.51 (m, 4H).

8c: A solution of **7c** (1.62 g, 2.35 mmol) and 10% Pd/C (160 mg) in dry MeOH (100 mL) was subjected to hydrogenolysis at 40 °C and atmospheric pressure. After 60 min, the solution was cooled, filtered (Celite), and concentrated in vacuo. Column chromatography on SiO_2 ($CHCl_3$) furnished a clear oil, which was characterized as **8c**: 0.78 g (65%); FAB MS: *m/z* 511 ($[M + H]^{\oplus}$); ^{1}H NMR ([D$_6$]acetone): δ = 3.26 (s, 3H), 3.41–3.47 (m, 2H), 3.51–3.67 (m, 16H), 3.87–3.91 (m, 2H), 4.16–4.32 (m, 5H), 6.73–6.85 (m, 6H), 6.97–7.13 (m, 2H), 7.66 (br. s, 2H). Single crystals of **8c** · $Ba(SCN)_2$ · Me_2CO (m.p. 140–141.5 °C), suitable for X-ray crystallography, were obtained by the slow evaporation of equimolar amounts of **8c** and $Ba(SCN)_2$ from acetone.

Received: May 28, 1990
Revised: August 10, 1990 [Z 3986 IE]
German version: *Angew. Chem. 102* (1990) 1463

[1] C. J. Pedersen, *Angew. Chem. 100* (1988) 1053; *Angew. Chem. Int. Ed. Engl. 27* (1988) 1021; D. J. Cram, *ibid. 100* (1988) 1041 and *27* (1988) 1009.

[2] J.-M. Lehn, *Angew. Chem. 100* (1988) 91; *Angew. Chem. Int. Ed. Engl. 27* (1988) 90.

[3] For a review, see F. Diederich, *Angew. Chem. 100* (1988) 372; *Angew. Chem. Int. Ed. Engl. 27* (1988) 362.

[4] For a review, see J. F. Stoddart, *Annu. Rep. Prog. Chem. Sect. B. 85* (1988) 353.

[5] D. J. Cram, *Angew. Chem. 98* (1986) 1041; *Angew. Chem. Int. Ed. Engl. 25* (1986) 1039.

[6] E. C. Constable, M. D. Ward, D. A. Tocher, *J. Am. Chem. Soc. 112* (1990) 1256; J.-M. Lehn, A. Rigault, *Angew. Chem. 100* (1988) 1121; *Angew. Chem. Int. Ed. Engl. 27* (1988) 1095.

[7] T. Iimori, W. C. Still, A. L. Rheingold, D. L. Staley, *J. Am. Chem. Soc. 111* (1989) 3439.

[8] A. Schepartz, J. P. McDevitt, *J. Am. Chem. Soc. 111* (1989) 5976.

[9] A. Echavarren, A. Galán, J.-M. Lehn, J. de Mendoza, *J. Am. Chem. Soc. 111* (1989) 4994; F. P. Schmidtchen, *Tetrahedron Lett. 30* (1989) 4493.

[10] S. M. Shirodkar, G. R. Weisman, *J. Chem. Soc. Chem. Commun. 1989*, 236.

[11] T. Tjivikua, P. Ballester, J. Rebek, Jr., *J. Am. Chem. Soc. 112* (1990) 1249. T. R. Kelly, C. Zhao, G. J. Bridger, *ibid. 111* (1989) 3744.

[12] For reviews, see F. Vögtle, E. Weber, *Angew. Chem. 91* (1979) 813; *Angew. Chem. Int. Ed. Engl. 18* (1979) 753; F. Vögtle, *Chimia 33* (1979) 239.

[13] B. Tümmler, G. Maass, F. Vögtle, H. Sieger, U. Heimann, E. Weber, *J. Am. Chem. Soc. 101* (1979) 2588.

[14] The rational approach towards the design of ligands for the selective complexation of metals has been reviewed recently. See, R. D. Hancock, A. E. Martell, *Chem. Rev. 89* (1989) 1875.

[15] The clogging of oil wells as a result of $BaSO_4$ scale formation has proved both a vexatious and costly problem (O. J. G. Vetter, *J. Petr. Techn. 1975*, 1515; *ibid. 1976* 1402). In the prevention and dissolution of such scales, the application of acyclic ethylenediaminetetraacetic acid and macrocyclic chelating agents (F. de Jong, D. N. Reinhoudt, G. J. Torny, A. van Zon, *Recl. J. R. Neth. Chem. Soc. 102* (1983) 164) is a very useful approach. Scorpion-like molecules offer a unique opportunity to include flexibility, selectivity, and chelate stability into the same compounds.

[16] "The wrapping of linear polyetheneglycol ligands around metal cations is dependent upon their length" (W. Saenger, I.-H. Suh, G. Weber, *Isr. J. Chem. 18* (1979) 253). To our knowledge, the scorpion-like mode of encapsulation represents an addition to the circular, helical, and S-like (where two metal ions are bound) modes of metal encapsulation.

[17] The synthesis of **1a** has been reported (M. Schmidt, R. Amstutz, G. Crass, D. Seebach, *Chem. Ber. 113* (1980) 1691). The higher homologues **1b–d** were synthesized in a similar manner.

[18] D. G. Parsons, *J. Chem. Soc. Perkin Trans. 1, 1978*, 451.

[19] a) The solvent extraction of aqueous metal picrates provides a facile technique for the rapid screening of the cation binding ability of neutral acyclic polyether ligands (K. E. Koenig, G. M. Lein, P. Stuckler, T. Kaneda, D. J. Cram, *J. Am. Chem. Soc. 101* (1979) 3553). Since the extracting ability of such ligands is generally low in comparison to that of their macrocyclic analogues, the technique was modified to increase the sensitivity of the detection of extracted picrate anion by UV spectrophotometry. In a typical experiment, a 5 mM solution of the appropriate aqueous metal picrate was partitioned with a 60 mM solution ($CHCl_3$) of the ligand. Interpretation and comparisons of K_a values should be confined to this closely related series of neutral acyclic polyether ligands. b) The assumed 1:1 stoichiometries of all the complexes were supported by FAB MS investigations. An expression for calculating K_a values from the experimental data obtained for extractions of divalent alkaline earth metal picrates was derived in a similar manner to that previously described for monovalent metal picrates (J. M. Timko, S. S. Moore, D. M. Walba, P. C. Hiberty, D. J. Cram, *J. Amer. Chem. Soc. 99* (1977) 4207). Values for distribution constants (K_d) for the alkaline earth metal picrates between chloroform and water were taken from the literature (T. Maeda, K. Kimura, T. Shono, *Fresenius Z. Anal. Chem. 313* (1982) 407).

[20] The T_1 measurements were carried out by the inversion recovery technique (Bruker AM 250 spectrometer). An equimolar solution (15 mM) of **7b** and $Ba(SCN)_2$ was used in this experiment. We thank Dr. *J. R. Bales* (BP Research, Sunbury, UK) for his assistance in obtaining these ^{1}H-NMR spectra.

[21] CHEMX (Chemical Design Limited, Oxford), the general purpose molecular modeling software, was used in our studies. Molecular mechanics calculations upon such highly flexible ligands would be inappropriate. We have, therefore, relied upon a multi-disciplinary approach, in which conformational analysis, distance geometry information (^{1}H NMR experiments, NOE, and T_1 measurements) and X-ray crystallographic data (especially Ba–O bond distances) have allowed us to develop a three-dimensional model with low resolution for **7b** · $Ba^{2\oplus}$ and **8b** · $Ba^{2\oplus}$ which were not wholly at variance with the solid state structure of **8c** · $Ba(SCN)_2$ · Me_2CO.

[22] F. Vögtle, W. M. Müller, W. Wehner, E. Buhleier, *Angew. Chem. 89* (1977) 564; *Angew. Chem. Int. Ed. Engl. 16* (1977) 548.

[23] B. L. Allwood, S. E. Fuller, P. C. Y. K. Ning, A. M. Z. Slawin, J. F. Stoddart, D. J. Williams, *J. Chem. Soc. Chem. Commun. 1984*, 1356.

[24] Nicolet R3m diffractometer, ω scans, $Cu_{K\alpha}$ radiation (graphite monochromator). The structure was solved by the heavy atom method and the non-hydrogen atoms were refined anisotropically. Further details of the crystal structure investigation can be obtained from the Cambridge Crystallographic Data Centre, University Chemical Laboratory, Lensfield Road, Cambridge CB2 1EW (UK). Any request should be accompanied by the full literature citation of this communication.

Artificial Receptors for Carbohydrate Derivatives**

By *Richard P. Bonar-Law, Anthony P. Davis,** and *Brian A. Murray*

There is widespread interest in the recognition and binding of neutral, polar molecules in organic solvents. Particular attention has been paid to derivatives of amino acids[1] and nucleobases,[2] but little has been published on the binding of the third major class of natural building blocks, the carbohydrates.[3] This is possibly because of the three-dimensional complexity of carbohydrate structures. In order to take full advantage of the potential binding sites on, for example, the pyranose nucleus, it is necessary to design receptors which can surround the nucleus on all sides with hydrogen-bond donor and/or acceptor functionality.[4] We have recently published syntheses of a series of "cholaphanes" **1a–e**.[5] Noting that their common framework is able to enclose a pyranose, and that **1a** in particular bears six functional groups with hydrogen-bond donor/acceptor properties (four hydroxyl and two secondary amide groups), we undertook to investigate these macrocycles as receptors for carbohydrate derivatives. We now report evidence that **1a** and **1e** bind to the lipophilic glucoside **2** in $CDCl_3$ with stability constants (K_a) in the region of 10^3 M^{-1}.[6]

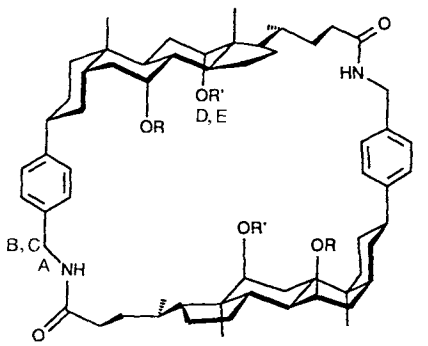

1a: R,R' = H
1b: R,R' = Ac
1c: R = Ac, R' = Bn
1d: R = Ac, R' = H
1e: R = H, R' = Bn

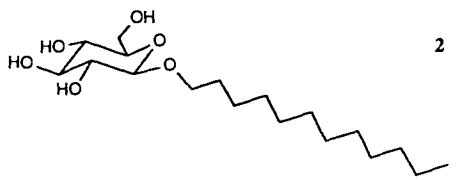

2

When glucoside **2** was added incrementally to a ca. 1 mM solution of the tetrahydroxycholaphane **1a** in $CDCl_3$, the ^1H NMR spectrum of the latter underwent a number of changes. Initially, the region from $\delta = 4.2$ to 5.8 contained a signal corresponding to the two amide NH protons (broad triplet) and an AB quartet corresponding to the four benzylic CH_2-N protons, each of which is further coupled to the amide protons (see Fig. 1a and Table 1). As **2** was added, the amide and the lower-field benzylic resonances moved downfield, the higher-field benzylic resonances moved upfield,

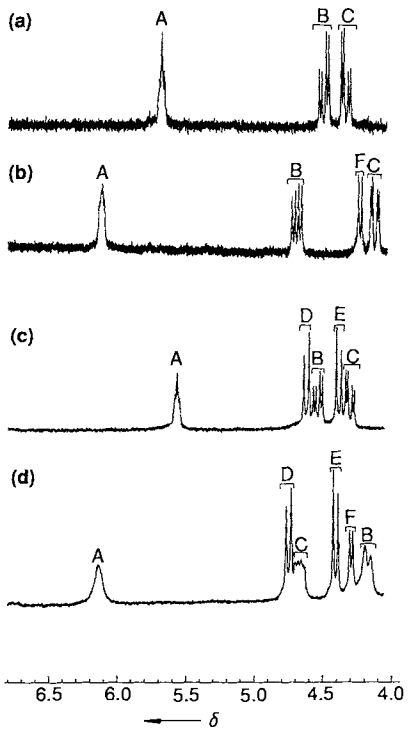

Fig. 1. Partial ^1H NMR spectra in $CDCl_3$ of a) **1a** (1.1 mM). b) **1a** (1.1. mM) + **2** (0.88 mM). c) **1e** (5.6 mM). d) **1e** (5.2 mM) + **2** (7.8 mM). Assignments: A = NH; B,C = CH_2N; D,E = CH_2 of the OBn group (**1e** only); F = anomeric CH (see also formulas **1** and **2**).

and there were substantial changes in the coupling constants between the amide and benzylic protons (Fig. 1b). The changes were analyzed using an iterative least-squares curve-fitting program with weighting of data points according to the error analysis of *Deranleau*.[7] They were found to be consistent with the formation of a 1:1 complex between **1a** and **2** with $K_a = 1740(\pm 200)$ M^{-1}. The calculated binding curve and chemical shifts for the amide resonance are shown in Figure 2, and the limiting values for the chemical shifts are given in Table 1.

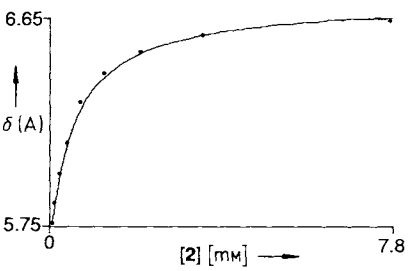

Fig. 2. Downfield shifts of the NH NMR signal of **1a** on incremental addition of **2**; experimental points and calculated binding curve.

Analysis of the carbohydrate resonances was less informative, because of overlap between the signals due to host and guest. However, the anomeric CH proton of **2** does stand out clearly as a sharp doublet F and can be seen to shift up field by $\Delta\delta > 0.1$ on complex formation. To confirm that we could discount self-association of host and guest, we recorded ^1H NMR spectra of each at various concentrations. As anticipated, for both cases there was virtually no change within the concentration range important for the binding experiment.

[*] Dr. A. P. Davis, R. P. Bonar-Law, Dr. B. A. Murray
Department of Chemistry, Trinity College
IRL-Dublin 2 (Ireland)

[**] This work was supported by EOLAS (the Irish science and technology agency), Loctite Corp. (provision of our molecular graphics facility) and Diamalt AG (gifts of cholic acid and methyl cholate). B.A.M. is an employee of BioResearch Ireland. We thank *Siobhan Stokes* and *Philippe Almargot* for NMR and IR spectra.

Table 1. Selected ^{1}H NMR data for hosts **1a** and **1e**, and corresponding values for complexes with **2** (by extrapolation; see text). A,B,C: see formula for **1**.

	δ(A)	δ(B/C)	(J(A,B/C), [Hz])	δ(CH_2O)		δ (21-Me)
1a	5.67	4.48(5.9)	4.34(5.1)			1.01
1a + **2**	6.75	4.8(>8.1)	3.9(<3.3)			0.97
1e	5.58	4.27(4.8)	4.51(6.0)	4.6	4.36	0.99
1e + **2**	6.37	4.71(>7)	4.04 [a]	4.75	4.37	0.75

[a] Signal broadened; J too small to be discernible.

Similar experiments were used to investigate the interaction of **2** with **1b–e** in $CDCl_3$. On addition of **2** the ^{1}H NMR spectra of **1b–d** underwent no significant changes, but the dibenzyl derivative **1e** showed evidence of binding in much the same manner as **1a** (Fig. 1c, 1d and Table 1). New features were the movement of the signals due to the $PhCH_2$-O protons and the doublet corresponding to the methyl group (21-Me) in the steroidal side chain (Table 1). Again, analysis of the data indicated that a 1:1 complex had been formed, with a binding constant of 700($\pm$100) M^{-1}.

We believe that the glucoside is located inside the macrocycle in both the above complexes for the following reasons: 1) The changes in the $H_{B,C}$ signals on complex formation clearly suggest a major alteration in the conformational properties of the macrocycles, probably the "freezing out" of one or a limited number of conformations (see below). This is most easily accommodated by the inclusion of the carbohydrate molecule in the macrocyles. 2) In the case of **1e**, the changes in the $PhCH_2$-O resonances and the 21-Me provide further support. They imply that conformational changes are occurring in widely separated regions of the macrocycle, and it is hard to see how such changes could be induced other than by an inclusion process. 3) The binding constants are sufficiently large to suggest that multiple hydrogen bonding interactions are involved. As a comparison, in a recent study by *Rebek* et al. involving the binding of adenine derivatives, association constants in the range 100 to 400 M^{-1} were measured for complexes in which two hydrogen bonds and one π-stacking interaction were postulated.[2a]

The association between **1e** and **2** was also studied by IR spectroscopy. Initially the IR spectrum of **1e** in $CHCl_3$ (7.26 mM) showed a single band in the N–H stretching region at 3446 cm^{-1}, and bands at 1662 cm^{-1} (C=O) and 1513 cm^{-1} (amide II). On incremental addition of **2** the carbonyl stretching band was only marginally affected, broadening somewhat and shifting to a slightly lower frequency (up to 10 cm^{-1}). In contrast the intensities of the N–H stretching and amide II bands decreased steadily and in concert with each other. These results are significant in that, when combined with the shift in the NH resonance, they suggest strongly that the amide groups act as hydrogen bond donors in complex formation.[8]

We have attempted to interpret our results with the assistance of computer-based molecular modeling.[9] Calculations on **1a** suggest that the cholaphane framework does have considerable flexibility; thus, 36 different conformations have been found within 4.5 kcal mol^{-1} of the baseline (which is as represented by **1**), and their structural variety is such as to suggest that there are many more. However, although their shapes vary considerably (e.g. NH···HN distances from 11.1 to 14.9 Å), all have open conformations with substantial cavities.

On addition of methyl β-D-glucopyranoside (a model for **2**), it becomes clear that there are many possibilities for formation of multiple hydrogen bonds between host and guest.

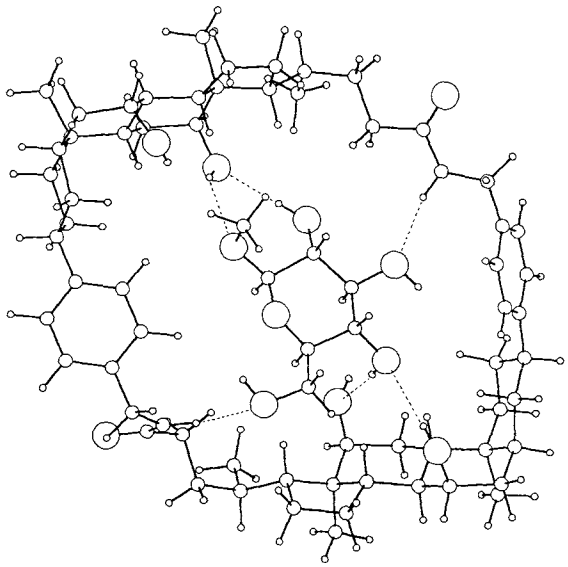

Fig. 3. A possible conformation for **1a** and methyl β-D-glucopyranoside, minimized within the CHARMm force field. Dotted lines represent intermolecular hydrogen bonds, ranging in length from 2.06 to 2.32 Å.

One example which is consistent with the IR data is shown in Figure 3. It is derived from a conformer of the macrocycle which is 3.4 kcal mol^{-1} above the baseline. Complex formation requires a further slight distortion of the macrocyclic framework (3.2. kcal mol^{-1}), but is promoted by the formation of six hydrogen bonds, as illustrated. Although this specific structure may not be important, it does demonstrate the ability of the glucoside to enter the cavity of **1a** and to form multiple hydrogen bonds with its host without causing undue distortion.

Similar studies on **1e** support the idea that complex formation would substantially reduce the conformational options of the O-benzyl groups, accounting for the movement of the CH_2-O NMR resonances. The shift of the 21-Me resonance probably results from the same process, the effect being transmitted via the diamagnetic anisotropy of the benzyl group.

Received: July 9, 1990 [Z 4059]
German version: *Angew. Chem. 102* (1990) 1497

CAS Registry numbers:
1a · **2**, 130197-63-6; **1e** · **2**, 130197-64-7.

[1] Recent examples: W. H. Pirkle, T. C. Pochopsky, *J. Am. Chem. Soc. 109* (1987) 5975; P. E. Sanderson, J. D. Kilburn, W. C. Still, *ibid. 111* (1989) 8314.

[2] a) K. Williams, B. Askew, P. Ballester, C. Buhr, K. S. Jeong, S. Jones, J. Rebek, Jr., *J. Am. Chem. Soc. 111* (1989) 1090; b) J. Rebek, Jr., *Angew. Chem. 102* (1990) 261; *Angew. Chem. Int. Ed. Engl. 29* (1990) 245, and references cited therein.

[3] For a notable exception, see: Y. Aoyama, Y. Tanaka, S. Sugahara, *J. Am. Chem. Soc. 111* (1989) 5397.

[4] The system reported in [3] is unable to fulfill this condition and is thought to bind its substrates by face-to-face interactions.

[5] R. P. Bonar-Law, A. P. Davis, *J. Chem. Soc. Chem. Commun. 1989*, 1050.

[6] A preliminary indication of (unquantified) binding between a similar glucoside and a flexible, non-macrocyclic host containing two cholic acid units has been reported by *C. J. Burrows* et al.: J. F. Kinneary, T. M. Roy, J. S. Albert, H. Yoon, T. R. Wagler, L. Shen, C. J. Burrows, *J. Inclusion Phenom. and Mol. Recognit. Chem. 7* (1989) 155.

[7] D. A. Deranleau, *J. Am. Chem. Soc. 91* (1969) 4044.

[8] D. Hadzi, S. Detoni, in S. Patai (Ed.): *The Chemistry of Acid Derivatives, Part 1*, Wiley, New York 1979, p. 214.

[9] Employing the QUANTA/CHARMm software package, implemented on an IRIS 4D20G workstation.

An Aluminaphosphacubane, a New Aluminum Phosphide Precursor

By *Alan H. Cowley*,** *Richard A. Jones*,* *Miguel A. Mardones, Jerry L. Atwood*,* and *Simon G. Bott*

There is a heightened interest in the chemistry of cubanes and their isolobal analogues. In the context of phosphorus-containing cubanes, salient developments include the syntheses of $[t\mathrm{BuE}(\mu_3\text{-P})]_4$ (E = C[1], Si[2]) **1**, $[\mathrm{PhSn}(\mu_3\text{-P})]_4$[3] **2**, and several organometallic derivatives of the general type $[(L_nM)_x(P)_{4-x}]$.[4] Conceptually, these novel compounds can be regarded as derivatives of the hypothetical cubane P_8.[5] Alternatively, cubanes **1** and **2** can be viewed as tetramers of triply-bonded monomers, RE≡P. In principle, a different class of phosphorus-containing cubane should be possible by tetramerization of monomers of the type RM≒PR′ where M represents a group 13 element. We report the first aluminaphosphacubane.

Treatment of equimolar quantities of $i\mathrm{Bu_2AlH}$ and $\mathrm{Ph_3SiPH_2}$[6] in toluene at 25 °C for 12 h resulted in the evolution of H_2 and the formation of white, crystalline **3**.

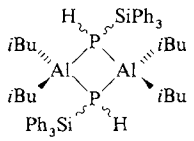

3

The dimeric nature of **3** was established by mass spectrometry (MS) which revealed a parent peak at *m/z* 864 followed by fragment ions corresponding to $[\mathrm{MH^{\oplus}} - i\mathrm{Bu} - \mathrm{Ph_3Si}]$ and $[\mathrm{M^{\oplus}} - 2i\mathrm{Bu} - \mathrm{Ph_3Si}]$. Like $[(\mathrm{Me_3Si})_2\mathrm{AlP(Ph)(SiMe_3)}]_2$,[7] **3** exists as a mixture of *syn* and *anti* isomers in approximately 1:2 abundance as evidenced by the presence of two ^{31}P-NMR peaks.[8] Compound **3** starts to melt at 80 °C; however, melting is accompanied by gas evolution (MS: isobutane) followed by resolidification. Refluxing **3** in toluene solution for 12 h, followed by concentration and cooling to − 20 °C, resulted in the isolation of white, crystalline $[i\mathrm{BuAl}(\mu_3\text{-}\mathrm{PSiPh_3})]_4$ (**4**) in 83% yield. Mass spectroscopy was not very useful for the characterization of **4**; the highest mass peak in EI or CI experiments occurred at *m/z* 259 and corresponds to $[\mathrm{Ph_3Si^{\oplus}}]$. The ^{31}P-NMR spectrum comprised a singlet at $\delta = -213.0$ and the ^{1}H- and ^{13}C{^{1}H}-NMR spectra were indicative of the presence of equal numbers of *i*Bu and $\mathrm{Ph_3Si}$ groups. The ^{27}Al-NMR signal for **4** was very broad ($\Delta W_{1/2}$ 4700 Hz) and no ^{31}P coupling was discernible. Elemental analytical data corresponded to the empirical composition $i\mathrm{BuAlPSiPh_3}$. An X-ray crystallographic study[9] revealed that **4** possesses a cubane structure (Fig. 1). There are no short intermolecular contacts and each molecule resides on a site of S_4 symmetry. As in the case of the recently isolated tetraphosphacubanes, $[t\mathrm{BuC}(\mu_3\text{-P})]_4$[1] and $[t\mathrm{BuSi}(\mu_3\text{-P})]_4$[2] the cube of **4** is distorted in the sense that the internal bond

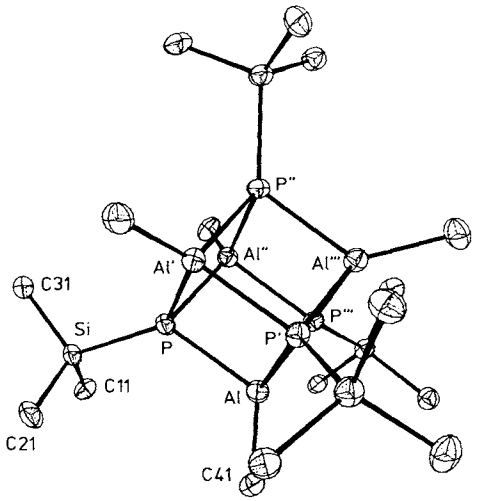

Fig. 1. View (ORTEP) of **4** showing the atom numbering scheme. Important bond distances [Å] and bond angles [°]: P–Al 2.409(4), P–Al′ 2.415(4), P–Al″ 2.417(4), P–Si 2.236(4), Al–C41 1.96(1), Al–P–Al′ 89.0(2), Al–P–Al″ 87.8(2), Al′–P–Al″ 87.7(2), Al–P–Si 127.3(2), Al′–P–Si 125.6(2), Al″–P–Si 126.8(2), P–Al–P′ 90.9(2), P–Al–P‴ 92.3(2), P′–Al–P‴ 92.2(2), P–Al–C41 120.6(4), P′–Al–C41 127.7(4), P‴–Al–C41 123.6(4).

angles at phosphorus are less than 90° (av. 88.2(2)°). The average Al–P bond distance in **4** (2.414(4) Å) is slightly less than those observed in Al_2P_2 dimers which span the range 2.433(4) to 2.475(1) Å.[7] The P–Si distance in **4** (2.236(4) Å) is slighly shorter than that in the diphosphene 2,4,6-$t\mathrm{Bu_3C_6H_2P}$ = $\mathrm{PSiPh_3}$ (2.269(2) Å).[6]

Preliminary work indicates that an analogous gallaphosphacubane $[t\mathrm{BuGa}(\mu_3\text{-}\mathrm{PSiPh_3})]_4$ ($\delta_{^{31}\mathrm{P}} = -185$) can be prepared by treatment of $[t\mathrm{BuGaCl_2}]_2$ with $\mathrm{Ph_3SiPLi_2}$ in $\mathrm{Et_2O}$. Interestingly, we have not been able to isolate cubanes when phosphorus substituents other than $\mathrm{Ph_3Si}$ are employed.

Cubane **4** is reactive toward both electrophiles and nucleophiles. For example, reaction of **4** with eight equivalents of EtOH affords $\mathrm{Ph_3SiPH_2}$[6] and $i\mathrm{BuAl(OEt)_2}$.[10] Even when less than eight equivalents are employed, complete cage degradation occurs and a proportionate quantity of unchanged **4** is left over. Similar results are obtained with H_2O. Treatment of **4** with four equivalents of MeLi in $\mathrm{Et_2O}$ also causes rupture of the Al_4P_4 cage. The NMR data for the MeLi reaction product correspond to those anticipated for the anion $[i\mathrm{BuMeAlPSiPh_3}]^{\ominus}$ **5**.[8] This was confirmed by the reaction of **5** with EtOH, which produced $[i\mathrm{BuMeAlOEt}]$.[10]

Thermolysis studies reveal that the new Al_4P_4 cubane **4** represents a potentially interesting precursor to aluminum phosphide. Temperature-programmed EI or CI mass spectrometry demonstrates that the decomposition of the cubane starts as low as 150 °C. The major volatiles are identified as $\mathrm{Ph_3SiH}$ and isobutylene. XPS (X-ray Photoelectron Spectroscopy) analysis[11] and X-ray diffraction of the residue that remained after heating to 500 °C indicates that it is aluminum phosphide.

Experimental Procedure

3: A toluene solution (25 wt.%) of $i\mathrm{Bu_2AlH}$ (13.4 mL, 20 mmol) was added to 5.84 g (20 mmol) of $\mathrm{Ph_3SiPH_2}$. The resulting clear solution, which evolved hydrogen, was stirred for 12 h at room temperature. Solvent evaporation afforded white, crystalline **3** in virtually quantitative yield (m.p. = 80 °C, decomp.). **4**: A toluene solution of **3** was refluxed for 12 h. The solvent and volatiles were removed in vacuo, following which the resulting white residue was redissolved in toluene. After filtration and concentration of the filtrate, colorless crystals of **4** formed in 83% yield by cooling to − 20 °C.

[*] Prof. Dr. A. H. Cowley, Prof. Dr. R. A. Jones, M. A. Mardones
Department of Chemistry
University of Texas at Austin
Austin, TX 78712 (USA)
Professor Dr. J. L. Atwood and Dr. S. G. Bott
Department of Chemistry
University of Alabama
Tuscaloosa, AL 35486 (USA)

[**] This work was supported by the National Science Foundation, the Robert A. Welch Foundation, and the U.S. Army Research Office.

Received: August 23, 1990 [Z 4148 IE]
German version: *Angew. Chem.* *102* (1990) 1504

CAS Registry numbers:
syn-**3**, 130149-56-3; *anti*-**3**, 130195-60-7; **4**, 130149-57-4; **5**, 130149-58-5; $[t\text{BuGa}(\mu_3\text{-PSiPh}_3)]_4$, 130149-59-6; $i\text{Bu}_2\text{AlH}$, 1191-15-7; Ph_3SiPH_2, 122623-38-5; Ph_3SiPLi_2, 130149-55-2; $[t\text{BuGaCl}_2]_2$, 127139-90-6; $i\text{BuAl(OEt)}_2$, 37167-69-4.

[1] T. Wettling, J. Schneider, O. Wagner, C. G. Kreiter, M. Regitz, *Angew. Chem. 101* (1989) 1035; *Angew. Chem. Int. Ed. Engl. 28* (1989) 1013.

[2] M. Baudler, G. Scholz, K.-F. Tebbe, M. Fehér, *Angew. Chem. 101* (1989) 352; *Angew. Chem. Int. Ed. Engl. 28* (1989) 339.

[3] H. Schumann, H. Benda, *Angew. Chem. 80* (1968) 846; *Angew. Chem. Int. Ed. Engl. 7* (1968) 813.

[4] See, for example, G. L. Simon, L. F. Dahl, *J. Am. Chem. Soc. 95* (1973) 2175; O. J. Scherer, T. Dave, J. Braun, G. Wolmershäuser, *J. Organomet. Chem. 350* (1988) C20.

[5] See, for example, E. A. Halevi, H. Bock, B. Rohr, *Inorg. Chem. 23* (1984) 4376. R. Ahlrichs, S. Brode, C. Ehrhardt, *J. Am. Chem. Soc. 107* (1985) 7260.

[6] A. H. Cowley, P. C. Knüppel, C. M. Nunn, *Organometallics 8* (1989) 2490.

[7] J. F. Janik, E. N. Duesler, W. F. McNamara, M. Westerhausen, R. T. Paine, *Organometallics 8* (1989) 506. For additional structural information on this class of compound, see S. A. Sangokoya, W. T. Pennington, G. H. Robinson, D. C. Hrncir, *J. Organomet. Chem. 385* (1990) 23.

[8] ^{31}P NMR (121.5 MHz, C_6D_6, 295 K, 85% H_3PO_4 external standard): **3**: $\delta = -216.8$ (*anti*), -217.6 (*syn*); **4**: $\delta = -213.0$.—^{1}H NMR (300.15 MHz, C_6D_6, 295 K) **3**: $\delta = 0.36$ (8H, d, broad. $J = 7.2$ Hz, CH_2Al), 0.80 (6H, d, $J = 6.6$ Hz, CH_3), 0.94 (6H, d, $J = 6.6$ Hz, CH_3), 0.97 (6H, d, $J = 6.6$ Hz, CH_3), 1.07 (6H, d, $J = 6.6$ Hz, CH_3), 1.84 (4H, m, $J = 6.6$ Hz, *H*-C(CH_3)$_2$), 7.13 (18H, m, phenyl H), 7.66 (12H, m, phenyl H); **4**: $\delta = 0.23$ (8H, d, broad. $J = 7.2$ Hz, CH_2Al), 0.39 (24H, d, $J = 6.6$ Hz, C(CH_3)$_2$), 1.24 (4H, m, $J = 6.6$ Hz, *H*C(CH_3)$_2$) 7.13 (36H, *o-p* phenyl H), 7.66 (24H, m, phenyl H).—^{27}Al NMR (78.21 MHz, C_6D_6, 295 K, $Al(NO_3)_3$ external standard) $\delta = 20$ (broad).

[9] **4**: tetragonal, space group $P\bar{4}2_1c$ (No. 114), $Z = 2$, $a = 15.721(2)$, $b = 17.186(3)$ Å; $V = 4248$ Å^3; $\varrho_{calcd} = 1.175$ g cm^{-3}; $2° < 2\theta < 50°$ ($Mo_{K\alpha}$, $\lambda = 0.71069$ Å; $\mu = 2.24$ cm^{-1}); $T = 24$ °C. 8249 reflections, $\theta/2\theta$ scan mode, of these 1911 reflections with $I > 6.0\sigma(I)$ were used to solve (direct methods) and refine (full-matrix, least squares) the structure of **3**. $R = 0.0507$, $Rw = 0.0499$. There is some disorder in the isobutyl groups. Further details of the crystal structure investigation can be obtained from the Fachinformationszentrum Karlsruhe, Gesellschaft für wissenschaftlich-technische Information mbH D-7514, Eggenstein-Leopoldshafen 2, FRG by quoting the depository number CSD-54883, the names of the authors, and the journal citation.

[10] Identified by comparison of ^{1}H- and ^{13}C{^{1}H}-NMR spectra with those of an authentic sample. See A. Alberola, R. Pedrosa, *An. Quim., Ser. C 76*, (1980) 21.

[11] XPS data were obtained on a VG Scientific Escalab Mark I instrument with a $Mg_{K\alpha}$ X-ray anode.

The Structure of Cyclic C_6S_6 and C_6O_6**

By *Gernot Frenking**

Dedicated to Professor Karl Dimroth on the occasion of his 80th birthday

Sülzle et al.[1] recently reported on the mass spectrometric investigation of benzo[1,2-*d*:3,4-*d'*:5,6-*d''*]-tri(1,3-dithiol-2-one) **1**, in which, after cleavage of three molecules of CO from the radical anion $\mathbf{1}^{\bullet\ominus}$ and subsequent charge exchange reactions, the fragments $C_6S_6^n$ (n = + 1, 0, − 1) were detected. The experimental findings provided no information about the structure of the $C_6S_6^n$ fragments, but, owing to the low tendency of radical anions to rearrange,[2] it was presumed that the six-membered ring structure of **1** remains intact. As possible structures the valence isomers **2a** and **2b** were proposed.[1]

2a and **2b** are not only aesthetically attractive, their relative stability is also of considerable interest for theoretical studies of molecular structures, since they afford important information about the influence of aromatic stabilization,

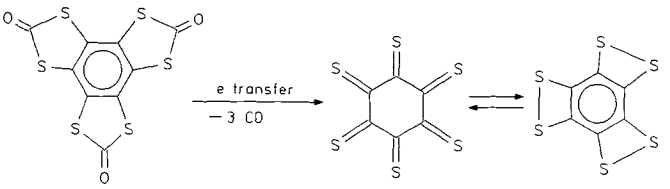

1 2a 2b

Fig. 1. Proposed structures **2a** and **2b** of C_6S_6 formed from **1**.

ring strain and the strength of the C–S double bond. We have therefore calculated the geometries and energies of the C_6S_6 isomers **2a** and **2b** as well as of the quinoid form **2c**.[3, 4] The optimized geometries are depicted in Figure 2, and the relative energies are listed in Table 1.[5] In addition, we report our results of theoretical studies on the analogous oxygen compound C_6O_6 in the isomeric forms **3a**, **3b**, and **3c**.

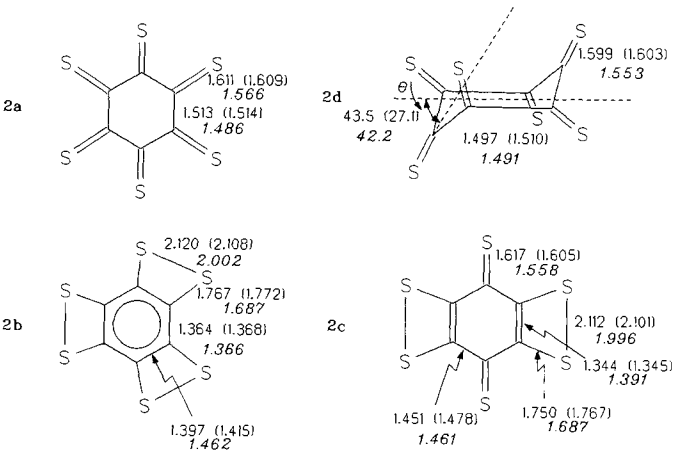

Fig. 2. Calculated bond lengths [Å] and angles [°] for **2a**–**2d**. Numerical data: 3-21G* basis set, in brackets: STO-3G basis set, italics: MNDO method.

Table 1. Calculated relative energies E_{rel} [kcal mol^{-1}] and zero point vibration energies ZPE [kcal mol^{-1}] with the number of imaginary frequencies *i*.

Cpd.	Symm.	HF/STO-3G			HF/ 3-21G*	HF/ 6-31G* [a]	MP2/ 3-21G*[a]	MNDO	
		E_{rel}	NSE	*i*	E_{rel}	E_{rel}	E_{rel}	E_{rel}	*i*
2a	D_{6h}	136.0	31.0	3	53.9	62.3	26.5	78.5	3
2b	D_{3h}	0.0	33.7	0	0.0	0.0	0.0	0.0	0
2c	D_{2h}	48.8	32.9	0	3.2	1.1	−10.1	28.4	0
2d	D_{3d}	130.8	30.9	0	30.0	34.7	3.1	66.6	0
3a	D_{6h}	0.0	38.6	0	0.0	0.0	0.0	6.5	3
3b	D_{3h}	88.9	42.8	0	241.0	294.1	233.9	316.6	0
3c	D_{2h}	64.7	41.6	0	163.5	192.4	148.0	205.9	0
3d	D_{3d}	– [b]			– [b]			0.0	0

[a] Energy calculation with 3-21G*-optimized geometries. [b] Optimization leads to the structure **3a**.

[*] Prof. Dr. G. Frenking
Fachbereich Chemie der Universität
Hans-Meerwein-Strasse, W-3550 Marburg (FRG)

[**] This work was supported by the Fonds der Chemischen Industrie, the Deutsche Forschungsgemeinschaft, and Convex and Silicon Graphics.

The optimization of the geometries of **2a–2c** were first carried out with the MNDO method and at the ab initio level with the STO-3G basis set. The calculation of the frequency of the optimized structure **2a** with D_{6h} symmetry yielded in both cases three imaginary frequencies, whose coordinates correspond to non planar modes. An optimization of the geometry without enforced planarity led to the chair-shaped structure **2d**, which is respectively 5.2 kcal mol^{-1} (STO-3G) and 11.9 kcal mol^{-1} (MNDO) energetically more favorable than **2a**. The calculation of the force constant matrix identified **2d** as minimum on the potential hypersurface. **2b**, however, is predicted by MNDO and STO-3G to be the energetically most favorable form (Table 1).

We have also optimized the geometries of **2a–2d** with the 3-21G* basis set. The data in Figure 2 and Table 1 show an increase in the stability of **2d** compared with **2a**; the chair form **2d** is now calculated to be 23.9 kcal mol^{-1} more favorable than the planar form **2a** and the bending angle θ is 43.5°. The energetically most favorable isomer at the 3-21G* level is still the aromatic form **2b**. However, the quinoid structure **2c** is calculated as lying only 3.2 kcal mol^{-1} higher (Table 1). A calculation of the energy with the 6-31G* basis set using the 3-21G*-optimized geometries changes this result only very slightly. The difference in the stability of **2b** and **2c** is still only 1.1 kcal mol^{-1}. However, inclusion of the correlation energy leads to a marked preference of structure **2c**. At the MP2/6-31G*//3-21G* level the quinoid form **2c** is calculated as lying 10.1 kcal mol^{-1} lower energetically than the aromatic form **2b**. If the zero-point energy (ZPE) is also taken into consideration this energy difference increases to 10.9 kcal mol^{-1}.[6] At the same theoretical level, i.e. MP2/6-31G*//3-21G* + ZPE, the aromatic form **2b** and the chair structure **2d** are energetically almost degenerate; **2b** is calculated as being 0.3 kcal mol^{-1} more favorable than **2d**. Our results are in agreement with the theoretical studies on dithial HSC–CSH, according to which the four-membered valence isomer is energetically almost degenerate with the dithial form.[7]

Table 1 also lists our calculated energies for the structurally analogous oxygen compounds C_6O_6 **3a–3d**, whose geometries are shown in Figure 3. Here the question of the energetically most favorable structure is clearly answered in favor of the hexaketo form (Table 1). The MNDO calculation again predicts the chair form **3d** as being the energetically most favorable minimum,[8] which, however, lies only 6.5 kcal mol^{-1} lower than the planar structure **3a**, whereas the ab initio calculations indicate the D_{6h} form **3a** as being the most stable isomer. The difference in energy between **3a** and **3b** or **3c** is more than 100 kcal mol^{-1} (Table 1).

The differences in energy of the series of C_6O_6 isomers relative to those of the C_6S_6 isomers can be explained quite easily. The ring strain of the four-membered rings in **3b** and **3c** is substantially greater than in **2b** and **2c** since the O–O bond is much shorter than the S–S bond. Moreover, the use of standard values for the bonding increments[9] of C–C, C–O, C–S, O–O, and S–S bonds gives an exothermic balance of -8 kcal mol^{-1} for the formation of **2c** from **2a** or **2d**, whereas the corresponding transition from **3a** to **3c** is 80 kcal mol^{-1} and endothermic.

These results show that of the three C_6S_6 isomers of **2a–2d** investigated, the quinoid form **2c** is the energetically most favorable,[6] and that the hexathioketone isomer prefers the nonplanar chair form **2d**. Although it cannot be ruled out that, under the experimental conditions of the neutralization-reionization mass spectrometry (NRMS),[10] the more energetic isomers **2b** or **2d** are generated from **1** in a kinetically controlled process,[1] it appears likely that the indirectly observed species C_6S_6 has the structure **2c**.

How great are the chances of generating from the precursor analogous to **1** but with oxygen instead of sulfur ("benzene tricarbonate") a fragment C_6O_6 which has structure **3c**? We have calculated (MP2/3-21G*//3-21G* + ZPE[11]) the reaction enthalpies of the decomposition into six molecules of CS and CO respectively for each of the most stable C_6S_6 and C_6O_6 isomers **2c** and **3a**.

$$\mathbf{2c} \rightarrow 6\,CS + 221.8 \text{ kcal mol}^{-1} \quad (a)$$

$$\mathbf{3a} \rightarrow 6\,CO + 27.5 \text{ kcal mol}^{-1} \quad (b)$$

The reaction enthalpies for the reactions (a) and (b) show that the decomposition of **2c** into six molecules of CS is not favored thermodynamically. In contrast, an extremely low C–C bond strength of 27.5/6 = 4.6 kcal mol^{-1} is calculated for **3a**. It appears unlikely that the same method by which C_6S_6 could be observed[1] also leads to indirect detection of C_6O_6 in the case of the analogous precursor benzene tricarbonate. In this instance other strategies should be examined.[12]

Received: June 19, 1990 [Z 4025 IE]
German version: *Angew. Chem. 102* (1990) 1516

CAS Registry numbers:
2a, 129917-29-9; **2b**, 123439-59-8; **2c**, 129917-30-2; **2c**, *ortho* isomer, 129917-31-3; **3a**, 527-31-1; **3b**, 129917-32-4; **3c**, 129917-33-5.

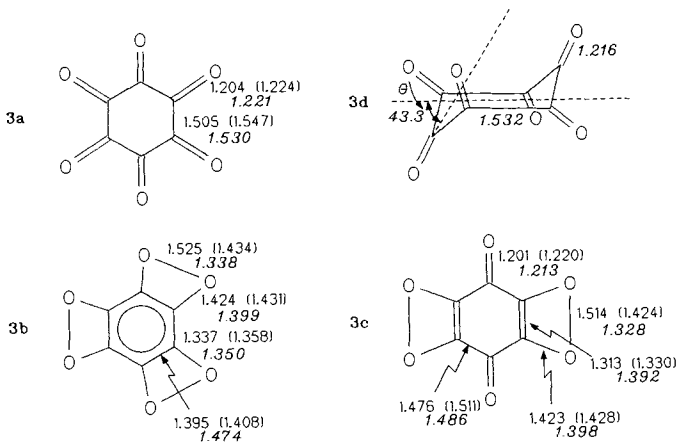

Fig. 3. Calculated bond lengths [Å] and angles [°] for **3a–3d**. Numerical data: see caption to Figure 2.

[1] D. Sülzle, N. Beye, E. Fanghänel, H. Schwarz, *Chem. Ber. 122* (1989) 2411.
[2] a) H. Budzikiewicz, *Angew. Chem. 93* (1981) 635; *Angew. Chem. Int. Ed. Engl. 20* (1981) 624; b) J. H. Bowie, *Mass Spectrom. Rev. 3* (1984) 161.
[3] MNDO: M. J. S. Dewar, W. Thiel, *J. Am. Chem. Soc. 99* (1977) 4899, 4907.
[4] Gaussian 88: M. J. Frisch, M. Head-Gordon, H. B. Schlegel, K. Raghavachari, J. S. Binkley, C. Gonzalez, D. J. DeFrees, D. J. Fox, R. A. Whiteside, R. Seeger, C. F. Melius, J. Baker, R. Martin, L. R. Kahn, J. J. P. Stewart, E. M. Fluder, S. Topiol, J. A. Pople, Gaussian Inc., Pittsburgh, PA, USA 1988.
[5] Calculated total energies (in Hartrees): **2a**: -2583.2645 (STO-3G), -2599.7452 (HF/3-21G*), -2612.0719 (HF/6-31G*), -2601.0464 (MP2/3-21G*); **3a**: -667.3394 (STO-3G), -672.4538 (HF/3-21G*), -676.2623 (HF/6-31G*), -673.7364 (MP2/3-21G*). The formation enthalpies calculated with MNDO are 182.7 kcal mol^{-1} for **2a** and -157.4 kcal mol^{-1} for **3a**.
[6] We have also carried out calculations for the *ortho* isomer corresponding to **2c**. This lies 11.3 kcal mol^{-1} higher energetically than **2c** (MP2/3-21G*//3-21G* + ZPE).
[7] a) J. D. Goddard, *J. Comput. Chem. 8* (1987) 369; b) R. Janoschek, A. B. Hess Jr., J. Fabian, *Z. Chem. 30* (1990) 176.
[8] The new semiempirical method AM1 (M. J. S. Dewar, E. G. Zoebisch, E. F. Healy, J. J. P. Stewart, *J. Am. Chem. Soc. 107* (1985) 3902) yields very similar results regarding the energetic stabilities. The relative energies for

C_6S_6 are 76.3 kcal mol^{-1} (**2a**), 0.0 kcal mol^{-1} (**2b**), 29.0 kcal mol^{-1} (**2c**), 64.4 kcal mol^{-1} (**2d**). The E_{rel} values for C_6O_6 are 5.9 kcal mol^{-1} (**3a**), 390.0 kcal mol^{-1} (**3b**), 263.9 kcal mol^{-1} (**3c**), 0.0 kcal mol^{-1} (**3d**). The enthalpies of formation calculated with AM1 are 232.2 kcal mol^{-1} for **2a** and -128.0 kcal mol^{-1} for **3a**.

[9] The following standard values were used: For the single bonds O–O 35 kcal mol^{-1}, S–S 64 kcal mol^{-1}; for the π bonds C=O 90 kcal mol^{-1}, C=S 63 kcal mol^{-1}, C–C 70 kcal mol^{-1}. W. Kutzelnigg, *Angew. Chem. 96* (1984) 262; *Angew. Chem. Int. Ed. Engl. 23* (1984) 272.

[10] C. Wesdemiotis, F. W. McLafferty, *Chem. Rev. 87* (1987) 485.

[11] Calculated values for CO: bond lengths 1.129 Å (HF/3-21G*), energy -112.3014 Hartree (MP2/3-21G*//3-21G*), ZPE 3.5 kcal mol^{-1} (STO-3G); for CS: bond lengths 1.523 Å (HF/3-21G*), energy -433.2461 Hartree (MP2/3-21G*//3-21G*), ZPE 2.3 kcal mol^{-1} (STO-3G).

[12] From ethylenetetracarboxylic acid derivatives a bis-anhydride of the formula C_6O_6 with two five-membered rings can be formed, which according to our calculations is 45.5 kcal mol^{-1} (MP2/3-21G*//3-21G* + ZPE) more stable than **3a** [13]. This anhydride is structurally related to the known anhydride of mellitic acid $C_{12}O_9$: N. N. Greenwood, A. Earnshaw: *Chemie der Elemente*, VCH, Weinheim 1988, p. 362.

[13] In the meantime the detection of C_6O_6 in the gas phase by NRMS experiments starting from ethylenetetracarboxylates has been made. The author thanks Dr. *D. Sülzle* for this information and for interesting discussions.

Isotope Effects Associated with α-Olefin Insertion in Zirconocene-Based Polymerisation Catalysts: Evidence for an α-Agostic Transition State**

By *Helmuth Krauledat* and *Hans-Herbert Brintzinger**

In memoriam Piero Pino

Efficient catalysts for the stereospecific polymerization of α-olefins are obtained from chiral *ansa*-zirconocene complexes by activation with methyl alumoxane (MAO).[1] A useful model for the stereochemical course of this catalysis has been derived by *Pino* et al.[2] from studies on the MAO-activated hydrooligomerization of olefins in the presence of H_2, which is catalyzed by a resolved *ansa*-zirconocene enantiomer, (*R*)-[ethylene bis(4,5,6,7-tetrahydro-1-indenyl]zirconium dichloride (*R*)-**1**. The absolute configuration of the hydrotrimer was found to be that expected from an insertion path in which the CH_2R alkyl chain of the $ZrCH_2CH_2R$ unit points into an open segment of the chiral ligand framework, while the olefin approaches with that enantioface[3]—*si* for the complex with (*R*) configuration—which places the two alkyl substituents at the incipient C–C bond in *trans* positions to each other (**I**). This model has been confirmed by *Kaminsky* et al. in a recent study on the enantioselective oligomerization of α-olefins with this catalyst system.[4]

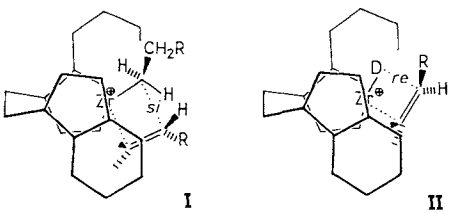

I II

An olefin approach with opposite enantiofacial preference—*re* for (*R*)-**1**—was indicated, however, by the prevailing product configuration for (*R*)-**1**-catalyzed α-olefin deuteration (**II**).[5] Here, the olefin substituent appears to take up the position which was occupied by the CH_2R group in **I**.

To test these models we studied the zirconocene/MAO-catalyzed hydrodimerization of 1-hexene, labeled with deuterium in its 1-*trans* position: the hydrodimerization product 6-deuterio-5-deuteriomethylundecane **2** must arise from two consecutive olefin insertions and final hydrogenolysis in the form of its *threo* isomer if both insertions proceed with opposite enantiofacial olefin orientation, and in the form of the *erythro* isomer if the two olefin insertions proceed with identical enantiofacial orientation.

Such a hydrodimerization, carried out with 0.1 mol-% rac-**1**, activated by MAO (200:1) under 20–15 atm of H_2 at -5 °C, affords ca. 10% 1-deuteriohexane, 5% hydrodimer **2** and 85% of higher hydrooligomers.[6] The D-NMR spectrum of **2** shows the signals of the *threo* ($\delta = 1.09$) and *erythro* ($\delta = 1.28$) diastereomers in a ratio of $(2.30 \pm 0.03):1$.[7] With (*Z*)- instead of (E)-1-deuterio-1-hexene, this ratio is inverted to $1:(2.55 \pm 0.10)$ in favor of the *erythro* isomer. These results confirm that olefin insertions into Zr–H and $Zr–CHDCH_2R$ units occur preferentially with opposite enantiofacial orientation.

For catalysis of the same reactions by MAO-activated $(C_5H_5)_2ZrCl_2$ one would expect that this achiral catalyst cannot induce any enantiofacial bias of the two α-olefin insertions. Yet repeated runs of these experiments consistently lead to a significant excess of the *erythro* product, with *threo*/*erythro* ratios of $1:(1.30 \pm 0.03)$.[8]

This surprising result is explained, in line with considerations of *Grubbs* et al.,[9] as outlined in Scheme 1: the asymmetric orientation of H and D atoms at the α-C atom of the first insertion product must influence the sense of insertion of the second olefin by a primary kinetic isotope effect,[10] when the $ZrCHDCH_2R$ unit is folded into an α-agostic bridge—either to $\overbrace{Zr \leftarrow H–CDCH_2R}$ or to $\overbrace{Zr \leftarrow D–CHCH_2R}$—in the transition state of the olefin insertion. Preference for H over D atoms in such an agostic bridge, together with preferentially *trans*-positioned alkyl groups at the incipient C–C bond, would indeed predict a preference for identical olefin orientations in both insertion steps for such an achiral catalyst.

Assuming a strict *trans* arrangement of the two alkyl residues and an energy lower by 500–600 J mol^{-1} for a metal–H–C- than for a metal–D–C-bridged species, as determined e.g. for $[HOs_3(CO)_{10}CH_2D]$ from temperature-dependent ^{1}H-NMR shifts of the CH_2D group,[11] Scheme 1 would yield, at a reaction temperature of 268 K, exactly the observed *threo*/*erythro* ratio of 1:1.3. The tenet of Scheme 1 is further supported by the observation that the $(C_5H_5)_2ZrCl_2$/MAO-catalyzed hydrodimerization of (Z)-1-deuterio-1-hexene gives the same *threo*/*erythro* ratio as that of its E isomer. This documents the chemical equivalence of the α-H/D positions in the first insertion product and distinguishes the isotopic differentiation in such an achiral catalyst from the stereotopic differentiation found for catalysis with rac-**1**, where inverted diastereomer ratios were observed for (*E*) and (*Z*) deuterated olefins.

That olefin insertions in Ziegler-Natta catalysis pass through a transition state involving an α-agostic distortion

[*] Prof. Dr. H. H. Brintzinger, Dipl. Chem. H. Krauledat
Fakultät für Chemie der Universität
Postfach 5560, D-7750 Konstanz (FRG)

[**] This work was supported by the Volkswagen-Stiftung and the Fonds der Chemischen Industrie. We thank BASF AG (Ludwigshafen) for gifts of chemicals, Prof. *G. Fink* (Max-Planck-Institut für Kohlenforschung, Mülheim a.d. Ruhr) for gas chromatographic (GC) separations, Dr. *H. Rüegger* and Dr. *D. Moskau* (Spectrospin AG, Fällanden, Switzerland) for D-NMR spectra, Prof. *J. E. Bercaw*, Dr. *W. E. Piers* and Prof. *R. H. Grubbs* (California Institute of Technology, Pasadena, USA) for communication of unpublished results [13] and helpful discussions.

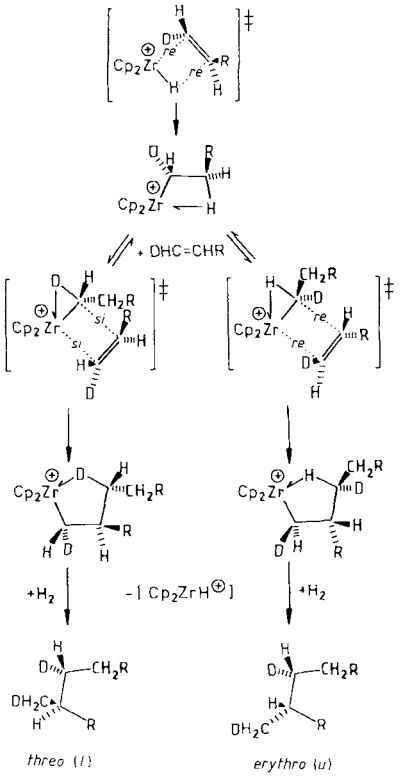

Scheme 1. Reaction paths with alternative α-agostic transition states leading to *threo*-**2** (left) and *erythro*-**2** (right) via two consecutive olefin insertions with opposite and identical olefin orientations, respectively.

of the migrating alkyl unit, has been proposed by *Brookhart* and *Green*.[12] The observations reported here constitute the first experimental evidence for such an α-agostic transition state in zirconocene-catalyzed olefin polymerizations.[13]

Experimental

(*E*)-1-deuterio-1-hexene: Reaction of 1-hexyne with 1 equiv. diisobutylaluminum hydride in toluene at 0 °C; cleavage with D_2O and fractional distillation [G. Wilke, H. Müller, *Justus Liebigs Ann. Chem. 629* (1960) 222; G. Zweifel, R. L. Miller, *J. Am. Chem. Soc. 92* (1970) 6678]; the ^{1}H-NMR spectrum (doublet of triplets, $\delta = 4.98$, $^3J = 17.1$, $^4J = 1.5$ Hz, 1H; symmetric multiplet, $\delta = 5.82$, 1H[14]) indicates that (*E*)-1-deuterio-1-hexene is the only olefin present. (*Z*)-1-deuterio-1-hexene: Cleavage with H_2O of the hydroalumination product of 1-deuterio-1-hexyne [G. W. Kabalka, R. J. Newton, J. Jacobus, *J. Org. Chem. 43* (1978) 1567]. ^{1}H NMR: $\delta = 4.91$ (d, $^3J = 10.4$ Hz), 5.80(m). The presence of ca. 15% [D_2]hexane, 10% toluene and 5% [D_1]butane, indicated by gas chromatography does not interfere with the catalysis or with the isolation of the hydrodimer **2**; traces of 1-hexyne have to be removed by prolonged stirring with and distilling from solvent-free *n*-butyllithium.

Hydrodimerizations: 3.5 mL (33 mmol) of (*E*)- or (*Z*)-1-deuterio-1-hexene, 430 mg MAO (6.6 mmol CH_3AlO, Schering AG, $M_r \approx 1300$, in 4.5 mL toluene) and 33 μmol of either rac-**1** or $(C_5H_5)_2ZrCl_2$ in 0.5 mL toluene (all under N_2) were exposed in a 50 mL autoclave at − 5 °C to initial H_2 pressures of 20 and 15 atm, respectively, for 16–20 h; during this time H_2 pressures fell by ca. 5 atm. After quenching with 10 mL 1.5 M aq. HCl and separation of the organic layer, **2** was isolated by fractional distillation. Admixtures of ca. 5% 6,7-[D_2]-*n*-dodecane (the tail-to-tail mis-insertion product) gave weak D-NMR signals just separable from the adjacent signal of *erythro*-**2**.

Received: July 5, 1990 [Z 4051 IE]
German Version: *Angew. Chem. 102* (1990) 1459

[1] W. Kaminsky, K. Külper, H. H. Brintzinger, F. R. W. P. Wild, *Angew. Chem. 97* (1985) 507; *Angew. Chem. Int. Ed. Engl. 24* (1985) 507.
[2] P. Pino, P. Cioni, J. Wei, *J. Am. Chem. Soc. 109* (1987) 6189; P. Pino, P. Cioni, M. Galimberti, J. Wei, N. Piccolrovazzi in W. Kaminsky, H. Sinn (Eds.): *Transition Metals and Organometallics as Catalysts for Olefin Polymerisation*, Springer, Berlin 1988, p. 269.
[3] The *re*/*si* designations are based throughout on $R \geq C_2H_5$; they are reversed for 1-deuterated α-olefins.
[4] W. Kaminsky, A. Ahlers, N. Möller-Lindenhof, *Angew. Chem. 101* (1989) 1304; *Angew. Chem. Int. Ed. Engl. 28* (1989) 1216.
[5] R. Waymouth, P. Pino, *J. Am. Chem. Soc. 112* (1990) 4911; P. Pino, M. Galimberti, *J. Organomet. Chem. 370* (1989) 1.
[6] Determined by gas chromatography with toluene as internal standard. Under 100 atm H_2, the respective yields are 61%, 10% and 29%. For **2** obtained from this reaction, the *threo*/*erythro* ratio is still 2.30:1, i.e., equal to that obtained with 20 atm H_2.
[7] Measured in C_6H_6 solution relative to $\delta(C_6H_5D) = 7.15$ on Bruker AMX-600 and AMX-500 NMR spectrometers operated at 92.1 and 76.8 MHz respectively with broad-band ^{1}H decoupling. The assignment of the signal at $\delta = 1.09$ to *threo*-**2** and that at $\delta = 1.28$ to *erythro*-**2** is based on closely similar D-NMR shifts for the *threo* ($\delta = 1.07$) and *erythro* ($\delta = 1.28$) diastereomers of 2-deuterio-3-methylpentane, prepared by hydroboration and subsequent deuterolysis with CH_3COOD from the (*Z*) and (*E*) isomers, respectively, of 3-methyl-2-pentene (c.f. G. W. Kabalka, R. J. Newton, J. Jacobus, *J. Org. Chem. 44* (1979) 4185).
[8] This reaction yields 35% 1-deuteriohexane, 45–50% **2** and 15–20% of hydrotrimer plus higher hydrooligomers.
[9] L. Clawson, J. Soto, S. L. Buchwald, M. L. Steigerwald, R. H. Grubbs, *J. Am. Chem. Soc. 107* (1985) 3377.
[10] Secondary (e.g. steric) isotope effects would be expected to be of smaller magnitude; see for example L. Melander, W. H. Saunders, Jr.: *Reaction Rates of Isotopic Molecules*, Wiley, New York 1980, p. 189.
[11] R. B. Calvert, J. R. Shapley, *J. Am. Chem. Soc. 100* (1978) 7726.
[12] M. Brookhart, M. L. H. Green, *J. Organomet. Chem. 250* (1983) 395; M. Brookhart, M. L. H. Green, L. Wong, *Prog. Inorg. Chem. 36* (1988) 1.
[13] A similar kinetic isotope effect due to α-CHD asymmetry has recently been observed for the hydrocyclization of (*E*,*E*)-1,6-dideuterio-1,5-hexadiene to 2-deuterio-1-deuteriomethylcyclopentane for which an achiral scandiocene catalyst gave, at − 10 °C, a *cis*/*trans* diastereomer ratio of 1:1.26 (J. E. Bercaw, W. E. Piers, *J. Am. Chem. Soc.*, in press). For the analogous cyclization reaction catalyzed by MAO-activated $(C_5H_5)_2ZrCl_2$, we find a *cis*/*trans* ratio of 1.01 ± 0.02, i.e. no indication for any α-agostic interaction. A *cis*/*trans* ratio of 1.0 has also been reported for the $Al(C_2H_5)Cl_2$-induced, stoichiometric cyclization of Cp_2TiCl–CHD–$(CH_2)_3$–$CH=CH_2$ to Cp_2TiCl–CH_2–$\overline{CH}$–$(CH_2)_3$–$\overline{CH}$D [9].
[14] Asahi Research Center: *Handbook of Proton NMR-Spectra and Data Vol. 2*, Academic Press, London 1985, p. 115.

2-Pentylcyclopent-2-en-1-one by Catalytic Pauson-Khand Reaction**

By *Valentin Rautenstrauch,** *Patrick Mégard, José Conesa*, and *Wilhelm Küster*

We report the preparation of 2-pentylcyclopent-2-en-1-one **1**, a precursor of methyl *trans*-dihydrojasmonate (Hedione®),[1] an important perfumery chemical, from hept-1-yne **2**, ethylene **3** and CO, by catalytic Pauson-Khand reaction (PKR) (Scheme 1).

Conventionally, PKRs are carried out by heating the complexes $[Co_2(CO)_6(alkyne)]$ (intramolecular PKRs: $[Co_2(CO)_6(alkenyne)]$) with alkenes (for exceptions, see below),[2] and **1** was obtained via this stoichiometric PKR, from $[Co_2(CO)_6(hept\text{-}1\text{-}yne)]$ **4** and **3**. The yields were 31–47% based on **4** (35–70% in the presence of 1 mol-equiv. of tributylphosphane oxide), but were irreproducible.[3] The complexes are prepared in a separate step, from the alkynes

[*] Prof. Dr. V. Rautenstrauch, P. Mégard (dec.), J. Conesa
Firmenich SA, Laboratoires de Recherche
CH-1211 Genève 8 (Switzerland)
Dr. W. Küster
Institut für Technische Chemie und Petrolchemie der Technischen Hochschule
D-5100 Aachen (FRG)

[**] Incorporated in this work is the Diplomarbeit of *W. Küster*, carried out under the direction of Professor *W. Keim*, whose help and advice are gratefully acknowledged.

or alkenynes and $[Co_2(CO)_8]$ **5**.[2] The yield of **4** was 80–85% (1 mol-equiv. or slight excess of **2**[3]).

A catalytic PKR that would instead allow the use of free alkyne and CO would be of great interest, especially for industrial applications. This has often been attempted,[4] but the only truly catalytic reactions described so far[4a] involve the strained, reactive alkenes norbornene and norbornadiene, in combination with acetylene and CO. The turnover numbers achieved were small (8 and 11) and the amounts of (pre)catalyst **5** used rather high (9.4 and 3.7 mol-% of the alkenes).

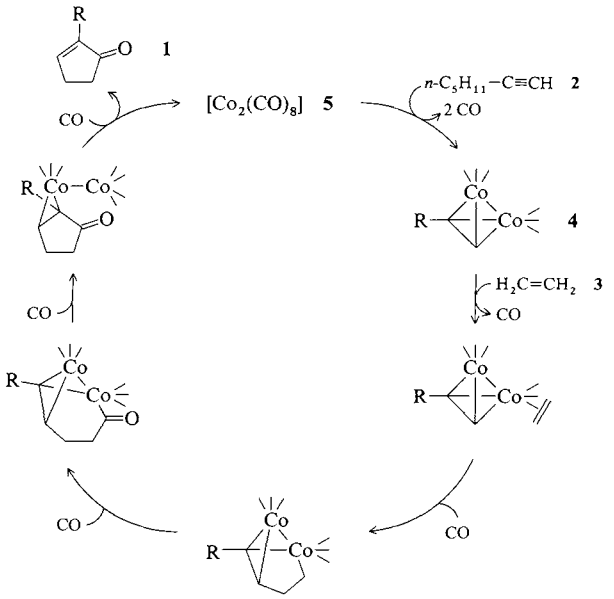

Scheme 1. Hypothetical mechanism for the synthesis of the cyclopentenone **1** via a catalytic Pauson-Khand reaction. R = n-C_5H_{11}. The CO ligands are indicated by dashes.

Our process is based on the fact that PKRs involving a 1-alkyne and **3** are uniquely favorable. The complexes $[Co_2(CO)_6$(1-alkyne)] react highly regioselectively and in the right sense, whereas 1-alkenes react completely unselectively.[2] As concerns regioselectivity, combination of **4** (or of **2** in a catalytic process) with **3** is therefore the best possible choice. **3** is also very reactive.[3] Kinetic data are lacking, but one can assume that **3** is the most reactive unstrained alkene component, and that alkene reactivity is a key factor. In view of the known catalytic reactions,[4a] it is certain that **3** is also the best possible choice with respect to reactivity. In the alternative combination of $[Co_2(CO)_6(C_2H_2)]$ (or acetylene) with hept-1-ene and CO, the regioselectivity with respect to, and the reactivity of, hept-1-ene are both unfavorable. Moreover, the reactivities of the alkynes towards cyclotrimerization, one of the prominent side reactions, also favor the first combination, **2** cyclotrimerizing less readily than acetylene. The second combination would be an alternative because it would produce 5-pentyl- along with 4-pentylcyclopent-2-en-1-one, and the former can be readily isomerized to **1**.[5]

Four types of prominent side reactions compete in our process: cyclotrimerization (CT) (**2** → **6** + **7**), cocyclotrimerization (CCT) (**2** + **3** → **8** + **9**), formation of **10** (spirofuranone (SF)-formation), which is trapped in situ by **3** as the Diels-Alder adduct **11**, and formation of the cyclopentadienones (CPs) **12** and **13** (→ → **14** + **15**, see below)].[6] None of these side reactions has previously been identified in PKRs, although CT had been suggested as an obvious possibility.[7]

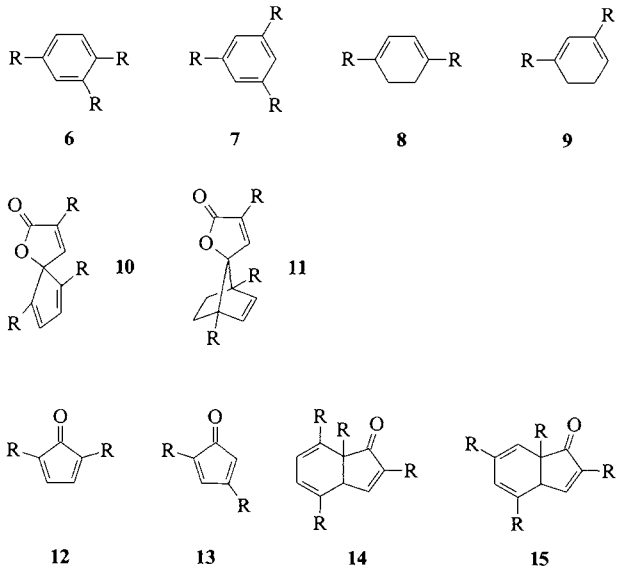

Our process is further based on the identification of three parameters that strongly affect the PKR and side reactions: 1) the concentration of **2**—CT, CCT and CP formation were all more or less suppressed at low concentrations of **2**. 2) The CO pressure—at high CO pressure, the PKR was favored, catalyst recycling improved, and CP formation favored at the expense of CT, but SF formation not favored; 3) the pressures of **3**—high pressures were needed, but the catalytic system broke down beyond a certain limit. The primary parameters are the concentrations of CO and **3** in the liquid phase. These are determined by the partial pressures and solubilities, but the solubility of **3** is much higher than that of CO.

In terms of statistical analysis, these parameters appear to interact.[8] We carried out two long series of experiments (some 40 runs in each) in which these and some other parameters were varied, and which led to the above deductions. The experiments were not statistically designed,[8] because other, unidentified and/or difficult-to-control parameters seem to play a role. This is suggested by the fact that we were unable to reproduce exactly the first series in the second series (about 5 months later, see below), although we could reproduce experiments when they were successive or close in time within each series. One of these parameters is clearly autoclave conditioning.

In one of our best experiments, we used a 0.80 M toluene solution of **2** (40 mmol, about 50 mL solution), 0.088 mmol **5** (0.0022 mol-equiv., 0.22 mol-%), partial pressures (room temperature) of 40 bar **3** and 100 bar CO [100 mL stainless steel autoclave, magnetically-linked high speed stirrer; about 9 mol-equiv. of **3** and 6 mol-equiv. of CO]. We heated to 150 °C for 16 h (310–360 bar total pressure at 150 °C) and obtained **1** in 47–49% isolated yield based on **2**. The conversion of **2** was ≥ 98% (GC), the overall turnover number about 220, the overall turnover rate about 0.04 s^{-1}, and the initial turnover rate about 0.2 s^{-1}. The regioselectivity was 98–99% (1–2% of **16**). All four side reactions were largely suppressed, but CCT and CP formation less than the other two. Based on the yield of **1** and approximate product ratios determined by gas chromatography, we estimate yields[9] of

about 8% for **8** + **9**, 7% for **14** + **15**, and 1% each for **6** + **7**, and **11**. The sum of these yields and that of **1**, about 65%, is a material balance with respect to **2**, which is clearly incomplete. Apart from the prominent side products, we also detected a background of trace products (GC) and may have overlooked products of high molecular weight.

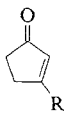

16

The irreproducibilities mentioned above were as follows: the maximum yield of **1** was close to 50% in the second series (the results above are from the second series), but close to 60% in the first; furthermore, small amounts of acetonitrile and $[Fe(CO)_5]$ had apparently improved the yield in the first series, which we were unable to reproduce exactly in the second.

Scheme 1 shows a working hypothesis for the mechanism of the catalytic PKR, which is based on the Schore-Magnus mechanism for the stoichiometric reaction.[10] There is little experimental evidence to support either one of these hypotheses, but they at least permit a first discussion. The kinetics of the first step, the reaction between **5** and alkynes, have been studied and a mechanism proposed[11b] which involves loss of a CO ($\rightarrow [Co_2(CO)_7]$), addition of the alkyne ($\rightarrow [Co_2(CO)_7(\text{alkyne})]$), and loss of the second CO (the sequence is not explicitly formulated).

How the Co_2 fragment is liberated from the cyclopentenone and recycled is unknown, but the ultimate fate of the fragment in the stoichiometric reaction is known: in isooctane as the solvent $[Co_4(CO)_{12}]$ was isolated,[4a] and in aromatic solvents the clusters $[Co_4(CO)_9(\text{arene})]$ ($[Co_4(CO)_{12}]$ reacts with arenes to give $[Co_4(CO)_9(\text{arene})]$).[2a, 12] The same clusters are primary products when **5** is thermolyzed (at or above room temperature) in the absence of CO; the end product is metallic Co.[11c, 12] In contrast, in the presence of CO, but effectively only at high CO pressures, an equilibrium favoring **5** is established (little $[Co_4(CO)_{12}]$, no decomposition to metallic Co); the kinetics of the back reaction $[Co_4(CO)_{12}] + 4\,CO \rightarrow 2\,\mathbf{5}$ have been investigated and a mechanism deduced.[11c, 13] All of this suggested that catalyst recycling in the PKR might only be efficient at high CO pressure. No systematic investigation of the PKR at high CO pressure is in the literature, but it has been established that CO at atmospheric pressure has little or no effect on the stoichiometric reaction.[2c] As reaction **5** + **2** → **4** + 2CO involves CO dissociation (see above), and the same is assumed in the next step, the insertion of **3** (Scheme 1), one might have expected that high CO pressure would block these dissociations.

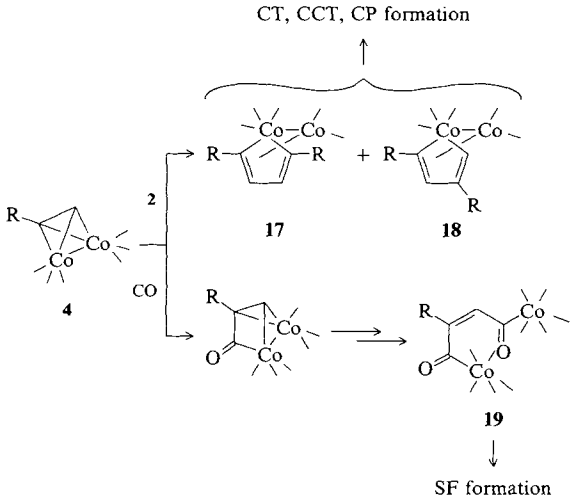

Scheme 2. Hypothetical reaction pathways to the prominent side products in the synthesis of **1**. R = n-C_5H_{11}. Dashes = CO ligands.

Scheme 2 shows the two pathways presumed to lead to the side reactions. One pathway involves the reaction of **4** with **2** to give **17** and **18**,[14] thought to be common intermediates in CT,[15] CCT[16] and CP formation. The other involves the reaction of **4** with CO to **19**, considered to be an intermediate in SF formation (for details, see [17]). Once the free CPs **12** and **13** are generated, they undergo mainly two Diels-Alder reactions, **12** + **12** and **12** + **13**, and the resulting adducts then decarbonylate to **14** and **15**.[17–19]

Received: June 15, 1990 [Z 4019 IE]
German version: *Angew. Chem. 102* (1990) 1441

CAS Registry numbers:
1, 25564-22-1; **2**, 628-71-7; **3**, 74-85-1.

[1] Reviews: E. P. Demole in E. T. Theimer (Ed.): *Fragrance Chemistry. The Science of the Sense of Smell*, Academic Press, New York 1982, p. 374; G. Ohloff: *Riechstoffe und Geruchssinn. Die molekulare Welt der Düfte*, Springer, Berlin 1990, pp. 149–152.

[2] Reviews: a) P. L. Pauson, I. U. Khand, *Ann. N.Y. Acad. Sci. 295* (1977) 2–14; b) P. L. Pauson, *Tetrahedron 41* (1985) 5855–5869; c) P. L. Pauson in A. de Meijere, H. tom Dieck (Eds.): *Organometallics in Organic Synthesis. Aspects of a Modern Interdisciplinary Field*, Springer, Berlin 1987, pp. 233–246; d) N. E. Schore, *Chem. Rev. 88* (1988) 1085–1119; e) N. E. Schore in B. M. Trost, I. Fleming (Eds.): *Comprehensive Organic Synthesis*, Pergamon, in press and *Org. React. N.Y.*, in press.

[3] D. C. Billington, I. M. Helps, P. L. Pauson, W. Thomson, D. Willison, *J. Organomet. Chem. 354* (1988) 233–242.

[4] a) I. U. Khand, G. R. Knox, P. L. Pauson, W. E. Watts, M. I. Foreman, *J. Chem. Soc. Perkin Trans. 1 1973*, 977–981; b) D. C. Billington, *Tetrahedron Lett. 24* (1983) 2905–2908; c) P. Magnus, L. M. Principe, M. J. Slater, *J. Org. Chem. 52* (1987) 1483–1486; d) D. C. Billington, W. J. Kerr, P. L. Pauson, C. F. Farnocchi, *J. Organomet. Chem. 356* (1988) 213–219.

[5] J. Tsuji, Y. Kobayashi, I. Shimizu, *Tetrahedron Lett. 1979*, 39–40; DE-A 3412713 (April 19, 1983), Sumitomo Chemical Co., Ltd.

[6] **6**:**7** = 90:10; **8**:**9** = 79:21; **14**:**15** = 60:40.

[7] For a notable instance, see: N. E. Schore, S. D. Najdi, *J. Am. Chem. Soc. 112* (1990) 441–442.

[8] G. E. P. Box, W. G. Hunter, J. S. Hunter: *Statistics for Experimenters. An Introduction to Design, Data Analysis, and Model Building*, Wiley, New York 1978; R. Caulcutt: *Statistics in Research and Development*, Chapman and Hall, London 1983; C. K. Bayne, I. B. Rubin: *Practical Experimental Designs and Optimization Methods for Chemists*, VCH, Weinheim 1986.

[9] Yields counted per unit **2** so as to be commensurate with that of **1**, for example a 100% yield of **11** when 1 mole of **2** gives 1/3 mol **11**.

[10] P. Magnus, L. M. Principe, *Tetrahedron Lett. 26* (1985) 4851–4854; B. E. La Belle, M. J. Knudsen, M. M. Olmstead, H. Hope, M. D. Yanuck, N. E. Schore, *J. Org. Chem. 50* (1985) 5215–5222; P. Magnus, C. Exon, P. Albaugh-Robertson, *Tetrahedron 41* (1985) 5861–5869.

[11] R. D. W. Kemmitt, D. R. Russell in G. Wilkinson, F. G. A. Stone, E. W. Abel (Eds.): *Comprehensive Organometallic Chemistry, Vol. 5*, Pergamon, Oxford 1982; a) pp. 192–209; c) pp. 3–8.

[12] I. U. Khand, G. R. Knox, P. L. Pauson, W. E. Watts, *J. Chem. Soc. Chem. Commun. 1971*, 36; *J. Chem. Soc. Perkin Trans. 1 1973*, 975–977.

[13] G. Bor, U. K. Dietler, P. Pino, A. Poe, *J. Organomet. Chem. 154* (1978) 301–315; G. Bor, U. K. Dietler, *ibid. 191* (1980) 295–302.

[14] One such cobaltacycle is known: a) M. A. Bennett, P. B. Donaldson, *Inorg. Chem. 17* (1978) 1995–2000; analogues from $[CpCoL_2]$: b) R. F. Heck: *Organotransition Metal Chemistry. A Mechanistic Approach*, Academic Press, New York 1974, pp. 176–182; c) Y. Wakatsuki, O. Nomura, K. Kitaura, K. Morokuma, H. Yamazaki, *J. Am. Chem. Soc. 105* (1983) 1907–1912; d) J. P. Collman, L. S. Hegedus, J. R. Norton, R. G. Finke: *Principles and Applications of Organotransition Metal Chemistry*, Univ. Science Books, CA-Mill Valley 1987, pp. 509–512, 613–615, 870–877.

[15] CT catalysis by **5**: [2d], p. 1097–1099; [11a]; [14a]; [14b]; by $[CpCoL_2]$: [2d], p. 1097; [11a]; [14b]; [14d].

[16] CCT catalysis by **5** is new; catalysis by $[CpCoL_2]$: [2d], pp. 1101–1103; [14b]; [14d]; see also D. W. Macomber, A. G. Verma, R. D. Rogers, *Organometallics 7* (1988) 1241–1253.
[17] V. Rautenstrauch, P. Mégard, B. Gamper, B. Bourdin, E. Walther, G. Bernardinelli, *Helv. Chim. Acta. 72* (1989) 811–824.
[18] Formation of $[Co_2(CO)_4(CP)_2]$ and the free CP from $[Co_2(CO)_6$(bulky alkyne)] and the alkyne: C. Hoogzand, W. Hübel, *Tetrahedron Lett. 1961*, 637–643; U. Kruerke, W. Hübel, *Chem. Ber. 94* (1961) 2829–2856. Analogous generation of the parent CP: N. E. Schore, B. E. La Belle, M. J. Knudsen, H. Hope, X.-J. Xu, *J. Organomet. Chem. 272* (1984) 435–446. CP complexes from $[CpCoL_2]$: [14b]; H. Yamazaki, N. Hagihara, *J. Organomet. Chem. 7* (1967) P22.
[19] C. H. DePuy, M. Isaks, K. L. Eilers, G. F. Morris, *J. Org. Chem. 29* (1964) 3503–3507. Diels-Alder reactions **12** + **3** and **13** + **3** may nevertheless come to the fore in our experiments (low concentrations of **5**, and thus of **12** and **13**). As trace products, some further dihydroindenones were generated by alternative Diels-Alder reactions, and also Diels-Alder adducts from dihydroindenones and **3**.

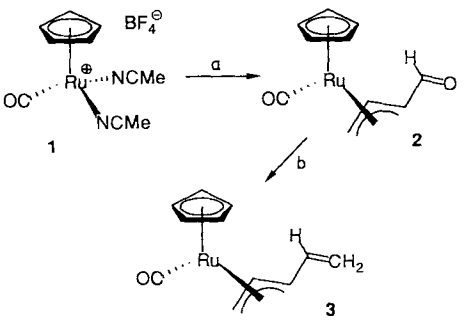

Scheme 1. a) 1-(Trimethylsilyloxy)buta-1,3-diene, CH_2Cl_2; b) $Ph_3P{=}CH_2$, THF, −78 °C.

s-trans-1,3-Dienes as Ligands for Cationic Group 8 Metal Centers**

By *Stephen A. Benyunes, Jeremy P. Day, Michael Green*, Abdul Wahab Al-Saadoon*, and *Tracey L. Waring*

Conjugated dienes, as ligands, have been of paramount importance during the development of organotransition metal chemistry.[1] Structural studies have long since established that, in contrast to the solution behavior of the free ligand, upon coordination to a metal center a 1,3-diene almost invariably adopts an *s-cis* conformation. Species in which the coordinated diene defies this generalization were first reported in 1980 by *Erker* et al.[2] Since then a variety of thermally stable neutral *s-trans*-diene complexes has been described.[3] Examples of these, however, are confined to the early transition metals in which the L_nM-diene moiety may be viewed as being predominantly metallacyclic in character. More recently we have described the first examples of species containing an *s-trans*-diene coordinated at a cationic molybdenum center.[4] Complexes of type $[Mo(\eta^4\text{-}C_4H_5R)(CO)_2(\eta\text{-}C_5Me_5)][CF_3SO_3]$ were generated at low temperature, and were found to undergo irreversible isomerization to their *s-cis* counterparts above − 30 °C. In extending our synthetic methodology to an analogous ruthenium system we have discovered that cationic *s-trans*-1,3-diene complexes of this type are surprisingly more stable, and with this insight we have selectively trapped *s-trans*-1,3-dienes with a $[Ru(CO)(\eta\text{-}C_5H_5)]^{\oplus}$ fragment.

As a continuation of the synthetic approach established for molybdenum, the reaction of 1-trimethylsilyloxybuta-1,3-diene with $[Ru(NCMe)_2(CO)(\eta\text{-}C_5H_5)][BF_4]$ **1**[5] was investigated. This gave, upon prolonged stirring, the oxo-functionalized allyl complex **2** as an *exo-syn*:*endo-syn* isomeric mixture[6] (4:1), which was purified by column chromatography. Reaction of **2** with the Wittig reagent $Ph_3P{=}CH_2$ resulted in a smooth transformation into the corresponding η^3-pentadienyl species **3** (Scheme 1). Characterization of *exo-syn*-**2** by means of a single-crystal X-ray diffraction analysis[7] revealed an unexpectedly short C^1–C^2 interatomic distance in the allyl ligand (1.46 Å). This observed increase in the bond order implies the presence of considerable π delocalization throughout the ligand, and hence a high degree of stereochemical rigidity. This latter feature was reflected accordingly in the low-temperature protonation of **2**: treatment of *syn*-**2** with CF_3SO_3H (CD_2Cl_2, −78 °C) gave only the *s-trans*-diene complex **4**, thereby demonstrating retention of the stereochemical integrity of the transoid C_4 ligand. In similar fashion, protonation of *syn*-**3** afforded exclusively the *s-trans*-diene complex **5** (Scheme 2). Complexes **4** and **5**

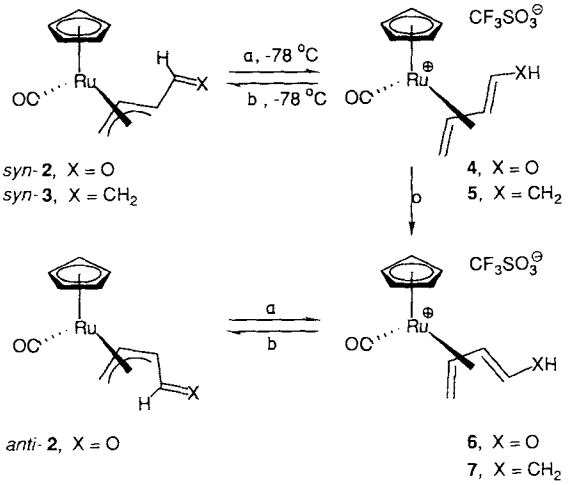

Scheme 2. a) CF_3SO_3H, CH_2Cl_2; b) NEt_3.

were not isolated, and were characterized in situ by comparison of their ^{1}H-NMR data with those of the known[5] *s-cis* isomerization products **6** and **7**. Identification as such was based on two spectroscopic features associated with the *s-trans* geometry: a) a higher value for $^3J(H^b\text{–}H^c)$ across the central C–C single bond and b) a marked upfield shift of the signals arising from the exposed protons H^a and H^e, both criteria being relative to the isomeric *s-cis* species (Table 1). In contrast with the analogous molybdenum complexes, the rate of isomerization of **4** and **5** was relatively slow, their stability in CH_2Cl_2 solution at 25 °C corresponding to a $t_{1/2}$ of 2 and 48 h, respectively. Reaction of the hydroxydiene cations **4** and **6** with NEt_3 gave only *syn*-**2** and *anti*-**2**, respectively, thus demonstrating again the previously established

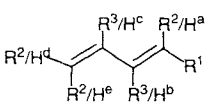

[*] Dr. S. A. Benyunes, Dr. J. P. Day, Prof. M. Green, Dr. A. W. Al-Saadoon and Dr. T. L. Waring
Department of Chemistry
King's College London
Strand, London WC2R 2LS (UK).

[**] This work was supported by the Science and Engineering Research Council (SERC) and the Government of Iraq.

Table 1: ^{1}H-NMR data (CD_2Cl_2, TMS, J in Hz) for the selected η^4-*s-trans* diene complexes **4**–**7**

	R^1	R^2	R^3	δH^a	δH^e	$^3J(H^b\text{–}H^e)$
4 (*s-trans*) [a]	OH	H	H	8.05	3.65	8.1
5 (*s-trans*) [a]	Me	H	H	4.94	4.31	7.7
6 (*s-cis*) [b]	OH	H	H	5.48	1.64	6.3
7 (*s-cis*) [b]	Me	H	H	2.65	1.65	5.8

[a] $T = -40\,^\circ C$, [b] $T = 25\,^\circ C$.

structural relationship (*syn*-allyl $\rightleftharpoons$ *s-trans*-diene, *anti*-allyl $\rightleftharpoons$ *s-cis*-diene) inherent in the protonation of **2** and **3**.

The unexpectedly high degree of thermal stability displayed by the cations **4** and **5** suggested that it might actually be possible to prepare such species by the selective capture of an *s-trans*-1,3-diene with an appropriate metal fragment. This was achieved via a simple extension of an existing procedure.[8] Addition of $HBF_4 \cdot OEt_2$ to allyl complex **8** (CH_2Cl_2, $-78\,^\circ C$) followed by an excess of 2,3-dimethylbuta-1,3-diene afforded a mixture of the *s-trans* and *s-cis* cations **9** and **10** (Scheme 3). Complex **9** proved unstable in

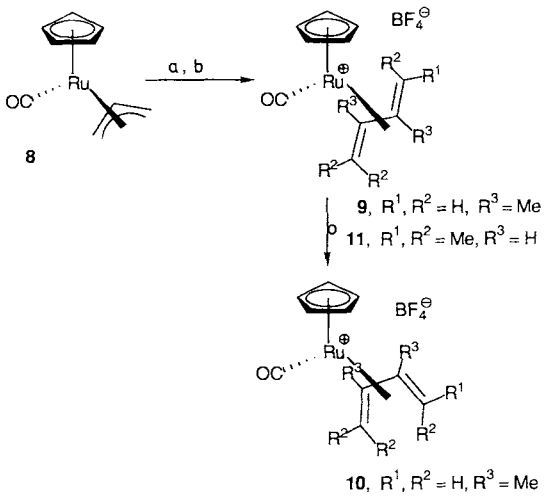

Scheme 3. a) $HBF_4 \cdot OEt_2$, CH_2Cl_2, $-78\,^\circ C$; b) Diene

solution at 25 °C, undergoing slow rearrangement to the *s-cis* isomer **10**. Substitution, in the above sequence of the more sterically demanding 2,5-dimethylhexa-2,4-diene gave only a single species **11** isolated as orange-yellow crystals. As was the case for **9**, the asymmetry present in the diene ligand, highlighted by ^{1}H and ^{13}C NMR, allowed **11** to be unequivocally assigned the predicted *s-trans* geometry. Solution studies show a complete absence of isomerization at 25 °C, and thus **11** can be regarded as an unprecedented example of a stable cationic *s-trans* diene complex. It is also the first example of an *s-trans*-1,3-diene complex of a metal from the right-hand side of the periodic table. Our studies might thus suggest that *s-trans*-1,3-dienes as ligands are less unusual than was originally thought.

Experimental

2: A solution of **1** (0.50 g, 1.38 mmol) in CH_2Cl_2 (30 mL) was treated with 1-trimethylsilyloxybuta-1,3-diene (0.50 g, 3.5 mmol) and the resulting mixture stirred for 3 d at 25 °C. After removal of solvent, the residue was chromatographed on alumina with Et_2O. **2** (0.18 g, 50%), was obtained as an orange-yellow solid in the form of a 4:1 *exo-syn*:*endo-syn* mixture.

exo-syn-**2**: IR (CH_2Cl_2): $\tilde{\nu}$ (C=O) = 1950 vs, 1650 s cm^{-1}; ^{1}H NMR (CD_2Cl_2): δ = 9.00 (d, 1H, CHO, J = 6.7 Hz), 4.30 (s, 5H, C_5H_5), 4.22 (ddd, 1H, CH, J = 11.1, 9.2, 7.0 Hz), 2.77 (dd, 1H, CH_2, J = 7.0, 1.4 Hz), 2.46 (dd, 1H, CH, J = 9.2, 6.7 Hz), 1.53 (dd, 1H, CH_2, J = 11.1, 1.5 Hz); MS: m/z 263 ($M^\oplus$).

3: A solution of **2** (250 mg, 0.95 mmol) in THF (40 mL) was cooled to $-78\,^\circ C$, and treated with a THF solution of $Ph_3P{=}CH_2$ (0.8 g, 2.9 mmol). The mixture was warmed to ambient temperature and stirred for 15 h. Solvent was then removed under reduced pressure, and the solid residue purified by column chromatography. Elution with Et_2O/hexane (1:1) afforded a bright yellow band, which following concentration and recrystallization from hexane gave yellow crystals of **3** (145 mg, 58%).

exo-syn-**3**: IR (CH_2Cl_2): $\tilde{\nu}$ (C=O) = 1940 vs cm^{-1}; ^{1}H NMR ($CDCl_3$): δ = 5.88 (dt, 1H, CH, J = 17.0, 10.1 Hz), 5.17 (dd, 1H, $=CH_2$, J = 16.9, 1.5 Hz), 4.97 (s, 5H, C_5H_5), 4.80 (dd, 1H, CH, J = 10.1, 1.5 Hz), 4.23 (ddd, 1H, CH, J = 10.3, 9.9, 6.9 Hz), 2.84 (t, 1H, =CH, J = 9.9 Hz), 2.81 (dd, 1H, CH_2, J = 6.8, 1.9 Hz), 1.29 (dd, 1H, CH_2, J = 10.5, 1.9 Hz); MS: m/z = 263 ($M^\oplus$).

4: A slight excess of CF_3SO_3H (8 µL, 0.09 mmol) was added slowly to a cooled ($-78\,^\circ C$) solution of **2** (21 mg, 0.08 mmol) in CD_2Cl_2 (0.5 mL) contained within a septum capped 5-mm NMR tube. This was transferred immediately to the pre-cooled ($-70\,^\circ C$) probe of the NMR spectrometer. Spectra were recorded whilst warming at 10 °C intervals, showing the instantaneous and quantitative generation of **4** as the only species present in solution.

exo-s-trans-**4**: ^{1}H NMR ($-40\,^\circ C$): δ = 8.05 (d, 1H, H^a, J_{ab} = 10.4 Hz), 5.59 (s, 5H, C_5H_5), 4.46 (ddd, 1H, H^c, J_{ce} = 11.5, J_{cb} = 8.1, J_{cd} = 6.9 Hz), 3.82 (dd, 1H, H^b, J_{ba} = 10.5, J_{bc} = 8.0 Hz), 3.65 (d, 1H, H^e, J_{ec} = 11.4 Hz), 3.32 (d, 1H, H^d, J_{dc} = 6.9 Hz). Warming the sample to 25 °C gave rise to a second set of signals corresponding to *endo-s-cis*-**6**: ^{1}H NMR: δ = 5.92 (ddd, 1H, H^c, J_{ce} = 11.2, J_{cd} = 8.2, J_{ch} = 6.4 Hz), 5.60 (dd, 1H, H^b, J_{ba} = 9.2, J_{bc} = 6.2 Hz), 5.55 (s, 5H, C_5H_5), 5.48 (d, 1H, H^a, J_{ab} = 9.2 Hz), 3.30 (dd, 1H, H^d, J_{dc} = 8.2, J_{de} = 2.1 Hz), 1.64 (dd, 1H, H^e, J_{ec} = 11.4, J_{ed} = 2.1 Hz).

5: The low-temperature protonation of **3** gave, in similar fashion, *exo-s-trans*-**5**. ^{1}H NMR: ($-40\,^\circ C$) δ = 5.65 (s, 5H, C_5H_5), 4.94 (dq, 1H, H^a, J_{ab} = 11.5, $J_{a\text{-}Me}$ = 6.4 Hz), 4.58 (dd, 1H, H^b, J_{ba} = 11.5, J_{bc} = 7.7 Hz), 4.31 (d, 1H, H^e, J_{ec} = 12.7 Hz), 4.22 (d, 1H, H^d, J_{dc} = 6.8 Hz), 4.15 (dt, 1H, H^c, J_{ce} = 12.7, $J_{ch \approx cd} \approx 7.0$ Hz), 1.86 (d, 3H, Me, $J_{Me\text{-}a}$ = 6.4 Hz).

11: To a cooled ($-78\,^\circ C$) solution of **8** (50 mg, 0.21 mmol) in CH_2Cl_2 (5 mL) was added successively $HBF_4 \cdot OEt_2$ (85%, 21 µL, 0.23 mmol) and 2,5-dimethylhexa-2,4-diene (70 mg, 0.64 mmol). The mixture was then allowed to warm to ambient temperature. Stirring was continued for 4 d, accompanied by a gradual change in color from orange to dark green. The resulting solution was filtered through celite and concentrated under reduced pressure. Addition of Et_2O gave a pale green powder, which upon recrystallization from CH_2Cl_2 ($-40\,^\circ C$) afforded orange-yellow crystals of **11** (53 mg, 64%). IR (CH_2Cl_2): $\tilde{\nu}$ (C=O) = 2004 vs cm^{-1}; ^{1}H NMR (CD_2Cl_2): δ = 5.36 (s, 5H, C_5H_5), 4.89 (d, 1H, CH, J = 9.4 Hz), 4.24 (d, 1H, CH, J = 9.4 Hz), 2.14 (s, 6H, 2 Me), 2.10 (s, 3H, Me), 2.02 (s, 3H, Me); ^{13}C-{^{1}H} NMR (CD_2Cl_2): δ = 119.5 (CMe_2), 110.0 (CMe_2), 90.8 (C_5H_5), 86.4 (CH), 75.3 (CH) 32.0 (Me), 31.5 (Me), 25.3 (Me), 24.7 (Me).

Received: June 15, 1990 [Z 4015 IE]
German version: *Angew. Chem. 102* (1990) 1505

CAS Registry numbers:
1, 101680-17-5; (*exo, syn*)-**2**, 130197-97-6; (*endo, syn*)-**2**, 130272-85-4; (*exo, syn*)-**3**, 130197-98-7; (*endo, syn*)-**3**, 130272-86-5; (*exo, s-trans*)-**4**, 130198-00-4; (*endo, s-trans*)-**4**, 130272-81-0; (*exo, s-trans*)-**5**, 130404-06-7; (*endo, s-trans*)-**5**, 130272-82-1; **8**, 31741-51-2; **9**, 130198-02-6; **10**, 130272-84-3; **11**, 130198-04-8; 1-(Trimethylsilyloxy)buta-1,3-diene, 6651-43-0; 2,5-Dimethylhexa-2,4-diene, 764-13-6; 2,3-Dimethylbuta-1,3-diene, 513-81-5.

[1] J. P. Collman, L. S. Hegedus, J. R. Norton, L. S. Finke (Eds): *Principles and Applications of Organotransition Metal Chemistry*, Univ. Science Books, CA-Mill Valley 1987.

[2] a) G. Erker, J. Wicher, J. Engel, F. Rosenfeldt, W. Dietrich, C. Krüger, *J. Am. Chem. Soc. 102* (1980) 6344–6346.

[3] a) A. Nakamura. H. Yasuda, *Angew. Chem. 99* (1987) 745–764; *Angew. Chem. Int. Ed. Engl. 26* (1987) 723–742; b) G. Erker, C. Krüger, G. Muller, *Adv. Organomet. Chem. 24* (1985) 1–39, and references cited therein; c) T. Okamoto, H. Yasuda, Y. Nakamura, Y. Kai, N. Kanehisa, N. Kasai, *J. Am. Chem. Soc. 110* (1988) 5008–5017; d) N. J. Christensen, A. D. Hunter, P. Legzdins, *Organometallics 8* (1989) 930–940.

[4] S. A. Benyunes, M. Green, M. J. Grimshire, *Organometallics 8* (1989) 2268–2270.

[5] M. Crocker, M. Green, C. E. Morton, K. R. Nagle, A. G. Orpen, *J. Chem. Soc., Dalton Trans. 1985*, 2145–2153.

[6] The terms *exo* and *endo* refer to the relative stereochemical arrangements of the η^5-C_5Me_5, and allyl or diene ligands. Complexes **2**–**7** are all present in the form of *exo-endo* isomeric mixtures. For simplification purposes, only one of these is illustrated.

[7] T. L. Waring *Ph. D. Thesis*, University of Bristol 1987.

[8] V. V. Krivykh, O. V. Gusev, M. I. Rybinskaya, *J. Organomet. Chem. 362* (1989) 351–362.

A Synthetic Equivalent for [2.2]Paracyclophane-1,9-diyne: Octaphenyl-1:2,9:10-dibenzo[2.2]paracyclophane-1,9-diene and Its Reduction to the Hexaanion**

By *Armin de Meijere,* Jürgen Heinze, Klaus Meerholz, Oliver Reiser*, and *Burkhard König*

Dedicated to Professor Marit Traetteberg on the occasion of her 60th birthday

The synthesis of unusual molecules that are not naturally occurring is not just a challenge, but often an opportunity to discover new properties and phenomena. 1:2,9:10-Dibenzo[2.2]paracyclophane-1,9-diene (**1a**), first synthesized by *Wong*,[1] contains two biphenyl units that are nonconjugated in the classical sense because the phenyl rings are mutually orthogonal. Reduction of **1a** with alkali metals gives a radical anion, $\mathbf{1a}^{\bullet\ominus}$, whose unpaired electron resides in the phane benzene rings.[2] The tetraphenyl derivative **1b**, which we synthesized,[3] behaves differently; the first two additional electrons reside in the lateral *ortho*-terphenyl units.[4] Compound **1c** can be reversibly reduced to the tetraanion.[5] Thus, octaphenyl-1:2,9:10-dibenzo[2.2]paracyclophane-1,9-diene (**7**), described here, was expected to extend this trend still further.

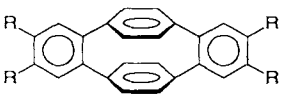

1a R = H
1b R = C_6H_5
1c R = p-$C_6H_4C(CH_3)_3$

The synthesis of **1a** developed by *Wong*[1] starts with 9,9-dibromo-1:2-benzo[2.2]paracyclophan-1-ene, which is obtained in five steps from *o*-terphenyl in only poor yield (0.3%). This route is therefore hardly suitable for a synthesis of **1a** in preparative quantities. However, we found that the concept of double dehydrobromination of a geminal dibromide can be applied to the isomeric mixture of 1,1,9,9- and 1,1,10,10-tetrabromo[2.2]paracyclophane (**5**), easily obtained in large amounts (90% yield) from commercially available [2.2]paracyclophane.[6] In this way, not only **1a** but also a series of interesting derivatives, such as **3b**, **7**, and **10**, are now readily available for the first time in large amounts. Treatment of **5** with potassium *tert*-butoxide in tetrahydrofuran (THF) results, via fourfold dehydrobromination, in the stepwise formation of a triple bond in each bridge of [2.2]paracyclophane. In the presence of furan (**4a**), the highly strained alkynes are immediately trapped and afford the two diastereomeric bis-endoxides *syn/anti*-**2a** (23% yield) in a ratio of about 1:1 (Scheme 1). The bis-endoxides *syn/anti*-**2a**[7] undergo facile deoxygenation upon treatment with low-valent titanium ($TiCl_4/LiAlH_4$) to give **3a** (= **1a**) (75%). Dibenzo[2.2]paracyclophanediene (**1a**) can thus be prepared in three steps in gram amounts from [2.2]paracyclophane. Use of 2,5-disubstituted furans **4b**[8] as trapping agents in this sequence leads, via the corresponding bis-endoxides **2b**,[7] to 3′,6′,3″,6″-tetrasubstituted dibenzo[2.2]paracyclophanedienes such as **3b**.[7]

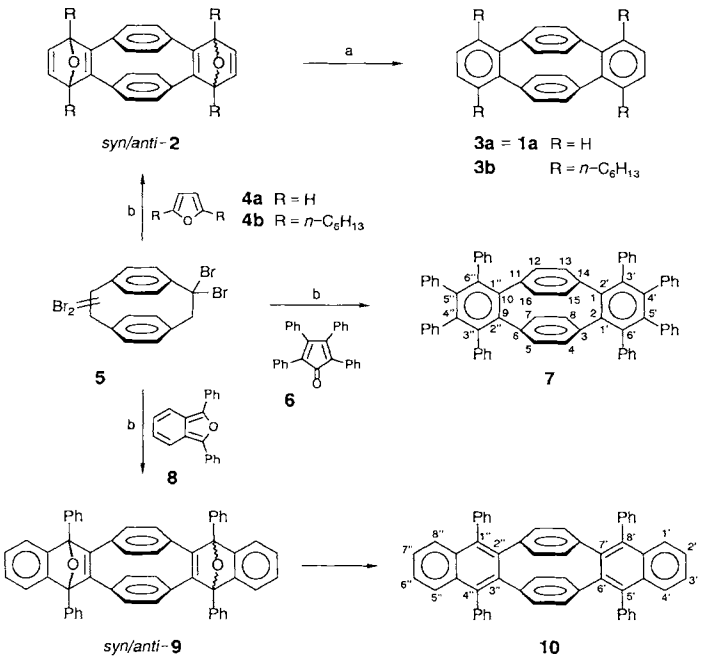

Scheme 1. a) $TiCl_4/LiAlH_4$, NEt_3, THF, room temperature 0.5 h; b) KO*t*Bu/THF, 22 °C, 4–5 h.

Analogously, reaction with 2,5-diphenylisobenzofuran (**8**) affords the dibenzo bis-endoxides *syn/anti*-**9**, which are deoxygenated by $TiCl_4/LiAlH_4$ to give dinaphtho[2.2]paracyclophane-1,9-diene (**10**).[7] Dropwise addition of a solution of potassium *tert*-butoxide in THF to a mixture of **5** and tetraphenylcyclopentadienone (tetracyclone, **6**) furnishes octaphenyldibenzo[2.2]paracyclophanediene (**7**)[7] in a yield of 69%. The high efficiency with which the ring-strained alkyne generated here is trapped by tetracyclone (**6**), a diene with inverse electron demand, is also known for other highly strained cycloalkynes.[9]

Compound **7** has a centrosymmetric structure in the crystal (Fig. 1). The interplanar angles in each of the four

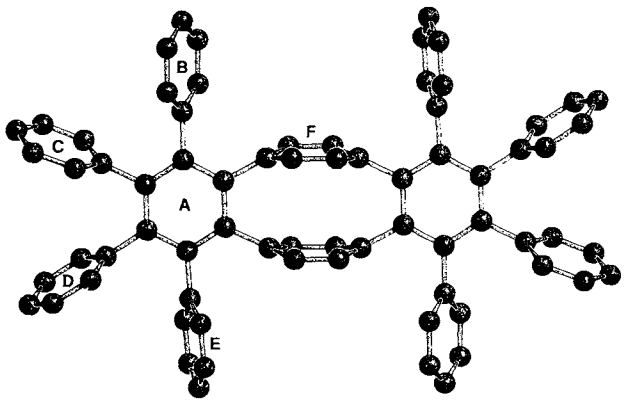

Fig. 1. Molecular structure of 7 (SCHAKAL drawing) [11]. Triclinic crystals of space group $P\bar{1}$, $Z = 1$, unit cell $a = 612.3(7)$, $b = 1137(1)$, $c = 1878(3)$ pm, $\alpha = 79.1(1)$, $\beta = 86.79(9)$, $\gamma = 81.4(1)°$, $\varrho_{calcd} = 1.12$ g cm^{-3}, 3959 evaluated reflections with $2\theta \leq 65°$, $Cu_{K\alpha}$, $R_w = 6.8\%$. C1-C2 142.7(5), C1-C14 150.2(5), C2-C3 149.8(5) pm; average CC bond length in ring A: 140.1(5), B: 137.6(6), C: 137.5(6), D: 136.1(8), E: 137.1(7), F: 139.1(5) pm; bond angles C14-C1-C2 117.0(1), C1-C2-C3 116.3(2)°; interplanar angles A/B: 63, A/C: 70, A/D: 78, A/E: 81°.

[*] Prof. Dr. A. de Meijere [+], Dr. O. Reiser, Dipl.-Chem. B. König
Institut für Organische Chemie der Universität
Martin-Luther-King-Platz 6, D-2000 Hamburg 13 (FRG)
Prof. Dr. J. Heinze, Dipl.-Chem. K. Meerholz
Institut für Physikalische Chemie der Universität Freiburg

[+] New address:
Institut für Organische Chemie der Universität
Tammannstrasse 2, D-3400 Göttingen (FRG)

[**] This work was supported by the Volkswagen-Stiftung, the Deutsche Forschungsgemeinschaft, the Fonds der Chemischen Industrie, BASF AG, Hoechst AG, Bayer AG, and Degussa AG. *B. K.* thanks the Studienstiftung des Deutschen Volkes for a doctoral fellowship.

biphenyl units formed by the two lateral benzene rings and their four phenyl substituents increase sequentially from 63.2° to 81.4°, presumably owing to intermolecular effects in the crystal. The same phenomenon has also been observed for hexaphenylbenzene,[10] for which the average value of the interplanar angle (67.2°) is slightly, but significantly, smaller than that in **7** (average value 73.2°). The geometry of the central framework in **7** corresponds to that in the parent compound **1a**.[12]

Whereas **1a** can be reduced to a dianion in two steps and the tetraphenyl derivative **1c** can be reduced to a tetraanion in four steps,[5] the cyclovoltammogram of the octaphenyl derivative **7**[13] shows three reversible two-electron reduction waves at $E^0 = -2.61$, -2.76, and -3.13 V versus Ag/AgCl. Only a few examples of reversibly formed hexaanions have been reported so far.[14] As expected, the reduction potentials of **7** are all more positive than those of hexaphenylbenzene, which is reduced in three steps at $E^0 = -2.73$, -3.10, and -3.23 V to only a trianion. Even in **1c**, the potential differences between mono- and dianion formation and tri- and tetraanion formation (70 and 85 mV, respectively) are very small owing to the weak interaction between the two substituted, lateral benzene rings.[5] It is not surprising, therefore, that formal 2e processes with $\Delta E^0 < 50$ mV are observed for **7**, which has still larger conjugated systems. Also noteworthy is the formation of the hexaanion over an extremely small potential range ($\Delta E^0 = 0.52$ V). Compound **7** is thus an efficient storer of charge, since Coulomb repulsions between the six excess charges are minimized by the unusual structure.

Received: July 30, 1990 [Z 4101 IE]
German version: *Angew. Chem. 102* (1990) 1443

CAS Registry numbers:
1a, 97315-26-9; *syn*-**2a**, 130248-91-8; *anti*-**2a**, 130322-52-0; *syn*-**2b**, 130248-92-9; *anti*-**2b**, 130322-53-1; **3b**, 130248-93-0; **4a**, 110-00-9; **4b**, 128912-39-0; **5** (1,1,9,9 isomer), 7567-81-9; **5** (1,1,10,10 isomer), 109764-60-5; **6**, 479-33-4; **7**, 130248-96-3; **8**, 5471-63-6; *syn*-**9**, 130248-94-1; *anti*-**9**, 130322-54-2; **10**, 130248-95-2; [2,2]paracyclophane-1,9-diyne, 130248-97-4.

[1] a) H. N. C. Wong, C. W. Chan, *J. Am. Chem. Soc. 107* (1985) 4790; b) H.-N. C. Wong, C. W. Chan, *ibid. 110* (1988) 463.
[2] F. Gerson, W. B. Martin Jr., H. N. C. Wong, C. W. Chan, *Helv. Chim. Acta 70* (1987) 79.
[3] A. de Meijere, S. Reichow, O. Reiser, *Angew. Chem. 98* (1987) 1285; *Angew. Chem. Int. Ed. Engl. 26* (1987) 1277.
[4] F. Gerson, A. de Meijere, O. Reiser, B. König, T. Wellauer, *J. Am. Chem. Soc. 112* (1990) 6827.
[5] A. de Meijere, J. Heinze, K. Meerholz, O. Reiser, B. König, unpublished results.
[6] M. Stöbbe, O. Reiser, R. Näder, A. de Meijere, *Chem. Ber. 120* (1987) 1667.
[7] All new compounds were fully characterized by spectroscopic methods (IR, ^{1}H NMR, ^{13}C NMR, MS, UV) and elemental analysis. The assignment of ^{13}C NMR data was aided by spectra recorded with the DEPT protocol; (+) and (−) designate tertiary/primary and secondary carbon atoms, respectively. Representative data for **2a**: ^{1}H NMR (250 MHz; $CDCl_3$): $\delta = 5.69$ (br. s, 4H, 3′(6′,3″,6″)-H), 6.14 and 6.17 (each dd, 4H, $^3J = 8.0$ Hz, $^4J = 1.9$ Hz), 7.45 (br. s, 4H, 4′(5′,4″,5″)-H). ^{13}C NMR (63 MHz; $CDCl_3$): $\delta = 85.26$ (+, C-3′(6′,3″,6″)), 127.90 and 130.71 (+, phane-C_6H_4), 136.21 (C_{quat}), 145.04 (+; C-4′(5′,4″,5″)), 160.51 (C_{quat}). MS (70 eV): m/z 336 ($M^{\oplus}$, 100%). **3b**: ^{1}H NMR (250 MHz; $CDCl_3$): $\delta = 0.85$ (t, 12H, CH_2-CH_3), 1.2–1.8 (m, 32H, -CH_2-); 2.79 (t, 8H, aryl-CH_2-), 6.65 (s, 8H, phane-C_6H_4), 7.28 (s, 4H, 4′(5′,4″,5″)-H). ^{13}C NMR (63 MHz, $CDCl_3$): $\delta = 14.03$ (+, CH_3), 22.61, 29.32, 31.63, 31.82 and 35.00 (-, -CH_2-), 127.51 and 132.23 (+, arene-C), 136.44, 139.95 and 144.24 (C_{quat}; arene-C). MS (70 eV): m/z 640 ($M^{\oplus}$, 100%). **7**: ^{1}H NMR: (400 MHz, $CDCl_3$): $\delta = 6.62$ (s, 8H, phane-C_6H_4), 6.85, 6.94 and 7.10 (m, 24/8/8H, phenyl-H). ^{13}C NMR: (63 MHz, $CDCl_3$): $\delta = 125.05$, 125.52, 126.35, 126.73, 130.64, 131.12 and 132.30 (+), 138.22, 139.46, 139.94, 140.37, 140.98 and 143.31 (C_{quat}). MS (70 eV): m/z 913 ($M^{\oplus} + 1$, 77%); 912 ($M^{\oplus}$, 10), 456 ($M^{2\oplus}$, 2). **10**: ^{1}H NMR (250 MHz, $CDCl_3$): $\delta = 6.42$ (s, 8H, phane-C_6H_4), 7.24–7.40 (br. m, 24H, phenyl-H and naphtho-H), 7.50 (m, 4H, naphtho-H). ^{13}C NMR (63 MHz, $CDCl_3$): $\delta = 126.06$, 126.89, 127.06, 127.98, 130.98, 130.69 and 132.77 (+), 131.93, 135.96, 139.34, 139.94 and 141.33 (C_{quat}). MS (70 eV): m/z 708 ($M^{\oplus}$, 100%), 354 ($M^{2\oplus}$, 6).
[8] Cf. a) V. Ramanathan, R. Levine, *J. Org. Chem. 27* (1962) 1216; b) G. Büchi, H. Wuest, *ibid. 31* (1966) 975.
[9] Vgl. a) H. Meier, T. Molz, U. Merkele, T. Echter, M. Lorch, *Liebigs Ann. Chem. 1982*, 914; b) A. Hohmann, A. Krebs, unpublished results; c) A. Hohmann, *Dissertation*, Universität Hamburg 1985.
[10] J. C. J. Bart, *Acta Crystallogr. Sect. B 24* (1968) 1277.
[11] Further details of the crystal structure investigation may be obtained from the Fachinformationszentrum Karlsruhe, Gesellschaft für wissenschaftlich-technische Information mbH, D-7514 Eggenstein-Leopoldshafen 2 (FRG), on quoting the depository number CSD-54703, the names of the authors, and the journal citation.
[12] H. N. C. Wong, C. W. Chan, T. C. W. Mak, *Acta Crystallogr. Sect. C 42* (1986) 703.
[13] Recorded with a scan rate of between 10 and 100 mV s^{-1} at -65 °C in dimethylamine/tetrahydrofuran 1:1, electrolyte 0.1 M tetrabutylammonium bromide.
[14] a) J. Heinze, *Angew. Chem. 96* (1984) 823; *Angew. Chem. Int. Ed. Engl. 23* (1984) 821; b) R. Cosmo, C. Kantz, K. Meerholz, J. Heinze, K. Müllen, *Angew. Chem. 101* (1989) 638; *Angew. Chem. Int. Ed. Engl. 28* (1989) 604.

$[Cu_4(ddtp)_2Br_4]$, a Unique Tetranuclear Copper(I) Complex with Bridging Thioethers and Bridging Bromides**

By *Adrianus L. E. Stoffels, Willem G. Haanstra, Willem L. Driessen,** and *Jan Reedijk*

The ligand 1,5-bis(3′,5′-dimethylpyrazolyl)-3-thiapentane (ddtp), which has three potential donor atoms, forms coordination compounds with a 1:1 stoichiometry, namely $M(ddtp)X_2$, with divalent first row transition metals and anions.[1] In contrast, when reacting $CuBr_2$ with ddtp in warm ethanol/acetone in air,[2] the solution decolorizes almost immediately. On cooling, colorless air-stable crystals of stoichiometry $Cu_2(ddtp)Br_2$ separate. Apparently a reduction to a Cu^I species has occurred. Cu^{II} compounds exhibit a d-d transition band in the VIS-NIR region and usually give rise to an EPR signal. Both phenomena were absent in the resulting ddtp copper bromide compound. The same compound was also prepared by reacting ddtp with CuBr in a nitrogen atmosphere,[3] as confirmed by a comparison of IR spectra and X-ray powder patterns.

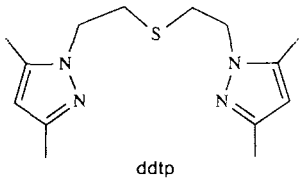

ddtp

Single-crystal X-ray structure analysis[4] shows that each copper ion resides in a distorted tetrahedral environment provided by a nitrogen, a bridging thioether and two bridging bromides (see Fig. 1). Two copper ions are linked by two bromides forming a Cu_2Br_2 fragment. The Cu···Cu distance

[*] Dr. W. L. Driessen, A. L. E. Stoffels, W. G. Haanstra, Dr. J. Reedijk
Department of Chemistry, Gorlaeus Laboratories,
Leiden University P.O. Box 9502,
NL-2300 RA Leiden (The Netherlands)

[**] We thank *S. Gorter* for providing the data set for the X-ray structure analysis and *R. A. G. de Graaff* for assistance in solving the X-ray structure. Further we also thank *M. van Roon* for providing an alternative reaction path to the title compound.—ddtp = 1,5-bis(3′,5′-dimethylpyrazolyl)-3-thiapentane

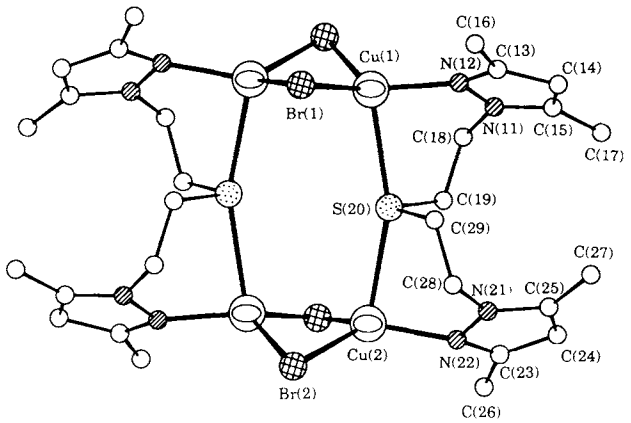

Fig. 1. Structure of the tetranuclear Cu^{I} complex $[Cu_4(ddtp)_2Br_4]$ (PLUTO projection [5]; hydrogen atoms are omitted for clarity).

(270 pm) is somewhat smaller than the Cu···Cu distances in other Cu^{I} compounds with comparable bridges (e.g. 274 and 286 pm[6]; 288 and 284 pm[7]). This distance and the acute Cu–Br–Cu angles (54.4 and 57.8°) suggest some $Cu^{I}\cdots Cu^{I}$ interaction. Two Cu_2Br_2 fragments are linked together by two ddtp ligands, bringing the four copper atoms into a rectangular arrangement. The ligand links the Cu_2Br_2 fragments together through its two ligating nitrogen atoms as well as through the thioether sulfur, which bridges two copper ions of different Cu_2Br_2 fragments. Thus Cu···Cu distances of 270 and 524 pm are observed in this complex. A striking feature is that the Cu–S–Cu angle (160.6°) is significantly larger than any other Cu–S–Cu angle reported so far. Some angles found in other X-ray structures are 79.4[7], 109.8[8], 112.2[8], 116.2[8] and 118.6°[9]. The C–S–Cu angles are 96.9 and 97.0° respectively. The Cu···S distances are 264 and 268 pm. The occurrence of both bromide and thioether bridges in a tetranuclear Cu^{I} compound, together with the relatively short Cu···Cu distances, make this air-stable compound truly unique.

Received: June 13, 1990 [Z 4014 IE]
German version: *Angew. Chem. 102* (1990) 1454

CAS Registry number: $[Cu_4(ddtp)_2Br_4]$, 130642-00-1.

[1] W. G. Haanstra, W. L. Driessen, A. L. E. Stoffels and J. Reedijk, *Inorg. Chim. Acta*, in press.

[2] *Method:* To a solution of $CuBr_2$ (670 mg, 3 mmol) in an ethanol/acetone (1:1 v/v) mixture (25 mL) at 70 °C was added a solution of ddtp (840 mg, 3 mmol) in a boiling ethanol/acetone (1:1 v/v) mixture (30 mL). Soon the solution turned milky and transparant crystals started to separate. The crystals were collected by decantation, washed with ether, and dried in air. Yield: 550 mg (65%).

[3] *Method:* Under a nitrogen atmosphere a warm solution of CuBr (390 mg, 2.72 mmol), in a 5 mL ethanol/acetonitrile (1:2 v/v) mixture, was added to a warm solution of ddtp (380 mg, 1.36 mmol) in 5 mL methanol. The crystals were collected by filtation, washed with ether, and dried in air. Yield: 540 mg (70% Cu).

[4] Crystal dimensions 0.20 × 0.20 × 0.15 mm, space group $P2_1/c$, $a = 871.5(3)$, $b = 1523.3(2)$, $c = 1479.9(2)$ pm, $\beta = 100.18(2)°$, $V = 1934 \times 10^6$ pm^3, $Z = 4$. Enraf-Nonius CAD-4 diffractometer with graphite monochromatized $Mo_{K\alpha}$ radiation, $\omega/2\theta$ scan, $2° \leq \theta \leq 27.5°$, 1314 independent reflections with $I > 2\sigma(I)$. The structure was solved using Patterson and difference Fourier methods. Non-hydrogen atoms were refined anisotropically and the hydrogen atoms placed at 96 pm from the parent atom and refined with one overall isotropic thermal parameter. The residuals after the last cycle of a full matrix refinement were $R = 0.035$ and $R_w = 0.056$ with $W = 1/\sigma^2$. Selected distances [pm] and bond angles [°]: Cu1-Cu2 270.6(2), Br1-Br2 395.4(2), Cu1-Br1 237.6(2), Cu1-Br2 250.8(2), Cu2-Br1 246.2(2), Cu2-Br2 246.1(2), Cu1-N12 197.4(8), Cu2-N22 200.2(9), Cu1-S20 268.4(4), Cu2-S20 264.5(4); Br1-Cu1-Br2 108.08(7), Br1-Cu2-Br2 106.86(7), Br1-Cu1-N12 127.2(3), Br2-Cu1-N12 114.5(3), Br1-Cu2-N22 122.2(3), Br2-Cu2-N22 122.3(3), Br1-Cu1-S20 104.5(1), Br2-Cu1-S20 113.6(1), Br1-Cu2-S20 102.2(1), Br2-Cu2-S20 110.15(9), C19-S20-C29 103.8(5), Cu1-Br1-Cu2 67.98(6), Cu1-Br2-Cu2 65.98(6), Cu1-S20-Cu2 160.6(1), N12-Cu1-S20 85.9(3), N22-Cu2-S20 88.6(3). Further details of the crystal structure investigations may be obtained from the director of the Cambridge Crystallographic Data Centre, University Chemical Laboratory, Lensfield Road, GB-Cambridge CB2 1EW, on quoting the complete journal citation.

[5] W. D. S. Motherwell and W. Clegg, *PLUTO, a program for plotting molecular and crystal structures*, Univ. of Cambridge, England 1978.

[6] J. C. Barnes, J. D. Paton, *Acta Crystallogr., Sect. B, 26* (1970) 1414.

[7] J. Willemse, W. P. Bosman, J. H. Noordik, J. A. Cras, *Recl. Trav. Chim. Pays-Bas 102* (1983) 477.

[8] E. W. Ainscough, A. M. Brodie, J. M. Husbands, *J. Chem. Soc. Dalton Trans. 1985* 151.

[9] J. S. Filippo, Jr., L. E. Zyontz, J. Potenza, *Inorg. Chem. 14* (1975) 1167.

Asymmetric Protonation of Enolates**

By *Dominique Potin, Kevin Williams*, and *Julius Rebek, Jr.**

An effective, chiral proton source is a desirable goal of modern organic synthesis, since it could lead to asymmetric carbonyl compounds from readily available enolates. Progress in this areas has been made by several groups, especially those of *Duhamel*,[1] *Hünig*[2] and *Fehr*,[3] using the chiral proton sources **1, 2** and **3**, respectively. If proton transfer

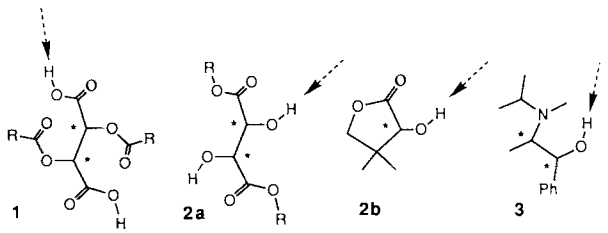

from these materials takes place along the expected trajectories (indicated by arrows), it would appear that the asymmetric centers are less than ideally placed to influence the course of the reaction. Even if intramolecular hydrogen bonding is involved (as seems to be a common feature of these sources), the enolate carbon could be quite remote from the asymmetric environment in the transition structure. We have prepared some new structures in which the proton is buried within an asymmetric environment; they have been useful as chiral auxiliaries in cycloadditions[4] and alkylation reactions.[5] Here we report their application to the asymmetric protonation of enolates.

The compounds are derivatives of Kemp's tricarboxylic acid **4**[6] and they are readily prepared as previously described.[4] Condensation of **4** with urea, followed by reaction with $SOCl_2$ gives the acid chloride **5a**, with which optically active amines can be acylated with formation of **5b**. Reduction with $NaBH_4$ followed by acid treatment gives the tricyclic lactams **6**. The diastereomers are obtained as an easily separable mixture,[7] and the X-ray crystal structure[8] of one of the diastereomers **6a** of the (*R*)-naphthylethyl series is shown in Figure 1. This reveals that the acidic NH bond

[*] Prof. J. Rebek Jr., D. Potin, K. Williams
Departments of Chemistry
University of Pittsburgh, Pittsburgh, PA 15260
and the Massachusetts Institute of Technology,
Cambridge, MA 02139 (USA)

[**] This work was supported by Hoechst Celanese and Rhône-Poulenc Sauté (Fellowship to *D. P.*).

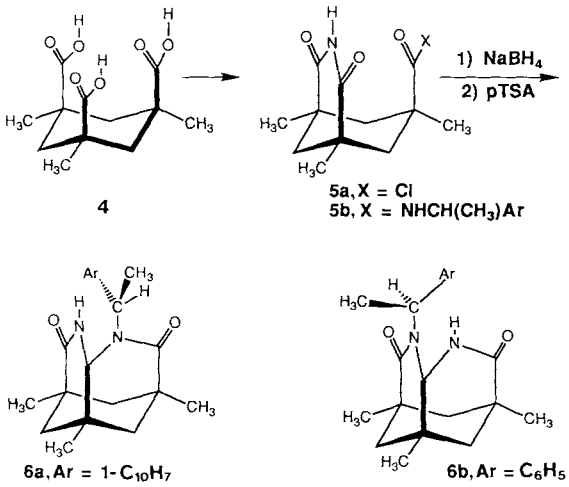

is buried within an asymmetric microenvironment; the NH signal in the ^{1}H-NMR spectrum of this diastereomer is shifted upfield ($\delta = 3.5$ in $CDCl_3$), indicating shielding by the aromatic surface. From (*S*)-phenethylamine the diastereomer **6b** was obtained.

Fig. 1. X-ray crystal structure of **6a** [8].

Initially, the test enolate **8a** described by *Hünig* et al.[2] in which the enolate geometry is fixed by means of a cyclic arrangement was protonated. An enantiomeric excess (*ee*) of up to 53% had been observed with the α-hydroxycarbonyl compound **2b**. The relatively weak basicity of **8a** and the weak acidity of the dilactams **6** led to unreproducible results.[9] However, a series of alkyl substituted enolates, **8b**–**8f**, were successfully protonated (Table 1).

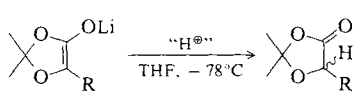

8 **9**

a, R = Ph; **b**, R = Me; **c**, R = Et; **d**, R = *n*Bu; **e**, R = *i*Pr; **f**, R = *t*Bu; **g**, R = Bn

In relating the stereochemistry of the product to the shape of the dilactam, a reasonable transition structure, **10**, can be proposed. The lithium is likely to be chelated between the two oxygens in the structure shown, and the second point of contact is at the proton to be transferred. Finally, steric interactions in **10** were also significant:[11] Larger groups R remain outside of the cavity, with selectivity according to their sizes; small groups, e.g. **8b**, show negligible preference. These considerations lead to the absolute stereochemistry observed for the products **9**.

Table 1. Asymmetric protonation of the enolates **8** with **6a** and **6b**.

Enolate	Proton source	*ee* [%] [a]/ Configuration [b]
8a	**6a**	0
8b	**6a**	9/(*R*)
8c	**6a**	28/(*S*)
8d	**6a**	33/(*S*)
8e	**6a**	76/(*S*)
8f	**6a**	91/(*S*)
8f	**6b**	72/(*R*)
8g	**6a**	50/(*S*)

[a] Determined by ^{1}H-NMR spectroscopy with (*S*)-1-(9-anthryl)-2,2,2-trifluoroethanol as the chiral shift reagent [10]. [b] Determined by polarimetry on **9**; cf T. Polonski, *Tetrahedron 39* (1983) 3131.

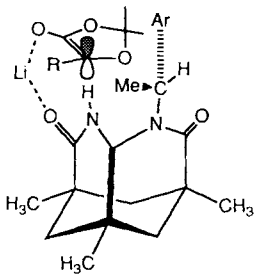

10

Experimental

In a typical experiment, the dioxolanone [12] (1 mmol) was added to a solution of lithium diisopropylamide (1.3–1.5 mmol) in THF (5 mL) at −78 °C. After the reaction mixture had been stirred for 20 min (−78 °C to −30 °C), the solution was cooled to −78 °C and transferred to a flask containing a suspension of the dilactam (1.7–7.8 mmol) in THF (5 mL) at −78 °C. After 10 min, the reaction mixture was allowed to warm to room temperature. It was then treated with 10 mL of CH_2Cl_2 and 3 mL of saturated NH_4Cl solution. The organic layer was washed with HCl (10%) and saturated $NaHCO_3$ solution, and dried over $MgSO_4$. After concentration, the dilactam was precipitated by addition of pentane (1 mL) and the supernatant solution was evaporated and the products **9** were distilled (yield > 80%).

Received: June 15, 1990 [Z 4020 IE]
German version: *Angew. Chem. 102* (1990) 1485

[1] a) L. Duhamel, P. Duhamel, J. C. Launay, J. C. Plaquevent, *Bull. Soc. Chim. Fr. 2 1984*, 421; b) L. Duhamel, J. C. Plaquevent, *Tetrahedron Lett. 21* (1980) 2521; c) L. Duhamel, S. Fouquay, J. C. Plaquevent, *ibid. 27* (1986) 4975.
[2] U. Gerlach, S. Hünig, *Angew. Chem. 99* (1987) 1323; *Angew. Chem. Int. Ed. Engl. 26* (1987) 1283.
[3] C. Fehr, J. Galindo, *J. Am. Chem. Soc. 110* (1988) 6909.
[4] D. P. Curran, K. S. Jeong, T. A. Heffner, J. Rebek, Jr., *J. Am. Chem. Soc. 111* (1989) 9238.
[5] K. S. Jeong, K. Parris, P. Ballester, J. Rebek, Jr., *Angew. Chem. 102* (1990) 550; *Angew. Chem. Int. Ed. Engl. 29* (1990) 555.
[6] D. S. Kemp, K. S. Petrakis, *J. Org. Chem. 46* (1981) 5140. For a convenient synthesis see J. Rebek, Jr., B. Askew, M. Killoran, D. Nemeth, F.-T. Lin, *J. Am. Chem. Soc. 109* (1987) 2426.

[7] The overall yield of **6a** from Kemp's tricarboxylic acid was 44%: m.p. 195–196 °C, $[\alpha]_D = 89.7°$ ($c = 1.51$, CH_2Cl_2). For **6b** (43%) m.p. 107–109 °C, $[\alpha]_D = -252°$ ($c = 1.04$, CH_2Cl_2). All the new compounds were characterized by a full complement of high-resolution spectra.
[8] Further details of the crystal structure investigation are available on request from the Director of the Cambridge Crystallographic Data Centre, University Chemical Laboratory, Lensfield Road, GB-Cambridge CB2 1EW (UK), on quoting the full journal citation.
[9] J. Rebek, Jr. *Chemtracts 2* (1989) 337; J. Rebek, Jr. *Angew. Chem. 102* (1990) 261; *Angew. Chem. Int. Ed. Engl. 29* (1990) 245. The results reported in these papers for protonation of **8a** are in error.
[10] W. H. Pirkle, D. L. Sikkenga, M. S. Pavlin, *J. Org. Chem. 42* (1977) 384.
[11] W. H. Pirkle, T. C. Pochapsky, *Chem. Rev. 89* (1989) 347; J. Rebek, Jr., B. Askew, P. Ballester, M. Doa, *J. Am. Chem. Soc. 109* (1987) 4119.
[12] M. Farines, J. Soulier, *Bull. Soc. Chim. Fr.* (1970) 332.

Chiral Lithium-1-oxyalkanides by Asymmetric Deprotonation; Enantioselective Synthesis of 2-Hydroxyalkanoic Acids and Secondary Alkanols**

By *Dieter Hoppe,* Folker Hintze*, and *Petra Tebben*

α-Lithiated ethers **4a** and acetals **4b** are of great preparative importance as umpoled synthetic building blocks[1] for the nucleophilic introduction of 1-oxyalkyl groups. As long as R^1 is not a stabilizing group like aryl, 1-alkenyl or 1-alkynyl, the lithium compounds **4** cannot be generated by simple deprotonation of **3** at low temperature. The reagents **4a** or **4b** are therefore prepared, in general, by transmetalation[3] of the stannanes **1** or by reductive cleavage of the monothioacetals **2**.[4] Some racemic α-lithioalkyl benzoates with sterically shielded carbonyl groups, such as **4c**, were generated by deprotonation;[5] however, the subsequent cleavage of the aroyl group presents difficulties.

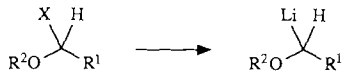

1, X = $SnBu_3$
2, X = SAr
3, X = H

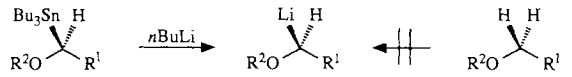

(*S*)-**1** (*S*)-**4** **3**

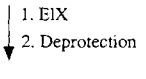

R^1 = Alkyl
a, R^2 = Alkyl
b, R^2 = 1-Alkoxyalkyl
c, R^2 = (2,4,6-*i*Pr)$_3$$C_6H_2C(=O)$

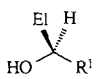

(*R*)- or (*S*)-**5**

The lithiodestannylation of (*S*)-**1** and subsequent electrophilic substitutions to (*R*)- or (*S*)-**5** proceed with retention of configuration,[6] i.e. the intermediate (*S*)-**4** is configurationally stable. The required non-racemic stannanes (*R*)- or (*S*)-**1** were obtained by optical resolution,[6a, b] asymmetric reduction of acylstannanes,[6d, e] or oxidation of α-trialkylstannyl boronates.[6f] We now report on the hitherto simplest entry to chiral synthetic building blocks of type **3**; it comprises an enantiotopically differentiating deprotonation of the precursor **3** in the presence of (-)sparteine[7] and is made possible by a protecting group R^2 of the carbamate type[9], which activates through chelate and dipole stabilization and which is cleavable under mild conditions.[8] We obtained the carbamates **10**[10] from the spirocyclic oxazolidine[11] **6** by acylation with the corresponding alkoxycarbonyl chlorides **7** (route A) or via the carbamoyl chloride (ClC=O for H in **6**) and reaction with sodium alkoxides **9** (route B) in yields of 87 to 95%. Treatment of the esters **10** with *sec*-butyllithium in ether/*N*,*N*,*N*′,*N*′-tetramethylethylenediamine (TMEDA) at −78 °C leads to the persistent lithium compounds *rac*-**11** · TMEDA, which were trapped as silanes[9] *rac*-**12** (Table 1).

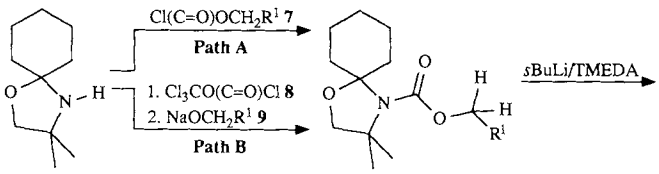

6 **10**

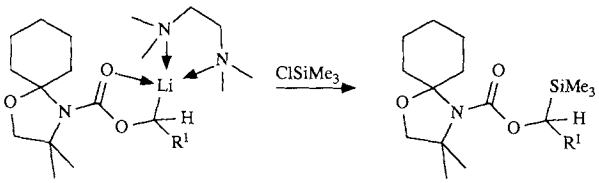

rac-**11**•TMEDA *rac*-**12**

a, R^1 = H **d**, R^1 = $(CH_2)_5CH_3$
b, R^1 = CH_3 **e**, R^1 = $CH(CH_3)_2$
c, R^1 = $(CH_2)_2CH_3$

The deprotonation of the carbamate **10b** under otherwise the same conditions in the presence of (−)-sparteine[7], (−)-**13**, instead of TMEDA leads to the uniformly configurated complex (*S*)-**11b** · (−)-**13** with high diastereomeric excess; i.e. the reagent discriminates between the enantiotopic α-protons in **10**. This is confirmed by carboxylation[12] to the

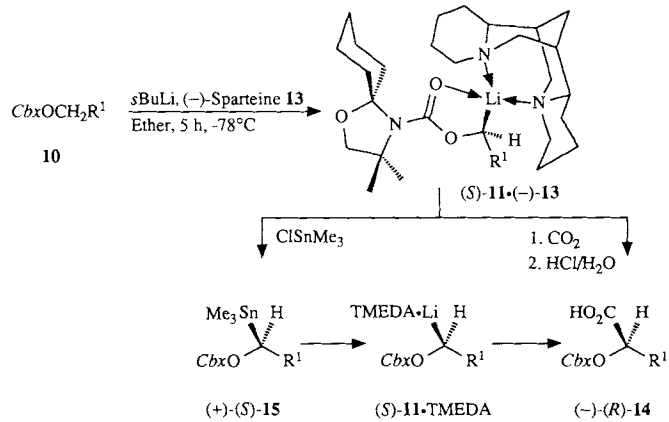

10 (*S*)-**11**•(−)-**13**

(+)-(*S*)-**15** (*S*)-**11**•TMEDA (−)-(*R*)-**14**

[*] Prof. Dr. D. Hoppe, F. Hintze, Dipl. Chem. P. Tebben
Institut für Organische Chemie der Universität
Olhausenerstraße 40, D-2300 Kiel 1

[**] This work was supported by the Deutsche Forschungsgemeinschaft and the Fonds der Chemischen Industrie.

(*R*)-lactic acid derivative (*R*)-**14b**,[10, 13] which is formed with > 95% *ee*.[14] Analogous results are achieved with the long-chain or β-branched carbamates **10c–e** (Table 1).

Table 1. Substitution products prepared from **10a–e**.

Product	R^1	Electrophile	Yield [%]	$[\alpha]_D^{22-23}$	*ee* [%]
rac-**12a**[a]	H	Me_3SiCl	97	–	–
rac-**12b**[a]	CH_3	Me_3SiCl	70	–	–
(*S*)-**12b**	CH_3	Me_3SiCl	67	−22.5[b]	–
rac-**14b**[a]	CH_3	CO_2	60	–	–
(*R*)-**14b**	CH_3	CO_2	75	−22.3[c]	>95
rac-**14c**[a]	$(CH_2)_2CH_3$	CO_2	65	–	–
(*R*)-**14c**	$(CH_2)_2CH_3$	CO_2	78	−12.6[c]	>95
rac-**14d**[a]	$(CH_2)_5CH_3$	CO_2	62	–	–
(*R*)-**14d**	$(CH_2)_5CH_3$	CO_2	70	−12.4[c]	>95
(*R*)-**14e**	$CH(CH_3)_2$	CO_2	52	−17.3[c]	>95
(*S*)-**15b**	CH_3	Me_3SnCl	76	+35.4[b]	>95
(*S*)-**15c**	$(CH_2)_2CH_3$	Me_3SnCl	62	+35.2[b]	>95
(*S*)-**15d**	$(CH_2)_5CH_3$	Me_3SnCl	86	+34.2[b]	>95
(*S*)-**15e**	$CH(CH_3)_2$	Me_3SnCl	62	+23.5[b]	>95
(*S*)-**16**	$(CH_2)_5CH_3$	CH_3I	81	+14.1[c]	96

[a] With TMEDA as ligand. [b] c = 1.4–2.8, CH_2Cl_2. [c] c = 1.1–1.9, acetone.

The reaction of (*S*)-**11b** · (−)**13** with trimethyltin chloride yields the stannane (+)-(*S*)-**15b**, whose transmetalation to (*S*)-**11b** · TMEDA in ether and reaction with carbon dioxide likewise leads to the carboxylic acid (*R*)-**14b** with > 95% *ee* (yield 63%). Restannylation of (*S*)-**11e** · TMEDA again afforded (+)-(*R*)-**15e** (yield 83%). The quoted (*S*)-configuration for **11** in the (−)-sparteine complex is based on the well-founded assumption that here, as in all the other cases investigated, the lithium α-oxyalkanide is substituted by electrophiles with retention.[6, 12, 15] In contrast, in the case of a similar benzyllithium derivative we observed an inversion for carboxylation and stannylation.[16] As checked with the complex **11d** · (−)-**13** (obtained from **10d**), the methylation also proceeds highly stereoselectively; the (*S*)-2-octylcarbamate (+)-(*S*)-**16** is obtained with 96% *ee*.[17] The *Cbx* group is cleaved under mild conditions, as was demonstrated on (*S*)-**16**. The methanolysis of the aminoketal **16** under acid catalysis leads to the urethane **17**, which, upon addition of barium hydroxide, is hydrolyzed to the alcohol (+)-(*S*)-**18**.

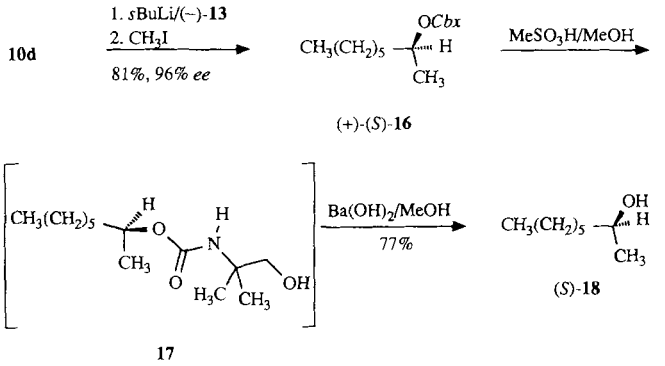

Table 2. Selected physical data of the compounds **10–18**.

10b: Route A; yield 87%; colorless solid; m.p. 42 °C; b.p. 100 °C/2.25 mbar; ^{1}H NMR ($CDCl_3$): δ = 4.06 (q, ^3J(H,H) = 7.1 Hz, 2H; OCH_2), 3.61 (s, 2H; CH_2), 2.00–2.40 (m, 2H; cyclohexyl), 1.40–1.70 (m, 8H; cyclohexyl), 1.30 (s, 6H; CH_3), 1.21 (t, ^3J(H,H) = 7.1 Hz, 3H; CH_3)

10d: Route B; yield 95%; colorless oil; R_F = 0.62 (ether/*n*-pentane 1:1); ^{1}H NMR ($CDCl_3$): δ = 4.07 (t, ^3J(H,H) = 6.6 Hz, 2H; OCH_2), 3.69 (s, 2H; CH_2), 2.00–2.50 (m, 2H; cyclohexyl), 1.70–1.48 (m; cyclohexyl, heptyl-CH_2, CH_3), 1.48–0.85 (m; cyclohexyl, heptyl-CH_3)

12a: colorless solid; m.p. 89 °C; ^{1}H NMR ($CDCl_3$): δ = 3.72 (s, 2H; CH_2), 3.69 (s, 2H; OCH_2), 2.10–2.50 (m, 2H; cyclohexyl), 1.70–1.35 (m, 14H; cyclohexyl, CH_3), 0.11 (s, 9H; $Si(CH_3)_3$)

(*S*)-**12b**: colorless oil; R_F = 0.64 (ether/*n*-pentane 1:1); ^{1}H NMR ($CDCl_3$): δ = 4.65 (q, ^3J(H,H) = 7.4 Hz, 1H; CH), 3.68 (s, 2H; CH_2), 2.50–2.10 (m, 2H; cyclohexyl), 1.70–1.35 (m, 14H; cyclohexyl, CH_3), 1.26 (d, ^3J(H,H) = 7.4 Hz, 3H; CH_3), 0.60 (s, 9H; $Si(CH_3)_3$)

(*R*)-**14b**: colorless crystals; m.p. 112 °C; ^{1}H NMR ($CDCl_3$): δ = 8.90–8.00 (br. s, 1H; COOH), 5.09/5.10 (q, ^3J(H,H) = 7.1 Hz, 1H; CH), 3.72/3.71 (s, 2H; CH_2), 2.50–2.05 (m, 2H; cyclohexyl), 1.55 (d, ^3J(H,H) = 7.1 Hz, 3H; CH_3), 1.85–1.00 (m, 14H; cyclohexyl, CH_3)

(*R*)-**14b**-methyl ester: colorless oil; R_F = 0.50 (ether/*n*-pentane 1:1); ^{1}H NMR ($CDCl_3$): δ = 5.09/5.10 (q, ^3J(H,H) = 7.1 Hz, 1H; CH), 3.75 (s, 3H; OCH_3), 3.72/3.71 (s, 2H; CH_2), 2.50–2.00 (m, 2H; cyclohexyl), 1.66–1.00 (m, 14H; cyclohexyl, CH_3), 1.51 (d, ^3J(H,H) = 7.1 Hz, 3H; CH_3)

(*S*)-**15b**: colorless solid; m.p. 34 °C; ^{1}H NMR ($CDCl_3$): δ = 4.58 (q, ^3J(H,H) = 7.6 Hz, 1H; CH), 3.68 (s, 2H; CH_2), 2.20–2.40 (m, 2H; cyclohexyl), 1.10–1.70 (m, 14H; cyclohexyl, CH_3), 1.53 (d, ^3J(H,H) = 7.6 Hz, 3H; CH_3), 0.099 (s, 9H; $Sn(CH_3)_3$)

(*S*)-**16**: colorless oil; R_F = 0.69 (ether/*n*-pentane 1:1); ^{1}H NMR ($CDCl_3$): δ = 4.84 (t, ^3J(H,H) = 6.2 Hz, 1H; CH), 3.68 (s, 2H; CH_2), 2.55–2.00 (m, 2H; cyclohexyl), 1.75–1.00 (m, 24H; cyclohexyl, heptyl-CH_2, CH_3), 1.12 (d, ^3J(H,H) = 6.2, 3H; CH_3), 0.88 (t, ^3J(H,H) = 6.7 Hz, 3H; heptyl-CH_3)

Experimental

A solution of 2.8 mmol of *s*BuLi (in cyclohexane/isopentane) in 8 mL of ether was cooled to −78 °C and treated with 2.9 mmol of (−)-sparteine, (−)-**13**. After 10 minutes' stirring and injection of a solution of 2.0 mmol of the carbamate **10** in 2 mL ether, the mixture was stirred for 5–6 h at −78 °C. After introduction of carbon dioxide (excess) into the solution of (*S*)-**11** · (−)-**13** (for the synthesis of **14**) or addition of 3.5 mmol of trimethyltin chloride or methyl iodide (for the synthesis of **15** or **16**), the reaction mixture was stirred for 16 h at −78 °C. Work-up was carried out as usual with 10 mL of ether/10 mL of 2N HCl, and the crude product was purified by flash chromatography on silica gel with ether/pentane mixtures. The racemates *rac*-**11** · TMEDA were generated in the same way, but with 2.9 mmol of TMEDA instead of (−)-sparteine.

For cleavage of the *Cbx* group a solution of 2 mmol of **16** in 10 mL of methanol was heated under reflux with 0.1 mL of methanesulfonic acid for 16 h. Finally, 1.0 g of $Ba(OH)_2 \cdot 8H_2O$ was added to the mixture, which was heated under reflux for a further 4 h before workup in the usual way in aqueous medium and purification of the crude product on silica gel by flash chromatography.

Received: July 5, 1990 [Z 4052 IE]
German version: *Angew. Chem. 102* (1990) 1457

[1] Reviews: a) D. Seebach, *Angew. Chem. 91* (1979) 259–278; *Angew. Chem. Int. Ed. Engl. 18* (1979) 239–258; b) J. E. Saavedra in T. A. Haase (Ed.): *Umpoled Synthons*, Wiley, New York 1987, p. 101.

[2] At high temperature Wittig rearrangements occur; review: T. Nakai, K. Mikami, *Chem. Rev. 86* (1986) 885–902.

[3] a) W. C. Still, A. Mitra, *J. Am. Chem. Soc. 100* (1978) 1927–1928; b) J. S. Sawyer, A. Kucerovy, T. L. Macdonald, G. J. McGarvey, *ibid. 110* (1988) 842–853.

[4] a) Review: T. Cohen, M. Bhupathy, *Acc. Chem. Res. 22* (1989) 152–161; b) T. Cohen, M. T. Lin, *J. Am. Chem. Soc. 106* (1984) 1130–1131; c) A. Fernandez-Mayoralas, A. Marra, M. Trumtel, A. Veyrières, P. Sinaÿ, *Tetrahedron Lett. 30* (1989) 2537–2540; d) S. D. Rychnovsky, D. E. Mickus, *ibid. 30* (1989) 3011–3014.

[5] a) P. Beak, B. G. McKinnie, *J. Am. Chem. Soc. 99* (1977) 5213; b) P. Beak, L. G. Carter, *J. Org. Chem. 46* (1981) 2363–2373; c) R. Schlecker, D. Seebach, W. Lubosch, *Helv. Chim. Acta 61* (1978) 512–526.

[6] a) W. C. Still, C. Sreekumar, *J. Am. Chem. Soc. 102* (1980) 1201–1202; b) V. J. Jephcote, A. J. Pratt, E. J. Thomas, *J. Chem. Soc. Chem. Commun. 1984*, 800–802; *J. Chem. Soc. Perkin Trans. 1 1989*, 1529–1535; c) P. Lesimple, J.-M. Beau, P. Sinaÿ, *J. Chem. Soc. Chem. Commun. 1985*, 894–895; d) J. A. Marshall, W. Y. Gung, *Tetrahedron 45* (1989) 1043–1052; e) J. M. Chong, E. K. Mar, *ibid. 45* (1989) 7709–7716; f) D. S. Matteson, P. B. Tripathy, A. Sarkur, K. N. Sadhu, *J. Am. Chem. Soc. 111* (1989) 4399–4402; g) R. J. Linderman, A. Ghannam, *ibid. 112* (1990) 2392–2398.

[7] For earlier attempts at the chiral modification of organolithium compounds by (−)-sparteine: a) H. Nozaki, T. Aratani, T. Toraya, R. Noyori, *Tetrahedron 27* (1971) 905–913; b) L. M. Engelhardt, W.-P. Leung, C. L.

Raston, G. Salem, P. Twiss, A. H. White, *J. Chem. Soc. Dalton Trans. 1988*, 2403–2409. Asymmetric deprotonations of 2-alkenyl carbamates: c) D. Hoppe, O. Zschage, *Angew. Chem. 101* (1989) 67–69; *Angew. Chem. Int. Ed. Engl. 28* (1989) 65–67; d) O. Zschage, J.-R. Schwark, D. Hoppe, *ibid. 102* (1990) 336–337 and *29* (1990) 296–297.

[8] N. G. Rondan, K. N. Houk, P. Beak, W. J. Zajdel, J. Chandrasekhar, P. von R. Schleyer, *J. Org. Chem. 46* (1981) 4108–4110; cf. also D. Seebach, J. Hansen, P. Seiler, J. M. Gromek, *J. Organomet. Chem. 285* (1985) 1–13.

[9] Review: D. Hoppe, *Angew. Chem. 96* (1984) 930–946; *Angew. Chem. Int. Ed. Engl. 23* (1984) 932–948.

[10] All the new compounds gave correct elemental analyses (C,H ± 0.3%)

[11] P. Mickon, A. Rassat, *Bull. Soc. Chim. Fr. 1971*, 3561–3567.

[12] During the preparation of the manuscript a paper concerning the carboxylation of enantiomerically enriched α-(benzyloxymethyl)alkanides of the type **4b** appeared in the literature: P. C.-M. Chan, J. M. Chong, *Tetrahedron Lett. 31* (1990) 1985–1988.

[13] Correlated as **14b**-methyl ester with a sample obtained from (*R*)-lactic acid.

[14] For the determination of the *ee* value the acids **14** were first converted with diazomethane into their methyl esters and subsequently measured with 5–8 mol-% tris-[(heptafluoropropylhydroxymethylene)-D-campherato] europium(III), $Eu(hfpc)_3$, on a 300 MHz spectrometer on the basis of the α-H signal. The absorption bands are in each case doubled, due to amide-*E*/*Z* isomerism. The enantiomeric(*S*)-**14** methyl esters were not detectable in any of the samples.

[15] Theoretical studies on the carboxylation: E. Kaufmann, S. Sieber, P. von R. Schleyer, *J. Am. Chem. Soc. 111* (1989) 4005–4008.

[16] D. Hoppe, A. Carstens, T. Krämer, *Angew. Chem. 102* (1990) 1455; *Angew. Chem. Int. Ed. Engl. 29* (1990) 1424.

[17] Determined gas-chromatographically on the alcohol **18** as (−)-(*S*)-phenylethylurethane, 98:2; W. H. Pirkle, M. S. Hoekstra, *J. Org. Chem. 39* (1974) 3904–3906.

Generation of a Configurationally Stable Chiral Benzyllithium Derivative, and the Capricious Stereochemistry of Its Electrophilic Substitution**

By *Dieter Hoppe,** *Axel Carstens*, and *Thomas Krämer*

Dedicated to Professor Jürgen Bestmann on the occasion of his 65th birthday

Chiral benzyl alkali metal derivatives **1A** undergo rapid racemization in solution via an ion pair **1B** with planar configurated carbanion; hence, the chiral information of the optically active precursor is generally lost during its generation.[1] Some α-sulfonylbenzyl anions constitute an exception.[2]

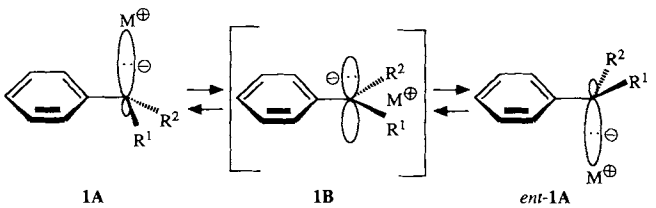

1A **1B** *ent*-**1A**

Short-lived benzyl anions have been trapped in situ with high enantiomeric excesses by deprotonation/reprotonation of optically active phenyl alkanes[1] as well as in the Haller-Bauer cleavage of tertiary benzyl phenyl ketones.[3] Chiral α-oxybenzyl anions are trapped as short-lived intermediates in the Brook[4] and reverse Brook rearrangement.[5]

[*] Prof. Dr. D. Hoppe, A. Carstens, Dr. T. Krämer
Institut für Organische Chemie der Universität
Olshausenstrasse 40, D-2300 Kiel 1 (FRG)

[**] This work was supported by the Deutsche Forschungsgemeinschaft and the Fonds der Chemischen Industrie.

Although non-racemic, heterosubstituted benzyllithium derivatives, e.g. carbanions derived from tetrahydroisoquinolines,[6,7] play an important role in enantioselective synthesis, knowledge of the stereochemical course of their electrophilic substitution is very limited. The reason for this is that the extent to which the chiral auxiliary influences the properties of the carbanionic center is unknown.[8] We now report on the generation of an enantiomerically enriched benzyllithium derivative which is practically configurationally stable at low temperatures, and which, like some allyllithium derivatives synthesized by us,[9] is free of such complications. Furthermore, we have investigated the stereochemistry of some important substitution reactions.

The *N*,*N*-diisopropyl carbamate[10,11] (*R*)-**2**, obtained from (*R*)-1-phenylethanol[12] (97% *ee*[13]), was deprotonated with *sec*-butyllithium/*N*,*N*,*N*′,*N*′-tetramethylethylenediamine (TMEDA) in hexane below −70 °C,[14] and after 30 min the intermediary lithium alkanide (*R*)-**3**[15,16] was trapped with chlorotrimethylsilane. The silane (−)-**4**[17] of unknown absolute configuration was obtained with 96% *ee*.[18] This means that maximally 1% racemization occurs over the two reaction steps. Protonation of (*R*)-**3** with methanol leads to the initial carbamate (*R*)-**2** again, whereas with acetic acid inversion takes place with formation of (*S*)-**2**.

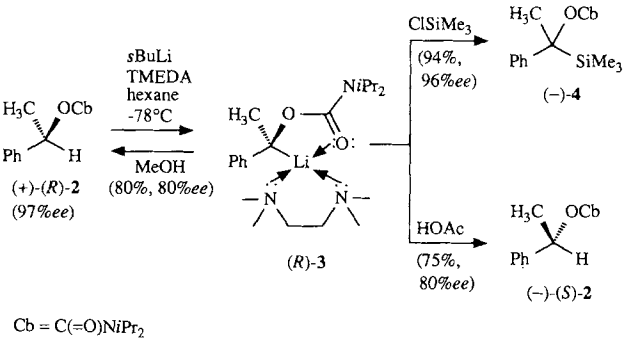

Cb = C(=O)N*i*Pr$_2$

The alkylation of (*R*)-**3** with *n*-propyl bromide proceeds with retention of the configuration; the tertiary carbamate[17,18] (−)-(*S*)-**5** was correlated stereochemically with the known carbinol (−)-(*S*)-**6**.[19]

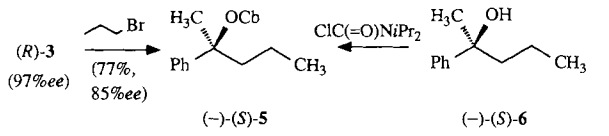

(*R*)-**3** reacts with dimethyl carbonate with retention of configuration, but with methoxycarbonyl chloride with inversion, to give the methyl ester[17,18] (−)-(*R*)-**7**[20] and (+)-(*S*)-**7**, respectively. Surprisingly, carbon dioxide like-

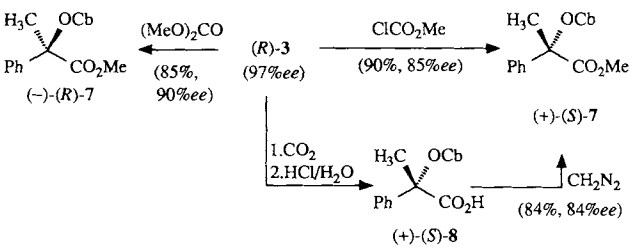

wise adds with inversion and furnishes the acid (+)-(*S*)-**8**; normally, the carboxylation of alkyllithium compounds proceeds with retention.[21]

A particularly unexpected result was that of the stannylation-lithiodestannylation sequence starting from (*R*)-**3**: it leads via (+)-(*R*)-**9**[17, 22] to the lithium compound (*S*)-**3** (detected by trapping with dimethyl carbonate as (+)-(*S*)-**7** or with chlorotrimethylstannane as (−)-(*S*)-**9**); i.e. one of the two reaction steps proceeds with inversion, the other with retention.

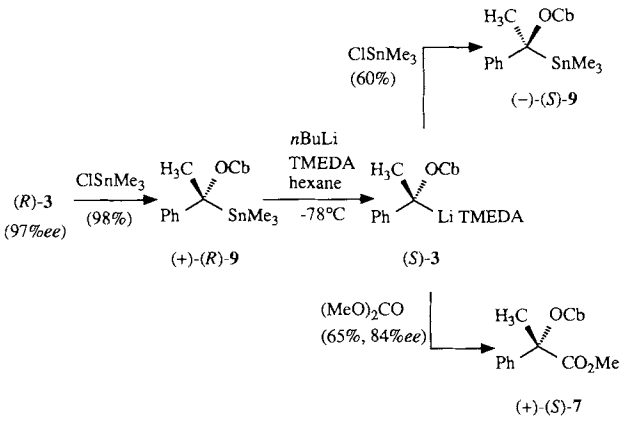

Table 1. Selected physical data of the new compounds **2**–**9**.

(*R*)-**2**: colorless oil; 97% *ee*; $[\alpha]_D^{20}$ + 5.1 (CH_2Cl_2, *c* = 1.2); ^{1}H NMR ($CDCl_3$): δ = 1.20 [d, *J* = 6.8 Hz, NCH(CH_3)$_2$], 1.55 (d, *J* = 6.6 Hz, 1-CH_3), 3.94 (m, NCH), 5.85 (q, 1-H), 7.22–7.44 (m, Ph)

(−)-**4**: colorless oil; 96% *ee*; $[\alpha]_D^{20}$ = − 17.3 (CH_2Cl_2, *c* = 1.0); ^{1}H NMR ($CDCl_3$): δ = 0.01 [s, Si(CH_3)$_3$], 1.24 [m, NCH(CH_3)$_2$], 1.90 (s, 1-CH_3), 3.93 (m, NCH), 7.07–7.30 (m, Ph)

(*S*)-**5**: colorless oil; 85% *ee*; $[\alpha]_D^{20}$ − 29.9 (CH_2Cl_2, *c* = 1.2); ^{1}H NMR ($CDCl_3$): δ = 0.87 (t, $J_{3,4}$ = 7.2 Hz, 4-CH_3), 1.15–1.32 [m, NCH(CH_3)$_2$ 3-H_2), 1.84 (s, 1-CH_3), 1.85–2.14 (m, 2-H_2), 3.77 and 4.04 (each m, NCH), 7.16–7.37 (m, Ph)

(*R*)-**7**: colorless crystals; m.p. 80 °C (ether/pentane); 90% *ee*; $[\alpha]_D^{20}$ −7.5 (CH_2Cl_2, *c* = 1.04); ^{1}H NMR ($CDCl_3$): δ = 1.28 [d, *J* = 6.6 Hz, NCH(CH_3)$_2$], 1.98 (s, 1-CH_3), 3.69 (s, OCH_3), 3.93 (m, NCH), 7.23–7.52 (m, Ph)

(*S*)-**7**: 85% *ee*; $[\alpha]_D^{20}$ + 6.9 (CH_2Cl_2, *c* = 1.05)

(*R*)-**9**: colorless crystals; m.p. 68 °C (ether/pentane); $[\alpha]_D^{20}$ +76.3 (CH_2Cl_2, *c* = 1.0); ^{1}H NMR ($CDCl_3$): δ = − 0.03 [s, Sn(CH_3)$_3$], 1.25 [m, NCH(CH_3)$_2$], 1.83 (s, 1-CH_3), 3.79 and 4.17 (each m, NCH), 7.05–7.34 (m, Ph)

Our experimental findings confirm the theoretical predictions of *Schleyer* et al.,[26] according to which the activation energies of front-side and back-side attack lie close to each another. Apparently the extent of the interaction of electrofugal and nucleofugal leaving groups as well as steric effects have a decisive influence thereby on the competing reaction paths. The energy difference between the two reaction channels could shrink further, and the antarafacial attack gain more significance by the mesomeric flattening of the carbanionic center in the benzyl position.[27] Besides insights into the course of electrophilic substitution reactions which chiral α-oxybenzyllithium of type **3** provides, they also facilitate principally new routes for the enantioselective synthesis of tertiary benzyl alcohols. In the preceding communication we report on a carbamoyl group cleavable under mild conditions.[24]

Received: June 15, 1990 [Z 4016 IE]
German version: *Angew. Chem. 102* (1990) 1455

[1] D. J. Cram, C. A. Kingsberg, B. Rickborn *J. Am. Chem. Soc. 83* (1960) 3688–3696, and references cited therein.
[2] H.-J. Gais, G. Hellmann, H. Günther, F. Lopez, H. J. Lindner, S. Braun, *Angew. Chem. 101* (1989) 1061–1063; *Angew. Chem. Int. Ed. Engl. 28* (1989) 1025–1027.
[3] a) D. J. Cram, J. L. Mateos, F. Hauck, A. Langemann, K. R. Kopecky, W. D. Nielsen, J. Allinger, *J. Am. Chem. Soc. 81* (1959) 5774–5784 and preceding work by this group; b) L. A. Paquette, J. P. Gilday, C. S. Ra, *ibid. 109* (1987) 6858–6960.
[4] A. G. Brook, J. D. Pescoe, *J. Am. Chem. Soc. 93* (1971) 6224–6227.
[5] A. Wright, R. West, *J. Am. Chem. Soc. 96* (1974) 3227–3232.
[6] a) A. I. Meyers, L. M. Fuentes, *J. Am. Chem. Soc. 105* (1983) 117–118; b) A. I. Meyers, L. M. Fuentes, Y. Kubota, *Tetrahedron 40* (1984) 1361–1370; c) A. I. Meyers, M. Boes, A. Dickmann, *Angew. Chem. 96* (1984) 448–449; *Angew. Chem. Int. Ed. Engl. 23* (1984) 458–460; d) Review: A. I. Meyers, D. A. Dickman, M. Boes, *Tetrahedron 43* (1987) 5095–5108.
[7] D. Seebach, I. M. P. Huber, *Chimia 39* (1985) 233–234.
[8] a) K. Rein, M. Goicoechea-Pappas, T. V. Anklekar, G. C. Hart, G. A. Smith, R. E. Gawley, *J. Am. Chem. Soc. 111* (1989) 2211–2217; b) M. F. Loewe, M. Boes, A. I. Meyers, *Tetrahedron Lett. 26* (1985) 3295–3298.
[9] a) D. Hoppe, T. Krämer, *Angew. Chem. 98* (1986) 171–173; *Angew. Chem. Int. Ed. Engl. 25* (1986) 160–162; b) O. Zschage, J.-R. Schwark, D. Hoppe, *ibid. 102* (1990) 336–337 and *29* (1990) 296–297. c) T. Krämer, J.-R. Schwark, D. Hoppe, *Tetrahedron Lett. 30* (1989) 7037–7040.
[10] Review: D. Hoppe, *Angew. Chem. 96* (1984) 930–946; *Angew. Chem. Int. Ed. Engl. 23* (1984) 932–948.
[11] D. Hoppe, A. Brönneke, *Synthesis 1982*, 1045–1048.
[12] K. Laumen, M. P. Schneider, *J. Chem. Soc. Chem. Commun. 1988*, 598–600. We thank Professor *Schneider* and Dr. *Laumen* for help with the enzymatic ester hydrolysis.
[13] W. H. Pirkle, M. S. Hoekstra, *J. Org. Chem. 39* (1974) 3904–3906.
[14] A solution of (*R*)-**2** (1 mmol) and TMEDA (1.1 mmol) in hexane (2 mL) was treated dropwise at −78 °C with a ca. 1.4 M solution of *sec*-butyllithium (1.1 mmol) in cyclohexane/isopentane and the mixture stirred for 30 min at this temperature. The resulting yellow solution of (*R*)-**3** was treated at −78 °C with 1.1 mmol of the electrophile, stirred for 30 min, allowed to warm to room temperature, neutralized with 2 mL of 2N HCl, and extracted three times with ether. Purification was performed by flash chromatography on silica gel with ether/pentane (1:4 to 1:8).
[15] We assign the lithium compound **3** the (*R*)-configuration, since we assume a deprotonation with retention of configuration. Although this assumption is plausible [9a] and finds theoretical support [16], it has to our knowledge, never been proven, since the absolute configuration of the trapping product was always determined and not that of the organometallic intermediate. For simplification an equilibrium of monomeric **3** with dimeric or tetrameric aggregates has not been taken into consideration; cf. references cited in [27].
[16] Review: M. H. Abraham, P. L. Grellier in F. R. Hartley, S. Patai (Eds.): *The Chemistry of the Metal-Carbon Bond, Vol. 2*, Wiley, Chichester 1985, pp. 25–149.
[17] All the new compounds gave correct C,H analyses (C,H ± 0.3%).
[18] Determined ^{1}H NMR spectroscopically in ca. 0.1 M $CDCl_3$ solution with 5–10 mol-% tris[(heptafluoropropylhydroxymethylene)-D-camphorato]-europium(III) (Eu(hfpc)$_3$).
[19] a) M. Tramontini, L. Angiolini, C. Fouquey, J. Jaques, *Tetrahedron 29* (1973) 4183–4187; W. Kirmse, P. Feyen, *Chem. Ber. 108* (1975) 71–78.
[20] (*R*)-**7** was correlated with a sample obtained from (*R*)-atrolactic acid; V. Prelog, *Helv. Chim. Acta 36* (1953) 308–325.
[21] E. Kaufmann, S. Sieber, P. von R. Schleyer, *J. Am. Chem. Soc. 111* (1989) 4005–4008, and references cited therein.
[22] The (*R*)-configuration of the stannane (+)-**9** is not strictly confirmed; it follows from the observed rotation using Brewsters rule [23]. In the sequence (+)-**9** → (*S*)-**3** → (−)-**9** only one of the two steps can proceed with inversion, and according to the derived assignment of configuration it must be the delithiostannylation. This is also supported by the fact that retention has always been established for lithiodestannylations of α-oxyalkylstannanes [24, 25].
[23] a) J. H. Brewster, *Top. Stereochem. 2* (1967) 1–72; b) *Tetrahedron Lett. 1959*, 23–28.
[24] D. Hoppe, F. Hintze, P. Tebben, *Angew. Chem. 102* (1990) 1457; *Angew. Chem. Int. Ed. Engl. 29* (1990) 1422.
[25] a) R. J. Linderman, A. Ghannam, *J. Am. Chem. Soc. 112* (1990) 2392–2398; b) P. C.-M. Chan, J. M. Chong, *Tetrahedron Lett. 31* (1990) 1985–1988, and references cited therein.
[26] E. D. Jemmis, J. Chandrasekhar, P. von R. Schleyer, *J. Am. Chem. Soc. 101* (1979) 527–533.
[27] X-ray structure analyses of monomeric benzyllithium-solvent adducts: a) W. Zarges, M. Marsch, K. Harms, G. Boche, *Chem. Ber. 122* (1989) 2303–2309; b) W. Zarges, M. Marsch, K. Harms, W. Koch, G. Frenking, G. Boche, *Chem. Ber. 123* (1990), in press.

Building Up Metal-Stabilized Fourfold Bridged Cyclobutadienophanes**

By *Rolf Gleiter** and *Volker Schehlmann*

The metal-induced [2+2] and [2+2+2] cycloaddition of two or three triple bonds is a very important method of synthesizing metal-stabilized cyclobutadienes,[1] benzenes[2] or 6π-heterocycles.[3] Using α,ω-diynes provides access to bicyclic aromatic systems.[2] A reaction between cyclic diynes and $[CpCoL_2]$ yields tricyclic cyclobutadiene complexes or, in one case, a fourfold bridged cyclophane of cyclobutadiene, capped by a CpCo unit on each side. Thus, while such a superphane (**2**) occurred as major product (together with **3** and **4**) when cyclodeca-1,6-diyne, **1**, was heated with $[CpCo(CO)_2]$,[4, 5a] no analogue could be detected when other medium-sized cyclic diynes were used.[5b, 6] We report here a new concept in the superphane synthesis based on a construction principle that uses masked cycloalkynes as building blocks.[6]

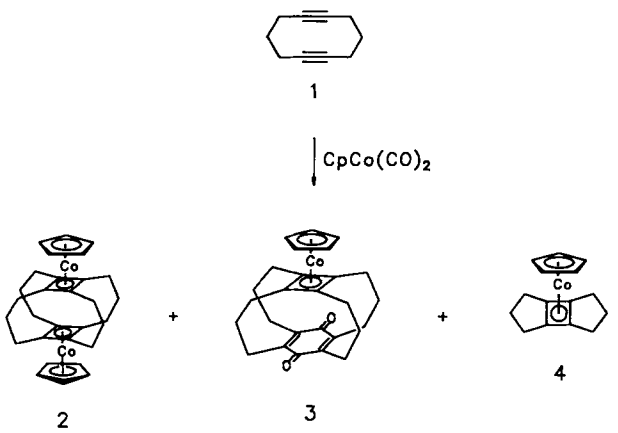

The starting point for our synthesis is 5-cyclodecynol **5**.[7] It can be transformed into a mixture of tricyclic cyclobutadiene complexes **6** in 40% yield by heating a very dilute solution in decalin with [CpCo(cod)] at 150–160 °C (Scheme 1). The alcohols **6** are oxidized to the isomeric ketones **7a** and **7b** in 83% yield via an Oppenauer oxidation with acetone. The isomers may be separated on silicagel using CH_2Cl_2 as eluent (Table 1). The structure of **7b** was determined by X-ray analysis.[8]

In the next step the mixture of diketones is transformed into the bisselena-diazoles **8a** and **8b** via a method first devised by *Lalezari* et al.[9] Without further purification the mixture **8a/8b** is treated with *n*BuLi at −40 °C to give the diyne **9** (Table 1, X-ray analysis[8]) in 70% yield. The reaction shown in Scheme 1 allows the preparation of 1–2 g of **9** in one synthetic run.

Scheme 2 shows that diyne **9** is the key compound in the synthesis of several metal-protected fourfold bridged cyclobutadienophanes. When **9** is heated in cyclooctane with $[CpCo(CO)_2]$ the superphane **2** is obtained in 80% yield. This reaction occurs relatively fast; this supports our earlier

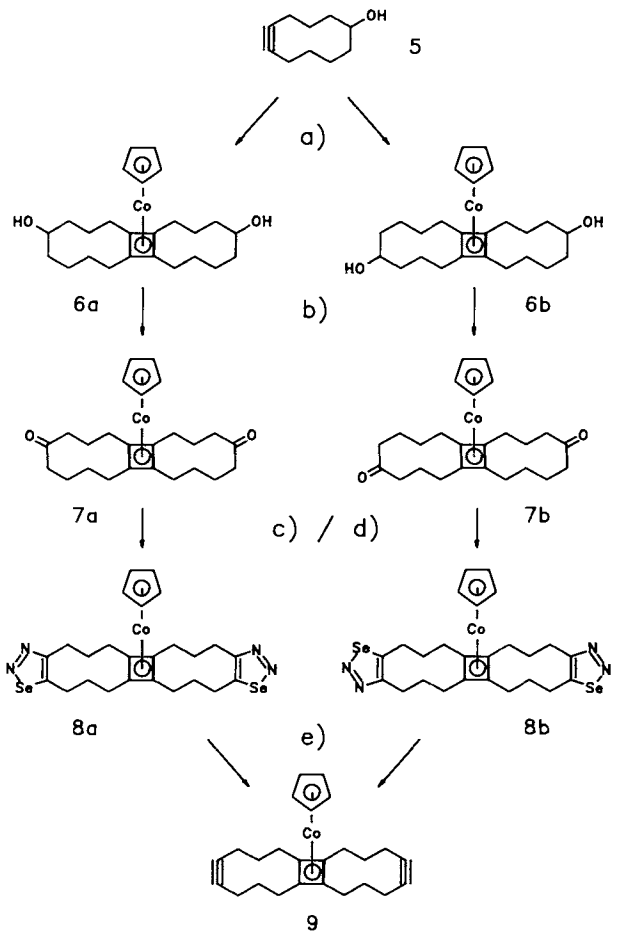

Scheme 1: a) [CpCo(cod)], decalin, 150–160 °C, high dilution, 7 d; b) Oppenauer oxidation, acetone/toluene, $Al(OiPr)_3$, 14 h reflux; c) Semicarbazide · HOAc, ethanol, 45 min. reflux; d) SeO_2, CH_3COOH, 4–5 h, 30–40 °C; e) BuLi, THF, −40 °C.

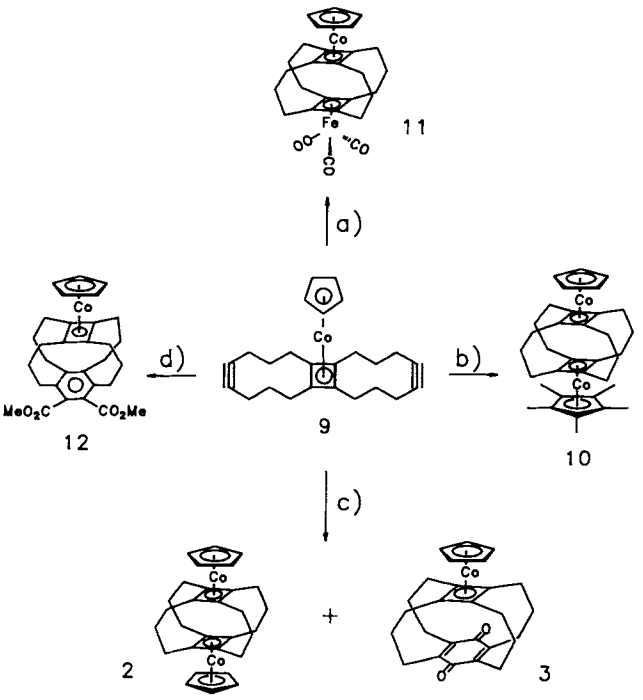

Scheme 2: a) $Fe(CO)_5$, toluene, 18 h reflux; b) $[Cp^*Co(CO)_2]$, decalin, 150–160 °C, 24 h; c) $[CpCo(CO)_2]$, cyclooctane, 2 h reflux; d) $[CpCo(CO)_2]$, DMAD, toluene, 24 h reflux.

[*] Prof. Dr. R. Gleiter, Dr. V. Schehlmann
Organisch-chemisches Institut der Univesität
Im Neuenheimer Feld 270 W-6900 Heidelberg (FRG)

[**] This work was supported by the Deutsche Forschungsgemeinschaft (Sonderforschungsbereich 247), the Volkswagen-Stiftung, the Fonds der Chemischen Industrie, and the BASF AG (Ludwigshafen)

Table 1. Spectroscopic data of the most important compounds.

7a: m.p. 147–148 °C; ^{1}H NMR (300 MHz, $CDCl_3$): δ = 4.44 (s, 5H), 2.87–2.98 (m, 2H), 2.47–2.56 (m, 2H), 1.33–2.44 (m, 24H); ^{13}C NMR (75.47 MHz, $CDCl_3$): δ = 213.3(s), 80.4 (d, Cp), 79.9(s), 78.6(s), 43.4(t), 37.6(t), 27.5(t), 24.5(t), 23.8 (t, 2C), 22.8(t); IR (KBr): $\tilde{\nu}$ [cm^{-1}] = 2946, 2908, 1703, 1441, 1422, 1371, 1222, 1103, 821, 805; MS (70 eV): *m/z* = 424(61%), 188(20), 151(22), 137(40), 129(23), 124(100), 115(22), 91(48), 79(25), 67(25), 59(90), 41(52); UV (pentane): λ_{max} [nm] (lgε) = 266(4.41), 300(3.22), 375(2.73).

7b: m.p. 170–172 °C; ^{1}H NMR (300 MHz, $CDCl_3$): δ = 4.42 (s, 5H), 2.96–3.07 (m, 2H), 1.35–2.54 (m, 26H); ^{13}C NMR (75.47 MHz, $CDCl_3$): δ = 213.3(s), 80.6 (d, Cp), 79.6(s), 79.0(s), 43.9(t), 36.8(t), 28.6(t), 23.9(t), 23.8(t), 23.5(t), 22.0(t); IR (KBr): $\tilde{\nu}$ [cm^{-1}] = 2932, 2910, 1704, 1443, 1420, 1369, 1103, 997,807; MS and UV spectra: as for isomer **7a**.

9: m.p. 106–108 °C; ^{1}H NMR (300 MHz, $CDCl_3$): δ = 4.49 (s, 5H), 1.50–2.50 (m, 24H); ^{13}C NMR (75.47 MHz, $CDCl_3$): δ = 82.3(s), 82.1(s), 80.0 (d, Cp), 27.8(t), 25.6(t), 19.2(t); IR ($CDCl_3$): $\tilde{\nu}$ [cm^{-1}] = 2928, 2234, 1430, 1255, 806; MS (70 eV): *m/z* 388(4%), 322(20), 308(18), 131(24), 119(27), 105(76), 91(100), 57(18), 43(18); UV (pentane): λ_{max} [nm] (lgε) = 266(4.38), 296(3.28), 378(2.73).

10: m.p. >300 °C; ^{1}H NMR (300 MHz, C_6D_6): δ = 4.56 (s, 5H), 2.21–2.25 (m, 8H), 1.80–1.84 (m, 8H), 1.76 (s, 15H), 1.52–1.61 (m, 8H); ^{13}C NMR (75.47 MHz, C_6D_6): δ = 87.0(s), 80.3 (d, Cp), 78.5(s), 74.0(s), 28.0(t), 26.9(t), 25.0(t), 9.5(q); IR(KBr): $\tilde{\nu}$ [cm^{-1}] = 2922, 2886, 1443, 1376, 1342, 994, 549, 495; MS (70 eV): *m/z* 582(10%), 457(27), 291(22), 259(100), 133(34), 124(25), 59(32); UV (hexane): λ_{max} [nm] (lgε) = 205(3.75), 243(3.35), 399(4.05).

11: m.p. >260 °C (decomp.); ^{1}H NMR (300 MHz, C_6D_6): δ = 4.46 (s, 5H), 2.05–2.13 (m, 16H), 1.33–1.43 (m, 8H); ^{13}C NMR (75.47 MHz, C_6D_6): δ = 217.4(s), 87.3(s), 80.5 (d, Cp), 78.7(s), 28.1(t), 26.3(t), 25.6(t); IR (C_6D_6): $\tilde{\nu}$ [cm^{-1}] = 2936, 2894, 2006, 1944, 1429, 1349, 1248, 1103, 1070, 736, 702, 605; MS (70 eV): *m/z* 528(17%), 500(8.6), 472(32), 444(41), 317(24), 124(100), 115(18), 84(21), 59(61), 56(48); UV (pentane): λ_{max} [nm] (lgε) = 202(4.62), 240 (s, 4.22), 288(4.61).

12: m.p. 175–179 °C; ^{1}H NMR (300 MHz, C_6D_6): δ = 4.38 (s, 5H), 3.50 (s, 6H), 3.06–3.19 (m, 2H), 2.79–2.88 (m, 2H), 2.52–2.62 (m, 2H), 2.26–2.43 (m, 4H), 2.06–2.11 (m, 4H), 1.66–1.99 (m, 10H); ^{13}C NMR (75.46 MHz, C_6D_6): δ = 169.9(s), 141.2(s), 135.6(s), 130.2(s), 80.5 (d, Cp), 80.4(s), 77.8(s), 51.8(q), 27.9(t), 26.8(t), 26.2(t), 24.9(t), 23.4(t), 22.1(t); IR ($CDCl_3$): $\tilde{\nu}$ [cm^{-1}] = 2928, 2848, 1737, 1707, 1432, 1266, 1220, 1195, 1177; MS (70 eV): *m/z* 530(35%), 249(27), 165(25), 153(20), 141(29), 128(36), 124(65), 115(41), 104(20), 91(56), 77(30), 65(21), 59(100), 55(34), 44(50), 41(38); UV (CH_3CN): λ_{max} [nm] (lgε) = 196(4.15), 266(4.06), 294(3.25).

assumption that **9** is an intermediate in the reaction **1** → **2**.[4] As a side product of this reaction we isolated the donor-acceptor-phane **3**[5] (1% yield). The reaction with [Cp*Co-$(CO)_2$][10] in decalin at 150–160 °C yields **10** (84%) and heating **9** with $Fe(CO)_5$ in toluene[11] leads to **11** (8%). Compound **11** is related to the recently synthesized [2,2](1,3)cyclobutadienophane which is capped with an $Fe(CO)_3$ unit on each side.[12] The structure of **11** has been confirmed by an X-ray study on single crystals.[8] Finally, heating with dimethylacetylenedicarboxylate (DMAD) and $[CpCo(CO)_2]$ gives the mixed cyclophane **12** in 5% yield.

Calculations using the AM1 method[14] on a model of **9** which does not contain the CpCo unit but allows minimization of all geometrical parameters[13] of the remaining hydrocarbon reproduces the molecular parameters calculated in the X-ray studies for the hydrocarbon unit very well. Besides the global minimum **A**, in which the acetylene units are 6.3 Å apart, the calculations predict two local minima, **B** and **C**, in which the triple bonds are separated by 3.9 and 4.6 Å, respectively (Scheme 3).

The calculated energy difference between **A** and **C** is 8.3 kcal mol^{-1} and between **A** and **B** 10.0 kcal mol^{-1}.

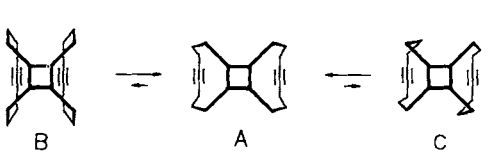

	B	A	C
d [Å]	3.9	6.3	4.6
$E_{rel.}$ [kcal mol^{-1}]	10.0	0.0	8.3

Scheme 3.

Received: July 23, 1990 [Z 4084 IE]
German version: *Angew. Chem. 102* (1990) 1450

[1] A Efraty, *Chem. Rev. 77* (1977) 691; N. E. Schore, *ibid. 88* (1988) 1081, and references cited therein.
[2] K. P. C. Vollhardt, *Acc. Chem. Res. 10* (1977) 1; *Angew. Chem. 96* (1984) 525; *Angew. Chem. Int. Ed. Engl. 23* (1984) 539, and references cited therein.
[3] H. Bönnemann, *Angew. Chem. 97* (1985) 264; *Angew. Chem. Int. Ed. Engl. 24* (1985) 248; H. Bönnemann, R. Goddard, J. Grub, R. Mynott, E. Raabe, S. Wendel, *Organometallics 8* (1989) 1941, and references cited therein.
[4] R. Gleiter, M. Karcher, M. L. Ziegler, B. Nuber, *Tetrahedron Lett. 28* (1987) 195.
[5] a) R. Gleiter, D. Kratz, *Tetrahedron Lett. 31* (1990) 5893; b) R. Gleiter, D. Kratz, M. L. Ziegler, B. Nuber, *ibid. 31* (1990) 6175.
[6] R. Gleiter, M. Karcher, D. Kratz, S. Rittinger, V. Schehlmann in H. Werner, G. Erker (Eds.): *Organometallics in Organic Synthesis 2*, Springer, Berlin 1989, p. 109.
[7] M. Hanack, C. E. Harding, J.-L. Derocque, *Chem. Ber. 105* (1972) 421.
[8] The X-ray analyses were carried out by M. L. Ziegler, B. Nuber.
[9] I. Lalezari, A. Shafiee, M. Yalpani, *Tetrahedron Lett. 1969*, 5105; *Angew. Chem. 82* (1970) 484; *Angew. Chem. Int. Ed. Engl. 9* (1970) 464; H. Petersen, H. Meier, *Chem. Ber. 113* (1980) 2383.
[10] R. B. King, A. Efraty, W. M. Douglas, *J. Organomet. Chem. 56* (1973) 345.
[11] R. B. King, I. Haiduc, C. W. Eavenson, *J. Am. Chem. Soc. 95* (1973) 2508.
[12] C. M. Adams, E. M. Holt, *Organometallics 9* (1990) 980.
[13] The minima have been characterized by inspection of the first and second derivative of the energy with respect to all geometrical variables.
[14] M. J. S. Dewar, E. G. Zoebisch, E. F. Healy, J. J. P. Stewart, *J. Am. Chem. Soc. 107* (1985) 3902.

Doubly Bridged Prismanes, Dewar Benzenes and Benzene Derivatives from Cyclooctyne and 1,8-Cyclotetradecadiyne: En Route to Propella[n_3]prismanes**

By *Rolf Gleiter** and *Björn Treptow*

Starting from 1,6-cyclodecadiyne we recently synthesized propella[3_4]prismane **1**.[1] En route to the homologous propella[n_3]prismane **2** we have now succeeded in the synthesis of **3** and **4**, each with two of the three methylene bridges. To

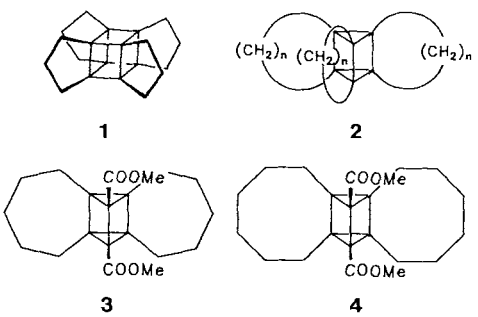

1 **2** **3** **4**

[*] Prof. Dr. R. Gleiter, Dipl. Chem. B. Treptow
Organisch-chem. Institut der Universität
Im Neuenheimer Feld 270, D-6900 Heidelberg (FRG)

[**] This work was supported by the Volkswagen-Stiftung, the Fonds der Chemischen Industrie, and BASF AG (Ludwigshafen).

our knowledge these are the first doubly bridged prismane derivatives.

As starting material we chose for **3** 1,8-cyclotetradecadiyne[2] **5** and for **4** cyclooctyne **9**.[3] The reaction with $AlCl_3$ in CH_2Cl_2 yields, as expected, the cyclobutadiene–$AlCl_3$ σ-complexes **6** and **10**, respectively. Addition of dimethyl acetylenedicarboxylate (DMAD) and dimethyl sulfoxide (DMSO) results in the formation of the two isomeric doubly bridged Dewar benzene derivatives **7**, **8** and **11**, **12**, respectively, as shown in Scheme 1.

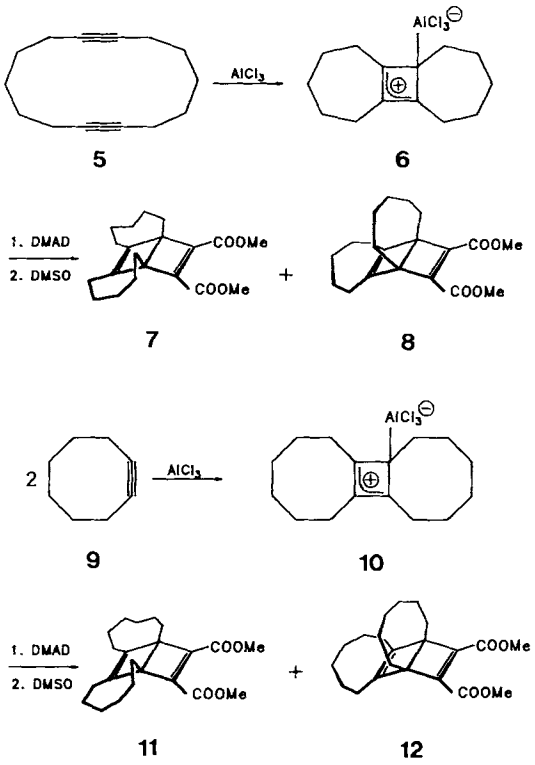

Scheme 1.

This route to Dewar benzenes was discovered in 1971[4], and the reaction has been thoroughly studied since then.[5] *Hogeveen* and et al. only briefly mentioned the reaction leading to the Dewar benzenes **7** and **8**.[5] If the reaction is carried out at low temperature (−50 °C) the addition of DMSO is necessary to release the cyclobutadiene,[6, 7] which now reacts in a Diels–Alder reaction with DMAD to form a 1:1 mixture of the isomeric products. At higher temperatures (0° to 10 °C) this ratio is shifted to 3:7 in favor of **8** and **12**, respectively. Separation of the isomeric Dewar benzenes by column chromatography is difficult and tedious. The Dewar-benzene isomers are characterized by NMR spectroscopy as follows (cf. Table 1): in the ^{13}C-NMR spectra of **7** and **8** with the pentamethylene chains we observe six methylene signals for **8**, two of them with lower intensity and five signals for **7**, all of them showing equal intensity. The characterization of **11** and **12** is more difficult and can only be achieved via the corresponding aromatic isomers **14** and **16**, which show different dynamic behaviors. Compound **14** shows the expected sharp ^{13}C-NMR signals. In **16**, however, the signals for the benzene ring and the *para* methylene chain exhibit considerable line broadening due to bridge flipping. This phenomenon is typical for [6]paracyclophanes and was thoroughly studied by *Tochtermann* and co-workers.[8] A low-temperature ^1H-NMR spectrum (253 K) of **16** reveals two signals at $\delta = -0.51$ and -0.75. They are assigned to the central protons of the *para* bridge, which point towards the aromatic ring. These resonances are in good agreement with those found for similar systems.[8] The assignment is also supported by the UV spectrum, which shows a bathochromic shift of about 30 nm relative to the transitions for the flat systems **13** and **14**. This shift is characteristic for a bent aromatic system[9]

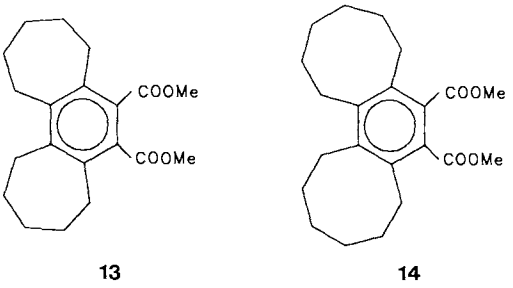

Irradiation[11] of **7** and **11** either at 250 nm or 300 nm leads quantitatively to the aromatic isomers **13** and **14**,[10] whereas irradiation[11] of **8** at 250 nm yields only polymeric material. We suggest that the corresponding [5]paracyclophane **15** is formed but decomposes immediately, because these compounds are unstable at temperatures above 0 °C.[12] The prismane **3** is isolated in 15% yield after 72 h when **8** is irradiated at 280 nm[11] (Scheme 2). Longer irradiation leads only to polymeric by-products and does not increase the yield.

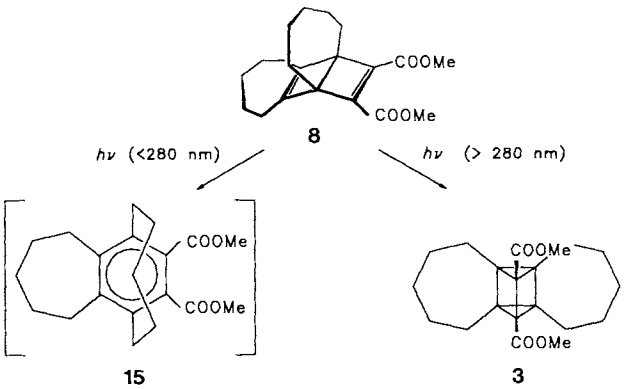

Scheme 2.

When **12** is irradiated[11] at 250 nm a rapid isomerization (100% after 1 h) to the [6]paracyclophane **16** takes place;[13] increasing the wavelength to 280 nm leads to prismane **4** (30% after 24 h).[13, 14] Monitoring by ^1H-NMR spectroscopy shows that at first a major part of **12** is transformed into the [6]paracyclophane **16** while the formation of the prismane commences slowly. A solution of **16** irradiated under similar conditions also led to the prismane[15] (Scheme 3).

There are two possible explanations for this behavior. First our prismanes may not be generated directly from the Dewar benzenes but via the paracyclophanes. This would also explain the unexpectedly low yield of prismane **3**, because the intermediate [5]paracyclophane **15** partly decomposes before it can react to the corresponding prismane. Second a photochemical equilibrium may exist between

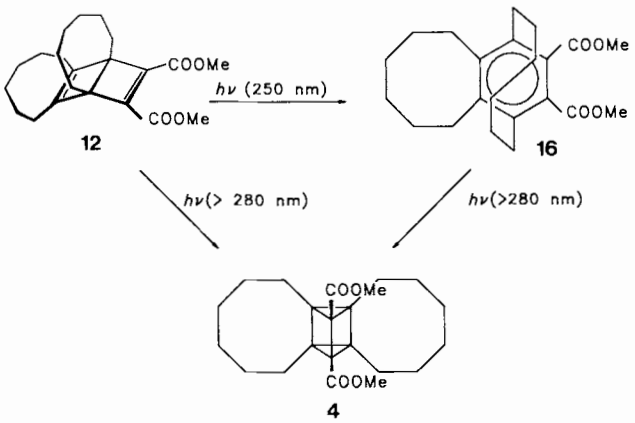

Scheme 3.

Dewar benzene and paracyclophane, both of which can isomerize to the corresponding prismane. We are continuing our irradiation experiments to clarify the kinetics of the process.

The prismanes **3** and **4** can easily be characterized by ^{13}C-NMR spectroscopy. A change from a Dewar benzene or a paracyclophane to a prismane creates a second plane of symmetry and thus reduces the number of ^{13}C signals. For both prismanes we observe one low field resonance assigned to the carboxyl groups and six further signals below $\delta = 60$ belonging to the core and the methylene chains (Table 1).

Table 1. Important spectroscopic data of **3, 4, 7, 8, 11–14**, and **16**.

3: ^1H NMR (300 MHz, $CDCl_3$): $\delta = 3.66$ (s, 6H), 1.73 (s, br, 20H); ^{13}C NMR (75.46 MHz, $CDCl_3$): $\delta = 169.7$, 57.0, 51.0, 42.2, 32.2, 30.8, 24.5; IR($CDCl_3$): $\tilde{\nu}$[cm^{-1}] = 2928, 2842, 1688, 1431, 1304, 1194; UV/VIS (acetonitrile): λ_{max}[nm](lg ε) = 208 (3.95), 248 sh (3.34); high resolution MS: $m/z(M^{\oplus})$: calcd 330.1831, found 330.1822.

4: ^1H NMR (200 MHz, $CDCl_3$): $\delta = 3.64$ (s, 6H), 1.95–1.1 (m, 24H); ^{13}C NMR (50.32 MHz, $CDCl_3$): $\delta = 169.8$, 57.0, 51.0, 43.0, 26.6, 25.6, 20.9; IR($CDCl_3$): $\tilde{\nu}$[cm^{-1}] = 2848, 1679, 1300, 1141; UV/VIS (acetonitrile): λ_{max}[nm](lg ε) = 195 (3.92), 250 sh (3.34); high resolution MS: $m/z(M^{\oplus})$: calcd 358.2144, found 358.2164.

7: ^1H NMR (200 MHz, CD_2Cl_2): $\delta = 3.73$ (s, 6H), 2.4–1.0 (m, 20H); ^{13}C NMR (50.32 MHz, CD_2Cl_2): $\delta = 163.7$, 150.4, 146.9, 60.7, 51.7, 31.6, 28.9, 28.7, 28.4, 27.6; high resolution MS: $m/z(M^{\oplus})$: calcd 330.1831, found 330.1842.

8: ^1H NMR (200 MHz, $CDCl_3$): $\delta = 3.76$ (s, 6H), 2.3–1.1 (m, 20H); ^{13}C NMR (50.32 MHz, $CDCl_3$): $\delta = 162.8$, 151.2, 147.7, 61.1, 51.5, 33.2, 29.2, 28.5, 28.4, 27.6, 26.5; IR($CDCl_3$): $\tilde{\nu}$[cm^{-1}] = 2834, 1704, 1618, 1307, 1202; UV/VIS (acetonitrile): λ_{max}[nm](lg ε) = 190 (4.41), 240 sh (3.84); high resolution MS: $m/z(M^{\oplus})$: calcd 330.1831, found 330.1862.

11: ^1H NMR (300 MHz, $CDCl_3$): $\delta = 3.77$ (s, 6H), 2.4–2.2 (m, 4H), 2.0–1.2 (m, 20H); ^{13}C NMR (75.46 MHz, $CDCl_3$): $\delta = 163.3$, 151.1, 148.5, 61.5, 51.6, 28.4, 28.0, 25.7, 25.1, 24.5, 23.6; high resolution MS: $m/z(M^{\oplus} - CH_3OH)$: calcd 326.1882, found 326.1871.

12: ^1H NMR (300 MHz, $CDCl_3$): $\delta = 3.78$ (s, 6H), 2.3–1.8 (m, 8H), 1.8–1.2 (m, 16H); ^{13}C NMR (75.46 MHz, $CDCl_3$): $\delta = 162.8$, 152.3, 147.1, 61.3, 51.6, 26.7, 26.6, 26.2, 25.3, 24.1, 23.8; IR($CDCl_3$): $\tilde{\nu}$[cm^{-1}] = 2928, 2846, 1701, 1232, 1191; UV/VIS (acetonitrile): λ_{max}[nm](lg ε) = 195 (4.12); high resolution MS: $m/z(M^{\oplus})$: calcd 358.2144, found 358.2115.

13: ^1H NMR (300 MHz, $CDCl_3$): $\delta = 3.84$ (s, 6H), 2.91–2.87 (m, 4H), 2.82–2.78 (m, 4H), 1.8–1.5 (m, 12H); ^{13}C NMR (75.47 MHz, $CDCl_3$): $\delta = 169.9$, 143.3, 139.0, 128.9, 52.2, 31.4, 30.8, 29.4, 27.2, 26.6; IR($CDCl_3$): $\tilde{\nu}$[cm^{-1}] = 2920, 2848, 1725, 1435, 1300, 1210, 1174; UV/VIS (acetonitrile): λ_{max}[nm](lg ε) = 213 (4.45), 240 (3.8), 285 (3.15).

14: ^1H NMR (200 MHz, $CDCl_3$): $\delta = 3.83$ (s, 6H), 2.9–2.83 (m, 4H), 2.81–2.75 (m, 4H), 1.85–1.55 (m, 8H), 1.5–1.2 (m, 8H); ^{13}C NMR (50.32 MHz, $CDCl_3$): $\delta = 170.6$, 142.4, 138.1, 130.9, 52.8, 32.1, 31.2, 30.6, 28.0, 27.2, 26.7; IR($CDCl_3$): $\tilde{\nu}$[cm^{-1}] = 2922, 1725, 1436, 1191; UV/VIS (CH_2Cl_2): λ_{max}[nm](lg ε) = 215 (4.47), 250 sh (3.65), 282 (3.06).

16: ^1H NMR (300 MHz, $CDCl_3$): $\delta = 3.81$ (s, 6H), 3.2–3.0 (m, 3H), 3.0–2.6 (m, 5H), 2.0–1.0 (m, 14H), 1.0–0.5 (m, 2H); ^{13}C NMR (75.46 MHz, $CDCl_3$): $\delta = 169.0$, 144.8 (br), 140.9 (br), 50.6, 33.9 (br), 32.3 (br), 31.8, 28.0, 26.4 (br), 26.0 (the missing aromatic signal can only be detected in a low temperature spectrum at 253 K as doublet at $\delta = 133.9$ and 127.4); IR($CDCl_3$): $\tilde{\nu}$[cm^{-1}] = 2926, 2846, 1709, 1434; UV/VIS (CH_2Cl_2): λ_{max}[nm](lg ε) = 247 (4.25), 280 (3.65), 333 (3.15).

Received: August 6, 1990 [Z 4115 IE]
German version: *Angew. Chem. 102* (1990) 1452

CAS Registry numbers:
2 (n = 3), 130434-00-3; **2** (n = 4), 130434-01-4; **3**, 130434-02-5; **4**, 130434-03-6; **5**, 1540-80-3; **6**, 130434-12-7; **7**, 130434-04-7; **8**, 130434-05-8; **9**, 1781-78-8; **10**, 130434-13-8; **11**, 130434-06-9; **12**, 130434-07-0; **13**, 130434-08-1; **14**, 130434-09-2; **15**, 130434-10-5; **16**, 130434-11-6.

[1] R. Gleiter, M. Karcher, *Angew. Chem. 100* (1988) 851; *Angew. Chem. Int. Ed. Engl. 27* (1988) 840.
[2] J. Dale, A. J. Hubert, G. S. D. King, *J. Chem. Soc. 1963*, 73.
[3] H. Bühl, H. Gugel, H. Kolshorn, H. Meier, *Synthesis 1978*, 536.
[4] J. B. Koster, G. J. Timmermans, H. van Bekkum, *Synthesis 1971*, 139; W. Schäfer, H. Hellmann, *Angew. Chem. 79* (1967) 566; *Angew. Chem. Int. Ed. Engl. 6* (1967) 518.
[5] H. Hogeveen, D. M. Kok in S. Patai, Z. Rappoport (Eds.): *The Chemistry of Triple-Bonded Functional Groups, Suppl. C, Part 2*. Wiley, New York 1983; Chap. 23, and references cited therein.
[6] P. B. J. Driessen, H. Hogeveen, *J. Am. Chem. Soc. 100* (1978) 1193.
[7] P. B. J. Driessen, H. Hogeveen, *J. Organomet. Chem. 156* (1978) 265.
[8] C. Wolff, J. Liebe, W. Tochtermann, *Tetrahedron Lett. 23* (1982) 1143; H. Günther, P. Schmitt, H. Fischer, W. Tochtermann, J. Liebe, C. Wolff *Helv. Chim. Acta 68* (1985) 801.
[9] N. L. Allinger, L. A. Freiberg, R. B. Hermann, M. A. Miller, *J. Am. Chem. Soc. 85* (1963) 1171.
[10] D. S. Greidinger, D. Ginsburg, *J. Org. Chem. 22* (1957) 1406.
[11] The irradiations were carried out under argon with high-pressure mercury lamps (Osram HBO 500 W and Phillips HPK 125 W) in dry diethyl ether at 10 °C.
[12] G. B. M. Kostermans, W. H. de Wolf, F. Bickelhaupt, *Tetrahedron Lett. 27* (1986) 1095; G. B. M. Kostermans, W. H. de Wolf, F. Bickelhaupt, *Tetrahedron 43* (1987) 2955.
[13] H. Dreeskamp, P. Kapahnke, W. Tochtermann, *Radiat. Phys. Chem. 32* (1988) 537.
[14] Y. Tobe, K. Kakiuchi, Y. Odaira, T. Hosaki, Y. Kai, N. Kasai, *J. Am. Chem. Soc. 105* (1983) 1376.
[15] J. Liebe, C. Wolff, C. Krieger, J. Weiss, W. Tochtermann, *Chem. Ber. 118* (1985) 4144.

Spontaneous Formation of Stable Phosphino(silyl)-carbenes from Unstable Diazo Compounds

By *Gregory R. Gillette, Antoine Baceiredo*, and *Guy Bertrand**

The ability of transition metals to stabilize electron-deficient species such as carbenes, nitrenes, and phosphinidenes is now well established. More seldomly, it has been shown that a similar role could be played by heavier main group elements.[1] We previously utilized this property in the synthesis of the first stable compound featuring all the characteristic reactions of simple carbenes, i.e. cyclopropanation, carbon-hydrogen insertion and carbene-carbene coupling.[2] However, the preparation of this species, namely the [bis(diisopropylamino)phosphanyl](trimethylsilyl)carbene **1b**, was rather tricky due to the drastic conditions used (250 °C under 10^{-2} torr) and to the narrow utilizable temperature range: below 240 °C the starting diazo **1a** is not decomposed and above 260 °C the carbene inserted into a C–H bond of a diisopropylamino substituent affording heterocycle **1c**. As a result of efforts to extend the chemistry of these carbene-like derivatives, we now report the surprisingly facile synthesis of new stable compounds of this type.

Several phosphinodiazomethanes[3] have previously been studied, but until now only the combination of two

[*] Dr. G. Bertrand, Dr. G. R. Gillette, Dr. A. Baceiredo
Laboratoire de Chimie de Coordination du CNRS, UP 8241
lié par conventions à l'Université
Paul Sabatier et à l'Institut National Polytechnique
205 route de Narbonne, F-31077 Toulouse Cédex (France)

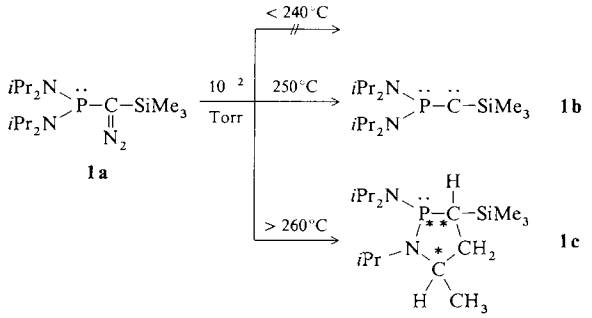

diisopropylamino substituents at phosphorus and a trimethylsilyl group at carbon led to a stable "carbene" after elimination of N_2.[2] It was of interest to know to what extent we could vary the nature of the substituents while retaining the kinetic stabilization of the carbene. We first chose to replace one of the diisopropylamino groups by a dimethylamino group. The diazo derivative **2a** was easily available from the lithium salt of the trimethylsilyldiazomethane[4] and the corresponding phosphorus chloride.[5] Photolysis of **2a** did not lead to the desired carbene but to its [2+2] cyclic dimer **2d** (involving its λ^5-phosphaacetylene form) as had already been observed by *Regitz* et al. for the bis(dimethylamino) analogue.[3d] However, the carbene-like nature of the intermediate was confirmed by a trapping experiment with *tert*-butylisocyanide, affording ketenimine **2e**. Diazo **2a** is stable up to 250 °C under vacuum, while thermolysis at 300 °C under 10^{-2} torr gave rise to a mixture of five-membered ring diastereoisomers **2c**, formally resulting from a CH insertion of the carbene.

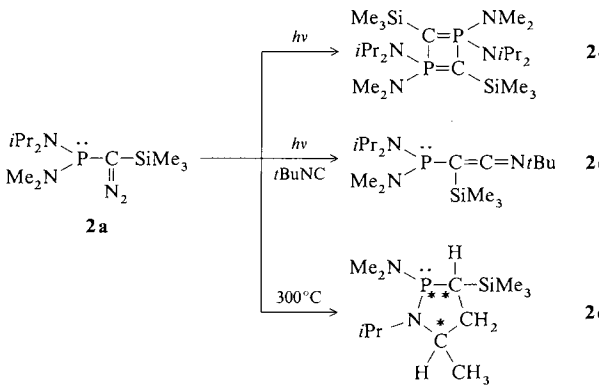

From these results the influence of the steric hindrance was obvious and thus we attempted to synthesize the [diisopropylamino(2,2,6,6-tetramethylpiperidino)phosphino](trimethylsilyl)diazomethane **3a** by the usual procedure. Surprisingly, after work-up we isolated the "carbene" **3b** in near quantitative yield. It appeared that the diazo compound **3a** was only stable for a short time at room temperature but could be spectroscopically characterized in solution. In marked contrast, "carbene" **3b** was perfectly stable for weeks in solution at room temperature, but appeared to be very poorly reactive (it did not react with *tert*-butylisocyanide).

A good compromise was found using both tetramethylpiperidino- and dimethylamino-substituents at phosphorus. In this case, we have i) a diazo compound **4a** which decomposed over a few days at room temperature or after 1 hour at 35 °C; ii) a "carbene" **4b**, stable for weeks at room temperature but also quite reactive, as demonstrated by its immediate reaction with *tert*-butylisocyanide at 20 °C to give **4e**. In other words, **4a** allows straightforward access to multi-gram quantities of a synthetically useful "carbene".

The generality of the influence of the tetramethylpiperidino group on the decomposition temperature of the diazo and on the stability of the "carbene" is shown by the results obtained with compounds **5** and **6**. No dramatic change was

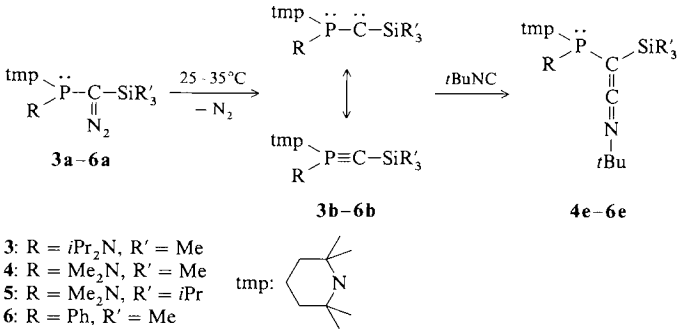

3: R = iPr$_2$N, R′ = Me
4: R = Me$_2$N, R′ = Me
5: R = Me$_2$N, R′ = iPr
6: R = Ph, R′ = Me

observed when the trimethylsilyl was replaced by a triisopropylsilyl group except for a decrease in reactivity of the carbene: reaction of **5b** with *t*BuNC required two days at room temperature. **6b** is of special interest since it is the first example of a relatively stable "carbene" (one day at room temperature, but weeks at −20 °C) with only one amino group at phosphorus.

All the carbenes are easily characterized by multinuclear NMR spectroscopy (Table 1). The most striking features are

Table 1. Selected spectroscopic data of the compounds **1**–**6** (coupling constants with phosphorus in brackets).

Cpd.	a		b			e	
	IR $\tilde{\nu}$ [cm^{-1}]	δ^{31}P	δ^{31}P	δ^{13}C	δ^{29}Si	IR: $\tilde{\nu}$ [cm^{-1}]	δ^{31}P
1 [2]	2010	+56.1	−40.0	142.7 (159)	−19.7 (59)	2020	+50.3
2	2035	+77.3		[a]		2020	+75.3
3	2020	+88.0	−49.7	145.5 (203)	−21.3 (70)	[b]	
4	2040	+83.8	−24.1	133.5 (147)	−13.2 (52)	2020	+75.4
5	2030	+88.7	−27.8	120.7 (181)	−2.8 (47)	2040, 2020	+88.6
6	2060	+25.0	−38.1	136.9 (147)	−17.0 (27)	1990	+27.4

[a] **2b** was not characterized. [b] **3b** does not react with *t*BuNC.

certainly the high-field chemical shift in ^{31}P (δ = −24.1 to −49.7), and in ^{29}Si (δ = −2.8 to −21.3), the low-field ^{13}C resonances (δ = 120.7 to 145.5), and the large $^1J_{PC}$ (147 to 203 Hz) and $^2J_{PSi}$ (27 to 70 Hz) coupling constants.

In summary, given the right set of substituents, it appears that phosphino(silyl)carbenes can be more "stable" than their corresponding diazo precursors!

Experimental

In a typical experiment, 4.72 mL of a solution of 1.6 M *n*BuLi in hexane (7.6 mmol) was added to a THF solution (10 mL) of trimethylsilyldiazomethane (0.86 g, 7.6 mmol), at −78 °C. The mixture was stirred, at −78 °C for 30 min, then chlorodimethylamino(2,2,6,6-tetramethylpiperidino)phosphane (1.92 g, 7.6 mmol) was added neat, via a syringe. The resulting solution was

slowly (3 h) warmed to room temperature and then the volatiles were removed in vacuo. Following treatment with pentane, filtration, and evaporation, 2.4 g (96%) of diazo **4a** was obtained. Carbene **4b** was prepared by heating a toluene solution (10 mL) of 2.4 g of diazo **4a**, at 35 °C for 1 h.

Received: July 6, 1990 [Z 4057 IE]
German version: *Angew. Chem. 102* (1990) 1486

CAS Registry numbers:
1a, 97135-48-3; **1b**, 115797-19-8; **1c**, 130195-59-4; **2a**, 130148-60-6; **2c**, 130148-62-8; **2d**, 130168-01-3; **2e**, 130148-61-7; **3a**, 130148-63-9; **3b**, 130148-66-2; **4a**, 130148-64-0; **4b**, 130148-67-3; **4e**, 130148-70-8; **5a**, 130148-65-1; **5b**, 130148-68-4; **5e**, 130148-71-9; **6a**, 130168-02-4; **6b**, 130148-69-5; **6e**, 130148-72-0; ^{29}Si, 14304-87-1.

[1] a) O. Glemser, R. Mews, *Angew. Chem. 92* (1980) 915; *Angew. Chem. Int. Ed. Engl. 19* (1980) 883; b) G. Bertrand, J. P. Majoral, A. Baceiredo, *Acc. Chem. Res. 19* (1986) 17; c) D. Christen, H. G. Mack, C. J. Marsden, H. Oberhammer, G. Schatte, K. Seppelt, H. Willner, *J. Am. Chem. Soc. 109* (1987) 4009.
[2] a) A. Igau, H. Grützmacher, A. Baceiredo, G. Bertrand, *J. Am. Chem. Soc. 110* (1988) 6463; b) A. Igau, A. Baceiredo, G. Trinquier, G. Bertrand, *Angew. Chem. 101* (1989) 617; *Angew. Chem. Int. Ed. Engl. 28* (1989) 621.
[3] a) H. Keller, M. Regitz, *Tetrahedron Lett. 29* (1988) 925; b) H. Keller, G. Maas, M. Regitz, *ibid. 27* (1986) 1903; c) T. Facklam, O. Wagner, H. Heydt, M. Regitz, *Angew. Chem. 102* (1990) 316; *Angew. Chem. Int. Ed. Engl. 29* (1990) 314; d) H. Keller, *Dissertation*, Universität Kaiserslautern, 1988; e) T. Facklam, *Dissertation*, Universität Kaiserslautern, 1989.
[4] T. Aoyama, S. Inove, T. Shioiri, *Tetrahedron Lett. 25* (1984) 433.
[5] J. Böske, E. Niecke, E. Ocando-Mavarez, J. P. Majoral, G. Bertrand, *Inorg. Chem. 25* (1986) 2695.

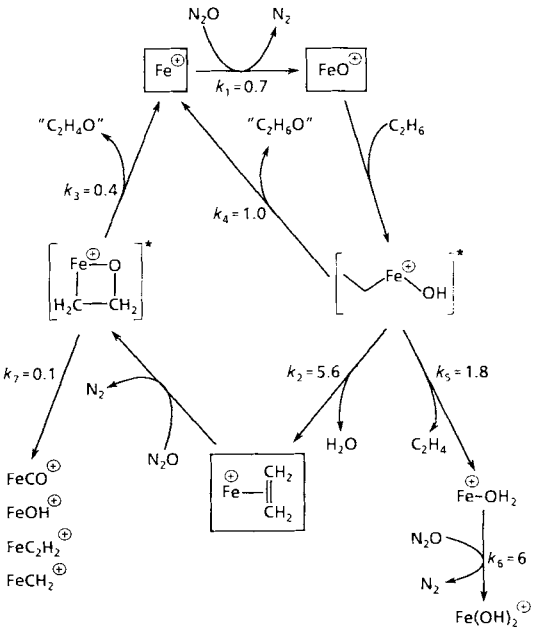

Scheme 1. Catalytic cycle for the $Fe^{\oplus}$-mediated oxidation of C_2H_6 by N_2O. The rate constants k_i, given in cm^3 molecule^{-1} s^{-1}, have to be multiplied by 10^{-10}.

$Fe^{\oplus}$-Catalyzed Gas-Phase Oxidation of Ethane by N_2O**

By *Detlef Schröder* and *Helmut Schwarz**

Dedicated to Professor Albert Eschenmoser on the occasion of his 65th birthday

Although thermodynamically favored, many oxidation reactions do not occur at room temperature unless the kinetic barriers are lowered by catalysts. This fact is a prerequisite for the origin and maintenance of life,[1] but it also poses an obstacle to the in vitro transformation of simple substrates to "more valuable" products.

Here we describe a model reaction in which oxidation of ethane by N_2O [Eq. (a)] is catalyzed by $Fe^{\oplus}$. Although the process is strongly exothermic ($\Delta H_r = -121$ kcal mol^{-1}), it does not occur in the absence of $Fe^{\oplus}$.

$$C_2H_6 + 2\,N_2O \rightarrow CH_3CHO + H_2O + 2\,N_2 \qquad (a)$$

The oxidation takes place in the gas phase and the individual steps of the $Fe^{\oplus}$-catalyzed cycle (Scheme 1) can be studied by Fourier transform ion cyclotron resonance (FT-ICR).[2]

The following observations were made concerning the individual reactions:

1. In the reaction of $FeO^{\oplus}$ with C_2H_6, already investigated by *Freiser* et al.,[7] the encounter complex $[FeO/C_2H_6]^{\oplus *}$ is not observed. Instead, the products of three reaction paths were found [Eq. (b)]. The corresponding rate constants k_i are given in Scheme 1. All processes are strongly exothermic.[8]

$$\begin{array}{lllll} FeO^{\oplus} + C_2H_6 & & & & \Delta H_r \\ \downarrow & & & & [\text{kcal mol}^{-1}] \\ & \xrightarrow{67\%} & Fe(C_2H_4)^{\oplus} + H_2O & -36 & \\ [FeO/C_2H_6]^{\oplus *} & \xrightarrow{21\%} & Fe(OH_2)^{\oplus} + C_2H_4 & -31 & (b) \\ & \xrightarrow{12\%} & Fe^{\oplus} + CH_3CH_2OH & -13 & \end{array}$$

A double resonance experiment demonstrates that $FeO^{\oplus}$ is the direct precursor of all products shown in Equation (b): irradiation at the resonance frequency of $FeO^{\oplus}$ results in suppression of the reactions. Collisional activation and labeling experiments provide indications of the structures of the $Fe(C_2H_4)^{\oplus}$ and $Fe(OH_2)^{\oplus}$ ions. The iron–hydrocarbon complex at m/z 84 specifically loses C_2H_4 upon collisional activation with argon; this finding is consistent with an Fe(ethylene)$^{\oplus}$ structure. The dominating reaction of the ion at m/z 74 with argon is loss of H_2O; in addition, ca. 10% loss of H$^{\bullet}$ or OH$^{\bullet}$ is observed. If, instead of an $Fe(OH_2)^{\oplus}$ complex, an $Fe(H)OH^{\oplus}$ structure were present, preferential H$^{\bullet}$ loss would be expected owing to the dissociation energies $D(M^{\oplus}\text{-}X)$ (X = H, OH).[9] Moreover, the thermochemical data favor the structure $Fe(OH_2)^{\oplus}$ over $Fe(H)OH^{\oplus}$ by more than 14 kcal mol^{-1}.[8] The role of $Fe(OH_2)^{\oplus}$ as a "sink" in the catalytic cycle will be discussed in greater detail later.

The encounter complex $(FeO/C_2H_6)^{\oplus *}$ presumably corresponds to $Fe(C_2H_5)OH^{\oplus *}$, as indicated by the product distribution obtained from the reaction of $FeO^{\oplus}$ with CH_3CD_3: decomposition of $(FeO/CH_3CD_3)^{\oplus *}$ yields almost exclusively HDO and $C_2H_2D_2$ as neutral molecules.

2. Reaction of "isolated" $Fe(C_2H_4)^{\oplus}$ with N_2O results in liberation of N_2 [Eq. (c)]. Since the liberated N_2 takes away

[*] Prof. Dr. H. Schwarz, Dipl.-Chem. D. Schröder
Institut für Organische Chemie der Technischen Universität
Strasse des 17. Juni 135, D-1000 Berlin 12 (FRG)

[**] This work was supported by the Deutsche Forschungsgemeinschaft, the Fonds der Chemischen Industrie, and the Gesellschaft von Freunden der Technischen Universität Berlin.

part of the excitation energy as translational and vibrational energy, it is not surprising that a signal for $Fe(C_2H_4O)^{\oplus}$ is observable. However, the main products are $Fe^{\oplus}$ and "C_2H_4O". The two reactions account for 88% of the product distribution; the products corresponding to k_7 in Scheme 1 ($\Sigma < 12\%$) are formed in nearly equal amounts ($X = CO, OH, C_2H_2, CH_2$).

$$Fe(C_2H_4)^{\oplus} + N_2O \xrightarrow{-N_2} \begin{cases} \xrightarrow{16\%} Fe(C_2H_4O)^{\oplus} \\ \xrightarrow{72\%} Fe^{\oplus} + C_2H_4O \\ \xrightarrow{<12\%} FeX^{\oplus} \end{cases} \quad (c)$$

3. The ion $Fe(C_2H_4O)^{\oplus}$ is most likely a ferraoxacyclobutane, since, upon collisional activation, the "isolated" ion decomposes practically exclusively to $FeCH_2^{\oplus}/CH_2O$ and $Fe^{\oplus}/C_2H_4O$. The formation of $FeCH_2^{\oplus}$ would not be possible from either an $Fe(CH_3CHO)^{\oplus}$ or an $Fe(CH_2=CHOH)^{\oplus}$ complex. That the metallacycle does not decompose to $FeO^{\oplus}/C_2H_4$ upon collisonal activation is due to the product stability for the two other conceivable cycloreversions; $FeO^{\oplus}/C_2H_4$ is at least 20 kcal mol^{-1} less favorable than $FeCH_2^{\oplus}/CH_2O$.

4. The central question posed by the reaction $FeC_2H_4^{\oplus} + N_2O \rightarrow Fe^{\oplus} + C_2H_4O$ [Eq. (c)] concerns the constitution of "C_2H_4O". Chemically reasonable structures for the neutral compound include oxirane, vinyl alcohol, and acetaldehyde. As shown by Scheme 2, the formation of each

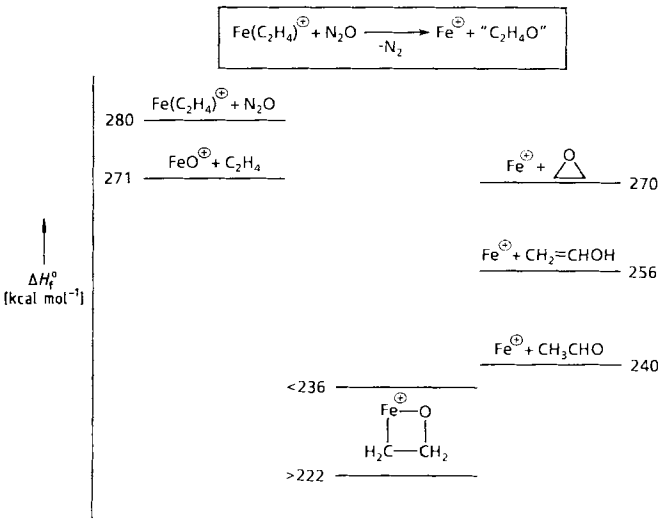

Scheme 2.

of the three isomers starting from $Fe(C_2H_4)^{\oplus}/N_2O$ would be exothermic. Since neutral species cannot be directly observed in ICR experiments, indirect evidence is necessary. Nonetheless, the appearance of a weak-intensity signal at m/z 43 ($CH_3CO^{\oplus}$) proves that, in the course of this reaction, oxygen must have been transferred to the C_2H_4 unit.

The enthalpy of formation ΔH_f° of the metallacycle $Fe(C_2H_4O)^{\oplus}$ can be estimated from the occurrence or absence of the ligand displacement reactions (d) and (e): $222 < \Delta H_f^{\circ}(FeC_2H_4O)^{\oplus} < 236$ kcal mol^{-1}.

The observation of the metallacycle $Fe(C_2H_4O)^{\oplus}$ despite the strong exothermicity of the reaction [Eq. (c)] must be due to the fact that the simultaneously formed nitrogen carries

$$Fe(C_2H_4)^{\oplus} + H_2C\overset{O}{\diagup\diagdown}CH_2 \longrightarrow \begin{matrix} {}^{\oplus}Fe-O \\ | \quad | \\ H_2C-CH_2 \end{matrix} + C_2H_4 \quad (d)$$

$$Fe(butadiene)^{\oplus} + H_2C\overset{O}{\diagup\diagdown}CH_2 \dashrightarrow \begin{matrix} {}^{\oplus}Fe-O \\ | \quad | \\ H_2C-CH_2 \end{matrix} + C_4H_6 \quad (e)$$

away a considerable part of the energy as kinetic energy. This assumption is supported by the observation that an encounter complex is *not* detectable in the reaction $FeO^{\oplus} + C_2H_4 \rightarrow Fe(C_2H_4O)^{\oplus}$, although this process is 9 kcal mol^{-1} less exothermic; instead, only subsequently formed products are observed. If at least 9 kcal mol^{-1} of internal energy is transferred to N_2 as translational energy on formation of $Fe(C_2H_4O)^{\oplus}$ from $Fe(C_2H_4)^{\oplus}$ and N_2O, however, then oxirane is necessarily ruled out for thermochemical reasons as the oxidation product of C_2H_4. This supposition is supported by an independent experiment: $Fe^{\oplus}$, thermalized with argon ($p \approx 5 \times 10^{-8}$ mbar) for about 20 s, reacts with added oxirane to give, among other products, $FeO^{\oplus}$ and C_2H_4 (25%); this means that $Fe(C_2H_4)^{\oplus}/N_2O$ would react via $Fe^{\oplus}/C_2H_4O$ to give $FeO^{\oplus}/C_2H_4$ if C_2H_4O corresponded to oxirane. This is not observed in the experiment [Eq. (c)].

The decision in favor of acetaldehyde is facilitated by a "mechanistic criterion". *Armentrout, Beauchamp* et al.[6, 10] have indicated that the weakest bond in a metallacycle of type **1** is the metal–carbon bond. Cleavage of this bond could lead, via diverse ion/dipole complexes, to a "metal-bound" diradical **3** (Scheme 3). Experimental data and MO

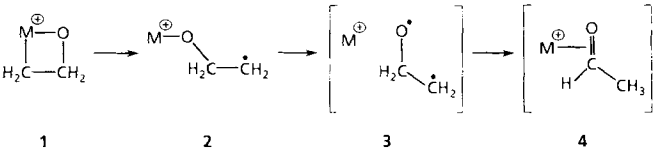

1 2 3 4

Scheme 3.

calculations[11] indicate that a free diradical $\dot{O}CH_2\dot{C}H_2$ should isomerize to CH_3CHO. If this also holds true in the presence of $M^{\oplus}$, then complex **4** would be formed in the present case. It should be mentioned that the side product $Fe(CO)^{\oplus}$ (4%) in reaction (c) could be formed from **4** by reductive elemination of CH_4. The main path, however, would be loss of CH_3CHO and regeneration of $Fe^{\oplus}$, which, in turn, could initiate a new cycle. *Beyond any doubt, $Fe^{\oplus}$ functions as a catalyst in reaction (a).* From the rate constants given in Scheme 1, each $Fe^{\oplus}$ ion is estimated to convert about 2.5 molecules of C_2H_6. Where are the "sinks" that keep the turnover number so small? (1) The metallacycle **1** (M = Fe) not only decomposes to $Fe^{\oplus}$ and CH_3CHO with a rate constant of $k_3 = 0.4 \times 10^{-10}$ cm^3 molecule^{-1} s^{-1}, but also affords other side products ($k_7 = 0.1 \times 10^{-10}$ cm^3 molecule^{-1} s^{-1}); common to all is the loss of $Fe^{\oplus}$. (2) A strong sink is the reaction path with the rate constants k_5: $Fe(OH_2)^{\oplus}$ undergoes rapid further reaction with N_2O to give $Fe(OH)_2^{\oplus}$, which, however, only reacts with C_2H_6/N_2O at an unmeasurably slow rate; thus, $Fe(OH)_2^{\oplus}$ represents a dead end. It is noteworthy that $FeO^{\oplus}$ reacts with C_2H_6 whereas $Fe(OH)_2^{\oplus}$ reacts only sluggishly: although both iron-containing ions have a formal oxidation state of + 3, the oxidation state of the metal is not the only governing factor for an efficient activation.

Finally, the result of a further test should be mentioned. This test my be regarded as a measure of the reliability of the k_i values in Scheme 1 (which themselves were derived from the reaction of "isolated" intermediates). Use of the so-derived rate constants for determination of the time dependence of the ions $Fe^{\oplus}$, $FeO^{\oplus}$, $Fe(C_2H_4)^{\oplus}$, and $Fe(OH)_2^{\oplus}$ appearing in the catalytic cycle gives the data shown in Figure 1. Theory (solid line) and experiment are in good agreement in view of the known errors involved in FTICR intensity measurements. Comparison of theory with experiment reveals the following: (1) No noticeable excitation occurs on "isolation" of the intermediates. (2) Additional intermediates need not be considered in modeling the catalytic cycle.

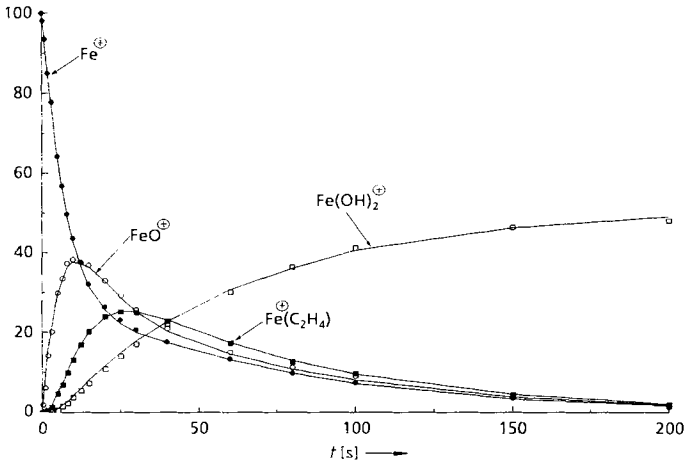

Fig. 1. Time dependence of ion abundance for $Fe^{\oplus}$, $FeO^{\oplus}$, $Fe(C_2H_4)^{\oplus}$, and $Fe(OH)_2^{\oplus}$ in the range $0 < t < 200$ s. The solid lines are based on a numerical solution of the respective differential equations using the k_i values given in Scheme 1 (see text). ●,■,○,□ = measured values.

Received: June 15, 1990 [Z 4017 IE]
German version: *Angew. Chem. 102* (1990) 1466

CAS Registry numbers:
$[FeOCH_2CH_2]^{\oplus}$, 129877-75-6; C_2H_6, 74-84-0; N_2O, 10024-97-2; $Fe^{\oplus}$, 14067-02-8; $FeO^{\oplus}$, 12434-84-3; $[Fe(H_2C=CH_2)]^{\oplus}$, 109801-95-8.

[1] A. Eschenmoser, *Angew. Chem. 100* (1988) 5; *Angew. Chem. Int. Ed. Engl. 27* (1988) 5.

[2] Conditions: $Fe^{\oplus}$ ions were generated from a stainless steel target in the external ion source of a Spectrospin CMS 47X mass spectrometer[3] by laser desorption/ionization using an Nd-YAG laser (Spectron Systems; $\lambda = 1064$ nm)[4]. The metal ions were transferred to the actual ICR cell by means of a system of electrical potentials and lenses. After deceleration, they were trapped in the magnetic field of a superconducting magnet (Oxford Instruments; maximum field strength 7.05 T). The isotope $^{56}Fe^{\oplus}$ was "isolated" by a double resonance experiment and allowed to react with N_2O ($p = 8 \times 10^{-8}$ mbar) to give $FeO^{\oplus}$[5]. Since this reaction is strongly exothermic (1.8 eV)[6], the products were formed with considerable excitation energy, which, however, was removed by collisions with the environment. $FeO^{\oplus}$ was "reisolated" and allowed to react with C_2H_6 ($p = 1.2 \times 10^{-8}$ mbar) as described by *Freiser*[7]. The main product was $FeC_2H_4^{\oplus}$ (70%), which, after renewed "isolation", was allowed to react again with N_2O. Mainly (>80%) "C_2H_4O" and $Fe^{\oplus}$ were thereby formed. The regenerated $Fe^{\oplus}$ completes the catalytic cycle and is available for a new cycle. It should be noted that the rate constants k_i are independent of the "age" of $Fe^{\oplus}$ within the error limits of ± 15%.

[3] Detailed description: a) K. Eller, H. Schwarz, *Int. J. Mass Spectrom. Ion Processes 93* (1989) 243; b) K. Eller, W. Zummack, H. Schwarz, *J. Am. Chem. Soc. 112* (1990) 621.

[4] a) B. S. Freiser, *Talanta 32* (1985) 697; b) B. S. Freiser, *Anal. Chim. Acta 178* (1985) 137.

[5] a) M. M. Kappes, R. H. Staley, *J. Am. Chem. Soc. 103* (1981) 1286; b) M. M. Kappes, R. H. Staley, *J. Phys. Chem. 85* (1981) 942.

[6] S. K. Loh, E. R. Fisher, L. Lian, R. H. Schultz, P. B. Armentrout, *J. Phys. Chem. 93* (1989) 3159.

[7] T. C. Jackson, D. B. Jacobson, B. S. Freiser, *J. Am. Chem. Soc. 106* (1984) 1252.

[8] All reaction enthalpies were estimated by using known ΔH_f values (kcal mol^{-1}): $Fe^{\oplus}$ 282; $FeO^{\oplus}$ 259; $Fe(C_2H_4)^{\oplus}$ 260; $Fe(H_2O)^{\oplus}$ 196; $Fe(H)OH^{\oplus}$ 211–223; Fe(butadiene)$^{\oplus}$ 261; N_2O 20; C_2H_4 12; C_2H_6 − 20; H_2O − 57; CH_2CH_2O − 12; $CH_2=C(H)OH$ − 26; CH_3CHO − 44; CH_3CH_2OH − 56; $CH_2=CH-CH=CH_2$ 27.

[9] T. F. Magnera, D. E. David, J. Michl, *J. Am. Chem. Soc. 111* (1989) 4100.

[10] a) L. F. Halle, P. B. Armentrout, J. L. Beauchamp, *Organometallics 2* (1983) 1829; b) H. Kang, J. L. Beauchamp, *J. Am. Chem. Soc. 108* (1986) 5663; c) E. R. Fisher, P. B. Armentrout, *J. Phys. Chem. 94* (1990) 1674.

[11] a) A. Lifshitz, H. Ben-Hamon, *J. Chem. Phys. 87* (1983) 1782; b) J. G. Serafin, C. M. Friend, *J. Am. Chem. Soc. 111* (1989) 6019; c) F. W. McLafferty, *Science (Washington D. C.) 247* (1990) 925; e) C. Wesdemiotis, B. Leyh, A. Fura, F. W. McLafferty, *J. Am. Chem. Soc.*, in press.

$FeO^{\oplus}$ Activates Methane**

By *Detlef Schröder* and *Helmut Schwarz**

Dedicated to Professor Rolf Huisgen on the occasion of his 70th birthday

The metal-mediated activation of methane is the most important of all CH bond activations.[1] This is due not only to the great economic interest in the direct conversion of methane to "valuable" products such as methanol, but also to the inherent scientific challenge, which still remains to be met in a general way. The approach used succesfully for many substrates, namely, to obtain information on the detailed steps of the activation of CH/CC bonds by "naked" transition-metal ions,[2] has failed for the simple reason that the oxidative addition of most metal ions $M^{\oplus}$ (M = Ti, V, Co, Fe, Nb, Rh, Sc, Y, La, Lu, Co, Ni, Zn, and U)[3] to CH_4 [Eq. (a)] is endothermic.[4]

$$CH_4 + M^{\oplus} \rightarrow H\text{-}M^{\oplus}\text{-}CH_3 \rightarrow \text{products} \qquad \text{(a)}$$

The only exceptions are those cases where either $M^{\oplus}$ is electronically excited (e.g., $Ti^{\oplus}$ [5] or $Cr^{\oplus}$ [6]) or the barrier to oxidative addition is overcome by kinetic excitation of $M^{\oplus}$.[2b, 7] The reaction of "naked" metal atoms M (M = Mn, Fe, Co, Ni, Zn) with CH_4 in a noble-gas matrix is also only possible after photochemical excitation of M.[8] The often useful approach of activating CH/CC bonds not by single metal ions but rather by homo- or heteronuclear ionic clusters[9] has also proved fruitless.[10]

A conceivable way of favorably influencing the reaction enthalpy for activation of methane is the use of $MO^{\oplus}$ instead of $M^{\oplus}$.[11] Indeed, *Freiser* et al.[12] were able to increase the propensity of alkanes to react by use of $FeO^{\oplus}$ instead of $Fe^{\oplus}$. The authors reported, however, that "cold" $FeO^{\oplus}$ did *not* react with CH_4 in the gas phase, even though all processes shown in Equation (b) are exothermic.[13]

We have not been able to confirm this result.[12] $FeO^{\oplus}$, generated under FTICR (Fourier transform ion cyclotron resonance) conditions[14] from $Fe^{\oplus}$ and N_2O, *affords all the products shown in Equation (b) in a ratio of 57:2:41.*[19] The possibility that excited $FeO^{\oplus}$ might be generated[20] and

[*] Prof. Dr. H. Schwarz, Dipl.-Chem. D. Schröder
Institut für Organische Chemie der Technischen Universität
Strasse des 17. Juni 135, D-1000 Berlin 12 (FRG)

[**] This work was supported by the Deutsche Forschungsgemeinschaft, the Volkswagen-Stiftung, and the Fonds der Chemischen Industrie.

$$\begin{array}{lll} & & \Delta H_r \\ & & [\text{kcal mol}^{-1}] \\ \text{FeO}^{\oplus} + \text{CH}_4 \xrightarrow{k_1} & \text{FeOH}^{\oplus} + \text{CH}_3^{\bullet} & -2 \\ & \text{FeCH}_2^{\oplus} + \text{H}_2\text{O} & -21 \\ & \text{Fe}^{\oplus} + \text{CH}_3\text{OH} & -7 \end{array} \quad \text{(b)}$$

thus be responsible for the activation of CH_4 is unsupported. This is directly shown by control experiments in which $FeO^{\oplus}$ was allowed to react with CH_4 under diverse conditions (variation of the trapping time or the quenching partner); no change in the product distribution or the rate constants k_1 was found. We obtained a value of $k_1 = 2.0 \times 10^{-10}$ cm^3 molecule^{-1} s^{-1}. Although this value is significantly smaller than that for the analogous reaction of $FeO^{\oplus}$ with C_2H_6 ($k = 8.4 \times 10^{-10}$ cm^3 molecule^{-1} s^{-1} [12, 21]), it is still two orders of magnitude greater than the rate constants for association reactions of $M^{\oplus}$ with CH_4.[3b]

The product distribution[22] obtained from the reaction of $FeO^{\oplus}$ with CH_2D_2 and with CD_4 [Eq. (c)] allows conclusions to be drawn concerning the reaction mechanism. A small isotope effect ($k_H/k_D = 4.6$) is found by comparing the rate constants for formation of $FeOD^{\oplus}$ and $FeOH^{\oplus}$ (reaction with CH_2D_2). Comparison of the distribution of the products $FeOX^{\oplus}$ (X = H, D) and $Fe^{\oplus}$ for CH_4, CH_2D_2, and CD_4 reveals that the formation of $Fe^{\oplus}$, which, for thermodynamic reasons, is necessarily coupled with the generation of CH_3OH, is likewise favored by an isotope effect.

$$\begin{array}{lll} & & \text{rel. amount [\%]} \\ \text{FeO}^{\oplus} + \text{CH}_2\text{D}_2 \longrightarrow & \text{FeOD}^{\oplus} + \text{CH}_2\text{D}^{\bullet} & 9 \\ & \text{FeOH}^{\oplus} + \text{CHD}_2^{\bullet} & 41 \\ & \text{Fe}^{\oplus} + \text{CH}_2\text{D}_2\text{O} & 50 \\ \text{FeO}^{\oplus} + \text{CD}_4 \longrightarrow & \text{FeOD}^{\oplus} + \text{CD}_3^{\bullet} & 35 \\ & \text{Fe}^{\oplus} + \text{CD}_3\text{OD} & 65 \end{array} \quad \text{(c)}$$

The observed isotope effects can be easily explained if the species $CH_3FeOH^{\oplus}$ (**1**) is postulated as central intermediate. Several paths for the formation of **1** are conceivable.

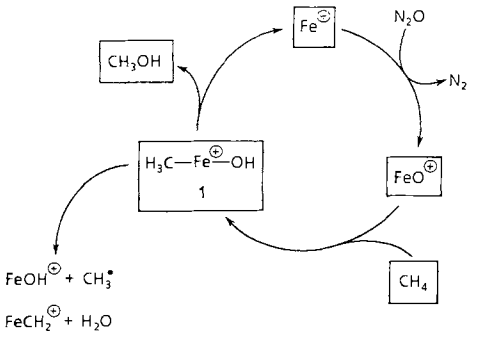

Scheme 1.

Although $Fe^{\oplus}$ is used in "equimolar" amounts in the experiments described here,[23] the chances of achieving a *catalytic* activation of CH_4 by $FeO^{\oplus}$ are not small, since $Fe^{\oplus}$ generated in the course of the reductive elimination of CH_3OH could be easily reintroduced into the cycle after reaction with, for example, N_2O (Scheme 1).[24]

Received: July 18, 1990 [Z 4073 IE]
German version: *Angew. Chem. 102* (1990) 1468

CAS Registry numbers:
D, 7782-39-0; $FeO^{\oplus}$, 12434-84-3; methane, 74-82-8.

[1] A. E. Shilov: *Activation of Saturated Hydrocarbons by Transition Metal Complexes*, Reidel, Boston 1984; D. J. Trevor, D. M. Cox, A. Kaldor, *J. Am. Chem. Soc. 112* (1990) 3742; H. D. Gesser, N. R. Hunter, C. B. Prakash, *Chem. Rev. 85* (1985) 235.

[2] Review article: a) H. Schwarz, *Acc. Chem. Res. 22* (1989) 282; b) P. B. Armentrout, J. L. Beauchamp, *Acc. Chem. Res. 22* (1989) 315, and references cited therein.

[3] Selected literature: a) N. Aristov, P. B. Armentrout, *J. Phys. Chem. 91* (1987) 6178; b) R. Tonkyn, M. Ronan, J. C. Weisshaar, *J. Phys. Chem. 92* (1988) 92; c) L. S. Sunderlin, P. B. Armentrout, *J. Am. Chem. Soc. 111* (1989) 3845.

[4] Exceptions are the transition-metal ions $M^{\oplus}$ = $Ta^{\oplus}$, $W^{\oplus}$, $Os^{\oplus}$, $Ir^{\oplus}$, and $Pt^{\oplus}$, which were recently shown to dehydrogenate methane with formation of $MCH_2^{\oplus}$. Furthermore, $Ta^{\oplus}$, $W^{\oplus}$, and $Pt^{\oplus}$ were capable of "polymerizing" methane ($M^{\oplus} + CH_4 \rightarrow MC_4H_8^{\oplus} + 4H_2$): J. L. Beauchamp, K. Irakura, *NATO ASI Fundam. Gas Phase Ion Chem.*, France 1990. We thank Prof. *J. L. Beauchamp*, Pasadena, for permission to mention these results.

[5] L. S. Sunderlin, P. B. Armentrout, *J. Phys. Chem. 92* (1988) 1209.

[6] L. F. Halle, P. B. Armentrout, J. L. Beauchamp, *J. Am. Chem. Soc. 103* (1981) 962; W. D. Reents, Jr., F. Strobel, R. B. Freas III, J. Wronka, D. P. Ridge, *J. Phys. Chem. 89* (1985) 5666; R. Georgiadis, P. B. Armentrout, *J. Phys. Chem. 92* (1988) 7060.

[7] R. H. Schultz, J. L. Elkind, P. B. Armentrout, *J. Am. Chem. Soc. 110* (1988) 411.

[8] Z. H. Kafafi, R. H. Hauge, J. L. Margrave, *J. Am. Chem. Soc. 107* (1985) 6134; J. M. Parnis, S. A. Mitchell, J. Garcia-Prieto, G. A. Ozin, *J. Am. Chem. Soc. 107* (1985) 8169; S.-C. Chang, R. H. Hauge, W. E. Billups, J. L. Margrave, Z. H. Kafafi, *Inorg. Chem. 27* (1988) 205, and references cited therein. A. B. Anderson, S. Baldwin, *Organometallics 6* (1987) 1621. For matrix experiments on photoinduced CH_4 activation of transition-metal fragments, see R. N. Perutz, *Pure Appl. Chem. 62* (1990) 1103.

[9] S. W. Buckner, B. S. Freiser, *Polyhedron 7* (1988) 1583; B. S. Freiser *Chemtracts: Anal. Phys. Chem. 1* (1989) 65.

[10] M. P. Irion, A. Selinger, *Ber. Bunsenges. Phys. Chem. 93* (1989) 1408; Y. Huang, B. S. Freiser, *J. Am. Chem. Soc. 110* (1988) 387, and references cited therein.

[11] K. K. Irikura, J. L. Beauchamp, *J. Am. Chem. Soc. 111* (1989) 75.

[12] T. C. Jackson, D. B. Jacobson, B. S. Freiser, *J. Am. Chem. Soc. 106* (1984) 1252.

[13] The reaction enthalpies were estimated by using known ΔH_f° values [kcal mol^{-1}]: $Fe^{\oplus}$ 282; $FeO^{\oplus}$ 259; $FeOH^{\oplus}$ 206; $FeCH_2^{\oplus}$ 278; $CH_3^{\bullet}$ 34; CH_3OH − 47; H_2O − 57.

[14] The following conditions were used: $Fe^{\oplus}$ ions were generated from a steel target in the external ion source of a Spectrospin CMS 47X FTICR instrument[15] by laser desorption/ionization using an Nd-YAG laser (Spectron Systems; λ = 1064 nm)[16]. The metal ions were transferred to the actual ICR cell by means of a system of electrical potentials and lenses. After deceleration, they were trapped in the magnetic field of a superconducting magnet (Oxford Instruments; maximum field strength 7.05 T). The isotope $^{56}Fe^{\oplus}$ was "isolated" by a double resonance experiment and allowed to react with pulsed-in N_2O ($p = 10^{-5}$ mbar) to give $FeO^{\oplus}$ [17]. This reaction is strongly exothermic[18]; the excess energy was removed by collision with argon (p: $0.2-2 \times 10^{-7}$ mbar). $FeO^{\oplus}$ was "reisolated" and allowed to react with CH_4 (p: $0.5-2 \times 10^{-8}$ mbar).

[15] Detailed description: K. Eller, H. Schwarz, *Int. J. Mass Spectrom. Ion Processes 93* (1989) 243; K. Eller, W. Zumack, H. Schwarz, *J. Am. Chem. Soc. 112* (1990) 621.

[16] B. S. Freiser, *Talanta 32* (1985) 697.

[17] M. M. Kappes, R. H. Staley, *J. Am. Chem. Soc. 103* (1981) 1286.

[18] S. K. Loh, E. R. Fisher, L. Lian, R. H. Schultz, P. B. Armentrout, *J. Phys. Chem. 93* (1989) 3159.

[19] The thermodynamically favored loss of H_2O is presumably kinetically hindered.

[20] There are four low-lying states for $FeO^{\oplus}$ ($^4\pi$, $^4\Delta$, $^4\Phi$, and $^6\Sigma^+$). An experimental assignment has not yet been reported (see also [18]).

[21] D. Schröder, H. Schwarz, *Angew. Chem. 102* (1990) 1466, *Angew. Chem. Int. Ed. Engl. 29* (1990) 1431.

[22] The intensity of the signals for $FeCHD^{\oplus}$ and $FeCD_2^{\oplus}$ is too weak for quantitative evaluation.

[23] Our results have prompted Prof. *B. S. Freiser*, Purdue University, to repeat the earlier investigations[12]. Perfect agreement with our results was obtained (*B. S. Freiser*, personal communication, June 13, 1990). We thank Prof. *B. S. Freiser* and Prof. *D. Jacobson* for promptly carrying out the control experiments.

[24] For the $Fe^{\oplus}$-mediated *catalytic* oxidation of C_2H_6 with N_2O, see[21].

Sterically Hindered Internal Rotation in an Acyclic α,β-Unsaturated Ketone. 2,2,5-Trimethyl-4-isopropylhex-4-en-3-one**

By *John M. Nuss,* Steven J. Bark, Daniel B. Borchardt,* and *Thomas Hellmann Morton**

Sterically hindered internal rotation has been widely studied in a variety of organic compounds. Surprisingly, such effects in the simplest conjugated systems have been detected in a comparatively small number of cases. Among hydrocarbons, only two examples of acyclic skew dienes have been reported, 2,3-di-*tert*-butyl-1,3-butadiene (**1**)[1] and 2,5-dimethyl-3,4-diisopropyl-2,4-hexadiene (**2**).[2] The former

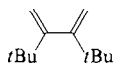

1

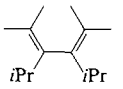

2

was characterized by the λ_{max} value of its $\pi \rightarrow \pi^*$ absorption, while hindered rotation in the latter was characterized by the chemical nonequivalence of its isopropyl methyl groups in the ^{1}H NMR spectrum and by its He(I) photoelectron spectrum.[3] From the absence of any line broadening in the ^{1}H NMR spectrum of **2** at low frequency (60 MHz) and high temperature (195 °C), an experimental barrier to planarization of $\Delta G > 110$ kJ mol^{-1} (26 kcal mol^{-1}) has been calculated.[2] From the photoelectron spectrum, the dihedral angle between the two double bonds of **2** is estimated to be $\theta = 90 \pm 5°$.[3]

To date no example of sterically hindered internal rotation about the sp^2–sp^2 single bond in an acyclic enone has been reported. We describe here the synthesis and spectroscopic properties of α,β-unsaturated ketone **3**, which exhibits a barrier to planarization of its π system. The following alter-

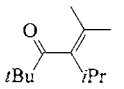

3

ations of the electronic spectrum might be anticipated as the result of preventing the carbonyl from being coplanar with the carbon–carbon double bond. Since $n \rightarrow \pi^*$ transitions are spatially forbidden, skewing, which brings the lone pair orbitals into better overlap with the π system of the double bond, ought to increase the extinction coefficient relative to that of a planar enone. At the same time, decreased overlap between the carbonyl and double-bond π systems should diminish the extinction coefficient of the $\pi \rightarrow \pi^*$ transition.

Compound **3** was synthesized from the vinyl iodide **4**.[4] Conversion to the corresponding vinyllithium **5** by addition of two equivalents of *tert*-butyllithium proceeds in good yield, as evidenced by recovery of the vinyltributylstannane **6** in 80% yield when the reaction mixture is quenched with tributyltin chloride. When pivaloyl chloride is added to a solution of **5** in THF at −78 °C and the mixture allowed to warm to room temperature, **3** is produced, but in a lower yield (55%) along with di-*tert*-butyl ketone as the major impurity. Purification of **3** by distillation and column chromatography affords a colorless liquid with a camphoraceous odor reminiscent of cineole (b.p. 104–105 °C at 25 Torr, $[n]_D^{20} = 1.4522$).[5]

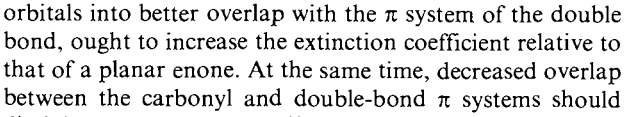

4, X = I
5, X = Li
6, X = Bu_3Sn

3 (a)

^{1}H NMR spectra at −99 °C and 25 °C are shown in Figure 1. By fitting[6] the observed spectra at eleven temperatures over the range, we calculated the following Arrhenius parameters for interconversion of the nonequivalent isopropyl methyl groups: $E_a = 45 \pm 3$ kJ mol^{-1}, $\lg A = 14.4 \pm 0.7$, where the experimental errors represent 95% confidence limits.

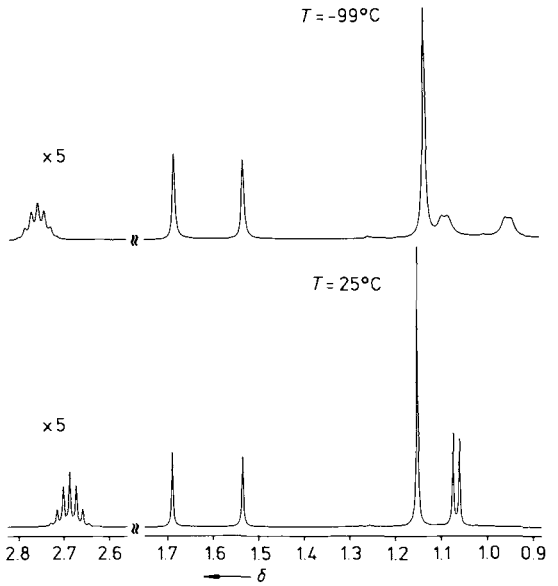

Fig. 1. 500-MHz ^{1}H NMR spectrum of **3** in $CFCl_3$. The doublets corresponding to the nonequivalent isopropyl methyl groups at $\delta = 0.95$ and 1.1 coalesce at −75 °C and sharpen to a doublet at $\delta = 1.08$ in the room temperature spectrum.

We infer that the nonequivalence of the isopropyl methyl resonances results from the chirality of the nonplanar enone. This inference is corroborated by the UV spectrum. The $n \rightarrow \pi^*$ transition of **3** ($\lambda_{max} = 318$ nm, $\varepsilon = 80$) has an extinction coefficient twice as large as that of mesityl oxide and exhibits partially resolved vibrational fine structure (six bands between 290 and 345 nm with a separation of 1100 cm^{-1}). The $\pi \rightarrow \pi^*$ transition of **3** ($\lambda_{max} = 242$ nm, $\varepsilon = 960$) is an order of magnitude less intense than the corresponding band in mesityl oxide.

Planarization of the enone is required in order for the isopropyl methyl groups to become chemically equivalent, and the barrier for **3** is much lower than for **2**. We have examined a number of molecular mechanics calculations of the relative planarization barriers and cannot find an obvious explanation. Although torsional potentials for aliphatic sp^2–sp^2 single bonds have not been well parameterized for force-field computations, we are nevertheless surprised that such calculations inevitably predict a planarization barrier for **2** that is less than twice as large as that for **3**, contrary to our experimental findings. The large preexponential A factor (which corresponds to a positive $\Delta S^{\ddagger}$) is also unusual. Although positive activation entropies have been reported for

[*] Prof. J. M. Nuss, Prof. T. H. Morton, S. J. Bark, Dr. D. B. Borchardt
Department of Chemistry, University of California
Riverside, CA 92521-0403 (USA)

[**] This work was supported by the National Science Foundation (CHE8802086) and the University of California, Riverside.

some conformational changes (e.g., six-member ring interconversions in the gas phase), solution-phase values of $\Delta S^{\neq}$ (from NMR studies) tend to be close to zero.[7] The hindered rotation in 2,2'-dimethylbiphenyl exhibits a negative activation entropy,[8] as do nearly all other hindered rotations for which activation parameters have been reported. Additional insight will be gained from studying homologues of compounds **1**–**3**.

Received: August 28, 1990 [Z 4158 IE]
German version: *Angew. Chem. 102* (1990) 1532

CAS Registry numbers:
3, 92605-05-5; **5**, 63883-73-8; $(CH_3)_3CCOCl$, 3282-30-2.

[1] H. Wynberg, A. DeGroot, D. W. Davies, *Tetrahedron Lett. 1963*, 1083.
[2] D. S. Bomse, T. H. Morton, *Tetrahedron Lett. 1974*, 3491.
[3] P. D. Mollere, K. N. Houk, D. S. Bomse, T. H. Morton, *J. Am. Chem. Soc. 98* (1976) 4732.
[4] D. M. Hilvert, M. D. Jacobs, T. H. Morton, *Org. Prep. Proced. Int. 13* (1981) 197.
[5] Compound **3** gave a satisfactory elemental analysis. Its IR and Raman spectra both show bands at 1678 and 1646 cm^{-1}. The mass spectrum shows no molecular ion; the highest mass ion is observed at *m/z* 125 and corresponds to $M^{\oplus}-t$Bu. ^{13}C NMR (75 MHz, $CDCl_3$, 25 °C): δ = 19.4, 21.7, 23.7, 27.7, 29.5, 43.9, 126.6, 141.9, 219.7.
[6] D. S. Stephenson, G. Binsch: DNMR5, Quantum Chemistry Program Exchange 365, Indiana University, Bloomington, IN 47405 (USA).
[7] P. S. Chu, N. S. True, *J. Phys. Chem. 89* (1985) 5613.
[8] W. Theilacker, H. Böhm, *Angew. Chem. 79* (1967) 232; *Angew. Chem. Int. Ed. Engl. 6* (1967) 251.

A 1-Silyl-1*H*-phosphirene/1,2-Dihydro-1,2-phosphasilete Rearrangement—The Decisive Step in the Synthesis of Heterocycles Containing 2-Phospha-1,3-diene Units**

By *Steffen Haber, Roland Boese*, and *Manfred Regitz**

Dedicated to Professor Wolfgang Kirmse on the occasion of his 60th birthday

1-Chloro-1*H*-phosphirenes such as **1** are readily accessible by [2 + 1] cycloaddition of chlorocarbenes (thermally generated from chlorodiazirines) to phosphaalkynes followed by [1,3] Cl shift.[1] We have used **1** to obtain the tris(trimethylsilyl)silyl-1*H*-phosphirene **3a**, which, via a previously unknown photochemical rearrangement, gives the dihydrophosphasilete **4a**. Compound **4a** provides an entry to the still unexplored chemistry of heterocycles containing 2-phospha-1,3-diene units.

The starting point for this sequence of reactions is the 1-chloro-1*H*-phosphirene **1**,[1] which undergoes smooth nucleophilic substitution with the lithiated silane **2a**[2] to give the 1-silyl-1*H*-phosphirene **3a**. Irradiation of **3a** in benzene results in ring expansion at the phenyl-substituted carbon of the three-membered ring and (Si → P) silyl shift to give the dihydrophosphasilete **4a**.[3] Dihydrodiphosphetes and dihydrometallaphosphetes (**4**, RP and metal complex fragments, respectively, instead of $M(SiMe_3)_2$) with comparable structures have already been prepared from 1*H*-phosphirenes by intermolecular insertion reactions.[4] The 1-germyl-1*H*-phosphirene/dihydrophosphagermete rearrangement (**3b** → **4b**), also previously unknown, can be carried out photochemically.[5]

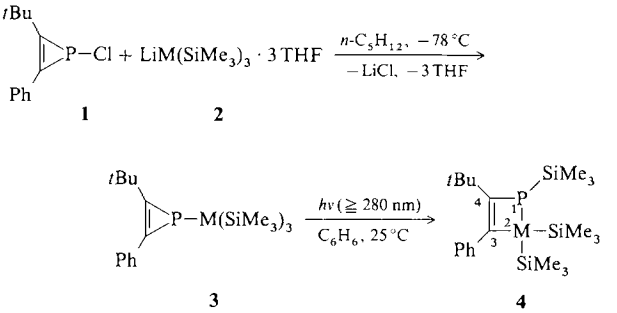

2a–**4a**: M = Si
2b–**4b**: M = Ge

The ring expansion **3a** → **4a** is accompanied by a downfield shift of the ^{31}P NMR signal (see Table 1). The signal of the C atom bearing the *t*Bu group (C4) in **4a** is also shifted downfield relative to that in **3a** and exhibits a $^1J(^{31}P,^{13}C)$ coupling of only 22.1 Hz, as also observed for 1,2-dihydro-1,2-diphosphetes.[6] In the ^1H NMR spectrum, the (Si → P) silyl shift is revealed by splitting of the $SiMe_3$ signal ($^3J(P,H)$ = 4 Hz).[7] These findings also hold true for **4b**.[5] The spectroscopic observations were confirmed by crystal structure analysis of **4a**.[8]

The 1,2-dihydro-1,2-phosphasilete ring is nearly planar, as shown by the torsional angles (see caption to Fig. 1). Notably, the exocyclic P–Si bond (2.259(1) Å) is significantly shorter than the P–Si bond in the ring (2.283(1) Å).

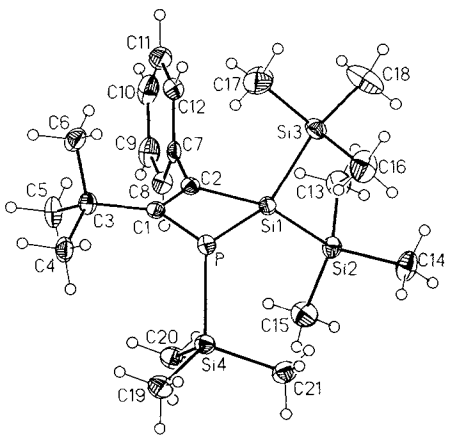

Fig. 1. Molecular structure of **4**[8]. Selected bond lengths [Å] and angles [°]: C1-C2 1.348(3), C1-P 1.879(2), C2-Si1 1.881(2), P-Si1 2.283(1), P-Si4 2.259(1), C1-C3 1.532(3), C2-C7 1.487(3), Si1-Si2 2.356(1), Si1-Si3 2.348(1); C1-P-Si1 73.5(1), P-Si1-C2 77.7(1), Si1-C2-C1 100.8(1), C2-C1-P 108.0(2), Si1-P-Si4 103.0(1), C1-P-Si4 103.7(1). Torsional angles: C1-C2-Si1-P 0.4, P-C1-C2-Si1 0.5, Si4-P-Si1-C2 –101.0, Si4-P-C1-C2 –100.1.

The reactivity of the silylphosphane component of **4a** may be exploited preparatively. Reaction with chlorobis(trimethylsilyl)methylenephosphane gives **5** (80%). Methyl pro-

[*] Prof. Dr. M. Regitz, Dipl.-Chem. S. Haber
Fachbereich Chemie der Universität
Erwin-Schrödinger-Strasse, D-6750 Kaiserslautern (FRG)
Dr. R. Boese
Institut für Anorganische Chemie der Universität-Gesamthochschule
Universitätsstrasse 5–7, D-4300 Essen 1 (FRG)

[**] Phosphorus Compounds with Unusual Coordination, Part 45. This work was supported by the Deutsche Forschungsgemeinschaft and the Fonds der Chemischen Industrie. Part 44: M. Ehle, O. Wagner, U. Bergstraßer, M. Regitz, *Tetrahedron Lett. 31* (1990), in press.

piolate undergoes insertion into the P–Si bond to afford **6** (95%);[9] likewise, diphenylketene yields **7** (70%).

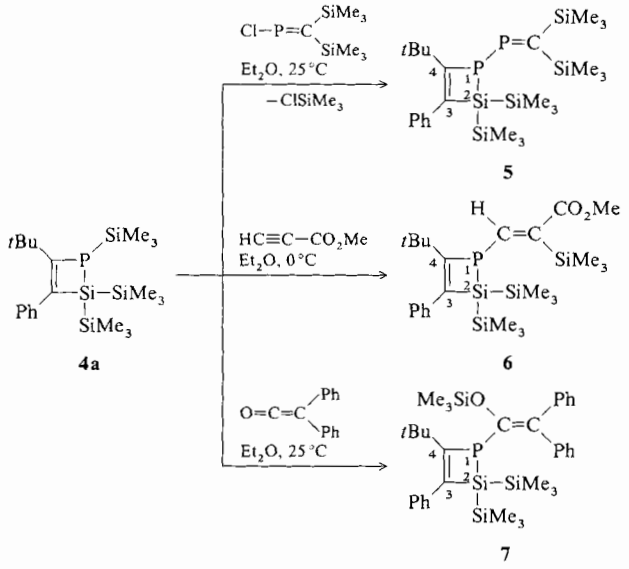

Table 1. Selected physical data for compounds **3**–**7** and **10**[a].

3a: bright yellow oil, b.p. 150 °C/10^{-3} mbar [b]; ^{1}H NMR: $\delta = 0.4$ (s, 27H, $SiMe_3$), 1.4 (s, 9H, *t*Bu), 7.1–7.9 (m, 5H, arene H). ^{13}C NMR: $\delta = 2.4$ (s, $Si(CH_3)_3$), 29.7 (s, $C(CH_3)_3$), 33.9 (d, ^2J(P,C) = 6.7 Hz, $C(CH_3)_3$), 111.5 (d, ^1J(P,C) = 45.3 Hz, =*C*-Ph), 130.9 (d, ^1J(P,C) = 56.2 Hz, =*C*-*t*Bu). ^{31}P NMR: $\delta = -205$.

4a: colorless crystals, m.p. 75 °C; ^{1}H NMR(CD_2Cl_2): $\delta = 0.2$–0.4 (broad, 18H, $Si(SiMe_3)_2$), 0.45 (d, ^3J(P,H) = 4.0 Hz, 9H, P-$SiMe_3$), 1.10 (s, 9H, *t*Bu), 7.0–7.2 (m, 5H, arene H). ^{13}C NMR: $\delta = 0.1$, 1.2 (each broad, Si-Si(CH_3)$_3$), 2.0 (d, ^2J(P,C) = 10.3 Hz, P-$Si(CH_3)_3$), 31.5 (d, ^3J(P,C) = 5.0 Hz, $C(CH_3)_3$), 40.9 (d, ^2J(P,C) = 13.7 Hz, $C(CH_3)_3$), 149.3 (d, ^2J(P,C) = 13.3 Hz, C3), 166.2 (d, ^1J(P,C) = 22.1 Hz, C4); ^{31}P NMR: $\delta = -130.7$.

5: bright yellow, nondistillable oil. ^{13}C NMR: $\delta = 0.35$, 1.4 (each s, $Si(CH_3)_3$), 1.9 (d, ^3J(P,C) = 12.4 Hz, $Si(CH_3)_3$), 3.0 (d, ^3J(P,C) = 8.9 Hz, $Si(CH_3)_3$), 31.6 (d, ^3J(P,C) = 4.7 Hz, $C(CH_3)_3$), 41.5 (d, ^2J(P,C) = 11.8 Hz, $C(CH_3)_3$), 152.4 (dd, ^2J(P,C) = 14.6 Hz, ^3J(P,C) = 5.8 Hz, C3), 168.9 (dd, ^1J(P,C) = 23.7, ^2J(P,C) = 6.8 Hz, C4), 211.2 (d, ^1J(P,C) = 96.4 Hz, P=C); ^{31}P NMR: $\delta = 459$, −38 (each d, each ^1J(P,P) = 270.5 Hz).

6: bright yellow oil, b.p. 200 °C/10^{-3} mbar [b]. ^{1}H NMR: $\delta = 0.4$, 0.5, 0.6 (each s, each 9H, $SiMe_3$), 1.2 (s, 9H, *t*Bu), 3.6 (s, 3H, CO_2Me), 7.0–7.3 (m, 5H, arene H), 8.7 (d, ^2J(P,H) = 5.0 Hz, 1H, CH-olefin). ^{13}C NMR: $\delta = -0.2$ (s, $Si(CH_3)_3$), 0.5 (s, $Si(CH_3)_3$), 1.0 (d, J(P,C) = 8.8 Hz, $Si(CH_3)_3$), 31.3 (d, ^3J(P,C) = 4.8 Hz, $C(CH_3)_3$), 41.4 (d, ^2J(P,C) = 12.7 Hz, $C(CH_3)_3$), 51.1 (s, CO_2CH_3), 142.9 (d, ^2J(P,C) = 28.5 Hz, =*C*-ester), 151.3 (d, ^2J(P,C) = 20.1 Hz, C3), 164.6 (d, ^1J(P,C) = 46.3 Hz, ^1J(C,H) = 154.0 Hz, =C-H), 169.2 (d, ^3J(P,C) = 14.6 Hz, CO_2CH_3), 169.7 (d, ^1J(P,C) = 17.0 Hz, C4). ^{31}P NMR: $\delta = -82$.

7: bright yellow oil, b.p. 220 °C/10^{-3} mbar [b], ^{1}H NMR(CD_2Cl_2): $\delta = 0.05$, 0.15, 0.40 (each s, each 9H, $SiMe_3$), 1.10 (s, 9H, *t*Bu), 7.0–7.4 (m, 15H, arene H). ^{13}C NMR(CD_2Cl_2): $\delta = 0.2$ (d, J(P,C) = 3.0 Hz, $Si(CH_3)_3$), 1.6 (s, $Si(CH_3)_3$), 2.5 (s, $Si(CH_3)_3$), 31.4 (d, ^3J(P,C) = 4.6 Hz, $C(CH_3)_3$), 41.5 (d, ^2J(P,C) = 15.0 Hz, $C(CH_3)_3$), 134.1 (d, ^2J(P,C) = 38.1 Hz, =CPh_2), 153.3 (d, ^1J(P,C) = 62.0 Hz, =*C*-$OSiMe_3$), 153.4 (d, ^2J(P,C) = 20.4 Hz, C3), 166.5 (d, ^1J(P,C) = 19.6 Hz, C4). ^{31}P NMR(CD_2Cl_2): $\delta = -58$.

10a: colorless crystals, m.p. 85 °C. ^{1}H NMR(CD_2Cl_2): $\delta = 0.15$ (s, 18H, $SiMe_3$), 1.15 (s, 9H, *t*Bu), 1.3 (d, ^4J(P,H) = 2.0 Hz, *t*Bu), 7.0–7.4 (m, 5H, arene H). ^{13}C NMR(CD_2Cl_2): $\delta = -0.62$ (s, $Si(CH_3)_3$), 29.1 (d, ^3J(P,C) = 13.7 Hz, $C(CH_3)_3$), 32.8 (d, ^3J(P,C) = 14.0 Hz, $C(CH_3)_3$), 42.8 (d, ^2J(P,C) = 27.3 Hz, $C(CH_3)_3$), 43.1 (d, ^2J(P,C) = 24.1 Hz, $C(CH_3)_3$), 125.6, 127.9, 128.2, 145.1 (each s, arene C), 134.6 (d, ^2J(P,C) = 7.3 Hz, C-5), 161.5 (d, ^1J(P,C) = 58.2 Hz, C6), 217.6 (d, ^1J(P,C) = 79.3 Hz, C2). ^{31}P NMR(CD_2Cl_2): $\delta = 91$.

10b: dark red crystals, m.p. 135 °C. ^{1}H NMR: $\delta = 0.40$ (s, 18H, $SiMe_3$), 1.5 (s, 9H, *t*Bu), 4.2–4.5 (m, 7H, Cp-H), 5.1 (m, 2H, Cp-H), 7.1–7.4 (m, 5H, arene H). ^{31}P NMR: $\delta = 92$.

[a] 90-MHz ^{1}H, 100.64-MHz ^{13}C, and 80.8-MHz ^{31}P NMR spectra in C_6D_6 (TMS(int.) or 85% H_3PO_4(ext.)). [b] Oven temperature for kugelrohr distillation.

The dihydrophosphasilete framework is still intact in **5**–**7**, as shown by comparison of the NMR chemical shifts of the ring carbon atoms (as well as their P coupling constants) and phosphorus atoms with the corresponding values for **4a** (Table 1).

Reaction of **4a** with the acyl chlorides **8a, b** undoubtedly results in initial formation of the *P*-acyl dihydrophosphasiletes **9a, b**, which, in contrast to **5**–**7**, are not isolable. Instead, they undergo spontaneous isomerization by 1,3-silyl shift[10] to give the dihydrooxaphospasilines **10a, b**, the first cyclic compounds containing a 2-phospha-1,3-diene partial structure.

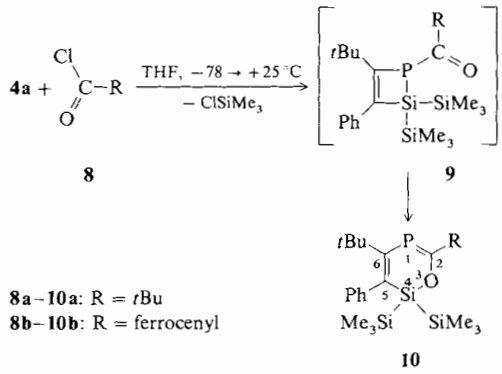

The transition from a $\lambda^3\sigma^3$ to a $\lambda^3\sigma^2$ phosphorus (**4a** → **10a,b**) is accompanied by a marked downfield shift of the ^{31}P NMR signal (Table 1). Otherwise, the NMR data for the 2-phospha-1,3-diene system of **10a,b** are in very good agreement with those for open-chain compounds containing the same structural unit, although in *s-trans* arrangement.[11, 12]

Experimental Procedure

4a: A solution of the 1-silyl-1*H*-phosphirene **3a** (1.5 g, 3.4 mmol) in 5 mL of benzene was irradiated in an NMR tube (diameter 10 mm) for 40 h (Heraeus TQ 150 high-pressure mercury lamp, ^{31}P NMR monitoring). After removal of the solvent, the crude product, a red-brown oil, was purified by kugelrohr distillation (150 °C oven temperature/10^{-3} mbar). Recrystallization from pentane at −78 °C afforded 0.5 g (34%) of colorless crystals of **4a** (m.p. 75 °C).

10b: A solution of **4a** (150 mg, 0.34 mmol) in 1 mL of tetrahydrofuran was treated slowly with a solution of **8b** (87 mg, 0.36 mmol) in 1 mL of tetrahydrofuran. After thawing, the solution was stirred for 24 h at 25 °C. Evaporation followed by column-chromatographic workup of the crude product on 12 g of silica gel (dried under vacuum) with 250 mL of pentane/ether (5/1) as eluent and recrystallization from pentane at −78 °C afforded 140 mg (70%) of dark red crystals of **10b** (m.p. 135 °C).

Received: June 29, 1990 [Z 4045 IE]
German version: *Angew. Chem. 102* (1990) 1523

CAS Registry numbers:
3a, 129943-63-1; **4a**, 129943-64-2; **5**, 129943-65-3; **6**, 129943-66-4; **7**, 129943-67-5; **8a**, 3282-30-2; **8b**, 1293-79-4; **10a**, 129964-83-6; **10b**, 129943-68-6; $ClP=C(SiMe_3)_2$, 79454-85-6; $HC\equiv CCO_2Me$, 922-67-8; $O=C=CPh_2$, 525-06-4.

[1] O. Wagner, M. Ehle, M Regitz, *Angew. Chem. 101* (1989) 227; *Angew. Chem. Int. Ed. Engl. 28* (1989) 225.
[2] G. Gutekunst, A. G. Brook, *J. Organomet. Chem. 225* (1982) 1; A. G. Brook, F. Abdesaken, H. Söllradt, *ibid. 299* (1986) 9.
[3] Distillative workup gave, in addition, 3,3-dimethyl-1-phenyl-1-butyne and hexakis(trimethylsilyl)disilane. Assuming a radical process, a homolysis of the P–Si bond of **3a** (→"P" loss) appears to compete with formation of **4a**, resulting in the aforementioned fragments.
[4] L. Ricard, M. Maigrot, C. Charrier, F. Mathey, *Angew. Chem. 99* (1987) 590; *Angew. Chem. Int. Ed. Engl. 26* (1987) 548; S. S. Al-Saaid, D.

Carmichael, P. B. Hitchcock, S. Lochschmidt, A. Marinetti, F. Mathey, J. F. Nixon, *J. Chem. Soc. Chem. Commun. 1988*, 1156.

[5] **3b**: bright yellow oil, b.p. 170 °C/10^{-3} mbar (kugelrohr distillation). ^{1}H NMR: δ = 0.40 (s, 27H, Ge(SiMe$_3$)$_3$), 1.35 (s, 9H, *t*Bu), 7.1–7.9 (m, 5H, arene-H). ^{13}C NMR: δ = 2.9 (s, Ge-Si(CH_3)$_3$), 29.6 (s, C(CH_3)$_3$), 113.2 (d, ^1J(P,C) = 48.9 Hz, =*C*Ph), 132.9 (d, ^1J(P,C) = 57.8 Hz, =*C*tBu). ^{31}P NMR: δ = – 189. **4b**: colorless crystals, m.p. 90 °C. ^{1}H NMR: δ = 0.25, 0.37 (each s, each 9H, Ge(SiMe$_3$)$_2$), 0.49 (d, ^3J(P,H) = 4.0 Hz, 9H, P-SiMe$_3$), 1.2 (s, 9H, *t*Bu), 7.0–7.2 (m, 5H, arene H). ^{13}C NMR: δ = 0.3 (s, Ge-Si(CH_3)$_3$), 0.6 (d, ^3J(P,C) = 2.6 Hz, Ge-Si(CH_3)$_3$), 1.9 (d, ^2J(P,C) = 7.0 Hz. P-Si(CH_3)$_3$), 31.7 (d, ^3J(P,C) = 6.2 Hz, C(CH_3)$_3$), 40.8 (d, ^2J(P,C) = 13.3 Hz, *C*(CH_3)$_3$), 151.3 (d, ^2J(P,C) = 14.1 Hz, C3), 163.7 (d, ^1J(P,C) = 23.4 Hz, C4). ^{31}P NMR: δ = – 92.

[6] C. Charrier, M. Maigrot, F. Mathey, F. Robert, Y. Jeannin, *Organometallics 5* (1986) 623.

[7] ^3J(P,H) in P(SiMe$_3$)$_3$ is 4.5 Hz: G. Fritz, H. Schäfer, W. Hölderich, *Z. Anorg. Allg. Chem. 407* (1974) 266.

[8] $C_{21}H_{41}PSi_4$: crystal dimensions 0.40 × 0.32 × 0.22 mm^3, Nicolet R3/mV four-circle diffractometer, Mo$_{K\alpha}$ radiation (graphite monochromator), measuring temperature 103 K, a = 9.437(1), b = 10.969(2), c = 26.800(4) Å, β = 99.36(1)°, monoclinic, space group $P2_1/n$, Z = 4; data collection of 4211 independent and 3340 observed ($F_o \geq 4\sigma(F)$) intensities, $2\theta_{max}$ = 48°, structure solution and refinement with SHELXTL-Plus (4.0), anisotropic displacement parameters for all non-hydrogen atoms, H atoms refined as rigid groups with groupwise isotropic displacement parameters, 252 parameters R = 0.033, R_w = 0.033, $w^{-1} = \sigma^2(F) + 2.4 \times 10^{-4}F_o^2$, maximal residual electron density 0.31 eÅ^{-3}. Further details of the crystal structure investigation may be obtained from the Fachinformationszentrum Karlsruhe, Gesellschaft für wissenschaftlich-technische Information mbH, D-7514 Eggenstein-Leopoldshafen 2 (FRG), on quoting the depository number CSD-320129, the names of the authors, and the journal citation.

[9] For this, we assume a *cis* configuration of the C–C double bond, which has been confirmed by crystal structure analysis for the insertion product obtained from dimethyl acetylene-dicarboxylate and **4a**. The orientation of the alkyne upon insertion is revealed by the ^2J(P,H) coupling of 5.0 Hz.

[10] G. Becker, *Z. Anorg. Allg. Chem. 430* (1977) 66. A silyl shift has not been used before to prepare cyclic phosphaalkenes.

[11] R. Appel, F. Knoch, H. Kunze, *Chem. Ber. 117* (1984) 3151.

[12] The X-ray analysis of **10b**, which has meanwhile been carried out, confirms the rearrangement.

Vanadium(-I) Dinitrogen Complexes with N_2 Coordinated End-on: Functional Models for the "Alternative Nitrogenase"**

By *Claus Woitha* and *Dieter Rehder**

Recently, the nitrogen-fixing bacterium *Azotobacter* was found to code not only for a molybdenum nitrogenase but also for "alternative nitrogenases" containing vanadium[1] or iron[2] instead of Mo in the active site. It has already been known for more than half a century that vanadium can play a role in the in vivo fixation of nitrogen.[3] However, the in vitro reduction of N_2 to NH_3 and/or N_2H_4 also occurs, for example, in alkaline $V^{2\oplus}$- and $Mg^{2\oplus}$-containing solutions[4] or in the system $V^{2\oplus}$/dicarboxylate.[5] In the latter case, a binuclear, N_2-bridged intermediate has been postulated. The structure of an N_2-bridged V^{II} complex, [(*o*-$Me_2NCH_2C_6H_4)_2V(NC_5H_4)]_2(\mu\text{-}N_2)$, was recently determined.[6] We have now synthesized and isolated a series of V^{-I} nitrogen complexes which contain N_2 coordinated in an end-on fashion and which are stable at room temperature.

Such complexes have only been identified previously in low-temperature matrices (e.g., $V(N_2)_6$[7] and $[CpV(NO)_2N_2]$[8]) or in solution below 220 K ($[V(CO)_5N_2]^{\ominus}$[9]). Multidentate phosphanes were used as supporting ligands to provide stabilization, as was the case for the comparable complexes of Mo^0 regarded as functional models of Mo nitrogenase.

The anionic vanadium complexes **2a–f** (Scheme 1), which have the composition $[Vp_n(N_2)_{6-n}]^{\ominus}$ (n indicates the number of *coordinated* phosphorus functions of one or more multidentate phosphanes p) are formed as their Na salts on reduction of $[VCl_3p_n(thf)_{3-n}]$[10] (**1**) with sodium sand in the presence of the phosphane under N_2 (see Eq. (a) for p_n = bis(dimethylphosphino)ethane, dmpe), when catalytic amounts of naphthalene are added.

$$VCl_3(thf)_3 + dmpe \longrightarrow [VCl_3dmpe(thf)] \xrightarrow[dmpe,\ Na]{N_2} \mathbf{2a}\text{-Na} + \mathbf{2c}\text{-Na} \qquad (a)$$

1a

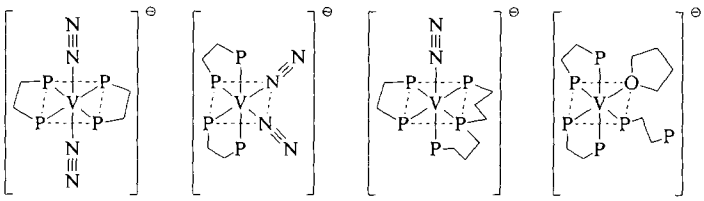

2a(b) **2c(d)** **2e(f)** **3**

Scheme 1. The formula numbers **2b,d,f** refer to the analogous $^{15}N_2$ complexes.

The composition of the reaction solution obtained according to Equation (a) can be determined from its ^{51}V NMR spectrum (Fig. 1, spectrum A).[11,12a] The main product is the *trans* complex **2a**, characterized by a quintet ($^1J(^{31}P,^{51}V)$ = 314 Hz) at $\delta(^{51}V)$ = – 1123. Also present is the *cis* isomer **2c** ($\delta(^{51}V)$ = – 978, A_2B_2X spin system, $J(^{31}P^A,^{51}V)$ = 316, $J(^{31}P^B,^{51}V)$ = 253 Hz). Carrying out the reaction at temperatures around 240 K results in an increase

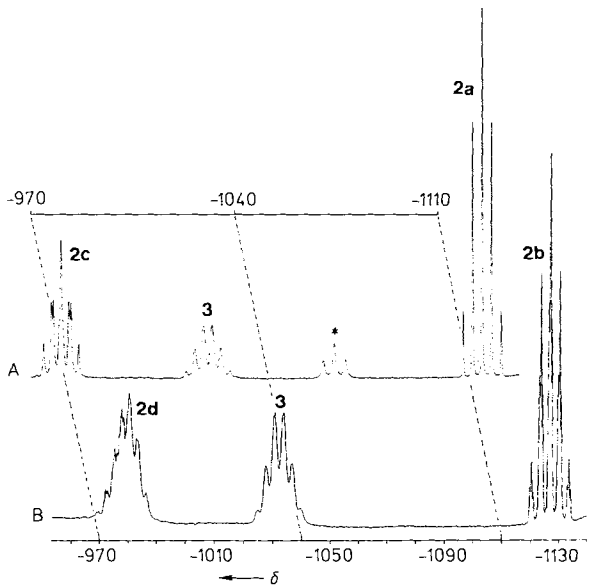

Fig. 1. 94.7-MHz $^{51}V\{^1H\}$ NMR spectrum of the reaction mixture formed on reduction of **1a** with Na under $^{14}N_2$ (A) and $^{15}N_2$ (B) at 273 K. In A, only a coupling pattern corresponding to $^{31}P,^{51}V$ coupling is observed. In B, $^{15}N,^{51}V$ coupling is also observed for the two nitrogen complexes **2b** and **2d**. Compound **3** (L = THF, preliminary formula) contains no nitrogen. The triplet marked with an asterisk is not assigned.

[*] Prof. Dr. D. Rehder, Dipl.-Chem. C. Woitha
Institut für Anorganische und Angewandte Chemie der Universität
Martin-Luther-King-Platz 6, D-2000 Hamburg 13 (FRG)

[**] This work was supported by the Deutsche Forschungsgemeinschaft and the Fonds der Chemischen Industrie.

in the amount of the *cis* isomer **2c**. In the IR spectrum of its solution in THF, **2a** is characterized by an intense, broad band for ν(NN) at 1763 cm^{-1} (Nujol: 1759 cm^{-1}). Complex **2c**, which can be precipitated from hexane at low temperatures as the pure Na salt, exhibits two equal-intensity bands (1791 and 1674 cm^{-1}) in the IR spectrum (Nujol).

Direct proof for the formation of N_2 complexes is provided by the reduction [Eq. (a)] under $^{15}N_2$. In the ^{51}V NMR spectrum, each component of the multiplet is further split into a triplet (Fig. 1, spectrum B: *trans*-$^{15}N_2$ complex **2b**, $J(^{15}N,^{51}V) = 57(1)$ Hz; *cis*-$^{15}N_2$ complex **2d**, $J(^{15}N,^{51}V) = 67(6)$ Hz).[12b] In the IR spectrum, the ν(NN) absorption for the *trans* complex is shifted to $\tilde{\nu} = 1695\ cm^{-1}$.

The values for the $^{31}P,^{51}V$ couplings lie in the region observed for other low-valent alkylphosphane complexes of vanadium.[14] $^{14/15}N,^{51}V$ coupling constants on the order of those determined here have only been observed sporadically so far and exclusively for V^V compounds.[15] The absence of fine splitting in the sextet observed at $\delta = -1032$ in the ^{51}V NMR spectrum of **3** (Fig. 1) shows that, in this case, no N_2 is coordinated. Compound **3** probably has the composition $[V(dmpe)_3(thf)]^{\ominus}$, five of the available P functions being coordinated to vanadium.[12c]

Nonetheless, it was also possible to prepare an anionic nitrogen complex containing only one N_2 ligand (**2e**) [Eq. (b)]. The tridentate phosphane bdpm (bis(3-dimethylphosphinopropyl)methylphosphane)[16] and dmpe were used.

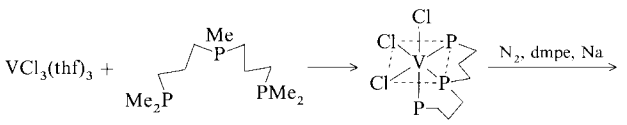

2e-Na ⟶ **2a**-Na

The complex anion **2e**, initially formed on reduction of **1b**, exhibits a characteristic N–N stretching vibration at $\tilde{\nu} = 1725\ cm^{-1}$ in the IR spectrum (THF). For the analogous $^{15}N_2$ complex, **2f**, ν(NN) is found at $\tilde{\nu} = 1678\ cm^{-1}$ in the IR spectrum (THF). Figure 2 shows the ^{51}V NMR spectrum of **2e**. The A_5BX spin system ($^1J(^{31}P^A,^{51}V) = 291$ Hz, $^1J(^{31}P^B,^{51}V) = 222$ Hz) clearly shows that the coupling pattern is governed not so much by the chemical nonequivalence of alkylphosphane functions in the end and middle positions but rather by their position with respect to the N_2 ligand. A similar argument explains the coupling pattern in the NMR spectrum of the hydrido complexes $HM_p(CO)_{6-n}$ (M = V, Nb, Ta; n = 2–4).[17] Compound **2e**-Na is soluble, but not stable, in hexane. Upon standing for several days, the hexane solution affords a precipitate of the pure Na salt, **2a**-Na.

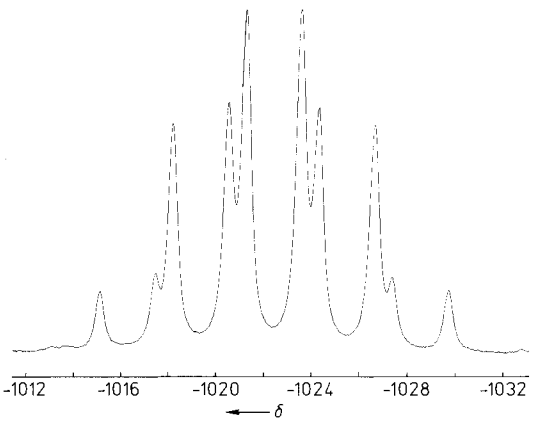

Fig. 2. 94.7-MHz $^{51}V\{^1H\}$ NMR spectrum of the anionic nitrogen complex **2e**.

The phosphane-stabilized V^{-1} dinitrogen complexes show spectroscopic similarities with the valence-isoelectronic Mo^0 complexes (e.g., *trans*-$[Mo(Et_2PCH_2CH_2PEt_2)_2(N_2)_2]$[13]), but also exhibit the differences expected for an anionic versus a neutral complex. For example, ν(NN) for the Mo complex lies at $\tilde{\nu} = 1928\ cm^{-1}$, about 170 cm^{-1} higher than for the V complex **2a**. The ^{15}N nucleus in the Mo complex ($\delta(^{15}N) = +338$[13]) is more strongly shielded than in **2b** ($\delta(^{15}N) = +423$[18]). Interestingly, the N_2 ligand in complexes **2a(b)** can be transformed into ammonia by reductive protonation, as observed for Mo complexes: When dry HCl gas is admitted into a THF solution of **2a**-Na at −30 °C, about 30% of the N_2 is converted into NH_4Cl (hydrazine is formed in only trace amounts). In addition, still not fully characterized chloro complexes, probably of V^{III}, are formed.

Experimental Procedure

$VCl_3(thf)_3$ (1 mmol)[19] was dissolved in 10 mL of THF. After addition of dmpe (2 mmol), the solution was stirred under inert atmosphere. The green solution of **1a** that was immediately formed was cooled to 273 K and then treated with sodium sand (8 mmol) and naphthalene (5 mg) and stirred for 5 h under N_2. The resulting brown solution contained, in addition to the main product **2a**, compounds **2c** and **3** (as well as a not further identified V^{-1} complex containing only one dmpe ligand, $\delta(^{51}V) = -1072$, $J(P,V) = 360$ Hz; cf. Fig. 1, A). Addition of about 100 mL of *n*-hexane resulted in precipitation of **2a**-Na as a pyrophoric, brown-black powder, which, however, was not completely homogeneous. When the reaction was carried out at 220–240 K, the main product was **2c**-Na, which could be precipitated from hexane at low temperatures as a pure substance. Compounds **2a**-Na and **2c**-Na are stable under N_2 at room temperature. The yields of **2a**-Na and **2c**-Na were 40%. In solution, **2c** is slowly transformed into **2a**. In vacuum, both complexes lose N_2. To synthesize the $^{15}N_2$ complexes **2b**, **2d**, and **2f**, $^{15}N_2$ (99%, Campro Scientific) was used.

Pure **2a**-Na was also obtained by an indirect route: $VCl_3(thf)_3$ (1 mmol) was dissolved in 20 mL of THF and treated with bdpm (1 mmol) and the reaction mixture was stirred for 1 h. The resulting solution, containing **1b**, was concentrated to 5 mL and then treated with dmpe (1 mmol), sodium sand (200 mg), and naphthalene (20 mg), after which it was stirred for one day at 198 K and one more day at 230 K under N_2. The main product was the nitrogen complex **2e**. Filtration through a short Celite column (2.5 × 1 cm) and treatment (at 198 K) with a large excess of *n*-hexane resulted in precipitation of small amounts of **2c**-Na. Microcrystalline **2a**-Na was obtained when the solution was allowed to stand for longer periods at room temperature.

Received: August 13, 1990 [Z 4132 IE]
German version: *Angew. Chem. 102* (1990) 1495

[1] B. J. Hales, E. E. Case, J. E. Morningstar, M. F. Dzeda, L. A. Mauterer, *Biochemistry 25* (1986) 7251.
[2] K. Schneider, A. Müller, *Eur. J. Biochem.*, in press.
[3] H. Bortels, *Zentralbl. Bakteriol. Parasitenk. Infektionskr. Abt. 2 95* (1936/37) 13.
[4] A. Shilov, N. Denisov, O. Efimov, N. Shuvalov, N. Shuvalova, A. Shilova, *Nature (London) 231* (1971) 460.
[5] B. Folkesson, R. Larsson *Acta. Chem. Scand. Ser. A33* (1979) 347.
[6] J. J.H. Ederna, A. Meetsma, S Gambarotta, *J. Am. Chem. Soc. 111* (1989) 6878.
[7] H. Huber, T. A. Ford, W. Klotzbücher, W. A. Ozin, *J. Am. Chem. Soc. 98* (1976) 3176.
[8] M. Herberhold, W. Kremnitz, H. Trampisch, R. B. Hitam, D. J. Taylor, A. J. Rest, *J. Chem. Soc. Dalton Trans. 1982*, 1261.
[9] K. Ihmels, D. Rehder, *Chem. Ber. 118* (1985) 895.
[10] E.g., $[VCl_3(dmpe)thf]$: J. Niemann, J. H. Teuben, J. C. Hoffmann, K. G. Caulton, *J. Organomet. Chem. 255* (1983) 193; $[VCl_3\{t\text{BuSi}(CH_2PMe_2)_3\}thf]$: T. G. Gardner, G. S. Girolami, *Organometallics 6* (1987) 2551.

[11] The ^{51}V NMR spectra were recorded with a Bruker AM 360 spectrometer at 94.726 MHz in 10-mm NMR tubes (THF solutions; total concentration c(V), ca. 0.05 M) at 298(1) K. Typical measurement parameters: sweep width 125 kHz, time domain 8200 K, pulse angle 20°, no relaxation delay, number of scans 25000. All $\delta(^{51}V)$ values are given with respect to $VOCl_3$ as external standard.

[12] a) The ^{31}P NMR spectra show signals of several kHz width due to the only partially relaxed scalar $^{51}V,^{31}P$ coupling ($J(^{51}V) = 7/2$); b) The $^{2}J(^{15}N,^{51}V)$ coupling is not resolved. In nitrogen complexes of W and Rh, it is several Hz[13]; c) Noncoordinated phosphorus: $^{31}P\{^{1}H\}$ NMR (32.4 MHz, THF, H_3PO_4): $\delta = -53.8$ (d, $^{3}J(P,P) = 26$ Hz); cf. uncomplexed dmpe: $\delta = -52.9$ (s).

[13] Summarized in S. Donavan-Mtunzi, R. L. Richards, J. Mason, *J. Chem. Soc. Dalton Trans. 1984*, 469.

[14] a) D. Rehder, *Magn. Reson. Rev. 9* (1984) 125; b) K. Ihmels, D. Rehder, *Organometallics 4* (1985) 1334.

[15] Examples of ^{1}J ($^{14}N,^{51}V$) are $V(NtBu)(OtBu)_3$, 105 Hz (F. Preuss, H. Noichl, J. Kaub, *Z. Naturforsch. B 41* (1986) 1085) and $VO(NEt_2)(OiPr)_2$, 105 Hz (W. Priebsch, D. Rehder, *Inorg. Chem. 24* (1985) 3058). The only reported example of a (nonresolved) $J(^{15}N,^{51}V)$ coupling is for $[FCl_2V(^{15}N_3S_2)]^{\ominus}$, 88 Hz (D. Rehder, D. Fenske, G. Baum, H. Borgholte, K. Dehnicke, *Z. Naturforsch. B 44* (1989) 1385).

[16] M. Antberg, C. Prengel, L. Dahlenburg, *Inorg. Chem. 23* (1984) 4170.

[17] S. Süßmilch, W. Glöckner, D. Rehder, *J. Organomet. Chem. 388* (1990) 95; D. Rehder, M. Fornalczyk, P. Oltmanns, *ibid. 331* (1987) 207; D. Rehder, P. Oltmanns, M. Hoch, C. Weidemann, W. Priebsch, *ibid. 308* (1986) 19.

[18] ^{15}N NMR (36.49 MHz, [D$_8$]-THF, ca. 1% Cr(acac)$_3$, 25 °C, NH_3(l)): $\delta = +423$ ($W_{1/2} = 470$ Hz; N$_\alpha$), $+421$ ($W_{1/2} = 130$ Hz; N$_\beta$). The $^{51}V,^{15}N$ couplings are not resolved. Both signals, which overlap, have shapes corresponding to partial decoupling of the two nuclei (due to quadrupole relaxation). The $^{31}P,^{15}N$ and $^{15}N\alpha,^{15}N\beta$ couplings, which are only several Hz in comparable Mo complexes[13], are also unresolved.

[19] a) Synthesis: J. P. Fackler, Jr., (Ed.): *Inorganic Synthesis, Vol. 21*, Wiley, New York 1982, p. 135. b) Structure: F. A. Cotton, S. A. Duraj, G. L. Powell, W. J. Roth, *Inorg. Chim. Acta 113* (1986) 81.

Lewis-Base-Dictated Structural Variations in Sodium Amide Chemistry: X-Ray Crystal Structures of Phenyl(2-pyridyl)amidosodium with Hexamethylphosphoric Triamide (HMPA) and with Pentamethyldiethylenetriamine (PMDETA)**

By *Philip C. Andrews, William Clegg*, and *Robert E. Mulvey**

Since their discovery nearly two centuries ago, sodium amides have been much utilized as reagents in, for example, amide transfer, metalation, and polymerization initiation.[1] Except for some silylated derivatives,[2] such as $[(Me_3Si)_2NNa]_\infty$,[2a] and for two adducts of *N*-sodioindole,[3] structural characterization of such species by X-ray diffraction has hitherto proved elusive. This dearth is in marked contrast to the recent growth in the number of lithium amide crystal structures.[4] Such an imbalance may reflect the greater sensitivity (to both moisture and oxygen) of heavier alkali-metal amides compared with their lithium counterparts. Reported here are the preparations and crystal structures of two adducts of the sodium amide $[Ph(2\text{-}NC_5H_4)NNa]_n$. The donor in **1** is hexamethylphosphoric triamide (HMPA) and in **2** pentamethyldiethylenetriamine (PMDETA).

$[Ph(2\text{-}NC_5H_4)N]Na \cdot 3\,HMPA \cdot Na[N(2\text{-}NC_5H_4)Ph]$ **1**

$[\{Ph(2\text{-}NC_5H_4)N\}Na \cdot PMDETA]_2$ **2**

The crystal structure of **1** determined by X-ray diffraction[5] reveals that the metal atoms are formally attached to the amido nitrogens (N(12) and N(22), Fig. 1), but that there are additional (anchimeric) coordinations with the pyridyl nitrogen atoms N(11) and N(21). These bidentate

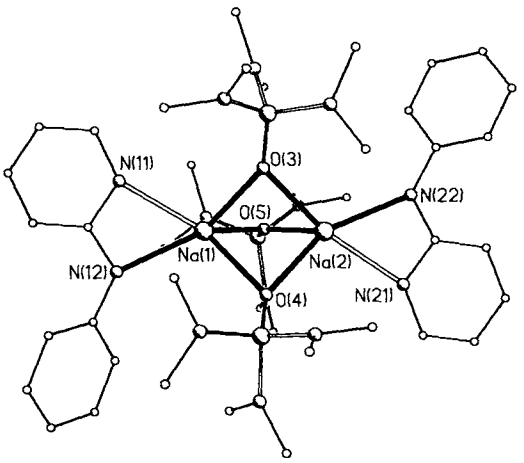

Fig. 1. Molecular structure of **1** without hydrogen atoms. Key distances [Å] and angles [°]. Na(1)-N(11) 2.459(5), Na(2)-N(21) 2.446(5), Na(1)-N(12) 2.439(7), Na(2)-N(22) 2.439(8), Na(1)-O(3) 2.381(6), Na(2)-O(3) 2.426(6), Na(1)-O(4) 2.436(5), Na(2)-O(4) 2.374(6), Na(1)-O(5) 2.347(5), Na(2)-O(5) 2.345(5), Na(1)···Na(2) 2.996(3); Na(1)-O(3)-Na(2) 77.1(2), Na(1)-O(4)-Na(2) 77.0(2), Na(1)-O(5)-Na(2) 79.4(2), N(11)-Na(1)-N(12) 55.4(2), N(21)-Na(2)-N(22) 55.1(2), O(3)-Na(1)-O(4) 78.7(2), O(3)-Na(1)-O(5) 87.1(2), O(4)-Na(1)-O(5) 87.3(2), O(3)-Na(2)-O(4) 79.1(2), O(3)-Na(2)-O(5) 86.1(2), O(4)-Na(2)-O(5) 88.8(2).

$[Ph(2\text{-}NC_5H_4)N]^{\ominus}$ anions occupy terminal positions and the oxygens of three neutral HMPA molecules each bridge the two metal centers. This donor usually binds to alkali metals in a terminal manner,[6] though it occasionally bridges in lithium systems.[7] However, this is the first example of μ_2-(HMPA)O–Na bonding. Four HMPA equivalents were available to every two equivalents of the metal in the reaction mixture producing **1**, but, by adopting bridging positions, only three HMPA equivalents are needed in order to render both sodium cations five-coordinate.

In keeping with the unpredictable structures of alkali-metal organometallics,[8] **2** prefers a dimeric arrangement that offers each metal atom an additional (sixth) coordination. Figure 2 shows that this crystal structure[9] is best viewed as a planar, centrosymmetric, rhomboidal $(N\text{-}Na)_2$ cyclic ring having nitrogen-bound phenyl and 2-pyridyl substituents. The *trans* positioning of these substituents above and below the ring plane allows each pyridyl nitrogen atom to interact with both cations through unsymmetrical Na–N–Na bridges. Overall, therefore, the six core atoms (Na,Na',N(1),N(1)',N(2),N(2)') generate a distorted octahedron. Each of its N–Na bonds is longer (by distances ranging from 0.040 to 0.346 Å) than the N–Na bonds in **1**, where the metal cations are only five-coordinate. Association appears preferential to complexation in **2** since PMDETA chelation here is incomplete with only two of its three potential donor

[*] Dr. R. E. Mulvey, P. C. Andrews
Department of Pure and Applied Chemistry
University of Strathclyde
Glasgow, G1 1XL (UK)
Dr. W. Clegg
Department of Chemistry
The University
Newcastle upon Tyne, NE1 7RU (UK)

[**] This work was supported by the UK Science and Engineering Research Council, by the Research Corporation Trust, and by the Royal Society (1983 Research Fellowship for *R.E.M.*)

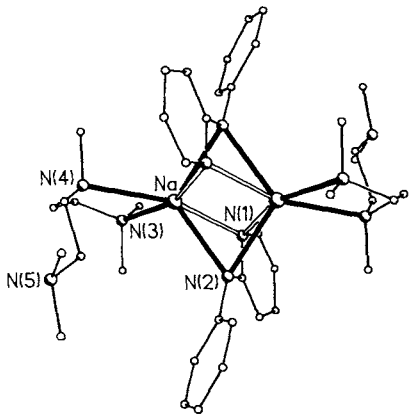

Fig. 2. Molecular structure of **2** without hydrogen atoms. Key distances [Å] and angles [°]: Na-N(1) 2.546(2), Na-N(1') 2.785(3), Na-N(2) 2.552(2), Na-N(2') 2.499(2), Na-N(3) 2.580(2), Na-N(4) 2.580(2), Na···Na' 2.946(1); Na-N(1)-Na' 66.9(1), Na-N(2)-Na' 71.3(1), N(1)-Na-N(2) 52.7(1), N(1')-Na-N(2') 50.4(1), N(1)-Na-N(1') 113.1(1), N(2)-Na-N(2') 108.7(1), N(1)-Na-N(2') 92.1(1), N(2)-Na-N(1') 85.7(1), N(3)-Na-N(4) 70.7(1).

atoms connecting to the metal. The crystal structure of **2** represents the first example where PMDETA binds to sodium in this bidentate manner. Even with the appreciably smaller lithium cation, such "partial" bonding has been reported only in the monomeric cyclopentadienyl derivative $(Me_3Si)_3C_5H_2Li \cdot PMDETA$.[10]

Experimental Procedure

1: One molar equivalent of phenyl(2-pyridyl)amine was added to a chilled suspension of PhNa in hexane under a dry, oxygen-free argon atmosphere. Stirring this mixture at 25 °C caused the precipitation of a solid, which redissolved on addition of HMPA (two molar equivalents per sodium). Cooling of the resulting orange solution afforded pale yellow plates which had 1.5 HMPA molecules per sodium and were identified as **1** [yield 72% based on amine, m.p. 100–102 C; satisfactory analyses (C,H,N,P,Na)].

2: One molar equivalent of PMDETA was added to a suspension of phenyl(2-pyridyl)amidosodium in chilled hexane under a dry, oxygen-free argon atmosphere. Stirring gave a pale brown solution which deposited pale brown crystals on refrigeration at −20 °C. These crystals were washed with hexane and identified as **2** [yield 84%, m.p. 89–91 °C; satisfactory analyses (C,H,N,Na)].

Single crystals of both **1** and **2** suitable for X-ray crystallography were sealed under argon in Lindemann capillary tubes prior to data collection.

Received: June 25, 1990 [Z 4032 IE]
German version: *Angew. Chem. 102* (1990) 1480

CAS Registry numbers:
1, 130495-58-8; **2**, 130495-57-7; PMDETA, 3030-47-5; NH(2-NC_5H_4)Ph, 6631-37-4; Na[N(2-NC_5H_4)Ph], 130468-98-3.

[1] M. F. Lappert, P. P. Power, A. R. Sanger, R. C. Srivastava: *Metal and Metalloid Amides*, Ellis Horwood-Wiley, Chichester 1980, pp. 24–44.

[2] a) R. Grüning, J. L. Atwood, *J. Organomet. Chem. 137* (1977) 101; b) T. D. Tilley, R. A. Andersen, A. Zalkin, *Inorg. Chem. 23* (1984) 2271; c) D. J. Brauer, H. Bürger, W. Geschwandtner, G. R. Liewald, C. Krüger, *J. Organomet. Chem. 248* (1983) 1.

[3] K. Gregory, M. Bremer, W. Bauer, P. von R. Schleyer, N. P. Lorenzen, J. Kopf, E. Weiss, *Organometallics 9* (1990) 1485.

[4] See, for example, D. R. Armstrong, D. Barr, W. Clegg, S. M. Hodgson, R. E. Mulvey, D. Reed, R. Snaith, D. S. Wright, *J. Am. Chem. Soc. 111* (1989) 4719 and references therein.

[5] **1**: $M_r = 922.0$, triclinic, space group $P\bar{1}$, $a = 11.034(2)$, $b = 11.475(2)$, $c = 21.292(4)$ Å, $\alpha = 96.59(1)$, $\beta = 98.80(2)$, $\gamma = 91.97(1)°$, $V = 2642.9$ Å^3, $Z = 2$, $\varrho_{calcd} = 1.158$ g cm^{-3}, $F(000) = 988$, $Cu_{K\alpha}$ radiation, $\lambda = 1.54184$ Å, $\mu = 1.57$ mm^{-1}. The structure was determined by direct methods and refined from 3845 unique observed reflections measured at room temperature with a Stoe-Siemens diffractometer ($2\theta_{max} = 110°$), with anisotropic thermal parameters and with isotropic H atoms in calculated positions: $R = 0.117$, $R_w = 0.109$, $S = 1.34$ for 545 parameters. Disorder was resolved for one phenyl group and is probably present, though unresolved, in the HMPA ligands, which were restrained in the refinement [9 b].

[6] See, for example, D. Barr, R. Snaith, W. Clegg, R. E. Mulvey, K. Wade, *J. Chem. Soc. Dalton Trans. 1987*, 2141 and references therein.

[7] D. Barr, W. Clegg, R. E. Mulvey, R. Snaith, *J. Chem. Soc. Chem. Commun. 1984*, 974.

[8] For a review of the crystal structures of heavier alkali-metal organic compounds, see C. Schade, P. von R. Schleyer, *Adv. Organomet. Chem. 27* (1987) 169.

[9] a) **2**: $M_r = 731.0$, triclinic, space group $P\bar{1}$, $a = 10.309(3)$, $b = 11.029(3)$, $c = 11.701(3)$ Å, $\alpha = 64.35(1)$, $\beta = 85.32(1)$, $\gamma = 64.22(1)°$, $V = 1070.6$ Å^3, $Z = 1$, $\varrho_{calcd} = 1.134$ g cm^{-3}, $F(000) = 396$, $Mo_{K\alpha}$ radiation, $\lambda = 0.71073$ Å, $\mu = 0.08$ mm^{-1}. The structure was determined and refined as described in [5] (2580 unique observed reflections, $2\theta_{max} = 50°$: $R = 0.038$, $R_w = 0.038$, $S = 1.01$ for 251 parameters, with no disorder). b) Further details of both crystal structure investigations can be obtained from the Director of the Cambridge Crystallographic Data Centre, University Chemical Laboratory, Lensfield Road, Cambridge, CB2 1EW (UK), by quoting the full journal citation.

[10] P. Jutzi, E. Schlüter, C. Krüger, S. Pohl, *Angew. Chem. 95* (1983) 1015; *Angew. Chem. Int. Ed. Engl. 22* (1983) 994.

Decameric and Dodecameric Sodium Amides and an Organosodium Amide with Stack Structures: $[Na_{10}(NMe_2)_{10}(tmeda)_4]$, $[Na_{12}(NMe_2)_{12}(tmeda)_4]$, and $[Na_{12}(NMe_2)_{10}(CH_2C_6H_4Me)_2(tmeda)_4]$**

By *Nis Peter Lorenzen, Jürgen Kopf, Falk Olbrich, Uwe Schümann*, and *Erwin Weiss**

Dedicated to Professor Fausto Calderazzo on the occasion of his 60th birthday

Alkali-metal organometallics exhibit a pronounced tendency to form oligomeric aggregates. Depending on the spatial demands of the organic groups, the ionic radius of the metal ion, and possible solvation (for example, by ethers or amines), various types of structures are found.[1] The alkali-metal amides, which are also synthetically valuable, show many structural similarities, as revealed particularly by recent investigations on lithium amides. Monomeric, dimeric, trimeric, tetrameric, and also ladder structures are known;[1c, 2] furthermore, a hexameric Li-Na imide with a stack structure was described recently.[2c]

Here we describe novel stack structures of sodium dimethylamide with aggregation numbers of 10 and 12 (**1**–**3**) the preparation of these oligomeric amides was not our actual goal; they were obtained in attempts to metalate hydrocarbons (4-methylbiphenyl, 1,2,4,5-tetramethylbenzene (durene), and *p*-xylene) by treating them with *n*-butylsodium in the presence of the chelating ligand tetramethylethylenediamine (TMEDA).

$[Na_{10}(NMe_2)_{10}(tmeda)_4]$ **1**

$[Na_{12}(NMe_2)_{12}(tmeda)_4]$ **2**

$[Na_{12}(NMe_2)_{10}(CH_2C_6H_4Me)_2(tmeda)_4]$ **3**

In this method,[3] TMEDA is used to transform *n*BuNa, which is insoluble in hydrocarbons, into a soluble form and to complex the resulting products. In addition, the activation energy is considerably lowered by the solvating ligand, re-

[*] Prof. Dr. E. Weiss, Dr. N. P. Lorenzen, Priv.-Doz. Dr. J. Kopf, Dipl.-Chem. F. Olbrich, Dr. U. Schümann
Institut für Anorganische und Angewandte Chemie der Universität
Martin-Luther-King-Platz 6, D-2000 Hamburg 13 (FRG)

[**] Metal-Alkyl and Metal-Aryl Compounds, Part 45. This work was supported by the Deutsche Forschungsgemeinschaft and the Fonds der Chemischen Industrie. We thank Dipl.-Chem. *Volker Jordan* for experimental help. Part 44: E. Weiss, S. Corbelin, J. K. Cockcroft, A. N. Fitch, *Chem. Ber. 123* (1990) 1629.

sulting in markedly shorter reaction times. The fragmentation of the ligand by highly reactive *n*-butylsodium partly counters these advantages in the reaction conditions.

The metalation of TMEDA by organolithium compounds and the subsequent fragmentation have already been investigated.[4] They require increased temperatures and proceed with preferential metalation of a terminal methyl group. We observed, in contrast, that treatment of TMEDA with *n*-butylsodium results to a large extent in amide formation and decomposition even at room temperature (yields of sodium dimethylamide: **1**, 34%; **2**, 48%). The limits of applicability of this metalation reaction are thus clearly evident. Here, the decomposition reaction apparently proceeds analogously to the ether cleavage, whereby the *N*-ligand in α position first is metalated and then decomposes with elimination of the amide [Eq. (a)].

$$Me_2NCH_2\text{-}CH_2NMe_2 + NaBu \xrightarrow[-BuH]{} Me_2NCH_2\text{-}CH(Na)NMe_2 \longrightarrow Me_2NCH{=}CH_2 + NaNMe_2 \quad (a)$$

The resulting amides **1** and **2** (Figs. 1, 2) have remarkable structures. They are oligomeric and correspond to the dode-

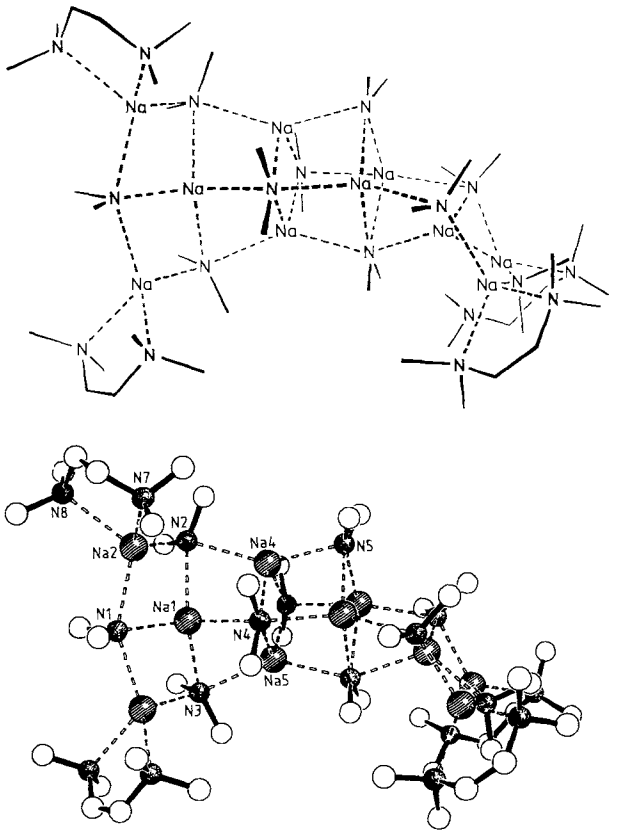

Fig. 1. Crystal structure of **1**. A twofold axis passes through the center of gravity of the molecule [6]; the asymmetric unit is thus formed by half of the molecule. The localized durene molecule present in the crystal of **1** is not shown [13]: Important distances [pm] and angles [°]: Na1-N1 235, Na1-N2 246, Na1-N3 246, Na-N4 248, Na2-N1 248, Na2-N2 242, Na2-N7 253, Na2-N8 254, Na4-N2 252, Na4-N4 258, Na4-N5 243, N-C (NMe_2, average) 144.4; N1-Na1-N2 102.2, N1-Na1-N3 102.8, N1-Na1-N4 119.4, N2-Na1-N3 141.7, N2-Na1-N4 96.9, N1-Na2-N2 99.3, N7-Na2-N8 73.0, N4-Na4-N5 94.3, Na4-N4-Na5 69.8.

cameric organolithium compound **4** (Fig. 3) we obtained earlier.[5] Such aggregates can arise by stacking of the cyclic basic unit $[(R_2Li_2)]_n$, provided that the groups R are not too

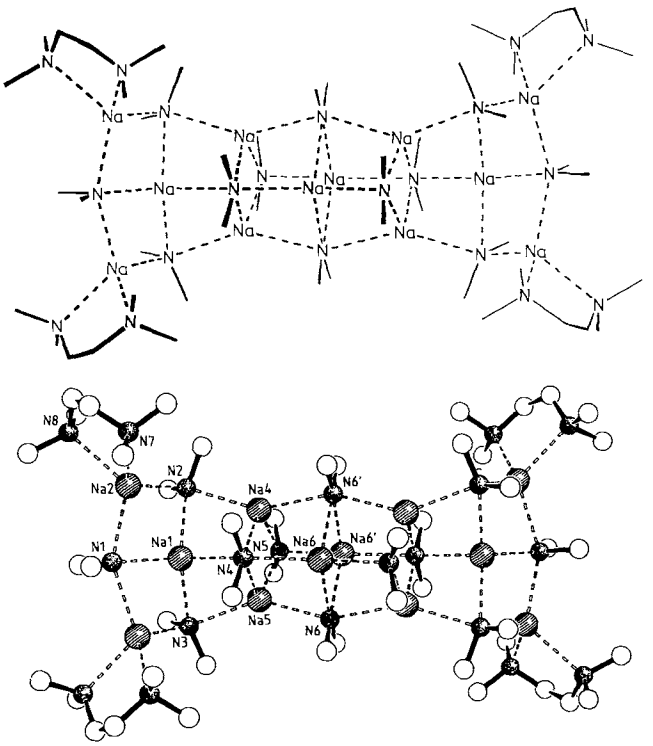

Fig. 2. Crystal structure of **2**. The unit cell contains two non-symmetry-related, but very similar molecules 1 and 2, each of which has a center of inversion at its center of gravity. Only molecule 1 is shown [7], but not the localized hexane molecule it contains [13]. Important distances [pm] and angles [°] for molecule 1 (the values for molecule 2 are very similar): Na1-N1 238, Na-N2 244, Na1-N3 245, Na1-N4 249, Na2-N1 248, Na2-N2 245, Na2-N7 259, Na2-N8 256, Na4-N4 255, Na4-N5 238, Na4-N2 252, Na4-N6' 260 Na5-N4 256, Na5-N5 242, Na5-N3 250, Na5-N6 250, N-C (NMe_2, average) 143.9; N1-Na1-N2 104.3, N1-Na1-N3 102.7, N1-Na1-N4 118.3, N2-Na1-N4 96.4, N2-Na1-N3 138.8, N1-Na2-N2 100.9, N7-Na2-N8 72.9, N4-Na4-N5 106.6, Na4-N4-Na5 71.0, N6'-Na6-N6 97.6, Na6-N6-Na6' 71.1.

sterically demanding. The terminal metal atoms of the stack are coordinatively saturated by solvent ligands (in this case, THF).

$[(LiC{\equiv}CtBu)_{12}(thf)]_4$ **4**

In a similar way, **1** and **2** could conceivably be formed by stacking of $Na_2(NR_2)_2$ rings. Here, however, the stacks are only ordered in their central portions with two roughly parallel rings (heterocubane system) in **1** and three parallel rings in **2**. At the ends of the stacks, the structures become more unsymmetric, although here, too, ring-shaped Na_2N_2 units

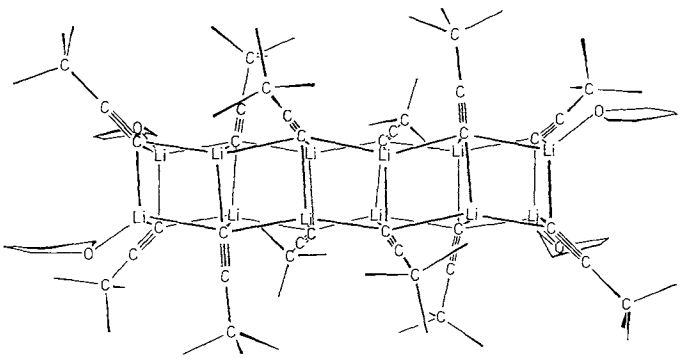

Fig. 3. Crystal structure of **4** [14].

are found and each Na atom is tetracoordinated by N atoms. The terminal Na atoms are coordinatively saturated by chelating TMEDA ligands. These ligands are sterically more demanding than THF and may therefore be responsible for the lower symmetry compared with **4**. Moreover, this results in more equal angles for the terminal pseudotetrahedral NaN_4 structural units of **1** and **2**, with strong deviations from tetrahedral angles occurring in the region of the four-membered ring stacks. In any case, the terminal structural units $Na_3(NMe_2)_3(tmeda)_2$ are particularly stable and are present in all the amide structures described here.

Further systematic investigations showed that solvated metal amides could be formed in high yields by direct synthesis from dimethyl-, diethyl-, or diphenylamine and *n*-butylsodium (or *n*-butyllithium) in the presence of TMEDA (or PMDTA = pentamethyldiethylenetriamine). The compounds characterized so far by X-ray analysis consist almost exclusively of dimers: for example, $[Na_2(NEt_2)_2(tmeda)_2]$, $[Na_2(NMe_2)_2(pmdta)_2]$, $[Na_2(NPh_2)_2(tmeda)_2]$, and $[Li_2(NPh_2)_2(tmeda)_2]$. The use of dimethylamine in excess results in formation of an oligomer $[Na_8(NMe_2)_8(HNMe_2)_2(pmdta)_2]$ with a complicated structure ($HNMe_2$ coordinated to a central $Na_2(NMe_2)_2$ four-membered ring).[8]

A further variant is offered by $[Na_{12}(NMe_2)_{10}(CH_2C_6H_4Me)_2(tmeda)_4]$ (**3**), which, in addition to amido groups, contains two *p*-xylyl moieties. Complex **3** was formed in an attempt to metalate *p*-xylene with *n*BuNa in the presence of TMEDA. Its structure is largely similar to that of **2** (Fig. 4). To the best of our knowledge, it is the first example of an alkali-metal complex containing organo and amido ligands; on the other hand, several mixed aggregates consisting of alkali amide and enolate[15a] or nitrile[15b] are known.

The compounds described here show that sodium amides can also have structures based on the "ring stacking principle". Similarly structured lithium amides have not yet been found. Based on theoretical model calculations, the suggestion has been made that further aggregation of lithium amide rings should lead preferentially to ladder structures and not to stacks. The results presented here indicate that this postulate is not valid for sodium amides.

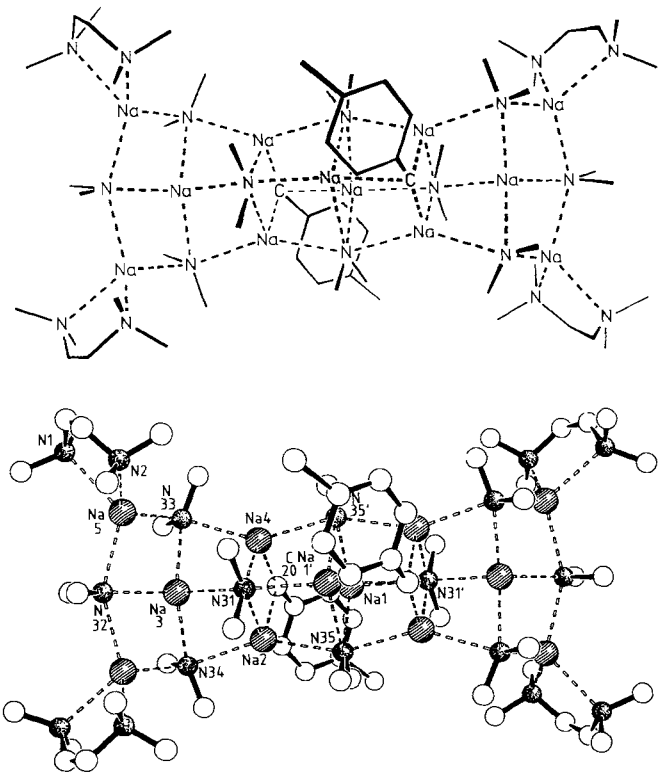

Fig. 4. Crystal structure of **3**. The *p*-xylyl and TMEDA groups are disordered. Therefore, the atomic positions are not exact [9, 13]. Important distances [pm] and angles [°]: Na1-C20 258, Na2-C20 259, Na4-C20 250, Na1-N35 253, Na1-N35′ 257, Na1-N31′ 244, Na2-N31 260, Na2-N35 254, Na3-N31 251, Na3-N33 245, Na3-N34 244, Na4-N35′ 252, Na4-N33 246, Na5-N33 241, Na5-N32 248, Na5-N1 256, Na5-N2 254; N35-Na1-N35′ 108.6, Na1-N35-Na1′ 71.5, C20-Na4-N31 108.2, C20-Na2-N31 103.5, Na2-N31-Na4 73.8; the other values are similar to those of **1** and **2**.

Experimental Procedure

1 · $C_{10}H_{14}$ ($C_{10}H_{14}$ = 1,2,4,5-tetramethylbenzene, durene): *n*-Butylsodium (1.2 g, 15 mmol) was suspended in 100 mL of hexane under inert atmosphere and largely dissolved by addition of TMEDA (9 mL, 60 mmol, dried over CaH_2). 1,2,4,5-Tetramethylbenzene (1.3 g, 10 mmol) was added to the dark brown, turbid solution, which was then stirred for a further 30 min at 20 °C. Clearing of the solution was accompanied by a lightening of the color. A yellow, finely crystalline precipitate formed and was collected by filtration. The filtrate was cooled to − 30 °C and afforded, after a few days, **1** as colorless, air-sensitive cubes with 1-cm edges; yield 0.74 g (34% based on *n*BuNa), correct elemental analyses for Na, C, H, N.

2 · 0.5 C_6H_{14} (C_6H_{14} = hexane): *n*-Butylsodium (0.8 g, 10 mmol) was suspended in 60 mL of hexane and largely dissolved by addition of TMEDA (6 mL, 40 mmol). 4-Methylbiphenyl (0.7 g, 4 mmol), dissolved in 20 mL of hexane, was added to the dark brown, stirred solution. The color lightened and an orange solid (0.5 g) precipitated and was removed by filtration. The filtrate was cooled to − 30 °C and afforded, after a few days, **2** as colorless cubes; yield 0.53 g (48%), correct analyses for Na, C, H, N.

3: *n*-Butylsodium (1.6 g, 20 mmol) was dissolved in 100 mL of benzene by addition of TMEDA (3 mL, 20 mmol) and the resulting solution was stirred overnight. Addition of *p*-xylene (2.4 mL, 19.4 mmol) resulted in transformation of the yellow-brown solution to an orange suspension. The reaction mixture was stirred overnight and the heterogeneous, brown-green precipitate (2.2 g) was removed by filtration. Upon long standing at 8 °C, the red-brown filtrate afforded **3** as brown cubes; yield 0.16 g (1.2%), correct analyses for Na, C, H, N; the heterogeneous main product has a different composition.

Received: July 19, 1990 [Z 4075 IE]
German version: *Angew. Chem. 102* (1990) 1481

CAS Registry numbers:
1, 130120-94-4; **1** · $C_{10}H_{14}$, 130120-95-5; **2**, 130120-96-6; **2** · 0.5 C_6H_{14}, 130120-97-7; **3**, 130145-29-8; $NaNMe_2$, 14314-59-1; BuNa, 3525-44-8.

[1] Review articles: a) W. Setzer, P. von R. Schleyer, *Adv. Organomet. Chem. 24* (1985) 353; b) C. Schade, P. von R. Schleyer, *ibid. 27* (1987) 169; c) R. Snaith, *Annu. Rep. Prog. Chem. Sect. A 82* (1985) 3; *ibid. A 83* (1986) 3; *ibid. A 84* (1987) 3, and references cited therein.

[2] a) D. R. Armstrong, D. Barr, W. Clegg, R. E. Mulvey, D. Reed, R. Snaith, K. Wade, *J. Chem. Soc. Chem. Commun. 1986*, 869; b) D. Barr, W. Clegg, S. M. Hodgson, G. R. Lamming, R. Mulvey, A. J. Scott, R. Snaith, D. S. Wright, *Angew. Chem. 101* (1989) 1279; *Angew. Chem. Int. Ed. Engl. 28* (1989) 124; c) D. Barr, W. Clegg, R. Mulvey, R. Snaith, *J. Chem. Soc. Chem. Commun 2989*, 57.

[3] a) H. Köster, E. Weiss, *J. Organomet. Chem. 168* (1979) 273; b) C. Schade, W. Bauer, P. von R. Schleyer, *ibid. 295* (1985) C25.

[4] W. N. Smith, *Adv. Chem. Ser. 130* (1974) 23, and references cited therein.

[5] M. Geissler, J. Kopf, B. Schubert, E. Weiss, W. Neugebauer, P. von R. Schleyer, *Angew. Chem. 99* (1987) 569; *Angew. Chem. Int. Ed. Engl. 26* (1987) 587.

[6] Crystal structure analysis of **1**: $[Na_{10}(NMe_2)_{10}(tmeda)_4] \cdot C_{10}H_{14}$, C2/c, $a = 2929(2)$, $b = 1271(1)$, $c = 2296(1)$ pm, $\beta = 91.10(5)°$, $V = 8544(1) \times 10^6$ pm^3, $\varrho_{calcd} = 0.987$ g cm^{-3}, $Z = 4$, crystal dimensions $0.3 \times 0.5 \times 0.3$ mm^3, 293 K, $Cu_{K\alpha}$ radiation, Enraf-Nonius CAD4, measuring range $2.25 < \theta < 60°$, 4077 symmetry-independent and significant reflections ($|F| > 4\sigma|F|$), structure solution by direct methods (SHELXS 86 [10]), 502 refined parameters, $R = 0.056$, $R_w = 0.052$ ($[\sigma^2(F) + 0.0001\ F^2]^{-1}$), all non-hydrogen atoms refined with anisotropic temperature factors, H atoms at calculated positions refined with isotropic temperature factors [13].

[7] Crystal structure analysis of **2**: $[Na_{12}(NMe_2)_{12}(tmeda)_4] \cdot 0.5\ C_6H_{14}$, $P\bar{1}$, $a = 1364.1(6)$, $b = 1645.6(13)$, $c = 2046.1(14)$ pm, $\alpha = 91.53(6)$, $\beta = 97.58(5)$, $\gamma = 104.90(5)°$, $V = 4391(5) \times 10^6$ pm^3, $\varrho_{calcd} = 0.993$ g cm^{-3}, $Z = 2$, crystal dimensions $0.4 \times 0.4 \times 0.4$ mm^3, 293 K, $Mo_{K\alpha}$ radiation, Syntex $P2_1$, measuring range $2.25 < \theta < 20°$, 3975 symmetry-independent

and significant reflections ($|F| > 4\sigma|F|$), structure solution by direct methods (SHELXS 86 [10]) and supplemental difference Fourier and LSQ calculations (SHELX 76) [11], 429 refined parameters, $R = 0.090$, $R_w = 0.076$ ($[\sigma^2(F) + 0.0002\,F^2]^{-1}$, all non-hydrogen atoms refined with anisotropic temperature factors, H at calculated positions refined with isotropic temperature factors [13].

[8] V. Jordan, E. Weiss, unpublished.

[9] Crystal structure analysis of **3**: $[Na_{12}(NMe_2)_{10}(CH_2C_6H_4Me)_2(tmeda)_4]$, $P2_1/n$, $a = 1337.3(6)$, $b = 1822.6(9)$, $c = 1970.2(13)$ pm, $\beta = 101.27(5)^\circ$, $V = 4709(4) \times 10^6$ pm^3, $\varrho_{calcd} = 0.98$ g cm^{-3}, $Z = 2$, crystal dimensions $0.4 \times 0.5 \times 0.7$ mm^3, 293 K, $Mo_{K\alpha}$ radiation, Syntex $P2_1$, measuring range $2 < \theta < 22^\circ$, 2012 symmetry-independent and significant reflections ($|F| > 5\sigma|F|$), structure solution by direct methods (MULTAN [12]) and supplemental difference Fourier and LSQ calculations (SHELX 76) [11], 491 refined parameters, $R = 0.074$, $R_w = 0.094$ ($[\sigma^2(F) + 0.002\,F^2]^{-1}$), all non-hydrogen atoms refined with anisotropic temperature factors, H at calculated positions refined with isotropic temperature factors. The $CH_2C_6H_4Me$ groups show (with the exception of the CH_2 groups) strong thermal motions or disorder, which was taken into account by use of a special model involving double C atomic positions with half occupation. This was also the case for the non-hydrogen atoms of the TMEDA ligands and is a frequently observed phenomenon [13].

[10] G. M. Sheldrick, *SHELXS 86, Program for Crystal Structure Solution*, Universität Göttingen 1986.

[11] G. M. Sheldrick, *SHELX 76, Program for Crystal Structure Determination*, University of Cambridge 1975.

[12] P. Main, S. E. Hull, L. Lessinger, G. Germain, J. P. Declerq, M. M. Woolfson, *MULTAN 78, A System of Computer Programs for the Automatic Solution of Crystal Structures from X-Ray Diffraction Data*, University of York, England 1978.

[13] Further details of the crystal structure investigations may be obtained from the Fachinformationszentrum Karlsruhe, Gesellschaft für wissenschaftlich-technische Information mbH, D-7514 Eggenstein-Leopoldshafen 2 (FRG), on quoting the depository number CSD-54819, the names of the authors, and the journal citation.

[14] Structure drawings: *SCHAKAL, a Fortran Program for the Graphical Representation of Molecular and Crystallographic Models*, [E. Keller, *J. Appl. Cryst. 22* (1989) 19].

[15] a) P. G. Williard, M. Hintze, *J. Am. Chem. Soc. 109* (1987) 5539; b) W. Zarges, M. Marsch, K. Harms, G. Boche, *Angew. Chem. 101* (1989) 1424; *Angew. Chem. Int. Ed. Engl. 28* (1989) 1392.

[16] D. R. Armstrong, D. Barr, W. Clegg, S. M. Hodgson, R. E. Mulvey, D. Reed, R. Snaith, D. S. Wright, *J. Am. Chem. Soc. 111* (1989) 4719.

Synthesis and Direct NMR Spectroscopic Observation of $[(\eta^4\text{-Arene})Cr(CO)_3]$ Dianions**

By *Hans G. Wey* and *Holger Butenschön**

Although a change in hapticity from η^6 to η^4 has not been achieved by reaction of $[(arene)Cr(CO)_3]$ complexes with bidentate phosphanes,[1] $[(\eta^4\text{-arene})Cr(CO)_3]$ dianions are known and have been used for the synthesis of functionalized cyclohexadienyl complexes[2] and for $Cr(CO)_3$ transfer under mild conditions.[3] The only compound of this type to be fully characterized so far is the $[(\eta^4\text{-naphthalene})Cr(CO)_3]$ dianion,[4] which is stable at room temperature and for which the η^4 coordination is facilitated by involvement of the decomplexed double bond in an aromatic system—a stabilization similar to the "indenyl effect".[5] The $[(\eta^4\text{-benzene})Cr(CO)_3]^{2\ominus}$ dianion has already been obtained by reaction of benzenetricarbonylchromium(0) (**1**) with naphthalenepotassium.[2, 3] However, its characterization was based only on its IR data and chemical reactivity. Here we describe the synthesis of $[(\eta^4\text{-arene})Cr(CO)_3]$ dianions by a method that does not involve paramagnetic naphthalenepotassium. This approach avoids contamination of the product by and undesired ligand exchange reactions with naphthalene.

Reaction of **1**[6] with lithium sand in THF at $-78\,^\circ C$ results in a color change from yellow to red to brown. Filtration to remove the excess lithium sand affords a solution that is stable for several days at $-78\,^\circ C$, but which decomposes above $-40\,^\circ C$ to give a black solid and benzene. Exposure to atmospheric oxygen results in re-formation of **1** (ca. 50%) with partial decomposition.

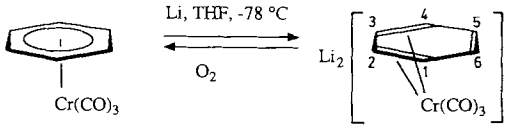

1 **2**

The solution could be easily investigated at $-80\,^\circ C$ by ^1H and ^{13}C NMR spectroscopy.[7] The starting material **1** was no longer detectable. The only signals observed were those fully consistent with the formation of **2**. Particularly useful is a comparison of the ^{13}C NMR data of **2** with those of **1** and benzene (**3**) (Table 1). In agreement with the corresponding

Table 1. Comparison of the ^{13}C NMR data for **1**, **2**, and **3** (75.5 MHz, $[D_8]THF$).

	C-1(4)	C-2(3)	C-5(6)	CO
δ (**3**)	128.0	128.0	128.0	-
δ (**1**)	95.5	95.5	95.5	235.0
δ (**2**)	55.6	87.5	124.5	245.8
δ (**2**) − δ (**1**)	−39.9	−8.0	29.0	10.8
δ (**2**) − δ (**3**)	−72.4	−40.5	−3.5	-

values for $[(\eta^4\text{-naphthalene})Cr(CO)_3]^{2\ominus}$,[4] the chemical shifts of the terminal C atoms of the coordinated diene in **2** (C-1(4)) differ from those of benzene by $\Delta\delta = -72.4$; for the internal C atoms (C-2(3)), $\Delta\delta = -40.5$. The similarity of the data for **2** with those for the $[(\eta^4\text{-naphthalene})Cr(CO)_3]$ dianion, which also extends to the $^1J_{CH}$ couplings of C-3 and C-4, poses the question whether the benzene ligand in **2**, like the naphthalene ligand, is bent.[4]

In our work on cyclobutabenzene complexes,[8] we were also interested in the question of which double bond in the η^6-cyclobutabenzene complex **4**,[9] whose cyclovoltammogram exhibits an irreversible reduction at 2.45 V (vs. SCE, mercury drop electrode, 0.1 M nBu_4NClO_4 in THF, 100 mV s^{-1}) at 25 °C, is preferentially decomplexed upon reduction. Reaction of **4** with lithium sand gives a brown-yellow solution, which no longer contains **4** and which de-

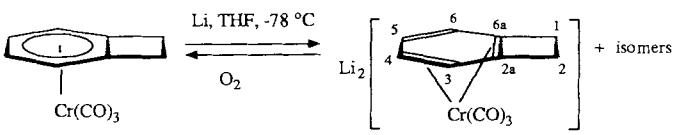

4 **5**

[*] Dr. H. Butenschön, Dr. H. G. Wey
Max-Planck-Institut für Kohlenforschung
Kaiser-Wilhelm-Platz 1, D-4330 Mülheim a.d. Ruhr 1 (FRG)

[**] *H. G. W.* thanks the Max-Planck-Gesellschaft for a doctoral fellowship and *H. B.* the Verband der Chemischen Industrie e. V. for a Liebig-Stipendium. We thank the director of the Max-Planck-Institut für Kohlenforschung, Prof. Dr. *G. Wilke*, for his supportive interest.

Table 2. Comparison of the ^{13}C NMR data of **4**, **5**, and **6** (75.5 MHz, $[D_8]$THF).

	C-1	C-2	C-2a	C-3	C-4	C-5	C-6	C-6a	CO
δ (**6**)	30.1	30.1	146.2	123.1	127.6	127.6	123.1	146.2	-
δ (**4**)	30.5	30.5	118.7	92.4	93.2	93.2	92.4	118.7	235.4
δ (**5**)	31.0 [a]	32.8 [a]	112.4	73.7 [c]	50.3	118.2 [b]	126.2 [b]	73.7 [c]	245.7
δ (**5**) − δ (**4**)	0.5	2.3	−6.3	−18.7	−42.9	25.0	33.8	−45.0	10.3
δ (**5**) − δ (**6**)	0.9	2.7	−33.8	−49.3	−77.3	−9.4	3.1	−72.5	

[a, b] Interchangeable assignment. [c] The signals in the gated spectrum are clearly differentiated as singlet (C-6a) and doublet (C-3).

composes above −60 °C to give a metal-containing solid and cyclobutabenzene (**6**). Exposure to atmospheric oxygen resulted in reoxidation to **4**.

NMR spectroscopic analysis shows that the solution contains one main component, whose ^{13}C NMR data are most consistent with **5**. Also present are at least two minor components, whose signals partly correspond to isomers of **5**. This is in agreement with the reoxidizability of the products to **4**. Because of the isomeric side products, the ^1H NMR spectrum is of little value. The η^4 coordination in **5** is shown, however, by comparing its ^{13}C NMR data with those for cyclobutabenzene (**6**) (Table 2). For **5** and **2**, the changes in the chemical shifts of the terminal C atoms ($\Delta\delta = -77.3$ and -72.5, respectively) and the inner C atoms ($\Delta\delta = -49.3$ and -33.8, respectively) of the coordinated diene unit relative to those of the free ligand are similar. Apparently, the most strained double bond of the ligand remains preferentially in the coordination sphere of the metal. Similar observations were made earlier for 4,7-dihydroacepentalene complexes.[10]

IR spectra of **2** and **5** in THF at −30 °C and of **2** at −100 °C in KBr were recorded.[11] Owing to the increase in electron density at the metal atom, the carbonyl bands display lower wave numbers than those in the starting materials. Small deviations from the data obtained by *Cooper* et al.[2] for $K_2[(\eta^4\text{-benzene})Cr(CO)_3]$ and by *Rieke* et al.[4] for $Na_2[(\eta^4\text{-naphthalene})Cr(CO)_3]$ may be due to differing measurement conditions and counterions.

This work thus represents the first synthesis and spectroscopic characterization of naphthalene-free solutions of $[(\eta^4\text{-arene})Cr(CO)_3]$ dianions whose decomplexed double bond is not stabilized by an aromatic system. In order to check whether the absence of stabilization facilitates the transfer of the $Cr(CO)_3$ group to other arenes, **2** was allowed to react with *ortho*-xylene and **6**, both in excess. However, the $Cr(CO)_3$ group was not transferred. Therefore, the transfer to naphthalene[3] presumably occurs because naphthalene readily undergoes η^4 coordination.

Experimental Procedure

2: Lithium sand (40 mg, 5.7 mmol) was activated on the surface by vigorous stirring under argon. It was then cooled to −78 °C and combined, under a stream of argon, with a solution of **1** (214 mg, 1.0 mmol) in 4 mL of $[D_8]$THF cooled to −78 °C. The initially yellow reaction solution turned red after a few minutes and then brown. The suspension was stirred for 16 h at −78 °C and then filtered at −78 °C to remove excess lithium sand. The brown-yellow solution is stable for several days under argon at −78 °C.

Received: April 9, 1990;
supplemented: September 3, 1990 [Z 3901 IE]
German version: *Angew. Chem. 102* (1990) 1469

CAS Registry numbers:
1, 12082-08-5; **2**, 129943-99-3; **4**, 99537-78-7; **5**, 129944-00-9.

[1] M. F. Semmelhack, W. Seufert, L. Keller, *J. Organomet. Chem. 226* (1982) 183.
[2] V. S. Leong, N. J. Cooper, *J. Am. Chem. Soc. 110* (1988) 2644.
[3] V. S. Leong, N. J. Cooper, *Organometallics 7* (1988) 2058.
[4] R. D. Rieke, W. P. Henry, J. S. Arney, *Inorg. Chem. 26* (1987) 420.
[5] L.-N. Ji, M. E. Rerek, F. Basolo, *Organometallics 3* (1984) 740.
[6] E. O. Fischer, K. Öfele, *Chem. Ber. 90* (1957) 2532.
[7] NMR data for dianions **2** and **5** (counterions $Li^{\oplus}$). **2**: ^1H NMR (200 MHz, $[D_8]$THF, −80 °C): $\delta = 1.57$ [br.s, 2H, 1(4)-H], 4.65 [br.s, 2H, 2(3)-H], 5.15 [br.s, 2H, 5(6)-H]. ^{13}C NMR (75.5 MHz, $[D_8]$THF, −80 °C): $\delta = 55.6$ [d, C-1(4), $^1J(C,H) = 150 \pm 2$ Hz], 87.5 [d, C-2(3), $^1J(C,H) = 163 \pm 2$ Hz], 124.5 [d, C-5(6), $^1J(C,H) = 154 \pm 2$ Hz], 245.8 (s, CO). **5**: ^{13}C NMR (75.5 MHz, $[D_8]$THF, −80 °C): $\delta = 31.0$ (t, C-1/C-2, $^1J(C,H) = 135$ Hz), 32.8 (t, C-1/C-2, $^1J(C,H) = 134$ Hz), 50.3 (d, C-4, $^1J(C,H) = 149$ Hz), 73.7 (d, C-3, $^1J(C,H) = 167$ Hz), 73.7 (s, C-6a), 112.4 (s, C-2a), 118.2 (d, C-5/C-6, $^1J(C,H) = 155$ Hz), 126.2 (d, C-5/C-6, $^1J(C,H) = 154$ Hz), 245.7 (s, CO). In addition to the signals assigned to **5**, other weaker signals are present and are probably due to isomers of **5**.
[8] a) H. G. Wey, H. Butenschön, *J. Organomet. Chem. 350* (1988) C8; b) H. G. Wey, P. Betz, H. Butenschön, *Chem. Ber.*, in press.
[9] D. E. F. Gracey, W. R. Jackson, W. B. Jennings, S. C. Rennison, R. Spratt, *J. Chem. Soc. B 1969*, 1210.
[10] a) H. Butenschön, A. de Meijere, *Tetrahedron 42* (1986) 1721; b) *Angew. Chem. 96* (1984) 722; *Angew. Chem. Int. Ed. Engl. 23* (1984) 707.
[11] Only the positions of the carbonyl bands are given. **2**: IR (THF, −30 °C): $\tilde{\nu}$[cm^{-1}] = 1845 m, 1810 m, 1790 s, 1765 s, 1765 m, 1735 m, 1710 m, 1665 m. The bands at 1845, 1735, and 1665 cm^{-1} disappear after only a few seconds, whereas the other bands given here as well as those of the starting material at 1960 and 1885 cm^{-1} become more intense. IR (KBr, −100 °C): $\tilde{\nu}$[cm^{-1}] = 3500 br, 3020 m, 2920 m, 2740 m, 1792 s, 1759 s, 1724 s, 1510 w, 1480 w, 1445 m, 1300 m, 1180 m, 1155 m, 1025 s, 750 m, 678 m, 635 m, 535 m. **4**: IR (THF, −30 °C): $\tilde{\nu}$[cm^{-1}] = 1842 m, 1795 m, 1790 m, 1750 m, 1735 m, 1708 m, 1665 m. The bands at 1842, 1790, 1735, and 1665 cm^{-1} disappear after only a few seconds, whereas the other bands given here as well as those of the starting material at 1957 and 1878 cm^{-1} become more intense.

Organoosmium Oxides: Efficient Syntheses and Structures**

By *Wolfgang A. Herrmann,* Stefan J. Eder, Paul Kiprof, Kristin Rypdal*, and *Petra Watzlowik*

The little explored organometallic oxides[1] offer application in homogeneous and heterogeneous catalysis, for example in the oxidation and metathesis of olefins and in aldehyde olefination.[2] The synthesis of compounds of general formula $R_aM_bO_c$ has so far been left largely to chance, since the usual oxide and halide precursors are not easily alkylated because they are strong oxidants. An exception is the methylation of dirhenium heptaoxide,[3] although extension to

[*] Prof. Dr. W. A. Herrmann, S. J. Eder, P. Kiprof, P. Watzlowik
Anorganisch-chemisches Institut der Technischen Universität München
Lichtenbergstrasse 4, W-8046 Garching (FRG)
Dr. K. Rypdal[†]
Department of Chemistry, University of Oslo
P. O. Box 1033 Blindern, N-0315 Oslo 3 (Norway)

[†] Electron diffraction analysis

[**] Multiple Bonds between Main-Group Elements and Transition Metals, Part 84. This work was supported by the Fonds der Chemischen Industrie (doctoral fellowship to *S. J. E.*) and the Deutsche Forschungsgemeinschaft. Part 83: I. A. Degnan, W. A. Herrmann, E. Herdtweck, *Chem. Ber. 123* (1990) 1347.

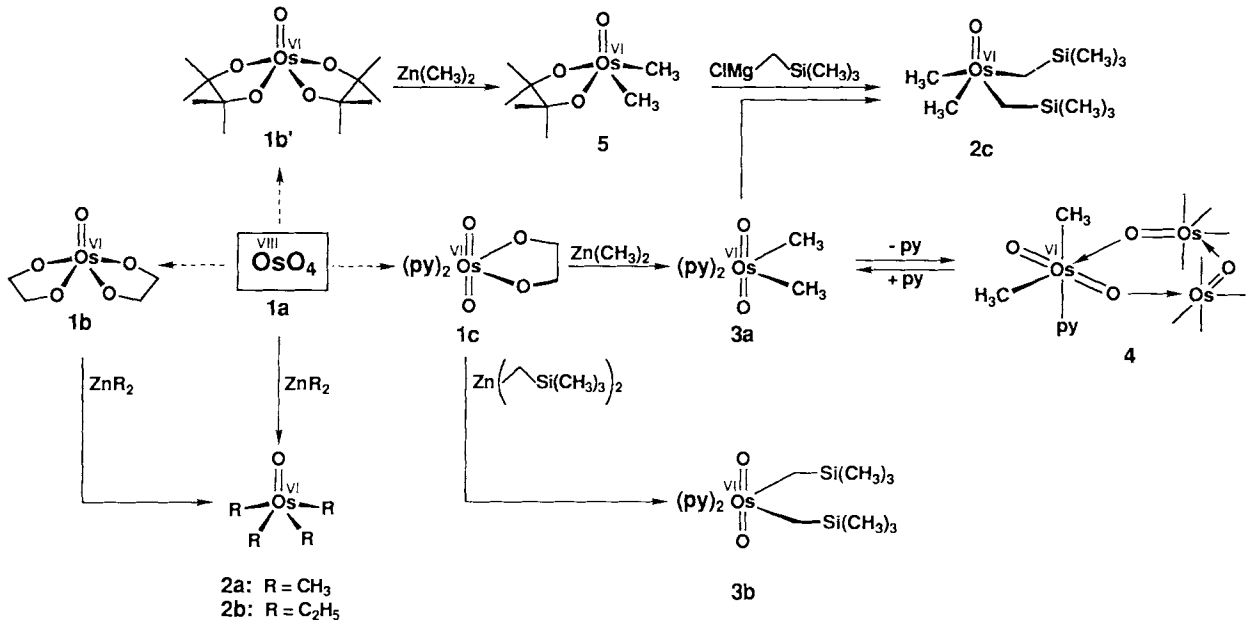

Scheme 1. Synthesis of selected new organoosmium oxides. All compounds were characterized by elemental analysis; for further data see [7–9, 11, 12].

even closely related osmium tetraoxide is not possible. Here we describe a simple, generalizable synthetic procedure, as exemplified by organoosmium oxides. It is based on the selective alkylation of glycolate complexes of metals in high oxidation states.

Alkylosmium oxides of unpredictable composition are formed in poor yields upon direct alkylation of osmium(VIII) oxide.[4] For example, treatment of OsO_4 (**1a**) with dimethylzinc affords tetramethyl(oxo)osmium(VI) (**2a**) in only 19% yield (Scheme 1).[4g] Only recently was a more efficient synthesis of a tetraalkylosmium oxide described.[5]

On the other hand, reaction of dimethylzinc and the air-stable glycolate complex **1b**, obtained by treatment of **1a** with 1,2-ethanediol (> 95% yield),[6] affords the methyl compound **2a** in 60% yield as a red solid that sublimes under vacuum without decomposition.[7a] Compound **2a**, the simplest alkylosmium oxide so far, has a square-pyramidal molecular structure of symmetry C_4 in the gas phase (Fig. 1). It is resistant to both oxidation and reduction: the cyclovoltammetric half-wave potentials are 2.2 V (irreversible) and −1.58 V (reversible), respectively, versus Ag/AgCl in acetonitrile. Diethylzinc reacts with **1a** to give the ethyl compound **2b**, which decomposes above −60 °C and preferentially loses *n*-butane, ethane, and ethylene at room temperature.[7b]

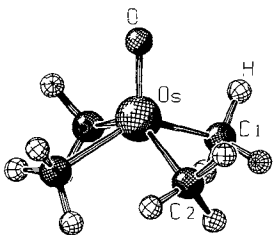

Fig. 1. Gas-phase structure of tetramethyl(oxo)osmium(VI) determined by electron diffraction. Selected bond lengths [pm] and angles [°]: Os-C 209.6(3), C-H 111.0(4), Os-O 168.1(4); C1-Os-C2 81.8(4), C1/C2/C3/C4-Os-O 112.2(5), Os-C-H 109(1); O-Os-C-H 24.(8).

The synthetic principle—exchange of a glycolate chelating ligand for two alkyl groups R—can be extended in a straightforward fashion to complex **1c**. As shown in Scheme 1, this reaction affords the dimethylosmium(VI) compound **3a** in 55% yield.[8a] Complex **3a** has a nearly undistorted octahedral molecular structure in the crystal with *trans* oxo and *cis* methyl groups (Fig. 2.) It is resistant to alkylzinc com-

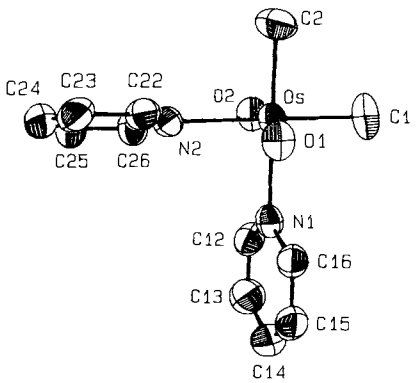

Fig. 2. Molecular structure of dimethyl(dioxo)bis(pyridine)osmium(VI) (**3a**) in the crystal (ORTEP plot without H atoms). Selected bond lengths [pm] and angles [°]: Os-O1 172.3(3), Os-O2 171.5(3), Os-C1 207.8(6), Os-C2 208.4(6), Os-N1 232.8(5), Os-N2 233.2(4); O1-Os-O2 164.8(2), C1-Os-C2 87.3(2), N1-Os-N2 88.9(1)[13].

pounds, but undergoes smooth alkylation on treatment with the Grignard reagent Me_3SiCH_2MgCl in a redox-neutral fashion and with retention of the *cis* configuration (!) (70% yield).[9] Organometallic oxides with *different* alkyl ligands are thus accessible for the first time by a direct and stereoselective reaction. Reaction of **1c** with bis(trimethylsilylmethyl) zinc gives complex **3b**[8b] (Scheme 1), which was also characterized by X-ray structure analysis.[10]

In vacuum, complex **3a** loses one molar equivalent of pyridine and affords the formally fivefold coordinated com-

plex $[OsO_2(CH_2)_3(py)]$. In the solid state, the latter complex forms the trinuclear compound **4**, which is octahedrally coordinated at osmium and has the same empirical formula (45% yield). The crystal structure (Fig. 3) is unusual in that an unsymmetrical, nearly planar Os_3O_3 six-membered ring, held together by O→Os donor bonds, is present.[11] However, these bonds stabilize only the solid-state structure. They are so weak that, even in chloroform or benzene, only monomers are present (vapor pressure osmometry). Addition of pyridine results in conversion of **4** back to **3a**.

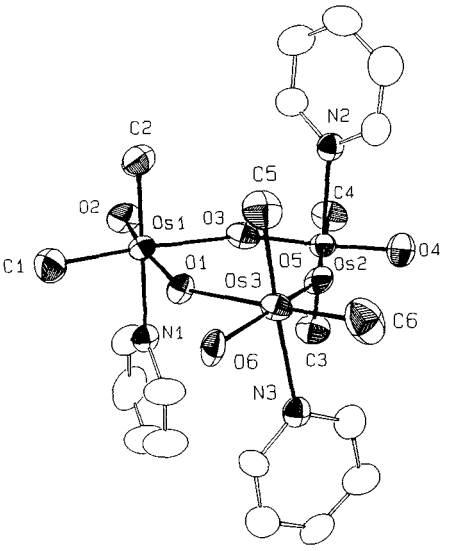

Fig. 3. Structure of trimeric dimethyl(dioxo)(pyridine)osmium(VI) (**4**) in the crystal (ORTEP plot without H atoms). Selected bond lengths [pm] and angles [°]: Os1-O1 173.5(3), Os1-O2 171.7(4), Os1-O3 231.2(4), Os3-O1 244.5(4), Os1-N1 232.4(6), Os1-C1 203.3(8), Os1-C2 207.0(7); O1-Os1-O2 164.3(2), C1-Os1-C2 89.1(3), O1-Os1-O3 81.9(2), Os1-O1-Os3 153.1(3)[13].

The constitution of the glycolate ligands may be used to control the selectivity of alkylation. The bulky bispinacolate complex **1b'** reacted with $Zn(CH_3)_2$ to give the dimethyl compound **5**, also characterized by an X-ray structure analysis,[10] in 55% yield.[12] The second chelating ligand here is only removed upon treatment with Grignard reagents (Scheme 1). This approach represents a second way to obtain mixed alkylated osmium oxides.

The glycolate derivatization—possibly with *reduction* (Scheme 1)—has proven useful in the efficient synthesis of alkyl(oxo) complexes of osmium in medium and high oxidation states. It is superior to the methods used so far with respect to yield, selectivity, and generizability. The route to a thorough exploration of this class of substances is thus open, and we have applied this technique to metals other than osmium.[14]

Received: July 26, 1990 [Z 4095 IE]
German version: *Angew. Chem. 102* (1990) 1460

CAS Registry numbers:
1a, 20816-12-0; **1b**, 54260-55-8; **1b**, 52782-38-4; **1c**, 39019-05-1; **2a**, 130149-61-0; **2b**, 130149-63-2; **2c**, 130149-64-3; **3a**, 130149-65-4; **3b**, 130149-67-6; **4**, 130149-66-5; **5**, 130149-62-1.

[1] Reviews: a) F. Bottomley, L. Sutin, *Adv. Organomet. Chem. 28* (1988) 339; b) W. A. Herrmann, *Angew. Chem. 100* (1988) 1269; *Angew. Chem. Int. Ed. Engl. 27* (1988) 1297.

[2] W. A. Herrmann, *J. Organomet. Chem. 382* (1990) 1, and references cited therein.

[3] W. A. Herrmann, J. G. Kuchler, J. K. Felixberger, E. Herdtweck, W. Wagner, *Angew. Chem. 100* (1988) 420; *Angew. Chem. Int. Ed. Engl. 27* (1988) 394.

[4] a) A. S. Alves, D. S. Moore, R. A. Andersen, G. Wilkinson, *Polyhedron 1* (1982) 83; b) R. P. Tooze, P. Stavropoulos, M. Motevalli, M. B. Hursthouse, G. Wilkinson, *J. Chem. Soc. Chem. Commun. 1985*, 1139; c) P. Stavropoulos, P. G. Edwards, T. Behling, G. Wilkinson, M. Motevalli, M. B. Hursthouse, *J. Chem. Soc. Dalton Trans. 1987*, 169; d) P. Stavropoulos, P. D. Savage, R. P. Tooze, G. Wilkinson, B. Hussain, M. Motevalli, M. B. Hursthouse, *ibid. 1987*, 557; e) C. J. Longley, P. D. Savage, G. Wilkinson, B. Hussain, M. B. Hursthouse, *Polyhedron 7* (1988) 1079; f) K. Mertis, G. Wilkinson, *J. Chem. Soc. Dalton Trans. 1976*, 1488; g) S. J. Eder, *Diplomarbeit*, Technische Universität München 1989.

[5] $[OsO(CH_2SiMe_3)_4]$ has a structure analogous to **2a** and is formed in 54% yield from $[OsO_2Cl_4]^{2\ominus}$: R. W. Marshman, W. S. Bigham, S. R. Wilson, P. A. Shapley, *Organometallics 9* (1990) 1341.

[6] a) R. J. Collin, J. Jones, W. P. Griffith, *J. Chem. Soc. Dalton Trans. 1974*, 1094; b) R. Criegee, *Justus Liebigs Ann. Chem. 522* (1936) 75; c) R. Criegee, B. Marchand, B. Wannowius, *ibid. 550* (1942) 99.

[7] a) **2a**: Red needles after sublimation under high vacuum onto a cold finger (0 °C), m.p. 74 °C. IR [cm^{-1}] ν(OsO) = 1013 vs (CS_2), 994 vs, br (KBr). ^1H NMR (270 MHz, [D_8]toluene, 20 °C): δ = 2.74 (s). ^{13}C NMR (67.9 MHz, [D_8]toluene, 20 °C): δ = 23.91. EI-MS (70 eV, ^{192}Os): molecular ion at *m/z* 268 ($M^{\oplus}$, 16%). ^{17}O NMR (C_6D_6, 20 °C, external standard H_2O): δ = 512. b) **2b**: Orange crystals, stable at −78 °C. ^1H NMR (400 MHz, $CDCl_3$, 20 °C): δ = 4.03 (q, $^3J(H,H)$ = 7.3 Hz, 8H; CH_2), 1.51 (t, 12H; CH_3). $\{^1H\}$ ^{13}C NMR (100.5 Hz, $CDCl_3$, 20 °C): δ = 40.30 (CH_2), 20.29 (CH_3). CI-MS (^{192}Os): *m/z* 324 ($M^{\oplus}$, 41%).

[8] a) **3a**: Red-brown, air-stable crystals, m.p. ≈ 235 °C. Red-brown cubes of dimensions 0.64 × 0.38 × 0.36 mm obtained from CS_2 solution (−25 °C); systematic absences, *h0l* (*l* = 2*n* + 1), *0k0* (*k* = 2*n* + 1); space group, monoclinic, P_1/c (No. 14). Lattice constants after least-squares refinement from 25 reflections at large diffraction angles: *a* = 674.0(1), *b* = 1479.4(2), *c* = 1355.1(2) pm, β = 92.27(<1)°, *V* = 1350 × 10^6 pm^3; empirical formula, $C_{12}H_{16}N_2O_2Os$ (410.5); *Z* = 4; F_{000} = 776; *P*(calcd) = 2.02 g cm^{-3}; Enraf-Nonius CAD-4 diffractometer, $Mo_{K\alpha}$ radiation (λ = 71.073 pm), graphite monochromator; *T* = 23 ± 3 °C; measuring range, 1.0 < θ < 25.0°; ω scan; scan width, (1.00 + 0.30 tanθ)° ± 25% before and after each reflection for background determination; *t*(max), 60 s; 2695 measured reflections (±*h*, +*k*, +*l*), 2082 unique reflections, 237 reflections with $I > 2.0\sigma(I)$ suppressed; 155 parameters after full-matrix least squares refinement; $R = \sum||F_o| - |F_c||/|F_o| = 0.035$; $R_w = [\sum w(||F_o| - |F_c||)^2/\sum w|F_o|^2]^{1/2} = 0.030$; GOF = $[\sum w(||F| - |F_c||)^2/(NO\text{-}NV)]^{1/2} = 1.964$ nur $w = 1/\sigma^2(F_o)$. Structure solution: Patterson methods, difference Fourier technique; empirical absorption correction, μ = 94.5 cm^{-1}, nine reflections; no decomposition; extinction, ε = 0.2525 × 10^{-6}, corrected; hydrogen atoms calculated for ideal geometry (*d*(C-H) = 95 pm) and included in the calculation of the structure factors with a collective isotropic temperature factor per C atom but not refined. Anomalous dispersion was taken into consideration. Shift/error < 0.01 in the last cycle of refinement; residual electron density, +1.10 $e_0Å$ for 99 pm and −1.10 $e_0Å^{-3}$ for 104 pm distance from osmium atom. IR (CS_2)[cm^{-1}] ν(OsO) = 866 (vs. ^1H NMR (270 MHz, C_6D_6, 20 °C): δ = 3.92 (s, 6H, CH_3), 8.84 (m, 4H, CH), 6.79 (m, 2H; CH), 6.57 (m, 4H; CH). ^{13}C NMR (100.5 MHz, C_6D_6, 20 °C): δ = −7.37 (q, $^1J(C,H)$ = 130 Hz; CH_3) 147.24 (*o*), 138.20 (*p*), 124.15 (*m*). ^{17}O NMR (54.2 MHz, C_6H_6/C_5H_5N, 20 °C, external standard H_2O): δ = 617, b) **3b**: brown crystals. ^1H NMR (400 MHz, CD_2Cl_2, 20 °C): δ = 0.07 (s, 18H; CH_3), 4.14 (s, 4H; CH_2), 8.58, 7.40 (2 m, 2 × 4H; CH), 7.80 (m, 2H; CH). ^{13}C NMR (100.5 MHz, CD_2Cl_2, 20 °C): δ = 0.34 (CH_3), 4.11 (CH_2), 124.6, 138.4, 148.3(CH).

[9] **2c**: brown oil. IR (CS_2) [cm^{-1}]: ν(OsO) = 1005 vs. ^1H NMR (400 MHz, $CDCl_3$, 20 °C): δ = 4.10 (d, $^2J(H,H)$ = 7.9 Hz; 2H; CH_2), 3.45 (d, $^2J(H,H)$ = 7.3 Hz, 2H; CH_2), 2.99 (s, 6H; $OsCH_3$), 0.09 (s, 18H; $SiCH_3$). $\{^1H\}$ ^{13}C NMR (100.5 MHz, $CDCl_3$, 20 °C): δ = 40.81 (t, $^1J(C,H)$ = 124 Hz; CH_2), 24.86 (q, $^1J(C,H)$ = 132 Hz; $OsCH_3$), 1.11 (t, $^1J(C,H)$ = 119 Hz; $SiCH_3$). EI-MS (70 eV, ^{192}Os): *m/z* 412 ($M^{\oplus}$, 7%).

[10] W. A. Herrmann, P. Kiprof, unpublished results, 1990.

[11] **4**: Dark, air-stable crystals, m.p. 83 °C; sublimation at 80 °C/ca. 10^{-3} Torr afforded red-brown prisms of dimensions 0.38 × 0.26 × 0.20 mm: *no* systematic absences; space group, triclinic, $P\bar{1}$ (No. 2). Lattice constants after least-squares refinement from 25 reflections at high diffraction angles: *a* = 972.6(1), *b* = 1090.9(1), *c* = 1415.0(1) pm, α = 85.03(<1), β = 76.41(1), γ = 67.71(1)°; *V* = 1350 × 10^6 pm^3; empirical formula, $C_{21}H_{33}N_3O_6Os_3$ (994.1); *Z* = 2; F_{000} = 912; ϱ(calcd) = 2.44 g cm^{-3}; Enraf-Nonius CAD-4 diffractometer, $Mo_{K\alpha}$ radiation (λ = 71.073 pm), graphite monochromator; *T* = 23 ± 3 °C; measuring range, 1.0 < θ < 25.0°; ω scan; scan width, (0.90 + 0.30 tan θ) ± 25% before and after each reflection for background determination; *t*(max): 60 s; 5028 measured reflections (−*h*, ±*k*, ±*l*), 4394 unique reflections, 4394 reflections with $I > 0.0\ \sigma(I)$ used; 299 parameters, full-matrix least-squares refinement; $R = \sum(||F_o| - |F_c||/\sum|F_o| = 0.048$; $R_w = [\sum w(||F_o| - |F_c||)^2/\sum w|F_o|^2]^{1/2} = 0.042$; GOF = $[\sum w(||F_o| - |F_c||)^2/(NO\text{-}NV)]^{1/2} = 3.951$ mit $w = 1/\sigma^2(F_o)$. Structure solution: Patterson methods, difference Fourier tech

nique; empirical absorption correction, $\mu = 141.5\ cm^{-1}$, eight reflections; decomposition, $-18.9\% \pm$ in 77.3 h for three control reflections, isotropic correction; extinction, $\varepsilon = 0.3526 \times 10^{-6}$, corrected; hydrogen atoms caculated for ideal geometry (d(C-H) = 95 pm) and included in the calculation of the structure factors with a collective isotropic temperature factor per C atom but not refined. Anomalous dispersion was taken into consideration. Shift/error < 0.01 in the last cycle of refinement; residual electron density: $+2.58\ e_0Å^{-3}$ for 85 pm and $-2.77\ e_0Å^{-3}$ for 91 pm distance from osmium atom. IR [cm^{-1}]: ν(OsO) = 904 vs (CS_2), 868 vs (KBr). ^{1}H NMR (400 MHz, C_6D_6, 20 °C): δ = 3.91 (s, 6H; CH_3) 8.35 (m, 2H; CH), 6.79 (m, 1H; CH), 6.51 (m, 2H; CH). {^{1}H}^{13}C NMR (100.5 MHz, C_6D_6, 20 °C): $\delta = -10.74$ (CH_3), 124.6, 139.0, 147.1 (CH). ^{17}O NMR (54.2 MHz, C_6H_6, 20 °C, external standard H_2O): δ = 745. FD-MS (CH_2Cl_2, ^{192}Os): m/z 333 (monomer; rel. int. 11%).

[12] **5**: red crystals, dec. above ca. 150 °C, sublimable at 50 °C/760 Torr. IR (KBr) [cm^{-1}] (ν(OsO, term.) = 950 vs, ν(OsO, ester) = 634 m. ^{1}H NMR (400 MHz, C_6D_6, 20 °C): δ = 0.93 (s, 6H; CCH_3), 1.27 (s, 6H; CCH_3), 3.87 (s, 6H; $OsCH_3$). ^{13}C NMR (100.5 MHz, C_6D_6, 20 °C): δ = 18.28 ($OsCH_3$), 24.63 (CCH_3), 25.80 (CCH_3), 90.94 (CCH_3). ^{17}O NMR (54.2 MHz, pentane, 20 °C, external standard H_2O): δ = 675. EI-MS (70 eV, ^{192}Os): m/z ($M^{\oplus}$, 5%)

[13] Further details of the crystal structure investigation of **3a** and **4** may be obtained from the Fachinformationszentrum Karlsruhe, Gesellschaft für wissenschaftlich-technische Information mbH, D-7514 Eggenstein-Leopoldshafen 2 (FRG), on quoting the depository number CSD-54862, the names of the authors and the journal citation.

[14] W. A. Herrmann, P. Watzlowik, P. Kiprof, unpublished results 1990.

$CsF{\cdot}Br_2$, an Alkali-Metal Halide Intercalation Compound**

By *Darryl D. DesMarteau,* Thomas Grelbig, Sun-Hee Hwang,* and *Konrad Seppelt*

Cesium fluoride is one of the strongest fluoride catalysts, since it combines a very large cation and a very small anion in a simple NaCl-type lattice. Therefore, the salt has a strong tendency to "increase" the size of its anion by forming intermediate or permanent anionic fluoride complexes. There are a large number of complex cesium fluorides $Cs_x^{\oplus}AF_y^{\ominus}$, where A can be almost any element of the periodic system. Many of their structures are known.

In the reactions of fluorinated nitriles with bromine in the presence of CsF, the CsF was found to absorb bromine, which was not readily removed at room temperature.[1, 2] Subsequent investigation revealed that CsF can absorb both Br_2 and I_2 to form complexes in which the ratio $CsF:X_2$ is 1:1 and 2:1.[3] The $CsF{\cdot}Br_2$ complex is very effective in oxidizing fluorinated nitriles and imines to *N*-bromo derivatives as well as in converting N–Cl bonds into N–Br bonds in *N,N*-dichloroamines.[1–3] This reactivity, combined with the novelty of the CsF–halogen complexes, made their structure determination of interest.

The halogen-rich 1:1 phases are formed with excess halogen at room temperature, and the 2:1 materials can be prepared by prolonged pumping at 10^{-2} mbar on the 1:1 phases. The supposition that the 1:1 materials might contain the polyhalide ions [Br-Br-F]$^{\ominus}$ and [I-I-F]$^{\ominus}$ (cf. $Br_3^{\ominus}$, $BrF_2^{\ominus}$, $ICl_2^{\ominus}$, $Cl_2F^{\ominus}$) was not in accord with the Raman spectra of $CsF{\cdot}Br_2$, since it shows only one line at $\tilde{\nu} = 292.5\ cm^{-1}$, which is almost unchanged from the Raman line of elemental Br_2 (317 cm^{-1}). No BrF stretching vibration could be seen.

In the case of $CsF \cdot Br_2$, we succeeded in growing single crystals and carrying out an X-ray analysis (Fig. 1). Much to our surprise the compound is a cesium fluoride intercalation compound with Br_2 as guest. The NaCl-type cesium fluoride lattice has opened along the (100) planes and the Br_2 molecules are stacked between the planes. The cesium and fluorine atoms are arranged in an eclipsed manner along [100], resulting in a primitive tetragonal cell. The Br–Br distance of 232.4 pm is only slightly longer than that in elemental bromine (228 pm) and the $Br \cdots F^{\ominus}$ contacts (252.1 pm) are about 40% longer than a normal Br–F bond (180 ± 10 pm). Any covalent bonding here must be very weak.

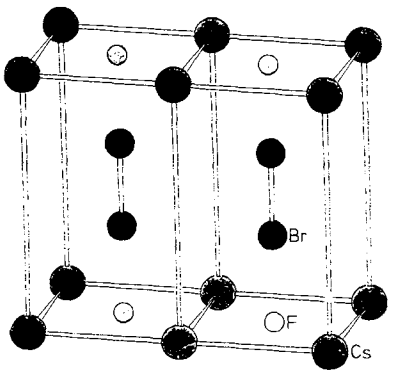

Fig. 1. Crystal structure of $CsF \cdot Br_2$ (two adjacent unit cells). The orange crystals were grown from CsF in a large excess of elemental bromine at 80 °C in a glass ampoule over four weeks. Enraf-Nonius CAD-4 diffractometer, $T = -153$ °C, $Mo_{K\alpha}$, graphite monochromator, $\omega/2\theta$ scan, DIFABS absorption correction. SHELX, full matrix, *P4/mmm* (No. 123), $a = 417.7(2)$, $c = 736.4(2)$ pm, $V = 128.5 \times 10^6$ pm^3, $Z = 1$. Reflections: 886 measured, 287 independant, 264 with $I \geq 3\sigma(I)$ within $2 \leq \theta \leq 40°$. $R = 3.15$, $R_w = 2.6$. Further details of the crystal structure investigation are available on request from the Fachinformationszentrum Karlsruhe, Gesellschaft für wissenschaftliche und technische Information mbH, D-7514 Eggenstein-Leopoldshafen 2 (FRG), on quoting the depository number CSD-54259, the names of the authors, and the journal citation.

If one considers the NaCl lattice to be very stable, this reaction is very surprising. But Madelung lattice energy calculations (MAPLE)[4] on CsF show that cleavage along (100) results in loss of only 6% of the energy; which explains the cleavability parallel to (100) for such crystals. If entropic terms are disregarded, this small loss of electrostatic energy could be compensated for by even very weak $Br \cdots F^{\ominus}$ interactions, which could amount to only a few kJ mol^{-1}.

The coordination of the $Cs^{\oplus}$ ions is square planar and the $Cs^{\oplus} \cdots F^{\ominus}$ distance of 300.1 pm in cesium fluoride is reduced to 294.0 pm in $CsF \cdot Br_2$. This is virtually identical to the $Cs^{\oplus} \cdots F^{\ominus}$ distance of 293.6 pm in the high-pressure CsF (CsCl-type) modification (48 kbar).[5] If the bromine atoms at a distance of 388 pm are included in the coordination of $Cs^{\oplus}$, the coordination number is 12 and the coordination polyhedron a square-based column.

Whether these features are retained in $CsF{\cdot}I_2$ and whether the 2:1 phases are intercalates where only every second layer is filled remain speculation until structural data are available.

[*] Prof. D. D. DesMarteau, S.-H. Huang
Department of Chemistry, Clemson University
Clemson, SC 29631 (USA)
Prof. K. Seppelt, T. Grelbig
Institut für Anorganische und Analytische Chemie der freien Universität
Fabeckstrasse 34–36, D-1000 Berlin 33 (FRG)

[**] This work was supported by the Fonds der Chemischen Industrie and the Alexander von Humboldt Stiftung. We thank Prof. *G. Meyer*, Hannover, for help with the MAPLE calculations.

Received: July 2, 1990 [Z 4048 IE]
German version: *Angew. Chem. 102* (1990) 1519

CAS Registry numbers:
$CsF \cdot Br_2$, 130147-11-4; $CsF \cdot I_2$, 130147-12-5; $2CsF \cdot Br_2$, 130147-13-6; $2CsF \cdot I_2$, 130147-14-7; CsF, 13400-13-0; bromine, 7726-95-6; iodine, 7753-56-2.

[1] B. A. O'Brien, D. D. DesMarteau, *J. Org. Chem. 49* (1984) 1467.
[2] Y. Y. Cheng, Q. C. Mir, B. A. O'Brien, D. D. DesMarteau, *Inorg. Chem. 23* (1984) 518.
[3] S. Y. Huang, *Ph. D. Thesis*, Clemson University, South Carolina, USA 1990.
[4] R. Hoppe, *Angew. Chem. 78* (1966) 52; *Angew. Chem. Int. Ed. Engl. 5* (1966) 95; *ibid. 82* (1970) 7 bzw. *9* (1970) 25.
[5] C. E. Weir, G. J. Piermarini, *J. Res. Natl. Bur. Stand. Sect. A 68* (1964) 105.

$(NBu_4)[Sn\{Pt(\mu\text{-}Cl)(C_6F_5)_2\}_3]$, an Unusual Cluster with Three $Pt^{II} \rightarrow Sn^{II}$ Bonds**

By *Rafael Usón,* Juan Forniés, Milagros Tomás,* and *Isabel Usón*

The insertion of $SnCl_2$ into M–Cl bonds to give $Cl_3Sn \rightarrow M$ bonds is well documented.[1] Adducts of the general type $[Cl_2Sn\{M(PMe_3)_3Cl\}_2]$ (M = Rh, Ir), displaying two $M \rightarrow SnCl_2$ bonds have been prepared recently and the structure of the rhodium complex has been solved by X-ray crystallography.[2] But, to the best of our knowledge, no complexes with bonds from a Pt^{II} moiety to an otherwise bare Sn^{II} center have, so far, been reported.

During the last few years we have shown that anionic pentahalophenyl complexes of platinum(II) are suitable precursors for the synthesis of heteronuclear complexes containing $Pt \rightarrow Ag$ bonds, since the basic platinum centers enable them to act as donor atoms to the electrophilic silver ions in silver salts ($AgClO_4$, $AgNO_3$) or silver complexes such as $[O_3ClOAgPPh_3]$.[3] Therefore, we have explored the use of anionic platinum(II) derivatives as Pt-donor ligands towards other electrophiles. Here we describe the synthesis of an unprecedented tetranuclear cluster containing three $Pt^{II} \rightarrow Sn^{II}$ bonds unsupported by any covalent bridging ligands; the Sn^{II} center is only linked to three Pt^{II} atoms and additionally displays short contacts to several *o*-F atoms of pentafluorophenyl groups.

Addition of $SnCl_2$ and $AgClO_4$ to a THF solution of the Pt complex **1**[4] at room temperature leads to precipitation of AgCl. The tetranuclear complex **2** can be obtained from the filtrate in 75% yield [Eq. (1)].

$$1.5(NBu_4)_2[Pt_2(\mu\text{-}Cl)_2(C_6F_5)_4] + SnCl_2 + 2\,AgClO_4 \xrightarrow{THF} \underset{\mathbf{1}}{} \quad (1)$$

$$2\,AgCl\downarrow + 2NBu_4ClO_4 + \underset{\mathbf{2}}{(NBu_4)[Sn\{Pt(\mu\text{-}Cl)(C_6F_5)_2\}_3]}$$

It is important to strictly maintain the given stoichiometry, since an excess of $AgClO_4$ also precipitates the bridging chloride ligands between the Pt^{II} atoms, leading to decomposition.

The structure of **2** has been established by a single-crystal X-ray study.[5] The unit cell (space group *Cc*) contains, in addition to the corresponding cations, two types of independent anions of the same composition (A and B) with very similar central cores but different orientations of the C_6F_5 groups (Fig. 1).

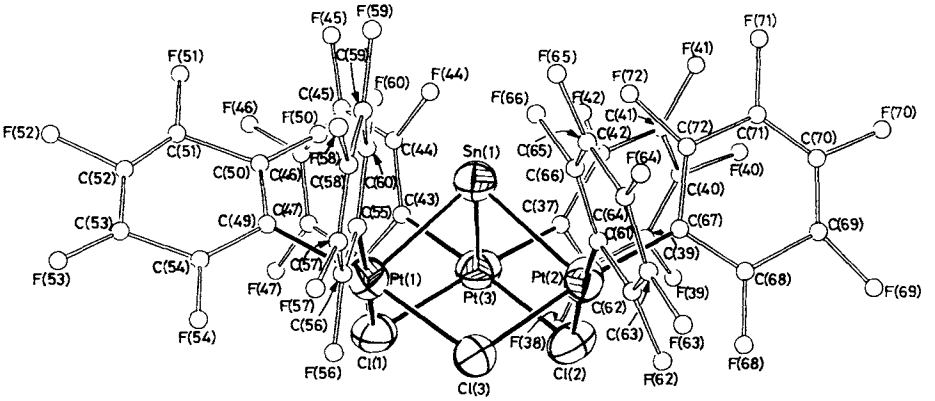

Fig. 1. Molecular structure of the anion in **2**. Selected bond lengths [Å] and bond angles [°]: anion A: Sn(1)-Pt(1) 2.732(2), Sn(1)-Pt(2) 2.742(3), Sn(1)-Pt(3) 2.704(2), Pt(1)-Cl(1) 2.414(6), Pt(1)-Cl(3) 2.373(7), Pt(2)-Cl(3) 2.401(7), Pt(2)-Cl(2), 2.415(6), Pt(3)-Cl(2) 2.372(7), Pt(3)-Cl(1) 2.426(8), Pt(1)-C(49) 2.029(23), Pt(1)-C(55) 2.068(23), Pt(2)-C(61) 1.943(19), Pt(2)-C(67) 1.968(23), Pt(3)-C(37) 1.981(24), Pt(3)-C(43) 2.028(24); Pt-Sn-Pt 87.7(30); Sn(1)-F(42) 2.9996(150), Sn(1)-F(44) 3.2526(166), Sn(1)-F(50) 2.9706(184), Sn(1)-F(60) 3.0491(132), Sn(1)-F(66) 3.0882(138), Sn(1)-F(72) 3.0946(153). anion B: Sn(2)-Pt(4) 2.733(2), Sn(2)-Pt(5) 2.703(3), Sn(2)-Pt(6) 2.734(2), Pt(4)-Cl(4) 2.439(7), Pt(4)-Cl(6) 2.417(7), Pt(5)-Cl(4) 2.386(7), Pt(5)-Cl5 2.404(7), Pt(6)-Cl(5) 2.422(7), Pt(6)-Cl(6) 2.396(7), Pt(4)-C(25) 1.989(25), Pt(4)-C(31) 1.960(23), Pt(5)-C(1) 2.007(23), Pt(5)-C(7) 2.048(23), Pt(6)-C(13) 1.957(23), Pt(6)-C(14) 1.962(27); Pt-Sn-Pt 88.1(9); Sn(2)-F(6) 2.8887(137), Sn(2)-F(8) 3.1309(132), Sn(2)-F(18) 3.0643(161), Sn(2)-F(24) 3.1668(133), Sn(2)-F(26) 3.0035(160), Sn(2)-F(32) 3.1930(136).

The cluster can be described as a $[Pt_3(\mu\text{-}Cl_3)(C_6F_5)_6]^{3\ominus}$ unit with a six-membered, puckered Pt_3Cl_3 ring in which the three Pt atoms are interconnected by three chloride bridges and linked to the Sn^{II} atom by platinum-to-tin donor–acceptor bonds. Thus, the Pt_3Cl_3 moiety acts as a tridentate ligand to the Sn atoms. Each platinum atom has square-pyramidal coordination with an apical Sn atom; the basal plane is defined by the *ipso*-C atoms of two C_6F_5 groups and two chloride ligands and the Pt–Sn bonds form angles of 10.63–

[*] Prof. R. Usón, Prof. J. Forniés, Dr. M. Tomás, I. Usón
Departamento de Química Inorgánica. Instituto de Ciencia de Materiales de Aragón
Universidad de Zaragoza.
E-50009 Zaragoza (Spain)

[**] We are grateful to the Spanish Comisión Interministerial de Ciencia y Tecnologia (CICYT) for financial support (project PB88-0076) and for a Formación de Personal Investigador (F.P.I.) grant to *I.U.*

13.66° with the perpendicular to each basal plane.[6] The Pt–Sn distances (2.703(3) to 2.742(3) Å) are within the expected range of 2.5[1] to 2.8[7,8] Å. Finally, short contacts between several *o*-F atoms and the Sn atom are present. As in the case of previously reported *o*-F···Ag contacts,[3] they are presumably responsible for the structure and stability of the cluster. The comparison parameter ρ (= experimental distances/sum of covalent radii)[9] has values between 1.42 and 1.59, which lie at the high end of the range found for *o*-F···Ag contacts, implying weak *o*-F···Sn interactions. Complex **2** behaves as 1:1 electrolyte in acetone solution; that is, the Pt → Sn bonds resist cleavage by this solvent.

We are studying the feasibility of preparing similar clusters. By substituting $PbCl_2$ for $SnCl_2$ in Equation (1), we have isolated a compound having the expected composition, but structural information is still lacking.

Experimental Procedure

A mixture of **1** (0.3 g, 0.1858 mmol), anhydrous $SnCl_2$ (0.0235 g, 0.1239 mmol), and $AgClO_4$ (0.0513 g, 0.2478 mmol) in THF (40 mL) was stirred at room temperature for 30 min. The suspension was evaporated to dryness and the residue treated with diethyl ether (50 mL). After filtration, a white residue (AgCl + NBu_4ClO_4) and a yellow solution were obtained. The solution was evaporated to dryness, the resulting oily residue was dissolved in CH_2Cl_2 (10 mL), and **2** (75% yield) was precipitaed by addition of pentane. Correct C,H,N analysis; m.p. 170 °C (dec.); molar conductivity (acetone $c \approx 5 \times 10^{-4}$ M), 128 S m^2 mol^{-1}. IR (Nujol), $\tilde{\nu}$ in cm^{-1}: C_6F_5 groups 1638 w, 1611 w, 1511 s, 1067 s, 964 s; X-sensitive [10] 813 s, 805 s; $NBu_4^{\oplus}$ 885; ν(Pt-Cl) 296 m,br.

Received: June 8, 1990 [Z 4004 IE]
German version: *Angew. Chem. 102* (1990) 1518

CAS Registry numbers:
1, 90590-30-0; **2**, 130246-95-6.

[1] M. S. Holt, W. L. Wilson, J. H. Nelson, *Chem. Rev. 89* (1989) 11, and references cited therein.
[2] D. M. T. Chan, T. B. Marder, *Angew. Chem. 100* (1988) 436; *Angew. Chem. Int. Ed. Engl. 27* (1988) 442.
[3] R. Usón, J. Forniés, M. Tomás, *J. Organomet. Chem. 358* (1988) 525.
[4] R. Usón, J. Forniés, F. Martínez, M. Tomás, *J. Chem. Soc. Dalton Trans. 1980*, 888.
[5] Crystals of **2** suitable for crystal structure investigation were obtained by slow diffusion of *n*-hexane into a solution of **2** in dichloromethane. X-ray structure analysis: $Pt_3SnCl_3F_{30}NC_{52}H_{36}$; space group *Cc*, a = 19.3966(12), b = 15.1882(17), c = 41.4803(25) Å, β = 93.799(5)°, V = 12193.3 Å^3, Z = 8 (two independent molecules in the assymmetric unit); Size 0.25 × 0.15 × 0.2 mm; $\mu(Mo_{K\alpha})$ = 78.06 cm^{-1}. Absorption correction (12 Ψ scans with transmission factors of 0.311–0.484). Siemens/Stoe four-circle diffractometer. Profile-fitted intensities [11], 4° ≤ 2θ ≤ 50°, ω scan. Total number of reflections 11521; 7545 unique reflections with $F_0 \geq 5\sigma(F_0)$; heavy-atom method. R = 0.052, R_w = 0.049 [12] Pt, Sn, Cl, and F atoms were treated as anisotropic. Weighting scheme: $\omega^{-1} = \sigma^2(F_0) + 0.00047\,F_0^2$; 1091 variables. The enantiomorph was chosen on the basis of a lower-weighted R factor. Further details of the crystal structure investigation are available from the Director of the Cambridge Crystallographic Data Centre, University Chemical Laboratory, Lensfield Road, GB-Cambridge CB2 1EW (England), on quoting the full journal citation.
[6] M. Nardelly, *Comput. Chem. 7* (1983) 95.
[7] R. U. Lindsey, Jr., G. W. Parshall, U. G. Stolberg, *Inorg. Chem. 5* (1966) 109.
[8] L. J. Guggenberger, *J. Chem. Soc. Chem. Commun. 1968*, 512.
[9] L. Pauling: *The Nature of Chemical Bond*, 3rd ed., Cornell Univ. Press, Ithaca, N.Y., USA, 1960, p. 403.
[10] R. Usón, J. Forniés, *Adv. Organometal. Chem. 26* (1988) 288, and references cited therein.
[11] W. Clegg, *Acta Crystallogr. Sect. A 39* (1983) 158.
[12] G. M. Sheldrick: *SHELX-76: Program of Crystal Structure Determination*, University of Cambridge, Cambridge (England), 1976.

Electrical and Magnetic Properties and X-Ray Structure of a Highly Conductive 4:1 Complex of Tetracyanoquinodimethane and a Tetrathiafulvalene Derivative**

By *Martin R. Bryce,* Adrian J. Moore, Masihul Hasan, Geoffrey J. Ashwell,* Alexander T. Fraser, William Clegg, Michael B. Hursthouse*, and *A. I. Karaulov*

Extended tetrathiafulvalene (TTF) derivatives have been identified by several groups to be promising donor molecules for the formation of new organic metals.[1–6] These large donors may be expected to form nonstoichiometric complexes with 7,7,8,8-tetracyano-*p*-quinodimethane (TCNQ) (by virtue of size mismatch) and they are known to form stable dication species; this is in marked contrast to TTF itself, for which the dication is destabilized by intramolecular Coulombic repulsion.[7] Although many extended TTF derivatives having alkenic, acetylenic, and quinonoid linking groups are known,[1–6] single crystals of neutral donors and their salts have been very difficult to obtain. Consequently, very little solid-state data are available for these materials. We now report the single-crystal X-ray structure of the donor 9,10-bis(4,5-dimethyl-1,3-dithiole)-2-ylidene-9,10-dihydroanthracene (**1**); we have recently reported the synthesis of this donor from anthraquinone.[8] *Yamashita* et al. have also synthesized analogues of this system.[5] We also present electrical, magnetic, and single-crystal X-ray data for a highly conducting 1:4 complex of **1** with TCNQ.

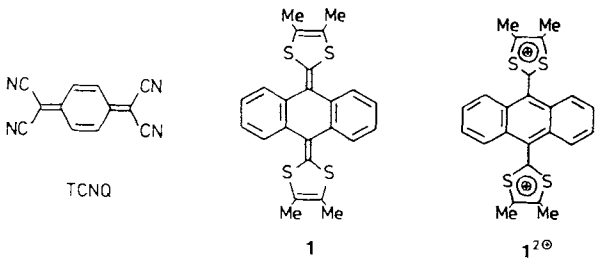

The crystal structure of the neutral donor **1** is shown in Figure 1a.[9] The molecule is butterfly-shaped with the central quinonoid ring severely distorted into a boat form.[10] Nonetheless, **1** forms a highly conductive 1:4 complex[11] with TCNQ, which is isolated from acetonitrile solution in 48% yield, and an insulating 1:2 salt with 2,5-dibromo-TCNQ. The 1:2 salt is diamagnetic with $\chi = -5.7 \times 10^{-4}$ emu mol^{-1}, the value being temperature-independent and consistent with that obtained from Pascal's constants. In contrast, the 1:4 TCNQ complex is paramagnetic. The susceptibility at 300 K, corrected for core diamagnetism, $\chi = 2.5 \times 10^{-3}$ emu mol^{-1}, corresponds to an effective mo-

[*] Dr. M. R. Bryce, Dr. A. J. Moore, Dr. M. Hasan
Department of Chemistry, University of Durham
GB-Durham, DH1 3LE (UK)
Dr. G. J. Ashwell, A. T. Fraser
Centre for Molecular Electronics, Cranfield Institute of Technology
Cranfield, GB-Bedford, MK43 0AL (UK)
Dr. W. Clegg
Department of Chemistry, University of Newcastle
GB-Newcastle upon Tyne, NE1 7RU (UK)
Professor M. B. Hursthouse, Dr. A. I. Karaulov
Department of Chemistry, Queen Mary College
Mile End Road, GB-London, E1 4NS (UK)

[**] This work was supported by SERC.

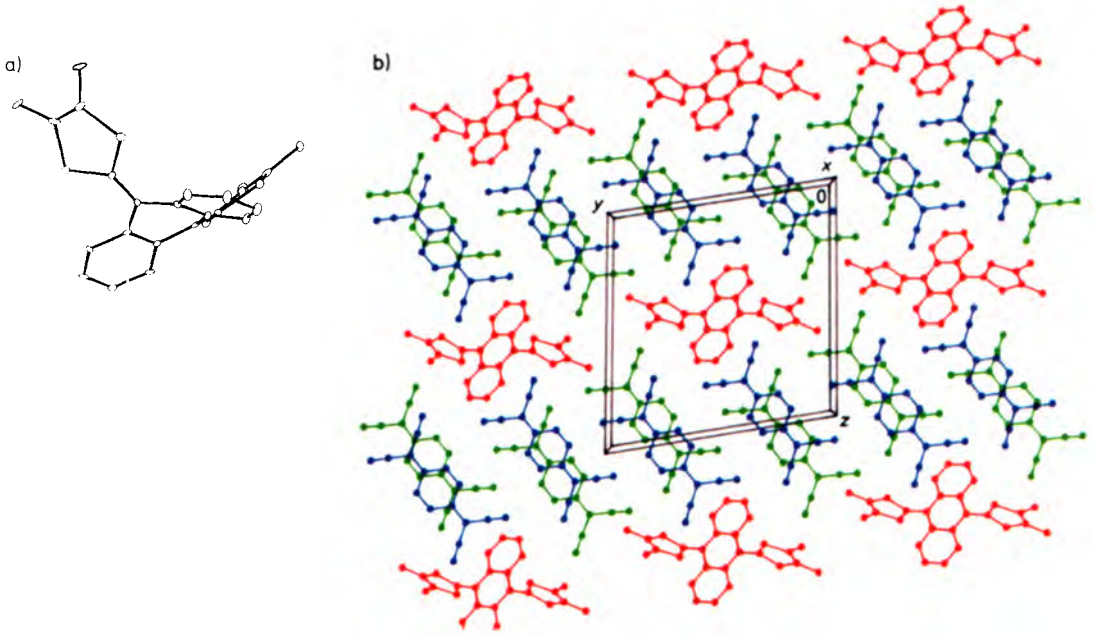

Fig. 1. Crystal structure of **1** (a) and the 1:4 complex $\mathbf{1}^{2\oplus}[(TCNQ)_4]^{2\ominus}$, projected along *a* (b).

ment of 2.45 μ_B. This value is lower than the 2.828 μ_B required of a triplet but is in close agreement with $\mu_{eff} = 2.449\ \mu_B$ for two independent spins per TCNQ formula unit. However, there is some uncertainty regarding the mechanism, since the effective moment is constant for a limited temperature range only.

The crystal structure of the 1:4 complex $\mathbf{1}^{2\oplus}[(TCNQ)_4]^{2\ominus}$, projected along *a*, is shown in Figure 1b.[12] The donor, in the dication form, adopts a dramatically different conformation from that of the neutral species, with dihedral angles of 86.0° between the planar anthracene group and the two dithiole rings. The dication is located on a center of symmetry. The TCNQ molecules stack plane-to-plane, parallel to *a*, with favorable ring-over-bond overlap and a uniform intermolecular spacing of 3.36 Å. The dimensions of the crystallographically independent molecules indicate that there is partial localization of charge onto alternate TCNQ molecules along the stacks.

$\mathbf{1}^{2\oplus}[(TCNQ)_4]^{2\ominus}$ is the first semimetallic TCNQ complex to be formed by a TTF-type donor that adopts such a nonplanar conformation.[13] The conductivity, $\sigma_{300K} = 60\ S\ cm^{-1}$, varies only slightly upon cooling to ca. 90 K but then decreases abruptly with a plateau between 50 and 70 K (Fig. 2a). This is mimicked by the susceptibility data, which show a plateau between ca. 40 and 80 K (Fig. 2b). In this temperature region, one sample showed an anomalous transition to a higher susceptibility state which persisted for several heating/cooling cycles. The effective moments, before and after switching, conformed to values for *two* and *four* spins per formula unit, respectively, signifying an unpairing of spins on the $\mathbf{1}^{2\oplus}$ stacks. Thus, we attribute the high conductivity to delocalized electrons on the uniform TCNQ stacks and the electrical and magnetic behavior in the 40–90 K region to structural transitions.

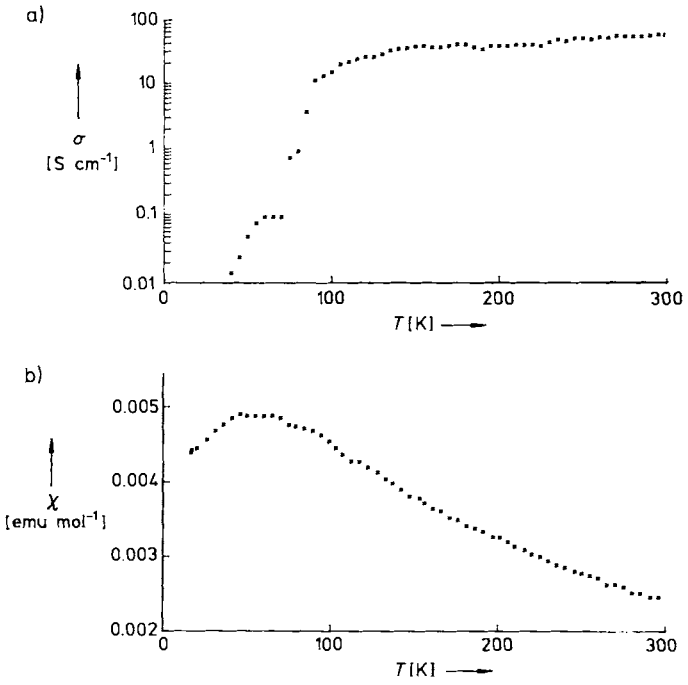

Fig. 2. Temperature dependence of the electrical conductivity σ (a) and the magnetic susceptibility corrected for core diamagnetism (b) of $\mathbf{1}^{2\oplus}[(TCNQ)_4]^{2\ominus}$. The data depicted correspond to cooling runs.

Received: May 16, 1990 [Z 3960 IE]
German version: *Angew. Chem. 102* (1990) 1493

CAS Registry numbers:
1, 117009-12-8; $\mathbf{1}^{2\oplus}\cdot$4TCNQ, 117009-13-9; **1** · 2(2,5-Br_2TCNQ), 130201-39-7.

[1] Z. Yoshida, T. Sugimoto. *Angew. Chem. 100* (1988) 1633; *Angew. Chem. Int. Ed. Engl. 27* (1988) 1573.
[2] M. R. Bryce, *J. Chem. Soc. Perkin Trans. 1 1985*, 1675.
[3] Y. Misaki, Y. Matsumura, T. Sugimoto, Z. Yoshida, *Tetrahedron Lett. 30* (1989) 5289.
[4] K. Takahashi, T. Nihira, *Tetrahedron Lett. 30* (1989) 5903.
[5] Y. Yamashita, Y. Kobayashi, T. Miyashi, *Angew. Chem. 101* (1989) 1090; *Angew. Chem. Int. Ed. Engl. 28* (1989) 1052.
[6] M. R. Bryce, A. J. Moore, D. Lorcy, A. S. Dhindsa, A. Robert, *J. Chem. Soc. Chem. Commun. 1990*, 470.

[7] S. Hünig, H. Berneth, *Top. Curr. Chem. 92* (1980) 1.
[8] M. R. Bryce, A. J. Moore, *Synth. Met. 25* (1988) 203.
[9] a) Crystal data for **1**: $M_r = 436.7$, monoclinic, space group $P2_1/c$, $a = 9.007$, $b = 12.719$, $c = 19.332$ Å, $\beta = 99.44°$, $V = 2184.7$ Å^3, $\varrho_{calcd} = 1.328$ g cm^{-3}, $Z = 4$, $F(000) = 912$, $\mu(Mo_{K\alpha}) = 4.3$ cm^{-1}, $\lambda = 0.71069$ Å. 3027 independent reflections of which 1691 were suppressed, weighting scheme $w = 6.0041/\sigma^2(F)$, $R = 0.082$, $R_w = 0.063$. Maximum electron density in final difference map, 0.34 e Å^{-3}. b) Further details of the crystal structure investigations are available on request from the Director of the Cambridge Crystallographic Data Centre, University Chemical laboratory, Lensfield Road, Cambridge, CB2 1EW (UK), on quoting the full journal citation.
[10] The analogous TCNQ derivative, 11,11,12,12-tetracyano-9,10-anthraquinodimethane, adopts a similar butterfly conformation in the neutral form; structural data for salts of this acceptor have not been reported. See A. Aumüller, S. Hünig, *Liebigs Ann. Chem. 1984*, 618; A. M. Kini, D. O. Cowan, F. Gerson, R. Mockel, *J. Am. Chem. Soc. 107* (1985) 556. For structural data on other severely distorted tetrathiafulvalene derivatives in which the TTF unit is incorporated into a cage see J. Röhrich, P. Wolf, V. Enkelmann, K. Müllen, *Angew. Chem. 100* (1988) 1429; *Angew. Chem. Int. Ed. Engl. 27* (1988) 1377; B. Girmay, J. D. Kilburn, A. E. Underhill, K. S. Varma, M. B. Hursthouse, M. E. Harman, J. Becher, G. Bojesen, *J. Chem. Soc. Chem. Commun. 1989*, 1406.
[11] This is a most unusual stoichiometry for a TCNQ complex. Cf. G. J. Ashwell, *Phys. Status Solidi B86* (1978) 705.
[12] Crystal data for $\mathbf{1}^{2\oplus}[(TCNQ)_4]^{2\ominus}$: $M_r = 1253.5$, triclinic, space group $P\bar{1}$, $a = 6.725(1)$, $b = 15.035(3)$, $c = 15.537(3)$ Å, $\alpha = 80.38(2)$, $\beta = 83.16(1)$, $\gamma = 87.15(1)°$, $V = 1537.1$ Å^3, $\varrho_{calcd} = 1.354$ g cm^{-3}, $Z = 1$, $F(000) = 644$, $\mu(Cu_{K\alpha}) = 18.5$ cm^{-1}, $\lambda = 1.54184$ Å. 3600 unique reflections of which 1007 were suppressed, weighting scheme $w^{-1} = \sigma^2(F)$, $R = 0.048$, $R_w = 0.052$. Maximum electron density in final difference map, 0.24 e Å^{-1}.
[13] Highly conducting salts of a severely distorted polyarene have been reported recently: P. Michel, A. Moradpour, M. Ribault, P. Petit, J.-J. Andre, *J. Chem. Soc. Chem. Commun. 1989*, 1173.

New Copper Clusters Containing Se and PEt_3 as Ligands: $[Cu_{70}Se_{35}(PEt_3)_{22}]$ and $[Cu_{20}Se_{13}(PEt_3)_{12}]$**

By *Dieter Fenske** and *Harald Krautscheid*

Dedicated to Professor Klaus Krogmann on the occasion of his 65th birthday

We recently reported on the reaction of CuCl with $Se(SiMe_3)_2$ in the presence of tertiary phosphanes such as $PtBu_3$ and $PiPr_3$.[1] High yields of clusters **1**–**3** were thereby obtained.

$[Cu_{29}Se_{15}(PiPr_3)_{12}]$ **1**

$[Cu_{30}Se_{15}(PiPr_3)_{12}]$ **2**

$[Cu_{36}Se_{18}(PtBu_3)_{12}]$ **3**

Apparently, the structures of the resulting cluster complexes are influenced by the phosphane used. We have therefore investigated which cluster complexes are formed on reaction of CuCl with $Se(SiMe_3)_2$ and PEt_3. Carried out in THF or toluene, this reaction results in a deep brown solution from which no crystalline products are isolable. On the other hand, crystals suitable for crystal structure analysis are obtained when the starting compounds are dissolved at -80 °C in diethyl ether and the reaction temperature is raised over several days to 20 °C. The resulting needles of **4** (yield ca. 60%) display a metallic luster. Although we have performed this reaction repeatedly, in only one case did we obtain black, octahedral crystals of composition **5**.[2]

$$CuCl + PEt_3 + Se(SiMe_3)_2 \rightarrow \underset{\mathbf{4}}{[Cu_{70}Se_{35}(PEt_3)_{22}]} + \underset{\mathbf{5}}{[Cu_{20}Se_{13}(PEt_3)_{12}]}$$

The IR spectra of **4** and **5** show the vibrational bands characteristic of PEt_3 ligands. Only one resonance signal ($\delta = -10$), providing no structural information, is found in the ^{31}P NMR spectrum (121.5 MHz, C_6D_6, 25 °C, H_3PO_4) of **4** owing to rapid exchange of the phosphane ligand.

The structures of **4** and **5** were determined by single-crystal investigations.[3] Cluster **5** (Fig. 1) consists of an undistorted

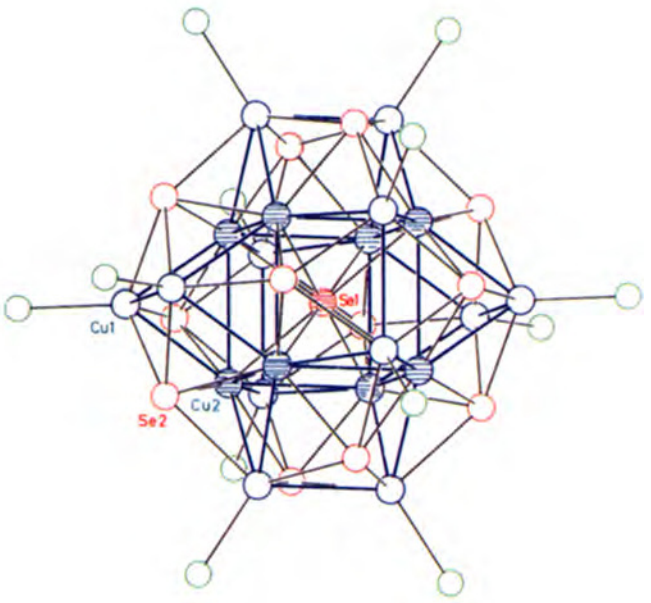

Fig. 1. Molecular structure of the cluster $[Cu_{20}Se_{13}(PEt_3)_{12}]$ (**5**) (C atoms omitted; Cu, blue; Cu1, open circles; Cu2, hatched; Se, red; Se1, hatched; Se2, open circles; P, green).

Cu_8 cube (Cu2, blue, hatched; Cu2-Cu2 300.8(3) pm), each of whose edges is bridged by a Cu1 atom (Cu1, blue, open circle; Cu1-Cu1 282.1(3) pm). The P atoms (green) of the PEt_3 ligands are bonded to each of these peripheral Cu1 atoms. In the resulting 20-atom Cu polyhedron, the shortest separations are those between Cu1 and Cu2 (267.8(3) pm). The μ_8-Se ligand Se1 (red, hatched; Se1-Cu2 260.5(3) pm) lies at the center of **5** and twelve μ_5-Se2 ligands cap all faces of the polyhedron (Se2, red, open circles; Cu1-Se2 247.7–260.1, Cu2-Se2 244.8(3) pm).

Alternatively, the Cu framework can be described in terms of six trigonal prisms, linked through common edges. Planes consisting of six Cu atoms result thereby. The Cu cluster is surrounded by twelve Se2 ligands, which form a nearly undistorted icosahedron (Se2 $\cdots$ Se2 392–415 pm). This structural principle is clearly illustrated in Figure 2 in which the faces of the Se icosahedron are drawn. However, the conceivable interpenetration of two dual polyhedra, an Se_{12} icosahedron and a Cu_{20} pentagonal dodecahedron, is only

[*] Prof. Dr. D. Fenske, Dipl-Chem. H. Krautscheid
Institut für Anorganische Chemie der Universität
Engesserstrasse, Geb.-Nr. 30.45, D-7500 Karlsruhe (FRG)

[**] This work was supported by the Deutsche Forschungsgemeinschaft, the Fonds der Chemischen Industrie, and Degussa AG. We thank Dr. *R. Kremer* and *W. Röthenbach* (Max-Planck-Institut für Festkörperforschung, Stuttgart) for help in measuring and interpreting the magnetic susceptibility data and the Guinier photographs and Dr. *T. Popp* for help in producing the figures.

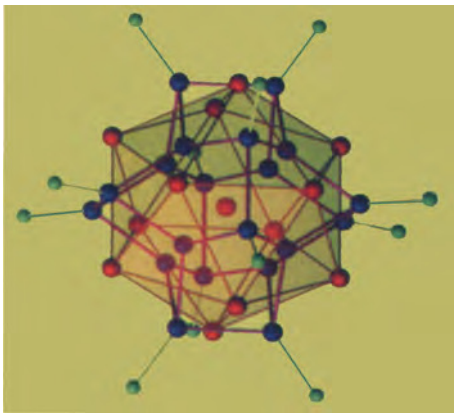

Fig. 2. Structure of the Se_{12} icosahedron (red) and the interpenetrating Cu_{20} polyhedron (Se, red; Cu, blue; P, green; Se–Cu bonds not shown).

realized in part, since, owing to the Cu–Cu interactions, the twelve Cu1 atoms lie above and the eight Cu2 atoms below the faces of the Se icosahedron.[12]

Thus, the bonding in **5** is different from that in the structurally related cluster $[Pd_{20}As_{12}(PPh_3)_{12}]$, in which the cluster center is unoccupied.[4] Consequently, the Pd–Pd bonds in the Pd_8 cube are significantly shorter (278.5–291.7 pm). The electron count in **5** gives 298 valence electrons. Assuming that all Cu–Cu distances less than 290 pm are bonding, the 18-electron rule is exceeded by only two electrons.

Comparison of the structures of **1**–**3** and **5** clearly reveals that use of PEt_3 ligands, which are not very sterically demanding, apparently can lead to a new cluster composition. In our attempts to isolate further copper complexes by reaction of CuCl with $Se(SiMe_3)_2$ and PEt_3, we were surprised to find only the $Cu_{70}Se_{35}$ cluster **4**, the largest cluster to be characterized so far by X-ray structure analysis.

Figure 3 shows that **4** contains a twofold axis through Se9, Se13, Cu31, Cu34, and Se19. The description of the structure of the Cu framework is problematic. Notable is the structural fragment shown in violet in Figure 4. It consists of two trigonal bipyramids that share a common vertex and in which two faces are bridged by Cu_2 units. Figure 4 clearly reveals that these Cu_{13} units (Cu6–Cu18 and Cu27–Cu33) are present three times in the Cu_{70} cluster and are linked through nearly planar layers of six (Cu21–Cu23) and seven (Cu19, Cu20, Cu23–Cu26) Cu atoms, respectively. Fifteen Cu atoms (Cu1-Cu5 and Cu34-Cu36) are bonded to the periphery of this structural fragment.

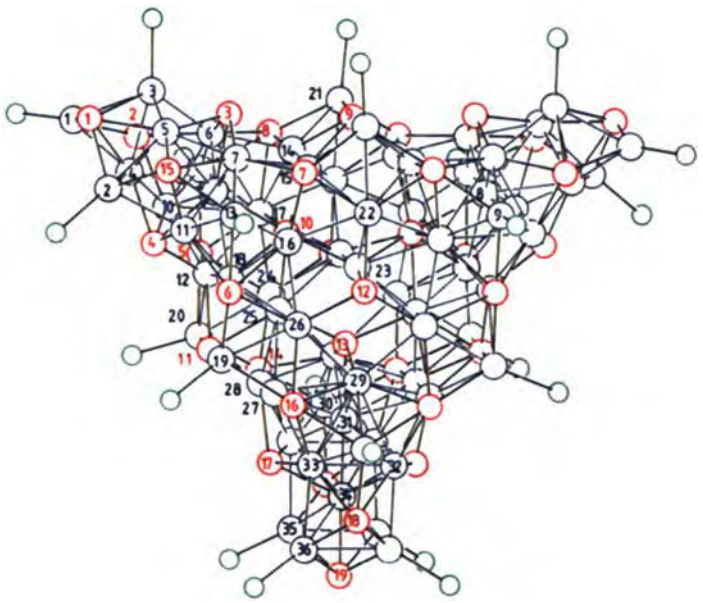

Fig. 3. Molecular structure of the cluster $[Cu_{70}Se_{35}(PEt_3)_{22}]$ (**4**) (C atoms omitted; Cu, blue; Se, red; P, green). Cu–Cu bonds up to 290 pm long and Cu–Se bonds up to 275 pm long are drawn. For clarity, the Cu atoms are labeled with blue numbers, the Se atoms with red numbers.

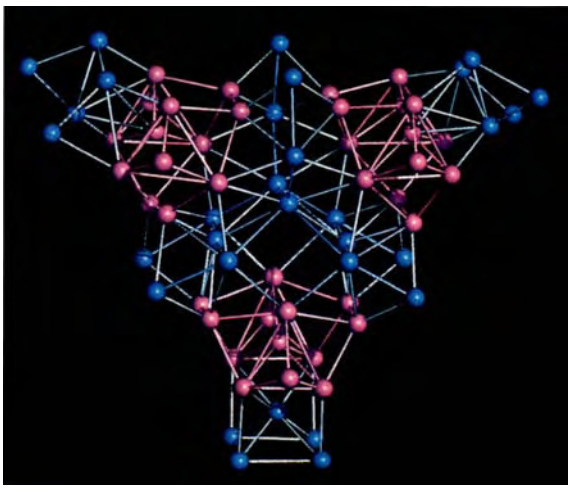

Fig. 4. Structure of the Cu_{70} framework in **4**.

The Se ligands are involved in different kinds of bonding. Se12 (Fig. 3) is present as a μ_4 bridge (Cu-Se12 233.6–240.1(5) pm). Se1, Se3, Se13, Se15, Se18, and Se19 serve as μ_5 ligands with Cu–Se distances of 236.4–268.8(5) pm. Se2, Se4–Se9, Se14, Se16, and Se 17 are μ_6-Se ligands (Cu-Se 234.2–273.2(5) pm). Se11 (Cu-Se 243.3–273.5(5) pm) and Se10 (Cu-Se 246.1–270.9(5) pm) function as μ_7 and μ_8 bridges, respectively.

The peripheral Cu atoms (Cu1–Cu3, Cu9, Cu13, Cu19–Cu21, Cu30, Cu35, and Cu36) are bonded to the P atoms of the PEt_3 ligands, which completely shield the surface of the cluster. Cu2, Cu35, and Cu36 are additionally surrounded by two Se and three Cu atoms (Cu-Cu 255.9–271.2(5) pm). Cu9, Cu13, Cu19–Cu21, and Cu30 form bonds to three Cu atoms (Cu-Cu 256.3–268.2(5) pm) and three Se atoms. Only Cu1 and Cu3 are bonded to two Cu and two Se atoms and to four Cu and three Se atoms (Cu-Cu 255.7–269.2(5) pm), respectively. All other Cu atoms inside the Cu cluster have coordination number 9 or 11. They are each bonded to three Se and six Cu atoms or to three Se and eight Cu atoms (Cu-Cu 242.5–289.6(5) pm). Similar Cu-Cu distances to those in **4** and **5** are also found in **1**–**3** and in other multinuclear copper complexes; they are indicative of only weak Cu-Cu interactions.[1, 5]

Cluster **4** contains 960 valence electrons. A comparison with the electron count calculated by rules such as the 18-electron rule is not possible, since the spectrum of Cu-Cu distances shows no clear boundary for possible Cu-Cu bonds. Overall, 210 Cu–Cu distances lie in the range 240–330 pm and 141 of these lie between 240 and 280 pm.

In the $Cu_{70}Se_{35}$ cluster, Cu has a formal charge of + 1. Accordingly, diamagnetic behavior would be expected. In fact, we find $\chi_{mol} = -2.73 \times 10^{-3}$ emu mol^{-1} at room temperature. Taking into consideration the diamagnetic increments for $Cu^{\oplus}$, $Se^{2\ominus}$, and PEt_3, a weak temperature-inde-

pendent paramagnetism of $\chi_{mol} = +1.77 \times 10^{-3}$ emu mol^{-1} [6] is obtained. This result is in agreement with the magnetic properties of Cu_2Se.[7]

The Cu:Se ratio is 2:1 in both **4** and Cu_2Se. Heating **4** to above 160°C results in loss of PEt_3 and formation of a (previously) unknown phase, which, on further warming, transforms into β-Cu_2Se (cubic). Cooling to below about 130°C affords α-Cu_2Se (monoclinic).[8] Accordingly, **4** may be regarded as a molecular precursor for the formation of binary copper selenides. This is consistent with findings made by *Steigerwald* et al. on the formation of NiTe from $[(cod)_2Ni]$ and Et_3PTe.[9]

Apparently, **4** and **5** are formed via a previously unknown and rather complex reaction path. Remarkably, however, **4** contains a Cu_9 unit (Fig. 3: Cu32–Cu36) whose structure is nearly identical with that of a Pd cluster of composition $[Pd_9As_8(PPh_3)_8]$. This compound is formed on reaction of $[PdCl_2(PPh_3)_2]$ with $As(SiMe_3)_3$ as part of a mixture also containing $[Pd_{20}As_{12}(PPh_3)_{12}]$, the Pd analogue of **5**.[4, 10] Possibly, the nine-atom metal cluster is an intermediate in the condensation to very large clusters. Further examples of metal clusters containing a large number of metal atoms are $[Au_{18}Ag_{19}Br_{11}(P\textit{p}\text{-}Tol_3)_{12}]^{2\oplus}$, $[Ni_{38}Pt_6(CO)_{48}H_{6-n}]^{n\ominus}$, $[Pd_{38}(CO)_{28}(PEt_3)_{12}]$, $[Au_{55}(PPh_3)_{12}Cl_6]$, $[Au_{13}Ag_{12}Br_8(P\textit{p}\text{-}Tol_3)_{10}]^{\ominus}$, and $[Ni_{34}Se_{22}(PPh_3)_{10}]$.[11]

Received: July 11, 1990 [Z 4063 IE]
German version: *Angew. Chem. 102* (1990) 1513

CAS Registry numbers:
4 · 5 Et_2O, 130295-80-6; **5**, 130246-65-0; $Se(SiMe_3)_2$, 4099-46-1.

[1] D. Fenske, H. Krautscheid, S. Balter, *Angew. Chem. 102* (1990) 799; *Angew. Chem. Int. Ed. Engl. 29* (1990) 796.

[2] Experimental procedure for **4** and **5**: CuCl (0.8 g, 8 mmol) was suspended in 100 mL of diethyl ether. After addition of PEt_3 (4.0 mL, 24 mmol), the CuCl dissolved. On addition of $Se(SiMe_3)_2$, the solution turned dark brown and **4** precipitated as microcrystals. Crystals of **4** and **5** suitable for crystal structure analysis were obtained by combining the starting materials at −80°C and then allowing the reaction mixture to warm over five days to room temperature. Yield: 60% **4** and 5% **5**.

[3] X-ray structure analyses: Stoe Stadi IV, $Mo_{K\alpha}$, empirical absorption correction; data collection and refinement: ω scan (profile analysis); **4** · 5 Et_2O: lattice constants: $a = 2778.9(20)$, $b = 3414.5(22)$, $c = 3094.3(20)$ pm, $\beta = 106.05(4)°$, $V = 28216 \times 10^6$ pm^3; space group $C2/c$ (No. 15), $Z = 4$, $\mu(Mo_{K\alpha}) = 95.7$ cm^{-1}, $2\theta_{max} = 50°$; 23230 reflections, 13751 unique with $I > 2\sigma(I)$, 1154 parameters (Se, Cu, P anisotropic; C, O isotropic), $R_1 = 0.072$, $R_2 = 0.060$. The C atoms of the PEt_3 groups are disordered but could be unambiguously localized. **5**: Crystals from diethyl ether, lattice constants (270 K): $a = b = c = 2321.0(8)$ pm, $\alpha = \beta = \gamma = 90$, $V = 12503 \times 10^6$ pm^3; space group $Fm3$ (No. 202), $Z = 4$, $\mu(Mo_{K\alpha}) = 71.0$ cm^{-1}, $2\theta_{max} = 50°$; 5730 reflections, 993 unique with $I > 2\sigma(I)$, 53 parameters (Se, Cu, P, C anisotropic), $R_1 = 0.083$, $R_2 = 0.059$. Further details of the crystal structure investigation may be obtained from the Fachinformationszentrum Karlsruhe, Gesellschaft für wissenschaftlich-technische Information mbH, D-7514 Eggenstein-Leopoldshafen 2 (FRG), on quoting the depository number CSD-54799, the names of the authors, and the journal citation.

[4] D. Fenske, H. Fleischer, C. Persau, *Angew. Chem. 101* (1989) 1740; *Angew. Chem. Int. Ed. Engl. 28* (1989) 1665.

[5] J. Beck, J. Strähle, *Angew. Chem. 97* (1985) 419; *Angew. Chem. Int. Ed. Engl. 24* (1985) 409; S. Gambarotta, C. Floriani, A. Chiesi-Villa, C. Guastini, *J. Chem. Soc. Chem. Commun. 1983*, 1156; J. A. J. Jarvis, B. T. Kilbourn, R. Pearce, M. F. Lappert, *ibid. 1973*, 475; H. Hartl, F. Mahdjour-Hassan-Abadi, *Angew. Chem. 96* (1984) 359; *Angew. Chem. Int. Ed. Engl. 23* (1984) 378; G. Henkel, P. Betz, B. Krebs, *J. Chem. Soc. Chem. Commun. 1984*, 314; P. Betz, B. Krebs, G. Henkel, *Angew. Chem. 96* (1984) 293; *Angew. Chem. Int. Ed. Engl. 23* (1984) 311; I. G. Dance, J. C. Calabrese, Inorg. Chim. Acta *19* (1976) L41; D. Coucouvanis, C. N. Murphy, S. K. Kanodia, *Inorg. Chem. 19* (1980) 2993; E. Block, M. Gernon, H. Kang, S. Liu, J. Zubieta, *J. Chem. Soc. Chem. Commun. 1988*, 1031.

[6] W. Klemm, *Z. Anorg. Allg. Chem. 244* (1940) 377; *ibid. 246* (1941) 347; P. Pascal, *C. R. Hebd. Seances Acad. Sci. 174* (1922) 457. Use of the molar susceptibilities of α-Cu_2Se and PEt_3 gives $\chi_{mol} = -2.67 \times 10^{-3}$ emu mol^{-1} for **4**.

[7] K. Okamoto, S. Kawai, R. Kiriyama, *Jpn. J. Appl. Phys. 8* (1969) 718.

[8] R. McLaren Murray, R. D. Heyding, *Can. J. Chem. 53* (1975) 878; A. L. N. Stevels, F. Jellinek, *Recl. Trav. Chim. Pay-Bas 90* (1971) 273; P. Rahlfs, *Z. Phys. Chem. Abt. B31* (1936) 157.

[9] J. G. Brennan, T. Siegrist, S. M. Stuczynski, M. L. Steigerwald, *J. Am. Chem. Soc. 111* (1989) 9240.

[10] D. Fenske, C. Persau, *Z. Anorg. Allg. Chem.*, in press.

[11] B. K. Teo, M. C. Hong, H. Zhang, D. B. Huang, *Angew. Chem. 99* (1987) 943; *Angew. Chem. Int. Ed. Engl. 26* (1987) 897; A. Ceriotti, F. Demartin, G. Longoni, M. Manassero, M. Marchionna, G. Piva, M. Sansoni, *ibid. 97* (1985) 708 and *24* (1985) 697; E. G. Mednikov, N. K. Eremenko, Y. L. Slovokhotov, Y. T. Struchkov, *J. Chem. Soc. Chem. Commun. 1987*, 218; G. Schmid, R. Pfeil, R. Boese, F. Bandermann, S. Meyer, G. H. M. Calis, J. W. A. van der Velden, *Chem. Ber. 114* (1981) 3634; J. P. Fackler, C. J. McNeal, R. E. P. Winpenny, *J. Am. Chem. Soc. 111* (1989) 6434; B. K. Teo, H. Zhang, X. Shi, *Inorg. Chem. 29* (1990) 2083; D. Fenske, J. Ohmer, J. Hachgenei, *Angew. Chem. 97* (1985) 993; *Angew. Chem. Int. Ed. Engl. 24* (1985) 993.

[12] We thank Prof. Dr. *P. Böttcher* (Universität Düsseldorf) for valuable suggestions in discussing this structure.

New Benzyl(β-oxido)phosphorus and -arsenic Ylides: Reactivity and Stereoselectivity in the Wittig Reaction**

By *Benaissa Boubia, André Mann, François D. Bellamy,* and *Charles Mioskowski**

Owing to its convenience and efficiency, the Wittig reaction is one of the most useful olefination methods used in organic chemistry. Generally, high selectivity for *E* or *Z* alkenes is achieved depending on the reaction conditions.[1] Furthermore, if the phosphorus atom bears other substituents than phenyl, the *E*/*Z* ratio can be increased or inverted.[2] Oxidophosphoranes show an increase in *E* selectivity.[3, 4] Particulary interesting are the β-oxido ylides, which were first prepared by *M. Schlosser* et al.[5] and subsequently developed by *E. J. Corey* et al.[6] and which have been used in the synthesis of natural compounds.[7] Depending on the order of addition of the aldehydes, trisubstituted olefins with controlled geometry are accessible. In general, the second aldehyde promotes the formation of the double bond, its oxygen atom being eliminated during the reaction as triphenylphosphane oxide. An exception is formaldehyde, which does not participate in the olefin formation.[1]

In view of the fact that Wittig condensation of semi-stabilized ylides gives mixtures of *E* and *Z* isomers, and taking into consideration the above-mentioned data, we have developed new benzyl ylides in order to form stereoselectively *E* isomers.[8] Since phosphorus and arsenic ylides behave differently in the Wittig condensation,[9] we have designed two new β-oxido benzyl ylides, **2a, b**, where the oxido and the ylide parts are two different appendages of P and As. The corresponding salts **1a, b** were easily prepared from the

[*] Dr. C. Mioskowski, Dr. B. Boubia
Université Louis Pasteur, Laboratoire de Chimie Bio-organique
associé au CNRS
Faculté de Pharmacie
74 route du Rhin, F-67401 Strasbourg (France)
Dr. A. Mann
Université Louis Pasteur, Centre de Neurochimie du CNRS
F-67084 Strasbourg (France)
Dr. F. D. Bellamy
Laboratoires Fournier
Dijon (France)

[**] This work was funded by the CNRS and the Laboratoires Fournier, Dijon. We thank Prof. *M. Schlosser* for suggesting the experiment described in [12].

known lithiodiphenylphosphane[10] and -arsane[11] by condensation with ethylene oxide followed by reaction with benzyl bromide. The ylides **2a, b** were obtained by addition of two equivalents of BuLi to the salts **1a, b** in THF or in a mixture of THF and HMPA (hexamethylphosphoramide) (85/15) at $-20\,^{\circ}C$.

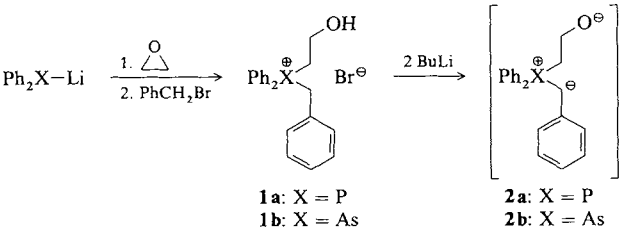

1a: X = P
1b: X = As

2a: X = P
2b: X = As

The reaction of these ylides with aldehydes (piperonal or hexanal) leads to the di(β-oxido) ylides **3a, b**, which can react further to give either olefins **4** and oxides **5** (pathway a) or ethylene and oxides **6** (pathway b) via oxaphosphetanes or oxaarsetanes **7a, b** and **8a, b**.

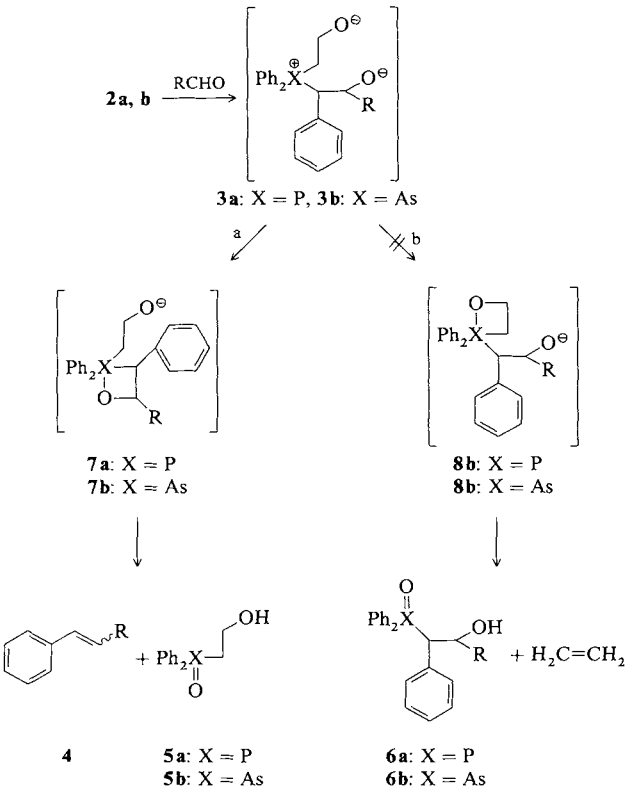

7a: X = P
7b: X = As

8b: X = P
8b: X = As

4

5a: X = P
5b: X = As

6a: X = P
6b: X = As

The ylides used here led only to products formed via pathway a. In the case of phosphorus ylide **2a**, the yields are high but the selectivities modest (see Table 1). In presence of HMPA, a slight increase in the *E*/*Z* ratio is observed. For the arsenic ylide **2b**, the reaction occurs only in the presence of HMPA; the yields are slightly lower, but the reaction is highly stereoselective with both piperonal and hexanal.[12]

No epoxidation occurs, in accord with observations made earlier with semi-stabilized arsenic ylides.[13] Moreover, the β-hydroxy oxides formed during the reactions are easier to remove from the reaction mixture than triphenylphosphane or -arsane oxides. This study shows that the arsenic ylide **2b** is a useful reagent for the stereoselective preparation of *E*-styrene derivatives **4**.

Table 1. Reaction conditions, yields, and *E*/*Z* ratio in the reaction of **2a, b** with hexanal or piperonal.

Ylide	Aldehyde	Solvent	*T* [°C]	*E*/*Z*	**4** [%]
2a	hexanal	THF	−78	65/35	91
2a	piperonal	THF	−78	75/25	73
2a	hexanal	THF/HMPA [a]	−78	85/15	87
2b	hexanal	THF	−78	–	–
2b	hexanal	THF	−20	–	–
2b	piperonal	THF/HMPA [a]	−78	100/0	65
2b	hexanal	THF/HMPA [a]	−78	100/0	65

[a] 85/15 (v/v).

Experimental Procedure

1a/b: Ph_2PLi [9] or Ph_2AsLi [10] (freshly prepared from triphenylphosphane or -arsane and Li in THF) were allowed to react with ethylene oxide at 0 °C. After extractive workup, the resulting phosphane or arsane was purified by chromatography on silica gel (ether/dichloromethane 5/95) (yield 65%). (β-Hydroxyethyl)diphenylphosphane: ^1H NMR (200 MHz, $CDCl_3$, 25 °C, TMS) $\delta = 7.50-7.39$ (m, 10H; Ar-H), 3.79 (td, 2H, $J = 7.0$, 9.0 Hz; CH_2-P), 2.41 (t, 2H, $J = 7.0$ Hz; CH_2-OH), 2.22 (s, 1H; OH). (β-Hydroxyethyl)diphenylarsane: ^1H NMR (200 MHz, $CDCl_3$, 25 °C, TMS) $\delta = 7.51-7.33$ (m, 10H; Ar-H), 3.85 (t, 2H, $J = 7.5$ Hz; CH_2-As), 2.36 (t, 2H, $J = 7.5$ Hz; CH_2-OH), 2.20 (s, 1H; OH).

Benzyl bromide (5.5 mmol) was added to a solution of the phosphane or arsane (5 mmol) dissolved in 20 mL of acetonitrile, and the mixture was refluxed for about 12 h under argon. The solvent was removed in vacuo and the resulting solid was taken up in dichloromethane. Addition of ether afforded white crystals in 75% yield for **1a** and 65% for **1b**.

1a: m.p. 172–174 °C. ^1H NMR (200 MHz, $CDCl_3$, 25 °C, TMS) $\delta = 7.76-7.52$ (m, 10H, Ar-H), 7.16–6.93 (m, 5H; Ar-H), 4.60 (d, 2H, $J = 15$ Hz; CH_2-Ar), 3.90 (td, 2H, $J = 5.5$, 20.0 Hz; CH_2-OH), 3.25 (td, 2H, $J = 5.5$, 12.0 Hz; CH_2-P).

1b: m.p. 146–148 °C. ^1H NMR (200 MHz, $CDCl_3$, 25 °C, TMS) $\delta = 7.66-7.48$ (m, 10H; Ar-H), 7.12–7.02 (m, 5H; Ar-H), 4.72 (s, 2H; CH_2-Ar), 4.05 (t, 2H, $J = 6$ Hz; CH_2OH), 3.48 (t, 2H, $J = 6$ Hz; CH_2-As).

Wittig olefination reaction: BuLi (2.2 mmol, 1.6 M in hexane) was added to a suspension of **1b** (1 mmol) in THF (10 mL) and HMPA (1.5 mL) at −20 °C. A yellow color appeared immediately and changed progressively to deep red. After 1 h, the mixture was chilled to −78 °C, the aldehyde (0.9 mmol) in THF (2 mL) was added, and the reaction mixture was allowed to warm up overnight. After extractive workup, the oily residue was purified by chromatography on silica gel and analyzed by gas chromatography to determe the stereoisomer composition.

Received: May 28, 1990 [Z 3988 IE]
German version: *Angew. Chem. 102* (1990) 1522

CAS Registry numbers:
1a, 130014-32-3; **1b**, 130014-33-4; (*E*)-**4** (R = pentyl), 10201-58-8; (*Z*)-**4** (R = pentyl), 10201-59-9; (*E*)-**4** (R = 1,3-benzodioxol-5-yl), 51003-16-8; (*Z*)-**4** (R = 1,3-benzodioxol-5-yl), 130014-34-5; Ph_2PLi, 4541-02-0; Ph_2AsLi, 19061-48-4; $PhCH_2Br$, 100-39-0; (β-hydroxyethyl)diphenylphosphane, 2360-04-5; (β-hydroxyethyl)diphenylarsane, 4645-25-4; ethylene oxide, 75-21-8; hexanal, 66-25-1; piperonal, 120-57-0.

[1] For an excellent review see: B. E. Marianoff, A. B. Reitz, *Chem. Rev. 89* (1989) 863.
[2] a) M. Schlosser, B. Schaub, *J. Am. Chem. Soc. 104* (1982) 5821; b) W. E. McEwen, J. V. Cooney, *J. Org. Chem. 48* (1983) 983; c) E. Vedejs, H. W. Fang, *ibid. 49* (1984) 210; d) E. Vedejs, C. F. Marth, *Tetrahedron Lett. 28* (1987) 3445; e) *J. Am. Chem. Soc. 110* (1988) 3948; f) S. Jeganathan, M. Tsukamoto, M. Schlosser, *Synthesis 1990*, 109.
[3] a) B. E. Marianoff, A. B. Reitz, B. A. Emsviller, *J. Am. Chem. Soc. 107* (1985) 217; b) M. Schlosser, H. B. Tuong, B. Schaub, *Tetrahedron Lett. 26* (1985) 311; c) carboxylate version: H. Daniel, M. Le Corre, *ibid. 28* (1987) 1165.
[4] An increase in *E* selectivity is described for lithio-oxido ylides in [3]. Under special conditions ("instant ylides"), high *Z* selectivity has been observed: B. Schaub, G. Blaser, M. Schlosser, *Tetrahedron Lett. 26* (1985) 307.

[5] a) M. Schlosser, K. F. Christmann, *Angew. Chem. 78* (1966) 115; *Angew. Chem. Int. Ed. Engl. 5* (1966) 126; b) *Justus Liebigs Ann. Chem. 708* (1967) 1; c) M. Schlosser, D. Coffinet, *Synthesis* 1972, 575.
[6] Di(β-oxido) ylides can be generated in two different ways: a) metalation of betaines: [5], E. J. Corey, P. Ulrich, A. Venkateswarlu, *Tetrahedron Lett. 1977*, 3229; b) from α-lithiomethylenetriphenylphosphoranes: E. J. Corey, J. Kang, *J. Am. Chem. Soc. 104* (1982) 4724.
[7] E. J. Corey, H. Yamamoto, *J. Am. Chem. Soc. 92* (1970) 226.
[8] Stereospecific *E* olefination of aldehydes has been achieved using bis(benzylic) arsenic ylides: B. Boubia, C. Mioskowski, F. Bellamy, *Tetrahedron Lett. 30* (1989) 5263.
[9] D. Lloyd, I. Gosney, R. A. Ormiston, *Chem. Soc. Rev. 16* (1987) 45; J. D. Hsi, M. Koreeda, *J. Org. Chem. 54* (1989) 3229.
[10] H. J. Cristau, Y. Ribeill, *Synthesis 1988*, 911.
[11] W. C. Still, V. J. Novack, *J. Am. Chem. Soc. 103* (1981) 1283.
[12] On account of the basicity of the arsenic ylides, we checked carefully that no isomerization of the final products had occurred under the reaction conditions. The Wittig reaction of **2b** and hexanal was performed in the presence of (*Z*)-1-(1,3-dioxaindan-5-yl)-1-heptene (purity > 99%). Gas-chromatographic analysis showed no trace of the *E* isomer.
[13] a) J. B. Ousset, C. Mioskowski, G. Solladié, *Tetrahedron Lett. 24* (1983) 4419 and references cited therein; b) *Synth. Commun. 1983*, 1193.

A Stereoselective π Cyclization to a Combined Bridgehead Olefin–Bridgehead Alcohol**

By *Uwe Vogt, Ulrike Eggert, Alexandra M. Z. Slawin, David J. Williams,* and *H. M. R. Hoffmann**

Bridgehead structure and bridgehead reactivity have contributed substantially to the evolution of concepts in organic chemistry. Starting from naturally occurring (−)-caryophyllene oxide (**1**), we describe a simple route to enantiomerically pure cage compounds in which the two bridgehead carbons are differentiated functionally.

Owing to the variety of its characteristic transformations and molecular rearrangements, caryophyllene has been considered unique among sesquiterpenes.[1, 2] The isomerization of its epoxide **1** has been investigated frequently in the past and shown to furnish allylic alcohols **2** and **3** in addition to

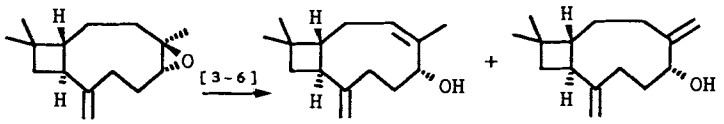

1 **2** **3**

unidentified products (Table 1).[3–6] Unfortunately, separation of the two isomers and isolation of pure **3** by chromatography are tedious, a situation not uncommon in caryophyllene chemistry. Further experiments to isomerize **1** with $Al(OiPr)_3$ in refluxing toluene[7] and with $KOtBu$ in refluxing pyridine[8] furnished both isomers (thin layer chromatography), with an increase in byproducts.

Table 1. Reported conversions of **1** into **3**.

Experimental conditions	2 [%]	3 [%]	Other products [%]	Ref.
PyHBr, pyridine, Δ	mixture			[3]
Al_2O_3	little	much		[4]
BuLi, Et_2O, Δ	8	58	34	[5]
Al_2O_3	4	50		[6]

Remarkably, treatment of **1** with $LiNiPr_2$ in refluxing THF gave the desired alcohol **3** in a clean, regio- and stereoselective reaction (90% yield). When **3** was treated with CH_3SO_2Cl/NEt_3 at −40 °C, a reactive secondary allylic mesylate, **3a**, was formed, which decomposed on attempted chromatography. However, **3a** could be isolated by crystallization at −20 °C in petroleum ether/ether. Hydrolysis of **3a** in H_2O/THF (1/10) gave a tertiary alcohol in 52% yield. Similarly, methanolysis afforded a tertiary methyl ether (39% yield). ^{13}C and ^1H NMR spectra (solvent $(CD_3)_2SO$) suggested structure **4a**[9] for the alcohol and **4b** for the methyl ether.

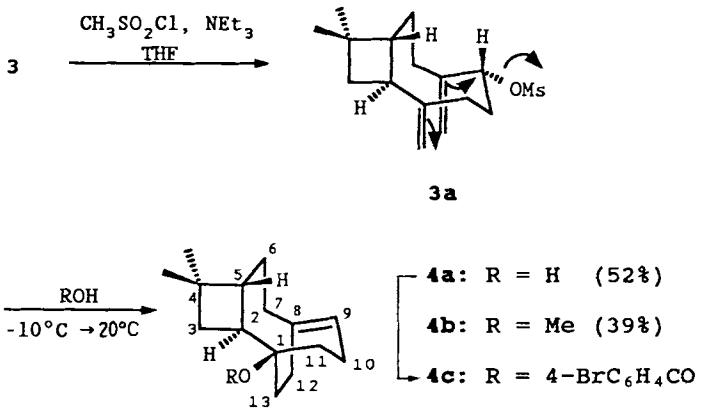

Structural assignment and absolute stereochemistry[10] were corroborated by preparation[11] of the crystalline *p*-bromobenzoate **4c** and X-ray diffraction analysis (Fig. 1). The NMR spectra and X-ray structure indicate that the cyclization is diastereoselective, giving enantiomerically pure **4a**, **b**.[10] Both **4a** and **4b** contain a *trans*-cyclononene moiety within the tricyclic framework. They also contain a (*Z*)-bicyclo[4.3.2]undec-1(9)-ene substructure, which has been calculated to be a "hyperstable" olefin.[12a]

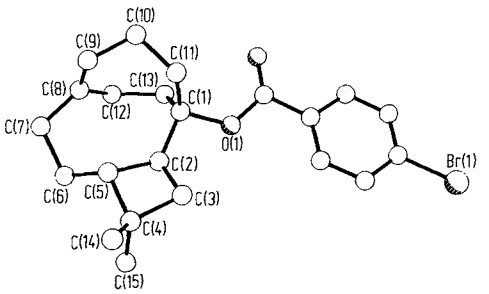

Fig. 1. Structure of one of the two independent molecules of **4c** in the crystal

The transformation of **3a** into **4a** and **4b** proceeds with ease and must have considerable driving force. Models show

[*] Prof. H. M. R. Hoffmann, Dr. U. Vogt [+], U. Eggert
Institut für Organische Chemie der Universität
Schneiderberg 1B, D-3000 Hannover (FRG)
A. M. Z. Slawin, Dr. D. J. Williams
Chemical Crystallography Laboratory
Department of Chemistry, Imperial College
GB-London SW7 2AY (UK)
[+] New address: FB-F2, Bayerwerk, D-5090 Leverkusen (FRG)

[**] We thank the Fonds der Chemischen Industrie and the Deutsche Forschungsgemeinschaft for support of our work.

that the reaction is stereoelectronically and also sterically favored. The leaving mesylate group in **3a** can adopt a quasi-axial position with respect to the allylic double bond. Transannular formation of the new carbon–carbon σ bond, which is antiperiplanar with respect to the departing mesylate group[10] involves two readily accessible, unsubstituted methylene termini. Nonetheless, it is a *bridgehead* cation that must be solvated and captured by the external nucleophile. The necessary stabilization of this tertiary cation is probably provided by a propellane-like interaction of the vacant p orbital with the π bond at the other bridgehead (estimated distance between bridgeheads[13] ca. 2.4 Å in the cation and 2.9 Å in **4c**).[14]

Although electrophilically induced π cyclization of polyenes is ubiquitous for building up natural products, both enzymatically and in vitro, the spontaneous formation of **4a, b** from **3a** is, to our knowledge, the first cyclization in which a bridgehead cation and a bridgehead olefin are simultaneously formed in a surprising, transannular fashion.

Received: May 25, 1990 [Z 3978 IE]
German version: *Angew. Chem. 102* (1990) 1530

[1] a) J. F. King, P. de Mayo in P. de Mayo (Ed.): *Molecular Rearrangements, Vol. 2*, Wiley, New York 1964, Chap. 13; b) V. P. Gatilova, D. V. Korchagina, T. V. Rybalova, Y. V. Gatilov, Z. V. Dubovenko, V. A. Barkhash, *Zh. Org. Khim. 25* (1989) 320.

[2] Total synthesis: E. J. Corey, R. B. Mitra, H. Uda, *J. Am. Chem. Soc. 86* (1964) 485.

[3] M. Holub, V. Herout, M. Horák, F. Šorm, *Collect. Czech. Chem. Commun. 24* (1959) 3730.

[4] E. W. Warnhoff, *Can. J. Chem. 42* (1964) 1664.

[5] K. H. Schulte-Elte, G. Ohloff, *Helv. Chim. Acta 51* (1968) 494; see also K. Gollnick, G. Schade, *Tetrahedron Lett. 1968*, 689.

[6] A. S. Gupta, S. Dev, *Tetrahedron 27* (1971) 635. These authors show that **1** is a constituent of the oleoresin of *Dipterocarpus pilosus*, a tall growing tree indigenous to Assam in India. β-Caryophyllene occurs in numerous essential oils; see also [9].

[7] S. Terao, M. Shiraishi, K. Kato, *Synthesis 1979*, 467.

[8] Z. Rykowski, K. Burak, *Rocz. Chem. 50* (1976) 1709; *Chem. Abstr. 86* (1977) 140258.

[9] Our route to **4a** could be biomimetic, since **4a** has been detected by GC-MS in clove oil and hop oil, used for flavoring beer; see T. Uchida, Y. Matsubara, A. Adachi, *Agric. Biol. Chem. 50* (1986) 1903.

[10] Absolute configuration of **4a**: 1*S*,2*S*,5*R*. The 1*R*,2*S*,5*R* epimer would have been detected in the NMR spectrum. Its formation is stereoelectronically unfavorable. For a concerted cyclization with transannular π participation to occur, the C–OMs σ bond would have to be cleaved in the nodal plane of the π system, generating an orthogonally twisted allyl cation. Other conformations of **3a**, which would cyclize to a very strained *trans*-cycloheptene substructure, can be excluded by the *trans*-cycloalkene rule [12b].

[11] *Experimental Procedure*: **3**: A solution (1.6 M in hexane) of *n*BuLi (12.4 mL, 19.8 mmol) was added dropwise to a solution of dry $HNiPr_2$ (2.0 g, 19.8 mmol) in absolute THF (50 mL) at 0 °C and stirred for 30 min. Compound **1** (3.96 g, 18 mmol) in absolute THF (15 mL) was added dropwise and the mixture was refluxed. After complete reaction, the solvent was evaporated, the residue taken up in *tert*-butyl methyl ether (MTBE), washed with cold dilute HCl, and dried ($MgSO_4$). Flash chromatography gave 3.56 g (90%) of a colorless oil. ^1H NMR (200 MHz, $CDCl_3$): δ = 5.05, 4.96 (s, C(2) = CH_2), 4.78, 4.76 (s, C(6) = CH_2), 4.08 (dd, J = 2, 7 Hz, H-5), 2.60–1.43 (m, 13H), 0.98 (s, CH_3). ^{13}C NMR (75 MHz, $CDCl_3$): δ = 152.38/151.26 (s, C-2, C-6), 113.29/109.03 (t, 2 = CH_2), 75.08 (d, C-5), 54.21/43.67 (d, C-1, C-9), 33.35 (s, C-10), 29.95/21.91 (q, C-14, C-15), 37.03/32.74/32.54/32.49/30.54 (t, 5C). **3a**: Allylic alcohol **3** (3.3 g, 15 mmol) in absolute THF (100 mL) was mixed with dry NEt_3 (2.9 mL, 21 mmol) and cooled to −40 °C. CH_3SO_2Cl (1.4 mL, 18 mmol) was added dropwise at −40 °C and the temperature was allowed to rise to −10 °C within 2 h. After filtration and removal of the solvent, the residue was taken up in 20 mL of petroleum ether/diethyl ether (1/1). Crystallization at −20 °C gave white crystals (3.32 g, 70%), m.p. 56–58 °C (dec.). **4a**: **3a** (0.6 g, 1.9 mmol) and K_2CO_3 (0.5 g) in THF/H_2O (22 mL, 10/1) were stirred for ca. 12 h at room temperature. After removal of solvent, the residue was taken up in H_2O and extracted with MTBE, and the organic phase was dried ($MgSO_4$). Column chromatography gave a white solid (220 mg, 52% based on **3a**), m.p. 140–143 °C. $[\alpha]_D^{22}$ = 15.7 ($CHCl_3$, c = 0.3 g per 100 mL). IR (KBr): $\tilde{\nu}$ [cm^{-1}] = 3365 (OH). ^1H NMR (200 MHz, $(CD_3)_2SO$): δ = 5.33 (bt, J = 6 Hz, H-9), 3.71 (s, OH), 2.38–1.22 (m, 16H), 0.93 (s, CH_3). ^{13}C NMR (50 MHz, $CDCl_3$): δ = 138.05 (C-8), 126.09 (C-9), 75.14 (C-1), 51.97, 47.74 (C-2, C-5), 29.99, 21.82 (C-14, C-15), 37.56/36.42/35.39/33.49/33.32/26.17/24.54/23.64 (8C). **4b**: Mesylate **3a** (157 mg, 0.5 mmol) and K_2CO_3 (50 mg) in MeOH (2 mL) were strirred for 2 h. Column chromatography gave 46 mg (39% based on **3a**) of white crystals, m.p. 65–66 °C. $[\alpha]_D^{22}$ = 49.7 ($CHCl_3$, c = 0.944 g per 100 mL). ^1H NMR (80 MHz, $CDCl_3$): δ = 5.41 (br. t, J = 7 Hz, H-9), 3.12 (s, OCH_3), 2.63–1.18 (m, 16H), 0.99, 0.98 (each s, CH_3). **4c**: A solution (1.6 M in hexane) of *n*BuLi (0.14 mL, 0.23 mmol) was added to **4a** in absolute THF (1 mL) and the solution was stirred for 0.5 h at room temperature. 4-BrC_6H_4COCl in absolute THF (1 mL) was added dropwise and the mixture was refluxed for 4 h. Flash chromatography and recrystallization (petroleum ether) gave white crystals (40 mg, 59%), m.p. 103–105 °C, which were used for X-ray crystallography [15].

[12] a) W. F. Maier, P. von R. Schleyer, *J. Am. Chem. Soc. 103* (1981) 1891; b) Review: P. M. Warner, *Chem. Rev. 89* (1989) 1067.

[13] R. W. Alder, *Tetrahedron 46* (1990) 683.

[14] The strained cyclobutane segment may also contribute to stabilization in that the *trans* junction, that is, the C(2)–C(5) σ bond, and the vacant p orbital of the bridgehead cation lie approximately in one plane and parallel to each other (models); see also I. Erden, A. de Meijere, *Tetrahedron Lett. 21* (1980) 3179.

[15] Nicolet R3m diffractometer, ω scans, $Cu_{K\alpha}$ radiation (graphite monochromator). The structure was solved by direct methods and refined anisotropically. Crystal data: orthorhombic, a = 8.233(2), b = 9.886(3), c = 48.210(12) Å, V = 3924 Å^3, space group $P2_12_12_1$, Z = 8 (there are two crystallographically independent molecules), ϱ = 1.37 g cm^{-3}, $\mu(Cu_{K\alpha})$ = 29 cm^{-1}. 2632 independent observed reflections with $|F_o| > 3\sigma(|F_o|)$, $2\theta \leq 116°$, R = 0.036, R_w = 0.037. The fused ring systems of the two independent molecules have virtually identical conformations with a maximum deviation of 0.1 Å for C(3) (from a least-squares fit of the two independent molecules). The absolute stereochemistry was confirmed by refinement of a free variable η, which multiplies all f''; this parameter was refined to a value of 1.06(4). Further details of the crystal structure investigation can be obtained from the Cambridge Crystallographic Data Centre, University Chemical Laboratory, Lensfield Road, Cambridge CB2 1EW (England), by quoting the full journal citation.

The 3-(3-Pyridyl)allyloxycarbonyl (Paloc) Moiety—a Stable, Amino-Protecting Group for Peptide Syntheses in Organic Media and in Water That Is Cleavable under Neutral Conditions**

By *Karsten von dem Bruch* and *Horst Kunz**

Peptides and peptide mimetics are currently attracting increasing interest as natural and natural-product-like active substances which exhibit selective biological activity and at the same time are biologically degradable.[1] The same applies in the case of glycopeptides, which embody partial structures of natural glycoproteins.[2] Since these compounds have a tendency to undergo transpeptidation or glycoside cleavage their synthesis requires methods which allow exactly specified transformations under very mild conditions. Enzymatic peptide synthesis[3] would undoubtedly be of interest for this purpose. A further prerequisite for the successful synthesis of such peptide-type substances are protecting groups which are stable in use and which, at the same time, can readily be removed under mild neutral conditions.

We report here on a novel amino protecting group, namely the 3-(3-pyridyl)allyloxycarbonyl (Paloc) residue, which combines the advantages of stability under various reaction conditions, cleavability under neutral conditions, and solu-

[*] Prof. Dr. H. Kunz, Dipl.-Chem. K. von dem Bruch
Institut für Organische Chemie der Universität
Johann-Joachim-Becher-Weg 18–20, D-6500 Mainz (FRG)

[**] This work was supported by the Deutsche Forschungsgemeinschaft and the Fonds der Chemischen Industrie. *K.v.d.B.* thanks the Fonds der Chemischen Industrie for a postgraduate grant.

bility in water. The Paloc group is so resistant towards trifluoroacetic acid that *tert*-butyl esters or ethers can be removed selectively. Moreover, it is stable under the conditions of the rhodium(I)-catalyzed isomerization and cleavage of allyl esters.[4] Nevertheless, like the allyl ester and the allyloxycarbonyl (Aloc) group,[6] it can be removed from the blocked amino function under neutral conditions by palladium(0)-catalyzed allyl transfer to weakly basic or neutral nucleophiles.

A suitable reagent for the introduction of the Paloc group is obtained by Meerwein-Ponndorf reduction of 3-(3-pyridyl)propenal **1**[7] to the 3-(3-pyridyl)allyl alcohol **2** and its subsequent reaction with bis-(4-nitrophenyl) carbonate[8] to give the 3-(3-pyridyl)allyl(4-nitrophenyl) carbonate (Paloc-ONp) **3** (Scheme 1).

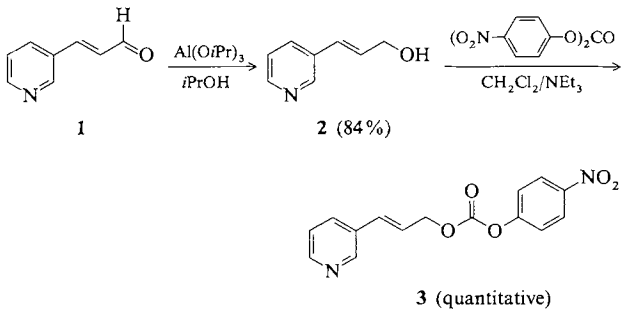

1 **2** (84%) **3** (quantitative)

Scheme 1.

When **3** is allowed to react with amino acids in water/dioxane under pH-stat conditions at pH 10 (Method A)[9] or with the amino acid trimethylsilyl esters (formed from the respective amino acids and equivalent amounts of trimethylchlorosilane) in the presence of two equivalents of ethyldiisopropylamine in chloroform/acetonitrile, the Paloc amino acids **4** are obtained in high yields (see Scheme 2 and Table 1). The Paloc compounds show characteristic UV absorption and IR and NMR spectra.[11]

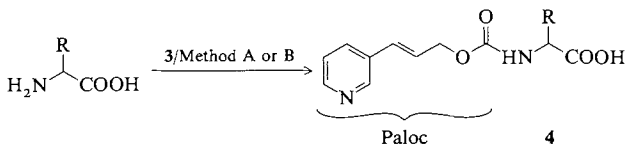

Scheme 2. A: H_2O/dioxane, pH-stat at pH 10, 4N NaOH; B: 1) 2 equiv. Me_3SiCl/2 equiv. *i*PrEtN in $CHCl_3$/MeCN (1:1); 2) **3**, reflux.

Table 1. Synthesis of 3-(3-pyridyl)allyloxycarbonyl (Paloc) amino acid **4** according to Scheme 2 [9, 10].

Compound	Amino acid	Method	Yield (%)	M.p. [°C]	$[\alpha]_D^{22}$ ($c = 2$, MeOH)
4a	Ala	A	82	115	−5.6
4b	Asp(OBzl)-OH	A	71	oil	+2.4
4c	Asp(OH)-O*t*Bu	A	68	oil	−13.0
4d	Gly	B	72	161	–
4e	Ile	A	89	oil	+8.3
4f	Leu	A	77	108	−11.1
4g	Lys(Z)	B [a]	65	99–101	−1.8
4h	Phe	B	72	102–104	−8.0
4i	Thr	A	80	Öl	+5.2
4j	Val	A	83	101–103	+3.2

[a] Twice the solvent volume.

Paloc amino acids **4** react smoothly with amino acid *tert*-butyl or allyl esters[4, 5] to form the Paloc dipeptide esters **5**. The solubility-promoting properties of the Paloc group permit the peptide condensations (Scheme 3) to be carried out both in an organic medium in the presence of condensation reagents such as ethyl-2-ethoxy-1,2-dihydroquinoline-1-carboxylate (EEDQ),[12] as well as in water, e.g. with 1-ethyl-3-(3′-dimethylaminopropyl)carbodiimide (DAEC)/1-hydroxybenzotriazole (HOBt) (Scheme 3 and Table 2).

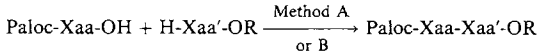

4 **5**

Scheme 3. A: EEDQ, CH_2Cl_2, 20 °C/20–60 h; B: DAEC/HOBt, H_2O/pH 5–6, 20 °C, 4 d.

Table 2. Synthesis of Paloc dipeptide esters **5** according to Scheme 3.

Compound	Xaa-Xaa′	OR	Method	Yield (%)	$[\alpha]_D^{22}$ ($c = 2$, MeOH)
5a	Ala-Gly	OAll	A	73	−15.7
			B	77	
5b	Asp(OBzl)-Ser(*t*Bu)	O*t*Bu	A	81	−0.8
5c	Gly-Thr	OAll	A	79	−3.5
5d	Gly-Thr(*t*Bu)	OAll	A	81	+10.4
5e	Ile-Leu	O*t*Bu	A	69	−39.3
			B	72	
5f	Ile-Thr(*t*Bu)	OAll	A	66	+0.5
5g	Leu-Ile	O*t*Bu	A	86	−22.5
5h	Phe-Val	O*t*Bu	A	90	−12.1
5i	Val-Ile	O*t*Bu	A	78	−24.0

Both in the case of the synthesis of the polar dipeptide ester **5a**, as well as in that of the unpolar, sterically hindered dipeptide ester **5e** a higher yield was obtained when the reaction was carried out in water. The high stability of the Paloc group towards acids is caused by protonation at the pyridine nitrogen atom and the resultant shielding against further proton attack. It enables *tert*-butyl protecting groups to be selectively removed from Paloc-protected peptides, e.g. with HCl in ether/dichloromethane (Scheme 4).

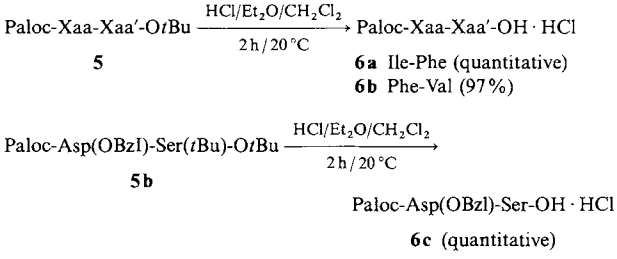

5 **5b**

Scheme 4.

The Paloc group is also stable during the cleavage of peptide allyl esters by rhodium(I)-catalyzed isomerization and subsequent hydrolysis of the resulting propenyl ester (Scheme 5). Not only the Paloc group but also protecting groups of the *tert*-butyl type are stable under these neutral conditions.

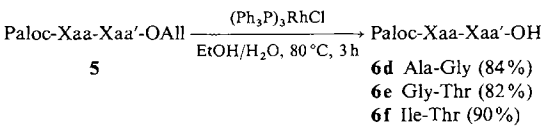

5

Scheme 5.

The Paloc group can be removed selectively and in high yield from the blocked amino functions of the peptides by palladium(0)-catalyzed allyl transfer to neutral or weakly basic nucleophiles, e.g. *N*-methylaniline (Scheme 6). Protected cysteine and methionine residues do not interfere with these reactions.[6] This deblocking requires longer reaction times than the cleavage of the unsubstituted Aloc group.[6] The very mild reaction conditions leave benzyl- and tert-*butyl*-type protecting groups intact (cf. **7d**). Furthermore, **7d** demonstrates that no transpeptidation of aspartic acid peptides occurs under the conditions of the Paloc cleavage.

Paloc-Xaa-Xaa'-O*t*Bu **5** $\xrightarrow[C_6H_5NHCH_3,\ THF,\ 20\,^\circ C,\ 10\,h]{(Ph_3P)_4Pd}$ H-Xaa-Xaa'-O*t*Bu

7a Val-Ile (89%)
7b Gly-Val (84%)
7c Ile-Leu (80%)
7d Asp(OBzl)-Ser(*t*Bu) (74%)

Scheme 6.

The solubilizing properties and stability of the Paloc group are advantageous for the synthesis of peptides by fragment condensation. As shown in Scheme 7 for the two Paloc tetrapeptide esters **8**, sterically hindered condensation agents such as isobutyl-2-isobutoxy-1,2-dihydroquinoline-1-carboxylate IIDQ[14] can be applied for this purpose. However, longer reaction times are necessary. Nevertheless, owing to the stability of the Paloc group no further undesired side reactions occur.

6a + **7b** $\xrightarrow[CH_2Cl_2,\ 3\,d]{IIDQ}$ Paloc-Ile-Phe-Gly-Val-O*t*Bu
8a (79%)

6d + **7a** $\xrightarrow[CH_2Cl_2,\ 3\,d]{IIDQ}$ Paloc-Ala-Gly-Val-Ile-O*t*Bu
8b (71%)

Scheme 7.

Stability, solubility properties, and cleavability under neutral conditions establish the Paloc group as valuable tool for the synthesis of demanding, sensitive peptide derivatives.

Received: July 24, 1990 [Z 4089 IE]
German version: *Angew. Chem. 102* (1990) 1520

CAS Registry numbers:
1, 28447-15-6; **2**, 69963-46-8; **3**, 129943-30-2; **4a**, 129943-31-3; **4b**, 129943-32-4; **4c**, 129943-33-5; **4d**, 129943-34-6; **4e**, 129943-35-7; **4f**, 129943-36-8; **4g**, 129943-37-9; **4h**, 129943-38-0; **4i**, 129943-39-1; **4j**, 129943-40-4; **5a**, 129943-42-6; **5b**, 129943-43-7; **5c**, 129943-44-8; **5d**, 129943-45-9; **5e**, 129943-46-0; **5f**, 129943-47-1; **5g**, 129943-48-2; **5h**, 129943-49-3; **5i**, 129943-50-6; **6a**, 129943-53-9; **6b**, 129943-54-0; **6c**, 129943-55-1; **6d**, 129943-56-2; **6e**, 129943-57-3; **6f**, 129943-58-4; **7a**, 104488-26-8; **7b**, 26560-53-2; **7c**, 28635-74-7; **7d**, 129943-60-8; **8a**, 129943-61-9; **8b**, 129943-62-0; Ala, 56-41-7; Asp(OBzl)-OH, 2177-63-1; Asp(OH)-O*t*Bu, 4125-93-3; Gly, 56-40-6; Ile, 73-32-5; Leu, 61-90-5; Lys(z), 1155-64-2; Phe, 63-91-2; Thr, 72-19-5; Val, 72-18-4; Gly-OAll, 59765-55-8; Ser(*t*Bu)-O*t*Bu 48067-24-9; Thr-OAll, 88224-10-6; Thr(*t*Bu)-OAll, 129943-41-5; Leu-O*t*Bu, 21691-53-2; Ile-O*t*Bu, 16874-08-1; Val-O*t*Bu, 13211-31-9; Paloc-Ile-Phe-O*t*Bu, 129943-51-7; Paloc-Ile-Thr-OAll, 129943-52-8; Paloc-Gly-Val-O*t*Bu, 129943-59-5.

[1] Review: J.-L. Fauchère, *Adv. Drug. Res. 15* (1986) 29.
[2] Review: H. Kunz, *Angew. Chem. 99* (1987) 297; *Angew. Chem. Int. Ed. Engl. 26* (1987) 294.
[3] Review: H.-D. Jakubke, P. Kuhl, A. Könnecke, *Angew. Chem. 97* (1985) 79; *Angew. Chem. Int. Ed. Engl. 24* (1985) 85.
[4] H. Waldmann, H. Kunz, *Liebigs Ann. Chem. 1983*, 1712.
[5] H. Kunz, H. Waldmann, *Angew. Chem. 96* (1984) 49; *Angew. Chem. Int. Ed. Engl. 23* (1984) 71.
[6] H. Kunz, C. Unverzagt, *Angew. Chem. 96* (1984) 426; *Angew. Chem. Int. Ed. Engl. 23* (1984) 436.
[7] M. Sakakibara, M. Matsui, *Agric. Biol. Chem. 43* (1979) 117.
[8] J. M. A. Hoeflacke, *Recl. Trav. Chim. Pays-Bas 40* (1961) 488.
[9] *Method A:* A solution of amino acid (25 mmol) in water (30 mL) was treated dropwise at constant pH 10 (addition of 4N NaOH) with a solution of **3** (7.5 g, 25 mmol) in dioxane (30 mL), the mixture stirred for 1 h, then adjusted to pH 4 with 6N HCl, and finally evaporated to dryness. The residue was digested with 250 mL of ethyl acetate, the mixture filtered over a small amount of silica gel and, after evaporating down, purified by flash chromatography on 100 g of silica gel (0.040–0.063 mesh) in ethyl acetate/glacial acetic acid (200:1). After removal of the solvent in vacuo and redistillation from toluene the Paloc amino acids **4** were obtained as colorless crystals or oils.
[10] *Method B:* A mixture of the amino acid (25 mmol) and trimethylchlorosilane (3.2 g, 25 mmol) in 100 mL of chloroform/acetonitrile (1:1) was heated under reflux for 2 h. After cooling, the mixture was treated with 8.7 mL of diisopropylethylamine (50 mmol) and stirred for 30 min. **3** (7.5 g, 25 mmol) was then added and the mixture refluxed for 12 h. After concentration in vacuo the concentrate was worked up as in **9**.
[11] UV: λ_{max} = 243 nm; IR(KBr): $\tilde{\nu}$ [cm^{-1}] = 1710–1680 (urethane), 980–960 (C=C); ^{1}H NMR (200 MHz, $CDCl_3$, 25 °C, TMS): δ = 8.65–8.55 (s, 1H, pyridine-2-H); 8.5–8.4 (d, J = 4.5 Hz, 1H, pyridine-6-H); 7.95–7.65 (d, J = 8 Hz, 1H, pyridine-4-H); 7.40–7.25 (dd, 1H, pyridine-5-H); 6.70–6.55 (d, J = 16 Hz, 1H, allyl-γ-H); 6.5–6.3 (dt, $J_{\alpha,\beta}$ = 5.5 Hz, 1H, allyl-β-H).
[12] B. Belleau, G. Malek, *J. Am. Chem. Soc. 90* (1968) 1651.
[13] W. König, R. Geiger, *Chem. Ber. 103* (1970) 788.
[14] Y. Kiso, H. Yajima, *J. Chem. Soc. Chem. Commun. 1972*, 942.

Synthesis and Transmission Electron Microscopic Investigation of Bi(Pb)–Sr–Ca–Cu–O Superconductors **

By *Jan-Henrik Müller, Martin Schwarz,* and *Reginald Gruehn* *

The preparation and investigation of ceramic high-temperature superconductors of the Bi(Pb)–Sr–Ca–Cu–O system are considerably more time-consuming and expensive than the preparation and characterization of specimens of the Y–Ba–Cu–O system. To obtain information, otherwise inaccessible, about the real structure of such specimens we resorted to the technique of high-resolution transmission electron microscopy.

For the synthesis of $Bi_2Sr_2Ca_2Cu_3O_{12-x}$ (Sample **A**, prepared from the oxides) the composition reported by *Endo* et al.[1] was chosen (nominal composition $Bi_{0.8}Pb_{0.2}Sr_{0.8}CaCu_{1.4}O_x$; T_c (R = 0) = 100 K). The phase purity was checked with X-ray powder patterns (Fig. 1, top) and the composition analytically. Measurements of the magnetic susceptibility on rod-shaped samples (2 × 2 × 10 mm) revealed a predominant superconducting domain (Fig. 1, bottom). The synthesis and characterization of the samples **B** (nominal composition as in the case of Sample

[*] Prof. Dr. R. Gruehn, J.-H. Müller
Institut für Anorganische und Analytische Chemie
der Justus-Liebig-Universität
Heinrich-Buff-Ring 58, W-6300 Giessen (FRG)
Dr. M. Schwarz
Hoechst AG
W-6230 Frankfurt am Main 80 (FRG)

[**] This work was supported by the Deutsche Forschungsgemeinschaft, the Fonds der Chemischen Industrie, and the Bundesministerium für Forschung und Technologie.

A; $T_c(R=0) = 105$ K) and **D** (nominal composition, $Bi_{4.3}Sr_{3.5}Ca_{3.5}Cu_6O_x$; T_c ($R=0$) = 95 K) were carried out in the same way as for Sample **A**. Sample **C** (composition $Bi_2Sr_{1.8}Ca_{0.2}Cu_2O_x$; $T_c \approx 90$ K (midpoint)[2] was characterized X-ray crystallographically by the Guinier method and was found to consist predominantly of the compound $Bi_2Sr_2CuO_x$.

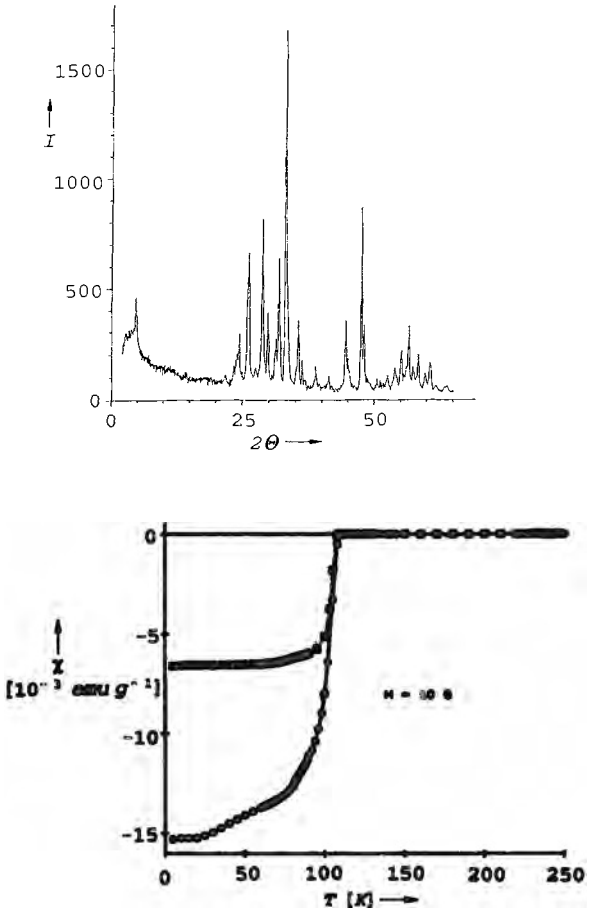

Fig. 1. Characterization of Sample **A**. Top: powder diffractogram; bottom: SQUID susceptometer measurement, shielding curve: —o—; Meissner curve: ··□·· (SQUID-VTS susceptometer, SHE Corp.).

Sample **A**: The layer structure to be expected on the basis of other investigations[3] is clearly recognizable *electron microscopically* upon viewing along [110] (transmission photograph Fig. 2a; corresponding electron diffraction pattern, Fig. 2b). However, the successive half unit cells staggered along [001] have different lengths, which can be characterized by the respective number (2 or 3) of the O–Cu–O layers. The contrasts change drastically on varying the defocus (Fig. 2d, e). The bright lines running perpendicular to the *c* direction appear to split. The layer pattern of Figure 2a is least pronounced in Figure 2e; instead finer details with a point resolution of about 3 Å are discernable. The Figures 2a, d, and e demonstrate the problem of assigning the structural units (e.g. half unit cells) or strongly diffracting heavy atoms (Bi) to the electron microscopically recorded contrasts: owing to the dependence of the contrasts on the defocusing, an unequivocal assignment of the structural details is not always possible. However, transmission images together with the electron diffraction can yield valuable information about the symmetry of the structure, as could also be shown by image simulation calculations (multi-slice method).[4]

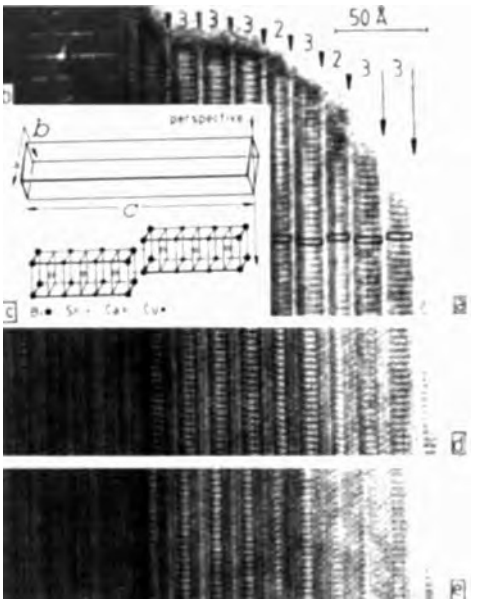

Fig. 2. Crystal fragment of Sample **A**; view along [110]. a) Transmission image with half unit cells indicated; b) corresponding electron diffraction pattern; c) structural model (after [3]) with two Cu "layers" in every half unit cell; d) and e) transmission images but, compared to (a), at different defocus values and with changed contrast.

A sequence of half unit cells with two, three and four O–Cu–O layers in another region of Sample **A** (Fig. 3) can also be interpreted in terms of substitution of three-layer half unit cells ($3 + 3 + 3 \rightarrow 2 + 3 + 4$). To this sequence are then attached further unit cells containing three O–Cu–O layers.

Fig. 3. Transmission photograph along [110] (other crystal fragment of Sample **A**).

A crystal fragment of Sample **B**, on the other hand (Fig. 4), shows extended regions of an undisturbed three-layer structure (three O–Cu–O layers per half unit cell); defects as are seen in Figures 2 and 3 are not found.

On viewing along [100], transmission and diffraction images (Fig. 5a and 5b, resp.) show a complicated superstructure (Sample **C**). Superstructures[8, 9] ("modulation"), which are possibly due to differences in the occupation and location of the oxygen positions adjacent to the Bi layers, have been observed in superconductors of the type $(BiO)_2Sr_2Ca_{n-1}Cu_nO_{2n+2}$ ($n \geq 1$).[3, 5-7] An influence on the positions of the metal atoms is assumed.[10] The electron microscopic photographs cannot as yet be satisfactorily evaluated, because, for example, a detailed model of the real structure of such a crystal is not accurately known. An attempt at a tentative interpretation of the modulated structure is described in Ref. [10].

A highly resolved transmission photograph along [001] (Fig. 6a) of an especially thin sample of **D** reveals a periodic change (superstructure with $5b \approx 27$ Å) of the contrast in the

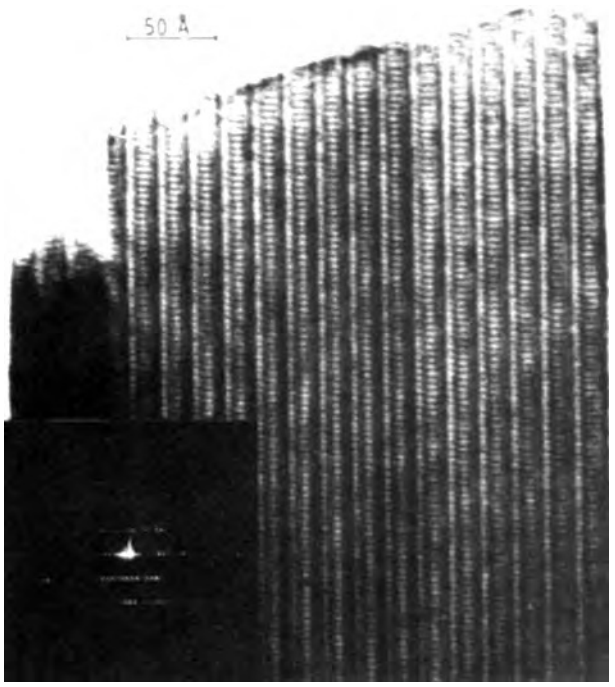

Fig. 4. Transmission and electron diffraction photographs along [110] (Sample **B**).

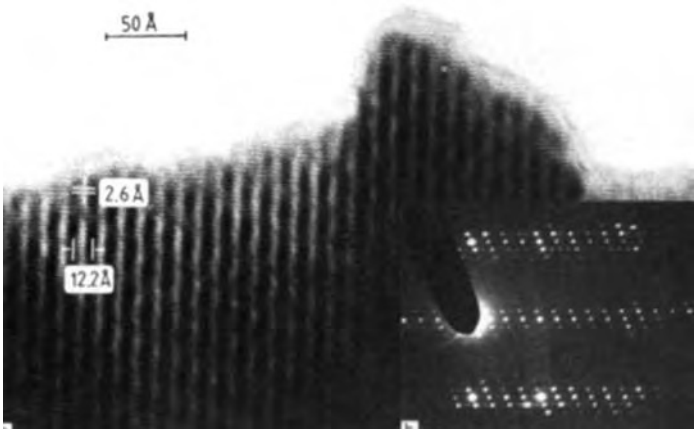

Fig. 5. Crystal fragment of Sample C; view along [100]. a) Transmission image; b) electron diffraction pattern.

direction of the *b* axis (horizontally in the image, "modulation"). The image contrast changes slightly every five unit cells (arrows in Fig. 6a). Periodic changes in contrast are also observed vertical to the *b* axis.

The electron diffraction pattern (Fig. 6b) shows intense reflections and very weak reflections which appear to be arranged crosswise. In Figure 6c, the reflections which illustrate the pattern of the superstructure in the direction b^* are shown (immediately adjacent reflections in the vertical direction have been omitted). The pattern (Fig. 6c) can be generated by rotation through 90° in the image plane and superposition with the original diagram ("rotated" twin in Fig. 6d). This type of defect, which differs markedly from the microtwinning in $YBa_2Cu_3O_{7-x}$,[11] has often been observed. This indicates that two or several crystal platelets (view perpendicular to {110}) have *not* rotated through 90° and, after that, superimposed coincidentally.

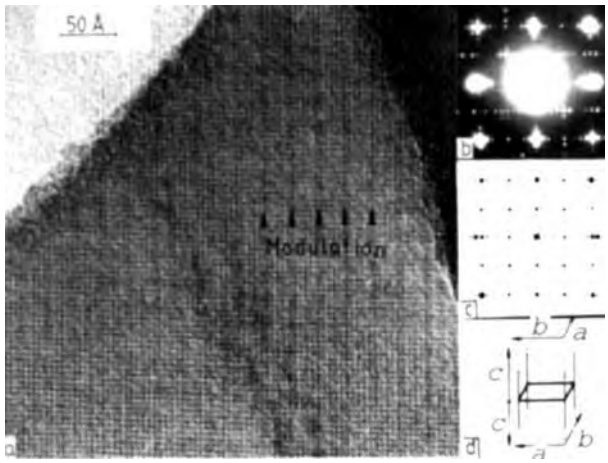

Fig. 6. Crystal fragment of Sample **D**; view along [001]. a) Transmission image; b) electron diffraction pattern; c) schematic diagram of the reflections of Figure 6 (cf. text); d) schematic drawing of a "rotated twin".

The electron microscopic investigation reveals the complicated real structure of the Bi(Pb)–Sr–Ca–Cu–O superconductor. A relationship between the observed structural defects and the preparative prehistory cannot be established on the basis of the present studies, since only a small number of crystal fragments found by chance have been examined. For example, according to the electron microscopic findings, sample **A**, which was characterized by X-ray powder patterns as a "three-layer compound", also contains crystal fragments which are made up by the "one-layer" compound and the "two-layer" compound.

Experimental

Synthesis of superconductors of the system Bi(Pb)–Sr–Ca–Cu–O: To suppress decomposition reactions, strontium was used in small excess and a part of the bismuth was substituted by lead. After preliminary reaction of the mixture at $T = 800$ °C, the powder was pressed to a tablet (13 mm × 3 mm; pressure $p =$ 50 bar) and sintered on a MgO support for 80 h at 846 °C (Sample **D**: 870 °C). Finally, the mixture was tempered a total of six times alternately for 3 h at 600 °C and 3 h at 846 °C (**D**: 870 °C), then cooled at a rate of 100 Kh^{-1} to room temperature. The samples were gently crushed and suspended in ethanol. One drop of the slurry was put on a Cu grid covered with a carbon coated perforated foil.[12]

Electron microscopic investigation: The electron microscopic investigation was carried out with a Philips EM-400-HMG (LaB_6 cathode, 120 kV; primary magnification of 4.4×10^5). With the help of electron diffraction, suitable crystals were so adjusted that the desired crystallographic direction lay in the direction of transmission. The crystal fragments had mainly the form of thin platelets (basal plane $\{110\}$[13]), so that normally only the view perpendicular to the basal plane, [001], could be used. Views along a diagonal of the unit cell were more difficult to obtain, and only in exceptional cases could an observation along one of the short axes be accomplished.

Received: July 23, 1990 [Z 4086 IE]
German version: *Angew. Chem. 102* (1990) 1448

CAS Registry numbers:
Bi–Pb–Sr–Ca–Cu–O system, 116739-98-1; Bi–Sr–Ca–Cu–O system, 114901-61-0.

[1] U. Endo, S. Koyama, T. Kawai, *Jpn. J. Appl. Phys. Lett. 27* (1988) L 1476, L 1861.
[2] V. Plies, Giessen, private communication.
[3] H. G. von Schnering, L. Walz, M. Schwarz, W. Becker, M. Hartweg, T. Popp, B. Hettich, P. Müller, G. Kämpf, *Angew. Chem. 100* (1988) 604; *Angew. Chem. Int. Ed. Engl. 27* (1988) 574.
[4] R. Gruehn, J.-H. Müller, unpublished.

[5] M. A. Subramanian, C. C. Torardi, J. C. Calabrese, J. Gopalkrishnan, K. J. Morrissey, T. R. Askew, R. B. Flippen, U. Chowdhry, A. W. Sleight, *Science 239* (1988) 1015.
[6] J. M. Tarascon, Y. Le Page, P. Barboux, B. G. Bagley, L. H. Greene, W. R. McKinnon, G. W. Hull, M. Giroud, D. M. Hwang, *Phys. Rev. B 37* (1988) 9382.
[7] P. Bordet, J. J. Capponi, C. Chaillout, J. Chevenas, A. W. Hewat, E. A. Hewat, J. L. Hodeau, M. Marezio, J. L. Tholence, D. Tran Qui, *Physica C 156* (1988) 189.
[8] Y. Gao, P. Lee, P. Coppens, M. A. Subramanian, A. W. Sleight, *Science 241* (1988) 954.
[9] Y. Le Page, W. R. McKinnon, J.-M. Tarascon, P. Barboux, *Phys. Rev. B 40* (1989) 6810.
[10] H. W. Zandbergen, W. A. Groen, F. C. Mijlhoff, G. Van Tendeloo, S. Amelinckx, *Physica C 156* (1988) 325.
[11] J.-H. Müller, V. Plies, R. Gruehn: *Naturwissenschaften 75* (1988) 196.
[12] R. Gruehn, W. Mertin, *Angew. Chem. 92* (1980) 531; *Angew. Chem. Int. Ed. Engl. 19* (1980) 505.
[13] For the structure determination cf. [3]: $(BiO)_2Sr_2Ca_{n-1}Cu_nO_{2n+2}$ ($n = 1$): $a = 5.392$, $b = 5.394$, $c = 24.537$ Å; ($n = 2$): $a = 5.395$, $b = 5.392$, $c = 30.628$ Å; ($n = 3$): $a = 5.407$, $b = 5.411$, $c = 37.054$ Å.

New Chiral C_3-Symmetric Tripodal Phosphanes**

By *Mark J. Burk** and *Richard L. Harlow*

Chiral ligands possessing a C_2 symmetry axis are known to induce a high degree of stereocontrol in a variety of transition-metal-catalyzed reactions.[1, 2] Despite the great success with C_2-symmetric ligands, chiral ligands possessing elements of higher symmetry[3] have been ignored to a large extent. The proper introduction of chirality into polydentate ligands should offer the opportunity to explore systems with higher order symmetry. Our objective has been the rational design of new chiral C_3-symmetric tris(phosphane) ligands which may be used in asymmetric catalysis.

The high optical yields obtained with catalysts bearing C_2-symmetric ligands have been attributed to a reduction in the number of possible diastereomeric transition states because of equivalent asymmetric environments imposed along the z axes (+ and −) of an intermediate square-planar metal complex.[1, 2] In addition to square-planar species, octahedral intermediates are known to be involved in many transition-metal-catalyzed reactions.[4] An octahedral intermediate bearing a chiral bidentate C_2-symmetric ligand (**A**) offers two nonequivalent (diastereotopic) coordination sites (axial and equatorial) for substrate binding. In contrast, a similar octahedral intermediate with a chiral tridentate C_3-symmetric ligand (**B**) offers only one type of site for substrate coordination; all the sites opposite a C_3-symmetric tripod ligand are equivalent (homotopic). The reduced number of competing asymmetric environments should lead to high enantioselectivity in catalytic reactions involving metal centers bearing chiral tripodal C_3-symmetric ligands. Furthermore, conformationally rigid polydentate ligands possessing a C_3 symmetry axis may provide a high degree of stereochemical control in notoriously difficult asymmetric catalytic reactions, such as those involving nonchelating or unfunctionalized substrates. We now report the first examples of homochiral C_3-symmetric polydentate phosphanes, as well as the preparation and structural characterization of several transition metal complexes bearing these ligands.

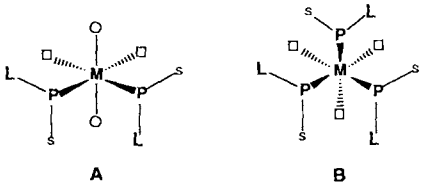

We recently described[5] an efficient route to (*R,R*) and (*S,S*)-2,5-disubstituted phospholanes such as **1**. Treatment of **1** with lithium metal was found to cleave the P–Ph bond of the phospholane selectively, providing a mixture of the lithium phosphide **2** and phenyllithium. As we wished to prepare chiral tripodal phosphanes, we examined the reaction between **2** and 1,1,1-tris(chloromethyl)ethane. The major product of this reaction, however, was the P–P coupled diphospholane dimer, **3**, presumably produced via initial lithium/halogen exchange. The desired C_3-symmetric triphospholane all-(*S*)-**4**[6] was obtained as a colorless crystalline solid upon reaction between the less hindered 1,3-dichloro-2-chloromethylpropane[7] and (*S,S*)-**2**. Analogously, either enantiomer of the C_3-symmetric triphospholanamine **5**[6] was readily prepared by treatment of the corresponding lithium phosphide (*R,R*) or (*S,S*)-**2** with tris(2-chloroethyl)amine. The high symmetry of **4** and **5** was indicated by the ^{31}P NMR spectra, which exhibited singlets at $\delta = -8.0$ and -3.4, respectively. The chiral nature of these phosphanes was confirmed by the large optical rotations, $[\alpha]_D^{20} = -329$ and $[\alpha]_D^{20} = -167$ (**c** = 1, hexane) for all-(*S*)-**4** and all-(*S*)-**5**, respectively.

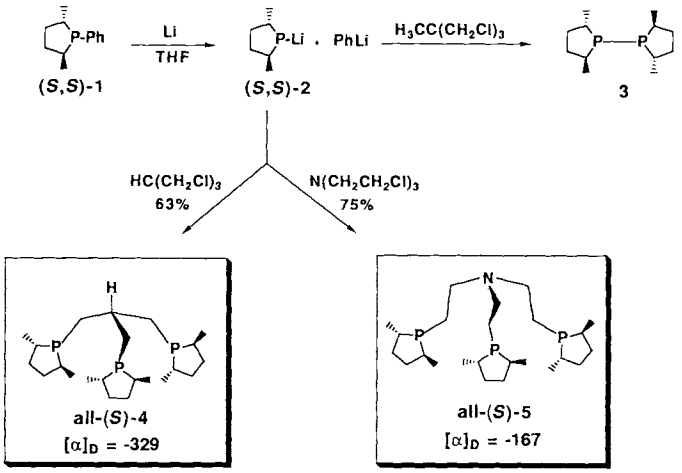

The C_3-symmetric rhodium complex $[(NP_3)Rh(CO)]^{\oplus}Cl^{\ominus}$ all-(*R*)-**6**[8] (NP_3 = **5**) was obtained as a bright yellow precipitate upon reaction of all-(*R*)-**5** with $[(CO)_2RhCl]_2$ in toluene. Its trigonal bipyramidal structure was ascertained by X-ray crystallography[9] (Fig. 1). The Rh atom is located 0.2 Å below the equatorial plane defined by the three P atoms. As is apparent from the view in Figure 1 (bottom), the molecule possesses a crystallographic C_3 symmetry axis which coincides with the apical N–Rh–CO axis of the complex; the chloride counterion also lies on this axis. Similarly, the chiral C_3-symmetric ligand, all-(*S*)-**4**, was reacted with $[(cod)_2Rh]^{\oplus}SbF_6^{\ominus}$ (cod = cyclooctadiene) to give the rhodium complex $[(cod)Rh(C_3P_3)]^{\oplus}SbF_6^{\ominus}$ (C_3P_3 = all-(*S*)-**4**), all-

[*] Dr. M. J. Burk, Dr. R. L. Harlow
Central Research and Development Department
E.I. du Pont de Nemours and Co, Experimental Station
Wilmington, DE 19880-0328 (USA)

[**] Contribution No. 5586 from the Central Research and Development Department. We wish to thank *John E. Feaster*, *Louis F. Lardear*, and *William J. Marshall* for expert technical assistance.

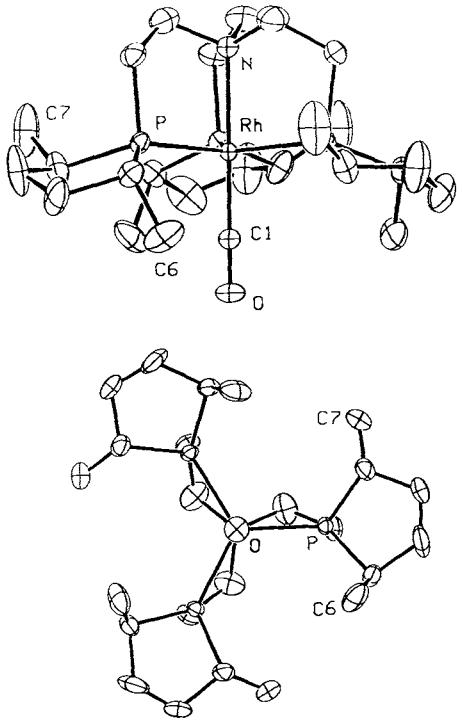

Fig. 1. ORTEP drawings of rhodium complex all-(*R*)-**6**. Hydrogen atoms and $Cl^{\ominus}$ anion are omitted for clarity. Top: Side view. Bottom: View looking down the crystallographic C_3 symmetry axis (N-Rh-CO axis).

(*S*)-**7**,[8] which was characterized by X-ray crystallography.[10] The ORTEP diagram (Fig. 2) reveals the C_3-symmetric environment imposed by the tripodal ligand all-(*S*)-**4**. These structural studies indicate that the electron-rich chiral C_3-symmetric tripodal phosphanes **4** and **5** produce a highly asymmetric environment when complexed to transition metal centers.

In preliminary studies the rhodium complex all-(*S*)-**7** was shown to act as a catalyst precursor for the enantioselective hydrogenation of methyl (z)-α-acetamidocinnamate (50 °C, 72 h, 89% *ee*) and dimethyl itaconate (50 °C, 20 h, 95% *ee*). Although activation of the catalyst through hydrogenation of the cod ligand of all-(*S*)-**7** occurs at 25 °C and 2 atm H_2, substrate hydrogenation was very slow under these conditions. The higher temperature required for reasonable reduction rates suggests that dissociation of one arm of the chelating substrates or the phosphane ligand in a five-coordinate (18-electron) intermediate is necessary for reaction with hydrogen. Further studies aimed at using the new C_3-symmetric chiral ligands **4** and **5** in asymmetric catalysis are in progress.

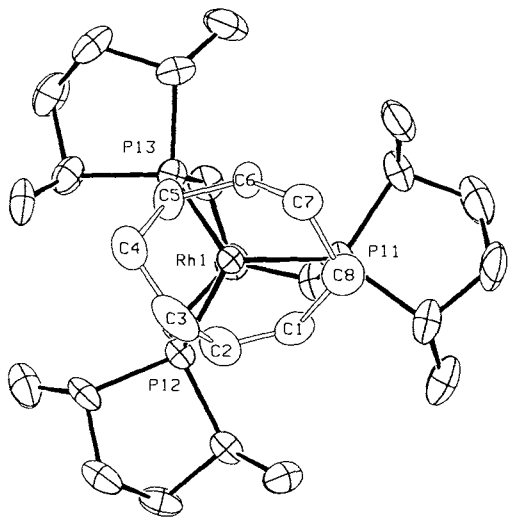

Fig. 2. ORTEP drawing of all-(*S*)-**7**. Hydrogen atoms and $SbF_6^{\ominus}$ anion are omitted for clarity.

Experimental Procedure

Preparation of all-(*S*)-**4**: Clean Li ribbon (0.55 g, 79 mmol) was added to a solution of (*S,S*)-**1** [5] (6.07 g, 32 mmol) in THF (200 mL) at 25 °C under Ar, and the mixture stirred for 15 h. The resulting brown/orange mixture was treated dropwise with a solution of 1,3-dichloro-2-(chloromethyl)propane [7] (1.70 g, 10.5 mmol) in THF (15 mL) at 25 °C. The reaction remained brown throughout the addition, and after stirring for 30 min, MeOH (3 mL) was added to quench the remaining PhLi. The mixture was stirred for a further 15 min and then filtered to remove precipitated lithium methoxide. The filtrate was concentrated in vacuo. The resulting solids were extracted with pentane (125 mL), and the pentane layer was filtered and concentrated to ca. 15 mL, during which time a colorless crystalline solid formed. Rapid filtration of the cold mixture afforded the product (1.0 g), which was dried in vacuo. The pentane filtrate was then evaporated down, and yielded a pale yellow solid, which was dissolved in a minimum amount of Et_2O (3 mL). This solution was treated with MeOH (15 mL), and the mixture was cooled to − 20 °C for 12 h. The resulting colorless crystals of all-(*S*)-**4** were filtered, washed with cold MeOH and dried in vacuo (1.65 g). Combined yield 2.65 g (63%).

Preparation of all-(*R*)-**5**: Clean Li ribbon (0.27 g, 39.0 mmol) was added to a solution of (*R,R*)-**1** [5] (3.0 g, 15.6 mmol) in THF (100 mL) at 25 °C under Ar, and the reaction mixture stirred for 15 h. To the resulting brown/orange mixture was added dropwise a solution of tris(2-chloroethyl)amine (1.06 g, 5.2 mmol) in THF (15 mL) at 25 °C. The procedure for isolation of the colorless crystalline product all-(*R*)-**5** was exactly as described above for all-(*S*)-**4**. Combined yield 1.73 g (75%).

Received: July 30, 1990 [Z 4104 IE]
German version: *Angew. Chem. 102* (1990) 1511

CAS Registry numbers:
(*R,R*)-**1**, 129647-10-5; (*S,S*)-**1**, 129705-29-9; (*S,S*)-**2**, 130296-22-9; **3**, 130296-23-0; all-(*S*)-**4**, 130296-24-1; all-(*R*)-**5**, 130296-25-2; all-(*S*)-**5**, 130404-32-9; all-(*R*)-**6**, 130296-27-4; all-(*S*)-**7**, 130326-20-4; $CH_3C(CH_2Cl)_3$, 1067-09-0; $HC(CH_2Cl)_3$, 66703-69-3; $N(CH_2CH_2Cl)_3$, 555-77-1; $[(CO)_2RhCl]_2$, 14523-22-9; $[(cod)_2Rh]^{\oplus}SbF_6^{\ominus}$, 130296-28-5; dimethyl itaconate, 617-52-7.

[1] J. K. Whitesell, *Chem. Rev. 89* (1989) 1581, and references therein.
[2] a) B. Bosnich (Ed.): *Asymmetric Catalysis*; Nijhoff, Dordrecht 1986; b) A. Pfaltz in R. Scheffold (Ed.): *Modern Synthetic Methods, Vol. 5*, Springer, Berlin 1989, p. 199 ff. c) H. B. Kagan in J. D. Morrison (Ed.): *Asymmetric Synthesis, Vol. 5*, Academic, New York 1985, Chap. 1. d) H. Brunner, *J. Organomet. Chem. 300* (1986) 39; e) *Angew. Chem. 95* (1983) 921; *Angew. Chem. Int. Ed. Engl. 22* (1983) 897; f) W. S. Knowles, *Acc. Chem. Res. 16* (1983) 106.
[3] For recent examples of phosphanes with C_3 symmetry, see: a) C. Bolm, W. M. Davis, R. L. Halterman, K. B. Sharpless, *Angew. Chem. 100* (1988) 882; *Angew. Chem. Int. Ed. Engl. 27* (1988) 835. b) C. Bolm, K. B. Sharpless, *Tetrahedron Lett. 29* (1988) 5101; c) B. Bogdanović, B. Henc, B. Meister, H. Pauling, G. Wilke, *Angew. Chem. 84* (1972) 1070; *Angew. Chem. Int. Ed. Engl. 11* (1972) 1023.
[4] a) J. P. Collman, L. S. Hegedus, J. R. Norton, R. G. Finke: *Principles and Applications of Organotransition Metal Chemistry*, Univ. Science Books, Mill Valley, CA 1987; b) J. K. Kochi: *Organometallic Mechanisms and Catalysis*, Academic, New York 1978.
[5] M. J. Burk, J. E. Feaster, R. L. Harlow, *Organometallics, 10* (1990) 2653.
[6] all-(*S*)-**4**: m.p. 115–118 °C; $[\alpha]_D^{25} = -329 \pm 4$ ($c = 1$, hexane); ^{1}H NMR (C_6D_6): $\delta = 1.0$–1.2 (m, 3H; CH, CH_2), 1.07 (dd, J(HH) = 7.2, J(PH) = 9.8 Hz, 9H; CH_3), 1.29 (dd, J(HH) = 7.0, J(PH) = 17.6 Hz, 9H; CH_3), 1.40 (m, 3H; CH, CH_2), 1.60 (m, 3H; CH_2), 1.80 (m, 3H; CH, CH_2), 1.9–2.2 (m, 13H; CH, CH_2); ^{31}P NMR (C_6D_6) $\delta = -8.0$; ^{13}C NMR (C_6D_6): $\delta = 14.89$ (CH_3), 21.51 (d, J(PC) = 30.7 Hz; CH_3), 31.85 (dt, J(PC) = 8.3, 22.1 Hz; bridge P–CH_2), 32.67 (q, J(PC) = 14.9 Hz; bridge CH), 34.12 (d, J(PC) = 11.6 Hz; ring CH), 37.30 (d, J(PC) = 3.8 Hz; ring CH_2), 37.47 (ring CH_2), 38.49 (d, J(PC) = 11.3 Hz; ring CH); HRMS (EI, direct insert): m/z 400.2583 ($M^{\oplus}$ exact mass calculated for $C_{22}H_{43}P_3$: 400.2578), 357.2021 ($M^{\oplus} - C_3H_7$), 315.1557 ($M^{\oplus} - C_6H_{13}$), 285.1896 ($M^{\oplus} - C_6H_{12}P$), 273.1104 ($M^{\oplus} - C_9H_{19}$), 232.0678 ($M^{\oplus} - C_{12}H_{24}$), 201.0955 ($M^{\oplus} - C_{12}H_{24}P$).—all-(*R*)-**5**: m.p. 55–58 °C; $[\alpha]_D^{25} = +167.4 \pm 2$ ($c = 1$, hexane); ^{1}H NMR (C_6D_6) $\delta = 1.0$–1.2 (m,

3H; CH, CH_2), 1.11 (dd, J(HH) = 7.2, J(PH) = 9.8 Hz, 9H; CH_3), 1.32 (dd, J(HH) = 7.0, J(PH) = 17.7 Hz, 9H; CH_3), 1.30–1.45 (m, 3H; CH, CH_2), 1.55 (m, 3H; CH_2), 1.70–2.15 (m, 15H; CH, CH_2), 2.80 (m, 6H; NCH_2); ^{31}P NMR (C_6D_6) δ = −3.4; ^{13}C NMR (C_6D_6) δ = 14.66 (CH_3), 21.34 (d, J(PC) = 31.0 Hz; CH_3), 22.02 (d, J(PC) = 22.8 Hz; bridge P-CH_2), 33.97 (d, J(PC) = 1.20 Hz; ring CH), 37.12 (d, J(PC) = 3.6 Hz; ring CH_2), 37.41 (ring CH_2), 38.41 (d, J(PC) = 11.3 Hz; ring CH), 51.73 (d, J(PC) = 25.6 Hz; bridge N-CH_2); HRMS (EI, direct insert): m/z 443.3035 ($M^{\oplus}$ exact mass calculated for $C_{24}H_{48}NP_3$: 443.3000), 328.2315 ($M^{\oplus}-C_6H_{12}P$), 314.2146 ($M^{\oplus}-C_7H_{14}P$), 242.1216 ($M^{\oplus}-C_{12}H_{26}P$).

[7] S. Latour, J. D. Wuest, *Synthesis 1987*, 742.

[8] Rhodium complex all-(*R*)-**6**: ^{1}H NMR (CD_2Cl_2): δ = 1.0–1.3 (m, 24H; CH_2, CH_3), 1.4 (m, 4H; CH_2), 1.65 (m, 4H; CH, CH_2), 2.20 (m, 8H; CH_2), 2.35 (m, 4H; CH, CH_2), 2.60 (m, 2H; NCH_2), 3.0 (m, 2H; NCH_2); ^{31}P NMR (CD_2Cl_2): δ = 69.5 (d, J(RhP) = 127 Hz); ^{13}C NMR (C_6D_6): δ = 13.11, 21.15, 27.48, 34.41, 35.34, 38.36, 38.51, 62.0; IR (CH_2Cl_2): $\tilde{\nu}$(CO) = 1985 cm^{-1}; correct elemental analysis (C,H,P)—Rhodium complex all-(*S*)-**7**: ^{1}H NMR (CD_2Cl_2): δ = 1.16 (dd, J(HH) = 7.4 Hz, J(PH) = 10.9 Hz, 9H; CH_3), 1.27 (dd, J(HH) = 7.0, J(PH) = 15.1 Hz, 9H; CH_3), 1.6–1.8 (m, 12H; CH_2), 2.0–2.2 (m, 11H; CH, cod-CH_2), 2.30 (m, 3H; CH), 2.65 (m, 6H; PCH_2), 3.15 (q br, 1H; CH), 3.85 (br, 2H; cod-CH), 4.20 (br, 2H; cod-CH); ^{31}P NMR (CD_2Cl_2): δ = 22.0 (d, J(RhP) = 99 Hz).

[9] Crystal data for all-(*R*)-**6**: cubic, $P2_13$ (No. 198), a = 14.298(0) Å, T = −70 °C, V = 2922.9 Å^3, $Mo_{K\alpha}$ radiation, μ_{calcd} = 8.46 cm^{-1}, ϱ_{calcd} = 1.386 g cm^{-3}, Z = 4, FW = 609.95. The structure was solved by direct methods and refined by a full-matrix least squares procedure to residuals of R = 0.036, R_w = 0.032, GOF = 0.98 for 2378 unique reflections with $I > 3.0\sigma(I)$ and 106 variables [10b].

[10] a) Crystal data for all-(*S*)-**7**: orthorhombic, $P2_12_12_1$ (No. 19), a = 12.126(2), b = 17.299(3), c = 32.146(7) Å, T = −110 °C, V = 6743.2 Å^3, $Mo_{K\alpha}$ radiation, μ_{calcd} = 14.85 cm^{-1}, ϱ_{calcd} = 1.673 g cm^{-3}, Z = 8, FW = 847.35. The structure was solved by direct methods and refined by a full-matrix least squares procedure to residuals of R = 0.037, R_w = 0.034, GOF = 1.09 for 5944 unique reflections with $I > 3.0\sigma(I)$ and 755 variables. b) Full structure details are available upon request from the director of the Cambridge Crystallographic Data Centre, University Chemical Laboratory, Lensfield Road, Cambridge, CB2 1EW, UK (England), on quoting the names of the authors and the full journal citation.

C_2S_2(Ethene-1,2-dithione), an Example for the Violation of Hund's Rule?**

By *Günther Maier,* Hans Peter Reisenauer, Jürgen Schrot,* and *Rudolf Janoschek*

Dedicated to Professor Karl Dimroth on the occasion of his 80th birthday

Of the open-chain oxides and sulfides of carbon having the general formula (S)O=(C_x)=O(S),[1] those with an even number of C atoms are characterized by the fact that only two instead of the four electrons required for a closed shell are available for the pairwise degenerate, highest occupied molecular orbitals in a linear atomic arrangement ($D_{\infty h}$). The electronic situation therefore resembles that in the O_2 and S_2 molecules, and should, according to Hund's rule, lead to a triplet ground state. The associated high reactivity is probably the reason why the first spectroscopic detection of a compound of this series (C_4O_2) (in a matrix) has been accomplished only recently.[2, 3] We now report on the synthesis and identification of matrix-isolated C_2S_2 **3**, and on quantum chemical calculations regarding its structure, the multiplicity of its ground state, and its electron-excitation and vibrational spectra.

As C_2S_2 precursors we chose the molecules **1**, **2** and **4**, made up exclusively of C, S and O atoms, and subjected these to a high-vacuum flash pyrolysis, with subsequent isolation of the products in an argon matrix, or to a direct photolysis in the matrix.

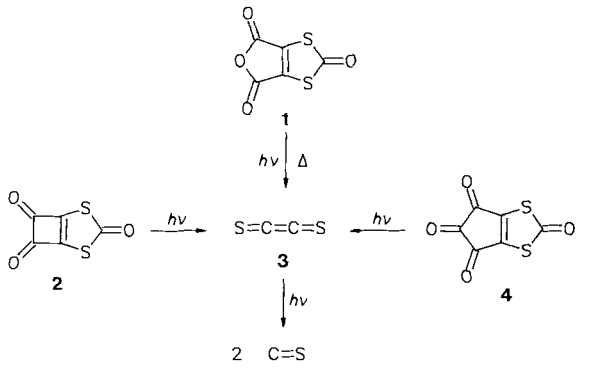

Brief irradiation of **1** with a mercury low-pressure lamp (254 nm) leads, as shown by the IR spectrum of the photolysis products (Fig. 1), to formation of CO_2, CO and small amounts of C_3OS,[4] COS, CS_2 and CS, as well as an unknown species showing an intense band at 1179 cm^{-1}. This

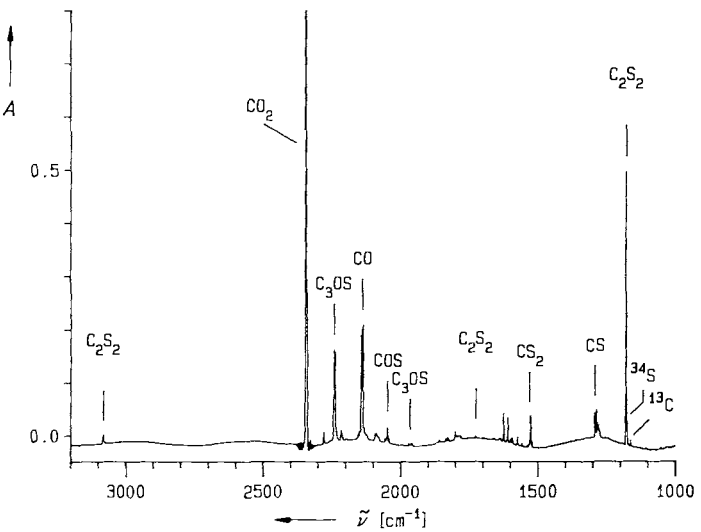

Fig. 1. IR spectrum of the photoproducts of **1** (Ar matrix, 12 K, after 15 min irradiation with λ = 254 nm). A = absorbance.

species also gives rise to a UV band with pronounced vibrational fine structure between 392 and 350 nm and to an additional intense end absorption beginning at about 230 nm (Fig. 2). On continuing the irradiation with 254-nm light these absorptions decrease only slowly, on irradiation with longer wavelength light (λ > 300 nm) very rapidly and in both cases in favor of the band characteristic for CS (Fig. 2). This observation in itself leaves little doubt that the photoproduct of **1** is C_2S_2 **3**.[14]

The IR spectrum is also as would be expected for C_2S_2. With $D_{\infty h}$ symmetry only one of the three stretching vibra-

[*] Prof. Dr. G. Maier, Dr. H. P. Reisenauer, Dipl.-Chem. J. Schrot
Institut für Organische Chemie der Universität
Heinrich-Buff-Ring 58, D-6300 Giessen (FRG)
Prof. Dr. R. Janoschek
Institut für Theoretische Chemie der Universität
Mozartgasse 14, A-8010 Graz (Austria)

[**] Heterocumulenes, Part 5. This work was supported by the Deutsche Forschungsgemeinschaft and the Fonds der Chemischen Industrie.—Part 4: [2].

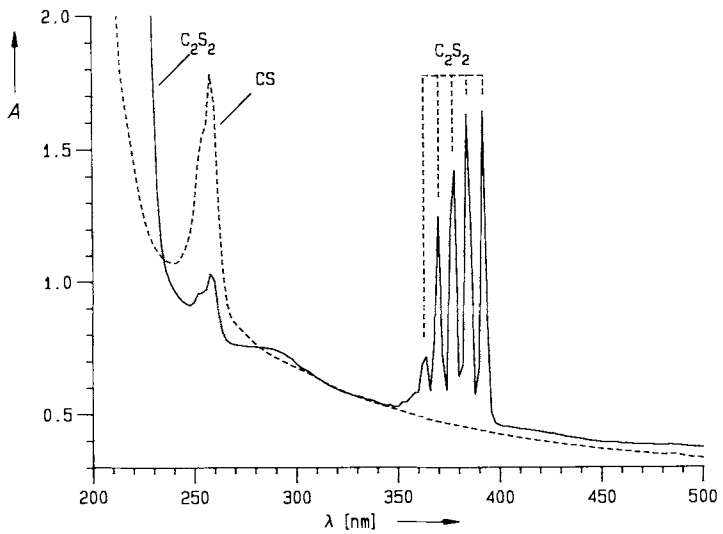

Fig. 2. UV/VIS spectra of the photoproducts of **1** (Ar matrix, 12 K); —— after 5 min irradiation with $\lambda = 254$ nm; --- after a further 6 min irradiation with $\lambda = 392 \pm 10$ nm.

tions (out-of-phase CS stretching vibration) and one of the two degenerate bending vibrations of C_2S_2 **3** are IR active. Since the latter is expected in the far IR region, only a single fundamental vibration should be observable above 300 cm^{-1}.

As indicated in Table 1 the observed position of the band at 1179 cm^{-1} ($\tilde{\nu}_3$) is in good agreement with the results of semiempirical PM3[5] and ab initio calculations.[6] Also informative are the weak bands of the ^{34}S and ^{13}C isotopomers at 1175 and 1162 cm^{-1}, respectively. From their relative intensities, which correspond to about double the natural abundances, and the fact that in each case only one isotope band is observable, if follows that two symmetry-equivalent atoms each of sulfur and carbon are present. In addition, the magnitude of the isotopic shift is in excellent agreement with the calculated values (Table 1). Two further weak absorptions which appear at 3083 and 1725 cm^{-1} and are best interpreted as combination bands ($\nu_1 + \nu_3$) and ($\nu_2 + \nu_3$) can also be assigned to C_2S_2 **3**. The position of the non-IR-active stretching vibrations which can be derived therefrom (1904 and 546 cm^{-1}) is also in agreement with the calculations. The experimental IR spectrum thus fits very well for a C_2S_2 **3** with linear or at least centrosymmetric structure.

Table 1. Observed IR spectrum and calculated fundamental vibrations [cm^{-1}] of C_2S_2.

	Experiment	Calculation		
		PM3		ab initio [6]
		$^1\Delta_g$	$^3\Sigma_g^-$	$^3\Sigma_g^-$
$\nu_1\ \Sigma_g$	(1904) [a]	2004	1984	2104
$\nu_2\ \Sigma_g$	(546) [a]	560	560	595
$\nu_3\ \Sigma_u$	1179.3	1160.5	1160.4	1262
^{34}S	1174.5	1155.8	1155.8	
^{13}C	1161.9	1143.1	1143.1	
$\nu_4\ \pi_g$	-	600	608	485
$\nu_5\ \pi_u$	-	219	217	199
$\nu_1 + \nu_3$	3082.8			
$\nu_2 + \nu_3$	1725.4			

[a] Calculated from combination bands.

The characteristic IR and UV bands of **3** can also be recorded after irradiation of the matrix-isolated precursor compounds **2** and **4**. In both cases, however, the yields of **3** are lower. Apparently the competing fragmentation, which leads to C_3OS and COS, gains more significance here. This is also true in general for the thermal cleavage of all three precursor molecules. In the pyrolysis of **1**, C_3OS and CS are the main products, and C_2S_2 **3** is formed in minor amounts only, while in the case of **2** and **4** the thermolysis leads exclusively to C_3OS and COS, and **3** is no longer detectable.

C_2S_2 **3** is a very reactive molecule. Without isolating matrix material it is incapable of existing at 77 K, as has been shown by pyrolysis of **1** and condensation of the products on a spectroscopic window cooled with liquid nitrogen. Under these conditions **3** polymerizes to a brown solid. Also its lifetime in the gas phase is apparently extremely short. After a flight of 30 cm in a 1 cm thick quartz tube at a pressure of about 10^{-4} mbar only ca. 10% of the C_2S_2 molecules formed are still detectable.

The experimental findings reported here give no answer to the important question of the multiplicity of the ground state of **3**.[7] What does theory say?—The C_2S_2 molecule with $D_{\infty h}$ symmetry has in the ground configuration $(\cdots(2\pi_g)^4(3\pi_u)^2(3\pi_g)^0(8\sigma_g)^0)$ 18 π-electrons, for which Hund's rule predicts a triplet ground state. Therefore, in the investigations carried out so far the lowest singlet state was disregarded.[3b, 6] Since we were recently unable to unequivocally rule out a singlet ground state for C_4O_2 (with $D_{\infty h}$ symmetry 14 π-electrons)[2] the ground state problem must also be very carefully investigated in the case of C_2S_2.

For the calculation of the structure of the lowest triplet and singlet states we used the MCSCF (*m*ulti*c*onfiguration *s*elf*c*onsistent *f*ield) method with a 3-21G(d) basis.[8] The configurations were chosen by the CAS(6,4) method, i.e. for the given spin multiplicity, all configurations were constructed (*c*omplete *a*ctive *s*pace) which are possible upon distribution of six electrons over four orbitals ($2\pi_g$, $3\pi_u$). In both states C_2S_2 is linear ($D_{\infty h}$) with bond lengths that hardly differ (Scheme 1). The almost identical structures of the two states are reflected in the frequencies calculated for harmonic vibrations according to the semiempirical PM3 method (Table 1): the singlet and the triplet state exhibit very similar vibrational spectra. The measured IR spectrum fits both equally well.

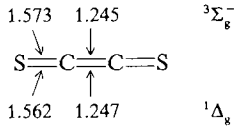

Scheme 1. Ab initio CAS (6,4)/3-21G(d) bond lengths [Å] for **3** in the lowest triplet state and in the lowest singlet state.

The calculation of the singlet–triplet energy difference of a molecule such as C_2S_2 **3** requires a well-balanced consideration of the electron correlation. Single calculations using conventional methods such as SCF-MP2 or extremely short MCSCF approaches are generally questionable. We have therefore repeated the calculation of the S–T difference in the MCSCF approximation with an increasing number of configurations, and using CAS(6,4) structures in all cases. As can be seen in Table 2 the S–T difference steadily decreases; with the CAS(6,6) *ansatz* (the active space consists of the six orbitals $2\pi_g$, $3\pi_u$, $3\pi_g$ of the above quoted electron configu-

Table 2. CASSCF-(3-21G(d)-basis) and RHF-CI(SD) calculations (6-31G(d)) of the singlet-triplet energy difference $\Delta E(S\text{-}T) = E(^1\Delta_g) - E(^3\Sigma_g^-)$ of **3**. For comparison: RMP2 ($^1\Delta_g$ with complex π-orbitals) and UMP2 ($^3\Sigma_g^-$, 6-31G basis set) yields 7.6 kcal mol^{-1}.

	Configurations used T	S	ΔE(S-T) [kcal mol^{-1}]
CAS(2,2)	1	3	11.9
CAS(6,4)	6	10	8.2
CAS(6,6)	189	175	−0.7
RHF	1	1	14.0
RHF-CI(SD)	ca. 20000		−2.1

ration) the singlet state is finally 0.7 kcal mol^{-1} more stable than the triplet state.

We have also carried out calculations for both states by the RHF-CI(SD) (*r*estricted *H*artree-*F*ock-*c*onfiguration *i*nteraction (*s*ingles *d*oubles)) method (6-31G(d)basis), whereby the active space for the configuration interaction consists of 9 occupied and 21 virtual orbitals.[9] The results showed that the singlet state is 2.1 kcal mol^{-1} more stable than the triplet state. The desirable combination CASSCF-CI(SD), a method in which the dynamic correlation (CI) is based on a variationally determined reference wave function (CASSCF), generally cannot be carried out because of the limited computer word length in systems with 44 electrons. Such a theoretical effort, however, was also not necessary for the previously reported examples of the violation of Hund's rule.

To our knowledge C_2S_2 **3** would thus provide the first example for the violation of Hund's rule in an equilibrium structure (geometry in the potential minimum). This would mean that also experimental evidence of a violation of Hund's rule could be found for the first time. Previously known violations of Hund's rule relate to highly symmetric transition structures of equilibrium reactions between structures with lower symmetry (square cyclobutadiene (D_{4h}), twisted ethylene(D_{2d})). In the case of these examples the violation of Hund's rule could be explained in terms of the dynamic spin polarization. A further special electronic property of C_2S_2 **3** concerns the near-degeneracy of the two states $^1\Delta_g(\cdots(2\pi_g)^4(3\pi_u)^2)$ and $^1\Delta_g^*(\cdots(2\pi_g)^2(3\pi_u)^4)$, which lie only 0.3 kcal mol^{-1} apart. This also explains the unusual sensitivity of the S–T difference to the size of the CAS and failure of the Møller-Plesset approximation.

For the MCSCF calculation of vertically excited electronic states the 3-21G(d) basis was extended by diffuse sp sets at all centers. The lowest symmetry-allowed electronic transitions for singlet and triplet terms are reproduced in Table 3.

Table 3. MCSCF calculations of the symmetry allowed vertical electronic transitions of **3**.

Initial state	$^3\Sigma_g^-$	$^3\Sigma_g^-$	$^3\Sigma_g^-$	$^1\Delta_g$	$^1\Delta_g$	$^1\Delta_g$
Final state	$^3\Pi_u$	$^3\Sigma_u^-$	$^3\Sigma_u^-$	$^1\Pi_u$	$^1\Delta_u$	$^1\Delta_u$
λ [nm]	212	275	567	229	295	687

The pattern is similar in both cases and is reconcilable within computational accuracy (44 electrons!) with the experimental spectrum. Accordingly the end absorption beginning at 230 nm can be assigned to a transition to a Π_u state with Rydberg character ($3\pi_u \rightarrow 8\sigma_g$) and the longer wavelength bands between 350 and 392 nm to a $3\pi_u \rightarrow 3\pi_g$ transition ($^3\Sigma_u^- \leftarrow {}^3\Sigma_g^-$ or $^1\Delta_u \leftarrow {}^1\Delta_g$). We have found no experimental evidence for the calculated $2\pi_g \rightarrow 3\pi_u$ transition ($^3\Sigma_u^- \leftarrow {}^3\Sigma_g^-$ or $^1\Delta_u \leftarrow {}^1\Delta_g$) at about 600 nm (the region up to 2600 nm was checked). Apparently this band has a very low intensity.

Summarizing: C_2S_2 **3** is a very reactive molecule, but capable of existence under matrix conditions. Upon photochemical excitation it decomposes into two molecules of CS. Its electronic structure is unusual. According to the calculations the $^1\Delta_g$ state and not the $^3\Sigma_g^-$ state is, contrary to Hund's rule, of lowest energy.

Experimental

1: A mixture of 1,3-dithiol-2-one-4,5-dicarboxylic acid monohydrate (5.20 g, 23 mmol) and thionyl chloride (25 mL) was heated at 50 °C for 1 h. After removal of the solvent by vacuum distillation and subsequent sublimation of the residue 2.50 g (57%) of **1** was obtained; m.p. 89 °C.—^{13}C NMR ($CDCl_3$): δ = 137.5, 155.5, 186.9.—IR(KBr): $\tilde{\nu}$ [cm^{-1}] = 1860, 1774, 1550, 1270, 1053, 880.—MS(70 eV): *m/z* 187.9208 ($M^{\oplus}$), 160, 116, 88, 84, 72, 56.—UV(CH_2Cl_2): λ_{max} [nm] (lg ε) = 342 (3.50), 240 (3.90).—Correct elemental analysis.

2: A suspension of dipotassium 1,2-dithioquadratate monohydrate (530 mg 2.2 mmol) [12] in acetonitrile (15 mL) was treated at 0 °C with a solution of phosgene in toluene (3 mL, 1.93 M) and the mixture stirred for 1 h at room temperature. After removal of the solvent by distillation and subsequent sublimation of the residue 130 mg (34%) of **2** was isolated; m.p. 124 °C (decomp.).—IR(KBr): $\tilde{\nu}$ [cm^{-1}] = 1800, 1765, 1755, 1732, 1713, 1665, 1150, 1125, 889.—UV(CH_3CN): λ_{max} [nm] (lg ε) = 270 (4.11), 218 (3.93).—MS(70 eV): *m/z* 171.9285 ($M^{\oplus}$), 144, 116, 88, 84, 56.—^{13}C NMR (CD_2Cl_2, Cr(acac)$_3$): δ = 182.7, 186.2, 190.9.

4: Analogously as described for **2**: 270 mg (1.0 mmol) of disodium 4,5-disulfido-4-cyclopentene-1,2,3-trione trihydrate [13] gave 85 mg (43%) of **4** as orange crystals; m.p. 140 °C (in a sealed tube).—^{13}C NMR (CD_3CN, Cr(acac)$_3$): δ = 159.6, 174.7, 182.9, 186.0.—IR(Nujol): $\tilde{\nu}$ [cm^{-1}] = 1770 (sh.), 1755 (sh.), 1710, 1260, 1240, 1160, 1095, 870, 725.—UV(CH_3CN): λ_{max} [nm] (lg ε) = 328 (4.04), 238 (3.98).—MS(70 eV): *m/z* 199.9236 ($M^{\oplus}$), 172, 144, 116, 88, 84, 56.

Received: August 6, 199 [Z 4116 IE]
German version: *Angew. Chem. 102* (1990) 1475

CAS Registry numbers:
1, 130201-15-9; **2**, 130201-16-0; **3**, 83917-77-5; **4**, 130201-17-1; 1,3-dithiol-2-one-4,5-dicarbonic acid, 5735-79-5; dipotassium-1,2-dithioquadratate, 52427-61-9; disodium-4,5-disulfido-4-cyclopentene-1,2,3-trione, 58149-12-5; phosgene, 75-44-5.

[1] The names carbon oxide/carbon sulfide should be reserved for such open-chain systems. A simple naming would then be: C_2O = dicarbon oxide, C_2O_2 = dicarbon dioxide etc. A general extension of these names to compounds of the elemental composition C_nO_x makes little sense. Mellitic anhydride ($C_{12}O_9$) also consists of only C and O atoms but chemically it is more appropriate to classify this compound in the group of "normal" anhydrides.

[2] G. Maier, H. P. Reisenauer, H. Balli, W. Brandt, R. Janoschek, *Angew. Chem. 102* (1990) 920; *Angew. Chem. Int. Ed. Engl. 29* (1990) 905.

[3] The existence of such species has also been proven by neutralization–reionization mass spectrometry. a) C_4O_2: D. Sülzle, H. Schwarz, *Angew. Chem. 102* (1990) 923; *Angew. Chem. Int. Ed. Engl. 29* (1990) 908; b) C_2S_2: D. Sülzle, H. Schwarz, *ibid. 100* (1988) 1384 and *27* (1988) 1337; c) C_2OS: D. Sülzle, J. K. Terlouw, H. Schwarz, *J. Am. Chem. Soc. 112* (1990) 628; d) C_4S_2: D. Sülzle, H. Schwarz, *Chem. Ber. 122* (1989) 1803; e) $S(C_x)S$ (x = 2–6): D. Sülzle, N. Beye, E. Fanghänel, H. Schwarz, *ibid. 123* (1990) 2069.

[4] F. M. Nicolaisen, J. J. Christiansen, *J. Mol. Struct. 52* (1979) 157.

[5] J. J. P. Stewart, *J. Comput. Chem. 10* (1989) 221.

[6] G. P. Raine, H. F. Schaefer III, R. C. Haddon, *J. Am. Chem. Soc. 105* (1983) 194.

[7] After irradiation of **1** in the matrix an extremely weak signal is recognizable in the ESR spectrum which could arise from a triplet species. Its assignment to **3** however is doubtful on the basis of previous findings.

[8] H. J. Werner, W. Meyer, *J. Chem. Phys. 74* (1981) 5794; H. J. Werner, E. A. Reinsch, *ibid. 76* (1982) 3144.

[9] M. Peterson, R. Poirier: *Program MONSTERGAUSS*, Toronto 1989.

[10] L. Salem: *Electrons in Chemical Reactions*, Wiley, New York 1982, p. 72, 86.

[11] R. Mayer, B. Gebhardt, *Chem. Ber. 97* (1964) 1298.

[12] D. Eggerding, R. West, *J. Org. Chem. 41* (1976) 3904; D. Coucouvanis, F. J. Hollander, D. Eggerding, R. West, *J. Am. Chem. Soc. 96* (1974) 3006; G. Seitz, K. Mann, R. Schmiedel, R. Matusch, *Chem. Ztg. 99* (1975) 90; *Chem. Ber. 112* (1979) 990.

[13] G. Seitz, K. Mann, R. Matusch, *Arch. Pharm. (Weinheim Ger.) 308* (1975) 792.

[14] Note added in proof (Nov. 28, 1990): The photocleavage is reversible. Upon irradiation (254 nm, Ar, 10 K) of the CS initially produced, C_2S_2 **3** is formed again.

Soluble, Oligomeric Bridged Phthalocyaninatoiron(II) Complexes

By *Michael Hanack*,* *Andreas Hirsch*, and *Helmut Lehmann*

Macrocyclic transition metal complexes can be linked by bidentate ligands to form axially bridged, stacked structures. A number of systems of this kind have been synthesized by us and have been the subject of intensive investigations, particularly with regard to their conductivity.[1] As macrocycles, we used, in particular, phthalocyanine (Pc),[1] tetrabenzoporphyrin (TBP)[2] and 2,3-naphthalocyanine (2,3-Nc);[1] as metal atoms we used Fe, Ru or Co. Besides neutral molecules such as pyrazine (pyz), tetrazine (tz) and 1,4-diisocyanobenzene (dib), anions such as cyanide or thiocyanate are suitable as bridging ligands L. Some compounds of this class also exhibit a relatively high electric conductivity without additional doping.[3] Most of the systems synthesized by us are practically insoluble in organic solvents. We have however, already been able to show, with $[t\mathrm{Bu_4PcMO}]_n$ (M = Si, Ge, Sn) as examples, that when peripherally substituted macrocycles are used the corresponding oligomers are soluble. This was corroborated with other examples.[5] We have also been able for the first time to synthesize soluble oligomers with a central transition metal atom.[6]

We report here on the synthesis and properties of soluble, bridged phthalocyaninatoiron complexes. As metallomacrocycles we used ($t\mathrm{Bu_4Pc}$)Fe **1** (mixture of the constitutional isomers) and ($\mathrm{R_8Pc}$)Fe **2** (R = 2-Et-$\mathrm{C_6H_{12}}$). Compounds **1** and **2** are readily soluble in almost all organic solvents. The metallocycles ($\mathrm{R_8Pc}$)Fe (R = $\mathrm{C_5H_{11}}$, $\mathrm{C_8H_{17}}$) prepared for comparison are more sparingly soluble, i.e. to achieve high solubilities the metallocycle should either be tetrasubstituted or have a branched alkyl chain.

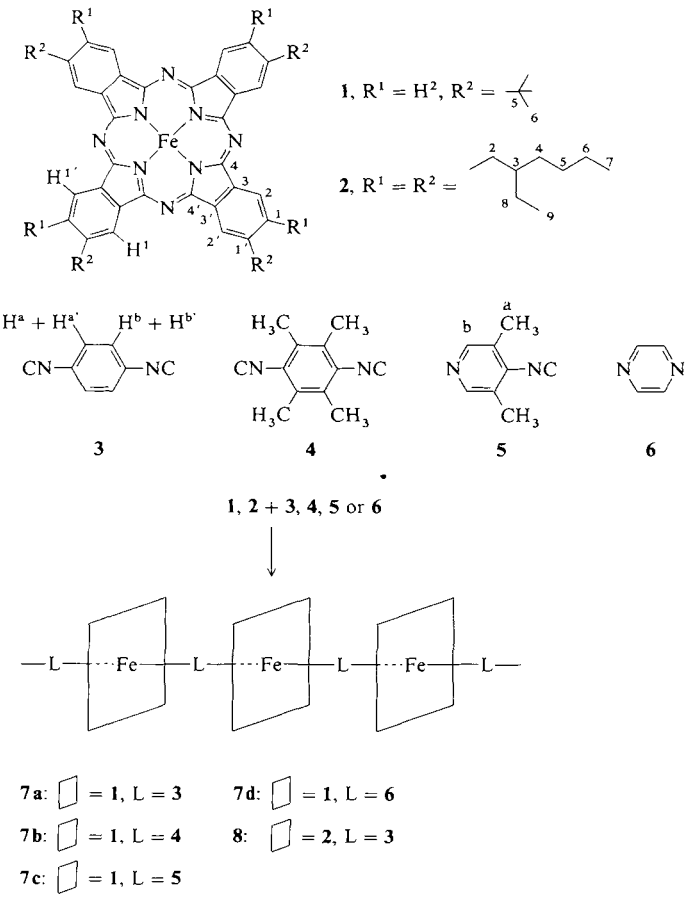

Scheme 1. Arbitrary position numbers.

Compounds **1** and **2** can be be converted into the bridged complexes **7a–d** and **8** by reaction with dib **3**, $\mathrm{Me_4}$dib **4**, $\mathrm{Me_2}$pyNC **5** and pyz **6** in acetone under reflux (Scheme 1). In contrast to the uncoordinated metallomacrocycles, **1** and **2**, and short-chain oligomers, the systems **7a–d** and **8** are sparingly soluble in acetone and can therefore be readily separated from short-chain oligomers. **7a–c** and **8** are soluble in $\mathrm{CHCl_3}$, whereas **7d** is relatively sparingly soluble.

The coordination of the isocyanides to the central iron atom of the phthalocyanine results in a characteristic shift of the NC valence vibration frequency compared to that of the uncoordinated ligand. The NC valence vibration frequency in **7a–c** and **8** is lowered by 20–30 $\mathrm{cm^{-1}}$ by the strong π-acceptor ability of **3–5** (Table 2).

The hexacoordination of the central iron atoms of **7a–d** and **8** is verified by their ^{57}Fe Mössbauer spectra. The measured isomer shifts δ and quadrupole splittings ΔE_Q (Table 1) correspond to the typical values for hexacoordinated $\mathrm{PcFe^{II}}$ complexes[7] and all insoluble systems $[\mathrm{PcFeL}]_n$ previously synthesized by us.[8] As reference compound the hexacoordinated monomer ($t\mathrm{Bu_4Pc}$)Fe(tBuNc)$_2$ **9** was prepared by reaction of **1** with *tert*-butyl isocyanide. Smaller isomer shifts and quadrupole splittings than in the pyz–bridged system **7d** were found for the dib-bridged oligomers **7a** and **8**, and the $\mathrm{Me_4}$dib-bridged oligomer **7b**. This can be explained in terms of a shorter M–L bond length in the isocyanide complex and a resulting higher electron density at the iron atoms along the z-axis.[8, 9] **7d** has hyperfine parameters which are characteristic for $\mathrm{PcFe^{II}}$ complexes coordinated biaxially with N-heterocycles.[7] In **7c**, both the heterocycle N-atom as well as the isocyanide group of the ambidentate bridging ligand **5** is coordinated to the central iron atom. Thus, **7c** has an intermediate ΔE (Table 1). The presence of identical iron centers, i.e. a regular head-to-tail arrangement of the bridging ligands is confirmed by the occurrence of only one doublet in the case of **7c**. Independent confirmation of this is also provided by the ^{1}H NMR spectra. In the formation of **7c** the strong *trans*-effect of the isocyanide ligand favors attachment of the heterocycle N-atom of **5** at the second axial position.

Table 1. ^{57}Fe Mössbauer spectroscopic data of **7a–d**, **8**, and **9**.

Compound		δ [a] [mm $\mathrm{s^{-1}}$]	ΔE_Q [mm $\mathrm{s^{-1}}$]
$[(t\mathrm{Bu_4Pc})\mathrm{Fe(dib)}]_n$	**7a**	0.09	0.72
$[(t\mathrm{Bu_4Pc})\mathrm{Fe(Me_4dib)}]_n$	**7b**	0.13	0.72
$[(t\mathrm{Bu_4Pc})\mathrm{Fe(Me_2pyNC)}]_n$	**7c**	0.12	1.24
$[(t\mathrm{Bu_4Pc})\mathrm{Fe(pyz)}]_n$	**7d**	0.24	1.99
$[\{(2\text{-Et-}\mathrm{C_6H_{12}})_8\mathrm{Pc}\}\mathrm{Fe}(dib)]_n$	**8**	0.11	0.67
$[(t\mathrm{Bu_4Pc})\mathrm{Fe}(t\mathrm{BuNC})]_2$	**9**	0.13	0.73

[a] Referred to α-iron.

Thermogravimetric measurements of **7a–d** and **8** showed that the ratio of macrocycle to L is 1:1 in all oligomers.[10] Since hexacoordinated complexes are present in each case the bridged structure of the oligomers is confirmed. Finally, the ^{1}H NMR spectra prove the bridged structure of the oligomers **7a–d** and **8**. The signals of the macrocycles **7a–d** and **8** are shifted upfield compared to those of the monomer **9** (Table 2). The signals of the inner macrocycle are shifted

[*] Prof. Dr. M. Hanack, Dr. A. Hirsch, Dr. H. Lehmann
Institut für Organische Chemie der Universität
Auf der Morgenstelle 18, W-7400 Tübingen (FRG)

Table 2. Selected spectroscopic data of **7a–d**, **8**, and **9** [a].

7a IR: ν [cm^{-1}] = 2099 (C ≡ N); ^{1}H NMR: δ = 1.49–1.62 (ns: n = number > 1, s = singlet; CH_3), 3.90–4.13 (m; H^a), 5.93 (s, H^a), 7.70–7.95 (m; H-2), 8.70–9.20 (m; H-1,1′); ^{13}C NMR (100 MHz, $CDCl_3$, 25 °C): δ = 31.8 (C-6), 35.4 (C-5), 117.1 (C-2′), 120.3 (C-2), 123.0 (C^b), 124.7 (C^a), 125.3 (C-1), 138.1 (C-3), 140.3 (C-3′), 146.4 (C-4, C-4′), 151.2 (C-1′), 158.9 (C^c).

7b IR: ν [cm^{-1}] = 2096 (C ≡ N); ^{1}H NMR: δ = – 0.97–0.80 (m; H$^{a\prime}$), 1.46–1.62 (ns; CH_3), 7.65–7.90 (m; H-2), 8.70–9.20 (m; H-1,1′).

7c IR: ν [cm^{-1}] = 2083 (C ≡ N); ^{1}H NMR: δ = – 1.89– – 1.63 (m; H$^{a\prime}$), – 0.18 (s; H^a) 0.42–0.87 (m; H$^{b\prime}$), 1.36–1.57 (ns; CH_3), 7.12 (s; H^b), 7.53–7.85 (m; H-2), 8.37–9.00 (m; H-1,1′).

7d ^{1}H NMR: δ = – 3.36–3.23 (ns, 2d; H$^{a\prime}$) 1.30–1.76 (nd; CH_3), 7.61 (d, ^3J (H,H) = 4.48 Hz; H^a), 7.49–7.85 (nd, ^3J (H,H) 7.92 Hz; H-2), 8.30–9.00 (nm; H-1,1′).

8 IR: ν [cm^{-1}] = 2097 (C ≡ N); ^{1}H NMR: δ = 0.73, 0.7 (2t; H-7,9), 1.0–1.5 (m; H-5,6,8), 1.69 (m; H-3), 2.74, 2.81 (d; H-2), 4.0 (m; H$^{a\prime}$), 8.55 (ns; H-1,1′, chain phthalocyanines), 8.8 (ns; H-1,1′, end-group phthalocyanines).

9 IR: ν [cm^{-1}] = 2143 (C ≡ N); ^{1}H NMR: δ = – 0.51 (s, 18H; CH_3), 1.76 (t, 36H; CH_3), 8.02 (d, ^3J (H,H) = 7.92 Hz, 4H; H-2), 9.22 (m, 4H; H-1), 9.34 (2s, 4H; H-1′).

[a] IR: KBr. ^{1}H NMR: 250 MHz, 400 MHz, $CDCl_3$. The bridge ligand protons marked with a prime correspond to the signals of inner units.

even further upfield by $\Delta\delta$ = 0.2–0.7 compared to those of the terminal macrocycles. This phenomenon is explained by the strong mutual influence of the phthalocyanine rings in close proximity through the ring current effect.[11] The magnitude of the upfield shift thus depends on the interplanar distance prescribed by the size of the bridging ligands. This increases along the series pyz < Me_2pyNC < dib, Me_4dib. Thus, the upfield shift of the inner compared to the terminal Pc-H 1,1′-protons is up to $\Delta\delta$ = 0.7 in the case of [(tBu$_4$Pc)Fe(pyz)]$_n$ **7d** and, in constrast, up to $\Delta\delta$ = 0.5 in the case of [(tBu$_4$Pc)Fe(Me_4dib)]$_n$ **7b**. Also the signals of inner bridging ligand protons are shifted upfield compared to those of terminal bridging ligand protons. Since the bridging ligands are situated between the aromatic systems of the macrocycles, the upfield shift in this instance is much more dependent on the interplanar distance. For example, in **7d** in the case of bridging dib ligands it is $\Delta\delta$ = 2 and in the case of bridging pyz ligands it reaches values of up to $\Delta\delta$ = 10. Due to the characteristic differences in the positions of the signals of terminal groups and bridging units, the average chain length in **7a–d** and **8** can be determined by the relevant intergration ratios. In **7d**, the average chain length is 4, longer chain oligomers are sparingly soluble. In the isocyanide-bridged systems **7a–c** the average chain lengths lie between 10 and 16, but can be increased by further boiling in $CHCl_3$. With an average number of at least 110 bridged phthalocyanine units, **8** represents the longest chain system in this series.

The ^{13}C NMR spectra of **7a–c** were recorded. Exemplary data, namely for **7a**, are collected in Table 2. The signals of terminal units are shifted downfield compared to those of the inner units and are seen in the spectra merely as shoulders of weak intensity. Spectra of short chain species show the signal splitting due to bridging much more clearly. The carbon atoms most strongly affected by the upfield shift of inner phthalocyanines are C4/4, C3, and C3′.

Experimental

2: A mixture of 4,5-dicyano-1,2-diisooctylbenzene (950 mg, 27 mmol) and $FeSO_4 \cdot H_2O$ (250 mg) in freshly distilled *N,N*-dimethylaminoethanol (7 mL) was boiled under reflux for 24 h in a nitrogen atmosphere. After completion of the reaction the mixture was treated with 70 mL of ethanol and the suspension heated to boiling.

The mixture was filtered and the residue boiled successively in 0.1N HCl and 0.1N NaOH, refiltered, washed thoroughly with H_2O, and finally taken up again in ethanol. The solvent was then removed under reduced pressure and the residue dried. 4,5-Dicyano-1,2-diisooctylbenzene was obtained from *o*-diisooctylbenzene, which was prepared via a Grignard reaction [12, 13]. *o*-Diisooctylbenzene was brominated in the 4- and 5-positions and the product transformed in a Rosenmund–von-Braun reaction into the desired compound.

7a–d and **8**: A mixture of 1 mmol of the relevant isocyanide **3**, **4**, or **5** or 3 mmol of pyrazine **6** in 50 mL of acetone was stirred under reflux for 2d in an N_2 atomosphere. After filtration, the residue was washed with acetone until the solution was colorless. The residue was then dried for 6 h at 70 °C in vacuo.

Received: August 7, 1990 [Z 4123 IE]
German version: *Angew. Chem. 102* (1990) 1499

CAS Registry numbers:
1, 18452-92-3; **2**, 130698-81-6; **3**, 935-16-0; **4**, 2999-48-6; **5**, 130670-82-5; **6**, 290-37-9; **7a**, 130670-84-7; **7b**, 130670-87-0; **7c**, 130670-88-1; **7d**, 130670-89-2; **8**, 130670-85-8; **9**, 130670-86-9; $FeSO_4$, 7720-78-7; 4,5-dicyano-1,2-diisooctylbenzene, 130670-83-6; *o*-diisooctylbenzene, 15433-62-2.

[1] a) M. Hanack, A. Datz, R. Fay, K. Fischer, U. Keppeler, J. Koch, J. Metz, M. Mezger, O. Schneider, H.-J. Schulze in T. Skotheim (Ed.): *Handbook of Conducting Polymers*, Marcel Dekker, New York 1986, p. 133; b) M. Hanack, S. Deger, A. Lange, *Coord. Chem. Rev. 83* (1988) 115.
[2] M. Hanack, C. Hedtmann-Rein, *Z. Naturforsch. B 40* (1985) 1087.
[3] a) O. Schneider, M. Hanack, *Angew. Chem. 95* (1983) 804; *Angew. Chem. Int. Ed. Engl. 22* (1983) 784; b) U. Keppeler, S. Deger, A. Lange, M. Hanack, *ibid. 99* (1987) 349 and *26* (1987) 344; c) J. Metz, M. Hanack, *J. Am. Chem. Soc. 105* (1983) 828.
[4] J. Metz, G. Pawlowski, M. Hanack, *Z. Naturforsch. B 38* (1983) 378.
[5] E. Orthmann, G. Wegner, *Angew. Chem. 98* (1986) 1114; *Angew. Chem. Int. Ed. Engl. 25* (1986) 1105.
[6] M. Hanack, P. Vermehren, *Synth. Met. 32* (1989) 257.
[7] a) F. Calderazzo, G. Pampaloni, D. Vitali, G. Pelizzi, I. Collamati, S. Frediani, A. M. Serra, *J. Organomet. Chem. 191* (1980) 217; b) B. W. Dale, R. J. P. Williams, P. R. Edwards, *Trans. Faraday. Soc. 64* (1968) 620.
[8] a) U. Keppeler, M. Hanack, *Chem. Ber. 119* (1986) 3363; b) A. Lange, *Dissertation*, Universität Tübingen 1988; c) M. Hanack, A. Lange, M. Rein, R. Behnisch, G. Renz, A. Leverenz, *Synth. Met. 29* (1989) F1.
[9] F. Calderazzo, S. Frediani, B. R. James, G. Pampaloni, K. J. Reimer, J. R. Sams, A. M. Serra, D. Vitali, *Inorg. Chem. 21* (1982) 2302.
[10] A. Hirsch, H. Lehmann, M. Hanack, unpublished.
[11] D. W. DeWulf, J. K. Leland, B. L. Wheeler, A. J. Bard, D. A. Batzel, D. R. Dininny, M. E. Kenney, *Inorg. Chem. 26* (1987) 266.
[12] M. Kumada, K. Tanao, K. Sunitani, *Org. Synth. Collect. Vol. VI* (1978) 407.
[13] a) E. A. Cuellar, T. J. Marks, *Inorg. Chem. 20* (1981) 3766; b) K. Ohta, L. Jacquemin, C. Sirlin, L. Bosio, J. Simon, *New J. Chem. 12* (1988) 751; c) H. Nishi, S. Ueno, *Nippon Kagako Kaishi 6* (1989) 983.

Amino Acid Esters as Chiral Auxiliary Groups in Lewis Acid Catalyzed Reactions of Electron-rich Siloxydienes with Imines**

By *Herbert Waldmann,** *Matthias Braun*, and *Martin Dräger*

Reactions of compounds containing C–N double bonds with dienes, particularly the Lewis acid catalyzed reactions of imines with electron-rich butadiene derivatives such as the Brassard diene **1**[1] and the Danishefsky diene **2**[2], open up a wide variety of possibilities for the synthesis of heterocycles and natural products.[3] Despite the great potential of this synthetic method only isolated efforts have thus far been made to carry out corresponding transformations asymmetrically using chiral auxiliary groups. In the case of **2**, highly diastereoselective tandem Mannich–Michael reactions have been reported to take place with chiral Schiff bases derived from a galactosylamine.[4] However, asymmetric aza-Diels–Alder reactions with imines, which, for instance, occur if **1** is treated with these heterodienophiles in the presence of Lewis acids[3b] have been the subject of very few investigations.[5]

[*] Dr. H. Waldmann, Dipl.-Chem. Matthias Braun
Institut für Organische Chemie der Universität
Becherweg 18–20, W-6500 Mainz
Prof. Dr. M. Dräger
Institut für Anorganische Chemie der Universität Mainz (FRG)

[**] This work was supported by the Deutsche Forschungsgemeinschaft.

We report here on the use of readily available amino acid esters as mediators of the chirality in the reactions of Schiff bases with the electron-rich siloxydienes **1** and **2**. These esters have already proven useful as chiral auxiliary groups in asymmetric Diels–Alder reactions,[5, 6] 1,3-dipolar cycloadditions,[7] and radical additions to carbonyl groups.[8]

The Brassard diene **1** undergoes cycloadditions with the amino acid ester imines **3** of aromatic and aliphatic aldehydes in the presence of Lewis acids ($TiCl_4$, $SnCl_4$, $EtAlCl_2$, $ZnCl_2$, $BF_3 \cdot OEt_2$) to form the α,β-unsaturated lactams **5/6** and the α,β-unsaturated esters **7/8** in good yields and with high diastereomeric excesses (Scheme 1, Table 1). The best results are achieved with 1.4 equivalents of $EtAlCl_2$ at −78 °C and with *tert*-butyl valinate as chiral auxiliary.

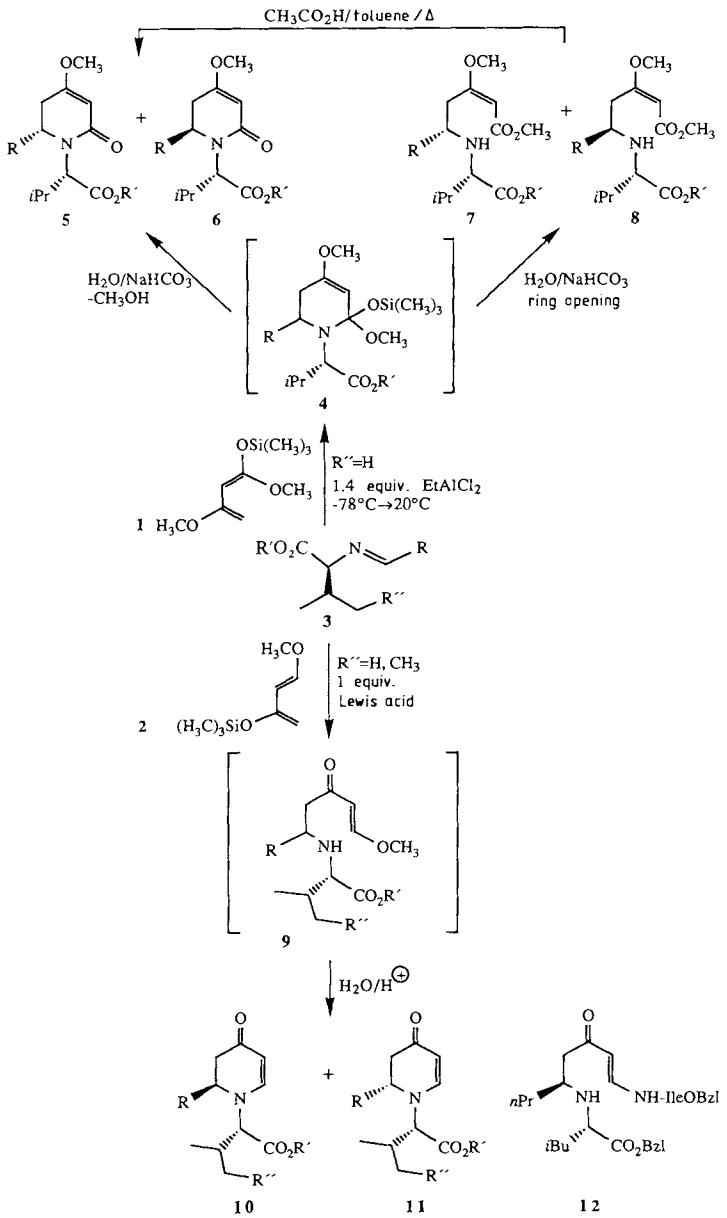

Scheme 1.

The primary adducts **4** with orthoester structure, expected to be formed as intermediates, could not be detected. Depending upon the nature of the imine substituents, hydrolysis with $NaHCO_3$ solution leads via elimination of methanol to the lactams **5/6** or via ring opening to the methyl esters **7/8**. Starting from aromatic aldehydes, only the esters **7/8** are always formed, while the imines of aliphatic aldehydes give mixtures of **5/6** and **7/8**. The methyl esters can, however, be converted into the lactams subsequently by simply warming in toluene in the presence of acetic acid. The absolute configuration of the major diastereomer was unequivocally established by an X-ray crystal structure analysis of the lactam **5d**, which revealed that, in this case, the (6*R*)-isomer is preferentially formed.[9] When the Danishefsky diene **2** is allowed to react with the amino acid ester imines **3** of aromatic and aliphatic aldehydes in the presence of an equimolar amount of different Lewis acids ($TiCl_4$, $BF_3 \cdot OEt_2$, $MeAlCl_2$, $EtAlCl_2$, Me_2AlCl, Et_2AlCl), the enaminones **10** and **11** are formed in good yields and with good diastereomeric excesses (Scheme 1, Table 2). The Schiff bases of aliphatic aldehydes give the best results when aluminum compounds are used as

Table 1. Yields and diastereomeric ratios *ds* in the synthesis of the cycloadducts **5/6** and **7/8**[a].

5/6 or **7/8**	R	Overall yield [b] [%]	**5/6**:**7/8**	*ds* [c] **5**/**7**:**6**/**8**
a	Ph	84	<2:98	97.5:2.5
a [d]	Ph	30	<2:98	94:6
b	3-Cl-Ph	64	<2:98	95:5
c	4-Cl-Ph	67	<2:98	97:3
d	*n*Pr	81	82:18	93:7
e [a]	*n*Pr	35	80:20	92:8
f	*i*Pr	60	46:54	96:4
g	*n*Bu	57	44:56	93:7
h	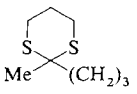	40	<2:98	96:4

[a] In the preparation of **5**–**8a**-**d** and **5**–**8f**-**g**, *tert*-butyl valinate was used as chiral auxiliary group, in the case of **5**–**8e**, benzyl valinate. All reactions were carried out in CH_2Cl_2 with $EtAlCl_2$ as Lewis acid. Imine, diene, and Lewis acid were employed in the ratio 1:1.3:1.4. [b] The α,β-unsaturated amides **5/6** and the α,β-unsaturated esters **7/8** were isolated as yellow oils and identified on the basis of their ^1H and ^{13}C NMR spectra [12]. The elemental analyses are in good agreement with the calculated values. [c] Determined from the crude reaction mixtures by HPLC. [d] $TiCl_4$ was used as Lewis acid.

Table 2. Yields and diastereomeric ratios *ds* in the synthesis of the enaminones **10** and **11**.

10/11	R	Amino acid ester	*T* [°C]	Lewis acid [a]	Yield [b] [%]	*ds* [c] **10**:**11**
a	Ph	Val-OMe	−20	$ZnCl_2$	45	92:8
b	4-MeO-Ph	Val-OMe	0	$ZnCl_2$	54	92:8
c	4-NO_2-Ph	Val-OMe	0	$ZnCl_2$	65	94:6
d	*n*Pr	Ile-OMe	−15	$ZnCl_2$	50	90:10
d	*n*Pr	Ile-OMe	−78 → 20	$EtAlCl_2$	80	94:6
d	*n*Pr	Ile-OMe	−78 → 20	$MeAlCl_2$	74	93:7
e	*n*Pr	Ile-OBzl	−13	$ZnCl_2$	65	90:10
f	*n*Bu	Ile-OMe	−78 → 20	Me_2AlCl	77	90:10
g	*i*Pr	Ile-OMe	−78 → 20	$EtAlCl_2$	47	97:3
h	$MeO_2C(CH_2)_3$	Ile-OBzl	−78 → 20	$EtAlCl_2$	46	93:7
i	$EtO_2C(CH_2)_2$	Val-OBzl	−78 → 20	$EtAlCl_2$	50	93:7
j	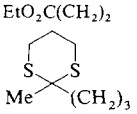	Ile-OMe	−78 → 20	$EtAlCl_2$	74	93:7

[a] All reactions with $ZnCl_2$ were carried out in THF, all reactions with aluminum Lewis acids in CH_2Cl_2. Imine, diene and Lewis acid were employed in the ratio 1:1.3:1. [b] All enaminones **10**/**11** were obtained as yellowish oils and identified on the basis of their ^1H and ^{13}C NMR spectra [14]. The elemental analyses are in good agreement with the calculated values. [c] Determined from the crude reaction mixtures by HPLC.

catalyst and dichloromethane as solvent (see **10d/11d** in Table 2). In the case of imines of aromatic aldehydes the best catalyst system is zinc chloride in tetrahydrofuran.

Particularly striking, and also unexpected, is that the chelating $ZnCl_2$ yields the same diastereomer in excess as the aluminum compounds, which generally are only capable of tetracoordination. An indication that the reactions of the Schiff bases **3** with the Danishefsky diene **2** proceed, in accord with the findings for the carbohydrate imines,[4] as tandem Mannich–Michael reactions is provided by the observation that, in the synthesis of **10e** with $ZnCl_2$, the vinylogous amide **12** can also be isolated (Scheme 1). This amide must be formed by nucleophilic attack of amino acid ester (present in the reaction mixture because of incomplete formation of imine) at the Mannich base intermediate, **9**.

In the asymmetric syntheses presented here the sterically demanding amino acids valine and isoleucine have proven to be especially suitable as chiral auxiliary groups. The size of the ester group has only a subordinate influence on the stereoselection; however, in the reactions with **1** the *tert*-butyl esters give the highest yields.

For the cleavage of the chiral auxiliary groups from the heterocycles we have used the principle of converting the α-C-atom into an acetal center, which liberates the desired heterocycle on treatment with aqueous acid or base.[10] Therefore the *tert*-butyl ester group and the enol ether structure on the α,β-unsaturated amides **5**/**6** were first removed simultaneously by treatment with trifluoroacetic acid (Scheme 2). The carboxylic acid formed in this way, e.g. from **5d**, is then converted with diphenylphosphorylazide[11] into the acid azide, which after heating to 80 °C undergoes a Curtius rearrangement. The isocyanate formed thereby is trapped as urethane **13** by added benzyl alcohol. After hydrogenolytic removal of the benzyl group and hydrolysis of the aminal structure the free amide **14** is formed.[12]

The same procedure has also proven useful in the case of the enaminones **10**/**11**. Thus **10d** and **10i**, after selective ester cleavage and Curtius rearrangement, furnished the aminals **15a**, **b** in ca. 50% yield, from which the vinylogous amides **16a**, **b** were released after hydrogenolysis. Enaminones such as **16a**, **b** are versatile intermediates for the synthesis of alkaloids.[4, 13] Thus, the indolizidine alkaloid (*R*)-δ-coniceine **18** could be synthesized from **16b** by lactam formation and subsequent reduction and deoxygenation of the enaminone system by known methods (Scheme 2).[4] In an analogous way, the *n*-propyl substituted vinylogous amide **16a**, after acylation at the nitrogen with Z-chloride in a similar sequence, affords the piperidine alkaloid (*S*)-coniine **17**. A comparison of the specific rotations measured for **17** and **18** with those given in the literature[14] confirmed the absolute configuration of the enaminones **10**/**11**.

The different steric courses of the reactions of the imines **3** with the dienes **1** and **2** in the presence of $EtAlCl_2$ indicate that these reactions proceed via different mechanisms (Scheme 1). In the tandem Mannich–Michael reactions with **2**, the amino acid esters should, in analogy to the Felkin–Anh model, assume the conformation shown in formula **A**, in which the *Re* side of the C=N bond is more freely accessible. The chelating $ZnCl_2$, which additionally coordinates the ester carbonyl group, is expected to reverse the direction of induction. NMR spectroscopic investigations, however, confirm that, in this case, the imine double bond isomerizes under the reaction conditions (− 20 °C to 0 °C), as previously observed by *Ojima* et al.[15] The resulting *cis*-imine is again preferentially attacked from the *Re* side. The Brassard diene **1** appears to undergo a cycloaddition with the imines **3** in the presence of $EtAlCl_2$, with the diene attacking the *Si* side of the C=N bond (formula **B**). The amino acid ester in B is actually present in an anti-Felkin–Anh conformation. However, in this arrangement the unfavorable steric interactions between the bulky substituents on C1 of the diene and the voluminous amino acid side chain are minimized.

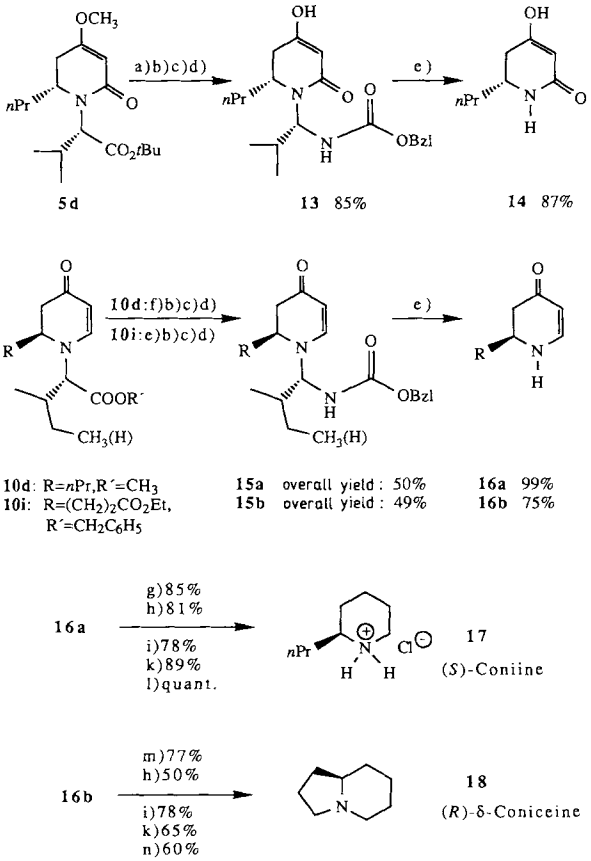

Scheme 2. a) CF_3CO_2H/H_2O (9:1), 81%, b) $(PhO)_2P(O)N_3$, c) toluene 80 °C, d) $PhCH_2OH$, e) H_2/Pd-C, f) NaOH/CH_3OH, g) Z-Cl, BuLi, h) L-selectride, THF, i) $HS(CH_2)_2SH/BF_3{\cdot}OEt_2$, k) Raney-Ni/ethanol/Δ, l) HCl/CH_3OH, m) DBU/benzene/Δ, n) $LiAlH_4$/THF.

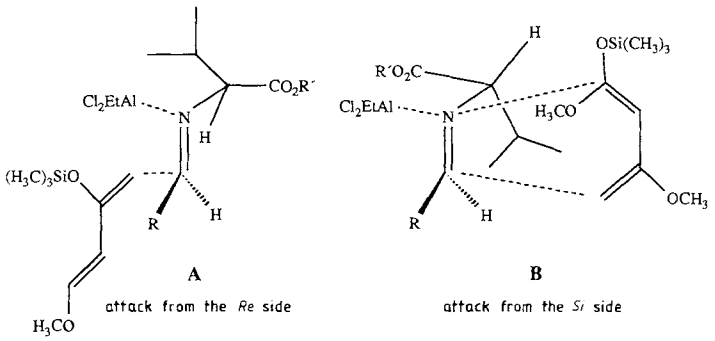

Received: July 30, 1990;
revised: October 8, 1990 [Z 4098/4099 IE]
German version: *Angew. Chem. 102* (1990) 1445

[1] J. Savard, P. Brassard, *Tetrahedron 40* (1984) 3455.
[2] J. Kervin Jr., S. Danishefsky, *Tetrahedron Lett. 23* (1982) 3739.
[3] a) S. Danishefsky, C. Vogel, *J. Org. Chem. 51* (1986) 3915, and references cited therein; b) M. Midland, J. McLoughlin, *Tetrahedron Lett. 29* (1988)

4653; c) Review: D. Boger, S. Weinreb, *Hetero Diels-Alder Methodology in Organic Synthesis*, Academic Press, New York 1987.
[4] H. Kunz, W. Pfrengle, *Angew. Chem. 101* (1989) 1041; *Angew. Chem. Int. Ed. Engl. 28* (1989) 1067.
[5] Purely thermal aza-Diels-Alder reactions were carried out with chiral immonium ions generated in situ in aqueous solution: S. Larson, P. Grieco, *J. Am. Chem. Soc. 107* (1985) 1768; H. Waldmann, *Angew. Chem. 100* (1988) 307; *Angew. Chem. Int. Ed. Engl. 27* (1988) 27; *Liebigs Ann. Chem. 1989*, 231. Lewis acid catalyzed asymmetric aza-Diels-Alder reactions were carried out with carbohydrate imines: W. Pfrengle, H. Kunz, *J. Org. Chem. 54* (1989) 4261.
[6] H. Waldmann, *Liebigs Ann. Chem. 1990*, 671; H. Waldmann, M. Dräger, *ibid. 1990*, 681.
[7] H. Waldmann, *Liebigs Ann. Chem. 1990*, 1013.
[8] H. Waldmann, SYNLETT *1990*, 627.
[9] Crystal structure analysis of **5d**: orthorhombic $P2_12_12_1$, $a = 9.993(2)$, $b = 11.339(1)$, $c = 17.272(7)$ Å, $V = 1957(1)$ Å^3, $Z = 4$, 2850 reflections (1425 Friedel pairs) with $I > 2\sigma(I)$, 212 variables, $R = 0.0706$; *t*Bu group statistically placed in two positions (55:45); establishment of the (*R*)-center by comparison with the (*S*)-valine center. Further details of the crystal structure investigations are available on request from the Fachinformationszentrum Karlsruhe, Gesellschaft für wissenschaftlich-technische Information mbH, W-7514 Eggenstein-Leopoldshafen 2 (FRG), on quoting the depository number CSD-54896, the names of the authors, and the journal citation.
[10] For the cleavage of the chemically very stable bond between the α-C-atom of the amino acid and the N atom, few methods have been examined, and these are not generally applicable: S. Yamada, N. Ikota, K. Achiwa, *Tetrahedron Lett. 1976*, 1001; A. Bose, M. Manhas, J. Vincent, K. Gala, I. Fernandez, *J. Org. Chem. 47* (1982) 4975. For further methods for converting the α-C-atoms of amino acids into acetal centers see: R. Lohmar, W. Steglich, *Angew. Chem. 90* (1978) 493; *Angew. Chem. Int. Ed. Engl. 17* (1978) 493; T. Shono, Y. Matsumura, K. Tsubata, K. Uchida, *J. Org. Chem. 51* (1986) 2590; D. Seebach, R. Charczuk, C. Gerber, P. Renaud, H. Berner, H. Schneider, *Helv. Chim. Acta 72* (1989) 401; K. Ginzel, P. Brungs, E. Steckhahn, *Tetrahedron 45* (1989) 1691; M. London, A. Radhakrishna, M. Almond, J. Blodgett, R. Bontin, *J. Org. Chem 49* (1984) 4272; H. Hoare, A. Olson, D. Koshland, Jr., *J. Am. Chem. Soc. 90* (1968) 1638.
[11] K. Nimoya, T. Shioiri, S. Yamada, *Tetrahedron 30* (1974) 2151.
[12] **5d**: $[\alpha]_D^{22}$ − 53.4 ($c = 1$, CH_2Cl_2); ^{13}C NMR (100 MHz, $CDCl_3$): δ = 165.4(C-4), 94.1 (C-3), 60.7 (C-α, Val), 55.4 (C-6). **14**: $[\alpha]_D^{22}$ − 25.4 ($c = 1$, CH_2Cl_2); ^{13}C NMR: δ = 160.0 (C-4), 94.0 (C-3), 50.4 (C-6).
[13] a) J. D. Brown, M. Foley, D. Comins, *J. Am. Chem. Soc. 110* (1988) 7445; b) D. Comins, D. LaMunyon, *Tetrahedron Lett. 30* (1989) 5053.
[14] **10d**: $[\alpha]_D^{22}$ − 178.4 ($c = 1$, CH_2Cl_2); ^{13}C NMR: δ = 191 (C-4), 149 (C-2), 98.9 (C-3), 69.7 (C-α, Ile). **16a**: $[\alpha]_D^{22}$ 325.5 ($c = 1$, CH_2Cl_2); ^1H NMR (400 MHz, $CDCl_3$): δ = 7.13 (d, J = 7 Hz, 1H; 2-H), 4.82 (d, 1H; 3-H), 3.56 (m, 1H; 6-H). (*S*)-Coniine hydrochloride **17**: m.p. 209 °C; $[\alpha]_D^{22}$ − 5.7 ($c = 0.53$, EtOH) [Lit. (W. H. Tallent, E. C. Horning, *J. Am. Chem. Soc. 78* (1956) 4467): m.p. − 215–17 °C; $[\alpha]_D^{22}$ − 6.9 ($c = 1.1$, EtOH)]. **10i**: $[\alpha]_D^{22}$ 55.8 ($c = 1$, CH_2Cl_2); ^1H NMR: δ = 7.0 (d, J = 6.4 Hz, 1H; 2-H), 4.99 (d, 1H; 3-H), 3.49 (m, 1H; 6-H), 3.39 (d, J = 11 Hz, 1H; α-H, Val). **16b**: $[\alpha]_D^{22}$ 229.1 ($c = 1$, CH_2Cl_2); ^1H NMR: δ = 7.13 (d, J = 7 Hz, 1H; 2-H), 5.59 (broad, 1H; NH), 3.65 (m, 1H; 6-H). (*R*)-δ-Coniceine **18**: $[\alpha]_D^{22}$ −7.9 ($c = 0.15$, EtOH) [Lit. (B. Ringdahl, A. Pinder, W. Pereira, N. Oppenheimer, J. Cymerman Craig, *J. Chem. Soc. Perkin, Trans 1 1984*, 1): $[\alpha]_D^{22}$ − 10.2 ($c = 1.76$, EtOH)].
[15] S. Brandstadter, I. Ojima, *Tetrahedron Lett. 29* (1988) 4653.

Oxidative Degradation of Aromatic Pollutants by Chemical Models of Ligninase Based on Porphyrin Complexes**

By *Gilles Labat, Jean-Louis Seris* and *Bernard Meunier**

Microorganisms in soils and waters convert many man-made organic chemicals into inorganic products.[1] However, some molecules are recalcitrant and are subject to biomagnification and accumulation in the tissues of plants and animals. Among these compounds, organohalide pollutants (e.g. DDT, lindane[2]) resist microbial destruction.[1, 3] The lack of penetration, coupled with the absence of a suitable extracellular enzyme (often a peroxidase rather than a monooxygenase), is the accepted basis for a molecule being recalcitrant. *Phanerochaete chrysosporium* is able to degrade not only lignin, the oxidation-resistant component of woody plants, but also organohalides, via an extracellular peroxidase, ligninase.[4] We recently developed a chemical ligninase model based on the association of a single oxygen atom donor with water-soluble iron and manganese porphyrin complexes.[5] This inorganic peroxide is also soluble in water at pH 7 and is an efficient oxidant for the generation of oxo-metalloporphyrin species.[6]

Here we report the high catalytic activity of the "metalloporphyrin/$KHSO_5$" system in the oxidation of 2,4,6-trichlorophenol[7] **1** (Table 1) and various substituted arenes

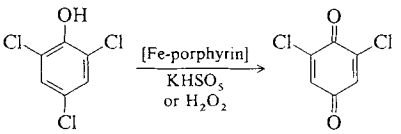

1 **2**

(Table 2). The data in the tables were obtained under the following experimental conditions: To 20 μmol of substrate and 60 nmol of metalloporphyrin[9] in 500 μL of acetonitrile and 1 mL of a buffer solution (0.1 M citrate-phosphate buffer for reactions at pH 3.0 or 0.5 M phosphate buffer at pH 6.0) were added 100 μmol of $KHSO_5$[11] (30.7 mg) in 500 μL of the required buffer (final volume: 2 mL). In some experiments, we replaced potassium monopersulfate by hydrogen peroxide as primary oxidant (12 μL of a 8.6 M solution of H_2O_2 in water). Catalysts adsorbed on Amerlite® were also used, namely FeTPPS-Ad and FeTMPS-Ad.[12] In that case, 2 μmol of metalloporphyrin adsorbed onto 100 mg of resin was added to the reaction mixture. Quinone formation was monitored by high-pressure liquid chromatography (HPLC) on a C_{18} μ-Bondapak analytical column (eluent: methanol/water, 1:1 v/v, flow rate 1 mL/min; UV detection at 280 nm).

Table 1. Oxidation of **1** to **2** catalyzed by iron porphyrins [9].

Run	Catalyst	% Catalyst per Substrate	pH	Oxidant	Yield of **2** [%] within 1 min	15 min
1	FeTPPS	0.3	3.0	$KHSO_5$	95[a]	-
2	FeTPPS	0.3	3.0	H_2O_2	11	68
3	FeTPPS	0.1	3.0	$KHSO_5$	90	92
4	FeTMPS	0.3	3.0	$KHSO_5$	95	-
5	FeTMPS	0.3	6.0	$KHSO_5$	25[b]	10[b]
6	FeTDCPPS	0.3	3.0	$KHSO_5$	92	-
7	FeTPPS-Ad	10	3.0	$KHSO_5$	11	30
8	FeTMPS-Ad	10	3.0	$KHSO_5$	15	36
9	MnTPPS	10	6.0	$KHSO_5$	25[b]	-

[a] 89% of **2** in 15 s: catalytic activity = 20 cycles per second. [b] **2** polymerizes at pH 6.0.

1 was oxidized to 2,6-dichloro-1,4-benzoquinone **2** by iron porphyrin catalysts (0.3% catalyst with respect to **1**) within 1 min at room temperature (Table 1 runs 1, 3 and 4). In run

[*] Dr. B. Meunier, Dr. G. Labat,
Laboratoire de Chimie de Coordination du CNRS
205 route de Narbonne, F-31077 Toulouse cedex (France)
Dr. J.-L. Seris
ELF-GRL
BP 34 Lacq, F-64170 Artix (France)

[**] The financial support of ELF-Aquitaine is gratefully acknowledged. Caroat® and Curox® were provided by Degussa and Interox, respectively.

1 with FeTPPS, 89% of the maximum yield of **2** formed within 15 s, corresponding to a catalytic activity of 20 cycles per second. The same oxidative dechlorination[4a] is performed by ligninase at only 1.5 cycles per second. At pH 6.0, the quinone tends to polymerize. So, the isolated yield of **2** is 25% after a reaction time of 1 min and only 10% after 10 min (run 5). With hydrogen peroxide, a non-pollutant oxidant, the reaction at pH 3 is slower than with $KHSO_5$, but **2** is still isolated with 68% yield after 15 min (run 2). A highly robust water-soluble porphyrin catalyst such as FeTDCPPS is also very efficient (run 6) and only 5% of the catalyst is lost at the end of the reaction. Supported metalloporphyrins can also be used although they are less active: a catalyst concentration of 10% of the substrate concentration is required to obtain 30–36% of **2** in 15 min (runs 7 and 8). Manganese complexes are apparently less active than iron complexes (run 9).

The high redox potential of **1** ($E_{1/2} = 1.7$ V; Ag/AgCl) indicates that the "FeTPPS/$KHSO_5$" peroxidase model is able to oxidize other oxidation-resistant molecules. We therefore investigated a series of methoxylated arenes as substrates (Table 2), some of which are oxidized by ligninase[13].

Table 2. Activity of the system FeTPPS/$KHSO_5$ in the oxidation of methoxyarenes to quinones for a 3:1000 catalyst:substrate ratio (reaction time: 5 min).

Substrate	$E_{1/2}$ [a]	Quinone	Yield [%]
anisole **3**	1.69	1,4-benzoquinone	20[b]
1,2-dimethoxybenzene **4**	1.36	2-methoxy-1,4-benzoquinone	30[b]
1,4-dimethoxybenzene **5**	1.25	1,4-benzoquinone	32[b]
2-methoxyphenol-(guaiacol) **6**	1.23	2-methoxy-1,4-benzoquinone	45
3,4,5-trimethoxyphenol **7**	0.96	2,6-dimethoxy-1,4-benzoquinone	63(43[c])
1,3,5-trimethoxybenzene **8**	1.45	2,6-dimethoxy-1,4-benzoquinone	55
5-chloro-1,3-dimethoxybenzene **9**	0.96	2-chloro-6-methoxy-1,4-benzoquinone	28[b]
1-methoxynaphthalene **10**	1.30	1,2- and 1,4-naphthoquinones[d]	22[b]

[a] $E_{1/2}$ [V] (Ag/AgCl) obtained by linear voltamperometry. [b] Other products are observed. [c] With H_2O_2 as oxidant. [d] The 1,4- to 1,2-quinone ratio is 1.75:1.

Reactions were performed as indicated above with the concentration of FeTPPS 0.3% that of the substrate at pH 3.0 and room temperature. Yields indicated in Table 2 correspond to the yield of isolated quinone after a reaction time of 5 min. All compounds were identified by their ^1H NMR, ^{13}C NMR, and UV-VIS spectra. All methoxylated arenes (**3–5**, **7–10**) are converted into quinones. In the case of horseradish peroxidase[14] or ligninase[13] such *O*-demethylation reactions have been shown to occur via a radical cation followed by the addition of a water molecule. Quinone yields range from 20 to 63% in 5 min (yield maxima are reached within 20–30 min). H_2O_2 can be used as the oxygen donor, as illustrated in the case of 3,4,5-trimethoxyphenol, with only a small decrease in the quinone yield (43% instead of 63%).

It must be noted that methoxylated benzene derivatives with an oxidation potential above 1.4 V are oxidized by FeTPPS/$KHSO_5$ ($E_{1/2}$ values referred to Ag/AgCl are listed in Table 2). We considered five methoxylated arenes, **6**, **5**, **4**, **8** and **3** (listed in order of increasing $E_{1/2}$ values) to scale the oxidation potential of this peroxidase model and to compare its oxidizing power with that of ligninase and horseradish peroxidase (Table 3). Horseradish peroxidase is only able to oxidize **6**, and ligninase **6** and dimethoxybenzenes (both substrates with $E_{1/2}$ values below 1.4 V), whereas "FeTPPS/$KHSO_5$" is able to oxidize all five compounds. This suggests that the redox potential of the high-valent iron–oxo species is above 1.7 V. The $E_{1/2}$ value for the corresponding active iron–oxo entity in cytochrome P-450 was recently estimated at 1.7–2.0 V (vs. calomel electrode, the difference of 45 mV between the two reference systems used is negligible compared to the values discussed here).[15] A value of 1.6 V was found in the case of a high-valent manganese–oxo porphyrin complex.[16]

Table 3. Comparison of the redox activity of the FeTPPS/$KHSO_5$ system and the peroxidases LiP or HRP in the catalytic oxidation of methoxybenzene derivatives [a].

Substrate	$E_{1/2}$ [b]	Oxidation by: FeTPPS/$KHSO_5$ [c]	LiP [d]	HRP
anisole **3**	1.69	+	–	–
1,3,5-trimethoxybenzene **8**	1.45	+	–	–
1,2-dimethoxybenzene **4**	1.36	+	+	–
1,4-dimethoxybenzene **5**	1.25	+	+	–
guaiacol **6**	1.23	+	+	+

[a] LiP = Ligninase, HRP = Horseradish peroxidase; + Oxidation, – no activity. [b] $E_{1/2}$ [V] (Ag/AgCl). [c] 0.3% catalyst, citrate-phosphate buffer at pH 3.0. [c] According to *Kirk* et al. [13].

To conclude, the "Fe-porphyrin/$KHSO_5$" system based on sulfonated porphyrin ligands is able to catalyze the oxidative dechlorination of phenols and the *O*-demethylation of methoxylated arenes which are usually considered as being recalcitrant to many microorganisms, except those producing ligninase. Since ligninase is a rather fragile enzyme (see [17] for the inactivation of ligninase by an excess of hydrogen peroxide), the peroxidase model described here might have a future in the oxidative degradation of organic pollutants.

Received: July 27, 1990 [Z 4097 IE]
German version: *Angew. Chem. 102* (1990) 1488

CAS Registry numbers:
1, 88-06-2; **3**, 100-66-3; **4**, 91-16-7; **5**, 150-78-8; **6**, 90-05-1; **7**, 642-71-7; **8**, 621-23-8; **9**, 7051-16-3; **10**, 2216-69-5; FeTPPS, 83006-36-4; FeTMPS, 130434-28-5; FeTDCPPS, 120751-65-7; MnTPPS, 73215-30-2; $KHSO_5$, 10058-23-8; Ligninase, 42613-30-9; Peroxidase, 9003-99-0.

[1] M. Alexander, *Science (Washington D.C.) 211* (1981) 132.
[2] DDT and lindane are 1,1,1-trichloro-2,2-bis(p-chlorophenyl)ethane and 1α,2α,3β,4α,5α,6β-hexachlorocyclohexane, respectively.
[3] W. Reineke in D. T. Gibson (Ed.): *Microbial Degradation of Aromatic Compounds*, Dekker, New York 1984, pp. 319–360.
[4] a) K. Lundquist, T. K. Kirk, W. J. Connors, *Arch. Microbiol. 112* (1977) 291; b) M. Tien, T. K. Kirk, *Science (Washington D.C.) 221* (1983) 661; c) J. K. Glenn, M. A. Morgan, M. B. Mayfield,, M. Kuwahara, M. H. Gold, *Biochem. Biophys. Res. Commun. 114* (1983) 1077; d) J. A. Bumpus, M. Tien, D. Wright, S. D. Aust, *Science (Washington D.C.) 228* (1985) 1434; e) K. E. Hammel, P. J. Tardoue, *Biochemistry 27* (1988) 6563.
[5] a) G. Labat, B. Meunier, *New J. Chem. 13* (1989) 801; b) *J. Org. Chem. 54* (1989) 5008.
[6] a) A. Robert, B. Meunier, *New. J. Chem. 12* (1988) 885; b) J. Bernadou, G. Pratviel, F. Bennis, M. Girardet, B. Meunier, *Biochemistry 28* (1989) 7268.
[7] **1** is among the major pollutants found in effluents from kraft paper mills [8].
[8] V. B. Huynh, H. M. Chang, T. W. Joyce, T. K. Kirk, *Tappi 68* (1985) 98.
[9] FeTPPS [10a], FeTMPS [10b], FeTDCPPS, [10b], and MnTPPS [10b] were prepared according to literature procedures. TPPS, TMPS and TDCPPS represent *meso*-tetrakis(4-sulfonatophenyl)porphyrinato, *meso*-tetrakis(3,5-disulfonatomesityl)porphyrinato, and *meso*-tetrakis(2,6-dichloro-3-sulfonatophenyl)porphyrinato ligands, respectively.

[10] a) T. S. Srivastava, M. Tsutsui, *J. Org. Chem. 38* (1973) 2103; b) G. Labat, PhD Thesis, Université Paul Sabatier, Toulouse, December 1989.
[11] Potassium monopersulfate, $KHSO_5$, is actually a triple salt, $2KHSO_5 + KHSO_4 + K_2SO_4$, commercially available under different trade names: Oxone®, Curox®, and Caroat® (Du Pont, Interox, and Degussa, respectively).
[12] For the preparation of these supported metalloporphyrin catalysts see [5] and references cited therein.
[13] P. J. Kersten, M. Tien, M. Kalyanaraman, T. K. Kirk, *J. Biol. Chem. 260* (1985) 2609.
[14] a) G. Meunier, B. Meunier, *J. Am. Chem. Soc. 107* (1985) 2558; b) *J. Biol. Chem. 260* (1985) 10576.
[15] T. L. Macdonald, N. G. Gutheim, R. B. Martin, F. P. Guengerich, *Biochemistry 28* (1989) 2071.
[16] O. Bortolini, M. Ricci, B. Meunier, P. Friant, I. Ascone, J. Goulon, *New J. Chem. 10* (1986) 39.
[17] H. Wariishi, M. H. Gold, *FEBS Lett. 243* (1989) 165.

π/σ Equilibria in Metal Complexes of Organic Carbonyl Compounds; Synthesis and Structure of Chiral Rhenium Complexes $[(\eta^5\text{-}C_5H_5)Re(NO)(PPh_3)(O{=}CHAr)]X$ **

By *N. Quirós Méndez, Atta M. Arif,* and *J. A. Gladysz* *

Interactions between metal fragments and organic carbonyl compounds pervade chemistry and biology.[1] Both π (η^2) and σ (η^1) binding modes have been recognized. However, few quantitative data on π/σ equilibria are available.[2] We have previously shown that the chiral rhenium fragment **1** binds aliphatic aldehydes to give the π complexes **2**,[3] and ketones to give the σ complexes **3**.[4, 5] Although we have

$[(\eta^5\text{-}C_5H_5)Re(NO)(PPh_3)]^{\oplus}$ **1**
$[(\eta^5\text{-}C_5H_5)Re(NO)(PPh_3)(\eta^2\text{-}O{=}CHR)]^{\oplus}\ BF_4^{\ominus}$ **2**
$[(\eta^5\text{-}C_5H_5)Re(NO)(PPh_3)(\eta^1\text{-}O{=}CRR')]^{\oplus}\ BF_4^{\ominus}$ **3**

previously suggested a rationale for this dichotomy[4b], we sought a series of compounds that would exhibit *both* binding modes and allow a rigorous study of equilibrium trends. In this communication, we report the synthesis and characterization of complexes of *aromatic* aldehydes, **4**. Depending

$[(\eta^5\text{-}C_5H_5)Re(NO)(PPh_3)(O{=}CHAr)]^{\oplus}\ BF_4^{\ominus}$ **4**

upon the aryl substituents, the temperature, and the solvent, either π or σ binding can dominate.

Reactions of dichloromethane complex **5**[6] with the aromatic aldehydes **6a–o** (2–3 equiv., Scheme 1) gave the substitution products **4a–o** (80–97%).[5] These exhibited different NMR properties. Some resembled π complexes, some resembled σ complexes, and others had peaks between the chemical shifts expected for these extremes. This behavior suggested rapidly equilibrating mixtures of π/σ isomers.

Low-temperature NMR spectra (CD_2Cl_2) did not show the decoalescence of π and σ isomers, although chemical shifts of some resonances changed markedly.[7] However, we noted earlier that the IR absorptions ν_{NO} of π complexes **2** (1740–1729 cm^{-1}) and σ complexes **3** (1697–1680 cm^{-1}) differ. Significantly, **4d–o** exhibited ν_{NO} in *both* regions, as illustrated by the representative spectra in Figure 1.[8] Area measurements gave the π/σ ratios in Scheme 1.[9]

Next, IR spectra of the benzaldehyde, *p*-methylbenzaldehyde, and *p*-methoxybenzaldehyde complexes **4i**, **l**, **o** were

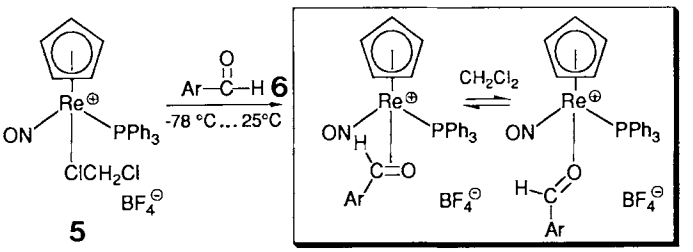

Ar	π-4/σ-4 (299 K)
a, C_6F_5	>96:<4
b, 4-$CF_3C_6H_4$	>96:<4
c, 3-$CF_3C_6H_4$	>96:<4
d, 3-$H_3COC_6H_4$	90:10
e, 2-$H_3COC_6H_4$	89:11
f, 4-ClC_6H_4	83:17
g, 4-FC_6H_4	83:17
h, 1-naphthyl	82:18
i, C_6H_5	84:16
j, 3,4,5-$(H_3CO)_3C_6H_2$	64:36
k, 4-$(C_6H_5)C_6H_4$	64:36
l, 4-$CH_3C_6H_4$	53:47
m, 2,4-$(H_3CO)_2C_6H_3$	25:75
n, 3,4-$(H_3CO)_2C_6H_3$	24:76
o, 4-$H_3COC_6H_4$	15:85

Scheme 1. Synthesis of aromatic aldehyde complexes **4**.

recorded in CH_2Cl_2 at temperatures ranging from 303 to 233 K. The π/σ ratios increased markedly at lower temperatures. Van't Hoff plots gave ΔH values of 3.6, 2.8, and 1.8 (±0.2) kcal mol^{-1}, and ΔS values of 9.2, 9.5, and 9.1 (±0.7) eu, respectively. Thus, π coordination is favored enthalpically, and σ coordination entropically.

The solvent dependence of these equilibria was investigated. First, IR spectra of **4i** were recorded in CH_2Cl_2/hexane (50:50 v/v). The π/σ ratio *decreased* to 1:1. Under identical conditions, aliphatic aldehyde complexes **2** exhibited small ν_{NO} shoulders suggestive of σ isomers. Next, IR spectra of **4o** in nitromethane showed an *increased* π/σ ratio of 36:64. Other complexes showed similar IR behavior in these sol-

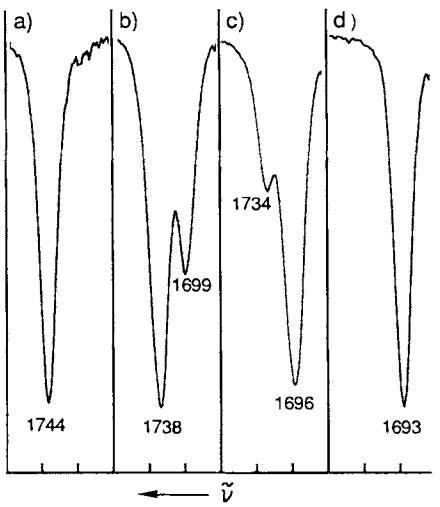

Fig. 1. IR spectra (1800 – 1650 cm^{-1}, CH_2Cl_2, 299 K; ν_{NO}) (a) of **2** with R = H, b) of **4l**, (c) of **4o**, and (d) of **3** with R = R' = Me.

[*] Prof. J. A. Gladysz, Mr. N. Quirós Méndez, Dr. A. M. Arif
Department of Chemistry
University of Utah
Salt Lake City, UT 84112 (USA)

[**] This research was supported by the Department of Energy.

vents. Thus, less polar solvents favor σ bonding, whereas more polar solvents favor π bonding. We attribute this to a greater resonance delocalization of the positive charge in the σ isomers.

The UV/VIS spectrum of **4a** (and the aliphatic ketone complexes **3**) in CH_2Cl_2 showed no visible absorptions. However visible absorptions were observed for **4b**, **i**, **l**, **o** (400–580 nm) and intensified as the proportion of σ isomers increased. Conjugated metal–ligand assemblies frequently give metal-to-ligand charge transfer absorptions.[10] **4o** exhibited a unique and intense UV band at 313 nm.

Finally, structures of **4b** and **4o** were determined (Fig. 2).[5b] Complex **4o** crystallizes as a σ isomer, with (1) conjugated aryl and C=O moieties (the angle between the plane of the ring and the C24–O bond is 6°), and (2) an eclipsed Re–O conformation that directs the aldehyde proton toward the nitrosyl ligand (N1,Re,O2 and C24 are coplanar). This orientation maximizes overlap of the HOMO, a d orbital, of **1** (Scheme 1) and the C=O π* acceptor lobes on oxygen (Fig. 2b). Accordingly, **4o** exhibits a low IR $\nu_{C=O}$ value[8b] and a considerably longer C=O bond length (1.271(8) Å) than those in other σ aldehyde and ketone complexes.[4] Complex **4b** crystallizes as a π isomer, with a Re–(C=O) conformation that allows a high degree of overlap of the HOMO of **1** and the C=O π* orbital. The geometric features of **4b** are similar to those previously found in the analogous phenylacetaldehyde complex,[3] but with somewhat more "slippage" of the carbonyl carbon away from the rhenium (Fig. 2d). Presumably, this distortion is yet more pronounced in π isomers of **4** without electron withdrawing substituents on the aryl ring.

In summary, these data clearly establish the importance of electronic effects in π/σ equilibria of aldehyde and ketone complexes. To a first approximation, electron-withdrawing arene substituents in **4** favor π binding, and electron-donating arene substituents favor σ binding. The acceptor substituents enhance π acidity and lower σ basicity, while the donor substituents have opposite effects.[11] Similar trends have been documented for selenobenzaldehyde complexes.[2b] However, other factors that may affect the equilibrium deserve emphasis. For example, complex **4e**, which has donor substituent in the *ortho* position of the arene ring, shows a much a higher π/σ ratio than the *para* substituted analog **4o**. In σ isomers, interactions are also possible between the arene ring and the phenyl rings of PPh_3.[4] Finally, stabilizing arene/C=O–Re conjugation as in **4o** (Fig. 2a) cannot occur with aliphatic aldehyde ligands. This accounts, at least in part, for the much higher π/σ ratios found for **2**. Future studies will probe other equilibria of π isomers of **4**,[7] and the effect of the binding mode on chemical reactivity.

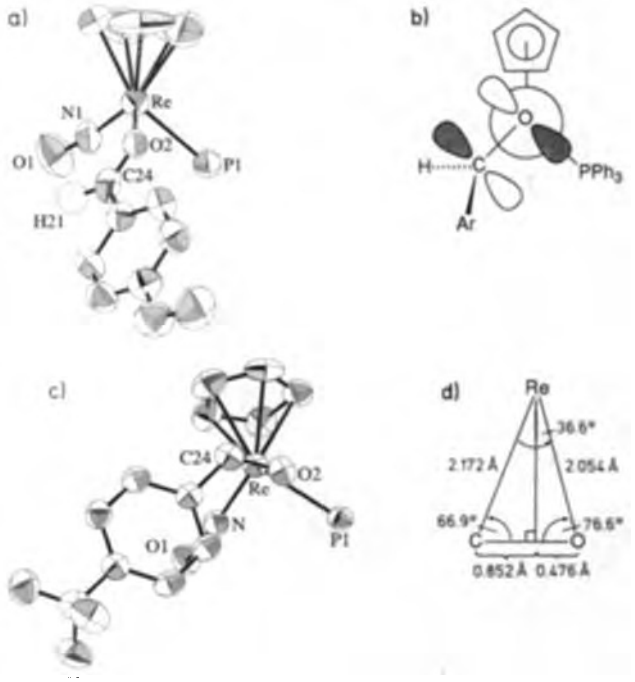

Fig. 2. Partial structures of **4o** (a, b) and **4b** (c, d) as $PF_6^\ominus$ salts, with phenyl rings omitted. Selected bond distances [Å] and angles [°]: **4o**, Re-N1, 1.731(6); N1-O1, 1.208(7); Re-P1, 2.397(2); Re-O2, 2.080(5); O2-C24, 1.271(8); N1-Re-P1, 92.0(2); N1-Re-O2, 102.9(2); P1-Re-O2, 83.3(1); Re-O2-C24, 129.5(4); Re-N1-O1, 170.3(6). **4b**, Re-N, 1.756(4); N-O1, 1.181(5); Re-P1, 2.446(1); Re-O2, 2.054(3); Re-C24, 2.172(4); C24-O2, 1.331(6); N-Re-P1, 89.8(1); C24-Re-O2, 36.6(2); Re-C24-O2, 66.9(2); Re-O2-C24, 76.6(2); Re-N-O1, 173.1(4).

Received: August 20, 1990 [Z 4142 IE]
German version: *Angew. Chem. 102* (1990) 1507

CAS Registry numbers:
4a π, 130575-77-8; **4b** π(PF_6), 130575-79-0; **4c** π, 130575-81-4; **4d** π, 130575-83-6; **4d** σ, 130575-85-8; **4e** π, 130575-87-0; **4e** σ, 130575-89-2; **4f** π, 130575-91-6; **4f** σ, 130575-93-8; **4g** π, 130575-95-0; **4g** σ, 130575-97-2; **4h** π, 130575-99-4; **4h** σ, 130576-01-1; **4i** π, 126186-43-4; **4i** σ, 130576-03-3; **4j** π, 130576-05-5; **4j** σ, 130576-07-7; **4k** π, 130576-09-9; **4k** σ, 130576-11-3; **4l** π, 130576-13-5; **4l** σ, 130576-15-7; **4m** π, 130576-17-9; **4m** σ, 130576-19-1; **4n** π, 130576-21-5; **4n** σ, 130576-23-7; **4o** π, 130576-25-9; **4o** σ(PF_6), 130576-27-1; **5**, 111470-01-0; **6a**, 653-37-2; **6b**, 455-19-6; **6c**, 454-89-7; **6d**, 591-31-1; **6e**, 135-02-4; **6f**, 104-88-1; **6g**, 459-57-4; **6h**, 90-15-3; **6i**, 100-52-7; **6j**, 86-81-7; **6k**, 3218-36-8; **6l**, 104-87-0; **6m**, 613-45-6; **6n**, 120-14-9; **6o**, 123-11-5.

[1] a) A. K. H. MacGibbon, S. C. Koerber, K. Pease, M. F. Dunn, *Biochemistry 26* (1987) 3058; b) P. Läuger, *Angew. Chem. 97* (1985) 939; *Angew. Chem. Int. Ed. Engl. 24* (1985) 905; c) D. A. Buckingham in A. W. Addison, W. R. Cullen, D. Dolphin, B. R. James (Eds.): *Biological Aspects of Inorganic Chemistry*, Wiley, New York 1977, Chapter 5.

[2] a) W. D. Harman, M. Sekine, H. Taube, *J. Am. Chem. Soc. 110* (1988) 2439; b) Studies of $(CO)_5M(Se=CHAr)$ complexes: H. Fischer, S. Zeuner, U. Gerbing, J. Riede, C. G. Kreiter, *J. Organomet. Chem. 377* (1989) 105.

[3] C. M. Garner, N. Quirós Méndez, J. M. Kowalczyk, J. M. Fernández, K. Emerson, R. D. Larsen, J. A. Gladysz, *J. Am. Chem. Soc. 112* (1990) 5146.

[4] a) J. M. Fernández, K. Emerson, R. D. Larsen, J. A. Gladysz, *J. Chem. Soc. Chem. Commun. 1988*, 37; b) D. M. Dalton, J. M. Fernández, K. Emerson, R. D. Larsen, A. M. Arif, J. A. Gladysz, *J. Am. Chem. Soc. 112* (1990), 9198.

[5] a) Distinguishing NMR features of π and σ complexes: δ(O=*C*) = 60–90 (**2**); 214–236 (**3**); δ(O=*CH*) = 5.2–5.4 (**2**); 8.4 (**4o** at 25 °C); (*P*Ph_3) 9–11 (**2**); 18–20 (**3**). Full characterization of **4a–o** has been given to the reviewers. b) Crystallographic data: **4b:** $a = 14.908(2)$, $b = 10.656(1)$, $c = 10.220(1)$ Å, $\alpha = 95.38(2)°$, $\beta = 74.74(2)°$, $\gamma = 93.64(2)°$, $Z = 2$, $\varrho_{obs} = 1.84$ g · cm^{-3}, space group $P\bar{1}$, 4508 observed reflections with $F > 3\sigma(F)$, $R = 0.0288$, $R_w = 0.0320$.—**4o**: $a = 11.780(2)$, $b = 14.691(3)$, $c = 11.035$ Å, $\alpha = 101.84(1)°$, $\beta = 111.36(1)°$, $\gamma = 82.32(1)°$, $Z = 2$, $\varrho_{obs} = 1.66$ g · cm^{-3}, space group $P\bar{1}$, 3958 observed reflections with $F > 3\sigma(F)$, $R = 0.0491$, $R_w = 0.0599$. Further details of the crystal structure investigations may be obtained from the Fachinformationszentrum Karlsruhe, Gesellschaft für wissenschaftlich-technische Information mbH, D-7514 Eggenstein-Leopoldshafen 2 (FRG), on quoting the depository number CSD-54893, the names of the authors, and the journal citation.

[6] J. M. Fernández, J. A. Gladysz, *Organometallics 8* (1989) 207.

[7] N. Quirós Méndez, C. L. Mayne, J. A. Gladysz, *Angew. Chem. 102* (1990) 1509; *Angew. Chem. Int. Ed. Engl. 29* (1990), 1475.

[8] a) The lower ν_{NO} values of the σ isomers of 4 indicate a more basic metal center. This shows σ aldehyde ligands to be poorer π acids than the corresponding π aldehyde ligands. b) Other IR data of interest ([cm^{-1}]): **4o**, ν_{CO} 1555 m; **6o** ν_{CO} 1686 m; **4i**, absorptions associated with Re-C-O, 1258/1007/820 w (assigned by use of **4i**-^{13}C isotope shifts and corresponding $PF_6^\ominus$ salts). These weaker bands are not suitable for π/σ equilibria measurements.

[9] a) An IR spectrum was recorded of a solution (CH_2Cl_2) that was 0.01 M in *both* the π formaldehyde complex **2** with R = H and σ acetone complex **3** with R = R′ = Me. The areas of the ν_{NO} absorptions (cut/weigh) agreed within 0.3%. For ν_{NO} absorptions that were not baseline-resolved, areas of the non-overlapping half of each band were measured. b) We assign error limits of ± 2 to each integer of the π/σ ratios in Scheme 1, and assume detection limits of < 4% when no σ isomer is observed (**4a–c**, **2**).

[10] G. L. Geoffroy, M. S. Wrighton: *Organometallic Photochemistry*, Academic Press, New York 1979, pp. 10–23.

[11] An interesting consequence is that the values of ν_{NO} decrease nearly monotonically in the series **4a–o** for *both* binding modes (π, $\tilde{\nu} = 1745–1733$; σ, $\tilde{\nu} = 1701–1692$ cm^{-1}).

Thermodynamic Aldehyde Enantioface Binding Selectivities in Complexes of Chiral Metal Fragments; Mechanism of Interconversion of Diastereomeric π-Aldehyde Complexes $[(\eta^5\text{-}C_5H_5)Re(NO)(PPh_3)(\eta^2\text{-}O{=}CHAr)]BF_4$ **

By *N. Quirós Méndez, Charles L. Mayne,* and *J. A. Gladysz* *

One of the most fundamental issues in asymmetric syntheses and separations is the "chiral recognition" event.[1] For example, a chiral receptor might selectively bind one enantioface of a prochiral organic molecule such as an aldehyde or monosubstituted alkene, giving predominantly one of two possible π diastereomers. In order for mechanisms of enantioselection to be fully delineated, data on kinetic and thermodynamic substrate binding selectivities, and diastereomer interconversion rates, are required.[2] In this communication, we report the first thermodynamic data on aldehyde enantioface binding selectivities in complexes of chiral metal fragments, as well as 2D-NMR experiments which show that the resulting π diastereomers interconvert by a novel intramolecular mechanism. Electronic effects evident in these data are probably broadly applicable to asymmetric transformations that proceed via metal π complexes.

Solution IR spectra show that the *p*-methoxybenzaldehyde complex **1f** is a temperature-dependent mixture of π and σ isomers.[3,4] Thus, variable temperature NMR spectra of **1f** were recorded. No signals decoalesced in CD_2Cl_2

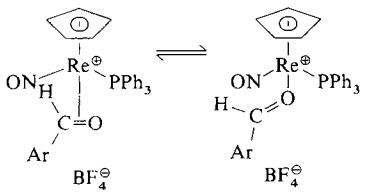

1

a, Ar = C_6F_5; **b**, Ar = 4-$CF_3C_6H_4$; **c**, Ar = 4-ClC_6H_4; **d**, Ar = C_6H_5; **e**, Ar = 4-$CH_3C_6H_4$; **f**, Ar = 4-$H_3COC_6H_4$

($^1H/^{13}C/^{31}P$), although some resonances broadened near the freezing point of the solution. However, ^{31}P NMR spectra in a lower-freezing solvent, $CDCl_2F$, showed decoalescence into *three* PPh_3 resonances (Figure 1; 136 K: δ = 22.8, 12.9, 9.4; areas 28:58:14). From data reported earlier,[3,5] the downfield resonance was assigned to σ isomer **III** (Scheme 1).[4a] The two upfield resonances were characteristic of π isomers, and were assigned to diastereomers of idealized structures **I** and **II** (81:19).[6] These differ in the enantioface of the aldehyde bound to the chiral rhenium fragment $[(\eta^5\text{-}C_5H_5)Re(NO)(PPh_3)]^{\oplus}$ **2**.

Low-temperature ^{31}P NMR spectra (CD_2Cl_2) were acquired for analogous pentafluorobenzaldehyde, 4-trifluoromethylbenzaldehyde, 4-chlorobenzaldehyde, benzaldehyde, and 4-methylbenzaldehyde complexes **1a–e**.[3] These exhibit much higher π/σ isomer ratios than **1f**.[4b] No peaks attributable to σ-isomers were observed. Resonances for π isomers **I** and **II**, however, decoalesced in each case, as summarized in Table 1.

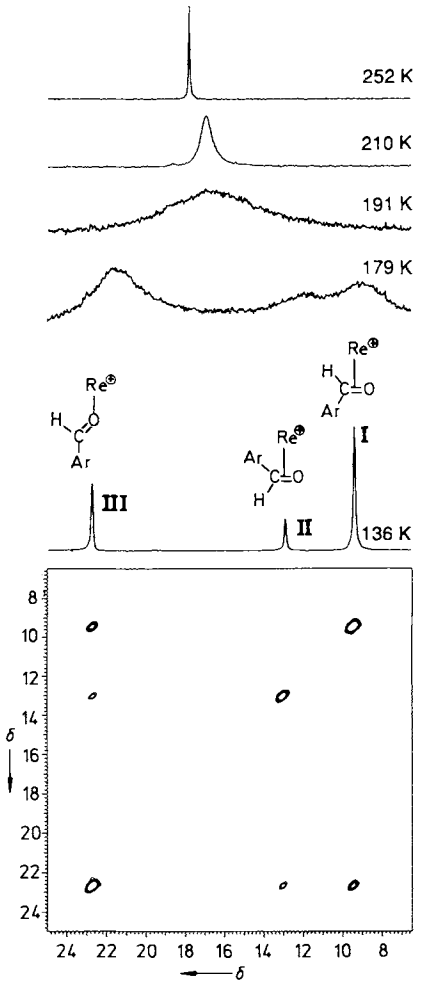

Fig. 1. ^{31}P NMR spectra of **1f** in $CDCl_2F$. Top: 1D spectra at several temperatures. Bottom: Chemical exchange map (mixing time 50 ms, 143 K).

Application of standard formulas[9] gave values for $\Delta G^{\neq}$ (T_c, **I** → **II**) of 9.8 to greater than 15.2 kcal mol^{-1}. Peak areas gave ΔG values (183 K, **I** → **II**; from **I**/**II** ratios) of 0.6 to 1.2 kcal mol^{-1}. The cyclopentadienyl ^1H and ^{13}C NMR resonances of isomers **I** and **II** also decoalesced, and gave nearly identical $\Delta G^{\neq}$ and ΔG (Table 1). The isomer ratios for **1a**, **b** were constant over the temperature range 273–183 K, as assayed by ^{31}P and ^1H NMR.

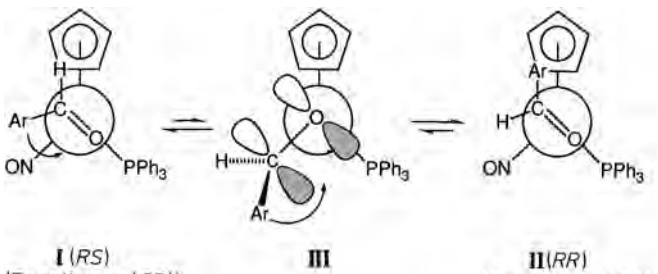

Scheme 1. Mechanism of interconversion of π diastereomers (**I**, **II**) of complexes of type **1**.

The data in Table 1 show several significant trends. First, enantioface binding selectivities increase as the π acidities of

[*] Prof. J. A. Gladysz, Mr. N. Quirós Méndez, Dr. C. L. Mayne
Department of Chemistry
University of Utah
Salt Lake City, UT 84112 (USA)

[**] This research was supported by the National Institutes of Health. Ar = aryl substituents.

Table 1. NMR data (183 K, CD_2Cl_2) for diastereomeric π-aldehyde complexes **1a–f**

1	^{31}P NMR			^{1}H NMR [a]			^{13}C NMR [a]			$\Delta G^{\neq}$
	δ [b]	I:II [c]	T_c [K]	δ [b]	I:II [c]	T_c [K]	δ [b]	I:II [c]	T_c [K]	[kcal mol^{-1}] [d]
a	9.31/11.00	96.4	>300	6.21/5.82	98:2	>300	99.4/101.1	98:2	>300	>15.2/16.0/15.9
b	9.07/11.71	89:11	277.7	6.18/5.61	91:9	274.4	98.7/101.1	95:5	274.0	13.2/13.5/13.8
c	8.93/11.62	88:12	246.2	6.14/5.61	87:13	241.2	99.5/101.9	88:12	240.7	11.6/11.7/11.6
d	9.11/11.70	84:16	233.6	6.10/5.55	86:14	231.4	99.5/102.0	88:12	231.9	10.9/11.1/11.2
e	9.26/11.74	83:17	211.8	6.08/5.54	82:18	213.6	98.4/100.9	82:18	212.6	9.8/10.1/10.1
f [e]	9.43/12.93	81:19	<185			<185			<185	<8.3/– /–

[a] Cyclopentadienyl resonance [b] The first value refers to isomer **I**, the second to isomer **II** [c] The diastereomer ratios were determined by integration; error limits—88:12 ≙ (88 ± 2):(12 ± 2). [d] For conversion of **I** to **II**, determined from ^{31}P, ^{1}H, and ^{13}C NMR data. [e] No decoalescence observed in ^{1}H and ^{13}C NMR spectra; the **I**:**II** ratio and limiting chemical shifts are taken from data in $CDCl_2F$ (see text).

the aldehydes increase (**1a** > **1b** > **1c** > **1d** > **1e** > **1f**).[3] Crystal structures show that aldehydes that are poorer π acceptors exhibit progressively greater "slippage" of the carbonyl carbon from the rhenium fragment **2**.[3, 7] This moves the carbon and rhenium stereocenters further apart, attenuating chiral recognition. Second, $\Delta G^{\neq}$ for the interconversion of π isomers (e.g., **I** → **II**) *increases* from **1f** to **1a** as ΔG for isomerization to σ isomers (**I** → **III**) *increases*.[3, 4b] We have previously shown that benzaldehyde does not readily dissociate from **1d** at room temperature.[7] These observations suggest that π isomers interconvert via σ isomers, as shown in Scheme 1.

This mechanistic possibility was probed via 2D ^{31}P NMR experiments. Complex **1f** gave the ^{31}P chemical exchange correlation map[10] shown in Figure 1. The diagonal peaks correspond to isomers **III**, **II** and **I**. Significantly, off-diagonal peaks are found *on σ/π intercepts, but not π/π intercepts*. Since the mixing time is quite short (50 ms), this indicates that π isomers **I** and **II** interconvert exclusively (within detection limits) via σ isomer **III**, as shown in Scheme 1. Analogous spectra with other mixing times corroborate these results, and analyses that will yield rates and activation parameters are in progress.

Some extensions of these experiments have been briefly investigated. First, low temperature ^{31}P and ^{1}H NMR spectra of complexes of **2** and aliphatic aldehydes O=CHR (R = CH_3, $CH(CH_3)_2$)[7] have been acquired and carefully analyzed in view of the new chemical shift data in Table 1. These show the reproducible decoalescence of small resonances that can be assigned to π isomers of the type **II** (**I**/**II** ca. 99/1). Thus, aliphatic aldehydes exhibit considerably greater thermodynamic enantioface binding selectivities than aromatic aldehydes. Accordingly, the corresponding crystal structures show less aldehyde ligand slippage.[7] Similarly, preliminary data suggest that aliphatic alkenes exhibit higher thermodynamic enantioface binding selectivities to **2** than styrene.[8, 11] The diastereomeric alkene complexes of **2** also interconvert by an intramolecular pathway (90–100 °C), and we have proposed a mechanism that is conceptually related to the mechanism in Scheme 1.[11]

In summary, this study has established (1) that a striking electronic effect, which is probably general for many π complexes of chiral metal fragments, influences the thermodynamic aldehyde enantioface binding selectivities, and (2) that the facile intramolecular equilibration of diastereomeric π aldehyde complexes proceeds via σ complexes. Both π aldehyde and σ ketone complexes of **2** undergo highly diastereoselective nucleophile additions.[5, 7] Future studies will investigate the relative reactivities of the π and σ isomers toward nucleophiles.

Received: August 20, 1990 [Z 4143 IE]
German version: *Angew. Chem. 102* (1990) 1509

CAS Registry numbers:
Ia, 130575-77-8; **Ib**, 130694-39-2; **Ic**, 130575-91-6; **Id**, 126186-43-4; **Ie**, 130576-13-5; **If**, 130576-25-9; **IIIa**, 130576-29-3; **IIIb**, 130576-31-7; **IIIc**, 130575-93-8; **IIId**, 130576-03-3; **IIIe**, 130576-15-7; **IIIf**, 130576-32-8.

[1] See, inter alia: a) W. H. Pirkle, T. C. Pochapsky, *Chem. Rev. 89* (1989) 347; b) S. Topiol, M. Sabio, *J. Am. Chem. Soc. 111* (1989) 4109; c) J. F. Garst, *J. Chem. Soc. Chem. Commun. 1990*, 211.
[2] For example, a highly stereoselective transformation need not proceed by the dominant substrate binding mode: B. McCulloch, J. Halpern, M. R. Thompson, C. R. Landis, *Organometallics 9* (1990) 1392, and references therein.
[3] N. Quirós Méndez, A. M. Arif, J. A. Gladysz, *Angew. Chem. 102* (1990) 1507, *Angew. Chem. Int. Ed. Engl. 29* (1990) 1473
[4] a) The crystal structures of the σ isomer of **1f** (**III**) and the major π isomer of **1b** (**I**) have been determined [3]; b) Equilibrium ratios (299 K, CH_2Cl_2, (**I** + **II**)/**III**) [3]: **1a** and **1b**, > 96: <4; **1c**, 83:17; **1d**, 84:16; **1e**, 53:47; **1f**, 15:85. For **I**–**III** see Scheme 1.
[5] D. M. Dalton, J. M. Fernández, K. Emerson, R. D. Larsen, A. M. Arif, J. A. Gladysz, *J. Am. Chem. Soc. 112* (1990) 9198.
[6] Factors in the assignment of **I** as the major π isomer include: a) crystal structures of π^2-O=CHR complexes of **2** show only isomer **I** [3,7]; b) intuitively, Ar/NO ligand steric interactions in **I** should be less than Ar/C_5H_5 ligand steric interactions in **II**; c) an analogous stability order and NMR chemical shift trends similar to those in Table 1 are found for diastereomers of complexes of **2** with monosubstituted alkenes H_2C=CHR [8].
[7] C. M. Garner, N. Quirós Méndez, J. M. Kowalczyk, J. M. Fernández, K. Emerson, R. D. Larsen, J. A. Gladysz, *J. Am. Chem. Soc. 112* (1990) 5146. Disorder prevents a rigorous analysis of the slippage of the propionaldehyde ligand in this paper.
[8] G. S. Bodner, T.-S. Peng, A. M. Arif, J. A. Gladysz, *Organometallics 9* (1990) 1191.
[9] J. Sandström, *Dynamic NMR Spectroscopy*, Academic Press, New York 1982, Chapter 7.
[10] a) R. R. Ernst, G. Bodenhausen, A. Wokaun: *Principles of Nuclear Magnetic Resonance in One and Two Dimensions*, Oxford University Press, New York 1987, Chapter 9; b) Y. Huang, S. Macura, R. R. Ernst, *J. Am. Chem. Soc. 103* (1981) 5327; c) R. Benn, *Angew. Chem. 94* (1982) 633; *Angew. Chem. Int. Ed. Engl. 21* (1982) 626.
[11] T.-S. Peng, J. A. Gladysz, *J. Chem. Soc. Chem. Commun. 1990*, 902.

Enantio- and Regiocontrolled Synthesis of a Central Ionophoric Antibiotic Building Block by Sequential Opening of Two Epoxide Rings with Cuprate Reagents**

By *Johann Mulzer** and *Bernd Schöllhorn*

Dedicated to Professor Helmut Vorbrüggen on the occasion of his 60th birthday

The synthesis of complex ionophoric antibiotics of the polypropionate type has been highly topical for several years

[*] Prof. Dr. J. Mulzer, Dipl.-Chem. B. Schöllhorn
Institut für Organische Chemie der Freien Universität
Takustrasse 3, W-1000 Berlin 33

[**] This work was supported by the Fonds der Chemischen Industrie and by the Graduiertenkolleg "Synthese und Strukturaufklärung niedermolekularer Verbindungen". *B. S.* thanks the Berlin Senate for a postgraduate grant.

now.[1] For such syntheses the availability of central chiral fragments (so-called "stereotriads" **1**[1] or "stereotetrads" **2**) is of decisive importance. Whereas numerous direct methods have been developed for the synthesis of triads, so far the tetrads have mainly been obtained by attachment of a further stereocenter to a triad.[1, 2] The simplest and more attractive access to such tetrads, however, would be the alternating substitution of hydroxy by methyl groups in polyols of the chiral pool, particularly if this can be achieved in a single synthetic operation.

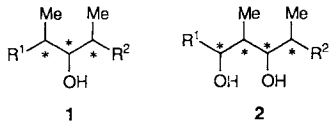

1 **2**

R^1, R^2 = CH_2OH, CH=O, $CH=CH_2$ etc.

This concept has been realized in the completely regio- and stereocontrolled synthesis of the stereotetrads **6a** and **9**. These tetrads are contained, e.g., in the ionophoric antibiotics zincophorin,[3] denticulatin A and B,[4] and, in enantiomeric form, also in ionomycin.[5] The key step in the synthesis is the sequential opening of two neighboring epoxide rings with cuprate reagents, which we use in two variants A and B. In both cases the ditosylate **3**, accessible in few steps from D-mannitol, serves as starting material. In variant A (Scheme 1) **3** is cyclized via **4** to give the epoxide **5**, which in

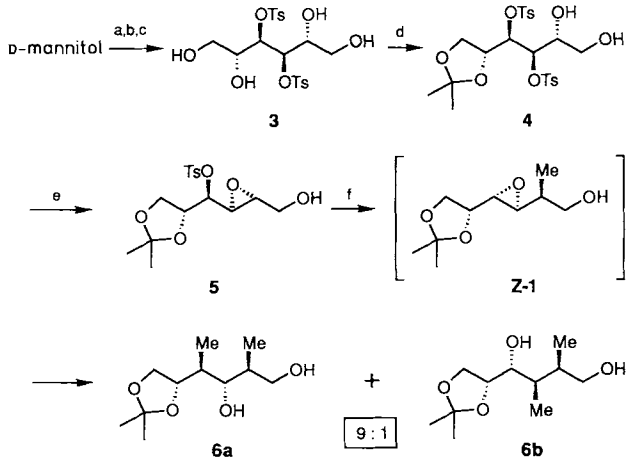

Scheme 1. a) Acetone/$ZnCl_2$, 22 °C, 4 h, 60%; b) *p*-toluenesulfonic acid chloride/dimethylaminopyridine (DMAP)/pyridine, 60 °C, 24 h, 85%; c) trifluoroacetic acid (TFA)/H_2O/MeOH, 50 °C, 12 h, 82%; d) 2,2'-dimethoxypropane (DMP)/*p*-toluenesulfonic acid/dimethylformamide (DMF), 22 °C, 12 h, 85%; e) K_2CO_3/MeOH/CH_2Cl_2, 22 °C, 1–2 h, 93%; f) $Me_2CNCuLi_2/Et_2O$, −78 °C, 3 h, **6a**: 72%, **6b**: 8%.

a tandem reaction with Lipshutz dimethyl cuprate,[6] immediately affords—presumably via the intermediate **Z-1**[7]—the tetrad **6a** (72%) (Table 1). Separation of **6a** from the regioisomer **6b** (8%) is unproblematical. The regiochemical control of the cuprate attack on **5** could be determined by the steric repulsion of the tosylate group. Possibly the primary hydroxyl group also steers the organometal into the neighboring position by complexation. In **Z-1** the steric repulsion by the methyl groups already present is presumably decisive for the site of the second attack by the cuprate. Lithium-

Table 1. Analytical data of some key compounds (correct combustion analyses for all compounds; ^1H and ^{13}C NMR spectra at 270 or 68 MHz with internal TMS standard, 25 °C)

6a: ^1H NMR ($CDCl_3$): δ = 0.80 (d, 3H, J = 6.8 Hz; 4-CH_3), 1.16 (d, 3H, J = 6.8 Hz; 2-CH_3), 1.38 (s, 3H; isopropylidene-CH_3), 1.42 (s, 3H; isopropylidene-CH_3), 1.86 (m, 1H; 2-H), 1.92 (m, 1H; 4-H), 3.15 (dd, 1H, J = 8.0, 2.8 Hz; 1-OH), 3.54–3.63 (m, 2H; 1-H_A, 3-H), ABM system: δ_A = 3.68, δ_B = 4.14, δ_M = 4.02 (J_{AB} = 8.1 Hz, J_{AM} = 8.1 Hz, $J_{M,4}$ = 8.6 Hz, J_{BM} = 5.9 Hz; 5-H, 6-H), 3.91 (dd, 1H, ^2J = 10.8 Hz, ^3J = 2.7 Hz; 1-H_B), 4.36 (s, broad, 1H; 3-OH); ^{13}C NMR ($CDCl_3$): δ = 13.0, 15.1, 25.8, 26.7, 35.9, 40.1, 65.4, 69.0, 80.2, 81.5, 109.6; $[\alpha]_D^{20}$ = + 24.0 (c = 1.8, $CHCl_3$)

7: ^1H NMR ([D_6]acetone): δ = 2.80 (s, 2H; 3-H, 4-H), 3.08 (m, 2H; 2-H, 5-H), AB-system: δ_A = 3.52, δ_B = 3.75 (2ddd, 4H, $^2J_{AB}$ = 11.3 Hz, $^3J_{A,OH}$ = $^3J_{B,OH}$ = 5.7 Hz, ^3J_B = 3.2 Hz, ^3J_A = 1.9 Hz; 1-H, 6-H), 3.92 (t, 2H, J = 5.7 Hz; OH); ^{13}C NMR ([D_6]DMSO): δ = 54.3, 56.1, 60.7; m.p. 91–93 °C; $[\alpha]_D^{20}$ = + 65.1 (c = 2.2, methanol)

8a: ^1H NMR ($CDCl_3$): δ = 1.07 (s, 18H; *t*Bu-CH_3), 2.93 (s, 2H; 3-H, 4-H), 3.11 (mc, 2H; 2-H, 5-H), 3.83 (ddd, 4H, ^2J = 15.0 Hz, ^3J = 4.0 Hz, ^3J = 3.0 Hz), 7.38 (mc, 12H; *o*- and *p*-arene-H), 7.66 (mc, 8H; *m*-arene-H); ^{13}C NMR ($CDCl_3$): δ = 19.3, 26.6, 53.4, 59.9, 62.8, 127.7, 129.8, 133.0, 133.2, 135.5; $[\alpha]_D^{20}$ = + 20.7 (c = 1.2, $CHCl_3$)

9: ^1H NMR ($CDCl_3$): δ = 0.76 (d, 3H; J = 7.0 Hz; CH_3), 1.00 (d, 3H, J = 7.0 Hz; CH_3), 1.05 (s, 9H; *t*Bu-CH_3), 1.08 (s, 9H; *t*Bu-CH_3), 1.85–2.03 (m, 2H; 3-H, 5-H), 3.52 (mc, 2H; 6-H), 3.64 (m, 2H; 1-H), 3.76 (d, 1H, J = 4.9 Hz; OH), 3.80 (m, 2H; 2-H, 4-H), 4.20 (s, broad, 1H; OH), 7.38 (m, 12H; *o*- and *p*-arene-H), 7.68 (m, 8H; *m*-arene-H); ^{13}C NMR ($CDCl_3$): δ = 13.7, 15.3, 19.2, 19.4, 27.0, 37.4, 38.7, 66.4, 67.1, 75.2, 80.5, 127.6, 129.6, 132.7, 133.0, 135.3; $[\alpha]_D^{20}$ = + 3.8 (c = 1.8, $CHCl_3$)

11: ^1H NMR ([D_6]DMSO): δ = 0.80 (d, 3H, J = 6.8 Hz; CH_3), 0.89 (d, 3H, J = 7.0 Hz; CH_3), 1.72 (mc, 1H; CH_3CH), 1.80 (mc, 1H; CH_3CH) 3.25 (m, 3H), 3.42 (mc, 1H), 3.53 (mc, 1H), 3.64 (mc, 1H), 4.32 (t, 1H, J = 5.1 Hz; OH), 4.52 (t, 1H, J = 5.4 Hz, OH), 4.56 (d, 1H, J = 4.3 Hz; OH), 4.76 (d, 1H, J = 5.7 Hz; OH); ^{13}C NMR ([D_4]methanol): δ = 13.1, 15.4, 38.9, 40.2, 64.4, 65.1, 75.2, 79.7; $[\alpha]_D^{20}$ = −7.0 (c = 2.1, methanol)

dimethyl homocuprate reacts less regioselectively (**6a**:**6b** = 7:1).

Variant B (Scheme 2) is used for the transformation of **3** into the C_2-symmetric bisepoxide **7** (Table 1). Decisive for the regiocontrol in the opening of the secondary product **8** with cuprate reagents are the two hydroxy protecting groups. Only the bulky *tert*-butyldiphenylsilyl moiety directs the attack to one of the two equivalent "inner" epoxide positions, and the unintercepted intermediate **Z-2** is formed. The attack of the second cuprate moiety is steered, as before, by the presence of the first methyl group, whose influence markedly dominates over that of the silyl group. As expected the transformation of **3** into **7** proceeds without Payne rear-

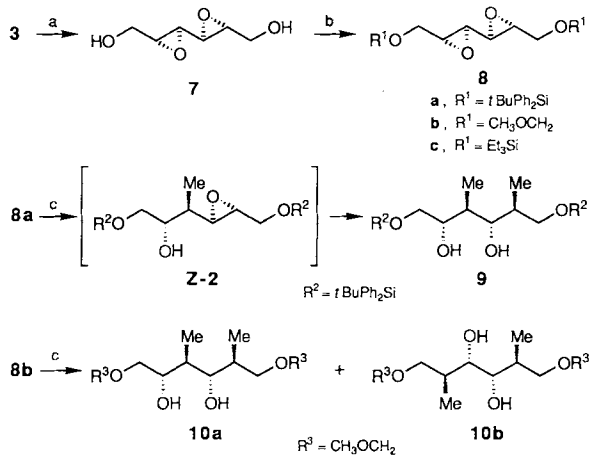

Scheme 2. a) K_2CO_3/MeOH, 22 °C, 3 h, 93%; b) **8a**: *t*$BuPh_2SiCl$/imidazole/DMF, 22 °C, 12 h, 95%; **8b**: CH_3OCH_2Cl/EtN(*i*Pr)$_2$/THF, 30–40 °C, 30 h, 86%; **8c**: Et_3SiCl/imidazole/DMF, 22 °C, 2 h, 96%; c) $Me_2CNCuLi_2/Et_2O$, −78 °C, 3 h, **9**: 67%, **10a**: 55%, **10b**: 28%.

rangement, since in this case a *cis*-epoxide would have been formed. Furthermore, in the course of the formation of **9** (Table 1) from **8a** (Table 1) a possible cyclization to give the tetrahydrofuran ring does not take place. Access to the enantiomeric tetrad *ent*-**9** was accomplished analogously by using the enantiomer *ent*-**7**, which is also accessible in few steps from D-mannitol.[8] From the bismethoxymethyl ether **8b**, on the other hand, two regioisomers **10a** and **10b** are obtained in the ratio 2:1 upon reaction with the cuprate. **7** and **8c** react in a regio-uncontrolled fashion. The configurations of **6a**, **9**, and **10a** were verified by degradation via **11** (Table 1) and **12** to the well-documented *meso* compound **13b**[9] (Scheme 3).

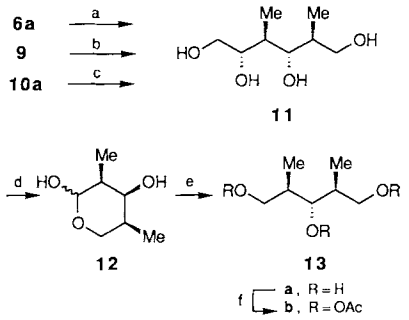

Scheme 3. a) TFA/H_2O/MeOH, 22 °C, 24 h, 88%; b) nBu_4NF/THF, 22 °C, 12 h, 92%; c) HCl(cat.)/MeOH, 60%, 12 h, 82%; d) H_5IO_6/THF, 22 °C, 1 h, 96%; e) $NaBH_4$/MeOH, 22 °C, 1–2 h, 87%; f) Ac_2O/DMAP/pyridine, 22 °C, 3 h, 96%.

Synthesis of the otherwise difficultly accessible *anti-anti*-triads **1**, which occur, e.g., in rifamycin **S**[10] or tirandamycin,[11] is possible via the semiacetal **12**. The structures of **6b** and **10b** were established by ^{1}H-^{1}H-COSY measurements.

The variants A and B complement each other with regards to the pattern of the protecting groups of the tetrads: In **6a** the 1,2-OH are differentiated from the 3,6-OH groups; in **9**, on the other hand, the 1,6-OH are distinguished from the 2,4-OH groups. In a further communication we shall report on the incorporation of both tetrads into polypropionate antibiotics and on the reaction of **5** and **8** with other nucleophiles.

Received: July, 28, 1990 [Z 4092 IE]
German version: *Angew. Chem. 102* (1990) 1529

CAS Registry numbers:
3, 20706-73-4; **4**, 129965-99-7; **5**, 129966-00-3; **6a**, 130059-98-2; **6b**, 129966-04-7; **7**, 20706-76-7; **8a**, 129966-01-4; **8b**, 129966-05-8; **8c**, 129966-06-9; **9**, 129966-02-5; **10a**, 129966-03-6; **10b**, 129966-07-0; **11**, 130059-99-3; **12** (isomer 1), 130060-00-3; **12** (isomer 2), 130060-01-4; **13a**, 94842-97-4; **13b**, 94942-09-3; D-mannitol, 69-65-8.

[1] R. W. Hoffmann, *Angew. Chem. 99* (1987) 503; *Angew. Chem. Int. Ed. Engl. 26* (1987) 489, and references cited therein.
[2] S. J. Danishefsky, D. F. Harvey, *J. Am. Chem. Soc. 107* (1985) 6647.
[3] a) H. A. Brooks, J. P. Poyser, D. Gardner, T. King, *J. Antibiot. 37* (1984) 1501; b) L. Radics, *J. Chem. Soc. Chem. Commun. 1984*, 599; c) U. Grafe, W. Schade, M. Roth, L. Radics, M. Incze, K. Ujszaszy, *J. Antibiot. 37* (1984) 836; S. J. Danishefsky, H. G. Selnick, R. E. Zelle, M. P. De Ninno, *J. Am. Chem. Soc. 110* (1988) 4368.
[4] F. E. Ziegler, M. R. Becker, *J. Org. Chem. 55* (1990) 2800.
[5] S. Hanessian, N. G. Cooke, B. DeHoff, Y. Sakito, *J. Am. Chem. Soc. 112* (1990) 5276; D. A. Evans, R. L. Dow, T. L. Shih, J. M. Takacs, R. Zahler, *ibid. 112* (1990) 5290.
[6] B. H. Lipshutz, *Synthesis 1987*, 325; B. H. Lipshutz, R. S. Wilhelm, J. A. Kozlowski, *Tetrahedron 40* (1984) 5005.
[7] Vgl. M. J. Kurth, M. A. Abreo, *Tetrahedron Lett. 28* (1987) 5631.
[8] C. Pietschmann, unpublished results, Berlin 1990.
[9] Y. Oikawa, T. Nishi, H. Itaya, O. Yanemitsu, *Tetrahedron Lett. 24* (1983) 1987.
[10] H. Nagaoka, W. Rutsch, G. Schmid, H. Iio, M. R. Johnson, Y. Kishi, *J. Am. Chem. Soc. 102* (1980) 7962; H. Nagaoka, Y. Kishi, *Tetrahedron 37* (1981) 3873; W. C. Still, J. C. Barrish, *J. Am. Chem. Soc. 105* (1983) 2487.
[11] P. J. Murphy, G. Procter, *Tetrahedron Lett. 31* (1990) 1059–1062.

Induction and Variation of Chirality in Discotic Liquid Crystalline Polymers **

By *Mark M. Green, Helmut Ringsdorf,* Jürgen Wagner,* and *Renate Wüstefeld*

Cholesteric[1] and chiral smectic phases[2] are of great importance, both scientifically and technologically. The chirality of these phases manifests itself in helical superstructures and in special physical properties such as selective reflection of polarized light[3] or ferroelectricity.[4] The influence of chirality has been studied in detail on calamitic (rod-shaped)[1–4] and lyotropic[5] liquid crystals. Chiral discotic (disk-shaped) liquid crystals, on the other hand, have scarcely received any attention, although chiral discotic compounds[6a–d] and phases are known. Special interest attaches to discotic-columnar phases, in which the chirality of the individual molecules can be enhanced first within the individual columns, and second by the arrangement of the columns (e.g. N_c phase) (Fig. 1). The helical order of disks[6a, c] or their side chains[7] is considered responsible for the first reinforcing effect. The helical order of columns leads to the second reinforcing effect that has so far only been demonstrated on lyotropic liquid crystals.[5]

The present work outlines several routes to chiral discotic-columnar phases (Fig. 2). To strengthen the interactions between the columns, main-chain polymers are synthesized in which chiral disk-shaped molecules are linked covalently (a in Fig. 2). If, in addition, these chiral polymers have electron-donor properties they can be doped with electron acceptors to form charge-transfer (CT) complexes;[8] as a consequence the interactions within the columns are strengthened (b in Fig. 2). If achiral polymers are used as starting material, chirality can be introduced by doping them with acceptor molecules (c in Fig. 2).

The chiral monomers for the *synthesis of the main chain polymers* were obtained analogously as described for achiral monomers with pentyloxy side chains.[9a] Triphenylene hexaacetate was allowed to react with (*S*)-(−)-2-methylbutyl

[*] Prof. Dr. H. Ringsdorf, Dipl.-Chem. R. Wüstefeld
Institut für Organische Chemie der Universität
J.-J.-Becher-Weg 18–20, W-6500 Mainz (FRG)
Prof. Dr. M. M. Green
Department of Chemistry and Polymer Chemistry
Polytechnic University
333 Jay Street, Brooklyn, NY 11201 (USA)
Dr. J. Wagner
Sektion Chemie der Humboldt-Universität
Hessische Strasse 1–2, O-1040 Berlin

[**] Part of this work was conducted at the IBM Almaden Research Center (San Jose, California) and at Osaka University (Osaka, Japan). *R. W.* is grateful to her hosts Dr. R. Twieg and Dr. C. G. Wilson (Almaden Research Center); J. W. and M. M. G. are grateful to Prof. Okamoto and Prof. Hatada (Osaka University).

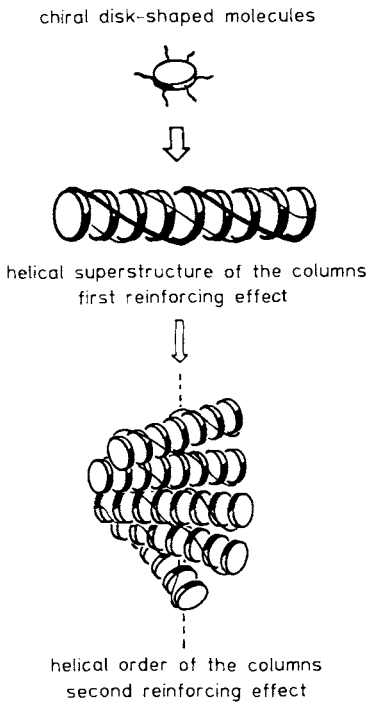

Fig. 1. Chirality in discotic columnar liquid crystals. Other than in the case of conventional calamitic (rod shaped) liquid crystals the chirality of the individual disk-shaped molecules can be doubly reinforced: by the helical superstructure of the columns and, e.g., in nematic columnar phases, and also by the helical ordering of the columns.

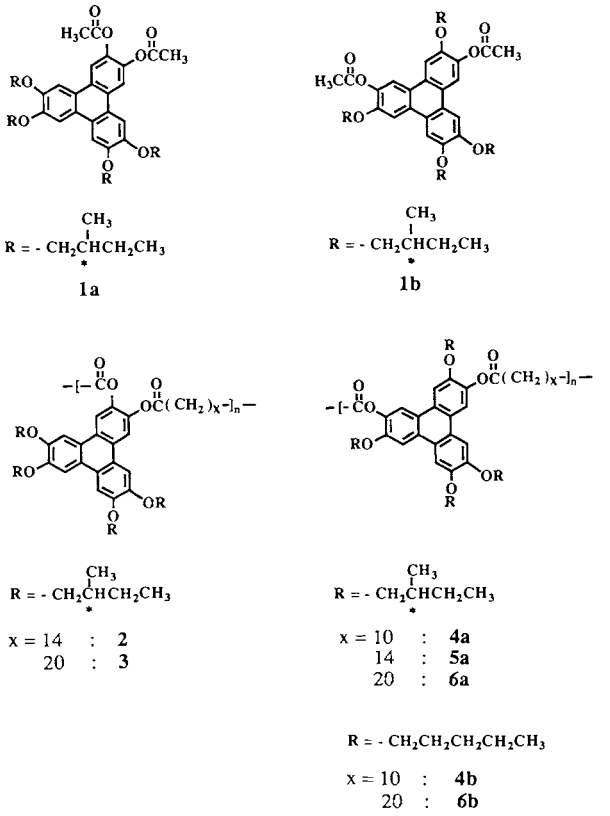

tosylate/K_2CO_3 to give a mixture of completely and incompletely etherified triphenylene acetates. The yield of diacetates (64 mol-%) was comparatively high (hexaether: 2 mol-%, monoacetate: 15 mol-%), since, with more than four side chains, the etherification is sterically hindered. For the first time, also the diacetate **1a** with two ortho acetyl groups was obtained which could be separated chromatographically from the remaining isomers **1b–d**.[10] For polymer synthesis both the *o*-diacetate **1a** (polymers **2** and **3**) as well as the mixture of the remaining isomers **1b–1d** (polymers **4a–6a**) were employed. Polycondensation was carried out in the melt by transesterification with the corresponding 1,ω-dicarboxylic acids (catalyst = *p*-toluenesulfonic acid).[9b]

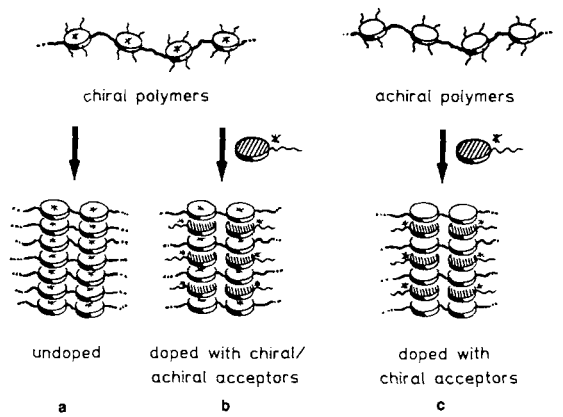

Fig. 2. Routes to chiral discotic-columnar polymer systems. a) The chiral polymer is liquid crystalline. b) The chiral polymer is not liquid crystalline, but can be converted by doping with achiral or chiral electron acceptors into a discotic liquid crystalline system. c) Chirality is introduced into an achiral polymer via doping with chiral electron acceptors.

The *phase behavior* of the monomeric diacetates and their polycondensates is shown in Table 1. Of all the compounds, only the main chain polymer **4a** (shortest spacer length) proved to be liquid crystalline. Analogously to the achiral polymers,[9a, b] the ratio of spacer length to side-chain length decides the mesomorphic properties. The structure of the starting monomer is, in contrast, less important: **2** and **5a** as well as **3** and **6a**, which were obtained from the *o*-diacetate **1a** and the diacetate mixture **1b–d** respectively, are amorphous and hardly differ in their glass temperatures.

Table 1. Characterization and phase behavior of the monomers **1a–d** and the polymers **2–6a**.

Compound	x [a]	M_r [b]	Phase behavior [c]
1a	–	689	k_1 180 k_2 195 i
1b–d	–	689	k 203 i
2	14	17000	g 105 i
3	20	15000	g 75 i
4a	10	19000	g 140 D_{ho} 192 i
5a	14	16000	g 108 i
6a	20	18000	g 79 i

[a] x = number of the CH_2 groups of the 1,ω-dicarboxylic acids used as spacers. [b] Relative molecular weight from gel-permeation chromatographic measurements versus polystyrene standards (UV detection, $CHCl_3$). [c] Phase transition temperatures [°C] from differential calorimetric measurements; g = glassy state; D_{ho} = *d*iscotic *h*exagonal *o*rdered phase; i = isotropic melt; k_1, k_2 = crystalline phases [12].

When the main chain polymers **2**, **3**, and **4a–6a** are treated with electron acceptors such as 2,4,7-trinitrofluorenone (TNF) or the enantiomeric 2-(2,4,5,7-tetranitro-9-fluorenylideneaminooxy)propionic acid propyl esters (−)- and

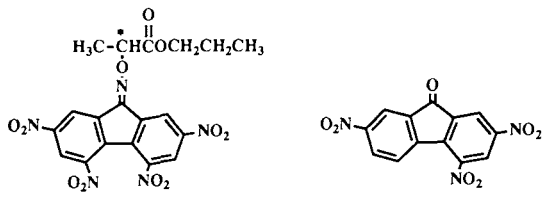

(−)-TAPAE
(+)-TAPAE

TNF

(+)-TAPAE, colored CT complexes (brownish red, violet, and green—depending on the dopant and polymer) and predominantly liquid crystalline phases are formed (see Table 2). Noticeably it is the first time that, besides the highly ordered D_{ho} and D_{ro} phases (in the case of **4a**, **5a**, **4b**), also a nematic-columnar N_c phase has been found for a chiral discotic system (**6a**/TNF) (cf. Fig. 1).[11]

Table 2. Phase behavior [a] of the chiral CT complexes.

Donor polymer	x	Undoped	Doped with electron acceptors TNF	TAPAE(+) [b]	TAPAE(−) [b]
4a	10	g 140 D_{ho} 192 i	g 118 D_{ho} 256 i	lc 235 i	lc 237 i
5a	14	g 108 i	g 83 D_{ro} 180 i	lc 157 i	lc 157 i
6a	20	g 79 i	g 60 N_c 116 i	amorph.	amorph.
4b	10	g 50 D_{ho} 195 i	g 40 D_{ho} 246 i	lc 220 i	lc 220 i

[a] Cf. [c] in Table 1; D_{ro} = *d*iscotic *r*ectangular *o*rdered phase; N_c = *n*ematic-*c*olumnar phase; lc = *l*iquid *c*rystalline [11]. [b] Glass point and mesophase type have not yet been determined.

Figures 3 and 4 show typical *UV and CD spectra* of thin films[12] of undoped and doped polymers in the region of $\lambda = 200-400$ nm. Doping was carried out with the chiral acceptors (+)-TAPAE or (−)-TAPAE, in each case in a molar ratio donor/acceptor of 3:1. None of the films shows anisotropy, so that orientational effects do not have to be considered upon interpreting the spectra. Instead, information is obtained about the chiral interactions between neighboring molecules within the columns (first reinforcement effect). Information about the chiral interactions between the columns (second reinforcement effect) cannot be gained from these measurements.

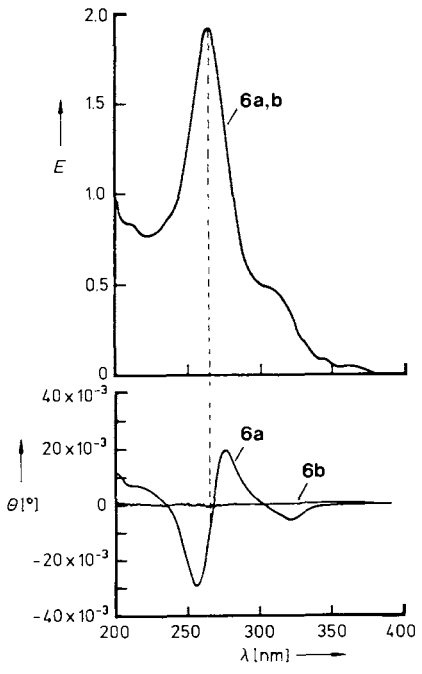

Fig. 3. UV (top) and CD spectra (bottom) of thin films of the *undoped* polymers; here as example, the chiral polymer **6a** and the achiral polymer **6b** with equal spacer lengths. The chiral polymers **4a** and **5a**, like **6a**, show an exciton splitting: the UV transition at $\lambda = 265$ nm splits in the CD spectrum into two transitions. UV absorption as extinction E, CD absorption as ellipticity θ in degrees [13].

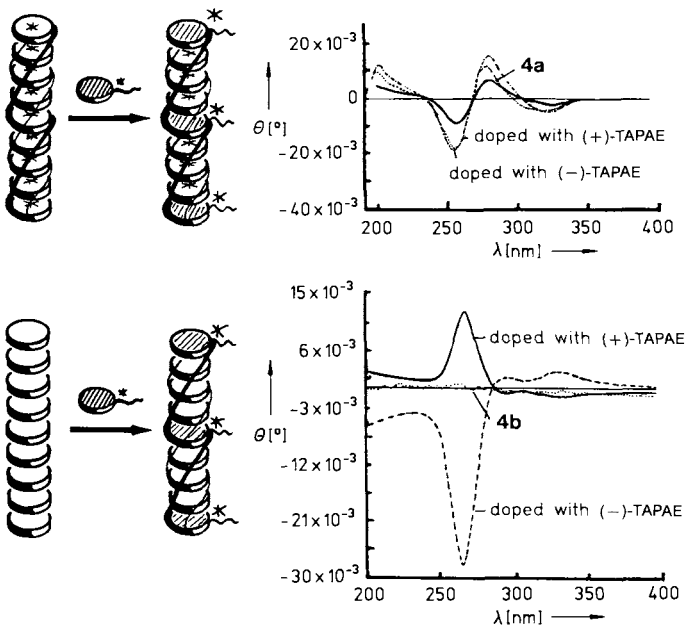

Fig. 4. CD spectra of thin films of *doped* polymers, and schematic representation of the acceptor's influence. Top: chiral polymer **4a**, undoped and doped with (−)-TAPAE or (+)-TAPAE. Doping leads, independently of the handedness of the acceptor, always to a slight increase in CD intensity. The acceptor is inserted into the column without noticeably influencing the interactions between the chiral triphenylene disks. Bottom: Polymers **4b**, undoped and doped with (−)-TAPAE or (+)-TAPAE. The doping leads to high CD intensities; the optical antipodes give mirror-image spectra. The acceptor induces chirality, which is enhanced via the cooperative interactions along the columns. In addition it now determines the handedness of the helix. CD adsorption as ellipticity θ in degrees [13].

The UV spectra of all polymer films are characterized by a broad band at $\lambda = 265$ nm with a shoulder at $\lambda = 310$ nm. They differ very little for chiral and achiral polymers. Larger differences appear only in the CD spectra, in which, as expected, only the chiral polymer systems—doped or undoped—show CD activity. Monomer **1a** was also investigated in solution (3 mM); it is not CD active. This lets us conclude that the CD activity of the polymers does not derive from individual triphenylenes, but from the resulting columnar superstructures that are present in the films. An indication of helical superstructures follows from the exciton splitting. The $\pi \rightarrow \pi^*$ transition of the UV absorption maximum at $\lambda = 265$ nm is split into two transitions in the CD spectrum, as is also found for $\pi \rightarrow \pi^*$ chromophores in helical polymers.[15]

If the *chiral* polymer is doped with the likewise chiral acceptors (−)-TAPAE or (+)-TAPAE, the structures of the CD spectra do not change. In the liquid crystalline systems **4a**/(+)-TAPAE and **4a**/(−)-TAPAE, the CD intensity increases slightly, and by the same amount for both optical antipodes (−)-TAPAE and (+)-TAPAE (Fig. 4, top). The following picture emerges: along the columns there are

strong interactions between the chiral methylbutyloxy side groups and thus also between the triphenylene chromophores, which are arranged in a helix. When (−)-TAPAE or (+)-TAPAE is added the CD spectrum does not change qualitatively, i.e. the CD activity still arises from the twisted triphenylene chromophores and not from the acceptors or triphenylene-acceptor pairs. Quantitatively the CD activity is increased only slightly by acceptor addition; (−)-TAPAE and (+)-TAPAE thus insert into the columns without substantially influencing the chiral interactions.[16]

If, however, the *achiral* polymers are doped with chiral acceptors, a completely different chiroptical behavior is observed (Fig. 4, bottom). Remarkable in this case is the high induced CD intensity, which, once again, arises from the triphenylene chromophores.[17] For the first time the CD spectra differ in the case of the optical antipodes (+)-TAPAE and (−)-TAPAE, namely in their sign. This difference is already known from induced cholesteric phases of enantiomeric calamitic or lyotropic liquid crystals.[18] The structure of the CD spectra is, there as also here in the case of **4b**/(+)-TAPAE and **4b**/(−)-TAPAE, virtually identical to that of the UV absorption spectra. Thus, the chiral acceptors induce—comparably with chiral dopants in calamitic liquid crystals—helical superstructures and, in addition, determine even the handedness of the helices. High CD intensities are obtained since the chirality of the acceptor is enhanced by cooperative interactions along the columns. Chiral doping thus signals a route on which the chiral discotic polymers with high optical activities are accessible at little synthetic expense. Due to CT interactions the chiral acceptor dopants can also be added in high concentrations (often up to molar ratios of 1:1) without destroying the LC phase. Moreover, the acceptors are incorporated into the columns and can, although not liquid crystalline themselves, be oriented with the mesogenic donors.

These first CD investigations show that the chiral discotic polymers prepared via various methods (see Fig. 2) are all optically active and that the high optical activities arise from the superstructures of the columns. The chirality can, as shown, be considerably influenced by the structure of the donor and of the acceptor. Furthermore, the temperature and the ratio donor/acceptor and thus concentrations of chiral groups can be varied. Via all three factors it should be possible to selectively influence the pitch of the helices along the columns. This is of fundamental importance for helical polymers. Moreover, in the case of discotic liquid crystals the connection between the helical superstructure of individual columns and the helical ordering of the columns is of interest (see Fig. 1.). This question is currently being investigated for the N_c phase of system **6a**/TNF. It also refers to helical polymers which may exhibit liquid crystalline ordering in nature as well.[19]

Received: June 27, 1990 [Z 4041 IE]
German version: *Angew. Chem. 102* (1990) 1525

[1] G. Solladié, R. G. Zimmermann, *Angew. Chem. 96* (1984) 335; *Angew. Chem. Int. Ed. Engl. 23* (1984) 348.
[2] G. W. Gray, J. G. W. Goodby: *Smectic Liquid Crystals-Textures and Structures*, Leonard Hill, Glasgow 1984.
[3] a) H. de Vries, *Acta Crystallogr. 4* (1951) 219; b) R. Steinsträsser, H. Krüger *Ullmanns Encykl. Tech. Chem. 4th edit. Vol. 11* (1976) 657.
[4] R. B. Meyer, L. Liebert, L. Strzelecki, P. Keller, *J. Phys. Lett. (Orsay Fr.) 36* (1975) L69.
[5] a) C. Robinson, J. C. Ward, *Nature (London) 180* (1957) 1183; b) K. Radley, A. Saupe, *Mol. Phys. 35* (1978) 1405; c) M. Acimis, L. W. Reeves, *Can. J. Chem. 58* (1980) 1533.
[6] a) N. L. Morris, R. G. Zimmermann, G. B. Jameson, A. W. Dalziel, P. M. Reuss, R. G. Weiss, *J. Am. Chem. Soc. 110* (1988) 2177; b) J. Malthête, C. Destrade, Nguyen Huu Tinh, J. Jacques, *Mol. Cryst. Liq. Cryst. 64* (1981) 233; c) J. Malthête, J. Jacques, Nguyen Huu Tinh, C. Destrade, *Nature (London) 298* (1982) 46; d) K. Yamamura, S. Ono, H. Ogoshi, H. Masuda, Y. Kuroda, *Synlett. 1989*, 18.
[7] a) A. M. Levelut, *J. Phys. Lett. (Orsay Fr.) 40* (1979) 81; b) P. A. Heiney, E. Fontes, W. H. de Jeu, *J. Phys. (Paris) 50* (1989) 461.
[8] a) H. Ringsdorf, R. Wüstefeld, E. Zerta, M. Ebert, J. H. Wendorff, *Angew. Chem. 101* (1989) 934; *Angew. Chem. Int. Ed. Engl. 28* (1989) 915; b) H. Ringsdorf, R. Wüstefeld, *Philos. Trans. R. Soc. London Ser. A 330* (1990) 95; c) H. Bengs, M. Ebert, O. Karthaus, B. Kohne, K. Praefcke, H. Ringsdorf, R. Wüstefeld, *Adv. Mater. 2* (1990) 141.
[9] a) W. Kreuder, H. Ringsdorf, *Makromol. Chem. Rapid Commun. 4* (1983) 807; b) W. Kreuder, H. Ringsdorf, P. Tschirner, *ibid. 6* (1985) 97.
[10] Composition of the isomeric mixture 73 mol-% **1b** and 27 mol-% **1c**/**1d** (**1c** and **1d** cannot be differentiated on the basis of the ^{1}H and ^{13}C NMR data).
[11] The phase types were determined by X-ray investigations: C. Baehr, M. Ebert, J. H. Wendorff, H. Ringsdorf, R. Wüstefeld, 19. Freiburger Arbeitstagung Flüssigkristalle, April 4–6, 1990, Tagungsband, P12.
[12] Preparation by spin coating of the polymer solutions (10 wt.-%) in cyclohexanone, 2d dry in vacuo. Film thickness 0.4–0.5 μm. CD and UV spectra were recorded at room temperature; the polymers are present either as liquid-crystalline or as completely amorphous glasses.
[13] The ellipticity is given by: $\theta = \theta_m cd \sim \Delta\varepsilon cd$; θ_m = molar ellipticity c = concentration, d = film thickness, and $\Delta\varepsilon = \varepsilon_L - \varepsilon_R$ with $\varepsilon_L, \varepsilon_R$ = molar extinction coefficient for left and right circularly polarized light respectively. Differences in the film thickness d play a role only in quantitative considerations and were taken into account by also comparing the intensity ratio I_{CD}/I_{UV}.
[14] Small differences are observed in the range 330 nm $< \lambda <$ 370 nm: the absorption bands of the chiral systems (λ = 345 nm, λ = 362 nm) are shifted hypsochromically compared to those of the achiral systems (λ = 350 nm, λ = 367 nm). It is not important whether the chirality is present in the polymer itself or first introduced via doping.
[15] a) Concerning exciton splitting in copolymers of styrene and chiral olefins: F. Ciardelli, P. Salvadori, *Pure Appl. Chem. 57* (1985) 931, and references cited therein; b) concerning exciton splitting in general: N. Harada, K. Nakanishi (Eds.): *Circular Dichroic Spectroscopy—Exciton Coupling in Organic Chemistry*, Oxford Univ. Press, Oxford 1983. c) For the first time an exciton splitting has also been found in the CD spectrum of a lyotropic liquid crystalline system: J. Wagner, M. Green, unpublished results from studies on chiral poly-2,6-dimethylheptylisocyanates and chirally doped polyhexylisocyanates.
[16] In the *amorphous* systems **6a**/(−)-TAPAE and **6a**/(+)-TAPAE the CD intensity is lower than in the undoped polymer **6a**. Insertion of the acceptor prevents the formation of helices and thus reduces the chiral interactions.
[17] The CD activity does not derive from the TAPAE acceptors. They show only slight CD activity, and their CD spectra differ significantly from those of the doped discotic polymers.
[18] F. D. Saeva in F. D. Saeva (Ed.): *Liquid Crystals, The Fourth State of Matter*, Dekker, New York 1979, p. 249–273.
[19] a) T. E. Strzelecka, M. W. Davidson, R. L. Rill, *Nature (London) 331* (1988) 457; b) Y. M. Yevdokimov, S. G. Skuridin, V. I. Salyanov, *Liq. Cryst. 11* (1988) 1443.

Multiple Bonds Between Metal Atoms in Ordered Assemblies: Liquid Crystals Containing Mo–Mo Quadruple Bonds**

By *Roger H. Cayton, Malcolm H. Chisholm,** and *Frank D. Darrington*

Compounds containing multiple bonds between metal atoms have been of considerable interest in terms of their

[*] Prof. M. H. Chisholm, Dr. R. H. Cayton
Department of Chemistry, Indiana University
Bloomington, IN 47405 (USA)
F. D. Darrington
Amoco Research Center
Naperville, IL 60566 (USA)

[**] This work was supported by the National Science Foundation (postdoctoral fellowship for *R. H. C.*). We thank *Jodie Wesemann* for help in the preparation of several of these compounds as well as Dr. *Ken Robinson* and Dr. *Cynthia Ontiveros* at AMOCO for their encouragement and assistance.

structure, reactivity, and electronic properties for some 25 years.[1] However, the field of macromolecular chemistry based on M–M multiple bonds is still in its infancy. We are interested in exploring the way in which chemical manipulations on a molecular level affect the macroscopic properties of bulk materials derived from dinuclear transition metal complexes containing electronically tunable M–M multiple bond systems. We describe here our preparation and characterization of the first examples of liquid crystalline compounds containing M–M quadruple bonds.[2]

Dimetal tetracarboxylates, $[M_2(O_2CR)_4]$, are known for numerous transition elements, and for certain MO configurations M–M multiple bonds result, e.g. $\sigma^2\pi^4\delta^2$ (M≡M) for M = Cr, Mo, W, and $\sigma^2\pi^4\delta^2\delta^{*2}\pi^{*2}$ (M=M) for M = Ru. In the absence of axial donor ligands these compounds form ladder structures **I** in the solid state, whereby the oxygen atom from one carboxylato ligand forms a weak intermolecular bond to the metal atom of a neighboring $[M_2(O_2CR)_4]$ unit.[3] In addition, for suitable substituents R, we believed that these compounds should exhibit thermotropic discotic liquid crystalline phases, **II**, wherein macroscopic order of the "disks" would be maintained by substituent interaction rather than the intermolecular M···O bonds. Discotic mesophases have been reported for $[Rh_2(O_2CR)_4]$ (M–M),[4] $[Cu_2(O_2CR)_4]$ (M···M),[5] and only just recently for $[Ru_2(O_2CR)_4]$ (M=M),[6] (R = C_nH_{2n+1}).

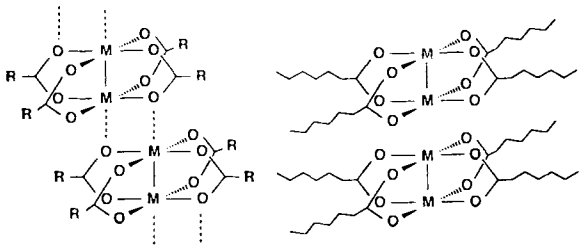

I II

We prepared a series of compounds of the composition $[Mo_2(O_2C(CH_2)_nCH_3)_4]$ where n = 1–11 and 16 by reaction of $[Mo(CO)_6]$ with the appropriate carboxylic acid in diglyme as solvent.[7] All the compounds were crystalline at room temperature and stable at temperatures up to 250 °C in an inert atmosphere. The phase behavior of these compounds was examined by differential scanning calorimetry (DSC) in the temperature range 22 °C–250 °C. The compounds for which n = 3 to 9 exhibit a liquid crystalline phase between their crystalline and isotropic liquid phases. The onset point, as well as the temperature range of the mesophase was found to vary significantly with hydrocarbyl chain length, as is evident in the phase–temperature profile for the series (Fig. 1). The shortest chain to exhibit a liquid crystal phase is for n = 3 (pentanoate), in which the mesophase first exists at 152 °C and is stable up to 174 °C. For n = 4 (hexanoate) the onset temperature is only 108 °C and the mesophase is stable over a range of 64 °C. With increasing chain length the onset temperatures vary only slightly, whereas the mesomorphic range decreases until n = 10 (dodecanoate), at which point the compound melts directly from its crystalline form to an isotropic liquid.

As shown by investigations with the polarizing microscope, a significant degree of order is maintained in the mesophase. Figure 2 shows $[Mo_2(O_2C(CH_2)_7CH_3)_4]$ in its mesomorphic temperature region as obtained by cooling the

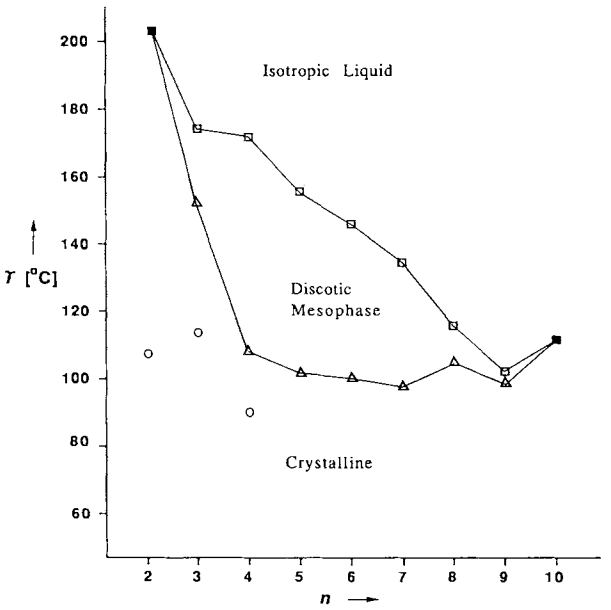

Fig. 1. Transition temperatures as a function of the carboxylate chain length for the complexes $[Mo_2(O_2C(CH_2)_nCH_3)_4]$, n = 2–10. □: LC↔IL; △: K↔LC; ○: C→C; ■: K↔IL. K = crystal, LC = liquid crystal, IL = isotropic liquid.

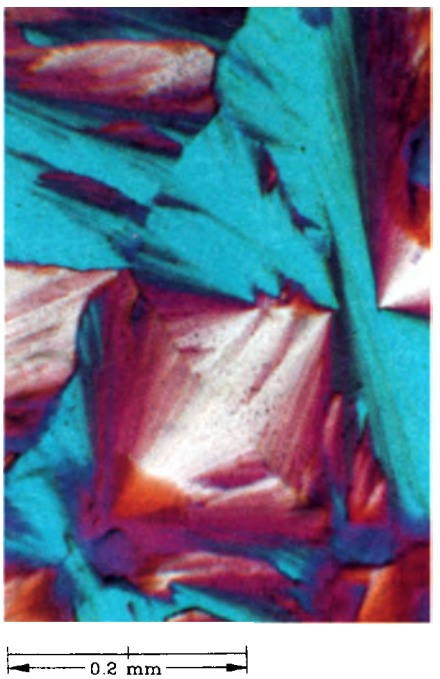

Fig. 2. View of the discotic mesophase of $[Mo_2(O_2C(CH_2)_7CH_3)_4]$ obtained by cooling the isotropic liquid phase.

isotropic liquid. The fan-like domains > 200 microns are indicative of a discotic mesophase.[8]

The endotherm associated with the crystal → liquid crystal transition is significantly larger than the liquid crystal → isotropic liquid endotherm (see Table 1). We were puzzled as to the interpretation of this phenomenon and in particular how it might relate to the weak metal–oxygen binding in the ladder structure. Accordingly we prepared the octanoates $[M_2(O_2C(CH_2)_6CH_3)_4]$ for the series of metals M = Cr, W, Ru and Rh. The tungsten complex was found to melt with-

Table 1. Phase transition temperatures [°C] and ΔH values [kcal mol^{-1}] in brackets for compounds of the composition $[M_2(O_2C(CH_2)_nCH_3)_4]$ [a].

M	n	Phase profile
Mo	2	K ⟷ 203 (5.2) ⟷ IL
Mo	3	K ⟷ 152 (4.0) ⟷ LC ⟷ 174 (0.6) ⟷ IL
Mo	4	K ⟷ 108 (5.1) ⟷ LC ⟷ 172 (0.6) ⟷ IL
Mo	5	K ⟷ 101 (10.4) ⟷ LC ⟷ 155 (0.6) ⟷ IL
Cr	6	K ⟷ 99 (10.1) ⟷ LC ⟷ >300 ⟷ decomp.
Mo	6	K ⟷ 100 (13.6) ⟷ LC ⟷ 147 (0.6) ⟷ IL
W	6	K ⟷ 90 (13.7) ⟷ IL
Ru	6	K ⟷ 107 (12.0) ⟷ LC ⟷ >290 ⟷ decomp.
Rh[b]	6	K ⟷ 95 (6.6) ⟷ LC ⟷ >220 ⟷ decomp.
Mo	7	K ⟷ 98 (12.0) ⟷ LC ⟷ 134 (0.4) ⟷ IL
Mo	8	K ⟷ 105 (12.8) ⟷ LC ⟷ 116 (0.3) ⟷ IL
Mo	9	K ⟷ 99 (19.0) ⟷ LC ⟷ 102 (0.2) ⟷ IL
Cr	10	K ⟷ 98 (17.7) ⟷ LC ⟷ >320 ⟷ decomp.
Mo	10	K ⟷ 111 (27.8) ⟷ IL
Ru	10	K ⟷ 103 (17.1) ⟷ LC ⟷ >290 ⟷ decomp.
Rh[b]	10	K ⟷ 100 (13.6) ⟷ LC ⟷ >220 ⟷ decomp.
Cr	16	K ⟷ 107 (18.6) ⟷ LC ⟷ >240 ⟷ decomp.
Mo	16	K ⟷ 112 (39.0) ⟷ IL
Ru	16	K ⟷ 103 (32.4) ⟷ LC ⟷ >240 ⟷ decomp.

[a] For abbreviations see caption to Figure 1. [b] Values from Ref. [4].

out showing a mesophase. The chromium, ruthenium and rhodium complexes (the latter being one previously shown to have a discotic phase) underwent a crystal–liquid crystal transition but did not melt before decomposition. Similar behavior was observed for the laurates (M = Cr, Ru, Rh) and stearates (M = Cr, Ru). It is known that axial ligation is stronger for M = Cr ≫ Mo > W, and in related compounds such as $M_2(O_2CMe)_2(CH_3CN)_6^{2\oplus}$[9] the axial binding to M = Rh is much stronger than that to M = Mo, as evidenced by the metal–ligand distances. The magnitude of the endotherms for the crystal–liquid crystal phase transition and the phase-transition temperature is very similar for all the octanoates. Thus we believe that in the liquid crystalline phase the axial M · · · O interactions are maintained, which is contrary to our initial expectations (see proposed structure **II**).

Given the redox activity and electronic tunability of the M–M manifold, these liquid crystalline materials based on dinuclear transition metal complexes should have interesting electronic, magnetic, and photophysical properties. Further studies are in progress.

Received: May 15, 1990 [Z 3959 IE]
German version: *Angew. Chem. 102* (1990) 1490

[1] F. A. Cotton, R. A. Walton: *Multiple Bonds Between Metal Atoms*, Wiley, New York 1982.

[2] For a recent review of metal-containing liquid crystals see: A. M. Giroud-Godquin, P. Maitlis, *Angew. Chem.*, in press; *Angew. Chem. Int. Ed. Engl.*, in press.

[3] See, for example, the crystal structure of $[W_2(O_2CCH_2CH_3)_4]$, M. H. Chisholm, H. T. Chiu, J. C. Huffman, *Polyhedron 3* (1984) 759.

[4] A. M. Giroud-Godquin, J. C. Marchon, D. Guillon, A. Skoulios, *J. Phys. Chem. 90* (1986) 5502.

[5] a) D. P. Strommen, A. M. Giroud-Godquin, J. C. Marchon, D. Guillon, A. Skoulios, *J. Phys. Lett. 45* (1981) L-681. b) A. M. Giroud-Godquin, J. M. Latour, J. C. Marchon, *Inorg. Chem. 24* (1985) 4454. c) H. Abied, D. Guillon, A. Skoulios, P. Weber, A. M. Giroud-Godquin, J. C. Marchon, *Liq. Cryst. 2* (1987) 269. d) A. M. Giroud-Godquin, P. Maldivi, J. C. Marchon, B. Marchon, *ibid. 2* (1987) 689. e) H. Abied, D. Guillon, A. Skoulios, H. Dexpert, A. M. Giroud-Godquin, J. C. Marchon, *J. Phys. (Les Ulis, Fr.) 49* (1988) 345. f) H. Abied, D. Guillon, A. Skoulios, A. M. Giroud-Godquin, P. Maldivi, J. C. Marchon, *Colloid Polym. Sci. 266* (1988) 579. g) A. M. Giroud-Godquin, P. Maldivi, J. C. Marchon, P. Aldebert, A. Peguy, D. Guillon, A. Skoulios, *J. Phys. (Les Ulis, Fr.) 50* (1989) 513.

[6] a) P. Maldivi, A. M. Giroud-Godquin, J. C. Marchon, D. Guillon, A. Skoulios, *Chem. Phys. Lett. 157* (1989) 552; b) J. C. Marchon, P. Maldivi, A. M. Giroud-Godquin, D. Guillon, A. Skoulios, D. P. Strommen, *Philos. Trans. R. Soc. London, A330* (1990) 109.

[7] In a typical preparation, 1.00 g (3.8 mmol) of $[Mo(CO)_6]$ was slurried in 15 mL of diglyme (dried and oxygen-free) under an N_2 atmosphere. To this mixture was added 3 equivalents of the carboxylic acid and the solution heated to reflux for 3 h. During this time, sublimed $[Mo(CO)_6]$ was continually shaken back into solution. The diglyme was removed in vacuo and the resulting yellow residue was recrystallized from hot toluene. ^{1}H NMR data indicate that all compounds are free from coordinated solvent.

[8] For a good review of discotic mesophases and their representative optical micrographs, see C. Destrade, P. Foucher, H. Gasparoux, N. H. Tinh, A. M. Levelut, J. Malthete, *Mol. Cryst. Liq. Cryst. 106* (1984) 121.

[9] C. D. Garner, W. Clegg, G. Pimblett, *J. Chem. Soc., Dalton Trans.* (1986) 1257.

Synthesis and Structure of $[Ba_3(OSiPh_3)_6(THF)] \cdot 0.5$ THF, a Trinuclear Barium Siloxide Containing Low-Coordinate Barium Ions

By *Kenneth G. Caulton,* Malcolm H. Chisholm, Simon R. Drake*, and *William E. Streib*

Alkoxides of barium are of interest as molecular precursors to solid-state materials such as the superconducting ternary oxide $YBa_2Cu_3O_{7-x}$.[1] Recently, we have shown that the reactions between barium metal and alcohols or phenols give oxo alkoxides and oxo aryloxides, respectively.[2, 3] Reasoning that the oxo group in these derivatives was derived from a C–O bond cleavage, we turned our attention to the use of a silanol for which Si–O bond cleavage by either a radical or cationic mechanism is less likely.[4] However, triphenyl silanol, which is known to form compounds with several alkali metals,[5, 6] failed to react with Ba granules in THF under conditions previously employed in the synthesis of barium alkoxides and aryloxides. Neither prolonged reflux nor the use of an ultrasonic gun had significant effect. The addition of trace amounts of $HgCl_2$ or I_2 (known to activate metal surfaces) or strong Lewis bases such as $Me_2NCH_2CH_2NMe_2$ or $(Me_2N)_3PO$ similarly failed to produce a reaction.

The alkaline-earth metals are known to dissolve in NH_3 to yield amide complexes,[7] which, though poorly characterized, have provided active systems for reactions with organic ligands containing acidic protons.[8, 9] Furthermore, NH_3-saturated solutions (rather than liquid NH_3) have found synthetic utility.[10] Barium metal granules in THF and triphenylsilanol react readily when gaseous ammonia is

[*] Prof. K. G. Caulton, Prof. M. H. Chisholm, Dr. S. R. Drake, Dr. W. E. Streib
Department of Chemistry and Molecular Structure Center
Indiana University
Bloomington, IN 47405 (USA)

[**] This work was supported by the National Science Foundation. *S.R.D.* is grateful to St. John's College, Cambridge (England), for a fellowship.

passed into the solution.[11] It is possible that a labile amido species is formed and leads by facile reaction with Ph_3SiOH to the title compound, siloxide **1**, though a radical pathway cannot be discounted. In any event, the reaction between barium and Ph_3SiOH is catalyzed by ammonia. Compound **1**, which is soluble in toluene, yielded crystals suitable for a single-crystal X-ray analysis from a toluene solution carefully layered with *n*-pentane.[12] The molecular structure of **1** and a ball-and-stick drawing of the M-OSi framework are shown in Figure 1.

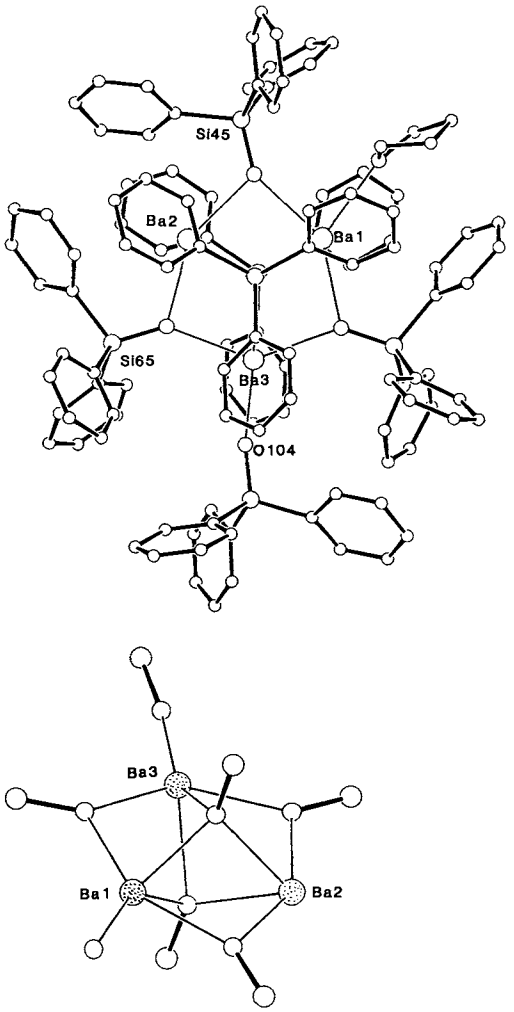

Fig. 1. Crystal structure of **1**. Top: Selected distances [Å], averaged where appropriate: Ba(1–3)-μ_3-$OSiPh_3$ 2.69(9), Ba(1-3)-μ_2-$OSiPh_3$ 2.64(4), Ba3-O104 2.472(4), Ba1-O(THF) 2.75(1). Bottom: Structure of $[Ba_3(OSi)_6O]$ core. ○ = O,Si; ⊜ = Ba.

In contrast to the recently reported structures of phenoxide, *tert*-butoxide, and methoxy-ethoxide complexes,[2, 3] there is no hydroxy or oxo ligand present in the compound. This is in accord with the prediction that the Si–O bond is stronger than the C–O bond.[4] Also worthy of mention is the low Lewis base (THF) content of **1**, which may be attributed to the steric bulkiness of the triphenylsilanol ligands and the solubility which these ligands impart to the resulting complex.

The three barium atoms form a triangle that is capped by two μ_3-$OSiPh_3$ ligands and further linked by three μ_2-$OSiPh_3$ moieties around the belt of the triangle. To achieve electrical neutrality (with Ba in a + 2 oxidation state), a sixth triphenylsiloxide ligand is terminally bonded to Ba3. In addition, one terminal THF molecule is ligated to Ba1. The barium atom coordination in **1** is exceptionally low for a dipositive cation as large as $Ba^{2\oplus}$.[13] Thus, Ba1 and Ba3, which are both ligated by terminal ligands (THF and Ph_3SiO, respectively), are five-coordinate, while Ba2 has the unprecedented coordination number 4 and a coordination geometry which constrains all four siloxide ligands into less than a hemisphere. The shortest Ba2–C(phenyl) distance is 3.31 Å, which is notably longer than the average Ba–C distance of 2.98 Å in Cp^*_2Ba($Cp^* = \eta^5$-C_5Me_5).[14] Moreover, Ba–C(phenyl) distances as short as 3.36 Å for Ba1 and Ba3 indicate that no significant phenyl–Ba2 interaction is operative. Four coordination of one of the barium metal centers in **1** represents the first observation of such a low coordination number (no such examples were found in a search of the Cambridge Crystallographic Data Base).[15] For barium, coordination numbers of 6–9 or greater are common.[13, 15, 16] Because the bonds between Ba2 and the oxygens of the μ_2- and μ_3-siloxide ligands are so short, the adjacent μ_2-siloxides (those containing Si45 and Si65) bend into the region of the empty hemisphere of Ba2. Whereas the terminal Ba–O104 bond is short (with a nearly linear Ba–O104–Si angle of 167.1°), the Ba–O(THF) bond is very long.

The ^1H and ^{13}C NMR spectra of **1** in $[D_8]$toluene reveal only one type of phenyl ring at ambient temperature.[17] Even at − 60 °C, only one phenyl group is identified by ^1H NMR spectroscopy. This suggests that the molecule may be fluxional, although the phenyl protons may not be sensitive probes for Ba–O interactions. Evidently, ^{29}Si NMR spectroscopy is more discriminating because the ^{29}Si NMR spectrum of **1** in $[D_8]$toluene shows two resonances in the integral ratio 2:4.[17] A plausible explanation for the 2:4 ^{29}Si NMR signals would be that the terminal $OSiPh_3$ is involved in a selective exchange with the μ-$OSiPh_3$ groups that lie in the Ba_3 plane. This $OSiPh_3$ exchange would not involve the μ_3-$OSiPh_3$ ligands that lie above and below the plane of the metal atoms.

Rather surprisingly, **1** is volatile and may be sublimed at 200–220 °C (10^{-2} Torr) to yield the THF-free compound, $[Ba(OSiPh_3)_2]_n$, which may also be obtained by stripping a toluene solution of **1** to dryness. This material is insoluble in nondonor media, but dissolves in THF, to regenerate **1** after crystallization from toluene.

Received: July 12, 1990 [Z 4065 IE]
German version: *Angew. Chem. 102* (1990) 1492

CAS Registry numbers:
1, 130168-42-2; **13a**, 7440-39-3.

[1] M. K. Wu, J. R. Ashburn, C. J. Thorng, P. H. Hor, R. L. Meng, L. Gao, Z. J. Huang, Y. Q. Wang, C. W. Chu, *Phys. Rev. Lett. 58* (1987) 908.
[2] K. G. Caulton, M. H. Chisholm, S. R. Drake, K. Folting, *J. Chem. Soc. Chem. Commun. 1990*, 1349.
[3] K. G. Caulton, M. H. Chisholm, S. R. Drake, J. C. Huffman, *J. Chem. Soc. Chem. Commun. 1990*, in press.
[4] R. E. Lapointe, P. T. Wolczanski, G. D. Van Duyne, *Organometallics 4* (1985) 1810.
[5] A. B. Goel, R. C. Mehrotra, *Indian J. Chem. Sect. A16* (1978) 428; D. C. Bradley, R. C. Mehrotra, D. P. Gaur: *Metal Alkoxides*, Academic Press, London 1978; G. A. Sigel, R. A. Bartlett, D. Decker, M. M. Olmstead, P. P. Power, *Inorg. Chem. 26* (1987) 1773.
[6] E. C. Ashby, A. B. Goel, *Inorg. Chem. 18* (1979) 1306.
[7] F. G. Cotrell, *J. Phys. Chem. 12* (1914) 85; W. Biltz, G. F. Hüttig, *Z. Anorg. Allg. Chem. 114* (1920) 241.
[8] G. R. Stevenson, L. E. Schock, *J. Am. Chem. Soc. 105* (1983) 3742; P. Jutzi, W. Leffers, G. Müller, B. Huber, *Chem. Ber. 122* (1989) 879.
[9] W. E. Linde in G. Wilkinson, F. G. A. Stone, E. W. Abel (Eds.): *Comprehensive Organometallic Chemistry, Vol. 1*, Pergamon, Oxford 1982, pp. 155–252.

[10] P. S. Belton, I. P. Parkin, J. D. Woollins, *J. Chem. Soc. Dalton Trans. 1990*, 514.

[11] All reactions were carried out under an argon atmosphere in dried and carefully deoxygenated solvents. **1**: Ba (1.37 g, 10 mmol) and Ph_3SiOH (5.56 g, 20 mmol) were weighed into a Schlenk tube in a glove box. After removal of the Schlenk tube from the glove box, 20 mL of THF was added, and ammonia gas was bubbled slowly into the reaction mixture for 7 min. The evolution of gas bubbles and the appearance of a pink color indicated that the barium metal was reacting. The solution was then stirred for 5 h, during which time all the metal was consumed, to yield a cloudy pink solution. The solvent and excess ammonia were removed under vacuum to yield a waxy solid, which was redissolved in 20 mL of THF. The solvent was removed once more, and the white powdery solid was redissolved in toluene (15 mL) and filtered. The filtrate was carefully layered with *n*-pentane (15 mL) and left to crystallize at 20 °C. Yield 6.15 g, 77% based on Ba. A small amount (< 30 mg) of a solid purple precipitate formed in the reaction was readily separated from the product by filtration.

[12] Crystal data for **1** at −169 °C: $a = 16.560(3)$, $b = 22.586(3)$, $c = 15.244(3)$ Å, $\alpha = 104.22(1)$, $\beta = 115.71(1)$, $\gamma = 88.82(1)°$, $Z = 2$, $\varrho_{calcd} = 1.456$ g cm^{-3}, space group $P\bar{1}$. Of the 15190 reflections collected ($Mo_{K\alpha}$, $6 \le 2\theta \le 45$), 13035 were unique and the 11231 having $F > 3\sigma(F)$ were used in the full-matrix least-squares refinement. Non-hydrogen atoms were refined anisotropically. The unit cell also contains a molecule of THF which is at a center of symmetry and is therefore disordered. Hydrogen atoms, except those on the disordered THF, were placed in calculated positions with d(C-H) = 0.95 Å and the thermal parameters were set to one plus the isotropic thermal parameter of the parent atom. The final residuals are $R = 0.041$ and $R_w = 0.045$. Further details of the crystal structure investigation may be obtained from the Fachinformationszentrum Karlsruhe, Gesellschaft für wissenschaftlich-technische Information mbH. D-7514 Eggenstein-Leopoldshafen 2 (FRG), on quoting the depository number CSD-54798, the names of the authors, and the journal citation.

[13] See, for example: D. Barr, A. T. Brooker, M. J. Doyle, S. R. Darke, P. R. Raithby, R. Snaith, D. S. Wright, *J. Chem. Soc. Chem. Commun. 1989*, 893, and references therein.

[14] R. A. Williams, T. P. Hanusa, J. C. Huffman, *Organometallics 29* (1990) 1128.

[15] Cambridge Crystallographic Data Base; Director: Dr. *O. Kennard*, University of Cambridge.

[16] For recent references see: R. Khattar, C. B. Knobler, M. F. Hawthorne, *Inorg. Chem. 29* (1990) 2191.

[17] Compound **1** slowly sublimes at 230–245 °C, > 250 °C dec. ^{1}H NMR (500 MHz, 20 °C, [D$_8$]toluene): $\delta = 1.20$ (m, THF), 3.06 (m, THF), 6.95 (m, Ph), 7.09 (m, Ph), 7.48 (s, br, Ph), 7.78 (s, Ph). ^{13}C NMR (126 MHz, 20 °C, [D$_8$]toluene): $\delta = 25.45$ (s, THF), 67.46 (s, THF), 128.29 (s, Ph), 129.66 (s, Ph), 130.31 (s, Ph), 135.44 (s, Ph). ^{29}Si NMR (99.336 MHz, 20 °C, [D$_8$]toluene, internal TMS as standard): $\delta = -17.51$(s), -20.84 in a ratio of 2:4. Correct elemental analysis.

Synthesis of Phospholyltetrahydroboratouranium Complexes. Crystal Structure of $[(\eta^5\text{-}C_4Me_4P)_2U(BH_4)_2]$

By *Denise Baudry,* Michel Ephritikhine, François Nief,* Louis Ricard,* and *François Mathey*

The phospholyl group is a heterocyclopentadienyl ligand that has recently been found capable of η^5-coordination to main group metals[1] as well as to rare earth[2] and early transition metals.[3] This ligand was of special interest to us in uranium chemistry because of its ability to bridge two metal centers.[4] Related pyrrolyl azacyclopentadienyl complexes of uranium have only recently appeared in the literature.[5] We report here the first synthesis of monomeric and dimeric uranium phospholyl complexes.

The phospholyl compounds were prepared similarly to other η^5-dienyltetrahydroborato complexes of uranium[6] (see Scheme 1). Thus, reaction of donor-free potassium 2,3,4,5-tetramethylphospholide **1**[7] (hereafter abbreviated as L) in THF with $[(Mes)U(BH_4)_3]$ (Mes = η^6-1,3,5-$(CH_3)_3C_6H_3$)[6a] afforded a red solution of $[L_2U(BH_4)_2]K$;[8] after removal of the solvent, a dark brown solution of $[(L_2UBH_4)_2]$ **2**[9] was obtained by extraction with toluene. The ^{31}P NMR spectrum of **2**,[10] which exhibited two signals at $\delta = 727$ and 3471, revealed the presence of two nonequivalent L ligands, whereas the ^{1}H NMR spectrum showed that the eight methyl groups in **2** are chemically nonequivalent. The neutral complex **2** adopts the dimeric structure shown in Scheme 1. We suppose that in this symmetric structure the phosphorus atom, which is σ–π bonded to uranium, gives rise to the large paramagnetic shift at $\delta = 3471$. The eight methyl groups of each L_2UBH_4 moiety are nonequivalent because of the chirality of the metal centers.

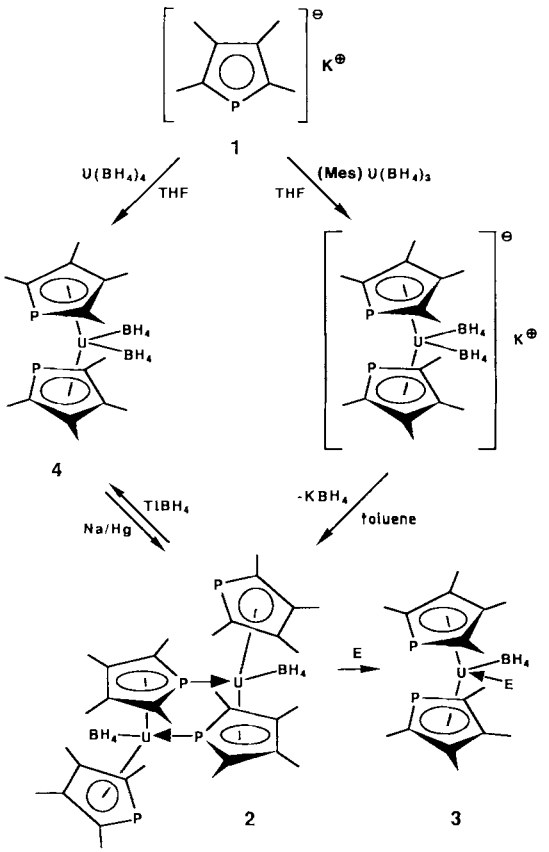

Scheme 1. Mes = η^6-1,3,5-$(CH_3)_3C_6H_3$. E = THF, PPh_3O.

Dimeric organouranium complexes are very rare,[11] and it is noteworthy that the phospholyl ligands rather than the borohydride groups are bridging in **2**. These bridges can be broken by dissolution of **2** in THF or by addition of one equivalent of PPh_3O in toluene, resulting in the formation of $[L_2U(BH_4)(OPPh_3)]$ **3**.[12]

Compound **2** was oxidized with $TlBH_4$ to the neutral U(IV) derivative $[L_2U(BH_4)_2]$ **4**,[13] which was also formed on reaction of $U(BH_4)_4$ with **1**. Reduction of **4** with sodium amalgam gives **2**.

[*] Dr. D. Baudry, Dr. M. Ephritikhine
Service de Chimie Moléculaire
DSM/DPhG, CEN/CEA Saclay, CNRS UA 331
91191 Gif sur Yvette Cedex (France)
Dr. F. Nief, Dr. L. Ricard, Prof. Dr. F. Mathey
Laboratoire de Chimie du Phosphore et des Métaux de Transition
DCPH Ecole Polytechnique
91128 Palaiseau Cedex (France)

The pseudotetrahedral structure of **4** in the crystal (Fig. 1)[14] shows that the phospholyl ligand is pentahapto bonded to the uranium atom. The ring geometry differs very little from that of related complexes of Li[1] or Zr.[3] The short U–B distance (255 pm) is typical for bonds with a tridentate BH_4 ligand.[6c] Finally, we should emphasize that,

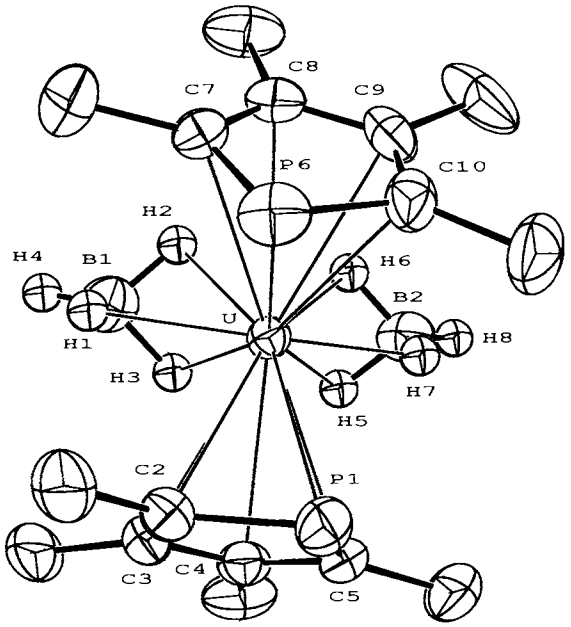

Fig. 1. Structure of **4** in the crystal. Selected mean bond lengths [pm] and angles [°]: U-P, 290.5 ± 0.8; U-C, 281.1 ± 4.3; U-B, 255.3 ± 0.1; U-H, 229 ± 20; P-C, 176.4 ± 1; C-C (cycle), 140.4 ± 2.1; B-H, 110 ± 15; B-U-B, 100.4(2); C-P-C, 90.4 ± 0.3; P-C-C (ring) and C-C-C (ring) 112.3 ± 0.7.

in contrast to two previous reports,[15, 16] we could detect the ^{31}P NMR signals for all the described compounds without major difficulty. We could also observe a resonance at $\delta = 2515$ ($W_{1/2} \approx 200$ Hz) for Cp_3UPPh_2.[15] Therefore, although there is not enough data available to establish correlations between ^{31}P NMR parameters and coordination modes of phosphorus, ^{31}P NMR should prove a valuable tool for the study of phosphorus-containing uranium compounds.

Experimental

^1H NMR (TMS int.): Bruker WP60 (60 MHz) and Bruker AC200 (200 MHz); ^{31}P NMR (85% H_3PO_4 int.): Bruker WP80 (32.4 MHz) and Bruker AM400 (162 MHz).

1: A solution of 1,4-bis(tetramethylphospholyl)butane [17] (5.16 g, 15.4 mmol) in dimethoxyethane (100 mL) was treated with K (1.8 g) at 50 °C for 3 h. After cooling, the reaction mixture was filtered and evaporated to dryness. The residue was rinsed with THF (2 × 50 mL) and dried in vacuo. Yield 3.20 g (17.9 mmol, 58%) of **1** as a white solid.—**2**: THF (20 mL) was condensed at −78 °C onto a mixture of [(Mes)U(BH_4)$_3$] (277 mg, 0.69 mmol) and **1** (245 mg, 1.37 mmol). After warming to room temperature, the solution was evaporated to dryness and extracted with toluene. The toluene solution was concentrated and **2** crystallized out on addition of cold (−78 °C) pentane (118 mg, 0.22 mmol, 32%).—**3**: A solution of **2** (150 mg, 0.28 mmol) and Ph_3PO (78 mg, 0.28 mmol) in toluene was stirred for 10 min at room temperature, then filtered. Evaporation of the cooled solution led to separation of microcrystals of **3**; these were washed with cold (−78 °C) toluene and pentane (84 mg, 0.11 mmol, 40%).—**4**: A mixture of U(BH_4)$_4$ (173 mg, 0.58 mmol) and **1** (207 mg, 1.16 mmol) in toluene (15 mL) was stirred of 2 h at room temperature. The solvent was then removed and the residue extracted with pentane. Upon cooling to −50 °C, dark brown crystals of **4** separated out (188 mg, 0.34 mmol, 59%).

Received: July 23, 1990 [Z 4085 IE]
German version: *Angew. Chem. 102* (1990) 1501

CAS Registry numbers:
1, 130149-60-9; **2**, 130168-03-5; **3** (E = $OPPh_3$), 130168-04-6; **3** (E = THF), 130168-07-9; **4**, 130168-05-7; $4^{\ominus}\cdot K^{\oplus}$, 130168-06-8; MesU($BH_4$)$_3$, 122627-85-4; U($BH_4$)$_4$, 47097-99-4; $TlBH_4$, 61204-71-5; Ph_3PO, 791-28-6; 1,4-Bis(tetramethylphospholyl)butane, 125706-15-2.

[1] K. Theopold, H. Douglas, *Angew. Chem. 101* (1989) 1394; *Angew. Chem. Int. Ed. Engl. 28* (1989) 1367.
[2] F. Nief, F. Mathey, *J. Chem. Soc. Chem. Commun. 1989*, 800.
[3] F. Nief, F. Mathey, L. Ricard, *Organometallics 7* (1988) 921; F. Nief, L. Ricard, F. Mathey, *ibid. 8* (1989) 1473.
[4] F. Nief, L. Ricard, F. Mathey, *J. Organomet. Chem. 384* (1990) 271.
[5] T. J. Marks, J. R. Kolb, *J. Organomet. Chem. 82* (1974) C35.
[6] a) D. Baudry, E. Bulot, M. Ephritikhine, *J. Chem. Soc. Chem. Commun. 1988*, 1369; b) *ibid. 1989*, 1316; c) D. Baudry, E. Bulot, P. Charpin, M. Ephritikhine, M. Lance, M. Nierlich, J. Vigner, *J. Organomet. Chem. 371* (1989) 163.
[7] **1**: ^1H NMR ([D_8]THF): $\delta = 1.87$ (CH_3), 2.09 (d, J(PH) 10.3 Hz, CH_3); $^{13}C\{^1H\}$NMR: $\delta = 13.9$ (CH_3), 16.1 (d, J(PC) 30.5 Hz, CH_3), 124.1 (C_2), 134.7 (d, J(PC) 36 Hz, C_3); $^{31}P\{^1H\}$NMR: $\delta = 74.1$. This compound has been described previously as an adduct with [18]crown-6: see Ref. [1].
[8] $[L_2U(BH_4)_2]^{\ominus}$: ^1H NMR ([D_8]THF, 303 K): $\delta = -13.29$ ($W_{1/2} = 15$ Hz, $4CH_3$), 4.08 ($W_{1/2} = 15$ Hz, $4CH_3$), 65.47 ($2BH_4$, $W_{1/2} = 300$ Hz); $^{31}P\{^1H\}$NMR (307 K): $\delta = 618$ ($W_{1/2} = 200$ Hz).
[9] **2**: ^1H NMR (C_6D_6, 303 K): $\delta = -46.80$, −40.95, −35.59, −20.08, −12.45, 5.57, 8.33, 13.45 ($2CH_3$ for each resonance, $W_{1/2} = 15$ Hz), 165 ($2BH_4$, $W_{1/2} = 300$ Hz); $^{31}P\{^1H\}$NMR (307 K): $\delta = 727$ ($W_{1/2} = 150$ Hz), 3471 ($W_{1/2} = 1000$ Hz).
[10] The positions of these unusually shifted resonances (although not unexpected owing to the paramagnetic nature of all U^{III} and U^{IV} complexes) have been verified by using different observation offset frequencies, running control samples, and recording the spectra at 32.4 MHz and 162 MHz.
[11] T. J. Marks, R. D. Ernst, in G. Wilkinson (Ed.): *Comprehensive Organometallic Chemistry, Vol. 3*, Pergamon, Oxford 1982, Chap. 21, *Cf.* the trimeric solid state structure of $(C_5Me_5)_2UCl$ with bridging chloride ligands: P. J. Fagan, J. M. Manriquez, T. J. Marks, C. S. Day, S. H. Vollmer, V. W. Day, *Organometallics 1* (1982) 170.
[12] **3**: ^1H NMR (C_6D_6, 303 K): $\delta = -18.99$, −8.76, −1.45, 3.49 ($2CH_3$ for each resonance, $W_{1/2} = 20$ Hz), 5.85 (3H para), 5.05 (6H meta), 0.16 (6H ortho), 86.94 ($1BH_4$, $W_{1/2} = 300$ Hz); $^{31}P\{^1H\}$NMR (307 K): $\delta = 86$ ($OPPh_3$, $W_{1/2} = 20$ Hz), 650 (PC_4Me_4, $W_{1/2} = 200$ Hz). Correct elemental analysis.
[13] **4**: ^1H NMR (C_6D_6, 303 K): $\delta = -36.73$ (q, $2BH_4$, J(BH) 86 Hz, −13.01 ($4CH_3$, $W_{1/2} = 12$ Hz), 35.13 ($4CH_3$, $W_{1/2} = 3$ Hz); $^{31}P\{^1H\}$NMR (307 K): $\delta = 960$ ($W_{1/2} = 200$ Hz). Correct elemental analysis.
[14] Crystals of **4** were grown at −18 °C from a pentane solution. Triclinic, $P\bar{1}$, $a = 803.1(1)$, $b = 873.7(1)$, $c = 1569.3(2)$ pm, $\alpha = 81.59(1)°$, $\beta = 80.66(1)°$, $\gamma = 72.89(1)°$, $Z = 2$, final $R = 0.026$. Further details of the crystal structure investigation are available on request from the Fachinformationszentrum Karlsruhe, Gesellschaft für wissenschaftlich-technische Information mbH, D-7514 Eggenstein-Leopoldshafen 2 (FRG), on quoting the depository number, CSD 54865, the names of the authors, and the journal citation.
[15] G. Paolucci, G. Rossetto, P. Zanella, R. D. Fischer, *J. Organomet. Chem. 284* (1985) 213.
[16] M. R. Duttera, V. W. Day, T. J. Marks, *J. Am. Chem. Soc. 106* (1984) 2907.
[17] C. Charrier, F. Mathey, *Tetrahedron. Lett 25* (1987) 5025.

Preparation and Structure of $[Se{=}W(PSe_4)(PSe_2)]^{2\ominus}$; a Cluster Containing a Heteroallylic $PSe_2^{\ominus}$ Unit**

By *Samuel C. O'Neal, William T. Pennington,* and *Joseph W. Kolis**

The chemistry of molecular transition-metal polyselenides and tellurides has recently been the subject of active investi-

[*] Prof. J. W. Kolis, S. C. O'Neal, W. T. Pennington
Department of Chemistry
Clemson University
Clemson SC 29634 (USA)

[**] This work was supported by the National Science Foundation (Grant No. CHE-8802217).

gation.[1] Part of the motivation for studies in this sector has derived from some obvious differences in chemistry from that of metal sulfides, as well as their use in generating new solids.[2] We are interested in using these elements to generate new three-dimensional cages which have novel structural and electronic characteristics.[3] However, since chalcogen atoms are generally divalent, the occurrence of true cages and clusters is somewhat limited. In contrast, compounds containing trivalent atoms of group 15 have recently been reported which possess extraordinary structural diversity.[4]

Cage compounds such as P_4S_3 are useful for generating novel three-dimensional clusters, either as a unit,[5] or as a source of unusual fragments.[6] In this communication we report the preparation of a tungsten phosphorus selenide cluster which displays several unusual features. The easily accessible $[Ph_4P]_2[WSe_4]$[7] readily reacts with phosphorus selenide glass, "P_4Se_4", and in reasonable yield to give the

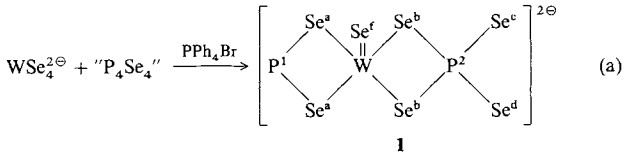

(a)

1

dianion **1** [Eq. (a)], which has been crystallized as its tetraphenylphosphonium salt with one DMF molecule per cluster. It has been characterized by a variety of spectroscopic methods and a single-crystal X-ray diffraction.[8] The structure of **1** is unusual in many respects (see Fig. 1). It

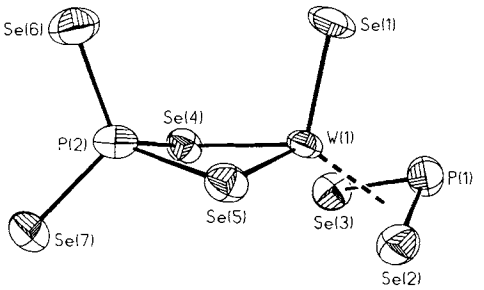

Fig. 1. Structure of **1** in the crystal (ORTEP), ellipsoids at the 50% probability level with important distances [pm]: W1-Se1 226.0(3), W1-Se2 252.6(3), W1-Se3 252.9(3), W1-Se4 248.9(3), W1-Se5 249.6(3), W1-P1 248.3(7), P1-Se2 222.9(7), P1-Se3 223.3(9), P2-Se4 228.0(7), P2-Se5 229.9(8), P2-Se6 212.7(6), P2-Se7 213.6(6).

contains a tetrahedral $PSe_4^{3\ominus}$ ligand coordinated in bidentate fashion to the metal center. This is in contrast to the metal phosphates which usually form bridges between different metal centers, but is common for dithiophosphate esters.[9] However, the coordination chemistry of the heavier phosphorus chalcogenides is not well developed and most examples are solid-state compounds derived from the sulfosalt class of minerals.[9]

The most interesting feature of the molecule is the very unusual bent PSe_2 moiety bound to the tungsten center. The group can be assigned a formal charge of -1, which would make it isoelectronic and isolobal with the allyl anion and $NO_2^{\ominus}$. The bond distances of 252.7(3) pm between tungsten and the $PSe_2^{\ominus}$ selenium atoms corresponds quite well with the length of a single bond. It is not much longer than the W–Se distances to the $PSe_4^{3\ominus}$ ligand (average 249.3(3) pm), but considerably longer than the double bond to the terminal selenide (226.0(3) pm). The distance between the tungsten and the phosphorus atom of the $PSe_2^{\ominus}$ ligand is 248.3(7) pm, which is clearly a bonding interaction.[10] The P–Se distances in the $PSe_2^{\ominus}$ group average 223.1(8) pm, which is between the formally double bonded terminal P–Se distances (213.2(6) pm), and the single bonded bridging distances (229.0(7) pm) of the coordinated $PSe_4^{3\ominus}$ group. In addition, the Se–P–Se angle is 102.3(3)° implying the existence of a stereoactive lone pair on the phosphorus atom.

Thus we can postulate a pseudo-allylic resonance structure which is coordinated to the tungsten center in a side bonded fashion. The single negative charge on the ligand implies a formal oxidation state of IV on the tungsten atom. The chemistry of low-coordinated phosphorus ligands has been extensively investigated,[11] but to our knowledge, the $PSe_2^{\ominus}$ group has not been reported in its free or complexed state.

We have performed multinuclear NMR characterization of this molecule and were able to assign all ^{31}P and ^{77}Se resonances on the basis of coupling and satellite peaks (see *Experimental* and Fig. 2). In the ^{31}P NMR spectrum the P(1)

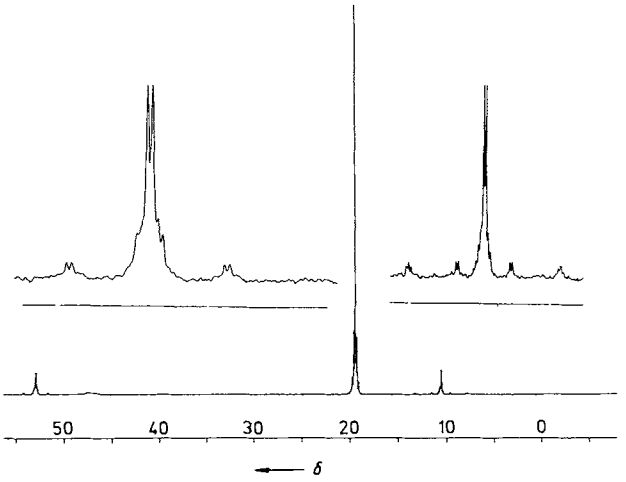

Fig. 2. ^{31}P NMR spectrum of $(PPh_4)_2 \cdot$ **1**, showing an expanded view of the satellites due to ^{77}Se coupling.

resonance appears 10.49 ppm upfield of the tetraphenylphosphonium signal. It has doublet satellite peaks with J_{P-Se} of 227.8 Hz and J_{P-Se} of 654.5 Hz. (All peaks are doublets due to long range coupling with the other phosphorus.) The satellites with the larger coupling can be assigned as the terminal phosphorus selenides. Since the two selenides are in a slightly different environment, their satellites show up as two superimposed doublets or a pseudo triplet. The resonance of P(1) (of the "$PSe_2^{\ominus}$ phosphorus") is downfield at $\delta = 52.85$ (with $J_{P-Se} = 309.4$ Hz). On the basis of these coupling constants, all of the selenium shifts, which show up as doublets due to coupling with the phosphorus, can be assigned with confidence. The terminal selenium bound to the tungsten appears far downfield, as is common with these groups.[12]

Experimental

The mixed polychalcogenide of stoichiometry P_4Se_4 was prepared by heating a mixture of equimolar amounts of red phosphorus and gray selenium in a quartz tube for 16 h at 450 °C followed by slow cooling to room temperature.

This was ground up and stored in an argon atmosphere. The "P_4Se_4" powder (0.40 g, 0.91 mmol) was added to a solution of 0.56 g (0.48 mmol) $[(C_6H_5)_4P]_2[WSe_4]$ in 10 mL DMF. The resulting red solution was stirred for 24 h at room temperature, then filtered, layered with 10 mL THF, and stored at 4 °C. Lustrous red crystals suitable for an X-ray diffraction analysis separated out. Yield 70%, correct analysis.—IR: ν [cm^{-1}] = 495(s), 441(s), 328(m), 123(m).—NMR data [for the designation of the P and Se atoms see Equation (a)]: ^{31}P NMR (DMF, H_3PO_4 ext.): δ = 52.85 (d, 1 P, P(1)) J(P(1)–P(2)) 9.8 Hz, J(P(1)–Se(a)) 309 Hz), δ = 10.49 (d,1 P, P(2)) J(P(2)–Se(b)) 227.8 Hz, J(P(2)–Se(c,d)) 654.5 Hz), 19.37 (s, 2 P, $Ph_4P^{\oplus}$), ^{77}Se NMR (DMF rel. to Me_2Se): δ = 1073 (d, 2 Se, Se(a)), 1210 (d, 2 Se, Se(b)), 993 (d, 2 Se, Se(c,d)), 2288 (s, 1 Se, Se(f)).

Received: June 13, 1990 [Z 4013 IE]
German version: *Angew. Chem. 102* (1990) 1502

CAS Registry numbers:
1, 130955-60-1; P_4Se_4, 56836-52-6; $[Ph_4P]_2[WSe_4]$, 112988-67-7.

[1] a) M. A. Ansari, J. A. Ibers, *Coord. Chem. Rev. 100* (1990) 223. b) M. Kanatzidis, *Comments Inorg. Chem. 10* (1990) 161; c) D. Fenske, J. Ohmer, J. Hachgenei, K. Merzweiler, *Angew. Chem. 100* (1988) 1300; *Angew. Chem. Int. Ed. Engl. 27* (1988) 1277; d) H. G. Gysling in S. Patai, Z. Rappaport (Eds.): *The Chemistry of Organic Selenium and Tellurium Compounds*, Wiley, New York 1986, p. 679; e) W. A. Herrmann, *Angew. Chem. 98* (1986) 57; *Angew. Chem. Int. Ed. Engl. 25* (1986) 56.

[2] J. G. Brennan, T. Siegrist, S. M. Stuczynski, M. L. Steigerwald, *J. Am. Chem. Soc. 111* (1989) 9240.

[3] a) W. A. Flomer, S. C. O'Neal, W. T. Pennington, D. Jeter, A. W. Cordes, J. W. Kolis, *Angew. Chem. 100* (1988) 1768; *Angew. Chem. Int. Ed. Engl. 27* (1988) 1702; b) W. A. Flomer, J. W. Kolis, *J. Am. Chem. Soc. 110* (1988) 3682.

[4] a) O. J. Scherer, *Comments Inorg. Chem. 6* (1987) 1; b) O. J. Scherer, M. Swarowsky, G. Wolmershäuser, *Organometallics 8* (1989) 841; c) M. DiVaira, P. Stoppioni, M. Peruzzini, *Polyhedron 6* (1987) 351; d) P. T. Wood, J. D. Woollins, *Transition Met. Chem. 11* (Weinheim, Germany) (1986) 358; e) A. J. DiMaio, A. L. Rheingold, *Chem. Rev. 90* (1990) 169; f) B. W. Eichhorn, R. C. Haushalter, J. C. Huffman, *Angew. Chem. 101* (1989) 1081; *Angew. Chem. Int. Ed. Engl. 28* (1989) 1032.

[5] a) A. W. Cordes, R. D. Joyner, R. D. Shores, E. D. Dill, *Inorg. Chem. 13* (1974) 132; b) C. A. Ghilardi, S. Midollini, A. Orlandini, *Angew. Chem. 95* (1983) 801; *Angew. Chem. Int. Ed. Engl. 22* (1983) 790.

[6] a) M. DiVaira, M. Peruzzini, P. Stoppioni, *J. Chem. Soc. Chem. Commun. 1983*, 903; b) M. DiVaira, M. Peruzzini, P. Stoppioni, *J. Chem Soc., Dalton Trans. 1985*, 291; c) *Polyhedron 4* (1986) 945; d) G. A. Zank, T. B. Rauchfuss, S. R. Wilson, A. L. Rheingold, *J. Am. Chem. Soc. 106* (1984) 7621.

[7] S. C. O'Neal, J. W. Kolis, *J. Am. Chem. Soc. 110* (1988) 1971.

[8] Crystal structure data: $[(C_6H_5)_4P]_2[Se{=}W(PSe_4)(PSe_2)] \cdot (CH_3)_2NCOH$, triclinic, space group $P\bar{1}$, a = 10.582(4), b = 13.770(5), c = 20.159(6) Å, α = 88.35(3)°, β = 77.00(3)°, γ = 70.28(3)°, V = 2692(2) Å^3, Z = 2, ϱ_{calc} 1.91 g cm^{-3}, $\mu Mo_{K\alpha}$ = 70.30 cm^{-1} (transmission factors: 0.47–1.00), T = 21 °C. Refined using 4395 reflections ($2\theta \leq 45°$) with $F_o^2 > 3\sigma(F_o^2)$ to R = 0.0702 and R_w = 0.0868 on 587 parameters (all non-hydrogen atoms refined anisotropically). Full structural details of the crystal structure investigation may be obtained from the Fachinformationszentrum Karlsruhe, Gesellschaft für wissenschaftlich-technische Information mbH, D-7514 Eggenstein-Leopoldshafen 2 (FRG), on quoting the depository number CSD-54 758, the names of the authors, and the journal citation.

[9] D. E. C. Corbridge: *The Structural Chemistry of Phosphorus*, Elsevier, Amsterdam, 1974.

[10] L. Aslanov, R. Mason, A. G. Wheeler, P. O. Whimp, *J. Chem Soc. D 1970*, 30.

[11] a) O. J. Scherer, *Angew. Chem. 102* (1990) 1137; *Angew. Chem. Int. Ed. Engl. 26* (1985) 1104, and references cited therein; b) J. F. Nixon, *Chem. Rev. 88* (1988) 1327.

[12] R. W. M. Wardle, S. Bhaduri, C.-N. Chau, J. A. Ibers, *Inorg. Chem. 27* (1988) 1747.

BOOK REVIEWS

Book Reviews are written by invitation from the editor. Suggestions for books to be reviewed and for book reviewers are welcome. Publishers should send brochures or (better) books to the following address: Redaktion Angewandte Chemie, Postfach 101161, D-6940 Weinheim, Federal Republic of Germany. The editor reserves the right of selecting which books will be reviewed. Uninvited books not chosen for review will not be returned.

Poets in the Laboratory

Cantor's Dilemma. By *C. Djerassi*. Doubleday, New York 1989. 230 pp., hardcover $ 18.95.—ISBN 0-385-26183-7

It is unusual for scientists to write fiction, the most familiar example being *C. P. Snow*, the Cambridge University chemist–spectroscopist, best known for his "Strangers and Brothers" series of novels and his influential and controversial book "The Two Cultures and the Scientific Revolution." *Carl Djerassi*, Professor of Chemistry at Stanford University, recipient of the US National Medal of Science and the first Wolf Prize in Chemistry and synthesizer of the first oral contraceptive, has followed *Baron Snow*'s example; he is the author of "The Futurist and Other Stories", and his short stories, essays, and poems have appeared in various magazines. As related in "Steroids Made It Possible", an autobiographical volume in *Jeffrey I. Seeman*'s "Profiles, Pathways and Dreams" series, following a cancer operation in 1985, *Djerassi* decided "to test the seriousness of [his] intellectual commitment to a new literary career... [proceeding] concurrently along two paths—one fictional, the other autobiographical."

The accelerating pace of research and increasing size of research groups has rendered more difficult the traditional mode of transmitting the methods, values, and ethics of science to scientific novices by personal contact with experienced researchers. One indirect but quite artistic means for accomplishing this goal is the medium of fiction, a method chosen by *Djerassi* in "Cantor's Dilemma," his first novel.

First and foremost, "Cantor's Dilemma" is an absorbing mystery that kept us engrossed through the final pages. We won't spoil the fun for potential readers by disclosing the outcome. It is a cautionary tale about I. C. Cantor, an internationally renowned "superstar" cell biologist and, like *Djerassi* himself, a true renaissance man, who pushes his best postdoc, Jeremiah Stafford, a young scientist with flawless laboratory technique into performing an *experimentum crucis* to prove Cantor's new theory of tumor formation. The

initial failure of one of the researchers in the laboratory of Kurt Krauss, a fellow cancer researcher and competitor of Cantor's, to replicate Stafford's work as well as an anonymous letter cause Cantor to doubt Jerry's results, so Cantor devises a second and simpler experimental proof, which he carries out himself. Cantor and Stafford jointly receive the Nobel Prize, and many of the later pages of the book are devoted to the elaborate Stockholm ceremonies. In the end Krauss attempts to blackmail Cantor into nominating him for the Nobel Prize.

The book reads like a veritable "Who's Who" of science. The names of familiar leading researchers, editors, and historians of science, historical and contemporary, appear on almost every page. *Djerassi* even slyly introduces an oblique reference to himself (p. 167). While telling his story, he deals with many personal and professional issues that researchers encounter in their work, issues neglected in traditional science courses, e.g., choosing a Ph.D. mentor, role models, hiring and tenure policies, laboratory notebooks, grantsmanship, refereemanship, the status of women in science, teacher-student relationships including sexual relations, nominations and awards, patents, competition, priority, jealousy, fraud, replication of experiments, credibility, retraction of published work, seminars, and lectures. Also unobtrusively and skillfully integrated into the story are countless other fascinating esoteric minutiae ranging from antique furniture and *Boccherini* string quartets to Nobel protocol and European dining habits.

After we each had read the book separately, we exchanged and compared our impressions. As a chemist, one reviewer marveled at the authoritative way in which *Djerassi* accurately presents a "behind the scenes" view of how science is done and how the scientific community works. He also admired the seemingly effortless manner in which the author dispenses nuggets of wisdom that should be invaluable to budding scientists. As a humanist, the other was disappointed at the picture of the scientific enterprise as predominantly award-oriented rather than as the idealistic search for truth generally perceived by the public. She also thought that the characters, especially the women, lacked depth. As we continued to discuss the book, more and more ambiguities surfaced; in particular, Cantor's final dilemma—whether or not to recommend Krauss—is unresolved. Nevertheless, we both enjoyed the book immensely and could not put it down until we had finished it.

According to *Djerassi*, "Publications, priorities, the order of the authors, the choice of the journal, the collegiality and the brutal competition, academic tenure, grantsmanship, the Nobel Prize, *Schadenfreude*... are soul and baggage of contemporary science. To illustrate them, I had Cantor and Stafford work on a totally fictitious theory of tumorigenesis.... Only by giving myself... the assurance that their science is pure fiction could I write about behavior and attitudes surely more common than we like to admit."

While *Djerassi*'s novel will be avidly read by chemists, it will also reach a wider audience. In view of the current rampant epidemic of antiscientific attitudes and chemophobia, many scientists may question the wisdom of washing science's dirty linen in public by giving the public an inside view of the darker side of science with Cromwellian warts. *Stephen G. Brush* has written an article, "Should the History of Science Be Rated X?" (*Science 183* (1974) 1164), subtitled "The way scientists behave (according to historians) might not be a good model for students." The same question might be raised with respect to "Cantor's Dilemma" and the nonscientific public. We recommend that you read it and answer the question yourself.

Gaps and Verges. By *R. Hoffmann*. University of Central Florida Press, Orlando 1990. Distributed by University Presses of Florida, 15 NW 15th St., Gainesville, FL 32603. x, 88 pp., hardcover, $ 14.95.—ISBN 0-8130-0943-X

As in *Hoffmann*'s first poetry volume ("The Metamict State", 1987), these poems are characterized by striking metaphors and vivid images, many drawn from scientific ideas and concepts: "disordered silica chains, rings and structural frustration"; "oxygenated salty soups, lightning-lit, when molecules swam to be shaped"; "membranes, assemblies of proteins and lipids that define the outer walls of cells"; and "lipid-tailored confinements, warm prisons where enzyme brews gel."

Not only do scientific and chemical metaphors and images occur in poems dealing with events from *Hoffmann*'s everyday life, but entire poems deal with scientific and academic themes. "Jerry-Built Forever" deals with an automobile exhaust suicide by describing in poetic but scientifically accurate detail the oxygen-carrying mechanism of hemoglobin and the competition between oxygen and carbon monoxide. "Modes of Representation" describes the artistic line cuts of laboratory experiments in old chemistry books. *Hoffmann* contrasts these simple but lucid drawings with the modern photoengraved illustrations in full color that grace the pages of the latest chemistry textbooks (and add tremendously to the cost!), whose introduction he connects with "a deterioration in the students' ability to follow a simple experimental procedure." "What we have learned about the Pineal" describes the functions and secretions of the pineal gland in animals and in humans. "Thèse pour Obtenir le Grade de Docteur ès-Sciences" depicts an oral thesis defense, a common academic rite of passage.

Many of the selections will appeal to nonscientists as well as to scientists. A number derive from *Hoffmann*'s frequent travels, e.g., "Svoloch" depicts his encounter with customs officials at Sheremetovo Airport and the confiscation of the cassette of a *Haydn* cello concerto played by *Mstislav Rostropovich*, who was then still *persona non grata* in his Russian homeland. "Eschatology" recalls the bishops' rooms at Maynooth, the Irish Pontifical Seminary where *Hoffmann* and other invited speakers at a scientific meeting were housed.

Although we found the meaning of a few of the poems obscure, particularly in Sections 1 and 6 of this six-part book, *Hoffmann*'s poignant autobiographical recollections of the Holocaust are readily accessible to Jew and non-Jew alike. "June 1944" recalls his escape after 15 months' hiding in an attic as a six-year-old with his mother to the Russian lines and the family home, while "Believing" sketches his experiences in Kraków at the age of eight as a Catholic, including confession and first communion (his family pretended to have converted during World War II).

The volume concludes with "Corral", a poem for *Carlos Fuentes* that portrays Sor *Juana Inés de la Cruz* (1651–1695), the intellectual prodigy, poet, scholar, and scientist, who retired to the convent of San Jerónimo because "it was not a time for learned women in Mexico". In this slim volume, which we heartily recommend to aficionados of *Hoffmann*'s verse, he masterly presents to a wider audience the image of a chemist both as a professional scientist and as a human being.

George B. Kauffman
Laurie M. Kauffman [NB 1119 IE]
California State University
Fresno, CA 93740 (USA)

Heats of Vaporization of Fluids. By *V. Majer, V. Svoboda* and *J. Pick*. Elsevier, Amsterdam 1988. 344 p., hard cover DFl 295.00.—ISBN 0-444-98920-X

The heat of vaporization is a thermodynamic quantity which plays an important part in the design of many chemical engineering processes. This book gives a very good survey of the methods now available for estimating or experimentally determining the heats of vaporization of pure substances and mixtures, with the emphasis on organic liquids.

It consists of eight chapters on pure substances, a further eight on mixtures, and four appendices, and covers all important aspects of the subject. First the fundamental thermodynamic relationships between the heat of vaporization and the vapor pressure, the specific heats, the phase composition and the p,V,T data are summarized briefly but in an easily comprehensible form. The various experimental methods based on these relationships for determining the heat of vaporization, either by direct calorimetric measurements or indirectly, are then described, together with many different experimental arrangements and their respective advantages and disadvantages. The empirical methods and correlations used for calculating heats of vaporization are discussed in detail, their application being illustrated by examples in every case. Azeotropic mixtures, mixtures containing non-volatile components, and those with components which associate, are given special treatment and the special points to be noted in these cases are explained. In addition there is a critical survey of the purposes to which heats of vaporization of pure substances can be applied. The appendices give details of methods recommended as suitable for calculating the p,V,T data that are usually needed in applying heats of vaporization in practical situations. Extensive bibliographies are appended to all the chapters.

The book aims to be a useful resource for all scientists and process development engineers who need data on heats of vaporization, and it fulfills this objective very well, though it assumes that the user already has a basic knowledge of thermodynamics. However, the price is very high, which could result in copies of the book being mainly confined to libraries.

Rüdiger N. Lichtenthaler [NB 1021 IE]
Physikalisch-chemisches Institut
der Universität Heidelberg (FRG)

C_4 Hydrocarbons and Derivatives—Resources, Production, Marketing. By *J. Schulze* and *M. Homann*. Springer, Berlin 1989. xi, 239 pp., hardcover, DM 228.00.—ISBN 3-540-19470-3

This book by *Schulze* and *Homann* offers a good and detailed insight into the industrial chemistry of C_4 compounds and their derivatives. The first half of the book is devoted to the chemistry and process technology of the compounds, and the second is concerned more with economic aspects such as the competitive situation and price structure for these chemicals. The book contains a great deal of detailed information and numerical data, since both authors have excellent connections with the chemical and petrochemicals industries; in fact one of them works in industry.

The book is divided into seven chapters. After an introductory chapter dealing with fundamentals such as the properties and specifications of the C_4 hydrocarbons, Chapter 2 describes the processes currently used for the separation or synthesis of C_4 hydrocarbons and the corresponding aldehydes and alcohols. This chapter is very concisely written and assumes that the reader already has some basic knowledge. For example, the several variants of the Mobil process are described in only a few sentences, the latest developments of the Fischer-Tropsch synthesis are covered in one short paragraph, and the production of 1-butene by the SHOP process is only mentioned in one sentence. By contrast Chapter 3, which describes processes for separating C_4 hydrocarbons and the wide-ranging chemistry based on these, including the latest developments, is very detailed. In Chapter 4 the industrial processes based on butane, butenes and butadiene are summarized in clear reaction schemes, supported by production figures. Chapter 5 is concerned with the market situation for C_4 products, and Chapter 6 evaluates the market prospects for derivatives of C_4 hydrocarbons, taking as examples motor fuels and C_4-based polymers. Chapter 7 then gives a further short survey of the most important cross-relationships and recent developments in industrial C_4 chemistry.

This book is an unqualified must for everyone who is involved with C_4 products and their marketing. The clear product charts and process flow diagrams, the extensive bibliography (over 350 references, covering publications up to 1987 in some parts), and the remarkably detailed numerical data make this book one of the most important available works of reference on C_4 chemicals. However, it is not very suitable for use as a student textbook, since considerable previous knowledge is assumed.

Arno Behr [NB 1087 IE]
Henkel KGaA
Düsseldorf (FRG)

Rings, Clusters and Polymers of Main Group and Transition Elements. Edited by *H. W. Roesky*. Elsevier, Amsterdam 1989. 560 pp., hardcover DFl 350.00. – ISBN 0-444-88172-7

This volume, edited by a leading authority in the field, *H. W. Roesky*, features 11 chapters on a variety of topics broadly described by the title. The book is in the type offset format, presumably to effect savings on the costs and on the time of the production process. Unfortunately, this has not resulted in a price that would tempt many chemists, even those active in the field, into a purchase. Nevertheless, the authors have maintained a standard of presentation of the material that is uniformly high, and there are only a few errors. A brief subject index is also provided. As might be expected the material is very much up to date (1989) and this is a very positive feature of the volume. In some respects, this collection of topics brings up to date and expands the relevant material for some of the chapters in the recently published two volume review monograph edited by *Haiduc* and *Sowerby* entitled "The Chemistry of Inorganic Homo- and Heterocycles".[*] The extremely rapid developments in some of the published areas described are readily apparent in a comparison of the two publications.

However, it would be a mistake to characterize this volume as solely an updated version of the *Haiduc* and *Sowerby* monograph. The majority of the topics are either unique or only have partial overlap with material previously published. Examples are the chapters on "Boron Hydride Clusters" by *N. N. Greenwood*, "Polysilanes" by *E. Hengge* and *H. Stüger* (which complements the corresponding chapter on "Cyclopolysilanes" in the previous monograph), "Germanium-

[*] *Angew. Chem. 100* (1988) 1017; *Angew. Chem. Int. Ed. Engl. 27* (1988) 1107

Carbon Rings" by *P. Mazerolles*, and "Rings with Phosphorus Carbon Multiple Bonds" by *E. Fluck* and *B. Neumüller*. Other chapters deal with the very active interface between main group and transition metal chemistry. Included in this category are "Multiple Bonds between Transition and Main Group Element Atoms" by *W. A. Herrmann*, "Organometallic π Systems" by *G. Huttner* and *H. Lang*, and "Clusters of Metals and Nonmetals" by *K. H. Whitmire*. A significant portion of this material has been reviewed earlier by these three authors but is here updated and expanded. Also included is a chapter by the editor on "Unsaturated 4,6 and 8-membered Metalloheterocycles and Metal Polymers". The timeliness of this chapter, in the light of recent developments in this field, can be gauged from the references, most of which date from the 1980's. Phosphorus-nitrogen ring systems are represented in a chapter entitled "Azaphospholes" by *A. Schmidpeter* and *K. Karaghiosoff*. The vast array of structural types and many novel classes of compound encompassed within the heading "Polynuclear Transition Metal Complexes with Sulfur Ligands" are reviewed by *B. Krebs* and *G. Henkel*. The review includes both sulfide and thiolate ligands. The huge scope of this chapter is reflected in over 400 references, even though 1,1-dithiolate and 1,2-dithiolenes, complexes with partial chalcogen spheres, and abiotic dithio ligands are excluded.

In summary, this book covers the very rapid developments in selected modern topics in the general area of inorganic rings, clusters and polymers. The distinguished list of authors who are all major contributors to their respective fields has ensured that the coverage is thorough. It is a book which every research library should have.

Philip P. Power [NB 1074 IE]
Department of Chemistry
University of California
Davis, CA (USA)

Fusarium Mycotoxins, Taxonomy and Pathogenicity. (Series: Topics in Secondary Metabolism, Vol. 2). Edited by *J. Chelkowski*. Elsevier, Amsterdam 1989. xiv, 492 pp., hardcover DFl 325.00.—ISBN 0-444-87468-2

This book of about 500 pages is based on a seminar on the topic named in the title which took place in September 1987 in Warsaw. It contains 26 contributions on various topics relating to molds of the genus *Fusarium* and their toxic metabolites. The emphasis in over half the articles is on the phytopathological aspects, whereas the chemical and analytical aspects are not adequately covered.

The problems of *Fusarium* taxonomy are discussed in detail, though it is regrettable that in Chapter 10 only the European species of *Fusarium* are treated. For those who are not experts in taxonomy Table 1 of this chapter is very useful, as this lists the different names used in the three "schools" for a given species. However, the list of *Fusarium* metabolites given in Chapter 1 is incomplete; it does not include the apotrichothecenes, nor fumonisin B_1 which is mentioned in Chapters 2 and 12. Not all the calonectrin derivatives are listed. In the bibliography one searches in vain for the "Natural Products Database" produced by *Berdy* et al.; on the other hand there are unnecessary references to many of the older original papers. For many compounds only the trivial name is given, not the systematic name nor the numbering. Instead of log ε the symbol ε_{mol} is used, although the values given for this are the same as those given in the literature for log ε. Chapter 2 gives a competent treatment of fusarin C. One wishes that all the chapters were so well written. Chapters 3 and 4—in very bad English and with many typographical errors—deal with the occurrence of *Fusarium* and mycotoxins in maize, wheat oats and rye, with special reference to Poland, while Chapter 5 contains a detailed discussion of problems in Mediterranean countries. Chapters 17 to 19 deal with subject matter which is similar, and in some cases is even the same. In Chapter 6 a new variant of the *Artemia-salina* bioassay procedure is described. The following chapter is a survey of the literature on trichothecene poisoning in fish. The chapters on the metabolism of trichothecenes in animals are lucid and comprehensible. Also interesting are the chapters on the hyperparasitism of *Fusarium* on some species of *Claviceps*, and the role of cutinase and cell-wall destroying enzymes in the process whereby plants become infected with *Fusarium*. A very nice conclusion is provided by the final chapter on the occurrence of *Fusarium* toxins in cereal crops and animal feeds in Europe. The latest literature (up to 1988) is covered, and the tables contain a great deal of clearly presented information.

Taken as a whole this multi-author volume is very non-uniform and is not well balanced. The treatments of many of the topics could have been shortened by leaving out all the information that is duplicated from one chapter to another. This editing should have been possible during the interval of two years between the seminar and the appearance of the book.

In my view the book can only be recommended for phytopathologists, since that is where the main emphasis of the contributions lies. Food chemists, biochemists and chemists will benefit little from it, especially as there is already a good choice of books on the mycotoxins field, including some that are better than this one.

Heidrun Anke [NB 1083 IE]
Lehrbereich Biotechnologie
der Universität Kaiserslautern (FRG)

Thermochemical Data of Pure Substances. Parts I and II. By *I. Barin*. VCH Verlagsgesellschaft, Weinheim/VCH Publishers, New York 1989. Part I: x, 87 pp. Index, pp. 1–816; Part II: vi, pp. 817–1739; hardcover DM 680.00.—ISBN 3-527-27812-5/0-89573-866-X

Anyone who had the experience of using a thermochemical data collection such as "Barin, Knacke and Kubaschewski" (1973, 1977) for everyday reference, whether for calculating reaction equilibria, estimating the ranges of conditions under which species exist, or determining the cell potentials of electrochemical chains, will welcome this updated work, with *I. Barin* as sole author.

Almost 2400 substances are covered, including 100 organic materials and, among inorganic substances, exotic species such as C_3, $PuC_{0.88}$ and Th_2N_2O. The wealth of compounds listed undoubtedly makes this collection of tables the most complete data compilation of its kind in existence, and when one also takes into account the attractive presentation, the relatively high price of DM 680 becomes justified. It is also of interest to the user to know that the thermodynamic information is also available in computer-readable form (though this is unfortunately not included in the price). Comparing this work with "Barin, Knacke and Kubaschewski", not only have some data been revised and new compounds included (thus confirming the need for this new version), but also a number of previously listed substances have been omitted. It would have been useful to give the reasons in these cases, since even a rejection of earlier data contains useful information.

A typical table lists the various thermochemical data for temperatures increasing in steps of 100 K above room temperature (extending up to 5000 K in the case of B_2O_3 for example), for the phase stable at each temperature at a pressure of 1 bar. The data listed include specific heats, enthalpies and entropies, and the auxiliary functions $(G\text{-}H_{298})/T$ and $(H\text{-}H_{298})$. A commendable feature is the inclusion also of the enthalpies of formation and free enthalpies of formation, and of the corresponding equilibrium constants; in the previous work the definition of these functions led to a serious potential source of error. Whereas the "Janaf" tables, for example, consistently use energies of formation (so that the values for elements are, by definition, zero at all temperatures), in "Barin, Knacke and Kubaschewski" the enthalpies of the elements are normalized to zero only at room temperature, and consequently the values at other temperatures differ from zero by amounts determined by their specific heats. The present work also lists at the top of each table the units employed, an arrangement which, although clumsy, is user-friendly. At the foot of each table the sources of the data are given; carefully checked sources such as the "Janaf" tables have been used wherever possible.

The precision and reliability of the listed data is a tiresome but unavoidable subject. The experienced themodynamicist is no doubt well aware that for important calculations one must consult the original papers. However, the occasional user may be tempted to assume precision values of up to 1 part in 10^6. For example, H-values are given to within 10^{-3} kJ mol^{-1}, whereas in the literature one frequently finds discrepancies of the order of 10 kJ mol^{-1}.

It is unreasonable to expect that error limits, reliability of data and inconsistencies in the thermodynamic literature can be taken into account and evaluated in every case, but the reader should certainly be given appropriate warnings on these points.

Much space (87 pages of Part I) is devoted to introductory explanations and comments to accompany the tables, including much useful information and worked examples. However, I preferred the introductory chapter on "Basic Principles" in the earlier work, as it was more concise and more appropriate to the book's purpose. In the present work this has been replaced by essentially a collection of formulas. One should not quarrel with the convention of introducing units into equations, but it is unfortunate that the logical notation of the physical-chemical literature has not been followed, particularly in a work of this nature: expressions of the form "t_c[°C] = T[K] -273.15" should really now be a thing of the past. Also the logical definitions in the chapter on "Entropy" are open to misunderstanding; the condition $\Delta S = 0$ does not necessarily imply a reversible adiabatic process, but can also apply to an (irreversible) steady state. The chapters on the pressure dependence of equilibrium constants and on normal potentials could lead to misunderstandings, and are—in view of the rigor of the statements—partly incorrect.

Joachim Maier [NB 1068 IE]
Max-Planck-Institut für Metallforschung, Stuttgart (FRG)

Registered names, trademarks, etc. used in this journal, even when not marked as such, are not to be considered unprotected by law.

© VCH Verlagsgesellschaft mbH, W-6940 Weinheim, 1990. – Printed in the Federal Republic of Germany by Konrad Triltsch Druck- und Verlagsanstalt Würzburg.

All rights reserved (including those of translation into foreign languages). No part of this issue may be reproduced in any form — by photoprint, microfilm, or any other means — nor transmitted or translated into a machine language without written permission from the publishers. Only single copies of contributions, or parts thereof, may be made for personal use. This journal was carefully produced in all its parts. Nevertheless, authors, editors and publisher do not warrant the information contained therein to be free of errors. Readers are advised to keep in mind that statements, data, illustrations, procedural details or other items may inadvertently be inaccurate.

Valid for users in the USA: The appearance of the code at the bottom of the first page of an article (serial) indicates the copyright owner's consent that copies of the article may be made for personal or internal use, or for the personal or internal use of specific clients. This consent is given on the condition, however, that the copier pay stated per-copy fee through the Copyright Clearance Center, Inc. (CCC), for copying beyond that permitted by Sections 107 or 108 of the U.S. Copyright Law. This consent does not extend to other kinds of copying, such as copying, for general distribution, for advertising or promotional purposes, for creating new collective works, or for resale. For copying from back volumes of this journal see 'Permissions to Photo-Copy: Publisher's Fee List' of the CCC.

Editorial office: Postfach 10 11 61, W-6490 Weinheim, Federal Republic of Germany, Telephone (06201) 60 22 55, Telex 465 516 vchwh d, Telefax (06201) 602 328.

Editor: *Peter Gölitz*

Associate editors: *D. I. Loewus, A. Stimson.* **Editorial assistant:** *E. Schweikart*

Publishers: VCH Verlagsgesellschaft mbH. (Managing Directors: *Hans Dirk Köhler, Dr. Hardy G. Sehrt.*), Pappelallee 3, W-6940 Weinheim, Federal Republic of Germany.

Advertising office (Advertising Manager *R. J. Roth*): Postfach 10 11 61, W-6940 Weinheim, Federal Republic of Germany, Telephone (0 62 01) 60 61 30, Telex 4 67 155, Telefax (0 62 01) 606 156.

AUTHOR INDEX [*Angew. Chem. Int. Ed. Engl. 29* (1990)]

The page numbers in square brackets refer to the German edition [*Angew. Chem. 102* (1990)] of Angewandte Chemie. Page numbers in round brackets indicate errata.

Abad, J.-A. 1125 [1184]
Abufarag, A. 1144 [1174]
Achternbosch, M. 783 [825]
Adam, M. 1126 [1157]
Adam, W. 890 [916]
Ahlers, M. 1269 [1310]
Ahmad, J. 306 [337]
Aichholz, R. 427 [439]
Albericio, F. 291 [311]
Alberto, R. 189 [208]
Albinati, A. 84 [71]
Allwohn, J. 398, 399, 1030, 1032 [435, 436, 1085, 1084]
Al-Saadoon, A. W. 1416 [1441]
Alsfasser, R. 898 [939]
Altenbach, H.-J. 67 [64]
Althaus, E. 531 [582]
Altman, S. 749 [735]
Ames, B. N. 1197 [1233]
Andersen, K. A. 921 [933]
Anderson, H. L. 1400 [1478]
Anderson, O. P. 921 [933]
Ando, W. 778 [813]
Andrews, P. C. 1440 [1480]
Arenz, T. 932 [929]
Arif, A. M. 287, 888, 1473 [307, 960, 1507]
Arlt, M. 672 [699]
Armstrong, D. R. 410 [443]
Artschwager-Perl, U. 1067 [1082]
Asensio, G. 1146 [1187]
Ashwell, G. J. 1450 [1493]
Astin, K. B. 306 [337]
Atwood, J. L. 1150, 1409 [1169, 1504]

Baceiredo, A. 659, 1123, 1429 [671, 1185, 1486]
Baciocchi, E. 658 [687]
Bahrmann, H. 391 [408]
Ballester, P. 555 [550]
Balli, H. 905 [920]
Balter, S. 796 [799]
Banert, K. 103, 1164 [90, 1166]
Barany, G. 291 [311]
Bardaji, E. 291 [311]
Bargon, J. 58 [70]
Bark, S. J. 1435 [1532]
Barr, D. 285, 410 [300, 443]
Barrans, R. E., Jr. 915 [953]
Barth, A. 929 [956]
Bartlett, J. S. 1404 [1463]
Basset, J.-M. 805 [803]
Bats, J. W. 106 [81]
Baudry, D. 1485 [1501]
Bauer, S. 1166 [1188]
Bäuerle, P. 419 [414]
Baumann, U. 541 [571]
Baumegger, A. 641 [722]
Baumgärtner, F. 189 [208]
Beck, J. 318 [331]
Beck, W. 293 [301]
Becker, S. 216, 406 [186, 426]
Beckhaus, H.-D. 320, 674 [313, 693]
Beckmann, S. 1395 [1439]
Beifuß, U. 527 [545]
Bell, T. W. 923 [931]
Bellamy, F. D. 1454 [1522]
Beller, M. 782 [812]
Benson, D. R. 191 [213]
Benyunes, S. A. 1416 [1441]
Berendsen, H. J. C. 992 [1020]
Berkessel, A. 106 [81]
Bernardinelli, G. 407 [421]
Berndt, A. 398, 399, 401, 1030, 1032 [435, 436, 438, 1085, 1084]
Bernstein, D. 181 [185]
Berti, C. 653 [684]
Bertrand, G. 659, 1123, 1429 [671, 1185, 1486]
Bertschy, H. 777 [828]
Besenyei, G. 1147 [1168]
Bestmann, H. J. 99 [95]
Betz, P. 322 [291]
Bevierre, M.-O. 655 [672]

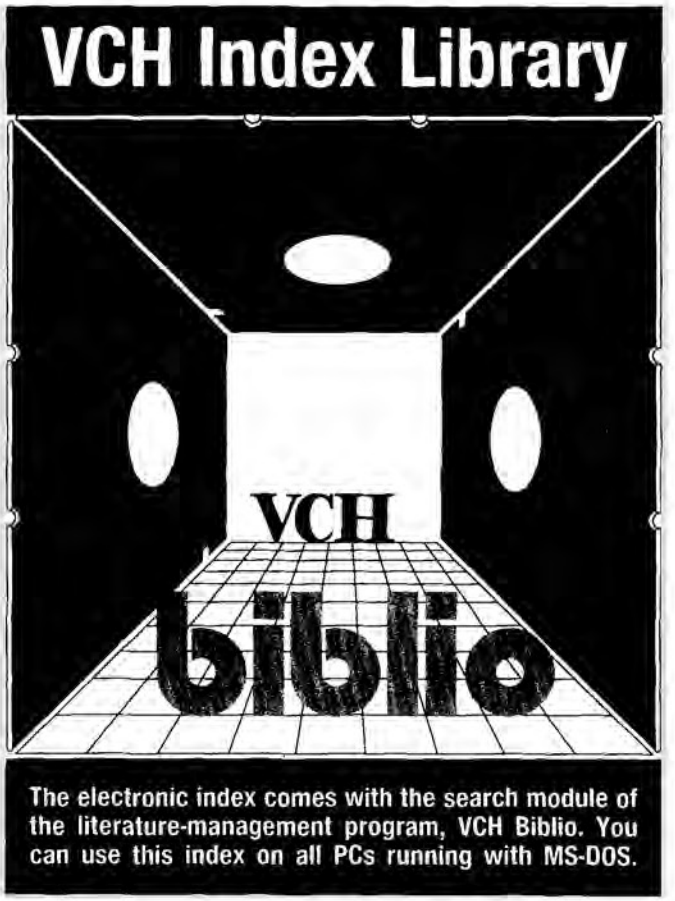

The electronic index comes with the search module of the literature-management program, VCH Biblio. You can use this index on all PCs running with MS-DOS.

ANGEWANDTE CHEMIE
International Edition in English

Soon available

At the press of a button

The annual index of "Angewandte" is soon available on 5 1/4" and 3 1/2" diskettes.

Yearly updates will keep this invaluable electronic library complete. You can search the cumulative contents in mere seconds.

Price: ca. DM 34.00 plus shipping and handling.

Special news! In honor of the 30th anniversary of "Angewandte Chemie I.E." the cumulative index will also be available on diskette.

VCH
Software
P.O. Box 101161
D-6940 Weinheim

VCH

Binger, P. 1037 [1070]
Bino, A. 811, 812 [841, 842]
Bishop, J. M. 716 [765]
Bissinger, P. 1399 [1473]
Blackburn, B. K. 639 [710]
Blake, A. J. 76, 197 [87, 203]
Blanche, F. 884 [947]
Blaser, H.-U. 558 [561]
Blatter, T. 1161 [1194]
Blumen, A. 113 [158]
Boche, G. 63, 308 [99, 334]
Bochmann, M. 638, 780 [703, 830]
Bock, H. 1042, 1044 [1095, 1099]
Bodenhausen, G. 374, 517 [392, 576]
Bodner, A. 68 [60]
Boese, R. 302, 317, 545, 549, 899, 900, 912, 1059, 1436 [318, 330, 568, 589, 909, 910, 914, 1059, 1523]
Bogdanović, B. 223 [239]
Bohle, D. S. 198 (938), 896 [202 (968), 938]
Böhm, G. 787 [832]
Böhmer, V. 280 [326]
Bohnen, A. 525 [548]
Bolm, C. 205 [206]
Bölz, U. 427 [439]
Bonar-Law, R. P. 1407 [1497]
Bönnemann, H. 273 [324]
Bonrath, W. 298 [295]
Borchardt, D. B. 1435 [1532]
Borrmann, H. 1395 [1439]
Bosold, F. 63 [99]
Bossek, U. 1055 [1093]
Bott, S. G. 1150, 1409 [1169, 1504]
Boubia, B. 1454 [1522]
Boury, B. 785 [818]
Brand, S. 665 [675]
Brand-Roth, B. 90 [93]
Brandt, L. 510, 1046 [584, 1062]
Brandt, W. 905 [920]
Braun, H. 783 [825]
Braun, M. 1468 [1445]
Braunstein, P. 1140 [1206]
Breitmaier, E. 385 [441]
Bremer, B. 531 [582]
Bremer, M. 311, 1132 [292, 1164]
Brett, W. A. 302 [318]
Brijoux, W. 273 [324]
Bringmann, G. 977 [1006]
Brintzinger, H.-H. 279, 1417 [339, 1505]
Broeker, G. K. 395 [405]
Brooker, A. T. 285, 410 [300, 443]
Bruch, K. von dem 1457 [1520]
Brumby, T. 665 [675]
Brunner, H. 652, 1131 [680, 1189]
Bryce, M. R. 1450 [1493]
Bucher, U. E. 548 [573]
Büchner, K. 918 [911]
Buchwald, S. L. 771 [820]
Bühl, M. 304, 886, 1059 [320, 962, 1059]
Bunz, U. 413 [418]
Bur, D. 205 [206]
Burk, M. J. 1462 [1511]
Burkart, G. 322 [291]
Butenschön, H. 1057, 1444 [1058, 1469]

Cameron, B. 884 [947]
Cantow, H.-J. 537 [551]
Capuano, V. L. 1134 [1162]
Cara, G. 1125 [1184]
Carcanague, D. R. 769 [836]
Carpenter, L. 785 [818]
Carstens, A. 1424 [1455]
Caulton, K. G. 1483 [1492]
Cayton, R. H. 1026, 1481 [1056, 1490]
Cech, T. R. 759 [745]
Chacon, S. T. 1026 [1056]
Chadha, R. 543 [586]
Channareddy, S. 199 [222]
Charalambous, E. 1137 [1172]
Charrier, C. 534 [575]
Chen, Q. 70 [100]
Chiang, Y. 792 [810]
Chin, J. 523 [580]
Chisholm, M. H. 1026, 1481, 1483 [1056, 1490, 1492]
Choplin, A. 805 [803]
Christl, M. 675, 1035 [704, 1090]
Clapés, P. 291 [311]
Clark, T. 648 [697]
Classen, H. G. 1090 [1122]
Clegg, W. 410, 1440, 1450 [443, 1480, 1493]
Cockcroft, J. K. 650 [728]
Collet, C. 535 [563]
Conesa, J. 1413 [1459]
Corain, B. 384 [404]
Corbelin, S. 650 [728]
Corriu, R. J. P. 785 [818]
Costello, J. F. 1404 [1463]
Cowley, A. H. 1150, 1409 [1169, 1504]
Cradock, S. 76 [87]
Cramer, R. E. 422 [455]
Crescenzi, M. 658 [687]
Crittell, C. M. 287 [307]
Crouzet, J. 884 [947]
Crowe, W. E. 256 [273]
Curci, R. 890 [916]
Custodero, E. 805 [803]

Dąbkowski, W. 522 [565]
Dahn, H. 647 [681]
Dange, O. 402 [429]
Darrington, F. D. 1481 [1490]
Davis, A. P. 1407 [1497]
Davis, W. M. 639, 918 [710, 911]
Day, J. P. 1416 [1441]
de Meijere, A. 1418 [1443]
DeFrees, D. J. 183 [198]
Dehmelt, H. 734 [774]
Dehnicke, K. 390 [420]
Deiseroth, H.-J. 1164 [1166]
Delville, A. 535 [563]
Deng, H.-B. 309 [328]
DesMarteau, D. D. 1448 [1519]
Diederich, F. 191, 769 [213, 836]
Dietrich-Buchecker, C. O. 1154 [1202]
Dietz, U. 680 [685]
Dixneuf, P. H. 215 [210]
Dogan, B. 320, 674 [313, 693]
Dohm, J. 902 [943]
Dolphin, D. 1028 [1073]
Döring, J. 88, 926 [85, 927]
Dötz, K. H. 176 [188]
Dougherty, D. A. 915 [953]
Doyle, M. J. 285 [300]
Dräger, M. 1468 [1445]
Drake, S. R. 285, 1483 [300, 1492]
Drauz, K. 417 [428]
Drechsler, M. 537 [551]
Driessen, W. L. 1419 [1454]
Drüeke, S. 68 [60]
Dulog, L. 415 [403]

Ebmeyer, F. 1148 [1191]
Ebsworth, E. A. V. 76 [87]
Eckert, H. 882 [950]
Economy, J. 1256 [1296]
Edelmann, F. T. 894 [941]
Eder, S. J. 1445 [1460]
Edstrom, E. D. 520 (–) [541 (850)]
Eggenberger, U. 374 [392]
Eggert, U. 1456 [1530]
Eguchi, J. 643 [709]
Eibl, M. 641 [722]
Eichberger, R. 670 [690]
Eickmeier, C. 1393 [1437]
Eisenmann, B. 87 [92]
Elbl-Weiser, K. 211 [183]
Eller, S. 1126 [1157]
Emsley, L. 517 [576]
Enders, D. 179 [226]
Ephritikhine, M. 1485 [1501]
Erker, G. 512, 1067 [543, 1082]
Ertl, G. 1219 [1258]
Estendorfer, S. 536 [547]

Facklam, T. 314 [316]
Falvello, L. R. 891 [952]
Fanwick, P. E. 395, 396, 664 [405, 407, 713]
Fennen, J. 665 [675]
Fenske, D. 390, 796, 1042, 1452 [420, 799, 1095, 1513]
Filippou, A. C. 207 (–) [224 (346)]
Fisch, K. 1131 [1189]
Fischer, D. 800 [835]
Fischer, P. 427 [439]
Fischer, R. 782 [812]
Fischer, R. D. 1126 [1157]
Fisher, R. A. 771 [820]
Fitch, A. N. 650 [728]
Flörke, U. 645 [720]
Forniés, J. 891, 1449 [952, 1518]
Foxman, B. M. 771 [820]
Franck, B. 1393, 1395 [1437, 1439]
Frank, W. 1158 [1178]
Franke, D. 882 [950]
Franklin, K. C. 76 [87]
Fraser, A. T. 1450 [1493]
Frauenrath, H. 932 [929]
Frechet, D. 884 [947]
Frenking, G. 1410 [1516]
Fries, A. 510 [584]
Fries, J. 1024 [1079]
Frim, R. 919 [919]
Fritz, H. 95 [105]
Fritz, M. 929 [956]
Fryzuk, M. D. 73 [67]
Fuchs, R. 783 [825]
Fuhrhop, J.-H. 672 [699]
Fujii, N. 801 [816]
Fujiwara, T. 662 [688]
Funakoshi, S. 801 [816]
Furaya, S. 1064 [1066]

Gade, L. H. 1137 [1172]
Gais, H.-J. 100 [96]
Galm, W. 686 [701]
Gamper, S. 295 [297]
Gante, J. 1025 [1081]
Ganter, C. 912 [914]
Gerdes, P. 179 [226]
Gersdorff, J. von 670 [690]
Gilje, J. W. 422 [455]
Gillette, G. R. 1429 [1486]
Girreser, U. 667 [718]
Gladysz, J. A. 1473, 1475 [1507, 1509]
Gleiter, R. 276, 413, 1048, 1426, 1427 [304, 418, 1071, 1450, 1452]
Glüsenkamp, K.-H. 782 [812]
Goddard III, W. A. 138 [119]

Goeke, A. 1024 [1079]
Göhrt, A. 527 [545]
Gold, L. S. 1197 [1233]
Gong, J. 396 [407]
Gorun, S. M. 1156 [1195]
Goto, M. 794 [823]
Granier, M. 659, 1123 [671, 1185]
Green, M. 1046, 1416 [1062, 1441]
Green, M. M. 1478 [1525]
Gregg, B. A. 82 [109]
Gregory, K. 410 [443]
Greig, J. A. 197 [203]
Grelbig, T. 1448 [1519]
Grierson, L. 653 [684]
Griesbeck, A. G. 803 [801]
Grimes, J. A.-M. 653 [684]
Groeger, U. 417 [428]
Gruehn, R. 1459 [1448]
Grünleitner, W. 207 (–) [224 (346)]
Grützmacher, H. 659 [671]
Guilhem, J. 1154 [1202]
Günther, E. 204 [220]
Günther, H. 1053 [1075]
Günther, W. 1050 [1068]

Haanstra, W. G. 1419 [1454]
Habashita, H. 801 [816]
Haber, S. 1436 [1523]
Hädrich, J. 320 [313]
Hagedorn, M. 103 [90]
Hager, R. 201 [204]
Hanack, M. 1467 [1499]
Harlow, R. L. 75, 1462 [89, 1511]
Harman, M. 638 [703]
Harms, K. 176, 308 [188, 334]
Harris, S. 194 [216]
Hartmann, R. 385 [441]
Hartweg, M. 65 [63]
Hasan, M. 1450 [1493]
Häselhoff, C. 322 [291]
Haslinger, E. 514 [562]
Haubold, W. 1044 [1099]
Haupt, H.-J. 645 [720]
Havlas, Z. 1042 [1095]
Heck, L. 1158 [1178]
Heeres, H. J. 420 [449]
Heid, S. 419 [414]
Heineke, D. 896 [938]
Heintz, R. A. 775 [805]
Heinze, J. 692, 1418 [695, 1443]
Heiß, H. 880 [935]
Helbig, J. 1090 [1122]
Heller, A. 82 [109]
Hellmann, G. 100 [96]
Hellwinkel, D. 689 [677]
Helmchen, G. 1024 [1079]
Hendrich, M. P. 921 [933]
Hendrickson, J. B. 1286 [1328]
Hengge, E. 641 [722]
Henkel, G. 531, 1143 [582, 1179]
Henkel, T. 1128 [1171]
Herberich, G. E. 317, 912 [330, 914]
Herbst, E. 595 [627]
Hergenrother, P. M. 1262 [1302]
Herrmann, G. 481 [469]
Herrmann, S. 388 [445]
Herrmann, W. A. 189, 391, 1445 [208, 408, 1460]
Hersperger, R. 185 [195]
Heydt, H. 314 [316]
Hill, J. E. 664 [713]
Hillebrecht, H. 537 [551]
Himbert, G. 86 [69]
Hintze, F. 1422 [1457]
Hirsch, A. 1467 [1499]
Hlineny, K. 884 [947]
Hochstrasser, R. 411 [454]
Hock, R. 1067 [1082]
Hodgson, S. M. 410 [443]
Hoffmann, H. M. R. 1456 [1530]
Hoffmann, K. 1158 [1178]
Hofmann, H. 648 [697]
Hofmann, P. 880 [935]
Hohenester, E. 641 [722]
Holder, A. J. 197 [203]
Hollenstein, S. 188 [194]
Holm, R. H. 840 [868]
Holman, T. R. 921 [933]
Holzapfel, W. 67 [64]
Hönle, W. 1395 [1439]
Hopf, H. 393 [425]
Hoppe, D. 296, 1422, 1424 [336, 1457, 1455]
Hoppe, R. 800 [835]
Horchler, K. 807 [821]
Hori, H. 424 [450]
Horváth, I. T. 194 [216]
Hostalek, M. 317 [330]
Hotzelmann, R. 645 [720]
Huang, J. 396 [407]
Huber, M. 670 [690]
Huber, P. 517 [576]
Huch, V. 216 [186]
Huffman, J. C. 1026 [1056]
Hummel, H.-U. 311 [292]
Hümmer, W. 1171 [1182]
Hünig, S. 204 [220]
Hunold, R. 398, 1032 [435, 1084]
Hursthouse, M. B. 638, 1450 [703, 1493]
Huttner, G. 929 [956]
Hwang, S.-H. 1448 [1519]
Hyde, T. I. 197 [203]

Ibuka, T. 801 [816]
Inoue, Y. 422 [455]
Irngartinger, H. 680, 1048 [685, 1071]
Ishihara, H. 530 [572]
Iyoda, M. 1062 [1077]

Jäger, V. 1169, 1171 [1180, 1182]
Jaggar, A. J. 780 [830]
Jähde, E. 782 [812]
Janiak, C. 775 [805]
Janoschek, R. 905, 1464 [920, 1475]
Jentzsch, W. 1228 [1267]
Jeong, K.-S. 555 [550]
Johnson, B. F. G. 1137 [1172]
Jonas, K. 322 [291]
Jones, P. G. 1125 [1184]
Jones, R. A. 1150, 1409 [1169, 1504]
Jordanov, J. 78 [74]
Joußen, E. 289 [314]
Joußen, T. 273 [324]
Juarez-Garcia, C. 921 [933]
Jutzi, P. 893 [913]
Jux, N. 1385, 1387 [1429, 1431]
Juza, M. 427 [439]

Kabe, Y. 778, 794 [813, 823]
Kabuto, C. 643 [709]
Kai, Y. 1062 [1077]
Kaim, W. 78 [74]
Kalthof, U. 1025 [1081]
Kammerer, J. 1038 [1087]
Kanatzidis, M. G. 914 [945]
Kandels, J. 58 [70]
Kanehisa, N. 1062 [1077]
Karaulov, A. I. 1450 [1493]
Karpitschka, E. M. 556 [559]
Karsch, H. H. 295 [297]
Kasack, V. 78 [74]
Kasai, N. 1062 [1077]
Kastrup, R. V. 194 [216]
Katakis, I. 82 [109]
Kato, S. 530 [572]
Kattner, L. 679 [717]
Kaufmann, D. 545 [568]
Kaupp, G. 933 [917]
Kawase, T. 794 [823]
Kazmaier, U. 514 [562]
Keim, W. 235 [251]
Keller, U. 295 [297]
Keller, W. 1044 [1099]
Kellner, J. 391 [408]
Kessler, H. 425, 546 [452, 588]
Kietzmann, R. 670 [690]
Kim, J. H. 523 [580]
Kim, J. S. 415 [403]
King, M. A. 888 [960]
Kipphardt, H. 179 [226]
Kiprof, P. 189, 207 (–), 1445 [208, 224 (346), 1460]
Kirmse, W. 661 [682]
Kirste, B. 670 [690]
Kirstein, G. 684 [706]
Klapötke, T. 677 [726]
Klärner, F.-G. 1025, 1061, 1067 [1081, 1097, 1082]
Kläui, W. 627 [661]
Klein, J. 87 [92]
Klenk, H. 417 [428]
Kling, A. 425 [452]
Klingebiel, U. 209 [218]
Klinowski, J. 553 [539]
Klötzer, W. 556 [559]
Klüfers, P. 783 [825]
Kluge, C. P. 1164 [1166]
Knauer, W. 293 [301]
Kneißl, G. 809 [827]
Ko, M. K. 1296 [1339]
Koch, K.-H. 525 [548]
Koch, P. 1385 [1429]
Koch, W. 183 [198]
Kochersperger, L. 1296 [1339]
Kohne, B. 177 [200]
Kolar, C. 809 [827]
Kolis, J. W. 1486 [1502]
Kölle, U. 773 [839]
König, B. 1418 [1443]
König, H. 1393 [1437]
König, W. A. 64 [84]
Konkol, W. 391 [408]
Konrad, W. 661 [682]
Kopf, J. 1441 [1481]
Koseki, K. 105 [66]
Kossakowski, J. 773 [839]
Köster, R. 302 [318]
Kotch, T. 1137 [1172]
Kottenhahn, M. 425 [452]
Kraft, A. 675 [704]
Krämer, A. 292 [333]
Krämer, T. 1424 [1455]
Kratky, C. 641 [722]
Kratz, D. 276 [304]
Krauledat, H. 1417 [1505]
Kräuter, G. 390 [420]
Krautscheid, H. 796, 1452 [799, 1513]
Krebs, B. 531 [582]
Kreitmeier, P. 927 [958]
Kresge, A. J. 792 [810]
Kreutzberg, J. 1143 [1179]
Kreutzer, M. 393 [425]

Kreuzer, E.-M. 289 [314]
Krickemeyer, E. 88, 926 [85, 927]
Krieger, C. 211 [183]
Krimm, S. 675 [704]
Krimmer, S. 427 [439]
Krüger, C. 322, 1067 [291, 1082]
Krügerke, T. 1128 [1171]
Kubiak, C. P. 395, 396 [405, 407]
Kuhn, N. 1143 [1179]
Kuhn, W. 1 [1]
Kula, M.-R. 386, 1139 [423, 1204]
Kulpe, J. A. 391 [408]
Kündig, E. P. 407 [421]
Kunz, H. 1050, 1457 [1068, 1520]
Kurreck, H. 670 [690]
Küster, W. 1413 [1459]
Kuwatani, Y. 1062 [1077]

Labat, G. 1471 [1488]
Lachmann, J. 880 [935]
Laszlo, P. 535 [563]
Lathrop, D. 882 [950]
Latscha, H. P. 799 [815]
Laube, T. 188 [194]
Lauer, G. 1024 [1079]
Laven, R. 317 [330]
Ledl, F. 536, 565 [547, 597]
Lee, S. C. 840 [868]
Lees, A. J. 1137 [1172]
Legon, A. C. 72 [76]
Lehmann, H. 1467 [1499]
Lehmkuhl, H. 289 [314]
Lehn, J.-M. 1304 [1347]
Lengweiler, T. 548 [573]
Lentz, D. 315 [308]
Leresche, J. 407 [421]
Levis, M. 1144 [1174]
Lewis, J. 1137 [1172]
Lex, J. 1385, 1387, 1390 [1429, 1431, 1434]
Lexa, D. 1028 [1073]
Lieberknecht, A. 514 [562]
Lindner, H. J. 100 [96]
Lindquist, S.-E. 82 [109]
Link, H. 556 [559]
Linti, G. 199, 682 [222, 715]
Lippard, S. J. 811, 812 [841, 842]
Lippert, B. 84 [71]
Litterst, E. 1048 [1071]
Liu, B. 183 [198]
Liu, J. 923 [931]
Liu, S. 70, 812 [100, 842]
Lochmann, L. 308 [334]
Lögers, M. 782 [812]
Lökös, M. 527 [545]
Lora, S. 384 [404]
Lorenzen, N. P. 300, 1441 [322, 1481]
Lowack, R. H. 1132 [1164]
Luche, O. 1144 [1174]
Lüttke, W. 525 [548]
Lutz, T. 1041 [1064]

Maercker, A. 667 [718]
Magonov, S. N. 537 [551]
Maier, G. 905, 1464 [920, 1475]
Maigrot, N. 534 [575]
Mann, A. 1454 [1522]
Mannschreck, A. 919 [919]
Mardones, M. A. 1150, 1409 [1169, 1504]
Marinetti, A. 1166 [1188]
Märkl, G. 927 [958]
Marks, T. J. 857 [886]
Marsch, M. 308 [334]
Masamune, S. 794 [823]
Maslak, P. 283 [302]
Massa, W. 398, 399, 1030, 1032 [435, 436, 1085, 1084]
Mathey, F. 534, 655, 1166, 1485 [575, 672, 1188, 1501]
Matros, Y. Sh. 1235 [1274]
Matsumoto, A. 1028 [1073]
Maxwell, R. 882 [950]
Mayne, C. L. 1475 [1509]
Mayr, H. 1371 [1415]
McKervey, A. M. 280 [326]
McManus, N. T. 73 [67]
McPartlin, M. 1137 [1172]
Meerholz, K. 692, 1418 [695, 1443]
Meetsma, A. 420 [449]
Mégard, P. 1413 [1459]
Mehani, S. 1404 [1463]
Melder, J.-P. 92, 95 [102, 105]
Mello, R. 890 [916]
Mendenhall, G. D. 362 [380]
Méndez, N. Q. 1473, 1475 [1507, 1509]
Mennekes, T. 899 [909]
Mercier, F. 655 [672]
Merwin, L. H. 807 [821]
Meunier, A. 777 [828]
Meunier, B. 1471 [1488]
Michaelis, S. 298 [295]
Michalski, J. 522 [565]
Michel, H. 401 [438]
Millar, J. M. 194 [216]
Minkwitz, R. 181, 688 [185, 692]
Mioskowski, C. 1454 [1522]
Miranda, M. A. 1146 [1187]
Miyashi, T. 643 [709]
Möbius, K. 670 [690]
Mohler, D. L. 1151 [1200]
Möhrke, A. 893 [913]
Möller, M. 1393 [1437]
Montavon, M. 556 [559]
Moore, A. J. 1450 [1493]
Mootz, D. 904 [949]
Morton, T. H. 1435 [1532]
Mosel, B. 531 [582]
Müllen, K. 525 [548]
Müller, A. 88, 926 [85, 927]
Müller, B. G. 406 [426]
Müller, G. 201, 295, 516, 880, 884 [204, 297, 569, 935, 947]
Müller, J.-H. 1459 [1448]
Müller, P. 1037 [1070]
Müller, W. 1269 [1310]
Müller-Warmuth, W. 531 [582]
Mulvey, R. E. 1440 [1480]
Mulzer, J. 431, 679, 1476 [433, 717, 1529]
Münck, E. 921 [933]
Muños, O. 385 [441]
Münzenberg, J. 61 [73]
Murata, I. 424 [450]
Murray, B. A. 1407 [1497]
Muschiol, M. 652 [680]
Müssner, R. 556 [559]
Mutter, M. 185 [195]
Mynott, R. 289, 1037 [314, 1070]
Myrabo, R. L. 549 [589]

Nakamura, A. 422 [455]
Nanz, D. 548 [573]
Narjes, K.-H. 1189 [1225]
Narvaez, J. N. 283 [302]
Naumann, M. 1061 [1097]
Navarro, R. 891 [952]
Naylor, A. M. 138 [119]
Neier, R. 777 [828]
Neiteler, P. 880 [935]
Németh, S. 1147 [1168]
Neumann, F. 429 [447]
Newman, D. A. 549 [589]
Nicholls, J. C. 780 [830]
Nicolaou, D. C. 1064 [1066]
Nicolaou, K. C. 1064 [1066]
Niedermeyer, U. 386 [423]
Nief, F. 1485 [1501]
Nieger, M. 1123 [1185]
Niethammer, D. 670 [690]
Noh, S. K. 775 [805]
Noltemeyer, M. 61, 669, 894 [73, 712, 941]
Nöth, H. 199, 682, 927 [222, 715, 958]
Nowicki, G. 688 [692]
Nowotny, H.-P. 939 [969]
Nuber, B. 68, 689, 787, 1055 [60, 677, 832, 1093]
Nuss, J. M. 1435 [1532]

O'Connor, J. M. 543 [586]
Oda, M. 1062 [1077]
Oeser, T. 680, 1048 [685, 1071]
Oguchi, Y. 801 [816]
Okada, J. 794 [823]
Olbrich, F. 1441 [1481]
O'Neal, S. C. 1486 [1502]
Oschkinat, H. 546 [588]
Oser, A. 1167 [1197]
Osterberg, C. E. 888 [960]
Oswald, B. 1140 [1206]
Owens, M. 280 [326]

Paetzold, P. 899, 900, 1059 [909, 910, 1059]
Paine, R. T. 682 [715]
Palma, G. 384 [404]
Paquette, L. A. 609 [642]
Park, Y. 914 [945]
Parkins, A. W. 1046 [1062]
Parris, K. 555 [550]
Pascard, C. 1154 [1202]
Paschalidis, C. 516 [569]
Paul, W. 739 [780]
Paulsen, H. 823 [851]
Paxinos, A. S. 1053 [1075]
Pearlstein, R. M. 639 [710]
Péchy, P. 647 [681]
Penk, M. 88, 926 [85, 927]
Pennington, W. T. 1486 [1502]
Perez-Prieto, J. 1146 [1187]
Perkins, M. J. 653 [684]
Peters, E.-M. 695, 803, 1164 [724, 801, 1166]
Peters, K. 65, 204, 695, 803 [63, 220, 724, 801]
Petrie, M. A. 1033 [1061]
Pfeifer, K.-H. 413 [418]
Philipsborn, W. von 548 [573]
Pieper, U. 209, 894 [218, 941]
Pilz, M. 399, 401, 1030, 1032 [436, 438, 1085, 1084]
Pinkos, R. 92, 95 [102, 105]
Pishko, M. V. 82 [109]
Plato, M. 670 [690]
Poganiuch, P. 812 [842]
Pohl, S. 90 [93]
Polborn, K. 682, 927 [715, 958]
Pörschke, K. R. 298 [295]
Potin, D. 1420 [1485]
Powell, A. K. 898 [939]
Power, P. P. 449, 1033, 1403 [527, 1061, 1484]

Praefcke, K. 177 [200]
Prasanna de Silva, A. 1173 [1159]
Prausnitz, J. M. 1246 [1286]
Prester, F. 652 [680]
Preugschat, D. 315 [308]
Prinzbach, H. 92, 95, 1038 [102, 105, 1087]
Pritchard, G. J. 282 [298]
Pritzkow, H. 60, 292, 659, 686, 799 [80, 333, 671, 701, 815]
Probst, T. 1397 [1471]
Profilet, R. D. 664 [713]
Pruszynski, P. 792 [810]
Pu, L. 543 [586]
Pugin, B. 558 [561]
Pyykkö, P. 213 [211]

Qing, W. 522 [565]
Quadbeck-Seeger, H.-J. 1177 [1213]
Quast, H. 695 [724]
Que, L., Jr. 921 [933]

Raabe, G. 773 [839]
Raatz, F. 805 [803]
Rabinovitz, M. 919 [919]
Rahbar, A. 1390 [1434]
Raithby, P. R. 285 [300]
Rajewsky, M. F. 782 [812]
Rall, K. 60 [80]
Ramdas, S. 1404 [1463]
Ramsey, N. F. 725 [790]
Rando, R. R. 461 [507]
Rankin, D. W. H. 201 [204]
Rardin, R. L. 812 [842]
Rasika Dias, H. V. 1033 [1061]
Ratliff, K. S. 395 [405]
Rautenstrauch, V. 1413 [1459]
Rebek, J., Jr. 245, 555, 1148, 1420 [261, 550, 1191, 1485]
Redenz-Stormanns, B. 900, 1059 [910, 1059]
Reedijk, J. 1419 [1454]
Rees, W. S., Jr. 918 [911]
Regitz, M. 314, 1436 [316, 1523]
Regnat, D. 695 [724]
Rego, C. A. 72 [76]
Rehage, H. 439 [497]
Rehder, D. 1438 [1495]
Reichert, A. 1269 [1310]
Reimann-Andersen, S. 60 [80]
Reißaus, E. 1164 [1166]
Reisenauer, H. P. 905, 1464 [920, 1475]
Reiser, O. 1418 [1443]
Reißig, H.-U. 1129 [1156]
Renaud, P. 433 [416]
Renn, O. 84 [71]
Rétey, J. 355 [373]
Rettig, S. J. 73 [67]
Reuchlein, H. 1035 [1090]
Ricard, L. 534, 655, 1166, 1485 [575, 672, 1188, 1501]
Richmond, T. G. 888 [960]
Riede, J. 1397 [1471]
Rieder, H. 204 [220]
Rieger, B. 279 [339]
Riepl, H. 391 [408]
Rihs, G. 1038 [1087]
Ringsdorf, H. 1269, 1478 [1310, 1525]
Rischer, M. 527 [545]
Rissanen, K. 902 [943]
Ritter, A. 223 [239]
Robertson, H. E. 201 [204]
Robl, C. 293 [301]
Rocha, J. 553 [539]
Rodewald, U. 1393 [1437]
Rodriguez-Val, E. 1387 [1431]
Roesky, H. W. 61, 669 [73, 712]
Rohlfing, R. 926 [927]
Rohr, J. 1051 [1091]
Röll, W. 279 [339]
Romanens, P. 407 [421]
Romero, A. 215 [210]
Ross II, C. 807 [821]
Rössner, E. 64 [84]
Roth, D. 99 [95]
Roth, E. 78 [74]
Roth, R. 1132 [1164]
Rothwell, I. P. 664 [713]
Rotter, H. W. 537 [551]
Rüchardt, C. 320, 674 [313, 693]
Ruf, D. 1159 [1192]
Ruiz, J. 1150 [1169]
Ruppert, K. 1042 [1095]
Ruppert, R. 388 [445]
Ruppmich, M. 86 [69]
Rütter, H. 904 [949]
Rypdal, K. 1445 [1460]

Saak, W. 90 [93]
Saalfrank, R. W. 311, 1041 [292, 1064]
Sabater, M. J. 1146 [1187]
Sailer, K. 933 [917]
Sam, F. O. 384 [404]
Samankumara Sandanayake, K. R. A. 1173 [1159]
Sander, W. 344 [362]
Sanders, J. K. M. 1400 [1478]
San-Martin, A. 385 [441]
Sattler, G. 689 [677]
Sauvage, J.-P. 1154 [1202]
Sawodny, W. 181 [185]
Scanlan, T. S. 1296 [1339]
Schäfer, H. J. 195 [228]
Schäfer, T. 176 [188]
Schehlmann, V. 1426 [1450]
Schepers, K. 531 [582]
Schepp, N. P. 792 [810]
Scherer, O. J. 1104 [1137]
Schleicher, E. 565 [597]
Schleyer, P. von R. 304, 886, 1059 [320, 962, 1059]
Schmickler, H. 1385, 1387, 1390 [1429, 1431, 1434]
Schmidbaur, H. 201, 516, 1090, 1397, 1399 [204, 569, 1122, 1471, 1473]
Schmidt, H.-G. 894 [941]
Schmidt, U. 514 [562]
Schmidt-Lukasch, G. 398 [435]
Schmieder, P. 546 [588]
Schmittel, M. 541, 1144 [571, 1174]
Schmuck, A. 213 [211]
Schneider, H.-J. 1159, 1161 [1192, 1194]
Schnering, H. G. von 65, 204, 695, 803, 1395 [63, 220, 724, 801, 1439]
Schnörer, H. 113 [158]
Schöllhorn, B. 431, 1476 [433, 1529]
Schreiber, S. L. 256 [273]
Schröder, D. 910, 1431, 1433 [925, 1466, 1468]
Schröder, M. 197 [203]
Schrot, J. 1464 [1475]
Schubert, H. 670 [690]
Schubert, S. 433 [416]
Schulten, H.-R. 280 [326]
Schultz, P. G. 1296 [1339]
Schulz, M. 1053 [1075]
Schulze, C. 509 [566]
Schumacher, R. 329 [347]
Schümann, U. 1441 [1481]
Schurig, V. 939 [969]
Schütz, J.-U. von 204 [220]
Schwark, J.-R. 296 [336]
Schwarz, C. 106 [81]
Schwarz, H. 402, 404, 509, 908, 910, 1431, 1433 [429, 431, 566, 923, 925, 1466, 1468]
Schwarz, M. 1459 [1448]
Schwederski, B. 78 [74]
Sebald, A. 807 [821]
Seebach, D. 1320 [1363]
Selle, A. 783 [825]
Sendlinger, S. C. 775 [805]
Seppelt, K. 213, 1128, 1448 [211, 1171, 1519]
Seris, J.-L. 1471 [1488]
Sessler, J. L. 1134 [1162]
Severin, T. 536 [547]
Seyferth, D. 918 [911]
Shambayati, S. 256 [273]
Sharpless, K. B. 639 [710]
Sheldrick, G. M. 527 [545]
Shokat, K. M. 1296 [1339]
Shoner, S. C. 1033, 1403 [1061, 1484]
Shore, S. G. 309 [328]
Sicilia, V. 891 [952]
Siebert, W. 292 [333]
Silberzahn, J. 799 [815]
Simándi, L. I. 1147 [1168]
Simon, H. 1053 [1075]
Simón-Fuentes, A. 1146 [1187]
Singer, D. 177 [200]
Singewald, N. 556 [559]
Skokotas, G. 1064 [1066]
Slawin, A. M. Z. 1404, 1456 [1463, 1530]
Smith, K. 282 [298]
Snaith, R. 285, 410 [300, 443]
Söderholm, S. 204 [220]
Solouki, B. 1044 [1099]
Somer, M. 65, 87 [63, 92]
Spindler, F. 558 [561]
Spliethoff, B. 223 [239]
Staab, H. A. 211 [183]
Stalke, D. 209, 894 [218, 941]
Stang, P. J. 287 [307]
Stark, A. 311 [292]
Stauffer, D. A. 915 [953]
Steckhan, E. 388 [445]
Steigelmann, O. 201, 516, 1397, 1399 [204, 569, 1471, 1473]
Steinke, D. 1139 [1204]
Steinrück, N. 402 [429]
Stibrany, R. T. 1156 [1195]
Stöckigt, D. 402 [429]
Stoddart, J. F. 1404 [1463]
Stoeckli-Evans, H. 429 [447]
Stoffel, W. 958 [987]
Stoffels, A. L. E. 1419 [1454]
Strazewski, P. 36 [37]
Strecker, B. 275 [310]
Streib, W. E. 1483 [1492]
Stürmer, R. 59 [62]
Suemune, H. 1064 [1066]
Sülzle, D. 404, 908 [431, 923]
Sundermeyer, W. 60 [80]
Sunko, D. E. 183 [198]
Suriano, J. A. 75 [89]
Süss-Fink, G. 429 [447]
Suzuki, T. 643 [709]
Szeimies, G. 413 [418]

Tamaoki, N. 105 [66]
Tamm, C. 36 [37]

Tanaka, K. 662 [688]
Tanaka, S. 643 [709]
Tatsumi, K. 422 [455]
Taylor, A. 197 [203]
Tebben, P. 1422 [1457]
Terem, B. 653 [684]
Terlouw, J. K. 404 [431]
Teuben, J. H. 420 [449]
Thaisrivongs, S. 1296 [1339]
Théolier, A. 805 [803]
Theopold, K. H. 775 [805]
Thibaut, D. 884 [947]
Thiele, G. 537 [551]
Thiem, J. 80 [78]
Thilgen, C. 1162 [1176]
Thömmes, J. 388 [445]
Tietze, L. F. 527, 665, 782 [545, 675, 812]
Tiripicchio, A. 896, 1140 [938, 1206]
Tiripicchio Camellini, M. 896, 1140 [938, 1206]
Toan, V. V. 647 [681]
Toda, F. 662 [688]
Tolman, W. B. 812 [842]
Tomalia, D. A. 138 [119]
Tomás, M. 891, 1449 [952, 1518]
Tornieporth-Oetting, I. 677 [726]
Torres, J. L. 291 [311]
Traub-Eberhard, U. 884 [947]
Treptow, B. 1427 [1452]
Trost, B. M. 520 (–) [541 (850)]
Tsumuraya, T. 778 [813]
Tumas, W. 75 [89]
Turowski, P. N. 811 [841]

Underiner, G. E. 529 [579]
Urmann, M. 1024 [1079]
Urwyler, B. 790 [807]
Usón, I. 1449 [1518]
Usón, R. 1449 [1518]
Uyehara, T. 801 [816]

Vahrenkamp, H. 198 (938), 896, 898 [202 (968), 938, 939]
Valencia, C. 291 [311]
Valentekovich, R. 191 [213]
Valet, G. 1167 [1197]
van der Zeijden, A. A. H. 512 [543]
van Dijk, C. 1053 [1075]
van Gunsteren, W. F. 992 [1020]
Vančik, H. 183 [198]
VanDoorne, W. 422 [455]
Varmus, H. E. 707 [756]
Vegas, A. 215 [210]
Veith, M. 216 [186]
Venanzi, L. M. 548 [573]
Venzmer, J. 1269 [1310]
Verevkin, S. 320, 674 [313, 693]
Veyssié, M. 439 [497]
Vicente, J. 1125 [1184]
Voelker, H. 669 [712]
Vogel, E. 1385, 1387, 1390 [1429, 1431, 1434]
Vogt, U. 1456 [1530]
Vogt, W. 280 [326]
Vögtle, F. 902, 1162 [943, 1176]
Völkl, C. 207 (–) [224 (346)]
Vollhardt, K. P. C. 549, 1151 [589, 1200]
Vuilhorgne, M. 884 [947]

Wadepohl, H. 686 [701]
Wagner, J. 1478 [1525]
Wagner, O. 314 [316]
Waldmann, H. 1468 [1445]
Walter, R. 977 [1006]
Walter, S. 209 [218]
Wandrey, C. 388 [445]
Waring, T. L. 1416 [1441]
Watzlowik, P. 1445 [1460]
Webb, K. 638 [703]
Weber, T. 1025 [1081]
Wedler, M. 894 [941]
Wehner, V. 1169 [1180]
Weidenbruch, M. 90 [93]
Weinges, K. 680 [685]
Weiper, A. 195 [228]
Weirich, R. 977 [1006]
Weiss, E. 300, 650, 1441 [322, 728, 1481]
Weiss, J. 68, 787, 1055 [60, 832, 1093]
Weiss, R. 1132 [1164]
Wenz, R. 1037 [1070]
Werner, H. 275, 510, 1077 [310, 584, 1109]
Werner, H.-P. 204 [220]
Werner, S. 1067 [1082]
Wesemann, L. 912 [914]
Wessel, T. 1395 [1439]
West, R. 529 [579]
Wey, H. G. 1444 [1469]
White, G. S. 73 [67]
Whitesides, G. M. 1209 [1247]
Wieczorek, C. 398 [435]
Wieghardt, K. 68, 645, 787, 1055 [60, 720, 832, 1093]
Wiel, A. 689 [677]
Wiemann, T. 80 [78]
Wienand, A. 1129 [1156]
Wijesekera, T. 1028 [1073]
Wilhelm, U. 783 [825]
Will, S. 1390 [1434]
Willershausen, P. 1030 [1085]
Williams, D. J. 1404, 1456 [1463, 1530]
Williams, K. 1420 [1485]
Willig, F. 670 [690]
Wirz, J. 411, 790, 792 [454, 807, 810]
Witt, M. 669 [712]
Wittneben, V. 88 [85]
Woelk, K. 58 [70]
Woitha, C. 1438 [1495]
Wolf, H. C. 204 [220]
Wolf, J. 510 [584]
Wolfender, J.-L. 429 [447]
Wolff, S. 1151 [1200]
Workman, D. P. 309 [328]
Wrackmeyer, B. 807 [821]
Wright, D. S. 285, 410 [300, 443]
Wulff, G. 684 [706]
Würthner, F. 419 [414]
Wüstefeld, R. 1478 [1525]

Yalpani, M. 302 [318]
Yamamoto, K. 424 [450]
Yamamoto, Y. 801 [816]
Yamaoka, T. 105 [66]
Yamashita, O. 794 [823]
Yamashita, Y. 643 [709]
Yamazaki, S. 424 [450]
Yannas, I. V. 20 [21]
Ye, L. 82 [109]
Yonkovich, S. 1296 [1339]
Yoshimi, M. 530 [572]

Zboron, M. 884 [947]
Zecca, M. 384 [404]
Zeeck, A. 64 [84]
Zehnder, M. 205 [206]
Zenneck, U. 126 [171]
Zimmermann, P. 1161 [1194]
Zolk, R. 279 [339]
Zschage, O. 296 [336]
Zsolnai, L. 929 [956]
Zubieta, J. 70 [100]

INDEX OF AUTHORS AND REVIEWERS OF BOOKS

This index lists separately the names of Authors/Editors and Reviewers, respectively, of books reviewed in *Angew. Chem. Int. Ed. Engl. 29* (1990).

Bookauthors

Agrawal, P. K. 1072
Allen, G. 699
Andersson, S. 1368
Andriska, V. 324
Ashfold, M. N. R. 936
Atkins, P. W. 1069
Atta-ur-Rahman 935
Baggott, J. E. 936
Barin, I. 1491
Bevington, J. C. 699
Birks, J. W. 436
Brandsma, L. 562
Brückner, R. 702
Büchel, K. H. 110
Büchner, W. 110
Buckingham, J. 561
Burguera, J. L. 819
Chanon, M. 704
Chelkowski, J. 1491
Cheng, X.-M. 435
Corey, E. J. 435
Cox, M. 701
Cox, P. A. 822
Datta, T. 111
Djerassi, C. 1488
Dugas, H. 815
Elschenbroich, C. 438
Emsley, J. 700
Falk, H. 1071
Farach, H. A. 111
Fox, M. A. 704
Friedrich, W. 112
Gale, R. J. 699
Glass, R. S. 815

Gutsche, C. D. 1075
Hahn, O. 219
Haines, A. H. 563
Harrison, P. J. 1072
Hellinger, U. 937
Hill, C. L. 700
Hill, M. J. 220
Hoffmann, R. 1489
Homann, M. 1490
Hyde, B. G. 1368
Iddon, B. 111
Ioffe, I. I. 222
Ismail, M. I. 817
Jaffe, H. W. 702
Kropf, H. 327
Kučera, A. 936
Kung, H. H. 1074
Laatsch, H. 560
Lachmann, H. 562
Langford, C. H. 1069
Larock, R. C. 435
Lindberg, T. 326
Lipatov, Y. S. 563
Lown, J. W. 559
Luckenbach, R. 109
Maier, J. P. 437
Mainzer, K. 821
Majer, V. 1490
Malhotra, R. 820
Martin, J. C. 820
Matolcsy, G. 324
Moore, G. L. 703
Moore, W. 697
Nádasy, M. 324
Narang, S. C. 820
Olah, G. A. 820
Omae, I. 1072
Otsuka, C. I. 327
Patai, S. 221, 821, 1070
Pick, J. 1490
Polster, J. 562
Poole, C. P. 111
Price, D. 111
Rabideau, P. W. 698
Rappoport, Z. 221, 1070
Regitz, M. 1369
Remers, W. A. 818
Richards, W. G. 1075
Roberts, R. M. 1069
Roesky, H. W. 1490
Rokach, J. 1073
Salzer, A. 438
Scheffold, R. 819
Schliebs, R. 110, 1490
Schulze, J. 1490
Shriver, D. F. 1069
Southon, I. W. 561
Sposito, G. 817
Stoddart, J. F. 1075
Struve, W. S. 816
Svoboda, V. 1490
Tullius, T. D. 1175
Verkruijsse, H. D. 562
Vögtle, F. 323
Wakefield, B. J. 111
Walker, J. M. 701
White, C. M. 325
Winter, G. 110
Woollins, J. D. 110
Yamamoto, Y. 1072
Yamanaka, T. 327

Reviewers

Altenbach, H.-J. 819
Anke, H. 1491
Baudler, M. 110
Bäuerle, P. 704
Bax, A. 935
Behr, A. 1490
Berscheid, H. G. 818
Boche, G. 562
Böhm, L. 699
Breitmaier, E. 1072
Broekaert, J. A. C. 703
Caulton, K. G. 110
Cherdron, H. 699
Christl, M. 702
Dietrich, B. 1075
Eckstein, F. 820
Ermer, O. 698
Feigel, M. 815
Fleissner, M. 699
Frimmel, F. H. 817
Gladysz, J. A. 438
Gossauer, A. 1071
Gruehn, R. 111
Gulick, W. M., Jr. 436
Hahn, T. 817
Henkelmann, J. 222
Herberhold, M. 111
Herrmann, G. 219
Heydt, H. 109
Hoffmann, H. 563
Hoffmann, H. M. R. 326
Holze, R. 699
Hopf, H. 1069
Janoschek, R. 697
Kaim, W. 704
Kauffman, G. B. 1488, 1489
Kauffman, L. M. 1488, 1489
Kirmse, W. 1369
Kleiböhmer, W. 325
Kleinermanns, K. 936
Kräutler, B. 112
Kreuder, W. 699
Krohn, K. 559, 821, 1070
Laatsch, H. 561
Lichtenthaler, R. N. 1490
Liebau, F. 702
Lippert, B. 1175
Loewus, D. I. 937
Lüning, U. 323
Maier, J. 1491
Maier, W. F. 1074
Märk, T. D. 437
Metzler, M. 220
Montforts, F.-P. 563
Neier, R. 435
Nesper, R. 1368
Neumann, W. P. 1072
Neumüller, B. 1069
Paquette, L. A. 435
Pommerening, G. 701
Power, P. P. 1490
Quack, M. 816, 821
Regitz, M. 109
Sander, W. 327
Schäfer, H. J. 700
Schmidtchen, F. P. 815
Schneller, A. 699
Schomburg, D. 1075
Schwedt, G. 822
Talsky, G. 562
Thauer, R. K. 327
Ullrich, V. 1073
Wachter, J. 700
Weber, E. 936
Weidenbruch, M. 221
Weinges, K. 560
Weissmüller, J. 324
Winter, F. 819
Ziegler, T. 820

SUBJECT INDEX

(A second page number to an entry indicates an erratum to the corresponding article.)

(R) = Review Article (C) = Short Communication (B) = Book Review (L) = Correspondence

Ab initio calculations
- Application of the Combined ab initio/IGLO/NMR Method to Resolve the B_6H_{12} Structural Question (C) 886
- C_4O_2 (1,2,3-Butatriene-1,4-dione), the First Dioxide of Carbon with an Even Number of C Atoms (C) 905
- C_2S_2(Ethene-1,2-dithione), an Example for the Violation of Hund's Rule? (C) 1464
- Lithium-Ion-Catalyzed Epoxidation by Triplet Dioxygen: An ab initio Study (C) 648
- On the Nature of Pyrazolylborane. An Ab Initio/IGLO/NMR Study (C) 304
- [PhLiNCH$_2$CH$_2$NLiPh] · 3HMPA, a Monomeric Dilithiumethylenediamide Complex with N_2Li_2 Double Bridging: Synthesis, Crystal Structure, and Model MO Calculations (C) 410
- The Structure of Cyclic C_6S_6 and C_6O_6 (C) 1410

Acetals
- Dependence of Anomeric Stabilization on Structure in Acetals (C) 320

Acetonitrile
- CH Activation of Acetonitrile by Alkyl Compounds of the Early Lanthanoids: Dimeric Cyanomethyl-Lanthanoid Complexes with CH_2CN Bridges (C) 420

Acrylamide
- Catalytic Hydration of Acrylonitrile to Acrylamide under Mild Conditions (C) 523

Acylation
- Asymmetric Nucleophilic Acylation via Metalated Chiral Amino Cyanides: Enantioselective Synthesis of 3-Substituted 4-Oxoesters by Asymmetric Michael Addition (C) 179

Adamantanes
- The First Clamped and Strongly Deformed Adamantane (C) 902

Aldol reactions
- A Novel Pyrrole Synthesis (C) 777

Alkali metal compounds
- About the $Li^{\oplus}$ Gegenion Effect on α-Sulfonyl Carbanions (C) 100
- Aspartic and Glutamic Acid as Ligands to Alkali and Alkaline-Earth Metals: Structural Chemistry as Related to Magnesium Therapy (R) 1090
- Borole Dianions: Metalation of 1-(Dialkylamino)-2,5-dihydro-1*H*-boroles and the Structure of $Li_2(C_4H_4BNEt_2)$ · TMEDA (C) 317
- Carbonylation of Doubly Lithiated *N*-Pivaloyl-anilines. A Novel Approach to Dioxindoles via Intramolecular Trapping of Aromatic Acyllithiums (C) 282
- Chiral Lithium-1-oxyalkanides by Asymmetric Deprotonation; Enantioselective Synthesis of 2-Hydroxyalkanoic Acids and Secondary Alkanols (C) 1422
- CsF · Br_2, an Alkali-Metal Halide Intercalation Compound (C) 1448
- $CsNa_2(OH)_3 \cdot 6H_2O$: Structural Differentiation in the Hydrate of a Ternary Alkali-Metal Hydroxide (C) 904
- Decameric and Dodecameric Sodium Amides and an Organosodium Amide with Stack Structures: $[Na_{10}(NMe_2)_{10}(tmeda)_4]$, $[Na_{12}(NMe_2)_{12}(tmeda)_4]$, and $[Na_{12}(NMe_2)_{10}(CH_2C_6H_4Me)_2(tmeda)_4]$ (C) 1441
- Generation of a Configurationally Stable Chiral Benzyllithium Derivative, and the Capricious Stereochemistry of Its Electrophilic Substitution (C) 1424
- Lewis-Base-Dictated Structural Variations in Sodium Amide Chemistry: X-Ray Crystal Structures of Phenyl(2-pyridyl)amidosodium with Hexamethylphosphoric Triamide (HMPA) and with Pentamethyldiethylenetriamine (PMDETA) (C) 1440
- Lithium Bis(di-*tert*-butylfluorosilyl)-amide as Contact Ion Pair with Linear Si–$N^{\ominus}$–Si Unit and as Ion Pair without $Li^{\oplus}$-Anion Contact (C) 209
- $Na_{10}\{Li_2[MnO_4]_4\}$, a Compound in Which LiO_4 and MnO_4 Tetrahedra Form Chains Consisting of Six- and Eight-Membered Rings (C) 800
- [*n*BuLi · LiO*t*Bu]$_4$, Solid-State Structure of an *n*-Butyllithium–Lithium *tert*-Butoxide Complex (C) 308
- [PhLiNCH$_2$CH$_2$NLiPh] · 3HMPA, a Monomeric Dilithiumethylenediamide Complex with N_2Li_2 Double Bridging: Synthesis, Crystal Structure, and Model MO Calculations (C) 410
- Preparation of an Enantiomerically Enriched Allyllithium Derivative by Deprotonation with Kinetic Resolution of Enantiomers (C) 296
- Reductive Scission of a Cyclopropane σ-Bond During the Action of Elemental Lithium on Cyclopropylacetylenes – A *cis*-1,2-Dilithioalkene as Intermediate (C) 667
- Structure Determination of $NaCD_3$ Powders at 1.5 and 300K by Neutron and Synchrotron–Radiation Diffraction (C) 650
- Synthesis and Structure Determination of Bicyclic $[Li(tmeda)]_2[S_6]$ (C) 422
- Synthesis and Structure of a Dimeric Lithium Diphenylcuprate: $[\{Li(OEt)_2\}(CuPh_2)]_2$ (C) 300
- 2,3,4,5-Tetramethyl-1-sodiopyrrole: An Azacyclopentadienyl Ligand in a Novel Bridging Function (C) 1143
- Tetraphenylallylsodium Diethyl Ether: A Contact Ion Pair with an Intramolecular $Na^{\oplus}$ Sandwich (C) 1042

Alkaline-earth metal compounds
- Aspartic and Glutamic Acid as Ligands to Alkali and Alkaline-Earth Metals: Structural Chemistry as Related to Magnesium Therapy (R) 1090

Alkaloids
- Dictionary of Alkaloids (B) 561
- Grahamine, an Unusual Tropane Alkaloid from *Schizanthus grahamii* (C) 385

Alkanes
- Activation and Functionalization of Alkanes (B) 700

Alkene complexes
- How Do Two C–C Double Bonds Add to One M–M Triple Bond? Structure and Bonding in Bis(η^2-ethylene)hexakis(neopentoxy)ditungsten (C) 1026

Alkenes
- CC Bond Formation by Addition of Carbenium Ions to Alkenes: Kinetics and Mechanism (R) 1371

Alkylidenebutenolides
- Facile Synthesis of 4-Acyl-5-alkyl-2,3-dioxo-2,3-dihydrofurans and Alkylidenebutenolides (C) 1041

Alkynes
- Ethynyl(phenyl)iodonium Triflate, [HC ≡ ClPh][OSO_2CF_3]: Preparation, Spectral Properties, Mechanism of Formation and X-Ray Molecular Structure (C) 287
- Novel Planar π-Systems (C) 393
- Synthesis of Cyclosilanylethynes (C) 641

Allosterism
- A Synthetic Allosteric System with High Cooperativity between Polar and Hydrophobic Binding Sites (C) 1159

Aluminum compounds
- An Aluminaphosphacubane, a New Aluminum Phosphide Precursor (C) 1409

Amino acids
- Aspartic and Glutamic Acid as Ligands to Alkali and Alkaline-Earth Metals: Structural Chemistry as Related to Magnesium Therapy (R) 1090

Aminofluorene
- The Ultimate Carcinogen, *O*-Acetyl-*N*-(2-fluorenyl)hydroxylamine ("*N*-Acetoxy-2-aminofluorene"), and Its Reaction in vitro to Form 2-[*N*-(Deoxyguanosin-8-yl)amino]fluorene (C) 63

Aminoreductones
- Formation of an Aminoreductone from Glucose (C) 536

Analytical methods
- Chemiluminescence Techniques for the Characterization of Materials (R) 362
- Die Technik der organischen Trennungsanalyse. Eine Einführung (B) 560
- Gas Chromatographic Separation of Enantiomers on Cyclodextrin Derivatives (R) 939
- NMR Microscopy—Fundamentals, Limits and Possible Applications (R) 1
- Spectrometric Titrations. Analysis of Chemical Equilibria (B) 562
- The Quartz Microbalance: A Novel Approach to the In-Situ Investigation of Interfacial Phenomena at the Solid/Liquid Junction (R) 329

Anomeric stabilization
- Dependence of Anomeric Stabilization on Structure in Acetals (C) 320

Anthracyclines
- Anthracycline- and Anthracenedione-Based Anticancer Agents (B) 559
- Semisynthetic Rhodomycins: Novel Glycosylation Methods for the Synthesis of Anthracycline Oligosaccharides (C) 809

Antibiotics
- Enantio- and Regiocontrolled Synthesis of a Central Ionophoric Antibiotic Building Block by Sequential Opening of Two Epoxide Rings with Cuprate Reagents (C) 1476
- The Chemistry of Antitumor Antibiotics. Vol.2 (B) 818

Antibodies
- Catalytic Antibodies: A New Class of Transition-State Analogues Used to Elicit Hydrolytic Antibodies (R) 1296

Antimony compounds
- The Synthesis and Structure of Stibaindoles (C) 771

Antitumor agents
- Golfomycin A, a Novel Designed Molecule with DNA-Cleaving Properties and Antitumor Activity (C) 1064
Antiviral agents
- [22]Coproporphyrin II for Photodynamic Therapy (C) 1395
- Nucleotide Analogues as Antiviral Agents (B) 820
Arene complexes
- $[H_2Ru_6(CO)_{16}(\mu\text{-}C_6H_4O)]$: Binding of Five Metal Atoms to a Phenol Molecule (C) 198, (L) 938
- Intramolecular Interconversion of *syn*- and *anti*-Tricarbonyl(1-ethoxy-1,2-dihydrocyclobutabenzene)chromium. Trapping of the *ortho*-Quinodimethane Intermediate (C) 407
- Synthesis and Direct NMR Spectroscopic Observation of $[(\eta^4\text{-Arene})Cr(CO)_3]$ Dianions (C) 1444
- Synthesis and Molecular Structure of *cis*-$[Pd(C_6F_5)_2(C_6H_5CH_2NMe_2)]$, an Intramolecular Coordination Compound Containing an Unusual η^1-Arene Ligand (C) 891
Arenes
- Mesolytic Cleavage of C–C Bonds. Comparison with Homolytic and Heterolytic Processes in the Same Substrate (C) 283
- ^{17}O NMR Spectroscopy of Benzoyl Compounds $Y\text{–}C_6H_4\text{–}COX$: Sensitivity to Ring Substituents as a Measure of the Electron Demand of the Carbonyl Group (C) 647
- Oligorylene as a Model for "Poly(perinaphthalene)" (C) 525
- The Directed Synthesis of Biaryl Compounds: Modern Concepts and Strategies (R) 977
- The Ultimate Carcinogen, *O*-Acetyl-*N*-(2-fluorenyl)hydroxylamine ("*N*-Acetoxy-2-aminofluorene"), and Its Reaction in vitro to Form 2-[*N*-(Deoxyguanosin-8-yl)amino]fluorene (C) 63
Aromatic nitration
- Clays Direct Aromatic Nitration (C) 535
Arsacyclobutenes
- Application of Titanacycles to Heterocycle Synthesis: Phospha- and Arsacyclobutenes (C) 75
Arsenic compounds
- A Compound with a Boron–Arsenic Double Bond (C) 1033
- $[H_6As_{10}Mo_{24}O_{90}]^{8\ominus}$, a Heteropolyanion Comprising Two Linked Spherical Fragments, and Reduced Keggin Anions as Its Degradation Products (C) 88
- Synthesis of Tetrachloroammonium Hexafluoroarsenate, $NCl_4^{\oplus}AsF_6^{\ominus}$ (C) 181
Artificial skin
- Biologically Active Analogues of the Extracellular Matrix: Artificial Skin and Nerves (R) 20
Asymmetric catalysis
- A Borate Propeller Compound as Chiral Catalyst for an Asymmetrically Induced Diels-Alder Reaction (C) 545
- Optically Active Bipyridines in Asymmetric Catalysis (C) 205
Asymmetric protonations
- Asymmetric Protonation of Enolates (C) 1420
Asymmetric syntheses
- Asymmetric Nucleophilic Acylation via Metalated Chiral Amino Cyanides: Enantioselective Synthesis of 3-Substituted 4-Oxoesters by Asymmetric Michael Addition (C) 179
- The Directed Synthesis of Biaryl Compounds: Modern Concepts and Strategies (R) 977
Atomic emission spectroscopy
- Introduction to Inductively Coupled Plasma Atomic Emission Spectroscopy (B) 703
Atomic spectroscopy
- Flow Injection Atomic Spectroscopy (B) 819
Aurophilicity
- Assembly of the $CAu_6^{2\oplus}$ Cluster with a Tailor-made Diphosphane Spanning the Octahedral Edges (C) 1399
Azadiboriridine-boranes
- Azadiboriridine-Borane: a Non-Classical Acid-Base Adduct (C) 1059
Azadiboriridines
- Boroboration of CO with Tri-*tert*-butylazadiboriridine (C) 900
Azides
- Zwitterions as Intermediates of the 1,3-Dipolar Cycloaddition of Electrophilic Azides to 5-Alkylidenedihydrotetrazoles – the Other Non-Concerted Limiting Case (C) 695
Azirines
- 2-Methylene-2*H*-azirines by Photolysis of 1-Azidoallenes (C) 103
Aziridimines
- Stable Aziridimines? A Structural Corrigendum (C) 1164
Azobenzenes
- [2.2](4,4')Azobenzenophane (C) 105

Barium compounds
- Synthesis and Structure of $[Ba_3(OSiPh_3)_6(THF)] \cdot 0.5$ THF, a Trinuclear Barium Siloxide Containing Low-Coordinate Barium Ions (C) 1483
Beilstein
- Beilstein Handbook of Organic Chemistry (B) 109
Betaines
- Electrostatic Control of the Molecular and Crystal Structure of an Olefinic Double Betaine (C) 1132
Biaryl compounds
- The Directed Synthesis of Biaryl Compounds: Modern Concepts and Strategies (R) 977
Bicyclopentanes
- The Bicyclo[1.1.1]pentane Framework—an Excellent Relay for π/σ Conjugation (C) 413
Bicyclopentasilanes
- A Bicyclo[1.1.1]pentasilane Derivative. Synthesis, Molecular Structure, and Comments on Structural Homology (C) 794
Bicyclopentenes
- Mechanism of the Cycloaddition of Bicyclo[2.1.0]pent-2-ene: a Non-concerted Homo-Diels-Alder Reaction (C) 1061
Biochemistry
- Replication Experiments with Nucleotide Base Analogues (R) 36
- The Myelin Membrane of the Central Nervous System—Essential Macromolecular Structure and Function (R) 958
Biological polymers
- Biologically Active Analogues of the Extracellular Matrix: Artificial Skin and Nerves (R) 20
Biomedicine
- NMR Microscopy—Fundamentals, Limits and Possible Applications (R) 1
Biomembrane processes
- Specific Interactions of Proteins with Functional Lipid Monolayers—Ways of Simulating Biomembrane Processes (R) 1269
Biomimetic catalysis
- Biomimetic Catalysis of an S_N2 Reaction Resulting from a Novel Form of Transition-State Stabilization (C) 915
Bioorganic chemistry
- Bioorganic Chemistry. A Chemical Approach to Enzyme Action (B) 815
Biosynthesis
- A Novel Type of Ring Contraction as Non-Enzymatic Step in the Later Stages of the Biosynthesis of Urdamycin H (C) 1051
- Hydrogenobyrinic Acid: Isolation, Biosynthesis, and Function (C) 884
Biotechnology
- The Language of Biotechnology. A Dictionary of Terms (B) 701
Bipyridines
- Optically Active Bipyridines in Asymmetric Catalysis (C) 205
Bismuth compounds
- Structure and Color of Substituted Pentaphenylbismuth (C) 213
Boron compounds
- A Bicyclic Isomer of the *closo*-Carbaborane $(CH)_2(BR)_4$ (C) 292
- A 1,2:2,1-Bis(2-silapropane-1,3-diyl)diborane(6): Stabilization Product of Bis(trisyl)diborane(2)? (C) 899
- A Borate Propeller Compound as Chiral Catalyst for an Asymmetrically Induced Diels-Alder Reaction (C) 545
- A Carbonyliron Complex of an Amino-9-fluorenylideneborane with Coordination at a Borabutadiene Unit (C) 199
- A Compound with a Boron–Arsenic Double Bond (C) 1033
- A Mesityl-bridged Methyleneborane (C) 399
- A New Route to Highly Enantiomerically Enriched (*Z*)-(1-Methyl-2-butenyl)-boronic Esters (C) 59
- An Allene-analogous Boranylidenephosphane with B = P Double Bond: 1,1-Diethylpropyl(2,2,6,6-tetramethylpiperidino)boranylidenephosphane-*P*-pentacarbonylchromium (C) 682
- Application of the Combined ab initio/IGLO/NMR Method to Resolve the B_6H_{12} Structural Question (C) 886
- Azadiboriridine-Borane: a Non-Classical Acid-Base Adduct (C) 1059
- Boroboration of CO with Tri-*tert*-butylazadiboriridine (C) 900
- Borole Dianions: Metalation of 1-(Dialkylamino)-2,5-dihydro-1*H*-boroles and the Structure of $Li_2(C_4H_4BNEt_2) \cdot TMEDA$ (C) 317
- Boron-Phosphorus Compounds and Multiple Bonding (R) 449
- $[BP_2]^{3\ominus}$ and $[BAs_2]^{3\ominus}$, Zintl Anions with Propadiene Structure (C) 65
- Compounds with a Boron–Carbon Triple Bond (C) 1032
- 2,3-Diboratabutadienes and 2-Borataallenes (C) 1030
- 1,2-Dimethyl-1,2-disila-*closo*-dodecaborane(12), the First Silicon Analogue of an *ortho*-Carborane (C) 918
- Lewis-Acid-Induced Transformation of a Terminal Carbonyl Ligand: Synthesis and Structure of the Alkyne-Cluster-Analogue $[(\mu\text{-}H)_3Os_3(CO)_9\{\mu_3,\eta^2\text{-}C(OBC_8H_{14})B(Cl)\}]$ (C) 309
- Measuring the Optical Activity of Chiral Imprints in Insoluble Highly Crosslinked Polymers (C) 684
- On the Nature of Pyrazolylborane. An Ab Initio/IGLO/NMR Study (C) 304
- Strong C–Sn Hyperconjugation in a Distannylmethyleneborane (C) 401
- Structure of a Non-classically Bridged Methyleneborane in the Crystal (C) 398
- Synthesis of Phospholyltetrahydroborato-uranium Complexes. Crystal Structure of $[(\eta^5\text{-}C_4Me_4P)_2U(BH_4)_2]$ (C) 1485

- The First Monomeric Diorgano(pyrazolyl)borane: A Nonclassical Boronium Ion in Solution? (C) 302
- Thermal Decomposition of the Nonmetal Octahedron $(ClB)_4P_2$ by Elimination of Its PP Octahedral Edge (C) 1044
- Unsaturated C_3B_2 Rings with Neighboring Boron Atoms: Derivatives of 4-Methylene-1,2-diboracyclopentane, Dilithium 2,3-diboratafulvene, and 1,2-Dibora-3-cyclopentene (C) 912

Boronic esters
- A New Route to Highly Enantiomerically Enriched (*Z*)-(1-Methyl-2-butenyl)-boronic Esters (C) 59

Bridgehead alcohol
- A Stereoselective π Cyclization to a Combined Bridgehead Olefin–Bridgehead Alcohol (C) 1456

Bromination
- Solvent and Structure Effects in the Photobromination of Benzyltrimethylsilanes. A Mechanistic Changeover from Hydrogen-Atom Transfer to Electron Transfer (C) 658

Bromine compounds
- Bromine Compounds. Chemistry and Applications (B) 111

Butadienes
- A Novel Synthesis of 2-Aminomethyl-1,3-butadienes from *N,O*-Acetals (C) 932

C_4 compounds
- C_4 Hydrocarbons and Derivatives—Resources, Production, Marketing (B) 1490

Cadmium compounds
- Synthesis, Structure, and Gas-Phase Decomposition of $[Cd(EC_6H_2tBu_3)_2]_2$ (E = S, Se): First Examples of Low-Coordinate Volatile Cadmium Chalcogenolato Complexes (C) 638

Cage compounds
- A Stereoselective π Cyclization to a Combined Bridgehead Olefin–Bridgehead Alcohol (C) 1456
- An Aluminaphosphacubane, a New Aluminum Phosphide Precursor (C) 1409
- Non-Metal Rings, Cages and Clusters (B) 110
- The Pagodane Route to Dodecahedranes: An Efficient Variant—New Substitution Patterns (C) 92
- The Pagodane Route to Dodecahedranes: Dodecahedradienes—Unusually "Pyramidalized", Isolable Olefins (C) 95
- Topologically Interesting Cages for Negative Ions with Extremely High "Coordination Number": An Unusual Property of V-O Clusters (C) 926

Calixarenes (B) 1075
- A New Type of Double Calix[4]arenes by Linkage via the Phenolic Hydroxy Groups (C) 280

Carbaboranes
- A Bicyclic Isomer of the *closo*-Carbaborane $(CH)_2(BR)_4$ (C) 292

Carbanions
- A Synthetic Equivalent for [2.2]Paracyclophane-1,9-diyne: Octaphenyl-1:2,9:10-dibenzo[2.2]para-cyclophane-1,9-diene and Its Reduction to the Hexaanion (C) 1418
- About the $Li^{\oplus}$ Gegenion Effect on α-Sulfonyl Carbanions (C) 100
- Chiral Lithium-1-oxyalkanides by Asymmetric Deprotonation; Enantioselective Synthesis of 2-Hydroxyalkanoic Acids and Secondary Alkanols (C) 1422
- Generation of a Configurationally Stable Chiral Benzyllithium Derivative, and the Capricious Stereochemistry of Its Electrophilic Substitution (C) 1424
- Helicene Dianions: Paratropicity of Twisted Phenanthrene Dianions (C) 919

Carbene complexes
- Coupling of an Iridium Vinylidene Complex with Aluminum Alkyls; Carbon-Carbon Bond Formation via Migratory Insertion of a Vinylidene Unit (C) 73
- Stereospecific Insertion of the Carbene Ligand of a Fischer Carbene Complex into Olefinic C–H Bonds (C) 1129
- Synthesis of Nitrogen Heterocycles by Diastereoselective Intramolecular Aminocarbene Annelation (C) 176

Carbenes
- Intramolecular Insertion of Arylcarbenes into C–Si Bonds (C) 661
- Spontaneous Formation of Stable Phosphino(silyl)carbenes from Unstable Diazo Compounds (C) 1429

Carbenium ions
- CC Bond Formation by Addition of Carbenium Ions to Alkenes: Kinetics and Mechanism (R) 1371

Carbides
- ^{13}C-MAS-NMR Spectra of Technical Calcium Carbide and Barium Carbide—Are the $C_2^{2\ominus}$ Ions in Ionic Carbides Surrounded Symmetrically? (C) 807

Carbido complexes
- Synthesis and Structure of the Novel μ_2-Carbido Complex $[(TPP)Fe{=}C{=}Re(CO)_4Re(CO)_5]$ (C) 318

Carbocations
- Experimental and Theoretical IR Spectra of the 2-Norbornyl Cation (C) 183

Carbohydrates
- Artificial Receptors for Carbohydrate Derivatives (C) 1407
- Concanavalin A Binds Pyranosides and Their Tetraacetates Stereoselectively (C) 672
- Cyclization of *N*-Protected 1-Amino-4-pentene-2,3-diols to *lyxo*-Configurated Deoxyimino Sugars (*cis*-Dihydroxypyrrolidines); Synthesis of Potential Glycosidase Inhibitors (C) 1171
- Facile Synthesis of a β(1-3)-Linked galgalactal Disaccharide and Its Use in *N*-Iodosuccinimide-Activated *O*-Glycopeptide Synthesis (C) 425
- Formation of an Aminoreductone from Glucose (C) 536
- Mixed Kolbe Electrolyses with Sugar Carboxylic Acids (C) 195
- New Aspects of the Maillard Reaction in Foods and in the Human Body (R) 565
- Syntheses, Conformations and X-Ray Structure Analyses of the Saccharide Chains from the Core Regions of Glycoproteins (R) 823
- Synthesis of D- and L-2-Amino-2-deoxyarabinose and 1,4-Dideoxy-1,4-iminolyxitol by $(C_2 + C_3)$-Nitroaldol Addition with 2-*O*-Benzylglyceraldehyde (C) 1169

Carbon oxides
- C_4O_2 (1,2,3-Butatriene-1,4-dione), the First Dioxide of Carbon with an Even Number of C Atoms (C) 905
- Identification of Butatrienedione, Its Radical Anion, and Its Radical Cation in the Gas Phase (C) 908
- The Structure of Cyclic C_6S_6 and C_6O_6 (C) 1410

Carbon sulfides
- C_2S_2(Ethene-1,2-dithione), an Example for the Violation of Hund's Rule? (C) 1464
- The Structure of Cyclic C_6S_6 and C_6O_6 (C) 1410

Carbon-carbon linkage
- Amino Acid Esters as Chiral Auxiliary Groups in Lewis Acid Catalyzed Reactions of Electron-rich Siloxydienes with Imines (C) 1468
- CC Bond Formation by Addition of Carbenium Ions to Alkenes: Kinetics and Mechanism (R) 1371
- Coupling of an Iridium Vinylidene Complex with Aluminum Alkyls; Carbon-Carbon Bond Formation via Migratory Insertion of a Vinylidene Unit (C) 73
- Enantioselective Catalysis with a New Zirconium Trichloride Lewis Acid Containing a "Dibornacyclopentadienyl" Ligand (C) 512
- Intramolecular Insertion of Arylcarbenes into C–Si Bonds (C) 661
- New Chiral Auxiliaries for Enolate Alkylations (C) 555
- Optically Active Bipyridines in Asymmetric Catalysis (C) 205
- Reductive Alkylation of Enamines with Chloromethyl *p*-Tolyl Sulfone via a Radical Chain Process (C) 433
- Rhodium-Catalyzed Synthesis of Trisubstituted Olefins from Ethene Derivatives and Diazoalkanes (C) 510
- Stereospecific Insertion of the Carbene Ligand of a Fischer Carbene Complex into Olefinic C–H Bonds (C) 1129

Carbonic acid
- Ionic Isomer Distinction by Neutralization-Reionization Mass Spectrometry (NRMS): Carbonic Acid Radical Cations, $(HO)_2CO^{\bullet\oplus}$ versus $(H_2O/CO_2)^{\bullet\oplus}$ Clusters (C) 404

Carbonyl complexes
- Complexes of Carbon Monoxide and Its Relatives: An Organometallic Family Celebrates Its Birthday (R) 1077

Carbonyl oxides
- Carbonyl Oxides: Zwitterions or Diradicals? (R) 344

Carbonylation
- A Novel Palladium-Catalyzed Carbonylation of Aromatic *N*-Chlorosulfonamidates to Arylsulfonyl Isocyanates (C) 1147
- Carbonylation of Doubly Lithiated *N*-Pivaloyl-anilines. A Novel Approach to Dioxindoles via Intramolecular Trapping of Aromatic Acyllithiums (C) 282

Carbyne complexes
- Alkyne Cleavage as a Novel Route to Low-Valent Carbyne-Metal Complexes (C) 207 (–)

Carcinogenicity
- Misconceptions on Pollution and the Causes of Cancer (R) 1197
- The Ultimate Carcinogen, *O*-Acetyl-*N*-(2-fluorenyl)hydroxylamine ("*N*-Acetoxy-2-aminofluorene"), and Its Reaction in vitro to Form 2-[*N*-(Deoxyguanosin-8-yl)amino]fluorene (C) 63

Catalysis
- A Novel Palladium-Catalyzed Carbonylation of Aromatic *N*-Chlorosulfonamidates to Arylsulfonyl Isocyanates (C) 1147
- A Surface Organometallic Approach for Controlling the Pore Opening Size of Zeolites: the Case of Mordenite Modified via Grafting of Dineopentylmagnesium (C) 805
- Application of Pattern Recognition to Catalytic Research (B) 222
- Catalytic Antibodies: A New Class of Transition-State Analogues Used to Elicit Hydrolytic Antibodies (R) 1296

- Catalytic Hydration of Acrylonitrile to Acrylamide under Mild Conditions (C) 523
- Catalytic Hydrosilylation or Hydrogenation at One Coordination Site of [Cp'Fe(CO)(X)] Fragments (C) 1131
- Clays Direct Aromatic Nitration (C) 535
- Continuous Generation of NADH from $NAD^{\oplus}$ and Formate Using a Homogeneous Catalyst with Enhanced Molecular Weight in a Membrane Reactor (C) 388
- Elementary Steps in Heterogeneous Catalysis (R) 1219
- Enantioselective Catalysis with a New Zirconium Trichloride Lewis Acid Containing a "Dibornacyclopentadienyl" Ligand (C) 512
- $Fe^{\oplus}$-Catalyzed Gas-Phase Oxidation of Ethane by N_2O (C) 1431
- $FeO^{\oplus}$ Activates Methane (C) 1433
- Isotope Effects Associated with α-Olefin Insertion in Zirconocene-Based Polymerisation Catalysts: Evidence for an α-Agostic Transition State (C) 1412
- Nickel: An Element with Wide Application in Industrial Homogeneous Catalysis (R) 235
- Optically Active Deltacyclanes and Deltacyclenes by Enantioselective Catalysis (C) 652
- Oxygen Activation with Transition Metal Complexes: Nickel-Catalyzed Oxidation of a Pentacoordinated Substrate (C) 106
- 2-Pentylcyclopent-2-en-1-one by Catalytic Pauson-Khand Reaction (C) 1413
- Radiation-Induced Copolymerization of *cis*-$[PdCl_2\{CN(CH_2)_3\text{-}OC(O)\text{-}CH=CH_2\}_2]$: A Novel Route to Organometallic Cross-linked Copolymers Useful for Catalytic Applications (C) 384
- Rhodium-Catalyzed Synthesis of Trisubstituted Olefins from Ethene Derivatives and Diazoalkanes (C) 510
- Stereo- and Regioselectivity of Chiral, Alkyl-substituted *ansa*-Zirconocene Catalysts in Methylalumoxane-activated Propene Polymerization (C) 279
- Transition Metal Oxides: Surface Chemistry and Catalysis (B) 1074
- Transition-Metal-Induced Generation of C_2H_4 from 1,7-Octadiene: Regiospecific Activation of Internal C–C Bonds instead of Metathesis-like Coupling of Terminal CH_2 Groups (C) 402
- Water-Soluble Metal Complexes of the Sulfonated Triphenylphosphane TPPTS: Preparation of the Pure Compounds and their Use in Catalysis (C) 391

C-C activation
- Kinetic Isotope Effects as a Mechanistic Tool for the Elucidation of the Rate-Determining Step(s) in the Transition-Metal-Ion-Mediated Activation of CH/CC Bonds. Ethylene Loss from Metastable 4-Octyne/$M^{\oplus}$ Complexes in the Gas Phase (C) 509
- Transition-Metal-Induced Generation of C_2H_4 from 1,7-Octadiene: Regiospecific Activation of Internal C–C Bonds instead of Metathesis-like Coupling of Terminal CH_2 Groups (C) 402

Central nervous system
- The Myelin Membrane of the Central Nervous System—Essential Macromolecular Structure and Function (R) 958

Ceramics
- A New Way to SiC Ceramic Precursors by Catalytic Preparation of Preceramic Polymers (C) 785

C-H activation
- CH Activation of Acetonitrile by Alkyl Compounds of the Early Lanthanoids: Dimeric Cyanomethyl-Lanthanoid Complexes with CH_2CN Bridges (C) 420
- Kinetic Isotope Effects as a Mechanistic Tool for the Elucidation of the Rate-Determining Step(s) in the Transition-Metal-Ion-Mediated Activation of CH/CC Bonds. Ethylene Loss from Metastable 4-Octyne/$M^{\oplus}$ Complexes in the Gas Phase (C) 509
- Novel Platinum Complexes Enable Selective C-H and C-Si Activation of Tetramethylsilane at Room Temperature (C) 880

Charge transfer complexes
- 4,7-Dimethyl-4,7-dihydro-[1,2,5]thiadiazolo[3,4-*b*]pyrazine, a Novel Electron Donor with a 12π-Electron Ring System (C) 643
- Electrical and Magnetic Properties and X-Ray Structure of a Highly Conductive 4:1 Complex of Tetracyanoquinodimethane and a Tetrathiafulvalene Derivative (C) 1450
- Novel S-Heteroquinoid Electron Acceptors. Synthesis of 2,5-Bis(cyanoimino)-2,5-dihydrothieno[3,2-*b*]thiophenes (DCNTTs) and Conductive Charge Transfer Complexes (C) 204
- Organometallic Host–Guest Systems Representing Novel Charge-Transfer "Ion Pairs" with Three-Dimensional Electron-Donor Networks (C) 1126

Chelate ligands
- A New Mode of Metal Encapsulation (C) 1404
- New Chiral C_3-Symmetric Tripodal Phosphanes (C) 1462

Chemical elements
- The Elements (B) 700
- The Elements—Their Origin, Abundance and Distribution (B) 822

Chemical equilibrium
- Spectrometric Titrations. Analysis of Chemical Equilibria (B) 562

Chemical process design
- Molecular Thermodynamics for Chemical Process Design (R) 1246

Chemical reactors
- Mathematical Modeling of Chemical Reactors—Development and Implementation of Novel Technologies (R) 1235

Chemiluminescence
- Chemiluminescence and Photochemical Reaction Detection in Chromatography (B) 436
- Chemiluminescence Techniques for the Characterization of Materials (R) 362

Chemistry today
- Chemistry for the Future—State of the Art and Perspectives (R) 1177
- Organic Synthesis—Where now? (R) 1320

Chemists as poets
- Cantor's Dilemma (B) 1488
- Gaps and Verges (B) 1489

Chemotherapy
- Anthracycline- and Anthracenedione-Based Anticancer Agents (B) 559
- Development of Tailor-Made Cytostatics Activable by Acid-Catalyzed Hydrolysis for Selective Tumor Therapy (C) 782

Chiral auxiliaries
- A Borate Propeller Compound as Chiral Catalyst for an Asymmetrically Induced Diels-Alder Reaction (C) 545
- Amino Acid Esters as Chiral Auxiliary Groups in Lewis Acid Catalyzed Reactions of Electron-rich Siloxydienes with Imines (C) 1468
- Asymmetric Protonation of Enolates (C) 1420
- New Chiral Auxiliaries for Enolate Alkylations (C) 555
- Structural Characterization of the Pseudoenantiomeric *cis*-Dioxo Osmium(VI) Esters of Chiral Diols with Cinchona Alkaloid Ligands (C) 639

Chirality
- Chiral Lithium-1-oxyalkanides by Asymmetric Deprotonation; Enantioselective Synthesis of 2-Hydroxyalkanoic Acids and Secondary Alkanols (C) 1422
- Generation of a Configurationally Stable Chiral Benzyllithium Derivative, and the Capricious Stereochemistry of Its Electrophilic Substitution (C) 1424
- Induction and Variation of Chirality in Discotic Liquid Crystalline Polymers (C) 1478

Chlorophenoles
- Oxidative Degradation of Aromatic Pollutants by Chemical Models of Lignase Based on Porphyrin Complexes (C) 1471

Chromatography
- Chemiluminescence and Photochemical Reaction Detection in Chromatography (B) 436
- Modern Supercritical Fluid Chromatography (B) 325

Chromium compounds
- A Paramagnetic μ-Methylene Complex with a Short Cr^{III}–Cr^{III} Bond (C) 775
- Dependence of the Magnetic Superexchange on the Cr···Cr Distance in Dinuclear Chromium(II) Complexes (C) 1055
- High-Pressure NMR Studies of $[(\eta^3\text{-}C_5H_5)(\eta^5\text{-}C_5H_5)Cr(CO)_2]$. Evidence for Concerted Ring Interchange (C) 194
- μ-Hydroxobis(μ-formato)hexaaquadichromium(III), an Intermediate in the Formation of Basic Chromium Carboxylates (C) 811
- Intramolecular Interconversion of *syn*- and *anti*-Tricarbonyl(1-ethoxy-1,2-dihydrocyclobutabenzene)chromium. Trapping of the *ortho*-Quinodimethane Intermediate (C) 407
- Synthesis and Direct NMR Spectroscopic Observation of $[(\eta^4\text{-Arene})Cr(CO)_3]$ Dianions (C) 1444
- Synthesis of Nitrogen Heterocycles by Diastereoselective Intramolecular Aminocarbene Annelation (C) 176

CIDNP
- NMR Study of Nuclear Spin Polarization during Chemical Reactions with Ortho Hydrogen (C) 58

Clusters
- Lewis-Acid-Induced Transformation of a Terminal Carbonyl Ligand: Synthesis and Structure of the Alkyne-Cluster-Analogue $[(\mu\text{-}H)_3Os_3(CO)_9\{\mu_3,\eta^2\text{-}C(OBC_8H_{14})B(Cl)\}]$ (C) 309
- New Copper Clusters Containing Se and PEt_3 as Ligands: $[Cu_{70}Se_{35}(PEt_3)_{22}]$ and $[Cu_{20}Se_{13}(PEt_3)_{12}]$ (C) 1452
- $[Ni_3(\mu_3\text{-}CNMe)(\mu_3\text{-}I)(CNMe)_2(Ph_2PCH_2PPh_2)_2]I$, a *triangulo* Nickel Cluster with an Unprecedented Symmetric Linear μ_3-η^1 Isocyanide Ligand (C) 395
- Nonmolecular Metal Chalcogenide/Halide Solids and Their Molecular Cluster Analogues (R) 840
- Novel Bonding Mode for a Cyanometalate Ligand: Synthesis and Crystal Structure of the Mn_4Pd_4 Cluster $[(OC)Pd(\mu\text{-}NC)Mn(\eta\text{-}C_5H_4Me)(CO)_2]_4$

Containing an Orthogonal Arrangement of Helical Units (C) 1140
- $[(Ph_3P)_2N]_2[Os_{18}Hg_2C_2(CO)_{42}]$ a Photochemically Generated High-Nuclearity Cluster Which Reversibly Incorporates Metallic Mercury into Its Metal Core (C) 1137
- Preparation and Structure of $[Se=W(PSe_4)(PSe_2)]^{2\ominus}$; a Cluster Containing a Heteroallylic $PSe_2^{\ominus}$ Unit (C) 1486
- Rings, Clusters and Polymers of Main Group and Transition Elements (B) 1490
- Synthesis and Structure of $(NBu_4)[Sn\{Pt(\mu\text{-}Cl)(C_6F_5)_2\}_3]$, an Unusual Cluster with Three $Pt^{II}\rightarrow Sn^{II}$ Bonds (C) 1449
- Synthesis and Structure of Novel Cu-Clusters: $[Cu_{30-x}Se_{15}(PiPr_3)_{12}]$ (x = 0,1) and $[Cu_{36}Se_{18}(PtBu_3)_{12}]$ (C) 796
- Topologically Interesting Cages for Negative Ions with Extremely High "Coordination Number": An Unusual Property of V-O Clusters (C) 926

Cobalt compounds
- Building Up Metal-Stabilized Fourfold Bridged Cyclobutadienophanes (C) 1426
- Catalytic Hydration of Acrylonitrile to Acrylamide under Mild Conditions (C) 523
- Cycloaddition Reactions of CpCo-Stabilized Cyclobutadiene Derivatives (C) 276
- Dicobalt Complexes with *syn*- and *anti*-Coordinated μ-Cycloheptatriene Bridges (C) 686
- Formation of Tetranuclear Chelate(4-) Ions of Divalent Metals (Mn, Co, Ni) with Idealized *T* Symmetry by Spontaneous Self-assembly (C) 311
- Heteronuclear Complexes Containing $CuCo(CO)_4$ Structural Units and Nitrogen Ligands (C) 783
- Ring-Opening of a Bicyclo[3.2.0]hepta-1,3-dienylcobalt(I) Complex Followed by Cycloaddition (C) 1057
- The Azide Homologues Et–PPP and Ph–AsAsAs as Bifacially Coordinated Ligands in Tripod-Cobalt Complexes: Synthesis, Structure and Molecular Dynamics (C) 929
- The Proton Catalyzed Transformation of a Cobaltacyclopentadiene into a η^4-Cyclobutadiene Complex (C) 1046
- The Tri-μ-amidobis[triammine-cobalt(III)] Cation: The First Triply Amido-bridged Complex (C) 1158
- *trans*-1,2-Difluoro-1,2-bis[(tetracarbonyl)cobaltio]ethene, a Difluoroethyne Complex with μ_2-η^1-η^1-Coordination (C) 315

Cobyrinic acid
- Hydrogenobyrinic Acid: Isolation, Biosynthesis, and Function (C) 884

Cocondensations
- Highly Reactive Intermediates from the Cocondensation Reactions of Iron, Cobalt and Nickel Vapor with Arenes (R) 126

Collisions
- Bimolecular Collisions (B) 936

Colloids
- Colloid Chemistry of Polymers (B) 563

Complexes with aldehyde ligands
- π/σ Equilibria in Metal Complexes of Organic Carbonyl Compounds; Synthesis and Structure of Chiral Rhenium Complexes $[(\eta^5\text{-}C_5H_5)Re(NO)(PPh_3)(O=CHAr)]X$ (C) 1473
- Thermodynamic Aldehyde Enantioface Binding Selectivities in Complexes of Chiral Metal Fragments; Mechanism of Interconversion of Diastereomeric π-Aldehyde Complexes $[(\eta^5\text{-}C_5H_5)Re(NO)(PPh_3)(\eta^2\text{-}O=CHAr)]BF_4$ (C) 1475

Complexes with arsenic ligands
- The Azide Homologues Et–PPP and Ph–AsAsAs as Bifacially Coordinated Ligands in Tripod-Cobalt Complexes: Synthesis, Structure and Molecular Dynamics (C) 929

Complexes with carbon ligands
- CH Activation of Acetonitrile by Alkyl Compounds of the Early Lanthanoids: Dimeric Cyanomethyl-Lanthanoid Complexes with CH_2CN Bridges (C) 420
- Complexes of Carbon Monoxide and Its Relatives: An Organometallic Family Celebrates Its Birthday (R) 1077
- (3,3-Diphenylallenylidene)trimethylphosphanetitanocene: The First Titanocene Carbene Complex with Three Cumulative Double Bonds (C) 1037
- $[\{Ni_2(\mu\text{-}CNMe)(CNMe)_4(Ph_2PCH_2PPh_2)\}_2Hg][NiCl_4]$, a Spirocyclic Ni_4Hg Cluster with an Hg^{II}-Center (C) 396
- $[Ni_3(\mu_3\text{-}CNMe)(\mu_3\text{-}I)(CNMe)_2(Ph_2PCH_2PPh_2)_2]I$, a *triangulo* Nickel Cluster with an Unprecedented Symmetric Linear μ_3-η^1 Isocyanide Ligand (C) 395
- Synthesis of Two Tl^{III} Diacetonyl Compounds and Crystal Structure of $[Tl\{CH_2C(O)Me\}_2(\mu\text{-}CF_3SO_3)(bpy)]_2$ (C) 1125
- The Proton Catalyzed Transformation of a Cobaltacyclopentadiene into a η^4-Cyclobutadiene Complex (C) 1046

Complexes with chalcogen ligands
- Low-Dimensional Compounds Incorporating Polychalcogenide Ligands. The Unusual Polymeric Structures of $[AuSe_5]_n^{n\ominus}$ and $[AuSe_{13}]_n^{3n\ominus}$ (C) 914
- Synthesis, Structure, and Gas-Phase Decomposition of $[Cd(EC_6H_2tBu_3)_2]_2$ (E = S, Se): First Examples of Low-Coordinate Volatile Cadmium Chalcogenolato Complexes (C) 638

Complexes with diene ligands
- *s-trans*-1,3-Dienes as Ligands for Cationic Group 8 Metal Centers (C) 1417

Complexes with hydrido ligands
- Synthesis and 2D-(^1H,^{103}Rh)-NMR Study of the First "Non-Classical" Polyhydrido Complex Stabilized by a Nitrogen Donor Ligand (C) 548

Complexes with nitrogen ligands
- Functional Tetrahedral Zinc Complexes (C) 898
- Heteronuclear Complexes Containing $CuCo(CO)_4$ Structural Units and Nitrogen Ligands (C) 783
- Ketenimine Complexes from Metal Isocyanides and Diazoalkanes (C) 275
- On a (1,4-Diazabutadiene)bis(ethene)-nickel(0) Complex and Related Compounds (C) 298
- $[PhLiNCH_2CH_2NLiPh]\cdot 3HMPA$, a Monomeric Dilithiumethylenediamide Complex with N_2Li_2 Double Bridging: Synthesis, Crystal Structure, and Model MO Calculations (C) 410
- Platinum in the Unusual Oxidation State +2.75: A Linear Tetranuclear Complex with the Model Nucleobase 1-Methylthymine (C) 84
- Synthesis and Structure of $Ph_2P(S)N=TiCl_2\cdot 3C_5H_5N$, the First Imidotitanium Complex (C) 669
- Synthesis, Structure, and Reactivity of Aryloxo(imido)titanium Complexes (C) 664
- The Tri-μ-amidobis[triamminecobalt-(III)] Cation: The First Triply Amido-bridged Complex (C) 1158
- Ytterbium(II) Benzamidinates, a New Class of Highly Reactive Lanthanoid(II) Complexes (C) 894

Complexes with oligocyclopentadienyl ligands
- On the Way to Ligating Oligocyclopentadienyls: Synthesis and Preliminary Reactions of the Two Isomeric Tercyclopentadienyls and Their Transition Metal Complexes (C) 549

Complexes with oxygen ligands
- Alkyltechnetium Oxides: First Examples and Reactions (C) 189
- Asymmetric Heterodinuclear $[L'Ru(\mu\text{-}O)(\mu\text{-}CH_3CO_2)_2ML]^{2\oplus}$ Complexes (M = Fe, Mn, V): Electronic Structure and Magnetic Properties (C) 645
- Coordination Chemistry of Polyoxomolybdates: The Structure of a Dodecanuclear Molybdate Cage Incorporating Hydrogen Squarate Ligands, $[(C_4H_9)_4N]_4[Mo_{12}O_{36}(C_4O_4H)_4]\cdot 10Et_2O$ (C) 70
- Formation of Tetranuclear Chelate(4-) Ions of Divalent Metals (Mn, Co, Ni) with Idealized *T* Symmetry by Spontaneous Self-assembly (C) 311
- μ-Hydroxobis(μ-formato)hexaaquadichromium(III), an Intermediate in the Formation of Basic Chromium Carboxylates (C) 811
- $[n\text{BuLi}\cdot \text{LiO}t\text{Bu}]_4$, Solid-State Structure of an *n*-Butyllithium–Lithium *tert*-Butoxide Complex (C) 308
- Organometallic Macrocycles: Synthesis and Molecular Structure of Trimeric Tartratodiruthenium Complexes (C) 429
- Structure–Magnetism Relationship in $[Ti^{III}\text{-}O\text{-}Ti^{III}]^{4\oplus}$ Complexes (C) 68
- Synthesis and Characterization of the Linear Trinuclear Complexes $[M^{II}_3(O_2CCH_3)_6(biphme)_2]$, M = Mn, Fe (C) 812
- Synthesis, Structure, and Catalase-Type Activity of a Novel Oxo-Bridged Tetranuclear Manganese Aggregate Exhibiting Short O···O Interactions (C) 1156
- The Coordination Chemistry and Organometallic Chemistry of Tridentate Oxygen Ligands with π-Donor Properties (R) 627
- The Re–Re Bond in Binuclear Di-μ-oxorhenium Complexes Containing the 1,4,7-Triazacyclononane Ligand (C) 787

Complexes with phosphorus ligands
- Assembly of the $CAu_6^{2\oplus}$ Cluster with a Tailor-made Diphosphane Spanning the Octahedral Edges (C) 1399
- Epoxidation of the P=C Double Bond of Phosphaalkene Complexes: X-Ray Crystal Structure Analysis of a Stable Oxaphosphirane Complex (C) 1166
- New Chiral C_3-Symmetric Tripodal Phosphanes (C) 1462
- Novel Diphosphinoiridium Catalysts for the Enantioselective Hydrogenation of *N*-Arylketimines (C) 558
- Synthesis of Phospholyltetrahydroboratouranium Complexes. Crystal Structure of $[(\eta^5\text{-}C_4Me_4P)_2U(BH_4)_2]$ (C) 1485
- The Azide Homologues Et–PPP and Ph–AsAsAs as Bifacially Coordinated Ligands in Tripod-Cobalt Complexes:

Synthesis, Structure and Molecular Dynamics (C) 929
- Water-Soluble Metal Complexes of the Sulfonated Triphenylphosphane TPPTS: Preparation of the Pure Compounds and their Use in Catalysis (C) 391
- $Zn^{II}Fe^{III}$ and $Fe^{II}Fe^{III}$ Complexes Containing a Novel (μ-Phenoxo)bis(μ-diphenylphosphato)dimetal(II,III) Core as Model Complexes for Active Sites of Purple Phosphatases (C) 531

Complexes with pnictogen ligands
- Complexes with Substituent-free Acyclic and Cyclic Phosphorus, Arsenic, Antimony, and Bismuth Ligands (R) 1104

Complexes with sulfur ligands
- Bis(1,4,7-trithiacyclononane)gold Dication: A Paramagnetic, Mononuclear Au^{II} Complex (C) 197
- $[Cu_4(ddtp)_2Br_4]$, a Unique Tetranuclear Copper(I) Complex with Bridging Thioethers and Bridging Bromides (C) 1419
- Oxygen Activation with Transition Metal Complexes: Nickel-Catalyzed Oxidation of a Pentacoordinated Substrate (C) 106
- Synthesis and Structure of $[Et_2OZn(SC_6H_2tBu_3)_2]$, the First T-Shaped Zinc Complex (C) 1403

Computer
- Computer Simulation of Molecular Dynamics: Methodology, Applications, and Perspectives in Chemistry (R) 992
- Organic Synthesis in the Age of Computers (R) 1286
- VCH TransDict, Übersetzersoftware, Version 2.2 (B) 937

Concanavalin A
- Concanavalin A Binds Pyranosides and Their Tetraacetates Stereoselectively (C) 672

Conformation
- On the Conformation and Structure of Organometal Complexes in the Solid State: Two Studies Relevant to Chemical Synthesis (R) 256
- Peptides as Conformational Switch: Medium-Induced Conformational Transitions of Designed Peptides (C) 185
- Restricted Rotation of an Unsubstituted η^5-Cyclopentadienyl Group in Solution Demonstrated by ^{13}C NMR Spectroscopy (C) 289

Conformational analysis
- Conformational Analysis of Medium-Sized Heterocycles (B) 815
- The Conformational Analysis of Cyclohexenes, Cyclohexadienes and Related Hydroaromatic Compounds (B) 698

Conformer separation
- Isolation of Conformational Isomers of α- and β-Ionones by Inclusion Complex Formation (C) 662

Coordination
- π/σ Equilibria in Metal Complexes of Organic Carbonyl Compounds; Synthesis and Structure of Chiral Rhenium Complexes $[(\eta^5\text{-}C_5H_5)\text{-}Re(NO)(PPh_3)(O=CHAr)]X$ (C) 1473
- A New Mode of Metal Encapsulation (C) 1404
- Complexes with Substituent-free Acyclic and Cyclic Phosphorus, Arsenic, Antimony, and Bismuth Ligands (R) 1104
- Cp*Ru(acac)--A Coordinatively Unsaturated, Stable 16-Valence-Electron Complex (C) 773
- Dicobalt Complexes with *syn*- and *anti*-Coordinated μ-Cycloheptatriene Bridges (C) 686
- Functional Tetrahedral Zinc Complexes (C) 898
- Ge^{II} and Sn^{II} Complexes of [2.2.2]Paracyclophane with Threefold Internal η^6 Coordination (C) 1397
- $[H_2Ru_6(CO)_{16}(\mu\text{-}C_6H_4O)]$: Binding of Five Metal Atoms to a Phenol Molecule (C) 198, (L) 938
- Lithium Bis(di-*tert*-butylfluorosilyl)-amide as Contact Ion Pair with Linear $Si\text{-}N^{\ominus}\text{-}Si$ Unit and as Ion Pair without $Li^{\oplus}$-Anion Contact (C) 209
- Novel Bonding Mode for a Cyanometalate Ligand: Synthesis and Crystal Structure of the Mn_4Pd_4 Cluster $[(OC)Pd(\mu\text{-}NC)Mn(\eta\text{-}C_5H_4Me)(CO)_2]_4$ Containing an Orthogonal Arrangement of Helical Units (C) 1140
- Ring-Opening of a Bicyclo[3.2.0]hepta-1,3-dienylcobalt(I) Complex Followed by Cycloaddition (C) 1057
- Synthesis and Direct NMR Spectroscopic Observation of $[(\eta^4\text{-Arene})Cr(CO)_3]$ Dianions (C) 1444
- Synthesis and Structure of $[Ba_3(OSiPh_3)_6(THF)] \cdot 0.5\ THF$, a Trinuclear Barium Siloxide Containing Low-Coordinate Barium Ions (C) 1483
- 2,3,4,5-Tetramethyl-1-sodiopyrrole: An Azacyclopentadienyl Ligand in a Novel Bridging Function (C) 1143
- Thermodynamic Aldehyde Enantioface Binding Selectivities in Complexes of Chiral Metal Fragments; Mechanism of Interconversion of Diastereomeric π-Aldehyde Complexes $[(\eta^5\text{-}C_5H_5)\text{-}Re(NO)(PPh_3)(\eta^2\text{-}O=CHAr)]BF_4$ (C) 1475
- Topologically Interesting Cages for Negative Ions with Extremely High "Coordination Number": An Unusual Property of V-O Clusters (C) 926

Cope rearrangements
- Stereocontrolled Construction of Complex Cyclic Ketones via Oxy-Cope Rearrangement (R) 609

Copper compounds
- Correlations between Magnetism and Structure in Dinuclear $Cu^{II}Fe^{III}$ Complexes with Integer Spin EPR Signals (C) 921
- $[Cu_4(ddtp)_2Br_4]$, a Unique Tetranuclear Copper(I) Complex with Bridging Thioethers and Bridging Bromides (C) 1419
- Heteronuclear Complexes Containing $CuCo(CO)_4$ Structural Units and Nitrogen Ligands (C) 783
- Highly Selective Synthesis of (*E*)-Alkene Isosteric Dipeptides With High Optical Purity via $RCu(CN)Li \cdot BF_3$ Mediated Reaction (C) 801
- New Copper Clusters Containing Se and PEt_3 as Ligands: $[Cu_{70}Se_{35}(PEt_3)_{22}]$ and $[Cu_{20}Se_{13}(PEt_3)_{12}]$ (C) 1452
- Structure of a Synthetic Trefoil Knot Coordinated to Two Copper(I) Centers (C) 1154
- Synthesis and Structure of a Dimeric Lithium Diphenylcuprate: $[\{Li(OEt)_2\}\{CuPh_2\}]_2$ (C) 300
- Synthesis and Structure of Novel Cu-Clusters: $[Cu_{30-x}Se_{15}(PiPr_3)_{12}]$ ($x = 0,1$) and $[Cu_{36}Se_{18}(PtBu_3)_{12}]$ (C) 796

Correspondence (L) 938

C-Si activation
- Novel Platinum Complexes Enable Selective C-H and C-Si Activation of Tetramethylsilane at Room Temperature (C) 880

Cumulenes
- Acetylene-Cumulene Porphyrinoids (C) 1385
- (3,3-Diphenylallenylidene)trimethylphosphanetitanocene: The First Titanocene Carbene Complex with Three Cumulative Double Bonds (C) 1037
- Nickel-Catalyzed Cyclodimerization of Hexapentaenes: [4]Radialenes and [5]Radialenones with Cumulated Double Bonds (C) 1062
- Ruthenium-containing Cumulenes: Generation of 2,3,4-Pentatrienylidene- and 3-Oxo-1,4-pentadienyl-Complexes (C) 215

Cyanines
- Vinylogous Cyanine-like Dications of Tetrakis(dimethylamino) Compounds (C) 211

Cyanohydrins
- Enzyme-Catalyzed Synthesis of (*S*)-Cyanohydrins (C) 386

Cycloadditions
- [4 + 2]-Cycloadditions of Phosphinodiazoalkanes: Synthesis of 1,2,4-λ^5-Diazaphosphinines (C) 314
- Cycloaddition Reactions of CpCo-Stabilized Cyclobutadiene Derivatives (C) 276
- Mechanism of the Cycloaddition of Bicyclo[2.1.0]pent-2-ene: a Non-concerted Homo-Diels-Alder Reaction (C) 1061
- Ring-Opening of a Bicyclo[3.2.0]hepta-1,3-dienylcobalt(I) Complex Followed by Cycloaddition (C) 1057
- Synthesis and Cycloadditions of Monomeric Selenobenzophenone (C) 1067
- Zwitterions as Intermediates of the 1,3-Dipolar Cycloaddition of Electrophilic Azides to 5-Alkylidenedihydrotetrazoles – the Other Non-Concerted Limiting Case (C) 695

Cyclobutadienes
- Cycloaddition Reactions of CpCo-Stabilized Cyclobutadiene Derivatives (C) 276

Cyclobutanes
- Synthesis and NMR Spectra of 2,3-Dihydro-1,3-methanoindene Derivatives and 1,2,3,5-Tetrahydro-1,3-methanopentalene (C) 1035

Cyclobutenes
- A 1,6-Diphospha-1,2,4,5-hexatetraene, Synthesis and Ring Closure Reactions to Cyclobutenes (C) 927

Cyclodextrins
- Gas Chromatographic Separation of Enantiomers on Cyclodextrin Derivatives (R) 939
- Permethyl-β-cyclodextrin, Chemically Bonded to Polysiloxane: a Chiral Stationary Phase with Wider Application Range for Enantiomer Separation by Capillary Gas Chromatography (C) 427

Cycloheptatrienes
- Dicobalt Complexes with *syn*- and *anti*-Coordinated μ-Cycloheptatriene Bridges (C) 686

Cyclopentenones
- 2-Pentylcyclopent-2-en-1-one by Catalytic Pauson-Khand Reaction (C) 1413

Cyclophanes
- A Spacious Cyclophane Host for Inclusion Complexation of Steroids and [m.n]Paracyclophanes (C) 769
- A Synthetic Equivalent for [2.2]Paracyclophane-1,9-diyne: Octaphenyl-1:2,9:10-dibenzo[2.2]para-cyclophane-1,9-diene and Its Reduction to the Hexaanion (C) 1418
- [2.2](4,4')Azobenzenophane (C) 105
- Building Up Metal-Stabilized Fourfold

Bridged Cyclobutadienophanes (C) 1426
- Catalytic Cyclophanes: A Porphyrin-Bridged Cyclophane as a Model for Cytochrome P-450 Enzymes (C) 191
- Ge^{II} and Sn^{II} Complexes of [2.2.2]Paracyclophane with Threefold Internal η^6 Coordination (C) 1397
- Heptasila[7]paracyclophane (C) 778
Cyclopropanes
- Reductive Scission of a Cyclopropane σ-Bond During the Action of Elemental Lithium on Cyclopropylacetylenes – A *cis*-1,2-Dilithioalkene as Intermediate (C) 667
Cycloreductions
- Synthesis of (±)-Phyllanthocin via a Metal-Catalyzed Cycloreduction (C) 520 (–)
Cyclovoltammetry
- Electrochemical Solid-State Studies on Oligomeric *p*-Phenylenes as Model Compounds for Conductive Polymers (C) 692
- Oligorylene as a Model for "Poly(perinaphthalene)" (C) 525

Deamidation
- Selective Deamidation of Peptide Amides (C) 1139
Deltacyclanes
- Optically Active Deltacyclanes and Deltacyclenes by Enantioselective Catalysis (C) 652
Dendrimers
- Starburst Dendrimers: Molecular-Level Control of Size, Shape, Surface Chemistry, Topology, and Flexibility from Atoms to Macroscopic Matter (R) 138
Diamines
- Cooperative Interactions in Molecular Recognition—the Binding of Diamines to a Tetracarboxylic Acid (C) 1148
Diastereoselectivity
- A New Route to Highly Enantiomerically Enriched (*Z*)-(1-Methyl-2-butenyl)-boronic Esters (C) 59
- Doubly Stereodifferentiating Hiyama Addition with Mismatched Reactants; Enantio- and Diastereo-controlled Synthesis of Dihydrocanadensolide (C) 679
- Highly Selective Synthesis of (*E*)-Alkene Isosteric Dipeptides With High Optical Purity via $RCu(CN)Li \cdot BF_3$ Mediated Reaction (C) 801
- Intramolecular Hetero-Diels–Alder Reactions of Oxadienes: Influence of Substituents of the Tether on the Diastereoselectivity (C) 665
- Synthesis of Nitrogen Heterocycles by Diastereoselective Intramolecular Aminocarbene Annelation (C) 176
Diazaphosphinines
- [4 + 2]-Cycloadditions of Phosphinodiazoalkanes: Synthesis of 1,2,4-λ^5-Diazaphosphinines (C) 314
Diazo compounds
- Spontaneous Formation of Stable Phosphino(silyl)carbenes from Unstable Diazo Compounds (C) 1429
Diazoalkanes
- Ketenimine Complexes from Metal Isocyanides and Diazoalkanes (C) 275
Dications
- Vinylogous Cyanine-like Dications of Tetrakis(dimethylamino) Compounds (C) 211
Dictionary
- Compact Wörterbuch der exakten Naturwissenschaften und der Technik. Band 1. Englisch-Deutsch (B) 936
- Dictionary of Alkaloids (B) 561
- The Language of Biotechnology. A Dictionary of Terms (B) 701
Diels–Alder reactions
- A Borate Propeller Compound as Chiral Catalyst for an Asymmetrically Induced Diels-Alder Reaction (C) 545
- Intramolecular Hetero-Diels–Alder Reactions of Oxadienes: Influence of Substituents of the Tether on the Diastereoselectivity (C) 665
- Novel Planar π-Systems (C) 393
- Synthesis of Enantiomerically Pure Heterosteroids by Intramolecular Hetero-Diels-Alder Reaction (C) 527
Dihydrocanadensolide
- Doubly Stereodifferentiating Hiyama Addition with Mismatched Reactants; Enantio- and Diastereo-controlled Synthesis of Dihydrocanadensolide (C) 679
Dihydrofurans
- Facile Synthesis of 4-Acyl-5-alkyl-2,3-dioxo-2,3-dihydrofurans and Alkylidenebutenolides (C) 1041
Dihydrooxathietes
- Isomerization of Benzoylalkylidene Sulfur Tetrafluorides C_6H_5-CO-CR = SF_4 to Dihydrooxathietes (C) 1128
Dihydroxypyrrolidines
- Cyclization of *N*-Protected 1-Amino-4-pentene-2,3-diols to *lyxo*-Configurated Deoxyimino Sugars (*cis*-Dihydroxypyrrolidines); Synthesis of Potential Glycosidase Inhibitors (C) 1171
- Synthesis of D- and L-2-Amino-2-deoxyarabinose and 1,4-Dideoxy-1,4-iminolyxitol by (C_2 + C_3)-Nitroaldol Addition with 2-*O*-Benzylglyceraldehyde (C) 1169
Diols
- Structural Characterization of the Pseudoenantiomeric *cis*-Dioxo Osmium(VI) Esters of Chiral Diols with Cinchona Alkaloid Ligands (C) 639
Dioxiranes
- O-Atom Insertion into Si–H Bonds by Dioxiranes: A Stereospecific and Direct Conversion of Silanes into Silanols (C) 890
1,4 Dipoles
- An *N*-Phosphino *C*-Thiophosphinoyl Nitrilimine as a Formal 1,4 Dipole: Synthesis of 1,2,3λ^5-Diaza- and 1,2,4,3λ^5-Triazaphosphinines (C) 1123
DNA
- Metal-DNA Chemistry (B) 1175
DNA cleavage
- Golfomycin A, a Novel Designed Molecule with DNA-Cleaving Properties and Antitumor Activity (C) 1064
DNA hybridization
- Nonradioactive Assay of DNA Hybridization by DNA-Template-Mediated Formation of a Ternary Tb^{III} Complex in Pure Liquid Phase (C) 1167
DNA replication
- Replication Experiments with Nucleotide Base Analogues (R) 36
Dodecahedranes
- The Pagodane Route to Dodecahedranes: An Efficient Variant—New Substitution Patterns (C) 92
- The Pagodane Route to Dodecahedranes: Dodecahedradienes—Unusually "Pyramidalized", Isolable Olefins (C) 95
Dynamics
- The Azide Homologues Et–PPP and Ph–AsAsAs as Bifacially Coordinated Ligands in Tripod-Cobalt Complexes: Synthesis, Structure and Molecular Dynamics (C) 929

Ecology
- Misconceptions on Pollution and the Causes of Cancer (R) 1197
- Oxidative Degradation of Aromatic Pollutants by Chemical Models of Ligninase Based on Porphyrin Complexes (C) 1471
Effective molarities
- Reactivity in Intramolecular Radical Reactions: A Comparison of Hydrogen Transfer with Alkene Addition (C) 653
Electrochemical reactors
- Electrochemical Reactors, Their Science and Technology. Part A: Fundamentals, Electrolysers, Batteries and Fuel Cells (B) 817
Electrochemistry
- Direct Electrical Communication between Graphite Electrodes and Surface Adsorbed Glucose Oxidase/Redox Polymer Complexes (C) 82
- Direct Electron Transfer between Carbon Electrodes, Immobilized Mediator and an Immobilized Viologen-accepting Pyridine Nucleotide Oxidoreductase (C) 1053
Electron transfer
- Electron Transfer between Covalently Linked Porphyrin and Quinone Units: Synthesis, Magnetic Resonance and Picosecond Fluorescence Spectroscopy (C) 670
- Phenyl-Linked Quinone-Substituted Porphyrin Trimers (C) 1134
- Photoinduced Electron Transfer. Parts A–D (B) 704
Enamines
- Reductive Alkylation of Enamines with Chloromethyl *p*-Tolyl Sulfone via a Radical Chain Process (C) 433
Enantiomer separation
- Gas Chromatographic Separation of Enantiomers on Cyclodextrin Derivatives (R) 939
- Permethyl-β-cyclodextrin, Chemically Bonded to Polysiloxane: a Chiral Stationary Phase with Wider Application Range for Enantiomer Separation by Capillary Gas Chromatography (C) 427
- Preparation of an Enantiomerically Enriched Allyllithium Derivative by Deprotonation with Kinetic Resolution of Enantiomers (C) 296
Enantioselectivity
- Enantioselective Catalysis with a New Zirconium Trichloride Lewis Acid Containing a "Dibornacyclopentadienyl" Ligand (C) 512
- Novel Diphosphinoiridium Catalysts for the Enantioselective Hydrogenation of *N*-Arylketimines (C) 558
- Optically Active Deltacyclanes and Deltacyclenes by Enantioselective Catalysis (C) 652
- Synthesis of Enantiomerically Pure Heterosteroids by Intramolecular Hetero-Diels-Alder Reaction (C) 527
- Thermodynamic Aldehyde Enantioface Binding Selectivities in Complexes of Chiral Metal Fragments; Mechanism of Interconversion of Diastereomeric π-Aldehyde Complexes $[(\eta^5\text{-}C_5H_5)\text{-}Re(NO)(PPh_3)(\eta^2\text{-}O = CHAr)]BF_4$ (C) 1475
Energy storage
- Active MgH_2–Mg Systems for Reversible Chemical Energy Storage (R) 223
Enols
- Asymmetric Protonation of Enolates (C) 1420
- New Chiral Auxiliaries for Enolate Alkylations (C) 555
- Stability and Cyclization of Enol Radical Cations: A Mechanistic Study of

One-Electron Oxidation of β,β-Dimesityl Enols (C) 541
Enones
- The Chemistry of Enones. Parts 1 and 2 (B) 1070
Enzyme catalysis
- Combined Chemoenzymatic Synthesis of *N*-Glycoprotein Building Blocks (C) 80
- Enzyme-Catalyzed Synthesis of (*S*)-Cyanohydrins (C) 386
- Enzymic Reaction Selectivity by Negative Catalysis or How Do Enzymes Deal with Highly Reactive Intermediates? (R) 355
- Isolation of an L-Stereospecific *N*-Acyl-L-proline-Acylase and its Use as Catalyst in Organic Synthesis (C) 417
Enzymes
- Bioorganic Chemistry. A Chemical Approach to Enzyme Action (B) 815
- Direct Electrical Communication between Graphite Electrodes and Surface Adsorbed Glucose Oxidase/Redox Polymer Complexes (C) 82
- Direct Electron Transfer between Carbon Electrodes, Immobilized Mediator and an Immobilized Viologen-accepting Pyridine Nucleotide Oxidoreductase (C) 1053
- Oxidative Degradation of Aromatic Pollutants by Chemical Models of Ligninase Based on Porphyrin Complexes (C) 1471
Epoxidation
- Epoxidation of the P = C Double Bond of Phosphaalkene Complexes: X-Ray Crystal Structure Analysis of a Stable Oxaphosphirane Complex (C) 1166
- Lithium-Ion-Catalyzed Epoxidation by Triplet Dioxygen: An ab initio Study (C) 648
Epoxides
- An Efficient Route to Linear Conjugated Triepoxides: *allo*-, *galacto*-, and *altro*-Type Trianhydrohexitols (C) 1038
- Enantio- and Regiocontrolled Synthesis of a Central Ionophoric Antibiotic Building Block by Sequential Opening of Two Epoxide Rings with Cuprate Reagents (C) 1476
ESR spectroscopy
- A Stable Triradical Compound and its Unusual Magnetic Properties (C) 415
- Ambident Behavior of the "New Vitamin" Methoxatin (Cofactor PQQ) towards Metals: Coordinative Stabilization of the Pyrrolide Form and the Semiquinone Form (C) 78
- Asymmetric Heterodinuclear $[L'Ru(\mu\text{-}O)(\mu\text{-}CH_3CO_2)_2ML]^{2\oplus}$ Complexes (M = Fe, Mn, V): Electronic Structure and Magnetic Properties (C) 645
- Bis(1,4,7-trithiacyclononane)gold Dication: A Paramagnetic, Mononuclear Au^{II} Complex (C) 197
- Correlations between Magnetism and Structure in Dinuclear $Cu^{II}Fe^{III}$ Complexes with Integer Spin EPR Signals (C) 921
- Structure–Magnetism Relationship in $[Ti^{III}\text{-}O\text{-}Ti^{III}]^{4\oplus}$ Complexes (C) 68
Ester cleavage
- Switching Reaction Mechanism by Monolayer Compression: An Ester Hydrolysis (C) 306
Esters
- Synergic Destabilization by Geminal Ester Groups (C) 674
Ethane
- $Fe^{\oplus}$-Catalyzed Gas-Phase Oxidation of Ethane by N_2O (C) 1431
Ethylene
- Transition-Metal-Induced Generation of C_2H_4 from 1,7-Octadiene: Regiospecific Activation of Internal C–C Bonds instead of Metathesis-like Coupling of Terminal CH_2 Groups (C) 402
Ethynol
- Reversible Photoisomerization of Ketene to Ethynol (C) 411
Ethynylethenes
- Novel Planar π-Systems (C) 393
Extracellular matrix
- Biologically Active Analogues of the Extracellular Matrix: Artificial Skin and Nerves (R) 20

Fenestins
- What Are the Structures of Fenestin A and Fenestin B? (C) 514
Flavonoids
- Carbon-13 NMR of Flavonoids (B) 1072
Fluorescence spectroscopy
- Electron Transfer between Covalently Linked Porphyrin and Quinone Units: Synthesis, Magnetic Resonance and Picosecond Fluorescence Spectroscopy (C) 670
- Fluorescence "Off–On" Signalling upon Linear Recognition and Binding of α,ω-Alkanediyldiammonium Ions by 9,10-Bis{(1-aza-4,7,10,13,16-pentaoxacyclooctadecyl)methyl}anthracene (C) 1173
Fluorine compounds
- Inverse Amine-Stabilized Sulfenes $F_2C = SO_2$ and $FHC = SO_2$ (C) 60
- Isomerization of Benzoylalkylidene Sulfur Tetrafluorides $C_6H_5\text{-}CO\text{-}CR = SF_4$ to Dihydrooxathietes (C) 1128
- Lithium Bis(di-*tert*-butylfluorosilyl)-amide as Contact Ion Pair with Linear $Si\text{–}N^{\ominus}\text{–}Si$ Unit and as Ion Pair without $Li^{\oplus}$-Anion Contact (C) 209
- Surprising Basicity of Low Valent Transition Metal Carbonyl Fluorides; Crystallographic Characterization of an $sp^2\text{-}CH\cdots F$ Hydrogen Bond (C) 888
- The Monofluorooxonium(0) Hexafluorometalate(VI)s $H_2OF^{\oplus}MF_6^{\ominus}$ (M = As,Sb) (C) 688
- *trans*-1,2-Difluoro-1,2-bis[(tetracarbonyl)cobaltio]ethene, a Difluoroethyne Complex with $\mu_2\text{-}\eta^1\text{-}\eta^1$-Coordination (C) 315
- Vanadium Tetrafluoride (C) 406
Force field calculations
- Computer Simulation of Molecular Dynamics: Methodology, Applications, and Perspectives in Chemistry (R) 992
- The Structure of Vicinal Pentaketones—X-Ray Structure Investigations and Calculations (C) 1048
Fractals
- Fractals and Related Hierarchical Models in Polymer Science (R) 113
Fragmentation
- Mesolytic Cleavage of C–C Bonds. Comparison with Homolytic and Heterolytic Processes in the Same Substrate (C) 283
Fulvalenes
- Electrical and Magnetic Properties and X-Ray Structure of a Highly Conductive 4:1 Complex of Tetracyanoquinodimethane and a Tetrathiafulvalene Derivative (C) 1450
Fulvenes
- Gas-Phase Thermolysis of 6-Cyclopropyl- and 6-Oxiranylpentafulvenes: Novel Routes to Dihydroindenes and Vinylcyclopentadienes (C) 803
- The Tautomeric Equilibrium between Cyclopentadienyl-1-carboxylic Acid and Fulvene-6,6-diol in Aqueous Solution (C) 790
Functional groups
- Patai's Guide to the Chemistry of Functional Groups (B) 821
Future of chemistry
- Chemistry for the Future—State of the Art and Perspectives (R) 1177
- Organic Synthesis—Where now? (R) 1320
- What Will Chemistry Do in the Next Twenty Years? (R) 1209

Gallium compounds
- Synthesis and Structure of a Diphosphadigalletane: A Novel Base-Stabilized Ga_2P_2 Ring System (C) 1150
Gas chromatography
- Gas Chromatographic Separation of Enantiomers on Cyclodextrin Derivatives (R) 939
- Permethyl-β-cyclodextrin, Chemically Bonded to Polysiloxane: a Chiral Stationary Phase with Wider Application Range for Enantiomer Separation by Capillary Gas Chromatography (C) 427
Gas-phase reactions
- Thermal Decomposition of the Nonmetal Octahedron $(ClB)_4P_2$ by Elimination of Its PP Octahedral Edge (C) 1044
Germanium compounds
- An Intramolecularly Lewis-Base-Stabilized Ge = N-Compound and a Related Ge-Fe Complex (C) 216
- Anions Isosteric with $CO_3^{2\ominus}$ in Cs_5SiP_3, Cs_5SiAs_3, Cs_5GeP_3, and Cs_5GeAs_3 (C) 87
- Ge^{II} and Sn^{II} Complexes of [2.2.2]Paracyclophane with Threefold Internal η^6 Coordination (C) 1397
Glycopeptides
- Facile Synthesis of a β(1-3)-Linked galgalactal Disaccharide and Its Use in *N*-Iodosuccinimide-Activated *O*-Glycopeptide Synthesis (C) 425
- Solid-Phase Synthesis of Glycopeptide Amides under Mild Conditions: Morphiceptin Analogues (C) 291
Glycoproteins
- Combined Chemoenzymatic Synthesis of *N*-Glycoprotein Building Blocks (C) 80
- Syntheses, Conformations and X-Ray Structure Analyses of the Saccharide Chains from the Core Regions of Glycoproteins (R) 823
- Synthesis of a β-Mannosyl-Chitobiosyl-Asparagine Conjugate—a Central Core Region Unit of the *N*-Glycoproteins (C) 1050
Glycosidase inhibitors
- Cyclization of *N*-Protected 1-Amino-4-pentene-2,3-diols to *lyxo*-Configurated Deoxyimino Sugars (*cis*-Dihydroxypyrrolidines); Synthesis of Potential Glycosidase Inhibitors (C) 1171
Glycosylation
- Semisynthetic Rhodomycins: Novel Glycosylation Methods for the Synthesis of Anthracycline Oligosaccharides (C) 809
Gold compounds
- Assembly of the $CAu_6^{2\oplus}$ Cluster with a Tailor-made Diphosphane Spanning the Octahedral Edges (C) 1399
- Bis(pentamethylcyclopentadienyl)silylene as Ligand in Gold(I) Chloride Complexes (C) 893
- Bis(1,4,7-trithiacyclononane)gold Dication: A Paramagnetic, Mononuclear Au^{II} Complex (C) 197
- Low-Dimensional Compounds Incorporating Polychalcogenide Ligands. The Unusual Polymeric Structures of $[AuSe_5]_n^{n\ominus}$ and $[AuSe_{13}]_n^{3n\ominus}$ (C) 914

Golfomycin A
- Golfomycin A, a Novel Designed Molecule with DNA-Cleaving Properties and Antitumor Activity (C) 1064
Grahamine
- Grahamine, an Unusual Tropane Alkaloid from *Schizanthus grahamii* (C) 385
Grob fragmentation
- X-Ray Structure Analysis of an Iminium Ion Generated by Grob Fragmentation (C) 188

Halogen compounds
- $CsF \cdot Br_2$, an Alkali-Metal Halide Intercalation Compound (C) 1448
- Ethynyl(phenyl)iodonium Triflate, $[HC \equiv CIPh][OSO_2CF_3]$: Preparation, Spectral Properties, Mechanism of Formation and X-Ray Molecular Structure (C) 287
- Facile Synthesis of 3-(ω-Haloalkyl)thiophenes as Key Building Blocks for Functionalized Thiophenes and Polythiophenes (C) 419
Heats of vaporization
- Heats of Vaporization of Fluids (B) 1490
Helicenes
- Helicene Dianions: Paratropicity of Twisted Phenanthrene Dianions (C) 919
Heteroallenes
- A Carbonyliron Complex of an Amino-9-fluorenylideneborane with Coordination at a Borabutadiene Unit (C) 199
- Preparation and Structure of $[Se = W(PSe_4)(PSe_2)]^{2\ominus}$; a Cluster Containing a Heteroallylic $PSe_2^{\ominus}$ Unit (C) 1486
Heteroarenes
- A First Step toward the Phosphorus Analogues of Polythiophenes (C) 655
- A Wagner–Meerwein Rearrangement as Intermediate Step in the Formation of Dihydroindolones from 2-Diazoacetoacetanilides (C) 86
- 5-Methyl-1,1,3,3-tetraphenyl-1λ^5,3λ^5-diphosphabenzene (C) 516
- Some Valenes of Benzannelated Five-Membered Heteroarenes – Synthesis and NMR Spectra (C) 675
- The Synthesis and Structure of Stibaindoles (C) 771
- Torand Synthesis by Trimerization—New Receptors for Guanidinium (C) 923
Heterocycles
- A Monocyclic Selenepine: Synthesis and Characterization of Diethyl 2,7-Di-*tert*-butyl-4,5-selenepinedicarboxylate (C) 424
- A 1-Silyl-1*H*-phosphirene/1,2-Dihydro-1,2-phosphasilete Rearrangement—The Decisive Step in the Synthesis of Heterocycles Containing 2-Phospha-1,3-diene Units (C) 1436
- Amino Acid Esters as Chiral Auxiliary Groups in Lewis Acid Catalyzed Reactions of Electron-rich Siloxydienes with Imines (C) 1468
- Application of Titanacycles to Heterocycle Synthesis: Phospha- and Arsacyclobutenes (C) 75
- Conformational Analysis of Medium-Sized Heterocycles (B) 815
- 4,7-Dimethyl-4,7-dihydro[1,2,5]thiadiazolo[3,4-*b*]pyrazine, a Novel Electron Donor with a 12π-Electron Ring System (C) 643
- Imidazo[1,2-*e*][1,3,5]triazepine Derivatives: First Representatives of a New Heterocyclic System (C) 933
- Novel S-Heteroquinoid Electron Acceptors. Synthesis of 2,5-Bis(cyanoimino)-2,5-dihydrothieno[3,2-*b*]thiophenes (DCNTTs) and Conductive Charge Transfer Complexes (C) 204
- Rings, Clusters and Polymers of Main Group and Transition Elements (B) 1490
- Synthesis and Structure of a 1λ^5,4λ^5-Diphosphapentalene (C) 799
- Synthesis of Nitrogen Heterocycles by Diastereoselective Intramolecular Aminocarbene Annelation (C) 176
- Unsaturated C_3B_2 Rings with Neighboring Boron Atoms: Derivatives of 4-Methylene-1,2-diboracyclopentane, Dilithium 2,3-diboratafulvene, and 1,2-Dibora-3-cyclopentene (C) 912
Heteropolyanions
- $[H_6As_{10}Mo_{24}O_{90}]^{8\ominus}$, a Heteropolyanion Comprising Two Linked Spherical Fragments, and Reduced Keggin Anions as Its Degradation Products (C) 88
Hexaalkynyltriphenylene
- Hexaalkynyltriphenylene: A New Type of Nematic-Discotic Hydrocarbon (C) 177
Hexapentaenes
- Nickel-Catalyzed Cyclodimerization of Hexapentaenes: [4]Radialenes and [5]Radialenones with Cumulated Double Bonds (C) 1062
Hexatrienes
- Macrocyclically Fixed Diarylhexatrienes (C) 1162
High pressure chemistry
- Peptide Synthesis under High Pressure (C) 1025
Hindered rotations
- Sterically Hindered Internal Rotation in an Acyclic α,β-Unsaturated Ketone 2,2,5-Trimethyl-4-isopropylhex-4-en-3-one (C) 1435
History of chemistry
- Chemistry for the Future—State of the Art and Perspectives (R) 1177
- Five Decades Ago: From the "Transuranics" to Nuclear Fission (R) 481
- Schrödinger—Life and Thought (B) 697
- Serendipity: Accidental Discoveries in Science (B) 1069
- Vom Radiothor zur Uranspaltung. Eine wissenschaftliche Selbstbiographie (B) 219
Hiyama addition
- Doubly Stereodifferentiating Hiyama Addition with Mismatched Reactants; Enantio- and Diastereo-controlled Synthesis of Dihydrocanadensolide (C) 679
Homo-Diels-Alder reactions
- Mechanism of the Cycloaddition of Bicyclo[2.1.0]pent-2-ene: a Non-concerted Homo-Diels-Alder Reaction (C) 1061
Hormaomycin
- Elucidation of the Structure of Hormaomycin (C) 64
Host-guest chemistry
- A New Mode of Metal Encapsulation (C) 1404
- A Spacious Cyclophane Host for Inclusion Complexation of Steroids and [m.n]Paracyclophanes (C) 769
- A Synthetic Allosteric System with High Cooperativity between Polar and Hydrophobic Binding Sites (C) 1159
- Amine-Template-Directed Synthesis of Cyclic Porphyrin Oligomers (C) 1400
- Biomimetic Catalysis of an S_N2 Reaction Resulting from a Novel Form of Transition-State Stabilization (C) 915
- Catalytic Cyclophanes: A Porphyrin-Bridged Cyclophane as a Model for Cytochrome P-450 Enzymes (C) 191
- Host-Guest Complexes with Closed, Half-open, and Stretched Receptors: Hydrophobic Cavity Effects and Induced Pole-Dipole Interactions (C) 1161
- Molecular Recognition with Model Systems (R) 245
- Organometallic Host–Guest Systems Representing Novel Charge-Transfer "Ion Pairs" with Three-Dimensional Electron-Donor Networks (C) 1126
- Supramolekulare Chemie (B) 323
- Torand Synthesis by Trimerization—New Receptors for Guanidinium (C) 923
Houben-Weyl
- Houben-Weyl. Methoden der Organischen Chemie. Band E13, Teil 1 und 2: Organische Peroxo-Verbindungen (B) 327
Hydration
- Catalytic Hydration of Acrylonitrile to Acrylamide under Mild Conditions (C) 523
Hydride transfer
- Iron(II)-Mediated Hydride and Methanide Transfer to Carbonyl Groups (C) 910
Hydroaromatic compounds
- The Conformational Analysis of Cyclohexenes, Cyclohexadienes and Related Hydroaromatic Compounds (B) 698
Hydrogen bonds
- Characterization by Microwave Spectroscopy of a Transient Hydrogen-Bonded Complex of Oxirane and Hydrogen Chloride Isolated in a Pulsed Jet (C) 72
- Cooperative Interactions in Molecular Recognition—the Binding of Diamines to a Tetracarboxylic Acid (C) 1148
- Surprising Basicity of Low Valent Transition Metal Carbonyl Fluorides; Crystallographic Characterization of an sp^2-CH $\cdots$ F Hydrogen Bond (C) 888
Hydrogen storage
- Active MgH_2–Mg Systems for Reversible Chemical Energy Storage (R) 223
Hydrogen transfer
- Reactivity in Intramolecular Radical Reactions: A Comparison of Hydrogen Transfer with Alkene Addition (C) 653
Hydrogenation
- Catalytic Hydrosilylation or Hydrogenation at One Coordination Site of [Cp'Fe(CO)(X)] Fragments (C) 1131
- Facile Hydrogenation of the Central Cyclohexatriene of Tris(benzocyclobutadieno)benzene: Synthesis, Structure, and Thermal and Photochemical Isomerization of all-*cis*-Tris(benzocyclobuta)cyclohexane (C) 1151
- Novel Diphosphinoiridium Catalysts for the Enantioselective Hydrogenation of *N*-Arylketimines (C) 558
Hydrogenobyrinic acid
- Hydrogenobyrinic Acid: Isolation, Biosynthesis, and Function (C) 884
Hydrosilylation
- Catalytic Hydrosilylation or Hydrogenation at One Coordination Site of [Cp'Fe(CO)(X)] Fragments (C) 1131
Hyperconjugation
- Strong C–Sn Hyperconjugation in a Distannylmethyleneborane (C) 401
Hypnophilin
- Synthesis of Enantiomerically Pure (−)-Hypnophilin (C) 680
Hypofluorous acid
- The Monofluorooxonium(0) Hexafluorometalate(VI)s $H_2OF^{\oplus}MF_6^{\ominus}$ (M = As,Sb) (C) 688

Imidazoles
- 1-Amino- and 1,3-Diaminoimidazolium Salts (C) 556

Imidazotriazepines
- Imidazo[1,2-*e*][1,3,5]triazepine Derivatives: First Representatives of a New Heterocyclic System (C) 933

Iminium ions
- X-Ray Structure Analysis of an Iminium Ion Generated by Grob Fragmentation (C) 188

Inclusion complexation
- Isolation of Conformational Isomers of α- and β-Ionones by Inclusion Complex Formation (C) 662

Indenes
- Gas-Phase Thermolysis of 6-Cyclopropyl- and 6-Oxiranylpentafulvenes: Novel Routes to Dihydroindenes and Vinylcyclopentadienes (C) 803
- Synthesis and NMR Spectra of 2,3-Dihydro-1,3-methanoindene Derivatives and 1,2,3,5-Tetrahydro-1,3-methanopentalene (C) 1035

Indoles
- A Wagner–Meerwein Rearrangement as Intermediate Step in the Formation of Dihydroindolones from 2-Diazoacetoacetanilides (C) 86
- Carbonylation of Doubly Lithiated *N*-Pivaloylanilines. A Novel Approach to Dioxindoles via Intramolecular Trapping of Aromatic Acyllithiums (C) 282

Industrial chemistry
- Industrial Inorganic Chemistry (B) 110
- Mathematical Modeling of Chemical Reactors—Development and Implementation of Novel Technologies (R) 1235
- Molecular Thermodynamics for Chemical Process Design (R) 1246
- What Does the Chemical Industry Expect from Physical and Industrial Chemistry? (R) 1228

Inorganic chemistry
- Industrial Inorganic Chemistry (B) 110
- Inorganic Chemistry (B) 1069

Intercalation compounds
- $CsF \cdot Br_2$, an Alkali-Metal Halide Intercalation Compound (C) 1448

Interfaces
- The Quartz Microbalance: A Novel Approach to the In-Situ Investigation of Interfacial Phenomena at the Solid/Liquid Junction (R) 329

Interstellar chemistry
- The Chemistry of Interstellar Space (R) 595

Ion traps
- Electromagnetic Traps for Charged and Neutral Particles (Nobel Lecture) (R) 739
- Experiments with an Isolated Subatomic Particle at Rest (Nobel Lecture) (R) 734

Ionones
- Isolation of Conformational Isomers of α- and β-Ionones by Inclusion Complex Formation (C) 662

Ions
- Ion and Cluster Ion Spectroscopy and Structure (B) 437

IR spectroscopy
- Experimental and Theoretical IR Spectra of the 2-Norbornyl Cation (C) 183
- The Monofluorooxonium(0) Hexafluorometalate(VI)s $H_2OF^{\oplus}MF_6^{\ominus}$ (M = As,Sb) (C) 688

Iridium compounds
- Coupling of an Iridium Vinylidene Complex with Aluminum Alkyls; Carbon-Carbon Bond Formation via Migratory Insertion of a Vinylidene Unit (C) 73
- Novel Diphosphinoiridium Catalysts for the Enantioselective Hydrogenation of *N*-Arylketimines (C) 558
- Synthesis and Structure of Annelated Carbon Rings Containing a Bridgehead Transition Metal (C) 543

Iron compounds
- A Carbonyliron Complex of an Amino-9-fluorenylideneborane with Coordination at a Borabutadiene Unit (C) 199
- Catalytic Hydrosilylation or Hydrogenation at One Coordination Site of [Cp'Fe(CO)(X)] Fragments (C) 1131
- Correlations between Magnetism and Structure in Dinuclear $Cu^{II}Fe^{III}$ Complexes with Integer Spin EPR Signals (C) 921
- Iron(II)-Mediated Hydride and Methanide Transfer to Carbonyl Groups (C) 910
- Soluble, Oligomeric Bridged Phthalocyaninatoiron(II) Complexes (C) 1467
- Synthesis and Characterization of the Linear Trinuclear Complexes $[M^{II}_3(O_2CCH_3)_6(biphme)_2]$, M = Mn, Fe (C) 812
- Synthesis and Structure of the Novel μ_2-Carbido Complex [(TPP)Fe = C = $Re(CO)_4Re(CO)_5$] (C) 318
- $Zn^{II}Fe^{III}$ and $Fe^{II}Fe^{III}$ Complexes Containing a Novel (μ-Phenoxo)bis(μ-diphenylphosphato)dimetal(II,III) Core as Model Complexes for Active Sites of Purple Phosphatases (C) 531

Isocorroles
- Isocorroles: Novel Tetrapyrrolic Macrocycles (C) 1390

Isocyanates
- A Novel Palladium-Catalyzed Carbonylation of Aromatic *N*-Chlorosulfonamidates to Arylsulfonyl Isocyanates (C) 1147

Isosterism
- Anions Isosteric with CO_3^{2-} in Cs_5SiP_3, Cs_5SiAs_3, Cs_5GeP_3, and Cs_5GeAs_3 (C) 87
- Highly Selective Synthesis of (*E*)-Alkene Isosteric Dipeptides With High Optical Purity via $RCu(CN)Li \cdot BF_3$ Mediated Reaction (C) 801

Isotope effects
- Kinetic Isotope Effects as a Mechanistic Tool for the Elucidation of the Rate-Determining Step(s) in the Transition-Metal-Ion-Mediated Activation of CH/CC Bonds. Ethylene Loss from Metastable 4-Octyne/$M^{\oplus}$ Complexes in the Gas Phase (C) 509

Jasmonoids
- Building Blocks for the Synthesis of Enantiomerically Pure Jasmonoids: Synthesis of (+)-Methyl Epijasmonate (C) 1024

Kaolinites
- Clays Direct Aromatic Nitration (C) 535
- Solid-State NMR Studies of the Structure and Reactivity of Metakaolinite (C) 553

Keggin anions
- $[H_6As_{10}Mo_{24}O_{90}]^{8\ominus}$, a Heteropolyanion Comprising Two Linked Spherical Fragments, and Reduced Keggin Anions as Its Degradation Products (C) 88

Ketenes
- Reversible Photoisomerization of Ketene to Ethynol (C) 411

Ketenimines
- A Cyclodimeric Silaketenimine (C) 90

Keto/enol equilibrium
- Stability and Cyclization of Enol Radical Cations: A Mechanistic Study of One-Electron Oxidation of β,β-Dimesityl Enols (C) 541
- The Enol of Mandelic Acid, Detection, Acidity in Aqueous Solution, and Estimation of the Keto-Enol Equilibrium Constant and Carbon Acidity of Mandelic Acid (C) 792
- The Tautomeric Equilibrium between Cyclopentadienyl-1-carboxylic Acid and Fulvene-6,6-diol in Aqueous Solution (C) 790

Ketones
- Stereocontrolled Construction of Complex Cyclic Ketones via Oxy-Cope Rearrangement (R) 609
- α-Umpolung of Ketones via Enol Radical Cations: A Mechanistic Study (C) 1144

Kinetics
- Bimolecular Collisions (B) 936

Knot compounds
- Structure of a Synthetic Trefoil Knot Coordinated to Two Copper(I) Centers (C) 1154

Kolbe electrolysis
- Mixed Kolbe Electrolyses with Sugar Carboxylic Acids (C) 195

β-Lactams
- A Facile Synthesis of β-Selenolactams (C) 530

Lanthanoid compounds
- CH Activation of Acetonitrile by Alkyl Compounds of the Early Lanthanoids: Dimeric Cyanomethyl-Lanthanoid Complexes with CH_2CN Bridges (C) 420
- The Ammonium Salt Route to Oligomeric Lanthanum Salt Complexes: Synthesis and X-Ray Crystal Structure of $La(NCS)_3 \cdot 4HMPA$ (C) 285
- Ytterbium(II) Benzamidinates, a New Class of Highly Reactive Lanthanoid(II) Complexes (C) 894

Leukotrienes
- Leukotrienes and Lipoxygenases. Chemical, Biological and Clinical Aspects (B) 1073

Lipids
- Specific Interactions of Proteins with Functional Lipid Monolayers—Ways of Simulating Biomembrane Processes (R) 1269

Lipoxygenases
- Leukotrienes and Lipoxygenases. Chemical, Biological and Clinical Aspects (B) 1073

Liquid crystals
- Advanced Materials: Trends and Possibilities in Liquid Crystalline Polymers (R) 1256
- Hexaalkynyltriphenylene: A New Type of Nematic-Discotic Hydrocarbon (C) 177
- Induction and Variation of Chirality in Discotic Liquid Crystalline Polymers (C) 1478
- Multiple Bonds Between Metal Atoms in Ordered Assemblies: Liquid Crystals Containing Mo–Mo Quadruple Bonds (C) 1481

Macrocycles
- A New Type of Double Calix[4]arenes by Linkage via the Phenolic Hydroxy Groups (C) 280
- Fluorescence "Off–On" Signalling upon Linear Recognition and Binding of α,ω-Alkanediyldiammonium Ions by 9,10-Bis{(1-aza-4,7,10,13,16-pentaoxacyclooctadecyl)methyl}anthracene (C) 1173

- Interfaces between Molecular and Polymeric "Metals": Electrically Conductive, Structure-Enforced Assemblies of Metallomacrocycles (R) 857
- Isocorroles: Novel Tetrapyrrolic Macrocycles (C) 1390
- Macrocyclically Fixed Diarylhexatrienes (C) 1162
- Organometallic Macrocycles: Synthesis and Molecular Structure of Trimeric Tartratodiruthenium Complexes (C) 429
- Soluble, Oligomeric Bridged Phthalocyaninatoiron(II) Complexes (C) 1467
- The First Clamped and Strongly Deformed Adamantane (C) 902
- Torand Synthesis by Trimerization—New Receptors for Guanidinium (C) 923

Macromolecular chemistry
- Starburst Dendrimers: Molecular-Level Control of Size, Shape, Surface Chemistry, Topology, and Flexibility from Atoms to Macroscopic Matter (R) 138

Magnesium compounds
- A Surface Organometallic Approach for Controlling the Pore Opening Size of Zeolites: the Case of Mordenite Modified via Grafting of Dineopentylmagnesium (C) 805
- Active MgH_2–Mg Systems for Reversible Chemical Energy Storage (R) 223

Magnesium therapy
- Aspartic and Glutamic Acid as Ligands to Alkali and Alkaline-Earth Metals: Structural Chemistry as Related to Magnesium Therapy (R) 1090

Magnetic resonance
- Experiments with Separated Oscillatory Fields and Hydrogen Masers (Nobel Lecture) (R) 725

Magnetic superexchange
- Dependence of the Magnetic Superexchange on the Cr···Cr Distance in Dinuclear Chromium(II) Complexes (C) 1055

Magnetism
- A Stable Triradical Compound and its Unusual Magnetic Properties (C) 415

Maillard reaction
- Formation of an Aminoreductone from Glucose (C) 536
- New Aspects of the Maillard Reaction in Foods and in the Human Body (R) 565

Mandelic acid
- The Enol of Mandelic Acid, Detection, Acidity in Aqueous Solution, and Estimation of the Keto-Enol Equilibrium Constant and Carbon Acidity of Mandelic Acid (C) 792

Manganese compounds
- First Coupling of a Metal Atom with Four Ethene Molecules to give a Metallaspiroalkane (C) 322
- $Na_{10}\{Li_2[MnO_4]_4\}$, a Compound in Which LiO_4 and MnO_4 Tetrahedra Form Chains Consisting of Six- and Eight-Membered Rings (C) 800
- Novel Bonding Mode for a Cyanometalate Ligand: Synthesis and Crystal Structure of the Mn_4Pd_4 Cluster $[(OC)Pd(\mu\text{-}NC)Mn(\eta\text{-}C_5H_4Me)(CO)_2]_4$ Containing an Orthogonal Arrangement of Helical Units (C) 1140
- Synthesis and Characterization of the Linear Trinuclear Complexes $[M^{II}_3(O_2CCH_3)_6(biphme)_2]$, M = Mn, Fe (C) 812
- Synthesis, Structure, and Catalase-Type Activity of a Novel Oxo-Bridged Tetranuclear Manganese Aggregate Exhibiting Short O···O Interactions (C) 1156

Mannich bases
- A Novel Synthesis of 2-Aminomethyl-1,3-butadienes from *N,O*-Acetals (C) 932

Masers
- Experiments with Separated Oscillatory Fields and Hydrogen Masers (Nobel Lecture) (R) 725

Mass spectrometry
- $Fe^{\oplus}$-Catalyzed Gas-Phase Oxidation of Ethane by N_2O (C) 1431
- $FeO^{\oplus}$ Activates Methane (C) 1433
- Identification of Butatrienedione, Its Radical Anion, and Its Radical Cation in the Gas Phase (C) 908
- Ionic Isomer Distinction by Neutralization-Reionization Mass Spectrometry (NRMS): Carbonic Acid Radical Cations, $(HO)_2CO^{\bullet\oplus}$ versus $(H_2O/CO_2)^{\bullet\oplus}$ Clusters (C) 404
- Iron(II)-Mediated Hydride and Methanide Transfer to Carbonyl Groups (C) 910
- Kinetic Isotope Effects as a Mechanistic Tool for the Elucidation of the Rate-Determining Step(s) in the Transition-Metal-Ion-Mediated Activation of CH/CC Bonds. Ethylene Loss from Metastable 4-Octyne/$M^{\oplus}$ Complexes in the Gas Phase (C) 509

Materials science
- Advanced Materials: Trends and Possibilities in Liquid Crystalline Polymers (R) 1256
- Interfaces between Molecular and Polymeric "Metals": Electrically Conductive, Structure-Enforced Assemblies of Metallomacrocycles (R) 857
- NMR Microscopy—Fundamentals, Limits and Possible Applications (R) 1
- Perspectives in the Development of High-Temperature Polymers (R) 1262

Matrix isolation
- Carbonyl Oxides: Zwitterions or Diradicals? (R) 344
- C_4O_2 (1,2,3-Butatriene-1,4-dione), the First Dioxide of Carbon with an Even Number of C Atoms (C) 905
- C_2S_2(Ethene-1,2-dithione), an Example for the Violation of Hund's Rule? (C) 1464

Membrane reactor
- Continuous Generation of NADH from $NAD^{\oplus}$ and Formate Using a Homogeneous Catalyst with Enhanced Molecular Weight in a Membrane Reactor (C) 388

Membranes
- The Chemistry of Vitamin A and Vision (R) 461
- Two-Dimensional Model Networks (R) 439

Mercury compounds
- $[\{Ni_2(\mu\text{-}CNMe)(CNMe)_4\text{-}(Ph_2PCH_2PPh_2)\}_2Hg][NiCl_4]$, a Spirocyclic Ni_4Hg Cluster with an Hg^{II}-Center (C) 396
- $[(Ph_3P)_2N]_2[Os_{18}Hg_2C_2(CO)_{42}]$ a Photochemically Generated High-Nuclearity Cluster Which Reversibly Incorporates Metallic Mercury into Its Metal Core (C) 1137

Metal powders
- The Preparation of Finely Divided Metal and Alloy Powders (C) 273

Metal-DNA chemistry
- Metal-DNA Chemistry (B) 1175

Metallacycles
- First Coupling of a Metal Atom with Four Ethene Molecules to give a Metallaspiroalkane (C) 322
- Synthesis and Structure of Annelated Carbon Rings Containing a Bridgehead Transition Metal (C) 543
- The Proton Catalyzed Transformation of a Cobaltacyclopentadiene into a η^4-Cyclobutadiene Complex (C) 1046

Metalloproteins
- Metalloproteins, Chemical Properties and Biological Effects (B) 327

Metal-metal bonds
- A Paramagnetic μ-Methylene Complex with a Short Cr^{III}–Cr^{III} Bond (C) 775
- How Do Two C–C Double Bonds Add to One M–M Triple Bond? Structure and Bonding in Bis(η^2-ethylene)hexakis(neopentoxy)ditungsten (C) 1026
- Multiple Bonds Between Metal Atoms in Ordered Assemblies: Liquid Crystals Containing Mo–Mo Quadruple Bonds (C) 1481
- Synthesis and Structure of (NBu_4)-$[Sn\{Pt(\mu\text{-}Cl)(C_6F_5)_2\}_3]$, an Unusual Cluster with Three $Pt^{II}\rightarrow Sn^{II}$ Bonds (C) 1449
- The Re–Re Bond in Binuclear Di-μ-oxorhenium Complexes Containing the 1,4,7-Triazacyclononane Ligand (C) 787

Metathesis
- Transition-Metal-Induced Generation of C_2H_4 from 1,7-Octadiene: Regiospecific Activation of Internal C–C Bonds instead of Metathesis-like Coupling of Terminal CH_2 Groups (C) 402

Methane
- $FeO^{\oplus}$ Activates Methane (C) 1433

Methoxatin
- Ambident Behavior of the "New Vitamin" Methoxatin (Cofactor PQQ) towards Metals: Coordinative Stabilization of the Pyrrolide Form and the Semiquinone Form (C) 78

Methylene complexes
- A Paramagnetic μ-Methylene Complex with a Short Cr^{III}–Cr^{III} Bond (C) 775

Methyleneboranes
- A Carbonyliron Complex of an Amino-9-fluorenylideneborane with Coordination at a Borabutadiene Unit (C) 199
- A Mesityl-bridged Methyleneborane (C) 399
- 2,3-Diboratabutadienes and 2-Borataallenes (C) 1030
- Strong C–Sn Hyperconjugation in a Distannylmethyleneborane (C) 401
- Structure of a Non-classically Bridged Methyleneborane in the Crystal (C) 398

Methylsodium
- Structure Determination of $NaCD_3$ Powders at 1.5 and 300K by Neutron and Synchrotron–Radiation Diffraction (C) 650

Michael additions
- Asymmetric Nucleophilic Acylation via Metalated Chiral Amino Cyanides: Enantioselective Synthesis of 3-Substituted 4-Oxoesters by Asymmetric Michael Addition (C) 179

Microwave spectroscopy
- Characterization by Microwave Spectroscopy of a Transient Hydrogen-Bonded Complex of Oxirane and Hydrogen Chloride Isolated in a Pulsed Jet (C) 72

Mixed-valence compounds
- Platinum in the Unusual Oxidation State +2.75: A Linear Tetranuclear Complex with the Model Nucleobase 1-Methylthymine (C) 84

Molecular beam experiments
- Experiments with Separated Oscillatory Fields and Hydrogen Masers (Nobel Lecture) (R) 725

Molecular design
- Computer-Aided Molecular Design (B) 1075
Molecular dynamics
- Computer Simulation of Molecular Dynamics: Methodology, Applications, and Perspectives in Chemistry (R) 992
Molecular recognition
- Artificial Receptors for Carbohydrate Derivatives (C) 1407
- Concanavalin A Binds Pyranosides and Their Tetraacetates Stereoselectively (C) 672
- Cooperative Interactions in Molecular Recognition—the Binding of Diamines to a Tetracarboxylic Acid (C) 1148
- Fluorescence "Off–On" Signalling upon Linear Recognition and Binding of α,ω-Alkanediyldiammonium Ions by 9,10-Bis{(1-aza-4,7,10,13,16-pentaoxacyclooctadecyl)methyl}anthracene (C) 1173
- Molecular Recognition with Model Systems (R) 245
- Perspectives in Supramolecular Chemistry—From Molecular Recognition towards Molecular Information Processing and Self-Organization (R) 1304
- Specific Interactions of Proteins with Functional Lipid Monolayers—Ways of Simulating Biomembrane Processes (R) 1269
Molecular spectroscopy
- Fundamentals of Molecular Spectroscopy (B) 816
Molybdenum compounds
- Coordination Chemistry of Polyoxomolybdates: The Structure of a Dodecanuclear Molybdate Cage Incorporating Hydrogen Squarate Ligands, $[(C_4H_9)_4N]_4[Mo_{12}O_{36}(C_4O_4H)_4] \cdot 10Et_2O$ (C) 70
- $[H_6As_{10}Mo_{24}O_{90}]^{8\ominus}$, a Heteropolyanion Comprising Two Linked Spherical Fragments, and Reduced Keggin Anions as Its Degradation Products (C) 88
- Multiple Bonds Between Metal Atoms in Ordered Assemblies: Liquid Crystals Containing Mo–Mo Quadruple Bonds (C) 1481
Morphiceptin
- Solid-Phase Synthesis of Glycopeptide Amides under Mild Conditions: Morphiceptin Analogues (C) 291
Multiple bonds
- A Compound with a Boron–Arsenic Double Bond (C) 1033
- An Allene-analogous Boranylidenephosphane with B = P Double Bond: 1,1-Diethylpropyl(2,2,6,6-tetramethylpiperidino)boranylidenephosphane-*P*-pentacarbonylchromium (C) 682
- An Intramolecularly Lewis-Base-Stabilized Ge = N-Compound and a Related Ge-Fe Complex (C) 216
- Boron-Phosphorus Compounds and Multiple Bonding (R) 449
- Compounds with a Boron–Carbon Triple Bond (C) 1032
- (3,3-Diphenylallenylidene)trimethylphosphanetitanocene: The First Titanocene Carbene Complex with Three Cumulative Double Bonds (C) 1037
- Inverse Amine-Stabilized Sulfenes $F_2C=SO_2$ and $FHC=SO_2$ (C) 60
- Nickel-Catalyzed Cyclodimerization of Hexapentaenes: [4]Radialenes and [5]Radialenones with Cumulated Double Bonds (C) 1062
- Synthesis and Structure of the Novel μ_2-Carbido Complex $[(TPP)Fe=C=Re(CO)_4Re(CO)_5]$ (C) 318
Mycotoxins
- Fusarium Mycotoxins, Taxonomy and Pathogenicity (B) 1491
Myelin membrane
- The Myelin Membrane of the Central Nervous System—Essential Macromolecular Structure and Function (R) 958

NADH
- Continuous Generation of NADH from $NAD^{\oplus}$ and Formate Using a Homogeneous Catalyst with Enhanced Molecular Weight in a Membrane Reactor (C) 388
Natural products
- Building Blocks for the Synthesis of Enantiomerically Pure Jasmonoids: Synthesis of (+)-Methyl Epijasmonate (C) 1024
- Combined Chemoenzymatic Synthesis of *N*-Glycoprotein Building Blocks (C) 80
- Elucidation of the Structure of Hormaomycin (C) 64
- Synthesis of (+)-Terrein from L-Tartaric Acid (C) 67
- Synthesis of Enantiomerically Pure (−)-Hypnophilin (C) 680
- Synthesis of (−)-Neplanocin A from (*R,R*)-Tartaric Acid (C) 99
- Vitamins (B) 112
Negative catalysis
- Enzymic Reaction Selectivity by Negative Catalysis or How Do Enzymes Deal with Highly Reactive Intermediates? (R) 355
Neplanocin A
- Synthesis of (−)-Neplanocin A from (*R,R*)-Tartaric Acid (C) 99
Nickel compounds
- Nickel: An Element with Wide Application in Industrial Homogeneous Catalysis (R) 235
- $[\{Ni_2(\mu\text{-CNMe})(CNMe)_4(Ph_2PCH_2PPh_2)\}_2Hg][NiCl_4]$, a Spirocyclic Ni_4Hg Cluster with an Hg^{II}-Center (C) 396
- $[Ni_3(\mu_3\text{-CNMe})(\mu_3\text{-I})(CNMe)_2(Ph_2PCH_2PPh_2)_2]I$, a *triangulo* Nickel Cluster with an Unprecedented Symmetric Linear μ_3-η^1 Isocyanide Ligand (C) 395
- On a (1,4-Diazabutadiene)bis(ethene)-nickel(0) Complex and Related Compounds (C) 298
- Oxygen Activation with Transition Metal Complexes: Nickel-Catalyzed Oxidation of a Pentacoordinated Substrate (C) 106
Nitration
- Nitration. Methods and Mechanisms (Organic Nitro Chemistry Series) (B) 820
Nitrenes
- Direct Evidence for a Nitrile Imine–Imidoylnitrene Rearrangement: X-Ray Crystal Structure of an Unusual Nitrene Complex (C) 659
Nitroaldol additions
- Synthesis of D- and L-2-Amino-2-deoxyarabinose and 1,4-Dideoxy-1,4-iminolyxitol by (C_2+C_3)-Nitroaldol Addition with 2-*O*-Benzylglyceraldehyde (C) 1169
Nitrogen compounds
- 1-Amino- and 1,3-Diaminoimidazolium Salts (C) 556
- An Intramolecularly Lewis-Base-Stabilized Ge = N-Compound and a Related Ge-Fe Complex (C) 216
- An *N*-Phosphino *C*-Thiophosphinoyl Nitrilimine as a Formal 1,4 Dipole: Synthesis of 1,2,3λ^5-Diaza- and 1,2,4,3λ^5-Triazaphosphinines (C) 1123
- [2.2](4,4')Azobenzenophane (C) 105
- Direct Evidence for a Nitrile Imine–Imidoylnitrene Rearrangement: X-Ray Crystal Structure of an Unusual Nitrene Complex (C) 659
- Imidazo[1,2-*e*][1,3,5]triazepine Derivatives: First Representatives of a New Heterocyclic System (C) 933
- 2-Methylene-2*H*-azirines by Photolysis of 1-Azidoallenes (C) 103
- Stable Azirinimines? A Structural Corrigendum (C) 1164
- Synthesis and Structure of the Stable Tellurium Nitride $(ClTeNSN)_3N$ (C) 61
- Synthesis of Tetrachloroammonium Hexafluoroarsenate, $NCl_4^{\oplus}AsF_6^{\ominus}$ (C) 181
- Synthesis of the First Silaamidide (C) 529
- Vinylogous Cyanine-like Dications of Tetrakis(dimethylamino) Compounds (C) 211
Nitrogen fixation
- Vanadium(-I) Dinitrogen Complexes with N_2 Coordinated End-on: Functional Models for the "Alternative Nitrogenase" (C) 1438
Nitrogen Triiodide (C) 677
Nitrogenases
- Vanadium(-I) Dinitrogen Complexes with N_2 Coordinated End-on: Functional Models for the "Alternative Nitrogenase" (C) 1438
Nitrosamines
- Nitrosamines. Toxicology and Microbiology (B) 220
Nitroxides
- A Stable Triradical Compound and its Unusual Magnetic Properties (C) 415
NMR spectroscopy
- Application of the Combined ab initio/IGLO/NMR Method to Resolve the B_6H_{12} Structural Question (C) 886
- Carbon-13 NMR of Flavonoids (B) 1072
- ^{13}C-MAS-NMR Spectra of Technical Calcium Carbide and Barium Carbide—Are the $C_2^{2\ominus}$ Ions in Ionic Carbides Surrounded Symmetrically? (C) 807
- Fast Heteronuclear 3D NMR Spectroscopy (C) 546
- Helicene Dianions: Paratropicity of Twisted Phenanthrene Dianions (C) 919
- Heteronuclear "X-Y" Decoupling in the MAS-NMR Spectroscopy of Inorganic Solids (C) 882
- High-Pressure NMR Studies of $[(\eta^3\text{-}C_5H_5)(\eta^5\text{-}C_5H_5)Cr(CO)_2]$. Evidence for Concerted Ring Interchange (C) 194
- Modern NMR Pulse Experiments: A Graphical Description of the Evolution of Spin Systems (R) 374
- NMR Microscopy—Fundamentals, Limits and Possible Applications (R) 1
- NMR Study of Nuclear Spin Polarization during Chemical Reactions with Ortho Hydrogen (C) 58
- ^{17}O NMR Spectroscopy of Benzoyl Compounds $Y-C_6H_4-COX$: Sensitivity to Ring Substituents as a Measure of the Electron Demand of the Carbonyl Group (C) 647
- One and Two Dimensional NMR Spectroscopy (B) 935
- Restricted Rotation of an Unsubstituted η^5-Cyclopentadienyl Group in Solution Demonstrated by ^{13}C NMR Spectroscopy (C) 289
- Solid-State NMR Studies of the Structure and Reactivity of Metakaolinite (C) 553
- Sterically Hindered Internal Rotation in an Acyclic α,β-Unsaturated Ketone

2,2,5-Trimethyl-4-isopropylhex-4-en-3-one (C) 1435
- Synthesis and 2D-(^{1}H,^{103}Rh)-NMR Study of the First "Non-Classical" Polyhydrido Complex Stabilized by a Nitrogen Donor Ligand (C) 548
- Synthesis and Direct NMR Spectroscopic Observation of [(η^4-Arene)Cr(CO)$_3$] Dianions (C) 1444
- Synthesis and NMR Spectra of 2,3-Dihydro-1,3-methanoindene Derivatives and 1,2,3,5-Tetrahydro-1,3-methanopentalene (C) 1035
- Unraveling Overlapping Multiplets in Two-Dimensional NMR Correlation Spectra by Selective Inversion of Coupling Partners (C) 517

Nobel lecture
- Electromagnetic Traps for Charged and Neutral Particles (Nobel Lecture) (R) 739
- Enzymatic Cleavage of RNA by RNA (Nobel Lecture) (R) 749
- Experiments with an Isolated Subatomic Particle at Rest (Nobel Lecture) (R) 734
- Experiments with Separated Oscillatory Fields and Hydrogen Masers (Nobel Lecture) (R) 725
- Retroviruses and Oncogenes I (Nobel Lecture) (R) 707
- Retroviruses and Oncogenes II (Nobel Lecture) (R) 716
- Self-splicing and Enzymatic Activity of an Intervening Sequence RNA from *Tetrahymena* (Nobel Lecture) (R) 759

Non-metal compounds
- Non-Metal Rings, Cages and Clusters (B) 110

Norbornyl cation
- Experimental and Theoretical IR Spectra of the 2-Norbornyl Cation (C) 183

Nuclear Fission
- Five Decades Ago: From the "Transuranics" to Nuclear Fission (R) 481

Nucleic acids
- Enzymatic Cleavage of RNA by RNA (Nobel Lecture) (R) 749
- Self-splicing and Enzymatic Activity of an Intervening Sequence RNA from *Tetrahymena* (Nobel Lecture) (R) 759

Nucleotide base analogues
- Replication Experiments with Nucleotide Base Analogues (R) 36

Nucleotides
- Bis(*N*,*N*-diisopropylamino)trimethylsiloxyphosphane: A Novel Flexible Phosphitylating Reagent in Nucleoside Chemistry and Its Application in the Synthesis of *P*-Modified Nucleotides (C) 522

Oligomers
- Amine-Template-Directed Synthesis of Cyclic Porphyrin Oligomers (C) 1400

Oligopyrroles
- The Chemistry of Linear Oligopyrroles and Bile Pigments (B) 1071

Oligorylenes
- Oligorylene as a Model for "Poly(perinaphthalene)" (C) 525

Oncogenes
- Retroviruses and Oncogenes I (Nobel Lecture) (R) 707
- Retroviruses and Oncogenes II (Nobel Lecture) (R) 716

Optical activity
- Measuring the Optical Activity of Chiral Imprints in Insoluble Highly Cross-linked Polymers (C) 684

Organic conductors
- Electrical and Magnetic Properties and X-Ray Structure of a Highly Conductive 4:1 Complex of Tetracyanoquinodimethane and a Tetrathiafulvalene Derivative (C) 1450
- Electrochemical Solid-State Studies on Oligomeric *p*-Phenylenes as Model Compounds for Conductive Polymers (C) 692
- Interfaces between Molecular and Polymeric "Metals": Electrically Conductive, Structure-Enforced Assemblies of Metallomacrocycles (R) 857

Organic synthesis
- Chemistry of Tin (B) 1072
- Comprehensive Organic Transformations (B) 435
- Organic Synthesis in the Age of Computers (R) 1286
- Organic Synthesis—Where now? (R) 1320
- Organisch-chemischer Denksport. Ein Seminar für Fortgeschrittene (B) 702
- Organotin Chemistry (B) 1072
- Organotin Compounds in Organic Synthesis (B) 1072
- Strategies and Tactics in Organic Synthesis. Vol. 2 (B) 326

Organometallic chemistry
- Organometallics. A Concise Introduction (B) 438
- Preparative Polar Organometallic Chemistry. Vol. 1 (B) 562

Ortho hydrogen
- NMR Study of Nuclear Spin Polarization during Chemical Reactions with Ortho Hydrogen (C) 58

Osmium compounds
- Direct Electrical Communication between Graphite Electrodes and Surface Adsorbed Glucose Oxidase/Redox Polymer Complexes (C) 82
- Lewis-Acid-Induced Transformation of a Terminal Carbonyl Ligand: Synthesis and Structure of the Alkyne-Cluster-Analogue [(μ-H)$_3$Os$_3$(CO)$_9${μ_3,η^2-C(OBC$_8$H$_{14}$)B(Cl)}] (C) 309
- Organoosmium Oxides: Efficient Syntheses and Structures (C) 1445
- [(Ph$_3$P)$_2$N]$_2$[Os$_{18}$Hg$_2$C$_2$(CO)$_{42}$] a Photochemically Generated High-Nuclearity Cluster Which Reversibly Incorporates Metallic Mercury into Its Metal Core (C) 1137
- Structural Characterization of the Pseudoenantiomeric *cis*-Dioxo Osmium(VI) Esters of Chiral Diols with Cinchona Alkaloid Ligands (C) 639

Oxadienes
- Intramolecular Hetero-Diels–Alder Reactions of Oxadienes: Influence of Substituents of the Tether on the Diastereoselectivity (C) 665

Oxetanones
- Isomerization versus Decarboxylation of Protonated Oxetanone: Comparison between Experimental Results and Theoretical Calculations (C) 1146

Oxidations
- Fe$^{\oplus}$-Catalyzed Gas-Phase Oxidation of Ethane by N_2O (C) 1431
- FeO$^{\oplus}$ Activates Methane (C) 1433
- Methods for the Oxidation of Organic Compounds—Alcohols, Alcohol Derivatives, Alkyl Halides, Nitroalkanes, Alkyl Azides, Carbonyl Compounds, Hydroxyarenes and Aminoarenes (B) 563

Oxidoreductases
- Direct Electrical Communication between Graphite Electrodes and Surface Adsorbed Glucose Oxidase/Redox Polymer Complexes (C) 82

Oxirane
- Characterization by Microwave Spectroscopy of a Transient Hydrogen-Bonded Complex of Oxirane and Hydrogen Chloride Isolated in a Pulsed Jet (C) 72

Oxoesters
- Asymmetric Nucleophilic Acylation via Metalated Chiral Amino Cyanides: Enantioselective Synthesis of 3-Substituted 4-Oxoesters by Asymmetric Michael Addition (C) 179

Oxygen activation
- Oxygen Activation with Transition Metal Complexes: Nickel-Catalyzed Oxidation of a Pentacoordinated Substrate (C) 106

Pagodane route
- The Pagodane Route to Dodecahedranes: An Efficient Variant—New Substitution Patterns (C) 92
- The Pagodane Route to Dodecahedranes: Dodecahedradienes—Unusually "Pyramidalized", Isolable Olefins (C) 95

Palladium compounds
- Novel Bonding Mode for a Cyanometalate Ligand: Synthesis and Crystal Structure of the Mn_4Pd_4 Cluster [(OC)Pd(μ-NC)Mn(η-C$_5$H$_4$Me)(CO)$_2$]$_4$ Containing an Orthogonal Arrangement of Helical Units (C) 1140
- Radiation-Induced Copolymerization of *cis*-[PdCl$_2${CN(CH$_2$)$_3$-OC(O)-CH = CH$_2$}$_2$]: A Novel Route to Organometallic Cross-linked Copolymers Useful for Catalytic Applications (C) 384
- Synthesis and Molecular Structure of *cis*-[Pd(C$_6$F$_5$)$_2$(C$_6$H$_5$CH$_2$NMe$_2$)], an Intramolecular Coordination Compound Containing an Unusual η^1-Arene Ligand (C) 891

Paloc
- The 3-(3-Pyridyl)allyloxycarbonyl (Paloc) Moiety—a Stable, Amino-Protecting Group for Peptide Syntheses in Organic Media and in Water That Is Cleavable under Neutral Conditions (C) 1457

Pauson-Khand reactions
- 2-Pentyl cyclopent-2-en-1-one by Catalytic Pauson-Khand Reaction (C) 1413

Pentaketones
- The Structure of Vicinal Pentaketones—X-Ray Structure Investigations and Calculations (C) 1048

Pentalenes
- Synthesis and NMR Spectra of 2,3-Dihydro-1,3-methanoindene Derivatives and 1,2,3,5-Tetrahydro-1,3-methanopentalene (C) 1035

Peptides
- Highly Selective Synthesis of (*E*)-Alkene Isosteric Dipeptides With High Optical Purity via RCu(CN)Li · BF$_3$ Mediated Reaction (C) 801
- Peptide Synthesis under High Pressure (C) 1025
- Peptides as Conformational Switch: Medium-Induced Conformational Transitions of Designed Peptides (C) 185
- Selective Deamidation of Peptide Amides (C) 1139
- The 3-(3-Pyridyl)allyloxycarbonyl (Paloc) Moiety—a Stable, Amino-Protecting Group for Peptide Syntheses in Organic Media and in Water That Is Cleavable under Neutral Conditions (C) 1457
- What Are the Structures of Fenestin A and Fenestin B? (C) 514

Peroxo compounds
- Houben-Weyl. Methoden der Organi-

schen Chemie. Band E13, Teil 1 und 2: Organische Peroxo-Verbindungen (B) 327
Pesticides
- Pesticide Chemistry (B) 324
Phenanthrenes
- Helicene Dianions: Paratropicity of Twisted Phenanthrene Dianions (C) 919
Phenylenes
- Electrochemical Solid-State Studies on Oligomeric *p*-Phenylenes as Model Compounds for Conductive Polymers (C) 692
Phosphaalkenes
- A 1,6-Diphospha-1,2,4,5-hexatetraene, Synthesis and Ring Closure Reactions to Cyclobutenes (C) 927
- Epoxidation of the P = C Double Bond of Phosphaalkene Complexes: X-Ray Crystal Structure Analysis of a Stable Oxaphosphirane Complex (C) 1166
Phosphatases
- $Zn^{II}Fe^{III}$ and $Fe^{II}Fe^{III}$ Complexes Containing a Novel (μ-Phenoxo)bis(μ-diphenylphosphato)dimetal(II,III) Core as Model Complexes for Active Sites of Purple Phosphatases (C) 531
Phosphoric acid amides
- Development of Tailor-Made Cytostatics Activable by Acid-Catalyzed Hydrolysis for Selective Tumor Therapy (C) 782
Phosphorus compounds
- [4 + 2]-Cycloadditions of Phosphinodiazoalkanes: Synthesis of 1,2,4-λ^5-Diazaphosphinines (C) 314
- A 1,6-Diphospha-1,2,4,5-hexatetraene, Synthesis and Ring Closure Reactions to Cyclobutenes (C) 927
- A First Step toward the Phosphorus Analogues of Polythiophenes (C) 655
- A New Route to 1,3-Diphospholide Ions. Synthesis and X-Ray Structure Analysis of a 1,3-Diphosphaferrocene (C) 534
- A 1-Silyl-1*H*-phosphirene/1,2-Dihydro-1,2-phos-phasilete Rearrangement—The Decisive Step in the Synthesis of Heterocycles Containing 2-Phospha-1,3-diene Units (C) 1436
- An Allene-analogous Boranylidenephosphane with B = P Double Bond: 1,1-Diethylpropyl(2,2,6,6-tetramethylpiperidino)boranylidenephosphane-*P*-pentacarbonylchromium (C) 682
- An Aluminaphosphacubane, a New Aluminum Phosphide Precursor (C) 1409
- An *N*-Phosphino *C*-Thiophosphinoyl Nitrilimine as a Formal 1,4 Dipole: Synthesis of 1,2,3λ^5-Diaza- and 1,2,4,3λ^5-Triazaphosphinines (C) 1123
- Bis(*N*,*N*-diisopropylamino)trimethylsiloxyphosphane: A Novel Flexible Phosphitylating Reagent in Nucleoside Chemistry and Its Application in the Synthesis of *P*-Modified Nucleotides (C) 522
- Boron-Phosphorus Compounds and Multiple Bonding (R) 449
- Direct Evidence for a Nitrile Imine–Imidoylnitrene Rearrangement: X-Ray Crystal Structure of an Unusual Nitrene Complex (C) 659
- 5-Methyl-1,1,3,3-tetraphenyl-1λ^5,3λ^5-diphosphabenzene (C) 516
- New Chiral C_3-Symmetric Tripodal Phosphanes (C) 1462
- Oxidative Addition of Phosphorus Ylides to $Ru_3(CO)_{12}$ (C) 896
- Ring Closure and Ring Expansion Reactions in Bridged Triarylphosphanes and Triarylarsanes with *o*-Isopropenyl Substituents. Novel Candidates for Turnstile Geometry (C) 689
- $Si[(Me_2P)_2C(SiMe_3)]_2$, a Stable σ-Bonded Compound Containing Divalent Silicon (C) 295
- Spontaneous Formation of Stable Phosphino(silyl)carbenes from Unstable Diazo Compounds (C) 1429
- Synthesis and Structure of a Diphosphadigalletane: A Novel Base-Stabilized Ga_2P_2 Ring System (C) 1150
- Synthesis and Structure of a 1λ^5,4λ^5-Diphosphapentalene (C) 799
- Thermal Decomposition of the Nonmetal Octahedron $(ClB)_4P_2$ by Elimination of Its PP Octahedral Edge (C) 1044
- Water-Soluble Metal Complexes of the Sulfonated Triphenylphosphane TPPTS: Preparation of the Pure Compounds and their Use in Catalysis (C) 391
Photochemistry
- A 1-Silyl-1*H*-phosphirene/1,2-Dihydro-1,2-phos-phasilete Rearrangement—The Decisive Step in the Synthesis of Heterocycles Containing 2-Phospha-1,3-diene Units (C) 1436
- Bimolecular Collisions (B) 936
- Chemiluminescence and Photochemical Reaction Detection in Chromatography (B) 436
- Facile Hydrogenation of the Central Cyclohexatriene of Tris(benzocyclobutadieno)benzene: Synthesis, Structure, and Thermal and Photochemical Isomerization of all-*cis*-Tris(benzocyclobuta)cyclohexane (C) 1151
- 2-Methylene-2*H*-azirines by Photolysis of 1-Azidoallenes (C) 103
- $[(Ph_3P)_2N]_2[Os_{18}Hg_2C_2(CO)_{42}]$ a Photochemically Generated High-Nuclearity Cluster Which Reversibly Incorporates Metallic Mercury into Its Metal Core (C) 1137
- Reversible Photoisomerization of Ketene to Ethynol (C) 411
- The Enol of Mandelic Acid, Detection, Acidity in Aqueous Solution, and Estimation of the Keto-Enol Equilibrium Constant and Carbon Acidity of Mandelic Acid (C) 792
- The Tautomeric Equilibrium between Cyclopentadienyl-1-carboxylic Acid and Fulvene-6,6-diol in Aqueous Solution (C) 790
Photoelectron spectroscopy
- The Bicyclo[1.1.1]pentane Framework—an Excellent Relay for π/σ Conjugation (C) 413
Photosensitizers
- [22]Coproporphyrin II for Photodynamic Therapy (C) 1395
Photosynthesis
- Phenyl-Linked Quinone-Substituted Porphyrin Trimers (C) 1134
- Synthesis, Structure, and Catalase-Type Activity of a Novel Oxo-Bridged Tetranuclear Manganese Aggregate Exhibiting Short O · · · O Interactions (C) 1156
Phyllanthocin
- Synthesis of (±)-Phyllanthocin via a Metal-Catalyzed Cycloreduction (C) 520 (–)
Pigments
- The Chemistry of Linear Oligopyrroles and Bile Pigments (B) 1071
Platinum compounds
- Novel Platinum Complexes Enable Selective C-H and C-Si Activation of Tetramethylsilane at Room Temperature (C) 880
- Platinum in the Unusual Oxidation State + 2.75: A Linear Tetranuclear Complex with the Model Nucleobase 1-Methylthymine (C) 84
- Synthesis and Structure of $(NBu_4)[Sn\{Pt(\mu\text{-}Cl)(C_6F_5)_2\}_3]$, an Unusual Cluster with Three $Pt^{II}\rightarrow Sn^{II}$ Bonds (C) 1449
Poetry
- Gaps and Verges (B) 1489
Pollutants
- Misconceptions on Pollution and the Causes of Cancer (R) 1197
Polyanions
- Coordination Chemistry of Polyoxomolybdates: The Structure of a Dodecanuclear Molybdate Cage Incorporating Hydrogen Squarate Ligands, $[(C_4H_9)_4N]_4[Mo_{12}O_{36}(C_4O_4H)_4]\cdot 10Et_2O$ (C) 70
- $Se_{10}^{2\ominus}$, a Bicyclic Polyselenide (C) 390
Polycations
- $Te_8^{2\oplus}$, a New Tellurium Polycation (C) 293
Polycycles
- Doubly Bridged Prismanes, Dewar Benzenes and Benzene Derivatives from Cyclooctyne and 1,8-Cyclotetradecadiyne: En Route to Propella[n_3]prismanes (C) 1427
- Ring Closure and Ring Expansion Reactions in Bridged Triarylphosphanes and Triarylarsanes with *o*-Isopropenyl Substituents. Novel Candidates for Turnstile Geometry (C) 689
Polyenes
- Macrocyclically Fixed Diarylhexatrienes (C) 1162
Polymerization
- Base-Free Cationic 14-Electron Titanium and Zirconium Alkyls: In situ Generation, Solution Structures, and Olefin Polymerization Activity (C) 780
- Isotope Effects Associated with α-Olefin Insertion in Zirconocene-Based Polymerisation Catalysts: Evidence for an α-Agostic Transition State (C) 1412
- Radiation-Induced Copolymerization of *cis*-$[PdCl_2\{CN(CH_2)_3\text{-}OC(O)\text{-}CH=CH_2\}_2]$: A Novel Route to Organometallic Cross-linked Copolymers Useful for Catalytic Applications (C) 384
- Stereo- and Regioselectivity of Chiral, Alkyl-substituted *ansa*-Zirconocene Catalysts in Methylalumoxane-activated Propene Polymerization (C) 279
- Two-Dimensional Model Networks (R) 439
Polymers
- Advanced Materials: Trends and Possibilities in Liquid Crystalline Polymers (R) 1256
- Chemiluminescence Techniques for the Characterization of Materials (R) 362
- Colloid Chemistry of Polymers (B) 563
- Comprehensive Polymer Science: The Synthesis, Characterization, Reactions and Applications of Polymers (B) 699
- Electrochemical Solid-State Studies on Oligomeric *p*-Phenylenes as Model Compounds for Conductive Polymers (C) 692
- Fractals and Related Hierarchical Models in Polymer Science (R) 113
- Induction and Variation of Chirality in Discotic Liquid Crystalline Polymers (C) 1478
- Measuring the Optical Activity of Chiral Imprints in Insoluble Highly Cross-linked Polymers (C) 684
- Perspectives in the Development of High-Temperature Polymers (R) 1262
- Rings, Clusters and Polymers of Main

Group and Transition Elements (B) 1490
Polyols
- Multiple 1,2-*O*,*O*-Shift of *tert*-Butyldiphenylsilyl Groups in Polyols (C) 431
Porphycenes
- Porphyrin Homologues: [22]Porphyrin-(2.2.2.2), a "Stretched Porphycene" (C) 1387
Porphyrins
- Acetylene-Cumulene Porphyrinoids (C) 1385
- Amine-Template-Directed Synthesis of Cyclic Porphyrin Oligomers (C) 1400
- Catalytic Cyclophanes: A Porphyrin-Bridged Cyclophane as a Model for Cytochrome P-450 Enzymes (C) 191
- [22]Coproporphyrin II for Photodynamic Therapy (C) 1395
- Electron Transfer between Covalently Linked Porphyrin and Quinone Units: Synthesis, Magnetic Resonance and Picosecond Fluorescence Spectroscopy (C) 670
- Isocorroles: Novel Tetrapyrrolic Macrocycles (C) 1390
- Oxidative Degradation of Aromatic Pollutants by Chemical Models of Ligninase Based on Porphyrin Complexes (C) 1471
- Perchlorinated and Highly Chlorinated *meso*-Tetraphenylporphyrins (C) 1028
- Phenyl-Linked Quinone-Substituted Porphyrin Trimers (C) 1134
- Porphyrin Homologues: [22]Porphyrin-(2.2.2.2), a "Stretched Porphycene" (C) 1387
- Synthesis of a Bisvinylogous Octaethylporphyrin (C) 1393
Powder metallurgy
- The Preparation of Finely Divided Metal and Alloy Powders (C) 273
Precision spectroscopy
- Electromagnetic Traps for Charged and Neutral Particles (Nobel Lecture) (R) 739
- Experiments with an Isolated Subatomic Particle at Rest (Nobel Lecture) (R) 734
- Experiments with Separated Oscillatory Fields and Hydrogen Masers (Nobel Lecture) (R) 725
Prismanes
- Doubly Bridged Prismanes, Dewar Benzenes and Benzene Derivatives from Cyclooctyne and 1,8-Cyclotetradecadiyne: En Route to Propella[N_3]prismanes (C) 1427
L-Proline
- Isolation of an L-Stereospecific *N*-Acyl-L-proline-Acylase and its Use as Catalyst in Organic Synthesis (C) 417
Prose
- Cantor's Dilemma (B) 1488
Protecting groups
- Multiple 1,2-*O*,*O*-Shift of *tert*-Butyldiphenylsilyl Groups in Polyols (C) 431
- Selective Deamidation of Peptide Amides (C) 1139
- The 3-(3-Pyridyl)allyloxycarbonyl (Paloc) Moiety—a Stable, Amino-Protecting Group for Peptide Syntheses in Organic Media and in Water That Is Cleavable under Neutral Conditions (C) 1457
Proteins
- Specific Interactions of Proteins with Functional Lipid Monolayers—Ways of Simulating Biomembrane Processes (R) 1269
Pyrazolylboranes
- On the Nature of Pyrazolylborane. An Ab Initio/IGLO/NMR Study (C) 304
- The First Monomeric Diorgano(pyrazolyl)borane: A Nonclassical Boronium Ion in Solution? (C) 302
Pyrroles
- A Novel Pyrrole Synthesis (C) 777
- 2,3,4,5-Tetramethyl-1-sodiopyrrole: An Azacyclopentadienyl Ligand in a Novel Bridging Function (C) 1143
- The Chemistry of Linear Oligopyrroles and Bile Pigments (B) 1071

Quartz microbalance
- The Quartz Microbalance: A Novel Approach to the In-Situ Investigation of Interfacial Phenomena at the Solid/Liquid Junction (R) 329
Quinodimethanes
- Intramolecular Interconversion of *syn*- and *anti*-Tricarbonyl(1-ethoxy-1,2-dihydrocyclobutabenzene)chromium. Trapping of the *ortho*-Quinodimethane Intermediate (C) 407

Radialenes
- Nickel-Catalyzed Cyclodimerization of Hexapentaenes: [4]Radialenes and [5]Radialenones with Cumulated Double Bonds (C) 1062
Radical cations
- Ionic Isomer Distinction by Neutralization-Reionization Mass Spectrometry (NRMS): Carbonic Acid Radical Cations, $(HO)_2CO^{\bullet\oplus}$ versus $(H_2O/CO_2)^{\bullet\oplus}$ Clusters (C) 404
- Stability and Cyclization of Enol Radical Cations: A Mechanistic Study of One-Electron Oxidation of β,β-Dimesityl Enols (C) 541
- α-Umpolung of Ketones via Enol Radical Cations: A Mechanistic Study (C) 1144
Radical chain reactions
- Reductive Alkylation of Enamines with Chloromethyl *p*-Tolyl Sulfone via a Radical Chain Process (C) 433
Radicals
- A Stable Triradical Compound and its Unusual Magnetic Properties (C) 415
- Reactivity in Intramolecular Radical Reactions: A Comparison of Hydrogen Transfer with Alkene Addition (C) 653
- Solvent and Structure Effects in the Photobromination of Benzyltrimethylsilanes. A Mechanistic Changeover from Hydrogen-Atom Transfer to Electron Transfer (C) 658
Radiochemistry
- Vom Radiothor zur Uranspaltung. Eine wissenschaftliche Selbstbiographie (B) 219
Raman spectroscopy
- Nitrogen Triiodide (C) 677
Reaction mechanisms
- CC Bond Formation by Addition of Carbenium Ions to Alkenes: Kinetics and Mechanism (R) 1371
- Elementary Steps in Heterogeneous Catalysis (R) 1219
- High-Pressure NMR Studies of $[(\eta^3\text{-}C_5H_5)(\eta^5\text{-}C_5H_5)Cr(CO)_2]$. Evidence for Concerted Ring Interchange (C) 194
- Isomerization versus Decarboxylation of Protonated Oxetanone: Comparison between Experimental Results and Theoretical Calculations (C) 1146
- Mesolytic Cleavage of C–C Bonds. Comparison with Homolytic and Heterolytic Processes in the Same Substrate (C) 283
- On the Conformation and Structure of Organometal Complexes in the Solid State: Two Studies Relevant to Chemical Synthesis (R) 256
- Solvent and Structure Effects in the Photobromination of Benzyltrimethylsilanes. A Mechanistic Changeover from Hydrogen-Atom Transfer to Electron Transfer (C) 658
- Stability and Cyclization of Enol Radical Cations: A Mechanistic Study of One-Electron Oxidation of β,β-Dimesityl Enols (C) 541
- Switching Reaction Mechanism by Monolayer Compression: An Ester Hydrolysis (C) 306
- α-Umpolung of Ketones via Enol Radical Cations: A Mechanistic Study (C) 1144
- Zwitterions as Intermediates of the 1,3-Dipolar Cycloaddition of Electrophilic Azides to 5-Alkylidenedihydrotetrazoles – the Other Non-Concerted Limiting Case (C) 695
Reactive intermediates
- Carbonyl Oxides: Zwitterions or Diradicals? (R) 344
- Enzymic Reaction Selectivity by Negative Catalysis or How Do Enzymes Deal with Highly Reactive Intermediates? (R) 355
Reagents
- A New Route to Highly Enantiomerically Enriched (*Z*)-(1-Methyl-2-butenyl)-boronic Esters (C) 59
- Bis(*N*,*N*-diisopropylamino)trimethylsilyoxyphosphane: A Novel Flexible Phosphitylating Reagent in Nucleoside Chemistry and Its Application in the Synthesis of *P*-Modified Nucleotides (C) 522
- Synthesis of (+)-Terrein from L-Tartaric Acid (C) 67
Rearrangements
- A 1-Silyl-1*H*-phosphirene/1,2-Dihydro-1,2-phos-phasilete Rearrangement—The Decisive Step in the Synthesis of Heterocycles Containing 2-Phospha-1,3-diene Units (C) 1436
- Gas-Phase Thermolysis of 6-Cyclopropyl- and 6-Oxiranylpentafulvenes: Novel Routes to Dihydroindenes and Vinylcyclopentadienes (C) 803
Reductions
- The Preparation of Finely Divided Metal and Alloy Powders (C) 273
Reductive scission
- Reductive Scission of a Cyclopropane σ-Bond During the Action of Elemental Lithium on Cyclopropylacetylenes – A *cis*-1,2-Dilithioalkene as Intermediate (C) 667
Research policy
- The Integrating Effect of the Research Policy of the European Communities (R) 1189
Restricted rotation
- Restricted Rotation of an Unsubstituted η^5-Cyclopentadienyl Group in Solution Demonstrated by ^{13}C NMR Spectroscopy (C) 289
Retroviruses
- Retroviruses and Oncogenes I (Nobel Lecture) (R) 707
- Retroviruses and Oncogenes II (Nobel Lecture) (R) 716
Rhenium compounds
- π/σ Equilibria in Metal Complexes of Organic Carbonyl Compounds; Synthesis and Structure of Chiral Rhenium Complexes $[(\eta^5\text{-}C_5H_5)Re(NO)(PPh_3)(O{=}CHAr)]X$ (C) 1473
- Synthesis and Structure of the Novel μ_2-Carbido Complex $[(TPP)Fe{=}C{=}Re(CO)_4Re(CO)_5]$ (C) 318

- The Re–Re Bond in Binuclear Di-μ-oxorhenium Complexes Containing the 1,4,7-Triazacyclononane Ligand (C) 787
- Thermodynamic Aldehyde Enantioface Binding Selectivities in Complexes of Chiral Metal Fragments; Mechanism of Interconversion of Diastereomeric π-Aldehyde Complexes $[(\eta^5\text{-}C_5H_5)Re(NO)(PPh_3)(\eta^2\text{-}O=CHAr)]BF_4$ (C) 1475

Rhodium compounds
- Continuous Generation of NADH from $NAD^{\oplus}$ and Formate Using a Homogeneous Catalyst with Enhanced Molecular Weight in a Membrane Reactor (C) 388
- Rhodium-Catalyzed Synthesis of Trisubstituted Olefins from Ethene Derivatives and Diazoalkanes (C) 510
- Synthesis and 2D-(^1H,^{103}Rh)-NMR Study of the First "Non-Classical" Polyhydrido Complex Stabilized by a Nitrogen Donor Ligand (C) 548

Rhodomycins
- Semisynthetic Rhodomycins: Novel Glycosylation Methods for the Synthesis of Anthracycline Oligosaccharides (C) 809

Ring contraction reactions
- A Novel Type of Ring Contraction as Non-Enzymatic Step in the Later Stages of the Biosynthesis of Urdamycin H (C) 1051

Ring expansion reactions
- Ring Closure and Ring Expansion Reactions in Bridged Triarylphosphanes and Triarylarsanes with *o*-Isopropenyl Substituents. Novel Candidates for Turnstile Geometry (C) 689

RNA cleavage
- Enzymatic Cleavage of RNA by RNA (Nobel Lecture) (R) 749
- Self-splicing and Enzymatic Activity of an Intervening Sequence RNA from *Tetrahymena* (Nobel Lecture) (R) 759

Ruthenium compounds
- Ambident Behavior of the "New Vitamin" Methoxatin (Cofactor PQQ) towards Metals: Coordinative Stabilization of the Pyrrolide Form and the Semiquinone Form (C) 78
- Asymmetric Heterodinuclear $[L'Ru(\mu\text{-}O)(\mu\text{-}CH_3CO_2)_2ML]^{2\oplus}$ Complexes (M = Fe, Mn, V): Electronic Structure and Magnetic Properties (C) 645
- Atomic Structure and Superstructure of α-$RuCl_3$ by Scanning Tunneling Microscopy (C) 537
- Cp*Ru(acac)—A Coordinatively Unsaturated, Stable 16-Valence-Electron Complex (C) 773
- $[H_2Ru_6(CO)_{16}(\mu\text{-}C_6H_4O)]$: Binding of Five Metal Atoms to a Phenol Molecule (C) 198, (L) (938)
- Organometallic Macrocycles: Synthesis and Molecular Structure of Trimeric Tartratodiruthenium Complexes (C) 429
- Oxidative Addition of Phosphorus Ylides to $Ru_3(CO)_{12}$ (C) 896
- Ruthenium-containing Cumulenes: Generation of 2,3,4-Pentatrienylidene- and 3-Oxo-1,4-pentadienyl-Complexes (C) 215
- *s-trans*-1,3-Dienes as Ligands for Cationic Group 8 Metal Centers (C) 1417

Sandwich complexes
- A New Route to 1,3-Diphospholide Ions. Synthesis and X-Ray Structure Analysis of a 1,3-Diphosphaferrocene (C) 534
- Building Up Metal-Stabilized Fourfold Bridged Cyclobutadienophanes (C) 1426
- Highly Reactive Intermediates from the Cocondensation Reactions of Iron, Cobalt and Nickel Vapor with Arenes (R) 126
- Tetraphenylallylsodium Diethyl Ether: A Contact Ion Pair with an Intramolecular $Na^{\oplus}$ Sandwich (C) 1042

Scanning tunneling microscopy
- Atomic Structure and Superstructure of α-$RuCl_3$ by Scanning Tunneling Microscopy (C) 537

Schrödinger
- Schrödinger—Life and Thought (B) 697

Selenium compounds
- A Facile Synthesis of β-Selenolactams (C) 530
- A Monocyclic Selenepine: Synthesis and Characterization of Diethyl 2,7-Di-*tert*-butyl-4,5-selenepinedicarboxylate (C) 424
- Low-Dimensional Compounds Incorporating Polychalcogenide Ligands. The Unusual Polymeric Structures of $[AuSe_5]_n^{n\ominus}$ and $[AuSe_{13}]_n^{3n\ominus}$ (C) 914
- New Copper Clusters Containing Se and PEt_3 as Ligands: $[Cu_{70}Se_{35}(PEt_3)_{22}]$ and $[Cu_{20}Se_{13}(PEt_3)_{12}]$ (C) 1452
- Preparation and Structure of $[Se=W(PSe_4)(PSe_2)]^{2\ominus}$; a Cluster Containing a Heteroallylic $PSe_2^{\ominus}$ Unit (C) 1486
- $Se_{10}^{2\ominus}$, a Bicyclic Polyselenide (C) 390
- Synthesis and Cycloadditions of Monomeric Selenobenzophenone (C) 1067
- Synthesis and Structure of Novel Cu-Clusters: $[Cu_{30-x}Se_{15}(PiPr_3)_{12}]$ (x = 0,1) and $[Cu_{36}Se_{18}(PtBu_3)_{12}]$ (C) 796

Self replication
- Molecular Recognition with Model Systems (R) 245

Self-assembly
- Formation of Tetranuclear Chelate(4-) Ions of Divalent Metals (Mn, Co, Ni) with Idealized *T* Symmetry by Spontaneous Self-assembly (C) 311
- Perspectives in Supramolecular Chemistry—From Molecular Recognition towards Molecular Information Processing and Self-Organization (R) 1304

Semi-empirical calculations
- Carbonyl Oxides: Zwitterions or Diradicals? (R) 344
- The First Monomeric Diorgano(pyrazolyl)borane: A Nonclassical Boronium Ion in Solution? (C) 302

Serendipity
- Serendipity: Accidental Discoveries in Science (B) 1069

Silicon compounds
- A Bicyclo[1.1.1]pentasilane Derivative. Synthesis, Molecular Structure, and Comments on Structural Homology (C) 794
- A 1,2:2,1-Bis(2-silapropane-1,3-diyl)diborane(6): Stabilization Product of Bis(trisyl)diborane(2)? (C) 899
- A Cyclodimeric Silaketenimine (C) 90
- A New Way to SiC Ceramic Precursors by Catalytic Preparation of Preceramic Polymers (C) 785
- Anions Isosteric with $CO_3^{2\ominus}$ in Cs_5SiP_3, Cs_5SiAs_3, Cs_5GeP_3, and Cs_5GeAs_3 (C) 87
- Bis(pentamethylcyclopentadienyl)silylene as Ligand in Gold(I) Chloride Complexes (C) 893
- 1,2-Dimethyl-1,2-disila-*closo*-dodecaborane(12), the First Silicon Analogue of an *ortho*-Carborane (C) 918
- Heptasila[7]paracyclophane (C) 778
- Intramolecular Insertion of Arylcarbenes into C–Si Bonds (C) 661
- O-Atom Insertion into Si–H Bonds by Dioxiranes: A Stereospecific and Direct Conversion of Silanes into Silanols (C) 890
- Permethyl-β-cyclodextrin, Chemically Bonded to Polysiloxane: a Chiral Stationary Phase with Wider Application Range for Enantiomer Separation by Capillary Gas Chromatography (C) 427
- $Si[(Me_2P)_2C(SiMe_3)]_2$, a Stable σ-Bonded Compound Containing Divalent Silicon (C) 295
- Structure of a 1:1 Adduct of Silyl Chloride and Dimethyl Ether at 100K (C) 76
- Synthesis of Cyclosilanylethynes (C) 641
- Synthesis of the First Silaamidide (C) 529
- Tetrasilylmethane, $C(SiH_3)_4$, the Si/C-Inverse of Tetramethylsilane, $Si(CH_3)_4$ (C) 201
- The Chemistry of Organic Silicon Compounds. Parts 1 and 2 (B) 221

Silyl migration
- Multiple 1,2-*O*,*O*-Shift of *tert*-Butyldiphenylsilyl Groups in Polyols (C) 431

Sodium amides
- Decameric and Dodecameric Sodium Amides and an Organosodium Amide with Stack Structures: $[Na_{10}(NMe_2)_{10}(tmeda)_4]$, $[Na_{12}(NMe_2)_{12}(tmeda)_4]$, and $[Na_{12}(NMe_2)_{10}(CH_2C_6H_4Me)_2(tmeda)_4]$ (C) 1441
- Lewis-Base-Dictated Structural Variations in Sodium Amide Chemistry: X-Ray Crystal Structures of Phenyl(2-pyridyl)amidosodium with Hexamethylphosphoric Triamide (HMPA) and with Pentamethyldiethylenetriamine (PMDETA) (C) 1440

Soils
- The Chemistry of Soils (B) 817

Solid state chemistry
- Crystal Chemistry and Refractivity (B) 702
- Heteronuclear "X-Y" Decoupling in the MAS-NMR Spectroscopy of Inorganic Solids (C) 882
- Introduction to Crystal Chemistry. Student Edition (B) 702
- Nonmolecular Metal Chalcogenide/Halide Solids and Their Molecular Cluster Analogues (R) 840

Solid-phase synthesis
- Solid-Phase Synthesis of Glycopeptide Amides under Mild Conditions: Morphiceptin Analogues (C) 291

Spectroelectrochemistry (B) 699

Spectroscopy
- Fundamentals of Molecular Spectroscopy (B) 816
- Ion and Cluster Ion Spectroscopy and Structure (B) 437

Spiro compounds
- First Coupling of a Metal Atom with Four Ethene Molecules to give a Metallaspiroalkane (C) 322

Squaric acid
- Coordination Chemistry of Polyoxomolybdates: The Structure of a Dodecanuclear Molybdate Cage Incorporating Hydrogen Squarate Ligands, $[(C_4H_9)_4N]_4[Mo_{12}O_{36}(C_4O_4H)_4]\cdot 10Et_2O$ (C) 70

Stacked structures
- Soluble, Oligomeric Bridged Phthalocyaninatoiron(II) Complexes (C) 1467

Stereotetrads
- Enantio- and Regiocontrolled Synthesis

of a Central Ionophoric Antibiotic Building Block by Sequential Opening of Two Epoxide Rings with Cuprate Reagents (C) 1476
Steroids
- A Spacious Cyclophane Host for Inclusion Complexation of Steroids and [m.n]Paracyclophanes (C) 769
- Synthesis of Enantiomerically Pure Heterosteroids by Intramolecular Hetero-Diels-Alder Reaction (C) 527
Stibaindoles
- The Synthesis and Structure of Stibaindoles (C) 771
Strained rings
- A Stereoselective π Cyclization to a Combined Bridgehead Olefin–Bridgehead Alcohol (C) 1456
- The Bicyclo[1.1.1]pentane Framework—an Excellent Relay for π/σ Conjugation (C) 413
- The First Clamped and Strongly Deformed Adamantane (C) 902
- The Pagodane Route to Dodecahedranes: Dodecahedradienes—Unusually "Pyramidalized", Isolable Olefins (C) 95
Structure elucidation
- About the $Li^{\oplus}$ Gegenion Effect on α-Sulfonyl Carbanions (C) 100
- $[BP_2]^{3\ominus}$ and $[BAs_2]^{3\ominus}$, Zintl Anions with Propadiene Structure (C) 65
- $CsNa_2(OH)_3 \cdot 6H_2O$: Structural Differentiation in the Hydrate of a Ternary Alkali-Metal Hydroxide (C) 904
- Decameric and Dodecameric Sodium Amides and an Organosodium Amide with Stack Structures: $[Na_{10}(NMe_2)_{10}(tmeda)_4]$, $[Na_{12}(NMe_2)_{12}(tmeda)_4]$, and $[Na_{12}(NMe_2)_{10}(CH_2C_6H_4Me)_2\text{-}(tmeda)_4]$ (C) 1441
- Electrostatic Control of the Molecular and Crystal Structure of an Olefinic Double Betaine (C) 1132
- Elucidation of the Structure of Hormaomycin (C) 64
- Ethynyl(phenyl)iodonium Triflate, $[HC{\equiv}CIPh][OSO_2CF_3]$: Preparation, Spectral Properties, Mechanism of Formation and X-Ray Molecular Structure (C) 287
- How Do Two C–C Double Bonds Add to One M–M Triple Bond? Structure and Bonding in Bis(η^2-ethylene)hexakis(neopentoxy)ditungsten (C) 1026
- Lewis-Base-Dictated Structural Variations in Sodium Amide Chemistry: X-Ray Crystal Structures of Phenyl(2-pyridyl)amidosodium with Hexamethylphosphoric Triamide (HMPA) and with Pentamethyldiethylenetriamine (PMDETA) (C) 1440
- $Na_{10}\{Li_2[MnO_4]_4\}$, a Compound in Which LiO_4 and MnO_4 Tetrahedra Form Chains Consisting of Six- and Eight-Membered Rings (C) 800
- $[n\text{BuLi} \cdot \text{LiO}t\text{Bu}]_4$, Solid-State Structure of an *n*-Butyllithium–Lithium *tert*-Butoxide Complex (C) 308
- On the Conformation and Structure of Organometal Complexes in the Solid State: Two Studies Relevant to Chemical Synthesis (R) 256
- Stable Azirinimines? A Structural Corrigendum (C) 1164
- Structural Characterization of the Pseudoenantiomeric *cis*-Dioxo Osmium(VI) Esters of Chiral Diols with Cinchona Alkaloid Ligands (C) 639
- Structure and Color of Substituted Pentaphenylbismuth (C) 213
- Structure Determination of $NaCD_3$ Powders at 1.5 and 300K by Neutron and Synchrotron–Radiation Diffraction (C) 650
- Structure of a 1:1 Adduct of Silyl Chloride and Dimethyl Ether at 100K (C) 76
- Structure of a Synthetic Trefoil Knot Coordinated to Two Copper(I) Centers (C) 1154
- Syntheses, Conformations and X-Ray Structure Analyses of the Saccharide Chains from the Core Regions of Glycoproteins (R) 823
- Synthesis and Structure of $[Et_2OZn(SC_6H_2tBu_3)_2]$, the First T-Shaped Zinc Complex (C) 1403
- The Ammonium Salt Route to Oligomeric Lanthanum Salt Complexes: Synthesis and X-Ray Crystal Structure of $La(NCS)_3 \cdot 4HMPA$ (C) 285
- The Structure of Vicinal Pentaketones—X-Ray Structure Investigations and Calculations (C) 1048
- What Are the Structures of Fenestin A and Fenestin B? (C) 514
- X-Ray Structure Analysis of an Iminium Ion Generated by Grob Fragmentation (C) 188
Substituent effects
- ^{17}O NMR Spectroscopy of Benzoyl Compounds $Y{-}C_6H_4{-}COX$: Sensitivity to Ring Substituents as a Measure of the Electron Demand of the Carbonyl Group (C) 647
- Synergic Destabilization by Geminal Ester Groups (C) 674
Sulfenes
- Inverse Amine-Stabilized Sulfenes $F_2C{=}SO_2$ and $FHC{=}SO_2$ (C) 60
Sulfur compounds
- A First Step toward the Phosphorus Analogues of Polythiophenes (C) 655
- A Novel Palladium-Catalyzed Carbonylation of Aromatic *N*-Chlorosulfonamidates to Arylsulfonyl Isocyanates (C) 1147
- Inverse Amine-Stabilized Sulfenes $F_2C{=}SO_2$ and $FHC{=}SO_2$ (C) 60
- Isomerization of Benzoylalkylidene Sulfur Tetrafluorides $C_6H_5\text{-}CO\text{-}CR{=}SF_4$ to Dihydrooxathietes (C) 1128
- Synthesis and Structure Determination of Bicyclic $[Li(tmeda)]_2[S_6]$ (C) 422
Superconductors
- Copper Oxide Superconductors (B) 111
- Synthesis and Transmission Electron Microscopic Investigation of Bi(Pb)–Sr–Ca–Cu–O Superconductors (C) 1459
Supercritical fluids
- Modern Supercritical Fluid Chromatography (B) 325
Supramolecular chemistry
- Perspectives in Supramolecular Chemistry—From Molecular Recognition towards Molecular Information Processing and Self-Organization (R) 1304
- Specific Interactions of Proteins with Functional Lipid Monolayers—Ways of Simulating Biomembrane Processes (R) 1269
Surface chemistry
- Transition Metal Oxides: Surface Chemistry and Catalysis (B) 1074
Symmetry
- Symmetrien der Natur. Ein Handbuch der Natur- und Wissenschaftsphilosophie (B) 821
Synergic interactions
- Synergic Destabilization by Geminal Ester Groups (C) 674
Synthesis design
- Organic Synthesis in the Age of Computers (R) 1286
Synthetic methods
- Activation and Functionalization of Alkanes (B) 700
- Highly Reactive Intermediates from the Cocondensation Reactions of Iron, Cobalt and Nickel Vapor with Arenes (R) 126
- Methods for the Oxidation of Organic Compounds—Alcohols, Alcohol Derivatives, Alkyl Halides, Nitroalkanes, Alkyl Azides, Carbonyl Compounds, Hydroxyarenes and Aminoarenes (B) 563
- Modern Synthetic Methods. Vol. 5 (B) 819
- Stereocontrolled Construction of Complex Cyclic Ketones via Oxy-Cope Rearrangement (R) 609
- Synthesis of a β-Mannosyl-Chitobiosyl-Asparagine Conjugate—a Central Core Region Unit of the *N*-Glycoproteins (C) 1050
- The Directed Synthesis of Biaryl Compounds: Modern Concepts and Strategies (R) 977
Synthetic strategy
- Starburst Dendrimers: Molecular-Level Control of Size, Shape, Surface Chemistry, Topology, and Flexibility from Atoms to Macroscopic Matter (R) 138
- The Logic of Chemical Synthesis (B) 435

Tautomerism

- The Enol of Mandelic Acid, Detection, Acidity in Aqueous Solution, and Estimation of the Keto-Enol Equilibrium Constant and Carbon Acidity of Mandelic Acid (C) 792
- The Tautomeric Equilibrium between Cyclopentadienyl-1-carboxylic Acid and Fulvene-6,6-diol in Aqueous Solution (C) 790
Technetium compounds
- Alkyltechnetium Oxides: First Examples and Reactions (C) 189
Tellurium compounds
- Synthesis and Structure of the Stable Tellurium Nitride $(ClTeNSN)_3N$ (C) 61
- $Te_8^{2\oplus}$, a New Tellurium Polycation (C) 293
Terbium compounds
- Nonradioactive Assay of DNA Hybridization by DNA-Template-Mediated Formation of a Ternary Tb^{III} Complex in Pure Liquid Phase (C) 1167
Tercyclopentadienyls
- On the Way to Ligating Oligocyclopentadienyls: Synthesis and Preliminary Reactions of the Two Isomeric Tercyclopentadienyls and Their Transition Metal Complexes (C) 549
Terrein
- Synthesis of (+)-Terrein from L-Tartaric Acid (C) 67
Tetracarboxylic acids
- Cooperative Interactions in Molecular Recognition—the Binding of Diamines to a Tetracarboxylic Acid (C) 1148
Tetrachloroammonium hexafluoroarsenate
- Synthesis of Tetrachloroammonium Hexafluoroarsenate, $NCl_4^{\oplus}AsF_6^{\ominus}$ (C) 181
Tetraphenylallylsodium diethyl ether
- Tetraphenylallylsodium Diethyl Ether: A Contact Ion Pair with an Intramolecular $Na^{\oplus}$ Sandwich (C) 1042
Tetrasilylmethane
- Tetrasilylmethane, $C(SiH_3)_4$, the Si/C-Inverse of Tetramethylsilane, $Si(CH_3)_4$ (C) 201
Tetrazoles
- Zwitterions as Intermediates of the 1,3-

Dipolar Cycloaddition of Electrophilic Azides to 5-Alkylidenedihydrotetrazoles – the Other Non-Concerted Limiting Case (C) 695
Thallium compounds
– Synthesis of Two Tl^{III} Diacetonyl Compounds and Crystal Structure of $[Tl\{CH_2C(O)Me\}_2(\mu\text{-}CF_3SO_3)(bpy)]_2$ (C) 1125
Theoretical chemistry
– Experimental and Theoretical IR Spectra of the 2-Norbornyl Cation (C) 183
– Fractals and Related Hierarchical Models in Polymer Science (R) 113
Thermochemistry
– Thermochemical Data of Pure Substances. Parts I and II (B) 1491
Thiadiazolopyrazines
– 4,7-Dimethyl-4,7-dihydro[1,2,5]thiadiazolo[3,4-*b*]pyrazine, a Novel Electron Donor with a 12π-Electron Ring System (C) 643
Thienothiophenes
– Novel S-Heteroquinoid Electron Acceptors. Synthesis of 2,5-Bis(cyanoimino)-2,5-dihydrothieno[3,2-*b*]thiophenes (DCNTTs) and Conductive Charge Transfer Complexes (C) 204
Thin films
– Two-Dimensional Model Networks (R) 439
Thiophenes
– Facile Synthesis of 3-(ω-Haloalkyl)thiophenes as Key Building Blocks for Functionalized Thiophenes and Polythiophenes (C) 419
Tin compounds
– Chemistry of Tin (B) 1072
– Ge^{II} and Sn^{II} Complexes of [2.2.2]Paracyclophane with Threefold Internal η^6 Coordination (C) 1397
– Organotin Chemistry (B) 1072
– Organotin Compounds in Organic Synthesis (B) 1072
– Strong C–Sn Hyperconjugation in a Distannylmethyleneborane (C) 401
– Synthesis and Structure of $(NBu_4)[Sn\{Pt(\mu\text{-}Cl)(C_6F_5)_2\}_3]$, an Unusual Cluster with Three $Pt^{II}\rightarrow Sn^{II}$ Bonds (C) 1449
Titanium compounds
– Application of Titanacycles to Heterocycle Synthesis: Phospha- and Arsacyclobutenes (C) 75
– Base-Free Cationic 14-Electron Titanium and Zirconium Alkyls: In situ Generation, Solution Structures, and Olefin Polymerization Activity (C) 780
– (3,3-Diphenylallenylidene)trimethylphosphanetitanocene: The First Titanocene Carbene Complex with Three Cumulative Double Bonds (C) 1037
– Structure–Magnetism Relationship in $[Ti^{III}\text{-}O\text{-}Ti^{III}]^{4\oplus}$ Complexes (C) 68
– Synthesis and Structure of $Ph_2P(S)N = TiCl_2 \cdot 3C_5H_5N$, the First Imidotitanium Complex (C) 669
– Synthesis, Structure, and Reactivity of Aryloxo(imido)titanium Complexes (C) 664
Torands
– Torand Synthesis by Trimerization—New Receptors for Guanidinium (C) 923
Translation
– VCH TransDict, Übersetzersoftware, Version 2.2 (B) 937
Transmission electron microscopy
– Synthesis and Transmission Electron Microscopic Investigation of Bi(Pb)–Sr–Ca–Cu–O Superconductors (C) 1459
Transuranics
– Five Decades Ago: From the "Transuranics" to Nuclear Fission (R) 481
Triepoxides
– An Efficient Route to Linear Conjugated Triepoxides: *allo*-, *galacto*-, and *altro*-Type Trianhydrohexitols (C) 1038
Trimethylisopropylhexenone
– Sterically Hindered Internal Rotation in an Acyclic α,β-Unsaturated Ketone 2,2,5-Trimethyl-4-isopropylhex-4-en-3-one (C) 1435
Triquinanes
– Synthesis of Enantiomerically Pure (−)-Hypnophilin (C) 680
Tris(benzocyclobutadieno)benzene
– Facile Hydrogenation of the Central Cyclohexatriene of Tris(benzocyclobutadieno)benzene: Synthesis, Structure, and Thermal and Photochemical Isomerization of all-*cis*-Tris(benzocyclobuta)cyclohexane (C) 1151
Tropanes
– Grahamine, an Unusual Tropane Alkaloid from *Schizanthus grahamii* (C) 385
Tungsten compounds
– Alkyne Cleavage as a Novel Route to Low-Valent Carbyne-Metal Complexes (C) 207 (–)
– How Do Two C–C Double Bonds Add to One M–M Triple Bond? Structure and Bonding in Bis(η^2-ethylene)hexakis(neopentoxy)ditungsten (C) 1026
– Preparation and Structure of $[Se = W(PSe_4)(PSe_2)]^{2\ominus}$; a Cluster Containing a Heteroallylic $PSe_2^{\ominus}$ Unit (C) 1486
– Surprising Basicity of Low Valent Transition Metal Carbonyl Fluorides; Crystallographic Characterization of an sp^2-CH···F Hydrogen Bond (C) 888

Umpolung
– α-Umpolung of Ketones via Enol Radical Cations: A Mechanistic Study (C) 1144
Uranium compounds
– Synthesis of Phospholyltetrahydroboratouranium Complexes. Crystal Structure of $[(\eta^5\text{-}C_4Me_4P)_2U(BH_4)_2]$ (C) 1485
Urdamycins
– A Novel Type of Ring Contraction as Non-Enzymatic Step in the Later Stages of the Biosynthesis of Urdamycin H (C) 1051

Valenes
– Some Valenes of Benzannelated Five-Membered Heteroarenes – Synthesis and NMR Spectra (C) 675
Vanadium compounds
– Topologically Interesting Cages for Negative Ions with Extremely High "Coordination Number": An Unusual Property of V-O Clusters (C) 926
– Vanadium Tetrafluoride (C) 406
– Vanadium(-I) Dinitrogen Complexes with N_2 Coordinated End-on: Functional Models for the "Alternative Nitrogenase" (C) 1438
Viologenes
– Direct Electron Transfer between Carbon Electrodes, Immobilized Mediator and an Immobilized Viologen-accepting Pyridine Nucleotide Oxidoreductase (C) 1053
– Organometallic Host–Guest Systems Representing Novel Charge-Transfer "Ion Pairs" with Three-Dimensional Electron-Donor Networks (C) 1126
Vision
– The Chemistry of Vitamin A and Vision (R) 461
Vitamin A
– The Chemistry of Vitamin A and Vision (R) 461
Vitamins (B) 112

Wagner–Meerwein rearrangements
– A Wagner–Meerwein Rearrangement as Intermediate Step in the Formation of Dihydroindolones from 2-Diazoacetoacetanilides (C) 86
Wittig reactions
– New Benzyl(β-oxido)phosphorus and -arsenic Ylides: Reactivity and Stereoselectivity in the Wittig Reaction (C) 1454

Ylides
– New Benzyl(β-oxido)phosphorus and -arsenic Ylides: Reactivity and Stereoselectivity in the Wittig Reaction (C) 1454

Zeolites
– A Surface Organometallic Approach for Controlling the Pore Opening Size of Zeolites: the Case of Mordenite Modified via Grafting of Dineopentylmagnesium (C) 805
Zinc compounds
– Functional Tetrahedral Zinc Complexes (C) 898
– Synthesis and Structure of $[Et_2OZn(SC_6H_2tBu_3)_2]$, the First T-Shaped Zinc Complex (C) 1403
– $Zn^{II}Fe^{III}$ and $Fe^{II}Fe^{III}$ Complexes Containing a Novel (μ-Phenoxo)bis(μ-diphenylphosphato)dimetal(II,III) Core as Model Complexes for Active Sites of Purple Phosphatases (C) 531
Zintl anions
– $[BP_2]^{3\ominus}$ and $[BAs_2]^{3\ominus}$, Zintl Anions with Propadiene Structure (C) 65
Zirconium compounds
– Base-Free Cationic 14-Electron Titanium and Zirconium Alkyls: In situ Generation, Solution Structures, and Olefin Polymerization Activity (C) 780
– Enantioselective Catalysis with a New Zirconium Trichloride Lewis Acid Containing a "Dibornacyclopentadienyl" Ligand (C) 512
– Isotope Effects Associated with α-Olefin Insertion in Zirconocene-Based Polymerisation Catalysts: Evidence for an α-Agostic Transition State (C) 1413
– Stereo- and Regioselectivity of Chiral, Alkyl-substituted *ansa*-Zirconocene Catalysts in Methylalumoxane-activated Propene Polymerization (C) 279
Zwitterions
– Zwitterions as Intermediates of the 1,3-Dipolar Cycloaddition of Electrophilic Azides to 5-Alkylidenedihydrotetrazoles – the Other Non-Concerted Limiting Case (C) 695